JPL Publication **25-1**

Chemical Kinetics and Photochemical Data for Use in Atmospheric Studies

Evaluation Number 20

NASA Panel for Data Evaluation:

J. B. Burkholder
Chemical Sciences Laboratory
National Oceanic and Atmospheric Administration (NOAA)

R. L. Caravan
Argonne National Laboratory

R. E. Huie
National Institute of Standards and Technology

V. L. Orkin
National Institute of Standards and Technology

C. J. Percival
Jet Propulsion Laboratory
California Institute of Technology

R. Sander
Max-Planck Institute for Chemistry

S. P. Sander
Jet Propulsion Laboratory
California Institute of Technology

D. M. Wilmouth
Harvard University
National Science Foundation

National Aeronautics and Space Administration

Jet Propulsion Laboratory
California Institute of Technology
Pasadena, California

2025

The research carried out at the Jet Propulsion Laboratory, California Institute of Technology, was under a contract with the National Aeronautics and Space Administration (NASA) under the Atmospheric Composition Program. Other panel members acknowledge support from their funding institutions: JBB (NASA and NOAA), RS (MPIC), VLO (NASA and NIST), DMW (NASA and NSF) and RLCs contributions at Argonne National Laboratory were supported by the U.S. Department of Energy, Office of Science, Basic Energy Sciences, Division of Chemical Sciences, Geosciences and Biosciences under Contract No. DE-AC02-06CH1135.

Reference herein to any specific commercial product, process, or service by trade name, trademark, manufacturer, or otherwise, does not constitute or imply its endorsement by the United States Government or the Jet Propulsion Laboratory, California Institute of Technology. Copyright 2025, California Institute of Technology. U.S. Government sponsorship acknowledged.

ABSTRACT

This is the twentieth in a series of evaluated sets of rate coefficients, photochemical processes, heterogeneous parameters, and thermochemical parameters compiled by the NASA Panel for Data Evaluation.

The data are to be used to model stratospheric and upper tropospheric processes, with particular emphasis on the ozone layer and its possible perturbation by anthropogenic and natural phenomena and in support of foundational laboratory studies.

The evaluation is available in electronic form from the following Internet URL:

https://science.jpl.nasa.gov/projects/data-evaluation/

This evaluation should be cited as:

J. B. Burkholder, R. L. Caravan, R. E. Huie, V. L. Orkin, C. J. Percival, R. Sander, S. P. Sander, and D. M. Wilmouth "Chemical Kinetics and Photochemical Data for Use in Atmospheric Studies, Evaluation No. 20," JPL Publication 25-1, Jet Propulsion Laboratory, Pasadena, 2025, https://science.jpl.nasa.gov/projects/data-evaluation/

Dr. Stanley P. Sander May 11, 1953 – March 23, 2025



The members of the NASA Panel for Data Evaluation dedicate this publication in memory of our long-time friend and colleague, Dr. Stanley P. Sander. Stan dedicated more than five decades to atmospheric science at the Jet Propulsion Laboratory, beginning his JPL career as a graduate research assistant in 1971. A leading figure in atmospheric chemistry, Stan made foundational contributions to our understanding of stratospheric ozone depletion, tropospheric air pollution, and climate science related to greenhouse gases.

His pioneering work in laboratory measurements—particularly of reaction rate constants, spectroscopy, and photochemistry—was designed to forge consensus among often disparate measurements. His steadfast application of the scientific method was essential for furthering scientific research, as well as for providing sound advice for use in air quality management and environmental policies. His expertise extended beyond Earth's atmosphere, with studies of methane chemistry on Mars, halogens on Venus, and hydrocarbons in Titan's atmosphere.

His work spans major aspects of atmospheric chemistry—from chlorine, bromine, and nitrogen oxides to sulfur compounds and peroxy radicals. The rate constants, cross sections, and photochemical data produced in his lab form the cornerstone of atmospheric modeling crucial to the scientific foundation of the Montreal Protocol on Substances that Deplete the Ozone Layer. He played a central role in the NASA Data Evaluations since joining as a panel member in 1987 and chairing/co-chairing the panel since 2000. Stan's contributions were recognized with numerous honors, including two NASA Exceptional Achievement Medals, a NASA Exceptional Service Medal, and being elected as a fellow for both the American Geophysical Union and the American Association for the Advancement of Science.

Stan was a rare combination of scientific brilliance, humility, and kindness. He was not only a leader in his field, but also a generous collaborator and cherished mentor. Those of us fortunate enough to have worked with Stan will always remember his kindness-first approach and steadfast resolve in the face of challenges. His loss is profoundly felt by the scientific community and by all who had the privilege of working with him. His legacy, however, will endure in those he mentored and the substantial contributions he made to scientific knowledge.

TABLE OF CONTENTS

INTRODUCTION v

I.1 Basis of the Recommendations ix
I.2 Scope of the Evaluation ix
I.3 Format of the Evaluation ix
I.4 Document Access x
I.5 Data Formats x
I.6 Units x
I.7 Noteworthy Changes/Updates in this Evaluation x
I.8 Acknowledgements xi
I.9 Bibliography xii

SECTION 1. BIMOLECULAR REACTIONS ..... 1-1 – 1-450

SECTION 2. TERMOLECULAR REACTIONS ..... 2-1 – 2-89

SECTION 3. EQUILIBRIUM CONSTANTS ..... 3-1 – 3-30

SECTION 4. PHOTOCHEMICAL AND SCATTERING DATA ..... 4-1 – 4-481

SECTION 5. HETEROGENEOUS PROCESSES ..... 5-1 – 5-239

SECTION 6. AQUEOUS CHEMISTRY ..... 6-1 – 6-62

SECTION 7. THERMODYNAMIC PARAMETERS ..... 7-1 – 7-141

INTRODUCTION

This compilation of kinetic and photochemical data is the 20th evaluation prepared by the NASA Panel for Data Evaluation. The Panel was established in 1977 by the NASA Upper Atmosphere Research Program Office for the purpose of providing a critical tabulation of the latest kinetic and photochemical data for use by modelers in simulations of atmospheric chemistry. Table I-1 lists this publication's editions:

Table I-1: Editions of this Publication

	Edition	Reference
1	NASA RP 1010, Chapter 1	Hudson et al.[1]
2	JPL Publication 79-27	DeMore et al.[14]
3	NASA RP 1049, Chapter 1	Hudson and Reed[2]
4	JPL Publication 81-3	DeMore et al.[12]
5	JPL Publication 82-57	DeMore et al.[10]
6	JPL Publication 83-62	DeMore et al.[11]
7	JPL Publication 85-37	DeMore et al.[5]
8	JPL Publication 87-41	DeMore et al.[6]
9	JPL Publication 90-1	DeMore et al.[7]
10	JPL Publication 92-20	DeMore et al.[8]
11	JPL Publication 94-26	DeMore et al.[9]
12	JPL Publication 97-4	DeMore et al.[13]
13	JPL Publication 00-3	Sander et al.[19]
14	JPL Publication 02-25	Sander et al.[18]
15	JPL Publication 06-2	Sander et al.[17]
16	JPL Publication 09-31	Sander et al.[15]
17	JPL Publication 10-6	Sander et al.[16]
18	JPL Publication 15-10	Burkholder et al.[4]
19	JPL Publication 19-5	Burkholder et al.[3]
20	JPL Publication 25-1	Burkholder et al.

The current document is not available in printed form. Editions 12-present are available for download from https://science.jpl.nasa.gov/projects/data-evaluation/

Contributions to the evaluation from past panel members are gratefully acknowledged. Past panel members and years of contribution are listed in Table I-2.

Table I-2: Past Panel Members

Panel Member	Years of Contribution
D. M. Golden	1977–2011
M. J. Molina	1977–2006
W. B. DeMore	1977–2000
R. F. Hampson	1977–2000
R. T. Watson	1977–1985
J. J. Margitan	1977–1985
L. J. Stief	1977–1981
D. Garvin	1977
C. J. Howard	1979–1997
M. J. Kurylo	1979–2019
F. Kaufman	1979–1981
A. R. Ravishankara	1982–2006

C. E. Kolb	1992–2019
G. K. Moortgat	2000–2011
R. R. Friedl	2000–2011
B. J. Finlayson-Pitts	2002–2006
P. H. Wine	2006–2019
J. P. D. Abbatt	2010–2019
J. R. Barker	2010–2019
C. Cappa	2019
J. D. Crounse	2019
T. S. Dibble	2019

Panel members, and their major areas of contribution for the current evaluation are listed in Table I-3.

Table I-3: Panel Member Areas of Major Contribution in the Current Evaluation

Panel Member	Contribution
J. B. Burkholder, Chair	Editorial $O(^1D)$ reactions, NO_x reactions, IO_x reactions, Photochemical and Scattering Data
R. L. Caravan	Criegee intermediate chemistry
R. E. Huie	Advisory
V. L. Orkin	OH reactions with halocarbons and hydrogen halides
C. J. Percival	Furanoid reactions
R. Sander	Henry's Law coefficients
S. P. Sander	Advisory
D. M. Wilmouth	Photochemical and Scattering Data

Each panel member concentrates their efforts on a given area or type of data. Nevertheless, the Panel's final recommendations represent a consensus of the entire Panel. Each member reviews the basis for all recommendations and is cognizant of the final decision in every case.

Current Panel members affiliation and contact information

J. B. Burkholder
Chemical Sciences Laboratory, R/CSD5
National Oceanic and Atmospheric Administration (NOAA)
325 Broadway
Boulder, CO 80305-3328
James.B.Burkholder@noaa.gov

R. L. Caravan
Chemical Sciences & Engineering Divsion
Argonne National Laboratory
9700 S Cass Avenue, Building 200
Lemont, IL 60439
caravarl@anl.gov

R. E. Huie
Chemical and Biochemical Reference Data Division
National Institute of Standards and Technology (NIST)
100 Bureau Drive, Stop 8320
Gaithersburg, MD 20899-8320
rehuie@verizon.net

V. L. Orkin
Chemical and Biochemical Reference Data Division
National Institute of Standards and Technology (NIST)
100 Bureau Drive, Stop 8320
Gaithersburg, MD 20899-8320
Vladimir.Orkin@nist.gov

C. J. Percival
Jet Propulsion Laboratory
California Institute of Technology
M/S 183-901
4800 Oak Grove Drive
Pasadena, CA 91109
carl.j.percival@jpl.nasa.gov

R. Sander
Max-Planck Institute for Chemistry
PO Box 3060
55020 Mainz, Germany
rolf.sander@mpic.de

D. M. Wilmouth
Harvard University
12 Oxford Street
Cambridge, MA 02138
wilmouth@huarp.harvard.edu
National Science Foundation (NSF)
dwilmout@nsf.gov

I.1 Basis of the Recommendations

In so far as possible, all recommendations are based on peer-reviewed published laboratory measurements. Recommendations are not adjusted to fit observations of atmospheric concentrations. The Panel considers the question of consistency of data with expectations based on the theory of reaction kinetics, and when a discrepancy appears to exist this fact is pointed out in the accompanying note. The major use of theoretical extrapolation of data is in connection with three-body reactions, in which the required pressure or temperature dependence is sometimes unavailable from laboratory measurements, that can be estimated by use of appropriate theoretical treatment. In some cases where no experimental data are available, the Panel may provide estimates of rate coefficient parameters based on analogy to similar reactions for which data are available.

I.2 Scope of the Evaluation

In the past (releases 1-12 of this evaluation), it was the practice of the Panel to re-evaluate the entire set of reactions with individual Panel members taking responsibility for specific chemical families or processes. In more recent evaluations, the upper troposphere and lower stratosphere (UT/LS) have become the primary areas of focus for model calculations and atmospheric measurements related to studies of ozone depletion and climate change. Because the UT/LS is a region of relatively high chemical and dynamical complexity, a different approach was adopted for subsequent evaluation releases. Specifically, the entire reaction set of the data evaluation is no longer re-evaluated for each release. Instead, specific subsets are chosen for re-evaluation, with Panel members working to develop recommendations for a given area. This approach makes it possible to treat each subset in greater depth, to examine the consistency of the recommended parameters within a given chemical family, and to expand the scope of the evaluation to new areas. Each release will contain new evaluations, but also the recommendations for every process that has been considered in the past. In this way, each release constitutes a complete set of recommendations.

It is recognized that important new laboratory data may be published that lie outside the specific subset chosen for re-evaluation. In order to ensure that these important data receive prompt consideration, each evaluation may also have a "special topics" category. Feedback from the atmospheric modeling community is solicited in the selection of reactions for this category.

For the current evaluation, the evaluation subsets include the following:

$O(^1D)$ reactions
NO_x reactions
Halocarbon reactions
Furanoid reactions
Criegee reactions
IO_x reactions
Photochemical and Scattering Data
Gas-liquid solubility (Henry's Law Constants)

I.3 Format of the Evaluation

Changes or additions to the data tables are indicated by gray shading. A new entry is completely shaded, whereas a changed entry is shaded only where it has changed.

The notes associated with each entry are an essential component of the evaluation. Thus, the reader is strongly encouraged to consult these notes as they contain important information that could not conveniently be included in the Table of recommended parameters. In several cases,

the note for a bimolecular reaction contains a three-parameter Arrhenius expression that better represents the accepted experimental data over a broader temperature range than the two-parameter Arrhenius expression given in the table, whose applicability is limited to a narrower temperature range as indicated in the note. In the Table of Thermochemical Properties, values in the original units are often given. Table entries for some reactions provide rate coefficient recommendations for individual reaction channels. In this case, the recommendation for the total reaction rate constant is given separately.

Notes in Tables 1–3 and the photochemistry and scattering section include a "time stamp" indicating the latest revision date for changes to the recommendation or note as well as the date of the most recent evaluation. In some cases, a reaction may have undergone a complete re-evaluation without changes to the recommendation or note. For such reactions, the date of the evaluation will be updated even though the re-evaluation did not result in any changes.

I.4 Document Access

This document is available online at https://science.jpl.nasa.gov/projects/data-evaluation/ in PDF format. This document is not available in printed form. A sign-up for email notification of new releases and errata is available on this web site.

I.5 Data Formats

In Table 1 (Rate Coefficients for Bimolecular Reactions) the reactions are grouped into the classes O_x, HO_x, NO_x, Organic Compounds, FO_x, ClO_x, BrO_x, IO_x, SO_x, and Metal Reactions. The data in Table 2.1 (Rate Coefficients for Association Reactions) are presented in the same order as in the bimolecular reactions section. The presentation of photochemical cross section data follows the same sequence. Most of the major Heterogeneous Processes Section tables follow the O_x, HO_x, NO_x, Organic Compounds, FO_x, ClO_x, BrO_x, IO_x, SO_x, and Metal Reactions listing sequence for the gaseous uptake species. There are minor deviations that usually occur in the order of halogen atom containing gases or how reactants with more than one halogen species are listed. The same sequence of gaseous heterogeneous reactants, with minor exceptions, is used in listing gas/surface mass accommodation and other reversible gas uptake coefficients, gas/surface reactive uptake kinetics and Henry's Law Constants for pure water, aqueous acids, and sea water or sea water simulations.

I.6 Units

Rate coefficients, k, are given in units of concentration expressed as molecules per cubic centimeter and time in seconds. That is, for first-, second-, and third-order reactions, units of k are s^{-1}, cm^3 $molecule^{-1}$ s^{-1}, and cm^6 $molecule^{-2}$ s^{-1}, respectively. Absorption cross sections are expressed as cm^2 $molecule^{-1}$, base e. For reactions in the aqueous phase, following the convention in that area of study, we use the concentration units mol L^{-1}. Thus, second-order rate constants are in units of L mol^{-1} s^{-1}. Thermodynamic quantities are expressed in units of Joules and moles. Thus, enthalpies are given in units of kJ mol^{-1} and entropies in units of J K^{-1} mol^{-1}. Henry's Law constants are given in units of mol L^{-1} atm^{-1}.

I.7 Noteworthy Changes/Updates in this Evaluation

1.7.1 Bimolecular Reactions (Section 1)

On the basis of an additional study, recommendations for the N + NO and NO_2 reactions and uncertainty estimates were revised and updated.

Several key OH + furanoid reactions were added to the evaluation.

Criegee intermediate reactions, in particular for *anti*- and *syn*-CH_3CHOO, have been updated or added to the evaluation.

A review and update of numerous FO_x and ClO_x reactions was conducted with an emphasis on halocarbon reactions. Many recommendations are based, in part, on studies using relative rate methods. In cases where significant revisions have been made to the recommended reference rate coefficient parameters after publication of the original study, rate coefficient recommendations given here were revised accordingly.

The O + CH_3I and CF_3I reactions were added to the evaluation.

Estimated uncertainty in several Metal reactions were revised.

1.7.2 Termolecular Reactions (Section 2)

No change

1.7.3 Equilibrium Constants (Section 3)

No change

1.7.4 Photochemical and Scattering Data (Section 4)

Fourteen molecules have been added to the photochemical data recommendations. In addition, numerous updates to the notes/recommendations were made throughout the section as indicated in Table 4-1.

A new section of Rayleigh scattering cross section recommendations for Ar, CH_4, CO_2, He, N_2, N_2O, O_2, and SF_6 was added.

1.7.5 Heterogeneous Processes (Section 5)

Henry's law recommendations were reviewed, expanded, and updated.

The section has been re-organized into Non-Equilibrium, Equilibrium, and Optical sub-sections.

1.7.6 Aqueous Chemistry (Section 6)

No change

1.7.7 Thermodynamic Parameters (Section 7)

No change

I.8 Acknowledgement

This work was supported in part by the NASA Atmospheric Composition Program.

I.9 Bibliography

(1) Chlorofluoromethanes and the Stratosphere. In *NASA Reference Publication 1010*; Hudson, R. D., Ed.; NASA: Washington, D.C, 1977.

(2) The Stratosphere: Present and Future. In *NASA Reference Publication 1049*; Hudson, R. D., Reed, E. I., Eds.; NASA: Washington, D.C, 1979.

(3) Burkholder, J. B.; Sander, S. P.; Abbatt, J.; Barker, J. R.; Cappa, C.; Crounse, J. D.; Dibble, T. S.; Huie, R. E.; Kolb, C. E.; Kurylo, M. J.; Orkin, V. L.; Percival, C. J.; Wilmouth, D. M.; Wine, P. H. Chemical Kinetics and Photochemical Data for Use in Atmospheric Studies, Evaluation No. 19, Jet Propulsion Laboratory Pasadena, CA, JPL Publication 19-5, **2019**, https://science.jpl.nasa.gov/projects/data-evaluation/.

(4) Burkholder, J. B.; Sander, S. P.; Abbatt, J. P. D.; Barker, J. R.; Huie, R. E.; Kolb, C. E.; Kurylo, M. J.; Orkin, V. L.; Wilmouth, D. M.; Wine, P. H. Chemical Kinetics and Photochemical Data for Use in Atmospheric Studies, Evaluation No. 18, Jet Propulsion Laboratory Pasadena, CA, JPL Publication 15-10, **2015**, https://science.jpl.nasa.gov/projects/data-evaluation/.

(5) DeMore, W. B.; Golden, D. M.; Hampson, R. F.; Howard, C. J.; Kurylo, M. J.; Margitan, J. J.; Molina, M. J.; Ravishankara, A. R.; Watson, R. T. Chemical Kinetics and Photochemical Data for Use in Stratospheric Modeling, Evaluation Number 7. **1985**.

(6) DeMore, W. B.; Golden, D. M.; Hampson, R. F.; Howard, C. J.; Kurylo, M. J.; Molina, M. J.; Ravishankara, A. R.; Sander, S. P. Chemical Kinetics and Photochemical Data for Use in Stratospheric Modeling, Evaluation Number 8. **1987**.

(7) DeMore, W. B.; Golden, D. M.; Hampson, R. F.; Howard, C. J.; Kurylo, M. J.; Molina, M. J.; Ravishankara, A. R.; Sander, S. P. Chemical Kinetics and Photochemical Data for Use in Stratospheric Modeling, Evaluation Number 9. **1990**.

(8) DeMore, W. B.; Golden, D. M.; Hampson, R. F.; Howard, C. J.; Kurylo, M. J.; Molina, M. J.; Ravishankara, A. R.; Sander, S. P. Chemical Kinetics and Photochemical Data for Use in Stratospheric Modeling, Evaluation Number 10. **1992**.

(9) DeMore, W. B.; Golden, D. M.; Hampson, R. F.; Howard, C. J.; Kurylo, M. J.; Molina, M. J.; Ravishankara, A. R.; Sander, S. P. Chemical Kinetics and Photochemical Data for Use in Stratospheric Modeling, Evaluation Number 11. **1994**.

(10) DeMore, W. B.; Golden, D. M.; Hampson, R. F.; Howard, C. J.; Kurylo, M. J.; Molina, M. J.; Ravishankara, A. R.; Watson, R. T. Chemical Kinetics and Photochemical Data for Use in Stratospheric Modeling, Evaluation Number 5. **1982**.

(11) DeMore, W. B.; Golden, D. M.; Hampson, R. F.; Howard, C. J.; Kurylo, M. J.; Molina, M. J.; Ravishankara, A. R.; Watson, R. T. Chemical Kinetics and Photochemical Data for Use in Stratospheric Modeling, Evaluation Number 6. **1983**.

(12) DeMore, W. B.; Golden, D. M.; Hampson, R. F.; Kurylo, M. J.; Margitan, J. J.; Molina, M. J.; Stief, L. J.; Watson, R. T. Chemical Kinetics and Photochemical Data for Use in Stratospheric Modeling, Evaluation Number 4. **1981**.

(13) DeMore, W. B.; Sander, S. P.; Golden, D. M.; Hampson, R. F.; Kurylo, M. J.; Howard, C. J.; Ravishankara, A. R.; Kolb, C. E.; Molina, M. J. Chemical Kinetics and Photochemical Data for Use in Stratospheric Modeling, Jet Propulsion Laboratory, California Institute of Technology Pasadena, CA, JPL Publication 97-4, **1997**, https://science.jpl.nasa.gov/projects/data-evaluation/.

(14) DeMore, W. B.; Stief, L. J.; Kaufman, F.; Golden, D. M.; Hampson, R. F.; Kurylo, M. J.; Margitan, J. J.; Molina, M. J.; Watson, R. T. Chemical Kinetics and Photochemical Data for Use in Stratospheric Modeling, Evaluation Number 2. **1979**.

(15) Sander, S. P.; Abbatt, J. P. D.; Barker, J. R.; Burkholder, J. B.; Friedl, R. R.; Golden, D. M.; Huie, R. E.; Kolb, C. E.; Kurylo, M. J.; Moortgat, G. K.; Orkin, V. L.; Wine, P. H. Chemical Kinetics and Photochemical Data for Use in Atmospheric Studies, Evaluation No. 16, Jet Propulsion Laboratory Pasadena, CA, JPL Publication 09-31, **2009**, https://science.jpl.nasa.gov/projects/data-evaluation/.

(16) Sander, S. P.; Abbatt, J. P. D.; Barker, J. R.; Burkholder, J. B.; Friedl, R. R.; Golden, D. M.; Huie, R. E.; Kolb, C. E.; Kurylo, M. J.; Moortgat, G. K.; Orkin, V. L.; Wine, P. H. Chemical Kinetics and Photochemical Data for Use in Atmospheric Studies, Evaluation No. 17, Jet Propulsion Laboratory Pasadena, CA, JPL Publication 10-6, **2011**, https://science.jpl.nasa.gov/projects/data-evaluation/.

(17) Sander, S. P.; Finlayson-Pitts, B. J.; Friedl, R. R.; Golden, D. M.; Huie, R. E.; Keller-Rudek, H.; Kolb, C. E.; Kurylo, M. J.; Molina, M. J.; Moortgat, G. K.; Orkin, V. L.; Ravishankara, A. R.; Wine, P. H. Chemical Kinetics and Photochemical Data for Use in Atmospheric Studies, Evaluation Number 15, Jet Propulsion Laboratory Pasadena, CA, JPL Publication 06-2, **2006**, https://science.jpl.nasa.gov/projects/data-evaluation/.

(18) Sander, S. P.; Finlayson-Pitts, B. J.; Friedl, R. R.; Golden, D. M.; Huie, R. E.; Kolb, C. E.; Kurylo, M. J.; Molina, M. J.; Moortgat, G. K.; Orkin, V. L.; Ravishankara, A. R. Chemical Kinetics and Photochemical Data for Use in Atmospheric Studies, Evaluation Number 14, Jet Propulsion Laboratory Pasadena, CA, JPL Publication 02-25, **2002**, https://science.jpl.nasa.gov/projects/data-evaluation/.

(19) Sander, S. P.; Friedl, R. R.; DeMore, W. B.; Golden, D. M.; Kurylo, M. J.; Hampson, R. F.; Huie, R. E.; Moortgat, G. K.; Ravishankara, A. R.; Kolb, C. E.; Molina, M. J. Chemical Kinetics and Photochemical Data for Use in Stratospheric Modeling, Evaluation Number 13, Jet Propulsion Laboratory, California Institute of Technology Pasadena, CA, JPL Publication 00-3, **2000**, https://science.jpl.nasa.gov/projects/data-evaluation/.

SECTION 1. BIMOLECULAR REACTIONS

Table of Contents

SECTION 1. BIMOLECULAR REACTIONS 1-1
1.1 Introduction 1-3
1.2 The Evaluation Procedure 1-4
1.3 Uncertainty Estimates 1-4
Rate Constants for Bimolecular Reactions
1.4 O_x Reactions 1-6
1.4.1 Table 1A: O_x Reactions 1-6
1.4.2 Notes: O_x Reactions 1-6
1.4.3 Bibliography – O_x Reactions 1-6
1.5 $O(^1D)$ Reactions 1-7
1.5.1 Table 1A: $O(^1D)$ Reactions 1-7
1.5.2 Notes: $O(^1D)$ Reactions 1-15
1.5.3 Bibliography – $O(^1D)$ Reactions 1-39
1.6 Singlet O_2 Reactions 1-43
1.6.1 Table 1A: Singlet O_2 Reactions 1-43
1.6.2 Notes: Singlet O_2 Reactions 1-44
1.6.3 Bibliography - Singlet O_2 Reactions 1-51
1.7 HO_x Reactions 1-54
1.7.1 Table 1B: HO_x Reactions 1-54
1.7.2 Notes: HO_x Reactions 1-55
1.7.3 Bibliography – HO_x Reactions 1-65
1.8 NO_x Reactions 1-71
1.8.1 Table 1C: NO_x Reactions 1-71
1.8.2 Notes: NO_x Reactions 1-73
1.8.3 Bibliography – NO_x Reactions 1-87
1.9 Reactions of Organic Compounds 1-95
1.9.1 Table 1D: Reactions of Organic Compounds 1-95
1.9.2 Notes: Reactions of Organic Compounds 1-101
1.9.3 Bibliography – Reactions of Organic Compounds 1-166
1.10 FO_x Reactions 1-190
1.10.1 Table 1E: FO_x Reactions 1-190
1.10.2 Notes: FO_x Reactions 1-196
1.10.3 Bibliography – FO_x Chemistry 1-239
1.11 ClO_x Reactions 1-250
1.11.1 Table 1F: ClO_x Reactions 1-250
1.11.2 Notes: ClO_x Reactions 1-258
1.11.3 Bibliography – ClO_x Reactions 1-317
1.12 BrO_x Reactions 1-338
1.12.1 Table 1G: BrO_x Reactions 1-338
1.12.2 Notes: BrO_x Reactions 1-341
1.12.3 Bibliography – BrO_x Reactions 1-360
1.13 IO_x Reactions 1-366
1.13.1 Table 1H: IO_x Reactions 1-366

1.13.2 Notes: IO_x Reactions 1-368
1.13.3 Bibliography – IO_x Reactions 1-377
1.14 SO_x Reactions 1-380
1.14.1 Table 1I: SO_x Reactions 1-380
1.14.2 Notes: SO_x Reactions 1-386
1.14.3 Bibliography – SO_x Reactions 1-429
1.15 Metal Reactions 1-443
1.15.1 Table 1J: Metal Reactions 1-443
1.15.2 Notes: Metal Reactions 1-445
1.15.3 Bibliography – Metal Reactions 1-450

1.1 Introduction

In Table 1 (Rate Constants for Bimolecular Reactions) the evaluated reactions are grouped into the classes O_x, $O(^1D)$, Singlet O_2, HO_x, NO_x, Organic Compounds, FO_x, ClO_x, BrO_x, IO_x, SO_x, and Metals. Some of the reactions in Table 1 are actually more complex than simple two-body, bimolecular, reactions. To explain the pressure and temperature dependences occasionally measured in reactions of this type, it is necessary to consider the bimolecular class of reactions in terms of two subcategories, direct (concerted) and indirect (nonconcerted) reactions.

A direct, or concerted, bimolecular reaction is one in which the reactants A and B proceed to products C and D without the intermediate formation of an AB adduct that has appreciable bonding, i.e., there is no bound intermediate; only the transition state $[AB]^{\#}$ lies between reactants and products.

$$A + B \rightarrow [AB]^{\#} \rightarrow C + D$$

The reaction of OH with CH_4 forming $H_2O + CH_3$ is an example of a reaction of this class.

The rate constants for these reactions can, in general, be reasonably well represented by the Arrhenius expression:

$$k(T) = A \times \exp(-E/RT)$$

over the temperature range of atmospheric interest. Very useful correlations between the expected structure of the transition state $[AB]^{\#}$ and the Arrhenius A-factor of the reaction rate constant can be made, especially in reactions that are constrained to follow a well-defined approach of the two reactants in order to minimize energy requirements in the making and breaking of bonds. The recommended parameters, A and E/R, are given in Table 1, as discussed below, and the applicable temperature range is discussed in the corresponding reaction note. Note that not all reactions have experimental rate constant data that covers the entire range of temperatures found in the troposphere and stratosphere. Rate constants for reactions of this type are not pressure dependent.

However, even for this class of reactions, deviation in the temperature dependence from the simple Arrhenius expression mentioned above may be apparent over the full range of the experimental data considered in the evaluation, and even over the more limited temperature range used to derive the Arrhenius expression recommendation. Deviation from Arrhenius behavior is typically exhibited as curvature in the Arrhenius plot - a concave upward curvature in $\ln(k(T))$ versus 1/T. There are several possible factors that may contribute to this curvature such as multiple reaction channels, the existence of reactant conformers, tunneling, and others. In cases where curvature was experimentally resolved, the reaction note includes the temperature range over which the Arrhenius parameters given in Table 1 are applicable and a recommended three-parameter expression may also be provided in the form:

$$k(T) = A \times (T/298)^n \times \exp(-E/RT)$$

where n is a fit parameter, that better represents the overall temperature dependence.

The indirect or nonconcerted class of bimolecular reactions is characterized by a more complex reaction path involving a potential well between reactants and products, leading to a bound adduct (or reaction complex) formed between the reactants A and B:

$$A + B \leftrightarrow [AB]^* \rightarrow C + D$$

The intermediate $[AB]^*$ is different from the transition state $[AB]^{\#}$, in that its lifetime substantially exceeds the characteristic time of intermolecular vibrations and, thus, it is considered a bound molecule. Of course, transition states are involved in all reactions, both forward and backward, but are not explicitly shown in the equation above. An example of a reaction of this class is $ClO + NO$, which normally produces $Cl + NO_2$. Reactions of the nonconcerted type can have more complex temperature dependences and can exhibit a pressure dependence if the lifetime of $[AB]^*$ is comparable to the rate of its collisional deactivation. This arises because the relative rate at which a complex $[AB]^*$ decomposes to products C + D or back to reactants A + B is a sensitive function of its internal energy. Thus, in reactions of this type, the distinction between the bimolecular and termolecular classification becomes less meaningful, and it is especially necessary to study such reactions under the temperature and pressure conditions in which they are to be used in model calculations, or, alternatively, to develop reliable theoretical bases for extrapolation of the experimental data. In several cases where sufficient data exist, reactions of this type are treated in Section 2 and included in the corresponding table for termolecular reactions.

As mentioned above, the recommended rate constant tabulation for bimolecular reactions (Table 1) is given in Arrhenius form, $k(T) = A \times \exp(-E/RT)$, and contains the following information:

1. Reaction stoichiometry and products (if known)

2. Temperature range of available kinetic data, not necessarily the temperature range for the recommended Arrhenius parameters
3. Arrhenius *A*-factor: ***A***
4. Recommended temperature dependence ("activation temperature"): ***E*/R**
5. Recommended rate constant at 298 K: ***k*(298 K)**
6. Rate constant uncertainty factor at 298 K: ***f*(298 K)** (see below)
7. A parameter used to calculate the rate constant uncertainty at temperatures other than 298 K: ***g*** (see below)
8. Index for a detailed note containing references to the literature, the basis of recommendation and, in several cases, alternative methods to calculate the rate constant

For a few reactions, the recommendations for *A*, *E*/R and *k*(298 K) are italicized in blue font. These represent estimates by the Panel in cases where there are either no literature data, where the existing data are judged to be of insufficient quality to base a recommendation, or where the recommendation is based on an extrapolation of very limited experimental data.

1.2 The Evaluation Procedure

The process of evaluating chemical kinetic data does not conform to a simple set of mathematical rules. There is no "one size fits all" algorithm that can be applied and each reaction must be examined on a case-by-case basis. Consideration of uncertainties in the kinetic and photochemical parameters used in atmospheric models plays a key role in determining the reliability of and uncertainty in the model results. Quite often the cause(s) of differences in experimental results from various laboratories can't be determined with confidence and making recommendations for the uncertainties of the rate constant is often more difficult than for making recommendations of the Arrhenius parameters themselves. In many cases, investigators suggest possible qualitative reasons for disagreements among datasets. Thus, data evaluators necessarily must consider a variety of factors in assigning a recommendation, including such aspects as the chemical complexity of the system, sensitivities and shortcomings of the experimental techniques employed, similarities or trends in reactivity, and the level of agreement among studies using different techniques.

A recommendation for *k*(298 K) is typically made by averaging the rate constants from those studies deemed to be of sufficiently high quality / reliability and free from chemical interferences that could have biased the results. In cases where a study provides reliable data over a range of temperatures of atmospheric interest, the value of *k*(298 K) used in the averaging process may have been obtained from a weighted non-linear least-squares fit of *k*(T) versus T. The reported data are either weighted using the reported uncertainties or equal relative uncertainties are assigned to the data at the different temperatures. In deriving a recommended Arrhenius temperature dependence (*E*/R), the selected data sets are examined to ascertain the temperature range over which a standard Arrhenius fit to the data provides an adequate representation. Each data set is then scaled by a constant factor so that the Arrhenius expressions describing the individual data sets give the recommended *k*(298 K) and a weighted non-linear least-squares fit to all of these scaled data is then made. This process helps avoid biases resulting from systematic errors associated with an individual data set or from the fact that the individual data sets may have been obtained over significantly different temperature ranges. In cases where the selected data sets have been obtained over similar ranges of temperature, a fit to the combined scaled data often yields a value for *E*/R not very different from that obtained by averaging the *E*/R values from the individual studies. The recommended Arrhenius pre-exponential factor "A" is then calculated based on the recommended values for *k*(298 K) and *E*/R. Results from relative rate measurements are recalculated using the currently recommended rate constants for the reference reactions.

1.3 Uncertainty Estimates

The parameters *f*(298 K) and *g* given in Table 1 can be used to calculate an estimated rate constant uncertainty at any given temperature, corresponding to approximately one standard deviation, from the following expression:

$$f(\mathrm{T}) = f(298\ \mathrm{K})\exp\left|g\left(\frac{1}{\mathrm{T}} - \frac{1}{298}\right)\right|$$

where the exponent is an absolute value.

Note that, since *f*(298 K) and *g* have been defined to correspond to approximately one standard deviation, *f*(T) yields a similar uncertainty interval. The more commonly used 95% confidence limits at a given temperature can be obtained by multiplying and dividing the recommended value of the rate constant at that temperature by the factor

f^2(T). It should be emphasized that the parameter g has been defined exclusively for use with f(298 K) in the above expression and should not be interpreted as the uncertainty in the Arrhenius activation temperature (E/R). Thus, the assignment of g is dependent on the value selected for f(298 K). For example, reactions for which f(298 K) is rather large may require only a small value of g to represent an adequate total rate constant uncertainty at other temperatures.

The uncertainty factor f(298 K), corresponding to approximately one standard deviation in the case of normally distributed data, was typically assigned such that all of the data used in deriving the average are encompassed within the band derived by multiplying and dividing k(298 K) by f^2(298 K), i.e., two standard deviations, which is considered a 95% confidence interval for the evaluation. In some cases, a slightly higher value of f(298 K) may be recommended to encompass outlying data that were not used in the averaging, but could not be entirely rejected. The uncertainty factor "g" was then selected for use in the f(T) expression described below such that f^2(T) encompasses all of the data used in the evaluation over the temperature range of the recommendation. Neither f(298 K) nor g is derived from a rigorous statistical treatment of the available data, which generally are too limited to permit such analyses, and more importantly, do not follow a normal statistical distribution. Rather, the uncertainty estimation is based on knowledge of the techniques, the difficulties of the experiments, and the potential for systematic errors.

This approach is based on the fact that rate constants are typically known with greater certainty at room temperature where the experimental data are more abundant and often more reliable. The overall uncertainty normally increases at other temperatures where there are fewer data. In addition, data obtained at temperatures significantly different from 298 K may be less accurate than at room temperature due to experimental difficulties or complications.

The uncertainty represented by f(T) is normally symmetric; i.e., the rate constant may be greater than or less than the recommended value, k(T), by the factor f(T). In a few cases in Table 1 asymmetric uncertainties are given. For these cases, the factors by which a rate constant is to be multiplied or divided to obtain, respectively, the upper and lower limits are not equal.

Finally, it is not possible to quantify "unknown" errors. The spread in results among different techniques for a given reaction may provide some basis for an uncertainty estimate, but the possibility of the same, or compensating, systematic errors in all the studies can't be disregarded. Comparisons among rate constants recommended for similar reactions or for reactions within a homologous series of compounds can also help in the assignment of uncertainty factors. For measurements subject to large systematic errors, the true rate constant may be much further from the recommended value than would be expected and allowed for with any reasonable values of f(T) based on the data available for the evaluation. For example, there have been cases in the past where the recommended rate constants have changed by factors well outside of the uncertainties that had been assigned in the absence of quantitative knowledge of systematic errors. However, as experimental techniques improve together with improved understanding of various reactive processes and with significant expansion of the kinetic and thermodynamic database for the recommendations, exceptionally large changes are becoming less likely.

Rate Constants for Bimolecular Reactions

1.4 O_x Reactions

1.4.1 Table 1A: O_x Reactions

Reaction	Temperature Range of Exp. Data(K) [a]	*A*-Factor	*E*/R	*k*(298 K) [b]	*f*(298 K) [c]	*g* [c]	Note
$O + O_2 \xrightarrow{M} O_3$		(See Table 2-1)					
$O + O_3 \rightarrow O_2 + O_2$	220–409	8.0×10^{-12}	2060	8.0×10^{-15}	1.10	200	A1

[a] Temperature range of available experimental data. This is not necessarily the range of temperature over which the recommended Arrhenius parameters are applicable. See the corresponding note for that information.

[b] Units are cm^3 $molecule^{-1}$ s^{-1}.

[c] *f*(298 K) is the uncertainty factor at 298 K. To calculate the uncertainty at other temperatures, use the expression:

$$f(\mathrm{T}) = f(298\ \mathrm{K})\exp\left|g\left(\frac{1}{\mathrm{T}} - \frac{1}{298}\right)\right|$$

Note that the exponent is an absolute value.

1.4.2 Notes: O_x Reactions

A1. **$O + O_3$**. The recommended rate expression is from Wine et al.[5] and is a linear least-squares fit of all data (unweighted) from Davis et al.,[2] McCrumb and Kaufman,[3] West et al.,[4] Arnold and Comes,[1] and Wine et al.[5] (Table: 83-62, Note: 83-62, Evaluation: 10-6)

(1) Arnold, I.; Comes, F. J. Temperature dependence of the reactions $O(^3P) + O_3 \rightarrow 2O_2$ and $O(^3P) + O_2 + M \rightarrow O_3 + M$. *Chem. Phys.* **1979**, *42*, 231-239, doi:10.1016/0301-0104(79)85182-4.

(2) Davis, D. D.; Wong, W.; Lephardt, J. A laser flash photolysis-resonance fluorescence kinetic study: Reaction of $O(^3P)$ with O_3. *Chem. Phys. Lett.* **1973**, *22*, 273-278, doi:10.1016/0009-2614(73)80091-0.

(3) McCrumb, J. L.; Kaufman, F. Kinetics of the $O + O_3$ reaction. *J. Chem. Phys.* **1972**, *57*, 1270-1276, doi:10.1063/1.1678386.

(4) West, G. A.; Weston, R. E., Jr.; Flynn, G. W. The influence of reactant vibrational excitation on the $O(^3P) + O_3^{\dagger}$ bimolecular reaction rate. *Chem. Phys. Lett.* **1978**, *56*, 429-433, doi:10.1016/0009-2614(78)89008-3.

(5) Wine, P. H.; Nicovich, J. M.; Thompson, R. J.; Ravishankara, A. R. Kinetics of $O(^3P_J)$ reactions with H_2O_2 and O_3. *J. Phys. Chem.* **1983**, *87*, 3948-3954, doi:10.1021/j100243a030.

1.5 $O(^1D)$ Reactions

1.5.1 Table 1A: $O(^1D)$ Reactions

Reaction	Branching Ratio [a]	Temperature Range of Exp. Data (K) [b]	Total Rate Coefficient: $O(^1D)$ Loss [c]					Note
			A-Factor [d]	*E*/R	*k*(298 K) [d]	*f*(298 K) [e]	*g* [e]	
$O(^1D)$ Reactions								A2
$O(^1D) + O_2$		104–424	3.3×10^{-11}	–55	3.95×10^{-11}	1.10	10	
$\rightarrow O(^3P) + O_2$	*0*							A3
$\rightarrow O(^3P) + O_2(^1\Sigma)$	0.80 ± 0.20							
$\rightarrow O(^3P) + O_2(^1\Delta)$	*0.20 (0.40-0)*							
$O(^1D) + O_3$		103–393	2.4×10^{-10}	0	2.4×10^{-10}	1.20	0	
$\rightarrow O(^3P) + O_3$	*0*							A4
$\rightarrow O_2 + O_2$	0.50 ± 0.03							
$\rightarrow O_2 + O(^3P) + O(^3P)$	0.50 ± 0.03							
$O(^1D) + H_2$		204–420	1.2×10^{-10}	0	1.2×10^{-10}	1.15	0	
$\rightarrow O(^3P) + H_2$	*<0.01*							A5
$\rightarrow OH + H$	$1.0\ ^{+0}_{-0.01}$							
$O(^1D) + H_2O$		217–453	1.74×10^{-10}	–45	2.02×10^{-10}	1.15	20	
$\rightarrow O(^3P) + H_2O$	<0.003							A6
$\rightarrow O_2 + H_2$	0.006 ± 0.006							
$\rightarrow OH + OH$	$1.0\ ^{+0}_{-0.015}$							
$O(^1D) + N_2$		104–673	2.15×10^{-11}	–110	3.1×10^{-11}	1.10	20	
$\rightarrow O(^3P) + N_2$	1.0							A7
$O(^1D) + N_2 \xrightarrow{M} N_2O$	(See Table 2-1)							
$O(^1D) + N_2O$		195–719	1.19×10^{-10}	–20	1.27×10^{-10}	1.10	25	
$\rightarrow O(^3P) + N_2O$	*<0.01*							A8
$\rightarrow N_2 + O_2$	0.39 (0.36-0.42)							
$\rightarrow NO + NO$	0.61 ± 0.03							
$O(^1D) + NH_3$		204–354	2.5×10^{-10}	0	2.5×10^{-10}	1.20	25	
$\rightarrow O(^3P) + NH_3$	*0*							A9
$\rightarrow$ Products	*1.0*							

Reaction	Branching Ratio [a]	Temperature Range of Exp. Data (K) [b]	Total Rate Coefficient: $O(^1D)$ Loss [c]					Note
			A-Factor [d]	*E*/R	*k*(298 K) [d]	*f*(298 K) [e]	*g* [e]	
$O(^1D) + HCN$ $\rightarrow O(^3P) + HCN$ $\rightarrow$ Products	 0.15×exp(200/T) 0.93×exp(-82/T)	193–430	1.08×10^{-10}	–105	1.54×10^{-10}	1.20	0	A10
$O(^1D) + CH_3CN$ $\rightarrow O(^3P) + CH_3CN$ $\rightarrow$ Products	 $0.035\ ^{+0.05}_{-0.035}$ $0.965\ ^{+0.035}_{-0.05}$	193–430	2.35×10^{-10}	0	2.35×10^{-10}	1.20	0	A11
$O(^1D) + CO_2$ $\rightarrow O(^3P) + CO_2$	 $1.0\ ^{+0}_{-0.01}$	195–370	7.5×10^{-11}	–115	1.1×10^{-10}	1.15	20	A12
$O(^1D) + CH_4$ $\rightarrow O(^3P) + CH_4$ $\rightarrow CH_3 + OH$ $\rightarrow CH_3O$ or $CH_2OH + H$ $\rightarrow CH_2O + H_2$	 <0.005 0.75 ± 0.15 0.20 ± 0.10 0.05 ± 0.05	198–413	1.75×10^{-10}	0	1.75×10^{-10}	1.15	5	A13
$O(^1D) + HCl$ $\rightarrow O(^3P) + HCl$ $\rightarrow H + ClO$ $\rightarrow Cl + OH$	 0.12 ± 0.04 0.20 ± 0.05 0.68 (0.63-0.73)	199–379	1.5×10^{-10}	0	1.5×10^{-10}	1.10	25	A14
$O(^1D) + HF$ $\rightarrow O(^3P) + HF$ $\rightarrow F + OH$	 0.70 ± 0.05 0.30 ± 0.05	298	*5.0×10^{-11}*	*0*	5.0×10^{-11}	1.50	25	A15
$O(^1D) + NF_3$ $\rightarrow O(^3P) + NF_3$ $\rightarrow$ Products	 $0.07^{+0.21}_{-0.07}$ $0.93^{+0.07}_{-0.21}$	199–356	2.0×10^{-11}	–44	2.3×10^{-11}	1.10	0	A16
$O(^1D) + HBr$ $\rightarrow O(^3P) + HBr$ $\rightarrow H + BrO$ $\rightarrow Br + OH$	 0.20 ± 0.07 0.20 ± 0.04 0.60 (0.49-0.71)	297	*1.5×10^{-10}*	*0*	1.5×10^{-10}	1.50	25	A17
$O(^1D) + Cl_2$ $\rightarrow O(^3P) + Cl_2$ $\rightarrow Cl + ClO$	 0.25 ± 0.10 0.75 ± 0.07	298	2.7×10^{-10}	*0*	2.7×10^{-10}	1.10	25	A18
$O(^1D) + CCl_2O$ $\rightarrow O(^3P) + CCl_2O$ $\rightarrow$ Products	 0.20 ± 0.04 0.80 ± 0.04	194–429	2.2×10^{-10}	–30	2.4×10^{-10}	1.10	25	A19

Reaction	Branching Ratio [a]	Temperature Range of Exp. Data (K) [b]	Total Rate Coefficient: $O(^1D)$ Loss [c]					Note
			A-Factor [d]	*E*/R	*k*(298 K) [d]	*f*(298 K) [e]	*g* [e]	
$O(^1D) + CClFO$		298	*1.9×10⁻¹⁰*	*0*	*1.9×10⁻¹⁰*	1.50	25	
$\rightarrow O(^3P) + CClFO$	*0.20*							A20
$\rightarrow$ Products	*0.80*							
$O(^1D) + CF_2O$		298	*7.4×10⁻¹¹*	*0*	7.4×10⁻¹¹	1.50	25	
$\rightarrow O(^3P) + CF_2O$	0.35							A21
$\rightarrow$ Products	0.65 ± 0.10							
$O(^1D) + CH_3Cl$		298	*2.6×10⁻¹⁰*	*0*	2.6×10⁻¹⁰	1.30	50	
$\rightarrow O(^3P) + CH_3Cl$	0.10							
$\rightarrow ClO$ + Products	0.46 ± 0.06							A22
$\rightarrow Cl$ + Products	*0.35*							
$\rightarrow H$ + Products	*0.09*							
$O(^1D) + CCl_4$ (CFC-10)		203–343	3.30×10⁻¹⁰	0	3.30×10⁻¹⁰	1.15	0	
$\rightarrow O(^3P) + CCl_4$	0.21 ± 0.04							A23
$\rightarrow ClO$ + Products	0.79 ± 0.04							
$O(^1D) + CH_3CCl_3$		298	*3.25×10⁻¹⁰*	*0*	*3.25×10⁻¹⁰*	1.40	0	
$\rightarrow O(^3P) + CH_3CCl_3$	*0.1*							A24
$\rightarrow$ Products	*0.9*							
$O(^1D) + CH_3Br$		297	*1.8×10⁻¹⁰*	*0*	1.8×10⁻¹⁰	1.15	50	
$\rightarrow O(^3P) + CH_3Br$	$0^{+0.07}_{-0}$							
$\rightarrow BrO$ + Products	0.44 ± 0.05							A25
$\rightarrow OH$ + Products	*0.56 (0.44-0.61)*							
$O(^1D) + CH_2Br_2$		297	*2.7×10⁻¹⁰*	*0*	2.7×10⁻¹⁰	1.20	25	
$\rightarrow O(^3P) + CH_2Br_2$	0.05 ± 0.07							A26
$\rightarrow$ Products	$0.95\ ^{+0.05}_{-0.10}$							
$O(^1D) + CHBr_3$		297	*6.6×10⁻¹⁰*	*0*	6.6×10⁻¹⁰	1.30	25	
$\rightarrow O(^3P) + CHBr_3$	0.30 ± 0.10							A27
$\rightarrow$ Products	0.70 ± 0.10							
$O(^1D) + CH_3F$ (HFC-41)		298	*1.5×10⁻¹⁰*	*0*	1.5×10⁻¹⁰	1.15	50	
$\rightarrow O(^3P) + CH_3F$	0.18 ± 0.07							A28
$\rightarrow$ Products	0.82 ± 0.07							
$O(^1D) + CH_2F_2$ (HFC-32)		298	*5.1×10⁻¹¹*	*0*	5.1×10⁻¹¹	1.20	50	
$\rightarrow O(^3P) + CH_2F_2$	0.70 ± 0.11							A29
$\rightarrow$ Products	0.30 ± 0.11							

Reaction	Branching Ratio [a]	Temperature Range of Exp. Data (K) [b]	Total Rate Coefficient: $O(^1D)$ Loss [c]					Note
			A-Factor [d]	*E*/R	*k*(298 K) [d]	*f*(298 K) [e]	*g* [e]	
$O(^1D) + CHF_3$ (HFC-23)		217–372	8.7×10^{-12}	–30	9.6×10^{-12}	1.05	0	
$\rightarrow O(^3P) + CHF_3$	0.75 ± 0.05							A30
→ Products	0.25 ± 0.05							
$O(^1D) + CHCl_2F$ (HCFC-21)		188–343	1.9×10^{-10}	0	1.9×10^{-10}	1.15	50	
$\rightarrow O(^3P) + CHCl_2F$	*0.20 ± 0.05*							
→ ClO + Products	0.74 ± 0.06							A31
→ OH + Products	*0.06 (0-0.17)*							
$O(^1D) + CHClF_2$ (HCFC-22)		173–373	1.02×10^{-10}	0	1.02×10^{-10}	1.07	0	
$\rightarrow O(^3P) + CHClF_2$	0.25 ± 0.05							
→ ClO + Products	0.56 ± 0.03							A32
→ OH + Products	0.05 ± 0.02							
→ Other Products	*0.14 (0.04-0.24)*							
$O(^1D) + CHF_2Br$		211–425	1.75×10^{-10}	–70	2.2×10^{-10}	1.15	25	
$\rightarrow O(^3P) + CHF_2Br$	0.40 ± 0.06							
→ BrO + Products	0.39 ± 0.07							A33
→ *Other Products*	*0.21 (0.08-0.34)*							
$O(^1D) + CCl_3F$ (CFC-11)		173–372	2.30×10^{-10}	0	2.30×10^{-10}	1.10	0	
$\rightarrow O(^3P) + CCl_3F$	0.10 ± 0.07							
→ ClO + Products	0.79 ± 0.04							A34
→ Other Products	*0.11 (0.0-0.22)*							
$O(^1D) + CCl_2F_2$ (CFC-12)		173–373	1.40×10^{-10}	–25	1.52×10^{-10}	1.15	0	
$\rightarrow O(^3P) + CCl_2F_2$	0.14 ± 0.07							
→ ClO + Products	0.76 ± 0.06							A35
→ *Other Products*	*0.10 (0-0.23)*							
$O(^1D) + CClF_3$ (CFC-13)		298	*8.7×10^{-11}*	*0*	8.7×10^{-11}	1.20	50	
$\rightarrow O(^3P) + CClF_3$	0.18 ± 0.06							
→ ClO + Products	0.82 ± 0.06							A36
$O(^1D)$ + 1,2-*c*-$C_4Cl_2F_6$ (*E*,*Z*)		296	*1.56×10^{-10}*	*0*	1.56×10^{-10}	1.10	*0*	
$\rightarrow O(^3P)$ + 1,2-*c*-$C_4Cl_2F_6$ (*E*,*Z*)	*0.12 ± 0.12*							
→ Products	$0.88\ ^{+0.12}_{-0.15}$							A37

Reaction	Branching Ratio [a]	Temperature Range of Exp. Data (K) [b]	Total Rate Coefficient: $O(^1D)$ Loss [c]					Note
			A-Factor [d]	*E*/R	*k*(298 K) [d]	*f*(298 K) [e]	*g* [e]	
$O(^1D) + CClBrF_2$ (Halon-1211) $\rightarrow O(^3P) + CClBrF_2$ $\rightarrow BrO + Products$ $\rightarrow Other\ Products$	0.35 ± 0.04 0.31 ± 0.06 *0.34 (0.24-0.44)*	297	*1.50×10⁻¹⁰*	*0*	1.50×10⁻¹⁰	1.20	50	A38
$O(^1D) + CBr_2F_2$ (Halon-1202) $\rightarrow O(^3P) + CBr_2F_2$ $\rightarrow Products$	0.55 ± 0.06 0.45 ± 0.06	297	*2.20×10⁻¹⁰*	*0*	2.20×10⁻¹⁰	1.20	50	A39
$O(^1D) + CBrF_3$ (Halon-1301) $\rightarrow O(^3P) + CBrF_3$ $\rightarrow BrO + Products$	0.55 ± 0.08 0.45 ± 0.08	297	*1.00×10⁻¹⁰*	*0*	1.00×10⁻¹⁰	1.20	50	A40
$O(^1D) + CF_4$ (PFC-14) $\rightarrow O(^3P) + CF_4$	–	297			<2×10⁻¹⁴			A41
$O(^1D) + CH_3CH_2F$ (HFC-161) $\rightarrow O(^3P) + CH_3CH_2F$ $\rightarrow Products$	0.18 ± 0.05 0.82 ± 0.05	297	*2.6×10⁻¹⁰*	*0*	2.6×10⁻¹⁰	1.20	25	A42
$O(^1D) + CH_3CHF_2$ (HFC-152a) $\rightarrow O(^3P) + CH_3CHF_2$ $\rightarrow OH + Products$ $\rightarrow Other\ Products$	0.45 ± 0.15 0.15 ± 0.02 *0.4 (0.18-0.62)*	297	*1.75×10⁻¹⁰*	*0*	1.75×10⁻¹⁰	1.20	50	A43
$O(^1D) + CH_3CCl_2F$ (HCFC-141b) $\rightarrow O(^3P) + CH_3CCl_2F$ $\rightarrow Products$	0.31 ± 0.05 0.69 ± 0.05	297	*2.60×10⁻¹⁰*	*0*	2.60×10⁻¹⁰	1.20	50	A44
$O(^1D) + CH_3CClF_2$ (HCFC-142b) $\rightarrow O(^3P) + CH_3CClF_2$ $\rightarrow Products$	0.35 ± 0.10 0.65 ± 0.10	217–373	2.0×10⁻¹⁰	0	2.0×10⁻¹⁰	1.10	0	A45
$O(^1D) + CH_3CF_3$ (HFC-143a) $\rightarrow O(^3P) + CH_3CF_3$ $\rightarrow OH + Products$ $\rightarrow Other\ Products$	0.35 ± 0.05 0.38 ± 0.06 *0.27 (0.16-0.38)*	217–373	5.6×10⁻¹¹	–20	6.0×10⁻¹¹	1.20	0	A46
$O(^1D) + CH_2ClCClF_2$ (HCFC-132b) $\rightarrow O(^3P) + CH_2ClCClF_2$ $\rightarrow Products$	*0.10* *0.90*	297	*1.6×10⁻¹⁰*	*0*	1.6×10⁻¹⁰	1.50	50	A47

Reaction	Branching Ratio [a]	Temperature Range of Exp. Data (K) [b]	Total Rate Coefficient: $O(^1D)$ Loss [c]					Note
			A-Factor [d]	*E*/R	*k*(298 K) [d]	*f*(298 K) [e]	*g* [e]	
$O(^1D) + CH_2ClCF_3$ (HCFC-133a) $\rightarrow O(^3P) + CH_2ClCF_3$ $\rightarrow$ Products	 0.20 ± 0.05 0.80 ± 0.05	297	*1.2×10⁻¹⁰*	*0*	1.2×10⁻¹⁰	1.25	50	A48
$O(^1D) + CH_2FCF_3$ (HFC-134a) $\rightarrow O(^3P) + CH_2FCF_3$ $\rightarrow$ OH + Products $\rightarrow$ Other Products	 0.65 ± 0.06 0.24 ± 0.04 *0.11 (0.01-0.21)*	297	*4.9×10⁻¹¹*	*0*	4.9×10⁻¹¹	1.15	50	A49
$O(^1D) + CHCl_2CF_3$ (HCFC-123) $\rightarrow O(^3P) + CHCl_2CF_3$ $\rightarrow$ Products	 0.21 ± 0.08 0.79 ± 0.08	297	*2.0×10⁻¹⁰*	*0*	2.0×10⁻¹⁰	1.20	50	A50
$O(^1D) + CHClFCF_3$ (HCFC-124) $\rightarrow O(^3P) + CHClFCF_3$ $\rightarrow$ Products	 0.31 ± 0.10 0.69 ± 0.10	297	*8.6×10⁻¹¹*	*0*	8.6×10⁻¹¹	1.20	50	A51
$O(^1D) + CHF_2CF_3$ (HFC-125) $\rightarrow O(^3P) + CHF_2CF_3$ $\rightarrow$ OH + Products $\rightarrow$ Other Products	 0.25 ± 0.05 0.60 ± 0.10 *0.15 (0-0.30)*	217–373	9.5×10⁻¹²	–25	1.03×10⁻¹¹	1.07	0	A52
$O(^1D) + CCl_3CF_3$ (CFC-113a) $\rightarrow O(^3P) + CCl_3CF_3$ $\rightarrow$ ClO + Products $\rightarrow$ Other Products	 *0.10* 0.79 ± 0.05 *0.11 (0-0.16)*	296	*2.6×10⁻¹⁰*	*0*	2.6×10⁻¹⁰	1.25	0	A53
$O(^1D) + CCl_2FCClF_2$ (CFC-113) $\rightarrow O(^3P) + CCl_2FCClF_2$ $\rightarrow$ ClO + Products $\rightarrow$ Other Products	 *0.10* 0.80 ± 0.05 *0.10 (0-0.15)*	217–373	2.32×10⁻¹⁰	0	2.32×10⁻¹⁰	1.10	0	A54
$O(^1D) + CCl_2FCF_3$ (CFC-114a) $\rightarrow O(^3P) + CCl_2FCF_3$ $\rightarrow$ ClO + Products $\rightarrow$ Other Products	 *0.10* 0.80 ± 0.05 *0.10 (0-0.15)*	296	*1.6×10⁻¹⁰*	*0*	1.6×10⁻¹⁰	1.20	0	A55
$O(^1D) + CClF_2CClF_2$ (CFC-114) $\rightarrow O(^3P) + CClF_2CClF_2$ $\rightarrow$ ClO + Products $\rightarrow$ Other Products	 *0.10* 0.85 ± 0.06 *0.05 (0-0.1)*	217–373	1.30×10⁻¹⁰	–25	1.41×10⁻¹⁰	1.10	0	A56

Reaction	Branching Ratio [a]	Temperature Range of Exp. Data (K) [b]	Total Rate Coefficient: $O(^1D)$ Loss [c]					Note
			A-Factor [d]	*E*/R	*k*(298 K) [d]	*f*(298 K) [e]	*g* [e]	
$O(^1D) + CClF_2CF_3$ (CFC-115)		217–373	5.4×10^{-11}	–30	6.0×10^{-11}	1.15	0	
$\rightarrow O(^3P) + CClF_2CF_3$	0.14 ± 0.06							A57
→ Products	0.86 ± 0.06							
$O(^1D) + CBrF_2CBrF_2$ (Halon-2402)		297	*1.60×10^{-10}*	*0*	1.60×10^{-10}	1.20	50	
$\rightarrow O(^3P) + CBrF_2CBrF_2$	0.25 ± 0.07							A58
→ Products	0.75 ± 0.07							
$O(^1D) + CF_3CF_3$ (CFC-116)		297			1.5×10^{-13}			
$\rightarrow O(^3P) + CF_3CF_3$								A59
→ Products	<0.2							
$O(^1D) + CF_3CHFCF_3$ (HFC-227ea)		217–373	7.9×10^{-12}	–70	1.0×10^{-11}	1.10	0	
$\rightarrow O(^3P) + CF_3CHFCF_3$	0.28 ± 0.07							A60
→ Products	0.72 ± 0.07							
$O(^1D) + CHF_2CH_2CF_3$ (HFC-245fa)			*1.5×10^{-10}*	*0*	*1.5×10^{-10}*	*1.30*	*0*	
$\rightarrow O(^3P) + CHF_2CH_2CF_3$	*0.5*							A61
→ Products	*0.5*							
$O(^1D) + CHF_2CF_2CF_2CHF_2$ (HFC-338pcc)		297	*1.8×10^{-11}*	*0*	1.8×10^{-11}	1.30	50	
$\rightarrow O(^3P) + CHF_2CF_2CF_2CHF_2$	$0.95^{+0.05}_{-0.09}$							A62
→ Products	$0.05^{+0.09}_{-0.05}$							
$O(^1D) + c\text{-}C_4F_8$		297			8×10^{-13}			
$\rightarrow O(^3P) + c\text{-}C_4F_8$								A63
→ Products	<0.04							
$O(^1D) + CF_3CHFCHFCF_2CF_3$ (HFC-43-10mee)		297	*2.1×10^{-10}*	*0*	2.1×10^{-10}	2.00	50	
$\rightarrow O(^3P) + CF_3CHFCHFCF_2CF_3$	0.90 ± 0.10							A64
→ Products	0.10 ± 0.10							
$O(^1D) + C_5F_{12}$ (PFC-41-12)		297			4×10^{-13}			
$\rightarrow O(^3P) + C_5F_{12}$								A65
→ Products	<0.12							
$O(^1D) + C_6F_{14}$ (PFC-51-14)		297			1×10^{-12}			
$\rightarrow O(^3P) + C_6F_{14}$								A66
→ Products	<0.16							

Reaction	Branching Ratio [a]	Temperature Range of Exp. Data (K) [b]	Total Rate Coefficient: $O(^1D)$ Loss [c]					Note
			A-Factor [d]	*E*/R	*k*(298 K) [d]	*f*(298 K) [e]	*g* [e]	
$O(^1D) + 1,2\text{-}(CF_3)_2c\text{-}C_4F_6$ $\rightarrow O(^3P) + 1,2\text{-}(CF_3)_2c\text{-}C_4F_6$ $\rightarrow$ Products	–	297			$<3\times10^{-13}$			A67
$O(^1D) + C_4F_{10}$ $\rightarrow O(^3P) + C_4F_{10}$ $\rightarrow$ Products	–	297			$<5\times10^{-13}$			A68
$O(^1D) + SF_6$ $\rightarrow O(^3P) + SF_6$ $\rightarrow$ Products	<0.7	297			1.8×10^{-14}			A69
$O(^1D) + SO_2$ $\rightarrow O(^3P) + SO_2$ $\rightarrow$ Products	0.24 ± 0.07 0.76 ± 0.07	298	*2.2×10^{-10}*	*0*	2.2×10^{-10}	1.30	30	A70
$O(^1D) + SO_2F_2$ $\rightarrow O(^3P) + SO_2F_2$ $\rightarrow$ Products	0.45 ± 0.04 0.55 ± 0.04	199–351	9×10^{-11}	–100	1.26×10^{-10}	1.30	30	A71
$O(^1D) + SF_5CF_3$ $\rightarrow O(^3P) + SF_5CF_3$ $\rightarrow$ Products	<0.3	296–300			2×10^{-13}			A72

Shaded areas indicate changes or additions since JPL19-5. Italicized blue entries denote estimates.

[a] Recommended product channel branching ratios are temperature independent unless noted otherwise.

[b] Temperature range of available experimental data. This is not necessarily the range of temperature over which the recommended Arrhenius parameters are applicable. See the corresponding note for such information.

[c] The total rate coefficient (i.e., $O(^1D)$ loss) is defined as $A \times \exp(-E/RT)$ in units of cm^3 $molecule^{-1}$ s^{-1}.
The rate coefficient for an individual reaction channel, if provided, is defined as Branching Ratio $\times A \times \exp(-E/RT)$ in units of cm^3 $molecule^{-1}$ s^{-1}.

[d] Units of cm^3 $molecule^{-1}$ s^{-1}.

[e] $f(298\ K)$ is the uncertainty factor at 298 K. To calculate the uncertainty at other temperatures, use the expression:

$$f(T) = f(298\ K)\exp\left|g\left(\frac{1}{T} - \frac{1}{298}\right)\right|$$

Note that the exponent is an absolute value.

1.5.2 Notes: O(^{1}D) Reactions

A2. **O(^{1}D) Reactions**. O(^{1}D) reactions are complex with several possible exothermic reaction pathways, which include (1) collisional (physical) quenching of O(^{1}D) to ground state oxygen atoms, O(^{3}P), (2) abstraction or addition-elimination reaction, and (3) reactive quenching to form O(^{3}P) and products other than the reactant, including stable and radical species. The recommended total rate coefficient parameters given in the table are for the disappearance of O(^{1}D). The details of deriving a recommended rate coefficient are given in the note for each reaction. In deriving recommended values, direct measurements are used whenever possible. However, rate coefficients measured via relative rate and competitive reaction techniques have also been included in the evaluation of measured elementary reaction rate coefficients. Note that ratios of rate coefficients for O(^{1}D) reactions measured using the same method (and often the same apparatus) may be more accurate and precise than the individual recommended rate coefficients. The ratios of rate coefficients can be obtained from the original references. The weight of the evidence indicates that the results from the studies of Heidner and Husain,[4] Heidner et al.,[3] and Fletcher and Husain[1,2] contain systematic errors and, therefore, are not considered in the determination of the recommendations.

The basis for the product branching ratio recommendations for deactivation and chemical reaction are described in the individual reaction notes. The collisional quenching channel and yield is listed as the first (possibly only) reaction pathway for each reaction given in the table. Reactive quenching channels, i.e., channels that produce O(^{3}P) and reaction products, are included for the O_2 and O_3 reactions, but have not been identified in the majority of the other experimental studies. Bromine, chlorine, and hydrogen are more easily displaced than fluorine from halocarbons and, therefore, typically account for major reaction product yields in the form of BrO, ClO, and OH radicals. The uncertainties in the recommended branching ratios are taken from the experimental studies (see notes) where possible. For some channels, a range of values is provided in parenthesis that is consistent with the other reported uncertainties and a total branching ratio of unity.
(Note: 25-1) Back to Table

(1) Fletcher, I. S.; Husain, D. Absolute reaction rates of oxygen (2^1D_2) with halogenated paraffins by atomic absorption spectroscopy in the vacuum ultraviolet. *J. Phys. Chem.* **1976**, *80*, 1837-1840, doi:10.1021/j100558a002.

(2) Fletcher, I. S.; Husain, D. The collisional quenching of electronically excited oxygen atoms, O(2^1D_2), by the gases NH_3, H_2O_2, C_2H_6, C_3H_8, and $C(CH_3)_4$, using time-resolved attenuation of atomic resonance radiation. *Can. J. Chem.* **1976**, *54*, 1765-1770, doi:10.1139/v76-251.

(3) Heidner, R. F., III ; Husain, D.; Wiesenfeld, J. R. Kinetic investigation of electronically excited oxygen atoms, O(2^1D_2), by time-resolved attenuation of atomic resonance radiation in the vacuum ultra-violet Part 2.-Collisional quenching by the atmospheric gases N_2, O_2, CO, CO_2, H_2O and O_3. *J. Chem. Soc. Faraday Trans. 2* **1973**, *69*, 927-938, doi:10.1039/f29736900927.

(4) Heidner, R. F., III; Husain, D. Electronically excited oxygen atoms, O(2^1D_2). A time-resolved study of the collisional quenching by the gases H_2, D_2, NO, N_2O, NO_2, CH_4, and C_3O_2 using atomic absorption spectroscopy in the vacuum ultraviolet. *Int. J. Chem. Kinet.* **1973**, *5*, 819-831, doi:10.1002/kin.550050509.

A3. **O(^{1}D) + O_2**. The recommended 298 K rate coefficient was derived from the studies of Blitz et al.,[4] Amimoto et al.,[11,2] Lee and Slanger,[10,11] Davidson et al.,[5,6] Dunlea and Ravishankara,[7] Streit et al.,[14] Strekowski et al.,[15] and Takahashi et al.[16] The temperature dependence was computed by normalizing the results of Strekowski et al., Dunlea and Ravishankara, and Streit et al. to the 298 K value recommended here. The low-temperature results from Grondin et al.[9] (50, 75, 127, and 296 K), obtained using a Laval nozzle-LIF technique, are in agreement with the recommendation at 296 and 127 K, but significantly lower at the lower temperatures. The recommendation is for the temperature range 100 to 400 K. The deactivation of O(^{1}D) by O_2 leads to the production of $O_2(^1\Sigma)$ with an efficiency of (80 ± 20)% (Noxon,[12] Biedenkapp and Bair,[3] Snelling,[13] and Lee and Slanger[10]). $O_2(^1\Sigma)$ is produced in the v = 0, 1, and 2 vibrational levels in the amounts 60%, 40%, and <3%, respectively (Gauthier and Snelling[8] and Lee and Slanger[10]). The fractional deactivation of O(^{1}D) that leads to the excitation of $O_2(^3\Sigma)$ to $O_2(^1\Delta)$ is expected to be ~20%. An $O_2(^1\Sigma)$ yield of (80 ± 20)% is recommended with the $O_2(^1\Delta)$ yield accounting for the balance of the reaction.
(Table: 06-2, Note: 15-10, Evaluated: 10-6) Back to Table

(1) Amimoto, S. T.; Force, A. P.; Gulotty, R. G., Jr.; Wiesenfeld, J. R. Collisional deactivation of O(2^1D_2) by the atmospheric gases. *J. Chem. Phys.* **1979**, *71*, 3640-3647, doi:10.1063/1.438807.

(2) Amimoto, S. T.; Force, A. P.; Wiesenfeld, J. R. Ozone photochemistry: Production and deactivation of O(2^1D_2) following photolysis at 248 nm. *Chem. Phys. Lett.* **1978**, *60*, 40-43, doi:10.1016/0009-2614(78)85705-4.

(3) Biedenkapp, D.; Bair, E. J. Ozone ultraviolet photolysis. I. The effect of molecular oxygen. *J. Chem. Phys.* **1970**, *52*, 6119-6125, doi:10.1063/1.1672914.
(4) Blitz, M. A.; Dillon, T. J.; Heard, D. E.; Pilling, M. J.; Trought, I. D. Laser induced fluorescence studies of the reactions of $O(^1D_2)$ with N_2, O_2, N_2O, CH_4, H_2, CO_2, Ar, Kr and *n*-C_4H_{10}. *Phys. Chem. Chem. Phys.* **2004**, *6*, 2162-2171, doi:10.1039/b400283k.
(5) Davidson, J. A.; Schiff, H. I.; Brown, T. J.; Howard, C. J. Temperature dependence of the rate constants for reactions of $O(^1D)$ atoms with a number of halocarbons. *J. Chem. Phys.* **1978**, *69*, 4277-4279, doi:10.1063/1.437113.
(6) Davidson, J. A.; Schiff, H. I.; Streit, G. E.; McAfee, J. R.; Schmeltekopf, A. L.; Howard, C. J. Temperature dependence of $O(^1D)$ rate constants for reactions with N_2O, H_2, CH_4, HCl, and NH_3. *J. Chem. Phys.* **1977**, *67*, 5021-5025, doi:10.1063/1.434724.
(7) Dunlea, E. J.; Ravishankara, A. R. Kinetics studies of the reactions of $O(^1D)$ with several atmospheric molecules. *Phys. Chem. Chem. Phys.* **2004**, *6*, 2152-2161, doi:10.1039/b400247d.
(8) Gauthier, M. J. E.; Snelling, D. R. Production de $O_2(b^1\Sigma_g^+)$, v' = 0,1 et 2 par la reaction $O(2^1D_2)$ + $O_2(X^3\Sigma_g^-)$. *Can. J. Chem.* **1974**, *52*, 4007-4015, doi:10.1139/v74-598.
(9) Grondin, R.; Loison, J.-C.; Hickson, K. M. Low temperature rate constants for the reactions of $O(^1D)$ with N_2, O_2, and Ar. *J. Phys. Chem. A* **2016**, *120*, 4838−4844, doi:10.1021/acs.jpca.5b12358.
(10) Lee, L. C.; Slanger, T. G. Observations on $O(^1D \rightarrow ^3P)$ and $O_2(b^1\Sigma_g^+ \rightarrow X^3\Sigma_g^-)$ following O_2 photodissociation. *J. Chem. Phys.* **1978**, *69*, 4053-4060, doi:10.1063/1.437136.
(11) Lee, L. C.; Slanger, T. G. Atmospheric OH production--The $O(^1D)$ + H_2O reaction rate. *Geophys. Res. Lett.* **1979**, *6*, 165-166, doi:10.1029/GL006i003p00165.
(12) Noxon, J. F. Optical emission from $O(^1D)$ and $O_2(b^1\Sigma_g)$ in ultraviolet photolysis of O_2 and CO_2. *J. Chem. Phys.* **1970**, *52*, 1852-1873, doi:10.1063/1.1673227.
(13) Snelling, D. R. The ultraviolet flash photolysis of ozone and the reactions of $O(^1D)$ and $O_2(^1\Sigma_g^+)$. *Can. J. Chem.* **1974**, *52*, 257-270, doi:10.1139/v74-042.
(14) Streit, G. E.; Howard, C. J.; Schmeltekopf, A. L.; Davidson, J. A.; Schiff, H. I. Temperature dependence of $O(^1D)$ rate constants for reactions with O_2, N_2, CO_2, O_3, and H_2O. *J. Chem. Phys.* **1976**, *65*, 4761-4764, doi:10.1063/1.432930.
(15) Strekowski, R. S.; Nicovich, J. M.; Wine, P. H. Temperature-dependent kinetics study of the reactions of $O(^1D_2)$ with N_2 and O_2. *Phys. Chem. Chem. Phys.* **2004**, *6*, 2145-2151, doi:10.1039/b400243a.
(16) Takahashi, K.; Takeuchi, Y.; Matsumi, Y. Rate constants of the $O(^1D)$ reactions with N_2, O_2, N_2O, and H_2O at 295 K. *Chem. Phys. Lett.* **2005**, *410*, 196-200, doi:10.1016/j.cplett.2005.05.062.

A4. **$O(^1D) + O_3$**. The room temperature rate coefficient was derived from the results of Davidson et al.,[4,5] Streit et al.,[8] Amimoto et al.,[1,2] Wine and Ravishankara,[10-12] Talukdar and Ravishankara,[9] and Dunlea and Ravishankara.[6] The reaction rate coefficient displays no significant temperature dependence between 103 and 383 K. The reaction of $O(^1D)$ with O_3 gives $O_2 + O_2$ or $O_2 + O + O$ as products. Davenport et al.[3] and Amimoto et al.[2] report that, on average, one ground state O atom is produced per $O(^1D)$ reacting with O_3. Dunlea et al.[7] have shown that the yield of $O(^3P)$ in this reaction is close to, but not exactly, unity. Dunlea et al. suggest a small, but significant decrease in the O atom yield with decreasing temperature. A $O(^3P)$ yield of unity at all temperatures is recommended until the results from the Dunlea et al. study are confirmed.
(Table: 25-1, Note: 25-1, Evaluated: 10-6) Back to Table

(1) Amimoto, S. T.; Force, A. P.; Gulotty, R. G., Jr.; Wiesenfeld, J. R. Collisional deactivation of $O(2^1D_2)$ by the atmospheric gases. *J. Chem. Phys.* **1979**, *71*, 3640-3647, doi:10.1063/1.438807.
(2) Amimoto, S. T.; Force, A. P.; Wiesenfeld, J. R. Ozone photochemistry: Production and deactivation of $O(2^1D_2)$ following photolysis at 248 nm. *Chem. Phys. Lett.* **1978**, *60*, 40-43, doi:10.1016/0009-2614(78)85705-4.
(3) Davenport, J.; Ridley, B.; Schiff, H. I.; Welge, K. H. communication. *Faraday Discuss. Chem. Soc.* **1972**, *53*, 230-231.
(4) Davidson, J. A.; Schiff, H. I.; Brown, T. J.; Howard, C. J. Temperature dependence of the rate constants for reactions of $O(^1D)$ atoms with a number of halocarbons. *J. Chem. Phys.* **1978**, *69*, 4277-4279, doi:10.1063/1.437113.
(5) Davidson, J. A.; Schiff, H. I.; Streit, G. E.; McAfee, J. R.; Schmeltekopf, A. L.; Howard, C. J. Temperature dependence of $O(^1D)$ rate constants for reactions with N_2O, H_2, CH_4, HCl, and NH_3. *J. Chem. Phys.* **1977**, *67*, 5021-5025, doi:10.1063/1.434724.
(6) Dunlea, E. J.; Ravishankara, A. R. Kinetics studies of the reactions of $O(^1D)$ with several atmospheric molecules. *Phys. Chem. Chem. Phys.* **2004**, *6*, 2152-2161, doi:10.1039/b400247d.
(7) Dunlea, E. J.; Ravishankara, A. R.; Strekowski, R. S.; Nicovich, J. M.; Wine, P. H. Temperature-dependent quantum yields for $O(^3P)$ and $O(^1D)$ production from photolysis of O_3 at 248 nm. *Phys. Chem. Chem. Phys.* **2004**, *6*, 5484-5489, doi:10.1039/b414326d.

(8) Streit, G. E.; Howard, C. J.; Schmeltekopf, A. L.; Davidson, J. A.; Schiff, H. I. Temperature dependence of $O(^1D)$ rate constants for reactions with O_2, N_2, CO_2, O_3, and H_2O. *J. Chem. Phys.* **1976**, *65*, 4761-4764, doi:10.1063/1.432930.
(9) Talukdar, R. K.; Ravishankara, A. R. Rate coefficients for $O(^1D) + H_2$, D_2, HD reactions and H atom yield in $O(^1D)$ + HD reaction. *Chem. Phys. Lett.* **1996**, *253*, 177-183, doi:10.1016/0009-2614(96)00203-5.
(10) Wine, P. H.; Ravishankara, A. R. Kinetics of $O(^1D)$ interactions with the atmospheric gases N_2, N_2O, H_2O, H_2, CO_2, and O_3. *Chem. Phys. Lett.* **1981**, *77*, 103-109, doi:10.1016/0009-2614(81)85609-6.
(11) Wine, P. H.; Ravishankara, A. R. O_3 photolysis at 248 nm and $O(^1D_2)$ quenching by H_2O, CH_4, H_2, and N_2O: $O(^3P_J)$ yields. *Chem. Phys.* **1982**, *69*, 365-373, doi:10.1016/0301-0104(82)88075-0.
(12) Wine, P. H.; Ravishankara, A. R. Reactive and non-reactive quenching of $O(^1D_2)$ by COF_2. *Chem. Phys. Lett.* **1983**, *96*, 129-132, doi:10.1016/0009-2614(83)80131-6.

A5. **$O(^1D) + H_2$**. The recommendation is based on the room temperature rate coefficient data from Davidson et al.,[2,3] Force and Wiesenfeld,[4,5] Wine and Ravishankara,[11] Talukdar and Ravishankara,[9] Blitz et al.,[1] and Vranckx et al.[10] Davidson et al. (200–350 K), Vranckx et al. (227–453 K), and Hickson and Suleimanov[6] (50–300 K) report that k is independent of temperature within the recommended $f(298\ K)$ uncertainty. Wine and Ravishankara[11] and Vranckx et al.[10] report the yield of $O(^3P)$ to be <4.9% and (0.7 ± 0.7)%, respectively. Hence, the major products of this reaction are H + OH with a recommended yield of unity. Koppe et al.[7] report a 2.7 times larger rate coefficient at a collisional energy of 0.12 eV. This does not agree with the observations of Davidson et al.[3] and Vranckx et al. who reported that k is independent of temperature and Matsumi et al.[8] who report no change in k when translationally hot $O(^1D)$ was moderated with Ar.
(Table: 25-1, Note: 25-1, Evaluated: 25-1) Back to Table

(1) Blitz, M. A.; Dillon, T. J.; Heard, D. E.; Pilling, M. J.; Trought, I. D. Laser induced fluorescence studies of the reactions of $O(^1D_2)$ with N_2, O_2, N_2O, CH_4, H_2, CO_2, Ar, Kr and n-C_4H_{10}. *Phys. Chem. Chem. Phys.* **2004**, *6*, 2162-2171, doi:10.1039/b400283k.
(2) Davidson, J. A.; Schiff, H. I.; Brown, T. J.; Howard, C. J. Temperature dependence of the rate constants for reactions of $O(^1D)$ atoms with a number of halocarbons. *J. Chem. Phys.* **1978**, *69*, 4277-4279, doi:10.1063/1.437113.
(3) Davidson, J. A.; Schiff, H. I.; Streit, G. E.; McAfee, J. R.; Schmeltekopf, A. L.; Howard, C. J. Temperature dependence of $O(^1D)$ rate constants for reactions with N_2O, H_2, CH_4, HCl, and NH_3. *J. Chem. Phys.* **1977**, *67*, 5021-5025, doi:10.1063/1.434724.
(4) Force, A. P.; Wiesenfeld, J. R. Collisional deactivation of $O(^1D_2)$ by the halomethanes. Direct determination of reaction efficiency. *J. Phys. Chem.* **1981**, *85*, 782-785, doi:10.1021/j150607a012.
(5) Force, A. P.; Wiesenfeld, J. R. Laser photolysis of O_3/H_2 mixtures: The yield of the $H + O_3 \rightarrow HO_2 + O$ reaction. *J. Chem. Phys.* **1981**, *74*, 1718-1723, doi:10.1063/1.441260.
(6) Hickson, K.; Suleimanov, Y. V. Low-temperature experimental and theoretical rate constants for the $O(^1D) + H_2$ reaction. *J. Phys. Chem. A* **2017**, *121*, 1916-1923, doi:10.1021/acs.jpca.7b00722.
(7) Koppe, S.; Laurent, T.; Naik, P. D.; Volpp, H.-R.; Wolfrum, J.; Arusi-Parpar, T.; Bar, I.; Rosenwaks, S. Absolute rate constants and reactive cross sections for the reactions of $O(^1D)$ with molecular hydrogen and deuterium. *Chem. Phys. Lett.* **1993**, *214*, 546-552, doi:10.1016/0009-2614(93)85681-D.
(8) Matsumi, Y.; Tonokura, K.; Inagaki, Y.; Kawasaki, M. Isotopic branching ratios and translational energy release of H and D atoms in reaction of $O(^1D)$ atoms with alkanes and akyl chlorides. *J. Phys. Chem.* **1993**, *97*, 6816-6821, doi:10.1021/j100128a012.
(9) Talukdar, R. K.; Ravishankara, A. R. Rate coefficients for $O(^1D) + H_2$, D_2, HD reactions and H atom yield in $O(^1D)$ + HD reaction. *Chem. Phys. Lett.* **1996**, *253*, 177-183, doi:10.1016/0009-2614(96)00203-5.
(10) Vranckx, S.; Peeters, J.; Carl, S. Kinetics of $O(^1D) + H_2O$ and $O(^1D) + H_2$: Absolute rate coefficients and $O(^3P)$ yields between 227 and 453 K. *Phys. Chem. Chem. Phys.* **2010**, *12*, 9213-9221, doi:10.1039/b923959f.
(11) Wine, P. H.; Ravishankara, A. R. O_3 photolysis at 248 nm and $O(^1D_2)$ quenching by H_2O, CH_4, H_2, and N_2O: $O(^3P_J)$ yields. *Chem. Phys.* **1982**, *69*, 365-373, doi:10.1016/0301-0104(82)88075-0.

A6. **$O(^1D) + H_2O$**. The recommended $k(298\ K)$ is based on the results of Davidson et al.,[3] Amimoto et al.,[1] Wine and Ravishankara,[13,14] Gericke and Comes,[6] Dunlea and Ravishankara,[5] Carl,[2] Takahashi et al.,[10] and Vranckx et al.,[12] but is weighted towards the study of Dunlea and Ravishankara because they used several different methods to quantify the water vapor concentration. The results of Lee and Slanger[8] and Dillon et al.[4] are consistent with the recommended value. The temperature dependence of the rate coefficient was derived from the data of Streit et al.[9] (217–353 K), Dunlea and Ravishankara (235–370 K), and Vranckx et al. (227–453 K) after normalizing the results from the two studies to the $k(298\ K)$ value recommended here. The $O_2 + H_2$

product yield was measured by Zellner et al.[15] to be (1 +0.5/–1)% and Glinski and Birks[7] to be (0.6 +0.7/–0.6)%. The yield of $O(^3P)$ from $O(^1D) + H_2O$ is reported to be less than (4.9 ± 3.2)% by Wine and Ravishankara,[14] (2 ± 1)% by Takahashi et al.,[11] <0.3% by Carl,[2] and 0.010 ± 0.003 by Vranckx et al.[12] The recommended yield of OH in this reaction is 2.0. To calculate the rates of OH production via $O(^1D)$ reactions in the atmosphere, the quantities of interest are the ratios of the rate coefficients for the reaction of $O(^1D)$ with H_2O to those with N_2 and O_2. Ratio data are given in the original references for this reaction.
(Table 25-1, Note: 25-1, Evaluated: 25-1) Back to Table

(1) Amimoto, S. T.; Force, A. P.; Gulotty, R. G., Jr.; Wiesenfeld, J. R. Collisional deactivation of $O(2^1D_2)$ by the atmospheric gases. *J. Chem. Phys.* **1979**, *71*, 3640-3647, doi:10.1063/1.438807.

(2) Carl, S. A. A highly sensitive method for time-resolved detection of $O(^1D)$ applied to precise determination of absolute $O(^1D)$ reaction rate constants and $O(^3P)$ yields. *Phys. Chem. Chem. Phys.* **2005**, *7*, 4051-4053, doi:10.1039/b513576c.

(3) Davidson, J. A.; Schiff, H. I.; Streit, G. E.; McAfee, J. R.; Schmeltekopf, A. L.; Howard, C. J. Temperature dependence of $O(^1D)$ rate constants for reactions with N_2O, H_2, CH_4, HCl, and NH_3. *J. Chem. Phys.* **1977**, *67*, 5021-5025, doi:10.1063/1.434724.

(4) Dillon, T. J.; Horowitz, A.; Crowley, J. N. The atmospheric chemistry of sulphuryl fluoride, SO_2F_2. *Atmos. Chem. Phys.* **2008**, *8*, 1547-1557, doi:10.5194/acp-8-1547-2008.

(5) Dunlea, E. J.; Ravishankara, A. R. Measurement of the rate coefficient for the reaction of $O(^1D)$ with H_2O and re-evaluation of the atmospheric OH production rate. *Phys. Chem. Chem. Phys.* **2004**, *6*, 3333-3340, doi:10.1039/b402483d.

(6) Gericke, K.-H.; Comes, F. J. Energy partitioning in the reaction $O(^1D) + H_2O \rightarrow OH + OH$ - The influence of $O(^1D)$ translation energy on the reaction rate constant. *Chem. Phys. Lett.* **1981**, *81*, 218-222, doi:10.1016/0009-2614(81)80239-4.

(7) Glinski, R. J.; Birks, J. W. Yields of molecular hydrogen in the elementary reactions $HO_2 + HO_2$ and $O(^1D_2) + H_2O$. *J. Phys. Chem.* **1985**, *89*, 3449-3453, doi:10.1021/j100262a006.

(8) Lee, L. C.; Slanger, T. G. Atmospheric OH production--The $O(^1D) + H_2O$ reaction rate. *Geophys. Res. Lett.* **1979**, *6*, 165-166, doi:10.1029/GL006i003p00165.

(9) Streit, G. E.; Howard, C. J.; Schmeltekopf, A. L.; Davidson, J. A.; Schiff, H. I. Temperature dependence of $O(^1D)$ rate constants for reactions with O_2, N_2, CO_2, O_3, and H_2O. *J. Chem. Phys.* **1976**, *65*, 4761-4764, doi:10.1063/1.432930.

(10) Takahashi, K.; Takeuchi, Y.; Matsumi, Y. Rate constants of the $O(^1D)$ reactions with N_2, O_2, N_2O, and H_2O at 295 K. *Chem. Phys. Lett.* **2005**, *410*, 196-200, doi:10.1016/j.cplett.2005.05.062.

(11) Takahashi, K.; Wada, R.; Matsumi, Y.; Kawasaki, M. Product branching ratios for $O(^3P)$ atom and ClO radical formation in the reactions of $O(^1D)$ with chlorinated compounds. *J. Phys. Chem.* **1996**, *100*, 10145-10149, doi:10.1021/jp952710a.

(12) Vranckx, S.; Peeters, J.; Carl, S. Kinetics of $O(^1D) + H_2O$ and $O(^1D) + H_2$: Absolute rate coefficients and $O(^3P)$ yields between 227 and 453 K. *Phys. Chem. Chem. Phys.* **2010**, *12*, 9213-9221, doi:10.1039/b923959f.

(13) Wine, P. H.; Ravishankara, A. R. Kinetics of $O(^1D)$ interactions with the atmospheric gases N_2, N_2O, H_2O, H_2, CO_2, and O_3. *Chem. Phys. Lett.* **1981**, *77*, 103-109, doi:10.1016/0009-2614(81)85609-6.

(14) Wine, P. H.; Ravishankara, A. R. O_3 photolysis at 248 nm and $O(^1D_2)$ quenching by H_2O, CH_4, H_2, and N_2O: $O(^3P_J)$ yields. *Chem. Phys.* **1982**, *69*, 365-373, doi:10.1016/0301-0104(82)88075-0.

(15) Zellner, R.; Wagner, G.; Himme, B. H_2 formation in the reaction of $O(^1D)$ with H_2O. *J. Phys. Chem.* **1980**, *84*, 3196-3198, doi:10.1021/j100461a013.

A7. **$O(^1D) + N_2$**. The rate coefficient recommendation for this reaction is taken from Ravishankara et al.,[5] which included the results from Strekowski et al.,[6] Blitz et al.,[1] and Dunlea and Ravishankara[3] in their analysis. The more recent results from Takahashi et al.[7] and Dillon et al.[2] are in agreement with the recommendation. The low-temperature results from Grondin et al.[4] (50, 75, 127, and 296 K), obtained using a Laval nozzle-LIF technique, are in agreement with the recommendation at 296 and 127 K, but significantly lower at the lower temperatures. The recommendation is for the temperature range 100 to 675 K. Strekowski et al. reported the rate coefficient for $O(^1D)$ removal by air and their results are in excellent agreement with the value derived using the current recommendation for $O(^1D)$ removal by N_2 and O_2. The reaction leads to 100% quenching of $O(^1D)$ to $O(^3P)$ with no significant reactive channels (see Table 2).
(Table: 06-2, Note: 25-1, Evaluated: 10-6) Back to Table

(1) Blitz, M. A.; Dillon, T. J.; Heard, D. E.; Pilling, M. J.; Trought, I. D. Laser induced fluorescence studies of the reactions of $O(^1D_2)$ with N_2, O_2, N_2O, CH_4, H_2, CO_2, Ar, Kr and *n*-C_4H_{10}. *Phys. Chem. Chem. Phys.* **2004**, *6*, 2162-2171, doi:10.1039/b400283k.

(2) Dillon, T. J.; Horowitz, A.; Crowley, J. N. The atmospheric chemistry of sulphuryl fluoride, SO_2F_2. *Atmos. Chem. Phys.* **2008**, *8*, 1547-1557, doi:10.5194/acp-8-1547-2008.

(3) Dunlea, E. J.; Ravishankara, A. R. Kinetics studies of the reactions of $O(^1D)$ with several atmospheric molecules. *Phys. Chem. Chem. Phys.* **2004**, *6*, 2152-2161, doi:10.1039/b400247d.
(4) Grondin, R.; Loison, J.-C.; Hickson, K. M. Low temperature rate constants for the reactions of $O(^1D)$ with N_2, O_2, and Ar. *J. Phys. Chem. A* **2016**, *120*, 4838−4844, doi:10.1021/acs.jpca.5b12358.
(5) Ravishankara, A. R.; Dunlea, E. J.; Blitz, M. A.; Dillon, T. J.; Heard, D. E.; Pilling, M. J.; Strekowski, R. S.; Nicovich, J. M.; Wine, P. H. Redetemination of the rate coefficient for the reaction of $O(^1D)$ with N_2. *Geophys. Res. Lett.* **2002**, *29*, 1745, doi:10.1029/2002GL014850.
(6) Strekowski, R. S.; Nicovich, J. M.; Wine, P. H. Temperature-dependent kinetics study of the reactions of $O(^1D_2)$ with N_2 and O_2. *Phys. Chem. Chem. Phys.* **2004**, *6*, 2145-2151, doi:10.1039/b400243a.
(7) Takahashi, K.; Takeuchi, Y.; Matsumi, Y. Rate constants of the $O(^1D)$ reactions with N_2, O_2, N_2O, and H_2O at 295 K. *Chem. Phys. Lett.* **2005**, *410*, 196-200, doi:10.1016/j.cplett.2005.05.062.

A8. **$O(^1D) + N_2O$**. This reaction has two reactive channels, one producing 2NO and the other producing $N_2 + O_2$. For atmospheric calculations of NO_x production, the rate coefficient for the channel that produces NO is critical, while the overall rate coefficient is important for deriving the loss rate of N_2O. The recommendation for the overall room temperature rate coefficient for the removal of $O(^1D)$ by N_2O was derived from a weighted average of the results from Davidson et al.,[6] Amimoto et al.,[1] Wine and Ravishankara,[13] Blitz et al.,[2] Dunlea and Ravishankara,[8] Carl,[5] Takahashi et al.,[11] Dillon et al.,[7] and Vranckx et al.[12] The temperature dependence of the rate coefficient was derived from the results of Davidson et al. (204–359 K), Dunlea and Ravishankara (220–370 K), and Vranckx et al. (227–715 K); only data at <400 K were considered in the evaluation, after normalization to the k(298 K) value recommended here for the overall rate coefficient. The recommended rate coefficients for the $N_2 + O_2$ and 2NO product channels were evaluated for 298 K, the only temperature at which such data are available. The branching ratio, R, k(NO + NO)/k(Total) is taken from Cantrell et al.[4] who reported R = 0.57 as well as an analysis of all measurements from 1957–1994 that led them to recommend R = 0.61 ± 0.06, where the uncertainty is the 95% confidence interval. Their recommended branching ratio agrees well with earlier measurements of the quantum yield from N_2O photolysis (Calvert and Pitts[3]). Dependencies of the branching ratio on $O(^1D)$ translational energy and temperature are at present not clearly resolved. The recommended rate coefficients for the two channels as a function of temperature were derived assuming that the branching ratio for the two channels is invariant with temperature.

The yield of $O(^3P)$ from $O(^1D) + N_2O$ (physical quenching or chemical reaction) has been determined to be <0.04, 0.04 ± 0.02, 0.056 ± 0.009, and 0.005 ± 0.002 by Wine and Ravishankara,[13] Nishida et al.,[10] Carl,[5] and Vranckx et al.[12] at 298 K, respectively. Vranckx et al. report a slight increase in the $O(^3P)$ yield with increasing temperature (248–600 K) and their reported yield supersedes the anomalously high value reported by Carl[5] from the same laboratory. A recommended $O(^3P)$ yield of <0.01 is based on the Vranckx et al. study. A direct measurement of the NO yield from the $O(^1D) + N_2O$ reaction in synthetic air by Greenblatt and Ravishankara[9] and the re-analysis by Dunlea and Ravishankara[8] agrees very well with the value predicted using the recommended $O(^1D)$ rate coefficients for N_2, O_2, and N_2O and the $O(^1D) + N_2O$ product branching ratio to give NO + NO. Better reactive channel branching ratio measurements at stratospheric temperatures and/or measurements of the NO yield in this reaction as a function of temperature below 298 K would be useful. (Table 09-31, Note: 15-10, Evaluated: 10-6) Back to Table

(1) Amimoto, S. T.; Force, A. P.; Gulotty, R. G., Jr.; Wiesenfeld, J. R. Collisional deactivation of $O(2^1D_2)$ by the atmospheric gases. *J. Chem. Phys.* **1979**, *71*, 3640-3647, doi:10.1063/1.438807.
(2) Blitz, M. A.; Dillon, T. J.; Heard, D. E.; Pilling, M. J.; Trought, I. D. Laser induced fluorescence studies of the reactions of $O(^1D_2)$ with N_2, O_2, N_2O, CH_4, H_2, CO_2, Ar, Kr and n-C_4H_{10}. *Phys. Chem. Chem. Phys.* **2004**, *6*, 2162-2171, doi:10.1039/b400283k.
(3) Calvert, J. G.; Pitts, J. N. Photochemistry; John Wiley & Sons, Inc.: New York, 1966; pp 783.
(4) Cantrell, C. A.; Shetter, R. E.; Calvert, J. G. Branching ratios for the $O(^1D) + N_2O$ reaction. *J. Geophys. Res.* **1994**, *99*, 3739-3743, doi:10.1029/93JD02659.
(5) Carl, S. A. A highly sensitive method for time-resolved detection of $O(^1D)$ applied to precise determination of absolute $O(^1D)$ reaction rate constants and $O(^3P)$ yields. *Phys. Chem. Chem. Phys.* **2005**, *7*, 4051-4053, doi:10.1039/b513576c.
(6) Davidson, J. A.; Howard, C. J.; Schiff, H. I.; Fehsenfeld, F. C. Measurements of the branching ratios for the reaction of $O(^1D_2)$ with N_2O. *J. Chem. Phys.* **1979**, *70*, 1697-1704, doi:10.1063/1.437686.
(7) Dillon, T. J.; Horowitz, A.; Crowley, J. N. The atmospheric chemistry of sulphuryl fluoride, SO_2F_2. *Atmos. Chem. Phys.* **2008**, *8*, 1547-1557, doi:10.5194/acp-8-1547-2008.
(8) Dunlea, E. J.; Ravishankara, A. R. Kinetics studies of the reactions of $O(^1D)$ with several atmospheric molecules. *Phys. Chem. Chem. Phys.* **2004**, *6*, 2152-2161, doi:10.1039/b400247d.
(9) Greenblatt, G. D.; Ravishankara, A. R. Laboratory studies on the stratospheric NO_x production rate. *J. Geophys. Res.* **1990**, *95*, 3539-3547, doi:10.1029/JD095iD04p03539.

(10) Nishida, S.; Takahashi, K.; Matsumi, Y.; Taniguchi, N.; Hayashida, S. Formation of $O(^3P)$ atoms in the photolysis of N_2O at 193 nm and $O(^3P) + N_2O$ product channel in the reaction of $O(^1D) + N_2O$ *J. Phys. Chem. A* **2004**, *108*, 2451-2456, doi:10.1021/jp037034o.
(11) Takahashi, K.; Takeuchi, Y.; Matsumi, Y. Rate constants of the $O(^1D)$ reactions with N_2, O_2, N_2O, and H_2O at 295 K. *Chem. Phys. Lett.* **2005**, *410*, 196-200, doi:10.1016/j.cplett.2005.05.062.
(12) Vranckx, S.; Peeters, J.; Carl, S. A. Absolute rate constant and $O(^3P)$ yield for the $O(^1D) + N_2O$ reaction in the temperature range 227 K to 719 K. *Atmos. Chem. Phys.* **2008**, *8*, 6261-6272, doi:10.5194/acp-8-6261-2008.
(13) Wine, P. H.; Ravishankara, A. R. O_3 photolysis at 248 nm and $O(^1D_2)$ quenching by H_2O, CH_4, H_2, and N_2O: $O(^3P_J)$ yields. *Chem. Phys.* **1982**, *69*, 365-373, doi:10.1016/0301-0104(82)88075-0.

A9. **$O(^1D) + NH_3$**. The recommended rate coefficient and temperature dependence is taken from Davidson et al.[1] Sanders et al.[2] have detected the products $NH(a^1\Delta)$ and OH formed in the reaction. They report that the yield of $NH(a^1\Delta)$ is in the range 3–15% of the amount of the OH detected. A unit reaction yield is recommended. Further studies are needed to quantify the reaction channel branching ratios.
(Table: 82-57, Note: 15-10, Evaluated: 10-6) Back to Table

(1) Davidson, J. A.; Schiff, H. I.; Streit, G. E.; McAfee, J. R.; Schmeltekopf, A. L.; Howard, C. J. Temperature dependence of $O(^1D)$ rate constants for reactions with N_2O, H_2, CH_4, HCl, and NH_3. *J. Chem. Phys.* **1977**, *67*, 5021-5025, doi:10.1063/1.434724.
(2) Sanders, N. D.; Butler, J. E.; McDonald, J. R. Product branching ratios in the reaction of $O(^1D_2)$ with NH_3. *J. Chem. Phys.* **1980**, *73*, 5381-5383, doi:10.1063/1.439927.

A10. **$O(^1D) + HCN$**. Strekowski et al.[1] measured the total rate coefficient over the temperature range 211 to 425 K. Their results, the only study available, are recommended. There are several possible exothermic product channel pathways. Strekowski et al. report a $O(^3P)$ yield at 298 K to be ~0.3 and observed the $O(^3P)$ yield to have a negative temperature dependence. A significant H atom product channel, ~0.35, was determined at 298 K. The recommended reactive yield was taken from this work.
(Table 15-10, Note: 15-10, Evaluated: 15-10) Back to Table

(1) Strekowski, R. S.; Nicovich, J. M.; Wine, P. H. Kinetic and mechanistic study of the reactions of $O(^1D_2)$ with HCN and CH_3CN. *ChemPhysChem* **2010**, *11*, 3942-3955, doi:10.1002/cphc.201000550.

A11. **$O(^1D) + CH_3CN$**. Strekowski et al.[2] (193–430 K) and Hickson and Loison[1] (296, 127, and 75 K) measured the total reaction rate coefficient. -Strekowski et al. used a pulse laser photolysis (PLP) – resonance fluorescence method, while Hickson and Loison used a supersonic flow reactor coupled with PLP and laser induced fluorescence detection methods. The 296 K values in the two studies are in good agreement. The extreme low-temperature data of Hickson and Loison show non-Arrhenius behavior. The results from the Strekowski et al. study is recommended over the temperature range of their measurements.

There are several possible exothermic product channel pathways. Strekowski et al. report a minor $O(^3P)$ collisional quenching yield. The measured $O(^3P)$ yield was independent of temperature over the 193–430 K temperature range to within the precision of the measurements. They also report a temperature independent H atom yield with a 298 K value of 0.16 ± 0.03. Hickson and Loison report a H atom yield of 0.177 ± 0.03 at 296 K. The recommended reactive yield was taken from the Strekowski et al. work, which encompasses the results from both studies.
(Table 15-10, Note: 25-1, Evaluated: 25-1) Back to Table

(1) Hickson, K. M.; Loison, J.-C. Kinetic study of the gas-phase $O(^1D) + CH_3OH$ and $O(^1D) + CH_3CN$ reactions: Low-temperature rate constants and atomic hydrogen product yields. *J. Phys. Chem. A* **2022**, *126*, 3903−3913, doi:10.1021/acs.jpca.2c01946.
(2) Strekowski, R. S.; Nicovich, J. M.; Wine, P. H. Kinetic and mechanistic study of the reactions of $O(^1D_2)$ with HCN and CH_3CN. *ChemPhysChem* **2010**, *11*, 3942-3955, doi:10.1002/cphc.201000550.

A12. **$O(^1D) + CO_2$**. k(298 K) was derived from the studies of Davidson et al.,[3] Streit et al.,[9] Amimoto et al.,[1] Dunlea and Ravishankara,[5] Shi and Barker,[8] and Blitz et al.[2] Temperature dependence was computed after normalizing the results of Dunlea and Ravishankara and Streit et al. (only the data in the range of 200 to 354 K) to the value of k(298 K) recommended here. The rate coefficient at 195 K reported by Blitz et al. is consistent with the recommendation.

This reaction produces $O(^3P)$ and CO_2, and is expected to proceed through the formation of a CO_3 complex (see for example DeMore and Dede[4]). This complex formation leads to isotopic scrambling (see for example Perri et al.[6]). There appears to be a small, but non-negligible, channel for $O(^1D)$ quenching. A reactive channel

to give CO and O_2 has been reported,[7] but needs better quantification. A quenching yield of unity is recommended.
(Table: 06-2, Note: 06-2, Evaluated: 10-6) Back to Table

(1) Amimoto, S. T.; Force, A. P.; Gulotty, R. G., Jr.; Wiesenfeld, J. R. Collisional deactivation of $O(2^1D_2)$ by the atmospheric gases. *J. Chem. Phys.* **1979**, *71*, 3640-3647, doi:10.1063/1.438807.

(2) Blitz, M. A.; Dillon, T. J.; Heard, D. E.; Pilling, M. J.; Trought, I. D. Laser induced fluorescence studies of the reactions of $O(^1D_2)$ with N_2, O_2, N_2O, CH_4, H_2, CO_2, Ar, Kr and *n*-C_4H_{10}. *Phys. Chem. Chem. Phys.* **2004**, *6*, 2162-2171, doi:10.1039/b400283k.

(3) Davidson, J. A.; Schiff, H. I.; Streit, G. E.; McAfee, J. R.; Schmeltekopf, A. L.; Howard, C. J. Temperature dependence of $O(^1D)$ rate constants for reactions with N_2O, H_2, CH_4, HCl, and NH_3. *J. Chem. Phys.* **1977**, *67*, 5021-5025, doi:10.1063/1.434724.

(4) DeMore, W. B.; Dede, C. Pressure dependence of carbon trioxide formation in the gas-phase reacion of $O(^1D)$ with carbon dioxide. *J. Phys. Chem.* **1970**, *74*, 2621-2625, doi:10.1021/j100707a006.

(5) Dunlea, E. J.; Ravishankara, A. R. Kinetics studies of the reactions of $O(^1D)$ with several atmospheric molecules. *Phys. Chem. Chem. Phys.* **2004**, *6*, 2152-2161, doi:10.1039/b400247d.

(6) Perri, M. J.; Van Wyngarden, A. L.; Boering, K. A.; Lin, J. J.; Lee, Y. T. Dynamics of the $O(^1D)$ + CO_2 oxygen isotope exchange reaction. *J. Chem. Phys.* **2003**, *119*, 8213-8216, doi:10.1063/1.1618737.

(7) Sedlacek, A. J.; Harding, D. R.; Weston Jr., R. E.; Kreutz, T. G.; Flynn, G. W. Probing the $O(^1D)$ + CO_2 reaction with second-derivative modulated diode laser spectroscopy. *J. Chem. Phys.* **1989**, *91*, 7550-7556, doi:10.1063/1.457278.

(8) Shi, J.; Barker, J. R. Kinetic studies of the deactivation of $O_2(^1\Sigma_g^+)$ and $O(^1D)$. *Int. J. Chem. Kinet.* **1990**, *20*, 1283-1301, doi:10.1002/kin.550221207.

(9) Streit, G. E.; Howard, C. J.; Schmeltekopf, A. L.; Davidson, J. A.; Schiff, H. I. Temperature dependence of $O(^1D)$ rate constants for reactions with O_2, N_2, CO_2, O_3, and H_2O. *J. Chem. Phys.* **1976**, *65*, 4761-4764, doi:10.1063/1.432930.

A13. $O(^1D) + CH_4$. The recommended overall rate coefficient for the removal of $O(^1D)$ by CH_4 at room temperature is a weighted average of the results from Davidson et al.,[4] Blitz et al.,[1] Dillon et al.,[5] and Vranckx et al.[12] The temperature dependence of the rate coefficient was derived from the results of Davidson et al. (198–357 K), Dillon et al. (223–297 K), and Vranckx et al. (227–450 K). Meng et al.[9] (50, 75, 127, and 298 K) report rate coefficients obtained using a supersonic flow reactor-LIF method. Their 298 K value agrees with the recommendation, while the low-temperature data is systematically lower than the recommended temperature dependence by ~20%, which is within the recommended uncertainty. The recommended rate coefficients for the product channels (a) CH_3 + OH, (b) CH_3O or CH_2OH + H and (c) CH_2O + H_2 were evaluated for 298 K, the only temperature at which such data are available. Lin and DeMore[6] analyzed the final products of N_2O/CH_4 photolysis mixtures and concluded that (a) accounted for about 90% and (c) accounted for about 9%. Casavecchia et al.[2] used a molecular beam experiment to observe H and CH_3O (or CH_2OH) products. They reported that the yield of H_2 was <25% of the yield of H from channel (b). Satyapal et al.[10] observed the production of H atoms in a pulsed laser experiment and reported an H atom yield of 25 ± 8%. Matsumi et al.[8] reported the H atom yield in low pressure gas mixtures to be (15 ± 3)%. Chen et al.[3] used laser infrared kinetic spectroscopy to study product formation and report yields of (67 ± 5)%, (30 ± 10)%, and 5% for channels a, b, and c, respectively. The yield of $O(^3P)$ via the physical quenching of $O(^1D)$ by CH_4 has been reported by several groups. Wine and Ravishankara,[13] Matsumi et al.,[7] and Takahashi et al.[11] reported $O(^3P)$ yields of <4.3%, <5%, and <1%, respectively. Vranckx et al.[12] reported the most sensitive $O(^3P)$ yield measurement to date and obtained a yield of 0.002 ± 0.003. We recommend the following branching ratios (a) (75 ± 15)%, (b) (20 ± 10)%, (c) (5 ± 5)%, and no $O(^1D)$ collisional quenching . It is assumed that the branching ratio for the three reactive channels is invariant with temperature.
(Table 09-31, Note: 25-1, Evaluated: 25-1) Back to Table

(1) Blitz, M. A.; Dillon, T. J.; Heard, D. E.; Pilling, M. J.; Trought, I. D. Laser induced fluorescence studies of the reactions of $O(^1D_2)$ with N_2, O_2, N_2O, CH_4, H_2, CO_2, Ar, Kr and *n*-C_4H_{10}. *Phys. Chem. Chem. Phys.* **2004**, *6*, 2162-2171, doi:10.1039/b400283k.

(2) Casavecchia, P.; Buss, R. J.; Sibener, S. J.; Lee, Y. T. A crossed molecular beam study of the $O(^1D_2)$ + CH_4 reaction. *J. Chem. Phys.* **1980**, *73*, 6351-6352, doi:10.1063/1.440102.

(3) Chen, H.-b.; Thweatt, W. D.; Wang, J.; Glass, G. P.; Curl, R. F. IR kinetic spectroscopy investigation of the CH_4 + $O(^1D)$ reaction. *J. Phys. Chem. A* **2005**, *109*, 2207-2216, doi:10.1021/jp045521d.

(4) Davidson, J. A.; Schiff, H. I.; Streit, G. E.; McAfee, J. R.; Schmeltekopf, A. L.; Howard, C. J. Temperature dependence of $O(^1D)$ rate constants for reactions with N_2O, H_2, CH_4, HCl, and NH_3. *J. Chem. Phys.* **1977**, *67*, 5021-5025, doi:10.1063/1.434724.

(5) Dillon, T. J.; Horowitz, A.; Crowley, J. N. Absolute rate coefficients for the reactions of $O(^1D)$ with a series of n-alkanes. *Chem. Phys. Lett.* **2007**, *443*, 12-16, doi:10.1016/j.cplett.2007.06.044.

(6) Lin, C. L.; DeMore, W. B. O(^{1}D) production in ozone photolysis near 3100 Å. *J. Photochem.* **1973/74**, *2*, 161-164, doi:10.1016/0047-2670(73)80014-0.
(7) Martin, D.; Jourdain, J. L.; Laverdet, G.; Le Bras, G. Kinetic study of the reaction of IO with CH_3SCH_3. *Int. J. Chem. Kinet.* **1987**, *19*, 503-512, doi:10.1002/kin.550190603.
(8) Matsumi, Y.; Nomura, S.; Kawasaki, M.; Imamura, T. Vibrational distribution of ClO radicals produced in the reaction Cl + O_3 → ClO + O_2. *J. Phys. Chem.* **1996**, *100*, 176-179, doi:10.1021/jp9518872.
(9) Meng, Q.; Hickson, K. M.; Shao, K.; Loison, J.-C.; Zhang, D. H. Theoretical and experimental investigations of rate coefficients of O(^{1}D) + CH_4 at low temperature. *Phys. Chem. Chem. Phys.* **2016**, *18*, 29286--29292, doi:10.1039/c6cp05517f.
(10) Satyapal, S.; Park, J.; Bersohn, R.; Katz, B. Dissociation of methanol and ethanol activated by a chemical reaction or by light. *J. Chem. Phys.* **1989**, *91*, 6873-6879, doi:10.1063/1.457356.
(11) Takahashi, K.; Wada, R.; Matsumi, Y.; Kawasaki, M. Product branching ratios for O(^{3}P) atom and ClO radical formation in the reactions of O(^{1}D) with chlorinated compounds. *J. Phys. Chem.* **1996**, *100*, 10145-10149, doi:10.1021/jp952710a.
(12) Vranckx, S.; Peeters, J.; Carl, S. A temperature dependence kinetic study of O(^{1}D) + CH_4: overall rate coefficient and product yields. *Phys. Chem. Chem. Phys.* **2008**, *10*, 5714-5722, doi: 10.1039/b804903c.
(13) Wine, P. H.; Ravishankara, A. R. O_3 photolysis at 248 nm and O(^{1}D$_2$) quenching by H_2O, CH_4, H_2, and N_2O: O(^{3}P$_J$) yields. *Chem. Phys.* **1982**, *69*, 365-373, doi:10.1016/0301-0104(82)88075-0.

A14. O(^{1}D) + HCl. The recommended room temperature rate coefficient is based on the measurements of Davidson et al.,[3] Wine et al.,[6] and Chichinin.[1] The temperature dependence is based on the measurements of Davidson et al. Product studies by Wine et al. indicate: O(^{3}P) + HCl (9 ± 5)%; H + ClO (24 ± 5)%; and OH + Cl (67 ± 10)%. Takahashi et al.[5] report that the O(^{3}P) yield is (15 ± 4)%. Chichinin[2] report the H + ClO channel to be (18 ± 4)%. Feierabend et al.[4] report a ClO yield of 0.20 ± 0.04 (2σ measurement precision). The recommended total reactive yield is based on an average of the Wine et al. and Takahashi et al. O(^{3}P) yield results with an estimated uncertainty that encompasses the range of the measurements at the 2σ level. The H + ClO channel branching ratio is the average of the Wine et al., Chichinin, and Feierabend et al. results with the balance of the reactive channel leading to the formation of Cl + OH.
(Table: 25-1, Note: 25-1, Evaluated: 10-6) Back to Table

(1) Chichinin, A. I. Collisions of O(^{1}D) with HCl, Cl_2, and $COCl_2$: Total quenching, channel specific rate constants, and yields of Cl(^{2}P$_{1/2}$). *J. Chem. Phys.* **1997**, *106*, 1057-1062, doi:10.1063/1.473181.
(2) Chichinin, A. I. Isotope effects in the deactivation of O(^{1}D) atom by XCl and XF (X = H,D). *Chem. Phys. Lett.* **2000**, *316*, 425-432, doi:10.1016/S0009-2614(99)01325-1.
(3) Davidson, J. A.; Schiff, H. I.; Streit, G. E.; McAfee, J. R.; Schmeltekopf, A. L.; Howard, C. J. Temperature dependence of O(^{1}*D*) rate constants for reactions with N_2O, H_2, CH_4, HCl, and NH_3. *J. Chem. Phys.* **1977**, *67*, 5021-5025, doi:10.1063/1.434724.
(4) Feierabend, K. J.; Papanastasiou, D. K.; Burkholder, J. B. ClO radical yields in the reaction of O(^{1}D) with Cl_2, HCl, chloromethanes and chlorofluoromethanes. *J. Phys. Chem. A* **2010**, *114*, 12052-12061, doi:10.1021/jp10776lt.
(5) Takahashi, K.; Wada, R.; Matsumi, Y.; Kawasaki, M. Product branching ratios for O(^{3}P) atom and ClO radical formation in the reactions of O(^{1}D) with chlorinated compounds. *J. Phys. Chem.* **1996**, *100*, 10145-10149, doi:10.1021/jp952710a.
(6) Wine, P. H.; Wells, J. R.; Ravishankara, A. R. Channel specific rate constants for reactions of O(^{1}*D*) with HCl and HBr. *J. Chem. Phys.* **1986**, *84*, 1349-1354, doi:10.1063/1.450526.

A15. O(^{1}D) + HF. The recommended values of k(298 K) and the reactive yield are those reported by Sorokin et al.,[1] the only study available. It is assumed that the rate coefficient and product yields are independent of temperature. The reactive products of this reaction are F + OH. The channel to give H + FO is endothermic and, hence, considered to be unimportant.
(Table: 06-2, Note: 06-2, Evaluated: 06-2) Back to Table

(1) Sorokin, V. I.; Gritsan, N. P.; Chichinin, A. I. Collisions of O(^{1}D) with HF, F_2, XeF_2, NF_3, and CF_4: Deactivation and reaction. *J. Chem. Phys.* **1998**, *108*, 8995-9003, doi:10.1063/1.476346.

A16. O(^{1}D) + NF_3. The recommended value for k(298 K) is based on the results of Zhao et al.,[4] Dillon et al.,[2] and the value reported by Baasandorj et al.[1] at 296 K. The k(298 K) value reported by Sorokin et al.[3] is a factor of two lower and not considered in the recommendation. The recommended Arrhenius parameters are derived from a fit to these data after normalization to k(298 K). Sorokin et al., Zhao et al., and Baasandorj et al. report reactive yields of 0.70, >0.95, and 0.87 +0.13/-0.15, respectively. The recommended reactive yield is an

average of the values reported by Zhao et al. and Baasandorj et al. The reactive yield is expected to be independent of temperature. Sorokin et al. observed a high FO radical reaction product yield. Dillon et al. observed a high F-atom yield and attribute the FO formation in the Sorokin et al. study to secondary chemistry. No recommendation is given for the reaction products.
(Table: 15-10, Note: 15-10, Evaluated: 15-10) Back to Table

(1) Baasandorj, M.; Hall, B. D.; Burkholder, J. B. Rate coefficients for the reaction of $O(^1D)$ with the atmospherically long-lived greenhouse gases NF_3, SF_5CF_3, CHF_3, C_2F_6, *c*-C_4F_8, *n*-C_5F_{12}, and *n*-C_6F_{14}. *Atmos. Chem. Phys.* **2012**, *12*, 11753-11764, doi:10.5194/acp-12-11753-2012.

(2) Dillon, T. J.; Vereecken, L.; Horowitz, A.; Khamaganov, V.; Crowley, J. N.; Lelieveld, J. Removal of the potent greenhouse gas NF_3 by reactions with the atmospheric oxidants $O(^1D)$, OH and O_3. *Phys. Chem. Chem. Phys.* **2011**, *13*, 18600-18608, doi:101039/c1cp22230a.

(3) Sorokin, V. I.; Gritsan, N. P.; Chichinin, A. I. Collisions of $O(^1D)$ with HF, F_2, XeF_2, NF_3, and CF_4: Deactivation and reaction. *J. Chem. Phys.* **1998**, *108*, 8995-9003, doi:10.1063/1.476346.

(4) Zhao, Z.; Laine, P. L.; Nicovich, J. M.; Wine, P. H. Reactive and non-reactive quenching of $O(^1D)$ by the potent greenhouse gases SO_2F_2, NF_3, and SF_5CF_3. *Proc. Nat. Acad. Sci.* **2010**, *107*, 6610-6615, doi:10.1073/pnas.0911228107.

A17. $O(^1D)$ + HBr. The recommended rate coefficient at 298 K was taken from Wine et al.[3] There are no reports on the temperature dependence of this rate coefficient. Because it is close to a collisional rate coefficient, the rate coefficient is assumed to be temperature independent. On the basis of $O(^3P)$ and $H(^2S)$ atom detection, Wine et al. reported physical quenching, HBr + $O(^3P)$, in this reaction to be (20 ± 7)%, which is recommended here assuming that no reactive quenching occurs, and the H + BrO reactive product channel to be <4.5%. In a crossed molecular beam study of this reaction, Balucani et al.[1] found the BrO yield to be >(14 ± 6)%. Using transient UV absorption spectroscopy, Cronkhite et al.[2] found the BrO yield to be (20 ± 4)%, which is recommended here. The balance of the reaction leads to the formation of Br + OH products.
(Table: 87-41, Note: 15-10, Evaluated: 10-6) Back to Table

(1) Balucani, N.; Beneventi, L.; Casavecchia, P.; Volpi, G. G.; Kruus, E. J.; Sloan, J. J. The dynamics of the reaction of $O(^1D)$ with HBr studied by crossed molecular beams and time-resolved Fourier transform spectroscopy. *Can. J. Chem.* **1994**, *72*, 888-902, doi:10.1139/v94-116.

(2) Cronkhite, J. M.; Wine, P. H. Branching ratios for BrO production from reactions of $O(^1D)$ with HBr, CF_3Br, CH_3Br, CF_2ClBr, and CF_2HBr. *Int. J. Chem. Kinet.* **1998**, *30*, 555-563, doi:10.1002/(SICI)1097-4601(1998)30:8<555::AID-KIN4>3.0.CO;2-R.

(3) Wine, P. H.; Wells, J. R.; Ravishankara, A. R. Channel specific rate constants for reactions of $O(^1D)$ with HCl and HBr. *J. Chem. Phys.* **1986**, *84*, 1349-1354, doi:10.1063/1.450526.

A18. $O(^1D)$ + Cl_2. The recommended *k*(298 K) is based on the studies of Wine et al.[6] and Sorokin et al.[4] There are no reports on the temperature dependence of this rate coefficient. The rate coefficient is assumed to be temperature independent because *k*(298 K) is close to a collisional rate coefficient. Wine et al. report a $O(^3P)$ yield of 0.25 ± 0.10. The Cl atom measurements of Chichinin[1] are consistent with a ClO + Cl yield of 0.7. These values are in excellent agreement with the directly measured ClO yield of 74 ± 15% by Takahashi et al.[5] and 77 ± 10% by Feierabend et al.[2] Feierabend et al. also reported no measurable (<10%) change in the ClO radical yield at 202 K. An indirect study by Freudenstein and Biedenkapp[3] is in reasonable agreement with the yield of ClO. Though energetically allowed, the formation of Cl_2O is expected to be negligible under atmospheric pressure and temperature conditions. On the basis of the Wine et al., Takahashi et al. and Feierabend et al. studies the recommended total reactive and Cl + ClO channel yield is 0.75 ± 0.07, independent of temperature.
(Table: 06-2, Note: 15-10, Evaluated: 15-10) Back to Table

(1) Chichinin, A. I. Collisions of $O(^1D)$ with HCl, Cl_2, and $COCl_2$: Total quenching, channel specific rate constants, and yields of $Cl(^2P_{1/2})$. *J. Chem. Phys.* **1997**, *106*, 1057-1062, doi:10.1063/1.473181.

(2) Feierabend, K. J.; Papanastasiou, D. K.; Burkholder, J. B. ClO radical yields in the reaction of $O(^1D)$ with Cl_2, HCl, chloromethanes and chlorofluoromethanes. *J. Phys. Chem. A* **2010**, *114*, 12052-12061, doi:10.1021/jp10776lt.

(3) Freudenstein, K.; Biedenkapp, D. Kinetics of reaction of electronically excited oxygen atoms with chlorine $O(^1D)$ + Cl_2. *Ber. Bunsenges. Phys. Chem.* **1976**, *80*, 42-48, doi:10.1002/bbpc.19760800110.

(4) Sorokin, V. I.; Gritsan, N. P.; Chichinin, A. I. Collisions of $O(^1D)$ with HF, F_2, XeF_2, NF_3, and CF_4: Deactivation and reaction. *J. Chem. Phys.* **1998**, *108*, 8995-9003, doi:10.1063/1.476346.

(5) Takahashi, K.; Wada, R.; Matsumi, Y.; Kawasaki, M. Product branching ratios for $O(^3P)$ atom and ClO radical formation in the reactions of $O(^1D)$ with chlorinated compounds. *J. Phys. Chem.* **1996**, *100*, 10145-10149, doi:10.1021/jp952710a.

(6) Wine, P. H.; Nicovich, J. M.; Ravishankara, A. R. Kinetics of the reactions of $O(^3P)$ and $O(^1D)$ with Cl_2. *J. Phys. Chem.* **1985**, *89*, 3914-3918, doi:10.1021/j100264a031.

A19. $O(^1D) + CCl_2O$. The recommended value of k(298 K) is derived from the values reported by Chichinin[1] and Strekowski et al.[3] The relative rate study of Jayanty et al.[2] is consistent with the recommended value. The temperature dependence is taken from Strekowski et al. There are three possible reactive channels: CO + ClO + Cl; CO_2 + 2 Cl; $CO_2 + Cl_2$. In the stratosphere, all these processes will lead to CO_2 and ClO. Chichinin reports that the above 3 reactions account for (80 ± 15)% of $O(^1D)$ loss with 20% leading to $O(^3P)$. Strekowski et al. report a $O(^3P)$ yield of 0.20 ± 0.04, which is the basis of the recommendation. The rate coefficient for the loss of CCl_2O via reaction with $O(^1D)$ may be greater than 80% of the overall rate coefficient recommended here due to reactive quenching of $O(^1D)$ to $O(^3P)$.
(Table: 06-2, Note: 15-10, Evaluated: 15-10) Back to Table

(1) Chichinin, A. I. Collisions of $O(^1D)$ with HCl, Cl_2, and $COCl_2$: Total quenching, channel specific rate constants, and yields of $Cl(^2P_{1/2})$. *J. Chem. Phys.* **1997**, *106*, 1057-1062, doi:10.1063/1.473181.
(2) Jayanty, R. K. M.; Simonaitis, R.; Heicklen, J. The reaction of $O(^1D)$ with CCl_2O, CFClO and CF_2O. *J. Photochem.* **1976**, *5*, 217-224, doi:10.1016/0047-2670(76)85018-6.
(3) Strekowski, R. S.; Nicovich, J. M.; Wine, P. H. Quenching of $O(^1D_2)$ by Cl_2CO: kinetics and $O(^3P_J)$ yield. *Chem. Phys. Lett.* **2000**, *330*, 354-360, doi:10.1016/S0009-2614(00)01105-2.

A20. $O(^1D) + CClFO$. The recommended rate coefficient is derived from data of Fletcher and Husain.[1] For consistency, the recommended value was derived using a scaling factor (0.5) that corrects for the difference between rate coefficients from the Husain laboratory and the recommendations for other $O(^1D)$ rate coefficients given in this evaluation. Based on consideration of similar $O(^1D)$ reactions, it is assumed that E/R equals zero and the A-factor has been set equal to k(298 K). The branching ratios are estimated based on measured values for similar compounds.
(Table: 82-57, Note: 15-10, Evaluated: 15-10) Back to Table

(1) Fletcher, I. S.; Husain, D. The collisional quenching of $O(2^1D_2)$ by $COCl_2$, COFCl and COF_2 using atomic absorption spectroscopy in the vacuum ultraviolet. *J. Photochem.* **1978**, *8*, 355-361, doi:10.1016/0047-2670(78)80158-0.

A21. $O(^1D) + CF_2O$. The recommendation is from the data of Wine and Ravishankara.[4] Their result is preferred over the value of Fletcher and Husain[2] because it appears to follow the pattern of decreased reactivity with increased fluorine substitution observed for other halocarbons. This reaction has only been studied at 298 K. Based on consideration of similar $O(^1D)$ reactions, it is assumed that E/R equals zero and the A-factor has been set equal to k(298 K). Wine and Ravishankara report (71 ± 7)% quenching of $O(^1D)$ to $O(^3P)$. Using relative rate methods, Atkinson et al.[1] and Jayanty et al.[3] measured reactive yields of 0.5 ± 0.15 and 0.70, respectively. The recommended reactive yield is an average of these studies.
(Table: 82-57, Note: 15-10, Evaluated: 15-10) Back to Table

(1) Atkinson, R.; Breuer, G. M.; Pitts Jr., J. N.; Sandoval, H. L. Tropospheric and stratospheric sinks for halocarbons: Photooxidation, $O(^1D)$ atom, and OH radical reactions. *J. Geophys. Res.* **1976**, *81*, 5765-5770, doi:10.1029/JC081i033p05765.
(2) Fletcher, I. S.; Husain, D. The collisional quenching of $O(2^1D_2)$ by $COCl_2$, COFCl and COF_2 using atomic absorption spectroscopy in the vacuum ultraviolet. *J. Photochem.* **1978**, *8*, 355-361, doi:10.1016/0047-2670(78)80158-0.
(3) Jayanty, R. K. M.; Simonaitis, R.; Heicklen, J. The reaction of $O(^1D)$ with CCl_2O, CFClO and CF_2O. *J. Photochem.* **1976**, *5*, 217-224, doi:10.1016/0047-2670(76)85018-6.
(4) Wine, P. H.; Ravishankara, A. R. Reactive and non-reactive quenching of $O(^1D_2)$ by COF_2. *Chem. Phys. Lett.* **1983**, *96*, 129-132, doi:10.1016/0009-2614(83)80131-6.

A22. $O(^1D) + CH_3Cl$. The k(298 K) recommendation is an average of the values reported by Matsumi et al.[3] and Force and Wiesenfeld.[2] There are no reports on the temperature dependence of this rate coefficient and it is assumed to be temperature independent. There have been several product channels observed for this reaction. Matsumi et al. observed the formation of H and Cl atoms with a 0.27 ratio. Force and Wiesenfeld reported an $O(^3P)$ yield of 0.09, which is the basis for the total reactive yield recommendation. Takahashi et al.[4] and Feierabend et al.[1] have reported ClO radical yields that are in excellent agreement, (0.47 ± 0.10) and (0.46 ± 0.06), respectively, which is recommended. The recommended product branching ratios for the H and Cl atom channels accounts for the remaining product yield in the ratio reported by Matsumi et al.
(Table 15-10, Note: 15-10, Evaluated: 15-10) Back to Table

(1) Feierabend, K. J.; Papanastasiou, D. K.; Burkholder, J. B. ClO radical yields in the reaction of $O(^1D)$ with Cl_2, HCl, chloromethanes and chlorofluoromethanes. *J. Phys. Chem. A* **2010**, *114*, 12052-12061, doi:10.1021/jp10776lt.
(2) Force, A. P.; Wiesenfeld, J. R. Collisional deactivation of $O(^1D_2)$ by the halomethanes. Direct determination of reaction efficiency. *J. Phys. Chem.* **1981**, *85*, 782-785, doi:10.1021/j150607a012.
(3) Matsumi, Y.; Tonokura, K.; Inagaki, Y.; Kawasaki, M. Isotopic branching ratios and translational energy release of H and D atoms in reaction of $O(^1D)$ atoms with alkanes and akyl chlorides. *J. Phys. Chem.* **1993**, *97*, 6816-6821, doi:10.1021/j100128a012.
(4) Takahashi, K.; Wada, R.; Matsumi, Y.; Kawasaki, M. Product branching ratios for $O(^3P)$ atom and ClO radical formation in the reactions of $O(^1D)$ with chlorinated compounds. *J. Phys. Chem.* **1996**, *100*, 10145-10149, doi:10.1021/jp952710a.

A23. **$O(^1D) + CCl_4$**. The recommended $k(298\ K)$ value is based on the data from Davidson et al.[1] and Force and Wiesenfeld.[3] The temperature independence of the rate coefficient is taken from Davidson et al. Force and Wiesenfeld reported this reaction to be (14 ± 6)% collisional quenching. Takahashi et al.[4] and Feierabend et al.[2] report ClO radical yields of (90 ± 19)% and (79 ± 4)%, respectively. The recommended value is taken from the more precise Feierabend et al. study. Additional product channels may also be possible.
(Table: 82-57, Note: 15-10, Evaluated: 15-10) Back to Table

(1) Davidson, J. A.; Schiff, H. I.; Brown, T. J.; Howard, C. J. Temperature dependence of the rate constants for reactions of $O(^1D)$ atoms with a number of halocarbons. *J. Chem. Phys.* **1978**, *69*, 4277-4279, doi:10.1063/1.437113.
(2) Feierabend, K. J.; Papanastasiou, D. K.; Burkholder, J. B. ClO radical yields in the reaction of $O(^1D)$ with Cl_2, HCl, chloromethanes and chlorofluoromethanes. *J. Phys. Chem. A* **2010**, *114*, 12052-12061, doi:10.1021/jp10776lt.
(3) Force, A. P.; Wiesenfeld, J. R. Collisional deactivation of $O(^1D_2)$ by the halomethanes. Direct determination of reaction efficiency. *J. Phys. Chem.* **1981**, *85*, 782-785, doi:10.1021/j150607a012.
(4) Takahashi, K.; Wada, R.; Matsumi, Y.; Kawasaki, M. Product branching ratios for $O(^3P)$ atom and ClO radical formation in the reactions of $O(^1D)$ with chlorinated compounds. *J. Phys. Chem.* **1996**, *100*, 10145-10149, doi:10.1021/jp952710a.

A24. **$O(^1D) + CH_3CCl_3$**. Nilsson et al.[1] reported a room temperature reactive rate coefficient of $(2.93 \pm 1.2) \times 10^{-10}$ cm^3 $molecule^{-1}$ s^{-1} (1σ error limit) that was obtained using a relative rate method with CH_4 as the reference compound. The recommended total rate coefficient was calculated assuming a 0.9 reactive yield.
(Table 15-10, Note: 15-10, Evaluated: 15-10) Back to Table

(1) Nilsson, E. J. K.; Andersen, V. F.; Nielsen, O. J.; Johnson, M. S. Rate coefficients for the chemical reactions of CH_2F_2, $CHClF_2$, CH_2FCF_3 and CH_3CCl_3 with $O(^1D)$ at 298 K. *Chem. Phys. Lett.* **2012**, *554*, 27-32, doi:10.1016/j.cplett.2012.10.001.

A25. **$O(^1D) + CH_3Br$**. The recommended rate coefficient at 298 K was taken from Thompson and Ravishankara.[2] There are no reports on the temperature dependence of this rate coefficient and it is assumed to be temperature independent. Thompson and Ravishankara report that the yield of $O(^3P)$ from physical quenching is (0 ± 7)%. On the basis of this single study, a unit reactive yield is recommended. Using transient UV absorption spectroscopy, Cronkhite et al.[1] measured the BrO yield to be (44 ± 5)%. The balance of the reaction is expected to lead to OH radical formation, although no experimental data are currently available.
(Table: 94-26, Note: 15-10, Evaluated: 10-6) Back to Table

(1) Cronkhite, J. M.; Wine, P. H. Branching ratios for BrO production from reactions of $O(^1D)$ with HBr, CF_3Br, CH_3Br, CF_2ClBr, and CF_2HBr. *Int. J. Chem. Kinet.* **1998**, *30*, 555-563, doi:10.1002/(SICI)1097-4601(1998)30:8<555::AID-KIN4>3.0.CO;2-R.
(2) Thompson, J. E.; Ravishankara, A. R. Kinetics of $O(^1D)$ reactions with bromocarbons. *Int. J. Chem. Kinet.* **1993**, *25*, 479-487, doi:10.1002/kin.550250607.

A26. **$O(^1D) + CH_2Br_2$**. The recommendation for $k(298\ K)$ is based on data from Thompson and Ravishankara,[1] the only study available. There are no reports on the temperature dependence of this rate coefficient and it is assumed to be temperature independent. They report that the yield of $O(^3P)$ from physical quenching is (5 ± 7)%. On the basis of this work, a reactive yield of $0.95\ ^{+0.05}_{-0.10}$ is recommended. There are no product studies available, although the major channels are expected to lead to BrO and OH radical formation.
(Table: 94-26, Note: 15-10, Evaluated: 10-6) Back to Table

(1) Thompson, J. E.; Ravishankara, A. R. Kinetics of $O(^1D)$ reactions with bromocarbons. *Int. J. Chem. Kinet.* **1993**, *25*, 479-487, doi:10.1002/kin.550250607.

A27. $O(^1D) + CHBr_3$. The recommendation for k(298 K) is based on data from Thompson and Ravishankara,[1] the only study available. The rate coefficient is large compared to analogous compounds. There are no reports on the temperature dependence of this rate coefficient and it is assumed to be temperature independent. They report that the yield of $O(^3P)$ from physical quenching is (32 ± 8)%. A reactive yield of 0.70 ± 0.1 is recommended. There are no product studies available, although the formation of BrO is expected to be a major product channel.
(Table: 94-26, Note: 15-10, Evaluated: 10-6) Back to Table

(1) Thompson, J. E.; Ravishankara, A. R. Kinetics of $O(^1D)$ reactions with bromocarbons. *Int. J. Chem. Kinet.* **1993**, *25*, 479-487, doi:10.1002/kin.550250607.

A28. $O(^1D) + CH_3F$ (HFC-41). The k(298 K) recommendation is the average of the measurements of Force and Wiesenfeld[2] and Schmoltner et al.[4] There are no reports on the temperature dependence of this rate coefficient and it is assumed to be temperature independent. The $O(^3P)$ product yield was reported to be (25 ± 3)% by Force and Wiesenfeld, (11 ± 5)% by Schmoltner et al., and (19 ± 5)% by Takahashi et al.[5] The recommended branching ratio is an average of these studies, with an uncertainty that encompasses the mean value from all studies at the 2σ level. Burks and Lin[1] reported observing vibrationally excited HF as a product. Park and Wiesenfeld[3] observed the formation of OH ($X^2\Pi$, ν" = 0, 1) in this reaction.
(Table: 94-26, 15-10, Evaluated: 10-6) Back to Table

(1) Burks, T. L.; Lin, M. C. The dynamics of formation of vibrationally excited HF in reactions of $O(2^1D_2)$ atoms with partially fluorinated alkanes. *Int. J. Chem. Kinet.* **1981**, *13*, 977-999, doi:10.1002/kin.550130918.
(2) Force, A. P.; Wiesenfeld, J. R. Collisional deactivation of $O(^1D_2)$ by the halomethanes. Direct determination of reaction efficiency. *J. Phys. Chem.* **1981**, *85*, 782-785, doi:10.1021/j150607a012.
(3) Park, C. R.; Wiesenfeld, J. R. Chemical dynamics of the reaction of $O(^1D_2)$ with CH_3F. *Chem. Phys. Lett.* **1991**, *186*, 170-176, doi:10.1016/S0009-2614(91)85124-F.
(4) Schmoltner, A. M.; Talukdar, R. K.; Warren, R. F.; Mellouki, A.; Goldfarb, L.; Gierczak, T.; McKeen, S. A.; Ravishankara, A. R. Rate coefficients for reactions of several hydrofluorocarbons with OH and $O(^1D)$ and their atmospheric lifetimes. *J. Phys. Chem.* **1993**, *97*, 8976-8982, doi:10.1021/j100137a023.
(5) Takahashi, K.; Wada, R.; Matsumi, Y.; Kawasaki, M. Product branching ratios for $O(^3P)$ atom and ClO radical formation in the reactions of $O(^1D)$ with chlorinated compounds. *J. Phys. Chem.* **1996**, *100*, 10145-10149, doi:10.1021/jp952710a.

A29. $O(^1D) + CH_2F_2$ (HFC-32). The k(298 K) recommendation is based on the measurement of Schmoltner et al.,[4] the only total rate coefficient study available. Using a relative rate technique, Green and Wayne[2] measured the loss of CH_2F_2 relative to the loss of N_2O. Their value when combined with the current recommendation for the $O(^1D) + N_2O$ reaction yields a rate coefficient for reactive loss of CH_2F_2 that is about three times the result of Schmoltner et al. Nilsson et al.[3] reported a 298 K reactive rate coefficient of $(4.78 \pm 1.02) \times 10^{-11}$ cm^3 molecule^{-1} s^{-1} in a relative rate experiment with the $O(^1D) + CH_4$ reaction as the reference. This corresponds to a reactive yield of 0.94 using the current total rate coefficient recommendation. Schmoltner et al. reported an $O(^3P)$ yield of (70 ± 11)%, which provides the basis of the reaction yield recommendation, assuming that it is due entirely to physical quenching. Burks and Lin[1] reported observing vibrationally excited HF as a product.
(Table: 94-26, Note: 15-10, Evaluated: 10-6) Back to Table

(1) Burks, T. L.; Lin, M. C. The dynamics of formation of vibrationally excited HF in reactions of $O(2^1D_2)$ atoms with partially fluorinated alkanes. *Int. J. Chem. Kinet.* **1981**, *13*, 977-999, doi:10.1002/kin.550130918.
(2) Green, R. G.; Wayne, R. P. Relative rate constants for the reactions of $O(^1D)$ atoms with fluorochlorocarbons and with N_2O. *J. Photochem.* **1976/77**, *6*, 371-374, doi:10.1016/0047-2670(76)85076-9.
(3) Nilsson, E. J. K.; Andersen, V. F.; Nielsen, O. J.; Johnson, M. S. Rate coefficients for the chemical reactions of CH_2F_2, $CHClF_2$, CH_2FCF_3 and CH_3CCl_3 with $O(^1D)$ at 298 K. *Chem. Phys. Lett.* **2012**, *554*, 27-32, doi:10.1016/j.cplett.2012.10.001.
(4) Schmoltner, A. M.; Talukdar, R. K.; Warren, R. F.; Mellouki, A.; Goldfarb, L.; Gierczak, T.; McKeen, S. A.; Ravishankara, A. R. Rate coefficients for reactions of several hydrofluorocarbons with OH and $O(^1D)$ and their atmospheric lifetimes. *J. Phys. Chem.* **1993**, *97*, 8976-8982, doi:10.1021/j100137a023.

A30. $O(^1D) + CHF_3$ (HFC-23). k(298 K) was measured by Force and Wiesenfeld[5] and Schmoltner et al.,[6] while Baasandorj et al.[2,3] measured the rate coefficient at 298 K and over the temperature range 217–373 K. The results from these studies are in good agreement and the results from the Baasandorj et al. study are recommended. The $O(^3P)$ product yield was reported to be (77 ± 15)% by Force and Wiesenfeld and (102 ± 3%) by Schmoltner et al. Using a relative rate technique, Baasandorj et al.[2,3] measured the reactive rate coefficient (relative to the $O(^1D) + NF_3$ reaction) at room temperature. They obtained a reactive yield of 0.25 ± 0.05, using the current k(298 K) recommendation for the HFC-23 reaction. This result is in good agreement with the Force and Wiesenfeld result. The reaction yield recommendation is based on the more precise Baasandorj et al. studies. There is no apparent explanation for the high quenching yield reported in the Schmoltner et al. study. Although physical quenching is the dominant process, detectable yields of vibrationally excited HF have been reported by Burks and Lin[4] and Aker et al.,[1] which indicate the formation of $HF + CF_2O$ products.
(Table: 15-10, Note: 15-10, Evaluated: 15-10) Back to Table

(1) Aker, P. M.; Niefer, B. I.; Sloan, J. J.; Heydtmann, H. The dynamics and microscopic kinetics of the reactions of $O(^1D_2)$ atoms with $CHCl_3$ and CHF_3. *J. Chem. Phys.* **1987**, *87*, 203-209, doi:10.1063/1.453616.

(2) Baasandorj, M.; Fleming, E. L.; Jackman, C. H.; Burkholder, J. B. $O(^1D)$ kinetic study of key ozone depleting substances and greenhouse gases. *J. Phys. Chem. A* **2013**, *117*, 2434-2445, doi:10.1021/jp312781c.

(3) Baasandorj, M.; Hall, B. D.; Burkholder, J. B. Rate coefficients for the reaction of $O(^1D)$ with the atmospherically long-lived greenhouse gases NF_3, SF_5CF_3, CHF_3, C_2F_6, *c*-C_4F_8, *n*-C_5F_{12}, and *n*-C_6F_{14}. *Atmos. Chem. Phys.* **2012**, *12*, 11753-11764, doi:10.5194/acp-12-11753-2012.

(4) Burks, T. L.; Lin, M. C. The dynamics of formation of vibrationally excited HF in reactions of $O(2^1D_2)$ atoms with partially fluorinated alkanes. *Int. J. Chem. Kinet.* **1981**, *13*, 977-999, doi:10.1002/kin.550130918.

(5) Force, A. P.; Wiesenfeld, J. R. Collisional deactivation of $O(^1D_2)$ by the halomethanes. Direct determination of reaction efficiency. *J. Phys. Chem.* **1981**, *85*, 782-785, doi:10.1021/j150607a012.

(6) Schmoltner, A. M.; Talukdar, R. K.; Warren, R. F.; Mellouki, A.; Goldfarb, L.; Gierczak, T.; McKeen, S. A.; Ravishankara, A. R. Rate coefficients for reactions of several hydrofluorocarbons with OH and $O(^1D)$ and their atmospheric lifetimes. *J. Phys. Chem.* **1993**, *97*, 8976-8982, doi:10.1021/j100137a023.

A31. $O(^1D) + CHCl_2F$ (HCFC-21). The recommendation is based on the total rate coefficient measurements of Davidson et al.[1] over the temperature range 188–343 K. Takahashi et al.[3] and Feierabend et al.[2] report the yield of ClO to be (74 ± 15)% and (73 ± 5)%, respectively. These studies are in excellent agreement and provide the recommendation for the ClO product channel branching ratio. It is expected that the OH radical, or other products, may also be formed in this reaction. An OH channel yield based on comparison with other HCFCs is estimated to be ~0.06.
(Table: 90-1, Note: 15-10, Evaluated: 15-10) Back to Table

(1) Davidson, J. A.; Schiff, H. I.; Brown, T. J.; Howard, C. J. Temperature dependence of the rate constants for reactions of $O(^1D)$ atoms with a number of halocarbons. *J. Chem. Phys.* **1978**, *69*, 4277-4279, doi:10.1063/1.437113.

(2) Feierabend, K. J.; Papanastasiou, D. K.; Burkholder, J. B. ClO radical yields in the reaction of $O(^1D)$ with Cl_2, HCl, chloromethanes and chlorofluoromethanes. *J. Phys. Chem. A* **2010**, *114*, 12052-12061, doi:10.1021/jp10776lt.

(3) Takahashi, K.; Wada, R.; Matsumi, Y.; Kawasaki, M. Product branching ratios for $O(^3P)$ atom and ClO radical formation in the reactions of $O(^1D)$ with chlorinated compounds. *J. Phys. Chem.* **1996**, *100*, 10145-10149, doi:10.1021/jp952710a.

A32. $O(^1D) + CHClF_2$ (HCFC-22). The rate coefficient recommendation is based on the measurements of Davidson et al.,[4] Warren et al.[8] and Baasandorj et al.[3] Davidson et al. (173–343 K) and Baasandorj et al. (217–373 K) determined that the rate coefficient has no temperature dependence between 173 and 343 K. Warren et al.[8] report an $O(^3P)$ yield of (28 ± 6)%, which they interpret to be due to collisional quenching of $O(^1D)$ to $O(^3P)$. Using a relative rate technique, Baasandorj et al. measured the reactive rate coefficient (relative to the $O(^1D) + NF_3$ reaction) at room temperature. They obtained a reaction yield of 0.75 ± 0.05, using the current k(298 K) recommendation for the NF_3 and HCFC-22 reactions, which is in good agreement with the Warren et al. result. A relative rate measurement by Green and Wayne,[6] with $O(^1D) + N_2O$ as the reference reaction, is ~25% higher than the recommended k(298 K) value. A relative rate measurement by Atkinson et al.[2] gives a rate coefficient about a factor of two too high. A relative rate measurement by Nilsson et al.,[7] with $O(^1D) + CH_4$ as the reference reaction, reported a reactive rate coefficient of (8.69 ± 1.72) × 10^{-11} cm^3 $molecule^{-1}$ s^{-1} corresponding to a

reactive yield of 0.85 ± 0.17 using the current total rate coefficient recommendation. The recommended total reactive yield of 0.75 is taken from the more precise Baasandorj et al. study.

This reaction has been shown to have multiple product channels. Addison et al.[1] reported the following product yields: ClO (55 ± 10)%, CF_2 (45 ± 10)%, O(^{3}P) (28 +10/ –15)%, and OH 5%, where the O(^{3}P) was interpreted to come from a branch yielding CF_2 and HCl. Feierabend et al.[5] reported a ClO radical yield of 0.56 ± 0.03, which agrees very well with the Addison et al. measurement and is the basis of the recommendation. An OH product channel yield of 0.05 is recommended and the balance of the reactive yield is assigned to other products.
(Table: 92-20, Note: 15-10, Evaluated: 15-10) Back to Table

(1) Addison, M. C.; Donovan, R. J.; Garraway, J. Reactions of O(2^1D_2) and O(2^3P_J) with halogenomethanes. *Faraday Disc.* **1979**, *67*, 286-296, doi:10.1039/dc9796700286.
(2) Atkinson, R.; Breuer, G. M.; Pitts Jr., J. N.; Sandoval, H. L. Tropospheric and stratospheric sinks for halocarbons: Photooxidation, O(^1D) atom, and OH radical reactions. *J. Geophys. Res.* **1976**, *81*, 5765-5770, doi:10.1029/JC081i033p05765.
(3) Baasandorj, M.; Fleming, E. L.; Jackman, C. H.; Burkholder, J. B. O(^{1}D) kinetic study of key ozone depleting substances and greenhouse gases. *J. Phys. Chem. A* **2013**, *117*, 2434-2445, doi:10.1021/jp312781c.
(4) Davidson, J. A.; Schiff, H. I.; Brown, T. J.; Howard, C. J. Temperature dependence of the rate constants for reactions of O(^1D) atoms with a number of halocarbons. *J. Chem. Phys.* **1978**, *69*, 4277-4279, doi:10.1063/1.437113.
(5) Feierabend, K. J.; Papanastasiou, D. K.; Burkholder, J. B. ClO radical yields in the reaction of O(^{1}D) with Cl_2, HCl, chloromethanes and chlorofluoromethanes. *J. Phys. Chem. A* **2010**, *114*, 12052-12061, doi:10.1021/jp10776lt.
(6) Green, R. G.; Wayne, R. P. Relative rate constants for the reactions of O(^{1}D) atoms with fluorochlorocarbons and with N_2O. *J. Photochem.* **1976/77**, *6*, 371-374, doi:10.1016/0047-2670(76)85076-9.
(7) Nilsson, E. J. K.; Andersen, V. F.; Nielsen, O. J.; Johnson, M. S. Rate coefficients for the chemical reactions of CH_2F_2, $CHClF_2$, CH_2FCF_3 and CH_3CCl_3 with O(^{1}D) at 298 K. *Chem. Phys. Lett.* **2012**, *554*, 27-32, doi:10.1016/j.cplett.2012.10.001.
(8) Warren, R.; Gierczak, T.; Ravishankara, A. R. A study of O(^{1}D) reactions with CFC substitutes. *Chem. Phys. Lett.* **1991**, *183*, 403-409, doi:10.1016/0009-2614(91)90402-U.

A33. O(^{1}D) + CHF_2Br. The recommended rate coefficient at room temperature and its temperature dependence are based on the study of Strekowski et al.[2] (211–425 K), which is the only available investigation of this reaction. They report a branching ratio for O(^{3}P) production of (39 ± 6)% independent of temperature and a branching ratio for H atom production of 2^{+1}_{-2}% at 298 K. Cronkhite et al.[1] report a BrO yield of (39 ± 7)% at room temperature. The recommended reactive yield is 0.60 with a significant yield, ~0.2, of unidentified reaction products.
(Table: 06-2, Note: 15-10, Evaluated: 10-6) Back to Table

(1) Cronkhite, J. M.; Wine, P. H. Branching ratios for BrO production from reactions of O(^{1}D) with HBr, CF_3Br, CH_3Br, CF_2ClBr, and CF_2HBr. *Int. J. Chem. Kinet.* **1998**, *30*, 555-563, doi:10.1002/(SICI)1097-4601(1998)30:8<555::AID-KIN4>3.0.CO;2-R.
(2) Strekowski, R. S.; Nicovich, J. M.; Wine, P. H. Kinetic and mechanistic study of the reaction of O(^{1}D) with CF_2HBr. *Int. J. Chem. Kinet.* **2001**, *33*, 262-270, doi:10.1002/kin.1019.abs.

A34. O(^{1}D) + CCl_3F (CFC-11). The recommended rate coefficient is based on the data from Davidson et al.[2] (173–343 K), Force et al.[4] (298 K), and Baasandorj et al.[1] (217–373 K), which are in good agreement and show the reaction to be independent of temperature between 173 and 373 K. Force and Wiesenfeld[4] reported this reaction to be (12 ± 4)% quenching of O(^{1}D) to O(^{3}P). Using a relative rate technique, Baasandorj et al. measured the reactive rate coefficient (relative to the O(^{1}D) + N_2O reaction) at room temperature and 240 K (no temperature dependence was observed). They obtained a reactive yield of 0.90 ± 0.07, using the current k(298 K) recommendation for the N_2O and their measured total rate coefficient, which is recommended here.

Takahashi et al.[5] and Feierabend et al.[3] report ClO yields of (88 ± 18)% and (79 ± 4)%, respectively, in good agreement with the results from the Force and Wiesenfeld and Baasandorj et al. studies. The more precise Feierabend et al. yield is recommended. On the basis of these recommendations, a ~10% yield of unidentified reaction products is possible.
(Table: 15-10, Note: 15-10, Evaluated: 15-10) Back to Table

(1) Baasandorj, M.; Fleming, E. L.; Jackman, C. H.; Burkholder, J. B. $O(^1D)$ kinetic study of key ozone depleting substances and greenhouse gases. *J. Phys. Chem. A* **2013**, *117*, 2434-2445, doi:10.1021/jp312781c.
(2) Davidson, J. A.; Schiff, H. I.; Brown, T. J.; Howard, C. J. Temperature dependence of the rate constants for reactions of $O(^1D)$ atoms with a number of halocarbons. *J. Chem. Phys.* **1978**, *69*, 4277-4279, doi:10.1063/1.437113.
(3) Feierabend, K. J.; Papanastasiou, D. K.; Burkholder, J. B. ClO radical yields in the reaction of $O(^1D)$ with Cl_2, HCl, chloromethanes and chlorofluoromethanes. *J. Phys. Chem. A* **2010**, *114*, 12052-12061, doi:10.1021/jp10776lt.
(4) Force, A. P.; Wiesenfeld, J. R. Collisional deactivation of $O(^1D_2)$ by the halomethanes. Direct determination of reaction efficiency. *J. Phys. Chem.* **1981**, *85*, 782-785, doi:10.1021/j150607a012.
(5) Takahashi, K.; Wada, R.; Matsumi, Y.; Kawasaki, M. Product branching ratios for $O(^3P)$ atom and ClO radical formation in the reactions of $O(^1D)$ with chlorinated compounds. *J. Phys. Chem.* **1996**, *100*, 10145-10149, doi:10.1021/jp952710a.

A35. $O(^1D) + CCl_2F_2$ (CFC-12). The recommended rate coefficient is based on the data from Davidson et al.[2] (173–343 K), Force et al.[4] (298 K), and Baasandorj et al.[1] (217–373 K), which are in good agreement and show the reaction to have a weak negative temperature dependence between 173 and 373 K.

Force and Wiesenfeld[4] report this reaction to be (14 ± 7)% quenching, which is assumed here to be due to physical quenching and is the basis for the recommendation. Takahashi et al.[5] report a ClO yield of (87 ± 18)% in good agreement with the Force and Wiesenfeld study. Takahashi et al.[5] and Feierabend et al.[3] report ~~a~~ ClO yields of (87 ± 18)% and (76 ± 6)%, respectively. The more precise Feierabend et al. yield is recommended. On the basis of the recommendations, there may be ~10% yield of unidentified reaction products.
(Table: 15-10, Note: 15-10, Evaluated: 15-10) Back to Table

(1) Baasandorj, M.; Fleming, E. L.; Jackman, C. H.; Burkholder, J. B. $O(^1D)$ kinetic study of key ozone depleting substances and greenhouse gases. *J. Phys. Chem. A* **2013**, *117*, 2434-2445, doi:10.1021/jp312781c.
(2) Davidson, J. A.; Schiff, H. I.; Brown, T. J.; Howard, C. J. Temperature dependence of the rate constants for reactions of $O(^1D)$ atoms with a number of halocarbons. *J. Chem. Phys.* **1978**, *69*, 4277-4279, doi:10.1063/1.437113.
(3) Feierabend, K. J.; Papanastasiou, D. K.; Burkholder, J. B. ClO radical yields in the reaction of $O(^1D)$ with Cl_2, HCl, chloromethanes and chlorofluoromethanes. *J. Phys. Chem. A* **2010**, *114*, 12052-12061, doi:10.1021/jp10776lt.
(4) Force, A. P.; Wiesenfeld, J. R. Collisional deactivation of $O(^1D_2)$ by the halomethanes. Direct determination of reaction efficiency. *J. Phys. Chem.* **1981**, *85*, 782-785, doi:10.1021/j150607a012.
(5) Takahashi, K.; Wada, R.; Matsumi, Y.; Kawasaki, M. Product branching ratios for $O(^3P)$ atom and ClO radical formation in the reactions of $O(^1D)$ with chlorinated compounds. *J. Phys. Chem.* **1996**, *100*, 10145-10149, doi:10.1021/jp952710a.

A36. $O(^1D) + CClF_3$ (CFC-13). The rate coefficient recommendation is based on the room temperature measurement by Ravishankara et al.[2] There are no reports on the temperature dependence of this rate coefficient and it is assumed to be temperature independent. Ravishankara et al. report (31 ± 10)% collisional quenching of $O(^1D)$ to $O(^3P)$. Takahashi et al.[3] report yields of $O(^3P)$ (16 ± 5)% and ClO (85 ± 18)%. Feierabend et al.[1] report a ClO radical yield of (82 ± 6)%, which is in good agreement with the Takahashi et al. work. The more precise Feierabend et al. ClO product channel yield is recommended for the reactive yield with the balance of the reaction yield assigned to physical quenching. The recommended quenching yield is less than the Ravishankara et al. value, but near to their estimated uncertainty limits.
(Table: 92-20, Note: 15-10, Evaluated: 10-6) Back to Table

(1) Feierabend, K. J.; Papanastasiou, D. K.; Burkholder, J. B. ClO radical yields in the reaction of $O(^1D)$ with Cl_2, HCl, chloromethanes and chlorofluoromethanes. *J. Phys. Chem. A* **2010**, *114*, 12052-12061, doi:10.1021/jp10776lt.
(2) Ravishankara, A. R.; Solomon, S.; Turnipseed, A. A.; Warren, R. F. Atmospheric lifetimes of long-lived halogenated species. *Science* **1993**, *259*, 194-199, doi:10.1126/science.259.5092.194.
(3) Takahashi, K.; Wada, R.; Matsumi, Y.; Kawasaki, M. Product branching ratios for $O(^3P)$ atom and ClO radical formation in the reactions of $O(^1D)$ with chlorinated compounds. *J. Phys. Chem.* **1996**, *100*, 10145-10149, doi:10.1021/jp952710a.

A37. O(^{1}D) + 1,2-*c*-$C_4Cl_2F_6$ (*E*,*Z*). Papdimitriou et al.[1] measured the total and reactive rate coefficients at 296 K for a 0.475:0.525 (*E*,*Z*) isomeric mixture. It is assumed that the isomers have equivalent reactivity and their results, the only study available, are recommended. The reactive rate coefficient was measured relative to the N_2O and CCl_2F_2 (CFC-12) reactions and the obtained rate coefficients agreed to within 10% using the current recommendations for the reference reactions. Consistent with the measured reactive yield and the observed trend for other CFCs, it is expected that the reaction is ~15% physical quenching. CF_2O and *c*-C_4F_6 products were observed, although not quantified.
(Table 15-10, Note: 15-10, Evaluated: 15-10) Back to Table

(1) Papadimitriou, V. C.; McGillen, M. R.; Smith, S. C.; Jubb, A. M.; Portmann, R. W.; Hall, B. D.; Fleming, E. L.; Jackman, C. H.; Burkholder, J. B. 1,2-Dichlorohexafluoro-cyclobutane (1,2-*c*-$C_4F_6Cl_2$, R-316c) a potent ozone depleting substance and greenhouse gas: Atmospheric loss processes, lifetimes, and ozone depletion and global warming potentials for the (*E*) and (*Z*) stereoisomers. *J. Phys. Chem. A* **2013**, *117*, 11049-11065, doi:10.1021/jp407823k.

A38. O(^{1}D) + $CClBrF_2$ (Halon-1211). The recommended rate coefficient at room temperature, *k*(298 K), is based on the data from Thompson and Ravishankara,[2] the only study available. There are no reports on the temperature dependence of this rate coefficient and it is assumed to be temperature independent. Thompson and Ravishankara report a O(^{3}P) yield of 0.36 ± 0.04. On the basis of this work a total reactive yield of 0.65 is recommended. Cronkhite et al.[1] report a BrO yield of 0.31 ± 0.06 at room temperature. On the basis of these studies, a ~0.34 yield of yet unidentified reaction products is possible.
(Table: 94-26, Note: 15-10, Evaluated: 10-6) Back to Table

(1) Cronkhite, J. M.; Wine, P. H. Branching ratios for BrO production from reactions of O(^{1}D) with HBr, CF_3Br, CH_3Br, CF_2ClBr, and CF_2HBr. *Int. J. Chem. Kinet.* **1998**, *30*, 555-563, doi:10.1002/(SICI)1097-4601(1998)30:8<555::AID-KIN4>3.0.CO;2-R.
(2) Thompson, J. E.; Ravishankara, A. R. Kinetics of O(^{1}D) reactions with bromocarbons. *Int. J. Chem. Kinet.* **1993**, *25*, 479-487, doi:10.1002/kin.550250607.

A39. O(^{1}D) + CBr_2F_2 (Halon-1202). The *k*(298 K) recommendation is based on data from Thompson and Ravishankara,[1] the only study available. There are no reports on the temperature dependence of this rate coefficient and it is assumed to be temperature independent. Thompson and Ravishankara report a O(^{3}P) yield of 0.54 ± 0.06. Assuming this to be physical quenching, a reactive yield of 0.45 is recommended.
(Table: 94-26, Note: 15-10, Evaluated: 10-6) Back to Table

(1) Thompson, J. E.; Ravishankara, A. R. Kinetics of O(^{1}D) reactions with bromocarbons. *Int. J. Chem. Kinet.* **1993**, *25*, 479-487, doi:10.1002/kin.550250607.

A40. O(^{1}D) + $CBrF_3$ (Halon-1301). The recommended rate coefficient at room temperature is based on data from Thompson and Ravishankara,[3] the only study available. There are no reports on the temperature dependence of this rate coefficient and it is assumed to be temperature independent. Thompson and Ravishankara report a O(^{3}P) yield of 0.59 ± 0.08. Lorenzen-Schmidt et al.[2] measured the $CBrF_3$ removal rate relative to N_2O and report that the rate coefficient for $CBrF_3$ loss in this reaction is $(4.0 \pm 0.4) \times 10^{-11}$ cm^3 molecule^{-1} s^{-1}, which is in excellent agreement with the results of Thompson and Ravishankara. Cronkhite et al.[1] report a BrO yield of 0.49 ± 0.07 at room temperature, which is greater than the inferred reactive yield from Thompson and Ravishankara. A reactive yield and BrO yield of 0.45 ± 0.08 is recommended, where the uncertainty limits encompass the results from the Cronkhite et al. and Thompson and Ravishankara studies.
(Table: 94-26, Note: 15-10, Evaluated: 10-6) Back to Table

(1) Cronkhite, J. M.; Wine, P. H. Branching ratios for BrO production from reactions of O(^{1}D) with HBr, CF_3Br, CH_3Br, CF_2ClBr, and CF_2HBr. *Int. J. Chem. Kinet.* **1998**, *30*, 555-563, doi:10.1002/(SICI)1097-4601(1998)30:8<555::AID-KIN4>3.0.CO;2-R.
(2) Lorenzen-Schmidt, H.; Weller, R.; Schrems, O. Kinetics and mechanisms of the reactions of O(^{1}D) atoms with CF_3Br and CF_3BrCF_2Br in the gas phase and in solid argon matrices. *Ber. Bunsenges. Phys. Chem.* **1994**, *98*, 1622-1629, doi:10.1002/bbpc.19940981220.
(3) Thompson, J. E.; Ravishankara, A. R. Kinetics of O(^{1}D) reactions with bromocarbons. *Int. J. Chem. Kinet.* **1993**, *25*, 479-487, doi:10.1002/kin.550250607.

A41. $O(^1D) + CF_4$ (CFC-14). The recommended rate coefficient upper limit is based on the work of Ravishankara et al.,[2] who report a (92 ± 8)% $O(^3P)$ yield. Force and Wiesenfeld[1] measured a quenching rate coefficient about 10 times larger. Shi and Barker[3] report an upper limit that is consistent with the recommendation. The small rate coefficient for this reaction makes it vulnerable to interference from reactant impurities. For this reason only an upper limit for the total rate coefficient is recommended with no reactive yield recommendation.
(Table: 92-20, Note: 10-6, Evaluated: 10-6) Back to Table

(1) Force, A. P.; Wiesenfeld, J. R. Collisional deactivation of $O(^1D_2)$ by the halomethanes. Direct determination of reaction efficiency. *J. Phys. Chem.* **1981**, *85*, 782-785, doi:10.1021/j150607a012.
(2) Ravishankara, A. R.; Solomon, S.; Turnipseed, A. A.; Warren, R. F. Atmospheric lifetimes of long-lived halogenated species. *Science* **1993**, *259*, 194-199, doi:10.1126/science.259.5092.194.
(3) Shi, J.; Barker, J. R. Kinetic studies of the deactivation of $O_2(^1\Sigma_g^+)$ and $O(^1D)$. *Int. J. Chem. Kinet.* **1990**, *20*, 1283-1301, doi:10.1002/kin.550221207.

A42. $O(^1D) + CH_3CH_2F$ (HFC-161). The $k(298\ K)$ recommendation is based on the data from Schmoltner et al.,[1] the only study available. There are no reports on the temperature dependence of this rate coefficient and it is assumed to be temperature independent. They report that the yield of $O(^3P)$ to be 0.18 ± 0.05. A reactive yield of 0.82 is recommended. Although no product studies are available, the OH radical is expected to be a major reaction product.
(Table: 94-26, Note: 15-10, Evaluated: 10-6) Back to Table

(1) Schmoltner, A. M.; Talukdar, R. K.; Warren, R. F.; Mellouki, A.; Goldfarb, L.; Gierczak, T.; McKeen, S. A.; Ravishankara, A. R. Rate coefficients for reactions of several hydrofluorocarbons with OH and $O(^1D)$ and their atmospheric lifetimes. *J. Phys. Chem.* **1993**, *97*, 8976-8982, doi:10.1021/j100137a023.

A43. $O(^1D) + CH_3CHF_2$ (HFC-152a). The recommended rate coefficient at room temperature is an average of the data from Warren et al.[2] and Kono and Matsumi,[1] which agree to within 25%. There are no reports on the temperature dependence of this rate coefficient and it is assumed to be temperature independent. Warren et al. report an $O(^3P)$ yield of 0.54 ± 0.07. Kono and Matsumi report an $O(^3P)$ yield of 0.34 ± 0.06, an OH yield of 0.15 ± 0.02, and that a large fraction of the reaction, ~0.50, leads to unidentified products. There is a significant discrepancy in the reactive yield between these two studies. The recommended physical quenching yield is an average of the Warren et al. and Kono and Matsumi results, 0.45 ± 0.15, where the uncertainty limit encompasses the results from both studies. The OH yield from the Kono and Matsumi study is recommended with the balance of the reactive yield assigned to unidentified products.
(Table: 10-6, Note: 15-10, Evaluated: 10-6) Back to Table

(1) Kono, M.; Matsumi, Y. Reaction processes of $O(^1D)$ with fluoroethane compounds. *J. Phys. Chem. A* **2001**, *105*, 65-69, doi:10.1021/jp001786q S1089-5639(00)01786-2.
(2) Warren, R.; Gierczak, T.; Ravishankara, A. R. A study of $O(^1D)$ reactions with CFC substitutes. *Chem. Phys. Lett.* **1991**, *183*, 403-409, doi:10.1016/0009-2614(91)90402-U.

A44. $O(^1D) + CH_3CCl_2F$ (HCFC-141b). The $k(298\ K)$ recommendation is based upon the measurement of Warren et al.,[1] the only study available. There are no reports on the temperature dependence of this rate coefficient and it is assumed to be temperature independent. Warren et al. report an $O(^3P)$ yield of 0.31 ± 0.05, which assuming physical quenching is the basis for the recommendation. ClO and OH radical reaction product channels are expected to be significant, although no product studies are currently available.
(Table: 92-20, Note: 15-10, Evaluated: 10-6) Back to Table

(1) Warren, R.; Gierczak, T.; Ravishankara, A. R. A study of $O(^1D)$ reactions with CFC substitutes. *Chem. Phys. Lett.* **1991**, *183*, 403-409, doi:10.1016/0009-2614(91)90402-U.

A45. $O(^1D) + CH_3CClF_2$ (HCFC-142b). Warren et al.[3] (298 K) and Baasandorj et al.[1] (217–373 K) measured the total rate coefficient for this reaction. The room temperature results from these studies are in reasonable agreement, to within 15%, and the average value from these studies is recommended. Baasandorj et al. reported the reaction to be temperature independent over the 217 to 373 K range.

Warren et al. report an $O(^3P)$ yield of 0.26 ± 0.05. Green and Wayne,[2] who measured the loss of CH_3CF_2Cl relative to the loss of N_2O, obtained a reactive yield of 0.75 ± 0.2 when the current recommendation for $O(^1D) + N_2O$ is used. Using a relative rate technique, Baasandorj et al. measured the reactive rate coefficient (relative to the $O(^1D)$ + HCFC-22 and CFC-115 reactions) at room temperature to be $(1.11 \pm 0.03) \times 10^{-11}$ cm^3 $molecule^{-1}$ s^{-1}. This corresponds to a reactive yield of 0.55 ± 0.05 using the current total rate coefficient recommendations. This is significantly less than reported by Warren et al. The recommended reactive yield is

an average of the Warren et al. and Baasandorj et al. results, where the uncertainty limit encompasses the results from both studies.
(Table: 15-10, Note: 15-10, Evaluated: 10-6) Back to Table

(1) Baasandorj, M.; Fleming, E. L.; Jackman, C. H.; Burkholder, J. B. O(^{1}D) kinetic study of key ozone depleting substances and greenhouse gases. *J. Phys. Chem. A* **2013**, *117*, 2434-2445, doi:10.1021/jp312781c.
(2) Green, R. G.; Wayne, R. P. Relative rate constants for the reactions of O(^{1}D) atoms with fluorochlorocarbons and with N_2O. *J. Photochem.* **1976/77**, *6*, 371-374, doi:10.1016/0047-2670(76)85076-9.
(3) Warren, R.; Gierczak, T.; Ravishankara, A. R. A study of O(^{1}D) reactions with CFC substitutes. *Chem. Phys. Lett.* **1991**, *183*, 403-409, doi:10.1016/0009-2614(91)90402-U.

A46. O(^{1}D) + CH_3CF_3 (HFC-143a). Kono and Matsumi[3] (298 K) and Baasandorj et al.[1] (217–373 K) have measured the total rate coefficient for this reaction. The room temperature results from these studies are in poor agreement with a ~50% difference. Baasandorj et al. reported the reaction to have a weak negative temperature dependence, $E/R = -20$ K, over the 217 to 373 K temperature range. The recommended k(298 K) is from the average of these two studies and the recommended temperature dependence is taken from Baasandorj et al.

Kono and Matsumi report an O(^{3}P) yield of 0.18 ± 0.04, an OH yield of 0.38 ± 0.06, and that ~0.40 of the reaction occurs through unidentified product channels. That is ~0.80 of the reaction leads to loss of CH_3CF_3. The relative rate coefficient measurement by Green and Wayne,[2] who measured the loss of CH_3CF_3 relative to N_2O, is in poor agreement with the results from Kono and Matsumi. Using the current recommendation for the O(^{1}D) + N_2O rate coefficient, the Green and Wayne reaction yield would be 1.05 ± 0.20. Using a relative rate technique, Baasandorj et al. measured the reactive rate coefficient (relative to the O(^{1}D) + NF_3, HCFC-22, and CFC-115 reactions) at room temperature to be $(3.91 \pm 0.11) \times 10^{-11}$ cm^3 molecule^{-1} s^{-1}. This corresponds to a reactive yield of 0.65 ± 0.05 using the current total rate coefficient recommendations. This is less than obtained from the Kono and Matsumi O(^{3}P) yield measurement. The recommended total reactive yield is taken from Baasandorj et al. due, in part, to the consistency of results obtained with multiple reference compounds, along with the OH yield from the Kono and Matsumi study.
(Table: 15-10, Note: 15-10, Evaluated: 15-10) Back to Table

(1) Baasandorj, M.; Fleming, E. L.; Jackman, C. H.; Burkholder, J. B. O(^{1}D) kinetic study of key ozone depleting substances and greenhouse gases. *J. Phys. Chem. A* **2013**, *117*, 2434-2445, doi:10.1021/jp312781c.
(2) Green, R. G.; Wayne, R. P. Relative rate constants for the reactions of O(^{1}D) atoms with fluorochlorocarbons and with N_2O. *J. Photochem.* **1976/77**, *6*, 371-374, doi:10.1016/0047-2670(76)85076-9.
(3) Kono, M.; Matsumi, Y. Reaction processes of O(^{1}D) with fluoroethane compounds. *J. Phys. Chem. A* **2001**, *105*, 65-69, doi:10.1021/jp001786q S1089-5639(00)01786-2.

A47. O(^{1}D) + $CH_2ClCClF_2$ (HCFC-132b). The recommendation is based on the room temperature relative rate measurement of Green and Wayne,[1] the only study available. There are no reports on the temperature dependence of this rate coefficient and it is assumed to be temperature independent. Green and Wayne measured the loss of CH_2ClCF_2Cl relative to the loss of N_2O. The recommendation for N_2O is used to obtain the recommended value. There are no product studies available for this reaction. On the basis of results obtained for other halocarbons, a reactive yield of 0.9 is estimated.
(Table: 90-1, Note: 15-10, Evaluated: 15-10) Back to Table

(1) Green, R. G.; Wayne, R. P. Relative rate constants for the reactions of O(^{1}D) atoms with fluorochlorocarbons and with N_2O. *J. Photochem.* **1976/77**, *6*, 371-374, doi:10.1016/0047-2670(76)85076-9.

A48. O(^{1}D) + CH_2ClCF_3 (HCFC-133a). The k(298 K) recommendation is based on the room temperature measurement of Warren et al.,[2] the only study available. There are no reports on the temperature dependence of this rate coefficient and it is assumed to be temperature independent. Warren et al. report an O(^{3}P) yield of 0.20 ± 0.05. Assuming that all O(^{3}P) production is via physical quenching, a reactive yield of 0.80 ± 0.05 is recommended. No product studies are currently available. The results from the Green and Wayne[1] study, who measured the loss of CH_2ClCF_3 relative to the loss of N_2O, agree with the recommendation when the current recommendation for N_2O is used.
(Table: 92-20, Note; 15-10, Evaluated: 10-6) Back to Table

(1) Green, R. G.; Wayne, R. P. Relative rate constants for the reactions of $O(^1D)$ atoms with fluorochlorocarbons and with N_2O. *J. Photochem.* **1976/77**, *6*, 371-374, doi:10.1016/0047-2670(76)85076-9.
(2) Warren, R.; Gierczak, T.; Ravishankara, A. R. A study of $O(^1D)$ reactions with CFC substitutes. *Chem. Phys. Lett.* **1991**, *183*, 403-409, doi:10.1016/0009-2614(91)90402-U.

A49. $O(^1D) + CH_2FCF_3$ (HFC-134a). The recommended total rate coefficient at room temperature is based on data from Warren et al.[3] and Kono and Matsumi,[1] which are in excellent agreement. There are no reports on the temperature dependence of this rate coefficient and it is assumed to be temperature independent. Warren et al.[3] reported an $O(^3P)$ yield of 0.94 +0.06/–0.01. Kono and Matsumi reported an $O(^3P)$ yield of 0.65 ± 0.06, an OH yield of 0.24 ± 0.04, and that a small fraction of the reaction, ~0.11, leads to other products. Nilsson et al.,[2] using a relative rate method with $O(^1D) + CH_4$ as the reference reaction, report a 298 K reactive rate coefficient of $(6.10 \pm 1.43) \times 10^{-11}$ cm^3 molecule^{-1} s^{-1}, which is greater than the recommended total rate coefficient. The product yields reported in the Kono and Matsumi study are recommended.
(Table: 92-20, Note: 10-6, Evaluated: 10-6) Back to Table

(1) Kono, M.; Matsumi, Y. Reaction processes of $O(^1D)$ with fluoroethane compounds. *J. Phys. Chem. A* **2001**, *105*, 65-69, doi:10.1021/jp001786q S1089-5639(00)01786-2.
(2) Nilsson, E. J. K.; Andersen, V. F.; Nielsen, O. J.; Johnson, M. S. Rate coefficients for the chemical reactions of CH_2F_2, $CHClF_2$, CH_2FCF_3 and CH_3CCl_3 with $O(^1D)$ at 298 K. *Chem. Phys. Lett.* **2012**, *554*, 27-32, doi:10.1016/j.cplett.2012.10.001.
(3) Warren, R.; Gierczak, T.; Ravishankara, A. R. A study of $O(^1D)$ reactions with CFC substitutes. *Chem. Phys. Lett.* **1991**, *183*, 403-409, doi:10.1016/0009-2614(91)90402-U.

A50. $O(^1D) + CHCl_2CF_3$ (HCFC-123). The k(298 K) recommendation is based on the room temperature measurement by Warren et al.,[2] the only study available. There are no reports on the temperature dependence of this rate coefficient and it is assumed to be temperature independent. The relative rate measurement of Green and Wayne,[1] who measured the loss of $CHCl_2CF_3$ relative to the loss of N_2O, agrees well with the recommendation when the current recommendation for N_2O is used. Warren et al. reported an $O(^3P)$ yield of 0.21 ± 0.08, which assuming it is due to physical quenching is the basis of the reactive yield recommendation.
(Table: 92-20, Note: 15-10, Evaluated: 10-6) Back to Table

(1) Green, R. G.; Wayne, R. P. Relative rate constants for the reactions of $O(^1D)$ atoms with fluorochlorocarbons and with N_2O. *J. Photochem.* **1976/77**, *6*, 371-374, doi:10.1016/0047-2670(76)85076-9.
(2) Warren, R.; Gierczak, T.; Ravishankara, A. R. A study of $O(^1D)$ reactions with CFC substitutes. *Chem. Phys. Lett.* **1991**, *183*, 403-409, doi:10.1016/0009-2614(91)90402-U.

A51. $O(^1D) + CHClFCF_3$ (HCFC-124). The k(298 K) recommendation is based on the room temperature measurement of Warren et al.,[1] the only study available. There are no reports on the temperature dependence of this rate coefficient and it is assumed to be temperature independent. Warren et al. reported an $O(^3P)$ yield of 0.31 ± 0.10, which assuming it is due to physical quenching is the basis of the reactive yield recommendation.
(Table: 92-20, Note: 15-10, Evaluated: 10-6) Back to Table

(1) Warren, R.; Gierczak, T.; Ravishankara, A. R. A study of $O(^1D)$ reactions with CFC substitutes. *Chem. Phys. Lett.* **1991**, *183*, 403-409, doi:10.1016/0009-2614(91)90402-U.

A52. $O(^1D) + CHF_2CF_3$ (HFC-125). The total rate coefficient has been measured by Warren et al.[4] (298 K), Kono and Matsumi[3] (298 K), and Baasandorj et al.[1] (217–373 K). The k(298 K) results from Kono and Matsumi and Baasandorj et al. are in excellent agreement, while the results from Warren et al. are nearly a factor of 10 greater. Baasandorj et al. report a weak negative temperature dependence, E/R = –25 K, for the reaction. The results from the Baasandorj et al. study are recommended.

Warren et al. reported an $O(^3P)$ yield of 0.85 + 0.15/–22. Kono and Matsumi reported an $O(^3P)$ yield of 0.24 ± 0.04, an OH yield of 0.60 ± 0.10, and that a fraction of the reaction, ~0.15, leads to other products. Green and Wayne[2] measured the loss of CHF_2CF_3 relative to the loss of N_2O and report a reactive rate coefficient that is significantly greater than the present k(298 K) recommendation. Using a relative rate technique, Baasandorj et al. measured the reactive rate coefficient (relative to the $O(^1D) + NF_3$ and HFC-23 reactions) at room temperature to be $(7.33 \pm 0.9) \times 10^{-12}$ cm^3 molecule^{-1} s^{-1}. This corresponds to a reactive yield of 0.73 ± 0.09 using the current total rate coefficient recommendation. This is in good agreement with that obtained from the Kono and Matsumi $O(^3P)$ yield measurement. The recommended total reactive yield of 0.75 ± 0.05 is taken from the Kono and Matsumi and Baasandorj et al. studies with an OH yield of 0.60 ± 0.10 from the Kono and Matsumi study.

(Table: 92-20, Note: 15-10, Evaluated: 15-10) Back to Table

(1) Baasandorj, M.; Fleming, E. L.; Jackman, C. H.; Burkholder, J. B. $O(^1D)$ kinetic study of key ozone depleting substances and greenhouse gases. *J. Phys. Chem. A* **2013**, *117*, 2434-2445, doi:10.1021/jp312781c.
(2) Green, R. G.; Wayne, R. P. Relative rate constants for the reactions of $O(^1D)$ atoms with fluorochlorocarbons and with N_2O. *J. Photochem.* **1976/77**, *6*, 371-374, doi:10.1016/0047-2670(76)85076-9.
(3) Kono, M.; Matsumi, Y. Reaction processes of $O(^1D)$ with fluoroethane compounds. *J. Phys. Chem. A* **2001**, *105*, 65-69, doi:10.1021/jp001786q S1089-5639(00)01786-2.
(4) Warren, R.; Gierczak, T.; Ravishankara, A. R. A study of $O(^1D)$ reactions with CFC substitutes. *Chem. Phys. Lett.* **1991**, *183*, 403-409, doi:10.1016/0009-2614(91)90402-U.

A53. **$O(^1D) + CCl_3CF_3$ (CFC-113a)**. The k(298 K) recommendation is taken from the measurement by Baasandorj et al.,[1] the only study available. There are no reports on the temperature dependence of this rate coefficient and it is assumed to be temperature independent. Baasandorj et al. reported a ClO radical yield of 0.79 ± 0.10 (2σ), which represents a lower-limit for the total reactive yield. A total reactive yield of 0.9 is estimated for this reaction with the balance assigned to physical quenching.
(Table: 92-20, Note: 15-10, Evaluated: 15-10) Back to Table

(1) Baasandorj, M.; Feierabend, K. J.; Burkholder, J. B. Rate coefficients and ClO radical yields in the reaction of $O(^1D)$ with $CClF_2CCl_2F$, CCl_3CF_3, $CClF_2CClF_2$, and CCl_2FCF_3. *Int. J. Chem. Kinet.* **2011**, *43*, 393-401, doi:10.1002/kin.20561.

A54. **$O(^1D) + CCl_2FCClF_2$ (CFC-113)**. The k(298 K) recommendation is taken from the studies of Baasandorj et al.[1] (298 K) and Baasandorj et al.[2] (217–373 K). Baasandorj et al.[2] found no temperature dependence to the reaction over the 217–373 K range. Baasandorj et al.[1] reported a ClO radical yield of 0.80 ± 0.10 (2σ), which may represent a lower-limit for the reactive yield. A reactive yield of 0.9 is estimated for this reaction.
(Table: 92-20, Note: 15-10, Evaluated: 15-10) Back to Table

(1) Baasandorj, M.; Feierabend, K. J.; Burkholder, J. B. Rate coefficients and ClO radical yields in the reaction of $O(^1D)$ with $CClF_2CCl_2F$, CCl_3CF_3, $CClF_2CClF_2$, and CCl_2FCF_3. *Int. J. Chem. Kinet.* **2011**, *43*, 393-401, doi:10.1002/kin.20561.
(2) Baasandorj, M.; Fleming, E. L.; Jackman, C. H.; Burkholder, J. B. $O(^1D)$ kinetic study of key ozone depleting substances and greenhouse gases. *J. Phys. Chem. A* **2013**, *117*, 2434-2445, doi:10.1021/jp312781c.

A55. **$O(^1D) + CCl_2FCF_3$ (CFC-114a)**. The k(298 K) recommendation is taken from the measurement by Baasandorj et al.,[1] the only study available. There are no reports on the temperature dependence of this rate coefficient and it is assumed to be temperature independent. Baasandorj et al.[1] reported a ClO radical yield of 0.79 ± 0.10 (2σ), which may represent a lower-limit for the reactive yield. A total reactive yield of 0.9 is estimated for this reaction.
(Table: 92-20, Note: 15-10, Evaluated: 15-10) Back to Table

(1) Baasandorj, M.; Feierabend, K. J.; Burkholder, J. B. Rate coefficients and ClO radical yields in the reaction of $O(^1D)$ with $CClF_2CCl_2F$, CCl_3CF_3, $CClF_2CClF_2$, and CCl_2FCF_3. *Int. J. Chem. Kinet.* **2011**, *43*, 393-401, doi:10.1002/kin.20561.

A56. **$O(^1D) + CClF_2CClF_2$ (CFC-114)**. The total rate coefficient has been measured by Ravishankara et al.[3] (298 K), Baasandorj et al.[1] (298 K), and Baasandorj et al.[2] (217–373 K). The k(298 K) results from these studies are in very good agreement. Baasandorj et al.[2] report a weak negative temperature dependence, E/R = –25 K, for the reaction over the 217–373 K range. The recommended rate coefficient is taken from this study. Ravishankara et al. reported the reaction to be (25 ± 9)% quenching of $O(^1D)$ to $O(^3P)$. Baasandorj et al.[1] reported a ClO radical yield of 0.85 ± 0.12 (2σ), which may represent a lower-limit for the reaction yield. The reaction yields from the Ravishankara et al. and Baasandorj et al. studies overlap, within the combined uncertainties, and a total reactive yield of 0.9 is recommended.
(Table: 92-20, Note: 15-10, Evaluated: 10-6) Back to Table

(1) Baasandorj, M.; Feierabend, K. J.; Burkholder, J. B. Rate coefficients and ClO radical yields in the reaction of $O(^1D)$ with $CClF_2CCl_2F$, CCl_3CF_3, $CClF_2CClF_2$, and CCl_2FCF_3. *Int. J. Chem. Kinet.* **2011**, *43*, 393-401, doi:10.1002/kin.20561.

(2) Baasandorj, M.; Fleming, E. L.; Jackman, C. H.; Burkholder, J. B. $O(^1D)$ kinetic study of key ozone depleting substances and greenhouse gases. *J. Phys. Chem. A* **2013**, *117*, 2434-2445, doi:10.1021/jp312781c.
(3) Ravishankara, A. R.; Solomon, S.; Turnipseed, A. A.; Warren, R. F. Atmospheric lifetimes of long-lived halogenated species. *Science* **1993**, *259*, 194-199, doi:10.1126/science.259.5092.194.

A57. $O(^1D) + CClF_2CF_3$ (CFC-115). The rate coefficient has been measured by Ravishankara et al.[2] (298 K) and Baasandorj et al.[1] (217–373 K). The k(298 K) values from these studies are in reasonable agreement and the average value is recommended. Baasandorj et al. measured a weak negative temperature dependence, $E/R = -30$ K, for the reaction, which is recommended.

Ravishankara et al. reported an $O(^3P)$ yield of 0.70 ± 0.07. Using a relative rate technique, Baasandorj et al. measured the reactive rate coefficient (relative to the $O(^1D) + NF_3$, HFC-22, and HFC-125 reactions) at room temperature to be $(5.16 \pm 0.9) \times 10^{-11}$ cm^3 molecule^{-1} s^{-1}. This corresponds to a reactive yield of 0.86 ± 0.06 using the current total rate coefficient recommendations. This is in poor agreement with the Ravishankara et al. value. The recommended reactive yield is taken from Baasandorj et al. due, in part, to the consistency of results obtained with multiple reference compounds. There are no product studies available for this reaction.
(Table: 92-20, Note: 15-10, Evaluated: 10-6) Back to Table

(1) Baasandorj, M.; Fleming, E. L.; Jackman, C. H.; Burkholder, J. B. $O(^1D)$ kinetic study of key ozone depleting substances and greenhouse gases. *J. Phys. Chem. A* **2013**, *117*, 2434-2445, doi:10.1021/jp312781c.
(2) Ravishankara, A. R.; Solomon, S.; Turnipseed, A. A.; Warren, R. F. Atmospheric lifetimes of long-lived halogenated species. *Science* **1993**, *259*, 194-199, doi:10.1126/science.259.5092.194.

A58. $O(^1D) + CBrF_2CBrF_2$ (Halon-2402). The k(298 K) recommendation is based on data from Thompson and Ravishankara,[2] the only study available. They reported an $O(^3P)$ yield of 0.25 ± 0.07. Lorenzen-Schmidt et al.[1] measured the Halon removal rate relative to the N_2O removal rate and report a reactive rate coefficient of $(8.8 \pm 1.2) \times 10^{-11}$ (a reactive yield of 0.55), which is significantly less than inferred by Thompson and Ravishankara. The Thompson and Ravishankara product yield is recommended with an uncertainty that encompasses the Lorenzen-Schmidt et al. result at the 2σ level. There are no product studies available for this reaction.
(Table: 94-26, Note: 15-10, Evaluated: 10-6) Back to Table

(1) Lorenzen-Schmidt, H.; Weller, R.; Schrems, O. Kinetics and mechanisms of the reactions of $O(^1D)$ atoms with CF_3Br and CF_3BrCF_2Br in the gas phase and in solid argon matrices. *Ber. Bunsenges. Phys. Chem.* **1994**, *98*, 1622-1629, doi:10.1002/bbpc.19940981220.
(2) Thompson, J. E.; Ravishankara, A. R. Kinetics of $O(^1D)$ reactions with bromocarbons. *Int. J. Chem. Kinet.* **1993**, *25*, 479-487, doi:10.1002/kin.550250607.

A59. $O(^1D) + CF_3CF_3$ (PFC-116). The k(298 K) recommendation is based on the work of Ravishankara et al.[2] The small rate coefficient for this reaction makes it vulnerable to interference from reactant impurities. For this reason, k(298 K) may be an upper limit. Ravishankara et al. report a $O(^3P)$ yield of 0.85 ± 0.15. Using a relative rate technique, Baasandorj et al.[1] measured the reactive rate coefficient for this reaction, relative to the $O(^1D) + CHF_3$ reaction, to be $<3 \times 10^{-14}$ cm^3 molecule^{-1} s^{-1}. On the basis of this study, an upper limit of 0.2 for the reactive yield is recommended.
(Table: 94-26, Note: 15-10, Evaluated: 15-10) Back to Table

(1) Baasandorj, M.; Hall, B. D.; Burkholder, J. B. Rate coefficients for the reaction of $O(^1D)$ with the atmospherically long-lived greenhouse gases NF_3, SF_5CF_3, CHF_3, C_2F_6, c-C_4F_8, n-C_5F_{12}, and n-C_6F_{14}. *Atmos. Chem. Phys.* **2012**, *12*, 11753-11764, doi:10.5194/acp-12-11753-2012.
(2) Ravishankara, A. R.; Solomon, S.; Turnipseed, A. A.; Warren, R. F. Atmospheric lifetimes of long-lived halogenated species. *Science* **1993**, *259*, 194-199, doi:10.1126/science.259.5092.194.

A60. $O(^1D) + CF_3CHFCF_3$ (HFC-227ea). Baasandorj et al.[1] measured the total rate coefficient over the temperature range 217 to 373 K. Their results, the only study available, are recommended. Using a relative rate technique, Baasandorj et al. measured the reactive rate coefficient for this reaction relative to the $O(^1D) + NF_3$, HFC-23, and HFC-125 reactions to be $(6.99 \pm 0.5) \times 10^{-12}$ cm^3 molecule^{-1} s^{-1}. On the basis of this study, a reactive yield of 0.72 ± 0.07 is recommended.
(Table 15-10, Note: 15-10, Evaluated: 15-10) Back to Table

(1) Baasandorj, M.; Fleming, E. L.; Jackman, C. H.; Burkholder, J. B. $O(^1D)$ kinetic study of key ozone depleting substances and greenhouse gases. *J. Phys. Chem. A* **2013**, *117*, 2434-2445, doi:10.1021/jp312781c.

A61. **$O(^1D) + CHF_2CH_2CF_3$ (HFC-245fa)**. There are no experimental studies of the rate coefficient for this reaction. The rate coefficient and product yield are estimated based on trends observed for other HFCs.
(Table 15-10, Note: 15-10, Evaluated: 15-10) Back to Table

A62. **$O(^1D) + CHF_2CF_2CF_2CHF_2$ (HFC-338pcc)**. The k(298 K) recommendation is based on data from Schmoltner et al.,[1] the only study available. There are no reports on the temperature dependence of this rate coefficient and it is assumed to be temperature independent. They reported an $O(^3P)$ yield of 0.97 ± 0.09. On the basis of this study, a reactive yield of $0.05^{+0.1}_{-0.05}$ is recommended.
(Table: 94-26, Note: 15-10, Evaluated: 10-6) Back to Table

(1) Schmoltner, A. M.; Talukdar, R. K.; Warren, R. F.; Mellouki, A.; Goldfarb, L.; Gierczak, T.; McKeen, S. A.; Ravishankara, A. R. Rate coefficients for reactions of several hydrofluorocarbons with OH and $O(^1D)$ and their atmospheric lifetimes. *J. Phys. Chem.* **1993**, *97*, 8976-8982, doi:10.1021/j100137a023.

A63. **$O(^1D) + c\text{-}C_4F_8$**. The k(298 K) recommendation for perfluorocyclobutane is based on the work of Ravishankara et al.,[2] the only study available. The small rate coefficient for this reaction makes it vulnerable to interference from reactant impurities. For this reason, k(298 K) may be an upper limit. Ravishankara et al. reported an $O(^3P)$ yield of 1.00 +0/-0.15. Using a relative rate technique, Baasandorj et al.[1] measured the reactive rate coefficient for this reaction relative to the $O(^1D) + CHF_3$ reaction to be $<3.5 \times 10^{-14}$ cm^3 molecule^{-1} s^{-1}. On the basis of the Baasandorj et al. study, an upper limit of 0.04 for the reaction yield is recommended.
(Table: 92-20, Note: 15-10, Evaluated: 10-6) Back to Table

(1) Baasandorj, M.; Hall, B. D.; Burkholder, J. B. Rate coefficients for the reaction of $O(^1D)$ with the atmospherically long-lived greenhouse gases NF_3, SF_5CF_3, CHF_3, C_2F_6, c-C_4F_8, n-C_5F_{12}, and n-C_6F_{14}. *Atmos. Chem. Phys.* **2012**, *12*, 11753-11764, doi:10.5194/acp-12-11753-2012.
(2) Ravishankara, A. R.; Solomon, S.; Turnipseed, A. A.; Warren, R. F. Atmospheric lifetimes of long-lived halogenated species. *Science* **1993**, *259*, 194-199, doi:10.1126/science.259.5092.194.

A64. **$O(^1D) + CF_3CHFCHFCF_2CF_3$ (HFC-43-10mee)**. The k(298 K) recommendation is based on data from Schmoltner et al.,[1] the only study available. There are no reports on the temperature dependence of this rate coefficient and it is assumed to be temperature independent. Schmoltner et al. report a $O(^3P)$ yield of 0.91 ± 0.04. The recommended branching ratio is taken from the Schmoltner et al. study with a larger uncertainty assigned because there is only a single study for this reaction.
(Table: 94-26, Note: 15-10, Evaluated: 10-6) Back to Table

(1) Schmoltner, A. M.; Talukdar, R. K.; Warren, R. F.; Mellouki, A.; Goldfarb, L.; Gierczak, T.; McKeen, S. A.; Ravishankara, A. R. Rate coefficients for reactions of several hydrofluorocarbons with OH and $O(^1D)$ and their atmospheric lifetimes. *J. Phys. Chem.* **1993**, *97*, 8976-8982, doi:10.1021/j100137a023.

A65. **$O(^1D) + C_5F_{12}$ (CFC-41-12)**. The k(298 K) recommendation is based on data from Ravishankara et al.,[2] the only total rate coefficient study available. There are no reports on the temperature dependence of this rate coefficient and it is assumed to be temperature independent. The small rate coefficient for this reaction makes it vulnerable to interference from reactant impurities. For this reason, k(298 K) may be an upper limit. Ravishankara et al. reported an $O(^3P)$ yield of 0.79 ± 0.12. Using a relative rate technique, Baasandorj et al.[1] measured the reactive rate coefficient for this reaction relative to the $O(^1D) + CHF_3$ reaction to be $<5 \times 10^{-14}$ cm^3 molecule^{-1} s^{-1}. On the basis of the Baasandorj et al. study, an upper limit of 0.12 for the reactive yield is recommended.
(Table: 94-26, Note: 15-10, Evaluated: 10-6) Back to Table

(1) Baasandorj, M.; Hall, B. D.; Burkholder, J. B. Rate coefficients for the reaction of $O(^1D)$ with the atmospherically long-lived greenhouse gases NF_3, SF_5CF_3, CHF_3, C_2F_6, c-C_4F_8, n-C_5F_{12}, and n-C_6F_{14}. *Atmos. Chem. Phys.* **2012**, *12*, 11753-11764, doi:10.5194/acp-12-11753-2012.
(2) Ravishankara, A. R.; Solomon, S.; Turnipseed, A. A.; Warren, R. F. Atmospheric lifetimes of long-lived halogenated species. *Science* **1993**, *259*, 194-199, doi:10.1126/science.259.5092.194.

A66. $O(^1D) + C_6F_{14}$ (PFC-51-14). The k(298 K) recommendation is based on data from Ravishankara et al.,[2] the only total rate coefficient study available. The small rate coefficient for this reaction makes it vulnerable to interference from reactant impurities. For this reason, k(298 K) may be an upper limit. Ravishankara et al. reported an $O(^3P)$ yield of 0.75 ± 0.09. Using a relative rate technique, Baasandorj et al.[1] measured the reactive rate coefficient for this reaction relative to the $O(^1D) + CHF_3$ reaction to be $<1.6 \times 10^{-13}$ cm^3 molecule^{-1} s^{-1}. On the basis of the Baasandorj et al. study, an upper limit of 0.16 for the reaction yield is recommended.
(Table: 94-26, Note: 15-10, Evaluated: 10-6) Back to Table

(1) Baasandorj, M.; Hall, B. D.; Burkholder, J. B. Rate coefficients for the reaction of $O(^1D)$ with the atmospherically long-lived greenhouse gases NF_3, SF_5CF_3, CHF_3, C_2F_6, c-C_4F_8, n-C_5F_{12}, and n-C_6F_{14}. *Atmos. Chem. Phys.* **2012**, *12*, 11753-11764, doi:10.5194/acp-12-11753-2012.
(2) Ravishankara, A. R.; Solomon, S.; Turnipseed, A. A.; Warren, R. F. Atmospheric lifetimes of long-lived halogenated species. *Science* **1993**, *259*, 194-199, doi:10.1126/science.259.5092.194.

A67. $O(^1D) + 1,2\text{-}(CF_3)_2c\text{-}C_4F_6$. The k(298 K) recommendation is based on data from Ravishankara et al.,[1] the only total rate coefficient study available. They reported an $O(^3P)$ yield of 0.84 ± 0.16. The small rate coefficient for this reaction makes it vulnerable to interference from reactant impurities. For this reason only an upper limit for the total rate coefficient and no reactive yield is recommended.
(Table: 94-26, Note: 15-10, Evaluated: 10-6) Back to Table

(1) Ravishankara, A. R.; Solomon, S.; Turnipseed, A. A.; Warren, R. F. Atmospheric lifetimes of long-lived halogenated species. *Science* **1993**, *259*, 194-199, doi:10.1126/science.259.5092.194.

A68. $O(^1D) + C_4F_{10}$. The k(298 K) recommendation is taken from the estimated upper limit for reactive loss given by Ravishankara et al.,[1] the only study available. The small rate coefficient for this reaction makes it vulnerable to interference from reactant impurities. For this reason an upper limit for the rate coefficient and no reactive yield is recommended.
(Table: 10-6, Note: 15-10, Evaluated: 10-6) Back to Table

(1) Ravishankara, A. R.; Solomon, S.; Turnipseed, A. A.; Warren, R. F. Atmospheric lifetimes of long-lived halogenated species. *Science* **1993**, *259*, 194-199, doi:10.1126/science.259.5092.194.

A69. $O(^1D) + SF_6$. The k(298 K) recommendation is based on the work of Ravishankara et al.,[1] the only study available. They reported an $O(^3P)$ yield of 0.32 ± 10. The small rate coefficient for this reaction makes it vulnerable to interference from reactant impurities. For this reason, k(298 K) may be an upper limit and a reactive yield upper limit of 0.7 is recommended.
(Table: 92-20, Note: 15-10, Evaluated: 10-6) Back to Table

(1) Ravishankara, A. R.; Solomon, S.; Turnipseed, A. A.; Warren, R. F. Atmospheric lifetimes of long-lived halogenated species. *Science* **1993**, *259*, 194-199, doi:10.1126/science.259.5092.194.

A70. $O(^1D) + SO_2$. The room temperature rate coefficient is taken from the work of Zhao et al.,[1] which is the only study for this reaction. Although no studies are available, the reaction rate coefficient is expected to have negligible temperature dependence. Zhao et al. reported the branching ratio for reactive loss to be 0.76 ± 0.12 (2σ), which is the basis of the recommendation.
(Table: 10-6, Note: 15-10, Evaluated: 10-6) Back to Table

(1) Zhao, Z.; Laine, P. L.; Nicovich, J. M.; Wine, P. H. Reactive and non-reactive quenching of $O(^1D)$ by the potent greenhouse gases SO_2F_2, NF_3, and SF_5CF_3. *Proc. Nat. Acad. Sci.* **2010**, *107*, 6610-6615, doi:10.1073/pnas.0911228107.

A71. $O(^1D) + SO_2F_2$. The recommendation is based on the measurements of Dillon et al.[1] and Zhao et al.,[2] which are in good agreement. Although Dillon et al. report a temperature independent rate coefficient over the temperature range 220–300 K, a weak negative temperature dependence is apparent in their data. Zhao et al. (199–351 K) report a negative temperature dependence, E/R = –98 K, that reproduces both data sets very well and is recommended. Dillon et al. reported a collisional quenching yield of 0.55 ± 0.04, independent of temperature. The results from Zhao et al. are in agreement with this result, but are less precise. The recommended reactive yield is taken from Dillon et al. Dillon et al. provide qualitative evidence that F atoms may be formed as a reaction product.
(Table: 10-6, Note: 15-10, Evaluated: 10-6) Back to Table

(1) Dillon, T. J.; Horowitz, A.; Crowley, J. N. The atmospheric chemistry of sulphuryl fluoride, SO_2F_2. *Atmos. Chem. Phys.* **2008**, *8*, 1547-1557, doi:10.5194/acp-8-1547-2008.

(2) Zhao, Z.; Laine, P. L.; Nicovich, J. M.; Wine, P. H. Reactive and non-reactive quenching of $O(^1D)$ by the potent greenhouse gases SO_2F_2, NF_3, and SF_5CF_3. *Proc. Nat. Acad. Sci.* **2010**, *107*, 6610-6615, doi:10.1073/pnas.0911228107.

A72. **$O(^1D) + SF_5CF_3$.** Zhao et al.[2] and Baasandorj et al.[1] have reported upper limits for the room temperature rate coefficient. There are no reports on the temperature dependence of this rate coefficient and it is assumed to be temperature independent. The determination of the small rate coefficient for this reaction makes it vulnerable to interference from reactant impurities. Baasandorj et al. reported a k(298 K) value that is greater than reported by Zhao et al., which is most likely due to the presence of sample impurities. For this reason only an upper limit for the rate coefficient is recommended. Using a relative rate technique, Baasandorj et al. measured the reactive rate coefficient for this reaction relative to the $O(^1D) + CHF_3$ reaction to be $<5.8 \times 10^{-14}$ cm^3 molecule^{-1} s^{-1}. On the basis of this study and the Zhao et al. k(298 K) value, an upper limit of 0.3 for the reaction yield is recommended.
(Table: 10-6, Note: 15-10, Evaluated: 10-6) Back to Table

(1) Baasandorj, M.; Hall, B. D.; Burkholder, J. B. Rate coefficients for the reaction of $O(^1D)$ with the atmospherically long-lived greenhouse gases NF_3, SF_5CF_3, CHF_3, C_2F_6, c-C_4F_8, n-C_5F_{12}, and n-C_6F_{14}. *Atmos. Chem. Phys.* **2012**, *12*, 11753-11764, doi:10.5194/acp-12-11753-2012.
(2) Zhao, Z.; Laine, P. L.; Nicovich, J. M.; Wine, P. H. Reactive and non-reactive quenching of $O(^1D)$ by the potent greenhouse gases SO_2F_2, NF_3, and SF_5CF_3. *Proc. Nat. Acad. Sci.* **2010**, *107*, 6610-6615, doi:10.1073/pnas.0911228107.

1.5.3 Bibliography – O(^{1}D) Reactions

Addison, M. C.; Donovan, R. J.; Garraway, J. Reactions of O(2^1D_2) and O(2^3P_J) with halogenomethanes. *Faraday Disc.* **1979**, *67*, 286-296, doi:10.1039/dc9796700286.

Aker, P. M.; Niefer, B. I.; Sloan, J. J.; Heydtmann, H. The dynamics and microscopic kinetics of the reactions of O($^1D_2$) atoms with $CHCl_3$ and CHF_3. *J. Chem. Phys.* **1987**, *87*, 203-209, doi:10.1063/1.453616.

Amimoto, S. T.; Force, A. P.; Gulotty, R. G., Jr.; Wiesenfeld, J. R. Collisional deactivation of O(2^1D_2) by the atmospheric gases. *J. Chem. Phys.* **1979**, *71*, 3640-3647, doi:10.1063/1.438807.

Amimoto, S. T.; Force, A. P.; Wiesenfeld, J. R. Ozone photochemistry: Production and deactivation of O(2^1D_2) following photolysis at 248 nm. *Chem. Phys. Lett.* **1978**, *60*, 40-43, doi:10.1016/0009-2614(78)85705-4.

Atkinson, R.; Breuer, G. M.; Pitts Jr., J. N.; Sandoval, H. L. Tropospheric and stratospheric sinks for halocarbons: Photooxidation, O(^1D) atom, and OH radical reactions. *J. Geophys. Res.* **1976**, *81*, 5765-5770, doi:10.1029/JC081i033p05765.

Baasandorj, M.; Feierabend, K. J.; Burkholder, J. B. Rate coefficients and ClO radical yields in the reaction of O(^{1}D) with $CClF_2CCl_2F$, CCl_3CF_3, $CClF_2CClF_2$, and CCl_2FCF_3. *Int. J. Chem. Kinet.* **2011**, *43*, 393-401, doi:10.1002/kin.20561.

Baasandorj, M.; Fleming, E. L.; Jackman, C. H.; Burkholder, J. B. O(^{1}D) kinetic study of key ozone depleting substances and greenhouse gases. *J. Phys. Chem. A* **2013**, *117*, 2434-2445, doi:10.1021/jp312781c.

Baasandorj, M.; Hall, B. D.; Burkholder, J. B. Rate coefficients for the reaction of O(^{1}D) with the atmospherically long-lived greenhouse gases NF_3, SF_5CF_3, CHF_3, C_2F_6, *c*-C_4F_8, *n*-C_5F_{12}, and *n*-C_6F_{14}. *Atmos. Chem. Phys.* **2012**, *12*, 11753-11764, doi:10.5194/acp-12-11753-2012.

Balucani, N.; Beneventi, L.; Casavecchia, P.; Volpi, G. G.; Kruus, E. J.; Sloan, J. J. The dynamics of the reaction of O(^{1}D) with HBr studied by crossed molecular beams and time-resolved Fourier transform spectroscopy. *Can. J. Chem.* **1994**, *72*, 888-902, doi:10.1139/v94-116.

Biedenkapp, D.; Bair, E. J. Ozone ultraviolet photolysis. I. The effect of molecular oxygen. *J. Chem. Phys.* **1970**, *52*, 6119-6125, doi:10.1063/1.1672914.

Blitz, M. A.; Dillon, T. J.; Heard, D. E.; Pilling, M. J.; Trought, I. D. Laser induced fluorescence studies of the reactions of O($^1D_2$) with N_2, O_2, N_2O, CH_4, H_2, CO_2, Ar, Kr and *n*-C_4H_{10}. *Phys. Chem. Chem. Phys.* **2004**, *6*, 2162-2171, doi:10.1039/b400283k.

Burks, T. L.; Lin, M. C. The dynamics of formation of vibrationally excited HF in reactions of O(2^1D_2) atoms with partially fluorinated alkanes. *Int. J. Chem. Kinet.* **1981**, *13*, 977-999, doi:10.1002/kin.550130918.

Calvert, J. G.; Pitts, J. N. Photochemistry; John Wiley & Sons, Inc.: New York, 1966; pp 783.

Cantrell, C. A.; Shetter, R. E.; Calvert, J. G. Branching ratios for the O(^{1}D) + N_2O reaction. *J. Geophys. Res.* **1994**, *99*, 3739-3743, doi:10.1029/93JD02659.

Carl, S. A. A highly sensitive method for time-resolved detection of O(^{1}D) applied to precise determination of absolute O(^{1}D) reaction rate constants and O(^{3}P) yields. *Phys. Chem. Chem. Phys.* **2005**, *7*, 4051-4053, doi:10.1039/b513576c.

Casavecchia, P.; Buss, R. J.; Sibener, S. J.; Lee, Y. T. A crossed molecular beam study of the O($^1D_2$) + CH_4 reaction. *J. Chem. Phys.* **1980**, *73*, 6351-6352, doi:10.1063/1.440102.

Chen, H.-b.; Thweatt, W. D.; Wang, J.; Glass, G. P.; Curl, R. F. IR kinetic spectroscopy investigation of the CH_4 + O(^{1}D) reaction. *J. Phys. Chem. A* **2005**, *109*, 2207-2216, doi:10.1021/jp045521d.

Chichinin, A. I. Collisions of O(^{1}D) with HCl, Cl_2, and $COCl_2$: Total quenching, channel specific rate constants, and yields of Cl($^2P_{1/2}$). *J. Chem. Phys.* **1997**, *106*, 1057-1062, doi:10.1063/1.473181.

Chichinin, A. I. Isotope effects in the deactivation of O(^{1}D) atom by XCl and XF (X = H,D). *Chem. Phys. Lett.* **2000**, *316*, 425-432, doi:10.1016/S0009-2614(99)01325-1.

Cronkhite, J. M.; Wine, P. H. Branching ratios for BrO production from reactions of O(^{1}D) with HBr, CF_3Br, CH_3Br, CF_2ClBr, and CF_2HBr. *Int. J. Chem. Kinet.* **1998**, *30*, 555-563, doi:10.1002/(SICI)1097-4601(1998)30:8<555::AID-KIN4>3.0.CO;2-R.

Davenport, J.; Ridley, B.; Schiff, H. I.; Welge, K. H. communication. *Faraday Discuss. Chem. Soc.* **1972**, *53*, 230-231.

Davidson, J. A.; Howard, C. J.; Schiff, H. I.; Fehsenfeld, F. C. Measurements of the branching ratios for the reaction of O($^1D_2$) with N_2O. *J. Chem. Phys.* **1979**, *70*, 1697-1704, doi:10.1063/1.437686.

Davidson, J. A.; Schiff, H. I.; Brown, T. J.; Howard, C. J. Temperature dependence of the rate constants for reactions of O(^1D) atoms with a number of halocarbons. *J. Chem. Phys.* **1978**, *69*, 4277-4279, doi:10.1063/1.437113.

Davidson, J. A.; Schiff, H. I.; Streit, G. E.; McAfee, J. R.; Schmeltekopf, A. L.; Howard, C. J. Temperature dependence of O(^1D) rate constants for reactions with N_2O, H_2, CH_4, HCl, and NH_3. *J. Chem. Phys.* **1977**, *67*, 5021-5025, doi:10.1063/1.434724.

DeMore, W. B.; Dede, C. Pressure dependence of carbon trioxide formation in the gas-phase reacion of O(^{1}D) with carbon dioxide. *J. Phys. Chem.* **1970**, *74*, 2621-2625, doi:10.1021/j100707a006.

Dillon, T. J.; Horowitz, A.; Crowley, J. N. Absolute rate coefficients for the reactions of $O(^1D)$ with a series of n-alkanes. *Chem. Phys. Lett.* **2007**, *443*, 12-16, doi:10.1016/j.cplett.2007.06.044.

Dillon, T. J.; Horowitz, A.; Crowley, J. N. The atmospheric chemistry of sulphuryl fluoride, SO_2F_2. *Atmos. Chem. Phys.* **2008**, *8*, 1547-1557, doi:10.5194/acp-8-1547-2008.

Dillon, T. J.; Vereecken, L.; Horowitz, A.; Khamaganov, V.; Crowley, J. N.; Lelieveld, J. Removal of the potent greenhouse gas NF_3 by reactions with the atmospheric oxidants $O(^1D)$, OH and O_3. *Phys. Chem. Chem. Phys.* **2011**, *13*, 18600-18608, doi:101039/c1cp22230a.

Dunlea, E. J.; Ravishankara, A. R. Kinetics studies of the reactions of $O(^1D)$ with several atmospheric molecules. *Phys. Chem. Chem. Phys.* **2004**, *6*, 2152-2161, doi:10.1039/b400247d.

Dunlea, E. J.; Ravishankara, A. R. Measurement of the rate coefficient for the reaction of $O(^1D)$ with H_2O and re-evaluation of the atmospheric OH production rate. *Phys. Chem. Chem. Phys.* **2004**, *6*, 3333-3340, doi:10.1039/b402483d.

Dunlea, E. J.; Ravishankara, A. R.; Strekowski, R. S.; Nicovich, J. M.; Wine, P. H. Temperature-dependent quantum yields for $O(^3P)$ and $O(^1D)$ production from photolysis of O_3 at 248 nm. *Phys. Chem. Chem. Phys.* **2004**, *6*, 5484-5489, doi:10.1039/b414326d.

Feierabend, K. J.; Papanastasiou, D. K.; Burkholder, J. B. ClO radical yields in the reaction of $O(^1D)$ with Cl_2, HCl, chloromethanes and chlorofluoromethanes. *J. Phys. Chem. A* **2010**, *114*, 12052-12061, doi:10.1021/jp10776lt.

Fletcher, I. S.; Husain, D. Absolute reaction rates of oxygen (2^1D_2) with halogenated paraffins by atomic absorption spectroscopy in the vacuum ultraviolet. *J. Phys. Chem.* **1976**, *80*, 1837-1840, doi:10.1021/j100558a002.

Fletcher, I. S.; Husain, D. The collisional quenching of electronically excited oxygen atoms, $O(2^1D_2)$, by the gases NH_3, H_2O_2, C_2H_6, C_3H_8, and $C(CH_3)_4$, using time-resolved attenuation of atomic resonance radiation. *Can. J. Chem.* **1976**, *54*, 1765-1770, doi:10.1139/v76-251.

Fletcher, I. S.; Husain, D. The collisional quenching of $O(2^1D_2)$ by $COCl_2$, COFCl and COF_2 using atomic absorption spectroscopy in the vacuum ultraviolet. *J. Photochem.* **1978**, *8*, 355-361, doi:10.1016/0047-2670(78)80158-0.

Force, A. P.; Wiesenfeld, J. R. Collisional deactivation of $O(^1D_2)$ by the halomethanes. Direct determination of reaction efficiency. *J. Phys. Chem.* **1981**, *85*, 782-785, doi:10.1021/j150607a012.

Force, A. P.; Wiesenfeld, J. R. Laser photolysis of O_3/H_2 mixtures: The yield of the $H + O_3 \rightarrow HO_2 + O$ reaction. *J. Chem. Phys.* **1981**, *74*, 1718-1723, doi:10.1063/1.441260.

Freudenstein, K.; Biedenkapp, D. Kinetics of reaction of electronically excited oxygen atoms with chlorine $O(^1D) + Cl_2$. *Ber. Bunsenges. Phys. Chem.* **1976**, *80*, 42-48, doi:10.1002/bbpc.19760800110.

Gauthier, M. J. E.; Snelling, D. R. Production de $O_2(b^1\Sigma_g^+)$, v' = 0,1 et 2 par la reaction $O(2^1D_2) + O_2(X^3\Sigma_g^-)$. *Can. J. Chem.* **1974**, *52*, 4007-4015, doi:10.1139/v74-598.

Gericke, K.-H.; Comes, F. J. Energy partitioning in the reaction $O(^1D) + H_2O \rightarrow OH + OH$ - The influence of $O(^1D)$ translation energy on the reaction rate constant. *Chem. Phys. Lett.* **1981**, *81*, 218-222, doi:10.1016/0009-2614(81)80239-4.

Glinski, R. J.; Birks, J. W. Yields of molecular hydrogen in the elementary reactions $HO_2 + HO_2$ and $O(^1D_2) + H_2O$. *J. Phys. Chem.* **1985**, *89*, 3449-3453, doi:10.1021/j100262a006.

Green, R. G.; Wayne, R. P. Relative rate constants for the reactions of $O(^1D)$ atoms with fluorochlorocarbons and with N_2O. *J. Photochem.* **1976/77**, *6*, 371-374, doi:10.1016/0047-2670(76)85076-9.

Greenblatt, G. D.; Ravishankara, A. R. Laboratory studies on the stratospheric NO_x production rate. *J. Geophys. Res.* **1990**, *95*, 3539-3547, doi:10.1029/JD095iD04p03539.

Heidner, R. F., III ; Husain, D.; Wiesenfeld, J. R. Kinetic investigation of electronically excited oxygen atoms, $O(2^1D_2)$, by time-resolved attenuation of atomic resonance radiation in the vacuum ultra-violet Part 2.- Collisional quenching by the atmospheric gases N_2, O_2, CO, CO_2, H_2O and O_3. *J. Chem. Soc. Faraday Trans. 2* **1973**, *69*, 927-938, doi:10.1039/f29736900927.

Heidner, R. F., III; Husain, D. Electronically excited oxygen atoms, $O(2^1D_2)$. A time-resolved study of the collisional quenching by the gases H_2, D_2, NO, N_2O, NO_2, CH_4, and C_3O_2 using atomic absorption spectroscopy in the vacuum ultraviolet. *Int. J. Chem. Kinet.* **1973**, *5*, 819-831, doi:10.1002/kin.550050509.

Jayanty, R. K. M.; Simonaitis, R.; Heicklen, J. The reaction of $O(^1D)$ with CCl_2O, CFClO and CF_2O. *J. Photochem.* **1976**, *5*, 217-224, doi:10.1016/0047-2670(76)85018-6.

Kono, M.; Matsumi, Y. Reaction processes of $O(^1D)$ with fluoroethane compounds. *J. Phys. Chem. A* **2001**, *105*, 65-69, doi:10.1021/jp001786q S1089-5639(00)01786-2.

Koppe, S.; Laurent, T.; Naik, P. D.; Volpp, H.-R.; Wolfrum, J.; Arusi-Parpar, T.; Bar, I.; Rosenwaks, S. Absolute rate constants and reactive cross sections for the reactions of $O(^1D)$ with molecular hydrogen and deuterium. *Chem. Phys. Lett.* **1993**, *214*, 546-552, doi:10.1016/0009-2614(93)85681-D.

Lee, L. C.; Slanger, T. G. Observations on $O(^1D \rightarrow ^3P)$ and $O_2(b^1\Sigma_g^+ \rightarrow X^3\Sigma_g^-)$ following O_2 photodissociation. *J. Chem. Phys.* **1978**, *69*, 4053-4060, doi:10.1063/1.437136.

Lee, L. C.; Slanger, T. G. Atmospheric OH production--The $O(^1D) + H_2O$ reaction rate. *Geophys. Res. Lett.* **1979**, *6*, 165-166, doi:10.1029/GL006i003p00165.

Lin, C. L.; DeMore, W. B. $O(^1D)$ production in ozone photolysis near 3100 Å. *J. Photochem.* **1973/74**, *2*, 161-164, doi:10.1016/0047-2670(73)80014-0.

Lorenzen-Schmidt, H.; Weller, R.; Schrems, O. Kinetics and mechanisms of the reactions of $O(^1D)$ atoms with CF_3Br and CF_3BrCF_2Br in the gas phase and in solid argon matrices. *Ber. Bunsenges. Phys. Chem.* **1994**, *98*, 1622-1629, doi:10.1002/bbpc.19940981220.

Martin, D.; Jourdain, J. L.; Laverdet, G.; Le Bras, G. Kinetic study of the reaction of IO with CH_3SCH_3. *Int. J. Chem. Kinet.* **1987**, *19*, 503-512, doi:10.1002/kin.550190603.

Matsumi, Y.; Nomura, S.; Kawasaki, M.; Imamura, T. Vibrational distribution of ClO radicals produced in the reaction $Cl + O_3 \rightarrow ClO + O_2$. *J. Phys. Chem.* **1996**, *100*, 176-179, doi:10.1021/jp9518872.

Matsumi, Y.; Tonokura, K.; Inagaki, Y.; Kawasaki, M. Isotopic branching ratios and translational energy release of H and D atoms in reaction of $O(^1D)$ atoms with alkanes and akyl chlorides. *J. Phys. Chem.* **1993**, *97*, 6816-6821, doi:10.1021/j100128a012.

Nilsson, E. J. K.; Andersen, V. F.; Nielsen, O. J.; Johnson, M. S. Rate coefficients for the chemical reactions of CH_2F_2, $CHClF_2$, CH_2FCF_3 and CH_3CCl_3 with $O(^1D)$ at 298 K. *Chem. Phys. Lett.* **2012**, *554*, 27-32, doi:10.1016/j.cplett.2012.10.001.

Nishida, S.; Takahashi, K.; Matsumi, Y.; Taniguchi, N.; Hayashida, S. Formation of $O(^3P)$ atoms in the photolysis of N_2O at 193 nm and $O(^3P) + N_2O$ product channel in the reaction of $O(^1D) + N_2O$ *J. Phys. Chem. A* **2004**, *108*, 2451-2456, doi:10.1021/jp037034o.

Noxon, J. F. Optical emission from $O(^1D)$ and $O_2(b^1\Sigma_g)$ in ultraviolet photolysis of O_2 and CO_2. *J. Chem. Phys.* **1970**, *52*, 1852-1873, doi:10.1063/1.1673227.

Papadimitriou, V. C.; McGillen, M. R.; Smith, S. C.; Jubb, A. M.; Portmann, R. W.; Hall, B. D.; Fleming, E. L.; Jackman, C. H.; Burkholder, J. B. 1,2-Dichlorohexafluoro-cyclobutane (1,2-*c*-$C_4F_6Cl_2$, R-316c) a potent ozone depleting substance and greenhouse gas: Atmospheric loss processes, lifetimes, and ozone depletion and global warming potentials for the (*E*) and (*Z*) stereoisomers. *J. Phys. Chem. A* **2013**, *117*, 11049-11065, doi:10.1021/jp407823k.

Park, C. R.; Wiesenfeld, J. R. Chemical dynamics of the reaction of $O(^1D_2)$ with CH_3F. *Chem. Phys. Lett.* **1991**, *186*, 170-176, doi:10.1016/S0009-2614(91)85124-F.

Perri, M. J.; Van Wyngarden, A. L.; Boering, K. A.; Lin, J. J.; Lee, Y. T. Dynamics of the $O(^1D) + CO_2$ oxygen isotope exchange reaction. *J. Chem. Phys.* **2003**, *119*, 8213-8216, doi:10.1063/1.1618737.

Ravishankara, A. R.; Dunlea, E. J.; Blitz, M. A.; Dillon, T. J.; Heard, D. E.; Pilling, M. J.; Strekowski, R. S.; Nicovich, J. M.; Wine, P. H. Redetemination of the rate coefficient for the reaction of $O(^1D)$ with N_2. *Geophys. Res. Lett.* **2002**, *29*, 1745, doi:10.1029/2002GL014850.

Ravishankara, A. R.; Solomon, S.; Turnipseed, A. A.; Warren, R. F. Atmospheric lifetimes of long-lived halogenated species. *Science* **1993**, *259*, 194-199, doi:10.1126/science.259.5092.194.

Sanders, N. D.; Butler, J. E.; McDonald, J. R. Product branching ratios in the reaction of $O(^1D_2)$ with NH_3. *J. Chem. Phys.* **1980**, *73*, 5381-5383, doi:10.1063/1.439927.

Satyapal, S.; Park, J.; Bersohn, R.; Katz, B. Dissociation of methanol and ethanol activated by a chemical reaction or by light. *J. Chem. Phys.* **1989**, *91*, 6873-6879, doi:10.1063/1.457356.

Schmoltner, A. M.; Talukdar, R. K.; Warren, R. F.; Mellouki, A.; Goldfarb, L.; Gierczak, T.; McKeen, S. A.; Ravishankara, A. R. Rate coefficients for reactions of several hydrofluorocarbons with OH and $O(^1D)$ and their atmospheric lifetimes. *J. Phys. Chem.* **1993**, *97*, 8976-8982, doi:10.1021/j100137a023.

Sedlacek, A. J.; Harding, D. R.; Weston Jr., R. E.; Kreutz, T. G.; Flynn, G. W. Probing the $O(^1D) + CO_2$ reaction with second-derivative modulated diode laser spectroscopy. *J. Chem. Phys.* **1989**, *91*, 7550-7556, doi:10.1063/1.457278.

Shi, J.; Barker, J. R. Kinetic studies of the deactivation of $O_2(^1\Sigma_g^+)$ and $O(^1D)$. *Int. J. Chem. Kinet.* **1990**, *20*, 1283-1301, doi:10.1002/kin.550221207.

Snelling, D. R. The ultraviolet flash photolysis of ozone and the reactions of $O(^1D)$ and $O_2(^1\Sigma_g^+)$. *Can. J. Chem.* **1974**, *52*, 257-270, doi:10.1139/v74-042.

Sorokin, V. I.; Gritsan, N. P.; Chichinin, A. I. Collisions of $O(^1D)$ with HF, F_2, XeF_2, NF_3, and CF_4: Deactivation and reaction. *J. Chem. Phys.* **1998**, *108*, 8995-9003, doi:10.1063/1.476346.

Streit, G. E.; Howard, C. J.; Schmeltekopf, A. L.; Davidson, J. A.; Schiff, H. I. Temperature dependence of $O(^1D)$ rate constants for reactions with O_2, N_2, CO_2, O_3, and H_2O. *J. Chem. Phys.* **1976**, *65*, 4761-4764, doi:10.1063/1.432930.

Strekowski, R. S.; Nicovich, J. M.; Wine, P. H. Quenching of $O(^1D_2)$ by Cl_2CO: kinetics and $O(^3P_J)$ yield. *Chem. Phys. Lett.* **2000**, *330*, 354-360, doi:10.1016/S0009-2614(00)01105-2.

Strekowski, R. S.; Nicovich, J. M.; Wine, P. H. Kinetic and mechanistic study of the reaction of $O(^1D)$ with CF_2HBr. *Int. J. Chem. Kinet.* **2001**, *33*, 262-270, doi:10.1002/kin.1019.abs.

Strekowski, R. S.; Nicovich, J. M.; Wine, P. H. Temperature-dependent kinetics study of the reactions of $O(^1D_2)$ with N_2 and O_2. *Phys. Chem. Chem. Phys.* **2004**, *6*, 2145-2151, doi:10.1039/b400243a.

Strekowski, R. S.; Nicovich, J. M.; Wine, P. H. Kinetic and mechanistic study of the reactions of $O(^1D_2)$ with HCN and CH_3CN. *ChemPhysChem* **2010**, *11*, 3942-3955, doi:10.1002/cphc.201000550.

Takahashi, K.; Takeuchi, Y.; Matsumi, Y. Rate constants of the $O(^1D)$ reactions with N_2, O_2, N_2O, and H_2O at 295 K. *Chem. Phys. Lett.* **2005**, *410*, 196-200, doi:10.1016/j.cplett.2005.05.062.

Takahashi, K.; Wada, R.; Matsumi, Y.; Kawasaki, M. Product branching ratios for $O(^3P)$ atom and ClO radical formation in the reactions of $O(^1D)$ with chlorinated compounds. *J. Phys. Chem.* **1996**, *100*, 10145-10149, doi:10.1021/jp952710a.

Talukdar, R. K.; Ravishankara, A. R. Rate coefficients for $O(^1D) + H_2$, D_2, HD reactions and H atom yield in $O(^1D)$ + HD reaction. *Chem. Phys. Lett.* **1996**, *253*, 177-183, doi:10.1016/0009-2614(96)00203-5.

Thompson, J. E.; Ravishankara, A. R. Kinetics of $O(^1D)$ reactions with bromocarbons. *Int. J. Chem. Kinet.* **1993**, *25*, 479-487, doi:10.1002/kin.550250607.

Vranckx, S.; Peeters, J.; Carl, S. A temperature dependence kinetic study of $O(^1D) + CH_4$: overall rate coefficient and product yields. *Phys. Chem. Chem. Phys.* **2008**, *10*, 5714-5722, doi: 10.1039/b804903c.

Vranckx, S.; Peeters, J.; Carl, S. Kinetics of $O(^1D) + H_2O$ and $O(^1D) + H_2$: Absolute rate coefficients and $O(^3P)$ yields between 227 and 453 K. *Phys. Chem. Chem. Phys.* **2010**, *12*, 9213-9221, doi:10.1039/b923959f.

Vranckx, S.; Peeters, J.; Carl, S. A. Absolute rate constant and $O(^3P)$ yield for the $O(^1D) + N_2O$ reaction in the temperature range 227 K to 719 K. *Atmos. Chem. Phys.* **2008**, *8*, 6261-6272, doi:10.5194/acp-8-6261-2008.

Warren, R.; Gierczak, T.; Ravishankara, A. R. A study of $O(^1D)$ reactions with CFC substitutes. *Chem. Phys. Lett.* **1991**, *183*, 403-409, doi:10.1016/0009-2614(91)90402-U.

Wine, P. H.; Nicovich, J. M.; Ravishankara, A. R. Kinetics of the reactions of $O(^3P)$ and $O(^1D)$ with Cl_2. *J. Phys. Chem.* **1985**, *89*, 3914-3918, doi:10.1021/j100264a031.

Wine, P. H.; Ravishankara, A. R. Kinetics of $O(^1D)$ interactions with the atmospheric gases N_2, N_2O, H_2O, H_2, CO_2, and O_3. *Chem. Phys. Lett.* **1981**, *77*, 103-109, doi:10.1016/0009-2614(81)85609-6.

Wine, P. H.; Ravishankara, A. R. O_3 photolysis at 248 nm and $O(^1D_2)$ quenching by H_2O, CH_4, H_2, and N_2O: $O(^3P_J)$ yields. *Chem. Phys.* **1982**, *69*, 365-373, doi:10.1016/0301-0104(82)88075-0.

Wine, P. H.; Ravishankara, A. R. Reactive and non-reactive quenching of $O(^1D_2)$ by COF_2. *Chem. Phys. Lett.* **1983**, *96*, 129-132, doi:10.1016/0009-2614(83)80131-6.

Wine, P. H.; Wells, J. R.; Ravishankara, A. R. Channel specific rate constants for reactions of $O(^1D)$ with HCl and HBr. *J. Chem. Phys.* **1986**, *84*, 1349-1354, doi:10.1063/1.450526.

Zellner, R.; Wagner, G.; Himme, B. H_2 formation in the reaction of $O(^1D)$ with H_2O. *J. Phys. Chem.* **1980**, *84*, 3196-3198, doi:10.1021/j100461a013.

Zhao, Z.; Laine, P. L.; Nicovich, J. M.; Wine, P. H. Reactive and non-reactive quenching of $O(^1D)$ by the potent greenhouse gases SO_2F_2, NF_3, and SF_5CF_3. *Proc. Nat. Acad. Sci.* **2010**, *107*, 6610-6615, doi:10.1073/pnas.0911228107.

1.6 Singlet O_2 Reactions

1.6.1 Table 1A: Singlet O_2 Reactions

Reaction	Temperature Range of Exp. Data (K) [a]	*A*-Factor	*E*/R	*k*(298 K)[b]	*f*(298 K)[c]	*g*	Notes
$O_2(^1\Delta) + O \rightarrow$ products	298			$<2\times10^{-16}$			A73
$O_2(^1\Delta) + O_2 \rightarrow$ products	100–450	3.6×10^{-18}	220	1.7×10^{-18}	1.2	100	A74
$O_2(^1\Delta) + O_3 \rightarrow O + 2O_2$	283–360	5.2×10^{-11}	2840	3.8×10^{-15}	1.2	500	A75
$O_2(^1\Delta) + H_2O \rightarrow$ products	298			4.8×10^{-18}	1.5		A76
$O_2(^1\Delta) + N \rightarrow NO + O$	195–300			$<9\times10^{-17}$			A77
$O_2(^1\Delta) + N_2 \rightarrow$ products	298			$<10^{-20}$			A78
$O_2(^1\Delta) + CO_2 \rightarrow$ products	298			$<2\times10^{-20}$			A79
$O_2(^1\Sigma) + O \rightarrow$ products	300			8×10^{-14}	5.0		A80
$O_2(^1\Sigma) + O_2 \rightarrow$ products	298			3.9×10^{-17}	1.5		A81
$O_2(^1\Sigma) + O_3 \rightarrow$ products	210–370	3.5×10^{-11}	135	2.2×10^{-11}	1.15	50	A82
$O_2(^1\Sigma) + H_2 \rightarrow$ products $O_2(^1\Sigma) + H_2 \rightarrow 2$ OH	173–393	6.4×10^{-12}	600	8.5×10^{-13} $<4\times10^{-17}$ (See Note)	1.15	100	A83
$O_2(^1\Sigma) + H_2O \rightarrow O_2 + H_2O$	250–370	3.9×10^{-12}	–125	5.9×10^{-12}	1.3	100	A84
$O_2(^1\Sigma) + N \rightarrow$ products	300			$<10^{-13}$			A85
$O_2(^1\Sigma) + N_2 \rightarrow$ products	203–370	1.8×10^{-15}	–45	2.1×10^{-15}	1.1	100	A86
$O_2(^1\Sigma) + N_2O \rightarrow$ products $O_2(^1\Sigma) + N_2O \rightarrow NO + NO_2$	210–370	7.0×10^{-14}	–75	9.0×10^{-14} $<2\times10^{-17}$ (See Note)	1.3	50	A87
$O_2(^1\Sigma) + CO_2 \rightarrow$ products	245–362	4.2×10^{-13}	0	4.2×10^{-13}	1.2	200	A88

Shaded areas indicate changes or additions since JPL19-5.

[a] Temperature range of available experimental data. This is not necessarily the range of temperature over which the recommended Arrhenius parameters are applicable. See the corresponding note for such information.

[b] Units are cm^3 $molecule^{-1}$ s^{-1}.

[c] *f*(298 K) is the uncertainty factor at 298 K. To calculate the uncertainty at other temperatures, use the expression:

$$f(\mathrm{T}) = f(298\ \mathrm{K})\exp\left|g\left(\frac{1}{\mathrm{T}} - \frac{1}{298}\right)\right|$$

Note that the exponent is an absolute value.

1.6.2 Notes: Singlet O_2 Reactions

A73. **$O_2(^1\Delta) + O$**. The recommendation is based on the upper limit reported by Clark and Wayne.[2] (Table: 92-20, Note: 92-20, Evaluation: 10-6) Back to Table

(1) Baasandorj, M.; Hall, B. D.; Burkholder, J. B. Rate coefficients for the reaction of $O(^1D)$ with the atmospherically long-lived greenhouse gases NF_3, SF_5CF_3, CHF_3, C_2F_6, *c*-C_4F_8, *n*-C_5F_{12}, and *n*-C_6F_{14}. *Atmos. Chem. Phys.* **2012**, *12*, 11753-11764, doi:10.5194/acp-12-11753-2012.

(2) Clark, I. D.; Wayne, R. P. The reaction of $O_2(^1\Delta_g)$ with atomic nitrogen and with atomic oxygen. *Chem. Phys. Lett.* **1969**, *3*, 405-407, doi:10.1016/0009-2614(69)80151-X.

(3) Zhao, Z.; Laine, P. L.; Nicovich, J. M.; Wine, P. H. Reactive and non-reactive quenching of $O(^1D)$ by the potent greenhouse gases SO_2F_2, NF_3, and SF_5CF_3. *Proc. Nat. Acad. Sci.* **2010**, *107*, 6610-6615, doi:10.1073/pnas.0911228107.

A74. **$O_2(^1\Delta) + O_2$**. The recommendation is the average of eight room temperature measurements: Steer et al.,[9] Findlay and Snelling,[5] Borrell et al.,[2] Leiss et al.,[6] Tachibana and Phelps,[10] Billington and Borrell,[1] Raja et al.,[8] and Wildt et al.[11] The temperature dependence is derived from the data of Findlay and Snelling and Billington and Borrell. Several other less direct measurements of the rate coefficient agree with the recommendation, including Clark and Wayne,[3] Findlay et al.,[4] and McLaren et al.[7] Wildt et al.[12] report observations of weak emission in the near IR due to collision-induced radiation. Wildt et al.[13] give rate coefficients for this process. (Table: 92-20, Note: 94-26, Evaluation: 10-6) Back to Table

(1) Billington, A. P.; Borrell, P. The low-temperature quenching of singlet molecular oxygen [$O_2(a\ ^1\Delta_g)$]. *J. Chem. Soc. Faraday Trans. 2* **1986**, *82*, 963-970, doi:10.1039/f29868200963.

(2) Borrell, P.; Borrell, P. M.; Pedley, M. D. Deactivation of singlet molecular oxygen, $O_2(^1\Delta_g)$, by oxygen. *Chem. Phys. Lett.* **1977**, *51*, 300-302, doi:10.1016/0009-2614(77)80407-7.

(3) Clark, I. D.; Wayne, R. P. Collisional quenching of $O_2(^1\Delta_g)$. *Proc. Roy. Soc. Lond. A.* **1969**, *314*, 111-127, doi:10.1098/rspa.1969.0218.

(4) Findlay, F. D.; Fortin, C. J.; Snelling, D. R. Deactivation of $O_2(^1\Delta_g)$. *Chem. Phys. Lett.* **1969**, *3*, 204-206, doi:10.1016/0009-2614(69)80026-6.

(5) Findlay, F. D.; Snelling, D. R. Collisional deactivation of $O_2(^1\Delta_g)$. *J. Chem. Phys.* **1971**, *55*, 545-551, doi:10.1063/1.1675786.

(6) Leiss, A.; Schurath, U.; Becker, K. H.; Fink, E. H. Revised quenching rate constants for metastable oxygen molecules $O_2(a^1\Delta_g)$. *J. Photochem.* **1978**, *8*, 211-214, doi:10.1016/0047-2670(78)80021-5.

(7) McLaren, I. A.; Morris, N. W.; Wayne, R. P. Is CO_2 a good quencher of $O_2(^1\Delta_g)$? A kinetic reappraisal. *J. Photochem.* **1981**, *16*, 311-319, doi:10.1016/0047-2670(81)80053-6.

(8) Raja, N.; Arora, P. K.; Chatha, J. P. S. Rate constants of $O_2(^1\Delta_g)$. *Int. J. Chem. Kinet.* **1986**, *18*, 505-512, doi:10.1002/kin.550180409.

(9) Steer, R. P.; Ackerman, R. A.; Pitts, J. N., Jr. Singlet oxygen in the environmental sciences. V. Rates of deactivation of $O_2(^1\Delta_g)$ by oxygen and nitrogen. *J. Chem. Phys.* **1969**, *51*, 843-844, doi:10.1063/1.1672082.

(10) Tachibana, K.; Phelps, A. V. Excitation of the $O_2(a\ ^1\Delta_g)$ state by low energy electrons. *J. Chem. Phys.* **1981**, *75*, 3315-3320, doi:10.1063/1.442483.

(11) Wildt, J.; Bednarek, G.; Fink, E. H.; Wayne, R. P. Laser excitation of $O_2(b^1\Sigma_g^+, v' = 0,1,2)$- Rates and channels of energy transfer and quenching. *Chem. Phys.* **1988**, *122*, 463-470, doi:10.1016/0301-0104(88)80027-2.

(12) Wildt, J.; Fink, E. H.; Biggs, P.; Wayne, R. P. The collision-induced radiation of $O_2(a^1\Delta_g)$. *Chem. Phys.* **1989**, *139*, 401-407, doi:10.1016/0301-0104(89)80152-1.

(13) Wildt, J.; Fink, E. H.; Biggs, P.; Wayne, R. P.; Vilesov, A. F. Collision-induced emission of $O_2(a^1\Delta_g \rightarrow X\ ^3\Sigma_g^-)$ in the gas phase. *Chem. Phys.* **1992**, *159*, 127-140, doi:10.1016/0301-0104(92)80065-4.

A75. **$O_2(^1\Delta) + O_3$**. The recommendation is the average of the room temperature measurements of Clark et al.,[4] Findlay and Snelling,[6] Becker et al.,[3] and Collins et al.[5] Several less direct measurements agree well with the recommendation (McNeal and Cook,[9] Wayne and Pitts,[12] and Arnold and Comes[2]). The temperature dependence is from the studies of Findlay and Snelling and Becker et al., which agree very well, although both covered a relatively small temperature range. An earlier study by Clark et al. covered a much larger range and found a much smaller temperature coefficient. The reason for this discrepancy is not clear. The yield of $O + 2O_2$ products appears to be close to unity, based on many studies of the quantum yield of O_3 destruction near the peak of the Hartley band, e.g. measurements of the number of O_3 molecules destroyed per photon absorbed (von Ellenrieder et al.,[11] Ravishankara et al.,[10] Lissi and Heicklen,[8] and references cited therein) and measurements of O_3 loss and O atom temporal profiles in pulsed experiments (Klais et al.[7] and Arnold and

Comes[2]). Anderson et al.[1] report that the rate coefficient for atom exchange between $O_2(^1\Delta)$ and O_3 is $<5 \times 10^{-16}$ at 300 K.
(Table: 92-20, Note: 94-26, Evaluation: 10-6) Back to Table

(1) Anderson, S. M.; Morton, J.; Mauersberger, K.; Yung, Y. L.; DeMore, W. B. A study of atom exchange between $O(^1D)$ and ozone. *Chem. Phys. Lett.* **1992**, *189*, 581-585, doi:10.1016/0009-2614(92)85254-8.
(2) Arnold, I.; Comes, F. J. Photolysis of ozone in the ultraviolet region. Reactions of $O(^1D)$, $O_2(^1\Delta_g)$ and $O_2^{\ddagger}$. *Chem. Phys.* **1980**, *47*, 125-130, doi:10.1016/0301-0104(80)80027-9.
(3) Becker, K. H.; Groth, W.; Schurath, U. Reactions of $O_2(^1\Delta_g)$ with ozone. *Chem. Phys. Lett.* **1972**, *14*, 489-492, doi:10.1016/0009-2614(72)80246-X.
(4) Clark, I. D.; Jones, I. T. N.; Wayne, R. P. The kinetics of the reaction between $O_2(^1\Delta_g)$ and ozone. *Proc. Roy. Soc. Lond. A.* **1970**, *317*, 407-416, doi:10.1098/rspa.1970.0124.
(5) Collins, R. J.; Husain, D.; Donovan, R. J. Kinetic and spectroscopic studies of $O_2(a^1\Delta_g)$ by time-resolved absorption spectroscopy in the vacuum ultra-violet. *J. Chem. Soc. Faraday Trans. 2* **1973**, *69*, 145-157, doi:10.1039/f29736900145.
(6) Findlay, F. D.; Snelling, D. R. Temperature dependence of the rate constant for the reaction $O_2(^1\Delta_g) + O_3 \rightarrow 2O_2 + O$. *J. Chem. Phys.* **1971**, *54*, 2750-2755, doi:10.1063/1.1675240.
(7) Klais, O.; Laufer, A. H.; Kurylo, M. J. Atmospheric quenching of vibrationally excited $O_2(^1\Delta)$. *J. Chem. Phys.* **1980**, *73*, 2696-2699, doi:10.1063/1.440483.
(8) Lissi, E.; Heicklen, J. The photolysis of ozone. *J. Photochem.* **1972**, *1*, 39-68, doi:10.1016/0047-2670(72)80004-2.
(9) McNeal, R. J.; Cook, G. R. Photoionization of electronically excited oxygen: Rate of the reaction. *J. Chem. Phys.* **1967**, *47*, 5385-5389, doi:10.1063/1.1701807.
(10) Ravishankara, A. R.; Wine, P. H.; Nicovich, J. M. Pulsed laser photolysis study of the reaction between $O(^3P)$ and HO_2. *J. Chem. Phys.* **1983**, *78*, 6629-6639, doi:10.1063/1.444661.
(11) von Ellenrieder, G.; Castellano, E.; Schumacher, H. J. The kinetics and the mechanism of the photochemical decomposition of ozone with light of 2537 Å wavelength. *Chem. Phys. Lett.* **1971**, *9*, 152-156, doi:10.1016/0009-2614(71)80211-7.
(12) Wayne, R. P.; Pitts, J. N., Jr. Rate constant for the reaction $O_2(^1\Delta_g) + O_3 \rightarrow 2O_2 + O$. *J. Chem. Phys.* **1969**, *50*, 3644-3645, doi:10.1063/1.1671606.

A76. $O_2(^1\Delta) + H_2O$. The recommendation is the average of the measurements reported by Becker et al.[1] and Findlay and Snelling.[3] An earlier study by Clark and Wayne[2] reported a value about three times larger.
(Table: 92-20, Note: 92-20, Evaluation: 10-6) Back to Table

(1) Becker, K. H.; Groth, W.; Schurath, U. The quenching of metastable $O_2(^1\Delta_g)$ and $O_2(^1\Sigma_g^+)$ molecules. *Chem. Phys. Lett.* **1971**, *8*, 259-262, doi:10.1016/0009-2614(71)85004-2.
(2) Clark, I. D.; Wayne, R. P. Collisional quenching of $O_2(^1\Delta_g)$. *Proc. Roy. Soc. Lond. A.* **1969**, *314*, 111-127, doi:10.1098/rspa.1969.0218.
(3) Findlay, F. D.; Snelling, D. R. Collisional deactivation of $O_2(^1\Delta_g)$. *J. Chem. Phys.* **1971**, *55*, 545-551, doi:10.1063/1.1675786.

A77. $O_2(^1\Delta) + N$. The recommendation is an upper limit based upon the measurement reported by Westenberg et al.,[4] who used ESR to detect $O_2(X^3\Sigma$ and $a^1\Delta)$, $O(^3P)$ and $N(^4S)$ with a discharge flow reactor. They used an excess of $O_2(^1\Delta)$ and measured the decay of N and the appearance of O at 195 and 300 K. They observed that the reaction of N with $O_2(^1\Delta)$ is somewhat slower than its reaction with $O_2(^3\Sigma)$. The recommended rate constant value for the latter provides the basis for the recommendation. Clark and Wayne[1,2] and Schmidt and Schiff[3] reported observations of an $O_2(^1\Delta)$ reaction with N that is about 30 times faster than the recommended limit. Schmidt and Schiff attribute the observed loss of $O_2(^1\Delta)$ in excess N to a rapid energy exchange with some constituent in discharged nitrogen, other than N.
(Table: 92-20, Note: 92-20, Evaluation: 10-6) Back to Table

(1) Clark, I. D.; Wayne, R. P. The reaction of $O_2(^1\Delta_g)$ with atomic nitrogen and with atomic oxygen. *Chem. Phys. Lett.* **1969**, *3*, 405-407, doi:10.1016/0009-2614(69)80151-X.
(2) Clark, I. D.; Wayne, R. P. Kinetics of the reaction between atomic nitrogen and molecular oxygen in the ground $(^3\Sigma_g^-)$ and first excited $(^1\Delta_g)$ states. *Proc. Roy. Soc. Lond. A.* **1970**, *316*, 539-550, doi:10.1098/rspa.1970.0095.
(3) Schmidt, C.; Schiff, H. I. Reactions of $O_2(^1\Delta_g)$ with atomic nitrogen and hydrogen. *Chem. Phys. Lett.* **1973**, *23*, 339-342, doi:10.1016/0009-2614(73)85092-4.

(4) Westenberg, A. A.; Roscoe, J. M.; deHaas, N. Rate measurements on N + $O_2(^1\Delta_g)$ → NO + O and H + $O_2(^1\Delta_g)$ → OH + O. *Chem. Phys. Lett.* **1970**, *7*, 597-599, doi:10.1016/0009-2614(70)87014-2.

A78. **$O_2(^1\Delta) + N_2$**. The recommendation is based upon the measurements by Findlay et al.[3] and Becker et al.[1] Other studies obtained higher values for an upper limit: Clark and Wayne[2] and Steer et al.[4]
(Table: 92-20, Note: 92-20, Evaluation: 10-6) Back to Table

(1) Becker, K. H.; Groth, W.; Schurath, U. The quenching of metastable $O_2(^1\Delta_g)$ and $O_2(^1\Sigma_g^+)$ molecules. *Chem. Phys. Lett.* **1971**, *8*, 259-262, doi:10.1016/0009-2614(71)85004-2.
(2) Clark, I. D.; Wayne, R. P. Collisional quenching of $O_2(^1\Delta_g)$. *Proc. Roy. Soc. Lond. A.* **1969**, *314*, 111-127, doi:10.1098/rspa.1969.0218.
(3) Findlay, F. D.; Fortin, C. J.; Snelling, D. R. Deactivation of $O_2(^1\Delta_g)$. *Chem. Phys. Lett.* **1969**, *3*, 204-206, doi:10.1016/0009-2614(69)80026-6.
(4) Steer, R. P.; Ackerman, R. A.; Pitts, J. N., Jr. Singlet oxygen in the environmental sciences. V. Rates of deactivation of $O_2(^1\Delta_g)$ by oxygen and nitrogen. *J. Chem. Phys.* **1969**, *51*, 843-844, doi:10.1063/1.1672082.

A79. **$O_2(^1\Delta) + CO_2$**. The recommendation is based on the measurements reported by Findlay and Snelling[2] and Leiss et al.[3] Upper limit rate coefficients reported by Becker et al.,[1] McLaren et al.,[4] and Singh et al.[5] are consistent with the recommendation.
(Table: 92-20, Note: 92-20, Evaluation: 10-6) Back to Table

(1) Becker, K. H.; Groth, W.; Schurath, U. The quenching of metastable $O_2(^1\Delta_g)$ and $O_2(^1\Sigma_g^+)$ molecules. *Chem. Phys. Lett.* **1971**, *8*, 259-262, doi:10.1016/0009-2614(71)85004-2.
(2) Findlay, F. D.; Snelling, D. R. Collisional deactivation of $O_2(^1\Delta_g)$. *J. Chem. Phys.* **1971**, *55*, 545-551, doi:10.1063/1.1675786.
(3) Leiss, A.; Schurath, U.; Becker, K. H.; Fink, E. H. Revised quenching rate constants for metastable oxygen molecules $O_2(a^1\Delta_g)$. *J. Photochem.* **1978**, *8*, 211-214, doi:10.1016/0047-2670(78)80021-5.
(4) McLaren, I. A.; Morris, N. W.; Wayne, R. P. Is CO_2 a good quencher of $O_2(^1\Delta_g)$? A kinetic reappraisal. *J. Photochem.* **1981**, *16*, 311-319, doi:10.1016/0047-2670(81)80053-6.
(5) Singh, J. P.; Setser, D. W. Electronic-to-vibrational energy-transfer studies of singlet molecular oxygen. 2. $O_2(b^1\Sigma_g^+)$. *J. Phys. Chem.* **1985**, *89*, 5353-5358, doi:10.1021/j100271a009.

A80. **$O_2(^1\Sigma) + O$**. The recommendation is based on the measurement reported by Slanger and Black.[1]
(Table: 92-20, Note: 92-20, Evaluation: 10-6) Back to Table

(1) Slanger, T. G.; Black, G. Interactions of O_2 ($b^1\Sigma_g^+$) with O(^3P) and O_3. *J. Chem. Phys.* **1979**, *70*, 3434-3438, doi:10.1063/1.437877.

A81. **$O_2(^1\Sigma) + O_2$**. The recommendation is the average of the room temperature values reported by Martin et al.,[5] Lawton et al.,[3] and Lawton and Phelps,[4] which are in excellent agreement. Measurements by Thomas and Thrush,[6] Chatha et al.,[1] and Knickelbein et al.[2] are in reasonable agreement with the recommendation. Knickelbein et al. report the yield of $O_2(^1\Delta)$ product to be approximately unity.
(Table: 92-20, Note: 92-20, Evaluation: 10-6) Back to Table

(1) Chatha, J. P. S.; Arora, P. K.; Raja, N.; Kulkarni, P. B.; Vohra, K. G. Collisional deactivation of $O_2(^1\Sigma_g^+)$. *Int. J. Chem. Kinet.* **1979**, *11*, 175-185, doi:10.1002/kin.550110209.
(2) Knickelbein, M. B.; Marsh, K. L.; Ulrich, O. E.; Busch, G. E. Energy transfer kinetics of singlet molecular oxygen: The deactivation channel for $O_2(b\ ^1\Sigma_g^+)$. *J. Chem. Phys.* **1987**, *87*, 2392-2393, doi:10.1063/1.453120.
(3) Lawton, S. A.; Novick, S. E.; Broida, H. P.; Phelps, A. V. Quenching of optically pumped $O_2(b^1\Sigma_g^+)$ by ground state O_2 molecules. *J. Chem. Phys.* **1977**, *66*, 1381-1382, doi:10.1063/1.434038.
(4) Lawton, S. A.; Phelps, A. V. Excitation of the $b\ ^1\Sigma_g^+$ state of O_2 by low energy electrons. *J. Chem. Phys.* **1978**, *69*, 1055-1068, doi:10.1063/1.436700.
(5) Martin, L. R.; Cohen, R. B.; Schatz, J. F. Quenching of laser induced fluorescence of O_2 ($b^1\Sigma_g^+$) by O_2 and N_2. *Chem. Phys. Lett.* **1976**, *41*, 394-396, doi:10.1016/0009-2614(76)80838-X.
(6) Thomas, R. G. O.; Thrush, B. A. Quenching of $O_2(^1\Sigma_g^+)$ by ground state O_2. *J. Chem. Soc. Faraday Trans. 2* **1975**, *71*, 664-667, doi:10.1039/f29757100664.

A82. **$O_2(^1\Sigma) + O_3$**. The recommendation is based on the room temperature measurements of Gilpin et al.,[6] Gauthier and Snelling,[5] Slanger and Black,[9] Choo and Leu,[3] Shi and Barker,[8] Turnipseed et al.,[11] and Dunlea et al.[4] Measurements by Snelling,[10] Amimoto and Wiesenfeld,[1] and Ogren et al.[7] are in agreement with the recommendation. The value from the study of Biedenkapp and Bair[2] is lower than the recommended value. The temperature dependence is taken from the results of Dunlea et al., who measured the rate coefficient between 210 and 370 K. The results of Choo and Leu, which encompassed 295–362 K, are consistent with the recommended value. This reaction has multiple product channels. The yield of $O + 2O_2$ products is reported to be (70 ± 20)% by Slanger and Black and Amimoto and Wiesenfeld. The remaining ~30% of the reaction is expected to lead to quenching to $O_2(^1\Delta$ or $^3\Sigma)$ while leaving ozone intact; the electronic state of O_2 that is produced in all these channels is not known.
(Table: 06-2, Note: 06-2, Evaluation: 10-6) Back to Table

(1) Amimoto, S. T.; Wiesenfeld, J. R. $O_2(b^1\Sigma_g^+)$ production and deactivation following quenching of $O(^1D_2)$ in O_3/O_2 mixtures. *J. Chem. Phys.* **1980**, *72*, 3899-3903, doi:10.1063/1.439671.

(2) Biedenkapp, D.; Bair, E. J. Ozone ultraviolet photolysis. I. The effect of molecular oxygen. *J. Chem. Phys.* **1970**, *52*, 6119-6125, doi:10.1063/1.1672914.

(3) Choo, K. Y.; Leu, M.-T. Rate constants for the quenching of metastable $O_2(^1\Sigma_g^+)$ molecules. *Int. J. Chem. Kinet.* **1985**, *17*, 1155-1167, doi:10.1002/kin.550171102.

(4) Dunlea, E. J.; Talukdar, R. K.; Ravishankara, A. R. Kinetic studies of $O_2(b^1\Sigma_g^+)$ with several atmospheric molecules. *J. Phys. Chem. A* **2005**, *109*, 3912-3920, doi:10.1021/jp044129x.

(5) Gauthier, M. J. E.; Snelling, D. R. La photolyse de l'ozone a 253.7 nm: Desactivation de $O(^1D)$ et de $O_2(^1\Sigma)$ par les gaz de l'atmosphere. *J. Photochem.* **1975**, *4*, 27-50, doi:10.1016/0047-2670(75)80012-8.

(6) Gilpin, R.; Schiff, H. I.; Welge, K. H. Photodissociation of O_3 in the Hartley band. Reactions of $O(^1D)$ and $O_2(^1\Sigma_g^+)$ with O_3 and O_2. *J. Chem. Phys.* **1971**, *55*, 1087-1093, doi:10.1063/1.1676190.

(7) Ogren, P. J.; Sworski, T. J.; Hochanadel, C. J.; Cassel, J. M. Flash photolysis of O_3 in O_2 and $O_2 + H_2$ mixtures. Kinetics of $O_2(^1\Sigma_g^+) + O_3$ and $O(^1D) + H_2$ reactions. *J. Phys. Chem.* **1982**, *86*, 238-242, doi:10.1021/j100391a021.

(8) Shi, J.; Barker, J. R. Kinetic studies of the deactivation of $O_2(^1\Sigma_g^+)$ and $O(^1D)$. *Int. J. Chem. Kinet.* **1990**, *20*, 1283-1301, doi:10.1002/kin.550221207.

(9) Slanger, T. G.; Black, G. Interactions of O_2 $(b^1\Sigma_g^+)$ with $O(^3P)$ and O_3. *J. Chem. Phys.* **1979**, *70*, 3434-3438, doi:10.1063/1.437877.

(10) Snelling, D. R. The ultraviolet flash photolysis of ozone and the reactions of $O(^1D)$ and $O_2(^1\Sigma_g^+)$. *Can. J. Chem.* **1974**, *52*, 257-270, doi:10.1139/v74-042.

(11) Turnipseed, A. A.; Vaghjiani, G. L.; Gierczak, T.; Thompson, J. E.; Ravishankara, A. R. The photochemistry of ozone at 193 and 222 nm. *J. Chem. Phys.* **1991**, *95*, 3244-3251, doi:10.1063/1.460881.

A83. **$O_2(^1\Sigma) + H_2$**. The rate coefficient for this reaction, at or around 298 K, has been measured by Kohse-Höinghaus and Stuhl,[6] Braithwaite et al.,[2] Choo and Leu,[3] Singh and Setser,[8] Wildt et al.,[10] Michelangeli et al.,[7] Borrell and Richards,[1] Hohmann et al.,[5] and Talukdar et al.[9] k(298 K) was derived from the results of all of the above studies except for the results of Singh and Setser and Borrell and Richards, which are clearly outside of the range of values obtained by others.

The temperature dependence of the rate coefficient was computed using the results of Braithwaite et al., Hohmann et al., and Talukdar et al. The results of Kohse-Höinghaus and Stuhl were not included, because they are assumed to be superseded by those of Hohmann et al. from the same group. It is suspected that the Kohse-Höinghaus and Stuhl study was hampered by impurities in their system, as discussed in Talukdar et al.

The rate coefficient for the reaction to produce 2 OH radicals is listed separately as an upper limit at 298 K and is based on the results of Talukdar et al. The same upper limit was shown to be valid even at 209 K. Therefore, this upper limit is recommended for all atmospheric calculations.

This reaction could also produce $O(^3P) + H_2O$. However, there is no evidence for the formation of $O(^3P)$ (Dunlea et al.[4]). Therefore, it is assumed that $O_2(^1\Sigma)$ is removed exclusively via quenching. The electronic state of O_2 that is produced is not known.
(Table: 06-2, Note: 06-2, Evaluation: 10-6) Back to Table

(1) Borrell, P.; Richards, D. S. Quenching of singlet molecular oxygen $O_2(a^1\Delta_g)$ and $O_2(b^1\Sigma_g^+)$ by H_2, D_2, HCl, and HBr. *J. Chem. Soc. Faraday Trans. 2* **1989**, *85*, 1401-1411, doi:10.1039/f29898501401.

(2) Braithwaite, M.; Ogryzlo, E. A.; Davidson, J. A.; Schiff, H. I. $O_2(^1\Sigma_g^+)$ relaxation in collisions Part 2.—Temperature dependence of the relaxation by hydrogen *J. Chem. Soc. Faraday Trans. II* **1976**, *72*, 2075-2081, doi:10.1039/f29767202075.

(3) Choo, K. Y.; Leu, M.-T. Rate constants for the quenching of metastable $O_2(^1\Sigma_g^+)$ molecules. *Int. J. Chem. Kinet.* **1985**, *17*, 1155-1167, doi:10.1002/kin.550171102.
(4) Dunlea, E. J. Atmospheric reactions of electronically excited atomic and molecular oxygen. Ph.D. Thesis, University of Colorado, Boulder, 2002.
(5) Hohmann, J.; Müller, G.; Schönnenbeck, G.; Stuhl, F. Temperature-dependent queching of $O_2(b^1\Sigma_g^+)$ by H_2, D_2, CO_2, HN_3, DN_3, HNCO, and DNCO. *Chem. Phys. Lett.* **1994**, *217*, 577-581, doi:10.1016/0009-2614(93)E1424-F.
(6) Kohse-Höinghaus, K.; Stuhl, F. H_2-laser photochemical study of the temperature dependent quenching of $O_2(b\ ^1\Sigma_g^+)$. *J. Chem. Phys.* **1980**, *72*, 3720-3726, doi:10.1063/1.439583.
(7) Michelangeli, D. V.; Choo, K.-Y.; Leu, M.-T. Yields of $O_2(^1\Sigma_g^+)$ and $O_2(^1\Delta_g)$ in the H + O_2 reaction system, and the quenching of $O_2(^1\Sigma_g^+)$ by atomic hydrogen. *Int. J. Chem. Kinet.* **1988**, *20*, 915-938, doi:10.1002/kin.550201202.
(8) Singh, J. P.; Setser, D. W. Electronic-to-vibrational energy-transfer studies of singlet molecular oxygen. 2. $O_2(b^1\Sigma_g^+)$. *J. Phys. Chem.* **1985**, *89*, 5353-5358, doi:10.1021/j100271a009.
(9) Talukdar, R. K.; Dunlea, E. J.; Brown, S. S.; Daniel, J. S.; Ravishankara, A. R. Kinetics of $O_2(^1\Sigma_g^+)$ reaction with H_2 and an upper limit for OH production. *J. Phys. Chem. A* **2002**, *106*, 8461-8470, doi:10.1021/jp020589j.
(10) Wildt, J.; Bednarek, G.; Fink, E. H.; Wayne, R. P. Laser excitation of $O_2(b^1\Sigma_g^+, v' = 0,1,2)$- Rates and channels of energy transfer and quenching. *Chem. Phys.* **1988**, *122*, 463-470, doi:10.1016/0301-0104(88)80027-2.

A84. **$O_2(^1\Sigma) + H_2O$**. The recommendation is the average of room temperature measurements reported by Stuhl and Niki,[8] Avilés et al.,[1] Shi and Barker,[7] and Dunlea et al.[3] Measurements reported by O'Brien and Myers[6] are lower, most likely due to an interference from $O_2(^1\Sigma)$ regeneration. The results of Derwent and Thrush[2] and Thomas and Thrush[9] are in agreement with the recommendation. The value reported by Gauthier and Snelling[5] has a very large uncertainty and hence overlaps with the recommendation. It is not clear why the results of Filseth et al.[4] are lower than all the other reported values; perhaps, they had an error in measuring water vapor concentration. The temperature dependence of the reaction is taken from the only reported value of Dunlea et al. Wildt et al.[10] report that the yield of $O_2(^1\Delta)$ is greater than 90%. There are no thermodynamically allowed reactive channels for this reaction. Therefore, the reaction products are written as $O_2 + H_2O$.[3]
(Table: 06-2, Note: 06-2, Evaluation: 10-6) Back to Table

(1) Avilés, R. G.; Muller, D. F.; Houston, P. L. Quenching of laser-excited $O_2(b^1\Sigma_g^+)$ by CO_2, H_2O, and I_2. *Appl. Phys. Lett.* **1980**, *37*, 358-360, doi:10.1063/1.91935.
(2) Derwent, R. G.; Thrush, B. A. Measurements on $O_2\ ^1\Delta_g$ and $O_2\ ^1\Sigma_g^+$ in discharge flow systems. *Trans. Faraday Soc.* **1971**, *67*, 2036-2043, doi:10.1039/tf9716702036.
(3) Dunlea, E. J.; Talukdar, R. K.; Ravishankara, A. R. Kinetic studies of $O_2(b^1\Sigma_g^+)$ with several atmospheric molecules. *J. Phys. Chem. A* **2005**, *109*, 3912-3920, doi:10.1021/jp044129x.
(4) Filseth, S. V.; Zia, A.; Welge, K. H. Flash photolytic production, reactive lifetime, and collisional quenching of $O_2(b^1\Sigma_g^+, v' = 0)$. *J. Chem. Phys.* **1970**, *52*, 5502-5510, doi:10.1063/1.1672816.
(5) Gauthier, M. J. E.; Snelling, D. R. La photolyse de l'ozone a 253.7 nm: Desactivation de $O(^1D)$ et de $O_2(^1\Sigma)$ par les gaz de l'atmosphere. *J. Photochem.* **1975**, *4*, 27-50, doi:10.1016/0047-2670(75)80012-8.
(6) O'Brien, R. J., Jr.; Myers, G. H. Direct flow measurement of $O_2(b^1\Sigma_g^+)$ quenching rates. *J. Chem. Phys.* **1970**, *53*, 3832-3835, doi:10.1063/1.1673848.
(7) Shi, J.; Barker, J. R. Kinetic studies of the deactivation of $O_2(^1\Sigma_g^+)$ and $O(^1D)$. *Int. J. Chem. Kinet.* **1990**, *20*, 1283-1301, doi:10.1002/kin.550221207.
(8) Stuhl, F.; Niki, H. Kinetic isotope effects in the quenching of $O_2(b^1\Sigma_g^-)$ by some deuterated compounds. *Chem. Phys. Lett.* **1970**, *7*, 473-474, doi:10.1016/0009-2614(70)80340-2.
(9) Thomas, R. G. O.; Thrush, B. A. Quenching of $O_2(^1\Sigma_g^+)$ by ground state O_2. *J. Chem. Soc. Faraday Trans. 2* **1975**, *71*, 664-667, doi:10.1039/f29757100664.
(10) Wildt, J.; Bednarek, G.; Fink, E. H.; Wayne, R. P. Laser excitation of $O_2(b^1\Sigma_g^+, v' = 0,1,2)$- Rates and channels of energy transfer and quenching. *Chem. Phys.* **1988**, *122*, 463-470, doi:10.1016/0301-0104(88)80027-2.

A85. **$O_2(^1\Sigma) + N$**. The recommendation is based on the upper limit reported by Slanger and Black.[1]
(Table: 92-20, Note: 92-20, Evaluation: 10-6) Back to Table

(1) Slanger, T. G.; Black, G. Interactions of O_2 $(b^1\Sigma_g^+)$ with $O(^3P)$ and O_3. *J. Chem. Phys.* **1979**, *70*, 3434-3438, doi:10.1063/1.437877.

A86. **$O_2(^1\Sigma) + N_2$.** The recommendation for room temperature is the average of measurements reported by Izod and Wayne,[5] Stuhl and Welge,[11] Filseth et al.,[4] Martin et al.,[7] Kohse-Höinghaus and Stuhl,[6] Choo and Leu,[2] Wildt et al.,[12] Shi and Barker,[10] and Dunlea et al.[3] Less direct measurements reported by Noxon,[9] Myers and O'Brien,[8] and Chatha et al.[1] are consistent with the recommendation. The temperature dependence of the rate coefficient is derived from the results of Kohse-Höinghaus and Stuhl between 203 and 349 K and of Dunlea et al. between 210 and 370 K.

There are no exothermic reaction channels. The channel to produce 2 NO molecules is endothermic by 5.6 kcal mol^{-1} at 298 K.
(Table: 06-2, Note: 06-2, Evaluation: 10-6) Back to Table

(1) Chatha, J. P. S.; Arora, P. K.; Raja, N.; Kulkarni, P. B.; Vohra, K. G. Collisional deactivation of $O_2(^1\Sigma_g^+)$. *Int. J. Chem. Kinet.* **1979**, *11*, 175-185, doi:10.1002/kin.550110209.

(2) Choo, K. Y.; Leu, M.-T. Rate constants for the quenching of metastable $O_2(^1\Sigma_g^+)$ molecules. *Int. J. Chem. Kinet.* **1985**, *17*, 1155-1167, doi:10.1002/kin.550171102.

(3) Dunlea, E. J.; Talukdar, R. K.; Ravishankara, A. R. Kinetic studies of $O_2(b^1\Sigma_g^+)$ with several atmospheric molecules. *J. Phys. Chem. A* **2005**, *109*, 3912-3920, doi:10.1021/jp044129x.

(4) Filseth, S. V.; Zia, A.; Welge, K. H. Flash photolytic production, reactive lifetime, and collisional quenching of $O_2(b^1\Sigma_g^+, v' = 0)$. *J. Chem. Phys.* **1970**, *52*, 5502-5510, doi:10.1063/1.1672816.

(5) Izod, T. P. J.; Wayne, R. P. The formation, reaction and deactivation of $O_2(^1\Sigma_g^+)$. *Proc. Roy. Soc. A* **1968**, *308*, 81-94, doi:10.1098/rspa.1968.0209.

(6) Kohse-Höinghaus, K.; Stuhl, F. H_2-laser photochemical study of the temperature dependent quenching of $O_2(b\ ^1\Sigma_g^+)$. *J. Chem. Phys.* **1980**, *72*, 3720-3726, doi:10.1063/1.439583.

(7) Martin, L. R.; Cohen, R. B.; Schatz, J. F. Quenching of laser induced fluorescence of O_2 $(b^1\Sigma_g^+)$ by O_2 and N_2. *Chem. Phys. Lett.* **1976**, *41*, 394-396, doi:10.1016/0009-2614(76)80838-X.

(8) Myers, G. H.; O'Brien, R. J., Jr. Quenching of $O_2(b^1\Sigma_g^+)$. *Ann. N.Y. Acad. Sci.* **1970**, *171*, 224-225, doi:10.1111/j.1749-6632.1970.tb39329.x.

(9) Noxon, J. F. Optical emission from $O(^1D)$ and $O_2(b^1\Sigma_g)$ in ultraviolet photolysis of O_2 and CO_2. *J. Chem. Phys.* **1970**, *52*, 1852-1873, doi:10.1063/1.1673227.

(10) Shi, J.; Barker, J. R. Kinetic studies of the deactivation of $O_2(^1\Sigma_g^+)$ and $O(^1D)$. *Int. J. Chem. Kinet.* **1990**, *20*, 1283-1301, doi:10.1002/kin.550221207.

(11) Stuhl, F.; Welge, K. H. Deactivation of $O(^1S)$ and $O_2(b^1\Sigma_g^+)$. *Can. J. Chem.* **1969**, *47*, 1870-1871, doi:10.1139/v69-306.

(12) Wildt, J.; Bednarek, G.; Fink, E. H.; Wayne, R. P. Laser excitation of $O_2(b^1\Sigma_g^+, v' = 0,1,2)$- Rates and channels of energy transfer and quenching. *Chem. Phys.* **1988**, *122*, 463-470, doi:10.1016/0301-0104(88)80027-2.

A87. **$O_2(^1\Sigma) + N_2O$.** The rate coefficient for the removal of $O_2(^1\Sigma)$ by N_2O at 298 K is derived from the studies of Filseth et al.,[3] Borrell et al.,[1] and Dunlea et al.[2] The results of Gauthier and Snelling[4] have a large uncertainty, which overlaps the recommended value within their quoted error bars. The temperature dependence of this rate coefficient is taken from Dunlea et al., the only temperature dependent study.

There are many possible reactive channels for this reaction:

$O_2(^1\Sigma_g^+) + N_2O$	$\rightarrow NO + NO_2$	$\Delta_{rxn}H_{298} = -27.6$ kcal/mol	(a)
	$\rightarrow N_2 + O_3$	$\Delta_{rxn}H_{298} = -23.0$ kcal/mol	(b)
	$\xrightarrow{M} N_2O_3$	$\Delta_{rxn}H_{298} = -37.3$ kcal/mol	(c)
	$\rightarrow O_2(^3\Sigma_g^-) + N_2O$	$\Delta_{rxn}H_{298} = -37.5$ kcal/mol	(d)
	$\rightarrow O_2(^1\Delta_g) + N_2O$	$\Delta_{rxn}H_{298} = -15.0$ kcal/mol	(e)

Dunlea et al. have placed upper limits of $<2 \times 10^{-4}$, $<1 \times 10^{-3}$, and $<3 \times 10^{-3}$ for channel (a + c), channel (b), and overall N_2O loss, respectively, from this reaction at 298 K. Based on these results, we recommend an upper limit for NO_x production of $<2 \times 10^{-17}$ cm^3 $molecule^{-1}$ s^{-1}. The upper limit for NO_x production from this reaction is assumed to be valid for all atmospheric temperatures.
(Table: 06-2, Note: 06-2, Evaluation: 10-6) Back to Table

(1) Borrell, P.; Borrell, P.; Grant, K. R. Inverse temperature dependences in the quenching of singlet oxygen $O_2(^1\Sigma_g^+)$ by CO_2 and N_2O studied with a discharge flow/shock tube. *J. Chem. Phys.* **1983**, *78*, 748-756, doi:10.1063/1.444827.

(2) Dunlea, E. J.; Talukdar, R. K.; Ravishankara, A. R. Kinetics and products of the reaction $O_2(^1\Sigma) + N_2O$. *Z. Phys. Chem.* **2010**, *224*, 989-1007, doi:10.1524/zpch.2010.6137.

(3) Filseth, S. V.; Zia, A.; Welge, K. H. Flash photolytic production, reactive lifetime, and collisional quenching of $O_2(b^1\Sigma_g^+, v' = 0)$. *J. Chem. Phys.* **1970**, *52*, 5502-5510, doi:10.1063/1.1672816.

(4) Gauthier, M. J. E.; Snelling, D. R. La photolyse de l'ozone a 253.7 nm: Desactivation de $O(^1D)$ et de $O_2(^1\Sigma)$ par les gaz de l'atmosphere. *J. Photochem.* **1975**, *4*, 27-50, doi:10.1016/0047-2670(75)80012-8.

A88. **$O_2(^1\Sigma) + CO_2$.** The recommendation is the average of measurements reported by Filseth et al.,[5] Davidson et al.,[3] Avilés et al.,[1] Muller and Houston,[7] Choo and Leu,[2] Wildt et al.,[10] Hohmann et al.,[6] Dunlea et al.,[4] and Shi and Barker[8] at room temperature. The temperature dependence is from the work of Choo and Leu. Muller and Houston and Singh and Setser[9] give evidence that $O_2(^1\Delta)$ is a product. Wildt et al. report a $O_2(^1\Delta)$ yield of ≥90%.
(Table: 92-20, Note: 06-2, Evaluated: 06-2) Back to Table

(1) Avilés, R. G.; Muller, D. F.; Houston, P. L. Quenching of laser-excited $O_2(b^1\Sigma_g^+)$ by CO_2, H_2O, and I_2. *Appl. Phys. Lett.* **1980**, *37*, 358-360, doi:10.1063/1.91935.
(2) Choo, K. Y.; Leu, M.-T. Rate constants for the quenching of metastable $O_2(^1\Sigma_g^+)$ molecules. *Int. J. Chem. Kinet.* **1985**, *17*, 1155-1167, doi:10.1002/kin.550171102.
(3) Davidson, J. A.; Kear, K. E.; Abrahamson, E. W. The photosensitized production and physical quenching of $O_2(^1\Sigma_g^+)$. *J. Photochem.* **1972/1973**, *1*, 307-316, doi:10.1016/0047-2670(72)80023-6.
(4) Dunlea, E. J.; Talukdar, R. K.; Ravishankara, A. R. Kinetic studies of $O_2(b^1\Sigma_g^+)$ with several atmospheric molecules. *J. Phys. Chem. A* **2005**, *109*, 3912-3920, doi:10.1021/jp044129x.
(5) Filseth, S. V.; Zia, A.; Welge, K. H. Flash photolytic production, reactive lifetime, and collisional quenching of $O_2(b^1\Sigma_g^+, v' = 0)$. *J. Chem. Phys.* **1970**, *52*, 5502-5510, doi:10.1063/1.1672816.
(6) Hohmann, J.; Müller, G.; Schönnenbeck, G.; Stuhl, F. Temperature-dependent queching of $O_2(b^1\Sigma_g^+)$ by H_2, D_2, CO_2, HN_3, DN_3, HNCO, and DNCO. *Chem. Phys. Lett.* **1994**, *217*, 577-581, doi:10.1016/0009-2614(93)E1424-F.
(7) Muller, D. F.; Houston, P. L. Direct observation of electronic-to-vibrational energy transfer for $O_2(^1\Sigma)$ to $CO_2(v_3)$. *J. Phys. Chem.* **1981**, *85*, 3563-3565, doi:10.1021/j150624a007.
(8) Shi, J.; Barker, J. R. Kinetic studies of the deactivation of $O_2(^1\Sigma_g^+)$ and $O(^1D)$. *Int. J. Chem. Kinet.* **1990**, *20*, 1283-1301, doi:10.1002/kin.550221207.
(9) Singh, J. P.; Setser, D. W. Electronic-to-vibrational energy-transfer studies of singlet molecular oxygen. 2. $O_2(b^1\Sigma_g^+)$. *J. Phys. Chem.* **1985**, *89*, 5353-5358, doi:10.1021/j100271a009.
(10) Wildt, J.; Bednarek, G.; Fink, E. H.; Wayne, R. P. Laser excitation of $O_2(b^1\Sigma_g^+, v' = 0,1,2)$- Rates and channels of energy transfer and quenching. *Chem. Phys.* **1988**, *122*, 463-470, doi:10.1016/0301-0104(88)80027-2.

1.6.3 Bibliography - Singlet O_2 Reactions

Amimoto, S. T.; Wiesenfeld, J. R. $O_2(b^1\Sigma_g^+)$ production and deactivation following quenching of $O(^1D_2)$ in O_3/O_2 mixtures. *J. Chem. Phys.* **1980**, *72*, 3899-3903, doi:10.1063/1.439671.

Anderson, S. M.; Morton, J.; Mauersberger, K.; Yung, Y. L.; DeMore, W. B. A study of atom exchange between $O(^1D)$ and ozone. *Chem. Phys. Lett.* **1992**, *189*, 581-585, doi:10.1016/0009-2614(92)85254-8.

Arnold, I.; Comes, F. J. Photolysis of ozone in the ultraviolet region. Reactions of $O(^1D)$, $O_2(^1\Delta_g)$ and $O_2^{\ddagger}$. *Chem. Phys.* **1980**, *47*, 125-130, doi:10.1016/0301-0104(80)80027-9.

Avilés, R. G.; Muller, D. F.; Houston, P. L. Quenching of laser-excited $O_2(b^1\Sigma_g^+)$ by CO_2, H_2O, and I_2. *Appl. Phys. Lett.* **1980**, *37*, 358-360, doi:10.1063/1.91935.

Becker, K. H.; Groth, W.; Schurath, U. The quenching of metastable $O_2(^1\Delta_g)$ and $O_2(^1\Sigma_g^+)$ molecules. *Chem. Phys. Lett.* **1971**, *8*, 259-262, doi:10.1016/0009-2614(71)85004-2.

Becker, K. H.; Groth, W.; Schurath, U. Reactions of $O_2(^1\Delta_g)$ with ozone. *Chem. Phys. Lett.* **1972**, *14*, 489-492, doi:10.1016/0009-2614(72)80246-X.

Biedenkapp, D.; Bair, E. J. Ozone ultraviolet photolysis. I. The effect of molecular oxygen. *J. Chem. Phys.* **1970**, *52*, 6119-6125, doi:10.1063/1.1672914.

Billington, A. P.; Borrell, P. The low-temperature quenching of singlet molecular oxygen [$O_2(a\ ^1\Delta_g)$]. *J. Chem. Soc. Faraday Trans. 2* **1986**, *82*, 963-970, doi:10.1039/f29868200963.

Borrell, P.; Borrell, P.; Grant, K. R. Inverse temperature dependences in the quenching of singlet oxygen $O_2(^1\Sigma_g^+)$ by CO_2 and N_2O studied with a discharge flow/shock tube. *J. Chem. Phys.* **1983**, *78*, 748-756, doi:10.1063/1.444827.

Borrell, P.; Borrell, P. M.; Pedley, M. D. Deactivation of singlet molecular oxygen, $O_2(^1\Delta_g)$, by oxygen. *Chem. Phys. Lett.* **1977**, *51*, 300-302, doi:10.1016/0009-2614(77)80407-7.

Borrell, P.; Richards, D. S. Quenching of singlet molecular oxygen $O_2(a^1\Delta_g)$ and $O_2(b^1\Sigma_g^+)$ by H_2, D_2, HCl, and HBr. *J. Chem. Soc. Faraday Trans. 2* **1989**, *85*, 1401-1411, doi:10.1039/f29898501401.

Braithwaite, M.; Ogryzlo, E. A.; Davidson, J. A.; Schiff, H. I. $O_2(^1\Sigma_g^+)$ relaxation in collisions Part 2.—Temperature dependence of the relaxation by hydrogen *J. Chem. Soc. Faraday Trans. II* **1976**, *72*, 2075-2081, doi:10.1039/f29767202075.

Chatha, J. P. S.; Arora, P. K.; Raja, N.; Kulkarni, P. B.; Vohra, K. G. Collisional deactivation of $O_2(^1\Sigma_g^+)$. *Int. J. Chem. Kinet.* **1979**, *11*, 175-185, doi:10.1002/kin.550110209.

Choo, K. Y.; Leu, M.-T. Rate constants for the quenching of metastable $O_2(^1\Sigma_g^+)$ molecules. *Int. J. Chem. Kinet.* **1985**, *17*, 1155-1167, doi:10.1002/kin.550171102.

Clark, I. D.; Jones, I. T. N.; Wayne, R. P. The kinetics of the reaction between $O_2(^1\Delta_g)$ and ozone. *Proc. Roy. Soc. Lond. A.* **1970**, *317*, 407-416, doi:10.1098/rspa.1970.0124.

Clark, I. D.; Wayne, R. P. Collisional quenching of $O_2(^1\Delta_g)$. *Proc. Roy. Soc. Lond. A.* **1969**, *314*, 111-127, doi:10.1098/rspa.1969.0218.

Clark, I. D.; Wayne, R. P. The reaction of $O_2(^1\Delta_g)$ with atomic nitrogen and with atomic oxygen. *Chem. Phys. Lett.* **1969**, *3*, 405-407, doi:10.1016/0009-2614(69)80151-X.

Clark, I. D.; Wayne, R. P. Kinetics of the reaction between atomic nitrogen and molecular oxygen in the ground ($^3\Sigma_g^-$) and first excited ($^1\Delta_g$) states. *Proc. Roy. Soc. Lond. A.* **1970**, *316*, 539-550, doi:10.1098/rspa.1970.0095.

Collins, R. J.; Husain, D.; Donovan, R. J. Kinetic and spectroscopic studies of $O_2(a^1\Delta_g)$ by time-resolved absorption spectroscopy in the vacuum ultra-violet. *J. Chem. Soc. Faraday Trans. 2* **1973**, *69*, 145-157, doi:10.1039/f29736900145.

Davidson, J. A.; Kear, K. E.; Abrahamson, E. W. The photosensitized production and physical quenching of $O_2(^1\Sigma_g^+)$. *J. Photochem.* **1972/1973**, *1*, 307-316, doi:10.1016/0047-2670(72)80023-6.

Derwent, R. G.; Thrush, B. A. Measurements on $O_2\ ^1\Delta_g$ and $O_2\ ^1\Sigma_g^+$ in discharge flow systems. *Trans. Faraday Soc.* **1971**, *67*, 2036-2043, doi:10.1039/tf9716702036.

Dunlea, E. J. Atmospheric reactions of electronically excited atomic and molecular oxygen. Ph.D. Thesis, University of Colorado, Boulder, 2002.

Dunlea, E. J.; Talukdar, R. K.; Ravishankara, A. R. Kinetic studies of $O_2(b^1\Sigma_g^+)$ with several atmospheric molecules. *J. Phys. Chem. A* **2005**, *109*, 3912-3920, doi:10.1021/jp044129x.

Dunlea, E. J.; Talukdar, R. K.; Ravishankara, A. R. Kinetics and products of the reaction $O_2(^1\Sigma) + N_2O$. *Z. Phys. Chem.* **2010**, *224*, 989-1007, doi:10.1524/zpch.2010.6137.

Filseth, S. V.; Zia, A.; Welge, K. H. Flash photolytic production, reactive lifetime, and collisional quenching of $O_2(b^1\Sigma_g^+, v' = 0)$. *J. Chem. Phys.* **1970**, *52*, 5502-5510, doi:10.1063/1.1672816.

Findlay, F. D.; Fortin, C. J.; Snelling, D. R. Deactivation of $O_2(^1\Delta_g)$. *Chem. Phys. Lett.* **1969**, *3*, 204-206, doi:10.1016/0009-2614(69)80026-6.
Findlay, F. D.; Snelling, D. R. Collisional deactivation of $O_2(^1\Delta_g)$. *J. Chem. Phys.* **1971**, *55*, 545-551, doi:10.1063/1.1675786.
Findlay, F. D.; Snelling, D. R. Temperature dependence of the rate constant for the reaction $O_2(^1\Delta_g) + O_3 \rightarrow 2O_2 + O$. *J. Chem. Phys.* **1971**, *54*, 2750-2755, doi:10.1063/1.1675240.
Gauthier, M. J. E.; Snelling, D. R. La photolyse de l'ozone a 253.7 nm: Desactivation de $O(^1D)$ et de $O_2(^1\Sigma)$ par les gaz de l'atmosphere. *J. Photochem.* **1975**, *4*, 27-50, doi:10.1016/0047-2670(75)80012-8.
Gilpin, R.; Schiff, H. I.; Welge, K. H. Photodissociation of O_3 in the Hartley band. Reactions of $O(^1D)$ and $O_2(^1\Sigma_g^+)$ with O_3 and O_2. *J. Chem. Phys.* **1971**, *55*, 1087-1093, doi:10.1063/1.1676190.
Hohmann, J.; Müller, G.; Schönnenbeck, G.; Stuhl, F. Temperature-dependent quecheing of $O_2(b^1\Sigma_g^+)$ by H_2, D_2, CO_2, HN_3, DN_3, HNCO, and DNCO. *Chem. Phys. Lett.* **1994**, *217*, 577-581, doi:10.1016/0009-2614(93)E1424-F.
Izod, T. P. J.; Wayne, R. P. The formation, reaction and deactivation of $O_2(^1\Sigma_g^+)$. *Proc. Roy. Soc. A* **1968**, *308*, 81-94, doi:10.1098/rspa.1968.0209.
Klais, O.; Laufer, A. H.; Kurylo, M. J. Atmospheric quenching of vibrationally excited $O_2(^1\Delta)$. *J. Chem. Phys.* **1980**, *73*, 2696-2699, doi:10.1063/1.440483.
Knickelbein, M. B.; Marsh, K. L.; Ulrich, O. E.; Busch, G. E. Energy transfer kinetics of singlet molecular oxygen: The deactivation channel for $O_2(b\ ^1\Sigma_g^+)$. *J. Chem. Phys.* **1987**, *87*, 2392-2393, doi:10.1063/1.453120.
Kohse-Höinghaus, K.; Stuhl, F. H_2-laser photochemical study of the temperature dependent quenching of $O_2(b\ ^1\Sigma_g^+)$. *J. Chem. Phys.* **1980**, *72*, 3720-3726, doi:10.1063/1.439583.
Lawton, S. A.; Novick, S. E.; Broida, H. P.; Phelps, A. V. Quenching of optically pumped $O_2(b^1\Sigma_g^+)$ by ground state O_2 molecules. *J. Chem. Phys.* **1977**, *66*, 1381-1382, doi:10.1063/1.434038.
Lawton, S. A.; Phelps, A. V. Excitation of the $b\ ^1\Sigma_g^+$ state of O_2 by low energy electrons. *J. Chem. Phys.* **1978**, *69*, 1055-1068, doi:10.1063/1.436700.
Leiss, A.; Schurath, U.; Becker, K. H.; Fink, E. H. Revised quenching rate constants for metastable oxygen molecules $O_2(a^1\Delta_g)$. *J. Photochem.* **1978**, *8*, 211-214, doi:10.1016/0047-2670(78)80021-5.
Lissi, E.; Heicklen, J. The photolysis of ozone. *J. Photochem.* **1972**, *1*, 39-68, doi:10.1016/0047-2670(72)80004-2.
Martin, L. R.; Cohen, R. B.; Schatz, J. F. Quenching of laser induced fluorescence of O_2 $(b^1\Sigma_g^+)$ by O_2 and N_2. *Chem. Phys. Lett.* **1976**, *41*, 394-396, doi:10.1016/0009-2614(76)80838-X.
McLaren, I. A.; Morris, N. W.; Wayne, R. P. Is CO_2 a good quencher of $O_2(^1\Delta_g)$? A kinetic reappraisal. *J. Photochem.* **1981**, *16*, 311-319, doi:10.1016/0047-2670(81)80053-6.
McNeal, R. J.; Cook, G. R. Photoionization of electronically excited oxygen: Rate of the reaction. *J. Chem. Phys.* **1967**, *47*, 5385-5389, doi:10.1063/1.1701807.
Michelangeli, D. V.; Choo, K.-Y.; Leu, M.-T. Yields of $O_2(^1\Sigma_g^+)$ and $O_2(^1\Delta_g)$ in the H + O_2 reaction system, and the quenching of $O_2(^1\Sigma_g^+)$ by atomic hydrogen. *Int. J. Chem. Kinet.* **1988**, *20*, 915-938, doi:10.1002/kin.550201202.
Muller, D. F.; Houston, P. L. Direct observation of electronic-to-vibrational energy transfer for $O_2(^1\Sigma)$ to $CO_2(v_3)$. *J. Phys. Chem.* **1981**, *85*, 3563-3565, doi:10.1021/j150624a007.
Myers, G. H.; O'Brien, R. J., Jr. Quenching of $O_2(b^1\Sigma_g^+)$. *Ann. N.Y. Acad. Sci.* **1970**, *171*, 224-225, doi:10.1111/j.1749-6632.1970.tb39329.x.
Noxon, J. F. Optical emission from $O(^1D)$ and $O_2(b^1\Sigma_g)$ in ultraviolet photolysis of O_2 and CO_2. *J. Chem. Phys.* **1970**, *52*, 1852-1873, doi:10.1063/1.1673227.
O'Brien, R. J., Jr.; Myers, G. H. Direct flow measurement of $O_2(b^1\Sigma_g^+)$ quenching rates. *J. Chem. Phys.* **1970**, *53*, 3832-3835, doi:10.1063/1.1673848.
Ogren, P. J.; Sworski, T. J.; Hochanadel, C. J.; Cassel, J. M. Flash photolysis of O_3 in O_2 and O_2 + H_2 mixtures. Kinetics of $O_2(^1\Sigma_g^+)$ + O_3 and $O(^1D)$ + H_2 reactions. *J. Phys. Chem.* **1982**, *86*, 238-242, doi:10.1021/j100391a021.
Raja, N.; Arora, P. K.; Chatha, J. P. S. Rate constants of $O_2(^1\Delta_g)$. *Int. J. Chem. Kinet.* **1986**, *18*, 505-512, doi:10.1002/kin.550180409.
Ravishankara, A. R.; Wine, P. H.; Nicovich, J. M. Pulsed laser photolysis study of the reaction between $O(^3P)$ and HO_2. *J. Chem. Phys.* **1983**, *78*, 6629-6639, doi:10.1063/1.444661.
Schmidt, C.; Schiff, H. I. Reactions of $O_2(^1\Delta_g)$ with atomic nitrogen and hydrogen. *Chem. Phys. Lett.* **1973**, *23*, 339-342, doi:10.1016/0009-2614(73)85092-4.
Shi, J.; Barker, J. R. Kinetic studies of the deactivation of $O_2(^1\Sigma_g^+)$ and $O(^1D)$. *Int. J. Chem. Kinet.* **1990**, *20*, 1283-1301, doi:10.1002/kin.550221207.

Singh, J. P.; Setser, D. W. Electronic-to-vibrational energy-transfer studies of singlet molecular oxygen. 2. $O_2(b^1\Sigma_g^+)$. *J. Phys. Chem.* **1985**, *89*, 5353-5358, doi:10.1021/j100271a009.
Slanger, T. G.; Black, G. Interactions of O_2 ($b^1\Sigma_g^+$) with $O(^3P)$ and O_3. *J. Chem. Phys.* **1979**, *70*, 3434-3438, doi:10.1063/1.437877.
Snelling, D. R. The ultraviolet flash photolysis of ozone and the reactions of $O(^1D)$ and $O_2(^1\Sigma_g^+)$. *Can. J. Chem.* **1974**, *52*, 257-270, doi:10.1139/v74-042.
Steer, R. P.; Ackerman, R. A.; Pitts, J. N., Jr. Singlet oxygen in the environmental sciences. V. Rates of deactivation of $O_2(^1\Delta_g)$ by oxygen and nitrogen. *J. Chem. Phys.* **1969**, *51*, 843-844, doi:10.1063/1.1672082.
Stuhl, F.; Niki, H. Kinetic isotope effects in the quenching of $O_2(b^1\Sigma_g^-)$ by some deuterated compounds. *Chem. Phys. Lett.* **1970**, *7*, 473-474, doi:10.1016/0009-2614(70)80340-2.
Stuhl, F.; Welge, K. H. Deactivation of $O(^1S)$ and $O_2(b^1\Sigma_g^+)$. *Can. J. Chem.* **1969**, *47*, 1870-1871, doi:10.1139/v69-306.
Tachibana, K.; Phelps, A. V. Excitation of the $O_2(a\ ^1\Delta_g)$ state by low energy electrons. *J. Chem. Phys.* **1981**, *75*, 3315-3320, doi:10.1063/1.442483.
Talukdar, R. K.; Dunlea, E. J.; Brown, S. S.; Daniel, J. S.; Ravishankara, A. R. Kinetics of $O_2(^1\Sigma_g^+)$ reaction with H_2 and an upper limit for OH production. *J. Phys. Chem. A* **2002**, *106*, 8461-8470, doi:10.1021/jp020589j.
Thomas, R. G. O.; Thrush, B. A. Quenching of $O_2(^1\Sigma_g^+)$ by ground state O_2. *J. Chem. Soc. Faraday Trans. 2* **1975**, *71*, 664-667, doi:10.1039/f29757100664.
Turnipseed, A. A.; Vaghjiani, G. L.; Gierczak, T.; Thompson, J. E.; Ravishankara, A. R. The photochemistry of ozone at 193 and 222 nm. *J. Chem. Phys.* **1991**, *95*, 3244-3251, doi:10.1063/1.460881.
von Ellenrieder, G.; Castellano, E.; Schumacher, H. J. The kinetics and the mechanism of the photochemical decomposition of ozone with light of 2537 Å wavelength. *Chem. Phys. Lett.* **1971**, *9*, 152-156, doi:10.1016/0009-2614(71)80211-7.
Wayne, R. P.; Pitts, J. N., Jr. Rate constant for the reaction $O_2(^1\Delta_g) + O_3 \rightarrow 2O_2 + O$. *J. Chem. Phys.* **1969**, *50*, 3644-3645, doi:10.1063/1.1671606.
Westenberg, A. A.; Roscoe, J. M.; deHaas, N. Rate measurements on $N + O_2(^1\Delta_g) \rightarrow NO + O$ and $H + O_2(^1\Delta_g) \rightarrow OH + O$. *Chem. Phys. Lett.* **1970**, *7*, 597-599, doi:10.1016/0009-2614(70)87014-2.
Wildt, J.; Bednarek, G.; Fink, E. H.; Wayne, R. P. Laser excitation of $O_2(b^1\Sigma_g^+, v' = 0,1,2)$- Rates and channels of energy transfer and quenching. *Chem. Phys.* **1988**, *122*, 463-470, doi:10.1016/0301-0104(88)80027-2.
Wildt, J.; Fink, E. H.; Biggs, P.; Wayne, R. P. The collision-induced radiation of $O_2(a^1\Delta_g)$. *Chem. Phys.* **1989**, *139*, 401-407, doi:10.1016/0301-0104(89)80152-1.
Wildt, J.; Fink, E. H.; Biggs, P.; Wayne, R. P.; Vilesov, A. F. Collision-induced emission of $O_2(a^1\Delta_g \rightarrow X\ ^3\Sigma_g^-)$ in the gas phase. *Chem. Phys.* **1992**, *159*, 127-140, doi:10.1016/0301-0104(92)80065-4.

1.7 HO_x Reactions

1.7.1 Table 1B: HO_x Reactions

Reaction	Temperature Range of Exp. Data (K) [a]	*A*-Factor	*E*/R	*k*(298 K) [b]	*f*(298 K) [c]	*g* [c]	Note
$O + OH \rightarrow O_2 + H$	136–515	1.8×10^{-11}	–180	3.3×10^{-11}	1.15	50	B1
$O + HO_2 \rightarrow OH + O_2$	229–391	3.0×10^{-11}	–200	5.9×10^{-11}	1.05	50	B2
$O + H_2O_2 \rightarrow OH + HO_2$	283–386	1.4×10^{-12}	2000	1.7×10^{-15}	1.20	100	B3
$H + O_2 \xrightarrow{M} HO_2$		(See Table 2-1)					
$H + O_3 \rightarrow OH + O_2$	196–424	1.4×10^{-10}	470	2.9×10^{-11}	1.10	40	B4
$H + HO_2 \rightarrow 2\ OH$ $\rightarrow O + H_2O$ $\rightarrow H_2 + O_2$	245–300	7.2×10^{-11} 1.6×10^{-12} 6.9×10^{-12}	0 0 0	7.2×10^{-11} 1.6×10^{-12} 6.9×10^{-12}	1.20 1.50 1.40	100 100 100	B5
$OH + O_3 \rightarrow HO_2 + O_2$	190–357	1.7×10^{-12}	940	7.3×10^{-14}	1.15	50	B6
$OH + H_2 \rightarrow H_2O + H$	200–1050	2.8×10^{-12}	1800	6.7×10^{-15}	1.05	100	B7
$OH + HD \rightarrow$ products	248–418	5.0×10^{-12}	2130	4.0×10^{-15}	1.15	50	B8
$OH + OH \rightarrow H_2O + O$ $\xrightarrow{M} H_2O_2$	233–580	1.8×10^{-12} (See Table 2-1)	0	1.8×10^{-12}	1.25	50	B9
$OH + HO_2 \rightarrow H_2O + O_2$	252–420	4.8×10^{-11}	–250	1.1×10^{-10}	1.15	50	B10
$OH + H_2O_2 \rightarrow H_2O + HO_2$		(See Note)					B11
$HO_2 + O_3 \rightarrow OH + 2O_2$	197–413	1.0×10^{-14}	490	1.9×10^{-15}	1.15	80	B12
$HO_2 + HO_2 \rightarrow H_2O_2 + O_2$ $\xrightarrow{M} H_2O_2 + O_2$	222–1120	3.0×10^{-13} 2.1×10^{-33} [M]	–460 –920	1.4×10^{-12} 4.6×10^{-32} [M]	1.15 1.20	100 200	B13
$HO_2 + HO_2 \cdot H_2O \rightarrow$ products	298–350	5.4×10^{-11}	410	1.4×10^{-11}	2.00	100	B14

Shaded areas indicate changes or additions since JPL19-5.

[a] Temperature range of available experimental data. This is not necessarily the range of temperature over which the recommended Arrhenius parameters are applicable. See the corresponding note for such information.

[b] Units are cm^3 $molecule^{-1}$ s^{-1}.

[c] $f(298\ K)$ is the uncertainty factor at 298 K. To calculate the uncertainty at other temperatures, use the expression:

$$f(T) = f(298\ K)\exp\left|g\left(\frac{1}{T} - \frac{1}{298}\right)\right|$$

Note that the exponent is an absolute value.

1.7.2 Notes: HO_x Reactions

B1. **O + OH**. The recommended rate coefficient was obtained from the studies of Westenberg et al.[8] (228–340 K), Lewis and Watson[4] (221–499 K), Howard and Smith[2] (250–515 K), Smith and Stewart[7] (158–294 K), and Robertson and Smith[5] (136–377 K). The recommendation is consistent with earlier work near room temperature as reviewed by Lewis and Watson,[4] and with the measurements of Brune et al.[1] (300 K), and Robertson and Smith[6] (295 K). The ratio $k(O + HO_2)/k(O + OH)$ measured by Keyser[3] agrees with the recommended values.
(Table: 10-6, Note: 10-6, Evaluated: 10-6) Back to Table

(1) Brune, W. H.; Schwab, J. J.; Anderson, J. G. Laser magnetic resonance, resonance fluorescence, and resonance absorption studies of the reaction kinetics of O + OH → H + O_2, O + HO_2 → OH + O_2, N + OH → H + NO, and N + HO_2 → products at 300 K between 1 and 5 torr. *J. Phys. Chem.* **1983**, *87*, 4503-4514, doi:10.1021/j100245a034.

(2) Howard, M. J.; Smith, I. W. M. Direct rate measurements on the reactions N + OH → NO + H and O + OH → O_2 + H from 250 to 515 K. *J. Chem. Soc. Faraday Trans. 2* **1981**, *77*, 997-1008, doi:10.1039/F29817700997.

(3) Keyser, L. F. Relative rate constants for the reactions of atomic oxygen with HO_2 and OH radicals. *J. Phys. Chem.* **1983**, *87*, 837-841, doi:10.1021/j100228a028.

(4) Lewis, R. S.; Watson, R. T. Temperature dependence of the reaction $O(^3P)$ + $OH(^2\Pi)$ → O_2 + H. *J. Phys. Chem.* **1980**, *84*, 3495-3503, doi:10.1021/j100463a002.

(5) Robertson, R.; Smith, G. P. Temperature dependence of O + OH at 136−377 K using ozone photolysis. *J. Phys. Chem. A* **2006**, *110*, 6673–6679, doi:10.1021/jp055863z.

(6) Robertson, R. G.; Smith, G. P. Photolytic measurement of the O + OH rate constant at 295 K. *Chem. Phys. Lett.* **2002**, *358*, 157-162, doi:10.1016/S0009-2614(02)00629-2.

(7) Smith, I. W. M.; Stewart, D. W. A. Low-temperature kinetics of reactions between neutral free radicals Rate constants for the reactions of OH radicals with N atoms (103 ≤ T/K ≤ 294) and with O atoms (158 ≤ T/K ≤ 294). *J. Chem. Soc. Faraday Trans.* **1994**, *90*, 3221-3227, doi:10.1039/ft9949003221.

(8) Westenberg, A. A.; deHaas, N.; Roscoe, J. M. Radical reactions in an electron spin resonance cavity homogeneous reactor. *J. Phys. Chem.* **1970**, *74*, 3431-3438, doi:10.1021/j100713a001.

B2. **O + HO_2**. The recommended values are based on the results of studies over a range of temperatures by Keyser[5] (229–372 K) and Nicovich and Wine[9] (266–391 K) and the room temperature studies of Sridharan et al.,[12] Ravishankara et al.,[10] and Brune et al.[1] Earlier studies by Hack et al.[4] (298 K) and Burrows et al.[2,3] (298, 293 K) are not considered because the OH + H_2O_2 reaction was important in these studies and the value used for its rate constant in their analyses has been shown to be in error. A study by Lii et al.[8] (298 K) is also not considered because of the insensitivity of the observed decays to O + HO_2. Data from Ravishankara et al.[10] (298 K) show no dependence on pressure between 10 and 500 Torr N_2. The ratio $k(O + HO_2)/k(O + OH)$ measured by Keyser[6] (299 K) agrees with the rate constants recommended here. Sridharan et al.[11] showed that the reaction products correspond to abstraction of an oxygen atom from HO_2 by the O reactant. Keyser et al.[7] reported <1% $O_2(^1\Delta)$ yield.
(Table: 06-2, Note: 06-2, Evaluated: 10-6) Back to Table

(1) Brune, W. H.; Schwab, J. J.; Anderson, J. G. Laser magnetic resonance, resonance fluorescence, and resonance absorption studies of the reaction kinetics of O + OH → H + O_2, O + HO_2 → OH + O_2, N + OH → H + NO, and N + HO_2 → products at 300 K between 1 and 5 torr. *J. Phys. Chem.* **1983**, *87*, 4503-4514, doi:10.1021/j100245a034.

(2) Burrows, J. P.; Cliff, D. I.; Harris, G. W.; Thrush, B. A.; Wilkinson, J. P. T. Atmospheric reactions of the HO_2 radical studied by laser magnetic-resonance spectroscopy. *Proc. Roy. Soc. Lond. A.* **1979**, *368*, 463-481, doi:10.1098/rspa.

(3) Burrows, J. P.; Harris, G. W.; Thrush, B. A. Rates of reaction of HO_2 with HO and O studied by laser magnetic resonance. *Nature* **1977**, *267*, 233-234, doi:10.1038/267233a0.

(4) Hack, W.; Preuss, A. W.; Temps, F.; Wagner, H. G. Reaction of O + HO_2 → OH + O_2 studied with a LMR-ESR spectrometer. *Ber. Bunsenges. Phys. Chem.* **1979**, *83*, 1275-1279, doi:10.1002/bbpc.19790831214.

(5) Keyser, L. F. Kinetics of the reaction O + HO_2 → OH + O_2 from 229 to 372 K. *J. Phys. Chem.* **1982**, *86*, 3439-3446, doi:10.1021/j100214a03.

(6) Keyser, L. F. Relative rate constants for the reactions of atomic oxygen with HO_2 and OH radicals. *J. Phys. Chem.* **1983**, *87*, 837-841, doi:10.1021/j100228a028.

(7) Keyser, L. F.; Choo, K. Y.; Leu, M. T. Yields of $O_2(b^1\Sigma_g^+)$ from reactions of HO_2. *Int. J. Chem. Kinet.* **1985**, *17*, 1169-1185, doi:10.1002/kin.550171103.

(8) Lii, R.-R.; Sauer, M. C., Jr.; Gordon, S. Rate constant of the reaction of O(^{3}P) with HO_2. *J. Phys. Chem.* **1980**, *84*, 817-819, doi:10.1021/j100445a002.
(9) Nicovich, J. M.; Wine, P. H. Temperature dependence of the O + HO_2 rate coefficient. *J. Phys. Chem.* **1987**, *91*, 5118-5123, doi:10.1021/j100303a049.
(10) Ravishankara, A. R.; Wine, P. H.; Nicovich, J. M. Pulsed laser photolysis study of the reaction between O(^3P) and HO_2. *J. Chem. Phys.* **1983**, *78*, 6629-6639, doi:10.1063/1.444661.
(11) Sridharan, U. C.; Klein, F. S.; Kaufman, F. Detailed course of the O + HO_2 reaction. *J. Chem. Phys.* **1985**, *82*, 592-593, doi:10.1063/1.448973.
(12) Sridharan, U. C.; Qiu, L. X.; Kaufman, F. Kinetics and product channels of the reactions of HO_2 with O and H atoms at 296 K. *J. Phys. Chem.* **1982**, *86*, 4569-4574, doi:10.1021/j100220a023.

B3. **O + H_2O_2**. There are two direct studies of the O + H_2O_2 reaction: Davis et al.[2] (283–368 K) and Wine et al.[4] (298–386 K). The recommended value is a fit to the combined data. An indirect measurement of the *E*/R value by Roscoe[3] is consistent with the recommendation. The *A* factor for both data sets is quite low compared to similar atom-molecule reactions. A somewhat higher activation barrier reported by Albers et al.[1] over the temperature range 370–800 K is suggestive of a non-linear temperature dependence.
(Table: 06-2, Note: 06-2, Evaluated: 10-6) Back to Table

(1) Albers, E. A.; Hoyermann, K.; Wagner, H. G.; Wolfrum, J. Absolute measurements of rate coefficients for the reactions of H and O atoms with H_2O_2 and H_2O. *Proc. Combust. Inst.* **1971**, *13*, 81-88.
(2) Davis, D. D.; Wong, W.; Schiff, R. A dye laser flash photolysis kinetics study of the reaction of ground-state atomic oxygen with hydrogen peroxide. *J. Phys. Chem.* **1974**, *78*, 463-464, doi:10.1021/j100597a033.
(3) Roscoe, J. M. The reaction of O(^3P) with H_2O_2. *Int. J. Chem. Kinet.* **1982**, *14*, 471-478, doi:10.1002/kin.550140504.
(4) Wine, P. H.; Nicovich, J. M.; Thompson, R. J.; Ravishankara, A. R. Kinetics of O(^3P_J) reactions with H_2O_2 and O_3. *J. Phys. Chem.* **1983**, *87*, 3948-3954, doi:10.1021/j100243a030.

B4. **H + O_3**. The recommendation is an average of the results of Lee et al.[8] (219–360 K) and Keyser[7] (196–424 K), which are in agreement over the 220–360 K range. Results by Seeley et al.[9] (298 K) and Finlayson-Pitts and Kleindienst[3] (299 K) agree well with the present recommendation. An earlier study by Clyne and Monkhouse[1] (298, 479, 638 K) is in very good agreement on the temperature dependence in the range 300–560 K, but lies about 60% below the recommended values. Although we have no reason not to believe the Clyne and Monkhouse values, we prefer the two studies that are in agreement, especially since they were carried out over the temperature range of interest. Reports of a channel forming HO_2 + O (Finlayson-Pitts and Kleindienst[3]: ~25%, and Force and Wiesenfeld[5] (298 K): ~40%) have been contradicted by other studies (Howard and Finlayson-Pitts[6] (298 K): <3%; Washida et al.[11] (298 K): <6%; Finlayson-Pitts et al.[4] (298 K): <2%; and Dodonov et al.[2] (298 K): <0.3%). Secondary chemistry is believed to be responsible for the observed O-atoms in this system. Washida et al.[10] (298 K) measured an upper limit (<0.1%) for the production of singlet molecular oxygen for the reaction.
(Table: 06-2, Note: 06-2, Evaluated: 10-6) Back to Table

(1) Clyne, M. A. A.; Monkhouse, P. Atomic resonance fluorescence for rate constants of rapid bimolecular reactions Part 5-Hydrogen atom reactions; H + NO_2 and H + O_3. *J. Chem. Soc. Faraday Trans. 2* **1977**, *73*, 298-309, doi:10.1039/F29777300298.
(2) Dodonov, A. F.; Zelenov, V. V.; Kukui, A. S.; Ponomarev, E. A.; Tal'Roze, V. L. Mass spectrometric investigation of elementary gas phase reactions passing in the H + O_3 + O_2 system-Channels of H + O_3 → OH(v) + O_2, H + O_2 → HO_2 + O reactions. *Khim. Fiz.* **1985**, *4*, 1335-1343.
(3) Finlayson-Pitts, B. J.; Kleindienst, T. E. The reaction of hydrogen atoms with ozone: Evidence for a second reaction path producing HO_2 and O(^3P). *J. Chem. Phys.* **1979**, *70*, 4804-4806, doi:10.1063/1.437271.
(4) Finlayson-Pitts, B. J.; Kleindienst, T. E.; Ezell, J. J.; Toohey, D. W. The production of O(^{3}P) and ground state OH in the reaction of hydrogen atoms with ozone. *J. Chem. Phys.* **1981**, *74*, 4533-4543, doi:10.1063/1.441642.
(5) Force, A. P.; Wiesenfeld, J. R. Laser photolysis of O_3/H_2 mixtures: The yield of the H + O_3 → HO_2 + O reaction. *J. Chem. Phys.* **1981**, *74*, 1718-1723, doi:10.1063/1.441260.
(6) Howard, C. J.; Finlayson-Pitts, B. J. Yields of HO_2 in the reaction of hydrogen atoms with ozone. *J. Chem. Phys.* **1980**, *72*, 3842-3843, doi:10.1063/1.439601.
(7) Keyser, L. F. Absolute rate constant and temperature dependence of the reaction between hydrogen (^{2}S) atoms and ozone. *J. Phys. Chem.* **1979**, *83*, 645-648, doi:10.1021/j100469a001.
(8) Lee, J. H.; Michael, J. V.; Payne, W. A.; Stief, L. J. Absolute rate of the reaction of hydrogen atoms with ozone from 219-360 K. *J. Chem. Phys.* **1978**, *69*, 350-353, doi:10.1063/1.436360.

(9) Seeley, J. V.; Jayne, J. T.; Molina, M. J. High pressure fast-flow technique for gas phase kinetics studies. *Int. J. Chem. Kinet.* **1993**, *25*, 571-594, doi:10.1002/kin.550250706.
(10) Washida, N.; Akimoto, H.; Okuda, M. Is O_2*($a^1\Delta_g$) formed in the O + O_3, H + O_3, and NO + O_3 reactions? *Bull. Chem. Soc. Jpn.* **1980**, *53*, 3496-3503, doi:10.1246/bcsj.53.3496.
(11) Washida, N.; Akimoto, H.; Okuda, M. O_2^* ($a^1\Delta_g$) in the reaction of H + O_3. *J. Chem. Phys.* **1980**, *72*, 5781-5783, doi:10.1063/1.439004.

B5. **H + HO_2**. There are five studies of this reaction: Hack et al.[2] (293 K), Hack et al.[1] (293 K), Thrush and Wilkinson[8] (298 K), Sridharan et al.[7] (296 K), and Keyser[4] (245–300 K). Related early work and combustion studies are referenced in Sridharan et al. All five studies used discharge flow systems. It is difficult to obtain a direct measurement of the rate constant for this reaction because both reactants are radicals and the products OH and O are reactive toward the HO_2 reactant. The recommendation is based on the kinetics and product data of Sridharan et al. and Keyser, because those measurements were the most direct and required the fewest corrections. Keyser found the rate coefficient and product yields to be independent of temperature for 245< T <300 K. The total rate constant measurements of, $(5.0 \pm 1.3) \times 10^{-11}$ cm^3 $molecule^{-1}$ s^{-1} by Thrush and Wilkinson[8] (298 K) and $(4.65 \pm 1) \times 10^{-11}$ by Hack et al.[1] (293 K) are significantly less than the recommended total rate constant, 8.05×10^{-11} cm^3 $molecule^{-1}$ s^{-1}. Hislop and Wayne[3] (298 K), Keyser et al.[5] (298 K), and Michelangeli et al.[6] (298 K) reported on the yield of $O_2(b^1\Sigma)$ formed in the H_2 + O_2 channel as $(2.8 \pm 1.3) \times 10^{-4}$, $<8 \times 10^{-3}$, and $<2.1 \times 10^{-2}$, respectively as a fraction of the overall reaction.
(Table: 06-2, Note: 06-2, Evaluated: 10-6) Back to Table

(1) Hack, W.; Preuss, A. W.; Wagner, H. G.; Hoyermann, K. Reactions of hydrogen atoms with hydroperoxyl radicals 2. Determination of the rate constant of the overall reaction. *Ber. Bunsenges. Phys. Chem.* **1979**, *83*, 212-217, doi:10.1002/bbpc.19790830306.
(2) Hack, W.; Wagner, H. G.; Hoyermann, K. Reactions of hydrogen atoms with hydroperoxyl radicals 1. Determination of specific rate constants of reaction channels. *Ber. Bunsenges. Phys. Chem.* **1978**, *82*, 713-719, doi:10.1002/bbpc.19780820710.
(3) Hislop, J. R.; Wayne, R. P. Production of $O_2(^1\Sigma_g^+)$ in the H + O_2 system. *J. Chem. Soc. Faraday Trans. 2* **1977**, *73*, 506-516, doi:10.1039/F29777300506.
(4) Keyser, L. F. Absolute rate constant and branching fractions for the H + HO_2 reaction from 245 to 300 K. *J. Phys. Chem.* **1986**, *90*, 2994-3003, doi:10.1021/j100404a040.
(5) Keyser, L. F.; Choo, K. Y.; Leu, M. T. Yields of $O_2(b^1\Sigma_g^+)$ from reactions of HO_2. *Int. J. Chem. Kinet.* **1985**, *17*, 1169-1185, doi:10.1002/kin.550171103.
(6) Michelangeli, D. V.; Choo, K.-Y.; Leu, M.-T. Yields of $O_2(^1\Sigma_g^+)$ and $O_2(^1\Delta_g)$ in the H + O_2 reaction system, and the quenching of $O_2(^1\Sigma_g^+)$ by atomic hydrogen. *Int. J. Chem. Kinet.* **1988**, *20*, 915-938, doi:10.1002/kin.550201202.
(7) Sridharan, U. C.; Qiu, L. X.; Kaufman, F. Kinetics and product channels of the reactions of HO_2 with O and H atoms at 296 K. *J. Phys. Chem.* **1982**, *86*, 4569-4574, doi:10.1021/j100220a023.
(8) Thrush, B. A.; Wilkinson, J. P. T. The rate of the reaction between H and HO_2. *Chem. Phys. Lett.* **1981**, *84*, 17-19, doi:10.1016/0009-2614(81)85360-2.

B6. **OH + O_3**. The recommended values are based on the results of studies over a range of temperatures by Anderson and Kaufman[1] (220–450 K), Ravishankara et al.[5] (238–357 K), Smith et al.[6] (240–295 K) and Nizkorodov et al.[4] (190–315 K) and the room temperature measurements of Kurylo,[3] Zahniser and Howard,[7] and Kulcke et al.[2] The recommended *E*/R and *k*(298 K) values are based on averages of the individual *E*/R and *k*(298 K) values obtained in the above mentioned studies. The value reported by Kulcke et al. has been corrected for a minor contribution from $k(HO_2 + O_3)$.
(Table: 02-25, Note: 10-6, Evaluated: 10-6) Back to Table

(1) Anderson, J. G.; Kaufman, F. Kinetics of the reaction OH (v=0) + O_3 → HO_2 + O_2. *Chem. Phys. Lett.* **1973**, *19*, 483-486, doi:10.1016/0009-2614(73)85131-0.
(2) Kulcke, A.; Blackman, B.; Chapman, W. B.; Kim, I. K.; Nesbitt, D. J. Time-resolved O_3 chemical chain reaction kinetics via high-resolution IR laser absorption methods. *J. Phys. Chem. A* **1998**, *102*, 1965-1972, doi:10.1021/jp972486k.
(3) Kurylo, M. J. Kinetics of the reactions OH(v=0) + NH_3 → H_2O + NH_2 and OH(v=0) + O_3 → HO_2 + O_2 at 298°K. *Chem. Phys. Lett.* **1973**, *23*, 467-471, doi:10.1016/0009-2614(73)89003-7.
(4) Nizkorodov, S. A.; Harper, W. W.; Blackmon, B. W.; Nesbitt, D. J. Temperature dependent kinetics of the OH/HO_2/O_3 chain reaction by time-resolved IR laser absorption spectroscopy. *J. Phys. Chem. A* **2000**, *104*, 3964-3973, doi:10.1021/jp9934984.
(5) Ravishankara, A. R.; Wine, P. H.; Langford, A. O. Absolute rate constant for the reaction OH(v = 0) + O_3 → HO_2 + O_2 over the temperature range 238-357°K. *J. Chem. Phys.* **1979**, *70*, 984-989, doi:10.1063/1.437488.

(6) Smith, C. A.; Molina, L. T.; Lamb, J. J.; Molina, M. J. Kinetics of the reaction of OH with pernitric and nitric acids. *Int. J. Chem. Kinet.* **1984**, *16*, 41-55, doi:10.1002/kin.550160107
(7) Zahniser, M. S.; Howard, C. J. Kinetics of the reaction of HO_2 with ozone. *J. Chem. Phys.* **1980**, *73*, 1620-1626, doi:10.1063/1.440343.

B7. **OH + H_2**. The OH + H_2 reaction has been the subject of numerous studies. The recommendation is fixed to the average of eleven studies at 298 K: Greiner,[2] Stuhl and Niki,[7] Westenberg and deHaas,[10] Smith and Zellner,[6] Atkinson et al.,[1] Overend et al.,[4] Tully and Ravishankara,[9] Zellner and Steinert,[11] Ravishankara et al.,[5] Talukdar et al.,[8] and Orkin et al.[3] The temperature dependent studies of Orkin et al. (200–480 K), Talukdar et al. (230–420 K), and Ravishankara et al. (250–1050 K) find that the reaction does not follow a simple Arrhenius expression over a large range of temperature. The recommended temperature dependence is based on the average of *E*/R values determined in the above-mentioned studies for temperatures below 300 K. Accordingly, the recommended Arrhenius expression is only valid between 200–300 K. Even over this range the simple Arrhenius expression likely overestimates, near 250 K, and underestimates, near 200 K, the data by approximately 10%.
(Table: 06-2, Note: 06-2, Evaluated: 10-6) Back to Table

(1) Atkinson, R.; Hansen, D. A.; Pitts, J. N., Jr. Rate constants for the reaction of OH radicals with CHF_2Cl, CF_2Cl_2, $CFCl_3$, and H_2 over the temperature range 297-434 °K. *J. Chem. Phys.* **1975**, *63*, 1703-1706, doi:10.1063/1.431566.
(2) Greiner, N. R. Hydroxyl radical kinetics by kinetic spectroscopy. V. Reaction with H_2 and CO in the range 300-500°K. *J. Chem. Phys.* **1969**, *51*, 5049-5051, doi:10.1063/1.1671902.
(3) Orkin, V. L.; Kozlov, S. N.; Poskrebyshev, G. A.; Huie, R. E.; Kurylo, M. J. Rate constant for the reaction of OH with H_2 between 200 and 480 K. *J. Phys. Chem. A* **2006**, *110*, 6978-6985, doi:10.1021/jp057035b.
(4) Overend, R. P.; Paraskevopoulos, G.; Cvetanović, R. J. Rates of OH radical reactions. I. Reactions with H_2, CH_4, C_2H_6, and C_3H_8 at 295 K. *Can. J. Phys.* **1975**, *53*, 3374-3382, doi:10.1139/v75-482.
(5) Ravishankara, A. R.; Nicovich, J. M.; Thompson, R. L.; Tully, F. P. Kinetic study of the reaction of OH with H_2 and D_2 from 250 to 1050 K. *J. Phys. Chem.* **1981**, *85*, 2498-2503, doi:10.1021/j150617a018.
(6) Smith, I. W. M.; Zellner, R. Rate measurements of reactions of OH by resonance absorption. Part 3. - Reactions of OH with H_2, D_2 and hydrogen and deuterium halides. *J. Chem. Soc. Faraday Trans. 2* **1974**, *70*, 1045-1056, doi:10.1039/F29747001045.
(7) Stuhl, F.; Niki, H. Pulsed vacuum-UV photochemical study of reactions of OH with H_2, D_2, and CO using a resonance-fluorescent detection method. *J. Chem. Phys.* **1972**, *57*, 3671-3677, doi:10.1063/1.1678825.
(8) Talukdar, R. K.; Gierczak, T.; Goldfarb, L.; Rudich, Y.; Madhava Rao, B. S.; Ravishankara, A. R. Kinetics of hydroxyl radical reactions with isotopically labeled hydrogen. *J. Phys. Chem.* **1996**, *100*, 3037-3043, doi:10.1021/jp9518724.
(9) Tully, F. P.; Ravishankara, A. R. Flash photolysis-resonance fluorescence kinetic study of the reactions $OH + H_2 \rightarrow H_2O + H$ and $OH + CH_4 \rightarrow H_2O + CH_3$ from 298 to 1020 K. *J. Phys. Chem.* **1980**, *84*, 3126-3130, doi:10.1021/j100460a031.
(10) Westenberg, A. A.; deHaas, N. Rates of CO + OH and H_2 + OH over an extended temperature range. *J. Chem. Phys.* **1973**, *58*, 4061-4065, doi:10.1063/1.1678961.
(11) Zellner, R.; Steinert, W. Vibrational rate enhancement in the reaction $OH + H_2(v=1) \rightarrow H_2O + H$. *Chem. Phys. Lett.* **1981**, *81*, 568-572, doi:10.1016/0009-2614(81)80465-4.

B8. **OH + HD**. The recommendation is based on direct measurements made by Talukdar et al.[2] (248–418 K) using pulsed photolysis-laser induced fluorescence. The recommendation is in excellent agreement with the ratio $k(OH + H_2)/k(OH + HD) = 1.65 \pm 0.05$ reported by Ehhalt et al.[1] (298 K) when combined with the recommended $k(OH + H_2)$.
(Table: 06-2, Note: 06-2, Evaluated: 10-6) Back to Table

(1) Ehhalt, D. H.; Davidson, J. A.; Cantrell, C. A.; Friedman, I.; Tyler, S. The kinetic isotope effect in the reaction of H_2 with OH. *J. Geophys. Res.* **1989**, *94*, 9831-9836, doi:10.1029/JD094iD07p09831.
(2) Talukdar, R. K.; Gierczak, T.; Goldfarb, L.; Rudich, Y.; Madhava Rao, B. S.; Ravishankara, A. R. Kinetics of hydroxyl radical reactions with isotopically labeled hydrogen. *J. Phys. Chem.* **1996**, *100*, 3037-3043, doi:10.1021/jp9518724.

B9. **OH + OH**. The recommendation for the OH + OH reaction is the average of eight measurements performed near 298 K at low bath gas pressures: Westenberg and deHaas,[9] McKenzie et al.,[6] Clyne and Down,[3] Trainor and von Rosenberg,[7] Farquharson and Smith,[4] Wagner and Zellner,[8] Bedjanian et al.,[2] and Bahng and MacDonald.[1] The rate coefficients reported in these studies fall in the range (1.4–2.7) × 10^{-12} cm^3 $molecule^{-1}$ s^{-1}. Wagner and Zellner (250–580 K) reported a slight positive temperature dependence of the rate coefficient in contrast with that reported by Bedjanian et al. (233–360 K), who report a small negative temperature dependence. The earlier work of Wagner and Zellner may have been complicated by an increased contribution of the OH + H reaction due to an underestimate of its reaction rate. Theoretical calculations by Harding and Wagner[5] suggest that tunneling substantially influences the reaction rate coefficient. In taking account of the tunneling contribution, the rate coefficient is found to have a minimum value near room temperature. In view of the predicted behavior and given that the experimental data are consistent with each other, within the stated uncertainties, the recommendation is a temperature independent value for the rate coefficient over the temperature range 200–300 K.
(Table: 10-6, Note: 10-6, Evaluated: 10-6) Back to Table

(1) Bahng, M.-K.; Macdonald, R. G. Determination of the rate constant for the $OH(X^2\Pi)$ + $OH(X^2\Pi)$ → $O(^3P)$ + H_2O reaction over the temperature range 293-373 K. *J. Phys. Chem. A* **2007**, *111*, 3850-3861, doi:10.1021/jp066359c.

(2) Bedjanian, Y.; Le Bras, G.; Poulet, G. Kinetic study of OH + OH and OD + OD reactions. *J. Phys. Chem.* **1999**, *103*, 7017-7025, doi:10.1021/jp991146r.

(3) Clyne, M. A. A.; Down, S. Kinetic behaviour of OH $X^2\Pi$ and $A^2\Sigma^+$ using molecular resonance fluorescence spectrometry. *J. Chem. Soc. Faraday Trans. 2* **1974**, *70*, 253-266, doi:10.1039/F29747000253.

(4) Farquharson, G. K.; Smith, R. H. Rate constants for the gaseous reactions OH + C_2H_4 and OH + OH. *Aust. J. Chem.* **1980**, *33*, 1425-1435, doi:10.1071/CH9801425.

(5) Harding, L. B.; Wagner, A. F. Theoretical study of the reaction rates of OH + OH ↔ H_2O + O. *Proc. Combust. Inst.* **1988**, *22*, 983-989, doi:10.1016/S0082-0784(89)80107-9.

(6) McKenzie, A.; Mulcahy, M. F. R.; Steven, J. R. Kinetics of decay of hydroxyl radicals at low pressure. *J. Chem. Phys.* **1973**, *59*, 3244-3254, doi:10.1063/1.1680466.

(7) Trainor, D. W.; von Rosenberg, C. W., Jr. Flash photolysis study of the gas phase recombination of hydroxyl radicals. *J. Chem. Phys.* **1974**, *61*, 1010-1015, doi:10.1063/1.1681968.

(8) Wagner, G.; Zellner, R. Temperature dependence of the reaction OH + OH → H_2O + O. *Ber. Bunsenges. Phys. Chem.* **1981**, *85*, 1122-1128, doi:10.1002/bbpc.19810851209.

(9) Westenberg, A. A.; deHaas, N. Rate of the reaction OH + OH → H_2O + O. *J. Chem. Phys.* **1973**, *58*, 4066-4071, doi:10.1063/1.1678962.

B10. **OH + HO_2**. A study by Keyser[8] (254–382 K) appears to resolve a discrepancy among low-pressure discharge flow experiments that all gave rate coefficients near 7 × 10^{-11} cm^3 $molecule^{-1}$ s^{-1}: Keyser[7] (299 K), Thrush and Wilkinson[16] (298 K), Sridharan et al.[13,14] (296, 252–420 K), Temps and Wagner[15] (298 K), Rozenshtein et al.[11] (298 K), and atmospheric pressure studies that gave rate coefficients near 11 × 10^{-11} cm^3 $molecule^{-1}$ s^{-1}: Lii et al.[10] (308 K), Hochanadel et al.[6] (296 K), DeMore[3] (298 K), Cox et al.[2] (308 K), Burrows et al.[1] (288–348 K), and Kurylo et al.[9] (298 K). Laboratory measurements using a discharge flow experiment and a chemical model analysis of the results by Keyser[8] demonstrate that the previous discharge flow measurements were probably subject to interference from small amounts of O and H. In the presence of excess HO_2, these atoms generate OH and result in a rate coefficient measurement that falls below the true value. The temperature dependence is from Keyser.[8] A flow tube study by Schwab et al.[12] (298 K) reported k = (8.0 +3/–4) × 10^{-11} cm^3 $molecule^{-1}$ s^{-1}. These workers measured the concentrations of HO_2, OH, O, and H and used a computer model of the relevant reactions to test for interference. A flow tube study by Dransfeld and Wagner[4] (298 K) employing an isotope labeled ^{18}OH reactant obtained k = (11 ± 2) × 10^{-11} cm^3 $molecule^{-1}$ s^{-1} in good agreement with the recommendation. They attributed about half of the reactive events to isotope scrambling because control experiments with ^{16}OH gave k = 6 × 10^{-11} cm^3 $molecule^{-1}$ s^{-1}. It should be noted that their control experiments were subject to the errors described by Keyser[8] due to the presence of small amounts of H and O, whereas their ^{18}OH measurements were not. Kurylo et al. found no evidence of significant scrambling in isotope studies of the OH and HO_2 reaction. An additional careful study of the reaction temperature dependence would be useful. Hippler and Troe[5] (1000–1250 K) have analyzed data for this reaction at temperatures up to 1250 K. In summary, this has historically been a difficult reaction to study. Earlier problems appear to have been resolved, as discussed above, and results now tend to converge on a central value, but the recommended value is still subject to a large uncertainty.
(Table: 06-2, Note: 06-2, Evaluated: 10-6) Back to Table

(1) Burrows, J. P.; Cox, R. A.; Derwent, R. G. Modulated photolysis of the ozone-water vapour system: Kinetics of the reaction of OH with HO_2. *J. Photochem.* **1981**, *16*, 147-168, doi:10.1016/0047-2670(81)80026-3.
(2) Cox, R. A.; Burrows, J. P.; Wallington, T. J. Rate coefficient for the reaction OH + HO_2 → H_2O + O_2 at 1 atmosphere pressure and 308 K. *Chem. Phys. Lett.* **1981**, *84*, 217-221, doi:10.1016/0009-2614(81)80329-6.
(3) DeMore, W. B. Rate constant and possible pressure dependence of the reaction OH + HO_2. *J. Phys. Chem.* **1982**, *86*, 121-126, doi:10.1021/j100390a025.
(4) Dransfeld, P.; Wagner, H. G. Comparative study of the reactions of ^{16}OH with $H^{16}O_2$. *Z. Naturforsch.* **1987**, *42a*, 471-476.
(5) Hippler, H.; Troe, J. Rate constants of the reaction HO + H_2O_2 → HO_2 + H_2O at T ≥ 1000 K. *Chem. Phys. Lett.* **1992**, *192*, 333-337, doi:10.1016/0009-2614(92)85478-S.
(6) Hochanadel, C. J.; Sworski, T. J.; Ogren, P. J. Rate constants for the reactions of HO_2 with OH and with HO_2. *J. Phys. Chem.* **1980**, *84*, 3274-3277, doi:10.1021/j100461a029.
(7) Keyser, L. F. Absolute rate constant of the reaction OH + HO_2 → H_2O + O_2. *J. Phys. Chem.* **1981**, *85*, 3667-3673, doi:10.1021/j150624a028.
(8) Keyser, L. F. Kinetics of the reaction OH + HO_2 → H_2O + O_2 from 254 to 382 K. *J. Phys. Chem.* **1988**, *92*, 1193-1200, doi:10.1021/j100316a037.
(9) Kurylo, M. J.; Klais, O.; Laufer, A. H. Mechanistic investigation of the HO + HO_2 reaction. *J. Phys. Chem.* **1981**, *85*, 3674-3678, doi:10.1021/j150624a029.
(10) Lii, R.-R.; Gorse, R. A., Jr.; Sauer, M. C., Jr.; Gordon, S. Rate constant for the reaction of OH with HO_2. *J. Phys. Chem.* **1980**, *84*, 819-821, doi:10.1021/j100445a003.
(11) Rozenshtein, V. B.; Gershenzon, Y. M.; Il'in, S. D.; Kishkovitch, O. P. Reactions of HO_2 with NO, OH and HO_2 studied by EPR/LMR spectroscopy. *Chem. Phys. Lett.* **1984**, *112*, 473-478, doi:10.1016/0009-2614(84)85572-4.
(12) Schwab, J. J.; Brune, W. H.; Anderson, J. G. Kinetics and mechanism of the OH + HO_2 reaction. *J. Phys. Chem.* **1989**, *93*, 1030-1035, doi:10.1021/j100340a005.
(13) Sridharan, U. C.; Qiu, L. X.; Kaufman, F. Kinetics of the reaction OH + HO_2 → H_2O + O_2 at 296 K. *J. Phys. Chem.* **1981**, *85*, 3361-3363, doi:10.1021/j150623a001.
(14) Sridharan, U. C.; Qiu, L. X.; Kaufman, F. Rate constant of the OH + HO_2 reaction from 252 to 420 K. *J. Phys. Chem.* **1984**, *88*, 1281-1282, doi:10.1021/j150651a006.
(15) Temps, F.; Wagner, H. G. Investigation of the reaction OH + HO_2 → H_2O + O_2 with the aid of a laser magnetic spectrometer. *Ber. Bunsenges. Phys. Chem.* **1982**, *86*, 119-125, doi:10.1002/bbpc.19820860206.
(16) Thrush, B. A.; Wilkinson, J. P. T. The rate of reaction of HO_2 radicals with HO and with NO. *Chem. Phys. Lett.* **1981**, *81*, 1-3, doi:10.1016/0009-2614(81)85314-6.

B11. OH + H_2O_2. The rate coefficient for this reaction shows non-Arrhenius behavior between 96 and 1250 K with a minimum value near room temperature. Data from a number of studies are in relatively good agreement between 300 and 500 K after normalization to account for the H_2O_2 UV absorption cross section recommendation in this evaluation. Hippler and Troe[1] (1000–1250 K) analyzed data for this reaction at temperatures up to 1250 K. The studies of Keyser[2] (245–423 K), Sridharan et al.[7] (250–459 K), Wine et al.[11] (273–410 K), Kurylo et al.[3] (250–370 K), Lamb et al.[4] (241–413 K), and Vaghjiani et al.[9] (273–410 K) show that the reaction displays a small positive temperature dependence (E/R = ~160 K) over the 300–500 K range. Measurements at room temperature by Marinelli and Johnston[5] (298 K), Riffault et al.[6] (298 K), Turnipseed et al.[8] (298 K), and Vakhtin et al.[10] (96–296 K) agree with the other studies. A value of 1.8×10^{-12} cm^3 molecule^{-1} s^{-1} is obtained by averaging the room temperature data. Lamb et al. and Vaghjiani report that k increases slightly with decreasing temperature for temperatures below 300 K while other studies show a slight positive temperature dependence. Vakhtin et al. used a pulsed Laval nozzle technique to study the reaction at very low temperatures (96–165 K) and report a significant increase in k with decreasing temperature. They suggest that the reaction mechanism includes the formation of a hydrogen-bonded complex. The recommendation is a temperature independent value of 1.8×10^{-12} cm^3 molecule^{-1} s^{-1} with f(298 K) = 1.15 and g = 45 over the temperature range of 200–300 K.
(Table: 06-2, Note: 10-6, Evaluated: 10-6) Back to Table

(1) Hippler, H.; Troe, J. Rate constants of the reaction HO + H_2O_2 → HO_2 + H_2O at T ≥ 1000 K. *Chem. Phys. Lett.* **1992**, *192*, 333-337, doi:10.1016/0009-2614(92)85478-S.
(2) Keyser, L. F. Absolute rate constant of the reaction OH + H_2O_2 → HO_2 + H_2O from 245 to 423 K. *J. Phys. Chem.* **1980**, *84*, 1659-1663, doi:10.1021/j100450a001.

(3) Kurylo, M. J.; Murphy, J. L.; Haller, G. S.; Cornett, K. D. A flash photolysis resonance fluorescence investigation of the reaction OH + H_2O_2 → HO_2 + H_2O. *Int. J. Chem. Kinet.* **1982**, *14*, 1149-1161, doi:10.1002/kin.550141008.
(4) Lamb, J. J.; Molina, L. T.; Smith, C. A.; Molina, M. J. Rate constant of the OH + H_2O_2 → HO_2 + H_2O reaction. *J. Phys. Chem.* **1983**, *87*, 4467-4470, doi:10.1021/j100245a028.
(5) Marinelli, W. J.; Johnston, H. S. Reaction rates of hydroxyl radical with nitric acid and with hydrogen peroxide. *J. Chem. Phys.* **1982**, *77*, 1225-1234, doi:10.1063/1.443998.
(6) Riffault, V.; Gierczak, T.; Burkholder, J. B.; Ravishankara, A. R. Quantum yields for OH production in the photodissociation of HNO_3 at 248 and 308 nm and H_2O_2 at 308 and 320 nm. *Phys. Chem. Chem. Phys.* **2006**, *8*, 1079-1085, doi:10.1039/b513760h.
(7) Sridharan, U. C.; Reimann, B.; Kaufman, F. Kinetics of the reaction OH + H_2O_2 → HO_2 + H_2O. *J. Chem. Phys.* **1980**, *73* 1286-1293, doi:10.1063/1.440240.
(8) Turnipseed, A. A.; Vaghjiani, G. L.; Gierczak, T.; Thompson, J. E.; Ravishankara, A. R. The photochemistry of ozone at 193 and 222 nm. *J. Chem. Phys.* **1991**, *95*, 3244-3251, doi:10.1063/1.460881.
(9) Vaghjiani, G. L.; Ravishankara, A. R.; Cohen, N. Reactions of OH and OD with H_2O_2 and D_2O_2. *J. Phys. Chem.* **1989**, *93*, 7833-7837, doi:10.1021/j100360a021.
(10) Vakhtin, A. B.; McCabe, D. C.; Ravishankara, A. R.; Leone, S. R. Low-temperature kinetics of the reaction of the OH radical with hydrogen peroxide. *J. Phys. Chem. A* **2003**, *17*, 10642-10647, doi:10.1021/jp030424q.
(11) Wine, P. H.; Semmes, D. H.; Ravishankara, A. R. A laser flash photolysis kinetics study of the reaction OH + H_2O_2 → HO_2 + H_2O. *J. Chem. Phys.* **1981**, *75*, 4390-4395, doi:10.1063/1.442602.

B12. **HO_2 + O_3.** The recommended values are based on results of studies over a range of temperatures by DeMore[1] (231–334 K), Zahniser and Howard[9] (245–365 K), Manzanares et al.[4] (298 K), Sinha et al.[7] (243–413 K), Wang et al.[8] (233–400 K), and Herndon et al.[3] (200–298 K). The data of Simonaitis and Heicklen[6] (225, 250, 298 K) and DeMore and Tschuikow-Roux[2] (273–342 K) were not considered. The temperature dependence studies show varying degrees of curvature in the Arrhenius plots, with the *E*/R decreasing at lower temperature. This is especially evident in the low temperature data of Herndon et al. where a number of measures were taken to control potential kinetic complications. The recommended *E*/R and *k*(298 K) values are based on averages of the individual *E*/R and *k*(298 K) values. Furthermore, only data at temperatures less than 298 K were used for the *E*/R determination. Accordingly, the recommendation is not valid for T>298 K. Additional temperature dependence data are needed for this reaction over a larger range to more fully characterize the non-linear behavior of the rate constant. The mechanism of the reaction has been studied using ^{18}O labeled HO_2 by Sinha et al., who reported that the reaction occurs (75 ± 10)% via H atom transfer at 297 K and by Nelson and Zahniser,[5] who reported branching ratios for H transfer vs O transfer over the range 226–355 K. They report that the H atom transfer decreases from (94 ± 5)% at (226 ± 11) K to (88 ± 5)% at (355 ± 8) K.
(Table: 00-3, Note: 00-3, Evaluated: 10-6) Back to Table

(1) DeMore, W. B. Reaction of HO_2 with O_3 and the effect of water vapor on HO_2 kinetics. *J. Phys. Chem.* **1979**, *83*, 1113-1118, doi:10.1021/j100472a001.
(2) DeMore, W. B.; Tschuikow-Roux, E. Temperature dependence of the reactions of OH and HO_2 with O_3 *J. Phys. Chem.* **1974**, *78*, 1447-1451, doi:10.1021/j100608a001.
(3) Herndon, S. C.; Villalta, P. W.; Nelson, D. D.; Jayne, J. T.; Zahniser, M. S. Rate constant measurements for the reaction of HO_2 with O_3 from 200 to 300 K using a turbulent flow reactor. *J. Phys. Chem. A* **2001**, *105*, 1583-1591, doi:10.1021/jp002383t.
(4) Manzanares, E. R.; Suto, M.; Lee, L. C.; Coffey, D. Reaction rate constant of HO_2 + O_3 measured by detecting HO_2 from photofragment fluorescence. *J. Chem. Phys.* **1986**, *85*, 5027-5034, doi:10.1063/1.451692.
(5) Nelson, D. D., Jr.; Zahniser, M. S. A mechanistic study of the reaction of HO_2 radical with ozone. *J. Phys. Chem.* **1994**, *98*, 2101-2104, doi:10.1021/j100059a020.
(6) Simonaitis, R.; Heicklen, J. Reaction of HO_2 with O_3. *J. Phys. Chem.* **1973**, *77*, 1932-1935, doi:10.1021/j100635a002.
(7) Sinha, A.; Lovejoy, E. R.; Howard, C. J. Kinetic study of the reaction of HO_2 with ozone. *J. Chem. Phys.* **1987**, *87*, 2122-2128, doi:10.1063/1.453136.
(8) Wang, X.; Suto, M.; Lee, L. C. Reaction rate constants of HO_2 + O_3 in the temperature range 233—400 K. *J. Chem. Phys.* **1988**, *88*, 896-899, doi:10.1063/1.454169.
(9) Zahniser, M. S.; Howard, C. J. Kinetics of the reaction of HO_2 with ozone. *J. Chem. Phys.* **1980**, *73*, 1620-1626, doi:10.1063/1.440343.

B13. **$HO_2 + HO_2$**. The overall rate coefficient for this reaction is the sum of a pressure-independent bimolecular component and a pressure-dependent termolecular component. Two separate expressions are given for these rate coefficients. Both components contribute to the overall loss of HO_2 under atmospheric conditions and have negative temperature dependencies. This reaction also has a dependence on H_2O that needs to be included in atmospheric model calculations. Christensen et al.[2,3] found that kinetic studies that used CH_3OH as an HO_2 radical precursor were possibly complicated by the formation of a weakly bound reactive HO_2-CH_3OH adduct, particularly important at low temperatures. The magnitude of the CH_3OH effect on the measured rate coefficients is dependent on the CH_3OH concentration and temperature in the particular study.

The recommended bimolecular and termolecular expressions for the $HO_2 + HO_2$ reaction were obtained from a global fit of the rate coefficient data that had negligible complications due to the presence of CH_3OH. The analysis included data obtained at low pressure (<30 Torr) from Thrush and Tyndall[27,28] (7–20 Torr, 298–358 K), Simonaitis and Heicklen[21] (5–770 Torr, 296 K), Sander[19] (1 Torr, 298 K), Takacs and Howard[24,25] (1–7 Torr, 252–391 K), Kurylo et al.[13] (25–600 Torr, 298 K), and Tang et al.[26] (30 Torr, 253–323 K) and data obtained at higher pressure (>30 Torr) from Sander et al.[20] (100–700 Torr, 298 K), Simonaitis and Heicklen, Kurylo et al., Christensen[3] (100 Torr, 222–295 K), Kircher and Sander[12] (100–700 Torr, 230–420 K) (only data above 298 K were used in the analysis), and Maricq and Szente[16] (200 Torr, 210–365 K). The rate coefficient data obtained using transient UV absorption detection of HO_2[12,13,16,20,21] were scaled to the currently recommended HO_2 absorption cross sections. Rate coefficient studies of Kurylo et al., Sander et al.[20] (298 K) and Kircher and Sander found little difference in the measured rate coefficient when N_2 or O_2 was used as the bath gas. The recommended termolecular expression applies to M = air. The experimental data is reproduced to within ±20% using the recommended parameters. The rate coefficient data reported by Maricq and Szente are systematically 20% higher than the current recommendation. Systematic discrepancies also exist in the low-temperature rate coefficient data where the results from Christensen et al. are ~25% lower than the current recommendation at 222 K. Hamilton and Lii[9] (298 K) and Sander et al. have reported the dependence of the rate coefficient on isotopic (H/D) substitution. Lightfoot et al.[14] (298–777 K) reported rate coefficients at atmospheric pressure that are in agreement with the recommended value at 298 K. This study indicates an upward curvature in the rate coefficient at temperatures above 500 K. A high temperature (750–1120 K) study by Hippler et al.[10] confirms the strong curvature. The current recommendation does not account for the non-Arrhenius behavior and is valid only for temperatures below 500 K.

Stone and Rowley[22] reported rate coefficient data at 760 Torr over the temperature range 236–309 K that were later shown by Christensen et al.[2] to be systematically overestimated due to the use of very high concentrations of CH_3OH. The Stone and Rowley data were not included in the present evaluation. The rate coefficient data and temperature dependence reported by Cox and Burrows[4] (3–760 Torr, 273–339 K) is in general agreement with this recommendation. Data from Rozenshtein et al.[18] (2.1–24.9 Torr, 298 K) are consistent with the low-pressure recommendation, but they report no change in the rate coefficient with pressure up to 1 atm. Results reported by Thrush and Wilkinson[29] (2–4 Torr, 298 K) and Dobis and Benson[6] (mTorr, 243–368 K) are inconsistent with the recommendation.

The $HO_2 + HO_2$ reaction exhibits a dependence on H_2O concentration due to the formation of a weakly bound reactive $HO_2 \bullet H_2O$ complex. English et al.[7] (~200 Torr, 263–303 K) report a bond energy of 6.9 kcal mol^{-1} for the complex (also see Table 3). There are numerous studies of the rate coefficient H_2O dependence (Hamilton[8] (295 K), Hochanadel et al.[11] (298 K), Hamilton and Lii,[9] Cox and Burrows,[4] DeMore[5] (231–334 K), Lii et al.[15] (298–373 K), Sander et al., Andersson et al.[1] (278, 299 K), Stone and Rowley[22] (760 Torr, 236–309 K), English et al., and Tang et al.) that are in good agreement. The effective rate coefficient in the presence of H_2O can be obtained by multiplying the recommended rate coefficient by the factor given by Lii et al. and Kircher and Sander: $[1 + 1.4 \times 10^{-21} [H_2O] \exp(2200/T)]$.

The major reaction products at 300 K have been identified as $H_2O_2 + O_2$ by Su et al.[23] (700 Torr, 298 K), Niki et al.[17] (700 Torr, 298 K), Sander et al.,[20] and Simonaitis and Heicklen.
(Table: 10-6, Note: 10-6, Evaluated: 10-6) Back to Table

(1) Andersson, B. Y.; Cox, R. A.; Jenkin, M. E. The effect of methanol on the self reaction of HO_2 radicals. *Int. J. Chem. Kinet.* **1988**, *20*, 283-295, doi:10.1002/kin.550200403.

(2) Christensen, L. E.; Okumura, M.; Hansen, J. C.; Sander, S. P.; Francisco, J. S. Experimental and ab initio study of the $HO_2 \bullet CH_3OH$ complex: Thermodynamics and kinetics of formation. *J. Phys. Chem. A* **2006**, *110*, 6948-6959, doi:10.1021/jp056579a.

(3) Christensen, L. E.; Okumura, M.; Sander, S. P.; Salawitch, R. J.; Toon, G. C.; Sen, B.; Blavier, J.-F.; Jucks, K. W. Kinetics of $HO_2 + HO_2 \rightarrow H_2O_2 + O_2$: Implications for stratospheric H_2O_2. *Geophys. Res. Lett.* **2002**, *29*, 1299, doi:1029/2001GL014525.

(4) Cox, R. A.; Burrows, J. P. Kinetics and mechanism of the disproportionation of HO_2 in the gas phase. *J. Phys. Chem.* **1979**, *83*, 2560-2568, doi:10.1021/j100483a002.

(5) DeMore, W. B. Reaction of HO_2 with O_3 and the effect of water vapor on HO_2 kinetics. *J. Phys. Chem.* **1979**, *83*, 1113-1118, doi:10.1021/j100472a001.
(6) Dobis, O.; Benson, S. W. Reaction of the ethyl radical with oxygen at millitorr pressures at 243-368 K and a study of the Cl + HO_2, ethyl + HO_2, and HO_2 + HO_2 reactions. *J. Am. Chem. Soc.* **1993**, *115*, 8798-8809, doi:10.1021/ja00072a038.
(7) English, A. M.; Hansen, J. C.; Szente, J. J.; Maricq, M. M. The effects of water vapor on the CH_3O_2 self-reaction and reaction with HO_2. *J. Phys. Chem. A* **2008**, *112*, 9220-9228, doi:10.1021/jp800727a.
(8) Hamilton, E. J., Jr. Water vapor dependence of the kinetics of the self-reaction of HO_2 in the gas phase. *J. Chem. Phys.* **1975**, *63*, 3682-3683, doi:10.1063/1.431772.
(9) Hamilton, E. J., Jr.; Lii, R.-R. The dependence on H_2O and on NH_3 of the kinetics of the self-reaction of HO_2 in the gas-phase formation of HO_2•H_2O and HO_2•NH_3 complexes. *Int. J. Chem. Kinet.* **1977**, *9*, 875-885, doi:10.1002/kin.550090604.
(10) Hippler, H.; Rahn, R.; Troe, J. Shock wave study of the reaction HO_2 + HO_2 → H_2O_2 + O_2: Confirmation of a rate constant minimum near 700 K. *J. Chem. Phys.* **1990**, *93*, 1755-1760, doi:10.1063/1.459102.
(11) Hochanadel, C. J.; Ghormley, J. A.; Ogren, P. J. Absorption spectrum and reaction kinetics of the HO_2 radical in the gas phase. *J. Chem. Phys.* **1972**, *56*, 4426-4432, doi:10.1063/1.1677885.
(12) Kircher, C. C.; Sander, S. P. Kinetics and mechanism of HO_2 and DO_2 disproportionations. *J. Phys. Chem.* **1984**, *88*, 2082-2091, doi:10.1021/j150654a029.
(13) Kurylo, M. J.; Ouellette, P. A.; Laufer, A. H. Measurements of the pressure dependence of the HO_2 radical self-disproportionation reaction at 298 K. *J. Phys. Chem.* **1986**, *90*, 437-440, doi:10.1021/j100275a017.
(14) Lightfoot, P. D.; Veyret, B.; Lesclaux, R. The rate constant for the HO_2 + HO_2 reaction at elevated temperatures. *Chem. Phys. Lett.* **1988**, *150*, 120-126, doi:10.1016/0009-2614(88)80407-X.
(15) Lii, R.-R.; Sauer, M. C., Jr.; Gordon, S. Temperature dependence of the gas-phase self-reaction of HO_2 in the presence of H_2O. *J. Phys. Chem.* **1981**, *85*, 2833-2834, doi:10.1021/j150619a027.
(16) Maricq, M. M.; Szente, J. J. A kinetic study of the reaction between ethylperoxy radicals and HO_2. *J. Phys. Chem.* **1994**, *98*, 2078-2082, doi:10.1021/j100059a016.
(17) Niki, H.; Maker, P. D.; Savage, C. M.; Breitenbach, L. P. An FTIR study of the mechanism for the gas phase reaction between HO_2 radicals. *Chem. Phys. Lett.* **1980**, *73*, 43-46, doi:10.1016/0009-2614(80)85198-0.
(18) Rozenshtein, V. B.; Gershenzon, Y. M.; Il'in, S. D.; Kishkovitch, O. P. Reactions of HO_2 with NO, OH and HO_2 studied by EPR/LMR spectroscopy. *Chem. Phys. Lett.* **1984**, *112*, 473-478, doi:10.1016/0009-2614(84)85572-4.
(19) Sander, S. P. Low-pressure study of the HO_2 + HO_2 reaction at 298 K. *J. Phys. Chem.* **1984**, *88*, 6018-6021, doi:10.1021/j150668a055.
(20) Sander, S. P.; Peterson, M.; Watson, R. T.; Patrick, R. Kinetics studies of the HO_2 + HO_2 and DO_2 + DO_2 reactions at 298 K. *J. Phys. Chem.* **1982**, *86*, 1236-1240, doi:10.1021/j100397a002.
(21) Simonaitis, R.; Heicklen, J. A kinetic study of the HO_2 + HO_2 reaction. *J. Phys. Chem.* **1982**, *86*, 3416-3418, doi:10.1021/j100214a030.
(22) Stone, D.; Rowley, D. M. Kinetics of the gas phase HO_2 self-reaction: Effects of temperature, pressure, water and methanol vapours. *Phys. Chem. Chem. Phys.* **2005**, *7*, 2156-2163, doi:10.1039/b502673c.
(23) Su, F.; Calvert, J. G.; Lindley, C. R.; Uselman, W. M.; Shaw, J. H. A Fourier transform infrared kinetic study of HOCl and its absolute integrated infrared band intensities. *J. Phys. Chem.* **1979**, *83*, 912-920, doi:10.1021/j100471a006.
(24) Takacs, G. A.; Howard, C. J. Room-temperature rate constant for the HO_2 + HO_2 reaction at low pressures. *J. Phys. Chem.* **1984**, *88*, 2110-2116, doi:10.1021/j150654a033.
(25) Takacs, G. A.; Howard, C. J. Temperature dependence of the reaction HO_2 + HO_2 at low pressures. *J. Phys. Chem.* **1986**, *90*, 687-690, doi:10.1021/j100276a041.
(26) Tang, Y.; Tyndall, G. S.; Orlando, J. J. Spectroscopic and kinetic properties of HO_2 radicals and the enhancement of the HO_2 self reaction by CH_3OH and H_2O. *J. Phys. Chem. A* **2010**, *114*, 369-378, doi:10.1021/jp905279b.
(27) Thrush, B. A.; Tyndall, G. S. The rate of reaction between HO_2 radicals at low pressures. *Chem. Phys. Lett.* **1982**, *92*, 232-235, doi:10.1016/0009-2614(82)80266-2.
(28) Thrush, B. A.; Tyndall, G. S. Reactions of HO_2 studied by flash photolysis with diode-laser spectroscopy. *J. Chem. Soc. Faraday Trans. 2* **1982**, *78*, 1469-1475, doi:10.1039/f29827801469.
(29) Thrush, B. A.; Wilkinson, J. P. T. Pressure dependence of the rate of reaction between HO_2 radicals. *Chem. Phys. Lett.* **1979**, *66*, 441-443, doi:10.1016/0009-2614(79)80312-7.

B14. **$HO_2 + HO_2$-H_2O**. The enhancement of the $HO_2 + HO_2$ reaction in the presence of H_2O vapor has been ascribed to the formation of a HO_2-H_2O complex and the higher reactivity of the complex over that of HO_2. The recommendation is based upon the studies of Kanno et al.[1,2] who analyzed the enhancement of HO_2 decays in the presence of H_2O. Enhancement factors were obtained at 298, 325, and 350 K and a total pressure of 50 Torr N_2. A pressure dependence of the rate coefficient has not been measured and a pressure independent value is recommended.
(Table: 10-6, Note: 10-6, Evaluated: 10-6) Back to Table

(1) Kanno, N.; Tonokura, K.; Koshi, M. Equilibrium constant of the HO_2-H_2O complex formation and kinetics of $HO_2 + HO_2$-H_2O: Implications for tropospheric chemistry. *J. Geophys. Res.* **2006**, *111*, D20312, doi:10.1029/2005JD006805.

(2) Kanno, N.; Tonokura, K.; Tezaki, A.; Koshi, M. Water dependence of the HO_2 self reaction: Kinetics of the HO_2−H_2O complex. *J. Phys. Chem. A* **2005**, *109*, 3153-3158, doi:10.1021/jp044592+.

1.7.3 Bibliography – HO_x Reactions

Albers, E. A.; Hoyermann, K.; Wagner, H. G.; Wolfrum, J. Absolute measurements of rate coefficients for the reactions of H and O atoms with H_2O_2 and H_2O. *Proc. Combust. Inst.* **1971**, *13*, 81-88.

Anderson, J. G.; Kaufman, F. Kinetics of the reaction OH (v=0) + O_3 → HO_2 + O_2. *Chem. Phys. Lett.* **1973**, *19*, 483-486, doi:10.1016/0009-2614(73)85131-0.

Andersson, B. Y.; Cox, R. A.; Jenkin, M. E. The effect of methanol on the self reaction of HO_2 radicals. *Int. J. Chem. Kinet.* **1988**, *20*, 283-295, doi:10.1002/kin.550200403.

Atkinson, R.; Hansen, D. A.; Pitts, J. N., Jr. Rate constants for the reaction of OH radicals with CHF_2Cl, CF_2Cl_2, $CFCl_3$, and H_2 over the temperature range 297-434 °K. *J. Chem. Phys.* **1975**, *63*, 1703-1706, doi:10.1063/1.431566.

Bahng, M.-K.; Macdonald, R. G. Determination of the rate constant for the OH($X^2\Pi$) + OH($X^2\Pi$) → O(^3P) + H_2O reaction over the temperature range 293-373 K. *J. Phys. Chem. A* **2007**, *111*, 3850-3861, doi:10.1021/jp066359c.

Bedjanian, Y.; Le Bras, G.; Poulet, G. Kinetic study of OH + OH and OD + OD reactions. *J. Phys. Chem.* **1999**, *103*, 7017-7025, doi:10.1021/jp991146r.

Brune, W. H.; Schwab, J. J.; Anderson, J. G. Laser magnetic resonance, resonance fluorescence, and resonance absorption studies of the reaction kinetics of O + OH → H + O_2, O + HO_2 → OH + O_2, N + OH → H + NO, and N + HO_2 → products at 300 K between 1 and 5 torr. *J. Phys. Chem.* **1983**, *87*, 4503-4514, doi:10.1021/j100245a034.

Burrows, J. P.; Cliff, D. I.; Harris, G. W.; Thrush, B. A.; Wilkinson, J. P. T. Atmospheric reactions of the HO_2 radical studied by laser magnetic-resonance spectroscopy. *Proc. Roy. Soc. Lond. A.* **1979**, *368*, 463-481, doi:10.1098/rspa.

Burrows, J. P.; Cox, R. A.; Derwent, R. G. Modulated photolysis of the ozone-water vapour system: Kinetics of the reaction of OH with HO_2. *J. Photochem.* **1981**, *16*, 147-168, doi:10.1016/0047-2670(81)80026-3.

Burrows, J. P.; Harris, G. W.; Thrush, B. A. Rates of reaction of HO_2 with HO and O studied by laser magnetic resonance. *Nature* **1977**, *267*, 233-234, doi:10.1038/267233a0.

Christensen, L. E.; Okumura, M.; Hansen, J. C.; Sander, S. P.; Francisco, J. S. Experimental and ab initio study of the HO_2•CH_3OH complex: Thermodynamics and kinetics of formation. *J. Phys. Chem. A* **2006**, *110*, 6948-6959, doi:10.1021/jp056579a.

Christensen, L. E.; Okumura, M.; Sander, S. P.; Salawitch, R. J.; Toon, G. C.; Sen, B.; Blavier, J.-F.; Jucks, K. W. Kinetics of HO_2 + HO_2 → H_2O_2 + O_2: Implications for stratospheric H_2O_2. *Geophys. Res. Lett.* **2002**, *29*, 1299, doi:1029/2001GL014525.

Clyne, M. A. A.; Down, S. Kinetic behaviour of OH $X^2\Pi$ and $A^2\Sigma^+$ using molecular resonance fluorescence spectrometry. *J. Chem. Soc. Faraday Trans. 2* **1974**, *70*, 253-266, doi:10.1039/F29747000253.

Clyne, M. A. A.; Monkhouse, P. Atomic resonance fluorescence for rate constants of rapid bimolecular reactions Part 5-Hydrogen atom reactions; H + NO_2 and H + O_3. *J. Chem. Soc. Faraday Trans. 2* **1977**, *73*, 298-309, doi:10.1039/F29777300298.

Cox, R. A.; Burrows, J. P. Kinetics and mechanism of the disproportionation of HO_2 in the gas phase. *J. Phys. Chem.* **1979**, *83*, 2560-2568, doi:10.1021/j100483a002.

Cox, R. A.; Burrows, J. P.; Wallington, T. J. Rate coefficient for the reaction OH + HO_2 → H_2O + O_2 at 1 atmosphere pressure and 308 K. *Chem. Phys. Lett.* **1981**, *84*, 217-221, doi:10.1016/0009-2614(81)80329-6.

Davis, D. D.; Wong, W.; Schiff, R. A dye laser flash photolysis kinetics study of the reaction of ground-state atomic oxygen with hydrogen peroxide. *J. Phys. Chem.* **1974**, *78*, 463-464, doi:10.1021/j100597a033.

DeMore, W. B. Reaction of HO_2 with O_3 and the effect of water vapor on HO_2 kinetics. *J. Phys. Chem.* **1979**, *83*, 1113-1118, doi:10.1021/j100472a001.

DeMore, W. B. Rate constant and possible pressure dependence of the reaction OH + HO_2. *J. Phys. Chem.* **1982**, *86*, 121-126, doi:10.1021/j100390a025.

DeMore, W. B.; Tschuikow-Roux, E. Temperature dependence of the reactions of OH and HO_2 with O_3 *J. Phys. Chem.* **1974**, *78*, 1447-1451, doi:10.1021/j100608a001.

Dobis, O.; Benson, S. W. Reaction of the ethyl radical with oxygen at millitorr pressures at 243-368 K and a study of the Cl + HO_2, ethyl + HO_2, and HO_2 + HO_2 reactions. *J. Am. Chem. Soc.* **1993**, *115*, 8798-8809, doi:10.1021/ja00072a038.

Dodonov, A. F.; Zelenov, V. V.; Kukui, A. S.; Ponomarev, E. A.; Tal'Roze, V. L. Mass spectrometric investigation of elementary gas phase reactions passing in the H + O_3 + O_2 system-Channels of H + O_3 → OH(v) + O_2, H + O_2 → HO_2 + O reactions. *Khim. Fiz.* **1985**, *4*, 1335-1343.

Dransfeld, P.; Wagner, H. G. Comparative study of the reactions of ^{16}OH with H$^{16}O_2$. *Z. Naturforsch.* **1987**, *42a*, 471-476.

Ehhalt, D. H.; Davidson, J. A.; Cantrell, C. A.; Friedman, I.; Tyler, S. The kinetic isotope effect in the reaction of H_2 with OH. *J. Geophys. Res.* **1989**, *94*, 9831-9836, doi:10.1029/JD094iD07p09831.

English, A. M.; Hansen, J. C.; Szente, J. J.; Maricq, M. M. The effects of water vapor on the CH_3O_2 self-reaction and reaction with HO_2. *J. Phys. Chem. A* **2008**, *112*, 9220-9228, doi:10.1021/jp800727a.

Farquharson, G. K.; Smith, R. H. Rate constants for the gaseous reactions OH + C_2H_4 and OH + OH. *Aust. J. Chem.* **1980**, *33*, 1425-1435, doi:10.1071/CH9801425.

Finlayson-Pitts, B. J.; Kleindienst, T. E. The reaction of hydrogen atoms with ozone: Evidence for a second reaction path producing HO_2 and O(^3P). *J. Chem. Phys.* **1979**, *70*, 4804-4806, doi:10.1063/1.437271.

Finlayson-Pitts, B. J.; Kleindienst, T. E.; Ezell, J. J.; Toohey, D. W. The production of O(^{3}P) and ground state OH in the reaction of hydrogen atoms with ozone. *J. Chem. Phys.* **1981**, *74*, 4533-4543, doi:10.1063/1.441642.

Force, A. P.; Wiesenfeld, J. R. Laser photolysis of O_3/H_2 mixtures: The yield of the H + O_3 → HO_2 + O reaction. *J. Chem. Phys.* **1981**, *74*, 1718-1723, doi:10.1063/1.441260.

Greiner, N. R. Hydroxyl radical kinetics by kinetic spectroscopy. V. Reaction with H_2 and CO in the range 300-500°K. *J. Chem. Phys.* **1969**, *51*, 5049-5051, doi:10.1063/1.1671902.

Hack, W.; Preuss, A. W.; Temps, F.; Wagner, H. G. Reaction of O + HO_2 → OH + O_2 studied with a LMR-ESR spectrometer. *Ber. Bunsenges. Phys. Chem.* **1979**, *83*, 1275-1279, doi:10.1002/bbpc.19790831214.

Hack, W.; Preuss, A. W.; Wagner, H. G.; Hoyermann, K. Reactions of hydrogen atoms with hydroperoxyl radicals 2. Determination of the rate constant of the overall reaction. *Ber. Bunsenges. Phys. Chem.* **1979**, *83*, 212-217, doi:10.1002/bbpc.19790830306.

Hack, W.; Wagner, H. G.; Hoyermann, K. Reactions of hydrogen atoms with hydroperoxyl radicals 1. Determination of specific rate constants of reaction channels. *Ber. Bunsenges. Phys. Chem.* **1978**, *82*, 713-719, doi:10.1002/bbpc.19780820710.

Hamilton, E. J., Jr. Water vapor dependence of the kinetics of the self-reaction of HO_2 in the gas phase. *J. Chem. Phys.* **1975**, *63*, 3682-3683, doi:10.1063/1.431772.

Hamilton, E. J., Jr.; Lii, R.-R. The dependence on H_2O and on NH_3 of the kinetics of the self-reaction of HO_2 in the gas-phase formation of HO_2•H_2O and HO_2•NH_3 complexes. *Int. J. Chem. Kinet.* **1977**, *9*, 875-885, doi:10.1002/kin.550090604.

Harding, L. B.; Wagner, A. F. Theoretical study of the reaction rates of OH + OH ↔ H_2O + O. *Proc. Combust. Inst.* **1988**, *22*, 983-989, doi:10.1016/S0082-0784(89)80107-9.

Herndon, S. C.; Villalta, P. W.; Nelson, D. D.; Jayne, J. T.; Zahniser, M. S. Rate constant measurements for the reaction of HO_2 with O_3 from 200 to 300 K using a turbulent flow reactor. *J. Phys. Chem. A* **2001**, *105*, 1583-1591, doi:10.1021/jp002383t.

Hippler, H.; Rahn, R.; Troe, J. Shock wave study of the reaction HO_2 + HO_2 → H_2O_2 + O_2: Confirmation of a rate constant minimum near 700 K. *J. Chem. Phys.* **1990**, *93*, 1755-1760, doi:10.1063/1.459102.

Hippler, H.; Troe, J. Rate constants of the reaction HO + H_2O_2 → HO_2 + H_2O at T ≥ 1000 K. *Chem. Phys. Lett.* **1992**, *192*, 333-337, doi:10.1016/0009-2614(92)85478-S.

Hislop, J. R.; Wayne, R. P. Production of $O_2(^1\Sigma_g^+)$ in the H + O_2 system. *J. Chem. Soc. Faraday Trans. 2* **1977**, *73*, 506-516, doi:10.1039/F29777300506.

Hochanadel, C. J.; Ghormley, J. A.; Ogren, P. J. Absorption spectrum and reaction kinetics of the HO_2 radical in the gas phase. *J. Chem. Phys.* **1972**, *56*, 4426-4432, doi:10.1063/1.1677885.

Hochanadel, C. J.; Sworski, T. J.; Ogren, P. J. Rate constants for the reactions of HO_2 with OH and with HO_2. *J. Phys. Chem.* **1980**, *84*, 3274-3277, doi:10.1021/j100461a029.

Howard, C. J.; Finlayson-Pitts, B. J. Yields of HO_2 in the reaction of hydrogen atoms with ozone. *J. Chem. Phys.* **1980**, *72*, 3842-3843, doi:10.1063/1.439601.

Howard, M. J.; Smith, I. W. M. Direct rate measurements on the reactions N + OH → NO + H and O + OH → O_2 + H from 250 to 515 K. *J. Chem. Soc. Faraday Trans. 2* **1981**, *77*, 997-1008, doi:10.1039/F29817700997.

Kanno, N.; Tonokura, K.; Koshi, M. Equilibrium constant of the HO_2-H_2O complex formation and kinetics of HO_2 + HO_2-H_2O: Implications for tropospheric chemistry. *J. Geophys. Res.* **2006**, *111*, D20312, doi:10.1029/2005JD006805.

Kanno, N.; Tonokura, K.; Tezaki, A.; Koshi, M. Water dependence of the HO_2 self reaction: Kinetics of the HO_2–H_2O complex. *J. Phys. Chem. A* **2005**, *109*, 3153-3158, doi:10.1021/jp044592+.
Keyser, L. F. Absolute rate constant and temperature dependence of the reaction between hydrogen (^2S) atoms and ozone. *J. Phys. Chem.* **1979**, *83*, 645-648, doi:10.1021/j100469a001.
Keyser, L. F. Absolute rate constant of the reaction OH + H_2O_2 → HO_2 + H_2O from 245 to 423 K. *J. Phys. Chem.* **1980**, *84*, 1659-1663, doi:10.1021/j100450a001.
Keyser, L. F. Absolute rate constant of the reaction OH + HO_2 → H_2O + O_2. *J. Phys. Chem.* **1981**, *85*, 3667-3673, doi:10.1021/j150624a028.
Keyser, L. F. Kinetics of the reaction O + HO_2 → OH + O_2 from 229 to 372 K. *J. Phys. Chem.* **1982**, *86*, 3439-3446, doi:10.1021/j100214a03.
Keyser, L. F. Relative rate constants for the reactions of atomic oxygen with HO_2 and OH radicals. *J. Phys. Chem.* **1983**, *87*, 837-841, doi:10.1021/j100228a028.
Keyser, L. F. Absolute rate constant and branching fractions for the H + HO_2 reaction from 245 to 300 K. *J. Phys. Chem.* **1986**, *90*, 2994-3003, doi:10.1021/j100404a040.
Keyser, L. F. Kinetics of the reaction OH + HO_2 → H_2O + O_2 from 254 to 382 K. *J. Phys. Chem.* **1988**, *92*, 1193-1200, doi:10.1021/j100316a037.
Keyser, L. F.; Choo, K. Y.; Leu, M. T. Yields of $O_2(b^1\Sigma_g^+)$ from reactions of HO_2. *Int. J. Chem. Kinet.* **1985**, *17*, 1169-1185, doi:10.1002/kin.550171103.
Kircher, C. C.; Sander, S. P. Kinetics and mechanism of HO_2 and DO_2 disproportionations. *J. Phys. Chem.* **1984**, *88*, 2082-2091, doi:10.1021/j150654a029.
Kulcke, A.; Blackman, B.; Chapman, W. B.; Kim, I. K.; Nesbitt, D. J. Time-resolved O_3 chemical chain reaction kinetics via high-resolution IR laser absorption methods. *J. Phys. Chem. A* **1998**, *102*, 1965-1972, doi:10.1021/jp972486k.
Kurylo, M. J. Kinetics of the reactions OH(v=0) + NH_3 → H_2O + NH_2 and OH(v=0) + O_3 → HO_2 + O_2 at 298°K. *Chem. Phys. Lett.* **1973**, *23*, 467-471, doi:10.1016/0009-2614(73)89003-7.
Kurylo, M. J.; Klais, O.; Laufer, A. H. Mechanistic investigation of the HO + HO_2 reaction. *J. Phys. Chem.* **1981**, *85*, 3674-3678, doi:10.1021/j150624a029.
Kurylo, M. J.; Murphy, J. L.; Haller, G. S.; Cornett, K. D. A flash photolysis resonance fluorescence investigation of the reaction OH + H_2O_2 → HO_2 + H_2O. *Int. J. Chem. Kinet.* **1982**, *14*, 1149-1161, doi:10.1002/kin.550141008.
Kurylo, M. J.; Ouellette, P. A.; Laufer, A. H. Measurements of the pressure dependence of the HO_2 radical self-disproportionation reaction at 298 K. *J. Phys. Chem.* **1986**, *90*, 437-440, doi:10.1021/j100275a017.
Lamb, J. J.; Molina, L. T.; Smith, C. A.; Molina, M. J. Rate constant of the OH + H_2O_2 → HO_2 + H_2O reaction. *J. Phys. Chem.* **1983**, *87*, 4467-4470, doi:10.1021/j100245a028.
Lee, J. H.; Michael, J. V.; Payne, W. A.; Stief, L. J. Absolute rate of the reaction of hydrogen atoms with ozone from 219-360 K. *J. Chem. Phys.* **1978**, *69*, 350-353, doi:10.1063/1.436360.
Lewis, R. S.; Watson, R. T. Temperature dependence of the reaction $O(^3P)$ + $OH(^2\Pi)$ → O_2 + H. *J. Phys. Chem.* **1980**, *84*, 3495-3503, doi:10.1021/j100463a002.
Lightfoot, P. D.; Veyret, B.; Lesclaux, R. The rate constant for the HO_2 + HO_2 reaction at elevated temperatures. *Chem. Phys. Lett.* **1988**, *150*, 120-126, doi:10.1016/0009-2614(88)80407-X.
Lii, R.-R.; Gorse, R. A., Jr.; Sauer, M. C., Jr.; Gordon, S. Rate constant for the reaction of OH with HO_2. *J. Phys. Chem.* **1980**, *84*, 819-821, doi:10.1021/j100445a003.
Lii, R.-R.; Sauer, M. C., Jr.; Gordon, S. Rate constant of the reaction of $O(^3P)$ with HO_2. *J. Phys. Chem.* **1980**, *84*, 817-819, doi:10.1021/j100445a002.
Lii, R.-R.; Sauer, M. C., Jr.; Gordon, S. Temperature dependence of the gas-phase self-reaction of HO_2 in the presence of H_2O. *J. Phys. Chem.* **1981**, *85*, 2833-2834, doi:10.1021/j150619a027.
Manzanares, E. R.; Suto, M.; Lee, L. C.; Coffey, D. Reaction rate constant of HO_2 + O_3 measured by detecting HO_2 from photofragment fluorescence. *J. Chem. Phys.* **1986**, *85*, 5027-5034, doi:10.1063/1.451692.
Maricq, M. M.; Szente, J. J. A kinetic study of the reaction between ethylperoxy radicals and HO_2. *J. Phys. Chem.* **1994**, *98*, 2078-2082, doi:10.1021/j100059a016.
Marinelli, W. J.; Johnston, H. S. Reaction rates of hydroxyl radical with nitric acid and with hydrogen peroxide. *J. Chem. Phys.* **1982**, *77*, 1225-1234, doi:10.1063/1.443998.
McKenzie, A.; Mulcahy, M. F. R.; Steven, J. R. Kinetics of decay of hydroxyl radicals at low pressure. *J. Chem. Phys.* **1973**, *59*, 3244-3254, doi:10.1063/1.1680466.

Michelangeli, D. V.; Choo, K.-Y.; Leu, M.-T. Yields of $O_2(^1\Sigma_g^+)$ and $O_2(^1\Delta_g)$ in the H + O_2 reaction system, and the quenching of $O_2(^1\Sigma_g^+)$ by atomic hydrogen. *Int. J. Chem. Kinet.* **1988**, *20*, 915-938, doi:10.1002/kin.550201202.

Nelson, D. D., Jr.; Zahniser, M. S. A mechanistic study of the reaction of HO_2 radical with ozone. *J. Phys. Chem.* **1994**, *98*, 2101-2104, doi:10.1021/j100059a020.

Nicovich, J. M.; Wine, P. H. Temperature dependence of the O + HO_2 rate coefficient. *J. Phys. Chem.* **1987**, *91*, 5118-5123, doi:10.1021/j100303a049.

Niki, H.; Maker, P. D.; Savage, C. M.; Breitenbach, L. P. An FTIR study of the mechanism for the gas phase reaction between HO_2 radicals. *Chem. Phys. Lett.* **1980**, *73*, 43-46, doi:10.1016/0009-2614(80)85198-0.

Nizkorodov, S. A.; Harper, W. W.; Blackmon, B. W.; Nesbitt, D. J. Temperature dependent kinetics of the $OH/HO_2/O_3$ chain reaction by time-resolved IR laser absorption spectroscopy. *J. Phys. Chem. A* **2000**, *104*, 3964-3973, doi:10.1021/jp9934984.

Orkin, V. L.; Kozlov, S. N.; Poskrebyshev, G. A.; Huie, R. E.; Kurylo, M. J. Rate constant for the reaction of OH with H_2 between 200 and 480 K. *J. Phys. Chem. A* **2006**, *110*, 6978-6985, doi:10.1021/jp057035b.

Overend, R. P.; Paraskevopoulos, G.; Cvetanović, R. J. Rates of OH radical reactions. I. Reactions with H_2, CH_4, C_2H_6, and C_3H_8 at 295 K. *Can. J. Phys.* **1975**, *53*, 3374-3382, doi:10.1139/v75-482.

Ravishankara, A. R.; Nicovich, J. M.; Thompson, R. L.; Tully, F. P. Kinetic study of the reaction of OH with H_2 and D_2 from 250 to 1050 K. *J. Phys. Chem.* **1981**, *85*, 2498-2503, doi:10.1021/j150617a018.

Ravishankara, A. R.; Wine, P. H.; Langford, A. O. Absolute rate constant for the reaction OH(v = 0) + O_3 → HO_2 + O_2 over the temperature range 238-357°K. *J. Chem. Phys.* **1979**, *70*, 984-989, doi:10.1063/1.437488.

Ravishankara, A. R.; Wine, P. H.; Nicovich, J. M. Pulsed laser photolysis study of the reaction between O(^3P) and HO_2. *J. Chem. Phys.* **1983**, *78*, 6629-6639, doi:10.1063/1.444661.

Riffault, V.; Gierczak, T.; Burkholder, J. B.; Ravishankara, A. R. Quantum yields for OH production in the photodissociation of HNO_3 at 248 and 308 nm and H_2O_2 at 308 and 320 nm. *Phys. Chem. Chem. Phys.* **2006**, *8*, 1079-1085, doi:10.1039/b513760h.

Robertson, R.; Smith, G. P. Temperature dependence of O + OH at 136−377 K using ozone photolysis. *J. Phys. Chem. A* **2006**, *110*, 6673–6679, doi:10.1021/jp055863z.

Robertson, R. G.; Smith, G. P. Photolytic measurement of the O + OH rate constant at 295 K. *Chem. Phys. Lett.* **2002**, *358*, 157-162, doi:10.1016/S0009-2614(02)00629-2.

Roscoe, J. M. The reaction of O(^3P) with H_2O_2. *Int. J. Chem. Kinet.* **1982**, *14*, 471-478, doi:10.1002/kin.550140504.

Rozenshtein, V. B.; Gershenzon, Y. M.; Il'in, S. D.; Kishkovitch, O. P. Reactions of HO_2 with NO, OH and HO_2 studied by EPR/LMR spectroscopy. *Chem. Phys. Lett.* **1984**, *112*, 473-478, doi:10.1016/0009-2614(84)85572-4.

Sander, S. P. Low-pressure study of the HO_2 + HO_2 reaction at 298 K. *J. Phys. Chem.* **1984**, *88*, 6018-6021, doi:10.1021/j150668a055.

Sander, S. P.; Peterson, M.; Watson, R. T.; Patrick, R. Kinetics studies of the HO_2 + HO_2 and DO_2 + DO_2 reactions at 298 K. *J. Phys. Chem.* **1982**, *86*, 1236-1240, doi:10.1021/j100397a002.

Schwab, J. J.; Brune, W. H.; Anderson, J. G. Kinetics and mechanism of the OH + HO_2 reaction. *J. Phys. Chem.* **1989**, *93*, 1030-1035, doi:10.1021/j100340a005.

Seeley, J. V.; Jayne, J. T.; Molina, M. J. High pressure fast-flow technique for gas phase kinetics studies. *Int. J. Chem. Kinet.* **1993**, *25*, 571-594, doi:10.1002/kin.550250706.

Simonaitis, R.; Heicklen, J. Reaction of HO_2 with O_3. *J. Phys. Chem.* **1973**, *77*, 1932-1935, doi:10.1021/j100635a002.

Simonaitis, R.; Heicklen, J. A kinetic study of the HO_2 + HO_2 reaction. *J. Phys. Chem.* **1982**, *86*, 3416-3418, doi:10.1021/j100214a030.

Sinha, A.; Lovejoy, E. R.; Howard, C. J. Kinetic study of the reaction of HO_2 with ozone. *J. Chem. Phys.* **1987**, *87*, 2122-2128, doi:10.1063/1.453136.

Smith, C. A.; Molina, L. T.; Lamb, J. J.; Molina, M. J. Kinetics of the reaction of OH with pernitric and nitric acids. *Int. J. Chem. Kinet.* **1984**, *16*, 41-55, doi:10.1002/kin.550160107.

Smith, I. W. M.; Stewart, D. W. A. Low-temperature kinetics of reactions between neutral free radicals Rate constants for the reactions of OH radicals with N atoms ($103 \le T/K \le 294$) and with O atoms ($158 \le T/K \le 294$). *J. Chem. Soc. Faraday Trans.* **1994**, *90*, 3221-3227, doi:10.1039/ft9949003221.

Smith, I. W. M.; Zellner, R. Rate measurements of reactions of OH by resonance absorption. Part 3. - Reactions of OH with H_2, D_2 and hydrogen and deuterium halides. *J. Chem. Soc. Faraday Trans. 2* **1974**, *70*, 1045-1056, doi:10.1039/F29747001045.

Sridharan, U. C.; Klein, F. S.; Kaufman, F. Detailed course of the O + HO_2 reaction. *J. Chem. Phys.* **1985**, *82*, 592-593, doi:10.1063/1.448973.
Sridharan, U. C.; Qiu, L. X.; Kaufman, F. Kinetics of the reaction OH + HO_2 → H_2O + O_2 at 296 K. *J. Phys. Chem.* **1981**, *85*, 3361-3363, doi:10.1021/j150623a001.
Sridharan, U. C.; Qiu, L. X.; Kaufman, F. Kinetics and product channels of the reactions of HO_2 with O and H atoms at 296 K. *J. Phys. Chem.* **1982**, *86*, 4569-4574, doi:10.1021/j100220a023.
Sridharan, U. C.; Qiu, L. X.; Kaufman, F. Rate constant of the OH + HO_2 reaction from 252 to 420 K. *J. Phys. Chem.* **1984**, *88*, 1281-1282, doi:10.1021/j150651a006.
Sridharan, U. C.; Reimann, B.; Kaufman, F. Kinetics of the reaction OH + H_2O_2 → HO_2 + H_2O. *J. Chem. Phys.* **1980**, *73* 1286-1293, doi:10.1063/1.440240.
Stone, D.; Rowley, D. M. Kinetics of the gas phase HO_2 self-reaction: Effects of temperature, pressure, water and methanol vapours. *Phys. Chem. Chem. Phys.* **2005**, *7*, 2156-2163, doi:10.1039/b502673c.
Stuhl, F.; Niki, H. Pulsed vacuum-UV photochemical study of reactions of OH with H_2, D_2, and CO using a resonance-fluorescent detection method. *J. Chem. Phys.* **1972**, *57*, 3671-3677, doi:10.1063/1.1678825.
Su, F.; Calvert, J. G.; Lindley, C. R.; Uselman, W. M.; Shaw, J. H. A Fourier transform infrared kinetic study of HOCl and its absolute integrated infrared band intensities. *J. Phys. Chem.* **1979**, *83*, 912-920, doi:10.1021/j100471a006.
Takacs, G. A.; Howard, C. J. Room-temperature rate constant for the HO_2 + HO_2 reaction at low pressures. *J. Phys. Chem.* **1984**, *88*, 2110-2116, doi:10.1021/j150654a033.
Takacs, G. A.; Howard, C. J. Temperature dependence of the reaction HO_2 + HO_2 at low pressures. *J. Phys. Chem.* **1986**, *90*, 687-690, doi:10.1021/j100276a041.
Talukdar, R. K.; Gierczak, T.; Goldfarb, L.; Rudich, Y.; Madhava Rao, B. S.; Ravishankara, A. R. Kinetics of hydroxyl radical reactions with isotopically labeled hydrogen. *J. Phys. Chem.* **1996**, *100*, 3037-3043, doi:10.1021/jp9518724.
Tang, Y.; Tyndall, G. S.; Orlando, J. J. Spectroscopic and kinetic properties of HO_2 radicals and the enhancement of the HO_2 self reaction by CH_3OH and H_2O. *J. Phys. Chem. A* **2010**, *114*, 369-378, doi:10.1021/jp905279b.
Temps, F.; Wagner, H. G. Investigation of the reaction OH + HO_2 → H_2O + O_2 with the aid of a laser magnetic spectrometer. *Ber. Bunsenges. Phys. Chem.* **1982**, *86*, 119-125, doi:10.1002/bbpc.19820860206.
Thrush, B. A.; Tyndall, G. S. The rate of reaction between HO_2 radicals at low pressures. *Chem. Phys. Lett.* **1982**, *92*, 232-235, doi:10.1016/0009-2614(82)80266-2.
Thrush, B. A.; Tyndall, G. S. Reactions of HO_2 studied by flash photolysis with diode-laser spectroscopy. *J. Chem. Soc. Faraday Trans. 2* **1982**, *78*, 1469-1475, doi:10.1039/f29827801469.
Thrush, B. A.; Wilkinson, J. P. T. Pressure dependence of the rate of reaction between HO_2 radicals. *Chem. Phys. Lett.* **1979**, *66*, 441-443, doi:10.1016/0009-2614(79)80312-7.
Thrush, B. A.; Wilkinson, J. P. T. The rate of reaction of HO_2 radicals with HO and with NO. *Chem. Phys. Lett.* **1981**, *81*, 1-3, doi:10.1016/0009-2614(81)85314-6.
Thrush, B. A.; Wilkinson, J. P. T. The rate of the reaction between H and HO_2. *Chem. Phys. Lett.* **1981**, *84*, 17-19, doi:10.1016/0009-2614(81)85360-2.
Trainor, D. W.; von Rosenberg, C. W., Jr. Flash photolysis study of the gas phase recombination of hydroxyl radicals. *J. Chem. Phys.* **1974**, *61*, 1010-1015, doi:10.1063/1.1681968.
Tully, F. P.; Ravishankara, A. R. Flash photolysis-resonance fluorescence kinetic study of the reactions OH + H_2 → H_2O + H and OH + CH_4 → H_2O + CH_3 from 298 to 1020 K. *J. Phys. Chem.* **1980**, *84*, 3126-3130, doi:10.1021/j100460a031.
Turnipseed, A. A.; Vaghjiani, G. L.; Gierczak, T.; Thompson, J. E.; Ravishankara, A. R. The photochemistry of ozone at 193 and 222 nm. *J. Chem. Phys.* **1991**, *95*, 3244-3251, doi:10.1063/1.460881.
Vaghjiani, G. L.; Ravishankara, A. R.; Cohen, N. Reactions of OH and OD with H_2O_2 and D_2O_2. *J. Phys. Chem.* **1989**, *93*, 7833-7837, doi:10.1021/j100360a021.
Vakhtin, A. B.; McCabe, D. C.; Ravishankara, A. R.; Leone, S. R. Low-temperature kinetics of the reaction of the OH radical with hydrogen peroxide. *J. Phys. Chem. A* **2003**, *17*, 10642-10647, doi:10.1021/jp030424q.
Wagner, G.; Zellner, R. Temperature dependence of the reaction OH + OH → H_2O + O. *Ber. Bunsenges. Phys. Chem.* **1981**, *85*, 1122-1128, doi:10.1002/bbpc.19810851209.
Wang, X.; Suto, M.; Lee, L. C. Reaction rate constants of HO_2 + O_3 in the temperature range 233—400 K. *J. Chem. Phys.* **1988**, *88*, 896-899, doi:10.1063/1.454169.
Washida, N.; Akimoto, H.; Okuda, M. Is O_2*($a^1\Delta_g$) formed in the O + O_3, H + O_3, and NO + O_3 reactions? *Bull. Chem. Soc. Jpn.* **1980**, *53*, 3496-3503, doi:10.1246/bcsj.53.3496.

Washida, N.; Akimoto, H.; Okuda, M. O_2^* ($a^1\Delta_g$) in the reaction of H + O_3. *J. Chem. Phys.* **1980**, *72*, 5781-5783, doi:10.1063/1.439004.
Westenberg, A. A.; deHaas, N. Rate of the reaction OH + OH → H_2O + O. *J. Chem. Phys.* **1973**, *58*, 4066-4071, doi:10.1063/1.1678962.
Westenberg, A. A.; deHaas, N. Rates of CO + OH and H_2 + OH over an extended temperature range. *J. Chem. Phys.* **1973**, *58*, 4061-4065, doi:10.1063/1.1678961.
Westenberg, A. A.; deHaas, N.; Roscoe, J. M. Radical reactions in an electron spin resonance cavity homogeneous reactor. *J. Phys. Chem.* **1970**, *74*, 3431-3438, doi:10.1021/j100713a001.
Wine, P. H.; Nicovich, J. M.; Thompson, R. J.; Ravishankara, A. R. Kinetics of O(^3P_J) reactions with H_2O_2 and O_3. *J. Phys. Chem.* **1983**, *87*, 3948-3954, doi:10.1021/j100243a030.
Wine, P. H.; Semmes, D. H.; Ravishankara, A. R. A laser flash photolysis kinetics study of the reaction OH + H_2O_2 → HO_2 + H_2O. *J. Chem. Phys.* **1981**, *75*, 4390-4395, doi:10.1063/1.442602.
Zahniser, M. S.; Howard, C. J. Kinetics of the reaction of HO_2 with ozone. *J. Chem. Phys.* **1980**, *73*, 1620-1626, doi:10.1063/1.440343.
Zellner, R.; Steinert, W. Vibrational rate enhancement in the reaction OH + H_2(v =1) → H_2O + H. *Chem. Phys. Lett.* **1981**, *81*, 568-572, doi:10.1016/0009-2614(81)80465-4.

1.8 NO_x Reactions

1.8.1 Table 1C: NO_x Reactions

Reaction	Temperature Range of Exp. Data (K) [a]	*A*-Factor	*E*/R	*k*(298 K) [b]	*f*(298 K) [c]	*g* [c]	Note
$O + NO \xrightarrow{M} NO_2$		(See Table 2-1)					
$O + NO_2 \rightarrow NO + O_2$		(See Table 2-1)					
$O + NO_2 \xrightarrow{M} NO_3$		(See Table 2-1)					
$O + NO_3 \rightarrow O_2 + NO_2$	298–329	1.3×10^{-11}	0	1.3×10^{-11}	1.50	50	C 1
$O + N_2O_5 \rightarrow$ products	223–300			$<3.0\times10^{-16}$			C 2
$O + HNO_3 \rightarrow OH + NO_3$	298			$<3.0\times10^{-17}$			C 3
$O + HO_2NO_2 \rightarrow$ products	228–297	7.8×10^{-11}	3400	8.6×10^{-16}	3.00	750	C 4
$H + NO_2 \rightarrow OH + NO$	195–2000	1.35×10^{-10}	0	1.35×10^{-10}	1.20	150	C 5
$OH + NO \xrightarrow{M} HONO$		(See Table 2-1)					
$OH + NO_2 \xrightarrow{M} HNO_3$		(See Table 2-1)					
$OH + NO_3 \rightarrow$ products	298			2.0×10^{-11}	1.50		C 6
$OH + HONO \rightarrow H_2O + NO_2$	278–1400	3.0×10^{-12}	–250	6.9×10^{-12}	1.30	100	C 7
$OH + HNO_3 \rightarrow H_2O + NO_3$		(See Table 2-1)					
$OH + HO_2NO_2 \rightarrow$ products	218–335	4.5×10^{-13}	–610	3.5×10^{-12}	1.30	50	C 8
$OH + NH_3 \rightarrow H_2O + NH_2$	228–2360	1.7×10^{-12}	710	1.6×10^{-13}	1.15	100	C 9
$HO_2 + NO \rightarrow NO_2 + OH$	193–1270	3.44×10^{-12}	–260	8.2×10^{-12}	1.10	0	C10
$NO_2^* + H_2O \rightarrow OH + HONO$		(See Note)					C11
$HO_2 + NO_2 \xrightarrow{M} HO_2NO_2$		(See Table 2-1)					
$HO_2 + NO_2 \rightarrow HONO + O_2$	296			$<5\times10^{-16}$			C12
$HO_2 + NO_3 \rightarrow$ products	263–343			3.5×10^{-12}	1.50		C13
$HO_2 + NH_2 \rightarrow$ products	298			4.8×10^{-11}	2.00		C14
$N + O_2 \rightarrow NO + O$	280–1220	3.3×10^{-12}	3150	8.5×10^{-17}	1.25	250	C15
$N + O_3 \rightarrow NO + O_2$	298			$<2.0\times10^{-16}$			C16

Reaction	Temperature Range of Exp. Data (K) [a]	*A*-Factor	*E*/R	*k*(298 K) [b]	*f*(298 K) [c]	*g* [c]	Note
$N + NO \rightarrow N_2 + O$	196–3660	2.0×10^{-11}	–165	3.48×10^{-11}	1.05	25	C17
$N + NO_2 \rightarrow$ products	223–700	5.8×10^{-12}	–220	1.2×10^{-11}	1.15	50	C18
$NO + O_3 \rightarrow NO_2 + O_2$	195–443	3.0×10^{-12}	1500	1.9×10^{-14}	1.07	130	C19
$NO + NO_3 \rightarrow 2NO_2$	209–703	1.7×10^{-11}	–125	2.6×10^{-11}	1.15	50	C20
$NO_2 + O_3 \rightarrow NO_3 + O_2$	231–362	1.2×10^{-13}	2450	3.2×10^{-17}	1.15	150	C21
$NO_2 + NO_3 \rightarrow NO + NO_2 + O_2$	236–538	(See Note)					C22
$NO_2 + NO_3 \xrightarrow{M} N_2O_5$		(See Table 2-1)					
$NO_3 + NO_3 \rightarrow 2NO_2 + O_2$	298–1100	8.5×10^{-13}	2450	2.3×10^{-16}	1.50	500	C23
$NH_2 + O_2 \rightarrow$ products	295–2300			$<6.0\times10^{-21}$			C24
$NH_2 + O_3 \rightarrow$ products	248–380	4.3×10^{-12}	930	1.9×10^{-13}	2.00	200	C25
$NH_2 + NO \rightarrow$ products	200–2500	4.0×10^{-12}	–450	1.8×10^{-11}	1.30	150	C26
$NH_2 + NO_2 \rightarrow N_2O + H_2O$ $\rightarrow H_2NO + NO$	295–910	6.0×10^{-12}	–385	2.2×10^{-11}	1.30	300	C27
$NH + NO \rightarrow N_2O + H$ $\rightarrow N_2 + OH$	269–3350	4.9×10^{-11}	0	4.9×10^{-11}	1.25	200	C28
$NH + NO_2 \rightarrow N_2O + OH$ $\rightarrow NO + HNO$	269–377	3.5×10^{-13}	–1140	1.6×10^{-11}	2.00	100	C29
$O_3 + HNO_2 \rightarrow O_2 + HNO_3$	226–300			$<5.0\times10^{-19}$			C30
$N_2O_5 + H_2O \rightarrow 2HNO_3$	290–298			$<2.0\times10^{-21}$			C31
$N_2(A,v) + O_2 \rightarrow$ products	80–560			2.5×10^{-12}, v=0	1.50		C32
$N_2(A,v) + O_3 \rightarrow$ products	298			4.1×10^{-11}, v=0	2.00		C33

Shaded areas indicate changes or additions since JPL19-5.

[a] Temperature range of available experimental data. This is not necessarily the range of temperature over which the recommended Arrhenius parameters are applicable. See the corresponding note for such information.

[b] Units are cm^3 $molecule^{-1}$ s^{-1}.

[c] f(298 K) is the uncertainty factor at 298 K. To calculate the uncertainty at other temperatures, use the expression:

$$f(\mathrm{T}) = f(298\ \mathrm{K})\exp\left|g\left(\frac{1}{\mathrm{T}} - \frac{1}{298}\right)\right|$$

Note that the exponent is an absolute value.

1.8.2 Notes: NO_x Reactions

C1. **O + NO_3.** The recommended k(298 K) is an average of the results from Graham and Johnston[2] (298 and 329 K) and Canosa-Mas et al.[1] (298 K). Over the limited temperature range of the Graham and Johnston study there was no measurable temperature dependence, which is the basis for the current recommendation.
(Table: 25-1, Note: 19-5, Evaluated: 19-5) Back to Table

(1) Canosa-Mas , C. E.; Carpenter, P. J.; Wayne, R. P. The reaction of NO_3 with atomic oxygen. *J. Chem. Soc. Faraday Trans 2* **1989**, *85*, 697-707, doi:10.1039/f29898500697.
(2) Graham, R. A.; Johnston, H. S. The photochemistry of NO_3 and the kinetics of the N_2O_5-O_3 system. *J. Phys. Chem.* **1978**, *82*, 254-268, doi:10.1021/j100492a002.

C2. **O + N_2O_5.** The recommendation is based on the study by Kaiser and Japar.[1] (223 and 300 K).
(Table: 82-57, Note: 82-57, Evaluated: 19-5) Back to Table

(1) Kaiser, E. W.; Japar, S. M. The kinetics of the gas phase reaction of O(^{3}P) with N_2O_5. *Chem. Phys. Lett.* **1978**, *54*, 265-268, doi:10.1016/0009-2614(78)80097-9.

C3. **O + HNO_3.** The upper limit reported by Chapman and Wayne[1] (300 K) is accepted.
(Table: 82-57, Note: 82-57, Evaluated: 19-5) Back to Table

(1) Chapman, C. J.; Wayne, R. P. The reaction of atomic oxygen and hydrogen with nitric acid. *Int. J. Chem. Kinet.* **1974**, *6*, 617-630, doi:10.1002/kin.550060502.

C4. **O + HO_2NO_2.** The recommended value is based on the study of Chang et al.[1] (228–297 K). The large uncertainty in E/R and k(298 K) are due to the fact that the recommendation is based on a single study.
(Table: 82-57, Note: 82-57, Evaluated: 19-5) Back to Table

(1) Chang, J. S.; Trevor, P. L.; Barker, J. R. O(^3P) + $HOONO_2$ → Products: Temperature-dependent rate constant. *Int. J. Chem. Kinet.* **1981**, *13*, 1151-1161, doi:10.1002/kin.550131106.

C5. **H + NO_2.** The recommended k(298 K) is derived from the studies of Wagner et al.[6] (243–461 K), Bemand and Clyne[2] (298 K), Clyne and Monkhouse[3] (298–653 K), Michael et al.[5] (195–400 K), and Ko and Fontijn[4] (296–755 K). The temperature dependence recommendation is from the studies of Wagner et al., Ko and Fontijn, and Michael et al. for temperatures <500 K. The data from Wategaonkar and Setser[7] (300 K) and Agrawalla et al.[1] (298 K) were not considered.
(Table: 19-5, Note: 19-5, Evaluated: 19-5) Back to Table

(1) Agrawalla, B. S.; Manocha, A. S.; Setser, D. W. Studies of H and O atom reactions by OH infrared chemiluminescence. *J. Phys. Chem.* **1981**, *85*, 2873-2877, doi:10.1021/j150620a004.
(2) Bemand, P. P.; Clyne, M. A. A. Atomic resonance fluorescence for rate constants of rapid bimolecular reactions Part 6.-Hydrogen atom reactions: H + Cl2 from 300 to 730 K and H + NO2 at 298 K. *J. Chem. Soc. Faraday Trans. 2* **1977**, *73*, 394-405, doi:10.1039/F29777300394.
(3) Clyne, M. A. A.; Monkhouse, P. Atomic resonance fluorescence for rate constants of rapid bimolecular reactions Part 5-Hydrogen atom reactions; H + NO_2 and H + O_3. *J. Chem. Soc. Faraday Trans. 2* **1977**, *73*, 298-309, doi:10.1039/F29777300298.
(4) Ko, T.; Fontijn, A. High temperature photochemistry kinetics study of the reaction H + NO_2 → OH + NO from 286 to 760 K. *J. Phys. Chem.* **1991**, *95*, 3984-3987, doi:10.1021/j100163a019.
(5) Michael, J. V.; Nava, D. F.; Payne, W. A.; Lee, J. H.; Stief, L. J. Rate constant for the reaction H + NO_2 from 195 to 400 K with FP-RF and DF-RF techniques. *J. Phys. Chem.* **1979**, *83*, 2818-2823, doi:10.1021/j100485a003.
(6) Wagner, H. G.; Welzbacher, U.; Zellner, R. Rate measurements for reactions H + NO_2 → OH + NO and H + NOCl → HCl + NO by Lyman-α fluorescence. *Ber. Bunsenges. Phys. Chem.* **1976**, *80*, 1023-1027, doi:10.1002/bbpc.19760801018
(7) Wategaonkar, S. J.; Setser, D. W. Infrared chemiluminescence studies of H atom reactions with Cl_2O, ClNO, F_2O, CF_3OF, ClO_2, NO_2, and ClO. *J. Chem. Phys.* **1989**, *90*, 251-264, doi:10.1063/1.456527.

C6. **OH + NO_3.** The recommendation is derived from an unweighted average of the results of Boodaghians et al.[2] (298 K), Mellouki et al.[3] (298 K), Becker et al.[1] (298 K), and Mellouki et al.[4] (297 K). There are no temperature dependence data available and no recommendation is given. The reaction products are expected to be HO_2 + NO_2.
(Table: 19-5, Note: 19-5, Evaluated: 19-5) Back to Table

(1) Becker, E.; Rahman, M. M.; Schindler, R. N. Determination of the rate constants for the gas phase reactions of NO_3 with H, OH and HO_2 radicals at 298 K. *Ber. Bunsenges. Phys. Chem.* **1992**, *96*, 776-783, doi:10.1002/bbpc.19920960608.
(2) Boodaghians, R. B.; Canosa-Mas, C. E.; Carpenter, P. J.; Wayne, R. P. The reactions of NO_3 with OH and H. *J. Chem. Soc. Faraday Trans. 2* **1988**, *84*, 931-948, doi:10.1039/F29888400931.
(3) Mellouki, A.; Le Bras, G.; Poulet, G. Kinetics of the reactions of NO_3 with OH and HO_2. *J. Phys. Chem.* **1988**, *92*, 2229-2234, doi:10.1021/j100319a029.
(4) Mellouki, A.; Talukdar, R. K.; Bopegedera, A. M. R. P.; Howard, C. J. Study of the kinetics of the reactions of NO_3 with HO_2 and OH. *Int. J. Chem. Kinet.* **1993**, *25*, 25-39, doi:10.1002/kin.550250104.

C7. **OH + HONO.** The recommendation is derived from the temperature dependence measurements of Burkholder et al.[1] (298–373 K). The results from Jenkin and Cox[3] (278–342 K), which supersede the earlier room temperature study of Cox et al.,[2] obtained using a molecular modulation technique are in reasonable agreement with the Burkholder et al. results, but show a positive temperature dependence, E/R = 450 K. The direct measurements of Burkholder et al., who used on line diode array UV absorption measurements to quantify the HONO and NO_2 concentration in their slow flow pulsed laser photolysis-laser induced fluorescence experiments, are preferred. The recommended uncertainty factors encompass the results from both studies and reflect increased uncertainty at temperatures below the range of the available experimental data.
(Table: 19-5, Note: 19-5, Evaluated: 19-5) Back to Table

(1) Burkholder, J. B.; Mellouki, A.; Talukdar, R.; Ravishankara, A. R. Rate coefficients for the reaction of OH with HONO between 298 and 373 K. *Int. J. Chem. Kinet.* **1992**, *24*, 711-725, doi:10.1002/kin.550240805.
(2) Cox, R. A.; Derwent, R. G.; Holt, P. M. Relative rate constants for the reactions of OH radicals with H_2, CH_4, CO, NO and HONO at atmospheric pressure and 296 K. *J. Chem. Soc. Faraday Trans. 1* **1976**, *72*, 2031-2043, doi:10.1039/F19767202031.
(3) Jenkin, M. E.; Cox, R. A. Kinetics of the gas-phase reaction of OH with nitrous acid. *Chem. Phys. Lett.* **1987**, *137*, 548-552, doi:10.1016/0009-2614(87)80627-9.

C8. **OH + HO_2NO_2.** The available studies for this reaction show significant scatter and relatively poor agreement. The recommendation is based on the study of Jiménez et al.[3] (218–335 K, 10–100 Torr (He)), who provide a thorough study over a range of temperature and pressure and accounting of secondary contributions to the observed OH radical loss. Jiménez et al. used a pulsed laser photolysis-laser induced fluorescence technique with the HO_2NO_2 concentration measured on line using diode array UV absorption. H_2O_2, HNO_3, and NO_2 impurities in their HO_2NO_2 sample were measured on line using mass spectrometry and UV/IR absorption measurements. Corrections for the impurity contributions to the observed pseudo first-order rate coefficient were in the range 5–25%. The impurities contributed <10% to the overall uncertainty in the measured rate coefficient. The room temperature data of Trevor et al.[6] (246–324 K), Barnes et al.[1] (295 K), Smith et al.[5] (240–300 K), and Barnes et al.[2] (268–295 K) are 15–50% greater than the recommended value, but with the possible exception of Smith et al. agree to within the combined range of estimated absolute uncertainties. Trevor et al. reported a temperature invariant value of 4.0×10^{-12} cm^3 molecule^{-1} s^{-1}. Smith et al. observed a negative temperature dependence with an E/R value of –(650 ± 30) K in good agreement with the Jiménez et al. study. Jiménez et al. report a weak non-Arrhenius behavior that is described by the expression $k(T) = 8.8 \times 10^{-19}$ T^2 exp(1130/T) cm^3 molecule^{-1} s^{-1}. The early Barnes et al.[1] study was carried out at room temperature and 1 Torr total pressure, while their later study was performed in the pressure range 1–300 Torr N_2 and temperature range 268–295 K. Within this limited temperature range no rate coefficient temperature dependence was observed. In addition, k(298 K) derived in Barnes et al.[1] was revised upward in the later study from 4.1×10^{-12} to 5.0×10^{-12} cm^3 molecule^{-1} s^{-1} due to a change in the reference reaction rate coefficient. No rate coefficient pressure dependence was observed in the Barnes et al. and Jiménez et al. studies. The less precise value for k(298 K) reported by Littlejohn and Johnston[4] (298 K) is in fair agreement with the recommended value. The recommended uncertainty factors are sufficient to encompass all of the available experimental data.

Jiménez et al.[3] reported that the HO_2 + HNO_3 and NO_3 + H_2O_2 reaction product channels have yields of <10% and <5%, respectively, at 298 K. They deduce that the major reaction pathway leads to the formation of H_2O, O_2, and NO_2.
(Table 19-5, Note: 19-5, Evaluated: 19-5) Back to Table

(1) Barnes, I.; Bastian, V.; Becker, K. H.; Fink, E. H.; Zabel, F. Rate constant of the reaction of OH with HO_2NO_2. *Chem. Phys. Lett.* **1981**, *83*, 459-464, doi:10.1016/0009-2614(81)85501-7.
(2) Barnes, I.; Bastian, V.; Becker, K. H.; Fink, E. H.; Zabel, F. Pressure dependence of the reaction of OH with HO_2NO_2. *Chem. Phys. Lett.* **1986**, *123*, 28-32, doi:10.1016/0009-2614(86)87007-5.

(3) Jiménez, E.; Gierczak, T.; Stark, H.; Burkholder, J. B.; Ravishankara, A. R. Reaction of OH with HO_2NO_2 (Peroxynitric Acid, PNA): Rate coefficients between 218 and 335 K and product yields at 298 K. *J. Phys. Chem. A* **2004**, *108*, doi:10.1021/jp0363489, pp. 0361139-0361149.
(4) Littlejohn, D.; Johnston, H. S. Rate constant for the reaction of hydroxyl radicals and peroxynitric acid. *EOS* **1980**, *61*, 966.
(5) Smith, C. A.; Molina, L. T.; Lamb, J. J.; Molina, M. J. Kinetics of the reaction of OH with pernitric and nitric acids. *Int. J. Chem. Kinet.* **1984**, *16*, 41-55, doi:10.1002/kin.550160107.
(6) Trevor, P. L.; Black, G.; Barker, J. R. Reaction rate constant for OH + $HOONO_2$ → products over the temperature range 246 to 324 K. *J. Phys. Chem.* **1982**, *86*, 1661-1669, doi:10.1021/j100206a035.

C9. OH + NH_3. The recommended k(298 K) is the average of the values reported by Stuhl[10] (298 K), Smith and Zellner[8] (228–472 K), Perry et al.[6] (298, 348, 426 K), Silver and Kolb[7] (294–1075 K), Stephens[9] (297–364 K), and Diau et al.[2] (273–433 K). The values reported by Pagsberg et al.[5] (300 K) and Cox et al.[1] (296 K) were not considered because these studies involved the analysis of a complex mechanism and the results are well outside the error limits implied by the above six direct studies. The results of Kurylo[4] (298 K) and Hack et al.[3] (298–669 K) were not considered because of their large discrepancies with the other direct studies (factors of 3.9 and 1.6 at room temperature, respectively). The kinetic data displays non-Arrhenius behavior at temperatures >300 K. The recommended temperature dependence is based on the data below 300 K from the studies of Smith and Zellner and Diau et al. with the A-factor taken to yield the recommended room temperature value. The non-Arrhenius behavior is reasonably well reproduced between 228 and 500 by:

$$k(228–500\ \text{K}) = 2.55 \times 10^{-13}\ (\text{T}/298)^2\ \exp(150/\text{T})\ \text{cm}^3\ \text{molecule}^{-1}\ \text{s}^{-1}$$

and falls within the range of the recommended uncertainty factors.
(Table: 19-5, Note: 19-5, Evaluated: 19-5) Back to Table

(1) Cox, R. A.; Derwent, R. G.; Holt, P. M. The photo-oxidation of ammonia in the presence of NO and NO_2. *Chemosphere* **1975**, *4*, 201-205, doi:10.1016/0045-6535(75)90063-6.
(2) Diau, E. W.-G.; Tso, T.-L.; Lee, Y.-P. Kinetics of the reaction OH + NH_3 in the range 273-433 K. *J. Phys. Chem.* **1990**, *94*, 5261-5265, doi:10.1021/j100376a018.
(3) Hack, W.; Hoyermann, K.; Wagner, H. G. Gas phase reactions of hydroxyl radical with ammonia and hydrazine. *Ber. Bunsenges. Phys. Chem.* **1974**, *78*, 386-391, doi:10.1002/bbpc.19740780415
(4) Kurylo, M. J. Kinetics of the reactions OH(v=0) + NH_3 → H_2O + NH_2 and OH(v=0) + O_3 → HO_2 + O_2 at 298°K. *Chem. Phys. Lett.* **1973**, *23*, 467-471, doi:10.1016/0009-2614(73)89003-7.
(5) Pagsberg, P. B.; Erikson, J.; Christensen, H. C. Pulse radiolysis of gaseous ammonia-oxygen mixtures. *J. Phys. Chem.* **1979**, *83*, 582-590, doi:10.1021/j100468a006.
(6) Perry, R. A.; Atkinson, R.; Pitts, J. N., Jr. Rate constants for the reactions OH + H_2S → H_2O + SH and OH + NH_3 → H_2O + NH_2 over the temperature range 297-427 °K. *J. Chem. Phys.* **1976**, *64*, 3237-3239, doi:10.1063/1.432663.
(7) Silver, J. A.; Kolb, C. E. Rate constant for the reaction NH_3 + OH → NH_2 + H_2O over a wide temperature range. *Chem. Phys. Lett.* **1980**, *75*, 191-195, doi:10.1016/0009-2614(80)80492-1.
(8) Smith, I. W. M.; Zellner, R. Rate measurements of OH by resonance absorption. IV. Reactions of OH with NH_3 and HNO_3. *Int. J. Chem. Kinet. Symp. No. 1* **1975**, 341-351.
(9) Stephens, R. D. Absolute rate constants for the reaction of hydroxyl radicals with ammonia from 297 to 364 K. *J. Phys. Chem.* **1984**, *88*, 3308-3313, doi:10.1021/j150659a034.
(10) Stuhl, F. Absolute rate constant for the reaction OH + NH_3 → NH_2 + H_2O. *J. Chem. Phys.* **1973**, *59*, 635-637, doi:10.1063/1.1680069.

C10. HO_2 +NO. The recommendation for the HO_2 + NO reaction is based on the average of eight measurements of the rate coefficient: Howard and Evenson[7] (296 K), Howard[6] (232–363 K), Hack et al.[5] (293 K), Jemi-Alade and Thrush[9] (297 K), Seeley et al.[12] (206–293 K), Bohn and Zetsch[2] (298 K), and Bardwell et al[1] (193–298 K). All of these studies are in quite good agreement. The results of Imamura and Washida[8] (298 K) and Leu[10] (269–426 K) were not considered due to the relatively large reported uncertainty limits. The result from Burrows et al.[3] (298 K) has been disregarded because of an error in the reference rate coefficient, k(OH + H_2O_2). The study of Rozenshtein et al.[11] (298 K) has been disregarded due to an inadequate treatment of possible secondary reactions. The Glaschick-Schimpf et al.[4] (298 K) result was not considered because of complications associated with the HO_2 detection method. The relative rate data of Thrush and Wilkinson[13] (298 K) was superseded by Jemi-Alade and Thrush[9] from the same laboratory and not included in the recommendation analysis. The recommended Arrhenius parameters are obtained from a fit to all the accepted data after normalization to the recommended k(298 K) value.
(Table: 19-5, Note: 19-5, Evaluated: 19-5) Back to Table

(1) Bardwell, M. W.; Bacak, A.; Raventos, M. T.; Percival, C. J.; Sanchez-Reyna, G.; Shallcross, D. E. Kinetics of the HO_2 + NO reaction: A temperature and pressure dependence study using chemical ionisation mass spectrometry. *Phys. Chem. Chem. Phys.* **2003**, *5*, 2381-2385, doi:10.1039/b300842h.
(2) Bohn, B.; Zetzsch, C. Rate constants of HO_2 + NO covering atmospheric conditions. 1. HO_2 formed by OH + H_2O_2. *J. Phys. Chem. A* **1997**, *101*, 1488-1493, doi:10.1021/jp961396x.
(3) Burrows, J. P.; Cliff, D. I.; Harris, G. W.; Thrush, B. A.; Wilkinson, J. P. T. Atmospheric reactions of the HO_2 radical studied by laser magnetic-resonance spectroscopy. *Proc. Roy. Soc. Lond. A.* **1979**, *368*, 463-481, doi:10.1098/rspa.
(4) Glaschick-Schimpf, I.; Leiss, A.; Monkhouse, P. B.; Schurath, U.; Becker, K. H.; Fink, E. H. A kinetic study of the reactions of HO_2/DO_2 radicals with niric oxide using near-infrared chemiluminescence detection. *Chem. Phys. Lett.* **1979**, *67*, 318-323, doi:10.1016/0009-2614(79)85170-2.
(5) Hack, W.; Preuss, A. W.; Temps, F.; Wagner, H. G.; Hoyermann, K. Direct determination of the rate constant of the reaction NO + HO_2 → NO_2 + OH with the LMR. *Int. J. Chem. Kinet.* **1980**, *12*, 851-860, doi:10.1002/kin.550121104.
(6) Howard, C. J. Temperature dependence of the reaction HO_2 + NO → OH + NO_2. *J. Chem. Phys.* **1979**, *71*, 2352-2359, doi:10.1063/1.438639.
(7) Howard, C. J.; Evenson, K. M. Kinetics of the reaction of HO_2 with NO. *Geophys. Res. Lett.* **1977**, *4*, 437-440, doi:10.1029/GL004i010p00437.
(8) Imamura, T.; Washida, N. Measurements of rate constants for HO_2 + NO and NH_2 + NO reactions by time-resolved photoizonization mass spectrometry. *Laser Chem.* **1995**, *16*, 43-51.
(9) Jemi-Alade, A. A.; Thrush, B. A. Reactions of HO_2 with NO and NO_2 studied by mid-infrared laser magnetic resonance. *J. Chem. Soc. Faraday Trans.* **1990**, *86*, 3355-3363, doi:10.1039/FT9908603355
(10) Leu, M. T. Rate constant for the reaction HO_2 + NO → OH + NO_2. *J. Chem. Phys.* **1979**, *70*, 1662-1666, doi:10.1063/1.437680.
(11) Rozenshtein, V. B.; Gershenzon, Y. M.; Il'in, S. D.; Kishkovitch, O. P. Reactions of HO_2 with NO, OH and HO_2 studied by EPR/LMR spectroscopy. *Chem. Phys. Lett.* **1984**, *112*, 473-478, doi:10.1016/0009-2614(84)85572-4.
(12) Seeley, J. V.; Meads, R. F.; Elrod, M. J.; Molina, M. J. Temperature and pressure dependence of the rate constant for the HO_2 + NO reaction. *J. Phys. Chem.* **1996**, *100*, 4026-4031, doi:10.1021/jp952553f.
(13) Thrush, B. A.; Wilkinson, J. P. T. The rate of reaction of HO_2 radicals with HO and with NO. *Chem. Phys. Lett.* **1981**, *81*, 1-3, doi:10.1016/0009-2614(81)85314-6.

C11. NO_2* + H_2O. The reaction of NO_2 with H_2O to produce OH and HONO is endothermic by about 40 kcal $mole^{-1}$ (ground state reactants and products). However, absorption of light by NO_2 at wavelengths less than 718 nm can exceed the thermodynamic threshold if all the NO_2 internal energy is available for reaction. Crowley and Carl[2] photolyzed NO_2/H_2O mixtures in the 430–450 nm spectral region and observed an OH action spectrum that mimicked the absorption features of NO_2. Because the dependence of the OH signal on photolysis laser energy was second order, they suggested that two-photon absorption of NO_2 produced $O(^1D)$ in their experiment which reacted with water vapor to produce OH. The energetic threshold for $O(^1D)$ production is 488 nm. When they performed the same experiment with 532 nm photolysis, no OH production was observed giving an upper limit for the OH branching fraction (reactive vs. unreactive quenching) of 7×10^{-5}. Li et al.[3] carried out laser pump/probe experiments at photolysis wavelengths between 560 and 640 nm in NO_2/H_2O mixtures. In contrast to Crowley and Carl, they found significant OH production in this wavelength range. Their experiments showed a unity slope dependence of OH production on laser energy, suggesting a one-photon process. Overtone pumping was used to check for the presence of HONO and HNO_3, which might be the source of the observed OH radicals. The rate constant for the NO_2* + H_2O reaction was determined to be 1.7×10^{-13} cm^3 $molecule^{-1}$ s^{-1} for NO_2 excitation at 565, 590 and 612.5 nm with an overall uncertainty of ±50%. This is large enough to have a significant impact on HO_x production in the troposphere. Carr et al.[1] performed a laser pump/probe experiment at 567.5 and 563.5 nm in NO_2/H_2O mixtures. These experiments failed to detect OH formation, resulting in an upper limit of 6×10^{-5} for the reactive branching fraction.

Although this reaction is potentially important, in view of the disagreement in the published results, the Panel makes no recommendation on this reaction until additional credible studies are carried out.
(Table: 10-6, Note: 10-6, Evaluated: 10-6) Back to Table

(1) Carr, S.; Heard, D. E.; Blitz, M. A. Comment on "Atmospheric hydroxyl radical production from electronically excited NO_2 and H_2O". *Science* **2009**, *324*, 336b, doi:10.1126/science.1166669.
(2) Crowley, J. N.; Carl, S. A. OH formation in the photoexcitation of NO_2 beyond the dissociation threshold in the presence of water vapor. *J. Phys. Chem. A* **1997**, *101*, 4178-4184, doi:10.1021/jp970319e.

(3) Li, S. P.; Matthews, J.; Sinha, A. Atmospheric hydroxyl radical production from electronically excited NO_2 and H_2O. *Science* **2008**, *319*, 1657-1660, doi:10.1126/science.1151443.

C12. $HO_2 + NO_2$. Tyndall et al.[2] (296 K) obtained an upper-limit to the rate coefficient for the HONO + O_2 product channel of 5×10^{-16} cm^3 $molecule^{-1}$ s^{-1} based on photolysis experiments at 760 Torr of N_2 in an environmental chamber with FTIR analysis. The results from this study are the basis of the recommendation. Dransfield et al.[1](296 K) reported no detectable HONO formation in a discharge-flow experiment with FTIR detection at 120 Torr of N_2 that is consistent with the Tyndall et al. results.
(Table: 19-5, Note: 19-5, Evaluated: 19-5) Back to Table

(1) Dransfield, T. J.; Donahue, N. M.; Anderson, J. G. High-pressure flow reactor product study of the reactions of HO_x + NO_2: The role of vibrationally excited intermediates. *J. Phys. Chem. A* **2001**, *105*, 1507-1514, doi:10.1021/jp002391+.
(2) Tyndall, G. S.; Orlando, J. J.; Calvert, J. G. Upper limit for the rate coefficient for the reaction HO_2 + NO_2 → HONO + O_2. *Environ. Sci. Technol.* **1995**, *29*, 202-206, doi:10.1021/es00001a026.

C13. $HO_2 + NO_3$. The recommended k(298 K) is based on a weighted average of the data of Hall et al.[2] (263–343 K), Mellouki et al.[3] (298 K), Becker et al.[1] (298 K), and Mellouki et al.[4] (297 K). There are insufficient data on which to base the temperature dependence of the rate coefficient. The measured branching ratios for the OH + NO_2 + O_2 channel range from 0.57 to 1.0. The most direct measurement is derived from the study of Mellouki et al.,[4] which obtained a value of 1.0 +0.0/–0.3 at 298 K**.**
(Table: 94-26, Note: 94-26, Evaluated: 19-5) Back to Table

(1) Becker, E.; Rahman, M. M.; Schindler, R. N. Determination of the rate constants for the gas phase reactions of NO_3 with H, OH and HO_2 radicals at 298 K. *Ber. Bunsenges. Phys. Chem.* **1992**, *96*, 776-783, doi:10.1002/bbpc.19920960608.
(2) Hall, I. W.; Wayne, R. P.; Cox, R. A.; Jenkin, M. E.; Hayman, G. D. Kinetics of the reaction of NO_3 with HO_2. *J. Phys. Chem.* **1988**, *92*, 5049-5054, doi:10.1021/j100328a043.
(3) Mellouki, A.; Le Bras, G.; Poulet, G. Kinetics of the reactions of NO_3 with OH and HO_2. *J. Phys. Chem.* **1988**, *92*, 2229-2234, doi:10.1021/j100319a029.
(4) Mellouki, A.; Talukdar, R. K.; Bopegedera, A. M. R. P.; Howard, C. J. Study of the kinetics of the reactions of NO_3 with HO_2 and OH. *Int. J. Chem. Kinet.* **1993**, *25*, 25-39, doi:10.1002/kin.550250104.

C14. $HO_2 + NH_2$. The 298 K relative rate studies of Cheskis and Sarkisov[1] and Pagsberg et al.[2] differ by nearly a factor of three. The recommended k(298 K) value is the average of the values reported in these studies. There are no temperature dependence studies available and no recommendation is given. The identity of the products is not known; however, it is suggested that the most probable reaction channels give either NH_3 + O_2 or HNO + H_2O as products.
(Table: 19-5, Note: 19-5, Evaluated: 19-5) Back to Table

(1) Cheskis, S. G.; Sarkisov, O. M. Flash photolysis of ammonia in the presence of oxygen. *Chem. Phys. Lett.* **1979**, *62*, 72-76, doi:10.1016/0009-2614(79)80415-7.
(2) Pagsberg, P. B.; Erikson, J.; Christensen, H. C. Pulse radiolysis of gaseous ammonia-oxygen mixtures. *J. Phys. Chem.* **1979**, *83*, 582-590, doi:10.1021/j100468a006.

C15. $N + O_2$. The recommended expression is derived from the data of Kistiakowsky and Volpi[5] (394–516 K), Wilson[7] (300–910 K), Becker et al.[2] (280–333 K), Westenberg et al.[6] (298 K), Clark and Wayne[3] (298 K), Winkler et al.[8] (298 K), Barnett et al.[1] (298 K), and Fernandez et al.[4] (404–1221 K). The rate coefficient data displays a non-Arrhenius behavior between 300 and 1200 K and the recommended Arrhenius expression was obtained from the experimental data at temperatures less than 500 K. k(298 K) is derived from the Arrhenius expression and is in agreement with the determinations at room temperature.
(Table: 25-1, Note: 19-5, Evaluated: 19-5) Back to Table

(1) Barnett, A. J.; Marston, G.; Wayne, R. P. Kinetics and chemiluminescence in the reaction of N atoms with O_2 and O_3. *J. Chem. Soc. Faraday Trans. 2* **1987**, *83*, 1453-1463, doi:10.1039/F29878301453.
(2) Becker, K. H.; Groth, W.; Kley, D. The rate constant of the aeronomic reaction N + O_2. *Z. Naturforsch* **1969**, *A24*, 1280-1281.
(3) Clark, I. D.; Wayne, R. P. Kinetics of the reaction between atomic nitrogen and molecular oxygen in the ground ($^3\Sigma_g^-$) and first excited ($^1\Delta_g$) states. *Proc. Roy. Soc. Lond. A.* **1970**, *316*, 539-550, doi:10.1098/rspa.1970.0095.
(4) Fernandez, A.; Goumri, A.; Fonijin, A. Kinetics of the reactions of N(^{4}S) atoms with O_2 and CO_2 over wide temperatures ranges. *J. Phys. Chem. A* **1998**, *102*, 168–172, doi:10.1021/jp972365k.

(5) Kistiakowsky, G. B.; Volpi, G. G. Reactions of nitrogen atoms. I. Oxygen and oxides of nitrogen. *J. Chem. Phys.* **1957**, *27*, 1141-1149, doi:10.1063/1.1743946.
(6) Westenberg, A. A.; Roscoe, J. M.; deHaas, N. Rate measurements on N + $O_2(^1\Delta_g)$ → NO + O and H + $O_2(^1\Delta_g)$ → OH + O. *Chem. Phys. Lett.* **1970**, *7*, 597-599, doi:10.1016/0009-2614(70)87014-2.
(7) Wilson, W. E. Rate constant for the reaction N + O_2 → NO + O. *J. Chem. Phys.* **1967**, *46*, 2017-2018, doi:10.1063/1.1840988.
(8) Winkler, I. C.; Stachnik, R. A.; Steinfeld, J. I.; Miller, S. M. Determination of NO (v = 0-7) product distribution from the N(^{4}S) + O_2 reaction using two-photon ionization. *J. Chem. Phys.* **1986**, *85*, 890-899, doi:10.1063/1.451840.

C16. **N + O_3.** The recommendation is based on the results of Barnett et al.[1] (298 K). The value of (1.0 ± 0.2) × 10^{-16} cm^3 $molecule^{-1}$ s^{-1} reported by Barnett et al. is considered an upper-limit rather than a determination. The low values reported by Barnett et al., Stief et al.[5] (298 K), and Garvin and Broida[3] cast doubt on the much greater rate coefficients reported by Phillips and Schiff[4] (298 K) and Chen and Taylor[2] (298 K).
(Table: 90-1, Note: 19-5, Evaluated: 19-5) Back to Table

(1) Barnett, A. J.; Marston, G.; Wayne, R. P. Kinetics and chemiluminescence in the reaction of N atoms with O_2 and O_3. *J. Chem. Soc. Faraday Trans. 2* **1987**, *83*, 1453-1463, doi:10.1039/F29878301453.
(2) Chen, M. C.; Taylor, H. A. Reaction of nitrogen atoms with ozone. *J. Chem. Phys.* **1961**, *34*, 1344-1347, doi:10.1063/1.1731742.
(3) Garvin, D.; Broida, H. P. "Atomic flame reactions involving N atoms, H atoms and ozone"; 9th Symposium (Int.) on Combustion, 1963.
(4) Phillips, L. F.; Schiff, H. I. Mass spectrometer studies of atoms reactions. I. Reactions in the atomic nitrogen-ozone system. *J. Chem. Phys.* **1962**, *36*, 1509-1517, doi:10.1063/1.1732772.
(5) Stief, L. J.; Payne, W. A.; Lee, J. H.; Michael, J. V. The reaction N(^4S) + O_3: An upper limit for the rate constant at 298 K. *J. Chem. Phys.* **1979**, *70*, 5241-5243, doi:10.1063/1.437317.

C17. **N + NO.** The recommended temperature dependence is based on the discharge flow-resonance fluorescence studies of Wennberg and Anderson[16] (213–339 K), flash photolysis-resonance fluorescence study of Lee et al.[10] (196–370 K), and the discharge flow-resonance fluorescence study of Papanastasiou et al.[13] (225–344 K). There is agreement between these studies and the more recent work of Nakayama et al.[12] (295 K). There is relatively poor agreement between these studies and the results of Clyne and McDermid[4] (298–670 K), Kistiakowsky and Volpi[9] (298 K, lower-limit), Herron[6] (298 K), Phillips and Schiff[14] (298 K), Lin et al.[11] (298 K), Sugawara et al.[15] (298 K), Cheah and Clyne[3] (298 K), Husain and Slater[7] (300 K), Clyne and Ono[5] (298 K), Brunning and Clyne[2] (289 K), Jeoung et al.[8] (298 K), and Bergeat et al.[1] (48–211 K).

The reaction displays a slight non-Arrhenius behavior at temperatures greater than 300 K that is represented by:

$$k(195–500\ K) = 1.3 \times 10^{-15}\ T^{1.5} \exp(500/T)$$

(Table: 25-1, Note: 25-1, Evaluated: 25-1) Back to Table

(1) Bergeat, A. H., K. M.; Daugey, N.; Caubet, P.; Costes, M. A low temperature investigation of the N($^4S^0$) + NO reaction. *Phys. Chem. Chem. Phys.* **2009**, *11*, 8149–8155, doi:10.1039/b905702a.
(2) Brunning, J.; Clyne, M. A. A. Elementary reactions of the SF radical Part 1.-Rate constants for the reactions F + OCS → SF + CO and SF + SF → SF_2 + S. *J. Chem. Soc. Faraday Trans 2* **1984**, *80*, 1001-1014, doi:10.1039/F29848001001.
(3) Cheah, C. T.; Clyne, M. A. A. Reactions forming electronically-excited free radicals Part 2.-Formation of N^{4}S, N ^{2}D and N ^{2}P atoms in the H + NF_2 reaction, and N atom reactions. *J. Chem. Soc. Faraday Trans. II* **1980**, *76*, 1543-1560, doi:10.1039/F29807601543.
(4) Clyne, M. A. A.; McDermid, I. S. Mass spectrometric determinations of the rates of elementary reactions of NO and of NO_2 with ground state N ^4S atoms. *J. Chem. Soc. Faraday Trans. 1* **1975**, *71*, 2189-2202, doi:10.1039/F19757102189.
(5) Clyne, M. A. A.; Ono, Y. Determination of the rate constant of reaction of N($^4S_{3/2}$) with NO_2 using resonance fluorescence in a discharge flow system. *Chem. Phys.* **1982**, *69*, 381-388, doi:10.1016/0301-0104(82)88077-4.
(6) Herron, J. T. Rate of the reaction NO + N. *J. Chem. Phys.* **1961**, *35*, 1138-1139, doi:10.1063/1.1701202.
(7) Husain, D.; Slater, N. K. H. Kinetic study of ground state atomic nitrogen, N($2^4S_{3/2}$), by time-resolved atomic resonance fluorescence. *J. Chem. Soc. Faraday Trans. II* **1980**, *76*, 606-619, doi:10.1039/F29807600606.

(8) Jeoung, S. C.; Choo, K. Y.; Benson, S. W. Very low pressure reactor chemiluminescence studies on N atom reactions with $CHCl_3$ and $CDCl_3$. *J. Phys. Chem.* **1991**, *95*, 7282-7290, doi:10.1021/j100172a035.
(9) Kistiakowsky, G. B.; Volpi, G. G. Reactions of nitrogen atoms. II. H_2, CO, NH_3, NO, and NO_2. *J. Chem. Phys.* **1958**, *28*, 665-668, doi:10.1063/1.1744209.
(10) Lee, J. H.; Michael, J. V.; Payne, W. A., Jr.; Stief, L. J. Absolute rate of the reaction of N(^4S) with NO from 196-400 K with DF-RF and FP-RF techniques. *J. Chem. Phys.* **1978**, *69*, 3069-3076, doi:10.1063/1.436998.
(11) Lin, C.-L.; Parkes, D. A.; Kaufman, F. Oscillator strength of the resonance transitions of ground-state N and O. *J. Chem. Phys.* **1970**, *53*, 3896-3900, doi:10.1063/1.1673858.
(12) Nakayama, T. T., K.; Matsumi, Y.; Shibuya K. N(^{4}S) Formation following the 193.3-nm ArF laser irradiation of NO and NO_2 and its application to kinetic studies of N(^{4}S) reactions with NO and NO_2. *J. Phys. Chem. A* **2005**, *109*, 10897–10902, doi:10.1021/jp054089c.
(13) Papanastasiou, D. K.; Bourgalais, J.; Gierczak, T.; Burkholder, J. B. N($^4S_{3/2}$) reaction with NO and NO_2: Temperature dependent rate coefficients and O(^{3}P) product yield. *Chem. Phys. Lett.* **2019**, *728*, 102-108, doi:10.1016/j.cplett.2019.04.081.
(14) Phillips, L. F.; Schiff, H. I. Mass spectrometer studies of atoms reactions. I. Reactions in the atomic nitrogen-ozone system. *J. Chem. Phys.* **1962**, *36*, 1509-1517, doi:10.1063/1.1732772.
(15) Sugawara, K.; Ishikawa, Y.; Sato, S. The rate constants of the reactions of the metastable nitrogen atoms, ^{2}D and ^{2}P, and the reactions of N(^{4}S) + NO → N_2 + O(^{3}P) and O(^{3}P) + NO + M → NO_2 + M. *Bull. Chem. Soc. Jpn.* **1980**, *53*, 3159-3164, doi:10.1246/bcsj.53.3159.
(16) Wennberg, P. O.; Anderson, J. G.; Weisenstein, D. K. Kinetics of reactions of ground state nitrogen atoms ($^4S_{3/2}$) with NO and NO_2. *J. Geophys. Res.* **1994**, *99*, 18839-18846, doi:10.1029/94JD01823.

C18. N + NO_2. The recommended k(298 K) is from the discharge flow-resonance fluorescence studies of Wennberg and Anderson[7] (223–366 K) and Papanastasiou et al.[6] (216–296 K). These studies had significantly better sensitivity for N(^{4}S) than the 293 K discharge flow-resonance fluorescence study of Clyne and Ono,[2] which reported a value about four times smaller. The room temperature study of Nakayama et al.[5] (295 K) reports k(298 K) a factor of 1.6 lower than that of Wennberg and Anderson and Papanastasiou et al. The results of Husain and Slater[3] (298 K) and Clyne and McDermid[1] (298 K) are not considered. The temperature dependence is obtained from the combined Wennberg and Anderson and Papanastasiou et al. studies. Papanastasiou et al. report a O(^{3}P) reaction product yield of 0.66 ± 0.06., while Wennberg and Anderson and Clyne and McDermid report atomic oxygen to be the principal reaction product. A study by Iwata et al.[4] suggested an upper limit of 3.3×10^{-13} cm^3 molecule^{-1} s^{-1} for the corresponding reaction involving N(^{2}D) and N(^{2}P) atoms (sum of all reaction channels).
(Table: 25-1, Note: 25-1, Evaluated: 25-1) Back to Table

(1) Clyne, M. A. A.; McDermid, I. S. Mass spectrometric determinations of the rates of elementary reactions of NO and of NO_2 with ground state N ^4S atoms. *J. Chem. Soc. Faraday Trans. 1* **1975**, *71*, 2189-2202, doi:10.1039/F19757102189.
(2) Clyne, M. A. A.; Ono, Y. Determination of the rate constant of reaction of N($^4S_{3/2}$) with NO_2 using resonance fluorescence in a discharge flow system. *Chem. Phys.* **1982**, *69*, 381-388, doi:10.1016/0301-0104(82)88077-4.
(3) Husain, D.; Slater, N. K. H. Kinetic study of ground state atomic nitrogen, N($2^4S_{3/2}$), by time-resolved atomic resonance fluorescence. *J. Chem. Soc. Faraday Trans. II* **1980**, *76*, 606-619, doi:10.1039/F29807600606.
(4) Iwata, R.; Ferrieri, R. A.; Wolf, A. P. Rate constant determination of the reaction of metastable N(^{2}D,^{2}P) with NO_2 using moderated nuclear recoil atoms. *J. Phys. Chem.* **1986**, *90*, 6722-6726, doi:10.1021/j100283a027.
(5) Nakayama, T.; K., T.; Matsumi, Y.; K., S. N(^{4}S) formation following the 193.3-nm ArF laser irradiation of NO and NO_2 and its application to kinetic studies of N(^{4}S) reactions with NO and NO_2. *J. Phys. Chem. A* **2005**, *109*, 10897–10902, doi:10.1021/jp054089c.
(6) Papanastasiou, D. K.; Bourgalais, J.; Gierczak, T.; Burkholder, J. B. N($^4S_{3/2}$) reaction with NO and NO_2: Temperature dependent rate coefficients and O(^{3}P) product yield. *Chem. Phys. Lett.* **2019**, *728*, 102-108, doi:10.1016/j.cplett.2019.04.081.
(7) Wennberg, P. O.; Anderson, J. G.; Weisenstein, D. K. Kinetics of reactions of ground state nitrogen atoms ($^4S_{3/2}$) with NO and NO_2. *J. Geophys. Res.* **1994**, *99*, 18839-18846, doi:10.1029/94JD01823.

C19. NO + O_3. The recommended values are based on the results of studies over a range of temperatures by Birks et al.[2] (203.5–361 K), Lippmann et al.[5] (283–443 K), Ray and Watson[8] (212–422 K), Michael et al.[6] (195–369 K), Borders and Birks[3] (203.8–353.2 K), and Moonen et al.[7] (298–328 K) and the room temperature studies of

Stedman and Niki[10] and Bemand et al.[1] The six temperature-dependent studies were given equal weighting in the recommendation by averaging over the E/R's from each individual data set. Following the Moonen et al. recommendation, their 200 K data point was excluded. All of the temperature dependence studies show some non-Arrhenius behavior, although increasing scatter between the data sets is evident at the lower temperatures. The non-Arrhenius behavior, between 204 and 440 K, is described well by the expression:

$$k(204\text{–}440\text{ K}) = 3.32 \times 10^{-13} \times (T/298)^{2.25} \times \exp(-850/T)\text{ cm}^3\text{ molecule}^{-1}\text{ s}^{-1}$$

This non-Arrhenius parameterization falls within the recommended range of uncertainty for temperatures less than 300 K.

Clough and Thrush,[4] Birks et al., Schurath et al.[9] (283–433 K), and Michael et al. have reported individual Arrhenius parameters for the two primary reaction channels producing ground and excited molecular oxygen. (Table: 19-5, Note: 19-5, Evaluated: 19-5) Back to Table

(1) Bemand, P. P.; Clyne, M. A. A.; Watson, R. T. Atomic resonance fluorescence and mass spectrometry for measurements of the rate constants for elementrary reactions: O ^3P_J + NO_2 → NO + O_2 and NO + O_3 → NO_2 + O_2. *J. Chem. Soc. Faraday Trans. 2* **1974**, *70*, 564-576, doi;10.1039/F29747000564.

(2) Birks, J. W.; Shoemaker, B.; Leck, T. J.; Hinton, D. M. Studies of reactions of importance in the stratosphere. I. Reaction of nitric oxide with ozone. *J. Chem. Phys.* **1976**, *65*, 5181-5185, doi:10.1063/1.433059.

(3) Borders, R. A.; Birks, J. W. High-precision measurements of activation energies over small temperature intervals: Curvature in the Arrhenius plot for the reaction NO + O_3 → NO_2 + O_2. *J. Phys. Chem.* **1982**, *86*, 3295-3302, doi:10.1021/j100214a007.

(4) Clough, P. N.; Thrush, B. A. Mechanism of chemiluminescent reaction between nitric oxide and ozone. *Trans. Faraday Soc.* **1967**, *63*, 915-925, doi:10.1039/TF9676300915.

(5) Lippmann, H. H.; Jesser, B.; Schurath, U. The rate constant of NO + O_3 → NO_2 + O_2 in the temperature range of 283–443 K. *Int. J. Chem. Kinet.* **1980**, *12*, 547-554, doi:10.1002/kin.550120805.

(6) Michael, J. V.; Allen, J. E., Jr.; Brobst, W. D. Temperature dependence of the NO + O_3 reaction rate from 195 to 369 K. *J. Phys. Chem.* **1981**, *85*, 4109-4117, doi:10.1021/j150626a032.

(7) Moonen, P. C.; Cape, J. N.; Storeton-West, R. L.; McColm, R. Measurement of the NO + O_3 reaction rate at atmospheric pressure using realistic mixing ratios. *J. Atmos. Chem.* **1998**, *29*, 299-314, doi:10.1023/A:100593601.

(8) Ray, G. W.; Watson, R. T. Kinetics of the reaction NO + O_3 → NO_2 + O_2 from 212 to 422 K. *J. Phys. Chem.* **1981**, *85* 1673-1676, doi:10.1021/j150612a015.

(9) Schurath, U.; Lippmann, H. H.; Jesser, B. Temperature dependence of the chemiluminescent reaction (1), NO + O_3 → $NO_2(^2A_1\text{-}^2B_{1,2})$ + O_2, and quenching of the excited product. *Ber. Bunsenges. Phys. Chem.* **1981**, *85*, 807-813, doi:10.1002/bbpc.19810850814.

(10) Stedman, D. H.; Niki, H. Kinetics and mechanism for the photolysis of nitrogen dioxide in air. *J. Phys. Chem.* **1973**, *77*, 2604-2609, doi:10.1021/j100640a005.

C20. NO + NO_3. The recommendation is based on the temperature dependent studies of Hammer et al.[2] (209–410 K), Sander and Kircher[3] (224–328 K), and Tyndall et al.[4] (223–353 K) and the room temperature study of Brown et al.,[1] which are in good agreement. The recommended temperature dependence is taken from an unweighted linear least-squares fit of the data from the three temperature dependence studies after scaling to the recommended k(298 K) value. The A-factor was adjusted to agree with the recommended k(298 K) value. (Table: 19-5, Note: 19-5, Evaluated: 19-5) Back to Table

(1) Brown, S. S.; Ravishankara, A. R.; Stark, H. Simultaneous kinetics and ring-down: Rate coefficients from single cavity loss temporal profiles. *J. Phys. Chem. A* **2000**, *104*, 7044-7052, doi:10.1021/jp0013715.

(2) Hammer, P. D.; Dlugokencky, E. J.; Howard, C. J. Kinetics of the gas-phase reaction NO + NO_3 → 2NO_2. *J. Phys. Chem.* **1986**, *90*, 2491-2496, doi:10.1021/j100402a045.

(3) Sander, S. P.; Kircher, C. C. Temperature dependence of the reaction NO + NO_3 → 2NO_2. *Chem. Phys. Lett.* **1986**, *126*, 149-152, doi:10.1016/S0009-2614(86)80029-X.

(4) Tyndall, G. S.; Orlando, J. J.; Cantrell, C. A.; Shetter, R. E.; Calvert, J. G. Rate coefficient for the reaction NO + NO_3 → 2NO_2 between 223 and 400 K. *J. Phys. Chem.* **1991**, *95*, 4381-4386, doi:10.1021/j100164a040.

C21. NO_2 + O_3. The recommended expression is derived from a least squares fit to the data of Davis et al.[2] (260–343 K), Graham and Johnston[3] (231–298 K), Huie and Herron[4] (259–362 K), and Cox and Coker[1] (298 K). The data of Verhees and Adema[6] (277–340 K) and Stedman and Niki[5] (298 K) were not considered because of systematic discrepancies with the other studies.

(Table: 90-1, Note: 19-5, Evaluated: 19-5) Back to Table

(1) Cox, R. A.; Coker, G. B. Kinetics of the reaction of nitrogen dioxide with ozone. *J. Atmos. Chem.* **1983**, *1*, 53-63.
(2) Davis, D. D.; Prusazcyk, J.; Dwyer, M.; Kim, P. A stop-flow time-of-flight mass spectrometry kinetics study. Reaction of ozone with nitrogen dioxide and sulfur dioxide. *J. Phys. Chem.* **1974**, *78*, 1775-1779, doi:10.1021/j100611a001.
(3) Graham, R. A.; Johnston, H. S. Kinetics of the gas-phase reaction between ozone and nitrogen dioxide. *J. Chem. Phys.* **1974**, *60*, 4628-4629, doi:10.1063/1.1680953.
(4) Huie, R. E.; Herron, J. T. The rate constant for the reaction $O_3 + NO_2 \rightarrow O_2 + NO_3$ over the temperature range 259-362 °K. *Chem. Phys. Lett.* **1974**, *27*, 411-414, doi:10.1016/0009-2614(74)90253-X.
(5) Stedman, D. H.; Niki, H. Kinetics and mechanism for the photolysis of nitrogen dioxide in air. *J. Phys. Chem.* **1973**, *77*, 2604-2609, doi:10.1021/j100640a005.
(6) Verhees, P. W. C.; Adema, E. H. The NO_2-O_3 system at sub-ppm concentrations: Influence of temperature and relative humidity. *J. Atmos. Chem.* **1985**, *2*, 387-403, doi:10.1007/BF00130750.

C22. **$NO_2 + NO_3$.** The existence of the reaction channel forming $NO + NO_2 + O_2$ has not been firmly established. However, studies of N_2O_5 thermal decomposition that monitor NO_2 (Daniels and Johnston[3] (288–338 K); Johnston and Tao[5] (338–396 K); Cantrell et al.[1] (243–397 K), and Wangberg et al.[6] (296–332 K)) and NO (Hjorth et al.[4] (296 K), Cantrell et al.[2] (273–313 K), and Wangberg et al.[6] (296–332 K)) require reaction(s) that decompose NO_3 into $NO + O_2$. The rate coefficient from the first three studies is obtained from the product kK_{eq}, where K_{eq} is the equilibrium constant for $NO_2 + NO_3 \rightarrow N_2O_5$, while for the latter two studies the rate coefficient is obtained from the ratio $k/k(NO + NO_3)$, where $k(NO + NO_3)$ is the rate constant for the reaction $NO + NO_3 \rightarrow 2NO_2$. Using K_{eq} and $k(NO + NO_3)$ from this evaluation, 4.35×10^{-14} exp (–1335/T) cm^3 $molecule^{-1}$ s^{-1} represents the available experimental data reasonably well. An overall uncertainty factor of 2 is recommended.
(Table: 25-1, Note: 19-5, Evaluated: 19-5) Back to Table

(1) Cantrell, C. A.; Davidson, J. A.; McDaniel, A. H.; Shetter, R. E.; Calvert, J. G. The equilibrium constant for $N_2O_5 \rightleftarrows NO_2 + NO_3$: Absolute determination by direct measurement from 243 to 397 K. *J. Chem. Phys.* **1988**, *88*, 4997-5006, doi:10.1063/1.454679.
(2) Cantrell, C. A.; Shetter, R. E.; McDaniel, A. H.; Calvert, J. G. The rate coefficient for the reaction $NO_2 + NO_3 \rightarrow NO + NO_2 + O_2$ from 273 to 313 K. *J. Geophys. Res.* **1990**, *95*, 20531-20537, doi:10.1029/JD095iD12p20531.
(3) Daniels, F.; Johnston, E. H. The thermal decomposition of gaseous nitrogen pentoxide. A monomolecular reaction. *J. Am. Chem. Soc.* **1921**, *43*, 53-71, doi:10.1021/ja01434a007.
(4) Hjorth, J.; Cappellani, F.; Nielsen, C. J.; Restelli, G. Determination of the $NO_3 + NO_2 \rightarrow NO + O_2 + NO_2$ rate constant by infrared diode laser and Fourier transform spectroscopy. *J. Phys. Chem.* **1989**, *93*, 5458-5461, doi:10.1021/j100351a028.
(5) Johnston, H. S.; Tao, Y.-S. Thermal decomposition of nitrogen pentoxide at high temperature. *J. Am. Chem. Soc.* **1951**, *73*, 2948-2949, doi:10.1021/ja01150a518.
(6) Wangberg, I.; Ljungstrom, E.; Olsson, B. E. R.; Davidsson, J. Temperature-dependence of the reaction $NO_3 + NO_2 \rightarrow NO + NO_2 + O_2$ in the range from 296 K to 332 K. *J. Phys. Chem.* **1992**, *96*, 7640-7645, doi:10.1021/j100198a029.

C23. **$NO_3 + NO_3$.** The recommended k(298 K) is from the studies of Graham and Johnston[2] (298–329 K) and Biggs et al.[1] (298 K). The temperature dependence is from Graham and Johnston.
(Table: 94-26, Note: 19-5, Evaluated: 19-5) Back to Table

(1) Biggs, P.; Canosa-Mas, C. E.; Monks, P. S.; Wayne, R. P.; Benter, T.; Schindler, R. N. The kinetics of the nitrate radical self-reaction. *Int. J. Chem. Kinet.* **1993**, *25*, 805-817, doi:10.1002/kin.550251002.
(2) Graham, R. A.; Johnston, H. S. The photochemistry of NO_3 and the kinetics of the N_2O_5-O_3 system. *J. Phys. Chem.* **1978**, *82*, 254-268, doi:10.1021/j100492a002.

C24. **$NH_2 + O_2$.** This reaction has several product channels which are energetically possible, including $NO + H_2O$ and HNO + OH. With the exception of the studies of Hack et al.[2] (295–353 K) and Jayanty et al.[3] (298 K) and several studies at high temperature, there is no evidence for a reaction. The following upper-limits have been measured at 298 K (cm^3 $molecule^{-1}$ s^{-1}): 3×10^{-18} (Lesclaux and Demissy[4]), 8×10^{-15} (Pagsberg et al.[8]), 1.5×10^{-17} (Cheskis and Sarkisov[1]), 3×10^{-18} (Lozovsky et al.[5]), 1×10^{-17} (Patrick and Golden[9]) and 7.7×10^{-18} (Michael et al.[7]), 6×10^{-21} (Tyndall et al.[10]), and 3×10^{-20} (Lozovsky et al.[6]). The recommendation is based on

the study of Tyndall et al., which was sensitive to reaction paths leading to the products NO, NO_2, and N_2O. The reaction forming NH_2O_2 cannot be ruled out, but it is apparently not important in the atmosphere.
(Table: 92-20, Note: 92-20, Evaluated: 19-5) Back to Table

(1) Cheskis, S. G.; Sarkisov, O. M. Flash photolysis of ammonia in the presence of oxygen. *Chem. Phys. Lett.* **1979**, *62*, 72-76, doi:10.1016/0009-2614(79)80415-7.
(2) Hack, W.; Horie, O.; Wagner, H. G. Determination of the rate of the reaction of NH_2 with O_2. *J. Phys. Chem.* **1982**, *86*, 765-771, doi:10.1021/j100394a036c.
(3) Jayanty, R. K. M.; Simonaitis, R.; Heicklen, J. Reaction of NH_2 with NO and O_2. *J. Phys. Chem.* **1976**, *80*, 433-437, doi:10.1021/j100546a001.
(4) Lesclaux, R.; Demissy, M. On the reaction of NH_2 radical with O_2, NO and NO_2. *Nouv. J. Chim.* **1977**, *1*, 443-444.
(5) Lozovsky, V. A.; Ioffe, M. A.; Sarkisov, O. M. On the reaction of the NH_2 radical with oxygen. *Chem. Phys. Lett.* **1984**, *110*, 651-654, doi:10.1016/0009-2614(84)85481-0.
(6) Lozovsky, V. A.; Sarkisov, O. M.; Okhrimchuk, A. G.; Enis, A. L. Upper limit of the rate constant for the reaction of NH_2 radicals with O_2 measured by intracavity dye laser spectroscopy. *Chem. Phys. Rep.* **1997**, *16*, 395-417.
(7) Michael, J. V.; Klemm, R. B.; Brobst, W. D.; Bosco, S. R.; Nava, D. F. Flash photolysis-laser induced fluorescence study of the rate constant for $NH_2 + O_2$ between 245 and 459 K. *J. Phys. Chem.* **1985**, *89*, 3335-3337, doi:10.1021/j100261a035.
(8) Pagsberg, P. B.; Erikson, J.; Christensen, H. C. Pulse radiolysis of gaseous ammonia-oxygen mixtures. *J. Phys. Chem.* **1979**, *83*, 582-590, doi:10.1021/j100468a006.
(9) Patrick, R.; Golden, D. M. Kinetics of the reactions of NH_2 radicals with O_3 and O_2. *J. Phys. Chem.* **1984**, *88*, 491-495, doi:10.1021/j150647a034.
(10) Tyndall, G. S.; Orlando, J. J.; Nickerson, K. E.; Cantrell, C. A.; Calvert, J. G. An upper limit for the rate coefficient of the reaction of NH_2 radicals with O_2 using FTIR product analysis. *J. Geophys. Res.* **1991**, *96*, 20761-20768, doi:10.1029/91JD02044.

C25. $NH_2 + O_3$. There is poor agreement among the studies of Cheskis et al.[2] (298 K), $k(298\text{ K}) = 1.5 \times 10^{-13}$ cm^3 molecule^{-1} s^{-1}, Patrick and Golden[5] (272–348 K), $k(298\text{ K}) = 3.25 \times 10^{-13}$ cm^3 molecule^{-1} s^{-1}, Hack et al.[3] (250–358 K), $k(298\text{ K}) = 1.84 \times 10^{-13}$ cm^3 molecule^{-1} s^{-1}, Bulatov et al.[1] (298 K), $k(298\text{ K}) = 1.2 \times 10^{-13}$ cm^3 molecule^{-1} s^{-1}, and Kurasawa and Lesclaux[4] (298–380 K), $k(298\text{ K}) = 0.62 \times 10^{-13}$ cm^3 molecule^{-1} s^{-1}. The very low value of Kurasawa and Lesclaux may be due to regeneration of NH_2 from secondary reactions (see Patrick and Golden), and it is disregarded here. The discharge flow value of Hack et al. is nearly a factor of two less than the recent Patrick and Golden flash photolysis value. The large discrepancy between Bulatov et al. and Patrick and Golden eludes explanation. The recommendation is the $k(298\text{ K})$ average of these four studies, and E/R is an average of the values reported by Patrick and Golden (1151 K) and Hack et al. (710 K).
(Table: 19-5, Note: 19-5, Evaluated: 19-5) Back to Table

(1) Bulatov, V. P.; Buloyan, A. A.; Cheskis, S. G.; Kozliner, M. Z.; Sarkisov, O. M.; Trostin, A. I. On the reaction of the NH_2 radical with ozone. *Chem. Phys. Lett.* **1980**, *74*, 288-292, doi:10.1016/0009-2614(80)85160-8.
(2) Cheskis, S. G.; Iogansen, A. A.; Sarkisov, O. M.; Titov, A. A. Laser photolysis of ozone in the presence of ammonia. Formation and decay of vibrationally excited NH_2 radicals. *Chem. Phys. Lett.* **1985**, *120*, 45-49, doi:/10.1016/0009-2614(85)87010-X.
(3) Hack, W.; Horie, O.; Wagner, H. G. The rate of the reaction of NH_2 with O_3. *Ber. Bunsenges. Phys. Chem.* **1981**, *85*, 72-78, doi:10.1002/bbpc.19810850115.
(4) Kurasawa, H.; Lesclaux, R. Rate constant for the reaction of NH_2 with ozone in relation to atmospheric processes. *Chem. Phys. Lett.* **1980**, *72*, 437-442, doi:10.1016/0009-2614(80)80325-3.
(5) Patrick, R.; Golden, D. M. Kinetics of the reactions of NH_2 radicals with O_3 and O_2. *J. Phys. Chem.* **1984**, *88*, 491-495, doi:10.1021/j150647a034.

C26. NH_2 + NO. The recommended $k(298\text{ K})$ is the average of the values reported by Lesclaux et al.[11] (300–500 K), Hancock et al.[9] (298 K), Sarkisov et al.[13] (298 K), Stief et al.[17] (216–480 K), Andresen et al.[1] (295 K), Whyte and Phillips[19] (298 K), Dreier and Wolfrum[5] (295 K), Atakan et al.[2] (294–1024 K), Wolf et al.[20] (293–612 K), Diau et al.[3] (297–673 K), Imamura and Washida[10] (298 K), and Yamasaki et al.[21] (298 K). The results of Gordon et al.[7] (298 K), Gehring et al.[6] (298 K), Hack et al.,[8] and Silver and Kolb[14] (294–1215 K) were not considered because they lie at least 2 standard deviations from the average of the previous group. The results tend to separate into two groups. The flash photolysis results average 1.8×10^{-11} cm^3 molecule^{-1} s^{-1} (except for the pulse radiolysis study of Gordon et al.), while those obtained using the discharge flow technique average 0.9×10^{-11} cm^3 molecule^{-1} s^{-1}. The apparent discrepancy cannot be due simply to a pressure effect as the

pressure ranges of the flash photolysis and discharge flow studies overlapped and none of the studies observed a pressure dependence for *k*. Whyte and Phillips have suggested that the difference may be due to decomposition of the adduct NH_2NO, which occurs on the timescale of the flow experiments, but not the flash experiments. There have been many studies of the temperature dependence but most have investigated the regime of interest to combustion and only two have gone below room temperature (Hack et al. (209–505 K) and Stief et al. (216–480 K). Each study reported *k* to decrease with increasing temperature. The recommended temperature dependence is taken from a fit to the Stief et al. data at room temperature and below. The reaction proceeds along a complex potential energy surface, which results in product branching ratios that are strongly dependent on temperature. *Ab initio* calculations by Walch[18] show the existence of four saddle points in the potential surface leading to $N_2 + H_2O$ without a reaction barrier. Elimination to form $OH + HN_2$ can occur at any point along the surface. While results from early studies on the branching ratio for OH formation differ significantly, the most recent studies (Hall et al., Dolson,[4] Silver and Kolb,[15] Atakan et al., Stephens et al.,[16] and Park and Lin[12]) agree on a value around 0.1 at 300 K, with $N_2 + H_2O$ making up the balance.
(Table: 97-4, Note: 19-5, Evaluated: 19-5) Back to Table

(1) Andresen, P.; Jacobs, A.; Kleinermanns, C.; Wolfrum, J. Direct investigations of the NH_2 + NO reaction by laser photolysis at different temperatures. In *19th Symp. (Intl.) Combustion*, 1982; pp 11-22.

(2) Atakan; Jacobs, B. A.; Wahl, M.; Weller, R.; Wolfrum, J. Kinetic measurements and product branching ratio for the reaction NH_2 + NO at 294-1027 K. *Chem. Phys. Lett.* **1989**, *155*, 609-613, doi:10.1016/0009-2614(89)87482-2.

(3) Diau, E. W.; Yu, T.; Wagner, M. A. G.; Lin, M. C. Kinetics of the NH_2 + NO reaction: Effects of temperature on the total rate constant and the OH/H_2O branching ratio. *J. Phys. Chem.* **1994**, *98*, 4034-4042, doi:10.1021/j100066a022.

(4) Dolson, D. A. Experimental determination of the OH product yield from NH_2 + NO at 300 K. *J. Phys. Chem.* **1986**, *90*, 6714-6718, doi:10.1021/j100283a025.

(5) Dreier, T.; Wolfrum, J. "Determination of the vibrational energy distribution in N_2 and H_2O formed in the NH_2 + NO reaction by cars and IR spectroscopy"; 20th International Symposium on Combustion, 1984.

(6) Gehring, M.; Hoyermann, K.; Sahaeke, H.; Wolfrum, J. "Direct studies of some elementary steps for the formation and destruction of nitric oxide in the H-N-O system"; 14th Symposium (Int.) on Combustion, 1973.

(7) Gordon, S.; Mulac, W.; Nangia, P. Pulse radiolysis of ammonia gas. 11. Rate of disappearance of the $NH_2(X^2B_1)$ radical. *J. Phys. Chem.* **1971**, *75* 2087-2093, doi:10.1021/j100683a004.

(8) Hack, W.; Schacke, H.; Schröter, M.; Wagner, H. G. "Reaction rates of NH_2-radicals with NO, NO_2, C_2H_2, C_2H_4 and other hydrocarbons"; 17th Symposium (Int.) on Combustion, 1979.

(9) Hancock, G.; Lange, W.; Lenzi, M.; Welge, K. H. Laser fluorescence of NH_2 and rate constant measurement of NH_2 + NO. *Chem. Phys. Lett.* **1975**, *33*, 168-172, doi:10.1016/0009-2614(75)85478-9.

(10) Imamura, T.; Washida, N. Measurements of rate constants for HO_2 + NO and NH_2 + NO reactions by time-resolved photoizonization mass spectrometry. *Laser Chem.* **1995**, *16*, 43-51.

(11) Lesclaux, R.; Khe, P. V.; Dezauzier, P.; Soulignac, J. C. Flash photolysis studies of the reaction of NH_2 radicals with NO. *Chem. Phys. Lett.* **1975**, *35*, 493-497, doi:10.1016/0009-2614(75)85650-8.

(12) Park, J.; Lin, M. C. Direct determination of product branching for the NH_2 + NO reaction at temperatures between 302 and 1060 *J. Phys. Chem.* **1996**, *100*, 3317-3319, doi:10.1021/jp9533741.

(13) Sarkisov, O. M.; Cheskis, S. G.; Sviridenkov, E. A. Study of NH_2 + NO reaction employing intraresonator laser spectroscopy. *Bull. Acad. Sci. USSR Chem.* **1978**, *Ser. 27*, 2336-2338, doi:10.1007/BF00946690.

(14) Silver, J. A.; Kolb, C. E. Kinetic measurements for the reaction of NH_2 + NO over the temperature range 294-1215 K. *J. Phys. Chem.* **1982**, *86*, 3240-3246, doi:10.1021/j100213a033.

(15) Silver, J. A.; Kolb, C. E. A reevaluation of the branching ratio for the reaction of NH_2 with NO. *J. Phys. Chem.* **1987**, *91*, 3713-3714, doi:10.1021/j100297a051.

(16) Stephens, J. W.; Morter, C. L.; Farhat, S. K.; Glass, G. P.; Curl, R. F. Branching ratio of the reaction NH_2 + NO at elevated temperatures. *J. Phys. Chem.* **1993**, *97*, 8944-8951, doi:10.1021/j100137a019.

(17) Stief, L. J.; Brobst, W. D.; Nava, D. F.; Borkowski, R. P.; Michael, J. V. Rate constant for the reaction NH_2 + NO from 216 to 480 K. *J. Chem. Soc. Faraday Trans. 2* **1982**, *78*, 1391-1401, doi:10.1039/F29827801391.

(18) Walch, S. P. Theoretical characterization of the reaction NH_2 + NO → products. *J. Chem. Phys.* **1993**, *99*, 5295-5300, doi:10.1063/1.465972.

(19) Whyte, A. R.; Phillips, L. F. Rates of reaction of NH_2 with N, NO and NO_2. *Chem. Phys. Lett.* **1983**, *102*, 451-454, doi:10.1016/0009-2614(83)87444-2.

(20) Wolf, M.; Yang, D. L.; Durant, J. L. Kinetic studies of NH_x radical reactions. *J. Photochem. Photobiol. A: Chem.* **1994**, *80*, 85-93, doi:i10.1016/1010-6030(93)01037-3.
(21) Yamasaki, K.; Watanabe, A.; Tanaka, A.; Sato, M.; Tokue, I. Kinetics of the reaction $NH_2(X^2B_1, v_2 = 0$ and 1) + NO. *J. Phys. Chem. A* **2002**, *106*, 6563-6569, doi:10.1021/jp013306g.

C27. $NH_2 + NO_2$. Hack et al.[2] (298 K), Kurasawa and Lesclaux[4] (298–505 K), Whyte and Phillips[10] (298 K), Xiang et al.[11] (298 K), Bulatov et al.[1] (295–620 K), Meunier et al.[6] (298 K), Park and Lin[7] (300–910 K), and Klippenstein et al.[3] (295–625 K) have reported rate coefficient data near room temperature. The results of Hack et al. and Meunier et al. are significantly less than the other studies and were not included in the recommendation. The results of Bulatov et al. are systematically less than the other studies at elevated temperatures and are not included in the recommendation. The recommended k(298 K) value is an average of the other studies listed above. The recommended temperature dependence is taken from the studies of Meunier et al., Park et al., and Klippenstein et al. for temperatures <500 K. Presently there are no kinetic measurements available for temperatures <295 K.

There have been several studies of the product branching yields. Hack et al. reported that the predominant reaction channel produces $N_2O + H_2O$ with a yield at 298 K of >95%. Using pulse radiolysis combined with infrared detection of N_2O and NO, Meunier et al. report (59 ± 3)% and (40 ± 5)% yields at 298 K for the $N_2O + H_2O$ and H_2NO + NO product channels, respectively. Using pulsed laser photolysis combined with time-resolved infrared diode laser detection of N_2O and NO products, Lindholm and Hershberger[5] report (24 ± 4)% and (76 ± 10)% yields at 298 K for the $N_2O + H_2O$ and H_2NO + NO product channels, respectively. This study supersedes that of Quandt and Hershberger.[8] Park and Lin[7] measured the $N_2O + H_2O$ product channel yield, using pulsed laser photolysis with mass spectroscopy detection, over the temperature range 300–900 K and report a (19 ± 2)% yield independent of temperature. Song et al.[9] reported a $N_2O + H_2O$ product channel yield of 0.17 ± 0.04 over the temperature range 1330–1527 K. A $N_2O + H_2O$ product channel yield of 20% is recommended with the H_2NO + NO channel as the balance of the reaction.
(Table: 19-5, Note: 19-5, Evaluated: 19-5) Back to Table

(1) Bulatov, V. P.; Ioffe, A. A.; Lozovsky, V. A.; Sarkisov, O. M. On the reaction of the NH_2 radical with NO_2 at 295–620 K. *Chem. Phys. Lett.* **1989**, *159*, 171–174, doi:10.1016/0009-2614(89)87403-2.
(2) Hack, W.; Schacke, H.; Schröter, M.; Wagner, H. G. "Reaction rates of NH_2-radicals with NO, NO_2, C_2H_2, C_2H_4 and other hydrocarbons"; 17th Symposium (Int.) on Combustion, 1979.
(3) Klippenstein, S. J.; Harding, L. B.; Glarborg, P.; Gao, Y.; Hu, H.; Marshall, P. Rate constant and branching fraction for the $NH_2 + NO_2$ reaction. *J. Phys. Chem. A* **2013**, *117*, 9011-9022, doi:10.1021/jp4068069.
(4) Kurasawa, H.; Lesclaux, R. Kinetics of the reaction of NH_2 with NO_2. *Chem. Phys. Lett.* **1979**, *66*, 602-607, doi:10.1016/0009-2614(79)80350-4.
(5) Lindholm, N.; Hershberger, J. F. Product branching ratios of the $NH_2(X^2B_1) + NO_2$ reaction. *J. Phys. Chem.* **1997**, *101*, 4991-4995, doi:10.1021/j100046a020.
(6) Meunier, H. P., P.; Sillesen, A. Kinetics and branching ratios of the reactions $NH_2 + NO_2 \rightarrow N_2O + H_2O$ and $NH_2 + NO_2 \rightarrow H_2NO$ + NO studied by pulse radiolysis combined with time-resolved infrared diode laser spectroscopy. *Chem. Phys. Lett.* **1996**, *261*, 277-282, doi:10.1016/0009-2614(96)00955-4.
(7) Park, J.; Lin, M. C. A mass spectrometric study of the $NH_2 + NO_2$ reaction. *J. Phys. Chem. A* **1997**, *101*, 2643-2647, doi:10.1021/jp963720u.
(8) Quandt, R. W.; Hershberger, J. F. Diode laser study of the product branching ratio of the $NH_2(X^2B_1) + NO_2$ reaction. *J. Phys. Chem.* **1996**, *100*, 9407-9411, doi:10.1021/jp960432p.
(9) Song, S.; Golden, D. M.; Hanson, R. K.; Bowman, C. T. A shock tube study of the $NH_2 + NO_2$ reaction. *Proc. Combustion Inst.* **2002**, *29*, 2163-2170, doi:10.1016/S1540-7489(02)80263-2.
(10) Whyte, A. R.; Phillips, L. F. Rates of reaction of NH_2 with N, NO and NO_2. *Chem. Phys. Lett.* **1983**, *102*, 451-454, doi:10.1016/0009-2614(83)87444-2.
(11) Xiang, T.; Torres, M. L.; Guillory, W. A. State-selected reaction and relaxation of $NH_2[X^2B_1(0,v_2,0)]$ radicals and NO_2. *J. Chem. Phys.* **1985**, *83*, 1623-1629, doi:10.1063/1.449399.

C28. NH + NO. The recommendation is derived from the room temperature results of Hansen et al.,[3] Cox et al.,[1] Harrison et al.,[4] and Okada et al.[5] The temperature dependence is from Harrison et al. (270–373 K). Several studies have reported product yield data for this reaction. Durant[2] used a discharge-flow technique with mass spectrometric detection of products and reported a N_2O + H branching yield of 0.8 ± 0.4 at 298 K. Okada et al. reported N_2O + H and OH + N_2 branching yields at 295 K of 0.65 and 0.30, respectively (Okada et al. supersedes the Yamasaki et al.[7] study from the same group). Quandt and Hershberger[6] measured the N_2O + H product branching yield at 298 K to be 0.77 ± 0.08.
(Table: 19-5, Note: 19-5, Evaluated: 19-5) Back to Table

(1) Cox, J. W.; Nelson, H. H.; McDonald, J. R. Temperature-dependent reaction kinetics of NH ($a^1\Delta$). *Chem. Phys.* **1985**, *96*, 175-182, doi:10.1016/0301-0104(85)80202-0.
(2) Durant, J. L., Jr. Product branching fractions in the reaction of NH (ND) ($^3\Sigma^-$) with NO. *J. Phys. Chem.* **1994**, *98*, 518-521, doi:10.1021/j100053a028.
(3) Hansen, I.; Hoinghaus, K.; Zetzsch, C.; Stuhl, F. Detection of NH ($X^3\Sigma^-$) by resonance fluorescence in the pulsed vacuum UV photolysis of NH_3 and its application to reactions of NH radicals. *Chem. Phys. Lett.* **1976**, *42*, 370-372.
(4) Harrison, J. A.; Whyte, A. R.; Phillips, L. F. Kinetics of reactions of NH with NO and NO_2. *Chem. Phys. Lett.* **1986**, *129*, 346-352, doi:10.1016/0009-2614(86)80356-6.
(5) Okada, S.; Tezaki, A.; Miyoshi, A.; Matsui, H. Product branching fractions in the reactions of NH($a^1\Delta$) and NH($X^3\Sigma^-$) with NO. *J. Chem. Phys.* **1994**, *101*, 9582-9588, doi:10.1063/1.467989.
(6) Quandt, R. W.; Hershberger, J. F. Product branching ratios of the NH ($^3\Sigma^-$) + NO and NH ($^3\Sigma^-$) + NO_2 reactions. *J. Phys. Chem.* **1995**, *99*, 16939-16944, doi:10.1021/j100046a020.
(7) Yamasaki, K.; Okada, S.; Koski, M.; Matsui, H. Selective product channels in the reactions of NH($a^1\Delta$) and NH($X^3\Sigma^-$) with NO. *J. Chem. Phys.* **1991**, *95*, 5087-5096, doi:10.1063/1.461676.

C29. NH + NO_2. The recommendation is derived from the low-pressure (1 Torr) pulsed laser photolysis-laser induced fluorescence temperature-dependence study of Harrison et al.[1] (269–377 K). The assigned uncertainty factors are relatively large to reflect the limited available data. Quandt and Hershberger[2] measured N_2O + OH and NO + HNO product branching ratios at 298 K to be 0.41 ± 0.15 and 0.59 ± 0.15, respectively, using pulsed laser photolysis of HN_3 to produce NH and time-resolved infrared diode laser spectroscopy to monitor N_2O and NO formation.
(Table: 19-5, Note: 19-5, Evaluated: 19-5) Back to Table

(1) Harrison, J. A.; Whyte, A. R.; Phillips, L. F. Kinetics of reactions of NH with NO and NO_2. *Chem. Phys. Lett.* **1986**, *129*, 346-352, doi:10.1016/0009-2614(86)80356-6.
(2) Quandt, R. W.; Hershberger, J. F. Product branching ratios of the NH ($^3\Sigma^-$) + NO and NH ($^3\Sigma^-$) + NO_2 reactions. *J. Phys. Chem.* **1995**, *99*, 16939-16944, doi:10.1021/j100046a020.

C30. O_3 + HNO_2. Based on Kaiser and Japar[1] (226 and 300 K) and Streit et al.[2] (298 K).
(Table: 82-57, Note: 82-57, Evaluated: 19-5) Back to Table

(1) Kaiser, E. W.; Japar, S. M. The kinetics of the gas phase reaction of nitrous acid with ozone. *Chem. Phys. Lett.* **1977**, *52*, 121-124, doi:10.1016/0009-2614(77)85133-6.
(2) Streit, G. E.; Wells, J. S.; Fehsenfeld, F. C.; Howard, C. J. A tunable diode laser study of the reactions of nitric and nitrous acids: HNO_3 + NO and HNO_2 + O_3. *J. Chem. Phys.* **1979**, *70*, 3439-3443, doi:10.1063/1.437878.

C31. N_2O_5 + H_2O. The recommended k(298 K) is based on the studies of Tuazon et al.[4] (298 K), Atkinson et al.[1] (298 K), and Hjorth et al.[2] (296 K). Sverdrup et al.[3] (298 K) obtained an upper limit that is a factor of four smaller than that obtained in the other studies, but the higher upper limit is recommended because of the difficulty of distinguishing between homogeneous and heterogeneous processes in the experiment. See the heterogeneous chemistry section of this evaluation for additional rate data for this reaction.
(Table: 85-37, Note: 90-1, Evaluated: 19-5) Back to Table

(1) Atkinson, R.; Tuazon, R. C.; Macleod, H.; Aschmann, S. M.; Winer, A. M. The gas-phase reaction of chlorine nitrate with water vapor. *Geophys. Res. Lett.* **1986**, *13*, 117-120, doi:10.1029/GL013i002p00117
(2) Hjorth, J.; Ottobrini, G.; Cappellani, F.; Restelli, G. A Fourier transform infrared study of the rate constant of the homogeneous gas-phase reaction N_2O_5 + H_2O and determination of absolute infrared band intensities of N_2O_5 and HNO_3. *J. Phys. Chem.* **1987**, *91*, 1565-1568, doi:10.1021/j100290a055.
(3) Sverdrup, G. M.; Spicer, C. W.; Ward, G. F. Investigation of the gas phase reaction of dinitrogen pentoxide with water vapor. *Int. J. Chem. Kinet.* **1987**, *19*, 191-205, doi:10.1002/kin.550190304.
(4) Tuazon, E. C.; Atkinson, R.; Plum, C. N.; Winer, A. M.; Pitts, J. N. The reaction of gas phase N_2O_5 with water vapor. *Geophys. Res. Lett.* **1983**, *10*, 953-956, doi:10.1029/GL010i010p00953/pdf.

C32. N_2(A,v) + O_2. Rate coefficients for the overall reaction for the v = 0, 1 and 2 vibrational levels of N_2(A) have been made by Dreyer et al.,[3] Zipf,[11] Piper et al.,[7] Iannuzzi and Kaufman,[6] Thomas and Kaufman,[10] Thomas et al.,[9]and De Sousa et al.[2] The results of these studies are in relatively good agreement. The recommended values are (2.5 ± 0.4), (4.0 ± 0.6), and (4.5 ± 0.6) (10^{-12} cm^3 $molecule^{-1}$ s^{-1}), from the work of De Sousa et al. The only temperature dependence data are from De Sousa et al., who obtained $k(T,v) = k(v,298\ K)(T/300)^{0.55}$

for v = 0,1,2. The observation of high N_2O production initially reported by Zipf[11] has not been reproduced by other groups, and the branching ratio for this channel is probably less than 0.02 (Iannuzzi et al.,[5] Black et al.,[1] De Sousa et al.,[2] and Fraser and Piper[4]). Thomas and Kaufman[8] report the 2NO product channel branching ratio to be <0.1%. The branching ratios for the other channels are poorly established, although there is strong evidence for the formation of both $O(^3P)$ and $O_2(B^3\Sigma_u^-)$.
(Table: 94-26, Note: 19-5, Evaluated: 19-5) Back to Table

(1) Black, G.; Hill, R. M.; Sharpless, R. L.; Slanger, T. G. Laboratory studies of N_2O relevant to stratospheric processes. *J. Photochem.* **1983**, *22*, 369-372.

(2) De Sousa, A. R.; Touzeau, M.; Petitdidier, M. Quenching reactions of metastable $N_2(A^3\Sigma, v=0, 1, 2)$ molecules by O_2. *Chem. Phys. Lett.* **1985**, *121*, 423-428, doi:10.1016/0009-2614(85)87207-9.

(3) Dreyer, J. W.; Perner, D.; Roy, C. R. Rate constants for the quenching of $N_2(A\ ^3\Sigma_u^+, v_A = 0\text{-}8)$ by CO, CO_2, NH_3, NO, and O_2. *J. Chem. Phys.* **1974**, *61*, 3164-3169, doi:10.1063/1.1682472.

(4) Fraser, M. E.; Piper, L. G. Product branching ratios from the $N_2(A^3\Sigma_u^+) + O_2$ interaction. *J. Phys. Chem.* **1989**, *93*, 1107-1111, doi:10.1021/j100340a017.

(5) Iannuzzi, M. P.; Jeffries, J. B.; Kaufman, F. Product channels of the $N_2(A^3\Sigma_u^+) + O_2$ interaction. *Chem. Phys. Lett.* **1982**, *87*, 570-574, doi:10.1016/0009-2614(82)83180-1.

(6) Iannuzzi, M. P.; Kaufman, F. Rate constants for the reaction of $N_2(A^3\Sigma_u^+, v = 0, 1, \text{and } 2)$ with O_2. *J. Phys. Chem.* **1981**, *85*, 2163-2165, doi:10.1021/j150615a005.

(7) Piper, L. G.; Caledonia, G. E.; Konnealy, J. P. Rate constants for deactivation of $N_2(A)v' = 0,1$ by O_2. *J. Chem. Phys.* **1981**, *74*, 2888-2895, doi:10.1063/1.441408.

(8) Thomas, J. M.; Kaufman, F. An upper limit on the formation of $NO(X^2\Pi_r)$ in the reactions $N_2(A^3\Sigma_u^+) + O(^3P)$ and $N2(A^3S_u^+) + O_2(X^3\Sigma_g^-)$ at 298 K. *J. Phys. Chem.* **1996**, *100*, 8901-8906, doi:10.1021/jp960164v.

(9) Thomas, J. M.; Kaufman, F.; Golde, M. F. Rate constants for electronic quenching of $N_2(A^3S_u^+, v=0\text{-}6)$ by O_2, NO, CO, N_2O, and C_2H_4. *J. Chem. Phys.* **1987**, *86*, 6885-6892, doi:10.1063/1.452388.

(10) Thomas, J. W.; Kaufman, F. Rate constants of the reactions of metastable $N_2(A\ ^3\Sigma_u^+)$ in $v = 0, 1, 2, \text{and } 3$ with ground state O_2 and O. *J. Chem. Phys.* **1985**, *83*, 2900-2903, doi:10.1063/1.449243.

(11) Zipf, E. C. A laboratory study on the formation of nitrous oxide by the reaction $N_2(A^3\Sigma_u^+) + O_2 \rightarrow N_2O + O$. *Nature (London)* **1980**, *287*, 523-525, doi:10.1038/287523a0.

C33. $N_2(A,v) + O_3$. The only study is that of Bohmer and Hack,[1] who obtained 298 K rate coefficients of 4.1 ± 1.0, 4.1 ± 1.2, 8.0 ± 2.3, and 10 ± 3.0 (10^{-11} cm^3 $molecule^{-1}$ s^{-1}) for the loss of the v = 0–3 vibrational levels of $N_2(A)$, respectively. This study determined that the $2NO + O(^3P)$ product channel accounts for about 20% of the reaction products.
(Table: 94-26, Note: 19-5, Evaluated: 19-5) Back to Table

(1) Bohmer, E.; Hack, W. Rate constants for the reactions of $N_2(A^3\Sigma_u^+, v')$ with $O_3(X^1A_1)$. *Ber. Bunsenges. Phys. Chem.* **1991**, *95*, 1688-1690, doi:10.1002/bbpc.19910951218.

1.8.3 Bibliography – NO_x Reactions

Agrawalla, B. S.; Manocha, A. S.; Setser, D. W. Studies of H and O atom reactions by OH infrared chemiluminescence. *J. Phys. Chem.* **1981**, *85*, 2873-2877, doi:10.1021/j150620a004.

Andresen, P.; Jacobs, A.; Kleinermanns, C.; Wolfrum, J. Direct investigations of the NH_2 + NO reaction by laser photolysis at different temperatures. In *19th Symp. (Intl.) Combustion*, 1982; pp 11-22.

Atakan; Jacobs, B. A.; Wahl, M.; Weller, R.; Wolfrum, J. Kinetic measurements and product branching ratio for the reaction NH_2 + NO at 294-1027 K. *Chem. Phys. Lett.* **1989**, *155*, 609-613, doi:10.1016/0009-2614(89)87482-2.

Atkinson, R.; Tuazon, R. C.; Macleod, H.; Aschmann, S. M.; Winer, A. M. The gas-phase reaction of chlorine nitrate with water vapor. *Geophys. Res. Lett.* **1986**, *13*, 117-120, doi:10.1029/GL013i002p00117.

Bardwell, M. W.; Bacak, A.; Raventos, M. T.; Percival, C. J.; Sanchez-Reyna, G.; Shallcross, D. E. Kinetics of the HO_2 + NO reaction: A temperature and pressure dependence study using chemical ionisation mass spectrometry. *Phys. Chem. Chem. Phys.* **2003**, *5*, 2381-2385, doi:10.1039/b300842h.

Barnes, I.; Bastian, V.; Becker, K. H.; Fink, E. H.; Zabel, F. Rate constant of the reaction of OH with HO_2NO_2. *Chem. Phys. Lett.* **1981**, *83*, 459-464, doi:10.1016/0009-2614(81)85501-7.

Barnes, I.; Bastian, V.; Becker, K. H.; Fink, E. H.; Zabel, F. Pressure dependence of the reaction of OH with HO_2NO_2. *Chem. Phys. Lett.* **1986**, *123*, 28-32, doi:10.1016/0009-2614(86)87007-5.

Barnett, A. J.; Marston, G.; Wayne, R. P. Kinetics and chemiluminescence in the reaction of N atoms with O_2 and O_3. *J. Chem. Soc. Faraday Trans. 2* **1987**, *83*, 1453-1463, doi:10.1039/F29878301453.

Becker, E.; Rahman, M. M.; Schindler, R. N. Determination of the rate constants for the gas phase reactions of NO_3 with H, OH and HO_2 radicals at 298 K. *Ber. Bunsenges. Phys. Chem.* **1992**, *96*, 776-783, doi:10.1002/bbpc.19920960608.

Becker, K. H.; Groth, W.; Kley, D. The rate constant of the aeronomic reaction N + O_2. *Z. Naturforsch* **1969**, *A24*, 1280-1281.

Bemand, P. P.; Clyne, M. A. A. Atomic resonance fluorescence for rate constants of rapid bimolecular reactions Part 6.-Hydrogen atom reactions: H + Cl_2 from 300 to 730 K and H + NO_2 at 298 K. *J. Chem. Soc. Faraday Trans. 2* **1977**, *73*, 394-405, doi:10.1039/F29777300394.

Bemand, P. P.; Clyne, M. A. A.; Watson, R. T. Atomic resonance fluorescence and mass spectrometry for measurements of the rate constants for elementrary reactions: O ^3P_J + NO_2 → NO + O_2 and NO + O_3 → NO_2 + O_2. *J. Chem. Soc. Faraday Trans. 2* **1974**, *70*, 564-576, doi;10.1039/F29747000564.

Bergeat, A. H., K. M.; Daugey, N.; Caubet, P.; Costes, M. A low temperature investigation of the N($^4S^0$) + NO reaction. *Phys. Chem. Chem. Phys.* **2009**, *11*, 8149–8155, doi:10.1039/b905702a.

Biggs, P.; Canosa-Mas, C. E.; Monks, P. S.; Wayne, R. P.; Benter, T.; Schindler, R. N. The kinetics of the nitrate radical self-reaction. *Int. J. Chem. Kinet.* **1993**, *25*, 805-817, doi:10.1002/kin.550251002.

Birks, J. W.; Shoemaker, B.; Leck, T. J.; Hinton, D. M. Studies of reactions of importance in the stratosphere. I. Reaction of nitric oxide with ozone. *J. Chem. Phys.* **1976**, *65*, 5181-5185, doi:10.1063/1.433059.

Black, G.; Hill, R. M.; Sharpless, R. L.; Slanger, T. G. Laboratory studies of N_2O relevant to stratospheric processes. *J. Photochem.* **1983**, *22*, 369-372.

Bohmer, E.; Hack, W. Rate constants for the reactions of $N_2(A^3\Sigma_u^+, v')$ with $O_3(X^1A_1)$. *Ber. Bunsenges. Phys. Chem.* **1991**, *95*, 1688-1690, doi:10.1002/bbpc.19910951218.

Bohn, B.; Zetzsch, C. Rate constants of HO_2 + NO covering atmospheric conditions. 1. HO_2 formed by OH + H_2O_2. *J. Phys. Chem. A* **1997**, *101*, 1488-1493, doi:10.1021/jp961396x.

Boodaghians, R. B.; Canosa-Mas, C. E.; Carpenter, P. J.; Wayne, R. P. The reactions of NO_3 with OH and H. *J. Chem. Soc. Faraday Trans. 2* **1988**, *84*, 931-948, doi:10.1039/F29888400931.

Borders, R. A.; Birks, J. W. High-precision measurements of activation energies over small temperature intervals: Curvature in the Arrhenius plot for the reaction NO + O_3 → NO_2 + O_2. *J. Phys. Chem.* **1982**, *86*, 3295-3302, doi:10.1021/j100214a007.

Brown, S. S.; Ravishankara, A. R.; Stark, H. Simultaneous kinetics and ring-down: Rate coefficients from single cavity loss temporal profiles. *J. Phys. Chem. A* **2000**, *104*, 7044-7052, doi:10.1021/jp0013715.

Brunning, J.; Clyne, M. A. A. Elementary reactions of the SF radical Part 1.-Rate constants for the reactions F + OCS → SF + CO and SF + SF → SF_2 + S. *J. Chem. Soc. Faraday Trans 2* **1984**, *80*, 1001-1014, doi:10.1039/F29848001001.

Bulatov, V. P.; Buloyan, A. A.; Cheskis, S. G.; Kozliner, M. Z.; Sarkisov, O. M.; Trostin, A. I. On the reaction of the NH_2 radical with ozone. *Chem. Phys. Lett.* **1980**, *74*, 288-292, doi:10.1016/0009-2614(80)85160-8.

Bulatov, V. P.; Ioffe, A. A.; Lozovsky, V. A.; Sarkisov, O. M. On the reaction of the NH_2 radical with NO_2 at 295–620 K. *Chem. Phys. Lett.* **1989**, *159*, 171–174, doi:10.1016/0009-2614(89)87403-2.

Burkholder, J. B.; Mellouki, A.; Talukdar, R.; Ravishankara, A. R. Rate coefficients for the reaction of OH with HONO between 298 and 373 K. *Int. J. Chem. Kinet.* **1992**, *24*, 711-725, doi:10.1002/kin.550240805.

Burrows, J. P.; Cliff, D. I.; Harris, G. W.; Thrush, B. A.; Wilkinson, J. P. T. Atmospheric reactions of the HO_2 radical studied by laser magnetic-resonance spectroscopy. *Proc. Roy. Soc. Lond. A.* **1979**, *368*, 463-481, doi:10.1098/rspa.

Canosa-Mas , C. E.; Carpenter, P. J.; Wayne, R. P. The reaction of NO_3 with atomic oxygen. *J. Chem. Soc. Faraday Trans 2* **1989**, *85*, 697-707, doi:10.1039/f29898500697.

Cantrell, C. A.; Davidson, J. A.; McDaniel, A. H.; Shetter, R. E.; Calvert, J. G. The equilibrium constant for $N_2O_5 \rightleftarrows NO_2 + NO_3$: Absolute determination by direct measurement from 243 to 397 K. *J. Chem. Phys.* **1988**, *88*, 4997-5006, doi:10.1063/1.454679.

Cantrell, C. A.; Shetter, R. E.; McDaniel, A. H.; Calvert, J. G. The rate coefficient for the reaction $NO_2 + NO_3 \rightarrow NO + NO_2 + O_2$ from 273 to 313 K. *J. Geophys. Res.* **1990**, *95*, 20531-20537, doi:10.1029/JD095iD12p20531.

Carr, S.; Heard, D. E.; Blitz, M. A. Comment on "Atmospheric hydroxyl radical production from electronically excited NO_2 and H_2O". *Science* **2009**, *324*, 336b, doi:10.1126/science.1166669.

Chang, J. S.; Trevor, P. L.; Barker, J. R. $O(^3P) + HOONO_2 \rightarrow$ Products: Temperature-dependent rate constant. *Int. J. Chem. Kinet.* **1981**, *13*, 1151-1161, doi:10.1002/kin.550131106.

Chapman, C. J.; Wayne, R. P. The reaction of atomic oxygen and hydrogen with nitric acid. *Int. J. Chem. Kinet.* **1974**, *6*, 617-630, doi:10.1002/kin.550060502.

Cheah, C. T.; Clyne, M. A. A. Reactions forming electronically-excited free radicals Part 2.-Formation of $N\,^4S$, $N\,^2D$ and $N\,^2P$ atoms in the $H + NF_2$ reaction, and N atom reactions. *J. Chem. Soc. Faraday Trans. II* **1980**, *76*, 1543-1560, doi:10.1039/F29807601543.

Chen, M. C.; Taylor, H. A. Reaction of nitrogen atoms with ozone. *J. Chem. Phys.* **1961**, *34*, 1344-1347, doi:10.1063/1.1731742.

Cheskis, S. G.; Iogansen, A. A.; Sarkisov, O. M.; Titov, A. A. Laser photolysis of ozone in the presence of ammonia. Formation and decay of vibrationally excited NH_2 radicals. *Chem. Phys. Lett.* **1985**, *120*, 45-49, doi:/10.1016/0009-2614(85)87010-X.

Cheskis, S. G.; Sarkisov, O. M. Flash photolysis of ammonia in the presence of oxygen. *Chem. Phys. Lett.* **1979**, *62*, 72-76, doi:10.1016/0009-2614(79)80415-7.

Clark, I. D.; Wayne, R. P. Kinetics of the reaction between atomic nitrogen and molecular oxygen in the ground ($^3\Sigma_g^-$) and first excited ($^1\Delta_g$) states. *Proc. Roy. Soc. Lond. A.* **1970**, *316*, 539-550, doi:10.1098/rspa.1970.0095.

Clough, P. N.; Thrush, B. A. Mechanism of chemiluminescent reaction between nitric oxide and ozone. *Trans. Faraday Soc.* **1967**, *63*, 915-925, doi:10.1039/TF9676300915.

Clyne, M. A. A.; McDermid, I. S. Mass spectrometric determinations of the rates of elementary reactions of NO and of NO_2 with ground state $N\,^4S$ atoms. *J. Chem. Soc. Faraday Trans. 1* **1975**, *71*, 2189-2202, doi:10.1039/F19757102189.

Clyne, M. A. A.; Monkhouse, P. Atomic resonance fluorescence for rate constants of rapid bimolecular reactions Part 5-Hydrogen atom reactions; $H + NO_2$ and $H + O_3$. *J. Chem. Soc. Faraday Trans. 2* **1977**, *73*, 298-309, doi:10.1039/F29777300298.

Clyne, M. A. A.; Ono, Y. Determination of the rate constant of reaction of $N(^4S_{3/2})$ with NO_2 using resonance fluorescence in a discharge flow system. *Chem. Phys.* **1982**, *69*, 381-388, doi:10.1016/0301-0104(82)88077-4.

Cox, J. W.; Nelson, H. H.; McDonald, J. R. Temperature-dependent reaction kinetics of NH ($a^1\Delta$). *Chem. Phys.* **1985**, *96*, 175-182, doi:10.1016/0301-0104(85)80202-0.

Cox, R. A.; Coker, G. B. Kinetics of the reaction of nitrogen dioxide with ozone. *J. Atmos. Chem.* **1983**, *1*, 53-63.

Cox, R. A.; Derwent, R. G.; Holt, P. M. The photo-oxidation of ammonia in the presence of NO and NO_2. *Chemosphere* **1975**, *4*, 201-205, doi:10.1016/0045-6535(75)90063-6.

Cox, R. A.; Derwent, R. G.; Holt, P. M. Relative rate constants for the reactions of OH radicals with H_2, CH_4, CO, NO and HONO at atmospheric pressure and 296 K. *J. Chem. Soc. Faraday Trans. 1* **1976**, *72*, 2031-2043, doi:10.1039/F19767202031.

Crowley, J. N.; Carl, S. A. OH formation in the photoexcitation of NO_2 beyond the dissociation threshold in the presence of water vapor. *J. Phys. Chem. A* **1997**, *101*, 4178-4184, doi:10.1021/jp970319e.

Daniels, F.; Johnston, E. H. The thermal decomposition of gaseous nitrogen pentoxide. A monomolecular reaction. *J. Am. Chem. Soc.* **1921**, *43*, 53-71, doi:10.1021/ja01434a007.
Davis, D. D.; Prusazcyk, J.; Dwyer, M.; Kim, P. A stop-flow time-of-flight mass spectrometry kinetics study. Reaction of ozone with nitrogen dioxide and sulfur dioxide. *J. Phys. Chem.* **1974**, *78*, 1775-1779, doi:10.1021/j100611a001.
De Sousa, A. R.; Touzeau, M.; Petitdidier, M. Quenching reactions of metastable $N_2(A^3\Sigma, v=0, 1, 2)$ molecules by O_2. *Chem. Phys. Lett.* **1985**, *121*, 423-428, doi:10.1016/0009-2614(85)87207-9.
Diau, E. W.; Yu, T.; Wagner, M. A. G.; Lin, M. C. Kinetics of the NH_2 + NO reaction: Effects of temperature on the total rate constant and the OH/H_2O branching ratio. *J. Phys. Chem.* **1994**, *98*, 4034-4042, doi:10.1021/j100066a022.
Diau, E. W.-G.; Tso, T.-L.; Lee, Y.-P. Kinetics of the reaction OH + NH_3 in the range 273-433 K. *J. Phys. Chem.* **1990**, *94*, 5261-5265, doi:10.1021/j100376a018.
Dolson, D. A. Experimental determination of the OH product yield from NH_2 + NO at 300 K. *J. Phys. Chem.* **1986**, *90*, 6714-6718, doi:10.1021/j100283a025.
Dransfield, T. J.; Donahue, N. M.; Anderson, J. G. High-pressure flow reactor product study of the reactions of HO_x + NO_2: The role of vibrationally excited intermediates. *J. Phys. Chem. A* **2001**, *105*, 1507-1514, doi:10.1021/jp002391+.
Dreier, T.; Wolfrum, J. "Determination of the vibrational energy distribution in N_2 and H_2O formed in the NH_2 + NO reaction by cars and IR spectroscopy"; 20th International Symposium on Combustion, 1984.
Dreyer, J. W.; Perner, D.; Roy, C. R. Rate constants for the quenching of $N_2(A\ ^3\Sigma_u^+, v_A = 0\text{-}8)$ by CO, CO_2, NH_3, NO, and O_2. *J. Chem. Phys.* **1974**, *61*, 3164-3169, doi:10.1063/1.1682472.
Durant, J. L., Jr. Product branching fractions in the reaction of NH (ND) ($^3\Sigma^-$) with NO. *J. Phys. Chem.* **1994**, *98*, 518-521, doi:10.1021/j100053a028.
Fernandez, A.; Goumri, A.; Fonijin, A. Kinetics of the reactions of N(^{4}S) atoms with O_2 and CO_2 over wide temperatures ranges. *J. Phys. Chem. A* **1998**, *102*, 168–172, doi:10.1021/jp972365k.
Fraser, M. E.; Piper, L. G. Product branching ratios from the $N_2(A^3\Sigma_u^+)$ + O_2 interaction. *J. Phys. Chem.* **1989**, *93*, 1107-1111, doi:10.1021/j100340a017.
Garvin, D.; Broida, H. P. "Atomic flame reactions involving N atoms, H atoms and ozone"; 9th Symposium (Int.) on Combustion, 1963.
Gehring, M.; Hoyermann, K.; Sahaeke, H.; Wolfrum, J. "Direct studies of some elementary steps for the formation and destruction of nitric oxide in the H-N-O system"; 14th Symposium (Int.) on Combustion, 1973.
Glaschick-Schimpf, I.; Leiss, A.; Monkhouse, P. B.; Schurath, U.; Becker, K. H.; Fink, E. H. A kinetic study of the reactions of HO_2/DO_2 radicals with niric oxide using near-infrared chemiluminescence detection. *Chem. Phys. Lett.* **1979**, *67*, 318-323, doi:10.1016/0009-2614(79)85170-2.
Gordon, S.; Mulac, W.; Nangia, P. Pulse radiolysis of ammonia gas. 11. Rate of disappearance of the $NH_2(X^2B_1)$ radical. *J. Phys. Chem.* **1971**, *75* 2087-2093, doi:10.1021/j100683a004.
Graham, R. A.; Johnston, H. S. Kinetics of the gas-phase reaction between ozone and nitrogen dioxide. *J. Chem. Phys.* **1974**, *60*, 4628-4629, doi:10.1063/1.1680953.
Graham, R. A.; Johnston, H. S. The photochemistry of NO_3 and the kinetics of the N_2O_5-O_3 system. *J. Phys. Chem.* **1978**, *82*, 254-268, doi:10.1021/j100492a002.
Hack, W.; Horie, O.; Wagner, H. G. The rate of the reaction of NH_2 with O_3. *Ber. Bunsenges. Phys. Chem.* **1981**, *85*, 72-78, doi:10.1002/bbpc.19810850115.
Hack, W.; Horie, O.; Wagner, H. G. Determination of the rate of the reaction of NH_2 with O_2. *J. Phys. Chem.* **1982**, *86*, 765-771, doi:10.1021/j100394a036c.
Hack, W.; Hoyermann, K.; Wagner, H. G. Gas phase reactions of hydroxyl radical with ammonia and hydrazine. *Ber. Bunsenges. Phys. Chem.* **1974**, *78*, 386-391, doi:10.1002/bbpc.19740780415.
Hack, W.; Preuss, A. W.; Temps, F.; Wagner, H. G.; Hoyermann, K. Direct determination of the rate constant of the reaction NO + HO_2 → NO_2 + OH with the LMR. *Int. J. Chem. Kinet.* **1980**, *12*, 851-860, doi:10.1002/kin.550121104.
Hack, W.; Schacke, H.; Schröter, M.; Wagner, H. G. "Reaction rates of NH_2-radicals with NO, NO_2, C_2H_2, C_2H_4 and other hydrocarbons"; 17th Symposium (Int.) on Combustion, 1979.
Hall, I. W.; Wayne, R. P.; Cox, R. A.; Jenkin, M. E.; Hayman, G. D. Kinetics of the reaction of NO_3 with HO_2. *J. Phys. Chem.* **1988**, *92*, 5049-5054, doi:10.1021/j100328a043.
Hammer, P. D.; Dlugokencky, E. J.; Howard, C. J. Kinetics of the gas-phase reaction NO + NO_3 → $2NO_2$. *J. Phys. Chem.* **1986**, *90*, 2491-2496, doi:10.1021/j100402a045.

Hancock, G.; Lange, W.; Lenzi, M.; Welge, K. H. Laser fluorescence of NH_2 and rate constant measurement of NH_2 + NO. *Chem. Phys. Lett.* **1975**, *33*, 168-172, doi:10.1016/0009-2614(75)85478-9.

Hansen, I.; Hoinghaus, K.; Zetzsch, C.; Stuhl, F. Detection of NH ($X^3\Sigma^-$) by resonance fluorescence in the pulsed vacuum UV photolysis of NH_3 and its application to reactions of NH radicals. *Chem. Phys. Lett.* **1976**, *42*, 370-372.

Harrison, J. A.; Whyte, A. R.; Phillips, L. F. Kinetics of reactions of NH with NO and NO_2. *Chem. Phys. Lett.* **1986**, *129*, 346-352, doi:10.1016/0009-2614(86)80356-6.

Herron, J. T. Rate of the reaction NO + N. *J. Chem. Phys.* **1961**, *35*, 1138-1139, doi:10.1063/1.1701202.

Hjorth, J.; Cappellani, F.; Nielsen, C. J.; Restelli, G. Determination of the $NO_3 + NO_2 \rightarrow NO + O_2 + NO_2$ rate constant by infrared diode laser and Fourier transform spectroscopy. *J. Phys. Chem.* **1989**, *93*, 5458-5461, doi:10.1021/j100351a028.

Hjorth, J.; Ottobrini, G.; Cappellani, F.; Restelli, G. A Fourier transform infrared study of the rate constant of the homogeneous gas-phase reaction $N_2O_5 + H_2O$ and determination of absolute infrared band intensities of N_2O_5 and HNO_3. *J. Phys. Chem.* **1987**, *91*, 1565-1568, doi:10.1021/j100290a055.

Howard, C. J. Temperature dependence of the reaction $HO_2 + NO \rightarrow OH + NO_2$. *J. Chem. Phys.* **1979**, *71*, 2352-2359, doi:10.1063/1.438639.

Howard, C. J.; Evenson, K. M. Kinetics of the reaction of HO_2 with NO. *Geophys. Res. Lett.* **1977**, *4*, 437-440, doi:10.1029/GL004i010p00437.

Huie, R. E.; Herron, J. T. The rate constant for the reaction $O_3 + NO_2 \rightarrow O_2 + NO_3$ over the temperature range 259-362 °K. *Chem. Phys. Lett.* **1974**, *27*, 411-414, doi:10.1016/0009-2614(74)90253-X.

Husain, D.; Slater, N. K. H. Kinetic study of ground state atomic nitrogen, N($2^4S_{3/2}$), by time-resolved atomic resonance fluorescence. *J. Chem. Soc. Faraday Trans. II* **1980**, *76*, 606-619, doi:10.1039/F29807600606.

Iannuzzi, M. P.; Jeffries, J. B.; Kaufman, F. Product channels of the $N_2(A^3\Sigma_u^+) + O_2$ interaction. *Chem. Phys. Lett.* **1982**, *87*, 570-574, doi:10.1016/0009-2614(82)83180-1.

Iannuzzi, M. P.; Kaufman, F. Rate constants for the reaction of $N_2(A^3\Sigma_u^+$, v = 0, 1, and 2) with O_2. *J. Phys. Chem.* **1981**, *85*, 2163-2165, doi:10.1021/j150615a005.

Imamura, T.; Washida, N. Measurements of rate constants for HO_2 + NO and NH_2 + NO reactions by time-resolved photoizonization mass spectrometry. *Laser Chem.* **1995**, *16*, 43-51.

Iwata, R.; Ferrieri, R. A.; Wolf, A. P. Rate constant determination of the reaction of metastable N(^{2}D,^{2}P) with NO_2 using moderated nuclear recoil atoms. *J. Phys. Chem.* **1986**, *90*, 6722-6726, doi:10.1021/j100283a027.

Jayanty, R. K. M.; Simonaitis, R.; Heicklen, J. Reaction of NH_2 with NO and O_2. *J. Phys. Chem.* **1976**, *80*, 433-437, doi:10.1021/j100546a001.

Jemi-Alade, A. A.; Thrush, B. A. Reactions of HO_2 with NO and NO_2 studied by mid-infrared laser magnetic resonance. *J. Chem. Soc. Faraday Trans.* **1990**, *86*, 3355-3363, doi:10.1039/FT9908603355

Jenkin, M. E.; Cox, R. A. Kinetics of the gas-phase reaction of OH with nitrous acid. *Chem. Phys. Lett.* **1987**, *137*, 548-552, doi:10.1016/0009-2614(87)80627-9.

Jeoung, S. C.; Choo, K. Y.; Benson, S. W. Very low pressure reactor chemiluminescence studies on N atom reactions with $CHCl_3$ and $CDCl_3$. *J. Phys. Chem.* **1991**, *95*, 7282-7290, doi:10.1021/j100172a035.

Jiménez, E.; Gierczak, T.; Stark, H.; Burkholder, J. B.; Ravishankara, A. R. Reaction of OH with HO_2NO_2 (Peroxynitric Acid, PNA): Rate coefficients between 218 and 335 K and product yields at 298 K. *J. Phys. Chem. A* **2004**, *108*, 1139-1149, doi:10.1021/jp0363489.

Johnston, H. S.; Tao, Y.-S. Thermal decomposition of nitrogen pentoxide at high temperature. *J. Am. Chem. Soc.* **1951**, *73*, 2948-2949, doi:10.1021/ja01150a518.

Kaiser, E. W.; Japar, S. M. The kinetics of the gas phase reaction of nitrous acid with ozone. *Chem. Phys. Lett.* **1977**, *52*, 121-124, doi:10.1016/0009-2614(77)85133-6.

Kaiser, E. W.; Japar, S. M. The kinetics of the gas phase reaction of O(^{3}P) with N_2O_5. *Chem. Phys. Lett.* **1978**, *54*, 265-268, doi:10.1016/0009-2614(78)80097-9.

Kistiakowsky, G. B.; Volpi, G. G. Reactions of nitrogen atoms. I. Oxygen and oxides of nitrogen. *J. Chem. Phys.* **1957**, *27*, 1141-1149, doi:10.1063/1.1743946.

Kistiakowsky, G. B.; Volpi, G. G. Reactions of nitrogen atoms. II. H_2, CO, NH_3, NO, and NO_2. *J. Chem. Phys.* **1958**, *28*, 665-668, doi:10.1063/1.1744209.

Klippenstein, S. J.; Harding, L. B.; Glarborg, P.; Gao, Y.; Hu, H.; Marshall, P. Rate constant and branching fraction for the $NH_2 + NO_2$ reaction. *J. Phys. Chem. A* **2013**, *117*, 9011-9022, doi:10.1021/jp4068069.

Ko, T.; Fontijn, A. High temperature photochemistry kinetics study of the reaction $H + NO_2 \rightarrow OH + NO$ from 286 to 760 K. *J. Phys. Chem.* **1991**, *95*, 3984-3987, doi:10.1021/j100163a019.

Kurasawa, H.; Lesclaux, R. Kinetics of the reaction of NH_2 with NO_2. *Chem. Phys. Lett.* **1979**, *66*, 602-607, doi:10.1016/0009-2614(79)80350-4.
Kurasawa, H.; Lesclaux, R. Rate constant for the reaction of NH_2 with ozone in relation to atmospheric processes. *Chem. Phys. Lett.* **1980**, *72*, 437-442, doi:10.1016/0009-2614(80)80325-3.
Kurylo, M. J. Kinetics of the reactions OH(v=0) + NH_3 → H_2O + NH_2 and OH(v=0) + O_3 → HO_2 + O_2 at 298°K. *Chem. Phys. Lett.* **1973**, *23*, 467-471, doi:10.1016/0009-2614(73)89003-7.
Lee, J. H.; Michael, J. V.; Payne, W. A., Jr.; Stief, L. J. Absolute rate of the reaction of N(^4S) with NO from 196-400 K with DF-RF and FP-RF techniques. *J. Chem. Phys.* **1978**, *69*, 3069-3076, doi:10.1063/1.436998.
Lesclaux, R.; Demissy, M. On the reaction of NH_2 radical with O_2, NO and NO_2. *Nouv. J. Chim.* **1977**, *1*, 443-444.
Lesclaux, R.; Khe, P. V.; Dezauzier, P.; Soulignac, J. C. Flash photolysis studies of the reaction of NH_2 radicals with NO. *Chem. Phys. Lett.* **1975**, *35*, 493-497, doi:10.1016/0009-2614(75)85650-8.
Leu, M. T. Rate constant for the reaction HO_2 + NO → OH + NO_2. *J. Chem. Phys.* **1979**, *70*, 1662-1666, doi:10.1063/1.437680.
Li, S. P.; Matthews, J.; Sinha, A. Atmospheric hydroxyl radical production from electronically excited NO_2 and H_2O. *Science* **2008**, *319*, 1657-1660, doi:10.1126/science.1151443.
Lin, C.-L.; Parkes, D. A.; Kaufman, F. Oscillator strength of the resonance transitions of ground-state N and O. *J. Chem. Phys.* **1970**, *53*, 3896-3900, doi:10.1063/1.1673858.
Lindholm, N.; Hershberger, J. F. Product branching ratios of the $NH_2(X^2B_1)$ + NO_2 reaction. *J. Phys. Chem.* **1997**, *101*, 4991-4995, doi:10.1021/j100046a020.
Lippmann, H. H.; Jesser, B.; Schurath, U. The rate constant of NO + O_3 → NO_2 + O_2 in the temperature range of 283–443 K. *Int. J. Chem. Kinet.* **1980**, *12*, 547-554, doi:10.1002/kin.550120805.
Littlejohn, D.; Johnston, H. S. Rate constant for the reaction of hydroxyl radicals and peroxynitric acid. *EOS* **1980**, *61*, 966.
Lozovsky, V. A.; Ioffe, M. A.; Sarkisov, O. M. On the reaction of the NH_2 radical with oxygen. *Chem. Phys. Lett.* **1984**, *110*, 651-654, doi:10.1016/0009-2614(84)85481-0.
Lozovsky, V. A.; Sarkisov, O. M.; Okhrimchuk, A. G.; Enis, A. L. Upper limit of the rate constant for the reaction of NH_2 radicals with O_2 measured by intracavity dye laser spectroscopy. *Chem. Phys. Rep.* **1997**, *16*, 395-417.
Mellouki, A.; Le Bras, G.; Poulet, G. Kinetics of the reactions of NO_3 with OH and HO_2. *J. Phys. Chem.* **1988**, *92*, 2229-2234, doi:10.1021/j100319a029.
Mellouki, A.; Talukdar, R. K.; Bopegedera, A. M. R. P.; Howard, C. J. Study of the kinetics of the reactions of NO_3 with HO_2 and OH. *Int. J. Chem. Kinet.* **1993**, *25*, 25-39, doi:10.1002/kin.550250104.
Meunier, H. P., P.; Sillesen, A. Kinetics and branching ratios of the reactions NH_2 + NO_2 → N_2O + H_2O and NH_2 + NO_2 → H_2NO + NO studied by pulse radiolysis combined with time-resolved infrared diode laser spectroscopy. *Chem. Phys. Lett.* **1996**, *261*, 277-282, doi:10.1016/0009-2614(96)00955-4.
Michael, J. V.; Allen, J. E., Jr.; Brobst, W. D. Temperature dependence of the NO + O_3 reaction rate from 195 to 369 K. *J. Phys. Chem.* **1981**, *85*, 4109-4117, doi:10.1021/j150626a032.
Michael, J. V.; Klemm, R. B.; Brobst, W. D.; Bosco, S. R.; Nava, D. F. Flash photolysis-laser induced fluorescence study of the rate constant for NH_2 + O_2 between 245 and 459 K. *J. Phys. Chem.* **1985**, *89*, 3335-3337, doi:10.1021/j100261a035.
Michael, J. V.; Nava, D. F.; Payne, W. A.; Lee, J. H.; Stief, L. J. Rate constant for the reaction H + NO_2 from 195 to 400 K with FP-RF and DF-RF techniques. *J. Phys. Chem.* **1979**, *83*, 2818-2823, doi:10.1021/j100485a003.
Moonen, P. C.; Cape, J. N.; Storeton-West, R. L.; McColm, R. Measurement of the NO + O_3 reaction rate at atmospheric pressure using realistic mixing ratios. *J. Atmos. Chem.* **1998**, *29*, 299-314, doi:10.1023/A:100593601.
Nakayama, T. T., K.; Matsumi, Y.; Shibuya K. N(^{4}S) Formation following the 193.3-nm ArF laser irradiation of NO and NO_2 and its application to kinetic studies of N(^{4}S) reactions with NO and NO_2. *J. Phys. Chem. A* **2005**, *109*, 10897–10902, doi:10.1021/jp054089c.
Okada, S.; Tezaki, A.; Miyoshi, A.; Matsui, H. Product branching fractions in the reactions of NH($a^1\Delta$) and NH($X^3\Sigma^-$) with NO. *J. Chem. Phys.* **1994**, *101*, 9582-9588, doi:10.1063/1.467989.
Pagsberg, P. B.; Erikson, J.; Christensen, H. C. Pulse radiolysis of gaseous ammonia-oxygen mixtures. *J. Phys. Chem.* **1979**, *83*, 582-590, doi:10.1021/j100468a006.
Park, J.; Lin, M. C. Direct determination of product branching for the NH_2 + NO reaction at temperatures between 302 and 1060 *J. Phys. Chem.* **1996**, *100*, 3317-3319, doi:10.1021/jp9533741.

Park, J.; Lin, M. C. A mass spectrometric study of the $NH_2 + NO_2$ reaction. *J. Phys. Chem. A* **1997**, *101*, 2643-2647, doi:10.1021/jp963720u.
Patrick, R.; Golden, D. M. Kinetics of the reactions of NH_2 radicals with O_3 and O_2. *J. Phys. Chem.* **1984**, *88*, 491-495, doi:10.1021/j150647a034.
Perry, R. A.; Atkinson, R.; Pitts, J. N., Jr. Rate constants for the reactions $OH + H_2S \rightarrow H_2O + SH$ and $OH + NH_3 \rightarrow H_2O + NH_2$ over the temperature range 297-427 °K. *J. Chem. Phys.* **1976**, *64*, 3237-3239, doi:10.1063/1.432663.
Phillips, L. F.; Schiff, H. I. Mass spectrometer studies of atoms reactions. I. Reactions in the atomic nitrogen-ozone system. *J. Chem. Phys.* **1962**, *36*, 1509-1517, doi:10.1063/1.1732772.
Piper, L. G.; Caledonia, G. E.; Konnealy, J. P. Rate constants for deactivation of $N_2(A)v' = 0,1$ by O_2. *J. Chem. Phys.* **1981**, *74*, 2888-2895, doi:10.1063/1.441408.
Quandt, R. W.; Hershberger, J. F. Product branching ratios of the NH ($^3\Sigma^-$) + NO and NH ($^3\Sigma^-$) + NO_2 reactions. *J. Phys. Chem.* **1995**, *99*, 16939-16944, doi:10.1021/j100046a020.
Quandt, R. W.; Hershberger, J. F. Diode laser study of the product branching ratio of the $NH_2(X^2B_1) + NO_2$ reaction. *J. Phys. Chem.* **1996**, *100*, 9407-9411, doi:10.1021/jp960432p.
Ray, G. W.; Watson, R. T. Kinetics of the reaction $NO + O_3 \rightarrow NO_2 + O_2$ from 212 to 422 K. *J. Phys. Chem.* **1981**, *85* 1673-1676, doi:10.1021/j150612a015.
Rozenshtein, V. B.; Gershenzon, Y. M.; Il'in, S. D.; Kishkovitch, O. P. Reactions of HO_2 with NO, OH and HO_2 studied by EPR/LMR spectroscopy. *Chem. Phys. Lett.* **1984**, *112*, 473-478, doi:10.1016/0009-2614(84)85572-4.
Sander, S. P.; Kircher, C. C. Temperature dependence of the reaction $NO + NO_3 \rightarrow 2NO_2$. *Chem. Phys. Lett.* **1986**, *126*, 149-152, doi:10.1016/S0009-2614(86)80029-X.
Sarkisov, O. M.; Cheskis, S. G.; Sviridenkov, E. A. Study of $NH_2 + NO$ reaction employing intraresonator laser spectroscopy. *Bull. Acad. Sci. USSR Chem.* **1978**, *Ser. 27*, 2336-2338, doi:10.1007/BF00946690.
Schurath, U.; Lippmann, H. H.; Jesser, B. Temperature dependence of the chemiluminescent reaction (1), $NO + O_3 \rightarrow NO_2(^2A_1\text{-}^2B_{1,2}) + O_2$, and quenching of the excited product. *Ber. Bunsenges. Phys. Chem.* **1981**, *85*, 807-813, doi:10.1002/bbpc.19810850814.
Seeley, J. V.; Meads, R. F.; Elrod, M. J.; Molina, M. J. Temperature and pressure dependence of the rate constant for the $HO_2 + NO$ reaction. *J. Phys. Chem.* **1996**, *100*, 4026-4031, doi:10.1021/jp952553f.
Silver, J. A.; Kolb, C. E. Rate constant for the reaction $NH_3 + OH \rightarrow NH_2 + H_2O$ over a wide temperature range. *Chem. Phys. Lett.* **1980**, *75*, 191-195, doi:10.1016/0009-2614(80)80492-1.
Silver, J. A.; Kolb, C. E. Kinetic measurements for the reaction of $NH_2 + NO$ over the temperature range 294-1215 K. *J. Phys. Chem.* **1982**, *86*, 3240-3246, doi:10.1021/j100213a033.
Silver, J. A.; Kolb, C. E. A reevaluation of the branching ratio for the reaction of NH_2 with NO. *J. Phys. Chem.* **1987**, *91*, 3713-3714, doi:10.1021/j100297a051.
Smith, C. A.; Molina, L. T.; Lamb, J. J.; Molina, M. J. Kinetics of the reaction of OH with pernitric and nitric acids. *Int. J. Chem. Kinet.* **1984**, *16*, 41-55, doi:10.1002/kin.550160107.
Smith, I. W. M.; Zellner, R. Rate measurements of OH by resonance absorption. IV. Reactions of OH with NH_3 and HNO_3. *Int. J. Chem. Kinet. Symp. No. 1* **1975**, 341-351.
Song, S.; Golden, D. M.; Hanson, R. K.; Bowman, C. T. A shock tube study of the $NH_2 + NO_2$ reaction. *Proc. Combustion Inst.* **2002**, *29*, 2163-2170, doi:10.1016/S1540-7489(02)80263-2.
Stedman, D. H.; Niki, H. Kinetics and mechanism for the photolysis of nitrogen dioxide in air. *J. Phys. Chem.* **1973**, *77*, 2604-2609, doi:10.1021/j100640a005.
Stephens, J. W.; Morter, C. L.; Farhat, S. K.; Glass, G. P.; Curl, R. F. Branching ratio of the reaction $NH_2 + NO$ at elevated temperatures. *J. Phys. Chem.* **1993**, *97*, 8944-8951, doi:10.1021/j100137a019.
Stephens, R. D. Absolute rate constants for the reaction of hydroxyl radicals with ammonia from 297 to 364 K. *J. Phys. Chem.* **1984**, *88*, 3308-3313, doi:10.1021/j150659a034.
Stief, L. J.; Brobst, W. D.; Nava, D. F.; Borkowski, R. P.; Michael, J. V. Rate constant for the reaction $NH_2 + NO$ from 216 to 480 K. *J. Chem. Soc. Faraday Trans. 2* **1982**, *78*, 1391-1401, doi:10.1039/F29827801391.
Stief, L. J.; Payne, W. A.; Lee, J. H.; Michael, J. V. The reaction $N(^4S) + O_3$: An upper limit for the rate constant at 298 K. *J. Chem. Phys.* **1979**, *70*, 5241-5243, doi:10.1063/1.437317.
Streit, G. E.; Wells, J. S.; Fehsenfeld, F. C.; Howard, C. J. A tunable diode laser study of the reactions of nitric and nitrous acids: $HNO_3 + NO$ and $HNO_2 + O_3$. *J. Chem. Phys.* **1979**, *70*, 3439-3443, doi:10.1063/1.437878.
Stuhl, F. Absolute rate constant for the reaction $OH + NH_3 \rightarrow NH_2 + H_2O$. *J. Chem. Phys.* **1973**, *59*, 635-637, doi:10.1063/1.1680069.

Sugawara, K.; Ishikawa, Y.; Sato, S. The rate constants of the reactions of the metastable nitrogen atoms, ^2D and ^2P, and the reactions of $N(^4S) + NO \rightarrow N_2 + O(^3P)$ and $O(^3P) + NO + M \rightarrow NO_2 + M$. *Bull. Chem. Soc. Jpn.* **1980**, *53*, 3159-3164, doi:10.1246/bcsj.53.3159.

Sverdrup, G. M.; Spicer, C. W.; Ward, G. F. Investigation of the gas phase reaction of dinitrogen pentoxide with water vapor. *Int. J. Chem. Kinet.* **1987**, *19*, 191-205, doi:10.1002/kin.550190304.

Thomas, J. M.; Kaufman, F. An upper limit on the formation of $NO(X^2\Pi_r)$ in the reactions $N_2(A^3\Sigma_u^+) + O(^3P)$ and $N2(A^3S_u^+) + O_2(X^3\Sigma_g^-)$ at 298 K. *J. Phys. Chem.* **1996**, *100*, 8901-8906, doi:10.1021/jp960164v.

Thomas, J. M.; Kaufman, F.; Golde, M. F. Rate constants for electronic quenching of $N_2(A^3S_u^+$, v=0-6) by O_2, NO, CO, N_2O, and C_2H_4. *J. Chem. Phys.* **1987**, *86*, 6885-6892, doi:10.1063/1.452388.

Thomas, J. W.; Kaufman, F. Rate constants of the reactions of metastable $N_2(A\ ^3\Sigma_u^+)$ in $v = 0$, 1, 2, and 3 with ground state O_2 and O. *J. Chem. Phys.* **1985**, *83*, 2900-2903, doi:10.1063/1.449243.

Thrush, B. A.; Wilkinson, J. P. T. The rate of reaction of HO_2 radicals with HO and with NO. *Chem. Phys. Lett.* **1981**, *81*, 1-3, doi:10.1016/0009-2614(81)85314-6.

Trevor, P. L.; Black, G.; Barker, J. R. Reaction rate constant for $OH + HOONO_2 \rightarrow$ products over the temperature range 246 to 324 K. *J. Phys. Chem.* **1982**, *86*, 1661-1669, doi:10.1021/j100206a035.

Tuazon, E. C.; Atkinson, R.; Plum, C. N.; Winer, A. M.; Pitts, J. N. The reaction of gas phase N_2O_5 with water vapor. *Geophys. Res. Lett.* **1983**, *10*, 953-956, doi:10.1029/GL010i010p00953/pdf.

Tyndall, G. S.; Orlando, J. J.; Calvert, J. G. Upper limit for the rate coefficient for the reaction $HO_2 + NO_2 \rightarrow$ HONO + O_2. *Environ. Sci. Technol.* **1995**, *29*, 202-206, doi:10.1021/es00001a026.

Tyndall, G. S.; Orlando, J. J.; Cantrell, C. A.; Shetter, R. E.; Calvert, J. G. Rate coefficient for the reaction NO + $NO_3 \rightarrow 2NO_2$ between 223 and 400 K. *J. Phys. Chem.* **1991**, *95*, 4381-4386, doi:10.1021/j100164a040.

Tyndall, G. S.; Orlando, J. J.; Nickerson, K. E.; Cantrell, C. A.; Calvert, J. G. An upper limit for the rate coefficient of the reaction of NH_2 radicals with O_2 using FTIR product analysis. *J. Geophys. Res.* **1991**, *96*, 20761-20768, doi:10.1029/91JD02044.

Verhees, P. W. C.; Adema, E. H. The NO_2-O_3 system at sub-ppm concentrations: Influence of temperature and relative humidity. *J. Atmos. Chem.* **1985**, *2*, 387-403, doi:10.1007/BF00130750.

Wagner, H. G.; Welzbacher, U.; Zellner, R. Rate measurements for reactions $H + NO_2 \rightarrow OH + NO$ and H + NOCl $\rightarrow$ HCl + NO by Lyman-α fluorescence. *Ber. Bunsenges. Phys. Chem.* **1976**, *80*, 1023-1027, doi:10.1002/bbpc.19760801018

Walch, S. P. Theoretical characterization of the reaction $NH_2 +$ NO $\rightarrow$ products. *J. Chem. Phys.* **1993**, *99*, 5295-5300, doi:10.1063/1.465972.

Wangberg, I.; Ljungstrom, E.; Olsson, B. E. R.; Davidsson, J. Temperature-dependence of the reaction $NO_3 + NO_2 \rightarrow NO + NO_2 + O_2$ in the range from 296 K to 332 K. *J. Phys. Chem.* **1992**, *96*, 7640-7645, doi:10.1021/j100198a029.

Wategaonkar, S. J.; Setser, D. W. Infrared chemiluminescence studies of H atom reactions with Cl_2O, ClNO, F_2O, CF_3OF, ClO_2, NO_2, and ClO. *J. Chem. Phys.* **1989**, *90*, 251-264, doi:10.1063/1.456527.

Wennberg, P. O.; Anderson, J. G.; Weisenstein, D. K. Kinetics of reactions of ground state nitrogen atoms ($^4S_{3/2}$) with NO and NO_2. *J. Geophys. Res.* **1994**, *99*, 18839-18846, doi:10.1029/94JD01823.

Westenberg, A. A.; Roscoe, J. M.; deHaas, N. Rate measurements on $N + O_2(^1\Delta_g) \rightarrow NO + O$ and $H + O_2(^1\Delta_g) \rightarrow$ OH + O. *Chem. Phys. Lett.* **1970**, *7*, 597-599, doi:10.1016/0009-2614(70)87014-2.

Whyte, A. R.; Phillips, L. F. Rates of reaction of NH_2 with N, NO and NO_2. *Chem. Phys. Lett.* **1983**, *102*, 451-454, doi:10.1016/0009-2614(83)87444-2.

Wilson, W. E. Rate constant for the reaction $N + O_2 \rightarrow NO + O$. *J. Chem. Phys.* **1967**, *46*, 2017-2018, doi:10.1063/1.1840988.

Winkler, I. C.; Stachnik, R. A.; Steinfeld, J. I.; Miller, S. M. Determination of NO (v = 0-7) product distribution from the $N(^4S) + O_2$ reaction using two-photon ionization. *J. Chem. Phys.* **1986**, *85*, 890-899, doi:10.1063/1.451840.

Wolf, M.; Yang, D. L.; Durant, J. L. Kinetic studies of NH_x radical reactions. *J. Photochem. Photobiol. A: Chem.* **1994**, *80*, 85-93, doi:i10.1016/1010-6030(93)01037-3.

Xiang, T.; Torres, M. L.; Guillory, W. A. State-selected reaction and relaxation of $NH_2[X^2B_1(0,\nu_2,0)]$ radicals and NO_2. *J. Chem. Phys.* **1985**, *83*, 1623-1629, doi:10.1063/1.449399.

Yamasaki, K.; Okada, S.; Koski, M.; Matsui, H. Selective product channels in the reactions of $NH(a^1\Delta)$ and $NH(X^3\Sigma^-)$ with NO. *J. Chem. Phys.* **1991**, *95*, 5087-5096, doi:10.1063/1.461676.

Yamasaki, K.; Watanabe, A.; Tanaka, A.; Sato, M.; Tokue, I. Kinetics of the reaction $NH_2(X^2B_1$, $\nu_2 = 0$ and 1) + NO. *J. Phys. Chem. A* **2002**, *106*, 6563-6569, doi:10.1021/jp013306g.

Zipf, E. C. A laboratory study on the formation of nitrous oxide by the reaction $N_2(A^3\Sigma_u^+) + O_2 \rightarrow N_2O + O$. *Nature (London)* **1980**, *287*, 523-525, doi:10.1038/287523a0.

1.9 Reactions of Organic Compounds

1.9.1 Table 1D: Reactions of Organic Compounds

Reaction	Temperature Range of Exp. Data (K) [a]	*A*-Factor	*E*/R	*k*(298 K) [b]	*f*(298 K) [c]	*g* [c]	Note
$O + CH_3 \rightarrow$ products	259–341	1.1×10^{-10}	0	1.1×10^{-10}	1.30	250	D 1
$O + HCN \rightarrow$ products	469–900	1.0×10^{-11}	4000	1.5×10^{-17}	10.0	0	D 2
$O + C_2H_2 \rightarrow$ products	(See Note)	3.0×10^{-11}	1600	1.4×10^{-13}	1.30	250	D 3
$O + H_2CO \rightarrow$ products	250–748	3.4×10^{-11}	1600	1.6×10^{-13}	1.25	250	D 4
$O + CH_3CHO \rightarrow CH_3CO + OH$	298–475	1.8×10^{-11}	1100	4.5×10^{-13}	1.25	200	D 5
$O_2 + HOCO \rightarrow HO_2 + CO_2$	298			2×10^{-12} (See Note)	2.00		D 6
$O_3 + C_2H_2 \rightarrow$ products	243–323	*1.0×10^{-14}*	*4100*	1.0×10^{-20}	3.00	500	D 7
$O_3 + C_2H_4 \rightarrow$ products	178–373	1.2×10^{-14}	2630	1.7×10^{-18}	1.25	100	D 8
$O_3 + C_3H_6 \rightarrow$ products	183–362	6.5×10^{-15}	1900	1.1×10^{-17}	1.15	200	D 9
$O_3 + CH_2{=}C(CH_3)CHO \rightarrow$ products	240–324	1.5×10^{-15}	2110	1.3×10^{-18}	1.10	200	D10
$O_3 + CH_3C(O)CH{=}CH_2 \rightarrow$ products	240–324	8.5×10^{-16}	1520	5.2×10^{-18}	1.15	100	D11
$O_3 + CH_2{=}C(CH_3)CH{=}CH_2 \rightarrow$ products	242–353	1.1×10^{-14}	2000	1.3×10^{-17}	1.10	200	D12
$OH + CO \rightarrow$ Products		(See Table 2-1)					D13
$OH + CH_4 \rightarrow CH_3 + H_2O$	178–2025	2.45×10^{-12}	1775	6.3×10^{-15}	1.10	100	D14
$OH + {}^{13}CH_4 \rightarrow {}^{13}CH_3 + H_2O$	273–353	See Note					D15
$OH + CH_3D \rightarrow$ products	249–420	3.5×10^{-12}	1950	5.0×10^{-15}	1.15	200	D16
$OH + H_2CO \rightarrow H_2O + HCO$	228–2500	5.5×10^{-12}	–125	8.5×10^{-12}	1.15	50	D17
$OH + CH_3OH \rightarrow$ products	210–1350	2.9×10^{-12}	345	9.1×10^{-13}	1.10	60	D18
$OH + CH_3OOH \rightarrow$ products	203–423	3.8×10^{-12}	–200	7.4×10^{-12}	1.40	150	D19
$OH + HC(O)OH \rightarrow$ products	296–445	4.0×10^{-13}	0	4.0×10^{-13}	1.20	100	D20
$OH + HC(O)C(O)H \rightarrow$ products	210–390	1.15×10^{-11}	*0*	1.15×10^{-11}	1.50	200	D21
$OH + HOCH_2CHO \rightarrow$ products	240–362	8.1×10^{-12}	0	8.1×10^{-12}	1.10	0	D22
$OH + C_2H_2 \xrightarrow{M}$ products		(See Table 2-1)					

Reaction	Temperature Range of Exp. Data (K) [a]	*A*-Factor	*E*/R	*k*(298 K) [b]	*f*(298 K) [c]	*g* [c]	Note
$OH + C_2H_4 \xrightarrow{M} products$		(See Table 2-1)					
$OH + C_2H_6 \rightarrow H_2O + C_2H_5$	226–2000	7.66×10^{-12}	1020	2.5×10^{-13}	1.05	20	D23
$OH + CH_3CHO \rightarrow products$	202–350	4.63×10^{-12}	–350	1.5×10^{-11}	1.05	20	D24
$OH + CH_3OC(O)H \rightarrow products$	233–372	8.43×10^{-12}	460	1.8×10^{-13}	1.15	50	D25
$OH + CH_3CH_2OH \rightarrow products$	216–498	3.35×10^{-12}	0	3.35×10^{-12}	1.05	20	D26
$OH + CH_3C(O)OH \rightarrow products$	229–802	3.15×10^{-14}	–920	6.9×10^{-13}	1.15	100	D27
$OH + C_3H_8 \rightarrow products$	190–908	9.19×10^{-12}	630	1.11×10^{-12}	1.03	20	D28
$OH + C_2H_5CHO \rightarrow C_2H_5CO + H_2O$	240–372	4.9×10^{-12}	–405	1.9×10^{-11}	1.05	80	D29
$OH + 1\text{–}C_3H_7OH \rightarrow products$	263–372	4.4×10^{-12}	–70	5.6×10^{-12}	1.05	80	D30
$OH + 2\text{–}C_3H_7OH \rightarrow products$	220–745	2.10×10^{-12}	–270	5.2×10^{-12}	1.03	20	D31
$OH + C_2H_5C(O)OH \rightarrow products$	240–445	1.2×10^{-12}	0	1.2×10^{-12}	1.10	200	D32
$OH + CH_3C(O)CH_3 \rightarrow H_2O + CH_3C(O)CH_2$ $\rightarrow CH_3 + CH_3C(O)OH$	242–1650	(See Note)		< 2% of k			D33
$OH + CH_3OCH_2OCH_3 \rightarrow products$	252–372	2.12×10^{-12}	-250	4.9×10^{-12}	1.10	50	D34
$OH + n\text{-}C_4H_{10} \rightarrow products$	185–509	1.02×10^{-11}	430	2.4×10^{-12}	1.03	20	D35
$OH + iso\text{-}C_4H_{10} \rightarrow products$	213–864	4.86×10^{-12}	250	2.1×10^{-12}	1.05	20	D36
$OH + n\text{-}C_5H_{12} \rightarrow products$	224–900	1.49×10^{-11}	400	3.9×10^{-12}	1.05	50	D37
$OH + iso\text{-}C_5H_{12} \rightarrow products$	213–407	6.55×10^{-12}	170	3.7×10^{-12}	1.07	20	D38
$OH + cyclo\text{-}C_5H_{10} \rightarrow products$	209–491	1.68×10^{-11}	370	4.85×10^{-12}	1.05	50	D39
$OH + CH_2=C(CH_3)CHO \rightarrow products$	234–423	9.6×10^{-12}	–360	3.2×10^{-11}	1.15	100	D40
$OH + CH_3C(O)CH=CH_2 \rightarrow products$	232–424	2.7×10^{-12}	–580	1.9×10^{-11}	1.07	100	D41
$OH + CH_2=C(CH_3)CH=CH_2 \rightarrow products$	240–422	3.0×10^{-11}	–360	9.9×10^{-11}	1.10	50	D42
$OH + CH_3CN \rightarrow products$	256–424	7.8×10^{-13}	1050	2.3×10^{-14}	1.50	200	D43
$OH + CH_3ONO_2 \rightarrow products$	221–423	8.0×10^{-13}	1000	2.8×10^{-14}	1.70	200	D44
$OH + CH_3C(O)O_2NO_2$ (PAN) $\rightarrow$ products	273–299			$<4\times10^{-14}$			D45
$OH + C_2H_5ONO_2 \rightarrow products$	298–373	1.0×10^{-12}	490	2.0×10^{-13}	1.40	150	D46
$OH + 1\text{–}C_3H_7ONO_2 \rightarrow products$	298–368	7.1×10^{-13}	0	7.1×10^{-13}	1.50	200	D47

Reaction	Temperature Range of Exp. Data (K) [a]	*A*-Factor	*E*/R	*k*(298 K) [b]	*f*(298 K) [c]	*g* [c]	Note
$OH + 2\text{–}C_3H_7ONO_2 \rightarrow$ products	295–299	1.2×10^{-12}	320	4.1×10^{-13}	1.50	200	D48
$HO_2 + CH_2O \rightarrow$ adduct	273–373	6.7×10^{-15}	–600	5.0×10^{-14}	5.00	600	D49
$HO_2 + CH_3O_2 \rightarrow CH_3OOH + O_2$	228–700	4.1×10^{-13}	–750	5.2×10^{-12}	1.30	150	D50
$HO_2 + C_2H_5O_2 \rightarrow C_2H_5OOH + O_2$	210–480	7.5×10^{-13}	–700	8.0×10^{-12}	1.50	250	D51
$HO_2 + CH_3C(O)O_2 \rightarrow$ products	253–403	4.3×10^{-13}	–1040	1.4×10^{-11}	2.00	500	D52
$HO_2 + CH_3C(O)CH_2O_2 \rightarrow$ products	298	*8.6×10^{-13}*	*–700*	9.0×10^{-12}	2.00	300	D53
$NO_3 + CO \rightarrow$ products	295–298			$<4.0\times10^{-19}$			D54
$NO_3 + CH_2O \rightarrow$ products	295–298			5.8×10^{-16}	1.30		D55
$NO_3 + CH_3CHO \rightarrow$ products	263–433	1.4×10^{-12}	1900	2.4×10^{-15}	1.30	300	D56
$NO_3 + CH_2{=}C(CH_3)CHO \rightarrow$ products	296–323			3.4×10^{-15}	1.25		D57
$NO_3 + CH_3C(O)CH{=}CH_2 \rightarrow$ products	296–323			$< 4\times10^{-16}$			D58
$NO_3 + CH_2{=}C(CH_3)CH{=}CH_2 \rightarrow$ products	251–381	3.5×10^{-12}	450	7.8×10^{-13}	1.25	100	D59
$CH_3 + O_2 \rightarrow$ products	298–3000			$<3.0\times10^{-16}$			D60
$CH_3 + O_2 \xrightarrow{M} CH_3O_2$		(See Table 2-1)					
$CH_3 + O_3 \rightarrow$ products	221–384	5.4×10^{-12}	220	2.6×10^{-12}	2.00	150	D61
$HCO + O_2 \rightarrow CO + HO_2$	200–2000	5.2×10^{-12}	0	5.2×10^{-12}	1.40	100	D62
$CH_2OH + O_2 \rightarrow CH_2O + HO_2$	215–2000	9.1×10^{-12}	0	9.1×10^{-12}	1.30	200	D63
$CH_3O + O_2 \rightarrow CH_2O + HO_2$	296–900	3.9×10^{-14}	900	1.9×10^{-15}	1.50	300	D64
$CH_3O + NO \rightarrow CH_2O + HNO$ $CH_3O + NO \xrightarrow{M} CH_3ONO$		(See Note) (See Table 2-1)					D65
$CH_3O + NO_2 \rightarrow CH_2O + HONO$	298–1100	1.1×10^{-11}	1200	2.0×10^{-13}	5.00	600	D66
$CH_3O + NO_2 \xrightarrow{M} CH_3ONO_2$		(See Table 2-1)					
$CH_3O_2 + O_3 \rightarrow$ products	298	*2.9×10^{-16}*	*1000*	1.0×10^{-17}	3.00	500	D67
$CH_3O_2 + CH_3O_2 \rightarrow$ products	248–700	9.5×10^{-14}	–390	3.5×10^{-13}	1.20	100	D68
$CH_3O_2 + NO \rightarrow CH_3O + NO_2$	193–429	2.8×10^{-12}	–300	7.7×10^{-12}	1.15	100	D69
$CH_3O_2 + NO_2 \xrightarrow{M} CH_3O_2NO_2$		(See Table 2-1)					
$CH_3O_2 + CH_3C(O)O_2 \rightarrow$ products	253–368	2.0×10^{-12}	–500	1.1×10^{-11}	1.50	250	D70

Reaction	Temperature Range of Exp. Data (K) [a]	*A*-Factor	*E*/R	*k*(298 K) [b]	*f*(298 K) [c]	*g* [c]	Note
$CH_3O_2 + CH_3C(O)CH_2O_2 \rightarrow$ products	298	*7.5×10⁻¹³*	*–500*	4.0×10⁻¹²	2.00	300	D71
$C_2H_5 + O_2 \rightarrow C_2H_4 + HO_2$				<2.0×10⁻¹⁴			D72
$C_2H_5 + O_2 \xrightarrow{M} C_2H_5O_2$		(See Table 2-1)					
$C_2H_5O + O_2 \rightarrow CH_3CHO + HO_2$	225–411	6.3×10⁻¹⁴	550	1.0×10⁻¹⁴	1.50	200	D73
$C_2H_5O + NO \xrightarrow{M}$ products		(See Table 2-1)					
$C_2H_5O + NO_2 \xrightarrow{M}$ products		(See Table 2-1)					
$C_2H_5O_2 + C_2H_5O_2 \rightarrow$ products	228–460	6.8×10⁻¹⁴	0	6.8×10⁻¹⁴	2.00	300	D74
$C_2H_5O_2 + NO \rightarrow$ products	220–355	2.6×10⁻¹²	–365	8.7×10⁻¹²	1.20	150	D75
$CH_3C(O)O_2 + CH_3C(O)O_2 \rightarrow$ products	209–368	2.55×10⁻¹²	–535	1.40×10⁻¹¹	1.10	50	D76
$CH_3C(O)O_2 + NO \rightarrow$ products	218–402	8.1×10⁻¹²	–270	2.0×10⁻¹¹	1.50	100	D77
$CH_3C(O)O_2 + NO_2 \xrightarrow{M}$ products		See Table 2-1					
$CH_3C(O)CH_2O_2 + NO \rightarrow$ products	298	*2.9×10⁻¹²*	*–300*	8.0×10⁻¹²	1.50	300	D78
$HOC_5H_8OO + NO \rightarrow HOC_5H_8O + NO_2$ (k_1)	295–300	(See Note)					
$\xrightarrow{M} HOC_5H_8ONO_2$ (k_2)	295–300	(See Note)					D79
$k_{total} = k_1 + k_2$	295–300	*2.7×10⁻¹²*	*–350*	8.8×10⁻¹²	1.15	300	
Criegee Intermediate Reactions							
$CH_2OO \rightarrow$ products		(See Note)					D80
$CH_2OO + O_3 \rightarrow$ products	298			3.6×10⁻¹³	1.11		D81
$CH_2OO + H_2O \rightarrow$ products	293–298			2.8×10⁻¹⁶	1.70		D82
$CH_2OO + (H_2O)_2 \rightarrow$ products	283–324	2.8×10⁻¹⁶	–3010	6.8×10⁻¹²	1.10	400	D83
$CH_2OO + NO \rightarrow$ products	298			<6.4×10⁻¹⁴			D84
$CH_2OO + NO_2 \rightarrow$ products	298			4.25×10⁻¹²	1.70		D85
$CH_2OO + HNO_3 \rightarrow$ products	298			5.4×10⁻¹⁰	1.20		D86
$CH_2OO + CH_2OO \rightarrow$ products	298			7.12×10⁻¹¹	1.40		D87
$CH_2OO + HC(O)OH \rightarrow$ products	298			1.1×10⁻¹⁰	1.10		D88
$CH_2OO + CH_3CHO \rightarrow$ products	298–494	2.5×10⁻¹⁴	–1180	1.3×10⁻¹²	1.40	100	D89
$CH_2OO + CH_3C(O)OH \rightarrow$ products	298			1.25×10⁻¹⁰	1.10		D90

Reaction	Temperature Range of Exp. Data (K) [a]	*A*-Factor	*E*/R	*k*(298 K) [b]	*f*(298 K) [c]	*g* [c]	Note
$CH_2OO + CH_2=CH_2 \rightarrow$ products	298–494	1.1×10^{-14}	850	6.6×10^{-16}	1.20	100	D91
$CH_2OO + CH_3C(O)CH_3 \rightarrow$ products	298–494	$6.\times10^{-15}$	–1132	2.9×10^{-13}	1.10	85	D92
$CH_2OO + CH_2=CHCH_3 \rightarrow$ products	298–494	8.0×10^{-15}	450	1.75×10^{-15}	1.20	100	D93
$CH_2OO + CH_2=CHCH_2CH_3 \rightarrow$ products	298–494	5.3×10^{-15}	380	1.5×10^{-15}	1.20	100	D94
$CH_2OO + (CH_3)_2C=CH_2 \rightarrow$ products	298–494	5.4×10^{-15}	400	1.4×10^{-15}	1.20	100	D95
$CH_2OO + CH_3CH=CHCH_3 \rightarrow$ products	298–494	2.5×10^{-15}	400	6.5×10^{-16}	1.20	100	D96
$CH_2OO + CF_3C(O)OH \rightarrow$ products	240–340	1.2×10^{-10}	–300	3.3×10^{-10}	1.20	200	D97
$CH_2OO + CF_3C(O)CF_3$ (HFA)$\rightarrow$ products	298			3.17×10^{-11}	1.10		D98
$CH_2OO + HCl \rightarrow$ products	298			4.6×10^{-11}	1.20		D99
$CH_2OO + H_2S \rightarrow$ products	278–318	1×10^{-14}	–580	4.6×10^{-11}	1.20	200	D100
$CH_2OO + SO_2 \rightarrow$ products	223–344	6.22×10^{-12}	–541	3.82×10^{-11}	1.1 0	110	D101
$CH_3CHOO \rightarrow$ products		(See Note)					D102
anti-$CH_3CHOO + H_2O \rightarrow$ products	288–328	1.05×10^{-14}	–50.32	1.31×10^{-14}	1.18	50	D103
syn-$CH_3CHOO + H_2O \rightarrow$ products	298			$<2\times10^{-16}$			D103
anti-$CH_3CHOO + (H_2O)_2 \rightarrow$ products	288–328	5.23×10^{-20}	–6124.18	4.40×10^{-14}	1.12	50	D103
syn-$CH_3CHOO + (H_2O)_2 \rightarrow$ products		(See Note)					D103
anti-$CH_3CHOO + HC(O)OH \rightarrow$ products	298			5.0×10^{-10}	1.30		D104
syn-$CH_3CHOO + HC(O)OH \rightarrow$ products	298			2.5×10^{-10}	1.06		D104
anti-$CH_3CHOO + SO_2 \rightarrow$ products	242–353	1.15×10^{-10}	*0*	1.15×10^{-10}	1.25		D105
syn-$CH_3CHOO + SO_2 \rightarrow$ products	242–353	2.44×10^{-12}	–750	3.02×10^{-11}	1.25	50	D105
Furanoid Reactions							
OH + Furan $\rightarrow$ products	254–425	1.36×10^{-11}	–330	4.11×10^{-11}	1.05	50	D106
OH + 2-Methyl Furan $\rightarrow$ products	298–668			9.95×10^{-10}	1.07		D107
OH + 3-Methyl Furan $\rightarrow$ products	273–368	3.2×10^{-11}	–325	9.5×10^{-11}	1.10	50	D108
OH + 2,5-Dimethyl Furan $\rightarrow$ products	298			1.24×10^{-11}	1.05		D109
OH + 2-ethyl Furan $\rightarrow$ products	300			2.1×10^{-11}	1.20		D110

Shaded areas indicate changes or additions since JPL19-5. Italicized *blue* entries denote estimates.

[a] Temperature range of available experimental data. This is not necessarily the range of temperature over which the recommended Arrhenius parameters are applicable. See the corresponding note for each reaction for such information.

[b] Units are cm^3 $molecule^{-1}$ s^{-1}.

[c] f(298 K) is the uncertainty factor at 298 K. To calculate the uncertainty at other temperatures, use the expression:

$$f(\mathrm{T}) = f(298\ \mathrm{K})\exp\left|g\left(\frac{1}{\mathrm{T}} - \frac{1}{298}\right)\right|$$

Note that the exponent is an absolute value.

1.9.2 Notes: Reactions of Organic Compounds

D1. **O + CH_3.** The recommended k(298 K) is the weighted average of the measurements by Washida and Bayes[3] (259–341 K), Washida[2] (298 K), and Plumb and Ryan[1] (295 K). The E/R value is based on the results of Washida and Bayes, who found k to be independent of temperature.
(Table: 83-62, Note: 83-62, Evaluated: 83-62) Back to Table

(1) Plumb, I. C.; Ryan, K. R. Kinetics of the reactions of CH_3 with $O(^3P)$ and O_2 at 295 K. *Int. J. Chem. Kinet.* **1982**, *14*, 861-874, doi:10.1002/kin.550140806.
(2) Washida, N. Reaction of methyl radicals with $O(^3P)$, O_2 and NO. *J. Chem. Phys.* **1980**, *73*, 1665-1672, doi:10.1063/1.440348.
(3) Washida, N.; Bayes, K. D. The reactions of methyl radicals with atomic and molecular oxygen. *Int. J. Chem. Kinet.* **1976**, *8*, 777-794, doi:10.1002/kin.550080512.

D2. **O + HCN.** Because it is a very slow reaction, there are no studies of this reaction below 450 K. Davies and Thrush[1] studied this reaction between 469 and 574 K while Perry and Melius[3] studied it between 540 and 900 K. Results of Perry and Melius are in agreement with those of Davies and Thrush. Our recommendation is based on these two studies. The higher-temperature (T>1000 K) combustion-related studies of Roth et al.,[4] Szekely et al.,[5] and Louge and Hanson[2] have not been considered. This reaction has two reaction pathways: O + HCN → H + NCO, $\Delta H = -2$ kcal/mol (k_a); and O + HCN → CO + NH (k_b), $\Delta H = -36$ kcal/mol. The branching ratio k_a/k_b for these two channels has been measured to be ~2 at 860 K. The branching ratio at lower temperatures, which is likely to vary significantly with temperature, is unknown.
(Table: 87-41, Note: 92-20, Evaluated: 92-20) Back to Table

(1) Davies, P. B.; Thrush, B. A. Reactions of oxygen atoms with hydrogen cyanide, cyanogen chloride and cyanogen bromide. *Trans. Faraday Soc.* **1968**, *64*, 1836-1843, doi:10.1039/tf9686401836.
(2) Louge, M. Y.; Hanson, R. K. *Twentieth Symposium (International) on Combustion* **1984**, 665-672.
(3) Perry, R. A.; Melius, C. F. In *Twentieth Symposium (International) on Combustion*; The Combustion Institute, 1984; pp 639-646.
(4) Roth, P.; Löhr, R.; Hermanns, H. D. Shock wave measurements on the kinetics of the reaction HCN + O. *Ber. Bunsenges. Phys. Chem.* **1980**, *84*, 835-840, doi:10.1002/bbpc.19800840903.
(5) Szekely, A.; Hanson, R. K.; Bowman, C. In *Twentieth Symposium (International) on Combustion*; The Combustion Institute, 1984; pp 647-654.

D3. **O + C_2H_2.** The recommended k(298 K) is an average of ten measurements (Arrington et al.[2] (195, 295 K), Sullivan and Warneck[8] (298 K), Brown and Thrush[3] (298 K), Hoyermann et al.[4,5] (295, 243–673 K), Westenberg and deHaas[10] (195–616 K), James and Glass[6] (273–729 K), Stuhl and Niki[7] (300 K), Westenberg and deHaas[11] (297 K), and Aleksandrov et al.[1] (298–608 K)). There is reasonably good agreement among these studies. Arrington et al. did not observe a temperature dependence, an observation that was later shown to be erroneous by Westenberg and deHaas.[10] Westenberg and deHaas,[10] Hoyermann et al.,[5] and Aleksandrov et al. are the only authors who have measured the temperature dependence below 500 K. Westenberg and deHaas observed a curved Arrhenius plot at temperatures higher than 450 K. In the range 194–450 K, Arrhenius behavior provides an adequate description and the E/R obtained by a fit of the data from these three groups in this temperature range is recommended. The A-factor was calculated to reproduce k(298 K). This reaction can have two sets of products, i.e., C_2HO + H or CH_2 + CO. Under molecular beam conditions C_2HO has been shown to be the major product. The study by Aleksandrov et al. using a discharge flow-resonance fluorescence method (under undefined pressure conditions) indicates that the C_2HO + H channel contributes no more than 7% to the net reaction at 298 K, while a similar study by Vinckier et al.[9] (300–600 K) suggests that both CH_2 and C_2HO are formed.
(Table: 82-57, Note: 82-57, Evaluated: 82-57) Back to Table

(1) Aleksandrov, E. N.; Arutyunov, V. S.; Kozlov, S. N. Investigation of the reaction of atomic oxygen with acetylene. *Kinetics and Catalysis* **1981**, *22*, 391-394.
(2) Arrington, C. A.; Brennen, W.; Glass, G. P.; Michael, J. V.; Niki, H. Reactions of atomic oxygen with acetylene. I. Kinetics and mechanisms. *J. Chem. Phys.* **1965**, *43*, 525-532, doi:10.1063/1.1696776.
(3) Brown, J. M.; Thrush, B. A. E.S.R. studies of the reactions of atomic oxygen and hydrogen with simple hydrocarbons. *Trans. Faraday Soc.* **1967**, *63*, 630-642, doi:10.1039/tf9676300630.
(4) Hoyermann, K.; Wagner, H. G.; Wolfrum, J. Untersuchung der reaktionen von C_2H_2 mit H- und O-atomen mittels elektronen-spin-resonanz. *Z. Phys. Chem.* **1967**, *55*, 72-78, doi:10.1524/zpch.1967.55.1_2.072.
(5) Hoyermann, K.; Wagner, H. G.; Wolfrum, J. O + C_2H_2 → CO + CH_2 reaction. *Z. Phys. Chem.* **1969**, *63*, 193-196, doi:10.1524/zpch.1969.63.1_4.193.

(6) James, G. S.; Glass, G. P. Some aspects of acetylene oxidation. *J. Chem. Phys.* **1970**, *50*, 2268-2269, doi:10.1063/1.1671368.
(7) Stuhl, F.; Niki, H. Determination of rate constants for reactions of O atoms with C_2H_2, C_2D_2, C_2H_4, and C_3H_6 using a pulse vacuum-UV photolysis-chemiluminesent method. *J. Chem. Phys.* **1971**, *55*, 3954-3957, doi:10.1063/1.1676684.
(8) Sullivan, J. O.; Warneck, P. Rate constant for the reaction of oxygen atoms with acetylene. *J. Phys. Chem.* **1965**, *69*, 1749-1750, doi:10.1021/j100889a507.
(9) Vinckier, C.; Schaekers, M.; Peeters, J. The ketyl radical in the oxidation of ethyne by atomic oxygen at 300-600 K. *J. Phys. Chem.* **1985**, *89*, 508-512, doi:10.1021/j100249a028.
(10) Westenberg, A. A.; deHaas, N. Absolute measurements of the O + C_2H_2 rate coefficient. *J. Phys. Chem.* **1969**, *73*, 1181-1186, doi:10.1021/j100725a001.
(11) Westenberg, A. A.; deHaas, N. A flash photolysis-resonance fluorescence study of the O + C_2H_2 and O + C_2H_3Cl reactions. *J. Chem. Phys.* **1977**, *66*, 4900-4905, doi:10.1063/1.433828.

D4. **O + H_2CO.** The recommended values for A, E/R ,and k(298 K) are the averages of those determined by Klemm[3] (250–498 K) using flash photolysis-resonance fluorescence, by Klemm et al.[4] (298–748 K) using discharge flow-resonance fluorescence, and Chang and Barker[1] (296–436 K) using discharge flow-mass spectrometry techniques. All three studies are in good agreement. The k(298 K) value is also consistent with the results of Niki et al.,[6] Herron and Penzhorn[2] (300 K), and Mack and Thrush[5] (300 K). Although the mechanism for O + H_2CO has been considered to be the abstraction reaction yielding OH + HCO, Chang and Barker suggest that an additional channel yielding H + HCO_2 may be occurring to the extent of 30% of the total reaction. This conclusion is based on an observation of CO_2 as a product of the reaction under conditions where reactions such as O + HCO → H + CO_2 and O + HCO → OH + CO apparently do not occur. This interesting suggestion needs independent confirmation.
(Table: 82-57, Note: 82-57, Evaluated: 82-57) Back to Table

(1) Chang, J. S.; Barker, J. R. Reaction rate and products for the reaction O(^{3}P) + H_2CO. *J. Phys. Chem.* **1979**, *83*, 3059-3064, doi:10.1021/j100487a001.
(2) Herron, J. T.; Penzhorn, R. D. Mass spectrometric study of the reactions of atomic oxygen with ethylene and formaldehyde. *J. Phys. Chem.* **1969**, *73*, 191-196, doi:10.1021/j100721a031.
(3) Klemm, R. B. Absolute rate parameters for the reactions of formaldehyde with O atoms and H atoms over the temperature range 250-500 K. *J. Chem. Phys.* **1979**, *71*, 1987-1993, doi:10.1063/1.438589.
(4) Klemm, R. B.; Skolnik, E. G.; Michael, J. V. Absolute rate parameters for the reaction of O(^3P) with H_2CO over the temperature range 250 to 750 K. *J. Chem. Phys.* **1980**, *72*, 1256-1264, doi:10.1063/1.439186.
(5) Mack, G. P. R.; Thrush, B. Reaction of oxygen atoms with carbonyl compounds Part 1.-Formaldehyde. *J. Chem. Soc. Faraday Trans. 1* **1973**, *69*, 208-215, doi:10.1039/f19736900208.
(6) Niki, H.; Daby, E. E.; Weinstock, B. In *Twelfth Symposium (International) on Combustion*; The Combustion Institute, 1969; pp 277.

D5. **O + CH_3CHO.** The recommended k(298 K) is the average of three measurements by Cadle and Powers[2] (299–476 K), Mack and Thrush[3] (195–573 K), and Singleton et al.[4] (298–472 K), which are in good agreement. Cadle and Powers and Singleton et al. studied this reaction as a function of temperature and obtained very similar Arrhenius parameters. The recommended E/R value was obtained by considering both sets of data. This reaction is known to proceed via H-atom abstraction (Mack and Thrush, Avery and Cvetanovic,[1] and Singleton et al.).
(Table: 87-41, Note: 87-41, Evaluated: 87-41) Back to Table

(1) Avery, H. E.; Cvetanovic, R. J. Reaction of oxygen atoms with acetaldehyde. *J. Chem. Phys.* **1965**, *43*, 3727-3733, doi:10.1063/1.1696542.
(2) Cadle, R. D.; Powers, J. W. The reaction of O(^{3}P) with acetaldehyde in a fast-flow system. *J. Phys. Chem.* **1967**, *71*, 1702-1706, doi:10.1021/j100865a023.
(3) Mack, G. P. R.; Thrush, B. Reaction of oxygen atoms with carbonyl compounds Part 2.-Acetaldehyde. *J. Chem. Soc. Faraday Trans. 1* **1974**, *70*, 178-186, doi:10.1039/f19747000178.
(4) Singleton, D. L.; Irwin, R. S.; Cvetanović, R. J. Arrhenius parameters for the reactions of O(^3P) atoms with several aldehydes and the trend in aldehydic C-H bond dissociation energies. *Can. J. Chem.* **1977**, *55*, 3321-3327, doi:10.1139/v77-463.

D6. **O_2 + HOCO.** HOCO is produced by the association of OH with CO (See Table 2). The rate coefficient for the reaction of O_2 with HOCO has been measured by Petty et al.[2] (293 K) and Nolte et al.[1] (298 K) and the recommendation is based on these measurements. There are no reports on the temperature dependence of this reaction; however, the value at 298 K would be appropriate for all atmospheric conditions. The products of this reaction are HO_2, as shown by Nolte et al., and CO_2, as seen in numerous previous studies where it has been known to be the product of the reaction of OH with CO in air.
(Table: 06-2, Note: 06-2, Evaluated: 06-2) Back to Table

(1) Nolte, J.; Grussdorf, J.; Temps, F.; Wagner, H. Kinetics of the reaction HOCO + O_2 in the gas phase. *Z. Naturforsch.* **1993**, *48*, 1234-1238.
(2) Petty, J. T.; Harrison, J. A.; Moore, C. B. Reactions of *trans*-HOCO studied by infrared spectroscopy. *J. Phys. Chem.* **1993**, *97*, 11194-11198, doi:10.1021/j100145a013.

D7. **O_3 + C_2H_2.** The database for this reaction is not well established. Room temperature measurements (Cadle and Schadt,[2] DeMore,[3] DeMore,[4] Stedman and Niki,[7] Pate et al.,[6] and Atkinson and Aschmann[1]) disagree by as much as an order of magnitude. It is probable that secondary reactions involving destruction of ozone by radical products resulted in erroneously high values for the rate constants in several of the previous measurements. The present recommendation for k(298 K) is based on the room temperature value of Atkinson and Aschmann,[1] which is the lowest value obtained and therefore perhaps the most accurate. The temperature dependence is estimated, based on an assumed A-factor of 10^{-14} cm^3 molecule^{-1} s^{-1} similar to that for the O_3 + C_2H_4 reaction and corresponding to the expected five-membered ring structure for the transition state (DeMore[3,4]). Further studies, particularly of the temperature dependence, are needed. Major products in the gas phase reaction are CO, CO_2, and HCOOH, and chemically-activated formic anhydride has been proposed as an intermediate of the reaction (DeMore,[4] and DeMore and Lin[5]). The anhydride intermediates in several alkyne ozonations have been isolated in low temperature solvent experiments (DeMore and Lin[5]).
(Table: 90-1, Note: 90-1, Evaluated: 90-1) Back to Table

(1) Atkinson, R.; Aschmann, S. M. Rate constants for the reactions of O_3 and OH radicals with a series of alkynes. *Int. J. Chem. Kinet.* **1984**, *16*, 259-268, doi:10.1002/kin.550160308.
(2) Cadle, R. D.; Schadt, C. Kinetics of the gas phase reaction between acetylene and ozone. *J. Chem. Phys.* **1953**, *21*, 163, doi:10.1063/1.1698576.
(3) DeMore, W. B. Arrhenius constants for the reactions of ozone with ethylene and acetylene. *Int. J. Chem. Kinet.* **1969**, *1*, 209-220, doi:10.1002/kin.550010207.
(4) DeMore, W. B. Rates and mechanism of alkyne ozonation. *Int. J. Chem. Kinet.* **1971**, *3*, 161-173, doi:10.1002/kin.550030208.
(5) DeMore, W. B.; Lin, C.-L. Intermediates in the ozonation of simple alkynes. *J. Org. Chem.* **1973**, *38*, 985-989, doi:10.1021/jo00945a028.
(6) Pate, C. T.; Atkinson, R.; Pitts, J. N., Jr. The gas phase reaction of O_3 with a series of aromatic hydrocarbons. *J. Environ. Sci. Health* **1976**, *A11*, 1-10, doi:10.1080/10934527609385750.
(7) Stedman, D. H.; Niki, H. Ozonolysis rates of some atmospheric gases. *Environ. Lett.* **1973**, *4*, 303-310, doi:10.1080/00139307309435501.

D8. **O_3 + C_2H_4.** The rate constant of this reaction is well established over a large temperature range, 178 to 360 K. The present recommendation is based on the data of DeMore[4] (178–233 K), Stedman et al.[9] (299 K), Herron and Huie[5] (235–362 K), Japar et al.[6,7] (299 K), Toby et al.[11] (303 K), Su et al.[10] (291–299 K), Adeniji et al.[1] (260–294 K), Kan et al.[8] (282–303 K), Atkinson et al.[2] (296 K), and Bahta et al.[3] (232–298 K).
(Table: 90-1, Note: 90-1, Evaluated: 90-1) Back to Table

(1) Adeniji, S. A.; Kerr, J. A.; Williams, M. R. Rate constants for ozone-alkene reactions under atmospheric conditions. *Int. J. Chem. Kinet.* **1981**, *13*, 209-217, doi:10.1002/kin.550130210.
(2) Atkinson, R.; Aschmann, S. M.; Fitz, D. R.; Winer, A. M.; Pitts, J. N., Jr. Rate constants for the gas-phase reactions of O_3 with selected organics at 296 K. *Int. J. Chem. Kinet.* **1982**, *14*, 13-18, doi:10.1002/kin.550140103.
(3) Bahta, A.; Simonaitis, R.; Heicklen, J. Reactions of ozone with olefins: Ethylene, allene, 1,3-butadiene, and *trans*-1,3-pentadiene. *Int. J. Chem. Kinet.* **1984**, *16*, 1227-1246, doi:10.1002/kin.550161006.
(4) DeMore, W. B. Arrhenius constants for the reactions of ozone with ethylene and acetylene. *Int. J. Chem. Kinet.* **1969**, *1*, 209-220, doi:10.1002/kin.550010207.
(5) Herron, J. T.; Huie, R. E. Rate constants for the reactions of ozone with ethene and propene, from 235.0 to 362.0 K. *J. Phys. Chem.* **1974**, *78*, 2085-2088, doi:10.1021/j100614a004.

(6) Japar, S. M.; Wu, C. H.; Niki, H. Rate constants for the reaction of ozone with olefins in the gas phase. *J. Phys. Chem.* **1974**, *78*, 2318-2320, doi:10.1021/j150671a003.
(7) Japar, S. M.; Wu, C. H.; Niki, H. Effect of molecular oxygen on the gas phase kinetics of the ozonolysis of olefins. *J. Phys. Chem.* **1976**, *80*, 2057-2062, doi:10.1021/j100560a002.
(8) Kan, C. S.; Su, F.; Calvert, J. G.; Shaw, J. H. Mechanism of the ozone-ethene reaction in dilute N_2/O_2 mixtures near 1-atm pressure. *J. Phys. Chem.* **1981**, *85*, 2359-2363, doi:10.1021/j150616a013.
(9) Stedman, D. H.; Wu, C. H.; Niki, H. Kinetics of gas-phase reactions of ozone with some olefins. *J. Phys. Chem.* **1973**, *77*, 2511-2514, doi:10.1021/j100907a004.
(10) Su, F.; Calvert, J. G.; Shaw, J. H. A FT TR spectroscopic study of the ozone-ethene reaction mechanism in O_2-rich mixtures. *J. Phys. Chem.* **1980**, *84*, 239-246, doi:10.1021/j100440a003.
(11) Toby, F. S.; Toby, S.; O'Neal, H. E. The kinetics of the gas-phase reaction between ozone and alkenes. *Int. J. Chem. Kinet.* **1976**, *8*, 25-35, doi:10.1002/kin.550080105.

D9. **$O_3 + C_3H_6$.** The rate constant of this reaction is well established over the temperature range 185 to 360 K. The present recommendation is based largely on the data of Herron and Huie[5] (235–362 K). (Note that a typographical error in Table 2 of that paper improperly lists the lowest temperature as 250 K, rather than the correct value, 235 K.) The recommended Arrhenius expression agrees within 25% with the low temperature data of DeMore[4] (185–195 K), and is consistent with, but slightly higher (about 10%) than the data of Treacy et al.[10] (240–324 K) and slightly lower (about 40%) than the data of Adeniji et al.[1] (260–294 K). Room temperature measurements by Cox and Penkett,[3] Stedman et al.,[9] Japar et al.,[6,7] and Atkinson et al.[2] and Neeb and Moorgat[8] are in good agreement (10% or better) with the recommendation.
(Table: 06-2, Note: 06-2, Evaluated: 06-2) Back to Table

(1) Adeniji, S. A.; Kerr, J. A.; Williams, M. R. Rate constants for ozone-alkene reactions under atmospheric conditions. *Int. J. Chem. Kinet.* **1981**, *13*, 209-217, doi:10.1002/kin.550130210.
(2) Atkinson, R.; Aschmann, S. M.; Fitz, D. R.; Winer, A. M.; Pitts, J. N., Jr. Rate constants for the gas-phase reactions of O_3 with selected organics at 296 K. *Int. J. Chem. Kinet.* **1982**, *14*, 13-18, doi:10.1002/kin.550140103.
(3) Cox, R. A.; Penkett, S. A. Aerosol formation from sulphur dioxide in the presence of ozone and olefinic hydrocarbons. *J. Chem. Soc. Faraday Trans. 1* **1972**, *68*, 1735-1753, doi:10.1039/f19726801735.
(4) DeMore, W. B. Arrhenius constants for the reactions of ozone with ethylene and acetylene. *Int. J. Chem. Kinet.* **1969**, *1*, 209-220, doi:10.1002/kin.550010207.
(5) Herron, J. T.; Huie, R. E. Rate constants for the reactions of ozone with ethene and propene, from 235.0 to 362.0 K. *J. Phys. Chem.* **1974**, *78*, 2085-2088, doi:10.1021/j100614a004.
(6) Japar, S. M.; Wu, C. H.; Niki, H. Rate constants for the reaction of ozone with olefins in the gas phase. *J. Phys. Chem.* **1974**, *78*, 2318-2320, doi:10.1021/j150671a003.
(7) Japar, S. M.; Wu, C. H.; Niki, H. Effect of molecular oxygen on the gas phase kinetics of the ozonolysis of olefins. *J. Phys. Chem.* **1976**, *80*, 2057-2062, doi:10.1021/j100560a002.
(8) Neeb, P.; Moorgat, G. K. Formation of OH radicals in the gas-phase reaction of propene, isobutene, and isoprene with O_3: Yields and mechanistic implications. *J. Phys. Chem. A* **1999**, *103*, 9003-9012, doi:10.1021/jp9903458.
(9) Stedman, D. H.; Wu, C. H.; Niki, H. Kinetics of gas-phase reactions of ozone with some olefins. *J. Phys. Chem.* **1973**, *77*, 2511-2514, doi:10.1021/j100907a004.
(10) Treacy, J.; El Hag, M.; O'Farrell, D.; Sidebottom, H. Reactions of ozone with unsaturated organic compounds. *Ber. Bunsenges. Phys. Chem.* **1992**, *96*, 422-427, doi:10.1002/bbpc.19920960337.

D10. **$O_3 + CH_2=C(CH_3)CHO$.** The recommended E/R is based on the single temperature dependence study by Treacy et al.[7] (240–324 K). The recommended 298 K rate constant is obtained from an unweighted fit to $\ln k = \ln A - E/RT$ of the ambient temperature results of Atkinson et al.,[2] Grosjean and Grosjean,[4] Kamens et al.,[5] Neeb et al.,[6] and Treacy et al. in conjunction with the recommended E/R. While OH was scavenged only in the studies of Grosjean and Grosjean and Neeb et al., the studies where OH was not scavenged report results that agree well with the studies where OH was scavenged. By monitoring the production of cyclohexanone + cyclohexanol under conditions where OH was >95% scavenged by cyclohexane, Aschmann et al.[1] report an upper limit OH yield of 20^{+10}_{-13} percent. Ozone + alkene reactions proceed via initial formation of a primary ozonide that decomposes to a carbonyl compound plus a Criegee biradical with two different carbonyl/Criegee pairs produced (depending on which O−O bond cleaves); the Criegee biradical/carbonyl pairs produced in this case are $CH_3C(O)CHO$ (methyl glyoxal) + $\bullet CH_2OO\bullet$ and H_2CO + $CH_3C\bullet(OO\bullet)CHO$. Grosjean et al.[3] report carbonyl product yields to be 58% $CH_3C(O)CHO$ and 12% H_2CO.
(Table: 15-10, Note: 15-10, Evaluated: 15-10) Back to Table

(1) Aschmann, S. M.; Arey, J.; Atkinson, R. OH radical formation from the gas-phase reactions of O_3 with methacrolein and methyl vinyl ketone. *Atmos. Environ.* **1996**, *30*, 2939-2943, doi: 10.1016/1352-2310(96)00013-1.
(2) Atkinson, R.; Aschmann, S. M.; Winer, A. M.; Pitts Jr., J. N. Rate constants for the gas-phase reactions of O_3 with a series of carbonyls at 296 K. *Int. J. Chem. Kinet.* **1981**, *13*, 1133-1142, doi:10.1002/kin.550131104.
(3) Grosjean, D.; Williams, E. L., II; Grosjean, E. Atmospheric chemistry of isoprene and of its carbonyl products. *Environ. Sci. Technol.* **1993**, *27*, 830-840, doi:10.1021/es00042a004.
(4) Grosjean, E.; Grosjean, D. Rate constants for the gas-phase reaction of ozone with unsaturated oxygenates. *Int. J. Chem. Kinet.* **1998**, *30*, 21-29, doi:10.1002/(SICI)1097-4601(1998)30:1<21::AID-KIN3>3.0.CO;2-W.
(5) Kamens, R. M.; Gery, M. W.; Jeffries, H. E.; Jackson, M.; Cole, E. I. Ozone-isoprene reactions: Product formation and aerosol potential. *Int. J. Chem. Kinet.* **1982**, *14*, 955-975, doi:10.1002/kin.550140902.
(6) Neeb, P.; Kolloff, A.; Koch, S.; Moortgat, G. K. Rate constants for the reactions of methylvinyl ketone, methacrolein, methacrylic acid, and acrylic acid with ozone. *Int. J. Chem. Kinet.* **1998**, *30*, 769-776, doi:10.1002/(SICI)1097-4601(1998)30:10<769::AID-KIN9>3.0.CO;2-T.
(7) Treacy, J.; El Hag, M.; O'Farrell, D.; Sidebottom, H. Reactions of ozone with unsaturated organic compounds. *Ber. Bunsenges. Phys. Chem.* **1992**, *96*, 422-427, doi:10.1002/bbpc.19920960337.

D11. $O_3 + CH_3C(O)CH=CH_2$. The recommended E/R is based on the single temperature dependence study by Treacy et al.[8] (240–324 K). The recommended 298 K rate constant is obtained from an unweighted fit to $\ln k = \ln A - E/RT$ of the ambient temperature results of Atkinson et al.,[2] Grosjean et al.,[3] Grosjean and Grosjean,[4] Kamens et al.,[5] Neeb et al.,[6] and Treacy et al.[8] in conjunction with the recommended E/R. While OH was scavenged only in the more recent studies of Grosjean et al., Grosjean and Grosjean, and Neeb et al., the studies where OH was not scavenged report results that agree well with the studies where OH was scavenged. The yield of OH is reported to be 0.16 ± 0.08 and 0.16 ± 0.05 by Aschmann et al.[1] and Paulson et al.,[7] respectively. Ozone + alkene reactions proceed via initial formation of a primary ozonide that decomposes to a carbonyl compound plus a Criegee biradical with two different carbonyl/Criegee pairs produced (depending on which O−O bond cleaves); the Criegee biradical/carbonyl pairs produced in this case are $CH_3C(O)CHO$ (methyl glyoxal) + $\bullet CH_2OO\bullet$ and H_2CO + $CH_3C(O)C\bullet HOO\bullet$. Grosjean et al.[3] report carbonyl product yields to be 87% $CH_3C(O)CHO$ and 5% H_2CO; these investigators also report a 5% yield of $CH_3C(O)C(O)OH$ (pyruvic acid). (Table: 15-10, Note: 15-10, Evaluated: 15-10) Back to Table

(1) Aschmann, S. M.; Arey, J.; Atkinson, R. OH radical formation from the gas-phase reactions of O_3 with methacrolein and methyl vinyl ketone. *Atmos. Environ.* **1996**, *30*, 2939-2943, doi: 10.1016/1352-2310(96)00013-1.
(2) Atkinson, R.; Aschmann, S. M.; Winer, A. M.; Pitts Jr., J. N. Rate constants for the gas-phase reactions of O_3 with a series of carbonyls at 296 K. *Int. J. Chem. Kinet.* **1981**, *13*, 1133-1142, doi:10.1002/kin.550131104.
(3) Grosjean, D.; Williams, E. L., II; Grosjean, E. Atmospheric chemistry of isoprene and of its carbonyl products. *Environ. Sci. Technol.* **1993**, *27*, 830-840, doi:10.1021/es00042a004.
(4) Grosjean, E.; Grosjean, D. Rate constants for the gas-phase reaction of ozone with unsaturated oxygenates. *Int. J. Chem. Kinet.* **1998**, *30*, 21-29, doi:10.1002/(SICI)1097-4601(1998)30:1<21::AID-KIN3>3.0.CO;2-W.
(5) Kamens, R. M.; Gery, M. W.; Jeffries, H. E.; Jackson, M.; Cole, E. I. Ozone-isoprene reactions: Product formation and aerosol potential. *Int. J. Chem. Kinet.* **1982**, *14*, 955-975, doi:10.1002/kin.550140902.
(6) Neeb, P.; Kolloff, A.; Koch, S.; Moortgat, G. K. Rate constants for the reactions of methylvinyl ketone, methacrolein, methacrylic acid, and acrylic acid with ozone. *Int. J. Chem. Kinet.* **1998**, *30*, 769-776, doi:10.1002/(SICI)1097-4601(1998)30:10<769::AID-KIN9>3.0.CO;2-T.
(7) Paulson, S. E.; Chung, M.; Sen, A. D.; Orzechowska, G. Measurement of OH radical formation from the reaction of ozone with several biogenic alkenes *J. Geophys. Res.* **1998**, *103*, 25533-25539, doi:10.1029/98JD01951.
(8) Treacy, J.; El Hag, M.; O'Farrell, D.; Sidebottom, H. Reactions of ozone with unsaturated organic compounds. *Ber. Bunsenges. Phys. Chem.* **1992**, *96*, 422-427, doi:10.1002/bbpc.19920960337.

D12. O_3 + CH_2=C(CH_3)CH=CH_2. The recommended E/R is based on an unweighted fit to the temperature-dependent rate constants reported by Khamaganov and Hites[13] (242–363 K) to ln k = ln A – E/RT, while the recommended A-factor is based on the ambient temperature rate constants reported by Greene and Atkinson,[6] Grosjean et al.,[7] Grosjean and Grosjean,[8] Neeb and Moortgat,[16] Klawatsch-Carrasco et al.,[14] and Karl et al.[12] In all of the above studies, measures were taken to prevent secondary consumption of reactants by OH radicals, which are known to be generated in ozone + alkene reactions. Results from early studies by Adeniji et al.[1] (260–294 K), Atkinson et al.[3] (276–324 K), and Treacy et al.[19] (240–324 K), while in reasonable agreement with other studies, are not used to arrive at the recommendation because OH radicals were not scavenged in those studies. The Arrhenius parameters reported by Avzianova and Ariya[4] (278–353 K) are not accepted because of inconsistencies in their paper that the authors were unable to resolve (private communication from Ariya). Donahue et al.[5] have directly detected OH as a product of the O_3 + isoprene reaction, and OH yields have been reported in a number of studies where OH production was monitored indirectly by following the loss of an OH scavenger or the production of a product of an OH + scavenger reaction.[2,9,10,15-18] At room temperature and atmospheric pressure of air, reported OH yields from seemingly careful studies range from 0.19 to 0.53 with an average value of 0.32. The chemical pathways leading to OH production are too complex to discuss in this note; the interested reader is referred to a review article by Johnson and Marston.[11] As discussed by Johnson and Marston, the reaction proceeds via initial formation of a primary ozonide that decomposes to a carbonyl compound plus a Criegee biradical with several different carbonyl/Criegee pairs produced; the Criegee biradicals can react unimolecularly from a chemically activated state or be collisionally deactivated and live long enough to undergo bimolecular reactions under atmospheric conditions.
(Table: 15-10, Note: 15-10, Evaluated: 15-10) Back to Table

(1) Adeniji, S. A.; Kerr, J. A.; Williams, M. R. Rate constants for ozone-alkene reactions under atmospheric conditions. *Int. J. Chem. Kinet.* **1981**, *13*, 209-217, doi:10.1002/kin.550130210.

(2) Atkinson, R.; Aschmann, S. M.; Arey, J.; Shorees, B. Formation of OH radicals in the gas phase reactions of O_3 with a series of terpenes. *J. Geophys. Res.* **1992**, *97*, 6065-6073, doi:10.1029/92JD00062.

(3) Atkinson, R.; Winer, A. M.; Pitts, J. N., Jr. Rate constants for the gas phase reactions of O_3 with the natural hydrocarbons isoprene and α- and β-pinene. *Atmos. Environ.* **1982**, *16*, 1017-1020, doi: 10.1016/004-6981(82)90187-1.

(4) Avzianova, E. V.; Ariya, P. A. Temperature-dependent kinetic study for ozonolysis of selected tropospheric alkenes. *Int. J. Chem. Kinet.* **2002**, *34*, 678-684, doi:10.1002/kin.10093.

(5) Donahue, N. M.; Kroll, J. H.; Anderson, J. G.; Demerjian, K. L. Direct observation of OH production from the ozonolysis of olefins *Geophys. Res. Lett.* **1998**, *25*, 59-62, doi:10.1029/97GL53560.

(6) Greene, C. R.; Atkinson, R. Rate constants for the gas-phase reactions of O_3 with a series of alkenes at 296 ± 2 K. *Int. J. Chem. Kinet.* **1992**, *24*, 803-811, doi:10.1002/kin.550240905.

(7) Grosjean, D.; Williams, E. L., II; Grosjean, E. Atmospheric chemistry of isoprene and of its carbonyl products. *Environ. Sci. Technol.* **1993**, *27*, 830-840, doi:10.1021/es00042a004.

(8) Grosjean, E.; Grosjean, D. Rate constants for the gas-phase reaction of ozone with 1,1-disubstituted alkenes. *Int. J. Chem. Kinet.* **1996**, *28*, 911-918, doi:10.1002/(SICI)1097-4601(1996)28:12<911::AID-KIN8>3.0.CO;2-Q.

(9) Gutbrod, R.; Kraka, E.; Schindler, R. N.; Cremer, D. Kinetic and theoretical investigation of the gas-phase ozonolysis of isoprene: Carbonyl oxides as an important source for OH radicals in the atmosphere *J. Am. Chem. Soc.* **1997**, *119*, 7330-7342, doi:10.1021/ja970050c.

(10) Gutbrod, R.; Meyer, S.; Rahman, M. M.; Schindler, R. N. On the use of CO as scavenger for OH radicals in the ozonolysis of simple alkenes and isoprene *Int. J. Chem. Kinet.* **1997**, *29*, 717-723, doi:10.1002/(SICI)1097-4601(1997)29:93.3.CO;2-I.

(11) Johnson, D.; Marston, G. The gas-phase ozonolysis of unsaturated volatile organic compounds in the troposphere. *Chem. Soc. Rev.* **2008**, *37*, 699-716, doi:10.1039/b704260b.

(12) Karl, M.; Brauers, T.; Dorn, H.-P.; Holland, F.; Komenda, M.; Poppe, D.; Rohrer, F.; Rupp, L.; Schaub, A.; Wahner, A. Kinetic Study of the OH-isoprene and O_3-isoprene reaction in the atmosphere simulation chamber, SAPHIR. *Geophys. Res. Lett.* **2004**, *31*, L05117, doi:10.1029/2003GL019189.

(13) Khamaganov, V. G.; Hites, R. A. Rate constants for the gas-phase reactions of ozone with isoprene, α- and β-pinene, and limonene as a function of temperature. *J. Phys. Chem. A* **2001**, *105*, 815-822, doi:10.1021/jp002730z.

(14) Klawatsch-Carrasco, N.; Doussin, J. F.; Carlier, P. Absolute rate constants for the gas-phase ozonolysis of isoprene and methylbutenol. *Int. J. Chem. Kinet.* **2004**, *36*, 152-156, doi:10.1002/kin.10175.

(15) Lewin, A. G.; Johnson, D.; Price, D. W.; Marston, G. Aspects of the kinetics and mechanism of the gas-phase reactions of ozone with conjugated dienes *Phys. Chem. Chem. Phys.* **2001**, *3*, 1253-1261, doi:10.1039/b010006o.

(16) Neeb, P.; Moorgat, G. K. Formation of OH radicals in the gas-phase reaction of propene, isobutene, and isoprene with O_3: Yields and mechanistic implications. *J. Phys. Chem. A* **1999**, *103*, 9003-9012, doi:10.1021/jp9903458.
(17) Paulson, S. E.; Chung, M.; Sen, A. D.; Orzechowska, G. Measurement of OH radical formation from the reaction of ozone with several biogenic alkenes *J. Geophys. Res.* **1998**, *103*, 25533-25539, doi:10.1029/98JD01951.
(18) Rickard, A. R.; Johnson, D.; McGill, C. D.; Marston, G. OH yields in the gas-phase reactions of ozone with alkenes *J. Phys. Chem. A* **1999**, *103*, 7656-7664, doi:10.1021/jp9916992.
(19) Treacy, J.; El Hag, M.; O'Farrell, D.; Sidebottom, H. Reactions of ozone with unsaturated organic compounds. *Ber. Bunsenges. Phys. Chem.* **1992**, *96*, 422-427, doi:10.1002/bbpc.19920960337.

D13. OH + CO. See note for the OH + CO reaction in Section 2.
Back to Table

D14. OH + CH_4. This reaction has been extensively studied by Vaghjiani and Ravishankara[8] (223–420 K), Saunders et al.,[6] Finlayson-Pitts et al.[3] (278–378 K), Dunlop and Tully[2] (293–800 K), Mellouki et al.[5] (233–343 K), and Gierczak et al.[4] (195–296 K), who measured the absolute rate coefficients for this reaction using discharge flow and pulsed photolysis techniques. Sharkey and Smith[7] (178–298 K) have reported a high value (7.7×10^{-15} cm^3 $molecule^{-1}$ s^{-1}) for k(298 K), and this value has not been considered here. The recommendation for k(298 K) was derived from the results of Vaghjiani and Ravishankara, Dunlop and Tully, Saunders et al., Mellouki et al., Finlayson-Pitts et al., and Gierczak et al. The temperature dependence of this rate coefficient has been measured by Vaghjiani and Ravishankara, Dunlop and Tully (above 298 K), Finlayson-Pitts et al., and Mellouki et al. Gierczak et al. have extended the measurements of k to 195 K, and it appears that the rate coefficient does not strictly follow an Arrhenius expression. The recommended E/R was obtained from these results using data below 300 K.

A more accurate representation of the rate constant as a function of temperature is obtained by using the three-parameter expression: $k(T) = 2.80 \times 10^{-14} T^{0.667} \exp(-1575/T)$ cm^3 $molecule^{-1}$ s^{-1}. This three-parameter fit may be preferred for lower stratosphere and upper troposphere calculations. A report on this rate coefficient by Bonard et al.[1] agrees very well with the value recommended here.
(Table: 97-4, Note: 06-2, Evaluated: 06-2) Back to Table

(1) Bonard, A.; Daële, V.; Delfau, J.-L.; Vovelle, C. Kinetics of OH radical reactions with methane in the temperature range 295-660 K and with dimethyl ether and methyl-*tert*-butyl ether in the temperature range 295-618 K. *J. Phys. Chem. A* **2002**, *106*, 4384-4389, doi:10.1021/jp012425t.
(2) Dunlop, J. R.; Tully, F. P. A kinetic study of OH radical reactions with methane and perdeuterated methane. *J. Phys. Chem.* **1993**, *97*, 11148-11150, doi:10.1021/j100145a003.
(3) Finlayson-Pitts, B. J.; Hernandez, S. K.; Berko, H. N. A new dark source of the gaseous hydroxyl radical for the relative rate measurements. *J. Phys. Chem.* **1993**, *97*, 1172-1177, doi:10.1021/j100108a012.
(4) Gierczak, T.; Talukdar, R. K.; Herndon, S. C.; Vaghjiani, G. L.; Ravishankara, A. R. Rate coefficients for the reactions of hydroxyl radicals with methane and deuterated methanes. *J. Phys. Chem. A* **1997**, *101*, 3125-3134, doi:10.1021/jp963892r.
(5) Mellouki, A.; Téton, S.; Laverdet, G.; Quilgars, A.; Le Bras, G. Kinetic studies of OH reactions with H_2O_2, C_3H_8, and CH_4 using the pulsed laser photolysis-laser induced fluorescence method. *J. Chim. Phys.* **1994**, *91*, 473-487, doi:10.1051/jcp/1994910473.
(6) Saunders, S. M.; Hughes, K. J.; Pilling, M. J.; Baulch, D. L.; Smurthwaite, P. I. "Reactions of hydroxyl radicals with selected hydrocarbons of importance in atmospheric chemistry"; Optical Methods in Atmospheric Chemistry, 1992, Berlin.
(7) Sharkey, P.; Smith, I. W. M. Kinetics of elementary reactions at low temperatures: Rate constants for the reactions of OH with HCl ($298 \geq T/K \geq 138$), CH_4 ($298 \geq T/K \geq 178$), and C_2H_6 ($298 \geq T/K \geq 138$). *J. Chem. Soc. Faraday Trans.* **1993**, *89*, 631-638, doi:10.1039/ft9938900631.
(8) Vaghjiani, G. L.; Ravishankara, A. R. New measurement of the rate coefficient for the reaction of OH with methane. *Nature* **1991**, *350*, 406-409, doi:10.1038/350406a0.

D15. OH + $^{13}CH_4$. This reaction has been studied relative to the OH + $^{12}CH_4$ reaction, since the ratio of the rate constants (the kinetic isotope effect, KIE) is the quantity needed for quantifying methane sources. Rust and Stevens[3] (298 K), Davidson et al.,[2] Cantrell et al.[1] (273–353 K), and Saueressig et al.[4] (296 K) have reported KIE = k_{12}/k_{13} at room temperature to be 1.0036 ± 0.0013, 1.010 ± 0.007, 1.0055 ± 0.0009, and 1.0039 ± 0.0004, respectively (all uncertainties are stated as 95% confidence intervals). Cantrell et al.'s data supersede the results of Davidson et al. The recommended value of KIE = 1.0039 +0.0015/-0.0010 is the result of the latest most comprehensive study by Saueressig et al. However, the more conservative uncertainty is recommended because

of the nature of these measurements and unresolved difference with the earlier result of Cantrell et al. Cantrell et al. find KIE = k_{12}/k_{13} to be independent of temperature between 273 and 353 K.
Note that the ratio of collision frequencies for these reactions (due to small difference in colliding masses) is 1.0155. Thus, the observed KIE cannot be explained by the slight change in the relative velocity of the colliding reactant molecules.
(Table: 19-5, Note: 19-5, Evaluated: 19-5) Back to Table

(1) Cantrell, C. A.; Shetter, R. E.; McDaniel, A. J.; Calvert, J. G.; Davidson, J. A.; Lowe, D. C.; Tyler, S. C.; Cicerone, R. J.; Greenberg, J. P. Carbon kinetic isotope effect in the oxidation of methane by the hydroxyl radical. *J. Geophys. Res.* **1990**, *95*, 22455-22462, doi:10.1029/JD095iD13p22455.
(2) Davidson, J. A.; Cantrell, C. A.; Tyler, S. C.; Shetter, R. E.; Cicerone, R. J.; Calvert, J. G. Carbon kinetic isotope effect in the reaction of CH_4 with HO. *J. Geophys. Res.* **1987**, *92*, 2195-2199, doi:10.1029/JD092iD02p02195.
(3) Rust, F.; Stevens, C. M. Carbon kinetic isotope effect in the oxidation of methane by hydroxyl. *Int. J. Chem. Kinet.* **1980**, *12*, 371-377, doi:10.1002/kin.550120602.
(4) Saueressig, G.; Crowley, J. N.; Bergamaschi, P.; Brühl, C.; Brenninkmeijer, C. A. M.; Fischer, H. Carbon 13 and D kinetic isotope effects in the reactions of CH_4 with $O(^1D)$ and OH: New laboratory measurements and their implications for the isotopic composition of stratospheric methane. *J. Geophys. Res.* **2001**, *106*, 23127-23138, doi:10.1029/2000JD000120.

D16. OH + CH_3D. The rate coefficient for this reaction has been measured between 249 and 422 K using a pulsed laser photolysis-laser induced fluorescence system by Gierczak et al.[3] The recommended values of k(298 K) and E/R are from this study. The recommendation agrees within about 10% at 298 K with the rate constant measured by DeMore[1] in a relative rate study over the temperature range 298–360 K. The difference, while small in an absolute sense, is nevertheless significant for the isotopic fractionation of atmospheric CH_3D and CH_4 by OH. An earlier result of Gordon and Mulac[4] at 416 K is in good agreement with the extrapolated data of both of these determinations. However, that measurement has not been explicitly included in this recommendation because the experiments were carried out at higher temperatures and therefore are less applicable to the atmosphere. The rate coefficients for the reactions of OH with other deuterated methanes have also been measured (Dunlop and Tully,[2] Gierczak et al.,[5] Gordon and Mulac[4]).
(Table: 94-26, Note: 94-26, Evaluated: 94-26) Back to Table

(1) DeMore, W. B. Rate constant ratio for the reaction of OH with CH_3D and CH_4. *J. Phys. Chem.* **1993**, *97*, 8564-8566, doi:10.1021/j100135a006.
(2) Dunlop, J. R.; Tully, F. P. A kinetic study of OH radical reactions with methane and perdeuterated methane. *J. Phys. Chem.* **1993**, *97*, 11148-11150, doi:10.1021/j100145a003.
(3) Gierczak, T.; Talukdar, R. K.; Herndon, S. C.; Vaghjiani, G. L.; Ravishankara, A. R. Rate coefficient for the reaction of hydroxyl radicals with methane and deuterated methanes. *J. Phys. Chem. A* **1997**, *101*, 3125-3134, doi:10.1021/jp963892r.
(4) Gordon, S.; Mulac, W. A. Reaction of the $OH(X^2\prod)$ radical produced by the pulse radiolysis of water vapor. *Int. J. Chem. Kinet.* **1975**, *Symp. 1*, 289-299.
(5) Talukdar, R. K.; Gierczak, T.; Goldfarb, L.; Rudich, Y.; Madhava Rao, B. S.; Ravishankara, A. R. Kinetics of hydroxyl radical reactions with isotopically labeled hydrogen. *J. Phys. Chem.* **1996**, *100*, 3037-3043, doi:10.1021/jp9518724.

D17. OH + H_2CO. The recommended k(298 K) is the average of those determined by Niki et al.[6] (299 K), Atkinson and Pitts[1] (299–426 K), Stief et al.[9] (228–362 K), Yetter et al.[11] (298 K), Temps and Wagner[10] (296 K), and Sivakumaran et al.[7] (202–399 K). The value reported by Morris and Niki[3] is expected to be superseded by the later report of Niki et al.,[6] although it agrees within the stated uncertainty. There are two relative values that are not in agreement with the recommendations. The value of Niki et al.[4] relative to the OH + C_2H_4 reaction is higher, while the value of Smith[8] relative to the OH + OH reaction is lower. The rate coefficients reported by Zabarnick et al.[12] (296–576 K) at and above 298 K are consistently higher than those recommended here, but overlap within the combined uncertainty. The temperature dependence was calculated from the data of Stief et al. obtained below 298 K and from the data of Sivakumaran et al. below 330 K after normalizing the results of both studies to k(298 K) recommended here. There is a clear indication that the Arrhenius plot of this rate coefficient is curved with a positive activation energy at temperatures above ~330 K. It is therefore important that the recommended rate coefficients be used only in the 200–300 K temperature range. The abstraction reaction shown in the table is the major channel (Temps and Wagner,[10] Niki et al.[5]); other channels may contribute to a small extent (Horowitz et al.[2]). There is no indication that this rate coefficient is pressure dependent at atmospheric pressures and temperatures.
(Table: 06-2, Note: 06-2, Evaluated: 06-2) Back to Table

(1) Atkinson, R.; Pitts Jr., J. N. Kinetics of the reactions of the OH radical with HCHO and CH_3CHO over the temperature range 299-426°K. *J. Chem. Phys.* **1978**, *68*, 3581-3590, doi:10.1063/1.436215.
(2) Horowitz, A.; Su, F.; Calvert, J. G. Unusual H_2-forming chain reaction in the 3130-Å photolysis of formaldehyde-oxygen mixtures at 25°C. *Int. J. Chem. Kinet.* **1978**, *10*, 1099-1117, doi:10.1002/kin.550101102.
(3) Morris, E. D., Jr.; Niki, H. Mass spectrometric study of the reaction of hydroxyl radical with formaldehyde. *J. Chem. Phys.* **1971**, *55*, 1991-1992, doi:10.1063/1.1676348.
(4) Niki, H.; Maker, P. D.; Savage, C. M.; Breitenbach, L. P. Relative rate constants for the reaction of hydroxyl radical with aldehydes. *J. Phys. Chem.* **1978**, *82*, 132-134, doi:10.1021/j100491a002.
(5) Niki, H.; Maker, P. D.; Savage, C. M.; Breitenbach, L. P. Fourier transform infrared spectroscopic study of the kinetics for the HO radical reaction of $^{13}C^{16}O$ and $^{12}C^{18}O$. *J. Phys. Chem.* **1984**, *88*, 2116-2119, doi:10.1021/j150654a034.
(6) Niki, H.; Maker, P. D.; Savage, C. M.; Breitenbach, L. P. Fourier transform infrared study of the kinetics and mechanism for the reaction of hydroxyl radical with formaldehyde. *J. Phys. Chem.* **1984**, *88*, 5342-5344, doi:10.1021/j150666a047.
(7) Sivakumaran, V.; Holscher, D.; Dillon, T. J.; Crowley, J. N. Reaction between OH and HCHO: temperature dependent rate coeffiecients (202-399 K) and product pathways (298 K). *Phys. Chem. Chem. Phys.* **2003**, *5*, 4821-4827, doi:10.1039/b306859e.
(8) Smith, R. H. Rate constant and activation energy for the gaseous reaction between hydroxyl and formaldehyde. *Int. J. Chem. Kinet.* **1978**, *10*, 519-528, doi:10.1002/kin.550100509.
(9) Stief, L. J.; Nava, D. F.; Payne, W. A.; Michael, J. V. Rate constant for the reaction of hydroxyl radical with formaldehyde over the temperature range 228-362 K. *J. Chem. Phys.* **1980**, *73*, 2254-2258, doi:10.1063/1.440374.
(10) Temps, F.; Wagner, H. G. Rate constants for the reactions of OH radicals with CH_2O and HCO. *Ber. Bunsenges Phys. Chem.* **1984**, *88*, 415-418, doi:10.1002/bbpc.19840880419.
(11) Yetter, R. A.; Rabitz, H.; Dryer, F. L.; Maki, R. G.; Klemm, R. B. Evaluation of the rate constant for the reaction OH + H_2CO: Application of modeling and sensitivity analysis techniques for determination of the product branching ratio. *J. Chem. Phys.* **1989**, *91*, 4088-4097, doi:10.1063/1.456838.
(12) Zabarnick, S.; Fleming, J. W.; Lin, M. C. Kinetics of hydroxyl radical reactions with formaldehyde and 1,3,5-trioxane between 290 and 600 K. *Int. J. Chem. Kinet.* **1988**, *20*, 117-129, doi:10.1002/kin.550200205.

D18. OH + CH_3OH. The recommended k(298 K) is the average of direct studies by Overend and Paraskevopoulos[10] (296 K), Ravishankara and Davis[12] (298 K), Hagele et al.[4] (295–420 K), Meier et al.[9] (300–1020 K), McCaulley et al.[8] (298 K), Wallington and Kurylo[14] (240–440 K), Hess and Tully[5] (293–865 K), Jimenez et al.[6] (235–360 K), and Dillon et al.[3] (216–368 K). When these measurements were not at exactly 298 K, their values were recalculated for 298 K by using the E/R recommended here. Indirect measurements by Campbell et al.,[2] Barnes et al.,[1] Tuazon et al.,[13] Picquet et al.,[11] and Klopffer et al.[7] are in good agreement with the recommended value. The temperature dependence of k has been measured by Hagele et al., Meier et al., Greenhill and O'Grady, Wallington and Kurylo, Hess and Tully, Jimenez et al., and Crowley et al. The recommended value of E/R was calculated using the results obtained at temperature below 330 K by Wallington and Kurylo, Meier et al., Hess and Tully, Jimenez et al., and Crowley et al. The results of Greenhill and O'Grady are in reasonable agreement with the recommendation at and above 298 K, but are clearly lower than the recommendation below 298 K. Hess and Tully report a curved Arrhenius plot over the temperature range 298–1000 K, while Meier et al. did not observe such a curvature. This reaction has two pathways: abstraction of the H-atom from the methyl group to give CH_2OH + H_2O or from the OH group to give CH_3O + H_2O. The results of Hagele et al., Meier et al., and Hess and Tully suggest that H abstraction from the methyl group is the dominant channel below room temperature. At 298 K, for example, the branching ratio for the formation of CH_2OH is about 0.85 and increases as the temperature decreases. In the Earth's atmosphere, the eventual products of OH + CH_3OH reaction are the same for both reaction channels: CH_2O and HO_2.
(Table: 06-2, Note: 06-2, Evaluated: 06-2) Back to Table

(1) Barnes, I.; Bastian, V.; Becker, K. H.; Fink, E. H.; Zabel, F. Reactivity studies of organic substances towards hydroxyl radicals under atmospheric conditions. *Atmos. Environ.* **1982**, *16*, 545-550, doi:10.1016/0004-6981(82)90163-9.
(2) Campbell, I. M.; McLaughlin, D. F.; Handy, B. J. Rate constants for reactions of hydroxyl radicals with alcohol vapours at 292 K. *Chem. Phys. Lett.* **1976**, *38*, 362-364, doi:10.1016/0009-2614(76)85174-3.

(3) Dillon, T. J.; Hölscher, D.; Sivakumaran, V.; Horowitz, A.; Crowley, J. N. Kinetics of the reactions of HO with methanol (210–351 K) and with ethanol (216–368 K). *Phys. Chem. Chem. Phys.* **2005**, *7*, 349-355, doi:10.1039/b413961e.
(4) Hägele, J.; Lorenz, K.; Rhäsa, D.; Zellner, R. Rate constants and CH_3O product yield of the reaction OH + CH_3OH → products. *Ber. Bunsenges. Phys. Chem.* **1983**, *87*, 1023-1026, doi:10.1002/bbpc.19830871112.
(5) Hess, W. P.; Tully, F. P. Hydrogen-atom abstractlon from methanol by OH. *J. Phys. Chem.* **1989**, *93*, 1944-1947, doi:10.1021/j100342a049.
(6) Jiménez, E.; Gilles, M. K.; Ravishankara, A. R. Kinetics of the reactions of hydroxyl radical with CH_3OH and C_2H_5OH between 235 and 360 K. *J. Photochem. Photobiol. A: Chem.* **2003**, *157*, 237-245, doi:10.1016/S1010-6030(03)00073-X.
(7) Klopffer, W.; Frank, R.; Kohl, E. G.; Haag, F. Quantitative erfassung der photochemischen transformationsprozesse in der troposphäre. *Chemiker-Zeitung* **1986**, *110*, 57-61.
(8) McCaulley, J. A.; Kelly, N.; Golde, M. F.; Kaufman, F. kinetic studies of the reactions of F and OH with CH_3OH. *J. Phys. Chem.* **1989**, *93*, 1014-1018, doi:10.1021/j100340a002.
(9) Meier, U.; Grotheer, H. H.; Just, T. Temperature dependence and branching ratio of the CH_3OH + OH reaction. *Chem. Phys. Lett.* **1984**, *106*, 97-101, doi:10.1016/0009-2614(84)87019-0.
(10) Overend, R.; Paraskevopoulos, G. Rates of OH radical reactions. 4. Reactions with methanol, ethanol, 1-propanol, and 2-propanol at 296 K. *J. Phys. Chem.* **1978**, *82*, 1329-1333, doi:10.1021/j100501a001.
(11) Picquet, B.; Heroux, S.; Chebbi, A.; Doussin, J.-F.; Durand-Jolibois, R.; Monod, A.; Loirat, H.; Carlier, P. Kinetics of the reactions of OH radicals with some oxygenated volatile organic compounds under simulated atmospheric conditions. *Int. J. Chem. Kinet.* **1998**, *30*, 839-847, doi:10.1002/(SICI)1097-4601(1998)30:11<839::AID-KIN6>3.0.CO;2-W.
(12) Ravishankara, A. R.; Davis, D. D. Kinetic rate constants for the reaction of OH with methanol, ethanol, and tetrahydrofuran at 298 K. *J. Phys. Chem.* **1978**, *82*, 2852-2853, doi:10.1021/j100515a022.
(13) Tuazon, E. C.; Carter, W. P. L.; Atkinson, R.; Pitts, J. N., Jr. The gas-phase reaction of hydrazine and ozone: A nonphotolytic source of OH radicals for measurement of relative OH radical rate constants. *Int. J. Chem. Kinet.* **1983**, *15*, 619-629, doi:10.1002/kin.550150704.
(14) Wallington, T. J.; Kurylo, M. J. The gas phase reactions of hydroxyl radicals with a series of aliphatic alcohols over the temperature range 240-440 K. *Int. J. Chem. Kinet.* **1987**, *19*, 1015-1023, doi:10.1002/kin.550191106.

D19. OH + CH_3OOH. The recommended k(298 K) is the average of the rate coefficients measured by Niki et al.[1] (298 K) and Vaghjiani and Ravishankara[2] (203–423 K), which differ by nearly a factor of two. Niki et al. measured the rate coefficient relative to that for OH with C_2H_4 (= 8.0×10^{-12} cm^3 $molecule^{-1}$ s^{-1}) by monitoring CH_3OOH disappearance using an FTIR system. Vaghjiani and Ravishankara monitored the disappearance of OH, OD, and ^{18}OH in excess CH_3OOH in a pulsed photolysis-LIF system. They report a negative activation energy with E/R = –190 K; the recommended E/R is based on their results. The reaction of OH with CH_3OOH occurs via abstraction of H from the oxygen end to produce the CH_3OO radical and from the CH_3 group to produce the CH_2OOH radical, as originally proposed by Niki et al. and confirmed by Vaghjiani and Ravishankara. CH_2OOH is unstable and falls apart to CH_2O and OH within a few microseconds. The possible reaction of CH_2OOH with O_2 is unimportant under atmospheric conditions (Vaghjiani and Ravishankara). The recommended branching ratios are,

OH + CH_3OOH → CH_3O_2 + H_2O	(a)	70%
OH + CH_3OOH → CH_2OOH + H_2O	(b)	30%,

(from Vaghjiani and Ravishankara) and are nearly independent of temperature.
(Table: 02-25, Note: 02-25, Evaluated: 02-25) Back to Table

(1) Niki, H.; Maker, P. D.; Savage, C. M.; Breitenbach, L. P. A Fourier transform infrared study of the kinetics and mechanism for the reaction HO + CH_3OOH. *J. Phys. Chem.* **1983**, *87*, 2190-2193, doi:10.1021/j100235a030.
(2) Vaghjiani, G. L.; Ravishankara, A. R. Kinetics and mechanism of OH reaction with CH_3OOH. *J. Phys. Chem.* **1989**, *93*, 1948-1959, doi:10.1021/j100342a050.

D20. OH + HC(O)OH. The recommended value of k(298 K) is the average of those measured by Zetzsch and Stuhl,[5] Wine et al.[4] (298–430 K), Jolly et al.[2] (296 K), Dagaut et al.[1] (298 K), and Singleton et al.[3] (297–445 K). The temperature dependence of k has been studied by Wine et al. and by Singleton et al., who observed k to be essentially independent of temperature.

Wine et al. found the rate coefficient for the OH + HC(O)OH reaction to be the same as that for OH + DC(O)OH reaction. Jolly et al. found the formic acid dimer to be unreactive toward OH, i.e., abstraction of the H atom attached to C was not the major pathway for the reaction. A comprehensive study of Singleton et al. showed that reactivity of HC(O)OH is essentially the same as that of DC(O)OH, but DC(O)OD reacts much slower than HC(O)OH and DC(O)OH. These observations show that the reaction proceeds via abstraction of the acidic H atom. Wine et al. and Jolly et al. also found that H atoms are produced in the reaction, which is consistent with the formation of HC(O)O, which would rapidly fall apart to CO_2 and H. End product studies are also consistent with the formation of CO_2 and H_2O in this reaction (Singleton et al.). The products of this reaction would be mostly HC(O)O and H_2O. The fate of HC(O)O in the atmosphere will be to give HO_2 either directly via reaction with O_2 or via thermal decomposition to H atom, which adds to O_2.

Wine et al. have suggested that, in the atmosphere, the formic acid could be hydrogen bonded to a water molecule and its reactivity with OH could be lowered because the hydrogen bonded water would obstruct the abstraction of the H atom. This suggestion needs to be checked.
(Table: 02-25, Note: 02-25, Evaluated: 02-25) Back to Table

(1) Dagaut, P.; Wallington, T. J.; Liu, R.; Kurylo, M. J. The gas phase reactions of hydroxyl radicals with a series of carboxylic acids over the temperature range 240-440 K. *Int. J. Chem. Kinet.* **1988**, *20*, 331-338, doi:10.1002/kin.550200406.

(2) Jolly, G. S.; McKenney, D. J.; Singleton, D. L.; Paraskevopoulos, G.; Bossard, A. R. Rate constant and mechanism for the reaction of hydroxyl radical with formic acid. *J. Phys. Chem.* **1986**, *90*, 6557-6562, doi:10.1021/j100282a028.

(3) Singleton, D. L.; Paraskevopoulos, G.; Irwin, R. S.; Jolly, G. S.; McKenney, D. J. Rate and mechanism of the reaction of hydroxyl radicals with formic and deuterated formic acids. *J. Am. Chem. Soc.* **1988**, *110*, 7786-7790, doi:10.1021/ja00231a032.

(4) Wine, P. H.; Astalos, R. J.; Mauldin, R. L., III Kinetic and mechanistic study of the OH + HCOOH reaction. *J. Phys. Chem.* **1985**, *89*, 2620-2624, doi:10.1021/j100258a037.

(5) Zetzsch, C.; Stuhl, F. In *Proceedings of the 2nd European Symposium on the Physico-Chemical Behaviour of Atmospheric Pollutants*; D. Reidel Publishing Co.: Dordrecht, Holland, 1982; pp 129-137.

D21. OH + HC(O)C(O)H. The only available data are from the 298 K relative rate study of Plum et al.[1] and the results are recommended here. Because the rate coefficient is so large, it is unlikely to have a substantial temperature dependence and an E/R of zero is recommended. This reaction is expected to proceed via H-abstraction to yield H_2O, CO and HCO.
(Table: 06-2, Note: 06-2, Evaluated: 06-2) Back to Table

(1) Plum, C. N.; Sanhueza, E.; Atkinson, R.; Carter, W. P. L.; Pitts, J. N., Jr. OH radical rate constant and photolysis rates of α-dicarbonyls. *Environ. Sci. Technol.* **1983**, *17*, 479-484, doi:10.1021/es00114a008.

D22. OH + $HOCH_2CHO$. The recommendation is based on the available results of two absolute rate constant measurements by Karunanandan et al.[3] (240–362 K) (laser pulsed photolysis with LIF detection of OH) and Butkovskaya et al.[2] (233–296 K) (a turbulent flow reactor with CI MS). The recommended k(298 K) is an average of the values from these studies. The recommended value of $E/R = 0$ is based on results of Karunanandan et al.

The available results of relative rate studies at 298 K by Niki et al.,[5] Bacher et al.,[1] Magneron et al.,[4] and Zhu and Zhu[6] are in good agreement with the recommended value of k(298 K), while being larger by 12–50%. The reported uncertainties of individual measurements overlap with the uncertainty recommended for this reaction rate constant.

There are three possible sites for H-abstraction: the alcohol group, the CH_2 group, and the carbonyl group. Of these, the likely pathways for abstraction are from the latter two sites:

$$OH + HOCH_2CHO \rightarrow H_2O + HOC(H)CHO \quad (a)$$
$$OH + HOCH_2CHO \rightarrow H_2O + HOCH_2CO \quad (b)$$

Niki et al., Magneron et al., and Butkovskaya et al. have shown that the branching ratio for channel (b) is 0.8 and for channel (a) is 0.2. It is unlikely that the branching ratio changes significantly with temperature.
(Table: 25-1, Note: 25-1, Evaluated: 25-1) Back to Table

(1) Bacher, C.; Tyndall, G. S.; Orlando, J. J. The atmospheric chemistry of glycolaldehyde. *J. Atmos. Chem.* **2001**, *39*, 171-189, doi:10.1023/A:1010689706869.
(2) Butkovskaya, N. I.; Pouvesle, N.; Kukui, A.; Le Bras, G. Mechanism of the OH-initiated oxidation of glycolaldehyde over the temperature range 233-296 K. *J. Phys. Chem. A* **2006**, *110*, 13492-13499, doi:10.1021/jp064993k.
(3) Karunanandan, R.; Holscher, D.; Dillon, T. J.; Horowitz, A.; Crowley, J. N.; Vereecken, L.; Peeters, J. Reaction of HO with glycolaldehyde, $HOCH_2CHO$: Rate coefficients (240-362 K) and mechanism. *J. Phys. Chem. A* **2007**, *111*, 897-908, doi:10.1021/jp0649504.
(4) Magneron, I.; Mellouki, A.; Le Bras, G.; Moortgat, G. K.; Horowitz, A.; Wirtz, K. Photolysis and OH-initiated oxidation of glycolaldehyde under atmospheric conditions. *J. Phys. Chem. A* **2005**, *109*, 4552-4561, doi:10.1021/jp044346y.
(5) Niki, H.; Maker, P. D.; Savage, C. M.; Hurley, M. D. Fourier transform infrared study of the kinetics and mechanisms for the Cl-atom- and HO-radical-initiated oxidation of glycolaldehyde. *J. Phys. Chem.* **1987**, *91*, 2174-2178, doi:10.1021/j100292a038.
(6) Zhu, C.; Zhu, L. Photolysis of glycolaldehyde in the 280-340nm region. *J. Phys. Chem. A* **2010**, *114*, 8384-8390, doi:10.1021/jp104497d.

D23. OH + C_2H_6. There are numerous studies of this reaction at 298 K (Greiner,[11] Horne and Norrish,[14] Greiner,[12] Overend et al.,[21] Howard and Evenson,[15] Leu,[18] Lee and Tang,[17] Tully et al.,[29] Jeong et al.,[16] Smith et al.,[25] Baulch et al.,[2] Schmidt et al.,[23] Edney et al.,[9] Tully et al.,[28] Nielsen et al.,[20] Stachnik et al.,[26] Wallington et al.,[30] Bourmada et al.,[3] Zabarnick et al.,[31] Abbatt et al.,[1] Schiffman et al.,[22] Dobe et al.,[7] Sharkey and Smith,[24] Finlayson-Pitts,[10] Talukdar et al.,[27] Crowley et al.,[6] Cavalli et al.,[4] Donahue et al.,[8] Clarke et al.,[5] Heathfield et al.,[13] and Li et al.[19]). The recommended k(298 K) is an average of the majority of the results reported at room temperature (Overend et al.,[21] Howard and Evenson,[15] Leu,[18] Lee and Tang,[17] Tully et al.,[29] Smith et al.,[25] Baulch et al.,[2] Schmidt et al.,[23] Tully et al.,[28] Stachnik et al.,[26] Wallington et al.,[30] Bourmada et al.,[3] Zabarnick et al.,[31] Abbatt et al.,[1] Schiffman et al.,[22] Dobe et al.,[7] Finlayson-Pitts,[10] Talukdar et al.,[27] Crowley et al.,[6] Cavalli et al.,[4] Donohue et al.,[8] Clarke et al.,[5] Heathfield et al.,[13] and Li et al.[19]). The room temperature studies not used were either of lower precision (as evidenced by data scatter) or yielded somewhat higher rate constants.

The temperature dependence of the rate coefficient below 298 K has been measured by Jeong et al.[16] (248–472 K), Stachnik et al.[26] (248, 297 K), Smith et al.[25] (240–295 K), Wallington et al.[30] (226–363 K), Talukdar et al.[27] (231–377 K), Crowley et al.[6] (247–303 K), and Clarke et al.[5] (180–360 K). The last six of these studies are in good agreement (the data from Jeong et al.[16] exhibit noticable upward curvature below 298 K). Thus the recommended value for E/R is derived from a combined fit to the data below 300 K from the aforementioned six studies after each data set was normalized to the recommended value for k(298 K).
(Table: 19-5, Note: 10-6, Evaluated: 10-6) Back to Table

(1) Abbatt, J. P. D.; Demerjian, K. L.; Anderson, J. G. A new approach to free-radical kinetics: Radially and axially resolved high-pressure discharge flow with results for OH + (C_2H_6, C_3H_8, n-C_4H_{10}, n-C_5H_{12}) → products at 297 K. *J. Phys. Chem.* **1990**, *94*, 4566-4575, doi:10.1021/j100374a039.
(2) Baulch, D. L.; Campbell, I. M.; Saunders, S. M. Rate constants for the reactions of hydroxyl radicals with propane and ethane. *J. Chem. Soc. Faraday Trans. 1* **1985**, *81*, 259-263, doi:10.1039/f19858100259.
(3) Bourmada, N.; Lafage, C.; Devolder, P. Absolute rate constants of the reactions of OH with cyclohexane and ethane at 296 ± 2 K by the discharge flow method. *Chem. Phys. Lett.* **1987**, *136*, 209-214, doi:10.1016/0009-2614(87)80443-8.
(4) Cavalli, F.; Glasius, M.; Hjorth, J.; Rindone, B.; Jensen, N. R. Atmospheric lifetimes, infrared spectra and degradation products of a series of hydrofluoroethers. *Atmos. Environ.* **1998**, *32*, 3767-3773, doi:10.1016/S1352-2310(98)00106-X.
(5) Clarke, J. S.; Kroll, J. H.; Donahue, N. M.; Anderson, J. G. Testing frontier orbital control: Kinetics of OH with ethane, propane, and cyclopropane from 180 to 360K. *J. Phys. Chem. A* **1998**, *102*, 9847-9857, doi:10.1021/jp982922i.
(6) Crowley, J. N.; Campuzano-Jost, P.; Moortgat, G. K. Temperature dependent rate constants for the gas-phase reaction between OH and CH_3OCl. *J. Phys. Chem.* **1996**, *100*, 3601-3606, doi:10.1021/jp953018i.
(7) Dóbé, S.; Turányi, T.; Iogansen, A. A.; Bérces, T. Rate constants of the reactions of OH radicals with cyclopropane and cyclobutane. *Int. J. Chem. Kinet.* **1992**, *24*, 191-198, doi:10.1002/kin.550240207.

(8) Donahue, N. M.; Anderson, J. G.; Demerjian, K. L. New rate constants for ten OH alkane reactions from 300 to 400 K: An assessment of accuracy. *J. Phys. Chem. A* **1998**, *102*, 3121-3126, doi:10.1021/jp980532q.
(9) Edney, E. O.; Kleindienst, T. E.; Corse, E. W. Room temperature rate constants for the reaction of OH with selected chlorinated and oxygenated hydrocarbons. *Int. J. Chem. Kinet.* **1986**, *18*, 1355-1371, doi:10.1002/kin.550181207.
(10) Finlayson-Pitts, B. J.; Hernandez, S. K.; Berko, H. N. A new dark source of the gaseous hydroxyl radical for the relative rate measurements. *J. Phys. Chem.* **1993**, *97*, 1172-1177, doi:10.1021/j100108a012.
(11) Greiner, N. R. Hydroxyl-radical kinetics by kinetic spectroscopy. II. Reactions with C_2H_6, C_3H_8, and *iso*-C_4H_{10} at 300°K. *J. Chem. Phys.* **1967**, *46*, 3389-3392, doi:10.1063/1.1841228.
(12) Greiner, N. R. Hydroxyl radical kinetics by kinetic spectrosopy. VII. The reaction with ethylene in the range 300-500 °K. *J. Chem. Phys.* **1970**, *53*, 1284-1285, doi:10.1063/1.1674133.
(13) Heathfield, A. E.; Anastasi, C.; Pagsberg, P.; McCulloch, A. Atmospheric lifetimes of selected fluorinated ether compounds. *Atmos. Environ.* **1998**, *32*, 711-717, doi:10.1016/S1352-2310(97)00330-0.
(14) Horne, D. G.; Norrish, R. G. W. Rate of H-abstraction by OH from hydrocarbons. *Nature (London)* **1967**, *215*, 1373-1374, doi:10.1038/2151373a0.
(15) Howard, C. J.; Evenson, K. M. Rate constants for the reactions of OH with ethane and some halogen substituted ethanes at 296 K. *J. Chem. Phys.* **1976**, *64*, 4303-4306, doi:10.1063/1.432115.
(16) Jeong, K. M.; Hsu, K. J.; Jeffries, J. B.; Kaufman, F. Kinetics of the reactions of OH with C_2H_6, CH_3CCl_3, $CH_2ClCHCl_2$, $CH_2ClCClF_2$, and CH_2FCF_3. *J. Phys. Chem.* **1984**, *88*, 1222-1226, doi:10.1021/j150650a041.
(17) Lee, J. H.; Tang, I. N. Absolute rate constants for the hydroxyl radical reactions with ethane, furan, and thiophene at room temperature. *J. Chem. Phys.* **1982**, *77*, 4459-4463, doi:10.1063/1.444367.
(18) Leu, M. T. Rate constant for the reaction $HO_2 + NO \rightarrow OH + NO_2$. *J. Chem. Phys.* **1979**, *70*, 1662-1666, doi:10.1063/1.437680.
(19) Li, Q.; Osborne, M. C.; Smith, I. W. M. Rate constants for the reactions of Cl atoms with HCOOH and with HOCO radicals. *Int. J. Chem. Kinet.* **2000**, *32*, 85-91, doi:10.1002/(SICI)1097-4601(2000)32:2<85::AID-KIN3>3.0.CO;2-I.
(20) Nielsen, O. J.; Munk, J.; Pagsberg, P.; Sillesen, A. Absolute rate constants for the gas-phase reaction of OH radicals with cyclohexane and ethane at 295 K. *Chem. Phys. Lett.* **1986**, *128*, 168-171, doi:10.1016/0009-2614(86)80319-0.
(21) Overend, R. P.; Paraskevopoulos, G.; Cvetanović, R. J. Rates of OH radical reactions. I. Reactions with H_2, CH_4, C_2H_6, and C_3H_8 at 295 K. *Can. J. Phys.* **1975**, *53*, 3374-3382, doi:10.1139/v75-482.
(22) Schiffman, A.; Nelson, D. D.; Robinson, M. S.; Nesbitt, D. J. High-resolution infrared flash kinetic spectroscopy of OH radicals. *J. Phys. Chem.* **1991**, *95*, 2629-2636, doi:10.1021/j100160a004.
(23) Schmidt, V.; Zhu, G. Y.; Becker, K. H.; Fink, E. H. Study of OH reactions at high pressures by excimer laser photolysis - dye laser fluorescence. *Ber. Bunsenges. Phys. Chem.* **1985**, *89*, 321-322, doi:10.1002/bbpc.19850890337.
(24) Sharkey, P.; Smith, I. W. M. Kinetics of elementary reactions at low temperatures: Rate constants for the reactions of OH with HCl ($298 \geq T/K \geq 138$), CH_4 ($298 \geq T/K \geq 178$), and C_2H_6 ($298 \geq T/K \geq 138$). *J. Chem. Soc. Faraday Trans.* **1993**, *89*, 631-638, doi:10.1039/ft9938900631.
(25) Smith, C. A.; Molina, L. T.; Lamb, J. J.; Molina, M. J. Kinetics of the reaction of OH with pernitric and nitric acids. *Int. J. Chem. Kinet.* **1984**, *16*, 41-55, doi:10.1002/kin.550160107.
(26) Stachnik, R. A.; Molina, L. T.; Molina, M. J. Pressure and temperature dependences of the reaction of OH with nitric acid. *J. Phys. Chem.* **1986**, *90*, 2777-2780, doi:10.1021/j100403a044.
(27) Talukdar, R. K.; Mellouki, A.; Gierczak, T.; Barone, S.; Chiang, S.-Y.; Ravishankara, A. R. Kinetics of the reactions of OH with alkanes. *Int. J. Chem. Kinet.* **1994**, *26*, 973-990, doi:10.1002/kin.550261003.
(28) Tully, F. P.; Droege, A. T.; Koszykowski, M. L.; Melius, C. F. Hydrogen-atom abstraction from alkanes by OH. 2. Ethane. *J. Phys. Chem.* **1986**, *90*, 691-698, doi:10.1021/j100276a042.
(29) Tully, F. P.; Ravishankara, A. R.; Carr, K. Kinetic study of the reactions of the hydroxyl radical with ethane and propane. *Int. J. Chem. Kinet.* **1983**, *15*, 1111-1118, doi:10.1002/kin.550151014.
(30) Wallington, T. J.; Neuman, D. M.; Kurylo, M. J. Kinetics of the gas phase reaction of hydroxyl radicals with ethane, benzene, and a series of halogenated benzenes over the temperature range 234–438 K. *Int. J. Chem. Kinet.* **1987**, *19*, 725-739, doi:10.1002/kin.550190806.
(31) Zabarnick, S.; Fleming, J. W.; Lin, M. C. Kinetics of hydroxyl radical reactions with formaldehyde and 1,3,5-trioxane between 290 and 600 K. *Int. J. Chem. Kinet.* **1988**, *20*, 117-129, doi:10.1002/kin.550200205.

D24. OH + CH_3CHO. There have been 10 studies (Atkinson and Pitts[1] (299–426 K), Blázquez et al.[3] (11.7–177.5), Dobe et al.[7] (297–517 K), Michael et al.[9] (244–528 K), Semmes et al.[13] (253–424 K), Sivakumaran and Crowley[14] (201–348 K), Taylor et al.[16] (297–860 K), Vöhringer-Martinez et al.[20] (60–300 K), Wang et al.[22] (999–1367 K), and Zhu et al.[23] (204–373 K) of the temperature dependence of the reaction from 11.7–1388 K, however only two studies have been performed at temperatures relevant to Earth's atmosphere Sivakumaran and Crowley[14] and Zhu et al.[23] The temperature dependence changes from negative to positive at approximately 600 K Taylor et al.[15] Furthermore, extremely low temperatures studies using the CRESU technique have shown that below 100 K the reaction displays non-Arrhenius behavior.[3] The recommended values for k(298 K) and E/R come from a combined fit to the data of Sivakumaran and Crowley[14] and Zhu et al.[23] at T ≤350 K. There are 14 other studies of this reaction that provide the room temperature rate constant (Morris et al.,[10] Niki et al.,[11] Atkinson and Pitts,[1] Kerr and Sheppard,[8] Semmes et al.,[13] Michael et al.,[9] Dobe et al.,[7] Balestra-Garcia et al.,[2] Scollard et al.,[12] Tyndall et al.,[18] Taylor et al.,[15] D'Anna et al.,[6] Wang et al.,[21] and Taylor et al.[16]). The average value of k(298 K) from all of these studies is identical to that derived from the above fit. The study by Michael et al.[9] also provided data down to 244 K. While these data are far more scattered than those from Sivakumaran and Crowley[14] and Zhu et al.,[23] they are encompassed by the 95% confidence limits of the recommendation.

Measurements of H_2O formation yields were conducted by Wang et al.,[21] Butkovskaya et al.,[4] and Vandenberk and Peeters.[19] These investigators reported values of ~100%, (97.7 ± 4.7)%, and (89 ± 6)%, respectively at about room temperature. Butkovskaya et al.[4] report identical yields at both 298 K and 248 K. Tyndall et al.[17] concluded that more than 90% of the reaction proceeds via H-atom abstraction based on no measurable detection of acidic acid formation. Cameron et al.[5] detected CH_3 and CH_3CO radicals and H-atoms. The major reaction pathway was determined to be $CH_3CHO + OH \rightarrow CH_3CO + H_2O$ with a measured yield of (93 ± 18)%. Butkovskaya et al.[4] detected CH_2CHO radicals to obtain a branching ratio for H-atom abstraction from the CH_3 group of $5.1^{+2.4}_{-1.7}$%. Vöhringer-Martinez et al.[20] studied the effect of water vapor on the reaction rate constant at temperatures between 300 K and 60 K. They found little-to no effect at 300 K and enhancements approaching a factor of 2 at temperatures below 100 K.
(Table: 10-6, Note: 10-6, Evaluated: 10-6) Back to Table

(1) Atkinson, R.; Pitts Jr., J. N. Kinetics of the reactions of the OH radical with HCHO and CH_3CHO over the temperature range 299-426°K. *J. Chem. Phys.* **1978**, *68*, 3581-3590, doi:10.1063/1.436215.

(2) Balestra-Garcia, C.; Le Bras, G.; MacLeod, H. Kinetic study of the reactions OH + mono-, di-, and trichloroacetaldehyde and acetaldehyde by laser photolysis-resonance fluorescence at 298 K. *J. Phys. Chem.* **1992**, *96*, 3312-3316, doi:10.1021/j100187a026.

(3) Blázquez, S.; González, D.; Neeman, E. M.; Ballesteros, B.; Agúndez, M.; Canosa, A.; Albaladejo, J.; Cernicharo, J.; Jiménez, E. Gas-phase kinetics of CH_3CHO with OH radicals between 11.7 and 177.5 K. *Phys. Chem. Chem. Phys.* **2020**, *22*, 20562-20572, doi:10.1039/D0CP03203D.

(4) Butkovskaya, N. I.; Kukui, A.; Le Bras, G. Branching fractions for H_2O forming channels of the reaction of OH radicals with acetaldehyde. *J. Phys. Chem. A* **2004**, *108*, 1160-1168, doi:10.1021/jp036740m.

(5) Cameron, M.; Sivakumaran, V.; Dillon, T. J.; Crowley, J. N. Reaction between OH and CH_3CHO. Part 1. Primary product yields of CH_3 (296 K), CH_3CO (296 K), and H (237-296 K). *Phys. Chem. Chem. Phys.* **2002**, *4*, 3628-3638, doi:10.1039/b202586h.

(6) D'Anna, B.; Andresen, O.; Gefen, Z.; Nielsen, C. J. Kinetic study of OH and NO_3 radical reactions with 14 aliphatic aldehydes. *Phys. Chem. Chem. Phys.* **2001**, *3*, 3057-3063, doi:10.1039/b103623h.

(7) Dóbé, S.; Khachatryan, L. A.; Bérces, T. Kinetics of reactions of hydroxyl radicals with a series of aliphatic aldehydes. *Ber. Bunsenges. Phys. Chem.* **1989**, *93*, 847-852, doi:10.1002/bbpc.19890930806.

(8) Kerr, J. A.; Sheppard, D. W. Kinetics of the reactions of hydroxyl radicals with aldehydes studied under atmospheric conditions. *Environ. Sci. Technol.* **1981**, *15*, 960-963, doi:10.1021/es00090a012.

(9) Michael, J. V.; Keil, D. G.; Klemm, R. B. Rate constants for the reaction of hydroxyl radicals with acetaldehyde from 244-528 K. *J. Chem. Phys.* **1985**, *83* 1630-1636, doi:10.1063/1.449400.

(10) Morris, E. D., Jr.; Stedman, D. H.; Niki, H. Mass spectrometric study of the reactions of the hydroxyl radical with ethylene, propylene, and acetaldehyde in a discharge-flow system. *J. Am. Chem. Soc.* **1971**, *93*, 3570-3572, doi:10.1021/ja00744a004.

(11) Niki, H.; Maker, P. D.; Savage, C. M.; Breitenbach, L. P. Relative rate constants for the reaction of hydroxyl radical with aldehydes. *J. Phys. Chem.* **1978**, *82*, 132-134, doi:10.1021/j100491a002.

(12) Scollard, D. J.; Treacy, J. J.; Sidebottom, H. W.; Balestra-Garcia, C.; Laverdet, G.; LeBras, G.; MacLeod, H.; Téton, S. Rate constants for the reactions of hydroxyl radicals and chlorine atoms with halogenated aldehydes. *J. Phys. Chem.* **1993**, *97*, 4683-4688, doi:10.1021/j100120a021.

(13) Semmes, D. H.; Ravishankara, A. R.; Gump-Perkins, C. A.; Wine, P. H. Kinetics of the reactions of hydroxyl radical with aliphatic aldehydes. *Int. J. Chem. Kinet.* **1985**, *17*, 303-313, doi:10.1002/kin.550170307.
(14) Sivakumaran, V.; Crowley, J. N. Reaction between OH and CH_3CHO - Part 2. Temperature dependent rate coefficients (201-348 K). *Phys. Chem. Chem. Phys.* **2003**, *5*, 106-111, doi:10.1039/b209303k.
(15) Taylor, P. H.; Rahman, M. S.; Arif, M.; Dellinger, B.; Marshall, P. Kinetic and mechanistric studies of the reaction of hydroxyl radicals with acetaldehyde over an extended temperature range. *Symp. Int. Combust. Proc.* **1996**, *26*, 497-504.
(16) Taylor, P. H.; Yamada, T.; Marshall, P. The reaction of OH with acetaldehyde and deuterated acetaldehyde: Further insight into the reaction mechanism at both low and elevated temperatures. *Int. J. Chem. Kinet.* **2006**, *38*, 489-495, doi:10.1002/kin.20179.
(17) Tyndall, G. R. S.; Orlando, J. J.; Wallington, T. J.; Hurley, M. D.; Goto, M.; Kawasaki, M. Mechanism of the reaction of OH radicals with acetone and acetaldehyde at 251 and 296 K. *Phys. Chem. Chem. Phys.* **2002**, *4*, 2189-2193, doi:10.1039/b111195g.
(18) Tyndall, G. S.; Stafelbach, T. A.; Orlando, J. J.; Calvert, J. G. Rate coefficients for reactions of OH radicals with mehylglyoxal and acetaldehyde. *Int. J. Chem. Kinet.* **1995**, *27*, 1009-1020, doi:10.1002/kin.550271006.
(19) Vandenberk, S.; Peeters, J. The reaction of acetaldehyde and propionaldehdye with hydroxyl radicals: experimental determination of the primary H_2O yield at room temperature. *J. Photochem. Photobiol. A: Chem.* **2003**, *157*, 269-274, doi:10.1016/S1010-6030(03)00063-7.
(20) Vöhringer-Martinez, E.; Hansmann, B.; Hernandez, H.; Francisco, J. S.; Troe, J.; Abel, B. Water catalysis of a radical-molecule gas-phase reaction. *Science* **2007**, *315*, 497-501, doi:10.1126/science.1134494.
(21) Wang, J.; Chen, H. B.; Glass, G. P.; Curl, R. F. Kinetic study of the reaction of acetaldehyde with OH. *J. Phys. Chem. A* **2003**, *107*, 10834-10844, doi:10.1021/jp036114p.
(22) Wang, S.; Davidson, D. F.; Hanson, R. K. High temperature measurements for the rate constants of C_1–C_4 aldehydes with OH in a shock tube. *Proc. Combust. Inst.* **2015**, *35*, 473-480, doi:10.1016/j.proci.2014.06.112.
(23) Zhu, L.; Talukdar, R. K.; Burkholder, J. B.; Ravishankara, A. R. Rate coefficients for the OH + acetaldehyde (CH_3CHO) Reaction Between 204 and 373 K. *Int. J. Chem. Kinet.* **2008**, *40*, 635-646, doi:10.1002/kin.20346.

D25. OH + $CH_3OC(O)H$. The recommended values for k(298 K) and E/R come from a fit to the data of Le Calve et al.[3] (233–372 K), who studied the reaction by using an absolute technique. Results of room temperature studies reported by Good et al.[1] (298 K) and Szilagyi et al.[4] are in very good agreement with the recommended value. The recommended uncertainty at 95% confidence interval also encompasses the room temperature result reported by Wallington et al.[5] (296 K), which is 25% larger than the recommended value.

Jimenez et al.[2] studied this reaction at very low temperatures between 22 and 64 K to find the substantially larger rate constant of OH disappearance, which increases with decreasing temperature from 1.2×10^{-11} cm^3 $molecule^{-1}$ s^{-1} at 64 K to 1.2×10^{-10} cm^3 $molecule^{-1}$ s^{-1} at 22 K. The large rate constant of the OH removal can be associated with either adduct formation at low temperatures or H-abstraction chemical reaction.
(Table: 19-5, Note: 19-5, Evaluated: 19-5) Back to Table

(1) Good, D. A.; Hanson, J.; Francisco, J. S.; Li, Z.; Jeong, G.-R. Kinetics and reaction mechanism of hydroxyl radical reaction with methyl formate. *J. Phys. Chem. A* **1999**, *103*, 10893-10898, doi:10.1021/jp991960e.
(2) Jiménez, E.; Antiñolo, M.; Ballesteros, B.; Canosa, A.; Albaladejo, J. First evidence of the dramatic enhancement of the reactivity of methyl formate ($HC(O)OCH_3$) with OH at temperatures of the interstellar medium: a gas-phase kinetic study between 22 K and 64 K. *Phys. Chem. Chem. Phys* **2016**, *18*, 2183-2191, doi:10.1039/c5cp06369h.
(3) Le Calve, S.; LeBras, G.; Mellouki, A. Temperature dependence for the rate coefficients of the reactions of the OH radical with a series of formates. *J. Phys. Chem. A* **1997**, *101*, 5489-5493, doi:10.1021/jp970554x.
(4) Szilagyi, I.; Dobe, S.; Berces, T.; Marta, F.; Viskolcz, B. Direct kinetic study of reactions of hydroxyl radicals with alkyl formates. *Z. Phys. Chem.* **2004**, *218*, 479-492, doi:10.1524/zpch.218.4.479.29198.
(5) Wallington, T. J.; Dagaut, P.; Liu, R.; Kurylo, M. J. The gas phase reactons of hydroxyl radicals with a series of esters over the temperature range 240-440 K. *Int. J. Chem. Kinet.* **1988**, *20*, 177-186, doi:10.1002/kin.550200210.

D26. OH + C_2H_5OH. There are numerous studies of the reaction rate constant at room temperature (Campbell et al.,[1] Overend and Paraskevopoulos,[13] Ravishankara and Davis,[16] Kerr and Stocker,[7] Greenhill and O'Grady,[4] Wallington and Kurylo,[18] Hess and Tully,[5] Nelson et al.,[10] Picquet et al.,[14] Oh and Andino,[11] Sorensen et al.,[17] Jimenez et al.,[6] Wu et al.,[19] Dillon et al.,[3] Kovacs et al.,[8] Rajakumar et al.,[15] Carr et al.,[2] and Orkin et al.[12]). The recommended k(298 K) is an average of the rate constants measured by Campbell et al.,[1] Kerr and Stocker,[7] Wallington and Kurylo,[18] Hess and Tully,[5] Nelson et al.,[10] Sorensen et al.,[17] Jimenez et al.,[6] Wu et al.,[19] Dillon et al.,[3] Kovacs et al.,[8] Rajakumar et al.,[15] and Orkin et al.[12] The room temperature studies not used were either of lower precision (as evidenced by data scatter) or yielded systematically higher or lower rate constants. Comprehensive studies of this reaction at sub-ambient temperatures were done by Jimenez et al.,[6] Dillon et al.,[3] and Orkin et al.[12] The last two studies resulted in indistinguishable rate constants at low temperatures and coincide with the recommended value of k(298 K). The analysis of the data at low temperatures suggests a temperature independent reaction rate constant between 210 and 298 K and provide the basis for the recommended E/R.

This reaction has three possible product channels: (a) $CH_3CH_2O + H_2O$, (b) $CH_3CHOH + H_2O$, and (c) $CH_2CH_2OH+H_2O$. At room temperature, channel (b) is the major pathway accounting for (75% ± 15%) of the reaction (Meier et al.[9]) which is consistent with the thermochemistry of these three possible pathways. The branching ration for channel (b) is expected to increase with decreasing temperature.
(Table: 10-6, Note: 10-6, Evaluated: 10-6) Back to Table

(1) Campbell, I. M.; McLaughlin, D. F.; Handy, B. J. Rate constants for reactions of hydroxyl radicals with alcohol vapours at 292 K. *Chem. Phys. Lett.* **1976**, *38*, 362-364, doi:10.1016/0009-2614(76)85174-3.

(2) Carr, S. A.; Baeza-Romero, M. T.; Blitz, M. A.; Price, B. J. S.; Seakins, P. W. Ketone photolysis in the presence of oxygen: A useful source of OH for flash photolysis kinetics experiments. *Int. J. Chem. Kinet.* **2008**, *40*, 504-514, doi:10.1002/kin.20330.

(3) Dillon, T. J.; Hölscher, D.; Sivakumaran, V.; Horowitz, A.; Crowley, J. N. Kinetics of the reactions of HO with methanol (210–351 K) and with ethanol (216–368 K). *Phys. Chem. Chem. Phys.* **2005**, *7*, 349-355, doi:10.1039/b413961e.

(4) Greenhill, P. G.; O'Grady, B. V. The rate constant of the reaction of hydroxyl radicals with methanol, ethanol and (D_3)methanol. *Aust. J. Chem.* **1986**, *39*, 1775-1787, doi:10.1071/CH9861775.

(5) Hess, W. P.; Tully, F. P. Catalytic conversion of alcohols to alkenes by OH. *Chem. Phys. Lett.* **1988**, *152*, 183-189, doi:10.1016/0009-2614(88)87352-4.

(6) Jiménez, E.; Gilles, M. K.; Ravishankara, A. R. Kinetics of the reactions of hydroxyl radical with CH_3OH and C_2H_5OH between 235 and 360 K. *J. Photochem. Photobiol. A: Chem.* **2003**, *157*, 237-245, doi:10.1016/S1010-6030(03)00073-X.

(7) Kerr, J. A.; Stocker, D. W. Kinetics of the reactions of hydroxyl radicals with alkyl nitrates and with some oxygen-containing organic compounds studied under simulated atmospheric conditions. *J. Atmos. Chem.* **1986**, *4*, 253-262, doi:10.1007/BF00052004.

(8) Kovács, G.; Szász-Vadász, T.; Papadimitriou, V. C.; Dóbé, S.; Bérces, T.; Márta, F. Absolute rate constants for the reactions of OH radicals with CH_3CH_2OH, CF_2HCH_2OH and CF_3CH_2OH. *React. Kinet. Catal. Lett.* **2005**, *87*, 129-138, doi:10.1007/s11144-006-0018-2.

(9) Meier, U.; Grotheer, H. H.; Riekert, G.; Just, T. Temperature dependence and branching ratio of the C_2H_5OH + OH reaction. *Chem. Phys. Lett.* **1985**, *115*, 221-225, doi:10.1016/0009-2614(85)80684-9.

(10) Nelson, L.; Rattigan, O.; Neavyn, R.; Sidebottom, H.; Treacy, J.; Nielsen, O. J. Absolute and relative rate constants for the reactions of hydroxyl radicals and chlorine atoms with a series of aliphatic alcohols and ethers at 298 K. *Int. J. Chem. Kinet.* **1990**, *22*, 1111-1126, doi:10.1002/kin.550221102.

(11) Oh, S.; Andino, J. M. Kinetics of the gas-phase reactions of hydroxyl radicals with C1-C6 aliphatic alcohols in the presence of ammonium sulfate aerosols. *Int. J. Chem. Kinet.* **2001**, *33*, 422-430, doi:10.1002/kin.1038.

(12) Orkin, V. L.; Khamaganov, V. G.; Martynova, L. E.; Kurylo, M. J. High-accuracy measurements of OH reaction rate constants and IR and UV absorption spectra: Ethanol and partially fluorinated ethyl alcohols. *J. Phys. Chem. A* **2011**, *115*, 8656-8668, doi:10.1021/jp202099t.

(13) Overend, R.; Paraskevopoulos, G. Rates of OH radical reactions. 4. Reactions with methanol, ethanol, 1-propanol, and 2-propanol at 296 K. *J. Phys. Chem.* **1978**, *82*, 1329-1333, doi:10.1021/j100501a001.

(14) Picquet, B.; Heroux, S.; Chebbi, A.; Doussin, J.-F.; Durand-Jolibois, R.; Monod, A.; Loirat, H.; Carlier, P. Kinetics of the reactions of OH radicals with some oxygenated volatile organic compounds under simulated atmospheric conditions. *Int. J. Chem. Kinet.* **1998**, *30*, 839-847, doi:10.1002/(SICI)1097-4601(1998)30:11<839::AID-KIN6>3.0.CO;2-W.

(15) Rajakumar, B.; Burkholder, J. B.; Portmann, R. W.; Ravishankara, A. R. Rate coefficients, for the OH + CFH_2CH_2OH reaction between 238 and 355 K. *Phys. Chem. Chem. Phys.* **2005**, *7*, 2498-2505, doi:10.1039/b503332b.
(16) Ravishankara, A. R.; Davis, D. D. Kinetic rate constants for the reaction of OH with methanol, ethanol, and tetrahydrofuran at 298 K. *J. Phys. Chem.* **1978**, *82*, 2852-2853, doi:10.1021/j100515a022.
(17) Sørensen, M.; Hurley, M. D.; Wallington, T. J.; Dibble, T. S.; Nielsen, O. J. Do aerosols act as catalysts in the OH radical initiated atmospheric oxidation of volatile organic compounds? *Atmos. Environ.* **2002**, *36*, 5947-5952, doi:10.1016/S1352-2310(02)00766-5.
(18) Wallington, T. J.; Kurylo, M. J. The gas phase reactions of hydroxyl radicals with a series of aliphatic alcohols over the temperature range 240-440 K. *Int. J. Chem. Kinet.* **1987**, *19*, 1015-1023, doi:10.1002/kin.550191106.
(19) Wu, H.; Mu, Y.; Zhang, X.; Jiang, G. Relative rate constants for the reactions of hydroxyl radicals and chlorine atoms with a series of aliphatic alcohols. *Int. J. Chem. Kinet.* **2003**, *35*, 81-87, doi:10.1002/kin.10109.

D27. OH + $CH_3C(O)OH$. The recommended values of k(298 K) and E/R are derived from a combined fit to the data of Singleton et al.[8] (297–446 K), Butkovskaya et al.[1] (229–300 K), Crunaire et al.[2] (296 K), Vimal and Stevens[9] (273–373 K), Khamaganov et al.[7] (287–802 K), Huang et al.[6] (255–355 K), and Huang et al.[5] (241–301 K) at T ≤300 K. Data from these studies are in reasonable agreement below 300 K. However, above 300 K there is not a consistent picture of the temperature dependence of the rate constant with E/R values ranging from ~ –500 K to ~–1000 K. In an earlier study by Dagaut et al.[3] (240–440 K) at room temperature and above, an E/R value of +170 K was obtained. For this reason data from this study were not included in the combined fit, although k(298 K) from this study is in good agreement with recommended value. All studies required corrections for the presence of acetic acid dimer especially at temperatures below 298 K and they assumed no reactivity between OH and the dimer. This latter assumption is based on results from Singleton et al.[8] However, in the same study Singleton et al.[8] found that the rate constant for the reaction of OH with the dimer of propionic acid is equal to or greater than that of the rate constant of OH with propionic acid monomer. This result suggests that uncertainties regarding the reactivity of acetic acid dimer may remain. Such uncertainties would propagate into uncertainties in the reactivity of the monomer, especially at lower temperatures.

Three studies give similar results for the reaction mechanism. Butkovskaya et al.[1] reported a yield of (64 ± 17)% over the temperature range of 300–249 K for H-atom abstraction from the carboxyl group, (OH + $CH_3C(O)OH \rightarrow CH_3 + CO_2 + H_2O$). At room temperature, De Smedt et al.[4] and Crunaire et al.[2] reported similar yields of (64 ± 14)% and (78 ± 13)%, respectively. Observations by Singleton et al.[8] regarding the decrease in reactivity upon D substitution on the carboxylic site and no change in reactivity upon substitution on the methyl group, are reasonably consistent with these mechanistic studies.
(Table: 10-6, Note: 10-6, Evaluated: 10-6) Back to Table

(1) Butkovskaya, N. I.; Kukui, A.; Pouvesle, N.; Le Bras, G. Rate constant and mechanism of the reaction of OH radicals with acetic acid in the temperature range of 229-300 K. *J. Phys. Chem. A* **2004**, *108*, 7021-7026, doi:10.1021/jp048444v.
(2) Crunaire, S.; Tarmoul, J.; Fittschen, C.; Tomas, A.; Lemoine, B.; Coddeville, P. Use of cw-CRDS for studying the atmospheric oxidation of acetic acid in a simulation chamber. *Appl. Phys. B* **2006**, *85*, 467-476, doi:10.1007/s00340-006-2319-6.
(3) Dagaut, P.; Wallington, T. J.; Liu, R.; Kurylo, M. J. The gas phase reactions of hydroxyl radicals with a series of carboxylic acids over the temperature range 240-440 K. *Int. J. Chem. Kinet.* **1988**, *20*, 331-338, doi:10.1002/kin.550200406.
(4) De Smedt, F.; Bui, X. V.; Nguyen, T. L.; Peeters, J.; Vereecken, L. Theoretical and experimental study of the product branching in the reaction of acetic acid with OH radicals. *J. Phys. Chem. A* **2005**, *109*, 2401-2409, doi:10.1021/jp044679v.
(5) Huang, Y.-w.; Dransfield, T. J.; Anderson, J. G. Experimental evidence for the pressure dependence of the reaction rate constant between acetic acid and hydroxyl radicals. *J. Phys. Chem. A* **2010**, *114*, 11538-11544, doi:10.1021/jp106446q.
(6) Huang, Y.-w.; Dransfield, T. J.; Miller, J. D.; Rojas, R. D.; Castillo, X. G.; Anderson, J. G. Experimental study of the kinetics of the reaction of acetic acid with hydroxyl radicals from 255 to 355 K. *J. Phys. Chem. A* **2009**, *113*, 423-430, doi:10.1021/jp808627w.
(7) Khamaganov, V. G.; Bui, V. X.; Carl, S. A.; Peeters, J. Absolute rate coefficient of the OH + $CH_3C(O)OH$ reaction at T = 287-802 K. The two faces of pre-reactive H-bonding. *J. Phys. Chem. A* **2006**, *110*, 12852-12859, doi:10.1021/jp064922l.
(8) Singleton, D. L.; Paraskevopoulos, G.; Irwin, R. S. Rates and mechanism of the reactions of hydroxyl radicals with acetic, deuterated acetic, and propionic acids in the gas phase. *J. Am. Chem. Soc.* **1989**, *111*, 5248-5251, doi:10.1021/ja00196a035.

(9) Vimal, D.; Stevens, P. S. Experimental and theoretical studies of the kinetics of the reactions of OH radicals with acetic acid, acetic acid-d_3 and acetic acid-d_4 at low pressure. *J. Phys. Chem. A* **2006**, *110*, 11509-11516, doi:10.1021/jp063224y.

D28. OH + C_3H_8. There are numerous studies of this reaction at room temperature. However, we have based our evaluation on only the more comprehensive studies in which the temperature dependence of the rate constant was determined over the range that included room temperature. Results of eight absolute studies by Droege and Tully[5] (293–854 K), Talukdar et al.[9] (233–376 K), Mellouki et al.[7] (233–363 K), Donahue et al.[4] (300–390 K), Clarke et al.[2] (190–360 K), Kozlov et al.[6] (210–480 K), Bryukov et al.[1] (296–908 K), Morin et al.,[8] (230–908 K) and one relative rate study by DeMore and Bayes[3] (227–428 K) have been analyzed to derive the current recommendation. The results of the latter study were re-calculated by using the current recommendation for the rate constant of a reference reaction, OH + C_2H_6. The recommended value of k(298 K) is an average of the nine values derived from the fit to these individual data sets. All of these values agree within ≈2% with the recommended $k(298\text{ K}) = 1.11 \times 10^{-12}$ cm^3 molecule^{-1} s^{-1}. Although a fit to the data from earlier study by Tully et al.[10] (297–690 K) yields the same k(298 K) as other studies considered here, these data were not used in making recommendation because they exhibit larger scattering and they are probably superseded by the later study of Droege and Tully. Due to the noticeable curvature in the Arrhenius plot over the studied temperature range, the recommended Arrhenius expression is only valid between 190 and 300 K. The recommended E/R was derived from a composite fit to the data from Talukdar et al, Mellouki et al., Clarke et al., Kozlov et al., and Morin et al. between 210 and 300 K after each data set was scaled to the recommended k(298 K).

The Arrhenius plot of the temperature dependence exhibits a noticeable curvature near room temperature and above. Therefore, we recommend the three-parameter expression derived from a fit to the data of Kozlov et al. over the temperature range from 210 to 480 K after data were scaled to match the recommended value of k(298 K).

$$k(210\text{–}480\text{ K}) = 1.99 \times 10^{-12}\,(T/298)^{1.81}\exp(-174/T)$$

This reaction has two possible channels, i.e., abstraction of the primary and the secondary H-atom. From the analysis of reactivity of various deuterated propanes, Droege and Tully estimated that OH reacts with -CH_2- groups approximately 2.5 times faster than with -CH_3 at room temperature; this difference decreases down to a factor of 1.1 at 500 K and a factor of 0.8 at 850 K. Based on their observations between 295 and 854 K the rate constants for these two reaction channels above room temperature can be presented as

$$k_{\text{primary}}(295\text{–}854\text{ K}) = 1.97 \times 10^{-11} \times (T/298)^{1.23}\exp(-675/T)$$

$$k_{\text{secondary}}(295\text{–}854\text{ K}) = 8.54 \times 10^{-13} \times (T/298)^{1.54}\exp(-19/T)$$

(Table: 19-5, Note: 19-5, Evaluated: 19-5) Back to Table

(1) Bryukov, M. G.; Knyazev, V. D.; Lomnicki, S. M.; McFerrin, C. A.; Dellinger, B. Temperature-dependent kinetics of the gas-phase reactions of OH with Cl_2, CH_4, and C_3H_8. *J. Phys. Chem. A* **2004**, *108*, 10464-10472, doi:10.1021/jp047340h.

(2) Clarke, J. S.; Kroll, J. H.; Donahue, N. M.; Anderson, J. G. Testing frontier orbital control: Kinetics of OH with ethane, propane, and cyclopropane from 180 to 360K. *J. Phys. Chem. A* **1998**, *102*, 9847-9857, doi:10.1021/jp982922i.

(3) DeMore, W. B.; Bayes, K. D. Rate constants for the reactions of hydroxyl radical with several alkanes, cycloalkanes, and dimethyl ether. *J. Phys. Chem. A* **1999**, *103*, 2649-2654, doi:10.1021/jp983273d.

(4) Donahue, N. M.; Anderson, J. G.; Demerjian, K. L. New rate constants for ten OH alkane reactions from 300 to 400 K: An assessment of accuracy. *J. Phys. Chem. A* **1998**, *102*, 3121-3126, doi:10.1021/jp980532q.

(5) Droege, A. T.; Tully, F. P. Hydrogen-atom abstraction from alkanes by OH. 3. Propane. *J. Phys. Chem.* **1986**, *90*, 1949-1954, doi:10.1021/j100400a042.

(6) Kozlov, S. N.; Orkin, V. L.; Huie, R. E.; Kurylo, M. J. OH reactivity and UV spectra of propane, n-propyl bromide, and isopropyl bromide. *J. Phys. Chem. A* **2003**, *107*, 1333-1338, doi:10.1021/jp021806j.

(7) Mellouki, A.; Téton, S.; Laverdet, G.; Quilgars, A.; Le Bras, G. Kinetic studies of OH reactions with H_2O_2, C_3H_8, and CH_4 using the pulsed laser photolysis-laser induced fluorescence method. *J. Chim. Phys.* **1994**, *91*, 473-487, doi:10.1051/jcp/1994910473.

(8) Morin, J.; Romanias, M. N.; Bedjanian, Y. Experimental study of the reactions of OH radicals with propane, n-pentane, and n-heptane over a wide temperature range. *Int. J. Chem. Kinet.* **2015**, *47*, 629-637, doi:10.1002/kin.20936.

(9) Talukdar, R. K.; Mellouki, A.; Gierczak, T.; Barone, S.; Chiang, S.-Y.; Ravishankara, A. R. Kinetics of the reactions of OH with alkanes. *Int. J. Chem. Kinet.* **1994**, *26*, 973-990, doi:10.1002/kin.550261003.

(10) Tully, F. P.; Ravishankara, A. R.; Carr, K. Kinetic study of the reactions of the hydroxyl radical with ethane and propane. *Int. J. Chem. Kinet.* **1983**, *15*, 1111-1118, doi:10.1002/kin.550151014.

D29. OH + C_2H_5CHO. The recommended k(298 K) is an average of the results from Niki et al.,[4] Audley et al.,[1] Kerr and Sheppard,[3] Semmes et al.,[6] Papagni,[5] Thevenet,[7] and D'Anna.[2] The temperature dependence has been measured by Thevenet (240–372 K). The E/R is taken from Thevenet and the A-factor is adjusted to reproduce k(298 K). Vandenberk and Peeters[8] measured unity yields of H_2O from the reaction and conclude that the reaction proceeds exclusively by H-abstraction of the aldehydic H-atom.
(Table: 06-2, Note: 06-2, Evaluated: 06-2) Back to Table

(1) Audley, G. J.; Baulch, D. L.; Campbell, I. M. Gas-phase reactions of hydroxyl radicals with aldehydes in flowing H_2O_2 + NO_2 + CO mixtures. *J. Chem. Soc. Faraday Trans. 1* **1981**, *77*, 2541-2549, doi:10.1039/f19817702541.
(2) D'Anna, B.; Andresen, O.; Gefen, Z.; Nielsen, C. J. Kinetic study of OH and NO_3 radical reactions with 14 aliphatic aldehydes. *Phys. Chem. Chem. Phys.* **2001**, *3*, 3057-3063, doi:10.1039/b103623h.
(3) Kerr, J. A.; Sheppard, D. W. Kinetics of the reactions of hydroxyl radicals with aldehydes studied under atmospheric conditions. *Environ. Sci. Technol.* **1981**, *15*, 960-963, doi:10.1021/es00090a012.
(4) Niki, H.; Maker, P. D.; Savage, C. M.; Breitenbach, L. P. Relative rate constants for the reaction of hydroxyl radical with aldehydes. *J. Phys. Chem.* **1978**, *82*, 132-134, doi:10.1021/j100491a002.
(5) Papagni, C.; Arey, J.; Atkinson, R. Rate constants for the gas-phase reactions of a series of C_3–C_6 aldehydes with OH and NO_3 radicals. *Int. J. Chem. Kinet.* **2000**, *32*, 79-84, doi:10.1002/(SICI)1097-4601(2000)32:2<79::AID-KIN2>3.0.CO;2-A.
(6) Semmes, D. H.; Ravishankara, A. R.; Gump-Perkins, C. A.; Wine, P. H. Kinetics of the reactions of hydroxyl radical with aliphatic aldehydes. *Int. J. Chem. Kinet.* **1985**, *17*, 303-313, doi:10.1002/kin.550170307.
(7) Thévenet, R.; Mellouki, A.; Le Bras, G. Kinetics of OH and Cl Reactions with a Series of Aldehydes. *Int. J. Chem. Kinet.* **2000**, *32*, 676-685, doi:10.1002/1097-4601(2000)32:11<676::AID-KIN3>3.0.CO;2-V.
(8) Vandenberk, S.; Peeters, J. The reaction of acetaldehyde and propionaldehdye with hydroxyl radicals: experimental determination of the primary H_2O yield at room temperature. *J. Photochem. Photobiol. A: Chem.* **2003**, *157*, 269-274, doi:10.1016/S1010-6030(03)00063-7.

D30. OH + 1-C_3H_7OH. There have been a number of room temperature measurements that are in excellent agreement. The recommended k(298 K) is an average of the results from absolute kinetics studies by Overend and Paraskevopoulos,[6] Wallington and Kurylo,[7] Nelson et al.,[4] and Yujing and Mellouki.[9] Relative rate studies of Nelson et al., Oh and Andino,[5] Wu et al.,[8] and Cheema et al.[3] are in excellent agreement with the recommended value. The indirect study of Campbell[2] is consistent with, but 30% lower than the recommended value. The reaction is observed to be nearly temperature independent; Yujing and Mellouki (263–372 K) find a slight positive temperature dependence while Cheema et al. (273–343 K) find a small negative temperature dependence. The recommended E/R value is based on the direct study of Yujing and Mellouki. End product studies carried out by Azad and Andino[1] support predictions based on the structure-activity relationship that identify the primary reaction channels as hydrogen abstraction by the OH radical from the α(~75%) and β(~20%) carbons.
(Table: 06-2, Note: 06-2, Evaluated: 06-2) Back to Table

(1) Azad, K.; Andino, J. M. Products of the gas-phase photooxidation reactions of 1-propanol with OH radicals. *Int. J. Chem. Kinet.* **1999**, *31*, 810-818, doi:10.1002/(SICI)1097-4601(1999)31:11<810::AID-JCK8>3.0.CO;2-W.
(2) Campbell, I. M.; McLaughlin, D. F.; Handy, B. J. Rate constants for reactions of hydroxyl radicals with alcohol vapours at 292 K. *Chem. Phys. Lett.* **1976**, *38*, 362-364, doi:10.1016/0009-2614(76)85174-3.
(3) Cheema, S. A.; Holbrook, K. A.; Oldershaw, G. A.; Walker, R. W. Kinetics and mechanism associated with the reactions of hydroxyl radicals and of chlorine atoms with 1-propanol under near-tropospheric conditions between 273 and 343 K. *Int. J. Chem. Kinet.* **2002**, *34*, 110-121, doi:10.1002/kin.10027.
(4) Nelson, L.; Rattigan, O.; Neavyn, R.; Sidebottom, H.; Treacy, J.; Nielsen, O. J. Absolute and relative rate constants for the reactions of hydroxyl radicals and chlorine atoms with a series of aliphatic alcohols and ethers at 298 K. *Int. J. Chem. Kinet.* **1990**, *22*, 1111-1126, doi:10.1002/kin.550221102.
(5) Oh, S.; Andino, J. M. Effects of ammonium sulfate aerosols on the gas-phase reactions of the hydroxyl radical with organic compounds. *Atmos. Environ.* **2000**, *34*, 2901-2908, doi:10.1016/S1352-2310(00)00071-6.

(6) Overend, R.; Paraskevopoulos, G. Rates of OH radical reactions. 4. Reactions with methanol, ethanol, 1-propanol, and 2-propanol at 296 K. *J. Phys. Chem.* **1978**, *82*, 1329-1333, doi:10.1021/j100501a001.
(7) Wallington, T. J.; Kurylo, M. J. The gas phase reactions of hydroxyl radicals with a series of aliphatic alcohols over the temperature range 240-440 K. *Int. J. Chem. Kinet.* **1987**, *19*, 1015-1023, doi:10.1002/kin.550191106.
(8) Wu, H.; Mu, Y.; Zhang, X.; Jiang, G. Relative rate constants for the reactions of hydroxyl radicals and chlorine atoms with a series of aliphatic alcohols. *Int. J. Chem. Kinet.* **2003**, *35*, 81-87, doi:10.1002/kin.10109.
(9) Yujing, M.; Mellouki, A. Temperature dependence for the rate constants of the reaction of OH radicals with selected alcohols. *Chem. Phys. Lett.* **2001**, *333*, 63-68, doi:10.1016/S0009-2614(00)01346-4.

D31. OH + 2-C_3H_7OH. The recommendation is based on results of the most comprehensive absolute measurements of temperature dependences extended to below room temperature, which are reported by Yujing and Mellouki[11] (253–372 K), Rajakumar et al.[8] (237–376 K), and Orkin et al.[6] (220–370 K). The recommended k(298 K) is an average of values derived from the data reported in these papers. The recommended uncertainty encompasses the earlier room temperature data of Klopffer et al.,[3] Overend and Paraskevopoulos,[7] Dunlop and Tully,[2] and the newer relative rate results of Wu et al.[10] (reference compound is C_3H_8). It barely overlaps with the reported uncertainties of the earlier results reported by Wallington and Kurylo[9] (240– 440 K) (absolute measurements) and Nelson et al.[5] (298 K) (both relative rate and absolute measurements). The result of a relative rate study by Lloyd et al.[4] (305 K) is, within its wide error limits, consistent with the recommendation.

The recommended E/R (to be used only below 298 K) is derived from a combined fit to the data below 298 K of Rajakumar et al. averaged at each temperature and Orkin et al. The Arrhenius plot of the temperature dependence exhibits a noticeable curvature near room temperature and above. Results reported by Dunlop and Tully, Rajakumar et al., and Orkin et al. reveal a "bowl" shaped temperature dependence with a minimum near 400 K. Therefore, we recommend the three-parameter expression derived from a fit to the data of Orkin et al. over the temperature range from 220 to 370 K after data were scaled to match the recommended value of k(298 K).

$$k(220–370\ \text{K}) = 3.55 \times 10^{-13}\ (\text{T}/298)^{2.06}\ \exp(+800/\text{T})$$

This expression combined with f(T) = 1.03 encompasses the data of Yujing and Mellouki, Rajakumar et al., and Orkin et al. and also the above room temperature data of Dunlop and Tully up to 587 K at 95% confidence intervals.

Caravan et al.[1] reported the OH removal rate constant at very low temperatures as large as to ~4×10^{-11} cm^3 molecule^{-1} s^{-1} at 138 K and ~$(6–7) \times 10^{-11}$ cm^3 molecule^{-1} s^{-1} at 90 K. Although reaction products were not experimentally observed, authors suggest that the increased OH removal rate constant describes an H-abstraction reaction rather than a non-reactive low-temperature adduct formation. These results are consistent with the trend observed for below room temperature data: although a very long extrapolation beyond the measurement range is always suspicious, the recommended three-parameter expression would yield ~2.4×10^{-11} cm^3 molecule^{-1} s^{-1} at 138 K.

By using isotopic substitution, Dunlop and Tully determined that the primary reaction channel below 400 K involves H atom abstraction by OH from the α-site. This result is in agreement with estimates based on the structure-activity relationship (Yujing and Mellouki).
(Table: 19-5, Note: 19-5, Evaluated: 19-5) Back to Table

(1) Caravan, R. L.; Shannon, R. J.; Lewis, T.; Blitz, M. A.; Heard, D. E. Measurements of rate coefficients for reactions of OH with ethanol and propan-2-ol at very low temperatures. *J. Phys. Chem. A* **2015**, *119*, 7130-7137, doi:10.1021/jp505790m.
(2) Dunlop, J. R.; Tully, F. P. Catalytic dehydration of alcohols by OH. 2-propanol: An intermediate case. *J. Phys. Chem.* **1993**, *97*, 6457-6464, doi:10.1021/j100126a021.
(3) Klopffer, V. W.; Frank, R.; Kohl, E.-G.; Haag, F. Quantitative erfassung der photochemischen transformationsprozeese in der troposphare. *Chem. Ztg.* **1986**, *110*, 57-62.
(4) Lloyd, A. C.; Darnall, K. R.; Winer, A. M.; Pitts Jr., J. N. Relative rate constants for the reactions of OH radicals with isopropyl alcohol, diethyl and di-*n*-propyl ether at 305 ± 2 K. *Chem. Phys. Lett.* **1976**, *42*, 205-209, doi:10.1016/0009-2614(76)80347-8.
(5) Nelson, L.; Rattigan, O.; Neavyn, R.; Sidebottom, H.; Treacy, J.; Nielsen, O. J. Absolute and relative rate constants for the reactions of hydroxyl radicals and chlorine atoms with a series of aliphatic alcohols and ethers at 298 K. *Int. J. Chem. Kinet.* **1990**, *22*, 1111-1126, doi:10.1002/kin.550221102.
(6) Orkin, V. L.; Khamaganov, V. G.; Kurylo, M. J. High accuracy measurements of OH reaction rate constants and IR absorption spectra: Substituted 2-propanols. *J. Phys. Chem. A* **2012**, *116*, 6188-6198, doi:10.1021/jp211534n.

(7) Overend, R.; Paraskevopoulos, G. Rates of OH radical reactions. 4. Reactions with methanol, ethanol, 1-propanol, and 2-propanol at 296 K. *J. Phys. Chem.* **1978**, *82*, 1329-1333, doi:10.1021/j100501a001.
(8) Rajakumar, B.; McCabe, D. C.; Talukdar, R. K.; Ravishankara, A. R. Rate coefficients for the reactions of OH with n-propanol and iso-propanol between 237 and 376 K. *Int. J. Chem. Kinet.* **2010**, *42*, 10-24, doi:10.1002/kin.20456.
(9) Wallington, T. J.; Kurylo, M. J. The gas phase reactions of hydroxyl radicals with a series of aliphatic alcohols over the temperature range 240-440 K. *Int. J. Chem. Kinet.* **1987**, *19*, 1015-1023, doi:10.1002/kin.550191106.
(10) Wu, H.; Mu, Y.; Zhang, X.; Jiang, G. Relative rate constants for the reactions of hydroxyl radicals and chlorine atoms with a series of aliphatic alcohols. *Int. J. Chem. Kinet.* **2003**, *35*, 81-87, doi:10.1002/kin.10109.
(11) Yujing, M.; Mellouki, A. Temperature dependence for the rate constants of the reaction of OH radicals with selected alcohols. *Chem. Phys. Lett.* **2001**, *333*, 63-68, doi:10.1016/S0009-2614(00)01346-4.

D32. OH + $C_2H_5C(O)OH$. Studies of this reaction have been confined to 298 K and above because of the tendency of propionic acid to dimerize at lower temperatures and higher concentrations. Kinetic isotope effects measured by Singleton et al.[2] are consistent with a two channel mechanism proposed previously for OH reaction with acetic acid. In the propionic acid case, the channel involving direct abstraction of an alkyl hydrogen is predominant, thus accounting for the observed temperature independence of the rate constant. The recommended temperature independent rate constant, is based on an average of the results of Singleton et al. (298–446 K) and Dagout et al.[1] (298–440 K). A room temperature measurement by Zetsch and Stuhl[3] is ~30% higher, but consistent with the recommendation. Further studies below 298 K would be desirable to investigate possible non-Arrhenius behavior.
(Table: 06-2, Note: 06-2, Evaluated: 06-2) Back to Table

(1) Dagaut, P.; Wallington, T. J.; Liu, R.; Kurylo, M. J. The gas phase reactions of hydroxyl radicals with a series of carboxylic acids over the temperature range 240-440 K. *Int. J. Chem. Kinet.* **1988**, *20*, 331-338, doi:10.1002/kin.550200406.
(2) Singleton, D. L.; Paraskevopoulos, G.; Irwin, R. S. Rates and mechanism of the reactions of hydroxyl radicals with acetic, deuterated acetic, and propionic acids in the gas phase. *J. Am. Chem. Soc.* **1989**, *111*, 5248-5251, doi:10.1021/ja00196a035.
(3) Zetzsch, C.; Stuhl, F. In *Proceedings of the 2nd European Symposium on the Physico-Chemical Behaviour of Atmospheric Pollutants*; D. Reidel Publishing Co.: Dordrecht, Holland, 1982; pp 129-137.

D33. OH + $CH_3C(O)CH_3$. The rate coefficient for this reaction has been measured at temperatures close to 298 K by Cox et al.,[2] Zetzsch,[14] Chiorboli et al.,[1] Kerr and Stocker,[5] Wallington and Kurylo,[11] Le Calve et al.,[6] Wollenhaupt et al.,[12] Gierczak et al.,[3] and Yamada et al.[13] Cox reported only an upper limit of $<5 \times 10^{-13}$ cm^3 molecule^{-1} s^{-1}, which is consistent with this recommendation. The primary aim of Chiorboli et al. was to examine the atmospheric degradation of styrene, which produces acetone. They employed a relative rate measurement and reported a value of k(298 K) that is almost three times greater than the recommended value. Because of possible complications in their system, we have not included their results in arriving at the recommended value. Wallington and Kurylo (240–440 K), Le Calve et al. (243–372 K), Wollenhaupt et al. (202–395 K), Gierczak et al. (199–383 K), and Yamada et al. (298–832 K) have reported k as a function of temperature; all these studies directly measured the rate constant using the pulsed photolysis method where the temporal profile of OH was measured using resonance fluorescence or laser induced fluorescence. The extensive data of Wollenhaupt et al. and Gierczak et al. seem to show that this rate coefficient does not follow an Arrhenius expression. The results of Le Calve et al. and Wallington et al. are in general agreement with the results of Wollenhaupt et al. and Gierczak et al. The non-Arrhenius behavior was not evident in the results of Wallington et al. and Le Calve et al. because they measured the rate constant at a few temperatures and did not explore temperature below 240 K, where the curvature becomes increasingly evident. Yamada et al. measured k only above room temperature and their values are consistently lower than those of all the others noted above. As they noted in their paper, Yamada et al. did not measure the acetone concentration in the reactor and, thus, could have overestimated its concentration leading to consistently lower values of k. We have not included data of Yamada et al.[13] in deriving the fit because of this possible systematic error and because they did not report k under atmospheric temperatures. The following recommendation reproduces all reported data, except that of Chiorboli et al. within the recommended uncertainty of 25% at all temperatures:

$$k(T) = 1.33 \times 10^{-13} + 3.82 \times 10^{-11} \exp(-2000/T) \text{ cm}^3 \text{ molecule}^{-1} \text{ s}^{-1}$$

This reaction can proceed via the abstraction of an H atom or via the formation of a complex that decomposes to give many different products, which include $CH_3 + CH_3C(O)OH$, $CH_3OH + CH_3C(O)$, $CH_4 + CH_3CO_2$, and

H_2O + $CH_3C(O)CH_2$. The branching ratios for the formation of different sets of products could vary with temperature. Wollenhaupt et al.[12] have deduced that CH_3 radicals are produced with a yield of ~50% at 298 K and ~30% at 233 K. A similar branching ratio has also been reported by Vasvari et al.[10] The results of Gierczak et al. on the OH + $CD_3C(O)CD_3$ reaction, whose rate coefficient nearly obeys an Arrhenius expression between 240 and 400 K and is nearly an order of magnitude smaller than the non-deuterated analog at 250 K, suggest that H abstraction may be the dominant channel. Vandenberk et al.,[9] Tyndall et al.,[8] and Talukdar et al.,[7] clearly show that $CH_3C(O)OH$ is a minor, if not negligible, product of this reaction and that the reaction proceeds to abstract an H atom. The results of Yamada et al. are consistent with this finding. Theoretical calculations of Henon et al.[4] and Vandenberk et al.[9] also suggest that formation of acetic acid is negligible**.** We recommend that the products of this reaction be taken as H_2O and $CH_3C(O)CH_2$.
(Table: 06-2, Note: 06-2, Evaluated: 06-2) Back to Table

(1) Chiorboli, C.; Bignozzi, C. A.; Maldotti, A.; Giardini, P. F.; Rossi, A.; Carassiti, V. Rate constants for the gas-phase reactions of OH radicals with β-dimethylstyrene and acetone. Mechanism of β-dimethylstyrene NO_x – air photooxidation. *Int. J. Chem. Kinet.* **1983**, *15*, 579-586, doi:10.1002/kin.550150608.

(2) Cox, R. A.; Derwent, R. G.; Williams, M. R. Atmospheric photooxidation reactions. Rates, reactivity, and mechanism for reaction of organic compounds with hydroxyl radicals. *Environ. Sci. Technol.* **1980**, *14*, 57-61, doi:10.1021/es60161a007.

(3) Gierczak, T.; Gilles, M. K.; Bauerle, S.; Ravishankara, A. R. Reaction of hydroxyl radical with acetone. 1. Kinetics of the reactions of OH, OD, and ^{18}OH with acetone and acetone-d_6. *J. Phys. Chem. A* **2003**, *107*, 5014-5020, doi:10.1021/jp027301a.

(4) Henon, E.; Canneaux, S.; Bohr, F.; Dobe, S. Features of the potential energy surface for the reaction of OH radical with acetone. *Phys. Chem. Chem. Phys.* **2003**, *5*, 333-341, doi:10.1039/b210247c.

(5) Kerr, J. A.; Stocker, D. W. Kinetics of the reactions of hydroxyl radicals with alkyl nitrates and with some oxygen-containing organic compounds studied under simulated atmospheric conditions. *J. Atmos. Chem.* **1986**, *4*, 253-262, doi:10.1007/BF00052004.

(6) Le Calve, S.; Hitier, D.; Le Bras, G.; Mellouki, A. Kinetic studies of OH reactions with a series of ketones. *J. Phys. Chem. A* **1998**, *102*, 4579-4584, doi:10.1021/jp980848y.

(7) Talukdar, R. K.; Gierczak, T.; McCabe, D. C.; Ravishankara, A. R. Reaction of hydroxyl radial with acetone. 2. Products and reaction mechanism. *J. Phys. Chem. A* **2003**, *107*, 5021-5032, doi:10.1021/jp0273023.

(8) Tyndall, G. R. S.; Orlando, J. J.; Wallington, T. J.; Hurley, M. D.; Goto, M.; Kawasaki, M. Mechanism of the reaction of OH radicals with acetone and acetaldehyde at 251 and 296 K. *Phys. Chem. Chem. Phys.* **2002**, *4*, 2189-2193, doi:10.1039/b111195g.

(9) Vandenberk, S.; Vereecken, L.; Peeters, J. The acetic acid forming channel in the acetone plus OH reaction: A combined experimental and theoretical investigation. *Phys. Chem. Chem. Phys.* **2002**, *4*, 461-466, doi:10.1039/b108161f.

(10) Vasvári, G.; Szilágyi, I.; Bencsura, A.; Dóbe, S.; Bérces, T.; Henon, E.; Canneaux, S.; Bohr, F. Reaction and complex formation between OH radical and acetone. *Phys. Chem. Chem. Phys.* **2001**, *3*, 551-555, doi:10.1039/b009601f.

(11) Wallington, T. J.; Kurylo, M. J. Flash photolysis resonance fluorescence investigation of the gas-phase reactions of OH radicals with a series of aliphatic ketones over the temperature range 240-440 K. *J. Phys. Chem.* **1987**, *91*, 5050-5054, doi:10.1021/j100303a033.

(12) Wollenhaupt, M.; Carl, S. A.; Horowitz, A.; Crowley, J. N. Rate coefficients for reaction of OH with acetone between 202 and 395 K. *J. Phys. Chem. A* **2000**, *104*, 2695-2705, doi:10.1021/jp993738f.

(13) Yamada, T.; Taylor, P. H.; Goumri, A.; Marshall, P. The reaction of OH with acetone and acetone-d_6 from 298 to 832 K: Rate coefficients and mechanism. *J. Chem. Phys.* **2003**, *119*, 10600-10606, doi:10.1063/1.1619950.

(14) Zetzsch, C. "Rate constants for the reactions of OH with acetone and methylethylketone in the gas phase"; 7th International Symposium on Gas Kinetics, 1982, Goettingen, Germany.

D34. OH + $CH_3OCH_2OCH_3$. The rate constant of this reaction has been measured at temperatures close to 298 K by Wallington et al.[3] (relative rate data with C_2H_4 and cyclohexane as reference compounds), Porter et al.[1] (average value derived from relative rate study with diethyl ether, di-n-butyl ether, di-n-propyl ether, and C_2H_5OH as reference compounds is reported), and Thuner et al.[2] (relative rate data with cyclohexane as the reference compound). Porter et al.[1] (252–372 K) reported the temperature dependence of the rate constant derived from an absolute study, which exhibits a noticeable curvature in the Arrhenius plot. The result of absolute rate measurements at 346 K reported by Wallington et al.[3] agrees with this dependence. The recommended k(298 K) is an average of all reported results. The recommended E/R is based on the temperature dependence reported by Porter et al.[1] below 298 K.

(Table: 19-5, Note: 19-5, Evaluated: 19-5) Back to Table

(1) Porter, E.; Wenger, J.; Treacy, J.; Sidebottom, H.; Mellouki, A.; Teton, S.; LeBras, G. Kinetic studies on the reactions of hydroxyl radicals with diethers and hydroxyethers. *J. Phys. Chem. A* **1997**, *101*, 5770-5775, doi:10.1021/jp971254i.

(2) Thüner, L. P.; Barnes, I.; Maurer, T.; Sauer, C. G.; Becker, K. H. Kinetic study of the reaction of OH with a series of acetals at 298 ± 4 K. *Int. J. Chem. Kinet.* **1999**, *31*, 797-803, doi:10.1002/(SICI)1097-4601(1999)31:11<797::AID-JCK6>3.0.CO;2-C.

(3) Wallington, T. J.; Hurley, M. D.; Ball, J. C.; Straccia, A. M.; Platz, J.; Christensen, L. K.; Sehested, J.; Nielsen, O. J. Atmospheric chemistry of dimethoxymethane ($CH_3OCH_2OCH_3$): Kinetics and mechanism of its reaction with OH radicals and fate of the alkoxy radicals $CH_3OCHO(•)OCH_3$ and $CH_3OCH_2OCH_2O(•)$. *J. Phys. Chem. A* **1997**, *101*, 5302-5308, doi:10.1021/jp9631184.

D35. OH + *n*-C_4H_{10}. There are numerous studies of this reaction at room temperature. However, we have based our evaluation only on the more comprehensive studies in which the temperature dependence of the rate constant was determined over a temperature range that included room temperature. Thus the recommended k(298 K) is an average of the five values derived from the fit to the data from the absolute studies of Droege and Tully[5] (294–509 K), Donahue et al.[3] (300–390 K), Talukdar et al.[8] (231–378 K), Donahue and Clarke[4] (185–295 K), and relative rate study of DeMore and Bayers[2] (235–361 K) recalculated using the current recommendations for the reference reaction OH + C_3H_8. The results of first three absolute studies are indicative of the curvature in the Arrhenius plot. Therefore, the recommended value for E/R was obtained from a combined fit to the data sets extended below room temperature by Talukdar et al., Donahue and Clarke, and DeMore and Bayers after scaling each one to the recommended k(298 K). Only data below 330 K have been used for this combined fit. The recommended uncertainty of k(298 K) encompasses the earlier obtained room temperature results of Schmidt et al.,[7] Barnes et al.,[1] and Schiffman et al.[6] All of these eight determinations at room temperature agree to within 4% with the recommended value.

From the analysis of reactivity of various deuterated *n*-butanes Droege and Tully estimated that OH reacts with -CH_2- groups approximately 6 times faster than with -CH_3 at room temperature; this difference decreases at 509 K down to a factor of ~3.

(Table: 19-5, Note: 19-5, Evaluated 19-5) Back to Table

(1) Barnes, I.; Bastian, V.; Becker, K. H.; Fink, E. H.; Nelsen, W. Oxidation of sulphur compounds in the atmosphere: I. Rate constants of OH radical reactions with sulphur dioxide, hydrogen sulphide, aliphatic thiols and thiophenol. *J. Atmos. Chem.* **1986**, *4*, 445-466, doi:10.1007/BF00053845.

(2) DeMore, W. B.; Bayes, K. D. Rate constants for the reactions of hydroxyl radical with several alkanes, cycloalkanes, and dimethyl ether. *J. Phys. Chem. A* **1999**, *103*, 2649-2654, doi:10.1021/jp983273d.

(3) Donahue, N. M.; Anderson, J. G.; Demerjian, K. L. New rate constants for ten OH alkane reactions from 300 to 400 K: An assessment of accuracy. *J. Phys. Chem. A* **1998**, *102*, 3121-3126, doi:10.1021/jp980532q.

(4) Donahue, N. M.; Clarke, J. S. Fitting multiple datasets in kinetics: *n*-butane + OH → products. *Int. J. Chem. Kinet.* **2004**, *36*, 259-272, doi:10.1002/kin.10194.

(5) Droege, A. T.; Tully, F. P. Hydrogen-atom abstraction from alkanes by OH. 5. n-Butane. *J. Phys. Chem.* **1986**, *90*, 5937-5941, doi:10.1021/j100280a096.

(6) Schiffman, A.; Nelson, D. D.; Robinson, M. S.; Nesbitt, D. J. High-resolution infrared flash kinetic spectroscopy of OH radicals. *J. Phys. Chem.* **1991**, *95*, 2629-2636, doi:10.1021/j100160a004.

(7) Schmidt, V.; Zhu, G. Y.; Becker, K. H.; Fink, E. H. Study of OH reactions at high pressures by excimer laser photolysis - dye laser fluorescence. *Ber. Bunsenges. Phys. Chem.* **1985**, *89*, 321-322, doi:10.1002/bbpc.19850890337.

(8) Talukdar, R. K.; Mellouki, A.; Gierczak, T.; Barone, S.; Chiang, S.-Y.; Ravishankara, A. R. Kinetics of the reactions of OH with alkanes. *Int. J. Chem. Kinet.* **1994**, *26*, 973-990, doi:10.1002/kin.550261003.

D36. OH + *iso*-C_4H_{10}. There a number of room temperature measurements of this reaction, which are in good agreement, whereas only two studies of temperature dependence extend to below room temperatures. The recommended k(298 K) is an average of four absolute measurements by Tully et al.,[9] Schiffman et al.,[6] Talukdar et al.,[8] Donahue et al.,[4] and three relative rate measurements by Darnall et al.,[3] Atkinson et al,[1] and Wilson et al.[10] Results of relative rate studies have been recalculated using the current recommendation for the rate constant of the reference reaction, OH + *n*-C_4H_{10}, which was used in all measurements. Room temperature results reported by Bohland et al.,[2] Schmidt et al.,[7] and Edney et al.[5] have not been used because of their reported large uncertainties, which, however, overlap the recommended value. Four studies of the temperature dependence of this reaction, Tully et al. (293–864 K), Talukdar et al. (213–372 K), Donahue et al. (300–390 K), and Wilson et al. (229–347 K), reveal curvature in an Arrhenius plot of the rate constant. Therefore, the recommended E/R was derived from a combined fit to the data below 300 K from Talukdar et al. and Wilson et al. after scaling each data set to the recommended k(298 K).

From the analysis of reactivity of various deuterated *iso*-butanes, Tully et al. estimated that at room temperature ≈70% of the reaction proceeds via H-abstraction from the central carbon atom yielding *tert*-butyl radical (*tert*-C_4H_9) with only ≈30% abstraction occurring from -CH_3 groups. This branching ratio decreases down to ≈50% at 500 K and ≈25% at 1000 K.
(Table: 19-5, Note: 19-5, Evaluated 19-5) Back to Table

(1) Atkinson, R.; Carter, W. P. L.; Aschmann, S. M.; Winer, A. M.; Pitts, J. N., Jr. Kinetics of the reaction of OH radicals with a series of branched alkanes at 297 ± 2 K. *Int. J. Chem. Kinet.* **1984**, *16*, 469-481, doi:10.1002/kin.550160413.

(2) Bohland, T.; Temps, F.; Wagner, H. G. An LMR-spectrometer operating up to mm-wavelengths for kinetic investigations with discharge flow and flash photolysis systems. *Z. Phys. Chem. (Neue Folge)* **1984**, *142*, 129-140.

(3) Darnall, K. R.; Atkinson, R.; Pitts, J. N., Jr. Rate constants for the reaction of the OH radical with selected alkanes at 300 K. *J. Phys. Chem.* **1978**, *82*, 1581-1584, doi:10.1021/j100503a001.

(4) Donahue, N. M.; Anderson, J. G.; Demerjian, K. L. New rate constants for ten OH alkane reactions from 300 to 400 K: An assessment of accuracy. *J. Phys. Chem. A* **1998**, *102*, 3121-3126, doi:10.1021/jp980532q.

(5) Edney, E. O.; Kleindienst, T. E.; Corse, E. W. Room temperature rate constants for the reaction of OH with selected chlorinated and oxygenated hydrocarbons. *Int. J. Chem. Kinet.* **1986**, *18*, 1355-1371, doi:10.1002/kin.550181207.

(6) Schiffman, A.; Nelson, D. D.; Robinson, M. S.; Nesbitt, D. J. High-resolution infrared flash kinetic spectroscopy of OH radicals. *J. Phys. Chem.* **1991**, *95*, 2629-2636, doi:10.1021/j100160a004.

(7) Schmidt, V.; Zhu, G. Y.; Becker, K. H.; Fink, E. H. Study of OH reactions at high pressures by excimer laser photolysis - dye laser fluorescence. *Ber. Bunsenges. Phys. Chem.* **1985**, *89*, 321-322, doi:10.1002/bbpc.19850890337.

(8) Talukdar, R. K.; Mellouki, A.; Gierczak, T.; Barone, S.; Chiang, S.-Y.; Ravishankara, A. R. Kinetics of the reactions of OH with alkanes. *Int. J. Chem. Kinet.* **1994**, *26*, 973-990, doi:10.1002/kin.550261003.

(9) Tully, F. P.; Goldsmith, J. E. M.; Droege, A. T. Hydrogen-atom abstraction from alkanes by OH. 4. Isobutane. *J. Phys. Chem.* **1986**, *90*, 5932-5937, doi:10.1021/j100280a095.

(10) Wilson, E. W.; Hamilton, W. A.; Kennington, H. R.; Evans, B.; Scott, N. W.; DeMore, W. B. Measurement and estimation of rate constants for the reactions of hydroxyl radical with several alkanes and cycloalkanes. *J. Phys. Chem. A* **2006**, *110*, 3593-3604, doi:10.1021/jp055841c.

D37. OH + *n*-C_5H_{12}. The recommended k(298 K) is an average of the values derived from the fit to the data from the temperature dependent absolute studies of Donahue et al.,[6] Talukdar et al.,[9] and Morin et al.[7] and relative rate studies of DeMore and Bayes[5] (with C_3H_8 and *n*-C_4H_{10} as reference compounds). The values derived from the individual studies agree with the recommended value of k(298 K) within ≈6%. Results of earlier studies at room temperature by Atkinson et al.,[2] (which probably supersedes the earlier study from the same group by Darnall et al.,[4] Nolting et al.,[8] and Abbatt et al.[1] (which is probably superseded by results of Donahue et al.) agree with the recommended value within the combined uncertainties, except the result of a relative study by Cox et al.,[3] which is 25% larger. All studies of the temperature dependence of this reaction by Donahue et al. (300–390 K), Talukdar et al. (231–378 K), DeMore and Bayes (233–364 K), and Morin et al. (248–900 K)

revealed the curvature of the Arrhenius plot of the rate constant. Therefore, the recommended value for E/R was derived from a combined fit to the data sets of Talukdar et al. and DeMore and Bayes below 300 K after scaling each one to the recommended k(298 K). The data of Morin et al. was not used because they have been obtained mainly at higher temperatures and have larger uncertainty.
(Table: 19-5, Note: 19-5, Evaluated 19-5) Back to Table

(1) Abbatt, J. P. D.; Demerjian, K. L.; Anderson, J. G. A new approach to free-radical kinetics: Radially and axially resolved high-pressure discharge flow with results for OH + (C_2H_6, C_3H_8, n-C_4H_{10}, n-C_5H_{12}) → products at 297 K. *J. Phys. Chem.* **1990**, *94*, 4566-4575, doi:10.1021/j100374a039.

(2) Atkinson, R.; Aschmann, S. M.; Carter, W. P. L.; Winer, A. M.; Pitts, J. N., Jr. Kinetics of the reaction of OH radicals with n-alkanes at 299 ± 2 K. *Int. J. Chem Kinet.* **1982**, *14*, 781-788, doi:10.1002/kin.550140706.

(3) Cox, R. A.; Derwent, R. G.; Williams, M. R. Atmospheric photooxidation reactions. Rates, reactivity, and mechanism for reaction of organic compounds with hydroxyl radicals. *Environ. Sci. Technol.* **1980**, *14*, 57-61, doi:10.1021/es60161a007.

(4) Darnall, K. R.; Atkinson, R.; Pitts, J. N., Jr. Rate constants for the reaction of the OH radical with selected alkanes at 300 K. *J. Phys. Chem.* **1978**, *82*, 1581-1584, doi:10.1021/j100503a001.

(5) DeMore, W. B.; Bayes, K. D. Rate constants for the reactions of hydroxyl radical with several alkanes, cycloalkanes, and dimethyl ether. *J. Phys. Chem. A* **1999**, *103*, 2649-2654, doi:10.1021/jp983273d.

(6) Donahue, N. M.; Anderson, J. G.; Demerjian, K. L. New rate constants for ten OH alkane reactions from 300 to 400 K: An assessment of accuracy. *J. Phys. Chem. A* **1998**, *102*, 3121-3126, doi:10.1021/jp980532q.

(7) Morin, J.; Romanias, M. N.; Bedjanian, Y. Experimental study of the reactions of OH radicals with propane, n-pentane, and n-heptane over a wide temperature range. *Int. J. Chem Kinet.* **2015**, *47*, 629-637, doi:10.1002/kin.20936.

(8) Nolting, F.; Behnke, W.; Zetzsch, C. A smog chamber for studies of the reactions of terpenes and alkanes with ozone and OH. *J. Atmos. Chem.* **1988**, *6*, 47-59, doi:10.1016/0021-8502(87)90011-5.

(9) Talukdar, R. K.; Mellouki, A.; Gierczak, T.; Barone, S.; Chiang, S.-Y.; Ravishankara, A. R. Kinetics of the reactions of OH with alkanes. *Int. J. Chem. Kinet.* **1994**, *26*, 973-990, doi:10.1002/kin.550261003.

D38. OH + *iso*-C_5H_{12}. Only relative rate data are available for this reaction. The recommended values for k(298 K) and E/R are based on results of Wilson et al.[5] (213–407 K). They used OH + n-C_4H_{10} and OH + *iso*-C_4H_{10} as the reference reactions and the rate constant of the latter reaction has been derived in the same study by using the first one as the reference. Therefore, all the results have been recalculated using the current recommendation for the rate constant of the reference reaction, OH + n-C_4H_{10}, below 330 K. Two photochemical sources were used to make OH for each set of reference rate measurements, direct H_2O photolysis and N_2O photolysis followed by the $O(^1D) + H_2$ reaction. There is an excellent agreement between room temperature rate constants derived from the four data sets and they agree with the recommended value of k(298 K) within less than 3%. The data exhibit the curvature in the Arrhenius plot and, therefore, the recommended value for E/R was derived from the combined fit to the two data sets that are extended below 300 K. There are four earlier relative rate studies of this reaction at room temperature. The value reported by Atkinson et al.[1] coincides with the recommendation and probably supersedes the earlier data from the same group obtained by using the same reference compound, n-C_4H_{10}, by Lloyd et al.[4] and Darnall et al.,[3] which are smaller by 35% and 10%, respectively. The room temperature value determined by Cox et al.[2] (a reference compound was C_2H_4) is ≈10% smaller than the recommended value whereas its reported uncertainty is ±10%.
(Table: 19-5, Note: 19-5, Evaluated 19-5) Back to Table

(1) Atkinson, R.; Carter, W. P. L.; Aschmann, S. M.; Winer, A. M.; Pitts, J. N., Jr. Kinetics of the reaction of OH radicals with a series of branched alkanes at 297 ± 2 K. *Int. J. Chem. Kinet.* **1984**, *16*, 469-481, doi:10.1002/kin.550160413.

(2) Cox, R. A.; Derwent, R. G.; Williams, M. R. Atmospheric photooxidation reactions. Rates, reactivity, and mechanism for reaction of organic compounds with hydroxyl radicals. *Environ. Sci. Technol.* **1980**, *14*, 57-61, doi:10.1021/es60161a007.

(3) Darnall, K. R.; Atkinson, R.; Pitts, J. N., Jr. Rate constants for the reaction of the OH radical with selected alkanes at 300 K. *J. Phys. Chem.* **1978**, *82*, 1581-1584, doi:10.1021/j100503a001.

(4) Lloyd, A. C.; Darnall, K. R.; Winer, A. M.; Pitts Jr., J. N. Relative rate constants for the reactions of OH radicals with isopropyl alcohol, diethyl and di-*n*-propyl ether at 305 ± 2 K. *Chem. Phys. Lett.* **1976**, *42*, 205-209, doi:10.1016/0009-2614(76)80347-8.
(5) Wilson, E. W.; Hamilton, W. A.; Kennington, H. R.; Evans, B.; Scott, N. W.; DeMore, W. B. Measurement and estimation of rate constants for the reactions of hydroxyl radical with several alkanes and cycloalkanes. *J. Phys. Chem. A* **2006**, *110*, 3593-3604, doi:10.1021/jp055841c.

D39. OH + *cyclo*-C_5H_{10}. The data available for this reaction near room temperature are in good agreement. The recommended k(298 K) is an average of k(298 K) values derived from relative rate studies by Atkinson et al.[1] (using OH + *cyclo*-C_6H_{12} as reference reaction), Kramp and Paulson[7] (measured by using four reference compounds, *n*-nonane, propene, *trans*-2 butene, and butadiene), DeMore and Bayes[2] (*n*-C_4H_{10}, and *n*-C_6H_{14} were used as reference compounds), Wilson et al.[9] (*n*-C_4H_{10}, and *cyclo*-C_6H_{12} were used as reference compounds), and Singh et al.[8] (*n*-C_6H_{14} and *cyclo*-C_6H_{12} were used as reference compounds) and absolute studies by Jolly et al.[6] (pulsed photolysis followed by the UV absorption measurements), Droege and Tully,[4] (pulsed photolysis–LIF), and Gennaco et al.,[5] (a turbulent flow reactor–LIF). Note, that the rate constants for reference reactions of OH with *n*-C_6H_{14}, and *cyclo*-C_6H_{12} used in recalculating the relative data of DeMore and Bayes and Wilson et al. have been derived from the results of relative rate measurements of these reactions reported in the same papers by using the currently recommended rate constants of their "primarily" reference reactions, OH + C_3H_8 and OH + *n*-C_4H_{10}. Thus, obtained values were also used for recalculating the results of Atkinson et al. and Singh et al. The recommended value for E/R was derived from the combined fit to thus recalculated results of relative studies by DeMore and Bayes (273–423 K), Singh et al. (240–340 K), and Wilson et al. (209–407 K) and absolute study of Gennaco et al. (250–351 K) after each data set was scaled to the recommended k(298 K). Results of Droege and Tully (295–491 K) extended to higher temperatures and exhibit a slightly stronger temperature dependence; they were not used in the fit. Data reported by Donahue et al.,[3] (a turbulent flow reactor–LIF) are highly scattered and therefore were not used in this evaluation; they exceed the recommended rate constant by 10–30% between 300 and 390 K.
(Table: 19-5, Note: 19-5, Evaluated 19-5) Back to Table

(1) Atkinson, R.; Aschmann, S. M.; Winer, A. M.; Pitts, J. N., Jr. Rate constants for the reaction of OH radicals with a series of alkanes and alkenes at 299 ± 2 K. *Int. J. Chem. Kinet.* **1982**, *14*, 507-514, 10.1002/kin.550140508.
(2) DeMore, W. B.; Bayes, K. D. Rate constants for the reactions of hydroxyl radical with several alkanes, cycloalkanes, and dimethyl ether. *J. Phys. Chem. A* **1999**, *103*, 2649-2654, doi:10.1021/jp983273d.
(3) Donahue, N. M.; Anderson, J. G.; Demerjian, K. L. New rate constants for ten OH alkane reactions from 300 to 400 K: An assessment of accuracy. *J. Phys. Chem. A* **1998**, *102*, 3121-3126, doi:10.1021/jp980532q.
(4) Droege, A. T.; Tully, F. P. Hydrogen-atom abstraction from alkanes by OH. 6. Cyclopentane and cyclohexane. *J. Phys. Chem.* **1987**, *91*, 1222-1225, doi:10.1021/j100289a037.
(5) Gennaco, M. A.; Huang, Y. W.; Hannun, R. A.; Dransfield, T. J. Absolute rate constants for the reaction of OH with cyclopentane and cycloheptane from 233 to 351 K. *J. Phys. Chem. A* **2012**, *116*, 12438-12443, doi:10.1021/jp3048482.
(6) Jolly, G. S.; Paraskevopoulos, G.; Singleton, D. L. Rates of OH radical reactions. XII. The reactions of OH with *c*-C_3H_6, *c*-C_5H_{10}, and *c*-C_7H_{14}. Correlation of hydroxyl rate constants with bond dissociation energies. *Int. J. Chem. Kinet.* **1985**, *17*, 1-10, doi:10.1002/kin.550170102.
(7) Kramp, F.; Paulson, S. E. On the uncertainties in the rate coefficients for OH reactions with hydrocarbons, and the rate coefficients of the 1,3,5-trimethylbenzene and m-xylene reactions with OH radicals in the gas phase. *J. Phys. Chem. A* **1998**, *102*, 2685-2690, doi:10.1021/jp973289o.
(8) Singh, S.; de Leon, M. F.; Li, Z. Kinetics study of the reaction of OH radicals with C5–C8 cycloalkanes at 240–340 K using the relative rate/discharge flow/mass spectrometry technique. *J. Phys. Chem. A* **2013**, *117*, 10863-10872, doi:10.1021/jp406923d.
(9) Wilson, E. W.; Hamilton, W. A.; Kennington, H. R.; Evans, B.; Scott, N. W.; DeMore, W. B. Measurement and estimation of rate constants for the reactions of hydroxyl radical with several alkanes and cycloalkanes. *J. Phys. Chem. A* **2006**, *110*, 3593-3604, doi:10.1021/jp055841c.

D40. OH + CH_2=C(CH_3)CHO (methacrolein). The recommended E/R is that obtained from an unweighted fit to $\ln k = \ln A - E/RT$ of the rate constants reported by Gierczak et al.[7] (234-373 K), which is the only study that reports rate constants at tempertures <295 K. The recommended k(298 K) is the average of ambient temperature rate constants obtained in the flash photolysis studies of Kleindienst et al.[9] (297–424 K), Gierczak et al., and Chuong and Stevens[2] (300–422 K), the turbulent flow reactor study of Chuong and Stevens[3] (300 K), and the relative rate study of Atkinson et al.[1] (299 K), with all rate constants adjusted to 298 K using the recommended E/R. In a second relative rate study, Edney et al.[6] obtain a value for k(298 K) that is significantly greater than the rate constants reported in all other studies. Temperature-dependent rate constants reported by Kleindienst et al. and Chuong and Stevens in their flash photolysis studies are encompassed by the recommended error limits for all temperatures below 400 K. Product studies by Tuazon and Atkinson[11] and Orlando and Tyndall[10] demonstrate that, in air at ~298 K and ~1 atm, abstraction of the aldehydic hydrogen accounts for 45-50% of overall reactivity and addition to the double bond accounts for the rest; more than 80% of addition is to the terminal carbon. Chuong and Stevens[3] observe OH recycling in the presence of O_2 and NO at 300 K and conclude that (i) methacrolein-based peroxy radicals (OH−methacrolein−OO) react with NO with $k \sim 2 \times 10^{-11}$ cm^3 $molecule^{-1}$ s^{-1} and (ii) the peroxy radical + NO reactions produce NO_2 with a yield of ~90% and organic nitrates with a yield of ~10%. A turbulent flow reactor study by Hsin and Elrod[8] obtains OH−methacrolein−OO + NO rate constants that are a factor of two slower than those reported by Chuong and Stevens. In a combined experimental/theoretical study, Crounse et al.[4] provide evidence that OH−methacrolein−OO undergoes a 1,4 H shift of the aldehydic hydrogen to OO at a rate of ~0.5 s^{-1} to form a radical that rapidly decomposes to recycle OH. In a theoretical study, da Silva concludes that chemically activated OH−methacrolein and OH−methacrolein−OO strongly impact product distributions and OH recycling.[5]
(Table: 15-10, Note: 15-10, Evaluated: 15-10) Back to Table

(1) Atkinson, R.; Aschmann, S. M.; Pitts Jr., J. N. Kinetics of the gas-phase reactions of OH radicals with a series of α,β-unsaturated carbonyls at 299 ± 2 K. *Int. J. Chem. Kinet.* **1983**, *15*, 75-81, doi:10.1002/kin.550150108.

(2) Chuong, B.; Stevens, P. S. Kinetics of the OH + methyl vinyl ketone and OH + methacrolein reactions at low pressure *J. Phys. Chem. A* **2003**, *107*, 2185-2191, doi:10.1021/jp026036q.

(3) Chuong, B.; Stevens, P. S. Measurements of the kinetics of the OH-initiated oxidation of methyl vinyl ketone and methacrolein. *Int. J. Chem. Kinet.* **2004**, *36*, 12-25, doi:10.1002/kin.10167.

(4) Crounse, J. D.; Knap, H. C.; Ørnso, K. B.; Jørgensen, S.; Paulot, F.; Kjaergaard, H. G.; Wennberg, P. O. Atmospheric fate of methacrolein. 1. Peroxy radical isomerization following addition of OH and O_2. *J. Phys. Chem. A* **2012**, *116*, 5756-5762, doi:10.1021/jp211560u.

(5) da Silva, G. Reaction of methacrolein with the hydroxyl radical in air: Incorporation of secondary O_2 addition into the MACR + OH master equation. *J. Phys. Chem. A* **2012**, *116*, 5317-5324, doi:10.1021/jp303806w.

(6) Edney, E. O.; Kleindienst, T. E.; Corse, E. W. Room temperature rate constants for the reaction of OH with selected chlorinated and oxygenated hydrocarbons. *Int. J. Chem. Kinet.* **1986**, *18*, 1355-1371, doi:10.1002/kin.550181207.

(7) Gierczak, T.; Burkholder, J. B.; Talukdar, R. K.; Mellouki, A.; Barone, S. B.; Ravishankara, A. R. Atmospheric fate of methyl vinyl ketone and methacrolein. *J. Photochem. Photobiol. A: Chem.* **1997**, *110*, 1-10, doi:10.1016/S1010-6030(97)00159-7.

(8) Hsin, H. Y.; Elrod, M. J. Overall rate constant measurements of the reaction of hydroxy- and chloroalkylperoxy radicals derived from methacrolein and methyl vinyl ketone with nitric oxide. *J. Phys. Chem. A* **2007**, *111*, 613-619, doi:10.1021/jp0665574.

(9) Kleindienst, T. E.; Harris, G. W.; Pitts, J. N., Jr. Rates and temperature dependences of the reaction of OH with isoprene, its oxidation products, and selected terpenes. *Environ. Sci. Technol.* **1982**, *16*, 844-846, doi:10.1021/es00106a004.

(10) Orlando, J. J.; Tyndall, G. S. Mechanism of the OH-initiated oxidation of methacrolein. *Geophys. Res. Lett.* **1999**, *26*, 2191-2194, doi:10.1029/1999GL900453.

(11) Tuazon, E. C.; Atkinson, R. A product study of the gas-phase reaction of methacrolein with the OH radical in the presence of NO_x. *Int. J. Chem. Kinet.* **1990**, *22*, 591-602, doi:10.1002/kin.550220604.

D41. OH + $CH_3C(O)CH=CH_2$ (Methyl Vinyl Ketone, MVK). The recommendation is based on the temperature-dependent flash photolysis studies of Kleindienst et al.[7] (298–424 K) and Gierczak et al.[4] (232–378 K), the room temperature turbulent flow reactor study of Chuong and Stevens,[3] and the room temperature relative rate studies of Atkinson et al.[1] and Holloway et al.[5] Chuong and Stevens[2] observe pressure-dependent rate constants in 1–5 Torr Helium over the temperature range 300–422 K. All data used to arrive at the recommendation were obtained under (presumably) high pressure limit conditions, i.e., P >16 Torr. All data points reported in each temperature dependent study were scaled by a factor equal to the ratio $k(298\ K)_{Arr}/k(298\ K)_{ave}$ where k(298

K)$_{Arr}$ is the 298 K rate constant obtained from the best fit Arrhenius expression describing the individual T-dependent data set and k(298 K)$_{ave}$ is the average of all reported high-P limit room temperature rate constants. The best fit Arrhenius expression for the scaled data is recommended. A product study by Tuazon and Atkinson[8] demonstrates that reactivity is dominated by addition to the double bond with 72 ± 28 % of the addition being to the terminal carbon. Chuong and Stevens[3] observe OH recycling in the presence of O_2 and NO at T = 300 K and conclude that (i) MVK-based peroxy radicals (OH-MVK-OO) react with NO with k ~2 × 10^{-11} cm^3 $molecule^{-1}$ s^{-1} and (ii) the peroxy radical + NO reactions produce NO_2 with a yield of ~90% and organic nitrates with a yield of ~10%. A turbulent flow reactor study by Hsin and Elrod[6] obtains OH-MVK-OO + NO rate constants that are more than a factor of two slower than those reported by Chuong and Stevens. (Table: 15-10, Note: 15-10, Evaluated: 15-10) Back to Table

(1) Atkinson, R.; Aschmann, S. M.; Pitts Jr., J. N. Kinetics of the gas-phase reactions of OH radicals with a series of α,β-unsaturated carbonyls at 299 ± 2 K. *Int. J. Chem. Kinet.* **1983**, *15*, 75-81, doi:10.1002/kin.550150108.

(2) Chuong, B.; Stevens, P. S. Kinetics of the OH + methyl vinyl ketone and OH + methacrolein reactions at low pressure *J. Phys. Chem. A* **2003**, *107*, 2185-2191, doi:10.1021/jp026036q.

(3) Chuong, B.; Stevens, P. S. Measurements of the kinetics of the OH-initiated oxidation of methyl vinyl ketone and methacrolein. *Int. J. Chem. Kinet.* **2004**, *36*, 12-25, doi:10.1002/kin.10167.

(4) Gierczak, T.; Burkholder, J. B.; Talukdar, R. K.; Mellouki, A.; Barone, S. B.; Ravishankara, A. R. Atmospheric fate of methyl vinyl ketone and methacrolein. *J. Photochem. Photobiol. A: Chem.* **1997**, *110*, 1-10, doi:10.1016/S1010-6030(97)00159-7.

(5) Holloway, A.-L.; Treacy, J.; Sidebottom, H.; Mellouki, A.; Daële, V.; Le Bras, G.; Barnes, I. Rate coefficients for the reactions of OH radicals with the keto/enol tautomers of 2,4-pentanedione and 3-methyl-2,4 pentanedione, allyl alcohol and methyl vinyl ketone using the enols and methyl nitrite as photolytic sources of OH. *J. Photochem. Photobiol. A Chem.* **2005**, *176*, 183-190, doi:10.1016/j.photochem.2005.08.031.

(6) Hsin, H. Y.; Elrod, M. J. Overall rate constant measurements of the reaction of hydroxy- and chloroalkylperoxy radicals derived from methacrolein and methyl vinyl ketone with nitric oxide. *J. Phys. Chem. A* **2007**, *111*, 613-619, doi:10.1021/jp0665574.

(7) Kleindienst, T. E.; Harris, G. W.; Pitts, J. N., Jr. Rates and temperature dependences of the reaction of OH with isoprene, its oxidation products, and selected terpenes. *Environ. Sci. Technol.* **1982**, *16*, 844-846, doi:10.1021/es00106a004.

(8) Tuazon, E. C.; Atkinson, R. A product study of the gas-phase reaction of methyl vinyl ketone with the OH radical in the presence of NO_x. *Int. J. Chem. Kinet.* **1989**, *21*, 1141-1152, doi:10.1002/kin.550211207.

D42. OH + CH_2=C(CH_3)CH=CH_2. The recommended E/R is the average of values obtained from the temperature-dependent data sets of Kleindienst et al.[12] (299–422 K), Campuzano-Jost et al.[2,3] (251–342 K; 276–342 K), Gill and Hites[7] (295–364 K), Park et al.[16] (279–336 K), and Hites and Turner[9] (323–413 K); each data set was analyzed using an unweighted fit to ln k = ln A – E/RT. The recommended k(298 K) is the average of the values obtained from the best fit Arrhenius expressions for the five temperature-dependent studies plus the ambient temperature results reported by Winer et al.[20] (based on data reported by Grimsrud et al.[8]), Cox et al.,[5] Ohta,[15] Atkinson and Aschmann,[1] Edney et al.,[6] Stevens et al.,[19] McGivern et al.,[13] Zhang et al.,[21] McQuaid et al.,[14] Iida et al.,[10] Karl et al.,[11] Singh and Li.[17] Ambient temperature results obtained at temperatures other than 298 K were adjusted using the recommended E/R. Only results obtained under (investigator-reported) high pressure limit conditions are considered; this excludes the data of Chuong and Stevens[4] at T >300 K and the data of Singh and Li at 340 K. Data from the Laval nozzle study of Spangenberg et al.[18] are not considered because the investigated T, P conditions are not relevant for application to atmospheric chemistry. Singh and Li report the Arrhenius expression k = 2.33 × 10^{-11} exp(444/T) $cm^3molecule^{-1}s^{-1}$ 240−340 K; their reported temperature dependence is not used to evaluate E/R because (high pressure limit) rate constants are reported only at 298 K. Although the detailed pressure-dependence remains a subject of disagreement,[4,10,11,13,19] it is clear that the reaction is in its high-pressure limit under all relevant atmospheric conditions.
(Table: 15-10, Note: 15-10, Evaluated: 15-10) Back to Table

(1) Atkinson, R.; Aschmann, S. M. Rate constants for the reaction of OH radicals with a series of alkenes and dialkenes at 295 ± 1 K. *Int. J. Chem. Kinet.* **1984**, *16*, 1175-1186, doi:10.1002/kin.550161002.

(2) Campuzano-Jost, P.; Williams, M. B.; D'Ottone, L.; Hynes, A. J. Kinetics of the OH-initiated oxidation of isoprene. *Geophys. Res. Lett.* **2000**, *27*, 693-696, doi:10.1029/1999GL010995.

(3) Campuzano-Jost, P.; Williams, M. B.; D'Ottone, L.; Hynes, A. J. Kinetics and mechanism of the reaction of the hydroxyl radical with h_8-isoprene and d_8-isoprene: Isoprene absorption cross sections, rate coefficients, and the mechanism of hydroperoxyl radical production. *J. Phys. Chem. A* **2004**, *108*, 1537-1551, doi:10.1021/jp0363601.

(4) Chuong, B.; Stevens, P. S. Kinetic study of the OH + isoprene and OH + ethylene reactions between 2 and 6 Torr and over the temperature range 300-423 K. *J. Phys. Chem. A* **2000**, *104*, 5230-5237, doi:10.1021/jp993613a.
(5) Cox, R. A.; Derwent, R. G.; Williams, M. R. Atmospheric photooxidation reactions. Rates, reactivity, and mechanism for reaction of organic compounds with hydroxyl radicals. *Environ. Sci. Technol.* **1980**, *14*, 57-61, doi:10.1021/es60161a007.
(6) Edney, E. O.; Kleindienst, T. E.; Corse, E. W. Room temperature rate constants for the reaction of OH with selected chlorinated and oxygenated hydrocarbons. *Int. J. Chem. Kinet.* **1986**, *18*, 1355-1371, doi:10.1002/kin.550181207.
(7) Gill, K. J.; Hites, R. A. Rate constants for the gas-phase reactions of the hydroxyl radical with isoprene, α- and β-pinene, and limonene as a function of temperature. *J. Phys. Chem. A* **2002**, *106*, 2538-2544, doi:10.1021/jp013532q.
(8) Grimsrud, E. P.; Westberg, H. H.; Rasmussen, R. A. Atmospheric reactivity of monoterpene hydrocarbons, NO_x photooxidation and ozonolysis. *Int. J. Chem. Kinet.* **1975**, *Symp 1*, 183-195.
(9) Hites, R. A.; Turner, A. M. Rate constants for the gas-phase β-myrcene + OH and isoprene + OH reactions as a function of temperature. *Int. J. Chem. Kinet.* **2009**, *41*, 407-413, doi:10.1002/kin.20413.
(10) Iida, Y.; Obi, K.; Imamura, T. Rate constant for the reaction of OH radicals with isoprene at 298 ± 2K. *Chem. Lett.* **2002**, *31*, 792-793, doi:10.1246/cl.2002.792.
(11) Karl, M.; Brauers, T.; Dorn, H.-P.; Holland, F.; Komenda, M.; Poppe, D.; Rohrer, F.; Rupp, L.; Schaub, A.; Wahner, A. Kinetic Study of the OH-isoprene and O_3-isoprene reaction in the atmosphere simulation chamber, SAPHIR. *Geophys. Res. Lett.* **2004**, *31*, L05117, doi:10.1029/2003GL019189.
(12) Kleindienst, T. E.; Harris, G. W.; Pitts, J. N., Jr. Rates and temperature dependences of the reaction of OH with isoprene, its oxidation products, and selected terpenes. *Environ. Sci. Technol.* **1982**, *16*, 844-846, doi:10.1021/es00106a004.
(13) McGivern, W. S.; Suh, I.; Clinkenbeard, A. D.; Zhang, R.; North, S. W. Experimental and computational study of the OH-isoprene reaction: Isomeric branching and low-pressure behavior. *J. Phys. Chem. A* **2000**, *104*, 6609-6616, doi:10.1021/jp001163c.
(14) McQuaid, J. B.; Stocker, D. W.; Pilling, M. J. Kinetics of the reactions of OH with 3-methyl-2-cyclohexen-1-one and 3,5,5-trimethyl-2-cyclohexen-1-one under simulated atmospheric conditions. *Int. J. Chem. Kinet.* **2002**, *34*, 7-11, doi:10.1002/kin.10018.
(15) Ohta, T. Rate constants for the reactions of diolefins with OH radicals in the gas phase. Estimate of the rate constants from those for monoolefins. *J. Phys. Chem.* **1983**, *87*, 1209-1213, doi:10.1021/j100230a023.
(16) Park, J.; Jongsma, C. G.; Zhang, R.; North, S. W. OH/OD initiated oxidation of isoprene in the presence of O_2 and NO. *J. Phys. Chem. A* **2004**, *108*, 10688-10697, doi:10.1021/jp040421t.
(17) Singh, S.; Li, Z. Kinetics investigation of OH reaction with isoprene at 240-340 K and 1-3 Torr using the relative rate/discharge flow/mass spectrometry technique. *J. Phys. Chem. A* **2007**, *111*, 11843-11851, doi:10.1021/jp074148h.
(18) Spangenberg, T.; Kohler, S.; Hansmann, B.; Wachsmuth, U.; Abel, B.; Smith, M. A. Low-temperature reactions of OH radicals with propene and isoprene in pulsed Laval nozzle expansions. *J. Phys. Chem. A* **2004**, *108*, 7527-7534, doi:10.1021/jp031228m.
(19) Stevens, P.; L'Esperance, D.; Chuong, B.; Martin, G. Measurements of the kinetics of the OH-initiated oxidation of isoprene: Radical propagation in the OH + isoprene + O_2 + NO reaction system. *Int. J. Chem. Kinet.* **1999**, *31*, 637-643, doi:10.1002/(SICI)1097-4601(1999)31:9<637::AID-KIN5>3.0.CO;2-O.
(20) Winer, A. M.; Lloyd, A. C.; Darnall, K. R.; Pitts, J. N., Jr. Relative rate constants for the reaction of the hydroxyl radical with selected ketones, chloroethenes, and monoterpene hydrocarbons. *J. Phys. Chem.* **1976**, *80*, 1635-1639, doi:10.1021/j100555a024.
(21) Zhang, R.; Suh, I.; Lei, W.; Clinkenbeard, A. D.; North, S. W. Kinetic studies of OH-initiated reactions of isoprene. *J. Geophys. Res.* **2000**, *105*, 24627-24635, doi:10.1029/2000JD900330.

D43. OH + CH_3CN. This rate coefficient has been measured as a function of temperature by Harris et al.[2] (298–424 K), Kurylo and Knable[4] (250–363 K), Rhasa[6] (295–520 K), and Hynes and Wine[3] (256–388 K). In addition, the 298 K value has been measured by Poulet et al.[5] The 298 K results of Harris et al. are in disagreement with all other measurements and therefore have not been included. The recommended 298 K value is a weighted average of all other studies. The temperature dependence was computed using the results of Kurylo and Knable, the lower temperature values (i.e., 295–391 K) of Rhasa, and the data of Hynes and Wine. Three points are worth noting: (a) Rhasa observed a curved Arrhenius plot even in the temperature range of 295 to 520 K, and therefore extrapolation of the recommended expression could lead to large errors; (b) Hynes and Wine observed a pressure dependent increase of k(298 K) that levels off at about 1 atmosphere, and this observation is contradictory to the results of other investigations; (c) Hynes and Wine have carried out

extensive pressure, temperature, O_2 concentration, and isotope variations in this reaction. Hynes and Wine postulate that the reaction proceeds via addition as well as abstraction pathways. They observe OH regeneration in the presence of O_2. The recommended k(298 K) and E/R are applicable for only lower tropospheric conditions. Because of the unresolved questions of pressure dependence, the recommended value may not be applicable under upper tropospheric and stratospheric conditions. At 296 K and 700 Torr air, Tyndall et al. observe that HC(O)CN, an expected end product when reaction is initiated by H-abstraction, is formed with a yield of 0.4 ± 0.2.[7] The OH regeneration in the presence of O_2 reported by Hynes and Wine has been explained theoretically by Galano as resulting from initial formation of a $CH_3C(OH)N$ adduct that rearranges and dissociates to OH + $CH_3C(O)NO$.[1] In agreement with the observations of Hynes and Wine and Tyndall et al., Galano's theoretical analysis predicts similar branching ratios for H-abstraction and addition.
(Table: 92-20, Note: 15-10, Evaluated: 92-20) Back to Table

(1) Galano, A. Mechanism of OH radical reactions with HCN and CH_3CN: OH regeneration in the presence of O_2. *J. Phys. Chem. A* **2007**, *111*, 5086-5091, doi:10.1021/jp0708345.
(2) Harris, G. W.; Kleindienst, T. E.; Pitts, J. N., Jr. Rate constants for the reaction of OH radicals with CH_3CN, C_2H_5CN and CH_2=CH-CN in the temperature range 298-424 K. *Chem. Phys. Lett.* **1981**, *80*, 479-483, doi:10.1016/0009-2614(81)85061-0.
(3) Hynes, A. J.; Wine, P. H. Kinetics and mechanism of the reaction of hydroxyl radicals with acetonitrile under atmospheric conditions. *J. Phys. Chem.* **1991**, *95*, 1232-1240, doi:10.1021/j100156a037.
(4) Kurylo, M. J.; Knable, G. L. A kinetics investigation of the gas-phase reactions of Cl(^{2}P) and OH($X^2\Pi$) with CH_3CN: Atmospheric significance and evidence for decreased reactivity between strong electrophiles. *J. Phys. Chem.* **1984**, *88*, 3305-3308, doi:10.1021/j150659a033.
(5) Poulet, G.; Laverdet, G.; Jourdain, J. L.; Le Bras, G. Kinetic study of the reactions of acetonitrile with Cl and OH radicals. *J. Phys. Chem.* **1984**, *88*, 6259-6263, doi:10.1021/j150669a041.
(6) Rhasa, D. In *Diplomarbeit* Univ. of Gottingen FRG, 1983.
(7) Tyndall, G. S.; Orlando, J. J.; Wallington, T. J.; Hurley, M. D. Products of the chlorine-atom- and hydroxyl-radical-initiated oxidation of CH_3CN. *J. Phys. Chem. A* **2001**, *105*, 5380-5384, doi:10.1021/jp004318p.

D44. OH + CH_3ONO_2. The rate coefficient for this reaction at 298 K has been measured by Kerr and Stocker,[4] Nielsen et al.,[5] Gaffney et al.,[2] Talukdar et al.,[7] Kakesu et al.,[3] and Shallcross et al.[6] The results of Kerr and Stocker and of Nielsen et al. are a factor of ten greater than those reported by the other groups. There are no obvious reasons for the reported differences, but the lower values are preferred for a number of reasons. Firstly, Talukdar et al. have carried out a large number of checks which ruled out possible effects in their system due to the regeneration of OH via secondary reactions, to bath gas pressure, and to formation of an adduct that could undergo further reaction in the presence of oxygen. Secondly, the lower values are more consistent with reactivity predictions of Atkinson and Aschmann,[1] who assumed that the series of nitrate reactions proceed by H-atom abstraction pathways. Kinetic measurements of Talukdar et al. performed with isotopically substituted hydroxyl radical (OH, ^{18}OH, and OD) and methyl nitrate (CH_3ONO_2 and CD_3ONO_2) are consistent with this reaction proceeding via an H-atom abstraction pathway. Accordingly, the recommended k(298 K) is based on an average of the values given by Gaffney et al, Talukdar et al., Kakesu et al., and Shallcross et al. Further verification of the reaction mechanism by identification of the products of the reaction is needed. The temperature dependence of the rate coefficient has been measured by Nielsen et al. (298–393 K), Talukdar et al.(221–414 K), and Shallcross et al. (298–423 K). While Nielsen et al. report a negative activation energy, Talukdar et al. and Shallcross et al. report positive values. For the reasons given above, the temperature dependence recommended here is based on an average of Talukdar et al. and Shallcross et al.
(Table: 06-2, Note: 06-2, Evaluated: 06-2) Back to Table

(1) Atkinson, R.; Aschmann, S. M. Rate constants for the reactions of the OH radical with the propyl and butyl nitrates and 1-nitobutane at 298 ± 2 K. *Int. J. Chem. Kinet.* **1989**, *21*, 1123-1129, doi:10.1002/kin.550211205.
(2) Gaffney, J. S.; Fajer, R.; Senum, G. I.; Lee, J. H. Measurement of the reactivity of OH with methyl nitrate: Implications for prediction of alkyl nitrate-OH reaction rates. *Int. J. Chem. Kinet.* **1986**, *18*, 399-407, doi:10.1002/kin.550180311.
(3) Kakesu, M.; Bandow, H.; Takenaka, N.; Maeda, Y.; Washida, N. Kinetic measurements of methyl and ethyl nitrate reactions with OH radicals. *Int. J. Chem. Kinet.* **1997**, *29*, 933-941, doi:10.1002/(SICI)1097-4601(1997)29:12<933::AID-KIN5>3.0.CO;2-N.
(4) Kerr, J. A.; Stocker, D. W. Kinetics of the reactions of hydroxyl radicals with alkyl nitrates and with some oxygen-containing organic compounds studied under simulated atmospheric conditions. *J. Atmos. Chem.* **1986**, *4*, 253-262, doi:10.1007/BF00052004.

(5) Nielsen, O. J.; Sidebottom, H. W.; Donlon, M.; Treacy, J. An absolute- and relative-rate study of the gas-phase reaction of OH radicals and Cl atoms with *n*-alkyl nitrates. *Chem. Phys. Lett.* **1991**, *178*, 163-170, doi:10.1016/0009-2614(91)87051-C.
(6) Shallcross, D. E.; Biggs, P.; Canosa-Mas, C. E.; Clemitshaw, K. C.; Harrison, M. G.; Alañón, M. R. L.; Pyle, J. A.; Vipond, A.; Wayne, R. P. Rate constants for the reaction between OH and CH_3ONO_2 and $C_2H_5ONO_2$ over a range of pressure and temperature. *J. Chem. Soc. Faraday Trans.* **1997**, *93*, 2807-2811, doi:10.1039/a701471f.
(7) Talukdar, R. K.; Herndon, S. C.; Burkholder, J. B.; Roberts, J. M.; Ravishankara, A. R. Atmospheric fate of several alkyl nitrates Part 1 Rate coefficients of the reactions alkyl nitrates with isotopically labelled hydroxyl radicals. *J. Chem. Soc. Faraday Trans.* **1997**, *93*, 2787-2796, doi:10.1039/A701780D.

D45. OH + $CH_3C(O)O_2NO_2$ (Peroxy Acetyl Nitrate, PAN). This reaction has been studied by four groups Winer et al.,[4] Wallington et al.,[3] Tsalkani et al.,[2] and Talukdar et al.[1] Winer et al. obtained only an upper limit for the rate coefficient. Tsalkani et al. noted that their system was very ill-behaved and obtained a value of k(298 K) that is a factor of ~2 lower than that obtained by Wallington et al. The pulsed photolysis study of Wallington et al. yielded consistent results, but PAN was not directly measured and photodissociation of H_2O in the vacuum UV, where PAN absorbs strongly, was used as the OH source. The recent study of Talukdar et al.[1] (253, 272, and 298 K) yielded much lower rate coefficients. These investigators measured the PAN concentration directly in their system, minimized secondary reactions due to the photodissociation of PAN, and carried out extensive tests for decomposition of PAN, impurities, and secondary reactions. The recommended upper limit is a factor of two higher than the highest value measured by Talukdar et al. at 298 K and at 272 K. The quoted upper limit is expected to be valid at all atmospheric temperatures. The products of the reaction are not known. Further measurements of the rate coefficients and information on the reaction pathways are needed.
(Table: 94-26, Note: 94-26, Evaluated: 94-26) Back to Table

(1) Talukdar, R. K.; Burkholder, J. B.; Schmoltner, A.-M.; Roberts, J. M.; Wilson, R. R.; Ravishankara, A. R. Investigation of the loss processes for peroxyacetyl nitrate in the atmosphere: UV photolysis and reaction with OH. *J. Geophys. Res.* **1995**, *100*, 14163-14173, doi:10.1029/95JD00545.
(2) Tsalkani, N.; Mellouki, A.; Poulet, G.; Toupance, G.; Le Bras, G. Rate constant measurement for the reactions of OH and C1 with peroxyacetyl nitrate at 298 K. *J. Atmos. Chem.* **1988**, *7*, 409-419, doi:10.1007/BF00058713.
(3) Wallington, T. J.; Atkinson, R.; Winer, A. M. Rate constants for the gas phase reaction of OH radicals with peroxyacetyl nitrate (PAN) at 273 and 297 K. *Geophys. Res. Lett.* **1984**, *1*, 861-864, doi:10.1029/GL011i009p00861.
(4) Winer, A. M.; Lloyd, A. C.; Darnall, K. R.; Atkinson, R.; Pitts, J. N., Jr. Rate constnts for the reaction of OH radicals with *n*-propyl acetate, *sec*-butyl acetate, tertrahydrofuran and peroxyacetyl nitrate. *Chem. Phys. Lett.* **1977**, *51*, 221-226, doi:10.1016/0009-2614(77)80388-6.

D46. OH + $C_2H_5ONO_2$. The rate constant for this reaction at 298 K has been measured by Kerr and Stocker,[2] Nielsen et al.,[3] Talukdar et al.,[5] Kakesu et al.,[1] and Shallcross et al.[4] As in the case of the reaction of OH with CH_3ONO_2, the results of Kerr and Stocker and of Nielsen et al. are greater (by a factor of 3) than those of the more recent studies. The reasons for the differences are not clear. Because of the exhaustive tests carried out (see the note for the OH + CH_3ONO_2 reaction), the values of Talukdar et al., Kakesu et al., and Shallcross et al. are recommended. Nielsen et al. (298–373 K), Talukdar et al. (223–394 K), and Shallcross et al. (298–373 K) have measured the rate constant as a function of temperature. As with the OH + CH_3ONO_2 reaction, Nielsen et al. report a negative activation energy while Talukdar et al. and Shallcross et al. have observed a small positive activation energy. Talukdar et al. note that the rate coefficient for this reaction does not strictly follow Arrhenius behavior, consistent with the abstraction of both the primary and the secondary H atoms. Above 298 K, E/R values measured by Shallcross et al. and Talukdar et al. are in excellent agreement. Only Talukdar et al. have kinetics data below 298 K and the recommended E/R value was obtained by fitting the rate coefficients measured by Talukdar et al. at or below 298 K. The large uncertainty encompasses the results of Kerr and Stocker and Nielsen et al.
(Table: 06-2, Note: 06-2, Evaluated: 06-2) Back to Table

(1) Kakesu, M.; Bandow, H.; Takenaka, N.; Maeda, Y.; Washida, N. Kinetic measurements of methyl and ethyl nitrate reactions with OH radicals. *Int. J. Chem. Kinet.* **1997**, *29*, 933-941, doi:10.1002/(SICI)1097-4601(1997)29:12<933::AID-KIN5>3.0.CO;2-N.
(2) Kerr, J. A.; Stocker, D. W. Kinetics of the reactions of hydroxyl radicals with alkyl nitrates and with some oxygen-containing organic compounds studied under simulated atmospheric conditions. *J. Atmos. Chem.* **1986**, *4*, 253-262, doi:10.1007/BF00052004.

(3) Nielsen, O. J.; Sidebottom, H. W.; Donlon, M.; Treacy, J. An absolute- and relative-rate study of the gas-phase reaction of OH radicals and Cl atoms with *n*-alkyl nitrates. *Chem. Phys. Lett.* **1991**, *178*, 163-170, doi:10.1016/0009-2614(91)87051-C.
(4) Shallcross, D. E.; Biggs, P.; Canosa-Mas, C. E.; Clemitshaw, K. C.; Harrison, M. G.; Alañón, M. R. L.; Pyle, J. A.; Vipond, A.; Wayne, R. P. Rate constants for the reaction between OH and CH_3ONO_2 and $C_2H_5ONO_2$ over a range of pressure and temperature. *J. Chem. Soc. Faraday Trans.* **1997**, *93*, 2807-2811, doi:10.1039/a701471f.
(5) Talukdar, R. K.; Herndon, S. C.; Burkholder, J. B.; Roberts, J. M.; Ravishankara, A. R. Atmospheric fate of several alkyl nitrates Part 1 Rate coefficients of the reactions alkyl nitrates with isotopically labelled hydroxyl radicals. *J. Chem. Soc. Faraday Trans.* **1997**, *93*, 2787-2796, doi:10.1039/A701780D.

D47. OH + 1-$C_3H_7ONO_2$. The reaction has been studied by Kerr and Stocker[2] and Atkinson and Aschmann[1] at room temperature and by Nielsen et al.[3] between 298 and 368 K. The results of the three studies are in good agreement at room temperature. Nielsen et al. find that the reaction is temperature independent within the measurement uncertainty over the range studied. However as discussed above, the Nielson et al. results for the analogous reactions of OH with CH_3ONO_2 and $C_2H_5ONO_2$, yield negative activation energies that disagree with the positive activation energies obtained by others. Judging from the *E*/R's for the analogous reactions, one might expect the *E*/R for this reaction to be on the order of 300 K. Accordingly, we place a large uncertainty on the recommended temperature dependence. A thorough investigation of the temperature dependence of this reaction is needed.
(Table: 02-25, Note: 02-25, Evaluated: 02-25) Back to Table

(1) Atkinson, R.; Aschmann, S. M. Rate constants for the reactions of the OH radical with the propyl and butyl nitrates and 1-nitobutane at 298 ± 2 K. *Int. J. Chem. Kinet.* **1989**, *21*, 1123-1129, doi:10.1002/kin.550211205.
(2) Kerr, J. A.; Stocker, D. W. Kinetics of the reactions of hydroxyl radicals with alkyl nitrates and with some oxygen-containing organic compounds studied under simulated atmospheric conditions. *J. Atmos. Chem.* **1986**, *4*, 253-262, doi:10.1007/BF00052004.
(3) Nielsen, O. J.; Sidebottom, H. W.; Donlon, M.; Treacy, J. An absolute- and relative-rate study of the gas-phase reaction of OH radicals and Cl atoms with *n*-alkyl nitrates. *Chem. Phys. Lett.* **1991**, *178*, 163-170, doi:10.1016/0009-2614(91)87051-C.

D48. OH + 2-$C_3H_7ONO_2$. The reaction has been studied by Atkinson and Aschmann,[1] Atkinson et al.,[2] and Becker and Wirtz[3] at room temperature and by Talukdar et al.[4] over the range 233 and 395 K. The results of Atkinson and Aschmann supersede those of Atkinson et al. There is fair agreement between the results of the three studies at room temperature, with roughly a factor of two spread in the values. The recommendation is based on an average of the room temperature values and the *E*/R measured by Talukdar et al.
(Table: 02-25, Note: 02-25, Evaluated: 02-25) Back to Table

(1) Atkinson, R.; Aschmann, S. M. Rate constants for the reactions of the OH radical with the propyl and butyl nitrates and 1-nitobutane at 298 ± 2 K. *Int. J. Chem. Kinet.* **1989**, *21*, 1123-1129, doi:10.1002/kin.550211205.
(2) Atkinson, R.; Aschmann, S. M.; Carter, W. P. L.; Winer, A. M. Kinetics of the gas-phase reactions of OH radicals with alkyl nitrates at 299 ± 2 K. *Int. J. Chem. Kinet.* **1982**, *14*, 919-926, doi:10.1002/kin.550140810.
(3) Becker, K. H.; Wirtz, K. Gas phase reactions of alkyl nitrates with hydroxyl radicals under tropospheric conditions in comparison with photolysis. *J. Atmos. Chem.* **1989**, *9*, 419-433, doi:10.1007/BF00114754.
(4) Talukdar, R. K.; Herndon, S. C.; Burkholder, J. B.; Roberts, J. M.; Ravishankara, A. R. Atmospheric fate of several alkyl nitrates Part 1 Rate coefficients of the reactions alkyl nitrates with isotopically labelled hydroxyl radicals. *J. Chem. Soc. Faraday Trans.* **1997**, *93*, 2787-2796, doi:10.1039/A701780D.

D49. HO_2 + CH_2O. There is sufficient evidence to suggest that HO_2 adds to CH_2O (Su et al.,[2,3] Veyret et al.,[5] Zabel et al.,[6] Barnes et al.,[1] and Veyret et al.[4]). The recommended k(298 K) is the average of values obtained by Su et al.,[2] Veyret et al.,[5] and Veyret et al.[4] The temperature dependence observed by Veyret et al.[4] (275–333 K) is recommended. The value reported by Barnes et al. at 273 K is consistent with this recommendation. The adduct HO_2•CH_2O seems to isomerize to $HOCH_2OO$ reasonably rapidly and reversibly. There significant discrepancies between measured values of the equilibrium constants for this reaction.
(Table: 90-1, Note: 90-1, Evaluated: 90-1) Back to Table

(1) Barnes, I.; Becker, K. H.; Fink, E. H.; Reimer, A.; Zabel, F.; Niki, H. FTIR spectroscopic study of the gas-phase reaction of HO_2 with H_2CO. *Chem. Phys. Lett.* **1985**, *115*, 1-8, doi:10.1016/0009-2614(85)80091-9.
(2) Su, F.; Calvert, J. G.; Shaw, J. H. Mechanism of the photooxidation of gaseous formaldehyde. *J. Phys. Chem.* **1979**, *83*, 3185-3191, doi:10.1021/j100488a001.
(3) Su, F.; Calvert, J. G.; Shaw, J. H.; Niki, H.; Maker, P. D.; Savage, C. M.; Breitenbach, L. D. Spectroscopic and kinetic studies of a new metastable species in the photooxidation of gaseous formaldehyde. *Chem. Phys. Lett.* **1979**, *65*, 221-225, doi:10.1016/0009-2614(79)87053-0.
(4) Veyret, B.; Lesclaux, R.; Rayez, M.-T.; Rayez, J.-C.; Cox, R. A.; Moortgat, G. K. Kinetics and mechanism of the photooxidation of formaldehyde. 1. Flash photolysis study. *J. Phys. Chem.* **1989**, *93*, 2368-2374, doi:10.1021/j100343a033.
(5) Veyret, B.; Rayez, J. C.; Lesclaux, R. Mechanism of the photooxidation of formaldehyde studied by flash photolysis of CH_2O-O_2-NO mixtures. *J. Phys. Chem.* **1982**, *86*, 3424-3430, doi:10.1021/j100214a032.
(6) Zabel, F.; Sahetchian, K. A.; Chachaty, C. ESR spectra of free radicals formed during the gas-phase photo-oxidation of formaldehyde: Thermal stability of the $HOCH_2OO$ radical. *Chem. Phys. Lett.* **1987**, *134*, 433-437, doi:10.1016/0009-2614(87)87168-3.

D50. $HO_2 + CH_3O_2$. This recommendation is taken from the evaluated review of Tyndall et al.[4] The kinetics of this reaction have been studied by using UV absorption following pulsed photolytic production of the radicals. These authors first analyzed the available data for the products of the reaction and concluded that the major products are CH_3OOH and O_2. They used this product yield information with their evaluated UV absorption cross sections for HO_2 and CH_3O_2 to reanalyze the UV absorption profiles measured in kinetics experiments by Dagaut et al.[1] and by Lightfoot et al.,[3] the two groups that carried out the most extensive studies. They found that rate coefficients reported by these two groups need to be increased by ~20%. The recommended value is based on the average of the corrected data from these two groups. The temperature dependence was evaluated by Tyndall et al. by assuming that the absorption cross sections of CH_3O_2 and HO_2 are independent of temperature at the wavelengths used for the kinetics studies. The products of this reaction are shown as $CH_3OOH + O_2$ in the table. However, Elrod et al.[2] have determined that the reaction also yields $CH_2O + H_2O + O_2$ with yields that range from 0.1 at 298 K to 0.3 at 220 K. In anticipation of further work, the recommended product yield for the CH_2O channel is zero. The uncertainties of both k(298 K) and E/R are those presented in Tyndall et al.
(Table: 02-25, Note: 06-2, Evaluated: 06-2) Back to Table

(1) Dagaut, P.; Wallington, T. J.; Kurylo, M. J. Temperature dependence of the rate constant for the HO_2 + CH_3O_2 gas-phase reaction. *J. Phys. Chem.* **1988**, *92*, 3833-3836, doi:10.1021/j100324a030.
(2) Elrod, M. J.; Ranschaert, D. L.; Schneider, N. J. Direct kinetics study of the termperature dependence of the CH_2O branching channel for the CH_3O_2 + HO_2 Reaction. *Int. J. Chem. Kinet.* **2001**, *33*, 363-376, doi:10.1002/kin.1030.
(3) Lightfoot, P. D.; Veyret, B.; Lesclaux, R. Flash photolysis study of the CH_3O_2 + HO_2 reaction between 248 and 573 K. *J. Phys. Chem.* **1990**, *94*, 708-714, doi:10.1021/j100365a036.
(4) Tyndall, G. S.; Cox, R. A.; Granier, C.; Lesclaux, R.; Moortgat, G. K.; Pilling, M. J.; Ravishankara, A. R.; Wallington, T. J. Atmospheric chemistry of small organic peroxy radicals. *J. Geophys. Res.* **2001**, *106*, 12157-12182, doi:10.1029/2000JD900746.

D51. $HO_2 + C_2H_5O_2$. The recommended k(298 K) is the weighted average of those measured by Cattell et al.,[1] Dagaut et al.,[2] Fenter et al.,[3] and Maricq and Szente.[4] In all experiments the rate coefficient was obtained by modeling the reaction system. Also, the calculated rate coefficients depended on the UV absorption cross sections of both $C_2H_5O_2$ and HO_2. The absorption cross section of $C_2H_5O_2$ is not well-defined. The value reported by Dagaut et al. would be ~30% higher if the cross sections used by Maricq and Szente were used. The recommended E/R is derived from the measurements of Dagaut et al. (228–380 K), Fenter et al. (248–480 K), and Maricq and Szente (210–363 K). Wallington and Japar[5] have shown that $C_2H_5O_2H$ and O_2 are the only products of this reaction.
(Table: 94-26, Note: 94-26, Evaluated: 94-26) Back to Table

(1) Cattell, F. C.; Cavanagh, J.; Cox, R. A.; Jenkin, M. E. A kinetics study of reactions of HO_2 and $C_2H_5O_2$ using diode laser absorption spectroscopy. *J. Chem. Soc. Faraday Trans. 2* **1986**, *82*, 1999-2018, doi:10.1039/f29868201999.
(2) Dagaut, P.; Wallington, T. J.; Kurylo, M. J. Flash photolysis kinetic absorption spectroscopy study of the gas-phase reactlon HO_2 + $C_2H_5O_2$ over the temperature range 228-380 K. *J. Phys. Chem.* **1988**, *92*, 3836-3839, doi:10.1021/j100324a031.

(3) Fenter, F. F.; Catoire, V.; Lesclaux, R.; Lightfoot, P. D. The ethylperoxy radical: Its ultraviolet spectrum, self-reaction, and reaction with HO_2, each studied as a function of temperature. *J. Phys. Chem.* **1993**, *97*, 3530-3538, doi:10.1021/j100116a016.
(4) Maricq, M. M.; Szente, J. J. A kinetic study of the reaction between ethylperoxy radicals and HO_2. *J. Phys. Chem.* **1994**, *98*, 2078-2082, doi:10.1021/j100059a016.
(5) Wallington, T. J.; Japar, S. M. FTIR product study of the reaction of $C_2H_5O_2 + HO_2$ in air at 295 K. *Chem. Phys. Lett.* **1990**, *166*, 495-499, doi:10.1016/0009-2614(90)87140-M.

D52. $HO_2 + CH_3C(O)O_2$. This recommendation is taken from the evaluated review of Tyndall et al.[5] This reaction has two sets of products:

$$CH_3C(O)O_2 + HO_2 \rightarrow CH_3C(O)O_2H + O_2 \quad (a)$$

$$CH_3C(O)O_2 + HO_2 \rightarrow CH_3C(O)OH + O_3 \quad (b)$$

The majority of the reaction proceeds via channel (a), but there is clear evidence for channel (b). Tyndall et al. reevaluated the available data on end products of this reaction, particularly those of Crawford et al.,[1] Moortgat et al.,[3] and Horie and Moortgat,[2] and concluded that channel (a) contributes ~80% while channel (b) contributes ~20% at 298 K. They also concluded that $k_a/k_b = 37 \times \exp(-660/T)$ with a large uncertainty in this value. They derived the overall rate coefficient for this reaction, which has been measured only by following the radical concentrations via UV absorption. They based their recommendation mostly on the results of Moortgat et al.[3] and Tomas et al.[4] The uncertainties of both k(298 K) and E/R are those presented in Tyndall et al.
(Table: 02-25, Note: 02-25, Evaluated: 02-25) Back to Table

(1) Crawford, M. A.; Wallington, T. J.; Szente, J. J.; Maricq, M. M.; Francisco, J. S. Kinetics and mechanism of the acetylperoxy + HO_2 reaction. *J. Phys. Chem. A* **1999**, *103*, 365-378, doi:10.1021/jp983150t.
(2) Horie, O.; Moortgat, G. K. Reactions of $CH_3C(O)O_2$ radicals with CH_3O_2 and HO_2 between 263 and 333 K A product study. *J. Chem. Soc. Faraday Trans.* **1992**, *88*, 3305-3312, doi:10.1039/ft9928803305.
(3) Moortgat, G.; Veyret, B.; Lesclaux, R. Absorption spectrum and kinetics of reactions of the acetylperoxy radical. *J. Phys. Chem.* **1989**, *93*, 2362-2368, doi:10.1021/j100343a032.
(4) Tomas, A. E.; Villenave, E.; Lesclaux, R. Reactions of the HO_2 radical with CH_3CHO and $CH_3C(O)O_2$ in the gas phase. *J. Phys. Chem. A* **2001**, *105*, 3505-3514, doi:10.1021/jp003762p.
(5) Tyndall, G. S.; Cox, R. A.; Granier, C.; Lesclaux, R.; Moortgat, G. K.; Pilling, M. J.; Ravishankara, A. R.; Wallington, T. J. Atmospheric chemistry of small organic peroxy radicals. *J. Geophys. Res.* **2001**, *106*, 12157-12182, doi:10.1029/2000JD900746.

D53. $HO_2 + CH_3C(O)CH_2O_2$. This recommendation is taken from the evaluated review of Tyndall et al.[2] This reaction has been studied by only Bridier et al.[1] and Tyndall et al. based their recommendation on this one study. The uncertainties of both k(298 K) and E/R are those presented in Tyndall et al.
(Table: 02-25, Note: 02-25, Evaluated: 02-25) Back to Table

(1) Bridier, I.; Veyret, B.; Lesclaux, R.; Jenkin, M. E. Flash photolysis study of the UV spectrum and kinetics of reactions of the acetonylperoxy radical. *J. Chem. Soc. Faraday Trans.* **1993**, *89*, 2993-2997, doi:10.1039/ft9938902993.
(2) Tyndall, G. S.; Cox, R. A.; Granier, C.; Lesclaux, R.; Moortgat, G. K.; Pilling, M. J.; Ravishankara, A. R.; Wallington, T. J. Atmospheric chemistry of small organic peroxy radicals. *J. Geophys. Res.* **2001**, *106*, 12157-12182, doi:10.1029/2000JD900746.

D54. $NO_3 + CH_2=C(CH_3)CHO$ (methacrolein). The recommendation is the average of the results of relative rate studies by Chew et al.[2] (298 K) and Canosa-Mas et al.[1] (296 K). The Chew et al. study supersedes an earlier study by the same group.[3] Chew et al. report two rate constants obtained using propene and 1-butene as reference compounds while Canosa-Mas et al. report a single rate constant obtained using propene as the reference. Two flow tube studies[1,4] report faster rate constants, presumably due to the presence of reactive impurities in methacrolein samples. Reaction can proceed via addition to the double bond or via abstraction of the aldehydic hydrogen atom. In 760 Torr O_2, Canosa-Mas et al. observe production of both methyl glyoxal ($CH_3C(O)CHO$), likely formed via reactions involving a primary addition product, and MPAN ($CH_2=C(CH_3)C(O)OONO_2$), likely formed via reactions involving the H-abstraction product. Product yields have not been reported.
(Table: 15-10, Note: 15-10, Evaluated: 15-10) Back to Table

(1) Canosa-Mas, C. E.; Carr, S.; King, M. D.; Shallcross, D. E.; Thompson, K. C.; Wayne, R. P. A kinetic study of the reactions of NO_3 with methyl vinyl ketone, methacrolein, acrolein, methyl acrylate and methyl methacrylate. *Phys. Chem. Chem. Phys.* **1999**, *1*, 4195-4202, doi:10.1039/a904613e.
(2) Chew, A. A.; Atkinson, R.; Aschmann, S. M. Kinetics of the gas-phase reactions of NO_3 radicals with a series of alcohols, glycol ethers, ethers and chloroalkanes. *J. Chem. Soc. Faraday Trans.* **1998**, *94*, 1083-1089, doi:10.1039/a708183i.
(3) Kwok, E. S. C.; Aschmann, S. M.; Arey, J.; Atkinson, R. Product formation from the reaction of the NO_3 radical with isoprene and rate constants for the reactions of methacrolein and methyl vinyl ketone with the NO_3 radical. *Int. J. Chem. Kinet.* **1996**, *28*, 925-934, doi:10.1002/(SICI)1097-4601(1996)28:12<925::AID-KIN10>3.0.CO;2-B.
(4) Rudich, Y.; Talukdar, R. K.; Fox, R. W.; Ravishankara, A. R. Rate coefficients for reactions of NO_3 with a few olefins and oxygenated olefins. *J. Phys. Chem.* **1996**, *100*, 5374-5381, doi:10.1021/jp953079g.

D55. $NO_3 + CH_3C(O)CH=CH_2$ (Methyl Vinyl Ketone, MVK). In a low pressure flow tube study where NO_3 was produced by thermal decomposition of N_2O_5 and detected by long path diode laser absorption at 662 nm, Rudich et al.[3] (298 K) measured a rate constant of $(1.0 \pm 0.2) \times 10^{-16}$ $cm^3molecule^{-1}$ s^{-1}; acknowledging that "our experiment is not suited to accurately measuring such low rate coefficients," Rudich et al. chose to report their result as an upper limit, i.e., $k < 1.2 \times 10^{-16}$ $cm^3molecule^{-1}$ s^{-1}. In units of 10^{-16} $cm^3molecule^{-1}$ s^{-1}, Canosa-Mas et al.[1] (296 K) report $k = 3.2 \pm 0.6$ based on a low pressure flow tube study where NO_3 was produced via the F + HNO_3 reaction and detected by laser induced fluorescence; these authors also obtained a rate constant of 5.3 ± 1.9 (corrected using updated information for the $NO_3 + C_2H_4$ reference reaction) from a relative rate study in 760 Torr N_2. Kwok et al.[2] (296 K) report $k < 6 \times 10^{-16}$ $cm^3molecule^{-1}$ s^{-1} based on a relative rate study in 740 Torr air using $NO_3 + C_3H_6$ as the reference reaction. The recommendation, $k < 4 \times 10^{-16}$ $cm^3molecule^{-1}$ s^{-1}, is consistent with the results reported in both absolute rate constant determinations. The initial step in the reaction of NO_3 with MVK is addition of NO_3 to the double bond. In 760 Torr O_2 bath gas, Canosa-Mas et al. observe methyl glyoxal ($CH_3C(O)CHO$) as a reaction product; they propose a pathway where NO_3 adds to the terminal carbon followed by formation of a peroxy radical that reacts with a second NO_3 to form (via multiple steps) $CH_3C(O)CHO + HCHO + 2NO_2 + O_2$.
(Table: 15-10, Note: 15-10, Evaluated: 15-10) Back to Table

(1) Canosa-Mas, C. E.; Carr, S.; King, M. D.; Shallcross, D. E.; Thompson, K. C.; Wayne, R. P. A kinetic study of the reactions of NO_3 with methyl vinyl ketone, methacrolein, acrolein, methyl acrylate and methyl methacrylate. *Phys. Chem. Chem. Phys.* **1999**, *1*, 4195-4202, doi:10.1039/a904613e.
(2) Kwok, E. S. C.; Aschmann, S. M.; Arey, J.; Atkinson, R. Product formation from the reaction of the NO_3 radical with isoprene and rate constants for the reactions of methacrolein and methyl vinyl ketone with the NO_3 radical. *Int. J. Chem. Kinet.* **1996**, *28*, 925-934, doi:10.1002/(SICI)1097-4601(1996)28:12<925::AID-KIN10>3.0.CO;2-B.
(3) Rudich, Y.; Talukdar, R. K.; Fox, R. W.; Ravishankara, A. R. Rate coefficients for reactions of NO_3 with a few olefins and oxygenated olefins. *J. Phys. Chem.* **1996**, *100*, 5374-5381, doi:10.1021/jp953079g.

D56. $NO_3 + CH_2=C(CH_3)CH=CH_2$. The recommended E/R is obtained from an unweighted fit of the single temperature-dependent data set of Dlugokencky and Howard[6] to $\ln k = \ln A - E/RT$ (E/R = 446 K, 251–381 K). The recommended 298 K rate constant is an unweighted average of ambient temperature results reported by Atkinson et al.,[1,2] Dlugokencky and Howard[6] (rate constant obtained from the best fit Arrhenius expression), Barnes et al.,[3] Wille et al.,[10] Ellermann et al.,[7] Berndt and Boge,[5] Suh et al.,[9] and Stabel et al.[8] Ambient temperature results obtained at temperatures other than 298 K were adjusted using the recommended E/R. The 298 K rate constant reported by Benter and Schindler[4] is not considered because (a) it is faster than all others in the literature and (b) it is superseded by a later study from the same group.[10]
(Table 15-10, Note: 15-10, Evaluated: 15-10) Back to Table

(1) Atkinson, R.; Aschmann, S. M.; Pitts, J. N., Jr. Rate constants for the gas-phase reactions of the NO_3 radical with a series of organic compounds at 296 ± 2 K. *J. Phys. Chem.* **1988**, *92*, 3454-3457, doi:10.1021/j100323a028.
(2) Atkinson, R.; Aschmann, S. M.; Winer, A. M.; Pitts, J. N., Jr. Kinetics of the gas-phase reactions of NO_3 radicals with a series of dialkenes, cycloalkenes, and monoterpenes at 295 ± 1 K. *Environ. Sci. Technol.* **1984**, *18*, 370-375, doi:10.1021/es00123a016.
(3) Barnes, I.; Bastian, V.; Becker, K. H.; Tong, Z. Kinetics and products of the reactions of NO_3 with monoalkenes, dialkenes, and monoterpenes. *J. Phys. Chem.* **1990**, *94*, 2413-2419, doi:10.1021/j100369a041.

(4) Benter, T.; Schindler, R. N. Absolute rate coefficients for the reaction of NO_3 radicals with simple dienes. *Chem. Phys. Lett.* **1988**, *145*, 67-70, doi:10.1016/0009-2614(88)85134-0.
(5) Berndt, T.; Böge, O. Gas-phase reaction of NO_3 radicals with isoprene: A kinetic and mechanistic Study. *Int. J. Chem. Kinet.* **1997**, *29*, 755-765, doi:10.1002/(SICI)1097-4601(1997)29:10<755::AID-KIN4>3.0.CO;2-L.
(6) Dlugokencky, E. J.; Howard, C. J. Studies of NO_3 radical reactions with some atmospheric organic compounds at low pressures. *J. Phys. Chem.* **1989**, *93*, 1091-1096, doi:10.1021/j100340a015.
(7) Ellermann, T.; Nielsen, O. J.; Skov, H. Absolute rate constants for the reaction of NO_3 radicals with a series of dienes at 295 K. *Chem. Phys. Lett.* **1992**, *200*, 224-229, doi:10.1016/0009-2614(92)80002-S.
(8) Stabel, J. R.; Johnson, M. S.; Langer, S. Rate coefficients for the gas-phase reaction of isoprene with NO_3 and NO_2. *Int. J. Chem. Kinet.* **2005**, *37*, 57-65, doi:10.1002/kin.20050.
(9) Suh, I.; Lei, W.; Zhang, R. Experimental and theoretical studies of isoprene reaction with NO_3. *J. Phys. Chem. A* **2001**, *105*, 6471-6478, doi:10.1021/jp0105950.
(10) Wille, U.; Becker, E.; Schindler, R. N.; Lancar, I. T.; Poulet, G.; Le Bras, G. A discharge flow mass-spectrometric study of the reaction between the NO_3 radical and isoprene. *J. Atmos. Chem.* **1991**, *13*, 183-193, doi:10.1007/BF00115972.

D57. NO_3 + CO. The upper limit is based on the results of Hjorth et al.[2] (295 K), who monitored isotopically labeled CO loss in the presence of NO_3 by FTIR. Burrows et al.[1] (298 K) obtained an upper limit of 4×10^{-16} cm^3 molecule^{-1} s^{-1}, which is consistent with the Hjorth et al. study. Products are expected to be $NO_2 + CO_2$, if the reaction occurs.
(Table: 87-41, Note: 92-20, Evaluated: 92-20) Back to Table

(1) Burrows, J. P.; Tyndall, G. S.; Moortgat, G. K. Absorption spectrum of NO_3 and kinetics of the reactions of NO_3 with NO_2, Cl, and several stable atmospheric species at 298 K. *J. Phys. Chem.* **1985**, *89*, 4848-4856, doi:10.1021/j100268a038.
(2) Hjorth, J.; Ottobrini, G.; Restelli, G. Reaction of the NO_3 radical with CO: Determination of an upper limit for the rate constant using FTIR spectroscopy. *Int. J. Chem. Kinet.* **1986**, *18*, 819-827, doi:10.1002/kin.550180802.

D58. NO_3 + CH_2O. There are three measurements of this rate coefficient at 298 K: Atkinson et al.,[1] Cantrell et al.,[2] and Hjorth et al.[3] The value reported by Atkinson et al.,[1] $k = (3.23 \pm 0.26) \times 10^{-16}$ cm^3 molecule^{-1} s^{-1}, is corrected to 5.8×10^{-16} cm^3 molecule^{-1} s^{-1} to account for the different value of the equilibrium constant for the $NO_3 + NO_2 \leftrightarrow N_2O_5$ reaction that was measured subsequent to this study by the same group using the same apparatus. This correction is in accordance with their suggestion (Tuazon et al.[4]). The values reported by Cantrell et al. and Hjorth et al., $k = 6.3 \times 10^{-16}$ cm^3 molecule^{-1} s^{-1} and $(5.4 \pm 1.1) \times 10^{-16}$ cm^3 molecule^{-1} s^{-1}, respectively, are in good agreement with the corrected value of Atkinson et al. The recommended value is the average of these three studies. Cantrell et al. have good evidence to suggest that HNO_3 and CHO are the products of this reaction. The temperature dependence of this rate coefficient is unknown, but comparison with the analogous $NO_3 + CH_3CHO$ reaction suggests a large E/R.
(Table: 90-1, Note: 90-1, Evaluated: 90-1) Back to Table

(1) Atkinson, R.; Plum, C. N.; Carter, W. P. L.; Winer, A. M.; Pitts, J. N., Jr. Rate constants for the gas-phase reactions of nitrate radicals with a series of organics in air at 298 ± 1 K. *J. Phys. Chem.* **1984**, *88*, 1210-1215, doi:10.1021/j150650a039.
(2) Cantrell, C. A.; Stockwell, W. R.; Anderson, L. G.; Busarow, K. L.; Perner, D.; Schmeltekopf, A.; Calvert, J. G.; Johnston, H. S. Kinetlc study of the NO_3-CH_2O reaction and its possible role in nighttime tropospheric chemistry. *J. Phys. Chem.* **1985**, *89*, 139-146, doi:10.1021/j100247a031.
(3) Hjorth, J.; Ottobrini, G.; Restelli, G. Reaction between NO_3 and CH_2O in air: A determination of the rate constant at 295 ± 2 K. *J. Phys. Chem.* **1988**, *92*, 2669-2672, doi:10.1021/j100320a053.
(4) Tuazon, E. C.; Sanhueza, E.; Atkinson, R.; Carter, W. P. L.; Winer, A. M.; Pitts, J. N., Jr. Direct determination of the equilibrium constant at 298 K for the $NO_2 + NO_3 \leftrightarrow N_2O_5$ reactions. *J. Phys. Chem.* **1984**, *88*, 3095-3098, doi:10.1021/j150658a033.

D59. NO_3 + CH_3CHO. There are four measurements of this rate constant: Morris and Niki,[4] Atkinson et al.,[1] Cantrell et al.,[2] and Dlugokencky and Howard.[3] The value reported by Atkinson et al., $k = (1.34 \pm 0.28) \times 10^{-15}$ cm^3 molecule^{-1} s^{-1}, is corrected to 2.4×10^{-15} cm^3 molecule^{-1} s^{-1} as discussed for the $NO_3 + H_2CO$ reaction above and as suggested by Tuazon et al.[5] The recommended value is the average of the values obtained by Atkinson et al., Cantrell et al., and Dlugokencky and Howard. The results of Morris and Niki agree with the recommended value when their original data are re-analyzed using a more recent value for the equilibrium constant for the reaction $NO_2 + NO_3 \leftrightarrow N_2O_5$ as shown by Dlugokencky and Howard. Dlugokencky and

Howard (264–374 K) have studied the temperature dependence of this reaction. Their measured value of E/R is recommended. The A-factor has been calculated to agree with the k(298 K) recommended here. Morris and Niki, and Cantrell et al. observed the formation of HNO_3 and PAN in their studies, which strongly suggests that HNO_3 and CH_3CO are the products of this reaction.
(Table: 87-41, Note: 87-41, Evaluated: 87-41) Back to Table

(1) Atkinson, R.; Plum, C. N.; Carter, W. P. L.; Winer, A. M.; Pitts, J. N., Jr. Rate constants for the gas-phase reactions of nitrate radicals with a series of organics in air at 298 ± 1 K. *J. Phys. Chem.* **1984**, *88*, 1210-1215, doi:10.1021/j150650a039.

(2) Cantrell, C. A.; Davidson, J. A.; Busarow, K. L.; Calvert, J. G. The CH_3CHO-NO_3 reaction and possible nighttime PAN generation. *J. Geophys. Res.* **1986**, *91*, 5347-5353, doi:10.1029/JD091iD05p05347.

(3) Dlugokencky, E. J.; Howard, C. J. Studies of NO_3 radical reactions with some atmospheric organic compounds at low pressures. *J. Phys. Chem.* **1989**, *93*, 1091-1096, doi:10.1021/j100340a015.

(4) Morris, E. D.; Niki, H. Reaction of the nitrate radical with acetaldehyde and propylene. *J. Phys. Chem.* **1974**, *78*, 1337-1338, doi:10.1021/j100606a600.

(5) Tuazon, E. C.; Sanhueza, E.; Atkinson, R.; Carter, W. P. L.; Winer, A. M.; Pitts, J. N., Jr. Direct determination of the equilibrium constant at 298 K for the $NO_2 + NO_3 \leftrightarrow N_2O_5$ reactions. *J. Phys. Chem.* **1984**, *88*, 3095-3098, doi:10.1021/j150658a033.

D60. $CH_3 + O_2$. This bimolecular reaction is not expected to be important, based on the results of Baldwin and Golden,[1] who found $k < 5 \times 10^{-17}$ cm^3 molecule^{-1} s^{-1} for temperatures up to 1200 K. Klais et al.[3] failed to detect OH (via $CH_3 + O_2 \rightarrow CH_2O + OH$) at 368 K and placed an upper limit of 3×10^{-16} cm^3 molecule^{-1} s^{-1} for this rate coefficient. Bhaskaran et al.[2] measured $k = 1 \times 10^{-11} \exp(-12{,}900/T)$ cm^3 molecule^{-1} s^{-1} for $1800 < T < 2200$ K. The latter two studies thus support the results of Baldwin and Golden. Studies by Selzer and Bayes[5] and Plumb and Ryan[4] confirm the low value for this rate coefficient. Previous studies of Washida and Bayes[6] are superseded by those of Selzer and Bayes. Plumb and Ryan have placed an upper limit of 3×10^{-16} cm^3 molecule^{-1} s^{-1} based on their inability to find HCHO in their experiments. A study by Zellner and Ewig[7] suggests that this reaction is important at combustion temperature but is unimportant for the atmosphere.
(Table: 83-62, Note: 83-62, Evaluated: 83-62) Back to Table

(1) Baldwin, A. C.; Golden, D. M. Reactions of methyl radicals of importance in combustion systems. *Chem. Phys. Lett.* **1978**, *55*, 350-352, doi:10.1016/0009-2614(78)87036-5.

(2) Bhaskaran, K. A.; Frank, P.; Just, T. In *12th International Shock Tube Symposium* Jerusalem., 1979.

(3) Klais, O.; Anderson, P. C.; Laufer, A. H.; Kurylo, M. J. An upper limit for the rate constant of the bimolecular reaction $CH_3 + O_2 \rightarrow OH + H_2CO$ at 368 K. *Chem. Phys. Lett.* **1979**, *66*, 598-601, doi:10.1016/0009-2614(79)80349-8.

(4) Plumb, I. C.; Ryan, K. R. Kinetics of the reactions of CH_3 with O(^{3}P) and O_2 at 295 K. *Int. J. Chem. Kinet.* **1982**, *14*, 861-874, doi:10.1002/kin.550140806.

(5) Selzer, E. A.; Bayes, K. D. Pressure dependence of the rate of reaction of methyl radicals with O_2. *J. Phys. Chem.* **1983**, *87*, 392-394, doi:10.1021/j100226a007.

(6) Washida, N.; Bayes, K. D. The reactions of methyl radicals with atomic and molecular oxygen. *Int. J. Chem. Kinet.* **1976**, *8*, 777-794, doi:10.1002/kin.550080512.

(7) Zellner, R.; Ewig, F. Computational study of the $CH_3 + O_2$ chain branching reaction. *J. Phys. Chem.* **1988**, *92*, 2971-2974, doi:10.1021/j100321a050.

D61. $CH_3 + O_3$. The recommended A-factor and E/R are those obtained from the results of Ogryzlo et al.[4] (243–384 K). The results of Simonaitis and Heicklen,[6] based on an analysis of a complex system, are not used. Washida et al.[7] used $O + C_2H_4$ as the source of CH_3. Studies on the $O + C_2H_4$ reaction (Schmoltner et al.,[5] Kleinermanns and Luntz,[3] Hunziker et al.,[1] and Inoue and Akimoto[2]) have shown this reaction to be a poor source of CH_3. Therefore, the results of Washida et al. are also not used.
(Table: 83-62, Note: 83-62, Evaluated: 83-62) Back to Table

(1) Hunziker, H. E.; Kneppe, H.; Wendt, H. R. Photochemical modulation spectroscopy of oxygen atom reactions with olefins. *J. Photochem.* **1981**, *17*, 377-387, doi:10.1016/0047-2670(81)85380-4.

(2) Inoue, G.; Akimoto, H. Laser-induced fluorescence of the C_2H_3O radical. *J. Chem. Phys.* **1981**, *74*, 425-433, doi:10.1063/1.440848.

(3) Kleinermanns, K.; Luntz, A. C. Laser-induced fluorescence of CH_2CHO produced in the crossed molecular beam reactions of O(^{3}P) with olefins. *J. Phys. Chem.* **1981**, *85*, 1966-1968, doi:10.1021/j150614a003.

(4) Ogryzlo, E. A.; Paltenghi, R.; Bayes, K. D. The rate of reaction of methyl radicals with ozone. *Int. J. Chem. Kinet.* **1981**, *13*, 667-675, doi:10.1002/kin.550130707.

(5) Schmoltner, A.-M.; Chu, P. M.; Brudzynski, R. J.; Lee, Y. T. Crossed molecular beam study of the reaction $O(^3P) + C_2H_4$. *J. Chem. Phys.* **1989**, *91*, 6926-6936, doi:10.1063/1.457309.
(6) Simonaitis, R.; Heicklen, J. Reactions of CH_3, CH_3O, and CH_3O_2 radicals with O_3. *J. Phys. Chem.* **1975**, *79*, 298-302, doi:10.1021/j100571a002.
(7) Washida, N.; Akimoto, H.; Okuda, M. Is $O_2^*(a^1\Delta_g)$ formed in the $O + O_3$, $H + O_3$, and $NO + O_3$ reactions? *Bull. Chem. Soc. Jpn.* **1980**, *53*, 3496-3503, doi:10.1246/bcsj.53.3496.

D62. HCO + O_2. The value of k(298 K) is the average of the determinations by Washida et al.,[12] Shibuya et al.,[8] Veyret and Lesclaux,[11] Langford and Moore,[3] Nesbitt et al.,[5] Temps et al.,[9] and Ninomiya et al.[6] There are three measurements of k where HCO was monitored via the intracavity dye laser absorption technique (Reilly et al.,[7] Nadtochenko et al.,[4] and Gill et al.[1]). Even though these studies agree with the recent measurements of Nesbitt et al., the only recent measurement to obtain a low value, they have not been included in deriving the recommended value of k(298 K). However, the uncertainty has been increased to overlap with those measurements. The main reason for not including them in the average is the possible depletion of O_2 in those static systems (as suggested by Veyret and Lesclaux). Also, these experiments were designed more for the study of photochemistry than kinetics. The temperature dependence of this rate coefficient has been measured by Veyret and Lesclaux (298–503 K), Timonen et al.[10] (295–713 K), and Nesbitt et al. (200–398 K). While Timonen et al. obtain a slightly positive activation energy, Veyret and Lesclaux, and Nesbitt et al. measure slightly negative activation energy. It is very likely that the Arrhenius expression is curved. We recommend an E/R value of zero, with an uncertainty of 100 K. Veyret and Lesclaux preferred a T^n form ($k = 5.5 \times 10^{-11}$ $T^{-(0.4\pm0.3)}$ cm^3 molecule^{-1} s^{-1}). Hsu et al.[2] suggest that this reaction proceeds via addition at low temperature and abstraction at higher temperatures.
(Table: 02-25, Note: 02-25, Evaluated: 02-25) Back to Table

(1) Gill, R. J.; Johnson, W. D.; Atkinson, G. H. The formation and decay mechanisms of HCO in the photodissociation of gas phase acetaldehyde. *Chem. Phys.* **1981**, *58*, 29-44, doi:10.1016/0301-0104(81)80042-0.
(2) Hsu, C.-C.; Mebel, A. M.; Lin, M. C. *Ab initio* molecular orbital study of the HCO + O_2 reaction: Direct versus indirect abstraction channels. *J. Chem. Phys.* **1996**, *105*, 2346-2352, doi:10.1063/1.472083.
(3) Langford, A. O.; Moore, C. B. Collision complex formation in the reactions of formyl radicals with nitric oxide and oxygen. *J. Chem. Phys.* **1984**, *80*, 4211-4221, doi:10.1063/1.447252.
(4) Nadtochenko, V. A.; Sarkisov, O. M.; Vedeneev, V. I. *Doklady Akademii Nauk SSSR* **1979**, *244*, 152.
(5) Nesbitt, F. L.; Gleason, J. F.; Stief, L. J. Temperature dependence of the rate constant for the reaction HCO + O_2 → HO_2 + CO at T = 200-398 K. *J. Phys. Chem. A* **1999**, *103*, 3038-3043, doi:10.1021/jp984781q.
(6) Ninomiya, Y.; Kawasaki, M.; Guschin, A.; Molina, L. T.; Molina, M. J.; Wallington, T. J. Atmospheric chemistry of n-$C_3F_7OCH_3$: Reaction with OH radicals and Cl atoms and atmospheric fate of n-$C_3F_7OCH_2O(\bullet)$ radicals. *Environ. Sci. Technol.* **2000**, *34*, 2973-2978, doi:10.1021/es991449z.
(7) Reilly, J. P.; Clark, J. H.; Moore, C. B.; Pimentel, G. C. HCO production, vibrational relaxation, chemical kinetics, and spectroscopy following laser photolysis of formaldehyde. *J. Chem. Phys.* **1978**, *69*, 4381-4394, doi:10.1063/1.436449.
(8) Shibuya, K.; Ebatu, T.; Obi, K.; Tanaka, I. Rate constant measurements for the reactions of HCO with NO and O_2 in the gas phase. *J. Phys. Chem.* **1977**, *81*, 2292-2294, doi:10.1021/j100539a019.
(9) Temps, F.; Wagner, H. G. Rate constants for the reactions of OH radicals with CH_2O and HCO. *Ber. Bunsenges Phys. Chem.* **1984**, *88*, 415-418, doi:10.1002/bbpc.19840880419.
(10) Timonen, R. S.; Ratajczak, E.; Gutman, D. Kinetics of the reactions of the formyl radical with oxygen, nitrogen dioxide, chlorine, and bromine. *J. Phys. Chem.* **1988**, *92*, 651-655, doi:10.1021/j100314a017.
(11) Veyret, B.; Lesclaux, R. Absolute rate constants for the reactions of HCO with O_2 and NO from 298 to 503 K. *J. Phys. Chem.* **1981**, *85*, 1918-1922, doi:10.1021/j150613a028.
(12) Washida, N.; Martinez, R. I.; Bayes, K. D. The oxidation of formyl radicals. *Z. Naturforsch.* **1974**, *29A*, 251-255.

D63. $CH_2OH + O_2$. The rate coefficient was first measured directly by Radford[7] by detecting the HO_2 product in a laser magnetic resonance spectrometer. The wall loss of CH_2OH could have introduced a large error in this measurement. Radford also showed that the previous measurement of Avramenko and Kolesnikova[1] was in error. Wang et al.[8] measured a value of 1.4×10^{-12} cm^3 molecule^{-1} s^{-1} by detecting the HO_2 product. Dobe et al.,[2] Grotheer et al.,[3] Payne et al.,[6] Grotheer et al.,[4] and Nesbitt et al.[5] have measured k(298 K) to be close to 1.0×10^{-11} cm^3 molecule^{-1} s^{-1} under conditions where wall losses are small. This reaction appears to exhibit a very complex temperature dependence. Based on the recent data of Grotheer et al.[4] (298–682 K) and Nesbitt et al.[5] (215–300 K), k appears to increase from 200 K to approximately 250 K in an Arrhenius fashion, levels

off at approximately 300 K, decreases from 300 to 500 K, and finally increases as temperature is increased. This complex temperature dependence is believed to be due to the formation of a $CH_2(OH)•O_2$ adduct which can isomerize to $CH_2O•HO_2$ or decompose to reactants. The $CH_2O•HO_2$ isomer can also decompose to CH_2O and HO_2 or reform the original adduct. At temperatures less than 250 K, the data of Nesbitt et al. suggests an E/R value of ~1700 K. For atmospheric purposes, the value $E/R = 0$ is appropriate.
(Table: 90-1, Note: 90-1, Evaluated: 90-1) Back to Table

(1) Avramenko, L. I.; Kolesnikova, R. V. A photochemical study of the mechanism of the reaction between oxygen atoms and acetaldehyde. *Bull. Acad. Sci. USSR, Div. Chem. Sci.* **1961**, 1141-1143.
(2) Dóbé, S.; Temps, F.; Böhland, T.; Wagner, H. G. The reaction of CH_2OH radicals with O_2 studied by laser magnetic resonance technique. *Z. Naturforsch.* **1985**, *40a*, 1289-1298.
(3) Grotheer, H.-H.; Riekert, G.; Meier, U.; Just, T. Kinetics of the reactions of CH_2OH radicals with O_2 and HO_2. *Ber. Bunsenges. Phys. Chem.* **1985**, *89*, 187-191, doi:10.1002/bbpc.19850890219.
(4) Grotheer, H. H.; Riekert, G.; Walter, D.; Just, T. Non-Arrhenius behavior of the reaction of hydroxymethyl radicals with molecular oxygen. *J. Phys. Chem.* **1988**, *92*, 4028-4030, doi:10.1021/j100325a007.
(5) Nesbitt, F. L.; Payne, W. A.; Stief, L. J. Temperature dependence for the absolute rate constant for the reaction $CH_2OH + O_2 \rightarrow HO_2 + H_2CO$ from 215 to 300 K. *J. Phys. Chem.* **1988**, *92*, 4030-4032, doi:10.1021/j100325a008.
(6) Payne, W. A.; Brunning, J.; Mitchell, M. B.; Stief, L. J. Kinetics of the reactions of atomic chlorine with methanol and the hydroxymethyl radical with molecular oxygen at 298 K. *Int. J. Chem. Kinet.* **1988**, *20*, 63-74, doi:10.1002/kin.550200108.
(7) Radford, H. E. The fast reaction of CH_2OH with O_2. *Chem. Phys. Lett.* **1980**, *71*, 195-197, doi:10.1016/0009-2614(80)80145-X.
(8) Wang, W. C.; Suto, M.; Lee, L. C. $CH_2OH + O_2$ reaction rate constant measured by detecting HO_2 from photofragment emission. *J. Chem. Phys.* **1984**, *81*, 3122-3126, doi:10.1063/1.448015.

D64. $CH_3O + O_2$. The recommended k(298 K) is the average of those reported by Lorenz et al.[5] (298–450 K) and Wantuck et al.[8] (298–973 K). The recommended E/R was obtained using the results of Gutman et al.[4] (413–608 K), Lorenz et al.[5] (298–450 K), and Wantuck et al.[8] (298–498 K). These investigators have measured k directly under pseudo–first order conditions by following CH_3O via laser induced fluorescence. Wantuck et al. measured k up to 973 K and found the Arrhenius plot to be curved; only their lower temperature data are used in the fit to obtain E/R. The A factor has been adjusted to reproduce the recommended k(298 K). The previous high temperature measurements (Barker et al.[1] and Batt and Robinson[2]) are in reasonable agreement with the derived expression. This value is consistent with the 298 K results of Cox et al.,[3] obtained from an end product analysis study, and with the upper limit measured by Sanders et al.[7] The A-factor appears low for a hydrogen atom transfer reaction. The reaction may be more complicated than a simple abstraction. At 298 K, the products of this reaction are HO_2 and CH_2O, as shown by Niki et al.[6]
(Table: 87-41, Note: 87-41, Evaluated: 87-41) Back to Table

(1) Barker, J. R.; Benson, S. W.; Golden, D. M. The decomposition of dimethyl peroxide and the rate constant for $CH_3O + O_2 \rightarrow CH_2O + HO_2$. *Int. J. Chem. Kinet.* **1977**, *9*, 31-53, doi:10.1002/kin.550090105.
(2) Batt, L.; Robinson, G. N. Reaction of methoxy radicals with oxygen. I. Using dimethyl peroxide as a thermal source of methoxy radicals. *Int. J. Chem. Kinet.* **1979**, *11*, 1045-1053, doi:10.1002/kin.550111003.
(3) Cox, R. A.; Derwent, R. G.; Kearsey, S. V.; Batt, L.; Patrick, K. G. Photolysis of methyl nitrite: Kinetics of the reaction of the methoxy radical with O_2. *J. Photochem.* **1980**, *13*, 149-163, doi:10.1016/0047-2670(80)85006-4.
(4) Gutman, D.; Sanders, N.; Butler, J. E. Kinetics of the reactions of methoxy and ethoxy radicals with oxygen. *J. Phys. Chem.* **1982**, *86*, 66-70, doi:10.1021/j100390a013.
(5) Lorenz, K.; Rhäsa, D.; Zellner, R.; Fritz, B. Laser photolysis - LIF kinetic studies of the reactions of CH_3O and CH_2CHO with O_2 between 300 K and 500 K. *Ber. Bunsenges. Phys. Chem.* **1985**, *89*, 341-342, doi:10.1002/bbpc.19850890346.
(6) Niki, H.; Maker, P. D.; Savage, C. M.; Breitenbach, L. P. Fourier transform infrared studies of the self-reaction of CH_3O_2 radicals. *J. Phys. Chem.* **1981**, *85*, 877-881, doi:10.1021/j150607a028.
(7) Sanders, N.; Butler, J. E.; Pasternack, L. R.; McDonald, J. R. CH_3O (X^2E) production from 266 nm photolysis of methyl nitrite and reaction with NO. *Chem. Phys.* **1980**, *48*, 203-208, doi:10.1016/0301-0104(80)80049-8.
(8) Wantuck, P. J.; Oldenberg, R. C.; Baughcum, S. L.; Winn, K. R. Removal rate constant measurements for CH_3O by O_2 over the 298-973 K range. *J. Phys. Chem.* **1987**, *91*, 4653-4655, doi:10.1021/j100302a004.

D65. $CH_3O + NO$. The reaction of CH_3O with NO proceeds mainly via addition to form CH_3ONO (Batt et al.,[1] Wiebe and Heicklen,[4] Frost and Smith,[2] and Ohmori et al.[3]). However, a fraction of the energized CH_3ONO adducts decomposes to $CH_2O + HNO$, and appear to be a bimolecular channel. This reaction has been investigated by direct detection of CH_3O via laser-induced fluorescence (Zellner,[5] Frost and Smith,[2] Ohmori et al.[3]). End-product studies (Batt et al.,[1] Wiebe and Heicklen[4]) are generally consistent with this conclusion. Since the fraction of the CH_3ONO adduct that falls apart to $CH_2O + HNO$ decreases with increasing pressure and decreasing temperature, it is not possible to derive a "bimolecular" rate coefficient. A value of $k < 8 \times 10^{-12}$ cm^3 $molecule^{-1}$ s^{-1} can be deduced from the work of Frost and Smith[2] and Ohmori et al.[3] for lower atmospheric conditions.
(Table: 97-4, Note: 97-4, Evaluated: 97-4) Back to Table

(1) Batt, L.; Milne, R. T.; McCulloch, R. D. The gas-phase pyrolysis of alkyl nitrites. V. Methyl nitrite. *Int. J. Chem. Kinet.* **1977**, *9*, 567-587, doi:10.1002/kin.550090406.
(2) Frost, M. J.; Smith, I. W. M. Rate Constants for the reactions of CH_3O and C_2H_5O with NO over a range of temperature and total pressure. *J. Chem. Soc. Faraday Trans.* **1990**, *86*, 1757-1762, doi:10.1039/ft9908601757.
(3) Ohmori, K.; Yamasaki, K.; Matsui, H. Pressure dependence of the rate constant for the reaction of CH_3O + NO. *Bull. Chem. Soc. Jpn.* **1993**, *66*, 51-56, doi:10.1246/bcsj.66.51.
(4) Wiebe, H. A.; Heicklen, J. Photolysis of methyl nitrite. *J. Am. Chem. Soc.* **1973**, *95*, 1-7, doi:10.1021/ja00782a001.
(5) Zellner, R. Recent advances in free radical kinetics of oxygenated hydrocarbon radicals. *J. Chim. Phys.* **1987**, *84*, 403-407.

D66. $CH_3O + NO_2$. The reaction of CH_3O with NO_2 proceeds mainly via the formation of CH_3ONO_2. However, a fraction of the energized adducts fall apart to yield $CH_2O + HNO_2$. The bimolecular rate coefficient reported here is for the fraction of the reaction that yields CH_2O and HNO_2. It is not meant to represent a bimolecular metathesis reaction. The recommended value was derived from the study of McCaulley et al.[1] and is discussed in the section on association reactions.
(Table: 97-4, Note: 97-4, Evaluated: 97-4) Back to Table

(1) McCaulley, J. A.; Anderson, S. M.; Jeffries, J. B.; Kaufman, F. Kinetics of the reaction of CH_3O with NO_2. *Chem. Phys. Lett.* **1985**, *115*, 180-186, doi:10.1016/0009-2614(85)80675-8.

D67. $CH_3O_2 + O_3$. This recommendation is taken from the evaluated review of Tyndall et al.[1] Their recommendation is based mostly on the recent study by Tyndall et al.[2] The temperature dependence is based on the assumption that the only possible reaction which can occur is the O atom transfer from the CH_3O_2 radical and that the activation energy of ~2 kcal mol^{-1} for this O-atom transfer is similar to that in the $HO_2 + O_3$ reaction. The uncertainties of both k(298 K) and E/R are those presented in Tyndall et al.
(Table: 02-25, Note: 02-25, Evaluated: 02-25) Back to Table

(1) Tyndall, G. S.; Cox, R. A.; Granier, C.; Lesclaux, R.; Moortgat, G. K.; Pilling, M. J.; Ravishankara, A. R.; Wallington, T. J. Atmospheric chemistry of small organic peroxy radicals. *J. Geophys. Res.* **2001**, *106*, 12157-12182, doi:10.1029/2000JD900746.
(2) Tyndall, G. S.; Wallington, T. J.; Ball, J. C. FTIR product study of the reactions $CH_3O_2 + CH_3O_2$ and $CH_3O_2 + O_3$. *J. Phys. Chem. A* **1998**, *102*, 2547-2554, doi:10.1021/jp972784h.

D68. $CH_3O_2 + CH_3O_2$. This recommendation is taken from the evaluated review of Tyndall et al.[1] There are two confirmed sets of products for this reaction.

$$CH_3O_2 + CH_3O_2 \rightarrow CH_3O + CH_3O + O_2 \qquad (a)$$

$$CH_3O_2 + CH_3O_2 \rightarrow CH_3OH + HCHO + O_2 \qquad (b)$$

The relative product yield, k_a/k_b, was evaluated by Tyndall et al. to be $(26.2 \pm 6.6) \times \exp((-1130 \pm 240)/T)$. They concluded that there was no evidence for the formation of the CH_3OOCH_3. The kinetics of this reaction have been studied by using UV absorption following pulsed photolytic production of the radicals. Tyndall et al. used the values of k/σ measured by a large number of groups along with the σ values from their evaluation to calculate k. (σ is the absorption cross section of the radical at the wavelength at which it was monitored.) They only used the kinetics data obtained at wavelengths larger than 240 nm, since the absorption by HO_2 radicals that are unavoidably produced in these measurements can significantly contribute to the measured UV profiles at shorter wavelengths. They noted that the values of k/σ measured by various groups were much more accurate than the values of σ measured by the same groups. The value of k obtained by this method was then

corrected using the above branching ratio for the production of CH_3O that leads to the unavoidable occurrence of the $CH_3O_2 + HO_2$ side reaction; this side reaction consumes another CH_3O_2 radical. The uncertainties of both k(298 K) and E/R are those presented in Tyndall et al.
(Table: 02-25, Note: 02-25, Evaluated: 02-25) Back to Table

(1) Tyndall, G. S.; Cox, R. A.; Granier, C.; Lesclaux, R.; Moortgat, G. K.; Pilling, M. J.; Ravishankara, A. R.; Wallington, T. J. Atmospheric chemistry of small organic peroxy radicals. *J. Geophys. Res.* **2001**, *106*, 12157-12182, doi:10.1029/2000JD900746.

D69. CH_3O_2 + NO. This recommendation is taken from the evaluated review of Tyndall et al.[1] They evaluated the available information to deduce that the main set of products under atmospheric conditions is $CH_3O + NO_2$. They noted, however, that a very small yield, <0.5%, of CH_3ONO_2 is also possible. The rate coefficient for the reaction at 298 K and its temperature dependence is based on numerous direct studies of this reaction that have been reported. The uncertainties of both k(298 K) and E/R are those presented in Tyndall et al.
(Table: 02-25, Note: 02-25, Evaluated: 02-25) Back to Table

(1) Tyndall, G. S.; Cox, R. A.; Granier, C.; Lesclaux, R.; Moortgat, G. K.; Pilling, M. J.; Ravishankara, A. R.; Wallington, T. J. Atmospheric chemistry of small organic peroxy radicals. *J. Geophys. Res.* **2001**, *106*, 12157-12182, doi:10.1029/2000JD900746.

D70. $CH_3O_2 + CH_3C(O)O_2$. This recommendation is taken from the evaluated review of Tyndall et al.[2] This reaction has two sets of products:

$$CH_3C(O)O_2 + CH_3O_2 \rightarrow CH_3 + CO_2 + CH_3O + O_2 \quad (a)$$

$$CH_3C(O)O_2 + CH_3O_2 \rightarrow CH_3C(O)OH + HCHO + O_2 \quad (b)$$

Tyndall et al. reanalyzed the previously available data on the branching ratios for this reaction and concluded that the branching ratio for channel (a) was $k_a/k = 0.9 \pm 0.1$ and $k_b/k = 0.1 \pm 0.1$ at 298 K. They also concluded that branching ratios could not be derived for other temperatures from the existing data and therefore did not make a recommendation for the temperature dependence. The recommendation from Tyndall et al. is based on the work of Roehl et al.[1] and Villenave et al.[3] Their recommended temperature dependence for the overall rate coefficient is based on analogy with other RO_2 reactions. The uncertainties of both k(298 K) and E/R are those presented in Tyndall et al.
(Table: 02-25, Note: 02-25, Evaluated: 02-25) Back to Table

(1) Roehl, C. M.; Bauer, D.; Moortgat, G. K. Absorption spectrum and kinetics of the acetylperoxy radical. *J. Phys. Chem.* **1996**, *100*, 4038-4047, doi:10.1021/jp9526298.
(2) Tyndall, G. S.; Cox, R. A.; Granier, C.; Lesclaux, R.; Moortgat, G. K.; Pilling, M. J.; Ravishankara, A. R.; Wallington, T. J. Atmospheric chemistry of small organic peroxy radicals. *J. Geophys. Res.* **2001**, *106*, 12157-12182, doi:10.1029/2000JD900746.
(3) Villenave, E.; Lesclaux, R. Kinetics of the cross reactions of CH_3O_2 and $C_2H_5O_2$ radicals with selected peroxy radicals. *J. Phys. Chem.* **1996**, *100*, 14372-14382, doi:10.1021/jp960765m.

D71. $CH_3O_2 + CH_3C(O)CH_2O_2$. This recommendation is taken from the evaluated review of Tyndall et al.[3] This reaction has three possible sets of products:

$$CH_3C(O)CH_2O_2 + CH_3O_2 \rightarrow CH_3C(O) + HCHO + CH_3O + O_2 \quad (a)$$

$$CH_3C(O)CH_2O_2 + CH_3O_2 \rightarrow CH_3C(O)CH_2OH + HCHO + O_2 \quad (b)$$

$$CH_3C(O)CH_2O_2 + CH_3O_2 \rightarrow CH_3C(O)CHO + CH_3OH + O_2 \quad (c)$$

The branching ratios for these channels, $k_a/k = 0.3 \pm 0.1$, $k_b/k = 0.2 \pm 0.1$, and $k_c/k = 0.5 \pm 0.1$, are based on the work of Bridier et al.[1] and Jenkin et al.[2] The overall rate coefficient for this reaction has been studied only at 298 K by Bridier et al. and the recommendation is based on this value. The recommended values of E/R and g are based on analogy with other RO_2 reactions. The uncertainties of both k(298 K) and E/R are those presented in Tyndall et al.
(Table: 02-25, Note: 02-25, Evaluated: 02-25) Back to Table

(1) Bridier, I.; Veyret, B.; Lesclaux, R.; Jenkin, M. E. Flash photolysis study of the UV spectrum and kinetics of reactions of the acetonylperoxy radical. *J. Chem. Soc. Faraday Trans.* **1993**, *89*, 2993-2997, doi:10.1039/ft9938902993.
(2) Jenkin, M. E.; Cox, R. A.; Emrich, M.; Moortgat, G. K. Mechanisms of the Cl-atom-initiated oxidation of acetone and hydroxyacetone in air. *J. Chem. Soc. Faraday Trans.* **1993**, *89*, 2983-2991, doi:10.1039/ft9938902983.

(3) Tyndall, G. S.; Cox, R. A.; Granier, C.; Lesclaux, R.; Moortgat, G. K.; Pilling, M. J.; Ravishankara, A. R.; Wallington, T. J. Atmospheric chemistry of small organic peroxy radicals. *J. Geophys. Res.* **2001**, *106*, 12157-12182, doi:10.1029/2000JD900746.

D72. **$C_2H_5 + O_2$.** This is a complex reaction that involves the formation of a $C_2H_5O_2$ adduct, which can either be stabilized by collisions or fall apart to HO_2 and C_2H_4 (Wagner et al.,[3] Bozzelli and Dean,[1] and Kaiser et al.[2]). The fraction of the energized adducts that fall apart to give HO_2 and C_2H_4 will decrease with increasing pressure and decreasing temperature, i.e., as the $C_2H_5O_2$ formation increases. The C_2H_4-formation channel cannot be separated from the addition reaction. We recommend a conservative upper limit as a guide to the extent of this reaction. This upper limit is applicable only for lower atmospheric pressure and temperature conditions. (Table: 94-26, Note: 94-26, Evaluated: 94-26) Back to Table

(1) Bozzelli, J. W.; Dean, A. M. Chemical activation analysis of the reaction of C_2H_5 with O_2. *J. Phys. Chem.* **1990**, *94*, 3313-3317, doi:10.1021/j100371a021.
(2) Kaiser, E. W.; Lorkovic, I. M.; Wallington, T. J. Pressure dependence of the C_2H_4 yield from the reaction $C_2H_5 + O_2$. *J. Phys. Chem.* **1990**, *94*, 3352-3354, doi:10.1021/j100371a030.
(3) Wagner, A. F.; Slagle, I. R.; Sarzynski, D.; Gutman, D. Experimental and theoretical studies of the $C_2H_5 + O_2$ reaction kinetics. *J. Phys. Chem.* **1990**, *94*, 1853-1868, doi:10.1021/j100368a026.

D73. **$C_2H_5O + O_2$.** The recommendation is based on the pulsed laser photolysis studies of Gutman et al.[1] and Hartmann et al.[2] In both these studies, removal of C_2H_5O in an excess of O_2 was directly monitored via laser induced fluorescence. Gutman et al. measured k at 296 and 353 K, while Hartmann et al. measured k at 5 temperatures between 295 and 411 K. The E/R is from Hartmann et al. The 298 K value deduced from an indirect study by Zabarnick and Heicklen[3] is in reasonable agreement with the recommended value. (Table: 92-20, Note: 92-20, Evaluated: 92-20) Back to Table

(1) Gutman, D.; Sanders, N.; Butler, J. E. Kinetics of the reactions of methoxy and ethoxy radicals with oxygen. *J. Phys. Chem.* **1982**, *86*, 66-70, doi:10.1021/j100390a013.
(2) Hartmann, D.; Karthäuser, J.; Sawerysyn, J. P.; Zellner, R. Kinetics and HO_2 yield of the reaction $C_2H_5O + O_2$ between 295 and 411 K. *Ber. Bunsenges. Phys. Chem.* **1990**, *94*, 639-645, doi:10.1002/bbpc.19900940604.
(3) Zabarnick, S.; Heicklen, J. Reactions of alkoxy radicals with O_2. I. C_2H_5O radicals. *Int. J. Chem. Kinet.* **1985**, *17*, 455-476, doi:10.1002/kin.550170502.

D74. **$C_2H_5O_2 + C_2H_5O_2$.** k(298 K) has been studied by Adachi et al.,[1] Anastasi et al.,[3] Munk et al.,[8] Cattell et al.,[5] Anastasi et al.,[2] Wallington et al.,[10] Bauer et al.,[4] and Fenter et al.[6] All the above determinations used UV absorption to monitor $C_2H_5O_2$ and hence measured k/σ, where σ is the absorption cross section of $C_2H_5O_2$ at the monitoring wavelength. These investigators also measured the σ that was used in evaluating the rate coefficient. There are large discrepancies in the measured values of σ. For this evaluation, we have used the cross sections recommended here and recalculated the values of k from each investigation. The recommended k is based on the results of Cattell et al., Wallington et al., Bauer et al., and Fenter et al. In all these experiments, the observed rate coefficient is higher than the true rate coefficient because of secondary reactions involving HO_2. HO_2 is formed by the reaction of CH_3CH_2O with O_2 and it reacts with $C_2H_5O_2$ to enhance the observed rate coefficient (see Wallington et al.[11] or Lightfoot et al.[7] for further discussion). Based on product branching ratios discussed below, which determine the magnitude of the necessary correction, the recommended rate coefficient is 0.6 times the average observed rate coefficient. The recommended E/R was obtained from the results of Anastasi et al., Wallington et al.[10] (228–380 K), Cattell et al. (266–348 K), Bauer et al. (218–333 K), and Fenter et al. (248–460 K). The observed products (Niki et al.[9]), suggest that at 298 K the channel to yield 2 $C_2H_5O + O_2$ accounts for about 60% of the reaction; the channel to yield $CH_3CHO + C_2H_5OH + O_2$ accounts for about 40% of the reaction; and the channel to yield $C_2H_5O_2C_2H_5 + O_2$ accounts for less than 5% of the reaction. These branching ratios were used to obtain the true rate coefficient from the observed rate coefficient. (Table: 94-26, Note: 94-26, Evaluated: 94-26) Back to Table

(1) Adachi, H.; Basco, N.; James, D. G. L. The ethylperoxy radical spectrum and rate constant for mutual interaction measured by flash photolysis and kinetic spectroscopy. *Int. J. Chem. Kinet.* **1979**, *11*, 1211-1229, doi:10.1002/kin.550111107.
(2) Anastasi, C.; Brown, M. J.; Smith, D. B.; Waddington, D. J. Joint French and Italian sections of the Combustion Institute, 1987, Amalfi, Italy.
(3) Anastasi, C.; Waddington, D. J.; Woolley, A. Reactions of oxygenated radicals in the gas phase Part 10.-Self-reactions of ethylperoxy radicals. *J. Chem. Soc. Faraday Trans. 1* **1983**, *79*, 505-516, doi:10.1039/f19837900505.

(4) Bauer, D.; Crowley, J. N.; Moortgat, G. K. The UV absorption spectrum of the ethylperoxy radical and its self-reaction kinetics between 218 and 333 K. *J. Photochem. Photobiol. A: Chem.* **1992**, *65*, 329-344, doi:10.1016/1010-6030(92)80015-N.
(5) Cattell, F. C.; Cavanagh, J.; Cox, R. A.; Jenkin, M. E. A kinetics study of reactions of HO_2 and $C_2H_5O_2$ using diode laser absorption spectroscopy. *J. Chem. Soc. Faraday Trans. 2* **1986**, *82*, 1999-2018, doi:10.1039/f29868201999.
(6) Fenter, F. F.; Catoire, V.; Lesclaux, R.; Lightfoot, P. D. The ethylperoxy radical: Its ultraviolet spectrum, self-reaction, and reaction with HO_2, each studied as a function of temperature. *J. Phys. Chem.* **1993**, *97*, 3530-3538, doi:10.1021/j100116a016.
(7) Lightfoot, P. D.; Cox, R. A.; Crowley, J. N.; Destriau, M.; Hayman, G. D.; Jenkin, M. E.; Moortgat, G. K.; Zabel, F. Organic peroxy radicals: Kinetics, spectroscopy and tropospheric chemistry. *Atmos. Environ.* **1992**, *26A*, 1805-1961, doi:10.1016/0960-1686(92)90423-I.
(8) Munk, J.; Pagsberg, P.; Ratajczak, E.; Sillesen, A. Spectrokinetic studies of ethyl and ethylperoxy radicals. *J. Phys. Chem.* **1986**, *90*, 2752-2757, doi:10.1021/j100403a038.
(9) Niki, H.; Maker, P. D.; Savage, C. M.; Breitenbach, L. P. Fourier transform infrared studies of the self-reaction of $C_2H_5O_2$ radicals. *J. Phys. Chem.* **1982**, *86*, 3825-3829, doi:10.1021/j100216a023.
(10) Wallington, T. J.; Dagaut, P.; Kurylo, M. J. Measurements of the gas phase UV absorption spectrum of $C_2H_5O_2$• radicals and of the temperature dependence of the rate constant for their self-reaction. *J. Photochem. Photobiol. A: Chem.* **1988**, *42*, 173-185, doi:10.1016/1010-6030(88)80061-3.
(11) Wallington, T. J.; Dagaut, P.; Kurylo, M. J. Ultraviolet absorption cross sections and reaction kinetics and mechanisms for peroxy radicals in the gas phase. *Chem. Rev.* **1992**, *92*, 667-710, doi:10.1021/cr00012a008.

D75. $C_2H_5O_2$ + NO. The recommended k(298 K) is obtained from the results of Plumb et al.,[6] Sehested et al.,[7] Daele et al.,[3] Eberhard and Howard,[4] and Maricq and Szente.[5] The value reported by Adachi and Basco,[1] which is a factor of three lower than the recommended value, was not used. The rate coefficient for the CH_3O_2 + NO reaction measured by Basco and co-workers (Adachi et al.[2]) using the same apparatus is also much lower than the value recommended here. The recommended temperature dependence is derived from Eberhardt and Howard[4] (207–403 K) and Maricq and Szente[5] (220–355 K), which are in good agreement.
(Table: 97-4, Note: 97-4, Evaluated: 97-4) Back to Table

(1) Adachi, H.; Basco, N. Kinetic spectroscopy study of the reaction of CH_3O_2 with NO. *Chem. Phys. Lett.* **1979**, *63*, 490-492, doi:10.1016/0009-2614(79)80696-X.
(2) Adachi, H.; Basco, N.; James, D. G. L. The ethylperoxy radical spectrum and rate constant for mutual interaction measured by flash photolysis and kinetic spectroscopy. *Int. J. Chem. Kinet.* **1979**, *11*, 1211-1229, doi:10.1002/kin.550111107.
(3) Daële, V.; Ray, A.; Vassalli, I.; Poulet, G.; Le Bras, G. Kinetic study of reactions of C_2H_5O and $C_2H_5O_2$ with NO at 298 K and 0.55 – 2 torr. *Int. J. Chem. Kinet.* **1995**, *27*, 1121-1133, doi:10.1002/kin.550271109.
(4) Eberhard, J.; Howard, C. J. Temperature-dependent kinetics studies of the reactions of $C_2H_5O_2$ and *n*-$C_3H_7O_2$ radicals with NO. *Int. J. Chem. Kinet.* **1996**, *28*, 731-740, doi:10.1002/(SICI)1097-4601(1996)28:10<731::AID-KIN3>3.0.CO;2-O.
(5) Maricq, M. M.; Szente, J. J. Kinetics of the reaction between ethylperoxy radicals and nitric oxide. *J. Phys. Chem.* **1996**, *100*, 12374-12379, doi:10.1021/jp9607935.
(6) Plumb, I. C.; Ryan, K. R.; Steven, J. R.; Mulcahy, M. F. R. Kinetics of the reaction of $C_2H_5O_2$ with NO at 295 K. *Int. J. Chem. Kinet.* **1982**, *14*, 183-194, doi:10.1002/kin.550140208.
(7) Sehested, J.; Nielsen, O. J.; Wallington, T. J. Absolute rate constants for the reaction of NO with a series of peroxy radicals in the gas phase at 295 K. *Chem. Phys. Lett.* **1993**, *213*, 457-464, doi:10.1016/0009-2614(93)89142-5.

D76. $CH_3C(O)O_2$ + $CH_3C(O)O_2$. This reaction has been studied by Addison et al.,[1] Basco and Parmar,[3] Moortgat et al.,[5] Maricq and Szente,[4] and Roehl et al.,[6] using UV absorption techniques and by Assali and Fittschen[2] used continuous-wave cavity ring-down spectroscopy (cw-CRDS) in the near-infrared. All studies have to use complex modelling of secondary chemistry to retrieve the self-reaction rate coefficient. The early studies using UV detection also need to account for the overlap of the UV absorptions due to acetylperoxy, methylperoxy, and hydroperoxy radicals. The recommended value is obtained from the data of Assali and Fittschen, Moortgat et al., Maricq and Szente, and Roehl et al. As pointed out by Moortgat et al., the six times lower value of k obtained by Addison et al. is likely due to the use of incorrect UV absorption cross sections for the peroxy radical. The k obtained by Basco and Parmar is ~2 times lower than the recommended value. This discrepancy is possibly due to neglecting the UV absorption of CH_3O_2 and other stable products in their data analysis. Moortgat et al. and Maricq and Szente studied the rate coefficient over the temperature range 253–368 K and

209–358 K respectively. The temperature dependence of both studies are in good agreement and the E/R is taken from a fit to both sets of data with the A-factor being adjusted to reproduce k(298 K). Addison et al. reported the formation of O_3, which was attributed to the reaction channel that produces $CH_3C(O)OCH_3C(O) + O_3$. Moortgat et al. place an upper limit of 2% for this channel. The main products of this reaction appear to be $CH_3C(O)O + O_2$. The $CH_3C(O)O$ radicals rapidly decompose to give CH_3 and CO_2.
(Table: 25-01, Note: 25-01, Evaluated: 25-01) Back to Table

(1) Addison, M. C.; Burrows, J. P.; Cox, R. A.; Patrick, R. Absorption spectrum and kinetics of the acetylperoxy radical. *Chem. Phys. Lett.* **1980**, *73*, 283-287, doi:10.1016/0009-2614(80)80373-3.
(2) Assali, M.; Fittschen, C. Rate constants and branching ratios for the self-reaction of acetyl peroxy ($CH_3C(O)O_2^{\bullet}$) and Its reaction with CH_3O_2. *Atmos.* **2022**, *13*, 186, doi:10.3390/atmos13020186.
(3) Basco, N.; Parmar, S. S. Spectra and reactions of acetyl and acetylperoxy radicals. *Int. J. Chem. Kinet.* **1985**, *17*, 891-900, doi:10.1002/kin.550170809.
(4) Maricq, M. M.; Szente, J. J. The $CH_3C(O)O_2$ radical. Its UV spectrum, self-reaction kinetics, and reaction with CH_2O_2. *J. Phys. Chem.* **1996**, *100*, 45407-44513, doi:10.1021/jp9533234.
(5) Moortgat, G.; Veyret, B.; Lesclaux, R. Absorption spectrum and kinetics of reactions of the acetylperoxy radical. *J. Phys. Chem.* **1989**, *93*, 2362-2368, doi:10.1021/j100343a032.
(6) Roehl, C. M.; Bauer, D.; Moortgat, G. K. Absorption spectrum and kinetics of the acetylperoxy radical. *J. Phys. Chem.* **1996**, *100*, 4038-4047, doi:10.1021/jp9526298.

D77. $CH_3C(O)O_2$ + NO. This recommendation is from Tyndall et al.[1] These authors have argued that the only set of products of importance in the atmosphere is the production of $CH_3 + CO_2 + NO_2$. This is because the alkoxy radical produced upon O abstraction from the peroxy radical by NO will be unstable towards decomposition to give CH_3 and CO_2. The rate coefficient for the reaction was deduced primarily from direct studies, but was found to be consistent with the relative rate studies. In the relative rate studies, this rate coefficient was measured relative to the rate coefficient for the reaction of $CH_3C(O)O_2$ with NO_2.
(Table: 02-25, Note: 10-6, Evaluated: 10-6) Back to Table

(1) Tyndall, G. S.; Cox, R. A.; Granier, C.; Lesclaux, R.; Moortgat, G. K.; Pilling, M. J.; Ravishankara, A. R.; Wallington, T. J. Atmospheric chemistry of small organic peroxy radicals. *J. Geophys. Res.* **2001**, *106*, 12157-12182, doi:10.1029/2000JD900746.

D78. $CH_3C(O)CH_2O_2$ + NO. This recommendation is from Tyndall et al.[4] They deduced, based on the results of Sehested et al.,[3] Jenkin et al.,[1] and Orlando et al.,[2] that the products of this reaction are $CH_3C(O)CH_2O + NO_2$. The $CH_3C(O)CH_2O$ radical decomposes rapidly to give $CH_3C(O) + CH_2O$. The only kinetics study of this reaction by Sehested et al. forms the basis for the rate coefficient at 298 K. This value is uncertain because of the corrections that had to be made in the study of Sehested et al. to account for the production of NO_2, the monitored species, via the reaction of peroxy radicals (such as $CH_3C(O)O_2$ and CH_3O_2) with NO. The temperature dependence of the reaction is derived based on analogy with other peroxy radical reactions.
(Table: 02-25, Note: 02-25, Evaluated: 02-25) Back to Table

(1) Jenkin, M. E.; Cox, R. A.; Emrich, M.; Moortgat, G. K. Mechanisms of the Cl-atom-initiated oxidation of acetone and hydroxyacetone in air. *J. Chem. Soc. Faraday Trans.* **1993**, *89*, 2983-2991, doi:10.1039/ft9938902983.
(2) Orlando, J. J.; Tyndall, G. S.; Vereecken, L.; Peeters, J. The atmospheric chemistry of the acetonoxy radical. *J. Phys. Chem. A* **2000**, *104*, 11578-11588, doi:10.1021/jp0026991.
(3) Sehested, J.; Christensen, L. K.; Nielsen, O. J.; Bilde, M.; Wallington, T. J.; Schneider, W. F.; Orlando, J. J.; Tyndall, G. S. Atmospheric chemistry of acetone: Kinetic study of the $CH_3C(O)CH_2O_2$ + NO/ NO_2 reactions and decomposition of $CH_3C(O)CH_2O_2NO_2$. *Int. J. Chem. Kinet.* **1998**, *30*, 475-489, doi:10.1002/(SICI)1097-4601(1998)30:7<475::AID-KIN4>3.0.CO;2-P.
(4) Tyndall, G. S.; Cox, R. A.; Granier, C.; Lesclaux, R.; Moortgat, G. K.; Pilling, M. J.; Ravishankara, A. R.; Wallington, T. J. Atmospheric chemistry of small organic peroxy radicals. *J. Geophys. Res.* **2001**, *106*, 12157-12182, doi:10.1029/2000JD900746.

D79. $HOC_5H_8O_2$ + NO. This reaction has been the subject of a number of studies due to its potential importance, particularly in the branching to and fate of $RONO_2$, in controlling NO_x lifetime (and thus O_3 production) in the lower terrestrial atmosphere in regions with high isoprene emissions. Six isomers of $HOC_5H_8O_2$ have been shown to form from reactions of OH and O_2 with isoprene. These isomers interconvert on timescales shorter than their lifetime in the atmosphere (see Note for isoprene + OH reaction). The recommendations provided here are bulk averages for the RO_2 distribution at short RO_2 lifetimes, i.e., the RO_2 distribution formed near the kinetic limit of $HOC_5H_8 + O_2$, as the majority of the experimental data are for conditions near this limit and are not isomer resolved.

Total rate coefficient: The recommendation for the overall rate coefficient is taken as the average of the Stevens et al.,[15] Chuong and Stevens,[2] Zhang et al.,[19] Miller et al.,[8] Park et al.,[9] and Ghosh et al.[6] studies. With the exception of the result from Reitz et al,[13] there is good agreement among the experimental determinations. The Reitz et al.[13] result is not in agreement with that of Zhang et al.[19] from the same group, using a different method, and it is stated in Zhang et al.[19] "…ongoing OH cycling studies in the North group have obtained a rate constant of less than the value reported by Reitz et al. …" Therefore, the result of Reitz et al.[13] is not included in the recommendation. From a lack of pressure dependence in k_{total} over experimental conditions (1.3–200 hPa), it is clear that the total reaction rate coefficient is in the high-pressure limit for reactions occurring in the atmosphere. As only room temperature results for this reaction have been reported, the temperature dependence E/R of –350 K is estimated from measurements of $CH_3CH_2CH_2O_2$[3,4] and $CH_3CH(O_2)CH_3$[5] peroxy radicals reacting with NO, and the observed invariance of the total RO_2 + NO rate coefficient for a number of RO_2.[8] The A-factor is calculated from the recommended 298 K rate coefficient and the estimated E/R. A high uncertainty has been assigned to the temperature dependence due to the estimation methods.

Reaction branching to $RONO_2$ ($k_2/(k_{total})$): In contrast to the good agreement between determinations for the total rate coefficient for $HOC_5H_8O_2$ with NO, reports of the branching fraction to stabilized $RONO_2$ are quite varied, ranging from 0.044 to 0.14 for conditions near room temperature and 1 atmosphere. The recommendation for the branching fraction at 297 K in 993 hPa of air is based on the average of the results from Tuazon, et al.[17] (corrected for $O(^3P)$ chemistry, see Paulson et al.[12]), Sprengnether, et al.,[14] and Teng et al.[16]:

$$k_2/k_{total}\ (297\ K,\ 993\ hPa) = 0.13 \pm 0.04$$

The branching fraction from Xiong et al.,[18] falls within the uncertainty of the recommendation, but is not used in the recommendation due to its dependence on the assumed (calculated) isoprene RO_2 isomer distribution. In addition, results from Chen et al.[1] and Lockwood, et al.[7] are not used to arrive at a recommendation as these results are superseded by the study of Xiong et al.[18] from the same group. It is stated in Xiong et al.[18]: "Previous IN studies conducted in our group using GC methods consistently resulted in lower IN yields (Chen et al.[1]; Lockwood et al.[7]). We partially attribute the discrepancy of our previous and current work to the possible loss of the 1,2-IN isomer in the GC column and metal sample injection system." Data reported by Paulot et al.[11] are consistent with the recommendation, but not used as this result was not based on authentic $RONO_2$ standards. Additional data at reduced pressures from Sprengnether et al.,[14] Chuong and Stevens,[2] and Patchen et al.[10] are not used at this time as there are not sufficient data to recommend the pressure dependence of the branching fraction for this reaction. However, based on studies of similar reactions it is expected that the pressure and temperature variation of the branching fraction for this reaction is significant for atmospheric conditions, and further study is required for evaluation of these parameters.
(Table: 19-5, Note: 19-5, Evaluated: 19-5) Back to Table

(1) Chen, X.; Hulbert, D.; Shepson, P. B. Measurement of the organic nitrate yield from OH reaction with isoprene. *J. Geophys. Res.* **1998**, *103*, 25563-25568, doi:10.1029/98jd01483.

(2) Chuong, B.; Stevens, P. S. Measurements of the kinetics of the OH-initiated oxidation of isoprene. *J. Geophys. Res.* **2002**, *107*, 4162, doi:10.1029/2001JD000865.

(3) Eberhard, J.; Howard, C. J. Temperature-dependent kinetics studies of the reactions of $C_2H_5O_2$ and *n*-$C_3H_7O_2$ radicals with NO. *Int. J. Chem. Kinet.* **1996**, *28*, 731-740, doi:10.1002/(SICI)1097-4601(1996)28:10<731::AID-KIN3>3.0.CO;2-O.

(4) Eberhard, J.; Howard, C. J. Rate coefficients for the reactions of some C_3 to C_5 hydrocarbon peroxy radicals with NO. *J. Phys. Chem. A* **1997**, *101*, 3360-3366, doi:10.1021/jp9640282.

(5) Eberhard, J.; Villalta, P. W.; Howard, C. J. Reaction of isopropyl peroxy radicals with NO over the temperature range 201-401 K. *J. Phys. Chem.* **1996**, *100*, 993-997, doi:10.1021/jp951824j.

(6) Ghosh, B.; Bugarin, A.; Connell, B. T.; North, S. W. Isomer-selective study of the OH-initiated oxidation of isoprene in the presence of O_2 and NO: 2. The major OH addition channel. *J. Phys. Chem. A* **2010**, *114*, 2553-2560, doi:10.1021/jp909052t.

(7) Lockwood, A. L.; Shepson, P. B.; Fiddler, M. N.; Alaghmand, M. Isoprene nitrates: preperation, seperation, identification, yields, and atmospheric chemistry. *Atmos. Chem. Phys.* **2010**, *10*, 6169-6178, doi:10.5194/acp-10-6169-2010.

(8) Miller, A. M.; Yeung, L. Y.; Kiep, A. C.; Elrod, M. J. Overall rate constant measurements of the reactions of alkene-derived hydroxyalkylperoxy radicals with nitric oxide. *Phys. Chem. Chem. Phys.* **2004**, *6*, 3402-3407, doi:10.1039/b402110j.

(9) Park, J.; Jongsma, C. G.; Zhang, R.; North, S. W. OH/OD initiated oxidation of isoprene in the presence of O_2 and NO. *J. Phys. Chem. A* **2004**, *108*, 10688-10697, doi:10.1021/jp040421t.

(10) Patchen, A. K.; Pennino, M. J.; Kiep, A. C.; Elrod, M. J. Direct kinetic study of the product-forming channels of the reaction of isoprene-derived hydroxyperoxy radicals with NO. *Int. J. Chem. Kinet.* **2007**, *39*, 353-361, doi:10.1002/kin.20248.
(11) Paulot, F.; Crounse, J. D.; Kjaergaard, H. G.; Kroll, J. H.; Seinfeld, J. H.; Wennberg, P. O. Isoprene photoxidation: new insights into the production of acids and organic nitrates. *Atmos. Chem. Phys.* **2009**, *9*, 1479-1501, doi:10.5194/acp-9-1479-2009.
(12) Paulson, S. E.; Flagan, R. C.; Seinfeld, J. H. Atmospheric photoxidation of isoprene Part I: The hydroxyl radical and ground state atomic oxygen reactions. *Int. J. Chem. Kinet.* **1992**, *24*, 79-101, doi:10.1002/kin.550240109.
(13) Reitz, J. E.; McGivern, W. S.; Church, M. C.; Wilson, M. D.; North, S. W. The fate of the hydroxyalkoxy radical in the OH-initiated oxidation of isoprene. *Int. J. Chem. Kinet.* **2002**, *34*, 255-261, doi:10.1002/kin.10050.
(14) Sprengnether, M.; Demerjian, K. L.; Donahue, N. M.; Anderson, J. G. Product analysis of the OH oxidation of isoprene and 1,3-butadiene in the presence of NO. *J. Geophys. Res.* **2002**, *107*, 4268, doi:10.1029/2001JD000716.
(15) Stevens, P.; L'Esperance, D.; Chuong, B.; Martin, G. Measurements of the kinetics of the OH-initiated oxidation of isoprene: Radical propogation in the OH + isoprene + O_2 + NO reaction system. *Int. J. Chem. Kinet.* **1999**, *31*, 637-643, doi:10.1002/(SICI)1097-4601(1999)31:9<637::AID-KIN5>3.0.CO;2-O.
(16) Teng, A. P.; Crounse, J. D.; Wennberg, P. O. Isoprene peroxy radical dynamics. *J. Am. Chem. Soc.* **2017**, *139*, 5367-5377, doi:10.1021/jacs.6b12838.
(17) Tuazon, E. C.; Atkinson, R. A product study of the gas-phase reaction of isoprene with the OH radical in the presence of NO_x. *Int. J. Chem. Kinet.* **1990**, *22*, 1221-1236, doi:10.1002/kin.550221202.
(18) Xiong, F.; McAvey, K. M.; Pratt, K. A.; Groff, C. J.; Hostetler, M. A.; Lipton, M. A.; Starn, T. K.; Seeley, J. V.; Bertman, S. B.; Teng, A. P.; Crounse, J. D.; Nguyen, T. B.; Wennberg, P. O.; Misztal, P. K.; Goldstein, A. H.; Guenther, A. B.; Koss, A. R.; Olson, K. F.; de Gouw, J. A.; Baumann, K.; Edgerton, E. S.; Feiner, P. A.; Zhang, L.; Miller, D. O.; Brune, W. H.; Shepson, P. B. Observation of isoprene hydroxynitrates in the southeastern United States and implications for the fate of NO_x. *Atmos. Chem. Phys.* **2015**, *15*, 11257-11272, doi:10.5194/acp-15-11257-2015.
(19) Zhang, D.; Zhang, R.; North, S. W. Experimental study of NO reaction with isoprene hydroxyalkyl peroxy radicals. *J. Phys. Chem. A* **2003**, *107*, 11013-11019, doi:10.1021/jp0360016.

D80. CH_2OO → products. Berndt et al.[1] generated CH_2OO from the ozonolysis of ethene in an atmospheric pressure flow tube and detected the CH_2OO via the titration of CH_2OO with SO_2 to produce sulfuric acid, which is detected via PTRMS found (0.19 ± 0.07) s^{-1}. The most complete study of the unimolecular decay of CH_2OO has been carried out by Stone et al.[2] who used a combination of time resolved cavity enhanced broadband UV absorption spectroscopy, for direct monitoring of CH_2OO, and laser induced fluorescence, for monitoring of OH decomposition products to study the decomposition between 450 and 650 K and pressures in the range of 2–350 Torr. They found that $k_0 = 3.2 \times 10^{-4} (T/298)^{-5.81} \exp(-12770/T)$ cm^3 s^{-1}, $k_\infty = 1.4 \times 10^{13} (T/298)^{0.06} \exp(-10010/T)$ s^{-1} and $F_c = 0.447$. This corresponds to a unimolecular decay of $k_1 = 1.1 \times 10^{-3}$ s^{-1}in Helium at 760 Torr and 298 K and they report a decay of $k_1 = 8.6 \times 10^{-3}$ s^{-1}in N_2 at 760 Torr and 298 K. Berndt et al. report a somewhat faster rate coefficient than those obtained by Stone et al. Berndt et al. employed the highly exothermic $C_2H_4 + O_3$ to generate CH_2OO suggesting that the reactions of non-thermalized CH_2OO could impact the kinetic results. Stone et al. could not observe a radical loss that could be unequivocally assigned to the unimolecular decay of CH_2OO at atmospheric temperatures, so we are unable to make a recommendation at this point.
(Table: 19-5, Note: 19-5, Evaluated: 19-5) Back to Table

(1) Berndt, T.; Kaethner, R.; Voigtlander, J.; Stratmann, F.; Pfeifle, M.; Reichle, P.; Sipila, M.; Kulmala, M.; Olzmann, M. Kinetics of the unimolecular reaction of CH_2OO and the bimolecular reactions with the water monomer, acetaldehyde and acetone under atmospheric conditions. *Phys. Chem. Chem. Phys.* **2015**, *17*, 19862-19873, doi:10.1039/C5CP02224J.
(2) Stone, D.; Au, K.; Sime, S.; Medeiros, D. J.; Blitz, M.; Seakins, P. W.; Decker, Z.; Sheps, L. Unimolecular decomposition kinetics of the stabilised Criegee intermediates CH_2OO and CD_2OO. *Phys. Chem. Chem. Phys.* **2018**, *20*, 24940-24954, doi:10.1039/C8CP05332D.

D81. $CH_3OO + O_3$. There are two direct kinetic studies of the reaction of CH_2OO with ozone in the literature, both utilizing laser flash photolysis of CH_2I_2/O_2. The first measurement was reported by Chang et al.,[1] who monitored CH_2OO in via mid-infrared absorption spectroscopy using the chirped pulse output of a QCL in experiments performed at 298 K and 30–100 Torr (O_2 bath gas). More recently, Onel et al.[3] utilized broadband UV-Vis absorption spectroscopy at 296 K, 300 Torr (N_2 bath gas), in which the full spectra between 300-450

nm were fit to obtain the time evolution of CH_2I_2, CH_2OO, and IO. There is a substantial difference in the two reported rate coefficients, with the value of Onel et al. being around a factor of 5 greater. Onel et al. attribute this difference to how the two studies treat the side reaction of CH_2OO + IO: Onel et al. directly measure IO, which enables them to extract a rate coefficient for CH_2OO + IO, alongside CH_2OO + O_3, from fits to the CH_2OO time profiles. Chang et al. are unable to directly detect IO in their system and thus utilize a combination of experiments in which the initial concentration of CH_2OO is varied, and kinetic simulations of their data to estimate the CH_2OO + IO rate coefficient, which is a factor of 2 slower than the value later reported by Onel et al. Through constraining the kinetic fits to their data, Onel et al. find that overestimation of the rate coefficient for CH_2OO + IO leads to an underestimation in the CH_2OO + O_3 rate coefficient, in accord with the discrepancy between the two datasets. The recommend value is taken from Onel et al.

Neither experiment reports on the reaction products, However, theoretical studies by Wei et al.,[6] Kjaergaard et al.,[2] and Vereecken et al.[4,5] agree that the dominant products are CH_2O + $2O_2$. Interestingly, Vereecken finds that the mechanism proceeds via oxygen scrambling between the CH_2OO and O_3 co-reactants. Kjaergaard et al. provide only a lower limit to the rate coefficient (10^{-18} cm^3 $molecule^{-1}$ s^{-1}). The predictions of Vereecken et al. at room temperature are ~five orders of magnitude faster, and in accord with the measurements of Onel et al. Vereecken predicts a modest negative temperature dependence (250–250 K).
(Table: 25-1, Note: 25-1, Evaluated: 25-1) Back to Table

(1) Chang, Y.-P.; Chang, H.-H.; Lin, J. J.-M. Kinetics of the simplest Criegee intermediate reaction with ozone studied using a mid-infrared quantum cascade laser spectrometer. *Phys. Chem. Chem. Phys.* **2018**, *20*, 97-102, doi:10.1039/c7cp06653h.

(2) Kjaergaard, H. G.; Kurtén, T.; Nielsen, L. B.; Jørgensen, S.; Wennberg, P. O. Criegee intermediates react with ozone. *J. Phys. Chem. Lett.* **2013**, *4*, 2525-2529, doi:10.1021/jz401205m.

(3) Onel, L.; Blitz, M.; Seakins, P.; Heard, D.; Stone, D. Kinetics of the gas phase reactions of the Criegee intermediate CH_2OO with O_3 and IO. *J. Phys. Chem. A* **2020**, *124*, 6287-6293, doi:10.1021/acs.jpca.0c04422.

(4) Vereecken, L.; Harder, H.; Novelli, A. The reactions of Criegee intermediates with alkenes, ozone, and carbonyl oxides. *Phys. Chem. Chem. Phys.* **2014**, *16*, 4039-4049, doi:10.1039/c3cp54514h.

(5) Vereecken, L.; Rickard, A.; Newland, M.; Bloss, W. Theoretical study of the reactions of Criegee intermediates with ozone, alkylhydroperoxides, and carbon monoxide. *Phys. Chem. Chem. Phys.* **2015**, *17*, 23847-23858, doi:10.1039/c5cp03862f.

(6) Wei, W.-m.; Zheng, R.-h.; Pan, Y.-l.; Wu, Y.-k.; Yang, F.; Hong, S. Ozone dissociation to oxygen affected by Criegee intermediate. *J. Phys. Chem. A* **2014**, *118*, 1644-1650, doi:10.1021/jp4121047.

D82. CH_2OO + H_2O → products. The recommendation is based on the results of Sheps et al.[11] and Berndt et al.[4] The recommendation is the average of the two rate coefficients with equal weighting given to the two methods. Berndt et al.[4] generated CH_2OO from the ozonolysis of ethene in an atmospheric pressure flow tube and detected the CH_2OO via the titration of CH_2OO with SO_2 to produce sulfuric acid, which is detected via PTRMS. Sheps et al. coupled CH_2OO production by UV laser flash photolysis of CH_2I_2/O_2 with either time-resolved MPIMS mass spectroscopic or UV spectroscopic monitoring of CH_2OO over the pressure range 30-100 Torr. They observe a well-defined quadratic dependence of the pseudo first-order CH_2OO decay rate coefficient on [H_2O], and obtained the recommended bimolecular rate coefficient by adding a linear term to the fit of decay coefficient as a function of [H_2O]. Chao et al.[5] also observed a well-defined quadratic dependence of the pseudo first-order CH_2OO decay rate coefficient on [H_2O], and obtained an upper limit bimolecular rate coefficient of $<1.5 \times 10^{-15}$ from estimation of the maximum possible contribution to the observed kinetics from a process whose pseudo first-order rate coefficient varied linearly as a function of [H_2O]. A similar experiment is reported by Lewis et al.,[6] but with more scatter in the data. A less sensitive upper limit is also reported by Welz et al.,[14] who observed no significant increase in the CH_2OO decay rate upon addition of up to 3×10^{16} H_2O per cm^3 to their reaction mixtures; Welz et al. produced CH_2OO in the same manner as Chao et al. and Lewis et al., but employed photoionization mass spectrometry as the CH_2OO detection technique and lower total pressures than the other studies. Theoretical work by Ryzhkov and Ariya[10] suggests that the CH_2OO + H_2O rate coefficient may be significantly slower than any of the experimental rate coefficients/upper limits. Experimental rate coefficients slower than the current recommendation are reported by Ouyang et al.[8] and Stone et al.[12] As discussed by Lewis et al., misinterpretation of complex chemical mechanisms are likely to have been a problem in the Ouyang et al. and Stone et al. studies; also, Chao et al. suggest that interferences to detected signals from reaction products could have been a problem in these studies. Suto et al.,[13] Newland et al.,[7] Becker et al.,[3] report significantly faster rate coefficients than those obtained in other studies based on competitive kinetics results with CH_2OO + SO_2 used as the reference reaction. Both Suto et al. and Becker et al. employed the highly exothermic C_2H_4 + O_3 reaction to generate CH_2OO, suggesting that reactions of non-thermalized CH_2OO could impact the competitive kinetics results. Also, the O_3 + C_2H_4 reaction is known to produce OH. Based on theoretical studies by Aplincourt and Ruiz-López,[2] Ryzhkov and Ariya,[9] and Anglada

et al.,[1] it is well-established that CH_2OO interacts with H_2O to form a hydrogen bonded complex that isomerizes rapidly to hydroxymethyl hydroperoxide (HMHP, $HOCH_2OOH$). HMHP is stable ~190 kJ mol^{-1} relative to $CH_2OO + H_2O$.
(Table: 19-5, Note: 19-5, Evaluated: 19-5) Back to Table

(1) Anglada, J. M.; González, J.; Torrent-Sucarrat, M. Effects of the substituents on the reactivity of carbonyl oxides. A theoretical study on the reaction of substituted carbonyl oxides with water. *Phys. Chem. Chem. Phys.* **2001**, *13*, 13034-13045, doi:10.1039/c1cp20872a.

(2) Aplincourt, P.; Ruiz-López, M. F. Theoretical investigation of reaction mechanisms for carboxylic acid formation in the atmosphere. *J. Am. Chem. Soc.* **2000**, *122*, 8990-8997, doi:10.1021/ja000731z.

(3) Becker, K. H.; Bechara, J.; Brockmann, K. J. Studies on the formation of H_2O_2 in the ozonolysis of alkenes. *Atmos. Environ.* **1993**, *27A*, 57-61, doi:10.1016/0960-1686(93)90070-F.

(4) Berndt, T.; Kaethner, R.; Voigtlander, J.; Stratmann, F.; Pfeifle, M.; Reichle, P.; Sipila, M.; Kulmala, M.; Olzmann, M. Kinetics of the unimolecular reaction of CH_2OO and the bimolecular reactions with the water monomer, acetaldehyde and acetone under atmospheric conditions. *Phys. Chem. Chem. Phys.* **2015**, *17*, 19862-19873, doi:10.1039/C5CP02224J.

(5) Chao, W.; Hsieh, J.-T.; Chang, C.-H.; Lin, J. J.-M. Direct kinetic measurement of the reaction of the simplest Criegee intermediate with water vapor. *Science* **2015**, *347*, 751-754, doi:10.1126/science.1261549.

(6) Lewis, T. R.; Blitz, M. A.; Heard, D. E.; Seakins, P. W. Direct evidence for a substantive reaction between the Criegee intermediate, CH_2OO, and the water vapour dimer. *Phys. Chem. Chem. Phys.* **2015**, *17*, 4859-4863, doi:10.1039/c4cp04750h.

(7) Newland, M. J.; Rickard, A. R.; Vereecken, L.; Muñoz, A.; Ródenas, M.; Bloss, W. J. Atmospheric isoprene ozonolysis: impacts of stabilised Criegee intermediate reactions with SO_2, H_2O and dimethyl sulfide. *Atmos. Chem. Phys.* **2015**, *15*, 9521-9536, doi:10.5194/acp-15-9521-2015.

(8) Ouyang, B.; McLeod, M. W.; Jones, R. L.; Bloss, W. J. NO_3 radical production from the reaction between the Criegee intermediate CH_2OO and NO_2. *Phys. Chem. Chem. Phys.* **2013**, *15*, 17070-17075, doi:10.1039/c3cp53024h.

(9) Ryzhkov, A. B.; Ariya, P. A. A theoretical study of the reactions of carbonyl oxide with water in atmosphere: the role of water dimer. *Chem. Phys. Lett.* **2003**, *367*, 423-429, doi:10.1016/S0009-2614(02)01685-8.

(10) Ryzhkov, A. B.; Ariya, P. A. A theoretical study of the reactions of parent and substituted Criegee intermediates with water and the water dimer. *Phys. Chem. Chem. Phys.* **2004**, *6*, 5042-5050, doi:10.1039/b408414d.

(11) Sheps, L.; Rotavera, B.; Eskola, A. J.; Osborn, D. L.; Taatjes, C. A.; Au, K.; Shallcross, D. E.; Khan, M. A. H.; Percival, C. J. The reaction of Criegee intermediate CH_2OO with water dimer: primary products and atmospheric impact. *Phys. Chem. Chem. Phys.* **2017**, *19*, 21970-21979, doi:10.1039/C7CP03265J.

(12) Stone, D.; Blitz, M.; Daubney, L.; Howes, N. U. M.; Seakins, P. Kinetics of CH_2OO reactions with SO_2, NO_2, NO, H_2O, and CH_3CHO as a function of pressure. *Phys. Chem. Chem. Phys.* **2014**, *16*, 1139-1149, doi:10.1039/c3cp54391a.

(13) Suto, M.; Manzanares, E. R.; Lee, L. C. Detection of sulfuric acid aerosols by ultraviolet scattering. *Environ. Sci. Technol.* **1985**, *19*, 815-820, doi:10.1021/es00139a008.

(14) Welz, O.; Savee, J. D.; Osborn, D. L.; Vasu, S. S.; Percival, C. J.; Shallcross, D. E.; Taatjes, C. A. Direct kinetic measurements of Criegee intermediate (CH_2OO) formed by reaction of CH_2I with O_2. *Science* **2012**, *335*, 204-207, doi:10.1126/science.1213229.

D83. $CH_2OO + (H_2O)_2$. The recommendation for k(298 K) is the average of the value reported by Chao et al.,[3] Sheps et al.,[8] and the value obtained from an Arrhenius expression describing the temperature dependent rate coefficients reported by Smith et al.[9] The Smith et al. study reports the only available temperature dependent data, so the recommended E/R is obtained from the Arrhenius fit to their data. As a result of the limited studies extrapolation of the experimental results to other temperatures is not recommended. All three studies produce CH_2OO by UV laser flash photolysis of CH_2I_2/O_2. Chao et al. and Smith et al. (same research group) utilize time-resolved UV spectroscopic monitoring of CH_2OO for kinetics, whereas Sheps et al., use a combination time-resolved MPIMS mass spectroscopic or UV spectroscopic monitoring of CH_2OO. All three studies well-defined quadratic dependence of the pseudo-first order CH_2OO decay rate coefficient on [H_2O], and the source

of information they used to obtain an equilibrium coefficient for 2 $H_2O \leftrightarrow (H_2O)_2$ is also the basis for the recommendation in Table 3 of this document.[7] A similar (to Chao et al., Smith et al. and Sheps et al.) experiment is reported by Lewis et al.,[5] but with more scatter in the data; these authors obtain a rate coefficient somewhat slower than the recommendation. Berndt et al.[2] report a somewhat faster rate coefficient than those obtained in the other studies based on competitive kinetics results with $CH_2OO + SO_2$ used as the reference reaction; these investigators employed the highly exothermic $C_2H_4 + O_3$ reaction to generate CH_2OO, suggesting that reactions of non-thermalized CH_2OO could impact the competitive kinetics results. Lewis et al. speculate that enhanced formation of $(H_2O)_2$ in the mass spectrometer sampling region could have been a problem in the Berndt et al. study. Unlike earlier studies that employed $O_3 + C_2H_4$ as the CH_2OO source,[1,10] Berndt et al. added propane to their reaction mixtures to scavenge OH radicals; this could explain why they observed a quadratic dependence of CH_2OO reactivity on $[H_2O]$ that was not observed in the earlier studies. The recommended uncertainty (f) is chosen so f^2 approximately brackets the results of the four experimental studies. The indirect study of Nguyen et al., report an approximate rate coefficient of $\sim 1 \times 10^{-12}$ cm^3 molecule^{-1} s^{-1}, which is in broad agreement with the direct studies. The theoretical work of Ryzhkov and Ariya,[6] shows that CH_2OO interacts with $(H_2O)_2$ to form hydrogen bonded ring complexes which isomerize rapidly to hydrogen bonded complexes of H_2O with hydroxymethyl hydroperoxide (HMHP, $HOCH_2OOH$) that are stable by ~190 kJ mol^{-1} relative to $CH_2OO + (H_2O)_2$; as discussed theoretically by Crehuet et al.,[4] these complexes can undergo unimolecular conversion to $HCOOH + 2\ H_2O$ or $H_2O_2 + H_2CO + H_2O$. Sheps et al., have quantified the branching ratio for the reaction using MPIMPS and found that $\Phi_3(CH_2O) = (40 \pm 10)\%$, $\Phi_3(HCOOH) < 10\%$ HMHP is then $(55 \pm 15)\%$. Theoretical analysis by Smith et al. confirms that the unusually large negative activation energy they observe experimentally is consistent with the mechanism described above.
(Table: 19-5, Note: 19-5, Evaluated: 19-5) Back to Table

(1) Becker, K. H.; Bechara, J.; Brockmann, K. J. Studies on the formation of H_2O_2 in the ozonolysis of alkenes. *Atmos. Environ.* **1993**, *27A*, 57-61, doi:10.1016/0960-1686(93)90070-F.

(2) Berndt, T.; Voightländer, J.; Stratmann, F.; Junninen, H.; Mauldin III, R. L.; Sipilä, M.; Kulmala, M.; Herrmann, H. Competing atmospheric reactions of CH_2OO with SO_2 and water vapour. *Phys. Chem. Chem. Phys.* **2014**, *16*, 19130-19136, doi:10.1039/c4cp02345e.

(3) Chao, W.; Hsieh, J.-T.; Chang, C.-H.; Lin, J. J.-M. Direct kinetic measurement of the reaction of the simplest Criegee intermediate with water vapor. *Science* **2015**, *347*, 751-754, doi:10.1126/science.1261549.

(4) Crehuet, R.; Anglada, J. M.; Bofill, J. M. Tropospheric formation of hydroxymethyl hydroperoxide, formic acid, H_2O_2, and OH from carbonyl oxide in the presence of water vapor: A theoretical study of the reaction mechanism. *Chem. Eur. J.* **2001**, *7*, 2227-2235, doi:10.1002/1521-3765(2001051817:10<2227::AID-CHEM2227>3.0.CO;2-O.

(5) Lewis, T. R.; Blitz, M. A.; Heard, D. E.; Seakins, P. W. Direct evidence for a substantive reaction between the Criegee intermediate, CH_2OO, and the water vapour dimer. *Phys. Chem. Chem. Phys.* **2015**, *17*, 4859-4863, doi:10.1039/c4cp04750h.

(6) Ryzhkov, A. B.; Ariya, P. A. A theoretical study of the reactions of carbonyl oxide with water in atmosphere: the role of water dimer. *Chem. Phys. Lett.* **2003**, *367*, 423-429, doi:10.1016/S0009-2614(02)01685-8.

(7) Ryzhkov, A. B.; Ariya, P. A. A theoretical study of the reactions of parent and substituted Criegee intermediates with water and the water dimer. *Phys. Chem. Chem. Phys.* **2004**, *6*, 5042-5050, doi:10.1039/b408414d.

(8) Sheps, L.; Rotavera, B.; Eskola, A. J.; Osborn, D. L.; Taatjes, C. A.; Au, K.; Shallcross, D. E.; Khan, M. A. H.; Percival, C. J. The reaction of Criegee intermediate CH_2OO with water dimer: primary products and atmospheric impact. *Phys. Chem. Chem. Phys.* **2017**, *19*, 21970-21979, doi:10.1039/C7CP03265J.

(9) Smith, M. C.; Chang, C.-H.; Chao, W.; Lin, L.-C.; Takahashi, K.; Boering, K. A.; Lin, J. J.-M. Strong negative temperature dependence of the simplest Criegee intermediate CH_2OO reaction with water dimer. *J. Phys. Chem. Lett.* **2015**, *6*, 2708-2713, doi:10.1021/acs.jpclett.5b01109.

(10) Suto, M.; Manzanares, E. R.; Lee, L. C. Detection of sulfuric acid aerosols by ultraviolet scattering. *Environ. Sci. Technol.* **1985**, *19*, 815-820, doi:10.1021/es00139a008.

D84. CH_2OO + NO. There have been two studies of the reaction of CH_2OO + NO, Welz et al.[2] directly observed CH_2OO via photoionization mass spectrometry and Stone et al.[1] follow CH_2OO via the laser induced fluorescence of the product HCHO. Welz et al.[2] report an upper limit of $<6\times 10^{-14}$ cm^3 $molecule^{-1}$ s^{-1} whereas Stone eta l., report an upper limit of $<2 \times 10^{-13}$ cm^3 $molecule^{-1}$ s^{-1}. Stone et al.[1] note that there are considerable uncertainties in their reported upper limit as their retrieved rate coefficients have increased uncertainty as a result of biexponential behavior and used relatively low concentrations of NO in their experiments. Thus the lower upper of limit Welz et al.[2] is recommended.
(Table: 19-5, Note: 19-5, Evaluated: 19-5) Back to Table

(1) Stone, D.; Blitz, M.; Daubney, L.; Howes, N. U. M.; Seakins, P. Kinetics of CH_2OO reactions with SO_2, NO_2, NO, H_2O, and CH_3CHO as a function of pressure. *Phys. Chem. Chem. Phys.* **2014**, *16*, 1139-1149, doi:10.1039/c3cp54391a.

(2) Welz, O.; Savee, J. D.; Osborn, D. L.; Vasu, S. S.; Percival, C. J.; Shallcross, D. E.; Taatjes, C. A. Direct kinetic measurements of Criegee intermediate (CH_2OO) formed by reaction of CH_2I with O_2. *Science* **2012**, *335*, 204-207, doi:10.1126/science.1213229.

D85. $CH_2OO + NO_2$. The recommendation is the average of the rate coefficients reported by Welz et al.[5] (7(+3/-2) $\times 10^{-12}$ cm^3 $molecule^{-1}$ s^{-1}) and Stone et al.[4] ($1.5 \pm 0.5 \times 10^{-12}$ cm^3 $molecule^{-1}$ s^{-1}) with equal weighting given to the two studies (independent of the number of rate coefficients reported in each study). There has been one published relative rate for the reaction of CH_2OO + NO_2. Ouyang et al.[3] report a relative rate of $k_{CH2OO+NO2}/k_{CH2OO+H2O}$ of $(2.8 \pm 1.1) \times 10^5$, however the relative rate coefficient may have been influenced by the much faster reaction of the water dimer with the Criegee intermediate so is not considered in the current evaluation.

Ouyang et al.[3] suggest that NO_3 is the major product from the reaction, however [2] and Caravan et al.[1] suggest that little or no NO_3 is formed via the reaction. Caravan et al.[1] observe the CH_2OO-NO_2 adduct, however, as of yet, there have been no quantitative evaluations of the branching ratio for the reaction.
(Table: 19-5, Note: 19-5, Evaluated: 19-5) Back to Table

(1) Caravan, R. L.; Khan, M. A. H.; Rotavera, B.; Papajak, E.; Antonov, I. O.; Chen, M.-W.; Au, K.; Chao, W.; Osborn, D. L.; Lin, J. J.-M.; Percival, C. J.; Shallcross, D. E.; Taatjes, C. A. Products of Criegee intermediate reactions with NO_2: experimental measurements and tropospheric implications. *Faraday Discuss.* **2017**, *200*, 313-330, doi:10.1039/C7FD00007C.

(2) Lewis, T. R.; Blitz, M. A.; Heard, D. E.; Seakins, P. W. Direct evidence for a substantive reaction between the Criegee intermediate, CH_2OO, and the water vapour dimer. *Phys. Chem. Chem. Phys.* **2015**, *17*, 4859-4863, doi:10.1039/c4cp04750h.

(3) Ouyang, B.; McLeod, M. W.; Jones, R. L.; Bloss, W. J. NO_3 radical production from the reaction between the Criegee intermediate CH_2OO and NO_2. *Phys. Chem. Chem. Phys.* **2013**, *15*, 17070-17075, doi:10.1039/c3cp53024h.

(4) Stone, D.; Blitz, M.; Daubney, L.; Howes, N. U. M.; Seakins, P. Kinetics of CH_2OO reactions with SO_2, NO_2, NO, H_2O, and CH_3CHO as a function of pressure. *Phys. Chem. Chem. Phys.* **2014**, *16*, 1139-1149, doi:10.1039/c3cp54391a.

(5) Welz, O.; Savee, J. D.; Osborn, D. L.; Vasu, S. S.; Percival, C. J.; Shallcross, D. E.; Taatjes, C. A. Direct kinetic measurements of Criegee intermediate (CH_2OO) formed by reaction of CH_2I with O_2. *Science* **2012**, *335*, 204-207, doi:10.1126/science.1213229.

D86. $CH_2OO + HNO_3 \rightarrow$ products. There has been one study of the reaction of CH_2OO + HNO_3 [1] using direct detection of CH_2OO via UV absorption spectroscopy. Foreman et al.[1] do not measure reaction products however suggest that the reaction product is nitrooxymethyl hydroperoxide (NMHP) using CCSD/cc-pVDZ quantum chemical calculations.
(Table: 19-5, Note: 19-5, Evaluated: 19-5) Back to Table

(1) Foreman, E. S.; Kapnas, K. M.; Murray, C. Reactions between Criegee intermediates and the inorganic acids HCl and HNO_3: Kinetics and atmospheric implications. *Angew. Chem. Int. Ed.* **2016**, *55*, 10419-10422, doi:10.1002/anie.201604662.

D87. $CH_2OO + CH_2OO$. There have been 4 experimental determinations of the CH_2OO self-reaction by Buras et al.,[1] Su et al.,[3] Ting et al.,[4] and Chhantyal-Pun et al.[2] The recommendation is the average of the rate coefficients reported by Buras et al.,[1] Ting et al.,[4] and Chhantyal-Pun et al.[2] with equal weighting given to the three studies (independent of the number of rate coefficients reported in each study). The studies report rate coefficients of $(6.0 \pm 2.1) \times 10^{-11}$ cm^3 molecule^{-1} s^{-1}, $(8.0 \pm 4) \times 10^{-11}$ cm^3 molecule^{-1} s^{-1}and $(7.35 \pm 0.63) \times 10^{-11}$ cm^3 molecule^{-1} s^{-1} respectively. Su et al.[3] report a rate coefficient that is a factor of 5 higher than the other studies. In the follow on study from the same group by Ting et al.[4] it was pointed out that the initial study ignored secondary chemistry and had large errors associated with absorption cross section and thus is not considered in the evaluation.
(Table: 19-5, Note: 19-5, Evaluated: 19-5) Back to Table

(1) Buras, Z. J.; Elsamra, R. M. I.; Green, W. H. Direct determination of the simplest Criegee intermediate (CH_2OO) self reaction rate. *J. Phys. Chem. Lett.* **2014**, *5*, 2224-2228, doi:10.1021/jz5008406.
(2) Chhantyal-Pun, R.; Davey, A.; Shallcross, D. E.; Percival, C. J.; Orr-Ewing, A. J. A kinetic study of the CH_2OO Criegee intermediate self-reaction, reaction with SO_2 and unimolecular reaction using cavity ring-down spectroscopy. *Phys. Chem. Chem. Phys.* **2015**, *17*, 3617-3626, doi:10.1039/c4cp04198d.
(3) Su, Y.-T.; Lin, H.-Y.; Putikam, R.; Matsui, H.; Lin, M. C.; Lee, Y.-P. Extremely rapid self-reaction of the simplest Criegee intermediate CH_2OO and its implications in atmospheric chemistry. *Nat. Chem.* **2014**, *6*, 477-483, doi:10.1038/NCHEM.1890.
(4) Ting, W.-L.; Chang, C.-H.; Lee, Y.-F.; Matsui, H.; Lee, Y.-P.; Lin, J. J.-M. Detailed mechanism of the $CH_2I + O_2$ reaction: Yield and self-reaction of the simplest Criegee intermediate CH_2OO. *J. Chem. Phys.* **2014**, *141*, 104308, doi:10.1063/1.4894405.

D88. $CH_2OO + HC(O)OH \rightarrow$ products. There have been two studies of the reaction of CH_2OO + HCOOH both reported in Welz et al.[2] using direct detection of CH_2OO either via photoionization mass spectrometry or UV absorption spectroscopy. Both methods report an identical rate coefficient. Neeb et al.[1] report a relative rate of $k_{CH2OO+HCOOH}/k_{CH2OO+H2O} = 14000$; however the reference rate coefficient is not well defined, as it is likely the reported relative rate has been influenced the much faster water dimer reaction, so is not considered in the current evaluation. Neeb et al.[1] suggest that the reaction forms HMPF ($HC(O)OCH_2OOH$) and Welz et al. [2] observe product peaks that are assumed to be dissociative ions from HMPF.
(Table: 19-5, Note: 19-5, Evaluated: 19-5) Back to Table

(1) Neeb, P.; Horie, O.; Moortgat, G. K. The ethene−ozone reaction in the gas phase. *J. Phys. Chem. A* **1998**, *102*, 6778-6785, doi:10.1021/jp981264z.
(2) Welz, O.; Eskola, A. J.; Sheps, L.; Rotavera, B.; Savee, J. D.; Scheer, A. M.; Osborn, D. L.; Lowe, D.; Booth, A. M.; Xiao, P.; Khan, M. A. H.; Percival, C. J.; Shallcross, D. E.; Taatjes, C. A. Rate coefficients of C1 and C2 Criegee intermediate reactions with formic and acetic acid near the collision limit: Direct kinetics measurements and atmospheric implications. *Angew. Chem. Int. Ed.* **2014**, *53*, 4547-4550, doi:10.1002/anie.201400964.

D89. $CH_2OO + CH_3CHO$. There have been four studies in total of this reaction. Two direct studies of the reaction of $CH_2OO + CH_3CHO$ [6] use CH_2OO production by UV laser flash photolysis of CH_2I_2/O_2. Taatjes et al.[6] detect the CH_2OO via photoionization mass spectrometry and Elsamra et al.[2] use laser absorption technique at 375 nm. Two indirect studies [1] generated CH_2OO from the ozonolysis of ethene in an atmospheric pressure flow tube and detected the CH_2OO via the titration of CH_2OO with SO_2 to produce sulphuric acid, which is detected via PTRMs and Stone et al.[5] follow CH_2OO via the laser induced fluorescence of the product HCHO. Earlier work by Horie et al.[3] in an atmospheric pressure FTIR relative rate study report a relative rate of CH_2OO with Hexafluoroacetone compared to CH_3CHO. Only an approximate relative rate is reported and their relative rate assumes 100% conversion to the propene ozonide, which as the authors note they found evidence for the formation of CO_2 and HCHO as well as the ozonide, as a result the relative rate study is not considered in this evaluation.

At room temperature the four studies agree within the stated experimental uncertainties. Taatjes et al., report a value of $(9.5 \pm 0.7) \times 10^{-13}$ cm^3 molecule^{-1} s^{-1}at 4 Torr; Berndt et al., report a value of $(1.7 \pm 0.5) \times 10^{-12}$ cm^3 molecule^{-1} s^{-1} at atmospheric pressure, Elsamra et al.[2] report a value of $(1.1 \pm 0.1) \times 10^{-12}$ cm^3 molecule^{-1} s^{-1} at 4. Torr and Stone et al., report a value of $(1.48 \pm 0.04) \times 10^{-12}$ cm^3 molecule^{-1} s^{-1} at 25 Torr. Stone et al.[5] suggest

that the difference between high pressure and low pressure studies could be as a result of a pressure dependent rate of reaction. Elsamra et al.[2] carried out experiments as a function of pressure from 4 to 50 Torr and suggest that there could be a very weak pressure dependence. However, within the quoted experimental error, the rate coefficients reported by Elsamra et al.[2] are in agreement. A weak pressure dependence is also suggested by theoretical calculations of Jalan et al.[4] However, given the associated uncertainty between the studies and the lack of a single study that covers a large range of pressures the recommendation is the average of the four rate coefficients with equal weighting given to the four methods. Elsamra et al.[2] study reports the only available temperature dependent data, so the recommended E/R is obtained from the Arrhenius fit to their data.

Horie et al.[3] observe propene ozonide as a reaction product. Whereas Taatjes et al.[6] do not observe any peaks (parent or dissociative) that can be associated with the ozonide in their photoionization mass spectra, however Taatjes et al.[6] observe acetic acid. It is possible that the barriers for isomerization or decomposition for the secondary ozonide are near or below the energy of the reactants and at the low pressures used by Taatjes et al.[6] that collisional stabilization of the secondary ozonide does not occur, explaining the difference with the experimental results of Horie et al.[3] Elsamra et al.[2] also attempted to quantify the reaction products using photoionization mass spectrometry but were not able to observe any products. As of yet, no quantitative assessment of the product branching ratios have been reported.
(Table: 19-5, Note: 19-5, Evaluated: 19-5) Back to Table

(1) Berndt, T.; Kaethner, R.; Voigtlander, J.; Stratmann, F.; Pfeifle, M.; Reichle, P.; Sipila, M.; Kulmala, M.; Olzmann, M. Kinetics of the unimolecular reaction of CH_2OO and the bimolecular reactions with the water monomer, acetaldehyde and acetone under atmospheric conditions. *Phys. Chem. Chem. Phys.* **2015**, *17*, 19862-19873, doi:10.1039/C5CP02224J.

(2) Elsamra, R. M. I.; Jalan, A.; Buras, Z. J.; Middaugh, J. E.; Green, W. H. Temperature- and pressure-dependent kinetics of CH_2OO + CH_3COCH_3 and CH_2OO + CH_3CHO: Direct measurements and theoretical analysis. *Int. J. Chem. Kinet.* **2016**, *48*, 474-488, doi: 10.1002/kin.21007.

(3) Horie, O.; Schäfer, C.; Moortgat, G. K. High reactivity of hexafluoro acetone toward criegee intermediates in the gas-phase ozonolysis of simple alkenes. *Int. J. Chem. Kinet.* **1999**, *31*, 261-269, doi:10.1002/(SICI)1097-4601(1999)31:4<261::AID-KIN3>3.0.CO;2-Z.

(4) Jalan, A.; Allen, J. W.; Green, W. H. Chemically activated formation of organic acids in reactions of the Criegee intermediate with aldehydes and ketones. *Phys. Chem. Chem. Phys.* **2013**, *15*, 16841-16852, doi:10.1039/C3CP52598H.

(5) Stone, D.; Blitz, M.; Daubney, L.; Howes, N. U. M.; Seakins, P. Kinetics of CH_2OO reactions with SO_2, NO_2, NO, H_2O, and CH_3CHO as a function of pressure. *Phys. Chem. Chem. Phys.* **2014**, *16*, 1139-1149, doi:10.1039/c3cp54391a.

(6) Taatjes, C. A.; Welz, O.; Eskola, A. J.; Savee, J. D.; Osborn, D. L.; Lee, E. P. F.; Dyke, J. M.; Mok, D. W. K.; Shallcross, D. E.; Percival, C. J. Direct measurement of Criegee intermediate (CH_2OO) reactions with acetone, acetaldehyde, and hexafluoroacetone. *Phys. Chem. Chem. Phys.* **2012**, *14*, 10391-10400, doi:10.1039/C2CP40294G.

D90. CH_2OO + $CH_3C(O)OH$ → products. There have been two studies of the reaction of CH_2OO + CH_3COOH at 298 K both reported in Welz et al.[1] using direct detection of CH_2OO either via photoionization mass spectrometry ($1.3 \pm 0.1 \times 10^{-10}$ cm^3 $molecule^{-1}$ s^{-1}) or UV absorption spectroscopy ($1.2 \pm 0.1 \times 10^{-10}$ cm^3 $molecule^{-1}$ s^{-1}). The recommendation is the average of the two rate coefficients reported by Welz et al.[1] with equal weighting given to the two methods. Welz et al.[1] suggest that reaction proceeds via the formation of the CH_2OO-CH_3COOH adduct, however the product ions that were detected are most probably produced via the dissociative ionization of the adduct and no attempt was made to assess the branching ratio so no recommendation on product formation can be made.
(Table: 19-5, Note: 19-5, Evaluated: 19-5) Back to Table

(1) Welz, O.; Eskola, A. J.; Sheps, L.; Rotavera, B.; Savee, J. D.; Scheer, A. M.; Osborn, D. L.; Lowe, D.; Booth, A. M.; Xiao, P.; Khan, M. A. H.; Percival, C. J.; Shallcross, D. E.; Taatjes, C. A. Rate coefficients of C1 and C2 Criegee intermediate reactions with formic and acetic acid near the collision limit: Direct kinetics measurements and atmospheric implications. *Angew. Chem. Int. Ed.* **2014**, *53*, 4547-4550, doi:10.1002/anie.201400964.

D91. $CH_2OO + CH_2{=}CH_2 \rightarrow$ products. There has been one study of the reaction of CH_2OO + ethene [1] using CH_2OO production by UV laser flash photolysis of CH_2I_2/O_2 and direct detection of CH_2OO via UV absorption spectroscopy at 350 nm. Buras et al.[1] measured the rate coefficient as a function of pressure from 10 to 50 Torr and within experimental error was found to be independent of pressure. The rate coefficient was measured at three temperatures and was found to have a positive temperature dependence. The temperature dependence was predicted using B3LYP/MG3s theoretical calculations and suggest that the reaction proceeds via the formation of a pre-reactive complex before a 1,3 cycloaddition to the double bond. The theoretical calculations suggest that Arrhenius plots should be significantly curved, however, it is not possible assess experimentally given the limited amount of temperatures that the rate coefficient was determined experimentally. The theoretical calculations are approximately an order of magnitude faster than the experimentally determined rate coefficients and agreement is only qualitative, suggesting that the Arrhenius plots should be curved. Buras et al.[1] suggest that the disagreement is as a result of inadequate estimation of flux through shallow/submerged saddle points.
(Table: 19-5, Note: 19-5, Evaluated: 19-5) Back to Table

(1) Buras, Z. J.; Elsamra, R. M. I.; Jalan, A.; Middaugh, J. E.; Green, W. H. Direct kinetic measurements of reactions between the simplest Criegee intermediate CH_2OO and alkenes. *J. Phys. Chem. A* **2014**, *118*, 1997-2006, doi:10.1021/jp4118985.

D92. $CH_2OO + CH_3C(O)CH_3$. There have been two direct studies of the reaction of CH_2OO + $CH_3C(O)CH_3$ [2,4] . The direct studies both produce CH_2OO via by UV laser flash photolysis of CH_2I_2/O_2 [2,4] . Taatjes et al.,[4] detect the CH_2OO via photoionization mass spectrometry and Elsamra et al.[2] use laser absorption technique at 375 nm. There has been a further indirect study by Berndt et al.,[1] which generated CH_2OO from the ozonolysis of ethene in an atmospheric pressure flow tube. Berndt et al., detected the CH_2OO via the titration of CH_2OO with SO_2 to produce sulphuric acid, and the subsequent sulphuric acid was detected via PTRMs. All three studies are in good agreement and the recommendation is the average of the three rate coefficients with equal weighting given to the three methods. Elsamra et al.[2] carried out experiments as a function of pressure and within experimental error, the rate coefficient is independent of pressure. Elsamra et al.[2] study reports the only available temperature dependent data, so the recommended *E*/R is obtained from the Arrhenius fit to their data. Elsamra et al. and Taatjes et al.[2,4] observe the secondary ozonide 3,3-dimethyl-1,2,4-trioxolane and methoxy methyl acetate as the main products of the reaction, however no quantification of the branching is reported. Elsamra et al.[2] show that the relative yield of the SOZ has a weak pressure dependence, which is consistent with the theoretical calculations of Jalan et al.[3]
(Table: 19-5, Note: 19-5, Evaluated: 19-5) Back to Table

(1) Berndt, T.; Kaethner, R.; Voigtlander, J.; Stratmann, F.; Pfeifle, M.; Reichle, P.; Sipila, M.; Kulmala, M.; Olzmann, M. Kinetics of the unimolecular reaction of CH_2OO and the bimolecular reactions with the water monomer, acetaldehyde and acetone under atmospheric conditions. *Phys. Chem. Chem. Phys.* **2015**, *17*, 19862-19873, doi:10.1039/C5CP02224J.
(2) Elsamra, R. M. I.; Jalan, A.; Buras, Z. J.; Middaugh, J. E.; Green, W. H. Temperature- and pressure-dependent kinetics of CH_2OO + CH_3COCH_3 and CH_2OO + CH_3CHO: Direct measurements and theoretical analysis. *Int. J. Chem. Kinet.* **2016**, *48*, 474-488, doi: 10.1002/kin.21007.
(3) Jalan, A.; Allen, J. W.; Green, W. H. Chemically activated formation of organic acids in reactions of the Criegee intermediate with aldehydes and ketones. *Phys. Chem. Chem. Phys.* **2013**, *15*, 16841-16852, doi:10.1039/C3CP52598H.
(4) Taatjes, C. A.; Welz, O.; Eskola, A. J.; Savee, J. D.; Osborn, D. L.; Lee, E. P. F.; Dyke, J. M.; Mok, D. W. K.; Shallcross, D. E.; Percival, C. J. Direct measurement of Criegee intermediate (CH_2OO) reactions with acetone, acetaldehyde, and hexafluoroacetone. *Phys. Chem. Chem. Phys.* **2012**, *14*, 10391-10400, doi:10.1039/C2CP40294G.

D93. $CH_2OO + CH_2{=}CHCH_3$. There has been one study of the reaction CH_2OO + $CH_2{=}CHCH_3$ (propene)[1] using CH_2OO production by UV laser flash photolysis of CH_2I_2/O_2 and direct detection of CH_2OO via UV absorption spectroscopy at 350 nm. Buras et al.[1] measured the rate coefficient as a function of pressure from 10 to 50 Torr and within experimental error found it to be independent of pressure. The rate coefficient was measured at three temperatures and was found to have a positive temperature dependence. The temperature dependence was predicted using B3LYP/MG3s theoretical calculations that suggest the reaction proceeds via the formation of a pre-reactive complex before a 1,3 cycloaddition to the double bond. The theoretical calculations suggest

that Arrhenius plots should be significantly curved; however, it is not possible assess this experimentally given the limited range of temperatures investigated. The theoretical calculations are approximately an order of magnitude faster than the experimentally determined rate coefficients and agreement is only qualitative, suggesting that the Arrhenius plots should be curved. Buras et al.[1] suggest that the disagreement is as a result of inadequate estimation of flux through shallow/submerged saddle points.
(Table: 19-5, Note: 19-5, Evaluated: 19-5) Back to Table

(1) Buras, Z. J.; Elsamra, R. M. I.; Jalan, A.; Middaugh, J. E.; Green, W. H. Direct kinetic measurements of reactions between the simplest Criegee intermediate CH_2OO and alkenes. *J. Phys. Chem. A* **2014**, *118*, 1997-2006, doi:10.1021/jp4118985.

D94. $CH_2OO + CH_2=CHCH_2CH_3$. There has been one study of the reaction of $CH_2OO + CH_2=CHCH_2CH_3$ (1-butene)[1] using CH_2OO production by UV laser flash photolysis of CH_2I_2/O_2 and direct detection of CH_2OO via uv absorption spectroscopy at 350 nm. Buras et al.[1] measured the rate coefficient as a function of pressure from 10 to 50 Torr and within experimental error was found to be independent of pressure. The rate coefficient was measured at three temperatures and was found to have a positive temperature dependence. The temperature dependence was predicted using B3LYP/MG3s theoretical calculations and suggest that the reaction proceeds via the formation of a pre-reactive complex before a 1,3 cycloaddition to the double bond. The theoretical calculations suggest that Arrhenius plots should be significantly curved, however, it is not possible assess experimentally given the limited amount of temperatures that the rate coefficient was determined experimentally. The theoretical calculations are approximately an order of magnitude faster than the experimentally determined rate coefficients and agreement is only qualitative, suggesting that the Arrhenius plots should be curved. Buras et al.[1] suggest that the disagreement is as a result of inadequate estimation of flux through shallow/submerged saddle points.
(Table: 19-5, Note: 19-5, Evaluated: 19-5) Back to Table

(1) Buras, Z. J.; Elsamra, R. M. I.; Jalan, A.; Middaugh, J. E.; Green, W. H. Direct kinetic measurements of reactions between the simplest Criegee intermediate CH_2OO and alkenes. *J. Phys. Chem. A* **2014**, *118*, 1997-2006, doi:10.1021/jp4118985.

D95. $CH_2OO + (CH_3)_2C=CH_2$ (*iso*-butene). There has been one study of the reaction of CH_2OO + *iso*-butene [1] using CH_2OO production by UV laser flash photolysis of CH_2I_2/O_2 and direct detection of CH_2OO via UV absorption spectroscopy at 350 nm. Buras et al.[1] measured the rate coefficient as a function of pressure from 10 to 50 Torr and within experimental error was found to be independent of pressure. The rate coefficient was measured at three temperatures and was found to have a positive temperature dependence. The temperature dependence was predicted using B3LYP/MG3s theoretical calculations and suggest that the reaction proceeds via the formation of a pre-reactive complex before a 1,3 cycloaddition to the double bond. The theoretical calculations suggest that Arrhenius plots should be significantly curved, however, it is not possible assess experimentally given the limited amount of temperatures that the rate coefficient was determined experimentally. The theoretical calculations are approximately an order of magnitude faster than the experimentally determined rate coefficients and agreement is only qualitative, suggesting that the Arrhenius plots should be curved. Buras et al.[1] suggest that the disagreement is as a result of inadequate estimation of flux through shallow/submerged saddle points.
(Table: 19-5, Note: 19-5, Evaluated: 19-5) Back to Table

(1) Buras, Z. J.; Elsamra, R. M. I.; Jalan, A.; Middaugh, J. E.; Green, W. H. Direct kinetic measurements of reactions between the simplest Criegee intermediate CH_2OO and alkenes. *J. Phys. Chem. A* **2014**, *118*, 1997-2006, doi:10.1021/jp4118985.

D96. $CH_2OO + CH_3CH=CHCH_3$. There has been one study of the reaction of $CH_2OO + CH_3CH=CHCH_3$ (2-butene)[1] using CH_2OO production by UV laser flash photolysis of CH_2I_2/O_2 and direct detection of CH_2OO via UV absorption spectroscopy at 350 nm.[1] Buras et al.[1] measured the rate coefficient as a function of pressure from 10 to 50 Torr and within experimental error was found to be independent of pressure. The 2-butene was used as supplied and no quantification of the fraction of *trans* versus *cis* isomers was stated. However, as pointed out by the authors the *trans* isomer is expected to be relatively more reactive than the *cis* isomer and the *trans* isomer is thermodynamically more stable. Thus, the measure rate coefficient should be more representative of the reactivity of the *trans* isomer. The rate coefficient was measured at three temperatures

and was found to have a positive temperature dependence. The temperature dependence was predicted using B3LYP/MG3s theoretical calculations and suggest that the reaction proceeds via the formation of a pre-reactive complex before a 1,3 cycloaddition to the double bond. The theoretical calculations suggest that Arrhenius plots should be significantly curved; however, it is not possible assess this experimentally given the limited range of temperatures investigated. The theoretical calculations are approximately an order of magnitude faster than the experimentally determined rate coefficients and agreement is only qualitative. Buras et al.[1] suggest that the disagreement is as a result of inadequate estimation of flux through shallow/submerged saddle points.
(Table: 19-5, Note: 19-5, Evaluated: 19-5) Back to Table

(1) Buras, Z. J.; Elsamra, R. M. I.; Jalan, A.; Middaugh, J. E.; Green, W. H. Direct kinetic measurements of reactions between the simplest Criegee intermediate CH_2OO and alkenes. *J. Phys. Chem. A* **2014**, *118*, 1997-2006, doi:10.1021/jp4118985.

D97. $CH_2OO + CF_3C(O)OH$. There has been one study of the reaction of CH_2OO + TFA (trifluoroacetic acid) [1] using CH_2OO production by UV laser flash photolysis of CH_2I_2/O_2 and detection of CH_2OO using cavity ring-down spectroscopy at 355 nm between 10 and 100 Torr. The recommended E/R is obtained from the Arrhenius fit to their data. Theoretical work at the DF-HF//DF-LCCSD(T)-F12a/aug-cc-pVTZ//B3LYP/6-31 + G(d) level suggest that the reaction proceeds via a pre-reactive complex and suggest that the temperature dependence is best described by a non-Arrhenius expression $k = AT^2 exp\left(\frac{\Delta H}{RT}\right) + k_r$ where k_r is the high temperature limit from the fit to the experimental data where $A = (3.8 \pm 2.6) \times 10^{-18}$ cm^3 s^{-1} K^{-2}, $\Delta H = (13.1 \pm 1.5)$ kJ mol^{-1} and $k_r = 2.5 \times 10^{-10}$ cm^3 s^{-1}. As a result of the apparent curvature of the temperature dependence, it is not recommended to extrapolate the Arrhenius expression beyond the experimental temperatures studied.
(Table: 19-5, Note: 19-5, Evaluated: 19-5) Back to Table

(1) Chhantyal-Pun, R.; McGillen, M. R.; Beames, J. M.; Khan, M. A. H.; Percival, C. J.; Shallcross, D. E.; Orr-Ewing, A. J. Temperature-dependence of the rates of reaction of trifluoroacetic acid with Criegee intermediates. *Angew. Chem. Int. Ed.* **2017**, *56*, 9044-9047, doi:10.1002/anie.201703700.

D98. $CH_2OO + CF_3C(O)CF_3$ (HFA) → products. There have been two studies of the reaction of CH_2OO + HFA Taatjes et al.[2] and Liu et al.[1] The Taatjes et al. study was carried out at 4 Torr who reported a value of $3.53 \pm 0.29 \times 10^{-11}$ cm^3 molecule^{-1} s^{-1} and the Liu et al. study was carried out at 50 Torr who reported a value of $3.33 \pm 0.27 \times 10^{-11}$ cm^3 molecule^{-1} s^{-1}. The two determinations of the rate coefficients are in good agreement and would suggest that the rate coefficient is pressure independent. The recommendation is the average of the two rate coefficients reported with equal weighting given to the two methods. Taatjes et al.[2] observe the secondary ozonide 3,3-di(trifluoromethyl)-1,2,3-trioxolane and (trifluoromethoxy)methyl trifluoroacetate as the main products of the reaction, however no quantification of the branching is reported.
(Table: 19-5, Note: 19-5, Evaluated: 19-5) Back to Table

(1) Liu, Y. D.; Bayes, K. D.; Sander, S. P. Measuring rate constants for reactions of the simplest Criegee intermediate (CH_2OO) by monitoring the OH radical. *J. Phys. Chem. A* **2014**, *118*, 741-747, doi:10.1021/jp407058b.
(2) Taatjes, C. A.; Welz, O.; Eskola, A. J.; Savee, J. D.; Osborn, D. L.; Lee, E. P. F.; Dyke, J. M.; Mok, D. W. K.; Shallcross, D. E.; Percival, C. J. Direct measurement of Criegee intermediate (CH_2OO) reactions with acetone, acetaldehyde, and hexafluoroacetone. *Phys. Chem. Chem. Phys.* **2012**, *14*, 10391-10400, doi:10.1039/C2CP40294G.

D99. $CH_2OO + HCl$ → products. There has been one study of the reaction of CH_2OO + HCl [1] using direct detection of CH_2OO via UV absorption spectroscopy. Foreman et al.[1] do not measure reaction products however suggest that the reaction product is chloromethyl hydroperoxide (CMHP) using CCSD/cc-pVDZ quantum chemical calculations.
(Table: 19-5, Note: 19-5, Evaluated: 19-5) Back to Table

(1) Foreman, E. S.; Kapnas, K. M.; Murray, C. Reactions between Criegee intermediates and the inorganic acids HCl and HNO_3: Kinetics and atmospheric implications. *Angew. Chem. Int. Ed.* **2016**, *55*, 10419-10422, doi:10.1002/anie.201604662.

D100. $CH_2OO + H_2S \rightarrow$ products. There has been one study of the reaction of $CH_2OO + H_2S$ [1] using direct detection of CH_2OO via UV absorption spectroscopy at 340 nm. Smith et al.[1] measure that rate coefficient as a function of pressure from 100 to 500 Torr and within experimental error was found to be independent of pressure. The rate coefficient was measured at three temperatures and was found to have a weak temperature dependence. The weak temperature dependence agrees with the theoretical QCISD(T)/CBS calculations. No reaction products are measured, however, QCISD(T)/CBS calculations suggest that the reaction proceeds via the formation of a complex.
(Table: 19-5, Note: 19-5, Evaluated: 19-5) Back to Table

(1) Smith, M. C.; Chao, W.; Kumar, M.; Francisco, J. S.; Takahashi, K.; Lin, J. J.-M. Temperature-dependent rate coefficients for the reaction of CH_2OO with hydrogen sulfide. *J. Phys. Chem. A* **2017**, *121*, 938-945, doi:10.1021/acs.jpca.6b12303.

D101. $CH_2OO + SO_2$. Several direct kinetic investigations of $CH_2OO + SO_2$ have been caried out at room temperature. In all studies, CH_2OO was produced by laser flash photolysis of CH_2I_2/O_2, while kinetic information was obtained by various techniques. In many studies, CH_2OO was monitored directly using photoionization mass spectrometry by Welz et al.[16] (298 K, 4 Torr He), Stone et al.[13] (295 K, 1.5 Torr He), and Howes et al.[3] (295 K, 2 Torr He), using cavity ring down spectroscopy by Chhantyal-Pun et al.[1] (298 K, 10–30 Torr N_2), using IR absorption spectroscopy by Mir et al.[9] (298 K, 20–100 Torr N_2), and Qui and Tonokura[11] (298 K, 7.7 Torr N_2), using broadband UV-Vis absorption spectroscopy by Howes et al.[3] (295 K, 50 Torr N_2), Onel et al.[10] (223–344 K, 85 Torr N_2), Winiberg et al.[17] (295 K, 50 Torr N_2), or using broadband UV-Vis cavity-enhanced spectrometry by Sheps[12] (295 K, 5 Torr He). Other studies Liu et al.[7] (295 K, 50–200 Torr Ar) and Liu et al.[8] (300 K, 10 Torr Ar) have utilized laser induced fluorescence (LIF) of OH and Stone et el.[13] (295 K, 500 Torr N_2) used LIF of HCHO, where OH and HCHO have been identified as tracers for CH_2OO kinetics.

The experimental data are all in reasonable agreement at room temperature, and the rate coefficient is independent of pressure between ~1.5–760 Torr. At present, only Onel et al. have explored the temperature dependence of the rate coefficient, and observe a negative temperature dependence.

The recommendation at room temperature is the median value of all the experimental data, and the E/R value is based on the fits of Onel et al., and the A-Factor is adjusted to reproduce the k(298K).

In an earlier mechanistic study of this reaction, whereby CH_2OO was produced via the ozonolysis of ethene, Hatakeyama et al.[2] suggested that, under their experimental conditions, an adduct between CH_2OO and SO_2 is formed, and that this adduct either undergoes further reaction with SO_2 leading to SO_3 + HCHO, or decomposes to HCOOH and SO_2. A number of direct experimental studies have since identified HCHO + SO_3 as the direct reaction products of $CH_2OO + SO_2$: SO_3 was detected via both photoionization mass spectrometry[16] and IR absorption spectroscopy,[15] and HCHO was observed via photoionization mass spectrometry[16] and laser induced fluorescence spectroscopy.[13] Theoretical studies are generally in agreement that the reaction proceeds via the formation of a secondary ozonide and subsequent decomposition to HCHO + SO_3.[4-6,14,15] There is little support for stabilization of the SOZ even at higher pressures, in accord with the experimental observations.[6] Vereecken et al.[14] predict the formation of other product channels at atmospheric pressure (formyl sulfinic ester (HC(=O)−OS(=O)OH) or SO_2 + a singlet bisoxy diradical ($H_2C(O•)O•$)), however, as of yet, no experimental evidence for these has been reported.
(Table: 25-1, Note: 25-1, Evaluated: 25-1) Back to Table

(1) Chhantyal-Pun, R.; Davey, A.; Shallcross, D. E.; Percival, C. J.; Orr-Ewing, A. J. A kinetic study of the CH_2OO Criegee intermediate self-reaction, reaction with SO_2 and unimolecular reaction using cavity ring-down spectroscopy. *Phys. Chem. Chem. Phys.* **2015**, *17*, 3617-3626, doi:10.1039/c4cp04198d.
(2) Hatekayama, S.; Kobayashi, H.; Lin, Z.-Y.; Takagi, H.; Akimoto, H. Mechanism for the reaction of CH_2OO with SO_2 *J. Phys. Chem.* **1986**, *90*, 4131-4135, doi:10.1021/j100408a059.
(3) Howes, N. U. M.; Mir, Z. S.; Blitz, M. A.; Hardman, S.; Lewis, T. R.; Stone, D.; Seakins, P. W. Kinetic studies of C1 and C2 Criegee intermediates with SO_2 using laser flash photolysis coupled with photoionization mass spectrometry and time resolved UV absorption spectroscopy. *Phys. Chem. Chem. Phys.* **2018**, *20*, 22218-22227, doi:10.1039/C8CP03115K.

(4) Jiang, L.; Xu, Y.-S.; Ding, A.-Z. Reaction of stabilized Criegee intermediates from ozonolysis of limonene with sulfur dioxide: Ab initio and DFT study. *J. Phys. Chem. A* **2010**, *114*, 12452-12461, doi:10.1021/jp107783z.
(5) Kurten, T.; Lane, J. R.; Jorgensen, S.; Kjaergaard, H. G. A computational study of the oxidation of SO_2 to SO_3 by gas-phase organic oxidants. *J. Phys. Chem. A* **2011**, *115*, 8669-8681, doi:10.1021/jp203907d.
(6) Kuwata, K. T.; Guinn, E. J.; Hermes, M. R.; Fernandez, J. A.; Mathison, J. M.; Huang, K. A computational re-examination of the Criegee intermediate–sulfur dioxide reaction. *J. Phys. Chem. A* **2015**, *119*, 10316-10335, doi:10.1021/acs.jpca.5b06565.
(7) Liu, Y.; Bayes, K. D.; Sander, S. P. Measuring rate constants for reactions of the simplest Criegee intermediate (CH_2OO) by monitoring the OH radical. *J. Phys. Chem. A* **2014**, *118*, 741-747, doi:10.1021/jp407058b.
(8) Liu, Y.; Liu, F.; Liu, S.; Dai, D.; Dong, W.; Yang, X. A kinetic study of the CH_2OO Criegee intermediate reaction with SO_2, $(H_2O)_2$, CH_2I_2 and I atoms using OH laser induced fluorescence. *Phys. Chem. Chem. Phys.* **2017**, *19*, 20786-20794, doi:10.1039/C7CP04336H.
(9) Mir, Z. S.; Jamieson, M.; Greenall, N. R.; Seakins, P. W.; Blitz, M. A.; Stone, D. Identification, monitoring, and reaction kinetics of reactive trace species using time-resolved mid-infrared quantum cascade laser absorption spectroscopy: development, characterisation, and initial results for the CH_2OO Criegee intermediate. *Atmos. Meas. Tech.* **2022**, *15*, 2875-2887, doi:10.5194/amt-15-2875-2022.
(10) Onel, L.; Lade, R.; Mortiboy, J.; Blitz, M. A.; Seakins, P. W.; Heard, D. E.; Stone, D. Kinetics of the gas phase reaction of the Criegee intermediate CH_2OO with SO_2 as a function of temperature. *Phys. Chem. Chem. Phys.* **2021**, *23*, 19415-19423, doi:10.1039/d1cp02932k.
(11) Qiu, J.; Tonokura, K. Detection of the simplest Criegee intermediate CH_2OO in the ν4 band using a continuous wave quantum cascade laser and its kinetics with SO_2 and NO_2. *Chem. Phys. Lett.* **2019**, *737*, 100019, doi:10.1016/j.cpletx.2019.100019.
(12) Sheps, L. Absolute ultraviolet absorption spectrum of a Criegee intermediate CH_2OO. *J. Phys. Chem. Lett.* **2013**, *4*, 4201-4205, doi:10.1021/jz402191w.
(13) Stone, D.; Blitz, M.; Daubney, L.; Howes, N. U. M.; Seakins, P. Kinetics of CH_2OO reactions with SO_2, NO_2, NO, H_2O, and CH_3CHO as a function of pressure. *Phys. Chem. Chem. Phys.* **2014**, *16*, 1139-1149, doi:10.1039/c3cp54391a.
(14) Vereecken, L.; Harder, H.; Novelli, A. The reaction of Criegee intermediates with NO, RO_2, and SO_2, and their fate in the atmosphere. *Phys. Chem. Chem. Phys.* **2012**, *14*, 14682-14695, doi:10.1039/c2cp42300f.
(15) Wang, Y.-Y.; Dash, M. R.; Chung, C.-Y.; Lee, Y.-P. Detection of transient infrared absorption of SO_3 and 1,3,2-dioxathietane-2,2-dioxide [cyc-$(CH_2)O(SO_2)O$] in the reaction $CH_2OO + SO_2$. *J. Chem. Phys.* **2018**, *148*, doi:10.1063/1.5019205.
(16) Welz, O.; Savee, J. D.; Osborn, D. L.; Vasu, S. S.; Percival, C. J.; Shallcross, D. E.; Taatjes, C. A. Direct kinetic measurements of Criegee intermediate (CH_2OO) formed by reaction of CH_2I with O_2. *Science* **2012**, *335*, 204-207, doi:10.1126/science.1213229.
(17) Winiberg, F. A. F.; Chao, W.; Caravan, R. L.; Markus, C. R.; Sander, S. P.; Percival, C. J. A white cell based broadband transient UV-vis absorption spectroscopy with pulsed laser photolysis reactors for chemical kinetics under variable temperatures and pressures. *Rev. Sci. Instrum.* **2023**, *94*, doi:10.1063/5.0164733.

D102. $CH_3CHOO \rightarrow$ products. There have been numerous ozonolysis and direct studies investigating the thermal unimolecular decomposition rates of the simplest asymmetric Criegee intermediate, CH_3CHOO. The unimolecular decomposition of *syn*-CH_3CHOO occurs via 1,4-hydrogen transfer leading to the formation of a vinyl hydroperoxide, which subsequently decomposes to form OH + vinoxy. This pathway is sterically restricted for *anti*-CH_3CHOO, which instead undergoes isomerization via 1,3-cyclization to form methyl dioxirane. For *syn*-CH_3CHOO, there is general agreement between the direct experimental studies, some of the ozonolysis experimental studies, and the theoretical predictions of Fang et al.[2] at 298 K. The data for *anti*-CH_3CHOO are more limited, and as such no recommendation is made currently.

A number of groups have studied the ozonolysis of *trans*-2-butene[1,3,8,9] or *cis*-2-butene ozonolysis[8] to determine the unimolecular decomposition rates of CH_3CHOO. Berndt et al.[1] (293–323 K, 760 Torr air) and Newland et al.[8] (296–303 K, ~1000 mbar air) both examined the ozonolysis of *trans*-2-butene in the presence of SO_2 and

water vapor. Berndt et al. utilized chemical ionization mass spectrometry to detect sulfuric acid following the formation of SO_3 via *syn*/*anti*-$CH_3CHOO + SO_2$. Newland et al., who performed additional studies on *cis*-2-butene ozonolysis, observed the change in [SO_2] via a fluorescence monitor. Using the recommendation for *syn*-$CH_3CHOO + SO_2$ and *anti*-$CH_3CHOO + SO_2$ from this document, we derive absolute rate coefficients of 100 s^{-1} (Berndt et al.) and ~362 s^{-1} (Newland et al.) for *syn*-CH_3CHOO and 31 s^{-1} (Berndt et al.) for *anti*-CH_3CHOO. Novelli et al.[9] (293 K, 2.6 Torr N_2) utilized fluorescence assay by gas expansion (FAGE) coupled with laser induced fluorescence spectroscopy to detect OH from the unimolecular decomposition of *syn*-CH_3CHOO following ozonolysis of propene or *trans*-2-butene. They determined a rate coefficient of ~20 s^{-1}, with an upper limit of 30 s^{-1}. Fenske et al.[3] (298 K, 760 Torr air) studied the ozonolysis of *trans*-2-butene in the presence of excess acetaldehyde, using FTIR to detect the secondary ozonide product from CH_3CHOO + acetaldehyde to determine the kinetics of the unimolecular decomposition reaction. Fenske determined a rate coefficient of 76 s^{-1}, with other loss processes (e.g., wall loss or reaction with ozone or *trans*-2-butene) expected to contribute minimally.

Six direct experimental studies have been conducted on CH_3CHOO decomposition, each of which utilized UV laser flash photolysis of CH_3CHI_2/O_2 to produce CH_3CHOO. This photolytic production method was coupled with photoionization mass spectrometry by Taatjes et al.[12] (298 K, 4 Torr He) and Howes et al.[4] (295 K, 1–2.5 Torr He), cavity enhanced broadband absorption spectroscopy by Sheps et al.[11] (293 K, 10 Torr He), broadband UV-Vis absorption spectroscopy by Robinson et al.[10] (297–331 K, 12–300 Torr N_2), and single wavelength UV absorption spectroscopy by Li et al.[6] (340 nm, 278–318 K, 100–700 Torr N_2) to detect and resolve *syn*- and *anti*-CH_3CHOO. By contrast, Zhou et al.[14] (298 K, 10–100 Torr Ar) followed the production of the OH product via laser-induced fluorescence spectroscopy to study exclusively the *syn* conformer. Taatjes et al. differentiated *anti* and *syn* conformers by the lower ionization energy of the *anti*-conformer, and the dominance of the *syn* conformer to the photoionization signal at higher ionization energies. Howes et al. used a fixed photoionization energy at which the *syn* conformer dominates the photoionization signal. The broadband capabilities of the experiments of both Sheps et al. and Robinson et al. allowed these authors to differentiate the conformers by their spectral differences. Li et al. exploited the strong conformer dependent reactivity of CH_3CHOO with water vapor, using water vapor as a scavenger for *anti*-CH_3CHOO in their experiments, which mitigated the contribution of *anti*-CH_3CHOO absorption at 340 nm.

Taatjes et al., Sheps et al., and Howes et al. report upper limits for *syn*-CH_3CHOO decomposition based on the observed loss in the absence of co-reactant (ranging from 150–250 s^{-1}). Li et al., Robinson et al., and Zhou et al. undertook more rigorous investigations to resolve unimolecular decomposition of *syn*-CH_3CHOO from its other experimental loss processes. The results of Robinson et al. and Li et al. are in reasonable agreement at 298 K, and are consistent with the upper limits reported by Taatjes et al., Sheps et al., and Howes et al. Both Robinson et al. and Li et al. report modest pressure dependence and positive temperature dependence, whereas Zhou et al. report a pressure independent rate coefficient (182 s^{-1} at 298 K). Li et al. interrogated this discrepancy, and propose that Zhou may have underestimated the loss of *syn*-CH_3CHOO via diffusion in their lower pressure experiments. This would result in the overestimation of Zhou's unimolecular decay rates, and apparent absence of pressure dependence. Our recommendation for the *syn* conformer is a result of a fit to the temperature- and pressure-dependent data of Robinson et al. and Li et al, yielding a value 154 s^{-1} at atmospheric temperature and pressure:

$$k_0 = 5.8 \times 10^{-16} (T/298)^{-23.55} \text{ cm}^3 \text{ molecule}^{-1} \text{ s}^{-1},$$

$$k_\infty = 172 (T/298)^{-16.31} \text{ s}^{-1}$$

for the temperature range 298–331 K. The fit is consistent with the upper limits reported by Taatjes et al. and Howes et al., and falls within the uncertainties of the chamber experiment data reported by Novelli et al., Newland et al., and Fenske et al. The recommended $f(298\text{ K})$ uncertainty factor is 1.1. The fit to the data at elevated temperatures is much more uncertain. The fit should not be extrapolated beyond the range of the experimental data.

At present, the only direct experimental report of the *anti*-CH_3CHOO unimolecular decomposition rate is the upper limit assigned by Taatjes et al. (250 s^{-1}), however this work did not examine the contributions of wall loss and other reactive removal processes. This upper limit is consistent with the theoretical predictions of Long et al., Kuwata et al.,[5] and Vereecken et al.,[13] all of whom also predict that the rate coefficient exhibits a positive temperature dependence. At the present time, no recommendation is made for the *anti*-CH_3CHOO unimolecular decay rate coefficient due to limited direct studies.

Five theoretical studies have examined the unimolecular decomposition kinetics of *syn*-CH_3CHOO.[2,5,7,10,13] The temperature dependence observed experimentally by Robinson et al. and Li et al. is supported by the trend predicted by Long et al.[7] and Fang et al.,[2] plus the Robinson et al.[10] master equation fits to their experimental data. However, there is significant variation in the magnitude of the predicted kinetics in the literature, highlighting the challenges associated with these calculations.
(Table: 25-1, Note: 25-1, Evaluated: 25-1) Back to Table

(1) Berndt, T.; Jokinen, T.; Sipilä, M.; Mauldin, R. L.; Herrmann, H.; Stratmann, F.; Junninen, H.; Kulmala, M. H_2SO_4 formation from the gas-phase reaction of stabilized Criegee Intermediates with SO_2: Influence of water vapour content and temperature. *Atmos. Environ.* **2014**, *89*, 603-612, doi:10.1016/j.atmosenv.2014.02.062.

(2) Fang, Y.; Liu, F.; Barber, V. P.; Klippenstein, S. J.; McCoy, A. B.; Lester, M. I. Communication: Real time observation of unimolecular decay of Criegee intermediates to OH radical products. *J. Chem. Phys.* **2016**, *144*, 061102, doi:10.1063/1.4941768.

(3) Fenske, J. D.; Hasson, A. S.; Ho, A. W.; Paulson, S. E. Measurement of absolute unimolecular and bimolecular rate constants for CH_3CHOO generated by the *trans*-2-Butene reaction with ozone in the gas phase. *J. Phys. Chem. A* **2000**, *104*, 9921-9932, doi:10.1021/jp0016636.

(4) Howes, N. U. M.; Mir, Z. S.; Blitz, M. A.; Hardman, S.; Lewis, T. R.; Stone, D.; Seakins, P. W. Kinetic studies of C1 and C2 Criegee intermediates with SO_2 using laser flash photolysis coupled with photoionization mass spectrometry and time resolved UV absorption spectroscopy. *Phys. Chem. Chem. Phys.* **2018**, *20*, 22218-22227, doi:10.1039/C8CP03115K.

(5) Kuwata, K. T.; Hermes, M. R.; Carlson, J.; Zogg, C. K. Computational studies of the isomerization and hydration reactions of acetaldehyde oxide and methyl vinyl carbonyl oxide *J. Phys. Chem. A* **2010**, *114*, 9192-9204, doi:10.1021/jp105358v.

(6) Li, Y.-L.; Kuo, M.-T.; Lin, J. J.-M. Unimolecular decomposition rates of a methyl-substituted Criegee intermediate *syn*-CH_3CHOO. *RSC Adv.* **2020**, *10*, 8518-8524, doi:10.1039/d0ra01406k.

(7) Long, B.; Bao, J. L.; Truhlar, D. G. Atmospheric chemistry of Criegee intermediates: Unimolecular reactions and reactions with water. *J. Am. Chem. Soc.* **2016**, *138*, 14409-14422, doi:10.1021/jacs.6b08655.

(8) Newland, M. J.; Rickard, A. R.; Alam, M. S.; Vereecken, L.; Muñoz, A.; Ródenas, M.; Bloss, W. J. Kinetics of stabilised Criegee intermediates derived from alkene ozonolysis: reactions with SO_2, H_2O and decomposition under boundary layer conditions. *Phys. Chem. Chem. Phys.* **2015**, *17*, 4076-4088, doi:10.1039/c4cp04186k.

(9) Novelli, A.; Vereecken, L.; Lelieveld, J.; Harder, H. Direct observation of OH formation from stabilised Criegee intermediates. *Phys. Chem, Chem. Phys.* **2014**, *16*, 19941-19951, doi:10.1039/C4CP02719A.

(10) Robinson, C.; Onel, L.; Newman, J.; Lade, R.; Au, K.; Sheps, L.; Heard, D. E.; Seakins, P. W.; Blitz, M. A.; Stone, D. Unimolecular kinetics of stabilized CH_3CHOO Criegee intermediates: *syn*-CH_3CHOO decomposition and *anti*-CH_3CHOO isomerization. *J. Phys. Chem. A* **2022**, *126*, 6984-6994, doi:10.1021/acs.jpca.2c05461.

(11) Sheps, L.; Scully, A. M.; Au, K. UV absorption probing of the conformer-dependent reactivity of a Criegee intermediate CH_3CHOO. *Phys. Chem. Chem. Phys.* **2014**, *16*, 26701-26706, doi:10.1039/c4cp04408h.

(12) Taatjes, C. A.; Welz, O.; Eskola, A. J.; Savee, J. D.; Scheer, A. M.; Shallcross, D. E.; Rotavera, B.; Lee, E. P. F.; Dyke, J. M.; Mok, D. K. W.; Osborn, D. L.; Percival, C. J. Direct measurements of conformer-dependent reactivity of the Criegee intermediate CH_3CHOO. *Science* **2013**, *340*, 177-180, doi:10.1126/science.1234689.

(13) Vereecken, L.; Novelli, A.; Taraborrelli, D. Unimolecular decay strongly limits the atmospheric impact of Criegee intermediates. *Phys. Chem. Chem. Phys.* **2017**, *19*, 31599-31612, doi:10.1039/c7cp05541b.

(14) Zhou, X.; Liu, Y.; Dong, W.; Yang, X. Unimolecular reaction rate measurement of *syn*-CH_3CHOO. *J. Phys. Chem. Lett.* **2019**, *10*, 4817-4821, doi:10.1021/acs.jpclett.9b01740.

D103. CH_3CHOO (*syn* and *anti* conformers) + H_2O, $(H_2O)_2$. Direct experimental measurements of the reaction of CH_3CHOO with water monomer at 298 K have been reported by Taatjes et al.,[9] Sheps et al.,[8] and Lin et al.,[5] with the latter also reporting rate coefficients between 288–328 K for *anti*, and at 288 K for *syn*. Experimental determinations on the reaction of CH_3CHOO with water dimer are more limited: only Lin et al.[5] have performed direct experimental measurements (288–328 K), and report rate coefficients for only the *anti* conformer. No direct measurements of the *syn* conformer with water dimer have been published at this time.

In all three studies, CH_3CHOO was produced by UV laser flash photolysis of CH_3CHI_2/O_2. Taatjes et al. monitored CH_3CHOO using time-resolved photoionization mass spectrometry; the *anti* and *syn* conformers were differentiated by the lower ionization energy of the *anti* conformer, and the dominance of the *syn* conformer to the signal at higher ionization energies. Sheps et al. used time-resolved broadband (300–450 nm) cavity-enhanced spectrometry to monitor both conformers simultaneously; they determined spectra of the individual conformers based on their very different reactivities toward H_2O and SO_2. Lin et al.[5] utilized time-resolved absorption spectroscopy at 368 nm, which is close to the peak of the absorption band for the *anti* conformer: they were also able to extract a rate coefficient for the *syn* conformer by fitting the slower component on the measured temporal profiles, but state that that due to the scatter in their data, this value should be considered with care. The water concentration was measured in the experiments of Lin et al.[5] using a humidity and temperature probe. The studies of Taatjes et al. and Sheps et al. employed relatively low total pressures of 4 Torr (He bath gas) and 5–20 Torr (He bath gas) respectively, whereas the experiments of Lin et al.[5] were performed at 500 Torr (N_2 bath gas).

There have been multiple theoretical studies of the $CH_3CHOO + H_2O$ reactions.[1-4,6,7,10] Theoretical kinetics calculations predict significant conformer-dependent reactivity for this system. There is general agreement that that reaction primarily proceeds via initial formation of a hydrogen-bonded complex that isomerizes to the hydroxyl hydroperoxide $CH_3CH(OH)OOH$. Reaction of *syn* is much slower than that for *anti* because the transition state for the isomerization reaction lies 22 kJ mol^{-1} higher in energy than reactants, whereas for *anti*, isomerization takes place rapidly over a "submerged" barrier that lies 7 kJ mol^{-1} lower in energy than reactants.[2] This conformer dependence is in accord with experimental observations.

Taatjes et al. and Sheps et al. were only able to obtain upper limits for the rate coefficient for *syn*-$CH_3CHOO + H_2O$. The values of Sheps et al. and Lin et al.[5] are in reasonable agreement, whilst that of Taatjes et al. is around a factor of 20 larger. Theoretical predictions by Long et al.[6] and Lin et al. indicate that the rate coefficient may be orders of magnitude smaller than the upper limits determined experimentally. Theoretical work by Long et al. and Lin et al.[4] predicts that the rate coefficient exhibits a positive temperature dependence consistent with the data determined at 288 K by Lin et al.[5]

The experimentally determined rate coefficients for *anti*-$CH_3CHOO + H_2O$ are significantly faster than for *syn*-CH_3CHOO, in accord with theory. There is agreement between the values of Taatjes et al. and Lin et al.,[5] while the value of Sheps is a factor of 2 larger. One possible explanation for this would be the possible contribution of *anti*-$CH_3CHOO + (H_2O)_2$, which would result in a faster removal of *anti*-CH_3CHOO. This is supported by the analysis of Lin et al.,[5] who found that for concentrations higher than 3×10^{16} cm^{-3}, the contribution of the reaction of *anti*- CH_3CHOO with water dimer must be accounted for. The data of Sheps et al. and Lin et al.[5] both show slight indication of upward curvature with increasing $[H_2O]$ in the plot of the pseudo-first order *anti*-CH_3CHOO decay rate vs. $[H_2O]$. Lin et al.[5] account for this in their analysis by fitting their bimolecular plot data with an expression that combines linear and quadratic dependencies on water concentration and the literature equilibrium constant for water monomer and dimer, to enable extraction of rate coefficients for the reactions of *anti*-CH_3CHOO with water monomer and dimer. Lin et al.[5] note that their measured effective rates are consistent with those of Sheps, possibly indicating the presence of water dimer in the experiments of Sheps.

The most recent theoretical investigations of *anti*-CH_3CHOO + water monomer differ substantially in their predicted rate coefficients: the values of Lin et al.[4] (which predate their experimental determinations) are substantially higher than those of Long et al. Experimentally, Lin et al.[4] predict a minor negative temperature dependence, in accord with the trend observed in their more recent experimental data. In contrast, Long et al. predict a minor positive temperature dependence.

Lin et al.[4] predict substantial negative temperature dependences for both the reactions of *anti*-CH_3CHOO and *syn*-CH_3CHOO with water dimer, with their predicted rate coefficients for being substantially larger for *anti.*

Lin's predicted rate coefficients and temperature dependence for *anti*-CH_3CHOO + water dimer are in reasonable agreement with their experimental data.[5]

For *syn*-CH_3CHOO + water monomer, the median values of all three experimental studies are recommended, while for the *anti*-CH_3CHOO + water monomer, the median value of the Taatjes et al. and Lin et al.[5] data are recommended. The experimental values of Lin et al.[5] are recommended for the reaction of *anti*-CH_3CHOO + water dimer. No recommendation is made for the reaction of *syn*-CH_3CHOO + water dimer.
(Table: 25-1, Note: 25-1, Evaluated: 25-1) Back to Table

(1) Anglada, J. M.; Aplincourt, P.; Bofill, J. M.; Cremer, D. Atmospheric formation of OH radicals and H_2O_2 from alkene ozonolysis under humid conditions. *ChemPhysChem* **2002**, *3*, 215-221, doi:10.1002/1439-7641(20020215)3:2<215::AID-CPHC215>3.0.CO;2-3.

(2) Anglada, J. M.; González, J.; Torrent-Sucarrat, M. Effects of the substituents on the reactivity of carbonyl oxides. A theoretical study on the reaction of substituted carbonyl oxides with water. *Phys. Chem. Chem. Phys.* **2011**, *13*, 13034-13045, doi:10.1039/c1cp20872a.

(3) Kuwata, K. T.; Hermes, M. R.; Carlson, J.; Zogg, C. K. Computational studies of the isomerization and hydration reactions of acetaldehyde oxide and methyl vinyl carbonyl oxide *J. Phys. Chem. A* **2010**, *114*, 9192-9204, doi:10.1021/jp105358v.

(4) Lin, L.-C.; Chao, W.; Chang, C.-H.; Takahashi, K.; Lin, J. J.-M. Competition between H_2O and $(H_2O)_2$ reactions with CH_2OO/CH_3CHOO. *Phys. Chem. Chem. Phys.* **2016**, *18*, 4557-4568, doi:10.1039/c6cp05171e.

(5) Lin, L.-C.; Chao, W.; Chang, C.-H.; Takahashi, K.; Lin, J. J.-M. Temperature dependence of the reaction of *anti*-CH_3CHOO with water vapor. *Phys. Chem. Chem. Phys.* **2016**, *18*, 28189-28197, doi:10.1039/C6CP05171E.

(6) Long, B.; Bao, J. L.; Truhlar, D. G. Atmospheric chemistry of Criegee intermediates: Unimolecular reactions and reactions with water. *J. Am. Chem. Soc.* **2016**, *138*, 14409-14422, doi:10.1021/jacs.6b08655.

(7) Ryzhkov, A. B.; Ariya, P. A. A theoretical study of the reactions of parent and substituted Criegee intermediates with water and the water dimer. *Phys. Chem. Chem. Phys.* **2004**, *6*, 5042-5050, doi:10.1039/b408414d.

(8) Sheps, L.; Scully, A. M.; Au, K. UV absorption probing of the conformer-dependent reactivity of a Criegee intermediate CH_3CHOO. *Phys. Chem. Chem. Phys.* **2014**, *16*, 26701-26706, doi:10.1039/c4cp04408h.

(9) Taatjes, C. A.; Welz, O.; Eskola, A. J.; Savee, J. D.; Scheer, A. M.; Shallcross, D. E.; Rotavera, B.; Lee, E. P. F.; Dyke, J. M.; Mok, D. K. W.; et al. Direct measurements of conformer-dependent reactivity of the Criegee intermediate CH_3CHOO. *Science* **2013**, *340*, 177-180, doi:10.1126/science.1234689.

(10) Vereecken, L.; Novelli, A.; Taraborrelli, D. Unimolecular decay strongly limits the atmospheric impact of Criegee intermediates. *Phys. Chem. Chem. Phys.* **2017**, *19*, 31599-31612, doi:10.1039/c7cp05541b.

D104. CH_3CHOO (*syn* and *anti* conformers) + HC(O)OH. There have been two direct kinetic studies of the reaction of CH_3CHOO with formic acid. Welz et al.[4] performed a conformer-resolved study at 298 K and 4 Torr (He) using multiplexed photoionization mass spectrometry coupled with tunable VUV radiation. They observed a rapid reaction with modest conformer dependence: the reaction of *anti* exceeds that of *syn* by approximately a factor of two. Behera and Lin[1] utilized Fourier- transform infrared (FTIR) spectroscopy to perform kinetic measurements of product formation at 298 K and 60 Torr, (O_2) yielding a conformer-unresolved rate coefficient that is in accord with the value obtained for *syn* by Welz et al. The recommended k(298 K) is taken from the direct studies of Welz et al.

The reaction is thought to predominantly lead to the formation of hydroperoxy ethylformate, in accord with the reaction of CH_2OO with formic acid. This is supported by the spectroscopic studies of Behera and Lin (FTIR) and Cabezas and Endo[2] (Fourier-transform microwave spectroscopy in a supersonic jet). Additional pathways include the dehydration of hydroperoxylethyl formate to formic acid anhydride (observed by Behera and Lin), and the acid-catalyzed isomerization of *syn*-CH_3CHOO to vinyl hydroperoxide (observed in the jet-cooled experiments of Liu et al.[3] using photoionization mass spectrometry).
(Table: 25-1, Note: 25-1, Evaluated: 25-1) Back to Table

(1) Behera, B.; Lee, Y.-P. Detailed mechanism and kinetics of reactions of *anti*- and *syn*-CH_3CHOO with HC(O)OH: infrared spectra of conformers of hydroperoxyethyl formate. *Phys. Chem. Chem. Phys.* **2024**, *26*, 2950-1966, doi:10.1039/D3CP04086K.

(2) Cabezas, C.; Endo, Y. Observation of hydroperoxyethyl formate from the reaction between methyl Criegee intermediate and formic acid. *Phys. Chem. Chem. Phys.* **2020**, *22*, 446-454, doi:10.1039/C9CP05030B.

(3) Liu, F.; Fang, Y.; Kumar, M.; Thompson, W. H.; Lester, M. I. Direct observation of vinyl hydroperoxide *Phys. Chem. Chem. Phys.* **2015**, *17*, 20490-20494, doi:10.1039/C5CP02917A.
(4) Welz, O.; Eskola, A. J.; Sheps, L.; Rotavera, B.; Savee, J. D.; Scheer, A. M.; Osborn, D. L.; Lowe, D.; Booth, A. M.; Xiao, P.; et al. Rate coefficients of C1 and C2 Criegee intermediate reactions with formic and acetic acid near the collision limit: Direct kinetics measurements and atmospheric implications. *Angew. Chem. Int. Ed.* **2014**, *53*, 4547-4550, doi:10.1002/anie.201400964.

D105. *syn-/anti*-$CH_3CHOO + SO_2$. Six direct experimental studies have been performed on the reaction of *syn*-CH_3CHOO with SO_2 at room temperature, each using UV laser flash photolysis of CH_3CHI_2/O_2 to produce CH_3CHOO. Experiments have utilized photoionization mass spectrometry (Taatjes et al.,[9] 298 K, 4 Torr He and Howes et al.,[2] 295 K, 1–2.5 Torr He), cavity enhanced broadband absorption spectroscopy (Sheps et al.,[7] 293 K, 10 Torr He), or broadband UV-Vis absorption spectroscopy (Smith et al.,[8] 295 K, 15-100 Torr, N_2, and Lade et al.,[4] 242–352 K, 10–600 Torr N_2) to directly monitor CH_3CHOO. Alternatively, laser induced fluorescence detection of OH (a tracer for CH_3CHOO) has also been utilized by Zhou et al.[11] (298 K, 10 Torr, Ar). Prior to the measurements of Lade et al., some discrepancy in the rate coefficient had been observed at room temperature, with the values of e.g., Sheps et al. and Howes et al. differing by a factor of ~1.7, which exceeds the uncertainty limits of the two measurements. Recently, Lade et al. observed that the reaction rate coefficient exhibited pressure dependence and a negative temperature dependence, in contrast to their measurements of *anti*-$CH_3CHOO + SO_2$. Invoking a mechanism involving chemical activation, plus a zero-pressure component, Lade et al. were able to fit their experimental data and capture the lower pressure data of Taatjes et al., Zhou et al., Howes et al., and Sheps et al. The mechanistic origin of the derived pressure dependence is unclear, but Lade propose that it could be due to the stabilization of the secondary ozonide intermediate, in competition with formation of $SO_3 + CH_3CHO$. Manonmani et al.[5] investigated the *syn*-$CH_3CHOO + SO_2$ reaction at 298 K and 200 Torr (He) and predicted a ~96% yield of $SO_3 + CH_3CHO$, however the pressure dependence of the yields were not reported. Theoretical investigations of SO_2 with more highly functionalized Criegee intermediates have differed in their predictions for the propensity for stabilization of the secondary ozonide vs. formation of the carbonyl + SO_3 co-product at higher pressures. For example, for $(CH_3)_2CHOO$, Vereecken et al.[10] predict that stabilization of the secondary ozonide would dominate at atmospheric pressure, whereas Kuwata et al.[3] predict decomposition to acetone and SO_3 with >95% yield. Further theoretical studies and product investigations are needed to further investigate the origin of the pressure dependence of this reaction. Further studies are also required to resolve the apparent pressure dependence of this reaction. At present, we recommend a pressure independent rate coefficient, which is the median of all the direct experimental values discussed above. The temperature dependence is based on the data of Lade et al., with the A factor scaled to give the recommended k(298 K).

Three experimental studies have been performed that unambiguously measure the reaction of *anti*-CH_3CHOO with SO_2 at room temperature. All studies utilize UV laser flash photolysis of CH_3CHI_2/O_2 to produce CH_3CHOO. Taatjes et al. (298 K, 4 Torr He) monitored CH_3CHOO using time-resolved photoionization mass spectrometry, using the lower photoionization energy of the *anti*-conformer to selectively probe its reaction with SO_2. Both Sheps et al. (293 K, 10 Torr He) and Lade et al. (242–352 K, 10–600 Torr N_2) used broadband UV-Vis absorption spectroscopy to simultaneously measure and differentiate the reactivity of both conformers with SO_2. Notably, all studies determine conformer-dependent reactivity, with k_{anti}/k_{syn} reported being between 2–7 at room temperature (3,5,7). This is partly attributed to lower steric hindrance of the *anti*-conformer. Lade et al. found the rate coefficient to be independent of both temperature and pressure, in contrast to their observations of *syn*-$CH_3CHOO + SO_2$. The value reported by Sheps et al. is around a factor of three greater than that of Taatjes et al., with the Lade et al. value close to the midpoint. The recommended rate coefficient is the median of the experimental values, and is independent of temperature and pressure.

In addition to the direct studies discussed above, Newland et al.[6] and Berndt et al.[1] conducted ozonolysis studies of butene in the presence of SO_2, such that the reactivity of CH_3CHOO with SO_2 could be examined. Because robust conformer resolution was not possible in either study, we do not include these data in our current evaluation, but summarize the findings herein. Newland et al. studied the ozonolysis of *trans*-but-2-ene and *cis*-2-butene and extracted relative rates of $CH_3CHOO + SO_2$ relative to H_2O for the *anti*-CH_3CHOO, and relative to unimolecular decomposition for *syn*-CH_3CHOO. Berndt et al. conducted a study of *trans*-2-butene ozonolysis at 298 K and 760 Torr, and monitored the formation of sulfuric acid in the presence of SO_2: their derived rate coefficient of conformationally unresolved $CH_3CHOO + SO_2$ is at least two orders of magnitude slower than those subsequently obtained via direct experiments.
(Table: 25-1, Note: 25-1, Evaluated: 25-1) Back to Table

(1) Berndt, T.; Jokinen, T.; Mauldin, R. L., III; Petäjä, T.; Herrmann, H.; Junninen, H.; Paasonen, P.; Worsnop, D. R.; Sipilä, M. Gas-phase ozonolysis of selected olefins: The yield of stabilized Criegee

intermediate and the reactivity toward SO_2. *J. Phys. Chem. Lett.* **2012**, *3*, 2892-2896, doi:10.1021/jz301158u.
(2) Howes, N. U. M.; Mir, Z. S.; Blitz, M. A.; Hardman, S.; Lewis, T. R.; Stone, D.; Seakins, P. W. Kinetic studies of C1 and C2 Criegee intermediates with SO_2 using laser flash photolysis coupled with photoionization mass spectrometry and time resolved UV absorption spectroscopy. *Phys. Chem. Chem. Phys.* **2018**, *20*, 22218-22227, doi:10.1039/C8CP03115K.
(3) Kuwata, K. T.; Guinn, E. J.; Hermes, M. R.; Fernandez, J. A.; Mathison, J. M.; Huang, K. A computational re-examination of the Criegee intermediate–sulfur dioxide reaction. *J. Phys. Chem. A* **2015**, *119*, 10316-10335, doi:10.1021/acs.jpca.5b06565.
(4) Lade, R. E.; Onel, L.; Blitz, M. A.; Seakins, P. W.; Stone, D. Kinetics of the gas-phase reactions of *syn*- and *anti*-CH_3CHOO Criegee intermediate conformers with SO_2 as a function of temperature and pressure. *J. Phys. Chem. A* **2024**, *128*, 2815-2824, doi:10.1021/acs.jpca.4c00199.
(5) Manonmani, G.; Sandhiya, L.; Senthilkumar, K. Reaction of Criegee intermediates with SO_2─ A possible route for sulfurous acid formation in the atmosphere. *ACS Earth Space Chem.* **2023**, *7*, 1890-1904, doi:10.1021/acsearthspacechem.3c00058.
(6) Newland, M. J.; Rickard, A. R.; Vereecken, L.; Muñoz, A.; Ródenas, M.; Bloss, W. J. Atmospheric isoprene ozonolysis: impacts of stabilised Criegee intermediate reactions with SO_2, H_2O and dimethyl sulfide. *Atmos. Chem. Phys.* **2015**, *15*, 9521-9536, doi:10.5194/acp-15-9521-2015.
(7) Sheps, L.; Scully, A. M.; Au, K. UV absorption probing of the conformer-dependent reactivity of a Criegee intermediate CH_3CHOO. *Phys. Chem. Chem. Phys.* **2014**, *16*, 26701-26706, doi:10.1039/c4cp04408h.
(8) Smith, M. C.; Ting, W.-L.; Chang, C.-H.; Takahashi, K.; Boering, K. A.; Lin, J. J.-M. UV absorption spectrum of the C2 Criegee intermediate CH_3CHOO. *J. Chem. Phys.* **2014**, *141*, 074302, doi:10.1063/1.4892582.
(9) Taatjes, C. A.; Welz, O.; Eskola, A. J.; Savee, J. D.; Scheer, A. M.; Shallcross, D. E.; Rotavera, B.; Lee, E. P. F.; Dyke, J. M.; Mok, D. K. W.; et al. Direct measurements of conformer-dependent reactivity of the Criegee intermediate CH_3CHOO. *Science* **2013**, *340*, 177-180, doi:10.1126/science.1234689.
(10) Vereecken, L.; Harder, H.; Novelli, A. The reaction of Criegee intermediates with NO, RO_2, and SO_2, and their fate in the atmosphere. *Phys. Chem. Chem. Phys.* **2012**, *14*, 14682-14695, doi:10.1039/c2cp42300f.
(11) Zhou, X.; Liu, Y.; Dong, W.; Yang, X. Unimolecular reaction rate measurement of *syn*-CH_3CHOO. *J. Phys. Chem. Lett.* **2019**, *10*, 4817-4821, doi:10.1021/acs.jpclett.9b01740.

D106. OH + Furan. There have been seven studies of the reaction of OH + Furan. Atkinson et al.[3] (298 K), Bierbach et al.[4] (300 K), and Tuazon et al.[8] performed measurements at room temperature using the relative rate technique, Lee and Tang[7] (298 K) measured the room temperature rate coefficient using a discharge flow resonance fluorescence technique. The temperature dependence was explored by Angelaki et al.[1] (273–353 K), using the relative rate technique; Wine and Thompson[10] (254–425 K), using a flash photolysis system and Whelan et al.[9] (294–668 K), using laser flash photolysis with time resolved OH LIF detection in a slow flow system. Whelan et al. experiments were performed using two separate apparatus for measurements at lower pressure (<200 mbar) and higher pressures (≥2 bar). The k(298 K) value from Lee and Tang value is an outlier being a factor of ~3 greater than all the other measurements and has not been included in the evaluation. Also, the rate coefficients of Whelan et al., are consistently lower than all other studies, so their data are not considered in this evaluation. The room temperature rate coefficients Atkinson et al., Bierbach et al., Angelaki et al., Tuazon et al., and Wine and Thompson are in good agreement and the recommendation is the average of the values, with equal weighting given to all studies.

The temperature-dependence studies of Angelaki et al. and Wine and Thompson are in excellent agreement. The E/R values are taken from a fit to the data of both studies and the A-factor is adjusted to reproduce the recommended value of k(298 K).

Bierbach et al.[5] reported a lower limit of 1,4-butenedial formation (>70%). Other reaction products with lower yields (<10%), included hydroxyfuranones, glyoxal, formic acid, and maleic anhydride. The mechanism in the presence of NO_x was studied by Gomez Alvarez et al.[6] and Aschmann et al.,[2] who report 1,4-butenedial yields of 100 ± 39% and 75 ± 5%, respectively.
(Table: 25-1, Note: 25-1, Evaluated: 25-1) Back to Table

(1) Angelaki, M. E.; Romanias, M. N.; Burkholder, J. B.; Papadimitriou, V. C. Rate coefficients for the gas-phase OH + furan (C_4H_4O) reaction between 273 and 353 K. *Int. J. Chem. Kinet.* **2023**, *56*, 119-139, doi:10.1002/kin.21697.

(2) Aschmann, S. M.; Nishino, N.; Arey, J.; Atkinson, R. Products of the OH radical-initiated reactions of furan, 2- and 3 methylfuran, and 2,3- and 2,5-dimethylfuran in the presence of NO. *J. Phys. Chem. A* **2014**, *118*, 457-466, doi:10.1021/jp410345k.
(3) Atkinson, R.; Aschmann, S. M.; Carter, W. P. L. Kinetics of the reactions of O_3 and OH radicals with furan and thiophene at 298 ± 2 K. *Int. J. Chem. Kinet.* **1983**, *15*, 51-61, doi:10.1002/kin.550150106.
(4) Bierbach, A.; Barnes, I.; Becker, K. H. Rate coefficients for the gas-phase reactions of hydroxyl radicals with furan, 2-methylfuran, 2-ethylfuran and 2,5-dimethylfuran at 300 ± 2 K. *Atmos. Environ. Part A* **1992**, *26*, 813-817, doi:10.1016/0960-1686(92)90241-C.
(5) Bierbach, A.; Barnes, I.; Becker, K. H. Product and kientic study of the OH-initiated gas-phase oxidation of furan, 2-methylfuran and furanladehydes at ≈300 K. *Atmos.Environ.* **1995**, *29*, 2651-2660, doi:10.1016/1352-2310(95)00096-H.
(6) Gómez Alvarez, E.; Borrás, E.; Viidanoja, J.; Hjorth, J. Unsaturated dicarbonyl products from the OH-initiated photo-oxidation of furan, 2-methylfuran and 3-methylfuran. *Atmos. Environ.* **2009**, *43*, 1603-1612, doi:10.1016/j.atmosenv.2008.12.019.
(7) Lee, J. H.; Tang, I. N. Absolute rate constants for the hydroxyl radical reactions with ethane, furan, and thiophene at room temperature. *J. Chem. Phys.* **1982**, *77*, 4459-4463, doi:10.1063/1.444367.
(8) Tuazon, E. C.; Atkinson, R.; Winer, A. M.; Pitts Jr., J. N. A study of the atmospheric reactions of 1,3-dichloropropene and other selected organochlorine compounds. *Arch Environ Contam Toxicol.* **1984**, *13*, 691-700.
(9) Whelan, C. A.; Eble, J.; Mir, Z. S.; Blitz, M. A.; Seakins, P. W.; Olzmann, M.; Stone, D. Kinetics of the reactions of hydroxyl radicals with furan and its alkylated derivatives 2-methyl furan and 2,5-dimethyl furan. *J. Phys. Chem. A* **2020**, *124*, 7416-7426, doi:10.1021/acs.jpca.0c06321.
(10) Wine, P. H.; Thompson, R. J. Kinetics of OH reactions with furan, thiophene, and tetrahydrothiophene. *Int J. Chem. Kinet.* **1984**, *16*, 867-878, doi:10.1002/kin.550160707.

D107. OH + 2- Methyl Furan. There have been three studies of the reaction of OH + 2-Methyl Furan at room temperature. Aschmann et al.[1] (296 K) and Bierbach et al.[2] (300 K) used the relative rate technique, and Whelan et al.[4] (294–668 K) measured absolute rate constants using laser flash photolysis with time resolved OH LIF detection in a slow flow system. Whelan et al. experiments were performed using two separate apparatus for measurements at lower pressure (<200 mbar) and higher pressures (≥2 bar). The rate coefficients at high pressures >2 bar are not considered in this evaluation. The recommended k(298 K) is the average of the three experimentally reported rate coefficients. Whelan et al. also report parameters for rate constants above room temperature, however no recommendation is currently made for Arrhenius parameters, as they would require extrapolation to atmospherically relevant conditions.

The dominant carbonyl formed from the reaction is 4-oxo-2-pentanal. In the absence of NO_x, Aschmann et al. reported a yield of ~70% and Bierbach et al.[3] report a yield of 80%. Bierbach et al. also report non-negligible yields of glyoxal (1.5−4.8%), methyl glyoxal (1.6−2.3%), formic acid (2.3–6%), and formaldehyde (1.4–2.3%). However, more studies are necessary to better quantify the product yields.
(Table: 25-1, Note: 25-1, Evaluated: 25-1) Back to Table

(1) Aschmann, S. M.; Nishino, N.; Arey, J.; Atkinson, R. Kinetics of the reactions of OH radicals with 2- and 3-methylfuran, 2,3- and 2,5-dimethylfuran, and *E*- and *Z*-3-Hexene-2,5-dione, and products of OH + 2,5-dimethylfuran. *Environ. Sci. Technol.* **2011**, *45*, 1859-1865, doi:10.1021/es103207k.
(2) Bierbach, A.; Barnes, I.; Becker, K. H. Rate coefficients for the gas-phase reactions of hydroxyl radicals with furan, 2-methylfuran, 2-ethylfuran and 2,5-dimethylfuran at 300 ± 2 K. *Atmos. Environ. Part A* **1992**, *26*, 813-817, doi:10.1016/0960-1686(92)90241-C.
(3) Bierbach, A.; Barnes, I.; Becker, K. H. Product and kientic study of the OH-initiated gas-phase oxidation of furan, 2-methylfuran and furanladehydes at ≈300 K. *Atmos.Environ.* **1995**, *29*, 2651-2660, doi:10.1016/1352-2310(95)00096-H.
(4) Whelan, C. A.; Eble, J.; Mir, Z. S.; Blitz, M. A.; Seakins, P. W.; Olzmann, M.; Stone, D. Kinetics of the reactions of hydroxyl radicals with furan and its alkylated derivatives 2-methyl furan and 2,5-dimethyl furan. *J. Phys. Chem. A* **2020**, *124*, 7416-7426, doi:10.1021/acs.jpca.0c06321.

D108. OH + 3-Methyl Furan. There have been four studies of the reaction of OH + 3-Methyl Furan. Aschmann et al.[1] (296 K), Atkinson et al.[2] (296 K), and Tapia et al.[4] (298 K) performed relative rate studies at room temperature, and Liljegren and Stevens[3] (273–368 K) studied the temperature dependence using a low-pressure discharge flow system with LIF detection of OH. All room temperature rate coefficients are in good agreement and the recommended value is the average of the four experimentally reported rate coefficients. The E/R is taken from Liljegren and Stevens and the A-factor is adjusted to reproduce k(298 K).

The reaction mechanism of the OH-initiated oxidation of 3-Methyl Furan was studied at atmospheric pressure and room temperature by Tapia et al., and Aschmann et al., who report 2-methylbutenedial as the major reaction product with yields of 45 ± 0.07% and 38 ± 2%, respectively. Other identified products included acetic acid, 3-furaldehyde, 3 methyl 2,5 furandione, 3methyl-2(3H) furnanone 3-furfural, 2-hydroxy-3-methyl-5(2H)-furanone, glyoxal, and methyl glyoxal.
(Table: 25-1, Note: 25-1, Evaluated: 25-1) Back to Table

(1) Aschmann, S. M.; Nishino, N.; Arey, J.; Atkinson, R. Kinetics of the reactions of OH radicals with 2- and 3-methylfuran, 2,3- and 2,5-dimethylfuran, and *E*- and *Z*-3-Hexene-2,5-dione, and products of OH + 2,5-dimethylfuran. *Environ. Sci. Technol.* **2011**, *45*, 1859-1865, doi:10.1021/es103207k.
(2) Atkinson, R.; Aschmann, S. M.; Tuazon, E. C.; Arey, J.; Zielinska, B. Formation of 3-methylfuran from the gas-phase reaction of OH radicals with isoprene and the rate constant for its reaction with the OH radical. *Int. J. Chem. Kinet.* **1989**, *21*, 593-604, doi:10.1002/kin.550210709.
(3) Liljegren, J.; Stevens, P. Measurements of the kinetics of the reaction of OH radicals with 3-methylfuran at low pressure. *Int. J. Chem. Kinet.* **2013**, *45*, 787-194, doi:10.1002/kin.20814.
(4) Tapia, A.; Villanueva, F.; Salgado, M. S.; Cabañas, B.; Martínez, E.; Martín, P. Atmospheric degradation of 3-methylfuran: kinetic and products study. *Atmos. Chem. Phys.* **2011**, *11*, 3227–3241, doi:10.5194/acp-11-3227-2011.

D109. OH + 2,5-Dimethyl Furan. There have been three studies of the reaction of OH + 2,5 -dimethyl Furan at room temperature. Two studies Aschmann et al.[1] (296 K) and Bierbach et al.[2] (300 K) were performed using the relative rate technique and an absolute study using laser flash photolysis with time resolved OH LIF detection in a slow flow system.[3] Whelan et al.[3] (294–668 K) also report high-pressure measurements, >2 bar, however these are not considered in this evaluation. The recommended value is the average of the three experimentally reported rate coefficients. Whelan et al. report rate coefficient parameters above room temperate, however, no recommendation is made for Arrhenius parameters as they would require extrapolation to atmospherically relevant conditions.

Aschmann et al., studied the reaction mechanism for 2,5-DMF + OH radicals. The observed yields for dicarbonyl products were 8 ± 2% for 3-methyl-4-oxo-2-pentenal (2,3-DMF) and 34 ± 3% for 3-hexene-2,5-dione (2,5-DMF).
(Table: 25-1, Note: 25-1, Evaluated: 25-1) Back to Table

(1) Aschmann, S. M.; Nishino, N.; Arey, J.; Atkinson, R. Kinetics of the reactions of OH radicals with 2- and 3-methylfuran, 2,3- and 2,5-dimethylfuran, and *E*- and *Z*-3-Hexene-2,5-dione, and products of OH + 2,5-dimethylfuran. *Environ. Sci. Technol.* **2011**, *45*, 1859-1865, doi:10.1021/es103207k.
(2) Bierbach, A.; Barnes, I.; Becker, K. H. Rate coefficients for the gas-phase reactions of hydroxyl radicals with furan, 2-methylfuran, 2-ethylfuran and 2,5-dimethylfuran at 300 ± 2 K. *Atmos. Environ. Part A* **1992**, *26*, 813-817, doi:10.1016/0960-1686(92)90241-C.
(3) Whelan, C. A.; Eble, J.; Mir, Z. S.; Blitz, M. A.; Seakins, P. W.; Olzmann, M.; Stone, D. Kinetics of the reactions of hydroxyl radicals with furan and its alkylated derivatives 2-methyl furan and 2,5-dimethyl furan. *J. Phys. Chem. A* **2020**, *124*, 7416-7426, doi:10.1021/acs.jpca.0c06321.

D110. OH + 2-ethyl Furan. There has been one study of the reaction of OH + 2-ethyl Furan, using the relative rate technique.[1] Bierbach et al. (300 K) did not measure reaction products for this reaction, but suggest that the reaction proceeds via addition at either the C2 or C3 position with addition at the C2 position most probably favored as it leads to an intermediate with an additional resonance structure.
(Table: 25-1, Note: 25-1, Evaluated: 25-1) Back to Table

(1) Bierbach, A.; Barnes, I.; Becker, K. H. Rate coefficients for the gas-phase reactions of hydroxyl radicals with furan, 2-methylfuran, 2-ethylfuran and 2,5-dimethylfuran at 300 ± 2 K. *Atmos. Environ. Part A* **1992**, *26*, 813-817, doi:10.1016/0960-1686(92)90241-C.

1.9.3 Bibliography – Reactions of Organic Compounds

Abbatt, J. P. D.; Demerjian, K. L.; Anderson, J. G. A new approach to free-radical kinetics: Radially and axially resolved high-pressure discharge flow with results for OH + (C_2H_6, C_3H_8, *n*-C_4H_{10}, *n*-C_5H_{12}) → products at 297 K. *J. Phys. Chem.* **1990**, *94*, 4566-4575, doi:10.1021/j100374a039.

Adachi, H.; Basco, N. Kinetic spectroscopy study of the reaction of CH_3O_2 with NO. *Chem. Phys. Lett.* **1979**, *63*, 490-492, doi:10.1016/0009-2614(79)80696-X.

Adachi, H.; Basco, N.; James, D. G. L. The ethylperoxy radical spectrum and rate constant for mutual interaction measured by flash photolysis and kinetic spectroscopy. *Int. J. Chem. Kinet.* **1979**, *11*, 1211-1229, doi:10.1002/kin.550111107.

Addison, M. C.; Burrows, J. P.; Cox, R. A.; Patrick, R. Absorption spectrum and kinetics of the acetylperoxy radical. *Chem. Phys. Lett.* **1980**, *73*, 283-287, doi:10.1016/0009-2614(80)80373-3.

Adeniji, S. A.; Kerr, J. A.; Williams, M. R. Rate constants for ozone-alkene reactions under atmospheric conditions. *Int. J. Chem. Kinet.* **1981**, *13*, 209-217, doi:10.1002/kin.550130210.

Aleksandrov, E. N.; Arutyunov, V. S.; Kozlov, S. N. Investigation of the reaction of atomic oxygen with acetylene. *Kinetics and Catalysis* **1981**, *22*, 391-394.

Anastasi, C.; Brown, M. J.; Smith, D. B.; Waddington, D. J. Joint French and Italian sections of the Combustion Institute, 1987, Amalfi, Italy.

Anastasi, C.; Waddington, D. J.; Woolley, A. Reactions of oxygenated radicals in the gas phase Part 10.-Self-reactions of ethylperoxy radicals. *J. Chem. Soc. Faraday Trans. 1* **1983**, *79*, 505-516, doi:10.1039/f19837900505.

Angelaki, M. E.; Romanias, M. N.; Burkholder, J. B.; Papadimitriou, V. C. Rate coefficients for the gas-phase OH + furan (C_4H_4O) reaction between 273 and 353 K. *Int. J. Chem. Kinet.* **2023**, *56*, 119-139, doi:10.1002/kin.21697.

Anglada, J. M.; Aplincourt, P.; Bofill, J. M.; Cremer, D. Atmospheric formation of OH radicals and H_2O_2 from alkene ozonolysis under humid conditions. *ChemPhysChem* **2002**, *3*, 215-221, doi:10.1002/1439-7641(20020215)3:2<215::AID-CPHC215>3.0.CO;2-3.

Anglada, J. M.; González, J.; Torrent-Sucarrat, M. Effects of the substituents on the reactivity of carbonyl oxides. A theoretical study on the reaction of substituted carbonyl oxides with water. *Phys. Chem. Chem. Phys.* **2011**, *13*, 13034-13045, doi:10.1039/c1cp20872a.

Anglada, J. M.; González, J.; Torrent-Sucarrat, M. Effects of the substituents on the reactivity of carbonyl oxides. A theoretical study on the reaction of substituted carbonyl oxides with water. *Phys. Chem. Chem. Phys.* **2001**, *13*, 13034-13045, doi:10.1039/c1cp20872a.

Aplincourt, P.; Ruiz-López, M. F. Theoretical investigation of reaction mechanisms for carboxylic acid formation in the atmosphere. *J. Am. Chem. Soc.* **2000**, *122*, 8990-8997, doi:10.1021/ja000731z.

Arrington, C. A.; Brennen, W.; Glass, G. P.; Michael, J. V.; Niki, H. Reactions of atomic oxygen with acetylene. I. Kinetics and mechanisms. *J. Chem. Phys.* **1965**, *43*, 525-532, doi:10.1063/1.1696776.

Aschmann, S. M.; Arey, J.; Atkinson, R. OH radical formation from the gas-phase reactions of O_3 with methacrolein and methyl vinyl ketone. *Atmos. Environ.* **1996**, *30*, 2939-2943, doi: 10.1016/1352-2310(96)00013-1.

Aschmann, S. M.; Nishino, N.; Arey, J.; Atkinson, R. Kinetics of the reactions of OH radicals with 2- and 3-methylfuran, 2,3- and 2,5-dimethylfuran, and *E*- and *Z*-3-Hexene-2,5-dione, and products of OH + 2,5-dimethylfuran. *Environ. Sci. Technol.* **2011**, *45*, 1859-1865, doi:10.1021/es103207k.

Aschmann, S. M.; Nishino, N.; Arey, J.; Atkinson, R. Products of the OH radical-initiated reactions of furan, 2- and 3 methylfuran, and 2,3- and 2,5-dimethylfuran in the presence of NO. *J. Phys. Chem. A* **2014**, *118*, 457-466, doi:10.1021/jp410345k.

Assali, M.; Fittschen, C. Rate constants and branching ratios for the self-reaction of acetyl peroxy ($CH_3C(O)O_2^{\bullet}$) and Its reaction with CH_3O_2. *Atmos.* **2022**, *13*, 186, doi:10.3390/atmos13020186.

Atkinson, R.; Aschmann, S. M. Rate constants for the reaction of OH radicals with a series of alkenes and dialkenes at 295 ± 1 K. *Int. J. Chem. Kinet.* **1984**, *16*, 1175-1186, doi:10.1002/kin.550161002.

Atkinson, R.; Aschmann, S. M. Rate constants for the reactions of O_3 and OH radicals with a series of alkynes. *Int. J. Chem. Kinet.* **1984**, *16*, 259-268, doi:10.1002/kin.550160308.

Atkinson, R.; Aschmann, S. M. Rate constants for the reactions of the OH radical with the propyl and butyl nitrates and 1-nitobutane at 298 ± 2 K. *Int. J. Chem. Kinet.* **1989**, *21*, 1123-1129, doi:10.1002/kin.550211205.

Atkinson, R.; Aschmann, S. M.; Arey, J.; Shorees, B. Formation of OH radicals in the gas phase reactions of O_3 with a series of terpenes. *J. Geophys. Res.* **1992**, *97*, 6065-6073, doi:10.1029/92JD00062.

Atkinson, R.; Aschmann, S. M.; Carter, W. P. L. Kinetics of the reactions of O_3 and OH radicals with furan and thiophene at 298 ± 2 K. *Int. J. Chem. Kinet.* **1983**, *15*, 51-61, doi:10.1002/kin.550150106.

Atkinson, R.; Aschmann, S. M.; Carter, W. P. L.; Winer, A. M. Kinetics of the gas-phase reactions of OH radicals with alkyl nitrates at 299 ± 2 K. *Int. J. Chem. Kinet.* **1982**, *14*, 919-926, doi:10.1002/kin.550140810.

Atkinson, R.; Aschmann, S. M.; Carter, W. P. L.; Winer, A. M.; Pitts, J. N., Jr. Kinetics of the reaction of OH radicals with n-alkanes at 299 ± 2 K. *Int. J. Chem Kinet.* **1982**, *14*, 781-788, doi:10.1002/kin.550140706.

Atkinson, R.; Aschmann, S. M.; Fitz, D. R.; Winer, A. M.; Pitts, J. N., Jr. Rate constants for the gas-phase reactions of O_3 with selected organics at 296 K. *Int. J. Chem. Kinet.* **1982**, *14*, 13-18, doi:10.1002/kin.550140103.

Atkinson, R.; Aschmann, S. M.; Pitts, J. N., Jr. Rate constants for the gas-phase reactions of the NO_3 radical with a series of organic compounds at 296 ± 2 K. *J. Phys. Chem.* **1988**, *92*, 3454-3457, doi:10.1021/j100323a028.

Atkinson, R.; Aschmann, S. M.; Pitts Jr., J. N. Kinetics of the gas-phase reactions of OH radicals with a series of α,β-unsaturated carbonyls at 299 ± 2 K. *Int. J. Chem. Kinet.* **1983**, *15*, 75-81, doi:10.1002/kin.550150108.

Atkinson, R.; Aschmann, S. M.; Tuazon, E. C.; Arey, J.; Zielinska, B. Formation of 3-methylfuran from the gas-phase reaction of OH radicals with isoprene and the rate constant for its reaction with the OH radical. *Int. J. Chem. Kinet.* **1989**, *21*, 593-604, doi:10.1002/kin.550210709.

Atkinson, R.; Aschmann, S. M.; Winer, A. M.; Pitts, J. N., Jr. Kinetics of the gas-phase reactions of NO_3 radicals with a series of dialkenes, cycloalkenes, and monoterpenes at 295 ± 1 K. *Environ. Sci. Technol.* **1984**, *18*, 370-375, doi:10.1021/es00123a016.

Atkinson, R.; Aschmann, S. M.; Winer, A. M.; Pitts Jr., J. N. Rate constants for the gas-phase reactions of O_3 with a series of carbonyls at 296 K. *Int. J. Chem. Kinet.* **1981**, *13*, 1133-1142, doi:10.1002/kin.550131104.

Atkinson, R.; Aschmann, S. M.; Winer, A. M.; Pitts, J. N., Jr. Rate constants for the reaction of OH radicals with a series of alkanes and alkenes at 299 ± 2 K. *Int. J. Chem. Kinet.* **1982**, *14*, 507-514, 10.1002/kin.550140508.

Atkinson, R.; Carter, W. P. L.; Aschmann, S. M.; Winer, A. M.; Pitts, J. N., Jr. Kinetics of the reaction of OH radicals with a series of branched alkanes at 297 ± 2 K. *Int. J. Chem. Kinet.* **1984**, *16*, 469-481, doi:10.1002/kin.550160413.

Atkinson, R.; Pitts Jr., J. N. Kinetics of the reactions of the OH radical with HCHO and CH_3CHO over the temperature range 299-426°K. *J. Chem. Phys.* **1978**, *68*, 3581-3590, doi:10.1063/1.436215.

Atkinson, R.; Plum, C. N.; Carter, W. P. L.; Winer, A. M.; Pitts, J. N., Jr. Rate constants for the gas-phase reactions of nitrate radicals with a series of organics in air at 298 ± 1 K. *J. Phys. Chem.* **1984**, *88*, 1210-1215, doi:10.1021/j150650a039.

Atkinson, R.; Winer, A. M.; Pitts, J. N., Jr. Rate constants for the gas phase reactions of O_3 with the natural hydrocarbons isoprene and α- and β-pinene. *Atmos. Environ.* **1982**, *16*, 1017-1020, doi: 10.1016/004-6981(82)90187-1.

Audley, G. J.; Baulch, D. L.; Campbell, I. M. Gas-phase reactions of hydroxyl radicals with aldehydes in flowing H_2O_2 + NO_2 + CO mixtures. *J. Chem. Soc. Faraday Trans. 1* **1981**, *77*, 2541-2549, doi:10.1039/f19817702541.

Avery, H. E.; Cvetanovic, R. J. Reaction of oxygen atoms with acetaldehyde. *J. Chem. Phys.* **1965**, *43*, 3727-3733, doi:10.1063/1.1696542.

Avramenko, L. I.; Kolesnikova, R. V. A photochemical study of the mechanism of the reaction between oxygen atoms and acetaldehyde. *Bull. Acad. Sci. USSR, Div. Chem. Sci.* **1961**, 1141-1143.

Avzianova, E. V.; Ariya, P. A. Temperature-dependent kinetic study for ozonolysis of selected tropospheric alkenes. *Int. J. Chem. Kinet.* **2002**, *34*, 678-684, doi:10.1002/kin.10093.

Azad, K.; Andino, J. M. Products of the gas-phase photooxidation reactions of 1-propanol with OH radicals. *Int. J. Chem. Kinet.* **1999**, *31*, 810-818, doi:10.1002/(SICI)1097-4601(1999)31:11<810::AID-JCK8>3.0.CO;2-W.

Bacher, C.; Tyndall, G. S.; Orlando, J. J. The atmospheric chemsitry of glycolaldehyde. *J. Atmos. Chem.* **2001**, *39*, 171-189, doi:10.1023/A:1010689706869.

Bahta, A.; Simonaitis, R.; Heicklen, J. Reactions of ozone with olefins: Ethylene, allene, 1,3-butadiene, and *trans*-1,3-pentadiene. *Int. J. Chem. Kinet.* **1984**, *16*, 1227-1246, doi:10.1002/kin.550161006.

Baldwin, A. C.; Golden, D. M. Reactions of methyl radicals of importance in combustion systems. *Chem. Phys. Lett.* **1978**, *55*, 350-352, doi:10.1016/0009-2614(78)87036-5.

Balestra-Garcia, C.; Le Bras, G.; MacLeod, H. Kinetic study of the reactions OH + mono-, di-, and trichloroacetaldehyde and acetaldehyde by laser photolysis-resonance fluorescence at 298 K. *J. Phys. Chem.* **1992**, *96*, 3312-3316, doi:10.1021/j100187a026.

Barker, J. R.; Benson, S. W.; Golden, D. M. The decomposition of dimethyl peroxide and the rate constant for $CH_3O + O_2 \rightarrow CH_2O + HO_2$. *Int. J. Chem. Kinet.* **1977**, *9*, 31-53, doi:10.1002/kin.550090105.

Barnes, I.; Bastian, V.; Becker, K. H.; Fink, E. H.; Nelsen, W. Oxidation of sulphur compounds in the atmosphere: I. Rate constants of OH radical reactions with sulphur dioxide, hydrogen sulphide, aliphatic thiols and thiophenol. *J. Atmos. Chem.* **1986**, *4*, 445-466, doi:10.1007/BF00053845.

Barnes, I.; Bastian, V.; Becker, K. H.; Fink, E. H.; Zabel, F. Reactivity studies of organic substances towards hydroxyl radicals under atmospheric conditions. *Atmos. Environ.* **1982**, *16*, 545-550, doi:10.1016/0004-6981(82)90163-9.

Barnes, I.; Bastian, V.; Becker, K. H.; Tong, Z. Kinetics and products of the reactions of NO_3 with monoalkenes, dialkenes, and monoterpenes. *J. Phys. Chem.* **1990**, *94*, 2413-2419, doi:10.1021/j100369a041.

Barnes, I.; Becker, K. H.; Fink, E. H.; Reimer, A.; Zabel, F.; Niki, H. FTIR spectroscopic study of the gas-phase reaction of HO_2 with H_2CO. *Chem. Phys. Lett.* **1985**, *115*, 1-8, doi:10.1016/0009-2614(85)80091-9.

Basco, N.; Parmar, S. S. Spectra and reactions of acetyl and acetylperoxy radicals. *Int. J. Chem. Kinet.* **1985**, *17*, 891-900, doi:10.1002/kin.550170809.

Batt, L.; Milne, R. T.; McCulloch, R. D. The gas-phase pyrolysis of alkyl nitrites. V. Methyl nitrite. *Int. J. Chem. Kinet.* **1977**, *9*, 567-587, doi:10.1002/kin.550090406.

Batt, L.; Robinson, G. N. Reaction of methoxy radicals with oxygen. I. Using dimethyl peroxide as a thermal source of methoxy radicals. *Int. J. Chem. Kinet.* **1979**, *11*, 1045-1053, doi:10.1002/kin.550111003.

Bauer, D.; Crowley, J. N.; Moortgat, G. K. The UV absorption spectrum of the ethylperoxy radical and its self-reaction kinetics between 218 and 333 K. *J. Photochem. Photobiol. A: Chem.* **1992**, *65*, 329-344, doi:10.1016/1010-6030(92)80015-N.

Baulch, D. L.; Campbell, I. M.; Saunders, S. M. Rate constants for the reactions of hydroxyl radicals with propane and ethane. *J. Chem. Soc. Faraday Trans. 1* **1985**, *81*, 259-263, doi:10.1039/f19858100259.

Becker, K. H.; Bechara, J.; Brockmann, K. J. Studies on the formation of H_2O_2 in the ozonolysis of alkenes. *Atmos. Environ.* **1993**, *27A*, 57-61, doi:10.1016/0960-1686(93)90070-F.

Becker, K. H.; Wirtz, K. Gas phase reactions of alkyl nitrates with hydroxyl radicals under tropospheric conditions in comparison with photolysis. *J. Atmos. Chem.* **1989**, *9*, 419-433, doi:10.1007/BF00114754.

Behera, B.; Lee, Y.-P. Detailed mechanism and kinetics of reactions of *anti*- and *syn*-CH_3CHOO with HC(O)OH: infrared spectra of conformers of hydroperoxyethyl formate. *Phys. Chem. Chem. Phys.* **2024**, *26*, 2950-1966, doi:10.1039/D3CP04086K.

Benter, T.; Schindler, R. N. Absolute rate coefficients for the reaction of NO_3 radicals with simple dienes. *Chem. Phys. Lett.* **1988**, *145*, 67-70, doi:10.1016/0009-2614(88)85134-0.

Berndt, T.; Böge, O. Gas-phase reaction of NO_3 radicals with isoprene: A kinetic and mechanistic Study. *Int. J. Chem. Kinet.* **1997**, *29*, 755-765, doi:10.1002/(SICI)1097-4601(1997)29:10<755::AID-KIN4>3.0.CO;2-L.

Berndt, T.; Jokinen, T.; Mauldin, R. L., III; Petäjä, T.; Herrmann, H.; Junninen, H.; Paasonen, P.; Worsnop, D. R.; Sipilä, M. Gas-phase ozonolysis of selected olefins: The yield of stabilized Criegee intermediate and the reactivity toward SO_2. *J. Phys. Chem. Lett.* **2012**, *3*, 2892-2896, doi:10.1021/jz301158u.

Berndt, T.; Jokinen, T.; Sipilä, M.; Mauldin, R. L.; Herrmann, H.; Stratmann, F.; Junninen, H.; Kulmala, M. H_2SO_4 formation from the gas-phase reaction of stabilized Criegee Intermediates with SO_2: Influence of water vapour content and temperature. *Atmos. Environ.* **2014**, *89*, 603-612, doi:10.1016/j.atm

Berndt, T.; Kaethner, R.; Voigtlander, J.; Stratmann, F.; Pfeifle, M.; Reichle, P.; Sipila, M.; Kulmala, M.; Olzmann, M. Kinetics of the unimolecular reaction of CH_2OO and the bimolecular reactions with the water monomer, acetaldehyde and acetone under atmospheric conditions. *Phys. Chem. Chem. Phys.* **2015**, *17*, 19862-19873, doi:10.1039/C5CP02224J.

Berndt, T.; Voightländer, J.; Stratmann, F.; Junninen, H.; Mauldin III, R. L.; Sipilä, M.; Kulmala, M.; Herrmann, H. Competing atmospheric reactions of CH_2OO with SO_2 and water vapour. *Phys. Chem. Chem. Phys.* **2014**, *16*, 19130-19136, doi:10.1039/c4cp02345e.

Bhaskaran, K. A.; Frank, P.; Just, T. In *12th International Shock Tube Symposium* Jerusalem., 1979.

Bierbach, A.; Barnes, I.; Becker, K. H. Rate coefficients for the gas-phase reactions of hydroxyl radicals with furan, 2-methylfuran, 2-ethylfuran and 2,5-dimethylfuran at 300 ± 2 K. *Atmos. Environ. Part A* **1992**, *26*, 813-817, doi:10.1016/0960-1686(92)90241-C.

Bierbach, A.; Barnes, I.; Becker, K. H. Product and kientic study of the OH-initiated gas-phase oxidation of furan, 2-methylfuran and furanladehydes at ≈300 K. *Atmos.Environ.* **1995**, *29*, 2651-2660, doi:10.1016/1352-2310(95)00096-H.

Bohland, T.; Temps, F.; Wagner, H. G. An LMR-spectrometer operating up to mm-wavelengths for kinetic investigations with discharge flow and flash photolysis systems. *Z. Phys. Chem. (Neue Folge)* **1984**, *142*, 129-140.

Bonard, A.; Daële, V.; Delfau, J.-L.; Vovelle, C. Kinetics of OH radical reactions with methane in the temperature range 295-660 K and with dimethyl ether and methyl-*tert*-butyl ether in the temperature range 295-618 K. *J. Phys. Chem. A* **2002**, *106*, 4384-4389, doi:10.1021/jp012425t.

Bourmada, N.; Lafage, C.; Devolder, P. Absolute rate constants of the reactions of OH with cyclohexane and ethane at 296 ± 2 K by the discharge flow method. *Chem. Phys. Lett.* **1987**, *136*, 209-214, doi:10.1016/0009-2614(87)80443-8.

Bozzelli, J. W.; Dean, A. M. Chemical activation analysis of the reaction of C_2H_5 with O_2. *J. Phys. Chem.* **1990**, *94*, 3313-3317, doi:10.1021/j100371a021.

Bridier, I.; Veyret, B.; Lesclaux, R.; Jenkin, M. E. Flash photolysis study of the UV spectrum and kinetics of reactions of the acetonylperoxy radical. *J. Chem. Soc. Faraday Trans.* **1993**, *89*, 2993-2997, doi:10.1039/ft9938902993.

Brown, J. M.; Thrush, B. A. E.S.R. studies of the reactions of atomic oxygen and hydrogen with simple hydrocarbons. *Trans. Faraday Soc.* **1967**, *63*, 630-642, doi:10.1039/tf9676300630.

Bryukov, M. G.; Knyazev, V. D.; Lomnicki, S. M.; McFerrin, C. A.; Dellinger, B. Temperature-dependent kinetics of the gas-phase reactions of OH with Cl_2, CH_4, and C_3H_8. *J. Phys. Chem. A* **2004**, *108*, 10464-10472, doi:10.1021/jp047340h.

Buras, Z. J.; Elsamra, R. M. I.; Green, W. H. Direct determination of the simplest Criegee intermediate (CH_2OO) self reaction rate. *J. Phys. Chem. Lett.* **2014**, *5*, 2224-2228, doi:10.1021/jz5008406.

Buras, Z. J.; Elsamra, R. M. I.; Jalan, A.; Middaugh, J. E.; Green, W. H. Direct kinetic measurements of reactions between the simplest Criegee intermediate CH_2OO and alkenes. *J. Phys. Chem. A* **2014**, *118*, 1997-2006, doi:10.1021/jp4118985.

Burrows, J. P.; Tyndall, G. S.; Moortgat, G. K. Absorption spectrum of NO_3 and kinetics of the reactions of NO_3 with NO_2, Cl, and several stable atmospheric species at 298 K. *J. Phys. Chem.* **1985**, *89*, 4848-4856, doi:10.1021/j100268a038.

Butkovskaya, N. I.; Kukui, A.; Le Bras, G. Branching fractions for H_2O forming channels of the reaction of OH radicals with acetaldehyde. *J. Phys. Chem. A* **2004**, *108*, 1160-1168, doi:10.1021/jp036740m.

Butkovskaya, N. I.; Kukui, A.; Pouvesle, N.; Le Bras, G. Rate constant and mechanism of the reaction of OH radicals with acetic acid in the temperature range of 229-300 K. *J. Phys. Chem. A* **2004**, *108*, 7021-7026, doi:10.1021/jp048444v.

Butkovskaya, N. I.; Pouvesle, N.; Kukui, A.; Le Bras, G. Mechanism of the OH-initiated oxidation of glycolaldehyde over the temperature range 233-296 K. *J. Phys. Chem. A* **2006**, *110*, 13492-13499, doi:10.1021/jp064993k.

Cabezas, C.; Endo, Y. Observation of hydroperoxyethyl formate from the reaction between methyl Criegee intermediate and formic acid. *Phys. Chem. Chem. Phys.* **2020**, *22*, 446-454, doi:10.1039/C9CP05030B.

Cadle, R. D.; Powers, J. W. The reaction of $O(^3P)$ with acetaldehyde in a fast-flow system. *J. Phys. Chem.* **1967**, *71*, 1702-1706, doi:10.1021/j100865a023.

Cadle, R. D.; Schadt, C. Kinetics of the gas phase reaction between acetylene and ozone. *J. Chem. Phys.* **1953**, *21*, 163, doi:10.1063/1.1698576.

Cameron, M.; Sivakumaran, V.; Dillon, T. J.; Crowley, J. N. Reaction between OH and CH_3CHO. Part 1. Primary product yields of CH_3 (296 K), CH_3CO (296 K), and H (237-296 K). *Phys. Chem. Chem. Phys.* **2002**, *4*, 3628-3638, doi:10.1039/b202586h.

Campbell, I. M.; McLaughlin, D. F.; Handy, B. J. Rate constants for reactions of hydroxyl radicals with alcohol vapours at 292 K. *Chem. Phys. Lett.* **1976**, *38*, 362-364, doi:10.1016/0009-2614(76)85174-3.

Campuzano-Jost, P.; Williams, M. B.; D'Ottone, L.; Hynes, A. J. Kinetics of the OH-initiated oxidation of isoprene. *Geophys. Res. Lett.* **2000**, *27*, 693-696, doi:10.1029/1999GL010995.

Campuzano-Jost, P.; Williams, M. B.; D'Ottone, L.; Hynes, A. J. Kinetics and mechanism of the reaction of the hydroxyl radical with h_8-isoprene and d_8-isoprene: Isoprene absorption cross sections, rate coefficients, and the mechanism of hydroperoxyl radical production. *J. Phys. Chem. A* **2004**, *108*, 1537-1551, doi:10.1021/jp0363601.

Canosa-Mas, C. E.; Carr, S.; King, M. D.; Shallcross, D. E.; Thompson, K. C.; Wayne, R. P. A kinetic study of the reactions of NO_3 with methyl vinyl ketone, methacrolein, acrolein, methyl acrylate and methyl methacrylate. *Phys. Chem. Chem. Phys.* **1999**, *1*, 4195-4202, doi:10.1039/a904613e.

Cantrell, C. A.; Davidson, J. A.; Busarow, K. L.; Calvert, J. G. The CH_3CHO-NO_3 reaction and possible nighttime PAN generation. *J. Geophys. Res.* **1986**, *91*, 5347-5353, doi:10.1029/JD091iD05p05347.

Cantrell, C. A.; Shetter, R. E.; McDaniel, A. J.; Calvert, J. G.; Davidson, J. A.; Lowe, D. C.; Tyler, S. C.; Cicerone, R. J.; Greenberg, J. P. Carbon kinetic isotope effect in the oxidation of methane by the hydroxyl radical. *J. Geophys. Res.* **1990**, *95*, 22455-22462, doi:10.1029/JD095iD13p22455.

Cantrell, C. A.; Stockwell, W. R.; Anderson, L. G.; Busarow, K. L.; Perner, D.; Schmeltekopf, A.; Calvert, J. G.; Johnston, H. S. Kinetlc study of the NO_3-CH_2O reaction and its possible role in nighttime tropospheric chemistry. *J. Phys. Chem.* **1985**, *89*, 139-146, doi:10.1021/j100247a031.

Caravan, R. L.; Khan, M. A. H.; Rotavera, B.; Papajak, E.; Antonov, I. O.; Chen, M.-W.; Au, K.; Chao, W.; Osborn, D. L.; Lin, J. J.-M.; Percival, C. J.; Shallcross, D. E.; Taatjes, C. A. Products of Criegee intermediate reactions with NO_2: experimental measurements and tropospheric implications. *Faraday Discuss.* **2017**, *200*, 313-330, doi:10.1039/C7FD00007C.

Caravan, R. L.; Shannon, R. J.; Lewis, T.; Blitz, M. A.; Heard, D. E. Measurements of rate coefficients for reactions of OH with ethanol and propan-2-ol at very low temperatures. *J. Phys. Chem. A* **2015**, *119*, 7130-7137, doi:10.1021/jp505790m.

Carr, S. A.; Baeza-Romero, M. T.; Blitz, M. A.; Price, B. J. S.; Seakins, P. W. Ketone photolysis in the presence of oxygen: A useful source of OH for flash photolysis kinetics experiments. *Int. J. Chem. Kinet.* **2008**, *40*, 504-514, doi:10.1002/kin.20330.

Cattell, F. C.; Cavanagh, J.; Cox, R. A.; Jenkin, M. E. A kinetics study of reactions of HO_2 and $C_2H_5O_2$ using diode laser absorption spectroscopy. *J. Chem. Soc. Faraday Trans. 2* **1986**, *82*, 1999-2018, doi:10.1039/f29868201999.

Cavalli, F.; Glasius, M.; Hjorth, J.; Rindone, B.; Jensen, N. R. Atmospheric lifetimes, infrared spectra and degradation products of a series of hydrofluoroethers. *Atmos. Environ.* **1998**, *32*, 3767-3773, doi:10.1016/S1352-2310(98)00106-X.

Chang, J. S.; Barker, J. R. Reaction rate and products for the reaction $O(^3P) + H_2CO$. *J. Phys. Chem.* **1979**, *83*, 3059-3064, doi:10.1021/j100487a001.

Chang, Y.-P.; Chang, H.-H.; Lin, J. J.-M. Kinetics of the simplest Criegee intermediate reaction with ozone studied using a mid-infrared quantum cascade laser spectrometer. *Phys. Chem. Chem. Phys.* **2018**, *20*, 97-102, doi:10.1039/c7cp06653h.

Chao, W.; Hsieh, J.-T.; Chang, C.-H.; Lin, J. J.-M. Direct kinetic measurement of the reaction of the simplest Criegee intermediate with water vapor. *Science* **2015**, *347*, 751-754, doi:10.1126/science.1261549.

Cheema, S. A.; Holbrook, K. A.; Oldershaw, G. A.; Walker, R. W. Kinetics and mechanism associated with the reactions of hydroxyl radicals and of chlorine atoms with 1-propanol under near-tropospheric conditions between 273 and 343 K. *Int. J. Chem. Kinet.* **2002**, *34*, 110-121, doi:10.1002/kin.10027.

Chen, X.; Hulbert, D.; Shepson, P. B. Measurement of the organic nitrate yield from OH reaction with isoprene. *J. Geophys. Res.* **1998**, *103*, 25563-25568, doi:10.1029/98jd01483.

Chew, A. A.; Atkinson, R.; Aschmann, S. M. Kinetics of the gas-phase reactions of NO_3 radicals with a series of alcohols, glycol ethers, ethers and chloroalkanes. *J. Chem. Soc. Faraday Trans.* **1998**, *94*, 1083-1089, doi:10.1039/a708183i.

Chhantyal-Pun, R.; Davey, A.; Shallcross, D. E.; Percival, C. J.; Orr-Ewing, A. J. A kinetic study of the CH_2OO Criegee intermediate self-reaction, reaction with SO_2 and unimolecular reaction using cavity ring-down spectroscopy. *Phys. Chem. Chem. Phys.* **2015**, *17*, 3617-3626, doi:10.1039/c4cp04198d.

Chhantyal-Pun, R.; McGillen, M. R.; Beames, J. M.; Khan, M. A. H.; Percival, C. J.; Shallcross, D. E.; Orr-Ewing, A. J. Temperature-dependence of the rates of reaction of trifluoroacetic acid with Criegee intermediates. *Angew. Chem. Int. Ed.* **2017**, *56*, 9044-9047, doi:10.1002/anie.201703700.

Chiorboli, C.; Bignozzi, C. A.; Maldotti, A.; Giardini, P. F.; Rossi, A.; Carassiti, V. Rate constants for the gas-phase reactions of OH radicals with β-dimethylstyrene and acetone. Mechanism of β-dimethylstyrene NO_x – air photooxidation. *Int. J. Chem. Kinet.* **1983**, *15*, 579-586, doi:10.1002/kin.550150608.

Chuong, B.; Stevens, P. S. Kinetic study of the OH + isoprene and OH + ethylene reactions between 2 and 6 Torr and over the temperature range 300-423 K. *J. Phys. Chem. A* **2000**, *104*, 5230-5237, doi:10.1021/jp993613a.

Chuong, B.; Stevens, P. S. Measurements of the kinetics of the OH-initiated oxidation of isoprene. *J. Geophys. Res.* **2002**, *107*, 4162, doi:10.1029/2001JD000865.

Chuong, B.; Stevens, P. S. Kinetics of the OH + methyl vinyl ketone and OH + methacrolein reactions at low pressure *J. Phys. Chem. A* **2003**, *107*, 2185-2191, doi:10.1021/jp026036q.
Chuong, B.; Stevens, P. S. Measurements of the kinetics of the OH-initiated oxidation of methyl vinyl ketone and methacrolein. *Int. J. Chem. Kinet.* **2004**, *36*, 12-25, doi:10.1002/kin.10167.
Clarke, J. S.; Kroll, J. H.; Donahue, N. M.; Anderson, J. G. Testing frontier orbital control: Kinetics of OH with ethane, propane, and cyclopropane from 180 to 360K. *J. Phys. Chem. A* **1998**, *102*, 9847-9857, doi:10.1021/jp982922i.
Cox, R. A.; Derwent, R. G.; Kearsey, S. V.; Batt, L.; Patrick, K. G. Photolysis of methyl nitrite: Kinetics of the reaction of the methoxy radical with O_2. *J. Photochem.* **1980**, *13*, 149-163, doi:10.1016/0047-2670(80)85006-4.
Cox, R. A.; Derwent, R. G.; Williams, M. R. Atmospheric photooxidation reactions. Rates, reactivity, and mechanism for reaction of organic compounds with hydroxyl radicals. *Environ. Sci. Technol.* **1980**, *14*, 57-61, doi:10.1021/es60161a007.
Cox, R. A.; Penkett, S. A. Aerosol formation from sulphur dioxide in the presence of ozone and olefinic hydrocarbons. *J. Chem. Soc. Faraday Trans. 1* **1972**, *68*, 1735-1753, doi:10.1039/f19726801735.
Crawford, M. A.; Wallington, T. J.; Szente, J. J.; Maricq, M. M.; Francisco, J. S. Kinetics and mechanism of the acetylperoxy + HO_2 reaction. *J. Phys. Chem. A* **1999**, *103*, 365-378, doi:10.1021/jp983150t.
Crehuet, R.; Anglada, J. M.; Bofill, J. M. Tropospheric formation of hydroxymethyl hydroperoxide, formic acid, H_2O_2, and OH from carbonyl oxide in the presence of water vapor: A theoretical study of the reaction mechanism. *Chem. Eur. J.* **2001**, *7*, 2227-2235, doi:10.1002/1521- 3765(2001051817:10<2227::AID-CHEM2227>3.0.CO;2-O.
Crounse, J. D.; Knap, H. C.; Ørnso, K. B.; Jørgensen, S.; Paulot, F.; Kjaergaard, H. G.; Wennberg, P. O. Atmospheric fate of methacrolein. 1. Peroxy radical isomerization following addition of OH and O_2. *J. Phys. Chem. A* **2012**, *116*, 5756-5762, doi:10.1021/jp211560u.
Crowley, J. N.; Campuzano-Jost, P.; Moortgat, G. K. Temperature dependent rate constants for the gas-phase reaction between OH and CH_3OCl. *J. Phys. Chem.* **1996**, *100*, 3601-3606, doi:10.1021/jp953018i.
Crunaire, S.; Tarmoul, J.; Fittschen, C.; Tomas, A.; Lemoine, B.; Coddeville, P. Use of cw-CRDS for studying the atmospheric oxidation of acetic acid in a simulation chamber. *Appl. Phys. B* **2006**, *85*, 467-476, doi:10.1007/s00340-006-2319-6.
D'Anna, B.; Andresen, O.; Gefen, Z.; Nielsen, C. J. Kinetic study of OH and NO_3 radical reactions with 14 aliphatic aldehydes. *Phys. Chem. Chem. Phys.* **2001**, *3*, 3057-3063, doi:10.1039/b103623h.
da Silva, G. Reaction of methacrolein with the hydroxyl radical in air: Incorporation of secondary O_2 addition into the MACR + OH master equation. *J. Phys. Chem. A* **2012**, *116*, 5317-5324, doi:10.1021/jp303806w.
Daële, V.; Ray, A.; Vassalli, I.; Poulet, G.; Le Bras, G. Kinetic study of reactions of C_2H_5O and $C_2H_5O_2$ with NO at 298 K and 0.55 – 2 torr. *Int. J. Chem. Kinet.* **1995**, *27*, 1121-1133, doi:10.1002/kin.550271109.
Dagaut, P.; Wallington, T. J.; Kurylo, M. J. Flash photolysis kinetic absorption spectroscopy study of the gas-phase reactlon HO_2 + $C_2H_5O_2$ over the temperature range 228-380 K. *J. Phys. Chem.* **1988**, *92*, 3836-3839, doi:10.1021/j100324a031.
Dagaut, P.; Wallington, T. J.; Kurylo, M. J. Temperature dependence of the rate constant for the HO_2 + CH_3O_2 gas-phase reaction. *J. Phys. Chem.* **1988**, *92*, 3833-3836, doi:10.1021/j100324a030.
Dagaut, P.; Wallington, T. J.; Liu, R.; Kurylo, M. J. The gas phase reactions of hydroxyl radicals with a series of carboxylic acids over the temperature range 240-440 K. *Int. J. Chem. Kinet.* **1988**, *20*, 331-338, doi:10.1002/kin.550200406.
Darnall, K. R.; Atkinson, R.; Pitts, J. N., Jr. Rate constants for the reaction of the OH radical with selected alkanes at 300 K. *J. Phys. Chem.* **1978**, *82*, 1581-1584, doi:10.1021/j100503a001.
Davidson, J. A.; Cantrell, C. A.; Tyler, S. C.; Shetter, R. E.; Cicerone, R. J.; Calvert, J. G. Carbon kinetic isotope effect in the reaction of CH_4 with HO. *J. Geophys. Res.* **1987**, *92*, 2195-2199, doi:10.1029/JD092iD02p02195.
Davies, P. B.; Thrush, B. A. Reactions of oxygen atoms with hydrogen cyanide, cyanogen chloride and cyanogen bromide. *Trans. Faraday Soc.* **1968**, *64*, 1836-1843, doi:10.1039/tf9686401836.
De Smedt, F.; Bui, X. V.; Nguyen, T. L.; Peeters, J.; Vereecken, L. Theoretical and experimental study of the product branching in the reaction of acetic acid with OH radicals. *J. Phys. Chem. A* **2005**, *109*, 2401-2409, doi:10.1021/jp044679v.
DeMore, W. B. Arrhenius constants for the reactions of ozone with ethylene and acetylene. *Int. J. Chem. Kinet.* **1969**, *1*, 209-220, doi:10.1002/kin.550010207.

DeMore, W. B. Rates and mechanism of alkyne ozonation. *Int. J. Chem. Kinet.* **1971**, *3*, 161-173, doi:10.1002/kin.550030208.
DeMore, W. B. Rate constant ratio for the reaction of OH with CH_3D and CH_4. *J. Phys. Chem.* **1993**, *97*, 8564-8566, doi:10.1021/j100135a006.
DeMore, W. B.; Bayes, K. D. Rate constants for the reactions of hydroxyl radical with several alkanes, cycloalkanes, and dimethyl ether. *J. Phys. Chem. A* **1999**, *103*, 2649-2654, doi:10.1021/jp983273d.
DeMore, W. B.; Lin, C.-L. Intermediates in the ozonation of simple alkynes. *J. Org. Chem.* **1973**, *38*, 985-989, doi:10.1021/jo00945a028.
Dillon, T. J.; Hölscher, D.; Sivakumaran, V.; Horowitz, A.; Crowley, J. N. Kinetics of the reactions of HO with methanol (210–351 K) and with ethanol (216–368 K). *Phys. Chem. Chem. Phys.* **2005**, *7*, 349-355, doi:10.1039/b413961e.
Dlugokencky, E. J.; Howard, C. J. Studies of NO_3 radical reactions with some atmospheric organic compounds at low pressures. *J. Phys. Chem.* **1989**, *93*, 1091-1096, doi:10.1021/j100340a015.
Dóbé, S.; Khachatryan, L. A.; Bérces, T. Kinetics of reactions of hydroxyl radicals with a series of aliphatic aldehydes. *Ber. Bunsenges. Phys. Chem.* **1989**, *93*, 847-852, doi:10.1002/bbpc.19890930806.
Dóbé, S.; Temps, F.; Böhland, T.; Wagner, H. G. The reaction of CH_2OH radicals with O_2 studied by laser magnetic resonance technique. *Z. Naturforsch.* **1985**, *40a*, 1289-1298.
Dóbé, S.; Turányi, T.; Iogansen, A. A.; Bérces, T. Rate constants of the reactions of OH radicals with cyclopropane and cyclobutane. *Int. J. Chem. Kinet.* **1992**, *24*, 191-198, doi:10.1002/kin.550240207.
Donahue, N. M.; Anderson, J. G.; Demerjian, K. L. New rate constants for ten OH alkane reactions from 300 to 400 K: An assessment of accuracy. *J. Phys. Chem. A* **1998**, *102*, 3121-3126, doi:10.1021/jp980532q.
Donahue, N. M.; Clarke, J. S. Fitting multiple datasets in kinetics: *n*-butane + OH → products. *Int. J. Chem. Kinet.* **2004**, *36*, 259-272, doi:10.1002/kin.10194.
Donahue, N. M.; Kroll, J. H.; Anderson, J. G.; Demerjian, K. L. Direct observation of OH production from the ozonolysis of olefins *Geophys. Res. Lett.* **1998**, *25*, 59-62, doi:10.1029/97GL53560.
Droege, A. T.; Tully, F. P. Hydrogen-atom abstraction from alkanes by OH. 3. Propane. *J. Phys. Chem.* **1986**, *90*, 1949-1954, doi:10.1021/j100400a042.
Droege, A. T.; Tully, F. P. Hydrogen-atom abstraction from alkanes by OH. 5. n-Butane. *J. Phys. Chem.* **1986**, *90*, 5937-5941, doi:10.1021/j100280a096.
Droege, A. T.; Tully, F. P. Hydrogen-atom abstraction from alkanes by OH. 6. Cyclopentane and cyclohexane. *J. Phys. Chem.* **1987**, *91*, 1222-1225, doi:10.1021/j100289a037.
Dunlop, J. R.; Tully, F. P. Catalytic dehydration of alcohols by OH. 2-propanol: An intermediate case. *J. Phys. Chem.* **1993**, *97*, 6457-6464, doi:10.1021/j100126a021.
Dunlop, J. R.; Tully, F. P. A kinetic study of OH radical reactions with methane and perdeuterated methane. *J. Phys. Chem.* **1993**, *97*, 11148-11150, doi:10.1021/j100145a003.
Eberhard, J.; Howard, C. J. Temperature-dependent kinetics studies of the reactions of $C_2H_5O_2$ and *n*-$C_3H_7O_2$ radicals with NO. *Int. J. Chem. Kinet.* **1996**, *28*, 731-740, doi:10.1002/(SICI)1097-4601(1996)28:10<731::AID-KIN3>3.0.CO;2-O.
Eberhard, J.; Howard, C. J. Rate coefficients for the reactions of some C_3 to C_5 hydrocarbon peroxy radicals with NO. *J. Phys. Chem. A* **1997**, *101*, 3360-3366, doi:10.1021/jp9640282.
Eberhard, J.; Villalta, P. W.; Howard, C. J. Reaction of isopropyl peroxy radicals with NO over the temperature range 201-401 K. *J. Phys. Chem.* **1996**, *100*, 993-997, doi:10.1021/jp951824j.
Edney, E. O.; Kleindienst, T. E.; Corse, E. W. Room temperature rate constants for the reaction of OH with selected chlorinated and oxygenated hydrocarbons. *Int. J. Chem. Kinet.* **1986**, *18*, 1355-1371, doi:10.1002/kin.550181207.
Ellermann, T.; Nielsen, O. J.; Skov, H. Absolute rate constants for the reaction of NO_3 radicals with a series of dienes at 295 K. *Chem. Phys. Lett.* **1992**, *200*, 224-229, doi:10.1016/0009-2614(92)80002-S.
Elrod, M. J.; Ranschaert, D. L.; Schneider, N. J. Direct kinetics study of the termperature dependence of the CH_2O branching channel for the CH_3O_2 + HO_2 Reaction. *Int. J. Chem. Kinet.* **2001**, *33*, 363-376, doi:10.1002/kin.1030.
Elsamra, R. M. I.; Jalan, A.; Buras, Z. J.; Middaugh, J. E.; Green, W. H. Temperature- and pressure-dependent kinetics of CH_2OO + CH_3COCH_3 and CH_2OO + CH_3CHO: Direct measurements and theoretical analysis. *Int. J. Chem. Kinet.* **2016**, *48*, 474-488, doi: 10.1002/kin.21007.
Fang, Y.; Liu, F.; Barber, V. P.; Klippenstein, S. J.; McCoy, A. B.; Lester, M. I. Communication: Real time observation of unimolecular decay of Criegee intermediates to OH radical products. *J. Chem. Phys.* **2016**, *144*, 061102, doi:10.1063/1.4941768.

Fenske, J. D.; Hasson, A. S.; Ho, A. W.; Paulson, S. E. Measurement of absolute unimolecular and bimolecular rate constants for CH_3CHOO generated by the *trans*-2-Butene reaction with ozone in the gas phase. *J. Phys. Chem. A* **2000**, *104*, 9921-9932, doi:10.1021/jp0016636.

Fenter, F. F.; Catoire, V.; Lesclaux, R.; Lightfoot, P. D. The ethylperoxy radical: Its ultraviolet spectrum, self-reaction, and reaction with HO_2, each studied as a function of temperature. *J. Phys. Chem.* **1993**, *97*, 3530-3538, doi:10.1021/j100116a016.

Finlayson-Pitts, B. J.; Hernandez, S. K.; Berko, H. N. A new dark source of the gaseous hydroxyl radical for the relative rate measurements. *J. Phys. Chem.* **1993**, *97*, 1172-1177, doi:10.1021/j100108a012.

Foreman, E. S.; Kapnas, K. M.; Murray, C. Reactions between Criegee intermediates and the inorganic acids HCl and HNO_3: Kinetics and atmospheric implications. *Angew. Chem. Int. Ed.* **2016**, *55*, 10419-10422, doi:10.1002/anie.201604662.

Frost, M. J.; Smith, I. W. M. Rate Constants for the reactions of CH_3O and C_2H_5O with NO over a range of temperature and total pressure. *J. Chem. Soc. Faraday Trans.* **1990**, *86*, 1757-1762, doi:10.1039/ft9908601757.

Gaffney, J. S.; Fajer, R.; Senum, G. I.; Lee, J. H. Measurement of the reactivity of OH with methyl nitrate: Implications for prediction of alkyl nitrate-OH reaction rates. *Int. J. Chem. Kinet.* **1986**, *18*, 399-407, doi:10.1002/kin.550180311.

Gennaco, M. A.; Huang, Y. W.; Hannun, R. A.; Dransfield, T. J. Absolute rate constants for the reaction of OH with cyclopentane and cycloheptane from 233 to 351 K. *J. Phys. Chem. A* **2012**, *116*, 12438-12443, doi:10.1021/jp3048482.

Ghosh, B.; Bugarin, A.; Connell, B. T.; North, S. W. Isomer-selective study of the OH-initiated oxidation of isoprene in the presence of O_2 and NO: 2. The major OH addition channel. *J. Phys. Chem. A* **2010**, *114*, 2553-2560, doi:10.1021/jp909052t.

Gierczak, T.; Burkholder, J. B.; Talukdar, R. K.; Mellouki, A.; Barone, S. B.; Ravishankara, A. R. Atmospheric fate of methyl vinyl ketone and methacrolein. *J. Photochem. Photobiol. A: Chem.* **1997**, *110*, 1-10, doi:10.1016/S1010-6030(97)00159-7.

Gierczak, T.; Gilles, M. K.; Bauerle, S.; Ravishankara, A. R. Reaction of hydroxyl radical with acetone. 1. Kinetics of the reactions of OH, OD, and ^{18}OH with acetone and acetone-d_6. *J. Phys. Chem. A* **2003**, *107*, 5014-5020, doi:10.1021/jp027301a.

Gierczak, T.; Talukdar, R. K.; Herndon, S. C.; Vaghjiani, G. L.; Ravishankara, A. R. Rate coefficient for the reaction of hydroxyl radicals with methane and deuterated methanes. *J. Phys. Chem. A* **1997**, *101*, 3125-3134, doi:10.1021/jp963892r.

Gierczak, T.; Talukdar, R. K.; Herndon, S. C.; Vaghjiani, G. L.; Ravishankara, A. R. Rate coefficients for the reactions of hydroxyl radicals with methane and deuterated methanes. *J. Phys. Chem. A* **1997**, *101*, 3125-3134, doi:10.1021/jp963892r.

Gill, K. J.; Hites, R. A. Rate constants for the gas-phase reactions of the hydroxyl radical with isoprene, α- and β-pinene, and limonene as a function of temperature. *J. Phys. Chem. A* **2002**, *106*, 2538-2544, doi:10.1021/jp013532q.

Gill, R. J.; Johnson, W. D.; Atkinson, G. H. The formation and decay mechanisms of HCO in the photodissociation of gas phase acetaldehyde. *Chem. Phys.* **1981**, *58*, 29-44, doi:10.1016/0301-0104(81)80042-0.

Gómez Alvarez, E.; Borrás, E.; Viidanoja, J.; Hjorth, J. Unsaturated dicarbonyl products from the OH-initiated photo-oxidation of furan, 2-methylfuran and 3-methylfuran. *Atmos. Environ.* **2009**, *43*, 1603-1612, doi:10.1016/j.atmosenv.2008.12.019.

Good, D. A.; Hanson, J.; Francisco, J. S.; Li, Z.; Jeong, G.-R. Kinetics and reaction mechanism of hydroxyl radical reaction with methyl formate. *J. Phys. Chem. A* **1999**, *103*, 10893-10898, doi:10.1021/jp991960e.

Gordon, S.; Mulac, W. A. Reaction of the $OH(X^2\prod)$ radical produced by the pulse radiolysis of water vapor. *Int. J. Chem. Kinet.* **1975**, *Symp. 1*, 289-299.

Greene, C. R.; Atkinson, R. Rate constants for the gas-phase reactions of O_3 with a series of alkenes at 296 ± 2 K. *Int. J. Chem. Kinet.* **1992**, *24*, 803-811, doi:10.1002/kin.550240905.

Greenhill, P. G.; O'Grady, B. V. The rate constant of the reaction of hydroxyl radicals with methanol, ethanol and (D_3)methanol. *Aust. J. Chem.* **1986**, *39*, 1775-1787, doi:10.1071/CH9861775.

Greiner, N. R. Hydroxyl-radical kinetics by kinetic spectroscopy. II. Reactions with C_2H_6, C_3H_8, and *iso*-C_4H_{10} at 300°K. *J. Chem. Phys.* **1967**, *46*, 3389-3392, doi:10.1063/1.1841228.

Greiner, N. R. Hydroxyl radical kinetics by kinetic spectrosopy. VII. The reaction with ethylene in the range 300-500 °K. *J. Chem. Phys.* **1970**, *53*, 1284-1285, doi:10.1063/1.1674133.

Grimsrud, E. P.; Westberg, H. H.; Rasmussen, R. A. Atmospheric reactivity of monoterpene hydrocarbons, NO_x photooxidation and ozonolysis. *Int. J. Chem. Kinet.* **1975**, *Symp 1*, 183-195.
Grosjean, D.; Williams, E. L., II; Grosjean, E. Atmospheric chemistry of isoprene and of its carbonyl products. *Environ. Sci. Technol.* **1993**, *27*, 830-840, doi:10.1021/es00042a004.
Grosjean, E.; Grosjean, D. Rate constants for the gas-phase reaction of ozone with 1,1-disubstituted alkenes. *Int. J. Chem. Kinet.* **1996**, *28*, 911-918, doi:10.1002/(SICI)1097-4601(1996)28:12<911::AID-KIN8>3.0.CO;2-Q.
Grosjean, E.; Grosjean, D. Rate constants for the gas-phase reaction of ozone with unsaturated oxygenates. *Int. J. Chem. Kinet.* **1998**, *30*, 21-29, doi:10.1002/(SICI)1097-4601(1998)30:1<21::AID-KIN3>3.0.CO;2-W.
Grotheer, H.-H.; Riekert, G.; Meier, U.; Just, T. Kinetics of the reactions of CH_2OH radicals with O_2 and HO_2. *Ber. Bunsenges. Phys. Chem.* **1985**, *89*, 187-191, doi:10.1002/bbpc.19850890219.
Grotheer, H. H.; Riekert, G.; Walter, D.; Just, T. Non-Arrhenius behavior of the reaction of hydroxymethyl radicals with molecular oxygen. *J. Phys. Chem.* **1988**, *92*, 4028-4030, doi:10.1021/j100325a007.
Gutbrod, R.; Kraka, E.; Schindler, R. N.; Cremer, D. Kinetic and theoretical investigation of the gas-phase ozonolysis of isoprene: Carbonyl oxides as an important source for OH radicals in the atmosphere *J. Am. Chem. Soc.* **1997**, *119*, 7330-7342, doi:10.1021/ja970050c.
Gutbrod, R.; Meyer, S.; Rahman, M. M.; Schindler, R. N. On the use of CO as scavenger for OH radicals in the ozonolysis of simple alkenes and isoprene *Int. J. Chem. Kinet.* **1997**, *29*, 717-723, doi:10.1002/(SICI)1097-4601(1997)29:93.3.CO;2-I.
Gutman, D.; Sanders, N.; Butler, J. E. Kinetics of the reactions of methoxy and ethoxy radicals with oxygen. *J. Phys. Chem.* **1982**, *86*, 66-70, doi:10.1021/j100390a013.
Hägele, J.; Lorenz, K.; Rhäsa, D.; Zellner, R. Rate constants and CH_3O product yield of the reaction OH + CH_3OH → products. *Ber. Bunsenges. Phys. Chem.* **1983**, *87*, 1023-1026, doi:10.1002/bbpc.19830871112.
Harris, G. W.; Kleindienst, T. E.; Pitts, J. N., Jr. Rate constants for the reaction of OH radicals with CH_3CN, C_2H_5CN and CH_2=CH-CN in the temperature range 298-424 K. *Chem. Phys. Lett.* **1981**, *80*, 479-483, doi:10.1016/0009-2614(81)85061-0.
Hartmann, D.; Karthäuser, J.; Sawerysyn, J. P.; Zellner, R. Kinetics and HO_2 yield of the reaction C_2H_5O + O_2 between 295 and 411 K. *Ber. Bunsenges. Phys. Chem.* **1990**, *94*, 639-645, doi:10.1002/bbpc.19900940604.
Hatekayama, S.; Kobayashi, H.; Lin, Z.-Y.; Takagi, H.; Akimoto, H. Mechanism for the reaction of CH_2OO with SO_2 *J. Phys. Chem.* **1986**, *90*, 4131-4135, doi:10.1021/j100408a059.
Heathfield, A. E.; Anastasi, C.; Pagsberg, P.; McCulloch, A. Atmospheric lifetimes of selected fluorinated ether compounds. *Atmos. Environ.* **1998**, *32*, 711-717, doi:10.1016/S1352-2310(97)00330-0.
Henon, E.; Canneaux, S.; Bohr, F.; Dobe, S. Features of the potential energy surface for the reaction of OH radical with acetone. *Phys. Chem. Chem. Phys.* **2003**, *5*, 333-341, doi:10.1039/b210247c.
Herron, J. T.; Huie, R. E. Rate constants for the reactions of ozone with ethene and propene, from 235.0 to 362.0 K. *J. Phys. Chem.* **1974**, *78*, 2085-2088, doi:10.1021/j100614a004.
Herron, J. T.; Penzhorn, R. D. Mass spectrometric study of the reactions of atomic oxygen with ethylene and formaldehyde. *J. Phys. Chem.* **1969**, *73*, 191-196, doi:10.1021/j100721a031.
Hess, W. P.; Tully, F. P. Catalytic conversion of alcohols to alkenes by OH. *Chem. Phys. Lett.* **1988**, *152*, 183-189, doi:10.1016/0009-2614(88)87352-4.
Hess, W. P.; Tully, F. P. Hydrogen-atom abstractlon from methanol by OH. *J. Phys. Chem.* **1989**, *93*, 1944-1947, doi:10.1021/j100342a049.
Hites, R. A.; Turner, A. M. Rate constants for the gas-phase β-myrcene + OH and isoprene + OH reactions as a function of temperature. *Int. J. Chem. Kinet.* **2009**, *41*, 407-413, doi:10.1002/kin.20413.
Hjorth, J.; Ottobrini, G.; Restelli, G. Reaction of the NO_3 radical with CO: Determination of an upper limit for the rate constant using FTIR spectroscopy. *Int. J. Chem. Kinet.* **1986**, *18*, 819-827, doi:10.1002/kin.550180802.
Hjorth, J.; Ottobrini, G.; Restelli, G. Reaction between NO_3 and CH_2O in air: A determination of the rate constant at 295 ± 2 K. *J. Phys. Chem.* **1988**, *92*, 2669-2672, doi:10.1021/j100320a053.
Holloway, A.-L.; Treacy, J.; Sidebottom, H.; Mellouki, A.; Daële, V.; Le Bras, G.; Barnes, I. Rate coefficients for the reactions of OH radicals with the keto/enol tautomers of 2,4-pentanedione and 3-methyl-2,4 pentanedione, allyl alcohol and methyl vinyl ketone using the enols and methyl nitrite as photolytic sources of OH. *J. Photochem. Photobiol. A Chem.* **2005**, *176*, 183-190, doi:10.1016/j.photochem.2005.08.031.

Horie, O.; Moortgat, G. K. Reactions of $CH_3C(O)O_2$ radicals with CH_3O_2 and HO_2 between 263 and 333 K A product study. *J. Chem. Soc. Faraday Trans.* **1992**, *88*, 3305-3312, doi:10.1039/ft9928803305.
Horie, O.; Schäfer, C.; Moortgat, G. K. High reactivity of hexafluoro acetone toward criegee intermediates in the gas-phase ozonolysis of simple alkenes. *Int. J. Chem. Kinet.* **1999**, *31*, 261-269, doi:10.1002/(SICI)1097-4601(1999)31:4<261::AID-KIN3>3.0.CO;2-Z.
Horne, D. G.; Norrish, R. G. W. Rate of H-abstraction by OH from hydrocarbons. *Nature (London)* **1967**, *215*, 1373-1374, doi:10.1038/2151373a0.
Horowitz, A.; Su, F.; Calvert, J. G. Unusual H_2-forming chain reaction in the 3130-Å photolysis of formaldehyde-oxygen mixtures at 25°C. *Int. J. Chem. Kinet.* **1978**, *10*, 1099-1117, doi:10.1002/kin.550101102.
Howard, C. J.; Evenson, K. M. Rate constants for the reactions of OH with ethane and some halogen substituted ethanes at 296 K. *J. Chem. Phys.* **1976**, *64*, 4303-4306, doi:10.1063/1.432115.
Howes, N. U. M.; Mir, Z. S.; Blitz, M. A.; Hardman, S.; Lewis, T. R.; Stone, D.; Seakins, P. W. Kinetic studies of C1 and C2 Criegee intermediates with SO_2 using laser flash photolysis coupled with photoionization mass spectrometry and time resolved UV absorption spectroscopy. *Phys. Chem. Chem. Phys.* **2018**, *20*, 22218-22227, doi:10.1039/C8CP03115K.
Hoyermann, K.; Wagner, H. G.; Wolfrum, J. Untersuchung der reaktionen von C_2H_2 mit H- und O-atomen mittels elektronen-spin-resonanz. *Z. Phys. Chem.* **1967**, *55*, 72-78, doi:10.1524/zpch.1967.55.1_2.072.
Hoyermann, K.; Wagner, H. G.; Wolfrum, J. $O + C_2H_2 \rightarrow CO + CH_2$ reaction. *Z. Phys. Chem.* **1969**, *63*, 193-196, doi:10.1524/zpch.1969.63.1_4.193.
Hsin, H. Y.; Elrod, M. J. Overall rate constant measurements of the reaction of hydroxy- and chloroalkylperoxy radicals derived from methacrolein and methyl vinyl ketone with nitric oxide. *J. Phys. Chem. A* **2007**, *111*, 613-619, doi:10.1021/jp0665574.
Hsu, C.-C.; Mebel, A. M.; Lin, M. C. *Ab initio* molecular orbital study of the $HCO + O_2$ reaction: Direct versus indirect abstraction channels. *J. Chem. Phys.* **1996**, *105*, 2346-2352, doi:10.1063/1.472083.
Huang, Y.-w.; Dransfield, T. J.; Anderson, J. G. Experimental evidence for the pressure dependence of the reaction rate constant between acetic acid and hydroxyl radicals. *J. Phys. Chem. A* **2010**, *114*, 11538-11544, doi:10.1021/jp106446q.
Huang, Y.-w.; Dransfield, T. J.; Miller, J. D.; Rojas, R. D.; Castillo, X. G.; Anderson, J. G. Experimental study of the kinetics of the reaction of acetic acid with hydroxyl radicals from 255 to 355 K. *J. Phys. Chem. A* **2009**, *113*, 423-430, doi:10.1021/jp808627w.
Hunziker, H. E.; Kneppe, H.; Wendt, H. R. Photochemical modulation spectroscopy of oxygen atom reactions with olefins. *J. Photochem.* **1981**, *17*, 377-387, doi:10.1016/0047-2670(81)85380-4.
Hynes, A. J.; Wine, P. H. Kinetics and mechanism of the reaction of hydroxyl radicals with acetonitrile under atmospheric conditions. *J. Phys. Chem.* **1991**, *95*, 1232-1240, doi:10.1021/j100156a037.
Iida, Y.; Obi, K.; Imamura, T. Rate constant for the reaction of OH radicals with isoprene at 298 ± 2K. *Chem. Lett.* **2002**, *31*, 792-793, doi:10.1246/cl.2002.792.
Inoue, G.; Akimoto, H. Laser-induced fluorescence of the C_2H_3O radical. *J. Chem. Phys.* **1981**, *74*, 425-433, doi:10.1063/1.440848.
Jalan, A.; Allen, J. W.; Green, W. H. Chemically activated formation of organic acids in reactions of the Criegee intermediate with aldehydes and ketones. *Phys. Chem. Chem. Phys.* **2013**, *15*, 16841-16852, doi:10.1039/C3CP52598H.
James, G. S.; Glass, G. P. Some aspects of acetylene oxidation. *J. Chem. Phys.* **1970**, *50*, 2268-2269, doi:10.1063/1.1671368.
Japar, S. M.; Wu, C. H.; Niki, H. Rate constants for the reaction of ozone with olefins in the gas phase. *J. Phys. Chem.* **1974**, *78*, 2318-2320, doi:10.1021/j150671a003.
Japar, S. M.; Wu, C. H.; Niki, H. Effect of molecular oxygen on the gas phase kinetics of the ozonolysis of olefins. *J. Phys. Chem.* **1976**, *80*, 2057-2062, doi:10.1021/j100560a002.
Jenkin, M. E.; Cox, R. A.; Emrich, M.; Moortgat, G. K. Mechanisms of the Cl-atom-initiated oxidation of acetone and hydroxyacetone in air. *J. Chem. Soc. Faraday Trans.* **1993**, *89*, 2983-2991, doi:10.1039/ft9938902983.
Jeong, K. M.; Hsu, K. J.; Jeffries, J. B.; Kaufman, F. Kinetics of the reactions of OH with C_2H_6, CH_3CCl_3, $CH_2ClCHCl_2$, $CH_2ClCClF_2$, and CH_2FCF_3. *J. Phys. Chem.* **1984**, *88*, 1222-1226, doi:10.1021/j150650a041.
Jiang, L.; Xu, Y.-S.; Ding, A.-Z. Reaction of stabilized Criegee intermediates from ozonolysis of limonene with sulfur dioxide: Ab initio and DFT study. *J. Phys. Chem. A* **2010**, *114*, 12452-12461, doi:10.1021/jp107783z.

Jiménez, E.; Antiñolo, M.; Ballesteros, B.; Canosa, A.; Albaladejo, J. First evidence of the dramatic enhancement of the reactivity of methyl formate ($HC(O)OCH_3$) with OH at temperatures of the interstellar medium: a gas-phase kinetic study between 22 K and 64 K. *Phys. Chem. Chem. Phys* **2016**, *18*, 2183-2191, doi:10.1039/c5cp06369h.

Jiménez, E.; Gilles, M. K.; Ravishankara, A. R. Kinetics of the reactions of hydroxyl radical with CH_3OH and C_2H_5OH between 235 and 360 K. *J. Photochem. Photobiol. A: Chem.* **2003**, *157*, 237-245, doi:10.1016/S1010-6030(03)00073-X.

Johnson, D.; Marston, G. The gas-phase ozonolysis of unsaturated volatile organic compounds in the troposphere. *Chem. Soc. Rev.* **2008**, *37*, 699-716, doi:10.1039/b704260b.

Jolly, G. S.; McKenney, D. J.; Singleton, D. L.; Paraskevopoulos, G.; Bossard, A. R. Rate constant and mechanism for the reaction of hydroxyl radical with formic acid. *J. Phys. Chem.* **1986**, *90*, 6557-6562, doi:10.1021/j100282a028.

Jolly, G. S.; Paraskevopoulos, G.; Singleton, D. L. Rates of OH radical reactions. XII. The reactions of OH with *c*-C_3H_6, *c*-C_5H_{10}, and *c*-C_7H_{14}. Correlation of hydroxyl rate constants with bond dissociation energies. *Int. J. Chem. Kinet.* **1985**, *17*, 1-10, doi:10.1002/kin.550170102.

Kaiser, E. W.; Lorkovic, I. M.; Wallington, T. J. Pressure dependence of the C_2H_4 yield from the reaction C_2H_5 + O_2. *J. Phys. Chem.* **1990**, *94*, 3352-3354, doi:10.1021/j100371a030.

Kakesu, M.; Bandow, H.; Takenaka, N.; Maeda, Y.; Washida, N. Kinetic measurements of methyl and ethyl nitrate reactions with OH radicals. *Int. J. Chem. Kinet.* **1997**, *29*, 933-941, doi:10.1002/(SICI)1097-4601(1997)29:12<933::AID-KIN5>3.0.CO;2-N.

Kamens, R. M.; Gery, M. W.; Jeffries, H. E.; Jackson, M.; Cole, E. I. Ozone-isoprene reactions: Product formation and aerosol potential. *Int. J. Chem. Kinet.* **1982**, *14*, 955-975, doi:10.1002/kin.550140902.

Kan, C. S.; Calvert, J. G.; Shaw, J. H. Oxidation of sulfur dioxide by methylperoxy radicals. *J. Phys. Chem.* **1981**, *85*, 1126-1132, doi:10.1021/j150609a011.

Karl, M.; Brauers, T.; Dorn, H.-P.; Holland, F.; Komenda, M.; Poppe, D.; Rohrer, F.; Rupp, L.; Schaub, A.; Wahner, A. Kinetic Study of the OH-isoprene and O_3-isoprene reaction in the atmosphere simulation chamber, SAPHIR. *Geophys. Res. Lett.* **2004**, *31*, L05117, doi:10.1029/2003GL019189.

Karunanandan, R.; Holscher, D.; Dillon, T. J.; Horowitz, A.; Crowley, J. N.; Vereecken, L.; Peeters, J. Reaction of HO with glycolaldehyde, $HOCH_2CHO$: Rate coefficients (240-362 K) and mechanism. *J. Phys. Chem. A* **2007**, *111*, 897-908, doi:10.1021/jp0649504.

Kerr, J. A.; Sheppard, D. W. Kinetics of the reactions of hydroxyl radicals with aldehydes studied under atmospheric conditions. *Environ. Sci. Technol.* **1981**, *15*, 960-963, doi:10.1021/es00090a012.

Kerr, J. A.; Stocker, D. W. Kinetics of the reactions of hydroxyl radicals with alkyl nitrates and with some oxygen-containing organic compounds studied under simulated atmospheric conditions. *J. Atmos. Chem.* **1986**, *4*, 253-262, doi:10.1007/BF00052004.

Khamaganov, V. G.; Bui, V. X.; Carl, S. A.; Peeters, J. Absolute rate coefficient of the OH + $CH_3C(O)OH$ reaction at T = 287-802 K. The two faces of pre-reactive H-bonding. *J. Phys. Chem. A* **2006**, *110*, 12852-12859, doi:10.1021/jp064922l.

Khamaganov, V. G.; Hites, R. A. Rate constants for the gas-phase reactions of ozone with isoprene, α- and β-pinene, and limonene as a function of temperature. *J. Phys. Chem. A* **2001**, *105*, 815-822, doi:10.1021/jp002730z.

Kjaergaard, H. G.; Kurtén, T.; Nielsen, L. B.; Jørgensen, S.; Wennberg, P. O. Criegee intermediates react with ozone. *J. Phys. Chem. Lett.* **2013**, *4*, 2525-2529, doi:10.1021/jz401205m.

Klais, O.; Anderson, P. C.; Laufer, A. H.; Kurylo, M. J. An upper limit for the rate constant of the bimolecular reaction $CH_3 + O_2 \rightarrow OH + H_2CO$ at 368 K. *Chem. Phys. Lett.* **1979**, *66*, 598-601, doi:10.1016/0009-2614(79)80349-8.

Klawatsch-Carrasco, N.; Doussin, J. F.; Carlier, P. Absolute rate constants for the gas-phase ozonolysis of isoprene and methylbutenol. *Int. J. Chem. Kinet.* **2004**, *36*, 152-156, doi:10.1002/kin.10175.

Kleindienst, T. E.; Harris, G. W.; Pitts, J. N., Jr. Rates and temperature dependences of the reaction of OH with isoprene, its oxidation products, and selected terpenes. *Environ. Sci. Technol.* **1982**, *16*, 844-846, doi:10.1021/es00106a004.

Kleinermanns, K.; Luntz, A. C. Laser-induced fluorescence of CH_2CHO produced in the crossed molecular beam reactions of $O(^3P)$ with olefins. *J. Phys. Chem.* **1981**, *85*, 1966-1968, doi:10.1021/j150614a003.

Klemm, R. B. Absolute rate parameters for the reactions of formaldehyde with O atoms and H atoms over the temperature range 250-500 K. *J. Chem. Phys.* **1979**, *71*, 1987-1993, doi:10.1063/1.438589.

Klemm, R. B.; Skolnik, E. G.; Michael, J. V. Absolute rate parameters for the reaction of $O(^3P)$ with H_2CO over the temperature range 250 to 750 K. *J. Chem. Phys.* **1980**, *72*, 1256-1264, doi:10.1063/1.439186.

Klopffer, V. W.; Frank, R.; Kohl, E.-G.; Haag, F. Quantitative erfassung der photochemischen transformationsprozeese in der troposphare. *Chem. Ztg.* **1986**, *110*, 57-62.

Klopffer, W.; Frank, R.; Kohl, E. G.; Haag, F. Quantitative erfassung der photochemischen transformationsprozesse in der troposphäre. *Chemiker-Zeitung* **1986**, *110*, 57-61.

Kovács, G.; Szász-Vadász, T.; Papadimitriou, V. C.; Dóbé, S.; Bérces, T.; Márta, F. Absolute rate constants for the reactions of OH radicals with CH_3CH_2OH, CF_2HCH_2OH and CF_3CH_2OH. *React. Kinet. Catal. Lett.* **2005**, *87*, 129-138, doi:10.1007/s11144-006-0018-2.

Kozlov, S. N.; Orkin, V. L.; Huie, R. E.; Kurylo, M. J. OH reactivity and UV spectra of propane, n-propyl bromide, and isopropyl bromide. *J. Phys. Chem. A* **2003**, *107*, 1333-1338, doi:10.1021/jp021806j.

Kramp, F.; Paulson, S. E. On the uncertainties in the rate coefficients for OH reactions with hydrocarbons, and the rate coefficients of the 1,3,5-trimethylbenzene and m-xylene reactions with OH radicals in the gas phase. *J. Phys. Chem. A* **1998**, *102*, 2685-2690, doi:10.1021/jp973289o.

Kurten, T.; Lane, J. R.; Jorgensen, S.; Kjaergaard, H. G. A computational study of the oxidation of SO_2 to SO_3 by gas-phase organic oxidants. *J. Phys. Chem. A* **2011**, *115*, 8669-8681, doi:10.1021/jp203907d.

Kurylo, M. J.; Knable, G. L. A kinetics investigation of the gas-phase reactions of $Cl(^2P)$ and $OH(X^2\Pi)$ with CH_3CN: Atmospheric significance and evidence for decreased reactivity between strong electrophiles. *J. Phys. Chem.* **1984**, *88*, 3305-3308, doi:10.1021/j150659a033.

Kuwata, K. T.; Guinn, E. J.; Hermes, M. R.; Fernandez, J. A.; Mathison, J. M.; Huang, K. A computational re-examination of the Criegee intermediate–sulfur dioxide reaction. *J. Phys. Chem. A* **2015**, *119*, 10316-10335, doi:10.1021/acs.jpca.5b06565.

Kuwata, K. T.; Hermes, M. R.; Carlson, J.; Zogg, C. K. Computational studies of the isomerization and hydration reactions of acetaldehyde oxide and methyl vinyl carbonyl oxide *J. Phys. Chem. A* **2010**, *114*, 9192-9204, doi:10.1021/jp105358v.

Kwok, E. S. C.; Aschmann, S. M.; Arey, J.; Atkinson, R. Product formation from the reaction of the NO_3 radical with isoprene and rate constants for the reactions of methacrolein and methyl vinyl ketone with the NO_3 radical. *Int. J. Chem. Kinet.* **1996**, *28*, 925-934, doi:10.1002/(SICI)1097-4601(1996)28:12<925::AID-KIN10>3.0.CO;2-B.

Lade, R. E.; Onel, L.; Blitz, M. A.; Seakins, P. W.; Stone, D. Kinetics of the gas-phase reactions of *syn*- and *anti*-CH_3CHOO Criegee intermediate conformers with SO_2 as a function of temperature and pressure. *J. Phys. Chem. A* **2024**, *128*, 2815-2824, doi:10.1021/acs.jpca.4c00199.

Langford, A. O.; Moore, C. B. Collision complex formation in the reactions of formyl radicals with nitric oxide and oxygen. *J. Chem. Phys.* **1984**, *80*, 4211-4221, doi:10.1063/1.447252.

Le Calve, S.; Hitier, D.; Le Bras, G.; Mellouki, A. Kinetic studies of OH reactions with a series of ketones. *J. Phys. Chem. A* **1998**, *102*, 4579-4584, doi:10.1021/jp980848y.

Le Calve, S.; LeBras, G.; Mellouki, A. Temperature dependence for the rate coefficients of the reactions of the OH radical with a series of formates. *J. Phys. Chem. A* **1997**, *101*, 5489-5493, doi:10.1021/jp970554x.

Lee, J. H.; Tang, I. N. Absolute rate constants for the hydroxyl radical reactions with ethane, furan, and thiophene at room temperature. *J. Chem. Phys.* **1982**, *77*, 4459-4463, doi:10.1063/1.444367.

Leu, M. T. Rate constant for the reaction $HO_2 + NO \rightarrow OH + NO_2$. *J. Chem. Phys.* **1979**, *70*, 1662-1666, doi:10.1063/1.437680.

Lewin, A. G.; Johnson, D.; Price, D. W.; Marston, G. Aspects of the kinetics and mechanism of the gas-phase reactions of ozone with conjugated dienes *Phys. Chem. Chem. Phys.* **2001**, *3*, 1253-1261, doi:10.1039/b010006o.

Lewis, T. R.; Blitz, M. A.; Heard, D. E.; Seakins, P. W. Direct evidence for a substantive reaction between the Criegee intermediate, CH_2OO, and the water vapour dimer. *Phys. Chem. Chem. Phys.* **2015**, *17*, 4859-4863, doi:10.1039/c4cp04750h.

Li, Y.-L.; Kuo, M.-T.; Lin, J. J.-M. Unimolecular decomposition rates of a methyl-substituted Criegee intermediate *syn*-CH_3CHOO. *RSC Adv.* **2020**, *10*, 8518-8524, doi:10.1039/d0ra01406k.

Li, Q.; Osborne, M. C.; Smith, I. W. M. Rate constants for the reactions of Cl atoms with HCOOH and with HOCO radicals. *Int. J. Chem. Kinet.* **2000**, *32*, 85-91, doi:10.1002/(SICI)1097-4601(2000)32:2<85::AID-KIN3>3.0.CO;2-I.

Lightfoot, P. D.; Cox, R. A.; Crowley, J. N.; Destriau, M.; Hayman, G. D.; Jenkin, M. E.; Moortgat, G. K.; Zabel, F. Organic peroxy radicals: Kinetics, spectroscopy and tropospheric chemistry. *Atmos. Environ.* **1992**, *26A*, 1805-1961, doi:10.1016/0960-1686(92)90423-I.

Lightfoot, P. D.; Veyret, B.; Lesclaux, R. Flash photolysis study of the CH_3O_2 + HO_2 reaction between 248 and 573 K. *J. Phys. Chem.* **1990**, *94*, 708-714, doi:10.1021/j100365a036.
Liljegren, J.; Stevens, P. Measurements of the kinetics of the reaction of OH radicals with 3-methylfuran at low pressure. *Int. J. Chem. Kinet.* **2013**, *45*, 787-194, doi:10.1002/kin.20814.
Lin, L.-C.; Chao, W.; Chang, C.-H.; Takahashi, K.; Lin, J. J.-M. Competition between H_2O and $(H_2O)_2$ reactions with CH_2OO/CH_3CHOO. *Phys. Chem. Chem. Phys.* **2016**, *18*, 4557-4568, doi:10.1039/c6cp05171e.
Lin, L.-C.; Chao, W.; Chang, C.-H.; Takahashi, K.; Lin, J. J.-M. Temperature dependence of the reaction of *anti*-CH_3CHOO with water vapor. *Phys. Chem. Chem. Phys.* **2016**, *18*, 28189-28197, doi:10.1039/C6CP05171E.
Liu, Y.; Bayes, K. D.; Sander, S. P. Measuring rate constants for reactions of the simplest Criegee intermediate (CH_2OO) by monitoring the OH radical. *J. Phys. Chem. A* **2014**, *118*, 741-747, doi:10.1021/jp407058b.
Liu, Y. D.; Bayes, K. D.; Sander, S. P. Measuring rate constants for reactions of the simplest Criegee intermediate (CH_2OO) by monitoring the OH radical. *J. Phys. Chem. A* **2014**, *118*, 741-747, doi:10.1021/jp407058b.
Liu, F.; Fang, Y.; Kumar, M.; Thompson, W. H.; Lester, M. I. Direct observation of vinyl hydroperoxide *Phys. Chem. Chem. Phys.* **2015**, *17*, 20490-20494, doi:10.1039/C5CP02917A.
Liu, Y.; Liu, F.; Liu, S.; Dai, D.; Dong, W.; Yang, X. A kinetic study of the CH_2OO Criegee intermediate reaction with SO_2, $(H_2O)_2$, CH_2I_2 and I atoms using OH laser induced fluorescence. *Phys. Chem. Chem. Phys.* **2017**, *19*, 20786-20794, doi:10.1039/C7CP04336H.
Lloyd, A. C.; Darnall, K. R.; Winer, A. M.; Pitts Jr., J. N. Relative rate constants for the reactions of OH radicals with isopropyl alcohol, diethyl and di-*n*-propyl ether at 305 ± 2 K. *Chem. Phys. Lett.* **1976**, *42*, 205-209, doi:10.1016/0009-2614(76)80347-8.
Lockwood, A. L.; Shepson, P. B.; Fiddler, M. N.; Alaghmand, M. Isoprene nitrates: preperation, seperation, identification, yields, and atmospheric chemistry. *Atmos. Chem. Phys.* **2010**, *10*, 6169-6178, doi:10.5194/acp-10-6169-2010.
Long, B.; Bao, J. L.; Truhlar, D. G. Atmospheric chemistry of Criegee intermediates: Unimolecular reactions and reactions with water. *J. Am. Chem. Soc.* **2016**, *138*, 14409-14422, doi:10.1021/jacs.6b08655.
Lorenz, K.; Rhäsa, D.; Zellner, R.; Fritz, B. Laser photolysis - LIF kinetic studies of the reactions of CH_3O and CH_2CHO with O_2 between 300 K and 500 K. *Ber. Bunsenges. Phys. Chem.* **1985**, *89*, 341-342, doi:10.1002/bbpc.19850890346.
Louge, M. Y.; Hanson, R. K. *Twentieth Symposium (International) on Combustion* **1984**, 665-672.
Mack, G. P. R.; Thrush, B. Reaction of oxygen atoms with carbonyl compounds Part 1.-Formaldehyde. *J. Chem. Soc. Faraday Trans. 1* **1973**, *69*, 208-215, doi:10.1039/f19736900208.
Mack, G. P. R.; Thrush, B. Reaction of oxygen atoms with carbonyl compounds Part 2.-Acetaldehyde. *J. Chem. Soc. Faraday Trans. 1* **1974**, *70*, 178-186, doi:10.1039/f19747000178.
Magneron, I.; Mellouki, A.; Le Bras, G.; Moortgat, G. K.; Horowitz, A.; Wirtz, K. Photolysis and OH-initiated oxidation of glycolaldehyde under atmospheric conditions. *J. Phys. Chem. A* **2005**, *109*, 4552-4561, doi:10.1021/jp044346y.
Manonmani, G.; Sandhiya, L.; Senthilkumar, K. Reaction of Criegee intermediates with SO_2─ A possible route for sulfurous acid formation in the atmosphere. *ACS Earth Space Chem.* **2023**, *7*, 1890-1904, doi:10.1021/acsearthspacechem.3c00058.
Maricq, M. M.; Szente, J. J. A kinetic study of the reaction between ethylperoxy radicals and HO_2. *J. Phys. Chem.* **1994**, *98*, 2078-2082, doi:10.1021/j100059a016.
Maricq, M. M.; Szente, J. J. Kinetics of the reaction between ethylperoxy radicals and nitric oxide. *J. Phys. Chem.* **1996**, *100*, 12374-12379, doi:10.1021/jp9607935.
Maricq, M. M.; Szente, J. J. The $CH_3C(O)O_2$ radical. Its UV spectrum, self-reaction kinetics, and reaction with CH_2O_2. *J. Phys. Chem.* **1996**, *100*, 45407-44513, doi:10.1021/jp9533234.
McCaulley, J. A.; Anderson, S. M.; Jeffries, J. B.; Kaufman, F. Kinetics of the reaction of CH_3O with NO_2. *Chem. Phys. Lett.* **1985**, *115*, 180-186, doi:10.1016/0009-2614(85)80675-8.
McGivern, W. S.; Suh, I.; Clinkenbeard, A. D.; Zhang, R.; North, S. W. Experimental and computational study of the OH-isoprene reaction: Isomeric branching and low-pressure behavior. *J. Phys. Chem. A* **2000**, *104*, 6609-6616, doi:10.1021/jp001163c.
McQuaid, J. B.; Stocker, D. W.; Pilling, M. J. Kinetics of the reactions of OH with 3-methyl-2-cyclohexen-1-one and 3,5,5-trimethyl-2-cyclohexen-1-one under simulated atmospheric conditions. *Int. J. Chem. Kinet.* **2002**, *34*, 7-11, doi:10.1002/kin.10018.

Meier, U.; Grotheer, H. H.; Just, T. Temperature dependence and branching ratio of the CH_3OH + OH reaction. *Chem. Phys. Lett.* **1984**, *106*, 97-101, doi:10.1016/0009-2614(84)87019-0.
Meier, U.; Grotheer, H. H.; Riekert, G.; Just, T. Temperature dependence and branching ratio of the C_2H_5OH + OH reaction. *Chem. Phys. Lett.* **1985**, *115*, 221-225, doi:10.1016/0009-2614(85)80684-9.
Mellouki, A.; Téton, S.; Laverdet, G.; Quilgars, A.; Le Bras, G. Kinetic studies of OH reactions with H_2O_2, C_3H_8, and CH_4 using the pulsed laser photolysis-laser induced fluorescence method. *J. Chim. Phys.* **1994**, *91*, 473-487, doi:10.1051/jcp/1994910473.
Michael, J. V.; Keil, D. G.; Klemm, R. B. Rate constants for the reaction of hydroxyl radicals with acetaldehyde from 244-528 K. *J. Chem. Phys.* **1985**, *83* 1630-1636, doi:10.1063/1.449400.
Miller, A. M.; Yeung, L. Y.; Kiep, A. C.; Elrod, M. J. Overall rate constant measurements of the reactions of alkene-derived hydroxyalkylperoxy radicals with nitric oxide. *Phys. Chem. Chem. Phys.* **2004**, *6*, 3402-3407, doi:10.1039/b402110j.
Mir, Z. S.; Jamieson, M.; Greenall, N. R.; Seakins, P. W.; Blitz, M. A.; Stone, D. Identification, monitoring, and reaction kinetics of reactive trace species using time-resolved mid-infrared quantum cascade laser absorption spectroscopy: development, characterisation, and initial results for the CH_2OO Criegee intermediate. *Atmos. Meas. Tech.* **2022**, *15*, 2875-2887, doi:10.5194/amt-15-2875-2022.
Moortgat, G.; Veyret, B.; Lesclaux, R. Absorption spectrum and kinetics of reactions of the acetylperoxy radical. *J. Phys. Chem.* **1989**, *93*, 2362-2368, doi:10.1021/j100343a032.
Morin, J.; Romanias, M. N.; Bedjanian, Y. Experimental study of the reactions of OH radicals with propane, n-pentane, and n-heptane over a wide temperature range. *Int. J. Chem. Kinet.* **2015**, *47*, 629-637, doi:10.1002/kin.20936.
Morin, J.; Romanias, M. N.; Bedjanian, Y. Experimental study of the reactions of OH radicals with propane, n-pentane, and n-heptane over a wide temperature range. *Int. J. Chem Kinet.* **2015**, *47*, 629-637, doi:10.1002/kin.20936.
Morris, E. D., Jr.; Niki, H. Mass spectrometric study of the reaction of hydroxyl radical with formaldehyde. *J. Chem. Phys.* **1971**, *55*, 1991-1992, doi:10.1063/1.1676348.
Morris, E. D., Jr.; Stedman, D. H.; Niki, H. Mass spectrometric study of the reactions of the hydroxyl radical with ethylene, propylene, and acetaldehyde in a discharge-flow system. *J. Am. Chem. Soc.* **1971**, *93*, 3570-3572, doi:10.1021/ja00744a004.
Morris, E. D.; Niki, H. Reaction of the nitrate radical with acetaldehyde and propylene. *J. Phys. Chem.* **1974**, *78*, 1337-1338, doi:10.1021/j100606a600.
Munk, J.; Pagsberg, P.; Ratajczak, E.; Sillesen, A. Spectrokinetic studies of ethyl and ethylperoxy radicals. *J. Phys. Chem.* **1986**, *90*, 2752-2757, doi:10.1021/j100403a038.
Nadtochenko, V. A.; Sarkisov, O. M.; Vedeneev, V. I. *Doklady Akademii Nauk SSSR* **1979**, *244*, 152.
Neeb, P.; Horie, O.; Moortgat, G. K. The ethene−ozone reaction in the gas phase. *J. Phys. Chem. A* **1998**, *102*, 6778-6785, doi:10.1021/jp981264z.
Neeb, P.; Kolloff, A.; Koch, S.; Moortgat, G. K. Rate constants for the reactions of methylvinyl ketone, methacrolein, methacrylic acid, and acrylic acid with ozone. *Int. J. Chem. Kinet.* **1998**, *30*, 769-776, doi:10.1002/(SICI)1097-4601(1998)30:10<769::AID-KIN9>3.0.CO;2-T.
Neeb, P.; Moorgat, G. K. Formation of OH radicals in the gas-phase reaction of propene, isobutene, and isoprene with O_3: Yields and mechanistic implications. *J. Phys. Chem. A* **1999**, *103*, 9003-9012, doi:10.1021/jp9903458.
Nelson, L.; Rattigan, O.; Neavyn, R.; Sidebottom, H.; Treacy, J.; Nielsen, O. J. Absolute and relative rate constants for the reactions of hydroxyl radicals and chlorine atoms with a series of aliphatic alcohols and ethers at 298 K. *Int. J. Chem. Kinet.* **1990**, *22*, 1111-1126, doi:10.1002/kin.550221102.
Nesbitt, F. L.; Gleason, J. F.; Stief, L. J. Temperature dependence of the rate constant for the reaction HCO + O_2 → HO_2 + CO at T = 200-398 K. *J. Phys. Chem. A* **1999**, *103*, 3038-3043, doi:10.1021/jp984781q.
Nesbitt, F. L.; Payne, W. A.; Stief, L. J. Temperature dependence for the absolute rate constant for the reaction CH_2OH + O_2 → HO_2 + H_2CO from 215 to 300 K. *J. Phys. Chem.* **1988**, *92*, 4030-4032, doi:10.1021/j100325a008.
Newland, M. J.; Rickard, A. R.; Alam, M. S.; Vereecken, L.; Muñoz, A.; Ródenas, M.; Bloss, W. J. Kinetics of stabilised Criegee intermediates derived from alkene ozonolysis: reactions with SO_2, H_2O and decomposition under boundary layer conditions. *Phys. Chem. Chem. Phys.* **2015**, *17*, 4076-4088, doi:10.1039/c4cp04186k.

Newland, M. J.; Rickard, A. R.; Vereecken, L.; Muñoz, A.; Ródenas, M.; Bloss, W. J. Atmospheric isoprene ozonolysis: impacts of stabilised Criegee intermediate reactions with SO_2, H_2O and dimethyl sulfide. *Atmos. Chem. Phys.* **2015**, *15*, 9521-9536, doi:10.5194/acp-15-9521-2015.

Nielsen, O. J.; Munk, J.; Pagsberg, P.; Sillesen, A. Absolute rate constants for the gas-phase reaction of OH radicals with cyclohexane and ethane at 295 K. *Chem. Phys. Lett.* **1986**, *128*, 168-171, doi:10.1016/0009-2614(86)80319-0.

Nielsen, O. J.; Sidebottom, H. W.; Donlon, M.; Treacy, J. An absolute- and relative-rate study of the gas-phase reaction of OH radicals and Cl atoms with *n*-alkyl nitrates. *Chem. Phys. Lett.* **1991**, *178*, 163-170, doi:10.1016/0009-2614(91)87051-C.

Niki, H.; Daby, E. E.; Weinstock, B. In *Twelfth Symposium (International) on Combustion*; The Combustion Institute, 1969; pp 277.

Niki, H.; Maker, P. D.; Savage, C. M.; Breitenbach, L. P. Relative rate constants for the reaction of hydroxyl radical with aldehydes. *J. Phys. Chem.* **1978**, *82*, 132-134, doi:10.1021/j100491a002.

Niki, H.; Maker, P. D.; Savage, C. M.; Breitenbach, L. P. Fourier transform infrared studies of the self-reaction of CH_3O_2 radicals. *J. Phys. Chem.* **1981**, *85*, 877-881, doi:10.1021/j150607a028.

Niki, H.; Maker, P. D.; Savage, C. M.; Breitenbach, L. P. Fourier transform infrared studies of the self-reaction of $C_2H_5O_2$ radicals. *J. Phys. Chem.* **1982**, *86*, 3825-3829, doi:10.1021/j100216a023.

Niki, H.; Maker, P. D.; Savage, C. M.; Breitenbach, L. P. A Fourier transform infrared study of the kinetics and mechanism for the reaction HO + CH_3OOH. *J. Phys. Chem.* **1983**, *87*, 2190-2193, doi:10.1021/j100235a030.

Niki, H.; Maker, P. D.; Savage, C. M.; Breitenbach, L. P. Fourier transform infrared spectroscopic study of the kinetics for the HO radical reaction of $^{13}C^{16}O$ and $^{12}C^{18}O$. *J. Phys. Chem.* **1984**, *88*, 2116-2119, doi:10.1021/j150654a034.

Niki, H.; Maker, P. D.; Savage, C. M.; Breitenbach, L. P. Fourier transform infrared study of the kinetics and mechanism for the reaction of hydroxyl radical with formaldehyde. *J. Phys. Chem.* **1984**, *88*, 5342-5344, doi:10.1021/j150666a047.

Niki, H.; Maker, P. D.; Savage, C. M.; Hurley, M. D. Fourier transform infrared study of the kinetics and mechanisms for the Cl-atom- and HO-radical-initiated oxidation of glycolaldehyde. *J. Phys. Chem.* **1987**, *91*, 2174-2178, doi:10.1021/j100292a038.

Ninomiya, Y.; Kawasaki, M.; Guschin, A.; Molina, L. T.; Molina, M. J.; Wallington, T. J. Atmospheric chemistry of *n*-$C_3F_7OCH_3$: Reaction with OH radicals and Cl atoms and atmospheric fate of *n*-$C_3F_7OCH_2O(\bullet)$ radicals. *Environ. Sci. Technol.* **2000**, *34*, 2973-2978, doi:10.1021/es991449z.

Nolte, J.; Grussdorf, J.; Temps, F.; Wagner, H. Kinetics of the reaction HOCO + O_2 in the gas phase. *Z. Naturforsch.* **1993**, *48*, 1234-1238.

Nolting, F.; Behnke, W.; Zetzsch, C. A smog chamber for studies of the reactions of terpenes and alkanes with ozone and OH. *J. Atmos. Chem.* **1988**, *6*, 47-59, doi:10.1016/0021-8502(87)90011-5.

Novelli, A.; Vereecken, L.; Lelieveld, J.; Harder, H. Direct observation of OH formation from stabilised Criegee intermediates. *Phys. Chem, Chem. Phys.* **2014**, *16*, 19941-19951, doi:10.1039/C4CP02719A.

Ogryzlo, E. A.; Paltenghi, R.; Bayes, K. D. The rate of reaction of methyl radicals with ozone. *Int. J. Chem. Kinet.* **1981**, *13*, 667-675, doi:10.1002/kin.550130707.

Oh, S.; Andino, J. M. Effects of ammonium sulfate aerosols on the gas-phase reactions of the hydroxyl radical with organic compounds. *Atmos. Environ.* **2000**, *34*, 2901-2908, doi:10.1016/S1352-2310(00)00071-6.

Oh, S.; Andino, J. M. Kinetics of the gas-phase reactions of hydroxyl radicals with C1-C6 aliphatic alcohols in the presence of ammonium sulfate aerosols. *Int. J. Chem. Kinet.* **2001**, *33*, 422-430, doi:10.1002/kin.1038.

Ohmori, K.; Yamasaki, K.; Matsui, H. Pressure dependence of the rate constant for the reaction of CH_3O + NO. *Bull. Chem. Soc. Jpn.* **1993**, *66*, 51-56, doi:10.1246/bcsj.66.51.

Ohta, T. Rate constants for the reactions of diolefins with OH radicals in the gas phase. Estimate of the rate constants from those for monoolefins. *J. Phys. Chem.* **1983**, *87*, 1209-1213, doi:10.1021/j100230a023.

Onel, L.; Blitz, M.; Seakins, P.; Heard, D.; Stone, D. Kinetics of the gas phase reactions of the Criegee intermediate CH_2OO with O_3 and IO. *J. Phys. Chem. A* **2020**, *124*, 6287-6293, doi:10.1021/acs.jpca.0c04422.

Onel, L.; Lade, R.; Mortiboy, J.; Blitz, M. A.; Seakins, P. W.; Heard, D. E.; Stone, D. Kinetics of the gas phase reaction of the Criegee intermediate CH_2OO with SO_2 as a function of temperature. *Phys. Chem. Chem. Phys.* **2021**, *23*, 19415-19423, doi:10.1039/d1cp02932k.

Orkin, V. L.; Khamaganov, V. G.; Kurylo, M. J. High accuracy measurements of OH reaction rate constants and IR absorption spectra: Substituted 2-propanols. *J. Phys. Chem. A* **2012**, *116*, 6188-6198, doi:10.1021/jp211534n.

Orkin, V. L.; Khamaganov, V. G.; Martynova, L. E.; Kurylo, M. J. High-accuracy measurements of OH reaction rate constants and IR and UV absorption spectra: Ethanol and partially fluorinated ethyl alcohols. *J. Phys. Chem. A* **2011**, *115*, 8656-8668, doi:10.1021/jp202099t.

Orlando, J. J.; Tyndall, G. S. Mechanism of the OH-initiated oxidation of methacrolein. *Geophys. Res. Lett.* **1999**, *26*, 2191-2194, doi:10.1029/1999GL900453.

Orlando, J. J.; Tyndall, G. S.; Vereecken, L.; Peeters, J. The atmospheric chemistry of the acetonoxy radical. *J. Phys. Chem. A* **2000**, *104*, 11578-11588, doi:10.1021/jp0026991.

Ouyang, B.; McLeod, M. W.; Jones, R. L.; Bloss, W. J. NO_3 radical production from the reaction between the Criegee intermediate CH_2OO and NO_2. *Phys. Chem. Chem. Phys.* **2013**, *15*, 17070-17075, doi:10.1039/c3cp53024h.

Overend, R.; Paraskevopoulos, G. Rates of OH radical reactions. 4. Reactions with methanol, ethanol, 1-propanol, and 2-propanol at 296 K. *J. Phys. Chem.* **1978**, *82*, 1329-1333, doi:10.1021/j100501a001.

Overend, R. P.; Paraskevopoulos, G.; Cvetanović, R. J. Rates of OH radical reactions. I. Reactions with H_2, CH_4, C_2H_6, and C_3H_8 at 295 K. *Can. J. Phys.* **1975**, *53*, 3374-3382, doi:10.1139/v75-482.

Papagni, C.; Arey, J.; Atkinson, R. Rate constants for the gas-phase reactions of a series of C_3–C_6 aldehydes with OH and NO_3 radicals. *Int. J. Chem. Kinet.* **2000**, *32*, 79-84, doi:10.1002/(SICI)1097-4601(2000)32:2<79::AID-KIN2>3.0.CO;2-A.

Park, J.; Jongsma, C. G.; Zhang, R.; North, S. W. OH/OD initiated oxidation of isoprene in the presence of O_2 and NO. *J. Phys. Chem. A* **2004**, *108*, 10688-10697, doi:10.1021/jp040421t.

Patchen, A. K.; Pennino, M. J.; Kiep, A. C.; Elrod, M. J. Direct kinetic study of the product-forming channels of the reaction of isoprene-derived hydroxyperoxy radicals with NO. *Int. J. Chem. Kinet.* **2007**, *39*, 353-361, doi:10.1002/kin.20248.

Pate, C. T.; Atkinson, R.; Pitts, J. N., Jr. The gas phase reaction of O_3 with a series of aromatic hydrocarbons. *J. Environ. Sci. Health* **1976**, *A11*, 1-10, doi:10.1080/10934527609385750.

Paulot, F.; Crounse, J. D.; Kjaergaard, H. G.; Kroll, J. H.; Seinfeld, J. H.; Wennberg, P. O. Isoprene photoxidation: new insights into the production of acids and organic nitrates. *Atmos. Chem. Phys.* **2009**, *9*, 1479-1501, doi:10.5194/acp-9-1479-2009.

Paulson, S. E.; Chung, M.; Sen, A. D.; Orzechowska, G. Measurement of OH radical formation from the reaction of ozone with several biogenic alkenes *J. Geophys. Res.* **1998**, *103*, 25533-25539, doi:10.1029/98JD01951.

Paulson, S. E.; Flagan, R. C.; Seinfeld, J. H. Atmospheric photoxidation of isoprene Part I: The hydroxyl radical and ground state atomic oxygen reactions. *Int. J. Chem. Kinet.* **1992**, *24*, 79-101, doi:10.1002/kin.550240109.

Payne, W. A.; Brunning, J.; Mitchell, M. B.; Stief, L. J. Kinetics of the reactions of atomic chlorine with methanol and the hydroxymethyl radical with molecular oxygen at 298 K. *Int. J. Chem. Kinet.* **1988**, *20*, 63-74, doi:10.1002/kin.550200108.

Perry, R. A.; Melius, C. F. In *Twentieth Symposium (International) on Combustion*; The Combustion Institute, 1984; pp 639-646.

Petty, J. T.; Harrison, J. A.; Moore, C. B. Reactions of *trans*-HOCO studied by infrared spectroscopy. *J. Phys. Chem.* **1993**, *97*, 11194-11198, doi:10.1021/j100145a013.

Picquet, B.; Heroux, S.; Chebbi, A.; Doussin, J.-F.; Durand-Jolibois, R.; Monod, A.; Loirat, H.; Carlier, P. Kinetics of the reactions of OH radicals with some oxygenated volatile organic compounds under simulated atmospheric conditions. *Int. J. Chem. Kinet.* **1998**, *30*, 839-847, doi:10.1002/(SICI)1097-4601(1998)30:11<839::AID-KIN6>3.0.CO;2-W.

Plum, C. N.; Sanhueza, E.; Atkinson, R.; Carter, W. P. L.; Pitts, J. N., Jr. OH radical rate constant and photolysis rates of α-dicarbonyls. *Environ. Sci. Technol.* **1983**, *17*, 479-484, doi:10.1021/es00114a008.

Plumb, I. C.; Ryan, K. R. Kinetics of the reactions of CH_3 with $O(^3P)$ and O_2 at 295 K. *Int. J. Chem. Kinet.* **1982**, *14*, 861-874, doi:10.1002/kin.550140806.

Plumb, I. C.; Ryan, K. R.; Steven, J. R.; Mulcahy, M. F. R. Kinetics of the reaction of $C_2H_5O_2$ with NO at 295 K. *Int. J. Chem. Kinet.* **1982**, *14*, 183-194, doi:10.1002/kin.550140208.

Porter, E.; Wenger, J.; Treacy, J.; Sidebottom, H.; Mellouki, A.; Teton, S.; LeBras, G. Kinetic studies on the reactions of hydroxyl radicals with diethers and hydroxyethers. *J. Phys. Chem. A* **1997**, *101*, 5770-5775, doi:10.1021/jp971254i.

Poulet, G.; Laverdet, G.; Jourdain, J. L.; Le Bras, G. Kinetic study of the reactions of acetonitrile with Cl and OH radicals. *J. Phys. Chem.* **1984**, *88*, 6259-6263, doi:10.1021/j150669a041.

Qiu, J.; Tonokura, K. Detection of the simplest Criegee intermediate CH_2OO in the ν4 band using a continuous wave quantum cascade laser and its kinetics with SO_2 and NO_2. *Chem. Phys. Lett.* **2019**, *737*, 100019, doi:10.1016/j.cpletx.2019.100019.

Radford, H. E. The fast reaction of CH_2OH with O_2. *Chem. Phys. Lett.* **1980**, *71*, 195-197, doi:10.1016/0009-2614(80)80145-X.

Rajakumar, B.; Burkholder, J. B.; Portmann, R. W.; Ravishankara, A. R. Rate coefficients, for the OH + CFH_2CH_2OH reaction between 238 and 355 K. *Phys. Chem. Chem. Phys.* **2005**, *7*, 2498-2505, doi:10.1039/b503332b.

Rajakumar, B.; McCabe, D. C.; Talukdar, R. K.; Ravishankara, A. R. Rate coefficients for the reactions of OH with n-propanol and iso-propanol between 237 and 376 K. *Int. J. Chem. Kinet.* **2010**, *42*, 10-24, doi:10.1002/kin.20456.

Ravishankara, A. R.; Davis, D. D. Kinetic rate constants for the reaction of OH with methanol, ethanol, and tetrahydrofuran at 298 K. *J. Phys. Chem.* **1978**, *82*, 2852-2853, doi:10.1021/j100515a022.

Reilly, J. P.; Clark, J. H.; Moore, C. B.; Pimentel, G. C. HCO production, vibrational relaxation, chemical kinetics, and spectroscopy following laser photolysis of formaldehyde. *J. Chem. Phys.* **1978**, *69*, 4381-4394, doi:10.1063/1.436449.

Reitz, J. E.; McGivern, W. S.; Church, M. C.; Wilson, M. D.; North, S. W. The fate of the hydroxyalkoxy radical in the OH-initiated oxidation of isoprene. *Int. J. Chem. Kinet.* **2002**, *34*, 255-261, doi:10.1002/kin.10050.

Rhasa, D. In *Diplomarbeit* Univ. of Gottingen FRG, 1983.

Rickard, A. R.; Johnson, D.; McGill, C. D.; Marston, G. OH yields in the gas-phase reactions of ozone with alkenes *J. Phys. Chem. A* **1999**, *103*, 7656-7664, doi:10.1021/jp9916992.

Robinson, C.; Onel, L.; Newman, J.; Lade, R.; Au, K.; Sheps, L.; Heard, D. E.; Seakins, P. W.; Blitz, M. A.; Stone, D. Unimolecular kinetics of stabilized CH_3CHOO Criegee intermediates: *syn*-CH_3CHOO decomposition and *anti*-CH_3CHOO isomerization. *J. Phys. Chem. A* **2022**, *126*, 6984-6994, doi:10.1021/acs.jpca.2c05461.

Roehl, C. M.; Bauer, D.; Moortgat, G. K. Absorption spectrum and kinetics of the acetylperoxy radical. *J. Phys. Chem.* **1996**, *100*, 4038-4047, doi:10.1021/jp9526298.

Roth, P.; Löhr, R.; Hermanns, H. D. Shock wave measurements on the kinetics of the reaction HCN + O. *Ber. Bunsenges. Phys. Chem.* **1980**, *84*, 835-840, doi:10.1002/bbpc.19800840903.

Rudich, Y.; Talukdar, R. K.; Fox, R. W.; Ravishankara, A. R. Rate coefficients for reactions of NO_3 with a few olefins and oxygenated olefins. *J. Phys. Chem.* **1996**, *100*, 5374-5381, doi:10.1021/jp953079g.

Rust, F.; Stevens, C. M. Carbon kinetic isotope effect in the oxidation of methane by hydroxyl. *Int. J. Chem. Kinet.* **1980**, *12*, 371-377, doi:10.1002/kin.550120602.

Ryzhkov, A. B.; Ariya, P. A. A theoretical study of the reactions of carbonyl oxide with water in atmosphere: the role of water dimer. *Chem. Phys. Lett.* **2003**, *367*, 423-429, doi:10.1016/S0009- 2614(02)01685-8.

Ryzhkov, A. B.; Ariya, P. A. A theoretical study of the reactions of parent and substituted Criegee intermediates with water and the water dimer. *Phys. Chem. Chem. Phys.* **2004**, *6*, 5042-5050, doi:10.1039/b408414d.

Sanders, N.; Butler, J. E.; Pasternack, L. R.; McDonald, J. R. CH_3O (X^2E) production from 266 nm photolysis of methyl nitrite and reaction with NO. *Chem. Phys.* **1980**, *48*, 203-208, doi:10.1016/0301-0104(80)80049-8.

Saueressig, G.; Crowley, J. N.; Bergamaschi, P.; Brühl, C.; Brenninkmeijer, C. A. M.; Fischer, H. Carbon 13 and D kinetic isotope effects in the reactions of CH_4 with $O(^1D)$ and OH: New laboratory measurements and their implications for the isotopic composition of stratospheric methane. *J. Geophys. Res.* **2001**, *106*, 23127-23138, doi:10.1029/2000JD000120.

Saunders, S. M.; Hughes, K. J.; Pilling, M. J.; Baulch, D. L.; Smurthwaite, P. I. "Reactions of hydroxyl radicals with selected hydrocarbons of importance in atmospheric chemistry"; Optical Methods in Atmospheric Chemistry, 1992, Berlin.

Schiffman, A.; Nelson, D. D.; Robinson, M. S.; Nesbitt, D. J. High-resolution infrared flash kinetic spectroscopy of OH radicals. *J. Phys. Chem.* **1991**, *95*, 2629-2636, doi:10.1021/j100160a004.

Schmidt, V.; Zhu, G. Y.; Becker, K. H.; Fink, E. H. Study of OH reactions at high pressures by excimer laser photolysis - dye laser fluorescence. *Ber. Bunsenges. Phys. Chem.* **1985**, *89*, 321-322, doi:10.1002/bbpc.19850890337.

Schmoltner, A.-M.; Chu, P. M.; Brudzynski, R. J.; Lee, Y. T. Crossed molecular beam study of the reaction $O(^3P)$ + C_2H_4. *J. Chem. Phys.* **1989**, *91*, 6926-6936, doi:10.1063/1.457309.

Scollard, D. J.; Treacy, J. J.; Sidebottom, H. W.; Balestra-Garcia, C.; Laverdet, G.; LeBras, G.; MacLeod, H.; Téton, S. Rate constants for the reactions of hydroxyl radicals and chlorine atoms with halogenated aldehydes. *J. Phys. Chem.* **1993**, *97*, 4683-4688, doi:10.1021/j100120a021.

Sehested, J.; Christensen, L. K.; Nielsen, O. J.; Bilde, M.; Wallington, T. J.; Schneider, W. F.; Orlando, J. J.; Tyndall, G. S. Atmospheric chemistry of acetone: Kinetic study of the $CH_3C(O)CH_2O_2$ + NO/ NO_2 reactions and decomposition of $CH_3C(O)CH_2O_2NO_2$. *Int. J. Chem. Kinet.* **1998**, *30*, 475-489, doi:10.1002/(SICI)1097-4601(1998)30:7<475::AID-KIN4>3.0.CO;2-P.

Sehested, J.; Nielsen, O. J.; Wallington, T. J. Absolute rate constants for the reaction of NO with a series of peroxy radicals in the gas phase at 295 K. *Chem. Phys. Lett.* **1993**, *213*, 457-464, doi:10.1016/0009-2614(93)89142-5.

Selzer, E. A.; Bayes, K. D. Pressure dependence of the rate of reaction of methyl radicals with O_2. *J. Phys. Chem.* **1983**, *87*, 392-394, doi:10.1021/j100226a007.

Semmes, D. H.; Ravishankara, A. R.; Gump-Perkins, C. A.; Wine, P. H. Kinetics of the reactions of hydroxyl radical with aliphatic aldehydes. *Int. J. Chem. Kinet.* **1985**, *17*, 303-313, doi:10.1002/kin.550170307.

Shallcross, D. E.; Biggs, P.; Canosa-Mas, C. E.; Clemitshaw, K. C.; Harrison, M. G.; Alañón, M. R. L.; Pyle, J. A.; Vipond, A.; Wayne, R. P. Rate constants for the reaction between OH and CH_3ONO_2 and $C_2H_5ONO_2$ over a range of pressure and temperature. *J. Chem. Soc. Faraday Trans.* **1997**, *93*, 2807-2811, doi:10.1039/a701471f.

Sharkey, P.; Smith, I. W. M. Kinetics of elementary reactions at low temperatures: Rate constants for the reactions of OH with HCl ($298 \geq T/K \geq 138$), CH_4 ($298 \geq T/K \geq 178$), and C_2H_6 ($298 \geq T/K \geq 138$). *J. Chem. Soc. Faraday Trans.* **1993**, *89*, 631-638, doi:10.1039/ft9938900631.

Sheps, L. Absolute ultraviolet absorption spectrum of a Criegee intermediate CH_2OO. *J. Phys. Chem. Lett.* **2013**, *4*, 4201-4205, doi:10.1021/jz402191w.

Sheps, L.; Rotavera, B.; Eskola, A. J.; Osborn, D. L.; Taatjes, C. A.; Au, K.; Shallcross, D. E.; Khan, M. A. H.; Percival, C. J. The reaction of Criegee intermediate CH_2OO with water dimer: primary products and atmospheric impact. *Phys. Chem. Chem. Phys.* **2017**, *19*, 21970-21979, doi:10.1039/C7CP03265J.

Sheps, L.; Scully, A. M.; Au, K. UV absorption probing of the conformer-dependent reactivity of a Criegee intermediate CH_3CHOO. *Phys. Chem. Chem. Phys.* **2014**, *16*, 26701-26706, doi:10.1039/c4cp04408h.

Shibuya, K.; Ebatu, T.; Obi, K.; Tanaka, I. Rate constant measurements for the reactions of HCO with NO and O_2 in the gas phase. *J. Phys. Chem.* **1977**, *81*, 2292-2294, doi:10.1021/j100539a019.

Simonaitis, R.; Heicklen, J. Reactions of CH_3, CH_3O, and CH_3O_2 radicals with O_3. *J. Phys. Chem.* **1975**, *79*, 298-302, doi:10.1021/j100571a002.

Singh, S.; de Leon, M. F.; Li, Z. Kinetics study of the reaction of OH radicals with C5–C8 cycloalkanes at 240–340 K using the relative rate/discharge flow/mass spectrometry technique. *J. Phys. Chem. A* **2013**, *117*, 10863-10872, doi:10.1021/jp406923d.

Singh, S.; Li, Z. Kinetics investigation of OH reaction with isoprene at 240-340 K and 1-3 Torr using the relative rate/discharge flow/mass spectrometry technique. *J. Phys. Chem. A* **2007**, *111*, 11843-11851, doi:10.1021/jp074148h.

Singleton, D. L.; Irwin, R. S.; Cvetanović, R. J. Arrhenius parameters for the reactions of $O(^3P)$ atoms with several aldehydes and the trend in aldehydic C-H bond dissociation energies. *Can. J. Chem.* **1977**, *55*, 3321-3327, doi:10.1139/v77-463.

Singleton, D. L.; Paraskevopoulos, G.; Irwin, R. S. Rates and mechanism of the reactions of hydroxyl radicals with acetic, deuterated acetic, and propionic acids in the gas phase. *J. Am. Chem. Soc.* **1989**, *111*, 5248-5251, doi:10.1021/ja00196a035.

Singleton, D. L.; Paraskevopoulos, G.; Irwin, R. S.; Jolly, G. S.; McKenney, D. J. Rate and mechanism of the reaction of hydroxyl radicals with formic and deuterated formic acids. *J. Am. Chem. Soc.* **1988**, *110*, 7786-7790, doi:10.1021/ja00231a032.

Sivakumaran, V.; Crowley, J. N. Reaction between OH and CH_3CHO - Part 2. Temperature dependent rate coefficients (201-348 K). *Phys. Chem. Chem. Phys.* **2003**, *5*, 106-111, doi:10.1039/b209303k.

Sivakumaran, V.; Holscher, D.; Dillon, T. J.; Crowley, J. N. Reaction between OH and HCHO: temperature dependent rate coeffiecients (202-399 K) and product pathways (298 K). *Phys. Chem. Chem. Phys.* **2003**, *5*, 4821-4827, doi:10.1039/b306859e.

Smith, R. H. Rate constant and activation energy for the gaseous reaction between hydroxyl and formaldehyde. *Int. J. Chem. Kinet.* **1978**, *10*, 519-528, doi:10.1002/kin.550100509.

Smith, M. C.; Chang, C.-H.; Chao, W.; Lin, L.-C.; Takahashi, K.; Boering, K. A.; Lin, J. J.-M. Strong negative temperature dependence of the simplest Criegee intermediate CH_2OO reaction with water dimer. *J. Phys. Chem. Lett.* **2015**, *6*, 2708-2713, doi:10.1021/acs.jpclett.5b01109.

Smith, M. C.; Chao, W.; Kumar, M.; Francisco, J. S.; Takahashi, K.; Lin, J. J.-M. Temperature-dependent rate coefficients for the reaction of CH_2OO with hydrogen sulfide. *J. Phys. Chem. A* **2017**, *121*, 938-945, doi:10.1021/acs.jpca.6b12303.

Smith, C. A.; Molina, L. T.; Lamb, J. J.; Molina, M. J. Kinetics of the reaction of OH with pernitric and nitric acids. *Int. J. Chem. Kinet.* **1984**, *16*, 41-55, doi:10.1002/kin.550160107.

Smith, M. C.; Ting, W.-L.; Chang, C.-H.; Takahashi, K.; Boering, K. A.; Lin, J. J.-M. UV absorption spectrum of the C2 Criegee intermediate CH_3CHOO. *J. Chem. Phys.* **2014**, *141*, 074302, doi:10.1063/1.4892582.

Sørensen, M.; Hurley, M. D.; Wallington, T. J.; Dibble, T. S.; Nielsen, O. J. Do aerosols act as catalysts in the OH radical initiated atmospheric oxidation of volatile organic compounds? *Atmos. Environ.* **2002**, *36*, 5947-5952, doi:10.1016/S1352-2310(02)00766-5.

Spangenberg, T.; Kohler, S.; Hansmann, B.; Wachsmuth, U.; Abel, B.; Smith, M. A. Low-temperature reactions of OH radicals with propene and isoprene in pulsed Laval nozzle expansions. *J. Phys. Chem. A* **2004**, *108*, 7527-7534, doi:10.1021/jp031228m.

Sprengnether, M.; Demerjian, K. L.; Donahue, N. M.; Anderson, J. G. Product analysis of the OH oxidation of isoprene and 1,3-butadiene in the presence of NO. *J. Geophys. Res.* **2002**, *107*, 4268, doi:10.1029/2001JD000716.

Stabel, J. R.; Johnson, M. S.; Langer, S. Rate coefficients for the gas-phase reaction of isoprene with NO_3 and NO_2. *Int. J. Chem. Kinet.* **2005**, *37*, 57-65, doi:10.1002/kin.20050.

Stachnik, R. A.; Molina, L. T.; Molina, M. J. Pressure and temperature dependences of the reaction of OH with nitric acid. *J. Phys. Chem.* **1986**, *90*, 2777-2780, doi:10.1021/j100403a044.

Stedman, D. H.; Niki, H. Ozonolysis rates of some atmospheric gases. *Environ. Lett.* **1973**, *4*, 303-310, doi:10.1080/00139307309435501.

Stedman, D. H.; Wu, C. H.; Niki, H. Kinetics of gas-phase reactions of ozone with some olefins. *J. Phys. Chem.* **1973**, *77*, 2511-2514, doi:10.1021/j100907a004.

Stevens, P.; L'Esperance, D.; Chuong, B.; Martin, G. Measurements of the kinetics of the OH-initiated oxidation of isoprene: Radical propogation in the OH + isoprene + O_2 + NO reaction system. *Int. J. Chem. Kinet.* **1999**, *31*, 637-643, doi:10.1002/(SICI)1097-4601(1999)31:9<637::AID-KIN5>3.0.CO;2-O.

Stevens, P.; L'Esperance, D.; Chuong, B.; Martin, G. Measurements of the kinetics of the OH-initiated oxidation of isoprene: Radical propagation in the OH + isoprene + O_2 + NO reaction system. *Int. J. Chem. Kinet.* **1999**, *31*, 637-643, doi:10.1002/(SICI)1097-4601(1999)31:9<637::AID-KIN5>3.0.CO;2-O.

Stief, L. J.; Nava, D. F.; Payne, W. A.; Michael, J. V. Rate constant for the reaction of hydroxyl radical with formaldehyde over the temperature range 228-362 K. *J. Chem. Phys.* **1980**, *73*, 2254-2258, doi:10.1063/1.440374.

Stone, D.; Au, K.; Sime, S.; Medeiros, D. J.; Blitz, M.; Seakins, P. W.; Decker, Z.; Sheps, L. Unimolecular decomposition kinetics of the stabilised Criegee intermediates CH_2OO and CD_2OO. *Phys. Chem. Chem. Phys.* **2018**, *20*, 24940-24954, doi:10.1039/C8CP05332D.

Stone, D.; Blitz, M.; Daubney, L.; Howes, N. U. M.; Seakins, P. Kinetics of CH_2OO reactions with SO_2, NO_2, NO, H_2O, and CH_3CHO as a function of pressure. *Phys. Chem. Chem. Phys.* **2014**, *16*, 1139-1149, doi:10.1039/c3cp54391a.

Stuhl, F.; Niki, H. Determination of rate constants for reactions of O atoms with C_2H_2, C_2D_2, C_2H_4, and C_3H_6 using a pulse vacuum-UV photolysis-chemiluminesent method. *J. Chem. Phys.* **1971**, *55*, 3954-3957, doi:10.1063/1.1676684.

Su, F.; Calvert, J. G.; Shaw, J. H. Mechanism of the photooxidation of gaseous formaldehyde. *J. Phys. Chem.* **1979**, *83*, 3185-3191, doi:10.1021/j100488a001.

Su, F.; Calvert, J. G.; Shaw, J. H. A FT TR spectroscopic study of the ozone-ethene reaction mechanism in O_2-rich mixtures. *J. Phys. Chem.* **1980**, *84*, 239-246, doi:10.1021/j100440a003.

Su, F.; Calvert, J. G.; Shaw, J. H.; Niki, H.; Maker, P. D.; Savage, C. M.; Breitenbach, L. D. Spectroscopic and kinetic studies of a new metastable species in the photooxidation of gaseous formaldehyde. *Chem. Phys. Lett.* **1979**, *65*, 221-225, doi:10.1016/0009-2614(79)87053-0.

Su, Y.-T.; Lin, H.-Y.; Putikam, R.; Matsui, H.; Lin, M. C.; Lee, Y.-P. Extremely rapid self-reaction of the simplest Criegee intermediate CH_2OO and its implications in atmospheric chemistry. *Nat. Chem.* **2014**, *6*, 477-483, doi:10.1038/NCHEM.1890.

Suh, I.; Lei, W.; Zhang, R. Experimental and theoretical studies of isoprene reaction with NO_3. *J. Phys. Chem. A* **2001**, *105*, 6471-6478, doi:10.1021/jp0105950.
Sullivan, J. O.; Warneck, P. Rate constant for the reaction of oxygen atoms with acetylene. *J. Phys. Chem.* **1965**, *69*, 1749-1750, doi:10.1021/j100889a507.
Suto, M.; Manzanares, E. R.; Lee, L. C. Detection of sulfuric acid aerosols by ultraviolet scattering. *Environ. Sci. Technol.* **1985**, *19*, 815-820, doi:10.1021/es00139a008.
Szekely, A.; Hanson, R. K.; Bowman, C. In *Twentieth Symposium (International) on Combustion*; The Combustion Institute, 1984; pp 647-654.
Szilagyi, I.; Dobe, S.; Berces, T.; Marta, F.; Viskolcz, B. Direct kinetic study of reactions of hydroxyl radicals with alkyl formates. *Z. Phys. Chem.* **2004**, *218*, 479-492, doi:10.1524/zpch.218.4.479.29198.
Taatjes, C. A.; Welz, O.; Eskola, A. J.; Savee, J. D.; Osborn, D. L.; Lee, E. P. F.; Dyke, J. M.; Mok, D. W. K.; Shallcross, D. E.; Percival, C. J. Direct measurement of Criegee intermediate (CH_2OO) reactions with acetone, acetaldehyde, and hexafluoroacetone. *Phys. Chem. Chem. Phys.* **2012**, *14*, 10391-10400, doi:10.1039/C2CP40294G.
Taatjes, C. A.; Welz, O.; Eskola, A. J.; Savee, J. D.; Scheer, A. M.; Shallcross, D. E.; Rotavera, B.; Lee, E. P. F.; Dyke, J. M.; Mok, D. K. W.; Osborn, D. L.; Percival, C. J. Direct measurements of conformer-dependent reactivity of the Criegee intermediate CH_3CHOO. *Science* **2013**, *340*, 177-180, doi:10.1126/science.1234689.
Talukdar, R. K.; Burkholder, J. B.; Schmoltner, A.-M.; Roberts, J. M.; Wilson, R. R.; Ravishankara, A. R. Investigation of the loss processes for peroxyacetyl nitrate in the atmosphere: UV photolysis and reaction with OH. *J. Geophys. Res.* **1995**, *100*, 14163-14173, doi:10.1029/95JD00545.
Talukdar, R. K.; Gierczak, T.; Goldfarb, L.; Rudich, Y.; Madhava Rao, B. S.; Ravishankara, A. R. Kinetics of hydroxyl radical reactions with isotopically labeled hydrogen. *J. Phys. Chem.* **1996**, *100*, 3037-3043, doi:10.1021/jp9518724.
Talukdar, R. K.; Gierczak, T.; McCabe, D. C.; Ravishankara, A. R. Reaction of hydroxyl radial with acetone. 2. Products and reaction mechanism. *J. Phys. Chem. A* **2003**, *107*, 5021-5032, doi:10.1021/jp0273023.
Talukdar, R. K.; Herndon, S. C.; Burkholder, J. B.; Roberts, J. M.; Ravishankara, A. R. Atmospheric fate of several alkyl nitrates Part 1 Rate coefficients of the reactions alkyl nitrates with isotopically labelled hydroxyl radicals. *J. Chem. Soc. Faraday Trans.* **1997**, *93*, 2787-2796, doi:10.1039/A701780D.
Talukdar, R. K.; Mellouki, A.; Gierczak, T.; Barone, S.; Chiang, S.-Y.; Ravishankara, A. R. Kinetics of the reactions of OH with alkanes. *Int. J. Chem. Kinet.* **1994**, *26*, 973-990, doi:10.1002/kin.550261003.
Tapia, A.; Villanueva, F.; Salgado, M. S.; Cabañas, B.; Martínez, E.; Martín, P. Atmospheric degradation of 3-methylfuran: kinetic and products study. *Atmos. Chem. Phys.* **2011**, *11*, 3227–3241, doi:10.5194/acp-11-3227-2011.
Taylor, P. H.; Rahman, M. S.; Arif, M.; Dellinger, B.; Marshall, P. Kinetic and mechanistric studies of the reaction of hydroxyl radicals with acetaldehyde over an extended temperature range. *Symp. Int. Combust. Proc.* **1996**, *26*, 497-504.
Taylor, P. H.; Yamada, T.; Marshall, P. The reaction of OH with acetaldehyde and deuterated acetaldehyde: Further insight into the reaction mechanism at both low and elevated temperatures. *Int. J. Chem. Kinet.* **2006**, *38*, 489-495, doi:10.1002/kin.20179.
Temps, F.; Wagner, H. G. Rate constants for the reactions of OH radicals with CH_2O and HCO. *Ber. Bunsenges Phys. Chem.* **1984**, *88*, 415-418, doi:10.1002/bbpc.19840880419.
Teng, A. P.; Crounse, J. D.; Wennberg, P. O. Isoprene peroxy radical dynamics. *J. Am. Chem. Soc.* **2017**, *139*, 5367-5377, doi:10.1021/jacs.6b12838.
Thévenet, R.; Mellouki, A.; Le Bras, G. Kinetics of OH and Cl Reactions with a Series of Aldehydes. *Int. J. Chem. Kinet.* **2000**, *32*, 676-685, doi:10.1002/1097-4601(2000)32:11<676::AID-KIN3>3.0.CO;2-V.
Thüner, L. P.; Barnes, I.; Maurer, T.; Sauer, C. G.; Becker, K. H. Kinetic study of the reaction of OH with a series of acetals at 298 ± 4 K. *Int. J. Chem. Kinet.* **1999**, *31*, 797-803, doi:10.1002/(SICI)1097-4601(1999)31:11<797::AID-JCK6>3.0.CO;2-C.
Timonen, R. S.; Ratajczak, E.; Gutman, D. Kinetics of the reactions of the formyl radical with oxygen, nitrogen dioxide, chlorine, and bromine. *J. Phys. Chem.* **1988**, *92*, 651-655, doi:10.1021/j100314a017.
Ting, W.-L.; Chang, C.-H.; Lee, Y.-F.; Matsui, H.; Lee, Y.-P.; Lin, J. J.-M. Detailed mechanism of the $CH_2I + O_2$ reaction: Yield and self-reaction of the simplest Criegee intermediate CH_2OO. *J. Chem. Phys.* **2014**, *141*, 104308, doi:10.1063/1.4894405.
Toby, F. S.; Toby, S.; O'Neal, H. E. The kinetics of the gas-phase reaction between ozone and alkenes. *Int. J. Chem. Kinet.* **1976**, *8*, 25-35, doi:10.1002/kin.550080105.

Tomas, A. E.; Villenave, E.; Lesclaux, R. Reactions of the HO_2 radical with CH_3CHO and $CH_3C(O)O_2$ in the gas phase. *J. Phys. Chem. A* **2001**, *105*, 3505-3514, doi:10.1021/jp003762p.

Treacy, J.; El Hag, M.; O'Farrell, D.; Sidebottom, H. Reactions of ozone with unsaturated organic compounds. *Ber. Bunsenges. Phys. Chem.* **1992**, *96*, 422-427, doi:10.1002/bbpc.19920960337.

Tsalkani, N.; Mellouki, A.; Poulet, G.; Toupance, G.; Le Bras, G. Rate constant measurement for the reactions of OH and C1 with peroxyacetyl nitrate at 298 K. *J. Atmos. Chem.* **1988**, *7*, 409-419, doi:10.1007/BF00058713.

Tuazon, E. C.; Atkinson, R. A product study of the gas-phase reaction of methyl vinyl ketone with the OH radical in the presence of NO_x. *Int. J. Chem. Kinet.* **1989**, *21*, 1141-1152, doi:10.1002/kin.550211207.

Tuazon, E. C.; Atkinson, R. A product study of the gas-phase reaction of isoprene with the OH radical in the presence of NO_x. *Int. J. Chem. Kinet.* **1990**, *22*, 1221-1236, doi:10.1002/kin.550221202.

Tuazon, E. C.; Atkinson, R. A product study of the gas-phase reaction of methacrolein with the OH radical in the presence of NO_x. *Int. J. Chem. Kinet.* **1990**, *22*, 591-602, doi:10.1002/kin.550220604.

Tuazon, E. C.; Atkinson, R.; Winer, A. M.; Pitts Jr., J. N. A study of the atmospheric reactions of 1,3-dichloropropene and other selected organochlorine compounds. *Arch Environ Contam Toxicol.* **1984**, *13*, 691-700.

Tuazon, E. C.; Carter, W. P. L.; Atkinson, R.; Pitts, J. N., Jr. The gas-phase reaction of hydrazine and ozone: A nonphotolytic source of OH radicals for measurement of relative OH radical rate constants. *Int. J. Chem. Kinet.* **1983**, *15*, 619-629, doi:10.1002/kin.550150704.

Tuazon, E. C.; Sanhueza, E.; Atkinson, R.; Carter, W. P. L.; Winer, A. M.; Pitts, J. N., Jr. Direct determination of the equilibrium constant at 298 K for the $NO_2 + NO_3 \leftrightarrow N_2O_5$ reactions. *J. Phys. Chem.* **1984**, *88*, 3095-3098, doi:10.1021/j150658a033.

Tully, F. P.; Droege, A. T.; Koszykowski, M. L.; Melius, C. F. Hydrogen-atom abstraction from alkanes by OH. 2. Ethane. *J. Phys. Chem.* **1986**, *90*, 691-698, doi:10.1021/j100276a042.

Tully, F. P.; Goldsmith, J. E. M.; Droege, A. T. Hydrogen-atom abstraction from alkanes by OH. 4. Isobutane. *J. Phys. Chem.* **1986**, *90*, 5932-5937, doi:10.1021/j100280a095.

Tully, F. P.; Ravishankara, A. R.; Carr, K. Kinetic study of the reactions of the hydroxyl radical with ethane and propane. *Int. J. Chem. Kinet.* **1983**, *15*, 1111-1118, doi:10.1002/kin.550151014.

Tyndall, G. R. S.; Orlando, J. J.; Wallington, T. J.; Hurley, M. D.; Goto, M.; Kawasaki, M. Mechanism of the reaction of OH radicals with acetone and acetaldehyde at 251 and 296 K. *Phys. Chem. Chem. Phys.* **2002**, *4*, 2189-2193, doi:10.1039/b111195g.

Tyndall, G. S.; Cox, R. A.; Granier, C.; Lesclaux, R.; Moortgat, G. K.; Pilling, M. J.; Ravishankara, A. R.; Wallington, T. J. Atmospheric chemistry of small organic peroxy radicals. *J. Geophys. Res.* **2001**, *106*, 12157-12182, doi:10.1029/2000JD900746.

Tyndall, G. S.; Orlando, J. J.; Wallington, T. J.; Hurley, M. D. Products of the chlorine-atom- and hydroxyl-radical-initiated oxidation of CH_3CN. *J. Phys. Chem. A* **2001**, *105*, 5380-5384, doi:10.1021/jp004318p.

Tyndall, G. S.; Stafelbach, T. A.; Orlando, J. J.; Calvert, J. G. Rate coefficients for reactions of OH radicals with mehylglyoxal and acetaldehyde. *Int. J. Chem. Kinet.* **1995**, *27*, 1009-1020, doi:10.1002/kin.550271006.

Tyndall, G. S.; Wallington, T. J.; Ball, J. C. FTIR product study of the reactions $CH_3O_2 + CH_3O_2$ and $CH_3O_2 + O_3$. *J. Phys. Chem. A* **1998**, *102*, 2547-2554, doi:10.1021/jp972784h.

Vaghjiani, G. L.; Ravishankara, A. R. Kinetics and mechanism of OH reaction with CH_3OOH. *J. Phys. Chem.* **1989**, *93*, 1948-1959, doi:10.1021/j100342a050.

Vaghjiani, G. L.; Ravishankara, A. R. New measurement of the rate coefficient for the reaction of OH with methane. *Nature* **1991**, *350*, 406-409, doi:10.1038/350406a0.

Vandenberk, S.; Peeters, J. The reaction of acetaldehyde and propionaldehdye with hydroxyl radicals: experimental determination of the primary H_2O yield at room temperature. *J. Photochem. Photobiol. A: Chem.* **2003**, *157*, 269-274, doi:10.1016/S1010-6030(03)00063-7.

Vandenberk, S.; Vereecken, L.; Peeters, J. The acetic acid forming channel in the acetone plus OH reaction: A combined experimental and theoretical investigation. *Phys. Chem. Chem. Phys.* **2002**, *4*, 461-466, doi:10.1039/b108161f.

Vasvári, G.; Szilágyi, I.; Bencsura, A.; Dóbe, S.; Bérces, T.; Henon, E.; Canneaux, S.; Bohr, F. Reaction and complex formation between OH radical and acetone. *Phys. Chem. Chem. Phys.* **2001**, *3*, 551-555, doi:10.1039/b009601f.

Vereecken, L.; Harder, H.; Novelli, A. The reaction of Criegee intermediates with NO, RO_2, and SO_2, and their fate in the atmosphere. *Phys. Chem. Chem. Phys.* **2012**, *14*, 14682-14695, doi:10.1039/c2cp42300f.

Vereecken, L.; Harder, H.; Novelli, A. The reactions of Criegee intermediates with alkenes, ozone, and carbonyl oxides. *Phys. Chem. Chem. Phys.* **2014**, *16*, 4039-4049, doi:10.1039/c3cp54514h.
Vereecken, L.; Novelli, A.; Taraborrelli, D. Unimolecular decay strongly limits the atmospheric impact of Criegee intermediates. *Phys. Chem. Chem. Phys.* **2017**, *19*, 31599-31612, doi:10.1039/c7cp05541b.
Vereecken, L.; Rickard, A.; Newland, M.; Bloss, W. Theoretical study of the reactions of Criegee intermediates with ozone, alkylhydroperoxides, and carbon monoxide. *Phys. Chem. Chem. Phys.* **2015**, *17*, 23847-23858, doi:10.1039/c5cp03862f.
Veyret, B.; Lesclaux, R. Absolute rate constants for the reactions of HCO with O_2 and NO from 298 to 503 K. *J. Phys. Chem.* **1981**, *85*, 1918-1922, doi:10.1021/j150613a028.
Veyret, B.; Lesclaux, R.; Rayez, M.-T.; Rayez, J.-C.; Cox, R. A.; Moortgat, G. K. Kinetics and mechanism of the photooxidation of formaldehyde. 1. Flash photolysis study. *J. Phys. Chem.* **1989**, *93*, 2368-2374, doi:10.1021/j100343a033.
Veyret, B.; Rayez, J. C.; Lesclaux, R. Mechanism of the photooxidation of formaldehyde studied by flash photolysis of CH_2O-O_2-NO mixtures. *J. Phys. Chem.* **1982**, *86*, 3424-3430, doi:10.1021/j100214a032.
Villenave, E.; Lesclaux, R. Kinetics of the cross reactions of CH_3O_2 and $C_2H_5O_2$ radicals with selected peroxy radicals. *J. Phys. Chem.* **1996**, *100*, 14372-14382, doi:10.1021/jp960765m.
Vimal, D.; Stevens, P. S. Experimental and theoretical studies of the kinetics of the reactions of OH radicals with acetic acid, acetic acid-d_3 and acetic acid-d_4 at low pressure. *J. Phys. Chem. A* **2006**, *110*, 11509-11516, doi:10.1021/jp063224y.
Vinckier, C.; Schaekers, M.; Peeters, J. The ketyl radical in the oxidation of ethyne by atomic oxygen at 300-600 K. *J. Phys. Chem.* **1985**, *89*, 508-512, doi:10.1021/j100249a028.
Vöhringer-Martinez, E.; Hansmann, B.; Hernandez, H.; Francisco, J. S.; Troe, J.; Abel, B. Water catalysis of a radical-molecule gas-phase reaction. *Science* **2007**, *315*, 497-501, doi:10.1126/science.1134494.
Wagner, A. F.; Slagle, I. R.; Sarzynski, D.; Gutman, D. Experimental and theoretical studies of the $C_2H_5 + O_2$ reaction kinetics. *J. Phys. Chem.* **1990**, *94*, 1853-1868, doi:10.1021/j100368a026.
Wallington, T. J.; Atkinson, R.; Winer, A. M. Rate constants for the gas phase reaction of OH radicals with peroxyacetyl nitrate (PAN) at 273 and 297 K. *Geophys. Res. Lett.* **1984**, *1*, 861-864, doi:10.1029/GL011i009p00861.
Wallington, T. J.; Dagaut, P.; Kurylo, M. J. Measurements of the gas phase UV absorption spectrum of $C_2H_5O_2$• radicals and of the temperature dependence of the rate constant for their self-reaction. *J. Photochem. Photobiol. A: Chem.* **1988**, *42*, 173-185, doi:10.1016/1010-6030(88)80061-3.
Wallington, T. J.; Dagaut, P.; Kurylo, M. J. Ultraviolet absorption cross sections and reaction kinetics and mechanisms for peroxy radicals in the gas phase. *Chem. Rev.* **1992**, *92*, 667-710, doi:10.1021/cr00012a008.
Wallington, T. J.; Dagaut, P.; Liu, R.; Kurylo, M. J. The gas phase reactons of hydroxyl radicals with a series of esters over the temperature range 240-440 K. *Int. J. Chem. Kinet.* **1988**, *20*, 177-186, doi:10.1002/kin.550200210.
Wallington, T. J.; Hurley, M. D.; Ball, J. C.; Straccia, A. M.; Platz, J.; Christensen, L. K.; Sehested, J.; Nielsen, O. J. Atmospheric chemistry of dimethoxymethane ($CH_3OCH_2OCH_3$): Kinetics and mechanism of its reaction with OH radicals and fate of the alkoxy radicals $CH_3OCHO(•)OCH_3$ and $CH_3OCH_2OCH_2O(•)$. *J. Phys. Chem. A* **1997**, *101*, 5302-5308, doi:10.1021/jp9631184.
Wallington, T. J.; Japar, S. M. FTIR product study of the reaction of $C_2H_5O_2 + HO_2$ in air at 295 K. *Chem. Phys. Lett.* **1990**, *166*, 495-499, doi:10.1016/0009-2614(90)87140-M.
Wallington, T. J.; Kurylo, M. J. Flash photolysis resonance fluorescence investigation of the gas-phase reactions of OH radicals with a series of aliphatic ketones over the temperature range 240-440 K. *J. Phys. Chem.* **1987**, *91*, 5050-5054, doi:10.1021/j100303a033.
Wallington, T. J.; Kurylo, M. J. The gas phase reactions of hydroxyl radicals with a series of aliphatic alcohols over the temperature range 240-440 K. *Int. J. Chem. Kinet.* **1987**, *19*, 1015-1023, doi:10.1002/kin.550191106.
Wallington, T. J.; Neuman, D. M.; Kurylo, M. J. Kinetics of the gas phase reaction of hydroxyl radicals with ethane, benzene, and a series of halogenated benzenes over the temperature range 234–438 K. *Int. J. Chem. Kinet.* **1987**, *19*, 725-739, doi:10.1002/kin.550190806.
Wang, J.; Chen, H. B.; Glass, G. P.; Curl, R. F. Kinetic study of the reaction of acetaldehyde with OH. *J. Phys. Chem. A* **2003**, *107*, 10834-10844, doi:10.1021/jp036114p.

Wang, Y.-Y.; Dash, M. R.; Chung, C.-Y.; Lee, Y.-P. Detection of transient infrared absorption of SO_3 and 1,3,2-dioxathietane-2,2-dioxide [cyc-$(CH_2)O(SO_2)O$] in the reaction $CH_2OO + SO_2$. *J. Chem. Phys.* **2018**, *148*, doi:10.1063/1.5019205.

Wang, W. C.; Suto, M.; Lee, L. C. $CH_2OH + O_2$ reaction rate constant measured by detecting HO_2 from photofragment emission. *J. Chem. Phys.* **1984**, *81*, 3122-3126, doi:10.1063/1.448015.

Wantuck, P. J.; Oldenberg, R. C.; Baughcum, S. L.; Winn, K. R. Removal rate constant measurements for CH_3O by O_2 over the 298-973 K range. *J. Phys. Chem.* **1987**, *91*, 4653-4655, doi:10.1021/j100302a004.

Washida, N. Reaction of methyl radicals with $O(^3P)$, O_2 and NO. *J. Chem. Phys.* **1980**, *73*, 1665-1672, doi:10.1063/1.440348.

Washida, N.; Akimoto, H.; Okuda, M. Is $O_2^*(a^1\Delta_g)$ formed in the $O + O_3$, $H + O_3$, and $NO + O_3$ reactions? *Bull. Chem. Soc. Jpn.* **1980**, *53*, 3496-3503, doi:10.1246/bcsj.53.3496.

Washida, N.; Bayes, K. D. The reactions of methyl radicals with atomic and molecular oxygen. *Int. J. Chem. Kinet.* **1976**, *8*, 777-794, doi:10.1002/kin.550080512.

Washida, N.; Martinez, R. I.; Bayes, K. D. The oxidation of formyl radicals. *Z. Naturforsch.* **1974**, *29A*, 251-255.

Wei, W.-m.; Zheng, R.-h.; Pan, Y.-l.; Wu, Y.-k.; Yang, F.; Hong, S. Ozone dissociation to oxygen affected by Criegee intermediate. *J. Phys. Chem. A* **2014**, *118*, 1644-1650, doi:10.1021/jp4121047.

Welz, O.; Eskola, A. J.; Sheps, L.; Rotavera, B.; Savee, J. D.; Scheer, A. M.; Osborn, D. L.; Lowe, D.; Booth, A. M.; Xiao, P.; Khan, M. A. H.; Percival, C. J.; Shallcross, D. E.; Taatjes, C. A. Rate coefficients of C1 and C2 Criegee intermediate reactions with formic and acetic acid near the collision limit: Direct kinetics measurements and atmospheric implications. *Angew. Chem. Int. Ed.* **2014**, *53*, 4547-4550, doi:10.1002/anie.201400964.

Welz, O.; Savee, J. D.; Osborn, D. L.; Vasu, S. S.; Percival, C. J.; Shallcross, D. E.; Taatjes, C. A. Direct kinetic measurements of Criegee intermediate (CH_2OO) formed by reaction of CH_2I with O_2. *Science* **2012**, *335*, 204-207, doi:10.1126/science.1213229.

Welz, O.; Savee, J. D.; Osborn, D. L.; Vasu, S. S.; Percival, C. J.; Shallcross, D. E.; Taatjes, C. A. Direct kinetic measurements of Criegee intermediate (CH_2OO) formed by reaction of CH_2I with O_2. *Science* **2012**, *335*, 204-207, doi:10.1126/science.1213229.

Westenberg, A. A.; deHaas, N. Absolute measurements of the $O + C_2H_2$ rate coefficient. *J. Phys. Chem.* **1969**, *73*, 1181-1186, doi:10.1021/j100725a001.

Westenberg, A. A.; deHaas, N. A flash photolysis-resonance fluorescence study of the $O + C_2H_2$ and $O + C_2H_3Cl$ reactions. *J. Chem. Phys.* **1977**, *66*, 4900-4905, doi:10.1063/1.433828.

Whelan, C. A.; Eble, J.; Mir, Z. S.; Blitz, M. A.; Seakins, P. W.; Olzmann, M.; Stone, D. Kinetics of the reactions of hydroxyl radicals with furan and its alkylated derivatives 2-methyl furan and 2,5-dimethyl furan. *J. Phys. Chem. A* **2020**, *124*, 7416-7426, doi:10.1021/acs.jpca.0c06321.

Wiebe, H. A.; Heicklen, J. Photolysis of methyl nitrite. *J. Am. Chem. Soc.* **1973**, *95*, 1-7, doi:10.1021/ja00782a001.

Wille, U.; Becker, E.; Schindler, R. N.; Lancar, I. T.; Poulet, G.; Le Bras, G. A discharge flow mass-spectrometric study of the reaction between the NO_3 radical and isoprene. *J. Atmos. Chem.* **1991**, *13*, 183-193, doi:10.1007/BF00115972.

Wilson, E. W.; Hamilton, W. A.; Kennington, H. R.; Evans, B.; Scott, N. W.; DeMore, W. B. Measurement and estimation of rate constants for the reactions of hydroxyl radical with several alkanes and cycloalkanes. *J. Phys. Chem. A* **2006**, *110*, 3593-3604, doi:10.1021/jp055841c.

Wine, P. H.; Astalos, R. J.; Mauldin, R. L., III Kinetic and mechanistic study of the OH + HCOOH reaction. *J. Phys. Chem.* **1985**, *89*, 2620-2624, doi:10.1021/j100258a037.

Wine, P. H.; Thompson, R. J. Kinetics of OH reactions with furan, thiophene, and tetrahydrothiophene. *Int J. Chem. Kinet.* **1984**, *16*, 867-878, doi:10.1002/kin.550160707.

Winer, A. M.; Lloyd, A. C.; Darnall, K. R.; Atkinson, R.; Pitts, J. N., Jr. Rate constnts for the reaction of OH radicals with *n*-propyl acetate, *sec*-butyl acetate, tertrahydrofuran and peroxyacetyl nitrate. *Chem. Phys. Lett.* **1977**, *51*, 221-226, doi:10.1016/0009-2614(77)80388-6.

Winer, A. M.; Lloyd, A. C.; Darnall, K. R.; Pitts, J. N., Jr. Relative rate constants for the reaction of the hydroxyl radical with selected ketones, chloroethenes, and monoterpene hydrocarbons. *J. Phys. Chem.* **1976**, *80*, 1635-1639, doi:10.1021/j100555a024.

Winiberg, F. A. F.; Chao, W.; Caravan, R. L.; Markus, C. R.; Sander, S. P.; Percival, C. J. A white cell based broadband transient UV-vis absorption spectroscopy with pulsed laser photolysis reactors for chemical kinetics under variable temperatures and pressures. *Rev. Sci. Instrum.* **2023**, *94*, doi:10.1063/5.0164733.

Wollenhaupt, M.; Carl, S. A.; Horowitz, A.; Crowley, J. N. Rate coefficients for reaction of OH with acetone between 202 and 395 K. *J. Phys. Chem. A* **2000**, *104*, 2695-2705, doi:10.1021/jp993738f.

Wu, H.; Mu, Y.; Zhang, X.; Jiang, G. Relative rate constants for the reactions of hydroxyl radicals and chlorine atoms with a series of aliphatic alcohols. *Int. J. Chem. Kinet.* **2003**, *35*, 81-87, doi:10.1002/kin.10109.

Xiong, F.; McAvey, K. M.; Pratt, K. A.; Groff, C. J.; Hostetler, M. A.; Lipton, M. A.; Starn, T. K.; Seeley, J. V.; Bertman, S. B.; Teng, A. P.; Crounse, J. D.; Nguyen, T. B.; Wennberg, P. O.; Misztal, P. K.; Goldstein, A. H.; Guenther, A. B.; Koss, A. R.; Olson, K. F.; de Gouw, J. A.; Baumann, K.; Edgerton, E. S.; Feiner, P. A.; Zhang, L.; Miller, D. O.; Brune, W. H.; Shepson, P. B. Observation of isoprene hydroxynitrates in the southeastern United States and implications for the fate of NO_x. *Atmos. Chem. Phys.* **2015**, *15*, 11257-11272, doi:10.5194/acp-15-11257-2015.

Yamada, T.; Taylor, P. H.; Goumri, A.; Marshall, P. The reaction of OH with acetone and acetone-d_6 from 298 to 832 K: Rate coefficients and mechanism. *J. Chem. Phys.* **2003**, *119*, 10600-10606, doi:10.1063/1.1619950.

Yetter, R. A.; Rabitz, H.; Dryer, F. L.; Maki, R. G.; Klemm, R. B. Evaluation of the rate constant for the reaction OH + H_2CO: Application of modeling and sensitivity analysis techniques for determination of the product branching ratio. *J. Chem. Phys.* **1989**, *91*, 4088-4097, doi:10.1063/1.456838.

Yujing, M.; Mellouki, A. Temperature dependence for the rate constants of the reaction of OH radicals with selected alcohols. *Chem. Phys. Lett.* **2001**, *333*, 63-68, doi:10.1016/S0009-2614(00)01346-4.

Zabarnick, S.; Fleming, J. W.; Lin, M. C. Kinetics of hydroxyl radical reactions with formaldehyde and 1,3,5-trioxane between 290 and 600 K. *Int. J. Chem. Kinet.* **1988**, *20*, 117-129, doi:10.1002/kin.550200205.

Zabarnick, S.; Heicklen, J. Reactions of alkoxy radicals with O_2. I. C_2H_5O radicals. *Int. J. Chem. Kinet.* **1985**, *17*, 455-476, doi:10.1002/kin.550170502.

Zabel, F.; Sahetchian, K. A.; Chachaty, C. ESR spectra of free radicals formed during the gas-phase photo-oxidation of formaldehyde: Thermal stability of the $HOCH_2OO$ radical. *Chem. Phys. Lett.* **1987**, *134*, 433-437, doi:10.1016/0009-2614(87)87168-3.

Zellner, R. Recent advances in free radical kinetics of oxygenated hydrocarbon radicals. *J. Chim. Phys.* **1987**, *84*, 403-407.

Zellner, R.; Ewig, F. Computational study of the $CH_3 + O_2$ chain branching reaction. *J. Phys. Chem.* **1988**, *92*, 2971-2974, doi:10.1021/j100321a050.

Zetzsch, C. "Rate constants for the reactions of OH with acetone and methylethylketone in the gas phase"; 7th International Symposium on Gas Kinetics, 1982, Goettingen, Germany.

Zetzsch, C.; Stuhl, F. In *Proceedings of the 2nd European Symposium on the Physico-Chemical Behaviour of Atmospheric Pollutants*; D. Reidel Publishing Co.: Dordrecht, Holland, 1982; pp 129-137.

Zhang, D.; Zhang, R.; North, S. W. Experimental study of NO reaction with isoprene hydroxyalkyl peroxy radicals. *J. Phys. Chem. A* **2003**, *107*, 11013-11019, doi:10.1021/jp0360016.

Zhang, R.; Suh, I.; Lei, W.; Clinkenbeard, A. D.; North, S. W. Kinetic studies of OH-initiated reactions of isoprene. *J. Geophys. Res.* **2000**, *105*, 24627-24635, doi:10.1029/2000JD900330.

Zhou, X.; Liu, Y.; Dong, W.; Yang, X. Unimolecular reaction rate measurement of *syn*-CH_3CHOO. *J. Phys. Chem. Lett.* **2019**, *10*, 4817-4821, doi:10.1021/acs.jpclett.9b01740.

Zhu, L.; Talukdar, R. K.; Burkholder, J. B.; Ravishankara, A. R. Rate coefficients for the OH + acetaldehyde (CH_3CHO) Reaction Between 204 and 373 K. *Int. J. Chem. Kinet.* **2008**, *40*, 635-646, doi:10.1002/kin.20346.

Zhu, C.; Zhu, L. Photolysis of glycolaldehyde in the 280-340nm region. *J. Phys. Chem. A* **2010**, *114*, 8384-8390, doi:10.1021/jp104497d.

1.10 FO_x Reactions

1.10.1 Table 1E: FO_x Reactions

Reaction	Temperature Range of Exp. Data (K) [a]	*A* Factor	*E*/R	*k*(298 K)[b]	*f*(298 K)[c]	*g* [c]	Note
$O + FO \rightarrow F + O_2$	298	*2.7×10⁻¹¹*	*0*	2.7×10^{-11}	3.00	250	E 1
$O + FO_2 \rightarrow FO + O_2$	–	*5.0×10⁻¹¹*	*0*	*5.0×10⁻¹¹*	5.00		E 2
$OH + CH_3F \rightarrow CH_2F + H_2O$ (HFC–41)	243–480	2.2×10^{-12}	1400	2.0×10^{-14}	1.10	150	E 3
$OH + CH_2F_2 \rightarrow CHF_2 + H_2O$ (HFC-32)	220–492	1.7×10^{-12}	1500	1.1×10^{-14}	1.07	100	E 4
$OH + CHF_3 \rightarrow CF_3 + H_2O$ (HFC-23)	253–1663	6.1×10^{-13}	2260	3.1×10^{-16}	1.15	100	E 5
$OH + CH_3CH_2F \rightarrow$ products (HFC-161)	210–480	2.5×10^{-12}	730	2.2×10^{-13}	1.07	50	E 6
$OH + CH_3CHF_2 \rightarrow$ products (HFC-152a)	210–480	8.7×10^{-13}	975	3.3×10^{-14}	1.07	50	E 7
$OH + CH_2FCH_2F \rightarrow CHFCH_2F + H_2O$ (HFC-152)	210–480	1.05×10^{-12}	710	9.7×10^{-14}	1.07	100	E 8
$OH + CH_3CF_3 \rightarrow CH_2CF_3 + H_2O$ (HFC-143a)	261–425	1.07×10^{-12}	2000	1.3×10^{-15}	1.10	100	E 9
$OH + CH_2FCHF_2 \rightarrow$ products (HFC-143)	278–441	3.9×10^{-12}	1620	1.7×10^{-14}	1.20	200	E10
$OH + CH_2FCF_3 \rightarrow CHFCF_3 + H_2O$ (HFC-134a)	220–473	1.03×10^{-12}	1620	4.5×10^{-15}	1.10	100	E11
$OH + CHF_2CHF_2 \rightarrow CF_2CHF_2 + H_2O$ (HFC-134)	294–434	1.6×10^{-12}	1660	6.1×10^{-15}	1.20	200	E12
$OH + CHF_2CF_3 \rightarrow CF_2CF_3 + H_2O$ (HFC-125)	220–441	5.16×10^{-13}	1670	1.9×10^{-15}	1.10	100	E13
$OH + CH_3CHFCH_3 \rightarrow$ products (HFC-281ea)	288–394	3.0×10^{-12}	490	5.8×10^{-13}	1.20	100	E14
$OH + CH_3CH_2CF_3 \rightarrow$ products (HFC-263fb)	238–375	3.7×10^{-12}	1290	4.9×10^{-14}	1.15	100	E15
$OH + CH_2FCF_2CHF_2 \rightarrow$ products (HFC-245ca)	260–365	2.1×10^{-12}	1620	9.2×10^{-15}	1.20	150	E16
$OH + CH_3CF_2CF_3 \rightarrow$ products (HFC-245cb)	287–370	4.2×10^{-13}	1680	1.5×10^{-15}	1.10	200	E17
$OH + CHF_2CHFCHF_2 \rightarrow$ products (HFC-245ea)	238–375	1.53×10^{-12}	1340	1.7×10^{-14}	1.10	150	E18
$OH + CH_2FCHFCF_3 \rightarrow$ products (HFC-245eb)	238–375	1.16×10^{-12}	1260	1.7×10^{-14}	1.15	100	E19
$OH + CHF_2CH_2CF_3 \rightarrow$ products (HFC-245fa)	273–370	6.1×10^{-13}	1330	7.0×10^{-15}	1.15	100	E20
$OH + CH_2FCF_2CF_3 \rightarrow CHFCF_2CF_3 + H_2O$	251–314	*1.03×10⁻¹²*	*1620*	*4.5×10⁻¹⁵*	2.00	200	E21
$OH + CHF_2CHFCF_3 \rightarrow$ products (HFC-236ea)	251–380	9.4×10^{-13}	1550	5.2×10^{-15}	1.20	200	E22
$OH + CF_3CH_2CF_3 \rightarrow CF_3CHCF_3 + H_2O$ (HFC–236fa)	251–413	1.45×10^{-12}	2500	3.3×10^{-16}	1.15	150	E23
$OH + CF_3CHFCF_3 \rightarrow CF_3CFCF_3 + H_2O$ (HFC-227ea)	250–463	4.8×10^{-13}	1680	1.7×10^{-15}	1.15	75	E24
$OH + CH_3CF_2CH_2CF_3 \rightarrow$ products (HFC-365mfc)	269–373	1.8×10^{-12}	1660	6.9×10^{-15}	1.30	100	E25

Reaction	Temperature Range of Exp. Data (K) [a]	*A* Factor	*E*/R	*k*(298 K)[b]	*f*(298 K)[c]	*g* [c]	Note
OH + $CF_3CH_2CH_2CF_3$ → products (HFC-356mff)	260–365	3.4×10^{-12}	1820	7.6×10^{-15}	1.20	300	E26
OH + $CH_2FCH_2CF_2CF_3$ → products (HFC-356mcf)	252–346	1.7×10^{-12}	1100	4.2×10^{-14}	1.30	150	E27
OH + $CHF_2CF_2CF_2CF_2H$ → products (HFC-338pcc)	232–419	7.7×10^{-13}	1540	4.4×10^{-15}	1.20	150	E28
OH + $CHF_2CF_2CF_2CF_3$ → products (HFC-329p)	296	*4.62×10^{-13}*	*1670*	1.7×10^{-15}	1.15	0	E29
OH + $CHF_2(CF_2)_4CF_3$ → products (HFC-52-13p)	250-430	5.16×10^{-13}	1670	1.9×10^{-15}	1.15	0	E30
OH + $CHF_2(CF_2)_6CF_3$ → products (HFC-72-17p)	253-328	6.92×10^{-13}	1670	2.55×10^{-15}	1.20	0	E31
OH + $CF_3CH_2CF_2CH_2CF_3$ → products (HFC-458mfcf)	278–354	1.1×10^{-12}	1800	2.6×10^{-15}	1.50	200	E32
OH + $CF_3CHFCHFCF_2CF_3$ → products (HFC-43-10mee)	250–400	5.2×10^{-13}	1500	3.4×10^{-15}	1.20	150	E33
OH + $CF_3CF_2CH_2CH_2CF_2CF_3$ → products	298	*3.5×10^{-12}*	*1800*	8.3×10^{-15}	1.50	300	E34
OH + CH_2=CHF → products	220–426	1.77×10^{-12}	–310	5.0×10^{-12}	1.07	20	E35
OH + (*Z*)-CHF=CHF → products	250–430	3.7×10^{-12}	–230	8.0×10^{-12}	1.10	0	E36
OH + (*E*)-CHF=CHF → products	250–430	4.0×10^{-12}	–255	9.4×10^{-12}	1.10	0	E37
OH + CH_2=CF_2 → products	219–373	1.7×10^{-12}	–150	2.8×10^{-12}	1.07	20	E38
OH + CHF=CF_2 → products	215–375	2.96×10^{-12}	–300	8.1×10^{-12}	1.07	20	E39
OH + CF_2=CF_2 → products	250–480	3.4×10^{-12}	–320	1.0×10^{-11}	1.07	20	E40
OH + CH_2=$CHCH_2F$ → products	228–430	2.97×10^{-12}	–440	1.3×10^{-11}	1.10	50	E41
OH + CH_2=$CFCH_3$ → products	250–430	3.28×10^{-12}	–490	1.7×10^{-11}	1.10	20	E42
OH + CH_2=$CHCF_3$ → products	252–370	8.2×10^{-13}	–170	1.45×10^{-12}	1.07	50	E43
OH + CH_2=$CFCF_3$ → products	207–430	1.1×10^{-12}	0	1.1×10^{-12}	1.02	10	E44
OH + (*E*)-CHF=$CHCF_3$ → products	220–430	7.1×10^{-13}	0	7.1×10^{-13}	1.03	20	E45
OH + (*E*)-CHF=$CHCF(CF_3)_2$ → products	214–380	1.1×10^{-12}	0	1.1×10^{-12}	1.07	0	E46
OH + (*Z*)-CHF=$CHCF_3$ → products	250–430	6.8×10^{-13}	–230	1.47×10^{-12}	1.10	0	E47
OH + CF_2=$CHCHF_2$ → products	223–373	7.47×10^{-13}	–360	2.5×10^{-12}	1.20	0	E48
OH + (*E*)-CHF=$CFCF_3$ → products	296	*1.65×10^{-12}*	*–100*	2.3×10^{-12}	1.30	50	E49
OH + (*Z*)-CHF=$CFCF_3$ → products	200–380	7.5×10^{-13}	–165	1.3×10^{-12}	1.07	50	E50
OH + CF_2=$CHCF_3$ → products	250–430	4.85×10^{-13}	–115	7.14×10^{-13}	1.15	0	E51
OH + CF_2=$CFCHF_2$ → products	250–430	1.43×10^{-12}	–485	7.3×10^{-12}	1.15	0	E52

Reaction	Temperature Range of Exp. Data (K) [a]	*A* Factor	*E*/R	*k*(298 K)[b]	*f*(298 K)[c]	*g* [c]	Note
OH + CF_2=$CFCF_3$ → products	250–489	5.34×10^{-13}	–415	2.15×10^{-12}	1.05	50	E53
OH + CF_2=$CFOCF_3$ → products	250–430	1.03×10^{-12}	–320	3.0×10^{-12}	1.10	50	E54
OH + CF_2=$CFOC_2F_5$ → products	207–300	6.0×10^{-13}	–480	3.0×10^{-12}	1.10	50	E55
OH + CF_2=$CFCF$=CF_2 → products	298	*4.0×10^{-12}*	*–300*	1.1×10^{-11}	1.15	100	E56
OH + CH_2=$CHCF_2CF_3$ → products	296	*7.9×10^{-13}*	*–170*	1.4×10^{-12}	1.20	50	E57
OH + (*E*)-CF_3CH=$CHCF_3$ → products	211–373	7.0×10^{-13}	500	1.3×10^{-13}	1.10	0	E58
OH + (*Z*)-CF_3CH=$CHCF_3$ → products	212–374	2.46×10^{-13}	–200	4.8×10^{-13}	1.07	20	E59
OH + (*E*)-CF_3CH=CHC_2F_5 → products	253–328	7.93×10^{-13}	645	9.1×10^{-14}	1.20	0	E60
OH + CH_2=$C(CF_3)_2$ → products	250–430	8.70×10^{-13}	25	8.0×10^{-13}	1.10	50	E61
OH + (*E*)-CF_3CF=$CFCF_3$ → products	230–370	3.17×10^{-13}	–180	5.8×10^{-13}	1.10	20	E62
OH + (*Z*)-CF_3CF=$CFCF_3$ → products	230–370	2.9×10^{-13}	–80	3.8×10^{-13}	1.10	20	E63
OH + CF_2=$CFCF_2CF_3$ → products	296	*4.47×10^{-13}*	*–415*	1.8×10^{-12}	1.15	50	E64
OH + *cyclo*-CH=$CHCF_2CF_2$- → products	253–328	4.50×10^{-13}	280	1.76×10^{-13}	1.10	0	E65
OH + *cyclo*-CH=$CFCF_2CF_2$- → products	253–328	5.4×10^{-13}	645	6.2×10^{-14}	1.10	0	E66
OH + *cyclo*-CF=$CFCF_2CF_2$- → products	253–328	3.25×10^{-13}	640	3.8×10^{-14}	1.10	0	E67
OH + *cyclo*-CH=$CHCF_2CF_2CF_2$- → products	253–328	3.7×10^{-13}	370	1.07×10^{-13}	1.15	0	E68
OH + *cyclo*-CH=$CFCF_2CF_2CF_2$- → products	242–370	3.7×10^{-13}	630	4.8×10^{-14}	1.10	0	E69
OH + *cyclo*-CF=$CFCF_2CF_2CF_2$- → products	242–372	3.56×10^{-13}	610	4.6×10^{-14}	1.10	0	E70
OH + (*E*)-CHF=$CHCF(CF_3)_2$→ products	214–380	3.2×10^{-13}	0	3.2×10^{-13}	1.05	0	E71
OH + $(CF_3)_2C$=$CFCF_2CF_3$ → products	250–370	7.1×10^{-14}	0	7.1×10^{-14}	1.05	50	E72
OH + $CF_3C{\equiv}CH$ → products	253–328	3.46×10^{-12}	835	2.1×10^{-13}	1.50	0	E73
OH + $CF_3C{\equiv}CCF_3$ → products	253–328	1.73×10^{-12}	940	7.4×10^{-14}	1.50	0	E74
OH + CF_3OH → CF_3O + H_2O	–			*<2×10^{-17}*			E75
OH + CH_2FCH_2OH → products	220–370	1.82×10^{-12}	210	9.0×10^{-13}	1.05	50	E76
OH + CHF_2CH_2OH → products	220–370	1.4×10^{-12}	500	2.6×10^{-13}	1.05	100	E77
OH + CF_3CH_2OH → products	220–430	8.6×10^{-13}	640	1.0×10^{-13}	1.05	100	E78
OH + $CF_3CH_2CH_2OH$ → products	263–358	*1.82×10^{-12}*	*210*	9.0×10^{-13}	1.10	50	E79

Reaction	Temperature Range of Exp. Data (K) [a]	*A* Factor	*E*/R	*k*(298 K)[b]	*f*(298 K)[c]	*g* [c]	Note
OH + $CF_3CF_2CH_2OH$ → products	250–430	1.16×10^{-12}	730	1.0×10^{-13}	1.05	100	E80
OH + $(CF_3)_2CHOH$ → products	220–430	4.05×10^{-13}	830	2.5×10^{-14}	1.05	100	E81
OH + $(CF_3)_2C(OH)CH_3$ → products	230–370	4.18×10^{-14}	520	7.3×10^{-15}	1.10	100	E82
OH + $(CF_3)_3COH$ → products	230–370	5.06×10^{-16}	-140	8.1×10^{-16}	1.20	100	E83
OH + $CF_3CHFCF_2CH_2OH$ → products	230–430	1.07×10^{-12}	640	1.25×10^{-13}	1.10	100	E84
OH + $CF_3CF_2CF_2CF_2CH_2OH$ → products	296	*1.16×10^{-12}*	*730*	1.0×10^{-13}	1.10	200	E85
OH + CH_3OCHF_2 → products (HFE-152a)	298–460	1.05×10^{-11}	1700	3.5×10^{-14}	1.30	200	E86
OH + CH_3OCF_3 → CH_2OCF_3 + H_2O (HFE-143a)	268–460	1.84×10^{-12}	1500	1.2×10^{-14}	1.10	150	E87
OH + CHF_2OCHF_2 → CF_2OCHF_2 +H_2O (HFE-134)	251–464	1.1×10^{-12}	1830	2.4×10^{-15}	1.10	150	E88
OH + CHF_2OCF_3 → CF_2OCF_3 + H_2O (HFE-125)	298–393	4.6×10^{-13}	2040	4.9×10^{-16}	1.20	200	E89
OH + $CH_3OCHFCF_3$ → products	253–328	2.05×10^{-12}	760	1.6×10^{-13}	1.15	50	E90
OH + $CH_2FOCH(CF_3)_2$ → products (Sevoflurane)	241–422	8.77×10^{-13}	960	3.5×10^{-14}	1.15	100	E91
OH + $CH_3OCF_2CHF_2$ → products	250–430	1.72×10^{-12}	1300	2.2×10^{-14}	1.10	200	E92
OH + $CH_3OCF_2CF_3$ → products	250–430	1.1×10^{-12}	1370	1.1×10^{-14}	1.20	150	E93
OH + $CHF_2OCH_2CF_3$ → products (HFE-245fa2)	292–460	2.9×10^{-12}	1660	1.1×10^{-14}	1.15	200	E94
OH + $CHF_2OCHFCF_3$ → products (Desflurane)	241–298	8.15×10^{-13}	1570	4.2×10^{-15}	1.15	100	E95
OH + $CHF_2OCF_2CHF_2$ → products	253–407	5.8×10^{-13}	1600	2.7×10^{-15}	1.20	50	E96
OH + $CF_3OCHFCF_3$ → products	250–430	3.1×10^{-13}	1680	1.1×10^{-15}	1.15	100	E97
OH + $CHF_2CF_2OCF_3$ → products	269–406	4.82×10^{-13}	1620	2.1×10^{-15}	1.10	100	E98
OH + $CH_3OCF_2CF_2CF_3$ → products	250–430	1.4×10^{-12}	1440	1.1×10^{-14}	1.15	150	E99
OH + $CH_3OCH(CF_3)_2$ → products (HFE-356mm1)	230–370	1.14×10^{-12}	470	2.35×10^{-13}	1.05	50	E100
OH + $CH_3OCF(CF_3)_2$ → products	250–430	1.3×10^{-12}	1330	1.5×10^{-14}	1.10	100	E101
OH + $CH_3OC_4F_9$ → products	253–328	1.17×10^{-12}	1390	1.1×10^{-14}	1.10	100	E102
OH + $CHF_2OCH_2CF_2CHF_2$ → products	250–430	1.82×10^{-12}	1410	1.6×10^{-14}	1.20	200	E103
OH + $CHF_2OCH_2CF_2CF_3$ → products	250–430	1.6×10^{-12}	1510	1.0×10^{-14}	1.30	200	E104
OH + $CHF_2OCH(CF_3)_2$ → products	284–398	1.03×10^{-12}	1760	2.8×10^{-15}	1.20	150	E105
OH + $CF_3OCH(CF_3)_2$ → products	296	*2.82×10^{-13}*	*2040*	3×10^{-16}	1.50	200	E106

Reaction	Temperature Range of Exp. Data (K) [a]	*A* Factor	*E*/R	*k*(298 K)[b]	*f*(298 K)[c]	*g* [c]	Note
$OH + CH_3CH_2OCF_2CHF_2 \rightarrow$ products	250–430	2.1×10^{-12}	670	2.2×10^{-13}	1.10	100	E107
$OH + CF_3CH_2OCH_2CF_3 \rightarrow$ products	268–409	2.8×10^{-12}	890	1.4×10^{-13}	1.10	100	E108
$OH + CF_3CH_2OCF_2CHF_2 \rightarrow$ products (HFE-347pcf2)	250–430	1.32×10^{-12}	1470	9.5×10^{-15}	1.07	50	E109
$OH + CF_3CHFCF_2OCF_3 \rightarrow$ products	270–406	3.94×10^{-13}	1590	1.9×10^{-15}	1.15	150	E110
$OH + CF_3CH_2OCF_2CHFCF_3 \rightarrow$ products	272–407	1.08×10^{-12}	1400	9.8×10^{-15}	1.15	150	E111
$OH + CHF_2CF_2OCHFCF_3 \rightarrow$ products	267–407	6.14×10^{-13}	1500	4.0×10^{-15}	1.15	150	E112
$OH + CF_3CHFCF_2OCH_2CF_2CF_3 \rightarrow$ products	253–328	5.36×10^{-13}	1345	5.9×10^{-15}	1.15	0	E113
$OH + CHF_2OCF_2OCHF_2 \rightarrow$ products	295	*1.0×10^{-12}*	*1800*	2.4×10^{-15}	1.40	200	E114
$OH + CHF_2OCF_2CF_2OCHF_2 \rightarrow$ products	295	*2.0×10^{-12}*	*1800*	4.7×10^{-15}	1.50	200	E115
$OH + CHF_2OCF_2CF_2OCF_2OCHF_2 \rightarrow$ products	295	*1.9×10^{-12}*	*1800*	4.6×10^{-15}	1.50	200	E116
$F + O_2 \xrightarrow{M} FO_2$		(See Table 2-1)					
$F + O_3 \rightarrow FO + O_2$	253–365	2.2×10^{-11}	230	1.0×10^{-11}	1.50	200	E117
$F + H_2 \rightarrow HF + H$	77–765	1.4×10^{-10}	500	2.6×10^{-11}	1.20	200	E118
$F + H_2O \rightarrow HF + OH$	240–373	1.4×10^{-11}	0	1.4×10^{-11}	1.30	200	E119
$F + NO \xrightarrow{M} FNO$		(See Table 2-1)					
$F + NO_2 \xrightarrow{M} FNO_2$		(See Table 2-1)					
$F + HNO_3 \rightarrow HF + NO_3$	260–373	6.0×10^{-12}	–400	2.3×10^{-11}	1.30	200	E120
$F + CH_4 \rightarrow HF + CH_3$	139–423	1.6×10^{-10}	260	6.7×10^{-11}	1.40	200	E121
$FO + O_3 \rightarrow$ products	298			$<1\times10^{-14}$			E122
$FO + NO \rightarrow NO_2 + F$	298–845	8.2×10^{-12}	–300	2.2×10^{-11}	1.50	200	E123
$FO + NO_2 \xrightarrow{M} FONO_2$		(See Table 2-1)					
$FO + FO \rightarrow 2F + O_2$	298–435	1.0×10^{-11}	0	1.0×10^{-11}	1.50	250	E124
$FO_2 + O_3 \rightarrow$ products	298			$<3.4\times10^{-16}$			E125
$FO_2 + NO \rightarrow FNO + O_2$	190–298	7.5×10^{-12}	690	7.5×10^{-13}	2.00	400	E126
$FO_2 + NO_2 \rightarrow$ products	260–315	3.8×10^{-11}	2040	4.0×10^{-14}	2.00	500	E127
$FO_2 + CO \rightarrow$ products	298			$<5.1\times10^{-16}$			E128
$FO_2 + CH_4 \rightarrow$ products	298			$<2\times10^{-16}$			E129

Reaction	Temperature Range of Exp. Data (K) [a]	*A* Factor	*E*/R	*k*(298 K)[b]	*f*(298 K)[c]	*g* [c]	Note
$CF_3 + O_2 \xrightarrow{M} CF_3O_2$		(See Table 2-1)					
$CF_3O + M \rightarrow F + CF_2O + M$		(See Table 2-1)					
$CF_3O + O_2 \rightarrow FO_2 + CF_2O$	373	*<3×10⁻¹¹*	*5000*	*<1.5×10⁻¹⁸*			E130
$CF_3O + O_3 \rightarrow CF_3O_2 + O_2$	210–353	*2×10⁻¹²*	*1400*	1.8×10⁻¹⁴	1.30	600	E131
$CF_3O + H_2O \rightarrow OH + CF_3OH$	296–381	*3×10⁻¹²*	*>3600*	*<2×10⁻¹⁷*			E132
$CF_3O + NO \rightarrow CF_2O + FNO$	213–393	3.7×10⁻¹¹	–110	5.4×10⁻¹¹	1.20	70	E133
$CF_3O + NO_2 \rightarrow$ products $\xrightarrow{M} CF_3ONO_2$	222–302	(See Note) (See Table 2-1)					E134
$CF_3O + CO \rightarrow$ products $\xrightarrow{M} CF_3OCO$	233–332	(See Note) (See Table 2-1)		<2×10⁻¹⁵			E135
$CF_3O + CH_4 \rightarrow CH_3 + CF_3OH$	231–573	2.6×10⁻¹²	1420	2.2×10⁻¹⁴	1.10	200	E136
$CF_3O + C_2H_6 \rightarrow C_2H_5 + CF_3OH$	233–573	4.9×10⁻¹²	400	1.3×10⁻¹²	1.20	100	E137
$CF_3O_2 + O_3 \rightarrow CF_3O + 2O_2$	210–353			<3×10⁻¹⁵			E138
$CF_3O_2 + CO \rightarrow CF_3O + CO_2$	296			<5×10⁻¹⁶			E139
$CF_3O_2 + NO \rightarrow CF_3O + NO_2$	230–430	5.4×10⁻¹²	–320	1.6×10⁻¹¹	1.10	150	E140
$CF_3O_2 + NO_2 \xrightarrow{M} CF_3O_2NO_2$		(See Table 2-1)					

Shaded areas indicate changes or additions since JPL19-5. Italicized blue data entries denote estimates.

[a] Temperature range of available experimental data. This is not necessarily the range of temperature over which the recommended Arrhenius parameters are applicable. See the corresponding note for each reaction for such information.

[b] Units are cm^3 $molecule^{-1}$ s^{-1}.

[c] *f*(298 K) is the uncertainty factor at 298 K. To calculate the uncertainty at other temperatures, use the expression:

$$f(\mathrm{T}) = f(298\ \mathrm{K})\exp\left|g\left(\frac{1}{\mathrm{T}} - \frac{1}{298}\right)\right|$$

Note that the exponent is an absolute value.

1.10.2 Notes: FO_x Reactions

E1. **O + FO.** The recommended value for k(298 K) is based on results of the room temperature study of Bedzhanyan et al.[1] The temperature dependence of the rate constant is expected to be small, as it is for the analogous ClO reaction.
(Table: 94-26, Note: 94-26, Evaluated: 94-26) Back to Table

(1) Bedzhanyan, Y. R.; Markin, E. M.; Politenkova, G. G.; Gershenzon, Y. M. Experimental study of elementary reactions of FO radicals. III. Reactions with oxygen and nitrogen atoms. *Kinetics and Catalysis* **1993**, *33*, 797-801.

E2. **O + FO_2.** The recommended Arrhenius parameters are estimated, as there are no experimental data. The rate constant for such a radical-atom process is expected to approach the gas collision frequency, and is not expected to exhibit a strong temperature dependence.
(Table: 82-57, Note: 82-57, Evaluated: 82-57) Back to Table

E3. **OH + CH_3F (HFC-41).** The recommended value for k(298 K) is an average of the values from Schmoltner et al.[8] (243–373 K), Nip et al.[7] (297 K), Hsu and DeMore[4] (298–363 K), and DeMore[2] (308–393 K) (with the relative rate constants from the last two studies listed above recalculated based on the current recommendations for the rate constants for the OH + CH_3CHF_2 and OH + CH_3Cl reference reactions, respectively.) The recalculation procedure for relative rate measurements referenced to the OH + CH_3CHF_2 reaction is discussed in the note for that reaction. The recommended value for E/R is an average of the values obtained in the studies of Schmoltner et al., Hsu and DeMore, and DeMore. The results of Howard and Evenson[3] (296 K), Jeong and Kaufman[5] (292–480 K), Bera and Hanrahan,[1] (298 K), and Wallington and Hurley[9] (296 K) appear to be systematically lower than those of the other studies over the temperature region of interest and were not used to derive the recommended parameters. The results from the study of Kowalczyk et al.[6] (298 K), although in good agreement with the recommended value for k(298 K), also were not used since the results reported in this study for several halocarbons vary widely (ranging from 10% agreement with recommendations to as much as 3 orders of magnitude disagreement with recommendations).
(Table: 15-10, Note: 15-10, Evaluated: 15-10) Back to Table

(1) Bera, R. K.; Hanrahan, R. J. Investigation of gas-phase reactions of OH radicals with fluoromethane and difluoromethane using Ar-sensitized pulse-radiolysis. *Radiation Phys. Chem.* **1988**, *32*, 579-584.
(2) DeMore, W. B. Experimental and estimated rate constants for the reactions of hydroxyl radicals with several halocarbons. *J. Phys. Chem.* **1996**, *100*, 5813-5820, doi:10.1021/jp953216+.
(3) Howard, C. J.; Evenson, K. M. Rate constants for the reactions of OH with CH_4 and fluorine, chlorine, and bromine substituted methanes at 296 K. *J. Chem. Phys.* **1976**, *64*, 197-202, doi:10.1063/1.431950.
(4) Hsu, K. J.; DeMore, W. B. Rate constants and temperature dependences for the reactions of hydroxyl radical with several halogenated methanes, ethanes, and propanes by relative rate measurements. *J. Phys. Chem.* **1995**, *99*, 1235-1244, doi:10.1021/j100004a025.
(5) Jeong, K. M.; Kaufman, F. Kinetics of the reaction of hydroxyl radical with methane and with nine Cl- and F-substituted methanes. 1. Experimental results, comparisons, and applications. *J. Phys. Chem.* **1982**, *86*, 1808-1815, doi:10.1021/j100207a016.
(6) Kowalczyk, J.; Jowko, A.; Symanowicz, M. Kinetics of radical reactions in freons. *J. Radioanal. Nucl. Chem.* **1998**, *232*, 75-78, doi:10.1007/BF02383716.
(7) Nip, W. S.; Singleton, D. L.; Overend, R.; Paraskevopoulos, G. Rates of OH radical reactions. 5. Reactions with CH_3F, CH_2F_2, CHF_3, CH_3CH_2F, and CH_3CHF_2 at 297 K. *J. Phys. Chem.* **1979**, *83*, 2440-2443, doi:10.1021/j100482a003.
(8) Schmoltner, A. M.; Talukdar, R. K.; Warren, R. F.; Mellouki, A.; Goldfarb, L.; Gierczak, T.; McKeen, S. A.; Ravishankara, A. R. Rate coefficients for reactions of several hydrofluorocarbons with OH and $O(^1D)$ and their atmospheric lifetimes. *J. Phys. Chem.* **1993**, *97*, 8976-8982, doi:10.1021/j100137a023.
(9) Wallington, T. J.; Hurley, M. D. Atmospheric chemistry of HC(O)F - Reaction with OH radicals. *Environ. Sci. Technol.* **1993**, *27*, 1448-1452, doi:10.1021/es00044a022.

E4. **OH + CH_2F_2 (HFC-32).** The recommended value of k(298 K) is an average from the studies of Nip et al.[7] (297 K), Jeong and Kaufman[5] (250–492 K), Talukdar et al.[9] (222–381 K), Hsu and DeMore[4] (297–333 K) (recalculated using the three-parameter expression given in the current recommendation for the rate constant for the OH + CH_3CHF_2 reference reaction), and Szilagyi et al.[8] (298 K). The recommended value for E/R is derived from a fit to the data from Jeong and Kaufman, Talukdar et al., and Hsu and DeMore below 400 K after scaling each data set to the recommended value for k(298 K). The results of Howard and Evenson[3] (296 K),

Clyne and Holt[2] (293–425 K), Bera and Hanrahan[1] (298 K), and Kowalczyk et al.[6] (298 K) are somewhat more scattered and were not used in deriving the recommended parameters.
(Table: 15-10, Note: 15-10, Evaluated: 15-10) Back to Table

(1) Bera, R. K.; Hanrahan, R. J. Investigation of gas-phase reactions of OH radicals with fluoromethane and difluoromethane using Ar-sensitized pulse-radiolysis. *Radiation Phys. Chem.* **1988**, *32*, 579-584.
(2) Clyne, M. A. A.; Holt, P. M. Reaction kinetics involving ground $X^2\Pi$ and excited $A^2\Sigma^+$ hydroxyl radicals Part 2.-Rate constants for reactions of OH $X^2\Pi$ with halogenomethanes and halogenoethanes. *J. Chem. Soc. Faraday Trans. 2* **1979**, *75*, 582-591, doi:10.1039/f29797500582.
(3) Howard, C. J.; Evenson, K. M. Rate constants for the reactions of OH with CH_4 and fluorine, chlorine, and bromine substituted methanes at 296 K. *J. Chem. Phys.* **1976**, *64*, 197-202, doi:10.1063/1.431950.
(4) Hsu, K. J.; DeMore, W. B. Rate constants and temperature dependences for the reactions of hydroxyl radical with several halogenated methanes, ethanes, and propanes by relative rate measurements. *J. Phys. Chem.* **1995**, *99*, 1235-1244, doi:10.1021/j100004a025.
(5) Jeong, K. M.; Kaufman, F. Kinetics of the reaction of hydroxyl radical with methane and with nine Cl- and F-substituted methanes. 1. Experimental results, comparisons, and applications. *J. Phys. Chem.* **1982**, *86*, 1808-1815, doi:10.1021/j100207a016.
(6) Kowalczyk, J.; Jowko, A.; Symanowicz, M. Kinetics of radical reactions in freons. *J. Radioanal. Nucl. Chem.* **1998**, *232*, 75-78, doi:10.1007/BF02383716.
(7) Nip, W. S.; Singleton, D. L.; Overend, R.; Paraskevopoulos, G. Rates of OH radical reactions. 5. Reactions with CH_3F, CH_2F_2, CHF_3, CH_3CH_2F, and CH_3CHF_2 at 297 K. *J. Phys. Chem.* **1979**, *83*, 2440-2443, doi:10.1021/j100482a003.
(8) Szilagyi, I.; Dobe, S.; Berces, T. Rate constant for the reaction of the OH-radical with CH_2F_2. *React. Kinet. Catal. Lett.* **2000**, *70*, 319-324, doi:10.1023/A:1010349118536.
(9) Talukdar, R.; Mellouki, A.; Gierczak, T.; Burkholder, J. B.; McKeen, S. A.; Ravishankara, A. R. Atmospheric fate of CF_2H_2, CH_3CF_3, CHF_2CF_3, and CH_3CFCl_2: Rate coefficients for reactions with OH and UV absorption cross sections of CH_3CFCl_2. *J. Phys. Chem.* **1991**, *95*, 5815-5821, doi:10.1021/j100168a021.

E5. OH + CHF_3 (HFC-23). The recommended value for k(298 K) is an average of the values reported in the absolute rate study of Schmoltner et al.[9] (252–374 K) and in the relative rate studies of Hsu and DeMore[5] (298–383 K) (recalculated based on the current recommendation for the rate constant for the OH + CHF_2CF_3 reference reaction) and of Chen et al.[2] (253–328 K) (two relative rate determinations recalculated based on the current recommendations for the rate constants for the OH + CHF_2CF_3 and OH + CHF_2Cl reference reactions). The recommended value for E/R is derived from a fit to the data from these same three studies after scaling each data set to the recommended value of k(298 K). The results of Jeong and Kaufman[6] (387–480 K) and Medhurst et al.[7] (298–753 K), being predominantly above room temperature, were not used in deriving the recommended parameters. The results from Clyne and Holt[3] (293–425 K)and Bera and Hanrahan[1] (298 K) were also not used due to their inconsistency with the other studies. The room temperature values of Howard and Evenson[4] (296 K) and Nip et al.[8] (297 K) are encompassed within the 2σ confidence limits.
(Table: 15-10, Note: 15-10, Evaluated: 15-10) Back to Table

(1) Bera, R. K.; Hanrahan, R. J. Investigation of gas-phase reactions of OH radicals with fluoromethane and difluoromethane using Ar-sensitized pulse-radiolysis. *Radiation Phys. Chem.* **1988**, *32*, 579-584.
(2) Chen, L.; Kutsuna, S.; Tokuhashi, K.; Sekiya, A. New technique for generating high concentrations of gaseous OH radicals in relative rate measurements. *Int. J. Chem. Kinet.* **2003**, *35*, 317-325, doi:10.1002/kin.10133.
(3) Clyne, M. A. A.; Holt, P. M. Reaction kinetics involving ground $X^2\Pi$ and excited $A^2\Sigma^+$ hydroxyl radicals Part 2.-Rate constants for reactions of OH $X^2\Pi$ with halogenomethanes and halogenoethanes. *J. Chem. Soc. Faraday Trans. 2* **1979**, *75*, 582-591, doi:10.1039/f29797500582.
(4) Howard, C. J.; Evenson, K. M. Rate constants for the reactions of OH with CH_4 and fluorine, chlorine, and bromine substituted methanes at 296 K. *J. Chem. Phys.* **1976**, *64*, 197-202, doi:10.1063/1.431950.
(5) Hsu, K. J.; DeMore, W. B. Rate constants and temperature dependences for the reactions of hydroxyl radical with several halogenated methanes, ethanes, and propanes by relative rate measurements. *J. Phys. Chem.* **1995**, *99*, 1235-1244, doi:10.1021/j100004a025.
(6) Jeong, K. M.; Kaufman, F. Kinetics of the reaction of hydroxyl radical with methane and with nine Cl- and F-substituted methanes. 1. Experimental results, comparisons, and applications. *J. Phys. Chem.* **1982**, *86*, 1808-1815, doi:10.1021/j100207a016.
(7) Medhurst, L. J.; Fleming, J.; Nelson, H. H. Reaction rate constants of OH + CHF_3 → products and $O(^3P)$ + CHF_3 → OH + CF_3 at 500−750 K. *Chem. Phys. Lett.* **1977**, *266*, 607-611, doi:10.1016/S0009-2614(97)00049-3.

(8) Nip, W. S.; Singleton, D. L.; Overend, R.; Paraskevopoulos, G. Rates of OH radical reactions. 5. Reactions with CH_3F, CH_2F_2, CHF_3, CH_3CH_2F, and CH_3CHF_2 at 297 K. *J. Phys. Chem.* **1979**, *83*, 2440-2443, doi:10.1021/j100482a003.
(9) Schmoltner, A. M.; Talukdar, R. K.; Warren, R. F.; Mellouki, A.; Goldfarb, L.; Gierczak, T.; McKeen, S. A.; Ravishankara, A. R. Rate coefficients for reactions of several hydrofluorocarbons with OH and O(^{1}D) and their atmospheric lifetimes. *J. Phys. Chem.* **1993**, *97*, 8976-8982, doi:10.1021/j100137a023.

E6. OH + CH_3CH_2F (HFC-161). The recommended value for k(298 K) is an average of the values from Nip et al.,[3] Schmoltner et al.[4] (243–373 K), and Kozlov et al.[2] (210–480 K). The value of E/R is derived from a fit to the data from the latter two studies at room temperature and below after scaling each data set to the value recommended for k(298 K). The relative rate study by Hsu and DeMore[1] (285–364 K) reports a temperature dependence that is markedly stronger than those of Schmoltner et al. and Kozlov et al., which are in excellent agreement. This difference is due to significantly lower rate constant values being in the Hsu and DeMore study in the region near room temperature. The Hsu and DeMore temperature dependence for HFC-161 is also significantly stronger than measured and recommended for HFC-152 and HFC-152a, where similar dependences would be expected. Curvature in the Arrhenius plot is evident from the study by Kozlov et al., which was conducted over an extended temperature range above and below room temperature. Singleton et al.[5] determined that 85 ± 3% of the abstraction by OH is from the fluorine-substituted methyl group at room temperature. Hence, curvature in the Arrhenius plot may be due to the increasing importance of hydrogen abstraction from the unsubstituted methyl group with increasing temperature, although similar curvature was observed in the case of OH + CH_2FCH_2F with two identical fluoromethyl groups. Due to such curvature, the recommended Arrhenius parameters should not be used for calculating rate constants above room temperature. Rather, one should use the three-parameter expression that is derived from a fit to the data of Kozlov et al. over the temperature range from 210 to 480 K after the data were scaled to match the recommended value of k(298 K):

$$k(210\text{–}480\ \text{K}) = 3.1 \times 10^{-13}\ (\text{T}/298)^{2.45}\ \exp(-103/\text{T})$$

(Table: 15-10, Note: 15-10, Evaluated: 15-10) Back to Table

(1) Hsu, K. J.; DeMore, W. B. Rate constants and temperature dependences for the reactions of hydroxyl radical with several halogenated methanes, ethanes, and propanes by relative rate measurements. *J. Phys. Chem.* **1995**, *99*, 1235-1244, doi:10.1021/j100004a025.
(2) Kozlov, S. N.; Orkin, V. L.; Kurylo, M. J. An investigation of the reactivity of OH with fluoroethanes: CH_3CH_2F (HFC-161), CH_2FCH_2F (HFC-152), and CH_3CHF_2 (HFC-152a). *J. Phys. Chem. A* **2003**, *107*, 2239-2246, doi:10.1021/jp022087b.
(3) Nip, W. S.; Singleton, D. L.; Overend, R.; Paraskevopoulos, G. Rates of OH radical reactions. 5. Reactions with CH_3F, CH_2F_2, CHF_3, CH_3CH_2F, and CH_3CHF_2 at 297 K. *J. Phys. Chem.* **1979**, *83*, 2440-2443, doi:10.1021/j100482a003.
(4) Schmoltner, A. M.; Talukdar, R. K.; Warren, R. F.; Mellouki, A.; Goldfarb, L.; Gierczak, T.; McKeen, S. A.; Ravishankara, A. R. Rate coefficients for reactions of several hydrofluorocarbons with OH and O(^{1}D) and their atmospheric lifetimes. *J. Phys. Chem.* **1993**, *97*, 8976-8982, doi:10.1021/j100137a023.
(5) Singleton, D. L.; Paraskevopoulos, G.; Irwin, R. S. Reaction of OH with CH_3CH_2F. The extent of H abstraction from the α and β positions. *J. Phys. Chem.* **1980**, *84*, 2339-2343, doi:10.1021/j100456a001.

E7. OH + CH_3CHF_2 (HFC-152a). The recommended value for k(298 K) is an average of the values from the absolute rate studies of Howard and Evenson[5] (296 K), Handwerk and Zellner[4] (293 K), Nip et al.[10] (297 K), Gierczak et al.[3] (212–349 K) (two different determinations), and Kozlov et al.[7] (210–480 K), and from the relative rate studies of Hsu and DeMore[6] (298– 358 K) (two determinations that have been recalculated based on the current recommendations for the rate constants of the OH + CH_4 and OH + CH_3CCl_3 reference reactions), Wilson et al.[12] (286–403 K) (two determinations that have been recalculated based on the current recommendations for the rate constants of the OH + C_2H_6 and OH + c-C_3H_6 reference reactions), and Taketani et al.[11] (295 K) (two determinations that have been recalculated based on the current recommendations for the rate constants of the OH + C_2H_2 and OH + C_2H_4 reference reactions). There are systematic differences in the temperature dependencies determined in the absolute studies (particularly below room temperature) and relative studies (conducted at room temperature and above). Curvature in the Arrhenius plot (as suggested by the data of Gierczak et al.) has been more clearly demonstrated in the study of Kozlov et al. and seems to explain the earlier cited differences between the relative and absolute rate data. This curvature may be due to the presence of two hydrogen-abstraction reaction channels, although similar curvature was observed in case of OH + CH_2FCH_2F with two identical fluoromethyl groups. Hence, care must be taken in deriving a recommended rate expression suitable for atmospheric modeling (in the temperature region below room temperature).

In spite of the noticeable Arrhenius curvature over the temperature range from 210 to 480 K, the data below 300 K can be well represented by a two-parameter Arrhenius expression. Thus, the recommended value for E/R is derived from a combined fit to the data ($T \leq 300$ K) of Gierczak et al. and Kozlov et al. after scaling each data set to the recommended value for k(298 K). The studies by Clyne and Holt[2] (298 K), Brown et al.[1] (220–423 K), and Nielsen[9] (293–388 K) all yield systematically higher rate constants and were not used in deriving the recommended parameters. The study by Liu et al.[8] is superseded by that of Kozlov et al. In light of the observed Arrhenius curvature, the Arrhenius parameters recommended for temperatures below 300 K are not suitable for use in recalculating rate constants from relative rate studies conducted at temperatures above 300 K in which the OH + CH_3CHF_2 reaction was the reference. For such purposes, we recommend use of the three-parameter expression derived from a fit to the data of Kozlov et al. over the temperature range from 210 to 480 K after the data were scaled to match the recommended value of k(298 K):

$$k(210\text{–}480\ \text{K}) = 7.57 \times 10^{-14}\ (T/298)^{3.02}\ \exp(-247/T)$$

The site-specific rate coefficients were estimated by Kozlov et al. (assuming that the observed curvature in the Arrhenius plot is entirely due to different reaction channels) to be 33% reaction at the CH_3 group and 67% H atom abstraction from the CHF_2 group.
(Table: 10-6, Note: 15-10, Evaluated: 15-10) Back to Table

(1) Brown, A. C.; Canosa-Mas, C. E.; Parr, A. D.; Wayne, R. P. Laboratory studies of some halogenated ethanes and ethers: Measurements of rates of reaction with OH and of infrared absorption cross-sections. *Atmos. Environ.* **1990**, *24A*, 2499-2511, doi:10.1016/0960-1686(90)90341-J.

(2) Clyne, M. A. A.; Holt, P. M. Reaction kinetics involving ground $X^2\Pi$ and excited $A^2\Sigma^+$ hydroxyl radicals Part 2.-Rate constants for reactions of OH $X^2\Pi$ with halogenomethanes and halogenoethanes. *J. Chem. Soc. Faraday Trans. 2* **1979**, *75*, 582-591, doi:10.1039/f29797500582.

(3) Gierczak, T.; Talukdar, R.; Vaghjiani, G. L.; Lovejoy, E. R.; Ravishankara, A. R. Atmospheric fate of hydrofluoroethanes and hydrofluorochloroethanes: 1. Rate coefficients for reactions with OH. *J. Geophys. Res.* **1991**, *96*, 5001-5011, doi:10.1029/90JD02736.

(4) Handwerk, V.; Zellner, R. Kinetics of the reactions of OH radicals with some halocarbons ($CHClF_2$, CH_2ClF, CH_2ClCF_3, CH_3CClF_2, CH_3CHF_2) in the temperature range 260-370 K. *Ber. Bunsenges. Phys. Chem.* **1978**, *82*, 1161-1166, doi:10.1002/bbpc.19780821117.

(5) Howard, C. J.; Evenson, K. M. Rate constants for the reactions of OH with ethane and some halogen substituted ethanes at 296 K. *J. Chem. Phys.* **1976**, *64*, 4303-4306, doi:10.1063/1.432115.

(6) Hsu, K. J.; DeMore, W. B. Rate constants and temperature dependences for the reactions of hydroxyl radical with several halogenated methanes, ethanes, and propanes by relative rate measurements. *J. Phys. Chem.* **1995**, *99*, 1235-1244, doi:10.1021/j100004a025.

(7) Kozlov, S. N.; Orkin, V. L.; Kurylo, M. J. An investigation of the reactivity of OH with fluoroethanes: CH_3CH_2F (HFC-161), CH_2FCH_2F (HFC-152), and CH_3CHF_2 (HFC-152a). *J. Phys. Chem. A* **2003**, *107*, 2239-2246, doi:10.1021/jp022087b.

(8) Liu, R.; Huie, R. E.; Kurylo, M. J. Rate constants for the reactions of the OH radical with some hydrochlorofluorocarbons over the temperature range 270-400 K. *J. Phys. Chem.* **1990**, *94*, 3247-3249, doi:10.1021/j100371a004.

(9) Nielsen, O. J. Rate constants for the gas-phase reactions of OH radicals with CH_3CHF_2 and $CHCl_2CF_3$ over the temperature range 295-388 K. *Chem. Phys. Lett.* **1991**, *187*, 286-290, doi:10.1016/0009-2614(91)90427-B.

(10) Nip, W. S.; Singleton, D. L.; Overend, R.; Paraskevopoulos, G. Rates of OH radical reactions. 5. Reactions with CH_3F, CH_2F_2, CHF_3, CH_3CH_2F, and CH_3CHF_2 at 297 K. *J. Phys. Chem.* **1979**, *83*, 2440-2443, doi:10.1021/j100482a003.

(11) Taketani, F.; Nakayama, T.; Takahashi, K.; Matsumi, Y.; Hurley, M. D.; Wallington, T. J.; Toft, A.; Sulbaek Andersen, M. P. Atmospheric chemistry of CH_3CHF_2 (HFC-152a): Kinetics, mechanisms, and products of Cl atom- and OH radical-initiated oxidation in the presence and absence of NO_x. *J. Phys. Chem. A* **2005**, *109*, 9061-9069, doi:10.1021/jp044218+.

(12) Wilson, E. W., Jr.; Jacoby, A. M.; Kukta, S. J.; Gilbert, L. E.; DeMore, W. B. Rate constants for reaction of CH_2FCH_2F (HFC-152) and CH_3CHF_2 (HFC-152a) with hydroxyl radicals. *J. Phys. Chem. A* **2003**, *107*, 9357-9361, doi:10.1021/jp027288u.

E8. OH + CH_2FCH_2F (HFC-152). The recommended value for k(298 K) is an average of the values from the absolute rate studies of Martin and Paraskevopoulos[2] (298 K) and Kozlov et al.[1] (210–480 K) and from the relative rate studies of Wilson et al.[3] (287–409 K) (three determinations recalculated using the current recommendations for the reference reactions of OH with HFC-152a, cyclopropane, and ethane). The value for E/R is from a fit to the data of Kozlov et al. at room temperature and below. The data above room temperature from Kozlov et al.[1] are in excellent agreement with the three relative rate data sets of Wilson et al. Together,

they show a pronounced curvature in the Arrhenius plot, which may indicate the existence of different conformers for HFC-152, each with differing temperature populations and reactivities. The data over the temperature range from 210 to 480 K can be represented by the three-parameter expression from Kozlov et al. after the latter was scaled to match the recommended k(298 K):

$$k(210–480\ \text{K}) = 4.23 \times 10^{-14}\ (\text{T}/298)^{3.85}\ \exp(+247/\text{T})$$

(Table: 10-6, Note: 15-10, Evaluated: 15-10) Back to Table

(1) Kozlov, S. N.; Orkin, V. L.; Kurylo, M. J. An investigation of the reactivity of OH with fluoroethanes: CH_3CH_2F (HFC-161), CH_2FCH_2F (HFC-152), and CH_3CHF_2 (HFC-152a). *J. Phys. Chem. A* **2003**, *107*, 2239-2246, doi:10.1021/jp022087b.

(2) Martin, J.-P.; Paraskevopoulos, G. A kinetic study of the reactions of OH radicals with fluoroethanes. Estimates of C-H bond strengths in fluoroalkanes. *Can. J. Chem.* **1983**, *61*, 861-865, doi:10.1139/v83-155.

(3) Wilson, E. W., Jr.; Jacoby, A. M.; Kukta, S. J.; Gilbert, L. E.; DeMore, W. B. Rate constants for reaction of CH_2FCH_2F (HFC-152) and CH_3CHF_2 (HFC-152a) with hydroxyl radicals. *J. Phys. Chem. A* **2003**, *107*, 9357-9361, doi:10.1021/jp027288u.

E9. OH + CH_3CF_3 (HFC-143a). The recommended value for k(298 K) is an average of the values from the absolute rate studies of Orkin et al.[4] (298–370 K) and Talukdar et al.[5] (223–374 K) (two different determinations by DF-LMR and LP-LIF), and from the relative rate study of Hsu and DeMore[2] (298–403 K) (two determinations that have been recalculated based on the current recommendations for the rate constants of the OH + CH_4 and OH + CHF_2CF_3 reference reactions). The value for E/R is from a combined fit of the data from these three studies after scaling each data set to the recommended value for k(298 K). The data of Clyne and Holt[1] (333–425 K) and from Martin and Paraskevopoulos[3] (298 K) were not used due to their inconsistency with the other studies.
(Table: 15-10, Note: 15-10, Evaluated: 15-10) Back to Table

(1) Clyne, M. A. A.; Holt, P. M. Reaction kinetics involving ground $X^2\Pi$ and excited $A^2\Sigma^+$ hydroxyl radicals Part 2.-Rate constants for reactions of OH $X^2\Pi$ with halogenomethanes and halogenoethanes. *J. Chem. Soc. Faraday Trans. 2* **1979**, *75*, 582-591, doi:10.1039/f29797500582.

(2) Hsu, K. J.; DeMore, W. B. Rate constants and temperature dependences for the reactions of hydroxyl radical with several halogenated methanes, ethanes, and propanes by relative rate measurements. *J. Phys. Chem.* **1995**, *99*, 1235-1244, doi:10.1021/j100004a025.

(3) Martin, J.-P.; Paraskevopoulos, G. A kinetic study of the reactions of OH radicals with fluoroethanes. Estimates of C-H bond strengths in fluoroalkanes. *Can. J. Chem.* **1983**, *61*, 861-865, doi:10.1139/v83-155.

(4) Orkin, V. L.; Huie, R. E.; Kurylo, M. J. Atmospheric lifetimes of HFC-143a and HFC-245fa. *J. Phys. Chem.* **1996**, *100*, 8907-8912, doi:10.1021/jp9601882.

(5) Talukdar, R.; Mellouki, A.; Gierczak, T.; Burkholder, J. B.; McKeen, S. A.; Ravishankara, A. R. Atmospheric fate of CF_2H_2, CH_3CF_3, CHF_2CF_3, and CH_3CFCl_2: Rate coefficients for reactions with OH and UV absorption cross sections of CH_3CFCl_2. *J. Phys. Chem.* **1991**, *95*, 5815-5821, doi:10.1021/j100168a021.

E10. OH + CH_2FCHF_2 (HFC-143). The recommended value for k(298 K) is an average of the room temperature values of Martin and Paraskevopoulos[3] (298 K) and Barry et al.[1] (278–323 K). The recommended temperature dependence is based on results of the relative rate study of Barry et al., which have been recalculated based on the current recommendation for the rate constant of the reference reaction OH + CH_3CCl_3. The significantly higher values reported by Clyne and Holt[2] (293–425 K) were not used in the derivation of the recommended parameters.
(Table: 02-25, Note: 02-25, Evaluated: 02-25) Back to Table

(1) Barry, J.; Sidebottom, H.; Treacy, J.; Franklin, J. Kinetics and mechanism for the atmospheric oxidation of 1,1,2-trifluoroethane (HFC 143). *Int. J. Chem. Kinet.* **1995**, *27*, 27-36, doi:10.1002/kin.550270105.

(2) Clyne, M. A. A.; Holt, P. M. Reaction kinetics involving ground $X^2\Pi$ and excited $A^2\Sigma^+$ hydroxyl radicals Part 2.-Rate constants for reactions of OH $X^2\Pi$ with halogenomethanes and halogenoethanes. *J. Chem. Soc. Faraday Trans. 2* **1979**, *75*, 582-591, doi:10.1039/f29797500582.

(3) Martin, J.-P.; Paraskevopoulos, G. A kinetic study of the reactions of OH radicals with fluoroethanes. Estimates of C-H bond strengths in fluoroalkanes. *Can. J. Chem.* **1983**, *61*, 861-865, doi:10.1139/v83-155.

E11. OH + CH_2FCF_3 (HFC-134a). The recommended value for k(298 K) is an average of the values derived from the absolute rate studies of Gierczak et al.[5] (223–450 K) (two determinations using discharge flow and pulsed photolysis), Leu and Lee[7] (255–424 K), Liu et al.[8] (270–400 K), and Orkin and Khamaganov[10] (298–460 K), from the relative rate study of DeMore[4] (298–358 K) (three determinations that have been recalculated based on the current recommendations for the rate constants of the reference reactions OH + CH_4, OH + CH_3CCl_3, and OH + CHF_2CF_3), and from the room temperature investigations of Bednarek et al.[1] (295 K) and Martin and Paraskevopoulos[9] (298 K). The value for E/R is derived from a combined fit (T ≤400 K) to the data from the first five investigations listed above after each data set was scaled to the recommended value of k(298 K), together with the single determination at 270 K by Zhang et al.[11] The data from Liu et al. above 350 K were excluded from the combined fit since they significantly exceed the results from the other studies at these temperatures, and subsequent experiments from the same laboratory have demonstrated that a systematic underestimation of the reaction cell temperature above 350 K may have been responsible. The data at 243 K and 223 K from the pulsed photolysis – LIF study by Gierczak et al. were also excluded from the combined fit since this data set (obtained at T <298 K) exhibits a substantially weaker Arrhenius temperature dependence (E/R = 1310 K) when compared with that from other studies conducted mainly above 270 K. This could be indicative of curvature in the Arrhenius plot at lower temperatures. Nevertheless, the "g" uncertainty factor was selected to encompass these low temperature data. The data of Brown et al.[2] (231–423 K), Clyne and Holt[3] (293–425 K), and Jeong et al.[6] (249–473 K) are considerably higher than those from all other studies and were not used in deriving the recommended parameters.
(Table: 15-10, Note: 15-10, Evaluated: 15-10) Back to Table

(1) Bednarek, G.; Breil, M.; Hoffman, A.; Kohlman, J. P.; Mörs, V.; Zellner, R. Rate and mechanism of the atmospheric degradation of 1,1,1,2-tetrafluoroethane (HFC-134a). *Ber. Bunsenges. Phys. Chem.* **1996**, *100*, 528-539, doi:10.1002/bbpc.19961000503.

(2) Brown, A. C.; Canosa-Mas, C. E.; Parr, A. D.; Wayne, R. P. Laboratory studies of some halogenated ethanes and ethers: Measurements of rates of reaction with OH and of infrared absorption cross-sections. *Atmos. Environ.* **1990**, *24A*, 2499-2511, doi:10.1016/0960-1686(90)90341-J.

(3) Clyne, M. A. A.; Holt, P. M. Reaction kinetics involving ground $X^2\Pi$ and excited $A^2\Sigma^+$ hydroxyl radicals Part 2.-Rate constants for reactions of OH $X^2\Pi$ with halogenomethanes and halogenoethanes. *J. Chem. Soc. Faraday Trans. 2* **1979**, *75*, 582-591, doi:10.1039/f29797500582.

(4) DeMore, W. B. Rate constants for the reactions of OH with HFC-134a (CF_3CH_2F) and HFC-134 (CHF_2CHF_2). *Geophys. Res. Lett.* **1993**, *20*, 1359-1362, doi:10.1029/93GL01336.

(5) Gierczak, T.; Talukdar, R.; Vaghjiani, G. L.; Lovejoy, E. R.; Ravishankara, A. R. Atmospheric fate of hydrofluoroethanes and hydrofluorochloroethanes: 1. Rate coefficients for reactions with OH. *J. Geophys. Res.* **1991**, *96*, 5001-5011, doi:10.1029/90JD02736.

(6) Jeong, K. M.; Hsu, K. J.; Jeffries, J. B.; Kaufman, F. Kinetics of the reactions of OH with C_2H_6, CH_3CCl_3, $CH_2ClCHCl_2$, $CH_2ClCClF_2$, and CH_2FCF_3. *J. Phys. Chem.* **1984**, *88*, 1222-1226, doi:10.1021/j150650a041.

(7) Leu, G.-H.; Lee, Y.-P. Temperature dependence of the rate coefficient of the reaction OH + CF_3CH_2F over the range 255-424 K. *J. Chin. Chem. Soc.* **1994**, *41*, 645-649, doi:10.1002/jccs.199400091.

(8) Liu, R.; Huie, R. E.; Kurylo, M. J. Rate constants for the reactions of the OH radical with some hydrochlorofluorocarbons over the temperature range 270-400 K. *J. Phys. Chem.* **1990**, *94*, 3247-3249, doi:10.1021/j100371a004.

(9) Martin, J.-P.; Paraskevopoulos, G. A kinetic study of the reactions of OH radicals with fluoroethanes. Estimates of C-H bond strengths in fluoroalkanes. *Can. J. Chem.* **1983**, *61*, 861-865, doi:10.1139/v83-155.

(10) Orkin, V. L.; Khamaganov, V. G. Determination of rate constants for reactions of some hydrohaloalkanes with OH radicals and their atmospheric lifetimes. *J. Atmos. Chem.* **1993**, *16*, 157-167, doi:10.1007/BF00702785.

(11) Zhang, Z.; Huie, R. E.; Kurylo, M. J. Rate constants for the reactions of OH with CH_3CFCl_2 (HCFC-141b), CH_3CF_2Cl (HCFC-l42b), and CH_2FCF_3 (HFC-134a). *J. Phys. Chem.* **1992**, *96*, 1533-1535, doi:10.1021/j100183a008.

E12. OH + CHF_2CHF_2 (HFC-134). The recommended Arrhenius parameters are based on results of the three relative rate measurements by DeMore[2] (298–358 K), which have been recalculated based on the current rate constant recommendations for the OH + CH_3CCl_3, OH + CH_2FCF_3, and OH + CHF_2CF_3 reference reactions. The room temperature value of Clyne and Holt[1] (293–425 K) agrees within the 2σ confidence limits.
(Table: 02-25, Note: 02-25, Evaluated: 02-25) Back to Table

(1) Clyne, M. A. A.; Holt, P. M. Reaction kinetics involving ground $X^2\Pi$ and excited $A^2\Sigma^+$ hydroxyl radicals Part 2.-Rate constants for reactions of OH $X^2\Pi$ with halogenomethanes and halogenoethanes. *J. Chem. Soc. Faraday Trans. 2* **1979**, *75*, 582-591, doi:10.1039/f29797500582.

(2) DeMore, W. B. Rate constants for the reactions of OH with HFC-134a (CF_3CH_2F) and HFC-134 (CHF_2CHF_2). *Geophys. Res. Lett.* **1993**, *20*, 1359-1362, doi:10.1029/93GL01336.

E13. OH + CHF_2CF_3 (HFC-125). The recommended values for both k(298 K) and E/R were derived from a fit (as described in the Introduction, Section 1.2) to the data reported by Talukdar et al.[5] (220–364 K). The recommended uncertainty was set to encompass the results of the relative rate studies by DeMore[3] (298–358 k), and Young et al.[6] (296 K). The temperature dependent data of Brown et al.[1] (226–423 K) and Clyne and Holt[2] (293–425 K) were not used in deriving the recommended parameters since they exhibit considerable scatter and the derived rate constants are systematically higher than those from the other studies, which may be indicative of impurity effects. The room temperature result reported by Martin and Paraskevopoulos[4] (298 K) was not used for similar reasons, although it barely overlaps with the recommended uncertainty interval.
(Table: 19-5, Note: 19-5, Evaluated: 19-5) Back to Table

(1) Brown, A. C.; Canosa-Mas, C. E.; Parr, A. D.; Wayne, R. P. Laboratory studies of some halogenated ethanes and ethers: Measurements of rates of reaction with OH and of infrared absorption cross-sections. *Atmos. Environ.* **1990**, *24A*, 2499-2511, doi:10.1016/0960-1686(90)90341-J.
(2) Clyne, M. A. A.; Holt, P. M. Reaction kinetics involving ground $X^2\Pi$ and excited $A^2\Sigma^+$ hydroxyl radicals Part 2.-Rate constants for reactions of OH $X^2\Pi$ with halogenomethanes and halogenoethanes. *J. Chem. Soc. Faraday Trans. 2* **1979**, *75*, 582-591, doi:10.1039/f29797500582.
(3) DeMore, W. B. Rate constants for the reactions of OH with HFC-134a (CF_3CH_2F) and HFC-134 (CHF_2CHF_2). *Geophys. Res. Lett.* **1993**, *20*, 1359-1362, doi:10.1029/93GL01336.
(4) Martin, J.-P.; Paraskevopoulos, G. A kinetic study of the reactions of OH radicals with fluoroethanes. Estimates of C-H bond strengths in fluoroalkanes. *Can. J. Chem.* **1983**, *61*, 861-865, doi:10.1139/v83-155.
(5) Talukdar, R.; Mellouki, A.; Gierczak, T.; Burkholder, J. B.; McKeen, S. A.; Ravishankara, A. R. Atmospheric fate of CF_2H_2, CH_3CF_3, CHF_2CF_3, and CH_3CFCl_2: Rate coefficients for reactions with OH and UV absorption cross sections of CH_3CFCl_2. *J. Phys. Chem.* **1991**, *95*, 5815-5821, doi:10.1021/j100168a021.
(6) Young, C. J.; Hurley, M. D.; Wallington, T. J.; Mabury, S. A. Atmospheric chemistry of CF_3CF_2H and $CF_3CF_2CF_2CF_2H$: Kinetics and products of gas-phase reactions with Cl atoms and OH radicals, infrared spectra, and formation of perfluorocarboxylic acids. *Chem. Phys. Lett.* **2009**, *473*, 251-256, doi:10.1016/j.cplett.2009.04.001.

E14. OH + CH_3CHFCH_3 (HFC-281ea). The recommended value for k(298 K) is an average of values derived from fits to each of five relative rate data sets of DeMore and Wilson[1] (270–424 K) (using infrared detection with C_2H_6, C_3H_8, and C_2H_5Cl as reference compounds and gas chromatography with C_2H_6 and C_3H_8 as reference compounds). All of the data were recalculated based on the current recommendations for the rate constants of the reference compounds reacting with OH. The recommended value for E/R is derived from the combined fit to all data from this study after each data set was scaled to the recommended value of k(298 K).
(Table: 02-25, Note: 15-10, Evaluated: 15-10) Back to Table

(1) DeMore, W. B.; Wilson, E. W., Jr. Rate constant and temperature dependence for the reaction of hydroxyl radicals with 2-fluoropropane (HFC-281ea). *J. Phys. Chem. A* **1999**, *103*, 573-576, doi:10.1021/jp9835521.

E15. OH + $CH_3CH_2CF_3$ (HFC-263fb). The recommended k(298 K) is an average of the values reported by Nelson et al.[1] (295 K) and by Rajakumar et al.[2] (238–373 K). The temperature dependence is from a fit to the data of Rajakumar et al.[2]
(Table: 10-6, Note: 10-6, Evaluated: 10-6) Back to Table

(1) Nelson, D. D.; Zahniser, M. S.; Kolb, C. E.; Magid, H. OH reaction kinetics and atmospheric lifetime estimates for several hydrofluorocarbons. *J. Phys. Chem.* **1995**, *99*, 16301-16306, doi:10.1021/j100044a016.
(2) Rajakumar, B.; Portmann, R. W.; Burkholder, J. B.; Ravishankara, A. R. Rate coefficients for the reactions of OH with $CF_3CH_2CH_3$ (HFC-263fb), CF_3CHFCH_2F (HFC-245eb), and $CHF_2CHFCHF_2$ (HFC-245ea) between 238 and 375 K. *J. Phys. Chem. A* **2006**, *110*, 6724 - 6731, doi:10.1021/jp056248y.

E16. OH + $CH_2FCF_2CHF_2$ (HFC-245ca). There is an approximate 50% difference between the absolute rate constant results of Zhang et al.[2] (260–365 K) and those derived from the relative rate data of Hsu and DeMore[1] (286– 364 K) (recalculated using the current recommendation for the rate constant of the OH + CH_4 reference reaction) over the common temperature region of the measurements. Both data sets, however, exhibit nearly identical temperature dependencies. The recommended value for k(298 K) is an average of the values from both studies. The recommended value for E/R is derived from a combined fit to the data from both studies after each data set was scaled to the recommended value of k(298 K).
(Table: 02-25, Note: 15-10, Evaluated: 15-10) Back to Table

(1) Hsu, K. J.; DeMore, W. B. Rate constants and temperature dependences for the reactions of hydroxyl radical with several halogenated methanes, ethanes, and propanes by relative rate measurements. *J. Phys. Chem.* **1995**, *99*, 1235-1244, doi:10.1021/j100004a025.
(2) Zhang, Z.; Padmaja, S.; Saini, R. D.; Huie, R. E.; Kurylo, M. J. Reactions of hydroxyl radicals with several hydrofluorocarbons: The temperature dependencies of the rate constants for $CHF_2CF_2CH_2F$ (HFC-245ca), $CF_3CHFCHF_2$ (HFC-236ea), CF_3CHFCF_3 (HFC-227ea), and $CF_3CH_2CH_2CF_3$ (HFC-356ffa). *J. Phys. Chem.* **1994**, *98*, 4312-4315, doi:10.1021/j100067a017.

E17. OH + $CH_3CF_2CF_3$ (HFC-245cb). The recommended Arrhenius parameters are based on the data of Orkin et al.[1] (287–370 K). The Arrhenius parameters for this reaction are expected to be similar to those for OH + CH_3CF_3 (HFC-143a). Hence, the 95% confidence limits have been selected to encompass the recommendation for the latter reaction.
(Table: 15-10, Note: 15-10), Evaluated: 15-10) Back to Table

(1) Orkin, V. L.; Huie, R. E.; Kurylo, M. J. Rate constants for the reactions of OH with HFC-245cb ($CH_3CF_2CF_3$) and some fluoroalkenes (CH_2CHCF_3, CH_2CFCF_3, CF_2CFCF_3, and CF_2CF_2). *J. Phys. Chem. A* **1997**, *101*, 9118-9124, doi:10.1021/jp971994r.

E18. OH + $CHF_2CHFCHF_2$ (HFC-245ea). Nelson et al.[1] (295 K) measured the room temperature rate constant for this reaction. Rajakumar et al.[2] (238–374 K) studied the temperature dependence in experiments conducted above and below room temperature. However, this study was complicated by the presence of a reactive impurity, as demonstrated by some additional low temperature results obtained with a purified sample. The recommended value for E/R was derived from a fit to the original data from Rajakumar et al. corrected for the effect of reactive impurities at T ≥298 K and the data obtained with the purified sample below 298 K. The recommended value for k(298 K) is an average of the value obtained from this fit and the value reported by Nelson et al., which are in excellent agreement.
(Table: 10-6, Note: 10-6, Evaluated: 10-6) Back to Table

(1) Nelson, D. D.; Zahniser, M. S.; Kolb, C. E.; Magid, H. OH reaction kinetics and atmospheric lifetime estimates for several hydrofluorocarbons. *J. Phys. Chem.* **1995**, *99*, 16301-16306, doi:10.1021/j100044a016.
(2) Rajakumar, B.; Portmann, R. W.; Burkholder, J. B.; Ravishankara, A. R. Rate coefficients for the reactions of OH with $CF_3CH_2CH_3$ (HFC-263fb), CF_3CHFCH_2F (HFC-245eb), and $CHF_2CHFCHF_2$ (HFC-245ea) between 238 and 375 K. *J. Phys. Chem. A* **2006**, *110*, 6724 - 6731, doi:10.1021/jp056248y.

E19. OH + $CH_2FCHFCF_3$ (HFC-245eb). The recommended value for k(298 K) is an average of the values reported by Nelson et al.[1] (295 K) and by Rajakumar et al.[2] (238–374 K). The recommended value for E/R was derived from a fit to the data from Rajakumar et al.
(Table: 10-6, Note: 10-6, Evaluated: 10-6) Back to Table

(1) Nelson, D. D.; Zahniser, M. S.; Kolb, C. E.; Magid, H. OH reaction kinetics and atmospheric lifetime estimates for several hydrofluorocarbons. *J. Phys. Chem.* **1995**, *99*, 16301-16306, doi:10.1021/j100044a016.
(2) Rajakumar, B.; Portmann, R. W.; Burkholder, J. B.; Ravishankara, A. R. Rate coefficients for the reactions of OH with $CF_3CH_2CH_3$ (HFC-263fb), CF_3CHFCH_2F (HFC-245eb), and $CHF_2CHFCHF_2$ (HFC-245ea) between 238 and 375 K. *J. Phys. Chem. A* **2006**, *110*, 6724 - 6731, doi:10.1021/jp056248y.

E20. OH + $CHF_2CH_2CF_3$ (HFC-245fa). The recommended value for k(298 K) is an average of values reported by Orkin et al.[2] (273–370 K) and Nelson et al.[1] (295 K), which are in good agreement. The temperature dependence is from Orkin et al.
(Table: 15-10, Note: 02-25, Evaluated: 15-10) Back to Table

(1) Nelson, D. D.; Zahniser, M. S.; Kolb, C. E.; Magid, H. OH reaction kinetics and atmospheric lifetime estimates for several hydrofluorocarbons. *J. Phys. Chem.* **1995**, *99*, 16301-16306, doi:10.1021/j100044a016.
(2) Orkin, V. L.; Huie, R. E.; Kurylo, M. J. Atmospheric lifetimes of HFC-143a and HFC-245fa. *J. Phys. Chem.* **1996**, *100*, 8907-8912, doi:10.1021/jp9601882.

E21. OH + $CH_2FCF_2CF_3$ (HFC-236cb). The recommended rate expression is estimated as being the same as that for the reaction of OH with CH_2FCF_3 (HFC-134a), since these reactions are expected to have similar Arrhenius parameters. This estimate is preferred over the results reported by Garland et al.[1] (256–314 K), the only published experimental study. The A-factor reported in that study is much lower than expected, and the reported E/R = 1107 K is lower than that reported for any similar halocarbon reaction.
(Table: 15-10, Note: 10-6, Evaluated: 15-10) Back to Table

(1) Garland, N. L.; Medhurst, L. J.; Nelson, H. H. Potential chlorofluorocarbon replacements: OH reaction rate constants between 250 and 315 K and infrared absorption spectra. *J. Geophys. Res.* **1993**, *98*, 23107-23111, doi:10.1029/93JD02550.

E22. OH + CHF_2CHFCF_3 (HFC-236ea). The recommended value for k(298 K) is an average of the values from the relative rate study of Hsu and DeMore[2] (298–380 K) (recalculated based on the current recommendation for the rate constant of the OH + CH_4 reference reaction) and from the absolute study of Nelson et al.[3] (295 K). The temperature dependence is from Hsu and DeMore[2] (298–380 K). The higher and somewhat more scattered values of Garland et al.[1] (251–311 K) and Zhang et al.[4] (260–365 K) were not used in deriving the recommended expression.
(Table: 02-25, Note: 02-25, Evaluated: 02-25) Back to Table

(1) Garland, N. L.; Medhurst, L. J.; Nelson, H. H. Potential chlorofluorocarbon replacements: OH reaction rate constants between 250 and 315 K and infrared absorption spectra. *J. Geophys. Res.* **1993**, *98*, 23107-23111, doi:10.1029/93JD02550.
(2) Hsu, K. J.; DeMore, W. B. Rate constants and temperature dependences for the reactions of hydroxyl radical with several halogenated methanes, ethanes, and propanes by relative rate measurements. *J. Phys. Chem.* **1995**, *99*, 1235-1244, doi:10.1021/j100004a025.
(3) Nelson, D. D.; Zahniser, M. S.; Kolb, C. E.; Magid, H. OH reaction kinetics and atmospheric lifetime estimates for several hydrofluorocarbons. *J. Phys. Chem.* **1995**, *99*, 16301-16306, doi:10.1021/j100044a016.
(4) Zhang, Z.; Padmaja, S.; Saini, R. D.; Huie, R. E.; Kurylo, M. J. Reactions of hydroxyl radicals with several hydrofluorocarbons: The temperature dependencies of the rate constants for $CHF_2CF_2CH_2F$ (HFC-245ca), $CF_3CHFCHF_2$ (HFC-236ea), CF_3CHFCF_3 (HFC-227ea), and $CF_3CH_2CH_2CF_3$ (HFC-356ffa). *J. Phys. Chem.* **1994**, *98*, 4312-4315, doi:10.1021/j100067a017.

E23. OH + $CF_3CH_2CF_3$ (HFC-236fa). The recommended rate expression is derived from a combined fit to the data from the relative rate study of Hsu and DeMore[5] (298–367 K) (recalculated based on the current recommendation for the rate constant of the reference reaction OH + CHF_2CF_3) and from the absolute rate study of Gierczak et al.[4] (269–398 K). The higher results of Nelson et al.[6] (295 K) and of Garland and Nelson[3] (281–337 K), which superseded the earlier results of Garland et al.[2] (257–311 K) were not used. A relative rate determination at room temperature by Barry et al.[1] (298 K) yields a rate constant in excellent agreement with the recommended value. However, the extremely small measured rate constant ratio (due to the use of OH + $CH_3CF_2CH_2CF_3$ as the reference) is associated with fairly large uncertainty. Hence, this determination was not directly used in the evaluation.
(Table: 02-25, Note: 02-25, Evaluated: 02-25) Back to Table

(1) Barry, J.; Locke, G.; Scollard, D.; Sidebottom, H.; Treacy, J.; Clerbaux, C.; Colin, R.; Franklin, J. 1,1,1,3,3,-pentafluorobutane (HFC-365mfc): Atmospheric degradation and contribution to radiative forcing. *Int. J. Chem. Kinet.* **1997**, *29*, 607-617, doi:10.1002/(SICI)1097-4601(1997)29:8<607::AID-KIN6>3.0.CO;2-Y.

(2) Garland, N. L.; Medhurst, L. J.; Nelson, H. H. Potential chlorofluorocarbon replacements: OH reaction rate constants between 250 and 315 K and infrared absorption spectra. *J. Geophys. Res.* **1993**, *98*, 23107-23111, doi:10.1029/93JD02550.
(3) Garland, N. L.; Nelson, H. H. Temperature dependent kinetics of the reaction OH + $CF_3CH_2CF_3$. *Chem. Phys. Lett.* **1996**, *248*, 296-300, doi:10.1016/0009-2614(95)01288-5.
(4) Gierczak, T.; Talukdar, R. K.; Burkholder, J. B.; Portmann, R. W.; Daniel, J. S.; Solomon, S.; Ravishankara, A. R. Atmospheric fate and greenhouse warming potentials of HFC 236fa and HFC 236ea. *J. Geophys. Res.* **1996**, *101*, 12905-12911, doi:10.1029/96JD00059.
(5) Hsu, K. J.; DeMore, W. B. Rate constants and temperature dependences for the reactions of hydroxyl radical with several halogenated methanes, ethanes, and propanes by relative rate measurements. *J. Phys. Chem.* **1995**, *99*, 1235-1244, doi:10.1021/j100004a025.
(6) Nelson, D. D.; Zahniser, M. S.; Kolb, C. E.; Magid, H. OH reaction kinetics and atmospheric lifetime estimates for several hydrofluorocarbons. *J. Phys. Chem.* **1995**, *99*, 16301-16306, doi:10.1021/j100044a016.

E24. OH + CF_3CHFCF_3 (HFC-227ea). The recommended value for k(298 K) is the average of values derived from the absolute rate studies of Nelson et al.[2] (294–369 K), Zellner et al.[5] (298–463 K), Zhang et al.[6] (270–365 K), and Tokuhashi et al.[3] (250–430 K), and from the relative rate studies of Hsu and DeMore[1] (296–398 K) (two determinations that have been recalculated based on the current recommendations for the rate constants of the reference reactions OH + CH_4 and OH + CHF_2CF_3) and Wallington et al.[4] (296 K) (two determinations that have been recalculated based on the current recommendations for the rate constants of the reference reactions OH + C_2H_4 and OH + C_2H_2). The recommended value for E/R is derived from a fit to the data below 400 K reported by Nelson et al., Zellner et al., Tokuhashi et al., and Hsu and DeMore after scaling each data set to the recommended value for k(298 K).
(Table: 15-10, Note: 15-10, Evaluated: 15-10) Back to Table

(1) Hsu, K. J.; DeMore, W. B. Rate constants and temperature dependences for the reactions of hydroxyl radical with several halogenated methanes, ethanes, and propanes by relative rate measurements. *J. Phys. Chem.* **1995**, *99*, 1235-1244, doi:10.1021/j100004a025.
(2) Nelson, D. D., Jr.; Zahniser, M. S.; Kolb, C. E. OH reaction kinetics and atmospheric lifetimes of CF_3CFHCF_3 and CF_3CH_2Br. *Geophys. Res. Lett.* **1993**, *20*, 197-200, doi:10.1029/93GL00239.
(3) Tokuhashi, K.; Chen, L.; Kutsuna, S.; Uchimaru, T.; Sugie, M.; Sekiya, A. Environmental assessment of CFC alternatives - Rate constants for the reactions of OH radicals with fluorinated compounds. *J. Fluor. Chem.* **2004**, *125*, 1801-1807, doi:10.1016/j.jfluchem.2004.09.013.
(4) Wallington, T. J.; Hurley, M. D.; Nielsen, O. J.; Sulbaek Andersen, M. P. Atmospheric chemistry of $CF_3CFHCF_2OCF_3$ and $CF_3CFHCF_2OCF_2H$: Reaction with Cl atoms and OH radicals, degradation mechanism, and global warming potentials. *J. Phys. Chem. A* **2004**, *108*, 11333-11338, doi:10.1021/jp046454q.
(5) Zellner, R.; Bednarek, G.; Hoffmann, A.; Kohlmann, J. P.; Mörs, V.; Saathoff, H. Rate and mechanism of the atmospheric degradation of 2H-heptafluoropropane (HFC-227). *Ber. Bunsenges. Phys. Chem.* **1994**, *98*, 141-146, doi:10.1002/bbpc.19940980202.
(6) Zhang, Z.; Padmaja, S.; Saini, R. D.; Huie, R. E.; Kurylo, M. J. Reactions of hydroxyl radicals with several hydrofluorocarbons: The temperature dependencies of the rate constants for $CHF_2CF_2CH_2F$ (HFC-245ca), $CF_3CHFCHF_2$ (HFC-236ea), CF_3CHFCF_3 (HFC-227ea), and $CF_3CH_2CH_2CF_3$ (HFC-356ffa). *J. Phys. Chem.* **1994**, *98*, 4312-4315, doi:10.1021/j100067a017.

E25. OH + $CH_3CF_2CH_2CF_3$ (HFC-365mfc). The recommended value of k(298 K) is an average of the values obtained from fits to the data from the absolute rate study of Mellouki et al.[2] (269–370 K) and of the relative rate study of Barry et al.[1] (278– 323 K) (recalculated using the current recommendation for the rate constant of the reference reaction OH + CH_3CCl_3). The value for E/R is an average of the values for this parameter from the same two studies.
(Table: 10-6, Note: 10-6, Evaluated: 10-6) Back to Table

(1) Barry, J.; Locke, G.; Scollard, D.; Sidebottom, H.; Treacy, J.; Clerbaux, C.; Colin, R.; Franklin, J. 1,1,1,3,3,-pentafluorobutane (HFC-365mfc): Atmospheric degradation and contribution to radiative forcing. *Int. J. Chem. Kinet.* **1997**, *29*, 607-617, doi:10.1002/(SICI)1097-4601(1997)29:8<607::AID-KIN6>3.0.CO;2-Y.
(2) Mellouki, A.; Teton, S.; Le Bras, G. Rate constant for the reaction of OH with HFC-365mfc ($CF_3CH_2CF_2CH_3$). *Geophys. Res. Lett.* **1995**, *22*, 389-392, doi:10.1029/94GL032.

E26. OH + $CF_3CH_2CH_2CF_3$ (HFC-356mff). The recommended value of k(298 K) is an average of the values from Nelson et al.[1] (296 K) and Zhang et al.[2] (260–365 K). The temperature dependence is from a fit to the data of Zhang et al., excluding the lowest temperature points (at 260 K), which are somewhat higher than an extrapolation from other data in that study.
(Table: 02-25, Note: 02-25, Evaluated: 02-25) Back to Table

(1) Nelson, D. D.; Zahniser, M. S.; Kolb, C. E.; Magid, H. OH reaction kinetics and atmospheric lifetime estimates for several hydrofluorocarbons. *J. Phys. Chem.* **1995**, *99*, 16301-16306, doi:10.1021/j100044a016.
(2) Zhang, Z.; Padmaja, S.; Saini, R. D.; Huie, R. E.; Kurylo, M. J. Reactions of hydroxyl radicals with several hydrofluorocarbons: The temperature dependencies of the rate constants for $CHF_2CF_2CH_2F$ (HFC-245ca), $CF_3CHFCHF_2$ (HFC-236ea), CF_3CHFCF_3 (HFC-227ea), and $CF_3CH_2CH_2CF_3$ (HFC-356ffa). *J. Phys. Chem.* **1994**, *98*, 4312-4315, doi:10.1021/j100067a017.

E27. OH + $CH_2FCH_2CF_2CF_3$ (HFC-356mcf). The recommended values for both k(298 K) and E/R are based on the data of Nelson et al.[1] (252–356 K).
(Table: 02-25, Note: 02-25, Evaluated: 02-25) Back to Table

(1) Nelson, D. D.; Zahniser, M. S.; Kolb, C. E.; Magid, H. OH reaction kinetics and atmospheric lifetime estimates for several hydrofluorocarbons. *J. Phys. Chem.* **1995**, *99*, 16301-16306, doi:10.1021/j100044a016.

E28. OH + $CHF_2CF_2CF_2CF_2H$ (HFC-338pcc). The recommended value for k(298 K) is an average of values derived from fits to the data of Schmoltner et al.[1] (232–378 K) and Zhang et al.[2] (245–419 K). The recommended value for E/R is derived from the combined fit to the data from both studies after each data set was scaled to the recommended value of k(298 K).
(Table: 02-25, Note: 15-10, Evaluated: 15-10) Back to Table

(1) Schmoltner, A. M.; Talukdar, R. K.; Warren, R. F.; Mellouki, A.; Goldfarb, L.; Gierczak, T.; McKeen, S. A.; Ravishankara, A. R. Rate coefficients for reactions of several hydrofluorocarbons with OH and $O(^1D)$ and their atmospheric lifetimes. *J. Phys. Chem.* **1993**, *97*, 8976-8982, doi:10.1021/j100137a023.
(2) Zhang, Z.; Saini, R. D.; Kurylo, M. J.; Huie, R. E. Rate constants for the reactions of the hydroxyl radical with $CHF_2CF_2CF_2CHF_2$ and $CF_3CHFCHFCF_2CF_3$. *Chem. Phys. Lett.* **1992**, *200*, 230-234, doi:10.1016/0009-2614(92)80003-T.

E29. OH + $CHF_2CF_2CF_2CF_3$ (HFC-329p). The recommended value for k(298 K) is an average of two relative rate measurements of Young et al.[1] (296 K) using C_2H_2 and C_2H_4 as reference compounds. Although the average values derived from these measurements are in good agreement (5%), the reported uncertainty due to data scattering is ~13%. In the same study, the reactivity of this compound was found to be indistinguishable from that of CHF_2CF_3. The value for E/R was estimated to be similar to that for the reactions of OH with CHF_2CF_3 and $CHF_2(CF_2)_4CF_3$ and the uncertainty was chosen to encompass the recommended values for these two reactions, which are ~12% larger.
(Table: 19-5, Note: 19-5, Evaluated: 19-5) Back to Table

(1) Young, C. J.; Hurley, M. D.; Wallington, T. J.; Mabury, S. A. Atmospheric chemistry of CF_3CF_2H and $CF_3CF_2CF_2CF_2H$: Kinetics and products of gas-phase reactions with Cl atoms and OH radicals, infrared spectra, and formation of perfluorocarboxylic acids. *Chem. Phys. Lett.* **2009**, *473*, 251-256, doi:10.1016/j.cplett.2009.04.001.

E30. OH + $CHF_2(CF_2)_4CF_3$ (HFC-52-13p). The recommended values for both k(298 K) and E/R are averages of values derived from relative rate data of Chen et al.[1] (250–430 K) that have been recalculated based on the current recommendations for the rate constants of the reference reactions and absolute data obtained in the same study (below 400 K) in the same study, which are ~20% smaller.
(Table: 19-5, Note: 19-5, Evaluated: 19-5) Back to Table

(1) Chen, L.; Tokuhashi, K.; Kutsuna, S.; Sekiya, A. Rate constants for the gas-phase reaction of $CF_3CF_2CF_2CF_2CF_2CHF_2$ with OH radicals at 250-430 K. *Int. J. Chem. Kinet.* **2004**, *33*, 26–33, doi:10.1002/kin.10170.

E31. OH + $CHF_2(CF_2)_6CF_3$ (HFC-72-17p). The recommended value for k(298 K) is an average of two values derived from relative rate data reported by Chen et al.[1] (254–328 K) that have been recalculated based on the current recommendations for the rate constants of the reference reactions with CHF_2CF_3 and CH_2FCF_3. The value for E/R was derived from a combined fit to recalculated data after each data set was normalized to the recommended value of k(298 K). The rate constants obtained exceed those for the similar reactions of OH with CHF_2CF_3 and $CHF_2(CF_2)_4CF_3$ by ~35%. Thus, the recommended uncertainties were chosen to encompass the values recommended for these latter reactions.
(Table: 19-5, Note: 19-5, Evaluated: 19-5) Back to Table

(1) Chen, L.; Uchimaru, T.; Kutsuna, S.; Tokuhashi, K.; Sekiya, A.; Okamoto, H. Kinetics and mechanism of gas-phase reaction of $CF_3CF_2CF_2CF_2CF_2CF_2CF_2H$ with OH radicals in an environmental reaction chamber at 253-328 K. *Chem. Phys. Lett.* **2011**, *501*, 263–266, doi:10.1016/j.cplett.2010.12.009.

E32. OH + $CF_3CH_2CF_2CH_2CF_3$ (HFC-458mfcf). The recommended values for both k(298 K) and E/R are based on the data of Nelson et al.[1] (278–354 K).
(Table: 02-25, Note: 02-25, Evaluated: 02-25) Back to Table

(1) Nelson, D. D.; Zahniser, M. S.; Kolb, C. E.; Magid, H. OH reaction kinetics and atmospheric lifetime estimates for several hydrofluorocarbons. *J. Phys. Chem.* **1995**, *99*, 16301-16306, doi:10.1021/j100044a016.

E33. OH + $CF_3CHFCHFCF_2CF_3$ (HFC-43-10mee). The recommended value for k(298 K) is an average of values derived from absolute studies by Schmoltner et al.[1] (251–375 K) and Zhang et al.[2] (250–400 K). The recommended value for E/R is derived from a combined fit to the data from Schmoltner et al. and Zhang et al. after scaling each data set to the recommended value for k(298 K).
(Table: 02-25, Note: 02-25, Evaluated: 02-25) Back to Table

(1) Schmoltner, A. M.; Talukdar, R. K.; Warren, R. F.; Mellouki, A.; Goldfarb, L.; Gierczak, T.; McKeen, S. A.; Ravishankara, A. R. Rate coefficients for reactions of several hydrofluorocarbons with OH and $O(^1D)$ and their atmospheric lifetimes. *J. Phys. Chem.* **1993**, *97*, 8976-8982, doi:10.1021/j100137a023.
(2) Zhang, Z.; Saini, R. D.; Kurylo, M. J.; Huie, R. E. Rate constants for the reactions of the hydroxyl radical with $CHF_2CF_2CF_2CHF_2$ and $CF_3CHFCHFCF_2CF_3$. *Chem. Phys. Lett.* **1992**, *200*, 230-234, doi:10.1016/0009-2614(92)80003-T.

E34. OH + $CF_3CF_2CH_2CH_2CF_2CF_3$ (HFC-55-10mcff). The recommended value for k(298 K) is that reported by Nelson et al.[1] (295 K). As expected, the rate constant is similar to that for OH + $CF_3CH_2CH_2CF_3$. Hence, the recommendation for E/R is estimated as being approximately the same as that for this reaction.
(Table: 02-25, Note: 02-25, Evaluated: 02-25) Back to Table

(1) Nelson, D. D.; Zahniser, M. S.; Kolb, C. E.; Magid, H. OH reaction kinetics and atmospheric lifetime estimates for several hydrofluorocarbons. *J. Phys. Chem.* **1995**, *99*, 16301-16306, doi:10.1021/j100044a016.

E35. OH + CH_2=CHF. The recommended values for k(298 K) and E/R are from the absolute study by Baasandorj et al.[1] (220–373 K). Data from the relative rate study by Chen et al.[2] (253–328 K) are in reasonable agreement with the recommendation, but are significantly more scattered. Baasandorj et al. found the rate constant to be pressure independent between 20 and 600 Torr, indicating that the high-pressure limit was achieved at these pressures for the reaction of this fluorinated alkene. Since this is the simplest of the halogenated alkenes, it implies that the recommendations for all of the halogenated alkene reactions included in Table 1 represent the high-pressure limits for the rate constants. The results of Perry et al.[3] (299–426 K) are ~10% larger at room temperature, with the agreement improving above room temperature. These data are encompassed within the recommended uncertainty.
(Table: 15-10, Note: 15-10, Evaluated: 15-10) Back to Table

(1) Baasandorj, M.; Knight, G.; Papadimitriou, V. C.; Talukdar, R. K.; Ravishankara, A. R.; Burkholder, J. B. Rate coefficients for the gas-phase reaction of the hydroxyl radical with CH_2=CHF and CH_2=CF_2. *J. Phys. Chem. A* **2010**, *114*, 4619-4633, doi:10.1021/jp100527z.
(2) Chen, L.; Uchimaru, T.; Kutsuna, S.; Tokuhashi, K.; Sekiya, A. Kinetics of the gas-phase reactions of CHX=CFX (X = H, F) with OH (253-328 K) and NO_3 (298 K) radicals and O_3 (236-308 K). *Int J. Chem. Kinet.* **2010**, *42*, 619-628, doi:10.1002/kin.20506.

(3) Perry, R. A.; Atkinson, R.; Pitts, J. N., Jr. Rate constants for the reaction of OH radicals with CH_2=CHF, CH_2=CHCl, and CH_2=CHBr over the temperature range 299-426 °K. *J. Chem. Phys.* **1977**, *67*, 458-462, doi:10.1063/1.434889.

E36. OH + *(Z)*-CHF=CHF. The recommended values for both k(298 K) and E/R are derived from a fit to the data from the absolute study by Tokuhashi et al.[1,2] (250–430 K).
(Table: 25-1, Note: 25-1, Evaluated: 25-1) Back to Table

(1) Tokuhashi, K.; Takizawa, K.; Kondo, S. Rate constants for the reactions of OH radicals with fluorinated ethenes: Kinetic measurements and correlation between structure and reactivity. *J. Phys. Chem. A* **2018**, *122*, 4593–4600, doi:10.1021/acs.jpca.7b11653.
(2) Tokuhashi, K.; Takizawa, K.; Kondo, S. Correction to "Rate constants for the reactions of OH radicals with fluorinated ethenes: Kinetic measurements and correlation between structure and reactivity". *J. Phys. Chem. A* **2019**, *123*, 382−383, doi:10.1021/acs.jpca.8b11536.

E37. OH + *(E)*-CHF=CHF. The recommended values for both k(298 K) and E/R are derived from a fit to the data from the absolute study by Tokuhashi et al.[1] (250–430 K).
(Table: 25-1, Note: 25-1, Evaluated: 25-1) Back to Table

(1) Tokuhashi, K.; Uchimaru, T.; Takizawa, K.; Kondo, S. Rate constants for the reactions of OH radicals with the (*E*)/(*Z*) isomers of CFCl=CFCl and (*E*)-CHF=CHF. *J. Phys. Chem. A* **2019**, *123*, 4834−4843, doi:10.1021/acs.jpca.9b02454.

E38. OH + CH_2=CF_2. The recommended value for k(298 K) is an average of values derived from the absolute study by Baasandorj et al.[1] (219–373 K) and the relative rate study by Chen et al.[2] (253–328 K). The value recommended for E/R is derived from a combined fit to the data from Baasandorj et al. and Chen et al. after scaling each data set to the recommended value for k(298 K). Baasandorj et al. found the rate constant to be pressure independent between 20 and 600 Torr, indicating that the high-pressure limit was achieved for the reaction of this fluorinated alkene. Howard[3] (296 K) studied this reaction at lower pressures and found a smaller rate constant that increased with pressure between 0.7 Torr and 7 Torr. This dependence is consistent with the recommended high-pressure limit from Baasandorj et al.
(Table: 15-10, Note: 15-10, Evaluated: 15-10) Back to Table

(1) Baasandorj, M.; Knight, G.; Papadimitriou, V. C.; Talukdar, R. K.; Ravishankara, A. R.; Burkholder, J. B. Rate coefficients for the gas-phase reaction of the hydroxyl radical with CH_2=CHF and CH_2=CF_2. *J. Phys. Chem. A* **2010**, *114*, 4619-4633, doi:10.1021/jp100527z.
(2) Chen, L.; Uchimaru, T.; Kutsuna, S.; Tokuhashi, K.; Sekiya, A. Kinetics of the gas-phase reactions of CHX=CFX (X = H, F) with OH (253-328 K) and NO_3 (298 K) radicals and O_3 (236-308 K). *Int J. Chem. Kinet.* **2010**, *42*, 619-628, doi:10.1002/kin.20506.
(3) Howard, C. J. Rate constants for the gas-phase reactions of OH radicals with ethylene and halogenated ethylene compounds. *J. Chem. Phys.* **1976**, *65*, 4771-4777, doi:10.1063/1.432932.

E39. OH + CHF=CF_2. The recommended value for k(298 K) is an average of the values derived from the results of relative rate study by Chen et al.[2] (253– 328 K), (average of two measurements with *n*-pentane and cyclohexane as reference compounds) and the absolute rate constant measurements by Baasandorj and Burkholder[1] (212–375 K) and Tokuhashi et al.[3] (250–430 K). The k(298 K) values derived from these individual studies differ from the recommended value by 2%, 7%, and 5%, respectively. The value for E/R was derived from a combined fit to the data from the same three studies after each data set was normalized to the recommended value of k(298 K).
(Table: 19-5, Note: 19-5, Evaluated: 19-5) Back to Table

(1) Baasandorj, M.; Burkholder, J. B. Rate coefficient for the gas-phase OH + CHF=CF_2 reaction between 212 and 375 K. *Int. J. Chem. Kinet.* **2016**, *48*, 714–723, doi:10.1002/kin.21027.
(2) Chen, L.; Uchimaru, T.; Kutsuna, S.; Tokuhashi, K.; Sekiya, A. Kinetics of the gas-phase reactions of CHX=CFX (X = H, F) with OH (253-328 K) and NO_3 (298 K) radicals and O_3 (236-308 K). *Int J. Chem. Kinet.* **2010**, *42*, 619-628, doi:10.1002/kin.20506.
(3) Tokuhashi, K.; Takizawa, K.; Kondo, S. Rate constants for the reactions of OH radicals with fluorinated ethenes: Kinetic measurements and correlation between structure and reactivity. *J. Phys. Chem. A* **2018**, *122*, 4593–4600, doi:10.1021/acs.jpca.7b11653.

E40. OH + CF_2=CF_2. The recommended value for k(298 K) is an average of the values determined in the studies of Acerboni et al.[1] (298 K) (two relative rate determinations referenced to the rate constants for the reactions of OH with propene and cyclohexane) and the absolute studies of Orkin et al.[2] (298 K) and Orkin et al.[3] (250–370 K). The value for E/R is derived from a fit to the data of Orkin et al.[3] The rate constant determined by Orkin et al.[4] (370, 480 K) at higher temperatures, are in good agreement with the recommended temperature dependence. As discussed for the OH + CH_2=CHF reaction, the recommended rate constant represents the high-pressure limit for this reaction.
(Table: 25-1, Note: 25-1, Evaluated: 10-6) Back to Table

(1) Acerboni, G.; Jensen, N. R.; Rindone, B.; Hjorth, J. Kinetics and products formation of the gas-phase reactions of tetrafluoroethylene with OH and NO_3 radicals and ozone. *Chem. Phys. Lett.* **1999**, *309*, 364-368, doi:10.1016/S0009-2614(99)00698-3.
(2) Orkin, V. L.; Huie, R. E.; Kurylo, M. J. Rate constants for the reactions of OH with HFC-245cb ($CH_3CF_2CF_3$) and some fluoroalkenes (CH_2CHCF_3, CH_2CFCF_3, CF_2CFCF_3, and CF_2CF_2). *J. Phys. Chem. A* **1997**, *101*, 9118-9124, doi:10.1021/jp971994r.
(3) Orkin, V. L.; Louis, F.; Huie, R. E.; Kurylo, M. J. Photochemistry of bromine-containing fluorinated alkenes: Reactivity toward OH and UV spectra. *J. Phys. Chem. A* **2002**, *106*, 10195-10199, doi:10.1021/jp014436s.
(4) Orkin, V. L.; Poskrebyshev, G. A.; Kurylo, M. J. Rate constants for the reactions between OH and perfluorinated alkenes. *J. Phys. Chem. A* **2011**, *115*, 6568-6574, doi:10.1021/jp201663j.

E41. OH + CH_2=$CHCH_2F$. The recommended values for both k(298 K) and E/R are derived from a fit to the data from the absolute study by Tokuhashi et al.[2] (250–430 K). The room temperature value, k(296 K), measured at 600 Torr total pressure in the absolute study by Albaladejo et al.[1] (228–388 K) coincides with the recommendation. However, their measurements resulted in unexpected increasing measured rate constant (up to 25%) with decreasing pressure from 600 to 100 Torr. The recommended uncertainty encompasses the results of this study below room temperature.
(Table: 25-1, Note: 25-1, Evaluated: 25-1) Back to Table

(1) Albaladejo, J.; Ballesteros, B.; Jimenez, E.; Diaz de Mera, Y.; Martinez, E. Gas-phase OH radical-initiated oxidation of the 3-halopropenes studied by PLP-LIF in the temperature range 228-388 K. *Atmos. Environ.* **2003**, *37*, 2919-2926, doi:10.1016/S1352-2310(03)00297-8.
(2) Tokuhashi, K.; Takizawa, K.; Kondo, S. Rate constants for reactions of OH radicals with (*Z*)-CF_3CCl=CHCl, CHF_2CF=CF_2, (*E*)-CF_3CH=CHF, (*Z*)-CF_3CH=CHF, CH_3CF=CH_2, and CH_2FCH=CH_2. *Atmos. Environ.* **2021**, *255*, 118428, doi:10.1016/j.atmosenv.2021.118428.

E42. OH + CH_2=$CFCH_3$. The recommended values for both k(298 K) and E/R are derived from a fit to the data from the absolute study by Tokuhashi et al.[2] (250–430 K). Results of relative rate studies at room temperature by Tovar et al.[3] (298 K) and Rivela et al.[1] (287–313 K) are in good agreement with the recommended value of k(298 K).
(Table: 25-1, Note: 25-1, Evaluated: 25-1) Back to Table

(1) Rivela, C. B.; Tovar, C. M.; Teruel, M. A.; Barnes, I.; Wiesen, P.; Blanco, M. B. CFCs replacements: Reactivity and atmospheric lifetimes of a series of Hydrofluoroolefins towards OH radicals and Cl atoms. *Chem. Phys. Lett.* **2019**, *714*, 190-196, doi:10.1016/j.cplett.2018.10.078.
(2) Tokuhashi, K.; Takizawa, K.; Kondo, S. Rate constants for reactions of OH radicals with (*Z*)-CF_3CCl=CHCl, CHF_2CF=CF_2, (*E*)-CF_3CH=CHF, (*Z*)-CF_3CH=CHF, CH_3CF=CH_2, and CH_2FCH=CH_2. *Atmos. Environ.* **2021**, *255*, 118428, doi:10.1016/j.atmosenv.2021.118428.
(3) Tovar, C. M.; Blanco, M. B.; Barnes, I.; Wiesen, P.; Teruel, M. A. Gas-phase reactivity study of a series of hydrofluoroolefins (HFOs) toward OH radicals and Cl atoms at atmospheric pressure and 298 K. *Atmos. Environ.* **2014**, *88*, 107-114, doi:10.1016/j.atmosenv.2014.01.060.

E43. OH + CH_2=$CHCF_3$. The recommended value for k(298 K) is an average of the values from the absolute rate constant measurements by Orkin et al.[2] (252–370 K) and González et al.[1] (263–338 K). The room temperature results from the two relative rate studies by Sulbaek Andersen et al.[3] (296 K) (recalculated using the current recommendations for the reference reactions OH + C_2H_4 and OH + C_2H_2) are somewhat lower but are encompassed within the combined reported uncertainties. The recommended value for E/R is derived from a combined fit to the data from Orkin et al. and González et al. after scaling each data set to the recommended value for k(298 K). González et al. found the rate constant to be pressure independent between 50 and 650, Torr indicating that the recommended rate constant represents the high-pressure limit for this reaction.
(Table: 15-10, Note: 15-10, Evaluated: 15-10) Back to Table

(1) González, S.; Jiménez, E.; Ballesteros, B.; Martinez, E.; Albaladejo, J. Hydroxyl radical reaction rate coefficients as a function of temperature and IR absorption cross sections for $CF_3CH=CH_2$ (HFO-1243zf), potential replacement of CF_3CH_2F (HFC-134a). *Environ. Sci. Pollut. Res.* **2014**, doi:10.1007/s11356-014-3426-2.
(2) Orkin, V. L.; Huie, R. E.; Kurylo, M. J. Rate constants for the reactions of OH with HFC-245cb ($CH_3CF_2CF_3$) and some fluoroalkenes (CH_2CHCF_3, CH_2CFCF_3, CF_2CFCF_3, and CF_2CF_2). *J. Phys. Chem. A* **1997**, *101*, 9118-9124, doi:10.1021/jp971994r.
(3) Sulbaek Andersen, M. P.; Nielsen, O. J.; Toft, A.; Nakayama, T.; Matsumi, Y.; Waterland, R. L.; Buck, R. C.; Hurley, M. D.; Wallington, T. J. Atmospheric chemistry of $C_xF_{2x+1}CH=CH_2$ (x=1, 2, 4, 6, and 8): Kinetics of gas-phase reactions with Cl atoms, OH radicals, and O_3. *J. Photochem. Photobiol. A: Chem.* **2005**, *176*, 124-128, doi:10.1016/j.jphotochem.2005.06.015.

E44. OH + CH_2=$CFCF_3$. The values of k(298 K) derived from results taken from the absolute reaction rate constant studies by Orkin et al.[2] (252–370 K), Papadimitriou et al.[4] (207–380 K), Orkin et al.[3] (220–370 K), and Tokuhashi et al.[5] (250–430 K), which agree to better than 1%. The data above room temperature exhibits slight curvature in the Arrhenius plot, as observed in the studies of Papadimitriou et al. and Orkin et al.[3] (220–370 K) extended to lower temperatures. The recommended Arrhenius parameters, most applicable for atmospheric conditions, were derived from a combined fit at T ≤300 K to the data of Papadimitriou et al. and Orkin et al.,[3] which agree to better than 2% at temperatures below 300 K. Above room temperature, the data of Orkin et al.,[2] Papadimitriou et al., and Orkin et al.[3] agree to better than 3%, but have a slight systematic deviation from the recommended Arrhenius expression with increasing temperature. The three-parameter expression derived from the fit to all of the data of Orkin et al.[3] can be used to represent k(T) over the entire temperature range from 207 to 430 K:

$$k(207–430\ \text{K}) = 5.5 \times 10^{-13}\ (\text{T}/298)^{0.87}\ \exp(+207/\text{T})$$

The two relative rate measurements at 298 K by Nielsen et al.[1] (recalculated using the current rate constant recommendations for the reference reactions OH + C_2H_4 and C_2H_2) lie noticeably outside the 95% uncertainty band assigned to k(298 K). Papadimitriou et al. (25 and 600 Torr) and Orkin et al.[3] (30 and 300 Torr) found the rate constant to be pressure independent, indicating that the recommendation is for the high-pressure limit for this reaction.
(Table: 25-1, Note: 25-1, Evaluated: 25-1) Back to Table

(1) Nielsen, O. J.; Javadi, M. S.; Sulbaek Andersen, M. P.; Hurley, M. D.; Wallington, T. J.; Singh, R. Atmospheric chemistry of $CF_3CF=CH_2$: Kinetics and mechanisms of gas-phase reactions with Cl atoms, OH radicals, and O_3. *Chem. Phys. Lett.* **2007**, *439*, 18-22, doi:10.1016/j.cplett.2007.03.053.
(2) Orkin, V. L.; Huie, R. E.; Kurylo, M. J. Rate constants for the reactions of OH with HFC-245cb ($CH_3CF_2CF_3$) and some fluoroalkenes (CH_2CHCF_3, CH_2CFCF_3, CF_2CFCF_3, and CF_2CF_2). *J. Phys. Chem. A* **1997**, *101*, 9118-9124, doi:10.1021/jp971994r.
(3) Orkin, V. L.; Martynova, L. E.; Ilichev, A. N. High-accuracy measurements of OH reaction rate constants and IR absorption spectra: CH_2=CF-CF_3 and *trans*-CHF=CH-CF_3. *J. Phys. Chem. A* **2010**, *114*, 5967-5979, doi:10.1021/jp9092817.
(4) Papadimitriou, V. C.; Talukdar, R. K.; Portmann, R. W.; Ravishankara, A. R.; Burkholder, J. B. $CF_3CF=CH_2$ and (Z)-$CF_3CF=CHF$: temperature dependent OH rate coefficients and global warming potentials. *Phys. Chem. Chem. Phys.* **2008**, *10*, 808-820, doi:10.1039/b714382f.
(5) Tokuhashi, K.; Takizawa, K.; Kondo, S. Rate constants for the reactions of OH radicals with $CF_3CX=CY_2$ (X = H, F, CF_3, Y=H, F, Cl). *Environ. Sci. Pollut. Res.* **2018**, *25*, 15204-15215, doi:10.1007/s11356-018-1700-4.

E45. OH + (*E*)-CHF=$CHCF_3$. Results of the three available absolute rate constant measurements, Orkin et al.[2] (220–370 K), Antinolo et al.[1] (263–358 K), and Tokuhashi et al.[4,5] (250–430 K), are in excellent agreement at room temperature and above. The recommended value of k(298 K) is the average of those derived from these data sets. Results of relative rate measurements of Zhang et al.[6] (253–328 K) at 298 K (recalculated based on the current recommendations for the rate constants for the OH + C_4H_{10} and n-C_5H_{12} reference reactions) are in excellent agreement with the recommended k(298 K). The two relative rate determinations by Sondergaard et al.[3] (296 K) (recalculated using the current recommendations for the rate constants of the reference reactions OH + C_2H_4 and C_2H_2) lie about 20% greater than the recommended value.

The data obtained by Orkin et al. (between 370 and 220 K) and by Antinolo et al. (between 358 and 263 K) exhibit a very weak temperature dependence and curvature in the Arrhenius plot. They are in excellent agreement over the overlapping temperature range. The Orkin et al. data are indicative of very weak increase in k(T) below room temperature. Both data sets are in very good agreement with those of Tokuhashi et al.

above room temperature. However, the below room temperature data of Tokuhashi et al. obtained at 273 and 250 K lie below those of Orkin et al.[1] thus suggesting a weak decrease of the rate constant below room temperature. Therefore, a temperature independent rate constant was recommended for below room temperature, while the recommended uncertainty encompasses all results below room temperature. The temperature dependent data from relative rate studies of Zhang at al. are too scattered to derive the temperature dependence and show different trends with different relative reactions.

The rate constant above room temperature, 313–430 K, can be represented by the Arrhenius expression derived from the fit to the data from all three absolute studies above room temperature

$$k(313–430\ \text{K}) = 1.12\times10^{-12}\times\exp(-140/T)$$

(Table: 25-1, Note: 25-1, Evaluated: 25-1) Back to Table

(1) Antiñolo, M.; Bravo, I. n.; Jiménez, E.; Ballesteros, B.; Albaladejo, J. Atmospheric chemistry of *E*- and *Z*-CF_3CH=CHF HFO-1234ze): OH reaction kinetics as a function of temperature and UV and IR absorption cross sections. *J. Phys. Chem. A* **2017**, *121*, 8322−8331, doi:10.1021/acs.jpca.7b06174.

(2) Orkin, V. L.; Martynova, L. E.; Ilichev, A. N. High-accuracy measurements of OH reaction rate constants and IR absorption spectra: CH_2=CF-CF_3 and *trans*-CHF=CH-CF_3. *J. Phys. Chem. A* **2010**, *114*, 5967-5979, doi:10.1021/jp9092817.

(3) Sondergaard, R.; Nielsen, O. J.; Hurley, M. D.; Wallington, T. J.; Singh, R. Atmospheric chemistry of *trans*-CF_3CH = CHF: Kinetics of the gas-phase reactions with Cl atoms, OH radicals, and O_3. *Chem. Phys. Lett.* **2007**, *443*, 199-204, doi:10.1016/j.cplett.2007.06.084.

(4) Tokuhashi, K.; Takizawa, K.; Kondo, S. Rate constants for reactions of OH radicals with (*Z*)-CF_3CCl=CHCl, CHF_2CF=CF_2, (*E*)-CF_3CH=CHF, (*Z*)-CF_3CH=CHF, CH_3CF=CH_2, and CH_2FCH=CH_2. *Atmos. Environ.* **2021**, *255*, 118428, doi:10.1016/j.atmosenv.2021.118428.

(5) Tokuhashi, K.; Takizawa, K.; Kondo, S. Corrigendum to “Rate constants for reactions of OH radicals with (*Z*)-CF_3CCl=CHCl, CHF_2CF=CF_2, (*E*)-CF_3CH=CHF, (*Z*)-CF_3CH=CHF, CH_3CF=CH_2, and CH_2FCH=CH_2” [Atmos. Environ. 255 (2021) 118428]. *Atmos. Environ.* **2023**, *310*, 119914, doi:10.1016/j.atmosenv.2023.119914.

(6) Zhang, N.; Chen, L.; Mizukado, J.; Quan, H.; Suda, H. Rate constants for the gas-phase reactions of (*Z*)-CF_3CH=CHF and (*E*)-CF_3CH=CHF with OH radicals at 253–328 K. *Chem. Phys. Lett.* **2015**, *621*, 78–84, doi:10.1016/j.cplett.2014.12.044.

E46. OH + *(E)*-CH_2=CHCF$(CF_3)_2$ (HFO-1438ezy(*E*)). The reaction was studied by Papadimitriou and Burkholder[1] (214–380 K) using absolute PLP-LIF measurements between 214 and 380 K and relative rate FTIR measurements at 296 K. The data exhibit weak curvature in the Arrhenius plot over the entire range of the study. The recommended values for both k(298 K) and E/R are derived from a fit to only the data obtained below room temperature in the absolute reaction rate study. Results of the room temperature relative rate study (CH_2=$CFCF_3$ and CH_2FCH_3 were reference compounds) are in good agreement. A three-parameter expression derived from the fit to all data of Papadimitriou and Burkholder can be used to represent k(T) from 214 to 380 K:

$$k(214\ \text{to}\ 380\ \text{K}) = 5.5\times10^{-14}\ (T/298)^{2.17}\ \exp(+530/T)$$

(Table: 25-1, Note: 25-1, Evaluated: 25-1) Back to Table

(1) Papadimitriou, V. C.; Burkholder, J. B. OH radical reaction rate coefficients, infrared spectrum, and global warming potential of $(CF_3)_2$CFCH=CHF (HFO-1438ezy(*E*)). *J. Phys. Chem. A* **2016**, *120*, 6618–6628, doi:10.1021/acs.jpca.6b06096.

E47. OH + (*Z*)-CHF=$CHCF_3$. The recommended values for both k(298 K) and E/R are derived from a fit to the results of the absolute study by Tokuhashi et al.[3] (250–430 K). Results of the relative rate study reported by Zhang et al.[4] (253–328 K) (using *n*-butane and *n*-pentane as reference compounds) are in good agreement with the recommended value of k(298 K), but show larger scatter outside room temperature, thus being 1–18% smaller than the recommended values. The rate constant measured by Antinolo et al.[1] (263–359 K) is temperature independent in contrast with data reported by Tokuhashi et al. and Zhang et al. Results of relative rate study of Nilsson et al.[2] (296 K), recalculated using the current recommendations for the rate constants of the reference reactions OH + C_2H_4 and C_2H_2, are 25–30% lower. The recommended uncertainty was chosen to encompass the results of Zhang et al. and the 298 K result of Antinolo et al.
(Table: 25-1, Note: 25-1, Evaluated: 25-1) Back to Table

(1) Antiñolo, M.; Bravo, I. n.; Jiménez, E.; Ballesteros, B.; Albaladejo, J. Atmospheric chemistry of *E*- and *Z*-CF_3CH=CHF HFO-1234ze): OH reaction kinetics as a function of temperature and UV and IR absorption cross sections. *J. Phys. Chem. A* **2017**, *121*, 8322−8331, doi:10.1021/acs.jpca.7b06174.
(2) Nilsson, E. J. K.; Nielsen, O. J.; Johnson, M. S.; Hurley, M. D.; Wallington, T. J. Atmospheric chemistry of *cis*-CF_3CH=CHF: Kinetics of reactions with OH radicals and O_3 and products of OH radical initiated oxidation. *Chem. Phys. Lett.* **2009**, *473*, 233–237, doi:10.1016/j.cplett.2009.03.076.
(3) Tokuhashi, K.; Takizawa, K.; Kondo, S. Rate constants for reactions of OH radicals with (*Z*)-CF_3CCl=CHCl, CHF_2CF=CF_2, (*E*)-CF_3CH=CHF, (*Z*)-CF_3CH=CHF, CH_3CF=CH_2, and CH_2FCH=CH_2. *Atmos. Environ.* **2021**, *255*, 118428, doi:10.1016/j.atmosenv.2021.118428.
(4) Zhang, N.; Chen, L.; Mizukado, J.; Quan, H.; Suda, H. Rate constants for the gas-phase reactions of (*Z*)-CF_3CH=CHF and (*E*)-CF_3CH=CHF with OH radicals at 253–328 K. *Chem. Phys. Lett.* **2015**, *621*, 78–84, doi:10.1016/j.cplett.2014.12.044.

E48. **OH + CF_2=$CHCHF_2$.** The recommended values for both k(298 K) and E/R are derived from a fit to the results of the absolute reaction rate study by Michelat et al.[1] (223–373 K).
(Table: 25-1, Note: 25-1, Evaluated: 25-1) Back to Table

(1) Michelat, L.; Mellouki, A.; Ravishankara, A. R.; El Othmani, H.; Papadimitriou, V. C.; Daële, V.; McGillen, M. R. Temperature-dependent structure-activity relationship of OH + haloalkene rate coefficients under atmospheric conditions and supporting measurements. *ACS Earth Space Chem.* **2022**, *6*, 3101-3114, doi:10.1021/acsearthspacechem.2c00296.

E49. **OH + (*E*)-CHF=$CFCF_3$.** The recommended value for k(298 K) is an average of the two relative rate determinations by Hurley et al.[1] (296 K), recalculated using the current recommendations for the rate constants of the reference reactions OH + C_2H_4 and C_2H_2. The value for E/R is estimated from that for similar fluorinated propenes. Based on the results obtained for other fluorinated alkenes, the recommended rate constant represents the high-pressure limit for this reaction.
(Table: 10-6, Note: 10-6, Evaluated: 10-6) Back to Table

(1) Hurley, M. D.; Ball, J. C.; Wallington, T. J. Atmospheric chemistry of the Z and E isomers of CF_3CF=CHF; Kinetics, mechanisms, and products of gas-phase reactions with Cl atoms, OH radicals, and O_3. *J. Phys. Chem. A* **2007**, *111*, 9789-9795, doi:10.1021/jp0753530.

E50. **OH + (*Z*)-CHF=$CFCF_3$.** The recommended value for k(298 K) is from Papadimitriou et al.[2] (206–380 K) who found the rate constant to be pressure independent between 25 and 600 Torr, indicating that the high-pressure limit is achieved for this reaction. The two room temperature values from the relative rate studies by Hurley et al.[1] (296 K) are in very good agreement with this recommendation. Papadimitriou et al. found weak curvature in the Arrhenius plot from 206 to 380 K. The recommended value for E/R is derived from a fit to their data at T ≤300 K. The data over the temperature range from 206 to 380 K can be represented by a three-parameter expression obtained from the fit to the data reported by Papadimitriou et al.

$$k(206–380\ \mathrm{K}) = 1.55 \times 10^{-13}\ (\mathrm{T}/298)^{1.92}\ \exp(+633/\mathrm{T})$$

(Table: 10-6, Note: 15-10, Evaluated: 15-10) Back to Table

(1) Hurley, M. D.; Ball, J. C.; Wallington, T. J. Atmospheric chemistry of the Z and E isomers of CF_3CF=CHF; Kinetics, mechanisms, and products of gas-phase reactions with Cl atoms, OH radicals, and O_3. *J. Phys. Chem. A* **2007**, *111*, 9789-9795, doi:10.1021/jp0753530.
(2) Papadimitriou, V. C.; Talukdar, R. K.; Portmann, R. W.; Ravishankara, A. R.; Burkholder, J. B. CF_3CF=CH_2 and (Z)-CF_3CF=CHF: temperature dependent OH rate coefficients and global warming potentials. *Phys. Chem. Chem. Phys.* **2008**, *10*, 808-820, doi:10.1039/b714382f.

E51. **OH + CF_2=$CHCF_3$.** The recommended Arrhenius parameters were derived from a combined fit to the data of Tokuhashi et al.[1] (250–430 K) from three series of pulse experiments with different OH precursors.
(Table: 25-1, Note: 25-1, Evaluated: 25-1) Back to Table

(1) Tokuhashi, K.; Takizawa, K.; Kondo, S. Rate constants for the reactions of OH radicals with CF_3CX=CY_2 (X = H, F, CF_3, Y=H, F, Cl). *Environ. Sci. Pollut. Res.* **2018**, *25*, 15204-15215, doi:10.1007/s11356-018-1700-4.

E52. OH + CF_2=CFCHF_2. The recommended Arrhenius parameters were derived from a combined fit to the data of Tokuhashi et al.[1] (250–430 K) from four series of pulse experiments with different OH precursors.
(Table: 25-1, Note: 25-1, Evaluated: 25-1) Back to Table

(1) Tokuhashi, K.; Takizawa, K.; Kondo, S. Rate constants for the reactions of OH radicals with $CF_3CX=CY_2$ (X = H, F, CF_3, Y=H, F, Cl). *Environ. Sci. Pollut. Res.* **2018**, *25*, 15204-15215, doi:10.1007/s11356-018-1700-4.

E53. OH + CF_2=CFCF_3. The recommended value for k(298 K) is an average of the values reported in the absolute rate constant investigations by McIlroy and Tully[3] (293–831 K), Orkin et al.[4] (252–370 K), Orkin et al.[5] (230–480 K), and Tokuhashi et al.[6] (250– 430 K) (two studies) and in the relative rate study by Mashino et al.[2] (296 K) (using two different reference gases). All of these individual k(298 K) values are in excellent agreement and lie within 3% of the recommended value. Results of the room temperature relative rate study by Acerboni et al.[1] (298 K) are internally inconsistent and exceed the recommended value by ~12% and ~60% when C_2H_4 and C_3H_6, respectively, were used as reference compounds. Although the first value overlaps the recommended k(298 K) within the reported uncertainty, the reason for the large difference when C_3H_6 was used as the reference compound is not clear, especially since the result for OH + C_2F_4 reported by the same group using the same reference reaction is in good agreement with other available data. The recommended value for E/R is derived from a fit of the data of Orkin et al.[5] at T ≤300 K. Based on results obtained for other fluorinated alkenes, the recommended rate constant represents the high-pressure limit for this reaction. The complete data set of Orkin et al.[5] between 230–480 K exhibits pronounced curvature in the Arrhenius plot and can be best fit by the three-parameter expression:

$$k(230–480\ \text{K}) = 9.75 \times 10^{-14}\ (\text{T}/298)^{1.94}\ \exp(+922/\text{T})$$

This expression encompasses all data from the studies used in deriving the recommendation within an f(T) factor of 1.05.
(Table: 15-10, Note: 15-10, Evaluated: 15-10) Back to Table

(1) Acerboni, G.; Beukes, J. A.; Jensen, N. R.; Hjorth, J.; Myhre, G.; Nielsen, C. J.; Sundet, J. K. Atmospheric degradation and global warming potentials of three perfluoroalkenes. *Atmos. Environ.* **2001**, *35*, 4113-4123, doi:10.1016/S1352-2310(01)00209-6.
(2) Mashino, M.; Ninomiya, Y.; Kawasaki, M.; Wallington, T. J.; Hurley, M. D. Atmospheric chemistry of $CF_3CF=CF_2$: Kinetics and mechanism of its reactions with OH radicals, Cl atoms, and ozone. *J. Phys. Chem. A* **2000**, *104*, 7255-7260, doi:10.1021/jp000498r.
(3) McIlroy, A.; Tully, F. P. Kinetic study of OH reactions with perfluoropropene and perfluorobenzene. *J. Phys. Chem.* **1993**, *97*, 610-614, doi:10.1021/j100105a013.
(4) Orkin, V. L.; Huie, R. E.; Kurylo, M. J. Rate constants for the reactions of OH with HFC-245cb ($CH_3CF_2CF_3$) and some fluoroalkenes (CH_2CHCF_3, CH_2CFCF_3, CF_2CFCF_3, and CF_2CF_2). *J. Phys. Chem. A* **1997**, *101*, 9118-9124, doi:10.1021/jp971994r.
(5) Orkin, V. L.; Poskrebyshev, G. A.; Kurylo, M. J. Rate constants for the reactions between OH and perfluorinated alkenes. *J. Phys. Chem. A* **2011**, *115*, 6568-6574, doi:10.1021/jp201663j.
(6) Tokuhashi, K.; Takahashi, A.; Kaise, M.; Kondo, S.; Sekiya, A.; Fujimoto, E. Rate constants for the reactions of OH radicals with $CF_3OCF=CF_2$ and $CF_3CF=CF_2$. *Chem. Phys. Lett.* **2000**, *325*, 189-195, doi:10.1016/S0009-2614(00)00626-6.

E54. OH + CF_2=CF-O-CF_3. The recommended values for k(298 K) and E/R were derived from a fit to the data of Tokuhashi et al.[3] (250–430 K). This recommendation is reasonably consistent with that for the similar reaction of OH with $CF_2=CFCF_3$, which was studied by several groups including Tokuhashi et al. Results of the relative rate study of Mashino et al.[2] (296 K), recalculated using the current recommendations for the rate constants of the reference reactions OH + C_2H_4 and C_2H_2, are 32% lower. Results of the absolute study by Li et al.[1] (253–348 K) exhibit an opposite temperature dependence of the rate constant with E/R = +870 K. Such behavior is inconsistent with recommended parameters of the similar reaction, OH + $CF_2=CFCF_3$, and other fast reactions of fluorinated alkenes, all of which exhibit a weak negative temperature dependence at room temperature and below, i.e., E/R <0.
(Table: 19-5, Note: 19-5, Evaluated: 19-5) Back to Table

(1) Li, Z.; Tao, Z.; Naik, V.; Good, D. A.; Hansen, J. C.; Jeong, G.-R.; Francisco, J. S.; Jain, A. K.; Wuebbles, D. J. Global warming potential assessment for $CF_3OCF=CF_2$. *J. Geophys. Res.* **2000**, *105*, 4019–4029, doi:10.1029/1999JD900943.

(2) Mashino, M.; Kawasaki, M.; Wallington, T. J.; Hurley, M. D. Atmospheric degradation of $CF_3OCF=CF_2$: Kinetics and mechanism of its reaction with OH radicals and Cl atoms. *J. Phys. Chem. A* **2000**, *104*, 2925–2930, doi:10.1021/jp000498r.
(3) Tokuhashi, K.; Takahashi, A.; Kaise, M.; Kondo, S.; Sekiya, A.; Fujimoto, E. Rate constants for the reactions of OH radicals with $CF_3OCF=CF_2$ and $CF_3CF=CF_2$. *Chem. Phys. Lett.* **2000**, *325*, 189-195, doi:10.1016/S0009-2614(00)00626-6.

E55. OH + CF_2=CF-O-C_2F_5. The recommended k(298 K) is an average of two values derived from the fit to the results of absolute rate constant measurements by Srinivasulu et al.[1] (207–300 K) and their relative rate measurement at 298 K (with the reference compound C_3H_8), which are in good agreement. The recommended value for E/R was derived from a fit to the results of the absolute measurements by Srinivasulu et al.
(Table: 25-1, Note: 25-1, Evaluated: 25-1) Back to Table

(1) Srinivasulu, G.; Bunkan, A. J. C.; Amedro, D.; Crowley, J. N. Absolute and relative-rate measurement of the rate coefficient for reaction of perfluoro ethyl vinyl ether ($C_2F_5OCF=CF_2$) with OH. *Phys. Chem. Chem. Phys.* **2018**, *20*, 3761-3767, doi:10.1039/c7cp08056e.

E56. OH + CF_2=CFCF=CF_2. Two relative rate studies of this reaction near room temperature have been conducted. There is approximately a 25–30% difference between the results from these studies using different reference compounds and approximately the same difference between the results when the same reference compound, C_2H_4, was used. Thus, the recommended value for k(298 K) is an average of all values determined in the relative rate studies of Acerboni et al.[1] (298 K) (using ethene, propene, and cyclohexane as reference compounds) and of Wallington and Hurley[2] (295 K) (using ethene and acetylene as reference compounds). The current recommendations for the rate constants of the reactions of OH with reference compounds were used to recalculate the results of each of the relative rate measurements. The recommended value for E/R is estimated as being approximately the same as that for OH + $CF_2=CF_2$.
(Table: 15-10, Note: 15-10, Evaluated: 15-10) Back to Table

(1) Acerboni, G.; Beukes, J. A.; Jensen, N. R.; Hjorth, J.; Myhre, G.; Nielsen, C. J.; Sundet, J. K. Atmospheric degradation and global warming potentials of three perfluoroalkenes. *Atmos. Environ.* **2001**, *35*, 4113-4123, doi:10.1016/S1352-2310(01)00209-6.
(2) Wallington, T. J.; Hurley, M. D. Atmospheric chemistry of hexafluorocyclobutene, octafluorocyclopentene, and hexafluoro-1,3-butadiene. *Chem. Phys. Lett.* **2011**, *507*, 19-23, doi:10.1016/j.cplett.2011.01.059.

E57. OH + CH_2=CHCF_2CF_3. The recommended value for k(298 K) is an average of the two relative rate study results by Sulbaek Andersen et al.[1] (296 K), which were recalculated using the current rate constant recommendations for the reference reactions OH + C_2H_4 and C_2H_2. The recommended value for E/R is estimated as being the same as that for OH + $CH_2=CHCF_3$. Sulbaek Andersen et al. determined the rate constants at 296 K for OH reactions with $CH_2=CHC_xF_{2x+1}$ (for x=1,2,4,6,8), and the recommendation given here covers all of these compounds. Based on results obtained for other fluorinated alkenes, the recommended rate constant represents the high-pressure limit for this reaction.
(Table: 15-10, Note: 15-10, Evaluated: 15-10) Back to Table

(1) Sulbaek Andersen, M. P.; Nielsen, O. J.; Toft, A.; Nakayama, T.; Matsumi, Y.; Waterland, R. L.; Buck, R. C.; Hurley, M. D.; Wallington, T. J. Atmospheric chemistry of $C_xF_{2x+1}CH=CH_2$ (x=1, 2, 4, 6, and 8): Kinetics of gas-phase reactions with Cl atoms, OH radicals, and O_3. *J. Photochem. Photobiol. A: Chem.* **2005**, *176*, 124-128, doi:10.1016/j.jphotochem.2005.06.015.

E58. OH + (*E*)-CF_3CH=CHCF_3. The recommended values for k(298 K) and E/R were derived from a fit to the data reported by Baasandorj et al.[1] (211–373 K). The result of a relative rate study at 296 K reported by Østerstrøm et al.[2] (296 K) is 18% greater than the recommended value when C_3H_8 was used as a reference compound, but 50% greater when C_2H_6 was used as the reference compound.
(Table: 19-5, Note: 19-5, Evaluated: 19-5) Back to Table

(1) Baasandorj, M.; Marshall, P.; Waterland, R. L.; Ravishankara, A. R.; Burkholder, J. B. Rate coefficient measurements and theoretical analysis of the OH + (*E*)-$CF_3CH=CHCF_3$ reaction. *J. Phys. Chem. A* **2018**, *122*, 4635–4646, doi:10.1021/acs.jpca.8b02771.
(2) Østerstrøm, F. F.; Andersen, S. T.; Sølling, T. I.; Nielsen, O. J.; Andersen, M. P. S. Atmospheric chemistry of *Z*- and *E*-$CF_3CH=CHCF_3$. *Phys. Chem. Chem. Phys.* **2017**, *19*, 735–750, doi:10.1039/c6cp07234h.

E59. OH + (*Z*)-$CF_3CH=CHCF_3$. The recommended values for both k(298 K) and E/R are derived from a fit to the data below 300 K of Baasandorj et al.[1] (212–374 K). The complete data set of Baasandorj et al. exhibits pronounced curvature in the Arrhenius plot and can be best fit by the three-parameter expression:

$$k(212–374\ K) = 3.68 \times 10^{-14}\ (T/298)^{2.33}\ \exp(+774/T)$$

The results of the 296 K relative rate study by Østerstrøm et al.[2] (296 K) are 10% and 16% smaller and overlap the recommended value within reported uncertainties when C_2H_6 and C_3H_8 were used as reference compounds, respectively.
(Table: 15-10, Note: 19-5, Evaluated: 19-5) Back to Table

(1) Baasandorj, M.; Ravishankara, A. R.; Burkholder, J. B. Atmospheric chemistry of (*Z*)-$CF_3CH=CHCF_3$: OH radical reaction rate coefficient and global warming potential. *J. Phys. Chem. A* **2011**, *115*, 10539-10549, doi:10.1021/jp206195g.

(2) Østerstrøm, F. F.; Andersen, S. T.; Sølling, T. I.; Nielsen, O. J.; Andersen, M. P. S. Atmospheric chemistry of *Z*- and *E*-$CF_3CH=CHCF_3$. *Phys. Chem. Chem. Phys.* **2017**, *19*, 735–750, doi:10.1039/c6cp07234h.

E60. OH + (*E*)-$CF_3CH=CHC_2F_5$. The recommended values for both k(298 K) and E/R are derived from a fit to the data from the relative rate study of Guo et al.[1] (253–328 K). Results obtained with two reference reactions, OH + CH_3CHFCH_3 and C_3H_8, are in the excellent agreement over the entire temperature range of the study.
(Table: 25-1, Note: 25-1, Evaluated: 25-1) Back to Table

(1) Guo, Q.; Zhang, N.; Uchimaru, T.; Chen, L.; Quan, H.; Mizukadob, J. Kinetics, products, and mechanism for the reaction of *E*−$CF_3CH=CHC_2F_5$ with OH radicals in gas phase and atmospheric implications. *Atmos. Environ.* **2018**, *185*, 7-14, doi:10.1016/j.atmosenv.2018.04.047.

E61. OH + $CH_2=C(CF_3)_2$. The recommended value of k(298 K) is an average of results from the absolute study by Tokuhashi et al.[3] (250–430 K) (three different sources of OH) and the relative rate study by Papadimitriou et al.[1] (298 K) (an average from measurements with three reference compounds: C_2H_4, C_2H_6, and C_3H_8). The value of E/R was derived from a combined fit to the data of Tokuhashi et al.

There are two other relative rate studies by Tovar et al.[4] (298 K) (relative C_3H_8 and C_4H_{10}) and Rivela et al.[2] (250–430 K). The recommended uncertainty overlaps the very scattered data of Tovar et al. Although the recommended uncertainty overlaps with the results of Rivela et al. at room temperature, these data exhibit an very strange strong negative temperature dependence with E/R = -3200 K.
(Table: 25-1, Note: 25-1, Evaluated: 25-1) Back to Table

(1) Papadimitriou, V. C.; Spitieri, C. S.; Papagiannakopoulos, P.; Cazaunau, M.; Lendar, M.; Daéle, V.; Mellouki, A. Atmospheric chemistry of $(CF_3)_2C=CH_2$: OH radicals, Cl atoms and O_3 rate coefficients, oxidation end-products and IR spectra. *Phys. Chem. Chem. Phys* **2015**, *17*, 25607-25620, doi:10.1039/c5cp03840e.

(2) Rivela, C. B.; Tovar, C. M.; Teruel, M. A.; Barnes, I.; Wiesen, P.; Blanco, M. B. CFCs replacements: Reactivity and atmospheric lifetimes of a series of Hydrofluoroolefins towards OH radicals and Cl atoms. *Chem. Phys. Lett.* **2019**, *714*, 190-196, doi:10.1016/j.cplett.2018.10.078.

(3) Tokuhashi, K.; Takizawa, K.; Kondo, S. Rate constants for the reactions of OH radicals with $CF_3CX=CY_2$ (X = H, F, CF_3, Y=H, F, Cl). *Environ. Sci. Pollut. Res.* **2018**, *25*, 15204-15215, doi:10.1007/s11356-018-1700-4.

(4) Tovar, C. M.; Blanco, M. B.; Barnes, I.; Wiesen, P.; Teruel, M. A. Gas-phase reactivity study of a series of hydrofluoroolefins (HFOs) toward OH radicals and Cl atoms at atmospheric pressure and 298 K. *Atmos. Environ.* **2014**, *88*, 107-114, doi:10.1016/j.atmosenv.2014.01.060.

E62. OH + (*E*)-$CF_3CF=CFCF_3$. The data reported by Orkin et al.[2] for this isomer exhibits curvature in the Arrhenius plot. The recommended values for both k(298 K) and E/R are derived from a fit to the data of Orkin et al.[2] (230–370 K) at T <300 K, the only temperature range where these recommended Arrhenius parameters should be used. The data over the broader temperature range from 230 to 370 K can be represented by the three-parameter expression obtained from the fit to the data reported by Orkin et al.:[2]

$$k(230–370\ K) = 7.5 \times 10^{-14}\ (T/298)^{1.68}\ \exp(+612/T)$$

Cometto et al.[1] and Young et al.[3] studied the reaction of OH with the industrial mixture of the two isomers, *(E)*-octafluoro-2-butene and *(Z)*-octafluoro-2-butene, at room temperature using a relative rate technique. They reported rate constants that are 35% and 25% lower than the recommended value, respectively, without including uncertainties in the reference rate constants. Orkin et al. separated and analyzed the individual isomer

abundance to find that the industrial mixture contains ~71% of the more reactive *(E)*-octafluoro-2-butene and ~ 29% of the less reactive *(Z)*-octafluoro-2-butene. Therefore, the result reported by Young et al. is in quantitative agreement with that calculated for such a mixture using the individual isomer rate constants of Orkin et al. The result reported by Cometto et al. appears too low for such a mixture based on the values recommended here.
(Table: 15-10, Note: 15-10, Evaluated: 15-10) Back to Table

(1) Cometto, P. M.; Taccone, R. A.; Nieto, J. D.; Dalmasso, P. R.; Lane, S. I. Kinetic study of OH radical reactions with $CF_3CCl=CCl_2$, $CF_3CCl=CClCF_3$ and $CF_3CF=CFCF_3$. *ChemPhysChem* **2010**, *11*, 4053-4059, doi:10.1002/cphc.201000430.
(2) Orkin, V. L.; Poskrebyshev, G. A.; Kurylo, M. J. Rate constants for the reactions between OH and perfluorinated alkenes. *J. Phys. Chem. A* **2011**, *115*, 6568-6574, doi:10.1021/jp201663j.
(3) Young, C. J.; Hurley, M. D.; Wallington, T. J.; Mabury, S. A. Atmospheric chemistry of perfluorobutenes ($CF_3CF=CFCF_3$ and $CF_3CF_2CF=CF_2$): Kinetics and mechanisms of reactions with OH radicals and chlorine atoms, IR spectra, global warming potentials, and oxidation to perfluorocarboxylic acids. *Atmos. Environ.* **2009**, *43*, 3717-3724, doi:10.1016/j.atmosenv.2009.04.025.

E63. OH + (*Z*)-$CF_3CF=CFCF_3$. The data reported by Orkin et al.[2] (230–370 K) for this isomer exhibits a weak temperature dependence and curvature in the Arrhenius plot. The recommended values for both k(298 K) and E/R are derived from a fit to the data of Orkin et al. at T <300 K, the only temperature range where these recommended Arrhenius parameters should be used. The data over the broader temperature range from 230 to 370 K can be represented by the three-parameter expression obtained from the fit to the data reported by Orkin et al.:

$$k(230–370\ \text{K}) = 3.0 \times 10^{-14}\ (\text{T}/298)^{2.61}\ \exp(+760/\text{T})$$

Cometto et al.[1] and Young et al.[3] studied the reaction of OH with the industrial mixture of the two isomers, *(E)*-octafluoro-2-butene and *(Z)*-octafluoro-2-butene, at room temperature using a relative rate technique. Orkin et al.[2] separated and analyzed the individual isomer abundance to find that the industrial mixture contains ~29% of the less reactive *(Z)*-octafluoro-2-butene and ~71% of the more reactive *(E)*-octafluoro-2-butene. The rate constant reported by Young et al. agrees with that calculated for such a mixture using the individual isomer rate constants measured by Orkin et al. within the total combined uncertainty. The result reported by Cometto et al. appears too low for such a mixture based on the values recommended here.
(Table: 15-10, Note: 15-10, Evaluated: 15-10) Back to Table

(1) Cometto, P. M.; Taccone, R. A.; Nieto, J. D.; Dalmasso, P. R.; Lane, S. I. Kinetic study of OH radical reactions with $CF_3CCl=CCl_2$, $CF_3CCl=CClCF_3$ and $CF_3CF=CFCF_3$. *ChemPhysChem* **2010**, *11*, 4053-4059, doi:10.1002/cphc.201000430.
(2) Orkin, V. L.; Poskrebyshev, G. A.; Kurylo, M. J. Rate constants for the reactions between OH and perfluorinated alkenes. *J. Phys. Chem. A* **2011**, *115*, 6568-6574, doi:10.1021/jp201663j.
(3) Young, C. J.; Hurley, M. D.; Wallington, T. J.; Mabury, S. A. Atmospheric chemistry of perfluorobutenes ($CF_3CF=CFCF_3$ and $CF_3CF_2CF=CF_2$): Kinetics and mechanisms of reactions with OH radicals and chlorine atoms, IR spectra, global warming potentials, and oxidation to perfluorocarboxylic acids. *Atmos. Environ.* **2009**, *43*, 3717-3724, doi:10.1016/j.atmosenv.2009.04.025.

E64. OH + $CF_2=CFCF_2CF_3$. The recommended value for k(298 K) is an average of two relative rate study results at 296 K reported by Young et al.,[1] recalculated using the current recommendations for the rate constants of the reference reactions OH + C_2H_4 and C_2H_2. These recalculated values differ from each other by 13%. The value for E/R is estimated to be the same as that for OH + $CF_2=CFCF_3$ and the uncertainty was chosen to encompass the recommended rate constants for this similar reaction.
(Table: 19-5, Note: 19-5, Evaluated: 19-5) Back to Table

(1) Young, C. J.; Hurley, M. D.; Wallington, T. J.; Mabury, S. A. Atmospheric chemistry of perfluorobutenes ($CF_3CF=CFCF_3$ and $CF_3CF_2CF=CF_2$): Kinetics and mechanisms of reactions with OH radicals and chlorine atoms, IR spectra, global warming potentials, and oxidation to perfluorocarboxylic acids. *Atmos. Environ.* **2009**, *43*, 3717-3724, doi:10.1016/j.atmosenv.2009.04.025.

E65. OH + *cyclo*-$CH=CHCF_2CF_2$-. There are two relative rate studies of this reaction, performed using an identical technique with GC monitoring of compounds' concentration over the same temperature range (253–328 K), Jia et al.[1] (OH + C_2H_6 and OH + CH_2FCH_2F reference reactions) and Zhang et al.[2] (OH + CH_3F and OH + CH_3CH_2F reference reactions). The recommended k(298 K) is an average of three values derived from the fits to the relative data sets reported by Jia et al. and Zhang et al. (only the OH + CH_3CH_2F reaction reference data) recalculated using the current recommendations for the rate constants of the reference reactions. The value for

E/R was derived from a combined fit to the same recalculated data after each data set was normalized to the recommended value of *k*(298 K). The results reported by Zhang et al. with OH + CH_3F as the reference reaction were not included, because the data exhibits a pronounced downward curvature of an Arrhenius dependence, with a noticeable deviation from the three other data sets, at temperatures below room temperature.
(Table: 25-1, Note: 25-1, Evaluated: 25-1) Back to Table

(1) Jia, X. Q.; Chen, L.; Mizukado, J.; Kutsuna, S.; Tokuhashi, K. Rate constants for the gas-phase reactions of cyclo-CX=CXCF_2CF_2- (X = H, F) with OH radicals at a temperature range of 253–328 K. *Chem. Phys.Lett.* **2013**, *572*, 21–25, doi:10.1016/j.cplett.2013.04.020.
(2) Zhang, W.; Guo, Q.; Quan, H. Atmospheric chemistry of cyc–CF_2CF_2CX=CX– (X=H, F): Kinetics, products, and mechanism of gas–phase reactions with OH radicals, and atmospheric implication. *Atmos. Environ.* **2025**, *349*, 121125, doi:10.1016/j.atmosenv.2025.121125.

E66. OH + *cyclo*-CH=CFCF_2CF_2-. There are two relative rate studies of this reaction, performed using an identical technique with GC monitoring of compounds' concentration over the same temperature range (253–328 K), Jia et al.[1] (OH + C_2H_6 and OH + CH_2FCH_2F reference reactions) and Zhang et al.[2] (OH + CH_3F and OH + CH_3CH_2F reference reactions). The recommended *k*(298 K) is an average of four values derived from the fits to the relative data sets reported by Jia et al. (253–328 K) and Zhang et al. (268–328 K) recalculated using the current recommendations for the rate constants of the reference reactions. The lowest temperature (253 K) data of Zhang et al. appear to be outliers. The value for *E*/R was derived from a combined fit to the same recalculated data after each data set was normalized to the recommended value of *k*(298 K).
(Table: 25-1, Note: 25-1, Evaluated: 25-1) Back to Table

(1) Jia, X. Q.; Chen, L.; Mizukado, J.; Kutsuna, S.; Tokuhashi, K. Rate constants for the gas-phase reactions of cyclo-CX=CXCF_2CF_2- (X = H, F) with OH radicals at a temperature range of 253–328 K. *Chem. Phys.Lett.* **2013**, *572*, 21–25, doi:10.1016/j.cplett.2013.04.020.
(2) Zhang, W.; Guo, Q.; Quan, H. Atmospheric chemistry of cyc–CF_2CF_2CX=CX– (X=H, F): Kinetics, products, and mechanism of gas–phase reactions with OH radicals, and atmospheric implication. *Atmos. Environ.* **2025**, *349*, 121125, doi:10.1016/j.atmosenv.2025.121125.

E67. OH + *cyclo*-CF=CFCF_2CF_2-. There are two relative rate studies of this reaction, performed using an identical technique with GC monitoring of compounds' concentration over the same temperature range (253–328 K), Jia et al.[1] (OH + C_2H_6 and OH + CH_2FCH_2F reference reactions) and Zhang et al.[3] (OH + CH_3F and OH + $CH_2FCHFCF_3$ reference reactions). The recommended *k*(298 K) is an average of four values derived from the fits to the relative data sets reported by Jia et al.[1] (253–328 K) and Zhang et al. (268–328 K) recalculated using the current recommendations for the rate constants of the reference reactions. The lowest temperature (253 K) data of Zhang et al. appear to be outliers and not considered in the recommendation. The value for *E*/R was derived from a combined fit to the same recalculated data after each data set was normalized to the recommended value of *k*(298 K). In a 296 K relative rate study, Wallington and Hurley[2] reported a rate constant, which is inexplicably larger by a factor of 2.2, was not considered in the recommendation.
(Table: 25-1, Note: 25-1, Evaluated: 25-1) Back to Table

(1) Jia, X. Q.; Chen, L.; Mizukado, J.; Kutsuna, S.; Tokuhashi, K. Rate constants for the gas-phase reactions of cyclo-CX=CXCF_2CF_2- (X = H, F) with OH radicals at a temperature range of 253–328 K. *Chem. Phys.Lett.* **2013**, *572*, 21–25, doi:10.1016/j.cplett.2013.04.020.
(2) Wallington, T. J.; Hurley, M. D. Atmospheric chemistry of hexafluorocyclobutene, octafluorocyclopentene, and hexafluoro-1,3-butadiene. *Chem. Phys. Lett.* **2011**, *507*, 19-23, doi:10.1016/j.cplett.2011.01.059.
(3) Zhang, W.; Guo, Q.; Quan, H. Atmospheric chemistry of cyc–CF_2CF_2CX=CX– (X=H, F): Kinetics, products, and mechanism of gas–phase reactions with OH radicals, and atmospheric implication. *Atmos. Environ.* **2025**, *349*, 121125, doi:10.1016/j.atmosenv.2025.121125.

E68. OH + *cyclo*-CH=CH$CF_2CF_2CF_2$-. The recommended values for *k*(298 K) and *E*/R were derived from a combined fit to the data from Guo et al.,[1] a relative rate study with C_3H_8 and CH_3CHFCH_3 as reference compounds. The reported *k*(298 K) values from this study agree within 3%.
(Table: 19-5, Note: 19-5, Evaluated: 19-5) Back to Table

(1) Guo, Q.; Zhang, N.; Uchimaru, T.; Chen, L.; Quana, H.; Mizukado, J. Atmospheric chemistry of cyc-$CF_2CF_2CF_2CH$=CH-: Kinetics, products, and mechanism of gas-phase reaction with OH radicals, and atmospheric implications. *Atmos. Environ.* **2018**, *179*, 69–75, doi:10.1016/j.atmosenv.2018.02.005.

E69. OH + *cyclo*-CH=CFCF$_2$CF$_2$CF$_2$-. The reaction was studied by Gierczak et al.[1] (242–370 K) using an absolute technique. Complementary relative rate measurements were done using OH + CH_2F_2, CH_3CHF_2, and $CHF_2CHFCHF_2$ as reference reactions at selected temperatures over the same range. Liu et al.[2] (298 K) reported results of relative rate measurements using OH + $CH_2FCHFCF_3$ and $CH_3CH_2CF_3$ as reference reactions. The recommended values of both k(298 K) and E/R are derived from the fit to the absolute rate data from Gierczak et al. Results of their relative rate measurements between 273 and 372 K are randomly within 6% of the recommended values. The value of k(298 K) derived by Liu et al. exceeds the recommendation by 8%.
(Table: 25-1, Note: 25-1, Evaluated: 25-1) Back to Table

(1) Gierczak, T.; Bernard, F. o.; Papanastasiou, D. K.; Burkholder, J. B. Atmospheric chemistry of c-C_5HF_7 and c-C_5F_8: Temperature-dependent OH reaction rate coefficients, degradation products, infrared spectra, and global warming potentials. *J. Phys. Chem. A* **2021**, *125*, 1050−1061, doi:10.1021/acs.jpca.0c10561.
(2) Liu, D.; Qin, S.; Li, W.; Zhang, D.; Guo, Z. Atmospheric chemistry of 1H-Heptafluorocyclopentene (*cyc*-$CF_2CF_2CF_2CF$=CH-): rate constant, products, and mechanism of gas-phase reactions with OH radicals, IR absorption spectrum, photochemical ozone creation potential, and global warming potential. *J. Phys. Chem. A* **2016**, *120*, 9557-9563, doi:10.1021/acs.jpca.6b10348.

E70. OH + *cyclo*-CF=CFCF$_2$CF$_2$CF$_2$-. The reaction was studied by Gierczak et al.[1] (242–370 K) using an absolute technique. Complementary relative rate measurements were done using OH + CH_2F_2, $CH_2FCHFCF_3$, and $CHF_2CHFCHF_2$ as reference reactions at selected temperatures over the same range. Zhang et al.[3] (253–328 K) reported results of relative rate measurements using OH + CH_2F_2 and CH_3F as reference reactions. The recommended values of k(298 K) and E/R are averages of values derived from the fit to the absolute rate data from Gierczak et al. and the combined fit to the data of Zhang et al. recalculated using the current recommendations for the rate constants of the reference reactions OH + CH_2F_2 and CH_3F. The difference between k(298 K) values derived from these studies is ca. 15% whereas E/R values are very similar. Wallington and Hurley[2] (296 K) reported a rate constant determined from relative rate measurements, which inexplicably exceeds the recommended value by a factor of 2.2.
(Table: 25-1, Note: 25-1, Evaluated: 25-1) Back to Table

(1) Gierczak, T.; Bernard, F. o.; Papanastasiou, D. K.; Burkholder, J. B. Atmospheric chemistry of c-C_5HF_7 and c-C_5F_8: Temperature-dependent OH reaction rate coefficients, degradation products, infrared spectra, and global warming potentials. *J. Phys. Chem. A* **2021**, *125*, 1050−1061, doi:10.1021/acs.jpca.0c10561.
(2) Wallington, T. J.; Hurley, M. D. Atmospheric chemistry of hexafluorocyclobutene, octafluorocyclopentene, and hexafluoro-1,3-butadiene. *Chem. Phys. Lett.* **2011**, *507*, 19-23, doi:10.1016/j.cplett.2011.01.059.
(3) Zhang, N.; Uchimaru, T.; Guo, Q.; Qing, F.; Chen, L.; Mizukado, J. Atmospheric chemistry of perfluorocyclopentene (cyc-$CF_2CF_2CF_2CF$=CF-): Kinetics, products, and mechanism of gas-phase reaction with OH radicals, and atmospheric implications. *Atmos. Environ.* **2017**, *160*, 46–54, doi:10.1016/j.atmosenv.2017.04.012.

E71. OH + (*E*)-CHF=CHCF(CF$_3$)$_2$. The reaction was studied by Papadimitriou and Burkholder[1] (214–380 K) using an absolute PLP-LIF technique and a relative rate FTIR technique at 296 K with two reference compounds, CH_3CH_2F and CH_2=$CFCF_3$. The data exhibit a noticeable curvature in the Arrhenius plot. The recommended value for k(298 K) is an average of results derived from all three measurements, which agree with the recommended value within 3%. The recommended value of E/R was derived from a fit to the data between 214 and 296 K, a range over which the rate constant is essentially temperature independent. The data over the broader temperature range from 214 to 380 K can be represented by a three-parameter expression derived from the data after scaling to the recommended k(298 K):

$$k(214–380\ \text{K}) = 5.44 \times 10^{-14}\ (T/298)^{2.17}\ \exp(+528/T)$$

(Table: 19-5, Note: 19-5, Evaluated: 19-5) Back to Table

(1) Papadimitriou, V. C.; Burkholder, J. B. OH radical reaction rate coefficients, infrared spectrum, and global warming potential of $(CF_3)_2CFCH$=CHF (HFO-1438ezy(*E*)). *J. Phys. Chem. A* **2016**, *120*, 6618–6628, doi:10.1021/acs.jpca.6b06096.

E72. OH + $(CF_3)_2C=CFCF_2CF_3$. The rate constant reported by Orkin et al.[2] (250–480 K) decreases with decreasing temperature and exhibits pronounced curvature in the Arrhenius plot between 250 and 370 K. The recommended values for both k(298 K) and E/R are derived from a fit to the data of Orkin et al. between ~300 and 250 K, the temperature region where the rate constant reached a minimum and became essentially temperature independent. The data over the complete temperature range from 370 to 250 K can be represented by the three-parameter expression reported by Orkin et al.

$$k(250–370\ \text{K}) = 2.17 \times 10^{-15}\ (\text{T}/298)^{3.90}\ \exp(+1044/\text{T})$$

The uncertainty parameters were chosen to encompass the possible increase of the rate constant at lower temperatures (below 250 K) following this three-parameter expression. Jubb et al.[1] (298 K) measured the rate constant ratio for $CH_3OC_7F_{13}$ to both $(CF_3)_2C=CFCF_2CF_3$ and (Z)-$CF_3CH=CHCF_3$, thereby enabling calculation of a room temperature rate constant for $(CF_3)_2C=CFCF_2CF_3$ from the current k(298 K) recommendation for (Z)-$CF_3CH=CHCF_3$. The resulting value is in excellent agreement with that recommended here.
(Table: 15-10, Note: 15-10, Evaluated: 15-10) Back to Table

(1) Jubb, A. M.; Gierczak, T.; Baasandorj, M.; Waterland, R. L.; Burkholder, J. B. Methyl-perfluoroheptene-ethers ($CH_3OC_7F_{13}$): Measured OH radical reaction rate coefficients for several isomers and enantiomers and their atmospheric lifetimes and global warming potentials. *Environ. Sci. Technol.* **2014**, *48*, 4954-4962, doi:10.1021/es500888v.
(2) Orkin, V. L.; Poskrebyshev, G. A.; Kurylo, M. J. Rate constants for the reactions between OH and perfluorinated alkenes. *J. Phys. Chem. A* **2011**, *115*, 6568-6574, doi:10.1021/jp201663j.

E73. OH + $CF_3C{\equiv}CH$. The recommended values for k(298 K) and E/R were derived from a combined fit to the data from Zhang et al.[1] (253–328 K), a relative rate study with C_2H_6 and C_3H_8 as reference compounds.
(Table: 25-1, Note: 25-1, Evaluated: 25-1) Back to Table

(1) Zhang, T.; Zhang, C.; Ma, X.; Quan, H. Atmospheric chemistry of $CF_3C{\equiv}CH$: Kinetics, products, mechanism of gas-phase reaction with OH radicals, and atmospheric implications-an effort for novel 'class' of refrigerant. *Atmos. Environ.* **2023**, *294*, 119467, doi:10.1016/j.atmosenv.2022.119467.

E74. OH + $CF_3C{\equiv}CCF_3$. The recommended values for k(298 K) and E/R were derived from a combined fit to the data from Zhang et al.[1] (253–328 K), a relative rate study with C_2H_6 and C_2H_5F as reference compounds.
(Table: 25-1, Note: 25-1, Evaluated: 25-1) Back to Table

(1) Zhang, Q.; Qin, S.; Guo, Z.; Ni, H.; Zhang, J. Atmospheric chemistry of $CF_3C{\equiv}CCF_3$: Kinetics, products, mechanism of gas-phase reaction with OH radicals, and atmospheric implications. *Atmos. Environ.* **2021**, *251*, 118264, doi:10.1016/j.atmosenv.2021.118264.

E75. OH + CF_3OH. There are no measurements of the rate coefficient of this reaction. The recommendation is based on the recommended limit for the reverse reaction rate coefficient and an estimated equilibrium constant. The thermochemistry of CF_3O and CF_3OH are taken from *ab initio* calculations (Montgomery et al.[2] and Schneider and Wallington[3]) and laboratory measurements (Huey et al.[1]) to estimate $\Delta G°_{298}(OH + CF_3OH \rightarrow CF_3O + H_2O)$ to be about (2 ± 4) kcal mol^{-1}. In considering the large uncertainty in the free energy change, the estimated rate coefficient limit is based on the assumption that the reaction is approximately thermoneutral.
(Table: 97-4, Note: 97-4, Evaluated: 97-4) Back to Table

(1) Huey, L. G.; Dunlea, E. J.; Howard, C. J. Gas-phase acidity of CF_3OH. *J. Phys. Chem.* **1996**, *100*, 6504-6508, doi:10.1021/jp953058m.
(2) Montgomery, J. A.; Michels, H. H.; Francisco, J. S. Ab initio calculation of the heats of formation of CF_3OH and CF_2O. *Chem. Phys. Lett.* **1994**, *220*, 391-396, doi:10.1016/0009-2614(94)00211-8.
(3) Schneider, W. F.; Wallington, T. J. Thermochemistry of COF_2 and related compounds. *J. Phys. Chem.* **1994**, *98*, 7448-7451, doi:10.1021/j100082a009.

E76. OH + CH_2FCH_2OH. The recommended values for k(298 K) and E/R are averages of the parameters derived from fits to the data of Rajakumar et al.[2] (238–355 K) and Orkin et al.[1] (220–370 K) for T <300 K with the former data corrected for an apparent error in the UV absorption cross section of CH_2FCH_2OH (which was used to determine the reactant concentration). When this correction is made, the data from these two studies are indistinguishable. The room temperature rate constant determined in the relative rate study of Sellevag et al.[3] (298 K) is about 50% greater than that recommended. The data over the temperature range 230 to 370 K from both Rajakumar et al. and Orkin et al. exhibit curvature in the Arrhenius plot (more evident in the higher

precision data from the latter study) and can be represented by the three-parameter expression reported by Orkin et al.:

$$k(230–370\ \text{K}) = 3.47 \times 10^{-14}\ (\text{T}/298)^{4.5}\ \exp(+977/\text{T})$$

(Table: 15-10, Note: 15-10, Evaluated: 15-10) Back to Table

(1) Orkin, V. L.; Khamaganov, V. G.; Martynova, L. E.; Kurylo, M. J. High-accuracy measurements of OH reaction rate constants and IR and UV absorption spectra: Ethanol and partially fluorinated ethyl alcohols. *J. Phys. Chem. A* **2011**, *115*, 8656-8668, doi:10.1021/jp202099t.

(2) Rajakumar, B.; Burkholder, J. B.; Portmann, R. W.; Ravishankara, A. R. Rate coefficients, for the OH + CFH_2CH_2OH reaction between 238 and 355 K. *Phys. Chem. Chem. Phys.* **2005**, *7*, 2498-2505, doi:10.1039/b503332b.

(3) Sellevåg, S. R.; Nielsen, C. J.; Søvde, O. A.; Myhre, G.; Sundet, J. K.; Stordal, F.; Isaksen, I. S. A. Atmospheric gas-phase degradation and global warming potentials of 2-fluoroethanol, 2,2-difluoroethanol, and 2,2,2-trifluoroethanol. *Atmos. Environ.* **2004**, *38*, 6725-6735, doi:10.1016/j.atmosenv.2004.09.023.

E77. OH + CHF_2CH_2OH. The recommended value of k(298 K) is an average of the values reported in the absolute rate studies of Kovacs et al.[1] (300 K) and Orkin et al.[2] (220–370 K). The value of E/R is derived from a fit at T ≤300 K to the data of Orkin et al., which are the only temperature dependent data available. The room temperature rate constant determined in the relative rate study of Sellevag et al.[3] (298 K) is about 80% greater than that recommended. The data over the temperature range from 220 to 370 K exhibit a curvature in the Arrhenius plot can be represented by a three-parameter expression that is derived from a fit to the data of Orkin et al. over the temperature range 220 to 370 K after the data were scaled to match the recommended value of k(298 K):

$$k(220–370\ \text{K}) = 3.73 \times 10^{-14}\ (\text{T}/298)^{4.25}\ \exp(+578/\text{T})$$

(Table: 10-6, Note: 15-10, Evaluated: 10-6) Back to Table

(1) Kovács, G.; Szász-Vadász, T.; Papadimitriou, V. C.; Dóbé, S.; Bérces, T.; Márta, F. Absolute rate constants for the reactions of OH radicals with CH_3CH_2OH, CF_2HCH_2OH and CF_3CH_2OH. *React. Kinet. Catal. Lett.* **2005**, *87*, 129-138, doi:10.1007/s11144-006-0018-2.

(2) Orkin, V. L.; Khamaganov, V. G.; Martynova, L. E.; Kurylo, M. J. High-accuracy measurements of OH reaction rate constants and IR and UV absorption spectra: Ethanol and partially fluorinated ethyl alcohols. *J. Phys. Chem. A* **2011**, *115*, 8656-8668, doi:10.1021/jp202099t.

(3) Sellevåg, S. R.; Nielsen, C. J.; Søvde, O. A.; Myhre, G.; Sundet, J. K.; Stordal, F.; Isaksen, I. S. A. Atmospheric gas-phase degradation and global warming potentials of 2-fluoroethanol, 2,2-difluoroethanol, and 2,2,2-trifluoroethanol. *Atmos. Environ.* **2004**, *38*, 6725-6735, doi:10.1016/j.atmosenv.2004.09.023.

E78. OH + CF_3CH_2OH. The recommended value for k(298 K) is an average of the values reported in the absolute studies of Wallington et al.[6] (298 K), Tokuhashi et al.[5] (250– 430 K) (two determinations), Kovacs et al.[2] (300 K), and Orkin et al.[3] (220–370 K), and the relative rate study of Hurley et al.[1] (296 K) (using OH + C_2H_2 as the reference reaction). The value of k(298 K) reported by Sellevag et al.[4] (298 K) is significantly larger than those from all of the other studies and was not used in deriving the recommended value. The recommended value for E/R is an average of the values derived from fits to the data below 300 K of Tokuhashi et al. and Orkin et al. The data over the temperature range from 220 to 370 K exhibit a curvature in the Arrhenius plot and can be represented by a three-parameter expression derived from a fit to the data of Orkin et al. after the data were scaled to match the recommended k(298 K):

$$k(220–370\ \text{K}) = 2.57 \times 10^{-14}\ (\text{T}/298)^{4.0}\ \exp(+405/\text{T})$$

(Table: 15-10, Note: 15-10, Evaluated: 15-10) Back to Table

(1) Hurley, M. D.; Wallington, T. J.; Sulbaek Andersen, M. P.; Ellis, D. A.; Martin, J. W.; Mabury, S. A. Atmospheric chemistry of fluorinated alcohols: Reaction with Cl atoms and OH radicals and atmospheric lifetimes. *J. Phys. Chem. A* **2004**, *108*, 1973-1979, doi:10.1021/jp0373088.

(2) Kovács, G.; Szász-Vadász, T.; Papadimitriou, V. C.; Dóbé, S.; Bérces, T.; Márta, F. Absolute rate constants for the reactions of OH radicals with CH_3CH_2OH, CF_2HCH_2OH and CF_3CH_2OH. *React. Kinet. Catal. Lett.* **2005**, *87*, 129-138, doi:10.1007/s11144-006-0018-2.

(3) Orkin, V. L.; Khamaganov, V. G.; Martynova, L. E.; Kurylo, M. J. High-accuracy measurements of OH reaction rate constants and IR and UV absorption spectra: Ethanol and partially fluorinated ethyl alcohols. *J. Phys. Chem. A* **2011**, *115*, 8656-8668, doi:10.1021/jp202099t.

(4) Sellevåg, S. R.; Nielsen, C. J.; Søvde, O. A.; Myhre, G.; Sundet, J. K.; Stordal, F.; Isaksen, I. S. A. Atmospheric gas-phase degradation and global warming potentials of 2-fluoroethanol, 2,2-difluoroethanol, and 2,2,2-trifluoroethanol. *Atmos. Environ.* **2004**, *38*, 6725-6735, doi:10.1016/j.atmosenv.2004.09.023.
(5) Tokuhashi, K.; Nagai, H.; Takahashi, A.; Kaise, M.; Kondo, S.; Sekiya, A.; Takahashi, M.; Gotoh, Y.; Suga, A. Measurement of the OH reaction rate constants for CF_3CH_2OH, $CF_3CF_2CH_2OH$, and $CF_3CH(OH)CF_3$. *J. Phys. Chem. A* **1999**, *103*, 2664-2672, doi:10.1021/jp983961x.
(6) Wallington, T. J.; Dagaut, P.; Kurylo, M. J. Correlation between gas-phase and solution-phase reactivities of hydroxyl radicals toward saturated organic compounds. *J. Phys. Chem.* **1988**, *92*, 5024-5028, doi:10.1021/j100328a039.

E79. OH + $CF_3CH_2CH_2OH$. The recommended value of k(298 K) is an average of all available results: absolute rate constant studies reported by Kelly et al.[4] (298 K), Jimenez et al.[3] (298 K), Antinolo et al.[1] (263–358 K), and the relative rate studies reported by Kelly et al. (average of three measurements) and Hurley et al.[2] (296 K) (average of two measurements). The temperature dependence was studied by Antinolo et al. The scatter in their temperature dependent data is too large to allow a reliable determination of E/R. Hence, the recommended value of E/R was estimated to be the same as that for the similar reaction of OH with CH_2FCH_2OH. The recommended uncertainty factor, f(298 K), assigned to represent the scatter of the room temperature data, adequately represents the uncertainty over the entire temperature range of atmospheric interest.
(Table: 19-5, Note: 19-5, Evaluated: 19-5) Back to Table

(1) Antiñolo, M.; Jiménez, E.; Albaladejo, J. Temperature effects on the removal of potential HFC replacements, $CF_3CH_2CH_2OH$ and $CF_3(CH_2)_2CH_2OH$, initiated by OH radicals. *Environ. Sci. Technol.* **2011**, *45*, 4323–4330, doi:10.1021/es103931s.
(2) Hurley, M. D.; Misner, J. A.; Ball, J. C.; Wallington, T. J.; Ellis, D. A.; Martin, J. W.; Mabury, S. A.; Andersen, M. P. S. Atmospheric chemistry of $CF_3CH_2CH_2OH$: Kinetics, mechanisms and products of Cl atom and OH radical initiated oxidation in the presence and absence of NO_X. *J. Phys. Chem. A* **2005**, *109*, 9816–9826, doi:10.1021/jp0535902.
(3) Jiménez, E.; Antinolo, M.; Ballesteros, B.; Martínez, E.; Albaladejo, J. Atmospheric lifetimes and global warming potentials of $CF_3CH_2CH_2OH$ and $CF_3(CH_2)_2CH_2OH$. *Chem. Phys. Chem.* **2010**, *11*, 4079–4087, doi:10.1002/cphc.201000365.
(4) Kelly, T.; Bossoutrot, V.; Magneron, I.; Wirtz, K.; Treacy, J.; Mellouki, A.; Sidebottom, H.; Le Bras, G. A kinetic and mechanistic study of the reactions of OH radicals and Cl atoms with 3,3,3-trifluoropropanol under atmospheric conditions. *J. Phys. Chem. A* **2005**, *109*, 347–355, doi:10.1021/jp0467402.

E80. OH + $CF_3CF_2CH_2OH$. The recommended value for k(298 K) is an average of the values derived from the data of Tokuhashi et al.[4] (250–430 K) (discharge flow and pulsed photolysis absolute studies) and from the relative rate studies of Chen et al.[2] (298–356 K) (recalculated based on the current recommendation for the rate constant for the OH + CH_2Cl_2 reference reaction) and Hurley et al.[3] (296 K) (recalculated based on the current recommendation for the rate constant for the OH + C_2H_2 reaction). The recommended value for E/R is derived from the combined fit to the temperature dependent data of Tokuhashi et al. (T <400 K) and Chen et al. after scaling each data set to the recommended value of k(298 K). The data reported by Antinolo et al. are scattered as in the case of their OH + $CF_3CH_2CH_2OH$ reaction data, and on average exceed the recommendation by 20%. Hence, these data were not used in deriving the recommendation.
(Table: 10-6, Note: 25-1, Evaluated: 15-10) Back to Table

(1) Antiñolo, M.; González, S.; Ballesteros, B.; Albaladejo, J.; Jiménez, E. Laboratory studies of $CHF_2CF_2CH_2OH$ and $CF_3CF_2CH_2OH$: UV and IR absorption cross sections and OH rate coefficients between 263 and 358 K. *J. Phys. Chem. A* **2012**, *116*, 6041–6050, doi:10.1021/jp2111633.
(2) Chen, L.; Fukuda, F.; Takenaka, N.; Bandow, H.; Maeda, Y. Kinetics of the gas-phase reaction of $CF_3CF_2CH_2OH$ with OH radicals and its atmospheric lifetime. *Int. J. Chem. Kinet.* **2000**, *25*, 73-78, doi:10.1002/(SICI)1097-4601(2000)32:2<73::AID-KIN1>3.0.CO;2-V.
(3) Hurley, M. D.; Wallington, T. J.; Sulbaek Andersen, M. P.; Ellis, D. A.; Martin, J. W.; Mabury, S. A. Atmospheric chemistry of fluorinated alcohols: Reaction with Cl atoms and OH radicals and atmospheric lifetimes. *J. Phys. Chem. A* **2004**, *108*, 1973, doi:10.1021/jp0373088.
(4) Tokuhashi, K.; Nagai, H.; Takahashi, A.; Kaise, M.; Kondo, S.; Sekiya, A.; Takahashi, M.; Gotoh, Y.; Suga, A. Measurement of the OH reaction rate constants for CF_3CH_2OH, $CF_3CF_2CH_2OH$, and $CF_3CH(OH)CF_3$. *J. Phys. Chem. A* **1999**, *103*, 2664-2672, doi:10.1021/jp983961x.

E81. OH + $(CF_3)_2CHOH$. The results of the absolute measurements reported by Tokuhashi et al.[2] (250–430 K) (three determinations) and Orkin et al.[1] (220–370 K) are in excellent agreement over the common temperature range of the measurements. The recommended k(298 K) is the same value obtained in both studies. The data from Orkin et al. exhibit a noticeable curvature in the Arrhenius plot between 220 and 370 K, which is most pronounced at lower temperatures. Because of this curvature, the recommended value for E/R is derived from a fit to the data from both studies only between 298 and 250 K. The data over the temperature range from 220 to 370 K can be represented by a three-parameter expression that is derived from a fit to the data of Orkin et al.:

$$k(220–370\ \text{K}) = 5.7 \times 10^{-16}\ (\text{T}/298)^{6.65}\ \exp(+1125/\text{T})$$

The g-factor is set to encompass the low temperature extrapolation of both the recommended two-parameter Arrhenius expression and the three-parameter expression from Orkin et al.
(Table: 15-10, Note: 15-10, Evaluated: 15-10) Back to Table

(1) Orkin, V. L.; Khamaganov, V. G.; Kurylo, M. J. High accuracy measurements of OH reaction rate constants and IR absorption spectra: Substituted 2-propanols. *J. Phys. Chem. A* **2012**, *116*, 6188-6198, doi:10.1021/jp211534n.
(2) Tokuhashi, K.; Nagai, H.; Takahashi, A.; Kaise, M.; Kondo, S.; Sekiya, A.; Takahashi, M.; Gotoh, Y.; Suga, A. Measurement of the OH reaction rate constants for CF_3CH_2OH, $CF_3CF_2CH_2OH$, and $CF_3CH(OH)CF_3$. *J. Phys. Chem. A* **1999**, *103*, 2664-2672, doi:10.1021/jp983961x.

E82. OH + $(CF_3)_2C(OH)CH_3$. The recommendation is based on results of the absolute study by Orkin et al.[2] (230–370 K). The reported data between 230 and 370 K exhibit surprisingly very weak temperature dependence and pronounced curvature in the Arrhenius plot with a minimum near 272 K. The data can be described by a three-parameter expression that is derived from a fit to the data of Orkin et al.

$$k(230–370\ \text{K}) = 1.90 \times 10^{-18}\ (\text{T}/298)^{11.5}\ \exp(+2476/\text{T}).$$

The recommended values of k(298 K) and E/R were derived from the fit of the Arrhenius expression to the data obtained between 230 and 298 K, which results in 5% underestimated k(298 K) when compared with the measured value because of the curvature in the Arrhenius plot. Kumar et al.[1] (268–363 K) reported results of relative rate measurements using OH +CH_4 and CH_3CN as reference reactions. Although these data have larger uncertainties, they are in good agreement with results of absolute measurements at below room temperatures.
(Table: 25-1, Note: 25-1, Evaluated: 25-1) Back to Table

(1) Kumar, A.; Gonu, S.; Vijayakumar, S.; Ramya, C. B.; Rajakumar, B. Experimental and computational investigations of the tropospheric photooxidation reactions of 1,1,1,3,3,3-hexafluoro-2-methyl-2-propanol initiated by OH radicals and Cl atoms. *J. Phys. Chem. A* **2021**, *125*, 523−535, doi:10.1021/acs.jpca.0c08130.
(2) Orkin, V. L.; Khamaganov, V. G.; Kurylo, M. J. High accuracy measurements of OH reaction rate constants and IR absorption spectra: Substituted 2-propanols. *J. Phys. Chem. A* **2012**, *116*, 6188-6198, doi:10.1021/jp211534n.

E83. OH + $(CF_3)_3COH$. The recommendation is based on results of the single available absolute study by Orkin et al.[1] (230–370 K). The reported data between 230 and 370 K exhibit a weak temperature dependence and pronounced curvature in the Arrhenius plot with a minimum near 272 K. The data can be described by a three-parameter expression that is derived from a fit to the data of Orkin et al.

$$k(230–370\ \text{K}) = 2.67 \times 10^{-20}\ (\text{T}/298)^{11.4}\ \exp(+3092/\text{T}).$$

The recommended values of k(298 K) and E/R were derived from the fit of the Arrhenius expression to the data obtained between 230 and 298 K, which results in 6% underestimated k(298 K) when compared with the measured value because of the curvature in the Arrhenius plot. Orkin et al. studied various purified samples of $(CF_3)_3COH$ to ensure that results were not affected by the presence of reactive impurities and estimated the total uncertainty of the reported results as 10%.
(Table: 25-1, Note: 25-1, Evaluated: 25-1) Back to Table

(1) Orkin, V. L.; Khamaganov, V. G.; Kurylo, M. J. High accuracy measurements of OH reaction rate constants and IR absorption spectra: Substituted 2-propanols. *J. Phys. Chem. A* **2012**, *116*, 6188-6198, doi:10.1021/jp211534n.

E84. OH + $CF_3CHFCF_2CH_2OH$. The recommended value of k(298 K) is an average of the values derived from the two relative rate studies of Chen et al.[1] (230– 430 K) (recalculated using the recommended rate constants for the reference reactions) and the two absolute rate studies of Chen et al. The recommended value for E/R is derived from a fit to all of the data (for T <~300 K) from both the relative rate and absolute rate determinations after scaling each data set to the recommended k(298 K).
(Table: 15-10, Note: 15-10, Evaluated: 15-10) Back to Table

(1) Chen, L.; Tokuhashi, K.; Kutsuna, S.; Sekiya, A.; Yonei, Y.; Yamamoto, A. Kinetic study of the gas-phase reaction of $CF_3CHFCF_2CH_2OH$ with OH radicals at 230–430 K. *Chem. Phys. Lett.* **2003**, *382*, 277-282, doi:10.1016/j.cplett.2003.09.162.

E85. OH + $CF_3CF_2CF_2CF_2CH_2OH$. The recommended value for k(298 K) is from the relative rate study of Hurley et al.[1] (296 K) (recalculated using the current recommendation for the rate constant of the OH + C_2H_2 reference reaction). The recommended value for E/R is estimated as being the same as that for the reaction of OH with $CF_3CF_2CH_2OH$.
(Table: 10-6, Note: 10-6, Evaluated: 10-6) Back to Table

(1) Hurley, M. D.; Wallington, T. J.; Sulbaek Andersen, M. P.; Ellis, D. A.; Martin, J. W.; Mabury, S. A. Atmospheric chemistry of fluorinated alcohols: Reaction with Cl atoms and OH radicals and atmospheric lifetimes. *J. Phys. Chem. A* **2004**, *108*, 1973, doi:10.1021/jp0373088.

E86. OH + CH_3OCHF_2 (HFE-152a). The recommended Arrhenius parameters are derived from a fit to the data of Orkin et al.[1] (298–460 K).
(Table: 15-10, Note: 15-10, Evaluated: 15-10) Back to Table

(1) Orkin, V. L.; Khamaganov, V. G.; Guschin, A. G. Photochemical properties of hydrofluoroethers CH_3OCHF_2, CH_3OCF_3, and $CHF_2OCH_2CF_3$: Reactivity toward OH, IR absorption cross sections, atmospheric lifetimes, and global warming potentials. *J. Phys. Chem. A* **2014**, *118*, 10770-10777, doi:10.1021/jp506377w.

E87. OH + CH_3OCF_3 (HFE-143a). The recommended value for k(298 K) is an average of the values derived in the studies of Orkin et al.[3] (298–460 K), Hsu and DeMore[2] (298– 381 K) (two relative rate determinations that have been recalculated based on the current recommendations for the rate constants of the OH + CH_3CHF_2 and CH_2F_2 reference reactions), and Chen et al.[1] (268–308 K) (two relative rate determinations that have been recalculated based on the current recommendations for the rate constants of the OH + CH_4 and CH_3CCl_3 reference reactions). The recalculation procedure for relative rate measurements referenced to the OH + CH_3CHF_2 reaction is discussed in the note for that reaction. The absolute room temperature result of Zhang et al.[4] (296 K) was not used in the derivation since it is significantly higher than the values of the other studies and was likely influenced by the presence of reactive impurities. The recommended value for E/R is derived from a fit to the data from Orkin et al., Hsu and DeMore, and Chen et al. (for T <400 K) after scaling each data set to the recommended k(298 K).
(Table: 10-6, Note: 15-10, Evaluated: 15-10) Back to Table

(1) Chen, L.; Kutsuna, S.; Nohara, K.; Takeuchi, K.; Ibusuki, T. Kinetics and mechanisms for the reactions of CF_3OCH_3 and $CF_3OC(O)H$ with OH radicals using an envirionmental reaction chamber. *J. Phys. Chem. A* **2001**, *105*, 10854-10859, doi:10.1021/jp010137r.
(2) Hsu, K. J.; DeMore, W. B. Temperature-dependent rate constants and substituent effects for the reactions of hydroxyl radicals with three partially fluorinated ethers. *J. Phys. Chem.* **1995**, *99*, 11141-11930, doi:10.1021/j100028a014.
(3) Orkin, V. L.; Khamaganov, V. G.; Guschin, A. G. Photochemical properties of hydrofluoroethers CH_3OCHF_2, CH_3OCF_3, and $CHF_2OCH_2CF_3$: Reactivity toward OH, IR absorption cross sections, atmospheric lifetimes, and global warming potentials. *J. Phys. Chem. A* **2014**, *118*, 10770-10777, doi:10.1021/jp506377w.
(4) Zhang, Z.; Saini, R. D.; Kurylo, M. J.; Huie, R. E. Rate constants for the reactions of the hydroxyl radical with several partially fluorinated ethers. *J. Phys. Chem.* **1992**, *96*, 9301-9304, doi:10.1021/j100202a045.

E88. OH + CHF_2OCHF_2 (HFE-134). The recommended value of k(298 K) is an average of the values derived in the relative rate studies of Hsu and DeMore[2] (298–368 K) (recalculated using the current recommendation for the rate constant of the OH + CH_3CCl_3 reference reaction) and Wilson et al.[4] (298–459 K) (recalculated using the current recommendation for the rate constant of the OH + CHF_2CF_3 reference reaction) and the absolute

study of Orkin et al.[3] (277–370 K). The recommended value for E/R is derived from a combined fit to the data from these three studies after scaling each data set to the recommended value of k(298 K). The more scattered data of Garland et al.[1] (269–312 K) were not used in derivation of the recommended value.
(Table: 15-10, Note: 15-10, Evaluated: 15-10) Back to Table

(1) Garland, N. L.; Medhurst, L. J.; Nelson, H. H. Potential chlorofluorocarbon replacements: OH reaction rate constants between 250 and 315 K and infrared absorption spectra. *J. Geophys. Res.* **1993**, *98*, 23107-23111, doi:10.1029/93JD02550.
(2) Hsu, K. J.; DeMore, W. B. Temperature-dependent rate constants and substituent effects for the reactions of hydroxyl radicals with three partially fluorinated ethers. *J. Phys. Chem.* **1995**, *99*, 11141-11930, doi:10.1021/j100028a014.
(3) Orkin, V. L.; Villenave, E.; Huie, R. E.; Kurylo, M. J. Atmospheric lifetimes and global warming potentials of hydrofluoroethers: Reactivity toward OH, UV spectra, and IR absorption cross sections. *J. Phys. Chem. A* **1999**, *103*, 9770-9779, doi:10.1021/jp991741t.
(4) Wilson, E. W., Jr.; Sawyer, A. A.; Sawyer, H. A. Rates of reaction for cyclopropane and difluoromethoxydifluoromethane with hydroxyl radicals. *J. Phys. Chem. A* **2001**, *105*, 1445-1448, doi:10.1021/jp002327s.

E89. OH + CHF_2OCF_3 (HFE-125). The recommended Arrhenius parameters are based on results of the relative rate study of Hsu and DeMore[1] (298–393 K) (recalculated using the current recommendation for the rate constant of the OH + CHF_3 reference reaction). Additional measurements by Hsu and DeMore relative to OH + CHF_2CF_3 and OH + CH_4 are encompassed well within the 2σ uncertainty limits, but were not used for assigning the recommended rate expression due to the large differences in reactivity between the two reference species and the target molecule. The room temperature result of Zhang et al.[2] (296 K) lies significantly higher than the recommended value, possibly due to the presence of reactive impurities in the sample.
(Table: 02-25, Note: 02-25, Evaluated: 02-25) Back to Table

(1) Hsu, K. J.; DeMore, W. B. Temperature-dependent rate constants and substituent effects for the reactions of hydroxyl radicals with three partially fluorinated ethers. *J. Phys. Chem.* **1995**, *99*, 11141-11930, doi:10.1021/j100028a014.
(2) Zhang, Z.; Saini, R. D.; Kurylo, M. J.; Huie, R. E. Rate constants for the reactions of the hydroxyl radical with several partially fluorinated ethers. *J. Phys. Chem.* **1992**, *96*, 9301-9304, doi:10.1021/j100202a045.

E90. OH + $CH_3OCHFCF_3$. The recommended value for k(298 K) is an average of values derived from two relative rate determinations by Chen et al.[1] (253–328 K) (recalculated using the current recommendations for the rate constants of the reference reactions OH + C_2H_6 and CH_3CHF_2). The recommended E/R is derived from a fit to these data after scaling each individual data set to the recommended k(298 K).
(Table: 10-6, Note: 10-6, Evaluated: 10-6) Back to Table

(1) Chen, L.; Kutsuna, S.; Tokuhashi, K.; Sekiya, A. Kinetics and mechanisms of $CF_3CHFOCH_3$, $CF_3CHFOC(O)H$, and $FC(O)OCH_3$ reactions with OH radicals. *J. Phys. Chem. A* **2006**, *110*, 12845-12851, doi:10.1021/jp064917h.

E91. OH + $CH_2FOCH(CF_3)_2$ (Sevoflurane). The recommended value for k(298 K) is an average of the values from the two studies (one relative rate and one absolute) by Sulbaek Andersen et al.[3] (243–298 K). The room temperature rate constants determined by Brown et al.[1] (299, 422 K) are approximately a factor of two higher than recommended here and may be indicative of impurity effects. The room temperature rate constant determined by Langbein et al.[2] (298 K) is approximately 30% lower than recommended and is encompassed within the 95% confidence limits. The recommended value for E/R is derived from an Arrhenius fit to the data from the absolute rate constant measurements of Sulbaek Andersen et al.[3]
(Table: 15-10, Note: 15-10, Evaluated: 15-10) Back to Table

(1) Brown, A. C.; Canosa-Mas, C. E.; Parr, A. D.; Wayne, R. P. Laboratory studies of some halogenated ethanes and ethers: Measurements of rates of reaction with OH and of infrared absorption cross-sections. *Atmos. Environ.* **1990**, *24A*, 2499-2511, doi:10.1016/0960-1686(90)90341-J.
(2) Langbein, T.; Sonntag, H.; Trapp, D.; Hoffmann, A.; Malms, W.; Röth, E.-P.; Mörs, V.; Zellner, R. Volatile anaesthetics and the atmosphere: atmospheric lifetimes and atmospheric effects of halothane, enflurane, isoflurane, desflurane and sevoflurane. *British J. Anaest.* **1999**, *82*, 66-73.
(3) Sulbaek Andersen, M. P.; Nielsen, O. J.; Karpichev, B.; Wallington, T. J.; Sander, S. P. Atmospheric chemistry of isoflurane, desflurane, and sevoflurane: Kinetics and mechanisms of reactions with

chlorine atoms and OH radicals and global warming potentials. *J. Phys. Chem. A* **2012**, *116*, 5806-5820, doi:10.1021/jp2077598.

E92. OH + $CH_3OCF_2CHF_2$. The recommended value for k(298 K) is an average of the values from the two absolute determinations by Tokuhashi et al.[3] (250–430 K) using pulsed photolysis and discharge flow techniques. The recommended value for E/R is derived from a fit to the pulsed photolysis data below 400 K. Results from a relative rate study by Kjaergaard et al.[2] (296 K) are in very good agreement with the recommendation (recalculated using the current recommendations for the rate constants of the OH + $CHCl_2F$ and CH_3F reference reactions). An absolute room temperature measurement by Heathfield et al.[1] (298 K) is nearly an order of magnitude higher than recommended, which may be due to reactive impurities.
(Table: 25-1, Note: 25-1, Evaluated: 25-1) Back to Table

(1) Heathfield, A. E.; Anastasi, C.; Pagsberg, P.; McCulloch, A. Atmospheric lifetimes of selected fluorinated ether compounds. *Atmos. Environ.* **1998**, *32*, 711-717, doi:10.1016/S1352-2310(97)00330-0.

(2) Kjærgaard, E. R.; Vogt, E.; Møller, K. H.; Nielsen, O. J.; Kjaergaard, H. G. Atmospheric Chemistry of $CH_3OCF_2CHF_2$. *J. Phys. Chem. A* **2021**, *125*, 10640−10648, doi:10.1021/acs.jpca.1c08973.

(3) Tokuhashi, K.; Takahashi, A.; Kaise, M.; Kondo, S.; Sekiya, A.; Yamashita, S.; Ito, H. Rate constants for the reactions of OH radicals with $CH_3OCF_2CHF_2$, $CHF_2OCH_2CF_2CHF_2$, $CHF_2OCH_2CF_2CF_3$, and $CF_3CH_2OCF_2CHF_2$ over the temperature range 250-430 K. *J. Phys. Chem. A* **2000**, *104*, 1165-1170, doi:10.1021/jp991421+.

E93. OH + $CH_3OCF_2CF_3$. The recommended Arrhenius parameters are derived from a fit to the data (below 400 K) of Tokuhashi et al.[1] (250–430 K) (three independent absolute measurement studies). The expression, as expected, is similar to those for the OH + CH_3OCF_3 and OH + $CH_3OCF_2CF_2CF_3$ reactions.
(Table: 02-25, Note: 02-25, Evaluated: 02-25) Back to Table

(1) Tokuhashi, K.; Takahashi, A.; Kaise, M.; Kondo, S.; Sekiya, A.; Yamashita, S.; Ito, H. Rate Constants for the Reactions of OH Radicals with $CH_3OCF_2CF_3$, $CH_3OCF_2CF_2CF_3$, and $CH_3OCF(CF_3)_2$. *Int. J. Chem. Kinet.* **1999**, *31*, 846-853, doi:10.1002/(SICI)1097-4601(1999)31:12<846::AID-KIN2>3.0.CO;2-4.

E94. OH + $CHF_2OCH_2CF_3$ (HFE-245fa2). The recommended value of k(298 K) is an average of the values reported in the absolute studies of Zhang et al.[3] (296 K) and Orkin et al.[1] (298–460 K) and in the relative rate study of Oyaro et al.[2] (298 K) (recalculated using the current recommendations for the rate constants of the OH + CH_3CCl_3 and CHF_2CH_2F reference reactions). The recommended value of E/R is derived from a fit to the data of Orkin et al.[1]
(Table: 10-6, Note: 15-10, Evaluated: 15-10) Back to Table

(1) Orkin, V. L.; Khamaganov, V. G.; Guschin, A. G. Photochemical properties of hydrofluoroethers CH_3OCHF_2, CH_3OCF_3, and $CHF_2OCH_2CF_3$: Reactivity toward OH, IR absorption cross sections, atmospheric lifetimes, and global warming potentials. *J. Phys. Chem. A* **2014**, *118*, 10770-10777, doi:10.1021/jp506377w.

(2) Oyaro, N.; Sellevag, S. R.; Nielsen, C. J. Atmospheric chemistry of hydrofluoroethers: Reaction of a series of hydrofluoroethers with OH radicals and Cl atoms, atmospheric lifetimes, and global warming potentials. *J. Phys. Chem. A* **2005**, *109*, 337-346, doi:10.1021/jp047860c.

(3) Zhang, Z.; Saini, R. D.; Kurylo, M. J.; Huie, R. E. Rate constants for the reactions of the hydroxyl radical with several partially fluorinated ethers. *J. Phys. Chem.* **1992**, *96*, 9301-9304, doi:10.1021/j100202a045.

E95. OH + $CHF_2OCHFCF_3$ (Desflurane). The recommended value for k(298 K) is an average of the values obtained in the absolute rate studies of Langbein et al.[1] (298 K) and Sulbaek Andersen et al.[3] (239–296 K). The values of the room temperature rate constant determined in the two relative rate studies of Oyaro et al.[2] (298 K) (relative to the reactions of OH with CH_3CCl_3 and CHF_2CH_2F) are approximately 50% greater than the recommended value. The recommendation for E/R is derived from a fit to the data of Sulbaek Andersen et al., which is the only study of the temperature dependence of this reaction.
(Table: 15-10, Note: 15-10, Evaluated: 15-10) Back to Table

(1) Langbein, T.; Sonntag, H.; Trapp, D.; Hoffmann, A.; Malms, W.; Röth, E.-P.; Mörs, V.; Zellner, R. Volatile anaesthetics and the atmosphere: atmospheric lifetimes and atmospheric effects of halothane, enflurane, isoflurane, desflurane and sevoflurane. *British J. Anaest.* **1999**, *82*, 66-73.

(2) Oyaro, N.; Sellevag, S. R.; Nielsen, C. J. Atmospheric chemistry of hydrofluoroethers: Reaction of a series of hydrofluoroethers with OH radicals and Cl atoms, atmospheric lifetimes, and global warming potentials. *J. Phys. Chem. A* **2005**, *109*, 337-346, doi:10.1021/jp047860c.
(3) Sulbaek Andersen, M. P.; Nielsen, O. J.; Karpichev, B.; Wallington, T. J.; Sander, S. P. Atmospheric chemistry of isoflurane, desflurane, and sevoflurane: Kinetics and mechanisms of reactions with chlorine atoms and OH radicals and global warming potentials. *J. Phys. Chem. A* **2012**, *116*, 5806-5820, doi:10.1021/jp2077598.

E96. OH + $CHF_2OCF_2CHF_2$. The recommended value for k(298 K) is an average of the relative rate determinations of Chen et al.[1] (253–328 K) (two studies that were recalculated using the current recommendations for the reference reactions of OH with $CH_3OCF_2CF_3$ and $CH_3OCF_2CF_2CF_3$) and Wilson et al.[2] (266–406 K) (two studies that were recalculated using the current recommendations for the reference reactions of OH with HFC-134a and HFC-143a). The recommended value for E/R is from a combined fit to the data of Chen et al. and Wilson et al. after each data set was scaled to the recommended value of k(298 K).
(Table: 10-6, Note: 10-6, Evaluated: 10-6) Back to Table

(1) Chen, L.; Kutsuna, S.; Tokuhashi, K.; Sekiya, A. Kinetics study of the gas-phase reactions of $CHF_2CF_2OCHF_2$ and $CF_3CHFCF_2OCH_2CF_2CF_3$ with OH radicals at 253-328 K. *Chem. Phys. Lett.* **2005**, *403*, 180-184, doi:10.1016/j.cplett.2005.01.002.
(2) Wilson, E. W., Jr.; Hamilton, W. A.; Mount, H. R.; DeMore, W. B. Rate constants for the reactions of hydroxyl radical with several fluoroethers by the relative rate method. *J. Phys. Chem. A* **2007**, *111*, 1610-1617, doi:10.1021/jp068355d.

E97. OH + $CF_3OCHFCF_3$. The recommended value for k(298 K) is an average of the values reported in the relative rate studies of Takahashi et al.[3] (296 K) (two studies that were recalculated using the current rate constant recommendations for the OH + C_2H_4 and C_2H_2 reference reactions) and Oyaro et al.[2] (298 K) (recalculated using the current recommended rate constant for the OH + HFC-143 reference reaction) and in the two absolute rate constant determinations of Tokuhashi et al.[4] (250–430 K). The k(298 K) value reported by Li et al.[1] (298 K) is approximately a factor of 5 greater than that recommended. The recommended value of E/R comes from a fit to the data of Tokuhashi et al. below 400 K.
(Table: 15-10, Note: 15-10, Evaluated: 15-10) Back to Table

(1) Li, Z.; Jeong, G.-R.; Hansen, J. C.; Good, D. A.; Francisco, J. S. Rate constant for the reactions of $CF_3OCHFCF_3$ with OH and Cl. *Chem. Phys. Lett.* **2000**, *320*, 70–76, doi:10.1016/S0009-2614(00)00192-5.
(2) Oyaro, N.; Sellevag, S. R.; Nielsen, C. J. Atmospheric chemistry of hydrofluoroethers: Reaction of a series of hydrofluoroethers with OH radicals and Cl atoms, atmospheric lifetimes, and global warming potentials. *J. Phys. Chem. A* **2005**, *109*, 337-346, doi:10.1021/jp047860c.
(3) Takahashi, K.; Matsumi, Y.; Wallington, T. J.; Hurley, M. D. Atmospheric chemistry of $CF_3CFHOCF_3$: Reaction with OH radicals, atmospheric lifetime, and global warming potential. *J. Geophys. Res.* **2002**, *107*, 4574, doi:10.1029/2002JD002125.
(4) Tokuhashi, K.; Chen, L.; Kutsuna, S.; Uchimaru, T.; Sugie, M.; Sekiya, A. Environmental assessment of CFC alternatives - Rate constants for the reactions of OH radicals with fluorinated compounds. *J. Fluor. Chem.* **2004**, *125*, 1801-1807, doi:10.1016/j.jfluchem.2004.09.013.

E98. OH + $CHF_2CF_2OCF_3$. The recommended value for k(298 K) is an average of the relative rate determinations of Sulbaek Andersen et al.[1] (296 K) (two studies that were recalculated using the current recommendations for the reference reactions of OH with C_2H_2 and C_2H_4) and those derived from Wilson et al.[2] (273–397 K) (two studies that were recalculated using the current recommendations for the reference reactions of OH with CHF_2CF_3 and CF_3CHFCF_3). The recommended value for E/R is from a combined fit to the data of Wilson et al. after each data set was scaled to the recommended value of k(298 K).
(Table: 25-1, Note: 25-1, Evaluated: 25-1) Back to Table

(1) Sulbaek Andersen, M. P.; Nielsen, O. J.; Wallington, T. J.; Hurley, M. D.; DeMore, W. B. Atmospheric chemistry of $CF_3OCF_2CF_2H$ and $CF_3OC(CF_3)_2H$: Reaction with Cl atoms and OH radicals, degradation mechanism, global warming potentials, and empirical relationship between k(OH) and k(Cl) for organic compounds. *J. Phys. Chem. A* **2005**, *109*, 3926-3934, doi:10.1021/jp044635m.
(2) Wilson, E. W., Jr.; Hamilton, W. A.; Mount, H. R.; DeMore, W. B. Rate constants for the reactions of hydroxyl radical with several fluoroethers by the relative rate method. *J. Phys. Chem. A* **2007**, *111*, 1610-1617, doi:10.1021/jp068355d.

E99. OH + $CH_3OCF_2CF_2CF_3$. The recommended value for k(298 K) is an average of the values reported by Tokuhashi et al.[2] (250–430 K) (two absolute measurement studies) and Ninomiya et al.[1] (295 K) (two relative rate determinations, which have been recalculated based on the current recommendations for the rate constants of the OH + CH_4 and CH_3Cl reference reactions). The recommended value for E/R is determined from a fit to the data (below 400 K) of Tokuhashi et al. The expression, as expected, is similar to those for the OH + CH_3OCF_3 and OH + $CH_3OCF_2CF_3$ reactions.

(Table: 02-25, Note: 02-25, Evaluated: 02-25) Back to Table

(1) Ninomiya, Y.; Kawasaki, M.; Guschin, A.; Molina, L. T.; Molina, M. J.; Wallington, T. J. Atmospheric chemistry of n-$C_3F_7OCH_3$: Reaction with OH radicals and Cl atoms and atmospheric fate of n-$C_3F_7OCH_2O(\bullet)$ radicals. *Environ. Sci. Technol.* **2000**, *34*, 2973-2978, doi:10.1021/es991449z.

(2) Tokuhashi, K.; Takahashi, A.; Kaise, M.; Kondo, S.; Sekiya, A.; Yamashita, S.; Ito, H. Rate Constants for the Reactions of OH Radicals with $CH_3OCF_2CF_3$, $CH_3OCF_2CF_2CF_3$, and $CH_3OCF(CF_3)_2$. *Int. J. Chem. Kinet.* **1999**, *31*, 846-853, doi:10.1002/(SICI)1097-4601(1999)31:12<846::AID-KIN2>3.0.CO;2-4.

E100. OH + $CH_3OCH(CF_3)_2$ (HFE-356mm1). The recommendations are based on the relative rate data of Chen et al.[1] (253–328 K) (recalculated using the recommended values for the rate constants of the reference reactions) and the rate constants measured by Orkin et al.[2] (230–370 K) using an absolute technique. The recommended value for k(298 K) is an average of values from these three studies, which are in excellent agreement.

The data of Orkin et al. over the entire temperature range of measurements exhibit a noticeable curvature in the Arrhenius plot. The recommended E/R is an average of the values derived from the two data sets of Chen et al. and the value derived from a fit to the data of Orkin et al. below 298 K. The data over the broader temperature range from 230 to 370 K can be represented by a three-parameter expression obtained from a fit to the Orkin et al. data after scaling to the recommended k(298 K):

$$k(230\text{–}370\ \text{K}) = 7.46 \times 10^{-14}\ (T/298)^{2.99}\ \exp(+342/T)$$

(Table: 19-5, Note: 19-5, Evaluated: 19-5) Back to Table

(1) Chen, L.; Kutsuna, S.; Tokuhashi, K.; Sekiya, A.; Tamai, R.; Hibino, Y. Kinetics and mechanism of $(CF_3)_2CHOCH_3$ reaction with OH radicals in an environmental reaction chamber. *J. Phys. Chem. A* **2005**, *109*, 4766-4771, doi:10.1021/jp050491f.

(2) Orkin, V. L.; Martynova, L. E.; Kurylo, M. J. Photochemical properties of CH_2=CH-CFCl-CF_2Br (4-bromo-3-chloro-3,4,4-trifluoro-1-butene) and CH_3-O-$CH(CF_3)_2$ (methyl hexafluoroisopropyl ether): OH reaction rate constants and UV and IR absorption spectra. *J. Phys. Chem. A* **2017**, *121*, 5675–5680, doi:10.1021/acs.jpca.7b04256.

E101. OH + $CH_3OCF(CF_3)_2$. The recommendation for k(298 K) is an average of the values from the absolute measurements of Tokuhashi et al.[2] (250–430 K) (three determinations) and Andersen et al.[1] (296 K). The recommended value for E/R is derived from a fit to the temperature-dependent data of Tokuhashi et al. below 400 K. The uncertainties, which were originally set to encompass the recommendations for the similar OH + CH_3OCF_3 and OH + $CH_3OCF_2CF_3$ reactions have been reduced slightly to account for the additional data point at 298 K.

(Table: 15-10, Note: 15-10, Evaluated: 15-10) Back to Table

(1) Andersen, L. L.; Østerstrøm, F. F.; Nielsen, O. J.; Sulbaek Andersen, M. P.; Wallington, T. J. Atmospheric chemistry of $(CF_3)_2CFOCH_3$. *Chem. Phys. Lett.* **2014**, *607*, 5-9, doi:10.1016/j.cplett.2014.05.036.

(2) Tokuhashi, K.; Takahashi, A.; Kaise, M.; Kondo, S.; Sekiya, A.; Yamashita, S.; Ito, H. Rate Constants for the Reactions of OH Radicals with $CH_3OCF_2CF_3$, $CH_3OCF_2CF_2CF_3$, and $CH_3OCF(CF_3)_2$. *Int. J. Chem. Kinet.* **1999**, *31*, 846-853, doi:10.1002/(SICI)1097-4601(1999)31:12<846::AID-KIN2>3.0.CO;2-4.

E102. OH + $CH_3OC_4F_9$. The recommended values for both k(298 K) and E/R were derived from the relative rate data reported by Chen et al.[3] (253–328 K), who studied both isomers, n-$CH_3OC_4F_9$ and iso-$CH_3OC_4F_9$, using two reference reactions. The results obtained with different reference compounds agree to within 5% and no difference in the reactivity of the isomers was observed. The recommended k(298 K) and E/R are the average of values derived from all four measurements. Results of relative rate measurements reported by Wallington et al.[5] (295 K) (recalculated using the current recommendation for the rate constant of the OH + CH_3Cl reference reaction) are in good agreement with the recommendation. Measurements in the same study using OH + CH_4 as the reference reaction exhibit considerably more scatter. These latter authors also reported no difference in

the reactivity of the isomers. A relative rate study by Cavalli et al.[2] (298 K) yielded a rate constant about 60% lower than recommended and the results of a relative rate study by Oyaro and Nielsen[4] (298 K) are 35% higher. The temperature dependent data reported by Bravo et al.[1] (288–368 K), are more than 60% higher and yield steeper temperature dependence.
(Table: 19-5, Note: 19-5, Evaluated: 19-5) Back to Table

(1) Bravo, I.; Díaz-de-Mera, Y.; Aranda, A.; Smith, K.; Shine, K. P.; Marston, G. Atmospheric chemistry of $C_4F_9OC_2H_5$ (HFE-7200), $C_4F_9OCH_3$ (HFE-7100), $C_3F_7OCH_3$ (HFE-7000) and $C_3F_7CH_2OH$: temperature dependence of the kinetics of their reactions with OH radicals, atmospheric lifetimes and global warming potentials. *Phys. Chem. Chem. Phys.* **2010**, *12*, 5115–5125, doi:10.1039/b923092k.

(2) Cavalli, F.; Glasius, M.; Hjorth, J.; Rindone, B.; Jensen, N. R. Atmospheric lifetimes, infrared spectra and degradation products of a series of hydrofluoroethers. *Atmos. Environ.* **1998**, *32*, 3767-3773, doi:10.1016/S1352-2310(98)00106-X.

(3) Chen, L.; Uchimaru, T.; Kutsuna, S.; Tokuhashi, K.; Sekiya, A. Kinetics and mechanism of gas-phase reactions of *n*-$C_4F_9OCH_3$, *i*-$C_4F_9OCH_3$, *n*-$C_4F_9OC(O)H$, and *i*-$C_4F_9OC(O)H$ with OH radicals in an environmental reaction chamber at 253-328 K. *Chem. Phys. Lett.* **2011**, *514*, 207–213, doi:10.1016/j.cplett.2011.08.049.

(4) Oyaro, N.; Nielsen, C. J. Kinetic study of the OH reaction with the hydrofluoroethers C_4F_9-O-CH_3 and C_4F_9-O-C_2H_5 by the relative rate method. *Asian Chem. Lett.* **2003**, *7*, 119–122.

(5) Wallington, T. J.; Schneider, W. F.; Sehested, J.; Bilde, M.; Platz, J.; Nielsen, O. J.; Christensen, L. K.; Molina, M. J.; Molina, L. T.; Wooldridge, P. W. Atmospheric chemistry of HFE-7100 ($C_4F_9OCH_3$): reaction with OH radicals, UV spectra and kinetic data for $C_4F_9OCH_2$• and $C_4F_9OCH_2O_2$• radicals, and the atmospheric fate of $C_4F_9OCH_2O$• radicals. *J. Phys. Chem. A* **1997**, *101*, 8264-8274, doi:10.1021/jp971353w.

E103. OH + $CHF_2OCH_2CF_2CHF_2$. The recommended value for k(298 K) is an average of the values from the two absolute determinations by Tokuhashi et al.[1] (250–430 K) using pulsed photolysis and discharge flow techniques. The recommended value for E/R is derived from a fit to the pulsed photolysis data.
(Table: 15-10, Note: 15-10, Evaluated: 15-10) Back to Table

(1) Tokuhashi, K.; Takahashi, A.; Kaise, M.; Kondo, S.; Sekiya, A.; Yamashita, S.; Ito, H. Rate constants for the reactions of OH radicals with $CH_3OCF_2CHF_2$, $CHF_2OCH_2CF_2CHF_2$, $CHF_2OCH_2CF_2CF_3$, and $CF_3CH_2OCF_2CHF_2$ over the temperature range 250-430 K. *J. Phys. Chem. A* **2000**, *104*, 1165-1170, doi:10.1021/jp991421+.

E104. OH + $CHF_2OCH_2CF_2CF_3$. The recommended value for k(298 K) is an average of the values from the two absolute determinations by Tokuhashi et al.[1] (250–430 K) using pulsed photolysis and discharge flow techniques. The recommended value for E/R is derived from a fit to the pulsed photolysis data below 400 K.
(Table: 02-25, Note: 15-10, Evaluated: 02-25) Back to Table

(1) Tokuhashi, K.; Takahashi, A.; Kaise, M.; Kondo, S.; Sekiya, A.; Yamashita, S.; Ito, H. Rate constants for the reactions of OH radicals with $CH_3OCF_2CHF_2$, $CHF_2OCH_2CF_2CHF_2$, $CHF_2OCH_2CF_2CF_3$, and $CF_3CH_2OCF_2CHF_2$ over the temperature range 250-430 K. *J. Phys. Chem. A* **2000**, *104*, 1165-1170, doi:10.1021/jp991421+.

E105. OH + $CHF_2OCH(CF_3)_2$. The recommended value for k(298 K) is an average of the values from the two relative rate determinations by Wilson et al.[1] (312–369 K), recalculated using the current rate constant recommendations for the OH + HFC-134a and OH + HFC-143a reference reactions. The recommended value for E/R is derived from a combined fit to the data after scaling each data set to the recommended value for k(298 K).
(Table: 10-6, Note: 15-10, Evaluated: 15-10) Back to Table

(1) Wilson, E. W., Jr.; Hamilton, W. A.; Mount, H. R.; DeMore, W. B. Rate constants for the reactions of hydroxyl radical with several fluoroethers by the relative rate method. *J. Phys. Chem. A* **2007**, *111*, 1610-1617, doi:10.1021/jp068355d.

E106. OH + $CF_3OCH(CF_3)_2$. The recommended value for k(298 K) is the result of the relative rate study of Sulbaek Andersen et al.[1] (296 K) (recalculated using the current recommendation for the reference reaction of OH with C_2H_2). The value for E/R is estimated to be the same as that for OH + CHF_2OCF_3 and the uncertainty was chosen to encompass the recommended rate constants for this similar reaction.
(Table: 25-1, Note: 25-1, Evaluated: 25-1) Back to Table

(1) Sulbaek Andersen, M. P.; Nielsen, O. J.; Wallington, T. J.; Hurley, M. D.; DeMore, W. B. Atmospheric chemistry of $CF_3OCF_2CF_2H$ and $CF_3OC(CF_3)_2H$: Reaction with Cl atoms and OH radicals, degradation mechanism, global warming potentials, and empirical relationship between k(OH) and k(Cl) for organic compounds. *J. Phys. Chem. A* **2005**, *109*, 3926-3934, doi:10.1021/jp044635m.

E107. OH + $CH_3CH_2OCF_2CHF_2$. The recommended parameters are from a combined fit to the data obtained by Tokuhashi et al.[2] (250–430 K) (three absolute determinations) below 400 K. A room temperature rate constant determined by Heathield et al.[1] (298 K) is about a factor of two greater than that recommended.
(Table: 10-6, Note: 10-6, Evaluated: 10-6) Back to Table

(1) Heathfield, A. E.; Anastasi, C.; Pagsberg, P.; McCulloch, A. Atmospheric lifetimes of selected fluorinated ether compounds. *Atmos. Environ.* **1998**, *32*, 711-717, doi:10.1016/S1352-2310(97)00330-0.
(2) Tokuhashi, K.; Takahashi, A.; Kaise, M.; Kondo, S. Rate constants for the reactions of OH radicals with CH_3OCF_2CHFCl, CHF_2OCF_2CHFCl, $CHF_2OCHClCF_3$, and $CH_3CH_2OCF_2CHF_2$. *J. Geophys. Res.* **1999**, *104*, 18681-18688, doi:10.1029/1999JD900278.

E108. OH + $CF_3CH_2OCH_2CF_3$. The recommended value for k(298 K) is an average of the rate constants measured in the absolute study of Orkin et al.[1] (277–370 K) and in the relative rate studies of Oyaro et al.[2] (298 K) and Wilson et al.[3] (268–409 K) (two determinations). The relative rate data were recalculated using the current rate constant recommendations for the OH reactions with the reference compounds ($CHCl_3$ for Oyaro et al. and HFC-152a and HFC-161 for Wilson et al.). The recommended value for E/R is an average of the values for this parameter derived from fits to the Orkin at al. and Wilson et al. data.
(Table: 10-6, Note: 10-6, Evaluated: 10-6) Back to Table

(1) Orkin, V. L.; Villenave, E.; Huie, R. E.; Kurylo, M. J. Atmospheric lifetimes and global warming potentials of hydrofluoroethers: Reactivity toward OH, UV spectra, and IR absorption cross sections. *J. Phys. Chem. A* **1999**, *103*, 9770-9779, doi:10.1021/jp991741t.
(2) Oyaro, N.; Sellevag, S. R.; Nielsen, C. J. Study of the OH and Cl-initiated oxidation, IR absorption cross-section, radiative forcing, and global warming potential of four C_4-hydrofluoroethers. *Environ. Sci. Technol.* **2004**, *38*, 5567-5576, doi:10.1021/es0497330.
(3) Wilson, E. W., Jr.; Hamilton, W. A.; Mount, H. R.; DeMore, W. B. Rate constants for the reactions of hydroxyl radical with several fluoroethers by the relative rate method. *J. Phys. Chem. A* **2007**, *111*, 1610-1617, doi:10.1021/jp068355d.

E109. OH + $CF_3CH_2OCF_2CHF_2$ (HFE-347pcf2). The recommended value for k(298 K) is an average of the rate constants measured in the absolute study of Tokuhashi et al.[3] (250–430 K) (three studies) and in the relative rate experiments of Chen et al.[1] (268–308 K) (two studies relative to OH + CH_3CCl_3 and OH + CHF_2Cl) and of Wilson et al.[4] (270– 407 K) (two studies relative to OH + HFC-152a and OH + HFC-32). All results of the relative rate studies were recalculated using the current recommendations for the reference reactions. The recommended value of E/R is from a combined fit to the data from all three groups after scaling each data set to the recommended k(298 K). The room temperature rate constant reported by Heathield et al.[2] (298 K) is about an order or magnitude greater than that from any of the other investigation and was not used to derive the recommendations given here.
(Table: 10-6, Note: 10-6, Evaluated: 19-5) Back to Table

(1) Chen, L.; Kutsuna, S.; Tokuhashi, K.; Sekiya, A.; Takeuchi, K.; Ibusuki, T. Kinetics for the gas-phase reactions of OH radicals with the hydrofluoroethers $CH_2FCF_2OCHF_2$, $CHF_2CF_2OCH_2CF_3$, $CF_3CHFCF_2OCH_2CF_3$, and $CF_3CHFCF_2OCH_2CF_2CHF_2$ at 268-308 K. *Int. J. Chem. Kinet.* **2003**, *35*, 239-245, doi:10.1002/kin.10124.
(2) Heathfield, A. E.; Anastasi, C.; Pagsberg, P.; McCulloch, A. Atmospheric lifetimes of selected fluorinated ether compounds. *Atmos. Environ.* **1998**, *32*, 711-717, doi:10.1016/S1352-2310(97)00330-0.
(3) Tokuhashi, K.; Takahashi, A.; Kaise, M.; Kondo, S.; Sekiya, A.; Yamashita, S.; Ito, H. Rate constants for the reactions of OH radicals with $CH_3OCF_2CHF_2$, $CHF_2OCH_2CF_2CHF_2$, $CHF_2OCH_2CF_2CF_3$, and $CF_3CH_2OCF_2CHF_2$ over the temperature range 250-430 K. *J. Phys. Chem. A* **2000**, *104*, 1165-1170, doi:10.1021/jp991421+.
(4) Wilson, E. W., Jr.; Hamilton, W. A.; Mount, H. R.; DeMore, W. B. Rate constants for the reactions of hydroxyl radical with several fluoroethers by the relative rate method. *J. Phys. Chem. A* **2007**, *111*, 1610-1617, doi:10.1021/jp068355d.

E110. OH + $CF_3CHFCF_2OCF_3$. The recommended value for k(298 K) is an average of two values derived from results of the relative rate study by Wilson et al.[1] (284–406 K) (two determinations that were recalculated using the current recommendations for the reference reactions of OH with CHF_2CF_3 and CF_3CHFCF_3). The recommended value for E/R is from a combined fit to the data of Wilson et al. after each data set was scaled to the recommended value of k(298 K).
(Table: 25-1, Note: 25-1, Evaluated: 25-1) Back to Table

(1) Wilson, E. W., Jr.; Hamilton, W. A.; Mount, H. R.; DeMore, W. B. Rate constants for the reactions of hydroxyl radical with several fluoroethers by the relative rate method. *J. Phys. Chem. A* **2007**, *111*, 1610-1617, doi:10.1021/jp068355d.

E111. OH + $CF_3CH_2OCF_2CHFCF_3$. The recommended value for k(298 K) is an average of two values derived from results of the relative rate study by Wilson et al.,[1] (270–404 K) which are in excellent agreement. (Two determinations were recalculated using the current recommendations for the reference reactions of OH with CH_2FCF_3 and CF_3CHFCF_3). The recommended value for E/R is from a combined fit to the data of Wilson et al. after each data set was scaled to the recommended value of k(298 K).
(Table: 25-1, Note: 25-1, Evaluated: 25-1) Back to Table

(1) Wilson, E. W., Jr.; Hamilton, W. A.; Mount, H. R.; DeMore, W. B. Rate constants for the reactions of hydroxyl radical with several fluoroethers by the relative rate method. *J. Phys. Chem. A* **2007**, *111*, 1610-1617, doi:10.1021/jp068355d.

E112. OH + $CHF_2CF_2OCHFCF_3$. The recommended value for k(298 K) was derived from results of the relative rate study by Wilson et al.[1] (270–407 K) (two determinations that were recalculated using the current recommendations for the reference reactions of OH with CH_2F_2 and CHF_2CF_3 yield the same value of k(298 K)). The recommended value for E/R is from a combined fit to the data of Wilson et al. Also, results of two other single temperature relative measurements by Wilson et al. at 347 K (relative OH + CH_2FCH_2F) and at 398 K (relative OH + CH_3CH_2F) are in good agreement with the recommended Arrhenius dependence.
(Table: 25-1, Note: 25-1, Evaluated: 25-1) Back to Table

(1) Wilson, E. W., Jr.; Hamilton, W. A.; Mount, H. R.; DeMore, W. B. Rate constants for the reactions of hydroxyl radical with several fluoroethers by the relative rate method. *J. Phys. Chem. A* **2007**, *111*, 1610-1617, doi:10.1021/jp068355d.

E113. OH + $CF_3CHFCF_2OCH_2CF_2F_3$. The recommended value for both k(298 K) and E/R were derived from a combined fit to the data from the relative rate determinations by Chen et al.[1] (253–328 K), recalculated using the current recommendation for the rate constant of the OH reference reactions with $CH_3OC_2F_5$ and $CH_3OC_3F_7$.
(Table: 25-1, Note: 19-5, Evaluated: 19-5) Back to Table

(1) Chen, L.; Kutsuna, S.; Tokuhashi, K.; Sekiya, A. Kinetics study of the gas-phase reactions of $CHF_2CF_2OCHF_2$ and $CF_3CHFCF_2OCH_2CF_2CF_3$ with OH radicals at 253-328 K. *Chem. Phys. Lett.* **2005**, *403*, 180-184, doi:10.1016/j.cplett.2005.01.002.

E114. OH + $CHF_2OCF_2OCHF_2$. The recommended value for k(298 K) is from the relative rate study by Cavalli et al.[1] (295 K), recalculated using the current recommendation for the rate constant of the reference reaction OH + CH_4. The value for k(298 K) is identical to that for OH + CHF_2OCHF_2, which might be expected to have a slightly higher rate constant. The value for E/R is estimated as being similar to that for the reaction of OH with CHF_2OCHF_2.
(Table: 10-6, Note: 10-6, Evaluated: 10-6) Back to Table

(1) Cavalli, F.; Glasius, M.; Hjorth, J.; Rindone, B.; Jensen, N. R. Atmospheric lifetimes, infrared spectra and degradation products of a series of hydrofluoroethers. *Atmos. Environ.* **1998**, *32*, 3767-3773, doi:10.1016/S1352-2310(98)00106-X.

E115. OH + $CHF_2OCF_2CF_2OCHF_2$. The recommended value for k(298 K) is from the relative rate study by Cavalli et al.[1] (295 K), recalculated using the current recommendation for the rate constant of the reference reaction OH + CH_4. However, the value for k(298 K) is a factor of two greater than that measured in the same study for OH + $CHF_2OCF_2OCHF_2$, which might be expected to have a similar rate constant. Hence, the recommended value for f(298 K) was chosen to encompass the rate constant recommended for the reaction of OH with $CHF_2OCF_2OCHF_2$. As with OH + $CHF_2OCF_2OCHF_2$, the value for E/R is estimated as being similar to that for the reaction of OH + CHF_2OCHF_2.
(Table: 10-6, Note: 10-6, Evaluated: 10-6) Back to Table

(1) Cavalli, F.; Glasius, M.; Hjorth, J.; Rindone, B.; Jensen, N. R. Atmospheric lifetimes, infrared spectra and degradation products of a series of hydrofluoroethers. *Atmos. Environ.* **1998**, *32*, 3767-3773, doi:10.1016/S1352-2310(98)00106-X.

E116. OH + $CHF_2OCF_2CF_2OCF_2OCHF_2$. The recommended value for k(298 K) is from the relative rate study by Cavalli et al.[1] (295 K), recalculated using the current recommendation for the rate constant of the reference reaction OH + CH_4. The value for k(298 K) is almost the same as that measured for OH + $CHF_2OCF_2CF_2OCHF_2$ in the same study. For both compounds, the measured values for k(298 K) are inexplicably a factor of two greater than that measured in the same study for OH + $CHF_2OCF_2OCHF_2$, which might be expected to have the same or even slightly higher rate constant. Hence, the recommended value for f(298 K) was selected accordingly. As with OH + $CHF_2OCF_2OCHF_2$ and OH + $CHF_2OCF_2CF_2OCHF_2$, the value for E/R is estimated as being similar to that for the reaction of OH + CHF_2OCHF_2.
(Table: 10-6, Note: 10-6, Evaluated: 10-6) Back to Table

(1) Cavalli, F.; Glasius, M.; Hjorth, J.; Rindone, B.; Jensen, N. R. Atmospheric lifetimes, infrared spectra and degradation products of a series of hydrofluoroethers. *Atmos. Environ.* **1998**, *32*, 3767-3773, doi:10.1016/S1352-2310(98)00106-X.

E117. F + O_3. The recommended parameters are based on results of the room temperature study of Bedzhanyan et al.[1] (298 K) and the temperature-dependent study of Wagner et al.[2] (253–365 K). The recommendation appears to be quite reasonable in view of the well-known reactivity of atomic chlorine with O_3.
(Table: 94-26, Note: 94-26, Evaluated: 94-26) Back to Table

(1) Bedzhanyan, Y. R.; Markin, E. M.; Gershenzon, Y. M. Experimental study of elementary reactions of FO radicals. I. Sources and measurement of absolute concentrations. The reaction F + O_3 → FO + O_2. *Kinetics and Catalysis* **1993**, *33*, 594-601.
(2) Wagner, H. G.; Zetzsch, C.; Warnatz, J. Synthesis of OF radical in gas phase by reaction of fluorine atoms with ozone. *Ber. Bunsenges. Phys. Chem.* **1972**, *76*, 526-530, doi:10.1002/bbpc.19720760613.

E118. F + H_2. The value of k(298 K) is well established with the results reported by Zhitneva and Pshezhetskii[10] (293 K), Heidner et al.[5,6] (295, 295–765 K), Wurzberg and Houston[9] (190–373 K), Dodonov et al.,[4] Clyne et al.[3] (298 K), Bozzelli,[1] Igoshin et al.[7] (194–294 K), Clyne and Hodgson[2] (298 K), and Stevens et al.[8] (240–373 K) being in excellent agreement (range of k being 2.3–3.0 × 10^{-11} cm^3 $molecule^{-1}$ s^{-1}). The recommended value at 298 K is taken to be the average of the values reported in these references. Values of E/R range from 433–595 K (Heidner et al.; Wurzberg and Houston; Igoshin et al.; and Stevens et al.). The recommended value of E/R is derived from a fit to the data in these studies.
(Table: 90-1, Note: 90-1, Evaluated: 90-1) Back to Table

(1) Bozzelli, J. W. *Ph.D. Thesis*; Dept. of Chemistry, Princeton University, 1973.
(2) Clyne, M. A. A.; Hodgson, A. Absolute rate constants for the reaction of fluorine atoms with H_2, CH_2Cl_2, CH_2ClF, CH_2F_2 and $CHCl_2$. *J. Chem. Soc. Faraday Trans. 2* **1985**, *81*, 443-455, doi:10.1039/f29858100443.
(3) Clyne, M. A. A.; McKenney, D. J.; Walker, R. F. Reaction kinetics of ground state fluorine, F(^{2}P), atoms. I. Measurement of fluorine atom concentrations and the rates of reactions F + CHF_3 and F + Cl_2 using mass spectrometry. *Can. J. Chem.* **1973**, *51*, 3596-3604, doi:10.1139/v73-535.
(4) Dodonov, A. F.; Lavrovskaya, G. K.; Morozov, I. I.; Tal'rose, V. L. *Dokl. Adak. Nauk USSR, 1971, Vol. 198, 622: Dokl. Phys. Chem. (Engl. Trans.)* **1971**, *198*, 440-442.
(5) Heidner, R. F.; Bott, J. F.; Gardner, C. E.; Melzer, J. E. Absolute rate coefficients for F + H_2 and F + D_2 at T = 295 K. *J. Chem. Phys.* **1979**, *70*, 4509-4514, doi:10.1063/1.437288.
(6) Heidner, R. F.; Bott, J. F.; Gardner, C. E.; Melzer, J. E. Absolute rate coefficients for F + H_2 and F + D_2 at T = 295-765 K. *J. Chem. Phys.* **1980**, *72*, 4815-4821, doi:10.1063/1.439819.
(7) Igoshin, V. I.; Kulakov, L. V.; Nikitin, A. I. Determination of the rate constant of the chemical reaction F + H_2(D_2) → HF(DF) + H(D) from the stimulated emission of the HF(DF) molecules. *Sov. J. Quant. Electron.* **1974**, *3*, 306.
(8) Stevens, P. S.; Brune, W. H.; Anderson, J. G. Kinetic and mechanistic investigations of F + H_2O/D_2O and F + H_2/D_2 over the temperature range 240-373 K. *J. Phys. Chem.* **1989**, *93*, 4068-4079, doi:10.1021/j100347a040.
(9) Wurzburg, E.; Houston, P. L. The temperature dependence of absolute rate constants for the F + H_2 and F + D_2 reactions. *J. Chem. Phys.* **1980**, *72*, 4811-4814, doi:10.1063/1.439818.
(10) Zhitneva, G. P.; Pshezhetskii, S. Y. Rate constant for the reaction of fluorine atoms with chlorine monofluoride. *Kinetika i Kataliz* **1978**, *19*, 228-231.

E119. F + H_2O. The recommended temperature-independent value for this rate constant is based on results reported in the study by Stevens et al.[2] (240–373 K) using a discharge flow system with chemical conversion of fluorine atoms to deuterium atoms and detection of the latter by resonance fluorescence. This value is in excellent agreement with the room temperature results of Frost et al.[1] (298 K) and Walther and Wagner[3] (243–369 K). In a limited temperature-dependent study, Walther and Wagner reported an *E*/R value of 400 K. Although these data have not been included in the derivation of the recommended value for *E*/R, with the exception of the one low temperature data point, they are encompassed within the indicated uncertainty limits.
(Table: 90-1, Note: 90-1, Evaluated: 90-1) Back to Table

(1) Frost, R. J.; Green, D. S.; Osborn, M. K.; Smith, I. W. M. Time-resolved vibrational chemiluminescence: Rate constants for the reactions of F atoms with H_2O and HCN, and for the relaxation of HF (v = 1) by H_2O and HCN. *Int. J. Chem. Kinet.* **1986**, *18*, 885-898, doi:10.1002/kin.550180808.

(2) Stevens, P. S.; Brune, W. H.; Anderson, J. G. Kinetic and mechanistic investigations of F + H_2O/D_2O and F + H_2/D_2 over the temperature range 240-373 K. *J. Phys. Chem.* **1989**, *93*, 4068-4079, doi:10.1021/j100347a040.

(3) Walther, C.-D.; Wagner, H. G. On the reactions of F atoms with H_2O, H_2O_2, and NH_3. *Ber. Bunsenges. Phys. Chem.* **1983**, *87*, 403-409, doi:10.1002/bbpc.19830870510.

E120. F + HNO_3. The recommendation is based on results of the temperature-dependent study of Wine et al.[4] (260–373 K) and the room temperature results of Mellouki et al.[2] (298 K), Rahman et al.[3] (298 K), and Becker et al.[1] (298 K). The rate constant values at room temperature are in good agreement. In the Wine et al. study below 320 K, the data were fit by the Arrhenius expression recommended here, whereas at higher temperatures a temperature-independent value was found, suggesting the occurrence of different mechanisms in the two temperature regimes.
(Table: 90-1, Note: 90-1, Evaluated: 90-1) Back to Table

(1) Becker, E.; Benter, T.; Kampf, R.; Schindler, R. N.; Wille, U. A redetermination of the rate constant of the reaction F + HNO_3 → HF + NO_3. *Ber. Bunsenges. Phys. Chem.* **1991**, *95*, 1168-1173, doi:10.1002/bbpc.19910951002.

(2) Mellouki, A.; Le Bras, G.; Poulet, G. Discharge flow kinetic study of NO_3 reactions with free radicals: The reaction of NO_3 with Cl. *J. Phys. Chem.* **1987**, *91*, 5760-5764, doi:10.1021/j100306a048.

(3) Rahman, M. M.; Becker, E.; Benter, T.; Schindler, R. N. A gas phase kinetic investigation of the system F + HNO_3 and the determination of absolute rate constants for the reaction of the NO_3 radical with CH_3SH, 2-methylpropene, 1,3-butadiene and 2,3-dimethyl-2-butene. *Ber. Bunsenges. Phys. Chem.* **1988**, *92*, 91-100, doi:10.1002/bbpc.198800018.

(4) Wine, P. H.; Wells, J. R.; Nicovich, J. M. Kinetics of the reactions of F(^{2}P) and Cl(^{2}P) with HNO_3. *J. Phys. Chem.* **1988**, *92*, 2223-2228, doi:10.1021/j100319a028.

E121. F + CH_4. The recommended value of k(298 K) is the average of the results of Wagner et al.[6] (253–352 K), Clyne et al.[1] (298 K), Kompa and Wanner[4] (298 K), Foon and Reid[3] (253–348 K), Fasano and Nogar[2] 298 K), and Persky et al.[5] (184–406 K). The temperature dependence is that reported by Persky et al. in a competitive study using F + D_2 as the reference reaction. These results are recommended over the temperature dependences reported in the earlier studies of Wagner et al. and Foon and Reid.
(Table: 97-4, Note: 97-4, Evaluated: 97-4) Back to Table

(1) Clyne, M. A. A.; McKenney, D. J.; Walker, R. F. Reaction kinetics of ground state fluorine, F(^{2}P), atoms. I. Measurement of fluorine atom concentrations and the rates of reactions F + CHF_3 and F + Cl_2 using mass spectrometry. *Can. J. Chem.* **1973**, *51*, 3596-3604, doi:10.1139/v73-535.

(2) Fasano, D. M.; Nogar, N. S. Rate determination for F + CH_4 by real-time competitive kinetics. *Chem. Phys. Lett.* **1982**, *92*, 411-414, doi:10.1016/0009-2614(82)83438-6.

(3) Foon, R.; Reid, G. P. Kinetics of the gas phase fluorination of hydrogen and alkanes. *Trans. Faraday Soc.* **1971**, *67*, 3513-3520, doi:10.1039/tf9716703513.

(4) Kompa, K. L.; Wanner, J. Study of some fluorine atom reactions using a chemical laser method. *Chem. Phys. Lett.* **1972**, *12*, 560-563, doi:10.1016/0009-2614(72)80008-3.

(5) Persky, A. Kinetics of the F + CH_4 reaction in the temperature range 184-406 K. *J. Phys. Chem.* **1996**, *100*, 689-693, doi:10.1021/jp9524035.

(6) Wagner, H. G.; Warnatz, J.; Zetzsch, C. On the reaction of F atoms with methane. *Anales Assoc. Quim. Argentina* **1971**, *59*, 169-177.

E122. FO + O_3. The recommended upper limit for k(298 K) is based on the results of Li et al.[2] (298 K) in a study using a discharge flow-mass spectrometric technique. FO was produced in the reaction of F atoms with excess O_3. No appreciable decay of FO, and only a small increase in FO_2, was detected, allowing an upper limit to the rate constant of 10^{-14} cm^3 $molecule^{-1}$ s^{-1} to be derived. A two orders of magnitude higher upper limit was derived by Sehested et al.[3] (295 K). A lower value of the upper limit was derived by Colussi and Grela[1] from a re-analysis of data on the quantum yields for ozone destruction in F_2/O_3 mixtures reported by Starrico et al.[4] The results of the recent, more direct, study of Li et al. are preferred over the earlier results of Starrico et al. There are two possible pathways which are exothermic, resulting in the production of F + $2O_2$ or FO_2 + O_2.
(Table: 97-4, Note: 97-4, Evaluated: 97-4) Back to Table

(1) Colussi, A. J.; Grela, M. A. Rate of the reaction between oxygen monofluoride and ozone. Implications for the atmospheric role of fluorine. *Chem. Phys. Lett.* **1994**, *229*, 134-138, doi:10.1016/0009-2614(94)01021-8.
(2) Li, Z.; Friedl, R. R.; Sander, S. P. Kinetics of FO_2 with NO, NO_2, O_3, CH_4 and C_2H_6. *J. Phys. Chem.* **1995**, *99*, 13445-13451, doi:10.1021/j100036a019.
(3) Sehested, J.; Sehested, K.; Nielsen, O. J.; Wallington, T. J. Atmospheric chemistry of FO_2 radicals: Reaction with CH_4, O_3, NO, NO_2, and CO at 295 K. *J. Phys. Chem.* **1994**, *98*, 6731-6739, doi:10.1021/j100078a014.
(4) Staricco, E. H.; Sicre, S. E.; Schumacher, H. J. Die photochemische reaktion zwisehen fluor und ozon. *Z. Phys. Chem. N.F.* **1962**, *31*, 385.

E123. FO + NO. The recommended parameters are based on results of the temperature-dependent study of Bedzhanyan et al.[1] (300–845 K) and the value reported by Ray and Watson[2] (298 K) using the discharge flow-mass spectrometric technique.
(Table: 94-26, Note: 94-26, Evaluated: 94-26) Back to Table

(1) Bedzhanyan, Y. R.; Markin, E. M.; Gershenzon, Y. M. Experimental study of elementary reactions of FO radicals. V. Reactions with H_2, CO, and NO. *Kinetics and Catalysis* **1993**, *34*, 1-3.
(2) Ray, G. W.; Watson, R. T. Kinetics study of the reactions of NO with FO, ClO, BrO, and IO at 298 K. *J. Phys. Chem.* **1981**, *85*, 2955-2960, doi:10.1021/j150620a022.

E124. FO + FO. The recommended parameters are based on the results of Bedzhanyan et al.[1] (300–435 K) and Clyne and Watson[2] (298 K). Wagner et al.,[3] in a less direct study, report a higher value. The results of Bedzhanyan et al. indicate the predominant reaction channel is that to produce 2F + O_2.
(Table: 94-26, Note: 94-26, Evaluated: 94-26) Back to Table

(1) Bedzhanyan, Y. R.; Markin, E. M.; Gershenzon, Y. M. Experimental study of elementary reactions of FO radicals. Kinetics and mechanism of the disproportionation reaction. *Kinetics and Catalysis* **1993**, *33*, 601-606.
(2) Clyne, M. A. A.; Watson, R. T. Kinetic studies of diatomic free radicals using mass spectrometry Part 1.-System description and applications to F atoms and FO radicals. *J. Chem. Soc. Faraday Trans. 1* **1974**, *70*, 1109-1123, doi:10.1039/f19747001109.
(3) Wagner, H. G.; Zetzsch, C.; Warnatz, J. Synthesis of OF radical in gas phase by reaction of fluorine atoms with ozone. *Ber. Bunsenges. Phys. Chem.* **1972**, *76*, 526-530, doi:10.1002/bbpc.19720760613.

E125. FO_2 + O_3. The recommended upper limit for k(298 K) is based on results of Sehested et al.[2] (295 K). A higher upper limit has been reported by Li et al.[1] (298 K).
(Table: 94-26, Note: 97-4, Evaluated: 97-4) Back to Table

(1) Li, Z.; Friedl, R. R.; Sander, S. P. Kinetics of FO_2 with NO, NO_2, O_3, CH_4 and C_2H_6. *J. Phys. Chem.* **1995**, *99*, 13445-13451, doi:10.1021/j100036a019.
(2) Sehested, J.; Sehested, K.; Nielsen, O. J.; Wallington, T. J. Atmospheric chemistry of FO_2 radicals: Reaction with CH_4, O_3, NO, NO_2, and CO at 295 K. *J. Phys. Chem.* **1994**, *98*, 6731-6739, doi:10.1021/j100078a014.

E126. FO_2 + NO. The recommended parameters are based on results of Li et al.[1] (190–298 K), the only temperature-dependent study. The recommended value for k(298 K) is nearly a factor of 2 less than that reported by Sehested et al.[2] (295 K).
(Table: 97-4, Note: 97-4, Evaluated: 97-4) Back to Table

(1) Li, Z.; Friedl, R. R.; Sander, S. P. Kinetics of FO_2 with NO, NO_2, O_3, CH_4 and C_2H_6. *J. Phys. Chem.* **1995**, *99*, 13445-13451, doi:10.1021/j100036a019.
(2) Sehested, J.; Sehested, K.; Nielsen, O. J.; Wallington, T. J. Atmospheric chemistry of FO_2 radicals: Reaction with CH_4, O_3, NO, NO_2, and CO at 295 K. *J. Phys. Chem.* **1994**, *98*, 6731-6739, doi:10.1021/j100078a014.

E127. FO_2 + NO_2. The recommended parameters are based on the results of Li et al.[1] (260–315 K), the only temperature-dependent study. The recommended value for k(298 K) is a factor of 2.5 less than the results of Sehested et al.[2] (295 K). This discrepancy might be attributable to a small NO impurity in the NO_2 sample used in the Sehested et al. study.
(Table: 97-4, Note: 97-4, Evaluated: 97-4) Back to Table

(1) Li, Z.; Friedl, R. R.; Sander, S. P. Kinetics of FO_2 with NO, NO_2, O_3, CH_4 and C_2H_6. *J. Phys. Chem.* **1995**, *99*, 13445-13451, doi:10.1021/j100036a019.
(2) Sehested, J.; Sehested, K.; Nielsen, O. J.; Wallington, T. J. Atmospheric chemistry of FO_2 radicals: Reaction with CH_4, O_3, NO, NO_2, and CO at 295 K. *J. Phys. Chem.* **1994**, *98*, 6731-6739, doi:10.1021/j100078a014.

E128. FO_2 + CO. The recommended upper limit for k(298 K) is based on results of Sehested et al.[1] (295 K), the only published study of this reaction.
(Table: 94-26, Note: 94-26, Evaluated: 94-26) Back to Table

(1) Sehested, J.; Sehested, K.; Nielsen, O. J.; Wallington, T. J. Atmospheric chemistry of FO_2 radicals: Reaction with CH_4, O_3, NO, NO_2, and CO at 295 K. *J. Phys. Chem.* **1994**, *98*, 6731-6739, doi:10.1021/j100078a014.

E129. FO_2 + CH_4. The recommended upper limit for k(298 K) is based on results of Li et al.[1] (298 K). This upper limit is a factor of 20 less than derived in the study by Sehested et al.[2] (295 K).
(Table: 97-4, Note: 97-4, Evaluated: 97-4) Back to Table

(1) Li, Z.; Friedl, R. R.; Sander, S. P. Kinetics of FO_2 with NO, NO_2, O_3, CH_4 and C_2H_6. *J. Phys. Chem.* **1995**, *99*, 13445-13451, doi:10.1021/j100036a019.
(2) Sehested, J.; Sehested, K.; Nielsen, O. J.; Wallington, T. J. Atmospheric chemistry of FO_2 radicals: Reaction with CH_4, O_3, NO, NO_2, and CO at 295 K. *J. Phys. Chem.* **1994**, *98*, 6731-6739, doi:10.1021/j100078a014.

E130. CF_3O + O_2. The recommendation is based on the results of Turnipseed et al.[1] (298, 373 K), who reported k(373 K) $\leq 4 \times 10^{-17}$ cm^3 molecule^{-1} s^{-1}. Assuming an E/R of 5000 K, which is equal to the reaction endothermicity, yields the recommended A and k(298 K) limits. By comparison to other reactions involving abstraction by O_2, the A- factor is likely to be much smaller.
(Table: 94-26, Note: 94-26, Evaluated: 94-26) Back to Table

(1) Turnipseed, A. A.; Barone, S. B.; Ravishankara, A. R. Kinetics of the reactions of CF_3O_x radicals with NO, O_3, and O_2. *J. Phys. Chem.* **1994**, *98*, 4594-4601, doi:10.1021/j100068a019.

E131. CF_3O + O_3. The recommended value for k(298 K) is based on the average of room temperature measurements reported by Turnipseed et al.[6] (298 K), Wallington and Ball[7] (296 K), and Bourbon et al.[1] Turnipseed et al. and Bourbon et al. made direct measurements using LIF detection of CF_3O with pulsed photolysis and flow tube reactors, respectively. Wallington and Ball used a competitive reaction scheme with IR absorption detection and CF_3O + CH_4 as the reference reaction. The recommended A factor is estimated by comparison to other CF_3O reactions, and the E/R is calculated to agree with the recommended k(298 K). Upper limits reported by Maricq and Szente[3] (210–353 K), Nielsen and Sehested[5] (295 K), and Wallington et al.[8] (295 K) are consistent with the k(298 K) recommendation. Measurements reported by Fockenberg et al.[2] (298 K) and Meller and Moortgat[4] (295 K) give rate coefficients about an order of magnitude less than the recommended value. Although the reason for this discrepancy is not known, both studies may have possibly been affected by significant secondary chemistry. The reaction products have not been observed.

(Table: 97-4, Note: 97-4, Evaluated: 97-4) Back to Table

(1) Bourbon, C.; Brioukov, M.; Devolder, P. Rate constant for the reaction $CF_3O + O_3 \rightarrow$ products by the fast flow absolute technique. *C. R. Acad. Sci. Paris* **1996**, *322*, 181-188.

(2) Fockenberg, C.; Saathoff, H.; Zellner, R. A laser photolysis/LIF study of the rate constant for the reaction $CF_3O + O_3 \rightarrow$ products. *Chem. Phys. Lett.* **1994**, *218*, 21-28, doi:10.1016/0009-2614(93)E1457-R.

(3) Maricq, M. M.; Szente, J. J. Upper limits for the rate constants of the reactions $CF_3O + O_3 \rightarrow CF_3O_2 + O_2$ and $CF_3O_2 + O_3 \rightarrow CF_3O + 2O_2$. *Chem. Phys. Lett.* **1993**, *213*, 449-456, doi:10.1016/0009-2614(93)89141-4.

(4) Meller, R.; Moortgat, G. K. Photolysis of $CF_3O_2CF_3$ in the presence of O_3 in oxygen: kinetic study of the reactions of CF_3O and CF_3O_2 radicals with O_3. *J. Photochem. Photobio. A: Chem.* **1995**, *86*, 15-25, doi:10.1016/1010-6030(94)03951-P.

(5) Nielsen, O. J.; Sehested, J. Upper limits for the rate constants of the reactions of CF_3O_2 and CF_3O radicals with ozone at 295 K. *Chem. Phys. Lett.* **1993**, *213*, 433-441, doi:10.1016/0009-2614(93)89139-9.

(6) Turnipseed, A. A.; Barone, S. B.; Ravishankara, A. R. Kinetics of the reactions of CF_3O_x radicals with NO, O_3, and O_2. *J. Phys. Chem.* **1994**, *98*, 4594-4601, doi:10.1021/j100068a019.

(7) Wallington, T. J.; Ball, J. C. Atmospheric chemistry of CF_3O radicals: reaction with O_3. *Chem. Phys. Lett.* **1995**, *234*, 187-194, doi:10.1016/0009-2614(95)00009-S.

(8) Wallington, T. J.; Hurley, M. D.; Schneider, W. F. Kinetic study of the reaction $CF_3O + O_3 \rightarrow CF_3O_2 + O_2$. *Chem. Phys. Lett.* **1993**, *213*, 442-448, doi:10.1016/0009-2614(93)89140-D.

E132. $CF_3O + H_2O$. The recommendation is based on the measurement of $k(381\text{ K}) \leq 2\times10^{-16}$ cm^3 molecule^{-1} s^{-1} reported by Turnipseed et al.[1] (298, 381 K). As for the reaction $CF_3O + O_3$, the A factor is estimated, and the E/R is calculated to fit k(381 K). The limits $k = (0.2–40) \times 10^{-17}$ cm^3 molecule^{-1} s^{-1} at 296 ± 2 K given by Wallington et al.[2] (296 K) are consistent with the recommendation.
(Table: 94-26, Note: 94-26, Evaluated: 94-26) Back to Table

(1) Turnipseed, A. A.; Barone, S. B.; Jensen, N. R.; Hanson, D. R.; Howard, C. J.; Ravishankara, A. R. Kinetics of the reactions of CF_3O radicals with CO and H_2O. *J. Phys. Chem.* **1995**, *99*, 6000-6009, doi:10.1021/j100016a041.

(2) Wallington, T. J.; Hurley, M. D.; Schneider, W. F.; Sehested, J.; Nielsen, O. J. Atmospheric chemistry of CF_3O radicals: Reaction with H_2O. *J. Phys. Chem.* **1993**, *97*, 7606-7611, doi:10.1021/j100131a033.

E133. $CF_3O + NO$. The recommended value for k(298 K) is based upon the room temperature rate coefficients reported by Sehested and Nielsen[7] (295 K), Turnipseed et al.[8] (233–360 K), and Jensen et al.,[6] (231–393 K)which are in very good agreement. An earlier low value given by Bevilacqua et al.[1] is superseded by Jensen et al. The temperature-dependence is derived from measurements by Turnipseed (233–360 K) and Jensen et al. (231–393 K). The room temperature results from Bourbon et al.[3] (298 K) and Bhatnagar and Carr[2] (293 K) and the results from the temperature dependence study by Dibble et al.[5] (213–353 K) are in good agreement with the recommendation. The reaction products have been reported by Chen et al.,[4] Bevilacqua et al., Bhatnagar and Carr, and Dibble et al.
(Table: 94-26, Note: 97-4, Evaluated: 97-4) Back to Table

(1) Bevilacqua, T. J.; Hanson, D. R.; Howard, C. J. Chemical ionization mass spectrometric studies of the gas-phase reactions $CF_3O_2 + NO$, $CF_3O + NO$, $CF_3O + RH$. *J. Phys. Chem.* **1993**, *97*, 3750-3757, doi:10.1021/j100117a020.

(2) Bhatnagar, A.; Carr, R. W. Flash photolysis time-resolved mass spectrometric investigations of the reactions of CF_3O_2 and CF_3O radicals with NO. *Chem. Phys. Lett.* **1994**, *231*, 454-459, doi:10.1016/0009-2614(94)01277-6.

(3) Bourbon, C.; Brioukov, M.; Hanoune, B.; Sawerysyn, J. P.; Devolder, P. Flow tube/LIF measurements of the rate constant for the reactions with NO of CF_3O and CF_3O_2 radicals. *Chem. Phys. Lett.* **1996**, *254*, 203-212, doi:10.1016/0009-2614(96)00277-1.

(4) Chen, J.; Zhu, T.; Niki, H. FTIR spectroscopic study of the reaction of CF_3O with NO: Evidence for $CF_3O + NO \rightarrow CF_2O + FNO$. *J. Phys. Chem.* **1992**, *96*, 6115-6117, doi:10.1021/j100194a004.

(5) Dibble, T. S.; Maricq, M. M.; Szente, J. J.; Francisco, J. S. Kinetics of the reaction of CF_3O with NO. *J. Phys. Chem.* **1995**, *99*, 17394-17402, doi:10.1021/j100048a014.

(6) Jensen, N. R.; Hanson, D. R.; Howard, C. J. Temperature dependence of the gas phase reactions of CF_3O with CH_4 and NO. *J. Phys. Chem.* **1994**, *98*, 8574-8579, doi:10.1021/j100085a042.

(7) Sehested, J.; Nielsen, O. J. Absolute rate constants for the reaction of CF_3O_2 and CF_3O radicals with NO at 295 K. *Chem. Phys. Lett.* **1993**, *206*, 369-375, doi:10.1016/0009-2614(93)85567-8.

(8) Turnipseed, A. A.; Barone, S. B.; Ravishankara, A. R. Kinetics of the reactions of CF_3O_x radicals with NO, O_3, and O_2. *J. Phys. Chem.* **1994**, *98*, 4594-4601, doi:10.1021/j100068a019.

E134. $CF_3O + NO_2$. There are no published measurements of the rate coefficient for this reaction. The reaction products have been reported by Chen et al.[1] (297 K), who used photolysis of CF_3NO to prepare CF_3O_2 and subsequently CF_3O in 700 Torr of air at 297 ± 2 K. They considered two product channels: (a) CF_3ONO_2 obtained via three-body recombination and (b) $CF_2O + FNO_2$ obtained via fluorine transfer. Products from both channels were observed and found to be thermally stable in their reactor. They report $k_a/(k_a + k_b) \geq 90\%$ and $k_b/(k_a + k_b) \leq 10\%$, thus the formation of CF_3ONO_2 is the dominant channel at 700 Torr and 297 K.
(Table: 94-26, Note: 94-26, Evaluated: 94-26) Back to Table

(1) Chen, J.; Young, V.; Zhu, T.; Niki, H. Long path Fourier transform infrared spectroscopic study of the reactions of CF_3OO and CF_3O radicals with NO_2. *J. Phys. Chem.* **1993**, *97*, 11696-11698, doi:10.1021/j100147a024.

E135. $CF_3O + CO$. The kinetics of this reaction were studied by Turnipseed et al.[1] (233–298 K), who used pulsed laser photolysis with pulsed laser-induced fluorescence detection and a flow tube reactor with chemical ionization detection to obtain data at temperatures from 233 to 332 K and at pressures from 0.8 to about 300 Torr in He and at about 300 Torr in SF_6. The reaction was found to be predominantly a three-body recombination, presumably producing CF_3OCO, as described in Table 2-1. The bimolecular reaction has at least two product channels: (a) $CF_2O + CFO$ and (b) $CF_3 + CO_2$. The recommended upper limit for the bimolecular rate coefficient is derived from the low-pressure results of Turnipseed et al., where the reaction was in the fall-off region. Their low-pressure data indicate that $k_b < 4 \times 10^{-16}$ cm^3 molecule^{-1} s^{-1} at 298 K. The fate of the CF_3OCO adduct is uncertain, and it may lead to the regeneration of CF_3 or CF_3O radicals in the atmosphere. Wallington and Ball[2] report a yield of 96 ± 8% CO_2 at one atmosphere and 296 ± 2 K.
(Table: 94-26, Note: 97-4, Evaluated: 97-4) Back to Table

(1) Turnipseed, A. A.; Barone, S. B.; Jensen, N. R.; Hanson, D. R.; Howard, C. J.; Ravishankara, A. R. Kinetics of the reactions of CF_3O radicals with CO and H_2O. *J. Phys. Chem.* **1995**, *99*, 6000-6009, doi:10.1021/j100016a041.
(2) Wallington, T. J.; Ball, J. C. Atmospheric chemistry of CF_3O radicals: Reactions with CH_4, CD_4, CH_3F, CF_3H, ^{13}CO, C_2H_5F, C_2D_6, C_2H_6, CH_3OH, *i*-C_4H_8, and C_2H_2. *J. Phys. Chem.* **1995**, *99*, 3201-3205, doi:10.1021/j100010a034.

E136. $CF_3O + CH_4$. The recommended value of k(298 K) is an average of the values reported in the absolute studies of Saathoff and Zellner[8] (298 K), Barone et al.[1] (247–360 K), Jensen et al.[6] (231–385 K), Bourbon et al.[4] (296–573 K), and Bednarek et al.[2] (235–401 K), which are all in excellent agreement. Kelly et al.[7] (298 K) used a relative method with FTIR detection to determine the ratio $k(CF_3O + CH_4)/k(CF_3O + C_2H_6) = R = 0.01 \pm 0.001$ at 298 ± 2 K. This ratio is considerably smaller than that calculated from the rate constants recommended in this evaluation, which is R = 0.017. However, a relative rate measurement reported by Wallington and Ball[9] (296 K) yields R = 0.0152 ± 0.0023 at 296 K, which is in good agreement with that calculated from the recommended rate coefficients. A relative rate measurement reported by Chen et al.[5] (297 K) using FTIR methods also gives a low result for the rate coefficient for this reaction, thus, in better agreement with the value of R from Kelly et al.[7] (298 K). The recommended temperature dependence is from the data of Barone et al., Jensen et al., and Bednarek et al., which agree very well. Measurements at higher temperatures by Bourbon et al. yield a higher value E/R (1606 K). The CF_3OH product was observed by Jensen et al. and Bevilacqua et al.[3]
(Table: 97-4, Note: 97-4, Evaluated: 97-4) Back to Table

(1) Barone, S. B.; Turnipseed, A. A.; Ravishankara, A. R. Kinetics of the reactions of the CF_3O radical with alkanes. *J. Phys. Chem.* **1994**, *98*, 4602-4608, doi:10.1021/j100068a020.
(2) Bednarek, G.; Kohlmann, J. P.; Saathoff, H.; Zellner, R. Temperature dependence and product distribution for the reaction of CF_3O radicals with methane. *Z. Phys. Chem.* **1995**, *188*, 1-15, doi:10.1524/zpch.1995.188.Part_1_2.001.
(3) Bevilacqua, T. J.; Hanson, D. R.; Howard, C. J. Chemical ionization mass spectrometric studies of the gas-phase reactions $CF_3O_2 + NO$, $CF_3O + NO$, $CF_3O + RH$. *J. Phys. Chem.* **1993**, *97*, 3750-3757, doi:10.1021/j100117a020.
(4) Bourbon, C.; Fittschen, C.; Sawerysyn, J. P.; Devolder, P. Temperature dependence of the gas phase reaction rates of CF_3O with methane, ethane, and isobutane. *J. Phys. Chem.* **1995**, *99*, 15102-15107, doi:10.1021/j100041a028.
(5) Chen, J.; Zhu, T.; Niki, H.; Mains, G. J. Long path FTIR spectroscopic study of the reactions of CF_3O radicals with ethane and propane. *Geophys. Res. Lett.* **1992**, *19*, 2215-2218, doi:10.1029/92GL02496.

(6) Jensen, N. R.; Hanson, D. R.; Howard, C. J. Temperature dependence of the gas phase reactions of CF_3O with CH_4 and NO. *J. Phys. Chem.* **1994**, *98*, 8574-8579, doi:10.1021/j100085a042.
(7) Kelly, C.; Treacy, J.; Sidebottom, H. W.; Nielsen, O. J. Rate constants for the reaction of CF_3O radicals with hydrocarbons at 298 K. *Chem. Phys. Lett.* **1993**, *207*, 498-503, doi:10.1016/0009-2614(93)89036-H.
(8) Saathoff, H.; Zellner, R. LIF detection of the CF_3O radical and kinetics of its reactions with CH_4 and C_2H_6. *Chem. Phys. Lett.* **1993**, *206*, 349-354, doi:10.1016/0009-2614(93)85563-4.
(9) Wallington, T. J.; Ball, J. C. Atmospheric chemistry of CF_3O radicals: Reactions with CH_4, CD_4, CH_3F, CF_3H, ^{13}CO, C_2H_5F, C_2D_6, C_2H_6, CH_3OH, *i*-C_4H_8, and C_2H_2. *J. Phys. Chem.* **1995**, *99*, 3201-3205, doi:10.1021/j100010a034.

E137. $CF_3O + C_2H_6$. The recommended value for k(298 K) is based on results reported by Saathoff and Zellner,[5] Barone et al.[1] (233–360 K), and Bourbon et al.[2] (295–573 K), which are in excellent agreement. Chen et al.[3] (297 K) measured the rate coefficient relative to that for the $CF_3O + NO$ reaction in 700 Torr of air at 297 K. Their ratio is in good agreement with the values recommended in this evaluation. Kelly et al.[4] (298 K) used a relative method with FTIR detection to determine the ratio $k(CF_3O + CH_4)/k(CF_3O + C_2H_6) = R = 0.01 \pm 0.001$ at 298 ± 2 K. This does not agree with the ratio calculated using the rate constants recommended in this evaluation, which is R = 0.017. However, a relative rate measurement reported by Wallington and Ball[6] (296 K) yields R = 0.0152 ± 0.0023 at 296 K in good agreement with that calculated using the recommended rate coefficients. The recommended temperature dependence is from the work of Barone et al.. Measurements by Bourbon et al. give a higher E/R (642 K). The products are inferred by analogy to other reactions of CF_3O with organic compounds.
(Table: 97-4, Note: 97-4, Evaluated: 97-4) Back to Table

(1) Barone, S. B.; Turnipseed, A. A.; Ravishankara, A. R. Kinetics of the reactions of the CF_3O radical with alkanes. *J. Phys. Chem.* **1994**, *98*, 4602-4608, doi:10.1021/j100068a020.
(2) Bourbon, C.; Fittschen, C.; Sawerysyn, J. P.; Devolder, P. Temperature dependence of the gas phase reaction rates of CF_3O with methane, ethane, and isobutane. *J. Phys. Chem.* **1995**, *99*, 15102-15107, doi:10.1021/j100041a028.
(3) Chen, J.; Zhu, T.; Niki, H.; Mains, G. J. Long path FTIR spectroscopic study of the reactions of CF_3O radicals with ethane and propane. *Geophys. Res. Lett.* **1992**, *19*, 2215-2218, doi:10.1029/92GL02496.
(4) Kelly, C.; Treacy, J.; Sidebottom, H. W.; Nielsen, O. J. Rate constants for the reaction of CF_3O radicals with hydrocarbons at 298 K. *Chem. Phys. Lett.* **1993**, *207*, 498-503, doi:10.1016/0009-2614(93)89036-H.
(5) Saathoff, H.; Zellner, R. LIF detection of the CF_3O radical and kinetics of its reactions with CH_4 and C_2H_6. *Chem. Phys. Lett.* **1993**, *206*, 349-354, doi:10.1016/0009-2614(93)85563-4.
(6) Wallington, T. J.; Ball, J. C. Atmospheric chemistry of CF_3O radicals: Reactions with CH_4, CD_4, CH_3F, CF_3H, ^{13}CO, C_2H_5F, C_2D_6, C_2H_6, CH_3OH, *i*-C_4H_8, and C_2H_2. *J. Phys. Chem.* **1995**, *99*, 3201-3205, doi:10.1021/j100010a034.

E138. $CF_3O_2 + O_3$. The recommended upper limit for k(298 K) is from the measurements reported by Ravishankara et al.[4] (298 K), who used chemical ionization detection of CF_3O_2 with a flow tube reactor. No measurable reaction was observed in their study. The less direct studies of Nielsen and Sehested[3] (295 K), Maricq and Szente[1] (210–353 K), and Turnipseed et al.[5] (298 K) report somewhat larger upper limits to the rate coefficient. An observable reaction was reported in an indirect measurement by Meller and Moortgat[2] (295 K). However, their result for the $CF_3O + O_3$ reaction is not consistent with the value recommended in this evaluation, suggesting that their study may have interference from unknown reactions. The products are assumed to be $CF_3O + 2O_2$.
(Table: 94-26, Note: 94-26, Evaluated: 94-26) Back to Table

(1) Maricq, M. M.; Szente, J. J. Upper limits for the rate constants of the reactions $CF_3O + O_3 \rightarrow CF_3O_2 + O_2$ and $CF_3O_2 + O_3 \rightarrow CF_3O + 2O_2$. *Chem. Phys. Lett.* **1993**, *213*, 449-456, doi:10.1016/0009-2614(93)89141-4.
(2) Meller, R.; Moortgat, G. K. Photolysis of $CF_3O_2CF_3$ in the presence of O_3 in oxygen: kinetic study of the reactions of CF_3O and CF_3O_2 radicals with O_3. *J. Photochem. Photobio. A: Chem.* **1995**, *86*, 15-25, doi:10.1016/1010-6030(94)03951-P.
(3) Nielsen, O. J.; Sehested, J. Upper limits for the rate constants of the reactions of CF_3O_2 and CF_3O radicals with ozone at 295 K. *Chem. Phys. Lett.* **1993**, *213*, 433-441, doi:10.1016/0009-2614(93)89139-9.
(4) Ravishankara, A. R.; Turnipseed, A. A.; Jensen, N. R.; Barone, S.; Mills, M.; Howard, C. J.; Solomon, S. Do hydrofluorocarbons destroy stratospheric ozone? *Science* **1994**, *263*, 71-75, doi:10.1126/science.263.5143.71.

(5) Turnipseed, A. A.; Barone, S. B.; Ravishankara, A. R. Kinetics of the reactions of CF_3O_x radicals with NO, O_3, and O_2. *J. Phys. Chem.* **1994**, *98*, 4594-4601, doi:10.1021/j100068a019.

E139. CF_3O_2 + CO. The recommended upper limit for k(298 K) is from Turnipseed et al.[2] (298 K), who used chemical ionization mass spectrometric detection of CF_3OO with a flow tube reactor. This result is at odds with an earlier study by Czarnowski and Schumacher,[1] who deduced a "fast reaction" when they observed the thermal decomposition of CF_3OOOCF_3 to accelerate in the presence of CO at 315–343 K. It is possible that the reaction of CF_3O with CO could account for their observations.
(Table: 94-26, Note: 94-26, Evaluated: 94-26) Back to Table

(1) Czarnowski, J.; Schumacher, H. J. The kinetics and the mechanism of the thermal decomposition of bis(trifluoromethyl) trioxide. The influence of carbon monoxide on its decomposition. *Int. J. Chem. Kinet.* **1981**, *13*, 639-649, doi:10.1002/kin.550130705.
(2) Turnipseed, A. A.; Barone, S. B.; Jensen, N. R.; Hanson, D. R.; Howard, C. J.; Ravishankara, A. R. Kinetics of the reactions of CF_3O radicals with CO and H_2O. *J. Phys. Chem.* **1995**, *99*, 6000-6009, doi:10.1021/j100016a041.

E140. CF_3O_2 + NO. The recommended value for k(298 K) is an average of the room temperature rate coefficients reported by Plumb and Ryan[6] (295 K), Dognon et al.[4] (230–430 K), Peeters et al.[5] (290 K), Bevilacqua et al.[1] (297 K), Sehested and Nielsen[7] (295 K), Turnipseed et al.[8] (298 K), Bourbon et al.[3] (298 K), and Bhatnagar and Carr[2] (293 K), all of which are in excellent agreement. The temperature dependence is derived from the results of Dognon et al. Several studies have confirmed the identity of the products.
(Table: 97-4, Note: 97-4, Evaluated: 97-4) Back to Table

(1) Bevilacqua, T. J.; Hanson, D. R.; Howard, C. J. Chemical ionization mass spectrometric studies of the gas-phase reactions CF_3O_2 + NO, CF_3O + NO, CF_3O + RH. *J. Phys. Chem.* **1993**, *97*, 3750-3757, doi:10.1021/j100117a020.
(2) Bhatnagar, A.; Carr, R. W. Flash photolysis time-resolved mass spectrometric investigations of the reactions of CF_3O_2 and CF_3O radicals with NO. *Chem. Phys. Lett.* **1994**, *231*, 454-459, doi:10.1016/0009-2614(94)01277-6.
(3) Bourbon, C.; Brioukov, M.; Hanoune, B.; Sawerysyn, J. P.; Devolder, P. Flow tube/LIF measurements of the rate constant for the reactions with NO of CF_3O and CF_3O_2 radicals. *Chem. Phys. Lett.* **1996**, *254*, 203-212, doi:10.1016/0009-2614(96)00277-1.
(4) Dognon, A. M.; Caralp, F.; Lesclaux, R. Réactions des radicaux chlorofluorométhyl péroxyles avec NO: Étude cinétique dans le domaine de température compris entre 230 et 430 K. *J. Chim. Phys.* **1985**, *82*, 349-352, doi:10.1051/jcp/1985820349.
(5) Peeters, J.; Vertommen, J.; Langhans, I. Rate constants of the reactions of CF_3O_2, i-$C_3H_7O_2$, and t-$C_4H_9O_2$ with NO. *Ber. Bunsenges. Phys. Chem.* **1992**, *96*, 431-436, doi:10.1002/bbpc.19920960339.
(6) Plumb, I. C.; Ryan, K. R. Kinetics of the reaction of CF_3O_2 with NO. *Chem. Phys. Lett.* **1982**, *92*, 236-238, doi:10.1016/0009-2614(82)80267-4.
(7) Sehested, J.; Nielsen, O. J. Absolute rate constants for the reaction of CF_3O_2 and CF_3O radicals with NO at 295 K. *Chem. Phys. Lett.* **1993**, *206*, 369-375, doi:10.1016/0009-2614(93)85567-8.
(8) Turnipseed, A. A.; Barone, S. B.; Ravishankara, A. R. Kinetics of the reactions of CF_3O_x radicals with NO, O_3, and O_2. *J. Phys. Chem.* **1994**, *98*, 4594-4601, doi:10.1021/j100068a019.

1.10.3 Bibliography – FO_x Chemistry

Acerboni, G.; Beukes, J. A.; Jensen, N. R.; Hjorth, J.; Myhre, G.; Nielsen, C. J.; Sundet, J. K. Atmospheric degradation and global warming potentials of three perfluoroalkenes. *Atmos. Environ.* **2001**, *35*, 4113-4123, doi:10.1016/S1352-2310(01)00209-6.

Acerboni, G.; Jensen, N. R.; Rindone, B.; Hjorth, J. Kinetics and products formation of the gas-phase reactions of tetrafluoroethylene with OH and NO_3 radicals and ozone. *Chem. Phys. Lett.* **1999**, *309*, 364-368, doi:10.1016/S0009-2614(99)00698-3.

Albaladejo, J.; Ballesteros, B.; Jimenez, E.; Diaz de Mera, Y.; Martinez, E. Gas-phase OH radical-initiated oxidation of the 3-halopropenes studied by PLP-LIF in the temperature range 228-388 K. *Atmos. Environ.* **2003**, *37*, 2919-2926, doi:10.1016/S1352-2310(03)00297-8.

Andersen, L. L.; Østerstrøm, F. F.; Nielsen, O. J.; Sulbaek Andersen, M. P.; Wallington, T. J. Atmospheric chemistry of $(CF_3)_2CFOCH_3$. *Chem. Phys. Lett.* **2014**, *607*, 5-9, doi:10.1016/j.cplett.2014.05.036.

Antiñolo, M.; Bravo, I. n.; Jiménez, E.; Ballesteros, B.; Albaladejo, J. Atmospheric chemistry of *E*- and *Z*-CF_3CH=CHF HFO-1234ze): OH reaction kinetics as a function of temperature and UV and IR absorption cross sections. *J. Phys. Chem. A* **2017**, *121*, 8322−8331, doi:10.1021/acs.jpca.7b06174.

Antiñolo, M.; González, S.; Ballesteros, B.; Albaladejo, J.; Jiménez, E. Laboratory studies of $CHF_2CF_2CH_2OH$ and $CF_3CF_2CH_2OH$: UV and IR absorption cross sections and OH rate coefficients between 263 and 358 K. *J. Phys. Chem. A* **2012**, *116*, 6041–6050, doi:10.1021/jp2111633.

Antiñolo, M.; Jiménez, E.; Albaladejo, J. Temperature effects on the removal of potential HFC replacements, $CF_3CH_2CH_2OH$ and $CF_3(CH_2)_2CH_2OH$, initiated by OH radicals. *Environ. Sci. Technol.* **2011**, *45*, 4323–4330, doi:10.1021/es103931s.

Baasandorj, M.; Burkholder, J. B. Rate coefficient for the gas-phase OH + $CHF=CF_2$ reaction between 212 and 375 K. *Int. J. Chem. Kinet.* **2016**, *48*, 714–723, doi:10.1002/kin.21027.

Baasandorj, M.; Knight, G.; Papadimitriou, V. C.; Talukdar, R. K.; Ravishankara, A. R.; Burkholder, J. B. Rate coefficients for the gas-phase reaction of the hydroxyl radical with CH_2=CHF and $CH_2=CF_2$. *J. Phys. Chem. A* **2010**, *114*, 4619-4633, doi:10.1021/jp100527z.

Baasandorj, M.; Marshall, P.; Waterland, R. L.; Ravishankara, A. R.; Burkholder, J. B. Rate coefficient measurements and theoretical analysis of the OH + (*E*)-$CF_3CH=CHCF_3$ reaction. *J. Phys. Chem. A* **2018**, *122*, 4635–4646, doi:10.1021/acs.jpca.8b02771.

Baasandorj, M.; Ravishankara, A. R.; Burkholder, J. B. Atmospheric chemistry of (*Z*)-$CF_3CH=CHCF_3$: OH radical reaction rate coefficient and global warming potential. *J. Phys. Chem. A* **2011**, *115*, 10539-10549, doi:10.1021/jp206195g.

Barone, S. B.; Turnipseed, A. A.; Ravishankara, A. R. Kinetics of the reactions of the CF_3O radical with alkanes. *J. Phys. Chem.* **1994**, *98*, 4602-4608, doi:10.1021/j100068a020.

Barry, J.; Locke, G.; Scollard, D.; Sidebottom, H.; Treacy, J.; Clerbaux, C.; Colin, R.; Franklin, J. 1,1,1,3,3,-pentafluorobutane (HFC-365mfc): Atmospheric degradation and contribution to radiative forcing. *Int. J. Chem. Kinet.* **1997**, *29*, 607-617, doi:10.1002/(SICI)1097-4601(1997)29:8<607::AID-KIN6>3.0.CO;2-Y.

Barry, J.; Sidebottom, H.; Treacy, J.; Franklin, J. Kinetics and mechanism for the atmospheric oxidation of 1,1,2-trifluoroethane (HFC 143). *Int. J. Chem. Kinet.* **1995**, *27*, 27-36, doi:10.1002/kin.550270105.

Becker, E.; Benter, T.; Kampf, R.; Schindler, R. N.; Wille, U. A redetermination of the rate constant of the reaction F + HNO_3 → HF + NO_3. *Ber. Bunsenges. Phys. Chem.* **1991**, *95*, 1168-1173, doi:10.1002/bbpc.19910951002.

Bednarek, G.; Breil, M.; Hoffman, A.; Kohlman, J. P.; Mörs, V.; Zellner, R. Rate and mechanism of the atmospheric degradation of 1,1,1,2-tetrafluoroethane (HFC-134a). *Ber. Bunsenges. Phys. Chem.* **1996**, *100*, 528-539, doi:10.1002/bbpc.19961000503.

Bednarek, G.; Kohlmann, J. P.; Saathoff, H.; Zellner, R. Temperature dependence and product distribution for the reaction of CF_3O radicals with methane. *Z. Phys. Chem.* **1995**, *188*, 1-15, doi:10.1524/zpch.1995.188.Part_1_2.001.

Bedzhanyan, Y. R.; Markin, E. M.; Gershenzon, Y. M. Experimental study of elementary reactions of FO radicals. I. Sources and measurement of absolute concentrations. The reaction F + O_3 → FO + O_2. *Kinetics and Catalysis* **1993**, *33*, 594-601.

Bedzhanyan, Y. R.; Markin, E. M.; Gershenzon, Y. M. Experimental study of elementary reactions of FO radicals. Kinetics and mechanism of the disproportionation reaction. *Kinetics and Catalysis* **1993**, *33*, 601-606.

Bedzhanyan, Y. R.; Markin, E. M.; Gershenzon, Y. M. Experimental study of elementary reactions of FO radicals. V. Reactions with H_2, CO, and NO. *Kinetics and Catalysis* **1993**, *34*, 1-3.

Bedzhanyan, Y. R.; Markin, E. M.; Politenkova, G. G.; Gershenzon, Y. M. Experimental study of elementary reactions of FO radicals. III. Reactions with oxygen and nitrogen atoms. *Kinetics and Catalysis* **1993**, *33*, 797-801.

Bera, R. K.; Hanrahan, R. J. Investigation of gas-phase reactions of OH radicals with fluoromethane and difluoromethane using Ar-sensitized pulse-radiolysis. *Radiation Phys. Chem.* **1988**, *32*, 579-584.

Bevilacqua, T. J.; Hanson, D. R.; Howard, C. J. Chemical ionization mass spectrometric studies of the gas-phase reactions CF_3O_2 + NO, CF_3O + NO, CF_3O + RH. *J. Phys. Chem.* **1993**, *97*, 3750-3757, doi:10.1021/j100117a020.

Bhatnagar, A.; Carr, R. W. Flash photolysis time-resolved mass spectrometric investigations of the reactions of CF_3O_2 and CF_3O radicals with NO. *Chem. Phys. Lett.* **1994**, *231*, 454-459, doi:10.1016/0009-2614(94)01277-6.

Bourbon, C.; Brioukov, M.; Devolder, P. Rate constant for the reaction $CF_3O + O_3 \rightarrow$ products by the fast flow absolute technique. *C. R. Acad. Sci. Paris* **1996**, *322*, 181-188.

Bourbon, C.; Brioukov, M.; Hanoune, B.; Sawerysyn, J. P.; Devolder, P. Flow tube/LIF measurements of the rate constant for the reactions with NO of CF_3O and CF_3O_2 radicals. *Chem. Phys. Lett.* **1996**, *254*, 203-212, doi:10.1016/0009-2614(96)00277-1.

Bourbon, C.; Fittschen, C.; Sawerysyn, J. P.; Devolder, P. Temperature dependence of the gas phase reaction rates of CF_3O with methane, ethane, and isobutane. *J. Phys. Chem.* **1995**, *99*, 15102-15107, doi:10.1021/j100041a028.

Bozzelli, J. W. *Ph.D. Thesis*; Dept. of Chemistry, Princeton University, 1973.

Bravo, I.; Díaz-de-Mera, Y.; Aranda, A.; Smith, K.; Shine, K. P.; Marston, G. Atmospheric chemistry of $C_4F_9OC_2H_5$ (HFE-7200), $C_4F_9OCH_3$ (HFE-7100), $C_3F_7OCH_3$ (HFE-7000) and $C_3F_7CH_2OH$: temperature dependence of the kinetics of their reactions with OH radicals, atmospheric lifetimes and global warming potentials. *Phys. Chem. Chem. Phys.* **2010**, *12*, 5115–5125, doi:10.1039/b923092k.

Brown, A. C.; Canosa-Mas, C. E.; Parr, A. D.; Wayne, R. P. Laboratory studies of some halogenated ethanes and ethers: Measurements of rates of reaction with OH and of infrared absorption cross-sections. *Atmos. Environ.* **1990**, *24A*, 2499-2511, doi:10.1016/0960-1686(90)90341-J.

Cavalli, F.; Glasius, M.; Hjorth, J.; Rindone, B.; Jensen, N. R. Atmospheric lifetimes, infrared spectra and degradation products of a series of hydrofluoroethers. *Atmos. Environ.* **1998**, *32*, 3767-3773, doi:10.1016/S1352-2310(98)00106-X.

Chen, L.; Fukuda, F.; Takenaka, N.; Bandow, H.; Maeda, Y. Kinetics of the gas-phase reaction of $CF_3CF_2CH_2OH$ with OH radicals and its atmospheric lifetime. *Int. J. Chem. Kinet.* **2000**, *25*, 73-78, doi:10.1002/(SICI)1097-4601(2000)32:2<73::AID-KIN1>3.0.CO;2-V.

Chen, J.; Young, V.; Zhu, T.; Niki, H. Long path Fourier transform infrared spectroscopic study of the reactions of CF_3OO and CF_3O radicals with NO_2. *J. Phys. Chem.* **1993**, *97*, 11696-11698, doi:10.1021/j100147a024.

Chen, J.; Zhu, T.; Niki, H. FTIR spectroscopic study of the reaction of CF_3O with NO: Evidence for CF_3O + NO $\rightarrow$ CF_2O + FNO. *J. Phys. Chem.* **1992**, *96*, 6115-6117, doi:10.1021/j100194a004.

Chen, J.; Zhu, T.; Niki, H.; Mains, G. J. Long path FTIR spectroscopic study of the reactions of CF_3O radicals with ethane and propane. *Geophys. Res. Lett.* **1992**, *19*, 2215-2218, doi:10.1029/92GL02496.

Chen, L.; Fukuda, F.; Takenaka, N.; Bandow, H.; Maeda, Y. Kinetics of the gas-phase reaction of $CF_3CF_2CH_2OH$ with OH radicals and its atmospheric lifetime. *Int. J. Chem. Kinet.* **2000**, *25*, 73-78, doi:10.1002/(SICI)1097-4601(2000)32:2<73::AID-KIN1>3.0.CO;2-V.

Chen, L.; Kutsuna, S.; Nohara, K.; Takeuchi, K.; Ibusuki, T. Kinetics and mechanisms for the reactions of CF_3OCH_3 and $CF_3OC(O)H$ with OH radicals using an envirionmental reaction chamber. *J. Phys. Chem. A* **2001**, *105*, 10854-10859, doi:10.1021/jp010137r.

Chen, L.; Kutsuna, S.; Tokuhashi, K.; Sekiya, A. New technique for generating high concentrations of gaseous OH radicals in relative rate measurements. *Int. J. Chem. Kinet.* **2003**, *35*, 317-325, doi:10.1002/kin.10133.

Chen, L.; Kutsuna, S.; Tokuhashi, K.; Sekiya, A. Kinetics study of the gas-phase reactions of $CHF_2CF_2OCHF_2$ and $CF_3CHFCF_2OCH_2CF_2CF_3$ with OH radicals at 253-328 K. *Chem. Phys. Lett.* **2005**, *403*, 180-184, doi:10.1016/j.cplett.2005.01.002.

Chen, L.; Kutsuna, S.; Tokuhashi, K.; Sekiya, A. Kinetics and mechanisms of $CF_3CHFOCH_3$, $CF_3CHFOC(O)H$, and $FC(O)OCH_3$ reactions with OH radicals. *J. Phys. Chem. A* **2006**, *110*, 12845-12851, doi:10.1021/jp064917h.

Chen, L.; Kutsuna, S.; Tokuhashi, K.; Sekiya, A.; Takeuchi, K.; Ibusuki, T. Kinetics for the gas-phase reactions of OH radicals with the hydrofluoroethers $CH_2FCF_2OCHF_2$, $CHF_2CF_2OCH_2CF_3$, $CF_3CHFCF_2OCH_2CF_3$, and $CF_3CHFCF_2OCH_2CF_2CHF_2$ at 268-308 K. *Int. J. Chem. Kinet.* **2003**, *35*, 239-245, doi:10.1002/kin.10124.

Chen, L.; Kutsuna, S.; Tokuhashi, K.; Sekiya, A.; Tamai, R.; Hibino, Y. Kinetics and mechanism of $(CF_3)_2CHOCH_3$ reaction with OH radicals in an environmental reaction chamber. *J. Phys. Chem. A* **2005**, *109*, 4766-4771, doi:10.1021/jp050491f.

Chen, L.; Tokuhashi, K.; Kutsuna, S.; Sekiya, A. Rate constants for the gas-phase reaction of $CF_3CF_2CF_2CF_2CF_2CHF_2$ with OH radicals at 250-430 K. *Int. J. Chem. Kinet.* **2004**, *33*, 26–33, doi:10.1002/kin.10170.

Chen, L.; Tokuhashi, K.; Kutsuna, S.; Sekiya, A.; Yonei, Y.; Yamamoto, A. Kinetic study of the gas-phase reaction of $CF_3CHFCF_2CH_2OH$ with OH radicals at 230–430 K. *Chem. Phys. Lett.* **2003**, *382*, 277-282, doi:10.1016/j.cplett.2003.09.162.

Chen, L.; Uchimaru, T.; Kutsuna, S.; Tokuhashi, K.; Sekiya, A. Kinetics of the gas-phase reactions of CHX=CFX (X = H, F) with OH (253-328 K) and NO_3 (298 K) radicals and O_3 (236-308 K). *Int J. Chem. Kinet.* **2010**, *42*, 619-628, doi:10.1002/kin.20506.

Chen, L.; Uchimaru, T.; Kutsuna, S.; Tokuhashi, K.; Sekiya, A. Kinetics and mechanism of gas-phase reactions of *n*-$C_4F_9OCH_3$, *i*-$C_4F_9OCH_3$, *n*-$C_4F_9OC(O)H$, and *i*-$C_4F_9OC(O)H$ with OH radicals in an environmental reaction chamber at 253-328 K. *Chem. Phys. Lett.* **2011**, *514*, 207–213, doi:10.1016/j.cplett.2011.08.049.

Chen, L.; Uchimaru, T.; Kutsuna, S.; Tokuhashi, K.; Sekiya, A.; Okamoto, H. Kinetics and mechanism of gas-phase reaction of $CF_3CF_2CF_2CF_2CF_2CF_2CF_2H$ with OH radicals in an environmental reaction chamber at 253-328 K. *Chem. Phys. Lett.* **2011**, *501*, 263–266, doi:10.1016/j.cplett.2010.12.009.

Clyne, M. A. A.; Hodgson, A. Absolute rate constants for the reaction of fluorine atoms with H_2, CH_2Cl_2, CH_2ClF, CH_2F_2 and $CHCl_2$. *J. Chem. Soc. Faraday Trans. 2* **1985**, *81*, 443-455, doi:10.1039/f29858100443.

Clyne, M. A. A.; Holt, P. M. Reaction kinetics involving ground $X^2\Pi$ and excited $A^2\Sigma^+$ hydroxyl radicals Part 2.-Rate constants for reactions of OH $X^2\Pi$ with halogenomethanes and halogenoethanes. *J. Chem. Soc. Faraday Trans. 2* **1979**, *75*, 582-591, doi:10.1039/f29797500582.

Clyne, M. A. A.; McKenney, D. J.; Walker, R. F. Reaction kinetics of ground state fluorine, $F(^2P)$, atoms. I. Measurement of fluorine atom concentrations and the rates of reactions F + CHF_3 and F + Cl_2 using mass spectrometry. *Can. J. Chem.* **1973**, *51*, 3596-3604, doi:10.1139/v73-535.

Clyne, M. A. A.; Watson, R. T. Kinetic studies of diatomic free radicals using mass spectrometry Part 1.-System description and applications to F atoms and FO radicals. *J. Chem. Soc. Faraday Trans. 1* **1974**, *70*, 1109-1123, doi:10.1039/f19747001109.

Colussi, A. J.; Grela, M. A. Rate of the reaction between oxygen monofluoride and ozone. Implications for the atmospheric role of fluorine. *Chem. Phys. Lett.* **1994**, *229*, 134-138, doi:10.1016/0009-2614(94)01021-8.

Cometto, P. M.; Taccone, R. A.; Nieto, J. D.; Dalmasso, P. R.; Lane, S. I. Kinetic study of OH radical reactions with $CF_3CCl=CCl_2$, $CF_3CCl=CClCF_3$ and $CF_3CF=CFCF_3$. *ChemPhysChem* **2010**, *11*, 4053-4059, doi:10.1002/cphc.201000430.

Czarnowski, J.; Schumacher, H. J. The kinetics and the mechanism of the thermal decomposition of bis(trifluoromethyl) trioxide. The influence of carbon monoxide on its decomposition. *Int. J. Chem. Kinet.* **1981**, *13*, 639-649, doi:10.1002/kin.550130705.

DeMore, W. B. Rate constants for the reactions of OH with HFC-134a (CF_3CH_2F) and HFC-134 (CHF_2CHF_2). *Geophys. Res. Lett.* **1993**, *20*, 1359-1362, doi:10.1029/93GL01336.

DeMore, W. B. Experimental and estimated rate constants for the reactions of hydroxyl radicals with several halocarbons. *J. Phys. Chem.* **1996**, *100*, 5813-5820, doi:10.1021/jp953216+.

DeMore, W. B.; Wilson, E. W., Jr. Rate constant and temperature dependence for the reaction of hydroxyl radicals with 2-fluoropropane (HFC-281ea). *J. Phys. Chem. A* **1999**, *103*, 573-576, doi:10.1021/jp9835521.

Dibble, T. S.; Maricq, M. M.; Szente, J. J.; Francisco, J. S. Kinetics of the reaction of CF_3O with NO. *J. Phys. Chem.* **1995**, *99*, 17394-17402, doi:10.1021/j100048a014.

Dodonov, A. F.; Lavrovskaya, G. K.; Morozov, I. I.; Tal'rose, V. L. *Dokl. Adak. Nauk USSR, 1971, Vol. 198, 622: Dokl. Phys. Chem. (Engl. Trans.)* **1971**, *198*, 440-442.

Dognon, A. M.; Caralp, F.; Lesclaux, R. Réactions des radicaux chlorofluorométhyl péroxyles avec NO: Étude cinétique dans le domaine de température compris entre 230 et 430 K. *J. Chim. Phys.* **1985**, *82*, 349-352, doi:10.1051/jcp/1985820349.

Fasano, D. M.; Nogar, N. S. Rate determination for F + CH_4 by real-time competitive kinetics. *Chem. Phys. Lett.* **1982**, *92*, 411-414, doi:10.1016/0009-2614(82)83438-6.

Fockenberg, C.; Saathoff, H.; Zellner, R. A laser photolysis/LIF study of the rate constant for the reaction CF_3O + O_3 → products. *Chem. Phys. Lett.* **1994**, *218*, 21-28, doi:10.1016/0009-2614(93)E1457-R.

Foon, R.; Reid, G. P. Kinetics of the gas phase fluorination of hydrogen and alkanes. *Trans. Faraday Soc.* **1971**, *67*, 3513-3520, doi:10.1039/tf9716703513.

Frost, R. J.; Green, D. S.; Osborn, M. K.; Smith, I. W. M. Time-resolved vibrational chemiluminescence: Rate constants for the reactions of F atoms with H_2O and HCN, and for the relaxation of HF (v = 1) by H_2O and HCN. *Int. J. Chem. Kinet.* **1986**, *18*, 885-898, doi:10.1002/kin.550180808.

Garland, N. L.; Medhurst, L. J.; Nelson, H. H. Potential chlorofluorocarbon replacements: OH reaction rate constants between 250 and 315 K and infrared absorption spectra. *J. Geophys. Res.* **1993**, *98*, 23107-23111, doi:10.1029/93JD02550.

Garland, N. L.; Nelson, H. H. Temperature dependent kinetics of the reaction OH + $CF_3CH_2CF_3$. *Chem. Phys. Lett.* **1996**, *248*, 296-300, doi:10.1016/0009-2614(95)01288-5.

Gierczak, T.; Bernard, F. o.; Papanastasiou, D. K.; Burkholder, J. B. Atmospheric chemistry of *c*-C_5HF_7 and *c*-C_5F_8: Temperature-dependent OH reaction rate coefficients, degradation products, infrared spectra, and global warming potentials. *J. Phys. Chem. A* **2021**, *125*, 1050−1061, doi:10.1021/acs.jpca.0c10561.

Gierczak, T.; Talukdar, R.; Vaghjiani, G. L.; Lovejoy, E. R.; Ravishankara, A. R. Atmospheric fate of hydrofluoroethanes and hydrofluorochloroethanes: 1. Rate coefficients for reactions with OH. *J. Geophys. Res.* **1991**, *96*, 5001-5011, doi:10.1029/90JD02736.

Gierczak, T.; Talukdar, R. K.; Burkholder, J. B.; Portmann, R. W.; Daniel, J. S.; Solomon, S.; Ravishankara, A. R. Atmospheric fate and greenhouse warming potentials of HFC 236fa and HFC 236ea. *J. Geophys. Res.* **1996**, *101*, 12905-12911, doi:10.1029/96JD00059.

González, S.; Jiménez, E.; Ballesteros, B.; Martinez, E.; Albaladejo, J. Hydroxyl radical reaction rate coefficients as a function of temperature and IR absorption cross sections for $CF_3CH=CH_2$ (HFO-1243zf), potential replacement of CF_3CH_2F (HFC-134a). *Environ. Sci. Pollut. Res.* **2014**, doi:10.1007/s11356-014-3426-2.

Guo, Q.; Zhang, N.; Uchimaru, T.; Chen, L.; Quan, H.; Mizukado, J. Atmospheric chemistry of cyc-$CF_2CF_2CF_2CH=CH$-: Kinetics, products, and mechanism of gas-phase reaction with OH radicals, and atmospheric implications. *Atmos. Environ.* **2018**, *179*, 69–75, doi:10.1016/j.atmosenv.2018.02.005.

Guo, Q.; Zhang, N.; Uchimaru, T.; Chen, L.; Quan, H.; Mizukadob, J. Kinetics, products, and mechanism for the reaction of *E*−$CF_3CH=CHC_2F_5$ with OH radicals in gas phase and atmospheric implications. *Atmos. Environ.* **2018**, *185*, 7-14, doi:10.1016/j.atmosenv.2018.04.047.

Handwerk, V.; Zellner, R. Kinetics of the reactions of OH radicals with some halocarbons ($CHClF_2$, CH_2ClF, CH_2ClCF_3, CH_3CClF_2, CH_3CHF_2) in the temperature range 260-370 K. *Ber. Bunsenges. Phys. Chem.* **1978**, *82*, 1161-1166, doi:10.1002/bbpc.19780821117.

Heathfield, A. E.; Anastasi, C.; Pagsberg, P.; McCulloch, A. Atmospheric lifetimes of selected fluorinated ether compounds. *Atmos. Environ.* **1998**, *32*, 711-717, doi:10.1016/S1352-2310(97)00330-0.

Heidner, R. F.; Bott, J. F.; Gardner, C. E.; Melzer, J. E. Absolute rate coefficients for F + H_2 and F + D_2 at T = 295 K. *J. Chem. Phys.* **1979**, *70*, 4509-4514, doi:10.1063/1.437288.

Heidner, R. F.; Bott, J. F.; Gardner, C. E.; Melzer, J. E. Absolute rate coefficients for F + H_2 and F + D_2 at T = 295-765 K. *J. Chem. Phys.* **1980**, *72*, 4815-4821, doi:10.1063/1.439819.

Howard, C. J. Rate constants for the gas-phase reactions of OH radicals with ethylene and halogenated ethylene compounds. *J. Chem. Phys.* **1976**, *65*, 4771-4777, doi:10.1063/1.432932.

Howard, C. J.; Evenson, K. M. Rate constants for the reactions of OH with CH_4 and fluorine, chlorine, and bromine substituted methanes at 296 K. *J. Chem. Phys.* **1976**, *64*, 197-202, doi:10.1063/1.431950.

Howard, C. J.; Evenson, K. M. Rate constants for the reactions of OH with ethane and some halogen substituted ethanes at 296 K. *J. Chem. Phys.* **1976**, *64*, 4303-4306, doi:10.1063/1.432115.

Hsu, K. J.; DeMore, W. B. Rate constants and temperature dependences for the reactions of hydroxyl radical with several halogenated methanes, ethanes, and propanes by relative rate measurements. *J. Phys. Chem.* **1995**, *99*, 1235-1244, doi:10.1021/j100004a025.

Hsu, K. J.; DeMore, W. B. Temperature-dependent rate constants and substituent effects for the reactions of hydroxyl radicals with three partially fluorinated ethers. *J. Phys. Chem.* **1995**, *99*, 11141-11930, doi:10.1021/j100028a014.

Huey, L. G.; Dunlea, E. J.; Howard, C. J. Gas-phase acidity of CF_3OH. *J. Phys. Chem.* **1996**, *100*, 6504-6508, doi:10.1021/jp953058m.

Hurley, M. D.; Ball, J. C.; Wallington, T. J. Atmospheric chemistry of the Z and E isomers of $CF_3CF=CHF$; Kinetics, mechanisms, and products of gas-phase reactions with Cl atoms, OH radicals, and O_3. *J. Phys. Chem. A* **2007**, *111*, 9789-9795, doi:10.1021/jp0753530.

Hurley, M. D.; Misner, J. A.; Ball, J. C.; Wallington, T. J.; Ellis, D. A.; Martin, J. W.; Mabury, S. A.; Andersen, M. P. S. Atmospheric chemistry of $CF_3CH_2CH_2OH$: Kinetics, mechanisms and products of Cl atom and OH radical initiated oxidation in the presence and absence of NO_X. *J. Phys. Chem. A* **2005**, *109*, 9816–9826, doi:10.1021/jp0535902.

Hurley, M. D.; Wallington, T. J.; Sulbaek Andersen, M. P.; Ellis, D. A.; Martin, J. W.; Mabury, S. A. Atmospheric chemistry of fluorinated alcohols: Reaction with Cl atoms and OH radicals and atmospheric lifetimes. *J. Phys. Chem. A* **2004**, *108*, 1973, doi:10.1021/jp0373088.

Igoshin, V. I.; Kulakov, L. V.; Nikitin, A. I. Determination of the rate constant of the chemical reaction $F + H_2(D_2) \rightarrow HF(DF) + H(D)$ from the stimulated emission of the HF(DF) molecules. *Sov. J. Quant. Electron.* **1974**, *3*, 306.

Jensen, N. R.; Hanson, D. R.; Howard, C. J. Temperature dependence of the gas phase reactions of CF_3O with CH_4 and NO. *J. Phys. Chem.* **1994**, *98*, 8574-8579, doi:10.1021/j100085a042.

Jeong, K. M.; Hsu, K. J.; Jeffries, J. B.; Kaufman, F. Kinetics of the reactions of OH with C_2H_6, CH_3CCl_3, $CH_2ClCHCl_2$, $CH_2ClCClF_2$, and CH_2FCF_3. *J. Phys. Chem.* **1984**, *88*, 1222-1226, doi:10.1021/j150650a041.

Jeong, K. M.; Kaufman, F. Kinetics of the reaction of hydroxyl radical with methane and with nine Cl- and F-substituted methanes. 1. Experimental results, comparisons, and applications. *J. Phys. Chem.* **1982**, *86*, 1808-1815, doi:10.1021/j100207a016.

Jia, X. Q.; Chen, L.; Mizukado, J.; Kutsuna, S.; Tokuhashi, K. Rate constants for the gas-phase reactions of cyclo-$CX=CXCF_2CF_2$- (X = H, F) with OH radicals at a temperature range of 253–328 K. *Chem. Phys.Lett.* **2013**, *572*, 21–25, doi:10.1016/j.cplett.2013.04.020.

Jiménez, E.; Antinolo, M.; Ballesteros, B.; Martínez, E.; Albaladejo, J. Atmospheric lifetimes and global warming potentials of $CF_3CH_2CH_2OH$ and $CF_3(CH_2)_2CH_2OH$. *Chem. Phys. Chem.* **2010**, *11*, 4079–4087, doi:10.1002/cphc.201000365.

Jubb, A. M.; Gierczak, T.; Baasandorj, M.; Waterland, R. L.; Burkholder, J. B. Methyl-perfluoroheptene-ethers ($CH_3OC_7F_{13}$): Measured OH radical reaction rate coefficients for several isomers and enantiomers and their atmospheric lifetimes and global warming potentials. *Environ. Sci. Technol.* **2014**, *48*, 4954-4962, doi:10.1021/es500888v.

Kelly, C.; Treacy, J.; Sidebottom, H. W.; Nielsen, O. J. Rate constants for the reaction of CF_3O radicals with hydrocarbons at 298 K. *Chem. Phys. Lett.* **1993**, *207*, 498-503, doi:10.1016/0009-2614(93)89036-H.

Kelly, T.; Bossoutrot, V.; Magneron, I.; Wirtz, K.; Treacy, J.; Mellouki, A.; Sidebottom, H.; Le Bras, G. A kinetic and mechanistic study of the reactions of OH radicals and Cl atoms with 3,3,3-trifluoropropanol under atmospheric conditions. *J. Phys. Chem. A* **2005**, *109*, 347–355, doi:10.1021/jp0467402.

Kompa, K. L.; Wanner, J. Study of some fluorine atom reactions using a chemical laser method. *Chem. Phys. Lett.* **1972**, *12*, 560-563, doi:10.1016/0009-2614(72)80008-3.

Kovács, G.; Szász-Vadász, T.; Papadimitriou, V. C.; Dóbé, S.; Bérces, T.; Márta, F. Absolute rate constants for the reactions of OH radicals with CH_3CH_2OH, CF_2HCH_2OH and CF_3CH_2OH. *React. Kinet. Catal. Lett.* **2005**, *87*, 129-138, doi:10.1007/s11144-006-0018-2.

Kowalczyk, J.; Jowko, A.; Symanowicz, M. Kinetics of radical reactions in freons. *J. Radioanal. Nucl. Chem.* **1998**, *232*, 75-78, doi:10.1007/BF02383716.

Kozlov, S. N.; Orkin, V. L.; Kurylo, M. J. An investigation of the reactivity of OH with fluoroethanes: CH_3CH_2F (HFC-161), CH_2FCH_2F (HFC-152), and CH_3CHF_2 (HFC-152a). *J. Phys. Chem. A* **2003**, *107*, 2239-2246, doi:10.1021/jp022087b.

Kumar, A.; Gonu, S.; Vijayakumar, S.; Ramya, C. B.; Rajakumar, B. Experimental and computational investigations of the tropospheric photooxidation reactions of 1,1,1,3,3,3-hexafluoro-2-methyl-2-propanol initiated by OH radicals and Cl atoms. *J. Phys. Chem. A* **2021**, *125*, 523−535, doi:10.1021/acs.jpca.0c08130.

Langbein, T.; Sonntag, H.; Trapp, D.; Hoffmann, A.; Malms, W.; Röth, E.-P.; Mörs, V.; Zellner, R. Volatile anaesthetics and the atmosphere: atmospheric lifetimes and atmospheric effects of halothane, enflurane, isoflurane, desflurane and sevoflurane. *British J. Anaest.* **1999**, *82*, 66-73.

Leu, G.-H.; Lee, Y.-P. Temperature dependence of the rate coefficient of the reaction $OH + CF_3CH_2F$ over the range 255-424 K. *J. Chin. Chem. Soc.* **1994**, *41*, 645-649, doi:10.1002/jccs.199400091.

Li, Z.; Friedl, R. R.; Sander, S. P. Kinetics of FO_2 with NO, NO_2, O_3, CH_4 and C_2H_6. *J. Phys. Chem.* **1995**, *99*, 13445-13451, doi:10.1021/j100036a019.

Li, Z.; Jeong, G.-R.; Hansen, J. C.; Good, D. A.; Francisco, J. S. Rate constant for the reactions of $CF_3OCHFCF_3$ with OH and Cl. *Chem. Phys. Lett.* **2000**, *320*, 70–76, doi:10.1016/S0009-2614(00)00192-5.

Li, Z.; Tao, Z.; Naik, V.; Good, D. A.; Hansen, J. C.; Jeong, G.-R.; Francisco, J. S.; Jain, A. K.; Wuebbles, D. J. Global warming potential assessment for $CF_3OCF=CF_2$. *J. Geophys. Res.* **2000**, *105*, 4019–4029, doi:10.1029/1999JD900943.

Liu, R.; Huie, R. E.; Kurylo, M. J. Rate constants for the reactions of the OH radical with some hydrochlorofluorocarbons over the temperature range 270-400 K. *J. Phys. Chem.* **1990**, *94*, 3247-3249, doi:10.1021/j100371a004.

Liu, D.; Qin, S.; Li, W.; Zhang, D.; Guo, Z. Atmospheric chemistry of 1H-Heptafluorocyclopentene (*cyc*-$CF_2CF_2CF_2CF=CH$-): rate constant, products, and mechanism of gas-phase reactions with OH radicals, IR absorption spectrum, photochemical ozone creation potential, and global warming potential. *J. Phys. Chem. A* **2016**, *120*, 9557-9563, doi:10.1021/acs.jpca.6b10348.

Maricq, M. M.; Szente, J. J. Upper limits for the rate constants of the reactions $CF_3O + O_3 \rightarrow CF_3O_2 + O_2$ and $CF_3O_2 + O_3 \rightarrow CF_3O + 2O_2$. *Chem. Phys. Lett.* **1993**, *213*, 449-456, doi:10.1016/0009-2614(93)89141-4.

Martin, J.-P.; Paraskevopoulos, G. A kinetic study of the reactions of OH radicals with fluoroethanes. Estimates of C-H bond strengths in fluoroalkanes. *Can. J. Chem.* **1983**, *61*, 861-865, doi:10.1139/v83-155.

Mashino, M.; Kawasaki, M.; Wallington, T. J.; Hurley, M. D. Atmospheric degradation of $CF_3OCF=CF_2$: Kinetics and mechanism of its reaction with OH radicals and Cl atoms. *J. Phys. Chem. A* **2000**, *104*, 2925–2930, doi:10.1021/jp000498r.

Mashino, M.; Ninomiya, Y.; Kawasaki, M.; Wallington, T. J.; Hurley, M. D. Atmospheric chemistry of $CF_3CF=CF_2$: Kinetics and mechanism of its reactions with OH radicals, Cl atoms, and ozone. *J. Phys. Chem. A* **2000**, *104*, 7255-7260, doi:10.1021/jp000498r.

McIlroy, A.; Tully, F. P. Kinetic study of OH reactions with perfluoropropene and perfluorobenzene. *J. Phys. Chem.* **1993**, *97*, 610-614, doi:10.1021/j100105a013.

Medhurst, L. J.; Fleming, J.; Nelson, H. H. Reaction rate constants of $OH + CHF_3 \rightarrow$ products and $O(^3P) + CHF_3 \rightarrow OH + CF_3$ at 500−750 K. *Chem. Phys. Lett.* **1977**, *266*, 607-611, doi:10.1016/S0009-2614(97)00049-3.

Meller, R.; Moortgat, G. K. Photolysis of $CF_3O_2CF_3$ in the presence of O_3 in oxygen: kinetic study of the reactions of CF_3O and CF_3O_2 radicals with O_3. *J. Photochem. Photobio. A: Chem.* **1995**, *86*, 15-25, doi:10.1016/1010-6030(94)03951-P.

Mellouki, A.; Le Bras, G.; Poulet, G. Discharge flow kinetic study of NO_3 reactions with free radicals: The reaction of NO_3 with Cl. *J. Phys. Chem.* **1987**, *91*, 5760-5764, doi:10.1021/j100306a048.

Mellouki, A.; Teton, S.; Le Bras, G. Rate constant for the reaction of OH with HFC-365mfc ($CF_3CH_2CF_2CH_3$). *Geophys. Res. Lett.* **1995**, *22*, 389-392, doi:10.1029/94GL03275.

Michelat, L.; Mellouki, A.; Ravishankara, A. R.; El Othmani, H.; Papadimitriou, V. C.; Daële, V.; McGillen, M. R. Temperature-dependent structure-activity relationship of OH + haloalkene rate coefficients under atmospheric conditions and supporting measurements. *ACS Earth Space Chem.* **2022**, *6*, 3101-3114, doi:10.1021/acsearthspacechem.2c00296.

Montgomery, J. A.; Michels, H. H.; Francisco, J. S. Ab initio calculation of the heats of formation of CF_3OH and CF_2O. *Chem. Phys. Lett.* **1994**, *220*, 391-396, doi:10.1016/0009-2614(94)00211-8.

Nelson, D. D., Jr.; Zahniser, M. S.; Kolb, C. E. OH reaction kinetics and atmospheric lifetimes of CF_3CFHCF_3 and CF_3CH_2Br. *Geophys. Res. Lett.* **1993**, *20*, 197-200, doi:10.1029/93GL00239.

Nelson, D. D.; Zahniser, M. S.; Kolb, C. E.; Magid, H. OH reaction kinetics and atmospheric lifetime estimates for several hydrofluorocarbons. *J. Phys. Chem.* **1995**, *99*, 16301-16306, doi:10.1021/j100044a016.

Nielsen, O. J. Rate constants for the gas-phase reactions of OH radicals with CH_3CHF_2 and $CHCl_2CF_3$ over the temperature range 295-388 K. *Chem. Phys. Lett.* **1991**, *187*, 286-290, doi:10.1016/0009-2614(91)90427-B.

Nielsen, O. J.; Javadi, M. S.; Sulbaek Andersen, M. P.; Hurley, M. D.; Wallington, T. J.; Singh, R. Atmospheric chemistry of $CF_3CF=CH_2$: Kinetics and mechanisms of gas-phase reactions with Cl atoms, OH radicals, and O_3. *Chem. Phys. Lett.* **2007**, *439*, 18-22, doi:10.1016/j.cplett.2007.03.053.

Nielsen, O. J.; Sehested, J. Upper limits for the rate constants of the reactions of CF_3O_2 and CF_3O radicals with ozone at 295 K. *Chem. Phys. Lett.* **1993**, *213*, 433-441, doi:10.1016/0009-2614(93)89139-9.

Nilsson, E. J. K.; Nielsen, O. J.; Johnson, M. S.; Hurley, M. D.; Wallington, T. J. Atmospheric chemistry of *cis*-$CF_3CH=CHF$: Kinetics of reactions with OH radicals and O_3 and products of OH radical initiated oxidation. *Chem. Phys. Lett.* **2009**, *473*, 233–237, doi:10.1016/j.cplett.2009.03.076.

Ninomiya, Y.; Kawasaki, M.; Guschin, A.; Molina, L. T.; Molina, M. J.; Wallington, T. J. Atmospheric chemistry of *n*-$C_3F_7OCH_3$: Reaction with OH radicals and Cl atoms and atmospheric fate of *n*-$C_3F_7OCH_2O(\bullet)$ radicals. *Environ. Sci. Technol.* **2000**, *34*, 2973-2978, doi:10.1021/es991449z.

Nip, W. S.; Singleton, D. L.; Overend, R.; Paraskevopoulos, G. Rates of OH radical reactions. 5. Reactions with CH_3F, CH_2F_2, CHF_3, CH_3CH_2F, and CH_3CHF_2 at 297 K. *J. Phys. Chem.* **1979**, *83*, 2440-2443, doi:10.1021/j100482a003.

Orkin, V. L.; Huie, R. E.; Kurylo, M. J. Atmospheric lifetimes of HFC-143a and HFC-245fa. *J. Phys. Chem.* **1996**, *100*, 8907-8912, doi:10.1021/jp9601882.

Orkin, V. L.; Huie, R. E.; Kurylo, M. J. Rate constants for the reactions of OH with HFC-245cb ($CH_3CF_2CF_3$) and some fluoroalkenes (CH_2CHCF_3, CH_2CFCF_3, CF_2CFCF_3, and CF_2CF_2). *J. Phys. Chem. A* **1997**, *101*, 9118-9124, doi:10.1021/jp971994r.

Orkin, V. L.; Khamaganov, V. G. Determination of rate constants for reactions of some hydrohaloalkanes with OH radicals and their atmospheric lifetimes. *J. Atmos. Chem.* **1993**, *16*, 157-167, doi:10.1007/BF00702785.

Orkin, V. L.; Khamaganov, V. G.; Guschin, A. G. Photochemical properties of hydrofluoroethers CH_3OCHF_2, CH_3OCF_3, and $CHF_2OCH_2CF_3$: Reactivity toward OH, IR absorption cross sections, atmospheric lifetimes, and global warming potentials. *J. Phys. Chem. A* **2014**, *118*, 10770-10777, doi:10.1021/jp506377w.

Orkin, V. L.; Khamaganov, V. G.; Kurylo, M. J. High accuracy measurements of OH reaction rate constants and IR absorption spectra: Substituted 2-propanols. *J. Phys. Chem. A* **2012**, *116*, 6188-6198, doi:10.1021/jp211534n.

Orkin, V. L.; Khamaganov, V. G.; Martynova, L. E.; Kurylo, M. J. High-accuracy measurements of OH reaction rate constants and IR and UV absorption spectra: Ethanol and partially fluorinated ethyl alcohols. *J. Phys. Chem. A* **2011**, *115*, 8656-8668, doi:10.1021/jp202099t.

Orkin, V. L.; Louis, F.; Huie, R. E.; Kurylo, M. J. Photochemistry of bromine-containing fluorinated alkenes: Reactivity toward OH and UV spectra. *J. Phys. Chem. A* **2002**, *106*, 10195-10199, doi:10.1021/jp014436s.

Orkin, V. L.; Martynova, L. E.; Ilichev, A. N. High-accuracy measurements of OH reaction rate constants and IR absorption spectra: CH_2=CF-CF_3 and *trans*-CHF=CH-CF_3. *J. Phys. Chem. A* **2010**, *114*, 5967-5979, doi:10.1021/jp9092817.

Orkin, V. L.; Martynova, L. E.; Kurylo, M. J. Photochemical properties of CH_2=CH-CFCl-CF_2Br (4-bromo-3-chloro-3,4,4-trifluoro-1-butene) and CH_3-O-CH$(CF_3)_2$ (methyl hexafluoroisopropyl ether): OH reaction rate constants and UV and IR absorption spectra. *J. Phys. Chem. A* **2017**, *121*, 5675–5680, doi:10.1021/acs.jpca.7b04256.

Orkin, V. L.; Martynova, L. E.; Ilichev, A. N. High-accuracy measurements of OH reaction rate constants and IR absorption spectra: CH_2=CF-CF_3 and *trans*-CHF=CH-CF_3. *J. Phys. Chem. A* **2010**, *114*, 5967-5979, doi:10.1021/jp9092817.

Orkin, V. L.; Poskrebyshev, G. A.; Kurylo, M. J. Rate constants for the reactions between OH and perfluorinated alkenes. *J. Phys. Chem. A* **2011**, *115*, 6568-6574, doi:10.1021/jp201663j.

Orkin, V. L.; Villenave, E.; Huie, R. E.; Kurylo, M. J. Atmospheric lifetimes and global warming potentials of hydrofluoroethers: Reactivity toward OH, UV spectra, and IR absorption cross sections. *J. Phys. Chem. A* **1999**, *103*, 9770-9779, doi:10.1021/jp991741t.

Østerstrøm, F. F.; Andersen, S. T.; Sølling, T. I.; Nielsen, O. J.; Andersen, M. P. S. Atmospheric chemistry of *Z*- and *E*-CF_3CH=$CHCF_3$. *Phys. Chem. Chem. Phys.* **2017**, *19*, 735–750, doi:10.1039/c6cp07234h.

Oyaro, N.; Nielsen, C. J. Kinetic study of the OH reaction with the hydrofluoroethers C_4F_9-O-CH_3 and C_4F_9-O-C_2H_5 by the relative rate method. *Asian Chem. Lett.* **2003**, *7*, 119–122.

Oyaro, N.; Sellevag, S. R.; Nielsen, C. J. Study of the OH and Cl-initiated oxidation, IR absorption cross-section, radiative forcing, and global warming potential of four C_4-hydrofluoroethers. *Environ. Sci. Technol.* **2004**, *38*, 5567-5576, doi:10.1021/es0497330.

Oyaro, N.; Sellevag, S. R.; Nielsen, C. J. Atmospheric chemistry of hydrofluoroethers: Reaction of a series of hydrofluoroethers with OH radicals and Cl atoms, atmospheric lifetimes, and global warming potentials. *J. Phys. Chem. A* **2005**, *109*, 337-346, doi:10.1021/jp047860c.

Papadimitriou, V. C.; Burkholder, J. B. OH radical reaction rate coefficients, infrared spectrum, and global warming potential of $(CF_3)_2$CFCH=CHF (HFO-1438ezy(*E*)). *J. Phys. Chem. A* **2016**, *120*, 6618–6628, doi:10.1021/acs.jpca.6b06096.

Papadimitriou, V. C.; Spitieri, C. S.; Papagiannakopoulos, P.; Cazaunau, M.; Lendar, M.; Daéle, V.; Mellouki, A. Atmospheric chemistry of $(CF_3)_2C=CH_2$: OH radicals, Cl atoms and O_3 rate coefficients, oxidation end-products and IR spectra. *Phys. Chem. Chem. Phys* **2015**, *17*, 25607-25620, doi:10.1039/c5cp03840e.

Papadimitriou, V. C.; Talukdar, R. K.; Portmann, R. W.; Ravishankara, A. R.; Burkholder, J. B. $CF_3CF=CH_2$ and (Z)-$CF_3CF=CHF$: temperature dependent OH rate coefficients and global warming potentials. *Phys. Chem. Chem. Phys.* **2008**, *10*, 808-820, doi:10.1039/b714382f.

Peeters, J.; Vertommen, J.; Langhans, I. Rate constants of the reactions of CF_3O_2, i-$C_3H_7O_2$, and t-$C_4H_9O_2$ with NO. *Ber. Bunsenges. Phys. Chem.* **1992**, *96*, 431-436, doi:10.1002/bbpc.19920960339.

Perry, R. A.; Atkinson, R.; Pitts, J. N., Jr. Rate constants for the reaction of OH radicals with $CH_2=CHF$, $CH_2=CHCl$, and $CH_2=CHBr$ over the temperature range 299-426 °K. *J. Chem. Phys.* **1977**, *67*, 458-462, doi:10.1063/1.434889.

Persky, A. Kinetics of the F + CH_4 reaction in the temperature range 184-406 K. *J. Phys. Chem.* **1996**, *100*, 689-693, doi:10.1021/jp9524035.

Plumb, I. C.; Ryan, K. R. Kinetics of the reaction of CF_3O_2 with NO. *Chem. Phys. Lett.* **1982**, *92*, 236-238, doi:10.1016/0009-2614(82)80267-4.

Rahman, M. M.; Becker, E.; Benter, T.; Schindler, R. N. A gas phase kinetic investigation of the system F + HNO_3 and the determination of absolute rate constants for the reaction of the NO_3 radical with CH_3SH, 2-methylpropene, 1,3-butadiene and 2,3-dimethyl-2-butene. *Ber. Bunsenges. Phys. Chem.* **1988**, *92*, 91-100, doi:10.1002/bbpc.198800018.

Rajakumar, B.; Burkholder, J. B.; Portmann, R. W.; Ravishankara, A. R. Rate coefficients, for the OH + CFH_2CH_2OH reaction between 238 and 355 K. *Phys. Chem. Chem. Phys.* **2005**, *7*, 2498-2505, doi:10.1039/b503332b.

Rajakumar, B.; Portmann, R. W.; Burkholder, J. B.; Ravishankara, A. R. Rate coefficients for the reactions of OH with $CF_3CH_2CH_3$ (HFC-263fb), CF_3CHFCH_2F (HFC-245eb), and $CHF_2CHFCHF_2$ (HFC-245ea) between 238 and 375 K. *J. Phys. Chem. A* **2006**, *110*, 6724 - 6731, doi:10.1021/jp056248y.

Ravishankara, A. R.; Turnipseed, A. A.; Jensen, N. R.; Barone, S.; Mills, M.; Howard, C. J.; Solomon, S. Do hydrofluorocarbons destroy stratospheric ozone? *Science* **1994**, *263*, 71-75, doi:10.1126/science.263.5143.71.

Ray, G. W.; Watson, R. T. Kinetics study of the reactions of NO with FO, ClO, BrO, and IO at 298 K. *J. Phys. Chem.* **1981**, *85*, 2955-2960, doi:10.1021/j150620a022.

Rivela, C. B.; Tovar, C. M.; Teruel, M. A.; Barnes, I.; Wiesen, P.; Blanco, M. B. CFCs replacements: Reactivity and atmospheric lifetimes of a series of Hydrofluoroolefins towards OH radicals and Cl atoms. *Chem. Phys. Lett.* **2019**, *714*, 190-196, doi:10.1016/j.cplett.2018.10.078.

Saathoff, H.; Zellner, R. LIF detection of the CF_3O radical and kinetics of its reactions with CH_4 and C_2H_6. *Chem. Phys. Lett.* **1993**, *206*, 349-354, doi:10.1016/0009-2614(93)85563-4.

Schmoltner, A. M.; Talukdar, R. K.; Warren, R. F.; Mellouki, A.; Goldfarb, L.; Gierczak, T.; McKeen, S. A.; Ravishankara, A. R. Rate coefficients for reactions of several hydrofluorocarbons with OH and $O(^1D)$ and their atmospheric lifetimes. *J. Phys. Chem.* **1993**, *97*, 8976-8982, doi:10.1021/j100137a023.

Schneider, W. F.; Wallington, T. J. Thermochemistry of COF_2 and related compounds. *J. Phys. Chem.* **1994**, *98*, 7448-7451, doi:10.1021/j100082a009.

Sehested, J.; Nielsen, O. J. Absolute rate constants for the reaction of CF_3O_2 and CF_3O radicals with NO at 295 K. *Chem. Phys. Lett.* **1993**, *206*, 369-375, doi:10.1016/0009-2614(93)85567-8.

Sehested, J.; Sehested, K.; Nielsen, O. J.; Wallington, T. J. Atmospheric chemistry of FO_2 radicals: Reaction with CH_4, O_3, NO, NO_2, and CO at 295 K. *J. Phys. Chem.* **1994**, *98*, 6731-6739, doi:10.1021/j100078a014.

Sellevåg, S. R.; Nielsen, C. J.; Søvde, O. A.; Myhre, G.; Sundet, J. K.; Stordal, F.; Isaksen, I. S. A. Atmospheric gas-phase degradation and global warming potentials of 2-fluoroethanol, 2,2-difluoroethanol, and 2,2,2-trifluoroethanol. *Atmos. Environ.* **2004**, *38*, 6725-6735, doi:10.1016/j.atmosenv.2004.09.023.

Singleton, D. L.; Paraskevopoulos, G.; Irwin, R. S. Reaction of OH with CH_3CH_2F. The extent of H abstraction from the α and β positions. *J. Phys. Chem.* **1980**, *84*, 2339-2343, doi:10.1021/j100456a001.

Sondergaard, R.; Nielsen, O. J.; Hurley, M. D.; Wallington, T. J.; Singh, R. Atmospheric chemistry of *trans*-$CF_3CH = CHF$: Kinetics of the gas-phase reactions with Cl atoms, OH radicals, and O_3. *Chem. Phys. Lett.* **2007**, *443*, 199-204, doi:10.1016/j.cplett.2007.06.084.

Srinivasulu, G.; Bunkan, A. J. C.; Amedro, D.; Crowley, J. N. Absolute and relative-rate measurement of the rate coefficient for reaction of perfluoro ethyl vinyl ether ($C_2F_5OCF=CF_2$) with OH. *Phys. Chem. Chem. Phys.* **2018**, *20*, 3761-3767, doi:10.1039/c7cp08056e.

Staricco, E. H.; Sicre, S. E.; Schumacher, H. J. Die photochemische reaktion zwisehen fluor und ozon. *Z. Phys. Chem. N.F.* **1962**, *31*, 385.

Stevens, P. S.; Brune, W. H.; Anderson, J. G. Kinetic and mechanistic investigations of F + H_2O/D_2O and F + H_2/D_2 over the temperature range 240-373 K. *J. Phys. Chem.* **1989**, *93*, 4068-4079, doi:10.1021/j100347a040.

Sulbaek Andersen, M. P.; Nielsen, O. J.; Karpichev, B.; Wallington, T. J.; Sander, S. P. Atmospheric chemistry of isoflurane, desflurane, and sevoflurane: Kinetics and mechanisms of reactions with chlorine atoms and OH radicals and global warming potentials. *J. Phys. Chem. A* **2012**, *116*, 5806-5820, doi:10.1021/jp2077598.

Sulbaek Andersen, M. P.; Nielsen, O. J.; Toft, A.; Nakayama, T.; Matsumi, Y.; Waterland, R. L.; Buck, R. C.; Hurley, M. D.; Wallington, T. J. Atmospheric chemistry of $C_xF_{2x+1}CH=CH_2$ (x=1, 2, 4, 6, and 8): Kinetics of gas-phase reactions with Cl atoms, OH radicals, and O_3. *J. Photochem. Photobiol. A: Chem.* **2005**, *176*, 124-128, doi:10.1016/j.jphotochem.2005.06.015.

Sulbaek Andersen, M. P.; Nielsen, O. J.; Wallington, T. J.; Hurley, M. D.; DeMore, W. B. Atmospheric chemistry of $CF_3OCF_2CF_2H$ and $CF_3OC(CF_3)_2H$: Reaction with Cl atoms and OH radicals, degradation mechanism, global warming potentials, and empirical relationship between *k*(OH) and *k*(Cl) for organic compounds. *J. Phys. Chem. A* **2005**, *109*, 3926-3934.

Szilagyi, I.; Dobe, S.; Berces, T. Rate constant for the reaction of the OH-radical with CH_2F_2. *React. Kinet. Catal. Lett.* **2000**, *70*, 319-324, doi:10.1023/A:1010349118536.

Takahashi, K.; Matsumi, Y.; Wallington, T. J.; Hurley, M. D. Atmospheric chemistry of $CF_3CFHOCF_3$: Reaction with OH radicals, atmospheric lifetime, and global warming potential. *J. Geophys. Res.* **2002**, *107*, 4574, doi:10.1029/2002JD002125.

Taketani, F.; Nakayama, T.; Takahashi, K.; Matsumi, Y.; Hurley, M. D.; Wallington, T. J.; Toft, A.; Sulbaek Andersen, M. P. Atmospheric chemistry of CH_3CHF_2 (HFC-152a): Kinetics, mechanisms, and products of Cl atom- and OH radical-initiated oxidation in the presence and absence of NO_x. *J. Phys. Chem. A* **2005**, *109*, 9061-9069, doi:10.1021/jp044218+.

Talukdar, R.; Mellouki, A.; Gierczak, T.; Burkholder, J. B.; McKeen, S. A.; Ravishankara, A. R. Atmospheric fate of CF_2H_2, CH_3CF_3, CHF_2CF_3, and CH_3CFCl_2: Rate coefficients for reactions with OH and UV absorption cross sections of CH_3CFCl_2. *J. Phys. Chem.* **1991**, *95*, 5815-5821, doi:10.1021/j100168a021.

Tokuhashi, K.; Chen, L.; Kutsuna, S.; Uchimaru, T.; Sugie, M.; Sekiya, A. Environmental assessment of CFC alternatives - Rate constants for the reactions of OH radicals with fluorinated compounds. *J. Fluor. Chem.* **2004**, *125*, 1801-1807, doi:10.1016/j.jfluchem.2004.09.013.

Tokuhashi, K.; Nagai, H.; Takahashi, A.; Kaise, M.; Kondo, S.; Sekiya, A.; Takahashi, M.; Gotoh, Y.; Suga, A. Measurement of the OH reaction rate constants for CF_3CH_2OH, $CF_3CF_2CH_2OH$, and $CF_3CH(OH)CF_3$. *J. Phys. Chem. A* **1999**, *103*, 2664-2672, doi:10.1021/jp983961x.

Tokuhashi, K.; Takahashi, A.; Kaise, M.; Kondo, S. Rate constants for the reactions of OH radicals with CH_3OCF_2CHFCl, CHF_2OCF_2CHFCl, $CHF_2OCHClCF_3$, and $CH_3CH_2OCF_2CHF_2$. *J. Geophys. Res.* **1999**, *104*, 18681-18688, doi:10.1029/1999JD900278.

Tokuhashi, K.; Takahashi, A.; Kaise, M.; Kondo, S.; Sekiya, A.; Fujimoto, E. Rate constants for the reactions of OH radicals with $CF_3OCF=CF_2$ and $CF_3CF=CF_2$. *Chem. Phys. Lett.* **2000**, *325*, 189-195, doi:10.1016/S0009-2614(00)00626-6.

Tokuhashi, K.; Takahashi, A.; Kaise, M.; Kondo, S.; Sekiya, A.; Yamashita, S.; Ito, H. Rate Constants for the Reactions of OH Radicals with $CH_3OCF_2CF_3$, $CH_3OCF_2CF_2CF_3$, and $CH_3OCF(CF_3)_2$. *Int. J. Chem. Kinet.* **1999**, *31*, 846-853, doi:10.1002/(SICI)1097-4601(1999)31:12<846::AID-KIN2>3.0.CO;2-4.

Tokuhashi, K.; Takahashi, A.; Kaise, M.; Kondo, S.; Sekiya, A.; Yamashita, S.; Ito, H. Rate constants for the reactions of OH radicals with $CH_3OCF_2CHF_2$, $CHF_2OCH_2CF_2CHF_2$, $CHF_2OCH_2CF_2CF_3$, and $CF_3CH_2OCF_2CHF_2$ over the temperature range 250-430 K. *J. Phys. Chem. A* **2000**, *104*, 1165-1170, doi:10.1021/jp991421+.

Tokuhashi, K.; Takizawa, K.; Kondo, S. Rate constants for the reactions of OH radicals with $CF_3CX=CY_2$ (X = H, F, CF_3, Y=H, F, Cl). *Environ. Sci. Pollut. Res.* **2018**, *25*, 15204-15215, doi:10.1007/s11356-018-1700-4.

Tokuhashi, K.; Takizawa, K.; Kondo, S. Rate constants for the reactions of OH radicals with fluorinated ethenes: Kinetic measurements and correlation between structure and reactivity. *J. Phys. Chem. A* **2018**, *122*, 4593–4600, doi:10.1021/acs.jpca.7b11653.

Tokuhashi, K.; Takizawa, K.; Kondo, S. Correction to "Rate constants for the reactions of OH radicals with fluorinated ethenes: Kinetic measurements and correlation between structure and reactivity". *J. Phys. Chem. A* **2019**, *123*, 382−383, doi:10.1021/acs.jpca.8b11536.

Tokuhashi, K.; Takizawa, K.; Kondo, S. Rate constants for reactions of OH radicals with (*Z*)-CF_3CCl=CHCl, CHF_2CF=CF_2, (*E*)-CF_3CH=CHF, (*Z*)-CF_3CH=CHF, CH_3CF=CH_2, and CH_2FCH=CH_2. *Atmos. Environ.* **2021**, *255*, 118428, doi:10.1016/j.atmosenv.2021.118428.

Tokuhashi, K.; Takizawa, K.; Kondo, S. Corrigendum to "Rate constants for reactions of OH radicals with (*Z*)-CF_3CCl=CHCl, CHF_2CF=CF_2, (*E*)-CF_3CH=CHF, (*Z*)-CF_3CH=CHF, CH_3CF=CH_2, and CH_2FCH=CH_2" [Atmos. Environ. 255 (2021) 118428]. *Atmos. Environ.* **2023**, *310*, 119914, doi:10.1016/j.atmosenv.2023.119914.

Tokuhashi, K.; Uchimaru, T.; Takizawa, K.; Kondo, S. Rate constants for the reactions of OH radicals with the (*E*)/(*Z*) isomers of CFCl=CFCl and (*E*)-CHF=CHF. *J. Phys. Chem. A* **2019**, *123*, 4834−4843, doi:10.1021/acs.jpca.9b02454.

Tovar, C. M.; Blanco, M. B.; Barnes, I.; Wiesen, P.; Teruel, M. A. Gas-phase reactivity study of a series of hydrofluoroolefins (HFOs) toward OH radicals and Cl atoms at atmospheric pressure and 298 K. *Atmos. Environ.* **2014**, *88*, 107-114, doi:10.1016/j.atmosenv.2014.01.060.

Turnipseed, A. A.; Barone, S. B.; Jensen, N. R.; Hanson, D. R.; Howard, C. J.; Ravishankara, A. R. Kinetics of the reactions of CF_3O radicals with CO and H_2O. *J. Phys. Chem.* **1995**, *99*, 6000-6009, doi:10.1021/j100016a041.

Turnipseed, A. A.; Barone, S. B.; Ravishankara, A. R. Kinetics of the reactions of CF_3O_x radicals with NO, O_3, and O_2. *J. Phys. Chem.* **1994**, *98*, 4594-4601, doi:10.1021/j100068a019.

Wagner, H. G.; Warnatz, J.; Zetzsch, C. On the reaction of F atoms with methane. *Anales Assoc. Quim. Argentina* **1971**, *59*, 169-177.

Wagner, H. G.; Zetzsch, C.; Warnatz, J. Synthesis of OF radical in gas phase by reaction of fluorine atoms with ozone. *Ber. Bunsenges. Phys. Chem.* **1972**, *76*, 526-530, doi:10.1002/bbpc.19720760613.

Wallington, T. J.; Ball, J. C. Atmospheric chemistry of CF_3O radicals: reaction with O_3. *Chem. Phys. Lett.* **1995**, *234*, 187-194, doi:10.1016/0009-2614(95)00009-S.

Wallington, T. J.; Ball, J. C. Atmospheric chemistry of CF_3O radicals: Reactions with CH_4, CD_4, CH_3F, CF_3H, ^{13}CO, C_2H_5F, C_2D_6, C_2H_6, CH_3OH, *i*-C_4H_8, and C_2H_2. *J. Phys. Chem.* **1995**, *99*, 3201-3205, doi:10.1021/j100010a034.

Wallington, T. J.; Dagaut, P.; Kurylo, M. J. Correlation between gas-phase and solution-phase reactivities of hydroxyl radicals toward saturated organic compounds. *J. Phys. Chem.* **1988**, *92*, 5024-5028, doi:10.1021/j100328a039.

Wallington, T. J.; Hurley, M. D. Atmospheric chemistry of HC(O)F - Reaction with OH radicals. *Environ. Sci. Technol.* **1993**, *27*, 1448-1452, doi:10.1021/es00044a022.

Wallington, T. J.; Hurley, M. D. Atmospheric chemistry of hexafluorocyclobutene, octafluorocyclopentene, and hexafluoro-1,3-butadiene. *Chem. Phys. Lett.* **2011**, *507*, 19-23, doi:10.1016/j.cplett.2011.01.059.

Wallington, T. J.; Hurley, M. D.; Nielsen, O. J.; Sulbaek Andersen, M. P. Atmospheric chemistry of $CF_3CFHCF_2OCF_3$ and $CF_3CFHCF_2OCF_2H$: Reaction with Cl atoms and OH radicals, degradation mechanism, and global warming potentials. *J. Phys. Chem. A* **2004**, *108*, 11333-11338, doi:10.1021/jp046454q.

Wallington, T. J.; Hurley, M. D.; Schneider, W. F. Kinetic study of the reaction $CF_3O + O_3 \rightarrow CF_3O_2 + O_2$. *Chem. Phys. Lett.* **1993**, *213*, 442-448, doi:10.1016/0009-2614(93)89140-D.

Wallington, T. J.; Hurley, M. D.; Schneider, W. F.; Sehested, J.; Nielsen, O. J. Atmospheric chemistry of CF_3O radicals: Reaction with H_2O. *J. Phys. Chem.* **1993**, *97*, 7606-7611, doi:10.1021/j100131a033.

Wallington, T. J.; Schneider, W. F.; Sehested, J.; Bilde, M.; Platz, J.; Nielsen, O. J.; Christensen, L. K.; Molina, M. J.; Molina, L. T.; Wooldridge, P. W. Atmospheric chemistry of HFE-7100 ($C_4F_9OCH_3$): reaction with OH radicals, UV spectra and kinetic data for $C_4F_9OCH_2$• and $C_4F_9OCH_2O_2$• radicals, and the atmospheric fate of $C_4F_9OCH_2O$• radicals. *J. Phys. Chem. A* **1997**, *101*, 8264-8274, doi:10.1021/jp971353w.

Walther, C.-D.; Wagner, H. G. On the reactions of F atoms with H_2O, H_2O_2, and NH_3. *Ber. Bunsenges. Phys. Chem.* **1983**, *87*, 403-409, doi:10.1002/bbpc.19830870510.

Wilson, E. W., Jr.; Hamilton, W. A.; Mount, H. R.; DeMore, W. B. Rate constants for the reactions of hydroxyl radical with several fluoroethers by the relative rate method. *J. Phys. Chem. A* **2007**, *111*, 1610-1617, doi:10.1021/jp068355d.

Wilson, E. W., Jr.; Jacoby, A. M.; Kukta, S. J.; Gilbert, L. E.; DeMore, W. B. Rate constants for reaction of CH_2FCH_2F (HFC-152) and CH_3CHF_2 (HFC-152a) with hydroxyl radicals. *J. Phys. Chem. A* **2003**, *107*, 9357-9361, doi:10.1021/jp027288u.

Wilson, E. W., Jr.; Sawyer, A. A.; Sawyer, H. A. Rates of reaction for cyclopropane and difluoromethoxydifluoromethane with hydroxyl radicals. *J. Phys. Chem. A* **2001**, *105*, 1445-1448, doi:10.1021/jp002327s.

Wine, P. H.; Wells, J. R.; Nicovich, J. M. Kinetics of the reactions of $F(^2P)$ and $Cl(^2P)$ with HNO_3. *J. Phys. Chem.* **1988**, *92*, 2223-2228, doi:10.1021/j100319a028.

Wurzburg, E.; Houston, P. L. The temperature dependence of absolute rate constants for the F + H_2 and F + D_2 reactions. *J. Chem. Phys.* **1980**, *72*, 4811-4814, doi:10.1063/1.439818.

Young, C. J.; Hurley, M. D.; Wallington, T. J.; Mabury, S. A. Atmospheric chemistry of CF_3CF_2H and $CF_3CF_2CF_2CF_2H$: Kinetics and products of gas-phase reactions with Cl atoms and OH radicals, infrared spectra, and formation of perfluorocarboxylic acids. *Chem. Phys. Lett.* **2009**, *473*, 251-256, doi:10.1016/j.cplett.2009.04.001.

Young, C. J.; Hurley, M. D.; Wallington, T. J.; Mabury, S. A. Atmospheric chemistry of perfluorobutenes ($CF_3CF=CFCF_3$ and $CF_3CF_2CF=CF_2$): Kinetics and mechanisms of reactions with OH radicals and chlorine atoms, IR spectra, global warming potentials, and oxidation to perfluorocarboxylic acids. *Atmos. Environ.* **2009**, *43*, 3717-3724, doi:10.1016/j.atmosenv.2009.04.025.

Zellner, R.; Bednarek, G.; Hoffmann, A.; Kohlmann, J. P.; Mörs, V.; Saathoff, H. Rate and mechanism of the atmospheric degradation of 2H-heptafluoropropane (HFC-227). *Ber. Bunsenges. Phys. Chem.* **1994**, *98*, 141-146, doi:10.1002/bbpc.19940980202.

Zhang, N.; Chen, L.; Mizukado, J.; Quan, H.; Suda, H. Rate constants for the gas-phase reactions of (*Z*)-$CF_3CH=CHF$ and (*E*)-$CF_3CH=CHF$ with OH radicals at 253–328 K. *Chem. Phys. Lett.* **2015**, *621*, 78–84, doi:10.1016/j.cplett.2014.12.044.

Zhang, N.; Uchimaru, T.; Guo, Q.; Qing, F.; Chen, L.; Mizukado, J. Atmospheric chemistry of perfluorocyclopentene (cyc-$CF_2CF_2CF_2CF=CF$-): Kinetics, products, and mechanism of gas-phase reaction with OH radicals, and atmospheric implications. *Atmos. Environ.* **2017**, *160*, 46–54, doi:10.1016/j.atmosenv.2017.04.012.

Zhang, Z.; Huie, R. E.; Kurylo, M. J. Rate constants for the reactions of OH with CH_3CFCl_2 (HCFC-141b), CH_3CF_2Cl (HCFC-l42b), and CH_2FCF_3 (HFC-134a). *J. Phys. Chem.* **1992**, *96*, 1533-1535, doi:10.1021/j100183a008.

Zhang, Z.; Padmaja, S.; Saini, R. D.; Huie, R. E.; Kurylo, M. J. Reactions of hydroxyl radicals with several hydrofluorocarbons: The temperature dependencies of the rate constants for $CHF_2CF_2CH_2F$ (HFC-245ca), $CF_3CHFCHF_2$ (HFC-236ea), CF_3CHFCF_3 (HFC-227ea), and $CF_3CH_2CH_2CF_3$ (HFC-356ffa). *J. Phys. Chem.* **1994**, *98*, 4312-4315, doi:10.1021/j100067a017.

Zhang, Z.; Saini, R. D.; Kurylo, M. J.; Huie, R. E. Rate constants for the reactions of the hydroxyl radical with $CHF_2CF_2CF_2CHF_2$ and $CF_3CHFCHFCF_2CF_3$. *Chem. Phys. Lett.* **1992**, *200*, 230-234, doi:10.1016/0009-2614(92)80003-T.

Zhang, Z.; Saini, R. D.; Kurylo, M. J.; Huie, R. E. Rate constants for the reactions of the hydroxyl radical with several partially fluorinated ethers. *J. Phys. Chem.* **1992**, *96*, 9301-9304, doi:10.1021/j100202a045.

Zhang, Q.; Qin, S.; Guo, Z.; Ni, H.; Zhang, J. Atmospheric chemistry of $CF_3C{\equiv}CCF_3$: Kinetics, products, mechanism of gas-phase reaction with OH radicals, and atmospheric implications. *Atmos. Environ.* **2021**, *251*, 118264, doi:10.1016/j.atmosenv.2021.118264.

Zhang, T.; Zhang, C.; Ma, X.; Quan, H. Atmospheric chemistry of $CF_3C{\equiv}CH$: Kinetics, products, mechanism of gas-phase reaction with OH radicals, and atmospheric implications-an effort for novel 'class' of refrigerant. *Atmos. Environ.* **2023**, *294*, 119467, doi:10.1016/j.atmosenv.2022.119467.

Zhitneva, G. P.; Pshezhetskii, S. Y. Rate constant for the reaction of fluorine atoms with chlorine monofluoride. *Kinetika i Kataliz* **1978**, *19*, 228-231.

1.11 ClO_x Reactions

1.11.1 Table 1F: ClO_x Reactions

Reaction	Temperature Range of Exp. Data (K) [a]	*A*-Factor	*E*/R	*k*(298 K) [b]	*f*(298 K) [c]	*g* [c]	Note
$O + ClO \rightarrow Cl + O_2$	220–1250	2.8×10^{-11}	–85	3.7×10^{-11}	1.05	50	F 1
$O + OClO \rightarrow ClO + O_2$	243–400	2.4×10^{-12}	960	1.0×10^{-13}	2.00	300	F 2
$O + OClO \xrightarrow{M} ClO_3$		(See Table 2-1)					
$O + Cl_2O \rightarrow ClO + ClO$	230–380	1.8×10^{-11}	475	3.66×10^{-12}	1.20	100	F 3
$O + HCl \rightarrow OH + Cl$	293–3197	1.0×10^{-11}	3300	1.5×10^{-16}	1.50	350	F 4
$O + HOCl \rightarrow OH + ClO$	213–298	1.7×10^{-13}	0	1.7×10^{-13}	3.00	300	F 5
$O + ClONO_2 \rightarrow$ products	202–325	3.6×10^{-12}	840	2.1×10^{-13}	1.20	100	F 6
$O_3 + OClO \rightarrow$ products	262–298	2.1×10^{-12}	4700	3.0×10^{-19}	2.50	1000	F 7
$O_3 + Cl_2O_2 \rightarrow$ products	195–217			$<1\times10^{-19}$			F 8
$OH + Cl_2 \rightarrow HOCl + Cl$	231–836	2.6×10^{-12}	1100	6.5×10^{-14}	1.10	200	F 9
$OH + ClO \rightarrow Cl + HO_2$	208–373	7.4×10^{-12}	–270	1.8×10^{-11}	1.20	50	F10
$\rightarrow HCl + O_2$	208–373	6.0×10^{-13}	–230	1.3×10^{-12}	1.70	100	
$OH + OClO \rightarrow HOCl + O_2$	242–473	1.4×10^{-12}	–600	1.0×10^{-11}	1.50	150	F11
$OH + Cl_2O \rightarrow HOCl + ClO$	223–383	4.7×10^{-12}	–140	7.5×10^{-12}	1.20	100	F12
$OH + Cl_2O_2 \rightarrow HOCl + ClOO$	223–318	6.0×10^{-13}	–670	5.7×10^{-12}	1.30	100	F13
$OH + HCl \rightarrow H_2O + Cl$	138–1060	1.8×10^{-12}	250	7.8×10^{-13}	1.10	50	F14
$OH + HOCl \rightarrow H_2O + ClO$	298	3.0×10^{-12}	500	5.0×10^{-13}	3.00	500	F15
$OH + ClNO_2 \rightarrow HOCl + NO_2$	259–348	2.4×10^{-12}	1250	3.6×10^{-14}	2.00	300	F16
$OH + ClONO_2 \rightarrow$ products	245–387	1.2×10^{-12}	330	3.9×10^{-13}	1.50	200	F17
$OH + CH_3Cl \rightarrow CH_2Cl + H_2O$	224–955	1.96×10^{-12}	1200	3.5×10^{-14}	1.10	50	F18
$OH + CH_2Cl_2 \rightarrow CHCl_2 + H_2O$	219–955	1.92×10^{-12}	880	1.0×10^{-13}	1.15	100	F19
$OH + CHCl_3 \rightarrow CCl_3 + H_2O$	249–775	2.2×10^{-12}	920	1.0×10^{-13}	1.15	150	F20
$OH + CCl_4 \rightarrow$ products	298	*1×10^{-11}*	*>6200*	*$<1\times10^{-20}$*			F21
$OH + CH_2FCl \rightarrow CHFCl + H_2O$ (HCFC-31)	245–486	2.4×10^{-12}	1210	4.1×10^{-14}	1.15	200	F22

Reaction	Temperature Range of Exp. Data (K) [a]	*A*-Factor	*E*/R	*k*(298 K) [b]	*f*(298 K) [c]	*g* [c]	Note
$OH + CHFCl_2 \rightarrow CFCl_2 + H_2O$ (HCFC-21)	241–810	1.52×10^{-12}	1170	3.0×10^{-14}	1.10	150	F23
$OH + CHF_2Cl \rightarrow CF_2Cl + H_2O$ (HCFC-22)	241–807	9.2×10^{-13}	1560	4.9×10^{-15}	1.07	100	F24
$OH + CFCl_3 \rightarrow$ products (CFC-11)	297–434	*1×10^{-11}*	*>9700*	*<1×10^{-25}*			F25
$OH + CF_2Cl_2 \rightarrow$ products (CFC-12)	293–480	*1×10^{-11}*	*>11900*	*<1×10^{-28}*			F26
$OH + CCl_2FCClF_2 \rightarrow$ products (CFC-113)	298	*1×10^{-11}*	*>6200*	*<1×10^{-20}*			F27
$OH + CClF_2CClF_2 \rightarrow$ products (CFC-114)	296	*1×10^{-11}*	*>6200*	*<1×10^{-20}*			F27
$OH + CF_3CClF_2 \rightarrow$ products (CFC-115)	–	*1×10^{-11}*	*>6200*	*<1×10^{-20}*			F27
$OH + CH_3CH_2Cl \rightarrow$ products	223–789	5.4×10^{-12}	800	3.7×10^{-13}	1.20	100	F28
$OH + CH_2ClCH_2Cl \rightarrow$ products	292–775	1.14×10^{-11}	1150	2.4×10^{-13}	1.10	200	F29
$OH + CH_3CCl_3 \rightarrow CH_2CCl_3 + H_2O$	243–761	1.64×10^{-12}	1520	1.0×10^{-14}	1.10	50	F30
$OH + CH_3CFCl_2 \rightarrow CH_2CFCl_2 + H_2O$ (HCFC-141b)	220–479	1.25×10^{-12}	1600	5.8×10^{-15}	1.07	100	F31
$OH + CH_3CF_2Cl \rightarrow CH_2CF_2Cl + H_2O$ (HCFC-142b)	220–808	1.3×10^{-12}	1770	3.4×10^{-15}	1.15	50	F32
$OH + CH_2ClCF_2Cl \rightarrow CHClCF_2Cl + H_2O$ (HCFC-132b)	249–788	2.76×10^{-12}	1500	1.8×10^{-14}	1.15	200	F33
$OH + CH_2FCFCl_2 \rightarrow CHFCFCl_2 + H_2O$ (HCFC-132c)	298–370	8.2×10^{-13}	1250	1.23×10^{-14}	1.15	100	F34
$OH + CH_2ClCF_3 \rightarrow CHClCF_3 + H_2O$ (HCFC-133a)	263–866	9.4×10^{-13}	1300	1.2×10^{-14}	1.10	100	F35
$OH + CHCl_2CF_2Cl \rightarrow CCl_2CF_2Cl + H_2O$ (HCFC-122)	298–460	7.7×10^{-13}	810	5.1×10^{-14}	1.20	150	F36
$OH + CHFClCFCl_2 \rightarrow CFClCFCl_2 + H_2O$	298–460	9.0×10^{-13}	1200	1.6×10^{-14}	1.10	100	F37
$OH + CHCl_2CF_3 \rightarrow CCl_2CF_3 + H_2O$ (HCFC-123)	213–866	7.4×10^{-13}	900	3.6×10^{-14}	1.10	100	F38
$OH + CHFClCF_2Cl \rightarrow CFClCF_2Cl + H_2O$ (HCFC-123a)	298–460	8.6×10^{-13}	1250	1.3×10^{-14}	1.30	200	F39
$OH + CHFClCF_3 \rightarrow CFClCF_3 + H_2O$ (HCFC-124)	210–867	7.1×10^{-13}	1300	9.0×10^{-15}	1.15	100	F40
$OH + CH_3CH_2CH_2Cl \rightarrow$ products	253–372	5.8×10^{-12}	530	9.8×10^{-13}	1.15	50	F41
$OH + CH_3CHClCH_3 \rightarrow$ products	233–372	2.35×10^{-12}	365	6.9×10^{-13}	1.15	50	F42
$OH + CH_3CF_2CFCl_2 \rightarrow$ products (HCFC-243cc)	295–367	7.7×10^{-13}	1720	2.4×10^{-15}	1.30	200	F43
$OH + CHCl_2CF_2CF_3 \rightarrow$ products (HCFC-225ca)	251–400	6.3×10^{-13}	960	2.5×10^{-14}	1.20	200	F44
$OH + CF_2ClCF_2CHFCl \rightarrow$ products (HCFC-225cb)	270–400	5.5×10^{-13}	1230	8.9×10^{-15}	1.10	150	F45

Reaction	Temperature Range of Exp. Data (K) [a]	*A*-Factor	*E*/R	*k*(298 K) [b]	*f*(298 K) [c]	*g* [c]	Note
OH + $CF_3CH_2CFCl_2$ → $CF_3CHCFCl_2$ + H_2O (HCFC-234fb)	298	*1.8×10⁻¹²*	*2300*	8.0×10⁻¹⁶	1.50	200	F46
OH + CH_2=CHCl → products	293–1173	1.3×10⁻¹²	–500	6.9×10⁻¹²	1.20	100	F47
OH + (*E*)-CHCl=CHCl → products	240–720	1.06×10⁻¹²	–230	2.3×10⁻¹²	1.10	100	F48
OH + (*Z*)-CHCl=CHCl → products	240–400	2.04×10⁻¹²	–70	2.6×10⁻¹²	1.10	100	F49
OH + CH_2=CCl_2 → products	240–750	2.17×10⁻¹²	–470	1.05×10⁻¹¹	1.10	100	F50
OH + CHCl=CCl_2 → products	234–1500	8.0×10⁻¹³	–300	2.2×10⁻¹²	1.20	100	F51
OH + CCl_2=CCl_2 → products	296–720	4.7×10⁻¹²	990	1.7×10⁻¹³	1.20	200	F52
OH + (*Z*)-CFCl=CFCl → products	250–430	1.75×10⁻¹²	–135	2.75×10⁻¹²	1.10	0	F53
OH + (*E*)-CFCl=CFCl → products	250–430	1.67×10⁻¹²	–140	2.67×10⁻¹²	1.10	0	F54
OH + CF_2=CFCl → products	296–364	1.06×10⁻¹²	–580	7.4×10⁻¹²	1.20	100	F55
OH + CH_2=$CHCH_2Cl$ → products	228–371	2.78×10⁻¹²	-540	1.7×10⁻¹¹	1.07	50	F56
OH + (*E*)-CHCl=$CHCF_3$ → products	213–376	9.0×10⁻¹³	280	3.5×10⁻¹³	1.07	20	F57
OH + (*Z*)-CHCl=$CHCF_3$ → products	213–376	3.67×10⁻¹³	–280	9.4×10⁻¹³	1.10	20	F58
OH + (*Z*)-CHCl=$CClCF_3$ → products	250–430	9.33×10⁻¹³	180	5.1×10⁻¹³	1.15	20	F59
OH + CCl_2=$CFCF_3$ → products	250–430	6.49×10⁻¹³	–200	1.27×10⁻¹²	1.15	0	F60
OH + CH_3OCF_2CHFCl → products	250–430	1.64×10⁻¹²	1130	3.7×10⁻¹⁴	1.20	0	F61
OH + $CHF_2OCHClCF_3$ → products (Isoflurane)	250–430	1.1×10⁻¹²	1275	1.5×10⁻¹⁴	1.07	50	F62
OH + CHF_2OCF_2CHFCl → products (Enflurane)	250–430	6.73×10⁻¹³	1200	1.2×10⁻¹⁴	1.10	100	F63
OH + CH_3OCl → products	250–341	2.5×10⁻¹²	370	7.1×10⁻¹³	2.00	150	F64
OH + CCl_3CHO → H_2O + CCl_3CO	298–520	9.1×10⁻¹²	580	1.3×10⁻¹²	1.30	200	F65
HO_2 + Cl → HCl + O_2	226–420	1.4×10⁻¹¹	–270	3.5×10⁻¹¹	1.20	100	F66
→ OH + ClO	226–420	3.6×10⁻¹¹	375	1.0×10⁻¹¹	1.40	150	
HO_2 + ClO → HOCl + O_2	203–364	2.6×10⁻¹²	–290	6.9×10⁻¹²	1.20	150	F67
H_2O + $ClONO_2$ → products	298			<2×10⁻²¹			F68
NO + OClO → NO_2 + ClO	220–367	*2.5×10⁻¹²*	*600*	3.4×10⁻¹³	2.00	300	F69
NO + Cl_2O_2 → products	220–298			<1×10⁻¹⁵			F70
NO_3 + OClO $\xrightarrow{M}$ O_2ClONO_2		(See Table 2-1)					

Reaction	Temperature Range of Exp. Data (K) [a]	*A*-Factor	*E*/R	*k*(298 K) [b]	*f*(298 K) [c]	*g* [c]	Note
$NO_3 + HCl \rightarrow HNO_3 + Cl$	298–473			$<5\times10^{-17}$			F71
$HO_2NO_2 + HCl \rightarrow$ products	296			$<1\times10^{-21}$			F72
$Cl + O_2 \xrightarrow{M} ClOO$		(See Table 2-1)					
$Cl + O_3 \rightarrow ClO + O_2$	184–1350	2.3×10^{-11}	200	1.2×10^{-11}	1.15	50	F73
$Cl + H_2 \rightarrow HCl + H$	199–3000	3.05×10^{-11}	2270	1.5×10^{-14}	1.10	100	F74
$Cl + H_2O_2 \rightarrow HCl + HO_2$	265–424	1.1×10^{-11}	980	4.1×10^{-13}	1.30	300	F75
$Cl + NO \xrightarrow{M} ClNO$		(See Table 2-1)					
$Cl + NO_2 \xrightarrow{M} ClONO\ (ClNO_2)$		(See Table 2-1)					
$Cl + NO_3 \rightarrow ClO + NO_2$	278–338	2.4×10^{-11}	0	2.4×10^{-11}	1.50	400	F76
$Cl + N_2O \rightarrow ClO + N_2$	773–1030	(See Note)					F77
$Cl + HNO_3 \rightarrow$ products	243–633			$<2\times10^{-16}$			F78
$Cl + HO_2NO_2 \rightarrow$ products	296–399			$<1\times10^{-13}$			F79
$Cl + CO \xrightarrow{M} ClCO$		(See Table 2-1)					
$Cl + CH_4 \rightarrow HCl + CH_3$	181–1550	7.1×10^{-12}	1270	1.0×10^{-13}	1.05	50	F80
$Cl + CH_3D \rightarrow$ products	223–343	7.46×10^{-12}	1400	6.8×10^{-14}	1.07	50	F81
$Cl + H_2CO \rightarrow HCl + HCO$	200–500	8.1×10^{-11}	30	7.3×10^{-11}	1.15	100	F82
$Cl + HC(O)OH \rightarrow$ products	298			2.0×10^{-13}	1.50		F83
$Cl + CH_3O_2 \rightarrow$ products	298			1.6×10^{-10}	1.50		F84
$Cl + CH_3OH \rightarrow CH_2OH + HCl$	200–573	5.5×10^{-11}	0	5.5×10^{-11}	1.20	100	F85
$Cl + CH_3OOH \rightarrow$ products	295			5.7×10^{-11}	2.00		F86
$Cl + CH_3ONO_2 \rightarrow$ products	298	*1.3×10^{-11}*	*1200*	2.3×10^{-13}	1.50	300	F87
$Cl + C_2H_2 \xrightarrow{M} ClC_2H_2$		(See Table 2-1)					
$Cl + C_2H_4 \xrightarrow{M} ClC_2H_4$		(See Table 2-1)					
$Cl + C_2H_6 \rightarrow HCl + C_2H_5$	48–1400	7.2×10^{-11}	70	5.7×10^{-11}	1.07	20	F88
$Cl + C_2H_5O_2 \rightarrow ClO + C_2H_5O$ $\rightarrow HCl + C_2H_4O_2$	298 298			7.4×10^{-11} 7.7×10^{-11}	2.000 2.00		F89
$Cl + CH_3CH_2OH \rightarrow$ products	266–600	9.6×10^{-11}	0	9.6×10^{-11}	1.20	100	F90

Reaction	Temperature Range of Exp. Data (K) [a]	*A*-Factor	*E*/R	*k*(298 K) [b]	*f*(298 K) [c]	*g* [c]	Note
Cl + $CH_3C(O)OH$ → products	298			2.8×10^{-14}	2.00		F91
Cl + CH_3CN → products	274–728	1.6×10^{-11}	2140	1.2×10^{-14}	2.00	300	F92
Cl + $C_2H_5ONO_2$ → products	298	*1.5×10^{-11}*	*400*	3.9×10^{-12}	1.50	200	F93
Cl + $CH_3CO_3NO_2$ → products	298			$<1\times10^{-14}$			F94
Cl + C_3H_8 → HCl + CH_3CHCH_3	48–1400	6.54×10^{-11}	–60	8.0×10^{-11}	1.10	20	F95
→ HCl + $CH_2CH_2CH_3$	48–1400	8.12×10^{-11}	90	6.0×10^{-11}	1.05	20	
Cl + $CH_3C(O)CH_3$ → $CH_3C(O)CH_2$ + HCl	210–440	1.63×10^{-11}	610	2.1×10^{-12}	1.07	50	F96
Cl + $CH_2=C(CH_3)CHO$ → products	296–298			2.2×10^{-10}	1.30		F97
Cl + $CH_3C(O)CH=CH_2$ → products	296–298			2.1×10^{-10}	1.10		F98
Cl + $CH_2=C(CH_3)CH=CH_2$ → products	233–320	7.6×10^{-11}	–500	4.1×10^{-10}	1.15	100	F99
Cl + $C_2H_5CO_3NO_2$ → products	295			1.1×10^{-12}	2.00		F100
Cl + 1-$C_3H_7ONO_2$ → products	295			2.3×10^{-11}	1.50		F101
Cl + 2-$C_3H_7ONO_2$ → products	295			4.0×10^{-12}	2.00		F102
Cl + OClO → ClO + ClO	229–588	3.4×10^{-11}	–160	5.8×10^{-11}	1.25	200	F103
Cl + ClOO → Cl_2 + O_2	160–306	2.3×10^{-10}	0	2.3×10^{-10}	2.00	200	F104
→ ClO + ClO	160–306	1.2×10^{-11}	0	1.2×10^{-11}	2.00	200	
Cl + Cl_2O → Cl_2 + ClO	233–373	6.2×10^{-11}	–130	9.6×10^{-11}	1.20	130	F105
Cl + Cl_2O_2 → products	217–298	7.6×10^{-11}	–65	1.0×10^{-10}	1.20	100	F106
Cl + HOCl → products	243–365	3.4×10^{-12}	130	2.2×10^{-12}	1.30	200	F107
Cl + ClNO → NO + Cl_2	220–450	5.8×10^{-11}	–100	8.1×10^{-11}	1.50	200	F108
Cl + $ClONO_2$ → products	195–298	6.5×10^{-12}	–135	1.0×10^{-11}	1.10	50	F109
Cl + CH_3Cl → HCl + CH_2Cl	233–843	2.03×10^{-11}	1110	4.9×10^{-13}	1.07	50	F110
Cl + CH_2Cl_2 → HCl + $CHCl_2$	273–790	7.4×10^{-12}	910	3.5×10^{-13}	1.07	100	F111
Cl + $CHCl_3$ → HCl + CCl_3	220–1010	3.3×10^{-12}	990	1.2×10^{-13}	1.15	100	F112
Cl + CH_3F → HCl + CH_2F (HFC-41)	216–368	1.96×10^{-11}	1200	3.5×10^{-13}	1.15	150	F113
Cl + CH_2F_2 → HCl + CHF_2 (HFC-32)	253–553	7.6×10^{-12}	1630	3.2×10^{-14}	1.08	100	F114
Cl + CHF_3 → HCl + CF_3 (HFC-23)	298			$<5\times10^{-16}$			F115

Reaction	Temperature Range of Exp. Data (K) [a]	*A*-Factor	*E*/R	*k*(298 K) [b]	*f*(298 K) [c]	*g* [c]	Note
$Cl + CH_2FCl \rightarrow HCl + CHFCl$ (HCFC-31)	273–298	*5.9×10⁻¹²*	*1200*	1.05×10^{-13}	1.10	200	F116
$Cl + CHFCl_2 \rightarrow HCl + CFCl_2$ (HCFC-21)	294–433	6.0×10^{-12}	1700	2.0×10^{-14}	1.20	200	F117
$Cl + CHF_2Cl \rightarrow HCl + CF_2Cl$ (HCFC-22)	296–411	5.9×10^{-12}	2430	1.7×10^{-15}	1.10	150	F118
$Cl + CH_3CCl_3 \rightarrow HCl + CH_2CCl_3$	253–423	3.0×10^{-12}	1730	9.0×10^{-15}	1.15	100	F119
$Cl + CH_3CH_2F \rightarrow HCl + CH_3CHF$ (HFC-161)	264–368	1.82×10^{-11}	330	6.0×10^{-12}	1.10	100	F120
$\rightarrow HCl + CH_2CH_2F$	264–368	1.4×10^{-11}	940	6.0×10^{-13}	1.15	100	
$Cl + CH_3CHF_2 \rightarrow HCl + CH_3CF_2$ (HFC-152a)	264–368	6.0×10^{-12}	950	2.5×10^{-13}	1.10	100	F121
$\rightarrow HCl + CH_2CHF_2$	264–368	6.5×10^{-12}	2320	2.7×10^{-15}	1.15	200	
$Cl + CH_2FCH_2F \rightarrow HCl + CHFCH_2F$ (HFC-152)	280–368	2.27×10^{-11}	1050	6.7×10^{-13}	1.15	200	F122
$Cl + CH_3CFCl_2 \rightarrow HCl + CH_2CFCl_2$ (HCFC-141b)	276–429	3.5×10^{-12}	2200	2.2×10^{-15}	1.15	200	F123
$Cl + CH_3CF_2Cl \rightarrow HCl + CH_2CF_2Cl$ (HCFC-142b)	295–673	1.35×10^{-12}	2400	4.3×10^{-16}	1.15	200	F124
$Cl + CH_3CF_3 \rightarrow HCl + CH_2CF_3$ (HFC-143a)	281–368	1.64×10^{-11}	3900	3.4×10^{-17}	1.50	300	F125
$Cl + CH_2FCHF_2 \rightarrow HCl + CH_2FCF_2$ (HFC-143)	281–368	6.8×10^{-12}	1670	2.5×10^{-14}	1.30	200	F126
$\rightarrow HCl + CHFCHF_2$	281–368	9.1×10^{-12}	1770	2.4×10^{-14}	1.30	200	
$Cl + CH_2ClCF_3 \rightarrow HCl + CHClCF_3$ (HCFC-133a)	296–500	1.83×10^{-12}	1680	6.5×10^{-15}	1.20	200	F127
$Cl + CH_2FCF_3 \rightarrow HCl + CHFCF_3$ (HFC-134a)	253–423	2.1×10^{-12}	2160	1.5×10^{-15}	1.10	200	F128
$Cl + CHF_2CHF_2 \rightarrow HCl + CF_2CHF_2$ (HFC-134)	280–368	7.0×10^{-12}	2430	2.0×10^{-15}	1.20	200	F129
$Cl + CHCl_2CF_3 \rightarrow HCl + CCl_2CF_3$ (HCFC-123)	276–382	5.0×10^{-12}	1800	1.2×10^{-14}	1.15	200	F130
$Cl + CHFClCF_3 \rightarrow HCl + CFClCF_3$ (HCFC-124)	276–376	1.13×10^{-12}	1800	2.7×10^{-15}	1.20	200	F131
$Cl + CHF_2CF_3 \rightarrow HCl + CF_2CF_3$ (HFC-125)	295–399	*1.85×10⁻¹²*	*2600*	3.0×10^{-16}	1.50	300	F132
$Cl + C_2Cl_4 \xrightarrow{M} C_2Cl_5$		(See Table 2-1)					
$ClO + O_3 \rightarrow ClOO + O_2$	223–413	2×10^{-12}	>3600	$<1.4\times10^{-17}$			F133
$\rightarrow OClO + O_2$	223–413	*1×10⁻¹²*	*>4000*	$<1.0\times10^{-18}$			
$ClO + H_2 \rightarrow$ products	294–670	*1×10⁻¹²*	*>4800*	*<1×10⁻¹⁹*			F134
$ClO + NO \rightarrow NO_2 + Cl$	202–415	6.4×10^{-12}	–290	1.7×10^{-11}	1.15	100	F135

Reaction	Temperature Range of Exp. Data (K) [a]	*A*-Factor	*E*/R	*k*(298 K) [b]	*f*(298 K) [c]	*g* [c]	Note
$ClO + NO_2 \xrightarrow{M} ClONO_2$		(See Table 2-1)					
$ClO + NO_3 \rightarrow ClOO + NO_2$	210–353	4.7×10^{-13}	0	4.7×10^{-13}	1.50	400	F136
$ClO + N_2O \rightarrow$ products	587	*1×10^{-12}*	*>4300*	*<6×10^{-19}*			F137
$ClO + CO \rightarrow$ products	587	*1×10^{-12}*	*>3700*	*<4×10^{-18}*			F138
$ClO + CH_4 \rightarrow$ products	670	*1×10^{-12}*	*>3700*	*<4×10^{-18}*			F139
$ClO + H_2CO \rightarrow$ products	298	*1×10^{-12}*	*>2100*	<1×10^{-15}			F140
$ClO + CH_3O_2 \rightarrow$ products	197–355	1.8×10^{-11}	600	2.4×10^{-12}	1.10	300 –20	F141
$ClO + ClO \rightarrow Cl_2 + O_2$	260–1250	1.0×10^{-12}	1590	4.8×10^{-15}	1.50	300	F142
$\rightarrow ClOO + Cl$	260–710	3.0×10^{-11}	2450	8.0×10^{-15}	1.50	500	
$\rightarrow OClO + Cl$	254–390	3.5×10^{-13}	1370	3.5×10^{-15}	1.50	300	
$ClO + ClO \xrightarrow{M} Cl_2O_2$		(See Table 2-1)					
$ClO + OClO \xrightarrow{M} Cl_2O_3$		(See Table 2-1)					
$HCl + ClONO_2 \rightarrow$ products	298			<1×10^{-20}			F143
$CH_2Cl + O_2 \xrightarrow{M} CH_2ClO_2$		(See Table 2-1)					
$CHCl_2 + O_2 \xrightarrow{M} CHCl_2O_2$		(See Table 2-1)					
$CCl_3 + O_2 \xrightarrow{M} CCl_3O_2$		(See Table 2-1)					
$CFCl_2 + O_2 \xrightarrow{M} CFCl_2O_2$		(See Table 2-1)					
$CF_2Cl + O_2 \xrightarrow{M} CF_2ClO_2$		(See Table 2-1)					
$CCl_3O_2 + NO_2 \xrightarrow{M} CCl_3O_2NO_2$		(See Table 2-1)					
$CFCl_2O_2 + NO_2 \xrightarrow{M} CFCl_2O_2NO_2$		(See Table 2-1)					
$CF_2ClO_2 + NO_2 \xrightarrow{M} CF_2ClO_2NO_2$		(See Table 2-1)					
$CH_2ClO + O_2 \rightarrow CHClO + HO_2$	264–336			6×10^{-14}	5.00		F144
$CH_2ClO_2 + HO_2 \rightarrow CH_2ClO_2H + O_2$	251–600	3.3×10^{-13}	–820	5.2×10^{-12}	1.50	200	F145
$CH_2ClO_2 + NO \rightarrow CH_2ClO + NO_2$	295	*7×10^{-12}*	*–300*	1.9×10^{-11}	1.50	200	F146
$CCl_3O_2 + NO \rightarrow CCl_2O + NO_2 + Cl$	228–413	7.3×10^{-12}	–270	1.8×10^{-11}	1.30	200	F147

Reaction	Temperature Range of Exp. Data (K) [a]	*A*-Factor	*E*/R	*k*(298 K) [b]	*f*(298 K) [c]	*g* [c]	Note
$CCl_2FO_2 + NO \rightarrow CClFO + NO_2 + Cl$	228–413	4.5×10^{-12}	–350	1.5×10^{-11}	1.30	200	F148
$CClF_2O_2 + NO \rightarrow CF_2O + NO_2 + Cl$	228–413	3.8×10^{-12}	–400	1.5×10^{-11}	1.20	200	F149

Shaded areas indicate changes or additions since JPL19-5. Italicized blue data entries denote estimates.

[a] Temperature range of available experimental data. This is not necessarily the range of temperature over which the recommended Arrhenius parameters are applicable. See the corresponding note for each reaction for such information.

[b] Units are cm^3 $molecule^{-1}$ s^{-1}.

[c] *f*(298 K) is the uncertainty factor at 298 K. To calculate the uncertainty at other temperatures, use the expression:

$$f(\mathrm{T}) = f(298\ \mathrm{K})\exp\left|g\left(\frac{1}{\mathrm{T}} - \frac{1}{298}\right)\right|$$

Note that the exponent is an absolute value.

1.11.2 Notes: ClO_x Reactions

F1. **O + ClO.** There have been six studies of this reaction over an extended temperature range using a variety of techniques: Leu[5] (295–422 K); Margitan[6] (241–298 K); Schwab et al.[10] (252–347 K); Ongstad and Birks[9] (224–387 K); Nicovich et al.[7] (231–367 K); and Goldfarb et al.[3] (227–362 K). The recommendation is based on a least squares fit to the data reported in these studies and in the earlier studies of Zahniser and Kaufman[11] (218–295 K) and Ongstad and Birks[8] (298 K). Values reported in the studies of Bemand et al.[1] (298 K) and Clyne and Nip[2] (220–426 K) are significantly higher and were not used in deriving the recommended value. Leu and Yung[4] were unable to detect $O_2(^1\Delta)$ or $O_2(^1\Sigma)$ and set upper limits to the branching ratios for their production of 4.4×10^{-4} and 2.5×10^{-2}, respectively.
(Table: 10-6, Note: 2025, Evaluated: 10-6) Back to Table

(1) Bemand, P. P.; Clyne, M. A. A.; Watson, R. T. Reactions of chlorine oxide radicals Part 4.-Rate constants for the reactions Cl + OClO, O + OClO, H + OClO, NO + OClO and O + ClO. *J. Chem. Soc. Faraday Trans. 1* **1973**, *69*, 1356-1374, doi:10.1039/f19736901356.

(2) Clyne, M. A. A.; Nip, W. S. Reactions of chlorine oxide radicals Part 6.-The reaction O + ClO → Cl + O_2 from 220 to 426 K. *J. Chem. Soc. Faraday Trans. 1* **1976**, *72*, 2211-2217, doi:10.1039/f19767202211.

(3) Goldfarb, L.; Burkholder, J. B.; Ravishankara, A. R. Kinetics of the O + ClO reaction. *J. Phys. Chem. A* **2001**, *105*, 5402-5409, doi:10.1021/jp0100351.

(4) Leu, M.-T.; Yung, Y. L. Determination of $O_2(a^1\Delta_g)$ and $O_2(b^1\Sigma_g^+)$ yields in the reaction O + ClO → Cl + O_2: Implications for photochemistry in the atmosphere of Venus. *Geophys. Res. Lett.* **1987**, *14*, 949-952, doi:10.1029/GL014i009p00949.

(5) Leu, M. T. Kinetics of the reaction O + ClO → Cl + O_2. *J. Phys. Chem.* **1984**, *88*, 1394-1398, doi:10.1021/j150651a032.

(6) Margitan, J. J. Kinetics of the reaction O + ClO → Cl + O_2. *J. Phys. Chem.* **1984**, *88*, 3638-3643, doi:10.1021/j150660a052.

(7) Nicovich, J. M.; Wine, P. H.; Ravishankara, A. R. Pulsed laser photolysis kinetics study of the $O(^3P)$ + ClO reaction. *J. Chem. Phys.* **1988**, *89*, 5670-5679, doi:10.1063/1.455574.

(8) Ongstad, A. P.; Birks, J. W. Studies of reactions of importance in the stratosphere. V. Rate constants for the reactions O + NO_2 → NO + O_2 and O + ClO → Cl + O_2 at 298 K. *J. Chem. Phys.* **1984**, *81*, 3922-3930, doi:10.1063/1.448185.

(9) Ongstad, A. P.; Birks, J. W. Studies of reactions of importance in the stratosphere. VI. Temperature dependence of the reactions O + NO_2 → NO + O_2 and O + ClO → Cl + O_2. *J. Chem. Phys.* **1986**, *85*, 3359-3368, doi:10.1063/1.450957.

(10) Schwab, J. J.; Toohey, D. W.; Brune, W. H.; Anderson, J. G. Reaction kinetics of O + ClO → Cl + O_2 between 252-347 K. *J. Geophys. Res.* **1984**, *89*, 9581-9587, doi:10.1029/JD089iD06p09581.

(11) Zahniser, M. S.; Kaufman, F. Kinetics of the reactions of ClO with O and with NO. *J. Chem. Phys.* **1977**, *66*, 3673-3681, doi:10.1063/1.434403.

F2. **O + OClO.** The recommended value is based on results of the DF-RF study of Gleason et al.[4] (200–400 K). Over the temperature range 240 to 400 K, their data are well fitted by the recommended Arrhenius expression, but at lower temperatures down to 200 K their data show an abrupt change to a negative temperature dependence. At 200 K, the value measured is a factor of 3 higher than that calculated from the Arrhenius expression. It appears that the earlier experiments of Bemand et al.[1] (298 K) were complicated by secondary chemistry. The low temperature data of Gleason et al. qualitatively support the results of Colussi[2] (298 K) and Colussi et al.[3] (248–312 K, 20–600 Torr Ar) over an extended pressure range that demonstrate the importance of the termolecular reaction O + OClO + M → ClO_3 + M (see entry for this reaction in Table 2-1). Mauldin et al.[5] (260 K, 100–400 Torr) also observed product formation at low temperatures and higher pressures that is consistent with adduct formation. It should be noted that the termolecular rate constants derived by Gleason et al. on the basis of their low temperature data are not consistent with the termolecular rate constant expression recommended in this evaluation (factor of 3 difference).
(Table: 10-6, Note: 10-6, Evaluated: 10-6) Back to Table

(1) Bemand, P. P.; Clyne, M. A. A.; Watson, R. T. Reactions of chlorine oxide radicals Part 4.-Rate constants for the reactions Cl + OClO, O + OClO, H + OClO, NO + OClO and O + ClO. *J. Chem. Soc. Faraday Trans. 1* **1973**, *69*, 1356-1374, doi:10.1039/f19736901356.

(2) Colussi, A. J. Formation and decay of (^3P_J)O atoms in the laser flash photolysis of chlorine dioxide (OClO) at 308 nm. *J. Phys. Chem.* **1990**, *94*, 8922-8926, doi:10.1021/j100389a014.

(3) Colussi, A. J.; Sander, S. P.; Friedl, R. R. Temperature dependence and mechanism of the reaction between $O(^3P)$ and chlorine dioxide. *J. Phys. Chem.* **1992**, *96*, 4442-4445, doi:10.1021/j100190a058.

(4) Gleason, J. F.; Nesbitt, F. L.; Stief, L. J. Temperature dependence of the reaction between O(^{3}P) and OClO at low pressure. *J. Phys. Chem.* **1994**, *98*, 126-131, doi:10.1021/j100052a022.
(5) Mauldin, R. L.; Burkholder, J. B.; Ravishankara, A. R. The reaction of O(^{3}P) with OClO. *Int. J. Chem. Kinet.* **1997**, *29*, 139-147, doi:10.1002/(SICI)1097-4601(1997)29:2<139::AID-KIN8>3.0.CO;2-V.

F3. **O + Cl_2O.** The studies of Stevens and Anderson[5] (230–380 K, DF-LMR/RF), Miziolek and Molina,[3] (236–295 K, DF-CL), Wecker et al.[6] (233–297 K, DF-ESR),and Papanastasiou and Burkholder[4] (230–357 K, PLP-RF) provide the basis for the recommended Arrhenius parameters. The results of Basco and Dogra[1] (298 K) and Freeman and Phillips[2] (298 K) are significantly greater, possibly due to data analysis difficulties, and are not considered in the recommendation. The results of Stevens and Anderson are in reasonable agreement with those from the Miziolek and Molina study, while the Wecker et al. and Papanastasiou and Burkholder results, which are in reasonable agreement, are about 30% lower at room temperature. The recommended k(298 K) is an average of these four studies at room temperature. The recommended E/R is taken from the Stevens and Anderson, Miziolek and Molina, and Papanastasiou and Burkholder studies, which are in excellent agreement. The recommended uncertainty factors encompass the range of the reported k(230–380 K) results.
(Table: 25-1, Note: 25-1, Evaluated: 25-1) Back to Table

(1) Basco, N.; Dogra, S. K. Reactions of halogen oxides studied by flash photolysis. I. The flash photolysis of chlorine dioxide. *Proc. Roy. Soc. Lond. A.* **1971**, *323*, 29-68, doi:10.1098/rspa.1971.0087.
(2) Freeman, C. G.; Phillips, L. F. Kinetics of chlorine oxide reactions. The reaction of oxygen atoms with Cl_2O. *J. Phys. Chem.* **1968**, *72*, 3025-3028, doi:10.1021/j100854a061.
(3) Miziolek, A. W.; Molina, M. J. The rate constant for the reaction of oxygen (^{3}P) atoms with dichlorine monoxide. *J. Phys. Chem.* **1978**, *82*, 1769-1771, doi:10.1021/j100505a001.
(4) Papanastasiou, D. K.; Burkholder, J. B. Rate coefficients for the O(^{3}P) + Cl_2O gas-phase reaction between 230 and 357 K. *Int. J. Chem Kinet.* **2011**, *43*, 312-321, doi:10.1002/kin.20556.
(5) Stevens, P. S.; Anderson, J. G. Kinetic and mechanistic study of X + ClOCl → products (X = Br, CI, F, O, OH, N) over the temperature range 240-373 K. *J. Phys. Chem.* **1992**, *96*, 1708-1718, doi:10.1021/j100183a040.
(6) Wecker, D.; Johanssen, R.; Schindler, R. N. ESR-spektroskopische untersuchungen der reaktion von O(^{3}P)-atomen mit dichlormonoxid. *Ber. Bunsenges. Phys. Chem.* **1982**, *86*, 532-538, doi:10.1002/bbpc.19820860612.

F4. **O + HCl.** The recommendation is based on the results of Brown and Smith[2] (293–440 K), Wong and Belles,[7] Ravishankara et al.[5] (250–402 K), Hack et al.[3] (293–718 K), Singleton and Cvetanovic[6] (330–600 K), and Mahmud et al.[4] (350–1480 K) near 300 K, but not on the results reported by Balakhnin et al.,[1] which are substantially higher. A large uncertainty is attached to the temperature dependence below room temperature due to the limited number and range (no data below 290 K) of measurements.
(Table: 10-6, Note: 10-6, Evaluated: 10-6) Back to Table

(1) Balakhnin, V. P.; Egorov, V. I.; Intezarova, E. I. *Kinetics and Catalysis* **1971**, *12*, 299.
(2) Brown, R. D. H.; Smith, I. W. M. Absolute rate constants for the reactions O(^3P) atoms with HCl and HBr. *Int. J. Chem. Kinet.* **1975**, *7*, 301-315, doi:10.1002/kin.550070211.
(3) Hack, W.; Mex, G.; Wagner, H. G. Determination of rate constant of reactions O + HCl in temperature range 293 to 718 K and OH + HCl at 293 K. *Ber. Bunsenges. Phys. Chem.* **1977**, *81*, 677-684, doi:10.1002/bbpc.19770810710.
(4) Mahmud, K.; Kim, J. S.; Fontijn, A. A high-temperature photochemical kinetics study of the O + HCl reaction from 350 K to 1480 K. *J. Phys. Chem.* **1990**, *94*, 2994-2998, doi:10.1021/j100370a048.
(5) Ravishankara, A. R.; Smith, G.; Watson, R. T.; Davis, D. D. A temperature dependent kinetics study of the reaction of HCl with OH and O(^{3}P). *J. Phys. Chem.* **1977**, *81*, 2220-2225, doi:10.1021/j100539a002.
(6) Singleton, D. L.; Cvetanovic, R. J. Temperature dependence of rate constants for the reaction of atomic oxygen with hydrogen chloride. *Int. J. Chem. Kinet.* **1981**, *13*, 945-956, doi:10.1002/kin.550130916
(7) Wong, E. L.; Belles, F. R.; NASA TN D-6495 NASA Washington, D. C., 1971.

F5. **O + HOCl.** The recommendation is based on results of Schindler et al.[1] (213–298 K). In this study the rate constant was found to be practically independent of temperature in the range 213–298 K. Product analysis indicated that Cl atom abstraction is the primary reaction channel, a conclusion that is supported by ab initio studies carried out by Xu and Lin,[3] Wang et al.,[2] and Schindler et al.
(Table: 97-4, Note: 10-6, Evaluated: 10-6) Back to Table

(1) Schindler, R. N.; Dethlefs, J.; Schmidt, M. Some results on the mechanism of the reaction between O(^{3}P) atoms and HOCl. An experimental and ab initio model study. *Ber. Bunsenges. Phys. Chem.* **1996**, *100*, 1242-1249, doi:10.1002/bbpc.19961000723.
(2) Wang, L.; Liu, J. Y.; Li, Z. S.; Sun, C. C. Ab initio and DFT theoretical studies and rate constants calculation on the reactions O (^{3}P) atoms with HOX (X = Cl, Br). *Chem. Phys. Lett.* **2005**, *411*, 225-232, doi:10.1016/j.cplett.2005.05.071.
(3) Xu, Z. F.; Lin, M. C. Computational studies on metathetical and redox processes of HOCl in the gas phase. 1. Reactions with H, O, HO, and HO_2. *J. Phys. Chem. A* **2009**, *113*, 8811-8817, doi:10.1021/jp905136h.

F6. **O + $ClONO_2$.** The recommended values are based on the results reported by Goldfarb et al.[2] (202–325 K), Molina et al.[4] (213–295 K), and Kurylo[3] (225–273 K). The room temperature results of Tyndall et al.[6] (298 K) and Adler-Golden and Wiesenfeld[1] (298 K) are in excellent agreement with the recommended value. The value reported by Ravishankara et al.[5] (245 K) is a factor of 2 greater than the results from the other studies, and this may possibly be attributed to (a) secondary kinetic complications, (b) the presence of NO_2 as a reactive impurity in the $ClONO_2$, or (c) formation of reactive photolytic products. Goldfarb et al. measured an essentially unit yield (±30%) of NO_2 from the reaction between the temperatures 248 and 298 K.
(Table: 10-6, Note: 10-6, Evaluated: 10-6) Back to Table

(1) Adler-Golden, S. M.; Wiesenfeld, J. R. Production of atomic oxygen following flash photolysis of $ClONO_2$. *Chem. Phys. Lett.* **1981**, *82*, 281-284, doi:10.1016/0009-2614(81)85156-1.
(2) Goldfarb, L.; Harwood, M. H.; Burkholder, J. B.; Ravishankara, A. R. Reaction of O(^{3}P) with $ClONO_2$: Rate coefficients and yield of NO_3 product. *J. Phys. Chem. A* **1998**, *102*, 8556-8563, doi:10.1021/jp9819386.
(3) Kurylo, M. J. Flash photolysis resonance fluorescence investigation of the reaction of O(^{3}P) atoms with $ClONO_2$. *Chem. Phys. Lett.* **1977**, *49*, 467-470, doi:10.1016/0009-2614(77)87016-4.
(4) Molina, L. T.; Spencer, J. E.; Molina, M. J. The rate constant for the reaction of O(^{3}P) atoms with $ClONO_2$. *Chem. Phys. Lett.* **1977**, *45*, 158-162, doi:10.1016/0009-2614(77)85233-0.
(5) Ravishankara, A. R.; Davis, D. D.; Smith, G.; Tesi, G.; Spencer, J. A study of the chemical degradation of $ClONO_2$ in the stratosphere. *Geophys. Res. Lett.* **1977**, *4*, 7-9, doi:10.1029/GL004i001p00007.
(6) Tyndall, G. S.; Kegley-Owen, C. S.; Orlando, J. J.; Calvert, J. G. Quantum yields for Cl($^2P_{3/2,1/2}$), ClO and O(^{3}P) in the photolysis of chlorine nitrate at 308 nm. *J. Chem. Soc. Faraday Trans.* **1997**, *93*, 2675-2682, doi:10.1039/a701585b.

F7. **O_3 + OClO.** The recommendation is based on results over the temperature range 262–296 K reported by Wongdontri-Stuper et al.[2] (253–296 K). The uncertainty limits encompass the somewhat lower room temperature result of Birks et al.[1] (298 K).
(Table: 90-1, Note: 90-1, Evaluated: 10-6) Back to Table

(1) Birks, J. W.; Shoemaker, B.; Leck, T. J.; Borders, R. A.; Hart, L. J. Studies of reactions of importance in the stratosphere. II. Reactions involving chlorine nitrate and chlorine dioxide. *J. Chem. Phys.* **1977**, *66*, 4591-4599, doi:10.1063/1.433716.
(2) Wongdontri-Stuper, W.; Jayanty, R. K. M.; Simonaitis, R.; Heicklen, J. The Cl_2 photosensitized decomposition of O_3: the reactions of ClO and OClO with O_3. *J. Photochem.* **1979**, *10*, 163-186, doi:10.1016/0047-2670(79)80004-0.

F8. **O_3 + Cl_2O_2.** The recommended upper-limit is taken from the study of DeMore and Tschuikow-Roux[1] (195–217 K) measured at 195 K.
(Table: 90-1, Note: 90-1, Evaluated: 10-6) Back to Table

(1) DeMore, W. B.; Tschuikow-Roux, E. Ultraviolet spectrum and chemical reactivity of the ClO dimer. *J. Phys. Chem.* **1990**, *94*, 5856-5860, doi:10.1021/j100378a046.

F9. **OH + Cl_2.** The recommended k(298 K) value is the average of the results reported by Bryokov et al.[2] (297–826 K), Gilles et al.[3] (231–354 K), Boodaghians et al.[1] (253–333 K), Loewenstein and Anderson,[5] (298 K), Ravishankara et al.[6] (298 K), and Leu and Lin[4] (298 K). The temperature dependence is based on an error-weighted average of the Gilles et al. and Boodaghians et al. E/R values. Loewenstein and Anderson determined that the exclusive products are Cl + HOCl.
(Table: 10-6, Note: 10-6, Evaluated: 10-6) Back to Table

(1) Boodaghians, R. B.; Hall, I. W.; Wayne, R. P. Kinetics of the reactions of the hydroxyl radical with molecular chlorine and bromine. *J. Chem. Soc. Faraday Trans. 2* **1987**, *83*, 529-538, doi:10.1039/f29878300529.
(2) Bryukov, M. G.; Knyazev, V. D.; Lomnicki, S. M.; McFerrin, C. A.; Dellinger, B. Temperature-dependent kinetics of the gas-phase reactions of OH with Cl_2, CH_4, and C_3H_8. *J. Phys. Chem. A* **2004**, *108*, 10464-10472, doi:10.1021/jp047340h.
(3) Gilles, M. K.; Burkholder, J. B.; Ravishankara, A. R. Rate coefficients for the reaction of OH with Cl_2, Br_2 and I_2 from 235 to 354 K. *Int. J. Chem. Kinet.* **1999**, *31*, 417-424, doi:10.1002/(SICI)1097-4601(1999)31:6<417::AID-KIN3>3.0.CO;2-A.
(4) Leu, M.-T.; Lin, C. L. Rate constants for the reactions of OH with ClO, Cl_2, and Cl_2O at 298K. *Geophys. Res. Lett.* **1979**, *6*, 425-428, doi:10.1029/GL006i006p00425.
(5) Loewenstein, L. M.; Anderson, J. G. Rate and product measurements for the reactions of OH with Cl_2, Br_2, and BrCl at 298 K. Trend interpretations. *J. Phys. Chem.* **1984**, *88*, 6277-6286, doi:10.1021/j150669a045.
(6) Ravishankara, A. R.; Eisele, F. L.; Wine, P. H. The kinetics of the reaction of OH with ClO. *J. Chem. Phys.* **1983**, *78*, 1140-1144, doi:10.1063/1.444906.

F10. OH + ClO. The reaction has two known product channels under atmospheric conditions: OH + ClO → Cl + HO_2 and OH + ClO → HCl + O_2. Most studies measured the rate coefficient for the overall reaction (OH + ClO → products), which is presumably the sum of the two channels. The assessment of the overall reaction (OH + ClO → products) is based on a fit to the data of Hills and Howard[3] (219–373 K), Lipson et al.[7] (208–298 K), Kegley-Owen et al.[4] (234–356 K), Poulet et al.[8] (298 K), Wang and Keyser[11] (218–298 K), and Bedjanian et al.[1] (230–360 K). Data reported in the studies of Burrows et al.[2] (243–298 K), Ravishankara et al.[9] (248–335 K) and Leu and Lin[5] (298 K) were not used in deriving the recommended value because the concentration of ClO was determined by an indirect method. The recommendation for the Cl + HO_2 channel is obtained from the equilibrium constant for this channel, combined with the recommended value for the reverse reaction. The minor reaction channel forming HCl poses significant experimental difficulties due to complications associated with the measurement of the HCl reaction product. Early studies inferred the HCl branching ratio without measuring HCl. These included the 298 K measurements of the yield of the Cl + HO_2 channel by Leu and Lin[5] (>0.65), Burrows et al.[2] (0.85 ± 0.2), and Hills and Howard[3] (0.86 ± 0.14). Poulet et al.[8] measured the Cl + HO_2 product yield to be 0.98 ± 0.12 using mass spectrometry, but their HCl sensitivity was marginal. These studies were not considered in the evaluation. Later studies by Lipson et al.[7] using mass spectrometry and by Wang and Keyser[12] using diode laser spectroscopy improved the precision of the HCl product channel measurements. Lipson et al.[6] measured rate constants for the HCl channel over the temperature range 207–298 K and reported a branching ratio of (7 ± 3) %, while Wang and Keyser[12] measured the HCl yield between 218–298 K, obtaining (9.0 ± 4.8) %, independent of temperature. The Wang and Keyser rate constant was computed from the HCl yield and their overall rate constant.[11] Measurements by Tyndall et al.[10] and Bedjanian et al.[1] were also considered. (Although the values for the HCl channel obtained by Lipson et al. from combining the values obtained in Lipson et al.[6,7] and Bedjanian et al.[1] are in agreement, their values for the overall reaction differ by 40–70%.) The recommendation for the HCl channel is unchanged from JPL 06-2, and the error limits have been reduced.
(Table: 09-31, Note: 09-31, Evaluated: 09-31) Back to Table

(1) Bedjanian, Y.; Riffault, V.; Le Bras, G. Kinetics and mechanism of the reaction of OH with ClO. *Int. J. Chem. Kinet.* **2001**, *33*, 587-599, doi:10.1002/kin.1054.
(2) Burrows, J. P.; Wallington, T. J.; Wayne, R. P. Kinetics of the reaction of OH with ClO. *J. Chem. Soc. Faraday Trans. 2* **1984**, *80*, 957-971, doi:10.1039/f29848000957.
(3) Hills, A. J.; Howard, C. J. Rate coefficient temperature dependence and branching ratio for the OH + ClO reaction. *J. Chem. Phys.* **1984**, *81*, 4458-4465, doi:10.1063/1.447414.
(4) Kegley-Owen, C. S.; Gilles, M. K.; Burkholder, J. B.; Ravishankara, A. R. Rate coefficient measurement for the reaction OH + ClO → products. *J. Phys. Chem. A* **1999**, *103*, 5040-5048, doi:10.1021/jp9904320.
(5) Leu, M.-T.; Lin, C. L. Rate constants for the reactions of OH with ClO, Cl_2, and Cl_2O at 298K. *Geophys. Res. Lett.* **1979**, *6*, 425-428, doi:10.1029/GL006i006p00425.
(6) Lipson, J. B.; Beiderhase, T. W.; Molina, L. T.; Molina, M. J.; Olzmann, M. Production of HCl in the OH + ClO reaction: Laboratory measurements and statistical rate theory calculations. *J. Phys. Chem. A* **1999**, *103*, 6540-6551, doi:10.1021/jp9847787.
(7) Lipson, J. B.; Elrod, M. J.; Beiderhase, T. W.; Molina, L. T.; Molina, M. J. Temperature dependence of the rate constant and branching ratio for the OH + ClO reaction. *J. Chem. Soc. Faraday Trans.* **1997**, *93*, 2665-2673, doi:10.1039/a701946g.

(8) Poulet, G.; Laverdet, G.; Le Bras, G. Rate constant and branching ratio for the reaction of OH with ClO. *J. Phys. Chem.* **1986**, *90*, 159-165, doi:10.1021/j100273a036.
(9) Ravishankara, A. R.; Eisele, F. L.; Wine, P. H. The kinetics of the reaction of OH with ClO. *J. Chem. Phys.* **1983**, *78*, 1140-1144, doi:10.1063/1.444906.
(10) Tyndall, G. S.; Kegley-Owen, C. S.; Orlando, J. J.; Fried, A. Tunable diode laser study of the reaction OH + ClO → HCl + O_2. *J. Phys. Chem. A* **2002**, *106*, 1567-1575, doi:10.1021/jp013410y.
(11) Wang, J. J.; Keyser, L. F. Absolute rate constant of the OH + ClO reaction at temperatures between 218 and 298 K. *J. Phys. Chem. A* **2001**, *105*, 10544-10552, doi:10.1021/jp012426l.
(12) Wang, J. J.; Keyser, L. F. HCl yield from the OH + ClO reaction at temperatures between 218 and 298 K. *J. Phys. Chem. A* **2001**, *105*, 6479-6489, doi:10.1021/jp0106449.

F11. OH + OClO. The recommendation is that reported by Gierczak et al.[1] (242–392 K). An earlier study by Poulet et al.[2] (298–473 K) is in fair agreement with the recommendation. Differences between the studies may lie in the methods used to determine the OClO concentration. Gierczak et al. used in situ optical measurements of OClO, whereas Poulet et al. relied on measured flows of dilute mixtures. The HOCl product was detected in the Poulet et al. study by modulated molecular beam mass spectrometry. The branching ratio for the channel to produce HOCl + O_2 was determined to be close to unity, but experimental uncertainty would allow it to be as low as 0.80.
(Table: 10-6, Note: 10-6, Evaluated: 10-6) Back to Table

(1) Gierczak, T.; Burkholder, J. B.; Ravishankara, A. R. Rate coefficients for the reaction of OH with OClO between 242 and 392 K. *Int. J. Chem. Kinet.* **2006**, *38*, 234-241, doi:10.1002/kin.20158.
(2) Poulet, G.; Zagogianni, H.; Le Bras, G. Kinetics and mechanism of the OH + ClO_2 reaction. *Int. J. Chem. Kinet.* **1986**, *18*, 847-859, doi:10.1002/kin.550180805.

F12. OH + Cl_2O. The reaction has been studied as a function of temperature by Stevens and Anderson[4] (236–383 K) and Hansen et al.[2] (223–307 K). The results of these two studies are in excellent agreement at temperatures below 300 K. Hansen et al. suggest that data taken above 300 K by Stevens and Anderson were complicated by wall decomposition of Cl_2O. The recommended value of E/R is the average of the individual E/R values from the two studies for data below 300 K. The recommended value for $k(298\ K)$ is an average of the results from Stevens and Anderson, Hansen et al., Ennis and Birks[1] (298 K), and Leu and Lin[3] (298 K).
(Table: 10-6, Note: 10-6, Evaluated: 10-6) Back to Table

(1) Ennis, C. A.; Birks, J. W. Rate constants for the reactions OH + HOCl → H_2O + ClO and H + HOCl → products. *J. Phys. Chem.* **1988**, *93*, 1119-1126, doi:10.1021/j100316a024.
(2) Hansen, J. C.; Friedl, R. R.; Sander, S. P. Kinetics of the OH + ClOOCl and OH + Cl_2O reactions: Experiment and theory. *J. Phys. Chem. A* **2008**, *112*, 9229-9237, doi:10.1021/jp8007706.
(3) Leu, M.-T.; Lin, C. L. Rate constants for the reactions of OH with ClO, Cl_2, and Cl_2O at 298K. *Geophys. Res. Lett.* **1979**, *6*, 425-428, doi:10.1029/GL006i006p00425.
(4) Stevens, P. S.; Anderson, J. G. Kinetic and mechanistic study of X + ClOCl → products (X = Br, CI, F, O, OH, N) over the temperature range 240-373 K. *J. Phys. Chem.* **1992**, *96*, 1708-1718, doi:10.1021/j100183a040.

F13. OH + Cl_2O_2. The recommendation is based on results from the study of Hansen et al.[1] (223–318 K) using a discharge flow technique coupled with direct detection of OH and Cl_2O_2 via resonance fluorescence and mass spectrometric techniques, respectively. Ab initio calculations by Hansen et al. support the finding of a negative temperature dependence.
(Table: 10-6, Note: 10-6, Evaluated: 10-6) Back to Table

(1) Hansen, J. C.; Friedl, R. R.; Sander, S. P. Kinetics of the OH + ClOOCl and OH + Cl_2O reactions: Experiment and theory. *J. Phys. Chem. A* **2008**, *112*, 9229-9237, doi:10.1021/jp8007706.

F14. OH + HCl. The recommendation is based on a least squares fit to the data over the temperature range 204–300 K reported in the studies of Molina et al.[8] (240–295 K), Keyser,[7] Ravishankara et al.[10] (240–1055 K), Battin-Leclerc et al.[1] (200–400 K), and Bryukov et al.[2] (298–1015 K). In these studies, particular attention was paid to the determination of the absolute concentration of HCl by UV and IR spectrophotometry. Earlier studies by Takacs and Glass[15] (295 K), Zahniser et al.[16] (224–460 K), Smith and Zellner[13] (220–480 K), Ravishankara et al.[9] (250–402 K), Hack et al.[4] (293–718 K), Husain et al.[5] (300 K), Cannon et al.[3] (298 K), Husain et al.[6] (300–700 K), and Smith and Williams[12] (298 K) had reported somewhat lower room temperature values. The data of Sharkey and Smith[11] (138–298 K) over the temperature range 138–216 K, Battin-Leclerc et al.[1] below 240 K, and Bryukov et al. over the temperature range 298–1015 K, depart from normal Arrhenius behavior. Quantum chemical and transition state calculations performed by Battin-Leclerc et al., Bryukov et al., and

Steckler et al.[14] generally support the existence of a weakly bound complex; however, a large tunneling effect is required to explain the low temperature data. Additional work at low temperature is needed to confirm the strong non-Arrhenius behavior.
(Table: 09-31, Note: 09-31, Evaluated: 09-31) Back to Table

(1) Battin-Leclerc, F.; Kim, I. K.; Talukdar, R. K.; Portmann, R. W.; Ravishankara, A. R.; Steckler, R.; Brown, D. Rate coefficients for the reactions of OH and OD with HCl and DCl between 200 and 400 K. *J. Phys. Chem. A* **1999**, *103*, 3237-3244, doi:10.1021/jp990177j.

(2) Bryukov, M. G.; Dellinger, B.; Knyazev, V. D. Kinetics of the gas-phase reaction of OH with HCl. *J. Phys. Chem. A* **2006**, *110*, 936-943, doi:10.1021/jp053615x.

(3) Cannon, B. D.; Robertshaw, J. S.; Smith, I. W. M.; Williams, M. D. A time-resolved LIF study of the kinetics of OH(v=0) and OH(v=1) with HCl and HBr. *Chem. Phys. Lett.* **1984**, *105*, 380-385, doi:10.1016/0009-2614(84)80045-7.

(4) Hack, W.; Mex, G.; Wagner, H. G. Determination of rate constant of reactions O + HCl in temperature range 293 to 718 K and OH + HCl at 293 K. *Ber. Bunsenges. Phys. Chem.* **1977**, *81*, 677-684, doi:10.1002/bbpc.19770810710.

(5) Husain, D.; Plane, J. M. C.; Slater, N. K. H. Kinetic investigation of the reactions of OH($X^2\Pi$) with the hydrogen halides, HCl, DCl, HBr and DBr by time-resolved resonance fluorescence ($A^2\Sigma^+$ - $X^2\Pi$). *J. Chem. Soc. Faraday Trans. 2* **1981**, *77*, 1949-1962, doi:10.1039/f29817701949.

(6) Husain, D.; Plane, J. M. C.; Xiang, C. C. Kinetic studies of the reactions of OH($X^2\Pi$) with hydrogen chloride and deuterium chloride at elevated temperatures by time-resolved resonance fluorescence ($A\ ^2\Sigma^+$ - $X\ ^2\Pi$). *J. Chem. Soc. Faraday Trans. 2* **1984**, *80*, 713-728, doi:10.1039/f29848000713.

(7) Keyser, L. F. High pressure flow kinetics: a study of the OH + HCl reaction from 2 to 100 torr. *J. Phys. Chem.* **1984**, *88*, 4750-4758, doi:10.1021/j150664a061.

(8) Molina, M. J.; Molina, L. T.; Smith, C. A. The rate of the reaction of OH with HCl. *Int. J. Chem. Kinet.* **1984**, *16*, 1151-1160, doi:10.1002/kin.550160910.

(9) Ravishankara, A. R.; Smith, G.; Watson, R. T.; Davis, D. D. A temperature dependent kinetics study of the reaction of HCl with OH and O(^{3}P). *J. Phys. Chem.* **1977**, *81*, 2220-2225, doi:10.1021/j100539a002.

(10) Ravishankara, A. R.; Wine, P. H.; Wells, J. R.; Thompson, R. L. Kinetic study of the reaction of OH with HCl from 240–1055 K. *Int. J. Chem. Kinet.* **1985**, *17*, 1281-1297, doi:10.1002/kin.550171206.

(11) Sharkey, P.; Smith, I. W. M. Kinetics of elementary reactions at low temperatures: Rate constants for the reactions of OH with HCl ($298 \geq T/K \geq 138$), CH_4 ($298 \geq T/K \geq 178$), and C_2H_6 ($298 \geq T/K \geq 138$). *J. Chem. Soc. Faraday Trans.* **1993**, *89*, 631-638, doi:10.1039/ft9938900631.

(12) Smith, I. W. M.; Williams, M. D. Effects of isotopic substitution and vibrational excitation on reaction rates Kinetics of OH(v = 0,1) and OD(v = 0,1) with HCl and DCl. *J. Chem. Soc. Faraday Trans. 2* **1986**, *82*, 1043-1055, doi:10.1039/f29868201043.

(13) Smith, I. W. M.; Zellner, R. Rate measurements of reactions of OH by resonance absorption. Part 3. - Reactions of OH with H_2, D_2 and hydrogen and deuterium halides. *J. Chem. Soc. Faraday Trans. 2* **1974**, *70*, 1045-1056, doi:10.1039/F29747001045.

(14) Steckler, R.; Thurman, G. M.; Watts, J. D.; Bartlett, R. J. *Ab initio* direct dynamics study of OH + HCl → Cl + H_2O. *J. Chem. Phys.* **1997**, *106*, 3926-3933, doi:10.1063/1.473981.

(15) Takacs, G. A.; Glass, G. P. Reactions of hydroxyl radicals with some hydrogen halides. *J. Phys. Chem.* **1973**, *77*, 1948-1951, doi:10.1021/j100635a005.

(16) Zahniser, M. S.; Kaufman, F.; Anderson, J. G. Kinetics of the reaction of OH with HCl. *Chem. Phys. Lett.* **1974**, *27*, 507-510, doi:10.1016/0009-2614(74)80292-7.

F15. OH + HOCl. In the only reported study of this system, Ennis and Birks[1] (298 K) reported the value of this rate constant at room temperature to lie in the range $(1.7–9.5) \times 10^{-13}$ cm^3 molecule^{-1} s^{-1}. A temperature-dependent expression has been estimated by choosing a pre-exponential factor by analogy with the OH + H_2O_2 reaction and selecting the midpoint of the experimental range for the room temperature rate constant. Theoretical calculations by Wang et al.,[2] however, suggest that tunneling may play an important role at lower temperatures and give rise to a significant curvature in the Arrhenius curve. The large uncertainty factor is needed to encompass the entire range.
(Table: 87-41, Note: 10-6, Evaluated: 10-6) Back to Table

(1) Ennis, C. A.; Birks, J. W. Rate constants for the reactions OH + HOCl → H_2O + ClO and H + HOCl → products. *J. Phys. Chem.* **1988**, *93*, 1119-1126, doi:10.1021/j100316a024.

(2) Wang, L.; Liu, J. Y.; Li, Z. S.; Sun, C. C. Direct ab initio dynamics studies on the hydrogen-abstraction reactions of OH radicals with HOX (X = F, Cl, and Br). *J. Comp. Chem.* **2004**, *25*, 558-564, doi:10.1002/jcc.10403.

F16. OH + $ClNO_2$. The recommendation is based on results of the direct studies of Ganske et al.[1,2] (259–348 K) using the discharge flow-resonance fluorescence technique. Mass spectrometric studies showed HOCl to be the major chlorine-containing product, with no evidence for a channel to produce $HONO_2$ + Cl.
(Table: 94-26, Note: 94-26, Evaluated: 94-26) Back to Table

(1) Ganske, J. A.; Berko, H. N.; Ezell, M. J.; Finlayson-Pitts, B. J. Kinetics of the gas-phase reaction of OH with $ClNO_2$ from 259 to 348 K. *J. Phys. Chem.* **1992**, *96*, 2568-2572, doi:10.1021/j100185a032.

(2) Ganske, J. A.; Ezell, M. J.; Berko, H. N.; Finlayson-Pitts, B. J. The reaction of OH with $ClNO_2$ at 298 K: kinetics and mechanisms. *Chem. Phys. Lett.* **1991**, *179*, 204-210, doi:10.1016/0009-2614(91)90317-3.

F17. OH + $ClONO_2$. The results reported by Zahniser et al.[2] (246–387 K) and Ravishankara et al.[1] (245 K) are in good agreement at ~245 K (within 25%), considering the difficulties associated with handling $ClONO_2$. The recommended value is that of Zahniser et al. Neither study reported data on the reaction products.
(Table: 82-57, Note: 82-57, Evaluated: 10-6) Back to Table

(1) Ravishankara, A. R.; Davis, D. D.; Smith, G.; Tesi, G.; Spencer, J. A study of the chemical degradation of $ClONO_2$ in the stratosphere. *Geophys. Res. Lett.* **1977**, *4*, 7-9, doi:10.1029/GL004i001p00007.

(2) Zahniser, M. S.; Chang, J.; Kaufman, F. Chlorine nitrate: Kinetics of formation by ClO + NO_2 + M and of reaction with OH. *J. Chem. Phys.* **1977**, *67*, 997-1003, doi:10.1063/1.434927.

F18. OH + CH_3Cl. The recommended k(298 K) is an average of the values from the relative rate study of Hsu and DeMore[6] (293–358 K) (recalculated based on the current recommendation for the rate constant of the OH + CH_3CHF_2 reference reaction, as described in the note for that reaction) and the absolute studies of Herndon et al.[4] (224–398 K) and Orkin et al.[8] (298–460 K). The recommended value for E/R was obtained from a fit to the data of Herndon et al. below room temperature. Data from the earlier studies of Howard and Evenson[5] (296 K), Perry et al.[10] (298–422 K), Davis et al.[3] (250–350 K), Paraskevopoulos et al.[9] (297 K), Jeong and Kaufman[7] (247–483 K), and Taylor et al.[11] (295– 800 K) (with the exception of their 295 K data point) are reasonably well encompassed within the recommended 2σ uncertainty limits. The room temperature value from Taylor et al. is inconsistent with the higher temperature results in the same study and with the other investigations and lies outside of the 2σ band, as do the higher room temperature values of Cox et al.[2] and Brown et al.[1]
(Table: 15-10, Note: 15-10, Evaluated: 15-10) Back to Table

(1) Brown, A. C.; Canosa-Mas, C. E.; Wayne, R. P. A kinetic study of the reactions of OH with CH_3I and CF_3I. *Atmos. Environ.* **1990**, *24A*, 361-367, doi:10.1016/0960-1686(90)90115-4.

(2) Cox, R. A.; Derwent, R. G.; Eggleton, A. E. J.; Lovelock, J. E. Photochemical oxidation of halocarbons in the troposphere. *Atmos. Environ.* **1976**, *10*, 305-308, doi:10.1016/0004-6981(76)90170-0.

(3) Davis, D. D.; Machado, G.; Conaway, B.; Oh, Y.; Watson, R. A temperature dependent kinetics study of the reaction of OH with CH_3Cl, CH_2Cl_2, $CHCl_3$, and CH_3Br. *J. Chem. Phys.* **1976**, *65*, 1268-1274, doi:10.1063/1.433236.

(4) Herndon, S. C.; Gierczak, T.; Talukdar, R. K.; Ravishankara, A. R. Kinetics of the reactions of OH with several alkyl halides. *Phys. Chem. Chem. Phys.* **2001**, *3*, 4529-4535, doi:10.1039/b105188c.

(5) Howard, C. J.; Evenson, K. M. Rate constants for the reactions of OH with CH_4 and fluorine, chlorine, and bromine substituted methanes at 296 K. *J. Chem. Phys.* **1976**, *64*, 197-202, doi:10.1063/1.431950.

(6) Hsu, K. J.; DeMore, W. B. Rate constants for the reactions of OH with CH_3Cl, CH_2Cl_2, $CHCl_3$, and CH_3Br. *Geophys. Res. Lett.* **1994**, *21*, 805-808, doi:10.1029/94GL00601.

(7) Jeong, K. M.; Kaufman, F. Kinetics of the reaction of hydroxyl radical with methane and with nine Cl- and F-substituted methanes. 1. Experimental results, comparisons, and applications. *J. Phys. Chem.* **1982**, *86*, 1808-1815, doi:10.1021/j100207a016.

(8) Orkin, V. L.; Khamaganov, V. G.; Kasimovskaya, E. E.; Guschin, A. G. Photochemical properties of some Cl-containing halogenated alkanes. *J. Phys. Chem. A* **2013**, *117*, 5483-5490, doi:10.1021/jp400408y.

(9) Paraskevopoulos, G.; Singleton, D. L.; Irwin, R. S. Rates of OH radical reactions. 8. Reactions with CH_2FCl, CHF_2Cl, $CHFCl_2$, CH_3CF_2Cl, CH_3Cl, and C_2H_5Cl at 297 K. *J. Phys. Chem.* **1981**, *85*, 561-564, doi:10.1021/j150605a021.

(10) Perry, R. A.; Atkinson, R.; Pitts, J. N., Jr. Rate constants for the reaction of OH radicals with $CHFCl_2$ and CH_3Cl over the temperature range 298-423 °K, and with CH_2Cl_2 at 298 °K. *J. Chem. Phys.* **1976**, *64*, 1618-1620, doi:10.1063/1.432335.

(11) Taylor, P. H.; D'Angelo, J. A.; Martin, M. C.; Kasner, J. H.; Dellinger, B. Laser photolysis/laser-induced fluorescence studies of reaction rates of OH with CH_3Cl, CH_2Cl_2, and $CHCl_3$ over an extended temperature range. *Int. J. Chem. Kinet.* **1989**, *21*, 829-846, doi:10.1002/kin.550210908

F19. OH + CH_2Cl_2. The recommended values for k(298 K) and E/R are derived from a combined fit to the data from the absolute studies of Villenave et al.[9] (277–370 K) and Herndon et al.[3] (219–394 K) and the relative rate study of Hsu and DeMore[5] (293–368 K) (two determinations, which have been recalculated based on the current recommendations for the rate constants of the OH + CH_3CHF_2 and CH_3CH_2F reference reactions). The renormalization procedure is discussed in the note for the OH + CH_3CHF_2 reaction. The lowest temperature data (219–220 K) of Herndon et al. were not used in the fit since they appear to be systematically higher than expected from the data at 227 K and above, a difference that could possibly be due to the presence of residual reactive stabilizer in the sample of CH_2Cl_2. The results of Cox et al.[1] and Davis et al.[2] (245–375 K) support the recommendation. The results from Taylor et al.[8] (298–775 K), Jeong and Kaufman[6] (251–455 K), Perry et al.[7] (298 K), and Howard and Evenson[4] (296 K) lie considerably higher than the recommendation and were not used in deriving the recommended parameters.
(Table: 15-10, Note: 15-10, Evaluated: 15-10) Back to Table

(1) Cox, R. A.; Derwent, R. G.; Eggleton, A. E. J.; Lovelock, J. E. Photochemical oxidation of halocarbons in the troposphere. *Atmos. Environ.* **1976**, *10*, 305-308, doi:10.1016/0004-6981(76)90170-0.
(2) Davis, D. D.; Machado, G.; Conaway, B.; Oh, Y.; Watson, R. A temperature dependent kinetics study of the reaction of OH with CH_3Cl, CH_2Cl_2, $CHCl_3$, and CH_3Br. *J. Chem. Phys.* **1976**, *65*, 1268-1274, doi:10.1063/1.433236.
(3) Herndon, S. C.; Gierczak, T.; Talukdar, R. K.; Ravishankara, A. R. Kinetics of the reactions of OH with several alkyl halides. *Phys. Chem. Chem. Phys.* **2001**, *3*, 4529-4535, doi:10.1039/b105188c.
(4) Howard, C. J.; Evenson, K. M. Rate constants for the reactions of OH with CH_4 and fluorine, chlorine, and bromine substituted methanes at 296 K. *J. Chem. Phys.* **1976**, *64*, 197-202, doi:10.1063/1.431950.
(5) Hsu, K. J.; DeMore, W. B. Rate constants for the reactions of OH with CH_3Cl, CH_2Cl_2, $CHCl_3$, and CH_3Br. *Geophys. Res. Lett.* **1994**, *21*, 805-808, doi:10.1029/94GL00601.
(6) Jeong, K. M.; Kaufman, F. Kinetics of the reaction of hydroxyl radical with methane and with nine Cl- and F-substituted methanes. 1. Experimental results, comparisons, and applications. *J. Phys. Chem.* **1982**, *86*, 1808-1815, doi:10.1021/j100207a016.
(7) Perry, R. A.; Atkinson, R.; Pitts, J. N., Jr. Rate constants for the reaction of OH radicals with $CHFCl_2$ and CH_3Cl over the temperature range 298-423 °K, and with CH_2Cl_2 at 298 °K. *J. Chem. Phys.* **1976**, *64*, 1618-1620, doi:10.1063/1.432335.
(8) Taylor, P. H.; Jiang, Z.; Dellinger, B. Determination of the gas-phase reactivity of hydroxyl with chlorinated methanes at high temperature: Effects of laser/thermal photochemistry. *Int. J. Chem. Kinet.* **1993**, *25*, 9-23, doi:10.1002/kin.550250103.
(9) Villenave, E.; Orkin, V. L.; Huie, R. E.; Kurylo, M. J. Rate constant for the reaction of OH radicals with dichloromethane. *J. Phys. Chem. A* **1997**, *101*, 8513-8517, doi:10.1021/jp9721614.

F20. OH + $CHCl_3$. The recommended k(298 K) is an average of the values from the relative rate study of Hsu and DeMore[3] (288–357 K) (which has been recalculated based on the current recommendation for the rate constant of the OH + CH_3CHF_2 reference reaction, as described in the note for that reaction) and the absolute studies of Taylor et al.[6] (295–774 K) (which superseded Taylor et al.[5]), Jeong and Kaufman[4] (249–487 K), Davis et al.,[1] (245–375 K), and Howard and Evenson[2] (296 K). The recommended value of E/R is an average of values for this parameter derived in the above temperature dependent studies.
(Table: 02-25, Note: 02-25, Evaluated: 02-25) Back to Table

(1) Davis, D. D.; Machado, G.; Conaway, B.; Oh, Y.; Watson, R. A temperature dependent kinetics study of the reaction of OH with CH_3Cl, CH_2Cl_2, $CHCl_3$, and CH_3Br. *J. Chem. Phys.* **1976**, *65*, 1268-1274, doi:10.1063/1.433236.
(2) Howard, C. J.; Evenson, K. M. Rate constants for the reactions of OH with CH_4 and fluorine, chlorine, and bromine substituted methanes at 296 K. *J. Chem. Phys.* **1976**, *64*, 197-202, doi:10.1063/1.431950.
(3) Hsu, K. J.; DeMore, W. B. Rate constants for the reactions of OH with CH_3Cl, CH_2Cl_2, $CHCl_3$, and CH_3Br. *Geophys. Res. Lett.* **1994**, *21*, 805-808, doi:10.1029/94GL00601.
(4) Jeong, K. M.; Kaufman, F. Kinetics of the reaction of hydroxyl radical with methane and with nine Cl- and F-substituted methanes. 1. Experimental results, comparisons, and applications. *J. Phys. Chem.* **1982**, *86*, 1808-1815, doi:10.1021/j100207a016.

(5) Taylor, P. H.; D'Angelo, J. A.; Martin, M. C.; Kasner, J. H.; Dellinger, B. Laser photolysis/laser-induced fluorescence studies of reaction rates of OH with CH_3Cl, CH_2Cl_2, and $CHCl_3$ over an extended temperature range. *Int. J. Chem. Kinet.* **1989**, *21*, 829-846, doi:10.1002/kin.550210908
(6) Taylor, P. H.; Jiang, Z.; Dellinger, B. Determination of the gas-phase reactivity of hydroxyl with chlorinated methanes at high temperature: Effects of laser/thermal photochemistry. *Int. J. Chem. Kinet.* **1993**, *25*, 9-23, doi:10.1002/kin.550250103.

F21. OH + CCl_4. The recommended k(298 K) was obtained by setting the Arrhenius pre-exponential factor (A) to 1×10^{-11} cm^3 molecule^{-1} s^{-1} and equating the activation energy (E) to the reaction endothermicity reported in this evaluation and in IUPAC. The JPL 10-6 evaluation had been based on upper-limits of the rate constant reported by Cox et al.[2] (298 K), Howard and Evenson[3] (296 K), and Clyne and Holt.[1] (293 K). None of these experimental studies indicated any evidence for reaction between these species.
(Table: 15-10, Note: 15-10, Evaluated: 15-10) Back to Table

(1) Clyne, M. A. A.; Holt, P. M. Reaction kinetics involving ground $X^2\Pi$ and excited $A^2\Sigma^+$ hydroxyl radicals Part 1.-Quenching kinetics of OH $A^2\Sigma^+$ and rate constants for reactions of OH $X^2\Pi$ with CH_3CCl_3 and CO. *J. Chem. Soc. Faraday Trans. 2* **1979**, *75*, 569-581, doi:10.1039/f29797500569.
(2) Cox, R. A.; Derwent, R. G.; Eggleton, A. E. J.; Lovelock, J. E. Photochemical oxidation of halocarbons in the troposphere. *Atmos. Environ.* **1976**, *10*, 305-308, doi:10.1016/0004-6981(76)90170-0.
(3) Howard, C. J.; Evenson, K. M. Rate constants for the reactions of OH with CH_4 and fluorine, chlorine, and bromine substituted methanes at 296 K. *J. Chem. Phys.* **1976**, *64*, 197-202, doi:10.1063/1.431950.

F22. OH + CH_2FCl (HCFC-31). The recommended k(298 K) is an average of the values from the relative rate study of DeMore[1] (293–371 K) (which has been recalculated based on the current recommendation for the rate constant of the OH + CH_2Cl_2 reference reaction) and the absolute rate studies of Howard and Evenson[3] (296 K), Paraskevopoulos et al.[5] (297 K), Watson et al.[6] (245–375 K), Handwerk and Zellner[2] (273–373 K), and Jeong and Kaufman[4] (250–486 K). The recommended value for E/R is an average of the values for this parameter derived from the data of DeMore, Watson et al., Handwerk and Zellner, and Jeong and Kaufman below 400 K.
(Table: 02-25, Note: 02-25, Evaluated: 02-25) Back to Table

(1) DeMore, W. B. Experimental and estimated rate constants for the reactions of hydroxyl radicals with several halocarbons. *J. Phys. Chem.* **1996**, *100*, 5813-5820, doi:10.1021/jp953216+.
(2) Handwerk, V.; Zellner, R. Kinetics of the reactions of OH radicals with some halocarbons ($CHClF_2$, CH_2ClF, CH_2ClCF_3, CH_3CClF_2, CH_3CHF_2) in the temperature range 260-370 K. *Ber. Bunsenges. Phys. Chem.* **1978**, *82*, 1161-1166, doi:10.1002/bbpc.19780821117.
(3) Howard, C. J.; Evenson, K. M. Rate constants for the reactions of OH with CH_4 and fluorine, chlorine, and bromine substituted methanes at 296 K. *J. Chem. Phys.* **1976**, *64*, 197-202, doi:10.1063/1.431950.
(4) Jeong, K. M.; Kaufman, F. Kinetics of the reaction of hydroxyl radical with methane and with nine Cl- and F-substituted methanes. 1. Experimental results, comparisons, and applications. *J. Phys. Chem.* **1982**, *86*, 1808-1815, doi:10.1021/j100207a016.
(5) Paraskevopoulos, G.; Singleton, D. L.; Irwin, R. S. Rates of OH radical reactions. 8. Reactions with CH_2FCl, CHF_2Cl, $CHFCl_2$, CH_3CF_2Cl, CH_3Cl, and C_2H_5Cl at 297 K. *J. Phys. Chem.* **1981**, *85*, 561-564, doi:10.1021/j150605a021.
(6) Watson, R. T.; Machado, G.; Conaway, B.; Wagner, S.; Davis, D. D. A temperature dependent kinetics study of the reaction of OH with CH_2ClF, $CHCl_2F$, $CHClF_2$, CH_3CCl_3, CH_3CF_2Cl, and $CF_2ClCFCl_2$. *J. Phys. Chem.* **1977**, *81*, 256-262, doi:10.1021/j100518a014.

F23. OH + $CHFCl_2$ (HCFC-21). The recommended k(298 K) is an average of the values from the studies of Howard and Evenson[4] (296 K), Paraskevopoulos et al.[6] (297 K), Perry et al.[7] (298–422 K), Watson et al.[8] (245–375 K), Chang and Kaufman[1] (241–396 K), Jeong and Kaufman[5] (250–483 K), and Fang et al.[3] (295–460 K). The recommended value for E/R is derived from a combined fit to the data from all but the first two studies listed above (which were only conducted at room temperature) after scaling each data set to the recommended value for k(298 K). The rate constants reported by Clyne and Holt[2] (293–413 K) are significantly higher than those from the other seven studies and were not used in deriving the recommended parameters.
(Table: 15-10, Note: 15-10, Evaluated: 02-25) Back to Table

(1) Chang, J. S.; Kaufman, F. Kinetics of the reactions of hydroxyl radicals with some halocarbons: $CHFCl_2$, CHF_2Cl, CH_3CCl_3, C_2HCl_3, and C_2Cl_4. *J. Chem. Phys.* **1977**, *66*, 4989-4994, doi:10.1063/1.433801.

(2) Clyne, M. A. A.; Holt, P. M. Reaction kinetics involving ground $X^2\Pi$ and excited $A^2\Sigma^+$ hydroxyl radicals Part 2.-Rate constants for reactions of OH $X^2\Pi$ with halogenomethanes and halogenoethanes. *J. Chem. Soc. Faraday Trans. 2* **1979**, *75*, 582-591, doi:10.1039/f29797500582.
(3) Fang, T. D.; Taylor, P. H.; Dellinger, B. Absolute rate measurements of the reaction of OH radicals with HCFC-21 ($CHFCl_2$) and HCFC-22 (CHF_2Cl) over an extended temperature range. *J. Phys. Chem.* **1996**, *100*, 4048-4054, doi:10.1021/jp952690c.
(4) Howard, C. J.; Evenson, K. M. Rate constants for the reactions of OH with CH_4 and fluorine, chlorine, and bromine substituted methanes at 296 K. *J. Chem. Phys.* **1976**, *64*, 197-202, doi:10.1063/1.431950.
(5) Jeong, K. M.; Kaufman, F. Kinetics of the reaction of hydroxyl radical with methane and with nine Cl- and F-substituted methanes. 1. Experimental results, comparisons, and applications. *J. Phys. Chem.* **1982**, *86*, 1808-1815, doi:10.1021/j100207a016.
(6) Paraskevopoulos, G.; Singleton, D. L.; Irwin, R. S. Rates of OH radical reactions. 8. Reactions with CH_2FCl, CHF_2Cl, $CHFCl_2$, CH_3CF_2Cl, CH_3Cl, and C_2H_5Cl at 297 K. *J. Phys. Chem.* **1981**, *85*, 561-564, doi:10.1021/j150605a021.
(7) Perry, R. A.; Atkinson, R.; Pitts, J. N., Jr. Rate constants for the reaction of OH radicals with $CHFCl_2$ and CH_3Cl over the temperature range 298-423 °K, and with CH_2Cl_2 at 298 °K. *J. Chem. Phys.* **1976**, *64*, 1618-1620, doi:10.1063/1.432335.
(8) Watson, R. T.; Machado, G.; Conaway, B.; Wagner, S.; Davis, D. D. A temperature dependent kinetics study of the reaction of OH with CH_2ClF, $CHCl_2F$, $CHClF_2$, CH_3CCl_3, CH_3CF_2Cl, and $CF_2ClCFCl_2$. *J. Phys. Chem.* **1977**, *81*, 256-262, doi:10.1021/j100518a014.

F24. OH + CHF_2Cl (HCFC-22). Studies of this reaction show very good agreement among both absolute and relative rate constant measurements. The recommended value for k(298 K) is an average of the values from the relative rate data of Hsu and DeMore[7] (298–366 K) (which has been recalculated based on the current recommendation for the rate constant of the OH + CH_4 reference reaction), and the absolute rate studies of Orkin and Khamaganov[9] (298–460 K), Fang et al.[4] (294–807 K), Atkinson et al.[1] (296–434 K), Watson et al.[11] (250–350 K), Chang and Kaufman[2] (253–427 K), Paraskevopoulos et al.[10] (297 K), and Jeong and Kaufman[8] (293–482 K). The recommended value for E/R is derived from a combined fit to these same data sets after scaling each one to the recommended value for k(298 K). The more scattered results of Handwerk and Zellner[5] (263–373 K) are in general agreement. The results from the studies of Howard and Evenson[6] (296 K) and Clyne and Holt[3] (294–426 K) are significantly different from those of the other studies and were not used in the derivation.
(Table: 15-10, Note: 15-10, Evaluated: 15-10) Back to Table

(1) Atkinson, R.; Hansen, D. A.; Pitts, J. N., Jr. Rate constants for the reaction of OH radicals with CHF_2Cl, CF_2Cl_2, $CFCl_3$, and H_2 over the temperature range 297-434 °K. *J. Chem. Phys.* **1975**, *63*, 1703-1706, doi:10.1063/1.431566.
(2) Chang, J. S.; Kaufman, F. Kinetics of the reactions of hydroxyl radicals with some halocarbons: $CHFCl_2$, CHF_2Cl, CH_3CCl_3, C_2HCl_3, and C_2Cl_4. *J. Chem. Phys.* **1977**, *66*, 4989-4994, doi:10.1063/1.433801.
(3) Clyne, M. A. A.; Holt, P. M. Reaction kinetics involving ground $X^2\Pi$ and excited $A^2\Sigma^+$ hydroxyl radicals Part 2.-Rate constants for reactions of OH $X^2\Pi$ with halogenomethanes and halogenoethanes. *J. Chem. Soc. Faraday Trans. 2* **1979**, *75*, 582-591, doi:10.1039/f29797500582.
(4) Fang, T. D.; Taylor, P. H.; Dellinger, B. Absolute rate measurements of the reaction of OH radicals with HCFC-21 ($CHFCl_2$) and HCFC-22 (CHF_2Cl) over an extended temperature range. *J. Phys. Chem.* **1996**, *100*, 4048-4054, doi:10.1021/jp952690c.
(5) Handwerk, V.; Zellner, R. Kinetics of the reactions of OH radicals with some halocarbons ($CHClF_2$, CH_2ClF, CH_2ClCF_3, CH_3CClF_2, CH_3CHF_2) in the temperature range 260-370 K. *Ber. Bunsenges. Phys. Chem.* **1978**, *82*, 1161-1166, doi:10.1002/bbpc.19780821117.
(6) Howard, C. J.; Evenson, K. M. Rate constants for the reactions of OH with CH_4 and fluorine, chlorine, and bromine substituted methanes at 296 K. *J. Chem. Phys.* **1976**, *64*, 197-202, doi:10.1063/1.431950.
(7) Hsu, K. J.; DeMore, W. B. Rate constants and temperature dependences for the reactions of hydroxyl radical with several halogenated methanes, ethanes, and propanes by relative rate measurements. *J. Phys. Chem.* **1995**, *99*, 1235-1244, doi:10.1021/j100004a025.
(8) Jeong, K. M.; Kaufman, F. Kinetics of the reaction of hydroxyl radical with methane and with nine Cl- and F-substituted methanes. 1. Experimental results, comparisons, and applications. *J. Phys. Chem.* **1982**, *86*, 1808-1815, doi:10.1021/j100207a016.
(9) Orkin, V. L.; Khamaganov, V. G. Determination of rate constants for reactions of some hydrohaloalkanes with OH radicals and their atmospheric lifetimes. *J. Atmos. Chem.* **1993**, *16*, 157-167, doi:10.1007/BF00702785.

(10) Paraskevopoulos, G.; Singleton, D. L.; Irwin, R. S. Rates of OH radical reactions. 8. Reactions with CH_2FCl, CHF_2Cl, $CHFCl_2$, CH_3CF_2Cl, CH_3Cl, and C_2H_5Cl at 297 K. *J. Phys. Chem.* **1981**, *85*, 561-564, doi:10.1021/j150605a021.
(11) Watson, R. T.; Machado, G.; Conaway, B.; Wagner, S.; Davis, D. D. A temperature dependent kinetics study of the reaction of OH with CH_2ClF, $CHCl_2F$, $CHClF_2$, CH_3CCl_3, CH_3CF_2Cl, and $CF_2ClCFCl_2$. *J. Phys. Chem.* **1977**, *81*, 256-262, doi:10.1021/j100518a014.

F25. OH + $CFCl_3$ (CFC-11). The recommended k(298 K) was obtained by setting the Arrhenius pre-exponential factor (A) to 1×10^{-11} cm^3 molecule^{-1} s^{-1} and equating the activation energy (E) to the reaction endothermicity reported in this evaluation and in IUPAC. The JPL 10-6 recommendation was based on the experimentally determined rate constant upper limits reported by Chang and Kaufman[2] at about 480 K and by Atkinson et al.,[1] Howard and Evenson,[5] Cox et al.,[4] and Clyne and Holt.[3] None of the investigators reported any evidence for reaction between these species.
(Table: 15-10, Note: 15-10, Evaluated: 15-10) Back to Table

(1) Atkinson, R.; Hansen, D. A.; Pitts, J. N., Jr. Rate constants for the reaction of OH radicals with CHF_2Cl, CF_2Cl_2, $CFCl_3$, and H_2 over the temperature range 297-434 °K. *J. Chem. Phys.* **1975**, *63*, 1703-1706, doi:10.1063/1.431566.
(2) Chang, J. S.; Kaufman, F. Upper limits of the rate constants for the reactions of $CFCl_3$ (F-11), CF_2Cl_2 (F-12), and N_2O with OH. Estimates of corresponding lower limits to their tropospheric lifetimes. *Geophys. Res. Lett.* **1977**, *4*, 192-194, doi:10.1029/GL004i005p00192.
(3) Clyne, M. A. A.; Holt, P. M. Reaction kinetics involving ground $X^2\Pi$ and excited $A^2\Sigma^+$ hydroxyl radicals Part 1.-Quenching kinetics of OH $A^2\Sigma^+$ and rate constants for reactions of OH $X^2\Pi$ with CH_3CCl_3 and CO. *J. Chem. Soc. Faraday Trans. 2* **1979**, *75*, 569-581, doi:10.1039/f29797500569.
(4) Cox, R. A.; Derwent, R. G.; Eggleton, A. E. J.; Lovelock, J. E. Photochemical oxidation of halocarbons in the troposphere. *Atmos. Environ.* **1976**, *10*, 305-308, doi:10.1016/0004-6981(76)90170-0.
(5) Howard, C. J.; Evenson, K. M. Rate constants for the reactions of OH with CH_4 and fluorine, chlorine, and bromine substituted methanes at 296 K. *J. Chem. Phys.* **1976**, *64*, 197-202, doi:10.1063/1.431950.

F26. OH + CF_2Cl_2 (CFC-12). The recommended k(298 K) was obtained by setting the Arrhenius pre-exponential factor (A) to 1×10^{-11} cm^3 molecule^{-1} s^{-1} and equating the activation energy (E) to the reaction endothermicity reported in this evaluation and in IUPAC. The JPL 10-6 recommendation was based on the experimentally determined rate constant upper limits reported by Chang and Kaufman[2] at about 480 K and by Atkinson et al.,[1] Howard and Evenson,[5] Cox et al.,[4] and Clyne and Holt.[3] None of the investigators reported any evidence for reaction between these species.
(Table: 15-10, Note: 15-10, Evaluated: 15-10) Back to Table

(1) Atkinson, R.; Hansen, D. A.; Pitts, J. N., Jr. Rate constants for the reaction of OH radicals with CHF_2Cl, CF_2Cl_2, $CFCl_3$, and H_2 over the temperature range 297-434 °K. *J. Chem. Phys.* **1975**, *63*, 1703-1706, doi:10.1063/1.431566.
(2) Chang, J. S.; Kaufman, F. Upper limits of the rate constants for the reactions of $CFCl_3$ (F-11), CF_2Cl_2 (F-12), and N_2O with OH. Estimates of corresponding lower limits to their tropospheric lifetimes. *Geophys. Res. Lett.* **1977**, *4*, 192-194, doi:10.1029/GL004i005p00192.
(3) Clyne, M. A. A.; Holt, P. M. Reaction kinetics involving ground $X^2\Pi$ and excited $A^2\Sigma^+$ hydroxyl radicals Part 2.-Rate constants for reactions of OH $X^2\Pi$ with halogenomethanes and halogenoethanes. *J. Chem. Soc. Faraday Trans. 2* **1979**, *75*, 582-591, doi:10.1039/f29797500582.
(4) Cox, R. A.; Derwent, R. G.; Eggleton, A. E. J.; Lovelock, J. E. Photochemical oxidation of halocarbons in the troposphere. *Atmos. Environ.* **1976**, *10*, 305-308, doi:10.1016/0004-6981(76)90170-0.
(5) Howard, C. J.; Evenson, K. M. Rate constants for the reactions of OH with CH_4 and fluorine, chlorine, and bromine substituted methanes at 296 K. *J. Chem. Phys.* **1976**, *64*, 197-202, doi:10.1063/1.431950.

F27. OH + CCl_2FCClF_2 (CFC-113), $CClF_2CClF_2$ (CFC-114), CF_3CClF_2 (CFC-115). The recommended kinetic parameters for these reactions are estimated as being the same as presently recommended for OH + CCl_4.
(Table: 15-10, Note: 15-10, Evaluated: 15-10) Back to Table

F28. OH + CH_3CH_2Cl. The recommended k(298 K) is an average of the values reported by Howard and Evenson[2] (296 K), Paraskevopoulos et al.[5] (297 K), Kasner et al.[3] (294–789 K), and Herndon et al.[1] (225-400 K). The recommended value for E/R is an average of the values for this parameter determined by Kasner et al. and

Herndon et al. Data from the study by Markert and Nielsen[4] (296–360 K) were not used to derive the recommended parameters, as they are somewhat more scattered.
(Table: 02-25, Note: 02-25, Evaluated: 02-25) Back to Table

(1) Herndon, S. C.; Gierczak, T.; Talukdar, R. K.; Ravishankara, A. R. Kinetics of the reactions of OH with several alkyl halides. *Phys. Chem. Chem. Phys.* **2001**, *3*, 4529-4535, doi:10.1039/b105188c.
(2) Howard, C. J.; Evenson, K. M. Rate constants for the reactions of OH with ethane and some halogen substituted ethanes at 296 K. *J. Chem. Phys.* **1976**, *64*, 4303-4306, doi:10.1063/1.432115.
(3) Kasner, J. H.; Taylor, P. H.; Dellinger, B. Laser photolysis/laser induced fluorescence study of OH-C_2H_5Cl rate constants from 294 to 789 K. *J. Phys. Chem.* **1990**, *94*, 3250-3253, doi:10.1021/j100371a005.
(4) Markert, F.; Nielsen, O. J. The reactions of OH radicals with chloroalkanes in the temperature range 295-360 K. *Chem. Phys. Lett.* **1992**, *194*, 123-127, doi:10.1016/0009-2614(92)85753-W.
(5) Paraskevopoulos, G.; Singleton, D. L.; Irwin, R. S. Rates of OH radical reactions. 8. Reactions with CH_2FCl, CHF_2Cl, $CHFCl_2$, CH_3CF_2Cl, CH_3Cl, and C_2H_5Cl at 297 K. *J. Phys. Chem.* **1981**, *85*, 561-564, doi:10.1021/j150605a021.

F29. OH + CH_2ClCH_2Cl. The recommended k(298 K) is an average of the values reported by Howard and Evenson[2] (296 K), Arnts et al.[1] (297 K), Taylor et al.[4] (292–775 K), and Qiu et al.[3] (292–363 K). The recommended value for E/R is an average of the values determined from fits to the data of Taylor et al.[4] (T <400 K) and Qiu et al.[3]
(Table: 15-10, Note: 15-10, Evaluated: 15-10) Back to Table

(1) Arnts, R. R.; Seila, R. L.; Bufalini, J. J. Determination of room temperature OH rate constants for acetylene, ethylene dichloride, ethylene dibromide, p-dichlorobenzene and carbon disulfide. *J. Air Pollut. Control Assoc.* **1989**, *39*, 453-460, doi:10.1080/08940630.1989.10466544.
(2) Howard, C. J.; Evenson, K. M. Rate constants for the reactions of OH with CH_4 and fluorine, chlorine, and bromine substituted methanes at 296 K. *J. Chem. Phys.* **1976**, *64*, 197-202, doi:10.1063/1.431950.
(3) Qiu, L. X.; Shi, S.-H.; Xing, S. B.; Chen, X. G. Rate constants for the reactions of OH with five halogen-substituted ethanes from 292 to 366 K. *J. Phys. Chem.* **1992**, *96*, 685-689, doi:10.1021/j100181a032.
(4) Taylor, P. H.; McCarron, S.; Dellinger, B. Investigation of 1,2-dichloroethane-hydroxyl kinetics over an extended temperature range: effect of chlorine substitution. *Chem. Phys. Lett.* **1991**, *177*, 27-32, doi:10.1016/0009-2614(91)90170-E.

F30. OH + CH_3CCl_3. The recommended k(298 K) is an average of the values from the absolute studies of Talukdar et al.[8] (243–379 K) and Finlayson-Pitts et al.[2] (278–378 K), and a relative rate study of DeMore[1] (277– 356 K) (recalculated based on the current recommendation for the rate constant of the OH + CH_4 reference reaction). The temperature dependence is a fit to the data between 243 and 379 K of Talukdar et al.[8] These studies indicate both a lower k(298 K) and E/R than were reported in earlier studies by Nelson et al.[7] (359–402 K), Jeong and Kaufman[3] (278–460 K), and Kurylo et al.[5] (253–363 K). More recent measurements by Jiang et al.[4] (298–761 K) and Lancar et al.[6] (298 K) yield rate constants that are slightly higher at 298 K than this recommendation.
(Table: 15-10, Note: 06-2, Evaluated: 15-10) Back to Table

(1) DeMore, W. B. Relative rate constants for the reactions of OH with methane and methyl chloroform. *Geophys. Res. Lett.* **1992**, *19*, 1367-1370, doi:10.1029/92GL01278.
(2) Finlayson-Pitts, B. J.; Ezell, M. J.; Jayaweera, T. M.; Berko, H. N.; Lai, C. C. Kinetics of the reactions of OH with methyl chloroform and methane: Implications for global tropospheric OH and the methane budget. *Geophys. Res. Lett.* **1992**, *19*, 1371-1374, doi:10.1029/92GL01279.
(3) Jeong, K. M.; Kaufman, F. Rates of the reactions of 1, 1, 1-trichloroethane (methyl chloroform) and 1, 1, 2-trichloroethane with OH. *Geophys. Res. Lett.* **1979**, *6*, 757-759, doi:10.1029/GL006i010p00757.
(4) Jiang, Z.; Taylor, P. H.; Dellinger, B. Laser photolysis/laser-induced fluorescence studies of the reaction of OH with 1,1,1-trichloroethane over an extended temperature range. *J. Phys. Chem.* **1992**, *96*, 8961-8964, doi:10.1021/j100201a048.
(5) Kurylo, M. J.; Anderson, P. C.; Klais, O. A flash photolysis resonance fluorescence investigation of the reaction OH + CH_3CCl_3 → H_2O + CH_2CCl_3. *Geophys. Res. Lett.* **1979**, *6*, 760-762, doi:10.1029/GL006i010p00760.
(6) Lancar, I.; Le Bras, G.; Poulet, G. Oxidation of CH_3CCl_3 and CH_3CFCl_2 in the atmosphere : kinetic study of OH reactions. *J. Chim. Phys.* **1993**, *90*, 1897-1908, doi:10.1051/jcp/1993901897.
(7) Nelson, L.; Shanahan, I.; Sidebottom, H. W.; Treacy, J.; Nielsen, O. J. Kinetics and mechanism for the oxidation of 1,1,1-trichloroethane. *Int. J. Chem. Kinet.* **1990**, *22*, 577-590, doi:10.1002/kin.550220603.

(8) Talukdar, R. K.; Mellouki, A.; Schmoltner, A.-M.; Watson, T.; Montzka, S.; Ravishankara, A. R. Kinetics of the OH reaction with methyl chloroform and its atmospheric implications. *Science* **1992**, *257*, 227-230, doi:10.1126/science.257.5067.227.

F31. OH + CH_3CFCl_2 (HCFC-141b). Studies of this reaction have shown that the presence of reactive impurities can have an appreciable effect on the accurate determination of its small rate constant. The recommended k(298 K) is the average of the values derived from the absolute studies of Talukdar et al.[7] (233– 393 K) (by DF-LMR and LP-LIF, for which only data obtained with the purer sample of HCFC-141b were considered) and Lancar et al.[4] (298–479 K) and from the relative rate study of Huder and DeMore[2] (298–360 K) (two determinations that were recalculated based on the current recommendations for the rate constants for the reference reactions OH + CH_4 and OH + CH_3CCl_3). The recommended value for E/R is derived from a combined Arrhenius fit below 400 K to the data of Talukdar et al. (without their lowest temperature data) and Lancar et al. after scaling each data set to the recommended k(298 K). Huder and DeMore reported only Arrhenius expressions derived from their relative rate measurements (i.e., no actual rate constants were tabulated). Their reported values for E/R are nearly identical to the value recommended here. The results of absolute measurements of Zhang et al.[8] (250–297 K) (which supersede those reported in Liu et al.[5]) were complicated by secondary chemistry that may not have been completely accounted for; nevertheless, they are encompassed within the recommended 2σ uncertainty limits. Earlier measurements by Brown et al.[1] (238–426 K) yielded significantly higher rate constants at every temperature, most likely due to the presence of very reactive impurities (such as CH_2=CCl_2) in their HCFC-141b sample. Talukdar et al. reported similar problems in their preliminary measurements. The room temperature result of Mörs et al.[6] (293 K) is 15% smaller than recommended but is encompassed within the recommended 2σ uncertainty limits. The room temperature rate constant reported by Kowalczyk et al.[3] (298 K) is inexplicably a factor of 8 smaller than recommended. The results reported by these authors for several other halocarbons vary widely (ranging from 10% agreement with recommendations to as much as 3 orders of magnitude disagreement).
(Table: 15-10, Note: 15-10, Evaluated: 15-10) Back to Table

(1) Brown, A. C.; Canosa-Mas, C. E.; Parr, A. D.; Wayne, R. P. Laboratory studies of some halogenated ethanes and ethers: Measurements of rates of reaction with OH and of infrared absorption cross-sections. *Atmos. Environ.* **1990**, *24A*, 2499-2511, doi:10.1016/0960-1686(90)90341-J.
(2) Huder, K.; DeMore, W. B. Rate constant for the reaction of OH with CH_3CCl_2F (HCFC-141b) determined by relative rate measurements with CH_4 and CH_3CCl_3. *Geophys. Res. Lett.* **1993**, *20*, 1575-1577, doi:10.1029/93GL01766.
(3) Kowalczyk, J.; Jowko, A.; Symanowicz, M. Kinetics of radical reactions in freons. *J. Radioanal. Nucl. Chem.* **1998**, *232*, 75-78, doi:10.1007/BF02383716.
(4) Lancar, I.; Le Bras, G.; Poulet, G. Oxidation of CH_3CCl_3 and CH_3CFCl_2 in the atmosphere : kinetic study of OH reactions. *J. Chim. Phys.* **1993**, *90*, 1897-1908, doi:10.1051/jcp/1993901897.
(5) Liu, R.; Huie, R. E.; Kurylo, M. J. Rate constants for the reactions of the OH radical with some hydrochlorofluorocarbons over the temperature range 270-400 K. *J. Phys. Chem.* **1990**, *94*, 3247-3249, doi:10.1021/j100371a004.
(6) Mörs, V.; Hoffman, A.; Malms, W.; Zellner, R. Time resolved studies of intermediate products in the oxidation of HCFC 141b ($CFCl_2CH_3$) and HCFC 142b (CF_2ClCH_3). *Ber. Bunsenges, Phys. Chem.* **1996**, *100*, 540-552, doi:10.1002/bbpc.19961000504.
(7) Talukdar, R.; Mellouki, A.; Gierczak, T.; Burkholder, J. B.; McKeen, S. A.; Ravishankara, A. R. Atmospheric fate of CF_2H_2, CH_3CF_3, CHF_2CF_3, and CH_3CFCl_2: Rate coefficients for reactions with OH and UV absorption cross sections of CH_3CFCl_2. *J. Phys. Chem.* **1991**, *95*, 5815-5821, doi:10.1021/j100168a021.
(8) Zhang, Z.; Huie, R. E.; Kurylo, M. J. Rate constants for the reactions of OH with CH_3CFCl_2 (HCFC-141b), CH_3CF_2Cl (HCFC-l42b), and CH_2FCF_3 (HFC-134a). *J. Phys. Chem.* **1992**, *96*, 1533-1535, doi:10.1021/j100183a008.

F32. OH + CH_3CF_2Cl (HCFC-142b). The recommended k(298 K) is an average of the values from Howard and Evenson[7] (296 K), Cox et al.[3] (298 K), Paraskevopoulos et al.[10] (297 K), Mörs et al.[9] (293 K), Watson et al.[11] (273–375 K), Handwerk and Zellner[6] (293, 373 K), Liu et al.[8] (270–400 K), Gierczak et al.[5] (223–427 K), and Fang et al.[4] (295–808 K). The recommended E/R is an average of values for this parameter derived from the last five studies listed above. The data from Brown et al.[1] (231–423 K) and Clyne and Holt[2] (293–425 K) were not used to derive the recommended parameters. The 270 K data of Zhang et al.[12] (270 K) are in reasonable agreement with the recommendation.
(Table: 15-10, Note: 02-25, Evaluated: 15-10) Back to Table

(1) Brown, A. C.; Canosa-Mas, C. E.; Parr, A. D.; Wayne, R. P. Laboratory studies of some halogenated ethanes and ethers: Measurements of rates of reaction with OH and of infrared absorption cross-sections. *Atmos. Environ.* **1990**, *24A*, 2499-2511, doi:10.1016/0960-1686(90)90341-J.
(2) Clyne, M. A. A.; Holt, P. M. Reaction kinetics involving ground $X^2\Pi$ and excited $A^2\Sigma^+$ hydroxyl radicals Part 2.-Rate constants for reactions of OH $X^2\Pi$ with halogenomethanes and halogenoethanes. *J. Chem. Soc. Faraday Trans. 2* **1979**, *75*, 582-591, doi:10.1039/f29797500582.
(3) Cox, R. A.; Derwent, R. G.; Eggleton, A. E. J.; Lovelock, J. E. Photochemical oxidation of halocarbons in the troposphere. *Atmos. Environ.* **1976**, *10*, 305-308, doi:10.1016/0004-6981(76)90170-0.
(4) Fang, T. D.; Taylor, P. H.; Dellinger, B.; Ehlers, C. J.; Berry, R. J. Kinetics of the OH + CH_3CF_2Cl reaction over an extended temperature range. *J. Phys. Chem. A* **1997**, *101*, 5758-5764, doi:10.1021/jp964095w.
(5) Gierczak, T.; Talukdar, R.; Vaghjiani, G. L.; Lovejoy, E. R.; Ravishankara, A. R. Atmospheric fate of hydrofluoroethanes and hydrofluorochloroethanes: 1. Rate coefficients for reactions with OH. *J. Geophys. Res.* **1991**, *96*, 5001-5011, doi:10.1029/90JD02736.
(6) Handwerk, V.; Zellner, R. Kinetics of the reactions of OH radicals with some halocarbons ($CHClF_2$, CH_2ClF, CH_2ClCF_3, CH_3CClF_2, CH_3CHF_2) in the temperature range 260-370 K. *Ber. Bunsenges. Phys. Chem.* **1978**, *82*, 1161-1166, doi:10.1002/bbpc.19780821117.
(7) Howard, C. J.; Evenson, K. M. Rate constants for the reactions of OH with ethane and some halogen substituted ethanes at 296 K. *J. Chem. Phys.* **1976**, *64*, 4303-4306, doi:10.1063/1.432115.
(8) Liu, R.; Huie, R. E.; Kurylo, M. J. Rate constants for the reactions of the OH radical with some hydrochlorofluorocarbons over the temperature range 270-400 K. *J. Phys. Chem.* **1990**, *94*, 3247-3249, doi:10.1021/j100371a004.
(9) Mörs, V.; Hoffman, A.; Malms, W.; Zellner, R. Time resolved studies of intermediate products in the oxidation of HCFC 141b ($CFCl_2CH_3$) and HCFC 142b (CF_2ClCH_3). *Ber. Bunsenges, Phys. Chem.* **1996**, *100*, 540-552, doi:10.1002/bbpc.19961000504.
(10) Paraskevopoulos, G.; Singleton, D. L.; Irwin, R. S. Rates of OH radical reactions. 8. Reactions with CH_2FCl, CHF_2Cl, $CHFCl_2$, CH_3CF_2Cl, CH_3Cl, and C_2H_5Cl at 297 K. *J. Phys. Chem.* **1981**, *85*, 561-564, doi:10.1021/j150605a021.
(11) Watson, R. T.; Machado, G.; Conaway, B.; Wagner, S.; Davis, D. D. A temperature dependent kinetics study of the reaction of OH with CH_2ClF, $CHCl_2F$, $CHClF_2$, CH_3CCl_3, CH_3CF_2Cl, and $CF_2ClCFCl_2$. *J. Phys. Chem.* **1977**, *81*, 256-262, doi:10.1021/j100518a014.
(12) Zhang, Z.; Huie, R. E.; Kurylo, M. J. Rate constants for the reactions of OH with CH_3CFCl_2 (HCFC-141b), CH_3CF_2Cl (HCFC-l42b), and CH_2FCF_3 (HFC-134a). *J. Phys. Chem.* **1992**, *96*, 1533-1535, doi:10.1021/j100183a008.

F33. OH + CH_2ClCF_2Cl (HCFC-132b). The recommended k(298 K) and E/R parameters are averages of those derived from the fits to the absolute data below 400 K from Fang et al.[1] (295–788 K), using a laser photolysis-laser induced fluorescence technique, and Watson et al.[3] (250–350 K), using a flash photolysis – resonance fluorescence technique, which were corrected by the authors for the presence of alkene impurities. The data of Jeong et al.[2] (249–473 K), using a discharge flow technique, indicating greater rate constants, may have been affected by such impurities; hence they were not included in deriving the recommendation.
(Table: 25-1, Note: 25-1, Evaluated: 25-1) Back to Table

(1) Fang, T. D.; Taylor, P. H.; Berry, R. J. Kinetics of the reaction of OH radicals with CH_2ClCF_2Cl and CH_2ClCF_3 over an extended temperature range. *J. Phys. Chem. A* **1999**, *103*, 2700-2704, doi:10.1021/jp984273g.
(2) Jeong, K. M.; Hsu, K. J.; Jeffries, J. B.; Kaufman, F. Kinetics of the reactions of OH with C_2H_6, CH_3CCl_3, $CH_2ClCHCl_2$, $CH_2ClCClF_2$, and CH_2FCF_3. *J. Phys. Chem.* **1984**, *88*, 1222-1226, doi:10.1021/j150650a041.
(3) Watson, R. T.; Ravishankara, A. R.; Machado, G.; Wagner, S.; Davis, D. D. A kinetics study of the temperature dependence of the reactions of OH($^2\Pi$) with CF_3CHCl_2, CF_3CHClF, and CF_2ClCH_2Cl. *Int. J. Chem. Kinet.* **1979**, *11*, 187-197, doi:10.1002/kin.550110210.

F34. OH + CH_2FCFCl_2 (HCFC-132c). The recommended Arrhenius parameters are derived from the data of Orkin et al.[1] (298–370 K).
(Table: 15-10, Note: 15-10, Evaluated: 15-10) Back to Table

(1) Orkin, V. L.; Khamaganov, V. G.; Kasimovskaya, E. E.; Guschin, A. G. Photochemical properties of some Cl-containing halogenated alkanes. *J. Phys. Chem. A* **2013**, *117*, 5483-5490, doi:10.1021/jp400408y.

F35. OH + CH_2ClCF_3 (HCFC-133a). The recommended parameters are derived from the data of McGillen et al.[6] (233–379 K), which is the only study to fully cover the lower temperatures of atmospheric interest. The value of the rate constant at room temperature from Howard and Evenson[5] (296 K) is in good agreement with the recommended value for k(298 K), while systematic differences exist with the k(298 K) values derived from the absolute measurements of Handwerk and Zellner[4] (263–373 K) (~50%) and Fang et al.[3] (~60%) and from the relative rate study of DeMore[2] (298–360 K) (~15%) using OH + CH_3CCl_3 as the reference reaction. Despite these systematic differences, the recommended temperature dependences derived from the last three studies listed above are in reasonable agreement with the recommended E/R The data of Clyne and Holt[1] (294–427 K) are quite scattered, and the values above room temperature are considerably higher than those from other studies. Hence, these data were not used in deriving the recommended parameters.
(Table: 15-10, Note: 15-10, Evaluated: 15-10) Back to Table

(1) Clyne, M. A. A.; Holt, P. M. Reaction kinetics involving ground $X^2\Pi$ and excited $A^2\Sigma^+$ hydroxyl radicals Part 2.-Rate constants for reactions of OH $X^2\Pi$ with halogenomethanes and halogenoethanes. *J. Chem. Soc. Faraday Trans. 2* **1979**, *75*, 582-591, doi:10.1039/f29797500582.

(2) DeMore, W. B. Regularities in Arrhenius parameters for rate constants of abstraction reactions of hydroxyl radical with C-H bonds. *J. Photochem. Photobiol. A: Chem.* **2005**, *176*, 129-135, doi:10.1016/j.jphotochem.2005.07.015.

(3) Fang, T. D.; Taylor, P. H.; Berry, R. J. Kinetics of the reaction of OH radicals with CH_2ClCF_2Cl and CH_2ClCF_3 over an extended temperature range. *J. Phys. Chem. A* **1999**, *103*, 2700-2704, doi:10.1021/jp984273g.

(4) Handwerk, V.; Zellner, R. Kinetics of the reactions of OH radicals with some halocarbons ($CHClF_2$, CH_2ClF, CH_2ClCF_3, CH_3CClF_2, CH_3CHF_2) in the temperature range 260-370 K. *Ber. Bunsenges. Phys. Chem.* **1978**, *82*, 1161-1166, doi:10.1002/bbpc.19780821117.

(5) Howard, C. J.; Evenson, K. M. Rate constants for the reactions of OH with ethane and some halogen substituted ethanes at 296 K. *J. Chem. Phys.* **1976**, *64*, 4303-4306, doi:10.1063/1.432115.

(6) McGillen, M. R.; Bernard, F.; Fleming, E. L.; Burkholder, J. B. HCFC-133a (CF_3CH_2Cl): OH rate coefficient, UV and infrared absorption spectra, and atmospheric implications. *Geophys. Res. Lett.* **2015**, *42*, 6098-6105, doi:10.1002/2015GL064939.

F36. OH + $CHCl_2CF_2Cl$ (HCFC-122). The recommended parameters are derived from a combined fit to the data of Orkin and Khamaganov[2] (298–460 K) (below 400 K) and DeMore[1] (303–371 K) (two determinations which have been recalculated based on the current recommendations for the rate constants of the OH + CH_2Cl_2 and $CHCl_2CF_3$ reference reactions).
(Table: 02-25, Note: 02-25, Evaluated: 02-25) Back to Table

(1) DeMore, W. B. Experimental and estimated rate constants for the reactions of hydroxyl radicals with several halocarbons. *J. Phys. Chem.* **1996**, *100*, 5813-5820, doi:10.1021/jp953216+.

(2) Orkin, V. L.; Khamaganov, V. G. Determination of rate constants for reactions of some hydrohaloalkanes with OH radicals and their atmospheric lifetimes. *J. Atmos. Chem.* **1993**, *16*, 157-167, doi:10.1007/BF00702785.

F37. OH + $CHFClCFCl_2$ (HCFC-122a). The recommended k(298 K) is an average of the results from the relative rate study of Hsu and DeMore[1] (294–362 K) (recalculated based on the current recommendation for the rate constant for the OH + CH_3CHF_2 reference reaction, as discussed in the note for that reaction) and from the absolute study of Orkin et al.[2] (298–460 K). The recommended value for E/R is derived from a combined fit to the data of both studies below 400 K after scaling both data sets to the recommended k(298 K).
(Table: 15-10, Note: 15-10, Evaluated: 15-10) Back to Table

(1) Hsu, K. J.; DeMore, W. B. Rate constants and temperature dependences for the reactions of hydroxyl radical with several halogenated methanes, ethanes, and propanes by relative rate measurements. *J. Phys. Chem.* **1995**, *99*, 1235-1244, doi:10.1021/j100004a025.

(2) Orkin, V. L.; Khamaganov, V. G.; Kasimovskaya, E. E.; Guschin, A. G. Photochemical properties of some Cl-containing halogenated alkanes. *J. Phys. Chem. A* **2013**, *117*, 5483-5490, doi:10.1021/jp400408y.

F38. OH + $CHCl_2CF_3$ (HCFC-123). The recommended k(298 K) is the average of the values from the absolute studies of Gierczak et al.[3] (213–380 K) (two determinations), Liu et al.[6] (270–400 K), and Yamada et al.[9] (296–866 K), and from the relative rate study by Hsu and DeMore[5] (298–359 K) (recalculated based on the current recommendation for the rate constant for the OH + CH_3CHF_2 reference reaction, as discussed in the note for that reaction). The recommendation for the temperature dependence is derived from a fit to the data of these

investigations after scaling each data set to the recommended value for k(298 K). The temperature dependence data of Nielsen[7] (295–385 K), Watson et al.[8] (245–375 K), Clyne and Holt[2] (293–429 K), and Brown et al.[1] (232–426 K) and the room temperature data of Howard and Evenson[4] (296 K) were not used in deriving the recommended parameters.
(Table: 15-10, Note: 02-25, Evaluated: 02-25) Back to Table

(1) Brown, A. C.; Canosa-Mas, C. E.; Parr, A. D.; Wayne, R. P. Laboratory studies of some halogenated ethanes and ethers: Measurements of rates of reaction with OH and of infrared absorption cross-sections. *Atmos. Environ.* **1990**, *24A*, 2499-2511, doi:10.1016/0960-1686(90)90341-J.

(2) Clyne, M. A. A.; Holt, P. M. Reaction kinetics involving ground $X^2\Pi$ and excited $A^2\Sigma^+$ hydroxyl radicals Part 2.-Rate constants for reactions of OH $X^2\Pi$ with halogenomethanes and halogenoethanes. *J. Chem. Soc. Faraday Trans. 2* **1979**, *75*, 582-591, doi:10.1039/f29797500582.

(3) Gierczak, T.; Talukdar, R.; Vaghjiani, G. L.; Lovejoy, E. R.; Ravishankara, A. R. Atmospheric fate of hydrofluoroethanes and hydrofluorochloroethanes: 1. Rate coefficients for reactions with OH. *J. Geophys. Res.* **1991**, *96*, 5001-5011, doi:10.1029/90JD02736.

(4) Howard, C. J.; Evenson, K. M. Rate constants for the reactions of OH with ethane and some halogen substituted ethanes at 296 K. *J. Chem. Phys.* **1976**, *64*, 4303-4306, doi:10.1063/1.432115.

(5) Hsu, K. J.; DeMore, W. B. Rate constants and temperature dependences for the reactions of hydroxyl radical with several halogenated methanes, ethanes, and propanes by relative rate measurements. *J. Phys. Chem.* **1995**, *99*, 1235-1244, doi:10.1021/j100004a025.

(6) Liu, R.; Huie, R. E.; Kurylo, M. J. Rate constants for the reactions of the OH radical with some hydrochlorofluorocarbons over the temperature range 270-400 K. *J. Phys. Chem.* **1990**, *94*, 3247-3249, doi:10.1021/j100371a004.

(7) Nielsen, O. J. Rate constants for the gas-phase reactions of OH radicals with CH_3CHF_2 and $CHCl_2CF_3$ over the temperature range 295-388 K. *Chem. Phys. Lett.* **1991**, *187*, 286-290, doi:10.1016/0009-2614(91)90427-B.

(8) Watson, R. T.; Ravishankara, A. R.; Machado, G.; Wagner, S.; Davis, D. D. A kinetics study of the temperature dependence of the reactions of OH($^2\Pi$) with CF_3CHCl_2, CF_3CHClF, and CF_2ClCH_2Cl. *Int. J. Chem. Kinet.* **1979**, *11*, 187-197, doi:10.1002/kin.550110210

(9) Yamada, T.; Fang, T. D.; Taylor, P. H.; Berry, R. J. Kinetics and thermochemistry of the OH radical reaction with CF_3CCl_2H and CF_3CFClH. *J. Phys. Chem. A* **2000**, *104*, 5013-5022, doi:10.1021/jp993577f.

F39. OH + $CHFClCF_2Cl$ (HCFC-123a). The recommended parameters are derived from the data of Orkin and Khamaganov.[1] (298–460 K).
(Table: 02-25, Note: 02-25, Evaluated: 02-25) Back to Table

(1) Orkin, V. L.; Khamaganov, V. G. Determination of rate constants for reactions of some hydrohaloalkanes with OH radicals and their atmospheric lifetimes. *J. Atmos. Chem.* **1993**, *16*, 157-167, doi:10.1007/BF00702785.

F40. OH + $CHFClCF_3$ (HCFC-124). The recommended value for k(298 K) is an average of the values from the studies of Watson et al.[4] (250–375 K), Gierczak et al.[1] (210– 425 K) (2 studies), Yamada et al.[5] (297–867 K), and Hsu and DeMore[3] (298–366 K) (two relative rate determinations, which have been recalculated based on the current recommendations for the rate constants of the OH + CH_4 and OH + CHF_2CHF_2 reference reactions). The room temperature rate constant of Howard and Evenson[2] (296 K) is considerably higher than these other values and was not included in the average. The recommended temperature dependence is an average of the dependencies derived from these same studies (but using only data below 400 K from Gierczak et al. and Yamada et al.).
(Table: 02-25, Note: 02-25, Evaluated: 02-25) Back to Table

(1) Gierczak, T.; Talukdar, R.; Vaghjiani, G. L.; Lovejoy, E. R.; Ravishankara, A. R. Atmospheric fate of hydrofluoroethanes and hydrofluorochloroethanes: 1. Rate coefficients for reactions with OH. *J. Geophys. Res.* **1991**, *96*, 5001-5011, doi:10.1029/90JD02736.

(2) Howard, C. J.; Evenson, K. M. Rate constants for the reactions of OH with ethane and some halogen substituted ethanes at 296 K. *J. Chem. Phys.* **1976**, *64*, 4303-4306, doi:10.1063/1.432115.

(3) Hsu, K. J.; DeMore, W. B. Rate constants and temperature dependences for the reactions of hydroxyl radical with several halogenated methanes, ethanes, and propanes by relative rate measurements. *J. Phys. Chem.* **1995**, *99*, 1235-1244, doi:10.1021/j100004a025.

(4) Watson, R. T.; Ravishankara, A. R.; Machado, G.; Wagner, S.; Davis, D. D. A kinetics study of the temperature dependence of the reactions of OH($^2\Pi$) with CF_3CHCl_2, CF_3CHClF, and CF_2ClCH_2Cl. *Int. J. Chem. Kinet.* **1979**, *11*, 187-197, doi:10.1002/kin.550110210

(5) Yamada, T.; Fang, T. D.; Taylor, P. H.; Berry, R. J. Kinetics and thermochemistry of the OH radical reaction with CF_3CCl_2H and CF_3CFClH. *J. Phys. Chem. A* **2000**, *104*, 5013-5022, doi:10.1021/jp993577f.

F41. OH + $CH_3CH_2CH_2Cl$. The recommended Arrhenius parameters are derived from the data of Yujing and Mellouki.[3] (253–372 K). The results from the investigations by Markert and Nielsen[2] (295–353 K) and Donaghy et al.[1] (303–308 K) exhibit considerably more scatter but are, to a large part, encompassed within the 2σ confidence limits of this recommendation.
(Table: 15-10, Note: 15-10, Evaluated: 15-10) Back to Table

(1) Donaghy, T.; Shanahan, I.; Hande, M.; Fitzpatrick, S. Rate constants and atmospheric lifetimes for the reactions of OH radicals and Cl atoms with haloalkanes. *Int. J. Chem. Kinet.* **1993**, *25*, 273-284, doi:10.1002/kin.550250407.
(2) Markert, F.; Nielsen, O. J. The reactions of OH radicals with chloroalkanes in the temperature range 295-360 K. *Chem. Phys. Lett.* **1992**, *194*, 123-127, doi:10.1016/0009-2614(92)85753-W.
(3) Yujing, M.; Mellouki, A. Rate constants for the reactions of OH with chlorinated propanes. *Phys. Chem. Chem. Phys* **2001**, *3*, 2614-2617, doi:10.1039/b102971c.

F42. OH + $CH_3CHClCH_3$. The recommended Arrhenius parameters are derived from the data of Yujing and Mellouki.[3] (233–372 K) The results from the investigations by Markert and Nielsen[2] (295–353 K) and by Donaghy et al.[1] (303 K) exhibit considerably more scatter but are, to a large part, encompassed within the 2σ confidence limits of this recommendation.
(Table: 15-10, Note: 15-10, Evaluated: 15-10) Back to Table

(1) Donaghy, T.; Shanahan, I.; Hande, M.; Fitzpatrick, S. Rate constants and atmospheric lifetimes for the reactions of OH radicals and Cl atoms with haloalkanes. *Int. J. Chem. Kinet.* **1993**, *25*, 273-284, doi:10.1002/kin.550250407.
(2) Markert, F.; Nielsen, O. J. The reactions of OH radicals with chloroalkanes in the temperature range 295-360 K. *Chem. Phys. Lett.* **1992**, *194*, 123-127, doi:10.1016/0009-2614(92)85753-W.
(3) Yujing, M.; Mellouki, A. Rate constants for the reactions of OH with chlorinated propanes. *Phys. Chem. Chem. Phys* **2001**, *3*, 2614-2617, doi:10.1039/b102971c.

F43. OH + $CH_3CF_2CFCl_2$ (HCFC-243cc). The recommended Arrhenius parameters are derived from the data of Nelson et al.[1] (295–367 K). The uncertainties have been assigned to reflect the assumption that the rate constant for this reaction should be less than that for OH + CH_3CF_2Cl.
(Table: 02-25, Note: 02-25, Evaluated:02-25) Back to Table

(1) Nelson, D. D., Jr.; Zahniser, M. S.; Kolb, C. E. Chemical kinetics of the reactions of the OH radical with several hydrochlorofluoropropanes. *J. Phys. Chem.* **1992**, *96*, 249-253, doi:10.1021/j100180a048.

F44. OH + $CHCl_2CF_2CF_3$ (HCFC-225ca). The recommended value for k(298 K) is an average of the values from Nelson et al.[2] (295–364 K) and Zhang et al.[3] (270–400 K). The recommendation for E/R is derived from the data of Nelson et al. The temperature-dependence data of Brown et al.[1] (251–393 K) were not considered because the relatively large rate constants at and below room temperature and the Arrhenius curvature are suggestive of sample impurities. The temperature dependence results of Zhang et al. are in reasonable agreement with those of Nelson et al. over the temperature range of measurement overlap. However, the complete Zhang et al. data set yields a value for E/R much larger than currently recommended for the OH + $CHCl_2CF_3$ (HCFC-123) reaction, for which the activation energy should be similar.
(Table: 02-25, Note: 02-25, Evaluated: 02-25) Back to Table

(1) Brown, A. C.; Canosa-Mas, C. E.; Parr, A. D.; Rothwell, K.; Wayne, R. P. Tropospheric lifetimes of three compounds for possible replacement of CFC and halons. *Nature* **1990**, *347*, 541-543, doi:10.1038/347541a0.
(2) Nelson, D. D., Jr.; Zahniser, M. S.; Kolb, C. E. Chemical kinetics of the reactions of the OH radical with several hydrochlorofluoropropanes. *J. Phys. Chem.* **1992**, *96*, 249-253, doi:10.1021/j100180a048.
(3) Zhang, Z.; Liu, R.; Huie, R. E.; Kurylo, M. J. Rate constants for the gas phase reactions of the OH radical with $CF_3CF_2CHCl_2$ (HCFC-225ca) and CF_2ClCF_2CHClF (HCFC-225cb). *Geophys. Res. Lett.* **1991**, *18*, 5-7, doi:10.1029/90GL02647.

F45. OH + CF_2ClCF_2CHFCl (HCFC-225cb). The recommended parameters are derived from a combined fit to the temperature-dependence data of Nelson et al.[1] (295–374 K) and Zhang et al.[2] (298–400 K), which are in excellent agreement.

(Table: 15-10, Note: 02-25, Evaluated: 02-25) Back to Table

(1) Nelson, D. D., Jr.; Zahniser, M. S.; Kolb, C. E. Chemical kinetics of the reactions of the OH radical with several hydrochlorofluoropropanes. *J. Phys. Chem.* **1992**, *96*, 249-253, doi:10.1021/j100180a048.
(2) Zhang, Z.; Liu, R.; Huie, R. E.; Kurylo, M. J. Rate constants for the gas phase reactions of the OH radical with $CF_3CF_2CHCl_2$ (HCFC-225ca) and CF_2ClCF_2CHClF (HCFC-225cb). *Geophys. Res. Lett.* **1991**, *18*, 5-7, doi:10.1029/90GL02647.

F46. OH + $CF_3CH_2CFCl_2$ (HCFC-234fb). The recommended k(298 K) is from the relative rate study of Barry et al.[1] (298 K). The value for E/R is estimated as being slightly less than that for OH + $CF_3CH_2CF_3$.
(Table: 10-6, Note: 10-6, Evaluated: 10-6) Back to Table

(1) Barry, J.; Locke, G.; Scollard, D.; Sidebottom, H.; Treacy, J.; Clerbaux, C.; Colin, R.; Franklin, J. 1,1,1,3,3,-pentafluorobutane (HFC-365mfc): Atmospheric degradation and contribution to radiative forcing. *Int. J. Chem. Kinet.* **1997**, *29*, 607-617, doi:10.1002/(SICI)1097-4601(1997)29:8<607::AID-KIN6>3.0.CO;2-Y.

F47. OH + CH_2=CHCl. The recommended value for k(298 K) is an average of the values reported by Howard[1] (296 K), Perry et al.[3] (299–422 K), Liu et al.[2] (313–1173 K), and Yamada et al.[4] (293–730 K). The recommended value for E/R is an average of the values for this parameter derived from fits to the data of Perry et al., Liu et al., and Yamada et al. at temperatures below about 400 K. In the 400–500 K region, the rate constant levels off before increasing at higher temperatures, suggesting the stronger importance of an abstraction mechanism at the higher temperatures. As discussed in note for the OH + CH_2=CHF reaction, the recommended rate constant represents the high-pressure limit for this reaction.
(Table: 02-25, Note: 10-6, Evaluated: 10-6) Back to Table

(1) Howard, C. J. Rate constants for the gas-phase reactions of OH radicals with ethylene and halogenated ethylene compounds. *J. Chem. Phys.* **1976**, *65*, 4771-4777, doi:10.1063/1.432932.
(2) Liu, A.; Mulac, W. A.; Jonah, C. D. Pulse radiolysis study of the gas-phase reaction of OH radicals with vinyl chloride at 1 atm and over the temperature range 313-1173 K. *J. Phys. Chem.* **1989**, *93*, 4092-4094, doi:10.1021/j100347a043.
(3) Perry, R. A.; Atkinson, R.; Pitts, J. N., Jr. Rate constants for the reaction of OH radicals with CH_2=CHF, CH_2=CHCl, and CH_2=CHBr over the temperature range 299-426 °K. *J. Chem. Phys.* **1977**, *67*, 458-462, doi:10.1063/1.434889.
(4) Yamada, T.; Siraj, M.; Taylor, P. H.; Peng, J.; Hu, X.; Marshall, P. Rate coefficients and mechanistic analysis for reaction of OH with vinyl chloride between 293 and 730 K. *J. Phys. Chem. A* **2001**, *105*, 9436-9444, doi:10.1021/jp011545y.

F48. OH + (E)-CHCl=CHCl. The recommended k(298 K) is an average of the values reported in the absolute studies of Abbatt and Anderson[1] (297–364 K), Zhang et al.[5] (240–400 K), Yamada et al.[4] (293–720 K), and Canosa-Mas et al.[2] (298 K). The recommended value for E/R is derived from a combined fit to the data below 400 K from the first three studies listed above after scaling to the recommended value for k(298 K). The data from the room temperature relative rate study of Tuazon et al.[3] (298 K) are significantly lower than those in the absolute studies and were not used in deriving the recommended value for k(298 K).
(Table: 15-10, Note: 15-10, Evaluated: 15-10) Back to Table

(1) Abbatt, J. P. D.; Anderson, J. G. High-pressure discharge flow kinetics and frontier orbital mechanistic analysis for OH + CH_2CCl_2, *cis*-CHClCHCl, *trans*-CHClCHCl, $CFClCF_2$, and CF_2CCl_2 → Products. *J. Phys. Chem.* **1991**, *95*, 2382-2390, doi:10.1021/j100159a049.
(2) Canosa-Mas, C. E.; Dillon, R. J.; Sidebotom, H.; Thompson, K. C.; Wayne, R. P. A study of the OH-initiated oxidation of chlorinated ethenes in the gas phase. *Phys. Chem. Chem. Phys.* **2001**, *3*, 542-550, doi:10.1039/b005392i.
(3) Tuazon, E. C.; Atkinson, R.; Aschmann, S. M.; Goodman, M. A.; Winer, A. M. Atmospheric reactions of chloroethenes with the OH radical. *Int. J. Chem. Kinet.* **1988**, *20*, 241-265, doi:10.1002/kin.550200305
(4) Yamada, T.; El-Sinawi, A.; Siraj, M.; Taylor, P. H.; Peng, J.; Hu, X.; Marshall, P. Rate coefficients and mechanistic analysis for the reaction of hydroxyl radicals with 1,1-dichloroethylene and *trans*-1,2-dichloroethylene over an extended temperature range. *J. Phys. Chem. A* **2001**, *105*, 7588-7597, doi:10.1021/jp0109067.
(5) Zhang, Z.; Liu, R. F.; Huie, R. E.; Kurylo, M. J. A gas-phase reactivity study of OH radicals with 1,l-dichloroethene and *cis*- and *trans*-l,2-dichloroethene over the temperature range 240-400 K. *J. Phys. Chem.* **1991**, *95*, 194-196, doi:10.1021/j100154a039.

F49. OH + (Z)-CHCl=CHCl. The recommended k(298 K) is an average of the values reported in the absolute rate studies of Abbatt and Anderson[1] (297–367 K) and Zhang et al.[3] (240–400 K). The recommended value for E/R is derived from a combined fit to the data of these two studies after scaling to the recommended value for k(298 K). The data from the room temperature relative rate study of Tuazon et al.[2] (298 K) were not used in deriving the recommended value for k(298 K). While in agreement with the recommended value, this same study yielded significantly different results than recommended for the trans isomer.
(Table: 15-10, Note: 15-10, Evaluated: 15-10) Back to Table

(1) Abbatt, J. P. D.; Anderson, J. G. High-pressure discharge flow kinetics and frontier orbital mechanistic analysis for OH + CH_2CCl_2, *cis*-CHClCHCl, *trans*-CHClCHCl, $CFClCF_2$, and CF_2CCl_2 → Products. *J. Phys. Chem.* **1991**, *95*, 2382-2390, doi:10.1021/j100159a049.

(2) Tuazon, E. C.; Atkinson, R.; Aschmann, S. M.; Goodman, M. A.; Winer, A. M. Atmospheric reactions of chloroethenes with the OH radical. *Int. J. Chem. Kinet.* **1988**, *20*, 241-265, doi:10.1002/kin.550200305

(3) Zhang, Z.; Liu, R. F.; Huie, R. E.; Kurylo, M. J. A gas-phase reactivity study of OH radicals with 1,l-dichloroethene and *cis*- and *trans*-l,2-dichloroethene over the temperature range 240-400 K. *J. Phys. Chem.* **1991**, *95*, 194-196, doi:10.1021/j100154a039.

F50. OH + CH_2=CCl_2. The recommended value for k(298 K) is an average of the values reported by Abbatt and Anderson[1] (297–368 K), Yamada et al.[6] (291–750 K), and Zhang et al.[7] (240–400 K). The room temperature results of Edney et al.[3] (294–298 K), Tuazon et al.,[5] (298 K) and Canosa-Mas et al.[2] (298 K) lie somewhat outside of the range of the other studies and were not used in deriving the recommendation. The recommended value for E/R is derived from a combined fit to the data of Abbatt and Anderson, Yamada et al., and Zhang et al. after scaling each data set to the value recommended for k(298 K). The data of Kirchner et al.[4] (295–300 K) were not used in deriving the recommended parameters since they were obtained at very low pressure, and the much stronger temperature dependence obtained may be indicative of a pressure dependence above room temperature. As discussed in the note for the OH + CH_2=CHF reaction, the recommended rate constant represents the high-pressure limit for this reaction.
(Table: 15-10, Note: 15-10, Evaluated: 15-10) Back to Table

(1) Abbatt, J. P. D.; Anderson, J. G. High-pressure discharge flow kinetics and frontier orbital mechanistic analysis for OH + CH_2CCl_2, *cis*-CHClCHCl, *trans*-CHClCHCl, $CFClCF_2$, and CF_2CCl_2 → Products. *J. Phys. Chem.* **1991**, *95*, 2382-2390, doi:10.1021/j100159a049.

(2) Canosa-Mas, C. E.; Dillon, R. J.; Sidebotom, H.; Thompson, K. C.; Wayne, R. P. A study of the OH-initiated oxidation of chlorinated ethenes in the gas phase. *Phys. Chem. Chem. Phys.* **2001**, *3*, 542-550, doi:10.1039/b005392i.

(3) Edney, E. O.; Kleindienst, T. E.; Corse, E. W. Room temperature rate constants for the reaction of OH with selected chlorinated and oxygenated hydrocarbons. *Int. J. Chem. Kinet.* **1986**, *18*, 1355-1371, doi:10.1002/kin.550181207.

(4) Kirchner, K.; Helf, D.; Ott, P.; Vogt, S. The reaction of OH radicals with 1,1-di-, tri- and tetrachloroethylene. *Ber. Bunsenges. Phys. Chem.* **1990**, *94*, 77-83, doi:10.1002/bbpc.19900940116.

(5) Tuazon, E. C.; Atkinson, R.; Aschmann, S. M.; Goodman, M. A.; Winer, A. M. Atmospheric reactions of chloroethenes with the OH radical. *Int. J. Chem. Kinet.* **1988**, *20*, 241-265, doi:10.1002/kin.550200305

(6) Yamada, T.; El-Sinawi, A.; Siraj, M.; Taylor, P. H.; Peng, J.; Hu, X.; Marshall, P. Rate coefficients and mechanistic analysis for the reaction of hydroxyl radicals with 1,1-dichloroethylene and *trans*-1,2-dichloroethylene over an extended temperature range. *J. Phys. Chem. A* **2001**, *105*, 7588-7597, doi:10.1021/jp0109067.

(7) Zhang, Z.; Liu, R. F.; Huie, R. E.; Kurylo, M. J. A gas-phase reactivity study of OH radicals with 1,l-dichloroethene and *cis*- and *trans*-l,2-dichloroethene over the temperature range 240-400 K. *J. Phys. Chem.* **1991**, *95*, 194-196, doi:10.1021/j100154a039.

F51. OH + CHCl=CCl_2. The recommended k(298 K) is the mean of the values reported by Howard[3] (296 K), Chang and Kaufman[1] (234–420 K), Kirchner et al.[5] (296–300 K), Klopffer et al.,[6] Edney et al.[2] (294–298 K), and Tichenor et al.[7] (291–650 K). The recommended value of E/R is an average of values for this parameter derived by Chang and Kaufman, Kirchner et al., and Tichenor et al. The value for k(298 K) derived from a relative rate study by Winer et al.[8] (305 K) is a factor of ~2 greater than the other values and is not considered in deriving the recommended value. An absolute study by Jiang et al.[4] (293–460 K) yielding a significantly higher value for k(298 K), as well as a considerably stronger temperature dependence (E/R = –970 K), is assumed to be

superseded by Tichenor et al. As discussed in the note for the OH + CH_2=CHF reaction, the recommended rate constant represents the high pressure limit for this reaction.
(Table: 02-25, Note: 10-6, Evaluated: 10-6) Back to Table

(1) Chang, J. S.; Kaufman, F. Kinetics of the reactions of hydroxyl radicals with some halocarbons: $CHFCl_2$, CHF_2Cl, CH_3CCl_3, C_2HCl_3, and C_2Cl_4. *J. Chem. Phys.* **1977**, *66*, 4989-4994, doi:10.1063/1.433801.
(2) Edney, E. O.; Kleindienst, T. E.; Corse, E. W. Room temperature rate constants for the reaction of OH with selected chlorinated and oxygenated hydrocarbons. *Int. J. Chem. Kinet.* **1986**, *18*, 1355-1371, doi:10.1002/kin.550181207.
(3) Howard, C. J. Rate constants for the gas-phase reactions of OH radicals with ethylene and halogenated ethylene compounds. *J. Chem. Phys.* **1976**, *65*, 4771-4777, doi:10.1063/1.432932.
(4) Jiang, Z.; Taylor, P. H.; Dellinger, B. Laser photolysis/laser-induced fluorescence studies of the reaction of OH with 1,1,1,2- and 1,1,2,2- tetrachloroethane over an extended temperature range. *J. Phys. Chem.* **1993**, *97*, 5050-5053, doi:10.1021/j100121a033.
(5) Kirchner, K.; Helf, D.; Ott, P.; Vogt, S. The reaction of OH radicals with 1,1-di-, tri- and tetrachloroethylene. *Ber. Bunsenges. Phys. Chem.* **1990**, *94*, 77-83, doi:10.1002/bbpc.19900940116.
(6) Klopffer, W.; Frank, R.; Kohl, E. G.; Haag, F. Quantitative erfassung der photochemischen transformationsprozesse in der troposphäre. *Chemiker-Zeitung* **1986**, *110*, 57-61.
(7) Tichenor, L. B.; El-Sinawi, A.; Yamada, T.; Taylor, P. H.; Peng, J. P.; Hu, X.; Marshall, P. Kinetic studies of the reaction of hydroxyl radicals with trichloroethylene and tetrachloroethylene. *Chemosphere* **2001**, *42*, 571-577, doi:10.1016/S0045-6535(00)00229-0.
(8) Winer, A. M.; Lloyd, A. C.; Darnall, K. R.; Pitts, J. N., Jr. Relative rate constants for the reaction of the hydroxyl radical with selected ketones, chloroethenes, and monoterpene hydrocarbons. *J. Phys. Chem.* **1976**, *80*, 1635-1639, doi:10.1021/j100555a024.

F52. OH + CCl_2=CCl_2. The recommended value for k(298 K) is the mean of the values reported by Howard[2] (296 K), Chang and Kaufman[1] (297–420 K), and Kirchner et al.[3] (296–301 K). The room temperature value reported by Winer et al.[5] (305 K) is more than a factor of 10 greater and was not used in deriving the recommendation. The recommended value for E/R is an average of values for this parameter derived by Chang and Kaufman and Kirchner et al. A study by Tichenor et al.[4] (296–714 K) yields a value for k(298 K) slightly lower than these other studies, but a temperature dependence less than half of that recommended. While the results of Tichenor et al. were not used in deriving the recommendations, they are encompassed within the 2σ confidence limits. As discussed in the note for the OH + CH_2=CHF reaction, the recommended rate constant represents the high-pressure limit for this reaction.
(Table: 02-25, Note: 10-6, Evaluated: 10-6) Back to Table

(1) Chang, J. S.; Kaufman, F. Kinetics of the reactions of hydroxyl radicals with some halocarbons: $CHFCl_2$, CHF_2Cl, CH_3CCl_3, C_2HCl_3, and C_2Cl_4. *J. Chem. Phys.* **1977**, *66*, 4989-4994, doi:10.1063/1.433801.
(2) Howard, C. J. Rate constants for the gas-phase reactions of OH radicals with ethylene and halogenated ethylene compounds. *J. Chem. Phys.* **1976**, *65*, 4771-4777, doi:10.1063/1.432932.
(3) Kirchner, K.; Helf, D.; Ott, P.; Vogt, S. The reaction of OH radicals with 1,1-di-, tri- and tetrachloroethylene. *Ber. Bunsenges. Phys. Chem.* **1990**, *94*, 77-83, doi:10.1002/bbpc.19900940116.
(4) Tichenor, L. B.; Graham, J. L.; Yamada, T.; Taylor, P. H.; Peng, J.; Hu, X.; Marshall, P. Kinetic and modeling studies of the reaction of hydroxyl radicals with tetrachloroethylene. *J. Phys. Chem. A* **2000**, *104*, 1700-1707, doi:10.1021/jp993203m.
(5) Winer, A. M.; Lloyd, A. C.; Darnall, K. R.; Pitts, J. N., Jr. Relative rate constants for the reaction of the hydroxyl radical with selected ketones, chloroethenes, and monoterpene hydrocarbons. *J. Phys. Chem.* **1976**, *80*, 1635-1639, doi:10.1021/j100555a024.

F53. OH + (*Z*)-CFCl=CFCl. Tokuhashi et al.[1] (250–430 K) used flash and laser photolysis combined with LIF OH radical detection in an absolute measurement of the rate coefficient. Measurements were performed at pressures between 5 and 200 Torr (Ar and He bath gas). No dependence of the reaction rate coefficient was observed and the reaction is assumed to be in the high-pressure limit over this range of pressure. This is the only available study of this reaction. The recommended Arrhenius parameters k(298 K) and E/R were derived from a fit of their data obtained using both photolysis methods that have reported 2σ precision of ~<5%, over the entire temperature range, and an estimated absolute uncertainty of ~10%.
(Table: 25-1, Note: 25-1, Evaluated: 25-1) Back to Table

(1) Tokuhashi, K.; Uchimaru, T.; Takizawa, K.; Kondo, S. Rate constants for the reactions of OH radicals with the (*E*)/(*Z*) isomers of CFCl=CFCl and (*E*)-CHF=CHF. *J. Phys. Chem. A* **2019**, *123*, 4834−4843, doi:10.1021/acs.jpca.9b02454.

F54. OH + (*E*)-CFCl=CFCl. Tokuhashi et al.[1] (250–430 K) used flash and laser photolysis combined with LIF OH radical detection in an absolute measurement of the rate coefficient. Measurements were performed at pressures between 5 and 200 Torr (Ar and He bath gas). No dependence of the reaction rate coefficient was observed and the reaction is assumed to be in the high-pressure limit over this range of pressure. This is the only available study of this reaction. The recommended Arrhenius parameters k(298 K) and E/R were derived from a fit of their data obtained using both photolysis methods that have reported 2σ precision of ~<5%, over the entire temperature range, and an estimated absolute uncertainty of ~10%.
(Table: 25-1, Note: 25-1, Evaluated: 25-1) Back to Table

(1) Tokuhashi, K.; Uchimaru, T.; Takizawa, K.; Kondo, S. Rate constants for the reactions of OH radicals with the (*E*)/(*Z*) isomers of CFCl=CFCl and (*E*)-CHF=CHF. *J. Phys. Chem. A* **2019**, *123*, 4834−4843, doi:10.1021/acs.jpca.9b02454.

F55. OH + CF_2=CFCl. The recommended Arrhenius parameters are derived from the data of Abbatt and Anderson[1] (297–364 K, 50–85 Torr (N_2)), using a discharge flow-LIF technique. Howard[2] (296 K, 0.7–7 Torr (He)), using a discharge flow-LMR technique, observed a weak pressure dependence measured k(296 K) at low-pressure. Howard estimated a 20% accuracy in the measured k(296 K). The Howard k(296 K) is consistent with the recommendation obtained at higher-pressure.
(Table: 15-10, Note: 25-1, Evaluated: 15-10) Back to Table

(1) Abbatt, J. P. D.; Anderson, J. G. High-pressure discharge flow kinetics and frontier orbital mechanistic analysis for OH + CH_2CCl_2, *cis*-CHClCHCl, *trans*-CHClCHCl, $CFClCF_2$, and CF_2CCl_2 → Products. *J. Phys. Chem.* **1991**, *95*, 2382-2390, doi:10.1021/j100159a049.
(2) Howard, C. J. Rate constants for the gas-phase reactions of OH radicals with ethylene and halogenated ethylene compounds. *J. Chem. Phys.* **1976**, *65*, 4771-4777, doi:10.1063/1.432932.

F56. OH + CH_2=CHCH$_2$Cl. The reaction was studied in two absolute studies by Albaladejo et al.[1] (228–388 K) and Sammaritano et al.[4] (253–371 K). Edney et al.[2,3] (298 K) and Tuazon et al.[5] (298 K) reported results of relative rate studies at room temperature with OH + n-C_4H_{10} and C_3H_6, respectively, as the reference reactions. The recommended value of k(298 K) is the average of values from the data of Tuazon et al., Albaladejo et al., and Sammaritano et al., which are in the excellent agreement. Results from the studies by Edney et al.[2,3] are of lower precision, but are agree with the recommendation and are encompassed by the recommended uncertainty. The recommended value of E/R was derived from a fit to the combined data from Sammaritano et al. and Albaladejo et al., except for their lowest temperature data point, after normalization to the recommended k(298 K) value.
(Table: 25-1, Note: 25-1, Evaluated: 25-1) Back to Table

(1) Albaladejo, J.; Ballesteros, B.; Jimenez, E.; Diaz de Mera, Y.; Martinez, E. Gas-phase OH radical-initiated oxidation of the 3-halopropenes studied by PLP-LIF in the temperature range 228-388 K. *Atmos. Environ.* **2003**, *37*, 2919-2926, doi:10.1016/S1352-2310(03)00297-8.
(2) Edney, E. O.; Kleindienst, T. E.; Corse, E. W. Room temperature rate constants for the reaction of OH with selected chlorinated and oxygenated hydrocarbons. *Int. J. Chem. Kinet.* **1986**, *18*, 1355-1371, doi:10.1002/kin.550181207.
(3) Edney, E. O.; Shepson, P. B.; Kleindienst, T. E.; Corse, E. W. The photooxidation of allyl chloride. *Int. J. Chem. Kinet.* **1986**, *18*, 597-608, doi:10.1002/kin.550180509.
(4) Sammaritano, M. A.; Vera, M. G.; Cometto, P. M.; Tejero, T. N.; Bauerfeldt, G. F.; Mellouki, A. Temperature dependence of rate coefficients for the gas phase reaction of OH with 3-chloropropene. A theoretical and experimental study. *Chem. Phys. Lett.* **2020**, *755*, 137757, doi:10.1016/j.cplett.2020.137757.
(5) Tuazon, E. C.; Atkinson, R.; Aschmann, S. M. Kinetics and products of the gas-phase reactions of the OH radical and O_3 with allyl chloride and benzyl chloride at room temperature. *Int J. Chem. Kinet.* **1990**, *22*, 981-998, doi:10.1002/kin.550220909.

F57. OH + (*E*)-CHCl=CHCF$_3$. The recommended k(298K) is an average of the values determined by Orkin et al.[2] (220–370 K) and Gierczak et al.[1] (213–376 K). The value reported in the room temperature relative rate study by Sulbaek-Andersen et al.[3] (295 K), while only about 15% greater than the recommended value, has much greater uncertainty due to uncertainties in the reference reaction rate constants. The data reported by Orkin et

al.[2] and Gierczak et al. exhibit somewhat different temperature dependences. Orkin et al. report significant curvature in the Arrhenius behavior over the temperature range 220–370 K that is best fit by a modified three-parameter Arrhenius expression:

$$k(T) = 1.03 \times 10^{-13} (T/298)^{2.29} \exp(+384/T)$$

This curvature was not observed in the data reported by Gierczak et al. The recommended value for E/R is an average of the E/R values derived from the individual fits to the Orkin et al.[2] and Gierczak et al. data for T <300 K.
(Table: 15-10, Note: 15-10, Evaluated: 15-10) Back to Table

(1) Gierczak, T.; Baasandorj, M.; Burkholder, J. B. OH + (*E*)- and (*Z*)-1-chloro-3,3,3-trifluoropropene-1 ($CF_3CH=CHCl$) reaction rate coefficients: Stereoisomer-dependent reactivity. *J. Phys. Chem. A* **2014**, *118*, 11015-11025, doi:10.1021/jp509127h.
(2) Orkin, V. L.; Martynova, L. E.; Kurylo, M. J. Photochemical properties of *trans*-1-chloro-3,3,3-trifluoropropene (*trans*-$CHCl=CHCF_3$): OH reaction rate constant, UV and IR absorption spectra, global warming potential, and ozone depletion potential. *J. Phys. Chem. A* **2014**, *118*, 5263-5271, doi:10.1021/jp5018949.
(3) Sulbaek Andersen, M. P.; Nilsson, E. J. K.; Nielsen, O. J.; Johnson, M. S.; Hurley, M. D.; Wallington, T. J. Atmospheric chemistry of *trans*-$CF_3CH=CHCl$: Kinetics of the gas-phase reactions with Cl atoms, OH radicals, and O_3. *J. Photochem. and Photobiol. A: Chem.* **2008**, *199*, 92-97, doi:10.1016/j.jphotochem.2008.05.013.

F58. OH + (*Z*)-$CHCl=CHCF_3$. The recommended Arrhenius parameters are derived from a fit to the data of Gierczak et al.[1] (218–373 K) for T <298 K. Above 298 K, the Arrhenius plot exhibits pronounced curvature such that the entire data set from 218–373 K is best fit by a modified three-parameter Arrhenius expression:

$$k(T) = 1.15 \times 10^{-13} (T/298)^{1.38} \exp(+628/T)$$

Below 298 K this expression and the simple Arrhenius parameterization yield nearly identical values for the rate constant.
(Table: 15-10, Note: 15-10, Evaluated: 15-10) Back to Table

(1) Gierczak, T.; Baasandorj, M.; Burkholder, J. B. OH + (*E*)- and (*Z*)-1-chloro-3,3,3-trifluoropropene-1 ($CF_3CH=CHCl$) reaction rate coefficients: Stereoisomer-dependent reactivity. *J. Phys. Chem. A* **2014**, *118*, 11015-11025, doi:10.1021/jp509127h.

F59. OH + (*Z*)-$CHCl=CClCF_3$. Tokuhashi et al.[1] (250–430 K) used flash and laser photolysis combined with LIF OH radical detection in an absolute measurement of the rate coefficient. Measurements were performed at pressures between 5 and 200 Torr (Ar and He bath gas). No dependence of the reaction rate coefficient was observed and the reaction is assumed to be in the high-pressure limit over this range of pressure. This is the only available study of this reaction. The recommended Arrhenius parameters k(298 K) and E/R were derived from a fit of their data obtained using both photolysis methods that have reported 2σ precision of ~<5%, over the entire temperature range, and an estimated absolute uncertainty of ~10%.
(Table: 25-1, Note: 25-1, Evaluated: 25-1) Back to Table

(1) Tokuhashi, K.; Takizawa, K.; Kondo, S. Rate constants for reactions of OH radicals with (*Z*)-$CF_3CCl=CHCl$, $CHF_2CF=CF_2$, (*E*)-$CF_3CH=CHF$, (*Z*)-$CF_3CH=CHF$, $CH_3CF=CH_2$, and $CH_2FCH=CH_2$. *Atmos. Environ.* **2021**, *255*, 118428, doi:10.1016/j.atmosenv.2021.118428.

F60. OH + $CCl_2=CFCF_3$. Tokuhashi et al.[1] (250–430 K) used flash and laser photolysis combined with LIF OH radical detection in an absolute measurement of the rate coefficient. Measurements were performed at pressures between 5 and 200 Torr (Ar and He bath gas). No dependence of the reaction rate coefficient was observed and the reaction is assumed to be in the high-pressure limit over this range of pressure. This is the only available study of this reaction. The recommended Arrhenius parameters k(298 K) and E/R were derived from a fit of their data obtained using both photolysis methods that have reported 2σ precision of ~<5%, over the entire temperature range, and an estimated absolute uncertainty of ~10%.
(Table: 25-1, Note: 25-1, Evaluated: 25-1) Back to Table

(1) Tokuhashi, K.; Takizawa, K.; Kondo, S. Rate constants for the reactions of OH radicals with $CF_3CX=CY_2$ (X = H, F, CF_3, Y=H, F, Cl). *Environ. Sci. Pollut. Res.* **2018**, *25*, 15204-15215, doi:10.1007/s11356-018-1700-4.

F61. OH + CH_3OCF_2CHFCl. The recommendation is based on the data reported by Tokuhashi et al.[2] (250–430 K), which exhibit a weak curvature in the Arrhenius plot between 250 and 430 K. The recommended values

for both k(298 K) and E/R were derived from a fit to the data from Tokuhashi et al. between 250 and 298 K. The only other study of this reaction by Heathfield et al.[1] (298 K) resulted in k(298 K), which is a factor of 4.5 larger. Such a high rate-constant is inconsistent with those measured for other haloethers. The data over the broader temperature range from 250 to 430 K can be represented by the three-parameter expression obtained from a fit to the data reported by Tokuhashi et al.:

$$k(T) = 3.39\times10^{-13}\ (T/298)^{1.87}\ \exp(-657/T)$$

(Table: 19-5, Note: 19-5, Evaluated: 19-5) Back to Table

(1) Heathfield, A. E.; Anastasi, C.; Pagsberg, P.; McCulloch, A. Atmospheric lifetimes of selected fluorinated ether compounds. *Atmos. Environ.* **1998**, *32*, 711-717, doi:10.1016/S1352-2310(97)00330-0.

(2) Tokuhashi, K.; Takahashi, A.; Kaise, M.; Kondo, S. Rate constants for the reactions of OH radicals with CH_3OCF_2CHFCl, CHF_2OCF_2CHFCl, $CHF_2OCHClCF_3$, and $CH_3CH_2OCF_2CHF_2$. *J. Geophys. Res.* **1999**, *104*, 18681-18688, doi:10.1029/1999JD900278.

F62. OH + $CHF_2OCHClCF_3$ (Isoflurane). The recommended k(298 K) is an average of the results from Tokuhashi et al.[5] (250–430 K), Langbein et al.[3] (298 K), and Sulbaek-Andersen et al.[4] (296 K). The recommended value for E/R is derived from a fit to the two temperature dependent data sets of Tokuhashi et al. The room temperature data determined in the discharge-flow experiments by Brown et al.[2] (298 K) and Beach et al.[1] (293–393 K) lie about 30% higher than recommended here. However, the data from Beach et al. above room temperature agree well with those of Tokuhashi et al.
(Table: 15-10, Note: 15-10, Evaluated: 15-10) Back to Table

(1) Beach, S. D.; Hickson, K. M.; Smith, I. W. M.; Tuckett, R. P. Rate constants and Arrhenius parameters for the reactions of OH radicals and Cl atoms with $CF_3CH_2OCHF_2$, $CF_3CHClOCHF_2$ and $CF_3CH_2OCClF_2$, using the discharge-flow/resonance fluorescence method. *Phys. Chem. Chem. Phys.* **2001**, *3*, 3064-3069, doi:10.1039/b103883b.

(2) Brown, A. C.; Canosa-Mas, C. E.; Parr, A. D.; Wayne, R. P. Laboratory studies of some halogenated ethanes and ethers: Measurements of rates of reaction with OH and of infrared absorption cross-sections. *Atmos. Environ.* **1990**, *24A*, 2499-2511, doi:10.1016/0960-1686(90)90341-J.

(3) Langbein, T.; Sonntag, H.; Trapp, D.; Hoffmann, A.; Malms, W.; Röth, E.-P.; Mörs, V.; Zellner, R. Volatile anaesthetics and the atmosphere: atmospheric lifetimes and atmospheric effects of halothane, enflurane, isoflurane, desflurane and sevoflurane. *British J. Anaest.* **1999**, *82*, 66-73.

(4) Sulbaek Andersen, M. P.; Nielsen, O. J.; Karpichev, B.; Wallington, T. J.; Sander, S. P. Atmospheric chemistry of isoflurane, desflurane, and sevoflurane: Kinetics and mechanisms of reactions with chlorine atoms and OH radicals and global warming potentials. *J. Phys. Chem. A* **2012**, *116*, 5806-5820, doi:10.1021/jp2077598.

(5) Tokuhashi, K.; Takahashi, A.; Kaise, M.; Kondo, S. Rate constants for the reactions of OH radicals with CH_3OCF_2CHFCl, CHF_2OCF_2CHFCl, $CHF_2OCHClCF_3$, and $CH_3CH_2OCF_2CHF_2$. *J. Geophys. Res.* **1999**, *104*, 18681-18688, doi:10.1029/1999JD900278.

F63. OH + CHF_2OCF_2CHFCl (Enflurane). The recommended k(298 K) is an average of the values from Tokuhashi et al.[4] (250–430 K) and Langbein et al.[3] (298 K). The recommended value for E/R is derived from a fit to the data below 400 K of Tokuhashi et al. (three absolute studies). The values of k determined in the discharge-flow experiments by Brown et al.[2] (302, 422 K) and Brown et al.[1] (298 K) lie about 30% higher than recommended here.
(Table: 15-10, Note: 15-10, Evaluated: 15-10) Back to Table

(1) Brown, A. C.; Canosa-Mas, C. E.; Parr, A. D.; Pierce, J. M. T.; Wayne, R. P. Tropospheric lifetimes of halogenated anaesthetics. *Nature* **1989**, *341*, 635-637, doi:10.1038/341635a0.

(2) Brown, A. C.; Canosa-Mas, C. E.; Parr, A. D.; Wayne, R. P. Laboratory studies of some halogenated ethanes and ethers: Measurements of rates of reaction with OH and of infrared absorption cross-sections. *Atmos. Environ.* **1990**, *24A*, 2499-2511, doi:10.1016/0960-1686(90)90341-J.

(3) Langbein, T.; Sonntag, H.; Trapp, D.; Hoffmann, A.; Malms, W.; Röth, E.-P.; Mörs, V.; Zellner, R. Volatile anaesthetics and the atmosphere: atmospheric lifetimes and atmospheric effects of halothane, enflurane, isoflurane, desflurane and sevoflurane. *British J. Anaest.* **1999**, *82*, 66-73.

(4) Tokuhashi, K.; Takahashi, A.; Kaise, M.; Kondo, S. Rate constants for the reactions of OH radicals with CH_3OCF_2CHFCl, CHF_2OCF_2CHFCl, $CHF_2OCHClCF_3$, and $CH_3CH_2OCF_2CHF_2$. *J. Geophys. Res.* **1999**, *104*, 18681-18688, doi:10.1029/1999JD900278.

F64. OH + CH_3OCl. The recommended Arrhenius parameters are derived from the data of Crowley et al.[1] (250–303 K), the only reported study of this reaction.
(Table: 02-25, Note: 02-25, Evaluated: 02-25) Back to Table

(1) Crowley, J. N.; Campuzano-Jost, P.; Moortgat, G. K. Temperature dependent rate constants for the gas-phase reaction between OH and CH_3OCl. *J. Phys. Chem.* **1996**, *100*, 3601-3606, doi:10.1021/jp953018i.

F65. OH + CCl_3CHO. The recommended k(298 K) is an average of the values reported by Barry et al.[2] (298 K) (using three independent techniques), Dobe et al.[3] (298–520 K), Nelson et al.[4] (298 K), Ballestra-Garcia et al.[1] (298 K), and Scollard et al.[5] (298 K). The temperature dependence is derived from the data of Dobe et al.
(Table: 02-25, Note: 02-25, Evaluated: 02-25) Back to Table

(1) Balestra-Garcia, C.; Le Bras, G.; MacLeod, H. Kinetic study of the reactions OH + mono-, di-, and trichloroacetaldehyde and acetaldehyde by laser photolysis-resonance fluorescence at 298 K. *J. Phys. Chem.* **1992**, *96*, 3312-3316, doi:10.1021/j100187a026.
(2) Barry, J.; Scollard, D. J.; Treacy, J. J.; Sidebottom, H. W.; Le Bras, G.; Poulet, G.; Teton, S.; Chichinin, A.; Canosa-Mas, C. E.; Kinnison, D. J.; Wayne, R. P.; Nielsen, O. J. Kinetic data for the reaction of hydroxyl radicals with 1,1,1-trichloroacetaldehyde at 298 ± 2 K. *Chem. Phys. Lett.* **1994**, *221*, 353-358, doi:10.1016/0009-2614(94)00274-6.
(3) Dóbé, S.; Khachatryan, L. A.; Bérces, T. Kinetics of reactions of hydroxyl radicals with a series of aliphatic aldehydes. *Ber. Bunsenges. Phys. Chem.* **1989**, *93*, 847-852, doi:10.1002/bbpc.19890930806.
(4) Nelson, L.; Shanahan, I.; Sidebottom, H. W.; Treacy, J.; Nielsen, O. J. Kinetics and mechanism for the oxidation of 1,1,1-trichloroethane. *Int. J. Chem. Kinet.* **1990**, *22*, 577-590, doi:10.1002/kin.550220603.
(5) Scollard, D. J.; Treacy, J. J.; Sidebottom, H. W.; Balestra-Garcia, C.; Laverdet, G.; LeBras, G.; MacLeod, H.; Téton, S. Rate constants for the reactions of hydroxyl radicals and chlorine atoms with halogenated aldehydes. *J. Phys. Chem.* **1993**, *97*, 4683-4688, doi:10.1021/j100120a021.

F66. HO_2 + Cl. The recommendations for the two reaction channels are based upon the results of Hickson and Keyser[5] (226–336 K), who measured both channels using the discharge flow-resonance fluorescence technique coupled with infrared diode laser spectroscopy, detecting HO, HO_2, Cl, and HCl; by Lee and Howard[6] (250–420 K), who measured the total rate constant and the OH + ClO channel using a discharge flow system with laser magnetic resonance detection of HO_2, OH, and ClO; and by Riffault et al.[9] (230–360 K), who measured the total rate constant and the OH + ClO channel using the discharge flow mass spectrometric technique. The studies of Lee and Howard and Riffault et al. suggest that the total rate constant is temperature independent with a value of $(4.2 \pm 0.7) \times 10^{-11}$ and $(4.4 \pm 0.6) \times 10^{-11}$ cm^3 molecule^{-1} s^{-1} over the temperature range 250–420 K and 230–360 K, respectively. The Hickson and Keyser study concludes that the HCl channel may be represented as $(1.4 \pm 0.3) \times 10^{-11} \exp[(269 \pm 58)/T]$ for temperatures from 256 to 296 K, while the OH channel is given by $(12.7 \pm 4.1) \times 10^{-11} \exp[-(801 \pm 94)/T]$ for temperatures of 226–336 K, the sum of which yields 4.3×10^{-11} cm^3 molecule^{-1} s^{-1} at 298 K with a small temperature dependence. These values for the total rate constant are in agreement with the results of indirect studies relative to Cl + H_2O_2 (Leu and DeMore[7] (295 K), Poulet et al.[8] (298 K), and Burrows et al.[1] (298 K)) or to Cl + H_2 (Cox[3] (274–338 K)). The contribution of the reaction channel producing OH + ClO (22% at room temperature) is much higher than the upper limit reported by Burrows et al. (1% of total reaction). Cattell and Cox[2] (308 K), using a molecular modulation-UV absorption technique over the pressure range 50–760 Torr, report results in good agreement with those of Lee and Howard both for the overall rate constant and for the relative contribution of the two reaction channels. A study by Dobis and Benson[4] (243–368 K) reports a total rate constant in good agreement with this recommendation but a much lower contribution (5 ± 3%) of the channel producing OH + ClO. The equilibrium constant for the channel producing ClO + OH can be calculated with excellent accuracy. The recommended value for this channel comes from the combination of this equilibrium constant and the rate constant for the reverse reaction.
(Table: 09-31, Note: 09-31, Evaluated: 09-31) Back to Table

(1) Burrows, J. P.; Cliff, D. I.; Harris, G. W.; Thrush, B. A.; Wilkinson, J. P. T. Atmospheric reactions of the HO_2 radical studied by laser magnetic-resonance spectroscopy. *Proc. Roy. Soc. Lond. A.* **1979**, *368*, 463-481, doi:10.1098/rspa.
(2) Cattell, F. C.; Cox, R. A. Pressure dependence of the reactions of HO_2 with Cl and ClO. *J. Chem. Soc. Faraday Trans. 2* **1986**, *82*, 1413-1426, doi:10.1039/f29868201413.
(3) Cox, R. A. Kinetics of the reaction Cl + HO_2 = HCl + O_2, using molecular modulation spectrometry. *Int. J. Chem. Kinet.* **1980**, *12*, 649-660, doi:10.1002/kin.550120906.
(4) Dobis, O.; Benson, S. W. Reaction of the ethyl radical with oxygen at millitorr pressures at 243-368 K and a study of the Cl + HO_2, ethyl + HO_2, and HO_2 + HO_2 reactions. *J. Am. Chem. Soc.* **1993**, *115*, 8798-8809, doi:10.1021/ja00072a038.

(5) Hickson, K. M.; Keyser, L. F. A kinetic and product study of the Cl + HO_2 reaction. *J. Phys. Chem. A* **2005**, *109*, 6887-6900, doi:10.1021/jp051176w.
(6) Lee, Y.-P.; Howard, C. J. Temperature dependence of the rate constant and the branching ratio for the reaction Cl + HO_2. *J. Chem. Phys.* **1982**, *77*, 756-763, doi:10.1063/1.443892.
(7) Leu, M.-T.; DeMore, W. B. Rate constants at 295 K for the reactions of atomic chlorine with H_2O_2, HO_2, O_3, CH_4 and HNO_3. *Chem. Phys. Lett.* **1976**, *41*, 121-124, doi:10.1016/0009-2614(76)85261-X.
(8) Poulet, G.; Le Bras, G.; Combourieu, J. Kinetic study of the reactions of Cl atoms with HNO_3, H_2O_2, and HO_2. *J. Chem. Phys.* **1978**, *69*, 767-773, doi:10.1063/1.436588.
(9) Riffault, V.; Bedjanian, Y.; Le Bras, G. Kinetics and mechanism of the reaction of Cl atoms with HO_2 radicals. *Int. J. Chem. Kinet.* **2001**, *33*, 317-327, doi:10.1002/kin.1026

F67. HO_2 + ClO. The recommended k(298 K) is based on studies by Hickson et al.[4] (220–336 K), Nickolaisen et al.[8] (203–364 K), Knight et al.[5] (215–298 K), and Stimpfle et al.[10] (235–393 K), which studied the reaction as a function of temperature. Earlier room temperature measurements by Reimann and Kaufman,[9] Leck et al.,[6] Burrows and Cox,[1] and Cattell and Cox[2] are slightly lower than the current recommendation. The studies of Cattell and Cox and Nickolaisen et al. were performed over extended pressure ranges and did not observe a pressure dependence. The most recent studies find the T-dependence to be characterized by linear Arrhenius behavior over the entire temperature range and do not support the finding of Stimpfle et al. of non-Arrhenius behavior. The recommended value for E/R is based on an average of individual E/R values for each of the first four studies listed above over their entire temperature ranges. The two most probable pairs of reaction products are (1) HOCl + O_2 and (2) HCl + O_3. Finkbeiner et al.[3] (210–300 K), using matrix isolation/ FTIR spectroscopy, studied product formation at 700 Torr. HOCl was observed to be the dominant product (>95% at all temperatures). Upper limits ranging from 0.3% to 2% have been determined for the channel (2) room temperature branching ratio by Leu[7] (248 and 298 K), Leck et al., Knight et al., and Finkbeiner et al. Slightly larger branching ratio (<5%) upper limit values for k_2/k were determined at temperatures below 250 K by Finkbeiner et al. and Leck et al. However, no direct evidence of product channels other than channel (1) was found. Theoretical calculations are in generally good agreement on the structures and relative energetics of the intermediates in this reaction system (see the summary in Hickson et al.). In particular, Xu et al.[11] reported quantum chemistry and master equation calculations that are in reasonable agreement with the experiments. For atmospheric conditions, their calculations identified only two significant channels: the pressure-independent abstraction reaction to form HOCl + O_2 and pressure-dependent formation of HOOOCl, which has thermal decomposition lifetimes ranging from hours to days under stratospheric conditions. At 250 K and 400 Torr of N_2, they calculate that the abstraction reaction constitutes ~60–70% of the total rate constant for ClO + HO_2, supporting the notion that a significant pressure-dependence exists. Further experimental studies on the formation, lifetime, and atmospheric fate of HOOOCl are warranted.
(Table: 09-31, Note: 10-6, Evaluated: 10-6) Back to Table

(1) Burrows, J. P.; Cox, R. A. Kinetics of chlorine oxide reactions using modulated photolysis. 4. The reactions Cl + Cl_2O → Cl_2 + ClO and ClO + HO_2 → products studied at 1 atm and 300 K. *J. Chem. Soc. Faraday Trans. 1* **1981**, *77*, 2465-2479, doi:10.1039/f19817702465.
(2) Cattell, F. C.; Cox, R. A. Pressure dependence of the reactions of HO_2 with Cl and ClO. *J. Chem. Soc. Faraday Trans. 2* **1986**, *82*, 1413-1426, doi:10.1039/f29868201413.
(3) Finkbeiner, M.; Crowley, J. N.; Horie, O.; Müller, R.; Moortgat, G. K.; Crutzen, P. J. Reaction between HO_2 and ClO: product formation between 210 and 300 K. *J. Phys. Chem.* **1995**, *99*, 16264-16275, doi:10.1021/j100044a011.
(4) Hickson, K. M.; Keyser, L. F.; Sander, S. P. Temperature dependence of the HO_2+ClO reaction. 2. Reaction kinetics using the discharge-flow resonance-fluorescence technique. *J. Phys. Chem. A* **2007**, *111*, 8126-8138, doi:10.1021/jp0689464.
(5) Knight, G. P.; Beiderhase, T.; Helleis, F.; Moortgat, G. K.; Crowley, J. N. Reaction of HO_2 with ClO: Flow tube studies of kinetics and product formation between 215 and 298 K. *J. Phys. Chem. A* **2000**, *104*, 1674-1685, doi:10.1021/jp9924631.
(6) Leck, T. J.; Cook, J. L.; Birks, J. W. Studies of reactions of importance in the stratosphere. III. Rate constant and products of the reaction between ClO and HO_2 radicals at 298 K. *J. Chem. Phys.* **1980**, *72*, 2364-2373, doi:10.1063/1.439484.
(7) Leu, M. T. Product distribution for the reaction of HO_2 with ClO. *Geophys. Res. Lett.* **1980**, *7*, 173-175, doi:10.1029/GL007i002p00173.
(8) Nickolaisen, S. L.; Roehl, C. M.; Blakeley, L. K.; Friedl, R. R.; Francisco, J. S.; Liu, R. F.; Sander, S. P. Temperature dependence of the HO_2 + ClO reaction. 1. Reaction kinetics by pulsed photolysis-ultraviolet absorption and ab initio studies of the potential surface. *J. Phys. Chem. A* **2000**, *104*, 308-319, doi:10.1021/jp992753h.

(9) Reimann, B.; Kaufman, F. Rate constant of the reaction $HO_2 + ClO \rightarrow HOCl + O_2$. *J. Chem. Phys.* **1978**, *69*, 2925-2926 doi:10.1063/1.436850.
(10) Stimpfle, R.; Perry, R.; Howard, C. J. Temperature dependence of the reaction of ClO and HO_2 radicals. *J. Chem. Phys.* **1979**, *71*, 5183-5190, doi:10.1063/1.438293.
(11) Xu, Z. F.; Zhu, R. S.; Lin, M. C. Ab initio studies of ClO_x reactions: VI. Theoretical prediction of total rate constant and product branching probabilities for the HO_2 + ClO reaction. *J. Phys. Chem. A* **2003**, *107*, 3841-3850, doi:10.1021/jp0221237.

F68. $H_2O + ClONO_2$. The recommendation is based on the upper limits to the homogeneous bimolecular rate constant reported by Atkinson et al.[1] (298 K) and Hatakeyama and Leu.[2,3] (296 K). Atkinson et al. observed by FTIR analysis the decay of $ClONO_2$ in the presence of H_2O in large-volume (2500 and 5800 liters) Teflon or Teflon-coated chambers. Their observed decay rate gives an upper limit to the homogeneous gas phase rate constant, and they conclude that the decay observed is due to heterogeneous processes. Hatakeyama and Leu (296 K), using a static photolysis system with FTIR analysis, derived a similar upper limit. Rowland et al.[4] (300 K) concluded that the decay they observed resulted from rapid heterogeneous processes. The homogeneous reaction is too slow to have any significant effect on atmospheric chemistry.
(Table: 87-41, Note: 87-41, Evaluated: 10-6) Back to Table

(1) Atkinson, R.; Tuazon, R. C.; Macleod, H.; Aschmann, S. M.; Winer, A. M. The gas-phase reaction of chlorine nitrate with water vapor. *Geophys. Res. Lett.* **1986**, *13*, 117-120, doi:10.1029/GL013i002p00117
(2) Hatakeyama, S.; Leu, M. T. Reactions of chlorine nitrate with HCl and H_2O. *Geophys. Res. Lett.* **1986**, *13*, 1343-1346, doi:10.1029/GL013i012p01343.
(3) Hatakeyama, S.; Leu, M. T. Rate constants for reactions between atmospheric reservoir species. 2. H_2O. *J. Phys. Chem.* **1989**, *93*, 5784-5789, doi:10.1021/j100352a027.
(4) Rowland, F. S.; Sato, H.; Khwaja, H.; Elliott, S. M. The hydrolysis of chlorine nitrate and its possible atmospheric significance. *J. Phys. Chem.* **1986**, *90*, 1985-1988, doi:10.1021/j100401a001.

F69. NO + OClO. The Arrhenius parameters are estimated based on 298 K data reported by Bemand et al.[1] Temperature dependent rate coefficient data by Li et al.[2] (220–367 K) are in good agreement with Bemand et al. at 298 K and display a negative temperature dependence over the range 220–367 K. However, the Li et al. data appear to be complicated by the secondary reaction of Cl with OClO.
(Table: 82-57, Note: 10-6, Evaluated: 10-6) Back to Table

(1) Bemand, P. P.; Clyne, M. A. A.; Watson, R. T. Reactions of chlorine oxide radicals Part 4.-Rate constants for the reactions Cl + OClO, O + OClO, H + OClO, NO + OClO and O + ClO. *J. Chem. Soc. Faraday Trans. 1* **1973**, *69*, 1356-1374, doi:10.1039/f19736901356.
(2) Li, Z. J.; Wuebbles, R. D.; Pylawka, N. J. Rate constant measurement for the reaction of OClO with NO at 220-367 K. *Chem. Phys. Lett.* **2002**, *354*, 491-497, doi:10.1016/S0009-2614(02)00181-1.

F70. NO + Cl_2O_2. The recommended upper limit is that determined by Ingham et al.[1] (220–298 K) in a study using a DF-MS technique.
(Table: 10-6, Note: 10-6, Evaluated: 10-6) Back to Table

(1) Ingham, T.; Sander, S. P.; Friedl, R. R. Kinetics and product studies of the reaction of Br, Cl, and NO with ClOOCl using discharge-flow mass spectrometry. *Faraday Discuss.* **2005**, *130*, 89-110, doi:10.1039/b500179j.

F71. NO_3 + HCl. The recommended upper limit is that reported by Mellouki et al.[3] (298 K) in a study using DF-EPR techniques. This upper limit shows that this reaction is of negligible importance in stratospheric chemistry. Somewhat lower upper-limits have been reported by Cantrell et al.[2] (298 K) and Canosa-Mas et al.[1] (333–473 K); the latter study also reports Arrhenius parameters at higher temperatures (333–473 K).
(Table: 90-1, Note: 25-1, Evaluated: 10-6) Back to Table

(1) Canosa-Mas, C. E.; Smith, S. J.; Toby, S.; Wayne, R. P. Laboratory studies of the reactions of the nitrate radical with chloroform, methanol, hydrogen chloride and hydrogen bromide. *J. Chem. Soc. Faraday Trans. 2* **1989**, *85*, 709-725, doi:10.1039/f29898500709.
(2) Cantrell, C. A.; Davidson, J. A.; Shetter, R. E.; Anderson, B. A.; Calvert, J. G. Reactions of NO_3 and N_2O_5 with molecular species of possible atmospheric interest. *J. Phys. Chem.* **1987**, *91*, 6017-6021, doi:10.1021/j100307a040.

(3) Mellouki, A.; Poulet, G.; Le Bras, G.; Singer, R.; Burrows, J. P.; Moortgat, G. K. Discharge flow kinetic study of the reactions of NO_3 with Br, BrO, HBr, and HCl. *J. Phys. Chem.* **1989**, *93*, 8017-8021, doi:10.1021/j100361a012.

F72. **HO_2NO_2 + HCl.** This upper limit is based on results of static photolysis-FTIR experiments reported by Leu et al.[1] (296 K).
(Table: 90-1, Note: 90-1, Evaluated: 10-6) Back to Table

(1) Leu, M.-T.; Hatkeyama, S.; Hsu, K. J. Rate constants for reactions between atmospheric reservoir species. 1. HCl. *J. Phys. Chem.* **1989**, *93*, 5778-5784, doi:10.1021/j100352a026.

F73. **Cl + O_3.** The results reported for k(298 K) by Watson et al.[13] (220–350 K), Zahniser et al.[14] (210–360 K), Kurylo and Braun[8] (213–298 K), Clyne and Nip[4] (221–629 K), Nicovich et al.[10] (189–345 K), Seeley et al.[11] (206–296 K), and Beach et al.[1] (184–298 K) are in good agreement, and have been used to determine the recommended value at this temperature. The values reported by Leu and DeMore[9] (295 K) (due to the large reported uncertainties) and Clyne and Watson[5] (298 K) (the value is inexplicably high) are not considered. The seven studies used for the k(298 K) recommendation report rate constants that agree to within 30-40% over the temperature range 205–300 K and all report similar values for the Arrhenius activation energy with the exception of Nicovich et al. and Seeley et al. who obtained significantly weaker temperature dependences. Nevertheless, there is no reason to prefer any one set of data over any other; therefore, the recommended E/R is the mean of the seven values for this parameter between 205 and 300 K. DeMore[7] (197–217 K) directly determined the ratio $k(Cl + O_3)/k(Cl + CH_4)$ to be within 15% of that calculated from the absolute rate constant values recommended here.

Vanderzanden and Birks[12] (298 K) have interpreted their observation of oxygen atoms in this system as evidence for some production (0.1–0.5%) of O_2 ($^1\Sigma$) in this reaction. The possible production of singlet molecular oxygen in this reaction has also been discussed by DeMore,[6] in connection with the Cl_2 photosensitized decomposition of ozone. However, Choo and Leu[3] (298 K) were unable to detect $O_2(^1\Sigma)$ or $O_2(^1\Delta)$ in the Cl + O_3 system and set upper limits to the branching ratios for their production of 5×10^{-4} and 2.5×10^{-2}, respectively. They suggested two possible mechanisms for the observed production of oxygen atoms, involving reactions of vibrationally excited ClO radicals with O_3 or with Cl atoms, respectively. Burkholder et al.[2] (298 K), in a study of infrared line intensities of the ClO radical, present evidence in support of the second mechanism. In their experiments with excess Cl atoms, the vibrationally excited ClO radicals produced in the Cl + O_3 reaction can react with Cl atoms to give Cl_2 and oxygen atoms, which can then remove additional ClO radicals. These authors point out the possibility for systematic error from assuming a 1:1 stoichiometry for [Cl]:$[O_3]_o$ when using the Cl + O_3 reaction as a quantitative source of ClO radicals for kinetic and spectroscopic studies.
(Table: 06-2, Note: 06-2, Evaluated: 06-2) Back to Table

(1) Beach, S. D.; Smith, I. W. M.; Tuckett, R. P. Rate constants for the reaction of Cl atoms with O_3 at temperatures from 298 to 184 K. *Int. J. Chem. Kinet.* **2002**, *34*, 104-109, doi:10.1002/kin.10033.
(2) Burkholder, J. B.; Hammer, P. D.; Howard, C. J.; Goldman, A. Infrared line intensity measurements in the ν = 0-1 band of the ClO radical. *J. Geophys. Res.* **1989**, *94*, 2225-2234, doi:10.1029/JD094iD02p02225.
(3) Choo, K. Y.; Leu, M. T. Determination of $O_2(^1\Sigma_g^+)$ and $O_2(^1\Delta_g)$ yields in Cl + O_2 and Cl + O_3 reactions. *J. Phys. Chem.* **1985**, *89*, 4832-4837, doi:10.1021/j100268a035.
(4) Clyne, M. A. A.; Nip, W. S. Study of elementary reactions by atomic resonance absorption with a non-reversed source Part 1.-The reaction Cl + O_3 → ClO + O_2. *J. Chem. Soc. Faraday Trans. 2* **1976**, *72*, 838-847, doi:10.1039/f29767200838.
(5) Clyne, M. A. A.; Watson, R. T. Kinetic studies of diatomic free radicals using mass spectrometry Part 2.-Rapid bimolecular reactions involving the ClO $X^2\Pi$ radical. *J. Chem. Soc. Faraday Trans. 1* **1974**, *70*, 2250-2259, doi:10.1039/f19747002250.
(6) DeMore, W. B. 182nd National Meeting of the American Chemical Society, 1981, New York.
(7) DeMore, W. B. Tests of stratospheric models: The reactions of atomic chlorine with O_3 and CH_4 at low temperature. *J. Geophys. Res.* **1991**, *96*, 4995-5000, doi:10.1029/90JD02737.
(8) Kurylo, M. J.; Braun, W. Flash photolysis resonance fluorescence study of the reaction Cl + O_3 → ClO + O_2 over the temperature range 213-298 K. *Chem. Phys. Lett.* **1976**, *37*, 232-235, doi:10.1016/0009-2614(76)80204-7.
(9) Leu, M.-T.; DeMore, W. B. Rate constants at 295 K for the reactions of atomic chlorine with H_2O_2, HO_2, O_3, CH_4 and HNO_3. *Chem. Phys. Lett.* **1976**, *41*, 121-124, doi:10.1016/0009-2614(76)85261-X.
(10) Nicovich, J. M.; Kreutter, K. D.; Wine, P. H. Kinetics of the reactions of Cl(^2P_J) and Br($^2P_{3/2}$) with O_3. *Int. J. Chem. Kinet.* **1990**, *22*, 399-414, doi:10.1002/kin.550220407.

(11) Seeley, J. V.; Jayne, J. T.; Molina, M. J. Kinetic studies of chlorine atom reactions using the turbulent flow tube technique. *J. Phys. Chem.* **1996**, *100*, 4019-4025, doi:10.1021/jp9525494.
(12) Vanderzanden, J. W.; Birks, J. W. Formation of oxygen atoms in the reaction of chlorine atoms with ozone. *Chem. Phys. Lett.* **1982**, *88*, 109-114, doi:10.1016/0009-2614(82)80080-8.
(13) Watson, R. T.; Machado, G.; Fischer, S.; Davis, D. D. A temperature dependence kinetics study of the reactions of $Cl(^2P_{3/2})$ with O_3, CH_4, and H_2O_2. *J. Chem. Phys.* **1976**, *65*, 2126-2138, doi:10.1063/1.433369.
(14) Zahniser, M. S.; Kaufman, F.; Anderson, J. G. Kinetics of the reaction $Cl + O_3 \rightarrow ClO + O_2$. *Chem. Phys. Lett.* **1976**, *37*, 226-231, doi:10.1016/0009-2614(76)80203-5.

F74. Cl + H_2. The recommended k(298 K) is an average of the values measured by Westenberg and deHaas[12] (251–456 K), Lee et al.[8] (200–500 K), Miller and Gordon[9] (200–500 K), and Kita and Stedman[6] (295–425 K). The value of k(298 K) derived in the flash photolysis - resonance fluorescence study of Davis et al.[4] (298 K) agrees with these studies but was likely overestimated by ~10% (the authors assumed that the fluorescence signal, I_f was proportional to $[Cl]^{0.9}$, whereas a linear relationship between I_f and [Cl] probably held under their experimental conditions). Room temperature determinations by Kumaran et al.[7] (296– 3000 K) (from a study that was actually focused primarily on high temperature measurements) and Eberhard et al.[5] (298 K) (focused on obtaining yields of HCl product in different vibrational levels) are both in reasonable agreement with the recommendation, as are the results from the relative rate studies by Su et al.[11] (298 K) and by Rodebush and Klingelhoefer[10] (273–372 K). The value for E/R is derived from a fit to the data at temperatures below 300 K reported by Westenberg and deHaas, Lee et al., and Miller and Gordon. The value is in good agreement with that determined by Adusei and Fontijn[1] (291–1283 K), although these data lie systematically lower than the results from other studies. Extrapolation above room temperature using the recommended Arrhenius parameters is in reasonable agreement with the data of Benson et al.[3] (351–1071 K) and Kita and Stedman. For a discussion of the large body of rate data at high temperatures, see the review by Baulch et al.[2] Miller and Gordon and Kita and Stedman also measured the rate of the reverse reaction and found the ratio to be in good agreement with equilibrium constant data.
(Table: 06-2, Note: 06-2, Evaluated: 06-2) Back to Table

(1) Adusei, G. Y.; Fontijn, A. Experimental studies of Cl-atom reactions at high temperatures: $Cl + H_2 \rightarrow HCl + H$ from 291 to 1283 K. *Int. Symp. on Combust.* **1994**, *25*, 801-808.
(2) Baulch, D. L.; Cox, R. A.; Hampson, R. F., Jr.; Kerr, J. A.; Troe, J.; Watson, R. T. Evaluated kinetic and photochemical data for atmospheric chemistry. *J. Phys. Chem. Ref. Data* **1980**, *9*, 295-471, doi:10.1063/1.555619.
(3) Benson, S. W.; Cruickshank, F. R.; Shaw, R. Iodine monochloride as a thermal source of chlorine atoms: The reaction of chlorine atoms with hydrogen. *Int. J. Chem. Kinet.* **1969**, *1*, 29-43, doi:10.1002/kin.550010105.
(4) Davis, D. D.; Braun, W.; Bass, A. M. Reactions of $Cl^2P_{3/2}$: Absolute rate constants for reaction with H_2, CH_4, C_2H_6, CH_2Cl_2, C_2Cl_4, and c-C_6H_{12}. *Int. J. Chem. Kinet.* **1970**, *2*, 101-114, doi:10.1002/kin.550020204
(5) Eberhard, J.; Yeh, P.-S.; Lee, Y.-P. Laser-photolysis/time-resolved Fourier-transform absorption spectroscopy: formation and quenching of HCl(v) in the chain reaction $Cl/Cl_2/H_2$. *J. Chem. Phys.* **1997**, *107*, 6499-6502, doi:10.1063/1.474264.
(6) Kita, D.; Stedman, D. H. Kinetic studies of reactions of hydrogen atoms with HCl, Cl_2 and NOCl, and chlorine atoms with H_2 and NOCl. *J. Chem. Soc. Faraday Trans. 2* **1982**, *78*, 1249-1259, doi:10.1039/f29827801249.
(7) Kumaran, S. S.; Lim, K. P.; Michael, J. V. Thermal rate constants for the $Cl + H_2$ and $Cl + D_2$ reactions between 296 and 3000 K. *J. Chem. Phys.* **1994**, *101*, 9487-9498, doi:10.1063/1.468486.
(8) Lee, J. H.; Michael, J. V.; Payne, W. A., Jr.; Stief, L. J. Absolute rate of the reaction of $Cl(^2P)$ with molecular hydrogen from 200-500 K. *J. Chem. Soc. Faraday Trans. 1* **1977**, *73*, 1530-1536, doi:10.1039/f19777301530.
(9) Miller, J. C.; Gordon, R. J. Kinetics of the Cl-H_2 system. I. Detailed balance in the $Cl + H_2$ reaction. *J. Chem. Phys.* **1981**, *75*, 5305-5310, doi:10.1063/1.441972.
(10) Rodebush, W. H.; Klingelhoefer, W. C., Jr. Atomic chlorine and its reaction with hydrogen. *J. Am. Chem. Soc.* **1933**, *55*, 130-142, doi:10.1021/ja01328a014.
(11) Su, F.; Calvert, J. G.; Lindley, C. R.; Uselman, W. M.; Shaw, J. H. A Fourier transform infrared kinetic study of HOCl and its absolute integrated infrared band intensities. *J. Phys. Chem.* **1979**, *83*, 912-920, doi:10.1021/j100471a006.
(12) Westenberg, A. A.; deHaas, N. Atom-molecule kinetics using ESR detection. IV. Results for $Cl + H_2 \rightleftarrows HCl + H$ in both directions. *J. Chem. Phys.* **1968**, *48*, 4405-4415, doi:10.1063/1.1668008.

F75. $Cl + H_2O_2$. The absolute rate coefficients determined at ~298 K by Watson et al.[6] (300 K), Leu and DeMore[3] (295 K), Michael et al.[4] (265–400 K), Poulet et al.[5] (298 K), and Keyser[2] (298–424 K) range in value from (3.6–6.2) × 10^{-13}. The studies of Michael et al., Keyser, and Poulet et al. are presently considered to be the most reliable. The recommended Arrhenius parameters are those reported by Keyser. The *A*-factor reported by Michael et al. is considerably lower than that expected from theoretical considerations and may possibly be attributed to decomposition of H_2O_2 at temperatures above 300 K. The data of Michael et al. at and below 300 K are in good agreement with the Arrhenius expression reported by Keyser. Heneghan and Benson[1] (300–350 K), using mass spectrometry, confirmed that this reaction proceeds only by the abstraction mechanism giving HCl and HO_2 as products.
(Table: 02-25, Note: 02-25, Evaluated: 10-6) Back to Table

(1) Heneghan, S. P.; Benson, S. W. Kinetic study of the reactions of Cl and Br with H_2O_2. *Int. J. Chem. Kinet.* **1983**, *15*, 1311-1319, doi:10.1002/kin.550151206.
(2) Keyser, L. F. Absolute rate constant of the reaction between chlorine (^2P) atoms and hydrogen peroxide from 298 to 424 K. *J. Phys. Chem.* **1980**, *84*, 11-14, doi:10.1021/j100438a004.
(3) Leu, M.-T.; DeMore, W. B. Rate constants at 295 K for the reactions of atomic chlorine with H_2O_2, HO_2, O_3, CH_4 and HNO_3. *Chem. Phys. Lett.* **1976**, *41*, 121-124, doi:10.1016/0009-2614(76)85261-X.
(4) Michael, J. V.; Whytock, D. A.; Lee, J. H.; Payne, W. A.; Stief, L. J. Absolute rate constant for the reaction of atomic chlorine with hydrogen peroxide vapor over the temperature range 265-400 K. *J. Chem. Phys.* **1977**, *67*, 3533-3536, doi:10.1063/1.435351.
(5) Poulet, G.; Le Bras, G.; Combourieu, J. Kinetic study of the reactions of Cl atoms with HNO_3, H_2O_2, and HO_2. *J. Chem. Phys.* **1978**, *69*, 767-773, doi:10.1063/1.436588.
(6) Watson, R. T.; Machado, G.; Fischer, S.; Davis, D. D. A temperature dependence kinetics study of the reactions of $Cl(^2P_{3/2})$ with O_3, CH_4, and H_2O_2. *J. Chem. Phys.* **1976**, *65*, 2126-2138, doi:10.1063/1.433369.

F76. $Cl + NO_3$. The recommended value at room temperature is based on the discharge flow-EPR study of Mellouki et al.[5] (298 K) and the discharge flow-mass spectrometric study of Becker et al.[1] (298 K). The results of these direct absolute rate studies are preferred over results of the earlier relative rate studies of Cox et al.[3] (296 K), Burrows et al.[2] (298 K), and Cox et al.[4] (278–338 K), in all of which NO_3 was monitored in the photolysis of Cl_2-$ClONO_2$-N_2 mixtures. Complications in the chemistry of the earlier systems probably contributed to the spread in reported values. This radical-radical reaction is expected to have negligible temperature dependence, which is consistent with the results from the study of Cox et al.[4] in which the complications must have been temperature independent.
(Table: 94-26, Note: 94-26, Evaluated: 10-6) Back to Table

(1) Becker, E.; Wille, U.; Rahman, M. M.; Schindler, R. H. An investigation of the reactions of NO_3 radicals with Cl and ClO. *Ber. Bunsenges. Phys. Chem.* **1991**, *95*, 1173-1179, doi:10.1002/bbpc.19910951003.
(2) Burrows, J. P.; Tyndall, G. S.; Moortgat, G. K. Absorption spectrum of NO_3 and kinetics of the reactions of NO_3 with NO_2, Cl, and several stable atmospheric species at 298 K. *J. Phys. Chem.* **1985**, *89*, 4848-4856, doi:10.1021/j100268a038.
(3) Cox, R. A.; Barton, R. A.; Ljungstrom, E.; Stocker, D. W. The reactions of Cl and ClO with the NO_3 radical. *Chem. Phys. Lett.* **1984**, *108*, 228-232, doi:10.1016/0009-2614(84)87054-2.
(4) Cox, R. A.; Fowles, M.; Moulton, D.; Wayne, R. P. Kinetics of the reactions of NO_3 radicals with Cl and ClO. *J. Phys. Chem.* **1987**, *91*, 3361-3365, doi:10.1021/j100296a051.
(5) Mellouki, A.; Le Bras, G.; Poulet, G. Discharge flow kinetic study of NO_3 reactions with free radicals: The reaction of NO_3 with Cl. *J. Phys. Chem.* **1987**, *91*, 5760-5764, doi:10.1021/j100306a048.

F77. $Cl + N_2O$. This rate coefficient has been determined in a study of the halogen-catalyzed decomposition of nitrous oxide at about 1000 K by Kaufman et al.[1] (876–1031 K). The largest value reported was 10^{-17} cm^3 $molecule^{-1}$ s^{-1}, with an activation energy of 34 kcal/mol. Extrapolation of these results to low temperature shows that this reaction cannot be of any significance in atmospheric chemistry. Kinetic isotope effects observed by Lesar et al.[2] are consistent with a reaction transition state where the chlorine atom is bonded to the oxygen atom of nitrous oxide with a planar trans arrangement of atoms.
(Table: 87-41, Note: 10-6, Evaluated: 10-6) Back to Table

(1) Kaufman, F.; Gerri, N. J.; Pascale, D. A. Halogen catalyzed decomposition of nitrous oxide. *J. Chem. Phys.* **1956**, *24*, 32-34, doi:10.1063/1.1700847.
(2) Lesar, A.; Hodošček, M.; Senegačnik, M. Experimental and theoretical studies of the decomposition of N_2O catalyzed by chlorine. *J. Chem. Phys.* **1996**, *105*, 917-926, doi:10.1063/1.471935.

F78. Cl + HNO_3. The recommended upper limit at room temperature is that reported in the study of Wine et al.[5] (298–400 K), in which long-path laser absorption spectroscopy was used to look for the appearance of NO_3 following the pulsed laser photolysis of Cl_2-HNO_3 mixtures, with no evidence for NO_3 production observed. In the same study, a less sensitive upper limit was derived from monitoring Cl atom decay by resonance fluorescence. A less sensitive upper limit was also found in the discharge flow-EPR study of Zagogianni et al.[6] (293 K). Higher values obtained in earlier studies (Leu and DeMore[3] (295 K), Kurylo et al.[2] (240–300 K), and Clark et al.[1] (298 K)), as well as the higher temperature results of Poulet et al.[4] (298–633 K) are not used.
(Table: 90-1, Note: 90-1, Evaluated: 10-6) Back to Table

(1) Clark, R. H.; Husain, D.; Jezequel, J. Y. The reaction of chlorine atoms, Cl(3 ^2P_J), with nitric acid in the gas phase. *J. Photochem.* **1982**, *18*, 39-46, doi:10.1016/0047-2670(82)80006-3.

(2) Kurylo, M. J.; Murphy, J. L.; Knable, G. L. Rate constant measurements for the reaction of Cl atoms with nitric acid over the temperature range 240-300 K. *Chem. Phys. Lett.* **1983**, *94*, 281-284, doi:10.1016/0009-2614(83)87088-2.

(3) Leu, M.-T.; DeMore, W. B. Rate constants at 295 K for the reactions of atomic chlorine with H_2O_2, HO_2, O_3, CH_4 and HNO_3. *Chem. Phys. Lett.* **1976**, *41*, 121-124, doi:10.1016/0009-2614(76)85261-X.

(4) Poulet, G.; Le Bras, G.; Combourieu, J. Kinetic study of the reactions of Cl atoms with HNO_3, H_2O_2, and HO_2. *J. Chem. Phys.* **1978**, *69*, 767-773, doi:10.1063/1.436588.

(5) Wine, P. H.; Wells, J. R.; Nicovich, J. M. Kinetics of the reactions of F(^{2}P) and Cl(^{2}P) with HNO_3. *J. Phys. Chem.* **1988**, *92*, 2223-2228, doi:10.1021/j100319a028.

(6) Zagogianni, H.; Mellouki, A.; Poulet, G. Réactivité des radicaux Cl et ClO avec HNO_3. *C. R. Acad. Sci. Paris* **1987**, *Series II 304*, 573-578.

F79. Cl + HO_2NO_2. The only study of this reaction is by Simonaitis and Leu[1] (296 K) using the low pressure discharge flow technique coupled with resonance fluorescence detection of Cl and mass spectrometric detection of HO_2NO_2 ion fragments. Consistent results were obtained monitoring either Cl or HO_2NO_2 decays and retrieved rate constants were less than 1×10^{-13} cm^3 molecule^{-1} s^{-1} for all conditions. Impurities in the HO_2NO_2 sample (especially H_2O_2) complicated the measurements. A limited temperature study over the 296–399 K range suggests that E/R is in the range of 500–1500 K. Given the experimental difficulties, only an upper limit is recommended for the reaction rate.
(Table: 02-25, Note: 02-25, Evaluated: 10-6) Back to Table

(1) Simonaitis, R.; Leu, M. T. Rate constant for the reaction Cl + HO_2NO_2 → Products. *Int. J. Chem. Kinet.* **1985**, *17*, 293-301, doi:10.1002/kin.550170306.

F80. Cl + CH_4. The recommended k(298 K) = 1.0×10^{-13} cm^3 molecule^{-1} s^{-1} was obtained as an average of the values derived from the absolute rate constant studies of Manning and Kurylo[15] (218–322 K), Whytock et al.[28] (200–500 K), Michael and Lee[17] (298 K), Lin et al.[14] (198–423 K), Zahniser et al.[29] (200–500 K), Keyser,[8] (220–423 K), Ravishankara and Wine[22] (221–375 K), Heneghan et al.[7] (233– 338 K) (which is assumed to supersede the results obtained by Baghal-Vayjooee et al.[1]), Dobis and Benson[6] (298 K), Sawerysyn et al.[23] (294 K), Lazarou et al.[11] (263–303 K), Beichert et al.[2] (298 K), Seeley et al.[25] (181–291 K), Pilgrim et al.[18] (292–800 K), Mellouki et al.[16] (297 K), Wang and Keyser[26] (218–298 K), and Bryukov et al.[3] (295–1104 K), all of which fall in the range $(0.9–1.13) \times 10^{-13}$ cm^3 molecule^{-1} s^{-1}. Other absolute studies by Davis et al.[5] (298 K), Clyne and Walker[4] (300–686 K), Poulet et al.[19] (295–490 K), Leu and DeMore[13] (295 K), Watson et al.[27] (218–298 K), and Schlyer et al.[24] (298 K) yield rate constant values slightly higher than those of the aforementioned studies. In some cases, this may be due to uncertainties in correcting the data for Cl atom loss via reaction with trace levels of ethane and propane in the methane samples used. Thus, these results were not used in deriving the recommended value for k(298 K). The values derived for k(298 K) from the competitive chlorination studies of Pritchard et al.[20] (273–488 K), Pritchard et al.[21] (273–573 K), Knox,[9] Knox and Nelson[10] (193–593 K), Lee and Rowland[12] (243–361 K), and Lin et al.[14] (198–296 K) are in the range $(0.8–1.6) \times 10^{-13}$ cm^3 molecule^{-1} s^{-1} when the original data are referenced to the presently recommended rate constant values for the reference reactions of Cl with H_2 and C_2H_6; these studies were not used in deriving the recommended value for k(298 K). In particular, the reference reaction Cl + C_2H_6 has a rate constant more than three orders of magnitude greater than that of Cl + CH_4, thus making it far from ideal for a competitive chlorination study.

Nine of the aforementioned absolute studies used in the derivation of k(298 K) were performed at temperatures below 300 K (Manning and Kurylo,[15] Whytock et al.,[28] Lin et al.,[14] Zahniser et al.,[29] Keyser,[8] Ravishankara and Wine,[22] Heneghan et al.,[7] Seeley et al., and Wang and Keyser[26]). The agreement among all studies below 300 K is reasonably good, with values of E/R ranging from 1170 K to 1320 K. The recommended E/R = 1270 K is derived from a combined fit to all data below 300 K from these nine studies after scaling each of the individual data sets to the recommended k(298 K). Systematic differences in activation energies are apparent when calculated using data obtained below 300 K versus data from above 300 K. Three studies have been

performed over the temperature region between 200 and 500 K (Whytock et al.,[28] Zahniser et al.,[29] and Keyser[8]), and in each case non-linear Arrhenius behavior was observed.

The curvature in the Arrhenius plot over the temperature range from 180 K to 410 K can be fit by the three-parameter expression:

$$k(180–410\ \text{K}) = 2.36 \times 10^{-12}\ (\text{T}/298)^{1.37}\ \exp(-939/\text{T}).$$

Below 307 K, this expression yields values for k(T) within 2% of those calculated using the Arrhenius parameters recommended above. The three-parameter expression is recommended for use in calculating the rate constants from the results of relative rate studies conducted both above and below room temperature in which the Cl + CH_4 reaction is used as the reference.

Ravishankara and Wine[22] observed that at temperatures below 240 K the apparent bimolecular rate constant was dependent on the chemical composition of the reaction mixture. They suggested that the effect was due to a non-equilibration of the $^2P_{1/2}$ and $^2P_{3/2}$ states of atomic chlorine when the mixture did not contain an efficient spin equilibrator, and thus the results obtained at lower pressure using the discharge flow and competitive chlorination techniques may be in error at the lower temperatures (<240 K). However, subsequent studies did not reproduce this observation. Therefore, only data obtained by Ravishankara and Wine[22] above 240 K were used here in the global fit.
(Table: 15-10, Note: 15-10, Evaluated: 15-10) Back to Table

(1) Baghal-Vayjooee, M. H.; Colussi, A. J.; Benson, S. W. Very low pressure reactor. A new technique for measuring rates and equilibria of radical-molecule reactions at low temperature. Heat of formation of the methyl radical. *J. Am. Chem. Soc.* **1978**, *100*, 3214-3215, doi:10.1021/ja00478a044.

(2) Beichert, P.; Wingen, L.; Lee, J.; Vogt, R.; Ezell, M. J.; Ragains, M.; Neavyn, R.; Finlayson-Pitts, B. J. Rate constants for the reactions of chlorine atoms with some simple alkanes at 298 K: Measurement of a self-consistent set using both absolute and relative rate methods. *J. Phys. Chem.* **1995**, *99*, 13156-13162, doi:10.1021/j100035a018.

(3) Bryukov, M. G.; Slagle, I. R.; Knyazev, V. D. Kinetics of reactions of Cl atoms with methane and chlorinated methanes. *J. Phys. Chem. A* **2002**, *106*, 10532-10542, doi:10.1021/jp0257909.

(4) Clyne, M. A. A.; Walker, R. F. Absolute rate constants for elementary reactions in the chlorination of CH_4, CD_4, CH_3Cl, CH_2Cl_2, $CHCl_3$, $CDCl_3$ and $CBrCl_3$. *J. Chem. Soc. Faraday Trans. 1* **1973**, *69*, 1547-1567, doi:10.1039/F19736901547.

(5) Davis, D. D.; Braun, W.; Bass, A. M. Reactions of Cl$^2P_{3/2}$: Absolute rate constants for reaction with H_2, CH_4, C_2H_6, CH_2Cl_2, C_2Cl_4, and c-C_6H_{12}. *Int. J. Chem. Kinet.* **1970**, *2*, 101-114, doi:10.1002/kin.550020204

(6) Dobis, O.; Benson, S. W. Analysis of flow dynamics in a new, very low pressure reactor. Application to the reaction: Cl + CH_4 ⇌ HCl + CH_3. *Int. J. Chem. Kinet.* **1987**, *19*, 691-708, doi:10.1002/kin.550190803.

(7) Heneghan, S. P.; Knoot, P. A.; Benson, S. W. The temperature coefficient of the rates in the system Cl + CH_4 ⇆ CH_3 + HCl, thermochemistry of the methyl radical. *Int. J. Chem. Kinet.* **1981**, *13*, 677-691, doi:10.1002/kin.550130708.

(8) Keyser, L. F. Absolute rate and temperature dependence of the reaction between chlorine (^2P) atoms and methane. *J. Chem. Phys.* **1978**, *69*, 214-218, doi:10.1063/1.436388.

(9) Knox, J. H. Application of gas phase partition chromatography to competitive chlorination reactions. *Chemistry and Industry* **1955**, 1631-1632.

(10) Knox, J. H.; Nelson, R. L. Competitive chlorination reaction in the gas phase: Hydrogen and C_1-C_5 saturated hydrocarbons. *Trans. Far. Soc.* **1959**, *55*, 937-946, doi:10.1039/tf9595500937.

(11) Lazarou, Y. G.; Michael, C.; Papagiannakopoulos, P. Kinetics of the reaction of chlorine atoms with dimethylnitramine. *J. Phys. Chem.* **1992**, *96*, 1705-1708, doi:10.1021/j100183a039.

(12) Lee, F. S. C.; Rowland, F. S. Competitive radiotracer evaluation of relative rate constants at stratospheric temperatures for reactions of ^{38}Cl with CH_4 and C_2H_6 vs. CH_2=CHBr. *J. Phys. Chem.* **1977**, *81*, 86-87, doi:10.1021/j100516a020.

(13) Leu, M.-T.; DeMore, W. B. Rate constants at 295 K for the reactions of atomic chlorine with H_2O_2, HO_2, O_3, CH_4 and HNO_3. *Chem. Phys. Lett.* **1976**, *41*, 121-124, doi:10.1016/0009-2614(76)85261-X.

(14) Lin, C. L.; Leu, M. T.; DeMore, W. B. Rate constant for the reaction of atomic chlorine with methane. *J. Phys. Chem.* **1978**, *82*, 1772-1777, doi:10.1021/j100505a002.

(15) Manning, R. G.; Kurylo, M. J. Flash photolysis resonance fluorescence investigation of the temperature dependencies of the reactions of Cl(^{2}P) atoms with CH_4, CH_3Cl, CH_3F, CH_3F^+, and C_2H_6. *J. Phys. Chem.* **1977**, *81*, 291-296, doi:10.1021/j100519a003.

(16) Mellouki, A. Kinetic studies of Cl atom reactions with series of alkanes using the pulsed laser photolysis resonance fluorescence method. *J. Chim. Phys.* **1998**, *95*, 513-522, doi:10.1051/jcp:1998165.
(17) Michael, J. V.; Lee, J. H. Selected rate constants for H, O, N, and Cl atoms with substrates at room temperatures. *Chem. Phys. Lett.* **1977**, *51*, 303-306, doi:10.1016/0009-2614(77)80408-9.
(18) Pilgrim, J. S.; McIlroy, A.; Taatjes, C. A. Kinetics of Cl atom reactions with methane, ethane, and propane from 292 to 800 K. *J. Phys. Chem. A* **1997**, *101*, 1873-1880, doi:10.1021/jp962916r.
(19) Poulet, G.; Le Bras, G.; Combourieu, J. Étude cinétique des réactions du chlore atomique et du radical ClO avec le méthane par la technique du réacteur a écoulement rapide, couplé a un spectromètre de masse. *J. Chim. Phys.* **1974**, *71*, 101-106, doi:10.1051/jcp/1974710101.
(20) Pritchard, H. O.; Pyke, J. B.; Trotman-Dickenson, A. F. A method for the study of chlorine atom reactions. The reaction Cl + CH_4 → CH_3 + HCl. *J. Am. Chem. Soc.* **1954**, *76*, 1201-1202, doi:10.1021/ja01633a100.
(21) Pritchard, H. O.; Pyke, J. B.; Trotman-Dickenson, A. F. The study of chlorine atom reactions in the gas phase. *J. Am. Chem. Soc.* **1955**, *77*, 2629-2633, doi:10.1021/ja01614a088.
(22) Ravishankara, A. R.; Wine, P. H. A laser flash photolysis-resonance fluorescence kinetics study of the reaction Cl(^2P) + CH_4 → CH_3 + HCl. *J. Chem. Phys.* **1980**, *72*, 25-30, doi:10.1063/1.438885.
(23) Sawerysyn, J.-P.; Lafage, C.; Meriaux, B.; Tighezza, A. Cinetique de la reaction des atomes de chlore avec le methane a 294 ± 1K: Une nouvelle etude par la technique du reacteur a ecoulement ratpide et a decharge couple a un spectrometre de masse. *J. Chim. Phys.* **1987**, *84*, 1187-1193.
(24) Schlyer, D. F.; Wolf, A. P.; Gaspar, P. P. Rate constants for the reactions of atomic chlorine with group 4 and group 5 hydrides. *J. Phys. Chem.* **1978**, *82*, 2633-2637, doi:10.1021/j100514a001.
(25) Seeley, J. V.; Jayne, J. T.; Molina, M. J. Kinetic studies of chlorine atom reactions using the turbulent flow tube technique. *J. Phys. Chem.* **1996**, *100*, 4019-4025, doi:10.1021/jp9525494.
(26) Wang, J. J.; Keyser, L. F. Kinetics of the Cl(^2P_J) + CH_4 reaction: Effects of secondary chemistry below 300 K. *J. Phys. Chem. A* **1999**, *103*, 7460-7469, doi:10.1021/jp9913259.
(27) Watson, R. T.; Machado, G.; Fischer, S.; Davis, D. D. A temperature dependence kinetics study of the reactions of Cl($^2P_{3/2}$) with O_3, CH_4, and H_2O_2. *J. Chem. Phys.* **1976**, *65*, 2126-2138, doi:10.1063/1.433369.
(28) Whytock, D. A.; Lee, J. H.; Michael, J. V.; Payne, W. A.; Stief, L. J. Absolute rate of the reaction of Cl(^2P) with methane from 200-500 K. *J. Chem. Phys.* **1977**, *66*, 2690-2695, doi:10.1063/1.434216.
(29) Zahniser, M. S.; Berquist, B. M.; Kaufman, F. Kinetics of the reaction Cl + CH_4 → CH_3 + HCl from 200° to 500° K. *Int. J. Chem. Kinet.* **1978**, *10*, 15-29, doi:10.1016/0009-2614(74)80292-7.

F81. Cl + CH_3D. The recommended value for k(298 K) is an average of the relative rate determinations by Feilberg et al.[2] (298 K), Sauer et al.[3] (248–343 K), Saueressig et al.[4] (296 K) (two measurements), and Tyler et al.[5] (273–350 K), all of which are in excellent agreement. The recommended value of E/R is derived from a combined fit to the data reported in the last three papers listed above after scaling each individual data set to the recommended k(298 K). The uncertainty in the data reported by Boone et al.[1] (298 K) (both in the measured rate constant ratio and in the temperature of the experiment) significantly exceeds those of other studies. Hence, these data were not used in the evaluation. However, this result is encompassed within the recommended 2σ uncertainty. The result originally reported by Wallington and Hurley[6] (295 K) was corrected in a personal communication from the authors as later reported by Saueressig et al. The corrected value is in excellent agreement with the recommendation at the temperature of the experiment. Note that a three-parameter expression recommended for the reaction Cl + CH_4 was used to derive the rate constants from the rate constant ratios reported in the original papers. The excellent agreement among all of the results reported for the reaction between Cl and CH_3D used in deriving this recommendation could be well encompassed within uncertainty limits calculated with f(298 K) = 1.03 and g = 50. However, all of the above-mentioned studies are relative rate measurements that utilize the same reference reaction, Cl + CH_4. Thus, all of these determinations can be affected by the same systematic uncertainty in the reference rate constant. The recommended uncertainty parameters, f(298 K) and g account for this added uncertainty.
(Table: 15-10, Note: 15-10, Evaluated: 15-10) Back to Table

(1) Boone, G. D.; Agyin, F.; Robichaud, D. J.; Tao, F.-M.; Hewitt, S. A. Rate constants for the reactions of chlorine atoms with deuterated methanes: Experiment and theory. *J. Phys. Chem. A* **2001**, *105*, 1456-1464, doi:10.1021/jp0027290.
(2) Feilberg, K. L.; Griffith, D. W. T.; Johnson, M. S.; Nielsen, C. J. The ^{13}C and D kinetic isotope effects in the reaction of CH_4 with Cl. *Int. J. Chem. Kinet.* **2005**, *37*, 110-118, doi:10.1002/kin.20058.
(3) Sauer, F.; Portmann, R. W.; Ravishankara, A. R.; Burkholder, J. B. Temperature dependence of the Cl atom reaction with deuterated methanes. *J. Phys. Chem. A* **2015**, *119*, 4396-4407, doi:10.1021/jp508721h.

(4) Saueressig, G.; Bergamaschi, P.; Crowley, J. N.; Fischer, H.; Harris, G. W. D/H kinetic isotope effect in the reaction CH_4 + Cl. *Geophys. Res. Lett.* **1996**, *23*, 3619-3622, doi:10.1029/96GL03292.
(5) Tyler, S. C.; Ajie, H. O.; Rice, A. L.; Cicerone, R. J. Experimentally determined kinetic isotope effects in the reaction of CH_4 with Cl: Implications for atmospheric CH_4. *Geophys. Res. Lett.* **2000**, *27*, 1715-1718, doi:10.1029/1999GL011168.
(6) Wallington, T. J.; Hurley, M. D. A kinetic study of the reaction of chlorine atoms with CF_3CHCl_2, CF_3CH_2F, $CFCl_2CH_3$, CF_2ClCH_3, CHF_2CH_3, CH_3D, CH_2D_2, CHD_3, CD_4, and CD_3Cl at 295 ± 2 K. *Chem. Phys. Lett.* **1992**, *189*, 437-442, doi:10.1016/0009-2614(92)85228-3.

F82. Cl + H_2CO. The results from five of the six published studies (Michael et al.[4] (200–500 K), Anderson and Kurylo[1] (223–323 K), Niki et al.[5] (298 K), Fasano and Nogar[2] (295 K), and Poulet et al.[6] (295 K)) are in good agreement at ~298 K, but are ~50% greater than the value reported by Foon et al.[3] (298 K). The recommended value at 298 K is obtained by combining the absolute values reported by Michael et al., Anderson and Kurylo, and Fasano and Nogar, with the values obtained by combining the ratio of $k(Cl + H_2CO)/k(Cl + C_2H_6)$ reported by Niki et al. (1.3 ± 0.1) and by Poulet et al. (1.16 ± 0.12) with the recommended value of 5.7×10^{-11} cm^3 $molecule^{-1}$ s^{-1} for $k(Cl + C_2H_6)$ at 298 K. The recommended value of E/R is obtained from a least-squares fit to all the data reported in Michael et al. and in Anderson and Kurylo. The A-factor was adjusted to agree with the recommended value at 298 K.
(Table: 82-57, Note: 82-57, Evaluated: 82-57) Back to Table

(1) Anderson, P. C.; Kurylo, M. J. Rate constant measurements for the reaction Cl + CH_2O → HCl + CHO. Implications regarding the removal of stratospheric chlorine. *J. Phys. Chem.* **1979**, *83*, 2055-2057, doi:10.1021/j100479a001.
(2) Fasano, D. M.; Nogar, N. S. The infrared chemiluminescent reaction of Cl atoms with H_2CO. *Int. J. Chem. Kinet.* **1981**, *13*, 325-332, doi:10.1002/kin.550130402.
(3) Foon, R.; Le Bras, G.; Combourieu, J. Étude cinétique par résonance paramagnetique électronique de la réaction des atomes de chlore acec le formaldéhyde. *C. R. Acad. Sci. Paris* **1979**, *Series C 288*, 241-243.
(4) Michael, J. V.; Nava, D. F.; Payne, W. A.; Stief, L. J. Rate constant for the reaction of atomic chlorine with formaldehyde from 200 to 500 K. *J. Chem. Phys.* **1979**, *70*, 1147-1150, doi:10.1063/1.437593.
(5) Niki, H.; Maker, P. D.; Breitenbach, L. P.; Savage, C. M. FTIR studies of the kinetics and mechanism for the reaction of Cl atom with formaldehyde. *Chem. Phys. Lett.* **1978**, *57*, 596-599, doi:10.1016/0009-2614(78)85328-7.
(6) Poulet, G.; Laverdet, G.; Le Bras, G. Discharge flow-mass spectrometric determination of the rate coefficients for the reactions of formaldehyde with bromine atoms and chlorine atoms. *J. Phys. Chem.* **1981**, *85*, 1892-1895, doi:10.1021/j150613a023.

F83. Cl + HC(O)OH. The room temperature kinetics of this reaction have been studied by Wallington et al.[3] (295 K) and Li et al.[1] (298 K). Wallington et al. used a relative rate technique at atmospheric pressure, while Li et al. employed flash photolysis at a pressure of 10 Torr. The results of the two studies are in excellent agreement and have been averaged together to derive the recommended value for k(298 K). Reaction products have been investigated by Tyndall et al.[2] at room temperature and 700 Torr pressure. They measured the CO_2 yield to be 96 ± 5% and suggested that the HOCO complex reacted with either O_2 or Cl_2 in their experiment to give the observed product.
(Table: 02-25, Note: 02-25, Evaluated: 02-25) Back to Table

(1) Li, Q.; Osborne, M. C.; Smith, I. W. M. Rate constants for the reactions of Cl atoms with HCOOH and with HOCO radicals. *Int. J. Chem. Kinet.* **2000**, *32*, 85-91, doi:10.1002/(SICI)1097-4601(2000)32:2<85::AID-KIN3>3.0.CO;2-I.
(2) Tyndall, G. S.; Wallington, T. J.; Potts, A. R. Product study of the reaction of Cl atoms with HCOOH. *Chem. Phys. Lett.* **1991**, *186*, 149-153, doi:10.1016/S0009-2614(91)85121-C.
(3) Wallington, T. J.; Andino, J. M.; Ball, J. C.; Japar, S. M. Fourier transform infrared studies of the reaction of C1 atoms with PAN, PPN, CH_3OOH, HCOOH, CH_3COCH_3 and $CH_3COC_2H_5$ at 295 ± 2 K. *J. Atmos. Chem.* **1990**, *10*, 301-313, doi:10.1007/BF00053865.

F84. Cl + CH_3O_2. The recommended k(298 K) is based on results of Maricq et al.[3] (298 K), Jungkamp et al.[2] (300 K), and Daële and Poulet.[1] (298 K). All three studies agree that this overall reaction is very fast. However, there is a discrepancy in the reported values of the branching ratios for the two pathways producing ClO + CH_3O (a) and HCl + CH_2O_2 (b). The branching ratio for the reaction channels producing HCl + CH_2O_2 (b) was reported to be 50% by both Maricq et al. and Jungkamp et al. but was reported to be 90% by Daële and Poulet. Because of this large discrepancy no branching ratios are recommended.

(Table: 97-4, Note: 97-4, Evaluated: 97-4) Back to Table

(1) Daële, V.; Poulet, G. Kinetics and products of the reactions of CH_3O_2 with Cl and ClO. *J. Chim. Phys.* **1996**, *93*, 1081-1099, doi:10.1051/jcp/1996931081.

(2) Jungkamp, T. P.; Kukui, A.; Schindler, R. N. Determination of rate constants and product branching ratios for the reactions of CH_3O_2 and CH_3O with Cl atoms at room temperature. *Ber. Bunsenges. Phys. Chem.* **1995**, *99*, 1057-1066, doi:10.1002/bbpc.199500031.

(3) Maricq, M. M.; Szente, J. J.; Kaiser, E. W.; Shi, J. Reaction of chlorine atoms with methylperoxy and ethylperoxy radicals. *J. Phys. Chem.* **1994**, *98*, 2083-2089, doi:10.1021/j100059a017.

F85. **Cl + CH_3OH.** This recommendation for k(298 K) is based on results of the absolute rate studies of Michael et al.[4] (200, 298, 500 K), Payne et al.[7] (298 K), Dobe et al.[1] (298 K), Pagsberg et al.[6] (298 K), and Tyndall et al.[10] (295 K), and results obtained in the competitive chlorination studies of Wallington et al.[11] (295 K), Lightfoot et al.[2] (248–573 K), Nelson et al.[5] (298 K), and Tyndall et al. The temperature independence of the rate constant was reported by Michael et al. in a direct study. This is consistent with the indirect results of Lightfoot et al., who deduced the rate coefficient for this reaction relative to that for methane as a function of temperature. This reaction can have two sets of products: CH_2OH + HCl, channel (a) and CH_3O + HCl, channel (b). Product analysis and isotopic substitution have established that the reaction proceeds via channel (a) rather than via channel (b); see Radford[8] (300 K), Radford et al.[9] (298 K), Meier et al.[3] (300–1020 K), and Payne et al. This reaction has been used in the laboratory as a source of CH_2OH and as a source of HO_2 by the reaction of CH_2OH with O_2.
(Table: 02-25, Note: 02-25, Evaluated: 02-25) Back to Table

(1) Dóbé, S.; Otting, M.; Temps, F.; Wagner, H. G.; Ziemer, H. Fast flow kinetic studies of the reaction $CH_2OH + HCl \rightleftharpoons CH_3OH + Cl$. The heat of formation of hydroxymethyl. *Ber. Bunsenges. Phys. Chem.* **1993**, *97*, 877-884, doi:10.1002/bbpc.19930970708.

(2) Lightfoot, P. D.; Veyret, B.; Lesclaux, R. Flash photolysis study of the $CH_3O_2 + HO_2$ reaction between 248 and 573 K. *J. Phys. Chem.* **1990**, *94*, 708-714, doi:10.1021/j100365a036.

(3) Meier, U.; Grotheer, H. H.; Just, T. Temperature dependence and branching ratio of the CH_3OH + OH reaction. *Chem. Phys. Lett.* **1984**, *106*, 97-101, doi:10.1016/0009-2614(84)87019-0.

(4) Michael, J. V.; Nava, D. F.; Payne, W. A.; Stief, L. J. Rate constants for the reaction of atomic chlorine with methanol and dimethyl ether from 200 to 500 K. *J. Chem. Phys.* **1979**, *70*, 3652-3656, doi:10.1063/1.437957.

(5) Nelson, L.; Rattigan, O.; Neavyn, R.; Sidebottom, H.; Treacy, J.; Nielsen, O. J. Absolute and relative rate constants for the reactions of hydroxyl radicals and chlorine atoms with a series of aliphatic alcohols and ethers at 298 K. *Int. J. Chem. Kinet.* **1990**, *22*, 1111-1126, doi:10.1002/kin.550221102.

(6) Pagsberg, P.; Munk, J.; Sillesen, A.; Anastasi, C. UV spectrum and kinetics of hydroxylmethyl radicals. *Chem. Phys. Lett.* **1988**, *146*, 375-381, doi:10.1016/0009-2614(88)87462-1.

(7) Payne, W. A.; Brunning, J.; Mitchell, M. B.; Stief, L. J. Kinetics of the reactions of atomic chlorine with methanol and the hydroxymethyl radical with molecular oxygen at 298 K. *Int. J. Chem. Kinet.* **1988**, *20*, 63-74, doi:10.1002/kin.550200108

(8) Radford, H. E. The fast reaction of CH_2OH with O_2. *Chem. Phys. Lett.* **1980**, *71*, 195-197, doi:10.1016/0009-2614(80)80145-X.

(9) Radford, H. E.; Evenson, K. M.; Jennings, D. A. Far-infrared LMR detection of hydroxymethyl. *Chem. Phys. Lett.* **1981**, *78*, 589-591, doi:10.1016/0009-2614(81)85264-5.

(10) Tyndall, G. S.; Orlando, J. J.; Kegley-Owen, C. S.; Wallington, T. J.; Hurley, M. D. Rate coefficients for the reactions of chlorine atoms with methanol and acetaldehyde. *Int. J. Chem. Kinet.* **1999**, *31*, 776-784, doi:10.1002/(SICI)1097-4601(1999)31:11<776::AID-JCK3>3.0.CO;2-Q.

(11) Wallington, T. J.; Skewes, L. M.; Siegl, W. O.; Wu, C. H.; Japar, S. M. Gas phase reaction of Cl atoms with a series of oxygenated organic species at 295 K. *Int. J. Chem. Kinet.* **1988**, *20*, 867-875, doi:10.1002/kin.550201105

F86. **Cl + CH_3OOH.** The recommended value for k(298 K) is taken from the only study of this reaction by Wallington et al.,[1] who measured the rate relative to Cl + C_2H_6 at 295 K and atmospheric pressure.
(Table: 02-25, Note: 02-25, Evaluated: 02-25) Back to Table

(1) Wallington, T. J.; Andino, J. M.; Ball, J. C.; Japar, S. M. Fourier transform infrared studies of the reaction of C1 atoms with PAN, PPN, CH_3OOH, HCOOH, CH_3COCH_3 and $CH_3COC_2H_5$ at 295 ± 2 K. *J. Atmos. Chem.* **1990**, *10*, 301-313, doi:10.1007/BF00053865.

F87. **Cl + CH_3ONO_2.** This reaction has been studied at 298 K by Nielsen et al.[1] using a relative rate technique. The reference compound was ethane. The recommended value is adjusted from that given by Nielsen et al. using

the currently recommended value for $k(Cl + C_2H_6)$. The temperature dependence is estimated by assuming an A-factor equal to approximately 20 times that of $OH + CH_3ONO_2$. This is consistent with observed Cl/OH A-factor ratios for primary H-abstraction from alkanes.
(Table: 02-25, Note: 02-25, Evaluated: 02-25) Back to Table

(1) Nielsen, O. J.; Sidebottom, H. W.; Donlon, M.; Treacy, J. An absolute- and relative-rate study of the gas-phase reaction of OH radicals and Cl atoms with *n*-alkyl nitrates. *Chem. Phys. Lett.* **1991**, *178*, 163-170, doi:10.1016/0009-2614(91)87051-C.

F88. $Cl + C_2H_6$. The recommended value for k(298 K) is an average of the absolute rate coefficients reported in the studies of Manning and Kurylo[17] (222–322 K), Lewis et al.[15] (220–604 K), Dobis and Benson[6] (203–343 K), Beichert et al.[3] (298 K), Pilgrim et al.[19] (292–800 K), Tyndall et al.[24] (297 K), Hitsuda et al.[9] (298 K), Bryukov et al.[4] (299–1002 K), and Hickson and Keyser[8] (177–353 K), all of which fall in the range $(5.3–6.1) \times 10^{-11}$ cm^3 molecule^{-1} s^{-1}. The value derived by Ray et al.[21] (298 K), in a study where the primary focus was not the determination of the rate constant for the target reaction, lies in the same range. A somewhat higher value reported by Davis et al.[5] (298 K) was probably overestimated by ~10% (the authors assumed that the fluorescence signal, I_f was proportional to $[Cl]^{0.9}$, whereas a linear relationship between I_f and [Cl] probably held under their experimental conditions). The rate constant reported by Schlyer et al.[22] (298 K) lies significantly lower than those from all other absolute studies, while the values from Mellouki et al.[18] (297 K) and Kaiser et al.[11] (298 K) lie slightly higher. Room temperature rate constants derived from the relative rate experiments of Pritchard et al.,[20] Knox and Nelson,[13] Atkinson and Aschmann,[1] Atkinson and Ashmann,[2] Tschuikow-Roux et al.,[23] Wallington et al.,[25] Beichert et al.,[3] Hooshiyar and Niki,[10] and Lin et al.[16] exhibit considerably more scatter even when recalculated based on the same (current) recommendations for the rate constants of the reference reactions. Nevertheless, most are encompassed within the 2σ uncertainty limits recommended for the value of k(298 K). The relative rate results of Kelly et al.[12] and Lee and Rowland[14] are significantly lower than other room temperature measurements. The recommended value for E/R is taken from a combined fit to the data of Manning and Kurylo,[17] Dobis and Benson,[6] and Hickson and Keyser[8] after scaling all three data sets to the recommended value of k(298 K). The data from Lewis et al.[15] and Lin et al.[16] below 300 K are encompassed by the 2σ uncertainty bands. The temperature dependent studies by Pilgrim et al. and Bryukov et al. did not extend below room temperature. An extrapolation of the recommended Arrhenius parameters and the 2σ uncertainty bands above room temperature encompasses the data of Pilgrim et al. but not those of Bryukov et al., which are characterized by a much stronger temperature dependence. The data obtained at very low temperatures (167–48 K) in Laval nozzle experiments by Hickson et al.[7] (48–167 K) strongly support the current recommendations.
(Table: 06-2, Note: 10-6, Evaluated: 10-6) Back to Table

(1) Atkinson, R.; Aschmann, S. M. Kinetics of the gas phase reaction of Cl atoms with a series of organics at 296 ± 2 K and atmospheric pressure. *Int. J. Chem. Kinet.* **1985**, *17*, 33-41, doi:10.1002/kin.550170105.
(2) Atkinson, R.; Aschmann, S. M. A structure-activity relationship for the estimation of rate constants for the gas-phase reactions of OH radicals with organic compounds. *Int. J. Chem. Kinet.* **1987**, *19*, 1097-1105, doi:10.1002/kin.550191206.
(3) Beichert, P.; Wingen, L.; Lee, J.; Vogt, R.; Ezell, M. J.; Ragains, M.; Neavyn, R.; Finlayson-Pitts, B. J. Rate constants for the reactions of chlorine atoms with some simple alkanes at 298 K: Measurement of a self-consistent set using both absolute and relative rate methods. *J. Phys. Chem.* **1995**, *99*, 13156-13162, doi:10.1021/j100035a018.
(4) Bryukov, M. G.; Slagle, I. R.; Knyazev, V. D. Kinetics of reactions of Cl atoms with ethane, chloroethane, and 1,1-dichloroethane. *J. Phys. Chem. A* **2003**, *107*, 6565-6573, doi:10.1021/jp0275138.
(5) Davis, D. D.; Braun, W.; Bass, A. M. Reactions of $Cl^2P_{3/2}$: Absolute rate constants for reaction with H_2, CH_4, C_2H_6, CH_2Cl_2, C_2Cl_4, and c-C_6H_{12}. *Int. J. Chem. Kinet.* **1970**, *2*, 101-114, doi:10.1002/kin.550020204
(6) Dobis, O.; Benson, S. W. Temperature coefficients of the rates of Cl atom reactions with C_2H_6, C_2H_5, and C_2H_4. The rates of disproportionation and recombination of ethyl radicals. *J. Am. Chem. Soc.* **1991**, *113*, 6377-6386, doi:10.1021/ja00017a004.
(7) Hickson, K. M.; Bergeat, A.; Costes, M. A low temperature study of the reactions of atomic chlorine with simple alkanes. *J. Phys. Chem. A* **2010**, *114*, 3038-3044, doi:10.1021/jp9061253.
(8) Hickson, K. M.; Keyser, L. F. Kinetics of the $Cl(^2P_J) + C_2H_6$ reaction between 177 and 353 K. *J. Phys. Chem. A* **2004**, *108*, 1150-1159, doi:10.1021/jp036458f.

(9) Hitsuda, K.; Takahashi, K.; Matsumi, Y.; Wallington, T. J. Kinetics of the reactions of $Cl(^2P_{1/2})$ and $Cl(^2P_{3/2})$ atoms with C_2H_6, C_2D_6, CH_3F, C_2H_5F, and CH_3CF_3 at 298 K. *J. Phys. Chem. A* **2001**, *105*, 5131-5136, doi:10.1021/jp003222s.
(10) Hooshiyar, P. A.; Niki, H. Rate constants for the gas-phase reactions of Cl-atoms with C_2-C_8 alkanes at $T = 296 \pm 2$ K. *Int. J. Chem. Kinet.* **1995**, *27*, 1197-1206, doi:10.1002/kin.550271206
(11) Kaiser, E. W.; Rimai, L.; Schwab, E.; Lim, E. C. Application of time-resolved infrared spectroscopy to the determination of absolute rate constants for Cl + C_2H_6 and Cl + C_2H_5Cl. *J. Phys. Chem.* **1992**, *96*, 303-306, doi:10.1021/j100180a057.
(12) Kelly, C. C.; Yu, W. H. S.; Wijnen, M. H. J. Competitive chlorination reactions with ICl. II. CH_4, C_2H_6, C_3H_8, and C_2H_5Cl. *Can. J. Chem.* **1970**, *48*, 603-606, doi:10.1139/v70-099.
(13) Knox, J. H.; Nelson, R. L. Competitive chlorination reaction in the gas phase: Hydrogen and C_1-C_5 saturated hydrocarbons. *Trans. Far. Soc.* **1959**, *55*, 937-946, doi:10.1039/tf9595500937.
(14) Lee, F. S. C.; Rowland, F. S. Competitive radiotracer evaluation of relative rate constants at stratospheric temperatures for reactions of ^{38}Cl with CH_4 and C_2H_6 vs. CH_2=CHBr. *J. Phys. Chem.* **1977**, *81*, 86-87, doi:10.1021/j100516a020.
(15) Lewis, R. S.; Sander, S. P.; Wagner, S.; Watson, R. T. Temperature-dependent rate constants for the reaction of ground-state chlorine with simple alkanes. *J. Phys. Chem.* **1980**, *84*, 2009-2015, doi:10.1021/j100453a004.
(16) Lin, C. L.; Leu, M. T.; DeMore, W. B. Rate constant for the reaction of atomic chlorine with methane. *J. Phys. Chem.* **1978**, *82*, 1772-1777, doi:10.1021/j100505a002.
(17) Manning, R. G.; Kurylo, M. J. Flash photolysis resonance fluorescence investigation of the temperature dependencies of the reactions of $Cl(^2P)$ atoms with CH_4, CH_3Cl, CH_3F, $CH_3F^{\dagger}$, and C_2H_6. *J. Phys. Chem.* **1977**, *81*, 291-296, doi:10.1021/j100519a003.
(18) Mellouki, A. Kinetic studies of Cl atom reactions with series of alkanes using the pulsed laser photolysis resonance fluorescence method. *J. Chim. Phys.* **1998**, *95*, 513-522, doi:10.1051/jcp:1998165.
(19) Pilgrim, J. S.; McIlroy, A.; Taatjes, C. A. Kinetics of Cl atom reactions with methane, ethane, and propane from 292 to 800 K. *J. Phys. Chem. A* **1997**, *101*, 1873-1880, doi:10.1021/jp962916r.
(20) Pritchard, H. O.; Pyke, J. B.; Trotman-Dickenson, A. F. The study of chlorine atom reactions in the gas phase. *J. Am. Chem. Soc.* **1955**, *77*, 2629-2633, doi:10.1021/ja01614a088.
(21) Ray, G. W.; Keyser, L. F.; Watson, R. T. Kinetics study of the $Cl(^2P) + Cl_2O \rightarrow Cl_2 + ClO$ reaction at 298 K. *J. Phys. Chem.* **1980**, *84*, 1674-1681, doi:10.1021/j100450a003.
(22) Schlyer, D. F.; Wolf, A. P.; Gaspar, P. P. Rate constants for the reactions of atomic chlorine with group 4 and group 5 hydrides. *J. Phys. Chem.* **1978**, *82*, 2633-2637, doi:10.1021/j100514a001.
(23) Tschuikow-Roux, E.; Faraji, F.; Paddison, S.; Niedzielski, J.; Miyokawa, K. Kinetics of photochlorination of halogen (F, Cl, Br) substituted methanes. *J. Phys. Chem.* **1988**, *92*, 1488-1495, doi:10.1021/j100317a023.
(24) Tyndall, G. S.; Orlando, J. J.; Wallington, T. J.; Dill, M.; Kaiser, E. W. Kinetics and mechanisms of the reactions of chlorine atoms with ethane, propane, and n-butane. *Int. J. Chem. Kinet.* **1997**, *29*, 43-55, doi:10.1002/(SICI)1097-4601(1997)29:1<43::AID-KIN6>3.0.CO;2-L.
(25) Wallington, T. J.; Skewes, L. M.; Siegl, W. O.; Wu, C. H.; Japar, S. M. Gas phase reaction of Cl atoms with a series of oxygenated organic species at 295 K. *Int. J. Chem. Kinet.* **1988**, *20*, 867-875, doi:10.1002/kin.550201105

F89. $Cl + C_2H_5O_2$. The recommended values of k(298 K) for the two reaction channels are based on results of Maricq et al.[1] (298 K).
(Table: 94-26, Note: 94-26, Evaluated: 94-26) Back to Table

(1) Maricq, M. M.; Szente, J. J.; Kaiser, E. W.; Shi, J. Reaction of chlorine atoms with methylperoxy and ethylperoxy radicals. *J. Phys. Chem.* **1994**, *98*, 2083-2089, doi:10.1021/j100059a017.

F90. $Cl + CH_3CH_2OH$. The rate coefficient for this reaction has been studied at 298 K by four groups using a relative rate technique: Nelson et al.[2] (298 K), Wallington et al.[4] (295 K), Edelbüttel -Einhaus et al.[1] (295 K), and Taatjes et al.[3] (295–600 K). Nelson et al. measured this rate constant relative to Cl + cyclohexane, while the others used Cl + C_2H_6 as the reference reaction. Taatjes et al. also measured this rate coefficient by measuring the temporal profile of the HCl product. The agreement between these five measurements is quite good, and the recommendation for k(298 K) is based on the average value. Taatjes et al. studied the temperature dependence of this rate coefficient above 298 K and found it to be essentially independent of temperature. We recommend the same temperature independence at atmospheric temperatures.

This reaction can have three sets of products: CH_2CH_2OH + HCl, channel (a); CH_3CHOH, channel (b); and CH_3CH_2O channel (c). Taatjes et al. have deduced that channel (c) is negligible and that channel (a) is about 8% at 298 K. Therefore, the majority of reaction is expected to occur via channel (b). It is very unlikely that these branching ratios will change significantly at lower atmospheric temperatures.
(Table: 02-25, Note: 02-25, Evaluated: 02-25) Back to Table

(1) Edelbüttel-Einhaus, J.; Hoyermann, K.; Rohde, G.; Seeba, J. The detection of the hydroxyethyl radical by REMPI/mass-spectrometry and the application to the study of the reactions CH_3CHOH + O and CH_3CHOH + H. *Proc. Combust. Inst.* **1992**, *24*, 661-668.
(2) Nelson, L.; Rattigan, O.; Neavyn, R.; Sidebottom, H.; Treacy, J.; Nielsen, O. J. Absolute and relative rate constants for the reactions of hydroxyl radicals and chlorine atoms with a series of aliphatic alcohols and ethers at 298 K. *Int. J. Chem. Kinet.* **1990**, *22*, 1111-1126, doi:10.1002/kin.550221102.
(3) Taatjes, C. A.; Christensen, L. K.; Hurley, M. D.; Wallington, T. J. Absolute and site-specific abstraction rate coefficients for reactions of Cl with CH_3CH_2OH, CH_3CD_2OH, and CD_3CH_2OH between 295 and 600 K. *J. Phys. Chem. A* **1999**, *103*, 9805-9814, doi:10.1021/jp992465l.
(4) Wallington, T. J.; Skewes, L. M.; Siegl, W. O.; Wu, C. H.; Japar, S. M. Gas phase reaction of Cl atoms with a series of oxygenated organic species at 295 K. *Int. J. Chem. Kinet.* **1988**, *20*, 867-875, doi:10.1002/kin.550201105

F91. Cl + $CH_3C(O)OH$. The recommended k(298 K) is based on the room temperature study by Koch and Moortgat[1] (298 K) using a relative rate technique. Deuterium substitution of the methyl hydrogens decreased the observed rate by a factor of 3.75. In addition, CO and CO_2 reaction products were observed in a stoichiometric ratio of 1:1. These observations were interpreted in terms of methyl hydrogen abstraction from acetic acid to form the $CH_2C(O)OH$ radical followed by reaction with O_2 to form a peroxy radical. Thermal decomposition of the peroxy radical produces HCHO, CO_2, and atomic H. In the laboratory system, the HCHO reacts with atomic chlorine to yield CO.
(Table: 02-25, Note: 02-25, Evaluated: 02-25) Back to Table

(1) Koch, S.; Moortgat, G. K. Rate and mechanism of the reaction Cl + CH_3COOH. *Chem. Phys. Lett.* **1990**, *173*, 531-536, doi:10.1016/0009-2614(90)87248-P.

F92. Cl + CH_3CN. The recommended Arrhenius parameters are based on the study by Tyndall et al.[4] (274–345 K), using both relative and absolute methods over a wide range of experimental conditions. These results are preferred over those of earlier studies by Kurylo and Knable[1] (298 K), Poulet et al.[3] (295–723 K), and Olbregts et al.[2] (370, 413 K). Product studies reported by Tyndall et al.[4] show that reaction proceeds predominantly, if not exclusively, by hydrogen atom abstraction.
(Table: 97-4, Note: 97-4, Evaluated: 97-4) Back to Table

(1) Kurylo, M. J.; Knable, G. L. A kinetics investigation of the gas-phase reactions of $Cl(^2P)$ and $OH(X^2\Pi)$ with CH_3CN: Atmospheric significance and evidence for decreased reactivity between strong electrophiles. *J. Phys. Chem.* **1984**, *88*, 3305-3308, doi:10.1021/j150659a033.
(2) Olbregts, J.; Brasseur, G.; Arijs, E. J. Reaction of acetonitrile and chlorine atoms. *J. Photochem.* **1984**, *24*, 315-322, doi:10.1016/0047-2670(84)80013-1.
(3) Poulet, G.; Laverdet, G.; Jourdain, J. L.; Le Bras, G. Kinetic study of the reactions of acetonitrile with Cl and OH radicals. *J. Phys. Chem.* **1984**, *88*, 6259-6263, doi:10.1021/j150669a041.
(4) Tyndall, G. S.; Orlando, J. J.; Wallington, T. J.; Sehested, J.; Nielsen, O. J. Kinetics of the reactions of acetonitrile with chlorine and fluorine atoms. *J. Phys. Chem.* **1996**, *100*, 660-668, doi:10.1021/jp9521417.

F93. Cl + $C_2H_5ONO_2$. Wallington et al.[2] (295 K) and Nielsen et al.[1] (298 K) have measured the rate of this reaction at room temperature relative to atomic chlorine reactions with ethyl chloride and ethane, respectively. The two studies are in excellent agreement, and the recommended value is based on an average of the two. The values given in Wallington et al. and Nielsen et al. were adjusted based on the currently accepted values of the reference rate constants. The temperature dependence is estimated by assuming an A-factor equal to approximately 20 times that of OH + CH_3ONO_2. This is consistent with observed Cl/OH A-factor ratios for primary H-abstraction from alkanes.
(Table: 02-25, Note: 02-25, Evaluated: 02-25) Back to Table

(1) Nielsen, O. J.; Sidebottom, H. W.; Donlon, M.; Treacy, J. An absolute- and relative-rate study of the gas-phase reaction of OH radicals and Cl atoms with *n*-alkyl nitrates. *Chem. Phys. Lett.* **1991**, *178*, 163-170, doi:10.1016/0009-2614(91)87051-C.

(2) Wallington, T. J.; Hinman, M. M.; Andino, J. M.; Siegl, W. O.; Japar, S. M. A relative rate study of the reaction of Cl atoms with a series of alkyl nitrates and nitro alkanes in air at 295 ± 2K. *Int. J. Chem. Kinet.* **1990**, *22*, 665-671, doi:10.1002/kin.550220702.

F94. **Cl + $CH_3CO_3NO_2$ (PAN).** The recommended upper limit for k(298 K) is based on results of the relative rate study of Wallington et al.[2] (295 K). In this study, no reaction of PAN was observed in the presence of Cl atoms. These results are preferred over the results of the direct study of Tsalkani et al.[1] (298 K) using a discharge flow system with EPR detection of Cl atom decay (in which the authors reported a rate constant of $(3.7 \pm 1.7) \times 10^{-13}$ cm^3 molecule^{-1} s^{-1}). In both studies, the major impurity in the PAN samples would be the alkane solvent. The presence of 0.1% tridecane in the PAN sample used by Tsalkani et al. could account for the observed Cl atom decay; however, solvent impurities in the PAN sample would be of no consequence in the relative rate study of Wallington et al.
(Table: 92-20, Note: 92-20, Evaluated: 92-20) Back to Table

(1) Tsalkani, N.; Mellouki, A.; Poulet, G.; Toupance, G.; Le Bras, G. Rate constant measurement for the reactions of OH and C1 with peroxyacetyl nitrate at 298 K. *J. Atmos. Chem.* **1988**, *7*, 409-419, doi:10.1007/BF00058713.
(2) Wallington, T. J.; Andino, J. M.; Ball, J. C.; Japar, S. M. Fourier transform infrared studies of the reaction of C1 atoms with PAN, PPN, CH_3OOH, HCOOH, CH_3COCH_3 and $CH_3COC_2H_5$ at 295 ± 2 K. *J. Atmos. Chem.* **1990**, *10*, 301-313, doi:10.1007/BF00053865.

F95. **Cl + C_3H_8.** The recommended values for k(298 K) and E/R for two individual reaction channels are presented in the Table. The recommended k(298 K) values are the means of the results from the competitive chlorination studies by Knox and Nelson[8] (193–593 K), Kelly et al.[7] (298 K), Tschuikow-Roux et al.[14] (281–368 K), Tyndall et al.[15] (297 K), and Sarzynski and Sztuba[13] (299–468 K). The recommended E/R values are based on the data of Sarzynski and Sztuba obtained between 300 and 400 K.

The recommended value for k(298 K) for the overall reaction given below is the mean of results of the competitive chlorination studies of Pritchard et al.,[12] (273–573 K), Knox and Nelson, Kelly et al., Tschuikow-Roux et al., Atkinson and Aschmann[1] (296 K), Wallington et al.[16] (295 K), Beichert et al.[2] (298 K), Hooshiyar and Niki[6] (296 K), Tyndall et al.[15] (297 K) (two determinations), and Sarzynski and Sztuba, and the absolute rate studies of Lewis et al.[9] (220–607 K), Beichert et al., Pilgrim et al.[11] (292–700 K), Mellouki[10] (297 K), Hitsuda et al.[5] (298 K), and Choi et al.[3] (195, 298 K). The recommended value of E/R = 0 for the overall reaction is based on the data obtained between 300 and 400 K by Sarzynski and Sztuba. The data obtained at very low temperatures (167–48 K) in Laval nozzle experiments by Hickson et al.,[4] the data of Pilgrim et al.,[11] extended to higher temperatures (292–700 K) , and the measurements by Choi et al. at 298 and 195 K exhibit no variation with temperature and, thus, support this recommendation.

$$A = 1.45 \times 10^{-10} \text{ cm}^3 \text{ molecule}^{-1} \text{ s}^{-1}$$
$$E/\text{R} = 0$$
$$k(298 \text{ K}) = 1.4 \times 10^{-10} \text{ cm}^3 \text{ molecule}^{-1} \text{ s}^{-1}$$
$$f(298 \text{ K}) = 1.05$$
$$g = 0$$

The sum of the recommended rate constant expressions for the two channels gives the same values as the rate constant expression recommended for the total reaction.
(Table: 15-10, Note: 15-10, Evaluated: 15-10) Back to Table

(1) Atkinson, R.; Aschmann, S. M. Kinetics of the gas phase reaction of Cl atoms with a series of organics at 296 ± 2 K and atmospheric pressure. *Int. J. Chem. Kinet.* **1985**, *17*, 33-41, doi:10.1002/kin.550170105.
(2) Beichert, P.; Wingen, L.; Lee, J.; Vogt, R.; Ezell, M. J.; Ragains, M.; Neavyn, R.; Finlayson-Pitts, B. J. Rate constants for the reactions of chlorine atoms with some simple alkanes at 298 K: Measurement of a self-consistent set using both absolute and relative rate methods. *J. Phys. Chem.* **1995**, *99*, 13156-13162, doi:10.1021/j100035a018.
(3) Choi, N.; Pilling, M. J.; Seakins, P. W.; Wang, L. Studies of site selective hydrogen atom abstractions by Cl atoms from isobutane and propane by laser flash photolysis/IR diode laser spectroscopy. *Phys. Chem. Chem. Phys.* **2006**, *8*, 2172–2178, doi:10.1039/b516531h.
(4) Hickson, K. M.; Bergeat, A.; Costes, M. A low temperature study of the reactions of atomic chlorine with simple alkanes. *J. Phys. Chem. A* **2010**, *114*, 3038-3044, doi:10.1021/jp9061253.
(5) Hitsuda, K.; Takahashi, K.; Matsumi, Y.; Wallington, T. J. Kinetics of the reactions of Cl($^2P_{1/2}$) and Cl($^2P_{3/2}$) atoms with C_2H_6, C_2D_6, CH_3F, C_2H_5F, and CH_3CF_3 at 298 K. *J. Phys. Chem. A* **2001**, *105*, 5131-5136, doi:10.1021/jp003222s.

(6) Hooshiyar, P. A.; Niki, H. Rate constants for the gas-phase reactions of Cl-atoms with C_2-C_8 alkanes at $T = 296 \pm 2$ K. *Int. J. Chem. Kinet.* **1995**, *27*, 1197-1206, doi:10.1002/kin.550271206
(7) Kelly, C. C.; Yu, W. H. S.; Wijnen, M. H. J. Competitive chlorination reactions with ICl. II. CH_4, C_2H_6, C_3H_8, and C_2H_5Cl. *Can. J. Chem.* **1970**, *48*, 603-606, doi:10.1139/v70-099.
(8) Knox, J. H.; Nelson, R. L. Competitive chlorination reaction in the gas phase: Hydrogen and C_1-C_5 saturated hydrocarbons. *Trans. Far. Soc.* **1959**, *55*, 937-946, doi:10.1039/tf9595500937.
(9) Lewis, R. S.; Sander, S. P.; Wagner, S.; Watson, R. T. Temperature-dependent rate constants for the reaction of ground-state chlorine with simple alkanes. *J. Phys. Chem.* **1980**, *84*, 2009-2015, doi:10.1021/j100453a004.
(10) Mellouki, A. Kinetic studies of Cl atom reactions with series of alkanes using the pulsed laser photolysis resonance fluorescence method. *J. Chim. Phys.* **1998**, *95*, 513-522, doi:10.1051/jcp:1998165.
(11) Pilgrim, J. S.; McIlroy, A.; Taatjes, C. A. Kinetics of Cl atom reactions with methane, ethane, and propane from 292 to 800 K. *J. Phys. Chem. A* **1997**, *101*, 1873-1880, doi:10.1021/jp962916r.
(12) Pritchard, H. O.; Pyke, J. B.; Trotman-Dickenson, A. F. The study of chlorine atom reactions in the gas phase. *J. Am. Chem. Soc.* **1955**, *77*, 2629-2633, doi:10.1021/ja01614a088.
(13) Sarzynski, D.; Sztuba, S. Gas-phase reactions of Cl atoms with propane, n-butane, and isobutane. *Int. J. Chem. Kinet.* **2002**, *34*, 651-658, doi:10.1002/kin.10096.
(14) Tschuikow-Roux, E.; Yano, T.; Niedzielski, J. Reactions of ground state chlorine atoms with fluorinated methanes and ethanes. *J. Chem. Phys.* **1985**, *82*, 65-74, doi:10.1063/1.448737.
(15) Tyndall, G. S.; Orlando, J. J.; Wallington, T. J.; Dill, M.; Kaiser, E. W. Kinetics and mechanisms of the reactions of chlorine atoms with ethane, propane, and n-butane. *Int. J. Chem. Kinet.* **1997**, *29*, 43-55, doi:10.1002/(SICI)1097-4601(1997)29:1<43::AID-KIN6>3.0.CO;2-L.
(16) Wallington, T. J.; Skewes, L. M.; Siegl, W. O.; Wu, C. H.; Japar, S. M. Gas phase reaction of Cl atoms with a series of oxygenated organic species at 295 K. *Int. J. Chem. Kinet.* **1988**, *20*, 867-875, doi:10.1002/kin.550201105

F96. **Cl + $CH_3C(O)CH_3$.** The recommended k(298 K) is an average of the values derived in the relative rate studies by Carr et al.[2] (298 K), Christensen et al.[3] (296 K), Martinez et al.[4] (298 K), Orlando et al.[7] (215–298 K), Romanias et al.[8] (273–363 K), and Wallington et al.[10] (295 K) and in the absolute rate studies by Romanias et al., Takahashi et al.[9] (295 K), and Zhao et al.[11] (216–369 K), all of which agree to within 15–20%. Room temperature rate constants reported by Notario et al.[5] (298 K) and Albaladejo et al.[1] (298 K) are about 40–50% greater than the recommended value, whereas the value reported by Olsson et al.[6] (294 K) is approximately 25% lower than recommended. Because of the level of disagreement with eight other studies, the results of the last three investigations listed above were not included in deriving the recommended value for k(298 K). The recommended value for E/R is derived from an Arrhenius fit to the data of Orlando et al. and Zhao et al. and the absolute rate data of Romanias et al. after scaling each data set to the recommended value for k(298 K). The relative rate data from Romanias et al. was not included due to uncertainties in the rate constants for the reference reactions. Nevertheless, the rate constant values derived from these relative rate experiments are in good agreement with the recommended rate expression. Although the data of Orlando et al. lie systematically about 13% lower than those of Zhao et al., the E/R values reported in both studies are nearly identical. End product studies clearly show that the products of this reaction are $CH_3C(O)CH_2$ and HCl.
(Table: 15-10, Note: 15-10, Evaluated: 15-10) Back to Table

(1) Albaladejo, J.; Notario, A.; Cuevas, C. A.; Ballesteros, B.; Martinez, E. A pulsed laser photolysis-resonance fluorescence kinetic study of the atmospheric Cl atom-initiated oxidation of propene and a series of 3-halopropenes at room temperature. *J. Atmos. Chem.* **2003**, *45*, 35-50, doi:10.1023/A:1024073012242.
(2) Carr, S.; Shallcross, D. E.; Canosa-Mas, C. E.; Wenger, J. C.; Sidebottom, H. W.; Treacy, J. J.; Wayne, R. P. A kinetic and mechanistic study of the gas-phase reactions of OH radicals and Cl atoms with some halogenated acetones and their atmospheric implications. *Phys. Chem. Chem. Phys.* **2003**, *5*, 3874-3883, doi:10.1039/b304298g.
(3) Christensen, L. K.; Ball, J. C.; Wallington, T. J. Atmospheric oxidation mechanism of methyl acetate. *J. Phys. Chem. A* **2000**, *104*, 345-351, doi:10.1021/jp993127n.
(4) Martinez, E.; Aranda, A.; Diaz de Mera, Y.; Rodriguez, A.; Rodriguez, D.; Notario, A. Mechanistic and kinetic study of the gas-phase reaction of atomic chlorine with cyclohexanone using an absolute and a relative technique; Influence of temperature. *J. Atmos. Chem.* **2004**, *48*, 283-299, doi:10.1023/B:JOCH.0000044424.22309.d8.
(5) Notario, A.; Mellouki, A.; Le Bras, G. Rate constants for the gas-phase reactions of chlorine atoms with a series of ketones. *Int. J. Chem. Kinet.* **2000**, *32*, 62-66, doi:10.1002/(SICI)1097-4601(2000)32:1<67::AID-JCK8>3.0.CO;2-M.

(6) Olsson, B.; Hallquist, M.; Ljungstrom, E.; Davidsson, J. A kinetic study of chlorine radical reactions with ketones by laser photolysis technique. *Int. J. Chem. Kinet.* **1997**, *29*, 195-201, doi:10.1002/(SICI)1097-4601(1997)29:3<195::AID-KIN6>3.0.CO;2-P.
(7) Orlando, J. J.; Tyndall, G. S.; Vereecken, L.; Peeters, J. The atmospheric chemistry of the acetonoxy radical. *J. Phys. Chem. A* **2000**, *104*, 11578-11588, doi:10.1021/jp0026991.
(8) Romanias, M. N.; Stefanopoulos, V. G.; Papanastasiou, D. K.; Papadimitriou, V. C.; Papagiannakopoulos, P. Temperature-dependent rate coefficients and mechanism for the gas-phase reaction of chlorine atoms with acetone. *Int. J. Chem. Kinet.* **2010**, *42*, 724-734, doi:10.1002/kin.20517.
(9) Takahashi, K.; Iwasaki, E.; Matsumi, Y.; Wallington, T. J. Pulsed laser photolysis vacuum UV laser-induced fluorescence kinetic study of the gas-phase reactions of $Cl(^2P_{3/2})$ atoms with C_3—C_6 ketones. *J. Phys. Chem. A* **2007**, *111*, 1271-1276, doi:10.1021/jp066410c.
(10) Wallington, T. J.; Andino, J. M.; Ball, J. C.; Japar, S. M. Fourier transform infrared studies of the reaction of C1 atoms with PAN, PPN, CH_3OOH, HCOOH, CH_3COCH_3 and $CH_3COC_2H_5$ at 295 ± 2 K. *J. Atmos. Chem.* **1990**, *10*, 301-313, doi:10.1007/BF00053865.
(11) Zhao, Z.; Huskey, D. T.; Nicovich, J. M.; Wine, P. H. Temperature-dependent kinetics study of the gas-phase reactions of atomic chlorine with acetone, 2-butanone, and 3-pentanone. *Int. J. Chem. Kinet.* **2008**, *40*, 259-267, doi:10.1002/kin.20321.

F97. Cl + CH_2=C(CH_3)CHO (Methacrolein). The recommendation is based on the relative rate studies of Kaiser et al.[4] (297 K) and Orlando et al.[5] (298 K) with the error limits adjusted to encompass the results of Canosa-Mas et al.[1,2] (298 K), and Wang et al.[7] (298 K). Kaiser et al. report that the 297 K rate coefficient is pressure dependent at P <100 Torr N_2, a result that is confirmed theoretically by Sun et al.,[6] who also calculate a 297 K high pressure limit rate constant in excellent agreement with the recommendation. The available information suggests that the rate constant measured by Canosa-Mas et al. in a low-pressure discharge flow study[1] is too fast. Experimental yields of HCl are reported by Canosa-Mas et al.[1] (18 ± 2%) and Kaiser et al. (27 ± 3%). Additional product studies by Kaiser et al. lead these authors to conclude that ~90% of the HCl production is via abstraction of the aldehydic hydrogen with the other 10% being attributable to abstraction of a methyl hydrogen. Sun et al. obtain a theoretical HCl yield of 12% with essentially all HCl production resulting from abstraction of the aldehydic hydrogen. Molar yields of carbon-containing products in NO_x-free air at ~1 atm and ~297 K have been reported by Kaiser et al. (44 ± 5% $ClCH_2C(O)CH_3$; 27 ± 3% CO_2; 14 ± 2% HCHO) and Orlando et al. (52 ± 4% CO; 42 ± 5% $ClCH_2C(O)CH_3$; 23 ± 2% CO; 18 ± 2% HCHO; ~5% ClCHO); the significant yield of $ClCH_2C(O)CH_3$ suggests that addition of Cl to the terminal carbon of the double bond is an important reaction pathway. A turbulent flow reactor study by Hsin and Elrod[3] (298 K) obtains a Cl-methacrolein-OO + NO rate constant of $(1.17 \pm 0.11) \times 10^{-11}$ cm^3 $molecule^{-1}$ s^{-1}.
(Table 15-10, Note: 15-10, Evaluated: 15-10) Back to Table

(1) Canosa-Mas, C. E.; Cotter, E. S. N.; Duffy, J.; Thompson, K. C.; Wayne, R. P. The reactions of atomic chlorine with acrolein, methacrolein, and methyl vinyl ketone. *Phys. Chem. Chem. Phys.* **2001**, *3*, 3075-3084, doi:10.1039/b101434j.
(2) Canosa-Mas, C. E.; Hutton-Squire, H. R.; King, M. D.; Stewart, D. J.; Thompson, K. C.; Wayne, R. P. Laboratory kinetic studies of the reactions of Cl atoms with species of biogenic origin: Δ^3-carene, isoprene, methacrolein and methyl vinyl ketone. *J. Atmos. Chem.* **1999**, *34*, 163-170, doi:10.1023/A:1006214423298.
(3) Hsin, H. Y.; Elrod, M. J. Overall rate constant measurements of the reaction of hydroxy- and chloroalkylperoxy radicals derived from methacrolein and methyl vinyl ketone with nitric oxide. *J. Phys. Chem. A* **2007**, *111*, 613-619, doi:10.1021/jp0665574.
(4) Kaiser, E. W.; Pala, I. R.; Wallington, T. J. Kinetics and mechanism of the reaction of methacrolein with chlorine atoms in 1-950 Torr of N_2 or N_2/O_2 diluent at 297 K. *J. Phys. Chem. A* **2010**, *114*, 6850-6860, doi:10.1021/jp103317c.
(5) Orlando, J. J.; Tyndall, G. S.; Apel, E. C.; Riemer, D. D.; Paulson, S. E. Rate coefficients and mechanisms of the reaction of Cl-atoms with a series of unsaturated hydrocarbons under atmospheric conditions. *Int. J. Chem. Kinet.* **2003**, *35*, 334-353, doi:10.1002/kin.10135.
(6) Sun, C.; Xu, B.; Zhang, S. Atmospheric reaction of Cl + methacrolein: A theoretical study on the mechanism, and pressure- and temperature-dependent rate constants. *J. Phys. Chem. A* **2014**, *118*, 3541-3551, doi:10.1021/jp500993k.
(7) Wang, W.; Ezell, M. J.; Ezell, A. A.; Soskin, G.; Finlayson-Pitts, B. J. Rate constants for the reactions of chlorine atoms with a series of unsaturated aldehydes and ketones at 298 K: structure and reactivity. *Phys. Chem. Chem. Phys.* **2002**, *4*, 1824-1831, doi:10.1039/b111557j.

F98. **Cl + $CH_3C(O)CH=CH_2$ (MVK).** The recommendation is based on the relative rate studies of Canosa-Mas et al.[2] (298 K), Finlayson-Pitts et al.[3] (298 K), Orlando et al.[5] (298 K), and Wang et al.[6] (298 K), all of which were carried out at room temperature using ~1 atm N_2 [2,3,6] or air[5] bath gas. In a low-pressure flow tube study, Canosa-Mas et al.[1] obtain rate constants that are about a factor of two slower than the recommended value. Product yields reported by Orlando et al. in NO_x-free air at 1 atm and 298 K are 75% $ClCH_2CHO$, 58 ± 5% CO_2, 47 ± 7% HCHO, 8% CH_3OH, 7 ± 1% ClCHO, and 6% $CH_3C(O)OOH$; the large observed yield of $ClCH_2CHO$ leads to the conclusion that the dominant reaction pathway is addition to the terminal carbon atom of the double bond. A turbulent flow reactor study by Hsin and Elrod[4] (298 K) obtained a Cl-MVK-OO + NO rate constant of $(1.14 \pm 0.14) \times 10^{-11}$ cm^3 $molecule^{-1}$ s^{-1}.
(Table 15-10, Note: 15-10, Evaluated: 15-10) Back to Table

(1) Canosa-Mas, C. E.; Cotter, E. S. N.; Duffy, J.; Thompson, K. C.; Wayne, R. P. The reactions of atomic chlorine with acrolein, methacrolein, and methyl vinyl ketone. *Phys. Chem. Chem. Phys.* **2001**, *3*, 3075-3084, doi:10.1039/b101434j.

(2) Canosa-Mas, C. E.; Hutton-Squire, H. R.; King, M. D.; Stewart, D. J.; Thompson, K. C.; Wayne, R. P. Laboratory kinetic studies of the reactions of Cl atoms with species of biogenic origin: Δ^3-carene, isoprene, methacrolein and methyl vinyl ketone. *J. Atmos. Chem.* **1999**, *34*, 163-170, doi:10.1023/A:1006214423298.

(3) Finlayson-Pitts, B. J.; Keoshian, C. J.; Buehler, B.; Ezell, A. A. Kinetics of reaction of chlorine atoms with some biogenic organics. *Int. J. Chem. Kinet.* **1999**, *31*, 491-499, doi:10.1002/(SICI)1097-4601(1999)31:7<491::AID-KIN4>3.0.CO;2-E.

(4) Hsin, H. Y.; Elrod, M. J. Overall rate constant measurements of the reaction of hydroxy- and chloroalkylperoxy radicals derived from methacrolein and methyl vinyl ketone with nitric oxide. *J. Phys. Chem. A* **2007**, *111*, 613-619, doi:10.1021/jp0665574.

(5) Orlando, J. J.; Tyndall, G. S.; Apel, E. C.; Riemer, D. D.; Paulson, S. E. Rate coefficients and mechanisms of the reaction of Cl-atoms with a series of unsaturated hydrocarbons under atmospheric conditions. *Int. J. Chem. Kinet.* **2003**, *35*, 334-353, doi:10.1002/kin.10135.

(6) Wang, W.; Ezell, M. J.; Ezell, A. A.; Soskin, G.; Finlayson-Pitts, B. J. Rate constants for the reactions of chlorine atoms with a series of unsaturated aldehydes and ketones at 298 K: structure and reactivity. *Phys. Chem. Chem. Phys.* **2002**, *4*, 1824-1831, doi:10.1039/b111557j.

F99. **Cl + $CH_2=C(CH_3)CH=CH_2$ (Isoprene).** The recommended 298 K rate constant is an average of room temperature results reported by Ragains and Finlayson-Pitts[10] (298 K), Fantechi et al.[4] (298 K), Notario et al.[7] (298 K), Bedjanian et al.[2] (233–320 K), Stutz et al.[11] (298 K), Finlayson-Pitts et al.[5] (298 K), Canosa-Mas et al.[3] (298 K), Suh and Zhang[12] (298 K), Albaladejo et al.[1] (298 K), Orlando et al.[8] (298 K), and Xing et al.[13] (297 K). The recommended *E*/R is based on the single temperature dependence study by Bedjanian et al., which covered the range 233–320 K. Although the atmospheric pressure relative rate studies of Ragains and Finlayson-Pitts, Fantechi et al., Finlayson-Pitts et al., and Canosa-Mas et al. suggest a 298 K rate constant that is nearly 20% faster than the recommended value, Bedjanian et al. report little or no pressure dependence over the range 0.25–3.0 Torr He, and Xing et al. report no pressure dependence at pressures above 1 Torr Ar. A recommended temperature-dependent yield for HCl is given by the expression 1.1exp(−595/T); the temperature dependence is that reported by Bedjanian et al. while the pre-exponential factor is adjusted to give a 298 K yield of 0.15, the average of values reported by Bedjanian et al., Ragains and Finlayson-Pitts, Fantechi et al., Suh and Zhang, and Xing et al. The reported 298 K HCl yields are in excellent agreement even though they were obtained under very different conditions of pressure and bath gas, i.e., 1 Torr He,[2] 10 Torr He,[12] 700 Torr N_2,[13] 740 Torr Air,[4] and 760 Torr N_2.[10] Molar yields of carbon-containing products in NO_x-free air at ~1 atm and ~297 K have been reported by Nordmeyer et al.[6] (298 K) (9 ± 5% $CH_3C(O)CH=CH_2$; unquantified but significant yields of $ClCH_2C(O)C(CH_3)=CH_2$ and its isomers), Fantechi et al. (4.4 ± 3.3% ClCHO; 1.1 ± 0.8% HCOOH; 25.7 ± 7.4% CO), and Orlando et al. (9.5 ± 1.0% HCHO; 5.1 ± 0.7% ClCHO; unquantified amount of $ClCH_2C(O)C(CH_3)=CH_2$). A turbulent flow reactor study by Patchen et al.[9] (298 K) obtains a Cl-isoprene-OO + NO rate constant of $(1.15 \pm 0.11) \times 10^{-11}$ cm^3 $molecule^{-1}$ s^{-1} (there are six isomers of Cl-isoprene-OO that could be generated, but the distribution in the Patchen et al. study is presumably the same as would be formed in the atmosphere).
(Table: 15-10, Note: 15-10, Evaluated: 15-10) Back to Table

(1) Albaladejo, J.; Notario, A.; Cuevas, C. A.; Ballesteros, B.; Martinez, E. A pulsed laser photolysis-resonance fluorescence kinetic study of the atmospheric Cl atom-initiated oxidation of propene and a series of 3-halopropenes at room temperature. *J. Atmos. Chem.* **2003**, *45*, 35-50, doi:10.1023/A:1024073012242.

(2) Bedjanian, Y.; Laverdet, G.; Le Bras, G. Low-pressure study of the reaction of Cl atoms with isoprene. *J. Phys. Chem. A* **1998**, *102*, 953-959, doi:10.1021/jp973336c.

(3) Canosa-Mas, C. E.; Hutton-Squire, H. R.; King, M. D.; Stewart, D. J.; Thompson, K. C.; Wayne, R. P. Laboratory kinetic studies of the reactions of Cl atoms with species of biogenic origin: Δ^3-carene, isoprene, methacrolein and methyl vinyl ketone. *J. Atmos. Chem.* **1999**, *34*, 163-170, doi:10.1023/A:1006214423298.
(4) Fantechi, G.; Jensen, N. R.; Saastad, O.; Hjorth, J.; Peeters, J. Reactions of Cl atoms with selected VOCs: Kinetics, products and mechanisms. *J. Atmos. Chem.* **1998**, *31*, 247-267, doi:10.1023/A:1006033910014.
(5) Finlayson-Pitts, B. J.; Keoshian, C. J.; Buehler, B.; Ezell, A. A. Kinetics of reaction of chlorine atoms with some biogenic organics. *Int. J. Chem. Kinet.* **1999**, *31*, 491-499, doi:10.1002/(SICI)1097-4601(1999)31:7<491::AID-KIN4>3.0.CO;2-E.
(6) Nordmeyer, T.; Wang, W.; Ragains, M. L.; Finlayson-Pitts, B. J.; Spicer, C. W.; Plastridge, R. A. Unique products of the reaction of isoprene with atomic chlorine: Potential markers of chlorine atom chemistry. *Geophys. Res. Lett.* **1997**, *24*, 1615-1618, doi:10.1029/97GL01547.
(7) Notario, A.; Le Bras, G.; Mellouki, A. Kinetics of Cl atom reactions with butadienes including isoprene. *Chem. Phys. Lett.* **1997**, *281*, 421-425, doi:10.1016/S0009-2614(97)01303-1.
(8) Orlando, J. J.; Tyndall, G. S.; Apel, E. C.; Riemer, D. D.; Paulson, S. E. Rate coefficients and mechanisms of the reaction of Cl-atoms with a series of unsaturated hydrocarbons under atmospheric conditions. *Int. J. Chem. Kinet.* **2003**, *35*, 334-353, doi:10.1002/kin.10135.
(9) Patchen, A. K.; Pennino, M. J.; Elrod, M. J. Overall rate constant measurements of the reaction of chloroalkylperoxy radicals with nitric oxide. *J. Phys. Chem. A* **2005**, *109*, 5865-5871, doi:10.1021/jp050388q.
(10) Ragains, M. L.; Finlayson Pitts, B. J. Kinetics and mechanism of the reaction of Cl atoms with 2-methyl-1,3-butadiene (isoprene) at 298 K. *J. Phys. Chem. A* **1997**, *101*, 1509-1517, doi:10.1021/jp962786m.
(11) Stutz, J.; Ezell, M. J.; Ezell, A. A.; Finlayson-Pitts, B. J. Rate constants and kinetic isotope effects in the reactions of atomic chlorine with n-butane and simple alkenes at room temperature. *J. Phys. Chem. A* **1998**, *102*, 8510-8519, doi:10.1021/jp981659i.
(12) Suh, I.; Zhang, R. Kinetic studies of isoprene reactions initiated by chlorine atom. *J. Phys. Chem. A* **2000**, *104*, 6590-6596, doi:10.1021/jp000605h.
(13) Xing, J.-H.; Takahashi, K.; Hurley, M. D.; Wallington, T. J. Kinetics of the reaction of chlorine atoms with isoprene (2-methyl 1,3-butadiene, CH_2=C(CH_3)CH=CH_2) at 297 ± 2 K. *Chem. Phys. Lett.* **2009**, *472*, 39-43, doi:10.1016/j.cplett.2009.03.002.

F100. Cl + $C_2H_5CO_3NO_2$. Wallington et al.[1] (295 K) have measured this rate constant relative to Cl + CH_3Cl. The recommended value of k(298 K) is adjusted from that given by Wallington et al. using the currently recommended value for the reference reaction rate constant.
(Table: 02-25, Note: 02-25, Evaluated: 02-25) Back to Table

(1) Wallington, T. J.; Andino, J. M.; Ball, J. C.; Japar, S. M. Fourier transform infrared studies of the reaction of C1 atoms with PAN, PPN, CH_3OOH, HCOOH, CH_3COCH_3 and $CH_3COC_2H_5$ at 295 ± 2 K. *J. Atmos. Chem.* **1990**, *10*, 301-313, doi:10.1007/BF00053865.

F101. Cl + 1-$C_3H_7ONO_2$. The recommended k(298 K) is based on studies by Wallington et al.[2] (295 K) and Nielsen et al.[1] (298 K), who measured the rate constant at room temperature relative to atomic chlorine reactions with ethyl chloride and ethane, respectively. The two studies are in excellent agreement, and the recommended value is based on an average of the two.
(Table: 10-6, Note: 10-6), Evaluated: 10-6) Back to Table

(1) Nielsen, O. J.; Sidebottom, H. W.; Donlon, M.; Treacy, J. An absolute- and relative-rate study of the gas-phase reaction of OH radicals and Cl atoms with *n*-alkyl nitrates. *Chem. Phys. Lett.* **1991**, *178*, 163-170, doi:10.1016/0009-2614(91)87051-C.
(2) Wallington, T. J.; Hinman, M. M.; Andino, J. M.; Siegl, W. O.; Japar, S. M. A relative rate study of the reaction of Cl atoms with a series of alkyl nitrates and nitro alkanes in air at 295 ± 2K. *Int. J. Chem. Kinet.* **1990**, *22*, 665-671, doi:10.1002/kin.550220702.

F102. Cl + 2-$C_3H_7ONO_2$. The recommended value of k(298 K) is taken from Wallington et al.[1] (295 K), who studied the reaction relative to Cl + C_2H_5Cl.
(Table: 10-6, Note: 10-6) Back to Table

(1) Wallington, T. J.; Hinman, M. M.; Andino, J. M.; Siegl, W. O.; Japar, S. M. A relative rate study of the reaction of Cl atoms with a series of alkyl nitrates and nitro alkanes in air at 295 ± 2K. *Int. J. Chem. Kinet.* **1990**, *22*, 665-671, doi:10.1002/kin.550220702.

F103. Cl + OClO. The recommended k(298 K) is the mean of the values reported by Toohey[2] and Bemand et al.[1] (298 K), which are in good agreement. The slight negative temperature dependence reported by Toohey is accepted, but with error limits that encompass the temperature independence reported in the Bemand et al. study.
(Table: 90-1, Note: 90-1, Evaluated: 10-6) Back to Table

(1) Bemand, P. P.; Clyne, M. A. A.; Watson, R. T. Reactions of chlorine oxide radicals Part 4.-Rate constants for the reactions Cl + OClO, O + OClO, H + OClO, NO + OClO and O + ClO. *J. Chem. Soc. Faraday Trans. 1* **1973**, *69*, 1356-1374, doi:10.1039/f19736901356.
(2) Toohey, D. W. Kinetic and Mechanistic Studies of Reactions of Bromine and Chlorine Species Important in the Earth's Stratosphere. Ph. D. Thesis, Harvard University, 1988.

F104. Cl + ClOO. The recommended Arrhenius parameters are based on the studies by Mauldin et al.[5] (191–250 K) and Baer et al.[2] (160–300 K), in which ClOO was formed by the pulsed photolysis of Cl_2/O_2 mixtures and its overall loss rate was monitored by UV absorption. In both studies k was found to be independent of temperature. These results are preferred over the results of the earlier, indirect studies of Johnston et al.[4] (298 K), Cox et al.[3] (298 K), and Ashford et al.[1] (298 K). The earlier studies did show that the predominant reaction pathway is that yielding $Cl_2 + O_2$ as products. From the branching ratio data of Cox et al., Ashford et al., and Nicholas and Norrish[6] (298 K), it can be estimated that this reaction channel constitutes 95% of the overall reaction with ClO + ClO the products of the minor (5%) reaction channel.
(Table: 92-20, Note: 92-20, Evaluated: 92-20) Back to Table

(1) Ashford, R. D.; Basco, N.; Hunt, J. E. The kinetics of ClO formation in the flash photolysis of chlorine-oxygen mixtures. *Int. J. Chem. Kinet.* **1978**, *10*, 1233-1244, doi:10.1002/kin.550101206.
(2) Baer, S.; Hippler, H.; Rahn, R.; Siefke, M.; Seitzinger, N.; Troe, J. Thermodynamic and kinetic properties of the reaction Cl + O_2 + M ⇌ ClOO + M in the range 160-300 K and 1-1000 bar. *J. Chem. Phys.* **1991**, *95*, 6463-6470, doi:10.1063/1.461543.
(3) Cox, R. A.; Derwent, R. G.; Eggleton, A. E. J.; Read, H. J. Kinetics of chlorine oxide radicals using modulated photolysis Part 2.-ClO and ClOO radical kinetics in the photolysis of Cl_2 + O_2 + N_2 mixtures. *J. Chem. Soc. Faraday Trans. I* **1979**, *75*, 1648-1666, doi:10.1039/f19797501648.
(4) Johnston, H. S.; Morris, E. D., Jr.; Van den Bogaerde, J. Molecular modulation kinetic spectrometry. ClOO and ClO_2 radicals in the photolysis of chlorine in oxygen. *J. Am. Chem. Soc.* **1969**, *91*, 7712-7727, doi:10.1021/ja50001a036.
(5) Mauldin, R. L., III; Burkholder, J. B.; Ravishankara, A. R. A photochemical, thermodynamic, and kinetic study of ClOO. *J. Phys. Chem.* **1992**, *96*, 2582-2588, doi:10.1021/j100185a035.
(6) Nicholas, J. E.; Norrish, R. G. W. Some reactions in the chlorine and oxygen system studied by flash photolysis. *Proc. Roy. Soc. A* **1968**, *307*, 391-397, doi:10.1098/rspa.1968.0197.

F105. Cl + Cl_2O. The recommended parameters are determined from results of the temperature-dependent study of Stevens and Anderson[4] (233–373 K) and the results of two independent absolute rate coefficient studies reported by Ray et al.[3] (298 K), which used the discharge flow-resonance fluorescence and discharge flow-mass spectrometric techniques. The recommended value for k(298 K) is in agreement with the results of Burrows and Cox[2] (300 K), who determined the ratio $k(Cl + Cl_2O)/k(Cl + H_2) = 6900$ in modulated photolysis experiments. The earlier value reported by Basco and Dogra[1] has been rejected.
(Table: 94-26, Note: 94-26, Evaluated: 10-6) Back to Table

(1) Basco, N.; Dogra, S. K. Reactions of halogen oxides studied by flash photolysis II. The flash photolysis of chlorine monoxide and of the ClO free radical. *Proc. Roy. Soc. Lond. A.* **1971**, *323*, 401-415, doi:10.1098/rspa.1971.0112.
(2) Burrows, J. P.; Cox, R. A. Kinetics of chlorine oxide reactions using modulated photolysis. 4. The reactions Cl + Cl_2O → Cl_2 + ClO and ClO + HO_2 → products studied at 1 atm and 300 K. *J. Chem. Soc. Faraday Trans. 1* **1981**, *77*, 2465-2479, doi:10.1039/f19817702465.
(3) Ray, G. W.; Keyser, L. F.; Watson, R. T. Kinetics study of the Cl(^{2}P) + Cl_2O → Cl_2 + ClO reaction at 298 K. *J. Phys. Chem.* **1980**, *84*, 1674-1681, doi:10.1021/j100450a003.
(4) Stevens, P. S.; Anderson, J. G. Kinetic and mechanistic study of X + ClOCl → products (X = Br, CI, F, O, OH, N) over the temperature range 240-373 K. *J. Phys. Chem.* **1992**, *96*, 1708-1718, doi:10.1021/j100183a040.

F106. Cl + Cl_2O_2. The recommended Arrhenius parameters are from Ingham et al.[2] in a study between 217 and 298 K using a DF-MS/RF technique. The room temperature value reported by Cox and Hayman[1] in a study using

a static photolysis technique with photodiode array UV spectroscopy is in excellent agreement with the recommended value.
(Table: 10-6, Note: 10-6, Evaluated: 10-6) Back to Table

(1) Cox, R. A.; Hayman, G. D. The stability and photochemistry of dimers of the ClO radical and implications for Antarctic ozone depletion. *Nature* **1988**, *332*, 796-800, doi:10.1038/332796a0.
(2) Ingham, T.; Sander, S. P.; Friedl, R. R. Kinetics and product studies of the reaction of Br, Cl, and NO with ClOOCl using discharge-flow mass spectrometry. *Faraday Discuss.* **2005**, *130*, 89-110, doi:10.1039/b500179j.

F107. Cl + HOCl. The recommended parameters are based on results over the temperature range 243–365 K reported by Cook et al.[1] and the room temperature result of Kukui et al.[3] The earlier work of Vogt and Schindler[4] (298 K) is thought to have been plagued by complexities with the F-atom titration procedure used for HOCl calibration. Ennis and Birks[2] (298 K) and Kukui et al. reported that the major reaction channel gives the products Cl_2 + OH with measured yields of 91 ± 6% and 96 ± 5%, respectively. Theoretical calculations by Wang et al.[5] lend support to the predominance of the Cl_2 + OH channel at all temperatures below 300 K.
(Table: 10-6, Note: 10-6, Evaluated: 10-6) Back to Table

(1) Cook, J. L.; Ennis, C. A.; Leck, T. J.; Birks, J. W. Studies of reactions of importance in the stratosphere. IV. Rate constant for the reaction Cl + HOCl → HCl + ClO over the temperature range 243-365 K. *J. Chem. Phys.* **1981**, *74*, 545-549, doi:10.1063/1.440807.
(2) Ennis, C. A.; Birks, J. W. Applications of a new laboratory source of gaseous HOCl: Product distribution in the Cl + HOCl reaction and equilibrium constant for the reaction Cl_2O + H_2O ⇌ 2HOCl. *J. Phys. Chem.* **1985**, *89*, 186-191, doi:10.1021/j100247a039.
(3) Kukui, A.; Roggenbuck, J.; Schindler, R. N. Mechanism and rate constants for the reactions of Cl atoms with HOCl, CH_3OCl and *tert*-C_4H_9OCl. *Ber. Bunsenges. Phys. Chem.* **1997**, *101*, 281-286, doi:10.1002/bbpc.19971010217.
(4) Vogt, R.; Schindler, R. N. A gas kinetic study of the reaction of HOCl with F-, Cl-, and H-atoms at room temperature. *Ber. Bunsenges. Phys. Chem.* **1993**, *97*, 819-829, doi:10.1002/bbpc.19930970612.
(5) Wang, L.; Liu, J. Y.; Li, Z. S.; Huang, X. R.; Sun, C. C. Theoretical study and rate constant calculation of the Cl + HOCl and H + HOCl reactions. *J. Phys. Chem. A* **2003**, *107*, 4921-4928, doi:10.1021/jp0277558.

F108. Cl + ClNO. The recommended k(298 K) is the mean of the values reported by Abbatt et al.,[1] (208–373 K), Chasovnikov et al.[2] (298 K), Nesbitt et al.[8] (298 K), and Kita and Stedman[6] (298 K). The room temperature result of Chesnokov[3] is in fair agreement with the recommended value. The laser photolysis-LMR study of Chasovnikov et al. provides rate data for each Cl atom spin state, and they attribute the low value reported by Nelson and Johnston[7] (298 K) in a laser flash photolysis-resonance fluorescence study to reaction of the Cl $^2P_{1/2}$ state. Adsorption and decomposition of ClNO on the walls of their static system may account for the very low value of Grimley and Houston[5] (298 K). The results of Clyne and Cruse[4] (298 K) in a discharge flow-resonance fluorescence study are significantly lower than all of the later studies. The recommended Arrhenius parameters are from the study of Abbatt et al.
(Table: 90-1, Note: 10-6, Evaluated: 10-6) Back to Table

(1) Abbatt, J. P. D.; Toohey, D. W.; Fenter, F. F.; Stevens, P. S.; Brune, W. H.; Anderson, J. G. Kinetics and mechanism of X + ClNO → XCI + NO (X = Cl, F, Br, OH, O, N) from 220 to 450 K. Correlation of reactivity and activation energy with electron affinity of X. *J. Phys. Chem.* **1989**, *93*, 1022-1029, doi:10.1021/j100340a004.
(2) Chasovnikov, S. A.; Chichinin, A. I.; Krasnoperov, L. N. Time-resolved LMR study on the reactions of Cl atoms in the ground ($^2P_{3/2}$) and excited ($^2P_{1/2}$) spin-orbital states with ClNO. *Chem. Phys.* **1987**, *116*, 91-99, doi:10.1016/0301-0104(87)80071-X.
(3) Chesnokov, E. N. Application of IR-chemiluminescence method for determination of rate constants of bimolecular reactions which are not leading to the formation of excited products. *Khim. Fiz.* **1991**, *10*, 204-212.
(4) Clyne, M. A. A.; Cruse, H. W. Atomic resonance fluorescence spectrometry for rate constants of rapid bimolecular reactions Part 1.-Reactions O + NO_2, Cl + ClNO, Br + ClNO. *J. Chem. Soc. Faraday Trans. 2* **1972**, *68*, 1281-1299, doi:10.1039/f29726801281.
(5) Grimley, A. J.; Houston, P. L. The photochemistry of nitrosyl halides: The X + NOX → X_2 + NO(v) reaction (X = Cl, Br). *J. Chem. Phys.* **1980**, *72*, 1471-1475, doi:10.1063/1.439371.
(6) Kita, D.; Stedman, D. H. Kinetic studies of reactions of hydrogen atoms with HCl, Cl_2 and NOCl, and chlorine atoms with H_2 and NOCl. *J. Chem. Soc. Faraday Trans. 2* **1982**, *78*, 1249-1259, doi:10.1039/f29827801249.

(7) Nelson, H. H.; Johnston, H. S. Kinetics of the reaction of Cl with ClNO and $ClNO_2$ and the photochemistry of $ClNO_2$. *J. Phys. Chem.* **1981**, *85*, 3891-3896, doi:10.1021/j150625a036.
(8) Nesbitt, F. L.; Nava, D. F.; Payne, W. A.; Stief, L. J. Absolute rate constant for the reaction of $Cl(^2P)$ with ClNO. *J. Phys. Chem.* **1987**, *91*, 5337-5340, doi:10.1021/j100304a039.

F109. Cl + $ClONO_2$. The recommended Arrhenius parameters are based on the results of Yokelson et al.[3] (195–354 K) and those of Margitan[2] (219–29 K), which are in excellent agreement. The slightly higher values of Kurylo et al.[1] (220–296 K) lie just outside the stated uncertainties. Yokelson et al. report that at 298 K, more than 95% of this reaction proceeds by the reaction channel giving $Cl_2 + NO_3$ as products.
(Table: 10-6, Note: 10-6, Evaluated: 10-6) Back to Table

(1) Kurylo, M. J.; Knable, G. L.; Murphy, J. L. A reinvestigation of the Cl + $ClONO_2$ reaction by flash photolysis resonance fluorescence. *Chem. Phys. Lett.* **1983**, *95*, 9-12, doi:10.1016/0009-2614(83)80800-8.
(2) Margitan, J. J. Chlorine nitrate photochemistry. Photolysis products and kinetics of the reaction Cl + $ClONO_2 \rightarrow Cl_2 + NO_3$. *J. Phys. Chem.* **1983**, *87*, 674-679, doi:10.1021/j100227a029.
(3) Yokelson, R. J.; Burkholder, J. B.; Goldfarb, L.; Fox, R. W.; Gilles, M. K.; Ravishankara, A. R. Temperature dependent rate coefficient for the Cl + $ClONO_2$ reaction. *J. Phys. Chem.* **1995**, *99*, 13976-13983, doi:10.1021/j100038a032.

F110. Cl + CH_3Cl. The recommended k(298 K) is the mean of results of the absolute rate studies of Manning and Kurylo[7] (233–322 K), Beichert et al.[1] (298 K), and Bryukov et al.[2,3] (300–843 K) and the relative rate studies of Wallington et al.[12] (295 K), Beichert et al., Orlando[8] (222–298 K) (two independent determinations), and Sarzyński et al.[10] (298–527 K). The recommended E/R is derived from a fit to the data below 300 K from Manning and Kurylo[7] (233–322 K) and from the two relative rate studies of Orlando after scaling each data set to the recommended value for k(298 K). While the 298 K results reported by Clyne and Walker[4] (300–604 K) are in good agreement, the value of the activation energy derived by these researchers is significantly higher than that recommended, similar to the situation encountered for the Cl + CH_4 reaction. Hence, it is assumed that the discharge flow-mass spectrometric studies of these authors were subject to a systematic error. The E/R obtained between 300 and 400 K by Bryukov et al.,[2,3] from a study primarily focused at higher temperatures, is in good agreement with that recommended here. The early relative rate studies by Pritchard et al.[9] (273–573 K), Goldfinger et al.,[5] Knox,[6] and Tschuikow-Roux et al.,[11] (273–368 K) were not used to derive the recommended parameters since they were performed at temperatures above 298 K and, with the exception of Pritchard et al., yield somewhat higher values for E/R.
(Table: 15-10, Note: 15-10, Evaluated: 15-10) Back to Table

(1) Beichert, P.; Wingen, L.; Lee, J.; Vogt, R.; Ezell, M. J.; Ragains, M.; Neavyn, R.; Finlayson-Pitts, B. J. Rate constants for the reactions of chlorine atoms with some simple alkanes at 298 K: Measurement of a self-consistent set using both absolute and relative rate methods. *J. Phys. Chem.* **1995**, *99*, 13156-13162, doi:10.1021/j100035a018.
(2) Bryukov, M. G.; Slagle, I. R.; Knyazev, V. D. Kinetics of reactions of Cl atoms with methane and chlorinated methanes. *J. Phys. Chem. A* **2002**, *106*, 10532-10542, doi:10.1021/jp0257909.
(3) Bryukov, M. G.; Slagle, I. R.; Knyazev, V. D. Kinetics of reactions of Cl atoms with ethane, chloroethane, and 1,1-dichloroethane. *J. Phys. Chem. A* **2003**, *107*, 6565-6573, doi:10.1021/jp0275138.
(4) Clyne, M. A. A.; Walker, R. F. Absolute rate constants for elementary reactions in the chlorination of CH_4, CD_4, CH_3Cl, CH_2Cl_2, $CHCl_3$, $CDCl_3$ and $CBrCl_3$. *J. Chem. Soc. Faraday Trans. 1* **1973**, *69*, 1547-1567, doi:10.1039/F19736901547.
(5) Goldfinger, P.; Huybrechts, G.; Martens, G. Elementary rate constants in atomic chlorination reactions. Part 2. - Experiments in competitive systems. *Trans. Faraday Soc.* **1961**, *57*, 2210-2219, doi:10.1039/tf9615702210.
(6) Knox, J. H. Application of gas phase partition chromatography to competitive chlorination reactions. *Chemistry and Industry* **1955**, 1631-1632.
(7) Manning, R. G.; Kurylo, M. J. Flash photolysis resonance fluorescence investigation of the temperature dependencies of the reactions of $Cl(^2P)$ atoms with CH_4, CH_3Cl, CH_3F, $CH_3F^{\dagger}$, and C_2H_6. *J. Phys. Chem.* **1977**, *81*, 291-296, doi:10.1021/j100519a003.
(8) Orlando, J. J. Temperature dependence of the rate coefficients for the reaction of chlorine atoms with chloromethanes. *Int. J. Chem. Kinet.* **1999**, *31*, 515-524, doi:10.1029/90JD02734.
(9) Pritchard, H. O.; Pyke, J. B.; Trotman-Dickenson, A. F. The study of chlorine atom reactions in the gas phase. *J. Am. Chem. Soc.* **1955**, *77*, 2629-2633, doi:10.1021/ja01614a088.

(10) Sarzyński, D.; Gola, A. A.; Dryś, A.; Jodkowski, J. T. Kinetic study of the reaction of chlorine atoms with chloromethane in the gas phase. *Chem. Phys. Lett.* **2009**, *476*, 138-142, doi:10/1016/j.cplett.2009.04.086.
(11) Tschuikow-Roux, E.; Faraji, F.; Paddison, S.; Niedzielski, J.; Miyokawa, K. Kinetics of photochlorination of halogen (F, Cl, Br) substituted methanes. *J. Phys. Chem.* **1988**, *92*, 1488-1495, doi:10.1021/j100317a023.
(12) Wallington, T. J.; Andino, J. M.; Ball, J. C.; Japar, S. M. Fourier transform infrared studies of the reaction of C1 atoms with PAN, PPN, CH_3OOH, HCOOH, CH_3COCH_3 and $CH_3COC_2H_5$ at 295 ± 2 K. *J. Atmos. Chem.* **1990**, *10*, 301-313, doi:10.1007/BF00053865.

F111. Cl + CH_2Cl_2. The recommended k(298 K) is an average of the values measured in the relative rate studies of Niki et al.,[7] (298 K), Beichert et al.[1] (298 K), Catoire et al.,[3] and Orlando[8] (222–298 K) (two independent determinations), and in the absolute rate study of Bryukov et al.[2] (293–810 K). For this evaluation, all of the relative rate measurements were recalculated based on the current recommendations for the rate constant of the reference reactions. The recommended value for E/R is derived from the data of Orlando and agrees with a fit to the data of Bryukov et al. (obtained at room temperature and above) up to 400 K. Above 400 K, these latter data increase more rapidly with temperature. The relative rate studies of Goldfinger et al.[5] (298 K), Knox,[6] and Tschuikow-Roux et al.[9] (273–368 K) were performed at temperatures above 298 K and yield significantly higher values for E/R, with the exception of one of the Knox et al. determinations (relative to CH_4), which gives a value of E/R in good agreement with that recommended. The results of Clyne and Walker[4] (300–604 K) are higher than those from any other study and were not used in deriving the recommended parameters. (Table: 06-2, Note: 06-2, Evaluated: 06-2) Back to Table

(1) Beichert, P.; Wingen, L.; Lee, J.; Vogt, R.; Ezell, M. J.; Ragains, M.; Neavyn, R.; Finlayson-Pitts, B. J. Rate constants for the reactions of chlorine atoms with some simple alkanes at 298 K: Measurement of a self-consistent set using both absolute and relative rate methods. *J. Phys. Chem.* **1995**, *99*, 13156-13162, doi:10.1021/j100035a018.
(2) Bryukov, M. G.; Slagle, I. R.; Knyazev, V. D. Kinetics of reactions of Cl atoms with ethane, chloroethane, and 1,1-dichloroethane. *J. Phys. Chem. A* **2003**, *107*, 6565-6573, doi:10.1021/jp0275138.
(3) Catoire, V.; Lesclaux, R.; Schneider, W. F.; Wallington, T. J. Kinetics and mechanisms of the self-reactions of CCl_3O_2 and $CHCl_2O_2$ radicals and their reactions with HO_2. *J. Phys. Chem.* **1996**, *100*, 14356-14371, doi:10.1021/jp960572z.
(4) Clyne, M. A. A.; Walker, R. F. Absolute rate constants for elementary reactions in the chlorination of CH_4, CD_4, CH_3Cl, CH_2Cl_2, $CHCl_3$, $CDCl_3$ and $CBrCl_3$. *J. Chem. Soc. Faraday Trans. 1* **1973**, *69*, 1547-1567, doi:10.1039/F19736901547.
(5) Goldfinger, P.; Huybrechts, G.; Martens, G. Elementary rate constants in atomic chlorination reactions. Part 2. - Experiments in competitive systems. *Trans. Faraday Soc.* **1961**, *57*, 2210-2219, doi:10.1039/tf9615702210.
(6) Knox, J. H. Competitive chlorinations Part 2.-Chloromethanes. *Trans. Faraday Soc.* **1962**, *58*, 275-283, doi:10.1039/tf9625800275.
(7) Niki, H.; Maker, P. D.; Savage, C. M.; Breitenbach, L. P. An FTIR study of the Cl atom-initiated oxidation of CH_2Cl_2 and CH_3Cl. *Int. J. Chem. Kinet.* **1980**, *12*, 1001-1012, doi:10.1002/kin.550121209.
(8) Orlando, J. J. Temperature dependence of the rate coefficients for the reaction of chlorine atoms with chloromethanes. *Int. J. Chem. Kinet.* **1999**, *31*, 515-524, doi:10.1029/90JD02734.
(9) Tschuikow-Roux, E.; Faraji, F.; Paddison, S.; Niedzielski, J.; Miyokawa, K. Kinetics of photochlorination of halogen (F, Cl, Br) substituted methanes. *J. Phys. Chem.* **1988**, *92*, 1488-1495, doi:10.1021/j100317a023.

F112. Cl + $CHCl_3$. The recommended k(298 K) is an average of the values measured in the relative rate studies of Beichert et al.[1] (298 K), Brahan et al.[2] (298 K) (two independent determinations), Catoire et al.,[4] and Orlando[9] (222–298 K) (two independent determinations). The recommended temperature dependence is derived from a fit to the two determinations by Orlando and agrees with a fit to the absolute rate data of Bryukov et al.[3] (obtained at room temperature and above) up to 400 K. Above 400 K, these latter data increase more rapidly with temperature. The room temperature value determined in the relative rate study by Yu and Wijnen[11] (298 K) is a factor of 50 greater than recommended and was not considered in the recommendation. The results of the absolute investigation of Clyne and Walker[5] (300–604 K) are also higher and more scattered than those from most other studies and were not used, nor was the room temperature value derived from the study by Jeoung et al.[7] (298 K), which is more than a factor of two lower than recommended. The relative rate study by Goldfinger et al.[6] performed near 500 K obtained values higher than those in more recent investigations. The

relative rate study of Knox[8] yields a similar temperature dependence to that recommended but with rate constant values systematically lower than other studies. The absolute study by Talhaoui et al.[10] (298–433 K) yielded a 298 K rate constant somewhat lower than recommended and a temperature dependence somewhat higher. For this evaluation, all of the relative rate measurements were recalculated based on the current recommendations for the rate constant of the reference reactions.
(Table: 06-2, Note: 06-2, Evaluated: 06-2) Back to Table

(1) Beichert, P.; Wingen, L.; Lee, J.; Vogt, R.; Ezell, M. J.; Ragains, M.; Neavyn, R.; Finlayson-Pitts, B. J. Rate constants for the reactions of chlorine atoms with some simple alkanes at 298 K: Measurement of a self-consistent set using both absolute and relative rate methods. *J. Phys. Chem.* **1995**, *99*, 13156-13162, doi:10.1021/j100035a018.

(2) Brahan, K. M.; Hewitt, A. D.; Boone, G. D.; Hewitt, S. A. Rate constant for the reaction of Cl with $CHCl_3$. *Int. J. Chem. Kinet.* **1996**, *28*, 397-404, doi:10.1002/(SICI)1097-4601(1996)28:6<397::AID-KIN1>3.0.CO;2-Q.

(3) Bryukov, M. G.; Slagle, I. R.; Knyazev, V. D. Kinetics of reactions of Cl atoms with ethane, chloroethane, and 1,1-dichloroethane. *J. Phys. Chem. A* **2003**, *107*, 6565-6573, doi:10.1021/jp0275138.

(4) Catoire, V.; Lesclaux, R.; Schneider, W. F.; Wallington, T. J. Kinetics and mechanisms of the self-reactions of CCl_3O_2 and $CHCl_2O_2$ radicals and their reactions with HO_2. *J. Phys. Chem.* **1996**, *100*, 14356-14371, doi:10.1021/jp960572z.

(5) Clyne, M. A. A.; Walker, R. F. Absolute rate constants for elementary reactions in the chlorination of CH_4, CD_4, CH_3Cl, CH_2Cl_2, $CHCl_3$, $CDCl_3$ and $CBrCl_3$. *J. Chem. Soc. Faraday Trans. 1* **1973**, *69*, 1547-1567, doi:10.1039/F19736901547.

(6) Goldfinger, P.; Huybrechts, G.; Martens, G. Elementary rate constants in atomic chlorination reactions. Part 2. - Experiments in competitive systems. *Trans. Faraday Soc.* **1961**, *57*, 2210-2219, doi:10.1039/tf9615702210.

(7) Jeoung, S. C.; Choo, K. Y.; Benson, S. W. Very low pressure reactor chemiluminescence studies on N atom reactions with $CHCl_3$ and $CDCl_3$. *J. Phys. Chem.* **1991**, *95*, 7282-7290, doi:10.1021/j100172a035.

(8) Knox, J. H. Competitive chlorinations Part 2.-Chloromethanes. *Trans. Faraday Soc.* **1962**, *58*, 275-283, doi:10.1039/tf9625800275.

(9) Orlando, J. J. Temperature dependence of the rate coefficients for the reaction of chlorine atoms with chloromethanes. *Int. J. Chem. Kinet.* **1999**, *31*, 515-524, doi:10.1029/90JD02734.

(10) Talhaoui, A.; Louis, F.; Meriaux, B.; Devolder, P.; Sawerysyn, J.-P. Temperature dependence of rate coefficients for the reactions of chlorine atoms with halomethanes of type $CHCl_{3-x}F_x$ (x = 0, 1, and 2). *J. Phys. Chem.* **1996**, *100*, 2107-2113, doi:10.1021/jp951814i.

(11) Yu, W. H. S.; Wijnen, M. H. J. Photolysis of chloroform in the presence of ethane at 25°C. *J. Chem. Phys.* **1970**, *52*, 2736-2739, doi:10.1063/1.1673626.

F113. Cl + CH_3F (HFC-41). The recommended k(298 K) is an average of the values from the absolute rate studies of Manning and Kurylo[2] (216–296 K) and Hitsuda et al.[1] (298 K) and the relative rate studies of Tschuikow-Roux et al.[3] (273–368 K), Tuazon et al.[4] (298 K), and Wallington et al.[5] (298 K). The recommended value for E/R is based on the study of Tschuikow-Roux et al. conducted at room temperature and above. However, in formulating this recommendation for E/R, the reported temperature dependence of Tschuikow-Roux et al. was reduced slightly (by approximately 100 K) to account for what appears to be a small systematic difference between the activation energies obtained in their similar investigations of the Cl + CH_3Cl and Cl + CH_3Br reactions above room temperature and the recommendations that are based on data at 300 K and below. The temperature dependence reported by Manning and Kurylo is significantly lower, seemingly due to a shift in their data below 250 K. This lower value of E/R is not consistent with the recommended values of E/R for Cl + CH_3Cl and Cl + CH_3Br when compared with those for OH + CH_3F, OH + CH_3Cl, and OH + CH_3Br. Hence, it appears that the Manning and Kurylo data may have been influenced by some systematic error at the lower temperatures.
(Table: 06-2, Note: 06-2, Evaluated: 06-2) Back to Table

(1) Hitsuda, K.; Takahashi, K.; Matsumi, Y.; Wallington, T. J. Kinetics of the reactions of Cl($^2P_{1/2}$) and Cl($^2P_{3/2}$) atoms with C_2H_6, C_2D_6, CH_3F, C_2H_5F, and CH_3CF_3 at 298 K. *J. Phys. Chem. A* **2001**, *105*, 5131-5136, doi:10.1021/jp003222s.

(2) Manning, R. G.; Kurylo, M. J. Flash photolysis resonance fluorescence investigation of the temperature dependencies of the reactions of Cl(^2P) atoms with CH_4, CH_3Cl, CH_3F, $CH_3F^{\dagger}$, and C_2H_6. *J. Phys. Chem.* **1977**, *81*, 291-296, doi:10.1021/j100519a003.

(3) Tschuikow-Roux, E.; Faraji, F.; Paddison, S.; Niedzielski, J.; Miyokawa, K. Kinetics of photochlorination of halogen (F, Cl, Br) substituted methanes. *J. Phys. Chem.* **1988**, *92*, 1488-1495, doi:10.1021/j100317a023.
(4) Tuazon, E. C.; Atkinson, R.; Corchnoy, S. B. Rate constants for the gas-phase reactions of Cl atoms with a series of hydrofluorocarbons and hydrochlorofluorocarbons at 298 ± 2 K. *Int. J. Chem. Kinet.* **1992**, *24*, 639-648, doi:10.1002/kin.550240704
(5) Wallington, T. J.; Ball, J. C.; Nielsen, O. J.; Bartkiewicz, E. Spectroscopic, kinetic, and mechanistic study of CH_2FO_2 radicals in the gas phase at 298 K. *J. Phys. Chem.* **1992**, *96*, 1241-1246, doi:10.1021/j100182a041.

F114. Cl + CH_2F_2 (HFC-32). The recommended k(298 K) is an average of the values from the relative rate study of Nielsen et al.[1] (298 K) and from an Arrhenius fit to the relative rate data of Nilsson et al.[2] (253–553 K) obtained in two independent studies, all recalculated using the rate constant for the reference reaction (Cl + CH_4) recommended in this evaluation. The recommended value for E/R is obtained from a fit to the data of Nilsson et al. below 410 K. The rate constants determined in the relative rate study of Tschuikow-Roux et al.[3] (281–368 K) lie systematically higher than those of Nielsen et al. and Nilsson et al. but yield a temperature dependence similar to that recommended here.
(Table: 15-10, Note: 15-10, Evaluated: 15-10) Back to Table

(1) Nielsen, O. J.; Ellermann, T.; Bartkiewicz, E.; Wallington, T. J.; Hurley, M. D. UV absorption spectra, kinetics and mechanisms of the self-reaction of CHF_2O_2 radicals in the gas phase at 298 K. *Chem. Phys. Lett.* **1992**, *192*, 82-88, doi:10.1016/0009-2614(92)85432-A.
(2) Nilsson, E. J. K.; Johnson, M. S.; Nielsen, O. J.; Kaiser, E. W.; Wallington, T. J. Kinetics of the gas-phase reactions of chlorine atoms with CH_2F_2, CH_3CCl_3, and CF_3CFH_2 over the temperature range 253-553 K. *Int. J. Chem Kinet.* **2009**, *41*, 401-406, doi:10.1002/kin.20398.
(3) Tschuikow-Roux, E.; Yano, T.; Niedzielski, J. Reactions of ground state chlorine atoms with fluorinated methanes and ethanes. *J. Chem. Phys.* **1985**, *82*, 65-74, doi:10.1063/1.448737.

F115. Cl + CHF_3 (HFC-23). The recommended upper-limit for k(298 K) is based on results from the absolute rate study by Jourdain et al.[2] Results from the relative rate study by Coomber and Whittle[1] yield an upper limit that is a factor of 50 smaller.
(Table: 06-2, Note: 15-10, Evaluated: 06-2) Back to Table

(1) Coomber, J. W.; Whittle, E. Photochlorination of methane and fluoroform Dissociation energy D(CF_3-H) and entropy of CF_3 radical. *Trans. Faraday Soc.* **1966**, *62*, 2183-2190, doi:10.1039/tf9666202183.
(2) Jourdain, J. L.; Poulet, G.; Barassin, J.; Le Bras, G.; Combourieu, J. Mecanismes chimiques de la pollution atmospherique par les composes halogenes: etude cinetique de reactions elementaires possibles. *Pollut. Atmos.* **1977**, *75*, 256-259.

F116. Cl + CH_2FCl (HCFC-31). The recommended value for k(298 K) is an average of the room temperature results from the absolute rate study by Jourdain et al.[1] and the relative rate studies by Tuazon et al.[3] (298 K) and Wallington et al.[4] (295 K). The temperature dependence is estimated from a comparison among the Cl and OH reactions with CH_2F_2, CH_2Cl_2, and CH_2FCl. The recommended value of E/R (essentially the same as that for the OH + CH_2FCl reaction) is slightly lower than that determined by Tschuikow-Roux et al.[2] (273–368 K), recalculated based on the current recommendation for the rate constant of the reference reaction (Cl + CH_4). However, as discussed for other Cl + halomethane reactions, there appears to be a small systematic overestimation in the temperature dependences determined by these authors.
(Table: 06-2, Note: 06-2, Evaluated: 06-2) Back to Table

(1) Jourdain, J. L.; Poulet, G.; Barassin, J.; Le Bras, G.; Combourieu, J. Mecanismes chimiques de la pollution atmospherique par les composes halogenes: etude cinetique de reactions elementaires possibles. *Pollut. Atmos.* **1977**, *75*, 256-259.
(2) Tschuikow-Roux, E.; Faraji, F.; Paddison, S.; Niedzielski, J.; Miyokawa, K. Kinetics of photochlorination of halogen (F, Cl, Br) substituted methanes. *J. Phys. Chem.* **1988**, *92*, 1488-1495, doi:10.1021/j100317a023.
(3) Tuazon, E. C.; Atkinson, R.; Corchnoy, S. B. Rate constants for the gas-phase reactions of Cl atoms with a series of hydrofluorocarbons and hydrochlorofluorocarbons at 298 ± 2 K. *Int. J. Chem. Kinet.* **1992**, *24*, 639-648, doi:10.1002/kin.550240704
(4) Wallington, T. J.; Hurley, M. D.; Schneider, W. F.; Sehested, J.; Nielsen, O. J. Mechanistic study of the gas-phase reaction of CH_2FO_2 radicals with HO_2. *Chem. Phys. Lett.* **1994**, *218*, 34-42, doi:10.1016/0009-2614(93)E1466-T.

F117. Cl + $CHFCl_2$ (HCFC-21). The recommended k(298 K) is the average of the results from the relative rate study of Tuazon et al.[4] (298 K) and the absolute rate study of Talhaoui et al.[3] (298–433 K). These results are preferred over the earlier room temperature results of Glavas and Heicklen.[1] (298 K). The room temperature value of Jourdain et al.[2] is approximately 50% higher than the recommendation. The recommended value for E/R is derived from the data of Talhaoui et al.
(Table: 06-2, Note: 06-2, Evaluated: 06-2) Back to Table

(1) Glavas, S.; Heicklen, J. Reactivity of chlorine atoms with NO, NO_2 and $HCCl_2F$ at room temperature and atmospheric pressure. *J. Photochem.* **1985**, *31*, 21-28, doi:10.1016/0047-2670(85)85070-X.
(2) Jourdain, J. L.; Poulet, G.; Barassin, J.; Le Bras, G.; Combourieu, J. Mecanismes chimiques de la pollution atmospherique par les composes halogenes: etude cinetique de reactions elementaires possibles. *Pollut. Atmos.* **1977**, *75*, 256-259.
(3) Talhaoui, A.; Louis, F.; Meriaux, B.; Devolder, P.; Sawerysyn, J.-P. Temperature dependence of rate coefficients for the reactions of chlorine atoms with halomethanes of type $CHCl_{3-x}F_x$ (x = 0, 1, and 2). *J. Phys. Chem.* **1996**, *100*, 2107-2113, doi:10.1021/jp951814i.
(4) Tuazon, E. C.; Atkinson, R.; Corchnoy, S. B. Rate constants for the gas-phase reactions of Cl atoms with a series of hydrofluorocarbons and hydrochlorofluorocarbons at 298 ± 2 K. *Int. J. Chem. Kinet.* **1992**, *24*, 639-648, doi:10.1002/kin.550240704

F118. Cl + CHF_2Cl (HCFC-22). The recommended k(298 K) is the mean of the values derived in the relative rate studies of Tuazon et al.[5] (298 K) and Sokolov et al.[3] (298 K) and in the absolute rate studies of Jourdain et al.[1] and Talhaoui et al.[4] (296–411 K) (which is assumed to supersede the earlier study by Sawerysyn et al.[2]). The recommended E/R is derived from the data reported by Talhaoui et al.
(Table: 15-10, Note: 15-10, Evaluated: 15-10) Back to Table

(1) Jourdain, J. L.; Poulet, G.; Barassin, J.; Le Bras, G.; Combourieu, J. Mecanismes chimiques de la pollution atmospherique par les composes halogenes: etude cinetique de reactions elementaires possibles. *Pollut. Atmos.* **1977**, *75*, 256-259.
(2) Sawerysyn, J. P.; Talhaoui, A.; Meriaux, B.; Devolder, P. Absolute rate constants for elementary reactions between chlorine atoms and CHF_2Cl, CH_3CFCl_2, CH_3CF_2Cl and CH_2FCF_3 at 297 ± 2 K. *Chem. Phys. Lett.* **1992**, *198*, 197-199, doi:10.1016/0009-2614(92)90071-T.
(3) Sokolov, O.; Hurley, M. D.; Wallington, T. J.; Kaiser, E. W.; Platz, J.; Nielsen, O. J.; Berho, F.; Rayez, M.-T.; Lesclaux, R. Kinetics and mechanism of the gas-phase reaction of Cl atoms with benzene. *J. Phys. Chem. A* **1998**, *102*, 10671-10681, doi:10.1021/jp9828080.
(4) Talhaoui, A.; Louis, F.; Meriaux, B.; Devolder, P.; Sawerysyn, J.-P. Temperature dependence of rate coefficients for the reactions of chlorine atoms with halomethanes of type $CHCl_{3-x}F_x$ (x = 0, 1, and 2). *J. Phys. Chem.* **1996**, *100*, 2107-2113, doi:10.1021/jp951814i.
(5) Tuazon, E. C.; Atkinson, R.; Corchnoy, S. B. Rate constants for the gas-phase reactions of Cl atoms with a series of hydrofluorocarbons and hydrochlorofluorocarbons at 298 ± 2 K. *Int. J. Chem. Kinet.* **1992**, *24*, 639-648, doi:10.1002/kin.550240704

F119. Cl + CH_3CCl_3. The recommended k(298 K) is an average of the results from the absolute rate study by Talhaoui et al.[4] (298–418 K) and the relative rate studies of Platz et al.[3] (296 K) and Nilsson et al.[2] (253–313 K), both recalculated using the rate constant for the reference reaction (Cl + CH_4) recommended in this evaluation. The recommended value for E/R is derived from a combined fit to the data of Talhaoui et al. and Nilsson et al. for T <400 K after scaling each data set to the recommended value for k(298 K). The results obtained by Cillien et al.[1] (323–423 K) in a relative rate study conducted over a very narrow temperature range above room temperature are encompassed by the recommended 2σ uncertainty. The results of the relative rate study of Tschuikow-Roux et al.[5] (281–368 K), although exhibiting a similar temperature dependence, lie systematically higher than the results of all other investigations.
(Table: 15-10, Note: 15-10, Evaluated: 15-10) Back to Table

(1) Cillien, C.; Goldfinger, P.; Huybrechts, G.; Martens, G. Hydrogen abstraction from chlorinated ethanes by chlorine atoms. *Trans. Faraday Soc.* **1967**, *63*, 1631-1635, doi:10.1039/TF9676301631.
(2) Nilsson, E. J. K.; Johnson, M. S.; Nielsen, O. J.; Kaiser, E. W.; Wallington, T. J. Kinetics of the gas-phase reactions of chlorine atoms with CH_2F_2, CH_3CCl_3, and CF_3CFH_2 over the temperature range 253-553 K. *Int. J. Chem Kinet.* **2009**, *41*, 401-406, doi:10.1002/kin.20398.
(3) Platz, J.; Nielson, O. J.; Sehested, J.; Wallington, T. J. Atmospheric chemistry of l,l,l-trichloroethane: UV absorption spectra and self-reaction kinetics of CCl_3CH_2 and $CCl_3CH_2O_2$ radicals, kinetics of the

reactions of the $CCl_3CH_2O_2$ Radical with NO and NO_2, and the fate of the alkoxy radical CCl_3CH_2O. *J. Phys. Chem.* **1995**, *99*, 6570-6579, doi:10.1021/j100017a044.
(4) Talhaoui, A.; Louis, F.; Devolder, P.; Meriaux, B.; Sawerysyn, J. P.; Rayez, M. T.; Rayez, J. C. Rate coefficients of the reactions of chlorine atoms with haloethanes of type $CH_3CCl_{3-x}F_x$ (x = 0, 1, and 2): Experimental and ab initio theoretical studies. *J. Phys. Chem.* **1996**, *100*, 13531-13538, doi:10.1021/jp9603243.
(5) Tschuikow-Roux, E.; Yano, T.; Niedzielski, J. Reactions of ground state chlorine atoms with fluorinated methanes and ethanes. *J. Chem. Phys.* **1985**, *82*, 65-74, doi:10.1063/1.448737.

F120. Cl + CH_3CH_2F (HFC-161). The recommended values for both k(298 K) and E/R for each of the two reaction channels are averages of the individual values derived in the relative rate studies of Cadman et al.[1] (281–368 K), Martens et al.[3] (254–333 K), and Tschuikow-Roux et al.[4] (281–368 K), with each recalculated based on the current recommendation for the rate constant of the reference reaction. The value for k(298 K) of the total reaction obtained from a sum of the two channels is in excellent agreement with the value obtained in the absolute rate study by Hitsuda et al.[2] (298 K). The parameters for the total reaction are:

$$A = 2.28 \times 10^{-11} \text{ cm}^3 \text{ molecule}^{-1} \text{ s}^{-1}$$
$$E/R = 370 \text{ K}$$
$$k(298 \text{ K}) = 6.6 \times 10^{-12} \text{ cm}^3 \text{ molecule}^{-1} \text{ s}^{-1}$$
$$f(298 \text{ K}) = 1.1$$
$$g = 100$$

(Table: 06-2, Note: 06-2, Evaluated: 06-2) Back to Table

(1) Cadman, P.; Kirk, A. W.; Trotman-Dickenson, A. F. Reactions of chlorine atoms with ethane, propane, isobutane, fluoroethane, 1,1-difluoroethane, 1,1,1-trifluoroethane and cyclopropane. *J. Chem. Soc. Faraday Trans. 1* **1976**, *72*, 1027-1032, doi:10.1039/f19767201027.
(2) Hitsuda, K.; Takahashi, K.; Matsumi, Y.; Wallington, T. J. Kinetics of the reactions of $Cl(^2P_{1/2})$ and $Cl(^2P_{3/2})$ atoms with C_2H_6, C_2D_6, CH_3F, C_2H_5F, and CH_3CF_3 at 298 K. *J. Phys. Chem. A* **2001**, *105*, 5131-5136, doi:10.1021/jp003222s.
(3) Martens, G. J.; Godfroid, M.; Delvaux, J.; Verbeyst, J. Gas-phase hydrogen abstraction from asymmetrically halogenated ethanes by chlorine atoms. *Int. J. Chem. Kinet.* **1976**, *8*, 153-158, doi:10.1002/kin.550080116.
(4) Tschuikow-Roux, E.; Yano, T.; Niedzielski, J. Reactions of ground state chlorine atoms with fluorinated methanes and ethanes. *J. Chem. Phys.* **1985**, *82*, 65-74, doi:10.1063/1.448737.

F121. Cl + CH_3CHF_2 (HFC-152a). The recommended values for k(298 K) for each of the two reaction channels are based on an average of the individual values from the relative rate studies of Cadman et al.[1] (281–368 K), Martens et al.[2] (254–333 K) and Yano and Tschuikow-Roux[6] (283–357 K) (with each recalculated based on the current recommendation for the rate constant of the appropriate reference reaction). The sum of these average values of k(298 K) for the two channels is 2.4×10^{-13} cm^3 molecule^{-1} s^{-1}. However, a more reliable value for $k(298 \text{ K}) = 2.5 \times 10^{-13}$ cm^3 molecule^{-1} s^{-1}for the overall reaction can be obtained from an average of the results from the relative rate studies of Wallington and Hurley[5] (295 K), Tuazon et al.[4] (298 K), and Taketani et al.[3] (295 K) and from the absolute study of Taketani et al.[3] Therefore, for consistency with the total rate constant recommendation, k(298 K) for each channel was scaled by a factor 1.04 (i.e., 2.5/2.4) to obtain the recommended values given in Table 1. The recommended value for E/R for each channel is an average of those determined by Cadman et al., Martens et al., and Yano and Tschuikow-Roux. There are no available experimental data on the temperature dependence of the rate constant of the total reaction. A simulated fit to the sum of the rate constants recommended for individual channels yields $E/R = 970$ K, which is recommended here. Thus, the recommended parameters for the total reaction are:

$$A = 6.5 \times 10^{-12} \text{ cm}^3 \text{ molecule}^{-1} \text{ s}^{-1}$$
$$E/R = 970 \text{ K}$$
$$k(298 \text{ K}) = 2.5 \times 10^{-13} \text{ cm}^3 \text{ molecule}^{-1} \text{ s}^{-1}$$
$$f(298 \text{ K}) = 1.1$$
$$g = 100$$

(Table: 15-10, Note: 15-10, Evaluated: 15-10) Back to Table

(1) Cadman, P.; Kirk, A. W.; Trotman-Dickenson, A. F. Reactions of chlorine atoms with ethane, propane, isobutane, fluoroethane, 1,1-difluoroethane, 1,1,1-trifluoroethane and cyclopropane. *J. Chem. Soc. Faraday Trans. 1* **1976**, *72*, 1027-1032, doi:10.1039/f19767201027.
(2) Martens, G. J.; Godfroid, M.; Delvaux, J.; Verbeyst, J. Gas-phase hydrogen abstraction from asymmetrically halogenated ethanes by chlorine atoms. *Int. J. Chem. Kinet.* **1976**, *8*, 153-158, doi:10.1002/kin.550080116.

(3) Taketani, F.; Nakayama, T.; Takahashi, K.; Matsumi, Y.; Hurley, M. D.; Wallington, T. J.; Toft, A.; Sulbaek Andersen, M. P. Atmospheric chemistry of CH_3CHF_2 (HFC-152a): Kinetics, mechanisms, and products of Cl atom- and OH radical-initiated oxidation in the presence and absence of NO_x. *J. Phys. Chem. A* **2005**, *109*, 9061-9069, doi:10.1021/jp044218+.
(4) Tuazon, E. C.; Atkinson, R.; Corchnoy, S. B. Rate constants for the gas-phase reactions of Cl atoms with a series of hydrofluorocarbons and hydrochlorofluorocarbons at 298 ± 2 K. *Int. J. Chem. Kinet.* **1992**, *24*, 639-648, doi:10.1002/kin.550240704
(5) Wallington, T. J.; Hurley, M. D. A kinetic study of the reaction of chlorine atoms with CF_3CHCl_2, CF_3CH_2F, $CFCl_2CH_3$, CF_2ClCH_3, CHF_2CH_3, CH_3D, CH_2D_2, CHD_3, CD_4, and CD_3Cl at 295 ± 2 K. *Chem. Phys. Lett.* **1992**, *189*, 437-442, doi:10.1016/0009-2614(92)85228-3.
(6) Yano, T.; Tschuikow-Roux, E. Competitive photochlorination of the fluoroethanes CH_3CHF_2, CH_2FCH_2F and CHF_2CHF_2. *J. Photochem.* **1986**, *32*, 25-37, doi:10.1016/0047-2670(86)85004-3.

F122. Cl + CH_2FCH_2F (HFC-152). The recommended k(298 K) is an average of the values derived in the relative rate studies of Yano and Tschuikow-Roux[2] (283–357 K) and Wallington et al.[1] (296 K) (two determinations), after recalculating each one based on the current recommendation for the rate constant of the appropriate reference reaction. The recommended temperature dependence was determined from a fit to the data of Yano and Tschuikow-Roux, which were obtained at room temperature and above. The temperature dependence may exhibit curvature below room temperature, similar to that for OH + CH_2FCH_2F. Such curvature is most probably encompassed by the assigned uncertainty parameters.
(Table: 06-2, Note: 06-2, Evaluated: 06-2) Back to Table

(1) Wallington, T. J.; Hurley, M. D.; Ball, J. C.; Ellerman, T.; Nielsen, O. J.; Sehested, J. Atmospheric chemistry of HFC-152: UV absorption spectrum of CH_2FCFHO_2 radicals, kinetics of the reaction $CH_2FCFHO_2 + NO \rightarrow CH_2FCHFO + NO_2$, and fate of the alkoxy radical CH_2FCFHO. *J. Phys. Chem.* **1994**, *98*, 5435-5440, doi:10.1021/j100072a008.
(2) Yano, T.; Tschuikow-Roux, E. Competitive photochlorination of the fluoroethanes CH_3CHF_2, CH_2FCH_2F and CHF_2CHF_2. *J. Photochem.* **1986**, *32*, 25-37, doi:10.1016/0047-2670(86)85004-3.

F123. Cl + CH_3CFCl_2 (HCFC-141b). The recommended k(298 K) is an average of the values derived in the absolute rate studies of Talhaoui et al.[2] (299–429 K) and Warren and Ravishankara[5] (298–397 K) and in the relative rate studies of Wallington and Hurley[4] (295 K) and Tuazon et al.[3] (298 K). The room temperature results of Talhaoui et al. are assumed to supersede those of Sawerysyn et al.[1] The recommended E/R is derived from the data of Talhaoui et al. The data of Warren and Ravishankara above room temperature exhibit considerable scatter, apparently due to Cl atom regeneration from decomposition of the radical product (CH_2-$CFCl_2$). Hence, this study was not used in deriving the recommended temperature dependence.
(Table: 15-10, Note: 15-10, Evaluated: 15-10) Back to Table

(1) Sawerysyn, J. P.; Talhaoui, A.; Meriaux, B.; Devolder, P. Absolute rate constants for elementary reactions between chlorine atoms and CHF_2Cl, CH_3CFCl_2, CH_3CF_2Cl and CH_2FCF_3 at 297 ± 2 K. *Chem. Phys. Lett.* **1992**, *198*, 197-199, doi:10.1016/0009-2614(92)90071-T.
(2) Talhaoui, A.; Louis, F.; Devolder, P.; Meriaux, B.; Sawerysyn, J. P.; Rayez, M. T.; Rayez, J. C. Rate coefficients of the reactions of chlorine atoms with haloethanes of type $CH_3CCl_{3-x}F_x$ (x = 0, 1, and 2): Experimental and ab initio theoretical studies. *J. Phys. Chem.* **1996**, *100*, 13531-13538, doi:10.1021/jp9603243.
(3) Tuazon, E. C.; Atkinson, R.; Corchnoy, S. B. Rate constants for the gas-phase reactions of Cl atoms with a series of hydrofluorocarbons and hydrochlorofluorocarbons at 298 ± 2 K. *Int. J. Chem. Kinet.* **1992**, *24*, 639-648, doi:10.1002/kin.550240704
(4) Wallington, T. J.; Hurley, M. D. A kinetic study of the reaction of chlorine atoms with CF_3CHCl_2, CF_3CH_2F, $CFCl_2CH_3$, CF_2ClCH_3, CHF_2CH_3, CH_3D, CH_2D_2, CHD_3, CD_4, and CD_3Cl at 295 ± 2 K. *Chem. Phys. Lett.* **1992**, *189*, 437-442, doi:10.1016/0009-2614(92)85228-3.
(5) Warren, R. F.; Ravishankara, A. R. Kinetics of $Cl(^2P)$ reactions with CF_3CHCl_2, CF_3CHFCl, and CH_3CFCl_2. *Int. J. Chem. Kinet.* **1993**, *25*, 833-844, doi:10.1002/kin.550251005.

F124. Cl + CH_3CF_2Cl (HCFC-142b). The recommended value for k(298 K) is an average of the results of the relative rate studies of Wallington and Hurley[5] (295 K) and Tuazon et al.[4] (298 K), both recalculated based on the current recommendation for the rate constant of the reference reaction (Cl + CH_4), and the absolute rate studies of Jourdain et al.[1] (298 K) and Talhaoui et al.[3] (296–438 K). The Talhaoui et al. study is assumed to supersede the earlier study by Sawerysyn et al.[2] The recommended temperature dependence is derived from the data of Talhaoui et al.
(Table: 06-2, Note: 06-2, Evaluated: 06-2) Back to Table

(1) Jourdain, J. L.; Poulet, G.; Barassin, J.; Le Bras, G.; Combourieu, J. Mecanismes chimiques de la pollution atmospherique par les composes halogenes: etude cinetique de reactions elementaires possibles. *Pollut. Atmos.* **1977**, *75*, 256-259.
(2) Sawerysyn, J. P.; Talhaoui, A.; Meriaux, B.; Devolder, P. Absolute rate constants for elementary reactions between chlorine atoms and CHF_2Cl, CH_3CFCl_2, CH_3CF_2Cl and CH_2FCF_3 at 297 ± 2 K. *Chem. Phys. Lett.* **1992**, *198*, 197-199, doi:10.1016/0009-2614(92)90071-T.
(3) Talhaoui, A.; Louis, F.; Devolder, P.; Meriaux, B.; Sawerysyn, J. P.; Rayez, M. T.; Rayez, J. C. Rate coefficients of the reactions of chlorine atoms with haloethanes of type $CH_3CCl_{3-x}F_x$ (x = 0, 1, and 2): Experimental and ab initio theoretical studies. *J. Phys. Chem.* **1996**, *100*, 13531-13538, doi:10.1021/jp9603243.
(4) Tuazon, E. C.; Atkinson, R.; Corchnoy, S. B. Rate constants for the gas-phase reactions of Cl atoms with a series of hydrofluorocarbons and hydrochlorofluorocarbons at 298 ± 2 K. *Int. J. Chem. Kinet.* **1992**, *24*, 639-648, doi:10.1002/kin.550240704
(5) Wallington, T. J.; Hurley, M. D. A kinetic study of the reaction of chlorine atoms with CF_3CHCl_2, CF_3CH_2F, $CFCl_2CH_3$, CF_2ClCH_3, CHF_2CH_3, CH_3D, CH_2D_2, CHD_3, CD_4, and CD_3Cl at 295 ± 2 K. *Chem. Phys. Lett.* **1992**, *189*, 437-442, doi:10.1016/0009-2614(92)85228-3.

F125. Cl + CH_3CF_3 (HFC-143a). The recommended value of k(298 K) is an average of the values from the relative rate studies of Tschuikow-Roux et al.[3] (281–368 K) and Nielsen et al.[2] (296 K), both recalculated based on the current recommendation for the rate constant of the reference reaction (Cl + CH_4). The recommended value for E/R is based on an Arrhenius fit of the relative rate data of Tschuikow-Roux et al., recalculated using the three-parameter fit for the Cl + CH_4 reaction given in the current recommendation. An upper limit for k(298 K) derived by Hitsuda et al.[1] (298 K) is more than two orders of magnitude larger than the recommended value. (Table: 15-10, Note: 15-10, Evaluated: 15-10) Back to Table

(1) Hitsuda, K.; Takahashi, K.; Matsumi, Y.; Wallington, T. J. Kinetics of the reactions of Cl($^2P_{1/2}$) and Cl($^2P_{3/2}$) atoms with C_2H_6, C_2D_6, CH_3F, C_2H_5F, and CH_3CF_3 at 298 K. *J. Phys. Chem. A* **2001**, *105*, 5131-5136, doi:10.1021/jp003222s.
(2) Nielsen, O. J.; Gamborg, E.; Sehested, J.; Wallington, T. J.; Hurley, M. D. Atmospheric chemistry of HFC-143a: Spectrokinetic investigation of the $CF_3CH_2O_2$• radical, its reactions with NO and NO_2, and the fate of CF_3CH_2O. *J. Phys. Chem.* **1994**, *98*, 9518-9525, doi:10.1021/j100089a026.
(3) Tschuikow-Roux, E.; Yano, T.; Niedzielski, J. Reactions of ground state chlorine atoms with fluorinated methanes and ethanes. *J. Chem. Phys.* **1985**, *82*, 65-74, doi:10.1063/1.448737.

F126. Cl + CH_2FCHF_2 (HFC-143). The recommended values for k(298 K) and E/R for each of the two reaction channels are based on results of the relative rate study of Tschuikow-Roux et al.[1] (281–368 K), recalculated based on the current recommendation for the rate constant of the reference reaction (Cl + CH_4). The recommended parameters for the total reaction are derived from the sum of the recommended rate expressions for the two reaction channels. The parameters for the total reaction are:

$$A = 1.57 \times 10^{-11} \text{ cm}^3 \text{ molecule}^{-1} \text{ s}^{-1}$$
$$E/\text{R} = 1720 \text{ K}$$
$$k(298 \text{ K}) = 4.9 \times 10^{-14}$$
$$f(298 \text{ K}) = 1.3$$
$$g = 200$$

(Table: 06-2, Note: 06-2, Evaluated: 06-2) Back to Table

(1) Tschuikow-Roux, E.; Yano, T.; Niedzielski, J. Reactions of ground state chlorine atoms with fluorinated methanes and ethanes. *J. Chem. Phys.* **1985**, *82*, 65-74, doi:10.1063/1.448737.

F127. Cl + CH_2ClCF_3 (HCFC-133a). The recommended value for k(298 K) is an average of the results from the absolute rate study of Jourdain et al.[1] (298–500 K) and the relative rate study of Mogelberg et al.[2] (296 K) (two determinations). The recommended value for E/R is derived from the data of Jourdain et al. (Table: 06-2, Note: 06-2, Evaluated: 06-2) Back to Table

(1) Jourdain, J. L.; Le Bras, G.; Combourieu, J. Étude cinétique des réactions du 1,1,1 trifluoro 2 chloroéthane avec les atomes de chlore et d'oxygène. *J. Chim. Phys.* **1978**, *75*, 318-323, doi:10.1051/jcp/1978750318.
(2) Mogelberg, T. E.; Nielsen, O. J.; Sehested, J.; Wallington, T. J. Atmospheric chemistry of HCFC-133a: the UV absorption spectra of CF_3CClH and CF_3CClHO_2 radicals, reactions of CF_3CClHO_2 with NO and NO_2, and fate of CF_3CClHO radicals. *J. Phys. Chem.* **1995**, *99*, 13437-13444, doi:10.1021/j100036a018.

F128. Cl + CH_2FCF_3 (HFC-134a). The recommended value for k(298 K) is an average of the results from the relative rate studies of Wallington and Hurley[6] (295 K), Tuazon et al.[5] (298 K), Kaiser[1] (263–365 K), and Nilsson et al.[3] (253– 313 K) (all recalculated using the current recommendations for the reference reactions) and from the absolute rate study of Louis et al.,[2] which is assumed to supersede the earlier study by Sawerysyn et al.[4] The recommended value for E/R is derived from a combined fit to the data of Kaiser et al., Louis et al., and Nilsson et al. below 400 K after scaling each data set to the recommended value for k(298 K).
(Table: 15-10, Note: 15-10, Evaluated: 15-10) Back to Table

(1) Kaiser, E. W. Relative rate constants for reactions of HFC 152a, 143, 143a, 134a, and HCFC 124 with F or Cl atoms and for CF_2CH_3, CF_2HCH_2, and CF_3CFH radicals with F_2, Cl_2, and O_2. *Int. J. Chem. Kinet.* **1993**, *25*, 667-680, doi:10.1002/kin.550250807

(2) Louis, F.; Talhaoui, A.; Sawerysyn, J.-P.; Rayez, M.-T.; Rayez, J.-C. Rate coefficients for the gas phase reactions of CF_3CH_2F (HFC-134a) with chlorine and fluorine atoms: experimental and ab initio theoretical studies. *J. Phys. Chem. A* **1997**, *101*, 8503-8507, doi:10.1021/jp972001s.

(3) Nilsson, E. J. K.; Johnson, M. S.; Nielsen, O. J.; Kaiser, E. W.; Wallington, T. J. Kinetics of the gas-phase reactions of chlorine atoms with CH_2F_2, CH_3CCl_3, and CF_3CFH_2 over the temperature range 253-553 K. *Int. J. Chem Kinet.* **2009**, *41*, 401-406, doi:10.1002/kin.20398.

(4) Sawerysyn, J. P.; Talhaoui, A.; Meriaux, B.; Devolder, P. Absolute rate constants for elementary reactions between chlorine atoms and CHF_2Cl, CH_3CFCl_2, CH_3CF_2Cl and CH_2FCF_3 at 297 ± 2 K. *Chem. Phys. Lett.* **1992**, *198*, 197-199, doi:10.1016/0009-2614(92)90071-T.

(5) Tuazon, E. C.; Atkinson, R.; Corchnoy, S. B. Rate constants for the gas-phase reactions of Cl atoms with a series of hydrofluorocarbons and hydrochlorofluorocarbons at 298 ± 2 K. *Int. J. Chem. Kinet.* **1992**, *24*, 639-648, doi:10.1002/kin.550240704

(6) Wallington, T. J.; Hurley, M. D. A kinetic study of the reaction of chlorine atoms with CF_3CHCl_2, CF_3CH_2F, $CFCl_2CH_3$, CF_2ClCH_3, CHF_2CH_3, CH_3D, CH_2D_2, CHD_3, CD_4, and CD_3Cl at 295 ± 2 K. *Chem. Phys. Lett.* **1992**, *189*, 437-442, doi:10.1016/0009-2614(92)85228-3.

F129. Cl + CHF_2CHF_2 (HFC-134). The recommended value for k(298 K) is an average of the results from the relative rate studies of Nielsen et al.[1] (298 K) and Yano and Tschuikow-Roux[2] (283–357 K), each recalculated based on the current recommendation for the rate constant of the appropriate reference reaction. The recommended value of E/R is derived from the data of Yano and Tschuikow-Roux.
(Table: 06-2, Note: 06-2, Evaluated: 06-2) Back to Table

(1) Nielsen, O. J.; Ellermann, T.; Sehested, J.; Wallington, T. J. Ultraviolet absorption spectrum and kinetics and mechanism of the self-reaction of $CHF_2CF_2O_2$ radicals in the gas phase at 298 K. *J. Phys. Chem.* **1992**, *96*, 10875-10879, doi:10.1021/j100205a050.

(2) Yano, T.; Tschuikow-Roux, E. Competitive photochlorination of the fluoroethanes CH_3CHF_2, CH_2FCH_2F and CHF_2CHF_2. *J. Photochem.* **1986**, *32*, 25-37, doi:10.1016/0047-2670(86)85004-3.

F130. Cl + $CHCl_2CF_3$ (HCFC-123). The recommended value for k(298 K) is an average of the results from the absolute rate study of Warren and Ravishankara[3] (276–382 K) and the relative rate studies of Wallington and Hurley[2] (295 K) and Tuazon et al.[1] (298 K), each recalculated based on the current recommendation for the rate constant of the appropriate reference reaction. The recommended value of E/R is derived from the data of Warren and Ravishankara.
(Table: 06-2, Note: 06-2, Evaluated: 06-2) Back to Table

(1) Tuazon, E. C.; Atkinson, R.; Corchnoy, S. B. Rate constants for the gas-phase reactions of Cl atoms with a series of hydrofluorocarbons and hydrochlorofluorocarbons at 298 ± 2 K. *Int. J. Chem. Kinet.* **1992**, *24*, 639-648, doi:10.1002/kin.550240704

(2) Wallington, T. J.; Hurley, M. D. A kinetic study of the reaction of chlorine atoms with CF_3CHCl_2, CF_3CH_2F, $CFCl_2CH_3$, CF_2ClCH_3, CHF_2CH_3, CH_3D, CH_2D_2, CHD_3, CD_4, and CD_3Cl at 295 ± 2 K. *Chem. Phys. Lett.* **1992**, *189*, 437-442, doi:10.1016/0009-2614(92)85228-3.

(3) Warren, R. F.; Ravishankara, A. R. Kinetics of $Cl(^2P)$ reactions with CF_3CHCl_2, CF_3CHFCl, and CH_3CFCl_2. *Int. J. Chem. Kinet.* **1993**, *25*, 833-844, doi:10.1002/kin.550251005.

F131. Cl + $CHFClCF_3$ (HCFC-124). The recommended value for k(298 K) is an average of the results from the absolute rate study by Warren and Ravishankara[2] (276–376 K) and the relative rate study by Tuazon et al.[1] (298 K). The recommended value for E/R is derived from the data of Warren and Ravishankara.
(Table: 06-2, Note: 06-2, Evaluated: 06-2) Back to Table

(1) Tuazon, E. C.; Atkinson, R.; Corchnoy, S. B. Rate constants for the gas-phase reactions of Cl atoms with a series of hydrofluorocarbons and hydrochlorofluorocarbons at 298 ± 2 K. *Int. J. Chem. Kinet.* **1992**, *24*, 639-648, doi:10.1002/kin.550240704
(2) Warren, R. F.; Ravishankara, A. R. Kinetics of Cl(^2P) reactions with CF_3CHCl_2, CF_3CHFCl, and CH_3CFCl_2. *Int. J. Chem. Kinet.* **1993**, *25*, 833-844, doi:10.1002/kin.550251005.

F132. Cl + CHF_2CF_3 (HFC-125). The recommended value for k(298 K) is an average of the results from the relative rate studies of Tuazon et al.[4] (298 K), Sehested et al.[3] (295 K), Edney and Driscoll[2] (298 K), and Young et al.[5] (296 K), all conducted only at room temperature and recalculated using the current recommendations for the rate constants of the reference reactions. The temperature dependence is estimated from a comparison among the Cl and OH reactions with CH_2FCF_3, CHF_2CHF_2, and CHF_2CF_3. The relative rate study by Coomber and Whittle[1] conducted between 303 K and 399 K corresponds to a value for k(298 K) a factor of 2.5 greater than that recommended. However, the value for E/R derived by these authors is only slightly lower than that estimated.
(Table: 15-10, Note: 15-10, Evaluated: 15-10) Back to Table

(1) Coomber, J. W.; Whittle, E. Photochlorination of methane and fluoroform Dissociation energy D(CF_3-H) and entropy of CF_3 radical. *Trans. Faraday Soc.* **1966**, *62*, 2183-2190, doi:10.1039/tf9666202183.
(2) Edney, E. O.; Driscoll, D. J. Chlorine initiated photooxidation studies of hydrochlorofluorocarbons (HCFCs) and hydrofluorocarbons (HFCs): results for HCFC-22 ($CHClF_2$); HFC-41 (CH_3F); HCFC-124 ($CClFHCF_3$); HFC-125 (CF_3CHF_2); HFC-134a (CF_3CH_2F); HCFC-142b ($CClF_2CH_3$); and HFC-152a (CHF_2CH_3). *Int. J. Chem. Kinet.* **1992**, *24*, 1067-1081, doi:10.1002/kin.550241205
(3) Sehested, J.; Ellermann, T.; Nielsen, O. J.; Wallington, T. J.; Hurley, M. D. UV absorption spectrum, and kinetics and mechanism of the self reaction of $CF_3CF_2O_2$ radicals in the gas phase at 295 K. *Int. J. Chem. Kinet.* **1993**, *25*, 701-717, doi:10.1002/kin.550250903.
(4) Tuazon, E. C.; Atkinson, R.; Corchnoy, S. B. Rate constants for the gas-phase reactions of Cl atoms with a series of hydrofluorocarbons and hydrochlorofluorocarbons at 298 ± 2 K. *Int. J. Chem. Kinet.* **1992**, *24*, 639-648, doi:10.1002/kin.550240704
(5) Young, C. J.; Hurley, M. D.; Wallington, T. J.; Mabury, S. A. Atmospheric chemistry of CF_3CF_2H and $CF_3CF_2CF_2CF_2H$: Kinetics and products of gas-phase reactions with Cl atoms and OH radicals, infrared spectra, and formation of perfluorocarboxylic acids. *Chem. Phys. Lett.* **2009**, *473*, 251-256, doi:10.1016/j.cplett.2009.04.001.

F133. ClO + O_3. There are two possible channels for this reaction: ClO + O_3 → ClOO + O_2 (k_1); and ClO + O_3 → OClO + O_2 (k_2). The recommended upper limit for k_1 at 298 K is based on results of Stevens and Anderson.[2] (233–413 K). These authors also report that $k_1 = (4 \pm 2) \times 10^{-16}$ cm^3 molecule^{-1} s^{-1} at 413 K. These data can be combined to derive the recommended Arrhenius parameters, $A = 2 \times 10^{-12}$ cm^3 molecule^{-1} s^{-1} and E/R >3600 K. The upper limit for k_2 is based on results reported by DeMore et al.[1] and Wongdontri-Stuper et al.[3] (254–296 K). The Arrhenius parameters for k_2 were estimated.
(Table: 92-20, Note: 92-20, Evaluated: 10-6) Back to Table

(1) DeMore, W. B.; Lin, C. L.; Jaffe, S. 12th Informal Conference on Photochemistry, 1976.
(2) Stevens, P. S.; Anderson, J. G. Kinetic measurements of the ClO + O_3 → ClOO + O_2 reaction. *Geophys. Res. Lett.* **1990**, *17*, 1287-1290, doi:10.1029/GL017i009p01287.
(3) Wongdontri-Stuper, W.; Jayanty, R. K. M.; Simonaitis, R.; Heicklen, J. The Cl_2 photosensitized decomposition of O_3: the reactions of ClO and OClO with O_3. *J. Photochem.* **1979**, *10*, 163-186, doi:10.1016/0047-2670(79)80004-0.

F134. ClO + H_2. The Arrhenius parameters are estimated based on the ~600 K data of Walker (reported in Clyne and Watson[1]).
(Table: 82-57, Note: 82-57, Evaluated: 10-6) Back to Table

(1) Clyne, M. A. A.; Watson, R. T. Kinetic studies of diatomic free radicals using mass spectrometry Part 2.-Rapid bimolecular reactions involving the ClO $X^2\Pi$ radical. *J. Chem. Soc. Faraday Trans. 1* **1974**, *70*, 2250-2259, doi:10.1039/f19747002250.

F135. ClO + NO. The absolute rate coefficients determined in the four discharge flow-mass spectrometric studies (Clyne and Watson[2] (298 K), Leu and DeMore[4] (226–415 K), Ray and Watson[5] (298 K), and Clyne and MacRobert[1] (295 K)) and the discharge flow laser magnetic resonance study of Lee et al.[3] (202–393 K) are in excellent agreement at room temperature, and are averaged to yield the recommended value for k(298 K). The value reported by Zahniser and Kaufman[7] (230–298 K) from a competitive study is not used in the derivation

of the recommended value, as it is about 33% higher. The magnitudes of the temperature dependences reported by Leu and DeMore and Lee et al. are in excellent agreement. Although the *E*/R value reported by Zahniser and Kaufman is in fair agreement with the other values, it is not considered as it is dependent upon the *E*/R value assumed for the Cl + O_3 reaction. The Arrhenius expression is derived from a least-squares fit to the data reported by Clyne and Watson, Leu and DeMore, Ray and Watson, Clyne and MacRobert, and Lee et al. Theoretical rate calculations by Sayin and McKee[6] give a reaction activation energy (~0.35 kcal/mol) over the temperature range 200–400 K that is supportive of the experimental values.
(Table: 82-57, Note: 10-6, Evaluated: 10-6) Back to Table

(1) Clyne, M. A. A.; MacRobert, A. J. Kinetic studies of free radical reactions by mass spectrometry. I. The reactions SO + NO_2 and ClO + NO. *Int. J. Chem. Kinet.* **1980**, *12*, 79-96, doi:10.1002/kin.550120202.
(2) Clyne, M. A. A.; Watson, R. T. Kinetic studies of diatomic free radicals using mass spectrometry Part 2.-Rapid bimolecular reactions involving the ClO $X^2\Pi$ radical. *J. Chem. Soc. Faraday Trans. 1* **1974**, *70*, 2250-2259, doi:10.1039/f19747002250.
(3) Lee, Y.-P.; Stimpfle, R. M.; Perry, R. A.; Mucha, J. A.; Evenson, K. M.; Jennings, D. A.; Howard, C. J. Laser magnetic resonance spectroscopy of ClO and kinetic studies of the reactions of ClO with NO and NO_2. *Int. J. Chem. Kinet.* **1982**, *14*, 711-732, doi:10.1002/kin.550140612.
(4) Leu, M.-T.; DeMore, W. B. Rate constant for the reaction ClO + NO → Cl + NO_2. *J. Phys. Chem.* **1978**, *82*, 2049-2052, doi:10.1021/j100508a001.
(5) Ray, G. W.; Watson, R. T. Kinetics study of the reactions of NO with FO, ClO, BrO, and IO at 298 K. *J. Phys. Chem.* **1981**, *85*, 2955-2960, doi:10.1021/j150620a022.
(6) Sayin, H.; McKee, M. L. Theoretical study of the mechanism of NO_2 production from NO + ClO. *J. Phys. Chem. A* **2005**, *109*, 4736-4743, doi:10.1021/jp050695w.
(7) Zahniser, M. S.; Kaufman, F. Kinetics of the reactions of ClO with O and with NO. *J. Chem. Phys.* **1977**, *66*, 3673-3681, doi:10.1063/1.434403.

F136. ClO + NO_3. The recommended parameters are based on results reported by Cox et al.[3] (296 K), Cox et al.[4] (278–338 K), Biggs et al.[2] (210–353 K), and Kukui et al.[6] (300 K). Biggs et al. report the rate constant to be independent of temperature, consistent with the results of Cox et al.[4] The study of Kukui et al. supersedes the earlier study of Becker et al.[1] (298 K) from the same laboratory, which had indicated the major products to be OClO + NO_2. There is now agreement among all studies that the major reaction channel forms ClOO + NO_2 (see Biggs et al., Cox et al.,[4] and Kukui et al.). From a study of the OClO/NO_3 system, Friedl et al.[5] conclude that at 220 K the formation of ClOO + NO_2 is favored.
(Table: 10-6, Note: 10-6, Evaluated: 10-6) Back to Table

(1) Becker, E.; Wille, U.; Rahman, M. M.; Schindler, R. H. An investigation of the reactions of NO_3 radicals with Cl and ClO. *Ber. Bunsenges. Phys. Chem.* **1991**, *95*, 1173-1179, doi:10.1002/bbpc.19910951003.
(2) Biggs, P.; Harwood, M. H.; Parr, A. D.; Wayne, R. P. Rate constant and products of the reaction between NO_3 and ClO over the temperature range 353-210 K. *J. Phys. Chem.* **1991**, *97*, 7746-7751, doi:10.1021/j100173a037.
(3) Cox, R. A.; Barton, R. A.; Ljungstrom, E.; Stocker, D. W. The reactions of Cl and ClO with the NO_3 radical. *Chem. Phys. Lett.* **1984**, *108*, 228-232, doi:10.1016/0009-2614(84)87054-2.
(4) Cox, R. A.; Fowles, M.; Moulton, D.; Wayne, R. P. Kinetics of the reactions of NO_3 radicals with Cl and ClO. *J. Phys. Chem.* **1987**, *91*, 3361-3365, doi:10.1021/j100296a051.
(5) Friedl, R. R.; Sander, S. P.; Yung, Y. L. Chloryl nitrate: A novel product of the OClO + NO_3 + M recombination. *J. Phys. Chem.* **1992**, *96*, 7490-7493, doi:10.1021/j100198a002.
(6) Kukui, A.; Jungkamp, T. P. W.; Schindler, R. N. Determination of the product branching ratio in the reaction of NO_3 with OCl at 300 K. *Ber. Bunsenges. Phys. Chem.* **1994**, *98*, 1619-1621, doi:10.1002/bbpc.19940981219.

F137. ClO + N_2O. The Arrhenius parameters are estimated based on the ~600 K data of Walker (reported in Clyne and Watson[1]).
(Table: 82-57, Note: 82-57, Evaluated: 10-6) Back to Table

(1) Clyne, M. A. A.; Watson, R. T. Kinetic studies of diatomic free radicals using mass spectrometry Part 2.-Rapid bimolecular reactions involving the ClO $X^2\Pi$ radical. *J. Chem. Soc. Faraday Trans. 1* **1974**, *70*, 2250-2259, doi:10.1039/f19747002250.

F138. ClO + CO. The Arrhenius parameters are estimated based on the ~600 K data of Walker (reported in Clyne and Watson[1]).

(Table: 82-57, Note: 82-57, Evaluated: 10-6) Back to Table

(1) Clyne, M. A. A.; Watson, R. T. Kinetic studies of diatomic free radicals using mass spectrometry Part 2.-Rapid bimolecular reactions involving the ClO $X^2\Pi$ radical. *J. Chem. Soc. Faraday Trans. 1* **1974**, *70*, 2250-2259, doi:10.1039/f19747002250.

F139. ClO + CH_4. The Arrhenius parameters are estimated based on the ~600 K data of Walker (reported in Clyne and Watson[1]).
(Table: 82-57, Note: 82-57) Back to Table

(1) Clyne, M. A. A.; Watson, R. T. Kinetic studies of diatomic free radicals using mass spectrometry Part 2.-Rapid bimolecular reactions involving the ClO $X^2\Pi$ radical. *J. Chem. Soc. Faraday Trans. 1* **1974**, *70*, 2250-2259, doi:10.1039/f19747002250.

F140. ClO + H_2CO. The Arrhenius parameters are estimated based on the upper limit for k(298 K) determined by Poulet et al.[1] (298 K) using the discharge flow-EPR technique.
(Table: 81-3, Note: 81-3, Evaluated: 81-3) Back to Table

(1) Poulet, G.; Le Bras, G.; Combourieu, J. E.P.R. study of the reactivity of ClO with H_2CO at 298 K. *Geophys. Res. Lett.* **1980**, *7*, 413-414, doi:10.1029/GL007i005p00413.

F141. ClO + CH_3O_2. The recommended value for k(298 K) is an average of values derived from the temperature dependent data of Helleis et al.[3] (225–355 K), Kukui et al.[6] (233–300 K), and Leather et al.[7] (223–298 K). Two other measurements at only room temperature by Simon et al.[8] and Kenner et al.[5] are 30% larger and 20% smaller, respectively, but overlap the recommended value within the reported uncertainties.

Helleis et al.[3] and Kukui et al. observed very weak temperature dependences of the rate constant with the reported E/R values of +114 K and –80 K, respectively. The data from these studies differ by less than 40% over the entire temperature range. In contrast, the study by Leather et al.[7] (223–298 K) yielded a much stronger temperature dependence with a reported E/R value of 626 K. Helleis et al.[3] and Kukui et al. used a low pressure discharge flow technique, whereas Leather et al. employed a turbulent flow reactor with substantially higher pressure. Thus, the data from this latter study should be free from possible interferences due to wall reactions. The combination of lower radical concentrations and higher total pressure in the Leather et al. study provides the basis for the temperature dependence recommended here. Thus, the recommended value for E/R is derived from a fit to the data of Leather et al. Nevertheless, in the absence of a definitive explanation for the difference between the results from the high and low pressure studies (which is as large as a factor of 2 to 3 at 200 K) values of the uncertainty parameters, f and g, were assigned to encompass the data from all three temperature dependence studies at the 95% confidence level. Note that assymetric values for "g" are assigned in the Table. To determine the upper band for f(T) one should use g = 300, whereas g = 20 should be used to determine the lower band of f(T).

There is general agreement that the only important reaction channels are those resulting in the production of ClOO + CH_3O (a) and CH_3OCl + O_2 (b). However, there is disagreement on their relative importance. At room temperature, Helleis et al.,[3] Simon et al.[8] (300 K), Kukui et al., and Helleis et al.[4] (215–295 K) report that reaction channel (a) is the major channel. However it is reported to be the minor channel by Biggs et al.[1] (298 K) and Daele and Poulet.[2] (298 K). Helleis et al.[4] (which supersedes the earlier data from Helleis et al.[3]) found that channel (b) increases from 14% at room temperature to 24% at 220 K whereas Kukui et al.[6] found this value to increase from 19% at room temperature to 43% at 230 K, i.e., indicating that both channels can be significant at the low temperatures of the polar stratosphere. All studies of the branching ratios were performed using a low-pressure discharge flow technique. Leather et al. provided no branching ratio information from their higher-pressure studies. Given the possibility of the influence of wall processes in the low-pressure studies, no recommendation on the branching ratio is made. Nevertheless, channel (a) appears to play a significant role.
(Table: 15-10, Note: 15-10, Evaluated: 15-10) Back to Table

(1) Biggs, P.; Canosa-Mas, C. E.; Fracheboud, J.-M.; Shallcross, D. E.; Wayne, R. P. Efficiency of formation of CH_3O in the reaction of CH_3O_2 with ClO. *Geophys. Res. Lett.* **1995**, *22*, 1221-1224, doi:10.1029/95GL01011.
(2) Daële, V.; Poulet, G. Kinetics and products of the reactions of CH_3O_2 with Cl and ClO. *J. Chim. Phys.* **1996**, *93*, 1081-1099, doi:10.1051/jcp/1996931081.
(3) Helleis, F.; Crowley, J. N.; Moortgat, G. K. Temperature-dependent rate constants and product branching ratios for the gas-phase reaction between CH_3O_2 and ClO. *J. Phys. Chem.* **1993**, *97*, 11464-11473, doi:10.1021/j100146a020.

(4) Helleis, F.; Crowley, J. N.; Moortgat, G. K. Temperature dependent CH_3OCl formation in the reaction of CH_3O_2 and ClO. *Geophys. Res. Lett.* **1994**, *21*, 1795-1798, doi:10.1029/94GL01280.
(5) Kenner, R. D.; Ryan, K. R.; Plumb, I. C. Kinetics of the reaction of CH_3O_2 with ClO at 293 K. *Geophys. Res. Lett.* **1993**, *20*, 1571-1574, doi:10.1029/93GL01891.
(6) Kukui, A. S.; Jungkamp, T. P. W.; Schindler, R. N. Determination of the rate constant and of product branching ratios in the reaction of CH_3O_2 with OCl between 233 K and 300 K. *Ber. Bunsenges. Phys. Chem.* **1994**, *98*, 1298-1302, doi:10.1002/bbpc.19940981013.
(7) Leather, K. E.; Bacak, A.; Wamsley, R.; Archibald, A. T.; Husk, A.; Shallcross, D. E.; Percival, C. J. Temperature and pressure dependence of the rate coefficient for the reaction between ClO and CH_3O_2 in the gas-phase. *Phys. Chem. Chem. Phys.* **2012**, *14*, 3425–3434, doi:10.1039/c2cp22834c.
(8) Simon, F. G.; Burrows, J. P.; Schneider, W.; Moortgat, G. K.; Crutzen, P. J. Study of the reaction ClO + CH_3O_2 → products at 300 K. *J. Phys. Chem.* **1989**, *93*, 7807-7813, doi:10.1021/j100360a017.

F142. ClO + ClO. There are three bimolecular channels for this reaction:

$$ClO + ClO \rightarrow Cl_2 + O_2 \ (k_1)$$
$$ClO + ClO \rightarrow ClOO + Cl \ (k_2)$$
$$ClO + ClO \rightarrow OClO + Cl \ (k_3)$$

The recommended values for the individual reaction channels are from the study of Nickolaisen et al.[8] (195–390 K). This study, using a flash photolysis/long path ultraviolet absorption technique, is the most comprehensive study of this system, covering a wide range of temperature and pressure. These results are preferred over the results of earlier studies of the total bimolecular rate coefficient at low pressures by Clyne and Coxon[1] (294–495 K), Clyne and White[3] (273–710 K), and Clyne et al.[2] (298 K), and those of other studies reported by Hayman et al.[5] (268–338 K), Cox and Derwent[4] (298 K), Simon et al.[9] (300 K), Horowitz et al.[6] (298 K), and Horowitz et al.[7] (285–331 K). The room temperature branching ratios are k_1:k_2:k_3 = 0.29:0.50:0.21. The reaction exhibits both bimolecular and termolecular reaction channels (see entry in Table 2-1). The termolecular reaction dominates at pressures higher than about 10 Torr. The equilibrium constant for formation of the ClO dimer, ClOOCl, is given in Table 3.
(Table: 94-26, Note: 97-4, Evaluated: 10-6) Back to Table

(1) Clyne, M. A. A.; Coxon, J. A. Kinetic studies of oxy-halogen radical systems. *Proc. Roy. Soc. A* **1968**, *303*, 207-231, doi:10.1098/rspa.1968.0048.
(2) Clyne, M. A. A.; McKenney, D. J.; Watson, R. T. Reactions of chlorine oxide radicals Part 5.−The reaction 2ClO ($X^2\Pi$) → products. *J. Chem. Soc. Faraday Trans. 1* **1975**, *71*, 322-335, doi:10.1039/f19757100322.
(3) Clyne, M. A. A.; White, I. F. Reactions of chlorine oxide radicals Part 3.-Kinetics of the decay reaction of the ClO($X^2\Pi$) radical. *Trans. Faraday Soc.* **1971**, *67*, 2068-2076, doi:10.1039/tf9716702068.
(4) Cox, R. A.; Derwent, R. G. Kinetics of chlorine oxide radical reactions using modulated photolysis Part 1.-Disproportionation of ClO in the Cl_2 photosensitised decomposition of ozone. *J. Chem. Soc. Faraday Trans. 1* **1979**, *75*, 1635-1647, doi:10.1039/f19797501635.
(5) Hayman, G. D.; Davies, J. M.; Cox, R. A. Kinetics of the reaction ClO + ClO → products and its potential relevance to Antarctic ozone. *Geophys. Res. Lett.* **1986**, *13*, 1347-1350, doi:10.1029/GL013i012p01347.
(6) Horowitz, A.; Bauer, D.; Crowley, J. N.; Moortgat, G. K. Determination of product branching ratio of the ClO self-reaction at 298 K. *Geophys. Res. Lett.* **1993**, *20*, 1423-1426, doi:10.1029/93GL01383.
(7) Horowitz, A.; Crowley, J. N.; Moortgat, G. K. Temperature dependence of the product branching ratios of the ClO self-reaction in oxygen. *J. Phys. Chem.* **1994**, *98*, 11924-11930, doi:10.1021/j100097a019.
(8) Nickolaisen, S. L.; Friedl, R. R.; Sander, S. P. Kinetics and mechanism of the ClO + ClO reaction: Pressure and temperature dependences of the bimolecular and termolecular channels and thermal decomposition of chlorine peroxide, ClOOCl. *J. Phys. Chem.* **1994**, *98*, 155-169, doi:10.1021/j100052a027.
(9) Simon, F. G.; Schneider, W.; Moortgat, G. K.; Burrows, J. P. A study of the ClO absorption cross-section between 240 and 310 nm and the kinetics of the self-reaction at 300 K. *J. Photochem. Photobiol. A: Chem.* **1990**, *55*, 1-23, doi:10.1016/1010-6030(90)80014-O.

F143. HCl + $ClONO_2$. Five studies of the kinetics of this system have been published, in which the following upper limits to the homogeneous bimolecular rate constant were reported: 10^{-19} cm^3 molecule^{-1} s^{-1} by a static wall-less long-path UV absorption technique and a steady-state flow FTIR technique (Molina et al.[6] (230–295 K)); 5×10^{-18} cm^3 molecule^{-1} s^{-1} using a flow reactor with FTIR analysis (Friedl et al.[3] (298 K)); 8.4×10^{-21} cm^3 molecule^{-1} s^{-1} using a static photolysis system with FTIR analysis (Hatakeyama and Leu[4] (296 K) and Leu et

al.[5] (296 K)); and 1.5×10^{-19} cm^3 molecule^{-1} s^{-1} by FTIR analysis of the decay of $ClONO_2$ in the presence of HCl in large-volume (2500 and 5800 liters) Teflon or Teflon-coated chambers (Atkinson et al.[1] (298 K)). Earlier, Birks et al.[2] (250–356 K) had reported a higher upper limit. All studies found this reaction to be catalyzed by surfaces. The differences in the reported upper limits can be accounted for in terms of the very different reactor characteristics and detection sensitivities of the various studies. The recommended upper limit for k(298 K) is based on the studies of Hatakeyama and Leu and Leu et al., which apparently are the most sensitive. The homogeneous reaction is too slow to have any significant effect on atmospheric chemistry.
(Table: 87-41, Note: 87-41, Evaluated: 10-6) Back to Table

(1) Atkinson, R.; Aschmann, S. M. A structure-activity relationship for the estimation of rate constants for the gas-phase reactions of OH radicals with organic compounds. *Int. J. Chem. Kinet.* **1987**, *19*, 1097-1105, doi:10.1002/kin.550191206.

(2) Birks, J. W.; Shoemaker, B.; Leck, T. J.; Borders, R. A.; Hart, L. J. Studies of reactions of importance in the stratosphere. II. Reactions involving chlorine nitrate and chlorine dioxide. *J. Chem. Phys.* **1977**, *66*, 4591-4599, doi:10.1063/1.433716.

(3) Friedl, R. R.; Goble, J. H.; Sander, S. P. A kinetics study of the homogeneous and heterogeneous components of the HCl + $ClONO_2$ reaction. *Geophys. Res. Lett.* **1986**, *13*, 1351-1354, doi:10.1029/GL013i012p01351.

(4) Hatakeyama, S.; Leu, M. T. Reactions of chlorine nitrate with HCl and H_2O. *Geophys. Res. Lett.* **1986**, *13*, 1343-1346, doi:10.1029/GL013i012p01343.

(5) Leu, M.-T.; Hatkeyama, S.; Hsu, K. J. Rate constants for reactions between atmospheric reservoir species. 1. HCl. *J. Phys. Chem.* **1989**, *93*, 5778-5784, doi:10.1021/j100352a026.

(6) Molina, L. T.; Molina, M. J.; Stachnik, R. A.; Tom, R. D. An upper limit to the rate of the HCl + $ClONO_2$ reaction. *J. Phys. Chem.* **1985**, *89*, 3779-3781, doi:10.1021/j100264a003.

F144. $CH_2ClO + O_2$. The CH_2ClO radical is reported to be resistant to unimolecular dissociation into Cl + CH_2O products, according to chain reaction/product analysis studies by Sanhueza and Heicklen[5] (302 K) and Niki et al.[4] (298 K), and kinetics studies by Catoire et al.[2] (251–600 K). The recommended value for k(298 K) is based on the work of Kaiser and Wallington[3] (296 K), in which the competition between reaction with O_2 and HCl elimination in a complex photochemical reaction system using FTIR detection of stable products was studied. The recommendation is a factor of 5 higher than estimated using the empirical relationship given by Atkinson and Carter.[1] The fate of CH_2ClO in the atmosphere is reaction with O_2.
(Table: 94-26, Note: 94-26, Evaluated: 94-26) Back to Table

(1) Atkinson, R.; Carter, W. P. L. Reactions of alkoxy radicals under atmospheric conditions: The relative importance of decomposition versus reaction with O_2. *J. Atmos. Chem.* **1991**, *13*, 195-210, doi:10.1007/BF00115973.

(2) Catoire, V.; Lesclaux, R.; Lightfoot, P. D.; Rayez, M. T. Kinetic study of the reactions of CH_2ClO_2 with itself and with HO_2, and theoretical study of the reactions of CH2ClO, between 251 and 600 K. *J. Phys. Chem.* **1994**, *98*, 2889-2898, doi:10.1021/j100062a027.

(3) Kaiser, E. W.; Wallington, T. J. FTIR product study of the Cl-initiated oxidation of CH_3Cl: Evidence for HCl elimination from the chloromethoxy radical. *J. Phys. Chem.* **1994**, *98*, 5679-5685, doi:10.1021/j100073a018.

(4) Niki, H.; Maker, P. D.; Savage, C. M.; Breitenbach, L. P. An FTIR study of the Cl atom-initiated oxidation of CH_2Cl_2 and CH_3Cl. *Int. J. Chem. Kinet.* **1980**, *12*, 1001-1012, doi:10.1002/kin.550121209.

(5) Sanhueza, E.; Heicklen, J. Chlorine-atom sensitized oxidation of dichloromethane and chloromethane. *J. Phys. Chem.* **1975**, *79*, 7-11, doi:10.1021/j100568a002.

F145. $CH_2ClO_2 + HO_2$. The recommended Arrhenius parameters are derived from the measurements of Catoire et al.,[1] in which pulsed photolysis with UV absorption detection was used at 1 atm pressure and 251–588 K.
(Table: 94-26, Note: 94-26, Evaluated: 94-26) Back to Table

(1) Catoire, V.; Lesclaux, R.; Lightfoot, P. D.; Rayez, M. T. Kinetic study of the reactions of CH_2ClO_2 with itself and with HO_2, and theoretical study of the reactions of CH2ClO, between 251 and 600 K. *J. Phys. Chem.* **1994**, *98*, 2889-2898, doi:10.1021/j100062a027.

F146. $CH_2ClO_2 + NO$. The recommended value for k(298 K) is from Sehested et al.[1] (295 K), who used pulsed radiolysis and UV absorption detection of NO_2 to measure the rate coefficient. The temperature dependence is estimated by analogy to similar RO_2 + NO reactions.
(Table: 94-26, Note: 94-26, Evaluated: 94-26) Back to Table

(1) Sehested, J.; Nielsen, O. J.; Wallington, T. J. Absolute rate constants for the reaction of NO with a series of peroxy radicals in the gas phase at 295 K. *Chem. Phys. Lett.* **1993**, *213*, 457-464, doi:10.1016/0009-2614(93)89142-5.

F147. CCl_3O_2 + NO. The recommended value for k(298 K) is an average of the values from Ryan and Plumb[3] (295 K) and Dognon et al.[1] (228–413 K), which are in good agreement. The temperature dependence is derived from the data of Dognon et al., which covered the temperature range 228–413 K. The CCl_3O primary product of the reaction of CCl_3O_2 with NO decomposes rapidly to eliminate Cl, according to Lesclaux et al.[2]
(Table: 94-26, Note: 94-26, Evaluated: 94-26) Back to Table

(1) Dognon, A. M.; Caralp, F.; Lesclaux, R. Réactions des radicaux chlorofluorométhyl péroxyles avec NO: Étude cinétique dans le domaine de température compris entre 230 et 430 K. *J. Chim. Phys.* **1985**, *82*, 349-352, doi:10.1051/jcp/1985820349.
(2) Lesclaux, R.; Dognon, A. M.; Caralp, F. Photo-oxidation of halomethanes at low temperature: The decomposition rate of CCl_3O and $CFCl_2O$ radicals. *J. Photochem. Photobiol. A: Chem.* **1987**, *41*, 1-11, doi:10.1016/1010-6030(87)80001-1.
(3) Ryan, K. R.; Plumb, I. C. Kinetics of the reactions of CCl_3 with O and O_2 and of CCl_3O_2 with NO at 295 K. *Int. J. Chem. Kinet.* **1984**, *16*, 591-602, doi:10.1002/kin.550160508.

F148. CCl_2FO_2 + NO. The recommended Arrhenius parameters are based on the measurements made by Dognon et al.[1] using pulsed photolysis with mass spectrometry detection at 1–10 Torr and 228–413 K. These results supersede the earlier study of Lesclaux and Caralp.[2] (298 K). The CCl_2FO radical primary product of the CCl_2FO_2 + NO reaction is reported by Lesclaux et al.[3] (233–253 K) and Wu and Carr[4] (238, 298 K) to rapidly decompose to eliminate Cl and to give the products indicated.
(Table: 94-26, Note: 94-26, Evaluated: 94-26) Back to Table

(1) Dognon, A. M.; Caralp, F.; Lesclaux, R. Réactions des radicaux chlorofluorométhyl péroxyles avec NO: Étude cinétique dans le domaine de température compris entre 230 et 430 K. *J. Chim. Phys.* **1985**, *82*, 349-352, doi:10.1051/jcp/1985820349.
(2) Lesclaux, R.; Caralp, F. Determination of the rate constants for the reactions of $CFCl_2O_2$ radical with NO and NO_2 by laser photolysis and time resolved mass spectrometry. *Int. J. Chem. Kinet.* **1984**, *16*, 1117-1128, doi:10.1002/kin.550160907
(3) Lesclaux, R.; Dognon, A. M.; Caralp, F. Photo-oxidation of halomethanes at low temperature: The decomposition rate of CCl_3O and $CFCl_2O$ radicals. *J. Photochem. Photobiol. A: Chem.* **1987**, *41*, 1-11, doi:10.1016/1010-6030(87)80001-1.
(4) Wu, F.; Carr, R. W. Time-resolved observation of the formation of CF_2O and CFClO in the CF_2Cl + O_2 and $CFCl_2$ + O_2 reactions. The unimolecular elimination of Cl atoms from CF_2ClO and $CFCl_2O$ radicals. *J. Phys. Chem.* **1992**, *96*, 1743-1748, doi:10.1021/j100183a046.

F149. $CClF_2O_2$ + NO. The recommended value for k(298 K) is an average of the determinations reported by Dognon et al.,[1] who used pulsed photolysis with mass spectrometry detection at 1–10 Torr and 228–413 K, and Sehested et al.[2] (295 K), who used pulsed radiolysis with UV absorption detection of the NO_2 product at 1 atm and 295 K. The recommended value for E/R is derived from the data of Dognon et al.[1] Wu and Carr[3] (238, 298 K) observed the $CClF_2O$ radical primary product to rapidly dissociate to CF_2O and Cl.
(Table: 94-26, Note: 94-26, Evaluated: 94-26) Back to Table

(1) Dognon, A. M.; Caralp, F.; Lesclaux, R. Réactions des radicaux chlorofluorométhyl péroxyles avec NO: Étude cinétique dans le domaine de température compris entre 230 et 430 K. *J. Chim. Phys.* **1985**, *82*, 349-352, doi:10.1051/jcp/1985820349.
(2) Sehested, J.; Nielsen, O. J.; Wallington, T. J. Absolute rate constants for the reaction of NO with a series of peroxy radicals in the gas phase at 295 K. *Chem. Phys. Lett.* **1993**, *213*, 457-464, doi:10.1016/0009-2614(93)89142-5.
(3) Wu, F.; Carr, R. W. Time-resolved observation of the formation of CF_2O and CFClO in the CF_2Cl + O_2 and $CFCl_2$ + O_2 reactions. The unimolecular elimination of Cl atoms from CF_2ClO and $CFCl_2O$ radicals. *J. Phys. Chem.* **1992**, *96*, 1743-1748, doi:10.1021/j100183a046.

1.11.3 Bibliography – ClO_x Reactions

Abbatt, J. P. D.; Anderson, J. G. High-pressure discharge flow kinetics and frontier orbital mechanistic analysis for OH + CH_2CCl_2, *cis*-CHClCHCl, *trans*-CHClCHCl, $CFClCF_2$, and CF_2CCl_2 → Products. *J. Phys. Chem.* **1991**, *95*, 2382-2390, doi:10.1021/j100159a049.

Abbatt, J. P. D.; Toohey, D. W.; Fenter, F. F.; Stevens, P. S.; Brune, W. H.; Anderson, J. G. Kinetics and mechanism of X + ClNO → XCI + NO (X = Cl, F, Br, OH, O, N) from 220 to 450 K. Correlation of reactivity and activation energy with electron affinity of X. *J. Phys. Chem.* **1989**, *93*, 1022-1029, doi:10.1021/j100340a004.

Adler-Golden, S. M.; Wiesenfeld, J. R. Production of atomic oxygen following flash photolysis of $ClONO_2$. *Chem. Phys. Lett.* **1981**, *82*, 281-284, doi:10.1016/0009-2614(81)85156-1.

Adusei, G. Y.; Fontijn, A. Experimental studies of Cl-atom reactions at high temperatures: Cl + H_2 → HCl + H from 291 to 1283 K. *Int. Symp. on Combust.* **1994**, *25*, 801-808.

Albaladejo, J.; Ballesteros, B.; Jimenez, E.; Diaz de Mera, Y.; Martinez, E. Gas-phase OH radical-initiated oxidation of the 3-halopropenes studied by PLP-LIF in the temperature range 228-388 K. *Atmos. Environ.* **2003**, *37*, 2919-2926, doi:10.1016/S1352-2310(03)00297-8.

Albaladejo, J.; Notario, A.; Cuevas, C. A.; Ballesteros, B.; Martinez, E. A pulsed laser photolysis-resonance fluorescence kinetic study of the atmospheric Cl atom-initiated oxidation of propene and a series of 3-halopropenes at room temperature. *J. Atmos. Chem.* **2003**, *45*, 35-50, doi:10.1023/A:1024073012242.

Anderson, P. C.; Kurylo, M. J. Rate constant measurements for the reaction Cl + CH_2O → HCl + CHO. Implications regarding the removal of stratospheric chlorine. *J. Phys. Chem.* **1979**, *83*, 2055-2057, doi:10.1021/j100479a001.

Arnts, R. R.; Seila, R. L.; Bufalini, J. J. Determination of room temperature OH rate constants for acetylene, ethylene dichloride, ethylene dibromide, p-dichlorobenzene and carbon disulfide. *J. Air Pollut. Control Assoc.* **1989**, *39*, 453-460, doi:10.1080/08940630.1989.10466544.

Ashford, R. D.; Basco, N.; Hunt, J. E. The kinetics of ClO formation in the flash photolysis of chlorine-oxygen mixtures. *Int. J. Chem. Kinet.* **1978**, *10*, 1233-1244, doi:10.1002/kin.550101206.

Atkinson, R.; Aschmann, S. M. Kinetics of the gas phase reaction of Cl atoms with a series of organics at 296 ± 2 K and atmospheric pressure. *Int. J. Chem. Kinet.* **1985**, *17*, 33-41, doi:10.1002/kin.550170105.

Atkinson, R.; Aschmann, S. M. A structure-activity relationship for the estimation of rate constants for the gas-phase reactions of OH radicals with organic compounds. *Int. J. Chem. Kinet.* **1987**, *19*, 1097-1105, doi:10.1002/kin.550191206.

Atkinson, R.; Carter, W. P. L. Reactions of alkoxy radicals under atmospheric conditions: The relative importance of decomposition versus reaction with O_2. *J. Atmos. Chem.* **1991**, *13*, 195-210, doi:10.1007/BF00115973.

Atkinson, R.; Hansen, D. A.; Pitts, J. N., Jr. Rate constants for the reaction of OH radicals with CHF_2Cl, CF_2Cl_2, $CFCl_3$, and H_2 over the temperature range 297-434 °K. *J. Chem. Phys.* **1975**, *63*, 1703-1706, doi:10.1063/1.431566.

Atkinson, R.; Tuazon, R. C.; Macleod, H.; Aschmann, S. M.; Winer, A. M. The gas-phase reaction of chlorine nitrate with water vapor. *Geophys. Res. Lett.* **1986**, *13*, 117-120, doi:10.1029/GL013i002p00117

Baer, S.; Hippler, H.; Rahn, R.; Siefke, M.; Seitzinger, N.; Troe, J. Thermodynamic and kinetic properties of the reaction Cl + O_2 + M ⇌ ClOO + M in the range 160-300 K and 1-1000 bar. *J. Chem. Phys.* **1991**, *95*, 6463-6470, doi:10.1063/1.461543.

Baghal-Vayjooee, M. H.; Colussi, A. J.; Benson, S. W. Very low pressure reactor. A new technique for measuring rates and equilibria of radical-molecule reactions at low temperature. Heat of formation of the methyl radical. *J. Am. Chem. Soc.* **1978**, *100*, 3214-3215, doi:10.1021/ja00478a044.

Balakhnin, V. P.; Egorov, V. I.; Intezarova, E. I. *Kinetics and Catalysis* **1971**, *12*, 299.

Balestra-Garcia, C.; Le Bras, G.; MacLeod, H. Kinetic study of the reactions OH + mono-, di-, and trichloroacetaldehyde and acetaldehyde by laser photolysis-resonance fluorescence at 298 K. *J. Phys. Chem.* **1992**, *96*, 3312-3316, doi:10.1021/j100187a026.

Barry, J.; Locke, G.; Scollard, D.; Sidebottom, H.; Treacy, J.; Clerbaux, C.; Colin, R.; Franklin, J. 1,1,1,3,3,-pentafluorobutane (HFC-365mfc): Atmospheric degradation and contribution to radiative forcing. *Int. J. Chem. Kinet.* **1997**, *29*, 607-617, doi:10.1002/(SICI)1097-4601(1997)29:8<607::AID-KIN6>3.0.CO;2-Y.

Barry, J.; Scollard, D. J.; Treacy, J. J.; Sidebottom, H. W.; Le Bras, G.; Poulet, G.; Teton, S.; Chichinin, A.; Canosa-Mas, C. E.; Kinnison, D. J.; Wayne, R. P.; Nielsen, O. J. Kinetic data for the reaction of hydroxyl

radicals with 1,1,1-trichloroacetaldehyde at 298 ± 2 K. *Chem. Phys. Lett.* **1994**, *221*, 353-358, doi:10.1016/0009-2614(94)00274-6.
Basco, N.; Dogra, S. K. Reactions of halogen oxides studied by flash photolysis II. The flash photolysis of chlorine monoxide and of the ClO free radical. *Proc. Roy. Soc. Lond. A.* **1971**, *323*, 401-415, doi:10.1098/rspa.1971.0112.
Basco, N.; Dogra, S. K. Reactions of halogen oxides studied by flash photolysis. I. The flash photolysis of chlorine dioxide. *Proc. Roy. Soc. Lond. A.* **1971**, *323*, 29-68, doi:10.1098/rspa.1971.0087.
Battin-Leclerc, F.; Kim, I. K.; Talukdar, R. K.; Portmann, R. W.; Ravishankara, A. R.; Steckler, R.; Brown, D. Rate coefficients for the reactions of OH and OD with HCl and DCl between 200 and 400 K. *J. Phys. Chem. A* **1999**, *103*, 3237-3244, doi:10.1021/jp990177j.
Baulch, D. L.; Cox, R. A.; Hampson, R. F., Jr.; Kerr, J. A.; Troe, J.; Watson, R. T. Evaluated kinetic and photochemical data for atmospheric chemistry. *J. Phys. Chem. Ref. Data* **1980**, *9*, 295-471, doi:10.1063/1.555619.
Beach, S. D.; Hickson, K. M.; Smith, I. W. M.; Tuckett, R. P. Rate constants and Arrhenius parameters for the reactions of OH radicals and Cl atoms with $CF_3CH_2OCHF_2$, $CF_3CHClOCHF_2$ and $CF_3CH_2OCClF_2$, using the discharge-flow/resonance fluorescence method. *Phys. Chem. Chem. Phys.* **2001**, *3*, 3064-3069, doi:10.1039/b103883b.
Beach, S. D.; Smith, I. W. M.; Tuckett, R. P. Rate constants for the reaction of Cl atoms with O_3 at temperatures from 298 to 184 K. *Int. J. Chem. Kinet.* **2002**, *34*, 104-109, doi:10.1002/kin.10033.
Becker, E.; Wille, U.; Rahman, M. M.; Schindler, R. H. An investigation of the reactions of NO_3 radicals with Cl and ClO. *Ber. Bunsenges. Phys. Chem.* **1991**, *95*, 1173-1179, doi:10.1002/bbpc.19910951003.
Bedjanian, Y.; Laverdet, G.; Le Bras, G. Low-pressure study of the reaction of Cl atoms with isoprene. *J. Phys. Chem. A* **1998**, *102*, 953-959, doi:10.1021/jp973336c.
Bedjanian, Y.; Riffault, V.; Le Bras, G. Kinetics and mechanism of the reaction of OH with ClO. *Int. J. Chem. Kinet.* **2001**, *33*, 587-599, doi:10.1002/kin.1054.
Beichert, P.; Wingen, L.; Lee, J.; Vogt, R.; Ezell, M. J.; Ragains, M.; Neavyn, R.; Finlayson-Pitts, B. J. Rate constants for the reactions of chlorine atoms with some simple alkanes at 298 K: Measurement of a self-consistent set using both absolute and relative rate methods. *J. Phys. Chem.* **1995**, *99*, 13156-13162, doi:10.1021/j100035a018.
Bemand, P. P.; Clyne, M. A. A.; Watson, R. T. Reactions of chlorine oxide radicals Part 4.-Rate constants for the reactions Cl + OClO, O + OClO, H + OClO, NO + OClO and O + ClO. *J. Chem. Soc. Faraday Trans. 1* **1973**, *69*, 1356-1374, doi:10.1039/f19736901356.
Benson, S. W.; Cruickshank, F. R.; Shaw, R. Iodine monochloride as a thermal source of chlorine atoms: The reaction of chlorine atoms with hydrogen. *Int. J. Chem. Kinet.* **1969**, *1*, 29-43, doi:10.1002/kin.550010105.
Biggs, P.; Canosa-Mas, C. E.; Fracheboud, J.-M.; Shallcross, D. E.; Wayne, R. P. Efficiency of formation of CH_3O in the reaction of CH_3O_2 with ClO. *Geophys. Res. Lett.* **1995**, *22*, 1221-1224, doi:10.1029/95GL01011.
Biggs, P.; Harwood, M. H.; Parr, A. D.; Wayne, R. P. Rate constant and products of the reaction between NO_3 and ClO over the temperature range 353-210 K. *J. Phys. Chem.* **1991**, *97*, 7746-7751, doi:10.1021/j100173a037.
Birks, J. W.; Shoemaker, B.; Leck, T. J.; Borders, R. A.; Hart, L. J. Studies of reactions of importance in the stratosphere. II. Reactions involving chlorine nitrate and chlorine dioxide. *J. Chem. Phys.* **1977**, *66*, 4591-4599, doi:10.1063/1.433716.
Boodaghians, R. B.; Hall, I. W.; Wayne, R. P. Kinetics of the reactions of the hydroxyl radical with molecular chlorine and bromine. *J. Chem. Soc. Faraday Trans. 2* **1987**, *83*, 529-538, doi:10.1039/f29878300529.
Boone, G. D.; Agyin, F.; Robichaud, D. J.; Tao, F.-M.; Hewitt, S. A. Rate constants for the reactions of chlorine atoms with deuterated methanes: Experiment and theory. *J. Phys. Chem. A* **2001**, *105*, 1456-1464, doi:10.1021/jp0027290.
Brahan, K. M.; Hewitt, A. D.; Boone, G. D.; Hewitt, S. A. Rate constant for the reaction of Cl with $CHCl_3$. *Int. J. Chem. Kinet.* **1996**, *28*, 397-404, doi:10.1002/(SICI)1097-4601(1996)28:6<397::AID-KIN1>3.0.CO;2-Q.
Brown, A. C.; Canosa-Mas, C. E.; Parr, A. D.; Pierce, J. M. T.; Wayne, R. P. Tropospheric lifetimes of halogenated anaesthetics. *Nature* **1989**, *341*, 635-637, doi:10.1038/341635a0.
Brown, A. C.; Canosa-Mas, C. E.; Parr, A. D.; Rothwell, K.; Wayne, R. P. Tropospheric lifetimes of three compounds for possible replacement of CFC and halons. *Nature* **1990**, *347*, 541-543, doi:10.1038/347541a0.

Brown, A. C.; Canosa-Mas, C. E.; Parr, A. D.; Wayne, R. P. Laboratory studies of some halogenated ethanes and ethers: Measurements of rates of reaction with OH and of infrared absorption cross-sections. *Atmos. Environ.* **1990**, *24A*, 2499-2511, doi:10.1016/0960-1686(90)90341-J.

Brown, A. C.; Canosa-Mas, C. E.; Wayne, R. P. A kinetic study of the reactions of OH with CH_3I and CF_3I. *Atmos. Environ.* **1990**, *24A*, 361-367, doi:10.1016/0960-1686(90)90115-4.

Brown, R. D. H.; Smith, I. W. M. Absolute rate constants for the reactions O(^3P) atoms with HCl and HBr. *Int. J. Chem. Kinet.* **1975**, *7*, 301-315, doi:10.1002/kin.550070211.

Bryukov, M. G.; Dellinger, B.; Knyazev, V. D. Kinetics of the gas-phase reaction of OH with HCl. *J. Phys. Chem. A* **2006**, *110*, 936-943, doi:10.1021/jp053615x.

Bryukov, M. G.; Knyazev, V. D.; Lomnicki, S. M.; McFerrin, C. A.; Dellinger, B. Temperature-dependent kinetics of the gas-phase reactions of OH with Cl_2, CH_4, and C_3H_8. *J. Phys. Chem. A* **2004**, *108*, 10464-10472, doi:10.1021/jp047340h.

Bryukov, M. G.; Slagle, I. R.; Knyazev, V. D. Kinetics of reactions of Cl atoms with methane and chlorinated methanes. *J. Phys. Chem. A* **2002**, *106*, 10532-10542, doi:10.1021/jp0257909.

Bryukov, M. G.; Slagle, I. R.; Knyazev, V. D. Kinetics of reactions of Cl atoms with ethane, chloroethane, and 1,1-dichloroethane. *J. Phys. Chem. A* **2003**, *107*, 6565-6573, doi:10.1021/jp0275138.

Burkholder, J. B.; Hammer, P. D.; Howard, C. J.; Goldman, A. Infrared line intensity measurements in the $\nu = 0$-1 band of the ClO radical. *J. Geophys. Res.* **1989**, *94*, 2225-2234, doi:10.1029/JD094iD02p02225.

Burrows, J. P.; Cliff, D. I.; Harris, G. W.; Thrush, B. A.; Wilkinson, J. P. T. Atmospheric reactions of the HO_2 radical studied by laser magnetic-resonance spectroscopy. *Proc. Roy. Soc. Lond. A.* **1979**, *368*, 463-481, doi:10.1098/rspa.

Burrows, J. P.; Cox, R. A. Kinetics of chlorine oxide reactions using modulated photolysis. 4. The reactions Cl + $Cl_2O \rightarrow Cl_2$ + ClO and ClO + $HO_2 \rightarrow$ products studied at 1 atm and 300 K. *J. Chem. Soc. Faraday Trans. 1* **1981**, *77*, 2465-2479, doi:10.1039/f19817702465.

Burrows, J. P.; Tyndall, G. S.; Moortgat, G. K. Absorption spectrum of NO_3 and kinetics of the reactions of NO_3 with NO_2, Cl, and several stable atmospheric species at 298 K. *J. Phys. Chem.* **1985**, *89*, 4848-4856, doi:10.1021/j100268a038.

Burrows, J. P.; Wallington, T. J.; Wayne, R. P. Kinetics of the reaction of OH with ClO. *J. Chem. Soc. Faraday Trans. 2* **1984**, *80*, 957-971, doi:10.1039/f29848000957.

Cadman, P.; Kirk, A. W.; Trotman-Dickenson, A. F. Reactions of chlorine atoms with ethane, propane, isobutane, fluoroethane, 1,1-difluoroethane, 1,1,1-trifluoroethane and cyclopropane. *J. Chem. Soc. Faraday Trans. 1* **1976**, *72*, 1027-1032, doi:10.1039/f19767201027.

Cannon, B. D.; Robertshaw, J. S.; Smith, I. W. M.; Williams, M. D. A time-resolved LIF study of the kinetics of OH(v=0) and OH(v=1) with HCl and HBr. *Chem. Phys. Lett.* **1984**, *105*, 380-385, doi:10.1016/0009-2614(84)80045-7.

Canosa-Mas, C. E.; Cotter, E. S. N.; Duffy, J.; Thompson, K. C.; Wayne, R. P. The reactions of atomic chlorine with acrolein, methacrolein, and methyl vinyl ketone. *Phys. Chem. Chem. Phys.* **2001**, *3*, 3075-3084, doi:10.1039/b101434j.

Canosa-Mas, C. E.; Dillon, R. J.; Sidebotom, H.; Thompson, K. C.; Wayne, R. P. A study of the OH-initiated oxidation of chlorinated ethenes in the gas phase. *Phys. Chem. Chem. Phys.* **2001**, *3*, 542-550, doi:10.1039/b005392i.

Canosa-Mas, C. E.; Hutton-Squire, H. R.; King, M. D.; Stewart, D. J.; Thompson, K. C.; Wayne, R. P. Laboratory kinetic studies of the reactions of Cl atoms with species of biogenic origin: Δ^3-carene, isoprene, methacrolein and methyl vinyl ketone. *J. Atmos. Chem.* **1999**, *34*, 163-170, doi:10.1023/A:1006214423298.

Canosa-Mas, C. E.; Smith, S. J.; Toby, S.; Wayne, R. P. Laboratory studies of the reactions of the nitrate radical with chloroform, methanol, hydrogen chloride and hydrogen bromide. *J. Chem. Soc. Faraday Trans. 2* **1989**, *85*, 709-725, doi:10.1039/f29898500709.

Cantrell, C. A.; Davidson, J. A.; Shetter, R. E.; Anderson, B. A.; Calvert, J. G. The temperature invariance of the NO_3 absorption cross section in the 662-nm region. *J. Phys. Chem.* **1987**, *91*, 5858-5863, doi:10.1021/j100307a009.

Cantrell, C. A.; Davidson, J. A.; Shetter, R. E.; Anderson, B. A.; Calvert, J. G. Reactions of NO_3 and N_2O_5 with molecular species of possible atmospheric interest. *J. Phys. Chem.* **1987**, *91*, 6017-6021, doi:10.1021/j100307a040.

Carr, S.; Shallcross, D. E.; Canosa-Mas, C. E.; Wenger, J. C.; Sidebottom, H. W.; Treacy, J. J.; Wayne, R. P. A kinetic and mechanistic study of the gas-phase reactions of OH radicals and Cl atoms with some

halogenated acetones and their atmospheric implications. *Phys. Chem. Chem. Phys.* **2003**, *5*, 3874-3883, doi:10.1039/b304298g.

Catoire, V.; Lesclaux, R.; Lightfoot, P. D.; Rayez, M.-T. Kinetic study of the reactions of CH_2ClO_2 with itself and with HO_2, and theoretical study of the reactions of CH_2ClO, between 251 and 600 K. *J. Phys. Chem.* **1994**, *98*, 2889-2898, doi:10.1021/j100062a027.

Catoire, V.; Lesclaux, R.; Schneider, W. F.; Wallington, T. J. Kinetics and mechanisms of the self-reactions of CCl_3O_2 and $CHCl_2O_2$ radicals and their reactions with HO_2. *J. Phys. Chem.* **1996**, *100*, 14356-14371, doi:10.1021/jp960572z.

Cattell, F. C.; Cox, R. A. Pressure dependence of the reactions of HO_2 with Cl and ClO. *J. Chem. Soc. Faraday Trans. 2* **1986**, *82*, 1413-1426, doi:10.1039/f29868201413.

Chang, J. S.; Kaufman, F. Kinetics of the reactions of hydroxyl radicals with some halocarbons: $CHFCl_2$, CHF_2Cl, CH_3CCl_3, C_2HCl_3, and C_2Cl_4. *J. Chem. Phys.* **1977**, *66*, 4989-4994, doi:10.1063/1.433801.

Chang, J. S.; Kaufman, F. Upper limits of the rate constants for the reactions of $CFCl_3$ (F-11), CF_2Cl_2 (F-12), and N_2O with OH. Estimates of corresponding lower limits to their tropospheric lifetimes. *Geophys. Res. Lett.* **1977**, *4*, 192-194, doi:10.1029/GL004i005p00192.

Chasovnikov, S. A.; Chichinin, A. I.; Krasnoperov, L. N. Time-resolved LMR study on the reactions of Cl atoms in the ground ($^2P_{3/2}$) and excited ($^2P_{1/2}$) spin-orbital states with ClNO. *Chem. Phys.* **1987**, *116*, 91-99, doi:10.1016/0301-0104(87)80071-X.

Chesnokov, E. N. Application of IR-chemiluminescence method for determination of rate constants of bimolecular reactions which are not leading to the formation of excited products. *Khim. Fiz.* **1991**, *10*, 204-212.

Choi, N.; Pilling, M. J.; Seakins, P. W.; Wang, L. Studies of site selective hydrogen atom abstractions by Cl atoms from isobutane and propane by laser flash photolysis/IR diode laser spectroscopy. *Phys. Chem. Chem. Phys.* **2006**, *8*, 2172–2178, doi:10.1039/b516531h.

Choo, K. Y.; Leu, M. T. Determination of $O_2(^1\Sigma_g^+)$ and $O_2(^1\Delta_g)$ yields in Cl + O_2 and Cl + O_3 reactions. *J. Phys. Chem.* **1985**, *89*, 4832-4837, doi:10.1021/j100268a035.

Christensen, L. K.; Ball, J. C.; Wallington, T. J. Atmospheric oxidation mechanism of methyl acetate. *J. Phys. Chem. A* **2000**, *104*, 345-351, doi:10.1021/jp993127n.

Cillien, C.; Goldfinger, P.; Huybrechts, G.; Martens, G. Hydrogen abstraction from chlorinated ethanes by chlorine atoms. *Trans. Faraday Soc.* **1967**, *63*, 1631-1635, doi:10.1039/TF9676301631.

Clark, R. H.; Husain, D.; Jezequel, J. Y. The reaction of chlorine atoms, Cl($3\ ^2P_J$), with nitric acid in the gas phase. *J. Photochem.* **1982**, *18*, 39-46, doi:10.1016/0047-2670(82)80006-3.

Clyne, M. A. A.; Coxon, J. A. Kinetic studies of oxy-halogen radical systems. *Proc. Roy. Soc. A* **1968**, *303*, 207-231, doi:10.1098/rspa.1968.0048.

Clyne, M. A. A.; Cruse, H. W. Atomic resonance fluorescence spectrometry for rate constants of rapid bimolecular reactions Part 1.-Reactions O + NO_2, Cl + ClNO, Br + ClNO. *J. Chem. Soc. Faraday Trans. 2* **1972**, *68*, 1281-1299, doi:10.1039/f29726801281.

Clyne, M. A. A.; Holt, P. M. Reaction kinetics involving ground $X^2\Pi$ and excited $A^2\Sigma^+$ hydroxyl radicals Part 1.-Quenching kinetics of OH $A^2\Sigma^+$ and rate constants for reactions of OH $X^2\Pi$ with CH_3CCl_3 and CO. *J. Chem. Soc. Faraday Trans. 2* **1979**, *75*, 569-581, doi:10.1039/f29797500569.

Clyne, M. A. A.; Holt, P. M. Reaction kinetics involving ground $X^2\Pi$ and excited $A^2\Sigma^+$ hydroxyl radicals Part 2.-Rate constants for reactions of OH $X^2\Pi$ with halogenomethanes and halogenoethanes. *J. Chem. Soc. Faraday Trans. 2* **1979**, *75*, 582-591, doi:10.1039/f29797500582.

Clyne, M. A. A.; MacRobert, A. J. Kinetic studies of free radical reactions by mass spectrometry. I. The reactions SO + NO_2 and ClO + NO. *Int. J. Chem. Kinet.* **1980**, *12*, 79-96, doi:10.1002/kin.550120202.

Clyne, M. A. A.; McKenney, D. J.; Watson, R. T. Reactions of chlorine oxide radicals Part 5.−The reaction 2ClO ($X^2\Pi$) → products. *J. Chem. Soc. Faraday Trans. 1* **1975**, *71*, 322-335, doi:10.1039/f19757100322.

Clyne, M. A. A.; Nip, W. S. Reactions of chlorine oxide radicals Part 6.-The reaction O + ClO → Cl + O_2 from 220 to 426 K. *J. Chem. Soc. Faraday Trans. 1* **1976**, *72*, 2211-2217, doi:10.1039/f19767202211.

Clyne, M. A. A.; Nip, W. S. Study of elementary reactions by atomic resonance absorption with a non-reversed source Part 1.-The reaction Cl + O_3 → ClO + O_2. *J. Chem. Soc. Faraday Trans. 2* **1976**, *72*, 838-847, doi:10.1039/f29767200838.

Clyne, M. A. A.; Walker, R. F. Absolute rate constants for elementary reactions in the chlorination of CH_4, CD_4, CH_3Cl, CH_2Cl_2, $CHCl_3$, $CDCl_3$ and $CBrCl_3$. *J. Chem. Soc. Faraday Trans. 1* **1973**, *69*, 1547-1567, doi:10.1039/F19736901547.

Clyne, M. A. A.; Watson, R. T. Kinetic studies of diatomic free radicals using mass spectrometry Part 2.-Rapid bimolecular reactions involving the ClO $X^2\Pi$ radical. *J. Chem. Soc. Faraday Trans. 1* **1974**, *70*, 2250-2259, doi:10.1039/f19747002250.

Clyne, M. A. A.; White, I. F. Reactions of chlorine oxide radicals Part 3.-Kinetics of the decay reaction of the ClO($X^2\Pi$) radical. *Trans. Faraday Soc.* **1971**, *67*, 2068-2076, doi:10.1039/tf9716702068.

Colussi, A. J. Formation and decay of (^3P_J)O atoms in the laser flash photolysis of chlorine dioxide (OClO) at 308 nm. *J. Phys. Chem.* **1990**, *94*, 8922-8926, doi:10.1021/j100389a014.

Colussi, A. J.; Sander, S. P.; Friedl, R. R. Temperature dependence and mechanism of the reaction between O(^{3}P) and chlorine dioxide. *J. Phys. Chem.* **1992**, *96*, 4442-4445, doi:10.1021/j100190a058.

Cook, J. L.; Ennis, C. A.; Leck, T. J.; Birks, J. W. Studies of reactions of importance in the stratosphere. IV. Rate constant for the reaction Cl + HOCl → HCl + ClO over the temperature range 243-365 K. *J. Chem. Phys.* **1981**, *74*, 545-549, doi:10.1063/1.440807.

Coomber, J. W.; Whittle, E. Photochlorination of methane and fluoroform Dissociation energy D(CF_3-H) and entropy of CF_3 radical. *Trans. Faraday Soc.* **1966**, *62*, 2183-2190, doi:10.1039/tf9666202183.

Cox, R. A. Kinetics of the reaction Cl + HO_2 = HCl + O_2, using molecular modulation spectrometry. *Int. J. Chem. Kinet.* **1980**, *12*, 649-660, doi:10.1002/kin.550120906.

Cox, R. A.; Barton, R. A.; Ljungstrom, E.; Stocker, D. W. The reactions of Cl and ClO with the NO_3 radical. *Chem. Phys. Lett.* **1984**, *108*, 228-232, doi:10.1016/0009-2614(84)87054-2.

Cox, R. A.; Derwent, R. G. Kinetics of chlorine oxide radical reactions using modulated photolysis Part 1.-Disproportionation of ClO in the Cl_2 photosensitised decomposition of ozone. *J. Chem. Soc. Faraday Trans. 1* **1979**, *75*, 1635-1647, doi:10.1039/f19797501635.

Cox, R. A.; Derwent, R. G.; Eggleton, A. E. J.; Lovelock, J. E. Photochemical oxidation of halocarbons in the troposphere. *Atmos. Environ.* **1976**, *10*, 305-308, doi:10.1016/0004-6981(76)90170-0.

Cox, R. A.; Derwent, R. G.; Eggleton, A. E. J.; Read, H. J. Kinetics of chlorine oxide radicals using modulated photolysis Part 2.-ClO and ClOO radical kinetics in the photolysis of Cl_2 + O_2 + N_2 mixtures. *J. Chem. Soc. Faraday Trans. I* **1979**, *75*, 1648-1666, doi:10.1039/f19797501648.

Cox, R. A.; Fowles, M.; Moulton, D.; Wayne, R. P. Kinetics of the reactions of NO_3 radicals with Cl and ClO. *J. Phys. Chem.* **1987**, *91*, 3361-3365, doi:10.1021/j100296a051.

Cox, R. A.; Hayman, G. D. The stability and photochemistry of dimers of the ClO radical and implications for Antarctic ozone depletion. *Nature* **1988**, *332*, 796-800, doi:10.1038/332796a0.

Crowley, J. N.; Campuzano-Jost, P.; Moortgat, G. K. Temperature dependent rate constants for the gas-phase reaction between OH and CH_3OCl. *J. Phys. Chem.* **1996**, *100*, 3601-3606, doi:10.1021/jp953018i.

Daële, V.; Poulet, G. Kinetics and products of the reactions of CH_3O_2 with Cl and ClO. *J. Chim. Phys.* **1996**, *93*, 1081-1099, doi:10.1051/jcp/1996931081.

Davis, D. D.; Braun, W.; Bass, A. M. Reactions of $Cl^2P_{3/2}$: Absolute rate constants for reaction with H_2, CH_4, C_2H_6, CH_2Cl_2, C_2Cl_4, and c-C_6H_{12}. *Int. J. Chem. Kinet.* **1970**, *2*, 101-114, doi:10.1002/kin.550020204

Davis, D. D.; Machado, G.; Conaway, B.; Oh, Y.; Watson, R. A temperature dependent kinetics study of the reaction of OH with CH_3Cl, CH_2Cl_2, $CHCl_3$, and CH_3Br. *J. Chem. Phys.* **1976**, *65*, 1268-1274, doi:10.1063/1.433236.

DeMore, W. B. 182nd National Meeting of the American Chemical Society, 1981, New York.

DeMore, W. B. Tests of stratospheric models: The reactions of atomic chlorine with O_3 and CH_4 at low temperature. *J. Geophys. Res.* **1991**, *96*, 4995-5000, doi:10.1029/90JD02737.

DeMore, W. B. Relative rate constants for the reactions of OH with methane and methyl chloroform. *Geophys. Res. Lett.* **1992**, *19*, 1367-1370, doi:10.1029/92GL01278.

DeMore, W. B. Experimental and estimated rate constants for the reactions of hydroxyl radicals with several halocarbons. *J. Phys. Chem.* **1996**, *100*, 5813-5820, doi:10.1021/jp953216+.

DeMore, W. B. Regularities in Arrhenius parameters for rate constants of abstraction reactions of hydroxyl radical with C-H bonds. *J. Photochem. Photobiol. A: Chem.* **2005**, *176*, 129-135, doi:10.1016/j.jphotochem.2005.07.015.

DeMore, W. B.; Lin, C. L.; Jaffe, S. 12th Informal Conference on Photochemistry, 1976.

DeMore, W. B.; Tschuikow-Roux, E. Ultraviolet spectrum and chemical reactivity of the ClO dimer. *J. Phys. Chem.* **1990**, *94*, 5856-5860, doi:10.1021/j100378a046.

Dóbé, S.; Khachatryan, L. A.; Bérces, T. Kinetics of reactions of hydroxyl radicals with a series of aliphatic aldehydes. *Ber. Bunsenges. Phys. Chem.* **1989**, *93*, 847-852, doi:10.1002/bbpc.19890930806.

Dóbé, S.; Otting, M.; Temps, F.; Wagner, H. G.; Ziemer, H. Fast flow kinetic studies of the reaction $CH_2OH + HCl \rightleftharpoons CH_3OH + Cl$. The heat of formation of hydroxymethyl. *Ber. Bunsenges. Phys. Chem.* **1993**, *97*, 877-884, doi:10.1002/bbpc.19930970708.

Dobis, O.; Benson, S. W. Analysis of flow dynamics in a new, very low pressure reactor. Application to the reaction: $Cl + CH_4 \rightleftharpoons HCl + CH_3$. *Int. J. Chem. Kinet.* **1987**, *19*, 691-708, doi:10.1002/kin.550190803.

Dobis, O.; Benson, S. W. Temperature coefficients of the rates of Cl atom reactions with C_2H_6, C_2H_5, and C_2H_4. The rates of disproportionation and recombination of ethyl radicals. *J. Am. Chem. Soc.* **1991**, *113*, 6377-6386, doi:10.1021/ja00017a004.

Dobis, O.; Benson, S. W. Reaction of the ethyl radical with oxygen at millitorr pressures at 243-368 K and a study of the $Cl + HO_2$, ethyl + HO_2, and $HO_2 + HO_2$ reactions. *J. Am. Chem. Soc.* **1993**, *115*, 8798-8809, doi:10.1021/ja00072a038.

Dognon, A. M.; Caralp, F.; Lesclaux, R. Réactions des radicaux chlorofluorométhyl péroxyles avec NO: Étude cinétique dans le domaine de température compris entre 230 et 430 K. *J. Chim. Phys.* **1985**, *82*, 349-352, doi:10.1051/jcp/1985820349.

Donaghy, T.; Shanahan, I.; Hande, M.; Fitzpatrick, S. Rate constants and atmospheric lifetimes for the reactions of OH radicals and Cl atoms with haloalkanes. *Int. J. Chem. Kinet.* **1993**, *25*, 273-284, doi:10.1002/kin.550250407.

Eberhard, J.; Yeh, P.-S.; Lee, Y.-P. Laser-photolysis/time-resolved Fourier-transform absorption spectroscopy: formation and quenching of HCl(v) in the chain reaction $Cl/Cl_2/H_2$. *J. Chem. Phys.* **1997**, *107*, 6499-6502, doi:10.1063/1.474264.

Edelbüttel-Einhaus, J.; Hoyermann, K.; Rohde, G.; Seeba, J. The detection of the hydroxyethyl radical by REMPI/mass-spectrometry and the application to the study of the reactions $CH_3CHOH + O$ and $CH_3CHOH + H$. *Proc. Combust. Inst.* **1992**, *24*, 661-668.

Edney, E. O.; Driscoll, D. J. Chlorine initiated photooxidation studies of hydrochlorofluorocarbons (HCFCs) and hydrofluorocarbons (HFCs): results for HCFC-22 ($CHClF_2$); HFC-41 (CH_3F); HCFC-124 ($CClFHCF_3$); HFC-125 (CF_3CHF_2); HFC-134a (CF_3CH_2F); HCFC-142b ($CClF_2CH_3$); and HFC-152a (CHF_2CH_3). *Int. J. Chem. Kinet.* **1992**, *24*, 1067-1081, doi:10.1002/kin.550241205.

Edney, E. O.; Kleindienst, T. E.; Corse, E. W. Room temperature rate constants for the reaction of OH with selected chlorinated and oxygenated hydrocarbons. *Int. J. Chem. Kinet.* **1986**, *18*, 1355-1371, doi:10.1002/kin.550181207.

Edney, E. O.; Shepson, P. B.; Kleindienst, T. E.; Corse, E. W. The photooxidation of allyl chloride. *Int. J. Chem. Kinet.* **1986**, *18*, 597-608, doi:10.1002/kin.550180509.

Ennis, C. A.; Birks, J. W. Applications of a new laboratory source of gaseous HOCl: Product distribution in the Cl + HOCl reaction and equilibrium constant for the reaction $Cl_2O + H_2O \rightleftharpoons 2HOCl$. *J. Phys. Chem.* **1985**, *89*, 186-191, doi:10.1021/j100247a039.

Ennis, C. A.; Birks, J. W. Rate constants for the reactions $OH + HOCl \rightarrow H_2O + ClO$ and $H + HOCl \rightarrow$ products. *J. Phys. Chem.* **1988**, *93*, 1119-1126, doi:10.1021/j100316a024.

Fang, T. D.; Taylor, P. H.; Berry, R. J. Kinetics of the reaction of OH radicals with CH_2ClCF_2Cl and CH_2ClCF_3 over an extended temperature range. *J. Phys. Chem. A* **1999**, *103*, 2700-2704, doi:10.1021/jp984273g.

Fang, T. D.; Taylor, P. H.; Dellinger, B. Absolute rate measurements of the reaction of OH radicals with HCFC-21 ($CHFCl_2$) and HCFC-22 (CHF_2Cl) over an extended temperature range. *J. Phys. Chem.* **1996**, *100*, 4048-4054, doi:10.1021/jp952690c.

Fang, T. D.; Taylor, P. H.; Dellinger, B.; Ehlers, C. J.; Berry, R. J. Kinetics of the $OH + CH_3CF_2Cl$ reaction over an extended temperature range. *J. Phys. Chem. A* **1997**, *101*, 5758-5764, doi:10.1021/jp964095w.

Fantechi, G.; Jensen, N. R.; Saastad, O.; Hjorth, J.; Peeters, J. Reactions of Cl atoms with selected VOCs: Kinetics, products and mechanisms. *J. Atmos. Chem.* **1998**, *31*, 247-267, doi:10.1023/A:1006033910014.

Fasano, D. M.; Nogar, N. S. The infrared chemiluminescent reaction of Cl atoms with H_2CO. *Int. J. Chem. Kinet.* **1981**, *13*, 325-332, doi:10.1002/kin.550130402.

Feilberg, K. L.; Griffith, D. W. T.; Johnson, M. S.; Nielsen, C. J. The ^{13}C and D kinetic isotope effects in the reaction of CH_4 with Cl. *Int. J. Chem. Kinet.* **2005**, *37*, 110-118, doi:10.1002/kin.20058.

Finkbeiner, M.; Crowley, J. N.; Horie, O.; Müller, R.; Moortgat, G. K.; Crutzen, P. J. Reaction between HO_2 and ClO: product formation between 210 and 300 K. *J. Phys. Chem.* **1995**, *99*, 16264-16275, doi:10.1021/j100044a011.

Finlayson-Pitts, B. J.; Ezell, M. J.; Jayaweera, T. M.; Berko, H. N.; Lai, C. C. Kinetics of the reactions of OH with methyl chloroform and methane: Implications for global tropospheric OH and the methane budget. *Geophys. Res. Lett.* **1992**, *19*, 1371-1374, doi:10.1029/92GL01279.

Finlayson-Pitts, B. J.; Keoshian, C. J.; Buehler, B.; Ezell, A. A. Kinetics of reaction of chlorine atoms with some biogenic organics. *Int. J. Chem. Kinet.* **1999**, *31*, 491-499, doi:10.1002/(SICI)1097-4601(1999)31:7<491::AID-KIN4>3.0.CO;2-E.

Foon, R.; Le Bras, G.; Combourieu, J. Étude cinétique par résonance paramagnetique électronique de la réaction des atomes de chlore acec le formaldéhyde. *C. R. Acad. Sci. Paris* **1979**, *Series C 288*, 241-243.

Freeman, C. G.; Phillips, L. F. Kinetics of chlorine oxide reactions. The reaction of oxygen atoms with Cl_2O. *J. Phys. Chem.* **1968**, *72*, 3025-3028, doi:10.1021/j100854a061.

Friedl, R. R.; Goble, J. H.; Sander, S. P. A kinetics study of the homogeneous and heterogeneous components of the HCl + $ClONO_2$ reaction. *Geophys. Res. Lett.* **1986**, *13*, 1351-1354, doi:10.1029/GL013i012p01351.

Friedl, R. R.; Sander, S. P.; Yung, Y. L. Chloryl nitrate: A novel product of the OClO + NO_3 + M recombination. *J. Phys. Chem.* **1992**, *96*, 7490-7493, doi:10.1021/j100198a002.

Ganske, J. A.; Berko, H. N.; Ezell, M. J.; Finlayson-Pitts, B. J. Kinetics of the gas-phase reaction of OH with $ClNO_2$ from 259 to 348 K. *J. Phys. Chem.* **1992**, *96*, 2568-2572, doi:10.1021/j100185a032.

Ganske, J. A.; Ezell, M. J.; Berko, H. N.; Finlayson-Pitts, B. J. The reaction of OH with $ClNO_2$ at 298 K: kinetics and mechanisms. *Chem. Phys. Lett.* **1991**, *179*, 204-210, doi:10.1016/0009-2614(91)90317-3.

Gierczak, T.; Baasandorj, M.; Burkholder, J. B. OH + (*E*)- and (*Z*)-1-chloro-3,3,3-trifluoropropene-1 (CF_3CH=$CHCl$) reaction rate coefficients: Stereoisomer-dependent reactivity. *J. Phys. Chem. A* **2014**, *118*, 11015-11025, doi:10.1021/jp509127h.

Gierczak, T.; Burkholder, J. B.; Ravishankara, A. R. Rate coefficients for the reaction of OH with OClO between 242 and 392 K. *Int. J. Chem. Kinet.* **2006**, *38*, 234-241, doi:10.1002/kin.20158.

Gierczak, T.; Talukdar, R.; Vaghjiani, G. L.; Lovejoy, E. R.; Ravishankara, A. R. Atmospheric fate of hydrofluoroethanes and hydrofluorochloroethanes: 1. Rate coefficients for reactions with OH. *J. Geophys. Res.* **1991**, *96*, 5001-5011, doi:10.1029/90JD02736.

Gilles, M. K.; Burkholder, J. B.; Ravishankara, A. R. Rate coefficients for the reaction of OH with Cl_2, Br_2 and I_2 from 235 to 354 K. *Int. J. Chem. Kinet.* **1999**, *31*, 417-424, doi:10.1002/(SICI)1097-4601(1999)31:6<417::AID-KIN3>3.0.CO;2-A.

Glavas, S.; Heicklen, J. Relative reactivity of chlorine atoms with NO, NO_2 and $HCCl_2F$ at room temperature and atmospheric pressure. *J. Photochem.* **1985**, *31*, 21-28, doi:10.1016/0047-2670(85)85070-X.

Gleason, J. F.; Nesbitt, F. L.; Stief, L. J. Temperature dependence of the reaction between $O(^3P)$ and OClO at low pressure. *J. Phys. Chem.* **1994**, *98*, 126-131, doi:10.1021/j100052a022.

Goldfarb, L.; Burkholder, J. B.; Ravishankara, A. R. Kinetics of the O + ClO reaction. *J. Phys. Chem. A* **2001**, *105*, 5402-5409, doi:10.1021/jp0100351.

Goldfarb, L.; Harwood, M. H.; Burkholder, J. B.; Ravishankara, A. R. Reaction of $O(^3P)$ with $ClONO_2$: Rate coefficients and yield of NO_3 product. *J. Phys. Chem. A* **1998**, *102*, 8556-8563, doi:10.1021/jp9819386.

Goldfinger, P.; Huybrechts, G.; Martens, G. Elementary rate constants in atomic chlorination reactions. Part 2. - Experiments in competitive systems. *Trans. Faraday Soc.* **1961**, *57*, 2210-2219, doi:10.1039/tf9615702210.

Grimley, A. J.; Houston, P. L. The photochemistry of nitrosyl halides: The X + NOX → X_2 + NO(v) reaction (X = Cl, Br). *J. Chem. Phys.* **1980**, *72*, 1471-1475, doi:10.1063/1.439371.

Hack, W.; Mex, G.; Wagner, H. G. Determination of rate constant of reactions O + HCl in temperature range 293 to 718 K and OH + HCl at 293 K. *Ber. Bunsenges. Phys. Chem.* **1977**, *81*, 677-684, doi:10.1002/bbpc.19770810710.

Handwerk, V.; Zellner, R. Kinetics of the reactions of OH radicals with some halocarbons ($CHClF_2$, CH_2ClF, CH_2ClCF_3, CH_3CClF_2, CH_3CHF_2) in the temperature range 260-370 K. *Ber. Bunsenges. Phys. Chem.* **1978**, *82*, 1161-1166, doi:10.1002/bbpc.19780821117.

Hansen, J. C.; Friedl, R. R.; Sander, S. P. Kinetics of the OH + ClOOCl and OH + Cl_2O reactions: Experiment and theory. *J. Phys. Chem. A* **2008**, *112*, 9229-9237, doi:10.1021/jp8007706.

Hatakeyama, S.; Leu, M. T. Reactions of chlorine nitrate with HCl and H_2O. *Geophys. Res. Lett.* **1986**, *13*, 1343-1346, doi:10.1029/GL013i012p01343.

Hatakeyama, S.; Leu, M. T. Rate constants for reactions between atmospheric reservoir species. 2. H_2O. *J. Phys. Chem.* **1989**, *93*, 5784-5789, doi:10.1021/j100352a027.

Hayman, G. D.; Davies, J. M.; Cox, R. A. Kinetics of the reaction ClO + ClO → products and its potential relevance to Antarctic ozone. *Geophys. Res. Lett.* **1986**, *13*, 1347-1350, doi:10.1029/GL013i012p01347.

Heathfield, A. E.; Anastasi, C.; Pagsberg, P.; McCulloch, A. Atmospheric lifetimes of selected fluorinated ether compounds. *Atmos. Environ.* **1998**, *32*, 711-717, doi:10.1016/S1352-2310(97)00330-0.

Helleis, F.; Crowley, J. N.; Moortgat, G. K. Temperature-dependent rate constants and product branching ratios for the gas-phase reaction between CH_3O_2 and ClO. *J. Phys. Chem.* **1993**, *97*, 11464-11473, doi:10.1021/j100146a020.
Helleis, F.; Crowley, J. N.; Moortgat, G. K. Temperature dependent CH_3OCl formation in the reaction of CH_3O_2 and ClO. *Geophys. Res. Lett.* **1994**, *21*, 1795-1798, doi:10.1029/94GL01280.
Heneghan, S. P.; Benson, S. W. Kinetic study of the reactions of Cl and Br with H_2O_2. *Int. J. Chem. Kinet.* **1983**, *15*, 1311-1319, doi:10.1002/kin.550151206.
Heneghan, S. P.; Knoot, P. A.; Benson, S. W. The temperature coefficient of the rates in the system Cl + CH_4 ⇆ CH_3 + HCl, thermochemistry of the methyl radical. *Int. J. Chem. Kinet.* **1981**, *13*, 677-691, doi:10.1002/kin.550130708.
Herndon, S. C.; Gierczak, T.; Talukdar, R. K.; Ravishankara, A. R. Kinetics of the reactions of OH with several alkyl halides. *Phys. Chem. Chem. Phys.* **2001**, *3*, 4529-4535, doi:10.1039/b105188c.
Hickson, K. M.; Bergeat, A.; Costes, M. A low temperature study of the reactions of atomic chlorine with simple alkanes. *J. Phys. Chem. A* **2010**, *114*, 3038-3044, doi:10.1021/jp9061253.
Hickson, K. M.; Keyser, L. F. Kinetics of the Cl(^2P_J) + C_2H_6 reaction between 177 and 353 K. *J. Phys. Chem. A* **2004**, *108*, 1150-1159, doi:10.1021/jp036458f.
Hickson, K. M.; Keyser, L. F. A kinetic and product study of the Cl + HO_2 reaction. *J. Phys. Chem. A* **2005**, *109*, 6887-6900, doi:10.1021/jp051176w.
Hickson, K. M.; Keyser, L. F.; Sander, S. P. Temperature dependence of the HO_2+ClO reaction. 2. Reaction kinetics using the discharge-flow resonance-fluorescence technique. *J. Phys. Chem. A* **2007**, *111*, 8126-8138, doi:10.1021/jp0689464.
Hills, A. J.; Howard, C. J. Rate coefficient temperature dependence and branching ratio for the OH + ClO reaction. *J. Chem. Phys.* **1984**, *81*, 4458-4465, doi:10.1063/1.447414.
Hitsuda, K.; Takahashi, K.; Matsumi, Y.; Wallington, T. J. Kinetics of the reactions of Cl($^2P_{1/2}$) and Cl($^2P_{3/2}$) atoms with C_2H_6, C_2D_6, CH_3F, C_2H_5F, and CH_3CF_3 at 298 K. *J. Phys. Chem. A* **2001**, *105*, 5131-5136, doi:10.1021/jp003222s.
Hooshiyar, P. A.; Niki, H. Rate constants for the gas-phase reactions of Cl-atoms with C_2-C_8 alkanes at $T = 296 \pm 2$ K. *Int. J. Chem. Kinet.* **1995**, *27*, 1197-1206, doi:10.1002/kin.550271206.
Horowitz, A.; Bauer, D.; Crowley, J. N.; Moortgat, G. K. Determination of product branching ratio of the ClO self-reaction at 298 K. *Geophys. Res. Lett.* **1993**, *20*, 1423-1426, doi:10.1029/93GL01383.
Horowitz, A.; Crowley, J. N.; Moortgat, G. K. Temperature dependence of the product branching ratios of the ClO self-reaction in oxygen. *J. Phys. Chem.* **1994**, *98*, 11924-11930, doi:10.1021/j100097a019.
Howard, C. J. Rate constants for the gas-phase reactions of OH radicals with ethylene and halogenated ethylene compounds. *J. Chem. Phys.* **1976**, *65*, 4771-4777, doi:10.1063/1.432932.
Howard, C. J.; Evenson, K. M. Rate constants for the reactions of OH with CH_4 and fluorine, chlorine, and bromine substituted methanes at 296 K. *J. Chem. Phys.* **1976**, *64*, 197-202, doi:10.1063/1.431950.
Howard, C. J.; Evenson, K. M. Rate constants for the reactions of OH with ethane and some halogen substituted ethanes at 296 K. *J. Chem. Phys.* **1976**, *64*, 4303-4306, doi:10.1063/1.432115.
Hsin, H. Y.; Elrod, M. J. Overall rate constant measurements of the reaction of hydroxy- and chloroalkylperoxy radicals derived from methacrolein and methyl vinyl ketone with nitric oxide. *J. Phys. Chem. A* **2007**, *111*, 613-619, doi:10.1021/jp0665574.
Hsu, K. J.; DeMore, W. B. Rate constants for the reactions of OH with CH_3Cl, CH_2Cl_2, $CHCl_3$, and CH_3Br. *Geophys. Res. Lett.* **1994**, *21*, 805-808, doi:10.1029/94GL00601.
Hsu, K. J.; DeMore, W. B. Rate constants and temperature dependences for the reactions of hydroxyl radical with several halogenated methanes, ethanes, and propanes by relative rate measurements. *J. Phys. Chem.* **1995**, *99*, 1235-1244, doi:10.1021/j100004a025.
Huder, K.; DeMore, W. B. Rate constant for the reaction of OH with CH_3CCl_2F (HCFC-141b) determined by relative rate measurements with CH_4 and CH_3CCl_3. *Geophys. Res. Lett.* **1993**, *20*, 1575-1577, doi:10.1029/93GL01766.
Husain, D.; Plane, J. M. C.; Slater, N. K. H. Kinetic investigation of the reactions of OH($X^2\Pi$) with the hydrogen halides, HCl, DCl, HBr and DBr by time-resolved resonance fluorescence ($A^2\Sigma^+$ - $X^2\Pi$). *J. Chem. Soc. Faraday Trans. 2* **1981**, *77*, 1949-1962, doi:10.1039/f29817701949.
Husain, D.; Plane, J. M. C.; Xiang, C. C. Kinetic studies of the reactions of OH($X^2\Pi$) with hydrogen chloride and deuterium chloride at elevated temperatures by time-resolved resonance fluorescence ($A\ ^2\Sigma^+$ - $X\ ^2\Pi$). *J. Chem. Soc. Faraday Trans. 2* **1984**, *80*, 713-728, doi:10.1039/f29848000713.

Ingham, T.; Sander, S. P.; Friedl, R. R. Kinetics and product studies of the reaction of Br, Cl, and NO with ClOOCl using discharge-flow mass spectrometry. *Faraday Discuss.* **2005**, *130*, 89-110, doi:10.1039/b500179j.

Jeong, K. M.; Hsu, K. J.; Jeffries, J. B.; Kaufman, F. Kinetics of the reactions of OH with C_2H_6, CH_3CCl_3, $CH_2ClCHCl_2$, $CH_2ClCClF_2$, and CH_2FCF_3. *J. Phys. Chem.* **1984**, *88*, 1222-1226, doi:10.1021/j150650a041.

Jeong, K. M.; Kaufman, F. Rates of the reactions of 1, 1, 1-trichloroethane (methyl chloroform) and 1, 1, 2-trichloroethane with OH. *Geophys. Res. Lett.* **1979**, *6*, 757-759, doi:10.1029/GL006i010p00757.

Jeong, K. M.; Kaufman, F. Kinetics of the reaction of hydroxyl radical with methane and with nine Cl- and F-substituted methanes. 1. Experimental results, comparisons, and applications. *J. Phys. Chem.* **1982**, *86*, 1808-1815, doi:10.1021/j100207a016.

Jeoung, S. C.; Choo, K. Y.; Benson, S. W. Very low pressure reactor chemiluminescence studies on N atom reactions with $CHCl_3$ and $CDCl_3$. *J. Phys. Chem.* **1991**, *95*, 7282-7290, doi:10.1021/j100172a035.

Jiang, Z.; Taylor, P. H.; Dellinger, B. Laser photolysis/laser-induced fluorescence studies of the reaction of OH with 1,1,1-trichloroethane over an extended temperature range. *J. Phys. Chem.* **1992**, *96*, 8961-8964, doi:10.1021/j100201a048.

Jiang, Z.; Taylor, P. H.; Dellinger, B. Laser photolysis/laser-induced fluorescence studies of the reaction of OH with 1,1,1,2- and 1,1,2,2- tetrachloroethane over an extended temperature range. *J. Phys. Chem.* **1993**, *97*, 5050-5053, doi:10.1021/j100121a033.

Johnston, H. S.; Morris, E. D., Jr.; Van den Bogaerde, J. Molecular modulation kinetic spectrometry. ClOO and ClO_2 radicals in the photolysis of chlorine in oxygen. *J. Am. Chem. Soc.* **1969**, *91*, 7712-7727, doi:10.1021/ja50001a036.

Jourdain, J. L.; Le Bras, G.; Combourieu, J. Étude cinétique des réactions du 1,1,1 trifluoro 2 chloroéthane avec les atomes de chlore et d'oxygène. *J. Chim. Phys.* **1978**, *75*, 318-323, doi:10.1051/jcp/1978750318.

Jourdain, J. L.; Poulet, G.; Barassin, J.; Le Bras, G.; Combourieu, J. Mecanismes chimiques de la pollution atmospherique par les composes halogenes: etude cinetique de reactions elementaires possibles. *Pollut. Atmos.* **1977**, *75*, 256-259.

Jungkamp, T. P.; Kukui, A.; Schindler, R. N. Determination of rate constants and product branching ratios for the reactions of CH_3O_2 and CH_3O with Cl atoms at room temperature. *Ber. Bunsenges. Phys. Chem.* **1995**, *99*, 1057-1066, doi:10.1002/bbpc.199500031.

Kaiser, E. W. Relative rate constants for reactions of HFC 152a, 143, 143a, 134a, and HCFC 124 with F or Cl atoms and for CF_2CH_3, CF_2HCH_2, and CF_3CFH radicals with F_2, Cl_2, and O_2. *Int. J. Chem. Kinet.* **1993**, *25*, 667-680, doi:10.1002/kin.550250807.

Kaiser, E. W.; Pala, I. R.; Wallington, T. J. Kinetics and mechanism of the reaction of methacrolein with chlorine atoms in 1-950 Torr of N_2 or N_2/O_2 diluent at 297 K. *J. Phys. Chem. A* **2010**, *114*, 6850-6860, doi:10.1021/jp103317c.

Kaiser, E. W.; Rimai, L.; Schwab, E.; Lim, E. C. Application of time-resolved infrared spectroscopy to the determination of absolute rate constants for Cl + C_2H_6 and Cl + C_2H_5Cl. *J. Phys. Chem.* **1992**, *96*, 303-306, doi:10.1021/j100180a057.

Kaiser, E. W.; Wallington, T. J. FTIR product study of the Cl-initiated oxidation of CH_3Cl: Evidence for HCl elimination from the chloromethoxy radical. *J. Phys. Chem.* **1994**, *98*, 5679-5685, doi:10.1021/j100073a018.

Kasner, J. H.; Taylor, P. H.; Dellinger, B. Laser photolysis/laser induced fluorescence study of OH-C_2H_5Cl rate constants from 294 to 789 K. *J. Phys. Chem.* **1990**, *94*, 3250-3253, doi:10.1021/j100371a005.

Kaufman, F.; Gerri, N. J.; Pascale, D. A. Halogen catalyzed decomposition of nitrous oxide. *J. Chem. Phys.* **1956**, *24*, 32-34, doi:10.1063/1.1700847.

Kegley-Owen, C. S.; Gilles, M. K.; Burkholder, J. B.; Ravishankara, A. R. Rate coefficient measurement for the reaction OH + ClO → products. *J. Phys. Chem. A* **1999**, *103*, 5040-5048, doi:10.1021/jp9904320.

Kelly, C. C.; Yu, W. H. S.; Wijnen, M. H. J. Competitive chlorination reactions with ICl. II. CH_4, C_2H_6, C_3H_8, and C_2H_5Cl. *Can. J. Chem.* **1970**, *48*, 603-606, doi:10.1139/v70-099.

Kenner, R. D.; Ryan, K. R.; Plumb, I. C. Kinetics of the reaction of CH_3O_2 with ClO at 293 K. *Geophys. Res. Lett.* **1993**, *20*, 1571-1574, doi:10.1029/93GL01891.

Keyser, L. F. Absolute rate and temperature dependence of the reaction between chlorine (^2P) atoms and methane. *J. Chem. Phys.* **1978**, *69*, 214-218, doi:10.1063/1.436388.

Keyser, L. F. Absolute rate constant of the reaction between chlorine (^{2}P) atoms and hydrogen peroxide from 298 to 424 K. *J. Phys. Chem.* **1980**, *84*, 11-14, doi:10.1021/j100438a004.

Keyser, L. F. High pressure flow kinetics: a study of the OH + HCl reaction from 2 to 100 torr. *J. Phys. Chem.* **1984**, *88*, 4750-4758, doi:10.1021/j150664a061.
Kirchner, K.; Helf, D.; Ott, P.; Vogt, S. The reaction of OH radicals with 1,1-di-, tri- and tetrachloroethylene. *Ber. Bunsenges. Phys. Chem.* **1990**, *94*, 77-83, doi:10.1002/bbpc.19900940116.
Kita, D.; Stedman, D. H. Kinetic studies of reactions of hydrogen atoms with HCl, Cl_2 and NOCl, and chlorine atoms with H_2 and NOCl. *J. Chem. Soc. Faraday Trans. 2* **1982**, *78*, 1249-1259, doi:10.1039/f29827801249.
Klopffer, W.; Frank, R.; Kohl, E. G.; Haag, F. Quantitative erfassung der photochemischen transformationsprozesse in der troposphäre. *Chemiker-Zeitung* **1986**, *110*, 57-61.
Knight, G. P.; Beiderhase, T.; Helleis, F.; Moortgat, G. K.; Crowley, J. N. Reaction of HO_2 with ClO: Flow tube studies of kinetics and product formation between 215 and 298 K. *J. Phys. Chem. A* **2000**, *104*, 1674-1685, doi:10.1021/jp9924631.
Knox, J. H. Application of gas phase partition chromatography to competitive chlorination reactions. *Chemistry and Industry* **1955**, 1631-1632.
Knox, J. H. Competitive chlorinations Part 2.-Chloromethanes. *Trans. Faraday Soc.* **1962**, *58*, 275-283, doi:10.1039/tf9625800275.
Knox, J. H.; Nelson, R. L. Competitive chlorination reaction in the gas phase: Hydrogen and C_1-C_5 saturated hydrocarbons. *Trans. Far. Soc.* **1959**, *55*, 937-946, doi:10.1039/tf9595500937.
Koch, S.; Moortgat, G. K. Rate and mechanism of the reaction Cl + CH_3COOH. *Chem. Phys. Lett.* **1990**, *173*, 531-536, doi:10.1016/0009-2614(90)87248-P.
Kowalczyk, J.; Jowko, A.; Symanowicz, M. Kinetics of radical reactions in freons. *J. Radioanal. Nucl. Chem.* **1998**, *232*, 75-78, doi:10.1007/BF02383716.
Kukui, A.; Jungkamp, T. P. W.; Schindler, R. N. Determination of the product branching ratio in the reaction of NO_3 with OCl at 300 K. *Ber. Bunsenges. Phys. Chem.* **1994**, *98*, 1619-1621, doi:10.1002/bbpc.19940981219.
Kukui, A.; Roggenbuck, J.; Schindler, R. N. Mechanism and rate constants for the reactions of Cl atoms with HOCl, CH_3OCl and *tert*-C_4H_9OCl. *Ber. Bunsenges. Phys. Chem.* **1997**, *101*, 281-286, doi:10.1002/bbpc.19971010217.
Kukui, A. S.; Jungkamp, T. P. W.; Schindler, R. N. Determination of the rate constant and of product branching ratios in the reaction of CH_3O_2 with OCl between 233 K and 300 K. *Ber. Bunsenges. Phys. Chem.* **1994**, *98*, 1298-1302, doi:10.1002/bbpc.19940981013.
Kumaran, S. S.; Lim, K. P.; Michael, J. V. Thermal rate constants for the Cl + H_2 and Cl + D_2 reactions between 296 and 3000 K. *J. Chem. Phys.* **1994**, *101*, 9487-9498, doi:10.1063/1.468486.
Kurylo, M. J. Flash photolysis resonance fluorescence investigation of the reaction of O(^{3}P) atoms with $ClONO_2$. *Chem. Phys. Lett.* **1977**, *49*, 467-470, doi:10.1016/0009-2614(77)87016-4.
Kurylo, M. J.; Anderson, P. C.; Klais, O. A flash photolysis resonance fluorescence investigation of the reaction OH + CH_3CCl_3 → H_2O + CH_2CCl_3. *Geophys. Res. Lett.* **1979**, *6*, 760-762, doi:10.1029/GL006i010p00760.
Kurylo, M. J.; Braun, W. Flash photolysis resonance fluorescence study of the reaction Cl + O_3 → ClO + O_2 over the temperature range 213-298 K. *Chem. Phys. Lett.* **1976**, *37*, 232-235, doi:10.1016/0009-2614(76)80204-7.
Kurylo, M. J.; Knable, G. L. A kinetics investigation of the gas-phase reactions of Cl(^{2}P) and OH($X^2\Pi$) with CH_3CN: Atmospheric significance and evidence for decreased reactivity between strong electrophiles. *J. Phys. Chem.* **1984**, *88*, 3305-3308, doi:10.1021/j150659a033.
Kurylo, M. J.; Knable, G. L.; Murphy, J. L. A reinvestigation of the Cl + $ClONO_2$ reaction by flash photolysis resonance fluorescence. *Chem. Phys. Lett.* **1983**, *95*, 9-12, doi:10.1016/0009-2614(83)80800-8.
Kurylo, M. J.; Murphy, J. L.; Knable, G. L. Rate constant measurements for the reaction of Cl atoms with nitric acid over the temperature range 240-300 K. *Chem. Phys. Lett.* **1983**, *94*, 281-284, doi:10.1016/0009-2614(83)87088-2.
Lancar, I.; Le Bras, G.; Poulet, G. Oxidation of CH_3CCl_3 and CH_3CFCl_2 in the atmosphere : kinetic study of OH reactions. *J. Chim. Phys.* **1993**, *90*, 1897-1908, doi:10.1051/jcp/1993901897.
Langbein, T.; Sonntag, H.; Trapp, D.; Hoffmann, A.; Malms, W.; Röth, E.-P.; Mörs, V.; Zellner, R. Volatile anaesthetics and the atmosphere: atmospheric lifetimes and atmospheric effects of halothane, enflurane, isoflurane, desflurane and sevoflurane. *British J. Anaest.* **1999**, *82*, 66-73.
Lazarou, Y. G.; Michael, C.; Papagiannakopoulos, P. Kinetics of the reaction of chlorine atoms with dimethylnitramine. *J. Phys. Chem.* **1992**, *96*, 1705-1708, doi:10.1021/j100183a039.

Leather, K. E.; Bacak, A.; Wamsley, R.; Archibald, A. T.; Husk, A.; Shallcross, D. E.; Percival, C. J. Temperature and pressure dependence of the rate coefficient for the reaction between ClO and CH_3O_2 in the gas-phase. *Phys. Chem. Chem. Phys.* **2012**, *14*, 3425–3434, doi:10.1039/c2cp22834c.

Leck, T. J.; Cook, J. L.; Birks, J. W. Studies of reactions of importance in the stratosphere. III. Rate constant and products of the reaction between ClO and HO_2 radicals at 298 K. *J. Chem. Phys.* **1980**, *72*, 2364-2373, doi:10.1063/1.439484.

Lee, F. S. C.; Rowland, F. S. Competitive radiotracer evaluation of relative rate constants at stratospheric temperatures for reactions of ^{38}Cl with CH_4 and C_2H_6 vs. CH_2=CHBr. *J. Phys. Chem.* **1977**, *81*, 86-87, doi:10.1021/j100516a020.

Lee, J. H.; Michael, J. V.; Payne, W. A., Jr.; Stief, L. J. Absolute rate of the reaction of Cl(^2P) with molecular hydrogen from 200-500 K. *J. Chem. Soc. Faraday Trans. 1* **1977**, *73*, 1530-1536, doi:10.1039/f19777301530.

Lee, Y.-P.; Howard, C. J. Temperature dependence of the rate constant and the branching ratio for the reaction Cl + HO_2. *J. Chem. Phys.* **1982**, *77*, 756-763, doi:10.1063/1.443892.

Lee, Y.-P.; Stimpfle, R. M.; Perry, R. A.; Mucha, J. A.; Evenson, K. M.; Jennings, D. A.; Howard, C. J. Laser magnetic resonance spectroscopy of ClO and kinetic studies of the reactions of ClO with NO and NO_2. *Int. J. Chem. Kinet.* **1982**, *14*, 711-732, doi:10.1002/kin.550140612.

Lesar, A.; Hodošček, M.; Senegačnik, M. Experimental and theoretical studies of the decomposition of N_2O catalyzed by chlorine. *J. Chem. Phys.* **1996**, *105*, 917-926, doi:10.1063/1.471935.

Lesclaux, R.; Caralp, F. Determination of the rate constants for the reactions of $CFCl_2O_2$ radical with NO and NO_2 by laser photolysis and time resolved mass spectrometry. *Int. J. Chem. Kinet.* **1984**, *16*, 1117-1128, doi:10.1002/kin.550160907.

Lesclaux, R.; Dognon, A. M.; Caralp, F. Photo-oxidation of halomethanes at low temperature: The decomposition rate of CCl_3O and $CFCl_2O$ radicals. *J. Photochem. Photobiol. A: Chem.* **1987**, *41*, 1-11, doi:10.1016/1010-6030(87)80001-1.

Leu, M.-T.; DeMore, W. B. Rate constants at 295 K for the reactions of atomic chlorine with H_2O_2, HO_2, O_3, CH_4 and HNO_3. *Chem. Phys. Lett.* **1976**, *41*, 121-124, doi:10.1016/0009-2614(76)85261-X.

Leu, M.-T.; DeMore, W. B. Rate constant for the reaction ClO + NO → Cl + NO_2. *J. Phys. Chem.* **1978**, *82*, 2049-2052, doi:10.1021/j100508a001.

Leu, M.-T.; Hatkeyama, S.; Hsu, K. J. Rate constants for reactions between atmospheric reservoir species. 1. HCl. *J. Phys. Chem.* **1989**, *93*, 5778-5784, doi:10.1021/j100352a026.

Leu, M.-T.; Lin, C. L. Rate constants for the reactions of OH with ClO, Cl_2, and Cl_2O at 298K. *Geophys. Res. Lett.* **1979**, *6*, 425-428, doi:10.1029/GL006i006p00425.

Leu, M.-T.; Yung, Y. L. Determination of $O_2(a^1\Delta_g)$ and $O_2(b^1\Sigma_g^+)$ yields in the reaction O + ClO → Cl + O_2: Implications for photochemistry in the atmosphere of Venus. *Geophys. Res. Lett.* **1987**, *14*, 949-952, doi:10.1029/GL014i009p00949.

Leu, M. T. Product distribution for the reaction of HO_2 with ClO. *Geophys. Res. Lett.* **1980**, *7*, 173-175, doi:10.1029/GL007i002p00173.

Leu, M. T. Kinetics of the reaction O + ClO → Cl + O_2. *J. Phys. Chem.* **1984**, *88*, 1394-1398, doi:10.1021/j150651a032.

Lewis, R. S.; Sander, S. P.; Wagner, S.; Watson, R. T. Temperature-dependent rate constants for the reaction of ground-state chlorine with simple alkanes. *J. Phys. Chem.* **1980**, *84*, 2009-2015, doi:10.1021/j100453a004.

Li, Q.; Osborne, M. C.; Smith, I. W. M. Rate constants for the reactions of Cl atoms with HCOOH and with HOCO radicals. *Int. J. Chem. Kinet.* **2000**, *32*, 85-91, doi:10.1002/(SICI)1097-4601(2000)32:2<85::AID-KIN3>3.0.CO;2-I.

Li, Z. J.; Wuebbles, R. D.; Pylawka, N. J. Rate constant measurement for the reaction of OClO with NO at 220-367 K. *Chem. Phys. Lett.* **2002**, *354*, 491-497, doi:10.1016/S0009-2614(02)00181-1.

Lightfoot, P. D.; Veyret, B.; Lesclaux, R. Flash photolysis study of the CH_3O_2 + HO_2 reaction between 248 and 573 K. *J. Phys. Chem.* **1990**, *94*, 708-714, doi:10.1021/j100365a036.

Lin, C. L.; Leu, M. T.; DeMore, W. B. Rate constant for the reaction of atomic chlorine with methane. *J. Phys. Chem.* **1978**, *82*, 1772-1777, doi:10.1021/j100505a002.

Lipson, J. B.; Beiderhase, T. W.; Molina, L. T.; Molina, M. J.; Olzmann, M. Production of HCl in the OH + ClO reaction: Laboratory measurements and statistical rate theory calculations. *J. Phys. Chem. A* **1999**, *103*, 6540-6551, doi:10.1021/jp9847787.

Lipson, J. B.; Elrod, M. J.; Beiderhase, T. W.; Molina, L. T.; Molina, M. J. Temperature dependence of the rate constant and branching ratio for the OH + ClO reaction. *J. Chem. Soc. Faraday Trans.* **1997**, *93*, 2665-2673, doi:10.1039/a701946g.

Liu, A.; Mulac, W. A.; Jonah, C. D. Pulse radiolysis study of the gas-phase reaction of OH radicals with vinyl chloride at 1 atm and over the temperature range 313-1173 K. *J. Phys. Chem.* **1989**, *93*, 4092-4094, doi:10.1021/j100347a043.

Liu, R.; Huie, R. E.; Kurylo, M. J. Rate constants for the reactions of the OH radical with some hydrochlorofluorocarbons over the temperature range 270-400 K. *J. Phys. Chem.* **1990**, *94*, 3247-3249, doi:10.1021/j100371a004.

Loewenstein, L. M.; Anderson, J. G. Rate and product measurements for the reactions of OH with Cl_2, Br_2, and BrCl at 298 K. Trend interpretations. *J. Phys. Chem.* **1984**, *88*, 6277-6286, doi:10.1021/j150669a045.

Louis, F.; Talhaoui, A.; Sawerysyn, J.-P.; Rayez, M.-T.; Rayez, J.-C. Rate coefficients for the gas phase reactions of CF_3CH_2F (HFC-134a) with chlorine and fluorine atoms: experimental and ab initio theoretical studies. *J. Phys. Chem. A* **1997**, *101*, 8503-8507, doi:10.1021/jp972001s.

Mahmud, K.; Kim, J. S.; Fontijn, A. A high-temperature photochemical kinetics study of the O + HCl reaction from 350 K to 1480 K. *J. Phys. Chem.* **1990**, *94*, 2994-2998, doi:10.1021/j100370a048.

Manning, R. G.; Kurylo, M. J. Flash photolysis resonance fluorescence investigation of the temperature dependencies of the reactions of $Cl(^2P)$ atoms with CH_4, CH_3Cl, CH_3F, $CH_3F^{\dagger}$, and C_2H_6. *J. Phys. Chem.* **1977**, *81*, 291-296, doi:10.1021/j100519a003.

Margitan, J. J. Chlorine nitrate photochemistry. Photolysis products and kinetics of the reaction $Cl + ClONO_2 \rightarrow Cl_2 + NO_3$. *J. Phys. Chem.* **1983**, *87*, 674-679, doi:10.1021/j100227a029.

Margitan, J. J. Kinetics of the reaction $O + ClO \rightarrow Cl + O_2$. *J. Phys. Chem.* **1984**, *88*, 3638-3643, doi:10.1021/j150660a052.

Maricq, M. M.; Szente, J. J.; Kaiser, E. W.; Shi, J. Reaction of chlorine atoms with methylperoxy and ethylperoxy radicals. *J. Phys. Chem.* **1994**, *98*, 2083-2089, doi:10.1021/j100059a017.

Markert, F.; Nielsen, O. J. The reactions of OH radicals with chloroalkanes in the temperature range 295-360 K. *Chem. Phys. Lett.* **1992**, *194*, 123-127, doi:10.1016/0009-2614(92)85753-W.

Martens, G. J.; Godfroid, M.; Delvaux, J.; Verbeyst, J. Gas-phase hydrogen abstraction from asymmetrically halogenated ethanes by chlorine atoms. *Int. J. Chem. Kinet.* **1976**, *8*, 153-158, doi:10.1002/kin.550080116.

Martinez, E.; Aranda, A.; Diaz de Mera, Y.; Rodriguez, A.; Rodriguez, D.; Notario, A. Mechanistic and kinetic study of the gas-phase reaction of atomic chlorine with cyclohexanone using an absolute and a relative technique; Influence of temperature. *J. Atmos. Chem.* **2004**, *48*, 283-299, doi:10.1023/B:JOCH.0000044424.22309.d8.

Mauldin, R. L.; Burkholder, J. B.; Ravishankara, A. R. The reaction of $O(^3P)$ with OClO. *Int. J. Chem. Kinet.* **1997**, *29*, 139-147, doi:10.1002/(SICI)1097-4601(1997)29:2<139::AID-KIN8>3.0.CO;2-V.

Mauldin, R. L., III; Burkholder, J. B.; Ravishankara, A. R. A photochemical, thermodynamic, and kinetic study of ClOO. *J. Phys. Chem.* **1992**, *96*, 2582-2588, doi:10.1021/j100185a035.

McGillen, M. R.; Bernard, F.; Fleming, E. L.; Burkholder, J. B. HCFC-133a (CF_3CH_2Cl): OH rate coefficient, UV and infrared absorption spectra, and atmospheric implications. *Geophys. Res. Lett.* **2015**, *42*, 6098-6105, doi:10.1002/2015GL064939.

Meier, U.; Grotheer, H. H.; Just, T. Temperature dependence and branching ratio of the CH_3OH + OH reaction. *Chem. Phys. Lett.* **1984**, *106*, 97-101, doi:10.1016/0009-2614(84)87019-0.

Mellouki, A. Kinetic studies of Cl atom reactions with series of alkanes using the pulsed laser photolysis resonance fluorescence method. *J. Chim. Phys.* **1998**, *95*, 513-522, doi:10.1051/jcp:1998165.

Mellouki, A.; Le Bras, G.; Poulet, G. Discharge flow kinetic study of NO_3 reactions with free radicals: The reaction of NO_3 with Cl. *J. Phys. Chem.* **1987**, *91*, 5760-5764, doi:10.1021/j100306a048.

Mellouki, A.; Poulet, G.; Le Bras, G.; Singer, R.; Burrows, J. P.; Moortgat, G. K. Discharge flow kinetic study of the reactions of NO_3 with Br, BrO, HBr, and HCl. *J. Phys. Chem.* **1989**, *93*, 8017-8021, doi:10.1021/j100361a012.

Michael, J. V.; Lee, J. H. Selected rate constants for H, O, N, and Cl atoms with substrates at room temperatures. *Chem. Phys. Lett.* **1977**, *51*, 303-306, doi:10.1016/0009-2614(77)80408-9.

Michael, J. V.; Nava, D. F.; Payne, W. A.; Stief, L. J. Rate constant for the reaction of atomic chlorine with formaldehyde from 200 to 500 K. *J. Chem. Phys.* **1979**, *70*, 1147-1150, doi:10.1063/1.437593.

Michael, J. V.; Nava, D. F.; Payne, W. A.; Stief, L. J. Rate constants for the reaction of atomic chlorine with methanol and dimethyl ether from 200 to 500 K. *J. Chem. Phys.* **1979**, *70*, 3652-3656, doi:10.1063/1.437957.

Michael, J. V.; Whytock, D. A.; Lee, J. H.; Payne, W. A.; Stief, L. J. Absolute rate constant for the reaction of atomic chlorine with hydrogen peroxide vapor over the temperature range 265-400 K. *J. Chem. Phys.* **1977**, *67*, 3533-3536, doi:10.1063/1.435351.

Miller, J. C.; Gordon, R. J. Kinetics of the Cl-H_2 system. I. Detailed balance in the Cl + H_2 reaction. *J. Chem. Phys.* **1981**, *75*, 5305-5310, doi:10.1063/1.441972.

Miziolek, A. W.; Molina, M. J. The rate constant for the reaction of oxygen (^{3}P) atoms with dichlorine monoxide. *J. Phys. Chem.* **1978**, *82*, 1769-1771, doi:10.1021/j100505a001.

Mogelberg, T. E.; Nielsen, O. J.; Sehested, J.; Wallington, T. J. Atmospheric chemistry of HCFC-133a: the UV absorption spectra of CF_3CClH and CF_3CClHO_2 radicals, reactions of CF_3CClHO_2 with NO and NO_2, and fate of CF_3CClHO radicals. *J. Phys. Chem.* **1995**, *99*, 13437-13444, doi:10.1021/j100036a018.

Molina, L. T.; Molina, M. J.; Stachnik, R. A.; Tom, R. D. An upper limit to the rate of the HCl + $ClONO_2$ reaction. *J. Phys. Chem.* **1985**, *89*, 3779-3781, doi:10.1021/j100264a003.

Molina, L. T.; Spencer, J. E.; Molina, M. J. The rate constant for the reaction of O(^{3}P) atoms with $ClONO_2$. *Chem. Phys. Lett.* **1977**, *45*, 158-162, doi:10.1016/0009-2614(77)85233-0.

Molina, M. J.; Molina, L. T.; Smith, C. A. The rate of the reaction of OH with HCl. *Int. J. Chem. Kinet.* **1984**, *16*, 1151-1160, doi:10.1002/kin.550160910.

Mörs, V.; Hoffman, A.; Malms, W.; Zellner, R. Time resolved studies of intermediate products in the oxidation of HCFC 141b ($CFCl_2CH_3$) and HCFC 142b (CF_2ClCH_3). *Ber. Bunsenges, Phys. Chem.* **1996**, *100*, 540-552, doi:10.1002/bbpc.19961000504.

Nelson, D. D., Jr.; Zahniser, M. S.; Kolb, C. E. Chemical kinetics of the reactions of the OH radical with several hydrochlorofluoropropanes. *J. Phys. Chem.* **1992**, *96*, 249-253, doi:10.1021/j100180a048.

Nelson, H. H.; Johnston, H. S. Kinetics of the reaction of Cl with ClNO and $ClNO_2$ and the photochemistry of $ClNO_2$. *J. Phys. Chem.* **1981**, *85*, 3891-3896, doi:10.1021/j150625a036.

Nelson, L.; Rattigan, O.; Neavyn, R.; Sidebottom, H.; Treacy, J.; Nielsen, O. J. Absolute and relative rate constants for the reactions of hydroxyl radicals and chlorine atoms with a series of aliphatic alcohols and ethers at 298 K. *Int. J. Chem. Kinet.* **1990**, *22*, 1111-1126, doi:10.1002/kin.550221102.

Nelson, L.; Shanahan, I.; Sidebottom, H. W.; Treacy, J.; Nielsen, O. J. Kinetics and mechanism for the oxidation of 1,1,1-trichloroethane. *Int. J. Chem. Kinet.* **1990**, *22*, 577-590, doi:10.1002/kin.550220603.

Nesbitt, F. L.; Nava, D. F.; Payne, W. A.; Stief, L. J. Absolute rate constant for the reaction of Cl(^{2}P) with ClNO. *J. Phys. Chem.* **1987**, *91*, 5337-5340, doi:10.1021/j100304a039.

Nicholas, J. E.; Norrish, R. G. W. Some reactions in the chlorine and oxygen system studied by flash photolysis. *Proc. Roy. Soc. A* **1968**, *307*, 391-397, doi:10.1098/rspa.1968.0197.

Nickolaisen, S. L.; Friedl, R. R.; Sander, S. P. Kinetics and mechanism of the ClO + ClO reaction: Pressure and temperature dependences of the bimolecular and termolecular channels and thermal decomposition of chlorine peroxide, ClOOCl. *J. Phys. Chem.* **1994**, *98*, 155-169, doi:10.1021/j100052a027.

Nickolaisen, S. L.; Roehl, C. M.; Blakeley, L. K.; Friedl, R. R.; Francisco, J. S.; Liu, R. F.; Sander, S. P. Temperature dependence of the HO_2 + ClO reaction. 1. Reaction kinetics by pulsed photolysis-ultraviolet absorption and ab initio studies of the potential surface. *J. Phys. Chem. A* **2000**, *104*, 308-319, doi:10.1021/jp992753h.

Nicovich, J. M.; Kreutter, K. D.; Wine, P. H. Kinetics of the reactions of Cl(^2P_J) and Br($^2P_{3/2}$) with O_3. *Int. J. Chem. Kinet.* **1990**, *22*, 399-414, doi:10.1002/kin.550220407.

Nicovich, J. M.; Wine, P. H.; Ravishankara, A. R. Pulsed laser photolysis kinetics study of the O(^3P) + ClO reaction. *J. Chem. Phys.* **1988**, *89*, 5670-5679, doi:10.1063/1.455574.

Nielsen, O. J. Rate constants for the gas-phase reactions of OH radicals with CH_3CHF_2 and $CHCl_2CF_3$ over the temperature range 295-388 K. *Chem. Phys. Lett.* **1991**, *187*, 286-290, doi:10.1016/0009-2614(91)90427-B.

Nielsen, O. J.; Ellermann, T.; Bartkiewicz, E.; Wallington, T. J.; Hurley, M. D. UV absorption spectra, kinetics and mechanisms of the self-reaction of CHF_2O_2 radicals in the gas phase at 298 K. *Chem. Phys. Lett.* **1992**, *192*, 82-88, doi:10.1016/0009-2614(92)85432-A.

Nielsen, O. J.; Ellermann, T.; Sehested, J.; Wallington, T. J. Ultraviolet absorption spectrum and kinetics and mechanism of the self-reaction of $CHF_2CF_2O_2$ radicals in the gas phase at 298 K. *J. Phys. Chem.* **1992**, *96*, 10875-10879, doi:10.1021/j100205a050.

Nielsen, O. J.; Gamborg, E.; Sehested, J.; Wallington, T. J.; Hurley, M. D. Atmospheric chemistry of HFC-143a: Spectrokinetic investigation of the $CF_3CH_2O_2$• radical, its reactions with NO and NO_2 and the fate of CF_3CH_2O. *J. Phys. Chem. A* **1994**, *98*, 9518-9525, doi:10.1021/j100089a026.

Nielsen, O. J.; Sidebottom, H. W.; Donlon, M.; Treacy, J. An absolute- and relative-rate study of the gas-phase reaction of OH radicals and Cl atoms with *n*-alkyl nitrates. *Chem. Phys. Lett.* **1991**, *178*, 163-170, doi:10.1016/0009-2614(91)87051-C.

Niki, H.; Maker, P. D.; Breitenbach, L. P.; Savage, C. M. FTIR studies of the kinetics and mechanism for the reaction of Cl atom with formaldehyde. *Chem. Phys. Lett.* **1978**, *57*, 596-599, doi:10.1016/0009-2614(78)85328-7.

Niki, H.; Maker, P. D.; Savage, C. M.; Breitenbach, L. P. An FTIR study of the Cl atom-initiated oxidation of CH_2Cl_2 and CH_3Cl. *Int. J. Chem. Kinet.* **1980**, *12*, 1001-1012, doi:10.1002/kin.550121209.

Nilsson, E. J. K.; Johnson, M. S.; Nielsen, O. J.; Kaiser, E. W.; Wallington, T. J. Kinetics of the gas-phase reactions of chlorine atoms with CH_2F_2, CH_3CCl_3, and CF_3CFH_2 over the temperature range 253-553 K. *Int. J. Chem Kinet.* **2009**, *41*, 401-406, doi:10.1002/kin.20398.

Nordmeyer, T.; Wang, W.; Ragains, M. L.; Finlayson-Pitts, B. J.; Spicer, C. W.; Plastridge, R. A. Unique products of the reaction of isoprene with atomic chlorine: Potential markers of chlorine atom chemistry. *Geophys. Res. Lett.* **1997**, *24*, 1615-1618, doi:10.1029/97GL01547.

Notario, A.; Le Bras, G.; Mellouki, A. Kinetics of Cl atom reactions with butadienes including isoprene. *Chem. Phys. Lett.* **1997**, *281*, 421-425, doi:10.1016/S0009-2614(97)01303-1.

Notario, A.; Mellouki, A.; Le Bras, G. Rate constants for the gas-phase reactions of chlorine atoms with a series of ketones. *Int. J. Chem. Kinet.* **2000**, *32*, 62-66, doi:10.1002/(SICI)1097-4601(2000)32:1<67::AID-JCK8>3.0.CO;2-M.

Olbregts, J.; Brasseur, G.; Arijs, E. J. Reaction of acetonitrile and chlorine atoms. *J. Photochem.* **1984**, *24*, 315-322, doi:10.1016/0047-2670(84)80013-1.

Olsson, B.; Hallquist, M.; Ljungstrom, E.; Davidsson, J. A kinetic study of chlorine radical reactions with ketones by laser photolysis technique. *Int. J. Chem. Kinet.* **1997**, *29*, 195-201, doi:10.1002/(SICI)1097-4601(1997)29:3<195::AID-KIN6>3.0.CO;2-P.

Ongstad, A. P.; Birks, J. W. Studies of reactions of importance in the stratosphere. V. Rate constants for the reactions $O + NO_2 \rightarrow NO + O_2$ and $O + ClO \rightarrow Cl + O_2$ at 298 K. *J. Chem. Phys.* **1984**, *81*, 3922-3930, doi:10.1063/1.448185.

Ongstad, A. P.; Birks, J. W. Studies of reactions of importance in the stratosphere. VI. Temperature dependence of the reactions $O + NO_2 \rightarrow NO + O_2$ and $O + ClO \rightarrow Cl + O_2$. *J. Chem. Phys.* **1986**, *85*, 3359-3368, doi:10.1063/1.450957.

Orkin, V. L.; Khamaganov, V. G. Determination of rate constants for reactions of some hydrohaloalkanes with OH radicals and their atmospheric lifetimes. *J. Atmos. Chem.* **1993**, *16*, 157-167, doi:10.1007/BF00702785.

Orkin, V. L.; Khamaganov, V. G.; Kasimovskaya, E. E.; Guschin, A. G. Photochemical properties of some Cl-containing halogenated alkanes. *J. Phys. Chem. A* **2013**, *117*, 5483-5490, doi:10.1021/jp400408y.

Orkin, V. L.; Martynova, L. E.; Kurylo, M. J. Photochemical properties of *trans*-1-chloro-3,3,3-trifluoropropene (*trans*-$CHCl=CHCF_3$): OH reaction rate constant, UV and IR absorption spectra, global warming potential, and ozone depletion potential. *J. Phys. Chem. A* **2014**, *118*, 5263-5271, doi:10.1021/jp5018949.

Orlando, J. J. Temperature dependence of the rate coefficients for the reaction of chlorine atoms with chloromethanes. *Int. J. Chem. Kinet.* **1999**, *31*, 515-524, doi:10.1029/90JD02734.

Orlando, J. J.; Tyndall, G. S.; Apel, E. C.; Riemer, D. D.; Paulson, S. E. Rate coefficients and mechanisms of the reaction of Cl-atoms with a series of unsaturated hydrocarbons under atmospheric conditions. *Int. J. Chem. Kinet.* **2003**, *35*, 334-353, doi:10.1002/kin.10135.

Orlando, J. J.; Tyndall, G. S.; Vereecken, L.; Peeters, J. The atmospheric chemistry of the acetonoxy radical. *J. Phys. Chem. A* **2000**, *104*, 11578-11588, doi:10.1021/jp0026991.

Pagsberg, P.; Munk, J.; Sillesen, A.; Anastasi, C. UV spectrum and kinetics of hydroxylmethyl radicals. *Chem. Phys. Lett.* **1988**, *146*, 375-381, doi:10.1016/0009-2614(88)87462-1.

Papanastasiou, D. K.; Burkholder, J. B. Rate coefficients for the $O(^3P) + Cl_2O$ gas-phase reaction between 230 and 357 K. *Int. J. Chem Kinet.* **2011**, *43*, 312-321, doi:10.1002/kin.20556.

Paraskevopoulos, G.; Singleton, D. L.; Irwin, R. S. Rates of OH radical reactions. 8. Reactions with CH_2FCl, CHF_2Cl, $CHFCl_2$, CH_3CF_2Cl, CH_3Cl, and C_2H_5Cl at 297 K. *J. Phys. Chem.* **1981**, *85*, 561-564, doi:10.1021/j150605a021.

Patchen, A. K.; Pennino, M. J.; Elrod, M. J. Overall rate constant measurements of the reaction of chloroalkylperoxy radicals with nitric oxide. *J. Phys. Chem. A* **2005**, *109*, 5865-5871, doi:10.1021/jp050388q.
Payne, W. A.; Brunning, J.; Mitchell, M. B.; Stief, L. J. Kinetics of the reactions of atomic chlorine with methanol and the hydroxymethyl radical with molecular oxygen at 298 K. *Int. J. Chem. Kinet.* **1988**, *20*, 63-74, doi:10.1002/kin.550200108.
Perry, R. A.; Atkinson, R.; Pitts, J. N., Jr. Rate constants for the reaction of OH radicals with $CHFCl_2$ and CH_3Cl over the temperature range 298-423 °K, and with CH_2Cl_2 at 298 °K. *J. Chem. Phys.* **1976**, *64*, 1618-1620, doi:10.1063/1.432335.
Perry, R. A.; Atkinson, R.; Pitts, J. N., Jr. Rate constants for the reaction of OH radicals with CH_2=CHF, CH_2=CHCl, and CH_2=CHBr over the temperature range 299-426 °K. *J. Chem. Phys.* **1977**, *67*, 458-462, doi:10.1063/1.434889.
Pilgrim, J. S.; McIlroy, A.; Taatjes, C. A. Kinetics of Cl atom reactions with methane, ethane, and propane from 292 to 800 K. *J. Phys. Chem. A* **1997**, *101*, 1873-1880, doi:10.1021/jp962916r.
Platz, J.; Nielson, O. J.; Sehested, J.; Wallington, T. J. Atmospheric chemistry of l,l,l-trichloroethane: UV absorption spectra and self-reaction kinetics of CCl_3CH_2 and $CCl_3CH_2O_2$ radicals, kinetics of the reactions of the $CCl_3CH_2O_2$ Radical with NO and NO_2, and the fate of the alkoxy radical CCl_3CH_2O. *J. Phys. Chem.* **1995**, *99*, 6570-6579, doi:10.1021/j100017a044.
Poulet, G.; Laverdet, G.; Jourdain, J. L.; Le Bras, G. Kinetic study of the reactions of acetonitrile with Cl and OH radicals. *J. Phys. Chem.* **1984**, *88*, 6259-6263, doi:10.1021/j150669a041.
Poulet, G.; Laverdet, G.; Le Bras, G. Discharge flow-mass spectrometric determination of the rate coefficients for the reactions of formaldehyde with bromine atoms and chlorine atoms. *J. Phys. Chem.* **1981**, *85*, 1892-1895, doi:10.1021/j150613a023.
Poulet, G.; Laverdet, G.; Le Bras, G. Rate constant and branching ratio for the reaction of OH with ClO. *J. Phys. Chem.* **1986**, *90*, 159-165, doi:10.1021/j100273a036.
Poulet, G.; Le Bras, G.; Combourieu, J. Étude cinétique des réactions du chlore atomique et du radical ClO avec le méthane par la technique du réacteur a écoulement rapide, couplé a un spectromètre de masse. *J. Chim. Phys.* **1974**, *71*, 101-106, doi:10.1051/jcp/1974710101.
Poulet, G.; Le Bras, G.; Combourieu, J. Kinetic study of the reactions of Cl atoms with HNO_3, H_2O_2, and HO_2. *J. Chem. Phys.* **1978**, *69*, 767-773, doi:10.1063/1.436588.
Poulet, G.; Le Bras, G.; Combourieu, J. E.P.R. study of the reactivity of ClO with H_2CO at 298 K. *Geophys. Res. Lett.* **1980**, *7*, 413-414, doi:10.1029/GL007i005p00413.
Poulet, G.; Zagogianni, H.; Le Bras, G. Kinetics and mechanism of the OH + ClO_2 reaction. *Int. J. Chem. Kinet.* **1986**, *18*, 847-859, doi:10.1002/kin.550180805.
Pritchard, H. O.; Pyke, J. B.; Trotman-Dickenson, A. F. A method for the study of chlorine atom reactions. The reaction Cl + CH_4 → CH_3 + HCl. *J. Am. Chem. Soc.* **1954**, *76*, 1201-1202, doi:10.1021/ja01633a100.
Pritchard, H. O.; Pyke, J. B.; Trotman-Dickenson, A. F. The study of chlorine atom reactions in the gas phase. *J. Am. Chem. Soc.* **1955**, *77*, 2629-2633, doi:10.1021/ja01614a088.
Qiu, L. X.; Shi, S.-H.; Xing, S. B.; Chen, X. G. Rate constants for the reactions of OH with five halogen-substituted ethanes from 292 to 366 K. *J. Phys. Chem.* **1992**, *96*, 685-689, doi:10.1021/j100181a032.
Radford, H. E. The fast reaction of CH_2OH with O_2. *Chem. Phys. Lett.* **1980**, *71*, 195-197, doi:10.1016/0009-2614(80)80145-X.
Radford, H. E.; Evenson, K. M.; Jennings, D. A. Far-infrared LMR detection of hydroxymethyl. *Chem. Phys. Lett.* **1981**, *78*, 589-591, doi:10.1016/0009-2614(81)85264-5.
Ragains, M. L.; Finlayson Pitts, B. J. Kinetics and mechanism of the reaction of Cl atoms with 2-methyl-1,3-butadiene (isoprene) at 298 K. *J. Phys. Chem. A* **1997**, *101*, 1509-1517, doi:10.1021/jp962786m.
Ravishankara, A. R.; Davis, D. D.; Smith, G.; Tesi, G.; Spencer, J. A study of the chemical degradation of $ClONO_2$ in the stratosphere. *Geophys. Res. Lett.* **1977**, *4*, 7-9, doi:10.1029/GL004i001p00007.
Ravishankara, A. R.; Eisele, F. L.; Wine, P. H. The kinetics of the reaction of OH with ClO. *J. Chem. Phys.* **1983**, *78*, 1140-1144, doi:10.1063/1.444906.
Ravishankara, A. R.; Smith, G.; Watson, R. T.; Davis, D. D. A temperature dependent kinetics study of the reaction of HCl with OH and O(^{3}P). *J. Phys. Chem.* **1977**, *81*, 2220-2225, doi:10.1021/j100539a002.
Ravishankara, A. R.; Wine, P. H. A laser flash photolysis-resonance fluorescence kinetics study of the reaction Cl(^2P) + CH_4 → CH_3 + HCl. *J. Chem. Phys.* **1980**, *72*, 25-30, doi:10.1063/1.438885.
Ravishankara, A. R.; Wine, P. H.; Wells, J. R.; Thompson, R. L. Kinetic study of the reaction of OH with HCl from 240–1055 K. *Int. J. Chem. Kinet.* **1985**, *17*, 1281-1297, doi:10.1002/kin.550171206.

Ray, G. W.; Keyser, L. F.; Watson, R. T. Kinetics study of the Cl(^{2}P) + Cl_2O → Cl_2 + ClO reaction at 298 K. *J. Phys. Chem.* **1980**, *84*, 1674-1681, doi:10.1021/j100450a003.
Ray, G. W.; Watson, R. T. Kinetics study of the reactions of NO with FO, ClO, BrO, and IO at 298 K. *J. Phys. Chem.* **1981**, *85*, 2955-2960, doi:10.1021/j150620a022.
Reimann, B.; Kaufman, F. Rate constant of the reaction HO_2 + ClO → HOCl + O_2. *J. Chem. Phys.* **1978**, *69*, 2925-2926 doi:10.1063/1.436850.
Riffault, V.; Bedjanian, Y.; Le Bras, G. Kinetics and mechanism of the reaction of Cl atoms with HO_2 radicals. *Int. J. Chem. Kinet.* **2001**, *33*, 317-327, doi:10.1002/kin.1026.
Rodebush, W. H.; Klingelhoefer, W. C., Jr. Atomic chlorine and its reaction with hydrogen. *J. Am. Chem. Soc.* **1933**, *55*, 130-142, doi:10.1021/ja01328a014.
Romanias, M. N.; Stefanopoulos, V. G.; Papanastasiou, D. K.; Papadimitriou, V. C.; Papagiannakopoulos, P. Temperature-dependent rate coefficients and mechanism for the gas-phase reaction of chlorine atoms with acetone. *Int. J. Chem. Kinet.* **2010**, *42*, 724-734, doi:10.1002/kin.20517.
Rowland, F. S.; Sato, H.; Khwaja, H.; Elliott, S. M. The hydrolysis of chlorine nitrate and its possible atmospheric significance. *J. Phys. Chem.* **1986**, *90*, 1985-1988, doi:10.1021/j100401a001.
Ryan, K. R.; Plumb, I. C. Kinetics of the reactions of CCl_3 with O and O_2 and of CCl_3O_2 with NO at 295 K. *Int. J. Chem. Kinet.* **1984**, *16*, 591-602, doi:10.1002/kin.550160508.
Sammaritano, M. A.; Vera, M. G.; Cometto, P. M.; Tejero, T. N.; Bauerfeldt, G. F.; Mellouki, A. Temperature dependence of rate coefficients for the gas phase reaction of OH with 3-chloropropene. A theoretical and experimental study. *Chem. Phys. Lett.* **2020**, *755*, 137757, doi:10.1016/j.cplett.2020.137757.
Sanhueza, E.; Heicklen, J. Chlorine-atom sensitized oxidation of dichloromethane and chloromethane. *J. Phys. Chem.* **1975**, *79*, 7-11, doi:10.1021/j100568a002.
Sarzyński, D.; Gola, A. A.; Dryś, A.; Jodkowski, J. T. Kinetic study of the reaction of chlorine atoms with chloromethane in the gas phase. *Chem. Phys. Lett.* **2009**, *476*, 138-142, doi:10/1016/j.cplett.2009.04.086.
Sarzynski, D.; Sztuba, S. Gas-phase reactions of Cl atoms with propane, n-butane, and isobutane. *Int. J. Chem. Kinet.* **2002**, *34*, 651-658, doi:10.1002/kin.10096.
Sauer, F.; Portmann, R. W.; Ravishankara, A. R.; Burkholder, J. B. Temperature dependence of the Cl atom reaction with deuterated methanes. *J. Phys. Chem. A* **2015**, *119*, 4396-4407, doi:10.1021/jp508721h.
Saueressig, G.; Bergamaschi, P.; Crowley, J. N.; Fischer, H.; Harris, G. W. D/H kinetic isotope effect in the reaction CH_4 + Cl. *Geophys. Res. Lett.* **1996**, *23*, 3619-3622, doi:10.1029/96GL03292.
Sawerysyn, J.-P.; Lafage, C.; Meriaux, B.; Tighezza, A. Cinetique de la reaction des atomes de chlore avec le methane a 294 ± 1K: Une nouvelle etude par la technique du reacteur a ecoulement ratpide et a decharge couple a un spectrometre de masse. *J. Chim. Phys.* **1987**, *84*, 1187-1193.
Sawerysyn, J. P.; Talhaoui, A.; Meriaux, B.; Devolder, P. Absolute rate constants for elementary reactions between chlorine atoms and CHF_2Cl, CH_3CFCl_2, CH_3CF_2Cl and CH_2FCF_3 at 297 ± 2 K. *Chem. Phys. Lett.* **1992**, *198*, 197-199, doi:10.1016/0009-2614(92)90071-T.
Sayin, H.; McKee, M. L. Theoretical study of the mechanism of NO_2 production from NO + ClO. *J. Phys. Chem. A* **2005**, *109*, 4736-4743, doi:10.1021/jp050695w.
Schindler, R. N.; Dethlefs, J.; Schmidt, M. Some results on the mechanism of the reaction between O(^{3}P) atoms and HOCl. An experimental and ab initio model study. *Ber. Bunsenges. Phys. Chem.* **1996**, *100*, 1242-1249, doi:10.1002/bbpc.19961000723.
Schlyer, D. F.; Wolf, A. P.; Gaspar, P. P. Rate constants for the reactions of atomic chlorine with group 4 and group 5 hydrides. *J. Phys. Chem.* **1978**, *82*, 2633-2637, doi:10.1021/j100514a001.
Schwab, J. J.; Toohey, D. W.; Brune, W. H.; Anderson, J. G. Reaction kinetics of O + ClO → Cl + O_2 between 252-347 K. *J. Geophys. Res.* **1984**, *89*, 9581-9587, doi:10.1029/JD089iD06p09581.
Scollard, D. J.; Treacy, J. J.; Sidebottom, H. W.; Balestra-Garcia, C.; Laverdet, G.; LeBras, G.; MacLeod, H.; Téton, S. Rate constants for the reactions of hydroxyl radicals and chlorine atoms with halogenated aldehydes. *J. Phys. Chem.* **1993**, *97*, 4683-4688, doi:10.1021/j100120a021.
Seeley, J. V.; Jayne, J. T.; Molina, M. J. Kinetic studies of chlorine atom reactions using the turbulent flow tube technique. *J. Phys. Chem.* **1996**, *100*, 4019-4025, doi:10.1021/jp9525494.
Sehested, J.; Ellermann, T.; Nielsen, O. J.; Wallington, T. J.; Hurley, M. D. UV absorption spectrum, and kinetics and mechanism of the self reaction of $CF_3CF_2O_2$ radicals in the gas phase at 295 K. *Int. J. Chem. Kinet.* **1993**, *25*, 701-717, doi:10.1002/kin.550250903.

Sehested, J.; Nielsen, O. J.; Wallington, T. J. Absolute rate constants for the reaction of NO with a series of peroxy radicals in the gas phase at 295 K. *Chem. Phys. Lett.* **1993**, *213*, 457-464, doi:10.1016/0009-2614(93)89142-5.

Sharkey, P.; Smith, I. W. M. Kinetics of elementary reactions at low temperatures: Rate constants for the reactions of OH with HCl (298 ≥ T/K ≥ 138), CH_4 (298 ≥ T/K ≥ 178), and C_2H_6 (298 ≥ T/K ≥ 138). *J. Chem. Soc. Faraday Trans.* **1993**, *89*, 631-638, doi:10.1039/ft9938900631.

Simon, F. G.; Burrows, J. P.; Schneider, W.; Moortgat, G. K.; Crutzen, P. J. Study of the reaction ClO + CH_3O_2 → products at 300 K. *J. Phys. Chem.* **1989**, *93*, 7807-7813, doi:10.1021/j100360a017.

Simon, F. G.; Schneider, W.; Moortgat, G. K.; Burrows, J. P. A study of the ClO absorption cross-section between 240 and 310 nm and the kinetics of the self-reaction at 300 K. *J. Photochem. Photobiol. A: Chem.* **1990**, *55*, 1-23, doi:10.1016/1010-6030(90)80014-O.

Simonaitis, R.; Leu, M. T. Rate constant for the reaction Cl + HO_2NO_2 → Products. *Int. J. Chem. Kinet.* **1985**, *17*, 293-301, doi:10.1002/kin.550170306.

Singleton, D. L.; Cvetanovic, R. J. Temperature dependence of rate constants for the reaction of atomic oxygen with hydrogen chloride. *Int. J. Chem. Kinet.* **1981**, *13*, 945-956, doi:10.1002/kin.550130916.

Smith, I. W. M.; Williams, M. D. Effects of isotopic substitution and vibrational excitation on reaction rates Kinetics of OH(v = 0,1) and OD(v = 0,1) with HCl and DCl. *J. Chem. Soc. Faraday Trans. 2* **1986**, *82*, 1043-1055, doi:10.1039/f29868201043.

Smith, I. W. M.; Zellner, R. Rate measurements of reactions of OH by resonance absorption. Part 3. - Reactions of OH with H_2, D_2 and hydrogen and deuterium halides. *J. Chem. Soc. Faraday Trans. 2* **1974**, *70*, 1045-1056, doi:10.1039/F29747001045.

Sokolov, O.; Hurley, M. D.; Wallington, T. J.; Kaiser, E. W.; Platz, J.; Nielsen, O. J.; Berho, F.; Rayez, M.-T.; Lesclaux, R. Kinetics and mechanism of the gas-phase reaction of Cl atoms with benzene. *J. Phys. Chem. A* **1998**, *102*, 10671-10681, doi:10.1021/jp9828080.

Steckler, R.; Thurman, G. M.; Watts, J. D.; Bartlett, R. J. *Ab initio* direct dynamics study of OH + HCl → Cl + H_2O. *J. Chem. Phys.* **1997**, *106*, 3926-3933, doi:10.1063/1.473981.

Stevens, P. S.; Anderson, J. G. Kinetic measurements of the ClO + O_3 → ClOO + O_2 reaction. *Geophys. Res. Lett.* **1990**, *17*, 1287-1290, doi:10.1029/GL017i009p01287.

Stevens, P. S.; Anderson, J. G. Kinetic and mechanistic study of X + ClOCl → products (X = Br, CI, F, O, OH, N) over the temperature range 240-373 K. *J. Phys. Chem.* **1992**, *96*, 1708-1718, doi:10.1021/j100183a040.

Stimpfle, R.; Perry, R.; Howard, C. J. Temperature dependence of the reaction of ClO and HO_2 radicals. *J. Chem. Phys.* **1979**, *71*, 5183-5190, doi:10.1063/1.438293.

Stutz, J.; Ezell, M. J.; Ezell, A. A.; Finlayson-Pitts, B. J. Rate constants and kinetic isotope effects in the reactions of atomic chlorine with n-butane and simple alkenes at room temperature. *J. Phys. Chem. A* **1998**, *102*, 8510-8519, doi:10.1021/jp981659i.

Su, F.; Calvert, J. G.; Lindley, C. R.; Uselman, W. M.; Shaw, J. H. A Fourier transform infrared kinetic study of HOCl and its absolute integrated infrared band intensities. *J. Phys. Chem.* **1979**, *83*, 912-920, doi:10.1021/j100471a006.

Suh, I.; Zhang, R. Kinetic studies of isoprene reactions initiated by chlorine atom. *J. Phys. Chem. A* **2000**, *104*, 6590-6596, doi:10.1021/jp000605h.

Sulbaek Andersen, M. P.; Nielsen, O. J.; Karpichev, B.; Wallington, T. J.; Sander, S. P. Atmospheric chemistry of isoflurane, desflurane, and sevoflurane: Kinetics and mechanisms of reactions with chlorine atoms and OH radicals and global warming potentials. *J. Phys. Chem. A* **2012**, *116*, 5806-5820, doi:10.1021/jp2077598.

Sulbaek Andersen, M. P.; Nilsson, E. J. K.; Nielsen, O. J.; Johnson, M. S.; Hurley, M. D.; Wallington, T. J. Atmospheric chemistry of *trans*-CF_3CH=CHCl: Kinetics of the gas-phase reactions with Cl atoms, OH radicals, and O_3. *J. Photochem. and Photobiol. A: Chem.* **2008**, *199*, 92-97, doi:10.1016/j.jphotochem.2008.05.013.

Sun, C.; Xu, B.; Zhang, S. Atmospheric reaction of Cl + methacrolein: A theoretical study on the mechanism, and pressure- and temperature-dependent rate constants. *J. Phys. Chem. A* **2014**, *118*, 3541-3551, doi:10.1021/jp500993k.

Taatjes, C. A.; Christensen, L. K.; Hurley, M. D.; Wallington, T. J. Absolute and site-specific abstraction rate coefficients for reactions of Cl with CH_3CH_2OH, CH_3CD_2OH, and CD_3CH_2OH between 295 and 600 K. *J. Phys. Chem. A* **1999**, *103*, 9805-9814, doi:10.1021/jp992465l.

Takacs, G. A.; Glass, G. P. Reactions of hydroxyl radicals with some hydrogen halides. *J. Phys. Chem.* **1973**, *77*, 1948-1951, doi:10.1021/j100635a005.

Takahashi, K.; Iwasaki, E.; Matsumi, Y.; Wallington, T. J. Pulsed laser photolysis vacuum UV laser-induced fluorescence kinetic study of the gas-phase reactions of Cl($^2P_{3/2}$) atoms with C_3—C_6 ketones. *J. Phys. Chem. A* **2007**, *111*, 1271-1276, doi:10.1021/jp066410c.

Taketani, F.; Nakayama, T.; Takahashi, K.; Matsumi, Y.; Hurley, M. D.; Wallington, T. J.; Toft, A.; Sulbaek Andersen, M. P. Atmospheric chemistry of CH_3CHF_2 (HFC-152a): Kinetics, mechanisms, and products of Cl atom- and OH radical-initiated oxidation in the presence and absence of NO_x. *J. Phys. Chem. A* **2005**, *109*, 9061-9069, doi:10.1021/jp044218+.

Talhaoui, A.; Louis, F.; Devolder, P.; Meriaux, B.; Sawerysyn, J. P.; Rayez, M. T.; Rayez, J. C. Rate coefficients of the reactions of chlorine atoms with haloethanes of type $CH_3CCl_{3-x}F_x$ (x = 0, 1, and 2): Experimental and ab initio theoretical studies. *J. Phys. Chem.* **1996**, *100*, 13531-13538, doi:10.1021/jp9603243.

Talhaoui, A.; Louis, F.; Meriaux, B.; Devolder, P.; Sawerysyn, J.-P. Temperature dependence of rate coefficients for the reactions of chlorine atoms with halomethanes of type $CHCl_{3-x}F_x$ (x = 0, 1, and 2). *J. Phys. Chem.* **1996**, *100*, 2107-2113, doi:10.1021/jp951814i.

Talukdar, R.; Mellouki, A.; Gierczak, T.; Burkholder, J. B.; McKeen, S. A.; Ravishankara, A. R. Atmospheric fate of CF_2H_2, CH_3CF_3, CHF_2CF_3, and CH_3CFCl_2: Rate coefficients for reactions with OH and UV absorption cross sections of CH_3CFCl_2. *J. Phys. Chem.* **1991**, *95*, 5815-5821, doi:10.1021/j100168a021.

Talukdar, R. K.; Mellouki, A.; Schmoltner, A.-M.; Watson, T.; Montzka, S.; Ravishankara, A. R. Kinetics of the OH reaction with methyl chloroform and its atmospheric implications. *Science* **1992**, *257*, 227-230, doi:10.1126/science.257.5067.227.

Taylor, P. H.; D'Angelo, J. A.; Martin, M. C.; Kasner, J. H.; Dellinger, B. Laser photolysis/laser-induced fluorescence studies of reaction rates of OH with CH_3Cl, CH_2Cl_2, and $CHCl_3$ over an extended temperature range. *Int. J. Chem. Kinet.* **1989**, *21*, 829-846, doi:10.1002/kin.550210908.

Taylor, P. H.; Jiang, Z.; Dellinger, B. Determination of the gas-phase reactivity of hydroxyl with chlorinated methanes at high temperature: Effects of laser/thermal photochemistry. *Int. J. Chem. Kinet.* **1993**, *25*, 9-23, doi:10.1002/kin.550250103.

Taylor, P. H.; McCarron, S.; Dellinger, B. Investigation of 1,2-dichloroethane-hydroxyl kinetics over an extended temperature range: effect of chlorine substitution. *Chem. Phys. Lett.* **1991**, *177*, 27-32, doi:10.1016/0009-2614(91)90170-E.

Tichenor, L. B.; El-Sinawi, A.; Yamada, T.; Taylor, P. H.; Peng, J. P.; Hu, X.; Marshall, P. Kinetic studies of the reaction of hydroxyl radicals with trichloroethylene and tetrachloroethylene. *Chemosphere* **2001**, *42*, 571-577, doi:10.1016/S0045-6535(00)00229-0.

Tichenor, L. B.; Graham, J. L.; Yamada, T.; Taylor, P. H.; Peng, J.; Hu, X.; Marshall, P. Kinetic and modeling studies of the reaction of hydroxyl radicals with tetrachloroethylene. *J. Phys. Chem. A* **2000**, *104*, 1700-1707, doi:10.1021/jp993203m.

Tokuhashi, K.; Takahashi, A.; Kaise, M.; Kondo, S. Rate constants for the reactions of OH radicals with CH_3OCF_2CHFCl, CHF_2OCF_2CHFCl, $CHF_2OCHClCF_3$, and $CH_3CH_2OCF_2CHF_2$. *J. Geophys. Res.* **1999**, *104*, 18681-18688, doi:10.1029/1999JD900278.

Tokuhashi, K.; Takizawa, K.; Kondo, S. Rate constants for the reactions of OH radicals with $CF_3CX{=}CY_2$ (X = H, F, CF_3, Y=H, F, Cl). *Environ. Sci. Pollut. Res.* **2018**, *25*, 15204-15215, doi:10.1007/s11356-018-1700-4.

Tokuhashi, K.; Takizawa, K.; Kondo, S. Rate constants for reactions of OH radicals with (*Z*)-$CF_3CCl{=}CHCl$, $CHF_2CF{=}CF_2$, (*E*)-$CF_3CH{=}CHF$, (*Z*)-$CF_3CH{=}CHF$, $CH_3CF{=}CH_2$, and $CH_2FCH{=}CH_2$. *Atmos. Environ.* **2021**, *255*, 118428, doi:10.1016/j.atmosenv.2021.118428.

Tokuhashi, K.; Uchimaru, T.; Takizawa, K.; Kondo, S. Rate constants for the reactions of OH radicals with the (*E*)/(*Z*) isomers of CFCl=CFCl and (*E*)-CHF=CHF. *J. Phys. Chem. A* **2019**, *123*, 4834−4843, doi:10.1021/acs.jpca.9b02454.

Toohey, D. W. Kinetic and Mechanistic Studies of Reactions of Bromine and Chlorine Species Important in the Earth's Stratosphere. Ph. D. Thesis, Harvard University, 1988.

Tsalkani, N.; Mellouki, A.; Poulet, G.; Toupance, G.; Le Bras, G. Rate constant measurement for the reactions of OH and C1 with peroxyacetyl nitrate at 298 K. *J. Atmos. Chem.* **1988**, *7*, 409-419, doi:10.1007/BF00058713.

Tschuikow-Roux, E.; Faraji, F.; Paddison, S.; Niedzielski, J.; Miyokawa, K. Kinetics of photochlorination of halogen (F, Cl, Br) substituted methanes. *J. Phys. Chem.* **1988**, *92*, 1488-1495, doi:10.1021/j100317a023.

Tschuikow-Roux, E.; Yano, T.; Niedzielski, J. Reactions of ground state chlorine atoms with fluorinated methanes and ethanes. *J. Chem. Phys.* **1985**, *82*, 65-74, doi:10.1063/1.448737.

Tuazon, E. C.; Atkinson, R.; Aschmann, S. M. Kinetics and products of the gas-phase reactions of the OH radical and O_3 with allyl chloride and benzyl chloride at room temperature. *Int J. Chem. Kinet.* **1990**, *22*, 981-998, doi:10.1002/kin.550220909.

Tuazon, E. C.; Atkinson, R.; Aschmann, S. M.; Goodman, M. A.; Winer, A. M. Atmospheric reactions of chloroethenes with the OH radical. *Int. J. Chem. Kinet.* **1988**, *20*, 241-265, doi:10.1002/kin.550200305

Tuazon, E. C.; Atkinson, R.; Corchnoy, S. B. Rate constants for the gas-phase reactions of Cl atoms with a series of hydrofluorocarbons and hydrochlorofluorocarbons at 298 ± 2 K. *Int. J. Chem. Kinet.* **1992**, *24*, 639-648, doi:10.1002/kin.550240704.

Tyler, S. C.; Ajie, H. O.; Rice, A. L.; Cicerone, R. J. Experimentally determined kinetic isotope effects in the reaction of CH_4 with Cl: Implications for atmospheric CH_4. *Geophys. Res. Lett.* **2000**, *27*, 1715-1718, doi:10.1029/1999GL011168.

Tyndall, G. S.; Kegley-Owen, C. S.; Orlando, J. J.; Calvert, J. G. Quantum yields for $Cl(^2P_{3/2,1/2})$, ClO and $O(^3P)$ in the photolysis of chlorine nitrate at 308 nm. *J. Chem. Soc. Faraday Trans.* **1997**, *93*, 2675-2682, doi:10.1039/a701585b.

Tyndall, G. S.; Kegley-Owen, C. S.; Orlando, J. J.; Fried, A. Tunable diode laser study of the reaction OH + ClO → HCl + O_2. *J. Phys. Chem. A* **2002**, *106*, 1567-1575, doi:10.1021/jp013410y.

Tyndall, G. S.; Orlando, J. J.; Kegley-Owen, C. S.; Wallington, T. J.; Hurley, M. D. Rate coefficients for the reactions of chlorine atoms with methanol and acetaldehyde. *Int. J. Chem. Kinet.* **1999**, *31*, 776-784, doi:10.1002/(SICI)1097-4601(1999)31:11<776::AID-JCK3>3.0.CO;2-Q.

Tyndall, G. S.; Orlando, J. J.; Wallington, T. J.; Dill, M.; Kaiser, E. W. Kinetics and mechanisms of the reactions of chlorine atoms with ethane, propane, and n-butane. *Int. J. Chem. Kinet.* **1997**, *29*, 43-55, doi:10.1002/(SICI)1097-4601(1997)29:1<43::AID-KIN6>3.0.CO;2-L.

Tyndall, G. S.; Orlando, J. J.; Wallington, T. J.; Sehested, J.; Nielsen, O. J. Kinetics of the reactions of acetonitrile with chlorine and fluorine atoms. *J. Phys. Chem.* **1996**, *100*, 660-668, doi:10.1021/jp9521417.

Tyndall, G. S.; Wallington, T. J.; Potts, A. R. Product study of the reaction of Cl atoms with HCOOH. *Chem. Phys. Lett.* **1991**, *186*, 149-153, doi:10.1016/S0009-2614(91)85121-C.

Vanderzanden, J. W.; Birks, J. W. Formation of oxygen atoms in the reaction of chlorine atoms with ozone. *Chem. Phys. Lett.* **1982**, *88*, 109-114, doi:10.1016/0009-2614(82)80080-8.

Villenave, E.; Orkin, V. L.; Huie, R. E.; Kurylo, M. J. Rate constant for the reaction of OH radicals with dichloromethane. *J. Phys. Chem. A* **1997**, *101*, 8513-8517, doi:10.1021/jp9721614.

Vogt, R.; Schindler, R. N. A gas kinetic study of the reaction of HOCl with F-, Cl-, and H-atoms at room temperature. *Ber. Bunsenges. Phys. Chem.* **1993**, *97*, 819-829, doi:10.1002/bbpc.19930970612.

Wallington, T. J.; Andino, J. M.; Ball, J. C.; Japar, S. M. Fourier transform infrared studies of the reaction of C1 atoms with PAN, PPN, CH_3OOH, HCOOH, CH_3COCH_3 and $CH_3COC_2H_5$ at 295 ± 2 K. *J. Atmos. Chem.* **1990**, *10*, 301-313, doi:10.1007/BF00053865.

Wallington, T. J.; Ball, J. C.; Nielsen, O. J.; Bartkiewicz, E. Spectroscopic, kinetic, and mechanistic study of CH_2FO_2 radicals in the gas phase at 298 K. *J. Phys. Chem.* **1992**, *96*, 1241-1246, doi:10.1021/j100182a041.

Wallington, T. J.; Hinman, M. M.; Andino, J. M.; Siegl, W. O.; Japar, S. M. A relative rate study of the reaction of Cl atoms with a series of alkyl nitrates and nitro alkanes in air at 295 ± 2K. *Int. J. Chem. Kinet.* **1990**, *22*, 665-671, doi:10.1002/kin.550220702.

Wallington, T. J.; Hurley, M. D. A kinetic study of the reaction of chlorine atoms with CF_3CHCl_2, CF_3CH_2F, $CFCl_2CH_3$, CF_2ClCH_3, CHF_2CH_3, CH_3D, CH_2D_2, CHD_3, CD_4, and CD_3Cl at 295 ± 2 K. *Chem. Phys. Lett.* **1992**, *189*, 437-442, doi:10.1016/0009-2614(92)85228-3.

Wallington, T. J.; Hurley, M. D.; Schneider, W. F.; Sehested, J.; Nielsen, O. J. Mechanistic study of the gas-phase reaction of CH_2FO_2 radicals with HO_2. *Chem. Phys. Lett.* **1994**, *218*, 34-42, doi:10.1016/0009-2614(93)E1466-T.

Wallington, T. J.; Skewes, L. M.; Siegl, W. O.; Wu, C. H.; Japar, S. M. Gas phase reaction of Cl atoms with a series of oxygenated organic species at 295 K. *Int. J. Chem. Kinet.* **1988**, *20*, 867-875, doi:10.1002/kin.550201105.

Wang, J. J.; Keyser, L. F. Kinetics of the $Cl(^2P_J)$ + CH_4 reaction: Effects of secondary chemistry below 300 K. *J. Phys. Chem. A* **1999**, *103*, 7460-7469, doi:10.1021/jp9913259.
Wang, J. J.; Keyser, L. F. Absolute rate constant of the OH + ClO reaction at temperatures between 218 and 298 K. *J. Phys. Chem. A* **2001**, *105*, 10544-10552, doi:10.1021/jp012426l.
Wang, J. J.; Keyser, L. F. HCl yield from the OH + ClO reaction at temperatures between 218 and 298 K. *J. Phys. Chem. A* **2001**, *105*, 6479-6489, doi:10.1021/jp0106449.
Wang, L.; Liu, J. Y.; Li, Z. S.; Huang, X. R.; Sun, C. C. Theoretical study and rate constant calculation of the Cl + HOCl and H + HOCl reactions. *J. Phys. Chem. A* **2003**, *107*, 4921-4928, doi:10.1021/jp0277558.
Wang, L.; Liu, J. Y.; Li, Z. S.; Sun, C. C. Direct ab initio dynamics studies on the hydrogen-abstraction reactions of OH radicals with HOX (X = F, Cl, and Br). *J. Comp. Chem.* **2004**, *25*, 558-564, doi:10.1002/jcc.10403.
Wang, L.; Liu, J. Y.; Li, Z. S.; Sun, C. C. Ab initio and DFT theoretical studies and rate constants calculation on the reactions O (^{3}P) atoms with HOX (X = Cl, Br). *Chem. Phys. Lett.* **2005**, *411*, 225-232, doi:10.1016/j.cplett.2005.05.071.
Wang, W.; Ezell, M. J.; Ezell, A. A.; Soskin, G.; Finlayson-Pitts, B. J. Rate constants for the reactions of chlorine atoms with a series of unsaturated aldehydes and ketones at 298 K: structure and reactivity. *Phys. Chem. Chem. Phys.* **2002**, *4*, 1824-1831, doi:10.1039/b111557j.
Warren, R. F.; Ravishankara, A. R. Kinetics of $Cl(^2P)$ reactions with CF_3CHCl_2, CF_3CHFCl, and CH_3CFCl_2. *Int. J. Chem. Kinet.* **1993**, *25*, 833-844, doi:10.1002/kin.550251005.
Watson, R. T.; Machado, G.; Conaway, B.; Wagner, S.; Davis, D. D. A temperature dependent kinetics study of the reaction of OH with CH_2ClF, $CHCl_2F$, $CHClF_2$, CH_3CCl_3, CH_3CF_2Cl, and $CF_2ClCFCl_2$. *J. Phys. Chem.* **1977**, *81*, 256-262, doi:10.1021/j100518a014.
Watson, R. T.; Machado, G.; Fischer, S.; Davis, D. D. A temperature dependence kinetics study of the reactions of $Cl(^2P_{3/2})$ with O_3, CH_4, and H_2O_2. *J. Chem. Phys.* **1976**, *65*, 2126-2138, doi:10.1063/1.433369.
Watson, R. T.; Ravishankara, A. R.; Machado, G.; Wagner, S.; Davis, D. D. A kinetics study of the temperature dependence of the reactions of $OH(^2\Pi)$ with CF_3CHCl_2, CF_3CHClF, and CF_2ClCH_2Cl. *Int. J. Chem. Kinet.* **1979**, *11*, 187-197, doi:10.1002/kin.550110210.
Wecker, D.; Johanssen, R.; Schindler, R. N. ESR-spektroskopische untersuchungen der reaktion von O(^{3}P)-atomen mit dichlormonoxid. *Ber. Bunsenges. Phys. Chem.* **1982**, *86*, 532-538, doi:10.1002/bbpc.19820860612.
Westenberg, A. A.; deHaas, N. Atom-molecule kinetics using ESR detection. IV. Results for Cl + H_2 ⇄ HCl + H in both directions. *J. Chem. Phys.* **1968**, *48*, 4405-4415, doi:10.1063/1.1668008.
Whytock, D. A.; Lee, J. H.; Michael, J. V.; Payne, W. A.; Stief, L. J. Absolute rate of the reaction of $Cl(^2P)$ with methane from 200-500 K. *J. Chem. Phys.* **1977**, *66*, 2690-2695, doi:10.1063/1.434216.
Wine, P. H.; Wells, J. R.; Nicovich, J. M. Kinetics of the reactions of F(^{2}P) and Cl(^{2}P) with HNO_3. *J. Phys. Chem.* **1988**, *92*, 2223-2228, doi:10.1021/j100319a028.
Winer, A. M.; Lloyd, A. C.; Darnall, K. R.; Pitts, J. N., Jr. Relative rate constants for the reaction of the hydroxyl radical with selected ketones, chloroethenes, and monoterpene hydrocarbons. *J. Phys. Chem.* **1976**, *80*, 1635-1639, doi:10.1021/j100555a024.
Wong, E. L.; Belles, F. R.; NASA TN D-6495 NASA Washington, D. C., 1971.
Wongdontri-Stuper, W.; Jayanty, R. K. M.; Simonaitis, R.; Heicklen, J. The Cl_2 photosensitized decomposition of O_3: the reactions of ClO and OClO with O_3. *J. Photochem.* **1979**, *10*, 163-186, doi:10.1016/0047-2670(79)80004-0.
Wu, F.; Carr, R. W. Time-resolved observation of the formation of CF_2O and CFClO in the CF_2Cl + O_2 and $CFCl_2$ + O_2 reactions. The unimolecular elimination of Cl atoms from CF_2ClO and $CFCl_2O$ radicals. *J. Phys. Chem.* **1992**, *96*, 1743-1748, doi:10.1021/j100183a046.
Xing, J.-H.; Takahashi, K.; Hurley, M. D.; Wallington, T. J. Kinetics of the reaction of chlorine atoms with isoprene (2-methyl 1,3-butadiene, CH_2=C(CH_3)CH=CH_2) at 297 ± 2 K. *Chem. Phys. Lett.* **2009**, *472*, 39-43, doi:10.1016/j.cplett.2009.03.002.
Xu, Z. F.; Lin, M. C. Computational studies on metathetical and redox processes of HOCl in the gas phase. 1. Reactions with H, O, HO, and HO_2. *J. Phys. Chem. A* **2009**, *113*, 8811-8817, doi:10.1021/jp905136h.
Xu, Z. F.; Zhu, R. S.; Lin, M. C. Ab initio studies of ClO_x reactions: VI. Theoretical prediction of total rate constant and product branching probabilities for the HO_2 + ClO reaction. *J. Phys. Chem. A* **2003**, *107*, 3841-3850, doi:10.1021/jp0221237.
Yamada, T.; El-Sinawi, A.; Siraj, M.; Taylor, P. H.; Peng, J.; Hu, X.; Marshall, P. Rate coefficients and mechanistic analysis for the reaction of hydroxyl radicals with 1,1-dichloroethylene and *trans*-1,2-dichloroethylene over an extended temperature range. *J. Phys. Chem. A* **2001**, *105*, 7588-7597, doi:10.1021/jp0109067.

Yamada, T.; Fang, T. D.; Taylor, P. H.; Berry, R. J. Kinetics and thermochemistry of the OH radical reaction with CF_3CCl_2H and CF_3CFClH. *J. Phys. Chem. A* **2000**, *104*, 5013-5022, doi:10.1021/jp993577f.

Yamada, T.; Siraj, M.; Taylor, P. H.; Peng, J.; Hu, X.; Marshall, P. Rate coefficients and mechanistic analysis for reaction of OH with vinyl chloride between 293 and 730 K. *J. Phys. Chem. A* **2001**, *105*, 9436-9444, doi:10.1021/jp011545y.

Yano, T.; Tschuikow-Roux, E. Competitive photochlorination of the fluoroethanes CH_3CHF_2, CH_2FCH_2F and CHF_2CHF_2. *J. Photochem.* **1986**, *32*, 25-37, doi:10.1016/0047-2670(86)85004-3.

Yokelson, R. J.; Burkholder, J. B.; Goldfarb, L.; Fox, R. W.; Gilles, M. K.; Ravishankara, A. R. Temperature dependent rate coefficient for the Cl + $ClONO_2$ reaction. *J. Phys. Chem.* **1995**, *99*, 13976-13983, doi:10.1021/j100038a032.

Young, C. J.; Hurley, M. D.; Wallington, T. J.; Mabury, S. A. Atmospheric chemistry of CF_3CF_2H and $CF_3CF_2CF_2CF_2H$: Kinetics and products of gas-phase reactions with Cl atoms and OH radicals, infrared spectra, and formation of perfluorocarboxylic acids. *Chem. Phys. Lett.* **2009**, *473*, 251-256, doi:10.1016/j.cplett.2009.04.001.

Yu, W. H. S.; Wijnen, M. H. J. Photolysis of chloroform in the presence of ethane at 25°C. *J. Chem. Phys.* **1970**, *52*, 2736-2739, doi:10.1063/1.1673626.

Yujing, M.; Mellouki, A. Rate constants for the reactions of OH with chlorinated propanes. *Phys. Chem. Chem. Phys* **2001**, *3*, 2614-2617, doi:10.1039/b102971c.

Zagogianni, H.; Mellouki, A.; Poulet, G. Réactivité des radicaux Cl et ClO avec HNO_3. *C. R. Acad. Sci. Paris* **1987**, *Series II 304*, 573-578.

Zahniser, M. S.; Berquist, B. M.; Kaufman, F. Kinetics of the reaction Cl + CH_4 → CH_3 + HCl from 200° to 500° K. *Int. J. Chem. Kinet.* **1978**, *10*, 15-29, doi:10.1016/0009-2614(74)80292-7.

Zahniser, M. S.; Chang, J.; Kaufman, F. Chlorine nitrate: Kinetics of formation by ClO + NO_2 + M and of reaction with OH. *J. Chem. Phys.* **1977**, *67*, 997-1003, doi:10.1063/1.434927.

Zahniser, M. S.; Kaufman, F. Kinetics of the reactions of ClO with O and with NO. *J. Chem. Phys.* **1977**, *66*, 3673-3681, doi:10.1063/1.434403.

Zahniser, M. S.; Kaufman, F.; Anderson, J. G. Kinetics of the reaction of OH with HCl. *Chem. Phys. Lett.* **1974**, *27*, 507-510, doi:10.1016/0009-2614(74)80292-7.

Zahniser, M. S.; Kaufman, F.; Anderson, J. G. Kinetics of the reaction Cl + O_3 → ClO + O_2. *Chem. Phys. Lett.* **1976**, *37*, 226-231, doi:10.1016/0009-2614(76)80203-5.

Zhang, Z.; Huie, R. E.; Kurylo, M. J. Rate constants for the reactions of OH with CH_3CFCl_2 (HCFC-141b), CH_3CF_2Cl (HCFC-l42b), and CH_2FCF_3 (HFC-134a). *J. Phys. Chem.* **1992**, *96*, 1533-1535, doi:10.1021/j100183a008.

Zhang, Z.; Liu, R.; Huie, R. E.; Kurylo, M. J. Rate constants for the gas phase reactions of the OH radical with $CF_3CF_2CHCl_2$ (HCFC-225ca) and CF_2ClCF_2CHClF (HCFC-225cb). *Geophys. Res. Lett.* **1991**, *18*, 5-7, doi:10.1029/90GL02647.

Zhang, Z.; Liu, R. F.; Huie, R. E.; Kurylo, M. J. A gas-phase reactivity study of OH radicals with 1,l-dichloroethene and *cis*- and *trans*-l,2-dichloroethene over the temperature range 240-400 K. *J. Phys. Chem.* **1991**, *95*, 194-196, doi:10.1021/j100154a039.

Zhao, Z.; Huskey, D. T.; Nicovich, J. M.; Wine, P. H. Temperature-dependent kinetics study of the gas-phase reactions of atomic chlorine with acetone, 2-butanone, and 3-pentanone. *Int. J. Chem. Kinet.* **2008**, *40*, 259-267, doi:10.1002/kin.20321.

1.12 BrO_x Reactions

1.12.1 Table 1G: BrO_x Reactions

Reaction	Temperature Range of Exp. Data (K) [a]	*A*-Factor	*E*/R	*k*(298 K) [b]	*f*(298 K) [c]	*g* [c]	Note
$O + BrO \rightarrow Br + O_2$	231–328	1.9×10^{-11}	–230	4.1×10^{-11}	1.5	150	G 1
$O + HBr \rightarrow OH + Br$	221–554	5.8×10^{-12}	1500	3.8×10^{-14}	1.3	200	G 2
$O + HOBr \rightarrow OH + BrO$	233–423	1.2×10^{-10}	430	2.8×10^{-11}	3.0	300	G 3
$O + BrONO_2 \rightarrow NO_3 + BrO$	227–339	1.9×10^{-11}	–215	3.9×10^{-11}	1.25	40	G 4
$OH + Br_2 \rightarrow HOBr + Br$	230–360	2.1×10^{-11}	–240	4.6×10^{-11}	1.1	50	G 5
$OH + BrO \rightarrow$ products	230–355	1.7×10^{-11}	–250	3.9×10^{-11}	1.4	100	G 6
$OH + HBr \rightarrow H_2O + Br$	235–960	6.2×10^{-12}	–170	1.1×10^{-11}	1.05	100	G 7
$OH + CH_3Br \rightarrow CH_2Br + H_2O$	233–400	1.42×10^{-12}	1150	3.0×10^{-14}	1.07	100	G 8
$OH + CH_2Br_2 \rightarrow CHBr_2 + H_2O$	244–375	2.0×10^{-12}	840	1.2×10^{-13}	1.1	100	G 9
$OH + CHBr_3 \rightarrow CBr_3 + H_2O$	230–370	9.0×10^{-13}	360	2.7×10^{-13}	1.05	20	G10
$OH + CH_2ClBr \rightarrow CHClBr + H_2O$	230–376	2.1×10^{-12}	880	1.1×10^{-13}	1.07	100	G11
$OH + CHClBr_2 \rightarrow CClBr_2 + H_2O$	230–330	9.0×10^{-13}	420	2.2×10^{-13}	1.07	20	G12
$OH + CHCl_2Br \rightarrow CCl_2Br + H_2O$	230–330	9.4×10^{-13}	510	1.7×10^{-13}	1.07	20	G13
$OH + CHF_2Br \rightarrow CF_2Br + H_2O$ (Halon-1201)	233–460	7.85×10^{-13}	1300	1.0×10^{-14}	1.07	100	G14
$OH + CF_2Br_2 \rightarrow$ products (Halon-1202)	298	*1×10^{-12}*	*>2200*	$<5\times10^{-16}$			G15
$OH + CF_3Br \rightarrow$ products (Halon-1301)	460	*1×10^{-12}*	*>3600*	*$<6\times10^{-18}$*			G16
$OH + CF_2ClBr \rightarrow$ products (Halon-1211)	373	*1×10^{-12}*	*>3500*	*$<8\times10^{-18}$*			G17
$OH + CH_3CH_2Br \rightarrow$ products	233–422	2.9×10^{-12}	640	3.4×10^{-13}	1.2	150	G18
$OH + CH_2BrCH_2Br \rightarrow$ products	292–366	1.75×10^{-11}	1290	2.3×10^{-13}	1.15	200	G19
$OH + CH_2BrCF_3 \rightarrow CHBrCF_3 + H_2O$ (Halon-2301)	280–460	9.5×10^{-13}	1200	1.7×10^{-14}	1.2	150	G20
$OH + CHFBrCF_3 \rightarrow CFBrCF_3 + H_2O$ (Halon-2401)	279–460	7.3×10^{-13}	1120	1.7×10^{-14}	1.2	100	G21
$OH + CHClBrCF_3 \rightarrow CClBrCF_3 + H_2O$ (Halothane, Halon-2311)	298–460	1.1×10^{-12}	940	4.7×10^{-14}	1.2	150	G22
$OH + CHFClCF_2Br \rightarrow CFClCF_2Br + H_2O$	315–372	8.4×10^{-13}	1220	1.4×10^{-14}	1.3	200	G23
$OH + CF_2BrCF_2Br \rightarrow$ products (Halon-2402)	460	*1×10^{-12}*	*>3600*	*$<6\times10^{-18}$*			G24

Reaction	Temperature Range of Exp. Data (K) [a]	*A*-Factor	*E*/R	*k*(298 K) [b]	*f*(298 K) [c]	*g* [c]	Note
$OH + CH_2BrCH_2CH_3 \rightarrow$ products	210–725	3.0×10^{-12}	330	1.0×10^{-12}	1.05	50	G25
$OH + CH_3CHBrCH_3 \rightarrow$ products	210–715	1.85×10^{-12}	270	7.5×10^{-13}	1.05	50	G26
$OH + CHBr=CF_2 \rightarrow$ products	250–370	1.3×10^{-12}	–370	4.5×10^{-12}	1.1	20	G27
$OH + CFBr=CF_2 \rightarrow$ products	250–370	2.0×10^{-12}	–400	7.6×10^{-12}	1.1	20	G28
$OH + CH_2=CBrCF_3 \rightarrow$ products	220–370	1.06×10^{-12}	–380	3.8×10^{-12}	1.05	20	G29
$OH + CH_2=CBrCF_2CF_3 \rightarrow$ products	250–370	9.5×10^{-12}	–370	3.3×10^{-12}	1.05	20	G30
$OH + CH_2=CHCF_2CF_2Br \rightarrow$ products	250–370	8.7×10^{-12}	–200	1.7×10^{-12}	1.1	20	G31
$OH + CH_2=CHCFClCF_2Br \rightarrow$ products	230–370	6.6×10^{-13}	–420	2.7×10^{-12}	1.1	0	G32
$HO_2 + Br \rightarrow HBr + O_2$	230–355	4.8×10^{-12}	310	1.7×10^{-12}	1.3	150	G33
$HO_2 + BrO \rightarrow$ products	210–360	4.5×10^{-12}	–460	2.1×10^{-11}	1.15	100	G34
$NO_3 + HBr \rightarrow HNO_3 + Br$	298			$<1.0\times10^{-16}$			G35
$Cl + CH_3Br \rightarrow HCl + CH_2Br$	210–700	1.46×10^{-11}	1040	4.45×10^{-13}	1.03	50	G36
$Cl + CH_2Br_2 \rightarrow HCl + CHBr_2$	222–395	6.8×10^{-12}	830	4.2×10^{-13}	1.1	50	G37
$Cl + CHBr_3 \rightarrow CBr_3 + HCl$	273–363	4.85×10^{-12}	850	2.8×10^{-13}	1.3	200	G38
$Cl + CH_2ClBr \rightarrow HCl + CHClBr$	298	*6.8×10^{-12}*	*870*	3.7×10^{-13}	1.2	100	G39
$Br + O_3 \rightarrow BrO + O_2$	195–422	1.6×10^{-11}	780	1.2×10^{-12}	1.15	100	G40
$Br + H_2O_2 \rightarrow HBr + HO_2$	298–378	*1×10^{-11}*	*>3000*	$<5\times10^{-16}$			G41
$Br + NO_2 \xrightarrow{M} BrNO_2$		(See Table 2-1)					
$Br + NO_3 \rightarrow BrO + NO_2$	298			1.6×10^{-11}	2.0		G42
$Br + H_2CO \rightarrow HBr + HCO$	223–480	1.7×10^{-11}	800	1.1×10^{-12}	1.2	125	G43
$Br + CH_2=C(CH_3)CHO \rightarrow$ products	301			2.3×10^{-11} (1 atm air)	1.5		G44
$Br + CH_3C(O)CH=CH_2 \rightarrow$ products	301			1.9×10^{-11} (1 atm air)	1.5		G45
$Br + CH_2=C(CH_3)CH=CH_2 \overset{M}{\leftrightarrow} X \overset{O_2}{\rightarrow}$ products	210–298	(See Note)					G46
$Br + CH_2=C(CH_3)CH=CH_2 \rightarrow CH_2=C(\cdot CH_2)CH=CH_2 + HBr$	526–673	1.2×10^{-11}	2100	1.0×10^{-14}	2.0	200	G47
$Br{-}CH_2=C(CH_3)CH=CH_2 + O_2 \rightarrow$ products	297			3.2×10^{-13}	1.5		G48
$Br + OClO \rightarrow BrO + ClO$	267–423	2.6×10^{-11}	1300	3.4×10^{-13}	2.0	300	G49

Reaction	Temperature Range of Exp. Data (K) [a]	*A*-Factor	*E*/R	*k*(298 K) [b]	*f*(298 K) [c]	*g* [c]	Note
$Br + Cl_2O \rightarrow BrCl + ClO$	220–402	2.1×10^{-11}	470	4.3×10^{-12}	1.3	150	G50
$Br + Cl_2O_2 \rightarrow$ products	223–298	5.9×10^{-12}	170	3.3×10^{-12}	1.3	200	G51
$BrO + O_3 \rightarrow$ products	298	*1×10^{-12}*	*>3200*	$<2\times10^{-17}$			G52
$BrO + NO \rightarrow NO_2 + Br$	224–425	8.8×10^{-12}	–260	2.1×10^{-11}	1.15	130	G53
$BrO + NO_2 \xrightarrow{M} BrONO_2$		(See Table 2-1)					
$BrO + NO_3 \rightarrow$ products	298			1.0×10^{-12}	3.0		G54
$BrO + ClO \rightarrow Br + OClO$	200–400	9.5×10^{-13}	–550	6.0×10^{-12}	1.2	100	G55
$\rightarrow Br + ClOO$		2.3×10^{-12}	–260	5.5×10^{-12}	1.2	100	
$\rightarrow BrCl + O_2$		4.1×10^{-13}	–290	1.1×10^{-12}	1.2	100	
$BrO + BrO \rightarrow$ products	220–348	1.5×10^{-12}	–230	3.2×10^{-12}	1.15	150	G56
$OBrO + O_3 \rightarrow$ products	298			$<1.5\times10^{-15}$			G57
$OBrO + NO \rightarrow$ products	240–350	2.4×10^{-13}	–610	1.8×10^{-12}	3	200	G58
$CH_2BrO_2 + NO \rightarrow CH_2O + NO_2 + Br$	298	*4×10^{-12}*	*–300*	1.1×10^{-11}	1.5	200	G59

Shaded areas indicate changes or additions since JPL19-5. Italicized blue data entries denote estimates.

[a] Temperature range of available experimental data. This is not necessarily the range of temperature over which the recommended Arrhenius parameters are applicable. See the corresponding note for such information.

[b] Units are cm^3 $molecule^{-1}$ s^{-1}.

[c] *f*(298 K) is the uncertainty factor at 298 K. To calculate the uncertainty at other temperatures, use the expression:

$$f(\mathrm{T}) = f(298\ \mathrm{K})\exp\left|g\left(\frac{1}{\mathrm{T}} - \frac{1}{298}\right)\right|$$

Note that the exponent is an absolute value.

1.12.2 Notes: BrO_x Reactions

G1. **O + BrO.** The preferred value is based on the value reported by Thorn et al.[2] (231–328 K) obtained using a dual laser flash photolysis-long path absorption-resonance fluorescence technique. Clyne et al.[1] (298 K) reported a value approximately 40% lower.
(Table: 97-4, Note: 97-4, Evaluated: 10-6) Back to Table

(1) Clyne, M. A. A.; Monkhouse, P. B.; Townsend, L. W. Reactions of O ^3P_J atoms with halogens: The rate constants for the elementary reactions O + BrCl, O + Br_2, and O + Cl_2. *Int. J. Chem. Kinet.* **1976**, *8*, 425-449, doi:10.1002/kin.550080309.

(2) Thorn, R. P.; Cronkhite, J. M.; Nicovich, J. M.; Wine, P. H. Laser flash photolysis studies of radical-radical reaction kinetics: The O(^3P_J) + BrO reaction. *J. Chem. Phys.* **1995**, *102*, 4131-4142, doi:10.1063/1.468541.

G2. **O + HBr.** Results of the flash photolysis-resonance fluorescence study of Nava et al.[2] (221–455 K) and the laser flash photolysis-resonance fluorescence study of Nicovich and Wine[3] (250–402 K) provide the only data at stratospheric temperatures. Other results reported include those of Singleton and Cvetanovic[4] (298–554 K) using a phase-shift technique, and discharge flow results of Brown and Smith[1] (267–430 K) and Takacs and Glass[5] (298 K). The recommended parameters are based on the results of Nava et al., Nicovich and Wine, and Singleton and Cvetanovic over the same temperature range, since these results are less subject to complications due to secondary chemistry than are the results obtained using discharge flow techniques. The uncertainty at 298 K has been set to encompass these latter results.
(Table: 90-1, Note: 90-1, Evaluated: 10-6) Back to Table

(1) Brown, R. D. H.; Smith, I. W. M. Absolute rate constants for the reactions O(^3P) atoms with HCl and HBr. *Int. J. Chem. Kinet.* **1975**, *7*, 301-315, doi:10.1002/kin.550070211.

(2) Nava, D. F.; Bosco, S. R.; Stief, L. J. Rate constant for the reaction of O(^3P) with HBr from 221 to 455 K. *J. Chem. Phys.* **1983**, *78*, 2443-2448, doi:10.1063/1.445047.

(3) Nicovich, J. M.; Wine, P. H. Kinetics of the reactions of O(^3P) and Cl(^2P) with HBr and Br_2. *Int. J. Chem. Kinet.* **1990**, *22*, 379-397, doi:10.1002/kin.550220406.

(4) Singleton, D. L.; Cvetanovic, R. J. Temperature dependence of rate constants for the reactions of oxygen atoms, O(^{3}P), with HBr and HI. *Can. J. Chem.* **1978**, *56*, 2934-2939, doi:10.1139/v78-481.

(5) Takacs, G. A.; Glass, G. P. Reaction of atomic oxygen with hydrogen bromide. *J. Phys. Chem.* **1973**, *77*, 1182-1186, doi:10.1021/j100628a020.

G3. **O + HOBr.** The recommended value for k(298 K) is the mean of results of Monks et al.[2] (298 K) and Kukui et al.[1] (300 K). The temperature dependence is from Nesbitt et al.[3] (233–423 K). The A-factor from that study has been adjusted to fit the recommended room temperature value. Kukui et al. determined that the Br atom abstraction channel is the only pathway at room temperature.
(Table: 97-4, Note: 97-4, Evaluated: 10-6) Back to Table

(1) Kukui, A.; Kirchner, U.; Benter, T.; Schindler, R. N. A gaskinetic investigation of HOBr reactions with Cl(^{2}P), O(^{3}P) and OH($^2\Pi$). The reaction of BrCl with OH($^2\Pi$). *Ber. Bunsenges. Phys. Chem.* **1996**, *100*, 455-461, doi:10.1002/bbpc.19961000409.

(2) Monks, P. S.; Nesbitt, F. L.; Scanlon, M.; Stief, L. J. HOBr kinetics: Reactions of halogen atoms, oxygen atoms, nitrogen atoms, and nitric oxide with HOBr. *J. Phys. Chem.* **1993**, *97*, 11699-11705, doi:10.1021/j100147a025.

(3) Nesbitt, F. L.; Monks, P. S.; Payne, W. A.; Stief, L. J.; Toumi, R. The reaction O(^{3}P) + HOBr: Temperature dependence of the rate constant and importance of the reaction as an HOBr stratospheric loss process. *Geophys. Res. Lett.* **1995**, *22*, 827-830, doi:10.1029/95GL00375.

G4. **O + $BrONO_2$.** The recommendation is based on the study of Soller et al.[2] using a laser flash photolysis–resonance fluorescence technique over the temperature range 227–339 K. The recommended uncertainty parameters are larger than those reported by Soller et al. pending independent confirmation of their results. Burkholder[1] has coupled laser flash photolysis with detection of NO_3 by long path absorption spectroscopy to show that the NO_3 yield is >0.85 at 298 K.
(Table: 06-2, Note: 06-2, Evaluated: 06-2) Back to Table

(1) Burkholder, J. B. NO_3 yield in the O(^{3}P) + $BrONO_2$ reaction. *J. Phys. Chem. A* **2000**, *104*, 6733-6737, doi:10.1021/jp9942926.

(2) Soller, R.; Nicovich, J. M.; Wine, P. H. Temperature-dependent rate coefficients for the reactions of Br($^2P_{3/2}$), Cl($^2P_{3/2}$), and O(^3P_J) with $BrONO_2$. *J. Phys. Chem. A* **2001**, *105*, 1416-1422, doi:10.1021/jp001947q.

G5. OH + Br_2. The recommended k(298 K) is the average of the values reported by Poulet et al.[5] (298 K), Loewenstein and Anderson[4] (298 K), Gilles et al.[3] (235–357 K), and Bedjanian et al.[1] (230–360 K). The temperature dependence is an average of the E/R values of Gilles et al. and Bedjanian et al. The room temperature results of Boodaghians et al.[2] (262–303 K) are 40% lower than the recommended value for k(298 K) and were not considered due to their large experimental uncertainty. Loewenstein and Anderson determined that the exclusive products are Br + HOBr.
(Table: 06-2, Note: 06-2, Evaluated: 06-2) Back to Table

(1) Bedjanian, Y.; Le Bras, G.; Poulet, G. Kinetic study of the reactions of Br_2 with OH and OD. *Int. J. Chem. Kinet.* **1999**, *31*, 698-704, doi:10.1002/(SICI)1097-4601(1999)31:10<698::AID-JCK3>3.0.CO;2-O.

(2) Boodaghians, R. B.; Hall, I. W.; Wayne, R. P. Kinetics of the reactions of the hydroxyl radical with molecular chlorine and bromine. *J. Chem. Soc. Faraday Trans. 2* **1987**, *83*, 529-538, doi:10.1039/f29878300529.

(3) Gilles, M. K.; Burkholder, J. B.; Ravishankara, A. R. Rate coefficients for the reaction of OH with Cl_2, Br_2 and I_2 from 235 to 354 K. *Int. J. Chem. Kinet.* **1999**, *31*, 417-424, doi:10.1002/(SICI)1097-4601(1999)31:6<417::AID-KIN3>3.0.CO;2-A.

(4) Loewenstein, L. M.; Anderson, J. G. Rate and product measurements for the reactions of OH with Cl_2, Br_2, and BrCl at 298 K. Trend interpretations. *J. Phys. Chem.* **1984**, *88*, 6277-6286, doi:10.1021/j150669a045.

(5) Poulet, G.; Laverdet, G.; Le Bras, G. Kinetics and products of the reaction of hydroxyl radical with molecular bromine. *Chem. Phys. Lett.* **1983**, *94*, 129-132, doi:10.1016/0009-2614(83)87225-X.

G6. OH + BrO. The recommended k(298 K) is an average of the results of Gilles et al.[2] (298 K) and Bedjanian et al.[1] (230–355 K). The only temperature-dependent study is from Bedjanian et al. The recommendation for E/R is based on their results. The likely products of this reaction are Br + HO_2. Bedjanian et al. attempted to measure the branching ratio for HBr formation, but there were significant problems from secondary chemistry. An upper limit of 3% was reported for the HBr yield.
(Table: 06-2, Note: 06-2, Evaluated: 06-2) Back to Table

(1) Bedjanian, Y.; Riffault, V.; Le Bras, G.; Poulet, G. Kinetics and mechanism of the OH and OD reactions with BrO. *J. Phys. Chem. A* **2001**, *105*, 6154-6166, doi:10.1021/jp010369q.

(2) Gilles, M. K.; McCabe, D. C.; Burkholder, J. B.; Ravishankara, A. R. Mesurement of the rate coefficient for the reaction of OH with BrO. *J. Phys. Chem. A* **2001**, *105*, 5849-5853, doi:10.1021/jp0039666.

G7. OH + HBr. The recommended k(298 K) is an average of the values derived from the data reported by Ravishankara et al.[9] (249–416 K) using FP-RF, Cannon et al.[4] (298 K) using FP-LIF, Ravishankara et al.[10] (298 K) using LFP-RF and LFP-LIF, Sims et al.[11] (23–295 K), Bedjanian et al.[3] (230–360 K) using DF-MS, Khamaganov et al.[8] (298–460 K) using DF-EPR, and Bedjanian[2] (235–960 K) using DF-MS. Although the earlier value obtained by Jourdain et al.[7] (298 K) using DF-EPR was not used in deriving the recommended k(298 K), it is only 16% smaller. Values reported by Takacs and Glass[13] (295 K) and Husain et al.[5] (300 K) as well as the preliminary value of Smith and Zellner[12] (298 K) are a factor of 2 lower and were not included in the derivation of the recommended value. The recommendation for the temperature dependence, the value of E/R, is derived from the fit to the most recent data of Bedjanian[2] obtained between 300 and 235 K, which are indicative of a weak negative temperature dependence. The data of Bedjanian exhibit a minimum near room temperature and a positive temperature dependence between 300 and 960 K. They are in good agreement with the greater than room temperature data reported by Ravishankara et al. and Bedjanian et al.[3] Bedjanian[2] also used DF-MS in a relative rate study between 340 and 920 K (OH + Br_2 was the reference reaction) to demonstrate the excellent agreement with results of his absolute rate constant measurements. The uncertainty g-factor was chosen to encompass the scattered results of the Laval nozzle studies by Atkinson et al.[1] and Jaramillo et al.[6] over the 185–242 K temperature range.
(Table: 25-1, Note: 25-1, Evaluated: 25-1) Back to Table

(1) Atkinson, D. B.; Jaramillo, V. I.; Smith, M. A. Low-temperature kinetic behavior of the bimolecular reaction OH + HBr (76-242 K). *J. Phys. Chem. A* **1997**, *101*, 3356-3359, doi:10.1021/jp963770z.

(2) Bedjanian, Y. Rate constant of the reaction of OH radicals with HBr over the temperature range 235-960 K. *J. Phys. Chem. A* **2021**, *125*, 1754-1759, doi:10.1021/acs.jpca.1c00251.

(3) Bedjanian, Y.; Riffault, V.; Le Bras, G.; Poulet, G. Kinetic study of the reactions of OH and OD with HBr and DBr. *J. Photochem. Photobiol. A: Chem.* **1999**, *128*, 15-25, doi:10.1016/S1010-6030(99)00159-8.

(4) Cannon, B. D.; Robertshaw, J. S.; Smith, I. W. M.; Williams, M. D. A time-resolved LIF study of the kinetics of OH(v=0) and OH(v=1) with HCl and HBr. *Chem. Phys. Lett.* **1984**, *105*, 380-385, doi:10.1016/0009-2614(84)80045-7.
(5) Husain, D.; Plane, J. M. C.; Slater, N. K. H. Kinetic investigation of the reactions of OH($X^2\Pi$) with the hydrogen halides, HCl, DCl, HBr and DBr by time-resolved resonance fluorescence ($A^2\Sigma^+$ - $X^2\Pi$). *J. Chem. Soc. Faraday Trans. 2* **1981**, *77*, 1949-1962, doi:10.1039/f29817701949.
(6) Jaramillo, V. I.; Gougeon, S.; Le Picard, S.; Canosa, A.; Smith, M.; Rowe, B. A consensus view of the temperature dependence of the gas phase reaction: OH + HBr → H_2O + Br. *Int. J. Chem. Kinet.* **2002**, *34*, 339-344, doi:10.1002/kin.10056.
(7) Jourdain, J. L.; Le Bras, G.; Combourieu, J. EPR determination of absolute rate constants for the reactions of H and OH radicals with hydrogen bromide. *Chem. Phys. Lett.* **1981**, *78*, 483-487, doi:10.1016/0009-2614(81)85242-6.
(8) Khamaganov, V. G.; Orkin, V. L.; Larin, I. K. Study of the reactions of OH with HCl, HBr, and HI between 298 K and 460 K. *Int. J. Chem. Kinet.* **2020**, *52*, 852-860, doi:10.1002/kin.21404.
(9) Ravishankara, A. R.; Wine, P. H.; Langford, A. O. Absolute rate constant for the reaction OH + HBr → H_2O + Br. *Chem. Phys. Lett.* **1979**, *63*, 479-484, doi:10.1016/0009-2614(79)80694-6.
(10) Ravishankara, A. R.; Wine, P. H.; Wells, J. R. The OH + HBr reaction revisited. *J. Chem. Phys.* **1985**, *83*, 447-448, doi:10.1063/1.449790.
(11) Sims, I. R.; Smith, I. W. M.; Clary, D. C.; Bocherel, P.; Rowe, B. R. Ultra-low temperature kinetics of neutral-neutral reactions: New experimental and theoretical results for OH + HBr between 295 and 23 K. *J. Chem. Phys.* **1994**, *101*, 1748-1751, doi:10.1063/1.467733.
(12) Smith, I. W. M.; Zellner, R. Rate measurements of reactions of OH by resonance absorption. Part 3. - Reactions of OH with H_2, D_2 and hydrogen and deuterium halides. *J. Chem. Soc. Faraday Trans. 2* **1974**, *70*, 1045-1056, doi:10.1039/F29747001045.
(13) Takacs, G. A.; Glass, G. P. Reactions of hydrogen atoms and hydroxyl radicals with hydrogen bromide. *J. Phys. Chem.* **1973**, *77*, 1060-1064, doi:10.1021/j100627a019.

G8. OH + CH_3Br. There are four studies of this reaction using different techniques that report 298 K rate constant values agreeing to within 10% and data that agree to better than 30% over a broad range of temperatures. The recommended k(298 K) was obtained from an average of the data from these four studies: the relative rate study of Hsu and DeMore[4] (298–360 K) (recalculated based on the recommendation for the rate constant for the OH + CH_3CHF_2 reference reaction given in the present evaluation and as discussed in the note for that reaction) and the absolute determinations by Chichinin et al.[1] (248–390 K), Mellouki et al.[5] (~230–380 K), and Zhang et al.[7] (250–400 K). The results of these extensive studies are preferred over the higher values reported in the earlier studies of Davis et al.[2] (244–350 K) and Howard and Evenson[3] (296 K). Although the room temperature value reported by Howard and Evenson is ~20% larger, it overlaps the recommended value within the reported experimental uncertainty. The data from Davis et al. yield a k(298 K) value that is more than 30% greater than recommended, with the difference between their measured rate constants and those recommended increasing at lower temperatures. This is suggestive of the presence of reactive impurities in the sample of methyl bromide. Also considered, but not used in deriving the recommended Arrhenius parameters are data from the relative rate and absolute studies of Nilsson et al.[6] (298–373 K). These data lie higher than the results from almost all of the previous measurements, and exceed the recommended value of k(298 K) by ~38% and 60%, respectively. The relative rate results barely overlap the recommended k(298 K) value within the combined 95% confidence limits when the uncertainties in the reference rate constants are included. While the high rate constants obtained in the absolute measurements of Nilsson et al. cannot be explained, significantly higher rate constant values were also previously obtained using the same apparatus for the OH reactions with HFC-152a and HCFC-123. The recommended value for E/R was derived from a fit to the data of Mellouki et al. below 300 K. The somewhat more scattered low temperature data of Chichinin et al. and Zhang et al. are encompassed within the recommended uncertainties.
(Table: 15-10, Note: 15-10, Evaluated: 15-10) Back to Table

(1) Chichinin, A.; Teton, S.; Le Bras, G.; Poulet, G. Kinetic investigation of the OH + CH_3Br reaction between 248 and 390 K. *J. Atmos. Chem.* **1994**, *18*, 239-245, doi:10.1007/BF00696781.
(2) Davis, D. D.; Machado, G.; Conaway, B.; Oh, Y.; Watson, R. A temperature dependent kinetics study of the reaction of OH with CH_3Cl, CH_2Cl_2, $CHCl_3$, and CH_3Br. *J. Chem. Phys.* **1976**, *65*, 1268-1274, doi:10.1063/1.433236.
(3) Howard, C. J.; Evenson, K. M. Rate constants for the reactions of OH with CH_4 and fluorine, chlorine, and bromine substituted methanes at 296 K. *J. Chem. Phys.* **1976**, *64*, 197-202, doi:10.1063/1.431950.
(4) Hsu, K. J.; DeMore, W. B. Rate constants for the reactions of OH with CH_3Cl, CH_2Cl_2, $CHCl_3$, and CH_3Br. *Geophys. Res. Lett.* **1994**, *21*, 805-808, doi:10.1029/94GL00601.

(5) Mellouki, A.; Talukdar, R. K.; Schmoltner, A.-M.; Gierczak, T.; Mills, M. J.; Soloman, S.; Ravishankara, A. R. Atmospheric lifetimes and ozone depletion potentials of methyl bromide (CH_3Br) and dibromomethane (CH_2Br_2). *Geophys. Res. Lett.* **1992**, *19*, 2059-2062, doi:10.1029/92GL01612.
(6) Nilsson, E. J. K.; Joelsson, I. M. T.; Heimdal, J.; Johnson, M. S.; Nielsen, O. J. Re-evaluation of the reaction rate coefficient of CH_3Br + OH with implications for the atmospheric budget of methyl bromide. *Atmos. Environ.* **2013**, *80*, 70-74, doi:10.1016/j.atmosenv.2013.07.046.
(7) Zhang, Z.; Saini, R. D.; Kurylo, M. J.; Huie, R. E. A temperature dependent kinetic study of the reaction of the hydroxyl radical with CH_3Br. *Geophys. Res. Lett.* **1992**, *19*, 2413-2416, doi:10.1029/92GL02929.

G9. OH + CH_2Br_2. The recommended k(298 K) is an average of the values from the absolute studies of Mellouki et al.[2] (~240–380 K) and Zhang et al.[4] (288–368 K) and from the relative rate measurements of DeMore[1] (293–375 K) (recalculated based on the recommendation for the rate constant for the OH + CH_2Cl_2 reference reaction given in this evaluation) and Orlando et al.[3] (298 K) (recalculated based on the recommendation for the rate constant for the OH + $CH_3C(O)CH_3$ reference reaction given in this evaluation). The recommended value of E/R is derived from an Arrhenius fit to the data of Mellouki et al. The uncertainty parameters reflect the latest understanding of the reactivities of this and similar compounds.
(Table: 02-25, Note: 15-10, Evaluated: 15-10) Back to Table

(1) DeMore, W. B. Experimental and estimated rate constants for the reactions of hydroxyl radicals with several halocarbons. *J. Phys. Chem.* **1996**, *100*, 5813-5820, doi:10.1021/jp953216+.
(2) Mellouki, A.; Talukdar, R. K.; Schmoltner, A.-M.; Gierczak, T.; Mills, M. J.; Soloman, S.; Ravishankara, A. R. Atmospheric lifetimes and ozone depletion potentials of methyl bromide (CH_3Br) and dibromomethane (CH_2Br_2). *Geophys. Res. Lett.* **1992**, *19*, 2059-2062, doi:10.1029/92GL01612.
(3) Orlando, J. J.; Tyndall, G. S.; Wallington, T. J.; Dill, M. Atmospheric chemistry of CH_2Br_2: Rate coefficients for its reaction with Cl atoms and OH and the chemistry of the $CHBr_2O$ radical. *Int. J. Chem. Kinet.* **1996**, *28*, 433-442, doi:10.1002/(SICI)1097-4601(1996)28:6<433::AID-KIN5>3.0.CO;2-W
(4) Zhang, D. Q.; Zhong, J. X.; Qiu, L. X. Kinetics of the reaction of hydroxyl radicals with CH_2Br_2 and its implications in the atmosphere. *J. Atmos. Chem.* **1997**, *27*, 209-215, doi:10.1023/A:1005821121158.

G10. OH + $CHBr_3$. The recommended Arrhenius parameters are derived from the data from the absolute rate constant study of Orkin et al.[2] (230–370 K). The results from the relative rate study of DeMore[1] (298– 366 K) (recalculated based on the recommendation for the rate constant for the OH + CH_2Cl_2 reference reaction given in this evaluation) lie systematically lower and exhibit a stronger temperature dependence. The results of the Orkin et al. investigation have been used in the rate constant recommendations for the OH reactions with $CHBr_3$, $CHClBr_2$, and $CHCl_2Br$. The observed systematic changes in the rate constants and temperature dependences found in this study are consistent with expectations based on increasing Cl atom substitution.
(Table: 15-10, Note: 15-10, Evaluated: 15-10) Back to Table

(1) DeMore, W. B. Experimental and estimated rate constants for the reactions of hydroxyl radicals with several halocarbons. *J. Phys. Chem.* **1996**, *100*, 5813-5820, doi:10.1021/jp953216+.
(2) Orkin, V. L.; Khamaganov, V. G.; Kozlov, S. N.; Kurylo, M. J. Measurements of rate constants for the OH reactions with bromoform ($CHBr_3$), $CHBr_2Cl$, $CHBrCl_2$, and epichlorohydrin (C_3H_5ClO). *J. Phys. Chem. A* **2013**, *117*, 3809-3818, doi:10.1021/jp3128753.

G11. OH + CH_2ClBr. The recommended k(298 K) is an average of the values from two relative rate studies by DeMore[2] (293–376 K) (recalculated based on the recommended rate constant for the OH + CH_2Cl_2 reference reaction) and Bilde et al.[1] (217– 296 K) (recalculated using the recommended rate constant for the OH + CH_2Br_2 reference reaction) and two absolute determinations by Orkin et al.[3] (277–370 K), all of which are in good agreement. The recommended E/R is obtained from a fit to the data of DeMore and Orkin et al. after scaling each data set to the recommended k(298 K).
(Table: 15-10, Note: 15-10, Evaluated: 15-10) Back to Table

(1) Bilde, M.; Wallington, T. J.; Ferronato, G.; Orlando, J. J.; Tyndall, G. S.; Estupinan, E.; Haberkorn, S. Atmospheric chemistry of CH_2BrCl, $CHBrCl_2$, $CHBr_2Cl$, $CF_3CHBrCl$, and CBr_2Cl_2. *J. Phys. Chem. A* **1998**, *102*, 1976-1986, doi:10.1021/jp9733375.
(2) DeMore, W. B. Experimental and estimated rate constants for the reactions of hydroxyl radicals with several halocarbons. *J. Phys. Chem.* **1996**, *100*, 5813-5820, doi:10.1021/jp953216+.

(3) Orkin, V. L.; Khamaganov, V. G.; Guschin, A. G.; Huie, R. E.; Kurylo, M. J. Atmospheric fate of chlorobromomethane: Rate constant for the reaction with OH, UV spectrum, and water solubility. *J. Phys. Chem. A* **1997**, *101*, 174-178, doi:10.1021/jp962428j.

G12. OH + $CHClBr_2$. The recommended Arrhenius parameters are derived from the data from the absolute rate study of Orkin et al.[1] (230–330 K). As discussed in the note for the reaction of OH with $CHBr_3$, the observed systematic changes in the rate constants for the OH reactions with $CHBr_3$, $CHClBr_2$, and $CHCl_2Br$ and the temperature dependences found in this study are consistent with expectations based on increasing Cl atom substitution and provide the basis for the assignment of the uncertainty parameters.
(Table: 15-10, Note: 15-10, Evaluated 15-10) Back to Table

(1) Orkin, V. L.; Khamaganov, V. G.; Kozlov, S. N.; Kurylo, M. J. Measurements of rate constants for the OH reactions with bromoform ($CHBr_3$), $CHBr_2Cl$, $CHBrCl_2$, and epichlorohydrin (C_3H_5ClO). *J. Phys. Chem. A* **2013**, *117*, 3809-3818, doi:10.1021/jp3128753.

G13. OH + $CHCl_2Br$. The recommended Arrhenius parameters are derived from the data from the absolute rate study of Orkin et al.[2] (230–330 K). As discussed in the note for the reaction of OH with $CHBr_3$, the observed systematic changes in the rate constants for the OH reactions with $CHBr_3$, $CHClBr_2$, and $CHCl_2Br$ and the temperature dependences found in this study are consistent with expectations based on increasing Cl atom substitution and provide the basis for the assignment of the uncertainty parameters. The room temperature rate constants determined in the relative rate study by Bilde et al.[1] (217–296 K) (recalculated using the recommended rate constants for the OH + CH_2Br_2 and CH_2ClBr reference reactions) lie approximately 20% and 50% lower, respectively, than recommended.
(Table: 15-10, Note: 15-10, Evaluated 15-10) Back to Table

(1) Bilde, M.; Wallington, T. J.; Ferronato, C.; Orlando, J. J.; Tyndall, G. S.; Estupiñan, E.; Haberkorn, S. Atmospheric chemistry of CH_2BrCl, $CHBrCl_2$, $CHBr_2Cl$, $CF_3CHBrCl$, and CBr_2Cl_2. *J. Phys. Chem. A* **1998**, *102*, 1976-1986, doi:10.1021/jp9733375.
(2) Orkin, V. L.; Khamaganov, V. G.; Kozlov, S. N.; Kurylo, M. J. Measurements of rate constants for the OH reactions with bromoform ($CHBr_3$), $CHBr_2Cl$, $CHBrCl_2$, and epichlorohydrin (C_3H_5ClO). *J. Phys. Chem. A* **2013**, *117*, 3809-3818, doi:10.1021/jp3128753.

G14. OH + CHF_2Br (Halon-1201). There are very consistent results from four studies of this reaction: Talukdar et al.[4] (233–432 K) (using two different measurement techniques, DF-LMR and PLP-LIF), Orkin and Khamaganov[3] (298– 460 K) (using DF-EPR), and Hsu and DeMore[2] (283–368 K) (relative rate measurements recalculated using the recommended rate constant for the OH + CH_4 reference reaction). Talukdar et al. noted a slight curvature in the Arrhenius plot at the higher temperatures, which is also supported by the data from Orkin and Khamaganov. Below 400 K, all four data sets exhibit nearly identical temperature dependences with E/R values ranging from 1271 to 1338 K^{-1}. The recommended k(298 K) is an average of the rate constants derived from each of the four studies. The recommended value for E/R is derived from a combined fit to the data from these four studies below 400 K after each data set was scaled to the recommended k(298 K). These data are preferred over the consistently higher results reported by Brown et al.[1] (275–420 K).
(Table: 15-10, Note: 15-10, Evaluated: 15-10) Back to Table

(1) Brown, A. C.; Canosa-Mas, C. E.; Parr, A. D.; Rothwell, K.; Wayne, R. P. Tropospheric lifetimes of three compounds for possible replacement of CFC and halons. *Nature* **1990**, *347*, 541-543, doi:10.1038/347541a0.
(2) Hsu, K. J.; DeMore, W. B. Rate constants and temperature dependences for the reactions of hydroxyl radical with several halogenated methanes, ethanes, and propanes by relative rate measurements. *J. Phys. Chem.* **1995**, *99*, 1235-1244, doi:10.1021/j100004a025.
(3) Orkin, V. L.; Khamaganov, V. G. Rate constants for reactions of OH radicals with some Br-containing haloalkanes. *J. Atmos. Chem.* **1993**, *16*, 169-178, doi:10.1007/BF00702786.
(4) Talukdar, R.; Mellouki, A.; Gierczak, T.; Burkholder, J. B.; McKeen, S. A.; Ravishankara, A. R. Atmospheric lifetime of CHF_2Br, a proposed substitute for halons. *Science* **1991**, *252*, 693-695, doi:10.1126/science.252.5006.693.

G15. OH + CF_2Br_2 (Halon-1202). The *A* factor was estimated and a lower limit for *E*/R was derived using the upper limit for the 298 K rate constant reported by Burkholder et al.[1] (293–424 K) in a study using pulsed photolysis-LIF and DF-LMR techniques.
(Table: 02-25, Note: 02-25, Evaluated: 15-10) Back to Table

(1) Burkholder, J. B.; Wilson, R. R.; Gierczak, T.; Talukdar, R.; McKeen, S. A.; Orlando, J. J.; Vaghjiani, G. L.; Ravishankara, A. R. Atmospheric fate of CF_3Br, CF_2Br_2, CF_2ClBr, and CF_2BrCF_2Br. *J. Geophys. Res.* **1991**, *96*, 5025-5043, doi:10.1029/90JD02735.

G16. OH + CF_3Br (Halon-1301). The *A*-factor was estimated and a lower limit for *E*/R was derived using the upper limit for the 460 K rate constant reported by Orkin and Khamaganov.[3] (298, 460 K). These parameters were then used to calculate an upper limit for *k*(298 K). The upper limit for *k*(298 K) determined by Burkholder et al.[1] (294–424 K) using pulsed photolysis-LIF and DF-LMR techniques at room temperature is understandably higher. A less sensitive upper limit was also reported by Le Bras and Combourieu[2] (298 K).
(Table: 02-25, Note: 02-25, Evaluated: 15-10) Back to Table

(1) Burkholder, J. B.; Wilson, R. R.; Gierczak, T.; Talukdar, R.; McKeen, S. A.; Orlando, J. J.; Vaghjiani, G. L.; Ravishankara, A. R. Atmospheric fate of CF_3Br, CF_2Br_2, CF_2ClBr, and CF_2BrCF_2Br. *J. Geophys. Res.* **1991**, *96*, 5025-5043, doi:10.1029/90JD02735.
(2) Le Bras, G.; Combourieu, J. EPR kinetic study of the reactions of CF_3Br with H atoms and OH radicals. *Int. J. Chem. Kinet.* **1978**, *10*, 1205-1213, doi:10.1002/kin.550101203.
(3) Orkin, V. L.; Khamaganov, V. G. Rate constants for reactions of OH radicals with some Br-containing haloalkanes. *J. Atmos. Chem.* **1993**, *16*, 169-178, doi:10.1007/BF00702786.

G17. OH + CF_2ClBr (Halon-1211). A lower limit for *E*/R was derived using an estimated *A* factor of 1×10^{-12} and the upper limit for the 373 K rate constant reported by Burkholder et al.[1] (293–424 K) in a study using pulsed photolysis-LIF and DF-LMR techniques. These parameters were then used to calculate an upper limit for *k*(298 K). A less sensitive upper limit was reported by Clyne and Holt[2] (298 K).
(Table: 15-10, Note: 15-10, Evaluated: 15-10) Back to Table

(1) Burkholder, J. B.; Wilson, R. R.; Gierczak, T.; Talukdar, R.; McKeen, S. A.; Orlando, J. J.; Vaghjiani, G. L.; Ravishankara, A. R. Atmospheric fate of CF_3Br, CF_2Br_2, CF_2ClBr, and CF_2BrCF_2Br. *J. Geophys. Res.* **1991**, *96*, 5025-5043, doi:10.1029/90JD02735.
(2) Clyne, M. A. A.; Holt, P. M. Reaction kinetics involving ground $X^2\Pi$ and excited $A^2\Sigma^+$ hydroxyl radicals Part 1.-Quenching kinetics of OH $A^2\Sigma^+$ and rate constants for reactions of OH $X^2\Pi$ with CH_3CCl_3 and CO. *J. Chem. Soc. Faraday Trans. 2* **1979**, *75*, 569-581, doi:10.1039/f29797500569.

G18. OH + CH_3CH_2Br. The recommended values for *k*(298 K) and *E*/R are derived from a fit to the data (T ≤300 K) of Herndon et al.[2] (223–422 K). These data suggest a curvature of the Arrhenius plot similar to that found for the OH reaction with CH_3CH_2F. The data of Qiu et al.[3] (292–366 K) (which include earlier data reported by the same research group in Xing et al.[4] (293–418 K)) were not used because they were obtained mainly above room temperature and exhibit a very steep temperature dependence resulting in a value for *E*/R that is larger than the *E*/R value obtained from data at T >298 K for the OH reaction with CH_3CH_2F. The *k*(300 K) value reported by Donaghy et al.[1] (300 K) seems too low for this reaction when compared with the recommendation for the presumably slower (and better studied) OH reaction with CH_3CH_2F.
(Table: 02-25, Note: 02-25, Evaluated: 02-25) Back to Table

(1) Donaghy, T.; Shanahan, I.; Hande, M.; Fitzpatrick, S. Rate constants and atmospheric lifetimes for the reactions of OH radicals and Cl atoms with haloalkanes. *Int. J. Chem. Kinet.* **1993**, *25*, 273-284, doi:10.1002/kin.550250407.
(2) Herndon, S. C.; Gierczak, T.; Talukdar, R. K.; Ravishankara, A. R. Kinetics of the reactions of OH with several alkyl halides. *Phys. Chem. Chem. Phys.* **2001**, *3*, 4529-4535, doi:10.1039/b105188c.
(3) Qiu, L. X.; Shi, S.-H.; Xing, S. B.; Chen, X. G. Rate constants for the reactions of OH with five halogen-substituted ethanes from 292 to 366 K. *J. Phys. Chem.* **1992**, *96*, 685-689, doi:10.1021/j100181a032.
(4) Xing, S. B.; Shi, S.-H.; Qiu, L. X. Kinetics studies of reactions of OH radicals with four haloethanes Part I. Experiment and BEBO calculation. *Int. J. Chem. Kinet.* **1992**, *24*, 1-10, doi:10.1002/kin.550240102.

G19. OH + CH_2BrCH_2Br. The recommended k(298 K) is an average of the values reported by Howard and Evenson[2] (296 K), Arnts et al.[1] (297 K), and Qiu et al.[3] (294–365 K). The recommended value for E/R is taken from the data of Qiu et al.
(Table: 15-10, Note: 15-10, Evaluated: 15-10) Back to Table

(1) Arnts, R. R.; Seila, R. L.; Bufalini, J. J. Determination of room temperature OH rate constants for acetylene, ethylene dichloride, ethylene dibromide, p-dichlorobenzene and carbon disulfide. *J. Air Pollut. Control Assoc.* **1989**, *39*, 453-460, doi:10.1080/08940630.1989.10466544.
(2) Howard, C. J.; Evenson, K. M. Rate constants for the reactions of OH with ethane and some halogen substituted ethanes at 296 K. *J. Chem. Phys.* **1976**, *64*, 4303-4306, doi:10.1063/1.432115.
(3) Qiu, L. X.; Shi, S.-H.; Xing, S. B.; Chen, X. G. Rate constants for the reactions of OH with five halogen-substituted ethanes from 292 to 366 K. *J. Phys. Chem.* **1992**, *96*, 685-689, doi:10.1021/j100181a032.

G20. OH + CH_2BrCF_3 (Halon-2301). The recommended k(298 K) is an average of the 298 K rate constants obtained from Arrhenius fits to the data of Nelson et al.[1] (~280–355 K) and Orkin and Khamaganov[2] (298–460 K). The recommended value of E/R was derived from a combined fit to both data sets (for T <400 K) after scaling each one to the recommended value of k(298 K).
(Table: 15-10, Note: 15-10, Evaluated: 15-10) Back to Table

(1) Nelson, D. D., Jr.; Zahniser, M. S.; Kolb, C. E. OH reaction kinetics and atmospheric lifetimes of CF_3CFHCF_3 and CF_3CH_2Br. *Geophys. Res. Lett.* **1993**, *20*, 197-200, doi:10.1029/93GL00239.
(2) Orkin, V. L.; Khamaganov, V. G. Rate constants for reactions of OH radicals with some Br-containing haloalkanes. *J. Atmos. Chem.* **1993**, *16*, 169-178, doi:10.1007/BF00702786.

G21. OH + $CHFBrCF_3$ (Halon-2401). The recommended Arrhenius parameters are derived from a combined fit to the data (below 400 K) of Orkin and Khamaganov[2] (298–460 K) and Brown et al.[1] (279–423 K), which are in good agreement.
(Table: 02-25, Note: 02-25, Evaluated: 02-25) Back to Table

(1) Brown, A. C.; Canosa-Mas, C. E.; Parr, A. D.; Rothwell, K.; Wayne, R. P. Tropospheric lifetimes of three compounds for possible replacement of CFC and halons. *Nature* **1990**, *347*, 541-543, doi:10.1038/347541a0.
(2) Orkin, V. L.; Khamaganov, V. G. Rate constants for reactions of OH radicals with some Br-containing haloalkanes. *J. Atmos. Chem.* **1993**, *16*, 169-178, doi:10.1007/BF00702786.

G22. OH + $CHClBrCF_3$ (Halothane, Halon-2311). The recommended Arrhenius parameters are derived from a fit to the data of Orkin and Khamaganov[2] (298–460 K, for T ≤400 K). The room temperature value measured by Brown et al.[1] (303 K) lies somewhat higher than this recommendation but is encompassed within the 2σ confidence limits.
(Table: 02-25, Note: 02-25, Evaluated: 02-25) Back to Table

(1) Brown, A. C.; Canosa-Mas, C. E.; Parr, A. D.; Wayne, R. P. Laboratory studies of some halogenated ethanes and ethers: Measurements of rates of reaction with OH and of infrared absorption cross-sections. *Atmos. Environ.* **1990**, *24A*, 2499-2511, doi:10.1016/0960-1686(90)90341-J.
(2) Orkin, V. L.; Khamaganov, V. G. Rate constants for reactions of OH radicals with some Br-containing haloalkanes. *J. Atmos. Chem.* **1993**, *16*, 169-178, doi:10.1007/BF00702786.

G23. OH + $CHFClCF_2Br$. The recommended Arrhenius parameters are derived from a fit to the data from the relative rate study of DeMore[1] (315–372 K) (recalculated based on the recommended rate constant for the OH + CH_3CCl_3 reference reaction).
(Table: 02-25, Note: 02-25, Evaluated: 02-25) Back to Table

(1) DeMore, W. B. Experimental and estimated rate constants for the reactions of hydroxyl radicals with several halocarbons. *J. Phys. Chem.* **1996**, *100*, 5813-5820, doi:10.1021/jp953216+.

G24. OH + CF_2BrCF_2Br (Halon-2402). The *A*-factor was estimated and a lower limit for *E*/R was derived by using the upper limit for the rate constant at 460 K reported by Orkin and Khamaganov[2] (298, 460 K). These parameters were then used to calculate a recommended upper limit for *k*(298 K). The upper limit for *k*(298 K) determined by Burkholder et al.[1] (295–424 K) in a study using pulsed photolysis-LIF and DF-LMR techniques at room temperature is understandably higher.
(Table: 02-25, Note: 02-25, Evaluated: 15-10) Back to Table

(1) Burkholder, J. B.; Wilson, R. R.; Gierczak, T.; Talukdar, R.; McKeen, S. A.; Orlando, J. J.; Vaghjiani, G. L.; Ravishankara, A. R. Atmospheric fate of CF_3Br, CF_2Br_2, CF_2ClBr, and CF_2BrCF_2Br. *J. Geophys. Res.* **1991**, *96*, 5025-5043, doi:10.1029/90JD02735.
(2) Orkin, V. L.; Khamaganov, V. G. Rate constants for reactions of OH radicals with some Br-containing haloalkanes. *J. Atmos. Chem.* **1993**, *16*, 169-178, doi:10.1007/BF00702786.

G25. OH + $CH_2BrCH_2CH_3$. The recommended *k*(298 K) is an average of *k*(298 K) values derived from fits to the data from the absolute studies of Téton et al.[8] (233–372 K), Nelson et al.[7] (271–363 K), Herndon et al.[5] (230–386 K), Gilles et al.[4] (230–360 K), Bryukov et al.[1] (297–725 K), and Kozlov et al.[6] (210–480 K) and the relative rate study of Donaghy et al.[3] (300 K) (recalculated using the rate coefficient for the OH + cyclohexane reference reaction from DeMore and Bayes[2]). Significant curvature in the Arrhenius plot has been observed over the 210 to 480 K temperature range, due to the three different hydrogen-abstraction reaction channels. These channels have been quantified in the study of Gilles et al. In spite of the noticeable Arrhenius curvature, the data below 300 K can be reasonably well represented by a two-parameter Arrhenius expression. The recommended value of *E*/R is an average of the *E*/R values obtained from fits to the data (for T ≤300 K) from Gilles et al. and Kozlov et al. The data over the 210–480 K temperature range can be represented by the three-parameter equation from Kozlov et al.

$$k(T) = 3.0 \times 10^{-13} (T/298)^{2.8} \exp(+369/T)$$

(Table: 10-6, Note: 15-10, Evaluated: 10-6) Back to Table

(1) Bryukov, M. G.; Vidrine, R. G.; Dellinger, B. Temperature-dependent kinetics study of the gas-phase reactions of OH with n- and i-propyl bromide. *J. Phys. Chem. A* **2007**, *111*, 6197-6203, doi:10.1021/jp072693c.
(2) DeMore, W. B.; Bayes, K. D. Rate constants for the reactions of hydroxyl radical with several alkanes, cycloalkanes, and dimethyl ether. *J. Phys. Chem. A* **1999**, *103*, 2649-2654, doi:10.1021/jp983273d.
(3) Donaghy, T.; Shanahan, I.; Hande, M.; Fitzpatrick, S. Rate constants and atmospheric lifetimes for the reactions of OH radicals and Cl atoms with haloalkanes. *Int. J. Chem. Kinet.* **1993**, *25*, 273-284, doi:10.1002/kin.550250407.
(4) Gilles, M. K.; Burkholder, J. B.; Gierczak, T.; Marshall, P.; Ravishankara, A. R. Rate coefficient and product branching measurements for the reaction OH + bromopropane from 230 to 360 K. *J. Phys. Chem. A* **2002**, *104*, 8945-8950, doi:10.1021/jp014736+.
(5) Herndon, S. C.; Gierczak, T.; Talukdar, R. K.; Ravishankara, A. R. Kinetics of the reactions of OH with several alkyl halides. *Phys. Chem. Chem. Phys.* **2001**, *3*, 4529-4535, doi:10.1039/b105188c.
(6) Kozlov, S. N.; Orkin, V. L.; Huie, R. E.; Kurylo, M. J. OH reactivity and UV spectra of propane, n-propyl bromide, and isopropyl bromide. *J. Phys. Chem. A* **2003**, *107*, 1333-1338, doi:10.1021/jp021806j.
(7) Nelson, D. D., Jr.; Wormhoudt, J. C.; Zahniser, M. S.; Kolb, C. E.; Ko, M. K. W.; Weisenstein, D. K. OH reaction kinetics and atmospheric impact of 1-bromopropane. *J. Phys. Chem. A* **1997**, *101*, 4987-4990, doi:10.1021/jp970874g.
(8) Téton, S.; El-Boudali, A.; Mellouki, A. Rate constants for the reactions of OH radicals with 1- and 2-bromopropane. *J. Chim. Phys.* **1996**, *93*, 274-282, doi:10.1051/jcp/1996930274.

G26. OH + $CH_3CHBrCH_3$. The recommendation for *k*(298 K) is an average of the values derived from the absolute studies of Herndon et al.[4] (215–402 K), Kozlov et al.[5] (210–480 K), and Bryukov et al.[1] (297–715 K) and from the relative rate study of Donaghy et al.[3] (298 K) (recalculated using the rate coefficient for the OH + cyclohexane reference reaction from DeMore and Bayes[2]). Significant curvature in the Arrhenius plot has been observed over the 210 to 480 K temperature range, presumably due to the existence of two different hydrogen-abstraction channels. In spite of the noticeable Arrhenius curvature, the data below 300 K can be reasonably well represented by a two-parameter Arrhenius fit. The recommended value for *E*/R is an average of the parameters derived from Arrhenius fits to the data (T ≤300 K) of Herndon et al. and Kozlov et al., which are in excellent agreement. The absolute temperature-dependent data of Téton et al.[6] (233–372 K) lie systematically

higher (15–30%) than those from the three more recent studies. The data over the 210–480 K temperature range can be represented by the three-parameter expression from Kozlov et al.[5]

$$k(T) = 1.66 \times 10^{-13} (T/298)^{2.95} \exp(+461/T)$$

(Table: 10-6, Note: 15-10, Evaluated: 10-6) Back to Table

(1) Bryukov, M. G.; Vidrine, R. G.; Dellinger, B. Temperature-dependent kinetics study of the gas-phase reactions of OH with n- and i-propyl bromide. *J. Phys. Chem. A* **2007**, *111*, 6197-6203, doi:10.1021/jp072693c.

(2) DeMore, W. B.; Bayes, K. D. Rate constants for the reactions of hydroxyl radical with several alkanes, cycloalkanes, and dimethyl ether. *J. Phys. Chem. A* **1999**, *103*, 2649-2654, doi:10.1021/jp983273d.

(3) Donaghy, T.; Shanahan, I.; Hande, M.; Fitzpatrick, S. Rate constants and atmospheric lifetimes for the reactions of OH radicals and Cl atoms with haloalkanes. *Int. J. Chem. Kinet.* **1993**, *25*, 273-284, doi:10.1002/kin.550250407.

(4) Herndon, S. C.; Gierczak, T.; Talukdar, R. K.; Ravishankara, A. R. Kinetics of the reactions of OH with several alkyl halides. *Phys. Chem. Chem. Phys.* **2001**, *3*, 4529-4535, doi:10.1039/b105188c.

(5) Kozlov, S. N.; Orkin, V. L.; Huie, R. E.; Kurylo, M. J. OH reactivity and UV spectra of propane, n-propyl bromide, and isopropyl bromide. *J. Phys. Chem. A* **2003**, *107*, 1333-1338, doi:10.1021/jp021806j.

(6) Téton, S.; El-Boudali, A.; Mellouki, A. Rate constants for the reactions of OH radicals with 1- and 2-bromopropane. *J. Chim. Phys.* **1996**, *93*, 274-282, doi:10.1051/jcp/1996930274.

G27. OH + $CHBr=CF_2$. The recommended Arrhenius parameters are derived from the data of Orkin et al.[1] (250–370 K).
(Table: 15-10, Note: 15-10, Evaluated: 15-10) Back to Table

(1) Orkin, V. L.; Louis, F.; Huie, R. E.; Kurylo, M. J. Photochemistry of bromine-containing fluorinated alkenes: Reactivity toward OH and UV spectra. *J. Phys. Chem. A* **2002**, *106*, 10195-10199, doi:10.1021/jp014436s.

G28. OH + $CFBr=CF_2$. The recommended Arrhenius parameters are derived from the data of Orkin et al.[1] (250–370 K).
(Table: 15-10, Note: 15-10, Evaluated: 15-10) Back to Table

(1) Orkin, V. L.; Louis, F.; Huie, R. E.; Kurylo, M. J. Photochemistry of bromine-containing fluorinated alkenes: Reactivity toward OH and UV spectra. *J. Phys. Chem. A* **2002**, *106*, 10195-10199, doi:10.1021/jp014436s.

G29. OH + $CH_2=CBrCF_3$. The recommended Arrhenius parameters are derived from a fit to the data (T <300 K) of Patten et al.[2] (220–370 K). Earlier, less extensive data from the same laboratory (Orkin et al.[1] (250–370 K)) are in excellent agreement. The room temperature data from the relative rate study of Sulbaek-Andersen et al.[3] (296 K) are also in very good agreement after recalculation using the latest recommended values for the reference reactions. While a standard Arrhenius parameterization provides a very good representation of the rate constants below room temperature, a pronounced curvature can be seen in the data over the full temperature range. Thus, the data over the complete temperature range (220–370 K) can be represented by the three-parameter equation:

$$k(T) = 4.85 \times 10^{-13} (T/298)^{0.92} \exp(+613/T)$$

(Table: 15-10, Note: 15-10, Evaluated: 15-10) Back to Table

(1) Orkin, V. L.; Louis, F.; Huie, R. E.; Kurylo, M. J. Photochemistry of bromine-containing fluorinated alkenes: Reactivity toward OH and UV spectra. *J. Phys. Chem. A* **2002**, *106*, 10195-10199, doi:10.1021/jp014436s.

(2) Patten, K. O.; Khamaganov, V. G.; Orkin, V. L.; Baughcum, S. L.; Wuebbles, D. J. OH reaction rate constant, IR absorption spectrum, ozone depletion potentials and global warming potentials of 2-bromo-3,3,3-trifluoropropene. *J. Geophys. Res.* **2011**, *116*, D24307, doi:10.1029/2011JD016518.

(3) Sulbaek-Andersen, M. P.; Hurley, M. D.; Wallington, T. J. Kinetics of the gas phase reactions of chlorine atoms and OH radicals with $CF_3CBr=CH_2$ and $CF_3CF_2CBr=CH_2$. *Chem. Phys. Lett.* **2009**, *482*, 20-23, doi:10.1016/j.cplett.2009.09.056.

G30. OH + CH_2=$CBrCF_2CF_3$. The recommended k(298 K) is an average of the values from the absolute rate study of Orkin et al.[1] (250–370 K) and the relative rate study of Sulbaek-Andersen et al.[2] (296 K) after recalculation using the latest recommended values for the reference reactions. The recommended value for E/R is derived from the data of Orkin et al.
(Table: 15-10, Note: 15-10, Evaluated: 15-10) Back to Table

(1) Orkin, V. L.; Louis, F.; Huie, R. E.; Kurylo, M. J. Photochemistry of bromine-containing fluorinated alkenes: Reactivity toward OH and UV spectra. *J. Phys. Chem. A* **2002**, *106*, 10195-10199, doi:10.1021/jp014436s.
(2) Sulbaek-Andersen, M. P.; Hurley, M. D.; Wallington, T. J. Kinetics of the gas phase reactions of chlorine atoms and OH radicals with CF_3CBr=CH_2 and CF_3CF_2CBr=CH_2. *Chem. Phys. Lett.* **2009**, *482*, 20-23, doi:10.1016/j.cplett.2009.09.056.

G31. OH + CH_2=$CHCF_2CF_2Br$. The recommended Arrhenius parameters are derived from the data of Orkin et al.[1] (250–370 K).
(Table: 15-10, Note: 15-10, Evaluated: 15-10) Back to Table

(1) Orkin, V. L.; Louis, F.; Huie, R. E.; Kurylo, M. J. Photochemistry of bromine-containing fluorinated alkenes: Reactivity toward OH and UV spectra. *J. Phys. Chem. A* **2002**, *106*, 10195-10199, doi:10.1021/jp014436s.

G32. OH + CH_2=$CHCFClCF_2Br$. The recommended values for both k(298 K) and E/R were derived from a fit to the data reported by Orkin et al.[1] (250–370 K).
(Table: 19-5, Note: 19-5, Evaluated: 19-5) Back to Table

(1) Orkin, V. L.; Martynova, L. E.; Kurylo, M. J. Photochemical properties of CH_2=CH-CFCl-CF_2Br (4-bromo-3-chloro-3,4,4-trifluoro-1-butene) and CH_3-O-$CH(CF_3)_2$ (methyl hexafluoroisopropyl ether): OH reaction rate constants and UV and IR absorption spectra. *J. Phys. Chem. A* **2017**, *121*, 5675–5680, doi:10.1021/acs.jpca.7b04256.

G33. HO_2 + Br. The recommended k(298 K) was obtained from an average of the results of Laverdet et al.[2] (296 K), Toohey et al.[5] (262–390 K), and Bedjanian et al.[1] (230–355 K). The results of Posey et al.[3] (298 K) were not considered because of problems with the experimental method. The results of Poulet et al.[4] (298 K) were also not considered because of complications associated with secondary reactions. The recommendation for the temperature dependence is based on the results of Bedjanian et al.
(Table: 06-2, Note: 06-2, Evaluated: 06-2) Back to Table

(1) Bedjanian, Y.; Riffault, V.; Le Bras, G.; Poulet, G. Kinetic study of the reactions of Br with HO_2 and DO_2. *J. Phys. Chem. A* **2001**, *105*, 573-578, doi:10.1021/jp002731r.
(2) Laverdet, G.; Le Bras, G.; Mellouki, A.; Poulet, G. The Br + HO_2 reaction revisited: absolute determination of the rate constant at 298 K. *Chem. Phys. Lett.* **1990**, *172*, 430-434, doi:10.1016/S0009-2614(90)87138-H.
(3) Posey, J.; Sherwell, J.; Kaufman, M. Kinetics of the reactions of atomic bromine with HO_2 and H_2O_2. *Chem. Phys. Lett.* **1981**, *77*, 476-479, doi:10.1016/0009-2614(81)85189-5.
(4) Poulet, G.; Laverdet, G.; Le Bras, G. Kinetics of the reactions of atomic bromine with HO_2 and HCO at 298 K. *J. Chem. Phys.* **1984**, *80*, 1922-1928, doi:10.1063/1.446953.
(5) Toohey, D. W.; Brune, W. H.; Anderson, J. G. Mechanism and kinetics of Br + HO_2 → HBr + O_2 and Br + H_2O_2 → products over the temperature range 260-390 K. *J. Phys. Chem.* **1987**, *91*, 1215-1222, doi:10.1021/j100289a036.

G34. HO_2 + BrO. The recommendation for E/R is based on results of the temperature-dependent studies of Elrod et al.[5] (210–298 K), Li et al.[7] (233–348 K), and Bedjanian et al.[1] (230–360 K). It is assumed that the Bedjanian et al. results supersede those of Larichev et al.[6] (233–344 K) since the same experimental technique was used, and the same research group was involved in both studies. The recommended k(298 K) is the mean of the values reported in these studies, as well as those of Cronkhite et al.[4] (296 K) and Bloss et al.[2] (298 K). The room temperature value of Bridier et al.[3] (298 K), which was not obtained under pseudo–first-order decay conditions, was not included in derivation of the recommendation. Bedjanian et al. have determined an upper limit of 0.4% for production of HBr and O_3 at 298 K. From a study of the reverse reaction above room temperature, Mellouki et al.[8] determined by extrapolation that the yield of HBr + O_3 is an insignificant fraction (<0.01%) of the total reaction down to 200 K.
(Table: 06-2, Note: 06-2, Evaluated: 06-2) Back to Table

(1) Bedjanian, Y.; Riffault, V.; Poulet, G. Kinetic study of the reactions of BrO radicals with HO_2 and DO_2. *J. Phys. Chem. A* **2001**, *105*, 3167-3175, doi:10.1021/jp0032255.
(2) Bloss, W. J.; Rowley, D. M.; Cox, R. A.; Jones, R. L. Rate coefficient for the BrO + HO_2 reaction at 298 K. *Phys. Chem. Chem. Phys.* **2002**, *4*, 3639-3647, doi:10.1039/b201653b.
(3) Bridier, I.; Veyret, B.; Lesclaux, R. Flash photolysis kinetic study of reactions of the BrO radical with BrO and HO_2. *Chem. Phys. Lett.* **1993**, *201*, 563-568, doi:10.1016/0009-2614(93)85118-8.
(4) Cronkhite, J. M.; Stickel, R. E.; Nicovich, J. M.; Wine, P. H. Laser flash photolysis studies of radical-radical reaction kinetics: The HO_2 + BrO reaction. *J. Phys. Chem. A* **1998**, *102*, 6651-6658, doi:10.1021/jp981456u.
(5) Elrod, M. J.; Meads, R. F.; Lipson, J. B.; Seeley, J. V.; Molina, M. J. Temperature dependence of the rate constant for the HO_2 + BrO reaction. *J. Phys. Chem.* **1996**, *100*, 5808-5812, doi:10.1021/jp953193z.
(6) Larichev, M.; Maguin, F.; Le Bras, G.; Poulet, G. Kinetics and mechanism of the BrO + HO_2 reaction. *J. Phys. Chem.* **1995**, *99*, 15911-15918, doi:10.1021/j100043a032.
(7) Li, Z.; Friedl, R. R.; Sander, S. P. Kinetics of the HO_2 + BrO reaction over the temperature range 233-348 K. *J. Chem. Soc. Faraday Trans.* **1997**, 2683-2691.
(8) Mellouki, A.; Talukdar, R. K.; Howard, C. J. Kinetics of the reactions of HBr with O_3 and HO_2: The yield of HBr from HO_2 + BrO. *J. Geophys. Res.* **1994**, *99*, 22949-22954, doi:10.1029/94JD02144.

G35. NO_3 + HBr. The recommendation accepts the upper limit reported by Mellouki et al.[2] (298 K) in a study using DF-EPR techniques. This upper limit shows that this reaction is of negligible importance in stratospheric chemistry. Canosa-Mas et al.[1] (298 K) reported a value that is consistent, within experimental error, with the upper limit of Mellouki et al.
(Table: 90-1, Note: 92-20, Evaluated: 10-6) Back to Table

(1) Canosa-Mas, C. E.; Smith, S. J.; Toby, S.; Wayne, R. P. Laboratory studies of the reactions of the nitrate radical with chloroform, methanol, hydrogen chloride and hydrogen bromide. *J. Chem. Soc. Faraday Trans. 2* **1989**, *85*, 709-725, doi:10.1039/f29898500709.
(2) Mellouki, A.; Poulet, G.; Le Bras, G.; Singer, R.; Burrows, J. P.; Moortgat, G. K. Discharge flow kinetic study of the reactions of NO_3 with Br, BrO, HBr, and HCl. *J. Phys. Chem.* **1989**, *93*, 8017-8021, doi:10.1021/j100361a012.

G36. Cl + CH_3Br. The recommended k(298 K) is an average of the results from the absolute rate studies of Gierczak et al.[1] (222–394 K), Kambanis et al.[3] (273–363 K), and Piety et al.,[5] (213–697 K) and from the relative rate study of Orlando et al.[4] (231–296 K). The recommended value for E/R is derived from a combined fit to the data from these same four studies restricted to temperatures of 400 K and below after scaling of each data set to the recommended value of k(298 K). Results of the relative rate study of Tschuikow-Roux et al.[6] (273–368 K) were not used in the derivation of the recommended values since they appear to be systematically higher than the results of the other investigations. The products of this reaction are expected to primarily be CH_2Br and HCl. The possible production of CH_3Cl + Br is very small in the atmosphere.[2] While a standard Arrhenius parameterization provides a very good representation of the rate constants below 400 K, a pronounced curvature can be seen in the data of Piety et al. particularly above 400 K. The data over the complete temperature range (210–700 K) can be represented by the three-parameter equation

$$k(T) = 4.60 \times 10^{-12} (T/298)^{1.2} \exp(-700/T)$$

(Table: 15-10, Note: 15-10, Evaluated: 15-10) Back to Table

(1) Gierczak, T.; Goldfarb, L.; Sueper, D.; Ravishankara, A. R. Kinetics of the reactions of Cl atoms with CH_3Br and CH_2Br_2. *Int. J. Chem. Kinet.* **1994**, *26*, 719-728, doi:10.1002/kin.550260705.
(2) Goliff, W. S.; Rowland, F. S. Methyl chloride formation by gas phase thermal chlorine atom reaction with methyl iodide and methyl bromide. *Geophys. Res. Lett.* **1997**, *23*, 3029-3032, doi:10.1029/97GL03093.
(3) Kambanis, K. G.; Lazarou, Y. G.; Papagiannakopoulos, P. J. Absolute rate constants for the reactions of Cl atoms with CH_3Br, CH_2Br_2, and $CHBr_3$. *J. Phys. Chem.* **1997**, *101*, 8496-8502, doi:10.1021/jp9719671.
(4) Orlando, J. J.; Tyndall, G. S.; Wallington, T. J.; Dill, M. Atmospheric chemistry of CH_2Br_2: Rate coefficients for its reaction with Cl atoms and OH and the chemistry of the $CHBr_2O$ radical. *Int. J. Chem. Kinet.* **1996**, *28*, 433-442, doi:10.1002/(SICI)1097-4601(1996)28:6<433::AID-KIN5>3.0.CO;2-W

(5) Piety, C. A.; Soller, R.; Nicovich, J. M.; McKee, M. L.; Wine, P. H. Kinetic and mechanistic study of the reaction of atomic chlorine with methyl bromide over an extended temperature range. *Chem. Phys.* **1998**, *231*, 155-169, doi:10.1016/S0301-0104(97)00356-X.
(6) Tschuikow-Roux, E.; Faraji, F.; Paddison, S.; Niedzielski, J.; Miyokawa, K. Kinetics of photochlorination of halogen (F, Cl, Br) substituted methanes. *J. Phys. Chem.* **1988**, *92*, 1488-1495, doi:10.1021/j100317a023.

G37. Cl + CH_2Br_2. The recommended k(298 K) is an average of the results from the absolute rate studies of Gierczak et al.[1] (222–395 K) and Kambanis et al.[2] (273–363 K) and from the relative rate experiments of Orlando et al.[3] (an average of three studies). The recommended value for E/R is based on a combined fit to the data (T <300 K) from these same studies after scaling each one to the recommended k(298 K). Results of the relative rate study of Tschuikow-Roux et al.[4] (273–368 K) were not used in derivation of the recommended parameters since they are significantly greater at 298 K and correspond to a temperature dependence substantially stronger than derived from the data of other investigations.
(Table: 06-2, Note: 06-2, Evaluated: 06-2) Back to Table

(1) Gierczak, T.; Goldfarb, L.; Sueper, D.; Ravishankara, A. R. Kinetics of the reactions of Cl atoms with CH_3Br and CH_2Br_2. *Int. J. Chem. Kinet.* **1994**, *26*, 719-728, doi:10.1002/kin.550260705.
(2) Kambanis, K. G.; Lazarou, Y. G.; Papagiannakopoulos, P. J. Absolute rate constants for the reactions of Cl atoms with CH_3Br, CH_2Br_2, and $CHBr_3$. *J. Phys. Chem.* **1997**, *101*, 8496-8502, doi:10.1021/jp9719671.
(3) Orlando, J. J.; Tyndall, G. S.; Wallington, T. J.; Dill, M. Atmospheric chemistry of CH_2Br_2: Rate coefficients for its reaction with Cl atoms and OH and the chemistry of the $CHBr_2O$ radical. *Int. J. Chem. Kinet.* **1996**, *28*, 433-442, doi:10.1002/(SICI)1097-4601(1996)28:6<433::AID-KIN5>3.0.CO;2-W.
(4) Tschuikow-Roux, E.; Faraji, F.; Paddison, S.; Niedzielski, J.; Miyokawa, K. Kinetics of photochlorination of halogen (F, Cl, Br) substituted methanes. *J. Phys. Chem.* **1988**, *92*, 1488-1495, doi:10.1021/j100317a023.

G38. Cl + $CHBr_3$. The recommended parameters are based on the only reported study of this reaction by Kambanis et al.[1] (273–363 K), which employed a very low pressure reactor and monitored reactants and products using mass spectrometry.
(Table: 06-2, Note: 06-2, Evaluated: 06-2) Back to Table

(1) Kambanis, K. G.; Lazarou, Y. G.; Papagiannakopoulos, P. J. Absolute rate constants for the reactions of Cl atoms with CH_3Br, CH_2Br_2, and $CHBr_3$. *J. Phys. Chem.* **1997**, *101*, 8496-8502, doi:10.1021/jp9719671.

G39. Cl + CH_2ClBr. The recommended k(298 K) is an average of two relative rate determinations by Bilde et al.[1] (217–296 K) (recalculated based on the recommended rate constants for the reference reactions). The temperature dependence is estimated from a comparison with the reactions of Cl with CH_2Cl_2 and CH_2Br_2. The relative rate investigation by Tschuikow-Roux et al.[2] (273–368 K) gives a value for k(298 K) only slightly larger than recommended, but a temperature dependence that is significantly stronger and inconsistent with that recommended for the Cl + CH_2Cl_2 and Cl + CH_2Br_2 reactions.
(Table: 06-2, Note: 06-2, Evaluated: 06-2) Back to Table

(1) Bilde, M.; Wallington, T. J.; Ferronato, G.; Orlando, J. J.; Tyndall, G. S.; Estupinan, E.; Haberkorn, S. Atmospheric chemistry of CH_2BrCl, $CHBrCl_2$, $CHBr_2Cl$, $CF_3CHBrCl$, and CBr_2Cl_2. *J. Phys. Chem. A* **1998**, *102*, 1976-1986, doi:10.1021/jp9733375.
(2) Tschuikow-Roux, E.; Faraji, F.; Paddison, S.; Niedzielski, J.; Miyokawa, K. Kinetics of photochlorination of halogen (F, Cl, Br) substituted methanes. *J. Phys. Chem.* **1988**, *92*, 1488-1495, doi:10.1021/j100317a023.

G40. Br + O_3. The results reported for k(298 K) by Clyne and Watson[1] (298 K), Leu and DeMore,[2] (224–422 K) Michael et al.[3] (200–360 K), Michael and Payne[4] (234–360 K), Toohey et al.,[7] (248–418 K), Nicovich et al.,[5] (195–392 K), and Ninomiya et al.[6] (298 K) are in excellent agreement. The recommended value at 298 K is derived as the mean of these seven values. There is less agreement among reported temperature dependences, with E/R values ranging from ~900 K^{-1} (Leu and DeMore and Toohey et al.) to ~600 K^{-1} (Michael et al. and Michael and Payne). The recommended value of E/R is an average of the E/R values from the five temperature-dependent studies (not including Clyne and Watson and Ninomiya et al., which were room temperature only).
(Table:09-31, Note: 09-31, Evaluated: 09-31) Back to Table

(1) Clyne, M. A. A.; Watson, R. T. Kinetic studies for diatomic free radicals using mass spectrometry Part 3.-Elementary reactions involving BrO $X^2\Pi$ radicals. *J. Chem. Soc. Faraday Trans. 1* **1975**, *71*, 336-350, doi:10.1039/f19757100336.
(2) Leu, M.-T.; DeMore, W. B. Rate constant for the reaction of atomic bromine with ozone. *Chem. Phys. Lett.* **1977**, *48*, 317-320, doi:10.1016/0009-2614(77)80323-0.
(3) Michael, J. V.; Lee, J. H.; Payne, W. A.; Stief, L. J. Absolute rate of the reaction of N(^4S) with NO from 196-400 K with DF-RF and FP-RF techniques. *J. Chem. Phys.* **1978**, *68*, 4093-4097, doi:10.1063/1.436322.
(4) Michael, J. V.; Payne, W. A. Absolute rate constants for the reaction of bromine atoms with ozone from 234 to 360 K. *Int. J. Chem. Kinet.* **1979**, *11*, 799-809, doi:10.1002/kin.550110711.
(5) Nicovich, J. M.; Kreutter, K. D.; Wine, P. H. Kinetics of the reactions of Cl(^2P_J) and Br($^2P_{3/2}$) with O_3. *Int. J. Chem. Kinet.* **1990**, *22*, 399-414, doi:10.1002/kin.550220407.
(6) Ninomiya, Y.; Hashimoto, S.; Kawasaki, M.; Wallington, T. J. Cavity ring-down study of BrO radicals: Kinetics of the Br + O_3 reaction and rate of relaxation of vibrationally excited BrO by collisions with N_2 and O_2. *Int. J. Chem. Kinet.* **2000**, *32*, 125-130, doi:10.1002/(SICI)1097-4601(2000)32:3<125::AID-KIN1>3.0.CO;2-4.
(7) Toohey, D. W.; Brune, W. H.; Anderson, J. G. Rate constant for the reaction Br + O_3 → BrO + O_2 from 248 to 418 K: Kinetics and mechanism. *Int. J. Chem. Kinet.* **1988**, *20*, 131-144, doi:10.1002/kin.550200206.

G41. Br + H_2O_2. The recommended upper limit for k(298 K) is based on results reported by Toohey et al.[5] using a discharge flow-resonance fluorescence-laser magnetic resonance technique. Their upper limit determined over the temperature range 298–378 K is consistent with less sensitive upper limits determined by Leu[2] (298–417 K) and Posey et al.[4] (298 K) using a discharge flow-mass spectrometric technique. The much higher value reported by Heneghan and Benson[1] (300–350 K) may result from the presence of excited Br atoms in their very low pressure reactor. The pre-exponential factor was estimated to be the same as that for the Cl + H_2O_2 rate constant, and the E/R value was fit to the upper limit at 298 K. Mellouki et al.[3] have measured the rate of the reverse reaction.
(Table: 87-41, Note: 94-26, Evaluated: 10-6) Back to Table

(1) Heneghan, S. P.; Benson, S. W. Kinetic study of the reactions of Cl and Br with H_2O_2. *Int. J. Chem. Kinet.* **1983**, *15*, 1311-1319, doi:10.1002/kin.550151206.
(2) Leu, M. T. Upper limits for the rate constant for the reaction Br + H_2O_2 → HBr + HO_2. *Chem. Phys. Lett.* **1980**, *69*, 37-39, doi:10.1016/0009-2614(80)80008-X.
(3) Mellouki, A.; Talukdar, R. K.; Howard, C. J. Kinetics of the reactions of HBr with O_3 and HO_2: The yield of HBr from HO_2 + BrO. *J. Geophys. Res.* **1994**, *99*, 22949-22954, doi:10.1029/94JD02144.
(4) Posey, J.; Sherwell, J.; Kaufman, M. Kinetics of the reactions of atomic bromine with HO_2 and H_2O_2. *Chem. Phys. Lett.* **1981**, *77*, 476-479, doi:10.1016/0009-2614(81)85189-5.
(5) Toohey, D. W.; Brune, W. H.; Anderson, J. G. Mechanism and kinetics of Br + HO_2 → HBr + O_2 and Br + H_2O_2 → products over the temperature range 260-390 K. *J. Phys. Chem.* **1987**, *91*, 1215-1222, doi:10.1021/j100289a036.

G42. Br + NO_3. The recommended k(298 K) is that reported by Mellouki et al.[1] (298 K) in a study using DF-EPR techniques.
(Table: 90-1, Note: 92-20, Evaluated: 10-6) Back to Table

(1) Mellouki, A.; Poulet, G.; Le Bras, G.; Singer, R.; Burrows, J. P.; Moortgat, G. K. Discharge flow kinetic study of the reactions of NO_3 with Br, BrO, HBr, and HCl. *J. Phys. Chem.* **1989**, *93*, 8017-8021, doi:10.1021/j100361a012.

G43. Br + H_2CO. There have been two direct studies of this rate constant as a function of temperature: Nava et al.[2] (223–480 K), using a flash photolysis–resonance fluorescence technique, and Poulet et al.[3] (295–480 K), using a discharge flow-mass spectrometric technique. These results are in reasonably good agreement. The recommended Arrhenius parameters were derived from a least-squares fit to the data reported in these two studies. The higher room temperature value of Le Bras et al.[1] (298 K), using a discharge flow–EPR technique, has been shown to be in error due to secondary chemistry (Poulet et al.). The relative rate study of Ramacher et al.[4] (250–296 K) is in good agreement with the recommendation.
(Table: 09-31, Note: 09-31, Evaluated: 09-31) Back to Table

(1) Le Bras, G.; Foon, R.; Combourieu, J. EPR kinetic study of the reactions of F and Br atoms with H_2CO. *Chem. Phys. Lett.* **1980**, *73*, 357-361, doi:10.1016/0009-2614(80)80388-5.

(2) Nava, D. F.; Michael, J. V.; Stief, L. J. Rate constant for the reaction of atomic bromine with formaldehyde from 223 to 480 K. *J. Phys. Chem.* **1981**, *85*, 1896-1899, doi:10.1021/j150613a024.
(3) Poulet, G.; Laverdet, G.; Le Bras, G. Discharge flow-mass spectrometric determination of the rate coefficients for the reactions of formaldehyde with bromine atoms and chlorine atoms. *J. Phys. Chem.* **1981**, *85*, 1892-1895, doi:10.1021/j150613a023.
(4) Ramacher, B.; Orlando, J. J.; Tyndall, G. S. Temperature-dependent rate coefficient measurements for the reaction of bromine atoms with a series of aldehydes. *Int. J. Chem. Kinet.* **2000**, *32*, 460-465, doi:10.1002/1097-4601(2000)32:8<460::AID-KIN2>3.0.CO;2-P.

G44. Br + CH_2=C(CH_3)CHO. A single relative rate study by Sauer et al.,[2] which employed air as the bath gas at 1 atm and 301 K, has been reported. The process studied by Sauer et al. is not an elementary reaction. The overall rate constant for loss of methacrolein (CH_2=C(CH_3)CHO) via a multi-reaction sequence was measured relative to the overall rate constant for loss of *trans*-2-butene via a similar multi-reaction sequence. The multi-reaction sequence involves addition of Br to the alkenes to form bromo-alkyl radicals that react with O_2 in competition with decomposition back to Br + alkene reactants. The rate constant for the reference reaction (Br + *trans*-2-butene) was measured relative to Br + propene, and the relative rate constants were put on an absolute scale by measuring the Br + propene rate constant relative to that of the well-studied H-abstraction reaction Br + CH_3CHO.[1] A complicated dependence of the overall rate constant on temperature, pressure, and [O_2] is likely, so the recommended rate constant and associated uncertainty are only appropriate for temperatures close to 301 K, pressures close to 1 atm, and O_2 mixing ratios close to those present in air. Sauer et al. report that, at 1 atm N_2 + O_2 and 301 K, the observed rate constant increases by nearly a factor of 4 as the O_2 partial pressure increases from 0.027 to 1.00 atm. In 900 mbar of synthetic air at 296 K, the following molar product yields are reported by Sauer et al.: HBr, ~0; $CH_3C(O)CH_2Br$, 0.60 ± 0.09; CO, 0.68 ± 0.08, CO_2, 0.10 ± 0.03; H_2CO, 0.08 ± 0.03. Small yields of CH_3OH and CH_3OOH are also reported. Sauer et al. conclude that the dominant reaction pathway is addition of Br to the terminal carbon atom of the double bond.
(Table 15-10, Note: 15-10, Evaluated: 15-10) Back to Table

(1) Bierbach, A.; Barnes, I.; Becker, K. H. Rate coefficients for the gas-phase reactions of bromine series of radicals with a alkenes, dienes, and aromatic hydrocarbons at 298 ± 2 K. *Int. J. Chem. Kinet.* **1996**, *28*, 565-577, doi:10.1002/(SICI)1097-4601(1996)28:8<565::AID-KIN2>3.0.CO;2-T.
(2) Sauer, C. G.; Barnes, I.; Becker, K. H. FT-IR kinetic and product study of the Br-radical initiated oxidation of α, β-unsaturated organic carbonyl compounds. *Atmos. Environ.* **1999**, *33*, 2969-2979, doi:10.1016/S1352-2310(99)00085-0.

G45. Br + $CH_3C(O)CH=CH_2$. A single relative rate study by Sauer et al.,[2] which employed air as the bath gas at 1 atm and 301 K, has been reported. The process studied by Sauer et al. is not an elementary reaction. The overall rate constant for loss of MVK ($CH_3C(O)CH=CH_2$) via a multi-reaction sequence was measured relative to the overall rate constant for loss of *trans*-2-butene via a similar multi-reaction sequence. The multi-reaction sequence involves addition of Br to the alkenes to form bromo-alkyl radicals that react with O_2 in competition with decomposition back to Br + alkene reactants. The rate constant for the reference reaction (Br + *trans*-2-butene) was measured relative to Br + propene, and the relative rate constants were put on an absolute scale by measuring the Br + propene rate constant relative to that of the well-studied H-abstraction reaction Br + CH_3CHO.[1] A complicated dependence of the overall rate constant on temperature, pressure, and [O_2] is likely, so the recommended rate constant and associated uncertainty are only appropriate for temperatures close to 301 K, pressures close to 1 atm, and O_2 mixing ratios close to those present in air. Sauer et al. report that, at 1 atm N_2 + O_2 and 301 K, the observed rate constant increases by about a factor of 2.5 as the O_2 partial pressure increases from 0.027 to 0.395 atm. In 900 mbar of synthetic air at 296 K, the following molar product yields are reported by Sauer et al.: HBr, ~0; CH_2BrCHO, 1.13 ± 0.21; CO_2, 0.61 ± 0.09; H_2CO, 0.39 ± 0.05. Small yields of CH_3OH, CH_3OOH, $CH_3C(O)OH$, and $CH_3C(O)OOH$ are also reported. Sauer et al. conclude that the dominant reaction pathway is addition of Br to the terminal carbon atom of the double bond.
(Table 15-10, Note: 15-10, Evaluated: 15-10) Back to Table

(1) Bierbach, A.; Barnes, I.; Becker, K. H. Rate coefficients for the gas-phase reactions of bromine series of radicals with a alkenes, dienes, and aromatic hydrocarbons at 298 ± 2 K. *Int. J. Chem. Kinet.* **1996**, *28*, 565-577, doi:10.1002/(SICI)1097-4601(1996)28:8<565::AID-KIN2>3.0.CO;2-T.
(2) Sauer, C. G.; Barnes, I.; Becker, K. H. FT-IR kinetic and product study of the Br-radical initiated oxidation of α, β-unsaturated organic carbonyl compounds. *Atmos. Environ.* **1999**, *33*, 2969-2979, doi:10.1016/S1352-2310(99)00085-0.

G46. Br + CH_2=C(CH_3)CH=CH_2 $\overset{M}{\leftrightarrow}$ adduct $\overset{O_2}{\leftrightarrow}$ products. One relative rate study by Bierbach et al.,[1] which employed air as the bath gas at 1 bar and 298 K, has been reported. The process studied by Bierbach et al. is not an elementary reaction. The overall rate constant for loss of isoprene via the above multi-reaction sequence was measured relative to the overall rate constant for loss of 1,3-butadiene via a similar multi-reaction sequence; a sequence of relative rate studies were carried out using progressively less reactive reference compounds (2,3-dimethyl-2-butene, *trans*-2-butene, propene, and acetaldehyde (CH_3CHO), with all relative rate constants being put on an absolute scale using the well-known rate constant for the elementary H-abstraction reaction of Br with CH_3CHO. A Br + CH_2=C(CH_3)CH=CH_2 rate constant of 7.4×10^{-11} cm^3 $molecule^{-1}$ s^{-1}, about a factor of three smaller than the gas kinetic collision rate constant, is reported by Bierbach et al. The uncertainty in the rate constant reported by Bierbach et al. is substantial because (i) five rate constant ratios had to be measured to extract the desired rate constant and (ii) all reactions studied except Br + CH_3CHO occurred via complex reaction sequences. Laine et al.[2] (227–673 K) have reported a laser flash photolysis–resonance fluorescence study where monitoring of Br kinetics as a function of temperature, pressure, [CH_2=C(CH_3)CH=CH_2], and [O_2] has allowed elementary rate constants for H abstraction, Br addition, adduct decomposition, and adduct reaction with O_2 to be deduced; these authors also estimated the temperature dependence of the adduct−O_2 unimolecular decomposition rate constant. The results of Laine et al. suggest that in the atmosphere CH_2=C(CH_3)CH=CH_2 is lost irreversibly on essentially every collision with Br at temperatures below 275 K. At higher temperatures, Laine et al. suggest that Br + CH_2=C(CH_3)CH=CH_2 may be regenerated via unimolecular reactions rapidly enough to compete with bimolecular reactions of the peroxy radical(s) both in the atmosphere and in environmental chambers. Until additional information becomes available, a recommendation that would prove useful for atmospheric modeling, particularly in warmer environments, cannot be made.
(Table: 15-10, Note: 15-10, Evaluated: 15-10) Back to Table

(1) Bierbach, A.; Barnes, I.; Becker, K. H. Rate coefficients for the gas-phase reactions of bromine series of radicals with a alkenes, dienes, and aromatic hydrocarbons at 298 ± 2 K. *Int. J. Chem. Kinet.* **1996**, *28*, 565-577, doi:10.1002/(SICI)1097-4601(1996)28:8<565::AID-KIN2>3.0.CO;2-T.
(2) Laine, P. L.; Sohn, Y. S.; Nicovich, J. M.; McKee, M. L.; Wine, P. H. Kinetics of elementary steps in the reactions of atomic bromine with isoprene and 1,3-butadiene under atmospheric conditions. *J. Phys. Chem. A* **2012**, *116*, 6341-6357, doi:10.1021/jp212127v.

G47. Br + CH_2=C(CH_3)CH=CH_2 → CH_2=C(·CH_2)CH=CH_2 + HBr. The recommendation is based on the results of Laine et al.[1] (526–673 K) at temperatures where adduct decomposition is so rapid that the adduct represents a negligible reservoir for Br. The estimated uncertainty is large because data are only available from a single study and because the long extrapolation to the atmospherically relevant temperature regime (200–300 K) is based on the assumption of Arrhenius behavior. The recommended uncertainty spans all values consistent with the 2σ error limits for *A* and *E*/R reported by Laine et al.
(Table: 15-10, Note: 15-10, Evaluated: 15-10). Back to Table

(1) Laine, P. L.; Sohn, Y. S.; Nicovich, J. M.; McKee, M. L.; Wine, P. H. Kinetics of elementary steps in the reactions of atomic bromine with isoprene and 1,3-butadiene under atmospheric conditions. *J. Phys. Chem. A* **2012**, *116*, 6341-6357, doi:10.1021/jp212127v.

G48. Br−CH_2=C(CH_3)CH=CH_2 + O_2 → products. The recommendation is based on the results of Laine et al.[1] (227–673 K), who extracted kinetic information from observation of the effect of added O_2 on the kinetics of Br equilibration with Br−CH_2=C(CH_3)CH=CH_2 following laser flash photolysis of CF_2Br_2/ CH_2=C(CH_3)CH=CH_2/N_2/O_2 mixtures. The obtained rate constant at 297 K was found to be independent of pressure over the range 50 to 700 Torr (mostly N_2). There are several possible isomers of Br−CH_2=C(CH_3)CH=CH_2; calculations (G4 method) reported by Laine et al. show that the energetically most stable isomer is $CH_2BrC^{\bullet}$(CH_3)CH=CH_2, but there is no experimental information concerning the distribution of isomers formed via Br addition to CH_2=C(CH_3)CH=CH_2. The rather large recommended uncertainty results from the somewhat indirect nature of the rate constant determination and the lack of a confirming study.
(Table: 15-10, Note: 15-10, Evaluated: 15-10) Back to Table

(1) Laine, P. L.; Sohn, Y. S.; Nicovich, J. M.; McKee, M. L.; Wine, P. H. Kinetics of elementary steps in the reactions of atomic bromine with isoprene and 1,3-butadiene under atmospheric conditions. *J. Phys. Chem. A* **2012**, *116*, 6341-6357, doi:10.1021/jp212127v.

G49. Br + OClO. The recommended value for k(298 K) is the mean of the values reported by Clyne and Watson[1] (298 K) and Toohey.[2] In the study of Clyne and Watson, correction for the effect of the rapid reverse reaction was required. The temperature dependence reported by Toohey[2] is accepted, but with increased error limits.
(Table: 90-1, Note: 90-1, Evaluated: 10-6) Back to Table

(1) Clyne, M. A. A.; Watson, R. T. Kinetic studies of diatomic free radicals using mass spectrometry Part 4.-The Br + OClO and BrO + ClO reactions. *J. Chem. Soc. Faraday Trans. 1* **1977**, *73*, 1169-1187, doi:10.1039/f19777301169.
(2) Toohey, D. W. Kinetic and Mechanistic Studies of Reactions of Bromine and Chlorine Species Important in the Earth's Stratosphere. Ph. D. Thesis, Harvard University, 1988.

G50. Br + Cl_2O. The recommended Arrhenius parameters are based on results reported by Stevens and Anderson[2] (240–373 K) and by Sander and Friedl[1] (220–400 K), which are in good agreement.
(Table: 94-26, Note: 94-26, Evaluated: 10-6) Back to Table

(1) Sander, S. P.; Friedl, R. R. Kinetics and product studies of the reaction ClO + BrO using flash photolysis-ultraviolet absorption. *J. Phys. Chem.* **1989**, *93*, 4764-4771, doi:10.1021/j100349a017.
(2) Stevens, P. S.; Anderson, J. G. Kinetic and mechanistic study of X + ClOCl → products (X = Br, CI, F, O, OH, N) over the temperature range 240-373 K. *J. Phys. Chem.* **1992**, *96*, 1708-1718, doi:10.1021/j100183a040.

G51. Br + Cl_2O_2. The recommended Arrhenius parameters are those determined in a study by Ingham et al.[1] (223–298 K) using a DF-MS/RF technique. Ingham et al. found that BrCl was the only major Br-containing product from the reaction.
(Table: 10-6, Note: 10-6, Evaluated: 10-6) Back to Table

(1) Ingham, T.; Sander, S. P.; Friedl, R. R. Kinetics and product studies of the reaction of Br, Cl, and NO with ClOOCl using discharge-flow mass spectrometry. *Faraday Discuss.* **2005**, *130*, 89-110, doi:10.1039/b500179j.

G52. BrO + O_3. The A factor was estimated to be similar to that estimated for the ClO + O_3 reaction and a lower limit for E/R was calculated using an upper limit for k(298 K) of 2×10^{-17} cm^3 molecule^{-1} s^{-1} based on the studies of Rattigan et al.[2] (298–343 K) and Rowley et al.[3] (298 K). The recommended upper limit for k(298 K) is a factor of 2.5 less than the upper limit of 5×10^{-17} derived by Mauldin et al.[1] (220–298 K). Both Rattigan et al. and Rowley et al. report a value of ~2×10^{-18} cm^3 molecule^{-1} s^{-1} at room temperature for the channel to produce OBrO + O_2.
(Table: 97-4, Note: 15-10, Evaluated: 10-6) Back to Table

(1) Mauldin, R. L., III; Wahner, A.; Ravishankara, A. R. Kinetics and mechanism of the self-reaction of the BrO radical. *J. Phys. Chem.* **1993**, *97*, 7585-7596, doi:10.1021/j100131a031.
(2) Rattigan, O. V.; Cox, R. A.; Jones, R. L. Br_2-sensitised decomposition of ozone: Kinetics of the reaction BrO + O_3 → products. *J. Chem. Soc. Faraday Trans.* **1995**, *91*, 4189-4197, doi:10.1039/ft9959104189.
(3) Rowley, D. M.; Harwood, M. H.; Freshwater, R. A.; Jones, R. L. A novel flash photolysis/UV absorption system employing charge-coupled device (CCD) detection: A study of the BrO + BrO reaction at 298 K. *J. Phys. Chem.* **1996**, *100*, 3020-3029, doi:10.1021/jp951825b.

G53. BrO + NO. The results of three low pressure mass spectrometric studies (Clyne and Watson[2] (298 K), Ray and Watson[4] (298 K), and Leu[3] (230–425 K)) and a high pressure UV absorption study (Watson et al.[5] (224–398 K)), which all used pseudo–first-order conditions, are in excellent agreement at 298 K and are thought to be much more reliable than an earlier low pressure UV absorption study (Clyne and Cruse[1] (293 K)). The results of the two temperature-dependent studies (Leu and Watson et al.) are in good agreement and both show a small negative temperature dependence. The preferred Arrhenius expression was derived from a least-squares fit to all the data reported in the four studies mentioned above. By combining the data reported by Watson et al. with those from the three mass spectrometric studies, it can be shown that this reaction does not exhibit any observable pressure dependence between 1 and 700 Torr total pressure. The temperature dependences of k for the analogous ClO and HO_2 reactions are also negative and are similar in magnitude.
(Table: 82-57, Note: 82-57, Evaluated: 10-6) Back to Table

(1) Clyne, M. A. A.; Cruse, H. W. Rates of elementary reactions involving the BrO ($X^2\Pi$) and IO ($X^2\Pi$) radicals Part 2.-Reactions of the BrO and IO radicals. *Trans. Faraday Soc.* **1970**, *66*, 2227-2236, doi:10.1039/tf9706602227.

(2) Clyne, M. A. A.; Watson, R. T. Kinetic studies for diatomic free radicals using mass spectrometry Part 3.-Elementary reactions involving BrO $X^2\Pi$ radicals. *J. Chem. Soc. Faraday Trans. 1* **1975**, *71*, 336-350, doi:10.1039/f19757100336.
(3) Leu, M. T. Rate constant for the reaction BrO + NO → Br + NO_2. *Chem. Phys. Lett.* **1979**, *61*, 275-279, doi:10.1016/0009-2614(79)80643-0.
(4) Ray, G. W.; Watson, R. T. Kinetics study of the reactions of NO with FO, ClO, BrO, and IO at 298 K. *J. Phys. Chem.* **1981**, *85*, 2955-2960, doi:10.1021/j150620a022.
(5) Watson, R. T.; Sander, S. P.; Yung, Y. L. Pressure and temperature dependence kinetics study of the NO + BrO → NO_2 + Br reaction. Implications for stratospheric bromine photochemistry. *J. Phys. Chem.* **1979**, *83*, 2936-2944, doi:10.1021/j100486a002.

G54. BrO + NO_3. The recommended value for k(298 K) is the geometric mean of the lower and upper limits reported by Mellouki et al.[1] (298 K) in a study using DF-EPR techniques. These reported limits are encompassed within the indicated uncertainty limits.
(Table: 90-1, Note: 92-20, Evaluated: 10-6) Back to Table

(1) Mellouki, A.; Poulet, G.; Le Bras, G.; Singer, R.; Burrows, J. P.; Moortgat, G. K. Discharge flow kinetic study of the reactions of NO_3 with Br, BrO, HBr, and HCl. *J. Phys. Chem.* **1989**, *93*, 8017-8021, doi:10.1021/j100361a012.

G55. BrO + ClO. Friedl and Sander[4] (220–400 K), using DF/MS techniques, measured the overall rate constant over the temperature range 220–400 K and also over this temperature range determined branching ratios for the reaction channels producing BrCl and OClO. The same authors in a separate study using flash photolysis–ultraviolet absorption techniques (Sander and Friedl[7] (220–400 K)) determined the overall rate constant over the temperature range 220–400 K and pressure range 50–750 Torr and also determined the branching ratio for OClO production at 220 K and 298 K. The results by these two independent techniques are in excellent agreement, with the overall rate constant showing a negative temperature dependence. Turnipseed et al.[9] (234–406 K) using DF/MS techniques also found a negative temperature dependence, reporting measurements of the overall rate constant and direct measurements of the branching ratios for the BrCl and OClO channels. Several other studies have reported only room temperature values: Toohey and Anderson,[8] using DF/RF/LMR techniques, reported room temperature values of the overall rate constant and the branching ratio for OClO production. They also found evidence for the direct production of BrCl in a vibrationally excited Π state. Poulet et al.[6] (298 K), using DF/MS techniques, reported room temperature values of the overall rate constant and branching ratios for OClO and BrCl production. Overall room temperature rate constant values reported also include a result from the DF/MS study of Clyne and Watson[2] (298 K) and a very low value derived in the flash photolysis study of Basco and Dogra.[1] The recommended Arrhenius expressions for the individual reaction channels are taken from the studies of Friedl and Sander and Turnipseed et al. These studies contain the most comprehensive sets of rate constant and branching ratio data. The overall rate constants reported in these two studies are in good agreement (20%) at room temperature and in excellent agreement at stratospheric temperatures. Both studies report that OClO production by channel (1) accounts for 60% of the overall reaction at 200 K and that the BrCl yield by channel (3) is about 8%, relatively independent of temperature. The recommended expressions are consistent with the body of data from all older studies except those of Hills et al.[5] (241–408 K) and Basco and Dogra. Recent results from Ferracci and Rowley[3] (246–314 K) using laser flash photolysis-absorption spectroscopy to measure the overall rate constant and branching ratio of the OClO channel are substantially higher than the recommended values and include a positive temperature dependence for the branching ratio of the OClO channel, in disagreement with past studies. Secondary chemistry is likely the cause of the discrepancies.
(Table:09-31, Note: 15-10, Evaluated: 09-31) Back to Table

(1) Basco, N.; Dogra, S. K. Reactions of halogen oxides studied by flash photolysis III. The production and reactions of BrO and ClO radicals in the halogen-sensitized decomposition of chlorine dioxide. *Proc. Roy. Soc. Lond. A.* **1971**, *323*, 417-429, doi:10.1098/rspa.1971.0113.
(2) Clyne, M. A. A.; Watson, R. T. Kinetic studies of diatomic free radicals using mass spectrometry Part 4.-The Br + OClO and BrO + ClO reactions. *J. Chem. Soc. Faraday Trans. 1* **1977**, *73*, 1169-1187, doi:10.1039/f19777301169.
(3) Ferracci, V.; Rowley, D. M. Kinetic studies of the BrO + ClO cross-reaction over the range T = 246–314 K. *Phys. Chem. Chem. Phys.* **2014**, *16*, 1182-1196, doi:10.1039/c3cp53440e.
(4) Friedl, R. R.; Sander, S. P. Kinetics and product studies of the reaction ClO + BrO using discharge-flow mass spectrometry. *J. Phys. Chem.* **1989**, *93*, 4756-4764, doi:10.1021/j100349a016.

(5) Hills, A. J.; Cicerone, R. J.; Calvert, J. G.; Birks, J. W. Temperature dependence of the rate constant and product channels for the BrO + ClO reaction. *J. Phys. Chem.* **1988**, *92*, 1853-1858, doi:10.1021/j100318a032.
(6) Poulet, G.; Lancar, I. T.; Laverdet, G.; Le Bras, G. Kinetics and products of the BrO + ClO reaction. *J. Phys. Chem.* **1990**, *94*, 278-284, doi:10.1021/j100364a046.
(7) Sander, S. P.; Friedl, R. R. Kinetics and product studies of the reaction ClO + BrO using flash photolysis-ultraviolet absorption. *J. Phys. Chem.* **1989**, *93*, 4764-4771, doi:10.1021/j100349a017.
(8) Toohey, D. W.; Anderson, J. G. Formation of BrCl($^3\Pi_0^+$) in the reaction of BrO with ClO. *J. Phys. Chem.* **1988**, *92*, 1705-1708, doi:10.1021/j100318a002.
(9) Turnipseed, A. A.; Birks, J. W.; Calvert, J. G. Kinetics and temperature dependence of the BrO + ClO reaction. *J. Phys. Chem.* **1991**, *95*, 4356-4364, doi:10.1021/j100164a035.

G56. BrO + BrO. Measurements of the overall rate constant can be divided into categories—those in which BrO was monitored by UV absorption and those in which BrO was monitored by mass spectrometry. Gilles et al.[4] (204–388 K) re-analyzed the results of the UV absorption studies and scaled the reported values of the rate constant to the UV absorption cross sections reported in their paper. When scaled in this manner, the room temperature rate constant values reported in the UV absorption studies (Sander and Watson[11] (223–338 K), Mauldin et al.[9] (220–298 K), Bridier et al.[1] (298 K), Rowley et al.[10] (298 K), Laszlo et al.[8] (298 K), and Gilles et al.) come into very good agreement among themselves and also with results of the mass spectrometric studies of Clyne and Watson[2] (298 K) and Lancar et al.[7] (298 K). This provides the basis for the recommended value for k(298 K). The temperature dependence is based on results of Sander and Watson, Turnipseed et al.[12] (253–400 K) and Gilles et al. The results of Harwood et al.[5] (222–298 K) are in good agreement with the recommendation.

There are two possible bimolecular channels for this reaction: BrO + BrO → 2Br + O_2 (k_1) and BrO + BrO → Br_2 + O_2 (k_2). The partitioning of the total rate constant into these two components, k_1 and k_2, has been determined at room temperature by Sander and Watson, Turnipseed et al., and Lancar et al., by Jaffe and Mainquist[6] (258–333 K), Cox et al.[3] (278–348 K), and Mauldin et al. All are in agreement that $k_1/k = 0.85 \pm 0.03$ at 298 K. From the values of $k_1/k = 0.85$ at 298 K (all studies) and 0.68 at 220 K (Mauldin et al. and Cox et al. extrapolated), one can derive the temperature-dependent expression $k_1/k = 1.60 \exp(-190/T)$. From the recommended Arrhenius expression for the overall rate constant $k = k_1 + k_2$ and the expression for the branching ratio k_1/k, one can derive the following Arrhenius expressions for the individual reaction channels:

$$k_1 = 2.4 \times 10^{-12} \exp(40/T) \text{ cm}^3 \text{ molecule}^{-1} \text{ s}^{-1}$$
$$k_2 = 2.8 \times 10^{-14} \exp(860/T) \text{ cm}^3 \text{ molecule}^{-1} \text{ s}^{-1}$$

(Table: 97-4, Note: 97-4, Evaluated: 10-6) Back to Table

(1) Bridier, I.; Veyret, B.; Lesclaux, R. Flash photolysis kinetic study of reactions of the BrO radical with BrO and HO_2. *Chem. Phys. Lett.* **1993**, *201*, 563-568, doi:10.1016/0009-2614(93)85118-8.
(2) Clyne, M. A. A.; Watson, R. T. Kinetic studies for diatomic free radicals using mass spectrometry Part 3.-Elementary reactions involving BrO $X^2\Pi$ radicals. *J. Chem. Soc. Faraday Trans. 1* **1975**, *71*, 336-350, doi:10.1039/f19757100336.
(3) Cox, R. A.; Sheppard, D. W.; Stevens, M. P. Absorption coefficients and kinetics of the BrO radical using molecular modulation. *J. Photochem.* **1982**, *19*, 189-207, doi:10.1016/0047-2670(82)80022-1.
(4) Gilles, M. K.; Turnipseed, A. A.; Burkholder, J. B.; Ravishankara, A. R. Kinetics of the IO radical. 2. Reaction of IO with BrO. *J. Phys. Chem. A* **1997**, *101*, 5526-5534, doi:10.1021/jp9709159.
(5) Harwood, M. H.; Rowley, D. M.; Cox, R. A.; Jones, R. L. Kinetics and mechanism of the BrO self-reaction: Temperature- and pressure-dependent studies. *J. Phys. Chem. A* **1998**, *102*, 1790-1802, doi:10.1021/jp973264p.
(6) Jaffe, S.; Mainquist, W. K. Bromine photosensitized decomposition of ozone. *J. Phys. Chem.* **1980**, *84*, 3277-3280, doi:10.1021/j100461a030.
(7) Lancar, I.; Laverdet, G.; Le Bras, G.; Poulet, G. Rate constant and products of the BrO + BrO reaction at 298 K. *Int. J. Chem. Kinet.* **1991**, *23*, 37-45, doi:10.1002/kin.550230105.
(8) Laszlo, B.; Huie, R. E.; Kurylo, M. J.; Miziolek, A. W. Kinetic studies of the reactions of BrO and IO radicals. *J. Geophys. Res.* **1997**, *102*, 1523-1532, doi:10.1029/96JD00458.
(9) Mauldin, R. L., III; Wahner, A.; Ravishankara, A. R. Kinetics and mechanism of the self-reaction of the BrO radical. *J. Phys. Chem.* **1993**, *97*, 7585-7596, doi:10.1021/j100131a031.
(10) Rowley, D. M.; Harwood, M. H.; Freshwater, R. A.; Jones, R. L. A novel flash photolysis/UV absorption system employing charge-coupled device (CCD) detection: A study of the BrO + BrO reaction at 298 K. *J. Phys. Chem.* **1996**, *100*, 3020-3029, doi:10.1021/jp951825b.

(11) Sander, S. P.; Watson, R. T. Kinetics and mechanism of the disproportionation of BrO radicals. *J. Phys. Chem.* **1981**, *85*, 4000-4007, doi:10.1021/j150626a010.
(12) Turnipseed, A. A.; Birks, J. W.; Calvert, J. G. Kinetics of the BrO + BrO reaction. *J. Phys. Chem.* **1990**, *94*, 7477-7482, doi:10.1021/j100382a032.

G57. $OBrO + O_3$. The upper limit for k(298 K) was determined by Li et al.[1] (240–350 K) using DF/MS.
(Table: 10-6, Note: 10-6, Evaluated: 10-6) Back to Table

(1) Li, Z. J.; Jeong, G. R.; Person, E. Kinetics of reactions of OBrO with NO, O_3, OClO, and ClO at 240-350 K. *Int. J. Chem. Kinet.* **2002**, *34*, 430-437, doi:10.1002/kin.10069.

G58. OBrO + NO. The recommended Arrhenius parameters are those determined by Li et al.[1] (240–350 K) using DF/MS to monitor the decay of OBrO in excess NO. A possible complication in these experiments may be related to secondary reactions of Br with OBrO and is reflected in the large uncertainty assigned to this recommendation.
(Table: 10-6, Note: 10-6, Evaluated: 10-6) Back to Table

(1) Li, Z. J.; Jeong, G. R.; Person, E. Kinetics of reactions of OBrO with NO, O_3, OClO, and ClO at 240-350 K. *Int. J. Chem. Kinet.* **2002**, *34*, 430-437, doi:10.1002/kin.10069.

G59. CH_2BrO_2 + NO. The recommended value for k(298 K) is based on the 298 K measurement of Sehested et al.,[4] who used pulsed radiolysis with UV absorption detection of the NO_2 product formation rate. The temperature dependence is estimated based on analogy to similar RO_2 + NO reactions. The CH_2BrO product has been shown to undergo rapid unimolecular decomposition to yield CH_2O + Br by Chen et al.[1] and Orlando et al.[3] The domination of this channel over the reaction of CH_2BrO with O_2 is consistent with the fate of other alkoxy radicals (Chen et al. and Orlando et al.), but contradicts the earlier result of Nielson et al.[2]
(Table: 94-26, Note: 97-4, Evaluated: 97-4) Back to Table

(1) Chen, J.; Catoire, V.; Niki, H. Mechanistic study of the $BrCH_2O$ radical degradation in 700 Torr air. *Chem. Phys. Lett.* **1995**, *245*, 519-528, doi:10.1016/0009-2614(95)01048-E.
(2) Nielsen, O. J.; Munk, J.; Locke, G.; Wallington, T. J. Ultraviolet absorption spectra and kinetics of the self-reaction of CH_2Br and CH_2BrO_2 radicals in the gas phase at 298 K. *J. Phys. Chem.* **1991**, *95*, 8714-8719, doi:10.1021/j100175a054.
(3) Orlando, J. J.; Tyndall, G. S.; Wallington, T. J. Atmospheric oxidation of CH_3Br: Chemistry of the CH_2BrO radical. *J. Phys. Chem.* **1996**, *100*, 7026-7033, doi:10.1021/jp951813q.
(4) Sehested, J.; Nielsen, O. J.; Wallington, T. J. Absolute rate constants for the reaction of NO with a series of peroxy radicals in the gas phase at 295 K. *Chem. Phys. Lett.* **1993**, *213*, 457-464, doi:10.1016/0009-2614(93)89142-5.

1.12.3 Bibliography – BrO_x Reactions

Arnts, R. R.; Seila, R. L.; Bufalini, J. J. Determination of room temperature OH rate constants for acetylene, ethylene dichloride, ethylene dibromide, p-dichlorobenzene and carbon disulfide. *J. Air Pollut. Control Assoc.* **1989**, *39*, 453-460, doi:10.1080/08940630.1989.10466544.

Atkinson, D. B.; Jaramillo, V. I.; Smith, M. A. Low-temperature kinetic behavior of the bimolecular reaction OH + HBr (76-242 K). *J. Phys. Chem. A* **1997**, *101*, 3356-3359, doi:10.1021/jp963770z.

Basco, N.; Dogra, S. K. Reactions of halogen oxides studied by flash photolysis III. The production and reactions of BrO and ClO radicals in the halogen-sensitized decomposition of chlorine dioxide. *Proc. Roy. Soc. Lond. A.* **1971**, *323*, 417-429, doi:10.1098/rspa.1971.0113.

Bedjanian, Y. Rate constant of the reaction of OH radicals with HBr over the temperature range 235-960 K. *J. Phys. Chem. A* **2021**, *125*, 1754-1759, doi:10.1021/acs.jpca.1c00251.

Bedjanian, Y.; Le Bras, G.; Poulet, G. Kinetic study of the reactions of Br_2 with OH and OD. *Int. J. Chem. Kinet.* **1999**, *31*, 698-704, doi:10.1002/(SICI)1097-4601(1999)31:10<698::AID-JCK3>3.0.CO;2-O.

Bedjanian, Y.; Riffault, V.; Le Bras, G.; Poulet, G. Kinetic study of the reactions of OH and OD with HBr and DBr. *J. Photochem. Photobiol. A: Chem.* **1999**, *128*, 15-25, doi:10.1016/S1010-6030(99)00159-8.

Bedjanian, Y.; Riffault, V.; Le Bras, G.; Poulet, G. Kinetic study of the reactions of Br with HO_2 and DO_2. *J. Phys. Chem. A* **2001**, *105*, 573-578, doi:10.1021/jp002731r.

Bedjanian, Y.; Riffault, V.; Le Bras, G.; Poulet, G. Kinetics and mechanism of the OH and OD reactions with BrO. *J. Phys. Chem. A* **2001**, *105*, 6154-6166, doi:10.1021/jp010369q.

Bedjanian, Y.; Riffault, V.; Poulet, G. Kinetic study of the reactions of BrO radicals with HO_2 and DO_2. *J. Phys. Chem. A* **2001**, *105*, 3167-3175, doi:10.1021/jp0032255.

Bierbach, A.; Barnes, I.; Becker, K. H. Rate coefficients for the gas-phase reactions of bromine series of radicals with a alkenes, dienes, and aromatic hydrocarbons at 298 ± 2 K. *Int. J. Chem. Kinet.* **1996**, *28*, 565-577, doi:10.1002/(SICI)1097-4601(1996)28:8<565::AID-KIN2>3.0.CO;2-T.

Bilde, M.; Wallington, T. J.; Ferronato, C.; Orlando, J. J.; Tyndall, G. S.; Estupiñan, E.; Haberkorn, S. Atmospheric chemistry of CH_2BrCl, $CHBrCl_2$, $CHBr_2Cl$, $CF_3CHBrCl$, and CBr_2Cl_2. *J. Phys. Chem. A* **1998**, *102*, 1976-1986, doi:10.1021/jp9733375.

Bilde, M.; Wallington, T. J.; Ferronato, G.; Orlando, J. J.; Tyndall, G. S.; Estupinan, E.; Haberkorn, S. Atmospheric chemistry of CH_2BrCl, $CHBrCl_2$, $CHBr_2Cl$, $CF_3CHBrCl$, and CBr_2Cl_2. *J. Phys. Chem. A* **1998**, *102*, 1976-1986, doi:10.1021/jp9733375.

Bloss, W. J.; Rowley, D. M.; Cox, R. A.; Jones, R. L. Rate coefficient for the BrO + HO_2 reaction at 298 K. *Phys. Chem. Chem. Phys.* **2002**, *4*, 3639-3647, doi:10.1039/b201653b.

Boodaghians, R. B.; Hall, I. W.; Wayne, R. P. Kinetics of the reactions of the hydroxyl radical with molecular chlorine and bromine. *J. Chem. Soc. Faraday Trans. 2* **1987**, *83*, 529-538, doi:10.1039/f29878300529.

Bridier, I.; Veyret, B.; Lesclaux, R. Flash photolysis kinetic study of reactions of the BrO radical with BrO and HO_2. *Chem. Phys. Lett.* **1993**, *201*, 563-568, doi:10.1016/0009-2614(93)85118-8.

Brown, A. C.; Canosa-Mas, C. E.; Parr, A. D.; Rothwell, K.; Wayne, R. P. Tropospheric lifetimes of three compounds for possible replacement of CFC and halons. *Nature* **1990**, *347*, 541-543, doi:10.1038/347541a0.

Brown, A. C.; Canosa-Mas, C. E.; Parr, A. D.; Wayne, R. P. Laboratory studies of some halogenated ethanes and ethers: Measurements of rates of reaction with OH and of infrared absorption cross-sections. *Atmos. Environ.* **1990**, *24A*, 2499-2511, doi:10.1016/0960-1686(90)90341-J.

Brown, R. D. H.; Smith, I. W. M. Absolute rate constants for the reactions O(^3P) atoms with HCl and HBr. *Int. J. Chem. Kinet.* **1975**, *7*, 301-315, doi:10.1002/kin.550070211.

Bryukov, M. G.; Vidrine, R. G.; Dellinger, B. Temperature-dependent kinetics study of the gas-phase reactions of OH with n- and i-propyl bromide. *J. Phys. Chem. A* **2007**, *111*, 6197-6203, doi:10.1021/jp072693c.

Burkholder, J. B. NO_3 yield in the O(^{3}P) + $BrONO_2$ reaction. *J. Phys. Chem. A* **2000**, *104*, 6733-6737, doi:10.1021/jp9942926.

Burkholder, J. B.; Wilson, R. R.; Gierczak, T.; Talukdar, R.; McKeen, S. A.; Orlando, J. J.; Vaghjiani, G. L.; Ravishankara, A. R. Atmospheric fate of CF_3Br, CF_2Br_2, CF_2ClBr, and CF_2BrCF_2Br. *J. Geophys. Res.* **1991**, *96*, 5025-5043, doi:10.1029/90JD02735.

Cannon, B. D.; Robertshaw, J. S.; Smith, I. W. M.; Williams, M. D. A time-resolved LIF study of the kinetics of OH(v=0) and OH(v=1) with HCl and HBr. *Chem. Phys. Lett.* **1984**, *105*, 380-385, doi:10.1016/0009-2614(84)80045-7.

Canosa-Mas, C. E.; Smith, S. J.; Toby, S.; Wayne, R. P. Laboratory studies of the reactions of the nitrate radical with chloroform, methanol, hydrogen chloride and hydrogen bromide. *J. Chem. Soc. Faraday Trans. 2* **1989**, *85*, 709-725, doi:10.1039/f29898500709.

Chen, J.; Catoire, V.; Niki, H. Mechanistic study of the $BrCH_2O$ radical degradation in 700 Torr air. *Chem. Phys. Lett.* **1995**, *245*, 519-528, doi:10.1016/0009-2614(95)01048-E.

Chichinin, A.; Teton, S.; Le Bras, G.; Poulet, G. Kinetic investigation of the OH + CH_3Br reaction between 248 and 390 K. *J. Atmos. Chem.* **1994**, *18*, 239-245, doi:10.1007/BF00696781.

Clyne, M. A. A.; Cruse, H. W. Rates of elementary reactions involving the BrO ($X^2\Pi$) and IO ($X^2\Pi$) radicals Part 2.-Reactions of the BrO and IO radicals. *Trans. Faraday Soc.* **1970**, *66*, 2227-2236, doi:10.1039/tf9706602227.

Clyne, M. A. A.; Holt, P. M. Reaction kinetics involving ground $X^2\Pi$ and excited $A^2\Sigma^+$ hydroxyl radicals Part 1.-Quenching kinetics of OH $A^2\Sigma^+$ and rate constants for reactions of OH $X^2\Pi$ with CH_3CCl_3 and CO. *J. Chem. Soc. Faraday Trans. 2* **1979**, *75*, 569-581, doi:10.1039/f29797500569.

Clyne, M. A. A.; Monkhouse, P. B.; Townsend, L. W. Reactions of O ^3P_J atoms with halogens: The rate constants for the elementary reactions O + BrCl, O + Br_2, and O + Cl_2. *Int. J. Chem. Kinet.* **1976**, *8*, 425-449, doi:10.1002/kin.550080309.

Clyne, M. A. A.; Watson, R. T. Kinetic studies for diatomic free radicals using mass spectrometry Part 3.-Elementary reactions involving BrO $X^2\Pi$ radicals. *J. Chem. Soc. Faraday Trans. 1* **1975**, *71*, 336-350, doi:10.1039/f19757100336.

Clyne, M. A. A.; Watson, R. T. Kinetic studies of diatomic free radicals using mass spectrometry Part 4.-The Br + OClO and BrO + ClO reactions. *J. Chem. Soc. Faraday Trans. 1* **1977**, *73*, 1169-1187, doi:10.1039/f19777301169.

Cox, R. A.; Sheppard, D. W.; Stevens, M. P. Absorption coefficients and kinetics of the BrO radical using molecular modulation. *J. Photochem.* **1982**, *19*, 189-207, doi:10.1016/0047-2670(82)80022-1.

Cronkhite, J. M.; Stickel, R. E.; Nicovich, J. M.; Wine, P. H. Laser flash photolysis studies of radical-radical reaction kinetics: The HO_2 + BrO reaction. *J. Phys. Chem. A* **1998**, *102*, 6651-6658, doi:10.1021/jp981456u.

Davis, D. D.; Machado, G.; Conaway, B.; Oh, Y.; Watson, R. A temperature dependent kinetics study of the reaction of OH with CH_3Cl, CH_2Cl_2, $CHCl_3$, and CH_3Br. *J. Chem. Phys.* **1976**, *65*, 1268-1274, doi:10.1063/1.433236.

DeMore, W. B. Experimental and estimated rate constants for the reactions of hydroxyl radicals with several halocarbons. *J. Phys. Chem.* **1996**, *100*, 5813-5820, doi:10.1021/jp953216+.

DeMore, W. B.; Bayes, K. D. Rate constants for the reactions of hydroxyl radical with several alkanes, cycloalkanes, and dimethyl ether. *J. Phys. Chem. A* **1999**, *103*, 2649-2654, doi:10.1021/jp983273d.

Donaghy, T.; Shanahan, I.; Hande, M.; Fitzpatrick, S. Rate constants and atmospheric lifetimes for the reactions of OH radicals and Cl atoms with haloalkanes. *Int. J. Chem. Kinet.* **1993**, *25*, 273-284, doi:10.1002/kin.550250407.

Elrod, M. J.; Meads, R. F.; Lipson, J. B.; Seeley, J. V.; Molina, M. J. Temperature dependence of the rate constant for the HO_2 + BrO reaction. *J. Phys. Chem.* **1996**, *100*, 5808-5812, doi:10.1021/jp953193z.

Ferracci, V.; Rowley, D. M. Kinetic studies of the BrO + ClO cross-reaction over the range T = 246–314 K. *Phys. Chem. Chem. Phys.* **2014**, *16*, 1182-1196, doi:10.1039/c3cp53440e.

Friedl, R. R.; Sander, S. P. Kinetics and product studies of the reaction ClO + BrO using discharge-flow mass spectrometry. *J. Phys. Chem.* **1989**, *93*, 4756-4764, doi:10.1021/j100349a016.

Gierczak, T.; Goldfarb, L.; Sueper, D.; Ravishankara, A. R. Kinetics of the reactions of Cl atoms with CH_3Br and CH_2Br_2. *Int. J. Chem. Kinet.* **1994**, *26*, 719-728, doi:10.1002/kin.550260705.

Gilles, M. K.; Burkholder, J. B.; Gierczak, T.; Marshall, P.; Ravishankara, A. R. Rate coefficient and product branching measurements for the reaction OH + bromopropane from 230 to 360 K. *J. Phys. Chem. A* **2002**, *104*, 8945-8950, doi:10.1021/jp014736+.

Gilles, M. K.; Burkholder, J. B.; Ravishankara, A. R. Rate coefficients for the reaction of OH with Cl_2, Br_2 and I_2 from 235 to 354 K. *Int. J. Chem. Kinet.* **1999**, *31*, 417-424, doi:10.1002/(SICI)1097-4601(1999)31:6<417::AID-KIN3>3.0.CO;2-A.

Gilles, M. K.; McCabe, D. C.; Burkholder, J. B.; Ravishankara, A. R. Mesurement of the rate coefficient for the reaction of OH with BrO. *J. Phys. Chem. A* **2001**, *105*, 5849-5853, doi:10.1021/jp0039666.

Gilles, M. K.; Turnipseed, A. A.; Burkholder, J. B.; Ravishankara, A. R. Kinetics of the IO radical. 2. Reaction of IO with BrO. *J. Phys. Chem. A* **1997**, *101*, 5526-5534, doi:10.1021/jp9709159.

Goliff, W. S.; Rowland, F. S. Methyl chloride formation by gas phase thermal chlorine atom reaction with methyl iodide and methyl bromide. *Geophys. Res. Lett.* **1997**, *23*, 3029-3032, doi:10.1029/97GL03093.

Harwood, M. H.; Rowley, D. M.; Cox, R. A.; Jones, R. L. Kinetics and mechanism of the BrO self-reaction: Temperature- and pressure-dependent studies. *J. Phys. Chem. A* **1998**, *102*, 1790-1802, doi:10.1021/jp973264p.

Heneghan, S. P.; Benson, S. W. Kinetic study of the reactions of Cl and Br with H_2O_2. *Int. J. Chem. Kinet.* **1983**, *15*, 1311-1319, doi:10.1002/kin.550151206.

Herndon, S. C.; Gierczak, T.; Talukdar, R. K.; Ravishankara, A. R. Kinetics of the reactions of OH with several alkyl halides. *Phys. Chem. Chem. Phys.* **2001**, *3*, 4529-4535, doi:10.1039/b105188c.

Hills, A. J.; Cicerone, R. J.; Calvert, J. G.; Birks, J. W. Temperature dependence of the rate constant and product channels for the BrO + ClO reaction. *J. Phys. Chem.* **1988**, *92*, 1853-1858, doi:10.1021/j100318a032.

Howard, C. J.; Evenson, K. M. Rate constants for the reactions of OH with CH_4 and fluorine, chlorine, and bromine substituted methanes at 296 K. *J. Chem. Phys.* **1976**, *64*, 197-202, doi:10.1063/1.431950.

Howard, C. J.; Evenson, K. M. Rate constants for the reactions of OH with ethane and some halogen substituted ethanes at 296 K. *J. Chem. Phys.* **1976**, *64*, 4303-4306, doi:10.1063/1.432115.

Hsu, K. J.; DeMore, W. B. Rate constants for the reactions of OH with CH_3Cl, CH_2Cl_2, $CHCl_3$, and CH_3Br. *Geophys. Res. Lett.* **1994**, *21*, 805-808, doi:10.1029/94GL00601.

Hsu, K. J.; DeMore, W. B. Rate constants and temperature dependences for the reactions of hydroxyl radical with several halogenated methanes, ethanes, and propanes by relative rate measurements. *J. Phys. Chem.* **1995**, *99*, 1235-1244, doi:10.1021/j100004a025.

Husain, D.; Plane, J. M. C.; Slater, N. K. H. Kinetic investigation of the reactions of OH($X^2\Pi$) with the hydrogen halides, HCl, DCl, HBr and DBr by time-resolved resonance fluorescence ($A^2\Sigma^+$ - $X^2\Pi$). *J. Chem. Soc. Faraday Trans. 2* **1981**, *77*, 1949-1962, doi:10.1039/f29817701949.

Ingham, T.; Sander, S. P.; Friedl, R. R. Kinetics and product studies of the reaction of Br, Cl, and NO with ClOOCl using discharge-flow mass spectrometry. *Faraday Discuss.* **2005**, *130*, 89-110, doi:10.1039/b500179j.

Jaffe, S.; Mainquist, W. K. Bromine photosensitized decomposition of ozone. *J. Phys. Chem.* **1980**, *84*, 3277-3280, doi:10.1021/j100461a030.

Jaramillo, V. I.; Gougeon, S.; Le Picard, S.; Canosa, A.; Smith, M.; Rowe, B. A consensus view of the temperature dependence of the gas phase reaction: OH + HBr → H_2O + Br. *Int. J. Chem. Kinet.* **2002**, *34*, 339-344, doi:10.1002/kin.10056.

Jourdain, J. L.; Le Bras, G.; Combourieu, J. EPR determination of absolute rate constants for the reactions of H and OH radicals with hydrogen bromide. *Chem. Phys. Lett.* **1981**, *78*, 483-487, doi:10.1016/0009-2614(81)85242-6.

Kambanis, K. G.; Lazarou, Y. G.; Papagiannakopoulos, P. J. Absolute rate constants for the reactions of Cl atoms with CH_3Br, CH_2Br_2, and $CHBr_3$. *J. Phys. Chem.* **1997**, *101*, 8496-8502, doi:10.1021/jp9719671.

Khamaganov, V. G.; Orkin, V. L.; Larin, I. K. Study of the reactions of OH with HCl, HBr, and HI between 298 K and 460 K. *Int. J. Chem. Kinet.* **2020**, *52*, 852-860, doi:10.1002/kin.21404.

Kozlov, S. N.; Orkin, V. L.; Huie, R. E.; Kurylo, M. J. OH reactivity and UV spectra of propane, n-propyl bromide, and isopropyl bromide. *J. Phys. Chem. A* **2003**, *107*, 1333-1338, doi:10.1021/jp021806j.

Kukui, A.; Kirchner, U.; Benter, T.; Schindler, R. N. A gaskinetic investigation of HOBr reactions with Cl(^{2}P), O(^{3}P) and OH($^2\Pi$). The reaction of BrCl with OH($^2\Pi$). *Ber. Bunsenges. Phys. Chem.* **1996**, *100*, 455-461, doi:10.1002/bbpc.19961000409.

Laine, P. L.; Sohn, Y. S.; Nicovich, J. M.; McKee, M. L.; Wine, P. H. Kinetics of elementary steps in the reactions of atomic bromine with isoprene and 1,3-butadiene under atmospheric conditions. *J. Phys. Chem. A* **2012**, *116*, 6341-6357, doi:10.1021/jp212127v.

Lancar, I.; Laverdet, G.; Le Bras, G.; Poulet, G. Rate constant and products of the BrO + BrO reaction at 298 K. *Int. J. Chem. Kinet.* **1991**, *23*, 37-45, doi:10.1002/kin.550230105.

Larichev, M.; Maguin, F.; Le Bras, G.; Poulet, G. Kinetics and mechanism of the BrO + HO_2 reaction. *J. Phys. Chem.* **1995**, *99*, 15911-15918, doi:10.1021/j100043a032.

Laszlo, B.; Huie, R. E.; Kurylo, M. J.; Miziolek, A. W. Kinetic studies of the reactions of BrO and IO radicals. *J. Geophys. Res.* **1997**, *102*, 1523-1532, doi:10.1029/96JD00458.

Laverdet, G.; Le Bras, G.; Mellouki, A.; Poulet, G. The Br + HO_2 reaction revisited: absolute determination of the rate constant at 298 K. *Chem. Phys. Lett.* **1990**, *172*, 430-434, doi:10.1016/S0009-2614(90)87138-H.

Le Bras, G.; Combourieu, J. EPR kinetic study of the reactions of CF_3Br with H atoms and OH radicals. *Int. J. Chem. Kinet.* **1978**, *10*, 1205-1213, doi:10.1002/kin.550101203.

Le Bras, G.; Foon, R.; Combourieu, J. EPR kinetic study of the reactions of F and Br atoms with H_2CO. *Chem. Phys. Lett.* **1980**, *73*, 357-361, doi:10.1016/0009-2614(80)80388-5.

Leu, M.-T.; DeMore, W. B. Rate constant for the reaction of atomic bromine with ozone. *Chem. Phys. Lett.* **1977**, *48*, 317-320, doi:10.1016/0009-2614(77)80323-0.

Leu, M. T. Rate constant for the reaction BrO + NO → Br + NO_2. *Chem. Phys. Lett.* **1979**, *61*, 275-279, doi:10.1016/0009-2614(79)80643-0.

Leu, M. T. Upper limits for the rate constant for the reaction Br + H_2O_2 → HBr + HO_2. *Chem. Phys. Lett.* **1980**, *69*, 37-39, doi:10.1016/0009-2614(80)80008-X.

Li, Z.; Friedl, R. R.; Sander, S. P. Kinetics of the HO_2 + BrO reaction over the temperature range 233-348 K. *J. Chem. Soc. Faraday Trans.* **1997**, 2683-2691.

Li, Z. J.; Jeong, G. R.; Person, E. Kinetics of reactions of OBrO with NO, O_3, OClO, and ClO at 240-350 K. *Int. J. Chem. Kinet.* **2002**, *34*, 430-437, doi:10.1002/kin.10069.

Loewenstein, L. M.; Anderson, J. G. Rate and product measurements for the reactions of OH with Cl_2, Br_2, and BrCl at 298 K. Trend interpretations. *J. Phys. Chem.* **1984**, *88*, 6277-6286, doi:10.1021/j150669a045.

Mauldin, R. L., III; Wahner, A.; Ravishankara, A. R. Kinetics and mechanism of the self-reaction of the BrO radical. *J. Phys. Chem.* **1993**, *97*, 7585-7596, doi:10.1021/j100131a031.

Mellouki, A.; Poulet, G.; Le Bras, G.; Singer, R.; Burrows, J. P.; Moortgat, G. K. Discharge flow kinetic study of the reactions of NO_3 with Br, BrO, HBr, and HCl. *J. Phys. Chem.* **1989**, *93*, 8017-8021, doi:10.1021/j100361a012.

Mellouki, A.; Talukdar, R. K.; Howard, C. J. Kinetics of the reactions of HBr with O_3 and HO_2: The yield of HBr from HO_2 + BrO. *J. Geophys. Res.* **1994**, *99*, 22949-22954, doi:10.1029/94JD02144.

Mellouki, A.; Talukdar, R. K.; Schmoltner, A.-M.; Gierczak, T.; Mills, M. J.; Soloman, S.; Ravishankara, A. R. Atmospheric lifetimes and ozone depletion potentials of methyl bromide (CH_3Br) and dibromomethane (CH_2Br_2). *Geophys. Res. Lett.* **1992**, *19*, 2059-2062, doi:10.1029/92GL01612.

Michael, J. V.; Lee, J. H.; Payne, W. A.; Stief, L. J. Absolute rate of the reaction of N(^4S) with NO from 196-400 K with DF-RF and FP-RF techniques. *J. Chem. Phys.* **1978**, *68*, 4093-4097, doi:10.1063/1.436322.

Michael, J. V.; Payne, W. A. Absolute rate constants for the reaction of bromine atoms with ozone from 234 to 360 K. *Int. J. Chem. Kinet.* **1979**, *11*, 799-809, doi:10.1002/kin.550110711.

Monks, P. S.; Nesbitt, F. L.; Scanlon, M.; Stief, L. J. HOBr kinetics: Reactions of halogen atoms, oxygen atoms, nitrogen atoms, and nitric oxide with HOBr. *J. Phys. Chem.* **1993**, *97*, 11699-11705, doi:10.1021/j100147a025.

Nava, D. F.; Bosco, S. R.; Stief, L. J. Rate constant for the reaction of O(^3P) with HBr from 221 to 455 K. *J. Chem. Phys.* **1983**, *78*, 2443-2448, doi:10.1063/1.445047.

Nava, D. F.; Michael, J. V.; Stief, L. J. Rate constant for the reaction of atomic bromine with formaldehyde from 223 to 480 K. *J. Phys. Chem.* **1981**, *85*, 1896-1899, doi:10.1021/j150613a024.

Nelson, D. D., Jr.; Wormhoudt, J. C.; Zahniser, M. S.; Kolb, C. E.; Ko, M. K. W.; Weisenstein, D. K. OH reaction kinetics and atmospheric impact of 1-bromopropane. *J. Phys. Chem. A* **1997**, *101*, 4987-4990, doi:10.1021/jp970874g.

Nelson, D. D., Jr.; Zahniser, M. S.; Kolb, C. E. OH reaction kinetics and atmospheric lifetimes of CF_3CFHCF_3 and CF_3CH_2Br. *Geophys. Res. Lett.* **1993**, *20*, 197-200, doi:10.1029/93GL00239.

Nesbitt, F. L.; Monks, P. S.; Payne, W. A.; Stief, L. J.; Toumi, R. The reaction O(^{3}P) + HOBr: Temperature dependence of the rate constant and importance of the reaction as an HOBr stratospheric loss process. *Geophys. Res. Lett.* **1995**, *22*, 827-830, doi:10.1029/95GL00375.

Nicovich, J. M.; Kreutter, K. D.; Wine, P. H. Kinetics of the reactions of Cl(^2P_J) and Br($^2P_{3/2}$) with O_3. *Int. J. Chem. Kinet.* **1990**, *22*, 399-414, doi:10.1002/kin.550220407.

Nicovich, J. M.; Wine, P. H. Kinetics of the reactions of O(^3P) and Cl(^2P) with HBr and Br_2. *Int. J. Chem. Kinet.* **1990**, *22*, 379-397, doi:10.1002/kin.550220406.

Nielsen, O. J.; Munk, J.; Locke, G.; Wallington, T. J. Ultraviolet absorption spectra and kinetics of the self-reaction of CH_2Br and CH_2BrO_2 radicals in the gas phase at 298 K. *J. Phys. Chem.* **1991**, *95*, 8714-8719, doi:10.1021/j100175a054.

Nilsson, E. J. K.; Joelsson, I. M. T.; Heimdal, J.; Johnson, M. S.; Nielsen, O. J. Re-evaluation of the reaction rate coefficient of CH_3Br + OH with implications for the atmospheric budget of methyl bromide. *Atmos. Environ.* **2013**, *80*, 70-74, doi:10.1016/j.atmosenv.2013.07.046.

Ninomiya, Y.; Hashimoto, S.; Kawasaki, M.; Wallington, T. J. Cavity ring-down study of BrO radicals: Kinetics of the Br + O_3 reaction and rate of relaxation of vibrationally excited BrO by collisions with N_2 and O_2. *Int. J. Chem. Kinet.* **2000**, *32*, 125-130, doi:10.1002/(SICI)1097-4601(2000)32:3<125::AID-KIN1>3.0.CO;2-4.

Orkin, V. L.; Khamaganov, V. G. Rate constants for reactions of OH radicals with some Br-containing haloalkanes. *J. Atmos. Chem.* **1993**, *16*, 169-178, doi:10.1007/BF00702786.

Orkin, V. L.; Khamaganov, V. G.; Guschin, A. G.; Huie, R. E.; Kurylo, M. J. Atmospheric fate of chlorobromomethane: Rate constant for the reaction with OH, UV spectrum, and water solubility. *J. Phys. Chem. A* **1997**, *101*, 174-178, doi:10.1021/jp962428j.

Orkin, V. L.; Khamaganov, V. G.; Kozlov, S. N.; Kurylo, M. J. Measurements of rate constants for the OH reactions with bromoform ($CHBr_3$), $CHBr_2Cl$, $CHBrCl_2$, and epichlorohydrin (C_3H_5ClO). *J. Phys. Chem. A* **2013**, *117*, 3809-3818, doi:10.1021/jp3128753.

Orkin, V. L.; Louis, F.; Huie, R. E.; Kurylo, M. J. Photochemistry of bromine-containing fluorinated alkenes: Reactivity toward OH and UV spectra. *J. Phys. Chem. A* **2002**, *106*, 10195-10199, doi:10.1021/jp014436s.

Orkin, V. L.; Martynova, L. E.; Kurylo, M. J. Photochemical properties of CH_2=CH-CFCl-CF_2Br (4-bromo-3-chloro-3,4,4-trifluoro-1-butene) and CH_3-O-CH(CF_3)$_2$ (methyl hexafluoroisopropyl ether): OH reaction rate constants and UV and IR absorption spectra. *J. Phys. Chem. A* **2017**, *121*, 5675–5680, doi:10.1021/acs.jpca.7b04256.

Orlando, J. J.; Tyndall, G. S.; Wallington, T. J. Atmospheric oxidation of CH_3Br: Chemistry of the CH_2BrO radical. *J. Phys. Chem.* **1996**, *100*, 7026-7033, doi:10.1021/jp951813q.

Orlando, J. J.; Tyndall, G. S.; Wallington, T. J.; Dill, M. Atmospheric chemistry of CH_2Br_2: Rate coefficients for its reaction with Cl atoms and OH and the chemistry of the $CHBr_2O$ radical. *Int. J. Chem. Kinet.* **1996**, *28*, 433-442, doi:10.1002/(SICI)1097-4601(1996)28:6<433::AID-KIN5>3.0.CO;2-W.

Patten, K. O.; Khamaganov, V. G.; Orkin, V. L.; Baughcum, S. L.; Wuebbles, D. J. OH reaction rate constant, IR absorption spectrum, ozone depletion potentials and global warming potentials of 2-bromo-3,3,3-trifluoropropene. *J. Geophys. Res.* **2011**, *116*, D24307, doi:10.1029/2011JD016518.

Piety, C. A.; Soller, R.; Nicovich, J. M.; McKee, M. L.; Wine, P. H. Kinetic and mechanistic study of the reaction of atomic chlorine with methyl bromide over an extended temperature range. *Chem. Phys.* **1998**, *231*, 155-169, doi:10.1016/S0301-0104(97)00356-X.

Posey, J.; Sherwell, J.; Kaufman, M. Kinetics of the reactions of atomic bromine with HO_2 and H_2O_2. *Chem. Phys. Lett.* **1981**, *77*, 476-479, doi:10.1016/0009-2614(81)85189-5.

Poulet, G.; Lancar, I. T.; Laverdet, G.; Le Bras, G. Kinetics and products of the BrO + ClO reaction. *J. Phys. Chem.* **1990**, *94*, 278-284, doi:10.1021/j100364a046.

Poulet, G.; Laverdet, G.; Le Bras, G. Discharge flow-mass spectrometric determination of the rate coefficients for the reactions of formaldehyde with bromine atoms and chlorine atoms. *J. Phys. Chem.* **1981**, *85*, 1892-1895, doi:10.1021/j150613a023.

Poulet, G.; Laverdet, G.; Le Bras, G. Kinetics and products of the reaction of hydroxyl radical with molecular bromine. *Chem. Phys. Lett.* **1983**, *94*, 129-132, doi:10.1016/0009-2614(83)87225-X.

Poulet, G.; Laverdet, G.; Le Bras, G. Kinetics of the reactions of atomic bromine with HO_2 and HCO at 298 K. *J. Chem. Phys.* **1984**, *80*, 1922-1928, doi:10.1063/1.446953.

Qiu, L. X.; Shi, S.-H.; Xing, S. B.; Chen, X. G. Rate constants for the reactions of OH with five halogen-substituted ethanes from 292 to 366 K. *J. Phys. Chem.* **1992**, *96*, 685-689, doi:10.1021/j100181a032.

Ramacher, B.; Orlando, J. J.; Tyndall, G. S. Temperature-dependent rate coefficient measurements for the reaction of bromine atoms with a series of aldehydes. *Int. J. Chem. Kinet.* **2000**, *32*, 460-465, doi:10.1002/1097-4601(2000)32:8<460::AID-KIN2>3.0.CO;2-P.

Rattigan, O. V.; Cox, R. A.; Jones, R. L. Br_2-sensitised decomposition of ozone: Kinetics of the reaction BrO + O_3 → products. *J. Chem. Soc. Faraday Trans.* **1995**, *91*, 4189-4197, doi:10.1039/ft9959104189.

Ravishankara, A. R.; Wine, P. H.; Langford, A. O. Absolute rate constant for the reaction OH + HBr → H_2O + Br. *Chem. Phys. Lett.* **1979**, *63*, 479-484, doi:10.1016/0009-2614(79)80694-6.

Ravishankara, A. R.; Wine, P. H.; Wells, J. R. The OH + HBr reaction revisited. *J. Chem. Phys.* **1985**, *83*, 447-448, doi:10.1063/1.449790.

Ray, G. W.; Watson, R. T. Kinetics study of the reactions of NO with FO, ClO, BrO, and IO at 298 K. *J. Phys. Chem.* **1981**, *85*, 2955-2960, doi:10.1021/j150620a022.

Rowley, D. M.; Harwood, M. H.; Freshwater, R. A.; Jones, R. L. A novel flash photolysis/UV absorption system employing charge-coupled device (CCD) detection: A study of the BrO + BrO reaction at 298 K. *J. Phys. Chem.* **1996**, *100*, 3020-3029, doi:10.1021/jp951825b.

Sander, S. P.; Friedl, R. R. Kinetics and product studies of the reaction ClO + BrO using flash photolysis-ultraviolet absorption. *J. Phys. Chem.* **1989**, *93*, 4764-4771, doi:10.1021/j100349a017.

Sander, S. P.; Watson, R. T. Kinetics and mechanism of the disproportionation of BrO radicals. *J. Phys. Chem.* **1981**, *85*, 4000-4007, doi:10.1021/j150626a010.

Sauer, C. G.; Barnes, I.; Becker, K. H. FT-IR kinetic and product study of the Br-radical initiated oxidation of α, β-unsaturated organic carbonyl compounds. *Atmos. Environ.* **1999**, *33*, 2969-2979, doi:10.1016/S1352-2310(99)00085-0.

Sehested, J.; Nielsen, O. J.; Wallington, T. J. Absolute rate constants for the reaction of NO with a series of peroxy radicals in the gas phase at 295 K. *Chem. Phys. Lett.* **1993**, *213*, 457-464, doi:10.1016/0009-2614(93)89142-5.

Sims, I. R.; Smith, I. W. M.; Clary, D. C.; Bocherel, P.; Rowe, B. R. Ultra-low temperature kinetics of neutral-neutral reactions: New experimental and theoretical results for OH + HBr between 295 and 23 K. *J. Chem. Phys.* **1994**, *101*, 1748-1751, doi:10.1063/1.467733.

Singleton, D. L.; Cvetanovic, R. J. Temperature dependence of rate constants for the reactions of oxygen atoms, O(^{3}P), with HBr and HI. *Can. J. Chem.* **1978**, *56*, 2934-2939, doi:10.1139/v78-481.

Smith, I. W. M.; Zellner, R. Rate measurements of reactions of OH by resonance absorption. Part 3. - Reactions of OH with H_2, D_2 and hydrogen and deuterium halides. *J. Chem. Soc. Faraday Trans. 2* **1974**, *70*, 1045-1056, doi:10.1039/F29747001045.

Soller, R.; Nicovich, J. M.; Wine, P. H. Temperature-dependent rate coefficients for the reactions of Br($^2P_{3/2}$), Cl($^2P_{3/2}$), and O(^3P_J) with $BrONO_2$. *J. Phys. Chem. A* **2001**, *105*, 1416-1422, doi:10.1021/jp001947q.

Stevens, P. S.; Anderson, J. G. Kinetic and mechanistic study of X + ClOCl → products (X = Br, CI, F, O, OH, N) over the temperature range 240-373 K. *J. Phys. Chem.* **1992**, *96*, 1708-1718, doi:10.1021/j100183a040.

Sulbaek-Andersen, M. P.; Hurley, M. D.; Wallington, T. J. Kinetics of the gas phase reactions of chlorine atoms and OH radicals with $CF_3CBr{=}CH_2$ and $CF_3CF_2CBr{=}CH_2$. *Chem. Phys. Lett.* **2009**, *482*, 20-23, doi:10.1016/j.cplett.2009.09.056.

Takacs, G. A.; Glass, G. P. Reaction of atomic oxygen with hydrogen bromide. *J. Phys. Chem.* **1973**, *77*, 1182-1186, doi:10.1021/j100628a020.

Takacs, G. A.; Glass, G. P. Reactions of hydrogen atoms and hydroxyl radicals with hydrogen bromide. *J. Phys. Chem.* **1973**, *77*, 1060-1064, doi:10.1021/j100627a019.
Talukdar, R.; Mellouki, A.; Gierczak, T.; Burkholder, J. B.; McKeen, S. A.; Ravishankara, A. R. Atmospheric lifetime of CHF_2Br, a proposed substitute for halons. *Science* **1991**, *252*, 693-695, doi:10.1126/science.252.5006.693.
Téton, S.; El-Boudali, A.; Mellouki, A. Rate constants for the reactions of OH radicals with 1- and 2-bromopropane. *J. Chim. Phys.* **1996**, *93*, 274-282, doi:10.1051/jcp/1996930274.
Thorn, R. P.; Cronkhite, J. M.; Nicovich, J. M.; Wine, P. H. Laser flash photolysis studies of radical-radical reaction kinetics: The $O(^3P_J)$ + BrO reaction. *J. Chem. Phys.* **1995**, *102*, 4131-4142, doi:10.1063/1.468541.
Toohey, D. W. Kinetic and Mechanistic Studies of Reactions of Bromine and Chlorine Species Important in the Earth's Stratosphere. Ph. D. Thesis, Harvard University, 1988.
Toohey, D. W.; Anderson, J. G. Formation of $BrCl(^3\Pi_{0^+})$ in the reaction of BrO with ClO. *J. Phys. Chem.* **1988**, *92*, 1705-1708, doi:10.1021/j100318a002.
Toohey, D. W.; Brune, W. H.; Anderson, J. G. Mechanism and kinetics of Br + HO_2 → HBr + O_2 and Br + H_2O_2 → products over the temperature range 260-390 K. *J. Phys. Chem.* **1987**, *91*, 1215-1222, doi:10.1021/j100289a036.
Toohey, D. W.; Brune, W. H.; Anderson, J. G. Rate constant for the reaction Br + O_3 → BrO + O_2 from 248 to 418 K: Kinetics and mechanism. *Int. J. Chem. Kinet.* **1988**, *20*, 131-144, doi:10.1002/kin.550200206.
Tschuikow-Roux, E.; Faraji, F.; Paddison, S.; Niedzielski, J.; Miyokawa, K. Kinetics of photochlorination of halogen (F, Cl, Br) substituted methanes. *J. Phys. Chem.* **1988**, *92*, 1488-1495, doi:10.1021/j100317a023.
Turnipseed, A. A.; Birks, J. W.; Calvert, J. G. Kinetics of the BrO + BrO reaction. *J. Phys. Chem.* **1990**, *94*, 7477-7482, doi:10.1021/j100382a032.
Turnipseed, A. A.; Birks, J. W.; Calvert, J. G. Kinetics and temperature dependence of the BrO + ClO reaction. *J. Phys. Chem.* **1991**, *95*, 4356-4364, doi:10.1021/j100164a035.
Watson, R. T.; Sander, S. P.; Yung, Y. L. Pressure and temperature dependence kinetics study of the NO + BrO → NO_2 + Br reaction. Implications for stratospheric bromine photochemistry. *J. Phys. Chem.* **1979**, *83*, 2936-2944, doi:10.1021/j100486a002.
Xing, S. B.; Shi, S.-H.; Qiu, L. X. Kinetics studies of reactions of OH radicals with four haloethanes Part I. Experiment and BEBO calculation. *Int. J. Chem. Kinet.* **1992**, *24*, 1-10, doi:10.1002/kin.550240102.
Zhang, D. Q.; Zhong, J. X.; Qiu, L. X. Kinetics of the reaction of hydroxyl radicals with CH_2Br_2 and its implications in the atmosphere. *J. Atmos. Chem.* **1997**, *27*, 209-215, doi:10.1023/A:1005821121158.
Zhang, Z.; Saini, R. D.; Kurylo, M. J.; Huie, R. E. A temperature dependent kinetic study of the reaction of the hydroxyl radical with CH_3Br. *Geophys. Res. Lett.* **1992**, *19*, 2413-2416, doi:10.1029/92GL02929.

1.13 IO_x Reactions

1.13.1 Table 1H: IO_x Reactions

Reaction	Temperature Range of Exp. Data (K) [a]	*A*-Factor	*E*/R	*k*(298 K) [b]	*f*(298 K) [c]	*g* [c]	Notes
$O + I_2 \rightarrow IO + I$	298	1.3×10^{-10}	0	1.3×10^{-10}	1.25	0	H1
$O + IO \rightarrow O_2 + I$	298	1.4×10^{-10}	0	1.4×10^{-10}	1.20	0	H2
$O + CH_3I \rightarrow$ products	213–364	1.08×10^{-11}	–158	1.84×10^{-11}	1.15	0	H3
$O + CF_3I \rightarrow$ products	213–523	1.0×10^{-11}	205	5.03×10^{-11}	1.15	0	H4
$OH + I_2 \rightarrow HOI + I$	240–348	2.1×10^{-10}	0	2.1×10^{-10}	1.25	0	H5
$OH + HI \rightarrow H_2O + I$	246–370	1.17×10^{-11}	–280	3.0×10^{-11}	+1.8/-1.15	100	H6
$OH + CH_3I \rightarrow H_2O + CH_2I$	271–423	3.5×10^{-12}	1100	8.7×10^{-14}	1.35	100	H7
$OH + CF_3I \rightarrow HOI + CF_3$	271–450	2.5×10^{-11}	2070	2.4×10^{-14}	1.30	200	H8
$HO_2 + I \rightarrow HI + O_2$	283–353	1.5×10^{-11}	1090	3.8×10^{-13}	2.00	0	H9
$HO_2 + IO \rightarrow$ products	273–373	1.3×10^{-11}	–570	8.8×10^{-11}	1.15	50	H10
$NO_3 + HI \rightarrow HNO_3 + I$		(See Note)					H11
$Cl + CH_3I \rightarrow CH_2I + HCl$	273–363	$2.9\text{x}10^{-11}$	1000	$1.0\text{x}10^{-12}$	1.50	250	H12
$I + O_3 \rightarrow IO + O_2$	231–368	2.0×10^{-11}	830	1.2×10^{-12}	1.20	100	H13
$I + NO \xrightarrow{M} INO$		(See Table 2-1)					
$I + NO_2 \xrightarrow{M} INO_2$		(See Table 2-1)					
$I + BrO \rightarrow IO + Br$	298			1.2×10^{-11}	2.00		H14
$IO + CH_3O_2 \rightarrow$ products		(See Note)					H15
$IO + NO \rightarrow I + NO_2$	240–370	8.6×10^{-12}	–230	1.9×10^{-11}	1.10	50	H16
$IO + NO_2 \xrightarrow{M} IONO_2$		(See Table 2-1)					
$IO + ClO \rightarrow I + OClO$	200–362	2.7×10^{-12}	–280	6.9×10^{-12}	1.30	150	H17
$\rightarrow I + Cl + O_2$	200–362	1.2×10^{-12}	–280	3.1×10^{-12}	1.30	150	
$\rightarrow ICl + O_2$	200–362	0.92×10^{-12}	–280	2.3×10^{-12}	1.30	150	

Reaction	Temperature Range of Exp. Data (K) [a]	*A*-Factor	*E*/R	*k*(298 K) [b]	*f*(298 K) [c]	*g* [c]	Notes
$IO + BrO \rightarrow Br + OIO$	204–388	4.4×10^{-12}	–760	5.6×10^{-11}	1.25	300	H18
$\rightarrow Br + I + O_2$	204–388	5.5×10^{-13}	–760	7.0×10^{-12}	1.50	300	
$\rightarrow I + OBrO$	204–388	4.4×10^{-13}	–760	5.6×10^{-12}	1.50	300	
$\rightarrow IBr + O_2$	204–388	1.1×10^{-13}	–760	1.4×10^{-12}	2.0	300	
$IO + IO \rightarrow$ products	250–373	1.5×10^{-11}	–500	8.0×10^{-11}	1.50	100	H19
$INO + INO \rightarrow I_2 + 2NO$	320–450	8.4×10^{-11}	2620	1.3×10^{-14}	2.50	600	H20
$INO_2 + INO_2 \rightarrow I_2 + 2NO_2$	320–450	2.9×10^{-11}	2600	4.7×10^{-15}	3.00	1000	H21

Shaded areas indicate changes or additions since JPL19-5.

[a] Temperature range of available experimental data. This is not necessarily the range of temperature over which the recommended Arrhenius parameters are applicable. See the corresponding note for such information.

[b] Units are cm^3 $molecule^{-1}$ s^{-1}.

[c] f(298 K) is the uncertainty factor at 298 K. To calculate the uncertainty at other temperatures, use the expression:

$$f(\mathrm{T}) = f(298\ \mathrm{K})\exp\left|g\left(\frac{1}{\mathrm{T}} - \frac{1}{298}\right)\right|$$

Note that the exponent is an absolute value.

1.13.2 Notes: IO_x Reactions

H1. **O + I_2.** Based on the room temperature data of Ray and Watson[4] (298 K), Laszlo et al.[2] (298 K), Turnipseed et al.[6] (298 K), Hölscher et al.[1] (295 K), and Tucceri et al.[5] (298 K). The recommended value of k(298 K) is derived from an unweighted average of the five studies. The molecular beam study of Parrish and Herschbach[3] suggests a zero activation energy, consistent with the near gas kinetic value of k(298 K).
(Table: 25-1, Note: 19-5, Evaluated: 19-5) Back to Table

(1) Hölscher, D.; Fockenberg, C.; Zellner, R. LIF detection of the IO-radical and kinetics of the reactions $I+O_3 \rightarrow IO+O_2$, $O(^3P)+I_2 \rightarrow IO+I$, $O(^3P)+CH_3I \rightarrow IO+CH_3$ and $O(^3P)+CF_3I \rightarrow IO+CF_3$ in the temperature range 230 to 310 K. *Ber. Bunsen-Ges. Phys. Chem. Chem. Phys.* **1998**, *102*, 716-722, doi:10.1002/bbpc.19981020503.

(2) Laszlo, B.; Kurylo, M. J.; Huie, R. E. Absorption cross sections, kinetics of formation, and self-reaction of the IO radical produced via the laser photolysis of $N_2O/I_2/N_2$ Mixtures. *J. Phys. Chem.* **1995**, *99*, 11701-11707, doi:10.1021/j100030a013.

(3) Parrish, D. D.; Herschbach, D. R. Molecular beam chemistry. Persistent collision complex in reaction of oxygen atoms with bromine molecules. *J. Am. Chem. Soc.* **1973**, *95*, 6133-6134, doi:10.1021/ja00799a059.

(4) Ray, G. W.; Watson, R. T. Kinetics study of the reactions of NO with FO, ClO, BrO, and IO at 298 K. *J. Phys. Chem.* **1981**, *85*, 2955-2960, doi:10.1021/j150620a022.

(5) Tucceri, M. E.; Dillon, T. J.; Crowley, J. N. A laser photolysis-resonance fluorescence study of the reactions: $I + O_3 \rightarrow IO + O_2$, $O + I_2 \rightarrow IO + I$, and $I + NO_2 + M \rightarrow INO_2 + M$ at 298 K. *Phys. Chem. Chem. Phys.* **2005**, *7*, 1657-1663, doi:10.1039/b502844b.

(6) Turnipseed, A. A.; Gilles, M. K.; Burkholder, J. B.; Ravishankara, A. R. LIF detection of IO and the rate coefficients for $I + O_3$ and IO + NO reactions. *Chem. Phys. Lett.* **1995**, *242*, 427-434, doi:10.1016/0009-2614(95)00774-X.

H2. **O + IO.** Based on the room temperature data of Canosa-Mas et al.[1] (296 K), Laszlo et al.[2] (298 K), and Payne et al.[3] (298 K), obtained from an unweighted average of the three studies. There are no temperature-dependence data. The reaction is near gas-kinetic at 298 K so the temperature dependence is likely to be small, or zero.
(Table: 19-5, Note: 19-5, Evaluated: 19-5) Back to Table

(1) Canosa-Mas, C. E.; Flugge, M. L.; Shah, D.; Vipond, A.; Wayne, R. P. Kinetics of the reactions of IO with HO_2 and $O(^3P)$. *J. Atmos. Chem.* **1999**, *34*, 153-162, doi:10.1023/a:1006262306459.

(2) Laszlo, B.; Kurylo, M. J.; Huie, R. E. Absorption cross sections, kinetics of formation, and self-reaction of the IO radical produced via the laser photolysis of $N_2O/I_2/N_2$ Mixtures. *J. Phys. Chem.* **1995**, *99*, 11701-11707, doi:10.1021/j100030a013.

(3) Payne, W. A.; Thorn, R. P.; Nesbitt, F. L.; Stief, L. J. Rate constant for the reaction of $O(^3P)$ with IO at T = 298 K. *J. Phys. Chem. A* **1998**, *102*, 6247-6250, doi:10.1021/jp9811530.

H3. **O + CH_3I.** The reaction has been studied by Gilles et al.[1] (213–364 K, >50 Torr), Hölscher et al.[2] (238–310 K, 100 Torr), Teruel et al.[4] (223–363 K), and Teruel[3] (298 K). Gilles et al. and Hölscher et al. measured the reaction rate coefficient using pulsed laser photolysis combined with time-resolved laser induced fluorescence detection of the IO reaction product. Teruel et al.[4] used pulsed laser photolysis combined with resonance fluorescence detection of $O(^3P)$. Teruel[3] (298 K, 1.56–3.26 Torr) measured the rate coefficient using a discharge flow method combined with resonance fluorescence detection of $O(^3P)$. The results from these studies are in good agreement. The lower-pressure measurement of Teruel is in agreement with the higher-pressure measurements. The recommended rate coefficient is a fit to the Gilles et al. data. The estimated f(298 K) uncertainty factor encompasses the range of kinetic data from all the studies.

Gilles et al. used multiple detection methods to determine the following 298 K reaction product yields: IO (0.44 ± 0.4), OH (0.16 ± 0.05), H (0.07 ± 0.02), CH_3O (<0.03), and HI (<0.05).
(New Entry) Back to Table

(1) Gilles, M. K.; Turnipseed, A. A.; Talukdar, R. K.; Rudich, Y.; Villalta, P. W.; Huey, L. G.; Burkholder, J. B.; Ravishankara, A. R. Reactions of $O(^3P)$ with alkyl iodides: Rate coefficients and reaction products. *J. Phys. Chem.* **1996**, *100*, 14005-14015, doi:10.1021/jp960688v.

(2) Hölscher, D.; Fockenberg, C.; Zellner, R. LIF detection of the IO-radical and kinetics of the reactions $I+O_3 \rightarrow IO+O_2$, $O(^3P)+I_2 \rightarrow IO+I$, $O(^3P)+CH_3I \rightarrow IO+CH_3$ and $O(^3P)+CF_3I \rightarrow IO+CF_3$ in the temperature range 230 to 310 K. *Ber. Bunsen-Ges. Phys. Chem. Chem. Phys.* **1998**, *102*, 716-722, doi:10.1002/bbpc.19981020503.

(3) Teruel, M. A. Low-pressure rate coefficients of the reaction of $O(^3P)$ with CF_3I and CH_3I. *J. Phys. Org. Chem.* **2008**, *21*, 1043-1047, doi:10.1002/poc.1393.

(4) Teruel, M. A.; Dillon, T. J.; Horowitz, A.; Crowley, J. N. Reaction of O(^{3}P) with the alkyl iodides:: CF_3I, CH_3I, CH_2I_2, C_2H_5I, 1-C_3H_7I and 2-C_3H_7I. *Phys. Chem. Chem. Phys.* **2004**, *6*, 2172-2178, doi:10.1039/b316402k.

H4. **O + CF_3I.** Rate coefficient data for this reaction has been reported in a number of studies over a range of temperature and bath gas pressure: Addison et al.[1] (300 K, 10 Torr), Watson et al.[9] (298 K, 10 Torr), Gilles et al.[5] (213–364 K, >50 Torr), Hölscher et al.[6] (233–295 K, 100 Torr), Atkinson et al.[2] (295 K, 9.4 and 30.1 Torr), Dillon and Heard[4] (223–523 K, 25 Torr), Teruel et al.[8] (223–363 K, 100 Torr), and Teruel[7] (298 K, 1.56–3.26 Torr). Addison et al. used flash photolysis with transient absorption detection. Watson et al. made an indirect measurement using the laser induced fluorescence (LIF) detection of an IF secondary chemistry product. Gilles et al., Hölscher et al., and Dillon and Heard measured the reaction rate coefficient using pulsed laser photolysis combined with LIF detection of the IO reaction product. Atkinson et al. used pulsed laser photolysis combined with cavity ring-down spectroscopy of IO. Teruel et al. used pulsed laser photolysis combined with resonance fluorescence detection of O(^{3}P). Teruel measured the rate coefficient at 298 K using a discharge flow method combined with resonance fluorescence detection of O(^{3}P). Except for the Addison et al. and Watson et al. studies, the results are in good agreement.

Dillon and Heard report a weak pressure dependence in k(223 K), but not at higher-temperatures, which is attributed to the formation of an O-CF_3I adduct. They report an association rate coefficient at 223 K of (5.5 ± 1.9) × 10^{-31} cm^6 molecule^{-2} s^{-1} for M = N_2.

The recommended k(298 K) is a standard deviation weighted average of all the studies, excluding the studies of Addison et al. and Watson et al. The recommended E/R is the average of the values reported in the Gilles et al., Dillon et al., and Teruel et al. studies. The estimated f(298 K) uncertainty factor encompasses the range of kinetic data from all the studies included in the average.

The Dillon and Heard and Teruel et al. studies show a slight non-Arrhenius behavior at temperatures greater than 300 K that is represented by the non-Arrhenius expression, after normalization to the recommended k(298 K) value:

$$k(195–500\ \text{K}) = 5.55 \times 10^{-12}\ T^{0.7}\ \exp(30/T)$$

Gilles et al. measured the IO product yield at 100 Torr (N_2) total pressure over the temperature range 250–370 K. No measurable temperature dependence was observed with a 298 K value of 0.83 ± 0.09 reported. A CF_3O product yield upper-limit of <0.01 was also reported. Bloss et al.[3] examined the pressure dependence of the IO yield and found a 20% decrease in the IO yield at 760 Torr and 220 K. The pressure and temperature dependence was also interpreted to be the result of the formation of a stabilized O-CF_3I adduct.
(New Entry) Back to Table

(1) Addison, M. C.; Donovan, R. J.; Garraway, J. Reactions of (2^1D_2) and O(2^3P_J) with halogenomethanes. *Faraday Disc. Chem. Soc.* **1980**, *67*, 286-296, doi:10.1039/DC9796700286.
(2) Atkinson, D. B.; Hudgens, J. W.; Orr-Ewing, A. J. Kinetic studies of the reactions of IO radicals determined by cavity ring-down spectroscopy. *J. Phys. Chem. A* **1999**, *103*, 6173-6180, doi:10.1021/jp9902497.
(3) Bloss, W. J.; Rowley, D. M.; Cox, R. A.; Jones, R. L. Kinetics and products of the IO self-reaction. *J. Phys. Chem. A* **2001**, *105*, 7840-7854, doi:10.1021/jp0044936.
(4) Dillon, T. J.; Heard, D. E. A laser-induced fluorescence study of the O(^{3}P) + CF_3I and IO + NO reactions - Evidence for an association channel for O + CF_3I at low temperatures. *J. Photochem. Photobiol. A-Chem.* **2003**, *157*, 223-230, doi:10.1016/s1010-6030(03)00056-x.
(5) Gilles, M. K.; Turnipseed, A. A.; Talukdar, R. K.; Rudich, Y.; Villalta, P. W.; Huey, L. G.; Burkholder, J. B.; Ravishankara, A. R. Reactions of O(^{3}P) with alkyl iodides: Rate coefficients and reaction products. *J. Phys. Chem.* **1996**, *100*, 14005-14015, doi:10.1021/jp960688v.
(6) Hölscher, D.; Fockenberg, C.; Zellner, R. LIF detection of the IO-radical and kinetics of the reactions $I+O_3 \rightarrow IO+O_2$, O(^{3}P)+$I_2 \rightarrow$IO+I, O(^{3}P)+$CH_3I \rightarrow IO+CH_3$ and O(^{3}P)+$CF_3I \rightarrow IO+CF_3$ in the temperature range 230 to 310 K. *Ber. Bunsen-Ges. Phys. Chem. Chem. Phys.* **1998**, *102*, 716-722, doi:10.1002/bbpc.19981020503.
(7) Teruel, M. A. Low-pressure rate coefficients of the reaction of O(^{3}P) with CF_3I and CH_3I. *J. Phys. Org. Chem.* **2008**, *21*, 1043-1047, doi:10.1002/poc.1393.
(8) Teruel, M. A.; Dillon, T. J.; Horowitz, A.; Crowley, J. N. Reaction of O(^{3}P) with the alkyl iodides:: CF_3I, CH_3I, CH_2I_2, C_2H_5I, 1-C_3H_7I and 2-C_3H_7I. *Phys. Chem. Chem. Phys.* **2004**, *6*, 2172-2178, doi:10.1039/b316402k.
(9) Watson, T. A.; Addison, M.; Wittig, C. Photolytic production of O(^{3}P) in the presence of CF_3I: The formation of IF($X^1\Sigma^+$). *Chem. Phys.* **1983**, *78*, 57-63, doi:10.1016/0301-0104(83)87006-2.

H5. OH + I_2. The rate coefficient has been measured by Loewenstein and Anderson[3] (298 K, using discharge-flow/RF measurements), Jenkin et al.[2] (294 K, using steady-state photolysis kinetic measurements), and Gilles et al.[1] (240–348 K, using pulsed laser photolysis/LIF measurements). The recommended k(298 K) and E/R values are taken from Gilles et al., which provides the most direct study over a range of temperature. The recommended uncertainty factors encompass the range of results from the Loewenstein and Anderson, Jenkin et al., and Gilles et al. studies.

Jenkin et al. derived k(294 K) relative to k(OH + C_2H_4) from steady-state photolysis experiments of HONO/C_2H_4/I_2 mixtures at 1 atm. The determined rate coefficient ratio yields the recommended k(298 K), when the current recommendation for the OH + C_2H_4 reaction is used. Loewenstein and Anderson observed significant dependences of their determined k(298 K) on the diameter of the flow rector, pressure, and carrier gas, Ar or He, that was attributed to heterogeneous reaction. As a result, they propose a factor of 2 uncertainty in their reported k(298 K).
(Table: 25-1, Note: 25-01, Evaluated: 25-1) Back to Table

(1) Gilles, M. K.; Burkholder, J. B.; Ravishankara, A. R. Rate coefficients for the reaction of OH with Cl_2, Br_2 and I_2 from 235 to 354 K. *Int. J. Chem. Kinet.* **1999**, *31*, 417-424, doi:10.1002/(SICI)1097-4601(1999)31:6<417::AID-KIN3>3.0.CO;2-A.
(2) Jenkin, M. E.; Clemitshaw, K. C.; Cox, R. A. Kinetics of the reaction of OH with I_2. *J. Chem. Soc. Faraday Trans. 2* **1984**, *80*, 1633-1641, doi:10.1039/f29848001633.
(3) Loewenstein, L. M.; Anderson, J. G. Rate and product measurements for the reactions of OH with I_2 and ICl at 298 K: Separation of gas-phase and surface reaction components. *J. Phys. Chem.* **1985**, *89*, 5371-5379, doi:10.1021/j100271a012.

H6. OH + HI. There are six studies of this reaction at room temperature performed using discharge-flow[3,4,7] and pulse photolysis[1,5,6] techniques with OH detection by using resonance fluorescence,[1,5] electron spin resonance,[3,4,7] and resonance absorption.[6] Authors of the latter studies[1,3-5] were aware of problems with handling the HI reactant. HI is unstable, tends to stick to the surfaces, and can decompose yielding molecular iodine, I_2, which reacts with OH ca. 7 times faster than HI itself.

Campuzano-Jost and Crowley[1] (246–353 K) used very dilute HI mixtures prepared in glass storage bulbs (0.013–0.025%). Such a small absolute amount of HI in the storage bulb (<0.25 Torr) raises a concern because I_2, if formed anywhere in the system, would partition into the gas phase. The HI containing flow in the Campuzano-Jost and Crowley study was passed through a cold trap (-110 ºC) before mixing with the main flow containing the OH precursor to remove possible traces of I_2. Campuzano-Jost and Crowley reported various problems in choosing the appropriate precursor for pulse photolytic production of OH. They found that HI forms complexes with OH precursors resulting in both large scattering of radiation and interfering secondary chemistry. The photolysis of H_2O_2 was found to be the most suitable source of OH and used in the measurements that yielded a rate constant that is about twice the currently recommended value. No other study of this reaction with H_2O_2 in the reactor has been reported.

Substantially less dilute mixtures of HI were used in other studies thus preventing formation of I_2 concentrations in gas phase comparable with the concentration of HI in the storage and delivery system. It can also be expected that the results of such experiments will be less affected by the possible loss of HI due to its adsorption on the walls before entering the reactor. Khamaganov et al.[3] (298–370 K) used pure undiluted HI thus eliminating the uncertainty in the HI content in the storage bulb and the transmitting line to the mixing point in front of the flow reactor. Measurements were performed immediately after a freeze-pump-thaw-boil purification cycle, which eliminated long-term preparation and storage of the mixture. Also, the decomposition of pure HI could not lead to a comparable concentration of I_2 in the gas phase, which could affect the results, since the saturated vapor pressure of I_2 is less than 0.3 Torr, while the pressure of pure HI was several hundred Torr, i.e., always $[I_2] << [HI]$ in the storage bulb and the main part of the reactant delivery line. HI was diluted with the carrier gas shortly before entering the flow reactor. Note that the contact time of all chemical components (HI and OH precursors) after their mixing before entering the reactor is much shorter in the discharge flow experiments than in the pulse photolysis experiments. This makes it less likely that any unwanted chemistry will occur that will influence the observed OH decay rates in the reactor. Specific test experiments performed by Khamaganov et al. demonstrated the homogeneous nature of the reaction with no wall effect on the measured rate constant.

Lancar et al.[4] (298 K) and MacLeod et al.[5] (298 K) used dilute mixtures of HI prepared in the storage bulbs. Their experiments, however, did not require as large a dilution as used by Campuzano-Jost and Crowley. Therefore, the potential impact of I_2 formation was minimized by its low vapor pressure similar to the experiments of Khamaganov et al. Note that MacLeod et al. used the photolysis of HNO_3 as the OH source, whereas Campuzano-Jost and Crowley found this to be problematic.

Rate coefficients reported in the earlier studies by Takacs and Glass[7] (295 K) and Smith and Zellner[6] (298 K) are less than the recommended value by a factor of two and three, respectively. The results reported by

these research groups exhibit a similar discrepancy from the recommended value for the better-established rate constant of the similar fast reaction between OH and HBr studied under the same conditions. However, they are in much better agreement with the recommended value for the substantially slower reaction between OH and HCl. The experimental conditions employed by Takacs and Glass were not favorable for quantitative discharge-flow experiments mainly due to very large [OH] decay rates; they also neglected the effect of OH diffusion. Smith and Zellner considered their results to be preliminary.

Recognizing that difficulties in handling HI gas in the storage and delivery system, rather than the measurement of OH decays, are the major source of error in the latter studies, the recommended k(298 K) is the average of the values obtained in three absolute rate coefficient studies by Lancar et al., MacLeod et al., and Khamaganov et al., which are in good agreement, within ca. 10% of the recommended value. These studies used three different experimental setups with different HI delivery systems. The experimental setups used by Lancar et al. and Khamaganov et al. were also employed to study a similarly fast reaction between OH and HBr resulting in good agreement with the recommended value of the rate coefficient.[2,3] However, there is no obvious explanation of the large discrepancy between results from these studies and those from the detailed study of Campuzano-Jost and Crowley, who used very diluted HI mixtures. Therefore, an asymmetrical uncertainty f(298 K) factor is recommended that encompasses the Campuzano-Jost and Crowley data.

The recommended E/R describes the weak negative temperature dependences observed by Khamaganov et al. at two temperatures, 298 and 370 K, and Campuzano-Jost and Crowley above 280 K, where their data exhibit less scatter.

(Table: 25-1, Note: 25-1, Evaluated: 25-1) Back to Table

(1) Campuzano-Jost, P.; Crowley, J. N. Kinetics of the reaction of OH with HI between 246 and 353 K. *J. Phys. Chem. A* **1999**, *103*, 2712 – 2719, doi:10.1021/jp984321x.

(2) Jourdain, J. L.; Le Bras, G.; Combourieu, J. EPR determination of absolute rate constants for the reactions of H and OH radicals with hydrogen bromide. *Chem. Phys. Lett.* **1981**, *78*, 483-487, doi:10.1016/0009-2614(81)85242-6.

(3) Khamaganov, V. G.; Orkin, V. L.; Larin, I. K. Study of the reactions of OH with HCl, HBr, and HI between 298 K and 460 K. *Int. J. Chem. Kinet.* **2020**, *52*, 852-860, doi:10.1002/kin.21404.

(4) Lancar, I.; Mellouki, A.; Poulet, G. Kinetics of the reactions of hydrogen iodide with hydroxyl and nitrate radicals. *Chem. Phys. Lett.* **1991**, *177*, 554-558, doi:10.1016/0009-2614(91)90083-L.

(5) MacLeod, H.; Balestra, C.; Jourdain, J. L.; Laverdet, G.; Le Bras, G. Kinetic study of the reaction OH + HI by laser photolysis-resonance fluorescence. *Int. J. Chem. Kinet.* **1990**, *22*, 1167-1176, doi:10.1002/kin.550221106.

(6) Smith, I. W. M.; Zellner, R. Rate measurements of reactions of OH by resonance absorption. Part 3. - Reactions of OH with H_2, D_2 and hydrogen and deuterium halides. *J. Chem. Soc. Faraday Trans. 2* **1974**, *70*, 1045-1056, doi:10.1039/F29747001045.

(7) Takacs, G. A.; Glass, G. P. Reactions of hydroxyl radicals with some hydrogen halides. *J. Phys. Chem.* **1973**, *77*, 1948-1951, doi:10.1021/j100635a005.

H7. OH + CH_3I. The reaction rate coefficient has been measured by Brown et al.[1] (271–423 K), Gilles et al.[3] (299 K), and Cotter et al.[2] (298 K). The k(298 K) recommendation is an average of the results from these three studies. The E/R recommendation is taken from Brown et al., the only study reporting temperature dependent data.

(Table: 25-01, Note: 25-01, Evaluated: 25-01) Back to Table

(1) Brown, A. C.; Canosa-Mas, C. E.; Wayne, R. P. A kinetic study of the reactions of OH with CH_3I and CF_3I. *Atmos. Environ.* **1990**, *24A*, 361-367, doi:10.1016/0960-1686(90)90115-4.

(2) Cotter, E. S. N.; Booth, N. J.; Canosa-Mas, C. E.; Gray, D. J.; Shallcross, D. E.; Wayne, R. P. Reactions of Cl atoms with CH_3I, C_2H_5I, 1-C_3H_7I, 2-C_3H_7I and CF_3I: kinetics and atmospheric relevance. *Phys. Chem. Chem. Phys.* **2001**, *3*, 402-408, doi:10.1039/B007608M.

(3) Gilles, M. K.; Turnipseed, A. A.; Talukdar, R. K.; Rudich, Y.; Villalta, P. W.; Huey, L. G.; Burkholder, J. B.; Ravishankara, A. R. Reactions of O(^{3}P) with alkyl iodides: Rate coefficients and reaction products. *J. Phys. Chem.* **1996**, *100*, 14005-14015, doi:10.1021/jp960688v.

H8. **OH + CF_3I.** The recommended rate expression is derived from a fit to the data of Gilles et al.[4] (272–370 K). The results from the studies by Garraway and Donovan[3] (298 K) and Berry et al.[1] (280–450 K) were not used in deriving the recommendation as the results were possibly influenced by reactant photolysis. The room temperature value from the discharge flow/resonance fluorescence study of Brown et al.[2] agrees within the 2σ limits.
(Table: 02-25, Note: 02-25, Evaluated: 02-25) Back to Table

(1) Berry, R.; Yuan, J.; Misra, A.; Marshall, P. Experimental and computational investigations of the reaction of OH with CF_3I and the enthalpy of formation of HOI. *J. Phys. Chem. A* **1998**, *102*, 5182-5188, doi:10.1021/jp980645+.
(2) Brown, A. C.; Canosa-Mas, C. E.; Wayne, R. P. A kinetic study of the reactions of OH with CH_3I and CF_3I. *Atmos. Environ.* **1990**, *24A*, 361-367, doi:10.1016/0960-1686(90)90115-4.
(3) Garraway, J.; Donovan, R. J. Gas phase reaction of OH with alkyl iodides. *J. Chem. Soc. Chem. Comm.* **1979**, 1108, doi:10.1039/C3979001108A.
(4) Gilles, M. K.; Talukdar, R. K.; Ravishankara, A. R. Rate coefficients for the OH + CF_3I reaction between 271 and 370 K. *J. Phys. Chem. A* **2000**, *104*, 8945-8950, doi:10.1021/jp001827i.

H9. **HO_2 + I.** Based on the data of Jenkin et al.[1] (283–353 K), the only reported study of this reaction.
(Table: 25-1, Note: 94-26, Evaluated: 94-26) Back to Table

(1) Jenkin, M. E.; Cox, R. A.; Mellouki, A.; Le Bras, G.; Poulet, G. Kinetics of the reaction of iodine atoms with HO_2 radicals. *J. Phys. Chem.* **1990**, *94*, 2927-2934, doi:10.1021/j100370a036.

H10. **HO_2 + IO.** The recommended k(298 K) is the average of values obtained from the Arrhenius expressions reported by Cronkhite et al.[2] (274–373 K) and Knight and Crowley[5] (273–353 K). The recommended room temperature uncertainty limits encompass the results of Maguin et al.[6] (298 K) and Canosa-Mas et al.[1] (296 K) and overlap with the uncertainty interval reported by Jenkin et al.[4] (298 K). The recommended E/R is obtained from a weighted fit ($1/k^2$ weighting factors) of the combined data of Cronkhite et al. and Knight and Crowley (one average rate constant per temperature studied) to the Arrhenius equation after scaling each individual set of rate constants by a constant factor so that the Arrhenius expressions describing the individual data sets each give the recommended k(298 K). In low pressure (~1 Torr He) flow tube studies, both Knight and Crowley and Maguin et al. observe HOI as a reaction product, but a quantitative HOI yield has not been reported. Computational results by Drougas and Kosmas[3] confirm the existence of energetically favorable pathways to HOI + $O_2(^1\Delta)$ products via both HOOIO and HOOOI intermediates. Drougas and Kosmas also predict that HOOIO can isomerize to the very stable $HOIO_2$ species (bound by ~220 kJ mol^{-1} relative to IO + HO_2). The predicted transition states for HOOIO isomerization and dissociation are approximately equal in energy to each other and to the HO_2 + IO reactants.
(Table: 25-1, Note: 15-10, Evaluated: 15-10) Back to Table

(1) Canosa-Mas, C.; Flugge, M. L.; Shah, D.; Vipond, A.; Wayne, R. P. Kinetics of the reactions of IO with HO_2 and $O(^3P)$. *J. Atmos. Chem.* **1999**, *34*, 153-162, doi:10.1023/a:1006262306459.
(2) Cronkhite, J. M.; Stickel, R. E.; Nicovich, J. M.; Wine, P. H. Laser flash photolysis studies of radical-radical reaction kinetics: The HO_2 + IO reaction. *J. Phys. Chem. A* **1999**, *103*, 3228-3236, doi:10.1021/jp990135v.
(3) Drougas, E.; Kosmas, A. M. Computational studies of (HIO_3) isomers and the HO_2 + IO reaction pathways. *J. Phys. Chem. A* **2005**, *109*, 3887-3892, doi:10.1021/jp044197j.
(4) Jenkin, M. E.; Cox, R. A.; Hayman, G. D. Kinetics of the reaction of IO radicals with HO_2 radicals at 298 K. *Chem. Phys. Lett.* **1991**, *177*, 272-278, doi:10.1016/0009-2614(91)85029-v.
(5) Knight, G. P.; Crowley, J. N. The reactions of IO with HO_2, NO and CH_3SCH_3: Flow tube studies of kinetics and product formation. *Phys. Chem. Chem. Phys.* **2001**, *3*, 393-401, doi:10.1039/b008447f.
(6) Maguin, F.; Laverdet, G.; Le Bras, G.; Poulet, G. Kinetic study of the reactions IO + HO_2 and IO + NO_2 at 298 K. *J. Phys. Chem.* **1992**, *96*, 1775-1780, doi:10.1021/j100183a052.

H11. **NO_3 + HI.** No recommendation is given, based on the potential for severe complications resulting from secondary chemistry in the only reported study of the reaction (Lancar et al.[1] (298 K)).
(Table: 94-26, Note: 94-26, Evaluated: 94-26) Back to Table

(1) Lancar, I.; Mellouki, A.; Poulet, G. Kinetics of the reactions of hydrogen iodide with hydroxyl and nitrate radicals. *Chem. Phys. Lett.* **1991**, *177*, 554-558, doi:10.1016/0009-2614(91)90083-L.

H12. Cl + CH_3I. This reaction, thought to be a simple H abstraction reaction, has been shown by Ayhens et al.[1] (218–694 K) to be quite complex. At low temperatures, Cl atom reversibly adds to CH_3I to form CH_3ICl. Thus, there are at least two channels for this reaction,

$$Cl + CH_3I \rightarrow CH_2I + HCl \quad (a)$$

$$Cl + CH_3I \leftrightarrow CH_3ICl \quad (b)$$

The rate coefficient for channel (a) has been measured by Ayhens et al. above 364 K, Kambanis et al.[5] (273–363 K), Bilde and Wallington[2] (298 K), and Cotter et al.[3] (298 K). The recommendation is based on these studies.

Under atmospheric conditions reaction (b) to form the adduct is about two orders of magnitude faster than reaction (a). However, the fate of the CH_3ICl adduct in the atmosphere is unclear. Its lifetime, based on the studies of Ayhens et al., can be as long as a few seconds at 200 K and a few hundred Torr pressure. Therefore, it is possible that it could react with O_2 or be photolyzed. At 298 K, in one atmosphere of O_2, it appears that the overall fate of the CH_3ClI is to decompose back to the reactants, based on the work of Bilde and Wallington. Therefore, if O_2 were to react with CH_3ICl, this rate coefficient has to be less than about 10^{-17} cm^3 $molecule^{-1}$ s^{-1}, using the rate coefficient for its decomposition measured by Ayhens et al. If the rate coefficient for $CH_3ICl + O_2$ were to remain approximately the same, i.e., 10^{-17} cm^3 $molecule^{-1}$ s^{-1}, at lower temperatures, the possible loss of CH_3ICl via reaction with O_2 cannot be ignored. Further, the possible atmospheric photolysis of CH_3ICl may be important if it has a J-value greater than 0.1 s^{-1}.

There is a third possible product channel for this reaction to yield CH_3Cl + I (Goliff and Rowland[4] (295 K)). Based on the results of Bilde and Wallington and Goliff and Rowland, we recommend that the rate coefficient for the $Cl + CH_3I \rightarrow CH_3Cl + I$ reaction to be less than $0.2k_a$ at 298 K. Since such a reaction is likely to have a significant barrier in the gas phase, even though it is exothermic by ~14 kcal mol^{-1} at 298 K, the branching ratio for the production of CH_3Cl and I in the atmosphere will be likely less than that at 298 K.
(Table: 02-25, Note: 25-1, Evaluated: 02-25) Back to Table

(1) Ayhens, Y. V.; Nicovich, J. M.; McKee, M. L.; Wine, P. H. Kinetic and mechanistic study of the reaction of atomic chlorine with methyl iodide over the temperature range 218-694 K. *J. Phys. Chem. A* **1997**, *101*, 9382-9390, doi:10.1021/jp9727097.

(2) Bilde, M.; Wallington, T. J. Atmospheric chemistry of CH_3I: Reaction with atomic chlorine at 1-700 Torr total pressure and 295 K. *J. Phys. Chem.* **1998**, *102*, 1550-1555, doi:10.1021/jp973303x.

(3) Cotter, E. S. N.; Booth, N. J.; Canosa-Mas, C. E.; Gray, D. J.; Shallcross, D. E.; Wayne, R. P. Reactions of Cl atoms with CH_3I, C_2H_5I, 1-C_3H_7I, 2-C_3H_7I and CF_3I: kinetics and atmospheric relevance. *Phys. Chem. Chem. Phys.* **2001**, *3*, 402-408, doi:10.1039/B007608M.

(4) Goliff, W. S.; Rowland, F. S. Methyl chloride formation by gas phase thermal chlorine atom reaction with methyl iodide and methyl bromide. *Geophys. Res. Lett.* **1997**, *23*, 3029-3032, doi:10.1029/97GL03093.

(5) Kambanis, K. G.; Lazarou, Y. G.; Papagiannakopoulos, P. Absolute reaction rate of chlorine atoms with iodomethane. *Chem. Phys. Lett.* **1997**, *268*, 498-504, doi:10.1016/S0009-2614(97)00212-1.

H13. I + O_3. The recommended k(298 K) is based on an unweighted average of the room temperature values of Jenkin et al.[3] (303 K), Sander[4] (298 K), Tucceri et al.[5] (298 K), Buben et al.[1] (231–337 K), Turnipseed et al.[6] (239–368 K), and Hölscher et al.[2] (243–295 K). The recommended E/R is obtained from the temperature-dependence studies of Buben et al., Turnipseed et al., and Hölscher et al.
(Table: 25-1, Note: 19-5, Evaluated: 19-5) Back to Table

(1) Buben, S. N.; Larin, I. K.; Messineva, N. A.; Trofimova, E. M. Study of processes with participation of atomic iodine: Determination of a constant of atomic iodine reaction rate with ozone in 231-337 K temperature range. *Khim. Fiz.* **1990**, *9*, 116-126.

(2) Hölscher, D.; Fockenberg, C.; Zellner, R. LIF detection of the IO-radical and kinetics of the reactions $I+O_3 \rightarrow IO+O_2$, $O(^3P)+I_2 \rightarrow IO+I$, $O(^3P)+CH_3I \rightarrow IO+CH_3$ and $O(^3P)+CF_3I \rightarrow IO+CF_3$ in the temperature range 230 to 310 K. *Ber. Bunsen-Ges. Phys. Chem. Chem. Phys.* **1998**, *102*, 716-722, doi:10.1002/bbpc.19981020503.

(3) Jenkin, M. E.; Cox, R. A. Kinetics study of the reactions $IO + NO_2 + M \rightarrow IONO_2 + M$, $IO + IO \rightarrow$ products, and $I + O_3 \rightarrow IO + O_2$. *J. Phys. Chem.* **1985**, *89*, 192-199, doi:10.1021/j100247a040.

(4) Sander, S. P. Kinetics and mechanism of the IO + IO reaction. *J. Phys. Chem.* **1986**, *90*, 2194-2199, doi:10.1021/j100401a039.

(5) Tucceri, M. E.; Dillon, T. J.; Crowley, J. N. A laser photolysis-resonance fluorescence study of the reactions: $I + O_3 \rightarrow IO + O_2$, $O + I_2 \rightarrow IO + I$, and $I + NO_2 + M \rightarrow INO_2 + M$ at 298 K. *Phys. Chem. Chem. Phys.* **2005**, *7*, 1657-1663, doi:10.1039/b502844b.

(6) Turnipseed, A. A.; Gilles, M. K.; Burkholder, J. B.; Ravishankara, A. R. LIF detection of IO and the rate coefficients for I + O_3 and IO + NO reactions. *Chem. Phys. Lett.* **1995**, *242*, 427-434, doi:10.1016/0009-2614(95)00774-X.

H14. I + BrO. Based on results of Laszlo et al.[1] (298 K), the only reported study of this rate constant. This value was derived from modeling the simultaneous decay of BrO and IO in a $Br_2/I_2/N_2O$ system.
(Table: 97-4, Note: 97-4, Evaluated: 97-4) Back to Table

(1) Laszlo, B.; Huie, R. E.; Kurylo, M. J.; Miziolek, A. W. Kinetic studies of the reactions of BrO and IO radicals. *J. Geophys. Res.* **1997**, *102*, 1523-1532, doi:10.1029/96JD00458.

H15. IO + CH_3O_2. There have been three room temperature studies (Bale et al.[1] (295 K), Dillon et al.[2] (298 K), and Dillon et al.[3] (296 K)) and one temperature dependence study (Enami et al.[4] (213–298 K)). This reaction is exceptionally difficult to study due to the almost unavoidable interference from secondary reactions. The results fall into two groups: Bale et al. and Enami et al. obtain relatively large rate constants at room temperature ($(6.0 \pm 1.3) \times 10^{-11}$ and $(7.0 \pm 3.0) \times 10^{-11}$ cm^3 $molecule^{-1}$ s^{-1}, respectively, while the two studies by Dillon et al. obtained much smaller rate constants ($(2 \pm 1) \times 10^{-12}$and $(3.4 \pm 1.4) \times 10^{-12}$ cm^3 $molecule^{-1}$ s^{-1}, respectively. Although Dillon et al.[3] make a compelling case for the rate constant being smaller than 1×10^{-11} cm^3 $molecule^{-1}$ s^{-1}, because of the difficulties caused by known and unknown secondary reactions, and the large disparity between the results of the two sets of studies, a recommendation is not be provided.
(Table: 19-5, Note: 19-5, Evaluated: 19-5) Back to Table

(1) Bale, C. S. E.; Canosa-Mas, C. E.; Shallcross, D. E.; Wayne, R. P. A discharge-flow study of the kinetics of the reactions of IO with CH_3O_2 and CF_3O_2. *Phys. Chem. Chem. Phys.* **2005**, *7*, 2164-2172, doi:10.1039/b501903f.
(2) Dillon, T. J.; Tucceri, M. E.; Crowley, J. N. Laser induced fluorescence studies of iodine oxide chemistry Part II. The reactions of IO with CH_3O_2, CF_3O_2 and O_3. *Phys. Chem. Chem. Phys.* **2006**, *8*, 5185-5198, doi:10.1039/b611116e.
(3) Dillon, T. J.; Tucceri, M. E.; Crowley, J. N. Rate coefficients for the reaction of iodine oxide with methyl peroxy radicals. *Chemphyschem* **2010**, *11*, 4011-4018, doi:10.1002/cphc.201000466.
(4) Enami, S.; Yamanaka, T.; Hashimoto, S.; Kawasaki, M.; Nakano, Y.; Ishiwata, T. Kinetic study of IO radical with RO_2 (R = CH_3, C_2H_5, and CF_3) using cavity ring-down spectroscopy. *J. Phys. Chem. A* **2006**, *110*, 9861-9866, doi:10.1021/jp0619336.

H16. IO + NO. The recommendation is based on the 298 K data of Ray and Watson,[7] Dillon et al.,[3] and Atkinson et al.,[1] and the temperature-dependence data of Hölscher et al.[4] (233–346 K), Knight et al.[6] (273–353 K), Turnipseed et al.[8] (237–346 K), and Daykin and Wine[2] (242–359 K). The result of Inoue et al.[5] (298 K) was excluded because it is several standard deviations above the other studies.
(Table: 19-5, Note: 19-5, Evaluated: 19-5) Back to Table

(1) Atkinson, D. B.; Hudgens, J. W.; Orr-Ewing, A. J. Kinetic studies of the reactions of IO radicals determined by cavity ring-down spectroscopy. *J. Phys. Chem. A* **1999**, *103*, 6173-6180, doi:10.1021/jp9902497.
(2) Daykin, E. P.; Wine, P. H. Kinetics of the reactions of IO Radicals with NO and NO_2. *J. Phys. Chem.* **1990**, *94*, 4528-4535, doi:10.1021/j100374a034.
(3) Dillon, T. J.; Heard, D. E. A laser-induced fluorescence study of the $O(^3P)$ + CF_3I and IO + NO reactions - Evidence for an association channel for O + CF_3I at low temperatures. *J. Photochem. Photobiol. A-Chem.* **2003**, *157*, 223-230, doi:10.1016/s1010-6030(03)00056-x.
(4) Hölscher, D.; Zellner, R. LIF study of the reactions of the IO radical with NO and NO_2 over an extended range of temperature and pressure. *Phys. Chem. Chem. Phys.* **2002**, *4*, 1839-1845, doi:10.1039/b110084j.
(5) Inoue, G.; Suzuki, M.; Washida, N. Laser induced fluorescence of IO radicals and rate constant for the reaction of IO + NO. *J. Chem. Phys.* **1983**, *79*, 4730-4735, doi:10.1063/1.445615.
(6) Knight, G. P.; Crowley, J. N. The reactions of IO with HO_2, NO and CH_3SCH_3: Flow tube studies of kinetics and product formation. *Phys. Chem. Chem. Phys.* **2001**, *3*, 393-401, doi:10.1039/b008447f.
(7) Ray, G. W.; Watson, R. T. Kinetics study of the reactions of NO with FO, ClO, BrO, and IO at 298 K. *J. Phys. Chem.* **1981**, *85*, 2955-2960, doi:10.1021/j150620a022.
(8) Turnipseed, A. A.; Gilles, M. K.; Burkholder, J. B.; Ravishankara, A. R. LIF detection of IO and the rate coefficients for I + O_3 and IO + NO reactions. *Chem. Phys. Lett.* **1995**, *242*, 427-434, doi:10.1016/0009-2614(95)00774-X.

H17. IO + ClO. Based on results of Turnipseed et al.[2] (200–362 K) and Bedjanian et al.[1] (298 K). Both studies carried out branching ratio measurements. Bedjanian et al. obtained channel-specific branching ratios at 298 K of (0.545 ± 0.026), (0.25 ± 0.018), and (0.195 ± 0.016) for the I + OClO, I + Cl + O_2, and ICl + O_2 channels, respectively. Turnipseed et al. measured the yield of the non-I atom producing channels to be 0.14 ± 0.04 at 298 K, which is consistent with the results of Bedjanian et al. To obtain the recommendations, the 298 K branching ratios from Bedjanian et al. are applied to the rate expression for the overall reaction, which is obtained by averaging the 298 K values from the two studies and adopting the *E*/R from Turnipseed et al. This rate expression is given by $k(T) = 4.82 \times 10^{-12} \exp(-280/T)$.
(Table: 19-5, Note: 19-5, Evaluated: 19-5) Back to Table

(1) Bedjanian, Y.; LeBras, G.; Poulet, G. Kinetics and mechanism of the IO + ClO reaction. *J. Phys. Chem. A* **1997**, *101*, 4088-4096, doi:10.1021/jp963947p.
(2) Turnipseed, A. A.; Gilles, M. K.; Burkholder, J. B.; Ravishankara, A. R. Kinetics of the IO radical. 1. Reaction of IO with ClO. *J. Phys. Chem. A* **1997**, *101*, 5517-5525, doi:10.1021/jp970914g.

H18. IO + BrO. There are four studies of this reaction from Gilles et al.[2] (204–388 K), Laszlo et al.[3] (298 K), Bedjanian et al.[1] (298 K), and Rowley et al.[4] (210–333 K). Gilles et al. measured the temperature dependence of the rate constant for the non-I atom product channels from 204–388 K. Laszlo et al. measured the 298 K rate constant for the overall reaction with no branching ratio information. Bedjanian et al. measured the 298 K rate constant for the overall reaction and found that the Br + OIO branching ratio is larger than 0.65. Upper limits for branching ratios were obtained for the other channels. Rowley et al. measured the temperature dependence of the overall reaction over the range 210–333 K, also finding that the Br + OIO branching ratio is larger than 0.65. To obtain the recommendations for the four channels, *E*/R was adopted from the Rowley et al. study, and *k*(298 K) for the overall reaction from the average of the Rowley et al., Bedjanian et al. and Laszlo et al. studies. The *k*(298 K) results of Gilles et al. was not considered because their technique was insensitive to the channels producing I atoms. The branching ratio ranges and upper-limits from Bedjanian et al. and Rowley et al. were used to derive channel-specific rate constant expressions assuming that the same *E*/R applies to each channel. This may be a poor assumption based on the much lower *E*/R (–260 K) obtained by Gilles et al. for the non-I atom channels than the *E*/R obtained by Rowley et al. (–760 K) for the overall reaction. However, until more precise channel-specific data can be obtained, this assumption has been adopted.
(Table: 19-5, Note: 19-5, Evaluated: 19-5) Back to Table

(1) Bedjanian, Y.; Le Bras, G.; Poulet, G. Kinetics and mechanism of the IO + BrO reaction. *J. Phys. Chem. A* **1998**, *102*, 10501-10511, doi:10.1021/jp982972n.
(2) Gilles, M. K.; Turnipseed, A. A.; Burkholder, J. B.; Ravishankara, A. R. Kinetics of the IO radical. 2. Reaction of IO with BrO. *J. Phys. Chem. A* **1997**, *101*, 5526-5534, doi:10.1021/jp9709159.
(3) Laszlo, B.; Huie, R. E.; Kurylo, M. J.; Miziolek, A. W. Kinetic studies of the reactions of BrO and IO radicals. *J. Geophys. Res.* **1997**, *102*, 1523-1532, doi:10.1029/96JD00458.
(4) Rowley, D. M.; Bloss, W. J.; Cox, R. A.; Jones, R. L. Kinetics and products of the IO + BrO reaction. *J. Phys. Chem. A* **2001**, *105*, 7855-7864, doi:10.1021/jp004494y.

H19. IO + IO. Sander[3] (250–373 K) reported a negative temperature dependence over the temperature range 250–373 K for the overall rate constant and for the absorption cross section at 427.2 nm. Harwood et al.[1] (253–320 K) reported that the overall rate constant and the absorption cross section to be independent of temperature from 253 to 320 K. The recommended room temperature value is the average of the values reported by Sander, Harwood et al., and Laszlo et al.[2] (298 K). The recommended temperature dependence is the average of the values reported by Sander and by Harwood et al., with an uncertainty sufficient to encompass the two reported values. The *A*-factor has been fitted to the recommended room temperature rate constant and the recommended temperature dependence. The overall rate constant for the decay of IO in the absence of ozone has been found to be independent of pressure by Sander, Laszlo et al., and Harwood et al. A comparison of the overall rate observed in excess ozone to that in the absence of ozone was interpreted by Sander and by Harwood et al. to imply that formation of the dimer I_2O_2 is the dominant reaction channel in the IO self-reaction.
(Table: 25-1, Note: 15-10, Evaluated: 97-4) Back to Table

(1) Harwood, M. H.; Burkholder, J. B.; Hunter, M.; Fox, R. W.; Ravishankara, A. R. Absorption cross sections and self-reaction kinetics of the IO radical. *J. Phys. Chem. A* **1997**, *101*, 853-863, doi:10.1021/jp962429b.
(2) Laszlo, B.; Kurylo, M. J.; Huie, R. E. Absorption cross sections, kinetics of formation, and self-reaction of the IO radical produced via the laser photolysis of $N_2O/I_2/N_2$ Mixtures. *J. Phys. Chem.* **1995**, *99*, 11701-11707, doi:10.1021/j100030a013.

(3) Sander, S. P. Kinetics and mechanism of the IO + IO reaction. *J. Phys. Chem.* **1986**, *90*, 2194-2199, doi:10.1021/j100401a039.

H20. INO + INO. Based on the data of Van den Bergh and Troe[1] (320–450 K).
(Table: 94-26, Note: 94-26, Evaluated: 94-26) Back to Table

(1) van den Bergh, H.; Troe, J. Kinetic and thermodynamic properties of INO and INO_2 intermediate complexes in iodine recombination. *J. Chem. Phys.* **1976**, *64*, 736-742, doi:10.1063/1.432220.

H21. INO_2 + INO_2. Based on the data of van den Bergh and Troe[1] (320–450 K).
(Table: 94-26, Note: 94-26, Evaluated: 94-26) Back to Table

(1) van den Bergh, H.; Troe, J. Kinetic and thermodynamic properties of INO and INO_2 intermediate complexes in iodine recombination. *J. Chem. Phys.* **1976**, *64*, 736-742, doi:10.1063/1.432220.

1.13.3 Bibliography – IO_x Reactions

Addison, M. C.; Donovan, R. J.; Garraway, J. Reactions of (2^1D_2) and O(2^3P_J) with halogenomethanes. *Faraday Disc. Chem. Soc.* **1980**, *67*, 286-296, doi:10.1039/DC9796700286.

Atkinson, D. B.; Hudgens, J. W.; Orr-Ewing, A. J. Kinetic studies of the reactions of IO radicals determined by cavity ring-down spectroscopy. *J. Phys. Chem. A* **1999**, *103*, 6173-6180, doi:10.1021/jp9902497.

Ayhens, Y. V.; Nicovich, J. M.; McKee, M. L.; Wine, P. H. Kinetic and mechanistic study of the reaction of atomic chlorine with methyl iodide over the temperature range 218-694 K. *J. Phys. Chem. A* **1997**, *101*, 9382-9390, doi:10.1021/jp9727097.

Bale, C. S. E.; Canosa-Mas, C. E.; Shallcross, D. E.; Wayne, R. P. A discharge-flow study of the kinetics of the reactions of IO with CH_3O_2 and CF_3O_2. *Phys. Chem. Chem. Phys.* **2005**, *7*, 2164-2172, doi:10.1039/b501903f.

Bedjanian, Y.; Le Bras, G.; Poulet, G. Kinetics and mechanism of the IO + BrO reaction. *J. Phys. Chem. A* **1998**, *102*, 10501-10511, doi:10.1021/jp982972n.

Bedjanian, Y.; LeBras, G.; Poulet, G. Kinetics and mechanism of the IO + ClO reaction. *J. Phys. Chem. A* **1997**, *101*, 4088-4096, doi:10.1021/jp963947p.

Berry, R.; Yuan, J.; Misra, A.; Marshall, P. Experimental and computational investigations of the reaction of OH with CF_3I and the enthalpy of formation of HOI. *J. Phys. Chem. A* **1998**, *102*, 5182-5188, doi:10.1021/jp980645+.

Bilde, M.; Wallington, T. J. Atmospheric chemistry of CH_3I: Reaction with atomic chlorine at 1-700 Torr total pressure and 295 K. *J. Phys. Chem.* **1998**, *102*, 1550-1555, doi:10.1021/jp973303x.

Bloss, W. J.; Rowley, D. M.; Cox, R. A.; Jones, R. L. Kinetics and products of the IO self-reaction. *J. Phys. Chem. A* **2001**, *105*, 7840-7854, doi:10.1021/jp0044936.

Brown, A. C.; Canosa-Mas, C. E.; Wayne, R. P. A kinetic study of the reactions of OH with CH_3I and CF_3I. *Atmos. Environ.* **1990**, *24A*, 361-367, doi:10.1016/0960-1686(90)90115-4.

Buben, S. N.; Larin, I. K.; Messineva, N. A.; Trofimova, E. M. Study of processes with participation of atomic iodine: Determination of a constant of atomic iodine reaction rate with ozone in 231-337 K temperature range. *Khim. Fiz.* **1990**, *9*, 116-126.

Campuzano-Jost, P.; Crowley, J. N. Kinetics of the reaction of OH with HI between 246 and 353 K. *J. Phys. Chem. A* **1999**, *103*, 2712 – 2719, doi:10.1021/jp984321x.

Canosa-Mas, C. E.; Flugge, M. L.; Shah, D.; Vipond, A.; Wayne, R. P. Kinetics of the reactions of IO with HO_2 and O(^{3}P). *J. Atmos. Chem.* **1999**, *34*, 153-162, doi:10.1023/a:1006262306459.

Cotter, E. S. N.; Booth, N. J.; Canosa-Mas, C. E.; Gray, D. J.; Shallcross, D. E.; Wayne, R. P. Reactions of Cl atoms with CH_3I, C_2H_5I, 1-C_3H_7I, 2-C_3H_7I and CF_3I: kinetics and atmospheric relevance. *Phys. Chem. Chem. Phys.* **2001**, *3*, 402-408, doi:10.1039/B007608M.

Cronkhite, J. M.; Stickel, R. E.; Nicovich, J. M.; Wine, P. H. Laser flash photolysis studies of radical-radical reaction kinetics: The HO_2 + IO reaction. *J. Phys. Chem. A* **1999**, *103*, 3228-3236, doi:10.1021/jp990135v.

Daykin, E. P.; Wine, P. H. Kinetics of the reactions of IO Radicals with NO and NO_2. *J. Phys. Chem.* **1990**, *94*, 4528-4535, doi:10.1021/j100374a034.

Dillon, T. J.; Heard, D. E. A laser-induced fluorescence study of the O(^{3}P) + CF_3I and IO + NO reactions - Evidence for an association channel for O + CF_3I at low temperatures. *J. Photochem. Photobiol. A-Chem.* **2003**, *157*, 223-230, doi:10.1016/s1010-6030(03)00056-x.

Dillon, T. J.; Tucceri, M. E.; Crowley, J. N. Laser induced fluorescence studies of iodine oxide chemistry Part II. The reactions of IO with CH_3O_2, CF_3O_2 and O_3. *Phys. Chem. Chem. Phys.* **2006**, *8*, 5185-5198, doi:10.1039/b611116e.

Dillon, T. J.; Tucceri, M. E.; Crowley, J. N. Rate coefficients for the reaction of iodine oxide with methyl peroxy radicals. *Chemphyschem* **2010**, *11*, 4011-4018, doi:10.1002/cphc.201000466.

Drougas, E.; Kosmas, A. M. Computational studies of (HIO_3) isomers and the HO_2 + IO reaction pathways. *J. Phys. Chem. A* **2005**, *109*, 3887-3892, doi:10.1021/jp044197j.

Enami, S.; Yamanaka, T.; Hashimoto, S.; Kawasaki, M.; Nakano, Y.; Ishiwata, T. Kinetic study of IO radical with RO_2 (R = CH_3, C_2H_5, and CF_3) using cavity ring-down spectroscopy. *J. Phys. Chem. A* **2006**, *110*, 9861-9866, doi:10.1021/jp0619336.

Garraway, J.; Donovan, R. J. Gas phase reaction of OH with alkyl iodides. *J. Chem. Soc. Chem. Comm.* **1979**, 1108, doi:10.1039/C3979001108A.

Gilles, M. K.; Talukdar, R. K.; Ravishankara, A. R. Rate coefficients for the OH + CF_3I reaction between 271 and 370 K. *J. Phys. Chem. A* **2000**, *104*, 8945-8950, doi:10.1021/jp001827i.
Gilles, M. K.; Turnipseed, A. A.; Burkholder, J. B.; Ravishankara, A. R. Kinetics of the IO radical. 2. Reaction of IO with BrO. *J. Phys. Chem. A* **1997**, *101*, 5526-5534, doi:10.1021/jp9709159.
Gilles, M. K.; Turnipseed, A. A.; Talukdar, R. K.; Rudich, Y.; Villalta, P. W.; Huey, L. G.; Burkholder, J. B.; Ravishankara, A. R. Reactions of $O(^3P)$ with alkyl iodides: Rate coefficients and reaction products. *J. Phys. Chem.* **1996**, *100*, 14005-14015, doi:10.1021/jp960688v.
Goliff, W. S.; Rowland, F. S. Methyl chloride formation by gas phase thermal chlorine atom reaction with methyl iodide and methyl bromide. *Geophys. Res. Lett.* **1997**, *23*, 3029-3032, doi:10.1029/97GL03093.
Harwood, M. H.; Burkholder, J. B.; Hunter, M.; Fox, R. W.; Ravishankara, A. R. Absorption cross sections and self-reaction kinetics of the IO radical. *J. Phys. Chem. A* **1997**, *101*, 853-863, doi:10.1021/jp962429b.
Hölscher, D.; Fockenberg, C.; Zellner, R. LIF detection of the IO-radical and kinetics of the reactions $I+O_3 \rightarrow IO+O_2$, $O(^3P)+I_2 \rightarrow IO+I$, $O(^3P)+CH_3I \rightarrow IO+CH_3$ and $O(^3P)+CF_3I \rightarrow IO+CF_3$ in the temperature range 230 to 310 K. *Ber. Bunsen-Ges. Phys. Chem. Chem. Phys.* **1998**, *102*, 716-722, doi:10.1002/bbpc.19981020503.
Hölscher, D.; Zellner, R. LIF study of the reactions of the IO radical with NO and NO_2 over an extended range of temperature and pressure. *Phys. Chem. Chem. Phys.* **2002**, *4*, 1839-1845, doi:10.1039/b110084j.
Inoue, G.; Suzuki, M.; Washida, N. Laser induced fluorescence of IO radicals and rate constant for the reaction of IO + NO. *J. Chem. Phys.* **1983**, *79*, 4730-4735, doi:10.1063/1.445615.
Jenkin, M. E.; Clemitshaw, K. C.; Cox, R. A. Kinetics of the reaction of OH with I_2. *J. Chem. Soc. Faraday Trans. 2* **1984**, *80*, 1633-1641, doi:10.1039/f29848001633.
Jenkin, M. E.; Cox, R. A. Kinetics study of the reactions $IO + NO_2 + M \rightarrow IONO_2 + M$, $IO + IO \rightarrow$ products, and $I + O_3 \rightarrow IO + O_2$. *J. Phys. Chem.* **1985**, *89*, 192-199, doi:10.1021/j100247a040.
Jenkin, M. E.; Cox, R. A.; Hayman, G. D. Kinetics of the reaction of IO radicals with HO_2 radicals at 298 K. *Chem. Phys. Lett.* **1991**, *177*, 272-278, doi:10.1016/0009-2614(91)85029-v.
Jenkin, M. E.; Cox, R. A.; Mellouki, A.; Le Bras, G.; Poulet, G. Kinetics of the reaction of iodine atoms with HO_2 radicals. *J. Phys. Chem.* **1990**, *94*, 2927-2934, doi:10.1021/j100370a036.
Khamaganov, V. G.; Orkin, V. L.; Larin, I. K. Study of the reactions of OH with HCl, HBr, and HI between 298 K and 460 K. *Int. J. Chem. Kinet.* **2020**, *52*, 852-860, doi:10.1002/kin.21404.
Kambanis, K. G.; Lazarou, Y. G.; Papagiannakopoulos, P. Absolute reaction rate of chlorine atoms with iodomethane. *Chem. Phys. Lett.* **1997**, *268*, 498-504, doi:10.1016/S0009-2614(97)00212-1.
Kambanis, K. G.; Lazarou, Y. G.; Papagiannakopoulos, P. J. Absolute rate constants for the reactions of Cl atoms with CH_3Br, CH_2Br_2, and $CHBr_3$. *J. Phys. Chem.* **1997**, *101*, 8496-8502, doi:10.1021/jp9719671.
Knight, G. P.; Crowley, J. N. The reactions of IO with HO_2, NO and CH_3SCH_3: Flow tube studies of kinetics and product formation. *Phys. Chem. Chem. Phys.* **2001**, *3*, 393-401, doi:10.1039/b008447f.
Lancar, I.; Mellouki, A.; Poulet, G. Kinetics of the reactions of hydrogen iodide with hydroxyl and nitrate radicals. *Chem. Phys. Lett.* **1991**, *177*, 554-558, doi:10.1016/0009-2614(91)90083-L.
Laszlo, B.; Huie, R. E.; Kurylo, M. J.; Miziolek, A. W. Kinetic studies of the reactions of BrO and IO radicals. *J. Geophys. Res.* **1997**, *102*, 1523-1532, doi:10.1029/96JD00458.
Laszlo, B.; Kurylo, M. J.; Huie, R. E. Absorption cross sections, kinetics of formation, and self-reaction of the IO radical produced via the laser photolysis of $N_2O/I_2/N_2$ Mixtures. *J. Phys. Chem.* **1995**, *99*, 11701-11707, doi:10.1021/j100030a013.
Loewenstein, L. M.; Anderson, J. G. Rate and product measurements for the reactions of OH with I_2 and ICl at 298 K: Separation of gas-phase and surface reaction components. *J. Phys. Chem.* **1985**, *89*, 5371-5379, doi:10.1021/j100271a012.
MacLeod, H.; Balestra, C.; Jourdain, J. L.; Laverdet, G.; Le Bras, G. Kinetic study of the reaction OH + HI by laser photolysis-resonance fluorescence. *Int. J. Chem. Kinet.* **1990**, *22*, 1167-1176, doi:10.1002/kin.550221106.
Maguin, F.; Laverdet, G.; Le Bras, G.; Poulet, G. Kinetic study of the reactions $IO + HO_2$ and $IO + NO_2$ at 298 K. *J. Phys. Chem.* **1992**, *96*, 1775-1780, doi:10.1021/j100183a052.
Payne, W. A.; Thorn, R. P.; Nesbitt, F. L.; Stief, L. J. Rate constant for the reaction of $O(^3P)$ with IO at $T = 298$ K. *J. Phys. Chem. A* **1998**, *102*, 6247-6250, doi:10.1021/jp9811530.
Ray, G. W.; Watson, R. T. Kinetics study of the reactions of NO with FO, ClO, BrO, and IO at 298 K. *J. Phys. Chem.* **1981**, *85*, 2955-2960, doi:10.1021/j150620a022.
Rowley, D. M.; Bloss, W. J.; Cox, R. A.; Jones, R. L. Kinetics and products of the IO + BrO reaction. *J. Phys. Chem. A* **2001**, *105*, 7855-7864, doi:10.1021/jp004494y.

Sander, S. P. Kinetics and mechanism of the IO + IO reaction. *J. Phys. Chem.* **1986**, *90*, 2194-2199, doi:10.1021/j100401a039.
Smith, I. W. M.; Zellner, R. Rate measurements of reactions of OH by resonance absorption. Part 3. - Reactions of OH with H_2, D_2 and hydrogen and deuterium halides. *J. Chem. Soc. Faraday Trans. 2* **1974**, *70*, 1045-1056, doi:10.1039/F29747001045.
Takacs, G. A.; Glass, G. P. Reactions of hydroxyl radicals with some hydrogen halides. *J. Phys. Chem.* **1973**, *77*, 1948-1951, doi:10.1021/j100635a005.
Teruel, M. A. Low-pressure rate coefficients of the reaction of $O(^3P)$ with CF_3I and CH_3I. *J. Phys. Org. Chem.* **2008**, *21*, 1043-1047, doi:10.1002/poc.1393.
Teruel, M. A.; Dillon, T. J.; Horowitz, A.; Crowley, J. N. Reaction of $O(^3P)$ with the alkyl iodides:: CF_3I, CH_3I, CH_2I_2, C_2H_5I, 1-C_3H_7I and 2-C_3H_7I. *Phys. Chem. Chem. Phys.* **2004**, *6*, 2172-2178, doi:10.1039/b316402k.
Tucceri, M. E.; Dillon, T. J.; Crowley, J. N. A laser photolysis-resonance fluorescence study of the reactions: $I + O_3 \rightarrow IO + O_2$, $O + I_2 \rightarrow IO + I$, and $I + NO_2 + M \rightarrow INO_2 + M$ at 298 K. *Phys. Chem. Chem. Phys.* **2005**, *7*, 1657-1663, doi:10.1039/b502844b.
Turnipseed, A. A.; Gilles, M. K.; Burkholder, J. B.; Ravishankara, A. R. LIF detection of IO and the rate coefficients for $I + O_3$ and IO + NO reactions. *Chem. Phys. Lett.* **1995**, *242*, 427-434, doi:10.1016/0009-2614(95)00774-X.
Turnipseed, A. A.; Gilles, M. K.; Burkholder, J. B.; Ravishankara, A. R. Kinetics of the IO radical. 1. Reaction of IO with ClO. *J. Phys. Chem. A* **1997**, *101*, 5517-5525, doi:10.1021/jp970914g.
van den Bergh, H.; Troe, J. Kinetic and thermodynamic properties of INO and INO_2 intermediate complexes in iodine recombination. *J. Chem. Phys.* **1976**, *64*, 736-742, doi:10.1063/1.432220.
Watson, T. A.; Addison, M.; Wittig, C. Photolytic production of $O(^3P)$ in the presence of CF_3I: The formation of $IF(X^1\Sigma^+)$. *Chem. Phys.* **1983**, *78*, 57-63, doi:10.1016/0301-0104(83)87006-2.

1.14 SO_x Reactions

1.14.1 Table 1I: SO_x Reactions

Reaction	Temperature Range of Exp. Data (K) [a]	*A*-Factor	*E*/R	*k*(298 K) [b]	*f*(298 K) [c]	*g* [c]	Note
$O + SH \rightarrow SO + H$	295			1.6×10^{-10}	5.00		I 1
$O + CS \rightarrow CO + S$	150–305	2.7×10^{-10}	760	2.1×10^{-11}	1.10	250	I 2
$O + H_2S \rightarrow OH + SH$	205–502	9.2×10^{-12}	1800	2.2×10^{-14}	1.70	550	I 3
$O + OCS \rightarrow CO + SO$	239–808	2.1×10^{-11}	2200	1.3×10^{-14}	1.15	150	I 4
$O + CS_2 \rightarrow CS + SO$	218–543	3.2×10^{-11}	650	3.6×10^{-12}	1.20	150	I 5
$O + SO_2 \xrightarrow{M} SO_3$		(See Table 2-1)					
$O + CH_3SCH_3 \rightarrow CH_3SO + CH_3$	252–557	1.3×10^{-11}	–410	5.0×10^{-11}	1.10	100	I 6
$O + CH_3SSCH_3 \rightarrow CH_3SO + CH_3S$	270–571	3.9×10^{-11}	–290	1.03×10^{-10}	1.10	100	I 7
$O + CH_3S(O)CH_3 \rightarrow$ products	266–383	2.0×10^{-12}	–440	8.8×10^{-12}	1.20	200	I 8
$O_3 + H_2S \rightarrow$ products	~298			$<2.0\times10^{-20}$			I 9
$O_3 + CH_3SCH_3 \rightarrow$ products	301			$<1.5\times10^{-19}$			I10
$O_3 + SO_2 \rightarrow SO_3 + O_2$	300, 360	3.0×10^{-12}	>7000	$<2.0\times10^{-22}$			I11
$O_3 + SO_2F_2 \rightarrow$ products	294-296			$<1.0\times10^{-23}$			I12
$OH + H_2S \rightarrow SH + H_2O$	228–885	3.3×10^{-12}	–100	4.6×10^{-12}	1.10	50	I13
$OH + OCS \rightarrow$ products	255–517	7.2×10^{-14}	1070	2.0×10^{-15}	2.00	200	I14
$OH + CS_2 \rightarrow SH + OCS$	251–520			$<2.0\times10^{-15}$			I15
$OH + CS_2 \rightarrow CS_2OH \xrightarrow{O_2}$ products		(See Note)		1.2×10^{-12} at P_{air} = 1 atm	1.25		I16
$CS_2OH + O_2 \rightarrow$ products	249–348	2.8×10^{-14}	0	2.8×10^{-14}	1.20	100	I17
$OH + CH_3SH \rightarrow CH_3S + H_2O$	244–430	9.9×10^{-12}	–360	3.3×10^{-11}	1.07	75	I18
$OH + CH_3SCH_3 \rightarrow H_2O + CH_2SCH_3$	248–573	1.2×10^{-11}	280	4.7×10^{-12}	1.10	100	I19
$OH + CH_3SCH_3 \xrightarrow{M} (CH_3)_2SOH \xrightarrow{O_2}$ products		(See Note)		2.0×10^{-12} at P_{air} = 1 atm	1.20		I20
$(CH_3)_2SOH + O_2 \rightarrow$ products	222–297	8.5×10^{-13}	0	8.5×10^{-13}	1.25	0	I21
$OH + CH_3SCH_2Cl \rightarrow$ products	298			2.5×10^{-12}	2.00		I22
$OH + CH_3SSCH_3 \rightarrow$ products	249–368	6.0×10^{-11}	–400	2.3×10^{-10}	1.20	200	I23

Reaction	Temperature Range of Exp. Data (K) [a]	*A*-Factor	*E*/R	*k*(298 K) [b]	*f*(298 K) [c]	*g* [c]	Note
$OH + CH_3S(O)CH_3 \rightarrow$ products	298–401	6.1×10^{-12}	–800	8.9×10^{-11}	1.20	500	I24
$OH + CH_3S(O)OH \rightarrow$ products	298			9.0×10^{-11}	1.40		I25
$OH + CH_3SO_3H \rightarrow CH_3SO_3 + H_2O$		(See Note)					I26
$OH + CH_3SC_2H_5$ H-abstraction rxns.	242–299	8.0×10^{-12}	0	8.0×10^{-12}	1.10	50	I27
$OH + CH_3SC_2H_5 \overset{M}{\leftrightarrow} CH_3S(OH)C_2H_5 \overset{O_2}{\rightarrow}$ products	242–346	(See Note)		2.3×10^{-12} at P_{air} = 1 atm	1.30		I28
$CH_3S(OH)C_2H_5 + O_2 \rightarrow$ products	242–296	1.0×10^{-12}	0	1.0×10^{-12}	1.50	0	I29
$OH + S \rightarrow H + SO$	298			6.6×10^{-11}	3.00		I30
$OH + SO \rightarrow H + SO_2$	295–703	2.6×10^{-11}	–330	7.9×10^{-11}	1.15	150	I31
$OH + SO_2 \overset{M}{\rightarrow} HOSO_2$		(See Table 2-1)					
$OH + SO_2F_2 \rightarrow$ products	294–333			$<1.0\times10^{-16}$			I32
$HO_2 + H_2S \rightarrow$ products	298			$<3.0\times10^{-15}$			I33
$HO_2 + CH_3SH \rightarrow$ products	298			$<4.0\times10^{-15}$			I33
$HO_2 + CH_3SCH_3 \rightarrow$ products	298			$<5.0\times10^{-15}$			I33
$HO_2 + SO_2 \rightarrow$ products	295–300			$<1.0\times10^{-18}$			I34
$NO_2 + SO_2 \rightarrow$ products	298			$<2.0\times10^{-26}$			I35
$NO_3 + H_2S \rightarrow$ products	298			$<8.0\times10^{-16}$			I36
$NO_3 + OCS \rightarrow$ products	297			$<1.0\times10^{-16}$			I37
$NO_3 + CS_2 \rightarrow$ products	297–298			$<4.0\times10^{-16}$			I38
$NO_3 + CH_3SH \rightarrow$ products	254–367	$4.4\text{x}10^{-13}$	–210	8.9×10^{-13}	1.25	200	I39
$NO_3 + CH_3SCH_3 \rightarrow CH_3SCH_2 + HNO_3$	256–376	1.9×10^{-13}	–530	1.1×10^{-12}	1.10	150	I40
$NO_3 + CH_3SSCH_3 \rightarrow$ products	280–382	$5.0\text{x}10^{-13}$	–60	6.1×10^{-13}	1.25	150	I41
$NO_3 + CH_3S(O)CH_3 \rightarrow$ products	295–298			2.9×10^{-13}	1.60		I42
$NO_3 + CH_3SC_2H_5 \rightarrow$ products	298			2.5×10^{-12}	1.50		I43
$NO_3 + SO_2 \rightarrow$ products	298–303			$<7.0\times10^{-21}$			I44
$N_2O_5 + CH_3SCH_3 \rightarrow$ products	296			$<1.0\times10^{-17}$			I45
$CH_3O_2 + SO_2 \rightarrow$ products	298–423			$<5.0\times10^{-17}$			I46

Reaction	Temperature Range of Exp. Data (K) [a]	*A*-Factor	*E*/R	*k*(298 K) [b]	*f*(298 K) [c]	*g* [c]	Note
$F + CH_3SCH_3 \rightarrow$ products	298			2.4×10^{-10}	2.00		I47
$Cl + H_2S \rightarrow HCl + SH$	202–914	3.4×10^{-11}	–225	7.3×10^{-11}	1.10	50	I48
$Cl + SO_2F_2 \rightarrow$ products	296–333			$<1.5\times10^{-18}$			I49
$Cl + OCS \rightarrow$ products	298			$<1.0\times10^{-16}$			I50
$Cl + CS_2 \rightarrow$ products		(See Table 2-1)					
$CS_2Cl + O_2 \rightarrow$ products	230–298			$<2.5\times10^{-16}$			I51
$Cl + CH_3SH \rightarrow CH_3S + HCl$	193–430	1.2×10^{-10}	–150	2.0×10^{-10}	1.10	100	I52
$Cl + CH_3SCH_3 \rightarrow CH_3SCH_2 + HCl$	240–421	9.4×10^{-11}	–190	1.8×10^{-10}	+1.2/ –2.5	0	I53
$Cl + CH_3SCH_3 \rightarrow$ products (P = 1 atm)	240–356	3.5×10^{-10}	0	3.5×10^{-10}	1.20	0	
$(CH_3)_2SCl + O_2 \rightarrow$ products	298			$<4.0\times10^{-18}$			I54
$(CH_3)_2SCl + NO \rightarrow$ products	298			1.2×10^{-11}	1.25		I54
$(CH_3)_2SCl + NO_2 \rightarrow$ products	298			2.7×10^{-11}	1.25		I54
$Cl + CH_3S(O)CH_3 \rightarrow CH_3S(O)CH_2 + HCl$	270–571	1.4×10^{-11}	0	1.4×10^{-11}	1.20	150	I55
$Cl + CH_3S(O)CH_3 \xrightarrow{M} CH_3(Cl)S(O)CH_3$		(See Note)					I55
$CH_3(Cl)S(O)CH_3 + O_2 \rightarrow$ products	296			$<3.0\times10^{-18}$			I56
$CH_3(Cl)S(O)CH_3 + NO \rightarrow$ products	296			1.2×10^{-11}	1.50		I56
$CH_3(Cl)S(O)CH_3 + NO_2 \rightarrow$ products	296			2.1×10^{-11}	1.50		I56
$Cl + CH_3SC_2H_5 \rightarrow$ products (P = 1 atm)	298			3.8×10^{-10}	1.20		I57
$Cl_2 + CH_3SCH_3 \rightarrow$ products	294–298			$<5.0\times10^{-14}$			I58
$ClO + OCS \rightarrow$ products	298			$<2.0\times10^{-16}$			I59
$ClO + CH_3SCH_3 \rightarrow$ products	259–335	2.1×10^{-15}	–340	6.6×10^{-15}	1.50	300	I60
$ClO + CH_3S(O)CH_3 \rightarrow$ products	298			$<2.0\times10^{-14}$			I61
$ClO + SO \rightarrow Cl + SO_2$	248–363	2.8×10^{-11}	0	2.8×10^{-11}	1.30	50	I62
$ClO + SO_2 \rightarrow Cl + SO_3$	298			$<4.0\times10^{-18}$			I59
$Br + H_2S \rightarrow HBr + SH$	319–431	1.4×10^{-11}	2750	1.4×10^{-15}	2.00	300	I63
$Br + CH_3SH \rightarrow CH_3S + HBr$	273–431	9.2×10^{-12}	390	2.5×10^{-12}	2.00	100	I63
$Br + CH_3SCH_3 \rightarrow CH_3SCH_2 + HBr$	386–604	9.0×10^{-11}	2390	3.0×10^{-14}	1.40	150	I64

Reaction	Temperature Range of Exp. Data (K) [a]	*A*-Factor	*E*/R	*k*(298 K) [b]	*f*(298 K) [c]	*g* [c]	Note
$Br + CH_3SCH_3 \xrightarrow{M} (CH_3)_2SBr$		(See Table 2-1)					
$Br + CH_3S(O)CH_3 \rightarrow$ products	298			1.2×10^{-14}	1.50		I65
$BrO + CH_3SH \rightarrow$ products		(See Note)					I66
$BrO + CH_3SCH_3 \rightarrow$ products	233–333	1.4×10^{-14}	–950	3.4×10^{-13}	1.25	200	I67
$BrO + CH_3SSCH_3 \rightarrow$ products	296			1.5×10^{-14}	2.00		I68
$BrO + CH_3S(O)CH_3 \rightarrow$ products	296–298			1.0×10^{-14}	2.00		I69
$BrO + SO \rightarrow Br + SO_2$	298			5.7×10^{-11}	1.40		I70
$IO + CH_3SH \rightarrow$ products	298			6.6×10^{-16}	2.00		I71
$IO + CH_3SCH_3 \rightarrow$ products	256–468	2.5×10^{-12}	1500	1.6×10^{-14}	1.50	400	I72
$S + O_2 \rightarrow SO + O$	252–878	1.6×10^{-12}	–100	2.2×10^{-12}	1.20	100	I73
$S + O_3 \rightarrow SO + O_2$	298			1.2×10^{-11}	2.00		I74
$SO + O_2 \rightarrow SO_2 + O$	230–585	1.6×10^{-13}	2280	7.6×10^{-17}	1.20	200	I75
$SO + O_3 \rightarrow SO_2 + O_2$	230–420	3.4×10^{-12}	1100	8.4×10^{-14}	1.10	150	I76
$SO + NO_2 \rightarrow SO_2 + NO$	210–363	1.4×10^{-11}	0	1.4×10^{-11}	1.20	50	I77
$SO + OClO \rightarrow SO_2 + ClO$	298			1.9×10^{-12}	3.00		I78
$SO_3 + 2\ H_2O \rightarrow$ products		(See Note)			1.20	200	I79
$SO_3 + NH_3 \rightarrow$ products		(See Table 2-1)					
$SO_3 + NO_2 \rightarrow$ products	298			1.0×10^{-19}	10.0		I80
$SH + O_2 \rightarrow OH + SO$	295–298			$<4.0\times10^{-19}$			I81
$SH + O_3 \rightarrow HSO + O_2$	296–431	9.0×10^{-12}	280	3.5×10^{-12}	1.20	200	I82
$SH + H_2O_2 \rightarrow$ products	298			$<5.0\times10^{-15}$			I83
$SH + NO \xrightarrow{M} HSNO$		(See Table 2-1)					
$SH + NO_2 \rightarrow HSO + NO$	221–415	2.9×10^{-11}	–250	6.7×10^{-11}	1.10	50	I84
$SH + N_2O \rightarrow HSO + N_2$	298			$<5.0\times10^{-16}$			I85
$SH + Cl_2 \rightarrow ClSH + Cl$	273–373	2.1×10^{-11}	800	1.4×10^{-12}	1.15	150	I86
$SH + BrCl \rightarrow$ products	298–373	1.9×10^{-11}	–290	5.0×10^{-11}	2.00	150	I87
$SH + Br_2 \rightarrow BrSH + Br$	273–373	5.7×10^{-11}	–160	9.7×10^{-11}	1.50	150	I87

Reaction	Temperature Range of Exp. Data (K) [a]	*A*-Factor	*E*/R	*k*(298 K) [b]	*f*(298 K) [c]	*g* [c]	Note
$SH + F_2 \rightarrow FSH + F$	298–373	5.3×10^{-11}	1440	4.2×10^{-13}	1.50	200	I87
$HSO + O_2 \rightarrow$ products	296			$<2.0\times10^{-17}$			I88
$HSO + O_3 \rightarrow$ products	273–423			1.0×10^{-13}	1.30		I89
$HSO + NO \rightarrow$ products	293–298			$<1.0\times10^{-15}$			I90
$HSO + NO_2 \rightarrow HSO_2 + NO$	293–298			9.6×10^{-12}	2.00		I90
$HSO_2 + O_2 \rightarrow HO_2 + SO_2$	296			3.0×10^{-13}	3.00		I91
$HOSO_2 + O_2 \rightarrow HO_2 + SO_3$	297–423	1.3×10^{-12}	330	4.3×10^{-13}	1.15	200	I92
$CS + O_2 \rightarrow OCS + O$	293–495			2.9×10^{-19}	2.00		I93
$CS + O_3 \rightarrow OCS + O_2$	298			3.0×10^{-16}	3.00		I94
$CS + NO_2 \rightarrow OCS + NO$	298			7.6×10^{-17}	3.00		I94
$CH_3S + O_2 \rightarrow$ products	298			$<3.0\times10^{-18}$			I95
$CH_3S + O_3 \rightarrow$ products	259–381	1.5×10^{-12}	–360	5.0×10^{-12}	1.15	100	I96
$CH_3S + NO \rightarrow$ products	295–503			$<1.0\times10^{-13}$			I97
$CH_3S + NO \xrightarrow{M}$ products		(See Table 2-1)					
$CH_3S + NO_2 \rightarrow CH_3SO + NO$	222–511	3.0×10^{-11}	–240	6.7×10^{-11}	1.20	150	I98
$CH_3S + CO \rightarrow$ products	208–295			$<1.4\times10^{-16}$ at all temps.			I99
$CH_3S + Br_2 \rightarrow CH_3SBr + Br$	298			1.7×10^{-10}	1.50		I100
$CH_2SH + O_2 \rightarrow$ products	298			6.5×10^{-12}	2.00		I101
$CH_2SH + O_3 \rightarrow$ products	298			3.5×10^{-11}	2.00		I102
$CH_2SH + NO \rightarrow$ products	298			1.9×10^{-11}	2.00		I103
$CH_2SH + NO_2 \rightarrow$ products	298			5.2×10^{-11}	2.00		I104
$CH_3SO + O_3 \rightarrow$ products	300			4.0×10^{-13}	1.50		I105
$CH_3SO + NO_2 \rightarrow CH_3SO_2 + NO$	297–300			1.2×10^{-11}	1.20		I106
$CH_3SOO + O_3 \rightarrow$ products	227			$<8.0\times10^{-13}$			I107
$CH_3SOO + NO \rightarrow$ products	227–256	1.1×10^{-11}	0	1.1×10^{-11}	2.00	100	I107
$CH_3SOO + NO_2 \rightarrow$ products	227–246	2.2×10^{-11}	0	2.2×10^{-11}	2.00	100	I107
$CH_3SO_2 + NO_2 \rightarrow$ products	298			2.2×10^{-12}	2.00		I108

Reaction	Temperature Range of Exp. Data (K) [a]	*A*-Factor	*E*/R	*k*(298 K) [b]	*f*(298 K) [c]	*g* [c]	Note
$CH_3SCH_2 + O_2 \xrightarrow{M} CH_3SCH_2O_2$		(See Table 2-1)					
$CH_3SCH_2 + NO_3 \rightarrow$ products	298			3.0×10^{-10}	2.00		I109
$CH_3SCH_2O_2 + NO \rightarrow CH_3S + CH_2O + NO_2$	261–400	4.9×10^{-12}	–260	1.2×10^{-11}	1.30	200	I110
$CH_3SCH_2O_2 + CH_3SCH_2O_2 \rightarrow$ products	298			1.0×10^{-11}	1.25		I111
$CH_3SS + O_3 \rightarrow$ products	300			4.6×10^{-13}	2.00		I112
$CH_3SS + NO_2 \rightarrow$ products	297			1.8×10^{-11}	2.00		I113
$CH_3SSO + NO_2 \rightarrow$ products	297			4.5×10^{-12}	2.00		I113

Shaded areas indicate changes or additions since JPL19-5.

[a] Temperature range of available experimental data. This is not necessarily the range of temperature over which the recommended Arrhenius parameters are applicable. See the corresponding note for such information.

[b] Units are cm^3 $molecule^{-1}$ s^{-1}.

[c] *f*(298 K) is the uncertainty factor at 298 K. To calculate the uncertainty at other temperatures, use the expression:

$$f(\mathrm{T}) = f(298\ \mathrm{K})\exp\left|g\left(\frac{1}{\mathrm{T}} - \frac{1}{298}\right)\right|$$

Note that the exponent is an absolute value.

1.14.2 Notes: SO_x Reactions

I1. **O + SH.** This recommendation accepts the results of Cupitt and Glass[1] (295 K). The large uncertainty reflects the absence of any confirming investigation.
(Table: 82-57, Note: 82-57, Evaluated: 82-57) Back to Table

(1) Cupitt, L. T.; Glass, G. P. Reactions of SH with atomic oxygen and hydrogen. *Int. J. Chem. Kinet.* **1975**, *Symp. 1*, 39-50.

I2. **O + CS.** The recommended k(298 K) is an average of the rate constants determined by Slagle et al.[4] (305 K), Bida et al.[1] (300 K), Lilenfeld and Richardson[3] (150–300 K), and Hancock and Smith[2] (298 K). The temperature dependence is that of Lilenfeld and Richardson, with the A-factor adjusted to yield the recommended k(298 K).
(Table: 94-26, Note: 94-26, Evaluated: 94-26) Back to Table

(1) Bida, G. T.; Breckenridge, W. H.; Kolln, W. S. A kinetic study of the very fast reaction: $O(^3P) + CS \rightarrow CO^{\ddagger} + S(^3P)$. *J. Chem. Phys.* **1976**, *64*, 3296-3302, doi:10.1063/1.432617.
(2) Hancock, G.; Smith, I. W. M. Infra-red chemiluminescence from vibrationally excited CO Part 1.-The reaction of atomic oxygen with carbon disulphide. *Trans. Faraday Soc.* **1971**, *67*, 2586-2597, doi:10.1039/tf9716702586.
(3) Lilenfeld, H. V.; Richardson, R. J. Temperature dependence of the rate constant for the reaction between carbon monosulfide and atomic oxygen. *J. Chem. Phys.* **1977**, *67*, 3991-3997, doi:10.1063/1.435416.
(4) Slagle, I. R.; Graham, R. E.; Gilbert, J. R.; Gutman, D. Direct determination of the rate constant for the reaction of oxygen atoms with carbon monosulphide. *Chem. Phys. Lett.* **1975**, *32*, 184-186, doi:10.1016/0009-2614(75)85196-7.

I3. **O + H_2S.** This recommendation is derived from an un-weighted least-squares fit of the data of Singleton et al.[4] (297–502 K) and Whytock et al.[8] (263–495 K). The results of Slagle et al.[6] (281–497 K) show very good agreement for E/R in the temperature region of overlap (300–500 K), but lie systematically higher at every temperature. The uncertainty factor at 298 K has been chosen to encompass the room temperature rate constant values of Slagle et al. and Hollinden et al.[3] (205–300 K). Other than the 263 K data point of Whytock et al. and the 281 K point of Slagle et al., the main body of rate constant data below 298 K comes from the study of Hollinden et al., which indicates a dramatic change in E/R in this temperature region. Thus, the parameter g was set to account for these observations. Such a non-linearity in the Arrhenius plot might indicate a change in the reaction mechanism from abstraction (as written) to addition. An addition channel (resulting in H atom displacement) has been proposed by Slagle et al., Singleton et al.,[4] and Singleton et al.[5] In the latter two studies, an upper limit of 20% was placed on the displacement channel. Direct observations of product HSO were made in the reactive scattering experiments of Clemo et al.[1] and Davidson et al.[2] A threshold energy of 3.3 kcal/mole was observed (similar to the activation energy measured in earlier studies), suggesting the importance of this direct displacement channel. Addition products from this reaction have been seen in a matrix by Smardzewski and Lin.[7] Further kinetic studies in the 200–300 K temperature range, as well as quantitative direct mechanistic information, could clarify these issues.
(Table: 82-57, Note: 82-57, Evaluated: 82-57) Back to Table

(1) Clemo, A. R.; Davidson, F. E.; Duncan, G. L.; Grice, R. Translational energy threshold functions for oxygen atom reactions. *Chem. Phys. Lett.* **1981**, *84*, 509-511, doi:10.1016/0009-2614(81)80396-X.
(2) Davidson, F. E.; Clemo, A. R.; Duncan, G. L.; Browett, R. J.; Hobson, J. H.; Grice, R. Reactive scattering of a supersonic oxygen atom beam: O + H_2S. *Mol. Phys.* **1982**, *46*, 33-40, doi:10.1080/00268978200101051.
(3) Hollinden, G. A.; Kurylo, M. J.; Timmons, R. B. Electron spin resonance study of the kinetics of the reaction of $O(^3P)$ atoms with H_2S. *J. Phys. Chem.* **1970**, *74*, 988-991, doi:10.1021/j100700a004.
(4) Singleton, D. L.; Irwin, R. S.; Nip, W. S.; Cvetanovic, R. J. Kinetics and mechanism of the reaction of oxygen atoms with hydrogen sulfide. *J. Phys. Chem.* **1979**, *83*, 2195-2200, doi:10.1021/j100480a003.
(5) Singleton, D. L.; Paraskevopoulos, G.; Irwin, R. S. Mechanism of the $O(^3P) + H_2S$ reaction. Abstraction or addition? *J. Phys. Chem.* **1982**, *86*, 2605-2609, doi:10.1021/j100211a011.
(6) Slagle, I. R.; Baiocchi, F.; Gutman, D. Study of the reactions of oxygen atoms with hydrogen sulfide, methanethiol, ethanethiol, and methyl sulfide. *J. Phys. Chem.* **1978**, *82* 1333-1336, doi:10.1021/j100501a002.
(7) Smardzewski, R. R.; Lin, M. C. Matrix reactions of oxygen atoms with H_2S molecules. *J. Chem. Phys.* **1977**, *66*, 3197-3204, doi:10.1063/1.434294.

(8) Whytock, D. A.; Timmons, R. B.; Lee, J. H.; Michael, J. V.; Payne, W. A.; Stief, L. J. Absolute rate of the reaction of O(^3P) with hydrogen sulfide over the temperature range 263 to 495 K. *J. Chem. Phys.* **1976**, *65*, 2052-2055, doi:10.1063/1.433387.

I4. **O + OCS.** The recommended k(298 K) is the average of the determinations by Westenberg and de Haas,[10] (273–808 K), Klemm and Stief[5] (263–502 K), Wei and Timmons[9] (239–404 K), Manning et al.[6] (298 K), and Breckenridge and Miller[1] (297 K). The recommended value of E/R is the average value taken from the first three listed studies. Hsu et al.[4] report that this reaction proceeds exclusively by a stripping mechanism. The vibrational and rotational state distributions in the SO and CO products have been reported by Chen et al.[2] and Nickolaisen et al.,[7] respectively. The kinetic isotope effect $k(^{34}S)/k(^{32}S)$ was reported by Hattori et al.[3] to be 0.9783 ± 0.0062 at 298 K. A theoretical calculation of potential energy surfaces and temperature-dependent rate coefficients (200–2500 K) has been reported by Saheb et al.[8]
(Table: 06-2, Note: 15-10, Evaluated: 06-2) Back to Table

(1) Breckenridge, W. H.; Miller, T. A. Kinetic study by EPR of the production and decay of SO($^1\Delta$) in the reaction of $O_2(^1\Delta_g)$ with SO($^3\Sigma^-$). *J. Chem. Phys.* **1972**, *56*, 465-474, doi:10.1063/1.1676891.
(2) Chen, X.; Wu, F.; Weiner, B. R. Internal energy distributions of the SO(X $^3\Sigma^-$) product from the O(^{3}P) + OCS reaction. *Chem. Phys. Lett.* **1995**, *247*, 313-320, doi:10.1016/S0009-2614(95)01265-6.
(3) Hattori, S.; Schmidt, J. A.; Mahler, D. W.; Danielache, S. O.; Johnson, M. S.; Yoshida, N. Isotope effect in the carbonyl sulfide reaction with O(^{3}P). *J. Phys. Chem. A* **2012**, *116*, 3521-3526, doi:10.1021/2120884.
(4) Hsu, D. S. Y.; Shaub, W. M.; Burks, T. L.; Lin, M. C. Dynamics of reactions of O(^{3}P) atoms with CS, CS_2 and OCS. *Chem. Phys.* **1979**, *44*, 143-150, doi:10.1016/0301-0104(79)80114-7.
(5) Klemm, R. B.; Stief, L. J. Absolute rate parameters for the reaction of ground state atomic oxygen with carbonyl sulfide. *J. Chem. Phys.* **1974**, *61*, 4900-4906, doi:10.1063/1.1681819.
(6) Manning, R. G.; Braun, W.; Kurylo, M. J. The effect of infrared laser excitation on reaction dynamics: O + $C_2H_4^\dagger$ and O + OCS†. *J. Chem. Phys.* **1976**, *65*, 2609-2615, doi:10.1063/1.433448.
(7) Nickolaisen, S. L.; Veney, D. W.; Cartland, H. E. CO(v,J) product state distributions from the reaction O(^{3}P) + OCS → CO + SO. *J. Chem. Phys.* **1994**, *100*, 4925-4931, doi:10.1063/1.467278.
(8) Saheb, V.; Alizadeh, M.; Rezaei, F.; Shahidi, S. Quantum chemical and theoretical kinetics studies on the reaction of carbonyl sulfide with H, OH, and O(^{3}P). *Comp. Theo. Chem.* **2012**, *994*, 25-33, 10.1016/j.comptc.2012.06.008.
(9) Wei, C. N.; Timmons, R. B. ESR study of the kinetics of the reactions of O(^3P) atoms with CS_2 and OCS. *J. Chem. Phys.* **1975**, *62*, 3240-3245, doi:10.1063/1.430875.
(10) Westenberg, A. A.; deHaas, N. Atom molecule using EST detection. V. Results for O + OCS, O + CS_2, O + NO, and H + C_2H_4. *J. Chem. Phys.* **1969**, *50*, 707-709, doi:10.1063/1.1671119.

I5. **O + CS_2.** The recommended k(298 K) is an average of the rate constants determined by Wei and Timmons[9] (218–293 K), Westenberg and de Haas[10] (227–538 K), Slagle et al.[8] (298 K), Callear and Smith,[3] Callear and Hedges,[2] Homann et al.[6] (300–920 K), Borissenko et al.[1] (300 K), and Graham and Gutman[5] (249–500 K). The E/R value is an average of the determinations by Wei and Timmons and Graham and Gutman. The g value has been set to encompass the temperature-dependent data of Westenberg and deHaas. The principal reaction products are thought to be CS + SO. However, Hsu et al.[7] report that 1.4% of the reaction at 298 K proceeds through a channel yielding CO + S_2 and calculate a rate constant for the overall process in agreement with that recommended. Graham and Gutman have found that 9.6% of the reaction proceeds to yield OCS + S at room temperature. Using time-resolved diode laser spectroscopy, Cooper and Hershberger[4] determined the branching ratios for the CO and OCS producing channels to be (3.0 ± 1.0)% and (8.5 ± 1.0)%, respectively.
(Table: 82-57, Note: 82-57, Evaluated: 82-57) Back to Table

(1) Borissenko, D.; Kukui, A.; Laverdet, G.; Le Bras, G. Experimental study of SO_2 formation in the reactions of CH_3SO radical with NO_2 and O_3 in relation with the atmospheric oxidation mechanism of dimethyl sulfide. *J. Phys. Chem. A* **2003**, *107*, 1155-1161, doi:10.1021/jp021701g.
(2) Callear, A. B.; Hedges, R. E. M. Flash spectroscopy with mercury resonance radiation Part 1.-An experimental method with microwave-pulse excitation. *Trans. Faraday Soc.* **1970**, *66*, 605-614, doi:10.1039/tf9706600605.
(3) Callear, A. B.; Smith, I. W. M. Measurement of the rate parameters for reaction of O(2^{3}P) with carbon disulphide and olefines, by flash spectroscopy. *Nature* **1967**, *213*, 382-383, doi:10.1038/213382a0.
(4) Cooper, W. F.; Hershberger, J. F. An infrared laser study of the O(^{3}P) + CS_2 reaction. *J. Phys. Chem.* **1992**, *96*, 5405-5410, doi:10.1021/j100192a041.

(5) Graham, R. A.; Gutman, D. J. Temperature dependence of rate constants and branching ratios for the reaction of oxygen atoms with carbon disulfide. *J. Phys. Chem.* **1977**, *81*, 207-209, doi:10.1021/j100518a005.
(6) Homann, K. H.; Krome, G.; Wagner, H. G. Carbon disulfide oxidation rate of elementary reactions .1. *Ber. Bunsenges. Phys. Chem.* **1968**, *72*, 998-1004, doi:10.1002/bbpc.19680720821.
(7) Hsu, D. S. Y.; Shaub, W. M.; Burks, T. L.; Lin, M. C. Dynamics of reactions of O(^{3}P) atoms with CS, CS_2 and OCS. *Chem. Phys.* **1979**, *44*, 143-150, doi:10.1016/0301-0104(79)80114-7.
(8) Slagle, I. R.; Gilbert, J. R.; Gutman, D. Kinetics of the reaction between oxygen atoms and carbon disulfide. *J. Chem. Phys.* **1974**, *61*, 704-709, doi:10.1063/1.1681949.
(9) Wei, C. N.; Timmons, R. B. ESR study of the kinetics of the reactions of O(^3P) atoms with CS_2 and OCS. *J. Chem. Phys.* **1975**, *62*, 3240-3245, doi:10.1063/1.430875.
(10) Westenberg, A. A.; deHaas, N. Atom molecule using EST detection. V. Results for O + OCS, O + CS_2, O + NO, and H + C_2H_4. *J. Chem. Phys.* **1969**, *50*, 707-709, doi:10.1063/1.1671119.

I6. **O + CH_3SCH_3.** This recommendation is based on a fit of the data from Nip et al.[4] (296–557 K), Lee et al.[3] (268–424 K), and Lee et al.[2](272–472 K). Product studies by Cvetanovic et al.[1] (300 K) indicate that the reaction proceeds almost entirely by addition followed by rapid fragmentation to CH_3SO + CH_3 products. Pavanaja et al.[5] (298 K) examined the pressure and reactant ratio dependencies of OH($A^2\Sigma^+$) and SO_2(^{3}B, ^{1}B) emissions in this reaction system. Their observations are consistent with initial product formation as written, followed by secondary generation of both OH and SO_2.
(Table: 94-26, Note: 97-4, Evaluated: 94-26) Back to Table

(1) Cvetanovic, R. J.; Singleton, D. L.; Irwin, R. S. Gas-phase reactions of O(^{3}P) atoms with methanethiol, ethanethiol, methyl sulfide, and dimethyl disulfide. 2. Reaction products and mechanisms. *J. Am. Chem. Soc.* **1981**, *103*, 3530-3539, doi:10.1021/ja00402a046.
(2) Lee, J. H.; Tang, I. N.; Klemm, R. B. Absolute rate constant for the reaction of O(^3P) with CH_3SCH_3 from 272 to 472 K. *J. Chem. Phys.* **1980**, *72*, 1793-1796, doi:10.1063/1.439295.
(3) Lee, J. H.; Timmons, R. B.; Stief, L. J. Absolute rate parameters for the reaction of ground state atomic oxygen with dimethyl sulfide and episulfide. *J. Chem. Phys.* **1976**, *64*, 300-305, doi:10.1063/1.431921.
(4) Nip, W. S.; Singleton, D. L.; Cvetanovic, R. J. Gas-phase reactions of O(^{3}P) atoms with methanethiol, ethanethiol, methyl sulfide, and dimethyl disulfide. 1. Rate constants and Arrhenius parameters. *J. Am. Chem. Soc.* **1981**, *103*, 3526-3530, doi:10.1021/ja00402a045.
(5) Pavanaja, U. B.; Upadhyaya, H. P.; Sapre, A. V.; Rao, K. V. S. R.; Mittal, J. P. Chemiluminescent reaction of oxygen atoms with dimethyl disulfide and dimethyl sulfide. *J. Chem. Soc. Faraday. Trans.* **1994**, *90*, 825-829, doi:10.1039/ft9949000825.

I7. **O + CH_3SSCH_3.** This recommendation averages the 298 K rate constants of Nip et al.[4] (298–571 K) and Borissenko et al.[1] (300 K), which are in good agreement with each other, but are about a factor of 2 lower than the value reported by Lee et al.[3] (270–329 K). The recommendation for E/R has been obtained from an unweighted Arrhenius fit that employs all available data, but scales the data of Lee et al. downward by a factor of 2.04 to bring their data into agreement with the other data at room temperature. Product studies by Cvetanovic et al.[2] (300 K) indicate that the reaction proceeds mainly by addition followed by rapid fragmentation to the products as written. Pavanaja et al.[5] (298 K) examined the pressure and reactant ratio dependencies of OH($A^2\Sigma^+$) and SO_2(^{3}B, ^{1}B) emissions in this reaction system. Their observations are consistent with initial product formation of CH_3SO + CH_3S, followed by secondary generation of both OH and SO_2.
(Table: 06-2, Note: 06-2, Evaluated: 06-2) Back to Table

(1) Borissenko, D.; Kukui, A.; Laverdet, G.; Le Bras, G. Experimental study of SO_2 formation in the reactions of CH_3SO radical with NO_2 and O_3 in relation with the atmospheric oxidation mechanism of dimethyl sulfide. *J. Phys. Chem. A* **2003**, *107*, 1155-1161, doi:10.1021/jp021701g.
(2) Cvetanovic, R. J.; Singleton, D. L.; Irwin, R. S. Gas-phase reactions of O(^{3}P) atoms with methanethiol, ethanethiol, methyl sulfide, and dimethyl disulfide. 2. Reaction products and mechanisms. *J. Am. Chem. Soc.* **1981**, *103*, 3530-3539, doi:10.1021/ja00402a046.
(3) Lee, J. H.; Tang, I. N. Absolute rate constant for the reaction of O(^3P) with CH_3SSCH_3 from 270 to 329 K. *J. Chem. Phys.* **1980**, *72*, 5718-5720, doi:10.1063/1.438990.
(4) Nip, W. S.; Singleton, D. L.; Cvetanovic, R. J. Gas-phase reactions of O(^{3}P) atoms with methanethiol, ethanethiol, methyl sulfide, and dimethyl disulfide. 1. Rate constants and Arrhenius parameters. *J. Am. Chem. Soc.* **1981**, *103*, 3526-3530, doi:10.1021/ja00402a045.
(5) Pavanaja, U. B.; Upadhyaya, H. P.; Sapre, A. V.; Rao, K. V. S. R.; Mittal, J. P. Chemiluminescent reaction of oxygen atoms with dimethyl disulfide and dimethyl sulfide. *J. Chem. Soc. Faraday. Trans.* **1994**, *90*, 825-829, doi:10.1039/ft9949000825.

I8. **O + $CH_3S(O)CH_3$.** The recommended 298 K rate constant is the average of values reported from a laser flash photolysis – resonance fluorescence study by Pope et al.[2] (266–383 K), and from a discharge flow − mass spectrometry study by Riffault et al.[3] (298 K). A rate constant reported by Barnes et al.[1] (with no details about how the rate constant was obtained) is somewhat greater than the recommendation, but in agreement to within the recommended uncertainty factor. The recommended value for *E*/R is from Pope et al. The recommended value for the parameter *g* is larger than the value reported by Pope et al. to reflect the fact that only a single temperature dependence study has been reported. In their study at one Torr total pressure, Riffault et al. found that the products SO_2 + 2 CH_3 are produced with near unit yield.
(Table: 06-2, Note: 06-2, Evaluated: 06-2) Back to Table

(1) Barnes, I.; Bastian, V.; Becker, K. H.; Martin, D. In *Biogenic Sulfur in the Environment*; ACS Symp. Ser, 1989; Vol. 393; pp 476-488.
(2) Pope, F. D.; Nicovich, J. M.; Wine, P. H. A temperature-dependent kinetics study of the reaction of $O(^3P_J)$ with $(CH_3)_2SO$. *Int. J. Chem. Kinet.* **2002**, *34*, 156-161, doi:10.1002/kin.10040.
(3) Riffault, V.; Bedjanian, Y.; Le Bras, G. Kinetics and mechanism of the O atom reaction with dimethyl sulfoxide. *J. Phys. Chem. A* **2003**, *107*, 5404-5411, doi:10.1021/jp0226127.

I9. **O_3 + H_2S.** This upper limit was determined by Becker et al.[1] (298 K) based on measurements of the rates of SO_2 production and O_3 consumption. The heterogeneous reaction between H_2S and O_3 occurs more rapidly than the gas phase reaction in most laboratory systems. A detailed potential energy surface for H_2S + $^1O_3$ has been reported by Mousavipour et al.[2]
(Table: 92-20, Note: 15-10, Evaluated: 92-20) Back to Table

(1) Becker, K. H.; Inocencio, M. A.; Schurath, U. The reaction of ozone with hydrogen sulfide and its organic derivatives. *Int. J. Chem. Kinet.* **1975**, *Symp. 1*, 205-220.
(2) Mousavipour, S. H.; Mortazavi, M.; Hematti, O. Multichannel RRKM-TST and direct dynamics CVT study of the reaction of hydrogen sulfide with ozone. *J. Phys. Chem. A* **2013**, *117*, 6744-6756, doi:10.1021/jp404738d.

I10. **O_3 + CH_3SCH_3.** The recommendation is based on the study of Du et al.[1] (301 K), which gives a more sensitive upper limit than an earlier study by Martinez and Herron[2] (296 K). Du et al. used cyclohexane to scavenge OH radicals and high levels of O_2 to scavenge oxygen atoms and convert more reactive carbon-centered radicals to less reactive peroxy radicals. Their reported rate constant is $(1.04 \pm 0.21) \times 10^{-19}$ cm^3 $molecule^{-1}$ s^{-1}. Because of the potential for interference from wall reaction or reactions involving radicals generated via secondary chemistry, the recommendation is an upper limit equal to the rate constant reported by Du et al. plus twice its reported uncertainty.
(Table: 10-6, Note: 10-6, Evaluated: 10-6) Back to Table

(1) Du, L.; Xu, Y.; Ge, M.; Long, J.; Yao, L.; Wang, W. Rate constant of the gas phase reaction of dimethyl sulfide (CH_3SCH_3) with ozone. *Chem. Phys. Lett.* **2007**, *436*, 36-40, doi:10.1016/j.cplett.2007.01.025.
(2) Martinez, R. I.; Herron, J. T. Stopped-flow study of the gas-phase reaction of ozone with organic sulfides: Dimethyl sulfide. *Int. J. Chem. Kinet.* **1978**, *10*, 433-452, doi:10.1002/kin.550100503.

I11. **O_3 + SO_2.** This recommendation is based on the limited data of Davis et al.[1] at 300 and 360 K in a stopped flow investigation using mass spectrometric and UV spectroscopic detection.
(Table: 85-37, Note: 85-37, Evaluated: 85-37) Back to Table

(1) Davis, D. D.; Prusazcyk, J.; Dwyer, M.; Kim, P. A stop-flow time-of-flight mass spectrometry kinetics study. Reaction of ozone with nitrogen dioxide and sulfur dioxide. *J. Phys. Chem.* **1974**, *78*, 1775-1779, doi:10.1021/j100611a001.

I12 **O_3 + SO_2F_2.** The recommended upper limit is based on the results of Dillon et al.[1] (294 K) and Sulbaek-Andersen et al.[2] (296 K).

(Table: 10-6, Note: 10-6, Evaluated: 10-6) Back to Table

(1) Dillon, T. J.; Horowitz, A.; Crowley, J. N. The atmospheric chemistry of sulphuryl fluoride, SO_2F_2. *Atmos. Chem. Phys.* **2008**, *8*, 1547-1557, doi:10.5194/acp-8-1547-2008.
(2) Sulbaek-Andersen, M. P.; Blake, D. R.; Rowland, F. S.; Hurley, M. D.; Wallington, T. J. Atmospheric chemistry of aulfuryl fluoride: Reaction with OH radicals, Cl Atoms and O_3, atmospheric lifetime, IR

spectrum, and global warming potential. *Environ. Sci. Technol.* **2009**, *43*, 1067-1070, doi:10.1021/es802439f.

I13. OH + H_2S. The recommended values for k(298 K) and E/R are derived from a composite un-weighted least-squares fit to the Arrhenius equation (ln k vs. T^{-1}) using the individual scaled data points at T ≤300 K only of Perry et al.[11] (297–427 K), Cox and Sheppard[3] (297 K), Wine et al.[16] (245–366 K), Leu and Smith[7] (228–518 K), Michael et al.[10] (228, 298, 437 K), Lin[8] (239–425 K), Lin et al.[9] (245–450 K), Wang and Lee[14] (300 K), Barnes et al.[1] (300 K), Lafage et al.[6] (243–463 K), and Wang et al.[13] The studies of Leu and Smith, Lin et al.,[9] Michael et al. and Lafage et al. show a non-Arrhenius temperature dependence of k with a minimum occurring near room temperature. Each data set is scaled by the ratio k(298 K)/<k(298 K)> where k(298 K) is the value obtained from the best fit Arrhenius expression or, for the studies that observed non-Arrhenius behavior, the best fit three-parameter expression of the form $k = A\ T^n \exp(-E/RT)$ and <k(298 K)> is the average of the k(298 K) values obtained as described above. The scaled data show a clear non-Arrhenius temperature dependence such that the following three-parameter expression is required over the full temperature range where data are available (228–518 K):

$$k(228–518\ \text{K}) = 7.95 \times 10^{-20}\ T^{+2.68} \exp(+783/T)\ \text{cm}^3\ \text{molecule}^{-1}\ \text{s}^{-1}$$

Lafage et al. and Michael et al. discuss the results in terms of a two-channel reaction scheme involving direct H atom abstraction and complex (adduct) formation. Lafage et al. analyzed their results above room temperature to yield an apparent E/R = 400 K for the abstraction channel, in good agreement with the E/R value determined above room temperature by Westenberg and de Haas[15] (298–885 K). The results of these latter workers lie systematically higher (by about 70%), presumably due to secondary reactions. The room temperature value measured by Stuhl[12] (298 K) lies just outside the 2σ error limit set for k(298 K). Theoretical work by Ellingson and Truhlar[5] and by Du and Zhang[4] supports the non-Arrhenius temperature dependence reported by some investigators (see above); Ellingson and Truhlar attribute the unusual temperature dependence to the existence of a pre- reactive complex (bound by 18 kJ mol^{-1}) with a submerged classical barrier on the reaction path. At low temperatures, the long-range attraction dominates and the rate constant decreases with increasing temperature. However, as the temperature is increased, the variational transition state vibrations transverse to the reaction path become tighter, the effective barrier becomes higher, and the temperature trend reverses. Du and Zhang find theoretically that there is no rate enhancement under atmospheric conditions due to catalysis by H_2O or $(H_2O)_2$. Butkovskaya and Setser[2] have observed infrared emission from vibrationally excited levels of the reaction product H_2O.
(Table: 19-5, Note: 19-5, Evaluated: 19-5) Back to Table

(1) Barnes, I.; Bastian, V.; Becker, K. H.; Fink, E. H.; Nelsen, W. Oxidation of sulphur compounds in the atmosphere: I. Rate constants of OH radical reactions with sulphur dioxide, hydrogen sulphide, aliphatic thiols and thiophenol. *J. Atmos. Chem.* **1986**, *4*, 445-466, doi:10.1007/BF00053845.
(2) Butkovskaya, N. I.; Setser, D. W. Chemical dynamics of the OH and OD radical reactions with H_2S, CH_3SCH_3, and CH_3SH studied by infrared chemiluminescence. *J. Phys. Chem. A* **1998**, *102*, 6395-6405, doi:10.1021/jp980256f.
(3) Cox, R. A.; Sheppard, D. Reactions of OH radicals with gaseous sulphur compounds. *Nature* **1980**, *284*, 330-331, doi:10.1038/284330a0.
(4) Du, B.; Zhang, W. The effect of $(H_2O)_n$ (n = 1-2) or H_2S on the hydrogen abstraction reaction of H_2S by OH radicals in the atmosphere. *Comput. Theor. Chem.* **2015**, *1069*, 77-85, doi:10.1016/j.comptc.2015.07.015.
(5) Ellingson, B. A.; Truhlar, D. G. Explanation of the unusual temperature dependence of the atmospherically important OH + H_2S → H_2O + HS reaction and prediction of the rate constant at combustion temperatures. *J. Am. Chem. Soc.* **2007**, *129*, 12765-12771, doi:10.1021/ja072538b.
(6) Lafage, C.; Pauwels, J.-F.; Carlier, M.; Devolder, P. Rate constant for the reaction OH + H_2S in the range 243-463 K by discharge-flow laser-induced fluorescence. *J. Chem. Soc. Faraday Trans. 2* **1987**, *83*, 731-739, doi:10.1039/f29878300731.
(7) Leu, M.-T.; Smith, R. H. Rate constants for the gas-phase reaction between hydroxyl and hydrogen sulfide over the temperature range 228-518 K. *J. Phys. Chem.* **1982**, *86*, 73-81, doi:10.1021/j100390a015.
(8) Lin, C. L. Temperature dependence of the rate constant for the reaction OH + H_2S. *Int. J. Chem. Kinet.* **1982**, *14*, 593-598, doi:10.1002/kin.550140514.
(9) Lin, Y.-L.; Wang, N.-S.; Lee, Y.-P. Temperature dependence of the rate constant for the reaction OH + H_2S in He, N_2, and O_2. *Int. J. Chem. Kinet.* **1985**, *17*, 1201-1214, doi:10.1002/kin.550171106.
(10) Michael, J. V.; Nava, D. F.; Brobst, W.; Borkowski, R. P.; Stief, L. J. Temperature dependence of the absolute rate constant for the reaction of hydroxyl radical with hydrogen sulfide. *J. Phys. Chem.* **1982**, *86*, 81-84, doi:10.1021/j100390a016.

(11) Perry, R. A.; Atkinson, R.; Pitts, J. N., Jr. Rate constants for the reactions OH + H_2S → H_2O + SH and OH + NH_3 → H_2O + NH_2 over the temperature range 297-427 °K. *J. Chem. Phys.* **1976**, *64*, 3237-3239, doi:10.1063/1.432663.
(12) Stuhl, F. Determination of rate constant for reaction OH + H_2S by a pulsed photolysis - resonance fluorescence method. *Ber. Bunsenges. Phys. Chem.* **1974**, *78*, 230-232, doi:10.1002/bbpc.19740780304.
(13) Wang, H.-T.; Zhang, Y.-J.; Mu, Y.-J. Rate constants for reactions of OH with several reduced sulfur compounds determined by relative rate constant method. *Acta Phys.-Chim. Sin.* **2008**, *24*, 945-950, doi:10.1016/S1872-1508(08)60041-8.
(14) Wang, N.-S.; Lee, Y.-P. Absolute rate constant measurement of the reaction OH + H_2S using discharge flow-resonance fluorescence technique. *Proc. Nat. Sci. Council (Taiwan)* **1985**, *9*, 87-94.
(15) Westenberg, A. A.; deHaas, N. Rate of the reaction OH + H_2S → SH + H_2O over an extended temperature range. *J. Chem. Phys.* **1973**, *59*, 6685-6686, doi:10.1063/1.1680055.
(16) Wine, P. H.; Kreutter, N. M.; Gump, C. A.; Ravishankara, A. R. Kinetics of OH reactions with the atmospheric sulfur compounds H_2S, CH_3SH, CH_3SCH_3, and CH_3SSCH_3. *J. Phys. Chem.* **1981**, *85*, 2660-2665, doi:10.1021/j150618a019.

I14. OH + OCS. The recommendation is based on the study of Wahner and Ravishankara[11] (245, 298 K) and the temperature dependent study of Cheng and Lee[2] (255−483 K). Because the data of Cheng and Lee suggest slight curvature in the Arrhenius plot, only their data at T≤ 423 K were used to arrive at the recommended Arrhenius parameters. The room temperature rate constants from the above-mentioned studies are a factor of 3 higher than the earlier determination by Leu and Smith[7] (300−517 K). As discussed in the later studies, this difference may be due to an overcorrection of the Leu and Smith data to account for OH reaction with H_2S impurities and also to possible regeneration of OH. The work by Wahner and Ravishankara supersedes the study of Ravishankara et al.[8] The Wahner and Ravishankara study minimized complications due to secondary and/or excited state reactions that presumably were interfering with the experiments of Atkinson et al.[1] (299−430 K) and Kurylo[5] (296 K). A relative rate study by Schmidt et al.[10] (296 K) suggests a somewhat faster k(298K) than recommended, but agrees with the recommended value within the (undesirably large) combined uncertainty limits. The upper limit for k(298 K) reported by Cox and Sheppard[3] (297 K) is too insensitive to permit comparison with more recent studies. The room temperature measurements of Wahner and Ravishankara demonstrate the lack of an effect of total pressure (or O_2 partial pressure) on the rate constant and are supported by the more limited pressure- and O_2-dependent studies of Cheng and Lee. A theoretical calculation of potential energy surfaces and temperature-dependent rate coefficients (200−2500 K) has been reported by Saheb et al.[9] Theoretical work by Schmidt et al. suggests that the 298 K rate constant is pressure-dependent, increasing by about a factor of two ($3.5-7.2 \times 10^{-16}$ cm^3 $molecule^{-1}$ s^{-1}) when air pressure increases from 10 Torr to 700 Torr. The theoretical results not only predict a pressure dependence that has not yet been observed experimentally, but also predict rate constants that are substantially smaller than those reported experimentally. Furthermore, the theoretical results provide mechanistic information that suggests potential problems with experimental studies where OH kinetics are directly monitored (see below).

Product observations by Leu and Smith indicate that SH is a primary product of this reaction and tentatively confirm the suggestion of Kurylo and Laufer[6] that the predominant reaction pathway is to produce SH + CO_2 through a complex (adduct) mechanism similar to that observed for the OH + CS_2 reaction. However, the absence of an O_2/pressure effect for OH + OCS is in marked contrast with the strong dependence seen in studies of OH + CS_2 (see note for the latter reaction). The theoretical analysis of Schmidt et al. (discussed briefly above) suggests that the pressure-independent channel involves transfer of the sulfur atom to OH to generate SOH + CO while the pressure-dependent channel involves formation of an energized OC(OH)S* adduct that can re-dissociate to OH + OCS reactants in competition with stabilization. Schmidt et al. suggest that dissociation of OC(OH)S* to CO_2 + SH can be important at elevated temperatures, but not under atmospheric conditions. Schmidt et al. further suggest that under atmospheric conditions both stabilized and un-stabilized adducts can react with O_2 to recycle OH. The possibility that the experiments of Cheng and Li and Wahner and Ravishankara were “blind” to the addition channel because OH, the monitored species in both studies, was rapidly regenerated is an important question that will require additional experimentation to address.

Low pressure (1–2.5 Torr) experiments by Greenblatt and Howard[4] have shown that the rate coefficient for oxygen atom exchange in the reaction of ^{18}OH with OCS is less than 10^{-17} cm^3 $molecule^{-1}$ s^{-1} at 296 and 373 K, suggesting that H atom migration in the energized complex is rather slow.
(Table: 19-5, Note: 19-5, Evaluated: 19-5) Back to Table

(1) Atkinson, R.; Perry, R. A.; Pitts Jr., J. N. Rate constants for the reaction of OH radicals with COS, CS_2 and CH_3SCH_3 over the temperature range 299-430 K. *Chem. Phys. Lett.* **1978**, *54*, 14-18, doi:10.1016/0009-2614(78)85653-X.

(2) Cheng, B.-M.; Lee, Y.-P. Rate constant of OH + OCS reaction over the temperature range 255-483 K. *Int. J. Chem. Kinet.* **1986**, *18*, 1303-1314, doi:10.1002/kin.550181202.
(3) Cox, R. A.; Sheppard, D. Reactions of OH radicals with gaseous sulphur compounds. *Nature* **1980**, *284*, 330-331, doi:10.1038/284330a0.
(4) Greenblatt, G. D.; Howard, C. J. Oxygen atom exchange in the interaction of ^{18}OH with several small molecules. *J. Phys. Chem.* **1989**, *93*, 1035-1042, doi:10.1021/j100340a006.
(5) Kurylo, M. J. Flash photolysis resonance fluorescence investigation of the reactions of OH radicals with OCS and CS_2. *Chem. Phys. Lett.* **1978**, *58*, 238-242, doi:10.1016/0009-2614(78)80285-1.
(6) Kurylo, M. J.; Laufer, A. H. Evidence for atom exchange in OH reactions with carbonyl compounds: $^{18}OH + CO_2 \rightarrow {}^{18}OCO + OH$; $^{18}OH + CO \rightarrow {}^{18}OC + OH$. *J. Chem. Phys.* **1979**, *70*, 2032-2033, doi:10.1063/1.437638.
(7) Leu, M.-T.; Smith, R. H. Kinetics of the gas-phase reaction between hydroxyl and carbonyl sulfide over the temperature range 300-517 K. *J. Phys. Chem.* **1981**, *85*, 2570-2575, doi:10.1021/j150617a031.
(8) Ravishankara, A. R.; Kreutter, N. M.; Shah, R. C.; Wine, P. H. Rate of reaction of OH with OCS. *Geophys. Res. Lett.* **1980**, *7*, 861-864, doi:10.1029/GL007i011p00861.
(9) Saheb, V.; Alizadeh, M.; Rezaei, F.; Shahidi, S. Quantum chemical and theoretical kinetics studies on the reaction of carbonyl sulfide with H, OH, and O(^{3}P). *Comp. Theo. Chem.* **2012**, *994*, 25-33, 10.1016/j.comptc.2012.06.008.
(10) Schmidt, J. A.; Kyte, M.; Østerstrøm, F. F.; Joelsson, L. M. T.; Knap, H. C.; Jørgensen, S.; Nielsen, O. J.; Murakami, T.; Johnson, M. S. On adduct formation and reactivity in the OCS + OH reaction: A combined theoretical and experimental study. *Chem. Phys. Lett.* **2017**, *675*, 111-117, doi:10.1016/j.cplett.2017.03.005.
(11) Wahner, A.; Ravishankara, A. R. The kinetics of the reaction of OH with COS. *J. Geophys. Res.* **1987**, *92*, 2189-2194, doi:10.1029/JD092iD02p02189.

I15. OH + CS_2 → SH + OCS. There is a consensus of experimental evidence that this reaction proceeds very slowly as a direct bimolecular process. Wine et al.[8] (251−363 K) set an upper limit on k(298 K) of 1.5×10^{-15} cm^3 $molecule^{-1}$ s^{-1}. A consistent upper limit is also reported by Iyer and Rowland[4] (298 K) for the rate of direct production of OCS, suggesting that OCS and SH are primary products of the bimolecular process. This mechanistic interpretation is further supported by the studies of Leu and Smith[6] (298−520 K) and Biermann et al.[2] (298 K), which set somewhat higher upper limits on k(298 K). The more rapid reaction rates measured by Atkinson et al.[1] (300, 424 K), Kurylo[5] (296 K), and Cox and Sheppard[3] (298 K) may be attributable to severe complications arising from excited state and secondary chemistry in their photolytic systems. The Cox and Sheppard study in particular may have been affected by the reaction of electronically excited CS_2 (produced via the 350 nm photolysis) with O_2 (in the 1-atm synthetic air mixture) as well as by the accelerating effect of O_2 on the OH + CS_2 reaction itself, which has been observed by other workers as summarized below. The possible importance of electronically excited CS_2 reactions in the tropospheric oxidation of CS_2 to OCS has been discussed by Wine et al.[7]
(Table: 06-2, Note: 06-2, Evaluated: 06-2) Back to Table

(1) Atkinson, R.; Perry, R. A.; Pitts Jr., J. N. Rate constants for the reaction of OH radicals with COS, CS_2 and CH_3SCH_3 over the temperature range 299-430 K. *Chem. Phys. Lett.* **1978**, *54*, 14-18, doi:10.1016/0009-2614(78)85653-X.
(2) Biermann, H. W.; Harris, G. W.; Pitts, J. N., Jr. Photoionization mass spectrometer studies of the collsionally stabillzed product distribution in the reaction of OH radicals with selected alkenes at 298 K. *J. Phys. Chem.* **1982**, *86*, 2958-2964, doi:10.1021/j100212a030.
(3) Cox, R. A.; Sheppard, D. Reactions of OH radicals with gaseous sulphur compounds. *Nature* **1980**, *284*, 330-331, doi:10.1038/284330a0.
(4) Iyer, R. S.; Rowland, F. S. A significant upper limit for the rate of formation of OCS from the reaction of OH with CS_2. *Geophys. Res. Lett.* **1980**, *7*, 797-800, doi:10.1029/GL007i010p00797.
(5) Kurylo, M. J. Flash photolysis resonance fluorescence investigation of the reactions of OH radicals with OCS and CS_2. *Chem. Phys. Lett.* **1978**, *58*, 238-242, doi:10.1016/0009-2614(78)80285-1.
(6) Leu, M.-T.; Smith, R. H. Rate constant for the reaction between OH and CS_2 at 298 and 520 K. *J. Phys. Chem.* **1982**, *86*, 958-961, doi:10.1021/j100395a024.
(7) Wine, P. H.; Chameides, W. L.; Ravishankara, A. R. Potential role of CS_2 photooxidation in tropospheric sulfur chemistry. *Geophys. Res. Lett.* **1981**, *8*, 543-546, doi:10.1029/GL008i005p00543.
(8) Wine, P. H.; Shah, R. C.; Ravishankara, A. R. Rate of reaction of OH with CS_2. *J. Phys. Chem.* **1980**, *84*, 2499-2503, doi:10.1021/j100457a003.

I16. $OH + CS_2 \rightarrow CS_2OH \xrightarrow{O_2}$ products. An accelerating effect of O_2 on the OH + CS_2 reaction rate has been observed by Jones et al.[3] (295 K), Barnes et al.[1] (264–293 K), and Hynes et al.[2] (251–348 K), along with a near unity product yield for SO_2 and OCS. In the latter two studies the effective bimolecular rate constant was found to be a function of total pressure (O_2 + N_2), and exhibited an appreciably negative temperature dependence. These observations are consistent with the formation of a long-lived adduct as postulated by Kurylo[4] (296 K) and Kurylo and Laufer[5] (296 K) followed by its reaction with O_2:

$$OH + CS_2 + M \underset{k_b}{\overset{k_a}{\rightleftharpoons}} CS_2OH + M$$

$$CS_2OH + O_2 \xrightarrow{k_c} \text{Products}$$

The effective second order rate constant for CS_2 or OH removal in the above reaction scheme can be expressed as

$$1/k_{eff} = (k_b/k_a k_c)(1/P_{O2}) + (1/k_a)(1/P_M)$$

where P_{O2} is the partial pressure of O_2 and P_M equals P_{O2} + P_{N2}. The validity of this expression requires that k_a and k_b are invariant with the P_{O_2}/P_{N_2} ratio. A $1/k$ vs $1/P_{O2}$ plot of the data of Jones et al.[3] taken at atmospheric pressure exhibits marked curvature, suggesting a more complex mechanistic involvement of O_2, whereas the data of Barnes et al. and Hynes et al. are more satisfactorily represented by this analytical expression. Nevertheless, while the qualitative features of the data from all three laboratories agree, there are some quantitative inconsistencies. First, under similar conditions of O_2 and N_2 pressures, the Barnes et al. rate constants lie approximately 60% higher than those of Jones et al. and up to a factor of 2 higher than those derived by Hynes et al. Secondly, two fits each of both the Barnes et al. and Hynes et al. data can be made: one at fixed P_M and varying P_{O2}, and the other at fixed P_{O2} and varying P_M (i.e., varying added N_2). Within each data set, rate constants calculated from both fits agree reasonably well for mole fractions of O_2 near 0.2 (equivalent to air) but disagree by more than a factor of 2 for measurements in a pure O_2 system. Finally, the temperature dependence (from 264–293 K) of the k_{eff} values from Barnes et al. varies systematically from an E/R of –1300 K for experiments in pure O_2 (at 700 Torr total pressure) to –2900 K for experiments in a 50 Torr O_2 plus 650 Torr N_2 mixture. An Arrhenius fit of the Hynes et al. data (from 251–348 K) recorded in synthetic air at 690 Torr yields an E/R = –3300 K, although the data show marked curvature over the temperature range of study. These observations suggest that k_a and k_b may not be independent of the identity of M. For this reason, we limit our recommendation to air mixtures (i.e., P_{O2}/P_{N2} = 0.25) at atmospheric pressure. Since most CS_2 is oxidized within the atmospheric boundary layer, such restriction does not limit the applicability of this recommendation in atmospheric modeling.

The present recommendation accepts the measurements of Hynes et al.,[2] which appear to be the most sensitive of the three investigations. Thus, k(298 K) is derived from the Arrhenius fit of the data near room temperature.

$$k(298\text{ K}) = 1.2 \times 10^{-12}\text{ cm}^3\text{ molecule}^{-1}\text{ s}^{-1}$$

To compute values of k below 298 K, we have accepted the analysis of Hynes et al.:

$$k(T) = (1.25 \times 10^{-16} \exp(4550/T))/(T + 1.81 \times 10^{-3} \exp(3400/T))\text{ cm}^3\text{ molecule}^{-1}\text{ s}^{-1}.$$

This recommendation is only valid for one atmosphere pressure of air. It is interesting to note that measurements by Hynes et al.[2] at approximately 250 K and 700 Torr total pressure result in k_{eff} values that are independent of the amount of O_2 for partial pressures between 145 and 680 Torr. This suggests that the adduct is quite stable with respect to dissociation into the reactants (OH + CS_2) at this low temperature and that the effective rate constant for reactant removal approaches the elementary rate constant for adduct formation.
(Table: 06-2, Note: 06-2, Evaluated: 06-2) Back to Table

(1) Barnes, I.; Becker, K. H.; Fink, E. H.; Reimer, A.; Zabel, F.; Niki, H. Rate constant and products of the reaction CS_2 + OH in the presence of O_2. *Int. J. Chem. Kinet.* **1983**, *15*, 631-645, doi:10.1002/kin.550150705.

(2) Hynes, A. J.; Wine, P. H.; Nicovich, J. M. Kinetics and mechanism of the reaction of OH with CS_2 under atmospheric conditions. *J. Phys. Chem.* **1988**, *92*, 3846-3852, doi:10.1021/j100324a034.

(3) Jones, B. M. R.; Burrows, J. P.; Cox, R. A.; Penkett, S. A. OCS formation in the reaction of OH with CS_2. *Chem. Phys. Lett.* **1982**, *88*, 372-376, doi:10.1016/0009-2614(82)83028-5.

(4) Kurylo, M. J. Flash photolysis resonance fluorescence investigation of the reactions of OH radicals with OCS and CS_2. *Chem. Phys. Lett.* **1978**, *58*, 238-242, doi:10.1016/0009-2614(78)80285-1.

(5) Kurylo, M. J.; Laufer, A. H. Evidence for atom exchange in OH reactions with carbonyl compounds: $^{18}OH + CO_2 \rightarrow {}^{18}OCO + OH$; $^{18}OH + CO \rightarrow {}^{18}OC + OH$. *J. Chem. Phys.* **1979**, *70*, 2032-2033, doi:10.1063/1.437638.

I17. $CS_2OH + O_2$. Three groups have obtained kinetic information about this reaction by observing either the perturbation of OH/CS_2OH equilibration kinetics upon addition of O_2, or by modeling the dependence of the observed rate constant for OH loss on [O_2]. Hynes et al.[2] (251−348 K), Murrells et al.[7] (249−318 K), and Diau and Lee[1] (298 K) agree quite well on the value of k, with an average value of 2.8×10^{-14} cm^3 molecule^{-1} s^{-1} independent of temperature and pressure being recommended. Diau and Lee also report rate constants for the reactions of the adduct (CS_2OH) with NO and NO_2 to be 7.3×10^{-13} and 4.2×10^{-11} cm^3 molecule^{-1} s^{-1}, respectively.

From a mechanistic viewpoint, the primary products of this reaction determine the products of CS_2 oxidation in air. Lovejoy et al.[4] have shown that the yields of HO_2 and SO_2 are equal and near unity. Further insight is provided by the mechanistic study of Stickel et al.,[8] who observe OCS and CO product yields of (0.83 ± 0.08) and (0.16 ± 0.03), respectively. The results from this study are interpreted to imply that OCS and CO are formed either as primary products of the $CS_2OH + O_2$ reaction or as products of a secondary reaction between a primary product and O_2. These same authors report an SO_2 yield of (1.15 ± 0.10), with the results suggesting that only about 75% of the SO_2 is formed as a prompt product, with the remainder generated via a slow reaction of SO (generated as a prompt product of the $CS_2OH + O_2$ reaction) with O_2. Insight into the specific reaction pathways can be gleaned from the study of Lovejoy et al.[3] (249−340 K) in which the rate constant for the reaction of $CS_2OD + O_2$ was found to be the same as that for $CS_2OH + O_2$, indicating that simple H atom abstraction is not the likely process. Rather, HO_2 production most likely involves complex formation followed by HO_2 elimination. Lovejoy et al.[5] (340 K) found that the ^{18}O atom in the ^{18}OH reactant is transferred predominantly (90 ± 20)% to the SO_2 product. These findings are consistent with an S–O-bonded CS_2–OH adduct and preservation of the S–O bond in the steps leading to SO_2 formation.

Theoretical studies by Zhang and Qin[9] and by McKee and Wine[6] have provided further insight into the reaction mechanism. The initial step is, indeed, formation of SCS−OH followed by addition of O_2 to the carbon atom. A key subsequent step appears to be an O atom transfer to the sulfur bearing the hydroxyl group which leads directly to HOSO + OCS. The reaction HOSO + O_2 → HO_2 + SO_2 is expected to occur rapidly under atmospheric conditions. One remaining problem is identification of the pathway for generation of CO, which is observed as a minor product.
(Table: 06-2, Note: 06-2, Evaluated: 06-2) Back to Table

(1) Diau, E. W.-G.; Lee, Y.-P. Kinetics of the reactions of CS_2OH with O_2, NO, and NO_2. *J. Phys. Chem.* **1991**, *95*, 7726-7732, doi:10.1021/j100173a033.

(2) Hynes, A. J.; Wine, P. H.; Nicovich, J. M. Kinetics and mechanism of the reaction of OH with CS_2 under atmospheric conditions. *J. Phys. Chem.* **1988**, *92*, 3846-3852, doi:10.1021/j100324a034.

(3) Lovejoy, E. R.; Kroeger, K. S.; Ravishankara, A. R. The kinetics of the $CS_2OH + O_2$ reaction. *Chem. Phys. Lett.* **1990**, *167*, 183-187, doi:10.1016/0009-2614(90)85002-T.

(4) Lovejoy, E. R.; Murrells, T. P.; Ravishankara, A. R.; Howard, C. J. Oxidation of CS_2 by reaction with OH. 2. Yields of HO_2 and SO_2 in oxygen. *J. Phys. Chem.* **1990**, *94*, 2386-2393, doi:10.1021/j100369a037.

(5) Lovejoy, E. R.; Ravishankara, A. R.; Howard, C. J. Yield of $^{16}OS^{18}O$ from the ^{18}OH initiated oxidation of CS_2 in $^{16}O_2$. *Int. J. Chem. Kinet.* **1994**, *26*, 551-560, doi:10.1002/kin.550260508.

(6) McKee, M. L.; Wine, P. H. Ab initio study of the atmospheric oxidation of CS_2. *J. Am. Chem. Soc.* **2001**, *123*, 2344-2353, doi:10.1021/ja003421p.

(7) Murrells, T. P.; Lovejoy, E. R.; Ravishankara, A. R. Oxidation of CS_2 by reaction with OH. 1. Equilibrium constant for the reaction OH + CS_2 ⇄ CS_2OH and the kinetics of the $CS_2OH + O_2$ reaction. *J. Phys. Chem.* **1990**, *94*, 2381-2386, doi:10.1021/j100369a036.

(8) Stickel, R. E.; Chin, M.; Daykin, E. P.; Hynes, A. J.; Wine, P. H.; Wallington, T. J. Mechanistic studies of the OH-initiated oxidation of CS_2 in the presence of O_2. *J. Phys. Chem.* **1993**, *97*, 13653-13661, doi:10.1021/j100153a038.

(9) Zhang, L.; Qin, Q.-Z. Theoretical studies on CS_2OH-O_2: a possible intermediate in the OH initiated oxidation of CS_2 by O_2. *J. Mol. Structure (Theochem)* **2000**, *531*, 375-379, doi:10.1016/S0166-1280(00)00455-3.

I18. OH + CH_3SH. This recommendation is based on a composite fit to the data of Atkinson et al.,[1] (300−423 K), Wine et al.[10] (244–366 K), Wine et al.[11] (254−430 K), and Hynes and Wine[5] (270, 300 K), which are in excellent agreement. The results from the relative rate study of Barnes et al.[2] (298 K) are in agreement with this recommendation and indicate that the higher value of Cox and Sheppard[4] (298 K) is due to complications resulting from the presence of O_2 and NO in their reaction system. MacLeod et al.[7,8] (298 K; 293 K) and Lee and Tang[6] (298 K) obtained rate constants at 298 K approximately 50% lower than recommended here. These authors also obtained lower values for the ethanethiol reaction in comparison with results from studies upon which the methanethiol recommendation is made. Wine et al.[11] present evidence that this reaction proceeds

via adduct formation to produce a species that is thermally stable over the temperature range and time scales of the kinetic measurements. Tyndall and Ravishankara[9] have determined the yield of CH_3S (via laser–induced fluorescence) to be unity, indicating that any adduct must be short lived (less than 100 μs). Longer lifetimes would have led to anomalies in the OH decay kinetics used for the rate constant determinations. Butkovskaya and Setser,[3] based on observations of IR emissions from the products of the reactions of OH and OD with CH_3SH and CH_3SD, conclude that H-abstraction from the methyl group occurs with a yield of 24 ± 8% for the OH reactions and 11 ± 4% for the OD reactions. Hynes and Wine[5] observed that the rate constant is independent of O_2 partial pressure.
(Table: 06-2, Note: 06-2, Evaluated: 06-2) Back to Table

(1) Atkinson, R.; Perry, R. A.; Pitts, J. N., Jr. Rate constants for the reaction of the OH radical with CH_3SH and CH_3NH_2 over the temperature range 299-426 °K. *J. Chem. Phys.* **1977**, *66*, 1578-1581, doi:10.1063/1.434076.
(2) Barnes, I.; Bastian, V.; Becker, K. H.; Fink, E. H.; Nelsen, W. Oxidation of sulphur compounds in the atmosphere: I. Rate constants of OH radical reactions with sulphur dioxide, hydrogen sulphide, aliphatic thiols and thiophenol. *J. Atmos. Chem.* **1986**, *4*, 445-466, doi:10.1007/BF00053845.
(3) Butkovskaya, N. I.; Setser, D. W. Product branching fractions and kinetic isotope effects for the reactions of OH and OD radicals with CH_3SH and CH_3SD. *J. Phys. Chem. A* **1999**, *103*, 6921-6929, doi:10.1021/jp9914828.
(4) Cox, R. A.; Sheppard, D. Reactions of OH radicals with gaseous sulphur compounds. *Nature* **1980**, *284*, 330-331, doi:10.1038/284330a0.
(5) Hynes, A. J.; Wine, P. H. Kinetics of the OH + CH_3SH reaction under atmospheric conditions. *J. Phys. Chem.* **1987**, *91*, 3672-3676, doi:10.1021/j100297a042.
(6) Lee, J. H.; Tang, I. N. Absolute rate constants for the hydroxyl radical reactions with CH_3SH adn C_2H_5SH at room temperature. *J. Chem. Phys.* **1983**, *78*, 6646-6649, doi:10.1063/1.444663.
(7) MacLeod, H.; Jourdain, J. L.; Poulet, G.; Le Bras, G. Kinetic study of reactions of some organic sulfur compounds with OH radicals. *Atmos. Environ.* **1984**, *18*, 2621-2626, doi:10.1016/0004-6981(84)90326-3.
(8) MacLeod, H.; Poulet, G.; Le Bras, G. Etude cinetique des reactions du radical OH avec CH_3SCH_3, CH_3SH et C_2H_5SH. *J. Chim. Phys.* **1983**, *80*, 287-292, doi:10.1051/jcp/1983800287.
(9) Tyndall, G. S.; Ravishankara, A. R. Kinetics of the reaction of CH_3S with O_3 at 298 K. *J. Phys. Chem.* **1989**, *93*, 4707-4710, doi:10.1021/j100349a006.
(10) Wine, P. H.; Kreutter, N. M.; Gump, C. A.; Ravishankara, A. R. Kinetics of OH reactions with the atmospheric sulfur compounds H_2S, CH_3SH, CH_3SCH_3, and CH_3SSCH_3. *J. Phys. Chem.* **1981**, *85*, 2660-2665, doi:10.1021/j150618a019.
(11) Wine, P. H.; Thompson, R. J.; Semmes, D. H. Kinetics of OH reactions with aliphatic thiols. *Int. J. Chem. Kinet.* **1984**, *16*, 1623-1636, doi:10.1002/kin.550161215.

I19. $OH + CH_3SCH_3 \rightarrow H_2O + CH_2SCH_3$. The OH + CH_3SCH_3 reaction is complex, proceeding by both H-abstraction and reversible addition pathways. In the presence of atmospheric levels of O_2, adduct reaction with O_2 makes the addition pathway partially irreversible. Only kinetic data obtained in the absence of O_2 and at low enough CH_3SCH_3 concentrations for the adduct to be a negligible reservoir for OH are considered in evaluation of the H-abstraction rate constant. Thus, this recommendation is based on the results of Hynes et al.[8] (250−310 K), Wine et al.[22] (248–363 K), Hsu et al.[7] (260–393 K), Abbatt et al.[1] (297–368 K), Barone et al.[6] (217–240 K), Turnipseed et al.[15] (298 K), Williams et al.[19-21] (261, 298 K; 240–245 K; 240–295 K), and Wang et al.[18] The earlier larger rate constant values of Atkinson et al.[3] (300−426 K) and Kurylo[10] (273–400 K) are presumably due to reactive impurities, while those of MacLeod et al.[11] (373, 573 K) were most likely overestimated because of heterogeneous reactions. Unlike other temperature dependence studies, the rate constants reported by Albu et al.[2] (250−299 K) suggest a significant negative activation energy, leading to suspicion of an interference from adduct reaction with impurity O_2. Absolute determinations lower than those recommended were obtained by Martin et al.[12] (273–318 K), Wallington et al.[17] (296 K), and Nielsen et al.[13] (295 K). The reasons for these differences are not readily apparent. Confirmation that H-abstraction is the dominant pathway under the experimental conditions specified above comes from the studies of Stickel et al.[14] (298–348 K) and Turnipseed et al. Stickel et al. used tunable diode laser spectroscopy to measure an HDO product yield of 0.84 ± 0.15 for the OD + CH_3SCH_3 reaction in 10−30 Torr N_2, while Turnipseed et al. used laser induced fluorescence observations of CH_3S production from OH + CH_3SCH_3 to show that the branching ratio for the CH_3S elimination channel is <0.04 and the direct H-abstraction yield is 0.84 ± 0.26. Further support for the dominance of the H-abstraction pathway comes from the work of Zhao et al.,[23] who obtained an upper limit yield of 0.07 for the methyl elimination channel in the OD + CH_3SCH_3 reaction. Barnes et al.,[4,5] Turnipseed et al., and Urbanski et al.[16] report that the abstraction product CH_3SCH_2 is converted predominantly to CH_3S under atmospheric conditions. Barnes et al.[4] measured a 0.7% yield of OCS under low NO_x conditions,

which they attribute to further oxidation of CH_3S. A theoretical study by Jorgensen and Kjaergaard[9] suggests that complexation of CH_3SCH_3 with a single water molecule can speed up the reaction by lowering the energy of the transition state relative to the energy of the reactants.
(Table: 10-6, Note: 15-10, Evaluated: 10-6) Back to Table

(1) Abbatt, J. P. D.; Fentner, F. F.; Anderson, J. G. High-pressure discharge flow kinetics study of OH + CH_3SCH_3, CH_3SSCH_3 → products from 297 to 368 K. *J. Phys. Chem.* **1992**, *96*, 1780-1785, doi:10.1021/j100183a053.

(2) Albu, M.; Barnes, I.; Becker, K. H.; Patroescu-Klotz, I.; Mocannu, R.; Benter, T. Rate coefficients for the gas-phase reaction of OH radicals withdimethyl sulfide: temperature and O_2 partial pressure dependnece. *Phys. Chem. Chem. Phys.* **2006**, *8*, 728-736, doi:10.1039/b512536g.

(3) Atkinson, R.; Perry, R. A.; Pitts Jr., J. N. Rate constants for the reaction of OH radicals with COS, CS_2 and CH_3SCH_3 over the temperature range 299-430 K. *Chem. Phys. Lett.* **1978**, *54*, 14-18, doi:10.1016/0009-2614(78)85653-X.

(4) Barnes, I.; Becker, K. H.; Patroescu, I. The tropospheric oxidation of dimethyl sulfide: A new source of carbonyl sulfide. *Geophys. Res. Lett.* **1994**, *21*, 2389-2392, doi:10.1029/94GL02499.

(5) Barnes, I.; Becker, K. H.; Patroescu, I. FTIR product study of the OH initiated oxidation of dimethyl sulphide: Observation of carbonyl sulphide and dimethyl sulphoxide. *Atmos. Environ.* **1996**, *30*, 1805-1814, doi:10.1016/1352-2310(95)00389-4.

(6) Barone, S. B.; Turnipseed, A. A.; Ravishankara, A. R. Reaction of OH with dimethyl sulfide (DMS). 1. Equilibrium constant for OH + DMS reaction and the kinetics of the OH•DMS + O_2 reaction. *J. Phys. Chem.* **1996**, *100*, 14694-14702, doi:10.1021/jp960866k.

(7) Hsu, Y.-C.; Chen, D.-S.; Lee, Y.-P. Rate constant for the reaction of OH radicals with dimethyl sulfide. *Int. J. Chem. Kinet.* **1987**, *19*, 1073-1082, doi:10.1002/kin.550191204.

(8) Hynes, A. J.; Wine, P. H.; Semmes, D. H. Kinetics and mechanism of OH reactions with organic sulfides. *J. Phys. Chem.* **1986**, *90*, 4148-4156, doi:10.1021/j100408a062.

(9) Jorgensen, S.; Kjaergaard, H. G. Effect of hydration on the hydrogen abstraction reaction by OH in DMS and its oxidation products. *J. Phys. Chem. A* **2010**, *114*, 4857-4863, doi:10.1021/jp910202n.

(10) Kurylo, M. J. Flash photolysis resonance fluorescence investigation of the reaction of OH radicals with dimethyl sulfide. *Chem. Phys. Lett.* **1978**, *58*, 233-237, doi:10.1016/0009-2614(78)80284-X.

(11) MacLeod, H.; Poulet, G.; Le Bras, G. Etude cinetique des reactions du radical OH avec CH_3SCH_3, CH_3SH et C_2H_5SH. *J. Chim. Phys.* **1983**, *80*, 287-292, doi:10.1051/jcp/1983800287.

(12) Martin, D.; Jourdain, J. L.; Le Bras, G. Kinetic study for the reactions of OH radicals with dimethylsulfide, diethylsulfide, tetrahydrothiophene, and thiophene. *Int. J. Chem. Kinet.* **1985**, *17*, 1247-1261, doi:10.1002/kin.550171202.

(13) Nielsen, O. J.; Sidebottom, H. W.; Nelson, L.; Treacy, J. J.; O'Farrell, D. J. An absolute and relative rate study of the reaction of OH radicals with dimethyl sulfide. *Int. J. Chem. Kinet.* **1989**, *21*, 1101-1112, doi:10.1002/kin.550211203.

(14) Stickel, R. E.; Zhao, Z.; Wine, P. H. Branching ratios for hydrogen transfer in the reactions of OD radicals with CH_3SCH_3 and $CH_3SC_2H_5$. *Chem. Phys. Lett.* **1993**, *212*, 312-318, doi:10.1016/0009-2614(93)89331-B.

(15) Turnipseed, A. A.; Barone, S. B.; Ravishankara, A. R. Reaction of OH with dimethyl sulfide. 2. Products and mechanisms. *J. Phys. Chem.* **1996**, *100*, 14703-14713, doi:10.1021/jp960867c.

(16) Urbanski, S. P.; Stickel, R. E.; Zhao, Z.; Wine, P. H. Mechanistric and kinetic study of formaldehyde production in the atmospheric oxidation of dimethyl sulfide. *J. Chem. Soc. Faraday Trans.* **1997**, *93*, 2813-2819, doi:10.1039/a701380i.

(17) Wallington, T. J.; Atkinson, R.; Tuazon, E. C.; Aschmann, S. M. The reaction of OH radicals with dimethyl sulfide. *Int. J. Chem. Kinet.* **1986**, *18*, 837-846, doi:10.1002/kin.550180804.

(18) Wang, H.-T.; Zhang, Y.-J.; Mu, Y.-J. Rate constants for reactions of OH with several reduced sulfur compounds determined by relative rate constant method. *Acta Phys.-Chim. Sin.* **2008**, *24*, 945-950, doi:10.1016/S1872-1508(08)60041-8.

(19) Williams, M. B.; Campuzano-Jost, P.; Bauer, D.; Hynes, A. J. Kinetic and mechanistic studies of the OH-initiated oxidation of dimethylsulfide at low temperature — A reevaluation of the rate coefficient and branching ratio. *Chem. Phys. Lett.* **2001**, *344*, 61-67, doi:10.1016/S0009-2614(01)00764-3.

(20) Williams, M. B.; Campuzano-Jost, P.; Cossairt, B. M.; Hynes, A. J.; Pounds, A. J. Experimental and theoretical studies of the reaction of the OH radical with alkyl sulfides: 1. Direct observations of the formation of the OH-DMS adduct-pressure dependence of the forward rate of addition and development of a predictive expression at low temperature. *J. Phys. Chem. A* **2007**, *111*, 89-104, doi:10.1021/jp063873+.

(21) Williams, M. B.; Campuzano-Jost, P.; Hynes, A. J.; Pounds, A. J. Experimental and theoretical studies of the reaction of the OH radical with alkyl sulfides: 3. Kinetics and mechanism of the OH initiated

oxidation of dimethyl, dipropyl, and dibutyl sulfides: Reactivity trends in the alkyl sulfides and development of a predictive expression for the reaction of OH with DMS. *J. Phys. Chem. A* **2009**, *113*, 6697-6709, doi:10.1021/Jp9010668.

(22) Wine, P. H.; Kreutter, N. M.; Gump, C. A.; Ravishankara, A. R. Kinetics of OH reactions with the atmospheric sulfur compounds H_2S, CH_3SH, CH_3SCH_3, and CH_3SSCH_3. *J. Phys. Chem.* **1981**, *85*, 2660-2665, doi:10.1021/j150618a019.

(23) Zhao, Z.; Stickel, R. E.; Wine, P. H. Branching ratios for methyl elimination in the reactions of OD radicals and Cl atoms with CH_3SCH_3. *Chem. Phys. Lett.* **1996**, *251*, 59-66, doi:10.1016/0009-2614(96)00059-0.

I20. OH + CH_3SCH_3⟶ $(CH_3)_2SOH$ → products. The OH + CH_3SCH_3 reaction is complex, proceeding by both direct H-abstraction and reversible addition pathways. A recommendation for the direct reaction is given separately in Table 1. The product of the reversible addition pathway reacts with O_2 creating an irreversible path as well. Mechanistically, this pathway is described by combining the rate constants k_f for the addition step, k_r for the reverse dissociation step, and k_{O2} for the adduct reaction with O_2. The equilibrium constant for the reversible addition process is $K_c = k_f/k_r$. Recommendations for K_c, k_f, and k_{O2} are found in Tables 3, 2, and 1, respectively. Subtracting the temperature-dependent H-abstraction rate constant from the overall irreversible rate constant (which depends on T, P, and P_{O2}) yields the rate constant for irreversible addition (k_{ia}), which can be expressed as:

$$k_{ia} = K_c\, k_{O2}\, [O_2] / (1 + (K_c\, k_{O2}\, [O_2] / k_f)).$$

Much of the kinetic data available for evaluating this reaction were obtained for OH + CD_3SCD_3. Although the methyl hydrogens are not directly involved in the reaction, the rate constants for OH addition reactions with CH_3SCH_3 and CD_3SCD_3 differ somewhat[6] as they are in the low-pressure limit where the value depends on the density of states, which are different for the two isotopomers. The recommended expression (units are cm^3 $molecule^{-1}$ s^{-1}),

$$k_{ia}(T,[O_2],[M]) = 8.2 \times 10^{-39}\, [O_2]\, \exp(+5376/T) / (1 + 1.05 \times 10^{-5}\, ([O_2] / [M])\, \exp(+3644/T)),$$

is based on the recommendations for K_c, k_f, and k_{O2} given elsewhere in this evaluation. It reproduces the data of Hynes et al.,[2] Williams et al.,[4-6] and Albu et al.[1] quite well for both isotopomers and for all mole fractions of O_2 in N_2/O_2 mixtures; however, it should be used with caution at temperatures below 240 K (where no data are available) or above 310 K (where k_{ia} is very small). The 298 K relative rate study of Wang et al.[3] suggests rate constants in air and pure O_2 at atmospheric pressure that are about a factor of two faster than those predicted by the above expression. Since the kinetic data of Hynes et al. and Williams et al. were obtained by monitoring OH loss, the overall rate constant for removal of CH_3SCH_3 would be underestimated if the adduct + O_2 reaction generated OH + dimethylsulfone ($CH_3(O)S(O)CH_3$) with a significant yield; the available data cannot rule out a small but significant branching ratio for this channel.
(Table: 10-6, Note: 10-6, Evaluated: 10-6) Back to Table

(1) Albu, M.; Barnes, I.; Becker, K. H.; Patroescu-Klotz, I.; Mocannu, R.; Benter, T. Rate coefficients for the gas-phase reaction of OH radicals withdimethyl sulfide: temperature and O_2 partial pressure dependnece. *Phys. Chem. Chem. Phys.* **2006**, *8*, 728-736, doi:10.1039/b512536g.

(2) Hynes, A. J.; Wine, P. H.; Semmes, D. H. Kinetics and mechanism of OH reactions with organic sulfides. *J. Phys. Chem.* **1986**, *90*, 4148-4156, doi:10.1021/j100408a062.

(3) Wang, H.-T.; Zhang, Y.-J.; Mu, Y.-J. Rate constants for reactions of OH with several reduced sulfur compounds determined by relative rate constant method. *Acta Phys.-Chim. Sin.* **2008**, *24*, 945-950, doi:10.1016/S1872-1508(08)60041-8.

(4) Williams, M. B.; Campuzano-Jost, P.; Bauer, D.; Hynes, A. J. Kinetic and mechanistic studies of the OH-initiated oxidation of dimethylsulfide at low temperature — A reevaluation of the rate coefficient and branching ratio. *Chem. Phys. Lett.* **2001**, *344*, 61-67, doi:10.1016/S0009-2614(01)00764-3.

(5) Williams, M. B.; Campuzano-Jost, P.; Cossairt, B. M.; Hynes, A. J.; Pounds, A. J. Experimental and theoretical studies of the reaction of the OH radical with alkyl sulfides: 1. Direct observations of the formation of the OH-DMS adduct-pressure dependence of the forward rate of addition and development of a predictive expression at low temperature. *J. Phys. Chem. A* **2007**, *111*, 89-104, doi:10.1021/jp063873+.

(6) Williams, M. B.; Campuzano-Jost, P.; Hynes, A. J.; Pounds, A. J. Experimental and theoretical studies of the reaction of the OH radical with alkyl sulfides: 3. Kinetics and mechanism of the OH initiated oxidation of dimethyl, dipropyl, and dibutyl sulfides: Reactivity trends in the alkyl sulfides and development of a predictive expression for the reaction of OH with DMS. *J. Phys. Chem. A* **2009**, *113*, 6697-6709, doi:10.1021/Jp9010668.

I21. **$(CH_3)_2SOH + O_2$.** All available kinetic data for this reaction were obtained by measuring k_{obs} for the OH + CH_3SCH_3 reaction as a function of O_2 partial pressure ($k_{obs} \equiv$ the sum of the rate constants for H-abstraction and irreversible addition). Much of the available data were obtained for OH + CD_3SCD_3. Since the methyl hydrogens are not directly involved in the reaction, the rate constant is expected to be virtually the same for CH_3SCH_3 as for CD_3SCD_3; hence, data for both reactants are used in the evaluation. The recommendation is based on the data of Hynes et al.[3] (250, 258, 267 K), Barone et al.[1] (217–240 K), and Williams et al.[8,9] (240–245 K; 240–295 K). The Hynes et al.[4] study supersedes an earlier report of a considerably faster rate constant. Over the range of experimental conditions where data are available (222–267 K and 30–200 Torr), the rate constant appears to be independent of temperature and pressure. By monitoring the regeneration of OH in the presence of NO, Hynes et al.[2] and Turnipseed et al.[7] have determined the yield for the HO_2 + $CH_3S(O)CH_3$ (DMSO) channel to be ~0.5. A theoretical study by Ramirez-Anguita et al.[5] suggests possible pathways for generating CH_3SOH + CH_3OO/CH_2OOH. A second theoretical study by the same authors supports the experimental finding that the rate constant has little temperature or pressure dependence.[6]
(Table: 10-6, Note: 15-10, Evaluated: 10-6) Back to Table

(1) Barone, S. B.; Turnipseed, A. A.; Ravishankara, A. R. Reaction of OH with dimethyl sulfide (DMS). 1. Equilibrium constant for OH + DMS reaction and the kinetics of the OH•DMS + O_2 reaction. *J. Phys. Chem.* **1996**, *100*, 14694-14702, doi:10.1021/jp960866k.

(2) Hynes, A. J.; Stickel, R. E.; Pounds, A. J.; Zhao, Z.; McKay, T.; Bradshaw, J. D.; Wine, P. H. *Dimethylsulfide: Oceans, Atmosphere, and Climate, ed. by G. Restelli and G. Angletti, Kluwer Academic Publishers, Brusse;Science* **1993**, 211-221.

(3) Hynes, A. J.; Stocker, R. B.; Pounds, A. J.; Mckay, T.; Bradshaw, J. D.; Nicovich, J. M.; Wine, P. H. A mechanistic study of the reaction of OH with dimethyl-d_6 sulfide. Direct observation of adduct formation and the kinetics of the adduct reaction with O_2. *J. Phys. Chem.* **1995**, *99*, 16967-16975, doi:10.1021/j100046a024.

(4) Hynes, A. J.; Wine, P. H.; Semmes, D. H. Kinetics and mechanism of OH reactions with organic sulfides. *J. Phys. Chem.* **1986**, *90*, 4148-4156, doi:10.1021/j100408a062.

(5) Ramirez-Anguita, J. M.; Gonzalez-Lafont, A.; Lluch, J. M. Formation pathways of CH_3SOH from $CH_3S(OH)CH_3$ in the presence of O_2: a theoretical study *Theor. Chem. Acc.* **2009**, *123*, 93-103, doi:10.1007/s00214-009-0547-7.

(6) Ramírez-Anguita, J. M.; González-Lafont, A.; Lluch, J. M. Variational transition-state theory study of the rate constant of the DMS•OH scavenging reaction by O_2. *J. Comput. Chem.* **2011**, *32*, 2104-2118, doi:10.1002/jcc.21793.

(7) Turnipseed, A. A.; Barone, S. B.; Ravishankara, A. R. Reaction of OH with dimethyl sulfide. 2. Products and mechanisms. *J. Phys. Chem.* **1996**, *100*, 14703-14713, doi:10.1021/jp960867c.

(8) Williams, M. B.; Campuzano-Jost, P.; Cossairt, B. M.; Hynes, A. J.; Pounds, A. J. Experimental and theoretical studies of the reaction of the OH radical with alkyl sulfides: 1. Direct observations of the formation of the OH-DMS adduct-pressure dependence of the forward rate of addition and development of a predictive expression at low temperature. *J. Phys. Chem. A* **2007**, *111*, 89-104, doi:10.1021/jp063873+.

(9) Williams, M. B.; Campuzano-Jost, P.; Hynes, A. J.; Pounds, A. J. Experimental and theoretical studies of the reaction of the OH radical with alkyl sulfides: 3. Kinetics and mechanism of the OH initiated oxidation of dimethyl, dipropyl, and dibutyl sulfides: Reactivity trends in the alkyl sulfides and development of a predictive expression for the reaction of OH with DMS. *J. Phys. Chem. A* **2009**, *113*, 6697-6709, doi:10.1021/Jp9010668.

I22. **OH + CH_3SCH_2Cl.** The recommendation is based on the low-pressure discharge flow resonance fluorescence study of Shallcross et al.[1] (298 K). The uncertainty reflects the fact that only one study performed under a limited range of experimental conditions has been reported. Shallcross et al. suggest that the likely reaction pathway is H-abstraction under the low-pressure conditions of their experiments. However, further experimental and/or theoretical research is needed before an addition-elimination pathway involving C−S bond cleavage can be ruled out. If H-abstraction dominates at low pressure, then under atmospheric conditions the rate constant could be significantly faster than reported by Shallcross et al. due to the occurrence of an irreversible addition channel at higher pressure and in the presence of O_2.
(Table: 10-6, Note: 10-6, Evaluated: 10-6) Back to Table

(1) Shallcross, D. E.; Vaughn, S.; Trease, D. R.; Canosa-Mas, C.; Ghosh, M. V.; Dyke, J. M.; Wayne, R. P. Kinetics of the reaction between OH radicals and monochlorodimethylsulphide (CH_3SCH_2Cl). *Atmos. Environ.* **2006**, *40*, 6899-6904, doi:10.1016/j.atmosenv.2006.06.037.

I23. **OH + CH_3SSCH_3.** This recommendation is based on the temperature–dependent studies of Wine et al.[7] (249–367 K) and Abbatt et al.[1](297–368 K) and the room temperature relative rate study of Cox and Sheppard[5] (298 K). Domine and Ravishankara[6] have observed both CH_3S (via laser–induced fluorescence) and CH_3SOH (via photo-ionization mass spectrometry) as products of this reaction. At 298 K, the yield of CH_3S alone was quantified at approximately 30%. An FTIR product study of the photooxidation of dimethyl disulfide by Barnes et al.[2] presents evidence that oxidation of the CH_3SOH product is the principal source of the methane sulfonic acid observed. Butkovskaya and Setser[3] have observed that HDO and D_2O are produced from OD + CH_3SSCH_3 in the same proportion and with the same vibrational state distributions as the products observed by the same investigators in a similar study of the OD + CH_3SD reaction,[4] leading these authors to suggest that the major product channel for OD + CH_3SSCH_3 is CH_3SD + CH_3SO.
(Table: 94-26, Note: 94-26, Evaluated: 94-26) Back to Table

(1) Abbatt, J. P. D.; Fentner, F. F.; Anderson, J. G. High-pressure discharge flow kinetics study of OH + CH_3SCH_3, CH_3SSCH_3 → products from 297 to 368 K. *J. Phys. Chem.* **1992**, *96*, 1780-1785, doi:10.1021/j100183a053.
(2) Barnes, I.; Becker, K. H.; Mihalopoulas, N. An FTIR product study of the photooxidation of dimethyl disulfide. *J. Atmos. Chem.* **1994**, *18*, 267-289, doi:10.1007/BF00696783.
(3) Butkovskaya, N. I.; Setser, D. W. Mechanism for the reaction of hydroxyl radicals with dimethyl disulfide. *Chem. Phys. Lett.* **1999**, *312*, 37-44, doi:10.1016/S0009-2614(99)00862-3.
(4) Butkovskaya, N. I.; Setser, D. W. Product branching fractions and kinetic isotope effects for the reactions of OH and OD radicals with CH_3SH and CH_3SD. *J. Phys. Chem. A* **1999**, *103*, 6921-6929, doi:10.1021/jp9914828.
(5) Cox, R. A.; Sheppard, D. Reactions of OH radicals with gaseous sulphur compounds. *Nature* **1980**, *284*, 330-331, doi:10.1038/284330a0.
(6) Domine, F.; Ravishankara, A. R. The yield of CH_3S from the reaction of OH with CH_3SSCH_3. *Int. J. Chem. Kinet.* **1992**, *24*, 943-951, doi:10.1002/kin.550241104.
(7) Wine, P. H.; Kreutter, N. M.; Gump, C. A.; Ravishankara, A. R. Kinetics of OH reactions with the atmospheric sulfur compounds H_2S, CH_3SH, CH_3SCH_3, and CH_3SSCH_3. *J. Phys. Chem.* **1981**, *85*, 2660-2665, doi:10.1021/j150618a019.

I24. **OH + $CH_3S(O)CH_3$.** The recommended k(298 K) is the average of the direct studies of Hynes and Wine[4] (298–401 K), Urbanski et al.[8] (298 K), and Kukui et al.[6] (298 K), which employed three different experimental approaches and are in excellent agreement. Competitive kinetics studies by Barnes et al.[2] and Falbe-Hanson et al.[3] (298 K) report rate constants in 1 atm. of air about a factor of 1.5 slower than those obtained in the direct studies. The recommended value for E/R is based on the only study of the temperature dependence,[4] where a significant negative activation energy was observed. The large uncertainty in E/R reflects the availability of very limited data (none below room temperature). The experimental studies of Urbanski et al., Kukui et al., and Arsene et al.[1] (284 K), as well as the theoretical study of Wang and Zhang,[9] provide strong evidence that the dominant reaction channel is production of CH_3 + $CH_3S(O)OH$ (MSIA, methanesulfinic acid). Arsene et al. attribute the failure to observe MSIA production in the chamber study of Sorensen et al.[7] (298 K) to loss via secondary gas phase and condensed phase oxidation before sampling. A theoretical study by Jorgensen and Kjaergaard[5] suggests that the H-abstraction may be more important under atmospheric conditions than previously thought because (i) complexation of $CH_3S(O)CH_3$ with a single water molecule can speed up the H-abstraction reaction by lowering the energy of the transition state relative to the energy of the reactants and (ii) under atmospheric conditions a significant fraction of $CH_3S(O)CH_3$ is complexed with H_2O. However, as mentioned above, experimental information suggests that methyl elimination, not H-abstraction, is the dominant reaction pathway.
(Table: 06-2, Note: 15-10, Evaluated: 06-2) Back to Table

(1) Arsene, C.; Barnes, I.; Becker, K. H.; Schneider, W. F.; Wallington, T. J.; Mihalopoulos, N.; Patroescu-Klotz, J. V. Formation of methane sulfinic acid in the gas-phase OH-radical initiated oxidation of dimethyl sulfoxide. *Environ. Sci. Technol.* **2002**, *36*, 5155-5163, doi:10.1021/es020035u.
(2) Barnes, I.; Bastian, V.; Becker, K. H.; Martin, D. In *Biogenic Sulfur in the Environment*; ACS Symp. Ser, 1989; Vol. 393; pp 476-488.
(3) Falbe-Hansen, H.; Sorensen, S.; Jensen, N. R.; Pedersen, T.; Hjorth, J. Atmospheric gas-phase reactions of dimethylsulphoxide and dimethylsulphone with OH and NO_3 radicals, Cl atoms and ozone. *Atmos. Environ.* **2000**, *34*, 1543-1551, doi:10.1016/S1352-2310(99)00407-0.
(4) Hynes, A. J.; Wine, P. H. The atmospheric chemistry of dimethylsulfoxide (DMSO) kinetics and mechanism of the OH + DMSO reaction. *J. Atmos. Chem.* **1996**, *24*, 23-37, doi:10.1007/BF00053821.
(5) Jorgensen, S.; Kjaergaard, H. G. Effect of hydration on the hydrogen abstraction reaction by OH in DMS and its oxidation products. *J. Phys. Chem. A* **2010**, *114*, 4857-4863, doi:10.1021/jp910202n.

(6) Kukui, A.; Borrisenko, D.; Laverdet, G.; Le Bras, G. Gas-phase reactions of OH radicals with dimethyl sulfoxide and methane sulfinic acid using turbulent flow reactor and chemical ionization mass spectrometry. *J. Phys. Chem. A* **2003**, *107*, 5732-5742, doi:10.1021/jp0276911.
(7) Sørensen, S.; Falbe-Hansen, H.; Mangoni, M.; Hjorth, J.; Jensen, N. R. Observation of DMSO and $CH_3S(O)OH$ from the gas phase reaction between DMS and OH. *J. Atmos. Chem.* **1996**, *24*, 299-315, doi:10.1007/BF00210288.
(8) Urbanski; Stickel, R. E.; Wine, P. H. Mechanistic and kinetic study of the gas-phase reaction of hydroxyl radical with dimethyl sulfoxide. *J. Phys. Chem. A* **1998**, *102*, 10522-10529, doi:10.1021/jp9833911.
(9) Wang, L.; Zhang, J. Ab initio study of reaction of dimethyl sulfoxide (DMSO) with OH radical. *Chem. Phys. Lett.* **2002**, *356*, 490-496, doi:10.1016/S0009-2614(02)00397-4.

I25. OH + $CH_3S(O)OH$. The recommendation is based on a turbulent flow reactor − chemical ionization mass spectrometry study by Kukui et al.[2] (298 K), which was carried out with OH in excess over $CH_3S(O)OH$ at total pressures of 200−400 Torr N_2. The large uncertainty factor results from the facts that (1) only a single room temperature study is reported in the literature and (2) $CH_3S(O)OH$ is a difficult species to study in the gas phase because of its low vapor pressure. Kukui et al. found that SO_2 was produced as a reaction product with near unit yield, suggesting that the dominant reaction channel (at least in the absence of O_2) is production of $CH_3 + SO_2 + H_2O$. Theoretical studies by Gonzalez-Garcia et al.[1] and Tian et al.[3] provide strong evidence that the $CH_3S(O)OH$−OH adduct is too short-lived to react with O_2 under atmospheric conditions.
(Table: 10-6, Note: 10-6, Evaluated: 10-6) Back to Table

(1) Gonzalez-Garcia, N.; Gonzalez-Lafont, A.; Lluch, J. M. Methanesulfinic acid reaction with OH: Mechanism, rate constants, and atmospheric implications. *J. Phys. Chem. A* **2007**, *111*, 7825-7832, doi:10.1021/jp0722455.
(2) Kukui, A.; Borrisenko, D.; Laverdet, G.; Le Bras, G. Gas-phase reactions of OH radicals with dimethyl sulfoxide and methane sulfinic acid using turbulent flow reactor and chemical ionization mass spectrometry. *J. Phys. Chem. A* **2003**, *107*, 5732-5742, doi:10.1021/jp0276911.
(3) Tian, Y.; Tian, Z.-M.; Wei, W.-M.; He, T.-J.; Chen, D.-M.; Liu, F.-C. Ab initio study of the reaction of OH radical with methyl sulfinic acid (MSIA). *Chem. Phys.* **2007**, *335*, 133-140, doi:10.1016/j.chemphys.2007.04.009.

I26. OH + CH_3SO_3H. No gas-phase experimental data are available for this reaction, but a detailed theoretical study has been reported by Jorgensen et al.[1] Equilibrium and transition state structures were optimized using B3LYP density functional theory with the aug-cc-pV(T+d)Z basis set. Energies of stable species and transition states were refined using CCSD(T)-F12A theory with the VDZ-F12 basis set. Two different mechanisms were identified for producing $CH_3SO_3 + H_2O$, hydrogen atom transfer and proton coupled electron transfer. The 298 K rate constant was calculated using conventional transition state theory and found to be 8.3×10^{-15} cm^3 $molecule^{-1}$ s^{-1}. Given that a 5 kJ mol^{-1} error in a transition state energy can cause a factor of ten error in a calculated rate constant, the uncertainty in the theoretical rate constant is estimated to be around one order of magnitude. The role of water complexation with both reactants was examined theoretically and found to have no effect on the predicted rate constant under tropospheric conditions.
(Table: 15-10, Note: 15-10, Evaluated: 15-10) Back to Table

(1) Jorgensen, S.; Jensen, C.; Kjaergaard, H. G.; Anglada, J. M. The gas-phase reaction of methane sulfonic acid with the hydroxyl radical without and with water vapor. *Phys. Chem. Chem. Phys.* **2013**, *15*, 5140-5150, doi:10.1039/c3cp44034f.

I27. OH + $CH_3SC_2H_5$ → H-abstraction products. The recommendation is based on the 299 K study of Hynes et al.[2] and the temperature dependent (242−296 K) study of Williams et al.[4] Oksdath-Mansilla et al.[3] obtained a 298 K rate constant from a relative rate study that is 40% faster than the recommended value. A theoretical study by Cao et al.[1] suggests that abstraction of the secondary hydrogen is dominant (92% at 200 K and 85% at 300 K), with abstraction of the methyl hydrogen accounting for 7% of overall reactivity at 200 K and 12% at 300 K.
(Table: 15-10, Note: 15-10, Evaluated: 15-10) Back to Table

(1) Cao, J.; Wang, W.; Zhang, Y.; Wang, W.; Zhang, T.; Lv, J.; Li, C. Computational study on the reaction of $CH_3SCH_2CH_3$ with OH radical: mechanism and enthalpy of formation. *Theor. Chem. Acc.* **2011**, *129*, 771-780, doi:10.1007/s00214-011-0934-8.
(2) Hynes, A. J.; Wine, P. H.; Semmes, D. H. Kinetics and mechanism of OH reactions with organic sulfides. *J. Phys. Chem.* **1986**, *90*, 4148-4156, doi:10.1021/j100408a062.

(3) Oksdath-Mansilla, G.; Penenory, A. B.; Albu, M.; Barnes, I.; Wiesen, P.; Teruel, M. A. FTIR relative kinetic study of the reactions of $CH_3CH_2SCH_2CH_3$ and $CH_3CH_2SCH_3$ with OH radicals and Cl atoms at atmospheric pressure. *Chem. Phys. Lett.* **2009**, *477*, 22-27, doi:10.1016/j.cplett.2009.06.035.
(4) Williams, M. B.; Campuzano-Jost, P.; Pounds, A. J.; Hynes, A. J. Experimental and theoretical studies of the reaction of the OH radical with alkyl sulfides: 2. Kinetics and mechanism of the OH initiated oxidation of methylethyl and diethyl sulfides; observations of a two channel oxidation mechanism. *Phys. Chem. Chem. Phys.* **2007**, *9*, 4370-4382, doi:10.1039/b703957n.

I28. **$OH + CH_3SC_2H_5 \overset{M}{\leftrightarrow} CH_3S(OH)C_2H_5 \overset{O_2}{\rightarrow}$ products.** The OH + $CH_3SC_2H_5$ reaction is complex, proceeding by both direct H-abstraction and reversible addition pathways. A recommendation for the H-abstraction reaction is given separately in Table 1. The product of the reversible addition pathway reacts with O_2 creating an irreversible addition path as well. Mechanistically, this pathway is described by combining the rate constants k_f for the addition step, k_r for the reverse dissociation step, and k_{O2} for the adduct reaction with O_2. The equilibrium constant for the reversible addition process is $K_c = k_f/k_r$. Subtracting the H-abstraction rate constant (which depends only on T) from the overall observed rate constant (which depends on T, P, and P_{O2}) yields the rate constant for irreversible addition (k_{ia}), which can be expressed as

$$k_{ia} = K_c\, k_{O2}\, [O_2] \,/\, (1 + (K_c\, k_{O2}\, [O_2] \,/\, k_f)).$$

The expression given below (units are cm^3 $molecule^{-1}$ s^{-1}) is obtained by substituting values for K_c, k_f, and k_{O2} that are derived from the results of Williams et al.[5] (240, 245 K) into the expression given above. Because data are available only over a limited range of experimental conditions, the expression below should be used only for air bath gas at P = 680 ± 80 Torr and T >240 K.

$$k_{ia}(T, 680 \pm 80 \text{ Torr air}) = 1.17 \times 10^{-38} \exp(+5290/T) \;/\; (7.25 \times 10^{-22}\, T \;+\; 3.59 \times 10^{-26} \exp(+4170/T)).$$

The expression reproduces the laser flash photolysis data of Williams et al.,[5] and the relative rate data of Oksdath-Mansilla et al.[1,2] quite well. The relative rate study of Wang et al.[4] suggests values for $k_{abstraction} + k_{ir}$ in 760 Torr air at 297−346 K that are faster than suggested by the above expression and are inconsistent with the results of the other available studies. Oksdath-Mansilla et al. report the following product yields in NO_x-free air at 760 Torr and 298 K (where irreversible addition is a minor but significant reaction pathway): SO_2, 51 ± 2%; CH_3CHO, 57 ± 3%; HCHO, 46 ± 4%.[3]
(Table: 15-10, Note: 15-10, Evaluated: 15-10) Back to Table

(1) Oksdath-Mansilla, G.; Penenory, A. B.; Albu, M.; Barnes, I.; Wiesen, P.; Teruel, M. A. FTIR relative kinetic study of the reactions of $CH_3CH_2SCH_2CH_3$ and $CH_3CH_2SCH_3$ with OH radicals and Cl atoms at atmospheric pressure. *Chem. Phys. Lett.* **2009**, *477*, 22-27, doi:10.1016/j.cplett.2009.06.035.
(2) Oksdath-Mansilla, G.; Penenory, A. B.; Albu, M.; Barnes, I.; Wiesen, P.; Teruel, M. A. $CH_3CH_2SCH_3$ + OH radicals: temperature-dependent rate coefficient and product identification under atmospheric pressure of air. *J. Phys. Org. Chem.* **2010**, *23*, 925-930, doi:10.1002/poc.1714.
(3) Oksdath-Mansilla, G.; Penenory, A. B.; Barnes, I.; Wiesen, P.; Teruel, M. A. Photodegradation of $(CH_3CH_2)_2S$ and $CH_3CH_2SCH_3$ initiated by OH radicals at atmospheric pressure. Product yields and mechanism in NO_x free air. *Atmos. Environ.* **2012**, *55*, 263-270, doi:10.1016/j.atmosenv.2012.02.086.
(4) Wang, K.; Ge, M. F.; Wang, W. G. Temperature dependent kinetics of the gas-phase reaction of OH radicals with EMS. *Chin. Sci. Bull.* **2011**, *56*, 391-396, doi:10.1007/s11434-010-4313-y.
(5) Williams, M. B.; Campuzano-Jost, P.; Pounds, A. J.; Hynes, A. J. Experimental and theoretical studies of the reaction of the OH radical with alkyl sulfides: 2. Kinetics and mechanism of the OH initiated oxidation of methylethyl and diethyl sulfides; observations of a two channel oxidation mechanism. *Phys. Chem. Chem. Phys.* **2007**, *9*, 4370-4382, doi:10.1039/b703957n.

I29. **$CH_3S(OH)C_2H_5 + O_2$.** The recommendation is based on the results of Williams et al.,[1] who extracted rate constants from measurements of k_{obs} for the OH + $CH_3SC_2H_5$ reaction as a function of O_2 partial pressure (k_{obs} ≡ the sum of the rate constants for H-abstraction and irreversible addition). The derived rate constants were found to be independent of temperature (242−296 K) and pressure (200−600 Torr N_2 + O_2).
(Table: 15-10, Note: 15-10, Evaluated: 15-10) Back to Table

(1) Williams, M. B.; Campuzano-Jost, P.; Pounds, A. J.; Hynes, A. J. Experimental and theoretical studies of the reaction of the OH radical with alkyl sulfides: 2. Kinetics and mechanism of the OH initiated oxidation of methylethyl and diethyl sulfides; observations of a two channel oxidation mechanism. *Phys. Chem. Chem. Phys.* **2007**, *9*, 4370-4382, doi:10.1039/b703957n.

I30. OH + S. This recommendation is based on the study by Jourdain et al.[1] (298 K). Their measured value for k(298 K) compares favorably with the recommended value of k(O + OH) when one considers the slightly greater exothermicity of the present reaction.
(Table: 82-57, Note: 82-57, Evaluated: 82-57) Back to Table

(1) Jourdain, J. L.; Le Bras, G.; Combourieu, J. Kinetic study of some elementrary reactions fo sulfur compounds including reactions of S and SO with OH radicals. *Int. J. Chem. Kinet.* **1979**, *11*, 569-577, doi:10.1002/kin.550110603.

I31. OH + SO. The recommendation is based on the results of Blitz et al.[1] (295−703 K) who report the only temperature dependent data. Earlier studies by Fair and Thrush[2] and Jourdain et al.[3] report room temperature rate constants that are less precise but in good agreement with the results of Blitz et al. Only Blitz et al. data at ≤503 K are used to obtain the recommended value for E/R since data at higher temperatures show a significant non-Arrhenius temperature dependence. The recommended value for g is conservative because only one temperature dependence study has been reported. High level electronic structure calculations by Rodriguez-Linares et al.[4] suggest that the evolution from reactants to H + SO_2 products involves multiple transition states.
(Table: 19-5, Note: 19-5, Evaluated: 19-5) Back to Table

(1) Blitz, M. A.; McKee, K. W.; Pilling, M. J. Temperature dependence of the reaction of OH and SO. *Proc. Combust. Inst.* **2000**, *28*, 2491-2497, doi:10.1016/S0082-0784(00)80664-5.
(2) Fair, R. W.; Thrush, B. A. Reaction of hydrogen atoms with hydrogen sulphide in the presence of molecular oxygen. *Trans. Faraday Soc.* **1969**, *65*, 1557-1570, doi:10.1039/tf9696501557.
(3) Jourdain, J. L.; Le Bras, G.; Combourieu, J. Kinetic study of some elementrary reactions fo sulfur compounds including reactions of S and SO with OH radicals. *Int. J. Chem. Kinet.* **1979**, *11*, 569-577, doi:10.1002/kin.550110603.
(4) Rodriguez-Linares, D.; Freitas, G. N.; Ballester, M. Y.; Nascimento, M. A. C.; Garrido, J. D. Coupled-cluster study of the lower energy region of the ground electronic state of the HSO_2 potential energy surface. *J. Phys. Chem. A* **2015**, *119*, 8734-8743, doi:10.1021/acs.jpca.5b04554.

I32. OH + SO_2F_2. The recommended upper limit is based on the relative rate experiments of Papadimitriou et al.[2] (296 K). Less sensitive upper limits are reported by Dillon et al.[1] (294 K) and Sulbaek-Andersen et al.[3] (296 K).
(Table: 10-6, Note: 10-6, Evaluated: 10-6) Back to Table

(1) Dillon, T. J.; Horowitz, A.; Crowley, J. N. The atmospheric chemistry of sulphuryl fluoride, SO_2F_2. *Atmos. Chem. Phys.* **2008**, *8*, 1547-1557, doi:10.5194/acp-8-1547-2008.
(2) Papadimitriou, V. C.; Portmann, R. W.; Fahey, D. W.; Muhle, J.; Weiss, R. F.; Burkholder, J. B. Experimental and theoretical study of the atmospheric chemistry and global warming potential of SO_2F_2. *J. Phys. Chem. A* **2008**, *112*, 12657-12666, doi:10.1021/jp806368u.
(3) Sulbaek-Andersen, M. P.; Blake, D. R.; Rowland, F. S.; Hurley, M. D.; Wallington, T. J. Atmospheric chemistry of aulfuryl fluoride: Reaction with OH radicals, Cl Atoms and O_3, atmospheric lifetime, IR spectrum, and global warming potential. *Environ. Sci. Technol.* **2009**, *43*, 1067-1070, doi:10.1021/es802439f.

I33. HO_2 + H_2S, HO_2 + CH_3SH, HO_2 + CH_3SCH_3. These upper limits are taken from the discharge flow laser magnetic resonance study of Mellouki and Ravishankara.[3] (298 K). The H_2S value disagrees with the rate constant reported by Bulatov et al.[2] by approximately three orders of magnitude. The reason for this difference is not readily apparent. However, the recommended upper limit is consistent with the values for CH_3SH and CH_3SCH_3, which respectively agree with upper limits from the work of Barnes et al.[1] (300 K) and Niki (reported as a private communication in the Mellouki and Ravishankara paper).
(Table: 94-26, Note: 94-26, Evaluated: 94-26) Back to Table

(1) Barnes, I.; Bastian, V.; Becker, K. H.; Fink, E. H.; Nelsen, W. Oxidation of sulphur compounds in the atmosphere: I. Rate constants of OH radical reactions with sulphur dioxide, hydrogen sulphide, aliphatic thiols and thiophenol. *J. Atmos. Chem.* **1986**, *4*, 445-466, doi:10.1007/BF00053845.
(2) Bulatov, V. P.; Vereschchuk, S. I.; Dzegilenko, F. N.; Sarkisov, O. M.; Khabarov, V. N. Photooxidative conversion of H_2S in the presence of O_2 and NO_2. *Khim. Fiz.* **1990**, *9*, 1214-1223.
(3) Mellouki, A.; Ravishankara, A. R. Does the HO_2 radical react with H_2S, CH_3SH, and CH_3SCH_3? *Int. J. Chem. Kinet.* **1994**, *26*, 355-365, doi:10.1002/kin.550260306.

I34. HO_2 + SO_2. This upper limit is based on the atmospheric pressure study of Graham et al.[2] (300 K). A low pressure laser magnetic resonance study by Burrows et al.[1] (298 K) places a somewhat higher upper limit on

k(298 K) of 4 × 10^{-17} cm^3 $molecule^{-1}$ s^{-1} (determined relative to OH + H_2O_2); their limit is based on the assumption that the products are OH and SO_3, an assumption that theoretical work by Wang and Hou[4] suggests is incorrect. Wang and Hou find that reaction proceeds via an energized HO_2SO_2 complex that is stabilized in competition with dissociation to O_2 + HOSO. At 300 K and 760 Torr N_2, calculated rate coefficients in units of 10^{-17} $cm^3molecule^{-1}s^{-1}$ are 1.1 for complex stabilization and 2.4 for production of O_2 + HOSO. However, at atmospheric temperatures, pressures, and O_2 partial pressures, both reactions are rapidly reversible, so there is no net reaction. The weight of evidence from the other cited studies suggests an error in the earliest determination by Payne et al.[3] (300 K).
(Table: 82-57, Note: 19-5, Evaluated: 19-5) Back to Table

(1) Burrows, J. P.; Cliff, D. I.; Harris, G. W.; Thrush, B. A.; Wilkinson, J. P. T. Atmospheric reactions of the HO_2 radical studied by laser magnetic-resonance spectroscopy. *Proc. Roy. Soc. Lond. A.* **1979**, *368*, 463-481, doi:10.1098/rspa.
(2) Graham, R. A.; Winer, A. M.; Atkinson, R.; Pitts, J. N., Jr. Rate constants for the reaction of HO_2 with HO_2, SO_2, CO, N_2O, *trans*-2-butene, and 2,3-dimethyl-2-butene at 300 K. *J. Phys. Chem.* **1979**, *83*, 1563-1567, doi:10.1021/j100475a002.
(3) Payne, W. A.; Stief, L. J.; Davis, D. D. A kinetics study of the reaction of HO_2 with SO_2 and NO. *J. Am. Chem. Soc.* **1973**, *95*, 7614-7619, doi:10.1021/ja00804a013.
(4) Wang, B.; Hou, H. Theoretical investigations on the SO_2 + HO_2 reaction and the SO_2−HO_2 radical complex. *Chem. Phys. Lett.* **2005**, *410*, 235-241, doi:10.1016/j.cplett.2005.05.091.

I35. NO_2 + SO_2. This recommendation is based on the study of Penzhorn and Canosa[2] (298 K) using second derivative UV spectroscopy. While these authors actually report a measured value for k(298 K), their observations of strong heterogeneous and water vapor catalyzed effects prompt us to accept their measurement as an upper limit. This value is approximately two orders of magnitude lower than that for a dark reaction observed by Jaffe and Klein[1] (298 K), much of which may have been due to heterogeneous processes. Penzhorn and Canosa suggest that the products of this reaction are NO + SO_3.
(Table: 85-37, Note: 85-37, Evaluated: 85-37) Back to Table

(1) Jaffe, S.; Klein, F. S. Photolysis of NO_2 in the presence of SO_2 at 3660Å. *Trans. Faraday Soc.* **1966**, *62*, 2150-2157, doi:10.1039/tf9666202150.
(2) Penzhorn, R. D.; Canosa, C. E. 2nd derivative UV spectroscopy study of the thermal and photochemical reaction of NO_2 with SO_2 and SO_3. *Ber. Bunsenges. Phys. Chem.* **1983**, *87*, 648-654, doi:10.1002/bbpc.19830870808.

I36. NO_3 + H_2S. This recommendation accepts the upper limit set by Dlugokencky and Howard[2] (298 K) based on experiments in which NO_3 loss was followed in the presence of large concentrations of H_2S. Less sensitive upper limits for the rate constant have been reported by Wallington et al.[3] (298 K) and Cantrell et al.[1] (298 K).
(Table: 90-1, Note: 90-1, Evaluated: 90-1) Back to Table

(1) Cantrell, C. A.; Davidson, J. A.; Shetter, R. E.; Anderson, B. A.; Calvert, J. G. Reactions of NO_3 and N_2O_5 with molecular species of possible atmospheric interest. *J. Phys. Chem.* **1987**, *91*, 6017-6021, doi:10.1021/j100307a040.
(2) Dlugokencky, E. J.; Howard, C. J. Laboratory studies of NO_3 radical reactions wlth some atmospheric sulfur compounds. *J. Phys. Chem.* **1988**, *92*, 1188-1193, doi:10.1021/j100316a036.
(3) Wallington, T. J.; Atkinson, R.; Winer, A. M.; Pitts, J. N., Jr. Absolute rate constants for the gas-phase reactions of the NO_3 radical with CH_3SH, CH_3SCH_3, CH_3SSCH_3, H_2S, SO_2, and CH_3OCH_3 over the temperature range 280-350 K. *J. Phys. Chem.* **1986**, *90*, 5393-5396, doi:10.1021/j100412a099.

I37. NO_3 + OCS. This upper limit is based on the relative rate data of MacLeod et al.[1] (297 K).
(Table: 90-1, Note: 90-1, Evaluated: 90-1) Back to Table

(1) MacLeod, H.; Aschmann, S. M.; Atkinson, R.; Tuazon, E. C.; Sweetman, J. A.; Winer, A. M.; Pitts, J. N., Jr. Kinetics and mechanisms of the gas phase reactions of the NO_3 radical with a series of reduced sulfur compounds. *J. Geophys. Res.* **1986**, *91*, 5338-5346, doi:10.1029/JD091iD05p05338.

I38. NO_3 + CS_2. This upper limit is based on the study of Burrows et al.[1] (298 K). A somewhat higher upper limit was derived in the relative rate study of MacLeod et al.[2] (297 K).
(Table: 90-1, Note: 90-1, Evaluated: 90-1) Back to Table

(1) Burrows, J. P.; Tyndall, G. S.; Moortgat, G. K. Absorption spectrum of NO_3 and kinetics of the reactions of NO_3 with NO_2, Cl, and several stable atmospheric species at 298 K. *J. Phys. Chem.* **1985**, *89*, 4848-4856, doi:10.1021/j100268a038.

(2) MacLeod, H.; Aschmann, S. M.; Atkinson, R.; Tuazon, E. C.; Sweetman, J. A.; Winer, A. M.; Pitts, J. N., Jr. Kinetics and mechanisms of the gas phase reactions of the NO_3 radical with a series of reduced sulfur compounds. *J. Geophys. Res.* **1986**, *91*, 5338-5346, doi:10.1029/JD091iD05p05338.

I39. **NO_3 + CH_3SH.** The recommended values are derived from a composite fit to the data of Wallington et al.[5] (280, 298, 350 K), Rahman et al.[4] (298 K), and Dlugokencky and Howard.[1] (254−367 K). The room temperature rate constant derived in the relative rate experiments of MacLeod et al.[3] (297 K) is in good agreement with the recommended value. The suite of investigations shows the rate constant to be pressure independent over the range 1–700 Torr. Dlugokencky and Howard place an upper limit of 5% on the production of NO_2 via this reaction at low pressure. Based on the product distribution observed in their investigation, Jensen et al.[2] propose a reaction mechanism initiated by abstraction of the hydrogen atom from the SH group, possibly after formation of an initial adduct as suggested by Wallington et al. and Dlugokencky and Howard. (Table: 15-10, Note: 94-26, Evaluated: 90-1) Back to Table

(1) Dlugokencky, E. J.; Howard, C. J. Laboratory studies of NO_3 radical reactions wlth some atmospheric sulfur compounds. *J. Phys. Chem.* **1988**, *92*, 1188-1193, doi:10.1021/j100316a036.
(2) Jensen, N. R.; Hjorth, J.; Lohse, C.; Skov, H.; Restelli, G. Products and mechanisms of the gas phase reactions of NO_3 with CH_3SCH_3, CD_3SCD_3, CH_3SH and CH_3SSCH_3. *J. Atmos. Chem.* **1992**, *14*, 95-108, doi:10.1007/BF00115226.
(3) MacLeod, H.; Aschmann, S. M.; Atkinson, R.; Tuazon, E. C.; Sweetman, J. A.; Winer, A. M.; Pitts, J. N., Jr. Kinetics and mechanisms of the gas phase reactions of the NO_3 radical with a series of reduced sulfur compounds. *J. Geophys. Res.* **1986**, *91*, 5338-5346, doi:10.1029/JD091iD05p05338.
(4) Rahman, M. M.; Becker, E.; Benter, T.; Schindler, R. N. A gas phase kinetic investigation of the system F + HNO_3 and the determination of absolute rate constants for the reaction of the NO_3 radical with CH_3SH, 2-methylpropene, 1,3-butadiene and 2,3-dimethyl-2-butene. *Ber. Bunsenges. Phys. Chem.* **1988**, *92*, 91-100, doi:10.1002/bbpc.198800018.
(5) Wallington, T. J.; Atkinson, R.; Winer, A. M.; Pitts, J. N., Jr. Absolute rate constants for the gas-phase reactions of the NO_3 radical with CH_3SH, CH_3SCH_3, CH_3SSCH_3, H_2S, SO_2, and CH_3OCH_3 over the temperature range 280-350 K. *J. Phys. Chem.* **1986**, *90*, 5393-5396, doi:10.1021/j100412a099.

I40. **NO_3 + CH_3SCH_3.** The recommended k(298 K) was obtained by averaging the rate constants reported by Tyndall et al.[11] (278−318 K), Dlugokencky and Howard[4] (256−376 K), and Daykin and Wine[3] (298 K). The recommended value of E/R is that reported by Dlugokencky and Howard. Tyndall et al. and Nakano et al.[9] (283−318 K) report data over rather narrow temperature ranges that are consistent with the Dlugokencky and Howard result. The relative rate study of Atkinson et al.[1] (296 K) yields a rate constant at room temperature that is about a factor two lower than the recommended value. Wallington et al.[12,13] (280, 298, 350 K; 298 K) also report rate constants that are somewhat lower than the recommended values; their results are suspect because their reaction mixtures contained F_2 in ten-fold excess over CH_3SCH_3, and it is now well-established that F_2 and CH_3SCH_3 react with each other rapidly.[7,8,10] The results of Nakano et al. are suspect because of the likely presence of background NO_3 associated with the use of N_2O_5 + hν as the NO_3 source. The experimental data from all investigations demonstrate the pressure independence of the rate constant over the range 1–740 Torr. Jensen et al.[5] propose a mechanism that involves hydrogen abstraction as the first step to explain their observed product distribution. In a later study, Jensen et al.[6] measured a kinetic isotope effect for the rate constant for CH_3SCH_3 vs. that for CD_3SCD_3 of $k_H/k_D = (3.8 \pm 0.6)$, in agreement with the kinetic isotope effect reported by Daykin and Wine; this provides further confirmation of the H-abstraction mechanism. Butkovskaya and Le Bras[2] utilized chemical titration of the primary radical produced from NO_3 + CH_3SCH_3 in a discharge flow mass spectrometry system to show that the reaction produces predominantly CH_3SCH_2 + HNO_3. An upper limit of 2% was placed on the reaction channel yielding CH_3 + CH_3SONO_2.
(Table: 10-6, Note: 10-6, Evaluated: 10-6) Back to Table

(1) Atkinson, R.; Pitts, J. N., Jr.; Aschmann, S. M. Tropospheric reactions of dimethyl sulfide with NO_3 and OH radicals. *J. Phys. Chem.* **1984**, *88*, 1584-1587, doi:10.1021/j150652a029.
(2) Butkovskaya, N. I.; Le Bras, G. Mechanism of the NO_3 + DMS reaction by discharge flow mass spectrometry. *J. Phys. Chem.* **1994**, *98*, 2582-2591, doi:10.1021/j100061a014.
(3) Daykin, E. P.; Wine, P. H. A study of the reactions of NO_3 radicals with organic sulfides: Reactivity trend at 298 K. *Int. J. Chem. Kinet.* **1990**, *22*, 1083-1094, doi:10.1002/kin.550221007.
(4) Dlugokencky, E. J.; Howard, C. J. Laboratory studies of NO_3 radical reactions wlth some atmospheric sulfur compounds. *J. Phys. Chem.* **1988**, *92*, 1188-1193, doi:10.1021/j100316a036.
(5) Jensen, N. R.; Hjorth, J.; Lohse, C.; Skov, H.; Restelli, G. Products and mechanism of the reaction between NO_3 and dimethlysulphide in air. *Atmos. Environ.* **1991**, *24A*, 1897-1904, doi:10.1016/0960-1686(91)90272-9.

(6) Jensen, N. R.; Hjorth, J.; Lohse, C.; Skov, H.; Restelli, G. Products and mechanisms of the gas phase reactions of NO_3 with CH_3SCH_3, CD_3SCD_3, CH_3SH and CH_3SSCH_3. *J. Atmos. Chem.* **1992**, *14*, 95-108, doi:10.1007/BF00115226.
(7) Lu, Y.-J.; Lee, L.; Pan, J.-W.; Witek, H. A.; Lin, J. J. Dynamics of the F_2 + CH_3SCH_3 reaction: A molecule-molecule reaction without entrance barrier. *J. Chem. Phys.* **2007**, *127*, 101101, doi:10.1063/1.2780145.
(8) Lu, Y.-J.; Lee, L.; Pan, J.-W.; Xie, T.; Witek, H. A.; Lin, J. J. Barrierless reactions between two closed-shell molecules. I. Dynamics of F_2 + CH_3SCH_3 reaction. *J. Chem. Phys.* **2008**, *128*, 104317, doi:10.1063/1.2837801.
(9) Nakano, Y.; Ishiwata, T.; Aloisio, S.; Kawasaki, M. Temperature and pressure dependence of the rate constants of the reaction of NO_3 radical with CH_3SCH_3. *J. Phys. Chem. A* **2006**, *110*, 7401-7405, doi:10.1021/jp0612230.
(10) Turnipseed, A. A.; Birks, J. W. Kinetics of the reaction of molecular fluorine with dimethyl sulfide. *J. Phys. Chem.* **1991**, *95*, 6569-6574, doi:10.1021/j100170a037.
(11) Tyndall, G. S.; Burrows, J. P.; Schneider, W.; Moortgat, G. K. Rate coefficient for the reaction between NO_3 radicals and dimethyl sulphide. *Chem. Phys. Lett.* **1986**, *130*, 463-466, doi:10.1016/0009-2614(86)80506-1.
(12) Wallington, T. J.; Atkinson, R.; Winer, A. M.; Pitts, J. N., Jr. Absolute rate constants for the gas-phase reactions of the NO_3 radical with CH_3SH, CH_3SCH_3, CH_3SSCH_3, H_2S, SO_2, and CH_3OCH_3 over the temperature range 280-350 K. *J. Phys. Chem.* **1986**, *90*, 5393-5396, doi:10.1021/j100412a099.
(13) Wallington, T. J.; Atkinson, R.; Winer, A. M.; Pitts Jr., J. N. Absolute rate constants for the gas-phase reactions of the NO_3 radical with CH_3SCH_3, NO_2, CO, and a series of alkanes at 298 ± 2 K. *J. Phys. Chem.* **1986**, *90*, 4640-4644, doi:10.1021/j100410a034.

I41. **NO_3 + CH_3SSCH_3.** The recommendation is based on the temperature dependent studies of Wallington et al.[5] (280, 298, 350 K) and Dlugokencky and Howard[2] (334, 382 K). All data points in each temperature dependent study were scaled by a factor equal to the ratio $k(298\ K)_{Arr}/k(298\ K)_{ave}$ where $k(298\ K)_{Arr}$ is the 298 K rate constant obtained from Arrhenius expression describing the individual T-dependent data set and $k(298\ K)_{ave}$ is the average of the two $k(298\ K)_{Arr}$ values. The best fit of the scaled data to $\ln k = \ln A - E/RT$ is recommended. The investigation by Atkinson et al.[1] (296 K) indicates that the relative rate technique cannot be considered as yielding reliable rate data for this reaction due to chemical complexities. Thus, the much lower room temperature results from the study of MacLeod et al.[4] (297 K) can be considered to be erroneous. Based on their observations of intermediate and end products, Jensen et al.[3] proposed a reaction mechanism in which the initial addition of NO_3 to one of the sulfur atoms results in formation of CH_3S + CH_3SO + NO_2.
(Table: 15-10, Note: 15-10, Evaluated: 15-10) Back to Table

(1) Atkinson, R.; Aschmann, S. M.; Pitts, J. N., Jr. Kinetics of the reaction of NO_3 radicals with CH_3SSCH_3. *J. Geophys. Res.* **1988**, *93*, 7125-7126, doi:10.1029/JD093iD06p07125.
(2) Dlugokencky, E. J.; Howard, C. J. Laboratory studies of NO_3 radical reactions wlth some atmospheric sulfur compounds. *J. Phys. Chem.* **1988**, *92*, 1188-1193, doi:10.1021/j100316a036.
(3) Jensen, N. R.; Hjorth, J.; Lohse, C.; Skov, H.; Restelli, G. Products and mechanisms of the gas phase reactions of NO_3 with CH_3SCH_3, CD_3SCD_3, CH_3SH and CH_3SSCH_3. *J. Atmos. Chem.* **1992**, *14*, 95-108, doi:10.1007/BF00115226.
(4) MacLeod, H.; Aschmann, S. M.; Atkinson, R.; Tuazon, E. C.; Sweetman, J. A.; Winer, A. M.; Pitts, J. N., Jr. Kinetics and mechanisms of the gas phase reactions of the NO_3 radical with a series of reduced sulfur compounds. *J. Geophys. Res.* **1986**, *91*, 5338-5346, doi:10.1029/JD091iD05p05338.
(5) Wallington, T. J.; Atkinson, R.; Winer, A. M.; Pitts, J. N., Jr. Absolute rate constants for the gas-phase reactions of the NO_3 radical with CH_3SH, CH_3SCH_3, CH_3SSCH_3, H_2S, SO_2, and CH_3OCH_3 over the temperature range 280-350 K. *J. Phys. Chem.* **1986**, *90*, 5393-5396, doi:10.1021/j100412a099.

I42. **NO_3 + $CH_3S(O)CH_3$.** The recommended $k(298\ K)$ is the geometric mean of the rate constants reported by Barnes et al.[1] and Falbe-Hansen et al.[2] (298 K) from similar competitive kinetics studies; the reported rate constants and associated 2σ uncertainties in units of 10^{-13} cm^3 $molecule^{-1}$ s^{-1} are 1.7 ± 0.6 (Barnes et al.) and 5.0 ± 3.8 (Falbe-Hansen et al.). In both studies, the only observed sulfur-containing end-product was dimethylsulfone ($CH_3(O)S(O)CH_3$). Barnes et al. suggest that reaction proceeds via formation of an adduct that rapidly decomposes to NO_2 + $CH_3(O)S(O)CH_3$.
(Table: 06-2, Note: 06-2, Evaluated: 06-2) Back to Table

(1) Barnes, I.; Bastian, V.; Becker, K. H.; Martin, D. In *Biogenic Sulfur in the Environment*; ACS Symp. Ser, 1989; Vol. 393; pp 476-488.

(2) Falbe-Hansen, H.; Sorensen, S.; Jensen, N. R.; Pedersen, T.; Hjorth, J. Atmospheric gas-phase reactions of dimethylsulphoxide and dimethylsulphone with OH and NO_3 radicals, Cl atoms and ozone. *Atmos. Environ.* **2000**, *34*, 1543-1551, doi:10.1016/S1352-2310(99)00407-0.

I43. **NO_3 + $CH_3SC_2H_5$.** The recommendation is the geometric mean of rate constants for NO_3 reactions with CH_3SCH_3 (k_1) and $C_2H_5SC_2H_5$ (k_2) reported by Daykin and Wine[1] (298 K), while the recommended uncertainty is large enough to include both k_1 and k_2 within its limits. Observation of the trend in rate constants for reactions of NO_3 radicals with CH_3SCH_3, CD_3SCD_3, and $C_2H_5SC_2H_5$ suggests that H-transfer is the dominant pathway for these reactions.[1] Products of the NO_3 + $CH_3SC_2H_5$ reaction measured in an environmental chamber by Jensen et al.[2] (298 K) using a combination of FTIR and ion chromatographic detection also supports H-transfer as the dominant pathway and suggests that yields of the H-transfer products $CH_2SCH_2CH_3$ and CH_3SCHCH_3 are approximately equal.
(Table: 15-10, Note: 15-10, Evaluated: 15-10) Back to Table

(1) Daykin, E. P.; Wine, P. H. A study of the reactions of NO_3 radicals with organic sulfides: Reactivity trend at 298 K. *Int. J. Chem. Kinet.* **1990**, *22*, 1083-1094, doi:10.1002/kin.550221007.
(2) Jensen, N. R.; Hjorth, J.; Lohse, C.; Skov, H.; Restelli, G. Reactions of the nitrate radical with a series of reduced organic sulfur compounds in air. *Int. J. Chem. Kinet.* **1992**, *24*, 839-850, doi:10.1002/kin550241002.

I44. **NO_3 + SO_2.** This recommended upper limit for k(298 K) is based on the study by Daubendiek and Calvert[3] (293 K). Considerably higher upper limits have been derived by Burrows et al.[1] (298 K), Wallington et al.[5] (298 K), Canosa–Mas et al.[2] (298 K), and Dlugokencky and Howard[4] (298 K).
(Table: 87-41, Note: 90-1, Evaluated: 90-1) Back to Table

(1) Burrows, J. P.; Tyndall, G. S.; Moortgat, G. K. Absorption spectrum of NO_3 and kinetics of the reactions of NO_3 with NO_2, Cl, and several stable atmospheric species at 298 K. *J. Phys. Chem.* **1985**, *89*, 4848-4856, doi:10.1021/j100268a038.
(2) Canosa-Mas, C.; Smith, S. J.; Toby, S.; Wayne, R. P. Reactivity of the nitrate radical towards alkynes and some other molecules. *J. Chem. Soc. Faraday Trans. 2* **1988**, *84*, 247-262, doi:10.1039/f29888400247.
(3) Daubendiek, R. L.; Calvert, J. G. Study of N_2O_5-SO_2-O_3 reaction system. *Environ. Lett.* **1975**, *8*, 103-116, doi:10.1080/00139307509437424.
(4) Dlugokencky, E. J.; Howard, C. J. Laboratory studies of NO_3 radical reactions wlth some atmospheric sulfur compounds. *J. Phys. Chem.* **1988**, *92*, 1188-1193, doi:10.1021/j100316a036.
(5) Wallington, T. J.; Atkinson, R.; Winer, A. M.; Pitts, J. N., Jr. Absolute rate constants for the gas-phase reactions of the NO_3 radical with CH_3SH, CH_3SCH_3, CH_3SSCH_3, H_2S, SO_2, and CH_3OCH_3 over the temperature range 280-350 K. *J. Phys. Chem.* **1986**, *90*, 5393-5396, doi:10.1021/j100412a099.

I45. **N_2O_5 + CH_3SCH_3.** This recommendation is based on the value estimated by Tyndall and Ravishankara[2] from the study by Atkinson et al.[1] (296 K).
(Table: 92-20, Note: 92-20, Evaluated: 92-20) Back to Table

(1) Atkinson, R.; Pitts, J. N., Jr.; Aschmann, S. M. Tropospheric reactions of dimethyl sulfide with NO_3 and OH radicals. *J. Phys. Chem.* **1984**, *88*, 1584-1587, doi:10.1021/j150652a029.
(2) Tyndall, G. S.; Ravishankara, A. R. Atmospheric oxidation of reduced sulfur species. *Int. J. Chem. Kinet.* **1991**, *23*, 483-527, doi:10.1002/kin.550230604.

I46. **CH_3O_2 + SO_2.** This recommendation accepts the results from the study of Sander and Watson[4] (298−423 K). These authors conducted experiments using much lower CH_3O_2 concentrations than employed in the earlier investigations of Sanhueza et al.[5] (298 K) and Kan et al.[3] (298 K), both of which resulted in k(298 K) values approximately 100 times greater. A later report by Kan et al.[2] (298 K) postulates that these differences are due to the reactive removal of the $CH_3O_2SO_2$ adduct at high CH_3O_2 concentrations prior to its reversible decomposition into CH_3O_2 and SO_2. They suggest that such behavior of $CH_3O_2SO_2$ or its equilibrated adduct with O_2 ($CH_3O_2SO_2O_2$) would be expected in the studies yielding high k values, while decomposition of $CH_3O_2SO_2$ into reactants would dominate in the Sander and Watson experiments. It does not appear likely that such secondary reactions involving CH_3O_2, NO, or other radical species would be rapid enough, if they occur under normal atmospheric conditions to compete with the adduct decomposition. This interpretation, however, does not explain the high rate constant derived by Cocks et al.[1] (298 K) under conditions of low [CH_3O_2].
(Table: 81-3, Note: 81-3, Evaluated: 81-3) Back to Table

(1) Cocks, A. T.; Fernanado, R. P.; Fletcher, I. S. The gas-phase reaction of the methylperoxy radical with sulphur dioxide. *Atmos. Environ.* **1986**, *20*, 2359-2366, doi:10.1016/0004-6981(86)90066-1.
(2) Kan, C. S.; Calvert, J. G.; Shaw, J. H. Oxidation of sulfur dioxide by methylperoxy radicals. *J. Phys. Chem.* **1981**, *85*, 1126-1132, doi:10.1021/j150609a011.
(3) Kan, C. S.; McQuigg, R. D.; Whitbeck, M. R.; Calvert, J. G. Kinetic flash spectroscopic study of the CH_3O_2-CH_3O_2 and CH_3O_2-SO_2 reactions. *Int. J. Chem. Kinet.* **1979**, *11*, 921-933, doi:10.1002/kin.550110811.
(4) Sander, S. P.; Watson, R. T. A kinetics study of the reaction of SO_2 with CH_3O_2. *Chem. Phys. Lett.* **1981**, *77*, 473-475, doi:10.1016/0009-2614(81)85188-3.
(5) Sanhueza, E.; Simonaitis, R.; Heicklen, J. The reaction of CH_3O_2 with SO_2. *Int. J. Chem. Kinet.* **1979**, *11*, 907-914, doi:10.1002/kin.550110809.

I47. **F + CH_3SCH_3.** This recommendation is based on the discharge flow mass spectrometric study by Butkovskaya et al.[1] (298 K). The uncertainty placed on this recommendation has been increased over that estimated by the authors to reflect the lack of confirming investigations. Titration of the primary organic radical products indicated that the reaction proceeds via two channels to produce HF + CH_3SCH_2 and CH_3 + CH_3SF with a branching ratio of approximately 0.8/0.2 respectively.
(Table: 97-4, Note: 97-4, Evaluated: 97-4) Back to Table

(1) Butkovskaya, N. I.; Poulet, G.; Le Bras, G. Discharge flow study of the reactions of chlorine and fluorine atoms with dimethyl sulfide. *J. Phys. Chem.* **1995**, *99*, 4536-4543, doi:10.1021/j100013a025.

I48. **Cl + H_2S.** This recommendation is based on the work of Nicovich et al.[10] (193–431 K), and Gao et al.[5] (290–914 K), who conducted careful studies with attention to sources of possible systematic error; only the Gao et al. data at ≤500 K are considered in arriving at the recommendation. The recommended rate constant at 298 K is in good agreement with that determined by Nesbitt and Leone[9] (298 K), who refined the data of Braithwaite and Leone[1] (296 K), but is significantly greater than the values reported by Clyne and Ono[4] (298 K), Clyne et al.[3] (296 K), Nava et al.,[8] (211–353 K) and Chen et al.[2] (298 K). The small, but clearly observed, negative activation energy determined by Nicovich et al. and Gao et al. contrasts with the lack of a temperature dependence observed by Nava et al. The Nicovich et al. study yields consistent results for both H_2S and CH_3SH as well as for D_2S and CD_3SD. In addition, Hossenlopp et al.[6] report a room temperature rate constant for Cl + D_2S that is in excellent agreement with the value reported by Nicovich et al. Lu et al.[7] (232–359 K) also measured a temperature–independent rate constant, but report a value at 298 K that is about 40% greater than those of Nicovich et al. and Gao et al. The presence of 4000 Torr of CF_3Cl bath gas in the Lu et al. study may suggest a slight pressure dependence of the rate constant, although Nicovich et al. observed no pressure dependence for pressures ranging up to 600 Torr N_2 and Gao et al. observed no pressure dependence over the range 30–100 Torr Ar. A theoretical study by Wilson and Hirst[11] suggests the dominance of an addition-elimination pathway with a small but significant fraction of reactive events occurring via a direct hydrogen abstraction mechanism.
(Table: 19-5, Note: 19-5, Evaluated: 19-5) Back to Table

(1) Braithwaite, M.; Leone, S. R. Laser-initiated chemical reactions: Cl + H_2S → HCl + HS: Rate constant, product energy distribution, and direct detection of a chain mechanism. *J. Chem. Phys.* **1978**, *69*, 839-845, doi:10.1063/1.43659.
(2) Chen, K. S.; Cheng, S. S.; Lee, Y. P. Reaction dynamics of Cl + H_2S: Rotational and vibrational distribution of HCl probed with time-resolved Fourier-transform spectroscopy. *J. Chem. Phys.* **2003**, *119*, 4229-4236, doi:10.1063/1.1592508.
(3) Clyne, M. A. A.; MacRobert, A. J.; Murrells, T. P.; Stief, L. J. Kinetics of the reactions of atomic chlorine with H_2S, HS and OCS. *J. Chem. Soc. Faraday Trans. 2* **1984**, *80*, 877-886, doi:10.1039/f29848000877.
(4) Clyne, M. A. A.; Ono, Y. Determination of the rate constant of reaction of ground-state Cl and H atoms with H_2S using resonance fluorescence in a discharge flow. *Chem. Phys. Lett.* **1983**, *94*, 597-602, doi:10.1016/0009-2614(83)85065-9.
(5) Gao, Y.; Alecu, A. A.; Goumri, A.; Marshall, P. High-temperature kinetics of the reaction between chlorine atoms and hydrogen sulfide. *Chem. Phys. Lett.* **2015**, *624*, 83-86, doi:10.1016/j.cplett.2015.02.011.
(6) Hossenlopp, J. M.; Hershberger, J. F.; Flynn, G. W. Kinetics and product vibrational energy disposal dynamics in the reaction of chlorine atoms with D_2S. *J. Phys. Chem.* **1990**, *94*, 1346-1351, doi:10.1021/j100367a029.

(7) Lu, E. C. C.; Iyer, R. S.; Rowland, F. S. Reaction rates for thermal chlorine atoms wlth H_2S from 232 to 359 K by a radiochemical technlque. *J. Phys. Chem.* **1986**, *90*, 1988-1990, doi:10.1021/j100401a002.
(8) Nava, D. F.; Brobst, W. D.; Stief, L. J. Temperature study of the rates of the reactions of atomic chlorine with H_2S and C_2H_4S. *J. Phys. Chem.* **1985**, *89*, 4703-4707, doi:10.1021/j100268a012.
(9) Nesbitt, D. J.; Leone, S. R. Laser-initiated chemical chain reactions. *J. Chem. Phys.* **1980**, *72*, 1722-1732, doi:10.1063/1.439284.
(10) Nicovich, J. M.; Wang, S.; Wine, P. H. Kinetics of the reactions of atomic chlorine with H_2S, D_2S, CH_3SH, and CD_3SD. *Int. J. Chem. Kinet.* **1995**, *27*, 359-368, doi:10.1002/kin.550270407
(11) Wilson, C.; Hirst, D. M. Ab initio study of the reaction of chlorine atoms with H_2S, CH_3SH, CH_3SCH_3 and CS_2. *J. Chem. Soc. Faraday Trans.* **1997**, *93*, 2831-2837, doi:10.1039/a701664f.

I49. **Cl + SO_2F_2 → products.** The recommended upper limit is a factor of 3 higher than that reported in the relative rate experiments of Sulbaek-Andersen et al.[2] (296 K) to account for a large uncertainty in the rate constant for the reference reaction they employed (Cl + CF_3CH_3). A less sensitive upper limit is reported by Papadimitriou et al.[1] (296 K).
(Table: 10-6, Note: 10-6, Evaluated: 10-6) Back to Table

(1) Papadimitriou, V. C.; Portmann, R. W.; Fahey, D. W.; Muhle, J.; Weiss, R. F.; Burkholder, J. B. Experimental and theoretical study of the atmospheric chemistry and global warming potential of SO_2F_2. *J. Phys. Chem. A* **2008**, *112*, 12657-12666, doi:10.1021/jp806368u.
(2) Sulbaek-Andersen, M. P.; Blake, D. R.; Rowland, F. S.; Hurley, M. D.; Wallington, T. J. Atmospheric chemistry of aulfuryl fluoride: Reaction with OH radicals, Cl Atoms and O_3, atmospheric lifetime, IR spectrum, and global warming potential. *Environ. Sci. Technol.* **2009**, *43*, 1067-1070, doi:10.1021/es802439f.

I50. **Cl + OCS.** This upper limit is based on the minimum detectable decrease in atomic chlorine measured by Eibling and Kaufman[2] (298 K). Based on the observation of product SCl, these authors set a lower limit on k(298 K) of 10^{-18} cm^3 molecule^{-1} s^{-1} for the SCl + CO reaction channel. Considerably higher upper limits on k(298 K) were determined in the studies of Clyne et al.[1] (296 K) and Nava et al.[3] (298 K).
(Table: 83-62, Note: 87-41, Evaluated: 83-62) Back to Table

(1) Clyne, M. A. A.; MacRobert, A. J.; Murrells, T. P.; Stief, L. J. Kinetics of the reactions of atomic chlorine with H_2S, HS and OCS. *J. Chem. Soc. Faraday Trans. 2* **1984**, *80*, 877-886, doi:10.1039/f29848000877.
(2) Eibling, R. E.; Kaufman, M. Kinetics studies relevant to possible couppling between the stratospheric chlorine and sulfur cycles. *Atmos. Environ.* **1983**, *17*, 429-431, doi:10.1016/0004-6981(83)90061-6.
(3) Nava, D. F.; Brobst, W. D.; Stief, L. J. Temperature study of the rates of the reactions of atomic chlorine with H_2S and C_2H_4S. *J. Phys. Chem.* **1985**, *89*, 4703-4707, doi:10.1021/j100268a012.

I51. **$CS_2Cl + O_2$.** This recommendation is based on the study of Nicovich et al.[2] (230, 293 K) who employed a laser flash photolysis resonance fluorescence technique to observe the effect of added O_2 on the kinetics of the Cl + CS_2 ↔ CS_2Cl equilibration reactions. Martin et al.[1] (293 K) report competitive kinetics results which they interpret as suggesting a fast $CS_2Cl + O_2$ reaction, but Wallington et al.[3] (298 K) have suggested that secondary production of OH in the photochemical system employed by Martin et al. is responsible for the observed dependence of the CS_2 loss rate on [O_2].
(Table: 06-2, Note: 06-2, Evaluated: 06-2) Back to Table

(1) Martin, D.; Barnes, I.; Becker, K. H. Rate constant and products of the reaction Cl + CS_2 in air. *Chem. Phys. Lett.* **1987**, *140*, 195-199, doi:10.1016/0009-2614(87)80813-8.
(2) Nicovich, J. M.; Shackelford, C. J.; Wine, P. H. Kinetics and thermochemistry of reversible adduct formation in the reaction of Cl(^2P_J) with CS_2. *J. Phys. Chem.* **1990**, *94*, 2896-2903, doi:10.1021/j100370a031.
(3) Wallington, T. J.; Andino, J. M.; Potts, A. R.; Wine, P. H. A competitive kinetics study of the reaction of Cl with CS_2 in air at 298 K. *Chem. Phys. Lett.* **1991**, *176*, 103-108, doi:10.1016/0009-2614(91)90018-5.

I52. **Cl + CH_3SH.** This recommendation is based on the results of Nicovich et al.[4] (193–431 K), who used laser flash photolysis with resonance fluorescence detection to study the reactions of Cl with H_2S, D_2S, CH_3SH, and CD_3SD. The room temperature determination by Nesbitt and Leone[2] (298 K) is in good agreement with the recommended value. The k(298 K) value from the study of Mellouki et al.[1] (298 K) is nearly a factor of 2 lower. However, the low sensitivity of EPR detection of Cl atoms did not permit these latter authors to conduct a precise determination of k under pseudo first–order conditions, and a more complex analysis of experiments conducted under second–order conditions was required. Nesbitt and Leone[3] (298 K) report that 2 ± 1% of the reaction occurs via abstraction of an H atom from the CH_3 group. A theoretical study by Wang et al. supports abstraction of H from the SH group as the dominant reaction pathway at atmospheric temperatures, but predicts that abstraction of H from the CH_3 group becomes important at higher temperatures.[5] A theoretical study by Wilson and Hirst[6] predicts a Cl−S adduct bond strength (298 K) of 57 kJ mol^{-1}, but is unable to deduce the relative importance of addition-elimination vs. direct hydrogen abstraction pathways.
(Table: 06-2, Note: 15-10, Evaluated: 06-2) Back to Table

(1) Mellouki, A.; Jourdain, J. L.; Le Bras, G. Discharge flow study of the $CH_3S + NO_2$ reaction mechanism using Cl + CH_3SH as the CH_3S source. *Chem. Phys. Lett.* **1988**, *148*, 231-236, doi:10.1016/0009-2614(88)80305-1.

(2) Nesbitt, D. J.; Leone, S. R. Laser-initiated chemical chain reactions. *J. Chem. Phys.* **1980**, *72*, 1722-1732, doi:10.1063/1.439284.

(3) Nesbitt, D. J.; Leone, S. R. Laser initiated chain reactions: A generalized extension to complex chemical chain systems. *J. Chem. Phys.* **1981**, *75*, 4949-4959, doi:10.1063/1.441883.

(4) Nicovich, J. M.; Wang, S.; Wine, P. H. Kinetics of the reactions of atomic chlorine with H_2S, D_2S, CH_3SH, and CD_3SD. *Int. J. Chem. Kinet.* **1995**, *27*, 359-368, doi:10.1002/kin.550270407.

(5) Wang, Y.-X.; Duan, X.-M.; Wang, Q.; Wang, L.; Liu, J.-Y.; Sun, C.-C. Direct *ab initio* dynamics studies of the reaction of methanethiol with chlorine atoms. *J. Theor. Comp. Chem.* **2010**, *9*, 265-277, doi:10.1142/S0219633610005669.

(6) Wilson, C.; Hirst, D. M. Ab initio study of the reaction of chlorine atoms with H_2S, CH_3SH, CH_3SCH_3 and CS_2. *J. Chem. Soc. Faraday Trans.* **1997**, *93*, 2831-2837, doi:10.1039/a701664f.

I53. **Cl + CH_3SCH_3.** Stickel et al.[9] (240–421 K) have used laser flash photolysis resonance fluorescence to measure the rate constant over the pressure range 3–700 Torr. The rate constant is near the gas-kinetic collision limit but increases with increasing pressure from a low-pressure limit of 1.8×10^{-10} to a value of 3.3×10^{-10} cm^3 $molecule^{-1}$ s^{-1} at 700 Torr. The yield of HCl at 297 K, measured by diode laser spectroscopy, decreased from near unity at low pressure to a value of approximately 0.5 at 203 Torr, suggesting that stabilization of a $(CH_3)_2SCl$ adduct becomes competitive with hydrogen atom abstraction with increasing pressure. These investigators also observed a negative temperature dependence for the reaction at low pressure. Butkovskaya et al.[2] (298 K) conducted a discharge flow mass spectrometry study, in which they determined that the reaction proceeds to form HCl + CH_3SCH_2 almost exclusively at 1 Torr total pressure. The sum of all other possible channels was estimated at less than 3%. Zhao et al.[13] (298 K) used laser photolysis coupled with CH_3 detection by time–resolved tunable diode laser absorption spectroscopy to determine an upper limit yield of 0.02 for CH_3 elimination at pressures in the range 10–30 Torr. Langer et al.[6] coupled cw photolysis with gas chromatographic detection of products to show that the yield of CH_3Cl is $(1.34 \pm 0.07) \times 10^{-3}$. Theoretical studies by Wilson and Hirst,[12] Resende and De Almeida,[8] and Thompson et al.[10] support the experimentally observed dominance of the H-abstraction pathway at low pressure. Diaz-de-Mera et al.[3] (259–364 K) have employed a discharge flow − mass spectrometry technique to measure rate constants at pressures of 0.5−1.0 Torr He. The 298 K rate constant reported by Diaz-de-Mera et al. is nearly a factor of 3 slower than the low-temperature limit value reported by Stickel et al. Furthermore, Diaz-de-Mera et al. report a small positive activation energy whereas Stickel et al. report a small negative activation energy. The present recommendation for the H-abstraction pathway is based on an extrapolated low-pressure limit rate constant obtained from the data of Stickel et al., with the uncertainty adjusted to encompass the result of Diaz-de-Mera et al. The data of Stickel et al. suggest that a high-pressure limit is reached at ~150 Torr. Urbanski and Wine[11] (298 K) have observed the UV-visible absorption spectrum of $(CH_3)_2SCl$ in 155 Torr O_2 and used absorbance rise−time data to derive a rate constant that agrees well with those measured by Stickel et al. at pressures of 150−750 Torr N_2. Enami et al.[4] (278–318 K) have observed the kinetics of adduct formation using cavity ring down spectroscopy, and derived rate constants over the pressure range 20−300 Torr N_2 that also agree well with those reported by Stickel et al. Room temperature competitive kinetics measurements by Nielsen et al.[7] at 740 Torr, Kinnison et al.[5] at 760 Torr, and Arsene et al.[1] at 750 Torr agree quite well with the results of Stickel et al., Urbanski and Wine, and Enami et al. Kinnison et al. and Arsene et al. report that the rate constant at atmospheric pressure is ~20% faster in synthetic air than in N_2 bath gas, suggesting that the $(CH_3)_2SCl$ adduct reacts with O_2; however, the results of Urbanski and Wine, and Enami et al. argue against the occurrence of such a reaction. Stickel et

al. report that the high-pressure rate constant in N_2 is independent of temperature whereas Arsene et al. report large negative activation energies in both N_2 and synthetic air bath gases. The large negative activation energies reported by Arsene et al. seem unlikely to result from a two-channel elementary reaction (H-abstraction and addition); hence, the recommended E/R is that reported by Stickel et al.
(Table: 10-6, Note: 15-10, Evaluated: 10-6) Back to Table

(1) Arsene, C.; Barnes, I.; Becker, K. H.; Benter, T. Gas-phase reaction of Cl with dimethyl sulfide: Temperature and oxygen partial pressure dependence of the rate coefficient. *Int. J. Chem. Kinet.* **2005**, *37*, 66-73, doi:10.1002/kin.20051.
(2) Butkovskaya, N. I.; Poulet, G.; Le Bras, G. Discharge flow study of the reactions of chlorine and fluorine atoms with dimethyl sulfide. *J. Phys. Chem.* **1995**, *99*, 4536-4543, doi:10.1021/j100013a025.
(3) Diaz-de-Mera, Y.; Aranda, A.; Rodriguez, D.; López, R.; Cabañas, B.; Martinez, E. Gas-phase reactions of chlorine atoms and ClO radicals with dimethyl sulfide. Rate coefficients and temperature dependences. *J. Phys. Chem. A* **2002**, *106*, 8627-8633, doi:10.1021/jp014570c.
(4) Enami, S.; Nakano, Y.; Hashimoto, S.; Kawasaki, M.; Aloisio, S.; Francisco, J. S. Reactions of Cl atoms with dimethyl sulfide: A theoretical calculation and an experimental study with cavity ring-down spectroscopy. *J. Phys. Chem. A* **2004**, *108*, 7785-7789, doi:10.1021/jp049772y.
(5) Kinnison, D. J.; Mengon, W.; Kerr, J. A. Rate coefficients for the room temperature reaction of Cl atoms with dimethyl sulfide and related alkyl sulfides. *J. Chem. Soc. Faraday Trans.* **1996**, *92*, 369-372, doi:10.1039/ft9969200369.
(6) Langer, S.; McGovney, B. T.; Finlayson-Pitts, B. J.; Moore, R. M. The dimethyl sulfide reaction with atomic chlorine and its implications for the budget of methyl chloride. *Geophys. Res. Lett.* **1996**, *23*, 1661-1664, doi:10.1029/96GL01427.
(7) Nielsen, O. J.; Sidebottom, H. W.; Nelson, L.; Rattigan, O.; Treacy, J. J.; O'Farrell, D. J. Rate constants for the reactions of OH radicals and Cl atoms with diethyl sulfide, Di-n-propyl sulfide, and Di-n-butyl sulfide. *Int. J. Chem. Kinet.* **1990**, *22*, 603-612, doi:10.1002/kin.550220605.
(8) Resende, S. M.; Almeida, W. B. D. Theoretical study of the atmospheric reaction between dimethyl sulfide and chlorine atoms. *J. Phys. Chem. A* **1997**, *101*, 9738-9744, doi:10.1021/jp971885c.
(9) Stickel, R. E.; Nicovich, J. M.; Wang, S.; Zhao, Z.; Wine, P. H. Kinetic and mechanistic study of the reaction of atomic chlorine with dimethyl sulfide. *J. Phys. Chem.* **1992**, *96*, 9875-9883, doi:10.1021/j100203a055.
(10) Thompson, K. C.; Canosa-Mas, C. E.; Wayne, R. P. Kinetics and mechanism of the reaction between atomic chlorine and dimethyl selenide; comparison with the reaction between atomic chlorine and dimethyl sulfide. *Phys. Chem. Chem. Phys.* **2002**, *4*, 4133-4139, doi:10.1039/b204657a.
(11) Urbanski, S. P.; Wine, P. H. Spectroscopic and kinetic study of the Cl-S$(CH_3)_2$ adduct. *J. Phys. Chem. A* **1999**, *103*, 10935-10944, doi:10.1021/jp992682m.
(12) Wilson, C.; Hirst, D. M. Ab initio study of the reaction of chlorine atoms with H_2S, CH_3SH, CH_3SCH_3 and CS_2. *J. Chem. Soc. Faraday Trans.* **1997**, *93*, 2831-2837, doi:10.1039/a701664f.
(13) Zhao, Z.; Stickel, R. E.; Wine, P. H. Branching ratios for methyl elimination in the reactions of OD radicals and Cl atoms with CH_3SCH_3. *Chem. Phys. Lett.* **1996**, *251*, 59-66, doi:10.1016/0009-2614(96)00059-0.

I54. **$(CH_3)_2SCl + O_2$, NO, NO_2.** The recommended k(298 K) are based on the study of Urbanski and Wine[2] (298 K) which combined laser flash photolytic production of $(CH_3)_2SCl$ with kinetic observations by time-resolved absorption spectroscopy. The recommended uncertainties for the NO and NO_2 reactions are larger than those reported by Urbanski and Wine pending independent confirmation of their results. As in the Urbanski and Wine study, Enami et al.[1] report no observable reaction between $(CH_3)_2SCl$ and O_2.
(Table: 06-2, Note: 06-2, Evaluated: 06-2) Back to Table

(1) Enami, S.; Nakano, Y.; Hashimoto, S.; Kawasaki, M.; Aloisio, S.; Francisco, J. S. Reactions of Cl atoms with dimethyl sulfide: A theoretical calculation and an experimental study with cavity ring-down spectroscopy. *J. Phys. Chem. A* **2004**, *108*, 7785-7789, doi:10.1021/jp049772y.
(2) Urbanski, S. P.; Wine, P. H. Spectroscopic and kinetic study of the Cl-S$(CH_3)_2$ adduct. *J. Phys. Chem. A* **1999**, *103*, 10935-10944, doi:10.1021/jp992682m.

I55. **$Cl + CH_3S(O)CH_3 \rightarrow CH_3S(O)CH_2 + HCl$.** The recommended k(298 K) for H-abstraction is based on the analysis of Nicovich et al.[4] (270–571 K), who fit the combined room temperature data of Nicovich et al., Martinez et al.[3] (273–335 K), and Riffault et al.[5] (298 K), which spanned an effective N_2 pressure range of 0.3−505 Torr, to the sum of a pressure-dependent component and a pressure-independent component and attributed the pressure-independent component to H-abstraction. The temperature dependence studies of Martinez et al. and Nicovich et al. suggest the possibility of curvature in the Arrhenius plot. The recommended

E/R (= 0) is appropriate for the 200−300 K temperature regime but not for higher temperatures. Vandresen and Resende[7] report a theoretical rate constant of 1.2×10^{-10} cm^3 molecule^{-1} s^{-1}, i.e., a factor of seven faster than the value suggested by experimental results. A theoretical study by Mao et al.[2] suggests that DMSO complexation with water affects the rate constant for the H-abstraction reaction. It has been predicted theoretically by Asatryan and Bozzelli[1] and confirmed experimentally by Taatjes et al.[6] that the peroxy radical formed via reaction of product •$CH_2S(O)CH_3$ with O_2 rapidly dissociates to produce the Criegee intermediate, CH_2OO.
(Table: 10-6, Note: 15-10, Evaluated: 10-6) Back to Table

(1) Asatryan, R.; Bozzelli, J. W. Formation of a Criegee intermediate in the low-temperature oxidation of dimethyl sulfoxide. *Phys. Chem. Chem. Phys.* **2008**, *10*, 1769-1780, doi:10.1039/b716179d.

(2) Mao, W.-X.; Long, Z.-W.; Long, B.; Wang, Y.-B.; Long, C.-Y.; Qin, S.-J. Theoretical study on the gas phase reaction of dimethyl sulfoxide with atomic chlorine in the presence of water. *Struct. Chem.* **2013**, *24*, 383-392, doi:10.1007/s11224-012-0086-z.

(3) Martinez, E.; Aranda, A.; Diaz-de-Mera, Y.; Rodriguez, D.; Reyes Lopez, M.; Albaladejo, J. Atmospheric DMSO degradation in the gas phase: Cl-DMSO reaction. Temperature dependence and products. *Environ. Sci. Technol.* **2002**, *36*, 1226-1230, doi:10.1021/es010169s.

(4) Nicovich, J. M.; Parthasarathy, S.; Pope, F. D.; Pegus, A. T.; McKee, M. L.; Wine, P. H. Kinetics, mechanism, and thermochemistry of the gas phase reaction of atomic chlorine with dimethyl sulfoxide. *J. Phys. Chem. A* **2006**, *110*, 6874-6885, doi:10.1021/jp0567467.

(5) Riffault, V.; Bedjanian, Y.; Le Bras, G. Kinetic and mechanistic study of the X and XO (X = Cl, Br) reactions with dimethyl sulfoxide. *Phys. Chem. Chem. Phys.* **2003**, *5*, 2828-2835, doi:10.1039/b302675b.

(6) Taatjes, C. A.; Meloni, G.; Selby, T. M.; Trevitt, A. J.; Osborn, D. L.; Percival, C. J.; Shallcross, D. E. Direct observation of the gas-phase Criegee intermediate (CH_2OO). *J. Am. Chem. Soc.* **2008**, *130*, 11883-11885, doi:10.1021/ja804165q.

(7) Vandresen, S.; Resende, S. M. The atmospheric reaction between DMSO and the chlorine radical. *J. Phys. Chem. A* **2004**, *108*, 2284-2289, doi:10.1021/jp036906j.

I56. **$CH_3(Cl)S(O)CH_3 + O_2$, NO, NO_2.** The recommendations are based on the study of Kleissas et al.[1] (296 K), which combined laser flash photolytic production of $CH_3(Cl)S(O)CH_3$ with kinetic observations by time-resolved absorption spectroscopy. The recommended uncertainties for the NO and NO_2 reactions are larger than those reported by Kleissas et al. pending independent confirmation of their results.
(Table: 10-6, Note: 10-6, Evaluated: 10-6) Back to Table

(1) Kleissas, K. M.; Nicovich, J. M.; Wine, P. H. Spectroscopy and kinetics of the gas phase addition complex of atomic chlorine with dimethyl sulfoxide. *J. Photochem. Photobiol. A: Chem.* **2007**, *187*, 1-9, doi:10.1016/j.jphotochem.2006.08.020.

I57. **Cl + $CH_3SC_2H_5$.** The recommended k(298 K) is the average of rate constants reported in two relative rate studies that employed a total of five different reference compounds;[1,2] all data were obtained at 298 K and 760 Torr air. Since both pressure independent H-abstraction pathways and a pressure dependent addition pathway are likely to be important, the recommended rate coefficient is only valid for ~1 atm $N_2 + O_2$. The following product yields are reported in 760 Torr of NO_x-free air: 43% for HCl, 55% for SO_2, 58% for CH_3CHO, and 58% for H_2CO.[3]
(Table: 15-10, Note: 15-10, Evaluated: 15-10) Back to Table

(1) Kinnison, D. J.; Mengon, W.; Kerr, J. A. Rate coefficients for the room temperature reaction of Cl atoms with dimethyl sulfide and related alkyl sulfides. *J. Chem. Soc. Faraday Trans.* **1996**, *92*, 369-372, doi:10.1039/ft9969200369.

(2) Oksdath-Mansilla, G.; Penenory, A. B.; Albu, M.; Barnes, I.; Wiesen, P.; Teruel, M. A. FTIR relative kinetic study of the reactions of $CH_3CH_2SCH_2CH_3$ and $CH_3CH_2SCH_3$ with OH radicals and Cl atoms at atmospheric pressure. *Chem. Phys. Lett.* **2009**, *477*, 22-27, doi:10.1016/j.cplett.2009.06.035.

(3) Oksdath-Mansilla, G.; Penenory, A. B.; Albu, M.; Barnes, I.; Wiesen, P.; Teruel, M. A. Product distribution study of the Cl-atom initiated oxidation of ethyl methyl sulfide and diethyl sulfide. *Atmos. Environ.* **2014**, *85*, 41-47, doi:10.1016/j.atmosenv.2013.11.063.

I58. **$Cl_2 + CH_3SCH_3$.** Dyke et al.[3] (294 K) have employed a flow tube technique with reactant and product detection by photoelectron spectroscopy to obtain a rate constant of $(3.4 \pm 0.7) \times 10^{-14}$ cm^3 molecule^{-1} s^{-1} at 1.6–3.0 Torr helium bath gas (the reported uncertainty is 1σ, precision); this rate constant is consistent with an upper limit value of 8×10^{-14} cm^3 molecule^{-1} s^{-1} at 298 K in 1 Torr helium reported by Butkovskaya et al.[1] Dyke et al.[2] have obtained the photoelectron spectrum of a reaction intermediate that they assign as $(CH_3)_2S{-}Cl_2$ (each Cl bound to S). A theoretical analysis suggests that the observed intermediate is stable by 26.3 kcal mol^{-1} relative to reactants and dissociates over a 29.0 kcal mol^{-1} barrier to the end products HCl + CH_3SCH_2Cl, both of which were observed by photoelectron spectroscopy.[2] Because it is not clear how Dyke et al. differentiated gas phase reaction of Cl_2 with CH_3SCH_3 from reaction on the flow tube walls in their investigation,[3] the recommendation treats their result plus two standard deviations as an upper limit for the gas phase rate constant.
(Table: 10-6, Note: 10-6, Evaluated: 10-6) Back to Table

(1) Butkovskaya, N. I.; Poulet, G.; Le Bras, G. Discharge flow study of the reactions of chlorine and fluorine atoms with dimethyl sulfide. *J. Phys. Chem.* **1995**, *99*, 4536-4543, doi:10.1021/j100013a025.

(2) Dyke, J. M.; Ghosh, M. V.; Goubet, M.; Lee, E. P. F.; Levita, G.; Miqueu, K.; Shallcross, D. E. A study of the atmospherically relevant reaction between molecular chlorine and dimethylsulfide (DMS): Establishing the reaction intermediate and measurement of absolute photoionization cross-sections. *Chem. Phys.* **2006**, *324*, 85-95, doi:10.1016/j.chemphys.2005.11.045.

(3) Dyke, J. M.; Ghosh, M. V.; Kinnison, D. J.; Levita, G.; Morris, A.; Shallcross, D. E. A kinetics and mechanistic study of the atmospherically relevant reaction between molecular chlorine and dimethyl sulfide (DMS). *Phys. Chem. Chem. Phys.* **2005**, *7*, 866-873, doi:10.1039/b415566a.

I59. **ClO + OCS; ClO + SO_2.** These recommendations are based on the discharge flow mass spectrometric data of Eibling and Kaufman.[1] (220–296 K). The upper limit on k(298 K) for ClO + OCS was set from the minimum detectable decrease in ClO. No products were observed. The upper limit on k(298 K) for ClO + SO_2 is based on the authors' estimate of their SO_3 detection limit. The upper limit for this same reaction based on the minimum detectable decrease in ClO was not used due to the potential problem of ClO reformation from the Cl + O_3 source reaction.
(Table: 83-62, Note: 83-62, Evaluated: 83-62) Back to Table

(1) Eibling, R. E.; Kaufman, M. Kinetics studies relevant to possible couppling between the stratospheric chlorine and sulfur cycles. *Atmos. Environ.* **1983**, *17*, 429-431, doi:10.1016/0004-6981(83)90061-6.

I60. **ClO + CH_3SCH_3.** The recommended k(298 K) is the average of the values reported in discharge flow mass spectrometry studies by Barnes et al.[1] (298 K) and Diaz-de-Mera et al.[2] (259–335 K). Barnes et al. prefer their more recent rate constant to one a factor of 4 higher that they determined using an earlier version of their apparatus. The recommendation for E/R is based on the temperature dependence observed by Diaz-de-Mera et al. The uncertainty factors reflect the fact that the two reported values for k(298 K) differ by more than a factor of two and that the activation energy is defined by data from a single study over a moderately narrow temperature range.
(Table: 06-2, Note: 06-2, Evaluated: 06-2) Back to Table

(1) Barnes, I.; Bastian, V.; Becker, K. H.; Overath, R. D. Kinetic studies of the reactions of IO, BrO, and ClO with dimethylsulfide. *Int. J. Chem. Kinet.* **1991**, *23*, 579-591, doi:10.1002/kin.550230704.

(2) Diaz-de-Mera, Y.; Aranda, A.; Rodriguez, D.; López, R.; Cabañas, B.; Martinez, E. Gas-phase reactions of chlorine atoms and ClO radicals with dimethyl sulfide. Rate coefficients and temperature dependences. *J. Phys. Chem. A* **2002**, *106*, 8627-8633, doi:10.1021/jp014570c.

I61. **ClO + $CH_3S(O)CH_3$.** The recommendation is based on the results of a low-pressure discharge flow mass spectrometry study by Riffault et al.[1] (298 K). These investigators were also able to establish an even lower upper limit of 2×10^{-15} cm^3 molecule^{-1} s^{-1} for the channel that produces Cl atoms
(Table: 06-2, Note: 06-2, Evaluated: 06-2) Back to Table

(1) Riffault, V.; Bedjanian, Y.; Le Bras, G. Kinetic and mechanistic study of the X and XO (X = Cl, Br) reactions with dimethyl sulfoxide. *Phys. Chem. Chem. Phys.* **2003**, *5*, 2828-2835, doi:10.1039/b302675b.

I62. **ClO + SO.** The recommended k(298 K) is an average of the determinations by Clyne and MacRobert[2] (295 K) and Brunning and Stief.[1] (210–363 K). The temperature independence is taken from the latter study with the A–factor recalculated to fit the k(298 K) recommendation.
(Table: 87-41, Note: 87-41, Evaluated: 87-41) Back to Table

(1) Brunning, J.; Stief, L. J. Kinetic studies of the reaction of the SO radical with NO_2 and ClO from 210 to 363 K. *J. Chem. Phys.* **1986**, *84*, 4371-4377, doi:10.1063/1.450059.

(2) Clyne, M. A. A.; MacRobert, A. J. Kinetic studies of free radical reactions by mass spectrometry. II. The reactions of SO + ClO, SO + OClO and SO + BrO. *Int. J. Chem. Kinet.* **1981**, *13*, 187-197, doi:10.1002/kin.550130208.

I63. **Br + H_2S, Br + CH_3SH.** These recommendations are based on the study by Nicovich et al.[1] (319–431 K for H_2S; 273–431 K for CH_3SH) who measured both the forward and reverse reactions by time–resolved resonance fluorescence detection of Br atoms. The uncertainties placed on these recommendations have been increased over those estimated by the authors to reflect the absence of any confirming investigations.
(Table: 94-26, Note: 94-26, Evaluated: 94-26) Back to Table

(1) Nicovich, J. M.; Kreutter, K. D.; van Dijk, C. A.; Wine, P. H. Temperature dependent kinetics studies of the reactions $Br(^2P_{3/2}) + H_2S \leftrightarrow SH + HBr$ and $Br(^2P_{3/2}) + CH_3SH \leftrightarrow CH_3S + HBr$. Heats of formation of SH and CH_3S radicals. *J. Phys. Chem.* **1992**, *96*, 2518-2528, doi:10.1021/j100185a025.

I64. **Br + CH_3SCH_3.** It is well-established based on studies by Wine et al.,[6] Ingham et al.[2] (298 K), and Nakano et al.[5] (278–333 K) that, under atmospheric conditions, attack of Br on CH_3SCH_3 occurs predominantly by addition to the sulfur atom. Above 375 K, adduct decomposition is so rapid that the addition channel is effectively negligible. Jefferson et al.[3] (386–604 K) report high temperature experiments where the individual hydrogen transfer reactions $Br + CH_3SCH_3 \rightarrow CH_3SCH_2 + HBr$ (forward reaction) and $CH_3SCH_2 + HBr \rightarrow Br + CH_3SCH_3$ (reverse reaction) were isolated in a laser flash photolysis resonance fluorescence system, and their kinetics were separately studied. These investigators determined Arrhenius expressions for the forward and reverse reactions to be $9.0 \times 10^{-11} \exp(-2386/T)$ and $8.6 \times 10^{-13} \exp(+836/T)$ cm^3 molecule^{-1} s^{-1}, respectively. Analysis of the equilibrium data also permitted determination of the heat of formation of CH_3SCH_2 (see Appendix 1). Extrapolation of the Jefferson et al. Arrhenius expression to 298 K gives a rate constant for the non-adduct-forming part of the $Br + CH_3SCH_3$ reaction (presumably direct hydrogen abstraction) of 3.0×10^{-14} cm^3 molecule^{-1} s^{-1}. This estimated rate constant agrees quite well with the value of $(4.9 \pm 2.0) \times 10^{-14}$ cm^3 molecule^{-1} s^{-1} obtained in a competitive kinetics study at atmospheric pressure in air by Ballesteros et al.[1] (296 K), and is consistent with an upper limit of 1×10^{-13} cm^3 molecule^{-1} s^{-1} reported in a similar study by Maurer et al.[4] (298 K). Direct comparison of the Jefferson et al. and Ballesteros et al. kinetic data is warranted only if essentially all adduct formation is reversible in the Ballesteros et al. experiment, which is possible based on the apparent absence of an adduct + O_2 pathway,[4,5] but is not yet well-established. The recommendation for the pressure-independent bimolecular reaction is based on extrapolation of the Arrhenius expression of Jefferson et al. to the atmospheric temperature regime. The large uncertainty reflects the need for a rather long extrapolation.
(Table: 06-2, Note: 06-2, Evaluated: 06-2) Back to Table

(1) Ballesteros, B., N. R. Jensen, and J. Hjorth FT-IR study of the kinetics and products of the reactions of dimethylsulphide, dimethylsulphoxide and dimethylsulphone with Br and BrO. *J. Atmos. Chem.* **2002**, *43*, 135-150, doi:10.1023/A:1019922224137.

(2) Ingham, T.; Bauer, D.; Sander, R.; Crutzen, P. J.; Crowley, J. N. Kinetics and products of the reactions BrO + DMS and Br + DMS at 298 K. *J. Phys. Chem. A* **1999**, *103*, 7199-7209, doi:10.1021/jp9905979.

(3) Jefferson, A.; Nicovich, J. M.; Wine, P. H. Temperature-dependent kinetics studies of the reactions $Br(^2P_{3/2}) + CH_3SCH_3 \leftrightarrow CH_3SCH_2 + HBr$. Heat of formation of the CH_3SCH_2 radical. *J. Phys. Chem.* **1994**, *98*, 7128-7135, doi:10.1021/j100080a006.

(4) Maurer, T., I. Barnes, and K. H. Becker FT-IR kinetic and product study of the Br-initiated oxidation of dimethyl sulfide. *Int. J. Chem. Kinet.* **1999**, *31*, 883-893, doi:10.1002/(SICI)1097-4601(1999)31:12<883::AID-KIN7>3.0.CO;2-V.

(5) Nakano, Y., M. Goto, S. Hashimoto, M. Kawasaki, and T. J. Wallington Cavity ring-down spectroscopic study of the reactions of Br atoms and BrO radicals with dimethyl sulfide. *J. Phys. Chem. A* **2001**, *105*, 11045-11050, doi:10.1021/jp012326f.

(6) Wine, P. H.; Nicovich, J. M.; Stickel, R. E.; Zhao, Z.; Shackelford, C. J.; Kreutter, K. D.; Daykin, E. P.; Wang, S. In *The Tropospheric Chemistry of Ozone in the Polar Regions*; Springer-Verlag: Berlin, 1993; Vol. I7; pp 385-395.

I65. **Br + $CH_3S(O)CH_3$.** The recommendation is based on the results of a low-pressure discharge flow mass spectrometry study by Riffault et al.[2] (298 K). These authors obtained an upper limit for the total rate constant of 1.5×10^{-14} cm^3 $molecule^{-1}$ s^{-1}, and also report channel–specific rate constants in units of 10^{-15} cm^3 $molecule^{-1}$ s^{-1} of 11 ± 3 for the H–abstraction channel and 1.2 ± 0.3 for the methyl elimination channel. A competitive kinetics study in 740 Torr air by Ballesteros et al.[1] (296 K) reports a less sensitive upper limit rate constant of 6×10^{-14} $cm^3 molecule^{-1} s^{-1}$.
(Table: 06-2, Note: 06-2, Evaluated: 06-2) Back to Table

(1) Ballesteros, B., N. R. Jensen, and J. Hjorth FT-IR study of the kinetics and products of the reactions of dimethylsulphide, dimethylsulphoxide and dimethylsulphone with Br and BrO. *J. Atmos. Chem.* **2002**, *43*, 135-150, doi:10.1023/A:1019922224137.

(2) Riffault, V.; Bedjanian, Y.; Le Bras, G. Kinetic and mechanistic study of the X and XO (X = Cl, Br) reactions with dimethyl sulfoxide. *Phys. Chem. Chem. Phys.* **2003**, *5*, 2828-2835, doi:10.1039/b302675b.

I66. **BrO + CH_3SH.** The recommendation is based on the low-pressure discharge flow mass spectrometry study of Aranda et al.[1] (259–333 K). A significant negative activation energy of -6.9 ± 2.0 kJ/mol was observed at 1.0 Torr He. At 298 K, reported rate coefficients in units of 10^{-14} cm^3 $molecule^{-1}$ s^{-1} increase with increasing helium pressure from 2.7 ± 0.5 at 0.5 Torr to 4.9 ± 0.4 at 3.0 Torr. HOBr was observed as a reaction product suggesting that an important reaction pathway is addition of BrO to CH_3SH followed by dissociation to HOBr + CH_3S in competition with dissociation to reactants. Until kinetic data are reported at higher pressures, no recommendation of appropriate rate constants for atmospheric modeling is made.
(Table: 10-6, Note: 10-6, Evaluated: 10-6) Back to Table

(1) Aranda, A.; Diaz de Mera, Y.; Rodríguez, D.; Salgado, S.; Martinez, E. Kinetic and products of the BrO + CH_3SH reaction: Temperature and pressure dependence. *Chem. Phys. Lett.* **2002**, *357*, 471-476, doi:10.1016/S0009-2614(02)00561-4.

I67. **BrO + CH_3SCH_3.** This recommendation is an average of results obtained in the discharge flow studies of Barnes et al.[2] (298 K) and Bedjanian et al.[3] (233–320 K), and the flash photolysis studies of Ingham et al.[4] (298 K) and Nakano et al.[5] (278–333 K). The flash photolysis studies were carried out at pressures of 60–200 Torr and give rate constants that are almost a factor of two greater than those obtained in the discharge flow studies at ~1 Torr. The error limits in the present evaluation are adjusted to include all available data. A new study to investigate the pressure dependence of the rate constant is needed. Both Bedjanian et al. and Ingham et al. have shown that DMSO ($CH_3S(O)CH_3$) is produced with near unit yield. Ballesteros et al.[1] (296 K) report that the rate constants for BrO + CH_3SCH_3 and BrO + CD_3SCD_3 are identical, a result that is consistent with reaction proceeding via formation of a short-lived adduct that rapidly decomposes to Br + DMSO.
(Table: 06-2, Note: 06-2, Evaluated: 06-2) Back to Table

(1) Ballesteros, B., N. R. Jensen, and J. Hjorth FT-IR study of the kinetics and products of the reactions of dimethylsulphide, dimethylsulphoxide and dimethylsulphone with Br and BrO. *J. Atmos. Chem.* **2002**, *43*, 135-150, doi:10.1023/A:1019922224137.

(2) Barnes, I.; Bastian, V.; Becker, K. H.; Overath, R. D. Kinetic studies of the reactions of IO, BrO, and ClO with dimethylsulfide. *Int. J. Chem. Kinet.* **1991**, *23*, 579-591, doi:10.1002/kin.550230704.

(3) Bedjanian, Y.; Poulet, G.; Le Bras, G. Kinetic study of the reaction of BrO radicals with dimethylsulfide. *Int. J. Chem. Kinet.* **1996**, *28*, 383-389, doi:10.1002/(SICI)1097-4601(1996)28:5<383::AID-KIN7>3.0.CO;2-R.

(4) Ingham, T.; Bauer, D.; Sander, R.; Crutzen, P. J.; Crowley, J. N. Kinetics and products of the reactions BrO + DMS and Br + DMS at 298 K. *J. Phys. Chem. A* **1999**, *103*, 7199-7209, doi:10.1021/jp9905979.

(5) Nakano, Y., M. Goto, S. Hashimoto, M. Kawasaki, and T. J. Wallington Cavity ring-down spectroscopic study of the reactions of Br atoms and BrO radicals with dimethyl sulfide. *J. Phys. Chem. A* **2001**, *105*, 11045-11050, doi:10.1021/jp012326f.

I68. **BrO + CH_3SSCH_3.** The recommendation is based on a competitive kinetics study in 740 Torr air by Ballesteros et al.[1] (296 K). The large uncertainty factor results from the fact that the reported rate constant is measured relative to an assumed value of 3.2×10^{-13} cm^3 $molecule^{-1}$ s^{-1} for the BrO + CH_3SCH_3 rate constant, which has an uncertain pressure dependence (see above), and from the fact that there is only a single study upon which to base a recommendation.
(Table: 06-2, Note: 06-2, Evaluated: 06-2) Back to Table

(1) Ballesteros, B., N. R. Jensen, and J. Hjorth FT-IR study of the kinetics and products of the reactions of dimethylsulphide, dimethylsulphoxide and dimethylsulphone with Br and BrO. *J. Atmos. Chem.* **2002**, *43*, 135-150, doi:10.1023/A:1019922224137.

I69. BrO + $CH_3S(O)CH_3$. The recommendation is based on a competitive kinetics study in 740 Torr air by Ballesteros et al.[1] (296 K). A low-pressure discharge flow mass spectrometry study by Riffault et al.[2] (298 K), gives an upper limit that is consistent with the recommendation. The large uncertainty factor results primarily from the fact that the reported rate constant is obtained from a series of competitive kinetics experiments that are referenced to an assumed value of 3.2×10^{-13} cm^3 $molecule^{-1}$ s^{-1} for the BrO + CH_3SCH_3 rate constant, which has an uncertain pressure dependence (see above).
(Table: 06-2, Note: 06-2, Evaluated: 06-2) Back to Table

(1) Ballesteros, B., N. R. Jensen, and J. Hjorth FT-IR study of the kinetics and products of the reactions of dimethylsulphide, dimethylsulphoxide and dimethylsulphone with Br and BrO. *J. Atmos. Chem.* **2002**, *43*, 135-150, doi:10.1023/A:1019922224137.
(2) Riffault, V.; Bedjanian, Y.; Le Bras, G. Kinetic and mechanistic study of the X and XO (X = Cl, Br) reactions with dimethyl sulfoxide. *Phys. Chem. Chem. Phys.* **2003**, *5*, 2828-2835, doi:10.1039/b302675b.

I70. BrO + SO. This recommendation is based on the measurements of Brunning and Stief[1] (298 K) performed under both excess BrO and excess SO conditions. The rate constant is supported by the lower limit assigned by Clyne and MacRobert[2] (295 K) from measurements of SO_2 production.
(Table: 87-41, Note: 87-41, Evaluated: 87-41) Back to Table

(1) Brunning, J.; Stief, L. J. Rate constant for the reaction SO + BrO → SO_2 + Br. *J. Chem. Phys.* **1986**, *85*, 2591-2594, doi:10.1063/1.451066.
(2) Clyne, M. A. A.; MacRobert, A. J. Kinetic studies of free radical reactions by mass spectrometry. II. The reactions of SO + ClO, SO + OClO and SO + BrO. *Int. J. Chem. Kinet.* **1981**, *13*, 187-197, doi:10.1002/kin.550130208.

I71. IO + CH_3SH. The recommended k(298 K) comes from the study by Maguin et al.[1] (298 K) using discharge flow mass spectrometry. The investigators establish a branching ratio near unity for the production of HOI. The uncertainty factor reflects the absence of confirming investigations.
(Table: 94-26, Note: 94-26, Evaluated: 94-26) Back to Table

(1) Maguin, F.; Mellouki, A.; Laverdet, G.; Poulet, G.; Le Bras, G. Kinetics of the reactions of the IO radical with dimethyl sulfide, methanethiol, ethylene, and propylene. *Int. J. Chem. Kinet.* **1991**, *23*, 237-245, doi:10.1002/kin.550230306.

I72. IO + CH_3SCH_3. The recommendation is based on the temperature-dependent studies of Gravestock et al.[5] (296–468 K) and Dillon et al.[4] (256–341 K) and the 298 K studies of Maguin et al.,[7] Barnes et al.,[1] and Knight et al.[6] All data points in each temperature dependent study were scaled by a factor equal to the ratio $k(298\ K)_{Arr}/k(298\ K)_{ave}$ where $k(298\ K)_{Arr}$ is the 298 K rate constant obtained from the best fit Arrhenius expression describing the individual temperature-dependent data set and $k(298\ K)_{ave}$ is the average of all reported 298 K rate constants (using $k(298\ K)_{Arr}$ from the temperature-dependent studies). The best fit of the scaled data to $\ln k = \ln A - E/RT$ is recommended. The studies of Maguin et al. and Barnes et al. supersede earlier, less direct measurements by the same groups,[2,8] which reported much greater rate constants. Nakano et al.[9] (273–312 K) employed a laser flash photolysis cavity ring down spectroscopy technique to investigate the temperature and pressure dependence of the rate constant. These investigators report that the 298 K rate constant increases from 1 to 25×10^{-14} cm^3 $molecule^{-1}$ s^{-1} as pressure increases from 5 to 100 Torr N_2, then levels off at higher pressure. Nakano et al. also investigated the temperature dependence of the rate constant at 100 Torr and observed a very strong negative temperature dependence, i.e., $E/R = -2230 \pm 460$ K. The pressure dependence reported by Nakano et al. is in conflict with the results of Daykin and Wine,[3] Gravestock et al., and Dillon et al. (no observed pressure–dependence at 297 ± 1 K) while the temperature dependence reported by Nakano et al. is in conflict with the results of Gravestock et al. and Dillon et al.
(Table: 15-10, Note: 15-10, Evaluated: 15-10) Back to Table

(1) Barnes, I.; Bastian, V.; Becker, K. H.; Overath, R. D. Kinetic studies of the reactions of IO, BrO, and ClO with dimethylsulfide. *Int. J. Chem. Kinet.* **1991**, *23*, 579-591, doi:10.1002/kin.550230704.
(2) Barnes, I.; Becker, K. H.; Carlier, P.; Mouvier, G. FTIR study of the DMS/NO_2/I_2/N_2 photolysis system: The reaction of IO radicals with DMS. *Int. J. Chem. Kinet.* **1987**, *19*, 489-501, doi:10.1002/kin.550190602.

(3) Daykin, E. P.; Wine, P. H. Rate of reaction of IO radicals with dimethylsulfide. *J. Geophys. Res.* **1990**, *95*, 18547-18553, doi:10.1029/JD095iD11p18547.
(4) Dillon, T. J.; Karunanandan, R.; Crowley, J. N. The reaction of IO with CH_3SCH_3: Products and temperature dependent rate coefficients by laser induced fluorescence. *Phys. Chem. Chem. Phys.* **2006**, *8*, 847-855, doi:10.1039/b514718b.
(5) Gravestock, T.; Blitz, M. A.; Heard, D. E. Kinetics study of the reaction of iodine monoxide radicals with dimethyl sulfide. *Phys. Chem. Chem. Phys* **2005**, *7*, 2173-2181, doi:10.1039/b502989a.
(6) Knight, G. P.; Crowley, J. N. The reactions of IO with HO_2, NO and CH_3SCH_3: Flow tube studies of kinetics and product formation. *Phys. Chem. Chem. Phys.* **2001**, *3*, 393-401, doi:10.1039/b008447f.
(7) Maguin, F.; Mellouki, A.; Laverdet, G.; Poulet, G.; Le Bras, G. Kinetics of the reactions of the IO radical with dimethyl sulfide, methanethiol, ethylene, and propylene. *Int. J. Chem. Kinet.* **1991**, *23*, 237-245, doi:10.1002/kin.550230306.
(8) Martin, D.; Jourdain, J. L.; Laverdet, G.; Le Bras, G. Kinetic study of the reaction of IO with CH_3SCH_3. *Int. J. Chem. Kinet.* **1987**, *19*, 503-512, doi:10.1002/kin.550190603.
(9) Nakano, Y.; Enami, S.; Nakamichi, S.; Aloisio, S.; Hashimoto, S.; Kawasaki, M. Temperature and pressure dependence study of the reaction of IO radicals with dimethyl sulfide by cavity ring-down laser spectroscopy. *J. Phys. Chem.* **2003**, *107*, 6381-6387, doi:10.1021/jp0345147.

I73. **$S + O_2$.** The recommended k(298 K) is the average of values reported by Fair and Thrush[5] (298 K), Fair et al.[6] (298 K), Donovan and Little[4] (295 K), Davis et al.[3] (298–422 K), Clyne and Townsend[1] (298 K), Clyne and Whitefield[2] (296–393 K), Miyoshi et al.[8] (293 K, 980–1610 K), and Lu et al.[7] (298–878 K). The recommended value for E/R is the average of E/R values obtained from the data sets of Davis et al. (25 Torr CO_2, E/R = +1 K), Davis et al. (20−200 Torr He, E/R = −204 K), Clyne and Whitefield (~1 Torr Ar, E/R = −129 K), and Lu et al. (50 Torr Ar, 298−505 K, E/R = −66 K). Lu et al. report non-Arrhenius behavior at T >505 K. A theoretical analysis by Lu et al. suggests that reaction occurs almost exclusively via a SOO(^{1}A′) intermediate at T <500 K, whereas other channels involving SOO(^{1}A″) as an intermediate and formation of SOO(^{3}A″) followed by isomerization to SO_2 before dissociation, become important at higher temperatures and account for the observed rapid increase of the rate constant with increasing temperature above 500 K. High temperature kinetic data reported by Saito et al.[9] (1900−2200 K), Tsuchiya et al. (980−1610 K),[10] and Woiki and Roth (1200−3500 K)[11] are reasonably consistent with the rate constants predicted theoretically by Lu et al.
(Table: 15-10, Note: 15-10, Evaluated: 15-10) Back to Table

(1) Clyne, M. A. A.; Townsend, L. W. Rate constant measurements for rapid reactions of ground state sulphur $3p^4(^3P_J)$ atoms. *Int. J. Chem. Kinet.* **1975**, *Symp. 1*, 73-84.
(2) Clyne, M. A. A.; Whitefield, P. D. Atomic resonance fluorescence for rate constants of rapid bimolecular reactions Part 7.-Sulphur atom reactions: $S + O_2 \rightarrow SO + O$ and $S + NO_2 \rightarrow SO + NO$ from 296 to 410 K. *J. Chem. Soc. Faraday Trans. 2* **1979**, *75*, 1327-1340, doi:10.1039/f29797501327.
(3) Davis, D. D.; Klemm, R. B.; Pilling, M. A flash photolysis-resonance fluorescence kinetics study of ground-state sulfur atoms I. Absolute rate parameters for reaction of S(^3P) with O_2($^3\Sigma$). *Int. J. Chem. Kinet.* **1972**, *4*, 367-382, doi:10.1002/kin.550040402
(4) Donovan, R. J.; Little, D. J. The rate of the reaction S(3^3P_J) + O_2. *Chem. Phys. Lett.* **1972**, *13*, 488-490, doi:10.1016/0009-2614(72)80087-3.
(5) Fair, R. W.; Thrush, B. A. Reaction of hydrogen atoms with hydrogen sulphide in the presence of molecular oxygen. *Trans. Faraday Soc.* **1969**, *65*, 1557-1570, doi:10.1039/tf9696501557.
(6) Fair, R. W.; van Roodaelaar, A.; Strausz, O. P. The reaction of S(^{3}P) atoms with molecular oxygen. *Can. J. Chem.* **1971**, *49*, 1659-1664, doi:10.1139/v71-270.
(7) Lu, C.-W.; Wu, Y.-J.; Lee, Y.-P.; Zhu, R. S.; Lin, M. C. Experimental and theoretical investigations of rate coefficients of the reaction S(^{3}P) + O_2 in the temperature range 298-878 K. *J. Chem. Phys.* **2004**, *121*, 8271-8278, doi:10.1063/1.1792611.
(8) Miyoshi, A.; Shina, H.; Tsuchiya, K.; Matsui, H. Kinetics and mechanism of the reaction of S(^{3}P) with O_2. *Symp. Int. Combust. Proc.* **1996**, *26*, 535-541.
(9) Saito, K.; Ueda, Y.; Ito, R.; Kakumoto, T.; Imamura, A. Measurements of the bimolecular rate constants for $S + O_2 \rightarrow SO + O$ and $CS_2 + O_2 \rightarrow CS + SO_2$ at high temperatures. *Int. J. Chem. Kinet.* **1986**, *18*, 871-884, doi:10.1002/kin.550180807.
(10) Tsuchiya, K.; Kamiya, K.; Matsui, H. Studies on the oxidation mechanism of H_2S based on direct examination of the key reactions. *Int. J. Chem. Kinet.* **1997**, *29*, 57-66, doi:10.1002/(SICI)1097-4601(1997)29:1<57::AID-KIN7>3.0.CO;2-K.
(11) Woiki, D.; Roth, P. Oxidation of S and SO by O_2 in high-temperature pyrolysis and photolysis reaction systems. *Int. J. Chem. Kinet.* **1995**, *27*, 59-71, doi:10.1002/kin.550270108.

I74. **S + O_3.** This recommendation accepts the only available experimental data of Clyne and Townsend.[1] (298 K). In this study the authors measure a value of the rate constant for S + O_2 in reasonable agreement with that recommended above.
(Table: 82-57, Note: 82-57, Evaluated: 82-57) Back to Table

(1) Clyne, M. A. A.; Townsend, L. W. Rate constant measurements for rapid reactions of ground state sulphur $3p^4(^3P_J)$ atoms. *Int. J. Chem. Kinet.* **1975**, *Symp. 1*, 73-84.

I75. **SO + O_2.** The recommended E/R is the average of values reported by Black et al. (E/R = 2370 K, 250–420 K)[1] and Schurath and Goede (E/R = 2180 K, 262–363 K),[5] while the recommended k(298 K) is the average of values computed from the Arrhenius expressions reported in the same two studies. The room temperature rate constant obtained from the Black et al. study[1] supersedes an earlier value as recommended by the authors. The recommended values for k(T) lie significantly higher than an extrapolation of the higher temperature data of Homann et al.,[4] but are consistent with the more recent high temperature study of Garland.[3] A room temperature upper limit on k set by Breckenridge and Miller[2] is consistent with the recommendation.
(Table: 15-10, Note: 15-10, Evaluated: 15-10) Back to Table

(1) Black, G.; Sharpless, R. L.; Slanger, T. G. Rate coefficients for SO reactions with O_2 and O_3 over the temperature range 230 to 420 K. *Chem. Phys. Lett.* **1982**, *93*, 598-602, doi:10.1016/0009-2614(82)83737-8.
(2) Breckenridge, W. H.; Miller, T. A. Kinetic study by EPR of the production and decay of $SO(^1\Delta)$ in the reaction of $O_2(^1\Delta_g)$ with $SO(^3\Sigma^-)$. *J. Chem. Phys.* **1972**, *56*, 465-474, doi:10.1063/1.1676891.
(3) Garland, N. L. Temperature dependence of the reaction: SO + O_2. *Chem. Phys. Lett.* **1998**, *290*, 385-390, doi:10.1016/S0009-2614(98)00553-3.
(4) Homann, K. H.; Krome, G.; Wagner, H. G. Carbon disulfide oxidation rate of elementary reactions .1. *Ber. Bunsenges. Phys. Chem.* **1968**, *72*, 998-1004, doi:10.1002/bbpc.19680720821.
(5) Schurath, U.; Goede, H.-J. Temperature Dependence of the Reactions SO + O_3 (1) and SO + O_2 (2). *Physico-Chemical Behaviour of Atmospheric Pollutants, Proc. 3rd European Symposium, Varese, Italy* **1984**, 227 - 239.

I76. **SO + O_3.** The recommended k(298 K) is an average of the determinations by Halstead and Thrush[3] (275–320 K), Robertshaw and Smith[4] (296 K), Schurath and Goede,[5] and Black et al.[1,2] (298 K, 230–420 K). The value of E/R is an average of the values reported by Halstead and Thrush, Schurath and Goede, and Black et al.[2], with the A-factor recalculated to fit the recommendation for k(298 K).
(Table: 06-2, Note: 06-2, Evaluated: 06-2) Back to Table

(1) Black, G.; Sharpless, R. L.; Slanger, T. G. Rate coefficients at 298 K for SO reactions with O_2, O_3, and NO_2. *Chem. Phys. Lett.* **1982**, *90*, 55-58, doi:10.1016/0009-2614(82)83324-1.
(2) Black, G.; Sharpless, R. L.; Slanger, T. G. Rate coefficients for SO reactions with O_2 and O_3 over the temperature range 230 to 420 K. *Chem. Phys. Lett.* **1982**, *93*, 598-602, doi:10.1016/0009-2614(82)83737-8.
(3) Halstead, C. J.; Thrush, B. A. The kinetics of elementary reactions involving the oxides of sulphur III. The chemilluminescent reaction between sulphur monoxide and ozone. *Proc. Roy. Soc. London A* **1966**, *295*, 380-398 doi:10.1098/rspa.1966.0248.
(4) Robertshaw, J. S.; Smith, I. W. M. Rate data for O + OCS → SO + CO and SO + O_3 → SO_2 + O_2 by a new time-resolved technique. *Int. J. Chem. Kinet.* **1980**, *12*, 729 -739, doi:10.1002/kin.550121006.
(5) Schurath, U.; Goede, H.-J. Temperature Dependence of the Reactions SO + O_3 (1) and SO + O_2 (2). *Physico-Chemical Behaviour of Atmospheric Pollutants, Proc. 3rd European Symposium, Varese, Italy* **1984**, 227 - 239.

I77. **SO + NO_2.** The recommended k(298 K) is an average of the determinations by Clyne and MacRobert[4] (295 K), Black et al.[1] (298 K), and Brunning and Stief[2] (210–363 K), which agree quite well with the rate constant calculated from the relative rate measurements of Clyne et al.[3] (298 K). The recommended value for E/R is taken from Brunning and Stief.
(Table: 82-57, Note: 82-57, Evaluated: 82-57) Back to Table

(1) Black, G.; Sharpless, R. L.; Slanger, T. G. Rate coefficients at 298 K for SO reactions with O_2, O_3, and NO_2. *Chem. Phys. Lett.* **1982**, *90*, 55-58, doi:10.1016/0009-2614(82)83324-1.
(2) Brunning, J.; Stief, L. J. Kinetic studies of the reaction of the SO radical with NO_2 and ClO from 210 to 363 K. *J. Chem. Phys.* **1986**, *84*, 4371-4377, doi:10.1063/1.450059.

(3) Clyne, M. A. A.; Halstead, C. J.; Thrush, B. A. The kinetics of elementary reactions involving the oxides of sulphur I. The nature of the sulphur dioxide afterglow. *Proc. Soc. London Ser. A.* **1966**, *295*, 355-362, doi:10.1098/rspa.1966.0246.
(4) Clyne, M. A. A.; MacRobert, A. J. Kinetic studies of free radical reactions by mass spectrometry. I. The reactions SO + NO_2 and ClO + NO. *Int. J. Chem. Kinet.* **1980**, *12*, 79-96, doi:10.1002/kin.550120202.

I78. **SO + OClO.** This recommendation is based on the room temperature study by Clyne and MacRobert–[1] (295 K). The uncertainty reflects the absence of any confirming investigation.
(Table: 82-57, Note: 82-57, Evaluated: 82-57) Back to Table

(1) Clyne, M. A. A.; MacRobert, A. J. Kinetic studies of free radical reactions by mass spectrometry. II. The reactions of SO + ClO, SO + OClO and SO + BrO. *Int. J. Chem. Kinet.* **1981**, *13*, 187-197, doi:10.1002/kin.550130208.

I79. **SO_3 + 2 H_2O.** Several research groups have attempted to quantify the rate of sulfuric acid formation via this reaction in the gas phase. Reiner and Arnold[6] (298 K) placed an upper limit of 2.4×10^{-15} cm^3 $molecule^{-1}$ s^{-1} on the rate constant, slightly lower than that determined by Wang et al.[8] (298 K). The inability to cite the results as other than an upper limit is due to the difficulty in excluding all heterogeneous effects from the experiments. The higher rate constant reported earlier by Castleman et al.[1] (298 K) may have resulted from an underestimation of the effects of such heterogeneous reactions. Subsequently, Reiner and Arnold[7] (298 K) sought to improve their rate constant determination by more detailed quantification of heterogeneous contributions. They derived a value of 1.2×10^{-15} cm^3 $molecule^{-1}$ s^{-1}, independent of pressure (from 31–260 mbar of synthetic air). Evidence was also obtained that H_2SO_4 was, indeed, the product of the reaction.

Kolb et al.[3] (243–333 K) attempted to measure the gas phase rate constant using a turbulent flow reactor designed to minimize wall effects. Their results, when analyzed as representing a bimolecular reaction, support a rate constant in the range $(1–7) \times 10^{-15}$ cm^3 $molecule^{-1}$ s^{-1}. However, a more detailed analysis of the data indicated that the gas phase reaction was second order in water vapor. The reaction rate was also observed to increase as the temperature was lowered from 333 to 243 K. These observations, together with calculations by Morokuma and Mugurama,[5] led the latter authors to suggest that SO_3 consumption likely involved its reaction with the water dimer or the reaction SO_3–H_2O + H_2O, leading to the formation of sulfuric acid.

A laminar flow reactor study by Lovejoy et al.[4] (250–360 K) also revealed SO_3 loss to be second order in water concentration and independent of pressure (from 20 to 80 Torr of N_2 at 300 K). These latter authors measured a strong negative temperature dependence for the rate constant and a significant kinetic isotope effect ($k_{H2O} \approx 2k_{D2O}$), leading them to describe the reaction as proceeding via the rapid association between SO_3 and H_2O followed by a slower reaction between the adduct and water to form sulfuric acid. Lovejoy at al.'s measurement of a −54 kJ mol^{-1} "activation" energy was viewed as energetically inconsistent with a SO_3 + water dimer reaction mechanism since it would require a large negative activation energy for the SO_3 + $(H_2O)_2$ step. Jayne et al.[2] (283–370 K) have carried out a turbulent flow reactor study in the pressure range 100 to 760 Torr N_2. Their results provide further support for a mechanism involving formation of an SO_3–H_2O adduct that reacts with a second H_2O to form H_2SO_4, and the rate constants they report agree quite well with those reported by Lovejoy et al. The recommended expression for first order loss of SO_3,

$$k^I = 8.5 \times 10^{-41} \exp(+6540/T) [H_2O]^2 \ s^{-1} \quad ([H_2O] \text{ in molecules cm}^{-3})$$

is the best fit of the combined data of Lovejoy et al. and Jayne et al. to an Arrhenius form.
(Table: 06-02, Note: 06-02, Evaluated: 06-2) Back to Table

(1) Castleman, A. W.; Davis, R. E.; Munkelwitz, H. R.; Tang, I. N.; Wood, W. P. Kinetics of association reactions pertaining to H_2SO_4 aerosol formation. *Int. J. Chem. Kinet.* **1975**, *Symp. 1*, 629-640.
(2) Jayne, J. T.; Poschl, U.; Chen, Y.; Dai, D.; Molina, L. T.; Worsnop, D. R.; Kolb, C. E.; Molina, M. J. Pressure and temperature dependence of the gas-phase reaction of SO_3 with H_2O and the heterogeneous reaction of SO_3 with H_2O/H_2SO_4 surfaces. *J. Phys. Chem. A* **1997**, *101*, 10000-10011, doi:10.1021/jp972549z.
(3) Kolb, C. E.; Jayne, J. T.; Worsnop, D. R.; Molina, M. J.; Meads, R. F.; Viggiano, A. A. Gas phase reaction of sulfur trioxide with water vapor. *J. Am. Chem. Soc.* **1994**, *116*, 10314-10315, doi:10.1021/ja00101a067.
(4) Lovejoy, E. R.; Hanson, D. R.; Huey, L. G. Kinetics and products of the gas-phase reaction of SO_3 with water. *J. Phys. Chem.* **1996**, *100*, 19911-19916, doi:10.1021/jp962414d.
(5) Morokuma, K.; Mugurama, C. Ab initio molecular orbital study of the mechanism of the gas phase reaction SO_3 + H_2O: Importance of the second water molecule. *J. Am. Chem. Soc.* **1994**, *116*, 10316-10317, doi:10.1021/ja00101a068.

(6) Reiner, T.; Arnold, F. Laboratory flow reactor measurements of the reaction $SO_3 + H_2O + M \rightarrow H_2SO_4 + M$: Implications for gaseous H_2SO_4 and aerosol formation in the plumes of jet aircraft. *Geophys. Res. Lett.* **1993**, *20*, 2659-2662, doi:10.1029/93GL02996.
(7) Reiner, T.; Arnold, F. Laboratory investigations of gaseous sulfuric acid formation via $SO_3 + H_2O + M \rightarrow H_2SO_4 + M$: Measurement of the rate constant and product indentification. *J. Chem. Phys.* **1994**, *101*, 7399-7407, doi:10.1063/1.468298.
(8) Wang, X.; Jin, Y. G.; Suto, M.; Lee, L. C. Rate constant of the gas phase reaction of SO_3 with H_2O. *J. Chem. Phys.* **1988**, *89*, 4853-4860, doi:10.1063/1.455680.

I80. **$SO_3 + NO_2$.** This recommendation is based on the study of Penzhorn and Canosa[1] (298 K) using second derivative UV spectroscopy. These authors observe the production of a white aerosol, which they interpret to be the adduct NSO_5. This claim is supported by ESCA spectra.
(Table: 85-37, Note: 85-37, Evaluated: 85-37) Back to Table

(1) Penzhorn, R. D.; Canosa, C. E. 2nd derivative UV spectroscopy study of the thermal and photochemical reaction of NO_2 with SO_2 and SO_3. *Ber. Bunsenges. Phys. Chem.* **1983**, *87*, 648-654, doi:10.1002/bbpc.19830870808.

I81. **$SH + O_2$.** This upper limit for k(298 K) is based on the study by Stachnik and Molina[6] (298 K) utilizing experiments sensitive to the production of OH. Somewhat higher upper limits of 1.0×10^{-17} and 1.5×10^{-17} cm^3 $molecule^{-1}$ s^{-1} were assigned by Friedl et al.[3] (298 K) and Wang et al.[8] (295 K) respectively from the sensitivities for OH detection and SH decay respectively. An even higher upper limit by Black[2] (298 K), based on the lack of SH decay, may have been complicated by SH regeneration. Much less sensitive upper limits have been calculated by Tiee et al.[7] (298 K) for the rate constant for the sum of the two $SH + O_2$ reaction channels (producing $OH + SO$ and $H + SO_2$). The HSO_2 potential energy surface has been studied theoretically by Ballester and Varandas,[1] Garrido et al.,[4] Resende and Ornellas,[5] and Zhou, et al.[9] Resende and Ornellas and Zhou et al. predict that at atmospheric temperatures (i) $OH + SO$ are the dominant bimolecular products and (ii) the rate constant is orders of magnitude slower than the upper limit reported by Stachnik and Molina.
(Table: 85-37, Note: 15-10, Evaluated: 15-10) Back to Table

(1) Ballester, M. Y.; Varandas, A. J. C. Double many-body expansion potential energy surface for ground state HSO_2. *Phys. Chem. Chem. Phys.* **2005**, *7*, 2305-2317, doi:10.1039/b500990a.
(2) Black, G. Reactions of HS with NO and NO_2 at 298 K. *J. Chem. Phys.* **1984**, *80*, 1103-1107, doi:10.1063/1.446838.
(3) Friedl, R. R.; Brune, W. H.; Anderson, J. G. Kinetics of SH with NO_2, O_3, O_2, and H_2O_2. *J. Phys. Chem.* **1985**, *89*, 5505-5510, doi:10.1021/j100271a038.
(4) Garrido, J. D.; Ballester, M. Y.; Orozco-González, Y.; Canuto, S. CASPT2 study of the potential energy surface of the HSO_2 system. *J. Phys. Chem. A* **2011**, *115*, 1453-1461, doi:10.1021/jp108460v.
(5) Resende, S. M.; Ornellas, F. R. The reaction of SH with O_2: A theoretical high level investigation. *Phys. Chem. Chem. Phys.* **2003**, *5*, 4617-4621, doi:10.1039/b308359d.
(6) Stachnik, R. A.; Molina, M. J. Kinetics of the reactions of SH radicals with NO_2 and O_2. *J. Phys. Chem.* **1987**, *91*, 4603-4606 doi:10.1021/j100301a035.
(7) Tiee, J. J.; Wampler, F. B.; Oldenborg, R. C.; Rice, W. W. Spectroscopy and reaction kinetics of the HS radicals. *Chem. Phys. Lett.* **1981**, *82*, 80-84, doi:10.1016/0009-2614(81)85111-1.
(8) Wang, N. S.; Lovejoy, E. R.; Howard, C. J. Temperature dependence of the rate constant for the reaction $HS + NO_2$. *J. Phys. Chem.* **1987**, *91*, 5743-5749, doi:10.1021/j100306a045.
(9) Zhou, C.; Sendt, K.; Haynes, B. S. Computational study of the reaction $SH + O_2$ *J. Phys. Chem. A* **2009**, *113*, 2975-2981, doi:10.1021/jp810105e.

I82. **$SH + O_3$.** The recommended k(298 K) is an average of the determinations by Friedl et al.[1] (298 K) (laser induced fluorescence detection of SH), Schonle et al.[4] (298 K) (mass spectrometric detection of reactant SH and product HSO) as revised by Schindler and Benter,[3] and Wang and Howard[5] (296–431 K) (laser magnetic resonance detection of SH). The temperature dependence is from Wang and Howard with the A–factor calculated to agree with the recommended value for k(298 K). The recommendation for g reflects the fact that the temperature dependence comes from measurements above room temperature and, thus, extrapolation to lower temperatures may be subject to additional uncertainties. Wang and Howard report observing a minor reaction channel that produces $H + SO + O_2$. A theoretical study by Resende and Ornellas[2] concludes that if reaction occurs on the ground state potential energy surface, the rate constant should be several orders of magnitude slower than the experimental value.
(Table: 06-2, Note: 06-2, Evaluated: 06-2) Back to Table

(1) Friedl, R. R.; Brune, W. H.; Anderson, J. G. Kinetics of SH with NO_2, O_3, O_2, and H_2O_2. *J. Phys. Chem.* **1985**, *89*, 5505-5510, doi:10.1021/j100271a038.
(2) Resende, S. M.; Ornellas, R. Does SH really react with O_3 in the ground state? *Chem. Phys. Lett.* **2001**, *349*, 123-130, doi:10.1016/S0009-2614(01)01177-0.
(3) Schindler, R. N.; Benter, T. Correction. *Ber. Bunsenges. Phys. Chem.* **1988**, *92*, 558, doi:10.1002/bbpc.198800126.
(4) Schonle, G.; Rahman, M. M.; Schindler, R. N. Kinetics of the reaction of atomic fluorine with H_2S and elementary reactions of the HS radical. *Ber. Bunsenges. Phys. Chem.* **1987**, *91*, 66-75, doi:10.1002/bbpc.19870910114.
(5) Wang, N. S.; Howard, C. J. Kinetics of the reactions of HS and HSO with O_3. *J. Phys. Chem.* **1990**, *94*, 8787-8794, doi:10.1021/j100388a009.

I83. **SH + H_2O_2.** This recommended upper limit for k(298 K) is based on the study of Friedl et al.[1] (298 K). Their value is calculated from the lack of SH decay (measured by laser induced fluorescence) and the lack of OH production (measured by resonance fluorescence). The three possible product channels are H_2S + HO_2, HSOH + OH, and HSO + H_2O.
(Table: 85-37, Note: 85-37, Evaluated: 85-37) Back to Table

(1) Friedl, R. R.; Brune, W. H.; Anderson, J. G. Kinetics of SH with NO_2, O_3, O_2, and H_2O_2. *J. Phys. Chem.* **1985**, *89*, 5505-5510, doi:10.1021/j100271a038.

I84. **SH + NO_2.** The recommendation is based on the temperature-dependent measurements of Wang et al.[10] (221–415 K) and Herndon and Ravishankara[5] (248–358 K). All data points in each study were scaled by a factor equal to the ratio $k(298\text{ K})_{Arr}/k(298\text{ K})_{ave}$ where $k(298\text{ K})_{Arr}$ is the 298 K rate constant obtained from the best fit Arrhenius expression describing the individual T-dependent data set and $k(298\text{ K})_{ave}$ is the average of the $k(298\text{ K})_{Arr}$ values from the two studies. The best fit of the scaled data to $\ln k = \ln A - E/RT$ is recommended. Wang et al. suggest that the lower values of k(298 K) reported by Black[1] (298 K), Friedl et al.[4] (298 K), and Bulatov et al.[2] are due to SH regeneration from the H_2S source compound. Herndon and Ravishankara suggest that simultaneous detection of SH and SO may have corrupted earlier studies where laser induced fluorescence was employed as the detection technique.[1,4] In the study by Stachnik and Molina,[9] attempts were made at minimizing SH regeneration, and the reported value of k(298 K) was significantly greater than that from the earlier studies, but still 30% less than that measured by Wang et al., who used two independent SH source reactions. A slightly larger rate constant measured by Schonle et al.,[8] as revised by Schindler and Benter,[7] is not recommended due to the somewhat more limited database for their determination. The reaction as written represents the most exothermic channel. In fact, HSO has been detected as a product by Leu and Smith,[6] Bulatov et al.,[2] Schonle et al.,[8] and Wang et al. The absence of a primary deuterium isotope effect, as observed by both Wang et al. and Herndon and Ravishankara, coupled with the large magnitude of the rate constant suggests that the (four–center intermediate) channels producing SO + HNO and OH + SNO are of minor importance. No evidence for a three–body combination reaction was found by either Black or Friedl et al. Based on a pressure independence of the rate constant between 30 and 300 Torr, Black set an upper limit of 7.0×10^{-31} cm^6 $molecule^{-2}$ s^{-1} for the termolecular rate constant. Similarly, Stachnik and Molina[9] (298 K) observed no change in decay rate between 100 and 730 Torr with O_2 (although these O_2 experiments were designed primarily to limit SH regeneration). The recommendation given here is supported by the discharge flow laser induced fluorescence study of the SD + NO_2 reaction by Fenter and Anderson.[3] These investigators report a 298 K rate constant of 6.8×10^{-11} cm^3 $molecule^{-1}$ s^{-1}, which compares favorably with the values of 7.3×10^{-11} and 6.6×10^{-11} cm^3 $molecule^{-1}$ s^{-1} determined by Wang et al. and Herndon and Ravishankara, respectively, in studies of the same reaction. Fenter and Anderson also obtained an E/R value of –210 K, very similar to the –279 K value derived by Herndon and Ravishankara for the SD reaction and the values –240 K and –270 K derived by Wang et al. and Herndon and Ravishankara, respectively, for the SH reaction.
(Table: 15-10, Note: 15-10, Evaluated: 15-10) Back to Table

(1) Black, G. Reactions of HS with NO and NO_2 at 298 K. *J. Chem. Phys.* **1984**, *80*, 1103-1107, doi:10.1063/1.446838.
(2) Bulatov, V. P.; Kozliner, M. Z.; Sarkisov, O. M. Determination of rate constants for the reactions of SH + NO_2 → HSO + NO and HSO + NO_2 → products. *Khim. Fiz.* **1984**, *3*, 1300-1305.
(3) Fenter, F. F.; Anderson, J. G. Kinetics of the DS-radical reactions with ClNO and NO_2. *Int. J. Chem. Kinet.* **1994**, *26*, 801-812, doi:10.1002/kin.550260803.
(4) Friedl, R. R.; Brune, W. H.; Anderson, J. G. Kinetics of SH with NO_2, O_3, O_2, and H_2O_2. *J. Phys. Chem.* **1985**, *89*, 5505-5510, doi:10.1021/j100271a038.
(5) Herndon, S. C.; Ravishankara, A. R. Kinetics of the reaction of SH and SD with NO_2. *J. Phys. Chem. A* **2006**, *110*, 106-113, doi:10.1021/jp053918r.

(6) Leu, M.-T.; Smith, R. H. Rate constants for the gas-phase reaction between hydroxyl and hydrogen sulfide over the temperature range 228-518 K. *J. Phys. Chem.* **1982**, *86*, 73-81, doi:10.1021/j100390a015.
(7) Schindler, R. N.; Benter, T. Correction. *Ber. Bunsenges. Phys. Chem.* **1988**, *92*, 558, doi:10.1002/bbpc.198800126.
(8) Schonle, G.; Rahman, M. M.; Schindler, R. N. Kinetics of the reaction of atomic fluorine with H_2S and elementary reactions of the HS radical. *Ber. Bunsenges. Phys. Chem.* **1987**, *91*, 66-75, doi:10.1002/bbpc.19870910114.
(9) Stachnik, R. A.; Molina, M. J. Kinetics of the reactions of SH radicals with NO_2 and O_2. *J. Phys. Chem.* **1987**, *91*, 4603-4606 doi:10.1021/j100301a035.
(10) Wang, N. S.; Lovejoy, E. R.; Howard, C. J. Temperature dependence of the rate constant for the reaction HS + NO_2. *J. Phys. Chem.* **1987**, *91*, 5743-5749, doi:10.1021/j100306a045.

I85. **SH + N_2O.** The recommendation is the upper limit rate constant reported by Herndon et al.[1] (298 K). As discussed by Herndon et al., the much greater (four orders of magnitude) rate constant reported by Ravichandran et al.[2] appears to result from mis−interpretation of the source of electronically excited HSO, chemiluminescence from which was employed by Ravichandran et al. to follow the reaction kinetics.
(Table: 06-02, Note: 06-02, Evaluated: 06-2) Back to Table

(1) Herndon, S. C.; Froyd, K. D.; Lovejoy, E. R.; Ravishankara, A. R. How rapidly does the SH radical react with N_2O? *J. Phys. Chem. A* **1999**, *103*, 6778-6785, doi:10.1021/jp9911853.
(2) Ravichandran, K.; Williams, R.; Fletcher, T. R. Atmospheric reactions of vibrationally excited greenhouse gases: SH + N_2O(*n*, 0, 0). *Chem. Phys. Lett.* **1994**, *217*, 375-380, doi:10.1016/0009-2614(93)E1411-9.

I86. **SH + Cl_2.** The recommended k(298 K) is the average of the one reported by Nesbitt and Leone[2] (298 K), who studied the kinetics of the Cl + H_2S → SH + HCl, SH + Cl_2 → ClSH + Cl chain reaction using a laser flash photolysis − IR emission technique, and the one reported by Fenter and Anderson,[1] who employed a discharge flow − laser induced fluorescence technique to study the SD + Cl_2 reaction over the temperature range 273−373 K; the Fenter and Anderson results are corrected for the secondary kinetic isotope effect using the theoretical results of Wang et al.,[3] who report $k_H / k_D = 1.11 \exp(-71/T)$. The recommended value for E/R is taken from the work of Fenter and Anderson corrected as described above for the secondary kinetic isotope effect. The recommended value for the parameter g reflects the absence of confirming studies.
(Table: 19-5, Note: 19-5, Evaluated: 19-5) Back to Table

(1) Fenter, F. F.; Anderson, J. G. Kinetics and mechanism of the reactions of the SD Radical with Br_2, BrCl, Cl_2, and F_2. *J. Phys. Chem.* **1991**, *95*, 3172-3180, doi:10.1021/j100161a041.
(2) Nesbitt, D. J.; Leone, S. R. Laser-initiated chemical chain reactions. *J. Chem. Phys.* **1980**, *72*, 1722-1732, doi:10.1063/1.439284.
(3) Wang, L.; Liu, J.-Y.; Li, Z.-S.; Sun, C.-C. Theoretical study and rate constant calculation for the reactions of SH (SD) with Cl_2, Br_2, and BrCl. *J. Comput. Chem.* **2004**, *26*, 184-193, doi:10.1002/jcc.20159.

I87. **SH + BrCl; SH + Br_2; SH + F_2.** The recommendations for these reactions are derived from the experimental data of Fenter and Anderson[1] for the SD reactions corrected for the secondary kinetic isotope effect using the theoretical results of Wang et al.[2,3] Wang et al. report $k_H / k_D = 0.81 \exp(-50/T)$ for BrCl and $1.08 \exp(-49/T)$ for Br_2;[2] their results for SH(SD) + F_2 suggest that $k_H / k_D = 1.036$, 1.048, and 1.056 at 298 K, 338 K, and 373 K, respectively,[3] the three temperatures where experimental SD rate constants are reported by Fenter and Anderson. The recommended uncertainties have been increased over those estimated by Fenter and Anderson to reflect the absence of any confirming investigations as well as uncertainty in the theoretical secondary kinetic isotope effects. For the SD + BrCl reaction, the channel producing ClSD + Br is reported by Fenter and Anderson to be described by the rate expression $k = 2.3 \times 10^{-11} \exp(+100/T)$ cm^3 molecule^{-1} s^{-1}, thereby accounting for 43% of overall reactivity at 298 K and 51% at 373 K. On the other hand, Wang et al.[2] predict theoretically that reaction proceeds almost exclusively to produce BrSD (BrSH) + Cl products at atmospheric temperatures, with the ClSD (ClSH) + Br channel becoming important only at higher temperatures.
(Table: 19-5, Note: 19-5, Evaluated: 19-5) Back to Table

(1) Fenter, F. F.; Anderson, J. G. Kinetics and mechanism of the reactions of the SD Radical with Br_2, BrCl, Cl_2, and F_2. *J. Phys. Chem.* **1991**, *95*, 3172-3180, doi:10.1021/j100161a041.
(2) Wang, L.; Liu, J.-Y.; Li, Z.-S.; Sun, C.-C. Theoretical study and rate constant calculation for the reactions of SH (SD) with Cl_2, Br_2, and BrCl. *J. Comput. Chem.* **2004**, *26*, 184-193, doi:10.1002/jcc.20159.

(3) Wang, L.; Liu, J.-Y.; Li, Z.-S.; Sun, C.-C. Dual-level direct dynamics study on the reactions of SH (SD) with F_2. *Int. J. Chem. Kinet.* **2005**, *37*, 710-716, doi:10.1002/kin.20124.

I88. HSO + O_2. This recommendation is based on the study by Lovejoy et al.[2] (296 K), who employed laser magnetic resonance monitoring of HSO in a discharge flow system. The upper limit thus derived for k(298 K) is nearly two orders of magnitude smaller than measured by Bulatov et al.[1]
(Table: 92-20, Note: 92-20, Evaluated: 92-20) Back to Table

(1) Bulatov, V. P.; Sarkisov, O. M.; Kozliner, M. Z.; Ergorov, V. G. Mechanism of hydrogen sulfide photooxidation in atmosphere. *Khim. Fiz.* **1986**, *5*, 1031-1036.
(2) Lovejoy, E. R.; Wang, N. S.; Howard, C. J. Kinetic studies of the reactions of HSO with NO_2, NO, and O_2. *J. Phys. Chem.* **1987**, *91*, 5749-5755, doi:10.1021/j100306a046.

I89. HSO + O_3. This recommended k(298 K) is based on the determinations by Friedl et al.[1] (298 K) and Wang and Howard[3] (296–405 K). In the first study, performed at higher O_3 concentrations, greater quantities of HSO were produced in the flow tube and SH approached a steady state due to its generation via HSO + O_3. The rate constant for this reaction was thus determined relative to SH + O_3 from measurements of the steady state SH concentration as a function of the initial SH concentration. In the second study, the rate constant and its branching ratio were measured at two temperatures. At room temperature, the overall rate constant is in excellent agreement with that of Friedl et al. More recently, Lee et al.[2] (273–423 K) determined a room temperature rate constant of 4.7×10^{-14} cm^3 molecule^{-1} s^{-1} for the sum of all reaction channels not producing HS. This value is approximately 30% greater than that measured by Wang and Howard for the same channels. Lee et al. derive an Arrhenius activation energy of 1120 K for these channels from data between 273and 423 K, in agreement with the more limited temperature-dependent data of Wang and Howard.

The lack of an isotope effect when SD was employed in the Friedl et al. study suggests that the products of the HSO + O_3 reaction are SH + $2O_2$ (analogous to those for HO_2 + O_3). However, Wang and Howard found that only 70% of the reaction leads to HS formation. In addition, their observations of HO_2 production in the presence of O_2 suggests the existence of a reaction channel producing HSO_2 + O_2 followed by HSO_2 + O_2 → HO_2 + SO_2. At the present time, no recommendation is given for the product channels. Further mechanistic work is suggested, since it is important to understand whether this reaction in the atmosphere leads to HS regeneration or to oxidation of the sulfur.
(Table: 92-20, Note: 94-26, Evaluated: 92-20) Back to Table

(1) Friedl, R. R.; Brune, W. H.; Anderson, J. G. Kinetics of SH with NO_2, O_3, O_2, and H_2O_2. *J. Phys. Chem.* **1985**, *89*, 5505-5510, doi:10.1021/j100271a038.
(2) Lee, Y.-Y.; Lee, Y.-P.; Wang, N. S. Kinetics of the reaction of HSO with O_3 at temperatures 273-423 K. *J. Chem. Phys.* **1994**, *100*, 387-392, doi:10.1063/1.466952.
(3) Wang, N. S.; Howard, C. J. Kinetics of the reactions of HS and HSO with O_3. *J. Phys. Chem.* **1990**, *94*, 8787-8794, doi:10.1021/j100388a009.

I90. HSO + NO; HSO + NO_2. The recommendations for these reactions are based on the study by Lovejoy et al.[3] (296 K) in which laser magnetic resonance was used to monitor HSO in a discharge flow system. Their upper limit for the NO reaction is a factor of 25 smaller than the rate constant measured by Bulatov et al.[2] using intracavity laser absorption at pressures between 10 and 100 Torr. Since it is unlikely that this reaction rate undergoes a factor of 25 increase between 1 Torr (the pressure of the Lovejoy et al. work) and 10 Torr, the higher rate constant may be due to secondary chemistry associated with the HSO production methods employed.

The recommendation for the NO_2 reaction is a factor of 2 higher than the rate constant reported by Bulatov et al.[1] Lovejoy et al. have attributed this difference to HSO regeneration under the experimental conditions used by Bulatov et al.[1] The product assignment for this reaction is discussed in the note for the HSO_2 + O_2 reaction.
(Table 87-41, Note: 87-41, Evaluated: 87-41) Back to Table

(1) Bulatov, V. P.; Kozliner, M. Z.; Sarkisov, O. M. Determination of rate constants for the reactions of SH + NO_2 → HSO + NO and HSO + NO_2 → products. *Khim. Fiz.* **1984**, *3*, 1300-1305.
(2) Bulatov, V. P.; Kozliner, M. Z.; Sarkisov, O. M. Reactions of SH and HSO radicals with nitrogen oxide. *Khim. Fiz.* **1985**, *4*, 1353-1357.
(3) Lovejoy, E. R.; Wang, N. S.; Howard, C. J. Kinetic studies of the reactions of HSO with NO_2, NO, and O_2. *J. Phys. Chem.* **1987**, *91*, 5749-5755, doi:10.1021/j100306a046.

I91. HSO_2 + O_2. This recommendation is based on the rate of HO_2 formation measured by Lovejoy et al.[1] (296 K) upon addition of O_2 to the HSO + NO_2 reaction system. While HSO_2 was not observed directly, a consideration

of the mechanistic possibilities for HSO + NO_2, coupled with measurements of the HO_2 production rate at various O_2 pressures, led these authors to suggest that HSO_2 is both a major product of the HSO + NO_2 reaction and a precursor for HO_2 via reaction with O_2.
(Table: 87-41, Note: 87-41, Evaluated: 87-41) Back to Table

(1) Lovejoy, E. R.; Wang, N. S.; Howard, C. J. Kinetic studies of the reactions of HSO with NO_2, NO, and O_2. *J. Phys. Chem.* **1987**, *91*, 5749-5755, doi:10.1021/j100306a046.

I92. **$HOSO_2 + O_2$.** This recommendation is based on the studies of Gleason et al.[3] (298 K) and Gleason and Howard[2] (297–423 K) in which the $HOSO_2$ reactant was monitored using a chemical ionization mass spectrometric technique. Gleason and Howard is the only temperature dependence investigation, and these authors report the same 297 K rate coefficient as the one reported by Gleason et al. The recommended uncertainty parameter *g* is increased from the *E*/R error limits quoted by Gleason and Howard to account for potential uncertainties in extrapolating their data to sub–ambient temperatures. The recommended value of *k*(298 K) derives further support from the studies of Margitan[6] (298 K) and Martin et al.[7] (298 K), both of whom used modeling fits of OH radical decays in the OH + SO_2 + M reaction system in the presence of O_2 and NO. In this latter analysis, the $HOSO_2$ reacts with O_2, yielding HO_2, which subsequently regenerates OH through its reaction with NO. Theoretical electronic structure and kinetics calculations by Huynh and coworkers[5] provides additional support for the recommendation. The infrared spectrum of $HOSO_2$ has been recorded in low temperature matrix isolation experiments by Hashimoto et al.[4] and Nagase et al.[8] Mass spectrometric detection of $HOSO_2$ in the gas phase has also been reported by Egsgaard et al.[1]
(Table: 06-2, Note: 19-5, Evaluated: 06-2) Back to Table

(1) Egsgaard, H.; Carlson, L.; Florencio, H.; Drewello, T.; Schwarz, H. Experimental evidence for the gaseous HSO_3 radical. The key intermediate in the oxidation of SO_2 in the atmosphere. *Chem. Phys. Lett.* **1988**, *148*, 537-540, doi:10.1016/0009-2614(88)80327-0.
(2) Gleason, J. F.; Howard, C. J. Temperature dependence of the gas-phase reaction $HOSO_2 + O_2 \rightarrow HO_2 + SO_3$. *J. Phys. Chem.* **1988**, *92*, 3414-3417, doi:10.1021/j100323a021.
(3) Gleason, J. F.; Sinha, A.; Howard, C. J. Kinetics of the gas-phase reaction $HOSO_2 + O_2 \rightarrow HO_2 + SO_3$. *J. Phys. Chem.* **1987**, *91*, 719-724, doi:10.1021/j100287a045.
(4) Hashimoto, S.; Inoue, G.; Akimoto, H. Infrared spectroscopic detection of the $HOSO_2$ radical in argon matrix at 11 K. *Chem. Phys. Lett.* **1984**, *107*, 198-202, doi:10.1016/0009-2614(84)85699-7.
(5) Mai, T. V.-T.; Duong, M. V.; Nguyen, H. T.; Huynh, L. K. Ab initio kinetics of the $HOSO_2 + 3O_2 \rightarrow SO_3 + HO_2$ reaction. *Phys. Chem. Chem. Phys.* **2018**, *20*, 6677-6687, doi:10.1039/c7cp07704a.
(6) Margitan, J. J. Mechanism of the atmospherlc oxidation of sulfur dioxide. Catalysis by hydroxyl radicals. *J. Phys. Chem.* **1984**, *88*, 3314-3318, doi:10.1021/j150659a035.
(7) Martin, D.; Jourdain, J. L.; Le Bras, G. Discharge flow measurements of the rate constants for the reactions OH + SO_2 + He and $HOSO_2 + O_2$ in relation with the atmospheric oxidation of SO_2. *J. Phys. Chem.* **1986**, *90*, 4143-4147, doi:10.1021/j100408a061.
(8) Nagase, S.; Hashimoto, S.; Akimoto, H. $HOSO_2$ and $HOSO_4$ radicals studied by ab initio calculation and matrix isolation technique. *J. Phys. Chem.* **1988**, *92*, 641-644, doi:10.1021/j100314a015.

I93. **CS + O_2.** The recommendation for *k*(298 K) is based on the work of Black et al.[1] (298 K) using laser induced fluorescence to monitor CS. This value agrees with the somewhat less precise determination by Richardson[2] (293, 495 K) using OCS formation rates. The latter author presents evidence that this reaction channel dominates over the one producing SO + CO by more than a factor of 10. Measurements by Richardson at 293 and 495 K yield an *E*/R of 1860 K. However, use of this activation energy with the recommended value of *k*(298 K) results in an unusually low Arrhenius *A*-factor of 1.5×10^{-16} cm^3 $molecule^{-1}$ s^{-1}. In view of this, no recommendation is given for the temperature dependence.
(Table: 85-37, Note: 85-37, Evaluated: 85-37) Back to Table

(1) Black, G.; Jusinski, L. E.; Slanger, T. G. Rate coefficients for CS reactions with O_2, O_3 and NO_2 at 298 K. *Chem. Phys. Lett.* **1983**, *102*, 64-68, doi:10.1016/0009-2614(83)80659-9.
(2) Richardson, R. J. CS-O_2 flame reaction chemistry. *J. Phys. Chem.* **1975**, *79*, 1153-1158, doi:10.1021/j100579a003.

I94. **CS + O_3; CS + NO_2.** The *k*(298 K) recommendations for both reactions accept the results of Black et al.[1] (298 K), who used laser–induced fluorescence to monitor the CS reactant. The uncertainty factors reflect the absence of any confirming measurements.
(Table: 85-37, Note: 85-37, Evaluated: 85-37) Back to Table

(1) Black, G.; Jusinski, L. E.; Slanger, T. G. Rate coefficients for CS reactions with O_2, O_3 and NO_2 at 298 K. *Chem. Phys. Lett.* **1983**, *102*, 64-68, doi:10.1016/0009-2614(83)80659-9.

I95. **$CH_3S + O_2$.** This upper limit is based on the study by Tyndall and Ravishankara[3] (298 K). Somewhat higher upper limits were derived in the earlier studies of Balla et al.[1] (298 K) and Black and Jusinski.[2]
(Table: 90-1, Note: 90-1, Evaluated: 90-1) Back to Table

(1) Balla, R. J.; Nelson, H. H.; McDonald, J. R. Kientics of the reaction of CH_3S with NO, NO_2 and O_2. *Chem. Phys.* **1986**, *109*, 101-107, doi:10.1016/0301-0104(86)80188-4.
(2) Black, G.; Jusinski, L. E. Laser-induced fluorescence studies of the CH_3S radical. *J. Chem. Soc. Faraday Trans. 2* **1986**, *86*, 2143-2151, doi:10.1039/f29868202143.
(3) Tyndall, G. S.; Ravishankara, A. R. Kinetics and mechanism of the reactions of CH_3S with O_2 and NO_2 at 298 K. *J. Phys. Chem.* **1989**, *93*, 2426-2435, doi:10.1021/j100343a041.

I96. **$CH_3S + O_3$.** The recommendation for k(298 K) is the average of room temperature rate constants reported by Tyndall and Ravishankara[5] (298 K), Domine et al. [2] (300 K), Turnipseed et al.[4] (295–359 K), and Martinez et al.[3] (259–381 K). The recommendation for E/R is the average of values obtained from least squares fits of the temperature-dependent data of Turnipseed et al. and Martinez et al. using only rate constants at temperatures below 345 K. A failure to observe significant reaction in the study by Black and Jusinski[1] is interpreted as due to rapid regeneration of CH_3S in their system. Tyndall and Ravishankara[5] corrected their measured 298 K rate constant downward by ~20% to account for CH_3S regeneration via the $CH_3SO + O_3$ reaction, but the magnitude of the correction is now highly uncertain in light of the results of Domine et al. and Turnipseed et al. Domine et al. measured the yield of CH_3SO to be 15%.
(Table: 06-2, Note: 06-2, Evaluated: 06-2) Back to Table

(1) Black, G.; Jusinski, L. E. Laser-induced fluorescence studies of the CH_3S radical. *J. Chem. Soc. Faraday Trans. 2* **1986**, *86*, 2143-2151, doi:10.1039/f29868202143.
(2) Domine, F.; Ravishankara, A. R.; Howard, C. J. Kinetics and mechanisms of the reactions of CH_3S, CH_3SO, and CH_3SS with O_3 at 300 K and low pressures. *J. Phys. Chem.* **1992**, *96*, 2171-2178, doi:10.1021/j100184a027.
(3) Martínez, E.; Albaladejo, A.; Notario, A.; Jiminéz, E. A study of the atmospheric reaction of CH_3S with O_3 as a function of temperature. *Atmos. Environ.* **2000**, *34*, 5295-5302, doi:10.1016/S1352-2310(00)00348-4.
(4) Turnipseed, A. A.; Barone, S. B.; Ravishankara, A. R. Reactions of CH_3S and CH_3SOO with O_3, NO_2, and NO. *J. Phys. Chem.* **1993**, *97*, 5926-5934, doi:10.1021/j100124a025.
(5) Tyndall, G. S.; Ravishankara, A. R. Kinetics of the reaction of CH_3S with O_3 at 298 K. *J. Phys. Chem.* **1989**, *93*, 4707-4710, doi:10.1021/j100349a006.

I97. **CH_3S + NO.** The upper limit for the bimolecular reaction between CH_3S and NO is based on estimates by Balla et al.[1] (295–503 K), who conducted a temperature dependence study of the termolecular reaction.
(Table: 92-20, Note: 92-20, Evaluated: 92-20) Back to Table

(1) Balla, R. J.; Nelson, H. H.; McDonald, J. R. Kientics of the reaction of CH_3S with NO, NO_2 and O_2. *Chem. Phys.* **1986**, *109*, 101-107, doi:10.1016/0301-0104(86)80188-4.

I98. **$CH_3S + NO_2$.** The recommendation for k(298 K) is the average of room temperature rate constants reported by Tyndall and Ravishankara[6] (298 K), Domine et al.[3] (297 K), Turnipseed et al.[5] (242–359 K), Martinez et al.[4] (263–381 K), and Chang et al.[2] (222–420 K). The recommendation for E/R is the average of values reported by Turnipseed et al., Martinez et al., and Chang et al. An earlier study by Balla et al.[1] (295–511 K) appears to have been affected by secondary reactions resulting from high radical concentrations. Tyndall and Ravishankara determined the NO yield to be (80 ± 20)%. Together with the unity yield of CH_3SO obtained by Domine et al., this implies that the primary reaction channel is as written.
(Table: 06-2, Note: 06-2, Evaluated: 06-2) Back to Table

(1) Balla, R. J.; Nelson, H. H.; McDonald, J. R. Kientics of the reaction of CH_3S with NO, NO_2 and O_2. *Chem. Phys.* **1986**, *109*, 101-107, doi:10.1016/0301-0104(86)80188-4.
(2) Chang, P.-F.; Wang, T. T.; Niann, S. W.; Hwang, Y.-L.; Lee, Y.-P. Temperature dependence of rate coefficients of reactions of NO_2 with CH_3S and C_2H_5S. *J. Phys. Chem. A* **2000**, *104*, 5525-5529, doi:10.1021/jp000294a.
(3) Domine, F.; Murrells, T. P.; Howard, C. J. Kinetics of the reactions of NO_2 with CH_3S, CH_3SO, CH_3SS, and CH_3SSO at 297 K and 1 Torr. *J. Phys. Chem.* **1990**, *94*, 5839-5847, doi:10.1021/j100378a043.

(4) Martinez, E.; Albaladejo, A.; Jiminez, E.; Notario, A.; Aranda, A. Kinetics of the reaction of CH_3S with NO_2 as a function of temperature. *Chem. Phys. Lett.* **1999**, *308*, 37-44, doi:10.1016/S0009-2614(99)00579-5.
(5) Turnipseed, A. A.; Barone, S. B.; Ravishankara, A. R. Reactions of CH_3S and CH_3SOO with O_3, NO_2, and NO. *J. Phys. Chem.* **1993**, *97*, 5926-5934, doi:10.1021/j100124a025.
(6) Tyndall, G. S.; Ravishankara, A. R. Kinetics and mechanism of the reactions of CH_3S with O_2 and NO_2 at 298 K. *J. Phys. Chem.* **1989**, *93*, 2426-2435, doi:10.1021/j100343a041.

I99. $CH_3S + CO$. The recommendation is based on the study of Koch et al.[1] (208–295 K), who generated CH_3S by laser flash photolysis of CH_3SSCH_3 and monitored the loss of CH_3S by laser induced fluorescence. The rate of loss of CH_3S was found to be independent of [CO] up to levels of approximately 10^{17} molecules cm^{-3}. No enhancement of the CH_3S loss rate was observed when O_2 was added to the reaction mixture, confirming that CH_3SOO is also unreactive toward CO. Electronic structure calculations are consistent with experimental observations, suggesting that there is a significant barrier (~12 kJ mol^{-1}) to formation of a very weakly bound (~9 kJ mol^{-1}) $CH_3S{-}CO$ adduct.
(Table: 15-10, Note: 15-10, Evaluated: 15-10) Back to Table

(1) Koch, L. C.; Marshall, P.; Ravishankara, A. R. An investigation of the reaction of CH_3S with CO. *J. Phys. Chem. A* **2004**, *108*, 5205-5212, doi:10.1021/jp049193t.

I100. $CH_3S + Br_2$. The recommendation is based on the study of Nicovich et al.[1] (298 K), who coupled laser flash photolysis of $Br_2/CH_3SH/H_2/N_2$ mixtures with resonance fluorescence detection of Br atoms to monitor the kinetics of Br approach to steady state ($Br + CH_3SH \rightarrow CH_3S + HBr$; $CH_3S + Br_2 \rightarrow CH_3SBr + Br$). The recommended uncertainty is larger than estimated by Nicovich et al. to reflect the slightly indirect nature of the rate constant determination and the lack of a confirming study.
(Table: 15-10, Note: 15-10, Evaluated: 15-10) Back to Table

(1) Nicovich, J. M.; Kreutter, K. D.; van Dijk, C. A.; Wine, P. H. Temperature dependent kinetics studies of the reactions $Br(^2P_{3/2}) + H_2S \leftrightarrow SH + HBr$ and $Br(^2P_{3/2}) + CH_3SH \leftrightarrow CH_3S + HBr$. Heats of formation of SH and CH_3S radicals. *J. Phys. Chem.* **1992**, *96*, 2518-2528, doi:10.1021/j100185a025.

I101. $CH_2SH + O_2$. This recommended k(298 K) is the average of the rate constants obtained by Rahman et al.[2] (298 K) in a fast flow mass spectrometry system and Anastasi et al.[1] (298 K) using a pulse radiolysis − kinetic absorption apparatus. The value of Anastasi et al. is nearly twice that of Rahman et al. It is difficult at present to indicate a preference for the results of one study over the other, and the value of f(298 K) has been chosen to reflect this uncertainty. Since this is a fast bimolecular reaction, one would expect the products to be $HO_2 + CH_2S$, by analogy with the reaction between CH_2OH and O_2.
(Table: 94-26, Note: 94-26, Evaluated: 94-26) Back to Table

(1) Anastasi, C.; Broomfield, M.; Nielsen, O. J.; Pagsberg, P. Kinetics and mechanisms of the reactions of CH_2SH radicals with O_2, NO, and NO_2. *J. Phys. Chem.* **1992**, *96*, 696-701, doi:10.1021/j100181a034.
(2) Rahman, M. M.; Becker, E.; Wille, U.; Schindler, R. N. Determination of rate constants for the reactions of the CH_2SH radical with O_2, O_3, and NO_2 at 298 K. *Ber. Bunsenges. Phys. Chem.* **1992**, *96*, 783-787, doi:10.1002/bbpc.19920960609.

I102. $CH_2SH + O_3$. The recommended k(298 K) comes from the study by Rahman et al.[1] (298 K) using fast flow mass spectrometry. The uncertainty factor reflects the absence of any confirming investigations.
(Table: 94-26, Note: 94-26, Evaluated: 94-26) Back to Table

(1) Rahman, M. M.; Becker, E.; Wille, U.; Schindler, R. N. Determination of rate constants for the reactions of the CH_2SH radical with O_2, O_3, and NO_2 at 298 K. *Ber. Bunsenges. Phys. Chem.* **1992**, *96*, 783-787, doi:10.1002/bbpc.19920960609.

I103. $CH_2SH + NO$. The recommended k(298 K) comes from the study by Anastasi et al.[1] (298 K) using a pulse radiolysis kinetic absorption apparatus. The uncertainty factor reflects the absence of any confirming investigations.
(Table: 94-26, Note: 94-26, Evaluated: 94-26) Back to Table

(1) Anastasi, C.; Broomfield, M.; Nielsen, O. J.; Pagsberg, P. Kinetics and mechanisms of the reactions of CH_2SH radicals with O_2, NO, and NO_2. *J. Phys. Chem.* **1992**, *96*, 696-701, doi:10.1021/j100181a034.

I104. $CH_2SH + NO_2$. The recommended k(298 K) is an average of the rate constants obtained by Rahman et al.[2] (298 K) in a fast flow mass spectrometry system and by Anastasi et al.[1] (298 K), using a pulse radiolysis kinetic absorption apparatus. The value of Rahman et al. is nearly twice that of Anastasi et al. It is difficult to indicate a preference for the results of one study over the other, and the value of f(298 K) has been chosen to reflect this uncertainty.
(Table: 94-26, Note: 94-26, Evaluated: 94-26) Back to Table

(1) Anastasi, C.; Broomfield, M.; Nielsen, O. J.; Pagsberg, P. Kinetics and mechanisms of the reactions of CH_2SH radicals with O_2, NO, and NO_2. *J. Phys. Chem.* **1992**, *96*, 696-701, doi:10.1021/j100181a034.
(2) Rahman, M. M.; Becker, E.; Wille, U.; Schindler, R. N. Determination of rate constants for the reactions of the CH_2SH radical with O_2, O_3, and NO_2 at 298 K. *Ber. Bunsenges. Phys. Chem.* **1992**, *96*, 783-787, doi:10.1002/bbpc.19920960609.

I105. $CH_3SO + O_3$. The recommended k(298 K) is an average of values reported by Domine et al.[2] (300 K) and Borissenko et al.[1] (300 K). It is supported by the study of Tyndall and Ravishankara[3] (298 K), in which the rate constant was derived from a complex analysis of the $CH_3S + O_3$ reaction system. Borissenko et al. measured the rate constant relative to the rate constant for the $CH_3SO + NO_2$ reaction; they report that the $CH_3SO + NO_2$ rate constant is greater by a factor of 47. Domine et al. place the direct yield of CH_2SO at approximately 10% and that of CH_3S at 13% at low pressure. Borissenko et al. report that the SO_2 yield is near unity in 100−600 Torr N_2.
(Table: 06-2, Note: 06-2, Evaluated: 06-2) Back to Table

(1) Borissenko, D.; Kukui, A.; Laverdet, G.; Le Bras, G. Experimental study of SO_2 formation in the reactions of CH_3SO radical with NO_2 and O_3 in relation with the atmospheric oxidation mechanism of dimethyl sulfide. *J. Phys. Chem. A* **2003**, *107*, 1155-1161, doi:10.1021/jp021701g.
(2) Domine, F.; Ravishankara, A. R.; Howard, C. J. Kinetics and mechanisms of the reactions of CH_3S, CH_3SO, and CH_3SS with O_3 at 300 K and low pressures. *J. Phys. Chem.* **1992**, *96*, 2171-2178, doi:10.1021/j100184a027.
(3) Tyndall, G. S.; Ravishankara, A. R. Kinetics of the reaction of CH_3S with O_3 at 298 K. *J. Phys. Chem.* **1989**, *93*, 4707-4710, doi:10.1021/j100349a006.

I106. $CH_3SO + NO_2$. This recommendation is based on the direct measurements of Domine et al.[2] (297 K). The results are supported by somewhat less direct measurements of Tyndall and Ravishankara[6] (298 K), Mellouki et al.[5] (298 K), and Kukui et al.[3] (300 K). The results of Kukui et al. suggest a small negative activation energy, but their data set is not extensive enough to warrant a recommendation for E/R without independent confirmation. Borissenko et al.[1] (298 K) report that the SO_2 yield drops from ~0.4 in 100 Torr N_2 to ~0.25 in 660 Torr N_2. A detailed theoretical singlet potential energy surface has been reported by Lesar.[4]
(Table: 06-2, Note: 15-10, Evaluated: 06-2) Back to Table

(1) Borissenko, D.; Kukui, A.; Laverdet, G.; Le Bras, G. Experimental study of SO_2 formation in the reactions of CH_3SO radical with NO_2 and O_3 in relation with the atmospheric oxidation mechanism of dimethyl sulfide. *J. Phys. Chem. A* **2003**, *107*, 1155-1161, doi:10.1021/jp021701g.
(2) Domine, F.; Murrells, T. P.; Howard, C. J. Kinetics of the reactions of NO_2 with CH_3S, CH_3SO, CH_3SS, and CH_3SSO at 297 K and 1 Torr. *J. Phys. Chem.* **1990**, *94*, 5839-5847, doi:10.1021/j100378a043.
(3) Kukui, A.; Bossoutrot, V.; Laverdet, G.; Le Bras, G. Mechanism of the reaction of CH_3SO with NO_2 in relation to atmospheric oxidation of dimethyl sulfide: Experimental and theoretical study. *J. Phys. Chem. A* **2000**, *104*, 935-946, doi:10.1021/jp993158i.
(4) Lesar, A. Product channels in the reaction of the CH_3SO radical with NO_2: DFT and ab initio studies. *Int. J. Quant. Chem.* **2011**, *112*, 1904-1912, doi:10.1002/qua.23154.
(5) Mellouki, A.; Jourdain, J. L.; Le Bras, G. Discharge flow study of the $CH_3S + NO_2$ reaction mechanism using Cl + CH_3SH as the CH_3S source. *Chem. Phys. Lett.* **1988**, *148*, 231-236, doi:10.1016/0009-2614(88)80305-1.
(6) Tyndall, G. S.; Ravishankara, A. R. Kinetics and mechanism of the reactions of CH_3S with O_2 and NO_2 at 298 K. *J. Phys. Chem.* **1989**, *93*, 2426-2435, doi:10.1021/j100343a041.

I107. $CH_3SOO + O_3$, $CH_3SOO + NO$, $CH_3SOO + NO_2$. These recommendations are based on the experiments of Turnipseed et al.[1] in which CH_3S was monitored by laser induced fluorescence in equilibrium with CH_3SOO. The upper limit for the O_3 reaction was determined from experiments at 227 K. The results for the NO and NO_2 reactions were independent of temperature over the ranges 227–256 K and 227–246 K, respectively. The uncertainties placed on these recommendations have been increased over those estimated by the authors to reflect the absence of any confirming investigations.

(Table: 94-26, Note: 94-26, Evaluated: 94-26) Back to Table

(1) Turnipseed, A. A.; Barone, S. B.; Ravishankara, A. R. Reactions of CH_3S and CH_3SOO with O_3, NO_2, and NO. *J. Phys. Chem.* **1993**, *97*, 5926-5934, doi:10.1021/j100124a025.

I108. $CH_3SO_2 + NO_2$. This recommendation is based on the study by Ray et al.[1] (298 K) using a discharge flow reactor equipped with laser induced fluorescence and mass spectrometric detection. The CH_3SO_2 was produced by the sequential oxidation of CH_3S and CH_3SO by NO_2 and is to be differentiated from the weakly bound adduct, CH_3SOO, formed by the reaction of CH_3S with O_2 at low temperature (Turnipseed et al.[2]). The uncertainty limit on the rate constant has been increased over that given by the authors to reflect the absence of any confirming investigation. However, some additional support for this recommendation does come from the study of the $CH_3S + NO_2$ reaction by Tyndall and Ravishankara.[3] These authors observed fluorescence from a product species tentatively identified as CH_3SO_2, produced by the reaction of CH_3SO with NO_2. Computer simulation of the rise and fall of the fluorescence signal yielded an approximate rate constant value for the reaction $CH_3SO_2 + NO_2$ of 7.0×10^{-12} cm^3 molecule^{-1} s^{-1}. However, an unambiguous differentiation between the production and disappearance rate constants was not possible.
(Table: 97-4, Note: 97-4, Evaluated: 97-4) Back to Table

(1) Ray, A.; Vassalli, I.; Laverdet, G.; Le Bras, G. Kinetics of the thermal decomposition of the CH_3SO_2 radical and its reaction with NO_2 at 1 Torr and 298 K. *J. Phys. Chem.* **1996**, *100*, 8895-8900, doi:10.1021/jp9600120.
(2) Turnipseed, A. A.; Barone, S. B.; Ravishankara, A. R. Reactions of CH_3S and CH_3SOO with O_3, NO_2, and NO. *J. Phys. Chem.* **1993**, *97*, 5926-5934, doi:10.1021/j100124a025.
(3) Tyndall, G. S.; Ravishankara, A. R. Kinetics and mechanism of the reactions of CH_3S with O_2 and NO_2 at 298 K. *J. Phys. Chem.* **1989**, *93*, 2426-2435, doi:10.1021/j100343a041.

I109. $CH_3SCH_2 + NO_3$. The recommended k(298 K) is based on the experiments of Butkovskaya and Le Bras[1] (298 K). The uncertainty factor reflects the absence of any confirming investigation.
(Table: 94-26, Note: 94-26, Evaluated: 94-26) Back to Table

(1) Butkovskaya, N. I.; Le Bras, G. Mechanism of the NO_3 + DMS reaction by discharge flow mass spectrometry. *J. Phys. Chem.* **1994**, *98*, 2582-2591, doi:10.1021/j100061a014.

I110. $CH_3SCH_2O_2 + NO$. The recommended k(298 K) is based on the experiments of Urbanski et al.[2] (261–400 K), which are less impacted by secondary chemistry complications than the experiments of Wallington et al.[3] (298 K) or Turnipseed et al.[1] (298 K); the error limits are chosen to encompass the rate constants reported in all three studies. The E/R value is taken from Urbanski et al., who report the only available temperature dependence data. The recommended value for the parameter g is larger than reported by Urbanski et al. pending independent confirmation of their result. Urbanski et al. observed that the reaction produces formaldehyde (H_2CO) with unit yield, suggesting that the CH_3SCH_2O product rapidly decomposes to $CH_3S + H_2CO$.
(Table: 06-2, Note: 19-5, Evaluated: 06-2) Back to Table

(1) Turnipseed, A. A.; Barone, S. B.; Ravishankara, A. R. Reaction of OH with dimethyl sulfide. 2. Products and mechanisms. *J. Phys. Chem.* **1996**, *100*, 14703-14713, doi:10.1021/jp960867c.
(2) Urbanski, S. P.; Stickel, R. E.; Zhao, Z.; Wine, P. H. Mechanistic and kinetic study of formaldehyde production in the atmospheric oxidation of dimethyl sulfide. *J. Chem. Soc. Faraday Trans.* **1997**, *93*, 2813-2819, doi:10.1039/a701380i.
(3) Wallington, T. J.; Ellermann, T.; Nielsen, O. J. Atmospheric chemistry of dimethyl sulfide: UV spectra and self-reaction kinetics of CH_3SCH_2 and $CH_3SCH_2O_2$ radicals and kinetics of the reactions $CH_3SCH_2 + O_2 \rightarrow CH_3SCH_2O_2$ and $CH_3SCH_2O_2 + NO \rightarrow CH_3SCH_2O + NO_2$. *J. Phys. Chem.* **1993**, *97*, 8442-8449, doi:10.1021/j100134a013.

I111. $CH_3SCH_2O_2 + CH_3SCH_2O_2$. The recommended k(298 K) is the average of values reported by Wallington et al.[2] (298 K) using a pulse radiolysis UV absorption technique and Urbanski et al.[1] (298 K) using a laser flash photolysis tunable diode laser absorption technique. Urbanski et al. observed that the reaction produces formaldehyde with unit yield, suggesting that the dominant reaction pathway is $2\ CH_3SCH_2O_2 \rightarrow 2\ CH_3SCH_2O + O_2$ (CH_3SCH_2O rapidly decomposes to $CH_3S + H_2CO$).
(Table 06-02, Note 06-02, Evaluated: 06-2) Back to Table

(1) Urbanski, S. P.; Stickel, R. E.; Zhao, Z.; Wine, P. H. Mechanistic and kinetic study of formaldehyde production in the atmospheric oxidation of dimethyl sulfide. *J. Chem. Soc. Faraday Trans.* **1997**, *93*, 2813-2819, doi:10.1039/a701380i.

(2) Wallington, T. J.; Ellermann, T.; Nielsen, O. J. Atmospheric chemistry of dimethyl sulfide: UV spectra and self-reaction kinetics of CH_3SCH_2 and $CH_3SCH_2O_2$ radicals and kinetics of the reactions $CH_3SCH_2 + O_2 \rightarrow CH_3SCH_2O_2$ and $CH_3SCH_2O_2 + NO \rightarrow CH_3SCH_2O + NO_2$. *J. Phys. Chem.* **1993**, *97*, 8442-8449, doi:10.1021/j100134a013.

I112. $CH_3SS + O_3$. The recommended k(298 K) is based on the discharge flow photoionization mass spectrometry study by Domine et al.[1] (300 K). The uncertainty factor reflects the absence of any confirming investigations. The rate constant ratio for the reactions of CH_3SS with O_3 and NO_2 is consistent with the rate constant ratio for the corresponding CH_3S reactions.
(Table: 92-20, Note: 92-20, Evaluated: 92-20) Back to Table

(1) Domine, F.; Ravishankara, A. R.; Howard, C. J. Kinetics and mechanisms of the reactions of CH_3S, CH_3SO, and CH_3SS with O_3 at 300 K and low pressures. *J. Phys. Chem.* **1992**, *96*, 2171-2178, doi:10.1021/j100184a027.

I113. $CH_3SS + NO_2$; $CH_3SSO + NO_2$. The recommended k(298 K) are based on the discharge flow photoionization mass spectrometry study by Domine et al.[1] (297 K). The rate constant ratio for these two reactions agrees with that observed for reactions of other RS/RSO radicals with NO_2. The assigned uncertainties reflect this agreement but acknowledge the absence of any confirming investigation. In the Domine et al. study, CH_3SSO was produced by reacting away all CH_3SS with high NO_2 concentrations. Thus, as expected, O atom transfer may be the primary channel in the CH_3SS reaction.
(Table: 92-20, Note: 92-20, Evaluated: 92-20) Back to Table

(1) Domine, F.; Murrells, T. P.; Howard, C. J. Kinetics of the reactions of NO_2 with CH_3S, CH_3SO, CH_3SS, and CH_3SSO at 297 K and 1 Torr. *J. Phys. Chem.* **1990**, *94*, 5839-5847, doi:10.1021/j100378a043.

1.14.3 Bibliography – SO_x Reactions

Abbatt, J. P. D.; Fentner, F. F.; Anderson, J. G. High-pressure discharge flow kinetics study of OH + CH_3SCH_3, CH_3SSCH_3 → products from 297 to 368 K. *J. Phys. Chem.* **1992**, *96*, 1780-1785, doi:10.1021/j100183a053.

Albu, M.; Barnes, I.; Becker, K. H.; Patroescu-Klotz, I.; Mocannu, R.; Benter, T. Rate coefficients for the gas-phase reaction of OH radicals withdimethyl sulfide: temperature and O_2 partial pressure dependnece. *Phys. Chem. Chem. Phys.* **2006**, *8*, 728-736, doi:10.1039/b512536g.

Anastasi, C.; Broomfield, M.; Nielsen, O. J.; Pagsberg, P. Kinetics and mechanisms of the reactions of CH_2SH radicals with O_2, NO, and NO_2. *J. Phys. Chem.* **1992**, *96*, 696-701, doi:10.1021/j100181a034.

Aranda, A.; Diaz de Mera, Y.; Rodríguez, D.; Salgado, S.; Martinez, E. Kinetic and products of the BrO + CH_3SH reaction: Temperature and pressure dependence. *Chem. Phys. Lett.* **2002**, *357*, 471-476, doi:10.1016/S0009-2614(02)00561-4.

Arsene, C.; Barnes, I.; Becker, K. H.; Benter, T. Gas-phase reaction of Cl with dimethyl sulfide: Temperature and oxygen partial pressure dependence of the rate coefficient. *Int. J. Chem. Kinet.* **2005**, *37*, 66-73, doi:10.1002/kin.20051.

Arsene, C.; Barnes, I.; Becker, K. H.; Schneider, W. F.; Wallington, T. J.; Mihalopoulos, N.; Patroescu-Klotz, J. V. Formation of methane sulfinic acid in the gas-phase OH-radical initiated oxidation of dimethyl sulfoxide. *Environ. Sci. Technol.* **2002**, *36*, 5155-5163, doi:10.1021/es020035u.

Asatryan, R.; Bozzelli, J. W. Formation of a Criegee intermediate in the low-temperature oxidation of dimethyl sulfoxide. *Phys. Chem. Chem. Phys.* **2008**, *10*, 1769-1780, doi:10.1039/b716179d.

Atkinson, R.; Aschmann, S. M.; Pitts, J. N., Jr. Kinetics of the reaction of NO_3 radicals with CH_3SSCH_3. *J. Geophys. Res.* **1988**, *93*, 7125-7126, doi:10.1029/JD093iD06p07125.

Atkinson, R.; Perry, R. A.; Pitts, J. N., Jr. Rate constants for the reaction of the OH radical with CH_3SH and CH_3NH_2 over the temperature range 299-426 °K. *J. Chem. Phys.* **1977**, *66*, 1578-1581, doi:10.1063/1.434076.

Atkinson, R.; Perry, R. A.; Pitts Jr., J. N. Rate constants for the reaction of OH radicals with COS, CS_2 and CH_3SCH_3 over the temperature range 299-430 K. *Chem. Phys. Lett.* **1978**, *54*, 14-18, doi:10.1016/0009-2614(78)85653-X.

Atkinson, R.; Pitts, J. N., Jr.; Aschmann, S. M. Tropospheric reactions of dimethyl sulfide with NO_3 and OH radicals. *J. Phys. Chem.* **1984**, *88*, 1584-1587, doi:10.1021/j150652a029.

Balla, R. J.; Nelson, H. H.; McDonald, J. R. Kientics of the reaction of CH_3S with NO, NO_2 and O_2. *Chem. Phys.* **1986**, *109*, 101-107, doi:10.1016/0301-0104(86)80188-4.

Ballester, M. Y.; Varandas, A. J. C. Double many-body expansion potential energy surface for ground state HSO_2. *Phys. Chem. Chem. Phys.* **2005**, *7*, 2305-2317, doi:10.1039/b500990a.

Ballesteros, B., N. R. Jensen, and J. Hjorth FT-IR study of the kinetics and products of the reactions of dimethylsulphide, dimethylsulphoxide and dimethylsulphone with Br and BrO. *J. Atmos. Chem.* **2002**, *43*, 135-150, doi:10.1023/A:1019922224137.

Barnes, I.; Bastian, V.; Becker, K. H.; Fink, E. H.; Nelsen, W. Oxidation of sulphur compounds in the atmosphere: I. Rate constants of OH radical reactions with sulphur dioxide, hydrogen sulphide, aliphatic thiols and thiophenol. *J. Atmos. Chem.* **1986**, *4*, 445-466, doi:10.1007/BF00053845.

Barnes, I.; Bastian, V.; Becker, K. H.; Martin, D. In *Biogenic Sulfur in the Environment*; ACS Symp. Ser, 1989; Vol. 393; pp 476-488.

Barnes, I.; Bastian, V.; Becker, K. H.; Overath, R. D. Kinetic studies of the reactions of IO, BrO, and ClO with dimethylsulfide. *Int. J. Chem. Kinet.* **1991**, *23*, 579-591, doi:10.1002/kin.550230704.

Barnes, I.; Becker, K. H.; Carlier, P.; Mouvier, G. FTIR study of the DMS/NO_2/I_2/N_2 photolysis system: The reaction of IO radicals with DMS. *Int. J. Chem. Kinet.* **1987**, *19*, 489-501, doi:10.1002/kin.550190602.

Barnes, I.; Becker, K. H.; Fink, E. H.; Reimer, A.; Zabel, F.; Niki, H. Rate constant and products of the reaction CS_2 + OH in the presence of O_2. *Int. J. Chem. Kinet.* **1983**, *15*, 631-645, doi:10.1002/kin.550150705.

Barnes, I.; Becker, K. H.; Mihalopoulas, N. An FTIR product study of the photooxidation of dimethyl disulfide. *J. Atmos. Chem.* **1994**, *18*, 267-289, doi:10.1007/BF00696783.

Barnes, I.; Becker, K. H.; Patroescu, I. The tropospheric oxidation of dimethyl sulfide: A new source of carbonyl sulfide. *Geophys. Res. Lett.* **1994**, *21*, 2389-2392, doi:10.1029/94GL02499.

Barnes, I.; Becker, K. H.; Patroescu, I. FTIR product study of the OH initiated oxidation of dimethyl sulphide: Observation of carbonyl sulphide and dimethyl sulphoxide. *Atmos. Environ.* **1996**, *30*, 1805-1814, doi:10.1016/1352-2310(95)00389-4.

Barone, S. B.; Turnipseed, A. A.; Ravishankara, A. R. Reaction of OH with dimethyl sulfide (DMS). 1. Equilibrium constant for OH + DMS reaction and the kinetics of the OH•DMS + O_2 reaction. *J. Phys. Chem.* **1996**, *100*, 14694-14702, doi:10.1021/jp960866k.

Becker, K. H.; Inocencio, M. A.; Schurath, U. The reaction of ozone with hydrogen sulfide and its organic derivatives. *Int. J. Chem. Kinet.* **1975**, *Symp. 1*, 205-220.

Bedjanian, Y.; Poulet, G.; Le Bras, G. Kinetic study of the reaction of BrO radicals with dimethylsulfide. *Int. J. Chem. Kinet.* **1996**, *28*, 383-389, doi:10.1002/(SICI)1097-4601(1996)28:5<383::AID-KIN7>3.0.CO;2-R.

Bida, G. T.; Breckenridge, W. H.; Kolln, W. S. A kinetic study of the very fast reaction: $O(^3P) + CS \rightarrow CO^{\ddagger} + S(^3P)$. *J. Chem. Phys.* **1976**, *64*, 3296-3302, doi:10.1063/1.432617.

Biermann, H. W.; Harris, G. W.; Pitts, J. N., Jr. Photoionization mass spectrometer studies of the collsionally stabillzed product distribution in the reaction of OH radicals with selected alkenes at 298 K. *J. Phys. Chem.* **1982**, *86*, 2958-2964, doi:10.1021/j100212a030.

Black, G. Reactions of HS with NO and NO_2 at 298 K. *J. Chem. Phys.* **1984**, *80*, 1103-1107, doi:10.1063/1.446838.

Black, G.; Jusinski, L. E. Laser-induced fluorescence studies of the CH_3S radical. *J. Chem. Soc. Faraday Trans. 2* **1986**, *86*, 2143-2151, doi:10.1039/f29868202143.

Black, G.; Jusinski, L. E.; Slanger, T. G. Rate coefficients for CS reactions with O_2, O_3 and NO_2 at 298 K. *Chem. Phys. Lett.* **1983**, *102*, 64-68, doi:10.1016/0009-2614(83)80659-9.

Black, G.; Sharpless, R. L.; Slanger, T. G. Rate coefficients at 298 K for SO reactions with O_2, O_3, and NO_2. *Chem. Phys. Lett.* **1982**, *90*, 55-58, doi:10.1016/0009-2614(82)83324-1.

Black, G.; Sharpless, R. L.; Slanger, T. G. Rate coefficients for SO reactions with O_2 and O_3 over the temperature range 230 to 420 K. *Chem. Phys. Lett.* **1982**, *93*, 598-602, doi:10.1016/0009-2614(82)83737-8.

Blitz, M. A.; McKee, K. W.; Pilling, M. J. Temperature dependence of the reaction of OH and SO. *Proc. Combust. Inst.* **2000**, *28*, 2491-2497, doi:10.1016/S0082-0784(00)80664-5.

Borissenko, D.; Kukui, A.; Laverdet, G.; Le Bras, G. Experimental study of SO_2 formation in the reactions of CH_3SO radical with NO_2 and O_3 in relation with the atmospheric oxidation mechanism of dimethyl sulfide. *J. Phys. Chem. A* **2003**, *107*, 1155-1161, doi:10.1021/jp021701g.

Braithwaite, M.; Leone, S. R. Laser-initiated chemical reactions: $Cl + H_2S \rightarrow HCl + HS$: Rate constant, product energy distribution, and direct detection of a chain mechanism. *J. Chem. Phys.* **1978**, *69*, 839-845, doi:10.1063/1.43659.

Breckenridge, W. H.; Miller, T. A. Kinetic study by EPR of the production and decay of $SO(^1\Delta)$ in the reaction of $O_2(^1\Delta_g)$ with $SO(^3\Sigma^-)$. *J. Chem. Phys.* **1972**, *56*, 465-474, doi:10.1063/1.1676891.

Brunning, J.; Stief, L. J. Kinetic studies of the reaction of the SO radical with NO_2 and ClO from 210 to 363 K. *J. Chem. Phys.* **1986**, *84*, 4371-4377, doi:10.1063/1.450059.

Brunning, J.; Stief, L. J. Rate constant for the reaction $SO + BrO \rightarrow SO_2 + Br$. *J. Chem. Phys.* **1986**, *85*, 2591-2594, doi:10.1063/1.451066.

Bulatov, V. P.; Kozliner, M. Z.; Sarkisov, O. M. Determination of rate constants for the reactions of $SH + NO_2 \rightarrow HSO + NO$ and $HSO + NO_2 \rightarrow$ products. *Khim. Fiz.* **1984**, *3*, 1300-1305.

Bulatov, V. P.; Kozliner, M. Z.; Sarkisov, O. M. Reactions of SH and HSO radicals with nitrogen oxide. *Khim. Fiz.* **1985**, *4*, 1353-1357.

Bulatov, V. P.; Sarkisov, O. M.; Kozliner, M. Z.; Ergorov, V. G. Mechanism of hydrogen sulfide photooxidation in atmosphere. *Khim. Fiz.* **1986**, *5*, 1031-1036.

Bulatov, V. P.; Vereschchuk, S. I.; Dzegilenko, F. N.; Sarkisov, O. M.; Khabarov, V. N. Photooxidative conversion of H_2S in the presence of O_2 and NO_2. *Khim. Fiz.* **1990**, *9*, 1214-1223.

Burrows, J. P.; Cliff, D. I.; Harris, G. W.; Thrush, B. A.; Wilkinson, J. P. T. Atmospheric reactions of the HO_2 radical studied by laser magnetic-resonance spectroscopy. *Proc. Roy. Soc. Lond. A.* **1979**, *368*, 463-481, doi:10.1098/rspa.

Burrows, J. P.; Tyndall, G. S.; Moortgat, G. K. Absorption spectrum of NO_3 and kinetics of the reactions of NO_3 with NO_2, Cl, and several stable atmospheric species at 298 K. *J. Phys. Chem.* **1985**, *89*, 4848-4856, doi:10.1021/j100268a038.

Butkovskaya, N. I.; Le Bras, G. Mechanism of the NO_3 + DMS reaction by discharge flow mass spectrometry. *J. Phys. Chem.* **1994**, *98*, 2582-2591, doi:10.1021/j100061a014.

Butkovskaya, N. I.; Poulet, G.; Le Bras, G. Discharge flow study of the reactions of chlorine and fluorine atoms with dimethyl sulfide. *J. Phys. Chem.* **1995**, *99*, 4536-4543, doi:10.1021/j100013a025.

Butkovskaya, N. I.; Setser, D. W. Chemical dynamics of the OH and OD radical reactions with H_2S, CH_3SCH_3, and CH_3SH studied by infrared chemiluminescence. *J. Phys. Chem. A* **1998**, *102*, 6395-6405, doi:10.1021/jp980256f.
Butkovskaya, N. I.; Setser, D. W. Mechanism for the reaction of hydroxyl radicals with dimethyl disulfide. *Chem. Phys. Lett.* **1999**, *312*, 37-44, doi:10.1016/S0009-2614(99)00862-3.
Butkovskaya, N. I.; Setser, D. W. Product branching fractions and kinetic isotope effects for the reactions of OH and OD radicals with CH_3SH and CH_3SD. *J. Phys. Chem. A* **1999**, *103*, 6921-6929, doi:10.1021/jp9914828.
Callear, A. B.; Hedges, R. E. M. Flash spectroscopy with mercury resonance radiation Part 1.-An experimental method with microwave-pulse excitation. *Trans. Faraday Soc.* **1970**, *66*, 605-614, doi:10.1039/tf9706600605.
Callear, A. B.; Smith, I. W. M. Measurement of the rate parameters for reaction of $O(2^3P)$ with carbon disulphide and olefines, by flash spectroscopy. *Nature* **1967**, *213*, 382-383, doi:10.1038/213382a0.
Canosa-Mas, C.; Smith, S. J.; Toby, S.; Wayne, R. P. Reactivity of the nitrate radical towards alkynes and some other molecules. *J. Chem. Soc. Faraday Trans. 2* **1988**, *84*, 247-262, doi:10.1039/f29888400247.
Cantrell, C. A.; Davidson, J. A.; Shetter, R. E.; Anderson, B. A.; Calvert, J. G. The temperature invariance of the NO_3 absorption cross section in the 662-nm region. *J. Phys. Chem.* **1987**, *91*, 5858-5863, doi:10.1021/j100307a009.
Cao, J.; Wang, W.; Zhang, Y.; Wang, W.; Zhang, T.; Lv, J.; Li, C. Computational study on the reaction of $CH_3SCH_2CH_3$ with OH radical: mechanism and enthalpy of formation. *Theor. Chem. Acc.* **2011**, *129*, 771-780, doi:10.1007/s00214-011-0934-8.
Castleman, A. W.; Davis, R. E.; Munkelwitz, H. R.; Tang, I. N.; Wood, W. P. Kinetics of association reactions pertaining to H_2SO_4 aerosol formation. *Int. J. Chem. Kinet.* **1975**, *Symp. 1*, 629-640.
Chang, P.-F.; Wang, T. T.; Niann, S. W.; Hwang, Y.-L.; Lee, Y.-P. Temperature dependence of rate coefficients of reactions of NO_2 with CH_3S and C_2H_5S. *J. Phys. Chem. A* **2000**, *104*, 5525-5529, doi:10.1021/jp000294a.
Chen, K. S.; Cheng, S. S.; Lee, Y. P. Reaction dynamics of Cl + H_2S: Rotational and vibrational distribution of HCl probed with time-resolved Fourier-transform spectroscopy. *J. Chem. Phys.* **2003**, *119*, 4229-4236, doi:10.1063/1.1592508.
Chen, X.; Wu, F.; Weiner, B. R. Internal energy distributions of the $SO(X\ ^3\Sigma^-)$ product from the $O(^3P)$ + OCS reaction. *Chem. Phys. Lett.* **1995**, *247*, 313-320, doi:10.1016/S0009-2614(95)01265-6.
Cheng, B.-M.; Lee, Y.-P. Rate constant of OH + OCS reaction over the temperature range 255-483 K. *Int. J. Chem. Kinet.* **1986**, *18*, 1303-1314, doi:10.1002/kin.550181202.
Clemo, A. R.; Davidson, F. E.; Duncan, G. L.; Grice, R. Translational energy threshold functions for oxygen atom reactions. *Chem. Phys. Lett.* **1981**, *84*, 509-511, doi:10.1016/0009-2614(81)80396-X.
Clyne, M. A. A.; Halstead, C. J.; Thrush, B. A. The kinetics of elementary reactions involving the oxides of sulphur I. The nature of the sulphur dioxide afterglow. *Proc. Soc. London Ser. A.* **1966**, *295*, 355-362, doi:10.1098/rspa.1966.0246.
Clyne, M. A. A.; MacRobert, A. J. Kinetic studies of free radical reactions by mass spectrometry. I. The reactions SO + NO_2 and ClO + NO. *Int. J. Chem. Kinet.* **1980**, *12*, 79-96, doi:10.1002/kin.550120202.
Clyne, M. A. A.; MacRobert, A. J. Kinetic studies of free radical reactions by mass spectrometry. II. The reactions of SO + ClO, SO + OClO and SO + BrO. *Int. J. Chem. Kinet.* **1981**, *13*, 187-197, doi:10.1002/kin.550130208.
Clyne, M. A. A.; MacRobert, A. J.; Murrells, T. P.; Stief, L. J. Kinetics of the reactions of atomic chlorine with H_2S, HS and OCS. *J. Chem. Soc. Faraday Trans. 2* **1984**, *80*, 877-886, doi:10.1039/f29848000877.
Clyne, M. A. A.; Ono, Y. Determination of the rate constant of reaction of ground-state Cl and H atoms with H_2S using resonance fluorescence in a discharge flow. *Chem. Phys. Lett.* **1983**, *94*, 597-602, doi:10.1016/0009-2614(83)85065-9.
Clyne, M. A. A.; Townsend, L. W. Rate constant measurements for rapid reactions of ground state sulphur $3p^4(^3P_J)$ atoms. *Int. J. Chem. Kinet.* **1975**, *Symp. 1*, 73-84.
Clyne, M. A. A.; Whitefield, P. D. Atomic resonance fluorescence for rate constants of rapid bimolecular reactions Part 7.-Sulphur atom reactions: $S + O_2 \rightarrow SO + O$ and $S + NO_2 \rightarrow SO + NO$ from 296 to 410 K. *J. Chem. Soc. Faraday Trans. 2* **1979**, *75*, 1327-1340, doi:10.1039/f29797501327.
Cocks, A. T.; Fernanado, R. P.; Fletcher, I. S. The gas-phase reaction of the methylperoxy radical with sulphur dioxide. *Atmos. Environ.* **1986**, *20*, 2359-2366, doi:10.1016/0004-6981(86)90066-1.

Cooper, W. F.; Hershberger, J. F. An infrared laser study of the $O(^3P) + CS_2$ reaction. *J. Phys. Chem.* **1992**, *96*, 5405-5410, doi:10.1021/j100192a041.
Cox, R. A.; Sheppard, D. Reactions of OH radicals with gaseous sulphur compounds. *Nature* **1980**, *284*, 330-331, doi:10.1038/284330a0.
Cupitt, L. T.; Glass, G. P. Reactions of SH with atomic oxygen and hydrogen. *Int. J. Chem. Kinet.* **1975**, *Symp. 1*, 39-50.
Cvetanovic, R. J.; Singleton, D. L.; Irwin, R. S. Gas-phase reactions of $O(^3P)$ atoms with methanethiol, ethanethiol, methyl sulfide, and dimethyl disulfide. 2. Reaction products and mechanisms. *J. Am. Chem. Soc.* **1981**, *103*, 3530-3539, doi:10.1021/ja00402a046.
Daubendiek, R. L.; Calvert, J. G. Study of N_2O_5-SO_2-O_3 reaction system. *Environ. Lett.* **1975**, *8*, 103-116, doi:10.1080/00139307509437424.
Davidson, F. E.; Clemo, A. R.; Duncan, G. L.; Browett, R. J.; Hobson, J. H.; Grice, R. Reactive scattering of a supersonic oxygen atom beam: O + H_2S. *Mol. Phys.* **1982**, *46*, 33-40, doi:10.1080/00268978200101051.
Davis, D. D.; Klemm, R. B.; Pilling, M. A flash photolysis-resonance fluorescence kinetics study of ground-state sulfur atoms I. Absolute rate parameters for reaction of $S(^3P)$ with $O_2(^3\Sigma)$. *Int. J. Chem. Kinet.* **1972**, *4*, 367-382, doi:10.1002/kin.550040402
Davis, D. D.; Prusazcyk, J.; Dwyer, M.; Kim, P. A stop-flow time-of-flight mass spectrometry kinetics study. Reaction of ozone with nitrogen dioxide and sulfur dioxide. *J. Phys. Chem.* **1974**, *78*, 1775-1779, doi:10.1021/j100611a001.
Daykin, E. P.; Wine, P. H. Rate of reaction of IO radicals with dimethylsulfide. *J. Geophys. Res.* **1990**, *95*, 18547-18553, doi:10.1029/JD095iD11p18547.
Daykin, E. P.; Wine, P. H. A study of the reactions of NO_3 radicals with organic sulfides: Reactivity trend at 298 K. *Int. J. Chem. Kinet.* **1990**, *22*, 1083-1094, doi:10.1002/kin.550221007.
Diau, E. W.-G.; Lee, Y.-P. Kinetics of the reactions of CS_2OH with O_2, NO, and NO_2. *J. Phys. Chem.* **1991**, *95*, 7726-7732, doi:10.1021/j100173a033.
Diaz-de-Mera, Y.; Aranda, A.; Rodriguez, D.; López, R.; Cabañas, B.; Martinez, E. Gas-phase reactions of chlorine atoms and ClO radicals with dimethyl sulfide. Rate coefficients and temperature dependences. *J. Phys. Chem. A* **2002**, *106*, 8627-8633, doi:10.1021/jp014570c.
Dillon, T. J.; Horowitz, A.; Crowley, J. N. The atmospheric chemistry of sulphuryl fluoride, SO_2F_2. *Atmos. Chem. Phys.* **2008**, *8*, 1547-1557, doi:10.5194/acp-8-1547-2008.
Dillon, T. J.; Karunanandan, R.; Crowley, J. N. The reaction of IO with CH_3SCH_3: Products and temperature dependent rate coefficients by laser induced fluorescence. *Phys. Chem. Chem. Phys.* **2006**, *8*, 847-855, doi:10.1039/b514718b.
Dlugokencky, E. J.; Howard, C. J. Laboratory studies of NO_3 radical reactions wlth some atmospheric sulfur compounds. *J. Phys. Chem.* **1988**, *92*, 1188-1193, doi:10.1021/j100316a036.
Domine, F.; Murrells, T. P.; Howard, C. J. Kinetics of the reactions of NO_2 with CH_3S, CH_3SO, CH_3SS, and CH_3SSO at 297 K and 1 Torr. *J. Phys. Chem.* **1990**, *94*, 5839-5847, doi:10.1021/j100378a043.
Domine, F.; Ravishankara, A. R. The yield of CH_3S from the reaction of OH with CH_3SSCH_3. *Int. J. Chem. Kinet.* **1992**, *24*, 943-951, doi:10.1002/kin.550241104.
Domine, F.; Ravishankara, A. R.; Howard, C. J. Kinetics and mechanisms of the reactions of CH_3S, CH_3SO, and CH_3SS with O_3 at 300 K and low pressures. *J. Phys. Chem.* **1992**, *96*, 2171-2178, doi:10.1021/j100184a027.
Donovan, R. J.; Little, D. J. The rate of the reaction $S(3^3P_J) + O_2$. *Chem. Phys. Lett.* **1972**, *13*, 488-490, doi:10.1016/0009-2614(72)80087-3.
Du, B.; Zhang, W. The effect of $(H_2O)_n$ (n = 1-2) or H_2S on the hydrogen abstraction reaction of H_2S by OH radicals in the atmosphere. *Comput. Theor. Chem.* **2015**, *1069*, 77-85, doi:10.1016/j.comptc.2015.07.015.
Du, L.; Xu, Y.; Ge, M.; Long, J.; Yao, L.; Wang, W. Rate constant of the gas phase reaction of dimethyl sulfide (CH_3SCH_3) with ozone. *Chem. Phys. Lett.* **2007**, *436*, 36-40, doi:10.1016/j.cplett.2007.01.025.
Dyke, J. M.; Ghosh, M. V.; Goubet, M.; Lee, E. P. F.; Levita, G.; Miqueu, K.; Shallcross, D. E. A study of the atmospherically relevant reaction between molecular chlorine and dimethylsulfide (DMS): Establishing the reaction intermediate and measurement of absolute photoionization cross-sections. *Chem. Phys.* **2006**, *324*, 85-95, doi:10.1016/j.chemphys.2005.11.045.
Dyke, J. M.; Ghosh, M. V.; Kinnison, D. J.; Levita, G.; Morris, A.; Shallcross, D. E. A kinetics and mechanistic study of the atmospherically relevant reaction between molecular chlorine and dimethyl sulfide (DMS). *Phys. Chem. Chem. Phys.* **2005**, *7*, 866-873, doi:10.1039/b415566a.

Egsgaard, H.; Carlson, L.; Florencio, H.; Drewello, T.; Schwarz, H. Experimental evidence for the gaseous HSO_3 radical. The key intermediate in the oxidation of SO_2 in the atmosphere. *Chem. Phys. Lett.* **1988**, *148*, 537-540, doi:10.1016/0009-2614(88)80327-0.

Eibling, R. E.; Kaufman, M. Kinetics studies relevant to possible couppling between the stratospheric chlorine and sulfur cycles. *Atmos. Environ.* **1983**, *17*, 429-431, doi:10.1016/0004-6981(83)90061-6.

Ellingson, B. A.; Truhlar, D. G. Explanation of the unusual temperature dependence of the atmospherically important OH + H_2S → H_2O + HS reaction and prediction of the rate constant at combustion temperatures. *J. Am. Chem. Soc.* **2007**, *129*, 12765-12771, doi:10.1021/ja072538b.

Enami, S.; Nakano, Y.; Hashimoto, S.; Kawasaki, M.; Aloisio, S.; Francisco, J. S. Reactions of Cl atoms with dimethyl sulfide: A theoretical calculation and an experimental study with cavity ring-down spectroscopy. *J. Phys. Chem. A* **2004**, *108*, 7785-7789, doi:10.1021/jp049772y.

Fair, R. W.; Thrush, B. A. Reaction of hydrogen atoms with hydrogen sulphide in the presence of molecular oxygen. *Trans. Faraday Soc.* **1969**, *65*, 1557-1570, doi:10.1039/tf9696501557.

Fair, R. W.; van Roodaelaar, A.; Strausz, O. P. The reaction of $S(^3P)$ atoms with molecular oxygen. *Can. J. Chem.* **1971**, *49*, 1659-1664, doi:10.1139/v71-270.

Falbe-Hansen, H.; Sorensen, S.; Jensen, N. R.; Pedersen, T.; Hjorth, J. Atmospheric gas-phase reactions of dimethylsulphoxide and dimethylsulphone with OH and NO_3 radicals, Cl atoms and ozone. *Atmos. Environ.* **2000**, *34*, 1543-1551, doi:10.1016/S1352-2310(99)00407-0.

Fenter, F. F.; Anderson, J. G. Kinetics and mechanism of the reactions of the SD Radical with Br_2, BrCl, Cl_2, and F_2. *J. Phys. Chem.* **1991**, *95*, 3172-3180, doi:10.1021/j100161a041.

Fenter, F. F.; Anderson, J. G. Kinetics of the DS-radical reactions with ClNO and NO_2. *Int. J. Chem. Kinet.* **1994**, *26*, 801-812, doi:10.1002/kin.550260803.

Friedl, R. R.; Brune, W. H.; Anderson, J. G. Kinetics of SH with NO_2, O_3, O_2, and H_2O_2. *J. Phys. Chem.* **1985**, *89*, 5505-5510, doi:10.1021/j100271a038.

Gao, Y.; Alecu, A. A.; Goumri, A.; Marshall, P. High-temperature kinetics of the reaction between chlorine atoms and hydrogen sulfide. *Chem. Phys. Lett.* **2015**, *624*, 83-86, doi:10.1016/j.cplett.2015.02.011.

Garland, N. L. Temperature dependence of the reaction: SO + O_2. *Chem. Phys. Lett.* **1998**, *290*, 385-390, doi:10.1016/S0009-2614(98)00553-3.

Garrido, J. D.; Ballester, M. Y.; Orozco-González, Y.; Canuto, S. CASPT2 study of the potential energy surface of the HSO_2 system. *J. Phys. Chem. A* **2011**, *115*, 1453-1461, doi:10.1021/jp108460v.

Gleason, J. F.; Howard, C. J. Temperature dependence of the gas-phase reaction $HOSO_2$ + O_2 → HO_2 + SO_3. *J. Phys. Chem.* **1988**, *92*, 3414-3417, doi:10.1021/j100323a021.

Gleason, J. F.; Sinha, A.; Howard, C. J. Kinetics of the gas-phase reaction $HOSO_2$ + O_2 → HO_2 + SO_3. *J. Phys. Chem.* **1987**, *91*, 719-724, doi:10.1021/j100287a045.

Gonzalez-Garcia, N.; Gonzalez-Lafont, A.; Lluch, J. M. Methanesulfinic acid reaction with OH: Mechanism, rate constants, and atmospheric implications. *J. Phys. Chem. A* **2007**, *111*, 7825-7832, doi:10.1021/jp0722455.

Graham, R. A.; Gutman, D. J. Temperature dependence of rate constants and branching ratios for the reaction of oxygen atoms with carbon disulfide. *J. Phys. Chem.* **1977**, *81*, 207-209, doi:10.1021/j100518a005.

Graham, R. A.; Winer, A. M.; Atkinson, R.; Pitts, J. N., Jr. Rate constants for the reaction of HO_2 with HO_2, SO_2, CO, N_2O, *trans*-2-butene, and 2,3-dimethyl-2-butene at 300 K. *J. Phys. Chem.* **1979**, *83*, 1563-1567, doi:10.1021/j100475a002.

Gravestock, T.; Blitz, M. A.; Heard, D. E. Kinetics study of the reaction of iodine monoxide radicals with dimethyl sulfide. *Phys. Chem. Chem. Phys* **2005**, *7*, 2173-2181, doi:10.1039/b502989a.

Greenblatt, G. D.; Howard, C. J. Oxygen atom exchange in the interaction of ^{18}OH with several small molecules. *J. Phys. Chem.* **1989**, *93*, 1035-1042, doi:10.1021/j100340a006.

Halstead, C. J.; Thrush, B. A. The kinetics of elementary reactions involving the oxides of sulphur III. The chemilluminescent reaction between sulphur monoxide and ozone. *Proc. Roy. Soc. London A* **1966**, *295*, 380-398 doi:10.1098/rspa.1966.0248.

Hancock, G.; Smith, I. W. M. Infra-red chemiluminescence from vibrationally excited CO Part 1.-The reaction of atomic oxygen with carbon disulphide. *Trans. Faraday Soc.* **1971**, *67*, 2586-2597, doi:10.1039/tf9716702586.

Hashimoto, S.; Inoue, G.; Akimoto, H. Infrared spectroscopic detection of the $HOSO_2$ radical in argon matrix at 11 K. *Chem. Phys. Lett.* **1984**, *107*, 198-202, doi:10.1016/0009-2614(84)85699-7.

Hattori, S.; Schmidt, J. A.; Mahler, D. W.; Danielache, S. O.; Johnson, M. S.; Yoshida, N. Isotope effect in the carbonyl sulfide reaction with $O(^3P)$. *J. Phys. Chem. A* **2012**, *116*, 3521-3526, doi:10.1021/2120884.

Herndon, S. C.; Froyd, K. D.; Lovejoy, E. R.; Ravishankara, A. R. How rapidly does the SH radical react with N_2O? *J. Phys. Chem. A* **1999**, *103*, 6778-6785, doi:10.1021/jp9911853.
Herndon, S. C.; Ravishankara, A. R. Kinetics of the reaction of SH and SD with NO_2. *J. Phys. Chem. A* **2006**, *110*, 106-113, doi:10.1021/jp053918r.
Hollinden, G. A.; Kurylo, M. J.; Timmons, R. B. Electron spin resonance study of the kinetics of the reaction of $O(^3P)$ atoms with H_2S. *J. Phys. Chem.* **1970**, *74*, 988-991, doi:10.1021/j100700a004.
Homann, K. H.; Krome, G.; Wagner, H. G. Carbon disulfide oxidation rate of elementary reactions .1. *Ber. Bunsenges. Phys. Chem.* **1968**, *72*, 998-1004, doi:10.1002/bbpc.19680720821.
Hossenlopp, J. M.; Hershberger, J. F.; Flynn, G. W. Kinetics and product vibrational energy disposal dynamics in the reaction of chlorine atoms with D_2S. *J. Phys. Chem.* **1990**, *94*, 1346-1351, doi:10.1021/j100367a029.
Hsu, D. S. Y.; Shaub, W. M.; Burks, T. L.; Lin, M. C. Dynamics of reactions of $O(^3P)$ atoms with CS, CS_2 and OCS. *Chem. Phys.* **1979**, *44*, 143-150, doi:10.1016/0301-0104(79)80114-7.
Hsu, Y.-C.; Chen, D.-S.; Lee, Y.-P. Rate constant for the reaction of OH radicals with dimethyl sulfide. *Int. J. Chem. Kinet.* **1987**, *19* 1073-1082, doi:10.1002/kin.550191204.
Hynes, A. J.; Stickel, R. E.; Pounds, A. J.; Zhao, Z.; McKay, T.; Bradshaw, J. D.; Wine, P. H. *Dimethylsulfide: Oceans, Atmosphere, and Climate, ed. by G. Restelli and G. Angletti, Kluwer Academic Publishers, Brusse;Science* **1993**, 211-221.
Hynes, A. J.; Stocker, R. B.; Pounds, A. J.; Mckay, T.; Bradshaw, J. D.; Nicovich, J. M.; Wine, P. H. A mechanistic study of the reaction of OH with dimethyl-d_6 sulfide. Direct observation of adduct formation and the kinetics of the adduct reaction with O_2. *J. Phys. Chem.* **1995**, *99*, 16967-16975, doi:10.1021/j100046a024.
Hynes, A. J.; Wine, P. H. Kinetics of the OH + CH_3SH reaction under atmospheric conditions. *J. Phys. Chem.* **1987**, *91*, 3672-3676, doi:10.1021/j100297a042.
Hynes, A. J.; Wine, P. H. The atmospheric chemistry of dimethylsulfoxide (DMSO) kinetics and mechanism of the OH + DMSO reaction. *J. Atmos. Chem.* **1996**, *24*, 23-37, doi:10.1007/BF00053821.
Hynes, A. J.; Wine, P. H.; Nicovich, J. M. Kinetics and mechanism of the reaction of OH with CS_2 under atmospheric conditions. *J. Phys. Chem.* **1988**, *92*, 3846-3852, doi:10.1021/j100324a034.
Hynes, A. J.; Wine, P. H.; Semmes, D. H. Kinetics and mechanism of OH reactions with organic sulfides. *J. Phys. Chem.* **1986**, *90*, 4148-4156, doi:10.1021/j100408a062.
Ingham, T.; Bauer, D.; Sander, R.; Crutzen, P. J.; Crowley, J. N. Kinetics and products of the reactions BrO + DMS and Br + DMS at 298 K. *J. Phys. Chem. A* **1999**, *103*, 7199-7209, doi:10.1021/jp9905979.
Iyer, R. S.; Rowland, F. S. A significant upper limit for the rate of formation of OCS from the reaction of OH with CS_2. *Geophys. Res. Lett.* **1980**, *7*, 797-800, doi:10.1029/GL007i010p00797.
Jaffe, S.; Klein, F. S. Photolysis of NO_2 in the presence of SO_2 at 3660Å. *Trans. Faraday Soc.* **1966**, *62*, 2150-2157, doi:10.1039/tf9666202150.
Jayne, J. T.; Poschl, U.; Chen, Y.; Dai, D.; Molina, L. T.; Worsnop, D. R.; Kolb, C. E.; Molina, M. J. Pressure and temperature dependence of the gas-phase reaction of SO_3 with H_2O and the heterogeneous reaction of SO_3 with H_2O/H_2SO_4 surfaces. *J. Phys. Chem. A* **1997**, *101*, 10000-10011, doi:10.1021/jp972549z.
Jefferson, A.; Nicovich, J. M.; Wine, P. H. Temperature-dependent kinetics studies of the reactions $Br(^2P_{3/2})$ + $CH_3SCH_3 \leftrightarrow CH_3SCH_2$ + HBr. Heat of formation of the CH_3SCH_2 radical. *J. Phys. Chem.* **1994**, *98*, 7128-7135, doi:10.1021/j100080a006.
Jensen, N. R.; Hjorth, J.; Lohse, C.; Skov, H.; Restelli, G. Products and mechanism of the reaction between NO_3 and dimethlysulphide in air. *Atmos. Environ.* **1991**, *24A*, 1897-1904, doi:10.1016/0960-1686(91)90272-9.
Jensen, N. R.; Hjorth, J.; Lohse, C.; Skov, H.; Restelli, G. Products and mechanisms of the gas phase reactions of NO_3 with CH_3SCH_3, CD_3SCD_3, CH_3SH and CH_3SSCH_3. *J. Atmos. Chem.* **1992**, *14*, 95-108, doi:10.1007/BF00115226.
Jensen, N. R.; Hjorth, J.; Lohse, C.; Skov, H.; Restelli, G. Reactions of the nitrate radical with a series of reduced organic sulfur compounds in air. *Int. J. Chem. Kinet.* **1992**, *24*, 839-850, doi:10.1002/kin550241002.
Jones, B. M. R.; Burrows, J. P.; Cox, R. A.; Penkett, S. A. OCS formation in the reaction of OH with CS_2. *Chem. Phys. Lett.* **1982**, *88*, 372-376, doi:10.1016/0009-2614(82)83028-5.
Jorgensen, S.; Jensen, C.; Kjaergaard, H. G.; Anglada, J. M. The gas-phase reaction of methane sulfonic acid with the hydroxyl radical without and with water vapor. *Phys. Chem. Chem. Phys.* **2013**, *15*, 5140-5150, doi:10.1039/c3cp44034f.
Jorgensen, S.; Kjaergaard, H. G. Effect of hydration on the hydrogen abstraction reaction by OH in DMS and its oxidation products. *J. Phys. Chem. A* **2010**, *114*, 4857-4863, doi:10.1021/jp910202n.

Jourdain, J. L.; Le Bras, G.; Combourieu, J. Kinetic study of some elementrary reactions fo sulfur compounds including reactions of S and SO with OH radicals. *Int. J. Chem. Kinet.* **1979**, *11*, 569-577, doi:10.1002/kin.550110603.

Kan, C. S.; Calvert, J. G.; Shaw, J. H. Oxidation of sulfur dioxide by methylperoxy radicals. *J. Phys. Chem.* **1981**, *85*, 1126-1132, doi:10.1021/j150609a011.

Kan, C. S.; McQuigg, R. D.; Whitbeck, M. R.; Calvert, J. G. Kinetic flash spectroscopic study of the CH_3O_2-CH_3O_2 and CH_3O_2-SO_2 reactions. *Int. J. Chem. Kinet.* **1979**, *11*, 921-933, doi:10.1002/kin.550110811.

Kinnison, D. J.; Mengon, W.; Kerr, J. A. Rate coefficients for the room temperature reaction of Cl atoms with dimethyl sulfide and related alkyl sulfides. *J. Chem. Soc. Faraday Trans.* **1996**, *92*, 369-372, doi:10.1039/ft9969200369.

Kleissas, K. M.; Nicovich, J. M.; Wine, P. H. Spectroscopy and kinetics of the gas phase addition complex of atomic chlorine with dimethyl sulfoxide. *J. Photochem. Photobiol. A: Chem.* **2007**, *187*, 1-9, doi:10.1016/j.jphotochem.2006.08.020.

Klemm, R. B.; Stief, L. J. Absolute rate parameters for the reaction of ground state atomic oxygen with carbonyl sulfide. *J. Chem. Phys.* **1974**, *61*, 4900-4906, doi:10.1063/1.1681819.

Knight, G. P.; Crowley, J. N. The reactions of IO with HO_2, NO and CH_3SCH_3: Flow tube studies of kinetics and product formation. *Phys. Chem. Chem. Phys.* **2001**, *3*, 393-401, doi:10.1039/b008447f.

Koch, L. C.; Marshall, P.; Ravishankara, A. R. An investigation of the reaction of CH_3S with CO. *J. Phys. Chem. A* **2004**, *108*, 5205-5212, doi:10.1021/jp049193t.

Kolb, C. E.; Jayne, J. T.; Worsnop, D. R.; Molina, M. J.; Meads, R. F.; Viggiano, A. A. Gas phase reaction of sulfur trioxide with water vapor. *J. Am. Chem. Soc.* **1994**, *116*, 10314-10315, doi:10.1021/ja00101a067.

Kukui, A.; Borrisenko, D.; Laverdet, G.; Le Bras, G. Gas-phase reactions of OH radicals with dimethyl sulfoxide and methane sulfinic acid using turbulent flow reactor and chemical ionization mass spectrometry. *J. Phys. Chem. A* **2003**, *107*, 5732-5742, doi:10.1021/jp0276911.

Kukui, A.; Bossoutrot, V.; Laverdet, G.; Le Bras, G. Mechanism of the reaction of CH_3SO with NO_2 in relation to atmospheric oxidation of dimethyl sulfide: Experimental and theoretical study. *J. Phys. Chem. A* **2000**, *104*, 935-946, doi:10.1021/jp993158i.

Kurylo, M. J. Flash photolysis resonance fluorescence investigation of the reaction of OH radicals with dimethyl sulfide. *Chem. Phys. Lett.* **1978**, *58*, 233-237, doi:10.1016/0009-2614(78)80284-X.

Kurylo, M. J. Flash photolysis resonance fluorescence investigation of the reactions of OH radicals with OCS and CS_2. *Chem. Phys. Lett.* **1978**, *58*, 238-242, doi:10.1016/0009-2614(78)80285-1.

Kurylo, M. J.; Laufer, A. H. Evidence for atom exchange in OH reactions with carbonyl compounds: $^{18}OH + CO_2 \rightarrow {}^{18}OCO + OH$; $^{18}OH + CO \rightarrow {}^{18}OC + OH$. *J. Chem. Phys.* **1979**, *70*, 2032-2033, doi:10.1063/1.437638.

Kuwata, K. T.; Hermes, M. R.; Carlson, J.; Zogg, C. K. Computational studies of the isomerization and hydration reactions of acetaldehyde oxide and methyl vinyl carbonyl oxide *J. Phys. Chem. A* **2010**, *114*, 9192-9204, doi:10.1021/jp105358v.

Lafage, C.; Pauwels, J.-F.; Carlier, M.; Devolder, P. Rate constant for the reaction OH + H_2S in the range 243-463 K by discharge-flow laser-induced fluorescence. *J. Chem. Soc. Faraday Trans. 2* **1987**, *83*, 731-739, doi:10.1039/f29878300731.

Langer, S.; McGovney, B. T.; Finlayson-Pitts, B. J.; Moore, R. M. The dimethyl sulfide reaction with atomic chlorine and its implications for the budget of methyl chloride. *Geophys. Res. Lett.* **1996**, *23*, 1661-1664, doi:10.1029/96GL01427.

Lee, J. H.; Tang, I. N. Absolute rate constant for the reaction of $O(^3P)$ with CH_3SSCH_3 from 270 to 329 K. *J. Chem. Phys.* **1980**, *72*, 5718-5720, doi:10.1063/1.438990.

Lee, J. H.; Tang, I. N. Absolute rate constants for the hydroxyl radical reactions with CH_3SH adn C_2H_5SH at room temperature. *J. Chem. Phys.* **1983**, *78*, 6646-6649, doi:10.1063/1.444663.

Lee, J. H.; Tang, I. N.; Klemm, R. B. Absolute rate constant for the reaction of $O(^3P)$ with CH_3SCH_3 from 272 to 472 K. *J. Chem. Phys.* **1980**, *72*, 1793-1796, doi:10.1063/1.439295.

Lee, J. H.; Timmons, R. B.; Stief, L. J. Absolute rate parameters for the reaction of ground state atomic oxygen with dimethyl sulfide and episulfide. *J. Chem. Phys.* **1976**, *64*, 300-305, doi:10.1063/1.431921.

Lee, Y.-Y.; Lee, Y.-P.; Wang, N. S. Kinetics of the reaction of HSO with O_3 at temperatures 273-423 K. *J. Chem. Phys.* **1994**, *100*, 387-392, doi:10.1063/1.466952.

Lesar, A. Product channels in the reaction of the CH_3SO radical with NO_2: DFT and ab initio studies. *Int. J. Quant. Chem.* **2011**, *112*, 1904-1912, doi:10.1002/qua.23154.

Leu, M.-T.; Smith, R. H. Kinetics of the gas-phase reaction between hydroxyl and carbonyl sulfide over the temperature range 300-517 K. *J. Phys. Chem.* **1981**, *85*, 2570-2575, doi:10.1021/j150617a031.

Leu, M.-T.; Smith, R. H. Rate constant for the reaction between OH and CS_2 at 298 and 520 K. *J. Phys. Chem.* **1982**, *86*, 958-961, doi:10.1021/j100395a024.
Leu, M.-T.; Smith, R. H. Rate constants for the gas-phase reaction between hydroxyl and hydrogen sulfide over the temperature range 228-518 K. *J. Phys. Chem.* **1982**, *86*, 73-81, doi:10.1021/j100390a015.
Lilenfeld, H. V.; Richardson, R. J. Temperature dependence of the rate constant for the reaction between carbon monosulfide and atomic oxygen. *J. Chem. Phys.* **1977**, *67*, 3991-3997, doi:10.1063/1.435416.
Lin, C. L. Temperature dependence of the rate constant for the reaction OH + H_2S. *Int. J. Chem. Kinet.* **1982**, *14*, 593-598, doi:10.1002/kin.550140514.
Lin, Y.-L.; Wang, N.-S.; Lee, Y.-P. Temperature dependence of the rate constant for the reaction OH + H_2S in He, N_2, and O_2. *Int. J. Chem. Kinet.* **1985**, *17*, 1201-1214, doi:10.1002/kin.550171106.
Lovejoy, E. R.; Hanson, D. R.; Huey, L. G. Kinetics and products of the gas-phase reaction of SO_3 with water. *J. Phys. Chem.* **1996**, *100*, 19911-19916, doi:10.1021/jp962414d.
Lovejoy, E. R.; Kroeger, K. S.; Ravishankara, A. R. The kinetics of the CS_2OH + O_2 reaction. *Chem. Phys. Lett.* **1990**, *167*, 183-187, doi:10.1016/0009-2614(90)85002-T.
Lovejoy, E. R.; Murrells, T. P.; Ravishankara, A. R.; Howard, C. J. Oxidation of CS_2 by reaction with OH. 2. Yields of HO_2 and SO_2 in oxygen. *J. Phys. Chem.* **1990**, *94*, 2386-2393, doi:10.1021/j100369a037.
Lovejoy, E. R.; Ravishankara, A. R.; Howard, C. J. Yield of $^{16}OS^{18}O$ from the ^{18}OH initiated oxidation of CS_2 in $^{16}O_2$. *Int. J. Chem. Kinet.* **1994**, *26*, 551-560, doi:10.1002/kin.550260508.
Lovejoy, E. R.; Wang, N. S.; Howard, C. J. Kinetic studies of the reactions of HSO with NO_2, NO, and O_2. *J. Phys. Chem.* **1987**, *91*, 5749-5755, doi:10.1021/j100306a046.
Lu, C.-W.; Wu, Y.-J.; Lee, Y.-P.; Zhu, R. S.; Lin, M. C. Experimental and theoretical investigations of rate coefficients of the reaction $S(^3P)$ + O_2 in the temperature range 298-878 K. *J. Chem. Phys.* **2004**, *121*, 8271-8278, doi:10.1063/1.1792611.
Lu, E. C. C.; Iyer, R. S.; Rowland, F. S. Reaction rates for thermal chlorine atoms wlth H_2S from 232 to 359 K by a radiochemical technlque. *J. Phys. Chem.* **1986**, *90*, 1988-1990, doi:10.1021/j100401a002.
Lu, Y.-J.; Lee, L.; Pan, J.-W.; Witek, H. A.; Lin, J. J. Dynamics of the F_2 + CH_3SCH_3 reaction: A molecule-molecule reaction without entrance barrier. *J. Chem. Phys.* **2007**, *127*, 101101, doi:10.1063/1.2780145.
Lu, Y.-J.; Lee, L.; Pan, J.-W.; Xie, T.; Witek, H. A.; Lin, J. J. Barrierless reactions between two closed-shell molecules. I. Dynamics of F_2 + CH_3SCH_3 reaction. *J. Chem. Phys.* **2008**, *128*, 104317, doi:10.1063/1.2837801.
MacLeod, H.; Aschmann, S. M.; Atkinson, R.; Tuazon, E. C.; Sweetman, J. A.; Winer, A. M.; Pitts, J. N., Jr. Kinetics and mechanisms of the gas phase reactions of the NO_3 radical with a series of reduced sulfur compounds. *J. Geophys. Res.* **1986**, *91*, 5338-5346, doi:10.1029/JD091iD05p05338.
MacLeod, H.; Jourdain, J. L.; Poulet, G.; Le Bras, G. Kinetic study of reactions of some organic sulfur compounds with OH radicals. *Atmos. Environ.* **1984**, *18*, 2621-2626, doi:10.1016/0004-6981(84)90326-3.
MacLeod, H.; Poulet, G.; Le Bras, G. Etude cinetique des reactions du radical OH avec CH_3SCH_3, CH_3SH et C_2H_5SH. *J. Chim. Phys.* **1983**, *80*, 287-292, doi:10.1051/jcp/1983800287.
Maguin, F.; Mellouki, A.; Laverdet, G.; Poulet, G.; Le Bras, G. Kinetics of the reactions of the IO radical with dimethyl sulfide, methanethiol, ethylene, and propylene. *Int. J. Chem. Kinet.* **1991**, *23*, 237-245, doi:10.1002/kin.550230306.
Mai, T. V.-T.; Duong, M. V.; Nguyen, H. T.; Huynh, L. K. Ab initio kinetics of the $HOSO_2$ + $3O_2$ → SO_3 + HO_2 reaction. *Phys. Chem. Chem. Phys.* **2018**, *20*, 6677-6687, doi:10.1039/c7cp07704a.
Manning, R. G.; Braun, W.; Kurylo, M. J. The effect of infrared laser excitation on reaction dynamics: O + $C_2H_4^\dagger$ and O + $OCS^\dagger$. *J. Chem. Phys.* **1976**, *65*, 2609-2615, doi:10.1063/1.433448.
Mao, W.-X.; Long, Z.-W.; Long, B.; Wang, Y.-B.; Long, C.-Y.; Qin, S.-J. Theoretical study on the gas phase reaction of dimethyl sulfoxide with atomic chlorine in the presence of water. *Struct. Chem.* **2013**, *24*, 383-392, doi:10.1007/s11224-012-0086-z.
Margitan, J. J. Mechanism of the atmospherlc oxidation of sulfur dioxide. Catalysis by hydroxyl radicals. *J. Phys. Chem.* **1984**, *88*, 3314-3318, doi:10.1021/j150659a035.
Martin, D.; Barnes, I.; Becker, K. H. Rate constant and products of the reaction Cl + CS_2 in air. *Chem. Phys. Lett.* **1987**, *140*, 195-199, doi:10.1016/0009-2614(87)80813-8.
Martin, D.; Jourdain, J. L.; Laverdet, G.; Le Bras, G. Kinetic study of the reaction of IO with CH_3SCH_3. *Int. J. Chem. Kinet.* **1987**, *19*, 503-512, doi:10.1002/kin.550190603.
Martin, D.; Jourdain, J. L.; Le Bras, G. Kinetic study for the reactions of OH radicals with dimethylsulfide, diethylsulfide, tetrahydrothiophene, and thiophene. *Int. J. Chem. Kinet.* **1985**, *17*, 1247-1261, doi:10.1002/kin.550171202.

Martin, D.; Jourdain, J. L.; Le Bras, G. Discharge flow measurements of the rate constants for the reactions OH + SO_2 + He and $HOSO_2$ + O_2 in relation with the atmospheric oxidation of SO_2. *J. Phys. Chem.* **1986**, *90*, 4143-4147, doi:10.1021/j100408a061.

Martinez, E.; Albaladejo, A.; Jiminez, E.; Notario, A.; Aranda, A. Kinetics of the reaction of CH_3S with NO_2 as a function of temperature. *Chem. Phys. Lett.* **1999**, *308*, 37-44, doi:10.1016/S0009-2614(99)00579-5.

Martinez, E.; Albaladejo, A.; Notario, A.; Jiminez, E. A study of the atmospheric reaction of CH_3S with O_3 as a function of temperature. *Atmos. Environ.* **2000**, *34*, 5295 - 5302, doi:10.1016/S1352-2310(00)00348-4.

Martinez, E.; Aranda, A.; Diaz-de-Mera, Y.; Rodriguez, D.; Reyes Lopez, M.; Albaladejo, J. Atmospheric DMSO degradation in the gas phase: Cl-DMSO reaction. Temperature dependence and products. *Environ. Sci. Technol.* **2002**, *36*, 1226-1230, doi:10.1021/es010169s.

Martinez, R. I.; Herron, J. T. Stopped-flow study of the gas-phase reaction of ozone with organic sulfides: Dimethyl sulfide. *Int. J. Chem. Kinet.* **1978**, *10*, 433-452, doi:10.1002/kin.550100503.

Maurer, T., I. Barnes, and K. H. Becker FT-IR kinetic and product study of the Br-initiated oxidation of dimethyl sulfide. *Int. J. Chem. Kinet.* **1999**, *31*, 883-893, doi:10.1002/(SICI)1097-4601(1999)31:12<883::AID-KIN7>3.0.CO;2-V.

McKee, M. L.; Wine, P. H. Ab initio study of the atmospheric oxidation of CS_2. *J. Am. Chem. Soc.* **2001**, *123*, 2344-2353, doi:10.1021/ja003421p.

Mellouki, A.; Jourdain, J. L.; Le Bras, G. Discharge flow study of the CH_3S + NO_2 reaction mechanism using Cl + CH_3SH as the CH_3S source. *Chem. Phys. Lett.* **1988**, *148*, 231-236, doi:10.1016/0009-2614(88)80305-1.

Mellouki, A.; Laverdet, G.; Jourdain, L.; Poulet, G. Kinetics of the reactions Br + NO_2 + M and I + NO_2 + M. *Int. J. Chem. Kinet.* **1989**, *21*, 1161-1172, doi:10.1002/kin.550211209.

Mellouki, A.; Ravishankara, A. R. Does the HO_2 radical react with H_2S, CH_3SH, and CH_3SCH_3? *Int. J. Chem. Kinet.* **1994**, *26*, 355-365, doi:10.1002/kin.550260306.

Michael, J. V.; Nava, D. F.; Brobst, W.; Borkowski, R. P.; Stief, L. J. Temperature dependence of the absolute rate constant for the reaction of hydroxyl radical with hydrogen sulfide. *J. Phys. Chem.* **1982**, *86*, 81-84, doi:10.1021/j100390a016.

Miyoshi, A.; Shina, H.; Tsuchiya, K.; Matsui, H. Kinetics and mechanism of the reaction of $S(^3P)$ with O_2. *Symp. Int. Combust. Proc.* **1996**, *26*, 535-541.

Morokuma, K.; Mugurama, C. Ab initio molecular orbital study of the mechanism of the gas phase reaction SO_3 + H_2O: Importance of the second water molecule. *J. Am. Chem. Soc.* **1994**, *116*, 10316-10317, doi:10.1021/ja00101a068.

Mousavipour, S. H.; Mortazavi, M.; Hematti, O. Multichannel RRKM-TST and direct dynamics CVT study of the reaction of hydrogen sulfide with ozone. *J. Phys. Chem. A* **2013**, *117*, 6744-6756, doi:10.1021/jp404738d.

Murrells, T. P.; Lovejoy, E. R.; Ravishankara, A. R. Oxidation of CS_2 by reaction with OH. 1. Equilibrium constant for the reaction OH + CS_2 ⇄ CS_2OH and the kinetics of the CS_2OH + O_2 reaction. *J. Phys. Chem.* **1990**, *94*, 2381-2386, doi:10.1021/j100369a036.

Nagase, S.; Hashimoto, S.; Akimoto, H. $HOSO_2$ and $HOSO_4$ radicals studied by ab initio calculation and matrix isolation technique. *J. Phys. Chem.* **1988**, *92*, 641-644, doi:10.1021/j100314a015.

Nakano, Y.; Enami, S.; Nakamichi, S.; Aloisio, S.; Hashimoto, S.; Kawasaki, M. Temperature and pressure dependence study of the reaction of IO radicals with dimethyl sulfide by cavity ring-down laser spectroscopy. *J. Phys. Chem.* **2003**, *107*, 6381-6387, doi:10.1021/jp0345147.

Nakano, Y.; Ishiwata, T.; Aloisio, S.; Kawasaki, M. Temperature and pressure dependence of the rate constants of the reaction of NO_3 radical with CH_3SCH_3. *J. Phys. Chem. A* **2006**, *110*, 7401-7405, doi:10.1021/jp0612230.

Nakano, Y., M. Goto, S. Hashimoto, M. Kawasaki, and T. J. Wallington Cavity ring-down spectroscopic study of the reactions of Br atoms and BrO radicals with dimethyl sulfide. *J. Phys. Chem. A* **2001**, *105*, 11045-11050, doi:10.1021/jp012326f.

Nava, D. F.; Brobst, W. D.; Stief, L. J. Temperature study of the rates of the reactions of atomic chlorine with H_2S and C_2H_4S. *J. Phys. Chem.* **1985**, *89*, 4703-4707, doi:10.1021/j100268a012.

Nesbitt, D. J.; Leone, S. R. Laser-initiated chemical chain reactions. *J. Chem. Phys.* **1980**, *72*, 1722-1732, doi:10.1063/1.439284.

Nesbitt, D. J.; Leone, S. R. Laser initiated chain reactions: A generalized extension to complex chemical chain systems. *J. Chem. Phys.* **1981**, *75*, 4949-4959, doi:10.1063/1.441883.

Nickolaisen, S. L.; Veney, D. W.; Cartland, H. E. CO(v,J) product state distributions from the reaction O(^{3}P) + OCS → CO + SO. *J. Chem. Phys.* **1994**, *100*, 4925-4931, doi:10.1063/1.467278.

Nicovich, J. M.; Kreutter, K. D.; van Dijk, C. A.; Wine, P. H. Temperature dependent kinetics studies of the reactions Br($^2P_{3/2}$) + H_2S ↔ SH + HBr and Br($^2P_{3/2}$) + CH_3SH ↔ CH_3S + HBr. Heats of formation of SH and CH_3S radicals. *J. Phys. Chem.* **1992**, *96*, 2518-2528, doi:10.1021/j100185a025.

Nicovich, J. M.; Parthasarathy, S.; Pope, F. D.; Pegus, A. T.; McKee, M. L.; Wine, P. H. Kinetics, mechanism, and thermochemistry of the gas phase reaction of atomic chlorine with dimethyl sulfoxide. *J. Phys. Chem. A* **2006**, *110*, 6874-6885, doi:10.1021/jp0567467.

Nicovich, J. M.; Shackelford, C. J.; Wine, P. H. Kinetics and thermochemistry of reversible adduct formation in the reaction of Cl(^2P_J) with CS_2. *J. Phys. Chem.* **1990**, *94*, 2896-2903, doi:10.1021/j100370a031.

Nicovich, J. M.; Wang, S.; Wine, P. H. Kinetics of the reactions of atomic chlorine with H_2S, D_2S, CH_3SH, and CD_3SD. *Int. J. Chem. Kinet.* **1995**, *27*, 359-368, doi:10.1002/kin.550270407.

Nielsen, O. J.; Sidebottom, H. W.; Nelson, L.; Rattigan, O.; Treacy, J. J.; O'Farrell, D. J. Rate constants for the reactions of OH radicals and Cl atoms with diethyl sulfide, Di-n-propyl sulfide, and Di-n-butyl sulfide. *Int. J. Chem. Kinet.* **1990**, *22*, 603-612, doi:10.1002/kin.550220605.

Nielsen, O. J.; Sidebottom, H. W.; Nelson, L.; Treacy, J. J.; O'Farrell, D. J. An absolute and relative rate study of the reaction of OH radicals with dimethyl sulfide. *Int. J. Chem. Kinet.* **1989**, *21*, 1101-1112, doi:10.1002/kin.550211203.

Nip, W. S.; Singleton, D. L.; Cvetanovic, R. J. Gas-phase reactions of O(^{3}P) atoms with methanethiol, ethanethiol, methyl sulfide, and dimethyl disulfide. 1. Rate constants and Arrhenius parameters. *J. Am. Chem. Soc.* **1981**, *103*, 3526-3530, doi:10.1021/ja00402a045.

Oksdath-Mansilla, G.; Penenory, A. B.; Albu, M.; Barnes, I.; Wiesen, P.; Teruel, M. A. FTIR relative kinetic study of the reactions of $CH_3CH_2SCH_2CH_3$ and $CH_3CH_2SCH_3$ with OH radicals and Cl atoms at atmospheric pressure. *Chem. Phys. Lett.* **2009**, *477*, 22-27, doi:10.1016/j.cplett.2009.06.035.

Oksdath-Mansilla, G.; Penenory, A. B.; Albu, M.; Barnes, I.; Wiesen, P.; Teruel, M. A. $CH_3CH_2SCH_3$ + OH radicals: temperature-dependent rate coefficient and product identification under atmospheric pressure of air. *J. Phys. Org. Chem.* **2010**, *23*, 925-930, doi:10.1002/poc.1714.

Oksdath-Mansilla, G.; Penenory, A. B.; Albu, M.; Barnes, I.; Wiesen, P.; Teruel, M. A. Product distribution study of the Cl-atom initiated oxidation of ethyl methyl sulfide and diethyl sulfide. *Atmos. Environ.* **2014**, *85*, 41-47, doi:10.1016/j.atmosenv.2013.11.063.

Oksdath-Mansilla, G.; Penenory, A. B.; Barnes, I.; Wiesen, P.; Teruel, M. A. Photodegradation of $(CH_3CH_2)_2S$ and $CH_3CH_2SCH_3$ initiated by OH radicals at atmospheric pressure. Product yields and mechanism in NO_x free air. *Atmos. Environ.* **2012**, *55*, 263-270, doi:10.1016/j.atmosenv.2012.02.086.

Papadimitriou, V. C.; Portmann, R. W.; Fahey, D. W.; Muhle, J.; Weiss, R. F.; Burkholder, J. B. Experimental and theoretical study of the atmospheric chemistry and global warming potential of SO_2F_2. *J. Phys. Chem. A* **2008**, *112*, 12657-12666, doi:10.1021/jp806368u.

Pavanaja, U. B.; Upadhyaya, H. P.; Sapre, A. V.; Rao, K. V. S. R.; Mittal, J. P. Chemiluminescent reaction of oxygen atoms with dimethyl disulfide and dimethyl sulfide. *J. Chem. Soc. Faraday. Trans.* **1994**, *90*, 825-829, doi:10.1039/ft9949000825.

Payne, W. A.; Stief, L. J.; Davis, D. D. A kinetics study of the reaction of HO_2 with SO_2 and NO. *J. Am. Chem. Soc.* **1973**, *95*, 7614-7619, doi:10.1021/ja00804a013.

Penzhorn, R. D.; Canosa, C. E. 2nd derivative UV spectroscopy study of the thermal and photochemical reaction of NO_2 with SO_2 and SO_3. *Ber. Bunsenges. Phys. Chem.* **1983**, *87*, 648-654, doi:10.1002/bbpc.19830870808.

Perry, R. A.; Atkinson, R.; Pitts, J. N., Jr. Rate constants for the reactions OH + H_2S → H_2O + SH and OH + NH_3 → H_2O + NH_2 over the temperature range 297-427 °K. *J. Chem. Phys.* **1976**, *64*, 3237-3239, doi:10.1063/1.432663.

Pope, F. D.; Nicovich, J. M.; Wine, P. H. A temperature-dependent kinetics study of the reaction of O(^3P_J) with $(CH_3)_2SO$. *Int. J. Chem. Kinet.* **2002**, *34*, 156-161, doi:10.1002/kin.10040.

Rahman, M. M.; Becker, E.; Benter, T.; Schindler, R. N. A gas phase kinetic investigation of the system F + HNO_3 and the determination of absolute rate constants for the reaction of the NO_3 radical with CH_3SH, 2-methylpropene, 1,3-butadiene and 2,3-dimethyl-2-butene. *Ber. Bunsenges. Phys. Chem.* **1988**, *92*, 91-100, doi:10.1002/bbpc.198800018.

Rahman, M. M.; Becker, E.; Wille, U.; Schindler, R. N. Determination of rate constants for the reactions of the CH_2SH radical with O_2, O_3, and NO_2 at 298 K. *Ber. Bunsenges. Phys. Chem.* **1992**, *96*, 783-787, doi:10.1002/bbpc.19920960609.

Ramirez-Anguita, J. M.; Gonzalez-Lafont, A.; Lluch, J. M. Formation pathways of CH_3SOH from $CH_3S(OH)CH_3$ in the presence of O_2: a theoretical study *Theor. Chem. Acc.* **2009**, *123*, 93-103, doi:10.1007/s00214-009-0547-7.

Ramírez-Anguita, J. M.; González-Lafont, A.; Lluch, J. M. Variational transition-state theory study of the rate constant of the DMS•OH scavenging reaction by O_2. *J. Comput. Chem.* **2011**, *32*, 2104-2118, doi:10.1002/jcc.21793.

Ravichandran, K.; Williams, R.; Fletcher, T. R. Atmospheric reactions of vibrationally excited greenhouse gases: SH + N_2O(*n*, 0, 0). *Chem. Phys. Lett.* **1994**, *217*, 375-380, doi:10.1016/0009-2614(93)E1411-9.

Ravishankara, A. R.; Kreutter, N. M.; Shah, R. C.; Wine, P. H. Rate of reaction of OH with OCS. *Geophys. Res. Lett.* **1980**, *7*, 861-864, doi:10.1029/GL007i011p00861.

Ray, A.; Vassalli, I.; Laverdet, G.; Le Bras, G. Kinetics of the thermal decomposition of the CH_3SO_2 radical and its reaction with NO_2 at 1 Torr and 298 K. *J. Phys. Chem.* **1996**, *100*, 8895-8900, doi:10.1021/jp9600120.

Reiner, T.; Arnold, F. Laboratory flow reactor measurements of the reaction $SO_3 + H_2O + M \rightarrow H_2SO_4 + M$: Implications for gaseous H_2SO_4 and aerosol formation in the plumes of jet aircraft. *Geophys. Res. Lett.* **1993**, *20*, 2659-2662, doi:10.1029/93GL02996.

Reiner, T.; Arnold, F. Laboratory investigations of gaseous sulfuric acid formation via $SO_3 + H_2O + M \rightarrow H_2SO_4 + M$: Measurement of the rate constant and product indentification. *J. Chem. Phys.* **1994**, *101*, 7399-7407, doi:10.1063/1.468298.

Resende, S. M.; Almeida, W. B. D. Theoretical study of the atmospheric reaction between dimethyl sulfide and chlorine atoms. *J. Phys. Chem. A* **1997**, *101*, 9738-9744, doi:10.1021/jp971885c.

Resende, S. M.; Ornellas, F. R. The reaction of SH with O_2: A theoretical high level investigation. *Phys. Chem. Chem. Phys.* **2003**, *5*, 4617-4621, doi:10.1039/b308359d.

Resende, S. M.; Ornellas, R. Does SH really react with O_3 in the ground state? *Chem. Phys. Lett.* **2001**, *349*, 123-130, doi:10.1016/S0009-2614(01)01177-0.

Richardson, R. J. CS-O_2 flame reaction chemistry. *J. Phys. Chem.* **1975**, *79*, 1153-1158, doi:10.1021/j100579a003.

Riffault, V.; Bedjanian, Y.; Le Bras, G. Kinetic and mechanistic study of the X and XO (X = Cl, Br) reactions with dimethyl sulfoxide. *Phys. Chem. Chem. Phys.* **2003**, *5*, 2828-2835, doi:10.1039/b302675b.

Riffault, V.; Bedjanian, Y.; Le Bras, G. Kinetics and mechanism of the O atom reaction with dimethyl sulfoxide. *J. Phys. Chem. A* **2003**, *107*, 5404-5411, doi:10.1021/jp0226127.

Robertshaw, J. S.; Smith, I. W. M. Rate data for O + OCS → SO + CO and SO + O_3 → SO_2 + O_2 by a new time-resolved technique. *Int. J. Chem. Kinet.* **1980**, *12*, 729 -739, doi:10.1002/kin.550121006.

Rodriguez-Linares, D.; Freitas, G. N.; Ballester, M. Y.; Nascimento, M. A. C.; Garrido, J. D. Coupled-cluster study of the lower energy region of the ground electronic state of the HSO_2 potential energy surface. *J. Phys. Chem. A* **2015**, *119*, 8734-8743, doi:10.1021/acs.jpca.5b04554.

Saheb, V.; Alizadeh, M.; Rezaei, F.; Shahidi, S. Quantum chemical and theoretical kinetics studies on the reaction of carbonyl sulfide with H, OH, and O(^{3}P). *Comp. Theo. Chem.* **2012**, *994*, 25-33, 10.1016/j.comptc.2012.06.008.

Saito, K.; Ueda, Y.; Ito, R.; Kakumoto, T.; Imamura, A. Measurements of the bimolecular rate constants for S + O_2 → SO + O and CS_2 + O_2 → CS + SO_2 at high temperatures. *Int. J. Chem. Kinet.* **1986**, *18*, 871-884, doi:10.1002/kin.550180807.

Sander, S. P.; Watson, R. T. A kinetics study of the reaction of SO_2 with CH_3O_2. *Chem. Phys. Lett.* **1981**, *77*, 473-475, doi:10.1016/0009-2614(81)85188-3.

Sanhueza, E.; Simonaitis, R.; Heicklen, J. The reaction of CH_3O_2 with SO_2. *Int. J. Chem. Kinet.* **1979**, *11*, 907-914, doi:10.1002/kin.550110809.

Schindler, R. N.; Benter, T. Correction. *Ber. Bunsenges. Phys. Chem.* **1988**, *92*, 558, doi:10.1002/bbpc.198800126.

Schmidt, J. A.; Kyte, M.; Østerstrøm, F. F.; Joelsson, L. M. T.; Knap, H. C.; Jørgensen, S.; Nielsen, O. J.; Murakami, T.; Johnson, M. S. On adduct formation and reactivity in the OCS + OH reaction: A combined theoretical and experimental study. *Chem. Phys. Lett.* **2017**, *675*, 111-117, doi:10.1016/j.cplett.2017.03.005.

Schonle, G.; Rahman, M. M.; Schindler, R. N. Kinetics of the reaction of atomic fluorine with H_2S and elementary reactions of the HS radical. *Ber. Bunsenges. Phys. Chem.* **1987**, *91*, 66-75, doi:10.1002/bbpc.19870910114.

Schurath, U.; Goede, H.-J. Temperature Dependence of the Reactions SO + O_3 (1) and SO + O_2 (2). *Physico-Chemical Behaviour of Atmospheric Pollutants, Proc. 3rd European Symposium, Varese, Italy* **1984**, 227 - 239.

Shallcross, D. E.; Vaughn, S.; Trease, D. R.; Canosa-Mas, C.; Ghosh, M. V.; Dyke, J. M.; Wayne, R. P. Kinetics of the reaction between OH radicals and monochlorodimethylsulphide (CH_3SCH_2Cl). *Atmos. Environ.* **2006**, *40*, 6899-6904, doi:10.1016/j.atmosenv.2006.06.037.

Sheps, L.; Scully, A. M.; Au, K. UV absorption probing of the conformer-dependent reactivity of a Criegee intermediate CH_3CHOO. *Phys. Chem. Chem. Phys.* **2014**, *16*, 26701-26706, doi:10.1039/c4cp04408h.

Singleton, D. L.; Irwin, R. S.; Nip, W. S.; Cvetanovic, R. J. Kinetics and mechanism of the reaction of oxygen atoms with hydrogen sulfide. *J. Phys. Chem.* **1979**, *83*, 2195-2200, doi:10.1021/j100480a003.

Singleton, D. L.; Paraskevopoulos, G.; Irwin, R. S. Mechanism of the $O(^3P) + H_2S$ reaction. Abstraction or addition? *J. Phys. Chem.* **1982**, *86*, 2605-2609, doi:10.1021/j100211a011.

Slagle, I. R.; Baiocchi, F.; Gutman, D. Study of the reactions of oxygen atoms with hydrogen sulfide, methanethiol, ethanethiol, and methyl sulfide. *J. Phys. Chem.* **1978**, *82* 1333-1336, doi:10.1021/j100501a002.

Slagle, I. R.; Gilbert, J. R.; Gutman, D. Kinetics of the reaction between oxygen atoms and carbon disulfide. *J. Chem. Phys.* **1974**, *61*, 704-709, doi:10.1063/1.1681949.

Slagle, I. R.; Graham, R. E.; Gilbert, J. R.; Gutman, D. Direct determination of the rate constant for the reaction of oxygen atoms with carbon monosulphide. *Chem. Phys. Lett.* **1975**, *32*, 184-186, doi:10.1016/0009-2614(75)85196-7.

Smardzewski, R. R.; Lin, M. C. Matrix reactions of oxygen atoms with H_2S molecules. *J. Chem. Phys.* **1977**, *66*, 3197-3204, doi:10.1063/1.434294.

Sørensen, S.; Falbe-Hansen, H.; Mangoni, M.; Hjorth, J.; Jensen, N. R. Observation of DMSO and $CH_3S(O)OH$ from the gas phase reaction between DMS and OH. *J. Atmos. Chem.* **1996**, *24*, 299-315, doi:10.1007/BF00210288.

Stachnik, R. A.; Molina, M. J. Kinetics of the reactions of SH radicals with NO_2 and O_2. *J. Phys. Chem.* **1987**, *91*, 4603-4606 doi:10.1021/j100301a035.

Stickel, R. E.; Chin, M.; Daykin, E. P.; Hynes, A. J.; Wine, P. H.; Wallington, T. J. Mechanistic studies of the OH-initiated oxidation of CS_2 in the presence of O_2. *J. Phys. Chem.* **1993**, *97*, 13653-13661, doi:10.1021/j100153a038.

Stickel, R. E.; Nicovich, J. M.; Wang, S.; Zhao, Z.; Wine, P. H. Kinetic and mechanistic study of the reaction of atomic chlorine with dimethyl sulfide. *J. Phys. Chem.* **1992**, *96*, 9875-9883, doi:10.1021/j100203a055.

Stickel, R. E.; Zhao, Z.; Wine, P. H. Branching ratios for hydrogen transfer in the reactions of OD radicals with CH_3SCH_3 and $CH_3SC_2H_5$. *Chem. Phys. Lett.* **1993**, *212*, 312-318, doi:10.1016/0009-2614(93)89331-B.

Stuhl, F. Determination of rate constant for reaction $OH + H_2S$ by a pulsed photolysis - resonance fluorescence method. *Ber. Bunsenges. Phys. Chem.* **1974**, *78*, 230-232, doi:10.1002/bbpc.19740780304.

Sulbaek-Andersen, M. P.; Blake, D. R.; Rowland, F. S.; Hurley, M. D.; Wallington, T. J. Atmospheric chemistry of aulfuryl fluoride: Reaction with OH radicals, Cl Atoms and O_3, atmospheric lifetime, IR spectrum, and global warming potential. *Environ. Sci. Technol.* **2009**, *43*, 1067-1070, doi:10.1021/es802439f.

Taatjes, C. A.; Meloni, G.; Selby, T. M.; Trevitt, A. J.; Osborn, D. L.; Percival, C. J.; Shallcross, D. E. Direct observation of the gas-phase Criegee intermediate (CH_2OO). *J. Am. Chem. Soc.* **2008**, *130*, 11883-11885, doi:10.1021/ja804165q.

Thompson, K. C.; Canosa-Mas, C. E.; Wayne, R. P. Kinetics and mechanism of the reaction between atomic chlorine and dimethyl selenide; comparison with the reaction between atomic chlorine and dimethyl sulfide. *Phys. Chem. Chem. Phys.* **2002**, *4*, 4133-4139, doi:10.1039/b204657a.

Tian, Y.; Tian, Z.-M.; Wei, W.-M.; He, T.-J.; Chen, D.-M.; Liu, F.-C. Ab initio study of the reaction of OH radical with methyl sulfinic acid (MSIA). *Chem. Phys.* **2007**, *335*, 133-140, doi:10.1016/j.chemphys.2007.04.009.

Tiee, J. J.; Wampler, F. B.; Oldenborg, R. C.; Rice, W. W. Spectroscopy and reaction kinetics of the HS radicals. *Chem. Phys. Lett.* **1981**, *82*, 80-84, doi:10.1016/0009-2614(81)85111-1.

Tsuchiya, K.; Kamiya, K.; Matsui, H. Studies on the oxidation mechanism of H_2S based on direct examination of the key reactions. *Int. J. Chem. Kinet.* **1997**, *29*, 57-66, doi:10.1002/(SICI)1097-4601(1997)29:1<57::AID-KIN7>3.0.CO;2-K.

Turnipseed, A. A.; Barone, S. B.; Ravishankara, A. R. Reactions of CH_3S and CH_3SOO with O_3, NO_2, and NO. *J. Phys. Chem.* **1993**, *97*, 5926-5934, doi:10.1021/j100124a025.

Turnipseed, A. A.; Barone, S. B.; Ravishankara, A. R. Reaction of OH with dimethyl sulfide. 2. Products and mechanisms. *J. Phys. Chem.* **1996**, *100*, 14703-14713, doi:10.1021/jp960867c.

Turnipseed, A. A.; Birks, J. W. Kinetics of the reaction of molecular fluorine with dimethyl sulfide. *J. Phys. Chem.* **1991**, *95*, 6569-6574, doi:10.1021/j100170a037.

Tyndall, G. S.; Burrows, J. P.; Schneider, W.; Moortgat, G. K. Rate coefficient for the reaction between NO_3 radicals and dimethyl sulphide. *Chem. Phys. Lett.* **1986**, *130*, 463-466, doi:10.1016/0009-2614(86)80506-1.

Tyndall, G. S.; Ravishankara, A. R. Kinetics and mechanism of the reactions of CH_3S with O_2 and NO_2 at 298 K. *J. Phys. Chem.* **1989**, *93*, 2426-2435, doi:10.1021/j100343a041.

Tyndall, G. S.; Ravishankara, A. R. Kinetics of the reaction of CH_3S with O_3 at 298 K. *J. Phys. Chem.* **1989**, *93*, 4707-4710, doi:10.1021/j100349a006.

Tyndall, G. S.; Ravishankara, A. R. Atmospheric oxidation of reduced sulfur species. *Int. J. Chem. Kinet.* **1991**, *23*, 483-527, doi:10.1002/kin.550230604.

Urbanski; Stickel, R. E.; Wine, P. H. Mechanistic and kinetic study of the gas-phase reaction of hydroxyl radical with dimethyl sulfoxide. *J. Phys. Chem. A* **1998**, *102*, 10522-10529, doi:10.1021/jp9833911.

Urbanski, S. P.; Stickel, R. E.; Zhao, Z.; Wine, P. H. Mechanistric and kinetic study of formaldehyde production in the atmospheric oxidation of dimethyl sulfide. *J. Chem. Soc. Faraday Trans.* **1997**, *93*, 2813-2819, doi:10.1039/a701380i.

Urbanski, S. P.; Wine, P. H. Spectroscopic and kinetic study of the Cl-S$(CH_3)_2$ adduct. *J. Phys. Chem. A* **1999**, *103*, 10935-10944, doi:10.1021/jp992682m.

Vandresen, S.; Resende, S. M. The atmospheric reaction between DMSO and the chlorine radical. *J. Phys. Chem. A* **2004**, *108*, 2284-2289, doi:10.1021/jp036906j.

Wahner, A.; Ravishankara, A. R. The kinetics of the reaction of OH with COS. *J. Geophys. Res.* **1987**, *92*, 2189-2194, doi:10.1029/JD092iD02p02189.

Wallington, T. J.; Andino, J. M.; Potts, A. R.; Wine, P. H. A competitive kinetics study of the reaction of Cl with CS_2 in air at 298 K. *Chem. Phys. Lett.* **1991**, *176*, 103-108, doi:10.1016/0009-2614(91)90018-5.

Wallington, T. J.; Atkinson, R.; Tuazon, E. C.; Aschmann, S. M. The reaction of OH radicals with dimethyl sulfide. *Int. J. Chem. Kinet.* **1986**, *18*, 837-846, doi:10.1002/kin.550180804.

Wallington, T. J.; Atkinson, R.; Winer, A. M.; Pitts, J. N., Jr. Absolute rate constants for the gas-phase reactions of the NO_3 radical with CH_3SH, CH_3SCH_3, CH_3SSCH_3, H_2S, SO_2, and CH_3OCH_3 over the temperature range 280-350 K. *J. Phys. Chem.* **1986**, *90*, 5393-5396, doi:10.1021/j100412a099.

Wallington, T. J.; Atkinson, R.; Winer, A. M.; Pitts Jr., J. N. Absolute rate constants for the gas-phase reactions of the NO_3 radical with CH_3SCH_3, NO_2, CO, and a series of alkanes at 298 ± 2 K. *J. Phys. Chem.* **1986**, *90*, 4640-4644, doi:10.1021/j100410a034.

Wallington, T. J.; Ellermann, T.; Nielsen, O. J. Atmospheric chemistry of dimethyl sulfide: UV spectra and self-reaction kinetics of CH_3SCH_2 and $CH_3SCH_2O_2$ radicals and kinetics of the reactions $CH_3SCH_2 + O_2 \rightarrow CH_3SCH_2O_2$ and $CH_3SCH_2O_2 + NO \rightarrow CH_3SCH_2O + NO_2$. *J. Phys. Chem.* **1993**, *97*, 8442-8449, doi:10.1021/j100134a013.

Wang, B.; Hou, H. Theoretical investigations on the $SO_2 + HO_2$ reaction and the $SO_2{-}HO_2$ radical complex. *Chem. Phys. Lett.* **2005**, *410*, 235-241, doi:10.1016/j.cplett.2005.05.091.

Wang, H.-T.; Zhang, Y.-J.; Mu, Y.-J. Rate constants for reactions of OH with several reduced sulfur compounds determined by relative rate constant method. *Acta Phys.-Chim. Sin.* **2008**, *24*, 945-950, doi:10.1016/S1872-1508(08)60041-8.

Wang, K.; Ge, M. F.; Wang, W. G. Temperature dependent kinetics of the gas-phase reaction of OH radicals with EMS. *Chin. Sci. Bull.* **2011**, *56*, 391-396, doi:10.1007/s11434-010-4313-y.

Wang, L.; Liu, J.-Y.; Li, Z.-S.; Sun, C.-C. Theoretical study and rate constant calculation for the reactions of SH (SD) with Cl_2, Br_2, and BrCl. *J. Comput. Chem.* **2004**, *26*, 184-193, doi:10.1002/jcc.20159.

Wang, L.; Liu, J.-Y.; Li, Z.-S.; Sun, C.-C. Dual-level direct dynamics study on the reactions of SH (SD) with F_2. *Int. J. Chem. Kinet.* **2005**, *37*, 710-716, doi:10.1002/kin.20124.

Wang, L.; Zhang, J. Ab initio study of reaction of dimethyl sulfoxide (DMSO) with OH radical. *Chem. Phys. Lett.* **2002**, *356*, 490-496, doi:10.1016/S0009-2614(02)00397-4.

Wang, N.-S.; Lee, Y.-P. Absolute rate constant measurement of the reaction OH + H_2S using discharge flow-resonance fluorescence technique. *Proc. Nat. Sci. Council (Taiwan)* **1985**, *9*, 87-94.

Wang, N. S.; Howard, C. J. Kinetics of the reactions of HS and HSO with O_3. *J. Phys. Chem.* **1990**, *94*, 8787-8794, doi:10.1021/j100388a009.

Wang, N. S.; Lovejoy, E. R.; Howard, C. J. Temperature dependence of the rate constant for the reaction HS + NO_2. *J. Phys. Chem.* **1987**, *91*, 5743-5749, doi:10.1021/j100306a045.

Wang, X.; Jin, Y. G.; Suto, M.; Lee, L. C. Rate constant of the gas phase reaction of SO_3 with H_2O. *J. Chem. Phys.* **1988**, *89*, 4853-4860, doi:10.1063/1.455680.

Wang, Y.-X.; Duan, X.-M.; Wang, Q.; Wang, L.; Liu, J.-Y.; Sun, C.-C. Direct *ab initio* dynamics studies of the reaction of methanethiol with chlorine atoms. *J. Theor. Comp. Chem.* **2010**, *9*, 265-277, doi:10.1142/S0219633610005669.

Wei, C. N.; Timmons, R. B. ESR study of the kinetics of the reactions of O(^3P) atoms with CS_2 and OCS. *J. Chem. Phys.* **1975**, *62*, 3240-3245, doi:10.1063/1.430875.

Westenberg, A. A.; deHaas, N. Atom molecule using EST detection. V. Results for O + OCS, O + CS_2, O + NO, and H + C_2H_4. *J. Chem. Phys.* **1969**, *50*, 707-709, doi:10.1063/1.1671119.

Westenberg, A. A.; deHaas, N. Rate of the reaction OH + H_2S → SH + H_2O over an extended temperature range. *J. Chem. Phys.* **1973**, *59*, 6685-6686, doi:10.1063/1.1680055.

Westenberg, A. A.; deHaas, N. Rate of the reaction OH + OH → H_2O + O. *J. Chem. Phys.* **1973**, *58*, 4066-4071, doi:10.1063/1.1678962.

Whytock, D. A.; Timmons, R. B.; Lee, J. H.; Michael, J. V.; Payne, W. A.; Stief, L. J. Absolute rate of the reaction of O(^3P) with hydrogen sulfide over the temperature range 263 to 495 K. *J. Chem. Phys.* **1976**, *65*, 2052-2055, doi:10.1063/1.433387.

Williams, M. B.; Campuzano-Jost, P.; Bauer, D.; Hynes, A. J. Kinetic and mechanistic studies of the OH-initiated oxidation of dimethylsulfide at low temperature — A reevaluation of the rate coefficient and branching ratio. *Chem. Phys. Lett.* **2001**, *344*, 61-67, doi:10.1016/S0009-2614(01)00764-3.

Williams, M. B.; Campuzano-Jost, P.; Cossairt, B. M.; Hynes, A. J.; Pounds, A. J. Experimental and theoretical studies of the reaction of the OH radical with alkyl sulfides: 1. Direct observations of the formation of the OH-DMS adduct-pressure dependence of the forward rate of addition and development of a predictive expression at low temperature. *J. Phys. Chem. A* **2007**, *111*, 89-104, doi:10.1021/jp063873+.

Williams, M. B.; Campuzano-Jost, P.; Hynes, A. J.; Pounds, A. J. Experimental and theoretical studies of the reaction of the OH radical with alkyl sulfides: 3. Kinetics and mechanism of the OH initiated oxidation of dimethyl, dipropyl, and dibutyl sulfides: Reactivity trends in the alkyl sulfides and development of a predictive expression for the reaction of OH with DMS. *J. Phys. Chem. A* **2009**, *113*, 6697-6709, doi:10.1021/Jp9010668.

Williams, M. B.; Campuzano-Jost, P.; Pounds, A. J.; Hynes, A. J. Experimental and theoretical studies of the reaction of the OH radical with alkyl sulfides: 2. Kinetics and mechanism of the OH initiated oxidation of methylethyl and diethyl sulfides; observations of a two channel oxidation mechanism. *Phys. Chem. Chem. Phys.* **2007**, *9*, 4370-4382, doi:10.1039/b703957n.

Wilson, C.; Hirst, D. M. Ab initio study of the reaction of chlorine atoms with H_2S, CH_3SH, CH_3SCH_3 and CS_2. *J. Chem. Soc. Faraday Trans.* **1997**, *93*, 2831-2837, doi:10.1039/a701664f.

Wine, P. H.; Chameides, W. L.; Ravishankara, A. R. Potential role of CS_2 photooxidation in tropospheric sulfur chemistry. *Geophys. Res. Lett.* **1981**, *8*, 543-546, doi:10.1029/GL008i005p00543.

Wine, P. H.; Kreutter, N. M.; Gump, C. A.; Ravishankara, A. R. Kinetics of OH reactions with the atmospheric sulfur compounds H_2S, CH_3SH, CH_3SCH_3, and CH_3SSCH_3. *J. Phys. Chem.* **1981**, *85*, 2660-2665, doi:10.1021/j150618a019.

Wine, P. H.; Nicovich, J. M.; Stickel, R. E.; Zhao, Z.; Shackelford, C. J.; Kreutter, K. D.; Daykin, E. P.; Wang, S. In *The Tropospheric Chemistry of Ozone in the Polar Regions*; Springer-Verlag: Berlin, 1993; Vol. I7; pp 385-395.

Wine, P. H.; Shah, R. C.; Ravishankara, A. R. Rate of reaction of OH with CS_2. *J. Phys. Chem.* **1980**, *84*, 2499-2503, doi:10.1021/j100457a003.

Wine, P. H.; Thompson, R. J.; Semmes, D. H. Kinetics of OH reactions with aliphatic thiols. *Int. J. Chem. Kinet.* **1984**, *16*, 1623-1636, doi:10.1002/kin.550161215.

Woiki, D.; Roth, P. Oxidation of S and SO by O_2 in high-temperature pyrolysis and photolysis reaction systems. *Int. J. Chem. Kinet.* **1995**, *27*, 59-71, doi:10.1002/kin.550270108.

Zhang, L.; Qin, Q.-Z. Theoretical studies on CS_2OH-O_2: a possible intermediate in the OH initiated oxidation of CS_2 by O_2. *J. Mol. Structure (Theochem)* **2000**, *531*, 375-379, doi:10.1016/S0166-1280(00)00455-3.

Zhao, Z.; Stickel, R. E.; Wine, P. H. Branching ratios for methyl elimination in the reactions of OD radicals and Cl atoms with CH_3SCH_3. *Chem. Phys. Lett.* **1996**, *251*, 59-66, doi:10.1016/0009-2614(96)00059-0.

Zhou, C.; Sendt, K.; Haynes, B. S. Computational study of the reaction SH + O_2 *J. Phys. Chem. A* **2009**, *113*, 2975-2981, doi:10.1021/jp810105e.

1.15 Metal Reactions

1.15.1 Table 1J: Metal Reactions

Reaction	Temperature Range of Exp. Data (K) [a]	*A*-Factor	*E*/R	*k*(298 K) [b]	*f*(298 K) [c]	*g* [c]	Notes
$Na + O_2 \xrightarrow{M} NaO_2$		(See Table 2-1)					
$Na + O_3 \rightarrow NaO + O_2$ $\rightarrow NaO_2 + O$	208–377	1.0×10^{-9}	95	7.3×10^{-10} $<4.0\times10^{-11}$	1.20	50	J 1
$Na + OH \xrightarrow{M} NaOH$		(See Table 2-1)					
$Na + N_2O \rightarrow NaO + N_2$	240–850	2.8×10^{-10}	1600	1.3×10^{-12}	1.20	400	J 2
$Na + Cl_2 \rightarrow NaCl + Cl$	294	*7.3×10^{-10}*	*0*	7.3×10^{-10}	1.30	200	J 3
$NaO + O \rightarrow Na + O_2$	290–573	4.4×10^{-10}	0	4.4×10^{-10}	1.50	200	J 4
$NaO + O_2 \xrightarrow{M} NaO_3$		(See Table 2-1)					
$NaO + O_3 \rightarrow NaO_2 + O_2$ $\rightarrow Na + 2O_2$	207–377 296	1.1×10^{-9} *6.0×10^{-11}*	570 *0*	1.6×10^{-10} 6.0×10^{-11}	1.50 3.00	300 0	J 5
$NaO + H_2 \rightarrow NaOH + H$	266–310	(See Note)					J 6
$NaO + H_2O \rightarrow NaOH + OH$	260–716	5.06×10^{-10}	240	2.3×10^{-10}	1.50	200	J 7
$NaO + NO \rightarrow Na + NO_2$	296	*1.5×10^{-10}*	*0*	1.5×10^{-10}	4.00	0	J 8
$NaO + CO \rightarrow Na + CO_2$	294–300	*1.6×10^{-10}*	*0*	1.6×10^{-10}	1.50	100	J 9
$NaO + CO_2 \xrightarrow{M} NaCO_3$		(See Table 2-1)					
$NaO + HCl \rightarrow$ products	308	*2.8×10^{-10}*	*0*	2.8×10^{-10}	3.00	0	J10
$NaO_2 + O \rightarrow NaO + O_2$	300	*2.2×10^{-11}*	*0*	2.2×10^{-11}	5.00	0	J11
$NaO_2 + NO \rightarrow NaO + NO_2$	296			$<10^{-14}$			J12
$NaO_2 + HCl \rightarrow$ products	295	*2.3×10^{-10}*	*0*	2.3×10^{-10}	3.00	0	J13
$NaOH + H \rightarrow Na + H_2O$	230–298	*3.8×10^{-11}*	*0*	3.8×10^{-11}	1.50	200	J14
$NaOH + CO_2 \xrightarrow{M} NaHCO_3$		(See Table 2-1)					
$NaOH + HCl \rightarrow NaCl + H_2O$	308	*2.8×10^{-10}*	*0*	2.8×10^{-10}	3.00	0	J15
$NaHCO_3 + H \rightarrow Na + H_2O + CO_2$	227–307	1.4×10^{-11}	1000	5×10^{-13}	2.00	0	J16
$Hg + Br \xrightarrow{M} HgBr$		(See Table 2-1)					
$HgBr + NO_2 \xrightarrow{M}$ *syn*-BrHgONO		(See Table 2-1)					

$HgBr + HO_2 \xrightarrow{M} BrHgOOH$		(See Table 2-1)					

Shaded areas indicate changes or additions since JPL19-5. Italicized entries in blue denote estimates.

[a] Temperature range of available experimental data. This is not necessarily the range of temperature over which the recommended Arrhenius parameters are applicable. See the corresponding note for such information.

[b] Units are cm^3 $molecule^{-1}$ s^{-1}.

[c] f(298 K) is the uncertainty factor at 298 K. To calculate the uncertainty at other temperatures, use the expression:

$$f(\mathrm{T}) = f(298\ \mathrm{K})\exp\left|g\left(\frac{1}{\mathrm{T}} - \frac{1}{298}\right)\right|$$, note that the exponent is an absolute value.

1.15.2 Notes: Metal Reactions

J1. **Na + O_3.** The recommendation is based on the measurements of Ager et al.,[1] Worsnop et al.[6] as corrected in Worsnop et al.,[7] and Plane et al.[3] The data of Worsnop et al. supersede earlier work from that laboratory (Silver and Kolb[5]). Measurements made by Husain et al.[2] at 500 K are somewhat lower, probably because they did not recognize that secondary chemistry, NaO + O_3 → Na + $2O_2$, interferes with the rate coefficient measurement. The temperature dependence is from the results of Worsnop et al.[7] (214–294 K) and Plane et al.[3] (208–377 K). Ager et al.[1] estimated that the NaO_2 + O product channel is ≤5%. Evidence that the NaO product is in the $^2\Sigma^+$ excited electronic state was reported by Shi et al.[4] and Wright et al.[8]
(Table: 94-26, Note: 94-26, Evaluated: 94-26) Back to Table

(1) Ager, J. W., III; Talcott, C. L.; Howard, C. J. Gas phase kinetics of the reactions of Na and NaO with O_3 and N_2O. *J. Chem. Phys.* **1986**, *85*, 5584-5592, doi:10.1063/1.451573.
(2) Husain, D.; Marshall, P.; Plane, J. M. C. Determination of the absolute 2nd order rate constant for the reaction Na + O_3 → NaO + O_2. *J. Chem. Soc. Chem. Comm.* **1985**, 1216-1218, doi:10.1039/C39850001216.
(3) Plane, J. M. C.; Nien, C.-F.; Allen, M. R.; Helmer, M. A kinetic investigation of the reactions Na + O_3 and NaO + O_3 over the temperature range 207-377 K. *J. Phys. Chem.* **1993**, *97*, 4459-4467, doi:10.1021/j100119a033.
(4) Shi, X.; Herschbach, D. R.; Worsnop, D. R.; Kolb, C. E. Molecular beam chemistry: Magnetic deflection analysis of monoxide electronic states from alkali-metal atom + ozone reactions. *J. Phys. Chem.* **1993**, *97*, 2113-2122, doi:10.1021/j100112a010.
(5) Silver, J. A.; Kolb, C. E. Determination of the absolute rate constants for the room temperature reactions of atomic sodium with ozone and nitrous oxide. *J. Phys. Chem.* **1986**, *90*, 3263-3266, doi:10.1021/j100405a042.
(6) Worsnop, D. R.; Zahniser, M. S.; Kolb, C. E. Low-temperature absolute rate constants for the reaction of atomic sodium with ozone and nitrous oxide. *J. Phys. Chem.* **1991**, *95*, 3960-3964, doi:10.1021/j100163a014.
(7) Worsnop, D. R.; Zahniser, M. S.; Kolb, C. E. Correction: Low-temperature absolute rate constants for the reaction of atomic sodium with ozone and nitrous oxide. *J. Phys. Chem.* **1992**, *96*, 9088, doi:10.1021/j100201a074.
(8) Wright, T. G.; Ellis, A. M.; Dyke, J. M. A study of the products of the gas-phase reactions M + N_2O and M + O_3 and where M = Na or K with ultraviolet photoelectron spectroscopy. *J. Chem. Phys.* **1993**, *98*, 2891-2907, doi:10.1063/1.464117.

J2. **Na + N_2O.** The recommendation incorporates the data of Husain and Marshall,[4] Ager et al.,[1] Plane and Rajasekhar,[5] and Worsnop et al.[7] Silver and Kolb[6] measured a rate coefficient at 295 K that is lower and is superseded by Worsnop et al. Helmer and Plane[3] report a measurement at 300 K in excellent agreement with the recommendation. Subsequently, Gómez Martin et al.[2] measured the rate constant for the Na + N_2O reaction at 295, 300, and 320 K; these near room temperature results are also in "excellant agreement" with the recommended 298 K value. Earlier, less direct studies were discussed by Ager et al.[1] The NaO product does not react significantly with N_2O at room temperature [k(for Na + N_2 + O_2 products) ≤10^{-16} cm^3 $molecule^{-1}$ s^{-1} and k(for NaO_2 + N_2 products) ≤2 × 10^{-15} cm^3 $molecule^{-1}$ s^{-1} (Ager et al.)]. Wright et al. [8] used UV photoelectron spectroscopy to determine the product NaO is formed predominantly in the excited $^2\Sigma^+$ state.
(Table: 92-20, Note: 19-5, Evaluated: 19-5) Back to Table

(1) Ager, J. W., III; Talcott, C. L.; Howard, C. J. Gas phase kinetics of the reactions of Na and NaO with O_3 and N_2O. *J. Chem. Phys.* **1986**, *85*, 5584-5592, doi:10.1063/1.451573.
(2) Gómez Martin, J. C.; Garraway, S. A.; Plane, J. M. C. Reaction kinetics of meteoric sodium reservoirs in the upper atmosphere. *J. Phys. Chem. A* **2016**, *120*, 1330-1346, doi:10.1021/acs.jpca.5b00622.
(3) Helmer, M.; Plane, J. M. C. A study of the reaction NaO_2 + O ---> NaO + O_2: Implications for the chemistry of sodium in the upper atmosphere. *J. Geophys. Res.* **1993**, *98*, 23207-23222, doi:10.1029/93JD02033.
(4) Husain, D.; Marshall, P. Kinetic study of the absolute rate constant for the reaction between Na + N_2O in the temperature range 349-917 K by time-resolved atomic resonance absorption spectroscopy at lambda = 589 nm ($Na(3^2P_J)$ - $Na(3^2S_{1/2})$ following pulsed irradiation. *Combust. and Flame* **1985**, *60*, 81-87, doi:10.1016/0010-2180(85)90120-8.
(5) Plane, J. M. C.; Rajasekhar, B. Kinetic study of the reactions Na + O_2 + N_2 and Na + N_2O over an extended temperature range. *J. Phys. Chem.* **1989**, *93*, 3135-3140, doi:10.1021/j100345a051.
(6) Silver, J. A.; Kolb, C. E. Determination of the absolute rate constants for the room temperature reactions of atomic sodium with ozone and nitrous oxide. *J. Phys. Chem.* **1986**, *90*, 3263-3266, doi:10.1021/j100405a042.

(7) Worsnop, D. R.; Zahniser, M. S.; Kolb, C. E. Low-temperature absolute rate constants for the reaction of atomic sodium with ozone and nitrous oxide. *J. Phys. Chem.* **1991**, *95*, 3960-3964, doi:10.1021/j100163a014.
(8) Wright, T. G.; Ellis, A. M.; Dyke, J. M. A study of the products of the gas-phase reactions M + N_2O and M + O_3 and where M = Na or K with ultraviolet photoelectron spectroscopy. *J. Chem. Phys.* **1993**, *98*, 2891-2907, doi:10.1063/1.464117.

J3. **Na + Cl_2**. Two room temperature measurements of the rate coefficient for this reaction are in excellent agreement: Silver[1] and Talcott et al.[2] The recommended value is the average of these results.
(Table 87-41, Note: 87-41, Evaluated: 87-41) Back to Table

(1) Silver, J. A. Room temperature rate constant for the reaction of Na with Cl_2. *J. Chem. Phys.* **1986**, *84*, 4718-4720, doi:10.1063/1.450003.
(2) Talcott, C. L.; Ager, J. W., III; Howard, C. J. Gas phase studies of Na diffusion in He and Ar and kinetics of Na + Cl_2 and Na + SF_6. *J. Chem. Phys.* **1986**, *84*, 6161-6169, doi:10.1063/1.450757.

J4. **NaO + O**. The recommendation is based on measurements by Plane and Husain[3] and Griffin et al.[1] The Na + O_3 reaction produces NaO predominately in the low laying A $^2\Sigma^+$ state, which can radiatively and collisionally decay slowly to the X $^2\Pi$ ground state. The Plane and Husain[3] experiment was configured so that the predominant reactant was NaO X $^2\Pi$ while the Griffin et al.[1] experiment was designed to maximize NaO A $^2\Sigma^+$ concentrations. While the two states may not have identical reaction rate constants, their energy difference is small compared to reaction exothermicity and both states show reaction rate constants near the collisional limit. Since this reaction in the atmosphere will probably proceed through a mixture of the two lowest NaO electronic states and data are available at only one temperature for each state, the recommended rate constant is an average of the two measurements. Plane and Husain[3] reported that ~0.01 of the Na product is in the 3^2P excited state, while Griffin et al.[1] report a Na 3^2P product branching ratio of 0.14 ± 0.04. This difference is consistent with the orbital correlation predictions of products for reaction of each NaO state as presented by Herschbach et al.[2]
(Table: 06-2, Note: 06-2, Evaluated: 06-2) Back to Table

(1) Griffin, J.; Worsnop, D. R.; Brown, R. C.; Kolb, C. E.; Herschbach, D. R. Chemical kinetics of the NaO ($A^2\Sigma^+$) + O(^{3}P) reaction. *J. Phys. Chem. A* **2001**, *105*, 1643-1648, doi:10.1021/jp002641m.
(2) Herschbach, D. R.; Kolb, C. E.; Worsnop, D. R.; Shi, X. Excitation mechanism of the mesospheric sodium nightglow. *Nature* **1992**, *356*, 414-416, doi:10.1038/356414a0.
(3) Plane, J. M. C.; Husain, D. Determination of the absolute rate constant for the reaction O + NaO → Na + O_2 by time-resolved atomic chemiluminescence at λ = 589 nm [Na($3\ ^2P_J$) → Na($3\ ^2S_{1/2}$) + hν]. *J. Chem. Soc. Faraday Trans. 2* **1986**, *82*, 2047-2052, doi:10.1039/f29868202047.

J5. **NaO + O_3.** This reaction was studied by Silver and Kolb,[3] Ager et al.,[1] and Plane et al.,[2] who agree on the rate coefficient and branching ratio. This agreement may be fortuitous because Silver and Kolb used an indirect method and an analysis based on their rate coefficient for the Na + O_3 reaction, which is about 1/2 of the recommended value. Ager et al. employed a somewhat more direct measurement, but the study is complicated by a chain reaction mechanism in the Na/O_3 system. Plane et al. reported rate coefficient measurements for the NaO_2 + O_2 product channel over the temperature range 207–377 K using pulsed photolysis LIF methods. The recommendation for that channel is based on all three studies, and the recommendation for the Na + $2O_2$ channel is based upon the results of Silver and Kolb and Ager et al. The latter reaction channel may also have a significant temperature dependence.
(Table: 25-1, Note: 94-26, Evaluated: 25-1) Back to Table

(1) Ager, J. W., III; Talcott, C. L.; Howard, C. J. Gas phase kinetics of the reactions of Na and NaO with O_3 and N_2O. *J. Chem. Phys.* **1986**, *85*, 5584-5592, doi:10.1063/1.451573.
(2) Plane, J. M. C.; Nien, C.-F.; Allen, M. R.; Helmer, M. A kinetic investigation of the reactions Na + O_3 and NaO + O_3 over the temperature range 207-377 K. *J. Phys. Chem.* **1993**, *97*, 4459-4467, doi:10.1021/j100119a033.
(3) Silver, J. A.; Kolb, C. E. Determination of the absolute rate constants for the room temperature reactions of atomic sodium with ozone and nitrous oxide. *J. Phys. Chem.* **1986**, *90*, 3263-3266, doi:10.1021/j100405a042.

J6. **NaO + H_2.** The prior recommendation was based on two 297 K and one 294 K measurements by Ager and Howard[1] who reported the NaOH + H product channel rate constant. They also reported evidence of a Na + H_2O product channel and that a small fraction of the Na from this channel is in the 3^2P excited state. Using direct mass spectral measurements of both NaO depletion and NaOH production in their flow reactor Gómez

Martin et al.[2] demonstrated that the Na + H_2O product channel is minor with a branching ratio estimate of (1.02 ± 0.14)%. They reported NaO + H_2 → NaOH + H rate constant measurements at 266 and 310 K that are ~5 times lower than Ager and Howard's three earlier measurements at 297, 297, and 294 K. Ager and Howard reported an averaged room temperature rate constant of (2.6 ± 1.0) × 10^{-11} cm^3 $molecule^{-1}$ s^{-1} compared to (4.9 ± 1.2) × 10^{-12} cm^3 $molecule^{-1}$ s^{-1} at 310 K and (6.0 ± 3.0) × 10^{-12} cm^3 $molecule^{-1}$ s^{-1} at 266 K reported by Gómez Martin et al. Gómez Martin et al. discuss possible reasons for the large discrepancy, but do not identify definative problems with either group's experiments. Because of the large unexplained discrepancy between the Ager and Howard and Gómez Martin et al. studies, no recommendation is given for this reaction.
(Table 19-5, Note: 19-5, Evaluated: 19-5) Back to Table

(1) Ager, J. W., III; Howard, C. J. Gas phase kinetics of the reactions of NaO with H_2, D_2, H_2O, and D_2O. *J. Chem. Phys.* **1987**, *87*, 921-925, doi:10.1063/1.453726.
(2) Gómez Martin, J. C.; Garraway, S. A.; Plane, J. M. C. Reaction kinetics of meteoric sodium reservoirs in the upper atmosphere. *J. Phys. Chem. A* **2016**, *120*, 1330-1346, doi:10.1021/acs.jpca.5b00622.

J7. **NaO + H_2O.** The prior recommendation was based on a room temperature (298 ± 1 K) measurement of (2.2 ± 0.4) × 10^{-10} cm^3 $molecule^{-1}$ s^{-1} by Ager and Howard[1] and a temperature dependent measurement by Cox and Plane[2] with the more extensive temperature dependent data favored. Cox and Plane's near room temperature (310 K) rate constants are (9.8 ± 2.4) and (9.3 ± 1.0) × 10^{-11} cm^3 $molecule^{-1}$ s^{-1}. While Gómez Martin et al.[3] reported a 310 K rate constant value of (2.4 ± 0.6) × 10^{-10} cm^3 $molecule^{-1}$ s^{-1}; in excellent agreement with Ager and Howard[1] and poor agreement with Cox and Plane.[2] Gómez Martin et al. discuss potential reasons for the discrepency with the earlier measurement and conclude their latter result is more likely to be correct. After reviewing the results of all three studies, they recommend a near room temperature value of k(300–310 K) = (2.3 ± 0.5) × 10^{-10} cm^3 $molecule^{-1}$ s^{-1} and an Arrhenius temperature dependence determined by a 2 kJ activation energy: k(260–716 K) = 5.06 × 10^{-10} exp (–240/T) cm^3 $molecule^{-1}$ s^{-1}; which is adopted here.
(Table: 19-5, Note: 19-5, Evaluated: 19-5) Back to Table

(1) Ager, J. W., III; Howard, C. J. Gas phase kinetics of the reactions of NaO with H_2, D_2, H_2O, and D_2O. *J. Chem. Phys.* **1987**, *87*, 921-925, doi:10.1063/1.453726.
(2) Cox, R. M.; Plane, J. M. C. An experimental and theoretical study of the reactions NaO + H_2O(D_2O) → NaOH(D) + OH(OD). *Phys. Chem, Chem. Phys.* **1999**, *1*, 4713-4720, doi:10.1039/A905601G.
(3) Gómez Martin, J. C.; Garraway, S. A.; Plane, J. M. C. Reaction kinetics of meteoric sodium reservoirs in the upper atmosphere. *J. Phys. Chem. A* **2016**, *120*, 1330-1346, doi:10.1021/acs.jpca.5b00622.

J8. **NaO + NO.** The recommendation is based on an indirect measurement reported by Ager et al.[1]
(Table 25-1, Note: 87-41, Evaluated: 25-1) Back to Table

(1) Ager, J. W., III; Talcott, C. L.; Howard, C. J. Gas phase kinetics of the reactions of Na and NaO with O_3 and N_2O. *J. Chem. Phys.* **1986**, *85*, 5584-5592, doi:10.1063/1.451573.

J9. **NaO + CO.** Two flow reactor studies have published room temperature rate constant measurements. Kolb et al.[2] reported k(294 K) = (2.1 ± 0.5) × 10^{-10} cm^3 $molecule^{-1}$ s^{-1} and 26 years later Gómez Martin et al.[1] reported k(300 K) = (1.2 ± 0.4) × 10^{-10} cm^3 $molecule^{-1}$ s^{-1}. These results overlap within their estimated errors. An averaged rate constant of k(294–300 K) = (1.6 ± 0.5) × 10^{-10} cm^3 $molecule^{-1}$ s^{-1} is recommended.
(Table 19-5, Note: 19-5, Evaluated: 19-5) Back to Table

(1) Gómez Martin, J. C.; Garraway, S. A.; Plane, J. M. C. Reaction kinetics of meteoric sodium reservoirs in the upper atmosphere. *J. Phys. Chem. A* **2016**, *120*, 1330-1346, doi:10.1021/acs.jpca.5b00622.
(2) Kolb, C. E.; Worsnop, D. R.; Zahniser, M. S.; Robinson, G. N.; Shi, X.; Herschbach, D. R. Chemical kinetics and dynamics of the mesopheric sodium nightglow. In *Gas Phase Metal Reactions*; Fontijn, A., Ed.; Elsevier: Amsterdam, The Netherlands, 1992; pp 15-27.

J10. **NaO + HCl.** There is only one indirect measurement of the rate coefficient for this reaction, that from the study by Silver et al.[1] They indicate that the products are NaCl and OH, although some NaOH and Cl production is not ruled out.
(Table: 25-1, Note: 85-37, Evaluated: 25-1) Back to Table

(1) Silver, J. A.; Stanton, A. D.; Zahniser, M. S.; Kolb, C. E. Gas-phase reaction rate of sodium hydroxide with hydrochloric acid. *J. Phys. Chem.* **1984**, *88*, 3123-3129, doi:10.1021/j150658a041.

J11. **NaO_2 + O.** The recommendation is based on a flow tube study at 300 K by Helmer and Plane.[1]
(Table: 25-1, Note: 94-26, Evaluated: 25-1) Back to Table

(1) Helmer, M.; Plane, J. M. C. A study of the reaction NaO_2 + O ---> NaO + O_2: Implications for the chemistry of sodium in the upper atmosphere. *J. Geophys. Res.* **1993**, *98*, 23207-23222, doi:10.1029/93JD02033.

J12. NaO_2 + NO. This reaction is endothermic. The upper limit recommended is from an experimental study by Ager et al.[1]
(Table 87-41, Note: 87-41, Evaluated: 87-41) Back to Table

(1) Ager, J. W., III; Talcott, C. L.; Howard, C. J. Gas phase kinetics of the reactions of Na and NaO with O_3 and N_2O. *J. Chem. Phys.* **1986**, *85*, 5584-5592, doi:10.1063/1.451573.

J13. NaO_2 + HCl. The recommendation is based on a measurement reported by Silver and Kolb.[1] They indicated that the products are NaCl + HO_2, but NaOOH + Cl may be possible products.
(Table 25-1, Note: 25-1, Evaluated: 87-41) Back to Table

(1) Silver, J. A.; Kolb, C. E. Gas-phase reaction rate of sodium superoxide with hydrochloric acid. *J. Phys. Chem.* **1986**, *90*, 3267-3269, doi:10.1021/j100405a043.

J14. NaOH + H. Gómez Martin et al.[1] report fast flow reactor measurements, presenting 12 measurements at 298 K and one at 230 K, with no evidence of significant temperature dependence. The weighted average of all measurements, including two sigma error estimates, is $k(230–298\ K) = (3.8 \pm 0.8) \times 10^{-11}$ cm^3 molecule^{-1} s^{-1}.
(Table 19-5, Note: 19-5, Evaluated: 19-5) Back to Table

(1) Gómez Martin, J. C.; Seaton, C.; de Miranda, M. P.; Plane, J. M. C. The reaction between sodium hydoxide and atomic hydrogen in atmospheric and flame chemistry. *J. Phys. Chem. A* **2017**, *121*, 7667-7674, doi:10.1021/acs.jpca.7b07808.

J15. NaOH + HCl. The recommendation is based on the study by Silver et al.,[1] which is the only published study of this reaction.
(Table: 25-1, Note: 85-37, Evaluated: 25-1) Back to Table

(1) Silver, J. A.; Stanton, A. D.; Zahniser, M. S.; Kolb, C. E. Gas-phase reaction rate of sodium hydroxide with hydrochloric acid. *J. Phys. Chem.* **1984**, *88*, 3123-3129, doi:10.1021/j150658a041.

J16. $NaHCO_3$ + H. The recommendation is based on measurements at 307 and 227 K by Cox et al.[2] Ager and Howard[1] did not observe this reaction and Cox et al. estimated k(300 K) to be $<2 \times 10^{-12}$ cm^3 molecule^{-1} s^{-1} from the Ager and Howard results.
(Table: 25-1, Note: 25-1, Evaluated: 25-1) Back to Table

(1) Ager, J. W., III; Howard, C. J. Rate coefficient for the gas phase reaction of NaOH with CO_2. *J. Geophys. Res.* **1987**, *92*, 6675-6678, doi:10.1029/JD092iD06p06675.
(2) Cox, R. M.; Self, D. E.; Plane, J. M. C. A study of the reaction between $NaHCO_3$ and H: Apparent closure on the chemistry of mesospheric Na. *J. Geophys. Res.* **2001**, *106*, 1733-1739, doi:10.1029/2000JD900579.

1.15.3 Bibliography – Metal Reactions

Ager, J. W., III; Howard, C. J. Gas phase kinetics of the reactions of NaO with H_2, D_2, H_2O, and D_2O. *J. Chem. Phys.* **1987**, *87*, 921-925, doi:10.1063/1.453726.

Ager, J. W., III; Howard, C. J. Rate coefficient for the gas phase reaction of NaOH with CO_2. *J. Geophys. Res.* **1987**, *92*, 6675-6678, doi:10.1029/JD092iD06p06675.

Ager, J. W., III; Talcott, C. L.; Howard, C. J. Gas phase kinetics of the reactions of Na and NaO with O_3 and N_2O. *J. Chem. Phys.* **1986**, *85*, 5584-5592, doi:10.1063/1.451573.

Cox, R. M.; Plane, J. M. C. An experimental and theoretical study of the reactions NaO + $H_2O(D_2O)$ → NaOH(D) + OH(OD). *Phys. Chem, Chem. Phys.* **1999**, *1*, 4713-4720, doi:10.1039/A905601G.

Cox, R. M.; Self, D. E.; Plane, J. M. C. A study of the reaction between $NaHCO_3$ and H: Apparent closure on the chemistry of mesospheric Na. *J. Geophys. Res.* **2001**, *106*, 1733-1739, doi:10.1029/2000JD900579.

Gómez Martin, J. C.; Garraway, S. A.; Plane, J. M. C. Reaction kinetics of meteoric sodium reservoirs in the upper atmosphere. *J. Phys. Chem. A* **2016**, *120*, 1330-1346, doi:10.1021/acs.jpca.5b00622.

Gómez Martin, J. C.; Seaton, C.; de Miranda, M. P.; Plane, J. M. C. The reaction between sodium hydoxide and atomic hydrogen in atmospheric and flame chemistry. *J. Phys. Chem. A* **2017**, *121*, 7667-7674, doi:10.1021/acs.jpca.7b07808.

Griffin, J.; Worsnop, D. R.; Brown, R. C.; Kolb, C. E.; Herschbach, D. R. Chemical kinetics of the NaO ($A^2\Sigma^+$) + O(^{3}P) reaction. *J. Phys. Chem. A* **2001**, *105*, 1643-1648, doi:10.1021/jp002641m.

Helmer, M.; Plane, J. M. C. A study of the reaction NaO_2 + O ---> NaO + O_2: Implications for the chemistry of sodium in the upper atmosphere. *J. Geophys. Res.* **1993**, *98*, 23207-23222, doi:10.1029/93JD02033.

Herschbach, D. R.; Kolb, C. E.; Worsnop, D. R.; Shi, X. Excitation mechanism of the mesospheric sodium nightglow. *Nature* **1992**, *356*, 414-416, doi:10.1038/356414a0.

Husain, D.; Marshall, P. Kinetic study of the absolute rate constant for the reaction between Na + N_2O in the temperature range 349-917 K by time-resolved atomic resonance absorption spectroscopy at lambda = 589 nm (Na(3^2P_J) - Na($3^2S_{1/2}$) following pulsed irradiation. *Combust. and Flame* **1985**, *60*, 81-87, doi:10.1016/0010-2180(85)90120-8.

Husain, D.; Marshall, P.; Plane, J. M. C. Determination of the absolute 2nd order rate constant for the reaction Na + O_3 → NaO + O_2. *J. Chem. Soc. Chem. Comm.* **1985**, 1216-1218, doi:10.1039/C39850001216.

Kolb, C. E.; Worsnop, D. R.; Zahniser, M. S.; Robinson, G. N.; Shi, X.; Herschbach, D. R. Chemical kinetics and dynamics of the mesopheric sodium nightglow. In *Gas Phase Metal Reactions*; Fontijn, A., Ed.; Elsevier: Amsterdam, The Netherlands, 1992; pp 15-27.

Plane, J. M. C.; Husain, D. Determination of the absolute rate constant for the reaction O + NaO → Na + O_2 by time-resolved atomic chemiluminescence at λ = 589 nm [Na($3\ ^2P_J$) → Na($3\ ^2S_{1/2}$) + hν]. *J. Chem. Soc. Faraday Trans. 2* **1986**, *82*, 2047-2052, doi:10.1039/f29868202047.

Plane, J. M. C.; Nien, C.-F.; Allen, M. R.; Helmer, M. A kinetic investigation of the reactions Na + O_3 and NaO + O_3 over the temperature range 207-377 K. *J. Phys. Chem.* **1993**, *97*, 4459-4467, doi:10.1021/j100119a033.

Plane, J. M. C.; Rajasekhar, B. Kinetic study of the reactions Na + O_2 + N_2 and Na + N_2O over an extended temperature range. *J. Phys. Chem.* **1989**, *93*, 3135-3140, doi:10.1021/j100345a051.

Shi, X.; Herschbach, D. R.; Worsnop, D. R.; Kolb, C. E. Molecular beam chemistry: Magnetic deflection analysis of monoxide electronic states from alkali-metal atom + ozone reactions. *J. Phys. Chem.* **1993**, *97*, 2113-2122, doi:10.1021/j100112a010.

Silver, J. A. Room temperature rate constant for the reaction of Na with Cl_2. *J. Chem. Phys.* **1986**, *84*, 4718-4720, doi:10.1063/1.450003.

Silver, J. A.; Kolb, C. E. Determination of the absolute rate constants for the room temperature reactions of atomic sodium with ozone and nitrous oxide. *J. Phys. Chem.* **1986**, *90*, 3263-3266, doi:10.1021/j100405a042.

Silver, J. A.; Kolb, C. E. Gas-phase reaction rate of sodium superoxide with hydrochloric acid. *J. Phys. Chem.* **1986**, *90*, 3267-3269, doi:10.1021/j100405a043.

Silver, J. A.; Stanton, A. D.; Zahniser, M. S.; Kolb, C. E. Gas-phase reaction rate of sodium hydroxide with hydrochloric acid. *J. Phys. Chem.* **1984**, *88*, 3123-3129, doi:10.1021/j150658a041.

Talcott, C. L.; Ager, J. W., III; Howard, C. J. Gas phase studies of Na diffusion in He and Ar and kinetics of Na + Cl_2 and Na + SF_6. *J. Chem. Phys.* **1986**, *84*, 6161-6169, doi:10.1063/1.450757.

Worsnop, D. R.; Zahniser, M. S.; Kolb, C. E. Low-temperature absolute rate constants for the reaction of atomic sodium with ozone and nitrous oxide. *J. Phys. Chem.* **1991**, *95*, 3960-3964, doi:10.1021/j100163a014.

Worsnop, D. R.; Zahniser, M. S.; Kolb, C. E. Correction: Low-temperature absolute rate constants for the reaction of atomic sodium with ozone and nitrous oxide. *J. Phys. Chem.* **1992**, *96*, 9088, doi:10.1021/j100201a074.

Wright, T. G.; Ellis, A. M.; Dyke, J. M. A study of the products of the gas-phase reactions M + N_2O and M + O_3 and where M = Na or K with ultraviolet photoelectron spectroscopy. *J. Chem. Phys.* **1993**, *98*, 2891-2907, doi:10.1063/1.464117.

SECTION 2. TERMOLECULAR REACTIONS

Table of Contents

SECTION 2. TERMOLECULAR REACTIONS 2-1
2.1 Introduction 2-1
2.2 Low-Pressure-Limiting Rate Constant, k^x_o(T) 2-3
2.3 Temperature Dependence of Low–Pressure Limiting Rate Constants: $(298/T)^n$ 2-3
2.4 High-Pressure-Limit Rate Constants, k_∞(T) 2-3
2.5 Temperature Dependence of High-Pressure-Limiting Rate Constants: $(298/T)^m$ 2-4
2.6 Uncertainty Estimates 2-4
2.7 Notes for Table 2-1: Termolecular Reactions 2-10
2.8 Notes for Table 2-2: Chemical Activation Reactions 2-56
2.9 Bibliography – Termolecular Reactions 2-65

Tables

Table 2-1 Rate Constants for Termolecular Reactions 2-5
Table 2-2 Rate Constants for Chemical Activation Reactions 2-55

2.1 Introduction

Recombination rate constants for simple association reactions of the type A + B ↔ [AB]* $\xrightarrow{M}$ AB (where the asterisk denotes rovibrational excitation) are pressure dependent. The low-pressure-limiting rate constants are given in the form:

$$k_0(T) = k_0^{298}\left(\frac{298}{T}\right)^n \text{ cm}^6 \text{ molecule}^{-2} \text{ s}^{-1}, \quad (2.1)$$

(where k_0^{298} has been adjusted for air as the third body). The limiting high-pressure rate constant is given in a similar form:

$$k_\infty(T) = k_\infty^{298}\left(\frac{298}{T}\right)^m \text{ cm}^3 \text{ molecule}^{-1} \text{ s}^{-1}. \quad (2.2)$$

To obtain the effective second-order rate constant for a given condition of temperature and pressure (altitude), the following formula is used:

$$k_f(T,[M]) = \left\{\frac{k_\infty(T)k_0(T)[M]}{k_\infty(T)+k_0(T)[M]}\right\} 0.6^{\left\{1+\left[log_{10}\left(\frac{k_0(T)[M]}{k_\infty(T)}\right)\right]^2\right\}^{-1}} \quad (2.3)$$

where [*M*] is the total gas concentration. The fixed value 0.6 that appears in this formula fits the data for all listed reactions adequately, although in principle this quantity is temperature-dependent and may be different for each reaction. However, there are rarely sufficient data to accommodate additional parameters. The four parameters, k_o(298 K), *n*, k_∞(298 K), and *m* are given in Table 2.1 for simple association reactions.

Some association reactions produce not only the recombination product, but additional products that appear to originate from a simple bimolecular reaction. For example, the reaction between OH and CO produces not only HOCO, the recombination product, but also H and CO_2, which resemble the products of a simple metathesis reaction. This is an example of a **chemical activation reaction**, which takes place on a potential energy surface that includes HOCO*, the rovibrationally excited free radical intermediate. The reactions involving this intermediate can be described with the following reaction scheme:

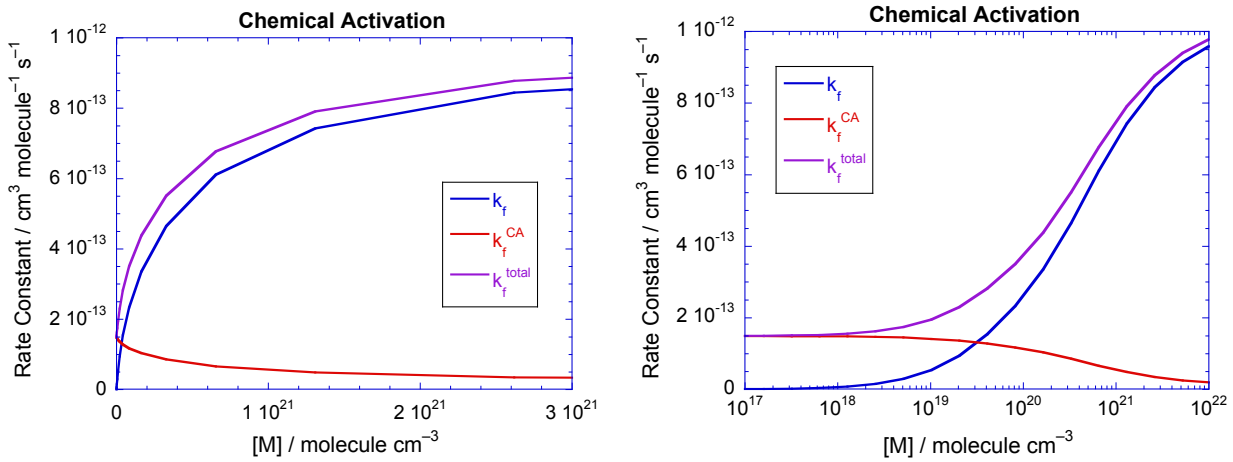
Chemical Activation

$$OH + CO \overset{(a,-a)}{\Longleftrightarrow} HOCO^* \xrightarrow{(b)} H + CO_2$$

$$M \downarrow (c)$$

$$HOCO$$

The net loss of reactants is thus the sum of two pressure-dependent processes, an association to yield HOCO and the chemical activation process yielding H and CO_2. In the limit of zero pressure (i.e., [M] = 0), the only products are H + CO_2. The yield of H + CO_2 is diminished and the yield of HOCO is increased as the pressure rises. In the limit of very high pressure, the only product is HOCO. The pressure-dependent rate constants are shown here in two common formats:



Figures: Two common formats showing the same chemical reaction rate constants as functions of pressure for a chemical activation system.

The chemical activation reaction scheme illustrated above is the basis for a model[1,2,5] that describes the contributions from the two coupled processes:

1) Eq. 2.3 ($k_f(T,[M])$) for the association reaction (e.g. for producing HOCO). This is the same expression that is used for simple association reactions.

2) Eq. 2.4 $k_f^{CA}(T,[M])$ for the formation of the "chemical activation products" (e.g. for producing H + CO_2):

$$k_f^{CA}(T,[M]) = k_{int}(T)\left[1 - \frac{k_f(T,[M])}{k_\infty(T)}\right] \tag{2.4}$$

where $k_{int}(T)$ is the second order rate constant at $[M] = 0$ (i.e., the zero-pressure intercept) given by the Arrhenius expression in Eq. 2.5.

$$k_{int}(T) = A\ exp(-B/T) \tag{2.5}$$

The total rate constant for loss of reactants is given by Eq. 2.6:

$$k_f^{total}(T,[M]) = k_f(T,[M]) + k_f^{CA}(T,[M]) \tag{2.6}$$

The six parameters, k_o(298 K), n, k_∞(298 K), m, A, and B, are listed in Table 2.2 for chemical activation systems.

The discussion that follows outlines the general methods we have used in establishing this table, and the notes to the table discuss specific data sources. Recent advances in theory have allowed direct calculation of rate constants for some reactions using RRKM/Master Equation methods.

2.2 Low-Pressure-Limiting Rate Constant, $k^x_o(T)$

Troe[4] has described a simple method for obtaining low-pressure-limiting rate constants. In essence this method depends on the definition:

$$k_o^x(T) \equiv \beta_x k_{o,sc}^x \tag{2.7}$$

Here sc signifies "strong" collisions, x denotes the bath gas, and β_x is an efficiency parameter ($0 < \beta_x < 1$), which provides a measure of energy transfer. The strong collision rate constant can be calculated with some accuracy from knowledge of molecular parameters available from experiment and more from theory.

The coefficient β_x is related to the average energy transferred in a collision with gas x, $\langle \Delta E \rangle_x$, via:

$$\frac{\beta_x}{\left(1-\sqrt{\beta_x}\right)} = \frac{\langle \Delta E \rangle_x}{F_E kT} \tag{2.8}$$

Notice that $\langle \Delta E \rangle$ is quite sensitive to β. F_E is the correction factor of the energy dependence of the density of states (a quantity of the order of 1.1 for most species of stratospheric interest).

For some of the reactions of possible stratospheric interest reviewed here, there exist data in the low-pressure limit (or very close thereto), and we have chosen to evaluate and unify this data by calculating $k_o^x(T)$ for the appropriate bath gas x and computing the value of β_x corresponding to the experimental value.[4] A compilation[3] gives details for many of the reactions considered here.

From the β_x values (most of which are for N_2, i.e., β_{N2}), we compute $\langle \Delta E \rangle_X$ according to the above equation. Values of $\langle \Delta E \rangle_{N2}$ of approximately 0.3–1 kcal mole^{-1} are generally expected. If multiple data exist, we average the values of $\langle \Delta E \rangle_{N2}$ and recommend a rate constant corresponding to the β_{N2} computed in the equation above.

Master equation calculations allow direct calculation of low-pressure rate constants and of β_x.

Where no data exist, we have sometimes estimated the low-pressure rate constant by taking $\beta_{N2} = 0.3$ at T = 298 K, a value based on those cases where data exist.

2.3 Temperature Dependence of Low–Pressure Limiting Rate Constants: $(298/T)^n$

The value of *n* recommended here comes from measurements or, in some cases, a calculation of $\langle \Delta E \rangle_{N2}$ from the data at 298 K, and a computation of $\beta_{N2}(200\ K)$ assuming that $\langle \Delta E \rangle_{N2}$ is independent of temperature in this range. This $\beta_{N2}(200\ K)$ value is combined with the computed value of $k_o^{sc}(200\ K)$ to give the expected value of the actual rate constant at 200 K. This latter, in combination with the value at 298 K, yields the value of ***n***.

This procedure can be directly compared with measured values of $k_o(200\ K)$ when those exist. Unfortunately, very few values at 200 K are available. There are often temperature-dependent studies, but some ambiguity exists when one attempts to extrapolate these down to 200 K. If data are to be extrapolated beyond the measured temperature range, a choice must be made as to the functional form of the temperature dependence.

There are two general ways of expressing the temperature dependence of rate constants. Either the Arrhenius expression:

$$k_o(T) = A \exp(-E/RT) \tag{2.9}$$

or the form:

$$k_o(T) = A' T^{-n} \tag{2.10}$$

is employed. Neither of these extrapolation techniques is soundly based, and since they often yield values that differ substantially, we have used the power law expression above as the basis of our recommendations.

2.4 High-Pressure-Limit Rate Constants, $k_\infty(T)$

High-pressure rate constants can often be obtained experimentally, but those for the relatively small species of stratospheric importance usually reach the high-pressure limit at inaccessibly high pressures. This leaves two sources

of these numbers, the first being estimates based upon theory, and the second being extrapolation of fall-off data up to higher pressures.

Stratospheric conditions generally render reactions of interest much closer to the low-pressure limit and thus are fairly insensitive to the high-pressure value. This means that while the extrapolation is long, and the value of $k_\infty(T)$ is often not very accurate, a "reasonable guess" of $k_\infty(T)$ will then suffice. In a few cases, we have declined to guess since the low-pressure limit is effective over the entire range of stratospheric conditions.

2.5 Temperature Dependence of High-Pressure-Limiting Rate Constants: $(298/T)^m$

Commonly, there are very few data upon which to base a recommendation for values of m. Values in Tables 2.1 and 2.2 are often estimated, based on models for the transition state of bond-association reactions and whatever data are available. In general, the temperature dependence of these rate constants is expected to be small.

2.6 Uncertainty Estimates

For three-body reactions (Tables 2.1 and 2.2) uncertainties are assigned using a procedure that is analogous to that employed for bimolecular reactions in Table 1-1. Values of $f(298\ K)$ are given for these rate constants at room temperature and assumed to be valid at all pressures. The additional uncertainty arising from the temperature extrapolation is expressed with a g-factor as in Table 1-1. Given that uncertainties for an expression with four parameters are expressed with only two parameters, a certain amount of arbitrariness is involved in their choice.

(1) Larson, C. W.; Stewart, R. H.; Golden, D. M. Pressure and temperature dependence of reactions proceeding via a bound complex. An approach for combustion and atmospheric chemistry modelers. Application to HO + CO → [HOCO] → H + CO_2. *Int. J. Chem. Kinet.* **1988**, *20*, 27-40, doi:10.1002/kin.550200105.

(2) Papadimitriou, V. C.; Karafas, E. S.; Gierczak, T.; Burkholder, J. B. $CH_3CO + O_2 + M$ (M = He, N_2) reaction rate coefficient measurements and implications for the OH radical product yield. *J. Phys. Chem. A* **2015**, *119*, 7481–7497, doi:10.1021/acs.jpca.5b00762.

(3) Patrick, R.; Golden, D. M. Third-order rate constants of atmospheric importance. *Int. J. Chem. Kinet.* **1983**, *15*, 1189-1227, doi:10.1002/kin.550151107.

(4) Troe, J. Theory of thermal unimolecular reactions at low pressures. I. Solutions of the master equation. *J. Chem. Phys.* **1977**, *66*, 4745-4757, doi:10.1063/1.433837.

(5) Tyndall, G. S.; Orlando, J. J.; Wallington, T. J.; Hurley, M. D. Pressure dependence of the rate coefficients and product yields for the reaction of CH_3CO radicals with O_2. *Int. J. Chem. Kinet.* **1997**, *29*, 655-663, doi:10.1002/(SICI)1097-4601(1997)29:9<655::AID-KIN2>3.0.CO;2-T.

Table 2-1 Rate Constants for Termolecular Reactions

Reaction	Low-Pressure Limit [a] $k_o(T) = k_o^{298}(T/298)^{-n}$		High-Pressure Limit [b] $k_\infty(T) = k_\infty^{298}(T/298)^{-m}$		k(T,[M])	*f*(298 K)	*g*	Note
	k_o^{300}	n	k_∞^{300}	m	298 K, 1 Atm			
O_x Reactions								
$O + O_2 \xrightarrow{M} O_3$	6.1×10^{-34}	2.4	–	–	1.5×10^{-14}	1.1	50	A1
$O(^1D)$ Reactions								
$O(^1D) + N_2 \xrightarrow{M} N_2O$	2.8×10^{-36}	0.9	–	–	6.9×10^{-17}	1.3	75	A2
HO_x Reactions								
$H + O_2 \xrightarrow{M} HO_2$	5.3×10^{-32}	1.8	9.5×10^{-11}	–0.4	1.15×10^{-12}	1.2	0	B1
$OH + OH \xrightarrow{M} H_2O_2$	6.9×10^{-31}	1.0	2.6×10^{-11}	0	6.3×10^{-12}	1.5	100	B2
NO_x Reactions								
$O + NO \xrightarrow{M} NO_2$	9.1×10^{-32}	1.5	3.0×10^{-11}	0.0	1.7×10^{-12}	1.2	100	C1
$O + NO_2 \xrightarrow{M} NO_3$	(See Table 2.2)							
$OH + NO \xrightarrow{M} HONO$	7.1×10^{-31}	2.6	3.6×10^{-11}	0.1	7.4×10^{-12}	1.2	50	C2
$OH + NO_2 \xrightarrow{M} HONO_2$	1.8×10^{-30}	3.0	2.8×10^{-11}	0	1.1×10^{-11}	1.3	100	C3
$\xrightarrow{M} HOONO$	9.3×10^{-32}	3.9	4.2×10^{-11}	0.5	1.8×10^{-12}	1.5	200	
$HO_2 + NO \xrightarrow{M} HONO_2$	(See Note)							C4
$HO_2 + NO_2 \xrightarrow{M} HO_2NO_2$	1.9×10^{-31}	3.4	4.0×10^{-12}	0.3	1.3×10^{-12}	1.06	400	C5
$NO_2 + NO_3 \xrightarrow{M} N_2O_5$	2.4×10^{-30}	3.0	1.6×10^{-12}	–0.1	1.3×10^{-12}	1.1	100	C6
$NO_3 \xrightarrow{M} NO + O_2$	(See Note)							C7
Hydrocarbon Reactions								
$OH + CO \xrightarrow{M} HOCO$ $\xrightarrow{M} H + CO_2$	(See Table 2.2)							
$CH_3 + O_2 \xrightarrow{M} CH_3O_2$	4.1×10^{-31}	3.6	1.2×10^{-12}	-1.1	8.1×10^{-13}	1.1	50	D1
$CH_3CH_2 + O_2 \xrightarrow{M} CH_3CH_2O_2$	(See Table 2.2)							
$OH + C_2H_2 \xrightarrow{M} HOCHCH$	5.5×10^{-30}	0.0	8.3×10^{-13}	–2	7.56×10^{-13}	1.1	50	D2

Reaction	Low-Pressure Limit [a] $k_o(T) = k_o^{298}(T/298)^{-n}$		High-Pressure Limit [b] $k_\infty(T) = k_\infty^{298}(T/298)^{-m}$		k(T,[M])	*f*(298 K)	*g*	Note
	k_o^{300}	n	k_∞^{300}	m	298 K, 1 Atm			
$OH + C_2H_4 \xrightarrow{M} HOCH_2CH_2$	1.1×10^{-28}	3.5	8.5×10^{-12}	1.75	7.9×10^{-12}	1.15	90	D3
$OH + CH_2{=}CHCH_3 \xrightarrow{M} HOC_3H_6$	4.7×10^{-27}	4	2.6×10^{-11}	1.3	2.5×10^{-11}	1.2	50	D4
OH + iso-Butene $\xrightarrow{M}$ Products	–	–	5.5×10^{-11}	1.4	5.5×10^{-11}	1.2	200	D5
OH + 1-Butene $\xrightarrow{M}$ Products	–	–	3.2×10^{-11}	1.4	3.2×10^{-11}	1.1	50	D6
OH + cis-2-Butene $\xrightarrow{M}$ Products	–	–	5.5×10^{-11}	1.2	5.5×10^{-11}	1.1	50	D7
OH + trans-2-Butene $\xrightarrow{M}$ Products	–	–	7.0×10^{-11}	1.2	7.0×10^{-11}	1.1	50	D8
$CH_3O + NO \xrightarrow{M} CH_3ONO$	2.3×10^{-29}	2.8	3.8×10^{-11}	0.6	2.9×10^{-11}	1.3	100	D9
$CH_3O + NO_2 \xrightarrow{M} CH_3ONO_2$	5.5×10^{-29}	4.4	1.9×10^{-11}	1.8	1.7×10^{-11}	1.1	0	D10
$C_2H_5O + NO \xrightarrow{M} C_2H_5ONO$	2.9×10^{-27}	4.0	5.0×10^{-11}	0.2	4.8×10^{-11}	1.2	50	D11
$C_2H_5O + NO_2 \xrightarrow{M} C_2H_5ONO_2$	2.1×10^{-27}	4.0	2.8×10^{-11}	1.0	2.7×10^{-11}	1.1	100	D12
$CH_3O_2 + NO_2 \xrightarrow{M} CH_3O_2NO_2$	1.0×10^{-30}	4.8	7.3×10^{-12}	2.1	3.8×10^{-12}	1.5	100	D13
$C_2H_5O_2 + NO_2 \xrightarrow{M} C_2H_5O_2NO_2$	1.2×10^{-29}	4.0	9.0×10^{-12}	0.0	7.5×10^{-12}	1.3	50	D14
$CH_3C(O)O_2 + NO_2 \xrightarrow{M} CH_3C(O)O_2NO_2$	7.3×10^{-29}	4.1	9.5×10^{-12}	1.6	8.7×10^{-12}	1.1	0	D15
$CH_3CH_2C(O)O_2 + NO_2 \xrightarrow{M} CH_3CH_2C(O)O_2NO_2$	9.6×10^{-28}	8.9	7.7×10^{-12}	0.2	7.4×10^{-12}	2.0	100	D16
$CH_3C(O)CH_2 + O_2 \xrightarrow{M} CH_3C(O)CH_2O_2$	3×10^{-29}		1.0×10^{-12}		9.4×10^{-13}	1.3		D17
$CH_2OO + CH_2OO \rightarrow$ Products (See Note)	0	0	7×10^{-11}	0	7.0×10^{-11}	1.5	100	D18
$OH + HCN \xrightarrow{M} HC(OH)N$	6.1×10^{-33}	1.5	9.8×10^{-15}	-4.6	7.4×10^{-15}	1.25	0	D19
FO_x Reactions								
$F + O_2 \xrightarrow{M} FO_2$	5.9×10^{-33}	1.7	1.0×10^{-10}	0	1.4×10^{-13}	1.3	100	E1
$F + NO \xrightarrow{M} FNO$	1.2×10^{-31}	0.5	2.8×10^{-10}	0	2.6×10^{-12}	1.4	200	E2
$F + NO_2 \xrightarrow{M} FNO_2$	1.5×10^{-30}	2.0	1.0×10^{-11}	0.0	5.4×10^{-12}	1.3	100	E3
$FO + NO_2 \xrightarrow{M} FONO_2$	2.6×10^{-31}	1.3	2.0×10^{-11}	1.5	3.2×10^{-12}	3	200	E4
$CF_3 + O_2 \xrightarrow{M} CF_3O_2$	3.1×10^{-29}	4.0	3.0×10^{-12}	1.0	2.8×10^{-12}	1.2	100	E5
$CF_3O + NO_2 \xrightarrow{M} CF_3ONO_2$	1.8×10^{-28}	6.9	1.1×10^{-11}	1	1.0×10^{-11}	1.1	50	E6

Reaction	Low-Pressure Limit [a] $k_o(T) = k_o^{298}(T/298)^{-n}$		High-Pressure Limit [b] $k_\infty(T) = k_\infty^{298}(T/298)^{-m}$		k(T,[M])	*f*(298 K)	*g*	Note
	k_o^{300}	n	k_∞^{300}	m	298 K, 1 Atm			
$CF_3O_2 + NO_2 \xrightarrow{M} CF_3O_2NO_2$	1.5×10^{-29}	2.2	9.7×10^{-12}	1	8.1×10^{-12}	1.1	50	E7
$CF_3O + CO \xrightarrow{M} CF_3OCO$	2.5×10^{-31}	2	6.7×10^{-14}	–1.2	6.0×10^{-14}	1.2	500	E8
$CF_3O \xrightarrow{M} CF_2O + F$	(See Note)							E9
ClO_x Reactions								
$Cl + O_2 \xrightarrow{M} ClOO$	2.2×10^{-33}	3.1	1.8×10^{-10}	0	5.3×10^{-14}	1.1	50	F1
$Cl + NO \xrightarrow{M} ClNO$	7.7×10^{-32}	1.8	–	–	1.9×10^{-12}	1.2	50	F2
$Cl + NO_2 \xrightarrow{M} ClONO$	1.3×10^{-30}	2	1×10^{-10}	1	1.6×10^{-11}	1.2	100	F3
$\xrightarrow{M} ClNO_2$	1.8×10^{-31}	2	1×10^{-10}	1	3.6×10^{-12}	1.3	100	
$Cl + CO \xrightarrow{M} ClCO$	1.3×10^{-33}	3.8	–	–	3.3×10^{-14}	1.1	50	F4
$Cl + C_2H_2 \xrightarrow{M} ClC_2H_2$	5.3×10^{-30}	2.4	2.2×10^{-10}	0.7	5.0×10^{-11}	1.1	50	F5
$Cl + C_2H_4 \xrightarrow{M} ClC_2H_4$	1.6×10^{-29}	3.3	3.1×10^{-10}	1.0	1.1×10^{-10}	1.5	50	F6
$Cl + C_2Cl_4 \xrightarrow{M} C_2Cl_5$	1.5×10^{-28}	8.5	4.0×10^{-11}	1.2	3.6×10^{-11}	1.12	50	F7
$ClO + NO_2 \xrightarrow{M} ClONO_2$	1.8×10^{-31}	3.4	1.5×10^{-11}	1.9	2.3×10^{-12}	1.3	50	F8
$OClO + NO_3 \xrightarrow{M} O_2ClONO_2$	(See Note)							F9
$ClO + ClO \xrightarrow{M} Cl_2O_2$	1.9×10^{-32}	3.6	3.7×10^{-12}	1.6	3.2×10^{-13}	1.15	0	F10
$ClO + OClO \xrightarrow{M} Cl_2O_3$	6.4×10^{-32}	4.7	2.4×10^{-11}	0	1.2×10^{-12}	1.1	25	F11
$OClO + O \xrightarrow{M} ClO_3$	3.0×10^{-31}	3.1	8.3×10^{-12}	0	2.3×10^{-12}	1.1	100	F12
$CH_2Cl + O_2 \xrightarrow{M} CH_2ClO_2$	1.9×10^{-30}	3.2	2.9×10^{-12}	1.2	2.2×10^{-12}	1.1	125	F13
$CHCl_2 + O_2 \xrightarrow{M} CHCl_2O_2$	1.3×10^{-30}	4.0	2.8×10^{-12}	1.4	2.0×10^{-12}	1.1	125	F14
$CCl_3 + O_2 \xrightarrow{M} CCl_3O_2$	8.3×10^{-31}	6	3.5×10^{-12}	1	2.2×10^{-12}	1.2	50	F15
$CFCl_2 + O_2 \xrightarrow{M} CFCl_2O_2$	5.1×10^{-30}	4.0	6.0×10^{-12}	1.0	4.8×10^{-12}	1.3	200	F16
$CF_2Cl + O_2 \xrightarrow{M} CF_2ClO_2$	5.4×10^{-29}	5.6	1.0×10^{-11}	0.8	9.1×10^{-12}	2	300	F17
$CCl_3O_2 + NO_2 \xrightarrow{M} CCl_3O_2NO_2$	3.0×10^{-29}	6.8	1.3×10^{-11}	1	1.1×10^{-11}	1.1	50	F18
$CFCl_2O_2 + NO_2 \xrightarrow{M} CFCl_2O_2NO_2$	2.3×10^{-29}	5.8	1.0×10^{-11}	1	8.7×10^{-12}	1.1	50	F19

Reaction	Low-Pressure Limit [a] $k_o(T) = k_o^{298}(T/298)^{-n}$		High-Pressure Limit [b] $k_\infty(T) = k_\infty^{298}(T/298)^{-m}$		k(T,[M])	*f*(298 K)	*g*	Note
	k_o^{300}	n	k_∞^{300}	m	298 K, 1 Atm			
$CF_2ClO_2 + NO_2 \xrightarrow{M} CF_2ClO_2NO_2$	1.1×10^{-29}	4.6	1.7×10^{-11}	1.2	1.3×10^{-11}	2	300	F20
BrO_x Reactions								
$Br + NO_2 \xrightarrow{M}$ Products	4.3×10^{-31}	2.4	2.7×10^{-11}	0	4.9×10^{-12}	1.1	50	G1
$BrO + NO_2 \xrightarrow{M} BrONO_2$	5.5×10^{-31}	3.1	6.6×10^{-12}	2.9	2.8×10^{-12}	1.2	400	G2
$Br + CH_2{=}CHCH{=}CH_2 \xrightarrow{M}$ Products	1.1×10^{-28}	4.8	2.1×10^{-10}	0.6	1.6×10^{-10}	1.5	100	G3
$Br + CH_2{=}C(CH_3)CH{=}CH_2 \xrightarrow{M}$ Products	1.1×10^{-27}	2.5	2.0×10^{-10}	1.1	1.8×10^{-10}	1.5	100	G4
IO_x Reactions								
$I + NO \xrightarrow{M} INO$	1.8×10^{-32}	1.0	1.7×10^{-11}	0	3.8×10^{-13}	1.3	150	H1
$I + NO_2 \xrightarrow{M} INO_2$	3.0×10^{-31}	1.0	6.6×10^{-11}	0	5.1×10^{-12}	1.2	300	H2
$IO + NO_2 \xrightarrow{M} IONO_2$	7.7×10^{-31}	3.5	7.7×10^{-12}	1.5	3.5×10^{-12}	1.3	50	H3
$CH_2I + O_2 \rightarrow$ Products	(See Table 2.2)							
SO_x Reactions								
$HS + NO \xrightarrow{M} HSNO$	2.4×10^{-31}	2.5	2.7×10^{-11}	0	3.4×10^{-12}	1.2	100	I1
$CH_3S + NO \xrightarrow{M} CH_3SNO$	3.3×10^{-29}	4.0	3.5×10^{-11}	1.8	2.8×10^{-11}	1.2	100	I2
$O + SO_2 \xrightarrow{M} SO_3$	1.8×10^{-33}	–2	4.1×10^{-14}	-1.8	1.3×10^{-14}	2	100	I3
$OH + SO_2 \xrightarrow{M} HOSO_2$	2.9×10^{-31}	4.1	1.7×10^{-12}	-0.2	9.5×10^{-13}	3, 1.08 (See Note)	100	I4
$CH_3S + O_2 \xrightarrow{M} CH_3SOO$	(See Note)							I5
$CH_3SCH_2 + O_2 \xrightarrow{M} CH_3SCH_2O_2$	(See Note)							I6
$CH_3 + SO_3 \xrightarrow{M} CH_3SO_3$	(See Note)		2.2×10^{-13}	0.2	2.2×10^{-13}	10	50	I7
$SO_3 + NH_3 \xrightarrow{M} H_3NSO_3$	3.7×10^{-30}	6.1	4.3×10^{-11}	0	1.9×10^{-11}	1.2	200	I8
$HO + CS_2 \xrightarrow{M} HO{-}{-}{-}CS_2$	5.0×10^{-31}	3.5	1.4×10^{-11}	1	4.0×10^{-12}	1.5	100	I9
$Cl + CS_2 \xrightarrow{M} Cl{-}{-}{-}CS_2$	6.0×10^{-31}	3.6	4.6×10^{-10}	0	1.2×10^{-11}	1.1	50	I10
$HO + (CH_3)_2S \xrightarrow{M} HO{-}{-}{-}(CH_3)_2S$	3.0×10^{-31}	6.24			7.4×10^{-12}	1.2		I11
$Cl + (CH_3)_2S \xrightarrow{M} Cl{-}{-}{-}(CH_3)_2S$	4.2×10^{-28}	7	2.0×10^{-10}	1	1.7×10^{-10}	1.1	50	I12

Reaction	Low-Pressure Limit [a] $k_o(T) = k_o^{298}(T/298)^{-n}$		High-Pressure Limit [b] $k_\infty(T) = k_\infty^{298}(T/298)^{-m}$		k(T,[M])	*f*(298 K)	*g*	Note
	k_o^{300}	n	k_∞^{300}	m	298 K, 1 Atm			
$Br + (CH_3)_2S \xrightarrow{M} Br\text{---}(CH_3)_2S$	3.8×10^{-29}	5.3	1.5×10^{-10}	2	9.6×10^{-11}	1.1	100	I13
Metal Reactions								
$Na + O_2 \xrightarrow{M} NaO_2$	3.2×10^{-30}	1.4	6.0×10^{-10}	0	5.3×10^{-11}	1.3	200	J1
$Na + OH \xrightarrow{M} NaOH$	(See Note)							J2
$NaO + O_2 \xrightarrow{M} NaO_3$	3.5×10^{-30}	2.0	5.7×10^{-10}	0	5.6×10^{-11}	1.3	200	J3
$NaO + CO_2 \xrightarrow{M} NaCO_3$	8.8×10^{-28}	*3.0*	6.5×10^{-10}	0.2	5.4×10^{-10}	1.3	200	J4
$NaOH + CO_2 \xrightarrow{M} NaHCO_3$	1.0×10^{-28}	*4.0*	6.8×10^{-10}	0.2	3.6×10^{-10}	1.5	200	J5
$Hg + Br \xrightarrow{M} HgBr$	1.5×10^{-32}	1.9	–	–	3.7×10^{-13}	1.5	100	J6
$Hg\,Br + HO_2 \xrightarrow{M}$ products	(See Note)							J7
$Hg\,Br + NO_2 \xrightarrow{M}$ products	(See Note)							J8

Shaded areas indicate changes or additions since JPL19-5**.**

The values quoted are suitable for air as the third body, M.

[a] Units are cm^6 $molecule^{-2}$ s^{-1}.

[b] Units are cm^3 $molecule^{-1}$ s^{-1}.

f(298 K) is the uncertainty factor at 298 K. To calculate the uncertainty at other temperatures, use the expression:

$$f(T) = f(298)\exp\left|g\left(\frac{1}{T}-\frac{1}{298}\right)\right|$$

Note that the exponent is an absolute value

2.7 Notes for Table 2-1: Termolecular Reactions

A1. **$O + O_2$.** Low pressure limit and T dependence are an average of Klais et al.,[10] Huie et al.,[7] and Lin and Leu.[11] These studies in N_2 and Ar are in the temperature range 200< T/K <268. The result is in agreement with the study of Hippler et al.[6] and the extrapolated recommendation fits their lower pressure N_2 data down to 100 K. High pressure studies by Croce de Cobos and Troe[2] are in agreement with this recommendation. Rawlins et al.[14] estimate values in Ar between 80 and 150 K from nascent vibrational distributions that are a factor of two higher than the recommendation extrapolated to 80 K. The temperature dependence of the rate constant determined from the experimental data are in excellent agreement with the value of n = 2.36 determined from the calculations of Patrick and Golden.[13] However there is some reason to believe that a radical-complex plays a role in this process.[6,8,12,19] Kaye[9] has calculated isotope effects for this reaction, using methods similar to those discussed in the Introduction of this document (see Troe[17] and Patrick and Golden[13]). Isotope effects have been reported by Anderson et al.[1] and Gross and Billing.[4] Measurements of isotopic fractionation by Mauersberger and colleagues[18] and Thiemens and co–workers[15] reveal distinctly non–statistical effects. Various attempts at theoretical explanations exist,[5] but the detailed knowledge of the potential energy surface required is unavailable. A summary of theoretical and experimental studies by Schinke et al.[16] goes into great detail on this subject as does a study by Gao and Marcus.[3]
(Table: 02-25, Note: 10-6, Evaluated 10-6) Back to Table

(1) Anderson, S. M.; Hulsebusch, D.; Mauersberger, K. Surprising rate coefficients for four isotopic variants of O + O_2 + M. *J. Chem. Phys.* **1997**, *107*, 5385-5392, doi:10.1063/1.474247.

(2) Croce de Cobos, A. E.; Troe, J. High-pressure range of the recombination O + O_2 → O_3. *Int. J. Chem. Kinet.* **1984**, *16*, 1519-1530, doi:10.1002/kin.550161206.

(3) Gao, Y. Q.; Marcus, R. A. An approximate theory of the ozone isotope effects: Rate constant ratios and pressure dependence. *J. Chem. Phys.* **2007**, *127*, 244316, doi:10.1063/1.2806189.

(4) Gross, A.; Billing, G. D. Isotope effects on the rate constants for the processes O_2 + O → O + O_2 and O_2 + O + Ar → O_3 + Ar On a modified ground-state potential energy surface for ozone. *Chem. Phys.* **1997**, *217*, 1-18, doi:10.1016/S0301-0104(97)84555-7.

(5) Hathorn, B. C.; Marcus, R. A. An intramolecular theory of the mass-independent isotope effect for ozone. II. Numerical implementation at low pressures using a loose transition state. *J. Chem. Phys.* **2000**, *113*, 9497-9509, doi:10.1063/1.1321045.

(6) Hippler, H.; Troe, J.; Willner, J. Temperature and pressure dependence of ozone formation rates in the range 1-1000 bar and 90-370 K. *J. Chem. Phys.* **1990**, *93*, 6560-6569, doi:10.1063/1.458972.

(7) Huie, R. E.; Herron, J. T.; Davis, D. D. Absolute rate constants for the reaction O + O_2 + M → O_3 + M over the temperature range 200-346°K. *J. Phys. Chem.* **1972**, *76*, 2653-2658, doi:10.1021/j100663a002.

(8) Ivanov, A. V.; Gershenzon, Y. M.; Gratpanche, F.; Devolder, P.; Saverysyn, J.-P. Heterogeneous loss of OH on NaCl and NH_4NO_3 at tropospheric temperatures. *Ann. Geophys.* **1996**, *14*, 659-664, doi:10.1007/s00585-996-0659-5.

(9) Kaye, J. A. Theoretical analysis of isotope effects on ozone formation in oxygen photochemistry. *J. Geophys. Res.* **1986**, *91*, 7865-7874, doi:10.1029/JD091iD07p07865.

(10) Klais, O.; Anderson, P. C.; Kurylo, M. J. A reinvestigation of the temperature dependence of the rate constant for the reaction O + O_2 + M → O_3 + M (for M = O_2, N_2, and Ar) by the flash photolysis resonance fluorescence technique. *Int. J. Chem. Kinet.* **1980**, *12*, 469-490, doi:10.1002/kin.550120704.

(11) Lin, C. L.; Leu, M. T. Temperature and third-body dependence of the rate constant for the reaction O + O_2 + M → O_3 + M. *Int. J. Chem. Kinet.* **1982**, *14*, 417-434, doi:10.1002/kin.550140408.

(12) Luther, K.; Oum, K.; Troe, J. Study of the recombination reaction CCl_3 + O_2 (+M) → CCl_3O_2 (+M) at pressures of 2-900 bar and temperatures of 260-346 K. *J. Phys. Chem. A* **2001**, *105*, 5535-5541, doi:10.1021/jp003844d.

(13) Patrick, R.; Golden, D. M. Third-order rate constants of atmospheric importance. *Int. J. Chem. Kinet.* **1983**, *15*, 1189-1227, doi:10.1002/kin.550151107.

(14) Rawlins, W. T.; Caledonia, G. E.; Armstrong, R. A. Dynamics of vibrationally excited ozone formed by three-body recombination. II. Kinetics and mechanism. *J. Chem. Phys.* **1987**, *87*, 5209-5213 doi:10.1063/1.453689.

(15) Savarino, J.; Thiemens, M. Mass-independent oxygen isotope (^{16}O, ^{17}O, ^{18}O) fractionation found in H_x, O_x reactions. *J. Phys. Chem. A* **1999**, *103*, 9221-9229, doi:10.1021/jp991221y.

(16) Schinke, R.; Grebenshchikov, S. Y.; Ivanov, M. V.; Fleurat-Lessard, P. Dynamical studies of the ozone isotope effect: A status report. *Ann. Rev. Phys. Chem.* **2006**, *57*, 625-661, doi:10.1146/annurev.physchem.57.032905.104542.
(17) Troe, J. Theory of thermal unimolecular reactions at low pressures. I. Solutions of the master equation. *J. Chem. Phys.* **1977**, *66*, 4745-4757, doi:10.1063/1.433837.
(18) Wolf, S.; Bitter, M.; Krankowsky, D.; Mauersberger, K. Multi-isotope study of fractionation effects in the ozone formation process. *J. Chem. Phys.* **2000**, *113*, 2684-2686, doi:10.1063/1.1305890.
(19) Zhu, R. S.; Lin, M. C. Ab initio studies of ClO_x reactions. VII. Isomers of Cl_2O_3 and their roles in the ClO + OClO reaction. *J. Chem. Phys.* **2003**, *118*, 8645-8655, doi:10.1063/1.1565315.

A2. **$O(^1D) + N_2$.** Recommended parameters (including *f* and *g*) are from Estupiñán et al.[1] whose detection capabilities were more advanced than those employed in earlier studies. Kajimoto and Cvetanovic[3] report a value at 296 K of 6.5×10^{-37} cm^6 s^{-1}. Maric and Burrows[4] extract $(8.8 \pm 3.3) \times 10^{-37}$ cm^6 s^{-1} from a study of the photolysis of synthetic air. Gaedtke et al.[2] report an approximate value of 10^{12} in molar units, which translates to 2.8×10^{-36} in molecular units. The rate constant is extremely low in this special system due to electronic curve crossing.
(Table: 06-2, Note: 06-2, Evaluated: 06-2) Back to Table

(1) Estupiñán, E. G.; Nicovich, J. M.; Li, J.; Cunnold, D. M.; Wine, P. H. Investigation of N_2O production from 266 and 532 nm laser flash photolysis of $O_3/N_2/O_2$ mixtures. *J. Phys. Chem. A* **2002**, *106*, 5880-5890, doi:10.1021/jp014242c.
(2) Gaedtke, H. K., H. Hippler, K. Luther, and J. Troe Addition reactions of oxygen atoms at high pressures. *Proc. Combust. Inst.* **1973**, *14*, 295-303.
(3) Kajimoto, O.; Cvetanovic, R. J. Formation of nitrous oxide in the reaction of $O(^1D_2)$ atoms with nitrogen. *J. Chem. Phys.* **1976**, *64*, 1005-1015, doi:10.1063/1.432308.
(4) Maric, D.; Burrows, J. P. Formation of N_2O in the photolysis/photoexciation of NO, NO_2 and air. *J. Photochem. Photobiol. A: Chem.* **1992**, *66*, 291-312, doi:10.1016/1010-6030(92)80002-D.

B1. **$H + O_2$.** Studies by Kurylo,[8] Wong and Davis,[13] Hsu et al.,[7] Hsu et al.,[6] Cobos et al.,[4] Pirraglia et al.,[10] Carleton et al.,[3] Troe,[12] Bates et al.,[1] Michael et al.,[9] and Fernandes et al.[5] have been considered. All are in good agreement. A theoretical study by Sellevåg et al.[11] contributes to knowledge of the reaction. The experimental/theoretical study by Fernandes et al.[5] provides an estimate of the high pressure limit, which is adopted in this recommendation. Because only a few measurements have been reported at low temperatures in the atmospheric range, data from a wider range of conditions were considered. Thus, the recommendation for the low-pressure limit is based on a least-squares analysis (using the adopted high-pressure limit) of all of the data from the studies listed above with T ≤500 K and N_2 concentration < 10^{20} molecules cm^3. The estimated error limits were chosen so that all of the data used for the recommendation fall within the 2σ error bounds. Two studies[1,9] have pointed out the large effect of water vapor as the collider gas. Baulch et al.[2] have evaluated this reaction over the temperature range 298< T/K <1500.
(Table: 19-5, Note: 19-5, Evaluated: 19-5) Back to Table

(1) Bates, R. W.; Golden, D. M.; Hanson, R. K.; Bowman, C. T. Experimental study and modeling of the reaction $H + O_2 + M \rightarrow HO_2 + M$ (M = Ar, N_2, H_2O) at elevated pressures and temperatures between 1050 and 1250 K. *Phys. Chem. Chem. Phys.* **2001**, *3*, 2337-2342, doi:10.1039/b010002l.
(2) Baulch, D. L.; Bowman, C. T.; Cobos, C. J.; Cox, R. A.; Just, T.; Kerr, J. A.; Pilling, M. J.; Stocker, D.; Troe, J.; Tsang, W.; Walker, R. W.; Warnatz, J. Evaluated kinetic data for combustion modeling: Supplement II. *J. Phys. Chem. Ref. Data* **2005**, *34*, 757-1397, doi:10.1063/1.1748524.
(3) Carleton, K. J.; Kessler, W. J.; Marinelli, W. J. $H + O_2 + M$ (= N_2, H_2O, Ar) three-body rate coefficients at 298-750 K. *J. Phys. Chem.* **1993**, *97*, 6412-6417, doi:10.1021/j100126a015.
(4) Cobos, C. J.; Hippler, H.; Troe, J. High-pressure falloff curves and specific rate constants for the reactions $H + O \rightleftharpoons HO + O$. *J. Phys. Chem.* **1985**, *89*, 342-349, doi:10.1021/j100248a033.
(5) Fernandes, R. X.; Luther, K.; Troe, J.; Ushakov, V. G. Experimental and modelling study of the recombination reaction $H + O_2$ (+M) = HO_2 (+M) between 300 and 900 K, 1.5 and 950 bar, and in the bath gases M = He, Ar, and N_2. *Phys. Chem. Chem. Phys.* **2008**, *10*, 4313-4321, doi:10.1039/b804553d.
(6) Hsu, K. J.; Anderson, S. M.; Durant, J. L.; Kaufman, F. Rate constants for $H + O_2 + M$ from 298 to 639 K for M = He, N_2, and H_2O. *J. Phys. Chem.* **1989**, *93*, 1018-1021, doi:10.1021/j100340a003.

(7) Hsu, K. J.; Durant, J. L.; Kaufman, F. Rate constants for H + O_2 + M at 298 K for M = He, N_2, and H_2O. *J. Phys. Chem.* **1987**, *91*, 1895-1899, doi:10.1021/j100291a043.
(8) Kurylo, M. J. Absolute rate constants for the reaction H + O_2 + M → HO_2 + M over the temperature range 203-404 K. *J. Phys. Chem.* **1972**, *76*, 3518-3526, doi:10.1021/j100668a002.
(9) Michael, J. V.; Su, M.-C.; Sutherland, J. W.; Carroll, J. J.; Wagner, A. F. Rate constants for H + O_2 + M → HO_2 + M in seven bath gases. *J. Phys. Chem. A* **2002**, *106*, 5297-5313, doi:10.1021/jp020229w.
(10) Pirraglia, A. N.; Michael, J. V.; Sutherland, J. W.; Klemm, R. B. A flash photolysis-shock tube kinetic study of the H atom reaction with O_2: H + O_2 ⇌ OH + O (962 K ≤ T ≤ 1705 K) and H + O_2 + Ar → HO_2 + Ar (746 K ≤ T ≤ 987 K). *J. Phys. Chem.* **1989**, *93*, 282-291, doi:10.1021/j100338a058.
(11) Sellevåg, S. R.; Geogievskii, Y.; Miller, J. A. The temperature and pressure dependence of the reactions H + O_2 (+M) → HO_2 (+M) and H + OH (+M) → H_2O (+M). *J. Phys. Chem. A* **2008**, *112*, 5085-5095, doi:10.1021/jp711800z.
(12) Troe, J. Detailed modeling of the temperature and pressure dependence of the reaction H + O_2 (+M) → HO_2 (+M). *Proc. Combust. Inst.* **2001**, *28*, 1463-1469.
(13) Wong, W. D.; Davis, D. A flash photolysis-resonance fluorescence study of the reaction of atomic hydrogen with molecular oxygen H + O_2 + M → HO_2 + M. *Int. J. Chem. Kinet.* **1974**, *6*, 401-416, doi:10.1002/kin.550060310.

B2. **OH + OH.** Recommended values are from fits of measurements by Zellner et al.[6] in N_2, by Forster et al.[2] and Fulle et al.[3] in 1–150 bar He scaled to N_2. A study by Fagerstrom et al.[1] in 85–1000 mbar SF_6 gives slightly different values. A pressure independent bimolecular channel to H_2O + O with a rate 1.8×10^{-12} is observed (see Table 1-1). Zellner et al. used somewhat different values for this rate constant to make substantial corrections to their measured values. Changing to the accepted value will make large changes in the Zellner et al. values and it is unclear how to evaluate this. Trainor and von Rosenberg[5] report a value at 300 K that is lower than recommended by a factor of 2.7. A theoretical study by Sellevåg et al.[4] recommends values for He that are compatible with the recommendation.
(Table: 02-25, Note: 10-6, Evaluated: 10-6) Back to Table

(1) Fagerstrom, K.; Lund, A.; Mahmound, G.; Jodkowski, J. T.; Ratajczak, E. Pressure and temperature dependence of the gas-phase reaction between methyl and hydroxyl radicals. *Chem. Phys. Lett.* **1994**, *224*, 43-50, doi:10.1016/0009-2614(94)00513-3.
(2) Forster, R.; Frost, M.; Fulle, D.; Hamann, H. F.; Hippler, H.; Schlepegreli; Troe, J. High pressure range of the addition of HO to HO, NO, NO_2, and CO. I. Saturated laser induced fluorescence measurements at 298 K. *J. Chem. Phys.* **1995**, *103*, 2949-2958, doi:10.1063/1.470482.
(3) Fulle, D.; Hamann, H. F.; Hippler, H.; Troe, J. High-pressure range of the addition of HO to HO. III. Saturated laser-induced fluorescence measurements between 200 and 700 K. *J. Chem. Phys.* **1996**, *105*, 1001-1006, doi:10.1063/1.471944.
(4) Sellevåg, S. R.; Georgievskii, Y.; Miller, J. A. Kinetics of the gas-phase recombination reaction of hydroxyl radicals to form hydrogen peroxide. *J. Phys. Chem. A* **2009**, *113*, 4457-4467, doi:10.1021/jp8110524.
(5) Trainor, D. W.; von Rosenberg, C. W., Jr. Flash photolysis study of the gas phase recombination of hydroxyl radicals. *J. Chem. Phys.* **1974**, *61*, 1010-1015, doi:10.1063/1.1681968.
(6) Zellner, R.; Ewig, F.; Paschke, R.; Wagner, G. Pressure and temperature dependence of the gas-phase recombination of hydroxyl radicals. *J. Phys. Chem.* **1988**, *92*, 4184-4190, doi:10.1021/j100325a038.

C1. **O + NO.** Low pressure limit and n from direct measurements of Schieferstein et al.[2] and their re–analysis of the data of Whytock et al.[3] Error limits encompass other studies. High pressure limit and *m* from fitting the data of Hippler et al.,[1] who report higher values for the high pressure limiting rate constant, to the format used in this compilation. Shock tube measurements by Yarwood et al.[4] in argon from 300–1300 K are consistent with the values in Table 2.
(Table: 06-2, Note: 06-2, Evaluated: 06-2) Back to Table

(1) Hippler, H.; Siefke, M.; Stark, H.; Troe, J. New studies of the unimolecular reaction NO_2 ⇌ O + NO. Part 1. High pressure range of the O + NO recombination between 200 and 400 K. *Phys. Chem. Chem. Phys.* **1999**, *1*, 57-61, doi:10.1039/a806520i.
(2) Schieferstein, M.; Kohse-Höinghaus, K.; Stuhl, F. Temperature dependence of the rate constants of the reaction O + NO + M → NO_2 + M (M = He, NO, N_2, CH_4). *Ber. Bunsenges. Phys. Chem.* **1983**, *87*, 361-366, doi:10.1002/bbpc.19830870419.
(3) Whytock, D. A.; Michael, J. V.; Payne, W. A. Absolute rate constants for O + NO + N_2 → NO_2 + N_2 from 217-500 K. *Chem. Phys. Lett.* **1976**, *42*, 466-471, doi:10.1016/0009-2614(76)80655-0.

(4) Yarwood, G.; Sutherland, J. W.; Wickramaaratchi, M. A.; Klemm, R. B. Direct rate constant measurements for the reaction O + NO + Ar → NO_2 + Ar at 300-1341 K. *J. Phys. Chem.* **1991**, *95*, 8771-8775, doi:10.1021/j100175a065.

C2. OH + NO. The low pressure limit rate constant has been reported by Anderson and Kaufman,[2] Stuhl and Niki,[17] Morley and Smith,[13] Westenberg and de Haas,[18] Anderson et al.,[3] Howard and Evenson,[12] Harris and Wayne,[11] Atkinson et al.,[6] Overend et al.,[14] Anastasi and Smith,[1] Burrows et al.,[7] and Atkinson and Smith.[4] The general agreement is good, and the recommended values of both the rate constant and the temperature dependence are weighted averages. Studies by Sharkey et al.[16] and Donahue et al.[8] in the transition regime between low and high pressure limits are in agreement and serve to reduce the uncertainty. These latter studies yield a value for the high pressure limiting rate constant in agreement with the results of Forster et al.,[9] whose study reached pressures of 100 bar in He. The temperature dependence of the high pressure limiting rate constant is from the data of Anastasi and Smith[1] and Sharkey et al. (both *cis*- and *trans*-HONO are expected to be formed.) Fulle et al.[10] report a high pressure limit in agreement with Forster et al.[9] Pagsberg et al.[15] report low pressure values in SF_6 that are compatible (i.e., the ratio of collision efficiencies is about a factor of two) with the recommendation. A study by Zabarnick[19] is noted. The error limits encompass the differences with the IUPAC[5] recommendation.
(Table: 06-2, Note: 06-2, Evaluated: 06-2) Back to Table

(1) Anastasi, C.; Smith, I. W. M. Rate measurements of reactions of OH by resonance absorption Part 6.-Rate constants for OH + NO(+M) → HNO_2(+M) over a wide range of temperature and pressure. *J. Chem. Soc. Faraday Trans. 2* **1978**, *74*, 1056-1064, doi:10.1039/f29787401056.

(2) Anderson, J. G.; Kaufman, F. Kinetics of the reaction OH + NO_2 + M → HNO_3 + M. *Chem. Phys. Lett.* **1972**, *16*, 375-379, doi:10.1016/0009-2614(72)80296-3.

(3) Anderson, J. G.; Margitan, J. J.; Kaufman, F. Gas phase recombination of OH with NO and NO_2. *J. Chem. Phys.* **1974**, *60*, 3310-3317, doi:10.1063/1.1681522.

(4) Atkinson, D. B.; Smith, M. A. Radical-molecule kinetics in pulsed uniform supersonic flows: Termolecular association of OH + NO between 90 and 220 K. *J. Phys. Chem.* **1994**, *98*, 5797-5800, doi:10.1021/j100074a001.

(5) IUPAC: Atmospheric Chemical Kinetic Data Evaluation. Atkinson, R.; Baulch, D. L.; Cox, R. A.; Crowley, J. N.; Hampson, J., R. F.; Hynes, R. G.; Jenkin, M. E.; Kerr, J. A.; Rossi, M. J.; Troe, J., 2004, http://www.iupac-kinetic.ch.cam.ac.uk.

(6) Atkinson, R.; Hansen, D. A.; Pitts, J., J. N. Rate constants for the reaction of the OH radical with H_2 and NO (M = Ar and N_2). *J. Chem. Phys.* **1975**, *62*, 3284-3288, doi:10.1063/1.430882.

(7) Burrows, J. P.; Wallington, T. J.; Wayne, R. P. Kinetics of the gas-phase reactions of OH with NO_2 and with NO. *J. Chem. Soc. Faraday Trans. 2* **1983**, *79*, 111-122, doi:10.1039/f29837900111.

(8) Donahue, N. M.; Dubey, M. K.; Mohrschladt, R.; Demerjian, K.; Anderson, J. G. High-pressure flow study of the reactions OH + NO_x → $HONO_x$: Errors in the falloff region. *J. Geophys. Res.* **1997**, *102*, 6159-6168, doi:10.1029/96JD02329.

(9) Forster, R.; Frost, M.; Fulle, D.; Hamann, H. F.; Hippler, H.; Schlepegreli; Troe, J. High pressure range of the addition of HO to HO, NO, NO_2, and CO. I. Saturated laser induced fluorescence measurements at 298 K. *J. Chem. Phys.* **1995**, *103*, 2949-2958, doi:10.1063/1.470482.

(10) Fulle, D. H.; Hamann, H. F.; Hippler, H.; Troe, J. Temperature and pressure dependence of the addition reactions of HO to NO and to NO_2. IV. Saturated laser-induced fluorescence measurements up to 1400 bar. *J. Chem. Phys.* **1998**, *108*, 5391-5397, doi:10.1063/1.475971.

(11) Harris, G. W.; Wayne, R. P. Reaction of hydroxyl radicals with NO, NO_2 and SO_2. *J. Chem. Soc. Faraday Trans. 1* **1975**, *71*, 610-617, doi:10.1039/f19757100610.

(12) Howard, C. J.; Evenson, K. M. Laser magnetic resonace study of the gas phase reactions of OH with CO, NO, and NO_2. *J. Chem. Phys.* **1974**, *61*, 1943-1952, doi:10.1063/1.1682195.

(13) Morley, C.; Smith, I. W. M. Rate measurements of reactions of OH by resonance absorption .1. Reactions of OH with NO_2 and NO. *J. Chem. Soc. Faraday Trans. 2* **1972**, *68*, 1016-1030, doi:10.1039/f29726801016.

(14) Overend, R. P.; Paraskevopoulos, G.; Black, C. Rates of OH radical reactions. II. The combination reaction OH + NO + M. *J. Chem. Phys.* **1976**, *64*, 4149-4154, doi:10.1063/1.431984.

(15) Pagsberg, P.; Bjergbakke, E.; Ratajczak, E.; Sillesen, A. Kinetics of the gas phase reaction OH + NO(+M) → HONO(+M) and the determination of the UV absorption cross sections of HONO. *Chem. Phys. Lett.* **1997**, *272*, 383-390, doi:10.1016/S0009-2614(97)00576-9.

(16) Sharkey, P.; Sims, I. R.; Smith, I. W. M.; Bocherl, P.; Rowe, B. R. Pressure and temperature dependence of the rate constants for the association reaction OH radicals with NO between 301 and 23 K. *J. Chem. Soc. Faraday Trans.* **1994**, *90*, 3609-3616, doi:10.1039/ft9949003609.

(17) Stuhl, F.; Niki, H. Flash Photochemical Study of the Reaction OH + NO + M Using Resonance Fluorescent Detection of OH. *J. Chem. Phys.* **1972**, *57*, 3677-3679, doi:10.1063/1.1678826.
(18) Westenberg, A. A.; deHaas, N. Rate measurement on OH + NO + M and OH + NO_2 + M. *J. Chem. Phys.* **1972**, *57*, 5375-5378, doi:10.1063/1.1678234.
(19) Zabarnick, S. Kinetics of the reaction OH + NO + M → HONO + M as a function of temperature and pressure in the presence of argon, SF_6 and N_2 bath gas. *Chem. Phys.* **1993**, *171*, 265-273, doi:10.1016/0301-0104(93)85149-3.

C3. **OH + NO_2.** This reaction has been the subject of detailed study. There are two product channels, one to $HONO_2$ (nitric acid) and the other to HOONO (pernitrous acid). (There are at least two conformers of HOONO, *cis-cis* and *trans-perp*, which are thought to be equilibrated under atmospheric conditions.) Golden and Smith[14] concluded that there were two pathways and they offered parameters in the format of this recommendation that were given in the note in JPL 02-25.[20] Experiments by Hippler and co-workers[11,12] up to about 100 bar at 300 K and the finding of a double exponential decay of OH at 430 K and 100 bar implicate a second pathway.[15] Nizkorodov and Wennberg[18] report 5% HOONO at 253 K and 20 Torr of an N_2/He buffer gas. Bean et al.[3] and Pollack et al.[19] report on the spectroscopy of the HOONO conformer. Mollner et al.[17] report the total rate constant at 298 K in N_2, O_2 and air from 50 to 900 Torr, and the branching ratio for the two pathways at 298 K in a mixture of N_2 and H_2 from 20 to 760 Torr. They find the efficiency of air to be 94% that of N_2 and by simultaneously fitting both the branching ratio and the total rate constant they obtained parameters at 298 K: $k_0 = 1.51 \times 10^{-30}$ and $k_\infty = 1.84 \times 10^{-30}$ for the $HONO_2$ pathway and $k_0 = 6.2 \times 10^{-32}$ and $k_\infty = 8.1 \times 10^{-11}$ for the HOONO pathway.

Golden et al.[13] have performed RRKM/master-equation calculations on an ab initio potential energy, which are the basis for the previous recommendation, which is retained for the current recommendation. Golden et al.[13] adjusted their calculations to agree with experiments: the low pressure limit and the high pressure limiting rate constants and their temperature dependences are from a fit to the data of Hippler et al.,[15] Anastasi and Smith,[1] Wine et al.,[21] Donahue et al.,[8] Dransfield et al.,[9] Brown et al.,[4] and D'Ottone et al.[7] Brown et al. report that O_2 is about 30% less efficient than N_2 as a collider and suggest that air might therefore have a total efficiency of 0.94 relative to N_2. The total rate constants reported by Mollner et al.[17] are in excellent agreement with the recommendation. Data from Anderson et al.,[2] Howard and Evenson,[16] Burrows et al.,[6] and Erler et al.[10] are in essential agreement. Data of Forster et al.[11] and Fulle et al.[12] are acknowledged to be about 30% too high.[15] Burkholder et al.[5] and Dransfield et al.[9] searched for the isomer HOONO, but were unable to detect it. The description of the reaction between HO and NO_2, as consisting of two product channels, requires that the data represent the sum of the two pathways. The branching ratios measured at 298 K by Mollner et al.[17] are about 25% lower than from the recommendation; Mollner et al. did not report branching ratios at other temperatures. The fate of HOONO has to be included in atmospheric models. If this fate involves rapid loss due to reaction or photolysis, the effect of the second pathway is the diminution of the $HONO_2$ forming rate constant. Evaluation of data, taking into account both pathways, indicates that the contribution of the HOONO forming reaction can be from 5 to 15% under atmospheric conditions at 298 K. The equilibrium constant is given in Table 3-1.
(Table: 06-2, Note: 15-10, Evaluated 15-10) Back to Table

(1) Anastasi, C.; Smith, I. W. M. Rate measurements of reactions of OH by resonance absorption Part 5.-Rate constants for OH + NO_2(+M) → HNO_3(+M) over a wide range of temperature and pressure. *J. Chem. Soc. Faraday Trans. 2* **1976**, *72*, 1459-1468, doi:10.1039/f29767201459.
(2) Anderson, J. G.; Margitan, J. J.; Kaufman, F. Gas phase recombination of OH with NO and NO_2. *J. Chem. Phys.* **1974**, *60*, 3310-3317, doi:10.1063/1.1681522.
(3) Bean, B. D.; Mollner, A. K.; Nizkorodov, S. A.; Nair, G.; Okumura, M.; Sander, S. P.; Peterson, K. A.; Francisco, J. S. Cavity ringdown spectroscopy of *cis-cis* HOONO and the HOONO/$HONO_2$ branching ratio in the reaction OH + NO_2 + M. *J. Phys. Chem. A* **2003**, *107*, 6974-6985, doi:10.1021/jp034407c.
(4) Brown, S. S.; Talukdar, R. K.; Ravishankara, A. R. Rate constants for the reaction OH + NO_2 + M → HNO_3 + M under atmospheric conditions. *Chem. Phys. Lett.* **1999**, *299*, 277-284, doi:10.1016/S0009-2614(98)01283-4.
(5) Burkholder, J. B.; Hammer, P. D.; Howard, C. J. Product analysis of the OH + NO_2 + M reaction. *J. Phys. Chem.* **1987**, *91*, 2136-2144, doi:10.1021/j100292a032.
(6) Burrows, J. P.; Wallington, T. J.; Wayne, R. P. Kinetics of the gas-phase reactions of OH with NO_2 and with NO. *J. Chem. Soc. Faraday Trans. 2* **1983**, *79*, 111-122, doi:10.1039/f29837900111.
(7) D'Ottone, L.; Campuzano-Jost, P.; Bauer, D.; Hynes, A. J. A pulsed laser photolysis-pulsed laser induced fluorescence study of the kinetics of the gas-phase reaction of OH with NO_2. *J. Phys. Chem. A* **2001**, *105*, 10538-10543, doi:10.1021/jp012250n.

(8) Donahue, N. M.; Dubey, M. K.; Mohrschladt, R.; Demerjian, K.; Anderson, J. G. High-pressure flow study of the reactions OH + NO_x → $HONO_x$: Errors in the falloff region. *J. Geophys. Res.* **1997**, *102*, 6159-6168, doi:10.1029/96JD02329.
(9) Dransfield, T. J.; Perkins, K. K.; Donahue, N. M.; Anderson, J. G.; Sprengnether, M. M.; Demerjian, K. Temperature and pressure dependent kinetics of the gas-phase reaction of the hydroxyl radical with nitrogen dioxide. *Geophys. Res. Lett.* **1999**, *26*, 687-690, doi:10.1029/1999GL900028.
(10) Erler, K.; Field, D.; Zellner, R.; Smith, I. W. M. Recombination reaction between hydroxyl radicals and nitrogen dioxide. OH + NO_2 + M (= He, CO_2) in temperature range 213-300 K. *Ber. Bunsenges. Phys. Chem.* **1977**, *81*, 22-26, doi:10.1002/bbpc.19770810107.
(11) Forster, R.; Frost, M.; Fulle, D.; Hamann, H. F.; Hippler, H.; Schlepegreli; Troe, J. High pressure range of the addition of HO to HO, NO, NO_2, and CO. I. Saturated laser induced fluorescence measurements at 298 K. *J. Chem. Phys.* **1995**, *103*, 2949-2958, doi:10.1063/1.470482.
(12) Fulle, D. H.; Hamann, H. F.; Hippler, H.; Troe, J. Temperature and pressure dependence of the addition reactions of HO to NO and to NO_2. IV. Saturated laser-induced fluorescence measurements up to 1400 bar. *J. Chem. Phys.* **1998**, *108*, 5391-5397, doi:10.1063/1.475971.
(13) Golden, D. M.; Barker, J. R.; Lohr, L. L. Master equation models for the pressure- and temperature-dependent reactions HO + NO_2 → $HONO_2$ and HO + NO_2 → HOONO. *J. Phys. Chem. A* **2003**, *107*, 11057-11071, doi:10.1021/jp0353183.
(14) Golden, D. M.; Smith, G. P. Reaction of OH + NO_2 + M: A new view. *J. Phys. Chem. A* **2000**, *104*, 3991-3997, doi:10.1021/jp9939928.
(15) Hippler, H.; Nasterlack, S.; Striebel, F. Reaction of OH + NO_2 + M: Kinetic evidence of isomer formation. *Phys. Chem. Chem. Phys.* **2002**, *4*, 2959-2964, doi:10.1039/b201932a.
(16) Howard, C. J.; Evenson, K. M. Laser magnetic resonace study of the gas phase reactions of OH with CO, NO, and NO_2. *J. Chem. Phys.* **1974**, *61*, 1943-1952, doi:10.1063/1.1682195.
(17) Mollner, A. K.; Valluvadasan, S.; Feng, L.; Sprague, M. K.; Okumura, M.; Milligan, D. B.; Bloss, W. J.; Sander, S. P.; Martien, P. T.; Harley, R. A.; McCoy, A. B.; Carter, W. P. L. Rate of gas phase association of hydroxyl radical and nitrogen dioxide. *Science* **2010**, *330*, 646-649, doi:10.1126/science.1193030.
(18) Nizkorodov, S. A.; Wennberg, P. O. First spectroscopic observation of gas-phase HOONO. *J. Phys. Chem. A* **2002**, *106*, 855-859, doi:10.1021/jp013598l.
(19) Pollack, I. B., I. M. Konen, E. X. J. Li, and M. I. Lester Spectroscopic characterization of HOONO and its binding energy via infrared action spectroscopy. *J. Chem. Phys.* **2003**, *119*, 9981-9984, doi:10.1063/1.1624246.
(20) Sander, S. P.; Finlayson-Pitts, B. J.; Friedl, R. R.; Golden, D. M.; Huie, R. E.; Kolb, C. E.; Kurylo, M. J.; Molina, M. J.; Moortgat, G. K.; Orkin, V. L.; Ravishankara, A. R. Chemical Kinetics and Photochemical Data for Use in Atmospheric Studies, Evaluation Number 14, Jet Propulsion Laboratory Pasadena, JPL Publication 02-25, 2002, http:\\jpldataeval.jpl.nasa.gov.
(21) Wine, P. H.; Kreutter, N. M.; Ravishankara, A. R. Flash photolysis-resonance fluorescence kinetics study of the reaction OH + NO_2 + M → HNO_3 + M. *J. Phys. Chem.* **1979**, *83*, 3191-3195, doi:10.1021/j100488a002.

C4. **HO_2 + NO.** Butkovskaya et al. studied this reaction in a high-pressure turbulent flow reactor coupled to a chemical ionization mass spectrometer.[2-4] Very small yields (<1%) of nitric acid were measured from 223 to 323 K and from 72 to 600 Torr of (mostly) N_2 and in the absence of water vapor. The yields were enhanced by the presence of water vapor.[3,4] In systems not including water vapor, they summarized the yield of nitric acid relative to the yield of NO_2 (from HO_2 + NO → OH + NO_2) as follows:

$$\beta(T,P) = (530 \pm 10)/T(K) + (6.4 \pm 1.3) \times 10^{-4} P(Torr) - (1.73 \pm 0.07)$$

At low temperatures, β extrapolated below 100 Torr has a large non-zero intercept at zero pressure,[2,4] which is not expected for a gas phase reaction. In the presence of water vapor, the chemical ionization mass spectrometer signals are affected significantly[3] and the yield of nitric acid increases linearly with added water vapor,[3,4] reaching an enhancement factor of ~8 at [H_2O] = 4×10^{17} molecule cm^{-3} and 298 K[3]:

$$f_{H_2O} \approx (1 + 2 \times 10^{-17} [H_2O])$$

where the concentration of H_2O is expressed in molecules cm^{-3}. If this effect is due to reaction of the hydrated HO_2 complex (i.e. $HO_2 \bullet H_2O$ + NO → HNO_3 + H_2O), then the rate constant of the complex with NO is ~6×10^{-13} cm^3 s^{-1} at 298 K in the presence of 200 Torr of N_2.[3]

Ab initio electronic structure calculations support the possibility of gas phase $HONO_2$ formation, but satisfactory simulations using master equations have been elusive.[1,5-7] The measured yields show a surprising

intercept at zero pressure, which might be indicative of wall reactions. However, Butkovskaya et al. have made great efforts to minimize wall reactions, and their analysis suggests that wall reactions should not be important.[3,4] Until the results have been confirmed by other groups and are better understood, no recommendation can be made. These rate parameters are provided for the purposes of model evaluation only and do not constitute a recommendation by the Panel.
(Table: 10-6, Note: 10-6, Evaluated 10-6) Back to Table

(1) Barker, J. R.; Lohr, L. L.; Shroll, R. M.; Reading, S. Modeling the organic nitrate yields in the reaction of alkyl peroxy radicals with nitric oxide. 2. Reaction simulations. *J. Phys. Chem. A* **2003**, *107*, 7434-7444, doi:10.1021/jp034638j.

(2) Butkovskaya, N.; Kukui, A.; Le Bras, G. HNO_3 forming channel of the HO_2 + NO reaction as a function of pressure and temperature in the ranges of 72-600 Torr and 223-323 K. *J. Phys. Chem. A* **2007**, *111*, 9047-9053, doi:10.1021/jp074117m.

(3) Butkovskaya, N.; Rayez, M.-T.; Rayez, J.-C.; Kukui, A.; Le Bras, G. Water vapor effect on the HNO_3 yield in the HO_2 + NO reaction: Experimental and theoretical evidence. *J. Phys. Chem. A* **2009**, *113*, 11327-11342, doi:10.1021/jp811428p.

(4) Butkovskaya, N. I.; Kukui, A.; Pouvesle, N.; Le Bras, G. Formation of nitric acid in the gas-phase HO_2 + NO reaction: Effects of temperature and water vapor *J. Phys. Chem. A* **2005**, *109*, 6509-6520, doi:10.1021/jp051534v.

(5) Golden, D. M.; Barker, J. R.; Lohr, L. L. Master equation models for the pressure- and temperature-dependent reactions HO + NO_2 → $HONO_2$ and HO + NO_2 → HOONO. *J. Phys. Chem. A* **2003**, *107*, 11057-11071, doi:10.1021/jp0353183.

(6) Zhang, J.; Donahue, N. M. Constraining the mechanism and kinetics of OH + NO_2 and HO_2 + NO using the multiple-well master equation. *J. Phys. Chem. A* **2006**, *110*, 6898-6911, doi:10.1021/jp0556512.

(7) Zhang, J. Y.; Dransfield, T.; Donahue, N. M. On the mechanism for nitrate formation via the peroxy radical plus NO reaction. *J. Phys. Chem. A* **2004**, *108*, 9082-9095, doi:10.1021/jp048096x.

C5. **HO_2 + NO_2.** Christensen et al.[2] report rate constants 219< T/K <298 and 45< P/Torr <200. They show that methanol, present in most other studies confounds the results by forming bound complexes with HO_2. They also suggest that some measurements yielded low rate constants as a result of perturbations to the NO_2/N_2O_4 equilibrium. Sander et al.[8] also noted that H_2O vapor enhances the reaction rate significantly. Bacak et al.[1] reported data obtained using CIMS, which is more sensitive and less prone to interference than UV and IR absorbance. They used initial radical concentrations 1000 times lower than previous work, eliminating potential interference from the HO_2 + HO_2 reaction. Rate constants measured by Bacak et al.[1] at 200 K, 223 K, and 298 K are quite similar to each other, suggesting very little temperature dependence (i.e., Bacak gives n = 0.2 and m = 0.5), which differs from previous work, leading them to conclude that previous work was affected by the HO_2 + HO_2 reaction at T <277 K. At ~298 K, rate constants measured by Sander et al.,[8] Kurylo et al.,[6,7] Christensen et al., and Bacak et al. are in excellent agreement, suggesting that at 298 K these studies were not affected by interferences. The recommendation is based on the data at T ≥277 K from Sander and Peterson,[8] Kurylo and Ouellette,[6,7] Christensen et al.,[2] and the data at 298 K of Bacak et al. The recommended parameters are similar to the previous recommendation; the exponent for k_∞ is small, as expected for a recombination reaction. The low-T data of Bacak et al. fall about a factor of two lower than the fit. Although CIMS experiments have the highest sensitivity and avoid spectral interference, the data are limited to only three temperatures and they have not been replicated at the lowest two temperatures. The error parameter g was chosen so that the CIMS data at low T fall within the error range. Other studies by Howard,[5] Simonaitis and Heicklen,[9] and Cox and Patrick[4] are in reasonable agreement with the recommendation, as is the value of Christensen et al.[3]
(Table: 15-10, Note: 15-10, Evaluated: 15-10) Back to Table

(1) Bacak, A.; Cooke, M. C.; Bardwell, M. W.; McGillen, M. R.; Archibald, A. T.; Huey, L. G.; Tanner, D.; Utembe, S. R.; Jenkin, M. E.; Derwent, R. G.; Shallcross, D. E.; Percival, C. J. Kinetics of the HO_2 + NO_2 Reaction: On the impact of new gas-phase kinetic data for the formation of HO_2NO_2 on HO_x, NO_x and HO_2NO_2 levels in the troposphere. *Atmos. Environ.* **2011**, *45*, 6414-6422, doi:10.1016/j.atmosenv.2011.08.008.

(2) Christensen, L. E.; Okumura, M.; Sander, S. P.; Friedl, R. R.; Miller, C. E.; Sloan, J. J. Measurements of the rate constant of HO_2 + NO_2 + N_2 → HO_2NO_2 + N_2 using near-infrared wavelength-modulation spectroscopy and UV-visible absorption spectroscopy. *J. Phys. Chem. A* **2004**, *108*, 80-91, doi:10.1021/jp035905o.

(3) Christensen, L. E.; Okumura, M.; Sander, S. P.; Salawitch, R. J.; Toon, G. C.; Sen, B.; Blavier, J.-F.; Jucks, K. W. Kinetics of $HO_2 + HO_2 \rightarrow H_2O_2 + O_2$: Implications for stratospheric H_2O_2. *Geophys. Res. Lett.* **2002**, *29*, 1299, doi:1029/2001GL014525.
(4) Cox, R. A.; Patrick, R. Kinetics of the reaction $HO_2 + NO_2(+M) = HO_2NO_2$ using molecular modulation spectrometry. *Int. J. Chem. Kinet.* **1979**, *11*, 635-648, doi:10.1002/kin.550110610.
(5) Howard, C. J. Kinetics of the reaction of HO_2 with NO_2. *J. Chem. Phys.* **1977**, *67*, 5258-5263, doi:10.1063/1.434703.
(6) Kurylo, M. J.; Ouellette, P. A. Pressure dependence of the rate constant for the reaction $HO_2 + NO_2 + M \rightarrow HO_2NO_2 + M$ (M = N_2, O_2) at 298 K. *J. Phys. Chem.* **1986**, *90*, 441-444, doi:10.1021/j100275a018.
(7) Kurylo, M. J.; Ouellette, P. A. Rate constants for the reaction $HO_2 + NO_2 + N_2 \rightarrow HO_2NO_2 + N_2$: The temperature dependence of the falloff parameters. *J. Phys. Chem.* **1987**, *91*, 3365-3368, doi:10.1021/j100296a052.
(8) Sander, S. P.; Peterson, M. Kinetics of the reaction $HO_2 + NO_2 + M \rightarrow HO_2NO_2 + M$. *J. Phys. Chem.* **1984**, *88*, 1566-1571, doi:10.1021/j150652a025.
(9) Simonaitis, R.; Heicklen, J. Temperature dependence of the reactions of HO_2 with NO and NO_2. *Int. J. Chem. Kinet.* **1978**, *10*, 67-87, doi:10.1002/kin.550100106.

C6. $NO_2 + NO_3$. The recommended limiting rate constants at 298 K (N_2 bath gas) and temperature exponents are the geometric mean of the corresponding rate constants and the average of the exponents, respectively, obtained by nonlinear least squares. The low pressure limit is based on the data of Kircher et al.,[9] Smith et al.,[12] Wallington et al.,[14] Orlando et al.,[11] and Nakano et al.,[10] combined with $k_{uni} \times K_{eq}$ data (recommended K_{eq} from Table 3-1); k_{uni} data were taken from Connell et al.[3] and Cantrell et al.[2] The high pressure limit is based on data from Kircher et al.,[9] Smith et al.,[12] Wallington et al.,[14] Hahn et al.,[6] and $k_{uni} \times K_{eq}$ (K_{eq} from Table 3-1); k_{uni} data were taken from Cantrell et al.[2] and Ide et al.[7] The recommendation is in good agreement with the data of Burrows et al.[1] and with k_{uni} (multiplied by K_{eq} from Table 3-1) reported by Viggiano et al.[13] Values from Croce de Cobos et al.[4] were excluded due to arguments given by Orlando et al.,[11] who point out that a reanalysis of these data using better values for the rate constant for $NO_3 + NO \rightarrow 2NO_2$ yields a negative value for $NO_2 + NO_3 + M$. The study of Fowles et al.[5] is noted, but not used. Johnston et al.[8] reviewed this reaction. The rate constant for the reverse reaction (k_{uni}) can be obtained as the ratio of the recommended recombination rate constant k_{rec} from this table, divided by the recommended K_{eq} from Table 3-1: $k_{uni} = k_{rec}/K_{eq}$.
(Table: 15-10, Note: 15-10, Evaluated: 15-10) Back to Table

(1) Burrows, J. P.; Tyndall, G. S.; Moortgat, G. K. Absorption spectrum of NO_3 and kinetics of the reactions of NO_3 with NO_2, Cl, and several stable atmospheric species at 298 K. *J. Phys. Chem.* **1985**, *89*, 4848-4856.
(2) Cantrell, C. A.; Shetter, R. E.; Calvert, J. G.; Tyndall, G. S.; Orlando, J. J. Measurement of rate coefficients for the unimolecular decomposition of N_2O_5. *J. Phys. Chem.* **1993**, *97*, 9141-9148, doi:10.1021/j100138a013.
(3) Connell, P. S.; Johnston, H. S. The thermal dissociation of N_2O_5 in N_2. *Geophys. Res. Lett.* **1979**, *6*, 553-556, doi:10.1029/GL006i007p00553.
(4) Croce de Cobos, A. E.; Hippler, H.; Troe, J. Study of the recombinatlon reaction $NO_2 + NO_3 + M \rightarrow N_2O_5 + M$ at high pressures. *J. Phys. Chem.* **1984**, *88*, 5083-5086, doi:10.1021/j150665a057.
(5) Fowles, M.; Mitchell, D. N.; Morgan, J. W. L.; Wayne, R. P. Kinetics and photochemistry of NO_3 Part 2.-Kinetics of the reaction $NO_2 + NO_3 + M$. *J. Chem. Soc. Faraday Trans. 2* **1982**, *78*, 1239-1248, doi:10.1039/f29827801239.
(6) Hahn, J.; Luther, K.; Troe, J. Experimental and theoretical study of the temperature and pressure dependences of the recombination reactions $O + NO_2(+ M) \rightarrow NO_3(+ M)$ and $NO_2 + NO_3(+M) \rightarrow N_2O_5(+M)$. *Phys. Chem. Chem. Phys.* **2000**, *2*, 5098-5104, doi:10.1039/b005756h.
(7) Ide, T.; Nakayama, T.; Takahashi, K.; Matsumi, Y. Thermal decomposition rate of N_2O_5 measured by cavity ring-down spectroscopy. *Int. J. Chem. Kinetics* **2008**, *40*, 679-684, doi:10.1002/kin.20351.
(8) Johnston, H. S.; Cantrell, C. A.; Calvert, J. G. Unimolecular decomposition of NO_3 to form NO and O_2 and a review of N_2O_5/NO_3 kinetics. *J. Geophys. Res.* **1986**, *91*, 5159-5172, doi:10.1029/JD091iD04p05159.
(9) Kircher, C. C.; Margitan, J. J.; Sander, S. P. Temperature and pressure dependence study of the reaction $NO_2 + NO_3 + M \rightarrow N_2O_5 + M$. *J. Phys. Chem.* **1984**, *88*, 4370-4375, doi:10.1021/j150663a037.
(10) Nakano, Y.; Sadamori, K.; Hosho, Y.; Ishiwata, T. Study of the pressure dependence of the rate constant of the reaction of NO_3 with NO_2. *Chem. Phys. Lett.* **2011**, *513*, 27-30, doi:10.1016/j.cplett.2011.07.060.

(11) Orlando, J. J.; Tyndall, G. S.; Cantrell, C. A.; Calvert, J. G. Temperature and pressure dependence of the rate coefficient for the reaction $NO_3 + NO_2 \rightarrow N_2O_5 + N_2$. *J. Chem. Soc. Faraday Trans.* **1991**, *87*, 2345-2349, doi:10.1039/ft9918702345.
(12) Smith, C. A.; Ravishankara, A. R.; Wine, P. H. Kinetics of the reaction $NO_2 + NO_3 + M$ at low pressures and 298 K. *J. Phys. Chem.* **1985**, *89*, 1423-1427, doi:10.1021/j100254a024.
(13) Viggiano, A. A.; Davidson, J. A.; Fehsenfeld, F. C.; Ferguson, E. E. Rate constants for the collisional dissociation of N_2O_5 by N_2. *J. Chem. Phys.* **1981**, *74*, 6113-6125, doi:10.1063/1.441055.
(14) Wallington, T. J.; Atkinson, R.; Winer, A. M.; Pitts, J. N., Jr. A study of the reaction $NO_3 + NO_2 + M \rightarrow N_2O_5 + M(M = N_2, O_2)$. *Int. J. Chem. Kinet.* **1987**, *19*, 243-249, doi:10.1002/kin.550190307.

C7. **$NO_3 + M$.** Johnston et al.[3] and Davidson et al.[1] have suggested significant thermal decomposition of NO_3. This has been disputed by Russell et al.[4] Davis et al.[2] claim that the barrier to thermal dissociation is 47.3 kcal mol^{-1}. This would seem to rule out such a process in the atmosphere.
(Table: 94-26, Note: 94-26, Evaluated: 94-26) Back to Table

(1) Davidson, J. A.; Cantrell, C. A.; Shetter, R. E.; McDaniel, A. H.; Calvert, J. G. The NO_3 radical decomposition and NO_3 scavenging in the troposphere. *J. Geophys. Res.* **1990**, *95*, 13963-13969, doi:10.1029/JD095iD09p13963.
(2) Davis, H. F.; Kim, B.; Johnston, H. S.; Lee, Y. T. Dissociation energy and photochemistry of NO_3. *J. Phys. Chem.* **1993**, *97*, 2172-2180, doi:10.1021/j100112a018.
(3) Johnston, H. S.; Cantrell, C. A.; Calvert, J. G. Unimolecular decomposition of NO_3 to form NO and O_2 and a review of N_2O_5/NO_3 kinetics. *J. Geophys. Res.* **1986**, *91*, 5159-5172, doi:10.1029/JD091iD04p05159.
(4) Russell, A. G.; Cass, G. R.; Seinfeld, J. H. On some aspects of nighttime atmospheric chemistry. *Environ. Sci. Technol.* **1986**, *20*, 1167-1172, doi:10.1021/es00153a013.

D1. **$CH_3 + O_2$.** Data from Kaiser[5] are fit to the NASA format. The ranges of this study were 3< P/Torr <11000 and 264< T/K <370. The rate constant was measured relative to the reaction $CH_3 + Cl_2 \rightarrow CH_3Cl + Cl$, k/cm^3 $molecule^{-1}$ $s^{-1} = 1.61 \times 10^{-12}exp(-530/RT)$. The recommended values are in good agreement with those from Selzer and Bayes.[12] These workers determined the rate constants as a function of pressure in N_2, Ar, O_2, and He. Plumb and Ryan[10] report a value in He which is consistent within error limits with the work of Selzer and Bayes. Pilling and Smith[9] have measured this process in Ar (32–490 Torr). Cobos et al.[2] have made measurements in Ar and N_2 from 0.25 to 150 atmospheres. They report parameters somewhat different than recommended here. The work of Laguna and Baughcum[7] seems to be in the fall–off region. Results of Pratt and Wood[11] in Ar are consistent with this recommendation, although the measurements are indirect. The suggested value accommodates the values of Keiffer et al.,[6] who measured the process in Ar between 20 and 600 Torr and in the range 334< T/K <582. Data of van den Bergh and Callear,[13] Hochanadel et al.,[4] Basco et al.,[1] Washida and Bayes,[15] Laufer and Bass,[8] and Washida[14] are also considered. A theoretical study by Zhu et al.[16] is in reasonable agreement with the recommendation. A study by Fernandes et al.[3] at pressures from 2–1000 bar and temperatures between 300 and 700 K presents a parameterization of the rate constant as a function of pressure and temperature which is in agreement with this recommendation at 300 K. If their parameters are used at 200 K the agreement is not as good, but is within the 95% uncertainty limit.
(Table: 06-2, Note: 10-6, Evaluated: 10-6) Back to Table

(1) Basco, N.; James, D. G. L.; James, F. C. A quantitative study of alkyl radical reactions by kinetic spectroscopy. II. Combination of the methyl radical with the oxygen molecule. *Int. J. Chem. Kinet.* **1972**, *4*, 129-149, doi:10.1002/kin.550040202.
(2) Cobos, C. J.; Hippler, H.; Luther, K.; Ravishankara, A. R.; Troe, J. High-pressure falloff curves and specific rate constants for the reaction $CH_3 + O_2 \rightleftharpoons CH_3O_2 \rightleftharpoons CH_3O + O$. *J. Phys. Chem.* **1985**, *89*, 4332-4338, doi:10.1021/j100266a036.
(3) Fernandes, R. X.; Luther, K.; Troe, J. Falloff curves for the reaction $CH_3 + O_2$ (+ M) $\rightarrow CH_3O_2$ (+ M) in the pressure range 2−1000 Bar and the temperature range 300−700 K. *J. Phys. Chem. A* **2006**, *110*, 4442-4449, doi:10.1021/jp056850o.
(4) Hochanadel, C. J.; Ghormley, J. A.; Boyle, J. W.; Ogren, P. J. Absorption spectrum and rates of formation and decay of the CH_3O_2 radical. *J. Phys. Chem.* **1977**, *81*, 3-7, doi:10.1021/j100516a002.
(5) Kaiser, E. W. Pressure dependence of the rate constants for the reactions $CH_3 + O_2$ and $CH_3 + NO$ from 3 to 10^4 Torr. *J. Phys. Chem.* **1993**, *97*, 11681-11688, doi:10.1021/j100147a022.
(6) Keiffer, M.; Pilling, M. J.; Smith, M. J. C. Pressure and temperature dependence of the reaction $CH_3 + O_2 + M \rightarrow CH_3O_2 + M$ over the range $334 \leq T/K \leq 582$. *J. Phys. Chem.* **1987**, *91*, 6028-6034, doi:10.1021/j100307a042.

(7) Laguna, G. A.; Baughcum, S. L. Real-time detection of methyl radicals by diode laser absorption at 608 cm^{-1}. *Chem. Phys. Lett.* **1982**, *88*, 568-571, doi:10.1016/0009-2614(82)85010-0.
(8) Laufer, A. H.; Bass, A. M. Rate constants of the combination of methyl radicals with nitric oxide and oxygen. *Int. J. Chem. Kinet.* **1975**, *7*, 639-648, doi:10.1002/kin.550070502.
(9) Pilling, M. J.; Smith, M. J. C. A laser flash photolysis study of the reaction $CH_3 + O_2 \rightarrow CH_3O_2$ at 298 K. *J. Phys. Chem.* **1985**, *89*, 4713-4720, doi:10.1021/j100268a014.
(10) Plumb, I. C.; Ryan, K. R. Kinetics of the reactions of CH_3 with $O(^3P)$ and O_2 at 295 K. *Int. J. Chem. Kinet.* **1982**, *14*, 861-874, doi:10.1002/kin.550140806.
(11) Pratt, G. L.; Wood, S. W. Kinetics of the reaction of methyl radicals with oxygen. *J. Chem. Soc. Faraday Trans. 1* **1984**, *80*, 3419-3427, doi:10.1039/f19848003419.
(12) Selzer, E. A.; Bayes, K. D. Pressure dependence of the rate of reaction of methyl radicals with O_2. *J. Phys. Chem.* **1983**, *87*, 392-394, doi:10.1021/j100226a007.
(13) van den Bergh, H. E.; Callear, A. B. Spectroscopic measurement of the rate of the gas-phase combination of methyl radicals with nitric oxide and oxygen at 295 K. *Trans. Faraday Soc.* **1971**, *67*, 2017-2024, doi:10.1039/tf9716702017.
(14) Washida, N. Reaction of methyl radicals with $O(^3P)$, O_2 and NO. *J. Chem. Phys.* **1980**, *73*, 1665-1672, doi:10.1063/1.440348.
(15) Washida, N.; Bayes, K. D. The reactions of methyl radicals with atomic and molecular oxygen. *Int. J. Chem. Kinet.* **1976**, *8*, 777-794, doi:10.1002/kin.550080512.
(16) Zhu, R., C.-C. Hsu and M. C. Lin *Ab initio* study of the $CH_3 + O_2$ reaction: Kinetics, mechanism and product branching probabilities. *J. Chem. Phys.* **2001**, *115*, 195-203, doi:10.1063/1.1376128.

D2. OH + C_2H_2. The rate constant for this complex process has been examined by Smith et al.[13] in the temperature range from 228 to 1400 K, and in the pressure range 1 to 760 Torr. Their analysis, which is cast in similar terms to those used here, is the source of the rate constants and temperature dependences at both limits. The negative value of m reflects the fact that their analysis includes a 1.2 kcal/mol barrier for the addition of OH to C_2H_2. The data analyzed include those of Pastrana and Carr,[1] Perry et al.,[10] Michael et al.,[8] and Perry and Williamson.[11] Other data of Wilson and Westenberg,[16] Breen and Glass,[3] Smith and Zellner,[14] and Davis et al.[4] were not included. Studies by Liu et al.[7] and Lai et al.[6] are in general agreement with the recommendation. Calculations of k_o via the methods of Patrick and Golden[9] yield values compatible with those of Smith et al.[13] A study by Sørensen et al.[15] at 298 K and pressures from 25 to 8000 Torr of bath gas suggests k_0/cm^6 $molecule^{-2}$ $s^{-1} = 2.92 \times 10^{-30}$, k_∞/cm^3 $molecule^{-1}$ $s^{-1} = 9.69 \times 10^{-13}$ and $F_c = 0.6$. No difference was found between air, N_2/O_2 mixtures or O_2 as the bath gas. These values yield rate constants as a function of pressure at 298 K in agreement with this recommendation, so the recommended values are unchanged from JPL 02-25. Earlier, Fulle et al.[5] reported a high pressure limiting rate constant of 2×10^{-12} cm^3 $molecule^{-1}$ s^{-1}, which is the basis for the IUPAC[2] recommendation. A theoretical study by Senosiain et al.[12] is in essential agreement with this recommendation.
(Table: 06-2, Note: 06-2, Evaluated: 06-2) Back to Table

(1) André, P. V.; Carr, R. W., Jr. Rate of the reaction of hydroxyl radical with acetylene. *Int. J. Chem. Kinet.* **1974**, *6*, 587-595, doi:10.1002/kin.550060414
(2) IUPAC: Atmospheric Chemical Kinetic Data Evaluation. Atkinson, R.; Baulch, D. L.; Cox, R. A.; Crowley, J. N.; Hampson, J., R. F.; Hynes, R. G.; Jenkin, M. E.; Kerr, J. A.; Rossi, M. J.; Troe, J., 2004, http://www.iupac-kinetic.ch.cam.ac.uk.
(3) Breen, J. E.; Glass, G. P. The reaction of the hydroxyl radical with acetylene. *Int. J. Chem. Kinet.* **1971**, *3*, 145-153, doi:10.1002/kin.550030206
(4) Davis, D. D.; Fischer, S.; Schiff, R.; Watson, R. T.; Bollinger, W. A kinetic study of the reaction of OH radicals with two C_2 hydrocarbons: C_2H_4 and C_2H_2. *J. Chem. Phys.* **1975**, *63*, 1707-1712, doi:10.1063/1.431567.
(5) Fulle, D.; Hamann, H. F.; Hippler, H.; Jänsch, C. P. The high pressure range of the addition of OH to C_2H_2 and C_2H_4. *Ber. Bunsenges. Phys. Chem.* **1997**, *101*, 1433-1442, doi:10.1002/bbpc.199700004.
(6) Lai, L.-H.; Hsu, Y.-C.; Lee, Y.-P. The enthalpy change and the detailed rate coefficients of the equilibrium reaction OH + C_2H_2 ⇌ (M) HOC_2H_2 over the temperature range 627-713 K. *J. Chem. Phys.* **1992**, *97*, 3092-3099, doi:10.1063/1.462996.
(7) Liu, A.; Mulac, W. A.; Jonah, C. D. Temperature dependence of the rate constants of the reactions of OH radicals with C_2H_2 and C_2D_2 at 1 atm in Ar and from 333 to 1273 K. *J. Phys. Chem.* **1988**, *92*, 5942-5945, doi:10.1021/j100332a020.
(8) Michael, J. V.; Nava, D. F.; Borkowski, R. P.; Payne, W. A.; Stief, L. J. Pressure dependence of the absolute rate constant for the reaction OH + C_2H_2 from 228 to 413 K. *J. Chem. Phys.* **1980**, *73*, 6108-6116, doi:10.1063/1.440147.

(9) Patrick, R.; Golden, D. M. Third-order rate constants of atmospheric importance. *Int. J. Chem. Kinet.* **1983**, *15*, 1189-1227, doi:10.1002/kin.550151107.
(10) Perry, R. A.; Atkinson, R.; Pitts, J. N., Jr. Kinetics of the reactions of OH radicals with C_2H_2 and CO. *J. Chem. Phys.* **1977**, *67*, 5577-5584, doi:10.1063/1.434755.
(11) Perry, R. A.; Williamson, D. Pressure and temperature dependence of the OH radical reaction with acetylene. *Chem. Phys. Lett.* **1982**, *93*, 331-334, doi:10.1016/0009-2614(82)83703-2.
(12) Senosiain, J. P.; Klippenstein, S. J.; Miller, J. A. The reaction of acetylene with hydroxyl radicals. *J. Phys. Chem. A* **2005**, *109*, 6045-6055 doi:10.1021/jp050737g.
(13) Smith, G. P.; Fairchild, P. W.; Crosley, D. R. The pressure and temperature dependence of the OH + C_2H_2 reaction above 800 K. *J. Chem. Phys.* **1984**, *81*, 2667-2677, doi:10.1063/1.447976.
(14) Smith, I. W. M.; Zellner, R. Rate measurements of reactions of OH by resonance absorption Part 2.-Reactions of OH with CO, C_2H_4 and C_2H_2. *J. Chem. Soc. Faraday Trans. 2* **1973**, *69*, 1617-1627, doi:10.1039/f29736901617.
(15) Sørensen, M.; Kaiser, E. W.; Hurley, M. D.; Wallington, T. J.; Nielsen, O. J. Kinetics of the reaction of OH radicals with acetylene in 25–8000 Torr of air at 296 K. *Int. J. Chem. Kinet.* **2003**, *35*, 191-197, doi:10.1002/kin.10119.
(16) Wilson, W. E.; Westenberg, A. A. Study of the reaction of hydroxyl radical with methane by quantitative ESR. *Proc. Combust. Inst.* **1967**, *11*, 1143-1150.

D3. **OH + C_2H_4.** The recommendation for the low pressure limit at 300 K is the average of fitted values from studies carried out over a significant range of pressure using synthetic air (Klein et al.[9]), N_2 (Vakhtin et al.[17] and Cleary et al.[2]), or Argon (Klein et al.[9]). All three colliders were treated as equivalent. The recommended temperature exponent (*n*) was taken from the master equation analysis by Golden,[6] who fitted the experimental rate constants in N_2, including those at very low temperatures (96, 110, and 165 K) reported by Vakhtin et al.[17] The recommendation for the high pressure limit at 300 K is the average of fitted values from eight data sets measured near 300 K using helium (Tully et al.,[16] Kuo and Lee,[10] and Cleary et al.[2]), argon (Klein et al.[9]), N_2 (Vakhtin et al.[17] and Cleary et al.[2]), and synthetic air (Klein et al.[9]). The recommended temperature exponent was from a least squares fit of the high pressure limiting values obtained from individual fits of data at 15 temperatures ranging from 200 K to 430 K, including data near 300 K.[2,9,10,16,17] In addition to the studies already mentioned, the recommended high pressure rate constants are in good agreement with the data of Davis et al.,[4] Howard,[8] Greiner,[7] Morris et al.,[12] and Overend and Paraskevopoulos[13] in helium, Atkinson et al.[1] in argon, and Lloyd et al.[11] and Cox[3] in nitrogen/oxygen mixtures. The parameters recommended are similar to the curve proposed by Klein et al.[9] at 298 K. Kuo and Lee[10] report a stronger temperature dependence for the low-pressure limit (n=4), but the present recommendation is in good agreement with their measured rate constants. Calculations of the type in Patrick and Golden[14] as described in Vakhtin et al.[17] yield $n = 4.2$, although they use a somewhat low value for energy transfer by nitrogen. The high-pressure limit temperature dependence has been determined by several workers. Zellner and Lorenz[18] report a value equivalent to $m = +0.8$ over the range ($296 < T/K < 524$) at about 1 atmosphere. A value of $m = +2.0$ fits the data ($540 < T/K < 670$) of Diau and Lee.[5] Cleary et al.[2] report values in N_2 at 295 K. They also report values in He between 200 and 400 K. They perform master equation calculations and report fitting parameters. Taylor et al.[15] report data at a single pressure and 69 and 86 K. Their data are well-accommodated by this recommendation and by the parameters in Cleary et al.[2]
(Table: 15-10, Note: 15-10, Evaluated: 15-10) Back to Table

(1) Atkinson, D. B.; Smith, M. A. Radical-molecule kinetics in pulsed uniform supersonic flows: Termolecular association of OH + NO between 90 and 220 K. *J. Phys. Chem.* **1994**, *98*, 5797-5800, doi:10.1021/j100074a001.
(2) Cleary, P. A.; Romero, M. T. B.; Blitz, M. A.; Heard, D. E.; Pilling, M. J.; Seakins, P. W.; Wang, L. Determination of the temperature and pressure dependence of the reaction OH + C_2H_4 from 200-400 K using experimental and master equation analyses. *Phys. Chem. Chem. Phys.* **2006**, *8*, 5633-5642, doi:10.1039/b612127f.
(3) Cox, R. A. Photolysis of gaseous nitrous acid-A Technique for obtaining kinetic data on atmospheric photooxidation reactions. *Int. J. Chem. Kinet.* **1975**, *1*, 379-398.
(4) Davis, D. D.; Fischer, S.; Schiff, R.; Watson, R. T.; Bollinger, W. A kinetic study of the reaction of OH radicals with two C_2 hydrocarbons: C_2H_4 and C_2H_2. *J. Chem. Phys.* **1975**, *63*, 1707-1712, doi:10.1063/1.431567.
(5) Diau, E. W.-G.; Lee, Y.-P. Detailed rate coefficients and the enthalpy change of the equilibrium reaction OH + C_2H_4 ⇄(M) HOC_2H_4 over the temperature range 544-673 K. *J. Chem. Phys.* **1992**, *96*, 377-386, doi:10.1063/1.462474.

(6) Golden, D. M. The reaction OH + C_2H_4: An example of rotational channel switching. *J. Phys. Chem. A* **2012**, *116*, 4259-4266, doi:10.1021/jp302009t.
(7) Greiner, N. R. Hydroxyl radical kinetics by kinetic spectrosopy. VII. The reaction with ethylene in the range 300-500 °K. *J. Chem. Phys.* **1970**, *53*, 1284-1285, doi:10.1063/1.1674133.
(8) Howard, C. J. Rate constants for the gas-phase reactions of OH radicals with ethylene and halogenated ethylene compounds. *J. Chem. Phys.* **1976**, *65*, 4771-4777, doi:10.1063/1.432932.
(9) Klein, T.; Barnes, I.; Becker, K. H.; Fink, E. H.; Zabel, F. Pressure dependence of the rate constants for the reactions of C_2H_4 and C_3H_8 with OH radicals at 295 K. *J. Phys. Chem.* **1984**, *88*, 5020-5025, doi:10.1021/j150665a046.
(10) Kuo, C. H.; Lee, Y.-P. Kinetics of the reaction OH + C_2H_4 in He, N_2, and O_2 at low pressure. *J. Phys. Chem.* **1991**, *95*, 1253-1257, doi:10.1021/j100156a040.
(11) Lloyd, A. C.; Darnall, K. R.; Winer, A. M.; Pitts, J. N., Jr. Relative rate constants for reaction of the hydroxyl radical with a series of alkanes, alkenes, and aromatic hydrocarbons. *J. Phys. Chem.* **1976**, *80*, 789-794, doi:10.1021/j100549a003.
(12) Morris, E. D., Jr.; Stedman, D. H.; Niki, H. Mass spectrometric study of the reactions of the hydroxyl radical with ethylene, propylene, and acetaldehyde in a discharge-flow system. *J. Am. Chem. Soc.* **1971**, *93*, 3570-3572, doi:10.1021/ja00744a004.
(13) Overend, R. P.; Paraskevopoulos, G. Rates of OH radical reactions. III. The reaction OH + C_2H_4 + M at 296 °K. *J. Chem. Phys.* **1977**, *67*, 674-679, doi:10.1063/1.434871.
(14) Patrick, R.; Golden, D. M. Third-order rate constants of atmospheric importance. *Int. J. Chem. Kinet.* **1983**, *15*, 1189-1227, doi:10.1002/kin.550151107.
(15) Taylor, S. E.; Goddard, A.; Blitz, M. A.; Cleary, P. A.; Heard, D. E. Pulsed Laval nozzle study of the kinetics of OH with unsaturated hydrocarbons at very low temperatures. *Phys. Chem. Chem. Phys.* **2008**, *10*, 422-437, doi:10.1039/b711411g.
(16) Tully, F. P. Laser photolysis/laser-induced fluorescence study of the reaction of hydroxyl radical with ethylene. *Chem. Phys. Lett.* **1983**, *96*, 148-153, doi:10.1016/0009-2614(83)80481-3.
(17) Vakhtin, A. B.; Murphy, J. E.; Leone, S. R. Low-temperature kinetics of reactions of OH radical with ethene, propene, and 1-butene. *J. Phys. Chem. A* **2003**, *107*, 10055-10062, doi:10.1021/jp030230a.
(18) Zellner, R.; Lorenz, K. Laser photolysis/resonance fluorescence study of the rate constants for the reactions of OH radicals with C_2H_4 and C_3H_6. *J. Phys. Chem.* **1984**, *88*, 984-989, doi:10.1021/j150649a028.

D4. OH + $CH_3CH=CH_2$ (propene). The following studies have been used to reach the recommendation: Spangenberg et al.[10] in a Laval nozzle expansion of N_2 with LIF detection of OH at 293 K and at individual points from 114 to 58 K; Vakhtin et al.[12,13] in a Laval nozzle expansion of N_2 with LIF detection of OH at 296 K and individual points at 96, 110, and 165 K; Nielsen et al.[6] in a pulse radiolysis experiment (kinetic UV absorbance of OH radical) at 298 K in 1 atm of air; Wallington[14] in a pulsed laser photolysis experiment with LIF detection of OH at 298 K in Argon; Schmidt et al.[9] with laser photolysis and LIF of OH at 295 K in 1 atm of air; Tully and Goldsmith[11] with laser photolysis and LIF detection of OH at 293 to 467 K in 25 to 600 Torr of He; Zellner and Lorenz[15] laser photolysis and resonance fluorescence detection of OH at 297 K in 1.3–130 mbar of Ar; Klein et al.[4] with a relative rate measurement (relevant to n-Hexane) at 295 K in 1.3–1000 mbar of air; Atkinson and Aschmann[1] from relative rate measurements at 295 K in 1 atm of air; Nip and Paraskevopoulos[7] with flash photolysis and resonance absorption at 297 K in 75 mbar of an H_2/N_2O mixture; Ravishankara et al.[8] with flash photolysis and resonance fluorescence of OH at 295 K in 20 and 200 Torr of He; and Atkinson and Pitts[2] by flash photolysis and resonance fluorescence of OH at 298–425 K in 25–100 Torr of Ar. Additional studies have been reviewed by Calvert et al.[3] The recommended high pressure rate constant at 298 K is the geometric mean of all of the studies listed above, except for the relative rate measurement of Klein et al.[4] The temperature exponent of k_∞ (parameter m) is the average of the values obtained from weighted least squares fits of data from Tully and Goldsmith[11] and from Vakhtin et al.;[13] the former extends upward from ~300 K and the latter extends downward. Pressure fall-off is only apparent at lower pressures and higher temperatures; most studies did not observe significant fall-off. Usable fall-off data near 300 K are available from Klein et al.[4] (Ar bath gas), Zellner and Lorenz[15] (Ar bath gas), and Vakhtin et al.[13] (N_2 bath gas). These fall-off data sets are for two different collider gases and provide only rough estimates of $k_0(298)$; the error factor associated with k_0 is at least ×3. Because no temperature-dependent fall-off data are available, the recommendation for the temperature exponent (parameter n) is based on the estimate by Calvert et al.[3] Loison et al.,[5] using a fast flow reactor coupled to a time of flight mass spectrometer, found that 71 ± 16% of the reaction near room temperature proceeds by addition of the OH to the terminal CH_2 group. (Table: 15-10, Note: 15-10, Evaluated: 15-10) Back to Table

(1) Atkinson, R.; Aschmann, S. M. Rate constants for the reaction of OH radicals with a series of alkenes and dialkenes at 295 ± 1 K. *Int. J. Chem. Kinet.* **1984**, *16*, 1175-1186, doi:10.1002/kin.550161002.
(2) Atkinson, R.; Pitts, J. N., Jr. Rate constants for the reaction of OH radicals with propylene and the butenes over the temperature range 297–425 °K. *J. Chem. Phys.* **1975**, *63*, 3591-3595, doi:10.1063/1.431800.
(3) Calvert, J. G.; Atkinson, R.; Kerr, J. A.; Madronich, S.; Moortgat, G. K.; Wallington, T. J.; Yarwood, G. *The Mechanisms of Atmospheric Oxidation of the Alkenes*; Oxford University Press: New York - Oxford, 2000.
(4) Klein, T.; Barnes, I.; Becker, K. H.; Fink, E. H.; Zabel, F. Pressure dependence of the rate constants for the reactions of C_2H_4 and C_3H_8 with OH radicals at 295 K. *J. Phys. Chem.* **1984**, *88*, 5020-5025, doi:10.1021/j150665a046.
(5) Loison, J.-C.; Daranlot, J.; Bergeat, A.; Caralp, F.; Mereau, R.; Hickson, K. M. Gas-phase kinetics of hydroxyl radical reactions with C_3H_6 and C_4H_8: Product branching ratios and OH addition site-specificity. *J. Phys. Chem. A* **2010**, *114*, 13326-13336, doi:10.1021/jp107217.
(6) Nielsen, O. J.; Jørgensen, O.; Donlon, M.; Sidebottom, H. W.; O'Farrell, D. J.; Treacy, J. Rate constants for the gas-phase reactions of OH radicals with nitroethene, 3-nitropropene and 1-nitrocyclohexene at 298 K and 1 atm. *Chem. Phys. Lett.* **1990**, *168*, 319-323, doi:10.1016/0009-2614(90)85618-M.
(7) Nip, W. S.; Paraskevopoulos, G. Rates of OH radical reactions. VI. Reactions with C_3H_6, 1-C_4H_8 and 1-C_5H_{10} at 297 K. *J. Chem. Phys.* **1979**, *71*, 2170-2174, doi:10.1063/1.438599.
(8) Ravishankara, A. R.; Wagner, S.; Fischer, S.; Smith, G.; Schiff, R.; Watson, R. T.; Tesi, G.; Davis, D. D. A kinetics study of the reactions of OH with several aromatic and olefinic compounds. *Int. J. Chem. Kinet.* **1978**, *10*, 783–804, doi:10.1002/kin.550100802.
(9) Schmidt, V.; Zhu, G. Y.; Becker, K. H.; Fink, E. H. Study of OH reactions at high pressures by excimer laser photolysis - dye laser fluorescence. *Ber. Bunsenges. Phys. Chem.* **1985**, *89*, 321-322, doi:10.1002/bbpc.19850890337.
(10) Spangenberg, T.; Kohler, S.; Hansmann, B.; Wachsmuth, U.; Abel, B.; Smith, M. A. Low-temperature reactions of OH radicals with propene and isoprene in pulsed Laval nozzle expansions. *J. Phys. Chem. A* **2004**, *108*, 7527-7534, doi:10.1021/jp031228m.
(11) Tully, F. P.; Goldsmith, J. E. M. Kinetic study of the hydroxyl radical-propene reaction. *Chem. Phys. Lett.* **1985**, *116*, 345-352, doi:10.1016/0009-2614(85)80182-2.
(12) Vakhtin, A. B.; Lee, S.; Heard, D. E.; Smith, I. W. M.; Leone, S. R. Low-temperature kinetics of reactions of the OH radical with propene and 1-butene studied by a pulsed laval nozzle apparatus combined with laser-induced fluorescence. *J. Phys. Chem. A* **2001**, *105*, 7889-7895, doi:10.1021/jp010809d.
(13) Vakhtin, A. B.; Murphy, J. E.; Leone, S. R. Low-temperature kinetics of reactions of OH radical with ethene, propene, and 1-butene. *J. Phys. Chem. A* **2003**, *107*, 10055-10062, doi:10.1021/jp030230a.
(14) Wallington, T. J. Kinetics of the gas phase reaction of OH radicals with pyrrole and thiophene. *Int. J. Chem. Kinet.* **1986**, *18*, 487-496, doi:10.1002/kin.550180407.
(15) Zellner, R.; Lorenz, K. Laser photolysis/resonance fluorescence study of the rate constants for the reactions of OH radicals with C_2H_4 and C_3H_6. *J. Phys. Chem.* **1984**, *88*, 984-989, doi:10.1021/j150649a028.

D5. **OH + CH_2=$C(CH_3)CH_3$ (*iso*-butene).** The rate constant is not dependent on pressure even at 1 Torr of helium, suggesting that it is very near the high-pressure limit in all of the reported studies. The recommended high pressure rate constant at 298 K is the geometric mean of the absolute rate constants reported by Atkinson and Pitts (flash photolysis (FP) with resonance fluorescence (RF) detection of OH)[2] and relative rate measurements reported by Wu et al.[8] (cited by Calvert et al.[4]), Barnes et al.,[3] Ohta,[6] and Atkinson and Aschmann.[1] The recommendation is in fair agreement with the early discharge-flow measurement of Morris and Niki.[5] The temperature dependence is based on the measurements of Atkinson and Pitts.[2] The estimated 2σ error limits are set to include all of the data used in the recommendation; because there is only one study of temperature dependence, f(298 K) and g were set to 1.2 and 200, respectively. Calvert et al.[4] reviewed the data published prior to 2000 and recommended rate constants in reasonable agreement with the present recommendation. The reaction proceeds mostly (>90%) by addition of OH to the two carbon atoms at the ends of the double bond.[4] Peeters et al.[7] reported that 85 ± 10% of the addition is to the terminal carbon atom, producing a tertiary free radical (the balance produces a primary free radical).
(Table: 15-10, Note: 15-10, Evaluated: 15-10) Back to Table

(1) Atkinson, R.; Aschmann, S. M. Rate constants for the reactions of O_3 and OH radicals with a series of alkynes. *Int. J. Chem. Kinet.* **1984**, *16*, 259-268, doi:10.1002/kin.550160308.

(2) Atkinson, R.; Pitts, J. N., Jr. Rate constants for the reaction of OH radicals with propylene and the butenes over the temperature range 297–425 °K. *J. Chem. Phys.* **1975**, *63*, 3591-3595, doi:10.1063/1.431800.
(3) Barnes, I.; Bastian, V.; Becker, K. H.; Fink, E. H.; Zabel, F. Reactivity studies of organic substances towards hydroxyl radicals under atmospheric conditions. *Atmos. Environ.* **1982**, *16*, 545-550, doi:10.1016/0004-6981(82)90163-9.
(4) Calvert, J. G.; Atkinson, R.; Kerr, J. A.; Madronich, S.; Moortgat, G. K.; Wallington, T. J.; Yarwood, G. *The Mechanisms of Atmospheric Oxidation of the Alkenes*; Oxford University Press: New York - Oxford, 2000.
(5) Morris, E. D., Jr.; Stedman, D. H.; Niki, H. Mass spectrometric study of the reactions of the hydroxyl radical with ethylene, propylene, and acetaldehyde in a discharge-flow system. *J. Am. Chem. Soc.* **1971**, *93*, 3570-3572, doi:10.1021/ja00744a004.
(6) Ohta, T. Rate constants for the reactions of OH radicals with alkyl substituted olefins. *Int. J. Chem. Kinet.* **1984**, *16*, 879-886, doi:10.1002/kin.550160708.
(7) Peeters, J.; Boullart, W.; Pultau, V.; Vandenberk, S.; Vereecken, L. Structure−activity relationship for the addition of OH to (poly)alkenes: Site-specific and total rate constants. *J. Phys. Chem. A* **2007**, *111*, 1618–1631, doi:10.1021/jp066973o.
(8) Wu, C. H.; Japar, S. M.; Niki, H. Relative reactivities of HO-hydrocarbon reactions from smog reactor studies. *J. Environ Sci. Health* **1976**, *A11*, 191-200, doi:10.1080/10934527609385765.

D6. OH + CH_2=$CH_2CH_2CH_3$ (1-butene). The rate constant is not dependent on pressure even at 1 Torr of helium, suggesting that it is very near the high-pressure limit in all of the studies. The recommended high pressure rate constant at 298 K is the geometric mean of the absolute rate constants reported by Atkinson and Pitts[2] (flash photolysis (FP) with resonance fluorescence (RF) detection of OH), Ravishankara et al.[13] (FP-RF), Nip and Paraskevopoulos[9] (FP with resonance absorption (RA) detection of OH), Biermann and Pitts[4] (discharge flow (DF) with mass spectrometry (MS) detection), Sims et al.[14] (Laval-Nozzle flow apparatus (LN) and laser induced fluorescence (LIF) detection of OH), Vakhtin et al.[15] (LN-LIF), and relative rate measurements reported by Wu et al.[17] (cited by Calvert et al.[5]), Lloyd et al.,[6] Winer et al.,[16] Barnes et al.,[3] Ohta,[10] and Atkinson and Aschmann.[1] The recommendation is in good agreement with the early discharge-flow measurement of Morris and Niki,[8] and in poor agreement with that of Pastrana and Carr,[11] which possibly was affected by secondary reactions. The temperature dependence is based on the measurements of Atkinson and Pitts,[2] Sims et al.,[14] and Vathkin et al.[15] Calvert et al. reviewed the data published prior to 2000 and recommended rate constants[5] in good agreement with the present recommendation. The estimated 2σ error limits are set to include all of the data used in the recommendation. The reaction proceeds mostly (>90%) by addition of OH to the two carbon atoms at the ends of the double bond.[5] Peeters et al.[12] measured product branching ratios in a multi-stage flow apparatus with mass spectrometric detection and concluded that 85 ± 10% of the OH addition reaction proceeds by addition to the terminal CH_2 group, producing a secondary free radical. Peeters et al. also developed a structure-activity relationship (SAR) for predicting the product distribution for OH + alkene reactions. Loison et al.[7] also used a flow apparatus with mass spectrometric detection, but with photoionization, and reported that 71 ± 16% of the addition reaction is to the terminal CH_2 group, in good agreement with Peeters et al. Furthermore, Loison et al. concluded that 8 ± 3% of the total reaction is due to abstraction.
(Table: 15-10, Note: 15-10, Evaluated: 15-10) Back to Table

(1) Atkinson, R.; Aschmann, S. M. Rate constants for the reactions of O_3 and OH radicals with a series of alkynes. *Int. J. Chem. Kinet.* **1984**, *16*, 259-268, doi:10.1002/kin.550160308.
(2) Atkinson, R.; Pitts, J. N., Jr. Rate constants for the reaction of OH radicals with propylene and the butenes over the temperature range 297–425 °K. *J. Chem. Phys.* **1975**, *63*, 3591-3595, doi:10.1063/1.431800.
(3) Barnes, I.; Bastian, V.; Becker, K. H.; Fink, E. H.; Zabel, F. Reactivity studies of organic substances towards hydroxyl radicals under atmospheric conditions. *Atmos. Environ.* **1982**, *16*, 545-550, doi:10.1016/0004-6981(82)90163-9.
(4) Biermann, H. W.; Harris, G. W.; Pitts, J. N., Jr. Photoionization mass spectrometer studies of the collsionally stabillzed product distribution in the reaction of OH radicals with selected alkenes at 298 K. *J. Phys. Chem.* **1982**, *86*, 2958-2964, doi:10.1021/j100212a030.
(5) Calvert, J. G.; Atkinson, R.; Kerr, J. A.; Madronich, S.; Moortgat, G. K.; Wallington, T. J.; Yarwood, G. *The Mechanisms of Atmospheric Oxidation of the Alkenes*; Oxford University Press: New York - Oxford, 2000.
(6) Lloyd, A. C.; Darnall, K. R.; Winer, A. M.; Pitts, J. N., Jr. Relative rate constants for reaction of the hydroxyl radical with a series of alkanes, alkenes, and aromatic hydrocarbons. *J. Phys. Chem.* **1976**, *80*, 789-794, doi:10.1021/j100549a003.

(7) Loison, J.-C.; Daranlot, J.; Bergeat, A.; Caralp, F.; Mereau, R.; Hickson, K. M. Gas-phase kinetics of hydroxyl radical reactions with C_3H_6 and C_4H_8: Product branching ratios and OH addition site-specificity. *J. Phys. Chem. A* **2010**, *114*, 13326–13336, doi:10.1021/jp107217.
(8) Morris, E. D., Jr.; Stedman, D. H.; Niki, H. Mass spectrometric study of the reactions of the hydroxyl radical with ethylene, propylene, and acetaldehyde in a discharge-flow system. *J. Am. Chem. Soc.* **1971**, *93*, 3570-3572, doi:10.1021/ja00744a004.
(9) Nip, W. S.; Paraskevopoulos, G. Rates of OH radical reactions. VI. Reactions with C_3H_6, 1-C_4H_8 and 1-C_5H_{10} at 297 K. *J. Chem. Phys.* **1979**, *71*, 2170-2174, doi:10.1063/1.438599.
(10) Ohta, T. Rate constants for the reactions of OH radicals with alkyl substituted olefins. *Int. J. Chem. Kinet.* **1984**, *16*, 879-886, doi:10.1002/kin.550160708.
(11) Pastrana, A. V.; Carr, R. W., Jr. Kinetics of the reaction of hydroxyl radicals with ethylene, propylene, 1-butene, and trans-2-butene. *J. Phys. Chem.* **1975**, *79*, 765–770, doi:10.1021/j100575a001.
(12) Peeters, J.; Boullart, W.; Pultau, V.; Vandenberk, S.; Vereecken, L. Structure−activity relationship for the addition of OH to (poly)alkenes: Site-specific and total rate constants. *J. Phys. Chem. A* **2007**, *111*, 1618–1631, doi:10.1021/jp066973o.
(13) Ravishankara, A. R.; Wagner, S.; Fischer, S.; Smith, G.; Schiff, R.; Watson, R. T.; Tesi, G.; Davis, D. D. A kinetics study of the reactions of OH with several aromatic and olefinic compounds. *Int. J. Chem. Kinet.* **1978**, *10*, 783–804, doi:10.1002/kin.550100802.
(14) Sims, I. R.; Smith, I. W. M.; Bocherel, P.; Defrance, A.; Travers, D.; Rowe, B. R. Ultra-low temperature kinetics of neutral-neutral reactions: Rate constants for the reactions of OH radicals with butenes between 295 and 23 K. *J. Chem. Soc. Faraday Trans.* **1994**, *90*, 1473-1478, doi:10.1039/FT9949001473.
(15) Vakhtin, A. B.; Lee, S.; Heard, D. E.; Smith, I. W. M.; Leone, S. R. Low-temperature kinetics of reactions of the OH radical with propene and 1-butene studied by a pulsed laval nozzle apparatus combined with laser-induced fluorescence. *J. Phys. Chem. A* **2001**, *105*, 7889-7895, doi:10.1021/jp010809d.
(16) Winer, A. M.; Lloyd, A. C.; Darnall, K. R.; Pitts, J. N., Jr. Relative rate constants for the reaction of the hydroxyl radical with selected ketones, chloroethenes, and monoterpene hydrocarbons. *J. Phys. Chem.* **1976**, *80*, 1635-1639, doi:10.1021/j100555a024.
(17) Wu, C. H.; Japar, S. M.; Niki, H. Relative reactivities of HO-hydrocarbon reactions from smog reactor studies. *J. Environ Sci. Health* **1976**, *A11*, 191-200, doi:10.1080/10934527609385765.

D7. **OH + *cis*-$CH_3CH=CHCH_3$ (*cis*-2-butene).** The rate constant is not dependent on pressure even at 1 Torr of helium, suggesting that it is very near the high-pressure limit in all of the studies. The recommended high pressure rate constant at 298 K is the geometric mean of the absolute rate constants reported by Atkinson and Pitts[2] (flash photolysis (FP) with resonance fluorescence (RF) detection of OH), Ravishankara et al.[7] (FP-RF), Sims et al.[8] (Laval-Nozzle flow apparatus (LN) and laser induced fluorescence (LIF) detection of OH), and relative rate measurements reported by Lloyd et al.,[4] Winer et al.,[9] Ohta,[6] and Atkinson and Aschmann.[1] The recommendation is in good agreement with the early discharge-flow measurement of Morris and Niki.[5] The temperature dependence is based on the measurements of Atkinson and Pitts[2] and Sims et al.[8] Calvert et al. reviewed the data published prior to 2000 and recommended rate constants[3] in good agreement with the present recommendation. The reaction proceeds mostly (>90%) by addition of OH to the two carbon atoms at the ends of the double bond.[3] The estimated 2σ error limits are set to include all of the data used in the recommendation. (Table: 15-10, Note: 15-10, Evaluated: 15-10) Back to Table

(1) Atkinson, R.; Aschmann, S. M. Rate constants for the reactions of O_3 and OH radicals with a series of alkynes. *Int. J. Chem. Kinet.* **1984**, *16*, 259-268, doi:10.1002/kin.550160308.
(2) Atkinson, R.; Pitts, J. N., Jr. Rate constants for the reaction of OH radicals with propylene and the butenes over the temperature range 297–425 °K. *J. Chem. Phys.* **1975**, *63*, 3591-3595, doi:10.1063/1.431800.
(3) Calvert, J. G.; Atkinson, R.; Kerr, J. A.; Madronich, S.; Moortgat, G. K.; Wallington, T. J.; Yarwood, G. *The Mechanisms of Atmospheric Oxidation of the Alkenes*; Oxford University Press: New York - Oxford, 2000.
(4) Lloyd, A. C.; Darnall, K. R.; Winer, A. M.; Pitts, J. N., Jr. Relative rate constants for reaction of the hydroxyl radical with a series of alkanes, alkenes, and aromatic hydrocarbons. *J. Phys. Chem.* **1976**, *80*, 789-794, doi:10.1021/j100549a003.
(5) Morris, E. D., Jr.; Niki, H. Reactivity of hydroxyl radicals with olefins. *J. Phys. Chem.* **1971**, *75*, 3640–3641, doi:10.1021/j100692a031.
(6) Ohta, T. Rate constants for the reactions of OH radicals with alkyl substituted olefins. *Int. J. Chem. Kinet.* **1984**, *16*, 879-886, doi:10.1002/kin.550160708.

(7) Ravishankara, A. R.; Wagner, S.; Fischer, S.; Smith, G.; Schiff, R.; Watson, R. T.; Tesi, G.; Davis, D. D. A kinetics study of the reactions of OH with several aromatic and olefinic compounds. *Int. J. Chem. Kinet.* **1978**, *10*, 783–804, doi:10.1002/kin.550100802.
(8) Sims, I. R.; Smith, I. W. M.; Bocherel, P.; Defrance, A.; Travers, D.; Rowe, B. R. Ultra-low temperature kinetics of neutral-neutral reactions: Rate constants for the reactions of OH radicals with butenes between 295 and 23 K. *J. Chem. Soc. Faraday Trans.* **1994**, *90*, 1473-1478, doi:10.1039/FT9949001473.
(9) Winer, A. M.; Lloyd, A. C.; Darnall, K. R.; Pitts, J. N., Jr. Relative rate constants for the reaction of the hydroxyl radical with selected ketones, chloroethenes, and monoterpene hydrocarbons. *J. Phys. Chem.* **1976**, *80*, 1635-1639, doi:10.1021/j100555a024.

D8. OH + *trans*-$CH_2CH=CHCH_3$ (*trans*-2-butene). The rate constant is not dependent on pressure even at 1 Torr of helium, suggesting that it is very near the high-pressure limit in all of the studies. The recommended high pressure rate constant at 298 K is the geometric mean of the absolute rate constants reported by Atkinson and Pitts[2] (flash photolysis (FP) with resonance fluorescence (RF) detection of OH), and Sims et al.[10] (Laval-Nozzle flow apparatus (LN) and laser induced fluorescence (LIF) detection of OH), and relative rate measurements reported by Wu et al.[11] (cited by Calvert et al.[3]), Ohta,[7] Atkinson and Aschmann,[1] Edney et al.,[4] and Rogers.[9] The recommendation is in good agreement with the early discharge-flow measurement of Morris and Niki,[6] and in poor agreement with that of Pastrana and Carr,[8] which possibly was affected by secondary reactions. The temperature dependence is based on the measurements of Atkinson and Pitts[2] and Sims et al.[10] The estimated 2σ error limits are set to include all of the data used in the recommendation. Calvert et al.[3] reviewed the data published prior to 2000 and recommended rate constants in reasonable agreement with the present recommendation. The reaction proceeds mostly (>90%) by addition of OH to the two carbon atoms at the ends of the double bond.[3] Loison et al.[5] used a flow apparatus with photoionization mass spectrometric detection and reported that 3 ± 1% of the total reaction proceeds by hydrogen abstraction.
(Table: 15-10, Note: 15-10, Evaluated: 15-10) Back to Table

(1) Atkinson, R.; Aschmann, S. M. Rate constants for the reactions of O_3 and OH radicals with a series of alkynes. *Int. J. Chem. Kinet.* **1984**, *16*, 259-268, doi:10.1002/kin.550160308.
(2) Atkinson, R.; Pitts, J. N., Jr. Rate constants for the reaction of OH radicals with propylene and the butenes over the temperature range 297–425 °K. *J. Chem. Phys.* **1975**, *63*, 3591-3595, doi:10.1063/1.431800.
(3) Calvert, J. G.; Atkinson, R.; Kerr, J. A.; Madronich, S.; Moortgat, G. K.; Wallington, T. J.; Yarwood, G. *The Mechanisms of Atmospheric Oxidation of the Alkenes*; Oxford University Press: New York - Oxford, 2000.
(4) Edney, E. O.; Kleindienst, T. E.; Corse, E. W. Room temperature rate constants for the reaction of OH with selected chlorinated and oxygenated hydrocarbons. *Int. J. Chem. Kinet.* **1986**, *18*, 1355-1371, doi:10.1002/kin.550181207.
(5) Loison, J.-C.; Daranlot, J.; Bergeat, A.; Caralp, F.; Mereau, R.; Hickson, K. M. Gas-phase kinetics of hydroxyl radical reactions with C_3H_6 and C_4H_8: Product branching ratios and OH addition site-specificity. *J. Phys. Chem. A* **2010**, *114*, 13326–13336, doi:10.1021/jp107217.
(6) Morris, E. D., Jr.; Niki, H. Reactivity of hydroxyl radicals with olefins. *J. Phys. Chem.* **1971**, *75*, 3640–3641, doi:10.1021/j100692a031.
(7) Ohta, T. Rate constants for the reactions of diolefins with OH radicals in the gas phase. Estimate of the rate constants from those for monoolefins. *J. Phys. Chem.* **1983**, *87*, 1209-1213, doi:10.1021/j100230a023.
(8) Pastrana, A. V.; Carr, R. W., Jr. Kinetics of the reaction of hydroxyl radicals with ethylene, propylene, 1-butene, and trans-2-butene. *J. Phys. Chem.* **1975**, *79*, 765–770, doi:10.1021/j100575a001.
(9) Rogers, J. D. Rate constant measurements for the reaction of the hydroxyl radical with cyclohexene, cyclopentene, and glutaraldehyde. *Environ. Sci. Technol.* **1989**, *23*, 177-181, doi:10.1021/es00179a006.
(10) Sims, I. R.; Smith, I. W. M.; Bocherel, P.; Defrance, A.; Travers, D.; Rowe, B. R. Ultra-low temperature kinetics of neutral-neutral reactions: Rate constants for the reactions of OH radicals with butenes between 295 and 23 K. *J. Chem. Soc. Faraday Trans.* **1994**, *90*, 1473-1478, doi:10.1039/FT9949001473.
(11) Wu, C. H.; Japar, S. M.; Niki, H. Relative reactivities of HO-hydrocarbon reactions from smog reactor studies. *J. Environ Sci. Health* **1976**, *A11*, 191-200, doi:10.1080/10934527609385765.

D9. CH_3O + NO. This reaction proceeds via a complex potential energy surface that includes both chemical activation and direct abstraction routes[1] to the disproportionation products CH_2O and HNO as well as the

combination to form CH_3NO. The chemical activation process would have inverse pressure dependence and the direct abstraction would be pressure independent. The recommended values take into account the results of Frost and Smith[4] in Ar and CF_4 and of Caralp et al.[1] in He and Ar. In both of these references the disproportionation process is subtracted from total loss of CH_3O with a pressure independent, temperature dependent value. At 300 K below one Torr the disproportionation process dominates. Temperature dependences are from the higher temperature results. The low pressure rate constant is consistent with the measurements of McCaulley et al.[5] and Daële et al.[2] in helium. Studies by Ohmori et al.[6] and Dobé et al.[3] are in general agreement with respect to both the addition and bimolecular pathways. (See the note in Table 1-1 for the bimolecular pathway.)
(Table: 06-2, Note: 06-2, Evaluated: 06-2) Back to Table

(1) Caralp, F., M-T. Rayez, W. Forst, N. Gomez, B. Delcroix, D. Fitschen and P. Devolder Kinetic and mechanistic study of the pressure and temperature dependence of the reaction CH_3O + NO. *J. Chem. Soc. Faraday Trans.* **1998**, *94*, 3321-3330, doi:10.1039/a807456i.
(2) Daële, V.; Laverdet, G.; Le Bras, G.; Poulet, G. Kinetics of the reactions CH_3O + NO, CH_3O + NO_3, and CH_3O_2 + NO_3. *J. Phys. Chem.* **1995**, *99*, 1470-1477, doi:10.1021/j100005a017.
(3) Dóbé, S.; Lendvay, G.; Szilágyi, I.; Bérces, T. Kinetics and mechanism of the reaction of CH_3O with NO. *Int. J. Chem. Kinet.* **1994**, *26*, 887-901, doi:10.1002/kin.550260903
(4) Frost, M. J.; Smith, I. W. M. Rate Constants for the reactions of CH_3O and C_2H_5O with NO over a range of temperature and total pressure. *J. Chem. Soc. Faraday Trans.* **1990**, *86*, 1757-1762, doi:10.1039/ft9908601757.
(5) McCaulley, J. A.; Moyle, A. M.; Golde, M. F.; Anderson, S. M.; Kaufman, F. Kinetics of the reactions of CH_3O and CD_3O with NO. *J. Chem Soc. Farad. Trans.* **1990**, *86*, 4001-4009, doi:10.1039/ft9908604001.
(6) Ohmori, K.; Yamasaki, K.; Matsui, H. Pressure dependence of the rate constant for the reaction of CH_3O + NO. *Bull. Chem. Soc. Jpn.* **1993**, *66*, 51-56, doi:10.1246/bcsj.66.51.

D10. CH_3O + NO_2. The recommended values are from the work mostly of Wollenhaupt and Crowley (in Ar).[6] Agreement is good with earlier work at 298 K from the study of Frost and Smith[2] in Ar (corrected by Frost and Smith[3]) and that of Biggs et al.[1] and Martinez et al.[4] in He. Low pressure results agree within a factor of two with the measurements of McCaulley et al.[5] in He. A minor bimolecular (chemical activation) pathway is also observed. (See Table 1-1.)
(Table: 02-25, Note: 06-2, Evaluated: 06-2) Back to Table

(1) Biggs, P.; Canosa-Mas, C. E.; Fracheboud, J. M.; Shallcross, D. E.; Wayne, R. P.; Caralp, F. Investigation into the pressure dependence between 1 and 10 Torr of the reactions of NO_2 with CH_3 and CH_3O. *J. Chem. Soc. Faraday Trans.* **1993**, *89*, 4163-4169, doi:10.1039/ft9938904163.
(2) Frost, M. J.; Smith, I. W. M. Rate constants for the reactions of CH_3O and C_2H_5O with NO_2 over a range of temperature and total pressure. *J. Chem. Soc. Faraday Trans.* **1990**, *86*, 1751-1756, doi:10.1039/ft9908601751.
(3) Frost, M. J.; Smith, I. W. M. Corrigendum to rate constants for the reductions of CH_3O and C_2H_5O with NO_2 over a range of temperature and total pressure. *J. Chem. Soc. Faraday Trans* **1993**, *89*, 4251, doi:10.1039/ft9938904251.
(4) Martinez, E.; Albaladejo, J.; Jiménez, E.; Notario, A.; Mera, Y. D. d. Temperature dependence of the limiting low- and high-pressure rate constants for the CH_3O + NO_2 + He reaction over the 250-390 K temperature range. *Chem. Phys. Lett.* **2000**, *329*, 191-199, doi:10.1016/S0009-2614(00)01012-5.
(5) McCaulley, J. A.; Anderson, S. M.; Jeffries, J. B.; Kaufman, F. Kinetics of the reaction of CH_3O with NO_2. *Chem. Phys. Lett.* **1985**, *115*, 180-186, doi:10.1016/0009-2614(85)80675-8.
(6) Wollenhaupt, M.; Crowley, J. N. Kinetic studies of the reactions CH_3 + NO_2 → products, CH_3O + NO_2 → products, and OH + $CH_3C(O)CH_3$ → $CH_3C(O)OH$ + CH_3, over a range of temperature and pressure. *J. Phys. Chem. A* **2000**, *104*, 6429-6438, doi:10.1021/jp0005726.

D11. C_2H_5O + NO. High-pressure data at 298 K in Ar from Frost and Smith[3] and in He between 286 and 388 K at pressures from 30 to 500 Torr, from Fitschen et al.[2] Low-pressure measurements in He are from Daele et el.[1] He experiments were scaled to N_2 by dividing by a factor of 2.5. Ar data were taken as equivalent to N_2 or air. The data were fit by subtracting an assumed pressure independent value of 1×10^{-11} from the measured rate constants to account for the route to form HNO and CH_3CHO. The low-pressure value agrees with theory. The bimolecular channel with an estimated rate constant of about 10^{-11} needs to be verified by direct studies. The temperature dependence of the low pressure limit is estimated and that of the high pressure limit is taken from Fitschen et al.[2] (The high pressure rate expression in Fitschen et al. seems to be in error.)

(Table: 06-2, Note: 06-2, Evaluated: 06-2) Back to Table

(1) Daële, V.; Ray, A.; Vassalli, I.; Poulet, G.; Le Bras, G. Kinetic study of reactions of C_2H_5O and $C_2H_5O_2$ with NO at 298 K and 0.55 – 2 torr. *Int. J. Chem. Kinet.* **1995**, *27*, 1121-1133, doi:10.1002/kin.550271109.

(2) Fittschen, C.; Frenzel, A.; Imrik, K.; Devolder, P. Rate constants for the reactions of C_2H_5O, i-C_3H_7O, and n-C_3H_7O with NO and O_2 as a function of temperature. *Int. J. Chem. Kinet.* **1999**, *31*, 860-866, doi:10.1002/(SICI)1097-4601(1999)31:12<860::AID-KIN4>3.0.CO;2-E.

(3) Frost, M. J.; Smith, I. W. M. Rate Constants for the reactions of CH_3O and C_2H_5O with NO over a range of temperature and total pressure. *J. Chem. Soc. Faraday Trans.* **1990**, *86*, 1757-1762, doi:10.1039/ft9908601757.

D12. $C_2H_5O + NO_2$. High-pressure rate constant at 298 K from Frost and Smith.[1] Other values estimated from similar reactions.
(Table: 06-2, Note: 92-20, Evaluated: 06-2) Back to Table

(1) Frost, M. J.; Smith, I. W. M. Rate constants for the reactions of CH_3O and C_2H_5O with NO_2 over a range of temperature and total pressure. *J. Chem. Soc. Faraday Trans.* **1990**, *86*, 1751-1756, doi:10.1039/ft9908601751.

D13. $CH_3O_2 + NO_2$. Golden[3] has re-evaluated the data for this reaction. The recommended parameters are from a fit to Percival[4] and temperature- and pressure-dependent data in Sander and Watson[6] and Ravishankara et al.[5] The temperature dependence of the high pressure rate constant is a little high, but results from the statistical fit to the data. The values recommended herein, were taken with the data in a study of the reverse reaction by Zabel et al.[7] to compute the value of the equilibrium constant in Table 3-1. Destriau and Troe[2] have fit the above data with k_∞ independent of temperature and $F_c = 0.36$. Bridier et al.[1] are in good agreement with this recommendation at one atmosphere and 298 K.
(Table: 06-2, Note: 06-2, Evaluated: 06-2) Back to Table

(1) Bridier, I.; Lesclaux, R.; Veyret, B. Flash photolysis kinetic study of the equilibrium $CH_3O_2 + NO_2 \leftrightarrow CH_3O_2NO_2$. *Chem. Phys. Lett.* **1992**, *191*, 259-263, doi:10.1016/0009-2614(92)85297-N.

(2) Destriau, M.; Troe, J. Thermal dissociation and recombination of alkyl and haloalkyl peroxyitrates: An SACM modelling study. *Int. J. Chem. Kinet.* **1990**, *22*, 915-934, doi:10.1002/kin.550220904.

(3) Golden, D. M. Evaluating data for atmospheric models, an example: $CH_3O_2 + NO_2 = CH_2O_2NO_2$. *Int. J. Chem. Kinet.* **2005**, *37*, 625-632, doi:10.1002/kin.20104.

(4) Percival, D. T.; Raventos-Duran, A.; Bacak, A. B. In *International Gas Kinetics Symposium* Bristol, UK, 2004.

(5) Ravishankara, A. R.; Eisele, F. L.; Wine, P. H. Pulsed laser photolysis-long path laser absorption kinetics study of the reaction of methylperoxy radicals with NO_2. *J. Chem. Phys.* **1980**, *73*, 3743-3749, doi:10.1063/1.440604.

(6) Sander, S. P.; Watson, R. T. Kinetic studies of the reactions of CH_3O_2 with NO, NO_2, and CH_3O_2 at 298 K. *J. Phys. Chem.* **1980**, *84*, 1664-1674, doi:10.1021/j100450a002.

(7) Zabel, F.; Reimer, A.; Becker, K. H.; Fink, E. H. Thermal decomposition of alkyl peroxynitrates. *J. Phys. Chem.* **1989**, *93*, 5500-5507, doi:10.1021/j100351a036.

D14. $C_2H_5O_2 + NO_2$. The only experimental study is that of Elfers et al.[3] who measured the rate constant relative to the $C_2H_5O_2 + NO$ reaction between 10 and 1000 mbar. Elfers et al. used a value of $k = 8.9 \times 10^{-12}$ cm^3 molecule^{-1} s^{-1} for the reference reaction. By comparison the recommended rate constant for the reference reaction from Table 1-1 of this evaluation is 1.1×10^{-11} cm^3 molecule^{-1} s^{-1} at 254 K. There are three data points. An evaluation of the Elfers et al. work by Destriau and Troe[2] cast the data in the format used in the IUPAC evaluation.[1] The parameters in Table 2 are adjusted to agree with the data corrected for the change in the reference reaction, using the simpler formula employed in this recommendation.
(Table: 02-25, Note: 02-25, Evaluated: 02-25) Back to Table

(1) Atkinson, R.; Baulch, D. L.; Cox, R. A.; Hampson, J., R. F.; Kerr, J. A.; Rossi, M. J.; Troe, J. Evaluated kinetic, photochemical and heterogeneous data for atmospheric chemistry: Supplement V. *J. Phys. Chem. Ref. Data* **1997**, *26*, 1329-1499, doi:10.1063/1.556010.

(2) Destriau, M.; Troe, J. Thermal dissociation and recombination of alkyl and haloalkyl peroxyitrates: An SACM modelling study. *Int. J. Chem. Kinet.* **1990**, *22*, 915-934, doi:10.1002/kin.550220904.

(3) Elfers, G.; Zabel, F.; Becker, K. H. Determination of the rate constant ratio for the reactions of the ehtylperoxy radical with NO and NO_2. *Chem. Phys. Lett.* **1990**, *168*, 14-19, doi:10.1016/0009-2614(90)85094-S.

D15. $CH_3C(O)O_2 + NO_2$. The recommended parameters are from the data of Bridier et al.,[1] who report in the format represented here, but using $F_c = 0.3$. Their values are: $k_0^{300} = (2.7 \pm 1.5) \times 10^{-28}$, $k_\infty^{300} = (12.1 \pm 2.0) \times 10^{-12}$, with $n = 7.1 \pm 1.7$ and $m = 0.9 \pm 0.15$. Bridier et al. also reported measured rate constants (k_{uni}) for the reverse reaction from 297 to 314 K and pressures from 7 to 600 Torr of N_2. Direct measurements of the recombination rate constant by Sehested et al.[6] are in excellent agreement with those of Bridier et al. The present recommendation is based on a non-linear least-squares analysis (assuming uniform relative errors) of the direct measurements reported by Bridier et al. for k_{rec} and k_{uni} (the latter multiplied by K_{eq}, which is recommended in Table 3). This recommendation is in very good agreement with previous ones and the 2σ parameter uncertainties encompass all of the values used in the least-squares analysis. Studies of the decomposition of $CH_3C(O)O_2NO_2$ (peroxyacetylnitrate, PAN) by Sehested et al.[6] are in excellent agreement with the recommendation and those by Roberts and Bertman,[4] Grosjean et al.,[2] and Orlando et al.[3] are in accord. Studies by Seefeld et al.[5] and Sehested et al.[6] of the relative rates of $CH_3C(O)O_2$ with NO and NO_2 are confirmatory. In the Roberts and Bertman[4] study it was shown that PAN decomposition yields only peroxyacetyl radical and NO_2; methyl nitrate was not detected. However, a study by von Ahsen et al.[7], which utilized matrix isolation of the PAN decomposition products, suggests a minor pathway due to O-O bond fission.
(Table: 19-5, Note: 19-5, Evaluated: 19-5) Back to Table

(1) Bridier, I.; Caralp, F.; Loirat, H.; Lesclaux, R.; Veyret, B.; Becker, K. H.; Reimer, A.; Zabel, F. Kinetic and theoretical studies of the reactions $CH_3C(O)O_2 + NO_2 + M \rightleftarrows CH_3C(O)O_2NO_2 + M$ between 248 and 393 K and between 30 and 760 Torr. *J. Phys. Chem.* **1991**, *95*, 3594-3600, doi:10.1021/j100162a031.
(2) Grosjean, D.; Grosjean, E.; Williams, E. L. Thermal decomposition of PAN, PPN and vinyl-PAN. *J. Air and Waste Manage. Assoc.* **1994**, *44*, 391-396.
(3) Orlando, J. J.; Tyndall, G. S.; Calvert, J. G. Thermal decomposition pathways for peroxy-acetyl nitrate (PAN): Implications for atmospheric methyl nitrate levels. *Atmos. Environ.* **1992**, *26A*, 3111-3118, doi:10.1016/0960-1686(92)90468-Z.
(4) Roberts, J. M.; Bertman, S. B. The thermal decomposition of peroxyacetic nitric anhydride (PAN) and peroxymethacrylic nitric anhydride (MPAN). *Int. J. Chem. Kinet.* **1992**, *24*, 297-307, doi:10.1002/kin.550240307.
(5) Seefeld, S.; Kinnison, D. J.; Kerr, J. A. Relative rate study of the reactions of acetylperoxy radicals with NO and NO_2: Peroxyacetyl nitrate formation under laboratory conditions related to the troposphere. *J. Phys. Chem. A* **1997**, *101*, 55-59, doi:10.1021/jp962266r.
(6) Sehested, J.; Christensen, L. K.; Mogelberg, T.; Nielsen, O. J.; Wallington, T. J.; Guschin, A.; Orlando, J. J.; Tyndall, G. S. Absolute and relative rate constants for the reactions $CH_3C(O)O_2 + NO$ and $CH_3C(O)O_2 + NO_2$ and thermal stability of $CH_3C(O)O_2NO_2$. *J. Phys. Chem. A* **1998**, *102*, 1779-1789, doi:10.1021/jp972881a.
(7) von Ahsen, S.; Wilner, H.; Francisco, J. S. Thermal decomposition of peroxy acetyl nitrate $CH_3C(O)OONO_2$. *J. Chem. Phys.* **2004**, *121*, 2048-2057, doi:10.1063/1.1767813.

D16. $CH_3CH_2C(O)O_2 + NO_2$. This reaction, forming peroxypropionyl nitrate (PPN), has been studied in the reverse direction by Schurath and Wipprecht,[4] Mineshos and Glavas,[3] Grosjean et al.,[1] and Kirchner et al.[2] Group additivity considerations indicate that the equilibrium constant for both PAN and PPN will be the same (both sides of the equilibrium for PPN differ from those for PAN by the group C-(C)(CO)$(H)_2$). Therefore, the recommended value for the association reaction is taken from the decomposition studies multiplied by the same equilibrium constant as for PAN. The resulting values are very similar to those for $CH_3C(O)O_2 + NO_2$ forming peroxyacetyl nitrate (PAN). Conservative error limits are estimated.
(Table: 02-25, Note: 06-2, Evaluated: 06-2) Back to Table

(1) Grosjean, D.; Grosjean, E.; Williams, E. L. Thermal decomposition of PAN, PPN and vinyl-PAN. *J. Air and Waste Manage. Assoc.* **1994**, *44*, 391-396.
(2) Kirchner, F.; Mayer-Figge, A.; Zabel, F.; Becker, K. H. Thermal stability of peroxynitrates. *Int. J. Chem. Kinet.* **1999**, *31*, 127-144, doi:10.1002/(SICI)1097-4601(1999)31:2<127::AID-KIN6>3.0.CO;2-L.
(3) Mineshos, G.; Glavas, S. Thermal decomposition of peroxypropionyl nitrate - Kinetics of the formation of nitrogenous products. *React. Kinet. Catal. Lett.* **1991**, *45*, 305-312, doi:10.1007/BF02070443.

(4) Schurath, U.; Wipprecht, V. 1st European Symposium on Physico-Chemical Behavior of Atmospheric Pollutants, 1979, Ispra.

D17. $CH_3C(O)CH_2 + O_2$. Cox et al.[1] reported a value of $k = (1.5 \pm 0.3) \times 10^{-12}$ cm^3 molecule^{-1} s^{-1} at 298 K and 1 atm of SF_6 in which a pulse radiolysis study was modeled. Studies in He at 298 K have been reported by Oguchi et al.,[5] Imrik et al.,[3] Kovacs et al.,[4] and Hassouna et al.[2] This data can be accommodated with $k_0 = 1.5 \times 10^{-29}$ cm^3 molecule^{-1} s^{-1}, $k_\infty = 1.0 \times 10^{-12}$ s^{-1} with $f = 1.15$. To account for the difference between He and N_2, $k_o = 3 \times 10^{-29}$, and $f = 1.3$ are estimated and recommended. Hassouna et al.report rate constants in the temperature range 291 to 400 K at 130 and 650 bar He showing a slight negative temperature dependence. They also report data at 10 bar He in the temperature range 459 to 520 K. These latter data exhibit biexponential decays from which the equilibrium constant is also extracted. (See Table 3-1.)
(Table:10-6, Note: 10-6, Evaluated: 10-6) Back to Table

(1) Cox, R. A.; Munk, J.; Nielsen, O. J.; Pagsberg, P.; Ratajczak, E. Ultraviolet absorption spectra and kientics of acetonyl and acetonylperoxy radicals. *Chem. Phys. Lett.* **1990**, *173*, 206-210, doi:10.1016/0009-2614(90)80079-S.
(2) Hassouna, M.; Delbos, E.; Devolder, P.; Viskolcz, B.; Fittschen, C. Rate and equilibrium constant of the reaction of 1-methylvinoxy radicals with O_2: $CH_3COCH_2 + O_2 \leftrightarrow CH_3COCH_2O_2$. *J. Phys. Chem. A* **2006**, *110*, 6667-6672, doi:10.1021/jp0558270.
(3) Imrik, K.; Farkas, E.; Vasvári, G.; Szilágyi, I.; Sarzyski, D.; Dóbé, S.; Bérces, T.; Márta, F. Laser spectrometry and kinetics of selected elementary reactions of the acetonyl radical. *Phys. Chem. Chem. Phys.* **2004**, *6*, 3958-3968, doi:10.1039/b404889j.
(4) Kovács, G.; Zádor, J.; Farkas, E.; Nádasdi, R.; Szilágyi, I.; Dóbé, S.; Bérces, T.; Márta, F.; Lendvay, G. Kinetics and mechanism of the reactions of CH_3CO and $CH_3C(O)CH_2$ radicals with O_2. Low-pressure discharge flow experiments and quantum chemical computations. *Phys. Chem. Chem. Phys.* **2007**, *9*, 4142-4154, doi:10.1039/b706216h.
(5) Oguchi, T.; Miyoshi, A.; Koshi, M.; Matsui, H.; Washida, N. Kinetic study on reactions of 1- and 2-methylvinoxy radicals with O_2. *J. Phys. Chem. A* **2000**, *105*, 378-382, doi:10.1021/jp001826q.

D18. $CH_2OO + CH_2OO$ (Criegee intermediate). The recommendation is the average of the rate constants reported near 298 K by Buras et al.[1] and Ting et al.[6] (the latter supersedes the report of Su et al.[5]). The reaction does not depend on pressure at least up to 1 atmosphere, because of the existence of low energy thresholds for subsequent isomerization and fragmentation.[7] The reaction products are thought to be $2\ H_2CO + O_2(^1\Delta_g)$. Because of the rapid reactions of CH_2OO and the complex mixtures of reactants present in the systems that have been studied, rate constants must be extracted from complicated mechanisms.[1-4,6,7] Ting et al.[6] have presented an analysis using perhaps the most comprehensive mechanism to date, but this field is changing very rapidly.
(Table 15-10, Note: 15-10, Evaluated: 15-10) Back to Table

(1) Buras, Z. J.; Elsamra, R. M. I.; Green, W. H. Direct determination of the simplest Criegee intermediate (CH_2OO) self reaction rate. *J. Phys. Chem. Lett.* **2014**, *5*, 2224-2228, doi:10.1021/jz5008406.
(2) Buras, Z. J.; Elsamra, R. M. I.; Jalan, A.; Middaugh, J. E.; Green, W. H. Direct kinetic measurements of reactions between the simplest Criegee intermediate CH_2OO and alkenes. *J. Phys. Chem. A* **2014**, *118*, 1997-2006, doi:10.1021/jp4118985.
(3) Gravestock, T. J.; Blitz, M. A.; Bloss, W. J.; Heard, D. E. A multidimensional study of the reaction $CH_2I + O_2$: Products and atmospheric implications. *ChemPhysChem* **2010**, *11*, 3928-3941, doi:10.1002/cphc.201000575.
(4) Huang, H.; Rotavera, B.; Eskola, A. J.; Taatjes, C. A. Correction to "Pressure-dependent I atom yield in the reaction of CH_2I with O_2 shows a remarkable apparent third-body efficiency for O_2". *J. Phys. Chem. Lett.* **2013**, *4*, 3824-3824, doi:10.1021/jz402266q.
(5) Su, Y.-T.; Lin, H.-Y.; Putikam, R.; Matsui, H.; Lin, M. C.; Lee, Y.-P. Extremely rapid self-reaction of the simplest Criegee intermediate CH_2OO and its implications in atmospheric chemistry. *Nat. Chem.* **2014**, *6*, 477-483, doi:10.1038/NCHEM.1890.
(6) Ting, W.-L.; Chang, C.-H.; Lee, Y.-F.; Matsui, H.; Lee, Y.-P.; Lin, J. J.-M. Detailed mechanism of the $CH_2I + O_2$ reaction: Yield and self-reaction of the simplest Criegee intermediate CH_2OO. *J. Chem. Phys.* **2014**, *141*, 104308, doi:10.1063/1.4894405.
(7) Vereecken, L.; Harder, H.; Novelli, A. The reactions of Criegee intermediates with alkenes, ozone, and carbonyl oxides. *Phys. Chem. Chem. Phys.* **2014**, *16*, 4039-4049, doi:10.1039/c3cp54514h.

D19. OH + HCN. The recommendation is based on the laser flash photolysis-laser induced fluorescence (FP-LIF) measurements of Strekowski.[6] A study by Fritz et al.[2] employed a laser flash photolysis-resonance absorption

apparatus. The Fritz et al. results are systematically greater than the Strekowski values. The results of Strekowski are preferred because the LIF technique is less subject to interference than resonance absorption. Furthermore, the activation energy of $k_\infty(T)$ measured by Strekowski (~13 kJ/mol) is consistent (within the expected error range) with the ab initio value (~14 kJ/mol) of Bunkan et al.,[1] while that from Fritz et al. (~5 kJ/mol) is not. The uncertainty factor (f) encompasses the data reported by Strekowski et al. and Fritz et al. The results reported by Fritz et al. and Strekowski suggest the reaction to be in the fall-off region under most atmospheric conditions. By contrast, Phillips[4,5] studied this reaction using a discharge flow apparatus at low pressures and found the rate coefficient to have reached the high pressure limit at ~10 Torr at 298 K. The results reported by Fritz et al. and Strekowski contradict this finding. Bunkan et al.[1] report the $^{12}C/^{13}C$ and $^{14}N/^{15}N$ kinetic isotope effects at 298 K and 1.00 atm to be 0.9733 ± 0.0012 and 0.9840 ± 0.0016, respectively (uncertainties are 1σ). The reaction mechanism has been investigated theoretically by Galano,[3] and Bunkan et al.[1] Galano[3] found that, under atmospheric conditions, HC(OH)N reacts with O_2 to generate nitroso formaldehyde (HC(O)NO) and regenerates an OH radical (a finding confirmed by Bunkan et al.[1]). Strekowski.[6] showed experimentally that >80% of the OH is regenerated when 100 Torr of O_2 is present at 295 K. Bunkan et al.[1] used theory to determine that the initial OH addition to the carbon atom in HCN has a barrier of 15.4 kJ/mol; when they adjusted it to 14.3 kJ mol^{-1}, the theoretical rate constant could be brought into agreement with the experiments of Strekowski.[6] Additional laboratory kinetic studies are desired to validate the Strekowski data and current recommendation.
(Table: 19-5, Note: 25-1, Evaluated: 19-5) Back to Table

(1) Bunkan, A. J.; Liang, C.-H.; Pilling, M. J.; Nielsen, C. J. Theoretical and experimental study of the OH radical reaction with HCN. *Mol. Phys.* **2013**, *111*, 1589-1598, doi:10.1080/00268976.2013.802036.
(2) Fritz, B.; Lorenz, K.; Steinert, W.; Zellner, R. Rate of oxidation of HCN by OH radicals at lower temperatures. *Oxidation Communications* **1984**, *6*, 363-370.
(3) Galano, A. Mechanism of OH radical reactions with HCN and CH_3CN: OH regeneration in the presence of O_2. *J. Phys. Chem. A* **2007**, *111*, 5086-5091, doi:10.1021/jp0708345.
(4) Phillips, L. F. Pressure dependence of the rate of reaction of OH with HCN. *Chem. Phys. Lett.* **1978**, *57*, 538-539, doi:10.1016/0009-2614(78)85316-0.
(5) Phillips, L. F. Rate of reaction of OH with HCN between 298 K and 563 K. *Aust. J. Chem.* **1979**, *32*, 2571-2577, doi:10.1071/CH9792571.
(6) Strekowski, R. Laser Flash Photolysis Studies of Some $O(^1D_2)$ and OH ($X^2\Pi$) Reactions of Atmospheric Interest, Georgia Institute of Technology, 2001.

E1. **F + O_2.** Values are taken from a study by Campuzano-Jost et al.,[2] with experiments from 100 to 420 K at pressures of He, Ar and N_2 from 1 to 1000 bar. (They used $F_c = 0.54(T/300)^{-0.09}$, but the results are essentially the same with $F_c = 0.6$.) A study by Pagsberg et al.[7] reports k_o in argon to be 4.38×10^{-33} $(T/300)^{-1.2}$. There is also good agreement with earlier values of Smith and Wrigley,[9] Smith and Wrigley,[10] Shamonina and Kotov,[8] Arutyunov et al.,[1] Wallington and Nielsen,[12] Wallington et al.,[11] and Ellerman et al.[5] The values are slightly lower than the values of Chen et al.[4] and Chegodaev et al.[3] Lyman and Holland[6] report a slightly lower value in Ar at 298 K. Campuzano-Jost et al.[2] and Pagsberg et al.[7] also determined the equilibrium constant and thus $\Delta H_{f,298}(FO_2) = 6.13 \pm 0.5$ kcal mol^{-1}. See F + O_2 in Table 3-1.
(Table: 06-2, Note: 06-2, Evaluated: 06-2) Back to Table

(1) Arutyunov, V. S.; Popov, L. S.; Chaikin, A. M. Measurement of the rate constant for the reaction of fluorine atoms with oxygen. *Kinet. Katal.* **1976**, *17*, 286-291.
(2) Campuzano-Jost, P.; Croce, A. E.; Hippler, H.; Siefke, M.; Troe, J. Kinetic and thermodynamic properties of the F + O_2 reaction system under high pressure and low temperature conditions. *J. Chem. Phys.* **1995**, *102*, 5317-5326, doi:10.1063/1.469258.
(3) Chegodaev, P. P.; Tubikov, B. I. *Dokl. Akad. Nauk. SSSR* **1973**, *210*, 647-649.
(4) Chen, H. L.; Trainor, D. W.; Center, R. E.; Fyfe, W. T. A flash photolysis, infrared chemiluminescence study of the rate constant for the recombination reaction F + O_2 + M. *J. Chem. Phys.* **1977**, *66*, 5513-5519, doi:10.1063/1.433872.
(5) Ellermann, T.; Sehested, J.; Nielson, O. J.; Pagsberg, P.; Wallington, T. J. Kinetics of the reaction of F atoms with O_2 and UV spectrum of FO_2 radicals in the gas phase at 295 K. *Chem. Phys. Lett.* **1994**, *218*, 287-294, doi:10.1016/0009-2614(94)00006-9.
(6) Lyman, J.; Holland, R. Oxygen fluoride chemical kinetics. *J. Phys. Chem.* **1988**, *92*, 7232-7241, doi:10.1021/j100337a015.
(7) Pagsberg, P.; Ratajczak, E.; Sillesen, A.; Jodkowski, J. T. Spectrokinetic studies of the gas-phase equilibrium F + O_2 ⇌ FO_2 between 295 and 359 K. *Chem. Phys. Lett.* **1987**, *141*, 88-94, doi:10.1016/0009-2614(87)80097-0.
(8) Shamonina, N. F.; Kotov, A. G. *Kinet. i Kataliz.* **1979**, *20*, 233.

(9) Smith, I. W. M.; Wrigley, D. J. Time-resolved vibrational chemiluminescence: Rate constants for the reaction F + HCl → HF + Cl and for the relaxation of HF(v=3) by HCl, CO_2, N_2O, CO, N_2 and O_2. *Chem. Phys. Lett.* **1980**, *70*, 481-486, doi:10.1016/0009-2614(80)80109-6.
(10) Smith, I. W. M.; Wrigley, D. J. Time resolved vibrational chemiluminescence: Rate constants for the reactions F + HBr, HI → HF + Br, I and for the relaxation of HF(v=4) and HF(v=6) by HBr, HI, CO_2, N_2O, CO, N_2 and O_2. *Chem. Phys.* **1981**, *63*, 321-336, doi:10.1016/0301-0104(81)87008-5.
(11) Wallington, T. J.; Mariq, M. M.; Ellerman, T.; Nielsen, O. J. Novel method for the measurement of gas-phase peroxy radical absorption spectra. *J. Phys. Chem.* **1992**, *96*, 982-986, doi:10.1021/j100181a080.
(12) Wallington, T. J.; Nielsen, O. J. UV absorption spectra and kinetics of the self reaction of $CFCl_2CH_2O_2$ and $CF_2ClCH_2O_2$ radicals in the gas phase at 298 K. *Int. J. Chem. Kinet.* **1991**, *23*, 785-798, doi:10.1002/kin.550230905.

E2. **F + NO.** A study by Pagsberg et al.,[2] taking into account data from Zetzsch,[6] Skolnik et al.,[4] Kim et al.,[1] Pagsberg et al.,[3] and Wallington et al.[5] reports rate constants for this reaction in several bath gases. Re-evaluating the data and converting to the form used in this compilation yields the recommended parameters.
(Table: 06-2, Note: 06-2, Evaluated: 06-2) Back to Table

(1) Kim, P.; MacLean, D. I.; Valence, W. G. ESR spectroscopic studies of the kinetics of the F + NO + M and F_2 + NO reactions. *J. Phys. Chem.* **1980**, *84*, 1806-1810, doi:10.1021/j100451a013.
(2) Pagsberg, P.; Sillesen, A.; Jodkowski, J. T.; Ratajczak, E. Kinetics of the reaction F + NO + M → FNO + M studied by pulse radiolysis combined with time-resolved IR and UV spectroscopy. *Chem. Phys. Lett.* **1996**, *249*, 358-364, doi:10.1016/0009-2614(95)01441-1.
(3) Pagsberg, P.; Sztuba, B.; Ratajczak, E.; Sillesen, A. Spectrokinetic studies of the gas phase reactions NH_2 + NO_x initiated by pulse radiolysis. *Acta Chem. Scand.* **1991**, *45*, 329-334, doi:10.3891/acta.chem.scand.45-0329.
(4) Skolnik, E. D.; Veysey, M. G.; Ahmed, M. G.; Jones, W. E. Rate constants for the reaction of fluorine atoms with nitric oxide in the presence of various third bodies. *Can. J. Chem.* **1975**, *53*, 3188-3193, doi:10.1139/v75-454.
(5) Wallington, T. J.; Ellerman, T.; Nielsen, O. J.; Sehested, J. Atmospheric chemistry of FCO_x radicals: UV spectra and self-reaction kinetics of FCO and $FC(O)O_2$ and kinetics of some reactions of FCO_x with O_2, O_3, and NO at 296 K. *J. Phys. Chem.* **1994**, *98*, 2346-2356, doi:10.1021/j100060a024.
(6) Zetzsch, C. Some combination reactions of fluorine atoms. In *First European Sym. on Combust*; Weinberg, F. S., Ed.; Academic Press London, 1973; Vol. 35; pp 35-40.

E3. **F + NO_2.** Fasano and Nogar[3] studied this reaction in N_2 at 300 K. Pagsberg et al.[5] studied the reaction in SF_6 and Zetzsch[7] studied it in He. The results from Fasano and Nogar[3] and Pagsberg et al.[5] were used to determine both the high and low pressure limits at 300 K. Treatment of the data for this system requires knowledge of the relative stabilities of FNO_2 and FONO. Patrick and Golden[6] assumed that the difference between these would be the same as between the $ClNO_2$ isomers. Theoretical work by Dixon and Christie,[2] Lee and Rice,[4] and Amos et al.[1] indicates that FNO_2 is 35–40 kcal mol^{-1} more stable than FONO, and therefore the measured rate refers to FNO_2 formation. The value of n = 2 is from Patrick and Golden, but consistent with Pagsberg et al.[5] who made a few measurements at 341 K. The value of m is a rough estimate from similar reactions, but is also consistent with Pagsberg et al.[5]
(Table: 06-2, Note: 06-2, Evaluated: 06-2) Back to Table

(1) Amos, R. D.; Murray, C. W.; Handy, N. C. Structures and vibrational frequencies of FOOF and FONO using density functional theory. *Chem. Phys. Lett.* **1993**, *202*, 489-494, doi:10.1016/0009-2614(93)90036-Z.
(2) Dixon, D. A.; Christe, K. O. Nitrosyl hypofluorite: Local denslty functional study of a problem case for theoretlcal methods. *J. Phys. Chem.* **1992**, *95*, 1018-1021, doi:10.1021/j100182a004.
(3) Fasano, D. M.; Nogar, N. S. Real-time kinetic study of the reaction F + NO_2. *J. Chem. Phys.* **1983**, *78*, 6688-6694, doi:10.1063/1.444668.
(4) Lee, T. J.; Rice, J. E. FONO: A difficult case for theory and experiment. *J. Chem. Phys.* **1992**, *97*, 4223-4232, doi:10.1063/1.463925.
(5) Pagsberg, P.; Sillesen, A.; Jodkowski, J. T.; Ratajczak, E. Kinetics of the F + NO_2 + M → FNO_2 + M reaction studied by pulse radiolysis combined with time-resolved IR and UV spectroscopy. *Chem. Phys. Lett.* **1996**, *252*, 165-171, doi:10.1016/S0009-2614(96)00161-3.
(6) Patrick, R.; Golden, D. M. Third-order rate constants of atmospheric importance. *Int. J. Chem. Kinet.* **1983**, *15*, 1189-1227, doi:10.1002/kin.550151107.

(7) Zetzsch, C. Some combination reactions of fluorine atoms. In *First European Sym. on Combust*; Weinberg, F. S., Ed.; Academic Press London, 1973; Vol. 35; pp 35-40.

E4. **$FO + NO_2$.** Low pressure limit from strong collision calculation and $\beta = 0.33$. T dependence from resultant $\langle \Delta E \rangle = 0.523$ kcal mol^{-1}, high-pressure limit and T dependence estimated. A theoretical study by Rayez and Destriau[2] indicates that the product is the single isomer $FONO_2$. Bedzhanyan et al.[1] report a value extracted from a complex mixture of bath gases.
(Table: 06-2, Note: 94-26, Evaluated: 06-2) Back to Table

(1) Bedzhanyan, Y. R.; Markin, E. M.; Gershenzon, Y. M. Experimental study of elementary reactions of FO radicals VI. Reaction with NO_2. *Kinetics and Catalysis* **1993**, *34*, 190-193.
(2) Rayez, M. T.; Destriau, M. Theoretical study of thermal dissociation and recombination reacitons of $XONO_2$ (X=F, Cl, Br, or I). *Chem. Phys. Lett.* **1993**, *206*, 278-284, doi:10.1016/0009-2614(93)85552-Y.

E5. **$CF_3 + O_2$.** Caralp et al.[3] have measured the rate constant in N_2 between 1 and 10 Torr. This supersedes the value from Caralp and Lesclaux.[2] Kaiser et al.[5] have extended the pressure range to 580 Torr measuring the reaction relative to the reaction of CF_3 with Cl_2. Breheny et al.[1] report values at 295 K from 2–110 Torr and they make a cogent argument for lowering the value of the rate constant used by Kaiser et al for their reference reaction by about 50%. This has the effect of lowering the Kaiser values. Each study recommends different parameters, but the data are well represented by the currently recommended values. Data of Ryan and Plumb[6] are in general agreement. Forst and Caralp[4] have examined this reaction theoretically.
(Table: 06-2, Note: 06-2, Evaluated: 06-2) Back to Table

(1) Breheny, C.; Hancock, G.; Morrell, C. The rate constant for the recombination reaction between CF_3 and O_2 measured between 2 and 110 Torr. *Z. Phys. Chem.* **2001**, *215*, 305-317, doi:10.1524/zpch.2001.215.3.305.
(2) Caralp, F.; Lesclaux, R. Rate constant for the reaction of the $CFCl_2$ radical with oxygen in the pressure range 0.2-12 Torr at 298 K. *Chem. Phys. Lett.* **1983**, *102*, 54-58, doi:10.1016/0009-2614(83)80657-5.
(3) Caralp, F.; Lesclaux, R.; Dognon, A. M. Kinetics of the reaction of CF_3 with O_2 over the temperature range 233-373 K. *Chem. Phys. Lett.* **1986**, *129*, 433-438, doi:10.1016/0009-2614(86)80224-X.
(4) Forst, W., and F. Caralp Microcanonical variational theory of radical recombination by inversion of interpolate partition function Part 2.-$CX_3 + O_2$ (X = H, F, Cl). *J. Chem. Soc. Faraday Trans.* **1991**, *87*, 2307-2315, doi:10.1039/ft9918702307.
(5) Kaiser, E. W.; Wallington, T. J.; Hurley, M. D. Kinetic study of the reaction of chlorine atoms with CF_3I and the reactions of CF_3 radicals with O_2, Cl_2 and NO at 296 K. *Int. J. Chem. Kinet.* **1995**, *27*, 205-218, doi:10.1002/kin.550270302.
(6) Ryan, K. R.; Plumb, I. C. Kinetics of the reactions of CF_3 with $O(^3P)$ and O_2 at 295 K. *J. Phys. Chem.* **1982**, *86*, 4678-4683, doi:10.1021/j100221a008.

E6. **$CF_3O + NO_2$.** Fockenberg et al.[2] report values (and large error limits) in nitrogen with 250< T/K <302 and 7< P/mbar <107. Their values, including two sigma errors are: $k_0 = (3.1 \pm 3.0) \times 10^{-28}$; $n = (2.0 \pm 2.0)$; $k_\infty = (1.5 \pm 0.5) \times 10^{-28}$; $m = (2.8 \pm 2.0)$. Because such large values for m are not physically justifiable, the recommendation is based on a fit forcing $m = 1$, which falls within the large error limits. The reaction products reported by Fockenberg et al. agree with those reported by Chen et al.,[1] who used photolysis of CF_3NO to prepare CF_3O_2 and subsequently CF_3O in 700 Torr of air at 297 ± 2 K. They considered two product channels: (a) CF_3ONO_2 obtained via three–body recombination and (b) $CF_2O + FNO_2$ obtained via fluorine transfer. Both products were observed and found to be thermally stable in their reactor. They report $k_a/(k_a+k_b) > 90\%$ and $k_b/(k_a+k_b) < 10\%$, thus the formation of CF_3ONO_2 is the dominant channel at 700 Torr and 297 K.
(Table: 06-2, Note: 15-10, Evaluated: 06-2) Back to Table

(1) Chen, J.; Young, V.; Zhu, T.; Niki, H. Long path Fourier transform infrared spectroscopic study of the reactions of CF_3OO and CF_3O radicals with NO_2. *J. Phys. Chem.* **1993**, *97*, 11696-11698, doi:10.1021/j100147a024.
(2) Fockenberg, C.; Somnitz, H.; Bednarek, G.; Zellner, R. Kinetic and mechanistic studies of the reactions of CF_3O radicals with NO and NO_2. *Ber. Bunsenges. Phys. Chem.* **1997**, *101*, 1411-1420, doi:10.1002/bbpc.199700001.

E7. **$CF_3O_2 + NO_2$.** The data are from experiments in O_2 of Caralp et al.,[1] who suggest a somewhat different fitting procedure than used here. A statistical best fit to the data yields a value of m = 5.7, but the values recommended

here fit the data just about as well. Destriau and Troe[2] use yet a different fitting procedure that does not represent the data quite as well as that recommended here. Reverse rate data are given by Köppenkastrop and Zabel.[3]
(Table: 06-2, Note: 06-2, Evaluated: 06-2) Back to Table

(1) Caralp, F.; Lesclaux, R.; Rayez, M. T.; Rayez, J.-C.; Forst, W. Kinetics of the combination reactions of chlorofluoromethylperoxy radicals with NO_2 in the temperature range 233-373 K. *J. Chem. Soc. Faraday Trans. 2* **1988**, *84*, 569-585, doi:10.1039/f29888400569.
(2) Destriau, M.; Troe, J. Thermal dissociation and recombination of alkyl and haloalkyl peroxyitrates: An SACM modelling study. *Int. J. Chem. Kinet.* **1990**, *22*, 915-934, doi:10.1002/kin.550220904.
(3) Köppenkastrop, D.; Zabel, F. Thermal decomposition of chlorofluoromethyl peroxynitrates. *Int. J. Chem. Kinet.* **1991**, *23*, 1-15, doi:10.1002/kin.550230102.

E8. **CF_3O + CO.** Values taken from Turnipseed et al.[1] The numbers were obtained for Ar as the bath gas and are assumed to hold for N_2 as well. The temperature dependence of the high-pressure rate constant was determined over the range 233< T/K <332 in SF_6. No temperature dependence of the low-pressure-limiting rate constant was reported. The value in the table is an estimate. Wallington and Ball[2] report values in good agreement with Turnipseed et al.[1]
(Table: 06-2, Note: 06-2, Evaluated: 06-2) Back to Table

(1) Turnipseed, A. A.; Barone, S. B.; Jensen, N. R.; Hanson, D. R.; Howard, C. J.; Ravishankara, A. R. Kinetics of the reactions of CF_3O radicals with CO and H_2O. *J. Phys. Chem.* **1995**, *99*, 6000-6009, doi:10.1021/j100016a041.
(2) Wallington, T. J.; Ball, J. C. Atmospheric chemistry of CF_3O radicals: Reactions with CH_4, CD_4, CH_3F, CF_3H, ^{13}CO, C_2H_5F, C_2D_6, C_2H_6, CH_3OH, *i*-C_4H_8, and C_2H_2. *J. Phys. Chem.* **1995**, *99*, 3201-3205, doi:10.1021/j100010a034.

E9. **CF_3O + M.** The activation energy for thermal decomposition of CF_3O to CF_2O + F has been reported to be 31 kcal mol^{-1} by Kennedy and Levy.[1] Thermochemical data yield $\Delta H^o(298)$ = 23 kcal mol^{-1}. This implies an intrinsic barrier of about 8 kcal mol^{-1} to elimination of F from CF_3O. Electronic structure calculations by Li and Francisco[2] support this observation. Adopting the *A*-factor for unimolecular dissociation, $A = 3 \times 10^{14}$ s^{-1} and E = 31 kcal mol^{-1} from Kennedy and Levy, k_∞(298 K) is about 6×10^{-9} s^{-1}. This corresponds to a lifetime of about 6 years; therefore, thermal decomposition of CF_3O is unimportant throughout the atmosphere.
(Table: 94-26, Note: 94-26) Back to Table

(1) Kennedy, R. C.; Levy, J. B. Bistrifluoromethyl peroxide. II. Kinetics of the decomposition to carbonyl fluoride and trifluoromethyl hypofluorite. *J. Phys. Chem.* **1972**, *76*, 3480-3488, doi:10.1021/j100667a032.
(2) Li, Z.; Francisco, J. S. Dissociation dynamics of perhaloalkoxy radicals. *J. Am. Chem. Soc.* **1989**, *111*, 5660-5667, doi:10.1021/ja00197a024.

F1. **Cl + O_2.** Nicovich et al.[3] measured the rate constant at 181< T/K < 200 and 15< P/Torr <40 in O_2. They reported $k_o = (9 \pm 3)\ 10^{-33}$ cm^6 $molecule^{-2}$ s^{-1} at T = 187 ± 6 K in O_2. The recommended low-pressure limiting parameters are from fitting their data over the entire range and assuming that O_2 and N_2 bath gases are equivalent. The value from the calculation at 300 K (i.e., 2.2×10^{-33} cm^6 $molecule^{-2}$ s^{-1}) compares with an older value of Nicholas and Norrish[2] of 1.7×10^{-33} in an $N_2 + O_2$ mixture. Baer et al.[1] report a value in O_2 of $k_o = 1.6 \times 10^{-33}(T/300)^{-2.9}$ cm^6 $molecule^{-2}$ s^{-1} in good agreement with the value recommended here. They also report a value in N_2 of $k_o = 1.4 \times 10^{-33}(T/300)^{-3.9}$ cm^6 $molecule^{-2}$ s^{-1}. A theoretical study by Zhu and Lin[4] suggests $k_o = 1.26 \times 10^{-16}$ $T^{-6.22}$ $\exp(-943/T)$ cm^6 $molecule^{-2}$ s^{-1} in O_2 (2.0×10^{-33} at 300 K) with $k_\infty(300) = 1.8 \times 10^{-10}$ s^{-1}, which is adopted here. The Nicovich et al.[3] data are so far from the high pressure limit, that the rate constant has little sensitivity to k_∞. Baer et al.[1] suggest $k_\infty = 2.7 \times 10^{-11}$ s^{-1}, but the data suggest a higher value.
(Table: 06-2, Note: 06-2, Evaluated: 06-2) Back to Table

(1) Baer, S.; Hippler, H.; Rahn, R.; Siefke, M.; Seitzinger, N.; Troe, J. Thermodynamic and kinetic properties of the reaction Cl + O_2 + M ⇌ ClOO + M in the range 160-300 K and 1-1000 bar. *J. Chem. Phys.* **1991**, *95*, 6463-6470, doi:10.1063/1.461543.
(2) Nicholas, J. E.; Norrish, R. G. W. Some reactions in the chlorine and oxygen system studied by flash photolysis. *Proc. Roy. Soc. A* **1968**, *307*, 391-397, doi:10.1098/rspa.1968.0197.
(3) Nicovich, J. M.; Kreutter, K. D.; Shackelford, C. J.; Wine, P. H. Thermochemistry and kinetics of the Cl + O_2 association reaction. *Chem. Phys. Lett.* **1991**, *179*, 367-373, doi:10.1016/0009-2614(91)85168-V.

(4) Zhu, R. S.; Lin, M. C. Ab initio studies of ClO_x reactions. VIII. Isomerization and decomposition of ClO_2 radicals and related bimolecular processes. *J. Chem. Phys.* **2003**, *119*, 2075-2082, doi:10.1063/1.1585027.

F2. **Cl + NO.** Low-pressure limit and temperature dependence is from re-evaluation of data from Lee et al.[3] The recommendation is also in good agreement with the data reported by Clark et al.[2] and by Ashmore and Spencer.[1] (Table: 06-2, Note: 06-2, Evaluated: 06-2) Back to Table

(1) Ashmore, P. G.; Spencer, M. S. Concurrent molecular and chlorine atom mechanisms in the reversible dissociation of nitrosyl chloride. *Trans. Faraday Soc.* **1959**, *55*, 1868-1883, doi:10.1039/tf9595501868.
(2) Clark, T. C.; Clyne, M. A. A.; Stedman, D. H. Mechanism of formation of triatomic molecules in atomic combination reactions Part 1.-Formation of ClNO and ClCO in reactions of atomic chlorine. *Trans. Faraday Soc.* **1966**, *62*, 3354-3365, doi:10.1039/tf9666203354.
(3) Lee, J. H.; Michael, J. V.; Payne, W. A., Jr.; Stief, L. J. The temperature dependence of the rate constant for Cl + NO + N_2 → NOCl + N_2. *J. Chem. Phys.* **1978**, *68*, 5410-5413, doi:10.1063/1.435716.

F3. **Cl + NO_2.** Low-pressure limit at 300 K from Leu[4] and Ravishankara et al.[7] The latter study extended the data to 200 Torr in He. A turbulent flow study by Seeley et al.[9] extended the results to 250 Torr of Ar and the high-pressure limit was chosen to fit these two studies after taking into account differences in collisional efficiencies of the bath gases. Leu[4] confirms the observation of Niki et al.[5] that both ClONO and $ClNO_2$ are formed, with the former dominating. This has been explained by Chang et al.,[1] with detailed calculations in Patrick and Golden.[6] The temperature dependence is as predicted in Patrick and Golden[6] and is the same as Leu's results in He. Ravishankara et al.[7] report a few data points in N_2 that may suggest a somewhat higher temperature dependence. The temperature dependence of the high-pressure limit is estimated. The uncertainty limits are estimated. Master Equation/RRKM studies by Zhu and Lin[10] and by Golden,[2] using potential energy surfaces computed by Lee,[3] Zhu and Lin,[10] and Sayin and McKee[8], report differences in their ability to fit the data. Zhu and Lin[10] claim to fit, while Golden[2] finds the calculations to under predict the low pressure data. (Table: 10-6, Note: 10-6, Evaluated: 10-6) Back to Table

(1) Chang, J. S.; Baldwin, A. C.; Golden, D. M. An explanation of the preferential formation of less stable isomers in three-body reactions: Cl + NO_2 + M; ClO + NO_2 + M. *J. Chem. Phys.* **1979**, *71*, 2021-2024, doi:10.1063/1.438593.
(2) Golden, D. M. The reaction Cl + NO_2 → ClONO and $ClNO_2$. *J. Phys. Chem. A* **2007**, *111*, 6772-6780, doi:10.1021/jp069000x.
(3) Lee, T. J. *Ab initio* characterization of $ClNO_2$, *cis*-ClONO, and *trans*-ClONO. *J. Phys. Chem.* **1994**, *98*, 111-115, doi:10.1021/j100052a019.
(4) Leu, M. T. Kinetics of the reaction Cl + NO_2 + M. *Int. J. Chem. Kinet.* **1984**, *16*, 1311-1320, doi:10.1002/kin.550161103.
(5) Niki, H.; Maker, P. D.; Savage, C. M.; Breitenbach, L. P. Fourier transform IR spectroscopic observation of chlorine nitrite, ClONO, formed via Cl + NO_2(+M) → ClONO(+M). *Chem. Phys. Lett.* **1978**, *59*, 78-79, doi:10.1016/0009-2614(78)85618-8.
(6) Patrick, R.; Golden, D. M. Third-order rate constants of atmospheric importance. *Int. J. Chem. Kinet.* **1983**, *15*, 1189-1227, doi:10.1002/kin.550151107.
(7) Ravishankara, A. R.; Smith, G. J.; Davis, D. D. A kinetics study of the reaction of Cl with NO_2. *Int. J. Chem. Kinet.* **1988**, *20*, 811-814, doi:10.1002/kin.550201005.
(8) Sayin, H.; McKee, M. L. Theoretical study of the mechanism of NO_2 production from NO + ClO. *J. Phys. Chem. A* **2005**, *109*, 4736-4743, doi:10.1021/jp050695w.
(9) Seeley, J. V.; Jayne, J. T.; Molina, M. J. Kinetic studies of chlorine atom reactions using the turbulent flow tube technique. *J. Phys. Chem.* **1996**, *100*, 4019-4025, doi:10.1021/jp9525494.
(10) Zhu, R. S.; Lin, M. C. Ab Initio studies of ClO_x reactions: Prediction of the rate constants of ClO + NO for the forward and reverse processes. *ChemPhysChem* **2004**, *5*, 1864-1870, doi:10.1002/cphc.200400305.

F4. **Cl + CO.** From Nicovich et al.,[2] who measured the process in N_2 for 185≤ T/K ≤260. Hewitt et al.[1] report a value at one atmosphere and 298 K with ^{13}CO in agreement with Nicovich et al.[2] (Table: 06-2, Note: 06-2, Evaluated: 06-2) Back to Table

(1) Hewitt, A. D.; Brahan, K. M.; Boone, G. D.; Hewitt, S. A. Kinetics and mechanism of the Cl + CO reaction in air. *Int. J. Chem. Kinet.* **1996**, *28*, 763-771, doi:10.1002/(SICI)1097-4601(1996)28:10<763::AID-KIN7>3.0.CO;2-L.

(2) Nicovich, J. M.; Kreutter, K. D.; Wine, P. H. Kinetics and thermochemistry of ClCO formation from the Cl + CO association reaction. *J. Chem. Phys.* **1990**, *92*, 3539-3544, doi:10.1063/1.457862.

F5. **Cl + C_2H_2.** The recommended values are a statistical fit to the work of Kaiser[4] in air. Kaiser and Wallington[3] extends the pressure range at 296 K to 0.3–6000 Torr. The data are in reasonable agreement with earlier measurements of Brunning and Stief[2] and Wallington et al.,[7] although the derived temperature dependence is less than obtained by Brunning and Stief.[2] These values are compatible with earlier studies of Poulet et al.,[6] Atkinson and Aschmann,[1] Lee and Rowland,[5] and Wallington et al.[8] Using FTIR, Zhu et al.[9] reported branching of 16% and 84% to the *trans* and *cis* adduct isomers, respectively, at 700 Torr N_2 and 295 K.
(Table: 06-2, Note: 06-2, Evaluated: 06-2) Back to Table

(1) Atkinson, R.; Aschmann, S. M. Kinetics of the gas phase reaction of Cl atoms with a series of organics at 296 ± 2 K and atmospheric pressure. *Int. J. Chem. Kinet.* **1985**, *17*, 33-41, doi:10.1002/kin.550170105.
(2) Brunning, J.; Stief, L. J. Pressure dependence of the absolute rate constant for the reaction Cl + C_2H_2 from 210-361 K. *J. Chem. Phys.* **1985**, *83*, 1005-1009, doi:10.1063/1.449463.
(3) Kaiser, E. W.; Wallington, T. J. Kinetics of the reactions of chlorine atoms with C_2H_4 (k_1) and C_2H_2 (k_2): A determination of $\Delta H_{f,298}°$ for C_2H_3. *J. Phys. Chem.* **1996**, *100*, 4111-4119, doi:10.1021/jp953178u.
(4) Kaiser, E. W. Pressure dependence of the reaction Cl + C_2H_2 over the temperature range 230 to 370 K. *Int. J. Chem. Kinet.* **1992**, *24*, 179-189, doi:10.1002/kin.550240206.
(5) Lee, F. S. C.; Rowland, F. S. Competitive radiotracer evaluation of relative rate constants at stratospheric temperatures for reactions of ^{38}Cl with CH_4 and C_2H_6 vs. CH_2=CHBr. *J. Phys. Chem.* **1977**, *81*, 86-87, doi:10.1021/j100516a020.
(6) Poulet, G.; Barassin, J.; Le Bras, G.; Combourieu, J. Étude cinetique de la réaction du chlore atomique avec l'acétylène. *Bull. Soc. Chim. Fr.* **1973**, *1*, 1-6.
(7) Wallington, T. J.; Andino, J. M.; Lorkovic, I. M.; Kaiser, E. W.; Marston, G. Pressure dependence of the reaction of chlorine atoms with ethene and acetylene in air at 295 K. *J. Phys. Chem.* **1990**, *94*, 3644-3648, doi:10.1021/j100372a052.
(8) Wallington, T. J.; Skewes, L. M.; Siegl, W. O. Kinetics of the gas phase reaction of chlorine atoms with a series of alkenes, alkynes and aromatic species at 295 K. *J. Photochem. Photobiol. A: Chem.* **1988**, *45*, 167-175, doi:10.1016/1010-6030(88)80126-6.
(9) Zhu, T.; Yarwood, G.; Chen, J.; Niki, H. FTIR study of the C1 + C_2H_2 reaction: Formation of *cis*- and *trans*-CHCl=CH radicals. *J. Phys. Chem.* **1994**, *98*, 5065-5067, doi:10.1021/j100070a020.

F6. **Cl + C_2H_4.** Values at 300 K are from a relative rate study by Wallington et al.[10] A relative rate study by Kaiser and Wallington[4] extends the pressure range to 0.3–6000 Torr and is compatible with earlier studies. Temperature dependence of k_o is taken from Kaiser and Wallington.[5] The temperature dependence of k_∞ is estimated. Values are in reasonable agreement with studies by Maricq et al.,[8] Lee and Rowland,[7] Iyer et al.,[3] Atkinson and Aschmann,[1] Atkinson and Aschmann,[2] and Wallington et al.[11] A study in He by Stutz et al.[9] is noted, as is a comment on it by Kaiser and Wallington.[5] Knyazev et al.[6] have done an extensive experimental and theoretical analysis. Their values agree with this recommendation.
(Table: 97-4, Note: 02-25, Evaluated: 06-2) Back to Table

(1) Atkinson, R.; Aschmann, S. M. Kinetics of the gas phase reaction of Cl atoms with a series of organics at 296 ± 2 K and atmospheric pressure. *Int. J. Chem. Kinet.* **1985**, *17*, 33-41, doi:10.1002/kin.550170105.
(2) Atkinson, R.; Aschmann, S. M. A structure-activity relationship for the estimation of rate constants for the gas-phase reactions of OH radicals with organic compounds. *Int. J. Chem. Kinet.* **1987**, *19*, 1097-1105, doi:10.1002/kin.550191206.
(3) Iyer, R. S.; Rogers, P. J.; Rowland, F. S. Thermal rate constant for addition of chlorine atoms to ethylene. *J. Phys. Chem.* **1983**, *87*, 3799-3801, doi:10.1021/j100243a001.
(4) Kaiser, E. W.; Wallington, T. J. Kinetics of the reactions of chlorine atoms with C_2H_4 (k_1) and C_2H_2 (k_2): A determination of $\Delta H_{f,298}°$ for C_2H_3. *J. Phys. Chem.* **1996**, *100*, 4111-4119, doi:10.1021/jp953178u.
(5) Kaiser, E. W.; Wallington, T. J. Comment on "Inverse kinetic isotope effect in the reaction of atomic chlorine with C_2H_4 and C_2D_4". *J. Phys. Chem. A* **1998**, *102*, 6054-6055, doi:10.1021/jp980578j.
(6) Knyazev, V. D.; Kalinovski, I. J.; Slagle, I. R. Kinetics of the $CH_2CH_2Cl \rightleftarrows C_2H_4$ + Cl reaction. *J. Phys. Chem. A* **1999**, *103*, 3216-3221, doi:10.1021/jp984207e.

(7) Lee, F. S. C.; Rowland, F. S. Competitive radiotracer evaluation of relative rate constants at stratospheric temperatures for reactions of ^{38}Cl with CH_4 and C_2H_6 vs. CH_2=CHBr. *J. Phys. Chem.* **1977**, *81*, 86-87, doi:10.1021/j100516a020.
(8) Maricq, M. M.; Szente, J. J.; Kaiser, E. W. A diode laser study of the Cl + C_2H_5 reaction. *J. Phys. Chem.* **1993**, *97*, 7970-7977, doi:10.1021/j100132a028.
(9) Stutz, J.; Ezell, M. J.; Finlayson-Pitts, B. J. Inverse kinetic isotope effect in the reaction of atomic chlorine with C_2H_4 and C_2D_4. *J. Phys. Chem. A* **1997**, *101*, 9187-9190, doi:10.1021/jp972935g.
(10) Wallington, T. J.; Andino, J. M.; Lorkovic, I. M.; Kaiser, E. W.; Marston, G. Pressure dependence of the reaction of chlorine atoms with ethene and acetylene in air at 295 K. *J. Phys. Chem.* **1990**, *94*, 3644-3648, doi:10.1021/j100372a052.
(11) Wallington, T. J.; Skewes, L. M.; Siegl, W. O.; Wu, C. H.; Japar, S. M. Gas phase reaction of Cl atoms with a series of oxygenated organic species at 295 K. *Int. J. Chem. Kinet.* **1988**, *20*, 867-875, doi:10.1002/kin.550201105

F7. **Cl + C_2Cl_4.** The recommendation is from the flash-photolysis study of Nicovich et al.[3] carried out at 231–390 K in 3–700 Torr N_2. A study by Thuner et al.[4] at 296 K and 2–700 Torr of air is in agreement, although agreement is poorer at pressures below 10 Torr. Results near room temperature and 1 atm by Atkinson and Aschmann[1] and by Morozov et al.[2] are also consistent. The scatter in the rate constants reported by Nicovich et al. is roughly independent of temperature.
(Table: 19-5, Note: 19-5, Evaluated: 02-25) Back to Table

(1) Atkinson, R.; Aschmann, S. M. Kinetics of the gas-phase reactions of Cl atoms with chloroethenes at 298 ± 2 K and atmospheric pressure. *Int. J. Chem. Kinet.* **1987**, *19*, 1097-1105, doi:10.1002/kin.550191206.
(2) Morozov, I. I.; Nielsen, C.; Morozova, O. S.; Vasiliev, E. S.; Loukhovitskaya, E. E. Reactios of chloroethenes with atomic chlorine in air at atmospheric pressure. *Russ. Chem. Bull., Int. Edition* **2010**, *59*, 754-760.
(3) Nicovich, J. M.; Wang, L.; McKee, M. L.; Wine, P. H. Kinetics and thermochemistry of the Cl(^2P_J) + C_2Cl_4 association reaction. *J. Phys. Chem.* **1996**, *100*, 680-688, doi:10.1021/jp952396k.
(4) Thuner, L. P.; Barnes, I.; Becker, K. H.; Wallington, T. J.; Christensen, L. K.; Orlando, J. J.; Ramacher, B. Atmospheric chemistry of tetrachloroethene (Cl_2C=CCl_2): Products of chlorine atom initiated oxidation. *J. Phys. Chem. A* **1999**, *103*, 8657-8663, doi:10.1021/jp991929c.

F8. **ClO + NO_2.** The low-pressure-limit recommendation and uncertainties are based on temperature-dependent values from Zahniser et al.,[15] Lee et al.,[8] Birks et al.,[2] Leu et al.,[9] Wallington and Cox,[14] Cox et al.,[3] and Molina et al.[10] All of these data were collected in N_2 bath gas, except for several points from Lee et al.[8] collected in O_2. The high-pressure-limit recommendation is based on the RRKM calculations of Smith and Golden.[12] There are several pressure-dependent data sets in the literature, such as Percival et al.,[11] Handwerk and Zellner,[7] Dasch et al.,[5] and Cox and Lewis;[4] however, they are too disparate to extract unambiguous values. These data are all reproduced within two-sigma error limits by the current recommendation. However, the value of m = 1.9 is somewhat large for a radical-radical process. If m = 1 is chosen the computed rate constant is lower by about 20% at 180 K and pressures above 500 Torr. Golden[6] attempted to fit the data with a master equation analysis and found that the usual energy transfer treatment at low pressures is insufficient to fit the data, but this appears to be due to a coding error.[1] Theoretical work by Zhu and Lin[16] find significant barriers to formation of the two ClOONO conformers from ClO + NO_2; these barriers are too large to enable formation of ClOONO. Most theoretical work, including rather precise work by Szakacs et al.[13] indicate that most stable ClOONO isomer is nearly isoenergetic with ClO + NO_2. Even in the absence of the barriers reported by Zhu and Lin, the thermodynamics make it unlikely that ClOONO would be formed.
(Table: 06-2, Note: 19-5, Evaluated: 10-6) Back to Table

(1) Barker, J. R. Personal communication. **2018**.
(2) Birks, J. W.; Shoemaker, B.; Leck, T. J.; Borders, R. A.; Hart, L. J. Studies of reactions of importance in the stratosphere. II. Reactions involving chlorine nitrate and chlorine dioxide. *J. Chem. Phys.* **1977**, *66*, 4591-4599, doi:10.1063/1.433716.
(3) Cox, R. A.; Burrows, J. P.; Coker, G. B. Product formation in the association reaction of ClO with NO_2 investigated by diode laser kinetic spectroscopy. *Int. J. Chem. Kinet.* **1984**, *16*, 445-467, doi:10.1002/kin.550160412.
(4) Cox, R. A.; Lewis, R. Kinetics of chlorine oxide radical reactions using modulated photolysis Part 3.-Pressure and temperature dependence of the reaction: ClO + NO_2(+M) → $ClONO_2$(+M). *J. Chem. Soc. Faraday Trans. 1* **1979**, *75*, 2649-2661, doi:10.1039/f19797502649.

(5) Dasch, W.; Sternberg, K.-H.; Schindler, R. N. Pressure dependence of the reaction ClO + NO_2 + N_2 → $ClONO_2$ + N_2 by laser flash photolysis. *Ber. Bunsenges. Phys. Chem.* **1981**, *85*, 611-615, doi:10.1002/bbpc.19810850717.
(6) Golden, D. M. Evaluation of data for atmospheric models: ME/RRKM calculations on the combination reaction ClO + NO_2 → $ClONO_2$, a recurring issue. *Int. J. Chem. Kinet.* **2009**, *41*, 573-581, doi:10.1002/kin.20432.
(7) Handwerk, V.; Zellner, R. Pressure and temperature dependence of the reaction ClO + NO_2 (+N_2) → $ClONO_2$ (+N_2). *Ber. Bunsenges. Phys. Chem.* **1984**, *88*, 405-409, doi:10.1002/bbpc.19840880417
(8) Lee, Y.-P.; Stimpfle, R. M.; Perry, R. A.; Mucha, J. A.; Evenson, K. M.; Jennings, D. A.; Howard, C. J. Laser magnetic resonance spectroscopy of ClO and kinetic studies of the reactions of ClO with NO and NO_2. *Int. J. Chem. Kinet.* **1982**, *14*, 711-732, doi:10.1002/kin.550140612.
(9) Leu, M. T. Kinetics of the reaction Cl + NO_2 + M. *Int. J. Chem. Kinet.* **1984**, *16*, 1311-1320, doi:10.1002/kin.550161103.
(10) Molina, M. J.; Molina, L. T.; Ishiwata, T. Kinetics of the ClO + NO_2 + M reaction. *J. Phys. Chem.* **1980**, *84*, 3100-3104, doi:10.1021/j100460a026.
(11) Percival, C. J.; Smith, G. D.; Molina, L. T.; Molina, M. J. Temperature and pressure dependence of the rate constant for the ClO + NO_2 reaction. *J. Phys. Chem. A* **1997**, *101*, 8830-8833, doi:10.1021/jp971907v.
(12) Smith, G. P.; Golden, D. M. Application of RRKM theory to the reactions OH + NO_2 + N_2 → $HONO_2$ + N_2 (1) and ClO + NO_2 + N_2 → $ClONO_2$ + N_2 (2); a modified gorin model transition state. *Int. J. Chem. Kinet.* **1978**, *10*, 489-501, doi:10.1002/kin.550100507.
(13) Szakács, P.; Csontos, J.; Das, S.; Kállay, M. High-accuracy theoretical thermochemistry of atmospherically important nitrogen oxide derivatives. *J. Phys. Chem. A* **2011**, *115*, 3144-3153, doi:10.1021/jp112116x.
(14) Wallington, T. J.; Cox, R. A. Kinetics and product of the gas-phase reaction of ClO with NO_2. *J. Chem. Soc. Faraday Trans. 2* **1986**, *82*, 275-289, doi:10.1039/f29868200275.
(15) Zahniser, M. S.; Chang, J.; Kaufman, F. Chlorine nitrate: Kinetics of formation by ClO + NO_2 + M and of reaction with OH. *J. Chem. Phys.* **1977**, *67*, 997-1003, doi:10.1063/1.434927.
(16) Zhu, R. S.; Lin, M. C. Ab initio studies of ClO_x reactions: Prediction of the rate constants of ClO + NO_2 for the forward and reverse processes. *ChemPhysChem* **2005**, *6*, 1514-1521, doi:10.1002/cphc.200400448.

F9. OClO + NO_3. Friedl et al.[2] studied this system at 1≤ P/Torr ≤5 for helium and 220≤ T/K ≤298. They deduced values for the rate constant consistent with their data of $k_o \approx 10^{-31}$ and $k_\infty \approx 10^{-11}$. They also suggest a value for the equilibrium constant: K/cm^3 molecule^{-1} = 1×10^{-28} exp (9300/T). Boyd et al.[1] raised the question of possible heterogeneous effects in this system. Parthiban et al.[3] in a theoretical study, support the finding of Friedl et al.[2] of the species O_2ClONO_2, but suggest a very different equilibrium constant. (See Table 3-1).
(Table: 94-26, Note: 06-2, Evaluated: 06-2) Back to Table

(1) Boyd, A. A.; Marston, G.; Wayne, R. P. Kinetic studies of the reaction between NO_3 and OClO at T = 300 K and P = 2-8 Torr. *J. Phys. Chem.* **1996**, *100*, 130-137, doi:10.1021/jp9509931.
(2) Friedl, R. R.; Sander, S. P.; Yung, Y. L. Chloryl nitrate: A novel product of the OClO + NO_3 + M recombination. *J. Phys. Chem.* **1992**, *96*, 7490-7493, doi:10.1021/j100198a002.
(3) Parthiban, S., T. J. Lee, S. Guha, and J. S. Francisco Theoretical study of chlorine nitrates: Implications for stratospheric chlorine chemistry. *J. Am. Chem. Soc.* **2003**, *125*, 10446-10458, doi:10.1021/ja010297g.

F10. ClO + ClO. The recommendation is based on a global non-linear least squares fit (all data were assumed to have the same relative error) of data from Sander et al.[15] (195–247 K), Nickolaisen et al.[13] (260–390 K), Bloss et al.[3] (183–245 K), Trolier et al.[19] (200–263 K), Boakes et al.,[4] and Ferracci and Rowley[7] (250–312 K). The Trolier et al. data have been corrected for values at the zero-pressure intercept as suggested in the Trolier et al. paper. With this adjustment most of the data are in reasonable agreement. Boakes et al.[4] report higher values and a zero-pressure intercept; they suggest disregarding their data at less than 100 Torr and report preferred parameters of 2.79×10^{-32}; 3.78; 3.44×10^{-12}; 1.73. Ferracci and Rowley[7] studied the reaction only at 760 Torr and found values in agreement with those of Boakes et al. The error limits represent an attempt to include most of the data within the 95% uncertainty band. The major dimerization product is chlorine peroxide (Birk et al.,[2] DeMore and Tschuikow-Roux,[6] Slanina and Uhlik,[16] Stanton et al.,[17] and Lee et al.[11]). Golden[8] has performed RRKM and master equation calculations using the potential energy surface in Zhu and Lin[21] and concluded that while a channel to form ClOClO might exist, the net yield is probably very small the best representation of the data remains that only a single channel is important. The k_o value for N_2 is not in accord with a simple

theory as explained in Patrick and Golden[14] and in some detail in Golden[8] (this finding was probably the result of a bug that was subsequently found in the master equation code). It has been suggested[18] that the "radical-complex" mechanism may apply here, although a study by Liu and Barker[12] suggests otherwise. Other previous rate constant measurements, such as those of Hayman et al.,[9] Cox and Derwent,[5] Basco and Hunt,[1] Walker,[20] and Johnston et al.,[10] range from (1–5) × 10^{-32} cm^6 $molecule^{-2}$ s^{-1}, with N_2 or O_2 as third bodies.
(Table 15-10, Note: 15-10, Evaluated: 15-10) Back to Table

(1) Basco, N.; Hunt, J. E. Mutual combination of ClO radicals. *Int. J. Chem. Kinet.* **1979**, *11*, 649-664, doi:10.1002/kin.550110611.
(2) Birk, M.; Friedl, R. R.; Cohen, E. A.; Pickett, H. M.; Sander, S. P. The rotational spectrum and structure of chlorine peroxide. *J. Chem. Phys.* **1989**, *91*, 6588-6597, doi:10.1063/1.457377.
(3) Bloss, W. J.; Nickolaisen, S. L.; Salawitch, R. J.; Friedl, R. R.; Sander, S. P. Kinetics of the ClO self-reaction and 210 nm absorption cross section of the ClO dimer. *J. Phys. Chem. A* **2001**, *105*, 11226-11239, doi:10.1021/jp012429y.
(4) Boakes, G.; Mok, W. H. H.; Rowley, D. M. Kinetic studies of the ClO + ClO association reaction as a function of temperature and pressure. *Phys. Chem. Chem. Phys.* **2005**, *7*, 4102-4113, doi:10.1039/b510308h.
(5) Cox, R. A.; Derwent, R. G. Kinetics of chlorine oxide radical reactions using modulated photolysis Part 1.-Disproportionation of ClO in the Cl_2 photosensitised decomposition of ozone. *J. Chem. Soc. Faraday Trans. 1* **1979**, *75*, 1635-1647, doi:10.1039/f19797501635.
(6) DeMore, W. B.; Tschuikow-Roux, E. Ultraviolet spectrum and chemical reactivity of the ClO dimer. *J. Phys. Chem.* **1990**, *94*, 5856-5860, doi:10.1021/j100378a046.
(7) Ferracci, V.; Rowley, D. M. Kinetic and thermochemical studies of the ClO + ClO + M ⇄ Cl_2O_2 + M reaction *Phys. Chem. Chem. Phys* **2010**, *12*, 11596-11608, doi:10.1039/c0cp00308e.
(8) Golden, D. M. Reaction ClO + ClO → products: Modeling and parameterization for use in atmospheric models. *Int. J. Chem. Kinet.* **2003**, *35*, 206-211, doi:10.1002/kin.10120.
(9) Hayman, G. D.; Davies, J. M.; Cox, R. A. Kinetics of the reaction ClO + ClO → products and its potential relevance to Antarctic ozone. *Geophys. Res. Lett.* **1986**, *13*, 1347-1350, doi:10.1029/GL013i012p01347.
(10) Johnston, H. S.; Morris, E. D., Jr.; Van den Bogaerde, J. Molecular modulation kinetic spectrometry. ClOO and ClO_2 radicals in the photolysis of chlorine in oxygen. *J. Am. Chem. Soc.* **1969**, *91*, 7712-7727, doi:10.1021/ja50001a036.
(11) Lee, T. J.; Rohlfing, C. M.; Rice, J. E. An extensive *ab initio* study of the structures, vibrational spectra, quadratic force fields, and relative energetics of three isomers of Cl_2O_2. *J. Chem. Phys.* **1992**, *97*, 6593-6605, doi:10.1063/1.463663.
(12) Liu, J. Y.; Barker, J. R. On the chaperon mechanism: Application to ClO + ClO (+N_2) → ClOOCl (+N_2). *J. Phys. Chem. A* **2007**, *111*, 8689-8698, doi:10.1021/jp072978p.
(13) Nickolaisen, S. L.; Friedl, R. R.; Sander, S. P. Kinetics and mechanism of the ClO + ClO reaction: Pressure and temperature dependences of the bimolecular and termolecular channels and thermal decomposition of chlorine peroxide, ClOOCl. *J. Phys. Chem.* **1994**, *98*, 155-169, doi:10.1021/j100052a027.
(14) Patrick, R.; Golden, D. M. Third-order rate constants of atmospheric importance. *Int. J. Chem. Kinet.* **1983**, *15*, 1189-1227, doi:10.1002/kin.550151107.
(15) Sander, S. P.; Friedl, R. P.; Yung, Y. L. Role of the ClO dimer in polar stratospheric chemistry; rate of formation and implications for ozone loss. *Science* **1989**, *245*, 1095-1098, doi:10.1126/science.245.4922.1095.
(16) Slanina, Z.; Uhlik, F. An estimation of dimerization energetics of the ClO radical. *Chem. Phys. Lett.* **1991**, *182*, 51-56, doi:10.1016/0009-2614(91)80102-4.
(17) Stanton, J. F.; Rittby, C. M. L.; Bartlett, R. J.; Toohey, D. W. Low-lying isomers of the chlorine oxide dimer: A theoretical study. *J. Phys. Chem.* **1991**, *95*, 2107-2110, doi:10.1021/j100159a004.
(18) Troe, J. Toward a quantitative analysis of association reactions in the atmosphere. *Chem. Rev.* **2003**, *104*, 4565-4576, doi:10.1021/cr020514b.
(19) Trolier, M.; Mauldin, R. L., III; Ravishankara, A. R. Rate coefficient for the termolecular channel of the self-reaction of ClO. *J. Phys. Chem.* **1990**, *94*, 4896-4907, doi:10.1021/j100375a027.
(20) Walker, R. W. Ph.D, Ph.D Thesis, Queen Mary College University of London, 1972.
(21) Zhu, R. S.; Lin, M. C. *Ab initio* studies of ClO_x reactions. IV. Kinetics and mechanism for the self-reaction of ClO radicals. *J. Chem. Phys.* **2003**, *118*, 4094-4106, doi:10.1063/1.1540623.

F11. ClO + OClO. Data are from Burkholder et al.,[1] who measured the rate constant in N_2 at 200≤ T/K ≤260 and densities from (1.1–10.9) × 10^{18} molecules cm^{-3}. They also measured the equilibrium constant (See Table 3-

1). Parr et al.[3] also report a value for the rate constant in reasonable agreement with the recommendation. Zhu and Lin[4] report an ab initio study of this system. Their parameters are somewhat different from those herein, but they fit the data equally well. Green et al.[2] report a value in He that is consistent with the values recommended herein.
(Table: 06-2, Note: 06-2, Evaluated: 06-2) Back to Table

(1) Burkholder, J. B.; Mauldin, R. L.; Yokelson, R. J.; Solomon, S.; Ravishankara, A. R. Kinetic, thermodynamic, and spectroscopic study of Cl_2O_3. *J. Phys. Chem.* **1993**, *97*, 7597-7605, doi:10.1021/j100131a032.
(2) Green, T. J.; Islam, M.; Guest, P.; Hickson, K.; Canosa-Mas, C. E.; Wayne, R. P. A discharge-flow study of Cl_2O_3. *Phys. Chem. Chem. Phys.* **2003**, *5*, 5409-5418, doi:10.1039/b311005b.
(3) Parr, A. D.; Wayne, R. P.; Hayman, G. D.; Jenkin, M. E.; Cox, R. A. The pressure dependence of the reaction between ClO and OClO at 226 K. *Geophys. Res. Lett.* **1990**, *17*, 2357-2360, doi:10.1029/GL017i013p02357.
(4) Zhu, R. S.; Lin, M. C. Ab initio studies of ClO_x reactions. VII. Isomers of Cl_2O_3 and their roles in the ClO + OClO reaction. *J. Chem. Phys.* **2003**, *118*, 8645-8655, doi:10.1063/1.1565315.

F12. **O + OClO.** The recommendation is based on data of Colussi et al.[2] and Colussi,[1] who measured the pressure dependence between 248 and 312 K in Ar. They interpret the intercept of their *k* vs [M] curves as a zero-pressure rate constant of $(1.6 \pm 0.4) \times 10^{-13}$ cm^3 molecule^{-1} s^{-1} with a negative activation energy corresponding to a chemical activation channel producing ClO + O_2. This interpretation is supported by a low pressure study by Gleason et al.,[3] as well as a theoretical study by Zhu and Lin,[4] which suggests a direct abstraction with a positive activation energy. (Zhu and Lin[4] point out that sym-ClO_3 has a positive barrier for dissociation to ClO + O_2.) The recommended values are fit to the data after subtracting the abstraction channel. See Table 1-1.
(Table: 06-2, Note: 06-2, Evaluated: 06-2) Back to Table

(1) Colussi, A. J. Formation and decay of (^3P_J)O atoms in the laser flash photolysis of chlorine dioxide (OClO) at 308 nm. *J. Phys. Chem.* **1990**, *94*, 8922-8926, doi:10.1021/j100389a014.
(2) Colussi, A. J.; Sander, S. P.; Friedl, R. R. Temperature dependence and mechanism of the reaction between O(^{3}P) and chlorine dioxide. *J. Phys. Chem.* **1992**, *96*, 4442-4445, doi:10.1021/j100190a058.
(3) Gleason, J. F.; Nesbitt, F. L.; Stief, L. J. Temperature dependence of the reaction between O(^{3}P) and OClO at low pressure. *J. Phys. Chem.* **1994**, *98*, 126-131, doi:10.1021/j100052a022.
(4) Zhu, R. S.; Lin, M. C. Ab initio studies of ClO_x reactions. 2. Unimolecular decomposition of s-ClO_3 and the bimolecular O + OClO reaction. *J. Phys. Chem. A* **2002**, *106*, 8386-8390, doi:10.1021/jp020015e.

F13. **$CH_2Cl + O_2$.** Measured by Fenter et al.[2] over the range 298≤ T/K ≤448 and 1≤P/Torr ≤760 in nitrogen. Two different techniques were employed: laser photolysis/photoionization mass spectrometry in the range 1–10 Torr and laser photolysis/UV absorption for the range 20–760 Torr. A study by Bilde et al.[1] in N_2 relative to the reaction $CH_2Cl + Cl_2 \rightarrow CH_2Cl_2 + Cl$ is in excellent agreement. Error limits transposed to the current format.
(Table: 06-2, Note: 06-2, Evaluated: 06-2) Back to Table

(1) Bilde, M.; Sehested, J.; Nielsen, O. J.; Wallington, T. J.; Meagher, R. J.; McIntosh, M. E.; Piety, C. A.; Nicovich, J. M.; Wine, P. H. Kinetics and mechanism of the gas phase reaction of atomic chlorine with CH_2ICl at 206-432 K. *J. Phys. Chem. A* **1997**, *101*, 8035-8041, doi:10.1021/jp9717960.
(2) Fenter, F. F.; Lightfoot, P. D.; Caralp, F.; Lesclaux, R.; Niranen, J. T.; Gutman, D. Kinetics of the $CHCl_2$ and CH_2Cl association reactions with molecular oxygen between 298 and 448 K and from 1 to 760 Torr of total pressure. *J. Phys. Chem.* **1993**, *97*, 4695-4703, doi:10.1021/j100120a023.

F14. **$CHCl_2 + O_2$.** Measured by Fenter et al.[1] over the range 298≤ T/K ≤383 and 1≤ P/Torr ≤760 in nitrogen. Two different techniques were employed: laser photolysis/photoionization mass spectrometry in the range1–10 Torr and laser photolysis/UV absorption for the range 20–760 Torr. A study by Nottingham et al.,[2] in He, is in agreement. Error limits transposed to the current format.
(Table: 94-26, Note: 94-26, Evaluated: 94-26) Back to Table

(1) Fenter, F. F.; Lightfoot, P. D.; Caralp, F.; Lesclaux, R.; Niranen, J. T.; Gutman, D. Kinetics of the $CHCl_2$ and CH_2Cl association reactions with molecular oxygen between 298 and 448 K and from 1 to 760 Torr of total pressure. *J. Phys. Chem.* **1993**, *97*, 4695-4703, doi:10.1021/j100120a023.
(2) Nottingham, W. C.; Rudolph, R. N.; Andrews, K. P.; Moore, J. H.; Tossell, J. A. Flowtube reactor study of the association reactions of $CHCl_2$ and CCl_3 with O_2 at low pressure. *Int. J. Chem. Kinet.* **1994**, *26*, 749-756, doi:10.1002/kin.550260709.

F15. **$CCl_3 + O_2$.** The recommendation incorporates studies by Fenter et al.,[3] Danis et al.,[2] and Luther et al.[5] (The data of Luther et al. above 100 bar are affected by slow diffusion.) Experimental data of Ryan and Plumb[8] have been considered in the evaluation. A study by Nottingham et al.,[6] in He, is in agreement. Forst and Caralp[4] have examined this reaction theoretically. A Patrick and Golden–type calculation using the thermochemistry of Russell et al.[7] yields $k_0^{300} = 1.5 \times 10^{-30}$, with $\beta = 0.3$. A value of $k_\infty^{300} = 5 \times 10^{-12}$ has been reported by Cooper et al.[1] The value of the rate constants recommended here differ only slightly from those of Luther et al., (who report $k_\infty^{300} = 5.2 \times 10^{-12}$; $m = 1.4$ and $k_0^{300} = 1.5 \times 10^{-30}$; $n = -6.3$; $F_c = 0.35 \times (T/300)^{-0.35}$ using the IUPAC formula) but yield an overall rate constant within their error limits.
(Table: 06-2, Note: 06-2, Evaluated: 06-2) Back to Table

(1) Cooper, R.; Cumming, J. B.; Gordon, S.; Mulac, W. A. The reactions of the halomethyl radicals CCl_3 and CF_3 with oxygen. *Radiation Phys. Chem.* **1980**, *16*, 169-174, doi:10.1016/0146-5724(80)90224-1.

(2) Danis, F.; Caralp, F.; Rayez, M.; Lesclaux, R. Kinetic study of the reaction $CCl_3 + O_2 + M \rightarrow CCl_3O_2 + M$ from 1 to 760 Torr and from 233 to 333 K. *J. Phys. Chem.* **1991**, *95*, 7300-7307, doi:10.1021/j100172a037.

(3) Fenter, F. F.; Lightfoot, P. D.; Niranen, J. T.; Gutman, D. Kinetics of the CCl_3 association reaction with molecular oxygen at 298 and 333 K and from 1 to 760 Torr of total pressure. *J. Phys. Chem.* **1993**, *97*, 5313-5320, doi:10.1021/j100122a023.

(4) Forst, W., and F. Caralp Microcanonical variational theory of radical recombination by inversion of interpolate partition function Part 2.-$CX_3 + O_2$ (X = H, F, Cl). *J. Chem. Soc. Faraday Trans.* **1991**, *87*, 2307-2315, doi:10.1039/ft9918702307.

(5) Luther, K.; Oum, K.; Troe, J. Study of the recombination reaction $CCl_3 + O_2$ (+M) $\rightarrow CCl_3O_2$ (+M) at pressures of 2-900 bar and temperatures of 260-346 K. *J. Phys. Chem. A* **2001**, *105*, 5535-5541, doi:10.1021/jp003844d.

(6) Nottingham, W. C.; Rudolph, R. N.; Andrews, K. P.; Moore, J. H.; Tossell, J. A. Flowtube reactor study of the association reactions of $CHCl_2$ and CCl_3 with O_2 at low pressure. *Int. J. Chem. Kinet.* **1994**, *26*, 749-756, doi:10.1002/kin.550260709.

(7) Russell, J. J.; Setula, J. A.; Gutman, D.; Danis, F.; F.Caralp; Lightfoot, P. D.; Lesclaux, R.; Melius, C. F.; Senkan, S. M. Kinetics and thermochemistry of the equilibrium $CCl_3 + O_2 \leftrightarrow CCl_3O_2$. *J. Phys. Chem.* **1990**, *94*, 3277-3283, doi:10.1021/j100371a012.

(8) Ryan, K. R.; Plumb, I. C. Kinetics of the reactions of CCl_3 with O and O_2 and of CCl_3O_2 with NO at 295 K. *Int. J. Chem. Kinet.* **1984**, *16*, 591-602, doi:10.1002/kin.550160508.

F16. **$CFCl_2 + O_2$.** Values for both low- and high-pressure limits at 300 K are from Caralp and Lesclaux.[1] Forst and Caralp[2] have examined this reaction theoretically. Temperature dependences are rough estimates based on their calculations and by analogy with similar reactions.
(Table: 06-2, Note: 06-2, Evaluated: 06-2) Back to Table

(1) Caralp, F.; Lesclaux, R. Rate constant for the reaction of the $CFCl_2$ radical with oxygen in the pressure range 0.2-12 Torr at 298 K. *Chem. Phys. Lett.* **1983**, *102*, 54-58, doi:10.1016/0009-2614(83)80657-5.

(2) Forst, W., and F. Caralp Microcanonical variational theory of radical recombination by inversion of interpolate partition function Part 2.-$CX_3 + O_2$ (X = H, F, Cl). *J. Chem. Soc. Faraday Trans.* **1991**, *87*, 2307-2315, doi:10.1039/ft9918702307.

F17. **$CF_2Cl + O_2$.** The recommended $k_0(300)$ and $k_\infty(300)$ are from the experimental work reported by Codnia and Azcárate,[1] and the recommended temperature exponents are taken from the theoretical predictions of Forst and Caralp.[2] Codnia and Azcárate used CO_2 laser IR multiphoton dissociation of CF_2Cl_2 to prepare CF_2Cl radicals in the presence of O_2 (and N_2 buffer gas) at 300 K. Subsequent fast reactions produced vibrationally excited CF_2O^*, which they monitored by measuring its spontaneous IR fluorescence near 1928 cm^{-1}. They showed that the growth and decay rates of the IR fluorescence intensity are due to the reactions of CF_2Cl radicals with O_2 and to the rate of collisional deactivation of CF_2O^*. Analysis of the reaction rates between CF_2Cl and O_2 revealed the existence of both the pressure-dependent recombination reaction and a direct bimolecular step (previously proposed by other workers; see Table 1-1) are important in the pressure range from 0 to 20 mbar of N_2. Separate control of O_2 concentrations enabled them to obtain the rate constant for the direct reaction (Table 1-1), as well as $k_0(300)$ and $k_\infty(300)$ for the recombination. The latter values are in rough agreement with the theoretical predictions of Forst and Caralp,[2] who predicted temperature exponents in approximate agreement with similar reactions. The estimated errors are relatively large because the reaction has been measured only once at 300 K and because the temperature dependence is based on theoretical predictions.
(Table: 10-6, Note: 10-6; Evaluated 10-6) Back to Table

(1) Codnia, J.; Azcarate, M. L. Rate measurement of the reaction of CF_2Cl radicals with O_2. *Photochem. Photobiol.* **2006**, *82*, 755–762, doi:10.1562/2006-01-04-RA-764.
(2) Forst, W., and F. Caralp Microcanonical variational theory of radical recombination by inversion of interpolate partition function Part 2.-$CX_3 + O_2$ (X = H, F, Cl). *J. Chem. Soc. Faraday Trans.* **1991**, *87*, 2307-2315, doi:10.1039/ft9918702307.

F18. **$CCl_3O_2 + NO_2$.** Statistical fit (constrained to $m = 1$) to experiments in O_2 of Caralp et al.,[1] who suggest a somewhat different fitting procedure, but the values recommended here fit the data just as well. Destriau and Troe[2] use yet a different fitting procedure that does not represent the data quite as well as that recommended herein. Reverse rate data are given by Köppenkastrop and Zabel.[3]
(Table: 06-2, Note: 06-2, Evaluated: 06-2) Back to Table

(1) Caralp, F.; Lesclaux, R.; Rayez, M. T.; Rayez, J.-C.; Forst, W. Kinetics of the combination reactions of chlorofluoromethylperoxy radicals with NO_2 in the temperature range 233-373 K. *J. Chem. Soc. Faraday Trans. 2* **1988**, *84*, 569-585, doi:10.1039/f29888400569.
(2) Destriau, M.; Troe, J. Thermal dissociation and recombination of alkyl and haloalkyl peroxyitrates: An SACM modelling study. *Int. J. Chem. Kinet.* **1990**, *22*, 915-934, doi:10.1002/kin.550220904.
(3) Köppenkastrop, D.; Zabel, F. Thermal decomposition of chlorofluoromethyl peroxynitrates. *Int. J. Chem. Kinet.* **1991**, *23*, 1-15, doi:10.1002/kin.550230102.

F19. **$CFCl_2O_2 + NO_2$.** Caralp et al.[1] studied this reaction at 233, 298, and 373 K at pressures of 0.013 to 0.13 atm. The reaction appears to be in the fall-off region. The recommended data are based on a fit with the constraint that m = 1. Caralp et al.[1] suggest a different fitting procedure, but the values recommended here fit the data just as well. Destriau and Troe[2] use yet a different fitting procedure that does not represent the data quite as well as that recommended herein. A study by Jowko et al.[3] in 1 atm of SF_6 at room temperature obtained an effective second order rate constant that is 15% lower than the value calculated from this recommendation. Data for the reverse reaction are reported by Köppenkastrop and Zabel.[4]
(Table: 06-2, Note: 19-5, Evaluated: 06-2) Back to Table

(1) Caralp, F.; Lesclaux, R.; Rayez, M. T.; Rayez, J.-C.; Forst, W. Kinetics of the combination reactions of chlorofluoromethylperoxy radicals with NO_2 in the temperature range 233-373 K. *J. Chem. Soc. Faraday Trans. 2* **1988**, *84*, 569-585, doi:10.1039/f29888400569.
(2) Destriau, M.; Troe, J. Thermal dissociation and recombination of alkyl and haloalkyl peroxyitrates: An SACM modelling study. *Int. J. Chem. Kinet.* **1990**, *22*, 915-934, doi:10.1002/kin.550220904.
(3) Jowko, A.; Wnorowski, K.; Kowalczyk, J.; Wojciechowski, K. The kinetics of the radical reactions in gaseous chloro- or fluorohydrocarbons. *Rad. Phys. Chem.* **2003**, *67*, 549-554, doi:10.1016/S0969-806X(03)00104-X.
(4) Köppenkastrop, D.; Zabel, F. Thermal decomposition of chlorofluoromethyl peroxynitrates. *Int. J. Chem. Kinet.* **1991**, *23*, 1-15, doi:10.1002/kin.550230102.

F20. **$CF_2ClO_2 + NO_2$.** A study by Xiong and Carr[5] of the reverse reaction, combined with the equilibrium constant, which was computed from correcting the study by Wu and Carr[4] of the forward reaction in a bath gas consisting of 80% CF_2ClBr + 20% O_2 for N_2 bath gas. (The study by Wu and Carr[4] supersedes the earlier work of Moore and Carr[3].) Xiong and Carr[5] report their parameterization differently than in this recommendation, but the values herein reproduce their results to a few percent. Reverse rate data are also given by Köppenkastrop and Zabel[2] and in a theoretical study by Forst and Caralp.[1]
(Table: 06-2, Note: 06-2, Evaluated: 06-2) Back to Table

(1) Forst, W.; Caralp, F. Microcanonical variational theory of radical recombination by inversion of interpolated partition function. 3. $CX_3O_2 + NO_2$ (X = H, F, Cl). *J. Phys. Chem.* **1992**, *96*, 6291-6298, doi:10.1021/j100194a036.
(2) Köppenkastrop, D.; Zabel, F. Thermal decomposition of chlorofluoromethyl peroxynitrates. *Int. J. Chem. Kinet.* **1991**, *23*, 1-15, doi:10.1002/kin.550230102.
(3) Moore, S. B.; Carr, R. W. Kinetics of the reactions of CF_2ClO_2 radicals with nitrogen dioxide. *J. Phys. Chem.* **1990**, *94*, 1393-1400, doi:10.1021/j100367a036.
(4) Wu, F.; Carr, R. W. An investigation of temperature and pressure dependence of the reaction of CF_2ClO_2 radicals with nitrogen dioxide by flash photolysis and time resolved mass spectrometry. *Int. J. Chem. Kinet.* **1991**, *23*, 701-715, doi:10.1002/kin.550230805.
(5) Xiong, J. Q.; Carr, R. W. Thermal decomposition of $CF_2ClO_2NO_2$. *J. Phys. Chem.* **1994**, *98*, 9811-9822, doi:10.1021/j100090a015.

G1. **Br + NO_2.** The recommended values are from a study by Kreutter et al.[2] They regarded the product as $BrNO_2$. Their k_o value in He agrees with the measurement of Mellouki et al.[4] at 300 K. Broske and Zabel[1] and Orlando and Burkholder[5] have shown that *cis*-BrONO is the major product in their studies. Orlando and Burkholder[5] suggest that isomerization to $BrNO_2$ is heterogeneous. Lee[3] calculated structure, frequencies and energetics for $BrNO_2$, *cis*-BrONO and *trans*-BrONO. A Patrick-and-Golden-type calculation using the Lee[3] results yields k_o(strong collision) ≈1.2, 2.5, and 2.1 in units of 1×10^{-31}cm^6 molecule^{-2} s^{-1} for *trans*-BrONO, *cis*-BrONO, and $BrNO_2$, respectively. The sum, 5.9×10^{-31}, multiplied by a collision efficiency in N_2 of 0.3 is a factor of about 2.5 lower than the observed k_o value. Also, the relative yield of $BrNO_2$ is somewhat too high since Orlando and Burkholder[5] measure BrONO >75%. Kreutter et al.[2] report an equilibrium constant, which, if *cis*-BrONO is assumed to be the product, suggests bond strengths for the BrONO compounds that are about 4 kcal mole^{-1} higher than the Lee[3] calculation. Computing k_o with these new values yields $k_o \approx 4.5$ and 6.4 in units of 1×10^{-31} for *trans*-BrONO and *cis*-BrONO, respectively. When the sum of the rate constants for the three channels is multiplied by the collision efficiency (0.3), the result is 3.9×10^{-31} and the yield of BrONO is 85%.
(Table: 06-2, Note: 06-2, Evaluated: 06-2) Back to Table

(1) Broske, R.; Zabel, F. Kinetics of the gas-phase reaction of $BrNO_2$ with NO. *J. Phys. Chem. A* **1998**, *102*, 8626-8631, doi:10.1021/jp982812b.
(2) Kreutter, K. D.; Nicovich, J. M.; Wine, P. H. Kinetics and thermochemistry of the Br($^2P_{3/2}$) + NO_2 association reaction. *J. Phys. Chem.* **1991**, *95*, 4020-4028, doi:10.1021/j100163a026.
(3) Lee, T. J. Characterization of $BrNO_2$, *cis*-BrONO, and *trans*-BrONO. Implications for atmospheric chemistry. *J. Phys. Chem.* **1996**, *100*, 19847-19852, doi:10.1021/jp962605g.
(4) Mellouki, A.; Laverdet, G.; Jourdain, J. L.; Poulet, G. Kinetics of the reactions Br + NO_2 + M and I + NO_2 + M. *Int. J. Chem. Kinet.* **1989**, *21*, 1161-1172, doi:10.1002/kin.550211209.
(5) Orlando, J. J.; Burkholder, J. B. Identification of BrONO as the major product in the gas-phase reaction of Br with NO_2. *J. Phys. Chem. A* **2000**, *104*, 2048-2053, doi:10.1021/jp993713g.

G2. **BrO + NO_2.** Recommended values are from a global least squares fit of data from Thorn et al.[10] and Sander et al.[9], which are in excellent agreement at 298 K. The recommended values differ only slightly from the previous recommendation. Danis et al.[1] give slightly lower values for the low-pressure-limiting rate constant and a smaller temperature dependence as well. This latter study may be hampered by heterogeneous effects, but can be accommodated within the error limits recommended. A theoretical study by Rayez and Destriau[8] suggests that the bond-dissociation energy in $BrONO_2$ is 8.5 kcal mol^{-1} higher than in $ClONO_2$, thus rationalizing the relative values of the low-pressure-limiting rate constants for these two processes. A more detailed theoretical study by Parthiban and Lee,[6] as well as a study by Orlando and Tyndall,[5] who measured $BrONO_2$ decomposition and thus an equilibrium constant, both determine only 1.6 kcal mol^{-1} for the above difference. A theoretical study by Zou et al.[12] agrees with the latter figure. A Patrick and Golden[7] type calculation, even with the stronger bond of Rayez and Destriau[8] yields a value for the low pressure limiting rate constant that is smaller than observed. Lessar et al.[4] calculate a potential energy surface for BrOONO. They find that the BrO–ONO bond strength is of the order of 7 kcal mol^{-1}, which is too weak to have any effect on the overall rate of BrO + NO_2. Walsh and Golden[2,11] have attempted to fit the data with a master equation analysis and found that the usual energy transfer treatment at low pressures is insufficient to fit the data (this was probably due to a bug that was found in that version of the master equation code). Kreycy et al.[3] analyzed atmospheric data and concluded that the recombination rate constant needed to fit the data near 200 K is smaller than the (previous) recommendation.
(Table: 15-10, Note: 15-10, Evaluated: 15-10) Back to Table

(1) Danis, F.; Caralp, F.; Masanet, J.; Lesclaux, R. Kinetics of the reaction BrO+NO_2+M → $BrONO_2$+M in the temperature range 263-343 K. *Chem. Phys. Lett.* **1990**, *167*, 450-456, doi:10.1016/0009-2614(90)85029-C.
(2) Golden, D. M. Pressure dependent reactions for atmospheric and combustion models. *Chem. Soc. Rev.* **2008**, *37*, 717-731, doi:10.1039/b704259k.
(3) Kreycy, S.; Camy-Peyret, C.; Chipperfield, M. P.; Dorf, M.; Feng, W.; Hossaini, R.; Kritten, L.; B.Werner; Pfeilsticker, K. Atmospheric test of the J($BrONO_2$)/$k_{BrO+NO2}$ ratio: implications for total stratospheric Br_y and bromine-mediated ozone loss. *Atmos. Chem. Phys.* **2013**, *13*, 6263-6274, doi:10.5194/acp-13-6263-2013.
(4) Lesar, A.; Prebil, S.; Mühlhaüser, M.; Hodošcek, M. Conformational potential energy surface of BrOONO. *Chem. Phys. Lett.* **2002**, *368*, 399-407, doi:10.1016/S0009-2614(02)01888-2.
(5) Orlando, J. J.; Tyndall, G. S. Rate coefficients for the thermal decomposition of $BrONO_2$ and the heat of formation of $BrONO_2$. *J. Phys. Chem.* **1996**, *100*, 19398-19405.

(6) Parthiban, P.; Lee, T. Ab initio investigation of the atmospheric molecule bromine nitrate: Equilibrium structure, vibrational spectrum, and heat of formation. *J. Chem. Phys.* **1998**, *109*, 525-530, doi:10.1063/1.476589.
(7) Patrick, R.; Golden, D. M. Third-order rate constants of atmospheric importance. *Int. J. Chem. Kinet.* **1983**, *15*, 1189-1227, doi:10.1002/kin.550151107.
(8) Rayez, M. T.; Destriau, M. Theoretical study of thermal dissociation and recombination reacitons of $XONO_2$ (X=F, Cl, Br, or I). *Chem. Phys. Lett.* **1993**, *206*, 278-284, doi:10.1016/0009-2614(93)85552-Y.
(9) Sander, S. P.; Ray, G. W.; Watson, R. T. Kinetics study of the pressure dependence of the BrO + NO_2 reaction at 298 K. *J. Phys. Chem.* **1981**, *85*, 199-210, doi:10.1021/j150602a018.
(10) Thorn, R. P.; Daykin, E. P.; Wine, P. H. Kinetics of the BrO + NO_2 association reaction. Temperature and pressure dependence in the falloff regime. *Int. J. Chem. Kinet.* **1993**, *25*, 521-537, doi:10.1002/kin.550250703.
(11) Walsh, R.; Golden, D. M. Evaluation of data for atmospheric models: Master equation/RRKM calculations on the combination reaction BrO + NO_2 → $BrONO_2$, a conundrum. *J. Phys. Chem. A* **2008**, *112*, 3891-3897, doi:10.1021/jp7116642.
(12) Zou, P.; Derecskei-Kovacs, A.; North, S. W. Theoretical calculation of $ClONO_2$ and $BrONO_2$ bond dissociation energies. *J. Phys. Chem. A* **2003**, *107*, 888-896, doi:10.1021/jp021961y.

G3. **Br + CH_2=CHCH=CH_2 (1,3-butadiene).** In a comprehensive study of the forward and reverse rates of this reaction (using laser flash photolysis of CF_2Br_2 precursor and atomic resonance fluorescence detection of Br-atoms), Laine et al.[2] determined the recombination rate constant from 227 to 298 K. The products are thought to consist of two isomers, but they were not identified in the experiments. Calculations (G4 method) reported by Laine et al. show that addition of Br to a terminal carbon atom is thermodynamically favored. The rate constants reported by Laine et al.[2] are about 2× as large as relative measurements at 298 K and 1 bar reported previously by Bierbach et al.[1] Bierbach et al. placed their rate constant on an absolute basis by employing a linked chain of relative rate measurements, which consisted of reactions of Br with 2,3-dimethyl-2-butene, trans-2-butene, propene, and terminated with an absolute rate constant for Br + acetaldehyde; thus the uncertainties may have accumulated. The current recommendation is based on the parameters measured in the direct experiments of Laine et al.[2] The recommended 2σ error bars encompass all of the data of Laine et al. (Table: 15-10, Note: 15-10, Evaluated: 15-10) Back to Table

(1) Bierbach, A.; Barnes, I.; Becker, K. H. Rate coefficients for the gas-phase reactions of bromine series of radicals with a alkenes, dienes, and aromatic hydrocarbons at 298 ± 2 K. *Int. J. Chem. Kinet.* **1996**, *28*, 565-577, doi:10.1002/(SICI)1097-4601(1996)28:8<565::AID-KIN2>3.0.CO;2-T.
(2) Laine, P. L.; Sohn, Y. S.; Nicovich, J. M.; McKee, M. L.; Wine, P. H. Kinetics of elementary steps in the reactions of atomic bromine with isoprene and 1,3-butadiene under atmospheric conditions. *J. Phys. Chem. A* **2012**, *116*, 6341-6357, doi:10.1021/jp212127v.

G4. **Br + CH_2=C(CH_3)CH=CH_2 (isoprene).** In a comprehensive study of the forward and reverse rates of this reaction (using laser flash photolysis of CF_2Br_2 precursor and atomic resonance fluorescence detection of Br-atoms), Laine et al.[2] determined the rate constant from 227 to 298 K. The products may consist of several isomers; calculations (G4 method) reported by Laine et al. show that the energetically most stable isomer is $BrH_2CC(CH_3)CH=CH_2$, but the identities of the isomers actually produced in the reaction are not known. Laine et al. also measured the rate constants for the reaction of Iso-Br + O_2 (see Table 1-1) and for the reaction of Br + 1,3-butadiene in both the presence and absence of O_2. They found that the apparent rate of the latter reaction is affected by the presence of O_2. Bierbach et al.[1] previously reported relative rate constants at 298 K and 1 bar of air. They placed their rate constants on an absolute basis by employing a linked chain of five relative rate measurements, consisting of reactions of Br with 1,3-butadiene, 2,3-dimethyl-2-butene, trans-2-butene, propene, and terminated with an absolute rate constant for Br + acetaldehyde; thus the uncertainties may have accumulated. The current recommendation is based on the parameters measured in the direct experiments of Laine et al.[2] in the absence of O_2. The recommended 2σ error bars encompass all of the data of Laine et al. (Table: 15-10, Note: 15-10, Evaluated: 15-10) Back to Table

(1) Bierbach, A.; Barnes, I.; Becker, K. H. Rate coefficients for the gas-phase reactions of bromine series of radicals with a alkenes, dienes, and aromatic hydrocarbons at 298 ± 2 K. *Int. J. Chem. Kinet.* **1996**, *28*, 565-577, doi:10.1002/(SICI)1097-4601(1996)28:8<565::AID-KIN2>3.0.CO;2-T.
(2) Laine, P. L.; Sohn, Y. S.; Nicovich, J. M.; McKee, M. L.; Wine, P. H. Kinetics of elementary steps in the reactions of atomic bromine with isoprene and 1,3-butadiene under atmospheric conditions. *J. Phys. Chem. A* **2012**, *116*, 6341-6357, doi:10.1021/jp212127v.

H1. **I + NO.** Evaluation taken from IUPAC.[3] The data are from van den Bergh et al.[4] and Basco and Hunt.[1] Error limits transposed to the current format. The heat of formation of INO is given as 120.0 ± 0.3 kJ/mole by Forte et al.[2]
(Table: 06-2, Note: 06-2, Evaluated: 06-2) Back to Table

(1) Basco, N.; Hunt, J. E. The recombination of iodine atoms in the presence of nitric oxide. *Int. J. Chem. Kinet.* **1978**, *10*, 733-743, doi:10.1002/kin.550100707.
(2) Forte, E.; Hippler, H.; van den Bergh, H. INO thermodynamic properties and ultraviolet spectrum. *Int. J. Chem. Kinet.* **1981**, *13*, 1227-1233.
(3) IUPAC *J. Phys. Chem. Ref. Data* **1992**, *21*, 1125-1568.
(4) van den Bergh, H.; Benoit-Guyot, N.; Troe, J. Collisional energy transfer in the reactions I + NO + M → INO + M and I + NO_2 + M → INO_2 + M. *Int. J. Chem. Kinet.* **1977**, *9*, 223-234, doi:10.1002/kin.550090207.

H2. **I + NO_2.** Evaluation taken from IUPAC.[2] The data are from van den Bergh et al.,[5] Mellouki et al.,[3] Buben et al.,[1] and van den Bergh and Troe.[6] IUPAC uses $F_c = 0.63$, which is essentially the same as the universal value adopted here of $F_c = 0.6$. (No evidence of possible isomers [INO_2 or IONO] is reported.) Error limits transposed to the current format. Tucceri et al.[4] used laser flash photolysis coupled to resonance-fluorescence detection of I atoms to measure the rate coefficients for the reaction: I + NO_2 + M → INO_2 + M. Rate coefficients at 298 K when combined with other datasets obtained at higher and lower pressures, were adequately described by a simplified Troe function with the parameters: k_0(He, 330 K) = 1.48×10^{-31} cm^6 molecule^{-2} s^{-1}, F_c(He) = 0.43, and $k_\infty = 1.1 \times 10^{-10}$ cm^3 molecule^{-1} s^{-1} for He as bath gas. In N_2 (or air) the following parameters were obtained $k_0(N_2, 300\ K) = 3.2 \times 10^{-31}$ cm^6 molecule^{-2} s^{-1}, $F_c(N_2) = 0.48$, with $k_\infty = 1.1 \times 10^{-10}$ cm^3 molecule^{-1} s^{-1}. These parameters essentially reproduce the values at 300 K from the parameters in the Table.
(Table: 10-6, Note: 10-6, Evaluated 10-6) Back to Table

(1) Buben, S. N.; Larin, I. K.; Messineva, N. A.; Trofimova, E. M. Measurement of the rate constant of the reaction I + NO_2 + M → INO_2 + M (M = He, N_2, Ar, O_2). *Kinetika i Kataliz* **1990**, *31*, 973.
(2) IUPAC *J. Phys. Chem. Ref. Data* **1992**, *21*, 1125-1568.
(3) Mellouki, A.; Laverdet, G.; Jourdain, L.; Poulet, G. Kinetics of the reactions Br + NO_2 + M and I + NO_2 + M. *Int. J. Chem. Kinet.* **1989**, *21*, 1161-1172, doi:10.1002/kin.550211209.
(4) Tucceri, M. E.; Dillon, T. J.; Crowley, J. N. A laser photolysis–resonance fluorescence study of the reactions: I + O_3 → IO + O_2, O + I_2 → IO + I, and I + NO_2 + M → INO_2 + M at 298 K. *Phys. Chem. Chem. Phys.* **2005**, *10*, 1657-1663, doi:10.1039/b502844b.
(5) van den Bergh, H.; Benoit-Guyot, N.; Troe, J. Collisional energy transfer in the reactions I + NO + M → INO + M and I + NO_2 + M → INO_2 + M. *Int. J. Chem. Kinet.* **1977**, *9*, 223-234, doi:10.1002/kin.550090207.
(6) van den Bergh, H.; Troe, J. Kinetic and thermodynamic properties of INO and INO_2 intermediate complexes in iodine recombination. *J. Chem. Phys.* **1976**, *64*, 736-742, doi:10.1063/1.432220.

H3. **IO + NO_2.** Data from Daykin and Wine,[2] Hölscher and Zellner,[5] Allan and Plane,[1] Jenkin and Cox,[6] and Dillon et al.[3] are considered. Dillon et al. suggest that the value from Hölscher and Zellner might be low at 298 K due to regeneration of IO, although their values at lower temperatures are in agreement with others. The recommendation takes this into consideration and accommodates the rest of the data. Two more studies at lower pressures are available, Larin et al.[8] and Maguin et al.[9] These latter do not agree very well with the above five studies and have larger experimental errors. The recommended k_o and k_∞ also agree with a theoretical study by Rayez and Destriau.[12] A computational study by Marshall[10] sets the bond dissociation energy as ΔH_0(IO-NO_2) = 113.6 ± 3.1 kJ mol^{-1} and suggests $k_o = (5.3–13.3) \times 10^{-31}$ cm^{6}molecule^{-1}s^{-1} for N_2 as the bath gas, while an ME/RRKM study by Golden[4] required ΔH_0(IO-NO_2) ~150 kJ mol^{-1} to fit the data. Papayannis and Kosmas[11] compute ΔH_0(IO-NO_2) = 137.6 or 131.7 kJ mol^{-1}, depending on spin orbit coupling corrections in IO. A computational study by Koltsoyannis and Plane[7] concludes that ΔH_0(IO-NO_2) = 117.9 kJ mol^{-1}. See Table 3-1 for the recommended K_{eq}.
(Table: 10-6, Note: 10-6, Evaluated: 10-6) Back to Table

(1) Allan, B. J.; Plane, J. M. C. A study of the recombination of IO with NO_2 and the stability of INO_3: Implications for the atmospheric chemistry of iodine. *J. Phys. Chem. A* **2002**, *106*, 8634-8641, doi:10.1021/jp020089q.
(2) Daykin, E. P.; Wine, P. H. Kinetics of the reactions of IO Radicals with NO and NO_2. *J. Phys. Chem.* **1990**, *94*, 4528-4535, doi:10.1021/j100374a034.

(3) Dillon, T. J.; Blitz, M. A.; Heard, D. E. Determination of the rate coefficients for the reactions IO + NO_2 +M (Air) → $IONO_2$ + M and $O(^3P)$ + NO_2 → O_2 + NO using laser-induced fluorescence spectroscopy. *J. Phys. Chem. A* **2006**, *110*, 6995-7002, doi:10.1021/jp057048p.
(4) Golden, D. M. Evaluating data for atmospheric models, an example: IO + NO_2 = $IONO_2$. *J. Phys. Chem. A* **2006**, *110*, 2940-2943, doi:10.1021/jp058221k.
(5) Hölscher, D.; Zellner, R. LIF study of the reactions of the IO radical with NO and NO_2 over an extended range of temperature and pressure. *Phys. Chem. Chem. Phys.* **2002**, *4*, 1839-1845, doi:10.1039/b110084j.
(6) Jenkin, M. E.; Cox, R. A. Kinetics study of the reactions IO + NO_2 + M → $IONO_2$ + M, IO + IO → products, and I + O_3 → IO + O_2. *J. Phys. Chem.* **1985**, *89*, 192-199, doi:10.1021/j100247a040.
(7) Kaltsoyannis , N.; Plane, J. M. C. Quantum chemical calculations on a selection of iodine-containing species (IO, OIO, INO_3, $(IO)_2$, I_2O_3, I_2O_4 and I_2O_5) of importance in the atmosphere. *Phys. Chem. Chem. Phys.* **2008**, *10*, 1723-1733, doi:10.1039/b715687c.
(8) Larin, I. K., D. V. Nevozhai, A. I. Spasskii, and E. M. Trofimova A study of the reaction IO + NO_2 + O_2 → $IONO_2$ + O_2. *Kinetics and Catalysis* **1998**, *39*, 666-672.
(9) Maguin, F.; Laverdet, G.; Le Bras, G.; Poulet, G. Kinetic study of the reactions IO + HO_2 and IO + NO_2 at 298 K. *J. Phys. Chem.* **1992**, *96*, 1775-1780, doi:10.1021/j100183a052.
(10) Marshall, P. Computational studies of the thermochemistry of the atmospheric iodine reservoirs HOI and $IONO_2$. *Advances in Quantum Chemistry* **2008**, 159-175.
(11) Papayannis, D. K.; Kosmas, A. M. Quantum mechanical characterization of (INO_3) isomers. *Chem. Phys. Lett.* **2004**, *398*, 75-81, doi:10.1016/j.cplett.2004.09.019.
(12) Rayez, M. T.; Destriau, M. Theoretical study of thermal dissociation and recombination reacitons of $XONO_2$ (X=F, Cl, Br, or I). *Chem. Phys. Lett.* **1993**, *206*, 278-284, doi:10.1016/0009-2614(93)85552-Y.

H4. **CH_2I + O_2.** The recommendation at 298 K is the average of measurements by Masaki et al.,[5] Eskola et al.,[2] Huang et al.,[3] Sheps,[6] and Stone et al.[7] Evidently, there is no pressure dependence up to at least 1 atm. The recommendation for the temperature dependence is taken from Eskola et al.[2] Among other products, this reaction produces significant yields of thermalized formaldehyde oxide (CH_2OO, the simplest carbonyl oxide, also known as a Criegee Intermediate).[1] Yields of CH_2OO in this reaction under one atmosphere of air near 300 K have been reported to be 0.15 ± 0.03,[3,4] ~0.18,[7] and ~0.30.[8]
(Table 15-10, Note: 15-10, Evaluated: 15-10) Back to Table

(1) Criegee, R. Mechanism of ozonolysis. *Angew. Chem. Int. Ed. Engl.* **1975**, *14*, 745-752, doi:10.1002/anie.197507451.
(2) Eskola, A. J.; Wojcik-Pastuszka, D.; Ratajczak, E.; Timonen, R. S. Kinetics of the reactions of CH_2Br and CH_2I radicals with molecular oxygen at atmospheric temperatures. *Phys. Chem. Chem. Phys.* **2006**, *8*, 416-1424, doi:10.1039/b516291b.
(3) Huang, H.; Eskola, A. J.; Taatjes, C. A. Pressure-dependent I-atom yield in the reaction of CH_2I with O_2 shows a remarkable apparent third-body efficiency for O_2. *J. Phys. Chem. Lett.* **2012**, *3*, 3399-3403, doi:10.1021/jz301585c.
(4) Huang, H.; Rotavera, B.; Eskola, A. J.; Taatjes, C. A. Correction to "Pressure-dependent I atom yield in the reaction of CH_2I with O_2 shows a remarkable apparent third-body efficiency for O_2". *J. Phys. Chem. Lett.* **2013**, *4*, 3824-3824, doi:10.1021/jz402266q.
(5) Masaki, A.; Tsunashima, N.; Washida, N. Rate constant for the reaction of CH_3O_2 with NO. *Chem. Phys. Lett.* **1994**, *218*, 523-528, doi:10.1016/0009-2614(94)00024-7.
(6) Sheps, L. Absolute ultraviolet absorption spectrum of a Criegee intermediate CH_2OO. *J. Phys. Chem. Lett.* **2013**, *4*, 4201-4205, doi:10.1021/jz402191w.
(7) Stone, D.; Blitz, M.; Daubney, L.; Ingham, T.; Seakins, P. CH_2OO Criegee biradical yields following photolysis of CH_2I_2 in O_2. *Phys. Chem. Chem. Phys.* **2013**, *15*, 19119-19124, doi:10.1039/c3cp52466c.
(8) Ting, W.-L.; Chang, C.-H.; Lee, Y.-F.; Matsui, H.; Lee, Y.-P.; Lin, J. J.-M. Detailed mechanism of the CH_2I + O_2 reaction: Yield and self-reaction of the simplest Criegee intermediate CH_2OO. *J. Chem. Phys.* **2014**, *141*, 104308, doi:10.1063/1.4894405.

I1. **HS + NO.** Data are from the work of Black et al.[1] The temperature dependence of k_∞ has been estimated and k_o has been adjusted to fit the data.
(Table: 06-2, Note: 06-2, Evaluated: 06-2) Back to Table

(1) Black, G.; Patrick, R.; Jusinski, L. E.; Slanger, T. G. Rate coefficients for the reaction HS + NO + M(M = He, Ar, and N_2) over the temperature range 250- 445 K. *J. Chem. Phys.* **1984**, *80*, 4065-4070, doi:10.1063/1.447287.

I2. **$CH_3S + NO$.** The recommended values are fit to the study by Balla et al.[1] The temperature range was 295 to 453 K and pressures of N_2 from 1.5 to 300 Torr. The recommended high-pressure limiting rate coefficient and temperature dependence provide a better fit to the data than reported by Balla et al.
(Table: 06-2, Note: 06-2, Evaluated: 06-2) Back to Table

(1) Balla, R. J.; Nelson, H. H.; McDonald, J. R. Kientics of the reaction of CH_3S with NO, NO_2 and O_2. *Chem. Phys.* **1986**, *109*, 101-107, doi:10.1016/0301-0104(86)80188-4.

I3. **$O + SO_2$.** Naidoo et al.[4] studied this spin-forbidden reaction in Ar over the temperature range 290< T/K <840 and pressure range 100< P/mbar <880. They fit the data very well using the IUPAC[1] format with $k_o = 9.5 \times 10^{-23}$ T^{-3} exp(–2400/T) cm^6 $molecule^{-2}$ s^{-1}, $k_\infty = 6.1 \times 10^{-13}$exp(–850/T) cm^3 $molecule^{-1}$ s^{-1} and $F_c = 0.558$exp(–T/316) + 0.442exp(–T/7442). The recommended values transpose the rate constants to the form used in this evaluation and are used with the standard value of $F_c = 0.6$. These parameters do not fit the higher temperatures as well as the values derived by Naidoo et al. (i.e. missing the values at 840 K by about 50% and those at 699 K by about 20%), but values at 289, 399 and 581 K are fit quite well and are adequate for atmospheric conditions. Earlier values are reported by Atkinson and Pitts[2] and Müller et al.[3]
(Table: 06-2, Note: 06-2, Evaluated: 06-2) Back to Table

(1) IUPAC: Atmospheric Chemical Kinetic Data Evaluation. Atkinson, R.; Baulch, D. L.; Cox, R. A.; Crowley, J. N.; Hampson, J., R. F.; Hynes, R. G.; Jenkin, M. E.; Kerr, J. A.; Rossi, M. J.; Troe, J., 2004, http://www.iupac-kinetic.ch.cam.ac.uk.

(2) Atkinson, R.; Pitts Jr., J. N. Kinetics of the reaction $O(^3P) + SO_2 + M \rightarrow SO_3 + M$ over the temperature range of 299°–440°K. *Int. J. Chem. Kinet.* **1978**, *10*, 1081-1090, doi:10.1002/kin.550101006.

(3) Müller, M. A.; Yetter, R. A.; Dryer, F. L. Kinetic modeling of the CO/ $H_2O/O_2/NO/SO_2$ system: Implications for high-pressure fall-off in the $SO_2 + O(+M) = SO_3(+M)$ reaction. *Int. J. Chem. Kinet.* **2000**, *32*, 317-339, doi:10.1002/(SICI)1097-4601(2000)32:6<317::AID-KIN1>3.0.CO;2-L.

(4) Naidoo, J., A. Goumri, and P. Marshall A kinetic study of the reaction of atomic oxygen with SO_2. *Proc. Combust. Inst.* **2005**, *30*, 1219-1225, doi:10.1016/j.proci.2004.08.214.

I4. **$OH + SO_2$.** The data for this reaction have been completely re–analyzed. The JPL10-15 recommendation was based on the results of Blitz et al.,[4] who determined the high pressure limit from measurements of OH(v=1) + SO_2 and fitted data by using a master equation approach. Recently, new results obtained by Blitz et al.[6] for OH(v=1,2,3) + SO_2 suggest that determination of the high pressure limit by using vibrational relaxation of OH(v) is more complicated than had been previously assumed.[4,11] The new findings by Blitz et al.[6] and Medeiros et al.[16] for k_∞(298 K) ($7 \pm 3 \times 10^{-13}$ and $5.9 \pm 0.8 \times 10^{-13}$, respectively) are a factor of 2–3 lower than most of the older data for this reaction. Blitz et al.[5] speculate that the older data are in error because of reactions of OH with SO_2 photolysis products in the flash photolysis experiments and regeneration of OH by secondary reactions in the flow tube experiments. Although Blitz et al.[6] did not offer any quantitative analysis in support of their reasoning, they rejected most of the older data and chose to retain only their own data, the measurements by Cox et al.,[7] and the data obtained by Wine et al.[24] in Ar bath gas (discarding data in He, N_2, and SF_6). The interpretation of Blitz et al.[5,6] is predicated on the existence of a pre–reactive complex, the existence of which is supported by theoretical calculations.[16,17] Their analysis is based on the premise that the capture rate constant for adduct formation is independent of the vibrational level of OH(v) and on the assumption that the measured rate constant for loss of OH(v) is due to both adduct formation and impulsive vibrational energy transfer, as described by Shin's extension of SSH theory.[19-22] Because these processes are not yet fully understood in this system and the analysis of Blitz and co-workers[5,6,16] is based on several simplifying assumptions, the reliability of the new interpretation cannot be determined. However, the measured deactivation rate constants of OH(v) may still be regarded as approximate upper limits to k_∞(T) for the recombination reaction.
The present recommendations for k_∞(298 K) and k_0(298 K) are based on a global non-linear least squares analysis of the experimental data (assuming uniform relative errors) for N_2 and O_2 collider gases near 298 K reported by Cox et al.[7] (with the measured relative rate constant corrected for current recommendations for the HO + CO reference reaction), Leu,[13] Wine et al.,[24] and Paraskevopoulos et al.[18] In their experiments, Wine et al.[24] and Paraskevopoulos et al.[18] used an SO_2 gas filter between the flash lamp and the reaction cell to attenuate wavelengths that might photolyze SO_2 in the reaction cell. When O_2 bath gas was studied by Leu,[13] there was some evidence that OH was being regenerated by secondary reactions; in that instance, Leu utilized the initial rate, which minimizes the effect. Because their data for O_2 and N_2 are in unexpected disagreement with each other, which possibly suggests the effects of secondary reactions,[5] the data of Lee et al.[12] were not included, although their results for N_2 are in good agreement with the recommendation. Data from Fulle et al.[8] were not included in the analysis, because in the relevant pressure range they are significantly higher than all of the other data.

The recommended value for k_∞(298 K) is consistent with regarding the measured rate constants for OH(v) deactivation as upper limits. The theoretical analysis of Somnitz,[23] the density functional theory calculations of Medeiros et al.[16], and the ab initio high level theoretical calculations of Long et al.[15] consistently predict that the reaction has a small intrinsic activation barrier of ~0.5 kcal/mol above the energy of the separate reactants. The recommended k_∞(298 K) is in reasonable agreement with the value (1.26×10^{-12}) computed by Long et al.[15] The recommended temperature exponent for k_∞(T) is based on the value predicted by Long et al.[15], multiplied by an adjustment factor of exp(90/T) to bring their value of k_∞(298 K) into agreement with the recommendation. This adjustment corresponds to lowering the predicted activation energy to ~0.3 kcal/mol. Data for N_2 and O_2 collider gases are available only near 298 K. The present recommendation for the low pressure temperature exponent was taken from the master equation analysis of Blitz et al.,[4] who re–evaluated the data of Wine et al.[24] (which are in very good agreement with the data of Paraskevopoulos et al.[18]) in several bath gases at pressures up to 150 Torr and temperatures between 260 and 420 K. The large error factor, f(298 K) =3, is a result of the uncertainty introduced by the studies by Blitz and coworkers; the much smaller uncertainty, f(298 K) = 1.08, is based on the least-squares analysis leading to the recommended parameters. The value for g applies mostly to the low-pressure limit. Earlier data listed in Harris and Wayne,[10] Harris et al.,[9] Baulch et al.,[3] Baulch et al.,[2] and Atkinson et al.[1] are noted. Blitz et al.[4] have calculated the entropy and measured a third law heat of formation for $HOSO_2$ (373 ± 6 kJ/mol). Medeiros et al.[16] have analyzed a set of selected data and compared heat of formation obtained from several different theoretical studies. See also Li and McKee.[14]

(Table: 19-5, Note: 19-5, Evaluated: 19-5) Back to Table

(1) Atkinson, R.; Baulch, D. L.; Cox, R. A.; Crowley, J. N.; Hampson, J., R. F.; Hynes, R. G.; Jenkin, M. E.; Kerr, J. A.; Rossi, M. J.; Troe, J. IUPAC: Atmospheric Chemical Kinetic Data Evaluation, 2004, http://www.iupac-kinetic.ch.cam.ac.uk.

(2) Baulch, D. L.; Cox, R. A.; Crutzen, P. J.; Hampson, R. F., Jr.; Kerr, J. A.; Troe, J.; Watson, R. T. Evaluated kinetic and photochemical data for atmospheric chemistry: Supplement 1. *J. Phys. Chem. Ref. Data* **1982**, *11*, 327-496, doi:10.1063/1.555664.

(3) Baulch, D. L.; Cox, R. A.; Hampson, R. F., Jr.; Kerr, J. A.; Troe, J.; Watson, R. T. Evaluated kinetic and photochemical data for atmospheric chemistry. *J. Phys. Chem. Ref. Data* **1980**, *9*, 295-471, doi:10.1063/1.555619.

(4) Blitz, M. A.; Huges, K. J.; Pilling, M. J. Determination of the high-pressure limiting rate coefficient and the enthalpy of reaction for OH + SO_2. *J. Phys. Chem. A* **2003**, *107*, 1971-1978, doi:10.1021/jp026524y.

(5) Blitz, M. A.; Salter, R. J.; Heard, D. E.; Seakins, P. W. An Experimental and Master Equation Study of the Kinetics of OH/ OD + SO_2: The Limiting High-Pressure Rate Coefficients. *J. Phys. Chem. A* **2017**, *121*, 3184−3191, doi:10.1021/acs.jpca.7b01295.

(6) Blitz, M. A.; Salter, R. J.; Heard, D. E.; Seakins, P. W. An Experimental Study of the Kinetics of OH/OD(v = 1,2,3) + SO_2: The Limiting High-Pressure Rate Coefficients as a Function of Temperature. *J. Phys. Chem. A* **2017**, *121*, 3175−3183, doi:10.1021/acs.jpca.7b01294.

(7) Cox, R. A. Photolysis of gaseous nitrous acid-A technique for obtaining kinetic data on atmospheric photooxidation reactions. *Int. J. Chem. Kinet. Symp.* **1975**, *1*, 379-398.

(8) Fulle, D.; Hamann, H. F.; Hippler, H. The pressure and temperature dependence of the recombination reaction HO+SO_2+M = $HOSO_2$+M. *Phys. Chem. Chem. Phys.* **1999**, *1999*, 2695-2702, doi:10.1039/a901596e.

(9) Harris, G. W.; Atkinson, R.; Pitts, J. N., Jr. Temperature dependence of the reaction OH + SO_2 + M → HSO_3 + M for M = Ar and SF_6. *Chem. Phys. Lett.* **1980**, *69*, 378-382, doi:10.1016/0009-2614(80)85085-8.

(10) Harris, G. W.; Wayne, R. P. Reaction of hydroxyl radicals with NO, NO_2 and SO_2. *J. Chem. Soc. Faraday Trans. 1* **1975**, *71*, 610-617, doi:10.1039/f19757100610.

(11) Jaffer, D. H.; Smith, I. W. M. Time-Resolved Measurements on the Relaxation of OH(v = 1) by NO, NO_2 AND O_2. *Faraday Discuss. Chem. Soc.* **1979**, *67*, 212−220, doi:10.1039/dc9796700212.

(12) Lee, Y.-Y.; Kao, W. C.; Lee, Y.-P. Kinetics of the reaction OH + SO_2 in He, N_2, and O_2 at low pressure. *J. Phys. Chem.* **1990**, *94*, 4535-4540, doi:10.1021/j100374a035.

(13) Leu, M. T. Rate constants for the reaction of OH with SO_2 at low pressure. *J. Phys. Chem.* **1982**, *86*, 4558-4562, doi:10.1021/j100220a021.

(14) Li, W.-K., and M. L. McKee Theoretical study of OH and H_2O addition to SO_2. *J. Phys. Chem. A* **1997**, *101*, 9778-9782, doi:10.1021/jp972389r.

(15) Long, B.; Bao, J. L.; Truhlar, D. G. Reaction of SO_2 with OH in the atmosphere. *Phys. Chem. Chem. Phys.* **2017**, *19*, 8091-8100, doi:10.1039/c7cp00497d.

(16) Medeiros, D. J.; Blitz, M. A.; Seakins, P. W. Exploring the features on the OH + SO_2 potential energy surface using theory and testing its accuracy by comparison to experimental data. *Phys. Chem. Chem. Phys.* **2018**, *20*, 8984-8990, doi:10.1039/c8cp00091c.
(17) Miriyala, V. M.; Bhasi, P.; Nhlabatsi, Z. P.; Sitha, S. Formation of a pre-reaction hydrogen-bonded complex and its significance in the potential energy surface of the OH + SO_2→ $HOSO_2$ reaction: A computational study. *J. Theor. Comput. Chem.* **2017**, *16*, 1750046, doi:10.1142/S0219633617500468.
(18) Paraskevopoulos, G.; Singleton, D. L.; Irwin, R. S. Rates of OH radical reactions. The reaction OH + SO_2 + N_2. *Chem. Phys. Lett.* **1983**, *100*, 83-87, doi:10.1016/0009-2614(83)87267-4.
(19) Shin, H. K. Temperature dependence of intermolecular energy transfer in polar molecules. *J. Amer. Chem. Soc.* **1968**, *90*, 3029-3039, doi:10.1021/ja01014a007.
(20) Shin, H. K. Deexciation of molecular vibration on collision: Vibration-to-rotation energy transfer in hydrogen halides. *J. Phys. Chem.* **1971**, *75*, 1079-1090, doi:10.1021/j100678a011.
(21) Shin, H. K. Vibration-rotation-translation energy transfer in HF-HF and DF-DF. *Chem. Phys. Lett.* **1971**, *10*, 81-85, doi:10.1016/0009-2614(71)80162-8.
(22) Shin, H. K. Temperature dependence of $V \rightarrow R$, T energy transfer probabilities in $CO_2(00^01)$ + HF/DF. *J. Chem. Phys.* **1974**, *60*, 3844-3851, doi:10.1063/1.1681329.
(23) Somnitz, H. Quantum chemical and dynamical characterisation of the reaction OH + SO_2 ⇌ $HOSO_2$ over an extended range of temperature and pressure. *Phys . Chem. Chem. Phys* . **2004**, *6*, 3844-3851, doi:10.1039/b317055a.
(24) Wine, P. H.; Thompson, R. J.; Ravishankara, A. R.; Semmes, D. H.; Gump, C. A.; Torabi, A.; Nicovich, J. M. Kinetics of the reaction OH + SO_2 + M → $HOSO_2$ + M. Temperature and pressure dependence in the falloff region. *J. Phys. Chem.* **1984**, *88*, 2095-2104, doi:10.1021/j150654a031.

I5. **$CH_3S + O_2$.** The Panel makes no recommendation, since only one direct measurement of the rate constant has been reported and helium bath gas is not appropriate for the atmosphere. The following is for information, only.

Turnipseed et al.[4] generated CH_3S radicals by pulsed laser photolysis of CH_3SCH_3 with O_2 in excess and used LIF of CH_3S to monitor the subsequent reaction. Biexponential decays were observed, signaling the reversible formation of a weakly bound complex. They obtained forward and reverse rate constants in 80 Torr of He bath gas at temperatures from 216 to 250 K; the values of $K_{eq} = k_{rec}/k_{uni}$ are in good agreement with the recommended K_{eq} (see Table 3-1). Assuming that k_{rec} is near the low-pressure limit, the data of Turnipseed et al. are described by $k_0(T) = 8 \times 10^{-32}\ (T/298)^{-5.7}$ in helium bath gas. The reaction has been implicated in three indirect studies,[1-3] which reported estimated ratios of rate constants.
(Table: 15-10; Note: 15-10; Evaluation 15-10) Back to Table

(1) Balla, R. J.; Heicklen, J. Oxidation of sulfur compounds III: The photolysis of $(CH_3S)_2$ in the presence of O_2. *J. Photochem.* **1985**, *29*, 297-310, doi:10.1016/0047-2670(85)85003-6.
(2) Grosjean, D. Photooxidation of methyl sulfide, ethyl sulfide, and methanethiol. *Environ. Sci. Technol.* **1984**, *18*, 460-468, doi:10.1021/es00124a013.
(3) Hatakeyama, S.; Akimoto, H. Reactions of hydroxyl radicals with methanethiol, dimethyl sulfide, and dimethyl disulfide in air. *J. Phys. Chem.* **1983**, *87*, 2387-2395, doi:10.1021/j100236a029.
(4) Turnipseed, A. A.; Barone, S. B.; Ravishankara, A. R. Observation of CH_3S addition to O_2 in the gas phase. *J. Phys. Chem.* **1992**, *96*, 7502-7505, doi:10.1021/j100198a006.

I6. **$CH_3SCH_2 + O_2$.** Wallington et al.[2] have employed a pulse radiolysis technique, obtaining $k = (5.7 \pm 0.4) \times 10^{-12}$ cm^3 $molecule^{-1}$ s^{-1} in 992 mbar of SF_6 at room temperature. A theoretical study by Resende and De Alemeida[1] yields a heat of formation of the product, $CH_3SCH_2O_2$, as 6.51 kcal mol^{-1}.
(Table: 94-26, Note: 06-2, Evaluated: 06-2) Back to Table

(1) Resende, S. M.; De Alemeida, W. B. Mechanism of the atmospheric reaction between the radical CH_3SCH_2 and O_2. *J. Phys. Chem. A* **1999**, *103*, 4191-4195, doi:10.1021/jp983524i.
(2) Wallington, T. J.; Ellermann, T.; Nielsen, O. J. Atmospheric chemistry of dimethyl sulfide: UV spectra and self-reaction kinetics of CH_3SCH_2 and $CH_3SCH_2O_2$ radicals and kinetics of the reactions $CH_3SCH_2 + O_2 \rightarrow CH_3SCH_2O_2$ and $CH_3SCH_2O_2 + NO \rightarrow CH_3SCH_2O + NO_2$. *J. Phys. Chem.* **1993**, *97*, 8442-8449, doi:10.1021/j100134a013.

I7. **$CH_3 + SO_3$.** (Also see Table 3-1) Because this reaction has never been investigated in laboratory experiments, the Panel makes no specific recommendation, but notes that the reaction has been investigated in theoretical studies. The results depend on both the level of theory and the size of the basis set. Salta et al.[2] commented that composite methods (e.g. G2, G3, and CBS–QB3) seem to be somewhat more reliable for this reaction than

single–point methods like B3LYP and CCSD(T), probably because the composite methods employ both high–level theory and empirical corrections for various effects. They prefer CBS–QB3 because it extrapolates to the complete basis set limit. For a summary of reported reaction enthalpies, which are uncertain, see the Note for this reaction in Table 3. Using a composite method (G3XMP2// B3LYP/6–311+G(3df,2p)), Cao et al.[1] found 63.5 kJ/mol for Δ_rH_0 for $CH_3SO_3 \rightarrow CH_3 + SO_3$ and a small intrinsic energy barrier (1.0 kJ/mol, including zero point energy); they report the total rate constant for dissociation is $k_{uni} = (1.40 \times 10^{12}) \times (T^{0.15}) \times \exp(-7831/T)$ s^{-1}. This rate constant may be too large, however, since $\Delta_fH_0(CH_3SO_3)$ reported by Cao et al.[1] is ~10 kJ/mol lower than computed by Salta et al.[2] and by Zhu et al.[3] using CBS-QB3. From the molecular parameters for CH_3, SO_3, and the transition state reported by Cao et al.,[1] we obtain $k_{rec}(T) = 2.2 \times 10^{-13} \times (T/298)^{-0.2}$ cm^3 s^{-1}. This value will not be affected by differences in the computed dissociation energy. Because the magnitude of the rate constant depends on the accuracy of geometrical parameters (symmetry and rotational constants), vibrational frequencies (which may be affected by anharmonicity), and computed barrier heights, we estimate an uncertainty factor $f(298\ K) = 10$ for $k_\infty(298\ K)$. The reaction is probably close to the high-pressure limit at 1 atm.

(Table: 19-5, Note: 19-5, Evaluated: 19-5) Back to Table

(1) Cao, J.; Wang, W.-L.; Gao, L.-J.; Fu, F. Mechanism and Thermodynamic Properties of CH_3SO_3 Decomposition. *Acta Phys.-Chim. Sin.* **2013**, *29*, 1161-1167, doi:10.3866/PKU.WHXB201304021.

(2) Salta, Z.; Kosmas, A. M.; Lesar, A. Computational investigation of the peroxy radicals $CH_3S(O)(n)OO$ and the peroxynitrates $CH_3S(O)(n)OONO_2$ (n=0, 1, 2). *Comput. Theo. Chem.* **2012**, *1001*, 67-76, doi:10.1016/j.comptc.2012.10.007.

(3) Zhu, B.; Zeng, X.; Beckers, H.; Francisco, J. S.; Willner, H. The Methylsulfonyloxyl Radical, CH_3SO_3. *Angew. Chem. Int. Ed.* **2015**, *54*, 11404 –11408, doi:10.1002/anie.201503776.

I8. **$SO_3 + NH_3$.** Recommendation is from Lovejoy.[1] This study covered 20–80 Torr from 280–340 K. An earlier study by Lovejoy and Hanson,[2] who studied this reaction from 10–400 Torr N_2 at 295 K is in agreement. Lovejoy and Hanson[2] observed that any incipient adduct rapidly becomes sulfamic acid (H_3NSO_3) which clusters efficiently with itself and sulfuric acid. The observed sulfamic acid dimerization rate constant exceeds 5×10^{-11} cm^3 $molecule^{-1}$ s^{-1}. Measurements of Shen et al.[3] at 1–2 Torr He are much higher than those of Lovejoy and Hanson[2] or Lovejoy.[1] Error limits have been adjusted to take into account the fact that the exponent of the temperature dependence of the low pressure rate constant is unusually large. Lovejoy[1] also reports an equilibrium constant and heat of formation of sulfamic acid of -24 ± 1 kcal mol^{-1}.
(Table: 06-2, Note: 06-2, Evaluated: 06-2) Back to Table

(1) Lovejoy, E. R. Kinetics and thermodynamics of the gas phase reaction $SO_3 + NH_3 + N_2 \leftrightarrow H_3NSO_3 + N_2$. *J. Phys. Chem. A* **1997**, *101*, 4950-4953, doi:10.1021/jp970652i.

(2) Lovejoy, E. R.; Hanson, D. R. Kinetics and products of the reaction $SO_3 + NH_3 + N_2$. *J. Phys. Chem.* **1996**, *100*, 4459-4465, doi:10.1021/jp952404x.

(3) Shen, G.; Suto, M.; Lee, L. C. Reaction rate constant of $SO_3 + NH_3$ in the gas phase. *J. Geophys. Res.* **1990**, *95*, 13981-13984, doi:10.1029/JD095iD09p13981.

I9. **HO + CS_2.** The data are from Hynes et al.[3] and Murrells et al.[4] The value $m = 1$ is constrained. The recommended rate constant is in reasonable agreement with the measurement of Bulatov et al.[1] Petris et al.[2] report experimental detection of CS_2OH. See Table 3-1 for the recommended equilibrium constant. The adduct reacts slowly with O_2. (See Table 1-1).
(Table: 06-2, Note: 15-10, Evaluated: 06-2) Back to Table

(1) Bulatov, V. P.; Buloyan, A. A.; Cheskis, S. G.; Kozliner, M. Z.; Sarkisov, O. M.; Trostin, A. I. On the reaction of the NH_2 radical with ozone. *Chem. Phys. Lett.* **1980**, *74*, 288-292, doi:10.1016/0009-2614(80)85160-8.

(2) de Petris, G.; Rosi, M.; Troiani, A. Direct experimental observation of CS_2OH. *ChemPhysChem* **2006**, *7*, 2352-2357, doi:10.1002/cphc.200600515.

(3) Hynes, A. J.; Wine, P. H.; Nicovich, J. M. Kinetics and mechanism of the reaction of OH with CS_2 under atmospheric conditions. *J. Phys. Chem.* **1988**, *92*, 3846-3852, doi:10.1021/j100324a034.

(4) Murrells, T. P.; Lovejoy, E. R.; Ravishankara, A. R. Oxidation of CS_2 by reaction with OH. 1. Equilibrium constant for the reaction OH + CS_2 ⇄ CS_2OH and the kinetics of the $CS_2OH + O_2$ reaction. *J. Phys. Chem.* **1990**, *94*, 2381-2386, doi:10.1021/j100369a036.

I10. **Cl + CS_2.** The data are from Nicovich et al.[2] Wallington et al.[3] have also studied this system. The value $m = 0$ is constrained. Nicovich et al.[2] confirm that the reaction proceeds via reversible adduct formation as suggested by Martin et al.[1] The much larger rate constant values determined by Martin et al. may possibly be

attributed to reactive impurities in the CS_2 sample. Nicovich et al. set an upper limit on the rate constant for the adduct (CS_2Cl) reacting with O_2 of 2.5×10^{-16} cm^3 molecule^{-1} s^{-1} at room temperature. Wang and Phillips[4] have reported a theoretical study of the adduct.
(Table: 06-2, Note: 06-2, Evaluated: 06-2) Back to Table

(1) Martin, D.; Jourdain, J. L.; Le Bras, G. Kinetic study for the reactions of OH radicals with dimethylsulfide, diethylsulfide, tetrahydrothiophene, and thiophene. *Int. J. Chem. Kinet.* **1985**, *17*, 1247-1261, doi:10.1002/kin.550171202.

(2) Nicovich, J. M.; Wine, P. H. Kinetics of the reactions of O(^3P) and Cl(^2P) with HBr and Br_2. *Int. J. Chem. Kinet.* **1990**, *22*, 379-397, doi:10.1002/kin.550220406.

(3) Wallington, T. J.; Andino, J. M.; Potts, A. R.; Wine, P. H. A competitive kinetics study of the reaction of Cl with CS_2 in air at 298 K. *Chem. Phys. Lett.* **1991**, *176*, 103-108, doi:10.1016/0009-2614(91)90018-5.

(4) Wang, D.; Phillips, D. L. Density functional theory study of CS_2/Cl adducts and their isomerization reactions. *Chem. Phys. Lett.* **2002**, *362*, 205-209, doi:10.1016/S0009-2614(02)01015-1.

I11. OH + CH_3SCH_3 → $(CH_3)_2SOH$ → products. The OH + CH_3SCH_3 reaction is complex, proceeding by both direct H-abstraction and reversible addition pathways. A recommendation for the direct reaction is discussed separately in Table 1-1. The product of the reversible addition pathway reacts with O_2 creating an irreversible path as well. Mechanistically, this pathway is described by combining the rate constants k_f for the addition step, k_r for the reverse dissociation step, and k_{O2} for the adduct reaction with O_2. This is discussed in detail in the notes for Table 1-1. The equilibrium constant for the reversible addition process is $K_c = k_f/k_r$. Recommendations for K_c, and k_{O2} are found in Tables 3-1, and 1-1, respectively. The value for k_f recommneded here is from Williams et al.[1] The discussion in Table 1-1 points out that this value taken with K_c and k_{O2} fits the extant data very well.
(Table: 10-6; Note: 10-6; Evaluated: 10-6) Back to Table

(1) Williams, M. B.; Campuzano-Jost, P.; Hynes, A. J.; Pounds, A. J. Experimental and theoretical studies of the reaction of the OH radical with alkyl sulfides: 3. Kinetics and mechanism of the OH initiated oxidation of dimethyl, dipropyl, and dibutyl sulfides: Reactivity trends in the alkyl sulfides and development of a predictive expression for the reaction of OH with DMS. *J. Phys. Chem. A* **2009**, *113*, 6697-6709, doi:10.1021/Jp9010668.

I12. Cl + $(CH_3)_2S$. [See Table 1-1] If the HCl yield at 297 K from Stickel et al.[4] is used as a measure of the abstraction reaction, the rate constant would be 1.64×10^{-10} cm^3 molecule^{-1} s^{-1}. Using this value the complete data set from Stickel et al.[4] can be fit with the form used in Table 2-1 with the addition of a term for the abstraction in the form $k_{abs} = 1.64 \times 10^{-10}(T/300)^a$. The value of "a" obtained in this manner is almost zero, so the data are fit with: $k_0 = 4 \times 10^{-28}(T/300)^{-7.0}$ and $k_\infty = 2 \times 10^{-10}$ $(T/300)^{-1}$ along with the temperature independent value of k_{abs}. These parameters are recommended herein. Enami et al.[2] propose $k_0 = 2.2 \times 10^{-28}$ and $k_\infty = 2.2 \times 10^{-10}$ at 298 K along with $k_{abs} = 1.8 \times 10^{-10}$. On the other hand, a study by Diaz-de-Mera et al.[1] performed in the temperature range 259< T/K <364 and in helium at pressures of 0.5< P/Torr <1 reports a value $k_{abs} = (2.0 \pm 1.2) \times 10^{-10} \exp[-(332 \pm 173)/T]$, which yields 6.6×10^{-11} cm^3 molecule^{-1} s^{-1} at room temperature. Several studies, both experimental by Urbanski and Wine[5] and theoretical by Resende and De Almeida[3] make it clear that at higher pressures an adduct Cl-S$(CH_3)_2$ is formed and this adduct does not yield CH_3 radicals or the products of the abstraction pathway.
(Table: 06-2, Note: 10-6, Evaluated 10-6) Back to Table

(1) Diaz-de-Mera, Y.; Aranda, A.; Rodriguez, D.; López, R.; Cabañas, B.; Martinez, E. Gas-phase reactions of chlorine atoms and ClO radicals with dimethyl sulfide. Rate coefficients and temperature dependences. *J. Phys. Chem. A* **2002**, *106*, 8627-8633, doi:10.1021/jp014570c.

(2) Enami, S.; Nakano, Y.; Hashimoto, S.; Kawasaki, M.; Aloisio, S.; Francisco, J. S. Reactions of Cl atoms with dimethyl sulfide: A theoretical calculation and an experimental study with cavity ring-down spectroscopy. *J. Phys. Chem. A* **2004**, *108*, 7785-7789, doi:10.1021/jp049772y.

(3) Resende, S. M.; Almeida, W. B. D. Theoretical study of the atmospheric reaction between dimethyl sulfide and chlorine atoms. *J. Phys. Chem. A* **1997**, *101*, 9738-9744, doi:10.1021/jp971885c.

(4) Stickel, R. E.; Nicovich, J. M.; Wang, S.; Zhao, Z.; Wine, P. H. Kinetic and mechanistic study of the reaction of atomic chlorine with dimethyl sulfide. *J. Phys. Chem.* **1992**, *96*, 9875-9883, doi:10.1021/j100203a055.

(5) Urbanski, S. P.; Wine, P. H. Spectroscopic and kinetic study of the Cl-S$(CH_3)_2$ adduct. *J. Phys. Chem. A* **1999**, *103*, 10935-10944, doi:10.1021/jp992682m.

I13. **Br + $(CH_3)_2S$.** Wine et al.[5] data for the adduct formation in N_2 at 25< P/Torr <600 and 263< T/K <310 are the basis for the recommendation. Studies by Ingham et al.[2] and Nakano et al.[4] are in agreement. Nakano et al.[4] is also in agreement with the value of the equilibrium constant. However, Maurer et al.[3] find a value at 300 K and 1 bar total pressure of a mixture of 5% O_2 and 95% N_2, only 2% as high as the value computed from the recommended parameters. This latter value is supported by Ballesteros et al.[1]
(Table: 06-2, Note: 06-2, Evaluated: 06-2) Back to Table

(1) Ballesteros, B., N. R. Jensen, and J. Hjorth FT-IR study of the kinetics and products of the reactions of dimethylsulphide, dimethylsulphoxide and dimethylsulphone with Br and BrO. *J. Atmos. Chem.* **2002**, *43*, 135-150, doi:10.1023/A:1019922224137.

(2) Ingham, T.; Bauer, D.; Sander, R.; Crutzen, P. J.; Crowley, J. N. Kinetics and products of the reactions BrO + DMS and Br + DMS at 298 K. *J. Phys. Chem. A* **1999**, *103*, 7199-7209, doi:10.1021/jp9905979.

(3) Maurer, T., I. Barnes, and K. H. Becker FT-IR kinetic and product study of the Br-initiated oxidation of dimethyl sulfide. *Int. J. Chem. Kinet.* **1999**, *31*, 883-893, doi:10.1002/(SICI)1097-4601(1999)31:12<883::AID-KIN7>3.0.CO;2-V.

(4) Nakano, Y., M. Goto, S. Hashimoto, M. Kawasaki, and T. J. Wallington Cavity ring-down spectroscopic study of the reactions of Br atoms and BrO radicals with dimethyl sulfide. *J. Phys. Chem. A* **2001**, *105*, 11045-11050, doi:10.1021/jp012326f.

(5) Wine, P. H.; Nicovich, J. M.; Stickel, R. E.; Zhao, Z.; Shackelford, C. J.; Kreutter, K. D.; Daykin, E. P.; Wang, S. In *The Tropospheric Chemistry of Ozone in the Polar Regions*; Springer-Verlag: Berlin, 1993; Vol. I7; pp 385-395.

J1. **Na + O_2.** A study by Plane and Rajasekhar[3] finds $k_o = (2.9 \pm 0.7) \times 10^{-30}$ cm^6 molecule^{-2} s^{-1}at 300 K with $n = 1.30 \pm 0.04$. They also estimate k_∞ to be about 6×10^{-10} cm^3 molecule^{-1} s^{-1} with a small positive temperature dependence. Another study by Helmer and Plane[1] yields $k_o = (3.1 \pm 0.2) \times 10^{-30}$ cm^6 molecule^{-2} s^{-1} at 300 K with $n = 1.52 \pm 0.27$. The recommended values are taken from these studies. They are consistent with values measured by Marshall et al.[2] at 600 K and those measured by Vinckier et al.[5] at higher temperature. The k_o value is about 60% higher than that of Silver et al.[4]
(Table: 06-2, Note: 06-2, Evaluated: 06-2) Back to Table

(1) Helmer, M.; Plane, J. M. C. A study of the reaction NaO_2 + O ---> NaO + O_2: Implications for the chemistry of sodium in the upper atmosphere. *J. Geophys. Res.* **1993**, *98*, 23207-23222, doi:10.1029/93JD02033.

(2) Marshall, P.; Narayan, A. S.; Fontijn, A. Kinetic and thermochemical studies of the recombination reaction Na + O_2 + N_2 from 590 to 1515 K by a modified high-temperature photochemistry technique. *J. Phys. Chem.* **1990**, *94*, 2998-3004, doi:10.1021/j100370a049.

(3) Plane, J. M. C.; Rajasekhar, B. Kinetic study of the reactions Na + O_2 + N_2 and Na + N_2O over an extended temperature range. *J. Phys. Chem.* **1989**, *93*, 3135-3140, doi:10.1021/j100345a051.

(4) Silver, J. A.; Zahniser, M. S.; Stanton, A. C.; Kolb, C. E. Temperature dependent termolecular reaction rate constants for potassium and sodium superoxide formation. *Proc. Combust. Inst.* **1984**, *20*, 605-612.

(5) Vinckier, C.; Dumoulin, A.; DeJaegere, S. Kinetic study of the Na + O_2 + He reaction in the temperature range 392-777 K. *J. Chem. Soc. Faraday Trans.* **1991**, *87*, 1075-1081, doi:10.1039/ft9918701075.

J2. **Na + OH.** This reaction was studied experimentally by Husain et al.[2] at 653 K in He. Jensen and Jones[3] inferred rate constants from Na-seeded flames at 1800–2200 K. Gómez-Martín et al.[1] applied theory to fit both sets of experimental data and obtained $k_0(T) = 2.4 \times 10^{-29}\ (T/298)^{-1.3}$ cm^6 molecule^{-2} s^{-1} in N_2 over the range 300–2400 K. They also estimated $k_\infty(T) = 9.4 \times 10^{-10}\ (T/300)^{0.2}$ cm^3 molecule^{-1} s^{-1} from a simple model. The only thermodynamically feasible product is NaOH.
(Table: 19-5, Note: 19-5, Evaluated: 19-5) Back to Table

(1) Gómez Martín, J. C.; Seaton, C.; de Miranda, M. P.; Plane, J. M. C. The reaction between sodium hydroxide and atomic hydrogen in atmospheric and flame chemistry. *J. Phys. Chem. A* **2017**, *121*, 7667–7674, doi:10.1021/acs.jpca.7b07808.

(2) Husain, D.; Plane, J. M. C.; Xiang, C. C. Determination of the absolute third-order rate constant for the reaction between Na + OH + He by time-resolved molecular resonance-fluorescence spectroscopy, $OH(A^2\Sigma^+\text{-}X^2\Pi$, coupled with steady atomic fluorescence spectroscopy, $Na(3\ ^2P_J\text{–}3\ ^2S_{1/2})$. *J. Chem. Soc., Faraday Trans. 2* **1984**, *80*, 1619−1631, doi:10.1039/f29848001619.

(3) Jensen, D. E.; Jones, G. A. Kinetics of flame inhibition by sodium. *J. Chem. Soc., Faraday Trans. 1* **1982**, *78*, 2843−2850, doi:10.1039/f19827802843.

J3. **NaO + O_2.** Ager and Howard[1] have measured the low-pressure limit at room temperature in several bath gases. Their value in N_2 is used in the recommendation. They performed a Troe calculation, as per Patrick and Golden[2], to obtain collision efficiency and temperature dependence. They obtained a high-pressure-limit rate constant by use of a simple model. The temperature dependence is estimated.
(Table: 06-2, Note: 06-2, Evaluated: 06-2) Back to Table

(1) Ager, J. W., III; Howard, C. J. The kinetics of NaO + O_2 and NaO + CO_2 + M and their role in atmospheric sodium chemistry. *Geophys. Res. Lett.* **1986**, *13*, 1395-1398, doi:10.1029/GL013i013p01395.
(2) Patrick, R.; Golden, D. M. Third-order rate constants of atmospheric importance. *Int. J. Chem. Kinet.* **1983**, *15*, 1189-1227, doi:10.1002/kin.550151107.

J4. **NaO + CO_2.** The recommendation is based on the work of Ager and Howard,[1] who measured the rate constant for this process in the "fall–off" regime and close to the low-pressure limit. The temperature dependence of k_0 is an estimate guided by the simulation results of Gómez Martín et al.[2] Ager and Howard calculated the high-pressure rate constant from a simple model. Gómez Martín et al. fit the data of Ager and Howard with an RRKM/Master Equation simulation and obtained $k_0(300)$ about 40% higher than Ager and Howard. The temperature dependence of k_∞ is taken from the assumption of a long range (R^{-6}) attractive potential, as used by Gómez Martín et al.
(Table: 06-2, Note: 19-5, Evaluated: 06-2) Back to Table

(1) Ager, J. W., III; Howard, C. J. The kinetics of NaO + O_2 and NaO + CO_2 + M and their role in atmospheric sodium chemistry. *Geophys. Res. Lett.* **1986**, *13*, 1395-1398, doi:10.1029/GL013i013p01395.
(2) Gómez Martin, J. C.; Garraway, S. A.; Plane, J. M. C. Reaction kinetics of meteoric sodium reservoirs in the upper atmosphere. *J. Phys. Chem. A* **2016**, *120*, 1330-1346, doi:10.1021/acs.jpca.5b00622.

J5. **NaOH + CO_2.** Ager and Howard[1] studied this reaction experimentally at 0.4–1.5 Torr in N_2/N_2O mixtures at 298 K. They detected NaOH by reacting it with atomic H to form Na, which was detected by resonance fluorescence. They reported a rate constant corrected for the effects of N_2O. Gomez Martin et al.[2] studied this reaction in 1–4 Torr N_2 and 300 K (and 2 Torr and 266 K) by photoionization time-of-flight mass spectrometry. Results of both sets of experiments are compatible with the reaction being in the low-pressure limit, but the value of $k_0(298)$ obtained by Gómez Martín et al. is about one-half that of Ager and Howard (for N_2 as the sole bath gas). However, Master Equation simulations by Gómez Martín et al. suggest that the reaction is not in the low-pressure limit under the conditions of their experiment. Both groups used simple models to obtain very similar estimates of k_∞(298 K). The recommendation for $k_0(298)$ is based on the average of the two sets of experimental results. The temperature dependence of k_0 is an estimate guided by the simulation results of Gómez Martín et al. The temperature-dependence of k_∞ is taken from the assumption of a long range (R^{-6}) attractive potential, as used by Gómez Martín et al.
(Table: 19-5, Note: 19-5, Evaluated: 19-5) Back to Table

(1) Ager, J. W., III; Howard, C. J. Gas phase kinetics of the reactions of NaO with H_2, D_2, H_2O, and D_2O. *J. Chem. Phys.* **1987**, *87*, 921-925, doi:10.1063/1.453726.
(2) Gómez Martin, J. C.; Garraway, S. A.; Plane, J. M. C. Reaction kinetics of meteoric sodium reservoirs in the upper atmosphere. *J. Phys. Chem. A* **2016**, *120*, 1330-1346, doi:10.1021/acs.jpca.5b00622.

J6. **Hg + Br.** The recommendation is based on the direct experiments of Donohoue et al.,[3] who used pulsed laser photolysis of Br_2 to generate an excess of Br atoms, which reacted with Hg^0 vapor; the Hg^0 and atomic Br were monitored simultaneously by pulsed laser induced fluorescence techniques. The recombination reaction rate constant at the low-pressure limit was measured in N_2 gas at temperatures from 243 to 293 K and N_2 pressures from 200 to 600 Torr (measurements were also carried out using He gas). In earlier studies, Greig et al.[6] analyzed the UV spectrum of HgBr and used their measured absorption coefficients to determine the recombination rate constant from 393 to 448 K in 200 Torr of CF_3Br (conditions not relevant to the atmosphere). Ariya et al.,[2] Spicer et al.,[9] and Sun et al.,[10] used relative rate techniques to obtain the rate constant. The first two studies are discussed in detail by Donohoue et al.,[3] who concluded that they were seriously affected by secondary reactions. Several theoretical calculations have been reported.[4,5,7,8,11] In particular, Goodsite et al.[4] used spectroscopic data, quantum chemistry calculations, and RRKM modeling to obtain theoretical rate constants. Later, using a corrected bond dissociation energy, they repeated the calculations[5] and showed that with a reasonable choice of an energy transfer parameter, the RRKM results are in very good agreement with the experiments of Donohoue et al.[3] A review of Hg atmospheric chemistry has appeared.[1]

(Table: 15-10; Note: 19-5; Evaluated: 15-10) Back to Table

(1) Ariya, P. A.; Amyot, M.; Dastoor, A.; Deeds, D.; Feinberg, A.; Kos, G.; Poulain, A.; Ryjkov, A.; Semeniuk, K.; Subir, M.; Toyota, K. Mercury physicochemical and biogeochemical transformation in the atmosphere and at atmospheric interfaces: A review and future directions. *Chem. Rev.* **2015**, *115*, 3760-3802, doi:10.1021/cr500667e.

(2) Ariya, P. A.; Khalizov, A.; Gidas, A. Reactions of gaseous mercury with atomic and molecular halogens: Kinetics, product studies, and atmospheric implications. *J. Phys. Chem. A* **2002**, *106*, 7310-7320, doi:10.1021/jp020719o.

(3) Donohoue, D. L.; Bauer, D.; Cossairt, B.; Hynes, A. J. Temperature and pressure dependent rate coefficients for the reaction of Hg with Br and the reaction of Br with Br: A pulsed laser photolysis-pulsed laser induced fluorescence study. *J. Phys. Chem. A* **2006**, *110*, 6623-6632, doi:10.1021/jp054688j.

(4) Goodsite, M. E.; Plane, J. M. C.; Skov, H. A theoretical study of the oxidation of Hg^0 to $HgBr_2$ in the troposphere. *Environ. Sci. Technol.* **2004**, *38*, 1772-1776, doi:10.1021/es034680s.

(5) Goodsite, M. E.; Plane, J. M. C.; Skov, H. Correction to a theoretical study of the oxidation of Hg^0 to $HgBr_2$ in the troposphere. *Environ. Sci. Technol.* **2012**, *46*, 5262-5262, doi:10.1021/es301201c.

(6) Greig, G.; Gunning, H. E.; Strausz, O. P. Reactions of metal atoms. II. The combination of mercury and bromine atoms and the dimerization of HgBr. *J. Chem. Phys.* **1970**, *52*, 3684-3690, doi:10.1063/1.1673544.

(7) Khalizov, A. F.; Viswanathan, B.; Larregaray, P.; Ariya, P. A. A theoretical study on the reactions of Hg with halogens: Atmospheric implications. *J. Phys. Chem. A* **2003**, *107*, 6360-6365, doi:10.1021/jp0350722.

(8) Shepler, B. C.; Balabanov, N. B.; Peterson, K. A. Hg + Br → HgBr recombination and collision-induced dissociation dynamics. *J. Chem. Phys.* **2007**, *107*, 164304, doi:10.1063/1.2777142.

(9) Spicer, C. W.; Satola, J.; Abbgy, A. A.; Plastridge, R. A.; Cowen, K. A. Kinetics of gas-phase elemental mercury reactions with halogen species, ozone, and nitrate radical under atmospheric conditions, Florida Department of Environmental Protection. **2002**.

(10) Sun, C.; Sommar, J.; Feng, X.; Lin, C.-J.; Ge, M.; Wang, W.; Yin, R.; Fu, X.; Shang, L. Study of mass-dependent and -independent fractionation of mercury isotope during gas-phase oxidation of elemental mercury vapor by atomic Cl and Br. *Environ. Sci. Technol.* **2016**, *50*, 9232-9241, doi:10.1021/acs.est.6b01668.

(11) Wilcox, J.; Okano, T. Ab initio-based mercury oxidation kinetics via bromine at postcombustion flue gas conditions. *Energy Fuels* **2011**, *25*, 1348-1356, doi:10.1021/ef101763r.

J7. HgBr + HO_2. The only data are from a theoretical study by Jiao and Dibble.[1] From their CASPT2 data we fit $k_\infty(T)$ to a power law to obtain $k_\infty(T) = 6.9 \times 10^{-11}\ (T/298)^{-2.4}$. These results are highly uncertain: perhaps by a factor of 3 ($f = 3$). Values in the low-pressure limit depend on assumed values of Lennard-Jones parameters and energy transfer (ΔE_{down}), which could lead to errors in k_0 of perhaps an additional factor of 3 ($f = 3$). Fitting the effective second order rate constants published by Jiao and Dibble to Equation 2.3 gives an expression of $k_0(T) = 2.3 \times 10^{-29}\ (T/298)^{-4.4}$. Their studies found sufficiently low rate constants to rule out significant formation of Hg + HOOBr or BrHgH + O_2 under tropospheric or stratospheric conditions. The formation of BrHgO + OH appears to be endothermic by 5 kcal/mole, which renders it negligible. This discussion is provided for the purposes of model evaluation only and does not constitute a recommendation by the Panel. (Table: 19-5; Note: 19-5; Evaluated: 19-5) Back to Table

(1) Jiao, Y.; Dibble, T. S. First kinetic study of the atmospherically important reactions BrHg• + NO_2 and BrHg• + HOO. *Phys. Chem. Chem. Phys.* **2017**, *19*, 1826-1838, doi:10.1039/C6CP06276H.

J8. HgBr + NO_2. The only data are from a theoretical study by Jiao and Dibble.[1] Their calculations indicate that significant amounts of the $BrHgNO_2$ isomer will also form, but will isomerize to more stable *syn*-BrHgONO in seconds or less. They suggest ~10% formation of Hg + $BrNO_2$ from these reactants. From their CASPT2 data we fit $k_\infty(T)$ to a power law to obtain $k_\infty(T) = 1.2 \times 10^{-10}\ (T/298)^{-1.9}$. These results are highly uncertain: perhaps by a factor of 3 ($f = 3$). Values in the low-pressure limit depend on assumed values of Lennard-Jones parameters and energy transfer (ΔE_{down}), which could lead to errors in k_0 of perhaps an additional factor of 3 ($f = 3$). Fitting to Equation 2.3 gives an expression of $k_0(T) = 7.1 \times 10^{-29}\ (T/298)^{-4.5}$. This discussion is provided for the purposes of model evaluation only and does not constitute a recommendation by the Panel. (Table: 19-5; Note: 19-5; Evaluated: 19-5) Back to Table

(1) Jiao, Y.; Dibble, T. S. First kinetic study of the atmospherically important reactions BrHg• + NO_2 and BrHg• + HOO. *Phys. Chem. Chem. Phys.* **2017**, *19*, 1826-1838, doi:10.1039/C6CP06276H.

Table 2-2 Rate Constants for Chemical Activation Reactions

Reactants $\xrightarrow{M}$ Association $\xrightarrow{M}$ Dissociation	$k_o(T) = k_o^{298}(298/T)^n$		$k_\infty(T) = k_\infty^{298}(298/T)^m$		$k_{int}(T) = A\ e^{-B/T}$		k_{total} (298 K, 1 atm)	$f(298)$	g	Note
	k_o^{298}	n	k_∞^{298}	m	A	B				
$O + NO_2$ $\xrightarrow{M} NO_3$ $\xrightarrow{M} NO + O_2$	3.4×10^{-31}	1.6	2.3×10^{-11}	0.2	5.3×10^{-12}	-200	1.26×10^{-11}	1.06	80	K1
$OH + HONO_2$ $\xrightarrow{M} OH{\bullet}HONO_2$ $\xrightarrow{M} H_2O + NO_3$	3.9×10^{-31}	7.2	1.5×10^{-13}	4.8	3.7×10^{-14}	-240	1.4×10^{-13}	1.12	50	K2
$OH + CO$ $\xrightarrow{M} HOCO$ $\xrightarrow{M} H + CO_2$	6.9×10^{-33}	2.1	1.1×10^{-12}	–1.3	1.85×10^{-13}	65	2.4×10^{-13}	1.05	25	K3
$CH_3CH_2 + O_2$ $\xrightarrow{M} CH_3CH_2O_2$ $\xrightarrow{M} C_2H_4 + HO_2$	1.3×10^{-28}	4.2	7.6×10^{-12}	1.4	1.8×10^{-13}	0	7.1×10^{-12}	1.15	50	K4
$CH_3C(O) + O_2$ $\xrightarrow{M} CH_3C(O)OO$ $\xrightarrow{M} CH_2C(O)O + OH$	2.0×10^{-29}	2.6	5.3×10^{-12}	0.7	6.6×10^{-14}	-800	4.8×10^{-12}	1.05	50	K5
$CH_2I + O_2$ $\xrightarrow{M} CH_2IO_2$ $\xrightarrow{M} CH_2OO + I$	4.9×10^{-31}	2.5	1.6×10^{-12}	1.6	2.9×10^{-13}	-460	1.5×10^{-12}	1.08	50	K6

2.8 Notes for Table 2-2: Chemical Activation Reactions

K1. **$O + NO_2$.** The recommended values are based on separate non-linear least squares analyses of (a) the total rate constant measured at low pressure over a range of temperatures and (b) the association rate constant for producing NO_3 measured at higher pressures. The measurements at low pressures (≤100 Torr in He, Ar, or N_2) consist of the those performed over a range of temperatures by Estupiñán et al.,[6] Gierczak et al.,[8] Ongstad and Birks,[10] Slanger et al.,[13] Geers-Muller and Stuhl,[7] and Avallone,[1] and the room temperature study of Paulson et al.[11] In the studies of Estupiñán et al.[6] and Gierczak et al.,[8] special emphasis was placed on accurate measurement of the NO_2 concentration and on measurements at low temperatures. The results of earlier studies by Davis et al.[5] and Bemand et al.[3] were not used in deriving the recommended values either because of possible complications from decomposition of NO_2 at higher temperatures or lack of direct NO_2 detection. The higher pressure studies consisted of those performed over a range of temperatures by Burkholder and Ravishankara[4] and by Hahn et al.[9] Near 300 K the highest pressure of Burkholder and Ravishankara is just a little lower than the lowest pressure studied by Hahn et al., but the rate constants reported by the latter are smaller by a factor of 2.2. Hahn et al.[9] cautioned that their results are less reliable at lower pressures, but the high pressure limit is more accurately known. Shiekh et al.[12] investigated the potential energy surface for the reaction using high level quantum chemistry methods and computed rate constants in reasonable agreement with the experiments.

The present recommendation at intermediate and high pressures is based on a least squares analysis of the data of Burkholder and Ravishankara,[4] constrained by the high pressure limit reported by Hahn et al.[9] The recommendation, which includes the measurements of Avallone,[1] is in good agreement with previous recommendations from this Panel and with the evaluation of Baulch et al.,[2] which fits the Hahn et al. values very well. It is also in reasonable agreement with parameters suggested by Burkholder and Ravishankara[4] and by Hahn et al.[9] The uncertainty factors listed in Table 2.2 are for the total rate constant, which has only been measured at relatively low pressures. The uncertainty factors increase with pressure, however, because the error parameters for the rate of production of NO_3 are estimated to be $f_{rec}(298) = 1.35$ and $g_{rec} = 100$.
(Table: 19-5, Note: 19-5, Evaluated: 19-5) Back to Table

(1) Avallone, L. M. Measurements of the temperature-dependent rate coefficient for the reaction $O(^3P) + NO_2 \rightarrow NO + O_2$. *J. Photochem. Photobiol. A,* **2003**, *157*, 231-236, doi:10.1016/S1010-6030(03)00058-3.

(2) Baulch, D. L.; Cox, R. A.; Hampson, R. F., Jr.; Kerr, J. A.; Troe, J.; Watson, R. T. Evaluated kinetic and photochemical data for atmospheric chemistry. *J. Phys. Chem. Ref. Data* **1980**, *9*, 295-471, doi:10.1063/1.555619.

(3) Bemand, P. P.; Clyne, M. A. A.; Watson, R. T. Atomic resonance fluorescence and mass spectrometry for measurements of the rate constants for elementrary reactions: $O\ ^3P_J + NO_2 \rightarrow NO + O_2$ and $NO + O_3 \rightarrow NO_2 + O_2$. *J. Chem. Soc. Faraday Trans. 2* **1974**, *70*, 564-576, doi;10.1039/F29747000564.

(4) Burkholder, J. B.; Ravishankara, A. R. Rate coefficient for the reaction: $O + NO_2 + M \rightarrow NO_3 + M$. *J. Phys. Chem. A* **2000**, *104*, 6752-6757, doi:10.1021/jp000169z.

(5) Davis, D. D.; Herron, J. T.; Huie, R. E. Absolute rate constants for the reaction $O(^3P) + NO_2 \rightarrow NO + O_2$ over the temperature range 230-339°K. *J. Chem. Phys.* **1973**, *58*, 530-535, doi:10.1063/1.1679233.

(6) Estupiñán, E. G., J. M. Nicovich and P.H. Wine A temperature-dependent kintetics study of the important stratospheric reaction $O(^3P) + NO_2 \rightarrow O_2 + NO$. *J. Phys. Chem. A* **2001**, *105*, 9697-9703, doi:10.1021/jp011940o.

(7) Geers-Müller, R.; Stuhl, F. On the kinetics of the reactions of oxygen atoms with NO_2, N_2O_4, and N_2O_3 at low temperatures. *Chem. Phys. Lett.* **1987**, *135*, 263-268, doi:10.1016/0009-2614(87)85153-9.

(8) Gierczak, T.; Burkholder, J. B.; Ravishankara, A. R. Temperature dependent rate coefficient for the reaction $O(^3P) + NO_2 \rightarrow NO + O_2$. *J. Phys. Chem. A* **1999**, *103*, 877-883, doi:10.1021/jp983962p.

(9) Hahn, J.; Luther, K.; Troe, J. Experimental and theoretical study of the temperature and pressure dependences of the recombination reactions $O + NO_2(+ M) \rightarrow NO_3(+ M)$ and $NO_2 + NO_3(+M) \rightarrow N_2O_5(+M)$. *Phys. Chem. Chem. Phys.* **2000**, *2*, 5098-5104, doi:10.1039/b005756h.

(10) Ongstad, A. P.; Birks, J. W. Studies of reactions of importance in the stratosphere. VI. Temperature dependence of the reactions $O + NO_2 \rightarrow NO + O_2$ and $O + ClO \rightarrow Cl + O_2$. *J. Chem. Phys.* **1986**, *85*, 3359-3368, doi:10.1063/1.450957.

(11) Paulson, S. E.; Orlando, J. J.; Tyndall, G. S.; Calvert, J. G. Rate coefficients for the reactions of $O(^3P)$ with selected biogenic hydrocarbons. *Int. J. Chem. Kinet.* **1995**, *27*, 997-1008, doi:10.1002/kin.550271005

(12) Shiekh, B. A.; Kaur, D.; Seth, B.; Mahajan, S. The theoretical-cum-statistical approach for the investigation of reaction $NO^2 + O(^3P) \rightarrow NO + O_2$ using SCTST and a full anharmonic VPT2 model. *Chem. Phys. Lett.* **2016**, *662*, 244-249, doi:10.1016/j.cplett.2016.08.058.
(13) Slanger, T. G.; Wood, B. J.; Black, G. Investigation of the rate coefficient for $O(^3P) + NO_2 \rightarrow O_2 + NO$. *Int. J. Chem. Kinet.* **1973**, *5*, 615-620, doi:10.1002/kin.550050411.

K2. OH + $HONO_2$. The recommendation is based on the data sets reported by Connell and Howard,[3] Brown et al.,[2] Dulitz et al.,[5] and Winiberg et al.[10] The first of these is the only data set at low pressure (assuming that the collision efficiency of He is 38% of that for N_2 [2,5]) and the other three studies are extensive both in the range and numbers of T,P (N_2 bath gas) combinations investigated. Connell and Howard[3] used a discharge flow apparatus with resonance fluorescence detection of OH radicals and UV absorption measurements of $HONO_2$. Brown et al.[2] performed rate constant measurements by using laser flash photolysis and $HONO_2$ concentrations obtained by UV absorption in an in-line absorption cell downstream from the reaction cell. Dulitz et al.[5] and Winiberg et al.[10] also used laser flash photolysis, but measured the $HONO_2$ concentrations in situ by different spectroscopic methods. In these two latter studies, measurements at extreme low temperatures were hampered by condensation of $HONO_2$ on the optical windows; this problem was apparently not as serious in the apparatus used by Brown et al.[2] Dulitz et al.[5] and Winiberg et al.[10] also found that their ex situ concentration measurements were subject to systematic errors (probably due to wall-deposition of $HONO_2$). The reported rate constants are similar in all three studies, but small systematic differences are apparent. Brown et al.,[2] Dulitz et al.,[5] and Winiberg et al.[10] analyzed their results in terms of the mechanism proposed by Smith et al.,[7] involving the formation of a bound, relatively long-lived HO•$HONO_2$ complex, in addition to the direct reaction channel forming $H_2O + NO_3$. Studies of the effects of isotopic substitution on the reactions OD + DNO_3, OH + DNO_3, OD + HNO_3, and $^{18}OH + HNO_3$ by Brown et al.[1] support the existence of an intermediate consisting of an H-bonded six-membered ring.

The isotopic studies of Brown et al.[1] and the theoretical calculations of Xia and Lin[11] support the assumption that the stabilized OH•$HONO_2$ complex ultimately reacts under atmospheric conditions to produce $H_2O + NO_3$. Thus, the effective reaction yield of NO_3 (per OH removed) is assumed to be unity at all temperatures and pressures. A global non-linear least squares analysis was performed in which all samples were first assumed to have identical relative errors, which were adjusted so that each of the four data sets had approximately equal weight. Because the number of data points differed widely in the four data sets (from 8 to 85), approximately equal weighting of the four sets was achieved by multiplying the relative error for each data point in a given data set by the square root of the number of data points in the set to which it belongs. The recommended rate constants are in good agreement with the four data sets used in the least squares analysis and in fair to good agreement with the data sets reported by Wine et al.,[9] Stachnik et al.,[8] Devolder et al.,[4] and Margitan and Watson.[6] The estimated error factors are based on fits to the data used in the least squares analysis.
(Table: 19-5, Note: 19-5, Evaluated: 19-5) Back to Table

(1) Brown, S. S.; Burkholder, J. B.; Talukdar, R. K.; Ravishankara, A. R. Reaction of hydroxyl radical with nitric acid: Insights into its mechanism. *J. Phys. Chem. A* **2001**, *105*, 1605-1614, doi:10.1021/jp002394m.
(2) Brown, S. S.; Talukdar, R. K.; Ravishankara, A. R. Reconsideration of the rate constant for the reaction of hydroxyl radicals with nitric acid. *J. Phys. Chem. A* **1999**, *103*, 3031-3037, doi:10.1021/jp984721k.
(3) Connell, P. S.; Howard, C. J. Kinetics study of the reaction HO + HNO_3. *Int. J. Chem. Kinet.* **1985**, *17*, 17-31, doi:10.1002/kin.550170104.
(4) Devolder, P.; Carlier, M.; Pauwels, J. F.; Sochet, L. R. Rate constant for the reaction of OH with nitric acid: A new investigation by discharge flow resonance fluorescence. *Chem. Phys. Lett.* **1984**, *111*, 94-99.
(5) Dulitz, K.; Amedro, D.; Dillon, T. J.; Pozzer, A.; Crowley, J. N. Temperature-(208–318 K) and pressure-(18–696 Torr) dependent rate coefficients for the reaction between OH and HNO_3. *Atmos. Chem. Phys.* **2018**, *18*, 2381–2394, doi:10.5194/acp-18-2381-20.
(6) Margitan, J. J.; Watson, R. T. Kinetics of the reaction of hydroxyl radicals with nitric acid. *J. Phys. Chem.* **1982**, *86*, 3819-3824, doi:10.1021/j100216a022.
(7) Smith, C. A.; Molina, L. T.; Lamb, J. J.; Molina, M. J. Kinetics of the reaction of OH with pernitric and nitric acids. *Int. J. Chem. Kinet.* **1984**, *16*, 41-55, doi:10.1002/kin.550160107

(8) Stachnik, R. A.; Molina, L. T.; Molina, M. J. Pressure and temperature dependences of the reaction of OH with nitric acid. *J. Phys. Chem.* **1986**, *90*, 2777-2780, doi:10.1021/j100403a044.
(9) Wine, P. H.; Ravishankara, A. R.; Kreutter, N. M.; Shah, R. C.; Nicovich, J. M.; Thompson, R. L.; Wuebbles, D. J. Rate of reactions of OH with HNO_3. *J. Geophys. Res.* **1981**, *86*, 1105-1112, doi:10.1029/JC086iC02p01105.
(10) Winiberg, F. A. F.; Percival, C. J.; Shannon, R.; Khan, A. H.; Shallcross, D. E.; Liu, Y.; Sander, S. P. Reaction kinetics of OH + HNO_3 under conditions relevant to the upper troposphere/lower stratosphere. *Phys . Chem. Chem. Phys.* **2018**, *20*, 24652, doi:10.1039/C8CP04193H.
(11) Xia, W. S.; Lin, M. C. A multifacet mechanism for the OH + HNO_3 reaction: An *ab initio* molecular orbital/statistical theory study. *J. Chem. Phys.* **2001**, *114*, 4522-4532, doi:10.1063/1.1337061.

K3. **HO + CO**. This reaction proceeds via initial formation of a chemically activated HOCO* intermediate, which can re-dissociate to HO + CO, dissociate to H + CO_2, and be collisionally stabilized to yield thermalized HOCO. In the presence of O_2, the H + CO_2 product set and the HOCO intermediate are both converted to HO_2 + CO_2 (DeMore,[9] Miyoshi et al.[17]). Miyoshi et al. report a rate constant for the reaction HOCO + $O_2 \rightarrow HO_2 + CO_2$ of $\sim 1.5 \times 10^{-12}$ cm^3 molecule^{-1} s^{-1} at 298 K (recommended Arrhenius parameters are given in Table 1-1). Therefore, for atmospheric purposes, the products can be taken to be HO_2 and CO_2. The recommended parameters are based on data from McCabe et al.[16] and Liu and Sander,[15] because these two comprehensive studies extended to much lower temperatures than the others. The parameters were obtained by taking the k_∞ parameters from Senosiain et al.[25] (as in previous recommendations) and then performing non-linear least squares fits to Eq. 2-5e, assuming uniform relative errors. The results from the two data sets were averaged to obtain the recommendation. The resulting fit is very similar to previous recommendations, except that the mathematical representation is both more efficient and slightly more accurate. Pressure and temperature dependent data from McCabe et al.,[16] Hynes et al.,[13] and Liu and Sander[15] are very well represented by the recommended parameters. The estimated error fraction, f(T), is based on the fits to the data of McCabe et al.[16] and Liu and Sander.[15] This reaction has been studied often by many workers. In general, the results are in keeping with the current recommendation. Values have been reported by Dreier and Wolfrum,[10] Husain et al.,[12] Ravishankara and Thompson,[24] Paraskevopoulos and Irwin,[22] Hofzumahaus and Stuhl.[11] The results of Jonah et al.[14] are too high and were not included. An increase in k with pressure has been observed by a large number of investigators, including Overend and Paraskevopoulos,[20] Perry et al.,[23] Chan et al.,[7] Biermann et al.,[2] Cox et al.,[8] Butler et al.,[6] Paraskevop and Irwin,[21,22] DeMore,[9] Hofzumahaus and Stuhl,[11] Hynes et al.,[13] McCabe et al.,[16] and Liu and Sander.[15] In addition, Niki et al.[19] have measured k relative to OH + C_2H_4 in one atmosphere of air by following CO_2 production using FTIR.

Previous controversy regarding the effect of small amounts of O_2 (Biermann et al.[2]) has been resolved and is attributed to secondary reactions (DeMore,[9] Hofzumahaus and Stuhl[11]). Liu and Sander[15] have demonstrated that modest levels of O_2 do not interfere with measuring the total rate constant. Currently, there are no indications to suggest that the presence of O_2 has any effect on the rate coefficient other than as a third body. The rate constant measurements (relative to OH + isobutane) of Butler et al.[6] were re-evaluated in the light of refinements in the rate coefficient for the OH + isobutane reaction; the corrected rate coefficient is in approximate agreement with the recommended value. Beno et al.[1] observe an enhancement of k with water vapor, which is in conflict with the flash photolysis studies; e.g. Ravishankara and Thompson,[24] Paraskevopoulos and Irwin,[22] Hynes et al.,[13] and McCabe et al.[16] Water is not expected to significantly change the rate coefficient for the reaction in the atmosphere and it is not expected to alter the products of the reaction.

Troe[26] has carried out extensive theoretical analysis of this reaction system. Senosiain et al.[25] performed empirical master equation calculations on a theoretical potential energy surface (the temperature exponent of k_∞ for the chemical activation pathway has a sign error in the reference). The recent ab initio calculations of Nguyen et al.[18] (also see Weston et al.[27]) fitted from 175–300 K predict $k_\infty(300) = 7.4 \times 10^{-13}$ cm^3 molecule^{-1} s^{-1}, n = -1.50, which are in good agreement with the entries in Table 2.2. Recently, time-resolved frequency comb spectroscopy has been used to directly monitor the concentrations of all of the reactants, products, and intermediates in the reaction of deuterated hydroxyl radical (DO + CO).[3-5] This enables determination of the branching ratio between the two reaction channels and the isomerization between the cis- and trans-DOCO products. Note, however, that the branching ratio between the two channels is not important in Earth's atmosphere because both H and HOCO react very rapidly with O_2 to form HO_2 + CO_2.
(Table: 19-5, Note: 19-5, Evaluation 15-10) Back to Table

(1) Beno, M. F.; Jonah, C. D.; Mulac, W. A. Rate constants for the reaction OH + CO as functions of temperature and water concentration. *Int. J. Chem. Kinet.* **1985**, *17*, 1091-1101, doi:10.1002/kin.550171006.
(2) Biermann, H. W.; Zetzsch, C.; Stuhl, F. Pressure dependence of reaction of HO with CO. *Ber. Bunsenges Phys. Chem.* **1978**, *82*, 633-639, doi:10.1002/bbpc.197800132.
(3) Bjork, B. J.; Bui, T. Q.; Heckl, O. H.; Changala, P. B.; Spaun, B.; Heu, P.; Follman, D.; Deutsch, C.; Cole, G. D.; Aspelmeyer, M.; Okumura, M.; Ye, J. Direct frequency comb measurement of OD + CO → DOCO kinetics. *Science* **2016**, *354*, 444-448, doi:10.1126/science.aag1862.
(4) Bui, T. Q.; Bjork, B. J.; Changala, P. B.; Heckl, O. H.; B.; Spaun, J. Y. OD + CO → D + CO_2 branching kinetics probed with time-resolved frequency comb spectroscopy. *Chem. Phys. Lett.* **2017**, *683*, 91–95, doi:10.1016/j.cplett.2017.04.061.
(5) Bui, T. Q.; Bjork, B. J.; Changala, P. B.; Nguyen, T. L.; Stanton, J. F.; Okumura, M.; Ye, J. Direct measurements of DOCO isomers in the kinetics of OD + CO. *Sci. Adv.* **2018**, *4*, eaao4777.
(6) Butler, R.; Solomon, I. J.; Snelson, A. Pressure dependence of the CO + OH rate constant in O_2 + N_2 mixtures. *Chem. Phys. Lett.* **1978**, *54*, 19-24, doi:10.1016/0009-2614(78)85654-1.
(7) Chan, W. H.; Uselman, W. M.; Calvert, J. G.; Shaw, J. H. The pressure dependence of the rate constant for the reaction: HO + CO → H + CO_2. *Chem. Phys. Lett.* **1977**, *45*, 240-244, doi:10.1016/0009-2614(77)80261-3.
(8) Cox, R. A.; Derwent, R. G.; Holt, P. M. Relative rate constants for the reactions of OH radicals with H_2, CH_4, CO, NO and HONO at atmospheric pressure and 296 K. *J. Chem. Soc. Faraday Trans. 1* **1976**, *72*, 2031-2043, doi:10.1039/F19767202031.
(9) DeMore, W. B. Rate constant for the OH + CO reaction: Pressure dependence and the effect of oxygen. *Int. J. Chem. Kinet.* **1984**, *16*, 1187-1200, doi:10.1002/kin.550161003.
(10) Dreier, T.; Wolfrum, J. Direct study of the reaction of vibrationally excited CO molecules with OH radicals. *Proc. Combust. Inst.* **1980**, *18*, 801-809.
(11) Hofzumahaus, A.; Stuhl, F. Rate constant of the reaction HO + CO in the presence of N_2 and O_2. *Ber. Bunsenges Phys. Chem.* **1984**, *88*, 557-561, doi:10.1002/bbpc.19840880612.
(12) Husain, D.; Plane, J. M. C.; Slater, N. K. H. Kinetic investigation of the reactions of OH($X^2\Pi$) with the hydrogen halides, HCl, DCl, HBr and DBr by time-resolved resonance fluorescence ($A^2\Sigma^+$ - $X^2\Pi$). *J. Chem. Soc. Faraday Trans. 2* **1981**, *77*, 1949-1962, doi:10.1039/f29817701949.
(13) Hynes, A. J.; Wine, P. H.; Ravishankara, A. R. Kinetics of the OH + CO reaction under atmospheric conditions. *J. Geophys. Res.* **1986**, *91*, 11815-11820, doi:10.1029/JD091iD11p11815.
(14) Jonah, C. D.; Mulac, W. A.; Zeglinski, P. Rate constants for the reaction of OH + CO, OD + CO, and OH + methane as a function of temperature. *J. Phys. Chem.* **1984**, *88*, 4100-4104, doi:10.1021/j150662a049.
(15) Liu, Y.; Sander, S. P. Rate constants for the OH + CO reaction at low temperatures. *J. Phys. Chem. A.* **2015**, *119*, 10060-10066, doi:10.1021/acs.jpca.5b07220.
(16) McCabe, D. C.; Gierczak, T.; Talukdar, R. K.; Ravishankara, A. R. Kinetics of the reaction OH + CO under atmospheric conditions. *Geophys. Res. Lett.* **2001**, *28*, 3135-3138, doi:10.1029/2000GL012719.
(17) Miyoshi, A.; Matsui, H.; Washida, N. Detection and reactions of the HOCO radical in gas phase. *J. Chem. Phys.* **1994**, *100*, 3532-3539, doi:10.1063/1.466395.
(18) Nguyen, T. L.; Xue, B.; Weston, R. E., Jr.; Barker, J. R.; Stanton, J. F. Reaction of HO with CO: Tunneling is indeed important *J. Phys. Chem. Lett.* **2012**, *3*, 1549-1553, doi:10.1021/jz300443a.
(19) Niki, H.; Maker, P. D.; Savage, C. M.; Breitenbach, L. P. Fourier transform infrared spectroscopic study of the kinetics for the HO radical reaction of $^{13}C^{16}O$ and $^{12}C^{18}O$. *J. Phys. Chem.* **1984**, *88*, 2116-2119, doi:10.1021/j150654a034.
(20) Overend, R. P.; Paraskevopoulos, G. The question of a pressure effect in the reaction OH + CO at room temperature. *Chem. Phys. Lett.* **1977**, *49*, 109-111, doi:10.1016/0009-2614(77)80452-1.
(21) Paraskevopoulos, G.; Irwin, R. S. XV Informal Conference on Photochemistry, 1982, Stanford, CA.
(22) Paraskevopoulos, G.; Irwin, R. S. The pressure dependence of the rate constant of the reaction of OH radicals with CO. *J. Chem. Phys.* **1984**, *80*, 259-266, doi:10.1063/1.446488.
(23) Perry, R. A.; Atkinson, R.; Pitts, J. N., Jr. Kinetics of the reactions of OH radicals with C_2H_2 and CO. *J. Chem. Phys.* **1977**, *67*, 5577-5584, doi:10.1063/1.434755.
(24) Ravishankara, A. R.; Thompson, R. L. Kinetic study of the reaction of OH with CO from 250 to 1040 K. *Chem. Phys. Lett.* **1983**, *99*, 377-381, doi:10.1016/0009-2614(83)80158-4.

(25) Senosiain, J. P., C. B. Musgrave and D. M. Golden Temperature and pressure dependence of the reaction of OH and CO: Master equation modeling on a high-level potential energy surface. *Int. J. Chem. Kinet.* **2003**, *35*, 464-474, doi:10.1002/kin.10144.
(26) Troe, J. "Modeling the temperature and pressure dependence of the reaction HO + CO = HOCO = H + CO_2"; Twenty-Seventh Symposium (International) on Combustion, 1998.
(27) Weston, R. E., Jr.; Nguyen, T. L.; Stanton, J. F.; Barker, J. R. HO + CO reaction rates and H/D kinetic isotope effects: Master equation models with ab initio SCTST rate constants. *J. Phys. Chem. A* **2013**, *117*, 821-835, doi:10.1021/jp311928w.

K4. **$C_2H_5 + O_2$.** Early direct mass spectrometric measurements of the title reaction were reported by Plumb and Ryan[18] and by Slagle et al.[21] at low pressures of He and by Munk et al.[16] at 1 atm of H_2. Plumb and Ryan and Munk et al. also reported branching fractions for the $HO_2 + C_2H_4$ reaction channel. Kaiser et al.[10] measured the total reaction rate constant relative to that for $C_2H_5 + Cl_2$, (calibrated at low He pressures to agree with the absolute measurements of Slagle et al.[21]) in order to obtain absolute rate constants and fall-off parameters at 298 K in He: $k_\infty = (9.2 \pm 0.9) \times 10^{-12}$ cm^3 molecule^{-1} s^{-1} and $k_o = (6.5 \pm 2.0) \times 10^{-29}$ cm^6 molecule^{-2} s^{-1}. Kaiser et al.[10] also measured the branching fraction to produce $HO_2 + C_2H_4$ at 298 K and N_2 pressures from 5 to 700 Torr. Later, Kaiser[8] reported branching fractions and used the relative rate technique to measure total rate constants as a function of temperature and pressure in He and O_2. Wagner et al.[23] performed measurements in He and carried out a detailed theoretical analysis of the reaction system. Dilger et al.[4] used the muon spin relaxation technique to measure the total rate constant from 259–425 K at N_2 pressures from 1.5 to 60 bar and recommended $k_\infty = (8.7 \pm 0.8) \times 10^{-12}$ cm^3 molecule^{-1} s^{-1} at 298 K; a least squares fit to their data gives a temperature exponent of m = 1.7. DeSain et al.[3] investigated the HO_2 yield (branching fraction of the chemical activation channel) by LIF in a pulsed photolytic Cl-initiated experiment and carried out modeling studies. Fernandes et al.[6] reported high pressure flash photolysis measurements in 100–1000 bar of Ar and 0.7–2 Torr of He and, after a theoretical analysis, recommended $k_\infty = (8.4 \pm 0.5) \times 10^{-12}$ cm^3 molecule^{-1} s^{-1} at 298 K and a complicated temperature dependence. k_∞ has been calculated by Wagner et al.,[23] Miller and Klippenstein,[15], Sheng et al.[20] and Knepp et al.[12] with k_∞(300 K) = 8, 10, 4 and 8 × 10^{-12} cm^3 molecule^{-1} s^{-1}, respectively. Although all studies cite some small temperature dependence, each study recommends neglecting it. A least squares fit of the prediction by Knepp et al.[12] gives a temperature exponent of m = 1.3.

For this evaluation, the relative measurements of Kaiser et al.[9] and Kaiser,[8] were re-computed using the more recent reference rate constant for $C_2H_5 + Cl_2$ from Eskola et al.[5] and for the experiments buffered with helium, the He pressures were scaled by a factor of 0.38 to make them comparable to N_2 pressures.[9] The recommendation is based on a least squares analysis of data for the total rate constant measured at T ≤ 425 K by Kaiser et al.,[9] Kaiser,[8] Dilger et al.,[4] and Fernandes et al.[6] combined with data for the branching ratio that were measured at T ≤ 425 K by Kaiser et al.,[9] Kaiser,[8] and Wagner et al.[23] The recommended parameters were obtained by performing a series of least squares analyses of the data for the total rate constant, while assuming fixed values for parameters A and B; the recommendation is an empirical compromise that gives a reasonable fit both to the total rate constant (average error ratio $f_{total}(298) = 1.15$) and to the branching ratio (average error factor $f_{branch}(298) = 1.8$). In order to account for errors associated with the relative rate measurement technique, the recommended error factor has been increased to $f(298) = 1.25$. The recommended high-pressure limit is in reasonable agreement with all of the experimental measurements and most of the theoretical studies. The recommended total rate constant is in good agreement the parameters reported by DeSain et al.[3] and with studies reported by Selzer and Bayes,[19] Pilling and Smith,[17] Cobos et al.,[2] Laguna and Baughcum,[13] Keiffer et al.,[11] Callear,[22] Hochanadel et al.,[7] Basco et al.,[1] Washida and Bayes,[25] Laufer and Bass,[14] and Washida.[24] The branching ratio data are quite scattered and show systematic deviations, but the branching ratio is small under atmospheric conditions and the recommendation falls within about a factor of 2 of most of the data.
(Table: 19-5, Note: 19-5, Evaluated: 19-5) Back to Table

(1) Basco, N.; James, D. G. L.; James, F. C. A quantitative study of alkyl radical reactions by kinetic spectroscopy. II. Combination of the methyl radical with the oxygen molecule. *Int. J. Chem. Kinet.* **1972**, *4*, 129-149, doi:10.1002/kin.550040202.
(2) Cobos, C. J.; Hippler, H.; Luther, K.; Ravishankara, A. R.; Troe, J. High-pressure falloff curves and specific rate constants for the reaction $CH_3 + O_2 \rightleftharpoons CH_3O_2 \rightleftharpoons CH_3O + O$. *J. Phys. Chem.* **1985**, *89*, 4332-4338, doi:10.1021/j100266a036.

(3) Desain, J. D.; Klippenstein, S. J.; Miller, J. A.; Taatjes, C. A. Measurements, theory, and modeling of OH formation in ethyl + O_2 and propyl + O_2 reactions. J. Phys. Chem. A 2003, 107, , DOI: . *J. Phys. Chem. A* **2003**, *107*, 4415-4427, doi:10.1021/jp0221946.

(4) Dilger, H.; Schwager, M.; Tregenna-Piggott, P. L. W.; Roduner, E.; Reid, I. D.; Arseneau, D. J.; Pan, J. J.; Senba, M.; Shelley, M.; Fleming, D. G. Addition kinetics and spin exchange in the gas phase reaction of the ethyl radical with oxygen. *J. Phys. Chem.* **1996**, *100*, 6561-6571, doi:10.1021/jp9525853.

(5) Eskola, A. J.; Lozovsky, V. A.; Timonen, R. S. Kinetics of the reactions of C_2H_5, n-C_3H_7, and n-C_4H_9 radicals with Cl_2 at the temperature range 190–360 K. *Int. J. Chem. Kinet.* **2007**, *39*, 614–619, doi:10.1002/kin.20272.

(6) Fernandes, R. X.; Luther, K.; Marowsky, G.; Rissanen, M. P.; Timonen, R.; Troe, J. R. Experimental and modeling study of the temperature and pressure dependence of the reaction $C_2H_5 + O_2$ (+ M) → $C_2H_5O_2$ (+ M). *J. Phys. Chem. A* **2015**, *119*, 7263−7269, doi:10.1021/jp511672v.

(7) Hochanadel, C. J.; Ghormley, J. A.; Boyle, J. W.; Ogren, P. J. Absorption spectrum and rates of formation and decay of the CH_3O_2 radical. *J. Phys. Chem.* **1977**, *81*, 3-7, doi:10.1021/j100516a002.

(8) Kaiser, E. W. Temperature and pressure dependence of the C_2H_4 yield from the reaction $C_2H_5 + O_2$. *J. Phys. Chem.* **1995**, *99*, 707-711, doi:10.1021/j100002a039.

(9) Kaiser, E. W.; Lorkovic, I. M.; Wallington, T. J. Pressure dependence of the C_2H_4 yield from the reaction $C_2H_5 + O_2$. *J. Phys. Chem.* **1990**, *94*, 3352-3354, doi:10.1021/j100371a030.

(10) Kaiser, E. W.; Wallington, T. J.; Andino, J. M. Pressure dependence of the reaction $C_2H_5 + O_2$. *Chem. Phys. Lett.* **1990**, *168*, 309-313, doi:10.1016/0009-2614(90)85616-K.

(11) Keiffer, M.; Pilling, M. J.; Smith, M. J. C. Pressure and temperature dependence of the reaction CH_3 + O_2 + M → CH_3O_2 + M over the range 334 ≤ T/K ≤ 582. *J. Phys. Chem.* **1987**, *91*, 6028-6034, doi:10.1021/j100307a042.

(12) Knepp, A. M.; Meloni, G.; Jusinski, L. E.; Taatjes, C. A.; Cavallotti, C.; Klippenstein, S. J. Theory, measurements, and modeling of OH and HO_2 formation in the reaction of cyclohexyl radicals with O_2. *Phys. Chem. Chem. Phys.* **2007**, *9*, 4315–4331, doi:10.1039/b705934e.

(13) Laguna, G. A.; Baughcum, S. L. Real-time detection of methyl radicals by diode laser absorption at 608 cm^{-1}. *Chem. Phys. Lett.* **1982**, *88*, 568-571, doi:10.1016/0009-2614(82)85010-0.

(14) Laufer, A. H.; Bass, A. M. Rate constants of the combination of methyl radicals with nitric oxide and oxygen. *Int. J. Chem. Kinet.* **1975**, *7*, 639-648, doi:10.1002/kin.550070502.

(15) Miller, J. A., and S. J. Klippenstein The reaction between ethyl and molecular oxygen II: Further analysis. *Int. J. Chem. Kinet.* **2001**, *33*, 654-668, doi:10.1002/kin.1063.

(16) Munk, J.; Pagsberg, P.; Ratajczak, E.; Sillesen, A. Spectrokinetic studies of ethyl and ethylperoxy radicals. *J. Phys. Chem.* **1986**, *90*, 2752-2757, doi:10.1021/j100403a038.

(17) Pilling, M. J.; Smith, M. J. C. A laser flash photolysis study of the reaction $CH_3 + O_2$ → CH_3O_2 at 298 K. *J. Phys. Chem.* **1985**, *89*, 4713-4720, doi:10.1021/j100268a014.

(18) Plumb, I. C.; Ryan, K. R. Kinetic studies of the reactios of C_2H_5 with O_2 at 295 K. *Int. J. Chem. Kinet.* **1981**, *13*, 1011-1028, doi:10.1002/kin.550131003.

(19) Selzer, E. A.; Bayes, K. D. Pressure dependence of the rate of reaction of methyl radicals with O_2. *J. Phys. Chem.* **1983**, *87*, 392-394, doi:10.1021/j100226a007.

(20) Sheng, C. Y., J. W. Bozzelli, A. M. Dean, and A. Y. Chang Detailed kinetics and thermochemistry of $C_2H_5 + O_2$: Reaction kinetics of the chemically-activated and stabilized CH_3CH_2OO• adduct. *J. Phys. Chem. A* **2002**, *106*, 7276-7293, doi:10.1021/jp014540+.

(21) Slagle, I. R.; Feng, Q.; Gutman, D. Kinetics of the reaction of ethyl radicals with molecular oxygen from 294 to 1002 K. *J. Phys. Chem.* **1984**, *88*, 3648, doi:10.1021/j150660a054.

(22) van den Bergh, H. E.; Callear, A. B. Spectroscopic measurement of the rate of the gas-phase combination of methyl radicals with nitric oxide and oxygen at 295 K. *Trans. Faraday Soc.* **1971**, *67*, 2017-2024, doi:10.1039/tf9716702017.

(23) Wagner, A. F.; Slagle, I. R.; Sarzynski, D.; Gutman, D. Experimental and theoretical studies of the $C_2H_5 + O_2$ reaction kinetics. *J. Phys. Chem.* **1990**, *94*, 1853-1868, doi:10.1021/j100368a026.

(24) Washida, N. Reaction of methyl radicals with O(^3P), O_2 and NO. *J. Chem. Phys.* **1980**, *73*, 1665-1672, doi:10.1063/1.440348.

(25) Washida, N.; Bayes, K. D. The reactions of methyl radicals with atomic and molecular oxygen. *Int. J. Chem. Kinet.* **1976**, *8*, 777-794, doi:10.1002/kin.550080512.

K5. **$CH_3C(O) + O_2$**. The recommendation is based on a least-squares analysis of the data obtained for N_2 bath gas by Papadimitriou et al.,[12] who measured rate constants at 241, 296, and 373 K by using three independent techniques: PLP-LIF of the OH product, PLP-CRDS of CH_3CO radical, and VLPR measurements of the total reaction rate relative to the rate of $CH_3CO + Cl_2$ (reference rate constant taken from Gierczak et al.[5]). Papadimitriou et al. analyzed their data with the chemical activation mechanism and critically compared their results for He bath gas with previous investigations that used He. Their total rate constants and yields of HO free radicals (first mentioned by Michael et al.[11]) in He bath gas are in reasonable agreement with investigations by Talukdar et al.,[15] McDade et al.,[10] Kovacs et al.,[8] Kaiser and Wallington,[7] and Groß et al.[6] Rate constants obtained by Tyndall et al.[16] in a relative rate study (adjusted by using the more recent reference rate constant from Gierczak et al.[5]) in N_2/O_2 bath gases at 298 K are more scattered and ~15% lower than those of Papadimitriou et al.[12] The rate constant measured by Sehested et al.[14] in 1 bar of SF_6 at 295 K ($(4.4 \pm 0.7) \times 10^{-12}$ cm^3 molecule^{-1} s^{-1}) is in reasonable agreement with the recommended k_∞(298 K). Branching ratios determined at Leeds by Blitz et al.,[1,2] Romero et al.,[13] and Carr et al.[3,4] are all self-consistent, but differ by a factor of ~3 from all other studies. Groß et al.[6] noted that the Leeds experiments required significant correction factors and sensitive curve-fitting, which may have led to systematic errors. The f(298 K) error factor is based on the fit to the N_2 bath gas data reported by Papadimitriou et al.[12] Theoretical master equation/RRKM simulations by Maranzana et al.[9] demonstrated that the simulations can separately reproduce either the Leeds results, or those of Talukdar et al.[15] and Kovacs et al.,[8] depending on the empirical parameter that describes collisional energy transfer. Theoretical calculations by Carr et al.[3,4] also confirmed that master equation calculations with empirical energy transfer parameters can fit the Leeds data.
(Table: 19-5, Note: 19-5, Evaluated: 19-5) Back to Table

(1) Blitz, M. A.; Heard, D. E.; Pilling, M. J. OH formation from $CH_3CO + O_2$: a convenient experimental marker for the acetyl radical. *Chem. Phys. Lett.* **2002**, *365*, 374-379.

(2) Blitz, M. A.; Heard, D. E.; Pilling, M. J.; Arnold, S. R.; Chipperfield, M. P. Pressure and temperature-dependent quantum yields for the photodissociation of acetone between 279 and 327.5 nm. *Geophys. Res. Lett.* **2004**, *31*, L06111, doi:1029/2003GL018793.

(3) Carr, S. A.; Baeza-Romero, M. T.; Blitz, M. A.; Pilling, M. J.; Heard, D. E.; Seakins, P. W. OH yields from the $CH_3CO + O_2$ reaction using an internal standard. *Chem. Phys. Lett.* **2007**, *445*, 108-112, doi:10.1016/j.cplett.2007.07.099.

(4) Carr, S. A.; Glowacki, D. R.; Liang, C.-H.; Baeza-Romero, M. T.; Blitz, M. A.; Pilling, M. J.; Seakins, P. W. Experimental and modeling studies of the pressure and temperature dependences of the kinetics and the OH yields in the acetyl + O_2 reaction. *J. Phys. Chem. A* **2011**, *115*, 1069–1085, doi:10.1021/jp1099199.

(5) Gierczak, T.; Rajakumar, B.; Flad, J. E.; Burkholder, J. B. Rate coefficients for the reaction of the acetyl radical, CH_3CO, with Cl_2 between 253 and 384 K. *Int. J. Chem. Kinet.* **2009**, *41*, 543-553, doi:10.1002/kin.20430.

(6) Groß, C. B. M.; Dillon, T. J.; Crowley, J. N. Pressure dependent OH yields in the reactions of CH_3CO and $HOCH_2CO$ with O_2. *Phys. Chem. Chem. Phys.* **2014**, *16*, 10990-10998, doi:10.1039/c4cp01108b.

(7) Kaiser, E. W.; Wallington, T. J. CH_3CO reactions with Cl_2 and O_2: More evidence for HCl elimination from the CH_3CHClO radical. *J. Phys. Chem.* **1995**, *99*, 8669–8672, doi:10.1021/j100021a035.

(8) Kovács, G.; Zádor, J.; Farkas, E.; Nádasdi, R.; Szilágyi, I.; Dóbé, S.; Bérces, T.; Márta, F.; Lendvay, G. Kinetics and mechanism of the reactions of CH_3CO and $CH_3C(O)CH_2$ radicals with O_2. Low-pressure discharge flow experiments and quantum chemical computations. *Phys. Chem. Chem. Phys.* **2007**, *9*, 4142-4154, doi:10.1039/b706216h.

(9) Maranzana, A.; Barker, J. R.; Tonachini, G. Master equation simulations of competing unimolecular and bimolecular reactions: Application to OH production in the reaction of acetyl radical with O_2. *Phys. Chem. Chem. Phys.* **2007**, *9*, 4129 - 4141, doi:10.1039/b705116f.

(10) McDade, C. E.; Lenhardt, T. M.; Bayes, K. D. The rate of reaction of acetyl and benzoyl radicals with O_2. *J. Photochem.* **1982**, *20*, 1-7, doi:10.1016/0047-2670(82)80042-7.

(11) Michael, J. V.; Keil, D. G.; Klemm, R. B. Rate constants for the reaction of hydroxyl radicals with acetaldehyde from 244-528 K. *J. Chem. Phys.* **1985**, *83* 1630-1636, doi:10.1063/1.449400.

(12) Papadimitriou, V. C.; Karafas, E. S.; Gierczak, T.; Burkholder, J. B. $CH_3CO + O_2 + M$ (M = He, N_2) reaction rate coefficient measurements and implications for the OH radical product yield. *J. Phys. Chem. A* **2015**, *119*, 7481–7497, doi:10.1021/acs.jpca.5b00762.

(13) Romero, M. T. B.; Blitz, M. A.; Heard, D. E.; Pilling, M. J.; Price, B.; Seakins, P. W. OH formation from the $C_2H_5CO + O_2$ reaction: An experimental marker for the propionyl radical. *Chem. Phys. Lett.* **2005**, *408*, 232-236, doi:10.1016/j.cplett.2005.04.018.
(14) Sehested, J.; Christensen, L. K.; Nielsen, O. J.; Wallington, T. J. Absolute rate constants for F + CH_3CHO and $CH_3CO + O_2$, relative rate study of CH_3CO + NO, and the product distribution of the F + CH_3CHO reaction. *Int. J. Chem. Kinet.* **1998**, *30*, 913-921.
(15) Talukdar, R. K.; Davis, M. E.; Zhu, L.; Ravishankara, A. R.; Burkholder, J. B. "Determination of the OH radical yield in the $CH_3CO + O_2$ reaction". *19th International Symposium on Gas Kinetics, 2006, Orleans, France.* **2006**.
(16) Tyndall, G. S.; Orlando, J. J.; Wallington, T. J.; Hurley, M. D. Pressure dependence of the rate coefficients and product yields for the reaction of CH_3CO radicals with O_2. *Int. J. Chem. Kinet.* **1997**, *29*, 655-663, doi:10.1002/(SICI)1097-4601(1997)29:9<655::AID-KIN2>3.0.CO;2-T.

K6. **$CH_2I + O_2$.** This reaction produces significant yields of thermalized formaldehyde oxide (CH_2OO), the simplest carbonyl oxide, which is also known as a Criegee Intermediate.[1] The recommendation for the total rate constant at 298 K is the average of measurements by Masaki et al.,[11] Eskola et al.,[5] Sheps,[12] and Stone et al.[13] The total rate constant displays very little pressure dependence from a few Torr up to at least 1 atm. The recommended parameter m is taken from fitting the data of Eskola et al.,[5] who used a flow tube coupled to a photoionization mass spectrometer. The recommended parameters A and B are based on assuming that the P = 0 rate constant is equal to the recommended k_∞(T) as expressed in Arrhenius form. The recommended low pressure k_0(298) and exponent n are based on the direct branching ratio measurements of Ting et al.[14] and of Huang et al.[10] obtained in N_2, O_2, and N_2+O_2 mixtures. Yields of the CH_2OO + I products in this reaction under one atmosphere of air near 300 K have been reported to be 0.15 ± 0.03,[8,9] ~0.18,[13] and ~0.35.[14] The only other major product is collisionally stabilized CH_2IO_2 free radical. Small yields (≤ 20%) of IO free radicals have been reported at low pressures by Enami et al.,[3,4] Dillon et al.,[2] Ting et al.,[14] and Foreman and Murray.[6] Gravestock et al.[7] and Stone et al.[13] have used several techniques to investigate the secondary reactions in this system. Foreman and Murray[6] concluded that the IO yields are due in part to reactions of vibrationally excited CH_2I free radicals produced by photolysis of CH_2I_2 at shorter wavelengths, and contributions from secondary reactions. Ting et al.[14] developed a detailed mechanism and concluded that yields of species other than CH_2OO and CH_2IO_2 are negligible at pressures ≥60 Torr. In the context of their detailed mechanism, Ting et al.[14] and Huang et al.[10] used time-resolved FTIR spectroscopy to investigate the yields of CH_2OO in N_2, O_2, and N_2 + O_2 mixtures; together, these studies covered the ranges of 295–343 K and [N_2] from 2–16 × 10^{18} molecules cm^{-3}. In addition, Huang et al.[10] used direct detection of both CH_2OO and CH_2IO_2 to obtain improved results. The error factor f(298) is based on fits to the total rate constants measured by Eskola et al.[5] and the fractional yields of CH_2OO measured by Ting et al.[14] and Huang et al.[10]
(Table: 19-5, Note: 19-5, Evaluated: 19-5) Back to Table

(1) Criegee, R. Mechanism of ozonolysis. *Angew. Chem. Int. Ed. Engl.* **1975**, *14*, 745-752, doi:10.1002/anie.197507451.
(2) Dillon, T. J.; Tucceri, M. E.; Sander, R.; Crowley, J. N. LIF studies of iodine oxide chemistry. *Phys. Chem. Chem. Phys.* **2008**, *10*, 1540−1554, doi:10.1039/B717386E.
(3) Enami, S.; Nakano, Y.; Hashimoto, S.; Kawasaki, M.; Aloisio, S.; Francisco, J. S. Reactions of Cl atoms with dimethyl sulfide: A theoretical calculation and an experimental study with cavity ring-down spectroscopy. *J. Phys. Chem. A* **2004**, *108*, 7785-7789, doi:10.1021/jp049772y.
(4) Enami, S.; Sakamoto, Y.; Yamanaka, T.; Hashimoto, S.; Kawasaki, M.; Tonokura, K.; Tachikawa, H. Reaction mechanisms of IO radical formation from the reaction of CH_3I with Cl atom in the presence of O_2. *Bull. Chem. Soc. Jpn.* **2008**, *81*, 1250−1257, doi:10.1246/bcsj.81.1250.
(5) Eskola, A. J.; Wojcik-Pastuszka, D.; Ratajczak, E.; Timonen, R. S. Kinetics of the reactions of CH_2Br and CH_2I radicals with molecular oxygen at atmospheric temperatures. *Phys. Chem. Chem. Phys.* **2006**, *8*, 416-1424, doi:10.1039/b516291b.
(6) Foreman, E. S.; Murray, C. Kinetics of IO production in the $CH_2I + O_2$ reaction studied by cavity ring-down spectroscopy. *J. Phys. Chem. A* **2015**, *119*, 8981−8990, doi:10.1021/acs.jpca.5b05058.
(7) Gravestock, T. J.; Blitz, M. A.; Bloss, W. J.; Heard, D. E. A multidimensional study of the reaction $CH_2I + O_2$: Products and atmospheric implications. *ChemPhysChem* **2010**, *11*, 3928-3941, doi:10.1002/cphc.201000575.

(8) Huang, H.; Eskola, A. J.; Taatjes, C. A. Pressure-dependent I-atom yield in the reaction of CH_2I with O_2 shows a remarkable apparent third-body efficiency for O_2. *J. Phys. Chem. Lett.* **2012**, *3*, 3399-3403, doi:10.1021/jz301585c.
(9) Huang, H.; Rotavera, B.; Eskola, A. J.; Taatjes, C. A. Correction to "Pressure-dependent I atom yield in the reaction of CH_2I with O_2 shows a remarkable apparent third-body efficiency for O_2". *J. Phys. Chem. Lett.* **2013**, *4*, 3824-3824, doi:10.1021/jz402266q.
(10) Huang, Y.-H.; Chen, L.-W.; Lee, Y.-P. Simultaneous infrared detection of the ICH_2OO radical and Criegee intermediate CH_2OO: The pressure dependence of the yield of CH_2OO in the reaction $CH_2I + O_2$. *J. Phys. Chem. Lett.* **2015**, *6*, 4610−4615, doi:10.1021/acs.jpclett.5b02298.
(11) Masaki, A.; Tsunashima, N.; Washida, N. Rate constant for the reaction of CH_3O_2 with NO. *Chem. Phys. Lett.* **1994**, *218*, 523-528, doi:10.1016/0009-2614(94)00024-7.
(12) Sheps, L. Absolute ultraviolet absorption spectrum of a Criegee intermediate CH_2OO. *J. Phys. Chem. Lett.* **2013**, *4*, 4201-4205, doi:10.1021/jz402191w.
(13) Stone, D.; Blitz, M.; Daubney, L.; Ingham, T.; Seakins, P. CH_2OO Criegee biradical yields following photolysis of CH_2I_2 in O_2. *Phys. Chem. Chem. Phys.* **2013**, *15*, 19119-19124, doi:10.1039/c3cp52466c.
(14) Ting, W.-L.; Chang, C.-H.; Lee, Y.-F.; Matsui, H.; Lee, Y.-P.; Lin, J. J.-M. Detailed mechanism of the $CH_2I + O_2$ reaction: Yield and self-reaction of the simplest Criegee intermediate CH_2OO. *J. Chem. Phys.* **2014**, *141*, 104308, doi:10.1063/1.4894405.

2.9 Bibliography – Termolecular Reactions

Ager, J. W., III; Howard, C. J. The kinetics of NaO + O_2 and NaO + CO_2 + M and their role in atmospheric sodium chemistry. *Geophys. Res. Lett.* **1986**, *13*, 1395-1398, doi:10.1029/GL013i013p01395.

Ager, J. W., III; Howard, C. J. Gas phase kinetics of the reactions of NaO with H_2, D_2, H_2O, and D_2O. *J. Chem. Phys.* **1987**, *87*, 921-925, doi:10.1063/1.453726.

Allan, B. J.; Plane, J. M. C. A study of the recombination of IO with NO_2 and the stability of INO_3: Implications for the atmospheric chemistry of iodine. *J. Phys. Chem. A* **2002**, *106*, 8634-8641, doi:10.1021/jp020089q.

Amos, R. D.; Murray, C. W.; Handy, N. C. Structures and vibrational frequencies of FOOF and FONO using density functional theory. *Chem. Phys. Lett.* **1993**, *202*, 489-494, doi:10.1016/0009-2614(93)90036-Z.

Anastasi, C.; Smith, I. W. M. Rate measurements of reactions of OH by resonance absorption Part 5.-Rate constants for OH + NO_2(+M) → HNO_3(+M) over a wide range of temperature and pressure. *J. Chem. Soc. Faraday Trans. 2* **1976**, *72*, 1459-1468, doi:10.1039/f29767201459.

Anastasi, C.; Smith, I. W. M. Rate measurements of reactions of OH by resonance absorption Part 6.-Rate constants for OH + NO(+M) → HNO_2(+M) over a wide range of temperature and pressure. *J. Chem. Soc. Faraday Trans. 2* **1978**, *74*, 1056-1064, doi:10.1039/f29787401056.

Anderson, J. G.; Kaufman, F. Kinetics of the reaction OH + NO_2 + M → HNO_3 + M. *Chem. Phys. Lett.* **1972**, *16*, 375-379, doi:10.1016/0009-2614(72)80296-3.

Anderson, J. G.; Margitan, J. J.; Kaufman, F. Gas phase recombination of OH with NO and NO_2. *J. Chem. Phys.* **1974**, *60*, 3310-3317, doi:10.1063/1.1681522.

Anderson, S. M.; Hulsebusch, D.; Mauersberger, K. Surprising rate coefficients for four isotopic variants of O + O_2 + M. *J. Chem. Phys.* **1997**, *107*, 5385-5392, doi:10.1063/1.474247.

André, P. V.; Carr, R. W., Jr. Rate of the reaction of hydroxyl radical with acetylene. *Int. J. Chem. Kinet.* **1974**, *6*, 587-595, doi:10.1002/kin.550060414.

Ariya, P. A.; Amyot, M.; Dastoor, A.; Deeds, D.; Feinberg, A.; Kos, G.; Poulain, A.; Ryjkov, A.; Semeniuk, K.; Subir, M.; Toyota, K. Mercury physicochemical and biogeochemical transformation in the atmosphere and at atmospheric interfaces: A review and future directions. *Chem. Rev.* **2015**, *115*, 3760-3802, doi:10.1021/cr500667e.

Ariya, P. A.; Khalizov, A.; Gidas, A. Reactions of gaseous mercury with atomic and molecular halogens: Kinetics, product studies, and atmospheric implications. *J. Phys. Chem. A* **2002**, *106*, 7310-7320, doi:10.1021/jp020719o.

Arutyunov, V. S.; Popov, L. S.; Chaikin, A. M. Measurement of the rate constant for the reaction of fluorine atoms with oxygen. *Kinet. Katal.* **1976**, *17*, 286-291.

Ashmore, P. G.; Spencer, M. S. Concurrent molecular and chlorine atom mechanisms in the reversible dissociation of nitrosyl chloride. *Trans. Faraday Soc.* **1959**, *55*, 1868-1883, doi:10.1039/tf9595501868.

Atkinson, D. B.; Smith, M. A. Radical-molecule kinetics in pulsed uniform supersonic flows: Termolecular association of OH + NO between 90 and 220 K. *J. Phys. Chem.* **1994**, *98*, 5797-5800, doi:10.1021/j100074a001.

Atkinson, R. A structure-activity relationship for the estimation of rate constants for the gas-phase reactions of OH radicals with organic compounds. *Int. J. Chem. Kinet.* **1987**, *19*, 799-828, doi:10.1002/kin.550190903.

Atkinson, R.; Aschmann, S. M. Rate constants for the reaction of OH radicals with a series of alkenes and dialkenes at 295 ± 1 K. *Int. J. Chem. Kinet.* **1984**, *16*, 1175-1186, doi:10.1002/kin.550161002.

Atkinson, R.; Aschmann, S. M. Rate constants for the reactions of O_3 and OH radicals with a series of alkynes. *Int. J. Chem. Kinet.* **1984**, *16*, 259-268, doi:10.1002/kin.550160308.

Atkinson, R.; Aschmann, S. M. Kinetics of the gas phase reaction of Cl atoms with a series of organics at 296 ± 2 K and atmospheric pressure. *Int. J. Chem. Kinet.* **1985**, *17*, 33-41, doi:10.1002/kin.550170105.

Atkinson, R.; Aschmann, S. M. Kinetics of the gas-phase reactions of Cl atoms with chloroethenes at 298 ± 2 K and atmospheric pressure. *Int. J. Chem. Kinet.* **1987**, *19*, 1097-1105, doi:10.1002/kin.550191206.

Atkinson, R.; Baulch, D. L.; Cox, R. A.; Crowley, J. N.; Hampson, J., R. F.; Hynes, R. G.; Jenkin, M. E.; Kerr, J. A.; Rossi, M. J.; Troe, J. IUPAC: Atmospheric Chemical Kinetic Data Evaluation, 2004, http://www.iupac-kinetic.ch.cam.ac.uk.

Atkinson, R.; Baulch, D. L.; Cox, R. A.; Hampson, J., R. F.; Kerr, J. A.; Rossi, M. J.; Troe, J. Evaluated kinetic, photochemical and heterogeneous data for atmospheric chemistry: Supplement V. *J. Phys. Chem. Ref. Data* **1997**, *26*, 1329-1499, doi:10.1063/1.556010.

Atkinson, R.; Hansen, D. A.; Pitts, J., J. N. Rate constants for the reaction of the OH radical with H_2 and NO (M = Ar and N_2). *J. Chem. Phys.* **1975**, *62*, 3284-3288, doi:10.1063/1.430882.

Atkinson, R.; Pitts, J. N., Jr. Rate constants for the reaction of OH radicals with propylene and the butenes over the temperature range 297–425 °K. *J. Chem. Phys.* **1975**, *63*, 3591-3595, doi:10.1063/1.431800.

Atkinson, R.; Pitts Jr., J. N. Kinetics of the reaction $O(^3P) + SO_2 + M \rightarrow SO_3 + M$ over the temperature range of 299°–440°K. *Int. J. Chem. Kinet.* **1978**, *10*, 1081-1090, doi:10.1002/kin.550101006.

Avallone, L. M. Measurements of the temperature-dependent rate coefficient for the reaction $O(^3P) + NO_2 \rightarrow NO + O_2$. *J. Photochem. Photobiol. A,* **2003**, *157*, 231-236, doi:10.1016/S1010-6030(03)00058-3.

Bacak, A.; Cooke, M. C.; Bardwell, M. W.; McGillen, M. R.; Archibald, A. T.; Huey, L. G.; Tanner, D.; Utembe, S. R.; Jenkin, M. E.; Derwent, R. G.; Shallcross, D. E.; Percival, C. J. Kinetics of the $HO_2 + NO_2$ Reaction: On the impact of new gas-phase kinetic data for the formation of HO_2NO_2 on HO_x, NO_x and HO_2NO_2 levels in the troposphere. *Atmos. Environ.* **2011**, *45*, 6414-6422, doi:10.1016/j.atmosenv.2011.08.008.

Baer, S.; Hippler, H.; Rahn, R.; Siefke, M.; Seitzinger, N.; Troe, J. Thermodynamic and kinetic properties of the reaction $Cl + O_2 + M \rightleftharpoons ClOO + M$ in the range 160-300 K and 1-1000 bar. *J. Chem. Phys.* **1991**, *95*, 6463-6470, doi:10.1063/1.461543.

Balla, R. J.; Heicklen, J. Oxidation of sulfur compounds III: The photolysis of $(CH_3S)_2$ in the presence of O_2. *J. Photochem.* **1985**, *29*, 297-310, doi:10.1016/0047-2670(85)85003-6.

Balla, R. J.; Nelson, H. H.; McDonald, J. R. Kientics of the reaction of CH_3S with NO, NO_2 and O_2. *Chem. Phys.* **1986**, *109*, 101-107, doi:10.1016/0301-0104(86)80188-4.

Ballesteros, B., N. R. Jensen, and J. Hjorth FT-IR study of the kinetics and products of the reactions of dimethylsulphide, dimethylsulphoxide and dimethylsulphone with Br and BrO. *J. Atmos. Chem.* **2002**, *43*, 135-150, doi:10.1023/A:1019922224137.

Barker, J. R. Personal communication. **2018**.

Barker, J. R.; Lohr, L. L.; Shroll, R. M.; Reading, S. Modeling the organic nitrate yields in the reaction of alkyl peroxy radicals with nitric oxide. 2. Reaction simulations. *J. Phys. Chem. A* **2003**, *107*, 7434-7444, doi:10.1021/jp034638j.

Barnes, I.; Bastian, V.; Becker, K. H.; Fink, E. H.; Zabel, F. Reactivity studies of organic substances towards hydroxyl radicals under atmospheric conditions. *Atmos. Environ.* **1982**, *16*, 545-550, doi:10.1016/0004-6981(82)90163-9.

Basco, N.; Hunt, J. E. The recombination of iodine atoms in the presence of nitric oxide. *Int. J. Chem. Kinet.* **1978**, *10*, 733-743, doi:10.1002/kin.550100707.

Basco, N.; Hunt, J. E. Mutual combination of ClO radicals. *Int. J. Chem. Kinet.* **1979**, *11*, 649-664, doi:10.1002/kin.550110611.

Basco, N.; James, D. G. L.; James, F. C. A quantitative study of alkyl radical reactions by kinetic spectroscopy. II. Combination of the methyl radical with the oxygen molecule. *Int. J. Chem. Kinet.* **1972**, *4*, 129-149, doi:10.1002/kin.550040202.

Bates, R. W.; Golden, D. M.; Hanson, R. K.; Bowman, C. T. Experimental study and modeling of the reaction $H + O_2 + M \rightarrow HO_2 + M$ (M = Ar, N_2, H_2O) at elevated pressures and temperatures between 1050 and 1250 K. *Phys. Chem. Chem. Phys.* **2001**, *3*, 2337-2342, doi:10.1039/b010002l.

Baulch, D. L.; Bowman, C. T.; Cobos, C. J.; Cox, R. A.; Just, T.; Kerr, J. A.; Pilling, M. J.; Stocker, D.; Troe, J.; Tsang, W.; Walker, R. W.; Warnatz, J. Evaluated kinetic data for combustion modeling: Supplement II. *J. Phys. Chem. Ref. Data* **2005**, *34*, 757-1397, doi:10.1063/1.1748524.

Baulch, D. L.; Cox, R. A.; Crutzen, P. J.; Hampson, R. F., Jr.; Kerr, J. A.; Troe, J.; Watson, R. T. Evaluated kinetic and photochemical data for atmospheric chemistry: Supplement 1. *J. Phys. Chem. Ref. Data* **1982**, *11*, 327-496, doi:10.1063/1.555664.

Baulch, D. L.; Cox, R. A.; Hampson, R. F., Jr.; Kerr, J. A.; Troe, J.; Watson, R. T. Evaluated kinetic and photochemical data for atmospheric chemistry. *J. Phys. Chem. Ref. Data* **1980**, *9*, 295-471, doi:10.1063/1.555619.

Bean, B. D.; Mollner, A. K.; Nizkorodov, S. A.; Nair, G.; Okumura, M.; Sander, S. P.; Peterson, K. A.; Francisco, J. S. Cavity ringdown spectroscopy of *cis-cis* HOONO and the $HOONO/HONO_2$ branching ratio in the reaction $OH + NO_2 + M$. *J. Phys. Chem. A* **2003**, *107*, 6974-6985, doi:10.1021/jp034407c.

Bedzhanyan, Y. R.; Markin, E. M.; Gershenzon, Y. M. Experimental study of elementary reactions of FO radicals VI. Reaction with NO_2. *Kinetics and Catalysis* **1993**, *34*, 190-193.

Bemand, P. P.; Clyne, M. A. A.; Watson, R. T. Atomic resonance fluorescence and mass spectrometry for measurements of the rate constants for elementrary reactions: $O\ ^3P_J + NO_2 \rightarrow NO + O_2$ and $NO + O_3 \rightarrow NO_2 + O_2$. *J. Chem. Soc. Faraday Trans. 2* **1974**, *70*, 564-576, doi;10.1039/F29747000564.

Beno, M. F.; Jonah, C. D.; Mulac, W. A. Rate constants for the reaction OH + CO as functions of temperature and water concentration. *Int. J. Chem. Kinet.* **1985**, *17*, 1091-1101, doi:10.1002/kin.550171006.

Bierbach, A.; Barnes, I.; Becker, K. H. Rate coefficients for the gas-phase reactions of bromine series of radicals with a alkenes, dienes, and aromatic hydrocarbons at 298 ± 2 K. *Int. J. Chem. Kinet.* **1996**, *28*, 565-577, doi:10.1002/(SICI)1097-4601(1996)28:8<565::AID-KIN2>3.0.CO;2-T.

Biermann, H. W.; Harris, G. W.; Pitts, J. N., Jr. Photoionization mass spectrometer studies of the collsionally stabillzed product distribution in the reaction of OH radicals with selected alkenes at 298 K. *J. Phys. Chem.* **1982**, *86*, 2958-2964, doi:10.1021/j100212a030.

Biermann, H. W.; Zetzsch, C.; Stuhl, F. Pressure dependence of reaction of HO with CO. *Ber. Bunsenges Phys. Chem.* **1978**, *82*, 633-639, doi:10.1002/bbpc.197800132.

Biggs, P.; Canosa-Mas, C. E.; Fracheboud, J. M.; Shallcross, D. E.; Wayne, R. P.; Caralp, F. Investigation into the pressure dependence between 1 and 10 Torr of the reactions of NO_2 with CH_3 and CH_3O. *J. Chem. Soc. Faraday Trans.* **1993**, *89*, 4163-4169, doi:10.1039/ft9938904163.

Bilde, M.; Sehested, J.; Nielsen, O. J.; Wallington, T. J.; Meagher, R. J.; McIntosh, M. E.; Piety, C. A.; Nicovich, J. M.; Wine, P. H. Kinetics and mechanism of the gas phase reaction of atomic chlorine with CH_2ICl at 206-432 K. *J. Phys. Chem. A* **1997**, *101*, 8035-8041, doi:10.1021/jp9717960.

Birk, M.; Friedl, R. R.; Cohen, E. A.; Pickett, H. M.; Sander, S. P. The rotational spectrum and structure of chlorine peroxide. *J. Chem. Phys.* **1989**, *91*, 6588-6597, doi:10.1063/1.457377.

Birks, J. W.; Shoemaker, B.; Leck, T. J.; Borders, R. A.; Hart, L. J. Studies of reactions of importance in the stratosphere. II. Reactions involving chlorine nitrate and chlorine dioxide. *J. Chem. Phys.* **1977**, *66*, 4591-4599, doi:10.1063/1.433716.

Bjork, B. J.; Bui, T. Q.; Heckl, O. H.; Changala, P. B.; Spaun, B.; Heu, P.; Follman, D.; Deutsch, C.; Cole, G. D.; Aspelmeyer, M.; Okumura, M.; Ye, J. Direct frequency comb measurement of OD + CO → DOCO kinetics. *Science* **2016**, *354*, 444-448, doi:10.1126/science.aag1862.

Black, G.; Patrick, R.; Jusinski, L. E.; Slanger, T. G. Rate coefficients for the reaction HS + NO + M(M = He, Ar, and N_2) over the temperature range 250- 445 K. *J. Chem. Phys.* **1984**, *80*, 4065-4070, doi:10.1063/1.447287.

Blitz, M. A.; Heard, D. E.; Pilling, M. J. OH formation from $CH_3CO + O_2$: a convenient experimental marker for the acetyl radical. *Chem. Phys. Lett.* **2002**, *365*, 374-379.

Blitz, M. A.; Heard, D. E.; Pilling, M. J.; Arnold, S. R.; Chipperfield, M. P. Pressure and temperature-dependent quantum yields for the photodissociation of acetone between 279 and 327.5 nm. *Geophys. Res. Lett.* **2004**, *31*, L06111, doi:1029/2003GL018793.

Blitz, M. A.; Huges, K. J.; Pilling, M. J. Determination of the high-pressure limiting rate coefficient and the enthalpy of reaction for OH + SO_2. *J. Phys. Chem. A* **2003**, *107*, 1971-1978, doi:10.1021/jp026524y.

Blitz, M. A.; Salter, R. J.; Heard, D. E.; Seakins, P. W. An Experimental and Master Equation Study of the Kinetics of OH/ OD + SO_2: The Limiting High-Pressure Rate Coefficients. *J. Phys. Chem. A* **2017**, *121*, 3184−3191, doi:10.1021/acs.jpca.7b01295.

Blitz, M. A.; Salter, R. J.; Heard, D. E.; Seakins, P. W. An Experimental Study of the Kinetics of OH/OD(v = 1,2,3) + SO_2: The Limiting High-Pressure Rate Coefficients as a Function of Temperature. *J. Phys. Chem. A* **2017**, *121*, 3175−3183, doi:10.1021/acs.jpca.7b01294.

Bloss, W. J.; Nickolaisen, S. L.; Salawitch, R. J.; Friedl, R. R.; Sander, S. P. Kinetics of the ClO self-reaction and 210 nm absorption cross section of the ClO dimer. *J. Phys. Chem. A* **2001**, *105*, 11226-11239, doi:10.1021/jp012429y.

Boakes, G.; Mok, W. H. H.; Rowley, D. M. Kinetic studies of the ClO + ClO association reaction as a function of temperature and pressure. *Phys. Chem. Chem. Phys.* **2005**, *7*, 4102-4113, doi:10.1039/b510308h.

Boyd, A. A.; Marston, G.; Wayne, R. P. Kinetic studies of the reaction between NO_3 and OClO at T = 300 K and P = 2-8 Torr. *J. Phys. Chem.* **1996**, *100*, 130-137, doi:10.1021/jp9509931.

Breen, J. E.; Glass, G. P. The reaction of the hydroxyl radical with acetylene. *Int. J. Chem. Kinet.* **1971**, *3*, 145-153, doi:10.1002/kin.550030206.

Breheny, C.; Hancock, G.; Morrell, C. The rate constant for the recombination reaction between CF_3 and O_2 measured between 2 and 110 Torr. *Z. Phys. Chem.* **2001**, *215*, 305-317, doi:10.1524/zpch.2001.215.3.305.

Bridier, I.; Caralp, F.; Loirat, H.; Lesclaux, R.; Veyret, B.; Becker, K. H.; Reimer, A.; Zabel, F. Kinetic and theoretical studies of the reactions $CH_3C(O)O_2 + NO_2 + M \rightleftarrows CH_3C(O)O_2NO_2 + M$ between 248 and 393 K and between 30 and 760 Torr. *J. Phys. Chem.* **1991**, *95*, 3594-3600, doi:10.1021/j100162a031.

Bridier, I.; Lesclaux, R.; Veyret, B. Flash photolysis kinetic study of the equilibrium $CH_3O_2 + NO_2 \leftrightarrow CH_3O_2NO_2$. *Chem. Phys. Lett.* **1992**, *191*, 259-263, doi:10.1016/0009-2614(92)85297-N.
Broske, R.; Zabel, F. Kinetics of the gas-phase reaction of $BrNO_2$ with NO. *J. Phys. Chem. A* **1998**, *102*, 8626-8631, doi:10.1021/jp982812b.
Brown, S. S.; Burkholder, J. B.; Talukdar, R. K.; Ravishankara, A. R. Reaction of hydroxyl radical with nitric acid: Insights into its mechanism. *J. Phys. Chem. A* **2001**, *105*, 1605-1614, doi:10.1021/jp002394m.
Brown, S. S.; Talukdar, R. K.; Ravishankara, A. R. Rate constants for the reaction $OH + NO_2 + M \rightarrow HNO_3 + M$ under atmospheric conditions. *Chem. Phys. Lett.* **1999**, *299*, 277-284, doi:10.1016/S0009-2614(98)01283-4.
Brown, S. S.; Talukdar, R. K.; Ravishankara, A. R. Reconsideration of the rate constant for the reaction of hydroxyl radicals with nitric acid. *J. Phys. Chem. A* **1999**, *103*, 3031-3037, doi:10.1021/jp984721k.
Brunning, J.; Stief, L. J. Pressure dependence of the absolute rate constant for the reaction $Cl + C_2H_2$ from 210-361 K. *J. Chem. Phys.* **1985**, *83*, 1005-1009, doi:10.1063/1.449463.
Buben, S. N.; Larin, I. K.; Messineva, N. A.; Trofimova, E. M. Measurement of the rate constant of the reaction $I + NO_2 + M \rightarrow INO_2 + M$ (M = He, N_2, Ar, O_2). *Kinetika i Kataliz* **1990**, *31*, 973.
Bui, T. Q.; Bjork, B. J.; Changala, P. B.; Heckl, O. H.; B.; Spaun, J. Y. $OD + CO \rightarrow D + CO_2$ branching kinetics probed with time-resolved frequency comb spectroscopy. *Chem. Phys. Lett.* **2017**, *683*, 91–95, doi:10.1016/j.cplett.2017.04.061.
Bui, T. Q.; Bjork, B. J.; Changala, P. B.; Nguyen, T. L.; Stanton, J. F.; Okumura, M.; Ye, J. Direct measurements of DOCO isomers in the kinetics of OD + CO. *Sci. Adv.* **2018**, *4*, eaao4777.
Bulatov, V. P.; Buloyan, A. A.; Cheskis, S. G.; Kozliner, M. Z.; Sarkisov, O. M.; Trostin, A. I. On the reaction of the NH_2 radical with ozone. *Chem. Phys. Lett.* **1980**, *74*, 288-292, doi:10.1016/0009-2614(80)85160-8.
Bunkan, A. J.; Liang, C.-H.; Pilling, M. J.; Nielsen, C. J. Theoretical and experimental study of the OH radical reaction with HCN. *Mol. Phys.* **2013**, *111*, 1589-1598, doi:10.1080/00268976.2013.802036.
Buras, Z. J.; Elsamra, R. M. I.; Green, W. H. Direct determination of the simplest Criegee intermediate (CH_2OO) self reaction rate. *J. Phys. Chem. Lett.* **2014**, *5*, 2224-2228, doi:10.1021/jz5008406.
Buras, Z. J.; Elsamra, R. M. I.; Jalan, A.; Middaugh, J. E.; Green, W. H. Direct kinetic measurements of reactions between the simplest Criegee intermediate CH_2OO and alkenes. *J. Phys. Chem. A* **2014**, *118*, 1997-2006, doi:10.1021/jp4118985.
Burkholder, J. B.; Hammer, P. D.; Howard, C. J. Product analysis of the $OH + NO_2 + M$ reaction. *J. Phys. Chem.* **1987**, *91*, 2136-2144, doi:10.1021/j100292a032.
Burkholder, J. B.; Mauldin, R. L.; Yokelson, R. J.; Solomon, S.; Ravishankara, A. R. Kinetic, thermodynamic, and spectroscopic study of Cl_2O_3. *J. Phys. Chem.* **1993**, *97*, 7597-7605, doi:10.1021/j100131a032.
Burkholder, J. B.; Ravishankara, A. R. Rate coefficient for the reaction: $O + NO_2 + M \rightarrow NO_3 + M$. *J. Phys. Chem. A* **2000**, *104*, 6752-6757, doi:10.1021/jp000169z.
Burrows, J. P.; Tyndall, G. S.; Moortgat, G. K. Absorption spectrum of NO_3 and kinetics of the reactions of NO_3 with NO_2, Cl, and several stable atmospheric species at 298 K. *J. Phys. Chem.* **1985**, *89*, 4848-4856, doi:10.1021/j100268a038.
Burrows, J. P.; Wallington, T. J.; Wayne, R. P. Kinetics of the gas-phase reactions of OH with NO_2 and with NO. *J. Chem. Soc. Faraday Trans. 2* **1983**, *79*, 111-122, doi:10.1039/f29837900111.
Butkovskaya, N.; Kukui, A.; Le Bras, G. HNO_3 forming channel of the $HO_2 + NO$ reaction as a function of pressure and temperature in the ranges of 72-600 Torr and 223-323 K. *J. Phys. Chem. A* **2007**, *111*, 9047-9053, doi:10.1021/jp074117m.
Butkovskaya, N.; Rayez, M.-T.; Rayez, J.-C.; Kukui, A.; Le Bras, G. Water vapor effect on the HNO_3 yield in the $HO_2 + NO$ reaction: Experimental and theoretical evidence. *J. Phys. Chem. A* **2009**, *113*, 11327-11342, doi:10.1021/jp811428p.
Butkovskaya, N. I.; Kukui, A.; Pouvesle, N.; Le Bras, G. Formation of nitric acid in the gas-phase $HO_2 + NO$ reaction: Effects of temperature and water vapor *J. Phys. Chem. A* **2005**, *109*, 6509-6520, doi:10.1021/jp051534v.
Butler, R.; Solomon, I. J.; Snelson, A. Pressure dependence of the $CO + OH$ rate constant in $O_2 + N_2$ mixtures. *Chem. Phys. Lett.* **1978**, *54*, 19-24, doi:10.1016/0009-2614(78)85654-1.
Calvert, J. G.; Atkinson, R.; Kerr, J. A.; Madronich, S.; Moortgat, G. K.; Wallington, T. J.; Yarwood, G. *The Mechanisms of Atmospheric Oxidation of the Alkenes*; Oxford University Press: New York - Oxford, 2000.

Campuzano-Jost, P.; Croce, A. E.; Hippler, H.; Siefke, M.; Troe, J. Kinetic and thermodynamic properties of the F + O_2 reaction system under high pressure and low temperature conditions. *J. Chem. Phys.* **1995**, *102*, 5317-5326, doi:10.1063/1.469258.

Cantrell, C. A.; Shetter, R. E.; Calvert, J. G.; Tyndall, G. S.; Orlando, J. J. Measurement of rate coefficients for the unimolecular decomposition of N_2O_5. *J. Phys. Chem.* **1993**, *97*, 9141-9148, doi:10.1021/j100138a013.

Cao, J.; Wang, W.-L.; Gao, L.-J.; Fu, F. Mechanism and Thermodynamic Properties of CH_3SO_3 Decomposition. *Acta Phys.-Chim. Sin.* **2013**, *29*, 1161-1167, doi:10.3866/PKU.WHXB201304021.

Caralp, F.; Lesclaux, R. Rate constant for the reaction of the $CFCl_2$ radical with oxygen in the pressure range 0.2-12 Torr at 298 K. *Chem. Phys. Lett.* **1983**, *102*, 54-58, doi:10.1016/0009-2614(83)80657-5.

Caralp, F.; Lesclaux, R.; Dognon, A. M. Kinetics of the reaction of CF_3 with O_2 over the temperature range 233-373 K. *Chem. Phys. Lett.* **1986**, *129*, 433-438, doi:10.1016/0009-2614(86)80224-X.

Caralp, F.; Lesclaux, R.; Rayez, M. T.; Rayez, J.-C.; Forst, W. Kinetics of the combination reactions of chlorofluoromethylperoxy radicals with NO_2 in the temperature range 233-373 K. *J. Chem. Soc. Faraday Trans. 2* **1988**, *84*, 569-585, doi:10.1039/f29888400569.

Caralp, F., M-T. Rayez, W. Forst, N. Gomez, B. Delcroix, D. Fitschen and P. Devolder Kinetic and mechanistic study of the pressure and temperature dependence of the reaction CH_3O + NO. *J. Chem. Soc. Faraday Trans.* **1998**, *94*, 3321-3330, doi:10.1039/a807456i.

Carleton, K. J.; Kessler, W. J.; Marinelli, W. J. H + O_2 + M (= N_2, H_2O, Ar) three-body rate coefficients at 298-750 K. *J. Phys. Chem.* **1993**, *97*, 6412-6417, doi:10.1021/j100126a015.

Carr, S. A.; Baeza-Romero, M. T.; Blitz, M. A.; Pilling, M. J.; Heard, D. E.; Seakins, P. W. OH yields from the CH_3CO + O_2 reaction using an internal standard. *Chem. Phys. Lett.* **2007**, *445*, 108-112, doi:10.1016/j.cplett.2007.07.099.

Carr, S. A.; Glowacki, D. R.; Liang, C.-H.; Baeza-Romero, M. T.; Blitz, M. A.; Pilling, M. J.; Seakins, P. W. Experimental and modeling studies of the pressure and temperature dependences of the kinetics and the OH yields in the acetyl + O_2 reaction. *J. Phys. Chem. A* **2011**, *115*, 1069–1085, doi:10.1021/jp1099199.

Chan, W. H.; Uselman, W. M.; Calvert, J. G.; Shaw, J. H. The pressure dependence of the rate constant for the reaction: HO + CO → H + CO_2. *Chem. Phys. Lett.* **1977**, *45*, 240-244, doi:10.1016/0009-2614(77)80261-3.

Chang, J. S.; Baldwin, A. C.; Golden, D. M. An explanation of the preferential formation of less stable isomers in three-body reactions: Cl + NO_2 + M; ClO + NO_2 + M. *J. Chem. Phys.* **1979**, *71*, 2021-2024, doi:10.1063/1.438593.

Chegodaev, P. P.; Tubikov, B. I. *Dokl. Akad. Nauk. SSSR* **1973**, *210*, 647-649.

Chen, H. L.; Trainor, D. W.; Center, R. E.; Fyfe, W. T. A flash photolysis, infrared chemiluminescence study of the rate constant for the recombination reaction F + O_2 + M. *J. Chem. Phys.* **1977**, *66*, 5513-5519, doi:10.1063/1.433872.

Chen, J.; Young, V.; Zhu, T.; Niki, H. Long path Fourier transform infrared spectroscopic study of the reactions of CF_3OO and CF_3O radicals with NO_2. *J. Phys. Chem.* **1993**, *97*, 11696-11698, doi:10.1021/j100147a024.

Christensen, L. E.; Okumura, M.; Sander, S. P.; Friedl, R. R.; Miller, C. E.; Sloan, J. J. Measurements of the rate constant of HO_2 + NO_2 + N_2 → HO_2NO_2 + N_2 using near-infrared wavelength-modulation spectroscopy and UV-visible absorption spectroscopy. *J. Phys. Chem. A* **2004**, *108*, 80-91, doi:10.1021/jp035905o.

Christensen, L. E.; Okumura, M.; Sander, S. P.; Salawitch, R. J.; Toon, G. C.; Sen, B.; Blavier, J.-F.; Jucks, K. W. Kinetics of HO_2 + HO_2 → H_2O_2 + O_2: Implications for stratospheric H_2O_2. *Geophys. Res. Lett.* **2002**, *29*, 1299, doi:1029/2001GL014525.

Clark, T. C.; Clyne, M. A. A.; Stedman, D. H. Mechanism of formation of triatomic molecules in atomic combination reactions Part 1.-Formation of ClNO and ClCO in reactions of atomic chlorine. *Trans. Faraday Soc.* **1966**, *62*, 3354-3365, doi:10.1039/tf9666203354.

Cleary, P. A.; Romero, M. T. B.; Blitz, M. A.; Heard, D. E.; Pilling, M. J.; Seakins, P. W.; Wang, L. Determination of the temperature and pressure dependence of the reaction OH + C_2H_4 from 200-400 K using experimental and master equation analyses. *Phys. Chem. Chem. Phys.* **2006**, *8*, 5633-5642, doi:10.1039/b612127f.

Cobos, C. J.; Hippler, H.; Luther, K.; Ravishankara, A. R.; Troe, J. High-pressure falloff curves and specific rate constants for the reaction CH_3 + O_2 ⇌ CH_3O_2 ⇌ CH_3O + O. *J. Phys. Chem.* **1985**, *89*, 4332-4338, doi:10.1021/j100266a036.

Cobos, C. J.; Hippler, H.; Troe, J. High-pressure falloff curves and specific rate constants for the reactions H + O ⇌ HO + O. *J. Phys. Chem.* **1985**, *89*, 342-349, doi:10.1021/j100248a033.
Codnia, J.; Azcarate, M. L. Rate measurement of the reaction of CF_2Cl radicals with O_2. *Photochem. Photobiol.* **2006**, *82*, 755–762, doi:10.1562/2006-01-04-RA-764.
Colussi, A. J. Formation and decay of (^3P_J)O atoms in the laser flash photolysis of chlorine dioxide (OClO) at 308 nm. *J. Phys. Chem.* **1990**, *94*, 8922-8926, doi:10.1021/j100389a014.
Colussi, A. J.; Sander, S. P.; Friedl, R. R. Temperature dependence and mechanism of the reaction between O(^{3}P) and chlorine dioxide. *J. Phys. Chem.* **1992**, *96*, 4442-4445, doi:10.1021/j100190a058.
Connell, P. S.; Howard, C. J. Kinetics study of the reaction HO + HNO_3. *Int. J. Chem. Kinet.* **1985**, *17*, 17-31, doi:10.1002/kin.550170104.
Connell, P. S.; Johnston, H. S. The thermal dissociation of N_2O_5 in N_2. *Geophys. Res. Lett.* **1979**, *6*, 553-556, doi:10.1029/GL006i007p00553.
Cooper, R.; Cumming, J. B.; Gordon, S.; Mulac, W. A. The reactions of the halomethyl radicals CCl_3 and CF_3 with oxygen. *Radiation Phys. Chem.* **1980**, *16*, 169-174, doi:10.1016/0146-5724(80)90224-1.
Cox, R. A. Photolysis of gaseous nitrous acid-A technique for obtaining kinetic data on atmospheric photooxidation reactions. *Int. J. Chem. Kinet. Symp.* **1975**, *1*, 379-398.
Cox, R. A.; Burrows, J. P.; Coker, G. B. Product formation in the association reaction of ClO with NO_2 investigated by diode laser kinetic spectroscopy. *Int. J. Chem. Kinet.* **1984**, *16*, 445-467, doi:10.1002/kin.550160412.
Cox, R. A.; Derwent, R. G. Kinetics of chlorine oxide radical reactions using modulated photolysis Part 1.-Disproportionation of ClO in the Cl_2 photosensitised decomposition of ozone. *J. Chem. Soc. Faraday Trans. 1* **1979**, *75*, 1635-1647, doi:10.1039/f19797501635.
Cox, R. A.; Derwent, R. G.; Holt, P. M. Relative rate constants for the reactions of OH radicals with H_2, CH_4, CO, NO and HONO at atmospheric pressure and 296 K. *J. Chem. Soc. Faraday Trans. 1* **1976**, *72*, 2031-2043, doi:10.1039/F19767202031.
Cox, R. A.; Lewis, R. Kinetics of chlorine oxide radical reactions using modulated photolysis Part 3.-Pressure and temperature dependence of the reaction: ClO + NO_2(+M) → $ClONO_2$(+M). *J. Chem. Soc. Faraday Trans. 1* **1979**, *75*, 2649-2661, doi:10.1039/f19797502649.
Cox, R. A.; Munk, J.; Nielsen, O. J.; Pagsberg, P.; Ratajczak, E. Ultraviolet absorption spectra and kientics of acetonyl and acetonylperoxy radicals. *Chem. Phys. Lett.* **1990**, *173*, 206-210, doi:10.1016/0009-2614(90)80079-S.
Cox, R. A.; Patrick, R. Kinetics of the reaction HO_2 + NO_2(+M) = HO_2NO_2 using molecular modulation spectrometry. *Int. J. Chem. Kinet.* **1979**, *11*, 635-648, doi:10.1002/kin.550110610.
Criegee, R. Mechanism of ozonolysis. *Angew. Chem. Int. Ed. Engl.* **1975**, *14*, 745-752, doi:10.1002/anie.197507451.
Croce de Cobos, A. E.; Hippler, H.; Troe, J. Study of the recombinatlon reaction NO_2 + NO_3 + M → N_2O_5 + M at high pressures. *J. Phys. Chem.* **1984**, *88*, 5083-5086, doi:10.1021/j150665a057.
Croce de Cobos, A. E.; Troe, J. High-pressure range of the recombination O + O_2 → O_3. *Int. J. Chem. Kinet.* **1984**, *16*, 1519-1530, doi:10.1002/kin.550161206.
D'Ottone, L.; Campuzano-Jost, P.; Bauer, D.; Hynes, A. J. A pulsed laser photolysis-pulsed laser induced fluorescence study of the kinetics of the gas-phase reaction of OH with NO_2. *J. Phys. Chem. A* **2001**, *105*, 10538-10543, doi:10.1021/jp012250n.
Daële, V.; Laverdet, G.; Le Bras, G.; Poulet, G. Kinetics of the reactions CH_3O + NO, CH_3O + NO_3, and CH_3O_2 + NO_3. *J. Phys. Chem.* **1995**, *99*, 1470-1477, doi:10.1021/j100005a017.
Daële, V.; Ray, A.; Vassalli, I.; Poulet, G.; Le Bras, G. Kinetic study of reactions of C_2H_5O and $C_2H_5O_2$ with NO at 298 K and 0.55 – 2 torr. *Int. J. Chem. Kinet.* **1995**, *27*, 1121-1133, doi:10.1002/kin.550271109.
Danis, F.; Caralp, F.; Masanet, J.; Lesclaux, R. Kinetics of the reaction BrO+NO_2+M → $BrONO_2$+M in the temperature range 263-343 K. *Chem. Phys. Lett.* **1990**, *167*, 450-456, doi:10.1016/0009-2614(90)85029-C.
Danis, F.; Caralp, F.; Rayez, M.; Lesclaux, R. Kinetic study of the reaction CCl_3 + O_2 + M → CCl_3O_2 + M from 1 to 760 Torr and from 233 to 333 K. *J. Phys. Chem.* **1991**, *95*, 7300-7307, doi:10.1021/j100172a037.
Dasch, W.; Sternberg, K.-H.; Schindler, R. N. Pressure dependence of the reaction ClO + NO_2 + N_2 → $ClONO_2$ + N_2 by laser flash photolysis. *Ber. Bunsenges. Phys. Chem.* **1981**, *85*, 611-615, doi:10.1002/bbpc.19810850717.
Davidson, J. A.; Cantrell, C. A.; Shetter, R. E.; McDaniel, A. H.; Calvert, J. G. The NO_3 radical decomposition and NO_3 scavenging in the troposphere. *J. Geophys. Res.* **1990**, *95*, 13963-13969, doi:10.1029/JD095iD09p13963.

Davis, D. D.; Fischer, S.; Schiff, R.; Watson, R. T.; Bollinger, W. A kinetic study of the reaction of OH radicals with two C_2 hydrocarbons: C_2H_4 and C_2H_2. *J. Chem. Phys.* **1975**, *63*, 1707-1712, doi:10.1063/1.431567.

Davis, D. D.; Herron, J. T.; Huie, R. E. Absolute rate constants for the reaction $O(^3P) + NO_2 \rightarrow NO + O_2$ over the temperature range 230-339°K. *J. Chem. Phys.* **1973**, *58*, 530-535, doi:10.1063/1.1679233.

Davis, H. F.; Kim, B.; Johnston, H. S.; Lee, Y. T. Dissociation energy and photochemistry of NO_3. *J. Phys. Chem.* **1993**, *97*, 2172-2180, doi:10.1021/j100112a018.

Daykin, E. P.; Wine, P. H. Kinetics of the reactions of IO Radicals with NO and NO_2. *J. Phys. Chem.* **1990**, *94*, 4528-4535, doi:10.1021/j100374a034.

de Petris, G.; Rosi, M.; Troiani, A. Direct experimental observation of CS_2OH. *ChemPhysChem* **2006**, *7*, 2352-2357, doi:10.1002/cphc.200600515.

DeMore, W. B. Rate constant for the OH + CO reaction: Pressure dependence and the effect of oxygen. *Int. J. Chem. Kinet.* **1984**, *16*, 1187-1200, doi:10.1002/kin.550161003.

DeMore, W. B.; Tschuikow-Roux, E. Ultraviolet spectrum and chemical reactivity of the ClO dimer. *J. Phys. Chem.* **1990**, *94*, 5856-5860, doi:10.1021/j100378a046.

Desain, J. D.; Klippenstein, S. J.; Miller, J. A.; Taatjes, C. A. Measurements, theory, and modeling of OH formation in ethyl + O2 and propyl + O2 reactions. J. Phys. Chem. A 2003, 107, , DOI: . *J. Phys. Chem. A* **2003**, *107*, 4415-4427, doi:10.1021/jp0221946.

Destriau, M.; Troe, J. Thermal dissociation and recombination of alkyl and haloalkyl peroxyitrates: An SACM modelling study. *Int. J. Chem. Kinet.* **1990**, *22*, 915-934, doi:10.1002/kin.550220904.

Devolder, P.; Carlier, M.; Pauwels, J. F.; Sochet, L. R. Rate constant for the reaction of OH with nitric acid: A new investigation by discharge flow resonance fluorescence. *Chem. Phys. Lett.* **1984**, *111*, 94-99.

Diau, E. W.-G.; Lee, Y.-P. Detailed rate coefficients and the enthalpy change of the equilibrium reaction $OH + C_2H_4 \rightleftarrows (M) HOC_2H_4$ over the temperature range 544-673 K. *J. Chem. Phys.* **1992**, *96*, 377-386, doi:10.1063/1.462474.

Diaz-de-Mera, Y.; Aranda, A.; Rodriguez, D.; López, R.; Cabañas, B.; Martinez, E. Gas-phase reactions of chlorine atoms and ClO radicals with dimethyl sulfide. Rate coefficients and temperature dependences. *J. Phys. Chem. A* **2002**, *106*, 8627-8633, doi:10.1021/jp014570c.

Dilger, H.; Schwager, M.; Tregenna-Piggott, P. L. W.; Roduner, E.; Reid, I. D.; Arseneau, D. J.; Pan, J. J.; Senba, M.; Shelley, M.; Fleming, D. G. Addition kinetics and spin exchange in the gas phase reaction of the ethyl radical with oxygen. *J. Phys. Chem.* **1996**, *100*, 6561-6571, doi:10.1021/jp9525853.

Dillon, T. J.; Blitz, M. A.; Heard, D. E. Determination of the rate coefficients for the reactions $IO + NO_2 + M$ (Air) $\rightarrow IONO_2 + M$ and $O(^3P) + NO_2 \rightarrow O_2 + NO$ using laser-induced fluorescence spectroscopy. *J. Phys. Chem. A* **2006**, *110*, 6995-7002, doi:10.1021/jp057048p.

Dillon, T. J.; Tucceri, M. E.; Sander, R.; Crowley, J. N. LIF studies of iodine oxide chemistry. *Phys. Chem. Chem. Phys.* **2008**, *10*, 1540−1554, doi:10.1039/B717386E.

Dixon, D. A.; Christe, K. O. Nitrosyl hypofluorite: Local denslty functional study of a problem case for theoretlcal methods. *J. Phys. Chem.* **1992**, *95*, 1018-1021, doi:10.1021/j100182a004.

Dóbé, S.; Lendvay, G.; Szilágyi, I.; Bérces, T. Kinetics and mechanism of the reaction of CH_3O with NO. *Int. J. Chem. Kinet.* **1994**, *26*, 887-901, doi:10.1002/kin.550260903.

Donahue, N. M.; Dubey, M. K.; Mohrschladt, R.; Demerjian, K.; Anderson, J. G. High-pressure flow study of the reactions $OH + NO_x \rightarrow HONO_x$: Errors in the falloff region. *J. Geophys. Res.* **1997**, *102*, 6159-6168, doi:10.1029/96JD02329.

Donohoue, D. L.; Bauer, D.; Cossairt, B.; Hynes, A. J. Temperature and pressure dependent rate coefficients for the reaction of Hg with Br and the reaction of Br with Br: A pulsed laser photolysis-pulsed laser induced fluorescence study. *J. Phys. Chem. A* **2006**, *110*, 6623-6632, doi:10.1021/jp054688j.

Dransfield, T. J.; Perkins, K. K.; Donahue, N. M.; Anderson, J. G.; Sprengnether, M. M.; Demerjian, K. Temperature and pressure dependent kinetics of the gas-phase reaction of the hydroxyl radical with nitrogen dioxide. *Geophys. Res. Lett.* **1999**, *26*, 687-690, doi:10.1029/1999GL900028.

Dreier, T.; Wolfrum, J. Direct study of the reaction of vibrationally excited CO molecules with OH radicals. *Proc. Combust. Inst.* **1980**, *18*, 801-809.

Dulitz, K.; Amedro, D.; Dillon, T. J.; Pozzer, A.; Crowley, J. N. Temperature-(208–318 K) and pressure-(18–696 Torr) dependent rate coefficients for the reaction between OH and HNO_3. *Atmos. Chem. Phys.* **2018**, *18*, 2381–2394, doi:10.5194/acp-18-2381-20.

Edney, E. O.; Kleindienst, T. E.; Corse, E. W. Room temperature rate constants for the reaction of OH with selected chlorinated and oxygenated hydrocarbons. *Int. J. Chem. Kinet.* **1986**, *18*, 1355-1371, doi:10.1002/kin.550181207.

Elfers, G.; Zabel, F.; Becker, K. H. Determination of the rate constant ratio for the reactions of the ehtylperoxy radical with NO and NO_2. *Chem. Phys. Lett.* **1990**, *168*, 14-19, doi:10.1016/0009-2614(90)85094-S.

Ellermann, T.; Sehested, J.; Nielson, O. J.; Pagsberg, P.; Wallington, T. J. Kinetics of the reaction of F atoms with O_2 and UV spectrum of FO_2 radicals in the gas phase at 295 K. *Chem. Phys. Lett.* **1994**, *218*, 287-294, doi:10.1016/0009-2614(94)00006-9.

Enami, S.; Nakano, Y.; Hashimoto, S.; Kawasaki, M.; Aloisio, S.; Francisco, J. S. Reactions of Cl atoms with dimethyl sulfide: A theoretical calculation and an experimental study with cavity ring-down spectroscopy. *J. Phys. Chem. A* **2004**, *108*, 7785-7789, doi:10.1021/jp049772y.

Enami, S.; Sakamoto, Y.; Yamanaka, T.; Hashimoto, S.; Kawasaki, M.; Tonokura, K.; Tachikawa, H. Reaction mechanisms of IO radical formation from the reaction of CH_3I with Cl atom in the presence of O_2. *Bull. Chem. Soc. Jpn.* **2008**, *81*, 1250−1257, doi:10.1246/bcsj.81.1250.

Erler, K.; Field, D.; Zellner, R.; Smith, I. W. M. Recombination reaction between hydroxyl radicals and nitrogen dioxide. OH + NO_2 + M (= He, CO_2) in temperature range 213-300 K. *Ber. Bunsenges. Phys. Chem.* **1977**, *81*, 22-26, doi:10.1002/bbpc.19770810107.

Eskola, A. J.; Lozovsky, V. A.; Timonen, R. S. Kinetics of the reactions of C_2H_5, n-C_3H_7, and n-C_4H_9 radicals with Cl_2 at the temperature range 190–360 K. *Int. J. Chem. Kinet.* **2007**, *39*, 614–619, doi:10.1002/kin.20272.

Eskola, A. J.; Wojcik-Pastuszka, D.; Ratajczak, E.; Timonen, R. S. Kinetics of the reactions of CH_2Br and CH_2I radicals with molecular oxygen at atmospheric temperatures. *Phys. Chem. Chem. Phys.* **2006**, *8*, 416-1424, doi:10.1039/b516291b.

Estupiñán, E. G., J. M. Nicovich and P.H. Wine A temperature-dependent kintetics study of the important stratospheric reaction $O(^3P)$ + NO_2 → O_2 + NO. *J. Phys. Chem. A* **2001**, *105*, 9697-9703, doi:10.1021/jp011940o.

Estupiñán, E. G.; Nicovich, J. M.; Li, J.; Cunnold, D. M.; Wine, P. H. Investigation of N_2O production from 266 and 532 nm laser flash photolysis of $O_3/N_2/O_2$ mixtures. *J. Phys. Chem. A* **2002**, *106*, 5880-5890, doi:10.1021/jp014242c.

Fagerstrom, K.; Lund, A.; Mahmound, G.; Jodkowski, J. T.; Ratajczak, E. Pressure and temperature dependence of the gas-phase reaction between methyl and hydroxyl radicals. *Chem. Phys. Lett.* **1994**, *224*, 43-50, doi:10.1016/0009-2614(94)00513-3.

Fasano, D. M.; Nogar, N. S. Real-time kinetic study of the reaction F + NO_2. *J. Chem. Phys.* **1983**, *78*, 6688-6694, doi:10.1063/1.444668.

Fenter, F. F.; Lightfoot, P. D.; Caralp, F.; Lesclaux, R.; Niranen, J. T.; Gutman, D. Kinetics of the $CHCl_2$ and CH_2Cl association reactions with molecular oxygen between 298 and 448 K and from 1 to 760 Torr of total pressure. *J. Phys. Chem.* **1993**, *97*, 4695-4703, doi:10.1021/j100120a023.

Fenter, F. F.; Lightfoot, P. D.; Niranen, J. T.; Gutman, D. Kinetics of the CCl_3 association reaction with molecular oxygen at 298 and 333 K and from 1 to 760 Torr of total pressure. *J. Phys. Chem.* **1993**, *97*, 5313-5320, doi:10.1021/j100122a023.

Fernandes, R. X.; Luther, K.; Marowsky, G.; Rissanen, M. P.; Timonen, R.; Troe, J. R. Experimental and modeling study of the temperature and pressure dependence of the reaction C_2H_5 + O_2 (+ M) → $C_2H_5O_2$ (+ M). *J. Phys. Chem. A* **2015**, *119*, 7263−7269, doi:10.1021/jp511672v.

Fernandes, R. X.; Luther, K.; Troe, J. Falloff curves for the reaction CH_3 + O_2 (+ M) → CH_3O_2 (+ M) in the pressure range 2−1000 Bar and the temperature range 300−700 K. *J. Phys. Chem. A* **2006**, *110*, 4442-4449, doi:10.1021/jp056850o.

Fernandes, R. X.; Luther, K.; Troe, J.; Ushakov, V. G. Experimental and modelling study of the recombination reaction H + O_2 (+M) = HO_2 (+M) between 300 and 900 K, 1.5 and 950 bar, and in the bath gases M = He, Ar, and N_2. *Phys. Chem. Chem. Phys.* **2008**, *10*, 4313-4321, doi:10.1039/b804553d.

Ferracci, V.; Rowley, D. M. Kinetic and thermochemical studies of the ClO + ClO + M ⇄ Cl_2O_2 + M reaction *Phys. Chem. Chem. Phys* **2010**, *12*, 11596-11608, doi:10.1039/c0cp00308e.

Fittschen, C.; Frenzel, A.; Imrik, K.; Devolder, P. Rate constants for the reactions of C_2H_5O, i-C_3H_7O, and n-C_3H_7O with NO and O_2 as a function of temperature. *Int. J. Chem. Kinet.* **1999**, *31*, 860-866, doi:10.1002/(SICI)1097-4601(1999)31:12<860::AID-KIN4>3.0.CO;2-E.

Fockenberg, C.; Somnitz, H.; Bednarek, G.; Zellner, R. Kinetic and mechanistic studies of the reactions of CF_3O radicals with NO and NO_2. *Ber. Bunsenges. Phys. Chem.* **1997**, *101*, 1411-1420, doi:10.1002/bbpc.199700001.

Foreman, E. S.; Murray, C. Kinetics of IO production in the $CH_2I + O_2$ reaction studied by cavity ring-down spectroscopy. *J. Phys. Chem. A* **2015**, *119*, 8981−8990, doi:10.1021/acs.jpca.5b05058.

Forst, W., and F. Caralp Microcanonical variational theory of radical recombination by inversion of interpolate partition function Part 2.-$CX_3 + O_2$ (X = H, F, Cl). *J. Chem. Soc. Faraday Trans.* **1991**, *87*, 2307-2315, doi:10.1039/ft9918702307.

Forst, W.; Caralp, F. Microcanonical variational theory of radical recombination by inversion of interpolated partition function. 3. $CX_3O_2 + NO_2$ (X = H, F, Cl). *J. Phys. Chem.* **1992**, *96*, 6291-6298, doi:10.1021/j100194a036.

Forster, R.; Frost, M.; Fulle, D.; Hamann, H. F.; Hippler, H.; Schlepegreli; Troe, J. High pressure range of the addition of HO to HO, NO, NO_2, and CO. I. Saturated laser induced fluorescence measurements at 298 K. *J. Chem. Phys.* **1995**, *103*, 2949-2958, doi:10.1063/1.470482.

Forte, E.; Hippler, H.; van den Bergh, H. INO thermodynamic properties and ultraviolet spectrum. *Int. J. Chem. Kinet.* **1981**, *13*, 1227-1233.

Fowles, M.; Mitchell, D. N.; Morgan, J. W. L.; Wayne, R. P. Kinetics and photochemistry of NO_3 Part 2.-Kinetics of the reaction $NO_2 + NO_3 + M$. *J. Chem. Soc. Faraday Trans. 2* **1982**, *78*, 1239-1248, doi:10.1039/f29827801239.

Friedl, R. R.; Sander, S. P.; Yung, Y. L. Chloryl nitrate: A novel product of the $OClO + NO_3 + M$ recombination. *J. Phys. Chem.* **1992**, *96*, 7490-7493, doi:10.1021/j100198a002.

Fritz, B.; Lorenz, K.; Steinert, W.; Zellner, R. Rate of oxidation of HCN by OH radicals at lower temperatures. *Oxidation Communications* **1984**, *6*, 363-370.

Frost, M. J.; Smith, I. W. M. Rate constants for the reactions of CH_3O and C_2H_5O with NO_2 over a range of temperature and total pressure. *J. Chem. Soc. Faraday Trans.* **1990**, *86*, 1751-1756, doi:10.1039/ft9908601751.

Frost, M. J.; Smith, I. W. M. Rate Constants for the reactions of CH_3O and C_2H_5O with NO over a range of temperature and total pressure. *J. Chem. Soc. Faraday Trans.* **1990**, *86*, 1757-1762, doi:10.1039/ft9908601757.

Frost, M. J.; Smith, I. W. M. Corrigendum to rate constants for the reductions of CH_3O and C_2H_5O with NO_2 over a range of temperature and total pressure. *J. Chem. Soc. Faraday Trans* **1993**, *89*, 4251, doi:10.1039/ft9938904251.

Fulle, D.; Hamann, H. F.; Hippler, H. The pressure and temperature dependence of the recombination reaction $HO+SO_2+M = HOSO_2+M$. *Phys. Chem. Chem. Phys.* **1999**, *1999*, 2695-2702, doi:10.1039/a901596e.

Fulle, D.; Hamann, H. F.; Hippler, H.; Jänsch, C. P. The high pressure range of the addition of OH to C_2H_2 and C_2H_4. *Ber. Bunsenges. Phys. Chem.* **1997**, *101*, 1433-1442, doi:10.1002/bbpc.199700004.

Fulle, D.; Hamann, H. F.; Hippler, H.; Troe, J. High-pressure range of the addition of HO to HO. III. Saturated laser-induced fluorescence measurements between 200 and 700 K. *J. Chem. Phys.* **1996**, *105*, 1001-1006, doi:10.1063/1.471944.

Fulle, D. H.; Hamann, H. F.; Hippler, H.; Troe, J. Temperature and pressure dependence of the addition reactions of HO to NO and to NO_2. IV. Saturated laser-induced fluorescence measurements up to 1400 bar. *J. Chem. Phys.* **1998**, *108*, 5391-5397, doi:10.1063/1.475971.

Gaedtke, H. K., H. Hippler, K. Luther, and J. Troe Addition reactions of oxygen atoms at high pressures. *Proc. Combust. Inst.* **1973**, *14*, 295-303.

Galano, A. Mechanism of OH radical reactions with HCN and CH_3CN: OH regeneration in the presence of O_2. *J. Phys. Chem. A* **2007**, *111*, 5086-5091, doi:10.1021/jp0708345.

Gao, Y. Q.; Marcus, R. A. An approximate theory of the ozone isotope effects: Rate constant ratios and pressure dependence. *J. Chem. Phys.* **2007**, *127*, 244316, doi:10.1063/1.2806189.

Geers-Müller, R.; Stuhl, F. On the kinetics of the reactions of oxygen atoms with NO_2, N_2O_4, and N_2O_3 at low temperatures. *Chem. Phys. Lett.* **1987**, *135*, 263-268, doi:10.1016/0009-2614(87)85153-9.

Gierczak, T.; Burkholder, J. B.; Ravishankara, A. R. Temperature dependent rate coefficient for the reaction $O(^3P) + NO_2 \rightarrow NO + O_2$. *J. Phys. Chem. A* **1999**, *103*, 877-883, doi:10.1021/jp983962p.

Gierczak, T.; Rajakumar, B.; Flad, J. E.; Burkholder, J. B. Rate coefficients for the reaction of the acetyl radical, CH_3CO, with Cl_2 between 253 and 384 K. *Int. J. Chem. Kinet.* **2009**, *41*, 543-553, doi:10.1002/kin.20430.

Gleason, J. F.; Nesbitt, F. L.; Stief, L. J. Temperature dependence of the reaction between $O(^3P)$ and OClO at low pressure. *J. Phys. Chem.* **1994**, *98*, 126-131, doi:10.1021/j100052a022.
Golden, D. M. Reaction ClO + ClO → products: Modeling and parameterization for use in atmospheric models. *Int. J. Chem. Kinet.* **2003**, *35*, 206-211, doi:10.1002/kin.10120.
Golden, D. M. Evaluating data for atmospheric models, an example: $CH_3O_2 + NO_2 = CH_2O_2NO_2$. *Int. J. Chem. Kinet.* **2005**, *37*, 625-632, doi:10.1002/kin.20104.
Golden, D. M. Evaluating data for atmospheric models, an example: $IO + NO_2 = IONO_2$. *J. Phys. Chem. A* **2006**, *110*, 2940-2943, doi:10.1021/jp058221k.
Golden, D. M. The reaction $Cl + NO_2 \rightarrow ClONO$ and $ClNO_2$. *J. Phys. Chem. A* **2007**, *111*, 6772-6780, doi:10.1021/jp069000x.
Golden, D. M. Pressure dependent reactions for atmospheric and combustion models. *Chem. Soc. Rev.* **2008**, *37*, 717-731, doi:10.1039/b704259k.
Golden, D. M. Evaluation of data for atmospheric models: ME/RRKM calculations on the combination reaction $ClO + NO_2 \rightarrow ClONO_2$, a recurring issue. *Int. J. Chem. Kinet.* **2009**, *41*, 573-581, doi:10.1002/kin.20432.
Golden, D. M. The reaction $OH + C_2H_4$: An example of rotational channel switching. *J. Phys. Chem. A* **2012**, *116*, 4259-4266, doi:10.1021/jp302009t.
Golden, D. M.; Barker, J. R.; Lohr, L. L. Master equation models for the pressure- and temperature-dependent reactions $HO + NO_2 \rightarrow HONO_2$ and $HO + NO_2 \rightarrow HOONO$. *J. Phys. Chem. A* **2003**, *107*, 11057-11071, doi:10.1021/jp0353183.
Golden, D. M.; Smith, G. P. Reaction of $OH + NO_2 + M$: A new view. *J. Phys. Chem. A* **2000**, *104*, 3991-3997, doi:10.1021/jp9939928.
Gómez Martin, J. C.; Garraway, S. A.; Plane, J. M. C. Reaction kinetics of meteoric sodium reservoirs in the upper atmosphere. *J. Phys. Chem. A* **2016**, *120*, 1330-1346, doi:10.1021/acs.jpca.5b00622.
Gómez Martín, J. C.; Seaton, C.; de Miranda, M. P.; Plane, J. M. C. The reaction between sodium hydroxide and atomic hydrogen in atmospheric and flame chemistry. *J. Phys. Chem. A* **2017**, *121*, 7667–7674, doi:10.1021/acs.jpca.7b07808.
Goodsite, M. E.; Plane, J. M. C.; Skov, H. A theoretical study of the oxidation of Hg^0 to $HgBr_2$ in the troposphere. *Environ. Sci. Technol.* **2004**, *38*, 1772-1776, doi:10.1021/es034680s.
Goodsite, M. E.; Plane, J. M. C.; Skov, H. Correction to a theoretical study of the oxidation of Hg^0 to $HgBr_2$ in the troposphere. *Environ. Sci. Technol.* **2012**, *46*, 5262-5262, doi:10.1021/es301201c.
Gravestock, T. J.; Blitz, M. A.; Bloss, W. J.; Heard, D. E. A multidimensional study of the reaction $CH_2I + O_2$: Products and atmospheric implications. *ChemPhysChem* **2010**, *11*, 3928-3941, doi:10.1002/cphc.201000575.
Green, T. J.; Islam, M.; Guest, P.; Hickson, K.; Canosa-Mas, C. E.; Wayne, R. P. A discharge-flow study of Cl_2O_3. *Phys. Chem. Chem. Phys.* **2003**, *5*, 5409-5418, doi:10.1039/b311005b.
Greig, G.; Gunning, H. E.; Strausz, O. P. Reactions of metal atoms. II. The combination of mercury and bromine atoms and the dimerization of HgBr. *J. Chem. Phys.* **1970**, *52*, 3684-3690, doi:10.1063/1.1673544.
Greiner, N. R. Hydroxyl radical kinetics by kinetic spectrosopy. VII. The reaction with ethylene in the range 300-500 °K. *J. Chem. Phys.* **1970**, *53*, 1284-1285, doi:10.1063/1.1674133.
Grosjean, D. Photooxidation of methyl sulfide, ethyl sulfide, and methanethiol. *Environ. Sci. Technol.* **1984**, *18*, 460-468, doi:10.1021/es00124a013.
Grosjean, D.; Grosjean, E.; Williams, E. L. Thermal decomposition of PAN, PPN and vinyl-PAN. *J. Air and Waste Manage. Assoc.* **1994**, *44*, 391-396.
Gross, A.; Billing, G. D. Isotope effects on the rate constants for the processes $O_2 + O \rightarrow O + O_2$ and $O_2 + O + Ar \rightarrow O_3 + Ar$ On a modified ground-state potential energy surface for ozone. *Chem. Phys.* **1997**, *217*, 1-18, doi:10.1016/S0301-0104(97)84555-7.
Groß, C. B. M.; Dillon, T. J.; Crowley, J. N. Pressure dependent OH yields in the reactions of CH_3CO and $HOCH_2CO$ with O_2. *Phys. Chem. Chem. Phys.* **2014**, *16*, 10990-10998, doi:10.1039/c4cp01108b.
Hahn, J.; Luther, K.; Troe, J. Experimental and theoretical study of the temperature and pressure dependences of the recombination reactions $O + NO_2(+ M) \rightarrow NO_3(+ M)$ and $NO_2 + NO_3(+M) \rightarrow N_2O_5(+M)$. *Phys. Chem. Chem. Phys.* **2000**, *2*, 5098-5104, doi:10.1039/b005756h.
Handwerk, V.; Zellner, R. Pressure and temperature dependence of the reaction $ClO + NO_2 (+N_2) \rightarrow ClONO_2 (+N_2)$. *Ber. Bunsenges. Phys. Chem.* **1984**, *88*, 405-409, doi:10.1002/bbpc.19840880417.
Harris, G. W.; Atkinson, R.; Pitts, J. N., Jr. Temperature dependence of the reaction $OH + SO_2 + M \rightarrow HSO_3 + M$ for M = Ar and SF_6. *Chem. Phys. Lett.* **1980**, *69*, 378-382, doi:10.1016/0009-2614(80)85085-8.

Harris, G. W.; Wayne, R. P. Reaction of hydroxyl radicals with NO, NO_2 and SO_2. *J. Chem. Soc. Faraday Trans. 1* **1975**, *71*, 610-617, doi:10.1039/f19757100610.

Hassouna, M.; Delbos, E.; Devolder, P.; Viskolcz, B.; Fittschen, C. Rate and equilibrium constant of the reaction of 1-methylvinoxy radicals with O_2: $CH_3COCH_2 + O_2 \leftrightarrow CH_3COCH_2O_2$. *J. Phys. Chem. A* **2006**, *110*, 6667-6672, doi:10.1021/jp0558270.

Hatakeyama, S.; Akimoto, H. Reactions of hydroxyl radicals with methanethiol, dimethyl sulfide, and dimethyl disulfide in air. *J. Phys. Chem.* **1983**, *87*, 2387-2395, doi:10.1021/j100236a029.

Hathorn, B. C.; Marcus, R. A. An intramolecular theory of the mass-independent isotope effect for ozone. II. Numerical implementation at low pressures using a loose transition state. *J. Chem. Phys.* **2000**, *113*, 9497-9509, doi:10.1063/1.1321045.

Hayman, G. D.; Davies, J. M.; Cox, R. A. Kinetics of the reaction ClO + ClO → products and its potential relevance to Antarctic ozone. *Geophys. Res. Lett.* **1986**, *13*, 1347-1350, doi:10.1029/GL013i012p01347.

Helmer, M.; Plane, J. M. C. A study of the reaction $NaO_2 + O$ ---> $NaO + O_2$: Implications for the chemistry of sodium in the upper atmosphere. *J. Geophys. Res.* **1993**, *98*, 23207-23222, doi:10.1029/93JD02033.

Hewitt, A. D.; Brahan, K. M.; Boone, G. D.; Hewitt, S. A. Kinetics and mechanism of the Cl + CO reaction in air. *Int. J. Chem. Kinet.* **1996**, *28*, 763-771, doi:10.1002/(SICI)1097-4601(1996)28:10<763::AID-KIN7>3.0.CO;2-L.

Hippler, H.; Nasterlack, S.; Striebel, F. Reaction of OH + NO_2 + M: Kinetic evidence of isomer formation. *Phys. Chem. Chem. Phys.* **2002**, *4*, 2959-2964, doi:10.1039/b201932a.

Hippler, H.; Siefke, M.; Stark, H.; Troe, J. New studies of the unimolecular reaction $NO_2 \rightleftharpoons O + NO$. Part 1. High pressure range of the O + NO recombination between 200 and 400 K. *Phys. Chem. Chem. Phys.* **1999**, *1*, 57-61, doi:10.1039/a806520i.

Hippler, H.; Troe, J.; Willner, J. Temperature and pressure dependence of ozone formation rates in the range 1-1000 bar and 90-370 K. *J. Chem. Phys.* **1990**, *93*, 6560-6569, doi:10.1063/1.458972.

Hochanadel, C. J.; Ghormley, J. A.; Boyle, J. W.; Ogren, P. J. Absorption spectrum and rates of formation and decay of the CH_3O_2 radical. *J. Phys. Chem.* **1977**, *81*, 3-7, doi:10.1021/j100516a002.

Hofzumahaus, A.; Stuhl, F. Rate constant of the reaction HO + CO in the presence of N_2 and O_2. *Ber. Bunsenges Phys. Chem.* **1984**, *88*, 557-561, doi:10.1002/bbpc.19840880612.

Hölscher, D.; Zellner, R. LIF study of the reactions of the IO radical with NO and NO_2 over an extended range of temperature and pressure. *Phys. Chem. Chem. Phys.* **2002**, *4*, 1839-1845, doi:10.1039/b110084j.

Howard, C. J. Rate constants for the gas-phase reactions of OH radicals with ethylene and halogenated ethylene compounds. *J. Chem. Phys.* **1976**, *65*, 4771-4777, doi:10.1063/1.432932.

Howard, C. J. Kinetics of the reaction of HO_2 with NO_2. *J. Chem. Phys.* **1977**, *67*, 5258-5263, doi:10.1063/1.434703.

Howard, C. J.; Evenson, K. M. Laser magnetic resonace study of the gas phase reactions of OH with CO, NO, and NO_2. *J. Chem. Phys.* **1974**, *61*, 1943-1952, doi:10.1063/1.1682195.

Hsu, K. J.; Anderson, S. M.; Durant, J. L.; Kaufman, F. Rate constants for H + O_2 + M from 298 to 639 K for M = He, N_2, and H_2O. *J. Phys. Chem.* **1989**, *93*, 1018-1021, doi:10.1021/j100340a003.

Hsu, K. J.; Durant, J. L.; Kaufman, F. Rate constants for H + O_2 + M at 298 K for M = He, N_2, and H_2O. *J. Phys. Chem.* **1987**, *91*, 1895-1899, doi:10.1021/j100291a043.

Huang, H.; Eskola, A. J.; Taatjes, C. A. Pressure-dependent I-atom yield in the reaction of CH_2I with O_2 shows a remarkable apparent third-body efficiency for O_2. *J. Phys. Chem. Lett.* **2012**, *3*, 3399-3403, doi:10.1021/jz301585c.

Huang, H.; Rotavera, B.; Eskola, A. J.; Taatjes, C. A. Correction to "Pressure-dependent I atom yield in the reaction of CH_2I with O_2 shows a remarkable apparent third-body efficiency for O_2". *J. Phys. Chem. Lett.* **2013**, *4*, 3824-3824, doi:10.1021/jz402266q.

Huang, Y.-H.; Chen, L.-W.; Lee, Y.-P. Simultaneous infrared detection of the ICH_2OO radical and Criegee intermediate CH_2OO: The pressure dependence of the yield of CH_2OO in the reaction $CH_2I + O_2$. *J. Phys. Chem. Lett.* **2015**, *6*, 4610−4615, doi:10.1021/acs.jpclett.5b02298.

Huie, R. E.; Herron, J. T.; Davis, D. D. Absolute rate constants for the reaction O + O_2 + M → O_3 + M over the temperature range 200-346°K. *J. Phys. Chem.* **1972**, *76*, 2653-2658, doi:10.1021/j100663a002.

Husain, D.; Plane, J. M. C.; Slater, N. K. H. Kinetic investigation of the reactions of OH($X^2\Pi$) with the hydrogen halides, HCl, DCl, HBr and DBr by time-resolved resonance fluorescence ($A^2\Sigma^+$ - $X^2\Pi$). *J. Chem. Soc. Faraday Trans. 2* **1981**, *77*, 1949-1962, doi:10.1039/f29817701949.

Husain, D.; Plane, J. M. C.; Xiang, C. C. Determination of the absolute third-order rate constant for the reaction between Na + OH + He by time-resolved molecular resonance-fluorescence spectroscopy, OH($A^2\Sigma^+$-

$X^2\Pi$, coupled with steady atomic fluorescence spectroscopy, Na($3\ ^2P_J$–$3\ ^2S_{1/2}$). *J. Chem. Soc., Faraday Trans. 2* **1984**, *80*, 1619−1631, doi:10.1039/f29848001619.
Hynes, A. J.; Wine, P. H.; Nicovich, J. M. Kinetics and mechanism of the reaction of OH with CS_2 under atmospheric conditions. *J. Phys. Chem.* **1988**, *92*, 3846-3852, doi:10.1021/j100324a034.
Hynes, A. J.; Wine, P. H.; Ravishankara, A. R. Kinetics of the OH + CO reaction under atmospheric conditions. *J. Geophys. Res.* **1986**, *91*, 11815-11820, doi:10.1029/JD091iD11p11815.
Ide, T.; Nakayama, T.; Takahashi, K.; Matsumi, Y. Thermal decomposition rate of N_2O_5 measured by cavity ring-down spectroscopy. *Int. J. Chem. Kinetics* **2008**, *40*, 679-684, doi:10.1002/kin.20351.
Imrik, K.; Farkas, E.; Vasvári, G.; Szilágyi, I.; Sarzyski, D.; Dóbé, S.; Bérces, T.; Márta, F. Laser spectrometry and kinetics of selected elementary reactions of the acetonyl radical. *Phys. Chem. Chem. Phys.* **2004**, *6*, 3958-3968, doi:10.1039/b404889j.
Ingham, T.; Bauer, D.; Sander, R.; Crutzen, P. J.; Crowley, J. N. Kinetics and products of the reactions BrO + DMS and Br + DMS at 298 K. *J. Phys. Chem. A* **1999**, *103*, 7199-7209, doi:10.1021/jp9905979.
IUPAC *J. Phys. Chem. Ref. Data* **1992**, *21*, 1125-1568.
IUPAC: Atmospheric Chemical Kinetic Data Evaluation. Atkinson, R.; Baulch, D. L.; Cox, R. A.; Crowley, J. N.; Hampson, J., R. F.; Hynes, R. G.; Jenkin, M. E.; Kerr, J. A.; Rossi, M. J.; Troe, J., 2004, http://www.iupac-kinetic.ch.cam.ac.uk.
Ivanov, A. V.; Gershenzon, Y. M.; Gratpanche, F.; Devolder, P.; Saverysyn, J.-P. Heterogeneous loss of OH on NaCl and NH_4NO_3 at tropospheric temperatures. *Ann. Geophys.* **1996**, *14*, 659-664, doi:10.1007/s00585-996-0659-5.
Iyer, R. S.; Rogers, P. J.; Rowland, F. S. Thermal rate constant for addition of chlorine atoms to ethylene. *J. Phys. Chem.* **1983**, *87*, 3799-3801, doi:10.1021/j100243a001.
Jaffer, D. H.; Smith, I. W. M. Time-Resolved Measurements on the Relaxation of OH(v = 1) by NO, NO_2 AND O_2. *Faraday Discuss. Chem. Soc.* **1979**, *67*, 212−220, doi:10.1039/dc9796700212.
Jenkin, M. E.; Cox, R. A. Kinetics study of the reactions IO + NO_2 + M → $IONO_2$ + M, IO + IO → products, and I + O_3 → IO + O_2. *J. Phys. Chem.* **1985**, *89*, 192-199, doi:10.1021/j100247a040.
Jensen, D. E.; Jones, G. A. Kinetics of flame inhibition by sodium. *J. Chem. Soc., Faraday Trans. 1* **1982**, *78*, 2843−2850, doi:10.1039/f19827802843.
Jiao, Y.; Dibble, T. S. First kinetic study of the atmospherically important reactions BrHg• + NO_2 and BrHg• + HOO. *Phys. Chem. Chem. Phys.* **2017**, *19*, 1826-1838, doi:10.1039/C6CP06276H.
Johnston, H. S.; Cantrell, C. A.; Calvert, J. G. Unimolecular decomposition of NO_3 to form NO and O_2 and a review of N_2O_5/NO_3 kinetics. *J. Geophys. Res.* **1986**, *91*, 5159-5172, doi:10.1029/JD091iD04p05159.
Johnston, H. S.; Morris, E. D., Jr.; Van den Bogaerde, J. Molecular modulation kinetic spectrometry. ClOO and ClO_2 radicals in the photolysis of chlorine in oxygen. *J. Am. Chem. Soc.* **1969**, *91*, 7712-7727, doi:10.1021/ja50001a036.
Jonah, C. D.; Mulac, W. A.; Zeglinski, P. Rate constants for the reaction of OH + CO, OD + CO, and OH + methane as a function of temperature. *J. Phys. Chem.* **1984**, *88*, 4100-4104, doi:10.1021/j150662a049.
Jowko, A.; Wnorowski, K.; Kowalczyk, J.; Wojciechowski, K. The kinetics of the radical reactions in gaseous chloro- or fluorohydrocarbons. *Rad. Phys. Chem.* **2003**, *67*, 549-554, doi:10.1016/S0969-806X(03)00104-X.
Kaiser, E. W.; Wallington, T. J. Kinetics of the reactions of chlorine atoms with C_2H_4 (k_1) and C_2H_2 (k_2): A determination of $\Delta H_{f,298}°$ for C_2H_3. *J. Phys. Chem.* **1996**, *100*, 4111-4119, doi:10.1021/jp953178u.
Kaiser, E. W. Pressure dependence of the reaction Cl + C_2H_2 over the temperature range 230 to 370 K. *Int. J. Chem. Kinet.* **1992**, *24*, 179-189, doi:10.1002/kin.550240206.
Kaiser, E. W. Pressure dependence of the rate constants for the reactions CH_3 + O_2 and CH_3 + NO from 3 to 10^4 Torr. *J. Phys. Chem.* **1993**, *97*, 11681-11688, doi:10.1021/j100147a022.
Kaiser, E. W. Temperature and pressure dependence of the C_2H_4 yield from the reaction C_2H_5 + O_2. *J. Phys. Chem.* **1995**, *99*, 707-711, doi:10.1021/j100002a039.
Kaiser, E. W.; Lorkovic, I. M.; Wallington, T. J. Pressure dependence of the C_2H_4 yield from the reaction C_2H_5 + O_2. *J. Phys. Chem.* **1990**, *94*, 3352-3354, doi:10.1021/j100371a030.
Kaiser, E. W.; Wallington, T. J. CH_3CO reactions with Cl_2 and O_2: More evidence for HCl elimination from the CH_3CHClO radical. *J. Phys. Chem.* **1995**, *99*, 8669–8672, doi:10.1021/j100021a035.
Kaiser, E. W.; Wallington, T. J. Comment on "Inverse kinetic isotope effect in the reaction of atomic chlorine with C_2H_4 and C_2D_4". *J. Phys. Chem. A* **1998**, *102*, 6054-6055, doi:10.1021/jp980578j.
Kaiser, E. W.; Wallington, T. J.; Andino, J. M. Pressure dependence of the reaction C_2H_5 + O_2. *Chem. Phys. Lett.* **1990**, *168*, 309-313, doi:10.1016/0009-2614(90)85616-K.

Kaiser, E. W.; Wallington, T. J.; Hurley, M. D. Kinetic study of the reaction of chlorine atoms with CF_3I and the reactions of CF_3 radicals with O_2, Cl_2 and NO at 296 K. *Int. J. Chem. Kinet.* **1995**, *27*, 205-218, doi:10.1002/kin.550270302.

Kajimoto, O.; Cvetanovic, R. J. Formation of nitrous oxide in the reaction of $O(^1D_2)$ atoms with nitrogen. *J. Chem. Phys.* **1976**, *64*, 1005-1015, doi:10.1063/1.432308.

Kaltsoyannis , N.; Plane, J. M. C. Quantum chemical calculations on a selection of iodine-containing species (IO, OIO, INO_3, $(IO)_2$, I_2O_3, I_2O_4 and I_2O_5) of importance in the atmosphere. *Phys. Chem. Chem. Phys.* **2008**, *10*, 1723-1733, doi:10.1039/b715687c.

Kaye, J. A. Theoretical analysis of isotope effects on ozone formation in oxygen photochemistry. *J. Geophys. Res.* **1986**, *91*, 7865-7874, doi:10.1029/JD091iD07p07865.

Keiffer, M.; Pilling, M. J.; Smith, M. J. C. Pressure and temperature dependence of the reaction $CH_3 + O_2 + M \rightarrow CH_3O_2 + M$ over the range $334 \leq T/K \leq 582$. *J. Phys. Chem.* **1987**, *91*, 6028-6034, doi:10.1021/j100307a042.

Kennedy, R. C.; Levy, J. B. Bistrifluoromethyl peroxide. II. Kinetics of the decomposition to carbonyl fluoride and trifluoromethyl hypofluorite. *J. Phys. Chem.* **1972**, *76*, 3480-3488, doi:10.1021/j100667a032.

Khalizov, A. F.; Viswanathan, B.; Larregaray, P.; Ariya, P. A. A theoretical study on the reactions of Hg with halogens: Atmospheric implications. *J. Phys. Chem. A* **2003**, *107*, 6360-6365, doi:10.1021/jp0350722.

Kim, P.; MacLean, D. I.; Valence, W. G. ESR spectroscopic studies of the kinetics of the F + NO + M and F_2 + NO reactions. *J. Phys. Chem.* **1980**, *84*, 1806-1810, doi:10.1021/j100451a013.

Kircher, C. C.; Margitan, J. J.; Sander, S. P. Temperature and pressure dependence study of the reaction $NO_2 + NO_3 + M \rightarrow N_2O_5 + M$. *J. Phys. Chem.* **1984**, *88*, 4370-4375, doi:10.1021/j150663a037.

Kirchner, F.; Mayer-Figge, A.; Zabel, F.; Becker, K. H. Thermal stability of peroxynitrates. *Int. J. Chem. Kinet.* **1999**, *31*, 127-144, doi:10.1002/(SICI)1097-4601(1999)31:2<127::AID-KIN6>3.0.CO;2-L.

Klais, O.; Anderson, P. C.; Kurylo, M. J. A reinvestigation of the temperature dependence of the rate constant for the reaction $O + O_2 + M \rightarrow O_3 + M$ (for M = O_2, N_2, and Ar) by the flash photolysis resonance fluorescence technique. *Int. J. Chem. Kinet.* **1980**, *12*, 469-490, doi:10.1002/kin.550120704.

Klein, T.; Barnes, I.; Becker, K. H.; Fink, E. H.; Zabel, F. Pressure dependence of the rate constants for the reactions of C_2H_4 and C_3H_8 with OH radicals at 295 K. *J. Phys. Chem.* **1984**, *88*, 5020-5025, doi:10.1021/j150665a046.

Knepp, A. M.; Meloni, G.; Jusinski, L. E.; Taatjes, C. A.; Cavallotti, C.; Klippenstein, S. J. Theory, measurements, and modeling of OH and HO_2 formation in the reaction of cyclohexyl radicals with O_2. *Phys. Chem. Chem. Phys.* **2007**, *9*, 4315–4331, doi:10.1039/b705934e.

Knyazev, V. D.; Kalinovski, I. J.; Slagle, I. R. Kinetics of the $CH_2CH_2Cl \rightleftarrows C_2H_4 + Cl$ reaction. *J. Phys. Chem. A* **1999**, *103*, 3216-3221, doi:10.1021/jp984207e.

Köppenkastrop, D.; Zabel, F. Thermal decomposition of chlorofluoromethyl peroxynitrates. *Int. J. Chem. Kinet.* **1991**, *23*, 1-15, doi:10.1002/kin.550230102.

Kovács, G.; Zádor, J.; Farkas, E.; Nádasdi, R.; Szilágyi, I.; Dóbé, S.; Bérces, T.; Márta, F.; Lendvay, G. Kinetics and mechanism of the reactions of CH_3CO and $CH_3C(O)CH_2$ radicals with O_2. Low-pressure discharge flow experiments and quantum chemical computations. *Phys. Chem. Chem. Phys.* **2007**, *9*, 4142-4154, doi:10.1039/b706216h.

Kreutter, K. D.; Nicovich, J. M.; Wine, P. H. Kinetics and thermochemistry of the $Br(^2P_{3/2}) + NO_2$ association reaction. *J. Phys. Chem.* **1991**, *95*, 4020-4028, doi:10.1021/j100163a026.

Kreycy, S.; Camy-Peyret, C.; Chipperfield, M. P.; Dorf, M.; Feng, W.; Hossaini, R.; Kritten, L.; B.Werner; Pfeilsticker, K. Atmospheric test of the $J(BrONO_2)/k_{BrO+NO2}$ ratio: implications for total stratospheric Br_y and bromine-mediated ozone loss. *Atmos. Chem. Phys.* **2013**, *13*, 6263-6274, doi:10.5194/acp-13-6263-2013.

Kuo, C. H.; Lee, Y.-P. Kinetics of the reaction OH + C_2H_4 in He, N_2, and O_2 at low pressure. *J. Phys. Chem.* **1991**, *95*, 1253-1257, doi:10.1021/j100156a040.

Kurylo, M. J. Absolute rate constants for the reaction $H + O_2 + M \rightarrow HO_2 + M$ over the temperature range 203-404 K. *J. Phys. Chem.* **1972**, *76*, 3518-3526, doi:10.1021/j100668a002.

Kurylo, M. J.; Ouellette, P. A. Pressure dependence of the rate constant for the reaction $HO_2 + NO_2 + M \rightarrow HO_2NO_2 + M$ (M = N_2, O_2) at 298 K. *J. Phys. Chem.* **1986**, *90*, 441-444, doi:10.1021/j100275a018.

Kurylo, M. J.; Ouellette, P. A. Rate constants for the reaction $HO_2 + NO_2 + N_2 \rightarrow HO_2NO_2 + N_2$: The temperature dependence of the falloff parameters. *J. Phys. Chem.* **1987**, *91*, 3365-3368, doi:10.1021/j100296a052.

Laguna, G. A.; Baughcum, S. L. Real-time detection of methyl radicals by diode laser absorption at 608 cm^{-1}. *Chem. Phys. Lett.* **1982**, *88*, 568-571, doi:10.1016/0009-2614(82)85010-0.

Lai, L.-H.; Hsu, Y.-C.; Lee, Y.-P. The enthalpy change and the detailed rate coefficients of the equilibrium reaction OH + C_2H_2 ⇌ (M) HOC_2H_2 over the temperature range 627-713 K. *J. Chem. Phys.* **1992**, *97*, 3092-3099, doi:10.1063/1.462996.

Laine, P. L.; Sohn, Y. S.; Nicovich, J. M.; McKee, M. L.; Wine, P. H. Kinetics of elementary steps in the reactions of atomic bromine with isoprene and 1,3-butadiene under atmospheric conditions. *J. Phys. Chem. A* **2012**, *116*, 6341-6357, doi:10.1021/jp212127v.

Larin, I. K., D. V. Nevozhai, A. I. Spasskii, and E. M. Trofimova A study of the reaction IO + NO_2 + O_2 → $IONO_2$ + O_2. *Kinetics and Catalysis* **1998**, *39*, 666-672.

Larson, C. W.; Stewart, R. H.; Golden, D. M. Pressure and temperature dependence of reactions proceeding via a bound complex. An approach for combustion and atmospheric chemistry modelers. Application to HO + CO → [HOCO] → H + CO_2. *Int. J. Chem. Kinet.* **1988**, *20*, 27-40, doi:10.1002/kin.550200105.

Laufer, A. H.; Bass, A. M. Rate constants of the combination of methyl radicals with nitric oxide and oxygen. *Int. J. Chem. Kinet.* **1975**, *7*, 639-648, doi:10.1002/kin.550070502.

Lee, F. S. C.; Rowland, F. S. Competitive radiotracer evaluation of relative rate constants at stratospheric temperatures for reactions of ^{38}Cl with CH_4 and C_2H_6 vs. CH_2=CHBr. *J. Phys. Chem.* **1977**, *81*, 86-87, doi:10.1021/j100516a020.

Lee, J. H.; Michael, J. V.; Payne, W. A., Jr.; Stief, L. J. The temperature dependence of the rate constant for Cl + NO + N_2 → NOCl + N_2. *J. Chem. Phys.* **1978**, *68*, 5410-5413, doi:10.1063/1.435716.

Lee, T. J. *Ab initio* characterization of $ClNO_2$, *cis*-ClONO, and *trans*-ClONO. *J. Phys. Chem.* **1994**, *98*, 111-115, doi:10.1021/j100052a019.

Lee, T. J. Characterization of $BrNO_2$, *cis*-BrONO, and *trans*-BrONO. Implications for atmospheric chemistry. *J. Phys. Chem.* **1996**, *100*, 19847-19852, doi:10.1021/jp962605g.

Lee, T. J.; Rice, J. E. FONO: A difficult case for theory and experiment. *J. Chem. Phys.* **1992**, *97*, 4223-4232, doi:10.1063/1.463925.

Lee, T. J.; Rohlfing, C. M.; Rice, J. E. An extensive *ab initio* study of the structures, vibrational spectra, quadratic force fields, and relative energetics of three isomers of Cl_2O_2. *J. Chem. Phys.* **1992**, *97*, 6593-6605, doi:10.1063/1.463663.

Lee, Y.-P.; Stimpfle, R. M.; Perry, R. A.; Mucha, J. A.; Evenson, K. M.; Jennings, D. A.; Howard, C. J. Laser magnetic resonance spectroscopy of ClO and kinetic studies of the reactions of ClO with NO and NO_2. *Int. J. Chem. Kinet.* **1982**, *14*, 711-732, doi:10.1002/kin.550140612.

Lee, Y.-Y.; Kao, W. C.; Lee, Y.-P. Kinetics of the reaction OH + SO_2 in He, N_2, and O_2 at low pressure. *J. Phys. Chem.* **1990**, *94*, 4535-4540, doi:10.1021/j100374a035.

Lesar, A.; Prebil, S.; Mühlhaüser, M.; Hodošcek, M. Conformational potential energy surface of BrOONO. *Chem. Phys. Lett.* **2002**, *368*, 399-407, doi:10.1016/S0009-2614(02)01888-2.

Leu, M. T. Rate constants for the reaction of OH with SO_2 at low pressure. *J. Phys. Chem.* **1982**, *86*, 4558-4562, doi:10.1021/j100220a021.

Leu, M. T. Kinetics of the reaction Cl + NO_2 + M. *Int. J. Chem. Kinet.* **1984**, *16*, 1311-1320, doi:10.1002/kin.550161103.

Li, W.-K., and M. L. McKee Theoretical study of OH and H_2O addition to SO_2. *J. Phys. Chem. A* **1997**, *101*, 9778-9782, doi:10.1021/jp972389r.

Li, Z.; Francisco, J. S. Dissociation dynamics of perhaloalkoxy radicals. *J. Am. Chem. Soc.* **1989**, *111*, 5660-5667, doi:10.1021/ja00197a024.

Lin, C. L.; Leu, M. T. Temperature and third-body dependence of the rate constant for the reaction O + O_2 + M → O_3 + M. *Int. J. Chem. Kinet.* **1982**, *14*, 417-434, doi:10.1002/kin.550140408.

Liu, A.; Mulac, W. A.; Jonah, C. D. Temperature dependence of the rate constants of the reactions of OH radicals with C_2H_2 and C_2D_2 at 1 atm in Ar and from 333 to 1273 K. *J. Phys. Chem.* **1988**, *92*, 5942-5945, doi:10.1021/j100332a020.

Liu, J. Y.; Barker, J. R. On the chaperon mechanism: Application to ClO + ClO (+N_2) → ClOOCl (+N_2). *J. Phys. Chem. A* **2007**, *111*, 8689-8698, doi:10.1021/jp072978p.

Liu, Y.; Sander, S. P. Rate constants for the OH + CO reaction at low temperatures. *J. Phys. Chem. A.* **2015**, *119*, 10060-10066, doi:10.1021/acs.jpca.5b07220.

Lloyd, A. C.; Darnall, K. R.; Winer, A. M.; Pitts, J. N., Jr. Relative rate constants for reaction of the hydroxyl radical with a series of alkanes, alkenes, and aromatic hydrocarbons. *J. Phys. Chem.* **1976**, *80*, 789-794, doi:10.1021/j100549a003.

Loison, J.-C.; Daranlot, J.; Bergeat, A.; Caralp, F.; Mereau, R.; Hickson, K. M. Gas-phase kinetics of hydroxyl radical reactions with C_3H_6 and C_4H_8: Product branching ratios and OH addition site-specificity. *J. Phys. Chem. A* **2010**, *114*, 13326-13336, doi:10.1021/jp107217.

Long, B.; Bao, J. L.; Truhlar, D. G. Reaction of SO_2 with OH in the atmosphere. *Phys. Chem. Chem. Phys.* **2017**, *19*, 8091-8100, doi:10.1039/c7cp00497d.

Lovejoy, E. R. Kinetics and thermodynamics of the gas phase reaction $SO_3 + NH_3 + N_2 \leftrightarrow H_3NSO_3 + N_2$. *J. Phys. Chem. A* **1997**, *101*, 4950-4953, doi:10.1021/jp970652i.

Lovejoy, E. R.; Hanson, D. R. Kinetics and products of the reaction $SO_3 + NH_3 + N_2$. *J. Phys. Chem.* **1996**, *100*, 4459-4465, doi:10.1021/jp952404x.

Luther, K.; Oum, K.; Troe, J. Study of the recombination reaction $CCl_3 + O_2$ (+M) → CCl_3O_2 (+M) at pressures of 2-900 bar and temperatures of 260-346 K. *J. Phys. Chem. A* **2001**, *105*, 5535-5541, doi:10.1021/jp003844d.

Lyman, J.; Holland, R. Oxygen fluoride chemical kinetics. *J. Phys. Chem.* **1988**, *92*, 7232-7241, doi:10.1021/j100337a015.

Maguin, F.; Laverdet, G.; Le Bras, G.; Poulet, G. Kinetic study of the reactions IO + HO_2 and IO + NO_2 at 298 K. *J. Phys. Chem.* **1992**, *96*, 1775-1780, doi:10.1021/j100183a052.

Maranzana, A.; Barker, J. R.; Tonachini, G. Master equation simulations of competing unimolecular and bimolecular reactions: Application to OH production in the reaction of acetyl radical with O_2. *Phys. Chem. Chem. Phys.* **2007**, *9*, 4129 - 4141, doi:10.1039/b705116f.

Margitan, J. J.; Watson, R. T. Kinetics of the reaction of hydroxyl radicals with nitric acid. *J. Phys. Chem.* **1982**, *86*, 3819-3824, doi:10.1021/j100216a022.

Maric, D.; Burrows, J. P. Formation of N_2O in the photolysis/photoexciation of NO, NO_2 and air. *J. Photochem. Photobiol. A: Chem.* **1992**, *66*, 291-312, doi:10.1016/1010-6030(92)80002-D.

Maricq, M. M.; Szente, J. J.; Kaiser, E. W. A diode laser study of the Cl + C_2H_5 reaction. *J. Phys. Chem.* **1993**, *97*, 7970-7977, doi:10.1021/j100132a028.

Marshall, P. Computational studies of the thermochemistry of the atmospheric iodine reservoirs HOI and $IONO_2$. *Advances in Quantum Chemistry* **2008**, 159-175.

Marshall, P.; Narayan, A. S.; Fontijn, A. Kinetic and thermochemical studies of the recombination reaction Na + O_2 + N_2 from 590 to 1515 K by a modified high-temperature photochemistry technique. *J. Phys. Chem.* **1990**, *94*, 2998-3004, doi:10.1021/j100370a049.

Martin, D.; Jourdain, J. L.; Le Bras, G. Kinetic study for the reactions of OH radicals with dimethylsulfide, diethylsulfide, tetrahydrothiophene, and thiophene. *Int. J. Chem. Kinet.* **1985**, *17*, 1247-1261, doi:10.1002/kin.550171202.

Martinez, E.; Albaladejo, J.; Jiménez, E.; Notario, A.; Mera, Y. D. d. Temperature dependence of the limiting low- and high-pressure rate constants for the CH_3O + NO_2 + He reaction over the 250-390 K temperature range. *Chem. Phys. Lett.* **2000**, *329*, 191-199, doi:10.1016/S0009-2614(00)01012-5.

Masaki, A.; Tsunashima, N.; Washida, N. Rate constant for the reaction of CH_3O_2 with NO. *Chem. Phys. Lett.* **1994**, *218*, 523-528, doi:10.1016/0009-2614(94)00024-7.

Maurer, T., I. Barnes, and K. H. Becker FT-IR kinetic and product study of the Br-initiated oxidation of dimethyl sulfide. *Int. J. Chem. Kinet.* **1999**, *31*, 883-893, doi:10.1002/(SICI)1097-4601(1999)31:12<883::AID-KIN7>3.0.CO;2-V.

McCabe, D. C.; Gierczak, T.; Talukdar, R. K.; Ravishankara, A. R. Kinetics of the reaction OH + CO under atmospheric conditions. *Geophys. Res. Lett.* **2001**, *28*, 3135-3138, doi:10.1029/2000GL012719.

McCaulley, J. A.; Anderson, S. M.; Jeffries, J. B.; Kaufman, F. Kinetics of the reaction of CH_3O with NO_2. *Chem. Phys. Lett.* **1985**, *115*, 180-186, doi:10.1016/0009-2614(85)80675-8.

McCaulley, J. A.; Moyle, A. M.; Golde, M. F.; Anderson, S. M.; Kaufman, F. Kinetics of the reactions of CH_3O and CD_3O with NO. *J. Chem Soc. Farad. Trans.* **1990**, *86*, 4001-4009, doi:10.1039/ft9908604001.

McDade, C. E.; Lenhardt, T. M.; Bayes, K. D. The rate of reaction of acetyl and benzoyl radicals with O_2. *J. Photochem.* **1982**, *20*, 1-7, doi:10.1016/0047-2670(82)80042-7.

Medeiros, D. J.; Blitz, M. A.; Seakins, P. W. Exploring the features on the OH + SO_2 potential energy surface using theory and testing its accuracy by comparison to experimental data. *Phys. Chem. Chem. Phys.* **2018**, *20*, 8984-8990, doi:10.1039/c8cp00091c.

Mellouki, A.; Laverdet, G.; Jourdain, J. L.; Poulet, G. Kinetics of the reactions Br + NO_2 + M and I + NO_2 + M. *Int. J. Chem. Kinet.* **1989**, *21*, 1161-1172, doi:10.1002/kin.550211209.

Michael, J. V.; Keil, D. G.; Klemm, R. B. Rate constants for the reaction of hydroxyl radicals with acetaldehyde from 244-528 K. *J. Chem. Phys.* **1985**, *83* 1630-1636, doi:10.1063/1.449400.

Michael, J. V.; Nava, D. F.; Borkowski, R. P.; Payne, W. A.; Stief, L. J. Pressure dependence of the absolute rate constant for the reaction OH + C_2H_2 from 228 to 413 K. *J. Chem. Phys.* **1980**, *73*, 6108-6116, doi:10.1063/1.440147.

Michael, J. V.; Su, M.-C.; Sutherland, J. W.; Carroll, J. J.; Wagner, A. F. Rate constants for H + O_2 + M → HO_2 + M in seven bath gases. *J. Phys. Chem. A* **2002**, *106*, 5297-5313, doi:10.1021/jp020229w.

Miller, J. A., and S. J. Klippenstein The reaction between ethyl and molecular oxygen II: Further analysis. *Int. J. Chem. Kinet.* **2001**, *33*, 654-668, doi:10.1002/kin.1063.

Mineshos, G.; Glavas, S. Thermal decomposition of peroxypropionyl nitrate - Kinetics of the formation of nitrogenous products. *React. Kinet. Catal. Lett.* **1991**, *45*, 305-312, doi:10.1007/BF02070443.

Miriyala, V. M.; Bhasi, P.; Nhlabatsi, Z. P.; Sitha, S. Formation of a pre-reaction hydrogen-bonded complex and its significance in the potential energy surface of the OH + SO_2→ $HOSO_2$ reaction: A computational study. *J. Theor. Comput. Chem.* **2017**, *16*, 1750046, doi:10.1142/S0219633617500468.

Miyoshi, A.; Matsui, H.; Washida, N. Detection and reactions of the HOCO radical in gas phase. *J. Chem. Phys.* **1994**, *100*, 3532-3539, doi:10.1063/1.466395.

Molina, M. J.; Molina, L. T.; Ishiwata, T. Kinetics of the ClO + NO_2 + M reaction. *J. Phys. Chem.* **1980**, *84*, 3100-3104, doi:10.1021/j100460a026.

Mollner, A. K.; Valluvadasan, S.; Feng, L.; Sprague, M. K.; Okumura, M.; Milligan, D. B.; Bloss, W. J.; Sander, S. P.; Martien, P. T.; Harley, R. A.; McCoy, A. B.; Carter, W. P. L. Rate of gas phase association of hydroxyl radical and nitrogen dioxide. *Science* **2010**, *330*, 646-649, doi:10.1126/science.1193030.

Moore, S. B.; Carr, R. W. Kinetics of the reactions of CF_2ClO_2 radicals with nitrogen dioxide. *J. Phys. Chem.* **1990**, *94*, 1393-1400, doi:10.1021/j100367a036.

Morley, C.; Smith, I. W. M. Rate measurements of reactions of OH by resonance absorption .1. Reactions of OH with NO_2 and NO. *J. Chem. Soc. Faraday Trans. 2* **1972**, *68*, 1016-1030, doi:10.1039/f29726801016.

Morozov, I. I.; Nielsen, C.; Morozova, O. S.; Vasiliev, E. S.; Loukhovitskaya, E. E. Reactios of chloroethenes with atomic chlorine in air at atmospheric pressure. *Russ. Chem. Bull., Int. Edition* **2010**, *59*, 754-760.

Morris, E. D., Jr.; Niki, H. Reactivity of hydroxyl radicals with olefins. *J. Phys. Chem.* **1971**, *75*, 3640–3641, doi:10.1021/j100692a031.

Morris, E. D., Jr.; Stedman, D. H.; Niki, H. Mass spectrometric study of the reactions of the hydroxyl radical with ethylene, propylene, and acetaldehyde in a discharge-flow system. *J. Am. Chem. Soc.* **1971**, *93*, 3570-3572, doi:10.1021/ja00744a004.

Müller, M. A.; Yetter, R. A.; Dryer, F. L. Kinetic modeling of the CO/ $H_2O/O_2/NO/SO_2$ system: Implications for high-pressure fall-off in the SO_2 + O(+M) = SO_3(+M) reaction. *Int. J. Chem. Kinet.* **2000**, *32*, 317-339, doi:10.1002/(SICI)1097-4601(2000)32:6<317::AID-KIN1>3.0.CO;2-L.

Munk, J.; Pagsberg, P.; Ratajczak, E.; Sillesen, A. Spectrokinetic studies of ethyl and ethylperoxy radicals. *J. Phys. Chem.* **1986**, *90*, 2752-2757, doi:10.1021/j100403a038.

Murrells, T. P.; Lovejoy, E. R.; Ravishankara, A. R. Oxidation of CS_2 by reaction with OH. 1. Equilibrium constant for the reaction OH + CS_2 ⇄ CS_2OH and the kinetics of the CS_2OH + O_2 reaction. *J. Phys. Chem.* **1990**, *94*, 2381-2386, doi:10.1021/j100369a036.

Naidoo, J., A. Goumri, and P. Marshall A kinetic study of the reaction of atomic oxygen with SO_2. *Proc. Combust. Inst.* **2005**, *30*, 1219-1225, doi:10.1016/j.proci.2004.08.214.

Nakano, Y., M. Goto, S. Hashimoto, M. Kawasaki, and T. J. Wallington Cavity ring-down spectroscopic study of the reactions of Br atoms and BrO radicals with dimethyl sulfide. *J. Phys. Chem. A* **2001**, *105*, 11045-11050, doi:10.1021/jp012326f.

Nakano, Y.; Sadamori, K.; Hosho, Y.; Ishiwata, T. Study of the pressure dependence of the rate constant of the reaction of NO_3 with NO_2. *Chem. Phys. Lett.* **2011**, *513*, 27-30, doi:10.1016/j.cplett.2011.07.060.

Nguyen, T. L.; Xue, B.; Weston, R. E., Jr.; Barker, J. R.; Stanton, J. F. Reaction of HO with CO: Tunneling is indeed important *J. Phys. Chem. Lett.* **2012**, *3*, 1549-1553, doi:10.1021/jz300443a.

Nicholas, J. E.; Norrish, R. G. W. Some reactions in the chlorine and oxygen system studied by flash photolysis. *Proc. Roy. Soc. A* **1968**, *307*, 391-397, doi:10.1098/rspa.1968.0197.

Nickolaisen, S. L.; Friedl, R. R.; Sander, S. P. Kinetics and mechanism of the ClO + ClO reaction: Pressure and temperature dependences of the bimolecular and termolecular channels and thermal decomposition of chlorine peroxide, ClOOCl. *J. Phys. Chem.* **1994**, *98*, 155-169, doi:10.1021/j100052a027.

Nicovich, J. M.; Kreutter, K. D.; Shackelford, C. J.; Wine, P. H. Thermochemistry and kinetics of the Cl + O_2 association reaction. *Chem. Phys. Lett.* **1991**, *179*, 367-373, doi:10.1016/0009-2614(91)85168-V.

Nicovich, J. M.; Kreutter, K. D.; Wine, P. H. Kinetics and thermochemistry of ClCO formation from the Cl + CO association reaction. *J. Chem. Phys.* **1990**, *92*, 3539-3544, doi:10.1063/1.457862.

Nicovich, J. M.; Wang, L.; McKee, M. L.; Wine, P. H. Kinetics and thermochemistry of the $Cl(^2P_J) + C_2Cl_4$ association reaction. *J. Phys. Chem.* **1996**, *100*, 680-688, doi:10.1021/jp952396k.

Nicovich, J. M.; Wine, P. H. Kinetics of the reactions of $O(^3P)$ and $Cl(^2P)$ with HBr and Br_2. *Int. J. Chem. Kinet.* **1990**, *22*, 379-397, doi:10.1002/kin.550220406.

Nielsen, O. J.; Jørgensen, O.; Donlon, M.; Sidebottom, H. W.; O'Farrell, D. J.; Treacy, J. Rate constants for the gas-phase reactions of OH radicals with nitroethene, 3-nitropropene and 1-nitrocyclohexene at 298 K and 1 atm. *Chem. Phys. Lett.* **1990**, *168*, 319-323, doi:10.1016/0009-2614(90)85618-M.

Niki, H.; Maker, P. D.; Savage, C. M.; Breitenbach, L. P. Fourier transform IR spectroscopic observation of chlorine nitrite, ClONO, formed via $Cl + NO_2(+M) \rightarrow ClONO(+M)$. *Chem. Phys. Lett.* **1978**, *59*, 78-79, doi:10.1016/0009-2614(78)85618-8.

Niki, H.; Maker, P. D.; Savage, C. M.; Breitenbach, L. P. Fourier transform infrared spectroscopic study of the kinetics for the HO radical reaction of $^{13}C^{16}O$ and $^{12}C^{18}O$. *J. Phys. Chem.* **1984**, *88*, 2116-2119, doi:10.1021/j150654a034.

Nip, W. S.; Paraskevopoulos, G. Rates of OH radical reactions. VI. Reactions with C_3H_6, 1-C_4H_8 and 1-C_5H_{10} at 297 K. *J. Chem. Phys.* **1979**, *71*, 2170-2174, doi:10.1063/1.438599.

Nizkorodov, S. A.; Wennberg, P. O. First spectroscopic observation of gas-phase HOONO. *J. Phys. Chem. A* **2002**, *106*, 855-859, doi:10.1021/jp013598l.

Nottingham, W. C.; Rudolph, R. N.; Andrews, K. P.; Moore, J. H.; Tossell, J. A. Flowtube reactor study of the association reactions of $CHCl_2$ and CCl_3 with O_2 at low pressure. *Int. J. Chem. Kinet.* **1994**, *26*, 749-756, doi:10.1002/kin.550260709.

Oguchi, T.; Miyoshi, A.; Koshi, M.; Matsui, H.; Washida, N. Kinetic study on reactions of 1- and 2-methylvinoxy radicals with O_2. *J. Phys. Chem. A* **2000**, *105*, 378-382, doi:10.1021/jp001826q.

Ohmori, K.; Yamasaki, K.; Matsui, H. Pressure dependence of the rate constant for the reaction $CH_3O + NO$. *Bull. Chem. Soc. Jpn.* **1993**, *66*, 51-56, doi:10.1246/bcsj.66.51.

Ohta, T. Rate constants for the reactions of diolefins with OH radicals in the gas phase. Estimate of the rate constants from those for monoolefins. *J. Phys. Chem.* **1983**, *87*, 1209-1213, doi:10.1021/j100230a023.

Ohta, T. Rate constants for the reactions of OH radicals with alkyl substituted olefins. *Int. J. Chem. Kinet.* **1984**, *16*, 879-886, doi:10.1002/kin.550160708.

Ongstad, A. P.; Birks, J. W. Studies of reactions of importance in the stratosphere. VI. Temperature dependence of the reactions $O + NO_2 \rightarrow NO + O_2$ and $O + ClO \rightarrow Cl + O_2$. *J. Chem. Phys.* **1986**, *85*, 3359-3368, doi:10.1063/1.450957.

Orlando, J. J.; Burkholder, J. B. Identification of BrONO as the major product in the gas-phase reaction of Br with NO_2. *J. Phys. Chem. A* **2000**, *104*, 2048-2053, doi:10.1021/jp993713g.

Orlando, J. J.; Tyndall, G. S. Rate coefficients for the thermal decomposition of $BrONO_2$ and the heat of formation of $BrONO_2$. *J. Phys. Chem.* **1996**, *100*, 19398-19405, doi:10.1021/jp9620274.

Orlando, J. J.; Tyndall, G. S.; Calvert, J. G. Thermal decomposition pathways for peroxy-acetyl nitrate (PAN): Implications for atmospheric methyl nitrate levels. *Atmos. Environ.* **1992**, *26A*, 3111-3118, doi:10.1016/0960-1686(92)90468-Z.

Orlando, J. J.; Tyndall, G. S.; Cantrell, C. A.; Calvert, J. G. Temperature and pressure dependence of the rate coefficient for the reaction $NO_3 + NO_2 \rightarrow N_2O_5 + N_2$. *J. Chem. Soc. Faraday Trans.* **1991**, *87*, 2345-2349, doi:10.1039/ft9918702345.

Overend, R. P.; Paraskevopoulos, G. The question of a pressure effect in the reaction OH + CO at room temperature. *Chem. Phys. Lett.* **1977**, *49*, 109-111, doi:10.1016/0009-2614(77)80452-1.

Overend, R. P.; Paraskevopoulos, G. Rates of OH radical reactions. III. The reaction $OH + C_2H_4 + M$ at 296 °K. *J. Chem. Phys.* **1977**, *67*, 674-679, doi:10.1063/1.434871.

Overend, R. P.; Paraskevopoulos, G.; Black, C. Rates of OH radical reactions. II. The combination reaction OH + NO + M. *J. Chem. Phys.* **1976**, *64*, 4149-4154, doi:10.1063/1.431984.

Pagsberg, P.; Bjergbakke, E.; Ratajczak, E.; Sillesen, A. Kinetics of the gas phase reaction $OH + NO(+M) \rightarrow HONO(+M)$ and the determination of the UV absorption cross sections of HONO. *Chem. Phys. Lett.* **1997**, *272*, 383-390, doi:10.1016/S0009-2614(97)00576-9.

Pagsberg, P.; Ratajczak, E.; Sillesen, A.; Jodkowski, J. T. Spectrokinetic studies of the gas-phase equilibrium $F + O_2 \rightleftharpoons FO_2$ between 295 and 359 K. *Chem. Phys. Lett.* **1987**, *141*, 88-94, doi:10.1016/0009-2614(87)80097-0.

Pagsberg, P.; Sillesen, A.; Jodkowski, J. T.; Ratajczak, E. Kinetics of the $F + NO_2 + M \rightarrow FNO_2 + M$ reaction studied by pulse radiolysis combined with time-resolved IR and UV spectroscopy. *Chem. Phys. Lett.* **1996**, *252*, 165-171, doi:10.1016/S0009-2614(96)00161-3.

Pagsberg, P.; Sillesen, A.; Jodkowski, J. T.; Ratajczak, E. Kinetics of the reaction F + NO + M → FNO + M studied by pulse radiolysis combined with time-resolved IR and UV spectroscopy. *Chem. Phys. Lett.* **1996**, *249*, 358-364, doi:10.1016/0009-2614(95)01441-1.

Pagsberg, P.; Sztuba, B.; Ratajczak, E.; Sillesen, A. Spectrokinetic studies of the gas phase reactions NH_2 + NO_x initiated by pulse radiolysis. *Acta Chem. Scand.* **1991**, *45*, 329-334, doi:10.3891/acta.chem.scand.45-0329.

Papadimitriou, V. C.; Karafas, E. S.; Gierczak, T.; Burkholder, J. B. CH_3CO + O_2 + M (M = He, N_2) reaction rate coefficient measurements and implications for the OH radical product yield. *J. Phys. Chem. A* **2015**, *119*, 7481–7497, doi:10.1021/acs.jpca.5b00762.

Papayannis, D. K.; Kosmas, A. M. Quantum mechanical characterization of (INO_3) isomers. *Chem. Phys. Lett.* **2004**, *398*, 75-81, doi:10.1016/j.cplett.2004.09.019.

Paraskevopoulos, G.; Irwin, R. S. XV Informal Conference on Photochemistry, 1982, Stanford, CA.

Paraskevopoulos, G.; Irwin, R. S. The pressure dependence of the rate constant of the reaction of OH radicals with CO. *J. Chem. Phys.* **1984**, *80*, 259-266, doi:10.1063/1.446488.

Paraskevopoulos, G.; Singleton, D. L.; Irwin, R. S. Rates of OH radical reactions. The reaction OH + SO_2 + N_2. *Chem. Phys. Lett.* **1983**, *100*, 83-87, doi:10.1016/0009-2614(83)87267-4.

Parr, A. D.; Wayne, R. P.; Hayman, G. D.; Jenkin, M. E.; Cox, R. A. The pressure dependence of the reaction between ClO and OClO at 226 K. *Geophys. Res. Lett.* **1990**, *17*, 2357-2360, doi:10.1029/GL017i013p02357.

Parthiban, P.; Lee, T. Ab initio investigation of the atmospheric molecule bromine nitrate: Equilibrium structure, vibrational spectrum, and heat of formation. *J. Chem. Phys.* **1998**, *109*, 525-530, doi:10.1063/1.476589.

Parthiban, S., T. J. Lee, S. Guha, and J. S. Francisco Theoretical study of chlorine nitrates: Implications for stratospheric chlorine chemistry. *J. Am. Chem. Soc.* **2003**, *125*, 10446-10458, doi:10.1021/ja010297g.

Pastrana, A. V.; Carr, R. W., Jr. Kinetics of the reaction of hydroxyl radicals with ethylene, propylene, 1-butene, and trans-2-butene. *J. Phys. Chem.* **1975**, *79*, 765–770, doi:10.1021/j100575a001.

Patrick, R.; Golden, D. M. Third-order rate constants of atmospheric importance. *Int. J. Chem. Kinet.* **1983**, *15*, 1189-1227, doi:10.1002/kin.550151107.

Paulson, S. E.; Orlando, J. J.; Tyndall, G. S.; Calvert, J. G. Rate coefficients for the reactions of O(^{3}P) with selected biogenic hydrocarbons. *Int. J. Chem. Kinet.* **1995**, *27*, 997-1008, doi:10.1002/kin.550271005

Peeters, J.; Boullart, W.; Pultau, V.; Vandenberk, S.; Vereecken, L. Structure−activity relationship for the addition of OH to (poly)alkenes: Site-specific and total rate constants. *J. Phys. Chem. A* **2007**, *111*, 1618–1631, doi:10.1021/jp066973o.

Percival, C. J.; Smith, G. D.; Molina, L. T.; Molina, M. J. Temperature and pressure dependence of the rate constant for the ClO + NO_2 reaction. *J. Phys. Chem. A* **1997**, *101*, 8830-8833, doi:10.1021/jp971907v.

Percival, D. T.; Raventos-Duran, A.; Bacak, A. B. In *International Gas Kinetics Symposium* Bristol, UK, 2004.

Perry, R. A.; Atkinson, R.; Pitts, J. N., Jr. Kinetics of the reactions of OH radicals with C_2H_2 and CO. *J. Chem. Phys.* **1977**, *67*, 5577-5584, doi:10.1063/1.434755.

Perry, R. A.; Williamson, D. Pressure and temperature dependence of the OH radical reaction with acetylene. *Chem. Phys. Lett.* **1982**, *93*, 331-334, doi:10.1016/0009-2614(82)83703-2.

Phillips, L. F. Pressure dependence of the rate of reaction of OH with HCN. *Chem. Phys. Lett.* **1978**, *57*, 538-539, doi:10.1016/0009-2614(78)85316-0.

Phillips, L. F. Rate of reaction of OH with HCN between 298 K and 563 K. *Aust. J. Chem.* **1979**, *32*, 2571-2577, doi:10.1071/CH9792571.

Pilling, M. J.; Smith, M. J. C. A laser flash photolysis study of the reaction CH_3 + O_2 → CH_3O_2 at 298 K. *J. Phys. Chem.* **1985**, *89*, 4713-4720, doi:10.1021/j100268a014.

Pirraglia, A. N.; Michael, J. V.; Sutherland, J. W.; Klemm, R. B. A flash photolysis-shock tube kinetic study of the H atom reaction with O_2: H + O_2 ⇌ OH + O (962 K ≤ T ≤ 1705 K) and H + O_2 + Ar → HO_2 + Ar (746 K ≤ T ≤ 987 K). *J. Phys. Chem.* **1989**, *93*, 282-291, doi:10.1021/j100338a058.

Plane, J. M. C.; Rajasekhar, B. Kinetic study of the reactions Na + O_2 + N_2 and Na + N_2O over an extended temperature range. *J. Phys. Chem.* **1989**, *93*, 3135-3140, doi:10.1021/j100345a051.

Plumb, I. C.; Ryan, K. R. Kinetic studies of the reactios of C_2H_5 with O_2 at 295 K. *Int. J. Chem. Kinet.* **1981**, *13*, 1011-1028, doi:10.1002/kin.550131003.

Plumb, I. C.; Ryan, K. R. Kinetics of the reactions of CH_3 with O(^{3}P) and O_2 at 295 K. *Int. J. Chem. Kinet.* **1982**, *14*, 861-874, doi:10.1002/kin.550140806.

Pollack, I. B., I. M. Konen, E. X. J. Li, and M. I. Lester Spectroscopic characterization of HOONO and its binding energy via infrared action spectroscopy. *J. Chem. Phys.* **2003**, *119*, 9981-9984, doi:10.1063/1.1624246.

Poulet, G.; Barassin, J.; Le Bras, G.; Combourieu, J. Étude cinetique de la réaction du chlore atomique avec l'acétylène. *Bull. Soc. Chim. Fr.* **1973**, *1*, 1-6.

Pratt, G. L.; Wood, S. W. Kinetics of the reaction of methyl radicals with oxygen. *J. Chem. Soc. Faraday Trans. 1* **1984**, *80*, 3419-3427, doi:10.1039/f19848003419.

Ravishankara, A. R.; Eisele, F. L.; Wine, P. H. Pulsed laser photolysis-long path laser absorption kinetics study of the reaction of methylperoxy radicals with NO_2. *J. Chem. Phys.* **1980**, *73*, 3743-3749, doi:10.1063/1.440604.

Ravishankara, A. R.; Smith, G. J.; Davis, D. D. A kinetics study of the reaction of Cl with NO_2. *Int. J. Chem. Kinet.* **1988**, *20*, 811-814, doi:10.1002/kin.550201005.

Ravishankara, A. R.; Thompson, R. L. Kinetic study of the reaction of OH with CO from 250 to 1040 K. *Chem. Phys. Lett.* **1983**, *99*, 377-381, doi:10.1016/0009-2614(83)80158-4.

Ravishankara, A. R.; Wagner, S.; Fischer, S.; Smith, G.; Schiff, R.; Watson, R. T.; Tesi, G.; Davis, D. D. A kinetics study of the reactions of OH with several aromatic and olefinic compounds. *Int. J. Chem. Kinet.* **1978**, *10*, 783–804, doi:10.1002/kin.550100802.

Rawlins, W. T.; Caledonia, G. E.; Armstrong, R. A. Dynamics of vibrationally excited ozone formed by three-body recombination. II. Kinetics and mechanism. *J. Chem. Phys.* **1987**, *87*, 5209-5213 doi:10.1063/1.453689.

Rayez, M. T.; Destriau, M. Theoretical study of thermal dissociation and recombination reacitons of $XONO_2$ (X=F, Cl, Br, or I). *Chem. Phys. Lett.* **1993**, *206*, 278-284, doi:10.1016/0009-2614(93)85552-Y.

Resende, S. M.; Almeida, W. B. D. Theoretical study of the atmospheric reaction between dimethyl sulfide and chlorine atoms. *J. Phys. Chem. A* **1997**, *101*, 9738-9744, doi:10.1021/jp971885c.

Resende, S. M.; De Alemeida, W. B. Mechanism of the atmospheric reaction between the radical CH_3SCH_2 and O_2. *J. Phys. Chem. A* **1999**, *103*, 4191-4195, doi:10.1021/jp983524i.

Roberts, J. M.; Bertman, S. B. The thermal decomposition of peroxyacetic nitric anhydride (PAN) and peroxymethacrylic nitric anhydride (MPAN). *Int. J. Chem. Kinet.* **1992**, *24*, 297-307, doi:10.1002/kin.550240307.

Rogers, J. D. Rate constant measurements for the reaction of the hydroxyl radical with cyclohexene, cyclopentene, and glutaraldehyde. *Environ. Sci. Technol.* **1989**, *23*, 177-181, doi:10.1021/es00179a006.

Romero, M. T. B.; Blitz, M. A.; Heard, D. E.; Pilling, M. J.; Price, B.; Seakins, P. W. OH formation from the $C_2H_5CO + O_2$ reaction: An experimental marker for the propionyl radical. *Chem. Phys. Lett.* **2005**, *408*, 232-236, doi:10.1016/j.cplett.2005.04.018.

Russell, A. G.; Cass, G. R.; Seinfeld, J. H. On some aspects of nighttime atmospheric chemistry. *Environ. Sci. Technol.* **1986**, *20*, 1167-1172, doi:10.1021/es00153a013.

Russell, J. J.; Setula, J. A.; Gutman, D.; Danis, F.; F.Caralp; Lightfoot, P. D.; Lesclaux, R.; Melius, C. F.; Senkan, S. M. Kinetics and thermochemistry of the equilibrium $CCl_3 + O_2 \leftrightarrow CCl_3O_2$. *J. Phys. Chem.* **1990**, *94*, 3277-3283, doi:10.1021/j100371a012.

Ryan, K. R.; Plumb, I. C. Kinetics of the reactions of CF_3 with $O(^3P)$ and O_2 at 295 K. *J. Phys. Chem.* **1982**, *86*, 4678-4683, doi:10.1021/j100221a008.

Ryan, K. R.; Plumb, I. C. Kinetics of the reactions of CCl_3 with O and O_2 and of CCl_3O_2 with NO at 295 K. *Int. J. Chem. Kinet.* **1984**, *16*, 591-602, doi:10.1002/kin.550160508.

Salta, Z.; Kosmas, A. M.; Lesar, A. atComputational investigation of the peroxy radicals $CH_3S(O)(n)OO$ and the peroxynitrates $CH_3S(O)(n)OONO_2$ (n=0, 1, 2). *Comput. Theo. Chem.* **2012**, *1001*, 67-76, doi:10.1016/j.comptc.2012.10.007.

Sander, S. P.; Finlayson-Pitts, B. J.; Friedl, R. R.; Golden, D. M.; Huie, R. E.; Kolb, C. E.; Kurylo, M. J.; Molina, M. J.; Moortgat, G. K.; Orkin, V. L.; Ravishankara, A. R. Chemical Kinetics and Photochemical Data for Use in Atmospheric Studies, Evaluation Number 14, Jet Propulsion Laboratory Pasadena, JPL Publication 02-25, 2002, http:\\jpldataeval.jpl.nasa.gov.

Sander, S. P.; Friedl, R. P.; Yung, Y. L. Role of the ClO dimer in polar stratospheric chemistry; rate of formation and implications for ozone loss. *Science* **1989**, *245*, 1095-1098, doi:10.1126/science.245.4922.1095.

Sander, S. P.; Peterson, M. Kinetics of the reaction $HO_2 + NO_2 + M \rightarrow HO_2NO_2 + M$. *J. Phys. Chem.* **1984**, *88*, 1566-1571, doi:10.1021/j150652a025.

Sander, S. P.; Ray, G. W.; Watson, R. T. Kinetics study of the pressure dependence of the $BrO + NO_2$ reaction at 298 K. *J. Phys. Chem.* **1981**, *85*, 199-210, doi:10.1021/j150602a018.

Sander, S. P.; Watson, R. T. Kinetic studies of the reactions of CH_3O_2 with NO, NO_2, and CH_3O_2 at 298 K. *J. Phys. Chem.* **1980**, *84*, 1664-1674, doi:10.1021/j100450a002.
Savarino, J.; Thiemens, M. Mass-independent oxygen isotope (^{16}O, ^{17}O, ^{18}O) fractionation found in H_x, O_x reactions. *J. Phys. Chem. A* **1999**, *103*, 9221-9229, doi:10.1021/jp991221y.
Sayin, H.; McKee, M. L. Theoretical study of the mechanism of NO_2 production from NO + ClO. *J. Phys. Chem. A* **2005**, *109*, 4736-4743, doi:10.1021/jp050695w.
Schieferstein, M.; Kohse-Höinghaus, K.; Stuhl, F. Temperature dependence of the rate constants of the reaction O + NO + M → NO_2 + M (M = He, NO, N_2, CH_4). *Ber. Bunsenges. Phys. Chem.* **1983**, *87*, 361-366, doi:10.1002/bbpc.19830870419.
Schinke, R.; Grebenshchikov, S. Y.; Ivanov, M. V.; Fleurat-Lessard, P. Dynamical studies of the ozone isotope effect: A status report. *Ann. Rev. Phys. Chem.* **2006**, *57*, 625-661, doi:10.1146/annurev.physchem.57.032905.104542.
Schmidt, V.; Zhu, G. Y.; Becker, K. H.; Fink, E. H. Study of OH reactions at high pressures by excimer laser photolysis - dye laser fluorescence. *Ber. Bunsenges. Phys. Chem.* **1985**, *89*, 321-322, doi:10.1002/bbpc.19850890337.
Schurath, U.; Wipprecht, V. 1st European Symposium on Physico-Chemical Behavior of Atmospheric Pollutants, 1979, Ispra.
Seefeld, S.; Kinnison, D. J.; Kerr, J. A. Relative rate study of the reactions of acetylperoxy radicals with NO and NO_2: Peroxyacetyl nitrate formation under laboratory conditions related to the troposphere. *J. Phys. Chem. A* **1997**, *101*, 55-59, doi:10.1021/jp962266r.
Seeley, J. V.; Jayne, J. T.; Molina, M. J. Kinetic studies of chlorine atom reactions using the turbulent flow tube technique. *J. Phys. Chem.* **1996**, *100*, 4019-4025, doi:10.1021/jp9525494.
Sehested, J.; Christensen, L. K.; Mogelberg, T.; Nielsen, O. J.; Wallington, T. J.; Guschin, A.; Orlando, J. J.; Tyndall, G. S. Absolute and relative rate constants for the reactions $CH_3C(O)O_2$ + NO and $CH_3C(O)O_2$ + NO_2 and thermal stability of $CH_3C(O)O_2NO_2$. *J. Phys. Chem. A* **1998**, *102*, 1779-1789, doi:10.1021/jp972881a.
Sehested, J.; Christensen, L. K.; Nielsen, O. J.; Wallington, T. J. Absolute rate constants for F + CH_3CHO and CH_3CO + O_2, relative rate study of CH_3CO + NO, and the product distribution of the F + CH_3CHO reaction. *Int. J. Chem. Kinet.* **1998**, *30*, 913-921.
Sellevåg, S. R.; Geogievskii, Y.; Miller, J. A. The temperature and pressure dependence of the reactions H + O_2 (+M) → HO_2 (+M) and H + OH (+M) → H_2O (+M). *J. Phys. Chem. A* **2008**, *112*, 5085-5095, doi:10.1021/jp711800z.
Sellevåg, S. R.; Georgievskii, Y.; Miller, J. A. Kinetics of the gas-phase recombination reaction of hydroxyl radicals to form hydrogen peroxide. *J. Phys. Chem. A* **2009**, *113*, 4457-4467, doi:10.1021/jp8110524.
Selzer, E. A.; Bayes, K. D. Pressure dependence of the rate of reaction of methyl radicals with O_2. *J. Phys. Chem.* **1983**, *87*, 392-394, doi:10.1021/j100226a007.
Senosiain, J. P., C. B. Musgrave and D. M. Golden Temperature and pressure dependence of the reaction of OH and CO: Master equation modeling on a high-level potential energy surface. *Int. J. Chem. Kinet.* **2003**, *35*, 464-474, doi:10.1002/kin.10144.
Senosiain, J. P.; Klippenstein, S. J.; Miller, J. A. The reaction of acetylene with hydroxyl radicals. *J. Phys. Chem. A* **2005**, *109*, 6045-6055 doi:10.1021/jp050737g.
Shamonina, N. F.; Kotov, A. G. *Kinet. i Kataliz.* **1979**, *20*, 233.
Sharkey, P.; Sims, I. R.; Smith, I. W. M.; Bocherl, P.; Rowe, B. R. Pressure and temperature dependence of the rate constants for the association reaction OH radicals with NO between 301 and 23 K. *J. Chem. Soc. Faraday Trans.* **1994**, *90*, 3609-3616, doi:10.1039/ft9949003609.
Shen, G.; Suto, M.; Lee, L. C. Reaction rate constant of SO_3 + NH_3 in the gas phase. *J. Geophys. Res.* **1990**, *95*, 13981-13984, doi:10.1029/JD095iD09p13981.
Sheng, C. Y., J. W. Bozzelli, A. M. Dean, and A. Y. Chang Detailed kinetics and thermochemistry of C_2H_5 + O_2: Reaction kinetics of the chemically-activated and stabilized CH_3CH_2OO• adduct. *J. Phys. Chem. A* **2002**, *106*, 7276-7293, doi:10.1021/jp014540+.
Shepler, B. C.; Balabanov, N. B.; Peterson, K. A. Hg + Br → HgBr recombination and collision-induced dissociation dynamics. *J. Chem. Phys.* **2007**, *107*, 164304, doi:10.1063/1.2777142.
Sheps, L. Absolute ultraviolet absorption spectrum of a Criegee intermediate CH_2OO. *J. Phys. Chem. Lett.* **2013**, *4*, 4201-4205, doi:10.1021/jz402191w.

Shiekh, B. A.; Kaur, D.; Seth, B.; Mahajan, S. The theoretical-cum-statistical approach for the investigation of reaction $NO^2 + O(^3P) \rightarrow NO + O_2$ using SCTST and a full anharmonic VPT2 model. *Chem. Phys. Lett.* **2016**, *662*, 244-249, doi:10.1016/j.cplett.2016.08.058.

Shin, H. K. Temperature dependence of intermolecular energy transfer in polar molecules. *J. Amer. Chem. Soc.* **1968**, *90*, 3029-3039, doi:10.1021/ja01014a007.

Shin, H. K. Deexciation of molecular vibration on collision: Vibration-to-rotation energy transfer in hydrogen halides. *J. Phys. Chem.* **1971**, *75*, 1079-1090, doi:10.1021/j100678a011.

Shin, H. K. Vibration-rotation-translation energy transfer in HF-HF and DF-DF. *Chem. Phys. Lett.* **1971**, *10*, 81-85, doi:10.1016/0009-2614(71)80162-8.

Shin, H. K. Temperature dependence of $V \rightarrow R, T$ energy transfer probabilities in $CO_2(00^01)$ + HF/DF. *J. Chem. Phys.* **1974**, *60*, 3844-3851, doi:10.1063/1.1681329.

Silver, J. A.; Zahniser, M. S.; Stanton, A. C.; Kolb, C. E. Temperature dependent termolecular reaction rate constants for potassium and sodium superoxide formation. *Proc. Combust. Inst.* **1984**, *20*, 605-612.

Simonaitis, R.; Heicklen, J. Temperature dependence of the reactions of HO_2 with NO and NO_2. *Int. J. Chem. Kinet.* **1978**, *10*, 67-87, doi:10.1002/kin.550100106.

Sims, I. R.; Smith, I. W. M.; Bocherel, P.; Defrance, A.; Travers, D.; Rowe, B. R. Ultra-low temperature kinetics of neutral-neutral reactions: Rate constants for the reactions of OH radicals with butenes between 295 and 23 K. *J. Chem. Soc. Faraday Trans.* **1994**, *90*, 1473-1478, doi:10.1039/FT9949001473.

Skolnik, E. D.; Veysey, M. G.; Ahmed, M. G.; Jones, W. E. Rate constants for the reaction of fluorine atoms with nitric oxide in the presence of various third bodies. *Can. J. Chem.* **1975**, *53*, 3188-3193, doi:10.1139/v75-454.

Slagle, I. R.; Feng, Q.; Gutman, D. Kinetics of the reaction of ethyl radicals with molecular oxygen from 294 to 1002 K. *J. Phys. Chem.* **1984**, *88*, 3648, doi:10.1021/j150660a054.

Slanger, T. G.; Wood, B. J.; Black, G. Investigation of the rate coefficient for $O(^3P) + NO_2 \rightarrow O_2 + NO$. *Int. J. Chem. Kinet.* **1973**, *5*, 615-620, doi:10.1002/kin.550050411.

Slanina, Z.; Uhlik, F. An estimation of dimerization energetics of the ClO radical. *Chem. Phys. Lett.* **1991**, *182*, 51-56, doi:10.1016/0009-2614(91)80102-4.

Smith, C. A.; Molina, L. T.; Lamb, J. J.; Molina, M. J. Kinetics of the reaction of OH with pernitric and nitric acids. *Int. J. Chem. Kinet.* **1984**, *16*, 41-55, doi:10.1002/kin.550160107

Smith, C. A.; Ravishankara, A. R.; Wine, P. H. Kinetics of the reaction $NO_2 + NO_3 + M$ at low pressures and 298 K. *J. Phys. Chem.* **1985**, *89*, 1423-1427, doi:10.1021/j100254a024.

Smith, G. P.; Fairchild, P. W.; Crosley, D. R. The pressure and temperature dependence of the OH + C_2H_2 reaction above 800 K. *J. Chem. Phys.* **1984**, *81*, 2667-2677, doi:10.1063/1.447976.

Smith, G. P.; Golden, D. M. Application of RRKM theory to the reactions $OH + NO_2 + N_2 \rightarrow HONO_2 + N_2$ (1) and $ClO + NO_2 + N_2 \rightarrow ClONO_2 + N_2$ (2); a modified gorin model transition state. *Int. J. Chem. Kinet.* **1978**, *10*, 489-501, doi:10.1002/kin.550100507.

Smith, I. W. M.; Wrigley, D. J. Time-resolved vibrational chemiluminescence: Rate constants for the reaction F + HCl → HF + Cl and for the relaxation of HF(v=3) by HCl, CO_2, N_2O, CO, N_2 and O_2. *Chem. Phys. Lett.* **1980**, *70*, 481-486, doi:10.1016/0009-2614(80)80109-6.

Smith, I. W. M.; Wrigley, D. J. Time resolved vibrational chemiluminescence: Rate constants for the reactions F + HBr, HI → HF + Br, I and for the relaxation of HF(v=4) and HF(v=6) by HBr, HI, CO_2, N_2O, CO, N_2 and O_2. *Chem. Phys.* **1981**, *63*, 321-336, doi:10.1016/0301-0104(81)87008-5.

Smith, I. W. M.; Zellner, R. Rate measurements of reactions of OH by resonance absorption Part 2.-Reactions of OH with CO, C_2H_4 and C_2H_2. *J. Chem. Soc. Faraday Trans. 2* **1973**, *69*, 1617-1627, doi:10.1039/f29736901617.

Somnitz, H. Quantum chemical and dynamical characterisation of the reaction $OH + SO_2 \rightleftharpoons HOSO_2$ over an extended range of temperature and pressure. *Phys . Chem. Chem. Phys* . **2004**, *6*, 3844-3851, doi:10.1039/b317055a.

Sørensen, M.; Kaiser, E. W.; Hurley, M. D.; Wallington, T. J.; Nielsen, O. J. Kinetics of the reaction of OH radicals with acetylene in 25–8000 Torr of air at 296 K. *Int. J. Chem. Kinet.* **2003**, *35*, 191-197, doi:10.1002/kin.10119.

Spangenberg, T.; Kohler, S.; Hansmann, B.; Wachsmuth, U.; Abel, B.; Smith, M. A. Low-temperature reactions of OH radicals with propene and isoprene in pulsed Laval nozzle expansions. *J. Phys. Chem. A* **2004**, *108*, 7527-7534, doi:10.1021/jp031228m.

Spicer, C. W.; Satola, J.; Abbgy, A. A.; Plastridge, R. A.; Cowen, K. A. Kinetics of gas-phase elemental mercury reactions with halogen species, ozone, and nitrate radical under atmospheric conditions, Florida Department of Environmental Protection. **2002**.

Stachnik, R. A.; Molina, L. T.; Molina, M. J. Pressure and temperature dependences of the reaction of OH with nitric acid. *J. Phys. Chem.* **1986**, *90*, 2777-2780, doi:10.1021/j100403a044.

Stanton, J. F.; Rittby, C. M. L.; Bartlett, R. J.; Toohey, D. W. Low-lying isomers of the chlorine oxide dimer: A theoretical study. *J. Phys. Chem.* **1991**, *95*, 2107-2110, doi:10.1021/j100159a004.

Stickel, R. E.; Nicovich, J. M.; Wang, S.; Zhao, Z.; Wine, P. H. Kinetic and mechanistic study of the reaction of atomic chlorine with dimethyl sulfide. *J. Phys. Chem.* **1992**, *96*, 9875-9883, doi:10.1021/j100203a055.

Stone, D.; Blitz, M.; Daubney, L.; Ingham, T.; Seakins, P. CH_2OO Criegee biradical yields following photolysis of CH_2I_2 in O_2. *Phys. Chem. Chem. Phys.* **2013**, *15*, 19119-19124, doi:10.1039/c3cp52466c.

Strekowski, R. Laser Flash Photolysis Studies of Some $O(^1D_2)$ and OH ($X^2\Pi$) Reactions of Atmospheric Interest, Georgia Institute of Technology, 2001.

Stuhl, F.; Niki, H. Flash photochemical study of the reaction OH + NO + M using resonance fluorescent detection of OH. *J. Chem. Phys.* **1972**, *57*, 3677-3679, doi:10.1063/1.1678826.

Stutz, J.; Ezell, M. J.; Finlayson-Pitts, B. J. Inverse kinetic isotope effect in the reaction of atomic chlorine with C_2H_4 and C_2D_4. *J. Phys. Chem. A* **1997**, *101*, 9187-9190, doi:10.1021/jp972935g.

Su, Y.-T.; Lin, H.-Y.; Putikam, R.; Matsui, H.; Lin, M. C.; Lee, Y.-P. Extremely rapid self-reaction of the simplest Criegee intermediate CH_2OO and its implications in atmospheric chemistry. *Nat. Chem.* **2014**, *6*, 477-483, doi:10.1038/NCHEM.1890.

Sun, C.; Sommar, J.; Feng, X.; Lin, C.-J.; Ge, M.; Wang, W.; Yin, R.; Fu, X.; Shang, L. Study of mass-dependent and -independent fractionation of mercury isotope during gas-phase oxidation of elemental mercury vapor by atomic Cl and Br. *Environ. Sci. Technol.* **2016**, *50*, 9232-9241, doi:10.1021/acs.est.6b01668.

Szakács, P.; Csontos, J.; Das, S.; Kállay, M. High-accuracy theoretical thermochemistry of atmospherically important nitrogen oxide derivatives. *J. Phys. Chem. A* **2011**, *115*, 3144-3153, doi:10.1021/jp112116x.

Talukdar, R. K.; Davis, M. E.; Zhu, L.; Ravishankara, A. R.; Burkholder, J. B. "Determination of the OH radical yield in the $CH_3CO + O_2$ reaction". *19th International Symposium on Gas Kinetics, 2006, Orleans, France.* **2006**.

Taylor, S. E.; Goddard, A.; Blitz, M. A.; Cleary, P. A.; Heard, D. E. Pulsed Laval nozzle study of the kinetics of OH with unsaturated hydrocarbons at very low temperatures. *Phys. Chem. Chem. Phys.* **2008**, *10*, 422-437, doi:10.1039/b711411g.

Thorn, R. P.; Daykin, E. P.; Wine, P. H. Kinetics of the $BrO + NO_2$ association reaction. Temperature and pressure dependence in the falloff regime. *Int. J. Chem. Kinet.* **1993**, *25*, 521-537, doi:10.1002/kin.550250703.

Thuner, L. P.; Barnes, I.; Becker, K. H.; Wallington, T. J.; Christensen, L. K.; Orlando, J. J.; Ramacher, B. Atmospheric chemistry of tetrachloroethene ($Cl_2C=CCl_2$): Products of chlorine atom initiated oxidation. *J. Phys. Chem. A* **1999**, *103*, 8657-8663, doi:10.1021/jp991929c.

Ting, W.-L.; Chang, C.-H.; Lee, Y.-F.; Matsui, H.; Lee, Y.-P.; Lin, J. J.-M. Detailed mechanism of the $CH_2I + O_2$ reaction: Yield and self-reaction of the simplest Criegee intermediate CH_2OO. *J. Chem. Phys.* **2014**, *141*, 104308, doi:10.1063/1.4894405.

Trainor, D. W.; von Rosenberg, C. W., Jr. Flash photolysis study of the gas phase recombination of hydroxyl radicals. *J. Chem. Phys.* **1974**, *61*, 1010-1015, doi:10.1063/1.1681968.

Troe, J. Theory of thermal unimolecular reactions at low pressures. I. Solutions of the master equation. *J. Chem. Phys.* **1977**, *66*, 4745-4757, doi:10.1063/1.433837.

Troe, J. "Modeling the temperature and pressure dependence of the reaction HO + CO = HOCO = H + CO_2"; Twenty-Seventh Symposium (International) on Combustion, 1998.

Troe, J. Detailed modeling of the temperature and pressure dependence of the reaction $H + O_2$ (+M) → HO_2 (+M). *Proc. Combust. Inst.* **2001**, *28*, 1463-1469.

Troe, J. Toward a quantitative analysis of association reactions in the atmosphere. *Chem. Rev.* **2003**, *104*, 4565-4576, doi:10.1021/cr020514b.

Trolier, M.; Mauldin, R. L., III; Ravishankara, A. R. Rate coefficient for the termolecular channel of the self-reaction of ClO. *J. Phys. Chem.* **1990**, *94*, 4896-4907, doi:10.1021/j100375a027.

Tucceri, M. E.; Dillon, T. J.; Crowley, J. N. A laser photolysis–resonance fluorescence study of the reactions: $I + O_3$ → $IO + O_2$, $O + I_2$ → IO + I, and $I + NO_2 + M$ → INO_2 + M at 298 K. *Phys. Chem. Chem. Phys.* **2005**, *10*, 1657-1663, doi:10.1039/b502844b.

Tully, F. P. Laser photolysis/laser-induced fluorescence study of the reaction of hydroxyl radical with ethylene. *Chem. Phys. Lett.* **1983**, *96*, 148-153, doi:10.1016/0009-2614(83)80481-3.

Tully, F. P.; Goldsmith, J. E. M. Kinetic study of the hydroxyl radical-propene reaction. *Chem. Phys. Lett.* **1985**, *116*, 345-352, doi:10.1016/0009-2614(85)80182-2.
Turnipseed, A. A.; Barone, S. B.; Jensen, N. R.; Hanson, D. R.; Howard, C. J.; Ravishankara, A. R. Kinetics of the reactions of CF_3O radicals with CO and H_2O. *J. Phys. Chem.* **1995**, *99*, 6000-6009, doi:10.1021/j100016a041.
Turnipseed, A. A.; Barone, S. B.; Ravishankara, A. R. Observation of CH_3S addition to O_2 in the gas phase. *J. Phys. Chem.* **1992**, *96*, 7502-7505, doi:10.1021/j100198a006.
Tyndall, G. S.; Orlando, J. J.; Wallington, T. J.; Hurley, M. D. Pressure dependence of the rate coefficients and product yields for the reaction of CH_3CO radicals with O_2. *Int. J. Chem. Kinet.* **1997**, *29*, 655-663, doi:10.1002/(SICI)1097-4601(1997)29:9<655::AID-KIN2>3.0.CO;2-T.
Urbanski, S. P.; Wine, P. H. Spectroscopic and kinetic study of the Cl-S$(CH_3)_2$ adduct. *J. Phys. Chem. A* **1999**, *103*, 10935-10944, doi:10.1021/jp992682m.
Vakhtin, A. B.; Lee, S.; Heard, D. E.; Smith, I. W. M.; Leone, S. R. Low-temperature kinetics of reactions of the OH radical with propene and 1-butene studied by a pulsed laval nozzle apparatus combined with laser-induced fluorescence. *J. Phys. Chem. A* **2001**, *105*, 7889-7895, doi:10.1021/jp010809d.
Vakhtin, A. B.; Murphy, J. E.; Leone, S. R. Low-temperature kinetics of reactions of OH radical with ethene, propene, and 1-butene. *J. Phys. Chem. A* **2003**, *107*, 10055-10062, doi:10.1021/jp030230a.
van den Bergh, H.; Benoit-Guyot, N.; Troe, J. Collisional energy transfer in the reactions I + NO + M → INO + M and I + NO_2 + M → INO_2 + M. *Int. J. Chem. Kinet.* **1977**, *9*, 223-234, doi:10.1002/kin.550090207.
van den Bergh, H.; Troe, J. Kinetic and thermodynamic properties of INO and INO_2 intermediate complexes in iodine recombination. *J. Chem. Phys.* **1976**, *64*, 736-742, doi:10.1063/1.432220.
van den Bergh, H. E.; Callear, A. B. Spectroscopic measurement of the rate of the gas-phase combination of methyl radicals with nitric oxide and oxygen at 295 K. *Trans. Faraday Soc.* **1971**, *67*, 2017-2024, doi:10.1039/tf9716702017.
Vereecken, L.; Harder, H.; Novelli, A. The reactions of Criegee intermediates with alkenes, ozone, and carbonyl oxides. *Phys. Chem. Chem. Phys.* **2014**, *16*, 4039-4049, doi:10.1039/c3cp54514h.
Viggiano, A. A.; Davidson, J. A.; Fehsenfeld, F. C.; Ferguson, E. E. Rate constants for the collisional dissociation of N_2O_5 by N_2. *J. Chem. Phys.* **1981**, *74*, 6113-6125, doi:10.1063/1.441055.
Vinckier, C.; Dumoulin, A.; DeJaegere, S. Kinetic study of the Na + O_2 + He reaction in the temperature range 392-777 K. *J. Chem. Soc. Faraday Trans.* **1991**, *87*, 1075-1081, doi:10.1039/ft9918701075.
von Ahsen, S.; Wilner, H.; Francisco, J. S. Thermal decomposition of peroxy acetyl nitrate $CH_3C(O)OONO_2$. *J. Chem. Phys.* **2004**, *121*, 2048-2057, doi:10.1063/1.1767813.
Wagner, A. F.; Slagle, I. R.; Sarzynski, D.; Gutman, D. Experimental and theoretical studies of the C_2H_5 + O_2 reaction kinetics. *J. Phys. Chem.* **1990**, *94*, 1853-1868, doi:10.1021/j100368a026.
Walker, R. W. Ph.D Thesis, Queen Mary College University of London, 1972.
Wallington, T. J. Kinetics of the gas phase reaction of OH radicals with pyrrole and thiophene. *Int. J. Chem. Kinet.* **1986**, *18*, 487-496, doi:10.1002/kin.550180407.
Wallington, T. J.; Andino, J. M.; Lorkovic, I. M.; Kaiser, E. W.; Marston, G. Pressure dependence of the reaction of chlorine atoms with ethene and acetylene in air at 295 K. *J. Phys. Chem.* **1990**, *94*, 3644-3648, doi:10.1021/j100372a052.
Wallington, T. J.; Andino, J. M.; Potts, A. R.; Wine, P. H. A competitive kinetics study of the reaction of Cl with CS_2 in air at 298 K. *Chem. Phys. Lett.* **1991**, *176*, 103-108, doi:10.1016/0009-2614(91)90018-5.
Wallington, T. J.; Atkinson, R.; Winer, A. M.; Pitts, J. N., Jr. A study of the reaction NO_3 + NO_2 + M → N_2O_5 + M(M = N_2, O_2). *Int. J. Chem. Kinet.* **1987**, *19*, 243-249, doi:10.1002/kin.550190307.
Wallington, T. J.; Ball, J. C. Atmospheric chemistry of CF_3O radicals: Reactions with CH_4, CD_4, CH_3F, CF_3H, ^{13}CO, C_2H_5F, C_2D_6, C_2H_6, CH_3OH, *i*-C_4H_8, and C_2H_2. *J. Phys. Chem.* **1995**, *99*, 3201-3205, doi:10.1021/j100010a034.
Wallington, T. J.; Cox, R. A. Kinetics and product of the gas-phase reaction of ClO with NO_2. *J. Chem. Soc. Faraday Trans. 2* **1986**, *82*, 275-289, doi:10.1039/f29868200275.
Wallington, T. J.; Ellerman, T.; Nielsen, O. J.; Sehested, J. Atmospheric chemistry of FCO_x radicals: UV spectra and self-reaction kinetics of FCO and $FC(O)O_2$ and kinetics of some reactions of FCO_x with O_2, O_3, and NO at 296 K. *J. Phys. Chem.* **1994**, *98*, 2346-2356, doi:10.1021/j100060a024.
Wallington, T. J.; Ellermann, T.; Nielsen, O. J. Atmospheric chemistry of dimethyl sulfide: UV spectra and self-reaction kinetics of CH_3SCH_2 and $CH_3SCH_2O_2$ radicals and kinetics of the reactions CH_3SCH_2 + O_2 → $CH_3SCH_2O_2$ and $CH_3SCH_2O_2$ + NO → CH_3SCH_2O + NO_2. *J. Phys. Chem.* **1993**, *97*, 8442-8449, doi:10.1021/j100134a013.

Wallington, T. J.; Mariq, M. M.; Ellerman, T.; Nielsen, O. J. Novel method for the measurement of gas-phase peroxy radical absorption spectra. *J. Phys. Chem.* **1992**, *96*, 982-986, doi:10.1021/j100181a080.
Wallington, T. J.; Nielsen, O. J. UV absorption spectra and kinetics of the self reaction of $CFCl_2CH_2O_2$ and $CF_2ClCH_2O_2$ radicals in the gas phase at 298 K. *Int. J. Chem. Kinet.* **1991**, *23*, 785-798, doi:10.1002/kin.550230905.
Wallington, T. J.; Skewes, L. M.; Siegl, W. O. Kinetics of the gas phase reaction of chlorine atoms with a series of alkenes, alkynes and aromatic species at 295 K. *J. Photochem. Photobiol. A: Chem.* **1988**, *45*, 167-175, doi:10.1016/1010-6030(88)80126-6.
Wallington, T. J.; Skewes, L. M.; Siegl, W. O.; Wu, C. H.; Japar, S. M. Gas phase reaction of Cl atoms with a series of oxygenated organic species at 295 K. *Int. J. Chem. Kinet.* **1988**, *20*, 867-875, doi:10.1002/kin.550201105.
Walsh, R.; Golden, D. M. Evaluation of data for atmospheric models: Master equation/RRKM calculations on the combination reaction $BrO + NO_2 \rightarrow BrONO_2$, a conundrum. *J. Phys. Chem. A* **2008**, *112*, 3891-3897, doi:10.1021/jp7116642.
Wang, D.; Phillips, D. L. Density functional theory study of CS_2/Cl adducts and their isomerization reactions. *Chem. Phys. Lett.* **2002**, *362*, 205-209, doi:10.1016/S0009-2614(02)01015-1.
Washida, N. Reaction of methyl radicals with $O(^3P)$, O_2 and NO. *J. Chem. Phys.* **1980**, *73*, 1665-1672, doi:10.1063/1.440348.
Washida, N.; Bayes, K. D. The reactions of methyl radicals with atomic and molecular oxygen. *Int. J. Chem. Kinet.* **1976**, *8*, 777-794, doi:10.1002/kin.550080512.
Westenberg, A. A.; deHaas, N. Rate measurement on OH + NO + M and OH + NO_2 + M. *J. Chem. Phys.* **1972**, *57*, 5375-5378, doi:10.1063/1.1678234.
Weston, R. E., Jr.; Nguyen, T. L.; Stanton, J. F.; Barker, J. R. HO + CO reaction rates and H/D kinetic isotope effects: Master equation models with ab initio SCTST rate constants. *J. Phys. Chem. A* **2013**, *117*, 821-835, doi:10.1021/jp311928w.
Whytock, D. A.; Michael, J. V.; Payne, W. A. Absolute rate constants for $O + NO + N_2 \rightarrow NO_2 + N_2$ from 217-500 K. *Chem. Phys. Lett.* **1976**, *42*, 466-471, doi:10.1016/0009-2614(76)80655-0.
Wilcox, J.; Okano, T. Ab initio-based mercury oxidation kinetics via bromine at postcombustion flue gas conditions. *Energy Fuels* **2011**, *25*, 1348-1356, doi:10.1021/ef101763r.
Williams, M. B.; Campuzano-Jost, P.; Hynes, A. J.; Pounds, A. J. Experimental and theoretical studies of the reaction of the OH radical with alkyl sulfides: 3. Kinetics and mechanism of the OH initiated oxidation of dimethyl, dipropyl, and dibutyl sulfides: Reactivity trends in the alkyl sulfides and development of a predictive expression for the reaction of OH with DMS. *J. Phys. Chem. A* **2009**, *113*, 6697-6709, doi:10.1021/Jp9010668.
Wilson, W. E.; Westenberg, A. A. Study of the reaction of hydroxyl radical with methane by quantitative ESR. *Proc. Combust. Inst.* **1967**, *11*, 1143-1150.
Wine, P. H.; Kreutter, N. M.; Ravishankara, A. R. Flash photolysis-resonance fluorescence kinetics study of the reaction $OH + NO_2 + M \rightarrow HNO_3 + M$. *J. Phys. Chem.* **1979**, *83*, 3191-3195, doi:10.1021/j100488a002.
Wine, P. H.; Nicovich, J. M.; Stickel, R. E.; Zhao, Z.; Shackelford, C. J.; Kreutter, K. D.; Daykin, E. P.; Wang, S. In *The Tropospheric Chemistry of Ozone in the Polar Regions*; Springer-Verlag: Berlin, 1993; Vol. I7; pp 385-395.
Wine, P. H.; Ravishankara, A. R.; Kreutter, N. M.; Shah, R. C.; Nicovich, J. M.; Thompson, R. L.; Wuebbles, D. J. Rate of reactions of OH with HNO_3. *J. Geophys. Res.* **1981**, *86*, 1105-1112, doi:10.1029/JC086iC02p01105.
Wine, P. H.; Thompson, R. J.; Ravishankara, A. R.; Semmes, D. H.; Gump, C. A.; Torabi, A.; Nicovich, J. M. Kinetics of the reaction $OH + SO_2 + M \rightarrow HOSO_2 + M$. Temperature and pressure dependence in the falloff region. *J. Phys. Chem.* **1984**, *88*, 2095-2104, doi:10.1021/j150654a031.
Winer, A. M.; Lloyd, A. C.; Darnall, K. R.; Pitts, J. N., Jr. Relative rate constants for the reaction of the hydroxyl radical with selected ketones, chloroethenes, and monoterpene hydrocarbons. *J. Phys. Chem.* **1976**, *80*, 1635-1639, doi:10.1021/j100555a024.
Winiberg, F. A. F.; Percival, C. J.; Shannon, R.; Khan, A. H.; Shallcross, D. E.; Liu, Y.; Sander, S. P. Reaction kinetics of $OH + HNO_3$ under conditions relevant to the upper troposphere/lower stratosphere. *Phys . Chem. Chem. Phys.* **2018**, *20*, 24652, doi:10.1039/C8CP04193H.
Wolf, S.; Bitter, M.; Krankowsky, D.; Mauersberger, K. Multi-isotope study of fractionation effects in the ozone formation process. *J. Chem. Phys.* **2000**, *113*, 2684-2686, doi:10.1063/1.1305890.

Wollenhaupt, M.; Crowley, J. N. Kinetic studies of the reactions $CH_3 + NO_2 \rightarrow$ products, $CH_3O + NO_2 \rightarrow$ products, and $OH + CH_3C(O)CH_3 \rightarrow CH_3C(O)OH + CH_3$, over a range of temperature and pressure. *J. Phys. Chem. A* **2000**, *104*, 6429-6438, doi:10.1021/jp0005726.

Wong, W. D.; Davis, D. A flash photolysis-resonance fluorescence study of the reaction of atomic hydrogen with molecular oxygen $H + O_2 + M \rightarrow HO_2 + M$. *Int. J. Chem. Kinet.* **1974**, *6*, 401-416, doi:10.1002/kin.550060310.

Wu, C. H.; Japar, S. M.; Niki, H. Relative reactivities of HO-hydrocarbon reactions from smog reactor studies. *J. Environ Sci. Health* **1976**, *A11*, 191-200, doi:10.1080/10934527609385765.

Wu, F.; Carr, R. W. An investigation of temperature and pressure dependence of the reaction of CF_2ClO_2 radicals with nitrogen dioxide by flash photolysis and time resolved mass spectrometry. *Int. J. Chem. Kinet.* **1991**, *23*, 701-715, doi:10.1002/kin.550230805.

Xia, W. S.; Lin, M. C. A multifacet mechanism for the $OH + HNO_3$ reaction: An *ab initio* molecular orbital/statistical theory study. *J. Chem. Phys.* **2001**, *114*, 4522-4532, doi:10.1063/1.1337061.

Xiong, J. Q.; Carr, R. W. Thermal decomposition of $CF_2ClO_2NO_2$. *J. Phys. Chem.* **1994**, *98*, 9811-9822, doi:10.1021/j100090a015.

Yarwood, G.; Sutherland, J. W.; Wickramaaratchi, M. A.; Klemm, R. B. Direct rate constant measurements for the reaction $O + NO + Ar \rightarrow NO_2 + Ar$ at 300-1341 K. *J. Phys. Chem.* **1991**, *95*, 8771-8775, doi:10.1021/j100175a065.

Zabarnick, S. Kinetics of the reaction $OH + NO + M \rightarrow HONO + M$ as a function of temperature and pressure in the presence of argon, SF_6 and N_2 bath gas. *Chem. Phys.* **1993**, *171*, 265-273, doi:10.1016/0301-0104(93)85149-3.

Zabel, F.; Reimer, A.; Becker, K. H.; Fink, E. H. Thermal decomposition of alkyl peroxynitrates. *J. Phys. Chem.* **1989**, *93*, 5500-5507, doi:10.1021/j100351a036.

Zahniser, M. S.; Chang, J.; Kaufman, F. Chlorine nitrate: Kinetics of formation by $ClO + NO_2 + M$ and of reaction with OH. *J. Chem. Phys.* **1977**, *67*, 997-1003, doi:10.1063/1.434927.

Zellner, R.; Ewig, F.; Paschke, R.; Wagner, G. Pressure and temperature dependence of the gas-phase recombination of hydroxyl radicals. *J. Phys. Chem.* **1988**, *92*, 4184-4190, doi:10.1021/j100325a038.

Zellner, R.; Lorenz, K. Laser photolysis/resonance fluorescence study of the rate constants for the reactions of OH radicals with C_2H_4 and C_3H_6. *J. Phys. Chem.* **1984**, *88*, 984-989, doi:10.1021/j150649a028.

Zetzsch, C. Some combination reactions of fluorine atoms. In *First European Sym. on Combust*; Weinberg, F. S., Ed.; Academic Press London, 1973; Vol. 35; pp 35-40.

Zhang, J.; Donahue, N. M. Constraining the mechanism and kinetics of $OH + NO_2$ and $HO_2 + NO$ using the multiple-well master equation. *J. Phys. Chem. A* **2006**, *110*, 6898-6911, doi:10.1021/jp0556512.

Zhang, J. Y.; Dransfield, T.; Donahue, N. M. On the mechanism for nitrate formation via the peroxy radical plus NO reaction. *J. Phys. Chem. A* **2004**, *108*, 9082-9095, doi:10.1021/jp048096x.

Zhu, B.; Zeng, X.; Beckers, H.; Francisco, J. S.; Willner, H. The Methylsulfonyloxyl Radical, CH_3SO_3. *Angew. Chem. Int. Ed.* **2015**, *54*, 11404 –11408, doi:10.1002/anie.201503776.

Zhu, R., C.-C. Hsu and M. C. Lin *Ab initio* study of the $CH_3 + O_2$ reaction: Kinetics, mechanism and product branching probabilities. *J. Chem. Phys.* **2001**, *115*, 195-203, doi:10.1063/1.1376128.

Zhu, R. S.; Lin, M. C. Ab initio studies of ClO_x reactions. 2. Unimolecular decomposition of s-ClO_3 and the bimolecular O + OClO reaction. *J. Phys. Chem. A* **2002**, *106*, 8386-8390, doi:10.1021/jp020015e.

Zhu, R. S.; Lin, M. C. *Ab initio* studies of ClO_x reactions. IV. Kinetics and mechanism for the self-reaction of ClO radicals. *J. Chem. Phys.* **2003**, *118*, 4094-4106, doi:10.1063/1.1540623.

Zhu, R. S.; Lin, M. C. Ab initio studies of ClO_x reactions. VII. Isomers of Cl_2O_3 and their roles in the ClO + OClO reaction. *J. Chem. Phys.* **2003**, *118*, 8645-8655, doi:10.1063/1.1565315.

Zhu, R. S.; Lin, M. C. Ab initio studies of ClO_x reactions. VIII. Isomerization and decomposition of ClO_2 radicals and related bimolecular processes. *J. Chem. Phys.* **2003**, *119*, 2075-2082, doi:10.1063/1.1585027.

Zhu, R. S.; Lin, M. C. Ab Initio studies of ClO_x reactions: Prediction of the rate constants of ClO + NO for the forward and reverse processes. *ChemPhysChem* **2004**, *5*, 1864-1870, doi:10.1002/cphc.200400305.

Zhu, R. S.; Lin, M. C. Ab initio studies of ClO_x reactions: Prediction of the rate constants of $ClO + NO_2$ for the forward and reverse processes. *ChemPhysChem* **2005**, *6*, 1514-1521, doi:10.1002/cphc.200400448.

Zhu, T.; Yarwood, G.; Chen, J.; Niki, H. FTIR study of the C1 + C_2H_2 reaction: Formation of *cis*- and *trans*-CHCl=CH radicals. *J. Phys. Chem.* **1994**, *98*, 5065-5067, doi:10.1021/j100070a020.

Zou, P.; Derecskei-Kovacs, A.; North, S. W. Theoretical calculation of $ClONO_2$ and $BrONO_2$ bond dissociation energies. *J. Phys. Chem. A* **2003**, *107*, 888-896, doi:10.1021/jp021961y.

SECTION 3. EQUILIBRIUM CONSTANTS

Table of Contents

SECTION 3. EQUILIBRIUM CONSTANTS 3-1
3.1 Format 3-1
3.2 Definitions 3-1
3.3 Notes to Table 3-1 3-5
3.4 Bibilography – Equilibrium Constants 3-23

Tables

TABLE 3-1. EQUILIBRIUM CONSTANTS 3-3

3.1 Format

Some three-body reactions form products that are thermally unstable at atmospheric temperatures. In such cases, the thermal decomposition reaction may compete with other loss processes, such as photodissociation or radical attack. Table 3-1 lists the equilibrium constants, $K_{eq}(T)$, for reactions that may fall in this category. Each reaction in Table 3-1 has six column entries, the first two being the parameters A and B that can be used to express $K_{eq}(T)$:

$$K_{eq}(T)/\text{cm}^3\,\text{molecule}^{-1} = A\,\exp(B/T)\ (200 < T < 300\ \text{K})$$

The third column entry is the calculated value of $K_{eq}(298\ \text{K})$, while the fourth and fifth columns contain the estimated uncertain factors $f(298\ \text{K})$ and g, respectively (see Table 3-1 footnote for uncertainty calculation method). The data sources for $K_{eq}(T)$ are described in the individual notes to Table 3-1, with a hyperlink to the note given in column six.

3.2 Definitions

When values of the heats of formation and entropies of all species in an equilibrium reaction are known at temperature T, the equilibrium constant, $K_{eq}(T)$, is given by the van't Hoff equation:

$$\ln\left(K_{eq}(T)\right) = \frac{\Delta S^\circ_T}{R} - \frac{\Delta H^\circ_T}{RT}$$

where $K_{eq}(T)$ is in units of bar^{-1} and the superscript "o" refers to a standard state of one bar. For $K_{eq}(T)$ in units of cm^3 molecule^{-1}:

$$\ln\left(K_{eq}(T)\right) = \frac{\Delta S^\circ_T}{R} - \frac{\Delta H^\circ_T}{RT} + \ln(T) - 50.37$$

When the entropy is known, or can be calculated from molecular properties, as a function of temperature, experimental values of $K_{eq}(T)$ can be used to extract a value for ΔH_0 enabling $K_{eq}(T)$ to be calculated over a wider temperature range (Third law method.). The parameters A (cm^3 molecule^{-1}) and B (K) in Table 3-1 are determined from a linear fit of $\ln(K_{eq}(T))$ vs 1/T. In some cases, $K_{eq}(T)$ was calculated directly from the forward and reverse reaction rate coefficients. When only thermochemical values at 298 K were available, they were treated as temperature independent and used to calculate $K_{eq}(200–300\ \text{K})$. The following equations were then used to calculate the parameters A and B:

$$B = \left(\frac{300 \times 200}{(300-200)}\right)\ln\left(\frac{K_{eq}^{200}}{K_{eq}^{300}}\right) = 600\ln\left(\frac{K_{eq}^{200}}{K_{eq}^{300}}\right)$$

$$\ln(A) = \ln\left(K_{eq}^{T}\right) - \frac{B}{T}$$

The relationships between the parameters *A* and *B* and the quantities $\Delta S^{o}(298\ K)$ and $\Delta H^{o}(298\ K)$ are:

$$A = \frac{eR'T}{N_{av}} \exp\left(\frac{\Delta S^{\circ}_{298\ K}}{R}\right) = 3.7 \times 10^{-22}\ T \exp\left(\frac{\Delta S^{\circ}_{298\ K}}{R}\right)$$

where $R' = 83.145\ cm^3\ bar\ mol^{-1}\ K^{-1}$, $N_{av} = 6.02 \times 10^{23}$ molecule mol^{-1} and

$$B = -\left(\frac{\Delta H^{\circ}_{298\ K} + RT}{R}\right)$$

Table 3-1. Equilibrium Constants

Reaction	A cm^3 molecule^{-1}	B K	K_{eq}(298 K)	f(298 K) [a]	g [a]	Note
$H_2O + H_2O \leftrightarrows (H_2O)_2$	8.9×10^{-24}	1622	2.0×10^{-21}	1.05	0	1
$HO + NO_2 \leftrightarrows HOONO$	3.5×10^{-27}	10135	2.2×10^{-12}	1.40	200	2
$HO_2 + NO_2 \leftrightarrows HO_2NO_2$	2.1×10^{-27}	10900	1.6×10^{-11}	1.30	100	3
$HO_2 + H_2O \leftrightarrows HO_2\bullet H_2O$	2.4×10^{-25}	4350	5.2×10^{-19}	2.00	200	4
$HO_2 + CH_3OH \leftrightarrows HO_2\bullet CH_3OH$	1.1×10^{-24}	4093	1.0×10^{-18}	1.20 (at 230 K)	100	5
$HO_2 + CH_2O \leftrightarrows HOCH_2OO$	6.3×10^{-27}	7488	5.2×10^{-16}	1.20	300	6
$HO_2 + CH_3CHO \leftrightarrows CH_3CH(OH)OO$	5.0×10^{-28}	7130	1.7×10^{-17}	2.00	0	7
$HO_2 + CH_3C(O)CH_3 \leftrightarrows HO_2\bullet CH_3C(O)CH_3$	1.8×10^{-24}	4040	1.4×10^{-18}	1.60	0	8
$NO + NO_2 \leftrightarrows N_2O_3$	3.3×10^{-27}	4667	2.1×10^{-20}	2.00	100	9
$NO_2 + NO_2 \leftrightarrows N_2O_4$	5.9×10^{-29}	6643	2.8×10^{-19}	1.40	100	10
$NO_2 + NO_3 \leftrightarrows N_2O_5$	3.0×10^{-27}	11066	4.0×10^{-11}	1.20	75	11
$CH_3O_2 + NO_2 \leftrightarrows CH_3O_2NO_2$	9.5×10^{-29}	11234	2.2×10^{-12}	1.30	500	12
$CH_3C(O)O_2 + NO_2 \leftrightarrows CH_3C(O)O_2NO_2$	6.8×10^{-29}	14063	2.13×10^{-8}	1.07	0	13
$CH_3CH_2C(O)O_2 + NO_2 \leftrightarrows CH_3CH_2C(O)O_2NO_2$	9.0×10^{-29}	14000	2.3×10^{-8}	10.0	800	14
$CH_3C(O)CH_2 + O_2 \leftrightarrows CH_3C(O)CH_2O_2$	6.3×10^{-27}	12200	3.8×10^{-9}	1.50	0	15
$F + O_2 \leftrightarrows FOO$	4.5×10^{-25}	6118	3.7×10^{-16}	1.50	300	16
$Cl + O_2 \leftrightarrows ClOO$	1.24×10^{-24}	2370	3.2×10^{-21}	1.70	100	17
$Cl + CO \leftrightarrows ClCO$	3.5×10^{-25}	3730	9.6×10^{-20}	1.20	200	18
$ClO + O_2 \leftrightarrows ClO\bullet O_2$	2.9×10^{-26}	<3700	$<7.2\times10^{-21}$			19
$ClO + ClO \leftrightarrows Cl_2O_2$ $ClO + ClO \leftrightarrows ClOClO$	2.16×10^{-27} 6.5×10^{-27}	8537 4460	6.0×10^{-15} 2.0×10^{-20}	1.20 2.00	20 600	20
$Cl + OClO \leftrightarrows ClClO_2$	2.2×10^{-26}	13100	3.1×10^{-7}	2.00	600	21
$ClO + OClO \leftrightarrows Cl_2O_3$	1.5×10^{-27}	7170	4.2×10^{-17}	1.20	400	22
$OClO + NO_3 \leftrightarrows O_2ClONO_2$	6.6×10^{-29}	3971	4.0×10^{-23}	2.30	250	23
$Br + CH_2{=}CHC(CH_3){=}CH_2 \leftrightarrows$ Product	4.2×10^{-24}	7480	3.3×10^{-13}	1.30	100	24

Reaction	A cm^3 molecule^{-1}	B K	K_{eq}(298 K)	f(298 K) [a]	g [a]	Note
Br + CH_2=CHCH=CH_2 ⇆ Product	1.1×10^{-24}	7520	8.6×10^{-14}	1.30	100	25
IO + NO_2 ⇆ $IONO_2$	5.0×10^{-28}	14120	1.9×10^{-7}	2.50	300	26
OH + CS_2 ⇆ CS_2OH	4.5×10^{-25}	5140	1.4×10^{-17}	1.40	300	27
OH + $(CH_3)_2S$ ⇆ HO–$(CH_3)_2S$	9.6×10^{-27}	5376	6.6×10^{-19}	1.40	0	28
CH_3 + SO_3 ⇆ CH_3SO_3	(See Note)		7.0×10^{-13}	60	1200	29
Cl + CS_2 ⇆ Cl–CS_2	1.8×10^{-25}	4982	3.3×10^{-18}	1.30	150	30
Br + $(CH_3)_2S$ ⇆ Br–$(CH_3)_2S$	3.4×10^{-25}	3021	4.6×10^{-15}	1.20	100	31
CH_3S + O_2 ⇆ CH_3SO_2	1.8×10^{-27}	5545	2.2×10^{-19}	1.40	300	32
CH_3S +O_2 ⇆ CH_3SOO	1.4×10^{-26}	4850	1.7×10^{-19}	1.20	0	33
Hg + Br ⇆ HgBr	9.1×10^{-24}	7800	2.1×10^{-12}	2.00	200	34

$K_{eq}(T) = A \exp(B/T)$ [200< T/K <300] in cm^3 molecule^{-1} units

Shaded areas indicate changes or additions since 19-5.

a f(298 K) is the uncertainty factor at 298 K, and g is a measure of the uncertainty in the quantity B. To calculate the uncertainty at temperatures other than 298 K, use the expression:

$$\boldsymbol{f(T) = f(298\ K)\exp\left|g\left(\frac{1}{T} - \frac{1}{298}\right)\right|}$$

3.3 Notes to Table 3-1

1. **$H_2O + H_2O \leftrightarrows (H_2O)_2$ (water dimer).** The recommendation is based on the optimized Active Thermochemical Tables of Ruscic,[1] which utilizes a comprehensive thermochemical network that includes all of the prior work related to this equilibrium. K_{eq} from Ruscic agrees very well with the recent work of Scribano et al.[2] and references cited therein. The error limit was set to encompass the exponential fit to the K_{eq} of Ruscic (which is not exactly exponential). For more accurate values, the following non-exponential fit falls within 2% of Ruscic's values:

$$K_{eq} = 1.92 \times 10^{-23} \exp[(1 + 43/T)\times 1216/T] \text{ cm}^3 \text{ molecule}^{-1}$$

(Table: 15-10; Note: 15-10; Evaluation 15-10) Back to Table

(1) Ruscic, B. Active thermochemical tables: Water and water dimer. *J. Phys. Chem. A* **2013**, *117*, 11940-11953, doi:10.1021/jp403197t.

(2) Scribano, Y.; Goldman, N.; Saykally, R. J.; Leforestier, C. Water dimers in the atmosphere III: Equilibrium constant from a flexible potential. *J. Phys. Chem. A* **2006**, *110*, 5411-5419, doi:10.1021/jp056759k.

2. **HO + $NO_2 \leftrightarrows$ HOONO.** The tabulated value is for the *cis*,*cis*-HOONO product channel (see below for formation of the *trans*,*perp*-HOONO isomer, which is unlikely to be important in the atmosphere). Using the data from Hippler et al.,[4] Golden et al.[2,3] performed a third law analysis using structures and frequencies from an ab initio quantum calculation to extract the heat of formation of *cis*-*cis*-HOONO ($\Delta H_f°(0\text{ K}) = -9.3$ kJ mol^{-1}). The data covers the temperature range 430< T/K <475 with 30% uncertainties. Most vibrational frequencies have been identified using matrix isolation spectroscopy[10] and the moments of inertia have been measured by microwave spectroscopy.[1] High level CCSD(T) calculations and spectral simulation of overtone and action spectra have examined the torsion in considerable detail.[9] Mathews and Sinha[8] measured overtone action spectra and carried out an analysis that gave $D_0 = 83.3 \pm 2.1$ kJ mol^{-1}. By using the observed frequencies (supplemented by the high level CCSD(T) calculations[10]), moments of inertia, and the potential energy and moment of inertia of the internal rotor,[9] a new third law analysis using the data from Hippler et al.[4] gives the entropy for reaction that differs from the previous analysis by –5.6 J K^{-1} mol^{-1} and a new estimate of $D_0 = 81.5 \pm 0.8$ kJ mol^{-1} and $\Delta H_f°(0\text{ K}) = -7.6$ kJ mol^{-1} ($\Delta H_f°(298\text{ K}) = -14.9$ kJ mol^{-1} and $S_f°(298) = 279$ J K^{-1} mol^{-1}).

For formation of the *trans*,*perp*-HOONO product channel (which is of negligible atmospheric importance), the reaction is written HO + NO_2 → *trans*,*perp*-HOONO. Konen et al.[5,6] used infrared overtone action spectroscopy in a molecular beam apparatus to determine $D_0 = 67.8 \pm 0.4$ kJ mol^{-1}. High level CCSD(T) calculations[5] supported by analysis[7] of the action spectra give vibrational frequencies and moments of inertia. These data are used to calculate $\Delta H_f°(0\text{ K}) = 6.1$ kJ mol^{-1} ($\Delta H_f°(298\text{ K}) = -0.5$ kJ mol^{-1} and $S_f°(298) = 291$ J K^{-1} mol^{-1}). Using these parameters, the equilibrium constant is given by $K_{eq}(trans,perp) = 1.33 \times 10^{-26} \exp(8390/T)$ with uncertainty factors set so that all of the data used for the recommendation fall within the 2σ error bounds.
(Table: 10-6, Note: 10-6, Evaluated: 10-6) Back to Table

(1) Fry, J.; Matthews, L. J.; Lane, J. R.; Sinha, A.; Kjaergaard, H. G.; Wennberg, P. O. OH-Stretch vibrational spectroscopy of hydroxymethyl hydroperoxide. *J. Phys. Chem. A* **2006**, *110*, 7072-7079, doi:10.1021/jp0612127.

(2) Golden, D. M.; Barker, J. R.; Lohr, L. L. Master equation models for the pressure- and temperature-dependent reactions HO + NO_2 → $HONO_2$ and HO + NO_2 → HOONO. *J. Phys. Chem. A* **2003**, *107*, 11057-11071, doi:10.1021/jp0353183.

(3) Golden, D. M.; Barker, J. R.; Lohr, L. L. Correction: Master equation models for the pressure- and temperature-dependent reactions HO + NO_2 → $HONO_2$ and HO + NO_2 → HOONO. *J. Phys. Chem. A* **2004**, *108*, 8552, doi:10.1021/jp040476v.

(4) Hippler, H.; Nasterlack, S.; Striebel, F. Reaction of OH + NO_2 + M: Kinetic evidence of isomer formation. *Phys. Chem. Chem. Phys.* **2002**, *4*, 2959-2964, doi:10.1039/b201932a.

(5) Konen, I. M.; Li, E. X. J.; Stephenson, T. A.; Lester, M. I. Second OH overtone excitation and statistical dissociation dynamics of peroxynitrous acid. *J. Chem. Phys.* **2005**, *123*, 204318, doi:10.1063/1.2126968.

(6) Konen, I. M.; Pollack, L. B.; Li, E. X. J.; Lester, M. I.; Varner, M. E.; Stanton, J. F. Infrared overtone spectroscopy and unimolecular decay dynamics of peroxynitrous acid. *J. Chem. Phys.* **2005**, *122*, 094320, doi:10.1063/1.1854094.

(7) Li, E. X.; Konan, I. M.; Lester, M. I.; McCoy, A. B. Spectroscopic characterization of peroxynitrous acid in cis-perp configurations. *J. Phys. Chem. A* **2006**, *110*, 5607-5613, doi:10.1021/jp056959w.

(8) Matthews, J.; Sinha, A. State-resolved unimolecular dissociation of *cis-cis* HOONO: Product state distributions and action spectrum in the $2\nu_{OH}$ band region. *J. Chem. Phys.* **2005**, *122*, 104313, doi:10.1063/1.858437.
(9) McCoy, A. B.; Fry, J. L.; Francisco, J. S.; Mollner, A. K.; Okumura, M. Role of OH-stretch/torsion coupling and quantum yield effects in the first OH overtone spectrum of *cis-cis* HOONO. *J. Chem. Phys.* **2005**, *122*, 104311, doi:10.1063/1.1859273.
(10) Zhang, X.; Nimlos, M. R.; Ellison, G. B.; Varner, M. E.; Stanton, J. F. Infrared absorption spectra of matrix-isolated *cis*, *cis*-HOONO and its *ab initio* CCSD(T) anharmonic vibrational bands. *J. Chem. Phys.* **2006**, *124*, 084305, doi:10.1063/1.2163343.

3. **$HO_2 + NO_2 \leftrightarrows HO_2NO_2$.** The value was obtained by combining the expression from Table 2-1 for the rate constant of the reaction as written with that from an average of the expressions from Graham et al.[3] and Zabel[4] for the reverse reaction. Values for the entropy and heat of formation of pernitric acid may be extracted. These values are: $S(298\ K) = 71.7$ cal mol^{-1} K^{-1} and $\Delta H_f(298\ K) = -12.9$ kcal mol^{-1}. If the entropy is calculated from the frequencies and moments of inertia given by Chen and Hamilton,[1] the value becomes 71.0 and the heat of formation is –13.1. The values in the Thermochemistry Section of this report reflect these results. A study of the thermal decomposition of HO_2NO_2 by Gierczak et al.[2] combined with values for the association reaction are in agreement.
(Table: 06-2, Note: 06-2, Evaluated: 06-2) Back to Table

(1) Chen, Z.; Hamilton, T. P. Ab initio study of pernitric acid: Comparison with experimental spectra. *J. Phys. Chem.* **1996**, *100*, 15731-15734, doi:10.1021/jp961772d.
(2) Gierczak, T.; Jimenez, E.; Riffault, V.; Burkholder, J. B.; Ravishankara, A. R. Thermal decomposition of HO_2NO_2 (peroxynitric acid, PNA): Rate coefficient and determination of the enthalpy of formation. *J. Phys. Chem. A* **2005**, *109*, 586-596, doi:10.1021/jp046632f.
(3) Graham, R. A.; Winer, A. M.; Pitts, J. N., Jr. Temperature dependence of the unimolecular decomposition of pernitric acid and its atmospheric implications. *Chem. Phys. Lett.* **1977**, *51*, 215-220, doi:10.1016/0009-2614(77)80387-4.
(4) Zabel, F. Unimolecular decomposition of peroxynitrates. *Z. Phys. Chem.* **1995**, *188*, 119-142, doi:10.1524/zpch.1995.188.Part_1_2.119.

4. **$HO_2 + H_2O \leftrightarrows HO_2{\bullet}H_2O$.** The influence of water vapor on the $HO_2 + HO_2$ bimolecular rate constant was first shown by Hamilton,[5] who invoked formation of a $HO_2{\bullet}H_2O$ complex with ~38 kJ mol^{-1} binding energy. Since then, several other groups have quantified the effect on the $HO_2 + HO_2$ reaction (see Table 1). Only two direct measurements of the equilibrium constant have been carried out. Aloisio et al.[1] used FTIR absorption spectroscopy around 1120 cm^{-1} to measure the depletion of gas phase HO_2 as it formed a complex with H_2O. They measured K_{eq} at 230 and 250 K, and obtained only an upper limit at room temperature. Kanno et al.[7,8] also monitored depletion of gas-phase HO_2, but with high resolution FM spectroscopy of the HO_2 A-X transition near 7020 cm^{-1} with apparently higher sensitivity than in the FTIR measurement of Aloisio et al., since they could measure K_{eq} up to much higher temperatures ($250 \le T \le 350$ K). The two studies are in rough agreement on parameter *B*, but differ on parameter *A* by a factor of 7. Kanno et al.'s results are in very good agreement with the parameter A derived from quantum chemistry calculations by Aloisio et al.[1] The indirect estimate of K_{eq} by Cox and Burrows[4] agrees better with Kanno et al., and the indirect estimate by Hamilton and Lii[6] is in better agreement with Aloisio et al. The current recommendation for K_{eq} is based on Kanno et al.[7,8] because their technique had higher sensitivity and because they measured K_{eq} over a much wider temperature range.

A 3rd Law analysis of the Kanno et al. experimental data was carried out using the harmonic frequencies calculated by Aloisio et al.[1] (who used B3LYP/6-311++G(3df,3pd)) and the microwave rotational constants from Suma et al.[10] This gives $S°_{298}(HO_2{\bullet}H_2O) = 314.6$ J K^{-1} mol^{-1} and $D_0 = 34.2 \pm 1.2$ kJ mol^{-1} (one sigma). Since the analysis is based only on the Kanno experiments, we adopt an estimated 95% confidence limit of ±3 kJ mol^{-1}. The results give $\Delta H_{f,0}(HO_2{\bullet}H_2O) = -259.6 \pm 3$ kJ mol^{-1} and $\Delta H_{f,298}(HO_2{\bullet}H_2O) = -268.0 \pm 3$ kJ mol^{-1}. The values of $f(298\ K)$ and g were chosen to include the data of Aloisio et al.[1] Several additional theoretical studies[2,3,9] have investigated complexes of $HO_2{\bullet}(H_2O)_n$ ($n \ge 1$).
(Table: 10-6, Note: 25-1, Evaluated: 10-6) Back to Table

(1) Aloisio, S.; Francisco, J. S.; Friedl, R. R. Experimental evidence for the existence of the HO_2-H_2O complex. *J. Phys. Chem. A* **2000**, *104*, 6597-6601, doi:10.1021/jp0006330.
(2) Alongi, K. S.; Dibble, T. S.; Shields, G. C.; Kirschner, K. N. Exploration of the potential energy surfaces, prediction of atmospheric concentrations, and prediction of vibrational spectra for the $HO_2{\cdots}(H_2O)_n$ (n = 1-2) hydrogen bonded complexes. *J. Phys. Chem. A* **2006**, *110*, 3686-3691, doi:10.1021/jp057165k.

(3) Belair, S. D.; Kais, S.; Francisco, J. S. Potential energy surface for the hydroperoxy and water (HO_2•H_2O) radical complex. *Molec. Phys.* **2002**, *100*, 247-253, doi:10.1080/00268970110086309.
(4) Cox, R. A.; Burrows, J. P. Kinetics and mechanism of the disproportionation of HO_2 in the gas phase. *J. Phys. Chem.* **1979**, *83*, 2560-2568, doi:10.1021/j100483a002.
(5) Hamilton, E. J., Jr. Water vapor dependence of the kinetics of the self-reaction of HO_2 in the gas phase. *J. Chem. Phys.* **1975**, *63*, 3682-3683, doi:10.1063/1.431772.
(6) Hamilton, E. J., Jr.; Lii, R.-R. The dependence on H_2O and on NH_3 of the kinetics of the self-reaction of HO_2 in the gas-phase formation of HO_2•H_2O and HO_2•NH_3 complexes. *Int. J. Chem. Kinet.* **1977**, *9*, 875-885, doi:10.1002/kin.550090604.
(7) Kanno, N.; Tonokura, K.; Koshi, M. Equilibrium constant of the HO_2-H_2O complex formation and kinetics of HO_2 + HO_2-H_2O: Implications for tropospheric chemistry. *J. Geophys. Res.* **2006**, *111*, D20312, doi:10.1029/2005JD006805.
(8) Kanno, N.; Tonokura, K.; Tezaki, A.; Koshi, M. Water dependence of the HO_2 self reaction: Kinetics of the HO_2−H_2O complex. *J. Phys. Chem. A* **2005**, *109*, 3153-3158, doi:10.1021/jp044592+.
(9) Shirts, R. B.; Kumbhani, S. R.; Burrell, E.; Hansen, J. C. An improved model to calculate equilibrium constants for formation of peroxy radical-water complexes. *Theor. Chem. Acc.* **2018**, *137*, 96.
(10) Suma, K.; Sumiyoshi, Y.; Endo, Y. The rotational spectrum of the water-hydroperoxy radical (H_2O-HO_2) complex. *Science* **2006**, *311*, 1278-1281, doi:10.1126/science.112402.

5. **HO_2 + CH_3OH ⇆ HO_2•CH_3OH.** The influence of CH_3OH on the HO_2 + HO_2 bimolecular rate constant was first shown by Andersson et al.,[1] who invoked formation of a HO_2•CH_3OH complex with ~25 kJ mol^{-1} binding energy to explain their results. Since then, several other groups have quantified the effect on the HO_2 + HO_2 reaction (see Table 1). The only direct measurement of the equilibrium constant was carried out by Christensen et al.[2] from 231 to 261 K. Their measurements are the basis for this recommendation. They obtained $\Delta_rH°$(246 K) = –37.4 ± 4.8 kJ mol^{-1} and $\Delta_rS°$(246 K) = –100 ± 19 J K^{-1} mol^{-1}. Christensen et al. also measured the forward and reverse rate constants and performed ab initio calculations, which are in reasonable agreement with the measured thermochemistry.
(Table: 10-6, Note: 10-6, Evaluated: 10-6) Back to Table

(1) Andersson, B. Y.; Cox, R. A.; Jenkin, M. E. The effect of methanol on the self reaction of HO_2 radicals. *Int. J. Chem. Kinet.* **1988**, *20*, 283-295, doi:10.1002/kin.550200403.
(2) Christensen, L. E.; Okumura, M.; Hansen, J. C.; Sander, S. P.; Francisco, J. S. Experimental and ab initio study of the HO_2•CH_3OH complex: Thermodynamics and kinetics of formation. *J. Phys. Chem. A* **2006**, *110*, 6948-6959, doi:10.1021/jp056579a.

6. **HO_2 + CH_2O ⇆ $HOCH_2OO$.** The recommendation is based on the data of Barnes et al.,[2] Burrows et al.,[4] Veyret et al.,[9] and Morajkar et al.[7] All of these measurements, which are in good agreement with each other, relied on optical absorption to monitor the free radicals. The early measurement of Su et al.[8] is considerably higher, for unknown reasons, as are the measurements of Zabel et al.,[10] who utilized electron spin resonance to monitor the radical concentrations. The temperature dependence reported by Zabel et al. is in good agreement with the current recommendation, although the reported absolute magnitude of Zabel et al.'s K_{eq} is systematically about a factor of 6 or 7 greater. Theoretical work on this reaction has been reported by Evleth et al.,[5] Aloisio and Francisco,[1] Benson,[3] and Hermans et al.[6]
(Table: 15-10, Note: 15-10, Evaluated: 15-10) Back to Table

(1) Aloisio, S.; Francisco, J. S. Complexes of hydroxyl and hydroperoxyl radical with formaldehyde, acetaldehyde, and acetone. *J. Phys. Chem. A* **2000**, *104*, 3211-3224, doi:10.1021/jp993789c.
(2) Barnes, I.; Becker, K. H.; Fink, E. H.; Reimer, A.; Zabel, F.; Niki, H. FTIR spectroscopic study of the gas-phase reaction of HO_2 with H_2CO. *Chem. Phys. Lett.* **1985**, *115*, 1-8, doi:10.1016/0009-2614(85)80091-9.
(3) Benson, S. W. Some observations on the kinetics and thermochemistry of the reactions of HO_2 radicals with aldehydes and ketones. *Int. J. Chem. Kinet.* **2001**, *33*, 509-512, doi:10.1002/kin.1047.
(4) Burrows, J. P.; Moortgat, G. K.; Tyndall, G. S.; Cox, R. A.; Jenkin, M. E.; Hayman, G. D.; Veyret, B. Kinetics and mechanism of the photooxidation of formaldehyde. 2. Molecular modulation studies. *J. Phys. Chem.* **1989**, *93*, 2375-2382, doi:10.1021/j100343a034.
(5) Evleth, E. M.; Melius, C. F.; Rayez, M. T.; Rayez, J. C.; Forst, W. Theoretical characterization of the reaction of hydroperoxy with formaldehyde. *J. Phys. Chem.* **1993**, *97*, 5040-5045, doi:10.1021/j100121a031.
(6) Hermans, I.; Muller, J. F.; Nguyen, T. L.; Jacobs, P. A.; Peeters, J. Kinetics of alpha-hydroxy-alkylperoxyl radicals in oxidation processes. HO_2 initiated oxidation of ketones/aldehydes near the tropopause. *J. Phys. Chem. A* **2005**, *109*, 4303-4311, doi:10.1021/jp044080v.

(7) Morajkar, P.; Schoemaecker, C.; Okumura, M.; Fittchen, C. Direct measurement of the equilibrium constants of the reaction of formaldehyde and acetaldehyde with HO_2 radicals. *Int. J. Chem. Kinet.* **2014**, *46*, 245-259, doi:10.1002/kin.20817.
(8) Su, F.; Calvert, J. G.; Shaw, J. H. Mechanism of the photooxidation of gaseous formaldehyde. *J. Phys. Chem.* **1979**, *83*, 3185-3191, doi:10.1021/j100488a001.
(9) Veyret, B.; Lesclaux, R.; Rayez, M.-T.; Rayez, J.-C.; Cox, R. A.; Moortgat, G. K. Kinetics and mechanism of the photooxidation of formaldehyde. 1. Flash photolysis study. *J. Phys. Chem.* **1989**, *93*, 2368-2374, doi:10.1021/j100343a033.
(10) Zabel, F.; Sahetchian, K. A.; Chachaty, C. ESR spectra of free radicals formed during the gas-phase photo-oxidation of formaldehyde: Thermal stability of the $HOCH_2OO$ radical. *Chem. Phys. Lett.* **1987**, *134*, 433-437, doi:10.1016/0009-2614(87)87168-3.

7. **$HO_2 + CH_3CHO \leftrightarrows CH_3CH(OH)OO$.** Tomas et al.[5] measured this equilibrium constant from 298 to 373 K by using flash photolysis with time resolved UV absorption spectroscopy to monitor all three species ($K_{eq} \approx 5.9 \times 10^{-17}$ cm^3 molecule^{-1} at 298 K). Moortgat et al.[3] obtained product quantum yields from the photo-oxidation of CH_3CHO in air. In carrying out their data analysis, which involved a complicated chemical mechanism, they estimated $K_{eq} \approx 1 \times 10^{-17}$ cm^3 molecule^{-1} at 298 K. Morajkar et al.[4] used laser flash photolysis with cavity ring-down spectroscopy (CRDS) at 297 K to monitor HO_2 radicals in real time; acetaldehyde concentrations were established by preparing gas mixtures (periodically checked in the cell by using laser induced fluorescence of OH and the known rate constant for OH + CH_3CHO). In their experiments, the HO_2 bi-exponential decays were used to extract $K_{eq} = (1.7 \pm 0.5) \times 10^{-17}$ cm^3 molecule^{-1} at 298 K without the necessity of measuring the concentration of $CH_3CH(OH)OO$ directly. The recommendation is based on the value obtained by Morajkar et al.[4] and the temperature dependence determined by Tomas et al.;[5] error bounds were set large enough to include almost all of the reported data. Theoretical calculations have been reported by Aloisia and Francisco[1] and by Hermans et al.[2]
(Table: 15-10, Note: 15-10, Evaluated: 15-10) Back to Table

(1) Aloisio, S.; Francisco, J. S. Complexes of hydroxyl and hydroperoxyl radical with formaldehyde, acetaldehyde, and acetone. *J. Phys. Chem. A* **2000**, *104*, 3211-3224, doi:10.1021/jp993789c.
(2) Hermans, I.; Muller, J. F.; Nguyen, T. L.; Jacobs, P. A.; Peeters, J. Kinetics of alpha-hydroxy-alkylperoxyl radicals in oxidation processes. HO_2 initiated oxidation of ketones/aldehydes near the tropopause. *J. Phys. Chem. A* **2005**, *109*, 4303-4311, doi:10.1021/jp044080v.
(3) Moortgat, G. K.; Meyrahn, H.; Warneck, P. Photolysis of acetaldehyde in air: CH_4, CO and CO_2 quantum yields. *ChemPhysChem* **2010**, *11*, 3896-3908, doi:10.1002/cphc.201000757.
(4) Morajkar, P.; Schoemaecker, C.; Okumura, M.; Fittchen, C. Direct measurement of the equilibrium constants of the reaction of formaldehyde and acetaldehyde with HO_2 radicals. *Int. J. Chem. Kinet.* **2014**, *46*, 245-259, doi:10.1002/kin.20817.
(5) Tomas, A. E.; Villenave, E.; Lesclaux, R. Reactions of the HO_2 radical with CH_3CHO and $CH_3C(O)O_2$ in the gas phase. *J. Phys. Chem. A* **2001**, *105*, 3505-3514, doi:10.1021/jp003762p.

8. **$HO_2 + CH_3C(O)CH_3 \leftrightarrows HO_2{\bullet}CH_3C(O)CH_3$.** The recommendation is based on the measured equilibrium constants that have been reported by Grieman et al.[4] and Dillon et al.[3] The two sets of data are in excellent agreement with each other. Both groups measured the HO_2 concentration with and without added acetone and identified the concentration difference with the concentration of the product (neither group observed the product adduct directly). Grieman et al. controlled the acetone concentration by temperature control of its vapor pressure and measured the HO_2 concentration by tunable IR diode laser absorption. Dillon et al used UV absorption to monitor the HO_2 and acetone concentrations. Both groups used information from theoretical calculations and other sources to determine that the product is the hydrogen bonded molecular complex (HBMC) and not the 2-hydroxyisopropylperoxyl radical isomer that is expected to be formed subsequently by a "tail-biting" cyclic hydrogen transfer reaction (analogous to the one that occurs in the reaction of HO_2 + CH_2O). Theoretical calculations at various levels of theory have been reported by Aloisio and Francisco,[1] Hermans et al.,[6] Hermans et al.,[5] Cours et al.,[2] and Dillon et al.[3]
(Table 15-10, Note 15-10, Evaluation 15-10) Back to Table

(1) Aloisio, S.; Francisco, J. S. Complexes of hydroxyl and hydroperoxyl radical with formaldehyde, acetaldehyde, and acetone. *J. Phys. Chem. A* **2000**, *104*, 3211-3224, doi:10.1021/jp993789c.
(2) Cours, T.; Canneaux, S.; Bohr, F. Features of the potential energy surface for the reaction of HO_2 radical with acetone. *Int. J. Quant. Chem.* **2007**, *107*, 1344-1354, doi:10.1002/qua.21269.
(3) Dillon, T. J.; Pozzer, A.; Vereecken, L.; Crowley, J. N.; Lelieveld, J. Does acetone react with HO_2 in the upper-troposphere? *Atmos. Chem. Phys.* **2012**, *12*, 1339-1351, doi:10.5194/acp-12-1339-2012.

(4) Grieman, F. J.; Noell, A. C.; Davis-Van Atta, C.; Okumura, M.; Sander, S. P. Determination of equilibrium constants for the reaction between acetone and HO_2 using infrared kinetic spectroscopy. *J. Phys. Chem. A* **2011**, *115*, 10527–10538, doi:10.1021/jp205347s.
(5) Hermans, I.; Muller, J. F.; Nguyen, T. L.; Jacobs, P. A.; Peeters, J. Kinetics of alpha-hydroxy-alkylperoxyl radicals in oxidation processes. HO_2 initiated oxidation of ketones/aldehydes near the tropopause. *J. Phys. Chem. A* **2005**, *109*, 4303-4311, doi:10.1021/jp044080v.
(6) Hermans, I.; Nguyen, T. L.; Jacobs, P. A.; Peeters, J. Tropopause chemistry revisited: HO_2*-initiated oxidation as an efficient acetone sink. *J. Am. Chem. Soc.* **2004**, *126*, 9908-9909, doi:10.1021/ja0467317.

9. **$NO + NO_2 \leftrightarrows N_2O_3$.** The data are from JANAF[2] and Chao et al.[1] This process is included because a measurement of the rate constant by Smith and Yarwood[4] and Markwalder et al.[3] shows that it is too slow to be an important process in most atmospheric and laboratory systems.
(Table: 94-26, Note: 94-26, Evaluated: 94-26) Back to Table

(1) Chao, J.; Wilhoit, R. C.; Zwolinski, B. J. Gas phase chemical equilibrium in dinitrogen trioxide and dinitrogen tetroxide. *Thermochim. Acta* **1974**, *10*, 359-371.
(2) JANAF *Thermochemical Tables*, Third ed.; National Bureau of Standards, 1985.
(3) Markwalder, B.; Gozel, P.; van den Bergh, H. Temperature-jump measurements on the kinetics of association and dissociation in weakly bound systems: $N_2O_4 + M = NO_2 + NO_2 + M$. *J. Chem. Phys.* **1992**, *97*, 5472-5479, doi:10.1063/1.463780.
(4) Smith, I. W. M.; Yarwood, G. Kinetic measurements on the system $NO + NO_2 \rightleftarrows N_2O_3$ by time-resolved infrared laser absorption. *Chem. Phys. Lett.* **1986**, *130*, 24-28, doi:10.1016/0009-2614(86)80418-3.

10. **$NO_2 + NO_2 \leftrightarrows N_2O_4$.** The data are from JANAF[8] and Vosper,[11] Chao et al.,[4] and Amoruso et al.[1] Rate data for this process are reported by Brunning et al.,[3] Borrell et al.,[2] Gozel et al.,[6] and Markwalder et al.[9] A direct study by Harwood and Jones[7] at low temperatures is in agreement with the recommendation. Estupiñán et al.,[5] Wollenhaupt and Crowley,[12] and Tuchler et al.[10] deduce values that are essentially in agreement, within uncertainties, with the recommendation.
(Table: 06-2, Note: 06-2, Evaluated: 06-2) Back to Table

(1) Amoruso, A.; Crescentini, L.; Fiocco, G.; Volpe, M. New measurements of the NO_2 absorption cross section in the 440- to 460-nm region and estimates of the NO_2-N_2O_4 equilibrium constant. *J. Geophys. Res.* **1993**, *98*, 16857-16863, doi:10.1029/93JD01582.
(2) Borrell, P.; Cobos, C. J.; Luther, K. Falloff curve and specific rate constants for the reaction $NO_2 + NO_2 \rightleftarrows N_2O_4$. *J. Phys. Chem.* **1988**, *92*, 4377-4384, doi:10.1021/j100326a027.
(3) Brunning, J.; Frost, M. J.; Smith, I. W. M. Kinetic measurements on the system: $2NO_2 \leftrightharpoons N_2O_4$ at (224 ± 2) K using time-resolved infrared laser absorption. *Int. J. Chem. Kinet.* **1988**, *20*, 957-965, doi:10.1002/kin.550201204.
(4) Chao, J.; Wilhoit, R. C.; Zwolinski, B. J. *Thermochim. Acta* **1974**, *10*, 361-371.
(5) Estupiñán, E. G., J. M. Nicovich and P.H. Wine A temperature-dependent kintetics study of the important stratospheric reaction $O(^3P) + NO_2 \rightarrow O_2 + NO$. *J. Phys. Chem. A* **2001**, *105*, 9697-9703, doi:10.1021/jp011940o.
(6) Gozel, P.; Calpani, B.; van den Bergh, H. Temperature jump measurements in gas kinetics. *Israel J. Chem.* **1984**, *24*, 210-213.
(7) Harwood, M. H.; Jones, R. L. Temperature dependent ultraviolet-visible absorption cross sections of NO_2 and N_2O_4: Low-temperature measurements of the equilibrium constant for $2NO_2 \rightleftharpoons N_2O_4$. *J. Geophys. Res.* **1994**, *99*, 22955-22964, doi:10.1029/94JD01635
(8) JANAF *Thermochemical Tables*, Third ed.; National Bureau of Standards, 1985.
(9) Markwalder, B.; Gozel, P.; van den Bergh, H. Temperature-jump measurements on the kinetics of association and dissociation in weakly bound systems: $N_2O_4 + M = NO_2 + NO_2 + M$. *J. Chem. Phys.* **1992**, *97*, 5472-5479, doi:10.1063/1.463780.
(10) Tuchler, M. F.; Schmidt, K. L.; Morgan, M. A CRDS approach to gas phase equilibrium constants: the case of $N_2O_4 \leftrightarrow 2NO_2$ at 283 K. *Chem. Phys. Lett.* **2005**, *401*, 393-399, doi:10.1016/j.cplett.2004.11.083.
(11) Vosper, A. J. Dissociation of dinitrogen tetroxide in gas phase. *J. Chem. Soc. A* **1970**, *1970*, 625-627, doi:10.1039/J19700000625.
(12) Wollenhaupt, M.; Crowley, J. N. Kinetic studies of the reactions $CH_3 + NO_2 \rightarrow$ products, $CH_3O + NO_2 \rightarrow$ products, and $OH + CH_3C(O)CH_3 \rightarrow CH_3C(O)OH + CH_3$, over a range of temperature and pressure. *J. Phys. Chem. A* **2000**, *104*, 6429-6438, doi:10.1021/jp0005726.

11. **$NO_2 + NO_3 \leftrightarrows N_2O_5$.** The recommendation is based on the direct measurements of K_{eq} reported by Cantrell et al.,[4] Hjorth et al.,[8] and Osthoff et al.[11] As pointed out by Osthoff et al., the differences among the direct measurements of K_{eq} differ mostly because of calibration errors in the absorption coefficients of NO_2, N_2O_5, and the NO_3 radical. The recommended parameters are based on the average of independent Third Law analyses of each experimental data set, carried out using the entropy of N_2O_5 computed by Alecu and Marshall.[1,2] Alecu and Marshall[1,2] employed a combination of M06-2X density functional theory and single point calculations at the CCSD(T)-F12a/cc-pVTZ-F12 level of theory, obtaining results in good general agreement with those computed by Glendening and Halpern.[6] From their results, Alecu and Marshall computed the entropy of N_2O_5 by using the multi-structural method to account for the combination of the two internal torsions in the molecule, obtaining $\Delta S_f^0(298\ K) = 353.45\ J\ K^{-1}\ mol^{-1}$.

The averaged Third Law analyses performed for this evaluation give $\Delta S_r^0 = -145.25\ J\ K^{-1}\ mol^{-1}$ and $\Delta H_r^0 = -94.25\ kJ\ mol^{-1}$ at 298.15 K. These results are in excellent agreement with a similar analysis reported by Alecu and Marshall[1,2] for the data of Osthoff et al. The current recommended values for K_{eq} are similar to a previous recommendation, which was based on the 'kinetics' K_{eq} reported by Cantrell et al.,[4] who carried out a thorough review of previous literature. Cantrell et al. used only their own measured rate constants for the decomposition reaction and the rate constants reported by Orlando et al.[10] for the recombination reaction to derive the 'kinetics' K_{eq}. The current recommendation is also in good agreement with the data of Burrows et al.[3] and with the room temperature data of Tuazon et al.[16] and of Perner et al.,[12] and with the exponential factor of Wängberg et al.[18] (although their absolute values of K_{eq} differ significantly, probably due to an unidentified calibration error). It is also in good agreement with the evaluation by Pritchard,[13] who reviewed the data of Cantrell et al.[4], Burrows et al.,[3] Graham and Johnston,[7] Wängberg et al.,[18] Schott and Davidson,[14] and the room temperature data of Tuazon et al.,[16] Perner et al.,[12] and Hjorth et al.[8] Pritchard also included the values given by Smith et al.,[15] and Kircher et al.,[9] who combined data on the forward reaction with decomposition data of Connell and Johnston[5] and Viggiano et al.[17]

(Table: 25-1, Note: 25-1, Evaluation: 25-1) Back to Table

(1) Alecu, I. M.; Marshall, P. Computational study of the thermochemistry of N_2O_5 and the kinetics of the reaction $N_2O_5 + H_2O \rightarrow 2\ HNO_3$. *J. Phys. Chem. A* **2014**, *118*, 11405−11416, doi:10.1021/jp509301t.

(2) Alecu, I. M.; Marshall, P. Correction to "Computational study of the thermochemistry of N_2O_5 and the kinetics of the reaction $N_2O_5 + H_2O \rightarrow 2\ HNO_3$". *J. Phys. Chem. A* **2016**, *120*, 10305−10305, doi:10.1021/acs.jpca.6b12514.

(3) Burrows, J. P.; Tyndall, G. S.; Moortgat, G. K. A study of the N_2O_5 equilibrium betwen 275 and 315 K and determination of the heat of formation of NO_3. *Chem. Phys. Lett.* **1985**, *119*, 193-198, doi:10.1016/0009-2614(85)80059-2.

(4) Cantrell, C. A.; Davidson, J. A.; McDaniel, A. H.; Shetter, R. E.; Calvert, J. G. The equilibrium constant for $N_2O_5 \rightleftarrows NO_2 + NO_3$: Absolute determination by direct measurement from 243 to 397 K. *J. Chem. Phys.* **1988**, *88*, 4997-5006, doi:10.1063/1.454679.

(5) Connell, P. S.; Johnston, H. S. The thermal dissociation of N_2O_5 in N_2. *Geophys. Res. Lett.* **1979**, *6*, 553-556, doi:10.1029/GL006i007p00553.

(6) Glendening, E. D.; Halpern, A. M. Ab initio calculations of nitrogen oxide reactions: Formation of N_2O_2, N_2O_3, N_2O_4, N_2O_5, and N_4O_2 from NO, NO_2, NO_3, and N_2O. *J. Chem. Phys.* **2007**, *127*, 164307, doi:10.1063/1.2777145.

(7) Graham, R. A.; Johnston, H. S. The photochemistry of NO_3 and the kinetics of the N_2O_5-O_3 system. *J. Phys. Chem.* **1978**, *82*, 254-268, doi:10.1021/j100492a002.

(8) Hjorth, J.; Nothholt, J.; Restelli, G. A spectroscoy study of the equilibrium $NO_2 + NO_3 + M \leftrightharpoons N_2O_5 + M$ and the kinetics of the $O_3/N_2O_5/NO_3/NO_2$/air system. *Int. J. Chem. Kinet.* **1992**, *24*, 51-65, doi:10.1002/kin.550240107.

(9) Kircher, C. C.; Margitan, J. J.; Sander, S. P. Temperature and pressure dependence study of the reaction $NO_2 + NO_3 + M \rightarrow N_2O_5 + M$. *J. Phys. Chem.* **1984**, *88*, 4370-4375, doi:10.1021/j150663a037.

(10) Orlando, J. J.; Tyndall, G. S.; Cantrell, C. A.; Calvert, J. G. Temperature and pressure dependence of the rate coefficient for the reaction $NO_3 + NO_2 \rightarrow N_2O_5 + N_2$. *J. Chem. Soc. Faraday Trans.* **1991**, *87*, 2345-2349, doi:10.1039/ft9918702345.

(11) Osthoff, H. D.; Pilling, M. J.; Ravishankara, A. R.; Brown, S. S. Temperature dependence of the NO_3 absorption cross-section above 298 K and determination of the equilibrium constant for $NO_3 + NO_2 \leftrightarrow N_2O_5$ at atmospherically relevant conditions. *Phys. Chem. Chem. Phys.* **2007**, *9*, 5785-5793, doi:10.1039/b709193a.

(12) Perner, D.; Schmeltekopf, A.; Winkler, R. H.; Johnston, H. S.; Calvert, J. G.; Cantrell, C. A.; Stockwell, W. R. A laboratory and field study of the equilibrium $N_2O_5 \rightleftharpoons NO_3 + NO_2$. *J. Geophys. Res.* **1985**, *90*, 3807-3812, doi:10.1029/JD090iD02p03807.

(13) Pritchard, H. O. The nitrogen pentoxide dissociation equilibrium. *Int. J. Chem. Kinet.* **1994**, *26*, 61-72, doi:10.1002/kin.550260108.
(14) Schott, G.; Davidson, N. Shock waves in chemical kinetics: The decomposition of N_2O_5 at high temperatures. *J. Am. Chem. Soc.* **1958**, *80*, 1841-1853, doi:10.1021/ja01541a019.
(15) Smith, C. A.; Ravishankara, A. R.; Wine, P. H. Kinetics of the reaction $NO_2 + NO_3 + M$ at low pressures and 298 K. *J. Phys. Chem.* **1985**, *89*, 1423-1427, doi:10.1021/j100254a024.
(16) Tuazon, E. C.; Sanhueza, E.; Atkinson, R.; Carter, W. P. L.; Winer, A. M.; Pitts, J. N., Jr. Direct determination of the equilibrium constant at 298 K for the $NO_2 + NO_3 \leftrightarrow N_2O_5$ reactions. *J. Phys. Chem.* **1984**, *88*, 3095-3098, doi:10.1021/j150658a033.
(17) Viggiano, A. A.; Davidson, J. A.; Fehsenfeld, F. C.; Ferguson, E. E. Rate constants for the collisional dissociation of N_2O_5 by N_2. *J. Chem. Phys.* **1981**, *74*, 6113-6125, doi:10.1063/1.441055.
(18) Wängberg, I.; Etzkorn, T.; Barnes, I.; Platt, U.; Becker, K. H. Absolute determination of the temperature behavior of the $NO_2 + NO_3 + (M) \leftrightarrow N_2O_5 + (M)$ equilibrium. *J. Phys. Chem. A* **1997**, *101*, 9694-9698, doi:10.1021/jp972203o.

12. **$CH_3O_2 + NO_2 \leftrightarrows CH_3O_2NO_2$.** Zabel et al.[4] have measured k(dissociation) as a function of pressure ($10 < P < 800$ Torr) and temperature ($253 < T < 272$ K). Bahta et al.[1] have measured k(dissociation) at 263 K. Using the values of k(recombination) suggested in this evaluation (Table-2), Golden[3] has re-evaluated the equilibrium constant. Bridier et al.[2] measure an equilibrium constant in good agreement with this recommendation, reducing the uncertainty even further.
(Table: 06-2, Note: 06-2, Evaluated: 06-2) Back to Table

(1) Bahta, A.; Simonaitis, R.; Heicklen, J. Thermal decomposition kinetics of $CH_3O_2NO_2$. *J. Phys. Chem.* **1982**, *86*, 1849-1853, doi:10.1021/j100207a022.
(2) Bridier, I.; Lesclaux, R.; Veyret, B. Flash photolysis kinetic study of the equilibrium $CH_3O_2 + NO_2 \leftrightarrow CH_3O_2NO_2$. *Chem. Phys. Lett.* **1992**, *191*, 259-263, doi:10.1016/0009-2614(92)85297-N.
(3) Golden, D. M. Evaluating data for atmospheric models, an example: $CH_3O_2 + NO_2 = CH_2O_2NO_2$. *Int. J. Chem. Kinet.* **2005**, *37*, 625-632, doi:10.1002/kin.20104.
(4) Zabel, F.; Reimer, A.; Becker, K. H.; Fink, E. H. Thermal decomposition of alkyl peroxynitrates. *J. Phys. Chem.* **1989**, *93*, 5500-5507, doi:10.1021/j100351a036.

13. **$CH_3C(O)O_2 + NO_2 \leftrightarrows CH_3C(O)O_2NO_2$.** The recommendation is derived from measurements of the rate constants in both directions. The recombination (forward) rate constants measured directly by Bridier et al.[1] were fit by non-linear least squares, weighted by assuming uniform relative errors. Direct measurements of the forward reaction by Sehested et al.[11] at 298 K are in excellent agreement. Relative rate measurements by Cox et al.,[4] Kirchner et al.,[6] Tuazon et al.,[12] Seefeld et al.,[10] and Sehested et al.[11] are confirmative. Measured rate constants for the reverse direction (unimolecular dissociation) taken from Bridier et al.[1] and from Sehested et al.[11] were used with the fitted expression for the forward rate constant to determine values for the "experimental" equilibrium constants, which were then used in a third law analysis. Data for the unimolecular decomposition reported by Roberts and Bertman[9] and by Kabir et al.[5] are in good agreement, but with larger scatter.

The third law analysis performed here employed vibrational frequencies for peroxyacetylnitrate reported by Coronel et al.[3] and rotational constants calculated by von Ahsen et al.[13]; the 1D hindered internal rotations of the CH_3 and NO_2 groups were treated explicitly. Parameters for acetyl radical were taken from Maranzana et al.[7], and those for NO_2 were taken from the JANAF Tables.[2] The recommended expression for the equilibrium constant was obtained by fitting the third law values for K_{eq} from 180 to 300 K, and is in good agreement with the previous recommendation, but is based on more experimental data and higher level theoretical calculations. The estimated error limits were chosen so that most of the data used for the recommendation fall within the 2σ error bounds. The third law value of the reaction enthalpy is reproduced in a theoretical study by Miller et al.[8] A theoretical study by Wei et al.[14] is noted.
(Table: 25-1, Note: 25-1, Evaluated 25-1) Back to Table

(1) Bridier, I.; Caralp, F.; Loirat, H.; Lesclaux, R.; Veyret, B.; Becker, K. H.; Reimer, A.; Zabel, F. Kinetic and theoretical studies of the reactions $CH_3C(O)O_2 + NO_2 + M \rightleftarrows CH_3C(O)O_2NO_2 + M$ between 248 and 393 K and between 30 and 760 Torr. *J. Phys. Chem.* **1991**, *95*, 3594-3600, doi:10.1021/j100162a031.
(2) Chase, M. W. NIST-JANAF thermochemical tables. *J. Phys. Chem. Ref. Data* **1998**, *Monograph 9*.
(3) Coronel, A. C.; Fernández, L. E.; Varetti, E. L. Scaled quantum mechanical force fields for the peroxynitrates. I. Acetyl peroxynitrate and trifluoroacetyl peroxynitrate. *Z. Anorg. Allg. Chem.* **2010**, *636*, 524–530, doi:10.1002/zaac.200900384.

(4) Cox, R. A.; Roffey, M. J. Thermal decomposition of peroxyacetylnitrate in the presence of nitric oxide. *Environ. Sci. Technol.* **1977**, *11*, 900-906, doi:10.1021/es60132a010.
(5) Kabir, M.; Jagiella, S.; Zabel, F. Thermal stability of n-acyl peroxynitrates. *Int. J. Chem. Kinet. 1–8, 2014* **2014**, *46*, 1-8, doi:10.1002/kin.20862.
(6) Kirchner, F.; Zabel, F.; Becker, K. H. Determination of the rate constant ratio for the reactions of the acetylperoxy radical with NO and NO_2. *Ber. Bunsenges. Phys. Chem.* **1990**, *94*, 1379-1382, doi:10.1002/bbpc.199000037.
(7) Maranzana, A.; Barker, J. R.; Tonachini, G. Master equation simulations of competing unimolecular and bimolecular reactions: Application to OH production in the reaction of acetyl radical with O_2. *Phys. Chem. Chem. Phys.* **2007**, *9*, 4129 - 4141, doi:10.1039/b705116f.
(8) Miller, C. E.; Lynton, J. I.; Keevil, D. M.; Franscisco, J. S. Dissociation pathways of peroxyacetyl nitrate (PAN). *J. Phys. Chem. A* **1999**, *103*, 11451-11459, doi:10.1021/jp992667h.
(9) Roberts, J. M.; Bertman, S. B. The thermal decomposition of peroxyacetic nitric anhydride (PAN) and peroxymethacrylic nitric anhydride (MPAN). *Int. J. Chem. Kinet.* **1992**, *24*, 297-307, doi:10.1002/kin.550240307.
(10) Seefeld, S.; Kinnison, D. J.; Kerr, J. A. Relative rate study of the reactions of acetylperoxy radicals with NO and NO_2: Peroxyacetyl nitrate formation under laboratory conditions related to the troposphere. *J. Phys. Chem. A* **1997**, *101*, 55-59, doi:10.1021/jp962266r.
(11) Sehested, J.; Christensen, L. K.; Mogelberg, T.; Nielsen, O. J.; Wallington, T. J.; Guschin, A.; Orlando, J. J.; Tyndall, G. S. Absolute and relative rate constants for the reactions $CH_3C(O)O_2$ + NO and $CH_3C(O)O_2$ + NO_2 and thermal stability of $CH_3C(O)O_2NO_2$. *J. Phys. Chem. A* **1998**, *102*, 1779-1789, doi:10.1021/jp972881a.
(12) Tuazon, E. C.; Carter, W. P. L.; Atkinson, R. Thermal decomposition of peroxyacetyl nitrate and reactions of acetyl peroxy radicals with NO and NO_2 over the temperature range 283-313 K. *J. Phys. Chem.* **1991**, *95*, 2434-2437, doi:10.1021/j100159a059.
(13) von Ahsen, S.; Wilner, H.; Francisco, J. S. Thermal decomposition of peroxy acetyl nitrate $CH_3C(O)OONO_2$. *J. Chem. Phys.* **2004**, *121*, 2048-2057, doi:10.1063/1.1767813.
(14) Wei, W.-M.; Tan, W.; Zheng, R.-H.; He, T.-J.; Chen, D.-M.; Liu, F.-C. Ab initio studies of isomerization and dissociation reactions of peroxyacetyl nitrate (PAN). *Chem. Phys.* **2005**, *312*, 241-259, doi:10.1016/j.chemphys.2004.12.007.

14. **$CH_3CH_2C(O)O_2 + NO_2 \leftrightarrows CH_3CH_2C(O)O_2NO_2$.** Assumed to be the same as for PAN. Both sides of the of the reaction differ from PAN by the group C–(C)(CO)$(H)_2$. Error limits are estimated and expanded from those for PAN.
(Table: 02-25, Note: 02-25, Evaluated: 02-25) Back to Table

15. **$CH_3C(O)CH_2 + O_2 \leftrightarrows CH_3C(O)CH_2O_2$.** Hassouna et al.[1] measured the rate constant and equilibrium constant for this reaction. The temperature range for the equilibrium measurements was 459< T <520 K. They extracted the entropy and enthalpy changes over this temperature range from a van't Hoff plot (Second Law). Values reported are $\Delta S = -143.0 \pm 4.0$ J mol^{-1} K^{-1} and $\Delta H = -105.0 \pm 2.0$ kJ mol^{-1}. The value in Table 3 is computed assuming that these thermochemical values are constant to 200 K. They also performed quantum calculations, which confirmed the enthalpy measurement. They suggest $\Delta H_{f,298}(CH_3C(O)CH_2) = -32.9 \pm 2.0$ kJ mol^{-1}.
(Table: 10-6, Note: 10-6, Evaluated: 10-6) Back to Table

(1) Hassouna, M.; Delbos, E.; Devolder, P.; Viskolcz, B.; Fittschen, C. Rate and equilibrium constant of the reaction of 1-methylvinoxy radicals with O_2: $CH_3COCH_2 + O_2 \leftrightarrow CH_3COCH_2O_2$. *J. Phys. Chem. A* **2006**, *110*, 6667-6672, doi:10.1021/jp0558270.

16. **$F + O_2 \leftrightarrows FOO$.** Taken from Campuzano-Jost et al.[1] There is good agreement with data from Pagsberg et al.[6] This corresponds to a value for $\Delta H_{f,298}(FO_2) = 6.13 \pm 0.5$ kcal mol^{-1}. There are several modern theoretical computations [2,3,5] of this value, ranging from 6 to 9 kcal mol^{-1}. Feller et al.[4] compute 5.8 ± 0.3 kcal mol^{-1}.
(Table: 10-6, Note: 10-6, Evaluated: 10-6) Back to Table

(1) Campuzano-Jost, P.; Croce, A. E.; Hippler, H.; Siefke, M.; Troe, J. Kinetic and thermodynamic properties of the F + O_2 reaction system under high pressure and low temperature conditions. *J. Chem. Phys.* **1995**, *102*, 5317-5326, doi:10.1063/1.469258.
(2) Denis, P. A., and O. N. Ventura CCSDT study of the fluoroperoxyl radical, FOO. *Chem. Phys. Lett.* **2004**, *385*, 292-297, doi:10.1016/j.cplett.2003.12.081.
(3) Feller, D.; Dixon, D. A. Coupled cluster theory and multireference configuration interaction study of FO, F_2O, FO_2, and FOOF. *J. Phys. Chem. A* **2003**, *107*, 9641-9651, doi:10.1021/jp030267v.

(4) Feller, D.; Peterson, K. A.; Dixon, D. A. A survey of factors contributing to accurate theoretical predictions of atomization energies and molecular structures. *J. Chem. Phys.* **2008**, *129*, 204105, doi:10.1063/1.3008061.
(5) Francisco, J. S., Y. Zhao, W. A. Lester, Jr., and I. H. Williams Theoretical studies of the structure and thermochemistry of FO_2 radical: Comparison of Møller-Plesset perturbation, complete-active-space self-consistent-field, and quadratic configuration interaction methods. *J. Chem. Phys.* **1992**, *96*, 2861-2867, doi:10.1063/1.461982.
(6) Pagsberg, P.; Ratajczak, E.; Sillesen, A.; Jodkowski, J. T. Spectrokinetic studies of the gas-phase equilibrium $F + O_2 \rightleftharpoons FO_2$ between 295 and 359 K. *Chem. Phys. Lett.* **1987**, *141*, 88-94, doi:10.1016/0009-2614(87)80097-0.

17. **$Cl + O_2 \leftrightarrows ClOO$.** The recommendation is based on Nicovich et al.,[8] Mauldin et al.,[6] Baer et al.,[3] and Suma et al.[11] The experimental determinations of K_{eq} by Baer et al. and Nicovich et al. do not rely on knowing the absolute value of the absorption cross section, and that of Nicovich et al. and Suma et al.[11] rely on kinetic modeling to determine K_c. As a result, this analysis weights the study of Baer et al. more heavily than the others. A third law analysis was carried out using known thermochemistry for Cl and O_2 (Active Thermochemical Tables Version 1.122 [9]) and entropy for ClOO was computed using the structure (determined by microwave spectroscopy) of Suma et al.[10] and the full set of anharmonicities (X_{ij}) from the neon matrix study of Müller and Willner.[7] Using vibrational frequencies from Müller and Willner results in $S°_{298}(ClOO)$ = 66.02 cal mol^{-1} K^{-1}. Using, instead, the harmonic vibrational frequencies from Abbott and Schaefer[2] and isotope shifts Abbott[1] (both from CCSDT(Q)/CBS calculations) leads to $S°_{298}(ClOO)$ = 66.32 cal mol^{-1} K^{-1}. Both lead to D_0 = 4.6 ± 0.2 kcal mol^{-1} and $\Delta H_{f,298\ K}(ClOO)$ = 23.8 ± 0.2 (2 s.d.) kcal mol^{-1}. The K_c recommendation is based on the average of the fits to these two third-law expressions. For comparison, the third law analysis of Suma et al. yielded D_0 = 4.7 ± 0.1 kcal mol^{-1} using all experimentally reported values of K_{eq}, except those of Baer et al., while Nicovich et al. and Mauldin et al.[6] reported similar values of D_0 (albeit with error bars of 0.5 kcal mol^{-1}). The recent high-level theoretical study by Abbot and Schaefer obtained D_0 = 4.8 kcal mol^{-1}.[2] The Active Thermochemical Tables Version 1.122 [9] gives D_0 = 3.8 kcal mol^{-1}, based largely on two theoretical papers by Karton et al.[4,5] Most of the uncertainty in the recommended K_{eq} derives from the differences among the experimental determinations.
(Table: 19-5, Note: 19-5, Evaluated: 19-5) Back to Table

(1) Abbott, A. S. personal communication. **2018**.
(2) Abbott, A. S.; Schaefer III, H. F. The structure and Cl−O dissociation energy of the ClOO radical: Finally, the right answers for the right reason. *J. Phys. Chem. A* **2018**, *122*, 2604-2610, doi:10.1021/acs.jpca.8b00394.
(3) Baer, S.; Hippler, H.; Rahn, R.; Siefke, M.; Seitzinger, N.; Troe, J. Thermodynamic and kinetic properties of the reaction $Cl + O_2 + M \rightleftharpoons ClOO + M$ in the range 160-300 K and 1-1000 bar. *J. Chem. Phys.* **1991**, *95*, 6463-6470, doi:10.1063/1.461543.
(4) Karton, A.; Daon, S.; Martin, J. M. L. W4-11: A high-confidence benchmark dataset for computational thermochemistry derived from first-principles W4 data. *Chem. Phys. Lett.* **2011**, *510*, 165-178, doi:10.1016/j.cplett.2011.05.007.
(5) Karton, A.; Parthiban, S.; Martin, J. M. L. Post-CCSD(T) ab Initio thermochemistry of halogen oxides and related hydrides XOX, XOOX, HOX, XO_n, and HXO_n (X) F, Cl), and evaluation of DFT methods for these systems. *J. Phys. Chem. A* **2009**, *113*, 4802-4816, doi:10.1021/jp8087435.
(6) Mauldin, R. L., III; Burkholder, J. B.; Ravishankara, A. R. A photochemical, thermodynamic, and kinetic study of ClOO. *J. Phys. Chem.* **1992**, *96*, 2582-2588, doi:10.1021/j100185a035.
(7) Müller, H. S. P.; Willner, H. Vibrational and electronic spectra of chlorine dioxide, OClO, and chlorine superoxide, ClOO, isolated in cryogenic matrices. *J. Phys. Chem.* **1993**, *97*, 10589-10598, doi:10.1021/j100143a013.
(8) Nicovich, J. M.; Kreutter, K. D.; Shackelford, C. J.; Wine, P. H. Thermochemistry and kinetics of the $Cl + O_2$ association reaction. *Chem. Phys. Lett.* **1991**, *179*, 367-373, doi:10.1016/0009-2614(91)85168-V.
(9) Ruscic, B. Active thermochemical tables: Thermochemistry for the 21st Century. *J. Phys. Conf. Ser.* **2005**, *16*, 561-570, doi:10.1088/1742-6596/16/1/078.
(10) Suma, K.; Sumiyoshi, Y.; Endo, Y. Fourier transform microwave spectroscopy and Fourier transform microwave–millimeter wave double resonance spectroscopy of the ClOO radical. *J. Chem. Phys.* **2004**, *121*, 8351-8359, doi:10.1063/1.1792591.
(11) Suma, K.; Sumiyoshi, Y.; Endo, Y.; Enami, S.; Aloisio, S.; Hashimoto, S.; Kawasaki, M.; Nishida, S.; Matsumi, Y. Equilibrium constants of the reaction of Cl with O_2 in the formation of ClOO. *J. Phys. Chem. A* **2004**, *108*, 8096-8099, doi:10.1021/jp049124e.

18. **Cl + CO ⇆ ClCO.** From fitting the data of Nicovich et al.[3] who measured both k and K_{eq} between 185 and 260 K in N_2. They report $\Delta H_{f,298}(ClCO) = -5.2 \pm 0.6$ kcal mol^{-1}. High-level calculations by Dixon et al.[2] obtained -4.6 ± 0.5 kcal mol^{-1}, whereas calculations by Davalos et al.[1] obtained –5.1 and –5.4 kcal mol^{-1} at the G3 and G4 levels of theory, respectively.
(Table: 06-2, Note: 19-5, Evaluated: 06-2) Back to Table

(1) Dávalos, J. Z.; Notario, R.; Cuevas, C. A.; Oliva, J. M.; Saiz-Lopez, A. Thermochemistry of halogen-containing organic compounds with influence on atmospheric chemistry. *Comp. Theor. Chem.* **2017**, *1099*, 36-44, doi:10.1016/j.comptc.2016.11.009.
(2) Dixon, D. A.; Peterson, K. A.; Francisco, J. S. The molecular structures and energetics of Cl_2CO, ClCO, Br_2CO, and BrCO. *J. Phys. Chem. A* **2000**, *104*, 6227-6332, doi:10.1021/jp0005571.
(3) Nicovich, J. M.; Kreutter, K. D.; Wine, P. H. Kinetics and thermochemistry of ClCO formation from the Cl + CO association reaction. *J. Chem. Phys.* **1990**, *92*, 3539-3544, doi:10.1063/1.457862.

19. **ClO + O_2 ⇆ ClO•O_2.** DeMore[2] reports K_{eq} <4 × 10^{-18} cm^3 molecule^{-1} at 197 K. His temperature dependence of the equilibrium constant is estimated using $S°_{298}(ClO•O_2)$ = 73 cal mol^{-1} K^{-1} and $\Delta H°_{298}$ <7.7 kcal mol^{-1}. A higher value of K_{eq} has been proposed by Prasad,[3] but it requires $S°(ClO·O_2)$ to be about 83 cal mol^{-1} K^{-1}, which seems unreasonably high. Carter and Andrews[1] found no experimental evidence for ClO•O_2 in matrix experiments. Prasad and Lee[4] discuss these issues and question the validity of the upper limit reported by DeMore.
(Table: 92-20, Note: 94-26, Evaluated: 94-26) Back to Table

(1) Carter, R. O.; Andrews, L. Matrix spectroscopic studies of chlorine atom-ozone reaction products. *J. Phys. Chem.* **1981**, *85*, 2351-2354, doi:10.1021/j150616a011.
(2) DeMore, W. B. Equilibrium constant for the reaction ClO + O_2 ↔ ClO•O_2. *Geophys. Res. Lett.* **1990**, *17*, 2353-2355, doi:10.1029/GL017i013p02353.
(3) Prasad, S. S. Possible existence and chemistry of $ClO·O_2$ in the stratosphere. *Nature* **1980**, *285*, 152.
(4) Prasad, S. S.; Lee, T. J. Atmospheric chemistry of the reaction ClO + O_2 ↔ ClO•O_2: Where it stands, what needs to be done, and why? *J. Geophys. Res.* **1994**, *99*, 8225-8230, doi:10.1029/93JD01809

20. **(a) ClO + ClO ⇆ ClOOCl.** The values of the equilibrium constant and the thermochemical parameters are from a third-law calculation based on the data of Hume at al.[13] (206 to 250 K) and Klobas and Wilmouth[16] (230–299 K). A second-law analysis of the data of Hume et al. is highly consistent with the third-law results, as are the second-law and third-law analyses by Klobas and Wilmouth. Results from both papers are statistically much more precise than previous studies, and the results of Hume et al. extend to temperatures which are more relevant to the stratosphere. The recommended value of K_{eq} is within 1% of the previous recommendation. All the data from Hume et al. and Klobas and Wilmouth falls within 14% of the recommended values, but the error limits were chosen to incorporate most of the error bars in these two studies, and, importantly, the uncertainties in the absorption cross section of ClOOCl and ClO. The recommended K_{eq} is generally consistent with the data of Cox and Hayman[8] and Nickolaisen et al.[18] The entropy of ClOOCl (302.9 J mol^{-1} K^{-1} at 298 K) was calculated from rotational constants measured by Birk et al.,[3] four vibrational frequencies measured by Jacobs et al.,[14] and two frequencies computed by Matus et al.[17] The entropy values are in close agreement with those calculated by Zhu and Lin [23] (symmetry number corrected by Golden[11] to account for optical isomers) or by treatment of the torsion as a hindered rotor,[2] in which case the symmetry number correction is not required. From the third-law analysis, the ClOOCl heat of formation at 0 K and 298 K are $\Delta H°_{f,0}$ = 133.3 ± 1 kJ mol^{-1} and $\Delta H°_{f,298}$ = 130.1 ± 1 kJ mol^{-1}, in good agreement with the analysis of Hume et al. A study of branching ratios of ClO + ClO channels in $Cl_2/O_2/O_3$ mixtures by Horowitz et al.[12] also finds the equilibrium constant in O_2 at 285 K to be in agreement with the recommendation. Values at single temperatures from Ellermann et al.[9] and from Boakes et al.[4] fall outside the 95% confidence limit. Broske and Zabel[5] measured the reverse reaction at four temperatures between 245 and 260 K. They used the parameters for the forward reaction recommended in JPL 02-25 to suggest van't Hoff parameters of 5.09 × 10^{-26} and 7584. van't Hoff parameters suggested by Plenge et al.,[19] who measured $\Delta H_{f,0}$(ClOOCl) =134.0 ± 2.80 kJ mol^{-1} by photoionization mass spectrometry and computed the entropy change for the reaction, are 1.92 × 10^{-27} and 8430. Ferracci and Rowley[10] report values of K_{eq} between 250 and 313 K that also fall within the 95% confidence limits. Several studies have derived values of K_{eq} using atmospheric measurements in the nighttime polar stratosphere under conditions where ClO and ClOOCl should be in equilibrium. These are summarized here but are not used in the derivation of the recommended equilibrium constants. Avallone and Toohey[1] used K_{eq} = 1.99 × 10^{-30} × T × exp(8854/T) derived from *in situ* aircraft experiments. The Avallone and Toohey[1] expression yields values that are quite close to those from the recommended expression. Atmospheric measurements from an airborne platform have also been used by von Hobe et al.[22] to deduce K_{eq} parameters of 3.61 × 10^{-27} and 8167, resulting in values which lie close to the lower 95% confidence limit. A reanalysis by

Canty et al.[6] of ER-2 data between 185 and 200 K, from Stimpfle et al.,[21] is consistent with the recommended K_{eq}. Santee et al.[20] report measurements in the Arctic and Antarctic night by satellite based instruments, which are close to the current recommendation. The recent analysis by Kleinböhl et al.[15] is also consistent with the current recommendation.
(Table 19-5, Note: 19-5, Evaluated: 19-5)

(b) ClO + ClO ⇆ ClOClO. Zhu and Lin[23] used the G2 composite method to calculate the bond dissociation energy D_0(ClO-ClO) = 49.8 kJ mol^{-1}. Matus et al.[17] used the CCSD(T)/aug-cc-pV(5+d)Z method extrapolated to the complete basis set limit and found that ClOClO is less strongly bound than ClOOCl by 33.9 kJ mol^{-1} at 298 K (Matus et al. estimate their errors to be less than 4.2 kJ mol^{-1}). Combining this value from Matus et al. with $\Delta H_{f,298}$(ClOOCl) = 130.1 ± 1 kJ mol^{-1} gives $\Delta H_{f,298}$(ClOClO) = 164.0 ± 5 kJ mol^{-1} ($\Delta H_{f,0}$ = 166.5 ± 5 kJ mol^{-1}) for ClOClO. The vibrational frequencies and moments of inertia calculated by Matus et al. are in good agreement with those of Zhu and Lin[23] and Chase[7]. The entropy of ClOClO was calculated using the harmonic frequencies from Matus et al.,[17] anharmonicities computed by Maranzana (2007, unpublished), and rotational constants from Chase,[7] giving $S°_{298}$(ClOClO) = 312.6 J K^{-1} mol^{-1}. Thermodynamic data for ClO radicals were taken from Chase.[7] The 1-sigma errors in $\Delta S_{r,298}$ and $\Delta H_{r,298}$ are estimated to be 6 J K^{-1} mol^{-1} and 6 kJ mol^{-1}, respectively. Using these parameters, the equilibrium constant is given by K_{eq}(ClOClO) = 6.5 × 10^{-27} × exp(4460/T) with uncertainty factors f(298 K) = 2 and g = 600.
(Table: 15-10, Note: 15-10, Evaluated: 15-10) Back to Table

(1) Avallone, L. M.; Toohey, D. W. Tests of halogen photochemistry using in situ measurements of ClO and BrO in the lower polar stratosphere. *J. Geophys. Res.* **2001**, *106*, 10411-10421, doi:10.1029/2000JD900831.

(2) Barker, J. R.; Ortiz, N. F.; Preses, J. M.; Lohr, L. L.; Maranzana, A.; Stimac, P. J.; Nguyen, T. L.; Kumar, T. J. D. MultiWell http://aoss.engin.umich.edu/multiwell/. University of Michigan: Ann Arbor, MI, 2011.

(3) Birk, M.; Friedl, R. R.; Cohen, E. A.; Pickett, H. M.; Sander, S. P. The rotational spectrum and structure of chlorine peroxide. *J. Chem. Phys.* **1989**, *91*, 6588-6597, doi:10.1063/1.457377.

(4) Boakes, G.; Mok, W. H. H.; Rowley, D. M. Kinetic studies of the ClO + ClO association reaction as a function of temperature and pressure. *Phys. Chem. Chem. Phys.* **2005**, *7*, 4102-4113, doi:10.1039/b510308h.

(5) Broske, R.; Zabel, F. Thermal decomposition of ClOOCl. *J. Phys. Chem. A* **2006**, *110*, 3280-3288, doi:10.1021/jp0550053.

(6) Canty, T. P.; Salawitch, R. J.; Wilmouth, D. M. The kinetics of the ClOOCl catalytic cycle. *J. Geophys. Res.* **2016**, *121*, 13768-13783, doi:10.1002/2016JD025710.

(7) Chase, M. W. NIST-JANAF thermochemical tables. *J. Phys. Chem. Ref. Data* **1998**, *Monograph 9*.

(8) Cox, R. A.; Hayman, G. D. The stability and photochemistry of dimers of the ClO radical and implications for Antarctic ozone depletion. *Nature* **1988**, *332*, 796-800, doi:10.1038/332796a0.

(9) Ellermann, T.; Johnsson, K.; Lund, A.; Pagsberg, P. Kinetics and equilibrium-constant of the reversible reaction ClO + ClO + M ↔ Cl_2O_2 + M at 295 K. *Acta Chem. Scand.* **1995**, *49*, 28-35, doi:10.3891/acta.chem.scand.49-0028.

(10) Ferracci, V.; Rowley, D. M. Kinetic and thermochemical studies of the ClO + ClO + M ⇄ Cl_2O_2 + M reaction *Phys. Chem. Chem. Phys* **2010**, *12*, 11596-11608, doi:10.1039/c0cp00308e.

(11) Golden, D. M. Reaction ClO + ClO → products: Modeling and parameterization for use in atmospheric models. *Int. J. Chem. Kinet.* **2003**, *35*, 206-211, doi:10.1002/kin.10120.

(12) Horowitz, A.; Crowley, J. N.; Moortgat, G. K. Temperature dependence of the product branching ratios of the ClO self-reaction in oxygen. *J. Phys. Chem.* **1994**, *98*, 11924-11930, doi:10.1021/j100097a019.

(13) Hume, K. L.; Bayes, K. D.; Sander, S. P. The equilibrium constant for the reaction ClO + ClO ↔ ClOOCl between 250 and 206 K. *J. Phys. Chem. A* **2015**, *119*, 4473-4481, doi:10.1021/jp510100n.

(14) Jacobs, J.; Kronberg, M.; Müller, H. S. P.; Willner, H. An experimental study on the photochemistry and vibrational spectroscopy of three isomers of Cl_2O_2 isolated in cryogenic matrices. *J. Am. Chem. Soc.* **1994**, *116*, 1106-1114, doi:10.1021/ja00082a038.

(15) Kleinböhl, A.; Khosravi, M.; J. Urban; Canty, T.; Salawitch, R. J.; G. C. Toon; Küllmann, H.; Notholt, J. Constraints for the photolysis rate and the equilibrium constant of ClO-dimer from airborne and balloon-borne measurements of chlorine compounds. *Geophys. Res. Atmos.* **2014**, *119*, 6916–6937, doi:10.1002/2013JD021433.

(16) Klobas, J. E.; Wilmouth, D. M. UV spectroscopic determination of the chlorine monoxide (ClO) / chlorine peroxide (ClOOCl) thermal equilibrium constant. *Atmos. Chem. Phys.* **2019**, *19*, 6205-6215, doi:10.5194/acp-19-6205-2019.

(17) Matus, M. H.; Nguyen, M. T.; Dixon, D. A.; Peterson, K. A.; Francisco, J. S. $ClClO_2$ is the most stable isomer of Cl_2O_2. Accurate coupled cluster energetics and electronic spectra of Cl_2O_2 isomers. *J. Phys. Chem. A* **2008**, *112*, 9623-9627, doi:10.1021/jp806220r.
(18) Nickolaisen, S. L.; Friedl, R. R.; Sander, S. P. Kinetics and mechanism of the ClO + ClO reaction: Pressure and temperature dependences of the bimolecular and termolecular channels and thermal decomposition of chlorine peroxide, ClOOCl. *J. Phys. Chem.* **1994**, *98*, 155-169, doi:10.1021/j100052a027.
(19) Plenge, J.; Kühl, S.; Vogel, B.; Müller, R.; Stroh, F.; von Hobe, M.; Flesch, R.; Rühl, E. Bond strength of chlorine peroxide. *J. Phys. Chem. A* **2005**, *109*, 6730-6734, doi:10.1021/jp044142h.
(20) Santee, M. L.; Sander, S. P.; Livesey, N. J.; Froidevaux, L. Constraining the chlorine monoxide (ClO)/chlorine peroxide (ClOOCl) equilibrium constant from Aura microwave limb sounder measurements of nighttime ClO. *Proc. Natl. Acad, Sci. USA* **2010**, *107*, 6588-6593, doi:10.1073/pnas.0912659107.
(21) Stimpfle, R. M.; Wilmouth, D. M.; Salawitch, R. J.; Anderson, J. G. First measurements of ClOOCl in the stratosphere: The coupling of ClOOCl and ClO in the Arctic polar vortex. *J. Geophys. Res.* **2004**, *109*, D03301, doi:10.1029/2003jd003811.
(22) von Hobe, M.; Grooss, J. U.; Muller, R.; Hrechanyy, S.; Winkler, U.; Stroh, F. A re-evaluation of the ClO/Cl_2O_2 equilibrium constant based on stratospheric in-situ observations. *Atmos. Chem. Phys.* **2005**, *5*, 693-702, doi:10.5194/acp-5-693-2005.
(23) Zhu, R. S.; Lin, M. C. *Ab initio* studies of ClO_x reactions. IV. Kinetics and mechanism for the self-reaction of ClO radicals. *J. Chem. Phys.* **2003**, *118*, 4094-4106, doi:10.1063/1.1540623.

21. $Cl + OClO \leftrightarrows ClClO_2$. Because of the high energy barriers calculated for other plausible pathways (ClO + ClO or isomerization of ClOOCl and ClOClO), this pathway seems to be the most relevant for formation and dissociation of $ClClO_2$ (chloryl chloride). Zhu and Lin[9] and found energy barriers of >19 kcal mol^{-1} separating $ClClO_2$ from ClOOCl and ClOClO; they did not identify any low energy paths from ClO + ClO to $ClClO_2$. Neither Zhu and Lin nor Grant et al.[2] reported pathways connecting Cl + ClOO to $ClClO_2$. It is noteworthy that Bröske and Zabel[1] did not see any evidence for formation of $ClClO_2$ when they measured the gas phase thermolysis of ClOOCl, although they were able to measure $ClClO_2$ produced in wall reactions. Thus, it seems unlikely that the gas phase isomerization reactions are fast enough to be significant. Experiments in cryogenic matrices by Jacobs et al.[4] and Müller and Willner[8] support the theoretical prediction that Cl + OClO produces both $ClClO_2$ and ClOClO. However, ClOClO is not observed when the reaction is carried out in the gas phase.[7] This is consistent with the fact that the equilibrium constant for ClOClO formation is enormously smaller than that for formation of $ClClO_2$: based on data from Matus et al.,[6] $K_{eq}(T)$ very roughly equals $7.0 \times 10^{-26} \times \exp(6200/T)$, corresponding to 9×10^{-17} at 298 K. The recommended K_{eq} for formation of $ClClO_2$ is based on a thermodynamic calculation using the spectroscopic data and theoretical energies. The vibrational frequencies and moments of inertia are known,[7,8] giving $S°_{298}(ClClO_2) = 294.4$ J K^{-1} mol^{-1}. The heat of formation of $ClClO_2$ has not been measured, but it has been calculated many times (see Zhu and Lin[9] for a summary of calculations up to 2003). We note high-level calculations by Horny et al.,[3] and Lee et al.,[5] but the best calculations appear to be those by Matus et al.[6] and Grant et al.[2] These authors concluded that $\Delta H_{f,0}(ClClO_2)$ is 5.1 kcal mol^{-1} below that of ClOOCl. Matus et al. estimate their relative errors to be less than ±1 kcal mol^{-1}. Coupled with the recommended value of 133.3 ± 1 kJ mol^{-1} for ClOOCl (see Note 14a), this gives $\Delta H_{f,0}(ClClO_2) = 112.0$ kJ mol^{-1} and $\Delta H_{f,298} = 107.9$ kJ mol^{-1}. The 1-sigma errors in $\Delta S_{r,298}$ and $\Delta H_{r,298}$ are estimated to be 6 J K^{-1} mol^{-1} and 5 kJ mol^{-1}, respectively.
(Table: 19-5, 19-5, Evaluated: 19-5) Back to Table

(1) Broske, R.; Zabel, F. Thermal decomposition of ClOOCl. *J. Phys. Chem. A* **2006**, *110*, 3280-3288, doi:10.1021/jp0550053.
(2) Grant, D. J.; III, E. B. G.; Matus, M. H.; Nguyen, M. T.; Peterson, K. A.; Francisco, J. S.; Dixon, D. A. Thermodynamic properties of the XO_2, X_2O, XYO, X_2O_2, and XYO_2 (X, Y = Cl, Br, and I) isomers. *J. Phys. Chem. A* **2010**, *114*, 4254-4265, doi:10.1021/jp911320p.
(3) Horný, Ľ.; Quack, M.; III, H. F. S.; Willeke, M. Chlorine peroxide (Cl_2O_2) and its isomers: structures, spectroscopy, formation and thermochemistry. *Mol. Phys.* **2016**, *114*, 1135-1147, doi:10.1080/00268976.2016.1143984.
(4) Jacobs, J.; Kronberg, M.; Müller, H. S. P.; Willner, H. An experimental study on the photochemistry and vibrational spectroscopy of three isomers of Cl_2O_2 isolated in cryogenic matrices. *J. Am. Chem. Soc.* **1994**, *116*, 1106-1114, doi:10.1021/ja00082a038.
(5) Lee, T. J.; Rohlfing, C. M.; Rice, J. E. An extensive *ab initio* study of the structures, vibrational spectra, quadratic force fields, and relative energetics of three isomers of Cl_2O_2. *J. Chem. Phys.* **1992**, *97*, 6593-6605, doi:10.1063/1.463663.

(6) Matus, M. H.; Nguyen, M. T.; Dixon, D. A.; Peterson, K. A.; Francisco, J. S. $ClClO_2$ is the most stable isomer of Cl_2O_2. Accurate coupled cluster energetics and electronic spectra of Cl_2O_2 isomers. *J. Phys. Chem. A* **2008**, *112*, 9623-9627, doi:10.1021/jp806220r.
(7) Müller, H. S. P.; Willner, H. Gas phase studies on chloryl chloride, $ClClO_2$. *Ber. Bunsenges. Phys. Chem.* **1992**, *96*, 427-431, doi:10.1002/bbpc.19920960338.
(8) Müller, H. S. P.; Willner, H. Synthesis and properties of chloryl chloride, $ClClO_2$. *Inorg. Chem.* **1992**, *31*, 2527-2534, doi:10.1021/ic00038a040.
(9) Zhu, R. S.; Lin, M. C. *Ab initio* studies of ClO_x reactions. IV. Kinetics and mechanism for the self-reaction of ClO radicals. *J. Chem. Phys.* **2003**, *118*, 4094-4106, doi:10.1063/1.1540623.

22. **ClO + OClO ⇆ Cl_2O_3.** Data are from Burkholder et al.,[2] Hayman and Cox,[5] and Green et al.[4] The best van't Hoff fit to all the data yields the recommended parameters. The 95% error limits encompass all the data. A calculation of the entropy and heat capacity from the structure and frequencies of ClOCl(O)O reported by Zhu and Lin[8] allows a "3rd Law" fit that gives K_{eq}/cm^3 molecule^{-1} = 1.6 × 10^{-27} exp(7155/T) for 232< T/K <298. By including the hindered rotor potential explicitly,[1] a new "3rd Law" fit obtained by fitting the data of Burkholder et al.[2] and Hayman and Cox,[5] including the lowest temperature point, gives the new recommendation: $S°_{298}$ (Cl_2O_3) = 337.8 J K^{-1} mol^{-1} (80.7 cal mol^{-1} K^{-1}) and $\Delta H_{f,0}$(Cl_2O_3) = 143.9 kJ mol^{-1} (34.4 kcal mol^{-1}) and $\Delta H_{f,298}$(Cl_2O_3) = 138.9 kJ mol^{-1} (33.2 kcal mol^{-1}). This compares to calculated values of $\Delta H_{f,0}$(Cl_2O_3) = 32.3 kcal mol^{-1} from Zhu and Lin[8] and 32.9 kcal mol^{-1} from Sicre and Cobos.[7] Burkholder et al.[2] reported that treating the lowest vibration as a free internal rotation increases the entropy of ClOCl(O)O by almost 9 cal mol^{-1} K^{-1}, but this value, repeated by Green et al.,[4] is not correct. Clark and Francisco,[3] who calculated structure and frequencies, concluded that $S°_{298}$(Cl_2O_3) = 78.5 cal mol^{-1} K^{-1}, based on harmonic frequencies. Li et al.[6] have also reported theoretical structure and frequencies in general agreement with Zhu and Lin[8] and Clark and Francisco,[3] but energetics that are quite different.
(Table: 10-6, Note: 10-6, Evaluated: 10-6) Back to Table

(1) Barker, J. R.; Ortiz, N. F.; Preses, J. M.; Lohr, L. L.; Maranzana, A.; Stimac, P. J.; Nguyen, T. L.; Kumar, T. J. D. MultiWell http://aoss.engin.umich.edu/multiwell/. University of Michigan: Ann Arbor, MI, 2011.
(2) Burkholder, J. B.; Mauldin, R. L.; Yokelson, R. J.; Solomon, S.; Ravishankara, A. R. Kinetic, thermodynamic, and spectroscopic study of Cl_2O_3. *J. Phys. Chem.* **1993**, *97*, 7597-7605, doi:10.1021/j100131a032.
(3) Clark, J.; Francisco, J. S. Study of the stability of Cl_2O_3 using ab initio methods. *J. Phys. Chem. A* **1997**, *101*, 7145-7153, doi:10.1021/jp971465n.
(4) Green, T. J.; Islam, M.; Guest, P.; Hickson, K.; Canosa-Mas, C. E.; Wayne, R. P. A discharge-flow study of Cl_2O_3. *Phys. Chem. Chem. Phys.* **2003**, *5*, 5409-5418, doi:10.1039/b311005b.
(5) Hayman, G. D.; Cox, R. A. UV absorption spectrum and thermochemistry of Cl_2O_3 formed in the photolysis of OClO-containing mixtures at low temperatures. *Chem. Phys. Lett.* **1989**, *155*, 1-7, doi:10.1016/S0009-2614(89)87350-6.
(6) Li, Q., S. Lu, Y. Xie, P. V. R. Schleyer and H. F. Schaefer, III Molecular structures, thermochemistry, and electron affinities for dichlorine oxides: Cl_2O_n/$Cl_2O_n^-$ (n = 1-4). *Int. J. Quant. Chem.* **2003**, *95*, 731-757, doi:10.1002/qua.10634.
(7) Sicre, J. E.; Cobos, C. J. Thermochemistry of the higher chlorine oxides ClO_x (x = 3,4) and Cl_2O_x (x = 3 - 7). *J. Mol. Struct. (Theochem)* **2003**, *620*, 215-226.
(8) Zhu, R. S.; Lin, M. C. Ab initio studies of ClO_x reactions. VII. Isomers of Cl_2O_3 and their roles in the ClO + OClO reaction. *J. Chem. Phys.* **2003**, *118*, 8645-8655, doi:10.1063/1.1565315.

23. **OClO + NO_3 ⇆ O_2ClONO_2.** From theoretical calculations of Parthiban et al.[2] This value replaces the value that was previously deduced by Friedl et al.[1] Uncertainties are based on an assumed ±1 kcal mol^{-1} uncertainty in the calculated heat of formation.
(Table: 10-6, Note: 15-10, Evaluated: 10-6) Back to Table

(1) Friedl, R. R.; Sander, S. P.; Yung, Y. L. Chloryl nitrate: A novel product of the OClO + NO_3 + M recombination. *J. Phys. Chem.* **1992**, *96*, 7490-7493, doi:10.1021/j100198a002.
(2) Parthiban, S., T. J. Lee, S. Guha, and J. S. Francisco Theoretical study of chlorine nitrates: Implications for stratospheric chlorine chemistry. *J. Am. Chem. Soc.* **2003**, *125*, 10446-10458, doi:10.1021/ja010297g.

24. **Br + CH_2=C(CH_3)CH=CH_2 (isoprene) ⇆ Product.** In a comprehensive study of the forward and reverse rates of this reaction (using laser flash photolysis of CF_2Br_2 precursor and atomic resonance fluorescence detection of Br-atoms), Laine et al.[1] determined K_{eq} from 210 to 298 K. The adduct(s) produced in the reaction

are not known, but may consist of several isomers; calculations (G4 method) reported by Laine et al. show that the energetically most stable isomer is $BrH_2CC(CH_3)CH{=}CH_2$. Analysis of the data by 2nd Law and by 3rd Law methods produced results in good mutual agreement. Laine et al. averaged the 2nd Law and 3rd Law results to obtain $\Delta_rH^{298} = -67.5 \pm 6.6$ kJ mol^{-1}, and $\Delta_rS^{298} = -93 \pm 16$ J K^{-1} mol^{-1}. The present recommendation is based on a 3rd Law analysis. The recommended error parameters are larger than the 40% 2σ relative errors (including both statistical and systematic) estimated by Laine et al.; they are set so that all of the K_{eq} data fall within the 2σ error limits and an extra margin was added because only one determination of K_{eq} has been reported for this reaction.
(Table: 15-10, Note: 15-10, Evaluated: 15-10) Back to Table

(1) Laine, P. L.; Sohn, Y. S.; Nicovich, J. M.; McKee, M. L.; Wine, P. H. Kinetics of elementary steps in the reactions of atomic bromine with isoprene and 1,3-butadiene under atmospheric conditions. *J. Phys. Chem. A* **2012**, *116*, 6341-6357, doi:10.1021/jp212127v.

25. Br + CH_2=CHCH=CH_2 (1,3-butadiene) ⇆ Product. In a comprehensive study of the forward and reverse rate constants of this reaction (using laser flash photolysis of CF_2Br_2 precursor and atomic resonance fluorescence detection of Br-atoms), Laine et al.[1] determined K_{eq} from 227 to 298 K; they estimated the 2σ relative error to be ~40%. The adduct(s) produced in the reaction were not measured directly, but calculations (G4 method) by Laine et al. predict that the adduct formed by addition of Br to the terminal carbon is favored thermodynamically. Analysis of the data by 2nd Law and by 3rd Law methods produced results in fair mutual agreement. Laine et al. averaged the 2nd Law and 3rd Law results to obtain $\Delta_rH^{298} = -64.5 \pm 8.5$kJ mol^{-1} and $\Delta_rS^{298} = -94 \pm 20$ J K^{-1} mol^{-1}, which provide the basis for the current recommendation. The recommended error parameters are larger than the 40% 2σ relative errors (including both statistical and systematic) estimated by Laine et al.; they are set so that all of the K_{eq} data of Laine et al. fall within the 2σ error limits and an extra margin was added because only one determination of K_{eq} has been reported for this reaction.
(Table: 15-10, Note: 15-10, Evaluated: 15-10) Back to Table

(1) Laine, P. L.; Sohn, Y. S.; Nicovich, J. M.; McKee, M. L.; Wine, P. H. Kinetics of elementary steps in the reactions of atomic bromine with isoprene and 1,3-butadiene under atmospheric conditions. *J. Phys. Chem. A* **2012**, *116*, 6341-6357, doi:10.1021/jp212127v.

26. IO + NO_2 ⇆ $IONO_2$. The parameters were computed based on a combination of experimental and theoretical data. The rovibrational parameters and electronic energy levels for IO radical and NO_2 were obtained from the NIST/JANAF tables;[2] rovibrational parameters for $IONO_2$ were obtained from Marshall.[5] The IO-NO_2 bond dissociation energy (D_0) is relatively uncertain, but estimates are provided by several recent publications. Golden[3] carried out RRKM/master equation calculations and concluded that D_0 is ~150 kJ mol^{-1}. Kaltsoyannis and Plane[4] obtained 117.9 kJ mol^{-1} from quantum chemical calculations at the CCSD(T)/aug-cc-pVTZ // B3LYP/aug-cc-pVTZ level of theory. Saiz-Lopes et al.[9] reported a rounded value of 118 kJ mol^{-1} in their recent review article. Marshall[5] obtained 113.6 (± 3.1) kJ mol^{-1} from quantum chemical calculations at the CCSD(T)/aug-cc-pVTZ // CCSD(T)/aug-cc-pVTZ level of theory. The $K_{eq} = A \times \exp(B/T)$ parameters computed based on D_0 from Golden, from Kaltsoyannis and Plane, and from Marshall are $A = 5.02 \times 10^{-28}$ (±~10%) and B = 18240, 14380, and13860. The recommendation is based on the average of the latter two. The entropy of $IONO_2$ computed using this model is S(298) = 320.95 J K^{-1} mol^{-1}. In earlier work, Rayez and Destriau[8] reported $D_0 = 134 \pm 13$ kJ mol^{-1}, Allan and Plane[1] reported $D_0 = 94.9$ kJ mol^{-1} and Papayannis and Kosmas[6,7] reported D_0 values from 131.4 to 137.6 kJ mol^{-1}.
(Table: 15-10, Note: 15-10, Evaluation: 15-10) Back to Table

(1) Allan, B. J.; Plane, J. M. C. A study of the recombination of IO with NO_2 and the stability of INO_3: Implications for the atmospheric chemistry of iodine. *J. Phys. Chem. A* **2002**, *106*, 8634-8641, doi:10.1021/jp020089q.
(2) Chase, M. W. NIST-JANAF thermochemical tables. *J. Phys. Chem. Ref. Data* **1998**, *Monograph 9*.
(3) Golden, D. M. Evaluating data for atmospheric models, an example: IO + NO_2 = $IONO_2$. *J. Phys. Chem. A* **2006**, *110*, 2940-2943, doi:10.1021/jp058221k.
(4) Kaltsoyannis , N.; Plane, J. M. C. Quantum chemical calculations on a selection of iodine-containing species (IO, OIO, INO_3, $(IO)_2$, I_2O_3, I_2O_4 and I_2O_5) of importance in the atmosphere. *Phys. Chem. Chem. Phys.* **2008**, *10*, 1723-1733, doi:10.1039/b715687c.
(5) Marshall, P. Computational studies of the thermochemistry of the atmospheric iodine reservoirs HOI and $IONO_2$. *Advances in Quantum Chemistry* **2008**, 159-175.
(6) Papayannis, D. K.; Kosmas, A. M. Quantum mechanical characterization of (INO_3) isomers. *Chem. Phys. Lett.* **2004**, *398*, 75-81, doi:10.1016/j.cplett.2004.09.019.

(7) Papayannis, D. K.; Kosmas, A. M. The conformational potential energy surface of IOONO and the isomerization and decomposition processes. *Chem. Phys.* **2005**, *315*, 251-258, doi:10.1016/j.chemphys.2005.04.014.
(8) Rayez, M. T.; Destriau, M. Theoretical study of thermal dissociation and recombination reacitons of $XONO_2$ (X=F, Cl, Br, or I). *Chem. Phys. Lett.* **1993**, *206*, 278-284, doi:10.1016/0009-2614(93)85552-Y.
(9) Saiz-Lopez, A.; Plane, J. M. C.; Baker, A. R.; Carpenter, L. J.; von Glasow, R.; Gomez Martín, J. C.; McFiggans, G.; Saunders, R. W. Atmospheric chemistry of iodine. *Chem. Rev.* **2012**, *112*, 1773-1804, doi:10.1021/cr200029u.

27. $OH + CS_2 \leftrightarrows CS_2OH$. Fit to the data of Murrells et al.,[4] Hynes et al.,[3] and Diau and Lee[2] between 246 and 318 K. Petris et al.[1] report experimental detection of CS_2OH.
(Table: 06-2, Note: 15-10, Evaluated 06-2) Back to Table

(1) de Petris, G.; Rosi, M.; Troiani, A. Direct experimental observation of CS_2OH. *ChemPhysChem* **2006**, *7*, 2352-2357, doi:10.1002/cphc.200600515.
(2) Diau, E. W.-G.; Lee, Y.-P. Kinetics of the reactions of CS_2OH with O_2, NO, and NO_2. *J. Phys. Chem.* **1991**, *95*, 7726-7732, doi:10.1021/j100173a033.
(3) Hynes, A. J.; Wine, P. H.; Nicovich, J. M. Kinetics and mechanism of the reaction of OH with CS_2 under atmospheric conditions. *J. Phys. Chem.* **1988**, *92*, 3846-3852, doi:10.1021/j100324a034.
(4) Murrells, T. P.; Lovejoy, E. R.; Ravishankara, A. R. Oxidation of CS_2 by reaction with OH. 1. Equilibrium constant for the reaction OH + CS_2 ⇄ CS_2OH and the kinetics of the CS_2OH + O_2 reaction. *J. Phys. Chem.* **1990**, *94*, 2381-2386, doi:10.1021/j100369a036.

28. $OH + (CH_3)_2S \leftrightarrows (CH_3)_2SOH$. This recommendation is based on the results of Hynes et al.[3] and Barone et al.,[1] who used deuterated dimethyl sulfide (DMS-d_6), and Williams et al.,[7] who used both DMS-d_6 and non-deuterated DMS-d_0, in studies of the rate constants for the reaction and found clear evidence for adduct formation. In each case, K_{eq} was obtained by analyzing the rate constant data, which showed double-exponential decays. Hynes et al.[3] measured K_{eq} from 250–267 K and reported an adduct bond energy of 13.0 ± 3.3 kcal mol^{-1} from a van't Hoff (2nd Law) analysis and a bond energy of 10.1 ± 1.1 kcal mol^{-1} based on a 3rd Law analysis using the theoretical molecular parameters computed by McKee.[4] Barone et al. measured K_{eq} from 217–240 K and reported bond energies of 10.2 and 10.7 ± 2.5 kcal mol^{-1} from 2nd and 3rd Law calculations, respectively. Williams et al. analyzed only their K_{eq} data for OH + DMS-d_6 (240–245 K) and obtained bond strengths of 10.9 ± 1.0 kcal mol^{-1} from a 2nd Law analysis and 10.5 kcal mol^{-1} from a 3rd Law analysis based on their own MP2/6-31+G(2d,p) quantum chemical calculations (in good agreement with McKee.[5] The present recommendation was obtained from a 3rd Law analysis of the data for OH + DMS-d_6 from all three DMD-d_6 studies combined with the data for OH + DMS-d_0 from Williams et al. The 61 data points covered the temperature range from 217–261 K. The 3rd Law analysis used the theoretical molecular parameters for DMS and HODMS computed by Williams et al.[7] and the properties of the OH radical from the JANAF[2] Tables and Ruscic et al.[6] to obtain the dissociation energy (without zero point energies) D_e = 55.5 ± 1.3 kJ mol^{-1} (2σ). When the zero-point energy differences are taken into account, this gives dissociation energies D_0(HO-DMS-d_6) = 43.2 ± 1.3 kJ mol^{-1} and D_0(HO-DMS-d_0) = 43.0 ± 1.3 kJ mol^{-1} (2σ).
(Table: 10-6, Note: 10-6, Evaluated: 10-6) Back to Table

(1) Barone, S. B.; Turnipseed, A. A.; Ravishankara, A. R. Reaction of OH with dimethyl sulfide (DMS). 1. Equilibrium constant for OH + DMS reaction and the kinetics of the OH•DMS + O_2 reaction. *J. Phys. Chem.* **1996**, *100*, 14694-14702, doi:10.1021/jp960866k.
(2) Chase, M. W. NIST-JANAF thermochemical tables. *J. Phys. Chem. Ref. Data* **1998**, *Monograph 9*.
(3) Hynes, A. J.; Wine, P. H.; Semmes, D. H. Kinetics and mechanism of OH reactions with organic sulfides. *J. Phys. Chem.* **1986**, *90*, 4148-4156, doi:10.1021/j100408a062.
(4) McKee, M. L. Computational study of addition and abstraction reactions between OH radical and dimethyl sulfide. A difficult case. *J. Phys. Chem.* **1993**, *97*, 10971-10976, doi:10.1021/j100144a013.
(5) McKee, M. L. Comparison of gas-phase and solution-phase reactions of dimethyl sulfide and 2-(methylthio)ethanol with hydroxyl radical. *J. Phys. Chem. A* **2003**, *107*, 6819-6827, doi:10.1021/jp034704h.
(6) Ruscic, B.; Pinzon, R. E.; Morton, M. L.; Srinivasan, N. K.; Su, M.-C.; Sutherland, J. W.; Michael, J. V. Active thermochemical tables: Accurate enthalpy of formation of hydroperoxyl radical, HO_2. *J. Phys. Chem. A* **2006**, *110*, 6592–6601, doi:10.1021/jp056311j.
(7) Williams, M. B.; Campuzano-Jost, P.; Cossairt, B. M.; Hynes, A. J.; Pounds, A. J. Experimental and theoretical studies of the reaction of the OH radical with alkyl sulfides: 1. Direct observations of the formation of the OH-DMS adduct-pressure dependence of the forward rate of addition and

development of a predictive expression at low temperature. *J. Phys. Chem. A* **2007**, *111*, 89-104, doi:10.1021/jp063873+.

29. **$CH_3 + SO_3 \leftrightarrows CH_3SO_3$.** Because this equilibrium has never been investigated in laboratory experiments, the Panel makes no specific recommendation, but notes that Δ_rH_0 and $\Delta_fH_{298}(CH_3SO_3)$ have been investigated in theoretical studies. The results depend on both the level of theory and the size of the basis set. Salta et al.[3] commented that composite methods (e.g. G2, G3, and CBS–QB3) seem to be somewhat more reliable than single–point methods like B3LYP and CCSD(T)), because the composite methods employ both high–level theory and empirical corrections for various effects. Salta et al. prefer CBS–QB3 because it extrapolates high level theory to the complete basis set limit. Single point calculations for $\Delta_fH_{298}(CH_3SO_3)$ have been reported by Resende and Almeida[2] (–244 kJ/mol, UCCSD(T)/cc–pVTZ//MP2/6–31G(d)) and for $\Delta_fH_0(CH_3SO_3)$ by Salta et al.[3] (–280 kJ/mol from G3 // MP2/6–311++G(d, p) and –291 kJ/mol from G3 // B3LYP/6–311++G(2d,2p)). Results for $\Delta_fH_0(CH_3SO_3)$ obtained using composite methods have been reported by Salta et al.[3] (–315 kJ/mol from CBS–QB3) and Cao et al.[1] (–308 kJ/mol from G3XMP2// B3LYP/6–311+G(3df,2p)). At the same level of theory, Cao et al. found 63.54 kJ/mol for Δ_rH_0 for $CH_3SO_3 \rightarrow CH_3 + SO_3$; they also found that the reaction has a small intrinsic energy barrier (~1 kJ/mol, including zero point energy); they report the total rate constant for dissociation is $k_{uni} = (1.4\times10^{+12}) \times (T^{0.15}) \times \exp(-7831/T)$ s^{-1}. Zhu et al.[4] reported values for Δ_rH_0 for $CH_3SO_3 \rightarrow CH_3 + SO_3$ obtained using both a single point method (CCSD(T)/6–311++G(2df,2pd)) and a composite method (CBS–QB3): 59.8 and 78 kJ/mol, respectively. From the data supplied in their paper (we treated the torsion as a hindered rotor) and molecular data for CH_3 and SO_3, we calculate that the corresponding values for $\Delta_fH_0(CH_3SO_3)$ are –303 and –318 kJ/mol, respectively. Evaluated in this way, their CBS-QB3 result is in reasonable agreement that of Salta et al. From Δ_rH_0 = 78 kJ/mol and other molecular parameters reported by of Zhu et al.[4] (and treating the torsion as a hindered internal rotor), $K_{eq}(T) = 9 \times 10^{-27} \exp(9550/T)$ and $S_{f,298}(CH_3SO_3)$ = 315 J K^{-1} mol^{-1}. The uncertainty in Δ_rH_0 is probably at least ±10 kJ/mol, suggesting $f(298\ K) = 60$ and $g = 1200$. When the expression for $K_{eq}(T)$ is used with $k_{rec,\infty}(T) = 2.2\times10^{-13} \times (T/298)^{-0.2}$ cm^3 s^{-1} (see Note in Table 2), the high pressure limit rate constant for unimolecular dissociation to $CH_3 + SO_3$ is $k_d^\infty = 2.1\times10^{+13} \times \exp(-9510/T$ s^{-1} ($k_d^\infty(298) = 0.3$ s^{-1}) with a combined uncertainty factor of $f(298\ K) = 600$.
(New Entry) Back to Table

(1) Cao, J.; Wang, W.-L.; Gao, L.-J.; Fu, F. Mechanism and thermodynamic properties of CH_3SO_3 decomposition. *Acta Phys.-Chim. Sin.* **2013**, *29*, 1161-1167, doi:10.3866/PKU.WHXB201304021.
(2) Resende, S. M.; De Alemeida, W. B. Thermodynamical analysis of the atmospheric fate of the $CH_3SCH_2O_2$ radical. *Phys. Chem. Chem. Phys* **1999**, *1*, 2953-2959, doi:10.1039/A902423I.
(3) Salta, Z.; Kosmas, A. M.; Lesar, A. Computational investigation of the peroxy radicals $CH_3S(O)_nOO$ and the peroxynitrates $CH_3S(O)_nOONO_2$ (n = 0, 1, 2). *Comput. Theo. Chem.* **2012**, 67-76, doi:10.1016/j.comptc.2012.10.007.
(4) Zhu, B.; Zeng, X.; Beckers, H.; Francisco, J. S.; Willner, H. The methylsulfonyloxyl radical, CH_3SO_3. *Angew. Chem. Int. Ed.* **2015**, *54*, 11404-11408, doi:10.1002/anie.201503776.

30. **$Cl + CS_2 \leftrightarrows Cl–CS_2$.** Fit to the data of Nicovich et al.[1] between 193 and 258 K.
(Table: 10-6, Note: 10-6, Evaluated: 10-6) Back to Table

(1) Nicovich, J. M.; Wine, P. H. Kinetics of the reactions of O(^3P) and Cl(^2P) with HBr and Br_2. *Int. J. Chem. Kinet.* **1990**, *22*, 379-397, doi:10.1002/kin.550220406.

31. **$Br + CH_3SCH_3 \leftrightarrows Br–(CH_3)_2S$.** Second Law fit to data of Wine et al.[2] and Nakano et al.[1] This corresponds to a bond dissociation energy in the adduct of 13.84 kcal mol^{-1}.
(Table: 06-2, Note: 06-2, Evaluated: 06-2) Back to Table

(1) Nakano, Y., M. Goto, S. Hashimoto, M. Kawasaki, and T. J. Wallington Cavity ring-down spectroscopic study of the reactions of Br atoms and BrO radicals with dimethyl sulfide. *J. Phys. Chem. A* **2001**, *105*, 11045-11050, doi:10.1021/jp012326f.
(2) Wine, P. H.; Nicovich, J. M.; Stickel, R. E.; Zhao, Z.; Shackelford, C. J.; Kreutter, K. D.; Daykin, E. P.; Wang, S. In *The Tropospheric Chemistry of Ozone in the Polar Regions*; Springer-Verlag: Berlin, 1993; Vol. I7; pp 385-395.

32. **$CH_3S + O_2 \leftrightarrows CH_3SO_2$.** Turnipseed et al.[1] report the equilibrium constant for 216≤ T ≤258 K. From a third law analysis using $\Delta S°_{237} = -36.8 \pm 2.6$ eu, they obtain $\Delta H°_{237} = -11.5 \pm 0.9$ kcal mol^{-1}.
(Table: 94-26, Note: 94-26, Evaluated: 94-26) Back to Table

(1) Turnipseed, A. A.; Barone, S. B.; Ravishankara, A. R. Observation of CH_3S addition to O_2 in the gas phase. *J. Phys. Chem.* **1992**, *96*, 7502-7505, doi:10.1021/j100198a006.

33. $CH_3S + O_2 \leftrightarrows CH_3SOO$. Turnipseed et al.[6] generated CH_3S radicals by pulsed laser photolysis of CH_3SCH_3 in an excess of O_2 and used LIF of CH_3S to monitor the subsequent reaction. Biexponential decays were observed, signaling the reversible formation of a weakly bound complex. The equilibrium constant was extracted in the data analysis over a range of temperatures from 216 to 258 K and a van't Hoff (2nd Law) analysis gives $K_{eq} = 7.9 \times 10^{-27} \exp(4978/T)$ cm^3 molecule^{-1}. In a different experimental system, Butkovskaya and Barnes[1] (cited by Chu and Lee[2]) measured $K_{eq} = 1.4 \times 10^{-19}$ at 298 K, in good agreement with the 2nd Law expression given above for K_{eq}. The molecular properties of CH_3SOO have been computed in several theoretical studies[4,5,7,8] and some vibrational transitions have been observed by FTIR.[2] The recommendation is based on a new 3rd Law analysis of the data of Turnipseed et al.[6] This analysis made use of vibrational frequencies and rotational constants obtained from Chu and Lee[2] and from the NIST CCCBDB database.[3] The value of K_{eq}(298 K) obtained by Butkovskaya and Barnes is in excellent agreement with the recommendation. The bond dissociation energies at 0 K and 298 K obtained in this 3rd Law analysis are 39.5 and 42.2 kJ mol^{-1}, respectively; the computed entropy of CH_3SOO at 298 K is 316.7 J K^{-1} mol^{-1}.
(Table: 15-10; Note: 15-10; Evaluation 15-10) Back to Table

(1) Butkovskaya, N. I.; Barnes, I. Model study of the photooxidation of $CH_3SO_2SCH_3$ at atmospheric pressure: Thermal decomposition of the CH_3SO_2 radical. *Global Atmospheric Change and its Impact on Regional Air Quality, NATO Science Series* **2002**, *16*, 147-152, doi:10.1007/978-94-010-0082-6_22.
(2) Chu, L.-K.; Lee, Y.-P. Transient infrared spectra of CH_3SOO and CH_3SO observed with a step-scan Fourier-transform spectrometer. *J. Chem. Phys.* **2010**, *133*, 184303, doi:10.1063/1.3495765.
(3) NIST Computational Chemistry Comparison and Benchmark Database, NIST Standard Reference Database Number 101, Release 16a, August 2013. Johnson, R. D., III 2013, http://cccbdb.nist.gov/.
(4) McKee, M. L. Theoretical study of the CH_3OO radical. *Chem. Phys. Lett.* **1993**, *211*, 643-648, doi:10.1016/0009-2614(93)80157-K.
(5) Salta, Z.; Kosmas, A. M.; Lesar, A. Computational investigation of the peroxy radicals $CH_3S(O)_nOO$ and the peroxynitrates $CH_3S(O)_nOONO_2$ (n = 0, 1, 2). *Comput. Theo. Chem.* **2012**, 67-76, doi:10.1016/j.comptc.2012.10.007.
(6) Turnipseed, A. A.; Barone, S. B.; Ravishankara, A. R. Observation of CH_3S addition to O_2 in the gas phase. *J. Phys. Chem.* **1992**, *96*, 7502-7505, doi:10.1021/j100198a006.
(7) Zhanga, H.-t.; Zhoua, Z.-y.; Jalbout, A. F. Vibrational mode analysis for the multi-channel reaction of $O_2 + CH_3S$. *J. Mol. Struct. (Theochem)* **2003**, *663*, 73-79, doi:10.1016/j.theochem.2003.08.068.
(8) Zhu, L.; Bozzelli, J. W. The multi-channel reaction of $CH_3SC + {}^3O_2$: Thermochemistry and kinetic barriers. *J. Mol. Struct. (Theochem)* **2005**, *728*, 147-157, doi:10.1016/j.theochem.2005.05.002.

34. Hg + Br $\leftrightarrows$ HgBr. This equilibrium constant has never been measured directly. Goodsite et al.[2] used statistical rate theory combined with atomic and molecular properties to calculate the forward and reverse rate constants, from which K_{eq} can be obtained. Later, Goodsite et al.[3] recomputed the rate constants with an updated HgBr bond dissociation energy (assumed to be 66.3 kJ mol^{-1}, which is the average of the spectroscopic determination by Tellinghuisen and Ashmore,[6] the computed value (CCSD(T)) from Shepler et al.,[5] and the JANAF value (from 1961). From the ratio of their forward and reverse rate constants we obtain $K_{eq} = 9.1 \times 10^{-24} \exp(7984/T)$. The spectroscopic determination of Tellinghuisen and Ashmore gives $D_0 = 5430 \pm 100$ cm^{-1} (65.0 ± 1.2 kJ mol^{-1}), where the estimated 1σ uncertainty arises from the extrapolation of the assigned vibrational levels to the dissociation limit. Dibble et al.[1] used this spectroscopic value in a direct statistical mechanics calculation, obtaining $K_{eq} = 9.1 \times 10^{-24} \exp(7801 \pm 201/T)$. Subsequent work by Jiao and Dibble[4] suggests the electronic degeneracy, g_e, of HgBr is 2, rather than the value of 4 cited by Dibble et al.[1] The agreement between the two sets of A-factors noted above suggests that Goodsite et al. also used $g_e = 4$. The recommendation is based on this revision of the calculation of Dibble et al.[1] The uncertainty at 298 K is assumed to be a factor of 2 in the absence of directly measured values of K_{eq}, and the uncertainty in the temperature dependence arises largely from the uncertainty in the spectroscopic value of D_0.[3]
(Table: 19-5; Note: 19-5; Evaluation; 19-5) Back to Table

(1) Dibble, T. S.; Zelie, M. J.; Mao, H. Thermodynamics of reactions of ClHg and BrHg radicals with atmospherically abundant free radicals. *Atmos. Chem. Phys.* **2012**, *12*, 10271-10279, doi:10.5194/acp-12-10271-2012.
(2) Goodsite, M. E.; Plane, J. M. C.; Skov, H. A theoretical study of the oxidation of Hg^0 to $HgBr_2$ in the troposphere. *Environ. Sci. Technol.* **2004**, *38*, 1772-1776, doi:10.1021/es034680s.
(3) Goodsite, M. E.; Plane, J. M. C.; Skov, H. Correction to a theoretical study of the oxidation of Hg^0 to $HgBr_2$ in the troposphere. *Environ. Sci. Technol.* **2012**, *46*, 5262-5262, doi:10.1021/es301201c.

(4) Jiao, Y.; Dibble, T. S. Structures, vibrational frequencies, and bond energies of the BrHgOX and BrHgXO species formed in atmospheric mercury depletion events. *J. Phys. Chem. A* **2017**, *121*, 7976-7985, doi:10.1021/acs.jpca.7b06829.
(5) Shepler, B. C.; Balabanov, N. B.; Peterson, K. A. Hg + Br → HgBr recombination and collision-induced dissociation dynamics. *J. Chem. Phys.* **2007**, *107*, 164304, doi:10.1063/1.2777142.
(6) Tellinghuisen, J.; Ashmore, J. G. Mixed representations for diatomic spectroscopic data: Application to HgBr. *Chem. Phys. Lett.* **1983**, *102*, 10-16, doi:10.1016/0009-2614(83)80647-2.

3.4 Bibilography – Equilibrium Constants

Abbott, A. S. personal communication. **2018**.

Abbott, A. S.; Schaefer III, H. F. The structure and Cl−O dissociation energy of the ClOO radical: Finally, the right answers for the right reason. *J. Phys. Chem. A* **2018**, *122*, 2604-2610, doi:10.1021/acs.jpca.8b00394.

Alecu, I. M.; Marshall, P. Computational study of the thermochemistry of N_2O_5 and the kinetics of the reaction $N_2O_5 + H_2O \rightarrow 2\ HNO_3$. *J. Phys. Chem. A* **2014**, *118*, 11405−11416, doi:10.1021/jp509301t.

Alecu, I. M.; Marshall, P. Correction to "Computational study of the thermochemistry of N_2O_5 and the kinetics of the reaction $N_2O_5 + H_2O \rightarrow 2\ HNO_3$". *J. Phys. Chem. A* **2016**, *120*, 10305−10305, doi:10.1021/acs.jpca.6b12514.

Allan, B. J.; Plane, J. M. C. A study of the recombination of IO with NO_2 and the stability of INO_3: Implications for the atmospheric chemistry of iodine. *J. Phys. Chem. A* **2002**, *106*, 8634-8641, doi:10.1021/jp020089q.

Aloisio, S.; Francisco, J. S. Complexes of hydroxyl and hydroperoxyl radical with formaldehyde, acetaldehyde, and acetone. *J. Phys. Chem. A* **2000**, *104*, 3211-3224, doi:10.1021/jp993789c.

Aloisio, S.; Francisco, J. S.; Friedl, R. R. Experimental evidence for the existence of the HO_2-H_2O complex. *J. Phys. Chem. A* **2000**, *104*, 6597-6601, doi:10.1021/jp0006330.

Alongi, K. S.; Dibble, T. S.; Shields, G. C.; Kirschner, K. N. Exploration of the potential energy surfaces, prediction of atmospheric concentrations, and prediction of vibrational spectra for the $HO_2\cdots(H_2O)_n$ (n = 1-2) hydrogen bonded complexes. *J. Phys. Chem. A* **2006**, *110*, 3686-3691, doi:10.1021/jp057165k.

Amoruso, A.; Crescentini, L.; Fiocco, G.; Volpe, M. New measurements of the NO_2 absorption cross section in the 440- to 460-nm region and estimates of the NO_2-N_2O_4 equilibrium constant. *J. Geophys. Res.* **1993**, *98*, 16857-16863, doi:10.1029/93JD01582.

Andersson, B. Y.; Cox, R. A.; Jenkin, M. E. The effect of methanol on the self reaction of HO_2 radicals. *Int. J. Chem. Kinet.* **1988**, *20*, 283-295, doi:10.1002/kin.550200403.

Avallone, L. M.; Toohey, D. W. Tests of halogen photochemistry using in situ measurements of ClO and BrO in the lower polar stratosphere. *J. Geophys. Res.* **2001**, *106*, 10411-10421, doi:10.1029/2000JD900831.

Baer, S.; Hippler, H.; Rahn, R.; Siefke, M.; Seitzinger, N.; Troe, J. Thermodynamic and kinetic properties of the reaction $Cl + O_2 + M \rightleftharpoons ClOO + M$ in the range 160-300 K and 1-1000 bar. *J. Chem. Phys.* **1991**, *95*, 6463-6470, doi:10.1063/1.461543.

Bahta, A.; Simonaitis, R.; Heicklen, J. Thermal decomposition kinetics of $CH_3O_2NO_2$. *J. Phys. Chem.* **1982**, *86*, 1849-1853, doi:10.1021/j100207a022.

Barker, J. R.; Ortiz, N. F.; Preses, J. M.; Lohr, L. L.; Maranzana, A.; Stimac, P. J.; Nguyen, T. L.; Kumar, T. J. D. MultiWell http://aoss.engin.umich.edu/multiwell/. University of Michigan: Ann Arbor, MI, 2011.

Barnes, I.; Becker, K. H.; Fink, E. H.; Reimer, A.; Zabel, F.; Niki, H. FTIR spectroscopic study of the gas-phase reaction of HO_2 with H_2CO. *Chem. Phys. Lett.* **1985**, *115*, 1-8, doi:10.1016/0009-2614(85)80091-9.

Barone, S. B.; Turnipseed, A. A.; Ravishankara, A. R. Reaction of OH with dimethyl sulfide (DMS). 1. Equilibrium constant for OH + DMS reaction and the kinetics of the OH•DMS + O_2 reaction. *J. Phys. Chem.* **1996**, *100*, 14694-14702, doi:10.1021/jp960866k.

Belair, S. D.; Kais, S.; Francisco, J. S. Potential energy surface for the hydroperoxy and water (HO_2•H_2O) radical complex. *Molec. Phys.* **2002**, *100*, 247-253, doi:10.1080/00268970110086309.

Benson, S. W. Some observations on the kinetics and thermochemistry of the reactions of HO_2 radicals with aldehydes and ketones. *Int. J. Chem. Kinet.* **2001**, *33*, 509-512, doi:10.1002/kin.1047.

Birk, M.; Friedl, R. R.; Cohen, E. A.; Pickett, H. M.; Sander, S. P. The rotational spectrum and structure of chlorine peroxide. *J. Chem. Phys.* **1989**, *91*, 6588-6597, doi:10.1063/1.457377.

Boakes, G.; Mok, W. H. H.; Rowley, D. M. Kinetic studies of the ClO + ClO association reaction as a function of temperature and pressure. *Phys. Chem. Chem. Phys.* **2005**, *7*, 4102-4113, doi:10.1039/b510308h.

Borrell, P.; Cobos, C. J.; Luther, K. Falloff curve and specific rate constants for the reaction $NO_2 + NO_2 \rightleftarrows N_2O_4$. *J. Phys. Chem.* **1988**, *92*, 4377-4384, doi:10.1021/j100326a027.

Bridier, I.; Caralp, F.; Loirat, H.; Lesclaux, R.; Veyret, B.; Becker, K. H.; Reimer, A.; Zabel, F. Kinetic and theoretical studies of the reactions $CH_3C(O)O_2 + NO_2 + M \rightleftarrows CH_3C(O)O_2NO_2 + M$ between 248 and 393 K and between 30 and 760 Torr. *J. Phys. Chem.* **1991**, *95*, 3594-3600, doi:10.1021/j100162a031.

Bridier, I.; Lesclaux, R.; Veyret, B. Flash photolysis kinetic study of the equilibrium $CH_3O_2 + NO_2 \leftrightarrow CH_3O_2NO_2$. *Chem. Phys. Lett.* **1992**, *191*, 259-263, doi:10.1016/0009-2614(92)85297-N.

Broske, R.; Zabel, F. Thermal decomposition of ClOOCl. *J. Phys. Chem. A* **2006**, *110*, 3280-3288, doi:10.1021/jp0550053.

Brunning, J.; Frost, M. J.; Smith, I. W. M. Kinetic measurements on the system: $2NO_2 \leftrightharpoons N_2O_4$ at (224 ± 2) K using time-resolved infrared laser absorption. *Int. J. Chem. Kinet.* **1988**, *20*, 957-965, doi:10.1002/kin.550201204.

Burkholder, J. B.; Mauldin, R. L.; Yokelson, R. J.; Solomon, S.; Ravishankara, A. R. Kinetic, thermodynamic, and spectroscopic study of Cl_2O_3. *J. Phys. Chem.* **1993**, *97*, 7597-7605, doi:10.1021/j100131a032.

Burrows, J. P.; Moortgat, G. K.; Tyndall, G. S.; Cox, R. A.; Jenkin, M. E.; Hayman, G. D.; Veyret, B. Kinetics and mechanism of the photooxidation of formaldehyde. 2. Molecular modulation studies. *J. Phys. Chem.* **1989**, *93*, 2375-2382, doi:10.1021/j100343a034.

Burrows, J. P.; Tyndall, G. S.; Moortgat, G. K. A study of the N_2O_5 equilibrium betwen 275 and 315 K and determination of the heat of formation of NO_3. *Chem. Phys. Lett.* **1985**, *119*, 193-198, doi:10.1016/0009-2614(85)80059-2.

Butkovskaya, N. I.; Barnes, I. Model study of the photooxidation of $CH_3SO_2SCH_3$ at atmospheric pressure: Thermal decomposition of the CH_3SO_2 radical. *Global Atmospheric Change and its Impact on Regional Air Quality, NATO Science Series* **2002**, *16*, 147-152, doi:10.1007/978-94-010-0082-6_22.

Campuzano-Jost, P.; Croce, A. E.; Hippler, H.; Siefke, M.; Troe, J. Kinetic and thermodynamic properties of the F + O_2 reaction system under high pressure and low temperature conditions. *J. Chem. Phys.* **1995**, *102*, 5317-5326, doi:10.1063/1.469258.

Cantrell, C. A.; Davidson, J. A.; McDaniel, A. H.; Shetter, R. E.; Calvert, J. G. The equilibrium constant for $N_2O_5 \rightleftarrows NO_2 + NO_3$: Absolute determination by direct measurement from 243 to 397 K. *J. Chem. Phys.* **1988**, *88*, 4997-5006, doi:10.1063/1.454679.

Canty, T. P.; Salawitch, R. J.; Wilmouth, D. M. The kinetics of the ClOOCl catalytic cycle. *J. Geophys. Res.* **2016**, *121*, 13768-13783, doi:10.1002/2016JD025710.

Cao, J.; Wang, W.-L.; Gao, L.-J.; Fu, F. Mechanism and thermodynamic properties of CH_3SO_3 decomposition. *Acta Phys.-Chim. Sin.* **2013**, *29*, 1161-1167, doi:10.3866/PKU.WHXB201304021.

Carter, R. O.; Andrews, L. Matrix spectroscopic studies of chlorine atom-ozone reaction products. *J. Phys. Chem.* **1981**, *85*, 2351-2354, doi:10.1021/j150616a011.

Chao, J.; Wilhoit, R. C.; Zwolinski, B. J. *Thermochim. Acta* **1974**, *10*, 361-371.

Chao, J.; Wilhoit, R. C.; Zwolinski, B. J. Gas phase chemical equilibrium in dinitrogen trioxide and dinitrogen tetroxide. *Thermochim. Acta* **1974**, *10*, 359-371.

Chase, M. W. NIST-JANAF thermochemical tables. *J. Phys. Chem. Ref. Data* **1998**, *Monograph 9*.

Chen, Z.; Hamilton, T. P. Ab initio study of pernitric acid: Comparison with experimental spectra. *J. Phys. Chem.* **1996**, *100*, 15731-15734, doi:10.1021/jp961772d.

Christensen, L. E.; Okumura, M.; Hansen, J. C.; Sander, S. P.; Francisco, J. S. Experimental and ab initio study of the HO_2•CH_3OH complex: Thermodynamics and kinetics of formation. *J. Phys. Chem. A* **2006**, *110*, 6948-6959, doi:10.1021/jp056579a.

Chu, L.-K.; Lee, Y.-P. Transient infrared spectra of CH_3SOO and CH_3SO observed with a step-scan Fourier-transform spectrometer. *J. Chem. Phys.* **2010**, *133*, 184303, doi:10.1063/1.3495765.

Clark, J.; Francisco, J. S. Study of the stability of Cl_2O_3 using ab initio methods. *J. Phys. Chem. A* **1997**, *101*, 7145-7153, doi:10.1021/jp971465n.

Connell, P. S.; Johnston, H. S. The thermal dissociation of N_2O_5 in N_2. *Geophys. Res. Lett.* **1979**, *6*, 553-556, doi:10.1029/GL006i007p00553.

Coronel, A. C.; Fernández, L. E.; Varetti, E. L. Scaled quantum mechanical force fields for the peroxynitrates. I. Acetyl peroxynitrate and trifluoroacetyl peroxynitrate. *Z. Anorg. Allg. Chem.* **2010**, *636*, 524–530, doi:10.1002/zaac.200900384.

Cours, T.; Canneaux, S.; Bohr, F. Features of the potential energy surface for the reaction of HO_2 radical with acetone. *Int. J. Quant. Chem.* **2007**, *107*, 1344-1354, doi:10.1002/qua.21269.

Cox, R. A.; Burrows, J. P. Kinetics and mechanism of the disproportionation of HO_2 in the gas phase. *J. Phys. Chem.* **1979**, *83*, 2560-2568, doi:10.1021/j100483a002.

Cox, R. A.; Hayman, G. D. The stability and photochemistry of dimers of the ClO radical and implications for Antarctic ozone depletion. *Nature* **1988**, *332*, 796-800, doi:10.1038/332796a0.

Cox, R. A.; Roffey, M. J. Thermal decomposition of peroxyacetylnitrate in the presence of nitric oxide. *Environ. Sci. Technol.* **1977**, *11*, 900-906, doi:10.1021/es60132a010.

Dávalos, J. Z.; Notario, R.; Cuevas, C. A.; Oliva, J. M.; Saiz-Lopez, A. Thermochemistry of halogen-containing organic compounds with influence on atmospheric chemistry. *Comp. Theor. Chem.* **2017**, *1099*, 36-44, doi:10.1016/j.comptc.2016.11.009.

de Petris, G.; Rosi, M.; Troiani, A. Direct experimental observation of CS_2OH. *ChemPhysChem* **2006**, *7*, 2352-2357, doi:10.1002/cphc.200600515.

DeMore, W. B. Equilibrium constant for the reaction ClO + $O_2 \leftrightarrow$ ClO•O_2. *Geophys. Res. Lett.* **1990**, *17*, 2353-2355, doi:10.1029/GL017i013p02353.

Denis, P. A., and O. N. Ventura CCSDT study of the fluoroperoxyl radical, FOO. *Chem. Phys. Lett.* **2004**, *385*, 292-297, doi:10.1016/j.cplett.2003.12.081.

Diau, E. W.-G.; Lee, Y.-P. Kinetics of the reactions of CS_2OH with O_2, NO, and NO_2. *J. Phys. Chem.* **1991**, *95*, 7726-7732, doi:10.1021/j100173a033.

Dibble, T. S.; Zelie, M. J.; Mao, H. Thermodynamics of reactions of ClHg and BrHg radicals with atmospherically abundant free radicals. *Atmos. Chem. Phys.* **2012**, *12*, 10271-10279, doi:10.5194/acp-12-10271-2012.

Dillon, T. J.; Pozzer, A.; Vereecken, L.; Crowley, J. N.; Lelieveld, J. Does acetone react with HO_2 in the upper-troposphere? *Atmos. Chem. Phys.* **2012**, *12*, 1339-1351, doi:10.5194/acp-12-1339-2012.

Dixon, D. A.; Peterson, K. A.; Francisco, J. S. The molecular structures and energetics of Cl_2CO, ClCO, Br_2CO, and BrCO. *J. Phys. Chem. A* **2000**, *104*, 6227-6332, doi:10.1021/jp0005571.

Ellermann, T.; Johnsson, K.; Lund, A.; Pagsberg, P. Kinetics and equilibrium-constant of the reversible reaction ClO + ClO + M ↔ Cl_2O_2 + M at 295 K. *Acta Chem. Scand.* **1995**, *49*, 28-35, doi:10.3891/acta.chem.scand.49-0028.

Estupiñán, E. G., J. M. Nicovich and P.H. Wine A temperature-dependent kintetics study of the important stratospheric reaction $O(^3P) + NO_2 \rightarrow O_2 + NO$. *J. Phys. Chem. A* **2001**, *105*, 9697-9703, doi:10.1021/jp011940o.

Evleth, E. M.; Melius, C. F.; Rayez, M. T.; Rayez, J. C.; Forst, W. Theoretical characterization of the reaction of hydroperoxy with formaldehyde. *J. Phys. Chem.* **1993**, *97*, 5040-5045, doi:10.1021/j100121a031.

Feller, D.; Dixon, D. A. Coupled cluster theory and multireference configuration interaction study of FO, F_2O, FO_2, and FOOF. *J. Phys. Chem. A* **2003**, *107*, 9641-9651, doi:10.1021/jp030267v.

Feller, D.; Peterson, K. A.; Dixon, D. A. A survey of factors contributing to accurate theoretical predictions of atomization energies and molecular structures. *J. Chem. Phys.* **2008**, *129*, 204105, doi:10.1063/1.3008061.

Ferracci, V.; Rowley, D. M. Kinetic and thermochemical studies of the ClO + ClO + M ⇄ Cl_2O_2 + M reaction *Phys. Chem. Chem. Phys* **2010**, *12*, 11596-11608, doi:10.1039/c0cp00308e.

Francisco, J. S., Y. Zhao, W. A. Lester, Jr., and I. H. Williams Theoretical studies of the structure and thermochemistry of FO_2 radical: Comparison of Møller-Plesset perturbation, complete-active-space self-consistent-field, and quadratic configuration interaction methods. *J. Chem. Phys.* **1992**, *96*, 2861-2867, doi:10.1063/1.461982.

Friedl, R. R.; Sander, S. P.; Yung, Y. L. Chloryl nitrate: A novel product of the OClO + NO_3 + M recombination. *J. Phys. Chem.* **1992**, *96*, 7490-7493, doi:10.1021/j100198a002.

Fry, J.; Matthews, L. J.; Lane, J. R.; Sinha, A.; Kjaergaard, H. G.; Wennberg, P. O. OH-Stretch vibrational spectroscopy of hydroxymethyl hydroperoxide. *J. Phys. Chem. A* **2006**, *110*, 7072-7079, doi:10.1021/jp0612127.

Gierczak, T.; Jimenez, E.; Riffault, V.; Burkholder, J. B.; Ravishankara, A. R. Thermal decomposition of HO_2NO_2 (peroxynitric acid, PNA): Rate coefficient and determination of the enthalpy of formation. *J. Phys. Chem. A* **2005**, *109*, 586-596, doi:10.1021/jp046632f.

Glendening, E. D.; Halpern, A. M. Ab initio calculations of nitrogen oxide reactions: Formation of N_2O_2, N_2O_3, N_2O_4, N_2O_5, and N_4O_2 from NO, NO_2, NO_3, and N_2O. *J. Chem. Phys.* **2007**, *127*, 164307, doi:10.1063/1.2777145.

Golden, D. M. Reaction ClO + ClO → products: Modeling and parameterization for use in atmospheric models. *Int. J. Chem. Kinet.* **2003**, *35*, 206-211, doi:10.1002/kin.10120.

Golden, D. M. Evaluating data for atmospheric models, an example: $CH_3O_2 + NO_2 = CH_2O_2NO_2$. *Int. J. Chem. Kinet.* **2005**, *37*, 625-632, doi:10.1002/kin.20104.

Golden, D. M. Evaluating data for atmospheric models, an example: IO + NO_2 = $IONO_2$. *J. Phys. Chem. A* **2006**, *110*, 2940-2943, doi:10.1021/jp058221k.

Golden, D. M.; Barker, J. R.; Lohr, L. L. Master equation models for the pressure- and temperature-dependent reactions HO + NO_2 → $HONO_2$ and HO + NO_2 → HOONO. *J. Phys. Chem. A* **2003**, *107*, 11057-11071, doi:10.1021/jp0353183.

Golden, D. M.; Barker, J. R.; Lohr, L. L. Correction: Master equation models for the pressure- and temperature-dependent reactions HO + NO_2 → $HONO_2$ and HO + NO_2 → HOONO. *J. Phys. Chem. A* **2004**, *108*, 8552, doi:10.1021/jp040476v.

Goodsite, M. E.; Plane, J. M. C.; Skov, H. A theoretical study of the oxidation of Hg^0 to $HgBr_2$ in the troposphere. *Environ. Sci. Technol.* **2004**, *38*, 1772-1776, doi:10.1021/es034680s.

Goodsite, M. E.; Plane, J. M. C.; Skov, H. Correction to a theoretical study of the oxidation of Hg^0 to $HgBr_2$ in the troposphere. *Environ. Sci. Technol.* **2012**, *46*, 5262-5262, doi:10.1021/es301201c.

Gozel, P.; Calpani, B.; van den Bergh, H. Temperature jump measurements in gas kinetics. *Israel J. Chem.* **1984**, *24*, 210-213.

Graham, R. A.; Johnston, H. S. The photochemistry of NO_3 and the kinetics of the N_2O_5-O_3 system. *J. Phys. Chem.* **1978**, *82*, 254-268, doi:10.1021/j100492a002.

Graham, R. A.; Winer, A. M.; Pitts, J. N., Jr. Temperature dependence of the unimolecular decomposition of pernitric acid and its atmospheric implications. *Chem. Phys. Lett.* **1977**, *51*, 215-220, doi:10.1016/0009-2614(77)80387-4.

Grant, D. J.; III, E. B. G.; Matus, M. H.; Nguyen, M. T.; Peterson, K. A.; Francisco, J. S.; Dixon, D. A. Thermodynamic properties of the XO_2, X_2O, XYO, X_2O_2, and XYO_2 (X, Y = Cl, Br, and I) isomers. *J. Phys. Chem. A* **2010**, *114*, 4254-4265, doi:10.1021/jp911320p.

Green, T. J.; Islam, M.; Guest, P.; Hickson, K.; Canosa-Mas, C. E.; Wayne, R. P. A discharge-flow study of Cl_2O_3. *Phys. Chem. Chem. Phys.* **2003**, *5*, 5409-5418, doi:10.1039/b311005b.

Grieman, F. J.; Noell, A. C.; Davis-Van Atta, C.; Okumura, M.; Sander, S. P. Determination of equilibrium constants for the reaction between acetone and HO_2 using infrared kinetic spectroscopy. *J. Phys. Chem. A* **2011**, *115*, 10527–10538, doi:10.1021/jp205347s.

Hamilton, E. J., Jr. Water vapor dependence of the kinetics of the self-reaction of HO_2 in the gas phase. *J. Chem. Phys.* **1975**, *63*, 3682-3683, doi:10.1063/1.431772.

Hamilton, E. J., Jr.; Lii, R.-R. The dependence on H_2O and on NH_3 of the kinetics of the self-reaction of HO_2 in the gas-phase formation of HO_2•H_2O and HO_2•NH_3 complexes. *Int. J. Chem. Kinet.* **1977**, *9*, 875-885, doi:10.1002/kin.550090604.

Harwood, M. H.; Jones, R. L. Temperature dependent ultraviolet-visible absorption cross sections of NO_2 and N_2O_4: Low-temperature measurements of the equilibrium constant for $2NO_2 \rightleftharpoons N_2O_4$. *J. Geophys. Res.* **1994**, *99*, 22955-22964, doi:10.1029/94JD01635

Hassouna, M.; Delbos, E.; Devolder, P.; Viskolcz, B.; Fittschen, C. Rate and equilibrium constant of the reaction of 1-methylvinoxy radicals with O_2: $CH_3COCH_2 + O_2 \leftrightarrow CH_3COCH_2O_2$. *J. Phys. Chem. A* **2006**, *110*, 6667-6672, doi:10.1021/jp0558270.

Hayman, G. D.; Cox, R. A. UV absorption spectrum and thermochemistry of Cl_2O_3 formed in the photolysis of OClO-containing mixtures at low temperatures. *Chem. Phys. Lett.* **1989**, *155*, 1-7, doi:10.1016/S0009-2614(89)87350-6.

Hermans, I.; Muller, J. F.; Nguyen, T. L.; Jacobs, P. A.; Peeters, J. Kinetics of alpha-hydroxy-alkylperoxyl radicals in oxidation processes. HO_2 initiated oxidation of ketones/aldehydes near the tropopause. *J. Phys. Chem. A* **2005**, *109*, 4303-4311, doi:10.1021/jp044080v.

Hermans, I.; Nguyen, T. L.; Jacobs, P. A.; Peeters, J. Tropopause chemistry revisited: HO_2*-initiated oxidation as an efficient acetone sink. *J. Am. Chem. Soc.* **2004**, *126*, 9908-9909, doi:10.1021/ja0467317.

Hippler, H.; Nasterlack, S.; Striebel, F. Reaction of OH + NO_2 + M: Kinetic evidence of isomer formation. *Phys. Chem. Chem. Phys.* **2002**, *4*, 2959-2964, doi:10.1039/b201932a.

Hjorth, J.; Nothholt, J.; Restelli, G. A spectroscoy study of the equilibrium $NO_2 + NO_3 + M \leftrightharpoons N_2O_5 + M$ and the kinetics of the $O_3/N_2O_5/NO_3/NO_2$/air system. *Int. J. Chem. Kinet.* **1992**, *24*, 51-65, doi:10.1002/kin.550240107.

Horný, Ľ.; Quack, M.; III, H. F. S.; Willeke, M. Chlorine peroxide (Cl_2O_2) and its isomers: structures, spectroscopy, formation and thermochemistry. *Mol. Phys.* **2016**, *114*, 1135-1147, doi:10.1080/00268976.2016.1143984.

Horowitz, A.; Crowley, J. N.; Moortgat, G. K. Temperature dependence of the product branching ratios of the ClO self-reaction in oxygen. *J. Phys. Chem.* **1994**, *98*, 11924-11930, doi:10.1021/j100097a019.

Hume, K. L.; Bayes, K. D.; Sander, S. P. The equilibrium constant for the reaction ClO + ClO ↔ ClOOCl between 250 and 206 K. *J. Phys. Chem. A* **2015**, *119*, 4473-4481, doi:10.1021/jp510100n.

Hynes, A. J.; Wine, P. H.; Nicovich, J. M. Kinetics and mechanism of the reaction of OH with CS_2 under atmospheric conditions. *J. Phys. Chem.* **1988**, *92*, 3846-3852, doi:10.1021/j100324a034.

Hynes, A. J.; Wine, P. H.; Semmes, D. H. Kinetics and mechanism of OH reactions with organic sulfides. *J. Phys. Chem.* **1986**, *90*, 4148-4156, doi:10.1021/j100408a062.

Jacobs, J.; Kronberg, M.; Müller, H. S. P.; Willner, H. An experimental study on the photochemistry and vibrational spectroscopy of three isomers of Cl_2O_2 isolated in cryogenic matrices. *J. Am. Chem. Soc.* **1994**, *116*, 1106-1114, doi:10.1021/ja00082a038.

JANAF *Thermochemical Tables*, Third ed.; National Bureau of Standards, 1985.

Jiao, Y.; Dibble, T. S. Structures, vibrational frequencies, and bond energies of the BrHgOX and BrHgXO species formed in atmospheric mercury depletion events. *J. Phys. Chem. A* **2017**, *121*, 7976-7985, doi:10.1021/acs.jpca.7b06829.

NIST Computational Chemistry Comparison and Benchmark Database, NIST Standard Reference Database Number 101, Release 16a, August 2013. Johnson, R. D., III 2013, http://cccbdb.nist.gov/.

Kabir, M.; Jagiella, S.; Zabel, F. Thermal stability of n-acyl peroxynitrates. *Int. J. Chem. Kinet. 1–8, 2014* **2014**, *46*, 1-8, doi:10.1002/kin.20862.

Kaltsoyannis , N.; Plane, J. M. C. Quantum chemical calculations on a selection of iodine-containing species (IO, OIO, INO_3, $(IO)_2$, I_2O_3, I_2O_4 and I_2O_5) of importance in the atmosphere. *Phys. Chem. Chem. Phys.* **2008**, *10*, 1723-1733, doi:10.1039/b715687c.

Kanno, N.; Tonokura, K.; Koshi, M. Equilibrium constant of the HO_2-H_2O complex formation and kinetics of HO_2 + HO_2-H_2O: Implications for tropospheric chemistry. *J. Geophys. Res.* **2006**, *111*, D20312, doi:10.1029/2005JD006805.

Kanno, N.; Tonokura, K.; Tezaki, A.; Koshi, M. Water dependence of the HO_2 self reaction: Kinetics of the HO_2–H_2O complex. *J. Phys. Chem. A* **2005**, *109*, 3153-3158, doi:10.1021/jp044592+.

Karton, A.; Daon, S.; Martin, J. M. L. W4-11: A high-confidence benchmark dataset for computational thermochemistry derived from first-principles W4 data. *Chem. Phys. Lett.* **2011**, *510*, 165-178, doi:10.1016/j.cplett.2011.05.007.

Karton, A.; Parthiban, S.; Martin, J. M. L. Post-CCSD(T) ab Initio thermochemistry of halogen oxides and related hydrides XOX, XOOX, HOX, XO_n, and HXO_n (X) F, Cl), and evaluation of DFT methods for these systems. *J. Phys. Chem. A* **2009**, *113*, 4802-4816, doi:10.1021/jp8087435.

Kircher, C. C.; Margitan, J. J.; Sander, S. P. Temperature and pressure dependence study of the reaction $NO_2 + NO_3 + M \rightarrow N_2O_5 + M$. *J. Phys. Chem.* **1984**, *88*, 4370-4375, doi:10.1021/j150663a037.

Kirchner, F.; Zabel, F.; Becker, K. H. Determination of the rate constant ratio for the reactions of the acetylperoxy radical with NO and NO_2. *Ber. Bunsenges. Phys. Chem.* **1990**, *94*, 1379-1382, doi:10.1002/bbpc.199000037.

Kleinböhl, A.; Khosravi, M.; J. Urban; Canty, T.; Salawitch, R. J.; G. C. Toon; Küllmann, H.; Notholt, J. Constraints for the photolysis rate and the equilibrium constant of ClO-dimer from airborne and balloon-borne measurements of chlorine compounds. *Geophys. Res. Atmos.* **2014**, *119*, 6916–6937, doi:10.1002/2013JD021433.

Klobas, J. E.; Wilmouth, D. M. UV spectroscopic determination of the chlorine monoxide (ClO) / chlorine peroxide (ClOOCl) thermal equilibrium constant. *Atmos. Chem. Phys.* **2019**, *19*, 6205-6215, doi:10.5194/acp-19-6205-2019.

Konen, I. M.; Li, E. X. J.; Stephenson, T. A.; Lester, M. I. Second OH overtone excitation and statistical dissociation dynamics of peroxynitrous acid. *J. Chem. Phys.* **2005**, *123*, 204318, doi:10.1063/1.2126968.

Konen, I. M.; Pollack, L. B.; Li, E. X. J.; Lester, M. I.; Varner, M. E.; Stanton, J. F. Infrared overtone spectroscopy and unimolecular decay dynamics of peroxynitrous acid. *J. Chem. Phys.* **2005**, *122*, 094320, doi:10.1063/1.1854094.

Laine, P. L.; Sohn, Y. S.; Nicovich, J. M.; McKee, M. L.; Wine, P. H. Kinetics of elementary steps in the reactions of atomic bromine with isoprene and 1,3-butadiene under atmospheric conditions. *J. Phys. Chem. A* **2012**, *116*, 6341-6357, doi:10.1021/jp212127v.

Lee, T. J.; Rohlfing, C. M.; Rice, J. E. An extensive *ab initio* study of the structures, vibrational spectra, quadratic force fields, and relative energetics of three isomers of Cl_2O_2. *J. Chem. Phys.* **1992**, *97*, 6593-6605, doi:10.1063/1.463663.

Li, E. X.; Konan, I. M.; Lester, M. I.; McCoy, A. B. Spectroscopic characterization of peroxynitrous acid in cis-perp configurations. *J. Phys. Chem. A* **2006**, *110*, 5607-5613, doi:10.1021/jp056959w.

Li, Q., S. Lu, Y. Xie, P. V. R. Schleyer and H. F. Schaefer, III Molecular structures, thermochemistry, and electron affinities for dichlorine oxides: $Cl_2O_n/Cl_2O_n^-$ (n = 1-4). *Int. J. Quant. Chem.* **2003**, *95*, 731-757, doi:10.1002/qua.10634.

Maranzana, A.; Barker, J. R.; Tonachini, G. Master equation simulations of competing unimolecular and bimolecular reactions: Application to OH production in the reaction of acetyl radical with O_2. *Phys. Chem. Chem. Phys.* **2007**, *9*, 4129 - 4141, doi:10.1039/b705116f.

Markwalder, B.; Gozel, P.; van den Bergh, H. Temperature-jump measurements on the kinetics of association and dissociation in weakly bound systems: $N_2O_4 + M = NO_2 + NO_2 + M$. *J. Chem. Phys.* **1992**, *97*, 5472-5479, doi:10.1063/1.463780.

Marshall, P. Computational studies of the thermochemistry of the atmospheric iodine reservoirs HOI and $IONO_2$. *Advances in Quantum Chemistry* **2008**, 159-175.

Matthews, J.; Sinha, A. State-resolved unimolecular dissociation of *cis-cis* HOONO: Product state distributions and action spectrum in the $2\nu_{OH}$ band region. *J. Chem. Phys.* **2005**, *122*, 104313, doi:10.1063/1.858437.

Matus, M. H.; Nguyen, M. T.; Dixon, D. A.; Peterson, K. A.; Francisco, J. S. $ClClO_2$ is the most stable isomer of Cl_2O_2. Accurate coupled cluster energetics and electronic spectra of Cl_2O_2 isomers. *J. Phys. Chem. A* **2008**, *112*, 9623-9627, doi:10.1021/jp806220r.

Mauldin, R. L., III; Burkholder, J. B.; Ravishankara, A. R. A photochemical, thermodynamic, and kinetic study of ClOO. *J. Phys. Chem.* **1992**, *96*, 2582-2588, doi:10.1021/j100185a035.

McCoy, A. B.; Fry, J. L.; Francisco, J. S.; Mollner, A. K.; Okumura, M. Role of OH-stretch/torsion coupling and quantum yield effects in the first OH overtone spectrum of *cis-cis* HOONO. *J. Chem. Phys.* **2005**, *122*, 104311, doi:10.1063/1.1859273.

McKee, M. L. Computational study of addition and abstraction reactions between OH radical and dimethyl sulfide. A difficult case. *J. Phys. Chem.* **1993**, *97*, 10971-10976, doi:10.1021/j100144a013.

McKee, M. L. Theoretical study of the CH_3OO radical. *Chem. Phys. Lett.* **1993**, *211*, 643-648, doi:10.1016/0009-2614(93)80157-K.

McKee, M. L. Comparison of gas-phase and solution-phase reactions of dimethyl sulfide and 2-(methylthio)ethanol with hydroxyl radical. *J. Phys. Chem. A* **2003**, *107*, 6819-6827, doi:10.1021/jp034704h.

Miller, C. E.; Lynton, J. I.; Keevil, D. M.; Franscisco, J. S. Dissociation pathways of peroxyacetyl nitrate (PAN). *J. Phys. Chem. A* **1999**, *103*, 11451-11459, doi:10.1021/jp992667h.

Moortgat, G. K.; Meyrahn, H.; Warneck, P. Photolysis of acetaldehyde in air: CH_4, CO and CO_2 quantum yields. *ChemPhysChem* **2010**, *11*, 3896-3908, doi:10.1002/cphc.201000757.

Morajkar, P.; Schoemaecker, C.; Okumura, M.; Fittchen, C. Direct measurement of the equilibrium constants of the reaction of formaldehyde and acetaldehyde with HO_2 radicals. *Int. J. Chem. Kinet.* **2014**, *46*, 245-259, doi:10.1002/kin.20817.

Müller, H. S. P.; Willner, H. Gas phase studies on chloryl chloride, $ClClO_2$. *Ber. Bunsenges. Phys. Chem.* **1992**, *96*, 427-431, doi:10.1002/bbpc.19920960338.

Müller, H. S. P.; Willner, H. Synthesis and properties of chloryl chloride, $ClClO_2$. *Inorg. Chem.* **1992**, *31*, 2527-2534, doi:10.1021/ic00038a040.

Müller, H. S. P.; Willner, H. Vibrational and electronic spectra of chlorine dioxide, OClO, and chlorine superoxide, ClOO, isolated in cryogenic matrices. *J. Phys. Chem.* **1993**, *97*, 10589-10598, doi:10.1021/j100143a013.

Murrells, T. P.; Lovejoy, E. R.; Ravishankara, A. R. Oxidation of CS_2 by reaction with OH. 1. Equilibrium constant for the reaction OH + CS_2 ⇄ CS_2OH and the kinetics of the CS_2OH + O_2 reaction. *J. Phys. Chem.* **1990**, *94*, 2381-2386, doi:10.1021/j100369a036.

Nakano, Y., M. Goto, S. Hashimoto, M. Kawasaki, and T. J. Wallington Cavity ring-down spectroscopic study of the reactions of Br atoms and BrO radicals with dimethyl sulfide. *J. Phys. Chem. A* **2001**, *105*, 11045-11050, doi:10.1021/jp012326f.

Nickolaisen, S. L.; Friedl, R. R.; Sander, S. P. Kinetics and mechanism of the ClO + ClO reaction: Pressure and temperature dependences of the bimolecular and termolecular channels and thermal decomposition of chlorine peroxide, ClOOCl. *J. Phys. Chem.* **1994**, *98*, 155-169, doi:10.1021/j100052a027.

Nicovich, J. M.; Kreutter, K. D.; Shackelford, C. J.; Wine, P. H. Thermochemistry and kinetics of the Cl + O_2 association reaction. *Chem. Phys. Lett.* **1991**, *179*, 367-373, doi:10.1016/0009-2614(91)85168-V.

Nicovich, J. M.; Kreutter, K. D.; Wine, P. H. Kinetics and thermochemistry of ClCO formation from the Cl + CO association reaction. *J. Chem. Phys.* **1990**, *92*, 3539-3544, doi:10.1063/1.457862.

Nicovich, J. M.; Wine, P. H. Kinetics of the reactions of O(^3P) and Cl(^2P) with HBr and Br_2. *Int. J. Chem. Kinet.* **1990**, *22*, 379-397, doi:10.1002/kin.550220406.

Orlando, J. J.; Tyndall, G. S.; Cantrell, C. A.; Calvert, J. G. Temperature and pressure dependence of the rate coefficient for the reaction NO_3 + NO_2 → N_2O_5 + N_2. *J. Chem. Soc. Faraday Trans.* **1991**, *87*, 2345-2349, doi:10.1039/ft9918702345.

Osthoff, H. D.; Pilling, M. J.; Ravishankara, A. R.; Brown, S. S. Temperature dependence of the NO_3 absorption cross-section above 298 K and determination of the equilibrium constant for NO_3 + NO_2 ↔ N_2O_5 at atmospherically relevant conditions. *Phys. Chem. Chem. Phys.* **2007**, *9*, 5785-5793, doi:10.1039/b709193a.

Pagsberg, P.; Ratajczak, E.; Sillesen, A.; Jodkowski, J. T. Spectrokinetic studies of the gas-phase equilibrium F + O_2 ⇌ FO_2 between 295 and 359 K. *Chem. Phys. Lett.* **1987**, *141*, 88-94, doi:10.1016/0009-2614(87)80097-0.

Papayannis, D. K.; Kosmas, A. M. Quantum mechanical characterization of (INO_3) isomers. *Chem. Phys. Lett.* **2004**, *398*, 75-81, doi:10.1016/j.cplett.2004.09.019.

Papayannis, D. K.; Kosmas, A. M. The conformational potential energy surface of IOONO and the isomerization and decomposition processes. *Chem. Phys.* **2005**, *315*, 251-258, doi:10.1016/j.chemphys.2005.04.014.

Parthiban, S., T. J. Lee, S. Guha, and J. S. Francisco Theoretical study of chlorine nitrates: Implications for stratospheric chlorine chemistry. *J. Am. Chem. Soc.* **2003**, *125*, 10446-10458, doi:10.1021/ja010297g.

Perner, D.; Schmeltekopf, A.; Winkler, R. H.; Johnston, H. S.; Calvert, J. G.; Cantrell, C. A.; Stockwell, W. R. A laboratory and field study of the equilibrium N_2O_5 ⇌ NO_3 + NO_2. *J. Geophys. Res.* **1985**, *90*, 3807-3812, doi:10.1029/JD090iD02p03807.

Plenge, J.; Kühl, S.; Vogel, B.; Müller, R.; Stroh, F.; von Hobe, M.; Flesch, R.; Rühl, E. Bond strength of chlorine peroxide. *J. Phys. Chem. A* **2005**, *109*, 6730-6734, doi:10.1021/jp044142h.

Prasad, S. S. Possible existence and chemistry of $ClO·O_2$ in the stratosphere. *Nature* **1980**, *285*, 152.

Prasad, S. S.; Lee, T. J. Atmospheric chemistry of the reaction ClO + O_2 ↔ $ClO•O_2$: Where it stands, what needs to be done, and why? *J. Geophys. Res.* **1994**, *99*, 8225-8230, doi:10.1029/93JD01809

Pritchard, H. O. The nitrogen pentoxide dissociation equilibrium. *Int. J. Chem. Kinet.* **1994**, *26*, 61-72, doi:10.1002/kin.550260108.

Rayez, M. T.; Destriau, M. Theoretical study of thermal dissociation and recombination reacitons of $XONO_2$ (X=F, Cl, Br, or I). *Chem. Phys. Lett.* **1993**, *206*, 278-284, doi:10.1016/0009-2614(93)85552-Y.

Resende, S. M.; De Alemeida, W. B. Thermodynamical analysis of the atmospheric fate of the $CH_3SCH_2O_2$ radical. *Phys. Chem. Chem. Phys* **1999**, *1*, 2953-2959, doi:10.1039/A902423I.

Roberts, J. M.; Bertman, S. B. The thermal decomposition of peroxyacetic nitric anhydride (PAN) and peroxymethacrylic nitric anhydride (MPAN). *Int. J. Chem. Kinet.* **1992**, *24*, 297-307, doi:10.1002/kin.550240307.

Ruscic, B. Active thermochemical tables: Thermochemistry for the 21st Century. *J. Phys. Conf. Ser.* **2005**, *16*, 561-570, doi:10.1088/1742-6596/16/1/078.
Ruscic, B. Active thermochemical tables: Water and water dimer. *J. Phys. Chem. A* **2013**, *117*, 11940-11953, doi:10.1021/jp403197t.
Ruscic, B.; Pinzon, R. E.; Morton, M. L.; Srinivasan, N. K.; Su, M.-C.; Sutherland, J. W.; Michael, J. V. Active thermochemical tables: Accurate enthalpy of formation of hydroperoxyl radical, HO_2. *J. Phys. Chem. A* **2006**, *110*, 6592–6601, doi:10.1021/jp056311j.
Saiz-Lopez, A.; Plane, J. M. C.; Baker, A. R.; Carpenter, L. J.; von Glasow, R.; Gomez Martín, J. C.; McFiggans, G.; Saunders, R. W. Atmospheric chemistry of iodine. *Chem. Rev.* **2012**, *112*, 1773-1804, doi:10.1021/cr200029u.
Salta, Z.; Kosmas, A. M.; Lesar, A. Computational investigation of the peroxy radicals $CH_3S(O)_nOO$ and the peroxynitrates $CH_3S(O)_nOONO_2$ (n = 0, 1, 2). *Comput. Theo. Chem.* **2012**, 67-76, doi:10.1016/j.comptc.2012.10.007.
Santee, M. L.; Sander, S. P.; Livesey, N. J.; Froidevaux, L. Constraining the chlorine monoxide (ClO)/chlorine peroxide (ClOOCl) equilibrium constant from Aura microwave limb sounder measurements of nighttime ClO. *Proc. Natl. Acad, Sci. USA* **2010**, *107*, 6588-6593, doi:10.1073/pnas.0912659107.
Schott, G.; Davidson, N. Shock waves in chemical kinetics: The decomposition of N_2O_5 at high temperatures. *J. Am. Chem. Soc.* **1958**, *80*, 1841-1853, doi:10.1021/ja01541a019.
Scribano, Y.; Goldman, N.; Saykally, R. J.; Leforestier, C. Water dimers in the atmosphere III: Equilibrium constant from a flexible potential. *J. Phys. Chem. A* **2006**, *110*, 5411-5419, doi:10.1021/jp056759k.
Seefeld, S.; Kinnison, D. J.; Kerr, J. A. Relative rate study of the reactions of acetylperoxy radicals with NO and NO_2: Peroxyacetyl nitrate formation under laboratory conditions related to the troposphere. *J. Phys. Chem. A* **1997**, *101*, 55-59, doi:10.1021/jp962266r.
Sehested, J.; Christensen, L. K.; Mogelberg, T.; Nielsen, O. J.; Wallington, T. J.; Guschin, A.; Orlando, J. J.; Tyndall, G. S. Absolute and relative rate constants for the reactions $CH_3C(O)O_2$ + NO and $CH_3C(O)O_2$ + NO_2 and thermal stability of $CH_3C(O)O_2NO_2$. *J. Phys. Chem. A* **1998**, *102*, 1779-1789, doi:10.1021/jp972881a.
Shepler, B. C.; Balabanov, N. B.; Peterson, K. A. Hg + Br → HgBr recombination and collision-induced dissociation dynamics. *J. Chem. Phys.* **2007**, *107*, 164304, doi:10.1063/1.2777142.
Shirts, R. B.; Kumbhani, S. R.; Burrell, E.; Hansen, J. C. An improved model to calculate equilibrium constants for formation of peroxy radical-water complexes. *Theor. Chem. Acc.* **2018**, *137*, 96, doi:10.1007/s00214-018-2262-8.
Sicre, J. E.; Cobos, C. J. Thermochemistry of the higher chlorine oxides ClO_x (x = 3,4) and Cl_2O_x (x = 3 - 7). *J. Mol. Struct. (Theochem)* **2003**, *620*, 215-226.
Smith, C. A.; Ravishankara, A. R.; Wine, P. H. Kinetics of the reaction NO_2 + NO_3 + M at low pressures and 298 K. *J. Phys. Chem.* **1985**, *89*, 1423-1427, doi:10.1021/j100254a024.
Smith, I. W. M.; Yarwood, G. Kinetic measurements on the system NO + NO_2 ⇄ N_2O_3 by time-resolved infrared laser absorption. *Chem. Phys. Lett.* **1986**, *130*, 24-28, doi:10.1016/0009-2614(86)80418-3.
Stimpfle, R. M.; Wilmouth, D. M.; Salawitch, R. J.; Anderson, J. G. First measurements of ClOOCl in the stratosphere: The coupling of ClOOCl and ClO in the Arctic polar vortex. *J. Geophys. Res.* **2004**, *109*, D03301, doi:10.1029/2003jd003811.
Su, F.; Calvert, J. G.; Shaw, J. H. Mechanism of the photooxidation of gaseous formaldehyde. *J. Phys. Chem.* **1979**, *83*, 3185-3191, doi:10.1021/j100488a001.
Suma, K.; Sumiyoshi, Y.; Endo, Y. Fourier transform microwave spectroscopy and Fourier transform microwave–millimeter wave double resonance spectroscopy of the ClOO radical. *J. Chem. Phys.* **2004**, *121*, 8351-8359, doi:10.1063/1.1792591.
Suma, K.; Sumiyoshi, Y.; Endo, Y. The rotational spectrum of the water-hydroperoxy radical (H_2O-HO_2) complex. *Science* **2006**, *311*, 1278-1281, doi:10.1126/science.112402.
Suma, K.; Sumiyoshi, Y.; Endo, Y.; Enami, S.; Aloisio, S.; Hashimoto, S.; Kawasaki, M.; Nishida, S.; Matsumi, Y. Equilibrium constants of the reaction of Cl with O_2 in the formation of ClOO. *J. Phys. Chem. A* **2004**, *108*, 8096-8099, doi:10.1021/jp049124e.
Tellinghuisen, J.; Ashmore, J. G. Mixed representations for diatomic spectroscopic data: Application to HgBr. *Chem. Phys. Lett.* **1983**, *102*, 10-16, doi:10.1016/0009-2614(83)80647-2.
Tomas, A. E.; Villenave, E.; Lesclaux, R. Reactions of the HO_2 radical with CH_3CHO and $CH_3C(O)O_2$ in the gas phase. *J. Phys. Chem. A* **2001**, *105*, 3505-3514, doi:10.1021/jp003762p.
Tuazon, E. C.; Carter, W. P. L.; Atkinson, R. Thermal decomposition of peroxyacetyl nitrate and reactions of acetyl peroxy radicals with NO and NO_2 over the temperature range 283-313 K. *J. Phys. Chem.* **1991**, *95*, 2434-2437, doi:10.1021/j100159a059.
Tuazon, E. C.; Sanhueza, E.; Atkinson, R.; Carter, W. P. L.; Winer, A. M.; Pitts, J. N., Jr. Direct determination of the equilibrium constant at 298 K for the NO_2 + NO_3 ↔ N_2O_5 reactions. *J. Phys. Chem.* **1984**, *88*, 3095-3098, doi:10.1021/j150658a033.

Tuchler, M. F.; Schmidt, K. L.; Morgan, M. A CRDS approach to gas phase equilibrium constants: the case of $N_2O_4 \leftrightarrow 2NO_2$ at 283 K. *Chem. Phys. Lett.* **2005**, *401*, 393-399, doi:10.1016/j.cplett.2004.11.083.

Turnipseed, A. A.; Barone, S. B.; Ravishankara, A. R. Observation of CH_3S addition to O_2 in the gas phase. *J. Phys. Chem.* **1992**, *96*, 7502-7505, doi:10.1021/j100198a006.

Veyret, B.; Lesclaux, R.; Rayez, M.-T.; Rayez, J.-C.; Cox, R. A.; Moortgat, G. K. Kinetics and mechanism of the photooxidation of formaldehyde. 1. Flash photolysis study. *J. Phys. Chem.* **1989**, *93*, 2368-2374, doi:10.1021/j100343a033.

Viggiano, A. A.; Davidson, J. A.; Fehsenfeld, F. C.; Ferguson, E. E. Rate constants for the collisional dissociation of N_2O_5 by N_2. *J. Chem. Phys.* **1981**, *74*, 6113-6125, doi:10.1063/1.441055.

von Ahsen, S.; Wilner, H.; Francisco, J. S. Thermal decomposition of peroxy acetyl nitrate $CH_3C(O)OONO_2$. *J. Chem. Phys.* **2004**, *121*, 2048-2057, doi:10.1063/1.1767813.

von Hobe, M.; Grooss, J. U.; Muller, R.; Hrechanyy, S.; Winkler, U.; Stroh, F. A re-evaluation of the ClO/Cl_2O_2 equilibrium constant based on stratospheric in-situ observations. *Atmos. Chem. Phys.* **2005**, *5*, 693-702, doi:10.5194/acp-5-693-2005.

Vosper, A. J. Dissociation of dinitrogen tetroxide in gas phase. *J. Chem. Soc. A* **1970**, *1970*, 625-627, doi:10.1039/J19700000625.

Wängberg, I.; Etzkorn, T.; Barnes, I.; Platt, U.; Becker, K. H. Absolute determination of the temperature behavior of the $NO_2 + NO_3 + (M) \leftrightarrow N_2O_5 + (M)$ equilibrium. *J. Phys. Chem. A* **1997**, *101*, 9694-9698, doi:10.1021/jp972203o.

Wei, W.-M.; Tan, W.; Zheng, R.-H.; He, T.-J.; Chen, D.-M.; Liu, F.-C. Ab initio studies of isomerization and dissociation reactions of peroxyacetyl nitrate (PAN). *Chem. Phys.* **2005**, *312*, 241-259, doi:10.1016/j.chemphys.2004.12.007.

Williams, M. B.; Campuzano-Jost, P.; Cossairt, B. M.; Hynes, A. J.; Pounds, A. J. Experimental and theoretical studies of the reaction of the OH radical with alkyl sulfides: 1. Direct observations of the formation of the OH-DMS adduct-pressure dependence of the forward rate of addition and development of a predictive expression at low temperature. *J. Phys. Chem. A* **2007**, *111*, 89-104, doi:10.1021/jp063873+.

Wine, P. H.; Nicovich, J. M.; Stickel, R. E.; Zhao, Z.; Shackelford, C. J.; Kreutter, K. D.; Daykin, E. P.; Wang, S. In *The Tropospheric Chemistry of Ozone in the Polar Regions*; Springer-Verlag: Berlin, 1993; Vol. I7; pp 385-395.

Wollenhaupt, M.; Crowley, J. N. Kinetic studies of the reactions $CH_3 + NO_2 \rightarrow$ products, $CH_3O + NO_2 \rightarrow$ products, and $OH + CH_3C(O)CH_3 \rightarrow CH_3C(O)OH + CH_3$, over a range of temperature and pressure. *J. Phys. Chem. A* **2000**, *104*, 6429-6438, doi:10.1021/jp0005726.

Zabel, F. Unimolecular decomposition of peroxynitrates. *Z. Phys. Chem.* **1995**, *188*, 119-142, doi:10.1524/zpch.1995.188.Part_1_2.119.

Zabel, F.; Reimer, A.; Becker, K. H.; Fink, E. H. Thermal decomposition of alkyl peroxynitrates. *J. Phys. Chem.* **1989**, *93*, 5500-5507, doi:10.1021/j100351a036.

Zabel, F.; Sahetchian, K. A.; Chachaty, C. ESR spectra of free radicals formed during the gas-phase photo-oxidation of formaldehyde: Thermal stability of the $HOCH_2OO$ radical. *Chem. Phys. Lett.* **1987**, *134*, 433-437, doi:10.1016/0009-2614(87)87168-3.

Zhang, X.; Nimlos, M. R.; Ellison, G. B.; Varner, M. E.; Stanton, J. F. Infrared absorption spectra of matrix-isolated *cis*, *cis*-HOONO and its *ab initio* CCSD(T) anharmonic vibrational bands. *J. Chem. Phys.* **2006**, *124*, 084305, doi:10.1063/1.2163343.

Zhanga, H.-t.; Zhoua, Z.-y.; Jalbout, A. F. Vibrational mode analysis for the multi-channel reaction of $O_2 + CH_3S$. *J. Mol. Struct. (Theochem)* **2003**, *663*, 73-79, doi:10.1016/j.theochem.2003.08.068.

Zhu, B.; Zeng, X.; Beckers, H.; Francisco, J. S.; Willner, H. The methylsulfonyloxyl radical, CH_3SO_3. *Angew. Chem. Int. Ed.* **2015**, *54*, 11404-11408, doi:10.1002/anie.201503776.

Zhu, L.; Bozzelli, J. W. The multi-channel reaction of $CH_3SC + {}^3O_2$: Thermochemistry and kinetic barriers. *J. Mol. Struct. (Theochem)* **2005**, *728*, 147-157, doi:10.1016/j.theochem.2005.05.002.

Zhu, R. S.; Lin, M. C. *Ab initio* studies of ClO_x reactions. IV. Kinetics and mechanism for the self-reaction of ClO radicals. *J. Chem. Phys.* **2003**, *118*, 4094-4106, doi:10.1063/1.1540623.

Zhu, R. S.; Lin, M. C. Ab initio studies of ClO_x reactions. VII. Isomers of Cl_2O_3 and their roles in the ClO + OClO reaction. *J. Chem. Phys.* **2003**, *118*, 8645-8655, doi:10.1063/1.1565315.

SECTION 4. PHOTOCHEMICAL AND SCATTERING DATA

Table of Contents

SECTION 4. PHOTOCHEMICAL AND SCATTERING DATA 4-1
4.1 Absorption Spectra and Uncertainty Estimates 4-2
4.2 Photodissociation Thresholds and Quantum Yields 4-2
4.3 Web Access to Recommended Data 4-3
SECTION 4A. O_X PHOTOCHEMISTRY 4-7
4.4 Bibliography – O_x Photochemistry 4-28
SECTION 4B. HO_X PHOTOCHEMISTRY 4-36
4.5 Bibliography – HO_x Photochemistry 4-47
SECTION 4C. NO_X PHOTOCHEMISTRY 4-51
4.6 Bibliography – NO_x Photochemistry 4-83
SECTION 4D. ORGANIC PHOTOCHEMISTRY 4-91
4.7 Bibliography – Organic Photochemistry 4-171
SECTION 4E. FO_X PHOTOCHEMISTRY 4-185
4.8 Bibliography – FO_x Photochemistry 4-219
SECTION 4F. ClO_X PHOTOCHEMISTRY 4-223
4.9 Bibliography – ClO_x Photochemistry 4-322
SECTION 4G. BrO_X PHOTOCHEMISTRY 4-334
4.10 Bibliography – BrO_x Photochemistry 4-393
SECTION 4H. IO_X PHOTOCHEMISTRY 4-399
4.11 Bibliography – IO_x Photochemistry 4-442
SECTION 4I. SO_X PHOTOCHEMISTRY 4-447
4.12 Bibliography – SO_x Photochemistry 4-461
SECTION 4J. METAL PHOTOCHEMISTRY 4-466
4.13 Bibliography – Metal Photochemistry 4-471
SECTION 4K. RAYLEIGH SCATTERING CROSS SECTIONS 4-472
4.14 Introduction 4-472
4.15 Notes 4-476

4.1 Absorption Spectra and Uncertainty Estimates

Table 4-1 lists the molecules included in this evaluation that have ultraviolet (UV) and vacuum ultraviolet (VUV) absorption spectra considered to be of laboratory and atmospheric photochemical interest. The linked Notes for each molecule contain a summary of the available studies and the basis for the absorption cross section, $\sigma(\lambda,T)$, recommendation and estimated uncertainty. The ultraviolet (UV) absorption spectra of O_2 and O_3 largely determine the extent of the penetration of solar radiation into the stratosphere and troposphere. Some comments and references to these spectra are presented. For further detail see WMO Report No. 11;[1] WMO Report No. 16[5] and the references cited in the Notes. The photodissociation of NO in the O_2 Schumann-Runge band spectral range is another important process requiring special treatment (see Frederick and Hudson,[3] Allen and Frederick,[2] WMO Report No. 11,[1] and Minschwaner and Siskind[4]).

Some species included in this evaluation have highly structured spectra, e.g., SO_2. Notes are provided for these molecules, but complete photochemical data are not always presented. CH_2O, NO_2, NO_3, ClO, BrO, OClO, and SO_2 are examples of molecules that have complicated spectra, often resolution dependent UV/vis absorption spectra, but in view of their importance to atmospheric chemistry a sample of the data is presented in the evaluation. In these cases, detailed information on the high-resolution spectra and the temperature dependence of the spectrum should be obtained from the original cited literature.

Absorption cross sections are defined by the following expression of Beer's Law:

$$I = I_o \exp(-\sigma(\lambda,T)\, n\, L)$$

where I_o and I are the incident and transmitted light intensity, respectively, $\sigma(\lambda,T)$ is the absorption cross section in cm^2 $molecule^{-1}$ at wavelength λ and temperature T, n is the concentration in molecule cm^{-3}, and L is the pathlength in cm.

Estimates of the uncertainty in $\sigma(\lambda,T)$ are provided within the Notes for many of the molecules included in this evaluation, but not all. The reported uncertainty factors are not rigorous values resulting from a detailed statistical error propagation analysis. Rather, they represent a consensus among the panel members as to the reliability of the data, taking into account the difficulty of the measurements and the agreement among the results reported by various groups. The uncertainty in $\sigma(\lambda,T)$ is, in most cases, expected to be wavelength and temperature dependent, e.g., the cross sections in wavelength regions with weak absorption or at low temperatures representative of the upper troposphere-lower stratosphere are usually more uncertain.

(1) *The Stratosphere 1981: Theory and Measurements*; National Aeronautics and Space Administration, 1982.

(2) Allen, M.; Frederick, J. E. Effective photodissociation cross sections for molecular oxygen and nitric oxide in the Schumann-Runge bands. *J. Atmos. Sci.* **1982**, *39*, 2066-2075, doi:10.1175/1520-0469(1982)039<2066:EPCSFM>2.0.CO;2.

(3) Frederick, J. E.; Hudson, R. D. Predissociation of nitric oxide in the mesosphere and stratosphere. *J. Atmos. Sci.* **1979**, *36*, 737-745.

(4) Minschwaner, K.; Siskind, D. E. A new calculation of nitric oxide photolysis in the stratosphere, mesosphere, and lower thermoosphere. *J. Geophys. Res.* **1993**, *98*, 20401-20412, doi:10.1029/93JD02007

(5) WMO *Atmospheric Ozone: 1985*; National Aeronautics and Space Administration: Geneva, Report No. 16, Chapter 7, 1986.

4.2 Photodissociation Thresholds and Quantum Yields

The threshold energies for the photolysis channels given in the Notes, and the corresponding wavelengths, were calculated using the 298 K heats of formation, ΔH_f(298 K) given in the Thermochemical Parameters section of this evaluation. Note that the threshold wavelengths do not account for possible photodissociation barriers.

The primary process in the photodissociation of chlorinated hydrocarbons is well established: absorption of ultraviolet radiation in the lowest frequency band is interpreted as an n–σ* transition involving excitation to a repulsive electronic state (anti-bonding in C–Cl), which dissociates by breaking the carbon-chlorine bond (Majer and Simons[1]). As expected, chlorofluoromethanes, which are a particular type of chlorinated hydrocarbons, behave in this fashion (Sandorfy[2]). The quantum yield for photodissociation is expected to be unity for these compounds. There are several studies that show specifically that this is the case for CF_2Cl_2, $CFCl_3$, and CCl_4. These studies also indicate that at shorter wavelengths two halogen atoms can be released simultaneously in the primary photolysis process.

The mechanism for the photodissociation of other classes of compounds, such as aldehydes and ketones, in many cases includes multiple product channels, where the different channels may have different impacts on atmospheric

chemistry. Photolysis quantum yields may also display a wavelength, pressure, and temperature dependence. Detailed quantum yield studies are presently not available for all molecules included in this evaluation. Quantum yield studies are cited and recommendations are made where possible.

(1) Majer, J. R.; Simons, J. P. Photochemical processes in halogenated compounds. In *Advances in Photochemistry*; Interscience, 1964; Vol. 2; pp 137-181.

(2) Sandorfy, C. U.V. absorption of fluorocabons. *Atmos. Environ.* **1976**, *10*, 343-351.

4.3 Web Access to Recommended Data

Many of the recommended cross sections given in this evaluation can be downloaded from the spectral atlas of the Max-Planck Institute for Chemistry at: http://www.uv-vis-spectral-atlas-mainz.org.[1]

(1) Keller-Rudek, H.; Moortgat, G. K.; Sander, R.; Sörensen, R. The MPI-Mainz UV/Vis spectral atlas of gaseous molecules of atmospheric interest. *Earth Syst. Sci. Data* **2013**, *5*, 365-373, doi:10.5194/essd-5-365-2013.

Table 4-1. Photochemical Processes

O_x Photochemistry

A1. $O_2 + h\nu \rightarrow O + O$
A2. $O_3 + h\nu \rightarrow O_2 + O$
$O_3 + h\nu \rightarrow O_2 + O(^1D)$

HO_x Photochemistry

B1. $HO_2 + h\nu \rightarrow$ Products
B2. $H_2O + h\nu \rightarrow$ Products
B3. $H_2O_2 + h\nu \rightarrow$ Products

NO_x Photochemistry

C1. $NO + h\nu \rightarrow$ Products
C2. $NO_2 + h\nu \rightarrow NO + O$
C3. $NO_3 + h\nu \rightarrow NO_2 + O$
$NO_3 + h\nu \rightarrow NO + O_2$
C4. $N_2O + h\nu \rightarrow$ Products
C5. $N_2O_3 + h\nu \rightarrow$ Products
C6. $N_2O_4 + h\nu \rightarrow NO_2 + NO_2$
C7. $N_2O_5 + h\nu \rightarrow$ Products
C8. $HONO + h\nu \rightarrow$ Products
C9. $HNO_3 + h\nu \rightarrow$ Products
C10. $HO_2NO_2 + h\nu \rightarrow$ Products

Organic Photochemistry

D1. $CH_3 + h\nu \rightarrow$ Products
D2. $CH_4 + h\nu \rightarrow$ Products
D3. $CH_2O + h\nu \rightarrow$ Products
D4. $CH_2OO + h\nu \rightarrow$ Products
D5. $CH_3O_2 + h\nu \rightarrow$ Products
D6. $CH_3OH + h\nu \rightarrow$ Products
D7. $CH_3OOH + h\nu \rightarrow$ Products
D8. $HC(O)OH + h\nu \rightarrow$ Products R,N
$(HC(O)OH)_2 + h\nu \rightarrow$ Products
D9. $HC(O)OOH + h\nu \rightarrow$ Products
D10. $HOCH_2OOH + h\nu \rightarrow$ Products
D11. $CH_3CO + h\nu \rightarrow$ Products
D12. $CH_3C(O)O_2 + h\nu \rightarrow$ Products
D13. $CH_3CHO + h\nu \rightarrow$ Products R
D14. $CH_3CHOO + h\nu \rightarrow$ Products
D15. $C_2H_5O_2 + h\nu \rightarrow$ Products
D16. $CH_3CH_2OH + h\nu \rightarrow$ Products N
D17. $HOCH_2CHO + h\nu \rightarrow$ Products N
D18. $HC(O)OCH_3 + h\nu \rightarrow$ Products R,N
D19. $CHOCHO + h\nu \rightarrow$ Products
D20. $CH_3C(O)OH + h\nu \rightarrow$ Products
D21. $CH_3C(O)OOH + h\nu \rightarrow$ Products
D22. $C_2H_5CHO + h\nu \rightarrow$ Products
D23. $CH_3CH_2CHOO + h\nu \rightarrow$ Products
D24. $(CH_3)_2COO + h\nu \rightarrow$ Products
D25. $(CH_3)_2CHOH + h\nu \rightarrow$ Products
D26. $CH_3C(O)CH_3 + h\nu \rightarrow$ Products
D27. $CH_3C(O)CH_2O_2 + h\nu \rightarrow$ Products
D28. $CH_3C(O)C(O)H + h\nu \rightarrow$ Products
D29. $CH_3C(O)CH_2OH + h\nu \rightarrow$ Products R,N
D30. $CH_2=CHCHO + h\nu \rightarrow$ Products
D31. $C_2H_5C(O)OH + h\nu \rightarrow$ Products
D32. $CH_3C(O)C(O)OH + h\nu \rightarrow$ Products
D33. $HC(O)OCH_2CH_3 + h\nu \rightarrow$ Products R,N
D34. $CH_3C(O)CH_2CH_3 + h\nu \rightarrow$ Products
D35. $CH_2C(CH_3)CHO + h\nu \rightarrow$ Products
D36. $CH_3C(O)C(O)CH_3 + h\nu \rightarrow$ Products
D37. $CH_3C(O)CH=CH_2 + h\nu \rightarrow$ Products
D38. $C_2H_2(CO)_2O + h\nu \rightarrow$ Products
D39. $CH_2=C(CH_3)CH=CH_2 + h\nu \rightarrow$ Products
D40. $CH_3ONO + h\nu \rightarrow$ Products
D41. $CH_3ONO_2 + h\nu \rightarrow$ Products
D42. $CH_3CH_2ONO_2 + h\nu \rightarrow$ Products
D43. $CH_3O_2NO_2 + h\nu \rightarrow$ Products
D44. $CH_3C(O)O_2NO_2 + h\nu \rightarrow$ Products
D45. $C_2H_5C(O)O_2NO_2 + h\nu \rightarrow$ Products
D46. $HCN + h\nu \rightarrow$ Products R,N
D47. $CH_3CN + h\nu \rightarrow$ Products

FO_x Photochemistry

E1. $HF + h\nu \rightarrow H + F$
E2. $FO_2 + h\nu \rightarrow F + O_2$
E3. $F_2O + h\nu \rightarrow$ Products
E4. $F_2O_2 + h\nu \rightarrow$ Products
E5. $FNO + h\nu \rightarrow F + NO$
E6. CHF_3 (HFC-23) $\rightarrow$ Products
E7. CH_2F_2 (HFC-32) $\rightarrow$ Products
E8. CHF_2CF_3 (HFC-125) $\rightarrow$ Products
E9. CH_2FCF_3 (HFC-134a) $\rightarrow$ Products
E10. CH_3CF_3 (HFC-143a) $\rightarrow$ Products
E11. CH_3CHF_2 (HFC-152a) $\rightarrow$ Products
E12. $CF_4 + h\nu \rightarrow$ Products
E13. $C_2F_6 + h\nu \rightarrow$ Products
E14. $c\text{-}C_4F_8 + h\nu \rightarrow$ Products
E15. $C_5F_{12} + h\nu \rightarrow$ Products
E16. $C_6F_{14} + h\nu \rightarrow$ Products
E17. $(CF_3)_2c\text{-}C_4F_6 + h\nu \rightarrow$ Products
E18. $CF_2O + h\nu \rightarrow$ Products
E19. $COHF + h\nu \rightarrow$ Products
E20. $CF_3O_2 + h\nu \rightarrow$ Products
E21. $CF_3OH + h\nu \rightarrow$ Products
E22. $CH_2FCH_2OH + h\nu \rightarrow$ Products
E23. $CHF_2CH_2OH + h\nu \rightarrow$ Products
E24. $CF_3CH_2OH + h\nu \rightarrow$ Products
E25. $CF_3OOCF_3 + h\nu \rightarrow$ Products
E26. $CF_3O_3CF_3 + h\nu \rightarrow$ Products
E27. $CF_3CHO + h\nu \rightarrow$ Products
E28. $CF_3C(O)F + h\nu \rightarrow$ Products
E29. $FC(O)C(O)F + h\nu \rightarrow$ Products
E30. $FC(O)CF_2C(O)F + h\nu \rightarrow$ Products
E31. $FC(O)CF_2CF_2C(O)F + h\nu \rightarrow$ Products
E32. $CF_3OONO_2 + h\nu \rightarrow$ Products
E33. $CF_3C(O)O_2NO_2 + h\nu \rightarrow$ Products
E34. $CF_3CH_2CHO + h\nu \rightarrow$ Products

E35. $(CF_3)_2CHOH + h\nu \rightarrow$ Products
E36. $CF_3C(O)OH + h\nu \rightarrow$ Products
E37. $CH_3C(O)F + h\nu \rightarrow$ Products R,N
E38. $CH_2=CHCF_3 + h\nu \rightarrow$ Products
E39. $CH_2=CFCF_3 + h\nu \rightarrow$ Products
E40. $CF_2=CF_2 + h\nu \rightarrow$ Products
E41. $CF_2=CFCF_3 + h\nu \rightarrow$ Products
E42. $NF_3 + h\nu \rightarrow$ Products

ClO_x Photochemistry

F1. $Cl_2 + h\nu \rightarrow Cl + Cl$ R,N
F2. $ClO + h\nu \rightarrow Cl + O$ N
F3. $ClOO + h\nu \rightarrow Cl + O_2$
F4. $OClO + h\nu \rightarrow$ Products
F5. $ClO_3 + h\nu \rightarrow$ Products
F6. $Cl_2O + h\nu \rightarrow$ Products
F7. $ClOOCl + h\nu \rightarrow$ Products
F8. $ClClO_2 + h\nu \rightarrow$ Products
F9. $Cl_2O_3 + h\nu \rightarrow$ Products
F10. $Cl_2O_4 + h\nu \rightarrow$ Products
F11. $Cl_2O_6 + h\nu \rightarrow$ Products
F12. $Cl_2O_7 + h\nu \rightarrow$ Products
F13. $HCl + h\nu \rightarrow H + Cl$
$DCl + h\nu \rightarrow$ Products
F14. $HOCl + h\nu \rightarrow$ Products
F15. $ClNO + h\nu \rightarrow Cl + NO$
F16. $ClNO_2 + h\nu \rightarrow$ Products
F17. $ClONO + h\nu \rightarrow$ Products
F18. $ClONO_2 + h\nu \rightarrow$ Products
F19. $CCl_4 + h\nu \rightarrow$ Products
F20. $CH_3OCl + h\nu \rightarrow$ Products
F21. $CHCl_3 + h\nu \rightarrow$ Products R,N
F22. $CH_2Cl_2 + h\nu \rightarrow$ Products R,N
F23. $CH_3Cl + h\nu \rightarrow$ Products N
F24. $CH_3CCl_3 + h\nu \rightarrow$ Products
F25. $CH_3CH_2Cl + h\nu \rightarrow$ Products
F26. $CH_3CHClCH_3 + h\nu \rightarrow$ Products
F27. $CH_2ClCH_2Cl + h\nu \rightarrow$ Products
F28. $CH_2ClCH_2CH_2Cl + h\nu \rightarrow$ Products
F29. $CH_2Cl(CH_2)_2CH_2Cl + h\nu \rightarrow$ Products
F30. $CCl_2O + h\nu \rightarrow$ Products R,N
F31. $HC(O)Cl + h\nu \rightarrow$ Products
F32. $ClC(O)F + h\nu \rightarrow$ Products
F33. $CFCl_3$ (CFC-11) $+ h\nu \rightarrow$ Products
F34. CF_2Cl_2 (CFC-12) $+ h\nu \rightarrow$ Products
F35. CF_3Cl (CFC-13) $+ h\nu \rightarrow$ Products
F36. CCl_2FCCl_2F (CFC-112) $+ h\nu \rightarrow$ Products
F37. CCl_3CClF_2 (CFC-112a) $+ h\nu \rightarrow$ Products
F38. $CF_2ClCFCl_2$ (CFC-113) $+ h\nu \rightarrow$ Products
F39. CCl_3CF_3 (CFC-113a) $+ h\nu \rightarrow$ Products
F40. CF_2ClCF_2Cl (CFC-114) $+ h\nu \rightarrow$ Products
F41. CCl_2FCF_3 (CFC-114a) $+ h\nu \rightarrow$ Products
F42. CF_3CF_2Cl (CFC-115)$+ h\nu \rightarrow$ Products R,N
F43. $CHFCl_2$ (HCFC-21) $+ h\nu \rightarrow$ Products
F44. CHF_2Cl (HCFC-22) $+ h\nu \rightarrow$ Products R,N
F45. CH_2FCl (HCFC-31) $+ h\nu \rightarrow$ Products
F46. $CHCl_2CClF_2$(HCFC-122) $+ h\nu \rightarrow$ Products
F47. $CHClFCCl_2F$ (HCFC-122a) $+ h\nu \rightarrow$ Products
F48. CF_3CHCl_2 (HCFC-123) $+ h\nu \rightarrow$ Products R,N
F49. $CHClFCClF_2$ (HCFC-123a) $+ h\nu \rightarrow$ Products
F50. CF_3CHFCl (HCFC-124) $+ h\nu \rightarrow$ Products
F51. CH_2FCCl_2F (HCFC-132c) $+ h\nu \rightarrow$ Products
F52. CF_3CH_2Cl (HCFC-133a) $+ h\nu \rightarrow$ Products R,N
F53. CH_3CFCl_2 (HCFC-141b) $+ h\nu \rightarrow$ Products R,N
F54. CH_3CF_2Cl (HCFC-142b) $+ h\nu \rightarrow$ Products R,N
F55. $CH_2ClCHO + h\nu \rightarrow$ Products
F56. $CHCl_2CHO + h\nu \rightarrow$ Products
F57. $CF_2ClCHO + h\nu \rightarrow$ Products
F58. $CFCl_2CHO + h\nu \rightarrow$ Products
F59. $CCl_3CHO + h\nu \rightarrow$ Products
F60. $CH_3C(O)Cl + h\nu \rightarrow$ Products
F61. $CH_2ClC(O)Cl + h\nu \rightarrow$ Products
F62. $CHCl_2C(O)Cl + h\nu \rightarrow$ Products
F63. $CCl_3C(O)Cl + h\nu \rightarrow$ Products
F64. $CF_3C(O)Cl + h\nu \rightarrow$ Products
F65. $CH_2=CHCl + h\nu \rightarrow$ Products
F66. $CHCl=CCl_2 + h\nu \rightarrow$ Products
F67. $CCl_2=CCl_2 + h\nu \rightarrow$ Products
F68. $CF_3CF_2CHCl_2$ (HCFC-225ca) $+ h\nu \rightarrow$ Products
F69. CF_2ClCF_2CHFCl (HCFC-225cb) $+ h\nu \rightarrow$ Products
F70. $CH_3C(O)CH_2Cl + h\nu \rightarrow$ Products
F71. 1,2-*c*-$C_4Cl_2F_6$(*E*) $+ h\nu \rightarrow$ Products
F72. 1,2-*c*-$C_4Cl_2F_6$(*Z*) $+ h\nu \rightarrow$ Products

BrO_x Photochemistry

G1. $Br_2 + h\nu \rightarrow Br + Br$
G2. $HBr + h\nu \rightarrow H + Br$
G3. $BrO + h\nu \rightarrow Br + O$ N
G4. $OBrO + h\nu \rightarrow$ Products N
G5. $Br_2O + h\nu \rightarrow$ Products
G6. $HOBr + h\nu \rightarrow$ Products
G7. $BrNO + h\nu \rightarrow Br + NO$
G8. *cis*-$BrONO + h\nu \rightarrow$ Products
G9. $BrNO_2 + h\nu \rightarrow$ Products
G10. $BrONO_2 + h\nu \rightarrow$ Products
G11. $BrCl + h\nu \rightarrow Br + Cl$
G12. $BrOCl + h\nu \rightarrow$ Products
G13. $CH_3Br + h\nu \rightarrow$ Products
G14. $CH_2Br_2 + h\nu \rightarrow$ Products
G15. $CHBr_3 + h\nu \rightarrow$ Products
G16. $CH_2BrCH_2Br + h\nu \rightarrow$ Products
G17. $C_2H_5Br + h\nu \rightarrow$ Products
G18. $CBr_2O + h\nu \rightarrow$ Products
G19. $HC(O)Br + h\nu \rightarrow$ Products
G20. CH_2ClBr (Halon-1011) $+ h\nu \rightarrow$ Products
G21. $CHClBr_2$ (Halon-1012) $+ h\nu \rightarrow$ Products
G22. $CHCl_2Br$ (Halon-1021) $+ h\nu \rightarrow$ Products
G23. CCl_3Br (Halon-1031) $+ h\nu \rightarrow$ Products
G24. CHF_2Br (Halon-1201) $+ h\nu \rightarrow$ Products
G25. CF_2Br_2 (Halon-1202) $+ h\nu \rightarrow$ Products
G26. CF_2ClBr (Halon-1211) $+ h\nu \rightarrow$ Products
G27. CF_3Br (Halon-1301) $+ h\nu \rightarrow$ Products R,N

G28. CH_2=CHBr + hν → Products
G29. CHBr=CF_2 + hν → Products
G30. CFBr=CF_2 + hν → Products
G31. CH_2=$CBrCF_3$ + hν → Products
G32. CF_3CH_2Br (Halon-2301) + hν → Products
G33. $CF_3CHClBr$ (Halon-2311) + hν → Products
G34. CF_3CHFBr (Halon-2401) + hν → Products R,N
G35. CF_2BrCF_2Br (Halon-2402) + hν → Products
G36. CF_3CF_2Br (Halon-2501) + hν → Products
G37. $CH_3CH_2CH_2Br$ + hν → Products
G38. $CH_3CHBrCH_3$ + hν → Products
G39. $CH_3C(O)CH_2Br$ + hν → Products
G40. CH_2=$CBrCF_2CF_3$ + hν → Products
G41. CH_2=$CHCF_2CF_2Br$ + hν → Products
G42. CH_2=$CHCFClCF_2Br$ + hν → Products

IO_x Photochemistry

H1. I_2 + hν → I + I
H2. IO + hν → I + $O(^3P)$, $O(^1D)$
H3. OIO + hν → Products
H4. HI + hν → H + I
H5. HOI + hν → OH + I
H6. ICl + hν → I + Cl
H7. IBr + hν → I + Br
H8. INO + hν → I + NO
H9. INO_2 + hν → Products
H10. $IONO_2$ + hν → Products
H11. CH_3I + hν → CH_3 + I R,N
H12. CH_2I_2 + hν → CH_2I + I
H13. C_2H_5I + hν → C_2H_5 + I N
H14. CH_3CHI_2 + hν → Products
H15. $CH_3CH_2CH_2I$ + hν → $CH_3CH_2CH_2$ + I R,N
H16. CH_3CHICH_3 + hν → Products
H17. *n*-C_4H_9I + hν → C_4H_9 + I R,N
H18. $(CH_3)_2CHCH_2I$ + hν → $(CH_3)_2CCH_2$ + I N
H19. $(CH_3)_3CI$ + hν → $(CH_3)_3C$ + I
H20. *n*-$C_5H_{11}I$ + hν → C_5H_{11} + I N
H21. CF_3I + hν → CF_3 + I
H22. CF_2I_2 + hν → Products
H23. C_2F_5I + hν → C_2F_5 + I
H24. *n*-C_3F_7I + hν → C_3F_7 + I R,N
H25. *n*-C_4F_9I + hν → C_4F_9 + I
H26. *n*-$C_6F_{13}I$ + hν → C_6F_{13} + I
H27. CH_2ICl + hν → Products
H28. CH_2BrI + hν → Products
H29. $CHClI_2$ + hν → Products
H30. CF_2BrCF_2I + hν → Products

SO_x Photochemistry

I1. SO_2 + hν → SO + O N
I2. SO_3 + hν → Products
I3. H_2S + hν → Products
I4. H_2SO_4 + hν → Products
I5. CS_2+ hν → CS + S
I6. $CH_3S(O)CH_3$ → Products
I7. $CH_3S(O)CH_2Cl$ → Products
I8. CH_3SSCH_3 + hν → Products
I9. OCS + hν → CO + S R,N
I10. SF_6 + hν → Products R,N
I11. SF_5CF_3 + hν → SF_5 + CF_3 R,N
I12. SO_2F_2 + hν → Products

Metal Photochemistry

J1. NaOH + hν → Products
J2. NaCl + hν → Na + Cl
J3. NaO + hν → Na + O
J4. NaO_2 + hν → Products
J5. NaO_3 + hν → Products
J6. $NaHCO_3$ + hν → Products

Rayleigh Scattering

K1. Ar
K2. CH_4
K3. CO_2
K4. He
K5. N_2
K6. N_2O
K7. O_2
K8. SF_6

Gray shading of a molecule indicates a new entry. Gray shaded R indicates a change to the recommendation and N a change to the note.

SECTION 4A. O_X PHOTOCHEMISTRY

A1. O_2 (molecular Oxygen)

Back to Index

$O_2 + h\nu$	$\rightarrow O(^3P) + O(^3P)$	494 kJ mol^{-1}	242.3 nm	(1)
	$\rightarrow O(^3P) + O(^1D)$	684 kJ mol^{-1}	175 nm	(2)
	$\rightarrow O(^1D) + O(^1D)$	873 kJ mol^{-1}	137 nm	(3)
	$\rightarrow O(^3P) + O(^1S)$	906 kJ mol^{-1}	132 nm	(4)
	$\rightarrow O(^1D) + O(^1S)$	1088 kJ mol^{-1}	110 nm	(5)

(Recommendation: 10-6, Note: 15-10, Evaluated: 10-6)

Absorption Cross Sections: The photodissociation of molecular oxygen in the stratosphere is due primarily to the absorption of solar radiation in the 200–240 nm wavelength region, i.e., within the Herzberg continuum, which arises from the $A^3\Sigma_u^+ \leftarrow X^3\Sigma_g^-$ transition. Between 240 and 300 nm the absorption spectrum is also due to the electronic transition from the ground $X^3\Sigma_g^-$ state to excited electronic states $A^3\Sigma_u^+ \leftarrow X^3\Sigma_g^-$ (Herzberg I), $c^1\Sigma_u^- \leftarrow X^3\Sigma_g^-$ (Herzberg II), and $A'^3\Delta_u \leftarrow X^3\Sigma_g^-$ (Herzberg III). The 175–205 nm region, the O_2 Schumann-Runge ($B^3\Sigma_g^- \leftarrow X^3\Sigma_g^-$) band spectral range, is also very important, since solar radiation penetrates efficiently into the stratosphere at these wavelengths. The Schumann-Runge band system is composed of rotational lines with widths on the order of 1 cm^{-1}. The peak absorption cross sections in the Schumann-Runge system span ~5 orders of magnitude.

Table 4A-1-1. Summary of O_2 Absorption Cross Section Studies

Study	Year	Molecule [a]	Wavelength (nm)	Resolution (nm)	Temperature (K)
Preston[70]	1940	O_2	121.567	0.01	298
Clark[22]	1952	O_2	8–103	0.01	295
Watanabe et al.[82]	1952	O_2	121.57	0.085	298
Weissler and Lee[85]	1952	O_2	30–131	0.01	295
Watanabe et al.[83]	1953	O_2	105–190	0.085	298
Aboud et al.[1]	1955	O_2	11–87	0.1	295
Lee[48]	1955	O_2	20–110	0.01	295
Wainfan et al.[80]	1955	O_2	47 – 99	0.5	295
Watanabe and Marmo[84]	1956	O_2	85–110 140–146	0.01	298
Tanaka et al.[78]	1959	O_2	140–149	0.01	298
Ditchburn and Young[27]	1962	O_2	185–250	0.01	298
Cook and Metzger[25]	1964	O_2	60–103	0.05	295
Cook et al.[24]	1964	O_2	83–103	0.05	295
Metzger and Cook[56]	1964	O_2	110–167	0.05	298
Huffman et al.[39]	1964	O_2	60–164	0.05	295
Samson and Cairns[71]	1964	O_2	30–104	0.01	298
Samson and Cairns[72]	1965	O_2	20–54	0.01	298
Goldstein and Mastrup[31]	1966	O_2	127–175	0.04	298
Blake et al.[12]	1966	O_2	125–235	0.02	298
Hudson et al.[35]	1966	O_2	159–195	0.0075	300, 600, 900
Matsunaga and Watanabe[55]	1967	O_2	58–108	0.03	298
Ogawa[64]	1968	O_2	121.6	0.009	298
Huffman[38]	1969	O_2	30–122	Review [b]	295
Ackerman et al.[4]	1969	O_2	176–191	0.001	300
Shardanand[74]	1969	O_2	200–280	0.25	298
Ackerman et al.[3]	1970	O_2	176–201	0.001	300
Ackerman[2]	1971	O_2	116–244	Review [b]	298
Bennett et al.[10]	1971	O_2	58.4	0.1	295
Hasson and Nichols[33]	1971	O_2	192–243	0.07	298
Ogawa[65]	1971	O_2	181–235	0.0075	298
Hudson and Mahle[36]	1972	O_2	176–210	0.1	150, 200, 250, 300

Study	Year	Molecule [a]	Wavelength (nm)	Resolution (nm)	Temperature (K)
Starr and Loewenstein[77]	1972	O_2	58.4	0.07	298
Brolley et al.[15]	1973	O_2	58.4	0.1	298
Ogawa and Ogawa[66]	1975	O_2 $O_2(a^1\Delta_g)$ [c]	108–160 108–152	0.014	298
Bertrand et al.[11]	1975	O_2	123.6, 147	0.1	298
Kockarts[45]	1976	O_2	176–203	J-calc-SR [d]	160 – 300
Shardanand and Prasad Rao[75]	1977	O_2	200–250	0.25	300
Cole and Dexter[23]	1978	O_2	5–34	0.02	298
Brion et al.[14]	1979	O_2	4–248 (e,e)	0.2	298
Frederick and Mentall[29]	1982	O_2	176–243	0.12	200, 250, 300
Herman and Mentall[34]	1982	O_2	187–225	0.12	not stated
Anderson and Hall[7]	1983	O_2	191–207	0.012	
Gibson et al.[30]	1983	O_2	140–174	0.01	295, 575
Lewis et al.[53]	1983	O_2	121.4–121.9	0.01	84, 203, 288, 366
Yoshino et al.[98]	1983	O_2	179.3–201.5	0.0013	300
Cheung et al.[19]	1984	O_2	193.5–204	0.0013	299
Cheung et al.[18]	1984	O_2	193.5–204	0.0013	300
Pirre et al.[68]	1984	O_2	202–220	0.01	not stated
Johnston et al.[42]	1984	O_2	205–225	0.2	206–327
Yoshino et al.[97]	1984	O_2	175–205	SR Atlas [e]	300
Kley[44]	1984	O_2	121.567	0.01	208–305
Cheung et al.[20]	1986	O_2	195–241	0.0013	298
Anderson and Hall[8]	1986	O_2	191–215	0.012	not stated
Jenouvrier et al.[41]	1986	O_2	205–240	0.05	298
Jenouvrier et al.[40]	1986	O_2	205–240	0.04	294
Lewis et al.[51]	1986	$^{16}O^{16}O$	175–205	0.004	295
Lewis et al.[52]	1986	$^{16}O^{16}O$	175–205	0.004	295
Nicolet and Kennes[61]	1986	O_2	200 – 244	J-calc-HC [f]	298
Saxon and Slanger[73]	1986	O_2	195–300	σ-calc-HC [g]	298
Yoshino et al.[96]	1987	O_2	179–198	0.0013	79
Wang et al.[81]	1987	O_2	130–160	0.01	295, 575
Yoshino et al.[88]	1988	O_2	205–240	recommended	298
Yoshino et al.[94]	1988	$^{18}O^{18}O$	183–196	0.0013	79
Murtagh[59]	1988	O_2	175–206	J-cal-SR [d]	150–300
Pirre et al.[69]	1988	O_2	200–217	0.01	not stated
Nicolet and Kennes[62]	1988	O_2	202–242	J-calc-HC [f]	not stated
Cheung et al.[17]	1989	$^{16}O^{18}O$	175–205	0.0013	78, 300
Yoshino et al.[95]	1989	$^{16}O^{18}O$	180–196	0.0013	79
Nicolet and Kennes[63]	1989	O_2	175–202	σ-cal-HC [g]	190–300
Cheung et al.[16]	1990	O_2	179–202	0.0013	79, 295
Chiu et al.[21]	1990	$^{18}O^{18}O$, $^{16}O^{18}O$	180–196	0.0013	79
Coquart et al.[26]	1990	O_2	196–205	0.065	219
Greenblatt et al.[32]	1990	O_2	330–1130	0.6	196, 296
Yoshino et al.[90]	1990	O_2	184–204	0.0013	295
Yoshino et al.[89]	1992	O_2	179–240	0.0013	300
Minschwaner et al.[57]	1992	O_2	175–205	σ-calc-SR [h]	130–500
Minschwaner et al.[58]	1993	O_2	175–205	σ-calc-SR [h]	205–300
Yoshino et al.[100]	1994	O_2	240–270	0.06 cm^{-1}	295
Huestis et al.[37]	1994	O_2	243–258	0.25 cm^{-1}	295
Yoshino et al.[91]	1995	O_2	240–270	0.06 cm^{-1}	295
Bao et al.[9]	1995	O_2	248–249	0.4 cm^{-1}	298
Oshima et al.[67]	1995	O_2	230–280	0.2	310

Study	Year	Molecule [a]	Wavelength (nm)	Resolution (nm)	Temperature (K)
Slanger et al.[76]	1996	O_2	242.1–244.2	0.2 cm^{-1}	298
Ahmed et al.[5]	1996	O_2	130, 165	0.05	295, 373, 473, 573
Amoruso et al.[6]	1996	O_2	208–240	0.001	280
Vattulainen et al.[79]	1997	O_2	195–260	0.5	293, 873, 1073
Kanik et al.[43]	1997	O_2	120, 149, 174	0.03	295,373, 473, 573
Yoshino et al.[99]	1998	O_2	240–270	0.06 cm^{-1}	295
Yoshino et al.[92]	1999	O_2	240–275	0.06 cm^{-1}	295
Fally et al.[28]	2000	O_2	240–294	2 cm^{-1}	288
Yoshino et al.[93]	2000	O_2	240–275	0.06 cm^{-1}	295
Bogumil et al.[13]	2003	O_2	234–440 650–800	0.24 0.48	203, 243, 293
Wu et al.[87]	2005	O_2	83, 92, 108	0.0008	295, 535
Yoshino et al.[101]	2005	O_2	130–173	0.066	78, 90, 295

[a] Entries labeled "O_2" refer to molecular oxygen with natural isotopic abundance; studies of specific isotopes are labeled accordingly
[b] Review: a status report on absorption cross section measurements
[c] Refers to the low lying metastable state of O_2
[d] J-calc-SR: a calculation of O_2 photodissociation coefficients in the Schumann-Runge bands
[e] SR Atlas: a detailed compendium of line assignments of the Schumann-Runge bands
[f] J-calc-HC: a calculation of O_2 photodissociation coefficients in the Herzberg Continuum
[g] σ-calc-HC: a calculation of absorption cross sections in the Herzberg Continuum
[h] σ-calc-SR: a calculation of absorption cross sections of the Schumann-Runge bands

Measurements of the absorption cross sections in the VUV have mainly been reported at low resolution during the period from 1952 to 1979 as listed in Table 4A-1-1. High resolution cross sections have been reported by Cole and Dexter,[23] Brion et al.,[14] Gibson et al.,[30] Ahmed et al.,[5] Wu et al.,[87] and Yoshino et al.[101]

At the Lyman-α wavelength (121.567 nm), absorption cross section values at 298 K were reported (in cm^2 $molecule^{-1}$) by Preston[70] (1.17×10^{-20}), Watanabe et al.[82] (1.23×10^{-20}), Ogawa[64] (1.03×10^{-20}), Kley[44] (1.13×10^{-20}), and Lewis et al.[53] (9.1×10^{-21}). The latter authors measured the temperature dependence of the cross sections in the range 84–366 K. A value of $(1.1 \pm 0.1) \times 10^{-20}$ cm^2 $molecule^{-1}$ is recommended at 298 K. Kley[44] measured the pressure dependence of the Lyman-α cross section in the pressure range 20–880 Torr and in the temperature range 208–305 K. The cross sections were parameterized by the following equation: $\sigma_{O2} = (1.13 \pm 0.09) \times 10^{-20} + (1.72 \pm 0.21) \times 10^{-23} \times P$ where P is the pressure in Torr.

In the Herzberg continuum (200–240 nm) Frederick and Mentall,[29] Herman and Mentall,[34] Anderson and Hall,[7,8] and Pirre et al.[68,69] estimated O_2 absorption cross sections from balloon measurements of solar irradiance in the stratosphere. These authors found the cross sections in the 200–210 nm range to be ~35% smaller than the smallest of the older laboratory results, which are those of Ditchburn and Young,[27] Hasson and Nichols,[33] Ogawa,[65] Shardanand,[74] and Shardanand and Prasad Rao.[75] The more recent laboratory studies (Johnston et al.,[42] Cheung et al.,[18-20] and Jenouvrier et al.[40,41]) confirm the lower values obtained from solar irradiance measurements. The recommended absorption cross section values between 205 and 240 nm are based on the data of Cheung et al.[20] and Jenouvrier et al.[40] and were evaluated by Yoshino et al.[88] as listed in Table 4A-1-2. The recommended values from 241–245 nm are from Fally et al.[28] (see below). Amoruso et al.[6] have also carried out cross section measurements in the wavelength range 208–240 nm of the Herzberg continuum; their values are ~15% lower than those reported by Yoshino et al.[88] Coquart et al.[26] have reported Herzberg continuum absorption cross sections at 219 K in the wavelength region 196–205 nm of the S-R bands, in agreement with the determinations of Cheung et al.[18,20] and Ogawa[65] and in line with the data of Yoshino et al.[88] Calculations of the absorption continua in the range 195–300 nm were performed by Saxon and Slanger.[73] Cross sections at elevated temperatures (up to 1073 K) and pressures (up to 6 bar) were reported by Vattulainen et al.[79]

Table 4A-1-2. Recommended Absorption Cross Sections of O_2 between 205 and 245 nm

λ (nm)	10^{24} σ (cm^2 $molecule^{-1}$)	λ (nm)	10^{24} σ (cm^2 $molecule^{-1}$)
205	7.35	226	3.21
206	7.13	227	2.98
207	7.05	228	2.77
208	6.86	229	2.63
209	6.68	230	2.43
210	6.51	231	2.25
211	6.24	232	2.10
212	6.05	233	1.94
213	5.89	234	1.78
214	5.72	235	1.63
215	5.59	236	1.48
216	5.35	237	1.34
217	5.13	238	1.22
218	4.88	239	1.10
219	4.64	240	1.01
220	4.46	241	0.88
221	4.26	242	0.81
222	4.09	243	0.39
223	3.89	244	0.13
224	3.67	245	0.05
225	3.45		

Note:
205–240 nm: Yoshino et al.[88]
241–245 nm: Fally et al.[28]

The penetration of solar radiation in the atmosphere in the Schumann-Runge wavelength region was based originally on laboratory cross section measurements using insufficient spectral resolution. Yoshino et al.[98] reported high resolution O_2 cross section measurements and band oscillator strengths of the (1,0)–(12,0) S-R bands in the wavelength range 179–202 nm at 300 K, obtaining the first set of results that were not limited by the instrument lineshape. Additional studies at other temperatures, wavelengths, and isotopic compositions have been carried out by Yoshino et al.,[90,94-97] Lewis et al.,[51,52] Cheung et al.,[16,17] and Chiu et al.[21] More recently, Yoshino et al.[89] reported cross sections of the S-R bands in the window region between the rotational lines for wavelengths between 180 and 195 nm; these measurements supersede the their earlier values reported in Yoshino et al.[98]

Absorption cross sections of the S-R continuum (130–175 nm) at room temperature were measured by Watanabe et al.,[83] Metzger and Cook,[56] and Ogawa and Ogawa.[66] Measurements of the temperature dependence were reported by Gibson et al.,[30] Hudson et al.,[35] Wang et al.,[81] Kanik et al.,[43] and Yoshino et al.[101]

Minschwaner et al.[57] have fit temperature dependent ($130<T<500$ K) O_2 cross sections between 175 and 204 nm with polynomial expressions, providing an accurate model of the Schumann-Runge band cross sections that incorporates the most recent laboratory data. Detailed photodissociation rates for the Herzberg continuum $\lambda >$ 200 nm were calculated by Nicolet and Kennes.[61] A parameterization in the Herzberg continuum was reported by Nicolet and Kennes.[62]

For parameterizations of the O_2 absorption in the Schumann-Runge bands used in atmospheric modeling calculations see Kockarts[45] and the review in WMO Report No. 16.[86] More recent work by Murtagh,[59] Nicolet and Kennes,[63] and Minschwaner et al.[57] incorporates results of the later laboratory measurements into efficient schemes for computing broadband transmission and photolysis rates. Transmission values obtained by Murtagh[59] agree well with the WMO[86] recommendations, although the high resolution calculations of Minschwaner et al.[58] differ with the WMO values by as much as 10–20% at some wavelengths.

Absorption cross section measurements in the region 240–300 nm were performed by Fally et al.[28] The different components of the spectrum, namely the discrete bands of the three Herzberg systems I, II, III (A, c, $A' \leftarrow X$), the Herzberg continuum, and the collision-induced Wulf bands were reported separately. The Herzberg continuum cross sections at 240 nm are in good agreement with the values reported by Yoshino et al.[88] and Jenouvrier et al.[40] The absorption cross sections measured by Fally et al.[28] in the range 241–245 nm

are entered in Table 4A-1-2. The absorption cross sections reported by Bogumil et al.[13] are roughly five times larger (at 241 nm) than those reported by Fally et al.[28] High resolution studies were performed by Yoshino et al.,[91,99,100] Huestis et al.,[37] Bao et al.,[9] and Slanger et al.[76] in the 242 to 248 nm range, where weak absorptions cross sections were reported for some vibrational bands in the Herzberg systems.

The O_2 cross section uncertainty factor is estimated to be 1.2 (1σ) for both the Schumann-Runge bands and continuum regions of its spectrum.

Photolysis Quantum yields and Product studies: The overall quantum yield for photodissociation channel (1), $O(^3P) + O(^3P)$, is unity, $\Phi(1) = 1$, for $175 < \lambda < 242$ nm. Above the threshold for channel (2), $O(^3P) + O(^1D)$, at 175 nm, Lee et al.[47] and Nee and Lee[60] determined the quantum yield of $O(^1D)$ to be unity. Thus, $\Phi(2) = 1$, in the wavelength range 139–175 nm. At 157 nm, both product channels (1) and (2) have been observed by Lin et al.,[54] with a relative yield for channel (1) of 0.55 ± 0.05. At wavelengths shorter than 139 nm Lee et al.[47] observed strong variations in $\Phi(O^1D)$, which was confirmed by Nee and Lee[60] (116–139 nm), Lee and Nee[49] (113–130 nm), and Lee and Nee[50] (105–113 nm). Lee et al.[47] reported $\Phi(O^1D) = \Phi(2) = 0.44 \pm 0.05$ at the Lyman-α line (121.567 nm). Lacoursière et al.[46] determined the $O(^1D)$ yield across the entire Lyman-α profile from 121.2 to 121.9 nm at a spectral resolution of 0.0012 nm, and found $\Phi(O^1D)$ to be strongly wavelength dependent in this window. $\Phi(O^1D)$ varied from 1.0 at 121.35 nm through a minimum of 0.48 near 121.62 nm. A strong temperature dependence was found by Lewis et al.[53] with a minimum yield of 0.28 near 121.62 nm at 84 K.

(1) Aboud, A. A.; Curtis, J. P.; Mercure, R.; Rense, W. A. Oxygen gas continuous absorption in the extreme ultraviolet *J. Opt. Soc. Am.* **1955**, *45*, 767-768, doi:10.1364/JOSA.45.000767.

(2) Ackerman, M. UV-solar radiation related to mesospheric processes. In *Mesospheric Models and Related Experiments*; Fiocco, G., Ed.; D. Reidel Publishing Company, Dordrecht, 1971; pp 149-159.

(3) Ackerman, M.; Biaumé, F.; Kockarts, B. Absorption cross sections of the Schumann-Runge bands of molecular oxygen. *Planet. Space Sci.* **1970**, *18*, 1639-1651, doi:10.1016/0032-0633(70)90038-3.

(4) Ackerman, M.; Biaumé, F.; Nicolet, M. Absorption in the spectral range of the Schumann-Runge bands. *Can. J. Chem.* **1969**, *47*, 1834-1940, doi:10.1139/v69-299.

(5) Ahmed, S. M.; Kanik, I.; Link, R. Temperature-dependent photoabsorption cross section measurements of O_2 at the O I-1304 Å triplet emission lines. *Chem. Phys. Lett.* **1996**, *259*, 545-553, doi:10.1016/0009-2614(96)00783-X.

(6) Amoruso, A.; Crescentini, L.; Silvia Cola, M.; Fiocco, G. Oxygen absorption cross-section in the Herzberg continuum. *J. Quant. Spectrosc. Radiat. Transf.* **1996**, *56*, 145-152, doi:10.1016/0022-4073(96)00012-X.

(7) Anderson, G. P.; Hall, L. A. Attenuation of solar irradiance in the stratosphere: Spectrometer measurements between 191 and 207 nm. *J. Geophys. Res.* **1983**, *88*, 6801-6806, doi:10.1029/JC088iC11p06801.

(8) Anderson, G. P.; Hall, L. A. Stratospheric determination of O_2 cross sections and photodissociation rate coefficients: 191-215 nm. *J. Geophys. Res.* **1986**, *91*, 14509-14514, doi:10.1029/JD091iD13p14509.

(9) Bao, Z.-C.; Yu, W. O.; Barker, J. R. Absolute integrated cross sections for some O_2 Herzberg I transitions near 248-249 nm. *J. Chem. Phys.* **1995**, *103*, 6-13, doi:10.1063/1.469624.

(10) Bennett, S. W.; Tellinghuisen, J. B.; Phillips, L. F. Absorption coefficients and ionization yields of some small molecules at 58.4 nm. *J. Phys. Chem.* **1971**, *75*, 719-721, doi:10.1021/j100675a019.

(11) Bertrand, C.; Collin, G. J.; Gagnon, H. Coefficients d'absorption et rendements quantiques ioniques de composés inorganiques et d'hydrocarbones insaturés. *J. Chim. Phys.* **1975**, *72*, 719-723, doi:10.1051/jcp/1975720719.

(12) Blake, A. J.; Carver, J. H.; Haddad, G. N. Photo-absorption cross sections of molecular oxygen between 1250 Å and 2350 Å. *J. Quant. Spectrosc. Radiat. Transf.* **1966**, *6*, 451-459, doi:10.1016/0022-4073(66)90010-0.

(13) Bogumil, K.; Orphal, J.; Homann, T.; Voigt, S.; Spietz, P.; Fleischmann, O. C.; Vogel, A.; Hartmann, M.; Kromminga, H.; Bovensmann, H.; et al. Measurements of molecular absorption spectra with the SCIAMACHY pre-flight model: instrument characterization and reference data for atmospheric remote sensing in the 230-2380 nm region. *J. Photochem. Photobiol. A: Chem.* **2003**, *157*, 167-184, doi:10.1016/S1010-6030(03)00062-5.

(14) Brion, C. E.; Tan, K. H.; van der Wiel, M. J.; van der Leeuw, P. E. Dipole oscillator-strengths for the photoabsorption, photoionization and fragmentation of molecular oxygen. *J. Electron Spectrosc. Relat. Phenom.* **1979**, *17*, 101-119, doi:10.1016/0368-2048(79)85032-X.

(15) Brolley, J. E.; Porter, L. E.; Sherman, R. H.; Theobald, J. K.; Fong, J. C. Photoabsorption cross sections of H_2, D_2, N_2, O_2, Ar, Kr, and Xe at the 584-Å line of neutral Helium. *J. Geophys. Res.* **1973**, *78*, 1627-1632, doi:10.1029/JA078i010p01627.

(16) Cheung, A. S. C.; Yoshino, K.; Esmond, J. R.; Chiu, S. S. L.; Freeman, D. E.; Parkinson, W. H. Predissociation linewidths of the (1,0)-(12,0) Schumann-Runge absorption bands of O_2 in the wavelength region 179-202 nm. *J. Chem. Phys.* **1990**, *92*, 842-849, doi:10.1063/1.458117.

(17) Cheung, A. S. C.; Yoshino, K.; Freeman, D. E.; Friedman, R. S.; Dalgarno, A.; Parkinson, W. H. The Schumann-Runge absorption bands of $^{16}O^{18}O$ in the wavelength region 175-205 nm and spectroscopic constants of isotopic oxygen molecules. *J. Mol. Spectrosc.* **1989**, *134*, 362-389, doi:10.1016/0022-2852(89)90323-8.

(18) Cheung, A. S. C.; Yoshino, K.; Parkinson, W. H.; Freeman, D. E. Herzberg continuum cross section of oxygen in the wavelength region 193.5 – 204.0 nm and band oscillator strengths of the (0,0) and (1,0) Schumann-Runge bands *Can. J. Phys.* **1984**, *62*, 1752-1762, doi:10.1139/p84-221.

(19) Cheung, A. S. C.; Yoshino, K.; Parkinson, W. H.; Freeman, D. E. Herzberg continuum cross section of oxygen in the wavelength region 193.5-204.0 nm: New laboratory measurements and stratospheric implications. *Geophys. Res. Lett.* **1984**, *11*, 580-582, doi:10.1029/GL011i006p00580.

(20) Cheung, A. S. C.; Yoshino, K.; Parkinson, W. H.; Guberman, S. L.; Freeman, D. E. Absorption cross-section measurements of oxygen in the wavelength region 195-241 nm of the Herzberg continuum. *Planet. Space Sci.* **1986**, *34*, 1007-1021, doi:10.1016/0032-0633(86)90011-5.

(21) Chiu, S. S. L.; Cheung, A. S. C.; Yoshino, K.; Esmond, J. R.; Freeman, D. E.; Parkinson, W. H. Predissociation linewidths of the (3,0)-(11,0) Schumann-Runge absorption bands of $^{18}O_2$ and $^{16}O^{18}O$ in the wavelength region 180-196 nm. *J. Chem. Phys.* **1990**, *93*, 5539-5543, doi:10.1063/1.459623.

(22) Clark, K. C. Ionospheric absorption by N_2 and O_2 of certain extreme ultraviolet solar wavelengths. *Phys. Rev.* **1952**, *87*, 271-276, doi:10.1103/PhysRev.87.271.

(23) Cole, B. E.; Dexter, R. N. Photoabsorption and photoionisation measurements on some atmospheric gases in the wavelength region 50-340 Å. *J. Phys. B: At. Mol. Phys.* **1978**, *11*, 1011-1023, doi:10.1088/0022-3700/11/6/013.

(24) Cook, G. R.; Ching, B. K.; Becker, R. A. Absorption by, and photo-ionization of, N_2 and O_2 in the 830-1000 Å range. *Discuss. Faraday Soc.* **1964**, *37*, 149-158, doi:10.1039/DF9643700149.

(25) Cook, G. R.; Metzger, P. H. Photoionization and absorption cross sections of O_2 and N_2 in the 600- to 1000-Å region. *J. Chem. Phys.* **1964**, *41*, 321-336, doi:10.1063/1.1725870.

(26) Coquart, B.; Merienne, M. F.; Jenouvrier, A. O_2 Herzberg continuum absorption cross-sections in the wavelength region 196-205 nm of the Schumann-Runge bands. *Planet. Space Sci.* **1990**, *38*, 287-300, doi:10.1016/0032-0633(90)90093-6.

(27) Ditchburn, R. W.; Young, P. A. The absorption of molecular oxygen between 1850 and 2500 Å. *J. Atmos. Terr. Phys.* **1962**, *24*, 127-139, doi:10.1016/0021-9169(62)90191-5.

(28) Fally, S.; Vandaele, A. C.; Carleer, M.; Hermans, C.; Jenouvrier, A.; Mérienne, M.-F.; Coquart, B.; Colin, R. Fourier transform spectroscopy of the O_2 Herzberg bands. III. Absorption cross sections of the collision-induced bands of the Herzberg continuum. *J. Mol. Spectrosc.* **2000**, *204*, 10-20, doi:10.1006/jmsp.2000.8204.

(29) Frederick, J. E.; Mentall, J. E. Solar irradiance in the stratosphere: Implications for the Herzberg continuum absorption of O_2. *Geophys. Res. Lett.* **1982**, *9*, 461-464, doi:10.1029/GL009i004p00461

(30) Gibson, S. T.; Gies, H. P. F.; Blake, A. J.; McCoy, D. G.; Rogers, P. J. Temperature dependence in the Schumann-Runge photoabsorption continuum of oxygen. *J. Quant. Spectrosc. Radiat. Transf.* **1983**, *30*, 385-393, doi:10.1016/0022-4073(83)90101-2.

(31) Goldstein, R.; Mastrup, F. N. Absorption coefficients of the O_2 Schumann-Runge continuum from 1270 Å ↔ 1745 Å using a new continuum source. *J. Opt. Soc. Am.* **1966**, *56*, 765-769, doi:10.1364/JOSA.56.000765.

(32) Greenblatt, G. D.; Orlando, J. J.; Burkholder, J. B.; Ravishankara, A. R. Absorption measurements of oxygen between 330 and 1140 nm. *J. Geophys. Res.* **1990**, *95*, 18577-18582, doi:10.1029/JD095iD11p18577.

(33) Hasson, V.; Nichols, R. W. Absolute spectral absorption measurements on molecular oxygen from 2640-1940 Å. *J. Phys. B. At. Mol. Phys.* **1971**, *4*, 1789-1797, doi:10.1088/0022-3700/4/12/025.

(34) Herman, J. R.; Mentall, J. E. O_2 absorption cross sections (187-225 nm) from stratospheric solar flux measurements. *J. Geophys. Res.* **1982**, *87*, 8967-8975, doi:10.1029/JC087iC11p08967.

(35) Hudson, R. D.; Carter, V. L.; Stein, J. A. An investigation of the effect of temperature on the Schumann-Runge absorption continuum of oxygen, 1580-1950 Å. *J. Geophys. Res.* **1966**, *71*, 2295-2298, doi:10.1029/JZ071i009p02295.

(36) Hudson, R. D.; Mahle, S. H. Photodissociation rates of molecular oxygen in the mesosphere and lower thermosphere. *J. Geophys. Res.* **1972**, *77*, 2902-2914, doi:10.1029/JA077i016p02902.

(37) Huestis, D. L.; Copeland, R. A.; Knutsen, K.; Slanger, T. G.; Jogma, R. T.; Boogaarts, M. G. H.; Meijer, G. Branch intensities and oscillator strengths for the Herzberg absorption systems in oxygen. *Can. J. Phys.* **1994**, 1109-1121, doi:10.1139/p94-145.

(38) Huffman, R. E. Absorption cross-sections of atmosperic gases for use in aeronomy. *Can. J. Chem.* **1969**, *47*, 1823-1834, doi:10.1139/v69-298.

(39) Huffman, R. E.; Tanaka, Y.; Larrabee, H. E. Nitrogen and oxygen absorption cross sections in the vacuum ultra-violet. *Discuss. Faraday Soc.* **1964**, *37*, 159-166, doi:10.1039/DF9643700159.

(40) Jenouvrier, A.; Coquart, B.; Merienne, M. F. Long pathlength measurements of oxygen absorption cross sections in the wavelength region 205-240 nm. *J. Quant. Spectrosc. Radiat. Transf.* **1986**, *36*, 349-354, doi:10.1016/0022-4073(86)90059-2.

(41) Jenouvrier, A.; Coquart, B.; Mérienne-Lafore, M. F. New measurements of the absorption cross-sections in the Herzberg continuum of molecular oxygen in the region between 205 and 240 nm. *Planet. Space Sci.* **1986**, *34*, 253-254, doi:10.1016/0032-0633(86)90119-4.

(42) Johnston, H. S.; Paige, M.; Yao, F. Oxygen absorption cross sections in the Herzberg continuum and between 206 and 327 K. *J. Geophys. Res.* **1984**, *89*, 11661-11665, doi:10.1029/JD089iD07p11661.

(43) Kanik, I.; Beegle, L.; Noren, C.; Ahmed, S. M.; Link, R. Temperature-dependent photoabsorption cross section measurements of O_2 at the NI airglow and auroral emission lines. *Chem. Phys. Lett.* **1997**, *279*, 297-302, doi:10.1016/S0009-2614(97)01077-4.

(44) Kley, D. Ly(α) absorption cross-section of H_2O and O_2. *J. Atmos. Chem.* **1984**, *2*, 203-210, doi:10.1007/BF00114132.

(45) Kockarts, G. Absorption and photodissociation in the Schumann-Runge bands of molecular oxygen in the terrestrial atmosphere. *Planet. Space Sci.* **1976**, *24*, 589-604, doi:10.1016/0032-0633(76)90137-9.

(46) Lacoursière, J.; Meyer, S. A.; Faris, G. W.; Slanger, T. G.; Lewis, B. R.; Gibson, S. T. The $O(^1D)$ yield from O_2 photooxidation near H Lyman-α (121.6 nm). *J. Chem. Phys.* **1999**, *110*, 1949-1958, doi:10.1063/1.477852.

(47) Lee, L. C.; Slanger, T. G.; Black, G.; Sharpless Quantum yields for the production of $O(^1D)$ from photodissociation of O_2 at 1160-1770 Å. *J. Chem. Phys.* **1977**, *67*, 5602-5606, doi:10.1063/1.434759.

(48) Lee, P. Photodissociation and photoionization of oxygen (O_2) as inferred from measured absorption coefficients. *J. Opt. Soc. Am.* **1955**, *45*, 703-709, doi:10.1364/JOSA.45.000703.

(49) Lee, P. C.; Nee, J. B. Detection of $O(^1D)$ produced in the photodissociation of O_2. I Identification of the $^3\Sigma_u^-$ and $^3\Pi_u$ Rydberg states in 113-130 nm. *J. Chem. Phys.* **2000**, *112*, 1763-1768, doi:10.1063/1.480739.

(50) Lee, P. C.; Nee, J. B. Detection of $O(^1D)$ produced in the photodissociation of O_2. II Identification of the $^3\Sigma_u^-$ and $^3\Pi_u$ Rydberg states in 105-113 nm. *J. Chem. Phys.* **2001**, *114*, 792-797, doi:10.1063/1.1330231.

(51) Lewis, B. R.; Berzins, L.; Carver, J. H. Oscillator strengths for the Schumann-Runge bands of $^{16}O_2$. *J. Quant. Spectrosc. Radiat. Transf.* **1986**, *36*, 209-232, doi:10.1016/0022-4073(86)90069-5.

(52) Lewis, B. R.; Berzins, L.; Carver, J. H.; Gibson, S. T. Rotational variation of predissociation linewidth in the Schumann-Runge bands of $^{16}O_2$. *J. Quant. Spectrosc. Radiat. Transf.* **1986**, *36*, 187-207, doi:10.1016/0022-4073(86)90068-3.

(53) Lewis, B. R.; Vardavas, I. M.; Carver, J. H. The aeronomic dissociation of water vapor by solar H Lyman α radiation. *J. Geophys. Res.* **1983**, *88*, 4935-4940, doi:10.1029/JA088iA06p04935.

(54) Lin, J. J.; Huang, D. W.; Lee, Y. T.; Yang, X. Photodissociation of O_2 at 157 nm: Experimental observation of anisotropy mixing in the $O_2 + h\nu \rightarrow O(^3P) + O(^3P)$ channel. *J. Chem. Phys.* **1998**, *109*, 1758-1762, doi:10.1063/1.476751.

(55) Matsunaga, F. M.; Watanabe, K. Total and photoionization coefficients and dissociation continua of O_2 in the 580-1070 Å region. *Sci. Light* **1967**, *16*, 31-42.

(56) Metzger, P. H.; Cook, G. R. A reinvestigation of the absorption cross sections of molecular oxygen in the 1050-1800 Å region. *J. Quant. Spectrosc. Radiat. Transf.* **1964**, *4*, 107-116, doi:10.1016/0022-4073(64)90057-3.

(57) Minschwaner, K.; Anderson, G. P.; Hall, L. A.; Yoshino, K. Polynomial coefficients for calculating O_2 Schumann-Runge cross sections at 0.5 cm^{-1} resolution. *J. Geophys. Res.* **1992**, *97*, 10103-10108, doi:10.1029/92JD00661.

(58) Minschwaner, K.; Salawitch, R. J.; McElroy, M. B. Absorption of solar radiation by O_2: Implications for O_3 and lifetimes of N_2O, $CFCl_3$, and CF_2Cl_2. *J. Geophys. Res.* **1993**, *98*, 10543-10561, doi:10.1029/93JD00223.

(59) Murtagh, D. P. The O_2 Schumann-Runge system - New calculations of photodissociation cross-sections. *Planet. Space Sci.* **1988**, *36*, 819-828, doi:10.1016/0032-0633(88)90087-6.

(60) Nee, J. B.; Lee, P. C. Detection of $O(^1D)$ produced in the photodissociation of O_2 in the Schumann-Runge continuum. *J. Phys. Chem. A* **1997**, *101*, 6653-6657, doi:10.1021/jp970439m.

(61) Nicolet, M.; Kennes, R. Aeronomic problems of the molecular oxygen photodissociation, I. The O_2 Herzberg continuum. *Planet. Space Sci.* **1986**, *34*, 1043-1059, doi:10.1016/0032-0633(86)90015-2.
(62) Nicolet, M.; Kennes, R. Aeronomic problems of the molecular oxygen photodissociation –IV. The various parameters for the Herzberg Continuum. *Planet. Space Sci.* **1988**, *36*, 1069-1076, doi:10.1016/0032-0633(88)90044-X.
(63) Nicolet, M.; Kennes, R. Aeronomic problems of molecular-oxygen photodissociation .6. Photodissociation frequency and transmittance in the spectral range of the Schumann-Runge bands. *Planet. Space Sci.* **1989**, *37*, 459-491, doi:10.1016/0032-0633(89)90125-6.
(64) Ogawa, M. Absorption coefficients of O_2 at the Lyman-alpha line and its vicinity. *J. Geophys. Res.* **1968**, *73*, 6759-6763, doi:10.1029/JA073i021p06759.
(65) Ogawa, M. Absorption cross sections of O_2 and CO_2 continua in the Schumann and far-uv regions. *J. Chem. Phys.* **1971**, *54*, 2550-2556, doi:10.1063/1.1675211.
(66) Ogawa, S.; Ogawa, M. Absorption cross sections of O_2 ($a\ ^1\Delta_g$) and $O_2(X\ ^3\Sigma_g^-)$ in the region from 1087 to 1700 Å. *Can. J. Phys.* **1975**, *53*, 1845-1852, doi:10.1139/p75-236.
(67) Oshima, Y.; Okamoto, Y.; Koda, S. Pressure effect of foreign gases on the Herzberg photoabsorption of oxygen. *J. Phys. Chem.* **1995**, *99*, 11830-11833, doi:10.1021/j100031a007.
(68) Pirre, M.; Rigaud, P.; Huguenin, D. New in situ measurements of the absorption cross-sections of O_2 in the Herzberg continuum. *Geophys. Res. Lett.* **1984**, *11*, 1199-1202, doi:10.1029/GL011i012p01199
(69) Pirre, M.; Rigaud, P.; Huguenin, D. *In situ* measurements of the absorption cross-sections of O_2 in the Herzberg continuum: The results of two different experiments. *Ann. Geophys.* **1988**, *6*, 535-540.
(70) Preston, W. M. The origin of radio fade-outs and the absorption coefficient of gases for light of wave-length 1215.7 Å. *Phys. Rev.* **1940**, *57*, 887-894, doi:10.1103/PhysRev.57.887.
(71) Samson, J. A. R.; Cairns, R. B. Absorption and photoionization cross sections of O_2 and N_2 at intense solar emission lines. *J. Geophys. Res.* **1964**, *69*, 4583-4590, doi:10.1029/JZ069i021p04583.
(72) Samson, J. A. R.; Cairns, R. B. Total absorption cross sections of H_2, N_2, and O_2 in the region 550-220 Å. *J. Opt. Soc. Am.* **1965**, *45*, 1035-1040, doi:10.1364/josa.55.001035.
(73) Saxon, R. P.; Slanger, T. G. Molecular oxygen absorption continua at 195-300 nm and O_2 radiative lifetimes. *J. Geophys. Res.* **1986**, *91*, 9877-9879, doi:10.1029/JD091iD09p09877.
(74) Shardanand Absorption cross sections of O_2 and O_4 between 2000 and 2800 Å. *Phys. Rev.* **1969**, *186*, 5-9, doi:10.1103/PhysRev.186.5.
(75) Shardanand; Rao, A. D. P. Collision-induced absorption of O_2 in the Herzberg continuum. *J. Quant. Spectrosc. Radiat. Transf.* **1977**, *17*, 433-439, doi:10.1016/0022-4073(77)90122-4.
(76) Slanger, T. G.; Huestis, D. L.; Cosby, P. C.; Naus, N.; Meijer, G. O_2 photoabsorption in the 40950-41300 cm^{-1} region: New Herzberg bands, new absorption lines, and improved spectroscopic data. *J. Chem. Phys.* **1996**, *105*, 9393-9402, doi:10.1063/1.472772.
(77) Starr, W. L.; Loewenstein, M. Total absorption cross sections of several gases of aeronomic interest at 584 Å. *J. Geophys. Res.* **1972**, *77*, 4790-4796, doi:10.1029/JA077i025p04790.
(78) Tanaka, Y.; Jursa, A. S.; LeBlanc, F. J.; Inn, E. C. Y. Spectroscopic study of the afterglows of N_2 and (N_2 + O_2) in the vacuum region. *Planet. Space Sci.* **1959**, *1*, 7-13, doi:10.1016/0032-0633(59)90016-9.
(79) Vattulainen, J.; Wallenius, L.; Stenberg, J.; Hernberg, R.; Linna, V. Experimental determination of SO_2, C_2H_2, and O_2 UV absorption cross sections at elevated temperatures and pressures. *Appl. Spectrosc.* **1997**, *57*, 1311-1315, doi:10.1366/0003702971942.
(80) Wainfan, N.; Walker, W. C.; Weissler, G. L. Photoionization efficiencies and cross sections in O_2, N_2, CO_2, A, H_2O, H_2, and CH_4. *Phys. Rev.* **1955**, *99*, 542-549, doi:10.1103/PhysRev.99.542.
(81) Wang, J.; McCoy, D. G.; Blake, A. J.; Torop, L. Effect of the close approach of potential curves in photoabsorption by atomic molecules – II. Temperature dependence of the O_2 cross section in the region 130-160 nm. *J. Quant. Spectrosc. Radiat. Transf.* **1987**, *38*, 19-27, doi:10.1016/0022-4073(87)90106-3.
(82) Watanabe, K.; Inn, E. C. Y.; Zelikoff, M. Absorption coefficients of gases in the vacuum ultraviolet. *J. Chem. Phys.* **1952**, *20*, 1969-1970, doi:10.1063/1.1700353.
(83) Watanabe, K.; Inn, E. C. Y.; Zelikoff, M. Absorption coefficients of oxygen in the vacuum ultraviolet. *J. Chem. Phys.* **1953**, *21*, 1026-1030, doi:10.1063/1.1699104.
(84) Watanabe, K.; Marmo, F. F. Photoionization and total absorption cross section of gases. II. O_2 and N_2 in the region 850-1500 Å. *J. Chem. Phys.* **1956**, *25*, 965-971, doi:10.1063/1.1743151.
(85) Weissler, G. L.; Lee, P. Absorption coefficients of oxygen in the vacuum ultraviolet. *J. Opt. Soc. Am.* **1952**, *42*, 200-203, doi:10.1364/JOSA.42.000200.
(86) WMO *Atmospheric Ozone: 1985*; National Aeronautics and Space Administration: Geneva, Report No. 16, Chapter 7, 1986.

(87) Wu, C. Y. R.; Judge, D. L.; Matsui, T. High-temperature ultrahigh-resolution absorption cross-section measurements of O_2 in the EUV region. *J. Electron Spectrosc. Related Phenom.* **2005**, *144-147*, 123-126, doi:10.1016/j.elspec.2005.01.047.

(88) Yoshino, K.; Cheung, A. S. C.; Esmond, J. R.; Parkinson, W. H.; Freeman, D. E.; Guberman, S. L.; Jenouvrier, A.; Coquart, B.; Merienne, M. F. Improved absorption cross sections of oxygen in the wavelength region 205-240 nm of the Herzberg continuum. *Planet. Space Sci.* **1988**, *36*, 1469-1475, doi:10.1016/0032-0633(88)90012-8.

(89) Yoshino, K.; Esmond, J. R.; Cheung, A. S.-C.; Freeman, D. E.; Parkinson, W. H. High resolution absorption cross sections in the transmission window region of the Schumann-Runge bands and Herzberg continuum of O_2. *Planet. Space Sci.* **1992**, *40*, 185-192, doi:10.1016/0032-0633(92)90056-T.

(90) Yoshino, K.; Esmond, J. R.; Cheung, A. S. C.; Freeman, D. E.; Parkinson, W. H. Band oscillator strengths of the (2,1)-(12,1) Schumann-Runge bands of O_2 from absolute absorption cross-section measurements at room temperature. *J. Geophys. Res.* **1990**, *95*, 11743-11746, doi:10.1029/JD095iD08p11743.

(91) Yoshino, K.; Esmond, J. R.; Murray, J. E.; Parkinson, W. H.; Thorne, A. P.; Learner, R. C. M.; Cox, G. Band oscillator strengths of the Herzberg I bands of O_2. *J. Chem. Phys.* **1995**, *103*, 1243-1249, doi:10.1063/1.469800.

(92) Yoshino, K.; Esmond, J. R.; Parkinson, W. H.; Thorne, A. P.; Learner, R. C. M.; Cox, G. Fourier transform spectroscopy annd cross-section measurements of the Herzberg II bands of O_2 at 295 K. *J. Chem. Phys.* **1999**, *111*, 2960-2967, doi:10.1063/1.479577.

(93) Yoshino, K.; Esmond, J. R.; Parkinson, W. H.; Thorne, A. P.; Learner, R. C. M.; Cox, G.; Cheung, A. S.-C. Fourier transform spectroscopy and cross section measurements of the Herzberg III bands of O_2 at 295 K. *J. Chem. Phys.* **2000**, *112*, 9791-9801, doi:10.1063/1.481702.

(94) Yoshino, K.; Freeman, D. E.; Esmond, J. R.; Friedman, R. S.; Parkinson, W. H. High-resolution absorption cross-sections and band oscillator-strengths of the Schumann-Runge absorption-bands of isotopic oxygen, $^{18}O_2$, at 79 K. *Planet. Space Sci.* **1988**, *36*, 1201-1210, doi:10.1016/0032-0633(88)90073-6.

(95) Yoshino, K.; Freeman, D. E.; Esmond, J. R.; Friedman, R. S.; Parkinson, W. H. High-resolution absorption cross-sections and band oscillator-strengths of the Schumann-Runge absorption-bands of isotopic oxygen, (OO)-$^{16}O^{18}O$, at 79-K. *Planet. Space Sci.* **1989**, *37*, 419-426, doi:10.1016/0032-0633(89)90123-2.

(96) Yoshino, K.; Freeman, D. E.; Esmond, J. R.; Parkinson, W. H. High-resolution absorption cross-sections and band oscillator-strengths of the Schumann-Runge bands of oxygen at 79-K. *Planet. Space Sci.* **1987**, *35*, 1067-1075, doi:10.1016/0032-0633(87)90011-0.

(97) Yoshino, K.; Freeman, D. E.; Parkinson, W. H. Atlas of the Schumann-Runge absorption bands of O_2 in the wavelength region 175-205 nm. *J. Phys. Chem. Ref. Data* **1984**, *13*, 207-227, doi:10.1063/1.555702.

(98) Yoshino, K.; Freeman, D. F.; Esmond, J. R.; Parkinson, W. H. High-resolution absorption cross-section measurements and band oscillator-strengths of the (1,0)-(12,0) Schumann-Runge bands of O_2. *Planet. Space Sci.* **1983**, *31*, 339-353 doi:10.1016/0032-0633(83)90085-5.

(99) Yoshino, K.; Huestis, D. L.; Nicholls, R. W. Comment on the Herzberg Continuum. *J. Quant. Spectrosc. Radiat. Transf.* **1998**, *60*, 1091.

(100) Yoshino, K.; Murray, J. E.; Esmond, J. R.; Sun, Y.; Parkinson, W. H.; Thorne, A. P.; Learner, R. C. M.; Cox, G. Fourier transform spectroscopy of the Herzberg I bands of O_2. *Can. J. Phys.* **1994**, *72*, 1101-1108, doi:10.1139/p94-144.

(101) Yoshino, K.; Parkinson, W. H.; Ito, K.; Matsui, T. Absolute absorption cross-section measurements of Schumann-Runge continuum of O_2 at 90 and 295 K. *J. Mol. Spectrosc.* **2005**, *229*, 238-243, doi:10.1016/j.jms.2004.08.020.

A2. O_3 (Ozone)

Back to Index

$O_3 + h\nu$	$\rightarrow O(^3P) + O_2(X^3\Sigma_g^-)$	101 kJ mol^{-1}	1180 nm	(1)
	$\rightarrow O(^3P) + O_2(a^1\Delta_g)$	195 kJ mol^{-1}	612 nm	(2)
	$\rightarrow O(^3P) + O_2(b^1\Sigma_g^+)$	258 kJ mol^{-1}	463 nm	(3)
	$\rightarrow O(^1D) + O_2(X^3\Sigma_g^-)$	291 kJ mol^{-1}	411 nm	(4)
	$\rightarrow O(^1D) + O_2(a^1\Delta_g)$	386 kJ mol^{-1}	310 nm	(5)
	$\rightarrow O(^1D) + O_2(b^1\Sigma_g^+)$	448 kJ mol^{-1}	267 nm	(6)
	$\rightarrow 3\ O(^3P)$	595 kJ mol^{-1}	201 nm	(7)
	$\rightarrow O(^1S) + O_2(a^1\Delta_g)$	610 kJ mol^{-1}	196 nm	(8)

(Recommendation: 10-6, Note: 15-10, Evaluated: 10-6)

Absorption Cross Sections. The O_3 absorption cross sections in the 200–790 nm region can be separated into four systems: the Hartley band (200–300 nm), the Huggins bands (300–370 nm), the Chappuis band (370–790 nm), and the Wulf bands extending towards longer wavelengths. The Hartley band is the strongest band and peaks around 255 nm. Although its overall shape is very smooth, there is residual vibrational structure in the region 250–260 nm. The Huggins band consists of a series of individual peaks and is marked with a drastic change of absorption cross sections (over more than five orders of magnitude) and strong temperature dependence. The Chappuis band is composed of a vibrational band progression superimposed on a continuous absorption in the visible region and is about a thousand times weaker than the Hartley band. The very weak near infrared part of the Chappuis band is clearly structured and corresponds to a different electronic transition (called the "Wulf bands").

Photolysis of ozone in the Hartley system occurs predominantly via the two spin-allowed channels (1) and (5) (Ball et al.[11]) whereas channels (2), (3) and (4) are spin forbidden. Channels (2) and (4) have been identified from photolysis in the Huggins band (Silvente et al.[64] and Denzer et al.[30]).

For the three main bands in the 200–790 nm region, there have been many different measurements of the absorption spectrum and cross sections at various experimental (temperature and pressure) and instrumental conditions (resolution) during the last century as given in Table 4A-2-1. The available measurements can be organized into three groups: (A) measurements of absolute cross sections at single wavelengths (e.g. at the Hg resonance line at 253.65 nm), (B) measurements of absolute cross sections over broad spectral regions (typically covering a few hundred nm), (C) measurements of relative O_3 absorption spectra over broad spectral regions that have been scaled to absolute spectra using results from other studies (Type A or B), (D) measurements of the O_3 cross section at a single wavelength relative to the O_3 cross section at another wavelength.

Table 4A-2-1. Summary of O_3 Absorption Cross Section Studies

Study	Year	Spectral Range (nm)	Type	Resolution (nm)	Temperature (K)
Ny and Choong[57]	1933	213–353	B	0.05	298
Vassy and Vassy[77]	1948	450–601	A	not stated	291, 231, 193, 168
Vigroux[79]	1953	230–793 245–345	B	0.05	291 181–393
Inn and Tanaka[41]	1953	200–750	B	0.5	290
Tanaka et al.[74]	1953	105–220	B	0.5	300
Ogawa and Cook[58]	1958	53–131	C	not stated	295
Inn and Tanaka[43]	1959	200–350 400–750	B	~0.05 0.5	273
Hearn[39]	1961	253.7–577.0	A	0.01-0.09	295
DeMore and Raper[29]	1964	210–300	B	0.2	77, 273
Vigroux[80]	1967	304–341	B	0.05	291
Griggs[37]	1968	200–360 450–850	B	0.1 0.5	303
Vigroux[81]	1969	230–270	B	0.1	291
Simons et al.[65]	1973	300–370	B	0.4	195, 300, 333
Astholz et al.[7]	1982	210–320	B	3	300, 500, 720, 900
Davenport[28]	1982	253–370	B	not stated	206, 225, 271, 298
McPeters and Bass[52]	1982	300–310	C	0.02	229, 245, 295

Study	Year	Spectral Range (nm)	Type	Resolution (nm)	Temperature (K)
Daumont et al.[27]	1983	310–350	B	0.012	223, 294
Brion et al.[19]	1983	310–350	B	0.012	223, 294
Brion et al.[20]	1984	310–350	B	0.012	223, 294
Freeman et al.[33]	1984	250–350	C*	0.002	195
Bass and Paur[13]	1985	230–350	C*	<0.025	200, 298
Paur and Bass[61]	1985	245–340	C*	<0.025	203, 218, 228, 243, 273, 298
Freeman et al.[34]	1985	281–335	A	0.003	195, 228, 293
Molina and Molina[53]	1986	185–350	B	0.07	226, 263, 298
Mauersberger et al.[50]	1986	253.7	A	not stated	297.5
Mauersberger et al.[51]	1987	253.7	A	not stated	297.5
Barnes and Mauersberger[12]	1987	237.7	A,C	not stated	195, 221, 237, 253, 273, 297, 318, 335, 351
Yoshino et al.[85]	1988	238.2–344.4	A, C*	0.13–0.003	195, 228, 295
Malicet et al.[45]	1989	253.36	A	not stated	229, 295
Cacciani et al.[25]	1989	339–355	B	0.012	220, 293
Amoruso et al.[3]	1990	590–610	B	0.05	230, 299
Daumont et al.[26]	1992	195–345	B*	0.01	295
Anderson and Mauersberger[5]	1992	543.5–632.8	A	not stated	295
Anderson et al.[4]	1993	750–975	A	not stated	295
Brion et al.[18]	1993	195–345 300–345	B*	0.01	218, 228, 243, 295, 273
Yoshino et al.[84]	1993	185–254	A, B	0.13–0.003	195, 228, 295
Burkholder and Talukdar[23]	1994	407–763	C*	0.2	220, 240, 260, 280, 298
Malicet et al.[46]	1995	195–345	C*	0.01	218, 228, 243, 273, 295,
Mason et al.[47]	1996	110–172	C*	0.05	298
Brion et al.[17]	1998	345–830 515–650	B*	0.01	295 218
Burrows et al.[24]	1999	231–794	B*	0.2–0.4	202, 221, 241, 273, 293
Voigt et al.[82]	2001	230–850	C*	5 cm^{-1}	203, 223, 246, 280, 293
Bogumil et al.[15]	2001	230–2400	C*	0.17–1.44	203, 293
Bogumil et al.[16]	2003	230–1070	C*	0.2–0.4	203, 223, 243, 273, 293
Enami et al.[32]	2004	759–768	A	0.002	214-5, 245, 260, 273, 296-8
El Helou et al.[31]	2005	540–1080	A	4 cm^{-1}	144, 150, 175, 222–225, 291–294
Fuchs et al.[35]	2009	404	D	0.5	296
Axson et al.[8]	2011	350–470	C	0.27–0.5	296
Petersen et al.[62]	2012	244.06 248.32 257.34	D	~0.002	295
Gorshelev et al.[36]	2014	213–1100	C	0.02–0.06	293
Serdyuchenko et al.[63]	2014	213–1100	C	0.02–0.06	193–293
Viallon et al.[78]	2015	244.06 248.32 253.65 257.34	A	~0.002 atomic line for 253.65	296

Earlier reviews of the measured absorption cross sections were presented by Inn and Tanaka,[42] Ackermann,[1] Hudson,[40] Nicolet,[55] Brion et al.,[21] Steinfeld et al.,[67] Bacis et al.,[9] Matsumi and Kawasaki,[49] and the WMO

Report No. 16,[83] which was the basis for the NASA/JPL 97-4 evaluation. Orphal[59,60] has recently critically reviewed the available laboratory measurements up to 2003, and the NASA/JPL 10-6 evaluation is partly based on that review. Relevant for that evaluation are the measurements of type B and C, particularly those studies whose data were digitally available (marked with an asterisk*). Unfortunately, the recommended data set for the NASA/JPL 97-4 evaluation of Molina and Molina[53] was not considered in his review.

In the Hartley and Huggins bands (about 240–325 nm) there is generally very good agreement (better than 2-3%) between the data measured at room temperature (293–300 K) by Bass and Paur[13] and Paur and Bass,[61] Molina and Molina,[53] Freeman et al.,[33] Yoshino et al.,[85] the Reims-team (Daumont et al.,[26] Brion et al.,[18] Malicet et al.,[46] and Brion et al.[17]), Yoshino et al.,[84] the Bremen-team (Burrows et al.,[24] Voigt et al.,[82] and Bogumil et al.,[16] Gorshelev et al.[36]), Petersen et al.,[62] and Viallon et al.[78] The older data by Ny and Choong,[57] Inn and Tanaka,[41] and Vigroux[79] are about 8% greater than the data of Molina and Molina.[53] The vibrational structure between 240 and 270 nm was observed in most studies, except those of Inn and Tanaka,[41] DeMore and Raper,[29] Davenport,[28] and Astholz et al.,[7] who used lower resolution instruments.

Measurements of absorption cross sections in the shorter wavelength VUV region were performed by Tanaka et al.,[74] Ogawa and Cook,[58] and Mason et al.[47] At the Lyman-α wavelength, 121.567 nm, an absorption cross section of 2.32×10^{-17} cm^2 molecule^{-1} was cited in the review by Ackermann.[1] Ogawa and Cook[58] measured 2.28×10^{-17} cm^2 molecule^{-1} whereas Mason et al.[47] reported 2.99×10^{-17} cm^2 molecule^{-1}. The latter more recent value is recommended and entered in Table 4A-2-2.

A comparison of the O_3 cross-sections at the Hg-line wavelength 253.7 nm was performed by Orphal[59,60] involving 13 absolute measurements and provided a mean value of $(114.1 \pm 0.9) \times 10^{-19}$ cm^2 molecule^{-1}. Viallon et al.[78] has since reported a cross section value of $(112.7 \pm 0.97) \times 10^{-19}$ cm^2 molecule^{-1}. The temperature dependence of the cross sections at 253.7 nm has been measured by Barnes and Mauersberger[12] between 195 and 351 K and by Malicet et al.[45] at 229 and 295 K. It has to be noted that the data of Bass and Paur[13] and Paur and Bass[61] are normalized to the absolute value 114.7×10^{-19} cm^2 molecule^{-1} at 253.7 nm and 295 K measured by Hearn.[39] In the range 230–260 nm, the data of the Reims-team (Daumont-Brion-Malicet-Brion) are generally lower (up to 2.5%) than the data of Molina and Molina,[53] Bass and Paur,[13] and the Bremen-team (Burrows-Voigt-Bogumil-Gorshelev-Serdyuchenko). Furthermore, the data of Voigt et al.[82] show a strong baseline shift below 255 nm and in the range 310–320 nm; in addition, the spectra are very noisy in the Hartley band maximum. The data of Bogumil et al.[15] contain periodic artifacts on the order of 0.5–1.0% in the range 240–270 nm and a stray light feature around 305 nm on the order of 2%.

Below 225 nm the room temperature cross sections of Molina and Molina,[53] DeMore and Raper,[29] and the Reims-team (Daumont-Brion-Malicet) agree within 1-2%, but are 2-5% larger than the measurements of Yoshino et al.[84] Other reported values measured by Ny and Choong,[57] Inn and Tanaka,[41] Astholz et al.,[7] and Griggs[37] differ up to 15%.

In the Huggins bands (310–350 nm) the studies differ in spectral resolution, which is mostly relevant only to atmospheric remote sensing. At wavelengths larger than 310 nm the vibrational structure becomes pronounced. In the range 310–340 nm, the agreement between the different studies is rather good (about 2%) for the data of Bass and Paur,[13] the Reims-team (Daumont-Brion-Malicet-Brion), Burrows et al.,[24] Gorshelev et al.,[36] and Serdyuchenko et al.,[63] although important differences (up to 13%) due to wavelength shifts and spectral resolution are reported by Orphal.[59,60] The data of Bass and Paur[13] and of the Reims-team (Daumont-Brion-Malicet-Brion) show wavelength shifts of more than 0.02 nm. The data of Voigt et al.[82] and Bogumil et al.[16] contain systematic baseline drifts. Above 312 nm, the data of Molina and Molina,[53] which are listed every 0.5 nm up to 350 nm, occasionally miss the maxima and minima of the peaks. The reported values by Cacciani et al.[25] are typically 5-8% lower than the values of Molina and Molina[53] in the range 339–355 nm.

The O_3 absorption cross sections in the 350–450 nm region between the Huggins and Chappuis bands are very small and the available measurements of absolute values scatter significantly. They have been measured by Brion et al.,[17] the Bremen team (Burrows-Voigt-Bogumil-Gorshelev-Serdyuchenko), Fuchs et al. (at 404 nm),[35] and Axson et al.[8] At the minimum near 378 nm, the reported absolute cross sections at 298 K vary between 5×10^{-23} cm^2 molecule^{-1} from Voigt et al.[82] and 5×10^{-24} cm^2 molecule^{-1} from Brion et al.[17]

Absorption cross section measurements of the Chappuis band of O_3 in the wavelength range 450–750 nm have been reported by Burkholder and Talukdar,[23] Brion et al.,[17] the Bremen team (Burrows-Voigt-Bogumil-Gorshelev-Serdyuchenko), El Helou et al.,[31] and at single wavelengths by Hearn,[39] Anderson and Mauersberger,[5] Anderson et al.,[4] and Enami et al.[32] At the peak of the Chappuis band near 602 nm, the values agree within a few percent, although the data of the Bremen-team (Burrows-Voigt-Bogumil) are consistently larger than those of Brion et al.[17] (by 2%) and Burkholder and Talukdar[23] (by 4%) (the latter data are scaled using the measurements of Anderson and Mauersberger[5]). Note that there are pronounced deviations of data

from Burkholder and Talukdar[23] in the region 425–490 nm. The older values of Vassy and Vassy,[77] Vigroux,[79] Inn and Tanaka,[41] Griggs,[37] and Amoruso et al.[3] deviate up to 20%.

Absorption cross sections in the Wulf band region (wavelength >750 nm) have been reported by Anderson et al.,[4] Burkholder and Talukdar,[23] the Bremen-team (Burrows-Voigt-Bogumil-Gorshelev-Serdyuchenko), Enami et al.,[32] and El Helou et al.[31] The data measured at room temperature by the latter group are in excellent agreement (within 0.25%) with those of Anderson et al.[4]

The temperature dependence of the O_3 cross sections has also been studied by several of the groups mentioned above and tabulated in Table 4A-2-1. In the critical review, Orphal [59,60] calculated and compared the integrated cross sections for 5 temperatures in the range 203–295 K in the different spectral regions of the O_3 spectrum. At all temperatures the agreement of the integrated cross sections in the Hartley band is better than 2% and less good agreement in the Chappuis band (4%). In particular, the integrated cross sections of Burkholder and Talukdar[23] lie systematically below the other measurements by about 3% and the data of Burrows et al.[24] are always higher by 2%. In the Huggins bands and the blue tail of the Chappuis band the integrated cross sections scatter by several percent (up to 5%), indicating systematic differences between the available data. The Hartley band integrated cross sections remain constant in the temperature range 203–293 K within the experimental uncertainties. The integrated cross sections in the Huggins bands decrease by more than 30% between 298 K and 203 K and the differential cross sections of the bands increase significantly.

In the Hartley band most studies report a slight (0.9–1.6%) increase of the cross section below 260 nm between room temperature and low temperatures 202–298 K, while Yoshino et al.[84] concluded that the temperature effect is negligible. Above 260 nm the cross section decreases significantly at lower temperatures. This effect is due to the changing populations of the various vibrational and rotational quantum states of ozone and has been analyzed by Simons et al.[65] The cross section values are not linearly proportional to the temperature; instead the effect is larger at the maxima than it is at the minima of the spectral features.

The absorption cross sections in the Huggins bands (310–350 nm) of O_3 decrease strongly with decreasing temperatures. Additionally, they depend on instrumental line shape and differences in wavelength calibration so that discrepancies up to 20% at the lowest temperatures are observed between the various studies. Comparison of the spectra obtained in the temperature range 220–229 K show good agreement (~3% at 325 nm, ~ 5% at 340 nm) with the data of Bass and Paur,[13] Molina and Molina,[53] the Brion team (Daumont-Brion-Malicet-Brion), and Burrows et al.[24] The data of Voigt et al.[82] and Bogumil et al.[16] display sudden baseline jumps and are consistently lower than the other cited data sets. Voigt et al.[82] observed in the region 335–380 nm the presence of "hot bands", which disappear with decreasing temperature, and "cold bands", which become more pronounced at lower temperatures.

In the Chappuis band, the available cross sections agree in showing a very small increase (1%) with decreasing temperature in the wavelength range 550–560 nm. However there is strong disagreement in the relative temperature dependence of the cross sections in the wings (400–550 nm and 650–790 nm) of the Chappuis band. Burkholder and Talukdar[23] report a decrease from 4% at 520 nm to 40% at 420 nm between 298 and 220 K, while Burrows et al.[24] observe a decrease at 420 nm to 70% at 221 K, and Bogumil et al.[16] a decrease of 20% at 223 K. These discrepancies could be due to baseline problems in the different measurements. It was also noted by the Bremen-team (Burrows-Voigt-Bogumil-Serdyuchenko) that in the wings the differential cross sections increase up to 10% between 298 and 203 K. In addition, the band structures between 400 and 500 nm shift toward shorter wavelengths with decreasing temperature. El Helou et al.[31] found the cross sections of the Wulf bands to be highly temperature dependent, increasing up to 91% upon reducing the temperature to 150 K.

Three different models have been proposed to reproduce the temperature dependence of the O_3 cross sections in the entire ultraviolet and visible regions within the experimental uncertainties. The first model was developed for the Hartley band by Adler-Golden[2] and uses an exponential function. The second model, developed by Bass and Paur,[13] uses a quadratic polynomial to be applied in the Hartley and Huggins bands. The third model of Voigt et al.[82] uses a double exponential function. The accuracy of the models was checked by Orphal,[59,60] who concluded that the experimental data are better reproduced using a quadratic polynomial.

The pressure dependence of the O_3 absorption cross sections was investigated by Hearn[39] in the Hartley band and by Voigt et al.[82] in the entire spectral region 240–790 nm. Both groups did not find experimental or theoretical support for pressure dependence, although Voigt et al. [82] proposed that temperature variations of the cross sections around 400 nm might be due to the formation of a weakly bound O_2-O_3 complex.

The recommended absorption cross sections are listed in Table 4A-2-2, averaged over atmospheric intervals at 218 K and at room temperature (293–298 K). It has to be noted that cross sections are listed over 500 cm^{-1} intervals in the region 185–300 nm, over 1 nm intervals in the region 300–321 nm, over 2 nm intervals in the

region 321.5–326.5 nm, and over 5 nm intervals in the region 330–825 nm. The 218 K values measured by the Reims-team (Daumont-Brion-Malicet-Brion) are only listed for the range 196–340 nm. The room temperature data were selected for the range 185–233 nm from the data of Molina and Molina,[53] for the range 323–310 nm from Burrows et al.,[24] and for the range 310–825 nm from the Reims team (Daumont-Brion-Malicet-Brion).

The uncertainty factor for the room temperature O_3 cross section is estimated to be 1.02 (1σ) near the peaks of the Hartley and Chappuis bands and the strong Huggins peaks. The estimated uncertainty in the 360–400 nm region is greater, 1.1 (1σ), primarily due to the spread in the available data sets.

Table 4A-2-2. Recommended Absorption Cross Sections of O_3 at 218 and 293–298 K

λ (nm)	10^{20} σ (cm^2 $molecule^{-1}$) 218 K	293–298 K	λ (nm)	10^{20} σ (cm^2 $molecule^{-1}$) 293–298 K
121.567 (Lyman α)		2990		
185.185–186.916		62.2	412.5–417.5	0.00295
186.916–188.679		57.6	417.5–422.5	0.00393
188.679–190.476		52.6	422.5–427.5	0.00656
190.476–192.308		47.7	427.5–432.5	0.00697
192.308–194.175		42.9	432.5–437.5	0.00882
194.175–196.078		38.5	437.5–442.5	0.0137
196.078–198.020	34.4	34.9	442.5–447.5	0.0165
198.020–200.000	32.0	32.4	447.5–452.5	0.0185
200.000–202.020	31.2	31.5	452.5–457.5	0.0218
202.020–204.082	32.4	32.6	457.5–462.5	0.0366
204.082–206.186	36.2	36.3	462.5–467.5	0.0367
206.186–208.333	43.2	43.3	467.5–472.5	0.0410
208.333–210.526	54.2	53.9	472.5–477.5	0.0481
210.526–212.766	69.6	69.3	477.5–482.5	0.0754
212.766–215.054	90.6	90.3	482.5–487.5	0.0813
215.054–217.391	119	118	487.5–492.5	0.0816
217.391–219.780	155	154	492.5–497.5	0.0908
219.780–222.222	201	199	497.5–502.5	0.121
222.222–224.719	256	255	502.5–507.5	0.160
224.719–227.273	323	322	507.5–512.5	0.158
227.273–229.885	403	401	512.5–517.5	0.166
229.885–232.558	492	490	517.5–522.5	0.183
232.558–235.294	589	590	522.5–527.5	0.219
235.294–238.095	692	693	527.5–532.5	0.267
238.095–240.964	799	802	532.5–537.5	0.287
240.964–243.902	905	908	537.5–542.5	0.295
243.902–246.914	995	1001	542.5–547.5	0.319
246.914–250.000	1074	1080	547.5–552.5	0.337
250.000–253.165	1116	1125	552.5–557.5	0.358
253.165–256.410	1136	1148	557.5–562.5	0.398
256.410–259.740	1105	1122	562.5–567.5	0.439
259.740–263.158	1047	1064	567.5–572.5	0.467
263.158–266.667	952	968	572.5–577.5	0.481
266.667–270.270	823	840	577.5–582.5	0.464
270.270–273.973	681	698	582.5–587.5	0.446
273.973–277.778	531	547	587.5–592.5	0.447
277.778–281.690	391	406	592.5–597.5	0.476
281.690–285.714	271	282	597.5–602.5	0.513
285.714–289.855	175	184	602.5–607.5	0.514
289.855–294.118	105	113	607.5–612.5	0.478
294.118–298.507	59.4	65.1	612.5–617.5	0.438
298.507–299.5	40.7	45.2	617.5–622.5	0.406

λ (nm)	10^{20} σ (cm^2 $molecule^{-1}$) 218 K	293–298 K	λ (nm)	10^{20} σ (cm^2 $molecule^{-1}$) 293–298 K
299.5–300.5	35.1	39.2	622.5–627.5	0.382
300.5–301.5	30.5	34.3	627.5–632.5	0.356
301.5–302.5	26.9	30.3	632.5–637.5	0.327
302.5–303.5	22.9	26.2	637.5–642.5	0.297
303.5–304.5	20.6	23.4	642.5–647.5	0.271
304.5–305.5	17.3	20.1	647.5–652.5	0.251
305.5–306.5	15.6	17.9	652.5–657.5	0.231
306.5–307.5	13.3	15.5	657.5–662.5	0.210
307.5–308.5	11.5	13.5	662.5–667.5	0.190
308.5–309.5	10.4	12.2	667.5–672.5	0.170
309.5–310.5	8.50	10.2	672.5–677.5	0.151
310.5–311.5	7.76	9.24	677.5–682.5	0.137
311.5–312.5	6.53	7.95	682.5–687.5	0.126
312.5–313.5	5.62	6.91	687.5–692.5	0.113
313.5–314.5	5.05	6.25	692.5–697.5	0.0989
314.5–315.5	4.08	5.19	697.5–702.5	0.0868
315.5–316.5	3.82	4.77	702.5–707.5	0.0784
316.5–317.5	3.11	4.02	707.5–712.5	0.0731
317.5–318.5	2.94	3.72	712.5–717.5	0.0696
318.5–319.5	2.11	2.89	717.5–722.5	0.0622
319.5–320.5	2.41	2.99	722.5–727.5	0.0543
320.5–321.5	1.43	2.10	727.5–732.5	0.0478
321.5–323.5	1.57	2.05	732.5–737.5	0.0442
323.5–325.5	1.02	1.41	737.5–742.5	0.0432
325.5–327.5	0.658	1.01	742.5–747.5	0.0447
327.5–332.5	0.483	0.697	747.5–752.5	0.0425
332.5–337.5	0.204	0.320	752.5–757.5	0.0338
337.5–342.5	0.0797	0.146	757.5–762.5	0.0286
342.5–347.5		0.0779	762.5–767.5	0.0262
347.5–352.5		0.0306	767.5–772.5	0.0260
352.5–357.5		0.0136	772.5–777.5	0.0294
357.5–362.5		0.00694	777.5–782.5	0.0318
362.5–367.5		0.00305	782.5–787.5	0.0262
367.5–372.5		0.00130	787.5–792.5	0.0208
372.5–377.5		0.000850	792.5–797.5	0.0173
377.5–382.5		0.000572	797.5–802.5	0.0157
382.5–387.5		0.000542	802.5–807.5	0.0156
387.5–392.5		0.000668	807.5–812.5	0.0186
392.5–397.5		0.000956	812.5–817.5	0.0221
397.5–402.5		0.00115	817.5–822.5	0.0206
402.5–407.5		0.00158	822.5–827.5	0.0145
407.5–412.5		0.00258		

Note:
T = 218 K, 196.078–342.5 nm, Reims team (1992-1995) (Daumont et al.,[26] Brion et al.,[18] Malicet et al.[46])
T = 298 K, 185.185–232.558 nm, Molina and Molina[53]
T = 293 K, 232.558–309.5 nm, Burrows et al.[24]
T = 295 K, 309.5–827.5 nm, Reims team (1992-1998) (Daumont et al.,[26] Brion et al.,[18] Malicet et al.,[46] Brion et al.[17]

Photolysis Quantum Yields and Product Studies. The recommendation for the $O(^1D)$ quantum yield from ozone photolysis as a function of wavelength and temperature, based on the review of Matsumi et al.,[48] is given by the expression (Eqn 4-1)

$$\Phi(\lambda,T)=\left(\frac{q_1}{q_1+q_2}\right)\times A_1\times\exp\left\{-\left(\frac{X_1-\lambda}{\omega_1}\right)^4\right\}+\left(\frac{q_2}{q_1+q_2}\right)\times A_2\times\left(\frac{T}{300}\right)^2\times\exp\left\{-\left(\frac{X_2-\lambda}{\omega_2}\right)^2\right\} \quad \text{Eqn 4-1}$$
$$+A_3\times\left(\frac{T}{300}\right)^{1.5}\times\exp\left\{-\left(\frac{X_3-\lambda}{\omega_3}\right)^2\right\}+c$$

where $q_i=\exp\left(-\frac{\nu_i}{RT}\right)$ and $X_{1–3}$, $A_{1–3}$, $\omega_{1–3}$, $\nu_{1–2}$ and c are best-fit parameters given in Table 4A-2-3, λ is in nm, T is in K, and R = 0.695 (cm^{-1} K^{-1}). The parameter c is assumed to be temperature and wavelength independent. This expression is valid only for the wavelength range 306–328 nm and temperature range 200–320 K.

Table 4A-2-3. Parameters for the Calculation of O(^{1}D) Quantum Yields

Parameter	i = 1	i = 2	i = 3
X_i (nm)	304.225	314.957	310.737
ω_i (nm)	5.576	6.601	2.187
A_i	0.8036	8.9061	0.1192
ν_i (cm^{-1})	0	825.518	–
c	0.0765	–	–

At room temperature (298 K) the uncertainties of the quantum yield values calculated with the above expression are estimated to be ±10% (1σ) for Φ(λ, 298 K) ≥0.4, while the uncertainties are estimated to be ±0.04 for Φ(λ, 298 K) <0.4. At temperatures other than room temperature, the uncertainties are estimated to be ±15% for Φ(λ, T) ≥0.4 and ±0.06 for Φ(λ, T) <0.4.

In the wavelength range 329–340 nm the recommended value of Φ(O^{1}D) = 0.08 ± 0.04, independent of temperature. For λ >340 nm, the quantum yield may be non-zero but no recommendation is made. For the wavelength range 220–305 nm, the recommended O(^{1}D) quantum yield is 0.90, independent of temperature, based on the study by Takahashi et al.[69] and the review by Matsumi and Kawasaki.[49] The quantum yield for O(^{1}D) formation in the range 193–225 nm was measured by Nishida et al.[56] who found that the O(^{1}D) yield decreased from 0.90 ± 0.12 (225 nm) to 0.48 ± 0.03 (193 nm). A simple expression in the wavelength range 193–225 nm was derived

$$\Phi_{O(^1D)}(\lambda) = 1.37 \times 10^{-2}\,\lambda - 2.16$$

Matsumi et al.[48] derived the recommended values for the temperature and wavelength dependences of Φ(O^{1}D) using the following procedure: the measured O(^{1}D) quantum yields at 298 K between 306 and 328 nm from eight studies (Talukdar et al.,[73] Takahashi et al.,[70] Ball et al.,[10] Armerding et al.,[6] Bauer et al.,[14] which superseded the data of Silvente et al.[64] from the same group, Brock and Watson,[22] Trolier and Wiesenfeld,[75] and Smith et al.[66] were normalized using Φ(O^{1}D) = 0.79 at 308 nm. This value was derived from the studies listed in Table 1 of Matsumi et al.[48] The renormalized data were then averaged. The wavelength dependence quantum yield data at various temperatures reported by Talukdar et al.,[72,73] Takahashi et al.,[70] Hancock and Hofzumahaus[38] (this includes all the data from the Oxford group), Bauer et al.,[14] and Smith et al.[66] were normalized to the value at 308 nm given above. These normalized data were used to obtain the best fit parameters for Eqn. 4-1 for the wavelength range 306–328 nm and temperature range 200–320 K. Because of the large number of studies upon which the 298 K evaluation is based, the averaged 298 K data were given a larger weight in the fitting procedure than the data at other temperatures. The recommended O(^{1}D) quantum yields calculated from Eqn. 4-1 using the fitting parameters given in Table 4A-2-3 are shown in Figure 4-1 for 200, 253, and 298 K in the wavelength range 306–328 nm (solid lines).

Products and yields from O_3 photodissociation at 157.6 nm were measured by Taherian and Slanger.[68] The primary atomic oxygen yield was measured to be 1.90 ± 0.30, of which 71% is O(^{3}P) and 29% O(^{1}D). Turnipseed et al.[76] measured the quantum yield for O(^{3}P) and O(^{1}D) formation from 193 nm photolysis to be 0.57 ± 0.14 and 0.46 ± 0.29, respectively, and at 222 nm they observed a quantum yield of 0.13 ± 0.02 for O(^{3}P) and 0.87 ± 0.04 for O(^{1}D).

Lee et al.[44] reported an upper limit of <0.1% for the quantum yield for the formation of O(^{1}S) via channel (8) in the 170–240 nm range. Takahashi et al.[71] measured the quantum yield of O(^{1}S) formation to be (2.5 ± 1.1)

$\times 10^{-3}$ in the 193 nm photolysis of O_3, while Nakayama et al.[54] reported $(1.4 \pm 0.4) \times 10^{-4}$ and $(5 \pm 3) \times 10^{-5}$ for the $O(^1S)$ formation at 215 and 220 nm, respectively.

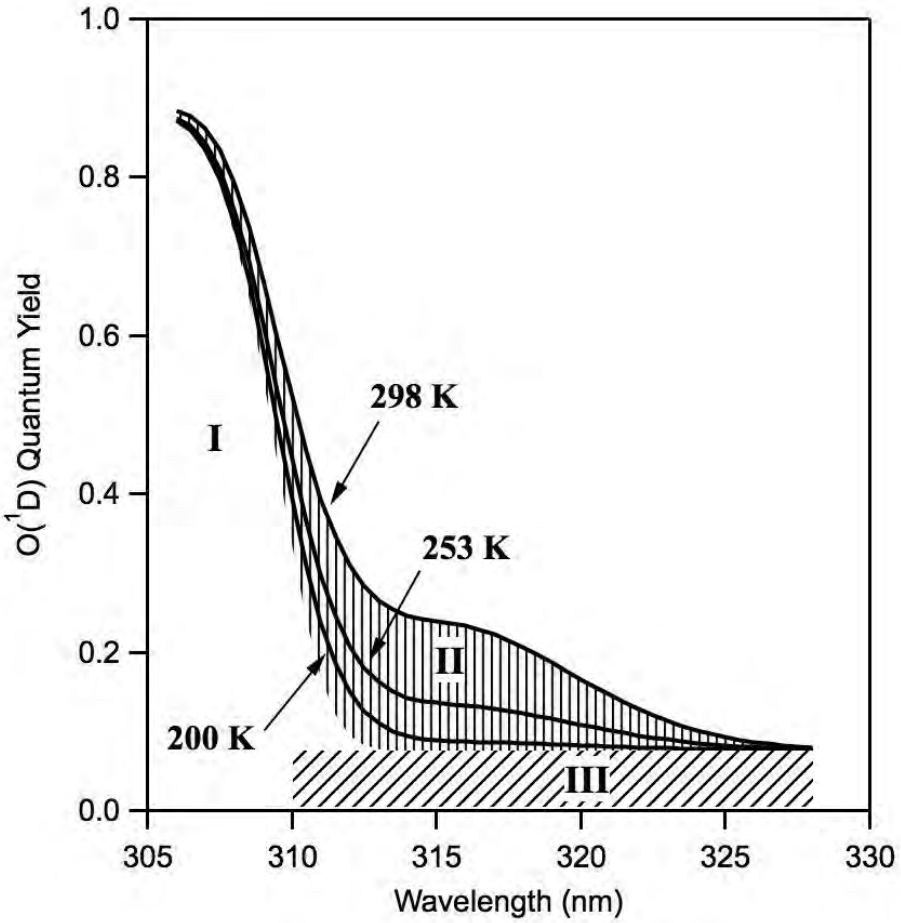


Figure 4A-1. Recommended $O(^1D)$ quantum yields calculated from Eqn. 4-1 using the fitting parameters given in Table 4A-2-3 for 200, 253 and 298 K in the wavelength range 306–328 nm (solid lines), based on Matsumi et al.[48] Contributions from different photolysis channels are indicated: region I corresponds to $O(^1D)$ formed via channel (5), $O(^1D) + O_2(a^1\Delta_g)$, region II (vertical hatching) represents the contribution of the hot-band excitation process via channel (5), while region III (diagonal hatching) corresponds to the contribution of $O(^1D)$ via the spin-forbidden channel (4), $O(^1D) + O_2(X^3\Sigma_g^-)$.

(1) Ackermann, M. In *Mesospheric Models and Related Experiments*; Fiocco, G., Ed., 1971; pp 149-159.

(2) Adler-Golden, S. M. Franck-Condon analysis of thermal and vibrational excitation effects on the ozone Hartley continuum. *J. Quant. Spectrosc. Radiat. Transf.* **1983**, *30*, 175-185, doi:10.1016/0022-4073(83)90099-7.

(3) Amoruso, A.; Cacciani, M.; di Sarra, A.; Fiocco, G. Absorption cross sections of ozone in the 590- to 610-nm region at $T = 230$ K and $T = 299$ K. *J. Geophys. Res.* **1990**, *95*, 20565-20568, doi:10.1029/JD095iD12p20565.

(4) Anderson, M.; Hupalo, P.; Mauersberger, K. Ozone absorption cross section measurements in the Wulf bands. *Geophys. Res. Lett.* **1993**, *20*, 1579-1582, doi:10.1029/93GL01765.

(5) Anderson, S. M.; Mauersberger, K. Laser measurements of ozone absorption cross sections in the Chappuis band. *Geophys. Res. Lett.* **1992**, *19*, 933-936, doi:10.1029/92GL00780.

(6) Armerding, W.; Comes, F. J.; Schulke, B. $O(^1D)$ quantum yields of ozone photolysis in the UV from 300 nm to its threshold at 355 nm. *J. Phys. Chem.* **1995**, *99*, 3137-3143, doi:10.1021/j100010a025.

(7) Astholz, D. C.; Croce, A. E.; Troe, J. Temperature dependence of the ozone absorption coefficient in the Hartley continuum. *J. Phys. Chem.* **1982**, *86*, 696-699, doi:10.1021/j100394a022.

(8) Axson, J. L.; Washenfelder, R. A.; Kahan, T. F.; Young, C. J.; Vaida, V.; Brown, S. S. Absolute ozone absorption cross section in the Huggins Chappuis minimum (350–470 nm) at 296 K. *Atmos. Chem. Phys.* **2011**, *11*, 11581-11590, doi:10.5194/acp-11-11581-2011.
(9) Bacis, A.; Bouvier, J.; Flaud, J. M. The ozone molecule: electronic spectroscopy. *Spectrochim. Acta, Part A* **1998**, *54*, 17-34, doi:10.1016/S1386-1425(97)00259-X.
(10) Ball, S. M.; Hancock, G.; Martin, S. E.; Pinot de Moira, J. C. A direct measurement of the O(^{1}D) quantum yields from the photodissociaiton of ozone between 300 and 328 nm. *Chem. Phys. Lett.* **1997**, *264*, 531-538, doi:10.1016/S0009-2614(96)01363-2.
(11) Ball, S. M.; Hancock, G.; Winterbottom, F. Product channels in the near-UV photodissociation of ozone. *Faraday Discuss.* **1995**, *100*, 215-227, doi:10.1039/FD9950000215.
(12) Barnes, J.; Mauersberger, K. Temperature dependence of the ozone absorption cross section at the 253.7-nm mercury line. *J. Geophys. Res.* **1987**, *92*, 14861-14864, doi:10.1029/JD092iD12p14861.
(13) Bass, A. M.; Paur, R. J. In *Atmospheric Ozone*; Zerefos, C. S., Ghazi, A., Eds., 1985; pp 606-610.
(14) Bauer, D.; D'Ottone, L.; Hynes, A. J. O ^{1}D quantum yields from O_3 photolysis in the near UV region between 305 and 375 nm. *Phys. Chem. Chem. Phys.* **2000**, *2*, 1421-1424, doi:10.1039/b000159g.
(15) Bogumil, K.; Orphal, J.; Burrows, J. P.; Flaud, J.-M. Vibrational progressions in the visible and near-ultraviolet absorption spectrum of ozone. *Chem. Phys. Lett.* **2001**, *349*, 241-248, doi:10.1016/S0009-2614(01)01191-5.
(16) Bogumil, K.; Orphal, J.; Homann, T.; Voigt, S.; Spietz, P.; Fleischmann, O. C.; Vogel, A.; Hartmann, M.; Kromminga, H.; Bovensmann, H.; et al. Measurements of molecular absorption spectra with the SCIAMACHY pre-flight model: instrument characterization and reference data for atmospheric remote-sensing in the 230-2380 nm region. *J. Photochem. Photobiol. A: Chem.* **2003**, *157*, 167-184, doi:10.1016/S1010-6030(03)00062-5.
(17) Brion, J.; Chakir, A.; Charbonnier, J.; Daumont, D.; Parisse, C.; Malicet, J. Absorption spectra measurements for the ozone molecule in the 350-830 nm region. *J. Atmos. Chem.* **1998**, *30*, 291-299, doi:10.1023/A:1006036924364.
(18) Brion, J.; Chakir, A.; Daumont, D.; Malicet, J.; Parisse, C. High-resolution laboratory absorption cross section of O_3 temperature effect. *Chem. Phys. Lett.* **1993**, *213*, 610-612, doi:10.1016/0009-2614(93)89169-I.
(19) Brion, J.; Daumont, D.; Malicet, J. Physique moléculaire - Nouvelles mesures des sections efficaces absolues de l'ozone à 294 et 223 K dans le domaine spectral 310-350 nm. *C. R. Acad. Sci. Paris* **1983**, *297*, 401-404, doi:10.1051/jphyslet:0198400450205700.
(20) Brion, J.; Daumont, D.; Malicet, J. New measurements of the absolute absorption cross-sections of ozone at 294 and 223 K in the 310-350 nm spectral range. *J. Physique. Lett.* **1984**, *45*, 57-60, doi:10.1051/jphyslet:0198400450205700.
(21) Brion, J.; Daumont, D.; Malicet, J.; Marché, P. Sections efficaces absolues de l'ozone a 298 K aux longueurs d'onde de la lampe au mercure : etude critique des donnees experimentales existantes. *J. Physique. Lett.* **1985**, *46*, 105-110, doi:10.1051/jphyslet:01985004603010500.
(22) Brock, J. C.; Watson, R. T. Laser flash photolysis of ozone: O(^{1}D) quantum yields in the fall-off region 297-325 nm. *Chem. Phys.* **1980**, *46*, 477-484, doi:10.1016/0301-0104(80)85223-2.
(23) Burkholder, J. B.; Talukdar, R. K. Temperature dependence of the ozone absorption spectrum over the wavelength range 410 to 760 nm. *Geophys. Res. Lett.* **1994**, *21*, 581-584, doi:10.1029/93GL02311.
(24) Burrows, J. P.; Richter, A.; Dehn, A.; Deters, B.; Himmelmann, S.; Voigt, S.; Orphal, J. Atmospheric remote-sensing reference data from GOME-2. Temperature-dependent absorption cross sections of O_3 in the 231-794 nm range. *J. Quant. Spectrosc. Radiat. Transf.* **1999**, *61*, 509-517, doi:10.1016/S0022-4073(98)00037-5.
(25) Cacciani, M.; di Sarra, A. D.; Fiocco, G.; Amoruso, A. Absolute determination of the cross sections of ozone in the wavelength region 339-355 nm at temperatures 220-293 K. *J. Geophys. Res.* **1989**, *94*, 8485-8490, doi:10.1029/JD094iD06p08485.
(26) Daumont, D.; Brion, J.; Charbonnier, J.; Malicet, J. Ozone UV spectroscopy I: Absorption cross-sections at room temperature. *J. Atmos. Chem.* **1992**, *15*, 145-155, doi:10.1007/BF00053756.
(27) Daumont, D.; Brion, J.; Malicet, J. Measurement of total atmospheric ozone - Consequences entailed by new values of O_3 absorption cross-sections at 223-K in the 310-350 nm spectral range. *Planet. Space Sci.* **1983**, *31*, 1229-1234, doi:10.1016/0032-0633(83)90114-9.
(28) Davenport, J. E. Parameter for ozone photolysis as a function of temperature at 280 - 330 nm. *National Technical Information Service, Report FAA-EE-80-44.* **1982**.
(29) DeMore, W. B.; Raper, O. Hartley band extinction coefficients of ozone in the gas phase and in liquid nitrogen, carbon monoxide, and argon. *J. Phys. Chem.* **1964**, *68*, 412-414, doi:10.1021/j100784a504.
(30) Denzer, W.; Hancock, G.; Pinot de Moira, J. C.; Tyley, P. L. Spin-forbidden dissociation of ozone in the Huggins bands. *Chem. Phys.* **1998**, *231*, 109-119, doi:10.1016/S0301-0104(97)00328-5.

(31) El Helou, Z.; Churassy, S.; Wannous, G.; Bacis, R.; Boursey, E. Absolute cross sections of ozone at atmospheric temperatures for the Wulf and the Chappuis bands. *J. Chem. Phys.* **2005**, *122*, 244311, doi:10.1063/1.193736.
(32) Enami, S.; Ueda, J.; Nakano, Y.; Hashimoto, S.; Kawasaki, M. Temperature-dependent absorption cross sections of ozone in the Wulf-Chappuis band at 759-768 nm. *J. Geophys. Res.* **2004**, *109*, D05309, doi:10.1029/2003JD004097.
(33) Freeman, D. E.; Yoshino, K.; Esmond, J. R.; Parkinson, W. H. High-resolution absorption cross-section measurements of ozone at 195-K in the wavelength region 240-350 nm. *Planet. Space Sci.* **1984**, *32*, 239-248, doi:10.1016/0032-0633(84)90158-2.
(34) Freeman, D. E.; Yoshino, K.; Esmond, J. R.; Parkinson, W. H. In *Atmospheric Ozone*; Zerefos, C. S., Ghazi, A., Eds., 1985; pp 622-624.
(35) Fuchs, H.; Dubé, W. P.; Lerner, B. M.; Wagner, N. L.; Williams, E. J.; Brown, S. S. A sensitive and versatile detector for atmospheric NO_2 and NO_x based on blue diode laser cavity ring-down spectroscopy. *Environ. Sci. Technol.* **2009**, *43*, 7831-7836, doi:10/1021/es902067h.
(36) Gorshelev, V.; Serdyuchenko, A.; Weber, M.; Chehade, W.; Burrows, J. P. High spectral resolution ozone absorption cross-sections – Part 1: Measurements, data analysis and comparison with previous measurements around 293 K. *Atmos. Meas. Tech.* **2014**, *7*, 609-624, doi:10/5194/amt-7-609-2014.
(37) Griggs, M. Absorption coefficients of ozone in the ultraviolet and visible regions. *J. Chem. Phys.* **1968**, *49*, 857-859, doi:10.1063/1.1670152.
(38) Hancock, G.; Hofzumahaus, A. Experimental Study of the Altitude Dependence of the Tropospheric Ozone Photolysis Frequency, J($O(^1D)$) Between 0 and 12 km Height (ATOP), EU R and D Programme Environment and Climate ENV4-CT95-0158, 1997,
(39) Hearn, A. G. Absorption of ozone in ultra-violet and visible regions of spectrum. *Proc. Phys. Soc. London* **1961**, *78*, 932-940, doi:10.1088/0370-1328/78/5/340.
(40) Hudson, R. D. Absorption cross sections of stratospheric molecules. *Can. J. Phys.* **1974**, *52*, 1465-1478, doi:10.1139/v74-218.
(41) Inn, E. C. Y.; Tanaka, Y. Absorption coefficient of ozone in the ultraviolet and visible regions. *J. Opt. Soc. Am.* **1953**, *43*, 870-873, doi:10.1364/JOSA.43.000870.
(42) Inn, E. C. Y.; Tanaka, Y. *Adv. Chem. Ser.* **1958**, *21*, 263-268, doi:10.1021/ba-1959-0021.ch037.
(43) Inn, E. C. Y.; Tanaka, Y. Ozone absorption coefficients in the visible and ultraviolet regions. *Adv. Chem. Ser.* **1959**, *21*, 263-268, doi:10.1021/ba-1959-0021.ch037.
(44) Lee, L. C.; Black, G.; Sharpless, R. L.; Slanger, T. G. $O(^1S)$ yield from O_3 photodissociation at 1700-2400 Å. *J. Chem. Phys.* **1980**, *73*, 256-258, doi:10.1063/1.439925.
(45) Malicet, J.; Brion, J.; Daumont, D. Temperature dependence of the absorption cross-section of ozone at 254 nm. *Chem. Phys. Lett.* **1989**, *158*, 293-296, doi:10.1016/0009-2614(89)87338-5.
(46) Malicet, J.; Daumont, D.; Charbonnier, J.; Parisse, C.; Chakir, A.; Brion, J. Ozone UV spectroscopy. II. Absorption cross-sections and temperature dependence. *J. Atmos. Chem.* **1995**, *21*, 263-273, doi:10.1007/BF00696758.
(47) Mason, N. J.; Gingell, J. M.; Davies, J. A.; Zhao, H.; Walker, I. C.; Siggel, M. R. F. VUV optical absorption and electron energy-loss spectroscopy of ozone. *J. Phys. B: At. Mol. Phys.* **1996**, *29*, 3075-3089, doi:10.1088/0953-4075/29/14/019.
(48) Matsumi, Y.; Comes, F. J.; Hancock, G.; Hofzumahaus, A.; Hynes, A. J.; Kawasaki, M.; Ravishankara, A. R. Quantum yields for production of $O(^1D)$ in the ultraviolet photolysis of ozone: Recommendation based on evaluation of laboratory data. *J. Geophys. Res.* **2002**, *107*, 4024, doi:10.1029/2001JD000510.
(49) Matsumi, Y.; Kawasaki, M. Photolysis of atmospheric ozone in the ultraviolet region. *Chem. Rev.* **2003**, *103*, 4767-4781, doi:10.1021/cr0205255.
(50) Mauersberger, K.; Barnes, J.; Hanson, D.; Morton, J. Measurement of the ozone absorption cross-section at the 253.7 nm mercury line. *Geophys. Res. Lett.* **1986**, *13*, 671-673, doi:10.1029/GL013i007p00671.
(51) Mauersberger, K.; Hanson, D.; Barnes, J.; Morton, J. Ozone vapor pressure and absorption cross-section measurements: Introduction of an ozone standard. *J. Geophys. Res.* **1987**, *92*, 8480-8482, doi:10.1029/JD092iD07p08480.
(52) McPeters, R. D.; Bass, A. M. Anomalous atmospheric spectral features between 300 and 310 nm interpreted in light of new ozone absorption coefficient measurements. *Geophys. Res. Lett.* **1982**, *9*, 227-230, doi:10.1029/GL009i003p00227.
(53) Molina, L. T.; Molina, M. J. Absolute absorption cross sections of ozone in the 185- to 350-nm wavelength range. *J. Geophys. Res.* **1986**, *91*, 14501-14508, doi:10.1029/JD091iD13p14501.

(54) Nakayama, T.; Takahashi, K.; Matsumi, Y.; Fujiwara, H. Laboratory study of $O(^1S)$ formation in the photolysis of O_3 and its atmospheric implications. *J. Atmos. Chem.* **2006**, *53*, 107-122, doi:10.1007/s10874-006-0597-3.
(55) Nicolet, M. The solar spectral irradiance and its action in the atmospheric photo-dissociation processes. *Planet. Space Sci.* **1981**, *29*, 951-974, doi:10.1016/0032-0633(81)90056-8.
(56) Nishida, S.; Taketani, F.; Takahashi, K.; Matsumi, Y. Quantum yield for $O(^1D)$ production from ozone photolysis in the wavelength range of 193-225 nm. *J. Phys. Chem. A* **2004**, *108*, 2710-2714, doi:10.1021/jp049979r.
(57) Ny, T.-Z.; Choong, S.-P. Sur l'absorption ultraviolette de l'ozone. *Chinese J. Phys.* **1933**, *1*, 38-54.
(58) Ogawa, M.; Cook, G. R. Absorption coefficients of O_3 in the vacuum ultraviolet region. *J. Chem. Phys.* **1958**, *28*, 173-174, doi:10.1063/1.1744071.
(59) Orphal, J. A Critical Review of the Absorption Cross-Sections of O_3 and NO_2 in the 240-790 nm Region, Part 1, Ozone, European Space Agency, ESA-ESTEC Noordwijk, ESA Technical Note MO-TN-ESA-GO-0302, 2002,
(60) Orphal, J. A critical review of the absorption cross-sections of O_3 and NO_2 in the ultraviolet and visible. *J. Photochem. Photobiol. A: Chem.* **2003**, *157*, 185-209, doi:10.1016/S1010-6030(03)00061-3.
(61) Paur, R. J.; Bass, A. M. In *Atmospheric Ozone*; Zerefos, C. S., Ghazi, A., Eds., 1985; pp 610-616.
(62) Petersen, M.; Viallon, J.; Moussay, P.; Wielgosz, R. I. Relative measurements of ozone absorption cross-sections at three wavelengths in the Hartley band using a well-defined UV laser beam. *J. Geophys. Res.* **2012**, *117*, D05301, doi:10.1029/2011jd016374.
(63) Serdyuchenko, A.; Gorshelev, V.; Weber, M.; Chehade, W.; Burrows, J. P. High spectral resolution ozone absorption cross-sections – Part 2: Temperature dependence. *Atmos. Meas. Tech.* **2014**, *7*, 625-636, doi:10.5194/amt-7-625-2014.
(64) Silvente, E.; Richter, R. C.; Zheng, M.; Saltzman, E. S.; Hynes, A. J. Relative quantum yields for $O(^1D)$ production in the photolysis of ozone between 301 and 336 nm: evidence for the participation of a spin-forbidden channel. *Chem. Phys. Lett.* **1997**, *264*, 309-315, doi:10.1016/S0009-2614(96)01342-5.
(65) Simons, J. W.; Paur, R. J.; Webster III, H. A.; Bair, E. J. Ozone ultraviolet photolysis. VI. The ultraviolet spectrum. *J. Chem. Phys.* **1973**, *59*, 1203-1208, doi:10.1063/1.1680169.
(66) Smith, G. D.; Molina, L. T.; Molina, M. J. Temperature dependence of $O(^1D)$ quantum yields from the photolysis of ozone between 295 and 338 nm. *J. Phys. Chem. A* **2000**, *104*, 8916-8921, doi:10.1021/jp001006d.
(67) Steinfeld, J. I.; Adler-Golden, S. M.; Gallagher, J. W. Critical survey of data on the spectroscopy and kinetics of ozone in the mesosphere and thermosphere. *J. Phys. Chem. Ref. Data* **1987**, *16*, 911-951, doi:10.1063/1.555796.
(68) Taherian, M. R.; Slanger, T. G. Products and yields from O_3 photodissociation at 1576 Å. *J. Chem. Phys.* **1985**, *83*, 6246-6250, doi:10.1063/1.449573.
(69) Takahashi, K.; Hayashi, S.; Matsumi, Y.; Taniguchi, N.; Hayashida, S. Quantum yields of (O^1D) formation in the photolysis of ozone between 230 and 308 nm. *J. Geophys. Res.* **2002**, *107*, 4440, doi:10.1029/2001JD002048.
(70) Takahashi, K.; Matsumi, Y.; Kawasaki, M. Photodissociation processs of ozone in the Huggins band at 308-326 nm: Direct observation of $O(^1D_2)$ and $O(^3P_j)$ products. *J. Phys. Chem.* **1996**, *100*, 4084-4089, doi:10.1021/jp9528065.
(71) Takahashi, T.; Nakayama, T.; Matsumi, Y. Vacuum ultraviolet laser-induced fluorescence detection of $O(^1S)$ atoms produced in the 193 nm photolysis of ozone. *J. Phys. Chem. A* **2003**, *107*, 9368-9373, doi:10.1021/jp0346864.
(72) Talukdar, R. K.; Gilles, M. K.; Battin-Leclerc, F.; Ravishankara, A. R.; Fracheboud, J.-M.; Orlando, J. J.; Tyndall, G. S. Photolysis of ozone at 308 and 248 nm: Quantum yield of $O(^1D)$ as a function of temperature. *Geophys. Res. Lett.* **1997**, *24*, 1091-1094, doi:10.1029/97GL00831.
(73) Talukdar, R. K.; Longfellow, C. A.; Gilles, M. K.; Ravishankara, A. R. Quantum yields of $O(^1D)$ in the photolysis of ozone between 289 and 329 nm as a function of temperature. *Geophys. Res. lett.* **1998**, *25*, 143-146, doi:10.1029/97GL03354.
(74) Tanaka, Y.; Inn, E. C. Y.; Watanabe, K. Absorption coefficients of gases in the vacuum ultraviolet. Part IV. Ozone. *J. Chem. Phys.* **1953**, *21*, 1651-1653, doi:10.1063/1.1698638.
(75) Trolier, M.; Wiesenfeld, J. R. Relative quantum yield of $O(^1D_2)$ following ozone photlysis between 275 and 325 nm. *J. Geophys. Res.* **1988**, *93*, 7119-7124, doi:10.1029/JD093iD06p07119.
(76) Turnipseed, A. A.; Vaghjiani, G. L.; Gierczak, T.; Thompson, J. E.; Ravishankara, A. R. The photochemistry of ozone at 193 and 222 nm. *J. Chem. Phys.* **1991**, *95*, 3244-3251, doi:10.1063/1.460881.
(77) Vassy, A.; Vassy, E. Effect of temperature on the absorption spectrum of ozone: Chappuis Bands. *J. Chem. Phys.* **1948**, *16*, 1163-1164, doi:10.1063/1.1746754.

(78) Viallon, J.; Lee, S.; Moussay, P.; Tworek, K.; Petersen, M.; Wielgosz, R. I. Accurate measurements of ozone absorption cross-sections in the Hartley band. *Atmos. Meas. Tech.* **2015**, *8*, 1245-1257, doi:10.5194/amt-8-1245-2015.
(79) Vigroux, E. Contribution a l'étude expérimentale de l'absorption de l'ozone. *Ann. Phys.* **1953**, *8*, 709-762.
(80) Vigroux, E. Physique de l'atmosphére. - Détermination des coefficients moyens d'absorption de l'ozone pour le spectrometre Dobson. *C. R. Acad. Sci. Paris* **1967**, *264*, 1290-1291.
(81) Vigroux, E. Coefficients d'absorption de l;ozone dans la bande de Hartley. *Ann. Geophys.* **1969**, *25*, 169-172.
(82) Voigt, S.; Orphal, J.; Bogumil, K.; Burrows, J. P. The temperature dependence (203-293 K) of the absorption cross sections of O_3 in the 230-850 nm region measured by Fourier-transform spectroscopy. *J. Photochem. Photobiol. A: Chem.* **2001**, *143*, 1-9, doi:10.1016/S1010-6030(01)00480-4.
(83) WMO *Atmospheric Ozone: 1985*; National Aeronautics and Space Administration: Geneva, Report No. 16, Chapter 7, 1986.
(84) Yoshino, K.; Esmond, J. R.; Freeman, D. E.; Parkinson, W. H. Measurements of absolute absorption cross sections of ozone in the 185- to 254-nm wavelength region and the temperature dependence. *J. Geophys. Res.* **1993**, *98*, 5205-5211, doi:10.1029/93JD00028.
(85) Yoshino, K.; Freeman, D. E.; Esmond, J. R.; Parkinson, W. H. Absolute absorption cross-section measurements of ozone in the wavelength region 238-335 nm and the temperature-dependence. *Planet. Space Sci.* **1988**, *36*, 395-398, doi:10.1016/0032-0633(88)90127-4.

4.4 Bibliography – O_x Photochemistry

Aboud, A. A.; Curtis, J. P.; Mercure, R.; Rense, W. A. Oxygen gas continuous absorption in the extreme ultraviolet *J. Opt. Soc. Am.* **1955**, *45*, 767-768, doi:10.1364/JOSA.45.000767.

Ackerman, M. UV-solar radiation related to mesospheric processes. In *Mesospheric Models and Related Experiments*; Fiocco, G., Ed.; D. Reidel Publishing Company, Dordrecht, 1971; pp 149-159.

Ackerman, M.; Biaumé, F.; Kockarts, B. Absorption cross sections of the Schumann-Runge bands of molecular oxygen. *Planet. Space Sci.* **1970**, *18*, 1639-1651, doi:10.1016/0032-0633(70)90038-3.

Ackerman, M.; Biaumé, F.; Nicolet, M. Absorption in the spectral range of the Schumann-Runge bands. *Can. J. Chem.* **1969**, *47*, 1834-1940, doi:10.1139/v69-299.

Ackermann, M. In *Mesospheric Models and Related Experiments*; Fiocco, G., Ed., 1971; pp 149-159.

Adler-Golden, S. M. Franck-Condon analysis of thermal and vibrational excitation effects on the ozone Hartley continuum. *J. Quant. Spectrosc. Radiat. Transf.* **1983**, *30*, 175-185, doi:10.1016/0022-4073(83)90099-7.

Ahmed, S. M.; Kanik, I.; Link, R. Temperature-dependent photoabsorption cross section measurements of O_2 at the O I-1304 Å triplet emission lines. *Chem. Phys. Lett.* **1996**, *259*, 545-553, doi:10.1016/0009-2614(96)00783-X.

Amoruso, A.; Cacciani, M.; di Sarra, A.; Fiocco, G. Absorption cross sections of ozone in the 590- to 610-nm region at $T = 230$ K and $T = 299$ K. *J. Geophys. Res.* **1990**, *95*, 20565-20568, doi:10.1029/JD095iD12p20565.

Amoruso, A.; Crescentini, L.; Silvia Cola, M.; Fiocco, G. Oxygen absorption cross-section in the Herzberg continuum. *J. Quant. Spectrosc. Radiat. Transf.* **1996**, *56*, 145-152, doi:10.1016/0022-4073(96)00012-X.

Anderson, G. P.; Hall, L. A. Attenuation of solar irradiance in the stratosphere: Spectrometer measurements between 191 and 207 nm. *J. Geophys. Res.* **1983**, *88*, 6801-6806, doi:10.1029/JC088iC11p06801.

Anderson, G. P.; Hall, L. A. Stratospheric determination of O_2 cross sections and photodissociation rate coefficients: 191-215 nm. *J. Geophys. Res.* **1986**, *91*, 14509-14514, doi:10.1029/JD091iD13p14509.

Anderson, M.; Hupalo, P.; Mauersberger, K. Ozone absorption cross section measurements in the Wulf bands. *Geophys. Res. Lett.* **1993**, *20*, 1579-1582, doi:10.1029/93GL01765.

Anderson, S. M.; Mauersberger, K. Laser measurements of ozone absorption cross sections in the Chappuis band. *Geophys. Res. Lett.* **1992**, *19*, 933-936, doi:10.1029/92GL00780.

Armerding, W.; Comes, F. J.; Schulke, B. O(^{1}D) quantum yields of ozone photolysis in the UV from 300 nm to its threshold at 355 nm. *J. Phys. Chem.* **1995**, *99*, 3137-3143, doi:10.1021/j100010a025.

Astholz, D. C.; Croce, A. E.; Troe, J. Temperature dependence of the ozone absorption coefficient in the Hartley continuum. *J. Phys. Chem.* **1982**, *86*, 696-699, doi:10.1021/j100394a022.

Axson, J. L.; Washenfelder, R. A.; Kahan, T. F.; Young, C. J.; Vaida, V.; Brown, S. S. Absolute ozone absorption cross section in the Huggins Chappuis minimum (350–470 nm) at 296 K. *Atmos. Chem. Phys.* **2011**, *11*, 11581-11590, doi:10.5194/acp-11-11581-2011.

Bacis, A.; Bouvier, J.; Flaud, J. M. The ozone molecule: electronic spectroscopy. *Spectrochim. Acta, Part A* **1998**, *54*, 17-34, doi:10.1016/S1386-1425(97)00259-X.

Ball, S. M.; Hancock, G.; Martin, S. E.; Pinot de Moira, J. C. A direct measurement of the O(^{1}D) quantum yields from the photodissociaiton of ozone between 300 and 328 nm. *Chem. Phys. Lett.* **1997**, *264*, 531-538, doi:10.1016/S0009-2614(96)01363-2.

Ball, S. M.; Hancock, G.; Winterbottom, F. Product channels in the near-UV photodissociation of ozone. *Faraday Discuss.* **1995**, *100*, 215-227, doi:10.1039/FD9950000215.

Bao, Z.-C.; Yu, W. O.; Barker, J. R. Absolute integrated cross sections for some O_2 Herzberg I transitions near 248-249 nm. *J. Chem. Phys.* **1995**, *103*, 6-13, doi:10.1063/1.469624.

Barnes, J.; Mauersberger, K. Temperature dependence of the ozone absorption cross section at the 253.7-nm mercury line. *J. Geophys. Res.* **1987**, *92*, 14861-14864, doi:10.1029/JD092iD12p14861.

Bass, A. M.; Paur, R. J. In *Atmospheric Ozone*; Zerefos, C. S., Ghazi, A., Eds., 1985; pp 606-610.

Bauer, D.; D'Ottone, L.; Hynes, A. J. O ^{1}D quantum yields from O_3 photolysis in the near UV region between 305 and 375 nm. *Phys. Chem. Chem. Phys.* **2000**, *2*, 1421-1424, doi:10.1039/b000159g.

Bennett, S. W.; Tellinghuisen, J. B.; Phillips, L. F. Absorption coefficients and ionization yields of some small molecules at 58.4 nm. *J. Phys. Chem.* **1971**, *75*, 719-721, doi:10.1021/j100675a019.

Bertrand, C.; Collin, G. J.; Gagnon, H. Coefficients d'absorption et rendements quantiques ioniques de composés inorganiques et d'hydrocarbones insaturés. *J. Chim. Phys.* **1975**, *72*, 719-723, doi:10.1051/jcp/1975720719.

Blake, A. J.; Carver, J. H.; Haddad, G. N. Photo-absorption cross sections of molecular oxygen between 1250 Å and 2350 Å. *J. Quant. Spectrosc. Radiat. Transf.* **1966**, *6*, 451-459, doi:10.1016/0022-4073(66)90010-0.

Bogumil, K.; Orphal, J.; Burrows, J. P.; Flaud, J.-M. Vibrational progressions in the visible and near-ultraviolet absorption spectrum of ozone. *Chem. Phys. Lett.* **2001**, *349*, 241-248, doi:10.1016/S0009-2614(01)01191-5.

Bogumil, K.; Orphal, J.; Homann, T.; Voigt, S.; Spietz, P.; Fleischmann, O. C.; Vogel, A.; Hartmann, M.; Kromminga, H.; Bovensmann, H.; Frerick, J.; Burrows, J. P. Measurements of molecular absorption

spectra with the SCIAMACHY pre-flight model: instrument characterization and reference data for atmospheric remote sensing in the 230-2380 nm region. *J. Photochem. Photobiol. A: Chem.* **2003**, *157*, 167-184, doi:10.1016/S1010-6030(03)00062-5.

Bogumil, K.; Orphal, J.; Homann, T.; Voigt, S.; Spietz, P.; Fleischmann, O. C.; Vogel, A.; Hartmann, M.; Kromminga, H.; Bovensmann, H.; Frerick, J.; Burrows, J. P. Measurements of molecular absorption spectra with the SCIAMACHY pre-flight model: instrument characterization and reference data for atmospheric remote-sensing in the 230-2380 nm region. *J. Photochem. Photobiol. A: Chem.* **2003**, *157*, 167-184, doi:10.1016/S1010-6030(03)00062-5.

Brion, C. E.; Tan, K. H.; van der Wiel, M. J.; van der Leeuw, P. E. Dipole oscillator-strengths for the photoabsorption, photoionization and fragmentation of molecular oxygen. *J. Electron Spectrosc. Relat. Phenom.* **1979**, *17*, 101-119, doi:10.1016/0368-2048(79)85032-X.

Brion, J.; Chakir, A.; Charbonnier, J.; Daumont, D.; Parisse, C.; Malicet, J. Absorption spectra measurements for the ozone molecule in the 350-830 nm region. *J. Atmos. Chem.* **1998**, *30*, 291-299, doi:10.1023/A:1006036924364.

Brion, J.; Chakir, A.; Daumont, D.; Malicet, J.; Parisse, C. High-resolution laboratory absorption cross section of O_3 temperature effect. *Chem. Phys. Lett.* **1993**, *213*, 610-612, doi:10.1016/0009-2614(93)89169-I.

Brion, J.; Daumont, D.; Malicet, J. Physique moléculaire - Nouvelles mesures des sections efficaces absolues de l'ozone à 294 et 223 K dans le domaine spectral 310-350 nm. *C. R. Acad. Sci. Paris* **1983**, *297*, 401-404, doi:10.1051/jphyslet:0198400450205700.

Brion, J.; Daumont, D.; Malicet, J. New measurements of the absolute absorption cross-sections of ozone at 294 and 223 K in the 310-350 nm spectral range. *J. Physique. Lett.* **1984**, *45*, 57-60, doi:10.1051/jphyslet:0198400450205700.

Brion, J.; Daumont, D.; Malicet, J.; Marché, P. Sections efficaces absolues de l'ozone a 298 K aux longueurs d'onde de la lampe au mercure : etude critique des donnees experimentales existantes. *J. Physique. Lett.* **1985**, *46*, 105-110, doi:10.1051/jphyslet:01985004603010500.

Brock, J. C.; Watson, R. T. Laser flash photolysis of ozone: $O(^1D)$ quantum yields in the fall-off region 297-325 nm. *Chem. Phys.* **1980**, *46*, 477-484, doi:10.1016/0301-0104(80)85223-2.

Brolley, J. E.; Porter, L. E.; Sherman, R. H.; Theobald, J. K.; Fong, J. C. Photoabsorption cross sections of H_2, D_2, N_2, O_2, Ar, Kr, and Xe at the 584-Å line of neutral Helium. *J. Geophys. Res.* **1973**, *78*, 1627-1632, doi:10.1029/JA078i010p01627.

Burkholder, J. B.; Talukdar, R. K. Temperature dependence of the ozone absorption spectrum over the wavelength range 410 to 760 nm. *Geophys. Res. Lett.* **1994**, *21*, 581-584, doi:10.1029/93GL02311.

Burrows, J. P.; Richter, A.; Dehn, A.; Deters, B.; Himmelmann, S.; Voigt, S.; Orphal, J. Atmospheric remote-sensing reference data from GOME-2. Temperature-dependent absorption cross sections of O_3 in the 231-794 nm range. *J. Quant. Spectrosc. Radiat. Transf.* **1999**, *61*, 509-517, doi:10.1016/S0022-4073(98)00037-5.

Cacciani, M.; di Sarra, A. D.; Fiocco, G.; Amoruso, A. Absolute determination of the cross sections of ozone in the wavelength region 339-355 nm at temperatures 220-293 K. *J. Geophys. Res.* **1989**, *94*, 8485-8490, doi:10.1029/JD094iD06p08485.

Cheung, A. S. C.; Yoshino, K.; Esmond, J. R.; Chiu, S. S. L.; Freeman, D. E.; Parkinson, W. H. Predissociation linewidths of the (1,0)-(12,0) Schumann-Runge absorption bands of O_2 in the wavelength region 179-202 nm. *J. Chem. Phys.* **1990**, *92*, 842-849, doi:10.1063/1.458117.

Cheung, A. S. C.; Yoshino, K.; Freeman, D. E.; Friedman, R. S.; Dalgarno, A.; Parkinson, W. H. The Schumann-Runge absorption bands of $^{16}O^{18}O$ in the wavelength region 175-205 nm and spectroscopic constants of isotopic oxygen molecules. *J. Mol. Spectrosc.* **1989**, *134*, 362-389, doi:10.1016/0022-2852(89)90323-8.

Cheung, A. S. C.; Yoshino, K.; Parkinson, W. H.; Freeman, D. E. Herzberg continuum cross section of oxygen in the wavelength region 193.5 – 204.0 nm and band oscillator strengths of the (0,0) and (1,0) Schumann-Runge bands *Can. J. Phys.* **1984**, *62*, 1752-1762, doi:10.1139/p84-221.

Cheung, A. S. C.; Yoshino, K.; Parkinson, W. H.; Freeman, D. E. Herzberg continuum cross section of oxygen in the wavelength region 193.5-204.0 nm: New laboratory measurements and stratospheric implications. *Geophys. Res. Lett.* **1984**, *11*, 580-582, doi:10.1029/GL011i006p00580.

Cheung, A. S. C.; Yoshino, K.; Parkinson, W. H.; Guberman, S. L.; Freeman, D. E. Absorption cross-section measurements of oxygen in the wavelength region 195-241 nm of the Herzberg continuum. *Planet. Space Sci.* **1986**, *34*, 1007-1021, doi:10.1016/0032-0633(86)90011-5.

Chiu, S. S. L.; Cheung, A. S. C.; Yoshino, K.; Esmond, J. R.; Freeman, D. E.; Parkinson, W. H. Predissociation linewidths of the (3,0)-(11,0) Schumann-Runge absorption bands of $^{18}O_2$ and $^{16}O^{18}O$ in the wavelength region 180-196 nm. *J. Chem. Phys.* **1990**, *93*, 5539-5543, doi:10.1063/1.459623.

Clark, K. C. Ionospheric absorption by N_2 and O_2 of certain extreme ultraviolet solar wavelengths. *Phys. Rev.* **1952**, *87*, 271-276, doi:10.1103/PhysRev.87.271.

Cole, B. E.; Dexter, R. N. Photoabsorption and photoionisation measurements on some atmospheric gases in the wavelength region 50-340 Å. *J. Phys. B: At. Mol. Phys.* **1978**, *11*, 1011-1023, doi:10.1088/0022-3700/11/6/013.

Cook, G. R.; Ching, B. K.; Becker, R. A. Absorption by, and photo-ionization of, N_2 and O_2 in the 830-1000 Å range. *Discuss. Faraday Soc.* **1964**, *37*, 149-158, doi:10.1039/DF9643700149.

Cook, G. R.; Metzger, P. H. Photoionization and absorption cross sections of O_2 and N_2 in the 600- to 1000-Å region. *J. Chem. Phys.* **1964**, *41*, 321-336, doi:10.1063/1.1725870.

Coquart, B.; Merienne, M. F.; Jenouvrier, A. O_2 Herzberg continuum absorption cross-sections in the wavelength region 196-205 nm of the Schumann-Runge bands. *Planet. Space Sci.* **1990**, *38*, 287-300, doi:10.1016/0032-0633(90)90093-6.

Daumont, D.; Brion, J.; Charbonnier, J.; Malicet, J. Ozone UV spectroscopy I: Absorption cross-sections at room temperature. *J. Atmos. Chem.* **1992**, *15*, 145-155, doi:10.1007/BF00053756.

Daumont, D.; Brion, J.; Malicet, J. Measurement of total atmospheric ozone - Consequences entailed by new values of O_3 absorption cross-sections at 223-K in the 310-350 nm spectral range. *Planet. Space Sci.* **1983**, *31*, 1229-1234, doi:10.1016/0032-0633(83)90114-9.

Davenport, J. E. Parameter for ozone photolysis as a function of temperature at 280 - 330 nm. *National Technical Information Service, Report FAA-EE-80-44.* **1982**.

DeMore, W. B.; Raper, O. Hartley band extinction coefficients of ozone in the gas phase and in liquid nitrogen, carbon monoxide, and argon. *J. Phys. Chem.* **1964**, *68*, 412-414, doi:10.1021/j100784a504.

Denzer, W.; Hancock, G.; Pinot de Moira, J. C.; Tyley, P. L. Spin-forbidden dissociation of ozone in the Huggins bands. *Chem. Phys.* **1988**, *231*, 109-119, doi:10.1016/S0301-0104(97)00328-5.

Ditchburn, R. W.; Young, P. A. The absorption of molecular oxygen between 1850 and 2500 Å. *J. Atmos. Terr. Phys.* **1962**, *24*, 127-139, doi:10.1016/0021-9169(62)90191-5.

El Helou, Z.; Churassy, S.; Wannous, G.; Bacis, R.; Boursey, E. Absolute cross sections of ozone at atmospheric temperatures for the Wulf and the Chappuis bands. *J. Chem. Phys.* **2005**, *122*, 244311, doi:10.1063/1.193736.

Enami, S.; Ueda, J.; Nakano, Y.; Hashimoto, S.; Kawasaki, M. Temperature-dependent absorption cross sections of ozone in the Wulf-Chappuis band at 759-768 nm. *J. Geophys. Res.* **2004**, *109*, D05309, doi:10.1029/2003JD004097.

Fally, S.; Vandaele, A. C.; Carleer, M.; Hermans, C.; Jenouvrier, A.; Mérienne, M.-F.; Coquart, B.; Colin, R. Fourier transform spectroscopy of the O_2 Herzberg bands. III. Absorption cross sections of the collision-induced bands of the Herzberg continuum. *J. Mol. Spectrosc.* **2000**, *204*, 10-20, doi:10.1006/jmsp.2000.8204.

Frederick, J. E.; Mentall, J. E. Solar irradiance in the stratosphere: Implications for the Herzberg continuum absorption of O_2. *Geophys. Res. Lett.* **1982**, *9*, 461-464, doi:10.1029/GL009i004p00461

Freeman, D. E.; Yoshino, K.; Esmond, J. R.; Parkinson, W. H. High-resolution absorption cross-section measurements of ozone at 195-K in the wavelength region 240-350 nm. *Planet. Space Sci.* **1984**, *32*, 239-248, doi:10.1016/0032-0633(84)90158-2.

Freeman, D. E.; Yoshino, K.; Esmond, J. R.; Parkinson, W. H. In *Atmospheric Ozone*; Zerefos, C. S., Ghazi, A., Eds., 1985; pp 622-624.

Fuchs, H.; Dubé, W. P.; Lerner, B. M.; Wagner, N. L.; Williams, E. J.; Brown, S. S. A sensitive and versatile detector for atmospheric NO_2 and NO_x based on blue diode laser cavity ring-down spectroscopy. *Environ. Sci. Technol.* **2009**, *43*, 7831-7836, doi:10/1021/es902067h.

Gibson, S. T.; Gies, H. P. F.; Blake, A. J.; McCoy, D. G.; Rogers, P. J. Temperature dependence in the Schumann-Runge photoabsorption continuum of oxygen. *J. Quant. Spectrosc. Radiat. Transf.* **1983**, *30*, 385-393, doi:10.1016/0022-4073(83)90101-2.

Goldstein, R.; Mastrup, F. N. Absorption coefficients of the O_2 Schumann-Runge continuum from 1270 Å ↔ 1745 Å using a new continuum source. *J. Opt. Soc. Am.* **1966**, *56*, 765-769, doi:10.1364/JOSA.56.000765.

Gorshelev, V.; Serdyuchenko, A.; Weber, M.; Chehade, W.; Burrows, J. P. High spectral resolution ozone absorption cross-sections – Part 1: Measurements, data analysis and comparison with previous measurements around 293 K. *Atmos. Meas. Tech.* **2014**, *7*, 609-624, doi:10/5194/amt-7-609-2014.

Greenblatt, G. D.; Orlando, J. J.; Burkholder, J. B.; Ravishankara, A. R. Absorption measurements of oxygen between 330 and 1140 nm. *J. Geophys. Res.* **1990**, *95*, 18577-18582, doi:10.1029/JD095iD11p18577.

Griggs, M. Absorption coefficients of ozone in the ultraviolet and visible regions. *J. Chem. Phys.* **1968**, *49*, 857-859, doi:10.1063/1.1670152.

Hancock, G.; Hofzumahaus, A. Experimental Study of the Altitude Dependence of the Tropospheric Ozone Photolysis Frequency, J(O(1D)) Between 0 and 12 km Height (ATOP), EU R and D Programme Environment and Climate ENV4-CT95-0158, 1997.

Hasson, V.; Nichols, R. W. Absolute spectral absorption measurements on molecular oxygen from 2640-1940 Å. *J. Phys. B. At. Mol. Phys.* **1971**, *4*, 1789-1797, doi:10.1088/0022-3700/4/12/025.

Hearn, A. G. Absorption of ozone in ultra-violet and visible regions of spectrum. *Proc. Phys. Soc. London* **1961**, *78*, 932-940, doi:10.1088/0370-1328/78/5/340.
Herman, J. R.; Mentall, J. E. O_2 absorption cross sections (187-225 nm) from stratospheric solar flux measurements. *J. Geophys. Res.* **1982**, *87*, 8967-8975, doi:10.1029/JC087iC11p08967.
Hudson, R. D. Absorption cross sections of stratospheric molecules. *Can. J. Phys.* **1974**, *52*, 1465-1478, doi:10.1139/v74-218.
Hudson, R. D.; Carter, V. L.; Stein, J. A. An investigation of the effect of temperature on the Schumann-Runge absorption continuum of oxygen, 1580-1950 Å. *J. Geophys. Res.* **1966**, *71*, 2295-2298, doi:10.1029/JZ071i009p02295.
Hudson, R. D.; Mahle, S. H. Photodissociation rates of molecular oxygen in the mesosphere and lower thermosphere. *J. Geophys. Res.* **1972**, *77*, 2902-2914, doi:10.1029/JA077i016p02902.
Huestis, D. L.; Copeland, R. A.; Knutsen, K.; Slanger, T. G.; Jogma, R. T.; Boogaarts, M. G. H.; Meijer, G. Branch intensities and oscillator strengths for the Herzberg absorption systems in oxygen. *Can. J. Phys.* **1994**, 1109-1121, doi:10.1139/p94-145.
Huffman, R. E. Absorption cross-sections of atmosperic gases for use in aeronomy. *Can. J. Chem.* **1969**, *47*, 1823-1834, doi:10.1139/v69-298.
Huffman, R. E.; Tanaka, Y.; Larrabee, H. E. Nitrogen and oxygen absorption cross sections in the vacuum ultra-violet. *Discuss. Faraday Soc.* **1964**, *37*, 159-166, doi:10.1039/DF9643700159.
Inn, E. C. Y.; Tanaka, Y. Absorption coefficient of ozone in the ultraviolet and visible regions. *J. Opt. Soc. Am.* **1953**, *43*, 870-873, doi:10.1364/JOSA.43.000870.
Inn, E. C. Y.; Tanaka, Y. *Adv. Chem. Ser.* **1958**, *21*, 263-268.
Inn, E. C. Y.; Tanaka, Y. Ozone absorption coefficients in the visible and ultraviolet regions. *Adv. Chem. Ser.* **1959**, *21*, 263-268, doi:10.1021/ba-1959-0021.ch037.
Jenouvrier, A.; Coquart, B.; Merienne, M. F. Long pathlength measurements of oxygen absorption cross sections in the wavelength region 205-240 nm. *J. Quant. Spectrosc. Radiat. Transf.* **1986**, *36*, 349-354, doi:10.1016/0022-4073(86)90059-2.
Jenouvrier, A.; Coquart, B.; Mérienne-Lafore, M. F. New measurements of the absorption cross-sections in the Herzberg continuum of molecular oxygen in the region between 205 and 240 nm. *Planet. Space Sci.* **1986**, *34*, 253-254.
Johnston, H. S.; Paige, M.; Yao, F. Oxygen absorption cross sections in the Herzberg continuum and between 206 and 327 K. *J. Geophys. Res.* **1984**, *89*, 11661-11665, doi:10.1029/JD089iD07p11661.
Kanik, I.; Beegle, L.; Noren, C.; Ahmed, S. M.; Link, R. Temperature-dependent photoabsorption cross section measurements of O_2 at the NI airglow and auroral emission lines. *Chem. Phys. Lett.* **1997**, *279*, 297-302, doi:10.1016/S0009-2614(97)01077-4.
Kley, D. Ly(α) absorption cross-section of H_2O and O_2. *J. Atmos. Chem.* **1984**, *2*, 203-210, doi:10.1007/BF00114132.
Kockarts, G. Absorption and photodissociation in the Schumann-Runge bands of molecular oxygen in the terrestrial atmosphere. *Planet. Space Sci.* **1976**, *24*, 589-604, doi:10.1016/0032-0633(76)90137-9.
Lacoursière, J.; Meyer, S. A.; Faris, G. W.; Slanger, T. G.; Lewis, B. R.; Gibson, S. T. The $O(^1D)$ yield from O_2 photooxidation near H Lyman-α (121.6 nm). *J. Chem. Phys.* **1999**, *110*, 1949-1958, doi:10.1063/1.477852.
Lee, L. C.; Black, G.; Sharpless, R. L.; Slanger, T. G. $O(^1S)$ yield from O_3 photodissociation at 1700-2400 Å. *J. Chem. Phys.* **1980**, *73*, 256-258, doi:10.1063/1.439925.
Lee, L. C.; Slanger, T. G.; Black, G.; Sharpless Quantum yields for the production of $O(^1D)$ from photodissociation of O_2 at 1160-1770 Å. *J. Chem. Phys.* **1977**, *67*, 5602-5606, doi:10.1063/1.434759.
Lee, P. Photodissociation and photoionization of oxygen (O_2) as inferred from measured absorption coefficients. *J. Opt. Soc. Am.* **1955**, *45*, 703-709, doi:10.1364/JOSA.45.000703.
Lee, P. C.; Nee, J. B. Detection of $O(^1D)$ produced in the photodissociation of O_2. I Identification of the $^3\Sigma_u^-$ and $^3\Pi_u$ Rydberg states in 113-130 nm. *J. Chem. Phys.* **2000**, *112*, 1763-1768, doi:10.1063/1.480739.
Lee, P. C.; Nee, J. B. Detection of $O(^1D)$ produced in the photodissociation of O_2. II Identification of the $^3\Sigma_u^-$ and $^3\Pi_u$ Rydberg states in 105-113 nm. *J. Chem. Phys.* **2001**, *114*, 792-797, doi:10.1063/1.1330231.
Lewis, B. R.; Berzins, L.; Carver, J. H. Oscillator strengths for the Schumann-Runge bands of $^{16}O_2$. *J. Quant. Spectrosc. Radiat. Transf.* **1986**, *36*, 209-232, doi:10.1016/0022-4073(86)90069-5.
Lewis, B. R.; Berzins, L.; Carver, J. H.; Gibson, S. T. Rotational variation of predissociation linewidth in the Schumann-Runge bands of $^{16}O_2$. *J. Quant. Spectrosc. Radiat. Transf.* **1986**, *36*, 187-207, doi:10.1016/0022-4073(86)90068-3.
Lewis, B. R.; Vardavas, I. M.; Carver, J. H. The aeronomic dissociation of water vapor by solar H Lyman α radiation. *J. Geophys. Res.* **1983**, *88*, 4935-4940, doi:10.1029/JA088iA06p04935.
Lin, J. J.; Huang, D. W.; Lee, Y. T.; Yang, X. Photodissociation of O_2 at 157 nm: Experimental observation of anisotropy mixing in the $O_2 + h\nu \rightarrow O(^3P) + O(^3P)$ channel. *J. Chem. Phys.* **1998**, *109*, 1758-1762, doi:10.1063/1.476751.

Malicet, J.; Brion, J.; Daumont, D. Temperature dependence of the absorption cross-section of ozone at 254 nm. *Chem. Phys. Lett.* **1989**, *158*, 293-296, doi:10.1016/0009-2614(89)87338-5.

Malicet, J.; Daumont, D.; Charbonnier, J.; Parisse, C.; Chakir, A.; Brion, J. Ozone UV spectroscopy. II. Absorption cross-sections and temperature dependence. *J. Atmos. Chem.* **1995**, *21*, 263-273, doi:10.1007/BF00696758.

Mason, N. J.; Gingell, J. M.; Davies, J. A.; Zhao, H.; Walker, I. C.; Siggel, M. R. F. VUV optical absorption and electron energy-loss spectroscopy of ozone. *J. Phys. B: At. Mol. Phys.* **1996**, *29*, 3075-3089, doi:10.1088/0953-4075/29/14/019.

Matsumi, Y.; Comes, F. J.; Hancock, G.; Hofzumahaus, A.; Hynes, A. J.; Kawasaki, M.; Ravishankara, A. R. Quantum yields for production of $O(^1D)$ in the ultraviolet photolysis of ozone: Recommendation based on evaluation of laboratory data. *J. Geophys. Res.* **2002**, *107*, 4024, doi:10.1029/2001JD000510.

Matsumi, Y.; Kawasaki, M. Photolysis of atmospheric ozone in the ultraviolet region. *Chem. Rev.* **2003**, *103*, 4767-4781, doi:10.1021/cr0205255.

Matsunaga, F. M.; Watanabe, K. Total and photoionization coefficients and dissociation continua of O_2 in the 580-1070 Å region. *Sci. Light* **1967**, *16*, 31-42.

Mauersberger, K.; Barnes, J.; Hanson, D.; Morton, J. Measurement of the ozone absorption cross-section at the 253.7 nm mercury line. *Geophys. Res. Lett.* **1986**, *13*, 671-673, doi:10.1029/GL013i007p00671.

Mauersberger, K.; Hanson, D.; Barnes, J.; Morton, J. Ozone vapor pressure and absorption cross-section measurements: Introduction of an ozone standard. *J. Geophys. Res.* **1987**, *92*, 8480-8482, doi:10.1029/JD092iD07p08480.

McPeters, R. D.; Bass, A. M. Anomalous atmospheric spectral features between 300 and 310 nm interpreted in light of new ozone absorption coefficient measurements. *Geophys. Res. Lett.* **1982**, *9*, 227-230, doi:10.1029/GL009i003p00227.

Metzger, P. H.; Cook, G. R. A reinvestigation of the absorption cross sections of molecular oxygen in the 1050-1800 Å region. *J. Quant. Spectrosc. Radiat. Transf.* **1964**, *4*, 107-116, doi:10.1016/0022-4073(64)90057-3.

Minschwaner, K.; Anderson, G. P.; Hall, L. A.; Yoshino, K. Polynomial coefficients for calculating O_2 Schumann-Runge cross sections at 0.5 cm^{-1} resolution. *J. Geophys. Res.* **1992**, *97*, 10103-10108, doi:10.1029/92JD00661.

Minschwaner, K.; Salawitch, R. J.; McElroy, M. B. Absorption of solar radiation by O_2: Implications for O_3 and lifetimes of N_2O, $CFCl_3$, and CF_2Cl_2. *J. Geophys. Res.* **1993**, *98*, 10543-10561, doi:10.1029/93JD00223.

Molina, L. T.; Molina, M. J. Absolute absorption cross sections of ozone in the 185- to 350-nm wavelength range. *J. Geophys. Res.* **1986**, *91*, 14501-14508, doi:10.1029/JD091iD13p14501.

Murtagh, D. P. The O_2 Schumann-Runge system - New calculations of photodissociation cross-sections. *Planet. Space Sci.* **1988**, *36*, 819-828, doi:10.1016/0032-0633(88)90087-6.

Nakayama, T.; Takahashi, K.; Matsumi, Y.; Fujiwara, H. Laboratory study of $O(^1S)$ formation in the photolysis of O_3 and its atmospheric implications. *J. Atmos. Chem.* **2006**, *53*, 107-122, doi:10.1007/s10874-006-0597-3.

Nee, J. B.; Lee, P. C. Detection of $O(^1D)$ produced in the photodissociation of O_2 in the Schumann-Runge continuum. *J. Phys. Chem. A* **1997**, *101*, 6653-6657, doi:10.1021/jp970439m.

Nicolet, M. The solar spectral irradiance and its action in the atmospheric photo-dissociation processes. *Planet. Space Sci.* **1981**, *29*, 951-974, doi:10.1016/0032-0633(81)90056-8.

Nicolet, M.; Kennes, R. Aeronomic problems of the molecular oxygen photodissociation, I. The O_2 Herzberg continuum. *Planet. Space Sci.* **1986**, *34*, 1043-1059, doi:10.1016/0032-0633(86)90015-2.

Nicolet, M.; Kennes, R. Aeronomic problems of the molecular oxygen photodissociation –IV. The various parameters for the Herzberg Continuum. *Planet. Space Sci.* **1988**, *36*, 1069-1076, doi:10.1016/0032-0633(88)90044-X.

Nicolet, M.; Kennes, R. Aeronomic problems of molecular-oxygen photodissociation .6. Photodissociation frequency and transmittance in the spectral range of the Schumann-Runge bands. *Planet. Space Sci.* **1989**, *37*, 459-491, doi:10.1016/0032-0633(89)90125-6.

Nishida, S.; Takahashi, K.; Matsumi, Y.; Taniguchi, N.; Hayashida, S. Formation of $O(^3P)$ atoms in the photolysis of N_2O at 193 nm and $O(^3P) + N_2O$ product channel in the reaction of $O(^1D) + N_2O$ *J. Phys. Chem. A* **2004**, *108*, 2451-2456, doi:10.1021/jp037034o.

Ny, T.-Z.; Choong, S.-P. Sur l'absorption ultraviolette de l'ozone. *Chinese J. Phys.* **1933**, *1*, 38-54.

Ogawa, M. Absorption coefficients of O_2 at the Lyman-alpha line and its vicinity. *J. Geophys. Res.* **1968**, *73*, 6759-6763, doi:10.1029/JA073i021p06759.

Ogawa, M. Absorption cross sections of O_2 and CO_2 continua in the Schumann and far-uv regions. *J. Chem. Phys.* **1971**, *54*, 2550-2556, doi:10.1063/1.1675211.

Ogawa, M.; Cook, G. R. Absorption coefficients of O_3 in the vacuum ultraviolet region. *J. Chem. Phys.* **1958**, *28*, 173-174, doi:10.1063/1.1744071.

Ogawa, S.; Ogawa, M. Absorption cross sections of O_2 ($a\ ^1\Delta_g$) and $O_2(X\ ^3\Sigma_g^-)$ in the region from 1087 to 1700 Å. *Can. J. Phys.* **1975**, *53*, 1845-1852, doi:10.1139/p75-236.

Orphal, J. A Critical Review of the Absorption Cross-Sections of O_3 and NO_2 in the 240-790 nm Region, Part 1, Ozone, European Space Agency, ESA-ESTEC Noordwijk, ESA Technical Note MO-TN-ESA-GO-0302, 2002,

Orphal, J. A critical review of the absorption cross-sections of O_3 and NO_2 in the ultraviolet and visible. *J. Photochem. Photobiol. A: Chem.* **2003**, *157*, 185-209, doi:10.1016/S1010-6030(03)00061-3.

Oshima, Y.; Okamoto, Y.; Koda, S. Pressure effect of foreign gases on the Herzberg photoabsorption of oxygen. *J. Phys. Chem.* **1995**, *99*, 11830-11833, doi:10.1021/j100031a007.

Paur, R. J.; Bass, A. M. In *Atmospheric Ozone*; Zerefos, C. S., Ghazi, A., Eds., 1985; pp 610-616.

Petersen, M.; Viallon, J.; Moussay, P.; Wielgosz, R. I. Relative measurements of ozone absorption cross-sections at three wavelengths in the Hartley band using a well-defined UV laser beam. *J. Geophys. Res.* **2012**, *117*, D05301, doi:10.1029/2011jd016374.

Pirre, M.; Rigaud, P.; Huguenin, D. New in situ measurements of the absorption cross-sections of O_2 in the Herzberg continuum. *Geophys. Res. Lett.* **1984**, *11*, 1199-1202, doi:10.1029/GL011i012p01199

Pirre, M.; Rigaud, P.; Huguenin, D. *In situ* measurements of the absorption cross-sections of O_2 in the Herzberg continuum: The results of two different experiments. *Ann. Geophys.* **1988**, *6*, 535-540.

Preston, W. M. The origin of radio fade-outs and the absorption coefficient of gases for light of wave-length 1215.7 Å. *Phys. Rev.* **1940**, *57*, 887-894, doi:10.1103/PhysRev.57.887.

Samson, J. A. R.; Cairns, R. B. Absorption and photoionization cross sections of O_2 and N_2 at intense solar emission lines. *J. Geophys. Res.* **1964**, *69*, 4583-4590, doi:10.1029/JZ069i021p04583.

Samson, J. A. R.; Cairns, R. B. Total absorption cross sections of H_2, N_2, and O_2 in the region 550-220 Å. *J. Opt. Soc. Am.* **1965**, *45*, 1035-1040, doi:10.1364/josa.55.001035.

Saxon, R. P.; Slanger, T. G. Molecular oxygen absorption continua at 195-300 nm and O_2 radiative lifetimes. *J. Geophys. Res.* **1986**, *91*, 9877-9879, doi:10.1029/JD091iD09p09877.

Serdyuchenko, A.; Gorshelev, V.; Weber, M.; Chehade, W.; Burrows, J. P. High spectral resolution ozone absorption cross-sections – Part 2: Temperature dependence. *Atmos. Meas. Tech.* **2014**, *7*, 625-636, doi:10.5194/amt-7-625-2014.

Shardanand Absorption cross sections of O_2 and O_4 between 2000 and 2800 Å. *Phys. Rev.* **1969**, *186*, 5-9, doi:10.1103/PhysRev.186.5.

Shardanand; Rao, A. D. P. Collision-induced absorption of O_2 in the Herzberg continuum. *J. Quant. Spectrosc. Radiat. Transf.* **1977**, *17*, 433-439, doi:10.1016/0022-4073(77)90122-4.

Silvente, E.; Richter, R. C.; Zheng, M.; Saltzman, E. S.; Hynes, A. J. Relative quantum yields for $O(^1D)$ production in the photolysis of ozone between 301 and 336 nm: evidence for the participation of a spin-forbidden channel. *Chem. Phys. Lett.* **1997**, *264*, 309-315, doi:10.1016/S0009-2614(96)01342-5.

Simons, J. W.; Paur, R. J.; Webster III, H. A.; Bair, E. J. Ozone ultraviolet photolysis. VI. The ultraviolet spectrum. *J. Chem. Phys.* **1973**, *59*, 1203-1208, doi:10.1063/1.1680169.

Slanger, T. G.; Huestis, D. L.; Cosby, P. C.; Naus, N.; Meijer, G. O_2 photoabsorption in the 40950-41300 cm^{-1} region: New Herzberg bands, new absorption lines, and improved spectroscopic data. *J. Chem. Phys.* **1996**, *105*, 9393-9402, doi:10.1063/1.472772.

Smith, G. D.; Molina, L. T.; Molina, M. J. Temperature dependence of $O(^1D)$ quantum yields from the photolysis of ozone between 295 and 338 nm. *J. Phys. Chem. A* **2000**, *104*, 8916-8921, doi:10.1021/jp001006d.

Starr, W. L.; Loewenstein, M. Total absorption cross sections of several gases of aeronomic interest at 584 Å. *J. Geophys. Res.* **1972**, *77*, 4790-4796, doi:10.1029/JA077i025p04790.

Steinfeld, J. I.; Adler-Golden, S. M.; Gallagher, J. W. Critical survey of data on the spectroscopy and kinetics of ozone in the mesosphere and thermosphere. *J. Phys. Chem. Ref. Data* **1987**, *16*, 911-951, doi:10.1063/1.555796.

Taherian, M. R.; Slanger, T. G. Products and yields from O_3 photodissociation at 1576 Å. *J. Chem. Phys.* **1985**, *83*, 6246-6250, doi:10.1063/1.449573.

Takahashi, K.; Hayashi, S.; Matsumi, Y.; Taniguchi, N.; Hayashida, S. Quantum yields of (O^1D) formation in the photolysis of ozone between 230 and 308 nm. *J. Geophys. Res.* **2002**, *107*, 4440, doi:10.1029/2001JD002048.

Takahashi, K.; Matsumi, Y.; Kawasaki, M. Photodissociation processs of ozone in the Huggins band at 308-326 nm: Direct observation of $O(^1D_2)$ and $O(^3P_j)$ products. *J. Phys. Chem.* **1996**, *100*, 4084-4089, doi:10.1021/jp9528065.

Takahashi, T.; Nakayama, T.; Matsumi, Y. Vacuum ultraviolet laser-induced fluorescence detection of $O(^1S)$ atoms produced in the 193 nm photolysis of ozone. *J. Phys. Chem. A* **2003**, *107*, 9368-9373, doi:10.1021/jp0346864.

Talukdar, R. K.; Gilles, M. K.; Battin-Leclerc, F.; Ravishankara, A. R.; Fracheboud, J.-M.; Orlando, J. J.; Tyndall, G. S. Photolysis of ozone at 308 and 248 nm: Quantum yield of $O(^1D)$ as a function of temperature. *Geophys. Res. Lett.* **1997**, *24*, 1091-1094, doi:10.1029/97GL00831.

Talukdar, R. K.; Longfellow, C. A.; Gilles, M. K.; Ravishankara, A. R. Quantum yields of $O(^1D)$ in the photolysis of ozone between 289 and 329 nm as a function of temperature. *Geophys. Res. lett.* **1998**, *25*, 143-146, doi:10.1029/97GL03354.

Tanaka, Y.; Inn, E. C. Y.; Watanabe, K. Absorption coefficients of gases in the vacuum ultraviolet. Part IV. Ozone. *J. Chem. Phys.* **1953**, *21*, 1651-1653, doi:10.1063/1.1698638.

Tanaka, Y.; Jursa, A. S.; LeBlanc, F. J.; Inn, E. C. Y. Spectroscopic study of the afterglows of N_2 and (N_2 + O_2) in the vacuum region. *Planet. Space Sci.* **1959**, *1*, 7-13, doi:10.1016/0032-0633(59)90016-9.

Trolier, M.; Wiesenfeld, J. R. Relative quantum yield of $O(^1D_2)$ following ozone photlysis between 275 and 325 nm. *J. Geophys. Res.* **1988**, *93*, 7119-7124, doi:10.1029/JD093iD06p07119.

Turnipseed, A. A.; Vaghjiani, G. L.; Gierczak, T.; Thompson, J. E.; Ravishankara, A. R. The photochemistry of ozone at 193 and 222 nm. *J. Chem. Phys.* **1991**, *95*, 3244-3251, doi:10.1063/1.460881.

Vassy, A.; Vassy, E. Effect of temperature on the absorption spectrum of ozone: Chappuis Bands. *J. Chem. Phys.* **1948**, *16*, 1163-1164, doi:10.1063/1.1746754.

Vattulainen, J.; Wallenius, L.; Stenberg, J.; Hernberg, R.; Linna, V. Experimental determination of SO_2, C_2H_2, and O_2 UV absorption cross sections at elevated temperatures and pressures. *Appl. Spectrosc.* **1997**, *57*, 1311-1315, doi:10.1366/0003702971942.

Viallon, J.; Lee, S.; Moussay, P.; Tworek, K.; Petersen, M.; Wielgosz, R. I. Accurate measurements of ozone absorption cross-sections in the Hartley band. *Atmos. Meas. Tech.* **2015**, *8*, 1245-1257, doi:10.5194/amt-8-1245-2015.

Vigroux, E. Contribution a l'étude expérimentale de l'absorption de l'ozone. *Ann. Phys.* **1953**, *8*, 709-762.

Vigroux, E. Physique de l'atmosphére. - Détermination des coefficients moyens d'absorption de l'ozone pour le spectrometre Dobson. Note. *C. R. Acad. Sci. Paris* **1967**, *264*, 1290-1291.

Vigroux, E. Coefficients d'absorption de l;ozone dans la bande de Hartley. *Ann. Geophys.* **1969**, *25*, 169-172.

Voigt, S.; Orphal, J.; Bogumil, K.; Burrows, J. P. The temperature dependence (203-293 K) of the absorption cross sections of O_3 in the 230-850 nm region measured by Fourier-transform spectroscopy. *J. Photochem. Photobiol. A: Chem.* **2001**, *143*, 1-9, doi:10.1016/S1010-6030(01)00480-4.

Wainfan, N.; Walker, W. C.; Weissler, G. L. Photoionization efficiencies and cross sections in O_2, N_2, CO_2, A, H_2O, H_2, and CH_4. *Phys. Rev.* **1955**, *99*, 542-549, doi:10.1103/PhysRev.99.542.

Wang, J.; McCoy, D. G.; Blake, A. J.; Torop, L. Effect of the close approach of potential curves in photoabsorption by atomic molecules – II. Temperature dependence of the O_2 cross section in the region 130-160 nm. *J. Quant. Spectrosc. Radiat. Transf.* **1987**, *38*, 19-27, doi:10.1016/0022-4073(87)90106-3.

Watanabe, K.; Inn, E. C. Y.; Zelikoff, M. Absorption coefficients of gases in the vacuum ultraviolet. *J. Chem. Phys.* **1952**, *20*, 1969-1970, doi:10.1063/1.1700353.

Watanabe, K.; Inn, E. C. Y.; Zelikoff, M. Absorption coefficients of oxygen in the vacuum ultraviolet. *J. Chem. Phys.* **1953**, *21*, 1026-1030, doi:10.1063/1.1699104.

Watanabe, K.; Marmo, F. F. Photoionization and total absorption cross section of gases. II. O_2 and N_2 in the region 850-1500 Å. *J. Chem. Phys.* **1956**, *25*, 965-971, doi:10.1063/1.1743151.

Weissler, G. L.; Lee, P. Absorption coefficients of oxygen in the vacuum ultraviolet. *J. Opt. Soc. Am.* **1952**, *42*, 200-203, doi:10.1364/JOSA.42.000200.

WMO *Atmospheric Ozone: 1985*; National Aeronautics and Space Administration: Geneva, Report No. 16, Chapter 7, 1986.

Wu, C. Y. R.; Judge, D. L.; Matsui, T. High-temperature ultrahigh-resolution absorption cross-section measurements of O_2 in the EUV region. *J. Electron Spectrosc. Related Phenom.* **2005**, *144-147*, 123-126, doi:10.1016/j.elspec.2005.01.047.

Yoshino, K.; Cheung, A. S. C.; Esmond, J. R.; Parkinson, W. H.; Freeman, D. E.; Guberman, S. L.; Jenouvrier, A.; Coquart, B.; Merienne, M. F. Improved absorption cross sections of oxygen in the wavelength region 205-240 nm of the Herzberg continuum. *Planet. Space Sci.* **1988**, *36*, 1469-1475, doi:10.1016/0032-0633(88)90012-8.

Yoshino, K.; Esmond, J. R.; Cheung, A. S.-C.; Freeman, D. E.; Parkinson, W. H. High resolution absorption cross sections in the transmission window region of the Schumann-Runge bands and Herzberg continuum of O_2. *Planet. Space Sci.* **1992**, *40*, 185-192, doi:10.1016/0032-0633(92)90056-T.

Yoshino, K.; Esmond, J. R.; Cheung, A. S. C.; Freeman, D. E.; Parkinson, W. H. Band oscillator strengths of the (2,1)-(12,1) Schumann-Runge bands of O_2 from absolute absorption cross-section measurements at room temperature. *J. Geophys. Res.* **1990**, *95*, 11743-11746, doi:10.1029/JD095iD08p11743.

Yoshino, K.; Esmond, J. R.; Freeman, D. E.; Parkinson, W. H. Measurements of absolute absorption cross sections of ozone in the 185- to 254-nm wavelength region and the temperature dependence. *J. Geophys. Res.* **1993**, *98*, 5205-5211, doi:10.1029/93JD00028.

Yoshino, K.; Esmond, J. R.; Murray, J. E.; Parkinson, W. H.; Thorne, A. P.; Learner, R. C. M.; Cox, G. Band oscillator strengths of the Herzberg I bands of O_2. *J. Chem. Phys.* **1995**, *103*, 1243-1249, doi:10.1063/1.469800.

Yoshino, K.; Esmond, J. R.; Parkinson, W. H.; Thorne, A. P.; Learner, R. C. M.; Cox, G. Fourier transform spectroscopy annd cross-section measurements of the Herzberg II bands of O_2 at 295 K. *J. Chem. Phys.* **1999**, *111*, 2960-2967, doi:10.1063/1.479577.

Yoshino, K.; Esmond, J. R.; Parkinson, W. H.; Thorne, A. P.; Learner, R. C. M.; Cox, G.; Cheung, A. S.-C. Fourier transform spectroscopy and cross section measurements of the Herzberg III bands of O_2 at 295 K. *J. Chem. Phys.* **2000**, *112*, 9791-9801, doi:10.1063/1.481702.

Yoshino, K.; Freeman, D. E.; Esmond, J. R.; Friedman, R. S.; Parkinson, W. H. High-resolution absorption cross-sections and band oscillator-strengths of the Schumann-Runge absorption-bands of isotopic oxygen, $^{18}O_2$, at 79 K. *Planet. Space Sci.* **1988**, *36*, 1201-1210, doi:10.1016/0032-0633(88)90073-6.

Yoshino, K.; Freeman, D. E.; Esmond, J. R.; Friedman, R. S.; Parkinson, W. H. High-resolution absorption cross-sections and band oscillator-strengths of the Schumann-Runge absorption-bands of isotopic oxygen, (OO)-$^{16}O^{18}O$, at 79-K. *Planet. Space Sci.* **1989**, *37*, 419-426, doi:10.1016/0032-0633(89)90123-2.

Yoshino, K.; Freeman, D. E.; Esmond, J. R.; Parkinson, W. H. High-resolution absorption cross-sections and band oscillator-strengths of the Schumann-Runge bands of oxygen at 79-K. *Planet. Space Sci.* **1987**, *35*, 1067-1075, doi:10.1016/0032-0633(87)90011-0.

Yoshino, K.; Freeman, D. E.; Esmond, J. R.; Parkinson, W. H. Absolute absorption cross-section measurements of ozone in the wavelength region 238-335 nm and the temperature-dependence. *Planet. Space Sci.* **1988**, *36*, 395-398, doi:10.1016/0032-0633(88)90127-4.

Yoshino, K.; Freeman, D. E.; Parkinson, W. H. Atlas of the Schumann-Runge absorption bands of O_2 in the wavelength region 175-205 nm. *J. Phys. Chem. Ref. Data* **1984**, *13*, 207-227, doi:10.1063/1.555702.

Yoshino, K.; Freeman, D. F.; Esmond, J. R.; Parkinson, W. H. High-resolution absorption cross-section measurements and band oscillator-strengths of the (1,0)-(12,0) Schumann-Runge bands of O_2. *Planet. Space Sci.* **1983**, *31*, 339-353 doi:10.1016/0032-0633(83)90085-5.

Yoshino, K.; Huestis, D. L.; Nicholls, R. W. Comment on the Herzberg Continuum. *J. Quant. Spectrosc. Radiat. Transf.* **1998**, *60*, 1091.

Yoshino, K.; Murray, J. E.; Esmond, J. R.; Sun, Y.; Parkinson, W. H.; Thorne, A. P.; Learner, R. C. M.; Cox, G. Fourier transform spectroscopy of the Herzberg I bands of O_2. *Can. J. Phys.* **1994**, *72*, 1101-1108, doi:10.1139/p94-144.

Yoshino, K.; Parkinson, W. H.; Ito, K.; Matsui, T. Absolute absorption cross-section measurements of Schumann-Runge continuum of O_2 at 90 and 295 K. *J. Mol. Spectrosc.* **2005**, *229*, 238-243, doi:10.1016/j.jms.2004.08.020.

.

SECTION 4B. HO_X PHOTOCHEMISTRY

B1. HO_2 (hydroperoxyl radical)

Back to Index

$HO_2 + h\nu \rightarrow OH + O(^3P)$	273 kJ mol^{-1}	438 nm	(1)
$\rightarrow OH + O(^1D)$	462 kJ mol^{-1}	259 nm	(2)

(Recommendation: 06-2; Note: 10-6; Evaluated: 10-6)

Absorption Cross Sections: UV absorption cross sections of HO_2 in the wavelength range 190–260 nm have been measured at room temperature by Paukert and Johnston,[12] Hochanadel et al.,[4] Cox and Burrows,[1] McAdam et al.,[10] Kurylo et al.,[5] Moortgat et al.,[11] Dagaut and Kurylo,[3] Lightfoot and Jemi-Alade,[8] who measured the cross sections at temperatures up to 777 K, Crowley et al.,[2] Maricq and Szente,[9] Roehl et al.,[13] and Sander et al.[14] The HO_2 absorption cross section studies have been evaluated in reviews by Lightfoot et al.,[7] Wallington et al.,[16] and Tyndall et al.[15] Discrepancies in the shape of the HO_2 spectrum and its absolute cross sections, particularly around 200 nm, exist among the available studies. Tyndall et al.[15] recommend absolute HO_2 cross sections based on a comparison of absorption cross sections for HO_2, CH_3O_2 and $C_2H_5O_2$ at 240 nm obtained by Roehl et al., Lightfoot and Jemi-Alade, and Maricq and Szente combined with the measurements by Crowley et al.[2] at 240 nm. Tyndall et al.[15] used the expression

$$\sigma = \frac{\sigma_{med}}{\left(1 - \frac{b}{\nu}\right)} \exp\left\{-a\left[\ln\frac{(\nu - b)}{(\nu_{med} - b)}\right]^2\right\}$$

where $\sigma_{med} = 1.64 \times 10^{-18}$ cm^2 molecule^{-1}, a = 4.91, b = 30612 cm^{-1} and ν_{med}= 50260 cm^{-1} that reproduces the HO_2 spectrum over the wavelength range 190–250 nm. They recommend that the spectrum be treated as temperature independent over the range 200–300 K. The recommended HO_2 cross sections in Table 4B-1 are taken from the Tyndall et al.[15] review.

Photolysis Quantum Yield and Product Studies: Lee[6] detected $O(^1D)$ as a primary photodissociation product of HO_2 at 193 and 248 nm with a quantum yield that is about 15 times larger at the longer wavelength. An absolute quantum yield for $O(^1D)$ production has not been reported.

Table 4B-1. Recommended Absorption Cross Sections of HO_2 at 298 K

λ (nm)	10^{20} σ (cm^2 molecule^{-1})
190	368
195	402
200	423
205	427
210	415
215	385
220	341
225	288
230	230
235	173
240	122
245	79.7
250	48.0
255	26.3
260	12.9

Note:
Tyndall et al.[15] review

(1) Cox, R. A.; Burrows, J. P. Kinetics and mechanism of the disproportionation of HO_2 in the gas phase. *J. Phys. Chem.* **1979**, *83*, 2560-2568, doi:10.1021/j100483a002.

(2) Crowley, J. N.; Simon, F. G.; Burrows, J. P.; Moortgat, G. K.; Jenkin, M. E.; Cox, R. A. The HO_2 radical UV absorption spectrum measured by molecular modulation, UV/diode-array spectroscopy. *J. Photochem. Photobiol. A: Chem.* **1991**, *60*, 1-10, doi:10.1016/1010-6030(91)90001-A.

(3) Dagaut, P.; Kurylo, M. J. The gas phase UV absorption spectrum of CH_3O_2 radicals: A reinvestigation. *J. Photochem. Photobiol. A: Chem.* **1990**, *51*, 133-140, doi:10.1016/1010-6030(90)87047-F.
(4) Hochanadel, C. J.; Ghormley, J. A.; Ogren, P. J. Absorption spectrum and reaction kinetics of the HO_2 radical in the gas phase. *J. Chem. Phys.* **1972**, *56*, 4426-4432, doi:10.1063/1.1677885.
(5) Kurylo, M. J.; Wallington, T. J.; Ouellette, P. A. Measurements of the UV absorption cross-sections for HO_2 and CH_3O_2 in the gas phase. *J. Photochem.* **1987**, *39*, 201-215, doi:10.1016/0047-2670(87)80032-1.
(6) Lee, L. C. Observation of $O(^1D)$ produced from photodissociation of HO_2 at 193 and 248 nm. *J. Chem. Phys.* **1982**, *76*, 4909-4915, doi:10.1063/1.442836.
(7) Lightfoot, P. D.; Cox, R. A.; Crowley, J. N.; Destriau, M.; Hayman, G. D.; Jenkin, M. E.; Moortgat, G. K.; Zabel, F. Organic peroxy radicals: Kinetics, spectroscopy and tropospheric chemistry. *Atmos. Environ.* **1992**, *26A*, 1805-1961, doi:10.1016/0960-1686(92)90423-I.
(8) Lightfoot, P. D.; Jemi-Alade, A. A. The temperature dependence of the UV spectra of the HO_2 and CH_3O_2 radicals. *J. Photochem. Photobiol. A: Chem.* **1991**, *59*, 1-10, doi:10.1016/1010-6030(91)87062-Z.
(9) Maricq, M. M.; Szente, J. J. A kinetic study of the reaction between ethylperoxy radicals and HO_2. *J. Phys. Chem.* **1994**, *98*, 2078-2082, doi:10.1021/j100059a016.
(10) McAdam, K.; Veyret, B.; Lesclaux, R. UV absorption spectra of HO_2 and CH_3O_2 radicals and the kinetics of their mutual reactions at 298 K. *Chem. Phys. Lett.* **1987**, *133*, 39-44, doi:10.1016/0009-2614(87)80049-0.
(11) Moortgat, G.; Veyret, B.; Lesclaux, R. Absorption spectrum and kinetics of reactions of the acetylperoxy radical. *J. Phys. Chem.* **1989**, *93*, 2362-2368, doi:10.1021/j100343a032.
(12) Paukert, T. T.; Johnston, H. S. Spectra and kinetics of the hydroperoxyl free radical in the gas phase. *J. Chem. Phys.* **1972**, *56*, 2824-2838, doi:10.1063/1.1677613.
(13) Roehl, C. M.; Bauer, D.; Moortgat, G. K. Absorption spectrum and kinetics of the acetylperoxy radical. *J. Phys. Chem.* **1996**, *100*, 4038-4047, doi:10.1021/jp9526298.
(14) Sander, S. P.; Peterson, M.; Watson, R. T.; Patrick, R. Kinetics studies of the $HO_2 + HO_2$ and $DO_2 + DO_2$ reactions at 298 K. *J. Phys. Chem.* **1982**, *86*, 1236-1240, doi:10.1021/j100397a002.
(15) Tyndall, G. S.; Cox, R. A.; Granier, C.; Lesclaux, R.; Moortgat, G. K.; Pilling, M. J.; Ravishankara, A. R.; Wallington, T. J. Atmospheric chemistry of small organic peroxy radicals. *J. Geophys. Res.* **2001**, *106*, 12157-12182, doi:10.1029/2000JD900746.
(16) Wallington, T. J.; Dagaut, P.; Kurylo, M. J. Ultraviolet absorption cross sections and reaction kinetics and mechanisms for peroxy radicals in the gas phase. *Chem. Rev.* **1992**, *92*, 667-710, doi:10.1021/cr00012a008.

B2. H_2O (water)

Back to Index

$H_2O + h\nu \rightarrow O(^3P) + H_2$	486 kJ mol^{-1}	246 nm	(1)
$\rightarrow OH(X^2\Pi) + H$	496 kJ mol^{-1}	242 nm	(2)
$\rightarrow O(^1D) + H_2$	684 kJ mol^{-1}	175 nm	(3)
$\rightarrow OH(A^2\Sigma^+) + H$	893 kJ mol^{-1}	134 nm	(4)
$\rightarrow O(^3P) + H + H$	927 kJ mol^{-1}	129 nm	(5)

(Recommendation: 10-6, Note: 10-6, Evaluated: 10-6)

Absorption Cross Sections: The VUV absorption spectrum of water vapor can be divided up into four main regions: (i) a broad continuum at wavelengths 145–190 nm with a maximum around 165 nm and the cross sections falling off rapidly toward longer wavelengths; (ii) a second continuum centered around 128 nm, which shows some diffuse vibrational structure; (iii) between 124–100 nm the absorption spectrum is dominated by progressions of sharp structured rovibronic peaks associated with Rydberg transitions; (iv) below 100 nm the spectrum is also a continuum consisting of two diffuse bands with maxima near 90 and 65 nm. In the atmosphere, water vapor is photodissociated mainly by the solar Lyman-α line (121.567 nm). The absorption cross sections and the photochemistry of water vapor were reviewed by Hudson,[22,23] Hudson and Kiefer,[24] Calvert and Pitts,[6] and Okabe.[38] Table 4B-2-1 summarizes the studies performed since 1950.

Table 4B-2-1. Summary of H_2O Vapor Absorption Cross Section Studies

Study	Year	Molecule	Wavelength (nm)	Resolution (nm)	Temperature (K)
Wilkinson and Johnston[53]	1950	H_2O	143–186	0.1	303
Watanabe and Zelikoff[52]	1953	H_2O	106–185	0.1	298
Wainfan et al.[50]	1955	H_2O	47–100	1.0	298
Harrison et al.[20]	1959	H_2O	154–200	0.3	295
Thompson et al.[47]	1963	H_2O	150–200	0.3	295
Metzger and Cook[34]	1964	H_2O	58.4–99	0.1	295
Watanabe and Jursa[51]	1964	H_2O	85–111	0.1	295
Laufer and McNesby[28]	1965	H_2O, D_2O	120–185	0.1	298
Schürgers and Welge[41]	1968	H_2O	120–183	0.25	298
de Reilhac and Damany[15]	1970	H_2O, D_2O	11.1–41.7	0.1	298
Bennett et al.[3]	1971	H_2O	58.4	0.1	295
Katayama et al.[26]	1973	H_2O, D_2O	58–105	0.05	298
Branton and Brion[4]	1974	H_2O	12-113, 138, 177, 248	0.1	298
Gürtler et al.[19]	1977	H_2O, D_2O	60–125	0.003	298
Phillips et al.[40]	1977	H_2O, D_2O	18–79	0.1	298
Tan et al.[44]	1978	H_2O	21-124, 138, 155, 177, 207	0.1	298
DeMore[16]	1979	H_2O	184.9	0.1	298
Lee[29]	1980	H_2O	105–137	0.2	294
Nicolet[37]	1981	H_2O	121.6	Calc J	230
Lewis et al.[31]	1983	H_2O	121.4–121.9	0.005	235, 292, 367
Kley[27]	1984	H_2O	121.6	0.005	298
Camy-Peyret et al.[7]	1985	H_2O	396.0–606.1	0.0127 cm^{-1}	300
Mandin et al.[32]	1986	H_2O	606.1–757.6	0.0127 cm^{-1}	300
Lee and Suto[30]	1986	H_2O, D_2O	50–190	0.2	295
Chan et al.[9]	1993	H_2O	6.2–206.6	0.5	298
Yoshino et al.[54]	1996	H_2O	120–188	0.0070	295
Brownsword et al.[5]	1997	H_2O	121.6	0.002	300
Cantrell et al.[8]	1997	H_2O, D_2O	184–193	0.2	273–353
Hofzumahaus et al.[21]	1997	H_2O	184.9	0.1	298
Creasey et al.[14]	2000	H_2O	184.9	0.1	298
Chung et al.[12]	2001	H_2O, D_2O HDO	140–195	0.1	295, 275, 250
The Harvard-Smithsonian Center for Astrophysics[1]	2001	H_2O	107.2–108.0 111.2–111.8 123.3–124.5	0.0002 0.0002 0.0007	295, 80 295 295, 80
Vatsa and Volpp[49]	2001	H_2O	121.567	0.0006	300
Coheur et al.[13]	2002	H_2O	385–758	0.06 cm^{-1}	291.3
Tanaka et al.[45]	2002	$H_2{}^{18}O$	606.5–688.7	0.06 cm^{-1}	298
Fally et al.[17]	2003	H_2O	384.6–769.2	0.06 cm^{-1}	289 ± 2
Mérienne et al.[33]	2003	H_2O	769.2–1081.1	0.03 cm^{-1}	292 ± 3
Parkinson and Yoshino[39]	2003	H_2O	181–199	0.0066	295
Cheng et al.[10]	2004	H_2O, D_2O HDO	125–145	0.01	300
Fillion et al.[18]	2004	H_2O, D_2O	99.9–113.9	0.01 cm^{-1}	298
Tanaka et al.[46]	2004	$H_2{}^{18}O$	584.1–688.7	0.06 cm^{-1}	298
Aldener et al.[2]	2005	H_2O	870–955	0.01 cm^{-1}	298
Mota et al.[36]	2005	H_2O	114.8–193.9	0.075	298
Kassi et al.[25]	2005	H_2O	747.5–751.2	0.06 cm^{-1}	298

The cross sections in the VUV band in the range 6 to 110 nm measured by Katayama et al.,[26] Gürtler et al.,[19] Phillips et al.,[40] Tan et al.,[44] Lee and Suto,[30] Chan et al.[9] are in good agreement, whereas the data of Wainfan

et al.,[50] Metzger and Cook,[34] de Reilhac and Damany,[15] Bennett et al.,[3] and Branton and Brion[4] show substantial deviations.

In the strong structured region between 100 and 125 nm, cross sections were measured at low resolution by Watanabe and Zelikoff,[52] Watanabe and Jursa,[51] Tan et al.,[44] Lee,[29] Lee and Suto,[30] Chan et al.,[9] and at high resolution by Gürtler et al.,[19] Lewis et al.,[31] The Harvard-Smithsonian Center for Astrophysics,[1] Fillion et al.,[18] and Mota et al.[36]

Absorption cross sections were reported at the Lyman-α wavelength, 121.567 nm, in units 10^{-17} cm^2 $molecule^{-1}$, to be 1.44 ± 0.04 by Watanabe and Zelikoff,[52] 1.4 ± 0.3 by Nicolet,[37] 1.5 ± 0.1 by Gürtler et al.,[19] 1.55 ± 0.1 by Lewis et al.,[31] 1.59 ± 0.1 by Kley,[27] 1.42 ± 0.1 by Lee,[29] 1.3 ± 0.05 by Chan et al.,[9] 1.4 ± 0.03 by Yoshino et al.,[54] 1.6 ± 0.1 by Brownsword et al.,[5] and 1.6 ± 0.1 by Vatsa and Volpp.[49] An average value (1.48 ± 0.10) × 10^{-17} cm^2 $molecule^{-1}$ for the absorption cross section at the Lyman-α wavelength 121.567 nm is recommended.

In the weak structured region between 125 and 140 nm, measurements at low resolution were reported by Watanabe and Zelikoff,[52] Laufer and McNesby,[28] Schürgers and Welge,[41] Branton and Brion,[4] Tan et al.,[44] Lee,[29] Lee and Suto,[30] Chan et al.,[9] and at high resolution by Yoshino et al.,[54] Cheng et al.,[10] and Mota et al.[36]

In the broad continuum at long wavelengths 145–190 nm, measurements at low resolution were performed by Wilkinson and Johnston,[53] Watanabe and Zelikoff,[52] Harrison et al.,[20] Thompson et al.,[47] Laufer and McNesby,[28] Schürgers and Welge,[41] Branton and Brion,[4] Tan et al.,[44] Lee and Suto,[30] Chan et al.,[9] and at high resolution by Yoshino et al.,[54] Chung et al.,[12] and Mota et al.[36]

In the tail of the absorption band in the wavelength range 185–200 nm, measurements were reported by Cantrell et al.,[8] Creasey et al.,[14] Chung et al.,[12] Parkinson and Yoshino,[39] and Mota et al.[36] At the 184.94 nm Hg line, absorption cross sections were measured, in units 10^{-20} cm^2 $molecule^{-1}$, to be 7.8 by DeMore,[16] 7.14 ± 0.2 by Cantrell et al.,[8] 7.22 ± 0.22 by Creasey et al.,[14] 10.1 ± 0.1 by Yoshino et al.,[54] 7.0 by Hofzumahaus et al.,[21] and 7.3 (a value measured by J. Crowley, cited by Hofzumahaus et al.[21]). Based on the latter studies, the recommended value for the absorption cross section at 184.94 nm is (7.1 ± 0.2) × 10^{-20} cm^2 $molecule^{-1}$ at 298 K.

High resolution spectra of water vapor and complete sets of line parameters have been measured in the visible region by Camy-Peyret et al.[7] (369–606 nm), Mandin et al.[32] (606–758 nm), Fally et al.[17] (385–769 nm), Coheur et al.[13] (385–769 nm), and for $H_2{}^{18}O$ by Tanaka et al.[46] (584–689 nm), and Tanaka et al.[45] (606–689 nm); in the near infrared by Mérienne et al.[33] (769–1081 nm), Aldener et al.[2] (926–952 nm), and Kassi et al.[25] (747–752 nm).

The recommended absorption cross sections listed in Table 4B-2-2 are taken from Yoshino et al. [54] for the range 121–182 nm, from Cantrell et al.[8] for the range 183–191 nm, and from the interpolated data of Parkinson and Yoshino[39] for the range 192–198 nm.

Photolysis Quantum Yield and Product Studies: Stief et al.[43] reported a relative quantum yield of process (2) $\Phi_2[H + OH(X^2\Pi)] = 0.89$ and process (3) $\Phi_3[H_2 + O(^1D)] = 0.11$ for the wavelength interval 105–145 nm, and $\Phi_2[H + OH(X^2\Pi)] \geq 0.99$ and $\Phi_3[H_2 + O(^1D)] \leq 0.01$ for the interval 145–185 nm. Lee[29] measured the quantum yield of the emission of $OH(A^2\Sigma^+) \rightarrow OH(X^2\Pi)$ produced in process (4), varying between 2 and 11% in the wavelength range 105–135 nm. The quantum yields show a maximum of 11% at 130 nm, decreasing slowly with decreasing wavelengths. Ung[48] measured the relative quantum yields $\Phi_2[H + OH(X^2\Pi)] = 0.92$ and $\Phi_3[H_2 + O(^1D)] = 0.08$ for the photolysis at 147 nm. At the Lyman-α wavelength (121.567 nm) a quantum yield for H atoms, Φ_H, of 1.02 was determined by Slanger and Black.[42] They also measured a quantum yield for processes (2) + (4), $\Phi_2[H + OH(X^2\Pi)] + \Phi_4[OH(A^2\Sigma^+) + H]$, of 0.78, for process (3), $\Phi_3[O(^1D) + H_2]$, of 0.10, and for process (5), $\Phi_5[O(^3P) + H + H]$, of 0.12. Chou et al.[11] photolyzed HTO at 174 nm and estimated $\Phi_1 \leq 0.003$ for the formation of $HT + O(^3P)$ and $\Phi_2 \sim 1$ for the processes leading to H + OT and T + OH. Mordaunt et al.[35] determined the absolute branching for the photodissociation channels at 121.567 nm as $\Phi_2[H + OH(X^2\Pi)] = 0.64$, $\Phi_3[O(^1D) + H_2] = 0.11$, $\Phi_4[OH(A^2\Sigma^+) + H] = 0.14$, and $\Phi_5[O(^3P) + H + H] = 0.11$.

Table 4B-2-2. Recommended Absorption Cross Sections of H_2O Vapor at 298 K

λ (nm)	10^{20} σ (cm^2)	λ (nm)	10^{20} σ (cm^2)	λ (nm)	10^{20} σ (cm^2)	λ (nm)	10^{20} σ (cm^2)
121.0	624	133.0	494	151	141	176	284
121.5	1276	133.5	513	152	165	177	240
121.567	1480	134.0	424	153	197	178	193
122.0	1689	134.5	382	154	211	179	140
122.5	826	135.0	367	155	236	180	90.0
123.0	283	135.5	310	156	266	181	54.6
123.5	589	136.0	251	157	295	182	32.9
124.0	1332	136.5	257	158	327	183	16.9
124.5	663	137.0	204	159	354	184	12.1
125.0	619	137.5	195	160	385	185	6.78
125.5	693	138.0	177	161	413	186	4.39
126.0	706	138.5	129	162	434	187	2.71
126.5	768	139.0	126	163	456	188	1.77
127.0	800	139.5	125	164	480	189	1.08
127.5	780	140	100	165	499	190	0.672
128.0	854	141	82.3	166	509	191	0.464
128.5	820	142	64.1	167	510	192	*0.30*
129.0	777	143	57.1	168	508	193	*0.21*
129.5	819	144	56.4	169	502	194	*0.16*
130.0	718	145	58.0	170	492	195	*0.13*
130.5	733	146	65.8	171	470	196	*0.11*
131.0	699	147	75.2	172	435	197	*0.10*
131.5	601	148	84.9	173	394	198	*0.09*
132.0	667	149	101	174	353		
132.5	538	150	120	175	319		

Note:
121.567 nm: average value (see note)
121–182 nm: data integrated from Yoshino et al.[54]
183–191 nm: Cantrell et al.[8]
192–198 nm: data interpolated from Parkinson and Yoshino[39]

(1) Harvard-Smithsonian Center for Astrophysics, "Atomic and Molecular Physics Database", **2009**, http://cfa-www.harvard.edu/amdata/ampdata/cfamols.html.

(2) Aldener, M.; Brown, S. S.; Stark, H.; Daniel, J. S.; Ravishankara, A. R. Near-IR absorption of water vapor: Pressure dependence of line strengths and an upper limit for continuum absorption. *J. Mol. Spectrosc.* **2005**, *232*, 223-230, doi:10.1016/j.jms.2005.04.011.

(3) Bennett, S. W.; Tellinghuisen, J. B.; Phillips, L. F. Absorption coefficients and ionization yields of some small molecules at 58.4 nm. *J. Phys. Chem.* **1971**, *75*, 719-721, doi:10.1021/j100675a019.

(4) Branton, G. R.; Brion, C. E. Total absorption and the energy dependence of the partial oscillator strengths for "Photoionization" of the valence orbitals of H_2O using an electron-electron coincidence method. *J. Electron Spectrosc. Relat. Phenom.* **1974**, *3*, 129-135, doi:10.1016/0368-2048(74)80004-6.

(5) Brownsword, R. A.; Hillenkamp, M.; Laurent, T.; Vatsa, R. K.; Volpp, H.-R.; Wolfrum, J. Photodissociation dynamics of the chloromethanes at the Lyman-α wavelength (121.6 nm). *J. Chem. Phys.* **1997**, *106*, 1359-1366, doi:10.1063/1.473304.

(6) Calvert, J. G.; Pitts, J. N. In *Photochemistry*; John Wiley & Sons, Inc.: New York, 1966; pp 230-231.

(7) Camy-Peyret, C.; Flaud, J.-M.; Mandin, J.-Y.; Chevillard, J.-P.; Brault, J.; Ramsay, D. A.; Vervloet, M.; Chauville, J. The high-resolution spectrum of water vapor between 16500 and 25250 cm^{-1}. *J. Mol. Spectrosc.* **1985**, *113*, 208-228, doi:10.1016/0022-2852(85)90131-6.

(8) Cantrell, C. A.; Zimmer, A.; Tyndall, G. S. Absorption cross sections for water vapor from 183 to 193 nm. *Geophys. Res. Lett.* **1997**, *24*, 2195-2198, 2687 (Erratum), doi:10.1029/97GL02100.

(9) Chan, W. F.; Cooper, G.; Brion, C. E. The electronic spectrum of water in the discrete and continuum regions. Absolute optical oscillator strengths for photoabsorption (6–200 eV). *Chem. Phys.* **1993**, *178*, 387-401, doi:10.1016/0301-0104(93)85078-M.

(10) Cheng, B.-M.; Chung, C.-Y.; Bahou, M.; Lee, Y.-P.; Lee, L. C.; van Harrevelt, R.; van Hemert, M. C. Quantitative spectroscopic and theoretical study of the optical absorption spectra of H_2O, HOD, and D_2O in the 125–145 nm region. *J. Chem. Phys.* **2004**, *120*, 224-229, doi:10.1063/1.1630304.
(11) Chou, C. C.; Lo, J. G.; Rowland, F. S. Primary processes in the photolysis of water vapor at 174 nm. *J. Chem. Phys.* **1974**, *60*, 1208-1210, doi:10.1063/1.1681183.
(12) Chung, C.-Y.; Chew, E. P.; Cheng, B.-M.; Bahou, M.; Lee, Y.-P. Temperature dependence of absorption cross-section of H_2O, HDO, and D_2O in the spectral region 140-193 nm. *Nucl. Instr. Meth. Phys. Res. A* **2001**, *467-468*, 1572-1576, doi:10.1016/S0168-9002(01)00762-8.
(13) Coheur, P.-F.; Fally, S.; Carleer, M.; Clerbaux, C.; Colin, R.; Jenouvrier, A.; Mérienne, M.-F.; Hermans, C.; Vandaele, A. C. New water vapor line parameters in the 26000–13000 cm^{-1} region. *J. Quant. Spectrosc. Radiat. Transf.* **2002**, *74*, 493-510, doi:10.1016/S0022-4073(01)00269-2.
(14) Creasey, D. J.; Heard, D. E.; Lee, J. D. Absorption cross-section measurements of water vapour and oxygen at 185 nm. Implications for the calibration of field instruments to measure OH, HO_2 and RO_2 radicals. *Geophys. Res. Lett.* **2000**, *27*, 1651-1654, doi:10.1029/1999GL011014.
(15) de Reilhac, L.; Damany, N. Spectres d'absorption de H_2O, NH_3 et CH_4 dans l'ultraviolet extrême (100-500 Å). *Spectrochim. Acta* **1970**, *26A*, 801-810, doi:10.1016/0584-8539(70)80276-8.
(16) DeMore, W. B. Reaction of HO_2 with O_3 and the effect of water vapor on HO_2 kinetics. *J. Phys. Chem.* **1979**, *83*, 1113-1118, doi:10.1021/j100472a001.
(17) Fally, S.; Coheur, P.-F.; Carleer, M.; Clerbaux, C.; Colin, R.; Jenouvrier, A.; Mérienne, M.-F.; Hermans, C.; Vandaele, A. C. Water vapor line broadening and shifting by air in the 26,000–13,000 cm^{-1} region. *J. Quant. Spectrosc. Radiat. Transf.* **2003**, *82*, 119-131, doi:10.1016/S0022-4073(03)00149-3.
(18) Fillion, J.-H.; Ruiz, J.; Yang, X.-F.; Castillejo, M.; Rostas, F.; Lemaire, J.-L. High resolution photoabsorption and photofragment fluorescence spectroscopy of water between 10.9 and 12 eV. *J. Chem. Phys.* **2004**, *120*, 6531-6541, doi:10.1063/1.1652566.
(19) Gürtler, P.; Saile, V.; Koch, E. E. Rydberg series in the absorption spectra of H_2O and D_2O in the vacuum ultraviolet. *Chem. Phys. Lett.* **1977**, *51*, 386-391, doi:10.1016/0009-2614(77)80427-2.
(20) Harrison, A. J.; Cederholm, B. J.; Terwilliger, M. A. Absorption of acyclic oxygen compounds in the vacuum ultraviolet. I. Alcohols. *J. Chem. Phys.* **1959**, *30*, 355-356, doi:10.1063/1.1729952.
(21) Hofzumahaus, A.; Brauers, T.; Aschmutat, U.; Brandenburger, U.; Dorn, H.-P.; Hausmann, M.; Hessling, M.; Holland, F.; Plass-Dülmer, C.; Sedlacek, M.; et al. Reply. *Geophys. Res. Lett.* **1997**, *24*, 3039-3040, doi:10.1029/97GL02947.
(22) Hudson, R. D. Critical review of ultraviolet photoabsorption cross sections for molecules of astrophysical and aeronomic interest. *Rev. Geophys. Space Phys.* **1971**, *9*, 305-399, doi:10.1029/RG009i002p00305.
(23) Hudson, R. D. Absorption cross sections of stratospheric molecules. *Can. J. Phys.* **1974**, *52*, 1465-1478, doi:10.1139/v74-218.
(24) Hudson, R. D.; Kieffer, L. J. Absorption Cross Sections of Stratospheric Molecules. In *The Natural Stratosphere of 1974*; CIAP, 1975; Vol. Monograph 1; pp (5-156)-(155-194).
(25) Kassi, S.; Macko, P.; Naumenko, O.; Campargue, A. The absorption spectrum of water near 750 nm by CW-CRDS: contribution to the search of water dimer absorption. *Phys. Chem. Chem. Phys.* **2005**, *7*, 2460-2467, doi:10.1039/b502172c.
(26) Katayama, D. H.; Huffman, R. E.; O'Bryan, C. L. Absorption and photoionization cross sections for H_2O and D_2O in the vacuum ultraviolet. *J. Chem. Phys.* **1973**, *59*, 4309-4319, doi:10.1063/1.1680627.
(27) Kley, D. Ly(α) absorption cross-section of H_2O and O_2. *J. Atmos. Chem.* **1984**, *2*, 203-210, doi:10.1007/BF00114132.
(28) Laufer, A. H.; McNesby, J. R. Deuterium isotope effect in vacuum-ultraviolet absorption coefficients of water and methane. *Can. J. Chem.* **1965**, *43*, 3487-3490, doi:10.1139/v65-495.
(29) Lee, L. C. OH($A\ ^2\Sigma^+ \leftarrow X\ ^2\Pi_i$) yield from H_2O photodissociation in 1050-1370 Å. *J. Chem. Phys.* **1980**, *72*, 4334-4340, doi:10.1063/1.439713.
(30) Lee, L. C.; Suto, M. Quantitative photoabsorption and fluorescence study of H_2O and D_2O at 50-190 nm. *Chem. Phys.* **1986**, *110*, 161-169, doi:10.1016/0301-0104(86)85154-0.
(31) Lewis, B. R.; Vardavas, I. M.; Carver, J. H. The aeronomic dissociation of water vapor by solar H Lyman α radiation. *J. Geophys. Res.* **1983**, *88*, 4935-4940, doi:10.1029/JA088iA06p04935.
(32) Mandin, J.-Y.; Chevillard, J.-P.; Camy-Peyret, C.; Flaud, J.-M.; Brault, J. W. The high-resolution spectrum of water vapor between 13200 and 16500 cm^{-1}. *J. Mol. Spectrosc.* **1986**, *116*, 167-190, doi:10.1016/0022-2852(86)90261-4.
(33) Mérienne, M.-F.; Jenouvrier, A.; Hermans, C.; Vandaele, A. C.; Carleer, M.; Clerbaux, C.; Coheur, P.-F.; Colin, R.; Fally, S.; Bach, M. Water vapor line parameters in the 13000-9250 cm^{-1} region. *J. Quant. Spectrosc. Radiat. Transf.* **2003**, *82*, 99-117, doi:10.1016/S0022-4073(03)00148-1.

(34) Metzger, P. H.; Cook, G. R. On the continuous absorption, photoionization, and fluorescence of H_2O, NH_3, CH_4, C_2H_2, C_2H_4, and C_2H_6 in the 600-to-1000-Å Region. *J. Chem. Phys.* **1964**, *41*, 642-648, doi:10.1063/1.1725939.
(35) Mordaunt, D. H.; Ashfold, M. N. R.; Dixon, R. N. Dissociation dynamics of $H_2O(D_2O)$ following photoexcitation at the Lyman-α wavelength (121.6 nm). *J. Chem. Phys.* **1994**, *100*, 7360-7375, doi:10.1063/1.466880.
(36) Mota, R.; Parafita, R.; Giuliani, A.; Hubin-Franskin, M.-J.; Lourenço, J. M. C.; Garcia, G.; Hoffmann, S. V.; Mason, N. J.; Ribeiro, P. A.; Raposo, M.; et al. Water VUV electronic state spectroscopy by synchrotron radiation. *Chem. Phys. Lett.* **2005**, *416*, 152-159, doi:10.1016/j.cplett.2005.09.073.
(37) Nicolet, M. The photodissociation of water vapor in the mesosphere. *J. Geophys. Res.* **1981**, *86*, 5203-5208, doi:10.1029/JC086iC06p05203.
(38) Okabe, H. In *Photochemistry of Small Molecules*; John Wiley and Sons Inc.: New York, 1978; pp 217.
(39) Parkinson, W. H.; Yoshino, K. Absorption cross-section measurements of water vapor in the wavelength region 181–199 nm. *Chem. Phys.* **2003**, *294*, 31-35, doi:10.1016/S0301-0104(03)00361-6.
(40) Phillips, E.; Lee, L. C.; Judge, D. L. Absolute photoabsorption cross sections for H_2O and D_2O from λ 180–790 Å. *J. Quant. Spectrosc. Radiat. Transf.* **1977**, *18*, 309-313, doi:10.1016/0022-4073(77)90061-9.
(41) Schürgers, M.; Welge, K. H. Absorptionskoeffizient von H_2O_2 und N_2H_4 zwischen 1200 und 2000 Å. *Z. Naturforsch.* **1968**, *23a*, 1508-1510.
(42) Slanger, T. G.; Black, G. Photodissociative channels at 1216 Å for H_2O, NH_3, and CH_4. *J. Chem. Phys.* **1982**, *77*, 2432-2437, doi:10.1063/1.444111.
(43) Stief, L. J.; Payne, W. A.; Klemm, R. B. A flash photolysis-resonance fluorescence study of the formation of $O(^1D)$ in the photolysis of water and the reaction of $O(^1D)$ with H_2, Ar, and He. *J. Chem. Phys.* **1975**, *62*, 4000-4008, doi:10.1063/1.430323.
(44) Tan, K. H.; Brion, C. E.; van der Leeuw, P. E.; van der Wiel, M. J. Absolute oscillator-strengths (10-60 eV) for photoabsorption, photoionization and fragmentation of H_2O. *Chem. Phys.* **1978**, *29*, 299-309, doi:10.1016/0301-0104(78)85080-0.
(45) Tanaka, M.; Brault, J. W.; Tennyson, J. Absorption spectrum of $H_2{}^{18}O$ in the range 12400-14520 cm^{-1}. *J. Mol. Spectrosc.* **2002**, *216*, 77-80, doi:10.1006/jmsp.2002.8670.
(46) Tanaka, M.; Sneep, M.; Ubachs, W.; Tennyson, J. Cavity ring-down spectroscopy of $H_2{}^{18}O$ in the range 16570-17120 cm^{-1}. *J. Mol. Spectrosc.* **2004**, *226*, 1-6, doi:10.1016/j.jms.2004.03.004.
(47) Thompson, B. A.; Harteck, P.; Reeves Jr., R. R. Ultraviolet absorption coefficients of CO_2, CO, O_2, H_2O, N_2O, NH_3, NO, SO_2, and CH_4 between 1850 and 4000 A. *J. Geophys. Res.* **1963**, *68*, 6431-6436, doi:10.1029/JZ068i024p06431.
(48) Ung, A. Y.-M. The photolysis of water vapor at 1470 Å. H_2 production in the primary process. *Chem. Phys. Lett.* **1974**, *28*, 603-607, doi:10.1016/0009-2614(74)80117-X.
(49) Vatsa, R. K.; Volpp, H.-R. Absorption cross-sections for some atmospherically important molecules at the H atom Lyman-α wavelength (121.567 nm). *Chem. Phys. Lett.* **2001**, *340*, 289-295, doi:10.1016/S0009-2614(01)00373-6.
(50) Wainfan, N.; Walker, W. C.; Weissler, G. L. Photoionization efficiencies and cross sections in O_2, N_2, CO_2, A, H_2O, H_2, and CH_4. *Phys. Rev.* **1955**, *99*, 542-549, doi:10.1103/PhysRev.99.542.
(51) Watanabe, K.; Jursa, A. S. Absorption and photoionization cross sections of H_2O and H_2S. *J. Chem. Phys.* **1964**, *41*, 1650-1653, doi:10.1063/1.1726138.
(52) Watanabe, K.; Zelikoff, M. Absorption coefficients of water vapor in the vacuum ultraviolet. *J. Opt. Soc. Am.* **1953**, *43*, 753-755, doi:10.1364/JOSA.43.000753.
(53) Wilkinson, P. G.; Johnston, H. L. The absorption spectra of methane, carbon dioxide, water vapor, and ethylene in the vacuum ultraviolet. *J. Chem. Phys.* **1950**, *18*, 190-193, doi:10.1063/1.1747586.
(54) Yoshino, K.; Esmond, J. R.; Parkinson, W. H.; Ito, K.; Matsui, T. Erratum Chem. Phys. 211, 387-391, 1996. *Chem. Phys.* **1997**, *215*, 429-430, doi:10.1016/S0301-0104(96)00381-3.

B3. H_2O_2 (hydrogen peroxide)

Back to Index

$H_2O_2 + h\nu \rightarrow OH + OH$	215 kJ mol^{-1}	557 nm	(1)
$\rightarrow H_2O + O(^1D)$	333 kJ mol^{-1}	359 nm	(2)
$\rightarrow H + HO_2$	369 kJ mol^{-1}	324 nm	(3)

(Recommendation: 90-1, Note: 15-10, Evaluated: 15-10)

Absorption Cross Sections: Absorption cross sections of hydrogen peroxide, H_2O_2, have been reported by a number of groups as summarized in Table 4B-3-1. The H_2O_2 spectrum is continuous and the absorption cross sections decrease monotonically from 180 nm toward longer wavelengths. The cross section data from the

studies performed after 1972 at wavelengths <350 nm are in reasonable agreement. Studies prior to 1977 are not considered for the recommendation. Nicovich and Wine[11] measured cross sections relative to the absolute values at 202.6 nm, $\sigma = 4.32 \times 10^{-19}$ cm^2, and 228.8 nm, $\sigma = 1.86 \times 10^{-19}$ cm^2, recommended in DeMore et al.[1] Knight et al.[7] normalized their spectra to the spectra of Nicovich and Wine[11] between 250 nm and 280 nm. The spectra measured by Knight et al.[7] at λ >290 nm are in excellent agreement with those reported by Nicovich and Wine[11] at all the temperatures studied. Kahan et al.[6] measured the absorption spectrum at 297 K between 353 and 410 nm, i.e., longer wavelengths than in previous studies, and quantified the spectrum using online absorption measurements at 213.9 nm (Zn line). Their absolute cross sections show a significant discontinuity with the recommended spectrum at shorter wavelengths. The Kahan et al. study demonstrates that H_2O_2 absorbs at the longer wavelengths and would contribute to the atmospheric photolysis loss of H_2O_2. However, due to the apparent disagreement with the previous absolute spectrum measurements at shorter wavelengths, a recommendation in this wavelength region is not given. The recommended 2σ uncertainty factors are 1.1 for the wavelength range 190 to 300 nm and 1.25 for the wavelength range 300 to 350 nm.

Vatsa and Volpp[21] measured the Lyman-α (121.567 nm) absorption cross section to be 9.8×10^{-18} cm^2 molecule^{-1}, which is recommended. Primarily because there is only a single study at Lyman-α rather large uncertainty factor of 1.4 is recommended.

Table 4B-3-1. Summary of H_2O_2 Absorption Cross Section Studies

Study	Year	Wavelength Range (nm)	Temperature (K)
Urey et al.[17]	1929	215–275	298
Fergusson et al.[2]	1936	220–290	298
Holt et al.[5]	1948	155–220	298
Schumb et al.[14]	1955	200–400	298
Schürgers and Welge[15]	1968	125–200	298
Troe[16]	1969	220–290	300
Hochenadel et al.[4]	1972	185–260	298
Molina et al.[10]	1977	210–350	296
Lin et al.[8]	1978	195–350	296
Molina and Molina[9]	1981	190–350	298
Nicovich and Wine[11]	1988	193–350	296, 285–381
Vaghjiani and Ravishankara[18]	1989	210–345	297
Vatsa and Volpp[21]	2001	121.567	300
Knight et al.[7]	2002	250–350	273, 296, 343
Kahan et al.[6]	2012	353–410	297

The recommended 298 K absorption cross section values for wavelengths <260 nm in Table 4B-5 are the mean of the data from Lin et al.,[8] Molina and Molina,[9] Nicovich and Wine,[11] and Vaghjiani and Ravishankara.[18] Molina and Molina[9] supersedes the results of Molina et al.[10]

The temperature dependence of the absorption spectrum has been measured by Nicovich and Wine[11] and Knight et al.[7] The results of Nicovich and Wine and Knight et al. are in excellent agreement. Nicovich and Wine[11] parameterized the temperature dependence for wavelengths >260 nm as the sum of two temperature dependent components, σ_0 and σ_1, using the expression given in Table 4B-3-2. In this parameterization, σ_0 represents absorption from the ground vibrational state and σ_1 represents absorption from the O-O stretch vibrational level. The expression given in Table 4B-3-2 is recommended and the 298 K cross section values obtained from this parameterization for wavelengths >260 nm are given in Table 4B-3-3.

Table 4B-3-2. Mathematical Expression for Absorption Cross Sections of H_2O_2 as a Function of Temperature

$$10^{21}\,\sigma(\lambda,T) = \chi \sum_{n=0}^{7} A_n \lambda^n + (1-\chi) \sum_{n=0}^{4} B_n \lambda^n$$

where T: temperature K; λ: nm; $\chi = (1 + \exp(-1265/T))^{-1}$

$A_0 = 6.4761 \times 10^4$ $B_0 = 6.8123 \times 10^3$

$A_1 = -9.2170972 \times 10^2$ $B_1 = -5.1351 \times 10^1$

$A_2 = 4.535649$ $B_2 = 1.1522 \times 10^{-1}$

$A_3 = -4.4589016 \times 10^{-3}$ $B_3 = -3.0493 \times 10^{-5}$

$A_4 = -4.035101 \times 10^{-5}$ $B_4 = -1.0924 \times 10^{-7}$

$A_5 = 1.6878206 \times 10^{-7}$

$A_6 = -2.652014 \times 10^{-10}$

$A_7 = 1.5534675 \times 10^{-13}$

Range 260–350 nm; 200–400 K

Table 4B-3-3. Recommended Absorption Cross Sections of H_2O_2 Vapor at 298 K

λ (nm)	$10^{20}\,\sigma$ (cm^2 $molecule^{-1}$)
190	67.2
195	56.4
200	47.5
205	40.8
210	35.7
215	30.7
220	25.8
225	21.7
230	18.2
235	15.0
240	12.4
245	10.2
250	8.3
255	6.7
260	5.3
265	4.2
270	3.3
275	2.6
280	2.0
285	1.5
290	1.2
295	0.90
300	0.68
305	0.51
310	0.38
315	0.28
320	0.20
325	0.15
330	0.11
335	0.084
340	0.064
345	0.049
350	0.036

Note:

<260 nm: mean of the data from Lin et al.,[8] Molina and Molina,[9] Nicovich and Wine,[11] and Vaghjiani and Ravishankara[18]

260–350 nm: Nicovich and Wine,[11] parameterization

Photolysis Quantum Yields and Product Studies. The photodissociation quantum yield is thought to be unity. At and above 248 nm, the major photodissociation process is that leading to OH, i.e., the quantum yield for OH production is 2 (Vaghjiani and Ravishankara,[19] Vaghjiani et al.,[20] Riffault et al.[12]). At 248 nm Vaghjiani and Ravishankara[19] reported $\Phi(OH) = 2.09 \pm 0.36$, $\Phi(O) < 0.002$, and $\Phi(H) < 0.0002$. Schiffman et al.[13] reported a slightly lower value for $\Phi(OH)$ at 248 nm of 1.58 ± 0.23; at 193 nm they obtained $\Phi(OH) = 1.22 \pm 0.13$. At 222 nm Vaghjiani et al.[20] measured $\Phi(OH) = 2.02 \pm 0.35$, $\Phi(O) < 0.002$, and $\Phi(H) = 0.024 \pm 0.012$. At 193 nm they obtained $\Phi(OH) = 1.51 \pm 0.18$, $\Phi(O) < 0.02$, and $\Phi(H) = 0.16 \pm 0.04$. Riffault et al.[12] reported $\Phi(OH)$ values of 1.93 ± 0.39 at 308 nm and 1.96 ± 0.50 at 320 nm. In addition, Gerlach-Meyer et al.[3] reported $\Phi(H) = 0.12 \pm 0.01$ and Schiffman et al.[13] reported $\Phi(OH) = 1.22 \pm 0.13$ for 193 nm photolysis in reasonable agreement with Vaghjiani et al.[20] An OH quantum yield of 2 for $\lambda > 230$ nm is recommended. For 193 nm $\Phi(OH) = 1.7$ and $\Phi(H) = 0.15$ are recommended.

(1) DeMore, W. B.; Golden, D. M.; Hampson, R. F.; Howard, C. J.; Kurylo, M. J.; Margitan, J. J.; Molina, M. J.; Ravishankara, A. R.; Watson, R. T. Chemical Kinetics and Photochemical Data for Use in Stratospheric Modeling, Evaluation Number 7, Jet Propulsion Laboratory, California Institute of Technology Pasadena CA, JPL Publication 85-37, 1985, http:\\jpldataeval.jpl.nasa.gov.

(2) Fergusson, W. C.; Slotin, L.; Style, D. W. G. The absorption spectrum of aqueous chlorine and hydrogen peroxide vapour. *Trans. Far. Soc.* **1936**, *32*, 956-962, doi:10.1039/tf9363200956.

(3) Gerlach-Meyer, U.; Linnebach, E.; Kleinermanns, K.; Wolfrum, J. H-atom photofragments from H_2O_2 dissociated at 193 nm. *Chem. Phys. Lett.* **1987**, *133*, 113-115, doi:10.1016/0009-2614(87)87031-8.

(4) Hochanadel, C. J.; Ghormley, J. A.; Ogren, P. J. Absorption spectrum and reaction kinetics of the HO_2 radical in the gas phase. *J. Chem. Phys.* **1972**, *56*, 4426-4432, doi:10.1063/1.1677885.

(5) Holt, R. B.; McLane, C. K.; Oldenberg, O. Ultraviolet absorption spectrum of hydrogen peroxide. *J. Chem. Phys.* **1948**, *16*, 225-229, doi:10.1063/1.1746843.

(6) Kahan, T. F.; Washenfelder, R. A.; Vaida, V.; Brown, S. S. Cavity-enhanced measurements of hydrogen peroxide absorption cross sections from 353 to 410 nm, J. Phys. Chem. A. *J. Phys. Chem. A* **2012**, *116*, 5941-5947, doi:10.1021/jp2104616.

(7) Knight, G.; Ravishankara, A. R.; Burkholder, J. B. UV absorption cross sections of HO_2NO_2 between 343 and 273 K. *Phys. Chem. Chem. Phys.* **2002**, *4*, 1432-1437, doi:10.1039/b108904h.

(8) Lin, C. L.; Rohatgi, N. K.; DeMore, W. B. Ultraviolet absorption cross sections of hydrogen peroxide. *Geophys. Res. Lett.* **1978**, *5*, 113-115, doi:10.1029/GL005i002p00113.

(9) Molina, L. T.; Molina, M. J. UV absorption cross sections of HO_2NO_2 vapor. *J. Photochem.* **1981**, *15*, 97-108, doi:10.1016/0047-2670(81)85002-2.

(10) Molina, L. T.; Schinke, S. D.; Molina, M. J. Ultraviolet absorption spectrum of hydrogen peroxide vapor. *Geophys. Res. Lett.* **1977**, *4*, 580-582, doi:10.1029/GL004i012p00580.

(11) Nicovich, J. M.; Wine, P. H. Temperature-dependent absorption cross sections for hydrogen peroxide vapor. *J. Geophys. Res.* **1988**, *93*, 2417-2421, doi:10.1029/JD093iD03p02417.

(12) Riffault, V.; Gierczak, T.; Burkholder, J. B.; Ravishankara, A. R. Quantum yields for OH production in the photodissociation of HNO_3 at 248 and 308 nm and H_2O_2 at 308 and 320 nm. *Phys. Chem. Chem. Phys.* **2006**, *8*, 1079-1085, doi:1010.1039/b513760h.

(13) Schiffman, A.; Nelson, D. D., Jr.; Nesbitt, D. J. Quantum yields for OH production from 193 and 248 nm photolysis of HNO_3 and H_2O_2. *J. Chem. Phys.* **1993**, *98*, 6935-6946, doi:10.1063/1.464735.

(14) Schumb, W. C.; Satterfield, C. N.; Wentworth, R. L. Hydrogen Peroxide; Reinhold Publishing Corporation: New York, 1955; pp 287-291.

(15) Schürgers, M.; Welge, K. H. Absorptionskoeffizient von H_2O_2 und N_2H_4 zwischen 1200 und 2000 Å. *Z. Naturforsch.* **1968**, *23a*, 1508-1510.

(16) Troe, J. Ultraviolettspektrum und reaktionen des HO_2-radikals im thermischen zerfall von H_2O_2. *Ber. Bunsenges. Phys. Chem.* **1969**, *73*, 946-952, doi:10.1002/bbpc.19690731003.

(17) Urey, H. C.; Dawsey, L. H.; Rice, F. O. The absorption spectrum and decomposition of hydrogen peroxide by light. *J. Am. Chem. Soc.* **1929**, *51*, 1371-1383, doi:10.1021/ja01380a011.

(18) Vaghjiani, G. L.; Ravishankara, A. R. Absorption cross sections of CH_3OOH, H_2O_2, and D_2O_2 vapors between 210 and 365 nm at 297 K. *J. Geophys. Res.* **1989**, *94*, 3487-3492, doi:10.1029/JD094iD03p03487.

(19) Vaghjiani, G. L.; Ravishankara, A. R. Photodissociation of H_2O_2 and CH_3OOH at 248 nm and 298 K: Quantum yields for OH, $O(^3P)$ and $H(^2S)$. *J. Chem. Phys.* **1990**, *92*, 996-1003, doi:10.1063/1.458081.

(20) Vaghjiani, G. L.; Turnipseed, A. A.; Warren, R. F.; Ravishankara, A. R. Photodissociation of H_2O_2 at 193 and 222 nm: Products and quantum yields. *J. Chem. Phys.* **1992**, *96*, 5878-5886, doi:10.1063/1.462684.

(21) Vatsa, R. K.; Volpp, H.-R. Absorption cross-sections for some atmospherically important molecules at the H atom Lyman-α wavelength (121.567 nm). *Chem. Phys. Lett.* **2001**, *340*, 289-295, doi:10.1016/S0009-2614(01)00373-6.

4.5 Bibliography – HO_x Photochemistry

Aldener, M.; Brown, S. S.; Stark, H.; Daniel, J. S.; Ravishankara, A. R. Near-IR absorption of water vapor: Pressure dependence of line strengths and an upper limit for continuum absorption. *J. Mol. Spectrosc.* **2005**, *232*, 223-230, doi:10.1016/j.jms.2005.04.011.

Bennett, S. W.; Tellinghuisen, J. B.; Phillips, L. F. Absorption coefficients and ionization yields of some small molecules at 58.4 nm. *J. Phys. Chem.* **1971**, *75*, 719-721, doi:10.1021/j100675a019.

Branton, G. R.; Brion, C. E. Total absorption and the energy dependence of the partial oscillator strengths for "Photoionization" of the valence orbitals of H_2O using an electron-electron coincidence method. *J. Electron Spectrosc. Relat. Phenom.* **1974**, *3*, 129-135, doi:10.1016/0368-2048(74)80004-6.

Brownsword, R. A.; Hillenkamp, M.; Laurent, T.; Vatsa, R. K.; Volpp, H.-R.; Wolfrum, J. Photodissociation dynamics of the chloromethanes at the Lyman-α wavelength (121.6 nm). *J. Chem. Phys.* **1997**, *106*, 1359-1366, doi:10.1063/1.473304.

Calvert, J. G.; Pitts, J. N. In *Photochemistry*; John Wiley & Sons, Inc.: New York, 1966; pp 230-231.

Camy-Peyret, C.; Flaud, J.-M.; Mandin, J.-Y.; Chevillard, J.-P.; Brault, J.; Ramsay, D. A.; Vervloet, M.; Chauville, J. The high-resolution spectrum of water vapor between 16500 and 25250 cm^{-1}. *J. Mol. Spectrosc.* **1985**, *113*, 208-228, doi:10.1016/0022-2852(85)90131-6.

Cantrell, C. A.; Zimmer, A.; Tyndall, G. S. Absorption cross sections for water vapor from 183 to 193 nm. *Geophys. Res. Lett.* **1997**, *24*, 2195-2198, 2687 (Erratum), doi:10.1029/97GL02100.

Chan, W. F.; Cooper, G.; Brion, C. E. The electronic spectrum of water in the discrete and continuum regions. Absolute optical oscillator strengths for photoabsorption (6–200 eV). *Chem. Phys.* **1993**, *178*, 387-401, doi:10.1016/0301-0104(93)85078-M.

Cheng, B.-M.; Chung, C.-Y.; Bahou, M.; Lee, Y.-P.; Lee, L. C.; van Harrevelt, R.; van Hemert, M. C. Quantitative spectroscopic and theoretical study of the optical absorption spectra of H_2O, HOD, and D_2O in the 125–145 nm region. *J. Chem. Phys.* **2004**, *120*, 224-229, doi:10.1063/1.1630304.

Chou, C. C.; Lo, J. G.; Rowland, F. S. Primary processes in the photolysis of water vapor at 174 nm. *J. Chem. Phys.* **1974**, *60*, 1208-1210, doi:10.1063/1.1681183.

Chung, C.-Y.; Chew, E. P.; Cheng, B.-M.; Bahou, M.; Lee, Y.-P. Temperature dependence of absorption cross-section of H_2O, HDO, and D_2O in the spectral region 140-193 nm. *Nucl. Instr. Meth. Phys. Res. A* **2001**, *467-468*, 1572-1576, doi:10.1016/S0168-9002(01)00762-8.

Coheur, P.-F.; Fally, S.; Carleer, M.; Clerbaux, C.; Colin, R.; Jenouvrier, A.; Mérienne, M.-F.; Hermans, C.; Vandaele, A. C. New water vapor line parameters in the 26000–13000 cm^{-1} region. *J. Quant. Spectrosc. Radiat. Transf.* **2002**, *74*, 493-510, doi:10.1016/S0022-4073(01)00269-2.

Cox, R. A.; Burrows, J. P. Kinetics and mechanism of the disproportionation of HO_2 in the gas phase. *J. Phys. Chem.* **1979**, *83*, 2560-2568, doi:10.1021/j100483a002.

Creasey, D. J.; Heard, D. E.; Lee, J. D. Absorption cross-section measurements of water vapour and oxygen at 185 nm. Implications for the calibration of field instruments to measure OH, HO_2 and RO_2 radicals. *Geophys. Res. Lett.* **2000**, *27*, 1651-1654, doi:10.1029/1999GL011014.

Crowley, J. N.; Simon, F. G.; Burrows, J. P.; Moortgat, G. K.; Jenkin, M. E.; Cox, R. A. The HO_2 radical UV absorption spectrum measured by molecular modulation, UV/diode-array spectroscopy. *J. Photochem. Photobiol. A: Chem.* **1991**, *60*, 1-10, doi:10.1016/1010-6030(91)90001-A.

Dagaut, P.; Kurylo, M. J. The gas phase UV absorption spectrum of CH_3O_2 radicals: A reinvestigation. *J. Photochem. Photobiol. A: Chem.* **1990**, *51*, 133-140, doi:10.1016/1010-6030(90)87047-F.

de Reilhac, L.; Damany, N. Spectres d'absorption de H_2O, NH_3 et CH_4 dans l'ultraviolet extrême (100-500 Å). *Spectrochim. Acta* **1970**, *26A*, 801-810, doi:10.1016/0584-8539(70)80276-8.

DeMore, W. B. Reaction of HO_2 with O_3 and the effect of water vapor on HO_2 kinetics. *J. Phys. Chem.* **1979**, *83*, 1113-1118, doi:10.1021/j100472a001.

DeMore, W. B.; Golden, D. M.; Hampson, R. F.; Howard, C. J.; Kurylo, M. J.; Margitan, J. J.; Molina, M. J.; Ravishankara, A. R.; Watson, R. T. Chemical Kinetics and Photochemical Data for Use in Stratospheric Modeling, Evaluation Number 7, Jet Propulsion Laboratory, California Institute of Technology Pasadena CA, JPL Publication 85-37, 1985, http:\\jpldataeval.jpl.nasa.gov.

Fally, S.; Coheur, P.-F.; Carleer, M.; Clerbaux, C.; Colin, R.; Jenouvrier, A.; Mérienne, M.-F.; Hermans, C.; Vandaele, A. C. Water vapor line broadening and shifting by air in the 26,000–13,000 cm^{-1} region. *J. Quant. Spectrosc. Radiat. Transf.* **2003**, *82*, 119-131, doi:10.1016/S0022-4073(03)00149-3.

Fergusson, W. C.; Slotin, L.; Style, D. W. G. The absorption spectrum of aqueous chlorine and hydrogen peroxide vapour. *Trans. Far. Soc.* **1936**, *32*, 956-962, doi:10.1039/tf9363200956.

Fillion, J.-H.; Ruiz, J.; Yang, X.-F.; Castillejo, M.; Rostas, F.; Lemaire, J.-L. High resolution photoabsorption and photofragment fluorescence spectroscopy of water between 10.9 and 12 eV. *J. Chem. Phys.* **2004**, *120*, 6531-6541, doi:10.1063/1.1652566.

Gerlach-Meyer, U.; Linnebach, E.; Kleinermanns, K.; Wolfrum, J. H-atom photofragments from H_2O_2 dissociated at 193 nm. *Chem. Phys. Lett.* **1987**, *133*, 113-115, doi:10.1016/0009-2614(87)87031-8.

Gürtler, P.; Saile, V.; Koch, E. E. Rydberg series in the absorption spectra of H_2O and D_2O in the vacuum ultraviolet. *Chem. Phys. Lett.* **1977**, *51*, 386-391, doi:10.1016/0009-2614(77)80427-2.

Harrison, A. J.; Cederholm, B. J.; Terwilliger, M. A. Absorption of acyclic oxygen compounds in the vacuum ultraviolet. I. Alcohols. *J. Chem. Phys.* **1959**, *30*, 355-356, doi:10.1063/1.1729952.

Harvard-Smithsonian Center for Astrophysics, "Atomic and Molecular Physics Database", **2009**, http://cfa-www.harvard.edu/amdata/ampdata/cfamols.html.

Hochanadel, C. J.; Ghormley, J. A.; Ogren, P. J. Absorption spectrum and reaction kinetics of the HO_2 radical in the gas phase. *J. Chem. Phys.* **1972**, *56*, 4426-4432, doi:10.1063/1.1677885.

Hofzumahaus, A.; Brauers, T.; Aschmutat, U.; Brandenburger, U.; Dorn, H.-P.; Hausmann, M.; Hessling, M.; Holland, F.; Plass-Dülmer, C.; Sedlacek, M.; Weber, M.; Ehhalt, D. H. Reply. *Geophys. Res. Lett.* **1997**, *24*, 3039-3040, doi:10.1029/97GL02947.

Holt, R. B.; McLane, C. K.; Oldenberg, O. Ultraviolet absorption spectrum of hydrogen peroxide. *J. Chem. Phys.* **1948**, *16*, 225-229, doi:10.1063/1.1746843.

Hudson, R. D. Critical review of ultraviolet photoabsorption cross sections for molecules of astrophysical and aeronomic interest. *Rev. Geophys. Space Phys.* **1971**, *9*, 305-399, doi:10.1029/RG009i002p00305.

Hudson, R. D. Absorption cross sections of stratospheric molecules. *Can. J. Phys.* **1974**, *52*, 1465-1478, doi:10.1139/v74-218.

Hudson, R. D.; Kieffer, L. J. Absorption Cross Sections of Stratospheric Molecules. In *The Natural Stratosphere of 1974*; CIAP, 1975; Vol. Monograph 1; pp (5-156)-(155-194).

Kahan, T. F.; Washenfelder, R. A.; Vaida, V.; Brown, S. S. Cavity-enhanced measurements of hydrogen peroxide absorption cross sections from 353 to 410 nm, J. Phys. Chem. A. *J. Phys. Chem. A* **2012**, *116*, 5941-5947, doi:10.1021/jp2104616.

Kassi, S.; Macko, P.; Naumenko, O.; Campargue, A. The absorption spectrum of water near 750 nm by CW-CRDS: contribution to the search of water dimer absorption. *Phys. Chem. Chem. Phys.* **2005**, *7*, 2460-2467, doi:10.1039/b502172c.

Katayama, D. H.; Huffman, R. E.; O'Bryan, C. L. Absorption and photoionization cross sections for H_2O and D_2O in the vacuum ultraviolet. *J. Chem. Phys.* **1973**, *59*, 4309-4319, doi:10.1063/1.1680627.

Kley, D. Ly(α) absorption cross-section of H_2O and O_2. *J. Atmos. Chem.* **1984**, *2*, 203-210, doi:10.1007/BF00114132.

Knight, G.; Ravishankara, A. R.; Burkholder, J. B. UV absorption cross sections of HO_2NO_2 between 343 and 273 K. *Phys. Chem. Chem. Phys.* **2002**, *4*, 1432-1437, doi:10.1039/b108904h.

Kurylo, M. J.; Wallington, T. J.; Ouellette, P. A. Measurements of the UV absorption cross-sections for HO_2 and CH_3O_2 in the gas phase. *J. Photochem.* **1987**, *39*, 201-215, doi:10.1016/0047-2670(87)80032-1.

Laufer, A. H.; McNesby, J. R. Deuterium isotope effect in vacuum-ultraviolet absorption coefficients of water and methane. *Can. J. Chem.* **1965**, *43*, 3487-3490, doi:10.1139/v65-495.

Lee, L. C. OH($A\ ^2\Sigma^+ \leftarrow X\ ^2\Pi_i$) yield from H_2O photodissociation in 1050-1370 Å. *J. Chem. Phys.* **1980**, *72*, 4334-4340, doi:10.1063/1.439713.

Lee, L. C. Observation of O(^{1}D) produced from photodissociation of HO_2 at 193 and 248 nm. *J. Chem. Phys.* **1982**, *76*, 4909-4915, doi:10.1063/1.442836.

Lee, L. C.; Suto, M. Quantitative photoabsorption and fluorescence study of H_2O and D_2O at 50-190 nm. *Chem. Phys.* **1986**, *110*, 161-169, doi:10.1016/0301-0104(86)85154-0.

Lewis, B. R.; Vardavas, I. M.; Carver, J. H. The aeronomic dissociation of water vapor by solar H Lyman α radiation. *J. Geophys. Res.* **1983**, *88*, 4935-4940, doi:10.1029/JA088iA06p04935.

Lightfoot, P. D.; Cox, R. A.; Crowley, J. N.; Destriau, M.; Hayman, G. D.; Jenkin, M. E.; Moortgat, G. K.; Zabel, F. Organic peroxy radicals: Kinetics, spectroscopy and tropospheric chemistry. *Atmos. Environ.* **1992**, *26A*, 1805-1961, doi:10.1016/0960-1686(92)90423-I.

Lightfoot, P. D.; Jemi-Alade, A. A. The temperature dependence of the UV spectra of the HO_2 and CH_3O_2 radicals. *J. Photochem. Photobiol. A: Chem.* **1991**, *59*, 1-10, doi:10.1016/1010-6030(91)87062-Z.

Lin, C. L.; Rohatgi, N. K.; DeMore, W. B. Ultraviolet absorption cross sections of hydrogen peroxide. *Geophys. Res. Lett.* **1978**, *5*, 113-115, doi:10.1029/GL005i002p00113.

Mandin, J.-Y.; Chevillard, J.-P.; Camy-Peyret, C.; Flaud, J.-M.; Brault, J. W. The high-resolution spectrum of water vapor between 13200 and 16500 cm^{-1}. *J. Mol. Spectrosc.* **1986**, *116*, 167-190, doi:10.1016/0022-2852(86)90261-4.

Maricq, M. M.; Szente, J. J. A kinetic study of the reaction between ethylperoxy radicals and HO_2. *J. Phys. Chem.* **1994**, *98*, 2078-2082, doi:10.1021/j100059a016.

McAdam, K.; Veyret, B.; Lesclaux, R. UV absorption spectra of HO_2 and CH_3O_2 radicals and the kinetics of their mutual reactions at 298 K. *Chem. Phys. Lett.* **1987**, *133*, 39-44, doi:10.1016/0009-2614(87)80049-0.

Mérienne, M.-F.; Jenouvrier, A.; Hermans, C.; Vandaele, A. C.; Carleer, M.; Clerbaux, C.; Coheur, P.-F.; Colin, R.; Fally, S.; Bach, M. Water vapor line parameters in the 13000-9250 cm^{-1} region. *J. Quant. Spectrosc. Radiat. Transf.* **2003**, *82*, 99-117, doi:10.1016/S0022-4073(03)00148-1.

Metzger, P. H.; Cook, G. R. On the continuous absorption, photoionization, and fluorescence of H_2O, NH_3, CH_4, C_2H_2, C_2H_4, and C_2H_6 in the 600-to-1000-Å Region. *J. Chem. Phys.* **1964**, *41*, 642-648, doi:10.1063/1.1725939.

Molina, L. T.; Molina, M. J. UV absorption cross sections of HO_2NO_2 vapor. *J. Photochem.* **1981**, *15*, 97-108, doi:10.1016/0047-2670(81)85002-2.

Molina, L. T.; Schinke, S. D.; Molina, M. J. Ultraviolet absorption spectrum of hydrogen peroxide vapor. *Geophys. Res. Lett.* **1977**, *4*, 580-582, doi:10.1029/GL004i012p00580.

Moortgat, G.; Veyret, B.; Lesclaux, R. Absorption spectrum and kinetics of reactions of the acetylperoxy radical. *J. Phys. Chem.* **1989**, *93*, 2362-2368, doi:10.1021/j100343a032.

Mordaunt, D. H.; Ashfold, M. N. R.; Dixon, R. N. Dissociation dynamics of $H_2O(D_2O)$ following photoexcitation at the Lyman-α wavelength (121.6 nm). *J. Chem. Phys.* **1994**, *100*, 7360-7375, doi:10.1063/1.466880.

Mota, R.; Parafita, R.; Giuliani, A.; Hubin-Franskin, M.-J.; Lourenço, J. M. C.; Garcia, G.; Hoffmann, S. V.; Mason, N. J.; Ribeiro, P. A.; Raposo, M.; Limão-Vieira, P. Water VUV electronic state spectroscopy by synchrotron radiation. *Chem. Phys. Lett.* **2005**, *416*, 152-159, doi:10.1016/j.cplett.2005.09.073.

Nicolet, M. The photodissociation of water vapor in the mesosphere. *J. Geophys. Res.* **1981**, *86*, 5203-5208, doi:10.1029/JC086iC06p05203.

Nicovich, J. M.; Wine, P. H. Temperature-dependent absorption cross sections for hydrogen peroxide vapor. *J. Geophys. Res.* **1988**, *93*, 2417-2421, doi:10.1029/JD093iD03p02417.

Okabe, H. In *Photochemistry of Small Molecules*; John Wiley and Sons Inc.: New York, 1978; pp 217.

Parkinson, W. H.; Yoshino, K. Absorption cross-section measurements of water vapor in the wavelength region 181–199 nm. *Chem. Phys.* **2003**, *294*, 31-35, doi:10.1016/S0301-0104(03)00361-6.

Paukert, T. T.; Johnston, H. S. Spectra and kinetics of the hydroperoxyl free radical in the gas phase. *J. Chem. Phys.* **1972**, *56*, 2824-2838, doi:10.1063/1.1677613.

Phillips, E.; Lee, L. C.; Judge, D. L. Absolute photoabsorption cross sections for H_2O and D_2O from λ 180–790 Å. *J. Quant. Spectrosc. Radiat. Transf.* **1977**, *18*, 309-313, doi:10.1016/0022-4073(77)90061-9.

Riffault, V.; Gierczak, T.; Burkholder, J. B.; Ravishankara, A. R. Quantum yields for OH production in the photodissociation of HNO_3 at 248 and 308 nm and H_2O_2 at 308 and 320 nm. *Phys. Chem. Chem. Phys.* **2006**, *8*, 1079-1085, doi:1010.1039/b513760h.

Roehl, C. M.; Bauer, D.; Moortgat, G. K. Absorption spectrum and kinetics of the acetylperoxy radical. *J. Phys. Chem.* **1996**, *100*, 4038-4047, doi:10.1021/jp9526298.

Sander, S. P.; Peterson, M.; Watson, R. T.; Patrick, R. Kinetics studies of the $HO_2 + HO_2$ and $DO_2 + DO_2$ reactions at 298 K. *J. Phys. Chem.* **1982**, *86*, 1236-1240, doi:10.1021/j100397a002.

Schiffman, A.; Nelson, D. D., Jr.; Nesbitt, D. J. Quantum yields for OH production from 193 and 248 nm photolysis of HNO_3 and H_2O_2. *J. Chem. Phys.* **1993**, *98*, 6935-6946, doi:10.1063/1.464735.

Schumb, W. C.; Satterfield, C. N.; Wentworth, R. L. Hydrogen Peroxide; Reinhold Publishing Corporation: New York, 1955; pp 287-291.

Schürgers, M.; Welge, K. H. Absorptionskoeffizient von H_2O_2 und N_2H_4 zwischen 1200 und 2000 Å. *Z. Naturforsch.* **1968**, *23a*, 1508-1510.

Slanger, T. G.; Black, G. Photodissociative channels at 1216 Å for H_2O, NH_3, and CH_4. *J. Chem. Phys.* **1982**, *77*, 2432-2437, doi:10.1063/1.444111.

Stief, L. J.; Payne, W. A.; Klemm, R. B. A flash photolysis-resonance fluorescence study of the formation of $O(^1D)$ in the photolysis of water and the reaction of $O(^1D)$ with H_2, Ar, and He. *J. Chem. Phys.* **1975**, *62*, 4000-4008, doi:10.1063/1.430323.

Tan, K. H.; Brion, C. E.; van der Leeuw, P. E.; van der Wiel, M. J. Absolute oscillator-strengths (10-60 eV) for photoabsorption, photoionization and fragmentation of H_2O. *Chem. Phys.* **1978**, *29*, 299-309, doi:10.1016/0301-0104(78)85080-0.

Tanaka, M.; Brault, J. W.; Tennyson, J. Absorption spectrum of $H_2{}^{18}O$ in the range 12400-14520 cm^{-1}. *J. Mol. Spectrosc.* **2002**, *216*, 77-80, doi:10.1006/jmsp.2002.8670.

Tanaka, M.; Sneep, M.; Ubachs, W.; Tennyson, J. Cavity ring-down spectroscopy of $H_2{}^{18}O$ in the range 16570-17120 cm^{-1}. *J. Mol. Spectrosc.* **2004**, *226*, 1-6, doi:10.1016/j.jms.2004.03.004.

Thompson, B. A.; Harteck, P.; Reeves Jr., R. R. Ultraviolet absorption coefficients of CO_2, CO, O_2, H_2O, N_2O, NH_3, NO, SO_2, and CH_4 between 1850 and 4000 A. *J. Geophys. Res.* **1963**, *68*, 6431-6436, doi:10.1029/JZ068i024p06431.

Troe, J. Ultraviolettspektrum und reaktionen des HO_2-radikals im thermischen zerfall von H_2O_2. *Ber. Bunsenges. Phys. Chem.* **1969**, *73*, 946-952, doi:10.1002/bbpc.19690731003.

Tyndall, G. S.; Cox, R. A.; Granier, C.; Lesclaux, R.; Moortgat, G. K.; Pilling, M. J.; Ravishankara, A. R.; Wallington, T. J. Atmospheric chemistry of small organic peroxy radicals. *J. Geophys. Res.* **2001**, *106*, 12157-12182, doi:10.1029/2000JD900746.

Ung, A. Y.-M. The photolysis of water vapor at 1470 Å. H_2 production in the primary process. *Chem. Phys. Lett.* **1974**, *28*, 603-607, doi:10.1016/0009-2614(74)80117-X.

Urey, H. C.; Dawsey, L. H.; Rice, F. O. The absorption spectrum and decomposition of hydrogen peroxide by light. *J. Am. Chem. Soc.* **1929**, *51*, 1371-1383, doi:10.1021/ja01380a011.

Vaghjiani, G. L.; Ravishankara, A. R. Absorption cross sections of CH_3OOH, H_2O_2, and D_2O_2 vapors between 210 and 365 nm at 297 K. *J. Geophys. Res.* **1989**, *94*, 3487-3492, doi:10.1029/JD094iD03p03487.

Vaghjiani, G. L.; Ravishankara, A. R. Photodissociation of H_2O_2 and CH_3OOH at 248 nm and 298 K: Quantum yields for OH, O(^3P) and H(^2S). *J. Chem. Phys.* **1990**, *92*, 996-1003, doi:10.1063/1.458081.

Vaghjiani, G. L.; Turnipseed, A. A.; Warren, R. F.; Ravishankara, A. R. Photodissociation of H_2O_2 at 193 and 222 nm: Products and quantum yields. *J. Chem. Phys.* **1992**, *96*, 5878-5886, doi:10.1063/1.462684.

Vatsa, R. K.; Volpp, H.-R. Absorption cross-sections for some atmospherically important molecules at the H atom Lyman-α wavelength (121.567 nm). *Chem. Phys. Lett.* **2001**, *340*, 289-295, doi:10.1016/S0009-2614(01)00373-6.

Wainfan, N.; Walker, W. C.; Weissler, G. L. Photoionization efficiencies and cross sections in O_2, N_2, CO_2, A, H_2O, H_2, and CH_4. *Phys. Rev.* **1955**, *99*, 542-549, doi:10.1103/PhysRev.99.542.

Wallington, T. J.; Dagaut, P.; Kurylo, M. J. Ultraviolet absorption cross sections and reaction kinetics and mechanisms for peroxy radicals in the gas phase. *Chem. Rev.* **1992**, *92*, 667-710, doi:10.1021/cr00012a008.

Watanabe, K.; Jursa, A. S. Absorption and photoionization cross sections of H_2O and H_2S. *J. Chem. Phys.* **1964**, *41*, 1650-1653, doi:10.1063/1.1726138.

Watanabe, K.; Zelikoff, M. Absorption coefficients of water vapor in the vacuum ultraviolet. *J. Opt. Soc. Am.* **1953**, *43*, 753-755, doi:10.1364/JOSA.43.000753.

Wilkinson, P. G.; Johnston, H. L. The absorption spectra of methane, carbon dioxide, water vapor, and ethylene in the vacuum ultraviolet. *J. Chem. Phys.* **1950**, *18*, 190-193, doi:10.1063/1.1747586.

Yoshino, K.; Esmond, J. R.; Parkinson, W. H.; Ito, K.; Matsui, T. Erratum Chem. Phys. 211, 387-391, 1996. *Chem. Phys.* **1997**, *215*, 429-430, doi:10.1016/S0301-0104(96)00381-3.

SECTION 4C. NO_X PHOTOCHEMISTRY

C1. NO (nitric oxide)

Back to Index

$NO + h\nu \rightarrow$ Products

(New)

Absorption Cross Sections: VUV/UV absorption cross sections of NO (nitric oxide) have been measured at room temperature by Bertrand et al.[1] (123.6 nm), Chan et al.[2] (41.32–228.55 nm, graphical data), Chung et al.[3] (90–134 nm, graphical data), Guest and Lee[4] (106.4–196.3 nm, graphical data), Iida et al.[5] (6.5–207 nm), Sun and Weissler[6] (37–131 nm), Thompson et al.[7] (186–227 nm, graphical data), Wang et al.[8] (197–235 nm), and Watanabe et al.[9] (58–135 nm). At wavelengths >150 nm, there are large discrepancies in the magnitude of the reported cross sections of Chan et al., Guest and Lee, Iida et al., Thompson et al., and Wang et al., which are due primarily to differences in the spectral resolution and pressure at which the spectra were obtained. No recommendation is given for this wavelength region.

For VUV wavelengths ≤135 nm, the available studies typically agree to within 50%. At the Lyman-α wavelength (121.567 nm), the cross section of Chung et al. is high relative to the other available studies, which all agree to within 25%. The recommended Lyman-α (121.567 nm) cross section given in Table 4C-1 is an average of the data of Chan et al., Guest and Lee, Iida et al., Sun and Weissler, and Watanabe et al. and has an estimated uncertainty factor (2σ) of 1.25.

Photolysis Quantum Yield and Product Studies: No recommendation.

Table 4C-1. Recommended Absorption Cross Section of NO (nitric oxide) at 298 K

λ (nm)	10^{20} σ (cm^2)
121.567	240

Note:
Average of Chan et al.,[2] Guest and Lee,[4] Iida et al.,[5] Sun and Weissler,[6] and Watanabe et al.[9]

(1) Bertrand, C.; Collin, G. J.; Gagnon, H. Coefficients d'absorption et rendements quantiques ioniques de composés inorganiques et d'hydrocarbones insaturés. *J. Chim. Phys.* **1975**, *72*, 719-723, doi:10.1051/jcp/1975720719.

(2) Chan, W. F.; Cooper, G.; Brion, C. E. Absolute optical oscillator strengths for the photoabsorption of nitric oxide (5-30 eV) at high resolution. *Chem. Phys.* **1993**, *170*, 111-121, doi:0.1016/0301-0104(93)80097-S.

(3) Chung, J.-S.; Kim, H. H.; Chung, J.-M. Measurement of photoabsorption cross sections of nitric oxide by using double-ionization chamber. *J. Opt. Soc. Korea* **2006**, *10*, 157-161, doi:10.3807/JOSK2006.10.4.157.

(4) Guest, J. A.; Lee, L. C. Quantitative absorption and fluorescence studies of NO between 1060 and 2000 Å. *J. Phys. B: At. Mol. Phys.* **1981**, *14*, 3401-3413, doi:10.1088/0022-3700/14/18/013.

(5) Iida, Y.; Carnovale, F.; Daviel, S.; Brion, C. E. Absolute oscillator-strengths for photoabsorption and the molecular and dissociative photoionization of nitric oxide. *Chem. Phys.* **1986**, *105*, 211-225, doi:10.1016/0301-0104(86)80070-2.

(6) Sun, H.; Weissler, G. L. Absorption coefficients of nitric oxide in the vacuum ultraviolet. *J. Chem. Phys.* **1955**, *23*, 1372-1373, doi:10.1063/1.1742309.

(7) Thompson, B. A.; Harteck, P.; Reeves Jr., R. R. Ultraviolet absorption coefficients of CO_2, CO, H_2O, N_2O, NH_3, NO, SO_2, and CH_4 between 1850 and 4000 Å. *J. Geophys. Res.* **1963**, *68*, 6431-6436, doi:10.1029/JZ068i024p06431.

(8) Wang, M.; Connolly, S. C.; Venables, D. S. Deep-ultraviolet absorption cross sections of strongly absorbing atmospheric species. *J. Quant. Spectrosc. Radiat. Transf.* **2024**, *323*, 109050, doi:10.1016/j.jqsrt.2024.109050.

(9) Watanabe, K.; Matsunaga, F. M.; Sakai, H. Absorption coefficient and photoionization yield of NO in the region 580-1350 Å. *Appl. Opt.* **1967**, *6*, 391-396, doi:10.1364/AO.6.000391.

C2. NO_2 (nitrogen dioxide)

Back to Index

$NO_2 + h\nu \rightarrow NO + O(^3P)$	301 kJ mol^{-1}	398 nm	(1)
$\rightarrow NO + O(^1D)$	490 kJ mol^{-1}	244 nm	(2)

(Recommendation: 06-2, Note: 10-6, Evaluated: 10-6)

Absorption Cross Sections: The UV/vis absorption spectrum of nitrogen dioxide, NO_2, in the 200–800 nm region can be separated into two principal systems: the D-X band below 250 nm and the broad B-X and A-X bands between 300 and 800 nm with a maximum around 400 nm. The forbidden C-X transition also contributes to the visible spectrum. There is enormous spectral fine structure superimposed on the broad visible system. Due to the complexity of the electronic states of NO_2, it is not presently possible to predict its spectrum from molecular quantum theory within the accuracy of the experimental measurements. The absorption spectrum and cross sections of NO_2 have been extensively studied during the last century as summarized in Table 4C-2-1.

Table 4C-2-1. Summary of NO_2 Absorption Cross Section Studies

Study	Year	λ Range (nm)	Type*	Resolution (nm)	Temperature (K)
Holmes and Daniels[21]	1934	265–436	B	1	298
Dixon[11]	1940	400–700	A	1.5 and 4.0	295
Hall and Blacet[16]	1952	240–500	A	0.2-0.5	298
Nakayama et al.[32]	1959	108–270	A	0.02	300
Jones and Bayes[24]	1973	297–579	B	0.2	300
Johnston and Graham[23]	1974	190–420	A	1.3	294
Bass et al.[2]	1976	185–410	B	0.015–0.04	235 and 298
Harker et al.[18]	1977	375–420	B	0.1	296
Hicks et al.[20]	1979	425–450 at single λ	B	0.04	235 and 298
Schneider et al.[39]	1987	200–700	A	0.04	298
Leroy et al.[28]	1987	427–450	B	0.04	235 and 298
Koffend et al.[27]	1987	391–414/ intervals	B	0.005	251 and 300
Calvert et al.[5]	1987	404.7	B	1.6	223, 273, 298, 325, 347, 370, 406, 496, 566
Davidson et al.[9]	1988	264–649	A	1.5 0.3–2.6 cm^{-1}	233, 243, 253, 263, 273, 298, and up to 397
Corcoran et al.[7]	1992	450–650 470–616	A, B	0.075 0.008	295, 573, 673
Amoruso et al.[1]	1993	440–460	B	0.134	220 and 298
Harwood and Jones[19]	1994	313–568	A	0.54	213, 225, 233, 243, 253, 263, 273, 298
Mérienne et al.[30]	1995	300–500	A	0.01–0.015	293
Coquart et al.[6]	1995	400–500	B	0.01	220, 240, 293
Vandaele et al.[43]	1996	380–830	A	2.0 cm^{-1}	294
Frost et al.[12]	1996	370–497	A	0.5–2.0 cm^{-1}	220
Jenouvrier et al.[22]	1996	200–300	B	0.01	293
Mihalcea et al.[31]	1996	395, 670	B	0.001	296-774
Harder et al.[17]	1997	350–585 (294 K) 350–560 (low T)	A	0.15 cm^{-1}	217, 230.2, 238.6, 293.8
Yoshino et al.[47]	1997	360–470	B	0.14 cm^{-1}	298.5
Mérienne et al.[29]	1997	200–400	A	0.05	220
Vandaele et al.[44]	1998	238–1000	A	2.0 cm^{-1}	220 and 294
Burrows et al.[4]	1998	231–794	C	0.2–0.4	221, 241,

Study	Year	λ Range (nm)	Type*	Resolution (nm)	Temperature (K)
					273, 293
Orphal et al.[36]	1998	667–1111	B	0.012 cm^{-1}	298
Gierczak et al.[15]	1999	413.4	B	1	259, 298, 323, 348, 385
Voigt et al.[45]	2002	250–800	A	0.5–1.0 cm^{-1}	223, 246, 260, 280, 293
Vandaele et al.[41]	2002	385–925	A	0.05–0.1 cm^{-1}	220, 240, 294
Bogumil et al.[3]	2003	230–1070	C	0.2–0.4	203, 223, 243, 273, 293
Nizkorodov et al.[33]	2004	415–525	B	0.06 cm^{-1}	215, 230, 250, 273, 298

* The studies summarized in Table 4C-2-1 are organized into three measurement categories: *Type A*, *absolute* cross section measurements over a broad spectral region (typically covering a few hundred nm); *Type B*, *absolute* cross section measurements at specific wavelengths or over narrow spectral ranges; and *Type C, relative* NO_2 absorption spectrum measurements over broad spectral region (typically a few hundred nm) that have been scaled to absolute cross section values using results from other studies.

In the earlier studies, the NO_2 ultraviolet-visible absorption cross section measurements were limited to lower spectral resolution. Since 1992, however, several sets of high resolution measurements, including temperature and pressure dependence studies, have been reported by several groups, which mainly aimed at improving the accuracy of atmospheric measurements, in particular, for the atmospheric remote sensing of NO_2. However, a number of laboratory measurements were also obtained at spectral resolutions that are limited by instrumental techniques.

The NASA/JPL 97-04[10] recommendation for the absorption cross sections of NO_2 was based on the work of Bass et al.,[2] Schneider et al.,[39] and Davidson et al.[9] Although at room temperature the agreement between these three sets of measurements is good (within 5% between 305 and 345 nm and within 10% at the longer wavelengths), serious non-uniform wavelength calibration errors are apparent in the wavelength range 400–500 nm as described by Schneider et al.[39] At shorter wavelengths and for temperatures below 298 K the agreement among these three sets of data is poor. A possible cause for the discrepancies is the presence of N_2O_4, which is the weakly bound NO_2 dimer present in equilibrium with the monomer. The ratio of the abundance of the two species is concentration and temperature dependent. Corrections were needed to account for the presence of N_2O_4 at wavelengths below 400 nm and especially near 200 nm where N_2O_4 absorbs strongly.

Kirmse et al.[26] analyzed the spectra reported between 1976 and 1995 and concatenated selected (and corrected) cross sections to create a "new standard" spectrum in the range 300–708 nm at a resolution of 0.05 nm, and another spectrum extending to 908 nm at a lower resolution of 1 nm. This high resolution "new standard" spectrum consisted of the Mérienne et al.[30] cross sections from 300 to 500 nm, the Corcoran et al.[7] cross sections from 500 to 600 nm, and the Schneider et al.[39] cross sections from 600 to 710 nm. A critical review and evaluation of the cross section studies was performed by Orphal[34] and Orphal,[37] covering most studies published since 1995. In his evaluations Orphal[34,37] considered baseline problems, wavelength calibration and integrated cross sections (after convolution of high resolution cross sections of 0.1 nm or better). In addition, Vandaele et al.[42] derived temperature and pressure dependent parameters from high resolution spectral data obtained since 1995.

At room temperature (295 ± 3 K) there is agreement to better than 2–3% among the absolute cross sections over the wavelength range covered by the measurements of Mérienne et al.,[30] Coquart et al.,[6] Vandaele et al.,[43] Jenouvrier et al.,[22] Yoshino et al.,[47] Mérienne et al.,[29] Vandaele et al.,[44] Bogumil et al.,[3] and Nizkorodov et al.[33] Many of these studies differ in spectral resolution, an issue relevant to atmospheric remote sensing applications. The cross sections of Harwood and Jones[19] are 6–8% below most of the other studies, while the data of Harder et al.[17] are systematically 2–5% higher than the data of Vandaele et al.[44] (1998) and show a systematic baseline drift of up to 10% at the lowest temperature.

The high pressure cross section data of Vandaele et al.[41] (2002) and Vandaele et al.[42] (2003) are nearly 4% smaller than the Vandaele et al.[43] (1996) and Vandaele et al.[44] (1998) data. The cross sections of Burrows et al.[4] are about 6–8% lower than most recent high resolution studies (Mérienne-95, Mérienne-97, Harder, Vandaele-96, Vandaele-98). The data of Voigt et al.[45] show several artificial peaks (probably Xenon lamp stray light) of a few percent and baseline shifts up to 10% (partly due to residual N_2O_4 absorption) at lower

temperatures. The spectra of Bogumil et al.[3] were scaled to absolute values using the integrated cross section of Vandaele et al.[44] (1998).

The temperature effect on the NO_2 absorption cross sections has been studied by only a few research teams, as given in Table 4C-2-1. The variation of the absorption consists mainly in an increase of the differential absorption cross sections with decreasing temperature. In his analysis of the temperature dependence of the cross sections in the 300–700 nm region, Orphal[35] (2003) observed a tilt in the baseline with decreasing temperature in the data of Davidson et al.,[9] Burrows et al.,[4] and Bogumil et al.[3] but less pronounced in the data of Harwood and Jones,[19] Harder et al.,[17] and Vandaele et al.[41] (2002). This is due to a change in the thermal population of the lower vibrational and rotational states causing large discrepancies in the relative change and the absolute magnitude of the absorption cross sections. The comparison of the high resolution absolute cross sections at temperatures below ambient reveals significant discrepancies in absolute magnitude of cross sections due to spectral resolution, baseline differences and possible wavelength calibration. For the temperatures 242 ± 2 and 220 ± 3 K, the overall agreement is within 15% in the region 350–500 nm, however outside this range the discrepancies are much larger. The integrated cross sections for the range 400–500 nm were calculated by Orphal[35] (2003) to be $(4.50 \pm 0.10) \times 10^{-17}$ cm^2 molecule^{-1} nm and are independent of temperature, as recently shown by Nizkorodov et al.[33] for the temperature range 215–298 K.

Orphal[35] (2003) and Vandaele et al.[42] (2003) compared the spectra after degrading the high resolution spectra to a lower resolution. At 220 K the best agreement (within 1.6%) is obtained between the data of Coquart et al.,[6] Mérienne et al.[29] (1997), and Vandaele et al.[44] (1998). The data of Harder et al.[17] differ by 3.7% from the Vandaele et al.[44] (1998) data below 500 nm but seem to contain more noise at longer wavelengths. The data of Voigt et al.[45] show larger disagreement, which is different in every temperature data set. At 223 K their data are 22% lower than the Vandaele et al.[44] (1998) values.

The temperature dependence of the NO_2 cross sections in the entire ultraviolet and visible regions can be reproduced within the experimental uncertainties using analytical expressions, at least at low and moderate spectral resolutions (i.e., 0.05 nm and less). Linear functions were proposed by Davidson et al.,[9] Kirmse et al.,[26] and Vandaele et al.[41] (2002), a quadratic polynomial by Burrows et al.,[4] and a double exponential function by Voigt et al.[45] For the high resolution spectra Nizkorodov et al.[33] concluded that a linear temperature dependence is not valid and a successful parameterization requires further work.

The NO_2 cross sections vary as a function of total pressure but these effects are only observed at high spectral resolution, i.e., better than 0.01 nm, as investigated by Harder et al.,[17] Wennberg et al.,[46] Vandaele et al.[44] (1998), Voigt et al.,[45] Vandaele et al.[41] (2002), and Nizkorodov et al.,[33] using NO_2/N_2 (or air) mixtures at total pressures up to 1 atm. Nizkorodov et al.[33] showed that a simple Lorentzian broadening model with linear dependence of the Lorentz width on pressure provides an adequate description of the pressure broadening effects in NO_2.

The current recommendation is based on the data of Vandaele et al.[44] (1998). Table 4C-2-2 lists recommended cross sections for 294 and 220 K averaged over atmospherically relevant intervals.

Photolysis Quantum Yield and Product Studies: A number of NO_2 photolysis quantum yield studies in the atmospherically important 300–470 nm region have been reported: Jones and Bayes[24] for the wavelength range 295–445 nm and at 492 nm, 546 nm and 579 nm; Gaedtke and Troe[13] in the range 313–416 nm; Harker et al.[18] for the range 375–420 nm at 1 nm intervals; Davenport[8] for the range 390–420 nm at 223 and 300 K; Gardner et al.[14] for the range 334–404 nm at 298 K, and at 404 nm at 273 and 370 K; and Roehl et al.[38] in the range 388–411 nm at 248 and 298 K. In the range 360–398 nm the Φ_1 values show a wide scatter, with differences of as much as 60%, especially for the data of Harker et al.[18] Although Gardner et al.[14] obtained values of Φ_1 between 0.89 ± 0.05 and 0.97 ± 0.06 in the range 379–397 nm, they made a critical assessment of the quantum yield data and recommended that Φ_1 is near unity at wavelengths up to and slightly beyond the dissociation limit of λ_0 = 397.95 nm (Jost et al.[25]) and then rapidly decreases to near zero at 424 nm. However, Roehl et al.[38] determined $\Phi_1 = (0.93 \pm 0.10)$ in the range 388–398 nm at 298 K, and $\Phi_1 = (0.90 \pm 0.10)$ at 248 K. Troe[40] conducted a critical reanalysis of the quantum yield data of Gardner et al.[14] and Roehl et al.[38] below λ_0 and concluded that certain secondary reactions were not correctly accounted for, and recommended corrections for both data sets. The recommended quantum yield values in Table 4C-2-3 are based on the data of Roehl et al.[38] as corrected by Troe.[40]

Table 4C-2-2. Recommended Absorption Cross Sections of NO_2 at 220 and 294 K

λ (nm)	10^{20} σ(220 K) (cm^2)	10^{20} σ(294 K) (cm^2)	λ (nm)	10^{20} σ(220 K) (cm^2)	10^{20} σ(294 K) (cm^2)
240.964–243.902	4.14	5.77	442.5–447.5	47.9	48.8
243.902–246.914	0.961	2.79	447.5–452.5	49.3	49.8
246.914–250.000	0.859	1.62	452.5–457.5	40.6	41.6
250.000–253.165	0.191	0.998	457.5–462.5	43.5	43.6
253.165–256.410	0.496	1.05	462.5–467.5	41.5	41.4
256.410–259.740	0.872	1.28	467.5–472.5	32.7	33.7
259.740–263.158	1.26	1.58	472.5–477.5	38.8	38.7
263.158–266.667	1.77	2.05	477.5–482.5	33.4	33.7
266.667–270.270	2.36	2.64	482.5–487.5	24.0	25.4
270.270–273.973	3.03	3.24	487.5–492.5	30.9	30.8
273.973–277.778	3.94	4.07	492.5–497.5	29.4	29.4
277.778–281.690	5.16	5.21	497.5–502.5	16.7	18.2
281.690–285.714	6.29	6.23	502.5 – 507.5	24.4	24.3
285.714–289.855	7.72	7.59	507.5–512.5	22.8	23.1
289.855–294.118	9.64	9.51	512.5–517.5	14.8	16.0
294.118–298.507	11.6	11.5	517.5–522.5	17.7	16.1
298.507–303.030	13.2	13.2	522.5–527.5	17.5	17.9
303.030–307.692	16.0	16.1	527.5–532.5	14.9	15.3
307.692–312.5	18.5	18.8	532.5–537.5	9.71	10.6
312.5–317.5	20.8	21.6	537.5–542.5	10.3	10.8
317.5–322.5	24.2	25.3	542.5–547.5	12.6	12.7
322.5–327.5	27.2	28.7	547.5–552.5	10.4	11.0
327.5–332.5	29.4	31.7	552.5–557.5	7.40	7.97
332.5–337.5	33.0	35.8	557.5–562.5	5.56	6.05
337.5–342.5	37.0	40.2	562.5–567.5	8.62	8.70
342.5–347.5	38.6	41.8	567.5–572.5	8.25	8.48
347.5–352.5	43.5	46.2	572.5–577.5	4.12	4.71
352.5–357.5	47.7	49.7	577.5–582.5	4.11	4.47
357.5–362.5	49.2	50.9	582.5–587.5	4.60	4.69
362.5–367.5	53.7	54.9	587.5–592.5	5.14	5.39
367.5–372.5	55.2	56.1	592.5–597.5	3.82	4.08
372.5–377.5	58.4	59.0	597.5–602.5	3.71	3.95
377.5–382.5	58.5	59.3	602.5–607.5	1.56	1.85
382.5–387.5	59.2	60.1	607.5–612.5	2.38	2.54
387.5–392.5	62.4	63.0	612.5–617.5	3.47	3.53
392.5–397.5	58.5	59.7	617.5–622.5	2.39	2.57
397.5–402.5	64.0	64.4	622.5–627.5	1.77	1.96
402.5–407.5	57.0	58.2	627.5–632.5	1.00	1.21
407.5–412.5	61.8	62.4	632.5–637.5	1.23	1.33
412.5–417.5	58.3	59.1	637.5–642.5	1.48	1.53
417.5–422.5	59.3	59.9	642.5–647.5	1.86	1.92
422.5–427.5	56.0	57.0	647.5–652.5	1.24	1.35
427.5–432.5	53.7	54.4	652.5–657.5	0.755	0.873
432.5–437.5	55.5	55.9	657.5–662.5	0.508	0.566
437.5–442.5	47.5	48.8			

Note:
Vandaele et al.[44] (1998)

Table 4C-2-3. Recommended Quantum Yields for NO_2 Photolysis

λ (nm)	Φ(298 K)	Φ(248 K)
300–398	1.00	1.00
399	0.95	0.94
400	0.88	0.86
401	0.75	0.69
402	0.62	0.56
403	0.53	0.44
404	0.44	0.34
405	0.37	0.28
406	0.30	0.22
407	0.26	0.18
408	0.22	0.14
409	0.18	0.12
410	0.15	0.10
411	0.13	0.08
412	0.11	0.07
413	0.09	0.06
414	0.08	0.04
415	0.06	0.03
416	0.05	0.02
417	0.04	0.02
418	0.03	0.02
419	0.02	0.01
420	0.02	0.01
422	0.01	0.01

Note:
Roehl et al.[38] as corrected by Troe[40]

(1) Amoruso, A.; Crescentini, L.; Fiocco, G.; Volpe, M. New measurements of the NO_2 absorption cross section in the 440- to 460-nm region and estimates of the NO_2-N_2O_4 equilibrium constant. *J. Geophys. Res.* **1993**, *98*, 16857-16863, doi:10.1029/93JD01582.

(2) Bass, A. M.; Ledford, A. E.; Laufer, A. H. Extinction coefficients of NO_2 and N_2O_4. *J. Res. Natl. Bur. Stand.* **1976**, *80A*, 143-166, doi:10.6028/jres.080A.017.

(3) Bogumil, K.; Orphal, J.; Homann, T.; Voigt, S.; Spietz, P.; Fleischmann, O. C.; Vogel, A.; Hartmann, M.; Kromminga, H.; Bovensmann, H.; et al. Measurements of molecular absorption spectra with the SCIAMACHY pre-flight model: instrument characterization and reference data for atmospheric remote-sensing in the 230-2380 nm region. *J. Photochem. Photobiol. A: Chem.* **2003**, *157*, 167-184, doi:10.1016/S1010-6030(03)00062-5.

(4) Burrows, J. P.; Dehn, A.; Deters, B.; Himmelmann, S.; Richter, A.; Voigt, S.; Orphal, J. Atmospheric remote-sensing reference data from GOME: Part 1. Temperature-dependent absorption cross-sections of NO_2 in the 231-794 nm range. *J. Quant. Spectrosc. Radiat. Transf.* **1998**, *60*, 1025-1031, doi:10.1016/S0022-4073(97)00197-0.

(5) Calvert, J. G.; Madronich, S.; Gardner, E. P.; Davidson, J. A.; Cantrell, C. A.; Shetter, R. E. Mechanism of NO_2 photodissociation in the energy-deficient region at 404.7 nm. *J. Phys. Chem.* **1987**, *91*, 6339-6341, doi:10.1021/j100309a006.

(6) Coquart, B.; Jenouvier, A.; Merienne, M. F. The NO_2 absorption spectrum. II. Cross-sections at low temperatures in the 400-500 nm region. *J. Atmos. Chem.* **1995**, *21*, 251-261, doi:10.1007/BF00696757.

(7) Corcoran, T. C.; Beiting, E. J.; Mitchell, M. O. High-resolution absolute absorption cross sections of NO_2 at 295, 573, and 673 K at visible wavelengths. *J. Mol. Spectrosc.* **1992**, *154*, 119-128, doi:10.1016/0022-2852(92)90033-K.

(8) Davenport, J. E. Determination of NO_2 Photolysis Parameters for Stratospheric Modeling, Federal Aviation Administration, Washington, DC. FAA-EQ-78-14, 1978,

(9) Davidson, J. A.; Cantrell, C. A.; McDaniel, A. H.; Shetter, R. E.; Madronich, S.; Calvert, J. G. Visible-ultraviolet absorption cross sections for NO_2 as a function of temperature. *J. Geophys. Res.* **1988**, *93*, 7105-7112, doi:10.1029/JD093iD06p07105.

(10) DeMore, W. B.; Sander, S. P.; Golden, D. M.; Hampson, R. F.; Kurylo, M. J.; Howard, C. J.; Ravishankara, A. R.; Kolb, C. E.; Molina, M. J. Chemical Kinetics and Photochemical Data for Use in Stratospheric Modeling. *JPL Publication 97-4* **1997**, *Evaluation 12*.
(11) Dixon, J. K. The absorption coefficient of nitrogen dioxide in the visible spectrum. *J. Chem. Phys.* **1940**, *8*, 157-160, doi:10.1063/1.1750622.
(12) Frost, G. J.; Goss, L. M.; Vaida, V. Measurements of high-resolution ultraviolet-visible absorption cross sections at stratospheric temperatures, 1. Nitrogen dioxide. *J. Geophys. Res.* **1996**, *101*, 3869-3877, doi:10.1029/95JD03388.
(13) Gaedtke, H.; Troe, J. Primary processes in photolysis of NO_2. *Ber. Bunsenges. Phys. Chem.* **1975**, *79*, 184-191, doi:10.1002/bbpc.19750790212.
(14) Gardner, E. P.; Sperry, P. D.; Calvert, J. G. Primary quantum yields of NO_2 photodissociation. *J. Geophys. Res.* **1987**, *92*, 6642-6652, doi:10.1029/JD092iD06p06642.
(15) Gierczak, T.; Burkholder, J. B.; Ravishankara, A. R. Temperature dependent rate coefficient for the reaction $O(^3P) + NO_2 \rightarrow NO + O_2$. *J. Phys. Chem. A* **1999**, *103*, 877-883, doi:10.1021/jp983962p.
(16) Hall, J., T. C.; Blacet, F. E. Separation of the absorption spectra of NO_2 and N_2O_4 in the range of 2400-5000A. *J. Chem. Phys.* **1952**, *20*, 1745-1749, doi:10.1063/1.1700281.
(17) Harder, J. W.; Brault, J. W.; Johnston, P. V.; Mount, G. H. Temperature dependent NO_2 cross sections at high spectral resolution. *J. Geophys. Res.* **1997**, *D102*, 3861-3879, doi:10.1029/96JD03086.
(18) Harker, A. B.; Ho, W.; Ratto, J. J. Photodissociation quantum yield of NO_2 in the region 375 to 420 nm. *Chem. Phys. Lett.* **1977**, *50*, 394-397, doi:10.1016/0009-2614(77)80351-5.
(19) Harwood, M. H.; Jones, R. L. Temperature dependent ultraviolet-visible absorption cross sections of NO_2 and N_2O_4: Low-temperature measurements of the equilibrium constant for $2NO_2 \rightleftharpoons N_2O_4$. *J. Geophys. Res.* **1994**, *99*, 22955-22964, doi:10.1029/94JD01635
(20) Hicks, E.; Leroy, B.; Rigaud, P.; Joudain, J.-L.; Le Bras, G. Near ultraviolet and visible absorption spectra of minor atmospheric components NO_2 and SO_2 between 200 and 300 K. *J. Chim. Phys.* **1979**, *76*, 693-698, doi:10.1051/jcp/1979760693.
(21) Holmes, H. H.; Daniels, F. The photolysis of nitrogen oxides: N_2O_5, N_2O_4 and NO_2. *J. Am. Chem. Soc.* **1934**, *56*, 630-637, doi:10.1021/ja01318a028.
(22) Jenouvrier, A.; Coquart, B.; Mérienne, M.-F. The NO_2 absorption spectrum. III: The 200-300 nm region at ambient temperature. *J. Atmos. Chem.* **1996**, *25*, 21-32, doi:10.1007/BF00053284.
(23) Johnston, H. S.; Graham, R. Photochemistry of NO_x and HNO_x compounds. *Can. J. Phys.* **1974**, *52*, 1415-1423, doi:10.1139/v74-214.
(24) Jones, I. T. N.; Bayes, K. Photolysis of nitrogen dioxide. *J. Chem. Phys.* **1973**, *59*, 4836-4844, doi:10.1063/1.1680696.
(25) Jost, R.; Nygard, J.; Pasinski, A.; Delon, A. The photodissociation threshold of NO_2: Precise determination of its energy and density of states. *J. Chem. Phys.* **1996**, *105*, 1287-1290, doi:10.1063/1.471992.
(26) Kirmse, B.; Delon, A.; Jost, R. NO_2 absorption cross section and its temperature dependence. *J. Geophys. Res.* **1997**, *D103*, 16089-16098, doi:10.1029/97JD00075.
(27) Koffend, J. B.; Holloway, J. S.; Kwok, M. A.; Heidner III, R. F. High resolution absorption spectroscopy of NO_2. *J. Quant. Spectrosc. Radiat. Transf.* **1987**, *37*, 449-453, doi:10.1016/S0022-4073(87)90103-8.
(28) Leroy, B.; Rigaud, P.; Hicks, E. Visible absorption cross-sections of NO_2 at 298 K and 235 K. *Ann. Geophys.* **1987**, *5A*, 247-250.
(29) Mérienne, M.-F.; Jenouvrier, A.; Coquart, B.; Lux, J. P. The NO_2 absorption spectrum. IV: The 200–400 nm region at 220 K. *J. Atmos. Chem.* **1997**, *27*, 219-232, doi:10.1023/A:1005829213463.
(30) Mérienne, M. F.; Jenouvrier, A.; Coquart, B. The NO_2 absorption spectrum. I. Absorption cross-sections at ambient temperature in the 300-500 nm region. *J. Atmos. Chem.* **1995**, *20*, 281-297, doi:10.1007/BF00694498.
(31) Mihalcea, R. M.; Baer, D. S.; Hanson, R. K. Tunable diode-laser absorption measurements of NO_2 near 670 and 395 nm. *Appl. Opt.* **1996**, *35*, 4059-4064, doi:10.1364/AO.35.004059.
(32) Nakayama, T.; Kitamura, M. T.; Watanabe, K. Ionization potential and absorption coefficients of nitrogen dioxide. *J. Chem. Phys.* **1959**, *30*, 1180-1186, doi:10.1063/1.1730152.
(33) Nizkorodov, S. A.; Sander, S. P.; Brown, L. R. Temperature and pressure dependence of high-resolution air-broadened absorption cross sections of NO_2 (415-525 nm) *J. Phys. Chem. A* **2004**, *108*, 4864-4872, doi:10.1021/jp049461n.
(34) Orphal, J. A Critical Review of the Absorption Cross-Sections of O_3 and NO_2 in the 240-790 nm Region, Part 1, Ozone, European Space Agency, ESA-ESTEC Noordwijk, ESA Technical Note MO-TN-ESA-GO-0302, 2002,

(35) Orphal, J. A critical review of the absorption cross-sections of O_3 and NO_2 in the ultraviolet and visible. *J. Photochem. Photobiol. A: Chem.* **2003**, *157*, 185-209, doi:10.1016/S1010-6030(03)00061-3.
(36) Orphal, J.; Dreher, S.; Voigt, S.; Burrows, J. P.; Jost, R.; Delon, A. The near-infrared bands of NO_2 observed by high-resolution Fourier-transform spectroscopy. *J. Chem. Phys.* **1998**, *109*, 10217-10221, doi:10.1063/1.477716.
(37) Orphal, J.; Fellows, C. E.; Flaud, J.-M. The visible absorption spectrum of NO_3 measured by high-resolution Fourier transform spectroscopy. *J. Geophys. Res.* **2003**, *108*, 4077, doi:10.1029/2002JD002489.
(38) Roehl, C. M.; Orlando, J. J.; Tyndall, G. S.; Shetter, R. E.; Vasquez, G. J.; Cantrell, C. A.; Calvert, J. G. Temperature dependence of the quantum yields for the photolysis of NO_2 near the dissociation limit. *J. Phys. Chem.* **1994**, *98*, 7837-7843, doi:10.1021/j100083a015.
(39) Schneider, W.; Moortgat, G. K.; Burrows, J. P.; Tyndall, G. Absorption cross-sections of NO_2 in the UV and visible region (200-700 nm) at 298 K. *J. Photochem. Photobiol. A: Chem.* **1987**, *40*, 195-217, doi:10.1016/1010-6030(87)85001-3.
(40) Troe, J. Are primary quantum yields of NO_2 photolysis at $\lambda \leq 398$ nm smaller than unity? *Z. Phys. Chem.* **2000**, *214*, 573-581, doi:10.1524/zpch.2000.214.5.573.
(41) Vandaele, A. C.; Hermans, C.; Fally, S.; Carleer, M.; Colin, R.; Mérienne, M.-F.; Jenouvrier, A.; Coquart, B. High-resolution Fourier transform measurement of the NO_2 visible and near-infrared absorption cross sections: Temperature and pressure effects. *J. Geophys. Res.* **2002**, *107*, 4384, doi:10.1029/2001JD000971.
(42) Vandaele, A. C.; Hermans, C.; Fally, S.; Carleer, M.; Merienne, M.-F. Absorption cross-sections of NO_2: simulation of temperature and pressure effects. *J. Quant. Spectrosc. Radiat. Transf.* **2003**, *76*, 373-391, doi:10.1016/S0022-4073(02)00064-X.
(43) Vandaele, A. C.; Hermans, C.; Simon, P. C.; Van Roozendael, M.; Guilmot, J. M.; Carleer, M.; Colin, R. Fourier transform measurement of NO_2 absorption cross-section in the visible range at room temperature. *J. Atmos. Chem.* **1966**, *25*, 289-305, doi:10.1007/BF00053797.
(44) Vandaele, A. C.; Hermans, D.; Simon, P. C.; Carleer, M.; Colin, R.; Fally, S.; Meriénne, M.-F.; Jenouvrier, A.; Coquart, B. Measurements of the NO_2 absorption cross-section from 42000 cm^{-1} to 10000 cm^{-1} (238-1000 nm) at 220 K and 294 K. *J. Quant. Spectrosc. Radiat. Transf.* **1998**, *59*, 171-184, doi:10.1016/S0022-4073(97)00168-4.
(45) Voigt, S.; Orphal, J.; Burrows, J. P. The temperature and pressure dependence of the absorption cross-sections of NO_2 in the 250-800 nm region measured by Fourier-transform spectroscopy. *J. Photochem. Photobiol. A: Chem.* **2002**, *149*, 1-7, doi:10.1016/S1010-6030(01)00650-5.
(46) Wennberg, P. O.; Brault, J. W.; Hanisco, T. F.; Salawitch, R. J.; Mount, G. H. The atmospheric column abundance of IO: Implications for stratospheric ozone. *J. Geophys. Res.* **1997**, *D102*, 8887-8898, doi:10.1029/96JD03712.
(47) Yoshino, K.; Esmond, J. R.; Parkinson, W. H. High-resolution absorption cross section measurements of NO_2 in the UV and visible region. *Chem. Phys.* **1997**, *221*, 169-174, doi:10.1016/S0301-0104(97)00149-3.

C3. NO_3 (nitrate radical)

Back to Index

$NO_3 + h\nu \rightarrow NO + O_2$	16 kJ mol^{-1}	7320 nm	(1)
$\rightarrow NO_2 + O(^3P)$	208 kJ mol^{-1}	574 nm	(2)

(Recommendation: 06-2; Note: 10-6; Evaluated: 10-6)

Absorption Cross Sections: The visible absorption spectrum of the NO_3 radical contains ~20 diffuse bands between 400 and 700 nm, Figure 4C-3-1. The most intense features are the bands for the 0-0 and 1-0 transitions in the symmetric N-O stretching vibration in the excited state that are centered at 662 and 623 nm, respectively. The absorption cross section of the 0-0 band at 662 nm is of special interest, since it is commonly used to monitor NO_3 both in the laboratory and in the atmosphere.

The absorption cross sections of NO_3 have been the subject of many laboratory studies. The spectroscopy of NO_3 has been reviewed by Wayne et al.[21] Although there is good agreement for the positions of the absorption features, the range in reported absolute cross sections is nearly a factor of two. The studies and reported cross sections values at the 662 nm peak are summarized in Table 4C-3-1.

Table 4C-3-1. Summary of NO_3 Absorption Cross Section Studies

	Study	Year	NO_3 source Technique	T (K)	λ (nm)	Resolution (nm)	σ(662 nm) (10^{-17} cm^2)
1	Schott and Davidson[19]	1958	N_2O_5 Shock pyrolysis	600, 650, 825, 1025	366–652	3.6	1.15 ± 0.4 [a]
2	Johnston and Graham[8]	1974	$N_2O_5 + O_3$ Equilibrium constant calculation	295	450–680	0.7	0.347 (±50%) 1.48 [b]
3	Graham and Johnston[6]	1978	$N_2O_5 + O_3$ Modulated photolysis	298	400–704	0.83	1.708
4	Mitchell et al.[11]	1980	$NO_2 + O_3$ Dual beam spectrometer	294 ± 4	498–671	0.05	1.21 ± 0.20
5	Marinelli et al.[10]	1982	$NO_2 + O_3$ Tunable dye laser abs.	296	654–671	0.05	1.90
6	Ravishankara and Wine[16]	1983	$F + HNO_3$ Discharge flow, dye laser	298	565–673	0.05	1.78 ± 0.23
7	Cox et al.[4]	1984	$Cl + ClONO_2$ Modulated photolysis, diode array spectrometer	296	662	0.4	1.63 ± 0.15
8	Burrows et al.[1]	1985	$F + HNO_3$, $Cl + HNO_3$ Modulated photolysis	298	615–670	1	1.85 ± 0.56
9	Ravishankara and Mauldin[15]	1986	$F + HNO_3$ Discharge flow, dye laser abs.	298	652.5–672.5	0.05	1.90 ± 0.22
				240			2.31 ± 0.23
				220			2.71 ± 0.27
10	Sander[17]	1986	$Cl + ClONO_2$ Flash photolysis, diode array spectrometer $F + HNO_3$ Discharge flow	298	220–700	~0.4	2.28 ± 0.12 2.28 ± 0.34 [c]
				250			2.62 ± 0.13
				230			2.70 ±0.14
				298			1.83 ± 0.27
11	Canosa-Mas et al.[2]	1987	$F + HNO_3$ Discharge flow	296 ± 3	662	1.1	2.23 ± 0.35
12	Cantrell et al.[3]	1987	$NO_2 + O_3$ Fourier transform spectroscopy	348	662	0.22 (5 cm^{-1})	2.06 ± 0.27
				323			2.13 ± 0.22
				298			2.02 ± 0.20
				271			2.08 ± 0.18
				253			1.84 ± 0.43
				232			2.22 ± 0.33
				215			2.02 ± 0.24
				215–348			2.06 ± 0.32 (average)
13	Yokelson et al.[22]	1994	$Cl + ClONO_2$ Flash photolysis, diode array spectrometer	298	440–720	~0.1	2.23 ± 0.09
				258			2.49 ± 0.13
				230			2.76 ± 0.13
				200			2.99 ± 0.14
14	Wängberg et al.[20]	1997	$N_2O_5 \leftrightarrow NO_3 + NO_3$ Differential optical absorption spectroscopy	279.6–294.2	603–682	0.42	scaled to 2.10 [d]
15	Orphal et al.[13]	2003	$N_2O_5 + O_3$ Fourier transform spectroscopy	294	465–794	0.6 cm^{-1} (0.026 nm at 662 nm)	2.18

	Study	Year	NO_3 source Technique	T (K)	λ (nm)	Resolution (nm)	σ(662 nm) (10^{-17} cm^2)
16	Osthoff et al.[14]	2007	$NO_3 + NO_3 \leftrightarrow N_2O_5$ Cavity ring-down spectroscopy	298 308 318 333 353 373 388	662.2 (vac)	0.5 cm^{-1}	2.30 ± 0.19 2.16 ± 0.18 1.98 ± 0.17 1.96 ± 0.16 1.68 ± 0.13 1.60 ± 0.13 1.55 ± 0.12

[a] Estimate for 300 K by Wayne et al.[21] from the data of Schott and Davidson.[19]

[b] Improvement by Graham and Johnston[6] using their more actual kinetic data.

[c] The overall uncertainty (± 15%) includes the uncertainty of the absorbance measurement (± 5%) and the uncertainty of σ($ClONO_2$) (± 10%). The value for σ(662 nm) obtained by the flash photolysis method is preferred by Sander[17] over that obtained by the discharge flow method.

[d] Recommendation by Wayne et al.[21]

The NASA/JPL 02-25[18] evaluation recommended a cross section value of (2.00 ± 0.25) × 10^{-17} cm^2 $molecule^{-1}$ at 662 nm derived from an average of the results from studies 5, 6, and 8-12 given in Table 4C-3-1. The recommendation by Wayne et al.[21] averaged the data of the more recent studies, studies 9-12, and resulted in a slightly higher value of (2.10 ± 0.20) × 10^{-17} cm^2 $molecule^{-1}$. Higher values for the absorption cross section at 662 nm were obtained in the more recent studies by Yokelson et al.[22] and Orphal et al.[13] Here, the results from Sander[17] and Yokelson et al.[22] are averaged to derive a recommended cross section of (2.25 ± 0.15) × 10^{-17} cm^2 $molecule^{-1}$ at 662 nm. The recommended absorption cross sections at other wavelengths in Table 4C-3-2 are taken from Sander[17] after normalization to this value, which is actually only a reduction of 1.3% from the originally reported data.

The studies of the absorption spectrum temperature dependence indicate an increase of the 662 nm peak absorption cross section with decreasing temperature. Ravishankara and Mauldin[15] reported an increase of 42% between 298 and 220 K. Sander[17] reported an increase of 17% between 298 and 230 K. Yokelson et al.[22] reported increases of 34% between 298 and 200 K and 24% between 298 and 230 K. Osthoff et al.[14] reported a decrease of 48% between 298 and 388 K. Cantrell et al.[3] reported a temperature independent cross section over the temperature range 210–348 K of 2.06 × 10^{-17} cm^2 $molecule^{-1}$ that is in disagreement with the findings from the other studies. Osthoff et al.[14] combined their data with the data from Yokelson et al.[22] and modified the parameterization given by Yokelson et al.[22] for the peak cross section temperature dependence slightly as:

$$\sigma(662\text{ nm}, T) = (4.582 \pm 0.096) - [(0.00796 \pm 0.0031) \times T] \times 10^{-17}\text{ cm}^2\text{ molecule}^{-1}$$

for the range 220–388 K. Orphal et al.[13] interpreted the temperature dependence as resulting from changes in the ground vibrational state population of NO_3 (D_{3h} symmetry) and derived a formula for the cross section ratio as function of temperature:

$$\sigma(T)/\sigma(298\text{ K}) = [1 - \exp(-1096.4/T) - 2\exp(-529.5/T)] / [1 - \exp(-1096.4/298.0) - 2\exp(-529.5/298.0)]$$

where the values of 1096.4 K and 529.5 K are the vibrational energies of 762 cm^{-1} and 368 cm^{-1} divided by the Boltzmann constant. There is excellent agreement between the calculated temperature dependence using the Orphal model and the empirical relationships from Yokelson et al.[22] and Osthoff et al.[14]

Photolysis Quantum Yield and Product Studies: The quantum yields Φ_1 and Φ_2 have been measured by Graham and Johnston,[6] and at higher spectral resolution by Magnotta and Johnston,[9] who report the product of the cross section times the quantum yield in the 400 to 630 nm range. The total quantum yield value, $\Phi_1 + \Phi_2$, computed from the results of Magnotta and Johnston[9] and the cross sections of Graham and Johnston,[6] is about 1.5 for λ <585 nm, based on the nearly constant yield of the major product $O(^3P)$, and a quantum yield for the NO production Φ_1 near zero. Because systematic errors seem to exist in these data, in their review Wayne et al.[21] normalized Φ_2 quantum yields to unity at λ <585 nm. The quantum yield for the NO production, Φ_1, increases from zero at 585 nm to a maximum of $\Phi_1 = 0.35$ at 595 nm, where $\Phi_2 = 0.65$. At longer wavelengths both Φ_1 and Φ_2 decrease to a value of zero at λ = 640 nm. Orlando et al.[12] measured the $O(^3P)$ and NO quantum yields in the photolysis of NO_3 between 570 and 635 nm. They qualitatively confirm the earlier measurements by Johnston and coworkers but provide more accurate data for both channels. The $O(^3P)$ quantum yield was found to be unity in the wavelength range 570–585 and to decrease to 0.1 at 635 nm. They observed anomalously low $O(^3P)$ yields in the region of the strong absorption band near 623 nm. The quantum yields for NO formation were <0.10 at 580 nm and 0.20 ± 0.10 near 590 nm. The wavelength dependence of Φ_1 and Φ_2 are similar to those recommended in the review of Wayne et al.[21]

In a molecular beam study, Davis et al.[5] investigated the photodissociation processes of NO_3 over the wavelength range 532–662 nm and determined a sharp threshold for the dissociation of internally cold NO_3 into NO_2 and $O(^3P)$ at 587 nm. At shorter wavelengths, e.g. 585 nm, the NO + O_2 yield dropped to <0.05. At excitation energies just below this threshold, i.e., $\lambda = 588$ nm, a large quantum yield (0.70 ± 0.10) for a concerted three-center rearrangement was observed, resulting in NO + $O_2(^3\Sigma_g^-, {}^1\Delta)$. The yield of this NO + O_2 process decreases at longer wavelengths to zero at 613 nm. At $\lambda > 588$ nm the O + NO_2 channel yield arises from vibrational excitation of the ground electronic state of NO_3. These results imply that for thermally equilibrated NO_3 the branching ratios for dissociation of both channels (1) and (2) will strongly depend on temperature, especially near the threshold wavelength.

Johnston et al.[7] re-analyzed the available laboratory data relevant to NO_3 photolysis, including quantum yield data for NO and NO_2 formation, fluorescence, and threshold energies reported in the molecular beam study. Their model reproduces the wavelength dependent quantum yield values for $\Phi(O + NO_2)$, $\Phi(NO + O_2)$ and Φ(fluorescence) at 190, 230, and 298 K. At 298 K the calculated $\Phi(O + NO_2)$ quantum yields agree reasonably well with those obtained by Orlando et al.,[12] but shows a systematic offset in the wavelength range 605–620 nm. The calculated $\Phi(NO + O_2)$ product yield agrees with those reported by Magnotta and Johnston[9] within the scatter of the experimental data.

The recommended quantum yields in Table 4C-3-3 over the wavelength range 685–640 nm at 190, 230, and 298 K are taken from Johnston et al.[7] For $\lambda < 585$ nm, $\Phi(O + NO_2) = 1$, and $\Phi(NO + O_2) = 0$ and for $\lambda > 640$ nm $\Phi(O + NO_2)$ and $\Phi(NO + O_2)$ are zero. Photodissiociation rates have been calculated by Johnston et al.[7] for overhead sun in the stratosphere to be

$$J(NO + O_2) = 0.0201\ s^{-1}$$

$$J(NO_2 + O) = 0.156\ s^{-1}$$

Table 4C-3-2. Recommended Absorption Cross Sections of NO_3 at 298 K

λ (nm)	10^{20} σ (cm^2)	λ (nm)	10^{20} σ (cm^2)	λ (nm)	10^{20} σ (cm^2)	λ (nm)	10^{20} σ (cm^2)	λ (nm)	10^{20} σ (cm^2)
403	2	461	41	519	165	577	362	635	154
404	0	462	42	520	180	578	354	636	181
405	3	463	43	521	196	579	347	637	222
406	2	464	51	522	206	580	358	638	217
407	1	465	54	523	189	581	380	639	169
408	3	466	58	524	176	582	351	640	132
409	0	467	61	525	169	583	314	641	108
410	1	468	60	526	175	584	302	642	99
411	2	469	62	527	193	585	310	643	104
412	5	470	63	528	225	586	355	644	102
413	5	471	66	529	257	587	446	645	92
414	2	472	69	530	239	588	540	646	80
415	6	473	66	531	224	589	656	647	75
416	7	474	66	532	216	590	638	648	66
417	8	475	73	533	209	591	583	649	58
418	5	476	84	534	218	592	548	650	53
419	9	477	83	535	247	593	490	651	59
420	9	478	78	536	275	594	449	652	65
421	9	479	78	537	276	595	460	653	76
422	10	480	75	538	251	596	495	654	88
423	12	481	76	539	219	597	467	655	105
424	10	482	76	540	225	598	393	656	142
425	8	483	77	541	219	599	333	657	184
426	15	484	83	542	201	600	296	658	260
427	15	485	88	543	180	601	307	659	436
428	13	486	98	544	183	602	355	660	798
429	12	487	99	545	210	603	408	661	1551
430	18	488	102	546	260	604	468	662	2250
431	14	489	103	547	312	605	467	663	1869

λ (nm)	10^{20} σ (cm^2)	λ (nm)	10^{20} σ (cm^2)	λ (nm)	10^{20} σ (cm^2)	λ (nm)	10^{20} σ (cm^2)	λ (nm)	10^{20} σ (cm^2)
432	16	490	111	548	320	606	355	664	1210
433	19	491	106	549	290	607	258	665	794
434	20	492	107	550	265	608	198	666	532
435	17	493	109	551	261	609	184	667	326
436	16	494	109	552	264	610	189	668	203
437	20	495	113	553	271	611	204	669	134
438	23	496	129	554	298	612	239	670	102
439	22	497	130	555	334	613	282	671	85
440	21	498	128	556	349	614	273	672	81
441	20	499	125	557	352	615	242	673	69
442	23	500	121	558	376	616	224	674	55
443	19	501	118	559	399	617	226	675	51
444	21	502	118	560	355	618	256	676	52
445	22	503	119	561	320	619	274	677	63
446	26	504	135	562	311	620	350	678	80
447	31	505	137	563	300	621	562	679	84
448	26	506	143	564	291	622	1090	680	74
449	30	507	137	565	292	623	1578	681	57
450	31	508	136	566	305	624	1291	682	42
451	33	509	145	567	301	625	898	683	33
452	36	510	162	568	305	626	783	684	28
453	34	511	186	569	310	627	806	685	19
454	38	512	189	570	299	628	789	686	17
455	38	513	172	571	296	629	748	687	13
456	38	514	169	572	294	630	724	688	13
457	42	515	170	573	298	631	518	689	13
458	39	516	167	574	306	632	350	690	11
459	45	517	160	575	330	633	233	691	8
460	42	518	154	576	350	634	176		

Note:
403–691 nm: data from Sander[17] normalized to 2.25×10^{-17} cm^2 $molecule^{-1}$ at 662 nm

Table 4C-3-3. Recommended Product Channel Quantum Yields in the Photolysis of NO_3 at 298, 230, and 190 K

λ (nm)	10^3 Φ($NO + O_2$)			10^3 Φ($NO_2 + O(^3P)$)		
	298 K	230 K	190 K	298 K	230 K	190 K
585	0.0	0.0	0.0	983.0	996.0	999.0
586	15.2	26.4	37.9	967.0	970.0	961.0
587	39.1	66.7	94.4	943.0	930.0	905.0
588	97.1	161.0	221.0	885.0	836.0	779.0
589	128.0	209.0	283.0	854.0	788.0	716.0
590	190.0	300.0	397.0	793.0	696.0	602.0
591	220.0	343.0	448.0	763.0	653.0	551.0
592	249.0	383.0	495.0	734.0	614.0	505.0
593	303.0	455.0	575.0	680.0	542.0	424.0
594	328.0	487.0	610.0	654.0	510.0	390.0
595	359.0	517.0	630.0	608.0	453.0	332.0
596	357.0	501.0	598.0	587.0	429.0	307.0
597	318.0	430.0	493.0	567.0	406.0	285.0
598	323.0	421.0	468.0	531.0	367.0	249.0
599	314.0	396.0	429.0	509.0	345.0	229.0
600	291.0	346.0	355.0	472.0	307.0	196.0
601	296.0	338.0	335.0	438.0	275.0	170.0
602	291.0	322.0	310.0	415.0	254.0	153.0
603	283.0	294.0	267.0	371.0	215.0	123.0
604	280.0	282.0	249.0	351.0	198.0	111.0

605	264.0	253.0	213.0	323.0	176.0	94.4
606	271.0	251.0	205.0	296.0	155.0	80.0
607	268.0	243.0	194.0	280.0	143.0	71.9
608	250.0	217.0	167.0	259.0	128.0	62.1
609	248.0	208.0	155.0	238.0	113.0	53.0
610	236.0	193.0	140.0	226.0	105.0	48.1
611	205.0	159.0	111.0	210.0	94.7	42.2
612	200.0	150.0	101.0	193.0	84.0	36.2
613	190.0	138.0	90.6	181.0	77.3	32.6
614	166.0	114.0	71.2	166.0	68.4	28.0
615	166.0	110.0	66.1	147.0	58.3	22.9
616	160.0	102.0	59.7	137.0	52.7	20.2
617	141.0	85.5	47.5	124.0	46.5	17.3
618	143.0	83.5	44.8	108.0	38.6	13.8
619	139.0	78.4	40.9	99.3	34.6	12.1
620	131.0	71.5	36.0	89.7	30.3	10.2
621	127.0	66.0	32.0	76.9	24.8	8.03
622	122.0	61.9	29.2	70.4	22.1	6.99
623	117.0	57.6	26.5	64.3	19.7	6.07
624	106.0	49.6	21.9	55.2	16.2	4.8
625	98.5	44.5	19.0	48.7	13.8	3.94
626	92.3	40.6	16.8	44.2	12.2	3.39
627	84.8	36.0	14.5	39.3	10.5	2.83
628	73.9	29.9	11.5	33.9	8.67	2.26
629	69.9	27.4	10.2	29.4	7.23	1.81
630	64.9	24.7	9.01	26.4	6.29	1.53
631	57.8	21.3	7.52	23.6	5.45	1.29
632	50.8	17.8	6.02	19.5	4.29	0.969
633	46.6	15.9	5.23	17.7	3.8	0.838
634	42.6	14.2	4.54	16.1	3.36	0.724
635	37.3	12.0	3.73	14.6	2.97	0.624
636	32.3	9.86	2.93	11.9	2.3	0.462
637	29.4	8.7	2.52	10.7	2.02	0.396
638	26.6	7.66	2.16	9.57	1.77	0.338
639	23.5	6.53	1.78	8.56	1.54	0.288
640	20.3	5.38	1.41	7.15	1.24	0.224

Note:
Johnston et al.[7]

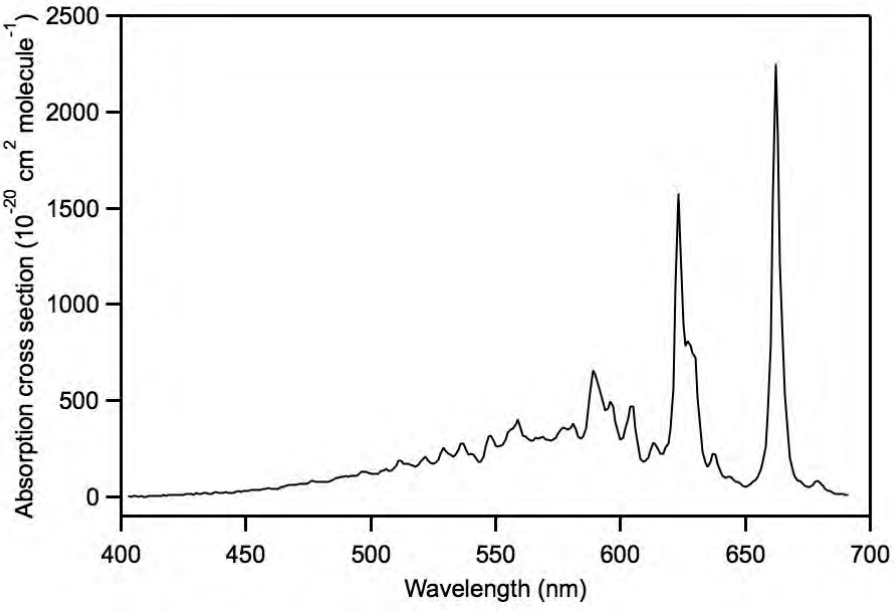


Figure 4C-3-1. Absorption Spectrum of NO_3

(1) Burrows, J. P.; Tyndall, G. S.; Moortgat, G. K. Absorption spectrum of NO_3 and kinetics of the reactions of NO_3 with NO_2, Cl, and several stable atmospheric species at 298 K. *J. Phys. Chem.* **1985**, *89*, 4848-4856, doi:10.1021/j100268a038.
(2) Canosa-Mas, C. E.; Fowles, M.; Houghton, P. J.; Wayne, R. P. Absolute absorption cross-section measurements on NO_3 Evaluation of the titration of NO_3 by NO in the determination of absolute concentrations. *J. Chem. Soc. Faraday Trans. 2* **1987**, *83*, 1465-1474, doi:10.1039/f29878301465.
(3) Cantrell, C. A.; Davidson, J. A.; Shetter, R. E.; Anderson, B. A.; Calvert, J. G. The temperature invariance of the NO_3 absorption cross section in the 662-nm region. *J. Phys. Chem.* **1987**, *91*, 5858-5863, doi:10.1021/j100307a009.
(4) Cox, R. A.; Barton, R. A.; Ljungstrom, E.; Stocker, D. W. The reactions of Cl and ClO with the NO_3 radical. *Chem. Phys. Lett.* **1984**, *108*, 228-232, doi:10.1016/0009-2614(84)87054-2.
(5) Davis, H. F.; Kim, B.; Johnston, H. S.; Lee, Y. T. Dissociation energy and photochemistry of NO_3. *J. Phys. Chem.* **1993**, *97*, 2172-2180, doi:10.1021/j100112a018.
(6) Graham, R. A.; Johnston, H. S. The photochemistry of NO_3 and the kinetics of the N_2O_5-O_3 system. *J. Phys. Chem.* **1978**, *82*, 254-268, doi:10.1021/j100492a002.
(7) Johnston, H. S.; Davis, H. F.; Lee, Y. T. NO_3 photolysis product channels: Quantum yields from observed energy thresholds. *J. Phys. Chem.* **1996**, *100*, 4713-4723, doi:10.1021/jp952692x.
(8) Johnston, H. S.; Graham, R. Photochemistry of NO_x and HNO_x compounds. *Can. J. Phys.* **1974**, *52*, 1415-1423, doi:10.1139/v74-214.
(9) Magnotta, F.; Johnston, H. S. Photodissociation quantum yields for the NO_3 free radical. *Geophys. Res. Lett.* **1980**, *7*, 769-772, doi:10.1029/GL007i010p00769.
(10) Marinelli, W. J.; Swanson, D. M.; Johnston, H. S. Absorption cross sections and line shape for the NO_3(0-0) band. *J. Chem. Phys.* **1982**, *76*, 2864-2870, doi:10.1063/1.443366.
(11) Mitchell, D. N.; Wayne, R. P.; Allen, P. J.; Harrison, R. P.; Twin, R. J. Kinetics and photochemistry of NO_3 Part 1.-Absolute absorption cross-section. *J. Chem. Soc. Faraday Trans. 2* **1980**, *76*, 785-793, doi:10.1039/f29807600785.
(12) Orlando, J. J.; Tyndall, G. S.; Moortgat, G. K.; Calvert, J. G. Quantum yields for NO_3 photolysis between 570 and 635 nm. *J. Phys. Chem.* **1993**, *97*, 10996-11000, doi:10.1021/j100144a017.
(13) Orphal, J.; Fellows, C. E.; Flaud, J.-M. The visible absorption spectrum of NO_3 measured by high-resolution Fourier transform spectroscopy. *J. Geophys. Res.* **2003**, *108*, 4077, doi:10.1029/2002JD002489.
(14) Osthoff, H. D.; Pilling, M. J.; Ravishankara, A. R.; Brown, S. S. Temperature dependence of the NO_3 absorption cross-section above 298 K and determination of the equilibrium constant for $NO_3 + NO_2 \leftrightarrow N_2O_5$ at atmospherically relevant conditions. *Phys. Chem. Chem. Phys.* **2007**, *9*, 5785-5793, doi:10.1039/b709193a.
(15) Ravishankara, A. R.; Mauldin, R. L. Temperature dependence of the NO_3 cross section in the 662-nm region. *J. Geophys. Res.* **1986**, *91*, 8709-8712, doi:10.1029/JD091iD08p08709.
(16) Ravishankara, A. R.; Wine, P. H. Absorption cross sections for NO_3 between 565 and 673 nm. *Chem. Phys. Lett.* **1983**, *101*, 73-78, doi:10.1016/0009-2614(83)80308-X.
(17) Sander, S. P. Temperature dependence of the NO_3 absorption spectrum. *J. Phys. Chem.* **1986**, *90*, 4135-4142, doi:10.1021/j100408a060.
(18) Sander, S. P.; Finlayson-Pitts, B. J.; Friedl, R. R.; Golden, D. M.; Huie, R. E.; Kolb, C. E.; Kurylo, M. J.; Molina, M. J.; Moortgat, G. K.; Orkin, V. L.; et al. Chemical Kinetics and Photochemical Data for Use in Atmospheric Studies, Evaluation Number 14, Jet Propulsion Laboratory Pasadena, JPL Publication 02-25, 2002, http:\\jpldataeval.jpl.nasa.gov.
(19) Schott, G.; Davidson, N. Shock waves in chemical kinetics: The decomposition of N_2O_5 at high temperatures. *J. Am. Chem. Soc.* **1958**, *80*, 1841-1853, doi:10.1021/ja01541a019.
(20) Wängberg, I.; Etzkorn, T.; Barnes, I.; Platt, U.; Becker, K. H. Absolute determination of the temperature behavior of the $NO_2 + NO_3 + (M) \leftrightarrow N_2O_5 + (M)$ equilibrium. *J. Phys. Chem. A* **1997**, *101*, 9694-9698, doi:10.1021/jp972203o.
(21) Wayne, R. P.; Barnes, I.; Burrows, J. P.; Canosa-Mas, C. E.; Hjorth, J.; Le Bras, G.; Moortgat, G. K.; Perner, D.; Poulet, G.; Restelli, G.; et al. The nitrate radical: Physics, chemistry, and the atmosphere. *Atmos. Environ.* **1991**, *25A*, 1-203, doi:10.1016/0960-1686(91)90192-A.
(22) Yokelson, R. J.; Burkholder, J. B.; Fox, R. W.; Talukdar, R. K.; Ravishankara, A. R. Temperature dependence of the NO_3 absorption spectrum. *J. Phys. Chem.* **1994**, *98*, 13144-13150, doi:10.1021/j100101a009.

C4. N_2O (nitrous oxide)

Back to Index

$N_2O + h\nu \rightarrow N_2 + O(^1D)$	356.5 kJ mol^{-1}	336 nm	(1)
$\rightarrow N_2 + O(^3P)$	168 kJ mol^{-1}	713 nm	(2)
$\rightarrow N(^4S) + NO(^2\Pi)$	482 kJ mol^{-1}	248 nm	(3)
$\rightarrow N_2 + O(^1S)$	571 kJ mol^{-1}	210 nm	(4)

(Recommendation: 06-2; Note: 15-10; Evaluated: 15-10)

Absorption Cross Sections: The VUV/UV absorption spectrum of nitrous oxide, N_2O, has been measured in numerous studies covering the wavelength range 108–315 nm at temperatures between 194 and 302 K. A summary of the available spectroscopic studies is given in Table 4C-4-1.

Table 4C-4-1. Summary of N_2O Cross Section Studies

Study	Year	Temperature (K)	Wavelength range (nm)	Resolution (nm)
Romand and Mayence[21]	1949	291	139–231	–
Zelikoff et al.[32]	1953	298	108–210	0.085
Zelikoff and Aschenbrand[31]	1954	298	184.9	–
Thompson et al.[26]	1963	298	190–240	–
Bates and Hays[1]	1967	298	190–315	–
Bertrand et al.[2]	1975	298	123.6	–
Johnston and Selwyn[12]	1975	298	210–300	–
Selwyn et al.[23]	1977	194, 225, 243, 263, 302	173–240	0.7, 0.075
Hitchcock et al.[9]	1980	298	16.8–155	0.5
Hubrich and Stuhl[10]	1980	208, 298	160–250	0.3
Selwyn and Johnston[24]	1981	150–500	172–197	0.003, 0.05, 0.07
Yoshino et al.[29]	1984	295–299	169.6–222.6	0.0006
Mérienne et al.[14]	1990	220, 240, 296	200–240	0.02
Chan et al.[4]	1994	298	6.1–168	0.5
Cantrell et al.[3]	1997	298, 353	184.9	<0.2
Creasey et al.[5]	2000	298	184.9	–
von Hessberg et al.[28]	2004	233, 283	180–218	0.7, 1.1
Rontu Carlon et al.[22]	2010	210–350	184.95, 202.206, 206.200, 213.857, 228.8	atomic lines
SPARC Evaluation[13]	2013	–	–	–

The N_2O spectrum has a broad absorption band between 160 and 260 nm with the peak near 182 nm (σ_{max} = (1.24–1.47) × 10^{-19} cm^2 molecule^{-1}) and a stronger but weaker band between 137 and 160 nm with the maximum near 145 nm (σ_{max} = (5-6) × 10^{-18} cm^2 molecule^{-1}). There is good agreement between the results from Selwyn et al.[23] and Hubrich and Stuhl.[10] The agreement over the entire 160–260 nm band is better than 15% and the difference at 182 nm is 5% with the data of Selwyn et al.[23] being greater. The results of Mérienne et al.[14] and Rontu Carlon et al.[22] are in excellent agreement, better than 5% and 3%, respectively, with those of Selwyn et al.[23] The results of Cantrell et al.[3] and Creasey et al.[5] at 184.9 nm are also in good agreement with the results of Selwyn et al.[23] The high resolution absorption spectrum reported by Yoshino et al.[29] shows the diffuse vibrational structure around the maximum and their absolute cross sections are close to those reported by Hubrich and Stuhl.[10] At wavelengths >250 nm, there are large discrepancies between the results from Bates and Hayes[1] and Johnston and Selwyn.[12] The recommended cross sections listed in Table 4C-4-2 are based on the room temperature results at 160, 165, and 170 nm of Hubrich and Stuhl[10] and the room temperature data between 173–240 nm from Selwyn et al.[23]

The VUV absorption spectrum of N_2O has been measured by Hitchcock et al.[9] (16.8–155 nm) and Chan et al.[4] (6.1–168 nm). The absorption cross section at 123.6 nm was measured by Bertrand et al.[2] The cross section results from Chan et al. and Hitchcock et al. agree to within 6% at 124 nm, while the value reported by Bertrand et al. is less by nearly a factor of 3. The reason for the difference is unknown. The recommended Lyman-α cross section is adopted from SPARC,[13] which used a linear interpolation of the Chan et al. cross section data at 118 and 124 nm to obtain a Lyman-α cross section of 2.4 × 10^{-17} cm^2 molecule^{-1} with an uncertainty factor of 1.5 (2σ).

The temperature dependence of the N_2O absorption cross section in the atmospherically relevant wavelength region has been measured by Selwyn et al.,[23] Hubrich and Stuhl,[10] Mérienne et al.,[14] and Rontu Carlon et al.[22] These studies report a decrease in absorption cross section with decreasing temperature. The Hubrich and Stuhl data has considerable scatter in the spectrum wavelength dependence and is not considered in the recommendation. The Rontu Carlon et al. study is in excellent agreement, to within 3%, with the NASA/JPL 10-6 recommendation at 202.206, 206.200, and 213.857 nm. There is a systematic difference in the cross section temperature dependence at 228.8 nm between the Mérienne et al. and Rontu Carlon et al. data and that of NASA/JPL 10-6, where the difference is ~18% at 210 K. The empirical cross section parameterization given by Selwyn et al.[23] given in Table 4C-4-3 is recommended.

On the basis of the Selwyn et al., Mérienne et al., and Rontu Carlon et al. studies, an uncertainty factor of 1.08 (2σ) is recommended for the 298 K absorption cross sections over the wavelength range 185–220 nm. The uncertainty factor at lower temperatures is estimated to be slightly greater with a value of 1.12 (2σ) at 200 K.

Isotopomer specific cross sections for $^{14}N^{14}NO$, $^{15}N^{14}NO$, $^{14}N^{15}NO$, $^{15}N^{15}NO$ over the wavelength range 181–218 nm have been reported by von Hessberg et al.[28] at 233 and 283 K. They observed a slight decrease in the absorption cross sections of $^{14}N^{15}NO$ and $^{15}N^{5}NO$ compared to those of $^{14}N^{14}NO$ and $^{15}N^{14}NO$. They also observed a systematic decrease in absorption cross section with decreasing temperature.

Photolysis Quantum Yield and Product Studies: The quantum yield for photodissociation is unity in the range 140–230 nm and the photoproducts are almost exclusively N_2 and $O(^1D)$ (Zelikoff and Aschenbrand,[31] Greiner,[7] Paraskevopoulos and Cvetanovic,[16] Preston and Barr,[17] and Simonaitis et al.[25]). The yield of $N(^4S)$ and $NO(^2\Pi)$ is less than 1% (Greenblatt and Ravishankara[6]). Nishida et al.[15] reported the yield of $O(^3P)$ at 193 nm to be 0.005 ± 0.002.

Several groups have investigated the isotopic fractionation of N_2O resulting from photolysis in the UV. Fractionation factors have been measured following photolysis at select wavelengths in the 193–213 nm range by Turatti et al.[27] (using high resolution FTIR spectroscopy), Röckmann et al.[19] (using a modified isotope ratio mass spectrometric technique), Rahn et al.[18] (utilizing isotope ratio mass spectrometry), and Zhang et al.[33] (using low resolution FTIR spectroscopy). Röckmann et al.[20] utilized a broadband photolysis source centered around 200 nm that simulated stratospheric actinic fluxes. The results are in reasonably good agreement and indicate that the fractionation factors increase with increasing wavelength between 193 and 213 nm. Furthermore, the fractionation factors show a clear dependence on the position of the ^{15}N atom, in agreement with the theoretical zero point energy model of Yung and Miller.[30] However, the Yung and Miller calculations underestimate the laboratory results by about a factor of two. A more detailed Hermite propagation model used by Johnson et al.[11] achieved better agreement with experimental enrichment factors. Analysis of the isotopic composition of stratospheric air samples yields results that are in qualitative agreement with the laboratory results, confirming that photolysis is the predominant sink for N_2O.[8,20] On the other hand, the fractionation factors measured in the atmospheric samples are smaller than those reported from the laboratory studies, indicating the influence of atmospheric diffusion and mixing (Röckmann et al.[20]).

Table 4C-4-2. Recommended Absorption Cross Sections of N_2O at 298 K

λ (nm)	$10^{20}\sigma$ (cm^2)	λ (nm)	$10^{20}\sigma$ (cm^2)	λ (nm)	$10^{20}\sigma$ (cm^2)	λ (nm)	$10^{20}\sigma$ (cm^2)
160	4.30	188	12.5	206	1.65	224	0.0375
165	5.61	189	11.7	207	1.38	225	0.0303
170	8.30	190	11.1	208	1.16	226	0.0239
173	11.3	191	10.4	209	0.980	227	0.0190
174	11.9	192	9.75	210	0.755	228	0.0151
175	12.6	193	8.95	211	0.619	229	0.0120
176	13.4	194	8.11	212	0.518	230	0.00955
177	14.0	195	7.57	213	0.421	231	0.00760
178	13.9	196	6.82	214	0.342	232	0.00605
179	14.4	197	6.10	215	0.276	233	0.00478
180	14.6	198	5.35	216	0.223	234	0.00360
181	14.6	199	4.70	217	0.179	235	0.00301
182	14.7	200	4.09	218	0.142	236	0.00240
183	14.6	201	3.58	219	0.115	237	0.00191
184	14.4	202	3.09	220	0.0922	238	0.00152
185	14.3	203	2.67	221	0.0739	239	0.00123
186	13.6	204	2.30	222	0.0588	240	0.00101
187	13.1	205	1.95	223	0.0474		

Note:
160–170 nm: Hubrich and Stuhl[10]
173–240 nm: Selwyn et al.[23]

Table 4C-4-3. Recommended Expression for the Absorption Cross Sections of N_2O as a Function of Temperature

$$\overline{\ln(\sigma(\lambda,T))} = \sum_{n=0}^{4} A_n \lambda^n + (T - 300)\exp\left(\sum_{n=0}^{3} B_n \lambda^n\right)$$

where T ≡ temperature (K) and λ ≡ wavelength (nm)

$A_0 = 68.21023$	$B_0 = 123.4014$
$A_1 = -4.071805$	$B_1 = -2.116255$
$A_2 = 4.301146 \times 10^{-2}$	$B_2 = 1.111572 \times 10^{-2}$
$A_3 = -1.777846 \times 10^{-4}$	$B_3 = -1.881058 \times 10^{-5}$
$A_4 = 2.520672 \times 10^{-7}$	

Ranges of applicability: 173 nm < λ < 240 nm; 194 K < T < 302 K

(1) Bates, D. R.; Hays, P. B. Atmospheric nitrous oxide. *Planet. Space Sci.* **1967**, *15*, 189-197, doi:10.1016/0032-0633(67)90074-8.

(2) Bertrand, C.; Collin, G. J.; Gagnon, H. Coefficients d'absorption et rendements quantiques ioniques de composés inorganiques et d'hydrocarbones insaturés. *J. Chim. Phys.* **1975**, *72*, 719-723, doi:10.1051/jcp/1975720719.

(3) Cantrell, C. A.; Zimmer, A.; Tyndall, G. S. Absorption cross sections for water vapor from 183 to 193 nm. *Geophys. Res. Lett.* **1997**, *24*, 2195-2198, 2687 (Erratum), doi:10.1029/97GL02100.

(4) Chan, W. F.; Cooper, G.; Brion, C. E. Discrete and continuum photoabsorption oscillator-strengths for the electronic spectrum of nitrous oxide (5.5-203 eV). *Chem. Phys.* **1994**, *180*, 77-88, doi:10.1016/0301-0104(93)E0386-A.

(5) Creasey, D. J.; Heard, D. E.; Lee, J. D. Absorption cross-section measurements of water vapour and oxygen at 185 nm. Implications for the calibration of field instruments to measure OH, HO_2 and RO_2 radicals. *Geophys. Res. Lett.* **2000**, *27*, 1651-1654, doi:10.1029/1999GL011014.

(6) Greenblatt, G. D.; Ravishankara, A. R. Laboratory studies on the stratospheric NO_x production rate. *J. Geophys. Res.* **1990**, *95*, 3539-3547, doi:10.1029/JD095iD04p03539.

(7) Greiner, N. R. Photochemistry of N_2O essential to a simplified vacuum-ultraviolet actinometer. *J. Chem. Phys.* **1967**, *47*, 4373-4377, doi:10.1063/1.1701640.

(8) Griffith, D. W. T.; Toon, G. C.; Sen, B.; Blavier, J.-F.; Toth, R. A. Vertical profiles of nitrous oxide isotopomer fractionation measured in the stratosphere. *Geophys. Res. Lett.* **2000**, *27*, 2485-2488, doi:10.1029/2000GL011797.

(9) Hitchcock, V. C.; Brion, E.; van der Wiel, M. J. Absolute oscillator-strengths for valence-shell ionic photofragmentation of N_2O and CO_2 (8-75 eV). *Chem. Phys.* **1980**, *45*, 461-478, doi:10.1016/0301-0104(80)87015-7.

(10) Hubrich, C.; Stuhl, F. The ultraviolet absorption of some halogenated methanes and ethanes of atmospheric interest. *J. Photochem.* **1980**, *12*, 93-107, doi:10.1016/0047-2670(80)85031-3.

(11) Johnson, M. S.; Billing, G. D.; Gruodis, A.; Janssen, M. H. M. Photolysis of nitrous oxide isotopomers studied by time-dependent hermite propagation. *J. Phys. Chem. A* **2001**, *105*, 8672-8680, doi:10.1021/jp011449x.

(12) Johnston, H. S.; Selwyn, G. S. New cross sections for the absorption of near ultraviolet radiation by nitrous oxide (N_2O). *Geophys. Res. Lett.* **1975**, *2*, 549-551, doi:10.1029/GL002i012p00549.

(13) Ko, M. K. W.; Newman, P. A.; Reimann, S.; Strahan, S. E.; Plumb, R. A.; Stolarski, R. S.; Burkholder, J. B.; Mellouki, W.; Engel, A.; Atlas, E. L.; Chipperfield, M.; Liang, Q. Lifetimes of Stratospheric Ozone-Depleting Substances, Their Replacements, and Related Species, SPARC Report No. 6, WCRP-15/2013, 2013, http://www.sparc-climate.org/publications/sparc-reports/sparc-report-no6/.

(14) Mérienne, M. F.; Coquart, B.; Jenouvrier, A. Temperature effect on the ultraviolet-absorption of $CFCl_3$, CF_2Cl_2 and N_2O. *Planet. Space Sci.* **1990**, *38*, 617-625, doi:10.1016/0032-0633(90)90067-Z.

(15) Nishida, S.; Takahashi, K.; Matsumi, Y.; Taniguchi, N.; Hayashida, S. Formation of $O(^3P)$ atoms in the photolysis of N_2O at 193 nm and $O(^3P) + N_2O$ product channel in the reaction of $O(^1D) + N_2O$ *J. Phys. Chem. A* **2004**, *108*, 2451-2456, doi:10.1021/jp037034o.

(16) Paraskevopoulos, G.; Cvetanovic, R. J. Competitive reactions of the excited oxygen atoms, $O(^1D)$. *J. Am. Chem. Soc.* **1969**, *91*, 7572-7577, doi:10.1021/ja50001a005.

(17) Preston, K. F.; Barr, R. F. Primary processes in the photolysis of nitrous oxide. *J. Chem. Phys.* **1971**, *54*, 3347-3348, doi:10.1063/1.1675349.

(18) Rahn, T.; Zhang, H.; Wahlen, M.; Blake, G. A. Stable isotope fractionation during ultraviolet photolysis of N_2O. *Geophys. Res. Lett.* **1998**, *25*, 4489-4492, doi:10.1029/1998GL900186.

(19) Röckmann, T. J.; Brenninkmeijer, C. A. M.; Wollenhaupt, M.; Crowley, J. N.; Crutzen, P. J. Measurement of the isotopic fractionaltion of $^{15}N^{14}N^{16}O$, $^{14}N^{15}N^{16}O$ and $^{14}N^{14}N^{18}O$ in the UV photolysis of nitrous oxide. *Geophys. Res. Lett.* **2000**, *27*, 1399-1402, doi:10.1029/1999GL011135.

(20) Röckmann, T. J.; Kaiser, J.; Brenninkmeijer, C. A. M.; Crowley, J. N.; Borchers, R.; Brand, W. A.; Crutzen, P. J. Isotopic enrichment of nitrous oxide ($^{15}N^{14}NO$, $^{14}N^{15}NO$, $^{14}N^{14}N^{18}O$) in the stratosphere and in the laboratory. *J. Geophys. Res.* **2001**, *106*, 10403-10410, doi:10.1029/2000JD900822.

(21) Romand, J.; Mayence, J. Spectre d'absorption de l'oxyde asoteux gaseux dans la région de Schumann. *Compt. Rend. Acad. Sci. Paris* **1949**, *228*, 998-1000.

(22) Rontu Carlon, N.; Papanastasiou, D. K.; Fleming, E. L.; Jackman, C. H.; Newman, P. A.; Burkholder, J. B. UV absorption cross sections of nitrous oxide (N_2O) and carbon tetrachloride (CCl_4) between 210 and 350 K and the atmospheric implications. *Atmos. Chem. Phys.* **2010**, *10*, 6137-6149, doi:10.5194/acp-10-6137-2010.

(23) Selwyn, G.; Podolske, J.; Johnston, H. S. Nitrous oxide ultraviolet absorption spectrum at stratospheric temperatures. *Geophys. Res. Lett.* **1977**, *4*, 427-430, doi:10.1029/GL004i010p00427.

(24) Selwyn, G. S.; Johnston, H. S. Ultraviolet absorption spectrum of nitrous oxide as function of temperature and isotopic substitution. *J. Chem. Phys.* **1981**, *74*, 3791-3803, doi:10.1063/1.441608.

(25) Simonaitis, R.; Greenberg, R. I.; Heicklen, J. The photolysis of N_2O at 2139 Å and 1849 Å. *Int. J. Chem. Kinet.* **1972**, *4*, 497-512, doi:10.1002/kin.550040504

(26) Thompson, B. A.; Harteck, P.; Reeves Jr., R. R. Ultraviolet absorption coefficients of CO_2, CO, O_2, H_2O, N_2O, NH_3, NO, SO_2, and CH_4 between 1850 and 4000 A. *J. Geophys. Res.* **1963**, *68*, 6431-6436, doi:10.1029/JZ068i024p06431.

(27) Turatti, F.; Griffith, D. W. T.; Wilson, S. R.; Esler, M. B.; Rahn, T.; Zhang, H.; Blake, G. A. Positionally dependent ^{15}N fractionation factors in the UV photolysis of N_2O determined by high resolution FTIR spectroscopy. *Geophys. Res. Lett.* **2000**, *27*, 2489-2492, doi:10.1029/2000GL011371.

(28) von Hessberg, P.; Kaiser, J.; Enghoff, M. B.; McLinden, C. A.; Sorensen, S. L.; Rockmann, T.; Johnson, M. S. Ultra-violet absorption cross sections of isotopically substituted nitrous oxide species: $^{14}N^{14}NO$, $^{15}N^{14}NO$, $^{14}N^{15}NO$ and $^{15}N^{15}NO$. *Atmos. Chem. Phys.* **2004**, *4*, 1237-1253, doi:10.5194/acp-4-1237-2004.

(29) Yoshino, K.; Freeman, D. E.; Parkinson, W. H. High resolution absorption cross-section measurements of N_2O at 295-299 K in the wavelength region 170-222 nm. *Planet. Space Sci.* **1984**, *32*, 1219-1222, doi:10.1016/0032-0633(84)90065-5.

(30) Yung, Y. L.; Miller, C. E. Isotopic fractionation of stratospheric nitrous oxide. *Science* **1997**, *278*, 1778-1780, doi:10.1126/science.278.5344.1778.
(31) Zelikoff, M.; Aschenbrand, L. M. Vacuum ultraviolet photochemistry, Part II. Nitrious oxide at 1849 A. *J. Chem. Phys.* **1954**, *22* 1685-1687, doi:10.1063/1.1739874.
(32) Zelikoff, M.; Watanabe, K.; Inn, E. C. Y. Absorption coefficients of gases in the vacuum ultraviolet. Part II. Nitrous oxide. *J. Chem. Phys.* **1953**, *21*, 1643-1647, doi:10.1063/1.1698636.
(33) Zhang, H.; Wennberg, P. O.; Wu, V. H.; Blake, G. A. Fractionation of $^{14}N^{15}N^{16}O$ and $^{15}N^{14}N^{16}O$ during photolysis at 213 nm. *Geophys. Res. Lett.* **2000**, *27*, 2481-2484, doi:10.1029/1999GL011236.

C5. N_2O_3 (dinitrogen trioxide)

Back to Index

$N_2O_3 + h\nu \rightarrow$ Products (1)

(Recommendation: 19-5; Note: 19-5; Evaluated: 19-5)

Absorption Cross Sections: UV absorption cross sections of N_2O_3 (dinitrogen trioxide) have been reported at 298 K by Stockwell et al.[2] (300–400 nm). The Stockwell et al. measurements are the only UV absorption data currently available for this molecule; however, the identification of the measured spectrum as N_2O_3(g) was considered tentative in the original paper and has not been confirmed. The reader is referred to the Stockwell et al. paper for further information and the Mainz spectral atlas[1] for the digitized cross section data. No recommendation for the absorption cross sections of N_2O_3 is made.

Photolysis Quantum Yield and Product Studies: No recommendation.

(1) Keller-Rudek, H.; Moortgat, G. K.; Sander, R.; Sörensen, R. The MPI-Mainz UV/VIS spectral atlas of gaseous molecules of atmospheric interest. *Earth Syst. Sci. Data* **2013**, *5*, 365-373, doi:10.5194/essd-5-365-2013.
(2) Stockwell, W. R.; Calvert, J. G. The near ultraviolet absorption spectrum of gaseous HONO and N_2O_3. *J. Photochem.* **1978**, *8*, 193-203, doi:10.1016/0047-2670(78)80019-7.

C6. N_2O_4 (dinitrogen tetraoxide)

Back to Index

$N_2O_4 + h\nu \rightarrow 2\ NO_2$ 57 kJ mol^{-1} 2090 nm (1)

(Recommendation: 06-2; Note: 10-6; Evaluated: 10-6)

Absorption Cross Sections: The UV/vis absorption spectrum of dinitrogen tetraoxide, N_2O_4, has been derived from absorption measurements of NO_2-N_2O_4 mixtures. The available studies are summarized in Table 4C-6-1. The N_2O_4 absorption spectrum consists of a band between 300 and 400 nm with a maximum at ~340 nm, a second less pronounced maximum near ~265 nm, and a strong absorption at shorter wavelengths with a maximum near 190 nm. For the wavelength region 185–360 nm, there is good agreement for the shape of the absorption spectrum but there are discrepancies in the absolute absorption cross sections. In the region below 240 nm, there is good agreement between the absorption cross sections of Bass et al.[1] and Schneider et al.[8] whereas the values reported by Mérienne et al.[6] are lower by ~30%. In the region between 250 and 300 nm, the results of Vandaele et al.[9] are systematically lower than the results of Mérienne et al.[6] by ~15% whereas the results of Bass et al.[1] are higher by ~30%. In the region 300–380 nm, Harwood and Jones[3] reported a systematic study of the temperature dependence of the N_2O_4 absorption spectrum. The absorption cross sections near the peak at 340 nm show a weak dependence on temperature over the range 213–253 K. There is good agreement between the results of Hall and Blacet,[2] the low-temperature data of Harwood and Jones,[3] and the results of Vandaele et al.[9] with the absorption cross sections at 340 nm agreeing to within 5%. Bass et al.[1] and Mérienne et al.[6] report cross section values at 340 nm that are 25% and 15% higher, respectively. The recommended cross section values in Table 4C-6-2 are averages over 2 nm intervals of the high resolution (0.01–0.03 nm) spectrum reported by Vandaele et al.[9] between 252 and 390 nm at 220 K.

Photolysis Quantum Yield and Product Studies: No recommendation.

Table 4C-6-1. Summary of N_2O_4 Absorption Cross Section Studies

Study	Year	Temperature (K)	Wavelength (nm)	10^{20} σ(340 nm) (cm^2)
Holmes and Daniels[4]	1934	273	265–405	~43
Hall and Blacet[2]*	1952	298	240–390	69
Nakayama et al.[7]	1959	300	197	–
Bass et al.[1]	1976	273	185–390	82.8
Schneider et al.[8]	1987	298	198–230	–
Harwood and Jones[3]	1994	213, 225 233, 243, 253, 273	320–405 320–430	64.2 66.5
Mérienne et al.[6]	1997	220	200–390	78.1
Vandaele et al.[9]	1998	220	250–455	68.1

* (as given in Johnston and Graham[5])

Table 4C-6-2. Recommended Absorption Cross Sections of N_2O_4 at 220 K

λ (nm)	10^{20} σ (cm^2)	λ (nm)	10^{20} σ (cm^2)	λ (nm)	10^{20} σ (cm^2)	λ (nm)	10^{20} σ (cm^2)
252	64.8	288	27.5	324	47.5	360	26.8
254	65.1	290	25.0	326	51.9	362	22.5
256	64.7	292	22.9	328	55.9	364	18.7
258	64.8	294	21.0	330	59.7	366	15.4
260	64.3	296	19.5	332	63.0	368	12.5
262	63.2	298	18.5	334	65.7	370	10.0
264	61.8	300	17.9	336	67.3	372	8.13
266	60.0	302	18.0	338	68.1	374	6.50
268	57.9	304	18.5	340	68.1	376	5.33
270	55.2	306	19.3	342	66.8	378	4.24
272	52.3	308	20.8	344	64.4	380	3.52
274	49.3	310	22.9	346	61.3	382	2.93
276	46.2	312	25.3	348	57.3	384	2.47
278	43.0	314	28.3	350	52.5	386	2.16
280	39.7	316	31.9	352	47.3	388	1.89
282	36.4	318	35.3	354	42.1	390	1.78
284	33.3	320	39.1	356	36.9		
286	30.3	322	43.2	358	31.7		

Note:
Vandaele et al.[9]

(1) Bass, A. M.; Ledford, A. E.; Laufer, A. H. Extinction coefficients of NO_2 and N_2O_4. *J. Res. Natl. Bur. Stand.* **1976**, *80A*, 143-166, doi:10.6028/jres.080A.017.

(2) Hall, J., T. C.; Blacet, F. E. Separation of the absorption spectra of NO_2 and N_2O_4 in the range of 2400-5000A. *J. Chem. Phys.* **1952**, *20*, 1745-1749, doi:10.1063/1.1700281.

(3) Harwood, M. H.; Jones, R. L. Temperature dependent ultraviolet-visible absorption cross sections of NO_2 and N_2O_4: Low-temperature measurements of the equilibrium constant for $2NO_2 \rightleftharpoons N_2O_4$. *J. Geophys. Res.* **1994**, *99*, 22955-22964, doi:10.1029/94JD01635

(4) Holmes, H. H.; Daniels, F. The photolysis of nitrogen oxides: N_2O_5, N_2O_4 and NO_2. *J. Am. Chem. Soc.* **1934**, *56*, 630-637, doi:10.1021/ja01318a028.

(5) Johnston, H. S.; Graham, R. Photochemistry of NO_x and HNO_x compounds. *Can. J. Phys.* **1974**, *52*, 1415-1423, doi:10.1139/v74-214.

(6) Mérienne, M.-F.; Jenouvrier, A.; Coquart, B.; Lux, J. P. The NO_2 absorption spectrum. IV: The 200–400 nm region at 220 K. *J. Atmos. Chem.* **1997**, *27*, 219-232, doi:10.1023/A:1005829213463.

(7) Nakayama, T.; Kitamura, M. T.; Watanabe, K. Ionization potential and absorption coefficients of nitrogen dioxide. *J. Chem. Phys.* **1959**, *30*, 1180-1186, doi:10.1063/1.1730152.

(8) Schneider, W.; Moortgat, G. K.; Burrows, J. P.; Tyndall, G. Absorption cross-sections of NO_2 in the UV and visible region (200-700 nm) at 298 K. *J. Photochem. Photobiol. A: Chem.* **1987**, *40*, 195-217, doi:10.1016/1010-6030(87)85001-3.

(9) Vandaele, A. C.; Hermans, D.; Simon, P. C.; Carleer, M.; Colin, R.; Fally, S.; Meriénne, M.-F.; Jenouvrier, A.; Coquart, B. Measurements of the NO_2 absorption cross-section from 42000 cm^{-1} to

10000 cm^{-1} (238-1000 nm) at 220 K and 294 K. *J. Quant. Spectrosc. Radiat. Transf.* **1998**, *59*, 171-184, doi:10.1016/S0022-4073(97)00168-4.

C7. N_2O_5 (dinitrogen pentoxide)

Back to Index

$N_2O_5 + h\nu \rightarrow NO_3 + NO_2$	95 kJ mol^{-1}	1255 nm	(1)
$\rightarrow NO_3 + NO + O(^3P)$	402 kJ mol^{-1}	298 nm	(2)
$\rightarrow NO_3 + NO_2^*$	–	–	(3)

(Recommendation: 06-2; Note: 15-10; Evaluated: 15-10)

Absorption Cross Sections: The UV/vis absorption spectrum of dinitrogen pentoxide, N_2O_5, exhibits an absorption maximum at 160 nm with continuously decreasing absorption cross sections toward longer wavelengths. The absorption cross sections of N_2O_5 have been measured in a number of studies that are summarized in Table 4C-7-1. The room temperature values from Yao et al.[14] and Harwood et al.[3-5] agree to within 10-20% at wavelengths above 250 nm. Below 250 nm, the cross sections reported by Yao et al.[14] that were recommended in the NASA/JPL 1997 evaluation are systematically higher than those reported by Harwood et al.[3] by up to a factor of ~2 at 208 nm. A possible explanation for this discrepancy was proposed by Harwood et al.[3] as due to contributions to the measured absorption by HNO_3 impurities. Harwood et al.[3] used N_2O_5 samples containing less than a 1% HNO_3 impurity. This explanation was later confirmed by the measurements of Osborne et al.[11] who also used thoroughly purified N_2O_5 samples and reported absorption cross sections in agreement with those of Harwood et al.[3] at 210–240 nm, but at a lower temperature.

The recommended absorption cross sections listed in Table 4C-7-2 are the mean of the data from Yao et al.[14] and Osborne[11] for 200–208 nm, the mean of the data from Yao et al.,[14] Osborne et al.,[11] and Harwood et al.[3] for 210–240 nm, the data of Harwood et al.[3] for 242–398 nm, and the data of Harwood et al.[4] for 400–420 nm.

The temperature dependence of the absorption spectrum was measured by Harwood et al.[3] and Yao et al.[14] and found to be significant for wavelengths >280 nm. The absorption cross sections decrease with decreasing temperature and the magnitude of the effect increases with increasing wavelength. Harwood et al.[4] parameterized the temperature dependence using the relationship

$$\log_{10}(\sigma) = A(\lambda) + 1000 \times B(\lambda)/T$$

which is valid over the temperature range 233–295 K. The A and B coefficients are given in Table 4C-7-2.

Table 4C-7-1. Summary of N_2O_5 Absorption Cross Section Studies

Study	Year	Temperature (K)	Wavelength (nm)
Holmes and Daniels[6]	1934	273	265, 280
Jones and Wulf[9]	1937	273	285–380
Johnston and Graham[8]	1974	298	210–290
Johnston et al.[7]	1974	298	200–360
Graham[2]	1975	298	205–310
Yao et al.[14]	1982	225, 243, 263, 277	290–380
Yao et al.[14]	1982	298-300	200–380
Harwood et al.[5]	1992	273, 295	280–380
Harwood et al.[4]	1993	233–295	240–420
Harwood et al.[3]	1998	295	208–398
Osborne et al.[11]	2000	195	152–240

Photolysis Quantum Yield and Product Studies: There are several studies of N_2O_5 primary photolysis products for wavelengths between 248 and 352.5 nm as summarized in Table 4C-7-3. The NO_3 radical is produced with unity quantum yield at wavelengths >300 nm. At shorter wavelengths the NO_3 quantum yield decreases to a value of ~0.71 at 248 nm and the $O(^3P)$ atom quantum increases. The study of Oh et al.[10] indicates that the primary photolysis products other than NO_3 are a wavelength dependent mixture of NO_2, NO_2* and NO + O, where NO_2* represents electronically excited NO_2 that is most likely the $^2B_1$ state. For atmospheric model calculations unit photolysis quantum yields of NO_3 and NO_2 are recommended for wavelengths >300 nm.

Table 4C-7-2. Recommended Absorption Cross Sections at 300 K and Temperature Coefficients for N_2O_5

λ (nm)	10^{20} σ (cm^2)	A	B (K)	λ (nm)	10^{20} σ (cm^2)	A	B (K)	λ (nm)	10^{20} σ (cm^2)	A	B (K)
200	910			270	16.2	–18.42	–0.104	340	0.368	–18.77	–0.492
202	842			272	14.9			342	0.328		
204	771			274	13.7			344	0.293		
206	682			276	12.4			346	0.262		
208	585			278	11.4			348	0.234		
210	480			280	10.5	–18.59	–0.112	350	0.210	–18.71	–0.583
212	381			282	9.59			352	0.188		
214	322			284	8.74			354	0.167		
216	267			286	7.94			356	0.149		
218	220			288	7.20			358	0.133		
220	181			290	6.52	–18.72	–0.135	360	0.120	–18.31	–0.770
222	151			292	5.88			362	0.107		
224	129			294	5.29			364	0.0958		
226	113			296	4.75			366	0.0852		
228	98.4			298	4.26			368	0.0763		
230	88.2			300	3.81	–18.84	–0.170	370	0.0685	–18.14	–0.885
232	80.5			302	3.40			372	0.0613		
234	74.0			304	3.03			374	0.0545		
236	69.2			306	2.70			376	0.0484		
238	64.6			308	2.40			378	0.0431		
240	59.8			310	2.13	–18.90	–0.226	380	0.0383	–18.01	–0.992
242	53.1			312	1.90			382	0.0341		
244	49.3			314	1.68			384	0.0305		
246	45.6			316	1.49			386	0.0278		
248	41.9			318	1.33			388	0.025		
250	38.6			320	1.18	–18.93	–0.294	390	0.0226	–18.42	–0.949
252	35.5			322	1.05			392	0.0202		
254	32.6			324	0.930			394	0.0182		
256	29.9			326	0.826			396	0.0165		
258	27.5			328	0.735			398	0.0150		
260	25.2	–18.27	–0.091	330	0.654	–18.87	–0.388	400	0.0135	–18.59	–0.966
262	23.1			332	0.582			410	0.008	–18.13	–1.160
264	21.1			334	0.518			420	0.005		
266	19.4			336	0.462						
268	17.8			338	0.412						

Note:

Absorption cross sections:

200–208 nm: mean of the data from Yao et al.[14] and Osborne et al.[11]

210 nm: smoothed value

212–234 nm: mean of the data from Yao et al.,[14] Osborne et al.,[11] and Harwood et al.[3]

236–240 nm: smoothed values

242–384 nm: data from Harwood et al.[3]

386–420 nm: smoothed extrapolation of Harwood et al.[3] and Harwood et al.[4] data

Temperature coefficients:

Harwood et al.[4] (260–410 nm), $\log_{10}(\sigma) = A(\lambda) + 1000B(\lambda)/T$; valid over the range 233–295 K

Table 4C-7-3. Summary of N_2O_5 Photolysis Quantum Yield Results

Reference	Year	λ (nm)	Φ(NO_3)	Φ(O^3P)
Swanson et al.[13]*	1984	248	0.73 ± 0.12	–
Ravishankara et al.[12]*	1986	248	0.77 ± 0.10	0.72 ± 0.09
Harwood et al.[3]	1998	248	0.64 ± 0.20	–
Ravishankara et al.[12]	1986	266	–	0.38 ± 0.08
Ravishankara et al.[12]	1986	287	–	0.21 ± 0.03
Ravishankara et al.[12]	1986	289	–	0.15 ± 0.03
Barker et al.[1]	1985	290	0.8 ± 0.2	< 0.1
Harwood et al.[3]	1998	308	0.96 ± 0.15	–
Swanson et al.[13]	1984	350	0.84 ± 0.09	–
Harwood et al.[3]	1998	352.5	1.03 ± 0.15	–

Note:

* The reported NO_3 quantum yields of (0.89 ± 0.15) by Swanson et al.[13] and (0.96 ± 0.13) by Ravishankara et al.[12] have been scaled using the currently recommended NO_3 absorption cross section at 662 nm.

(1) Barker, J. R.; Brouwer, L.; Patrick, R.; Rossi, M. J.; Trevor, P. L.; Golden, D. M. N_2O_5 photolysis products investigated by fluorescence and optoacoustic techniques. *Int. J. Chem. Kinet.* **1985**, *17*, 991-1006, doi:10.1002/kin.550170906.

(2) Graham, R. A. Photochemistry of NO_3 and the Kinetics of the N_2O_5-O_3 System. Ph. D. Thesis, University of California, Berkeley, CA, 1975.

(3) Harwood, M. H.; Burkholder, J. B.; Ravishankara, A. R. Photodissociation of $BrONO_2$ and N_2O_5: Quantum yields for NO_3 production at 248, 308, and 352.5 nm. *J. Phys. Chem. A* **1998**, *102*, 1309-1317, doi:10.1021/jp9729829.

(4) Harwood, M. H.; Jones, R. L.; Cox, R. A.; Lutman, E.; Rattigan, O. V. Temperature-dependent absorption cross-sections of N_2O_5. *J. Photochem. Photobiol. A: Chem.* **1993**, *73*, 167-175, doi:10.1016/1010-6030(93)90001-2.

(5) Harwood, M. H.; Rattigan, O. V.; Jones, R. L.; Cox, R. A. *Proc. SPIE Int. Soc. Opt. Eng.* **1992**, *1715*, 113-124.

(6) Holmes, H. H.; Daniels, F. The photolysis of nitrogen oxides: N_2O_5, N_2O_4 and NO_2. *J. Am. Chem. Soc.* **1934**, *56*, 630-637, doi:10.1021/ja01318a028.

(7) Johnston, H. S.; Chang, S.; Whitten, G. Photolysis of nitric acid vapor. *J. Phys. Chem.* **1974**, *78*, 1-7, doi:10.1021/j100594a001.

(8) Johnston, H. S.; Graham, R. Photochemistry of NO_x and HNO_x compounds. *Can. J. Phys.* **1974**, *52*, 1415-1423, doi:10.1139/v74-214.

(9) Jones, E. L.; Wulf, O. R. The absorption coefficient of nitrogen pentoxide in the ultraviolet and the visible absorption spectrum of NO_3. *J. Chem. Phys.* **1937**, *5*, 873-877, doi:10.1063/1.1749956.

(10) Oh, D.; Sisk, W.; Young, A.; Johnston, H. Nitrogen dioxide fluorescence from N_2O_5 photolysis. *J. Chem. Phys.* **1986**, *85*, 7146-7158, doi:10.1063/1.451348.

(11) Osbourne, B. A.; Marston, G.; Kaminski, L.; Jones, N. C.; Gingell, J. M.; Mason, N. J.; Walker, I. C.; Delwiche, J.; Hubin-Franskin, M.-J. Vacuum ultraviolet spectrum of dinitrogen pentoxide. *J. Quant. Spectrosc. Radiat. Transf.* **2000**, *64*, 67-74, doi:10.1016/S0022-4073(99)00104-1.

(12) Ravishankara, A. R.; Wine, P. H.; Smith, C. A.; Barbone, P. E.; Torabi, A. N_2O_5 photolysis: Quantum yields for NO_3 and $O(^3P)$. *J. Geophys. Res.* **1986**, *91*, 5355-5360, doi:10.1029/JD091iD05p05355.

(13) Swanson, D.; Kan, B.; Johnston, H. S. NO_3 quantum yields from N_2O_5 photolysis. *J. Phys. Chem.* **1984**, *88*, 3115-3118, doi:10.1021/j150658a038.

(14) Yao, F.; Wilson, I.; Johnston, H. Temperature-dependent ultraviolet absorptlon spectrum for dinitrogen pentoxide. *J. Phys. Chem.* **1982**, *86*, 3611-3615, doi:10.1021/j100215a023.

C8. HONO (nitrous acid)

Back to Index

$HONO + h\nu$	$\rightarrow OH + NO$	207 kJ mol^{-1}	579 nm	(1)
	$\rightarrow H + NO_2$	330 kJ mol^{-1}	362 nm	(2)

(Recommendation: 06-2; Note: 10-6; Evaluated: 10-6)

Absorption Cross Sections: The UV absorption spectrum of nitrous acid, HONO, consists of a highly structured absorption band between 300 and 400 nm due to vibrational progressions in the $A^1A'' \leftarrow X^1A'$ transition, with a maximum intensity near 354 nm and a stronger continuous absorption band at shorter wavelengths with a maximum near 205 nm. A summary of the HONO room temperature absorption cross section studies for the near UV band is given in Table 4C-8-1.

Table 4C-8-1. Summary of HONO Absorption Cross Section Studies

Study	Year	Wavelength Range (nm)	Resolution (nm)	10^{20} σ (354 nm) (cm^2)
Johnston and Graham[8]	1974	300–399	0.87	12.3
Cox and Derwent[5]	1976	200–394	<0.1	56.0
Perner[12]	1977	310–388	0.6	55.2
Stockwell and Calvert[13]	1978	310–396	<1	49.6
Platt et al.[11]	1980	336–376	0.8	47
Kenner et al.[9]	1986	184–274	0.38	–
Vasudev[15]	1990	310–393	–	(49.7)*
Bongartz et al.[3]	1991	300–400	0.1 (λ<375 nm) 0.8 (λ<375 nm)	64.2**
Bongartz et al.[2]	1994	300–400	0.1 (λ<375 nm) 0.8 (λ<375 nm)	54.9**
Febo et al.[6]	1996	50–380	1	49.7**
Pagsberg et al.[10]	1997	348–376	0.06	50.2
Brust et al.[4]	2000	323–394	0.5	38.9
Stutz et al.[14]	2000	291–404	0.061 ± 0.003	52.2
Wang and Zhang[16]	2000	352.2 354.2 357.0	<0.1	48.9
Gratien et al.[7]	2009	300–400	0.18	–

Notes:
* Normalized to the spectrum of Stockwell and Calvert[13]
** Bongartz et al.[2] corrected their 1991 results by a factor of 0.855

There is good agreement among the various data sets for the peak positions and discrepancies in the peak cross sections are generally a consequence of the differences in measurement spectral resolution. Stutz et al.[14] normalized the cross section data from earlier studies to a resolution of 1 nm, resulting in an agreement of better than 10% between their results and those of Bongartz et al.,[2] Pagsberg et al.,[10] and Vasudev.[15] The measurements of Stockwell and Calvert[13] are in reasonable agreement with the more recent studies. The cross sections from Cox and Derwent[5] are greater by ~26% (presumably due to uncorrected NO_2 absorption) and those from Johnston and Graham[8] are less by 70% (presumably due to non-equilibrium of the $NO/NO_2/H_2O$ mixture during the measurement) than the more recent studies. The source of the discrepancy with the measurements of Brust et al.[4] is unknown. Gratien et al.[7] performed simultaneous measurements of HONO absorption spectra in the IR and UV and confirmed that the UV cross sections of Bongartz et al.[2] and Stutz et al.[14] are consistent to within 5% with independent infrared studies and that the UV cross sections of Brust et al.[4] are underestimated by ~22%.

The short wavelength absorption band was measured by Cox and Derwent[5] (200–300 nm, <0.1 nm resolution) and Kenner et al.[9] (184–274 nm, 0.38 nm resolution). The reported spectra are in quantitative agreement over the wavelength range 220–270 nm. The sharp peak at 215 nm reported by Cox and Derwent[5], however, was not observed by Kenner et al.,[9] who provide a number of arguments for the correctness of their results.

The recommended absorption cross sections in Table 4C-8-2 are a combination of data as follows: for the wavelength region 184–274 nm data was taken from Kenner et al.[9] as read from a figure in their paper; for the wavelength region 296–396 nm data was taken from Stutz et al.;[14] for the wavelength regions 296–325 nm and

371–396 nm averages over 1 nm intervals of the Stutz et al.[14] high resolution spectrum are reported; and for the highly structured region 326–370 nm averages over 0.5 nm intervals were used.

Photolysis Quantum Yield and Product Studies: The photolysis quantum yield of HONO at wavelengths above the dissociation threshold are unity. The OH radical quantum yield at 365 ± 5 nm was determined by Cox and Derwent[5] to be (0.92 ± 0.16). Wollenhaupt et al.[17] determined an upper limit of 0.01 for the quantum yield of H atom formation for photolysis at 351 nm. The OH(A) quantum yield from HONO laser photolysis at 193 nm was measured to be 1.8×10^{-5} by Kenner et al.[9] The H + NO_2 (X^2A_1, A^2B_2, B^2B_1, C^2A_2) product channels in the photodissociation of HONO at 193.3 nm were examined by Amaral et al.[1] and branching ratios of the NO_2 electronic states estimated to be $X^2A_1 : A^2B_2 : B^2B_1/C^2A_2 \approx 0.13 : 0.21 : 0.66$, respectively.

Table 4C-8-2. Recommended Absorption Cross Sections of HONO at 298 K

λ (nm)	10^{20} σ (cm^2)	λ (nm)	10^{20} σ (cm^2)	λ (nm)	10^{20} σ (cm^2)	λ (nm)	10^{20} σ (cm^2)
184	85.0	296	0.326	335.5	6.55	360.0	6.87
186	95.0	297	0.565	336.0	5.33	360.5	6.32
188	106	298	0.517	336.5	4.36	361.0	6.05
190	124	299	0.429	337.0	4.23	361.5	5.95
192	143	300	0.617	337.5	5.13	362.0	5.98
194	162	301	0.690	338.0	9.38	362.5	6.35
196	179	302	0.579	338.5	16.52	363.0	7.39
198	196	303	0.925	339.0	14.32	363.5	9.22
200	210	304	1.04	339.5	9.96	364.0	11.49
202	219	305	1.57	340.0	7.79	364.5	12.71
204	223	306	1.29	340.5	8.51	365.0	12.82
205	224	307	0.916	341.0	16.13	365.5	13.19
206	223	308	1.45	341.5	31.52	366.0	14.84
208	220	309	2.01	342.0	29.40	366.5	18.43
210	213	310	1.51	342.5	18.47	367.0	25.08
212	204	311	2.07	343.0	11.43	367.5	35.18
214	193	312	2.42	343.5	8.29	368.0	43.56
216	179	313	2.25	344.0	7.59	368.5	41.37
218	164	314	3.35	344.5	8.18	369.0	31.45
220	150	315	2.54	345.0	8.77	369.5	21.72
222	135	316	1.61	345.5	9.10	370	15.05
224	121	317	3.21	346.0	9.64	371	9.49
226	108	318	4.49	346.5	8.87	372	7.96
228	94.5	319	3.19	347.0	7.80	373	6.30
230	84.5	320	4.66	347.5	7.06	374	4.59
232	74.0	321	5.96	348.0	6.63	375	3.55
234	66.0	322	4.05	348.5	6.26	376	3.36
236	58.0	323	4.56	349.0	6.00	377	3.66
238	50.0	324	5.89	349.5	6.47	378	4.33
240	43.0	325	4.05	350.0	9.06	379	5.66
242	37.0	326	2.65	350.5	14.95	380	7.21
244	32.0	326.5	3.55	351.0	16.94	381	9.13
246	27.5	327.0	6.44	351.5	14.07	382	12.44
248	23.5	327.5	10.26	352.0	12.42	383	17.03
250	20.0	328.0	9.22	352.5	12.81	384	19.47
252	17.0	328.5	6.38	353.0	16.34	385	16.09
254	14.5	329.0	5.20	353.5	28.49	386	10.52
256	12.3	329.5	6.12	354.0	48.73	387	6.59
258	10.3	330.0	9.92	354.5	44.34	388	4.30
260	8.6	330.5	15.06	355.0	27.64	389	2.81
262	7.3	331.0	14.32	355.5	16.40	390	1.71
264	6.2	331.5	9.88	356.0	11.13	391	0.992
266	5.3	332.0	6.94	356.5	9.35	392	0.731
268	4.3	332.5	6.00	357.0	9.45	393	0.597

270	3.7	333.0	6.31	357.5	10.08	394	0.528
272	3.0	333.5	7.11	358.0	9.84	395	0.403
274	2.5	334.0	8.35	358.5	9.02	396	0.237
		334.5	8.37	359.0	8.37		
		335.0	7.71	359.5	7.67		

Note:
184–274 nm: Kenner et al.[9]
296–325 nm: Stutz et al.[14] (average over 1 nm intervals)
326–370 nm: Stutz et al.[14] (average over 0.5 nm intervals)
371–396 nm: Stutz et al.[14] (average over 1 nm intervals)

(1) Amaral, G.; Xu, K.; Zhang, J. H + NO_2 channels in the photodissociation of HONO at 193.3 nm. *J. Phys. Chem. A* **2001**, *105*, 1465-1475, doi:10.1021/jp002521e.
(2) Bongartz, A.; Kames, J.; Schurath, U.; George, C.; Mirabel, P.; Ponche, J. L. Experimental determination of HONO mass accommodation coefficients using two different techniques. *J. Atmos. Chem.* **1994**, *18*, 149-169, doi:10.1007/BF00696812.
(3) Bongartz, A.; Kames, J.; Welter, F.; Schurath, U. Near-UV absorption cross sections and trans/cis equilibrium of nitrous acid. *J. Phys. Chem.* **1991**, *95*, 1076-1082, doi:10.1021/j100156a012.
(4) Brust, A. S.; Becker, K. H.; Kleffmann, J.; Wiesen, P. UV absorption cross sections of nitrous acid. *Atmos. Environ.* **2000**, *34*, 13-19, doi:10.1016/S1352-2310(99)00322-2.
(5) Cox, R. A.; Derwent, R. G. The ultra-violet absorption spectrum of gaseous nitrous acid. *J. Photochem.* **1976**, *6*, 23-34, doi:10.1016/0047-2670(76)87004-9.
(6) Febo, A.; Perrino, C.; Allegrini, I. Measurement of nitrous acid in Milan, Italy, by DOAS and diffusion denuders. *Atmos. Environ.* **1996**, *30*, 3599-3609, doi:10.1016/1352-2310(96)00069-6.
(7) Gratien, A.; Lefort, M.; Picquet-Varrault, B.; Orphal, J.; Doussin, J.-F.; Flaud, J.-M. Experimental intercomparison of the absorption cross-sections of nitrous acid (HONO) in the ultraviolet and mid-infrared spectral regions. *J. Quant. Spectrosc. Radiat. Transf.* **2009**, *110*, 256-263, doi:10.1016/j.jqsrt.2008.11.003.
(8) Johnston, H. S.; Graham, R. Photochemistry of NO_x and HNO_x compounds. *Can. J. Phys.* **1974**, *52*, 1415-1423, doi:10.1139/v74-214.
(9) Kenner, R. D.; Rohrer, F.; Stuhl, F. OH(A) production in the 193-nm photolysis of HONO. *J. Phys. Chem.* **1986**, *90*, 2635-2639, doi:10.1021/j100403a015.
(10) Pagsberg, P.; Bjergbakke, E.; Ratajczak, E.; Sillesen, A. Kinetics of the gas phase reaction OH + NO(+M) → HONO(+M) and the determination of the UV absorption cross sections of HONO. *Chem. Phys. Lett.* **1997**, *272*, 383-390, doi:10.1016/S0009-2614(97)00576-9.
(11) Platt, U.; Perner, D.; Harris, G. W.; Winer, A. M.; Pitts Jr., J. N. Observations of nitrous acid in an urban atmosphere by differential optical absorption. *Nature* **1980**, *285*, 312-314, doi:10.1038/285312a0.
(12) Röth, E. P.; Ruhnke, R.; Moortgat, G.; Meller, R.; Schneider, W. UV/VIS-Absorption Cross Sections and Quantum Yields for Use in Photochemistry and Atmospheric Modeling, Forschungszentrum Jülich Publication, Part 1 : Inorganic Substances (jül-3340), Part 2: Organic Substances (jül-3341). **1997**.
(13) Stockwell, W. R.; Calvert, J. G. The near ultraviolet absorption spectrum of gaseous HONO and N_2O_3. *J. Photochem.* **1978**, *8*, 193-203, doi:10.1016/0047-2670(78)80019-7.
(14) Stutz, J.; Kim, E. S.; Platt, U.; Bruno, P.; Perrino, C.; Febo, A. UV-visible absorption cross sections of nitrous acid. *J. Geophys. Res.* **2000**, *105*, 14585-14592, doi:10.1029/2000JD900003.
(15) Vasudev, R. Absorption spectrum and solar photodissociation of gaseous nitrous acid in the actinic wavelength region. *Geophys. Res. Lett.* **1990**, *17*, 2153-2155, doi:10.1029/GL017i012p02153.
(16) Wang, L.; Zhang, J. Detection of nitrous acid by cavity ring-down spectroscopy. *Environ. Sci. Technol.* **2000**, *34*, 4221-4227, doi:10.1021/es0011055.
(17) Wollenhaupt, M.; Carl, S. A.; Horowitz, A.; Crowley, J. N. Rate coefficients for reaction of OH with acetone between 202 and 395 K. *J. Phys. Chem. A* **2000**, *104*, 2695-2705, doi:10.1021/jp993738f.

C9. HNO_3 (nitric acid)

Back to Index

$HNO_3 + h\nu$	→ $OH + NO_2$	206 kJ mol^{-1}	581 nm	(1)
	→ $HONO + O(^3P)$	305 kJ mol^{-1}	392 nm	(2)
	→ $H + NO_3$	427 kJ mol^{-1}	280 nm	(3)
	→ $OH + NO_2{}^*(1^2B_2)$	–	–	(4)
	→ $HONO + O(^1D)$	494 kJ mol^{-1}	242 nm	(5)
	→ $HONO\ (a^3A) + O(^3P)$	–	–	(6)

(Recommendation: 06-2; Note: 15-10; Evaluated: 15-10)

Absorption Cross Sections: The UV absorption spectrum of nitric acid, HNO_3, consists of a strong absorption band between 150 and 240 nm with the maximum near 183 nm and a second band near 270 nm that appears as a shoulder on the long wavelength wing of the strong band. The recommended absorption cross sections and their temperature dependence for the region 192–350 nm listed in Table 4C-9 are taken from the work of Burkholder et al.[3] The temperature effect is very important for estimates of atmospheric photodissociation rate coefficients. The results of Burkholder et al.[3] agree well (to within 10% above 200 nm) with those of Rattigan et al.[15,16] at room temperature, whereas Rattigan et al.[15,16] report significantly smaller cross section values at 239 K (15–30% smaller in the range 220–330 nm and ~50% smaller at 330 nm). The recommended room temperature absorption cross sections are also in very good agreement with the data of Molina and Molina[12] (<15% difference up to 310 nm) and in good agreement with the values reported by Biaume[1] and Johnston and Graham,[8] except at long wavelength. Okabe[14] reported cross sections in the 110–190 nm range that are 20–30% lower than those of Burkholder et al.,[3] Biaume,[1] and Johnston and Graham[8] in the region 185–190 nm. Suto and Lee[19] reported cross sections between 105 and 210 nm that are 10–20% higher than those of Burkholder et al.,[3] Biaume,[1] and Johnston and Graham[8] in the region 185–190 nm, but show excellent agreement with the results of Molina and Molina[12] above 185 nm and Burkholder et al.[3] above 189 nm.

On the basis of the results from the Biaume, Burkholder et al., Johnston and Graham, and Rattigan et al. studies, uncertainty factors for the HNO_3 room temperature absorption cross sections in the wavelength regions 190-200 nm, 205–330 nm, and 335–350 nm are 1.1, 1.06, and 1.2 (2σ), respectively. The uncertainty factors at temperatures <298 K are expected to be greater in the 335–350 nm region, but are difficult to estimate without additional studies.

Photolysis Quantum Yield and Product Studies: There have been a number of room temperature HNO_3 photolysis studies conducted at wavelengths between 193 and 320 nm from which quantum yields have been derived. On the basis of end-product analysis, Johnston et al.[7] reported a quantum yield of ~1 for the OH + NO_2 channel in the 200–315 nm range. Margitan and Watson[11] used atomic resonance fluorescence to determine the quantum yield for O atom production at 266 nm to be 0.03 and that for H atom production to be ≤0.002. Jolly et al.[9] measured a quantum yield for OH production of 0.89 ± 0.08 at 222 nm. Turnipseed et al.[20] reported OH quantum yields of (0.95 ± 0.09) at 248, (0.90 ± 0.11) at 222 nm, and 0.33 ± 0.06 at 193 nm. Turnipseed et al.[20] also reported quantum yields for production of O atoms, $O(^3P) + O(^1D)$, to be 0.031 ± 0.01, 0.20 ± 0.03 and 0.81 ±0.13 at 248, 222, and 193 nm, respectively. Both $O(^3P)$ and $O(^1D)$ atom formation was observed at 222 and 193 nm but only $O(^3P)$ was detected at 248 nm. At 193 and 222 nm the $O(^1D)$ yield was determined to be 40% of the total O atom yield, yielding $\Phi(O(^1D)) = 0.28 \pm 0.07$ at 193 nm. Turnipseed et al.[20] reported upper limits for $\Phi(H(^2S))$ of ≤0.002 at 238 nm, ≤0.01 at 222 nm, and ≤0.012 at 193 nm. Riffault et al.[17] reported Φ(OH) values of 0.88 ± 0.09 at 248 nm and 1.05 ± 0.29 at 308 nm. Schiffman et al.[18] reported $\Phi(OH) = 0.47 \pm 0.06$ at 193 nm, which is larger than the value reported by Turnipseed et al.[20] At 248 nm they report $\Phi(OH) = 0.75 \pm 0.10$, which is a smaller value than reported in other studies.

Felder et al.[6] used molecular beam/photofragment translational spectroscopy and reported the yield for (OH + NO_2) to be $\Phi(OH) = 0.6 \pm 0.1$ and for (O + HONO) to be $\Phi(HONO) = 0.4 \pm 0.1$ at 193 nm. Myers et al.[13] also used this technique to measure the primary processes in the photolysis at 193 nm from the different photofragment ions and found evidence for all channels except 4. They determined the branching ratio (OH + NO_2)/(O+HONO) to be 0.50 ± 0.05, $\Phi(OH) = 0.33 \pm 0.04$ (in excellent agreement with the value obtained by Turnipseed et al.[20]). They also reported $\Phi(O(^3P) + O(^1D)) = 0.67 \pm 0.04$, which is lower than the 0.81 ± 0.13 value reported by Turnipseed et al.[20] but the latter authors included the contribution of the secondary dissociation of NO_2 produced in channel (1). Their primary yield of $O(^1D)$ formation of 0.54 ± 0.04 is much larger than the $\Phi O(^1D)$ yield of 0.28 ± 0.07 measured by Turnipseed et al.[20] and this discrepancy remains unexplained. In a study using LIF and REMPI–TOF techniques, Li et al.[10] found evidence for the ($O(^3P)$ + HONO) channel with a yield of ~0.06.

Band strengths for the OH stretch vibrational overtones of HNO_3 have been reported by Donaldson et al.,[5] Zhang et al.,[21] and Brown et al.[2] Photodissociation of HNO_3 by excitation of the $3\nu_{OH}$ (~983 nm), $4\nu_{OH}$ (~755 nm) and $5\nu_{OH}$ (~618 nm) overtones is a possible source of atmospheric OH radicals. There is good agreement among the various studies. Band strengths (in units of 10^{-20} cm^2 molecule^{-1} cm^{-1}) of 2.63 for $3\nu_{OH}$ and 0.237 for $4\nu_{OH}$ were reported by Donaldson et al.[5] Zhang et al.[21] obtained band strengths of (2.9 ± 0.7) for $3\nu_{OH}$ and (0.28 ± 0.10) for $4\nu_{OH}$. Brown et al.[2] measured the band strengths for $4\nu_{OH}$ to be (0.225 ± 0.015) at 296 K and (0.223 ± 0.015) at 251 K and for $5\nu_{OH}$ to be (0.0257 ± 0.015) at 296 K and (0.0241 ± 0.035) at 251 K. Although the contribution to the overall atmospheric OH production rate from HNO_3 overtone photodissociation is small, it is larger than estimated by Donaldson et al.[4]

Table 4C-9. Recommended Absorption Cross Sections at 298 K and Temperature Coefficients for HNO_3

λ (nm)	$10^{20}\sigma$ (cm^2)	10^3 B (K^{-1})	λ (nm)	$10^{20}\sigma$ (cm^2)	10^3 B (K^{-1})	λ (nm)	$10^{20}\sigma$ (cm^2)	10^3 B (K^{-1})
192	1225	0	246	2.06	1.61	300	0.263	3.10
194	1095	0	248	2.00	1.44	302	0.208	3.24
196	940	1.70	250	1.97	1.34	304	0.167	3.52
198	770	1.65	252	1.96	1.23	306	0.133	3.77
200	588	1.66	254	1.95	1.18	308	0.105	3.91
202	447	1.69	256	1.95	1.14	310	0.0814	4.23
204	328	1.74	258	1.93	1.12	312	0.0628	4.70
206	231	1.77	260	1.91	1.14	314	0.0468	5.15
208	156	1.85	262	1.87	1.14	316	0.0362	5.25
210	104	1.97	264	1.83	1.18	318	0.0271	5.74
212	67.5	2.08	266	1.77	1.22	320	0.0197	6.45
214	43.9	2.17	268	1.70	1.25	322	0.0154	6.70
216	29.2	2.17	270	1.62	1.45	324	0.0108	7.16
218	20.0	2.21	272	1.53	1.49	326	0.00820	7.55
220	14.9	2.15	274	1.44	1.56	328	0.00613	8.16
222	11.8	2.06	276	1.33	1.64	330	0.00431	9.75
224	9.61	1.96	278	1.23	1.69	332	0.00319	9.93
226	8.02	1.84	280	1.12	1.78	334	0.00243	9.60
228	6.82	1.78	282	1.01	1.87	336	0.00196	10.5
230	5.75	1.80	284	0.909	1.94	338	0.00142	10.8
232	4.87	1.86	286	0.807	2.04	340	0.00103	11.8
234	4.14	1.90	288	0.709	2.15	342	0.00086	11.8
236	3.36	1.97	290	0.615	2.27	344	0.00069	9.30
238	2.93	1.97	292	0.532	2.38	346	0.00050	12.1
240	2.58	1.97	294	0.453	2.52	348	0.00042	11.9
242	2.34	1.88	296	0.381	2.70	350	0.00042	9.30
244	2.16	1.75	298	0.316	2.92			

Note:

Absorption cross sections

192–350 nm: Burkholder et al.[3]

Temperature coefficients

Burkholder et al.[3]

$\sigma(\lambda, T) = \sigma(\lambda, 298\ K) \exp(B(\lambda)(T - 298))$, T in K

(1) Biaume, F. Nitric acid vapour absorption cross-section spectrum and its photodissociation in the stratosphere. *J. Photochem.* **1973**, *2*, 139-149, doi:10.1016/0047-2670(73)80012-7.

(2) Brown, S. S.; Wilson, R. W.; Ravishankara, A. R. Absolute intensities for third and fourth overtone absorptions in HNO_3 and H_2O_2 measured by cavity ring down spectroscopy. *J. Phys. Chem. A* **2000**, *104*, 4963-4976, doi:10.1021/jp000439d.

(3) Burkholder, J. B.; Talukdar, R. K.; Ravishankara, A. R.; Solomon, S. Temperature dependence of the HNO_3 UV absorption cross sections. *J. Geophys. Res.* **1993**, *98*, 22937-22948, doi:10.1029/93JD02178.

(4) Donaldson, D. J.; Frost, G. J.; Rosenlof, K. H.; Tuck, A. F.; Vaida, V. Atmospheric radical production by excitation of vibrational overtones *via* absorption of visible light. *Geophys. Res. Lett.* **1997**, *24*, 2651-2654, doi:10.1029/97GL02663.

(5) Donaldson, J.; Orlando, J. J.; Amann, S.; Tyndall, G. S.; Proos, R. J.; Henry, B. R.; Vaida, V. Absolute intensities of nitric acid overtones. *J. Phys. Chem.* **1998**, *102*, 5171-5174, doi:10.1021/jp980811d.

(6) Felder, P.; Yang, X.; Huber, J. R. Photodissociation of nitric acid in a cold molecular beam at 193 nm. *Chem. Phys. Lett.* **1993**, *215*, 221-227, doi:10.1016/0009-2614(93)89292-P.

(7) Johnston, H. S.; Chang, S.; Whitten, G. Photolysis of nitric acid vapor. *J. Phys. Chem.* **1974**, *78*, 1-7, doi:10.1021/j100594a001.

(8) Johnston, H. S.; Graham, R. Gas-phase ultraviolet absorption spectrum of nitric acid vapor. *J. Phys. Chem.* **1973**, *77*, 62-63, doi:10.1021/j100620a013.

(9) Jolly, G. S.; Singleton, D. L.; McKenney, D. J.; Paraskevopoulos, G. Laser photolysis of HNO_3 at 222 nm: Direct determination of the primary quantum yield of OH. *J. Chem. Phys.* **1986**, *84*, 6662-6667, doi:10.1063/1.450719.
(10) Li, Q.; Carter, R. T.; Huber, J. R. The photodissociation dynamics of nitric acid studied at 193 nm by LIF and REMPI-TOF methods. *Chem. Phys. Lett.* **2001**, *334*, 39-46, doi:10.1016/S0009-2614(00)01445-7.
(11) Margitan, J. J.; Watson, R. T. Kinetics of the reaction of hydroxyl radicals with nitric acid. *J. Phys. Chem.* **1982**, *86*, 3819-3824, doi:10.1021/j100216a022.
(12) Molina, L. T.; Molina, M. J. UV absorption cross sections of HO_2NO_2 vapor. *J. Photochem.* **1981**, *15*, 97-108, doi:10.1016/0047-2670(81)85002-2.
(13) Myers, T. L.; Forde, N. R.; Hu, B.; Kitchen, D. C.; Butler, L. J. The influence of local electronic character and nonadiabaticity in the photodissociation of nitric acid at 193 nm. *J. Chem. Phys.* **1997**, *81*, 5361-5373, doi:10.1063/1.474246.
(14) Okabe, H. Photodissociation of nitric acid and water in the vacuum ultraviolet; vibrational and rotational distributions of OH $^2\Sigma^+$. *J. Chem. Phys.* **1980**, *72*, 6642-6650, doi:10.1063/1.439123.
(15) Rattigan, O.; Lutman, E.; Jones, R. L.; Cox, R. A. Temperature dependent absorption cross sections and atmospheric photolysis rates of nitric acid. *Ber. Bunsenges. Phys. Chem.* **1992**, *96*, 399-404, doi:10.1002/bbpc.19920960331.
(16) Rattigan, O.; Lutman, E.; Jones, R. L.; Cox, R. A.; Clemitshaw, K.; Williams, J. Corrigendum: Temperature-dependent absorption cross-sections of gaseous nitric acid and methyl nitrate. *J. Photochem. Photobiol. A: Chem.* **1992**, *69*, 125-126, doi:10.1016/1010-6030(92)85269-Z.
(17) Riffault, V.; Gierczak, T.; Burkholder, J. B.; Ravishankara, A. R. Quantum yields for OH production in the photodissociation of HNO_3 at 248 and 308 nm and H_2O_2 at 308 and 320 nm. *Phys. Chem. Chem. Phys.* **2006**, *8*, 1079-1085, doi:1010.1039/b513760h.
(18) Schiffman, A.; Nelson, D. D., Jr.; Nesbitt, D. J. Quantum yields for OH production from 193 and 248 nm photolysis of HNO_3 and H_2O_2. *J. Chem. Phys.* **1993**, *98*, 6935-6946, doi:10.1063/1.464735.
(19) Suto, M.; Lee, L. C. Photoabsorption and photodissociation of $HONO_2$ in the 105-220 nm region. *J. Chem. Phys.* **1984**, *81*, 1294-1297, doi:10.1063/1.447816.
(20) Turnipseed, A. A.; Vaghjiani, G. L.; Thompson, J. E.; Ravishankara, A. R. Photodissociation of HNO_3 at 193, 222, and 248 nm: Products and quantum yields. *J. Chem. Phys.* **1992**, *96*, 5887-5895, doi:10.1063/1.462685.
(21) Zhang, H.; Roehl, C. M.; Sander, S. P.; Wennberg, P. O. Intensity of the second and third OH overtones of H_2O_2, HNO_3, and HO_2NO_2. *J. Geophys. Res.* **2000**, *105*, 14593-14598, doi:10.1029/2000JD900118.

C10. HO_2NO_2 (peroxynitric acid)

Back to Index

$HO_2NO_2 + h\nu$	$\rightarrow HO_2 + NO_2$	99 kJ mol^{-1}	1207 nm	(1)
	$\rightarrow OH + NO_3$	165 kJ mol^{-1}	726 nm	(2)
	$\rightarrow O(^3P) + HNO_3$	168 kJ mol^{-1}	713 nm	(3)
	$\rightarrow H + NO_2 + O_2$	305 kJ mol^{-1}	393 nm	(4)
	$\rightarrow HO_2 + NO + O(^3P)$	353 kJ mol^{-1}	339 nm	(5)
	$\rightarrow OH + NO_2 + O$	373 kJ mol^{-1}	321 nm	(6)
	$\rightarrow H + O(^3P) + NO_3$	594 kJ mol^{-1}	201 nm	(7)
	$\rightarrow HONO + O_2(^1\Sigma)$	131 kJ mol^{-1}	911 nm	(8)
	$\rightarrow HONO + O_2(^1\Delta)$	69 kJ mol^{-1}	1744 nm	(9)

(Recommendation: 06-2; Note: 15-10; Evaluated: 15-10)

Absorption Cross Sections: The gas-phase UV absorption spectrum of peroxynitric acid, HO_2NO_2, has been reported by Cox and Patrick[1] (195–265 nm; 284 K), Morel et al.[9] (200–290 nm; 298 K), Graham et al.[3] (190–330 nm; 269 K), Molina and Molina[8] (190–330 nm; 298 K), Singer et al.[13] (210–329 nm; 253, 273, and 298 K), and Knight et al.[5] (220–350 nm; 273, 296, 318, and 343 K). There is very good agreement (to within 5%) between the results of Molina and Molina[8] and Singer et al.[13] over the range 210–290 nm, but differences of ~15–60% exist in the wavelength range critical for atmospheric photodissociation ($\lambda \geq 290$ nm). The cross section values from Cox and Patrick,[1] Graham et al.,[3] and Morel et al.[9] are systematically greater than those of Molina and Molina[8] at wavelengths >200 nm. Knight et al.[5] used the data of Molina and Molina[8] and Singer et al.[13] in the 250–270 nm region for normalization to provide absolute cross section data for the long wavelength region. The recommended room temperature absorption cross section data in Table 4C-10-1 are a combination of data from Molina and Molina[8] in the region 190–205 nm, the mean of the data from Molina

and Molina[8] and Singer et al.[13] in the region 210–275 nm, and the data from Knight et al.[5] in the region 280–350 nm.

The temperature dependence of the absorption spectrum was examined by Singer et al.,[13] who found no temperature dependence between 253 and 298 K, and by Knight et al.,[5] who reported a systematic increase of the absorption cross sections with increasing temperature. Knight et al.[5] parameterized the temperature dependence using a two component model

$$\sigma(T, \lambda) = \sigma_0(\lambda)/Q + \sigma_1(\lambda)\ (1–1/Q)$$

where the partition function is given by $Q = 1 + \exp(-\Delta E/(0.69T))$ with $\Delta E = 988$ cm^{-1} (O-O stretching vibration) and T is in K. The Knight et al. parameterization is recommended.

On the basis of the results from the Molina and Molina, Singer et al., and Knight et al. studies, an uncertainty factor for the HO_2NO_2 room temperature absorption cross sections in the wavelength region 190–350 nm, is estimated to be 1.2 (2σ). The uncertainty factor at temperatures <298 K is expected to be greater in the long wavelength region, but is difficult to estimate without additional studies.

Photolysis Quantum Yield and Product Studies: HO_2NO_2 photodissociates in the UV with a unit quantum yield. MacLeod et al.[6] measured the quantum yield of OH radicals at 248 nm as $\Phi(OH) = 0.34 \pm 0.16$ (the sum of channels 2 and 5), relative to the OH yield in the photolysis of H_2O_2. Roehl et al.[10] determined the quantum yield of NO_2 in the photolysis at 248 nm (relative to the NO_2 yield in the photolysis of HNO_3) to be $\Phi(NO_2) = 0.56 \pm 0.17$ (the sum of channels 1,4 and 5). Jimenez et al.[4] measured the yield of OH and HO_2 (from channels 1 and 6) at 193 and 248 nm (relative to the photolysis of H_2O_2) and the yield of NO_3 (relative to the photolysis of $ClONO_2$) at 193, 248 and 308 nm over a pressure range of 10 to 84 Torr. Jimenez et al.[4] reported $\Phi_{193}(OH) = 0.21 \pm 0.12$, $\Phi_{248}(OH) = 0.085 \pm 0.08$, $\Phi_{193}(HO_2) = 0.56 \pm 0.02$, $\Phi_{248}(HO_2) = 0.89 \pm 0.26$, $\Phi_{193}(NO_3) = 0.35 \pm 0.03$, $\Phi_{248}(NO_3) = 0.08 \pm 0.03$ and $\Phi_{308}(NO_3) = 0.05 \pm 0.02$. Assuming that only channel (2) contributes to OH and NO_3 production, these results imply that at 248 nm the yields of OH and NO_3 are nearly identical, 0.08. This lower yield is in disagreement with the earlier 248 nm results of MacLeod et al.[6] and Roehl et al.[10] The high HO_2 yield (0.89 ± 0.26) measured at 248 nm by Jimenez et al.[4] overlaps within the experimental uncertainties with the NO_2 yield (0.56 ± 0.17) of Roehl et al.,[10] assuming that the HO_2 arises from channel (1). It cannot however not be excluded that the difference in NO_2 yields reflects the contribution of channel (6). The recommended quantum yields are given in Table 4C-10-2 where the values below 200 nm are taken from Jimenez et al.[4] and the values above 200 nm represent an average of the results from Jimenez et al., Roehl et al. and MacLeod et al. The estimated uncertainty in the recommended quantum yields is ±0.2.

The photodissociation of HO_2NO_2 via excitation of the OH stretch vibrational overtones $2\nu_1$, $3\nu_1$, and $4\nu_1$ in the near IR and visible is a possible atmospheric HO_x source.[15 12 2] The band strengths (in units of 10^{-20} cm^2 molecule^{-1} cm^{-1}) of (3.8 ± 0.11) for $3\nu_1$ and (0.30 ± 0.18) for $4\nu_1$ have been reported by Zhang et al.[16] and (3.3 ± 0.7) for $3\nu_1$ by Roehl et al.[11] Stark et al.[14] report greater values for the $3\nu_1$ and $4\nu_1$ band strengths of (5.7 ± 1.1) and (0.49 ± 0.09), respectively. Roehl et al.[11] also measured absolute integrated band strengths and photodissociation quantum yields for 3 dissociative bands in the infrared region: $2\nu_1 + \nu_3$ (8242 cm^{-1}), $2\nu_1$ (6900 cm^{-1}) and $\nu_1 + 2\nu_3$ (6252 cm^{-1}) as a function of temperature. Matthews et al.[7] photolysed HO_2NO_2 at 390 nm in its first OH-stretching overtone ($2\nu_1$) and reported a quantum yield of 0.30 at 298 K. The temperature dependent cross sections and dissociation quantum yields from Roehl et al.[11] are summarized in Table 4C-10-3.

Table 4C-10-1. Recommended Absorption Cross Sections of HO_2NO_2 at 298 K

λ (nm)	10^{20} σ (cm^2)	λ (nm)	10^{20} σ (cm^2)	λ (nm)	10^{20} σ (cm^2)	λ (nm)	10^{20} σ (cm^2)
190	1010	260	28.50	300	1.52	328	0.110
195	816	265	23.00	302	1.28	330	0.0926
200	563	270	18.05	304	1.05	332	0.0788
205	367	275	13.40	306	0.853	334	0.0650
210	239	280	9.29	308	0.702	336	0.0540
215	161	282	8.11	310	0.551	338	0.0456
220	117.5	284	6.93	312	0.465	340	0.0372
225	93.50	286	5.86	314	0.380	342	0.0320
230	79.20	288	4.91	316	0.313	344	0.0268
235	68.25	290	3.95	318	0.265	346	0.0228
240	58.10	292	3.37	320	0.216	348	0.0198
245	48.95	294	2.78	322	0.184	350	0.0168
250	41.25	296	2.30	324	0.152		
255	35.00	298	1.91	326	0.128		

Note:
190–205 nm: Molina and Molina[8]
210–275 nm: mean of the data from Molina and Molina[8] and Singer et al.[13]
280–350 nm: Knight et al.[5]

Table 4C-10-2. Recommended HO_2NO_2 Photolysis Quantum Yields

λ (nm)	Φ (OH)	Φ(NO_3)	Φ(HO_2)	Φ(NO_2)
<200	0.3	0.3	0.7	0.7
>200	0.2	0.2	0.8	0.8

Table 4C-10-3. Photodissociation Band Strengths and Quantum Yields for Several Overtone and Combination Bands of HO_2NO_2

Band	Band center (cm^{-1})	$\int \sigma_{diss} \Phi_\nu \, d\nu$ cm^2 $molecule^{-1}$ cm^{-1}	Quantum yield
$4\nu_1$	13105	3.0×10^{-21} (a)	1
$3\nu_1$	10090	3.3×10^{-20} (b)	1
$2\nu_1 + \nu_3$	8240	1.21×10^{-21} (b)	0.76
$2\nu_1$	6900	$4.09 \times 10^{-18} \exp(-826.5/T)$ (195 K> T >224 K) (b)	0.14
$\nu_1 + 2\nu_3$	6250	$1.87 \times 10^{-19} \exp(-1410.7/T)$ (195 K> T >240 K) (b)	0.02

Note:
a) Data from Zhang et al.[16]
b) Data from Roehl et al.[11]

(1) Cox, R. A.; Patrick, R. Kinetics of the reaction $HO_2 + NO_2(+M) = HO_2NO_2$ using molecular modulation spectrometry. *Int. J. Chem. Kinet.* **1979**, *11*, 635-648, doi:10.1002/kin.550110610.

(2) Evans, J. T.; Chipperfield, M. P.; Oelhaf, H.; Stowasser, M.; Wetzel, G. Effect of near-IR photolysis of HO_2NO_2 on stratospheric chemistry. *Geophys. Res. Lett.* **2003**, *29*, 1223, doi:10.1029/2002GL016470.

(3) Graham, R. A.; Winer, A. M.; Pitts, J. N., Jr. Ultraviolet and infrared absorption cross sections of gas phase HO_2NO_2. *Geophys. Res. Lett.* **1978**, *5*, 909-911, doi:10.1029/GL005i011p00909.

(4) Jiménez, E.; Gierczak, T.; Stark, H.; Burkholder, J. B.; Ravishankara, A. R. Quantum yields of OH, HO_2 and NO_3 in the UV photolysis of HO_2NO_2. *Phys. Chem. Chem. Phys.* **2005**, *7*, 342-348, doi:10.1039/b413429j.

(5) Knight, G.; Ravishankara, A. R.; Burkholder, J. B. UV absorption cross sections of HO_2NO_2 between 343 and 273 K. *Phys. Chem. Chem. Phys.* **2002**, *4*, 1432-1437, doi:10.1039/b108904h.

(6) MacLeod, H.; Smith, G. P.; Golden, D. M. Photodissociation of pernitric acid (HO_2NO_2) at 248 nm. *J. Geophys. Res.* **1988**, *93*, 3813-3823, doi:10.1029/JD093iD04p03813.
(7) Matthews, J.; Sharma, R.; Sinha, A. Photodissociation of vibrationally excited pernitric acid: HO_2NO_2 ($2\nu_1$) + 390 nm. *J. Phys. Chem. A* **2004**, *108*, 8134–8139, doi:10.1021/jp040285s.
(8) Molina, L. T.; Molina, M. J. UV absorption cross sections of HO_2NO_2 vapor. *J. Photochem.* **1981**, *15*, 97-108, doi:10.1016/0047-2670(81)85002-2.
(9) Morel, O.; Simonaitis, R.; Heicklen, J. Ultraviolet absorption spectra of HO_2NO_2, $CCl_3O_2NO_2$, $CCl_2FO_2NO_2$, and $CH_3O_2NO_2$. *Chem. Phys. Lett.* **1980**, *73*, 38-41, doi:10.1016/0009-2614(80)85197-9.
(10) Roehl, C. M.; Mazely, T. L.; Friedl, R. R.; Li, Y. M.; Francisco, J. S.; Sander, S. P. NO_2 quantum yield from the 248 nm photodissociation of peroxynitric acid (HO_2NO_2). *J. Phys. Chem. A* **2001**, *105*, 1592-1598, doi:10.1021/jp001982x.
(11) Roehl, C. M.; Nizkorodov, S. A.; Zhang, H.; Blake, G. A.; Wennberg, P. O. Photodissociation of peroxynitric acid in the near-IR. *J. Phys. Chem. A* **2002**, *106*, 3766-3772, doi:10.1021/jp013536v.
(12) Salawitch, R. J.; Wennberg, P. O.; Toon, G. C.; Sen, B.; Blavier, J.-F. Near IR photolysis of HO_2NO_2: Implications for HO_x. *Geophys. Res. Lett.* **2002**, *29*, 1-4, doi:10.1029/2002GL015006.
(13) Singer, R. J.; Crowley, J. N.; Burrows, J. P.; Schneider, W.; Moortgat, G. K. Measurement of the absorption cross-section of peroxynitric acid between 210 and 330 nm in the range 253-298 K. *J. Photochem. Photobiol. A: Chem.* **1989**, *48*, 17-32, doi:10.1016/1010-6030(89)87086-8.
(14) Stark, H.; Brown, S. S.; Burkholder, J. B.; Aldener, M.; Riffault, V.; Gierczak, T.; Ravishankara, A. R. Overtone dissociation of peroxynitric acid (HO_2NO_2): Absorption cross sections and photolysis products. *J. Phys. Chem. A* **2008**, *112*, 9296–9303, doi:10.1021/jp802259z.
(15) Wennberg, P. O.; Salawitch, R. J.; Donaldson, D. J.; Hanisco, T. F.; Lanzendorf, E. J.; Perkins, K. K.; Lloyd, S. A.; Vaida, V.; Gao, R. S.; Hintsa, E. J.; Cohen, R. C.; Swartz, W. H.; Kusterer, T. L.; Anderson, D. E. Twilight observations suggest unknown sources of HO_x. *Geophys. Res. Lett.* **1999**, *26*, 1373-1376, doi:10.1029/1999GL900255.
(16) Zhang, H.; Roehl, C. M.; Sander, S. P.; Wennberg, P. O. Intensity of the second and third OH overtones of H_2O_2, HNO_3, and HO_2NO_2. *J. Geophys. Res.* **2000**, *105*, 14593-14598, doi:10.1029/2000JD900118.

4.6 Bibliography – NO_x Photochemistry

Amaral, G.; Xu, K.; Zhang, J. H + NO_2 channels in the photodissociation of HONO at 193.3 nm. *J. Phys. Chem. A* **2001**, *105*, 1465-1475, doi:10.1021/jp002521e.

Amoruso, A.; Crescentini, L.; Fiocco, G.; Volpe, M. New measurements of the NO_2 absorption cross section in the 440- to 460-nm region and estimates of the NO_2-N_2O_4 equilibrium constant. *J. Geophys. Res.* **1993**, *98*, 16857-16863, doi:10.1029/93JD01582.

Barker, J. R.; Brouwer, L.; Patrick, R.; Rossi, M. J.; Trevor, P. L.; Golden, D. M. N_2O_5 photolysis products investigated by fluorescence and optoacoustic techniques. *Int. J. Chem. Kinet.* **1985**, *17*, 991-1006, doi:10.1002/kin.550170906.

Bass, A. M.; Ledford, A. E.; Laufer, A. H. Extinction coefficients of NO_2 and N_2O_4. *J. Res. Natl. Bur. Stand.* **1976**, *80A*, 143-166, doi:10.6028/jres.080A.017.

Bates, D. R.; Hays, P. B. Atmospheric nitrous oxide. *Planet. Space Sci.* **1967**, *15*, 189-197, doi:10.1016/0032-0633(67)90074-8.

Bertrand, C.; Collin, G. J.; Gagnon, H. Coefficients d'absorption et rendements quantiques ioniques de composés inorganiques et d'hydrocarbones insaturés. *J. Chim. Phys.* **1975**, *72*, 719-723, doi:10.1051/jcp/1975720719.

Biaume, F. Nitric acid vapour absorption cross-section spectrum and its photodissociation in the stratosphere. *J. Photochem.* **1973**, *2*, 139-149, doi:10.1016/0047-2670(73)80012-7.

Bogumil, K.; Orphal, J.; Homann, T.; Voigt, S.; Spietz, P.; Fleischmann, O. C.; Vogel, A.; Hartmann, M.; Kromminga, H.; Bovensmann, H.; Frerick, J.; Burrows, J. P. Measurements of molecular absorption spectra with the SCIAMACHY pre-flight model: instrument characterization and reference data for atmospheric remote-sensing in the 230-2380 nm region. *J. Photochem. Photobiol. A: Chem.* **2003**, *157*, 167-184, doi:10.1016/S1010-6030(03)00062-5.

Bongartz, A.; Kames, J.; Schurath, U.; George, C.; Mirabel, P.; Ponche, J. L. Experimental determination of HONO mass accommodation coefficients using two different techniques. *J. Atmos. Chem.* **1994**, *18*, 149-169, doi:10.1007/BF00696812.

Bongartz, A.; Kames, J.; Welter, F.; Schurath, U. Near-UV absorption cross sections and trans/cis equilibrium of nitrous acid. *J. Phys. Chem.* **1991**, *95*, 1076-1082, doi:10.1021/j100156a012.

Brown, S. S.; Wilson, R. W.; Ravishankara, A. R. Absolute intensities for third and fourth overtone absorptions in HNO_3 and H_2O_2 measured by cavity ring down spectroscopy. *J. Phys. Chem. A* **2000**, *104*, 4963-4976, doi:10.1021/jp000439d.

Brust, A. S.; Becker, K. H.; Kleffmann, J.; Wiesen, P. UV absorption cross sections of nitrous acid. *Atmos. Environ.* **2000**, *34*, 13-19, doi:10.1016/S1352-2310(99)00322-2.

Burkholder, J. B.; Talukdar, R. K.; Ravishankara, A. R.; Solomon, S. Temperature dependence of the HNO_3 UV absorption cross sections. *J. Geophys. Res.* **1993**, *98*, 22937-22948, doi:10.1029/93JD02178.

Burrows, J. P.; Dehn, A.; Deters, B.; Himmelmann, S.; Richter, A.; Voigt, S.; Orphal, J. Atmospheric remote-sensing reference data from GOME: Part 1. Temperature-dependent absorption cross-sections of NO_2 in the 231-794 nm range. *J. Quant. Spectrosc. Radiat. Transf.* **1998**, *60*, 1025-1031, doi:10.1016/S0022-4073(97)00197-0.

Burrows, J. P.; Tyndall, G. S.; Moortgat, G. K. Absorption spectrum of NO_3 and kinetics of the reactions of NO_3 with NO_2, Cl, and several stable atmospheric species at 298 K. *J. Phys. Chem.* **1985**, *89*, 4848-4856, doi:10.1021/j100268a038.

Calvert, J. G.; Madronich, S.; Gardner, E. P.; Davidson, J. A.; Cantrell, C. A.; Shetter, R. E. Mechanism of NO_2 photodissociation in the energy-deficient region at 404.7 nm. *J. Phys. Chem.* **1987**, *91*, 6339-6341, doi:10.1021/j100309a006.

Canosa-Mas, C. E.; Fowles, M.; Houghton, P. J.; Wayne, R. P. Absolute absorption cross-section measurements on NO_3 Evaluation of the titration of NO_3 by NO in the determination of absolute concentrations. *J. Chem. Soc. Faraday Trans. 2* **1987**, *83*, 1465-1474, doi:10.1039/f29878301465.

Cantrell, C. A.; Davidson, J. A.; Shetter, R. E.; Anderson, B. A.; Calvert, J. G. The temperature invariance of the NO_3 absorption cross section in the 662-nm region. *J. Phys. Chem.* **1987**, *91*, 5858-5863, doi:10.1021/j100307a009.

Cantrell, C. A.; Zimmer, A.; Tyndall, G. S. Absorption cross sections for water vapor from 183 to 193 nm. *Geophys. Res. Lett.* **1997**, *24*, 2195-2198, 2687 (Erratum), doi:10.1029/97GL02100.

Chan, W. F.; Cooper, G.; Brion, C. E. Absolute optical oscillator strengths for the photoabsorption of nitric oxide (5-30 eV) at high resolution. *Chem. Phys.* **1993**, *170*, 111-121, doi:0.1016/0301-0104(93)80097-S.

Chan, W. F.; Cooper, G.; Brion, C. E. Discrete and continuum photoabsorption oscillator-strengths for the electronic spectrum of nitrous oxide (5.5-203 eV). *Chem. Phys.* **1994**, *180*, 77-88, doi:10.1016/0301-0104(93)E0386-A.

Chung, J.-S.; Kim, H. H.; Chung, J.-M. Measurement of photoabsorption cross sections of nitric oxide by using double-ionization chamber. *J. Opt. Soc. Korea* **2006**, *10*, 157-161, doi:10.3807/JOSK2006.10.4.157.
Coquart, B.; Jenouvier, A.; Merienne, M. F. The NO_2 absorption spectrum. II. Cross-sections at low temperatures in the 400-500 nm region. *J. Atmos. Chem.* **1995**, *21*, 251-261, doi:10.1007/BF00696757.
Corcoran, T. C.; Beiting, E. J.; Mitchell, M. O. High-resolution absolute absorption cross sections of NO_2 at 295, 573, and 673 K at visible wavelengths. *J. Mol. Spectrosc.* **1992**, *154*, 119-128, doi:10.1016/0022-2852(92)90033-K.
Cox, R. A.; Barton, R. A.; Ljungstrom, E.; Stocker, D. W. The reactions of Cl and ClO with the NO_3 radical. *Chem. Phys. Lett.* **1984**, *108*, 228-232, doi:10.1016/0009-2614(84)87054-2.
Cox, R. A.; Derwent, R. G. The ultra-violet absorption spectrum of gaseous nitrous acid. *J. Photochem.* **1976**, *6*, 23-34, doi:10.1016/0047-2670(76)87004-9.
Cox, R. A.; Patrick, R. Kinetics of the reaction $HO_2 + NO_2(+M) = HO_2NO_2$ using molecular modulation spectrometry. *Int. J. Chem. Kinet.* **1979**, *11*, 635-648, doi:10.1002/kin.550110610.
Creasey, D. J.; Heard, D. E.; Lee, J. D. Absorption cross-section measurements of water vapour and oxygen at 185 nm. Implications for the calibration of field instruments to measure OH, HO_2 and RO_2 radicals. *Geophys. Res. Lett.* **2000**, *27*, 1651-1654, doi:10.1029/1999GL011014.
Davenport, J. E. Determination of NO_2 Photolysis Parameters for Stratospheric Modeling, Federal Aviation Administration, Washington, DC. FAA-EQ-78-14, 1978,
Davidson, J. A.; Cantrell, C. A.; McDaniel, A. H.; Shetter, R. E.; Madronich, S.; Calvert, J. G. Visible-ultraviolet absorption cross sections for NO_2 as a function of temperature. *J. Geophys. Res.* **1988**, *93*, 7105-7112, doi:10.1029/JD093iD06p07105.
Davis, H. F.; Kim, B.; Johnston, H. S.; Lee, Y. T. Dissociation energy and photochemistry of NO_3. *J. Phys. Chem.* **1993**, *97*, 2172-2180, doi:10.1021/j100112a018.
DeMore, W. B.; Sander, S. P.; Golden, D. M.; Hampson, R. F.; Kurylo, M. J.; Howard, C. J.; Ravishankara, A. R.; Kolb, C. E.; Molina, M. J. Chemical Kinetics and Photochemical Data for Use in Stratospheric Modeling. *JPL Publication 97-4* **1997**, *Evaluation 12*.
Dixon, J. K. The absorption coefficient of nitrogen dioxide in the visible spectrum. *J. Chem. Phys.* **1940**, *8*, 157-160, doi:10.1063/1.1750622.
Donaldson, D. J.; Frost, G. J.; Rosenlof, K. H.; Tuck, A. F.; Vaida, V. Atmospheric radical production by excitation of vibrational overtones *via* absorption of visible light. *Geophys. Res. Lett.* **1997**, *24*, 2651-2654, doi:10.1029/97GL02663.
Donaldson, J.; Orlando, J. J.; Amann, S.; Tyndall, G. S.; Proos, R. J.; Henry, B. R.; Vaida, V. Absolute intensities of nitric acid overtones. *J. Phys. Chem.* **1998**, *102*, 5171-5174, doi:10.1021/jp980811d.
Evans, J. T.; Chipperfield, M. P.; Oelhaf, H.; Stowasser, M.; Wetzel, G. Effect of near-IR photolysis of HO_2NO_2 on stratospheric chemistry. *Geophys. Res. Lett.* **2003**, *29*, 1223, doi:10.1029/2002GL016470.
Febo, A.; Perrino, C.; Allegrini, I. Measurement of nitrous acid in Milan, Italy, by DOAS and diffusion denuders. *Atmos. Environ.* **1996**, *30*, 3599-3609, doi:10.1016/1352-2310(96)00069-6.
Felder, P.; Yang, X.; Huber, J. R. Photodissociation of nitric acid in a cold molecular beam at 193 nm. *Chem. Phys. Lett.* **1993**, *215*, 221-227, doi:10.1016/0009-2614(93)89292-P.
Frost, G. J.; Goss, L. M.; Vaida, V. Measurements of high-resolution ultraviolet-visible absorption cross sections at stratospheric temperatures, 1. Nitrogen dioxide. *J. Geophys. Res.* **1996**, *101*, 3869-3877, doi:10.1029/95JD03388.
Gaedtke, H.; Troe, J. Primary processes in photolysis of NO_2. *Ber. Bunsenges. Phys. Chem.* **1975**, *79*, 184-191, doi:10.1002/bbpc.19750790212.
Gardner, E. P.; Sperry, P. D.; Calvert, J. G. Primary quantum yields of NO_2 photodissociation. *J. Geophys. Res.* **1987**, *92*, 6642-6652, doi:10.1029/JD092iD06p06642.
Gierczak, T.; Burkholder, J. B.; Ravishankara, A. R. Temperature dependent rate coefficient for the reaction $O(^3P) + NO_2 \rightarrow NO + O_2$. *J. Phys. Chem. A* **1999**, *103*, 877-883, doi:10.1021/jp983962p.
Graham, R. A. Photochemistry of NO_3 and the Kinetics of the N_2O_5-O_3 System. Ph. D. Thesis, University of California, Berkeley, CA, 1975.
Graham, R. A.; Johnston, H. S. The photochemistry of NO_3 and the kinetics of the N_2O_5-O_3 system. *J. Phys. Chem.* **1978**, *82*, 254-268, doi:10.1021/j100492a002.
Graham, R. A.; Winer, A. M.; Pitts, J. N., Jr. Ultraviolet and infrared absorption cross sections of gas phase HO_2NO_2. *Geophys. Res. Lett.* **1978**, *5*, 909-911, doi:10.1029/GL005i011p00909.
Gratien, A.; Lefort, M.; Picquet-Varrault, B.; Orphal, J.; Doussin, J.-F.; Flaud, J.-M. Experimental intercomparison of the absorption cross-sections of nitrous acid (HONO) in the ultraviolet and mid-infrared spectral regions. *J. Quant. Spectrosc. Radiat. Transf.* **2009**, *110*, 256-263, doi:10.1016/j.jqsrt.2008.11.003.
Greenblatt, G. D.; Ravishankara, A. R. Laboratory studies on the stratospheric NO_x production rate. *J. Geophys. Res.* **1990**, *95*, 3539-3547, doi:10.1029/JD095iD04p03539.

Greiner, N. R. Photochemistry of N_2O essential to a simplified vacuum-ultraviolet actinometer. *J. Chem. Phys.* **1967**, *47*, 4373-4377, doi:10.1063/1.1701640.
Griffith, D. W. T.; Toon, G. C.; Sen, B.; Blavier, J.-F.; Toth, R. A. Vertical profiles of nitrous oxide isotopomer fractionation measured in the stratosphere. *Geophys. Res. Lett.* **2000**, *27*, 2485-2488, doi:10.1029/2000GL011797.
Guest, J. A.; Lee, L. C. Quantitative absorption and fluorescence studies of NO between 1060 and 2000 Å. *J. Phys. B: At. Mol. Phys.* **1981**, *14*, 3401-3413, doi:10.1088/0022-3700/14/18/013.
Hall, J., T. C.; Blacet, F. E. Separation of the absorption spectra of NO_2 and N_2O_4 in the range of 2400-5000A. *J. Chem. Phys.* **1952**, *20*, 1745-1749, doi:10.1063/1.1700281.
Harder, J. W.; Brault, J. W.; Johnston, P. V.; Mount, G. H. Temperature dependent NO_2 cross sections at high spectral resolution. *J. Geophys. Res.* **1997**, *D102*, 3861-3879, doi:10.1029/96JD03086.
Harker, A. B.; Ho, W.; Ratto, J. J. Photodissociation quantum yield of NO_2 in the region 375 to 420 nm. *Chem. Phys. Lett.* **1977**, *50*, 394-397, doi:10.1016/0009-2614(77)80351-5.
Harwood, M. H.; Burkholder, J. B.; Ravishankara, A. R. Photodissociation of $BrONO_2$ and N_2O_5: Quantum yields for NO_3 production at 248, 308, and 352.5 nm. *J. Phys. Chem. A* **1998**, *102*, 1309-1317, doi:10.1021/jp9729829.
Harwood, M. H.; Jones, R. L. Temperature dependent ultraviolet-visible absorption cross sections of NO_2 and N_2O_4: Low-temperature measurements of the equilibrium constant for $2NO_2 \rightleftharpoons N_2O_4$. *J. Geophys. Res.* **1994**, *99*, 22955-22964, doi:10.1029/94JD01635.
Harwood, M. H.; Jones, R. L.; Cox, R. A.; Lutman, E.; Rattigan, O. V. Temperature-dependent absorption cross-sections of N_2O_5. *J. Photochem. Photobiol. A: Chem.* **1993**, *73*, 167-175, doi:10.1016/1010-6030(93)90001-2.
Harwood, M. H.; Rattigan, O. V.; Jones, R. L.; Cox, R. A. *Proc. SPIE Int. Soc. Opt. Eng.* **1992**, *1715*, 113-124.
Hicks, E.; Leroy, B.; Rigaud, P.; Joudain, J.-L.; Le Bras, G. Near ultraviolet and visible absorption spectra of minor atmospheric components NO_2 and SO_2 between 200 and 300 K. *J. Chim. Phys.* **1979**, *76*, 693-698, doi:10.1051/jcp/1979760693.
Hitchcock, V. C.; Brion, E.; van der Wiel, M. J. Absolute oscillator-strengths for valence-shell ionic photofragmentation of N_2O and CO_2 (8-75 eV). *Chem. Phys.* **1980**, *45*, 461-478, doi:10.1016/0301-0104(80)87015-7.
Holmes, H. H.; Daniels, F. The photolysis of nitrogen oxides: N_2O_5, N_2O_4 and NO_2. *J. Am. Chem. Soc.* **1934**, *56*, 630-637, doi:10.1021/ja01318a028.
Hubrich, C.; Stuhl, F. The ultraviolet absorption of some halogenated methanes and ethanes of atmospheric interest. *J. Photochem.* **1980**, *12*, 93-107, doi:10.1016/0047-2670(80)85031-3.
Iida, Y.; Carnovale, F.; Daviel, S.; Brion, C. E. Absolute oscillator-strengths for photoabsorption and the molecular and dissociative photoionization of nitric oxide. *Chem. Phys.* **1986**, *105*, 211-225, doi:10.1016/0301-0104(86)80070-2.
Jenouvrier, A.; Coquart, B.; Mérienne, M.-F. The NO_2 absorption spectrum. III: The 200-300 nm region at ambient temperature. *J. Atmos. Chem.* **1996**, *25*, 21-32, doi:10.1007/BF00053284.
Jiménez, E.; Gierczak, T.; Stark, H.; Burkholder, J. B.; Ravishankara, A. R. Quantum yields of OH, HO_2 and NO_3 in the UV photolysis of HO_2NO_2. *Phys. Chem. Chem. Phys.* **2005**, *7*, 342-348, doi:10.1039/b413429j.
Johnson, M. S.; Billing, G. D.; Gruodis, A.; Janssen, M. H. M. Photolysis of nitrous oxide isotopomers studied by time-dependent hermite propagation. *J. Phys. Chem. A* **2001**, *105*, 8672-8680, doi:10.1021/jp011449x.
Johnston, H. S.; Chang, S.; Whitten, G. Photolysis of nitric acid vapor. *J. Phys. Chem.* **1974**, *78*, 1-7, doi:10.1021/j100594a001.
Johnston, H. S.; Davis, H. F.; Lee, Y. T. NO_3 photolysis product channels: Quantum yields from observed energy thresholds. *J. Phys. Chem.* **1996**, *100*, 4713-4723, doi:10.1021/jp952692x.
Johnston, H. S.; Graham, R. Gas-phase ultraviolet absorption spectrum of nitric acid vapor. *J. Phys. Chem.* **1973**, *77*, 62-63, doi:10.1021/j100620a013.
Johnston, H. S.; Graham, R. Photochemistry of NO_x and HNO_x compounds. *Can. J. Phys.* **1974**, *52*, 1415-1423, doi:10.1139/v74-214.
Johnston, H. S.; Selwyn, G. S. New cross sections for the absorption of near ultraviolet radiation by nitrous oxide (N_2O). *Geophys. Res. Lett.* **1975**, *2*, 549-551, doi:10.1029/GL002i012p00549.
Jolly, G. S.; Singleton, D. L.; McKenney, D. J.; Paraskevopoulos, G. Laser photolysis of HNO_3 at 222 nm: Direct determination of the primary quantum yield of OH. *J. Chem. Phys.* **1986**, *84*, 6662-6667, doi:10.1063/1.450719.
Jones, E. L.; Wulf, O. R. The absorption coefficient of nitrogen pentoxide in the ultraviolet and the visible absorption spectrum of NO_3. *J. Chem. Phys.* **1937**, *5*, 873-877, doi:10.1063/1.1749956.
Jones, I. T. N.; Bayes, K. Photolysis of nitrogen dioxide. *J. Chem. Phys.* **1973**, *59*, 4836-4844, doi:10.1063/1.1680696.

Jost, R.; Nygard, J.; Pasinski, A.; Delon, A. The photodissociation threshold of NO_2: Precise determination of its energy and density of states. *J. Chem. Phys.* **1996**, *105*, 1287-1290, doi:10.1063/1.471992.

Keller-Rudek, H.; Moortgat, G. K.; Sander, R.; Sörensen, R. The MPI-Mainz UV/VIS spectral atlas of gaseous molecules of atmospheric interest. *Earth Syst. Sci. Data* **2013**, *5*, 365-373, doi:10.5194/essd-5-365-2013.

Kenner, R. D.; Rohrer, F.; Stuhl, F. OH(A) production in the 193-nm photolysis of HONO. *J. Phys. Chem.* **1986**, *90*, 2635-2639, doi:10.1021/j100403a015.

Kirmse, B.; Delon, A.; Jost, R. NO_2 absorption cross section and its temperature dependence. *J. Geophys. Res.* **1997**, *D103*, 16089-16098, doi:10.1029/97JD00075.

Knight, G.; Ravishankara, A. R.; Burkholder, J. B. UV absorption cross sections of HO_2NO_2 between 343 and 273 K. *Phys. Chem. Chem. Phys.* **2002**, *4*, 1432-1437, doi:10.1039/b108904h.

Ko, M. K. W.; Newman, P. A.; Reimann, S.; Strahan, S. E.; Plumb, R. A.; Stolarski, R. S.; Burkholder, J. B.; Mellouki, W.; Engel, A.; Atlas, E. L.; Chipperfield, M.; Liang, Q. Lifetimes of Stratospheric Ozone-Depleting Substances, Their Replacements, and Related Species, SPARC Report No. 6, WCRP-15/2013, 2013, http://www.sparc-climate.org/publications/sparc-reports/sparc-report-no6/.

Koffend, J. B.; Holloway, J. S.; Kwok, M. A.; Heidner III, R. F. High resolution absorption spectroscopy of NO_2. *J. Quant. Spectrosc. Radiat. Transf.* **1987**, *37*, 449-453, doi:10.1016/S0022-4073(87)90103-8.

Leroy, B.; Rigaud, P.; Hicks, E. Visible absorption cross-sections of NO_2 at 298 K and 235 K. *Ann. Geophys.* **1987**, *5A*, 247-250.

Li, Q.; Carter, R. T.; Huber, J. R. The photodissociation dynamics of nitric acid studied at 193 nm by LIF and REMPI-TOF methods. *Chem. Phys. Lett.* **2001**, *334*, 39-46, doi:10.1016/S0009-2614(00)01445-7.

MacLeod, H.; Smith, G. P.; Golden, D. M. Photodissociation of pernitric acid (HO_2NO_2) at 248 nm. *J. Geophys. Res.* **1988**, *93*, 3813-3823, doi:10.1029/JD093iD04p03813.

Magnotta, F.; Johnston, H. S. Photodissociation quantum yields for the NO_3 free radical. *Geophys. Res. Lett.* **1980**, *7*, 769-772, doi:10.1029/GL007i010p00769.

Margitan, J. J.; Watson, R. T. Kinetics of the reaction of hydroxyl radicals with nitric acid. *J. Phys. Chem.* **1982**, *86*, 3819-3824, doi:10.1021/j100216a022.

Marinelli, W. J.; Swanson, D. M.; Johnston, H. S. Absorption cross sections and line shape for the NO_3(0-0) band. *J. Chem. Phys.* **1982**, *76*, 2864-2870, doi:10.1063/1.443366.

Matthews, J.; Sharma, R.; Sinha, A. Photodissociation of vibrationally excited pernitric acid: HO_2NO_2 ($2\nu_1$) + 390 nm. *J. Phys. Chem. A* **2004**, *108*, 8134–8139, doi:10.1021/jp040285s.

Mérienne, M.-F.; Jenouvrier, A.; Coquart, B.; Lux, J. P. The NO_2 absorption spectrum. IV: The 200–400 nm region at 220 K. *J. Atmos. Chem.* **1997**, *27*, 219-232, doi:10.1023/A:1005829213463.

Mérienne, M. F.; Coquart, B.; Jenouvrier, A. Temperature effect on the ultraviolet-absorption of $CFCl_3$, CF_2Cl_2 and N_2O. *Planet. Space Sci.* **1990**, *38*, 617-625, doi:10.1016/0032-0633(90)90067-Z.

Mérienne, M. F.; Jenouvrier, A.; Coquart, B. The NO_2 absorption spectrum. I. Absorption cross-sections at ambient temperature in the 300-500 nm region. *J. Atmos. Chem.* **1995**, *20*, 281-297, doi:10.1007/BF00694498.

Mihalcea, R. M.; Baer, D. S.; Hanson, R. K. Tunable diode-laser absorption measurements of NO_2 near 670 and 395 nm. *Appl. Opt.* **1996**, *35*, 4059-4064, doi:10.1364/AO.35.004059.

Mitchell, D. N.; Wayne, R. P.; Allen, P. J.; Harrison, R. P.; Twin, R. J. Kinetics and photochemistry of NO_3 Part 1.-Absolute absorption cross-section. *J. Chem. Soc. Faraday Trans. 2* **1980**, *76*, 785-793, doi:10.1039/f29807600785.

Molina, L. T.; Molina, M. J. UV absorption cross sections of HO_2NO_2 vapor. *J. Photochem.* **1981**, *15*, 97-108, doi:10.1016/0047-2670(81)85002-2.

Morel, O.; Simonaitis, R.; Heicklen, J. Ultraviolet absorption spectra of HO_2NO_2, $CCl_3O_2NO_2$, $CCl_2FO_2NO_2$, and $CH_3O_2NO_2$. *Chem. Phys. Lett.* **1980**, *73*, 38-41, doi:10.1016/0009-2614(80)85197-9.

Myers, T. L.; Forde, N. R.; Hu, B.; Kitchen, D. C.; Butler, L. J. The influence of local electronic character and nonadiabaticity in the photodissociation of nitric acid at 193 nm. *J. Chem. Phys.* **1997**, *81*, 5361-5373, doi:10.1063/1.474246.

Nakayama, T.; Kitamura, M. T.; Watanabe, K. Ionization potential and absorption coefficients of nitrogen dioxide. *J. Chem. Phys.* **1959**, *30*, 1180-1186, doi:10.1063/1.1730152.

Nishida, S.; Takahashi, K.; Matsumi, Y.; Taniguchi, N.; Hayashida, S. Formation of $O(^3P)$ atoms in the photolysis of N_2O at 193 nm and $O(^3P) + N_2O$ product channel in the reaction of $O(^1D) + N_2O$ *J. Phys. Chem. A* **2004**, *108*, 2451-2456, doi:10.1021/jp037034o.

Nizkorodov, S. A.; Sander, S. P.; Brown, L. R. Temperature and pressure dependence of high-resolution air-broadened absorption cross sections of NO_2 (415-525 nm) *J. Phys. Chem. A* **2004**, *108*, 4864-4872, doi:10.1021/jp049461n.

Oh, D.; Sisk, W.; Young, A.; Johnston, H. Nitrogen dioxide fluorescence from N_2O_5 photolysis. *J. Chem. Phys.* **1986**, *85*, 7146-7158, doi:10.1063/1.451348.

Okabe, H. Photodissociation of nitric acid and water in the vacuum ultraviolet; vibrational and rotational distributions of OH $^2\Sigma^+$. *J. Chem. Phys.* **1980**, *72*, 6642-6650, doi:10.1063/1.439123.

Orlando, J. J.; Tyndall, G. S.; Moortgat, G. K.; Calvert, J. G. Quantum yields for NO_3 photolysis between 570 and 635 nm. *J. Phys. Chem.* **1993**, *97*, 10996-11000, doi:10.1021/j100144a017.

Orphal, J. A Critical Review of the Absorption Cross-Sections of O_3 and NO_2 in the 240-790 nm Region, Part 1, Ozone, European Space Agency, ESA-ESTEC Noordwijk, ESA Technical Note MO-TN-ESA-GO-0302, 2002,

Orphal, J. A critical review of the absorption cross-sections of O_3 and NO_2 in the ultraviolet and visible. *J. Photochem. Photobiol. A: Chem.* **2003**, *157*, 185-209, doi:10.1016/S1010-6030(03)00061-3.

Orphal, J.; Dreher, S.; Voigt, S.; Burrows, J. P.; Jost, R.; Delon, A. The near-infrared bands of NO_2 observed by high-resolution Fourier-transform spectroscopy. *J. Chem. Phys.* **1998**, *109*, 10217-10221, doi:10.1063/1.477716.

Orphal, J.; Fellows, C. E.; Flaud, J.-M. The visible absorption spectrum of NO_3 measured by high-resolution Fourier transform spectroscopy. *J. Geophys. Res.* **2003**, *108*, 4077, doi:10.1029/2002JD002489.

Osbourne, B. A.; Marston, G.; Kaminski, L.; Jones, N. C.; Gingell, J. M.; Mason, N. J.; Walker, I. C.; Delwiche, J.; Hubin-Franskin, M.-J. Vacuum ultraviolet spectrum of dinitrogen pentoxide. *J. Quant. Spectrosc. Radiat. Transf.* **2000**, *64*, 67-74, doi:10.1016/S0022-4073(99)00104-1.

Osthoff, H. D.; Pilling, M. J.; Ravishankara, A. R.; Brown, S. S. Temperature dependence of the NO_3 absorption cross-section above 298 K and determination of the equilibrium constant for $NO_3 + NO_2 \leftrightarrow N_2O_5$ at atmospherically relevant conditions. *Phys. Chem. Chem. Phys.* **2007**, *9*, 5785-5793, doi:10.1039/b709193a.

Pagsberg, P.; Bjergbakke, E.; Ratajczak, E.; Sillesen, A. Kinetics of the gas phase reaction OH + NO(+M) → HONO(+M) and the determination of the UV absorption cross sections of HONO. *Chem. Phys. Lett.* **1997**, *272*, 383-390, doi:10.1016/S0009-2614(97)00576-9.

Paraskevopoulos, G.; Cvetanovic, R. J. Competitive reactions of the excited oxygen atoms, O(^{1}D). *J. Am. Chem. Soc.* **1969**, *91*, 7572-7577, doi:10.1021/ja50001a005.

Platt, U.; Perner, D.; Harris, G. W.; Winer, A. M.; Pitts Jr., J. N. Observations of nitrous acid in an urban atmosphere by differential optical absorption. *Nature* **1980**, *285*, 312-314, doi:10.1038/285312a0.

Preston, K. F.; Barr, R. F. Primary processes in the photolysis of nitrous oxide. *J. Chem. Phys.* **1971**, *54*, 3347-3348, doi:10.1063/1.1675349.

Rahn, T.; Zhang, H.; Wahlen, M.; Blake, G. A. Stable isotope fractionation during ultraviolet photolysis of N_2O. *Geophys. Res. Lett.* **1998**, *25*, 4489-4492, doi:10.1029/1998GL900186.

Rattigan, O.; Lutman, E.; Jones, R. L.; Cox, R. A. Temperature dependent absorption cross sections and atmospheric photolysis rates of nitric acid. *Ber. Bunsenges. Phys. Chem.* **1992**, *96*, 399-404, doi:10.1002/bbpc.19920960331.

Rattigan, O.; Lutman, E.; Jones, R. L.; Cox, R. A.; Clemitshaw, K.; Williams, J. Corrigendum: Temperature-dependent absorption cross-sections of gaseous nitric acid and methyl nitrate. *J. Photochem. Photobiol. A: Chem.* **1992**, *69*, 125-126, doi:10.1016/1010-6030(92)85269-Z.

Ravishankara, A. R.; Mauldin, R. L. Temperature dependence of the NO_3 cross section in the 662-nm region. *J. Geophys. Res.* **1986**, *91*, 8709-8712, doi:10.1029/JD091iD08p08709.

Ravishankara, A. R.; Wine, P. H. Absorption cross sections for NO_3 between 565 and 673 nm. *Chem. Phys. Lett.* **1983**, *101*, 73-78, doi:10.1016/0009-2614(83)80308-X.

Ravishankara, A. R.; Wine, P. H.; Smith, C. A.; Barbone, P. E.; Torabi, A. N_2O_5 photolysis: Quantum yields for NO_3 and O(^3P). *J. Geophys. Res.* **1986**, *91*, 5355-5360, doi:10.1029/JD091iD05p05355.

Riffault, V.; Gierczak, T.; Burkholder, J. B.; Ravishankara, A. R. Quantum yields for OH production in the photodissociation of HNO_3 at 248 and 308 nm and H_2O_2 at 308 and 320 nm. *Phys. Chem. Chem. Phys.* **2006**, *8*, 1079-1085, doi:1010.1039/b513760h.

Röckmann, T. J.; Brenninkmeijer, C. A. M.; Wollenhaupt, M.; Crowley, J. N.; Crutzen, P. J. Measurement of the isotopic fractionaltion of $^{15}N^{14}N^{16}O$, $^{14}N^{15}N^{16}O$ and $^{14}N^{14}N^{18}O$ in the UV photolysis of nitrous oxide. *Geophys. Res. Lett.* **2000**, *27*, 1399-1402, doi:10.1029/1999GL011135.

Röckmann, T. J.; Kaiser, J.; Brenninkmeijer, C. A. M.; Crowley, J. N.; Borchers, R.; Brand, W. A.; Crutzen, P. J. Isotopic enrichment of nitrous oxide ($^{15}N^{14}NO$, $^{14}N^{15}NO$, $^{14}N^{14}N^{18}O$) in the stratosphere and in the laboratory. *J. Geophys. Res.* **2001**, *106*, 10403-10410, doi:10.1029/2000JD900822.

Roehl, C. M.; Mazely, T. L.; Friedl, R. R.; Li, Y. M.; Francisco, J. S.; Sander, S. P. NO_2 quantum yield from the 248 nm photodissociation of peroxynitric acid (HO_2NO_2). *J. Phys. Chem. A* **2001**, *105*, 1592-1598, doi:10.1021/jp001982x.

Roehl, C. M.; Nizkorodov, S. A.; Zhang, H.; Blake, G. A.; Wennberg, P. O. Photodissociation of peroxynitric acid in the near-IR. *J. Phys. Chem. A* **2002**, *106*, 3766-3772, doi:10.1021/jp013536v.

Roehl, C. M.; Orlando, J. J.; Tyndall, G. S.; Shetter, R. E.; Vasquez, G. J.; Cantrell, C. A.; Calvert, J. G. Temperature dependence of the quantum yields for the photolysis of NO_2 near the dissociation limit. *J. Phys. Chem.* **1994**, *98*, 7837-7843, doi:10.1021/j100083a015.

Romand, J.; Mayence, J. Spectre d'absorption de l'oxyde asoteux gaseux dans la région de Schumann. *Compt. Rend. Acad. Sci. Paris* **1949**, *228*, 998-1000.

Rontu Carlon, N.; Papanastasiou, D. K.; Fleming, E. L.; Jackman, C. H.; Newman, P. A.; Burkholder, J. B. UV absorption cross sections of nitrous oxide (N_2O) and carbon tetrachloride (CCl_4) between 210 and 350 K and the atmospheric implications. *Atmos. Chem. Phys.* **2010**, *10*, 6137-6149, doi:10.5194/acp-10-6137-2010.

Röth, E. P.; Ruhnke, R.; Moortgat, G.; Meller, R.; Schneider, W. UV/VIS-Absorption Cross Sections and Quantum Yields for Use in Photochemistry and Atmospheric Modeling, Forschungszentrum Jülich Publication, Part 1 : Inorganic Substances (jül-3340), Part 2: Organic Substances (jül-3341). **1997**.

Salawitch, R. J.; Wennberg, P. O.; Toon, G. C.; Sen, B.; Blavier, J.-F. Near IR photolysis of HO_2NO_2: Implications for HO_x. *Geophys. Res. Lett.* **2002**, *29*, 1-4, doi:10.1029/2002GL015006.

Sander, S. P. Temperature dependence of the NO_3 absorption spectrum. *J. Phys. Chem.* **1986**, *90*, 4135-4142, doi:10.1021/j100408a060.

Sander, S. P.; Finlayson-Pitts, B. J.; Friedl, R. R.; Golden, D. M.; Huie, R. E.; Kolb, C. E.; Kurylo, M. J.; Molina, M. J.; Moortgat, G. K.; Orkin, V. L.; Ravishankara, A. R. Chemical Kinetics and Photochemical Data for Use in Atmospheric Studies, Evaluation Number 14, Jet Propulsion Laboratory Pasadena, JPL Publication 02-25, 2002, http:\\jpldataeval.jpl.nasa.gov.

Schiffman, A.; Nelson, D. D., Jr.; Nesbitt, D. J. Quantum yields for OH production from 193 and 248 nm photolysis of HNO_3 and H_2O_2. *J. Chem. Phys.* **1993**, *98*, 6935-6946, doi:10.1063/1.464735.

Schneider, W.; Moortgat, G. K.; Burrows, J. P.; Tyndall, G. Absorption cross-sections of NO_2 in the UV and visible region (200-700 nm) at 298 K. *J. Photochem. Photobiol. A: Chem.* **1987**, *40*, 195-217, doi:10.1016/1010-6030(87)85001-3.

Schott, G.; Davidson, N. Shock waves in chemical kinetics: The decomposition of N_2O_5 at high temperatures. *J. Am. Chem. Soc.* **1958**, *80*, 1841-1853, doi:10.1021/ja01541a019.

Selwyn, G.; Podolske, J.; Johnston, H. S. Nitrous oxide ultraviolet absorption spectrum at stratospheric temperatures. *Geophys. Res. Lett.* **1977**, *4*, 427-430, doi:10.1029/GL004i010p00427.

Selwyn, G. S.; Johnston, H. S. Ultraviolet absorption spectrum of nitrous oxide as function of temperature and isotopic substitution. *J. Chem. Phys.* **1981**, *74*, 3791-3803, doi:10.1063/1.441608.

Simonaitis, R.; Greenberg, R. I.; Heicklen, J. The photolysis of N_2O at 2139 Å and 1849 Å. *Int. J. Chem. Kinet.* **1972**, *4*, 497-512, doi:10.1002/kin.550040504

Singer, R. J.; Crowley, J. N.; Burrows, J. P.; Schneider, W.; Moortgat, G. K. Measurement of the absorption cross-section of peroxynitric acid between 210 and 330 nm in the range 253-298 K. *J. Photochem. Photobiol. A: Chem.* **1989**, *48*, 17-32, doi:10.1016/1010-6030(89)87086-8.

Stark, H.; Brown, S. S.; Burkholder, J. B.; Aldener, M.; Riffault, V.; Gierczak, T.; Ravishankara, A. R. Overtone dissociation of peroxynitric acid (HO_2NO_2): Absorption cross sections and photolysis products. *J. Phys. Chem. A* **2008**, *112*, 9296–9303, doi:10.1021/jp802259z.

Stockwell, W. R.; Calvert, J. G. The near ultraviolet absorption spectrum of gaseous HONO and N_2O_3. *J. Photochem.* **1978**, *8*, 193-203, doi:10.1016/0047-2670(78)80019-7.

Stutz, J.; Kim, E. S.; Platt, U.; Bruno, P.; Perrino, C.; Febo, A. UV-visible absorption cross sections of nitrous acid. *J. Geophys. Res.* **2000**, *105*, 14585-14592, doi:10.1029/2000JD900003.

Sun, H.; Weissler, G. L. Absorption coefficients of nitric oxide in the vacuum ultraviolet. *J. Chem. Phys.* **1955**, *23*, 1372-1373, doi:10.1063/1.1742309.

Suto, M.; Lee, L. C. Photoabsorption and photodissociation of $HONO_2$ in the 105-220 nm region. *J. Chem. Phys.* **1984**, *81*, 1294-1297, doi:10.1063/1.447816.

Swanson, D.; Kan, B.; Johnston, H. S. NO_3 quantum yields from N_2O_5 photolysis. *J. Phys. Chem.* **1984**, *88*, 3115-3118, doi:10.1021/j150658a038.

Thompson, B. A.; Harteck, P.; Reeves Jr., R. R. Ultraviolet absorption coefficients of CO_2, CO, O_2, H_2O, N_2O, NH_3, NO, SO_2, and CH_4 between 1850 and 4000 A. *J. Geophys. Res.* **1963**, *68*, 6431-6436, doi:10.1029/JZ068i024p06431.

Troe, J. Are primary quantum yields of NO_2 photolysis at $\lambda \leq 398$ nm smaller than unity? *Z. Phys. Chem.* **2000**, *214*, 573-581, doi:10.1524/zpch.2000.214.5.573.

Turatti, F.; Griffith, D. W. T.; Wilson, S. R.; Esler, M. B.; Rahn, T.; Zhang, H.; Blake, G. A. Positionally dependent ^{15}N fractionation factors in the UV photolysis of N_2O determined by high resolution FTIR spectroscopy. *Geophys. Res. Lett.* **2000**, *27*, 2489-2492, doi:10.1029/2000GL011371.

Turnipseed, A. A.; Vaghjiani, G. L.; Thompson, J. E.; Ravishankara, A. R. Photodissociation of HNO_3 at 193, 222, and 248 nm: Products and quantum yields. *J. Chem. Phys.* **1992**, *96*, 5887-5895, doi:10.1063/1.462685.

Vandaele, A. C.; Hermans, C.; Fally, S.; Carleer, M.; Colin, R.; Mérienne, M.-F.; Jenouvrier, A.; Coquart, B. High-resolution Fourier transform measurement of the NO_2 visible and near-infrared absorption cross sections: Temperature and pressure effects. *J. Geophys. Res.* **2002**, *107*, 4384, doi:10.1029/2001JD000971.

Vandaele, A. C.; Hermans, C.; Fally, S.; Carleer, M.; Merienne, M.-F. Absorption cross-sections of NO_2: simulation of temperature and pressure effects. *J. Quant. Spectrosc. Radiat. Transf.* **2003**, *76*, 373-391, doi:10.1016/S0022-4073(02)00064-X.

Vandaele, A. C.; Hermans, C.; Simon, P. C.; Van Roozendael, M.; Guilmot, J. M.; Carleer, M.; Colin, R. Fourier transform measurement of NO_2 absorption cross-section in the visible range at room temperature. *J. Atmos. Chem.* **1966**, *25*, 289-305, doi:10.1007/BF00053797.

Vandaele, A. C.; Hermans, D.; Simon, P. C.; Carleer, M.; Colin, R.; Fally, S.; Meriénne, M.-F.; Jenouvrier, A.; Coquart, B. Measurements of the NO_2 absorption cross-section from 42000 cm^{-1} to 10000 cm^{-1} (238-1000 nm) at 220 K and 294 K. *J. Quant. Spectrosc. Radiat. Transf.* **1998**, *59*, 171-184, doi:10.1016/S0022-4073(97)00168-4.

Vasudev, R. Absorption spectrum and solar photodissociation of gaseous nitrous acid in the actinic wavelength region. *Geophys. Res. Lett.* **1990**, *17*, 2153-2155, doi:10.1029/GL017i012p02153.

Voigt, S.; Orphal, J.; Burrows, J. P. The temperature and pressure dependence of the absorption cross-sections of NO_2 in the 250-800 nm region measured by Fourier-transform spectroscopy. *J. Photochem. Photobiol. A: Chem.* **2002**, *149*, 1-7, doi:10.1016/S1010-6030(01)00650-5.

von Hessberg, P.; Kaiser, J.; Enghoff, M. B.; McLinden, C. A.; Sorensen, S. L.; Rockmann, T.; Johnson, M. S. Ultra-violet absorption cross sections of isotopically substituted nitrous oxide species: $^{14}N^{14}NO$, $^{15}N^{14}NO$, $^{14}N^{15}NO$ and $^{15}N^{15}NO$. *Atmos. Chem. Phys.* **2004**, *4*, 1237-1253, doi:10.5194/acp-4-1237-2004.

Wang, L.; Zhang, J. Detection of nitrous acid by cavity ring-down spectroscopy. *Environ. Sci. Technol.* **2000**, *34*, 4221-4227, doi:10.1021/es0011055.

Wang, M.; Connolly, S. C.; Venables, D. S. Deep-ultraviolet absorption cross sections of strongly absorbing atmospheric species. *J. Quant. Spectrosc. Radiat. Transf.* **2024**, *323*, 109050, doi:10.1016/j.jqsrt.2024.109050.

Wangberg, I.; Etzkorn, T.; Barnes, I.; Platt, U.; Becker, K. H. Absolute determination of the temperature behavior of the $NO_2 + NO_3 + (M) \leftrightarrow N_2O_5 + (M)$ equilibrium. *J. Phys. Chem. A* **1997**, *101*, 9694-9698, doi:10.1021/jp972203o.

Watanabe, K.; Matsunaga, F. M.; Sakai, H. Absorption coefficient and photoionization yield of NO in the region 580-1350 Å. *Appl. Opt.* **1967**, *6*, 391-396, doi:10.1364/AO.6.000391.

Wayne, R. P.; Barnes, I.; Burrows, J. P.; Canosa-Mas, C. E.; Hjorth, J.; Le Bras, G.; Moortgat, G. K.; Perner, D.; Poulet, G.; Restelli, G.; Sidebottom, H. The nitrate radical: Physics, chemistry, and the atmosphere. *Atmos. Environ.* **1991**, *25A*, 1-203, doi:10.1016/0960-1686(91)90192-A.

Wennberg, P. O.; Brault, J. W.; Hanisco, T. F.; Salawitch, R. J.; Mount, G. H. The atmospheric column abundance of IO: Implications for stratospheric ozone. *J. Geophys. Res.* **1997**, *D102*, 8887-8898, doi:10.1029/96JD03712.

Wennberg, P. O.; Salawitch, R. J.; Donaldson, D. J.; Hanisco, T. F.; Lanzendorf, E. J.; Perkins, K. K.; Lloyd, S. A.; Vaida, V.; Gao, R. S.; Hintsa, E. J.; Cohen, R. C.; Swartz, W. H.; Kusterer, T. L.; Anderson, D. E. Twilight observations suggest unknown sources of HO_x. *Geophys. Res. Lett.* **1999**, *26*, 1373-1376, doi:10.1029/1999GL900255.

Wollenhaupt, M.; Carl, S. A.; Horowitz, A.; Crowley, J. N. Rate coefficients for reaction of OH with acetone between 202 and 395 K. *J. Phys. Chem. A* **2000**, *104*, 2695-2705, doi:10.1021/jp993738f.

Yao, F.; Wilson, I.; Johnston, H. Temperature-dependent ultraviolet absorptlon spectrum for dinitrogen pentoxide. *J. Phys. Chem.* **1982**, *86*, 3611-3615, doi:10.1021/j100215a023.

Yokelson, R. J.; Burkholder, J. B.; Fox, R. W.; Talukdar, R. K.; Ravishankara, A. R. Temperature dependence of the NO_3 absorption spectrum. *J. Phys. Chem.* **1994**, *98*, 13144-13150, doi:10.1021/j100101a009.

Yoshino, K.; Esmond, J. R.; Parkinson, W. H. High-resolution absorption cross section measurements of NO_2 in the UV and visible region. *Chem. Phys.* **1997**, *221*, 169-174, doi:10.1016/S0301-0104(97)00149-3.

Yoshino, K.; Freeman, D. E.; Parkinson, W. H. High resolution absorption cross-section measurements of N_2O at 295-299 K in the wavelength region 170-222 nm. *Planet. Space Sci.* **1984**, *32*, 1219-1222, doi:10.1016/0032-0633(84)90065-5.

Yung, Y. L.; Miller, C. E. Isotopic fractionation of stratospheric nitrous oxide. *Science* **1997**, *278*, 1778-1780, doi:10.1126/science.278.5344.1778.

Zelikoff, M.; Aschenbrand, L. M. Vacuum ultraviolet photochemistry, Part II. Nitrious oxide at 1849 A. *J. Chem. Phys.* **1954**, *22* 1685-1687, doi:10.1063/1.1739874.

Zelikoff, M.; Watanabe, K.; Inn, E. C. Y. Absorption coefficients of gases in the vacuum ultraviolet. Part II. Nitrous oxide. *J. Chem. Phys.* **1953**, *21*, 1643-1647, doi:10.1063/1.1698636.

Zhang, H.; Roehl, C. M.; Sander, S. P.; Wennberg, P. O. Intensity of the second and third OH overtones of H_2O_2, HNO_3, and HO_2NO_2. *J. Geophys. Res.* **2000**, *105*, 14593-14598, doi:10.1029/2000JD900118.
Zhang, H.; Wennberg, P. O.; Wu, V. H.; Blake, G. A. Fractionation of $^{14}N^{15}N^{16}O$ and $^{15}N^{14}N^{16}O$ during photolysis at 213 nm. *Geophys. Res. Lett.* **2000**, *27*, 2481-2484, doi:10.1029/1999GL011236.

SECTION 4D. ORGANIC PHOTOCHEMISTRY

D1. CH_3 (methyl radical)

Back to Index

$CH_3 + h\nu \rightarrow$ Products

(New)

Absorption Cross Sections: UV absorption cross sections of CH_3 (methyl radical) have been measured at room temperature by Adachi et al.[1] (215.2–217.0 nm, graphical data), Basco et al.[2] (216.4 nm), Cameron et al.[3] (216.4 nm; 200–240 nm, graphical data), Khamaganov et al.[4] (214.4–218.6 nm), MacPherson et al.[5] (216.36 nm), Parkes and Quinn[6] (216.5 nm), and Slagle et al.[7] (216.36 nm). There are no reported measurements below room temperature, but several absorption measurements have been obtained of shock-heated methyl radicals at much higher temperatures (up to 2510 K).

The methyl radical has a narrow absorption band centered at 216.4 nm (~2 nm fwhm). All 7 room temperature studies agree to within 16% near the absorption peak. Of the studies that report data over a range of wavelengths, the shape of the absorption band differs significantly in the studies of Khamaganov et al. and Cameron et al., which Khamaganov et al. attribute to the lower spectral resolution of the Cameron et al. study (0.5 and 1.2 nm, respectively). The spectrum of Adachi et al. is blue shifted by ~0.2 nm relative to the studies of Khamaganov et al. and Cameron et al. The recommended cross section given in Table 4D-1 is for the absorption peak at 216.4 nm and is based on an average of all 7 studies. The recommended uncertainty factor (2σ) is 1.15.

Photolysis Quantum Yield and Product Studies: No recommendation.

Table 4D-1. Recommended Absorption Cross Section of CH_3 (methyl radical) at 298 K

λ (nm)	10^{20} σ (cm^2)
216.4	3800

Note:
Average of Adachi et al.,[1] Basco et al.,[2] Cameron et al.,[3] Khamaganov et al.,[4] MacPherson et al.,[5] Parkes and Quinn,[6] and Slagle et al.[7]

(1) Adachi, H.; Basco, N.; James, D. G. L. Mutual interactions of the methyl and methylperoxy radicals studied by flash photolysis and kinetic spectroscopy. *Int. J. Chem. Kinet.* **1980**, *12*, 949-977, doi:10.1002/kin.550121206.

(2) Basco, N.; James, D. G. L.; Suart, R. D. A quantitative study of alkyl radical reactions by kinetic spectroscopy. Part I. Mutual combination of methyl radicals and combination of methyl radicals with nitric acid. *Int. J. Chem. Kinet.* **1970**, *2*, 215-234 doi:10.1002/kin.550020307.

(3) Cameron, M.; Sivakumaran, V.; Dillon, T. J.; Crowley, J. N. Reaction between OH and CH_3CHO. Part 1. Primary product yields of CH_3 (296 K), CH_3CO (296 K), and H (237-296 K). *Phys. Chem. Chem. Phys.* **2002**, *4*, 3628-3638, doi:10.1039/b202586h.

(4) Khamaganov, V.; Karunanandan, R.; Rodriguez, A.; Crowley, J. N. Photolysis of $CH_3C(O)CH_3$ (248 nm, 266 nm), $CH_3C(O)C_2H_5$ (248 nm) and $CH_3C(O)Br$ (248 nm): pressure dependent quantum yields of CH_3 formation. *Phys. Chem. Chem. Phys.* **2007**, *9*, 4098-4113, doi:10.1039/b701382e.

(5) Macpherson, M. T.; Pilling, M. J.; Smith, M. J. C. Determination of the absorption cross section for CH_3 at 216.36 nm and the absolute rate constant for methyl radical recombination over the temperature range 296-577 K. *J. Phys. Chem.* **1985**, *89*, 2268-2274, doi:10.1021/j100257a024.

(6) Parkes, D. A.; Quinn, C. P. Study of the spectra and recombination kinetics of alkyl radicals by molecular modulation spectrometry. Part 2. - The recombination of ethyl, isopropyl and t-butyl radicals at room temperature and t-butyl radicals between 250 and 450 K. *J. Chem. Soc. Faraday Trans. I* **1976**, *72*, 1952-1971, doi:10.1039/F19767201952.

(7) Slagle, I. R.; Gutman, D.; Davies, J. W.; Pilling, M. J. Study of the recombination reaction $CH_3 + CH_3 \rightarrow C_2H_6$. 1. Experiment. *J. Phys. Chem.* **1988**, *92*, 2455-2462, doi:10.1021/j100320a015.

D2. CH_4 (methane)

Back to Index

$CH_4 + h\nu \rightarrow$ Products (1)

(Recommendation: 15-10; Note: 15-10; Evaluated: 15-10)

Absorption Cross Sections. CH_4 (methane) has negligible UV absorption. Its VUV absorption spectrum has been extensively studied at and around Lyman-α, 121.567 nm, including studies by Watanabe et al.[15] (120–144 nm), Ditchburn[6] (27–151 nm), Sun and Weissler[13] (37–131 nm), Laufer and McNesby[9] (113–143 nm), Backx et al.[2] (13.8–144 nm), Mount et al.[12] (137–160 nm), Lee and Chiang[11] (106–142 nm), Lee et al.[10] (120–153 nm), Au et al.[1] (5.6–165 nm), Brownsword et al.[3] (121.6 nm), Vatsa and Volpp[14] (121.567 nm), Kameta et al.[7] (52–125 nm), and Chen and Wu[5] (120–142 nm). The measured, or interpolated, values are in reasonable agreement at 121.567 nm, to within 20%. The recommended Lyman-α cross section at 298 K, adopted from Chapter 3[4] in the SPARC[8] (2013) lifetime report, is 1.85×10^{-17} cm^2 molecule^{-1} with an uncertainty factor of 1.3 (2σ).

Photolysis Quantum Yield and Product Studies: No recommendation.

(1) Au, J. W.; Cooper, G.; Burton, G. R.; Olney, T. N.; Brion, C. E. The valence shell photoabsorption of the linear alkanes, C_nH_{2n+2} (n=1-8): Absolute oscillator strengths (7-220 eV). *Chem. Phys.* **1993**, *173*, 209-239, doi:10.1016/0301-0104(93)80142-V.

(2) Backx, C.; Wight, G. R.; Tol, R. R.; van der Wiel, M. J. Electron-electron coincidence measurements of CH_4. *J. Phys. B: Atom. Mol. Phys.* **1975**, *8*, 3007-3019, doi:10.1088/0022-3700/8/18/020.

(3) Brownsword, R. A.; Hillenkamp, M.; Laurent, T.; Vatsa, R. K.; Volpp, H.-R.; Wolfrum, J. Quantum yield for H atom formation in the methane dissociation after photoexcitation at the Lyman-α (121.6 nm) wavelength. *Chem. Phys. Lett.* **1997**, *266*, 259-266, doi:10.1016/S0009-2614(96)01526-6.

(4) Burkholder, J. B.; Mellouki, W.; Fleming, E. L.; George, C.; Heard, D. E.; Jackman, C. H.; Kurylo, M. J.; Orkin, V. L.; Swartz, W. H.; Wallington, T. J. Chapter 3: Evaluation of Atmospheric Loss Processes. In Lifetimes of Stratospheric Ozone-Depleting Substances, Their Replacements, and Related Species; Ko, M. K. W., Newman, P. A., Reimann, S., Strahan, S. E., Eds., 2013, http://www.sparc-climate.org/publications/sparc-reports/sparc-report-no6/.

(5) Chen, F. Z.; Wu, C. Y. R. Temperature-dependent photoabsorption cross sections in the VUV-UV region. I. Methane and ethane. *J. Quant. Spectrosc. Radiat. Transf.* **2004**, *85*, 195-209, doi:10.1016/S0022-4073(03)00225-5.

(6) Ditchburn, R. W. Absorption cross-sections in the vacuum ultra-violet III. Methane. *Proc. Roy. Soc. London A* **1955**, *229*, 44-62, doi:10.1098/rspa.1955.0073.

(7) Kameta, K.; Kouchi, N.; Ukai, M.; Hatano, Y. Photoabsorption, photoionization, and neutral-dissociation cross sections of simple hydrocarbons in the vacuum ultraviolet range. *J. Electron Spectrosc. Related Phenom.* **2002**, *123*, 225-238.

(8) Ko, M. K. W.; Newman, P. A.; Reimann, S.; Strahan, S. E.; Plumb, R. A.; Stolarski, R. S.; Burkholder, J. B.; Mellouki, W.; Engel, A.; Atlas, E. L.; et al. Lifetimes of Stratospheric Ozone-Depleting Substances, Their Replacements, and Related Species, SPARC Report No. 6, WCRP-15/2013, 2013, http://www.sparc-climate.org/publications/sparc-reports/sparc-report-no6/.

(9) Laufer, A. H.; McNesby, J. R. Deuterium isotope effect in vacuum-ultraviolet absorption coefficients of water and methane. *Can. J. Chem.* **1965**, *43*, 3487-3490, doi:10.1139/v65-495.

(10) Lee, A. Y. T.; Yung, Y. L.; Cheng, B. M.; Bahou, M.; Chung, C.-Y.; Lee, Y. P. Enhancement of deuterated ethane on Jupiter. *Astrophys. J.* **2001**, *551*, L93-L96, doi:10.1086/319827.

(11) Lee, L. C.; Chiang, C. C. Fluorescence yield from photodissociation of CH_4 at 1060-1420 Å. *J. Chem. Phys.* **1983**, *78*, 688-691, doi:10.1063/1.444812.

(12) Mount, G. H.; Warden, E. S.; Moos, H. W. Photoabsorption cross sections of methane from 1400 to 1850 Å. *Astrophys. J.* **1977**, *214*, L47-L49, doi:10.1086/182440

(13) Sun, H.; Weissler, G. L. Absorption cross sections of methane and ammonia in the vacuum ultraviolet. *J. Chem. Phys.* **1955**, *23*, 1160-1164, doi:10.1063/1.1742205.

(14) Vatsa, R. K.; Volpp, H.-R. Absorption cross-sections for some atmospherically important molecules at the H atom Lyman-α wavelength (121.567 nm). *Chem. Phys. Lett.* **2001**, *340*, 289-295, doi:10.1016/S0009-2614(01)00373-6.

(15) Watanabe, K.; Zelikoff, M.; Inn, E. C. I. *Air Force Cambridge Research Center Technical Report* **1953**, *53-23*.

D3. CH_2O (formaldehyde)

Back to Index

$CH_2O + h\nu$	$\rightarrow H + HCO$	363 kJ mol^{-1}	330 nm	(1)
	$\rightarrow H_2 + CO$	331 kJ mol^{-1}	361 nm	(2)
	$\rightarrow H + H + CO$	423 kJ mol^{-1}	283 nm	(3)

(Recommendation: 15-10, Note: 15-10, Evaluated: 15-10)

Absorption Cross Sections. The UV absorption spectrum of formaldehyde (CH_2O) displays a highly structured absorption band (the formally electric-dipole forbidden $S_1 \leftarrow S_0$ transition gives rise to the $\tilde{A}^1A_2 - X^1A_1$ band system, which becomes allowed through vibronic coupling) between 240 and 380 nm. The absorption spectrum of formaldehyde has been measured in many studies at temperatures between 222 and 353 K as summarized in Table 4D-3-1.

Table 4D-3-1. Summary of CH_2O Absorption Cross Section Studies

Study	Year	Temperature (K)	Wavelength range (nm)	Resolution (nm)	Medium
McMillan[5]	1966	348	202–374	1	air
McQuigg and Calvert[22]	1969	300	220–370	1	air
Calvert et al.[4]	1972	298	290–360	1	air
Bass et al.[1]	1980	223, 296	258–360	0.05	air
Moortgat et al.[25]	1980	285	215–370	0.5	air
Moortgat et al.[26]	1983	220–353	253–353	5	air
Cantrell et al.[6]	1990	223, 233, 243, 253,263, 273, 283, 293, 296	300–385.8	1.0 cm^{-1} (~0.011)	vacuum
Rogers[31]	1990	296	235–365	0.01–0.04	vacuum
Meller and Moortgat[23]	2000	223, 298	224–373	~0.025	air
Chen and Zhu[8]	2003	293	290–330	0.0014	
Bogumil et al.[2]	2003	293	247–400	0.25	air
Pope et al.[29]	2005	263, 294	313–320	0.1 cm^{-1} (~0.001)	air/vacuum
Pope et al.[30]	2005	294	308–320	0.1 cm^{-1}	air/vacuum
Co et al.[11]	2005	220, 298	351–356	0.0003	vacuum
Smith et al.[32]	2006	245, 294	300–340	0.0035	air/vacuum
Gratien et al.[17]	2007	296	240–370	0.15	air
Gratien et al.[18]	2007	294	300–360	0.18	air
Gorrotxategi Carbajo et al.[16]	2008	245, 294	300–330	0.0035	air/vacuum
Tatum Ernst et al.[35]	2012	294 ± 2	304–330	0.09 cm^{-1} (~0.001)	air

Meller and Moortgat[23] have reviewed the cross section studies prior to 2000 including descriptions of the techniques, experimental details of CH_2O generation and the absorption measurements, and a comparison of the various results. The CH_2O absorption cross sections are a strong function of the measurement resolution and this needs to be considered when comparing results from the various studies. Low resolution spectra were obtained by McMillan[5] and Moortgat et al.[25] whereas medium resolution measurements were reported by Bass et al.,[1] Rogers,[31] and Bogumil et al.[2] The spectrum reported by Cantrell et al.[6] was measured with a resolution of 0.011 nm over the 300–358 nm region in the temperature range 223–293 K using Fourier transform spectroscopy. Meller and Moortgat[23] reported a spectrum at ~0.025 nm resolution over the entire UV absorption band (224–373 nm) at 298 and 223 K using diode array spectroscopy. In general, the agreement between the medium and higher resolution data is good, although the cross section data of Bass et al.[1] and Rogers[31] are systematically lower than those of Meller and Moortgat[23]. The spectrum reported by Bogumil et al.[2] that was obtained using the SCIAMACHY pre-flight satellite instrument agrees with the data of Meller and Moortgat.[23] The low resolution absorption cross sections reported by Chen and Zhu[7,8] and Chen et al.[9] in the 280–330 nm region deviate substantially, up to 50%, from those reported by Meller and Moortgat.[23]

A high resolution CH_2O spectrum, near the Doppler broadening limit of 0.07 cm^{-1}, was measured by Pope et al.[29,30] in the range 308–320 nm using tunable UV laser absorption spectroscopy at 263 and 294 K. In a later study from the same laboratory, Smith et al.[32] extended the high resolution measurements (0.35 cm^{-1}) from 300 to 340 nm at 294 and 245 K. The high resolution CH_2O spectrum measured by Pope et al.[29,30] is in excellent

agreement with the spectral features reported by Cantrell et al.[6] and Meller and Moortgat[23] after convolution with the lower resolution instrument functions. Rotationally resolved absorption cross sections in the narrow spectral region 351–356 nm were measured by Co et al.[11] using Fourier Transform spectroscopy with an apodized resolution of 0.027 cm^{-1}. They observed a strong pressure dependence of the rotational lines over the pressure range 75 to 400 Torr and determined a pressure broadening coefficient in dry air of 1.8×10^{-4} cm^{-1} $Torr^{-1}$ for several isolated lines in the $2^0_0 4^1_0$ band.

Gratien et al.[17,18] measured UV (0.15 nm resolution) and IR absorption cross sections simultaneously and compared the Integrated Band Intensities (IBI) of the main vibronic bands with previously published UV and IR data. The IBIs measured by Gratien et al.[18] in the region 300–360 nm compare well (within ~7%) with the IBI data derived from Meller and Moortgat,[23] but are ~20% lower than the IBIs calculated from the Cantrell et al.[6] and Rogers[31] data. Gratien et al.[18] attribute the difference to the IR band strength given in the HITRAN database, which is based on the data from Cantrell et al.[6] In a second study, Gratien et al.[17] compared the IBIs of 9 different band sections in the 300 to 360 nm region with more recent studies. In general, the IBI data of Gratien et al.[17] are in excellent agreement (within 2%) with the high resolution results of Smith et al.[32] It was also shown that the IBI data for 8 band sections measured by Smith et al.[32] are 2 to 14% larger than the data of Meller and Moortgat.[23] The IBIs for the bands studied by Pope et al.[29,30] (313.5–316.5 and 316.5–319.7 nm) are 4 and 13% larger, respectively, than the data of Meller and Moortgat.[23] On the other hand the IBI for the 351.7–355.5 nm band studied by Co et al.[11] is 12% larger than the values of Cantrell et al.[6] and Rogers,[31] but in excellent agreement with those of Meller and Moortgat[23] and Gratien et al.[17]

The study by Tatum Ernst et al.[35] used tunable UV laser absorption to measure the CH_2O spectrum at high resolution (0.09 cm^{-1}) over the wavelength range 304–330 nm at 294 K. Significant differences exist in the resolved line peak heights and depth between lines obtained in this study and the high resolution studies of Pope et al.,[29,30] and Smith et al.[32] (the Tatum Ernst et al. dataset shows greater spectrum structure). This leads to discrepancies in the band strengths between this work and previous high resolution studies that is not presently understood. Tatum Ernst et al.[35] estimate the cross section uncertainty in their study to be ~10% (1σ).

In general, the consistency between the absorption cross section data of Smith et al.,[32] Gratien et al.,[17] and Pope et al.[29,30] in the range 300 to 360 nm demonstrate that the previously recommended absorption cross sections reported by Meller and Moortgat[23] are too low by about 7–10%. The presently recommended cross sections in Table 4D-3-2 where taken from Meller and Moortgat[23] averaged over 1 nm intervals and scaled up by 8%. Table 4D-3-3 includes the scaled data averaged over intervals used in atmospheric modeling. Higher resolution cross section data can be obtained from the (studies cited in Table 4D-3-1). The estimated cross section uncertainty is expected to be a function of wavelength and measurement resolution. The recommended uncertainty factor for the band strengths is estimated to be 1.1 (2σ).

The temperature dependence of the CH_2O absorption cross sections has been studied by Bass et al.,[1] Moortgat et al.,[25] Cantrell et al.,[6] Meller and Moortgat,[23] Pope et al.,[29,30] Co et al.,[11] and Smith et al.[32] (see Table 4D-3-1). Temperature effects are the strongest at the maximum of the absorption bands where the lower temperatures result in larger absorptions. This effect is reversed in the wings of the absorption bands where higher temperatures result in a higher absorption. A linear parameterization of the absorption cross section temperature dependence between 223 and 323 K was derived by Meller and Moortgat:[23]

$$\sigma(\lambda, T) = \sigma(\lambda, 298\ K) + \Gamma(\lambda) \times (T - 298)$$

Values of $\Gamma(\lambda)$ from Meller and Moortgat[23] where scaled up by 8% and the values averaged over 1nm intervals and intervals used in atmospheric modeling are listed in Table 4D-3-2 and Table 4D-3-3, respectively.

VUV absorption cross sections for the wavelength region 60–185 nm have been obtained by Gentieu and Mentall,[14] Mentall et al.,[24] and Glicker and Stief[15] using optical methods and by Cooper et al.[12] for the region 6–261 nm using (e,e) dipole spectroscopy.

Photolysis Quantum Yields and Product Studies: The quantum yield studies by McQuigg et al.[22] and Calvert et al.[4] established that over the wavelength range 290–360 nm the radical yield increases with decreasing wavelength. More precise wavelength dependent quantum yield studies using monochromatic light sources were performed by Lewis et al.,[20] Marling,[21] Horowitz and Calvert,[19] Clark et al.,[10] Moortgat et al.,[27] and Tang et al.[34] Moortgat and Warneck[28] and Moortgat et al.[25,26] measured the yields of CO and H_2 in air (giving $\Phi_1(H + HCO) + \Phi_2(H_2 + CO)$ and $\Phi_2(H_2 + CO)$) as a function of wavelength (253–353 nm) and pressure (380–800 Torr) at 300 K and 220 K. These studies showed that the yield of CO was essentially unity between 290 and 330 nm at all pressures with no systematic temperature dependence. For $\lambda > 330$ nm, both temperature and pressure have a significant effect on $\Phi_2(H_2 + CO)$ but a negligible effect on $\Phi_1(H + HCO)$. At $\lambda < 290$ nm the total CO yield was found to decrease to a value of 0.76 at 240 nm.

Smith et al.[33] measured relative quantum yields at 50 mbar for the production of the radical products H and HCO using NO-chemical amplification and subsequent detection of NO_2 with chemical ionization mass spectrometry. These authors measured the quantum yields in the range 269 to 339 nm with sufficient resolution (±0.62 nm) to observe structure in the wavelength dependence, that was previously unreported, that is believed to provide evidence for a competition among the various dissociation pathways. The measured Φ_1(H + HCO) yields were normalized to a value of 0.753 at 303.75 nm based on the NASA/JPL 97-4 recommendation[13] and agree with the previous determinations reported by Horowitz and Calvert[19] and Moortgat et al.[26] However at λ >320 nm the Φ_1(H + HCO) yields reported by Smith et al.[33] are larger than the values recommended by DeMore et al.[13] resulting in a larger (~8%) overall rate of radical production.

Pope et al.[29,30] and Gorrotxategi Carbajo et al.[16] used cavity ring-down spectroscopy to measure HCO radical absorption coefficients and CH_2O absorption cross sections from which absolute HCO quantum yields were calculated. The absolute HCO radical signal was calibrated against the HCO radical produced from the Cl + HCHO $\rightarrow$ HCO + Cl_2 reaction following the photolysis of $Cl_2/CH_2O/N_2$ mixtures. In the 303–309 nm range Φ_{HCO} ~0.6 ± 0.1 was obtained, which is 25% lower than the NASA/JPL 06-2 recommendation and the data reported by Smith et al.[33] In the wavelength range 314–330 nm the Φ_{HCO} values (0.06 to 0.11) agree to within the quoted uncertainties with the NASA/JPL 06-2 recommendation.

The experimental technique used by Gorrotxategi Carbajo et al.[16] measured the product of the high resolution absolute absorption cross section (identical as measured by Smith et al.[32]) and the absolute HCO quantum yield, $\Phi_{HCO}(\lambda)\sigma_{CH2O}(\lambda)$, in the interval 302.6–331.0 nm with a wavelength resolution of 0.005 nm. It is important to note that a separate calculation of the product $\Phi_{HCO}\sigma_{CH2O}$ using single data of Φ_{HCO} and σ_{CH2O} at a given wavelength result in much lower $\Phi_{HCO}\sigma_{CH2O}$ values (up to a factor 2) than obtained by the direct combined technique.

Tatum Ernst et al.[36] used pulsed laser photolysis combined with pulsed laser induced fluorescence detection of OH radicals (conversion of H + HCO to OH by reaction with NO_2) to determine a high resolution action spectrum, i.e., the product of the CH_2O cross section and H + HCO quantum yield, over the wavelength range 304 to 329 nm. Φ_1(H + HCO) yields were determined using the CH_2O cross section data reported in Tatum Ernst et al.[36] and an absolute value of 0.69 at 31750 cm^{-1}. The quantum yields for the individual absorption bands in this region are in reasonable agreement with previous determinations and earlier NASA/JPL recommendations, although differences between individual absorption bands that were not noted in previous studies were reported.

Troe[37] used theoretical calculations to evaluate the quantum yields for the molecular and radical photolysis processes at λ >310 nm. An analytical representation was provided that enables extrapolation into temperature and pressure ranges that are not easily accessible experimentally.

The recommended quantum yields at standard pressure (1 atmosphere) and 300 K are listed in Table 4D-2-4 are based on a polynomial fit over the wavelength range 250–338 nm of the data for Φ_1(H + HCO) from Lewis et al.,[20] Marling,[21] Horowitz and Calvert,[19] Clark et al.,[10] Tang et al.,[34] Moortgat et al.,[26] Smith et al.,[33] Pope et al.,[29,30] Gorrotxategi Carbajo et al.,[16] and Tatum Ernst et al.:[36]

$$\Phi_1(\mathrm{H} + \mathrm{HCO}) = a_0 + a_1\lambda + a_2\lambda^2 + a_3\lambda^3 + a_4\lambda^4$$

where

a_o = 557.95835182

a_1 = –7.31994058026

a_2 = 0.03553521598

$a_3 = -7.54849718 \times 10^{-5}$

$a_4 = 5.91001021 \times 10^{-8}$

$\Phi_2(H_2 + CO)$ was optimized using the quantum data for CO from Moortgat et al.[26] and the relation $\Phi_2(H_2 + CO) = \Phi_{tot} - \Phi_1(H + HCO)$. The pressure and temperature dependence of $\Phi_2(H_2 + CO)$ for wavelengths >330 nm is based on the algorithm cited in Calvert et al.[3] The pressure dependence of $\Phi_2(H_2 + CO)$ is represented in Stern-Volmer form:

$$\Phi_2(\mathrm{H_2} + \mathrm{CO}) = \left[\frac{1}{\frac{1}{(1 - \Phi_1(\lambda)} + \alpha(\lambda, T) \times P}\right]$$

where pressure, P, is in atmospheres and $\alpha(\lambda,T)$ is the quenching coefficient whose values at 300 K are calculated from Φ_1 and Φ_2:

$$\alpha(\lambda, 300\ \mathrm{K}) = \frac{1}{\Phi_2(\lambda, 300\ \mathrm{K})} - \frac{1}{(1 - \Phi_1(\lambda)}$$

At temperatures between 220 and 300 K the quenching coefficient $\alpha(\lambda,T)$ can be calculated using:

$$\alpha(\lambda, T) = \alpha(\lambda, 300\ \mathrm{K}) \times \left[1 + 0.05 \times (\lambda - 329) \times \left(\frac{(300 - T)}{80}\right)\right]$$

The formulae given above for the pressure and temperature dependence of the quantum yields are recommended.

Table 4D-3-2. Recommended Absorption Cross Sections of CH_2O at 298 K and Temperature Coefficients Averaged over 1 nm Intervals

λ (nm)	10^{20} σ (cm^2)	10^{24} Γ(λ) ($cm^2\ K^{-1}$)	λ (nm)	10^{20} σ (cm^2)	$10^{24}\cdot$Γ(λ) ($cm^2\ K^{-1}$)	λ (nm)	10^{20} σ (cm^2)	$10^{24}\cdot$Γ(λ) ($cm^2\ K^{-1}$)
226	0.0193	–	276	2.800	-2.203	326	7.42	-6.091
227	0.0182	–	277	1.70	2.088	327	4.72	5.875
228	0.0191	–	278	1.11	1.541	328	1.32	5.472
229	0.0205	–	279	2.65	-2.751	329	3.37	-3.615
230	0.0221	–	280	2.53	-0.7344	330	4.17	-2.347
231	0.0356	–	281	1.68	0.6048	331	1.52	4.220
232	0.0362	–	282	1.05	0.8737	332	0.374	1.935
233	0.0283	–	283	0.778	0.0054	333	0.231	0.4633
234	0.0351	–	284	4.61	-9.418	334	0.172	-0.2462
235	0.0392	–	285	4.37	-1.944	335	0.104	-0.0054
236	0.0582	–	286	2.26	1.714	336	0.136	0.3510
237	0.0833	–	287	1.24	0.8208	337	0.414	0.3553
238	0.0614	–	288	3.42	-5.084	338	2.07	1.728
239	0.0737	–	289	3.48	-1.310	339	5.94	-7.114
240	0.0845	–	290	1.26	1.844	340	3.40	5.962
241	0.0837	–	291	1.99	-1.253	341	1.06	6.332
242	0.133	–	292	0.860	1.247	342	0.544	1.313
243	0.172	–	293	3.36	-5.300	343	2.07	-3.226
244	0.118	–	294	7.72	-11.03	344	1.37	0.2020
245	0.142	–	295	4.38	4.133	345	0.471	2.986
246	0.176	–	296	2.68	2.290	346	0.128	0.5843
247	0.163	–	297	1.47	1.498	347	0.0476	-0.3035
248	0.253	–	298	4.56	-5.328	348	0.0818	-0.7171
249	0.343	–	299	3.42	1.598	349	0.0408	-0.6048
250	0.278	0.219	300	1.04	4.608	350	0.0389	-0.7862
251	0.220	0.191	301	1.76	-2.779	351	0.0966	-0.1307
252	0.364	-0.0778	302	0.920	-2.511	352	0.790	0.3974
253	0.312	0.109	303	3.26	-3.888	353	2.46	-5.746
254	0.369	0.148	304	7.81	-5.213	354	1.78	0.6480
255	0.486	0.294	305	5.12	4.507	355	0.752	2.652
256	0.679	0.182	306	4.63	0.3456	356	0.160	-0.4190
257	0.478	0.950	307	1.92	3.442	357	0.0372	–
258	0.332	0.736	308	1.49	0.3596	358	0.0201	–
259	0.667	0.0907	309	3.52	-4.176	359	0.0120	–
260	0.652	0.483	310	1.88	2.549	360	0.009396	–
261	0.713	0.100	311	0.498	0.081	361	0.0108	–
262	0.650	0.686	312	1.28	-1.325	362	0.0228	–
263	1.17	-0.878	313	0.974	-1.554	363	0.0152	–
264	1.02	0.626	314	6.10	0.7776	364	0.0102	–
265	0.572	1.084	315	6.00	2.794	365	0.009504	–
266	0.581	0.466	316	2.74	5.141	366	0.00918	–

λ (nm)	10^{20} σ (cm^2)	10^{24} Γ(λ) (cm^2 K^{-1})	λ (nm)	10^{20} σ (cm^2)	10^{24}·Γ(λ) (cm^2 K^{-1})	λ (nm)	10^{20} σ (cm^2)	10^{24}·Γ(λ) (cm^2 K^{-1})
267	1.47	-0.950	317	6.25	-2.664	367	0.009828	–
268	1.34	-0.130	318	3.40	3.572	368	0.0154	–
269	1.07	1.205	319	1.05	2.735	369	0.0321	–
270	1.04	0.808	320	1.28	0.2592	370	0.0687	–
271	2.10	-1.412	321	1.73	-2.362	371	0.0618	–
272	1.54	1.080	322	0.779	0.1609	372	0.0213	–
273	0.875	1.326	323	0.353	0.4201	373	0.0122	–
274	0.710	0.941	324	0.930	-0.4925	374	0.009828	–
275	2.32	-2.952	325	1.66	2.390	375	0.009396	–

Note:
Meller and Moortgat[23] (scaled, see text)
$\sigma(\lambda, T) = \sigma(\lambda, 298\ K) + \Gamma(\lambda)(T - 298)$ for the temperature range 223–323 K

Table 4D-3-3. Recommended Absorption Cross Sections of CH_2O at 298 K and 223 K and Temperature Dependence Coefficients Averaged over Intervals Used in Atmospheric Models

λ (nm)	λ range (nm)	10^{20} σ(298 K) (cm^2)	10^{20} σ(223 K) (cm^2)	10^{24} Γ(λ) (cm^2 K^{-1})
226.0	224.7–227.3	0.0179	–	–
228.6	227.3–229.9	0.0195	–	–
231.2	229.9–232.6	0.0327	–	–
233.9	232.6–235.3	0.0338	–	–
236.7	235.3–238.1	0.0675	–	–
239.5	238.2–241.0	0.076	–	–
242.4	241.0–243.9	0.136	–	–
245.4	243.9–246.9	0.150	–	–
248.5	246.9–250.0	0.274	–	–
251.6	250.0–253.2	0.292	0.286	0.7776
254.8	253.2–256.4	0.485	0.470	1.912
258.1	256.4–259.7	0.516	0.473	5.778
261.4	259.7–263.2	0.754	0.742	1.566
264.9	263.2–266.7	0.795	0.754	5.400
268.5	266.7–270.3	1.22	1.20	3.024
272.1	270.3–274.0	1.40	1.37	4.180
275.9	274.0–277.8	1.99	2.04	-6.188
279.7	277.8–281.7	2.01	2.04	-3.888
283.7	281.7–285.7	2.75	2.94	-24.08
287.7	285.7–289.9	2.52	2.57	-8.068
292.0	289.9–294.1	2.87	3.16	-37.69
296.3	294.1–298.5	3.54	3.49	6.188
300.8	298.5–303.0	1.73	1.71	3.024
305.4	303.0–307.7	4.77	4.78	-1.868
310.1	307.7–312.5	1.76	1.80	-5.908
315	312.5–317.5	4.42	4.35	9.072
320	317.5–322.5	1.65	1.59	8.780
325	322.5–327.5	3.01	2.98	4.180
330	327.5–332.5	2.15	2.06	11.34
335	332.5–337.5	0.212	0.198	1.847
340	337.5–342.5	2.58	2.46	16.42
345	342.5–347.5	0.819	0.815	0.5184
350	347.5–352.5	0.210	0.238	-3.672
355	352.5–357.5	1.04	–	–
360	357.5–362.5	0.015	–	–
365	362.5–367.5	0.0108	–	–

370	367.5–372.5	0.0399	–	–

Note:
Absorption cross sections and temperature coefficients: Meller and Moortgat[23] (scaled, see text)
$\sigma(\lambda, T) = \sigma(\lambda, 298\ K) + \Gamma(\lambda)(T - 298)$ for the temperature range 223–323 K

Table 4D-3-4. Recommended CH_2O Photolysis Quantum Yields at 300 K and 1 Atmosphere

λ (nm)	Φ (H + HCO)	Φ (H_2 + CO)	λ (nm)	Φ (H + HCO)	Φ (H_2 + CO)	λ (nm)	Φ (H + HCO)	Φ (H_2 + CO)
250	0.310	0.490	288	0.669	0.291	326	0.463	0.537
251	0.308	0.492	289	0.680	0.284	327	0.435	0.565
252	0.307	0.493	290	0.690	0.278	328	0.406	0.594
253	0.306	0.494	291	0.700	0.272	329	0.375	0.625
254	0.305	0.495	292	0.710	0.266	330	0.343	0.657
255	0.304	0.496	293	0.718	0.262	331	0.310	0.690
256	0.304	0.496	294	0.726	0.259	332	0.276	0.714
257	0.303	0.497	295	0.734	0.256	333	0.240	0.730
258	0.303	0.497	296	0.740	0.254	334	0.203	0.737
259	0.304	0.496	297	0.746	0.252	335	0.165	0.735
260	0.307	0.493	298	0.751	0.249	336	0.126	0.724
261	0.312	0.490	299	0.755	0.245	337	0.085	0.705
262	0.318	0.487	300	0.758	0.242	338	0.043	0.687
263	0.325	0.485	301	0.761	0.239	339	0.0	0.665
264	0.333	0.482	302	0.762	0.238	340	–	0.645
265	0.343	0.477	303	0.762	0.238	341	–	0.620
266	0.354	0.471	304	0.762	0.238	342	–	0.590
267	0.365	0.465	305	0.760	0.240	343	–	0.560
268	0.377	0.458	306	0.758	0.242	344	–	0.530
269	0.390	0.450	307	0.754	0.246	345	–	0.505
270	0.404	0.441	308	0.749	0.251	346	–	0.480
271	0.418	0.432	309	0.744	0.256	347	–	0.450
272	0.433	0.422	310	0.737	0.263	348	–	0.425
273	0.448	0.412	311	0.729	0.271	349	–	0.400
274	0.464	0.401	312	0.720	0.280	350	–	0.375
275	0.479	0.391	313	0.709	0.291	351	–	0.350
276	0.495	0.380	314	0.698	0.302	352	–	0.320
277	0.512	0.371	315	0.685	0.315	353	–	0.285
278	0.528	0.362	316	0.671	0.329	354	–	0.250
279	0.544	0.356	317	0.656	0.344	355	–	0.220
280	0.560	0.347	318	0.639	0.361	356	–	0.190
281	0.576	0.337	319	0.622	0.378	357	–	0.160
282	0.591	0.329	320	0.603	0.397	358	–	0.130
283	0.606	0.321	321	0.583	0.417	359	–	0.09
284	0.620	0.313	322	0.561	0.439	360	–	0.04
285	0.633	0.307	323	0.539	0.461	361	–	0.0
286	0.645	0.302	324	0.515	0.485	–	–	–
287	0.657	0.296	325	0.489	0.511	–	–	–

Note:
The recommended quantum yields are based on a fit of the data for Φ(H + HCO) from Lewis et al.,[20] Marling,[21] Horowitz and Calvert,[19] Clark et al.,[10] Tang et al.,[34] Moortgat et al.,[26] Smith et al.,[33] Pope et al.,[29,30] and Gorrotxategi Carbajo et al.[16] and for Φ(H_2 + CO) from Moortgat et al.,[26] see text for details.

(1) Bass, A. M.; Glasgow, L. C.; Miller, C.; Jesson, J. P.; Filken, S. L. Temperature-dependent absorption cross-sections for formaldehyde (CH_2O) - The effect of formaldehyde on stratospheric chlorine chemistry. *Planet. Space Sci.* **1980**, *28*, 675-679, doi:10.1016/0032-0633(80)90112-9.

(2) Bogumil, K.; Orphal, J.; Homann, T.; Voigt, S.; Spietz, P.; Fleischmann, O. C.; Vogel, A.; Hartmann, M.; Kromminga, H.; Bovensmann, H.; et al. Measurements of molecular absorption spectra with the SCIAMACHY pre-flight model: instrument characterization and reference data for atmospheric

remote-sensing in the 230-2380 nm region. *J. Photochem. Photobiol. A: Chem.* **2003**, *157*, 167-184, doi:10.1016/S1010-6030(03)00062-5.
(3) Calvert, J. G.; Atkinson, R.; Kerr, J. A.; Madronich, S.; Moortgat, G. K.; Wallington, T. J.; Yarwood, G. *The Mechanisms of Atmospheric Oxidation of the Alkenes*; Oxford University Press: New York - Oxford, 2000.
(4) Calvert, J. G.; Kerr, J. A.; Demerjian, K. L.; McQuigg, R. D. Photolysis of formaldehyde as a hydrogen atom source in the lower stratosphere. *Science* **1972**, *175*, 751-752, doi:10.1126/science.175.4023.751.
(5) Calvert, J. G.; Pitts Jr., J. N. In *Photochemistry*; John Wiley & Sons, Inc.: New York, 1966; pp 368.
(6) Cantrell, C. A.; Davidson, J. A.; McDaniel, A. H.; Shetter, R. E.; Calvert, J. G. Temperature-dependent formaldehyde cross sections in the near-ultraviolet spectral region. *J. Phys. Chem.* **1990**, *94*, 3902-3908, doi:10.1021/j100373a008.
(7) Chen, Y.; Zhu, L. The wavelength dependence of the photodissociation of propionaldehyde in the 280-330 nm region. *J. Phys. Chem. A* **2001**, *105*, 9689-9696, doi:10.1021/jp011445s.
(8) Chen, Y.; Zhu, L. Wavelength-dependent photolysis of glyoxal in the 290-420 nm region. *J. Phys. Chem. A* **2003**, *107*, 4643-4651, doi:10.1021/jp022440d.
(9) Chen, Y.; Zhu, L.; Francisco, J. S. Wavelength-dependent photolysis of *n*-butyraldehyde and *i*-butyraldehyde in the 280-330-nm region. *J. Phys. Chem. A* **2002**, *106*, 7755-7763, doi:10.1021/jp014544e.
(10) Clark, J. H.; Moore, C. B.; Nogar, N. S. The photochemistry of formaldehyde: Absolute quantum yields, radical reactions, and NO reactions. *J. Chem. Phys.* **1978**, *68*, 1264-1271, doi:10.1063/1.435848.
(11) Co, D.; Hanisco, T. F.; Anderson, J. G.; Keutsch, F. N. Rotationally resolved absorption cross sections of formaldehyde in the 28100-28500 cm^{-1} (351-356 nm) spectral region: Implications for in situ LIF measurements. *J. Phys. Chem. A* **2005**, *109*, 10675-10682, doi:10.1021/jp053466i.
(12) Cooper, G.; Anderson, J. E.; Brion, C. E. Absolute photoabsorption and photoionization of formaldehyde in the VUV and soft X-ray regions (3-200 eV). *Chem. Phys.* **1996**, *209*, 61-77, doi:10.1016/0301-0104(96)00079-1.
(13) DeMore, W. B.; Sander, S. P.; Golden, D. M.; Hampson, R. F.; Kurylo, M. J.; Howard, C. J.; Ravishankara, A. R.; Kolb, C. E.; Molina, M. J. Chemical Kinetics and Photochemical Data for Use in Stratospheric Modeling, Evaluation Number 12, Jet Propulsion Laboratory, California Institute of Technology Pasadena, CA, JPL Publication 97-4, 1997,
(14) Gentieu, E. P.; Mentall, J. E. Formaldehyde absorption coefficients in the vacuum ultraviolet (650 to 1850 Å). *Science* **1970**, *169*, 681-683, doi:10.1126/science.169.3946.68.
(15) Glicker, S.; Stief, L. J. Photolysis of formaldehyde at 1470 and 1236 Å. *J. Chem. Phys.* **1971**, *54*, 2852-2857, doi:10.1063/1.1675264.
(16) Gorrotxategi Carbajo, P.; Smith, S. C.; Holloway, A.-L.; Smith, C. A.; Pope, F. D.; Shallcross, D. E.; Orr-Ewing, A. J. Ultraviolet photolysis of HCHO: Absolute HCO quantum yields by direct detection of the radical photoproduct. *J. Phys. Chem. A* **2008**, *112*, 12437-12448, doi:10.1021/jp8070508.
(17) Gratien, A.; Nilsson, E.; Doussin, J.-F.; Johnson, M. S.; Nielsen, C. J.; Stenstrøm, Y.; Picquet-Varrault, B. UV and IR absorption cross sections of HCHO, HCDO, and DCDO. *J. Phys. Chem. A* **2007**, *111*, 11506-11513, doi:10.1021/jp074288r.
(18) Gratien, A.; Picquet-Varrault, B.; Orphal, J.; Perraudin, E.; Doussin, J.-F. Laboratory intercomparison of the formaldehyde absorption cross sections in the infrared (1660-1820 cm^{-1}) and ultraviolet (300-360 nm) spectral regions. *J. Geophys. Res.* **2007**, *112*, D053005, doi:10.1029/2006JD007201.
(19) Horowitz, A.; Calvert, J. G. Wavelength dependence of the quantum efficiencies of the primary processes in formaldehyde photolysis at 25°C. *Int. J. Chem. Kinet.* **1978**, *10*, 805-819, doi:10.1002/kin.550100803.
(20) Lewis, R. S.; Tang, K. Y.; Lee, E. K. C. Photoexcited chemiluminescence spectroscopy: Detection of hydrogen atoms produced from single vibronic level photolysis of formaldehyde. *J. Chem. Phys.* **1976**, *65*, 2910-2911, doi:10.1063/1.433399.
(21) Marling, L. Isotope separation of oxygen-17, oxygen-18, carbon-13, and deuterium by ion laser induced formaldehyde photopredissociation. *J. Chem. Phys.* **1977**, *66*, 4200-4225, doi:10.1063/1.434496.
(22) McQuigg, R. D.; Calvert, J. G. The photodecomposition of CH_2O, CD_2O, CHDO, and CH_2O-CD_2O mixtures at xenon flash lamp intensities. *J. Am. Chem. Soc.* **1969**, *91*, 1590-1599, doi:10.1021/ja01035a002.
(23) Meller, R.; Moortgat, G. K. Temperature dependence of the absorption cross sections of formaldehyde between 223 and 323 K in the wavelength range 225-375 nm. *J. Geophys. Res.* **2000**, *105*, 7089-7101, doi:10.1029/1999JD901074.

(24) Mentall, J. E.; Gentieu, E. P.; Krauss, M.; Neumann, D. Photoionization and absorption spectrum of formaldehyde in the vacuum ultraviolet. *J. Chem. Phys.* **1971**, *55*, 5471-5479, doi:10.1063/1.1675711.
(25) Moortgat, G. K.; Klippel, W.; MÖbus, K. H.; Seiler, W.; Warneck, P. Federal Aviation Administration, Washington, DC FAA-EE-80-47, 1980,
(26) Moortgat, G. K.; Seiler, W.; Warneck, P. Photodissociation of HCHO in air: CO and H_2 quantum yields at 220 and 300 K. *J. Chem. Phys.* **1983**, *78*, 1185-1190, doi:10.1063/1.444911.
(27) Moortgat, G. K.; Slemr, F.; Seiler, W.; Warneck, P. Photolysis of formaldehyde: Relative quantum yields of H_2 and CO in the wavelength range 270 - 360 nm. *Chem. Phys. Lett.* **1978**, *54*, 444-447, doi:10.1016/0009-2614(78)85257-9.
(28) Moortgat, G. K.; Warneck, P. CO and H_2 quantum yields in the photodecomposition of formaldehyde in air. *J. Chem. Phys.* **1979**, *70*, 3639-3651, doi:10.1063/1.437956.
(29) Pope, F. D.; Smith, C. A.; Ashfold, N. M. R.; Orr-Ewing, A. J. High-resolution absorption cross sections of formaldehyde at wavelengths from 313 to 320 nm. *Phys. Chem. Chem. Phys.* **2005**, *7*, 79-84, doi:10.1039/b414183k.
(30) Pope, F. D.; Smith, C. A.; Davis, P. R.; Shallcross, D. E.; Ashfold, M. N. R.; Orr-Ewing, A. J. Photochemistry of formaldehyde under troposheric conditions. *J. Chem. Soc., Faraday Disc* **2005**, *130*, 59-73, doi:10.1039/b419227c.
(31) Rogers, J. D. Ultraviolet absorption cross sections and atmospheric photodissociation rate constants of formaldehyde. *J. Phys. Chem.* **1990**, *94*, 4011-4015, doi:10.1021/j100373a025.
(32) Smith, C. A.; Pope, F. D.; Cronin, B.; Parkes, C. B.; Orr-Ewing, A. J. Absorption cross sections of formaldehyde at wavelengths from 300 to 340 nm and at 294 and 245 K. *J. Phys. Chem. A* **2006**, *110*, 11645-11653, doi:10.1021/jp063713y.
(33) Smith, G. D.; Molina, L. T.; Molina, M. J. Measurement of radical quantum yields from formaldehyde photolysis between 269 and 339 nm. *J. Phys. Chem. A* **2002**, *106*, 1233-1240, doi:10.1021/jp013180n.
(34) Tang, K. Y.; Fairchild, P. W.; Lee, E. K. C. Laser-induced photodecomposition of formaldehyde (A^1A_2) from its single vibronic levels. Determination of the quantum yield of H atom by HNO* (A^1A'') chemiluminescence. *J. Phys. Chem.* **1979**, *83*, 569-573, doi:10.1021/j100468a003.
(35) Tatum Ernest, C.; Bauer, D.; Hynes, A. J. High-resolution absorption cross sections of formaldehyde in the 30285−32890 cm^{-1} (304−330 nm) spectral region. *J. Phys. Chem. A* **2012**, *116*, 5910-5922, doi:10.1021/jp210008g.
(36) Tatum Ernest, C.; Bauer, D.; Hynes, A. J. Radical quantum yields from formaldehyde photolysis in the 30 400−32 890 cm^{-1} (304−329 nm) spectral region: Detection of radical photoproducts using pulsed laser photolysis−pulsed laser induced fluorescence. *J. Phys. Chem. A* **2012**, *116*, 6983-6995, doi:10.1021/jp2117399.
(37) Troe, J. Analysis of quantum yields for the photolysis of formaldehyde at λ > 310 nm. *J. Phys. Chem. A* **2007**, *111*, 3868-3874, doi:10.1021/jp066886w.

D4. CH_2OO (formaldehyde oxide)

Back to Index

$CH_2OO + h\nu \rightarrow$ Products (1)

(Recommendation: 19-5; Note: 19-5; Evaluated: 19-5)

Absorption Cross Sections: UV absorption cross sections of the simplest Criegee intermediate CH_2OO (formaldehyde oxide) have been reported at room temperature by Beames et al.[1] (281–410 nm), Sheps et al.[4] (295.156–449.421 nm), Buras et al.[2] (375 nm), Ting et al.[5] (280–483.8 nm), and Foreman et al.[3] (362–476 nm). The cross section values of Ting et al., Foreman et al., and Buras et al. are in good agreement at wavelengths less than 400 nm, and are substantially lower than the values of Beames et al. and Sheps et al. At wavelengths greater than 410 nm, the cross sections of Foreman et al. are significantly greater than those of Ting et al. The discrepancy is approximately a factor of 2 at 420 nm and increases at longer wavelengths.

Ting et al. used SO_2 scavenging and self-reaction of CH_2OO to measure the shape of the absorption spectrum and assigned absolute cross sections at 308.4 and 351.8 nm based on molecular beam laser-depletion measurements. Their use of a reference molecule to effectively calibrate the laser fluence leads to more accurate results relative to the estimated laser fluence (without correction for beam non-uniformity) used for the Beames et al. action spectrum. Ting et al. also postulate that a temperature dependence of the CH_2OO cross sections at wavelengths greater than 360 nm could explain why the Beames et al. spectrum is weaker there.

The recommended cross sections given in Table 4D-4 are from Ting et al. and are 5 nm averages of their data (reported every ~0.6 nm) between 285–350 nm, 1 nm averages between 350–425 nm, and 5 nm averages between 425–450 nm. The wavelength-dependent averaging serves to maintain the vibrational structure on the long wavelength side of the peak cross section, which can be important for spectroscopic identification.

Estimated uncertainty factors (2σ) are recommended to be 1.2 at wavelengths less than 400 nm and increase linearly to 3.0 at 450 nm, primarily due to the discrepancy with Foreman et al. Although cross section data exist out to 484 nm, no recommendation is made for wavelengths longer than 450 nm due to the large uncertainties.

Photolysis Quantum Yield and Product Studies: No recommendation.

Table 4D-4. Recommended Absorption Cross Sections of CH_2OO (formaldehdye oxide) at 295 K

λ (nm)	10^{20} σ (cm^2)	λ (nm)	10^{20} σ (cm^2)	λ (nm)	10^{20} σ (cm^2)
285	304	369	840	401	325
290	389	370	854	402	315
295	477	371	867	403	223
300	570	372	870	404	193
305	672	373	864	405	190
310	779	374	805	406	185
315	902	375	759	407	223
320	987	376	736	408	225
325	1080	377	691	409	239
330	1150	378	681	410	234
335	1200	379	697	411	211
340	1230	380	718	412	140
345	1210	381	707	413	143
350	1190	382	670	414	128
351	1200	383	604	415	111
352	1170	384	576	416	83.0
353	1150	385	512	417	103
354	1130	386	470	418	89.0
355	1120	387	501	419	104
356	1130	388	537	420	120
357	1140	389	546	421	103
358	1130	390	531	422	88.5
359	1100	391	482	423	104
360	1060	392	407	424	69.5
361	1010	393	395	425	57.3
362	1030	394	340	430	27.3
363	1020	395	297	435	29.8
364	1010	396	336	440	7.44
365	1010	397	346	445	6.44
366	958	398	371	450	0.889
367	886	399	378		
368	888	400	340		

Note:
5 nm and 1 nm averages of Ting et al.[5]

(1) Beames, J. M.; Liu, F.; Lu, L.; Lester, M. I. Ultraviolet spectrum and photochemistry of the simplest Criegee intermediate CH_2OO. *J. Am. Chem. Soc.* **2012**, *134*, 20045-20048, doi:10.1021/ja310603j.

(2) Buras, Z. J.; Elsamra, R. M. I.; Green, W. H. Direct determination of the simplest Criegee intermediate (CH_2OO) self reaction rate. *J. Phys. Chem. Lett.* **2014**, *5*, 2224-2228, doi:10.1021/jz5008406.

(3) Foreman, E. S.; Kapnas, K. M.; Jou, Y.; Kalinowski, J.; Feng, D.; Gerber, R. B.; Murray, C. High resolution absolute absorption cross sections of the $B^1A'–X^1A'$ transition of the CH_2OO biradical. *Phys. Chem. Chem. Phys.* **2015**, *17*, 32539-32546, doi:10.1039/c5cp04977f.

(4) Sheps, L. Absolute ultraviolet absorption spectrum of a Criegee intermediate CH_2OO. *J. Phys. Chem. Lett.* **2013**, *4*, 4201-4205, doi:10.1021/jz402191w.

(5) Ting, W.-L.; Chen, Y.-H.; Chao, W.; Smith, M. C.; Lin, J. J.-M. The UV absorption spectrum of the simplest Criegee intermediate CH_2OO. *Phys. Chem. Chem. Phys.* **2014**, *16*, 10438-10443, doi:10.1039/c4cp00877d.

D5. CH_3O_2 (methylperoxy radical)

Back to Index

$CH_3O_2 + h\nu \rightarrow$ Products (1)

(Recommendation: 06-2, Note: 10-6, Evaluated: 10-6)

Absorption Cross Sections: The UV absorption cross sections of the methylperoxy radical, CH_3O_2, in the 195–310 nm region have been measured at room temperature by Parkes et al.,[21] Hochanadel et al.,[8] Parkes,[20] Anastasi et al.,[2] Kan et al.,[11] Cox and Tyndall[3,4] at 250 nm only; Adachi et al.,[1] Sander and Watson[24] at 250 nm only, Pilling and Smith[22] at 254 nm only, Kurylo et al.,[12] McAdam et al.,[17] Jenkin et al.,[10] Wallington et al.,[27] Moortgat et al.,[18] Dagaut and Kurylo,[5] Simon et al.,[25] Jenkin and Cox,[9] Lightfoot and Jemi-Alade[14] who measured the cross sections up to 777 K, Maricq and Wallington,[16] Wallington et al.,[29] Roehl et al.,[23] Fahr et al.,[6] and Nielsen et al.[19] The absorption cross sections have been evaluated in earlier reviews by Lightfoot et al.[13] and Wallington et al.,[28] who noted significant discrepancies in both the shapes of the spectra and the absolute magnitude of the cross section values. The ultraviolet absorption spectra have recently been reevaluated by Tyndall et al.,[26] who fit the absorption spectra to a semi-logarithmic Gaussian distribution function suggested by Lightfoot et al.[13] and Maric et al.:[15]

$$\sigma = \sigma_{max} \exp^{-a\left[\ln\left(\frac{\lambda_{max}}{\lambda}\right)\right]^2}$$

Screening of the data suggested that most spectra published before 1987 did not constrain the shape of the spectrum very well as indicated by the large relative uncertainty of the width parameter a. The shape was determined by averaging the individual fitting parameters from McAdam et al.,[17] Moortgat et al.,[18] Simon et al.,[25] Lightfoot and Jemi-Alade,[14] Jenkin and Cox,[9] and Maricq and Wallington,[16], which were judged to be most reliable by Tyndall et al.[26] Absolute cross sections were based on relative measurements of absorption cross sections of CH_3O_2 and $C_2H_5O_2$ at 240 nm taken under identical conditions (Wallington et al.,[28] Maricq and Wallington,[16] Fenter et al.,[7] and Roehl et al.[23]), combined with independent calibrations by Dagaut and Kurylo,[5] Simon et al.,[25] and Lightfoot and Jemi-Alade.[14] The fit parameters are: $\sigma_{max} = 4.26 \times 10^{-18}$ cm^2 molecule^{-1}; a = 44.4; $\lambda_{max} = 237.3$ nm. Table 4D-5 lists the recommended cross sections, which are taken from the review by Tyndall et al.[26] The shape of the UV spectrum measured by Nielsen et al.[19] is in excellent agreement with the recommendation of Tyndall et al.[26]

Photolysis Quantum Yield and Product Studies: No recommendation. The loss of CH_3O_2 due to photolysis in the stratosphere and troposphere is expected to be negligible.

Table 4D-5. Recommended Absorption Cross Sections of CH_3O_2, $C_2H_5O_2$, and $CH_3C(O)O_2$ at 298 K

λ (nm)	10^{20} σ (cm^2)		
	CH_3O_2	$C_2H_5O_2$	$CH_3C(O)O_2$
195.0			389
200.0			564
205.0	165		665
210.0	219	195	656
215.0	276	257	564
220.0	330	319	451
225.0	376	374	366
230.0	408	418	326
235.0	424	444	319
240.0	424	452	326
245.0	407	440	330
250.0	378	412	322
255.0	339	372	300
260.0	294	324	268
265.0	248	273	229
270.0	203	222	187
275.0	162	176	147
280.0	126	136	111
285.0	96.1	102	81.2
290.0	71.5	74.6	57.3
295.0	52.0	53.3	
300.0		37.3	

Note:
Tyndall et al.[26] review

(1) Adachi, H.; Basco, N.; James, D. G. L. Mutual interactions of the methyl and methylperoxy radicals studied by flash photolysis and kinetic spectroscopy. *Int. J. Chem. Kinet.* **1980**, *12*, 949-977, doi:10.1002/kin.550121206.

(2) Anastasi, C.; Smith, I. W. M.; Parkes, D. A. Flash photolysis study of the spectra of CH_3O_2 and $C(CH_3)_3O_2$ radicals and the kinetics of their mutual reaction and with NO. *J. Chem. Soc. Faraday Trans. 1* **1978**, *74*, 1693-1701, doi:10.1039/f19787401693.

(3) Cox, R. A.; Tyndall, G. Rate constants for reactions of CH_3O_2 in the gas phase. *Chem. Phys. Lett.* **1979**, *65*, 357-360, doi:10.1016/0047-2670(82)80022-1.

(4) Cox, R. A.; Tyndall, G. S. Rate constants for the reactions of CH_3O_2 with HO_2, NO and NO_2 using molecular modulation spectrometry. *J. Chem. Soc. Faraday Trans. II* **1980**, *76*, 153-163, doi:10.1039/f29807600153.

(5) Dagaut, P.; Kurylo, M. J. The gas phase UV absorption spectrum of CH_3O_2 radicals: A reinvestigation. *J. Photochem. Photobiol. A: Chem.* **1990**, *51*, 133-140, doi:10.1016/1010-6030(90)87047-F.

(6) Fahr, A.; Laufer, A. H.; Kraus, M.; Osman, R. Gas phase absorption spectrum and cross sections of vinylperoxy ($C_2H_3O_2$) radical. *J. Phys. Chem. A* **1997**, *101*, 4879-4886, doi:10.1021/jp964005n.

(7) Fenter, F. F.; Catoire, V.; Lesclaux, R.; Lightfoot, P. D. The ethylperoxy radical: Its ultraviolet spectrum, self-reaction, and reaction with HO_2, each studied as a function of temperature. *J. Phys. Chem.* **1993**, *97*, 3530-3538, doi:10.1021/j100116a016.

(8) Hochanadel, C. J.; Ghormley, J. A.; Boyle, J. W.; Ogren, P. J. Absorption spectrum and rates of formation and decay of the CH_3O_2 radical. *J. Phys. Chem.* **1977**, *81*, 3-7, doi:10.1021/j100516a002.

(9) Jenkin, M. E.; Cox, R. A. Kinetics of reactions of CH_3O_2 and $HOCH_2CH_2O_2$ radicals produced by the photolysis of iodomethane and 2-iodoethanol. *J. Phys. Chem.* **1991**, *95*, 3229-3237, doi:10.1021/j100161a049.

(10) Jenkin, M. E.; Cox, R. A.; Hayman, G.; Whyte, L. J. Kinetic study of the reactions CH_3O_2 + CH_3O_2 and CH_3O_2 + HO_2 using molecular modulation spectroscopy. *J. Chem. Soc. Faraday Trans. 2* **1988**, *84*, 913-930, doi:10.1039/f29888400913.

(11) Kan, C. S.; McQuigg, R. D.; Whitbeck, M. R.; Calvert, J. G. Kinetic flash spectroscopic study of the CH_3O_2-CH_3O_2 and CH_3O_2-SO_2 reactions. *Int. J. Chem. Kinet.* **1979**, *11*, 921-933, doi:10.1002/kin.550110811.

(12) Kurylo, M. J.; Wallington, T. J.; Ouellette, P. A. Measurements of the UV absorption cross-sections for HO_2 and CH_3O_2 in the gas phase. *J. Photochem.* **1987**, *39*, 201-215, doi:10.1016/0047-2670(87)80032-1.
(13) Lightfoot, P. D.; Cox, R. A.; Crowley, J. N.; Destriau, M.; Hayman, G. D.; Jenkin, M. E.; Moortgat, G. K.; Zabel, F. Organic peroxy radicals: Kinetics, spectroscopy and tropospheric chemistry. *Atmos. Environ.* **1992**, *26A*, 1805-1961, doi:10.1016/0960-1686(92)90423-I.
(14) Lightfoot, P. D.; Jemi-Alade, A. A. The temperature dependence of the UV spectra of the HO_2 and CH_3O_2 radicals. *J. Photochem. Photobiol. A: Chem.* **1991**, *59*, 1-10, doi:10.1016/1010-6030(91)87062-Z.
(15) Maric, D.; Crowley, J. N.; Burrows, J. P. Application of a Gaussian distribution function to describe molecular UV-visible absorption continua. 2. The UV spectra of RO_2• radicals. *J. Phys. Chem.* **1997**, *101*, 2561-2567, doi:10.1021/jp961715k.
(16) Maricq, M. M.; Wallington, T. J. Absolute ultraviolet cross sections of methyl and ethyl peroxy radicals. *J. Phys. Chem.* **1992**, *96*, 982-986, doi:10.1021/j100181a081.
(17) McAdam, K.; Veyret, B.; Lesclaux, R. UV absorption spectra of HO_2 and CH_3O_2 radicals and the kinetics of their mutual reactions at 298 K. *Chem. Phys. Lett.* **1987**, *133*, 39-44, doi:10.1016/0009-2614(87)80049-0.
(18) Moortgat, G.; Veyret, B.; Lesclaux, R. Absorption spectrum and kinetics of reactions of the acetylperoxy radical. *J. Phys. Chem.* **1989**, *93*, 2362-2368, doi:10.1021/j100343a032.
(19) Nielsen, O. J.; Johnson, M. S.; Wallington, T. J.; Christensen, L. K.; Platz, J. UV absorption cross sections of HO_2, CH_3O_2, $C_2H_5O_2$ and $CH_3C(O)CH_2O_2$ radicals and mechanism of the reactions of F and Cl atoms with $CH_3C(O)CH_3$. *Int. J. Chem. Kinet.* **2002**, *34*, 283-291, doi:10.1002/kin.10037.
(20) Parkes, D. A. The oxidation of methyl radicals at room temperature. *Int. J. Chem. Kinet.* **1977**, *9*, 451-469, doi:10.1002/kin.550090313
(21) Parkes, D. A.; Paul, D. M.; Quinn, C. P.; Robson, R. C. The ultraviolet absorption by alkylperoxy radicals and their mutual reactions. *Chem. Phys. Lett.* **1973**, *23*, 425-429, doi:10.1016/0009-2614(73)85115-2.
(22) Pilling, M. J.; Smith, M. J. C. A laser flash photolysis study of the reaction $CH_3 + O_2 \rightarrow CH_3O_2$ at 298 K. *J. Phys. Chem.* **1985**, *89*, 4713-4720, doi:10.1021/j100268a014.
(23) Roehl, C. M.; Bauer, D.; Moortgat, G. K. Absorption spectrum and kinetics of the acetylperoxy radical. *J. Phys. Chem.* **1996**, *100*, 4038-4047, doi:10.1021/jp9526298.
(24) Sander, S. P.; Watson, R. T. Temperature dependence of the self-reaction of CH_3O_2 radicals. *J. Phys. Chem.* **1981**, *85*, 2960-2964, doi:10.1021/j150620a023.
(25) Simon, F.-G.; Schneider, W.; Moortgat, G. K. UV-Absorption spectrum of the methylperoxy radical and the kinetics of its disproportionation reaction at 300 K. *Int. J. Chem. Kinet.* **1990**, *22*, 791-813, doi:10.1002/kin.550220802
(26) Tyndall, G. S.; Cox, R. A.; Granier, C.; Lesclaux, R.; Moortgat, G. K.; Pilling, M. J.; Ravishankara, A. R.; Wallington, T. J. Atmospheric chemistry of small organic peroxy radicals. *J. Geophys. Res.* **2001**, *106*, 12157-12182, doi:10.1029/2000JD900746.
(27) Wallington, T. J.; Dagaut, P.; Kurylo, M. J. Measurements of the gas phase UV absorption spectrum of $C_2H_5O_2$• radicals and of the temperature dependence of the rate constant for their self-reaction. *J. Photochem. Photobiol. A: Chem.* **1988**, *42*, 173-185, doi:10.1016/1010-6030(88)80061-3.
(28) Wallington, T. J.; Dagaut, P.; Kurylo, M. J. Ultraviolet absorption cross sections and reaction kinetics and mechanisms for peroxy radicals in the gas phase. *Chem. Rev.* **1992**, *92*, 667-710, doi:10.1021/cr00012a008.
(29) Wallington, T. J.; Mariq, M. M.; Ellerman, T.; Nielsen, O. J. Novel method for the measurement of gas-phase peroxy radical absorption spectra. *J. Phys. Chem.* **1992**, *96*, 982-986, doi:10.1021/j100181a080.

D6. CH_3OH (methanol, methyl alcohol)

Back to Index

$CH_3OH + h\nu \rightarrow$ Products

(New)

Absorption Cross Sections: VUV/UV absorption cross sections of CH_3OH (methanol) have been measured at room temperature by Burton et al.[1] (15.5–207 nm), Cheng et al.[2] (107–219.5 nm), Dillon et al.[3] (185 nm), Harrison et al.[5] (161–197.1 nm, graphical data), Jiménez et al.[6] (185 nm), Lange et al.[7] (115–220.5 nm), Nee et al.[8] (106.1–197.6 nm, graphical data), Ogawa and Cook[9] (50.8–174.9 nm), Person and Nicole[10] (105.25–124.35 nm, graphical data), Salahub and Sandorfy[11] (120–204.6 nm), and Tsubomura et al.[12] (164–185 nm, graphical data). Flowerday et al.[4] have also reported very small absorption cross sections of CH_3OH in the visible region

(445–456 nm and 505–516 nm) at room temperature using a cavity-enhanced technique. The data of Cheng et al., Dillon et al., Harrison et al., Lange et al., Nee et al., and Salahub and Sandorfy are in good agreement between 165–192 nm. Over this same range, the studies of Burton et al., Ogawa and Cook, and Tsubomura et al. disagree substantially with other studies. At UV wavelengths >192 nm, fewer studies are available, and the cross section data generally diverge as wavelength increases.

For VUV data in the 110–165 nm range, the studies of Cheng et al., Harrison et al., Lange et al., Person and Nicole, and Salahub and Sandorfy are generally in good agreement. At wavelengths shorter than 110 nm, the data of Ogawa and Cook are consistently 10–20% higher than the cross sections of Burton et al.

The recommended cross sections given in Table 4D-6 for 166–219 nm are from Cheng et al. at 1 nm intervals, interpolated to integer wavelengths. For the range 220–230 nm, the recommended values were obtained from a log-linear fit (209–219 nm) and extrapolation of the Cheng et al. data, $\log \sigma(\lambda) = 10.5034 - 0.14807\ \lambda$. Estimated uncertainty factors (2σ) of 1.1 for λ = 166–192 nm, 1.2 for λ = 193–208 nm, and 1.3 for λ = 209–219 nm are recommended. The recommended Lyman-α (121.567 nm) cross section is an average of the data of Lange et al., Cheng et al., Person and Nicole, Salahub and Sandorfy, and Nee et al. and given an estimated uncertainty factor (2σ) of 1.05.

Photolysis Quantum Yield and Product Studies: No recommendation.

Table 4D-6. Recommended Absorption Cross Sections of CH_3OH (methanol) at 298 K

λ (nm)	10^{20} σ (cm^2)	λ (nm)	10^{20} σ (cm^2)	λ (nm)	10^{20} σ (cm^2)
121.567	1300	185	60.6	205	1.42
166	22.0	186	59.4	206	1.01
167	23.1	187	57.3	207	0.715
168	24.8	188	54.3	208	0.505
169	26.8	189	50.9	209	0.360
170	29.1	190	46.9	210	0.255
171	31.8	191	42.1	211	0.180
172	34.8	192	37.5	212	0.130
173	37.9	193	32.7	213	0.0930
174	41.1	194	27.5	214	0.0660
175	44.2	195	22.9	215	0.0480
176	47.5	196	18.7	216	0.0335
177	50.5	197	15.0	217	0.0230
178	53.2	198	11.7	218	0.0165
179	55.7	199	8.93	219	0.0120
180	57.7	200	6.72	220	*0.00847*
181	59.7	201	4.91	225	*0.00154*
182	61.3	202	3.60	230	*0.000280*
183	61.7	203	2.68		
184	61.3	204	1.98		

Note:
121.567 nm: average of Lange et al.,[7] Cheng et al.,[2] Person and Nicole,[10] Salahub and Sandorfy,[11] and Nee et al.[8]
166–219 nm: Cheng et al.[2] data interpolated to 1 nm integer wavelengths
220–230 nm: extrapolation of Cheng et al.[2] data, $\log \sigma(\lambda) = 10.5034 - 0.14807\ \lambda$

(1) Burton, G. R.; Chan, W. F.; Cooper, G.; Brion, C. E. Absolute oscillator strengths for photoabsorption (6-360 eV) and ionic photofragmentation (10-80 eV) of methanol. *Chem. Phys.* **1992**, *167*, 349-367, doi:10.1016/0301-0104(92)80208-D.

(2) Cheng, B.-M.; Bahou, M.; Lee, Y.-P.; Lee, L. C. Experimental and theoretical studies on VUV absorption cross sections and photodissociation of CH_3OH, CH_3OD, CD_3OH, and CD_3OD. *J. Chem. Phys.* **2002**, *117*, 1633-1640, doi:10.1063/1.1485769.

(3) Dillon, T. J.; Hölscher, D.; Sivakumaran, V.; Horowitz, A.; Crowley, J. N. Kinetics of the reactions of HO with methanol (210–351 K) and with ethanol (216–368 K). *Phys. Chem. Chem. Phys.* **2005**, *7*, 349-355, doi:10.1039/b413961e.

(4) Flowerday, C. E.; Bhardwaj, N.; Thalman, R.; Asplund, M. C.; Sevy, E. T.; Hansen, J. C. Absorption cross-sections for the 5th and 6th vibrational overtones in a series of short chained alcohols using

incoherent broadband cavity enhanced-absorption spectroscopy (IBBCEAS). *J. Mol. Spectrosc.* **2023**, *392*, 111746, doi:10.1016/j.jms.2023.111746.
(5) Harrison, A. J.; Cederholm, B. J.; Terwilliger, M. A. Absorption of acyclic oxygen compounds in the vacuum ultraviolet. I. Alcohols. *J. Chem. Phys.* **1959**, *30*, 355-356, doi:10.1063/1.1729952.
(6) Jiménez, E.; Gilles, M. K.; Ravishankara, A. R. Kinetics of the reaction of the hydroxyl radical with CH_3OH and C_2H_5OH between 235 and 360 K. *J. Photochem. Photobiol. A: Photochem.* **2003**, *157*, 237-245, doi:10.1016/S1010-6030(03)00073-X.
(7) Lange, E.; Lozano, A. I.; Jones, N. C.; Hoffmann, S. V.; Kumar, S.; Smialek, M. A.; Duflot, D.; Brunger, M. J.; Limão-Vieira, P. Absolute photoabsorption cross-sections of methanol for terrestrial and astrophysical relevance. *J .Phys. Chem. A* **2020**, *124*, 8496-8508, doi:10.1021/acs.jpca.0c06615.
(8) Nee, J. B.; Suto, M.; Lee, L. C. Photoabsorption cross section of HF at 107-145 nm. *J. Phys. B: At. Mol. Phys.* **1985**, *18*, L293-L294, doi:10.1088/0022-3700/18/10/006.
(9) Ogawa, M.; Cook, G. R. Absorption coefficients of methyl, ethyl, *n*-propyl, and *n*-butyl alcohols. *J. Chem. Phys.* **1958**, *28*, 747-748, doi:10.1063/1.1744253.
(10) Person, J. C.; Nicole, P. P. Isotope effects in the photoionization yields and in the absorption cross sections for methanol, ethanol, methyl bromide, and ethyl bromide. *J. Chem. Phys.* **1971**, *55*, 3390-3397, doi:10.1063/1.1676590.
(11) Salahub, D. R.; Sandorfy, C. The far-ultraviolet spectra of some simple alcohols and fluoroalcohols. *Chem. Phys. Lett.* **1971**, *8*, 71-74, doi:10.1016/0009-2614(71)80578-X.
(12) Tsubomura, H.; Kimura, K.; Kaya, K.; Tanaka, J.; Nagakura, S. Vacuum ultraviolet absorption spectra of saturated organic compounds with non-bonding electrons. *Bull. Chem. Soc. Japan* **1964**, *37*, 417-423, doi:10.1246/bcsj.37.417.

D7. CH_3OOH (methylhydroperoxide)

Back to Index

$CH_3OOH + h\nu \rightarrow$	$CH_3O + OH$	185 kJ mol^{-1}	645 nm	(1)
$\rightarrow$	$CH_3 + HO_2$	292 kJ mol^{-1}	410 nm	(2)
$\rightarrow$	$CH_3O_2 + H$	358 kJ mol^{-1}	334 nm	(3)
$\rightarrow$	$CH_3OH + O(^3P)$	179 kJ mol^{-1}	670 nm	(4)

(Recommendation: 10-6, Note: 10-6, Evaluated: 10-6)

Absorption Cross Sections: The absorption spectrum of CH_3OOH (methylhydroperoxide) was measured at room temperature by Cox and Tyndall[2] (210–280 nm), Nozière et al.[5] (220–250 nm), Molina and Arguello[4] (210–350 nm), Vaghjiani and Ravishankara[8] (210–365 nm), Blitz et al.[1] (210–355 nm), Matthews et al.[3] (365–405 nm), and Roehl et al.[6] (305–365 nm).

Vaghjiani and Ravishankara[8] measured the cross sections of CH_3OOH by monitoring the CH_3OOH concentration via trapping and titration. These results are recommended and are listed in Table 4D-7. The earlier results of Molina and Arguello[4] are consistently 40% higher than the values shown in Table 4D-7. This difference is believed to be due to difficulty in trapping CH_3OOH and measuring its concentration. The results of Blitz et al.[1] are consistently 30% smaller than the data of Vaghjiani and Ravishankara[8] in the range 225–325 nm and are unreliable above 325 nm due to baseline problems during their measurements. The absorption cross sections of Roehl et al.[6] determined using action spectroscopy are 8-21 % greater than those measured by Vaghjiani and Ravishankara.[8] Similar absorption measurements were performed by Matthews et al.[3] in the weak tail of the absorption band up to 405 nm. Their cross sections were normalized to the value of Vaghjiani and Ravishankara[8] at 355 nm and are included in the recommendation in Table 4D-7.

Matthews et al.[3] also measured the absorption of the $5\nu_{OH}$ overtone band near 620 nm as $(3.6 \pm 0.4) \times 10^{-24}$ cm^2 molecule^{-1}.

Photolysis Quantum Yields and Product Studies: CH_3OOH dissociates to give CH_3O with unit quantum yield $\Phi_1 = 1.00 \pm 0.18$ (Vaghjiani and Ravishankara[9]). These authors also observed some production of H (quantum yield of 0.038 ± 0.007) and O atoms (quantum yield <0.007) at shorter wavelengths (i.e., 193 nm).

Thelen et al.[7] report unit quantum yields for OH production at 248 and 193 nm that are in agreement with the results of Vaghjiani and Ravishankara.[8] Quantum yields for OH and CH_3O were also measured by Blitz et al.[1] in the wavelength range 223–355 nm. These authors have shown that the quantum yield for both OH ands CH_3O production is unity across this range of wavelengths.

Table 4D-7. Recommended Absorption Cross Sections of CH_3OOH at 298 K

λ	10^{20} σ	λ	10^{20} σ

(nm)	(cm^2)	(nm)	(cm^2)
210	31.2	310	0.239
215	20.9	315	0.182
220	15.4	320	0.137
225	12.2	325	0.105
230	9.62	330	0.079
235	7.61	335	0.061
240	6.05	340	0.047
245	4.88	345	0.035
250	3.98	350	0.027
255	3.23	355	0.021
260	2.56	360	0.016
265	2.11	365	0.012
270	1.70	370	0.0075
275	1.39	375	0.0052
280	1.09	380	0.0040
285	0.863	385	0.0025
290	0.691	390	0.0014
295	0.551	395	0.0010
300	0.413	400	0.0006
305	0.313	405	0.0003

Note:
210–365 nm: data of Vaghjiani and Ravishankara[9]
370–405, 620 nm: data of Matthews et al.[3]

(1) Blitz, M. A.; Heard, D. E.; Pilling, M. J. Wavelength dependent photodissociation of CH_3OOH. Quantum yields for CH_3O and OH, measurement of the OH + CH_3OOH rate constant. *J. Photochem. Photobiol. A: Chem.* **2005**, *176*, 107-113, doi:10.1016/j.jphotochem.2005.09.017.

(2) Cox, R. A.; Tyndall, G. Rate constants for reactions of CH_3O_2 in the gas phase. *Chem. Phys. Lett.* **1979**, *65*, 357-360, doi:10.1016/0047-2670(82)80022-1.

(3) Matthews, J.; Sinha, A.; Francisco, J. S. The importance of weak absorption features in promoting tropospheric radical production. *Proc. Natl. Acad. Sci.* **2005**, *102*, 7449-7452, doi:10.1073/pnas.0502687102.

(4) Molina, M. J.; Arguello, G. Ultraviolet absorption spectrum of methylhydroperoxide vapor. *Geophys. Res. Lett.* **1979**, *6*, 953-955, doi:10.1029/GL006i012p00953.

(5) Nozière, B.; Lesclaux, R.; Hurley, M. D.; Dearth, M. A.; Wallington, T. J. A kinetic and mechanistic study of the self-reaction and reaction with HO_2 of the benzylperoxy radical. *J. Phys. Chem.* **1994**, *98*, 2864-2873, doi:10.1021/j100062a023.

(6) Roehl, C. M.; Marka, Z.; Fry, J. L.; Wennberg, P. O. Near-UV photolysis cross sections of CH_3OOH and $HOCH_2OOH$ determined via action spectroscopy. *Atmos. Chem. Phys.* **2007**, *7*, 713-720, doi:10.5194/acp-7-713-2007.

(7) Thelen, M.-A.; Felder, P.; Huber, J. R. The photofragmentation of methyl hydroperoxide CH_3OOH at 193 and 248 nm in a cold molecular beam. *Chem. Phys. Lett.* **1993**, *213*, 275-281, doi:10.1016/0009-2614(93)85132-8.

(8) Vaghjiani, G. L.; Ravishankara, A. R. Absorption cross sections of CH_3OOH, H_2O_2, and D_2O_2 vapors between 210 and 365 nm at 297 K. *J. Geophys. Res.* **1989**, *94*, 3487-3492, doi:10.1029/JD094iD03p03487.

(9) Vaghjiani, G. L.; Ravishankara, A. R. Photodissociation of H_2O_2 and CH_3OOH at 248 nm and 298 K: Quantum yields for OH, $O(^3P)$ and $H(^2S)$. *J. Chem. Phys.* **1990**, *92*, 996-1003, doi:10.1063/1.458081.

D8. HC(O)OH (formic acid)

Back to Index

$HC(O)OH + h\nu \rightarrow HCO + OH$	422 kJ mol^{-1}	260 nm	(1)
$\rightarrow H + COOH$	408 kJ mol^{-1}	293 nm	(2)
$\rightarrow HCOO + H$	470 kJ mol^{-1}	254 nm	(3)
$\rightarrow H_2 + CO_2$	–15 kJ mol^{-1}	All	(4)
$\rightarrow H_2O + CO$	264 kJ mol^{-1}	454 nm	(5)

$(HC(O)OH)_2$ (formic acid dimer)

$(HC(O)OH)_2 + h\nu \rightarrow HCO + OH + HCOOH$		(6)
$\rightarrow CO + H_2O + HCOOH$		(7)
$\rightarrow H_2 + CO_2 + HCOOH$		(8)

(Recommendation: 25-1, Note: 25-1, Evaluated: 25-1)

Absorption Cross Sections: The UV absorption spectrum of formic acid, HC(O)OH, and formic acid dimer, $(HC(O)OH)_2$, have been measured near 300 K for a range of sample pressures by McMillan[2] (200–249 nm; 35.2, 16.4, and 2.45 Torr), Singleton et al.[10] (195–250 nm; 29 pressures between 0.5 and 22 Torr), Singleton et al.,[12] and Nagakura et al.[8] (154–191 nm). Jolly et al.[6] reported cross sections at 222 nm in connection with their quantum yield measurements. Singleton et al.[12] also measured spectra at 356.2 K. The absorption spectrum of the dimer has a broad maximum near 205 nm and a monotonic decrease in intensity with increasing wavelength. The absorption maximum of the monomer is shifted to longer wavelengths, with a peak cross section near 215 nm, about one third the magnitude of the peak cross section for the dimer. The decrease in cross sections with increasing wavelength is more rapid for the dimer than for the monomer, resulting in monomer cross sections being greater at 250 nm by approximately a factor 10. The absorption spectra reported by McMillan[2] were derived assuming monomers only in spite of undefined amounts of monomer and dimer contributions, resulting in a reported spectra that lies between those reported by Singleton et al.[10] for the monomer and the dimer. The recommended absorption cross sections in Table 4D-8 are taken from Singleton et al.[10] measured with a resolution of 1 nm.

The VUV spectrum of HC(O)OH has been measured by several groups.[1,3,4,7,9,13] The recommended Lyman-α (121.567 nm) absorption cross section for HC(O)OH of 1.31×10^{-17} cm^2 molecule^{-1} is an average of the measurements in this wavelength region by Suto et al.,[13] Leach et al.,[7] and Randi et al.[9]

Photolysis Quantum Yield and Product Studies: In the pre-1966 studies considered in Calvert and Pitts,[2] yields of final products CO, CO_2, H_2, H_2O (suggested as due to the molecular elimination channels 4 and 5) were determined. However, in the experiments considered it would be difficult to distinguish between primary photolytic products and products formed by subsequent secondary free-radical reactions. Jolly et al.[6] determined the quantum yield of OH formation at 222 nm for the monomer to be 1.05 ± 0.14 and essentially zero for the dimer. In a follow-up study, Singleton et al.[12] re-determined the OH quantum yields at 222 nm to be 0.704 ± 0.048 at 298 K and 0.771 ± 0.030 at 356.2 K for the monomer, and 0.153 ± 0.028 at 298 K for the dimer (the OH yield for the dimer at elevated temperatures was assumed to be zero). Photodissociation into the other radical channels, 2 and 3, is minor and has been discussed by He and Fang.[5] Photodissociation quantum yields for the dimer were determined at 222 nm by Singleton et al.[11] to be $\Phi_6 = 0.15$, $\Phi_7 = 0.81$ and $\Phi_8 = 0.04$.

Table 4D-8. Recommended Absorption Cross Sections of HC(O)OH and $(HC(O)OH)_2$ at 302 K

λ (nm)	10^{20} σ (cm^2) monomer	dimer	λ (nm)	10^{20} σ (cm^2) monomer	dimer
195	9.18	27.4	223	11.9	17.0
196	9.96	29.1	224	11.3	15.5
197	9.57	30.8	225	10.9	14.1
198	10.0	32.2	226	9.87	12.7
199	10.7	33.3	227	10.4	11.3
200	10.7	34.6	228	9.24	10.1
201	11.5	35.4	229	9.15	8.87
202	11.9	36.2	230	8.12	7.78
203	12.5	36.7	231	7.18	6.77
204	12.5	37.3	232	7.07	5.87
205	13.8	37.4	233	6.44	5.01
206	13.6	37.4	234	6.68	4.26
207	13.7	37.2	235	5.24	3.58
208	13.6	36.9	236	5.40	2.95
209	14.1	36.2	237	4.10	2.46
210	14.4	35.5	238	4.32	2.03
211	14.2	34.6	239	3.58	1.63
212	13.6	33.6	240	3.79	1.31
213	14.3	32.4	241	2.79	1.02
214	14.9	31.0	242	2.83	0.795
215	15.0	29.4	243	1.98	0.659
216	13.7	28.1	244	2.10	0.490
217	13.6	26.7	245	1.73	0.337
218	13.4	25.1	246	1.79	0.267
219	13.5	23.4	247	1.18	0.190
220	12.9	21.8	248	1.23	0.134
221	11.6	20.2	249	0.855	0.093
222	12.4	18.6	250	0.861	0.072

Note:
Singleton et al.[10]

(1) Barnes, E. E.; Simpson, W. T. Correlations among electronic transitions for carbonyl and carboxyl in the vacuum ultraviolet. *J. Chem. Phys.* **1963**, *39*, 670-675, doi:10.1063/1.1734305.

(2) Calvert, J. G.; Pitts Jr., J. N. In *Photochemistry*; John Wiley & Sons, Inc.: New York, 1966; pp 368.

(3) Doner, A. C.; Moran, H. A.; Webb, A. R.; Christianson, M. G.; Koritzke, A. L.; Dewey, N. S.; Hartness, S. W.; Rotavera, B. Machine learning models for binary molecular classification using VUV absorption spectra. *J. Quant. Spectrosc. Radiat. Transf.* **2023**, *297*, 108438, doi:10.1016/j.jqsrt.2022.108438.

(4) Fujimoto, M. M.; Tanaka, H. K.; Marinho, R. R. T.; Medina, A.; Prudente, F. V.; Homem, M. G. P. Cross sections and asymmetry parameters for formic acid in the vacuum-ultraviolet energy range. *J. Phys. Chem. A* **2020**, *124*, 6478-6485, doi:10.1021/acs.jpca.0c03520.

(5) He, H.-Y.; Fang, W.-H. A CASSCF/MR-CI study toward the understanding of wavelength-dependent and geometrically memorized photodissociation of formic acid. *J. Am. Chem. Soc.* **2003**, *125*, 16139-16147, doi:10.1021/ja0363157.

(6) Jolly, G. S.; Singleton, D. L.; Paraskevopoulos, G. Direct determination of the quantum yield of OH in the laser photolysis of formic acid. *J. Phys. Chem.* **1987**, *91*, 3463-3465, doi:10.1021/j100297a001.

(7) Leach, S.; Schwell, M.; Dulieu, F.; Chotin, J.-L.; Jochims, H.-W.; Baumgärtel, H. Photophysical studies of formic acid in the VUV. Absorption spectrum in the 6-22 eV region. *Phys. Chem. Chem. Phys.* **2002**, *4*, 5025-5039, doi:10.1039/b205729h.

(8) Nagakura, S.; Kaya, K.; Tsubomura, H. Vacuum ultraviolet absorption spectra and electronic structures of formic acid, acetic acid and ethyl acetate. *J. Mol. Spectrosc.* **1964**, *13*, 1-8, doi:10.1016/0022-2852(64)90049-9.

(9) Randi, P. A. S.; Pastega, D. F.; Bettega, M. H. F.; Jones, N. C.; Hoffmann, S. V.; Eden, S.; Barbosa, A. S.; Limão-Vieira, P. Electronically excited states of formic acid investigated by theoretical and experimental methods. *Spectrochim. Acta A: Mol. Biomol. Spectrosc.* **2023**, *289*, 122237, doi:10.1016/j.saa.2022.122237.
(10) Singleton, D. L.; Paraskevopoulos, G.; Irwin, R. S. UV absorption cross-sections of the monomer and dimer of formic acid. *J. Photochem.* **1987**, *37*, 209-216, doi:10.1016/0047-2670(87)85001-3.
(11) Singleton, D. L.; Paraskevopoulos, G.; Irwin, R. S. Laser photolysis of formic acid vapor at 222 nm. Quantum yields of stable products. *Res. Chem. Intermediates* **1989**, *12*, 1-12, doi:10.1163/156856789X00131.
(12) Singleton, D. L.; Paraskevopoulos, G.; Irwin, R. S. Laser photolysis of carboxyclic acids in the gas phase. Direct determination of the OH quantum yield at 222 nm. *J. Phys. Chem.* **1990**, *94*, 695-699, doi:10.1021/j100365a034.
(13) Suto, M.; Wang, X.; Lee, L. C. Fluorescence yields from photodissociative excitation of HCOOH, $HCOOCH_3$, and CH_3COOH in the vacuum-ultraviolet region. *J. Phys. Chem.* **1988**, *92*, 3764-3768, doi:10.1021/j100324a015.

D9. HC(O)OOH (peroxyformic acid, performic acid, PFA)

Back to Index

$HC(O)OOH + h\nu \rightarrow$ Products (1)

(Recommendation: 19-5; Note: 19-5; Evaluated: 19-5)

Absorption Cross Sections: UV absorption cross sections of HC(O)OOH (peroxyformic acid) have been reported at room temperature by Indulkar et al.[1] at 282 and 355 nm. The Indulkar et al. measurements are the only UV absorption data currently available for this molecule. The absorption cross sections in this study were estimated by comparing the OH yield from PFA to that from H_2O_2 for which the cross sections at 282 and 355 nm are known. Indulkar et al. used a Gaussian function to interpolate between the two measured points and estimated the absorption cross sections for PFA over the entire 282–355 nm range. The recommended cross sections given in Table 4D-9 are the 282 nm and 355 nm values from Indulkar et al. An estimated uncertainty factor (2σ) of 1.5 is recommended.

Photolysis Quantum Yield and Product Studies: The quantum yield for OH formation from PFA was assumed to be unity by Indulkar et al.[1] at 282 and 355 nm. At 282 nm, this assumption was based on molecular orbital calculations indicating that O–O bond breakage is dominant, and at 355 nm, the OH fragmentation channel is the only one energetically open.

Table 4D-9. Recommended Absorption Cross Sections of HC(O)OOH (peroxyformic acid) at 298 K

λ (nm)	10^{20} σ (cm^2)
282	0.80
355	0.0034

Note:
Indulkar et al.[1]

(1) Indulkar, Y. N.; Louie, M. K.; Sinha, A. UV photochemistry of peroxyformic acid (HC(O)OOH): An experimental and computational study investigating 355 nm photolysis. *J. Phys. Chem. A* **2014**, *118*, 5939-5949, doi:10.1021/jp5039688.

D10. $HOCH_2OOH$ (hydroxymethyl hydroperoxide)

Back to Index

$HOCH_2OOH + h\nu \rightarrow HOCH_2O + OH$ 116 kJ mol^{-1} 1028 nm (1)

(Recommendation: 10-2, Note: 10-6, Evaluated: 10-6)

Absorption Cross Sections: The UV absorption spectrum of hydroxymethyl hydroperoxide, $HOCH_2OOH$, was measured at 298 K by Bauerle and Moortgat[1] in the range 205–360 nm, using a combination of diode array and FTIR spectroscopy. The absorption cross sections were also determined via action spectroscopy of the OH product by Roehl et al.[3] in the range 310–360 nm. The cross sections measured by Roehl et al.[3] were normalized to the value of Bauerle and Moortgat[1] at 320 nm. Their values are in reasonable agreement (within 20%) between 310 and 340 nm but are lower than those of Bauerle and Moortgat[1] at longer wavelengths (e.g. 33%

at 350 nm). The recommended cross sections listed in Table 4D-10 are taken from Bauerle and Moortgat[1] in the range 205–305 nm, and from the average of the values of Bauerle and Moortgat[1] and Roehl et al.[3] for the region 310–380 nm.

Photolysis Quantum Yields and Product Studies: The photolysis process is assumed to occur with unity quantum yield, Φ_1, at wavelengths greater than 290 nm, in analogy with CH_3OOH. Overtone photodissociation spectrum and quantum yields were obtained in the OH-stretching region for the $4\nu_{OH}$ (centered at 750 and 738 nm for the OO–H and RO–H bands, respectively) and $5\nu_{OH}$ (centered at 617 and 604 nm for the OO–H and RO–H bands, respectively) transitions by Fry et al.[2] Overtone photodissociation is not expected to be significant under atmospheric conditions.

Table 4D-10. Recommended Absorption Cross Sections of $HOCH_2OOH$ at 298 K

λ (nm)	10^{20} σ (cm^2)	λ (nm)	10^{20} σ (cm^2)
205	26.9	285	0.75
210	22.6	290	0.63
215	18.7	295	0.51
220	15.5	300	0.40
225	12.5	305	0.29
230	10.1	310	0.23
235	7.89	315	0.18
240	5.98	320	0.13
245	4.68	325	0.098
250	3.78	330	0.072
255	2.88	335	0.056
260	2.31	340	0.042
265	1.81	345	0.032
270	1.48	350	0.025
275	1.21	355	0.019
280	0.93	360	0.014

Note:
205–305 nm: Bauerle and Moortgat[1]
310–380 nm: average of data from Bauerle and Moortgat[1] and Roehl et al.[3]

(1) Bauerle, S.; Moortgat, G. K. Absorption cross-sections of $HOCH_2OOH$ vapor between 205 and 360 nm at 298 K. *Chem. Phys. Lett.* **1999**, *309*, 43-48, doi:10.1016/S0009-2614(99)00652-1.

(2) Fry, J.; Matthews, L. J.; Lane, J. R.; Sinha, A.; Kjaergaard, H. G.; Wennberg, P. O. OH-Stretch vibrational spectroscopy of hydroxymethyl hydroperoxide. *J. Phys. Chem. A* **2006**, *110*, 7072-7079, doi:10.1021/jp0612127.

(3) Roehl, C. M.; Marka, Z.; Fry, J. L.; Wennberg, P. O. Near-UV photolysis cross sections of CH_3OOH and $HOCH_2OOH$ determined via action spectroscopy. *Atmos. Chem. Phys.* **2007**, *7*, 713-720, doi:10.5194/acp-7-713-2007.

D11. CH_3CO (acetyl radical)

Back to Index

$CH_3CO + h\nu \rightarrow$ Products (1)

(Recommendation: 10-6, Note: 10-6, Evaluated: 10-6)

Absorption Cross Sections. The UV absorption spectrum of the acetyl radical, CH_3CO, has been measured by Adachi et al.,[1,2] Parkes,[7] Anastasi and Maw,[3] Basco and Parmar,[4] Maricq and Szente,[6] and Cameron et al.[5] The spectrum has a very broad band in the range 190–270 nm with maximum near 215 nm. The shapes and magnitudes of the reported spectra differ substantially in the different studies. Adachi et al.[1,2] and Basco and Parmar[4] report a peak cross section of 3.75×10^{-17} cm^2 molecule^{-1} whereas Maricq and Szente[6] report a value of 1.07×10^{-17} cm^2 molecule^{-1} at 216 nm and Ansatasi and Maw[3] a value of 0.7×10^{-17} cm^2 molecule^{-1} at 223 nm. Cameron et al.[5] measured a cross section of $(1.4 \pm 0.2) \times 10^{-17}$ cm^2 molecule^{-1} at 220 nm. Cameron et al.[5] also measured the spectrum using diode array spectroscopy in the range 190–247 nm; the shape of the spectrum being in reasonable agreement with the spectrum measured by Maricq and Szente.[6] The spectrum by Cameron et al.[5] is given by the equation:

$$\sigma = \sigma_{max} \exp^{-a\left[\ln\left(\frac{\lambda_{max}}{\lambda}\right)\right]^2}$$

where

$\sigma_{max} = 1.549 \times 10^{-17}$ $\quad$ $a = 129.19$ $\quad$ $\lambda_{max} = 213.985$

The visible absorption spectrum of CH_3CO was measured by Rajakumar et al.[8] in the wavelength range 490–660 nm using cavity ring-down spectroscopy. The spectrum has a broad continuous band with a broad peak at 535 nm. The spectrum obtained with the H_2O_2 photolysis source (in the presence of CH_3CHO) was used as a reference and fit with an empirical polynomial expression:

$$\sigma(\lambda) = A + B\lambda + C\lambda^2 + D\lambda^3 + E\lambda^4$$

yielding the parameters (σ in units of cm^2 molecule^{-1}, λ in nm)

$A = -6.6124 \times 10^{-17}$ $\quad$ $D = 1.02141 \times 10^{-24}$
$B = 4.1946 \times 10^{-19}$ $\quad$ $E = -3.93411 \times 10^{-28}$
$C = -9.865 \times 10^{-22}$

The recommended UV absorption cross sections in Table 4D-11-1 were calculated using the equation from Cameron et al.[5] The recommended cross sections in the visible region in Table 4D-11-2 were calculated using the polynomial expression from Rajakumar et al.[8]

Table 4D-11-1. Recommended UV Absorption Cross Sections of CH_3CO at 298 K

λ (nm)	$10^{20}\,\sigma$ (cm^2)	λ (nm)	$10^{20}\,\sigma$ (cm^2)	λ (nm)	$10^{20}\,\sigma$ (cm^2)
190	250	210	1480	230	790
192	339	212	1530	232	666
194	447	214	1550	234	551
196	572	216	1530	236	449
198	711	218	1480	238	359
200	859	220	1400	240	283
202	1010	222	1300	242	219
204	1150	224	1180	244	167
206	1290	226	1050	246	126
208	1400	228	921	248	93.1

Note:
using expression from Cameron et al.[5]

Table 4D-11-2. Vis Absorption Cross Sections of CH_3CO at 298 K

λ (nm)	10^{20} σ (cm^2)	λ (nm)	10^{20} σ (cm^2)	λ (nm)	10^{20} σ (cm^2)
500	7.41	555	10.22	610	4.65
505	8.36	560	9.87	615	4.05
510	9.31	565	9.38	620	3.57
515	9.96	570	8.96	625	3.11
520	10.45	575	8.44	630	2.96
525	10.78	580	7.90	635	2.30
530	10.97	585	7.34	640	1.95
535	11.03	590	6.78	645	1.64
540	10.97	595	6.21	650	1.36
545	10.82	600	5.65	655	1.11
550	10.58	605	5.10	660	0.94

Note:
using expression from Rajakumar et al.[8]

(1) Adachi, H.; Basco, N.; James, D. G. L. The acetyl radical studied by flash photolysis and kinetic spectroscopy. *Chem. Phys. Lett.* **1978**, *59*, 502-505, doi:10.1016/0009-2614(78)85028-3.

(2) Adachi, H.; Basco, N.; James, D. G. L. The acetyl radicals CH_3CO and CD_3CO studied by flash photolysis and kinetic spectroscopy. *Int. J. Chem. Kinet.* **1981**, *13*, 1251-1276, doi:10.1002/kin.550131206.

(3) Anastasi, C.; Maw, P. R. Reaction kinetics in acetyl chemistry over a wide range of temperature and pressure. *J. Chem. Soc. Faraday Trans. 1* **1982**, *78*, 2423-2433, doi:10.1039/f19827802423.

(4) Basco, N.; Parmar, S. S. Spectra and reactions of acetyl and acetylperoxy radicals. *Int. J. Chem. Kinet.* **1985**, *17*, 891-900, doi:10.1002/kin.550170809.

(5) Cameron, M.; Sivakumaran, V.; Dillon, T. J.; Crowley, J. N. Reaction between OH and CH_3CHO. Part 1. Primary product yields of CH_3 (296 K), CH_3CO (296 K), and H (237-296 K). *Phys. Chem. Chem. Phys.* **2002**, *4*, 3628-3638, doi:10.1039/b202586h.

(6) Maricq, M. M.; Szente, J. J. The UV spectrum of acetyl and the kinetics of the chain reaction between acetaldehyde and chlorine. *Chem. Phys. Lett.* **1996**, *253*, 333-339, doi:10.1016/0009-2614(96)00155-8.

(7) Parkes, D. A. The ultraviolet absorption spectra of the acetyl radical and the kinetics of the CH_3 + CO reaction at room temperature. *Chem. Phys. Lett.* **1981**, *77*, 527-532, doi:10.1016/0009-2614(81)85201-3.

(8) Rajakumar, B.; Flad, J. E.; Gierczak, T.; Ravishankara, A. R.; Burkholder, J. B. Visible absorption spectrum of the CH_3CO radical. *J. Phys. Chem. A* **2007**, *111*, 8950-8958, doi:10.1021/jp073339h.

D12. $CH_3C(O)O_2$ (acetylperoxy radical)

Back to Index

$CH_3C(O)O_2 + h\nu \rightarrow$ Products (1)

(Recommendation: 06-2, Note: 10-6, Evaluated: 10-6)

Absorption Cross Sections: The UV absorption spectrum of the acetylperoxy radical, $CH_3C(O)O_2$, is continuous with two absorption bands in the 185–300 nm region. The band centered at 245 nm is overlapped by a stronger band that peaks near 207 nm. Absorption cross sections have been measured at room temperature by Addison et al.,[1] Basco and Parmer,[2] Moortgat et al.,[5] Maricq and Szente,[4] and Roehl et al.[6] The absorption cross sections have been evaluated in reviews by Lightfoot et al.,[3] Wallington et al.,[8] and Tyndall et al.[7] and significant discrepancies in the both the shapes of the spectra and the absolute magnitude of the cross section values have been noted. Tyndall et al.[7] fit the absorption spectrum reasonably well to the sum of two Gaussian shaped absorption bands:

$$\sigma = \sigma_{max1} \exp^{-a_1\left[\ln\left(\frac{\lambda_{max1}}{\lambda}\right)\right]^2} + \sigma_{max2} \exp^{-a_2\left[\ln\left(\frac{\lambda_{max2}}{\lambda}\right)\right]^2}$$

The optimized fit parameters were determined by averaging the fit parameters from Maricq and Szente[4] and Roehl et al.,[6] which were judged to be the most reliable. It should be noted that the data from Maricq and Szente were adjusted for their overcorrection for the contribution of CH_3O_2. Absolute cross sections were based on relative measurements to the absorption cross sections of $C_2H_5O_2$ at 240 nm. The fitting parameters are:

$\sigma_{max1} = 6.29 \times 10^{-18}$ cm^2 molecule^{-1} $\sigma_{max2} = 3.26 \times 10^{-18}$ cm^2 molecule^{-1}
$\lambda_{max1} = 206.0$ nm $\lambda_{max2} = 246.1$ nm
$a_1 = 168.0$ $a_2 = 64.2$.

The recommended absorption cross sections in Table 4D-5 are taken from the review by Tyndall et al.[7]

Photolysis Quantum Yield and Product Studies: The loss of $CH_3C(O)O_2$ in the stratosphere and troposphere due to photolysis is expected to be negligible.

(1) Addison, M. C.; Burrows, J. P.; Cox, R. A.; Patrick, R. Absorption spectrum and kinetics of the acetylperoxy radical. *Chem. Phys. Lett.* **1980**, *73*, 283-287, doi:10.1016/0009-2614(80)80373-3.
(2) Basco, N.; Parmar, S. S. Spectra and reactions of acetyl and acetylperoxy radicals. *Int. J. Chem. Kinet.* **1985**, *17*, 891-900, doi:10.1002/kin.550170809.
(3) Lightfoot, P. D.; Cox, R. A.; Crowley, J. N.; Destriau, M.; Hayman, G. D.; Jenkin, M. E.; Moortgat, G. K.; Zabel, F. Organic peroxy radicals: Kinetics, spectroscopy and tropospheric chemistry. *Atmos. Environ.* **1992**, *26A*, 1805-1961, doi:10.1016/0960-1686(92)90423-I.
(4) Maricq, M. M.; Szente, J. J. The $CH_3C(O)O_2$ radical. Its UV spectrum, self-reaction kinetics, and reaction with CH_3O_2. *J. Phys. Chem.* **1996**, *100*, 4507-4513, doi:10.1021/jp9533234.
(5) Moortgat, G.; Veyret, B.; Lesclaux, R. Absorption spectrum and kinetics of reactions of the acetylperoxy radical. *J. Phys. Chem.* **1989**, *93*, 2362-2368, doi:10.1021/j100343a032.
(6) Roehl, C. M.; Bauer, D.; Moortgat, G. K. Absorption spectrum and kinetics of the acetylperoxy radical. *J. Phys. Chem.* **1996**, *100*, 4038-4047, doi:10.1021/jp9526298.
(7) Tyndall, G. S.; Cox, R. A.; Granier, C.; Lesclaux, R.; Moortgat, G. K.; Pilling, M. J.; Ravishankara, A. R.; Wallington, T. J. Atmospheric chemistry of small organic peroxy radicals. *J. Geophys. Res.* **2001**, *106*, 12157-12182, doi:10.1029/2000JD900746.
(8) Wallington, T. J.; Dagaut, P.; Kurylo, M. J. Ultraviolet absorption cross sections and reaction kinetics and mechanisms for peroxy radicals in the gas phase. *Chem. Rev.* **1992**, *92*, 667-710, doi:10.1021/cr00012a008.

D13. CH_3CHO (acetaldehyde)

Back to Index

$CH_3CHO + h\nu$	$\rightarrow CH_3 + HCO$	357 kJ mol^{-1}	335 nm	(1)
	$\rightarrow CH_4 + CO$	–19 kJ mol^{-1}	All	(2)
	$\rightarrow CH_3CO + H$	374 kJ mol^{-1}	320 nm	(3)

(Recommendation: 06-2, Note: 10-6, Evaluated: 10-6)

Absorption Cross Sections: The UV absorption spectrum of acetaldehyde, CH_3CHO, has been measured at room temperature by McMillan[4] (200–345 nm), Meyrahn et al.[14] (221–345 nm), Schneider and Moortgat[15] (197–362 nm), Libuda et al.[8,9] (235–360 nm), Martinez et al.[12] (202–365 nm), Limão-Vieira et al.[10] (240–350 nm), and Weaver et al.[16] (290–355 nm). The spectrum at wavelengths >200 nm consists of an absorption band with a peak at 290 nm and diffuse vibrational structure (~12 maxima or shoulders) at wavelengths >260 nm. The agreement between the various cross section studies is very good, mostly 5% or better, except for the results from Meyrahn et al.,[14] which are lower by ~10% in the structured region around the absorption maximum. The recommended cross sections in Table 4D-13-1 are based on the data of Libuda et al.[8,9] (1 nm averages of 0.6 nm resolution data) and Martinez et al.[12] (4 nm averages of 0.5 nm resolution data at 202–278 nm and 1 nm averages at 280–360 nm), for which the agreement is within 5% between 255 and 325 nm.

Spectrum measurements in the VUV have been reported by Lake and Harrison[7] (150–180 nm), Lucazeau and Sandorfy[11] (118–189 nm), Brint et al.[2] (120–180 nm), and Limão-Vieira et al.[10] (113–200 nm).

Photolysis Quantum Yield and Product Studies: The photodissociation quantum yield of CH_3CHO and the product quantum yields are wavelength and pressure dependent. Quantum yield measurements have been reported by Calvert and Pitts[4] and Weaver et al.[16] at isolated wavelengths between 290 and 332 nm. Quantum yields of CO, CH_4 and CO_2 were determined in the photolysis of trace concentrations of CH_3CHO in air and N_2 in the spectral range 250–330 nm at 1 atmospheric pressure by Meyrahn et al.,[14] which allowed the determination of $(\Phi_1 + \Phi_2)$, Φ_2, and Φ_3. The product quantum yield pressure dependence was also investigated by Meyrahn[13] at 270, 303.4 and 313 nm. Horowitz et al.[6] and Horowitz and Calvert[5] measured the quantum yields of CO, CH_4 and H_2 formation at 290, 300, 313, 320 and 332 nm in the presence of various pressures of O_2 and CO_2 from which Φ_1 and Φ_2 were derived. There is evidence from the studies of Meyrahn et al.[13,14] and Horowitz et al.[6] that some CO_2 is formed from secondary reactions of the CH_3CO radical that is produced in channel (3). The quantum yield for channel 3 was estimated to be 0.025 at 300 nm and to decrease to zero at

320 nm. Both Meyrahn et al.[13,14] and Horowitz et al.[5,6] observed a pressure dependence of the product yields, from which Stern-Volmer quenching coefficients were derived. These data were summarized by Calvert et al.[3]

The quantum yield recommendation given in Table 4D-13-2 for room temperature and atmospheric pressure are based on the evaluation by Atkinson and Lloyd[1] and the measurements by Horowitz and Calvert,[5] Meyrahn et al.,[14] and Meyrahn.[13]

Table 4D-13-1. Recommended Absorption Cross Sections of CH_3CHO at 298 K

λ (nm)	10^{20} σ (cm^2)	λ (nm)	10^{20} σ (cm^2)	λ (nm)	10^{20} σ (cm^2)	λ (nm)	10^{20} σ (cm^2)
202	0.056	286	4.41	312	2.52	338	0.212
206	0.053	287	4.56	313	2.47	339	0.206
210	0.049	288	4.69	314	2.38	340	0.135
214	0.048	289	4.74	315	2.20	341	0.0664
218	0.052	290	4.86	316	2.07	342	0.0416
222	0.065	291	4.75	317	2.08	343	0.0305
226	0.096	292	4.66	318	1.98	344	0.0267
230	0.151	293	4.51	319	1.84	345	0.0210
234	0.241	294	4.31	320	1.70	346	0.0199
238	0.375	295	4.26	321	1.48	347	0.0149
242	0.639	296	4.24	322	1.38	348	0.0159
246	0.887	297	4.37	323	1.23	349	0.0978
250	1.18	298	4.41	324	1.06	350	0.00774
254	1.57	299	4.26	325	1.15	351	0.00695
258	2.03	300	4.15	326	1.09	352	0.00497
262	2.45	301	3.97	327	0.808	353	0.00552
266	3.06	302	3.87	328	0.715	354	0.00436
270	3.38	303	3.70	329	0.741	355	0.00500
274	4.03	304	3.46	330	0.699	356	0.00518
278	4.15	305	3.43	331	0.560	357	0.00345
280	4.48	306	3.41	332	0.496	358	0.00428
281	4.65	307	3.36	333	0.420	359	0.00207
282	4.66	308	3.31	334	0.333	360	0.00275
283	4.70	309	3.11	335	0.350		
284	4.58	310	2.92	336	0.227		
285	4.46	311	2.73	337	0.219		

Note:
202–238 nm: Martinez et al.[12]
240–360 nm: mean of data from Martinez et al.[12] and Libuda et al.[8,9]

Table 4D-13-2. Recommended CH_3CHO Photolysis Quantum Yields at 1 bar Total Pressure

λ (nm)	Φ_1 ($CH_3 + HCO$)	Φ_2 $CH_4 + CO$	λ (nm)	Φ_1 ($CH_3 + HCO$)
256	0.29	0.48	296	0.47
258	0.30	0.47	298	0.45
260	0.31	0.45	300	0.43
262	0.32	0.43	302	0.40
264	0.34	0.40	304	0.38
266	0.36	0.37	306	0.35
268	0.38	0.33	308	0.31
270	0.41	0.29	310	0.28
272	0.44	0.25	312	0.24
274	0.48	0.20	314	0.19
276	0.53	0.14	316	0.15
278	0.56	0.09	318	0.12
280	0.58	0.06	320	0.10
282	0.59	0.04	322	0.07
284	0.59	0.03	324	0.05
286	0.58	0.02	326	0.03
288	0.56	0.01	328	0.02
290	0.54	0.01	330	0.01
292	0.52	0.005	332	0
294	0.50	0		

(1) Atkinson, R.; Lloyd, A. C. Evaluation of kinetic and mechanistic data for modeling photochemical smog. *J. Phys. Chem. Ref. Data* **1984**, *13*, 315-444, doi:10.1063/1.555710.

(2) Brint, P.; O'Toole, L.; Mayhew, C. A.; Dussa, W. Vacuum-ultraviolet absorption spectrum of acetaldehyde, CH_3CHO, and the related deuterides CH_3CDO and CD_3CDO. *J. Chem. Soc. Faraday Trans.* **1990**, *86*, 3349-3354, doi:10.1039/FT9908603349.

(3) Calvert, J. G.; Atkinson, R.; Kerr, J. A.; Madronich, S.; Moortgat, G. K.; Wallington, T. J.; Yarwood, G. *The Mechanisms of Atmospheric Oxidation of the Alkenes*; Oxford University Press: New York - Oxford, 2000.

(4) Calvert, J. G.; Pitts Jr., J. N. In *Photochemistry*; John Wiley & Sons, Inc.: New York, 1966; pp 368.

(5) Horowitz, A.; Calvert, J. G. Wavelength dependence of the primary processes in acetaldehyde photolysis. *J. Phys. Chem.* **1982**, *86*, 3105-3114, doi:10.1021/j100213a011.

(6) Horowitz, A.; Kershner, C. J.; Calvert, J. G. Primary processes in the photolysis of acetaldehyde at 3000 Å and 25 °C. *J. Phys. Chem.* **1982**, *86*, 3094-3104, doi:10.1021/j100213a010.

(7) Lake, J. S.; Harrison, A. J. Absorption of acyclic oxygen compounds in the vacuum ultraviolet. III. Acetone and acetaldehyde. *J. Chem. Phys.* **1959**, *30*, 361-362, doi:10.1063/1.1729955.

(8) Libuda, H. G. Spektroskopische und kinetische Untersuchungen an halogenierten Carbonylverbindungen von atmosphärischem Interesse. PhD-Thesis, University of Wuppertal, Germany, 1992.

(9) Libuda, H. G.; Zabel, F.; Becker, K. H. "UV spectra of some organic chlorine and bromine compounds of atmospheric interest"; Kinetics and Mechanisms for the Reactions of Halogenated Organic Compounds in the Troposphere. STEP-HALOCSIDE/AFEAS WORKSHOP, 1991, Dublin, Ireland.

(10) Limão-Vieira, P.; Eden, S.; Mason, N. J.; Hoffmann, S. V. Electronic state spectroscopy of acetaldehyde, CH_3CHO, by high-resolution VUV photoabsorption. *Chem. Phys. Lett.* **2003**, *376*, 737-747, doi:10.1016/S0009-2614(03)01070-4.

(11) Lucazeau, G.; Sandorfy, C. On the far-ultraviolet spectra of some simple aldehydes. *J. Mol. Spectrosc.* **1970**, *35*, 214-231, doi:10.1016/0022-2852(70)90199-2.

(12) Martinez, R. D.; Buitrago, A. A.; Howell, N. W.; Hearn, C. H.; Joens, J. A. The near UV absorption spectra of several aliphatic aldehydes and ketones. *Atmos. Environ.* **1992**, *26A*, 785-792, doi:10.1016/0960-1686(92)90238-G.

(13) Meyrahn, H. Bildungswege und Analytik des Peroxyacetylnitrats (PAN) in der Atmosphäre. PhD-Thesis, Johann-Gutenberg-Universität, 1984.

(14) Meyrahn, H.; Moortgat, G. K.; Warneck, P. Photolysis of CH_3CHO in the range 250 - 330 nm. *J. Photochem.* **1981**, *17*, 138, doi:10.1016/0047-2670(81)85266-5.

(15) Röth, E. P.; Ruhnke, R.; Moortgat, G.; Meller, R.; Schneider, W. UV/VIS-Absorption Cross Sections and Quantum Yields for Use in Photochemistry and Atmospheric Modeling, Forschungszentrum Jülich Publication, Part 1 : Inorganic Substances (jül-3340), Part 2: Organic Substances (jül-3341). **1997**.
(16) Weaver, J.; Meagher, J.; Heicklen, J. Photo-oxidation of CH_3CHO vapor at 3130 Å. *J. Photochem.* **1976**, *6*, 111-126, doi:10.1016/0047-2670(76)85054-X.

D14. CH_3CHOO (acetaldehyde oxide)

Back to Index

$CH_3CHOO + h\nu \rightarrow$ Products (1)

(Recommendation: 19-5; Note: 19-5; Evaluated: 19-5)

Absorption Cross Sections: UV absorption cross sections of the Criegee intermediate CH_3CHOO (acetaldehyde oxide) have been reported at room temperature by Beames et al.[1] (280–372 nm), Smith et al.[3] (280.2–440.6 nm), and Sheps et al.[2] (300–450 nm). The cross section values of Smith et al. and Beames et al. are in substantial disagreement, with the cross sections of Smith et al. lower by up to a factor of ~4.5. In addition, the spectral shape of these two studies are also significantly different. Smith et al. used SO_2 scavenging and self-reaction of CH_3CHOO to measure the shape of the absorption spectrum and assigned absolute cross sections at 308.4 and 351.8 nm based on molecular beam laser-depletion measurements. Beames et al. also used laser depletion in a molecular beam to determine absolute cross sections, but experimental factors, such as inhomogeneity of the laser beam and laser-molecular beam overlap, led to larger uncertainties (estimated by Beames et al. to be on the order of a factor of 2).

Sheps et al. presented UV absorption spectra for both conformers of acetaldehyde oxide, *syn*- and *anti*-CH_3CHOO, by separating them based on their decay times in the presence of H_2O. The UV spectrum of *syn*-CH_3CHOO is centered at 323 nm with FWHM of ~40 nm, and *anti*-CH_3CHOO is centered at ~360 nm with FWHM ~55 nm. The *syn*-CH_3CHOO conformer is more stable and thus more populated, reported to be 70% relative to 30% for the *anti*-CH_3CHOO.

Sheps et al. did not measure absolute cross sections, rather they scaled their measured spectrum of *syn*-CH_3CHOO to the cross section value of Smith et al. at 308.4 nm (a wavelength where absorption by the *syn*-conformer dominates). Sheps et al. found that their spectral shape was less intense on the low-energy side relative to the spectrum of Smith et al. However, summing the absorptions attributed to both *syn*- and *anti*-conformers in the Sheps et al. study led to good overall agreement with Smith et al., suggesting that the spectrum of Smith et al. contains unresolved contributions from both conformers. Sheps et al. estimated that the peak cross section for *anti*-CH_3CHOO is similar to the *syn*-conformer, but it should be noted that Sheps et al. considered their derivation of the cross sections for *anti*-CH_3CHOO to be a qualitative guide with large uncertainties. Theoretical UV spectra calculated by Sršeň et al.[4]show the *anti*-conformer to have a peak cross section slightly greater than *syn*-CH_3CHOO. Relative to the experimental spectra of Sheps et al., the calculated spectra of Sršeň et al. are shifted slightly to shorter wavelengths for the *anti*-conformer but are in good agreement for the *syn*-conformer.

The recommended cross sections given in Table 4D-14 are from Smith et al. and represent 5 nm averages of their data (reported every ~0.6 nm) between 285–435 nm. Estimated uncertainty factors (2σ) are recommended to be 1.2 below 390 nm and increase linearly to 1.4 at 435 nm.

Photolysis Quantum Yield and Product Studies: No recommendation.

Table 4D-14. Recommended Absorption Cross Sections of CH_3CHOO (acetaldehdye oxide) at 295 K

λ (nm)	10^{20} σ (cm^2)	λ (nm)	10^{20} σ (cm^2)	λ (nm)	10^{20} σ (cm^2)
285	494	340	1200	395	202
290	630	345	1080	400	171
295	762	350	1000	405	141
300	872	355	854	410	109
305	977	360	748	415	73.1
310	1080	365	648	420	70.2
315	1150	370	519	425	61.7
320	1220	375	447	430	48.1
325	1270	380	368	435	26.1
330	1270	385	299		
335	1250	390	251		

Note:
5 nm averages of Smith et al.[3]

(1) Beames, J. M.; Liu, F.; Lu, L.; Lester, M. I. UV spectroscopic characterization of an alkyl substituted Criegee intermediate CH_3CHOO. *J. Chem. Phys.* **2013**, *138*, 244307, doi:10.1063/1.4810865.

(2) Sheps, L.; Scully, A. M.; Au, K. UV absorption probing of the conformer-dependent reactivity of a Criegee intermediate CH_3CHOO. *Phys. Chem. Chem. Phys.* **2014**, *16*, 26701-26706, doi:10.1039/c4cp04408h.

(3) Smith, M. C.; Ting, W.-L.; Chang, C.-H.; Takahashi, K.; Boering, K. A.; Lin, J. J.-M. UV absorption spectrum of the C2 Criegee intermediate CH_3CHOO. *J. Chem. Phys.* **2014**, *141*, 074302, doi:10.1063/1.4892582.

(4) Sršeň, S.; Hollas, D.; Slaviček, P. UV absorption of Criegee intermediates: quantitative cross sections from high-level *ab initio* theory. *Phys. Chem. Chem. Phys.* **2018**, *20*, 6421-6430, doi:10.1039/c8cp00199e.

D15. $C_2H_5O_2$ (ethylperoxy radical)

Back to Index

$C_2H_5O_2 + h\nu \rightarrow$ Products (1)

(Recommendation: 06-2, Note: 10-6, Evaluated: 10-6)

Absorption Cross Sections: The absorption cross sections of the ethylperoxy radical, $C_2H_5O_2$, in the 200–310 nm region have been measured at room temperature by Adachi et al.,[1] Cattell et al.,[4] Wallington et al.,[14] Bauer et al.,[3] Maricq and Wallington,[9] Fenter et al.,[6] Munk et al.,[10] and Nielsen et al.[11] and as a function of temperature by Anastasi et al.,[2] Fenter et al.,[6] and Fauvet et al.[5] The absorption cross sections have been evaluated in reviews by Lightfoot et al.[7] and Wallington et al.,[15] who noted significant discrepancies in the both the shapes of the spectra and the absolute magnitude of the cross section values. The ultraviolet absorption spectra have recently been reevaluated by Tyndall et al.,[13] who fit the absorption spectra to a semi-logarithmic Gaussian distribution function suggested by Lightfoot et al.[7] and Maric et al.:[8]

$$\sigma = \sigma_{max} \exp^{-a\left[\ln\left(\frac{\lambda_{max}}{\lambda}\right)\right]^2}$$

The shape was determined by averaging the individual fitting parameters from Wallington et al.,[15] Bauer et al.,[3] Maricq and Wallington,[9] and Fenter et al.,[6] which were judged to be most reliable by Tyndall et al.[13] Absolute cross sections were based on relative measurements of absorption cross sections of CH_3O_2 and $C_2H_5O_2$ at 240 nm taken under identical conditions (Wallington et al.,[15] Maricq and Wallington,[9] Fenter et al.,[6] Roehl et al.[12]) and Nielsen et al.[11] combined with independent calibrations. The fitting parameters are $\sigma_{max} = 4.52 \times 10^{-18}$ cm^2 $molecule^{-1}$, a = 49.0, λ_{max} = 239.4 nm. Table 4D-5 lists the recommended cross sections, which are taken from the review by Tyndall et al.

Photolysis Quantum Yield and Product Studies: No recommendation. The loss of $C_2H_5O_2$ due to photolysis in the stratosphere and troposphere is expected to be negligible.

(1) Adachi, H.; Basco, N.; James, D. G. L. The ethylperoxy radical spectrum and rate constant for mutual interaction measured by flash photolysis and kinetic spectroscopy. *Int. J. Chem. Kinet.* **1979**, *11*, 1211-1229, doi:10.1002/kin.550111107.
(2) Anastasi, C.; Waddington, D. J.; Woolley, A. Reactions of oxygenated radicals in the gas phase Part 10.-Self-reactions of ethylperoxy radicals. *J. Chem. Soc. Faraday Trans. 1* **1983**, *79*, 505-516, doi:10.1039/f19837900505.
(3) Bauer, D.; Crowley, J. N.; Moortgat, G. K. The UV spectrum of the ethylperoxy radical and its self-reaction kinetics between 218 and 333 K. *J. Photochem. Photobiol. A: Chem.* **1992**, *65*, 329-344, doi:10.1016/1010-6030(92)80015-N.
(4) Cattell, F. C.; Cavanagh, J.; Cox, R. A.; Jenkin, M. E. A kinetics study of reactions of HO_2 and $C_2H_5O_2$ using diode laser absorption spectroscopy. *J. Chem. Soc. Faraday Trans. 2* **1986**, *82*, 1999-2018, doi:10.1039/f29868201999.
(5) Fauvet, S.; Ganne, J. P.; Brion, J.; Daumont, D.; Malicet, J.; Chakir, A. Study of $C_2H_5O_2$ using modulated photolysis: Ultra-violet spectrum and self-reaction kinetics in the temperature range 233-363 K. *J. Chim. Phys.* **1997**, *94*, 484-502, doi:10.1051/jcp/1997940484.
(6) Fenter, F. F.; Catoire, V.; Lesclaux, R.; Lightfoot, P. D. The ethylperoxy radical: Its ultraviolet spectrum, self-reaction, and reaction with HO_2, each studied as a function of temperature. *J. Phys. Chem.* **1993**, *97*, 3530-3538, doi:10.1021/j100116a016.
(7) Lightfoot, P. D.; Cox, R. A.; Crowley, J. N.; Destriau, M.; Hayman, G. D.; Jenkin, M. E.; Moortgat, G. K.; Zabel, F. Organic peroxy radicals: Kinetics, spectroscopy and tropospheric chemistry. *Atmos. Environ.* **1992**, *26A*, 1805-1961, doi:10.1016/0960-1686(92)90423-I.
(8) Maric, D.; Crowley, J. N.; Burrows, J. P. Application of a Gaussian distribution function to describe molecular UV-visible absorption continua. 2. The UV spectra of RO_2• radicals. *J. Phys. Chem.* **1997**, *101*, 2561-2567, doi:10.1021/jp961715k.
(9) Maricq, M. M.; Wallington, T. J. Absolute ultraviolet cross sections of methyl and ethyl peroxy radicals. *J. Phys. Chem.* **1992**, *96*, 982-986, doi:10.1021/j100181a081.
(10) Munk, J.; Pagsberg, P.; Ratajczak, E.; Sillesen, A. Spectrokinetic studies of ethyl and ethylperoxy radicals. *J. Phys. Chem.* **1986**, *90*, 2752-2757, doi:10.1021/j100403a038.
(11) Nielsen, O. J.; Johnson, M. S.; Wallington, T. J.; Christensen, L. K.; Platz, J. UV absorption cross sections of HO_2, CH_3O_2, $C_2H_5O_2$ and $CH_3C(O)CH_2O_2$ radicals and mechanism of the reactions of F and Cl atoms with $CH_3C(O)CH_3$. *Int. J. Chem. Kinet.* **2002**, *34*, 283-291, doi:10.1002/kin.10037.
(12) Roehl, C. M.; Bauer, D.; Moortgat, G. K. Absorption spectrum and kinetics of the acetylperoxy radical. *J. Phys. Chem.* **1996**, *100*, 4038-4047, doi:10.1021/jp9526298.
(13) Tyndall, G. S.; Cox, R. A.; Granier, C.; Lesclaux, R.; Moortgat, G. K.; Pilling, M. J.; Ravishankara, A. R.; Wallington, T. J. Atmospheric chemistry of small organic peroxy radicals. *J. Geophys. Res.* **2001**, *106*, 12157-12182, doi:10.1029/2000JD900746.
(14) Wallington, T. J.; Dagaut, P.; Kurylo, M. J. Measurements of the gas phase UV absorption spectrum of $C_2H_5O_2$• radicals and of the temperature dependence of the rate constant for their self-reaction. *J. Photochem. Photobiol. A: Chem.* **1988**, *42*, 173-185, doi:10.1016/1010-6030(88)80061-3.
(15) Wallington, T. J.; Dagaut, P.; Kurylo, M. J. Ultraviolet absorption cross sections and reaction kinetics and mechanisms for peroxy radicals in the gas phase. *Chem. Rev.* **1992**, *92*, 667-710, doi:10.1021/cr00012a008.

D16. CH_3CH_2OH (ethanol, ethyl alcohol)

Back to Index

$CH_3CH_2OH + h\nu \rightarrow$ Products (1)

(Recommendation: 19-5, Note: 25-1, Evaluated: 25-1)

Absorption Cross Sections: UV absorption cross sections of CH_3CH_2OH (ethanol) have been measured at room temperature by Ogawa and Cook[5] (50.8–174.9 nm), Harrison et al.[4] (168 nm, 181 nm), Tsubomura et al.[9] (164.9–185.6 nm), Salahub and Sandorfy[7] (120.5–208.3 nm), Han et al.[3] (46–200 nm), Feng and Brion[2] (6.2–248.0 nm), Dillon et al.[1] (184.9 nm), and Orkin et al.[6] (161.7–216.0 nm). Three studies have continuous wavelength coverage from 165–200 nm: Salahub and Sandorfy, Han et al., and Orkin et al., which are all in good agreement near the peak cross section at 182 nm, but generally diverge toward shorter and longer wavelengths. Three studies report single wavelength cross section measurements near the 182 nm peak: Feng and Brion (177.12 nm), Harrison et al. (181 nm), and Dillon et al. (184.9 nm), which all agree to within 10% with the three studies that have continuous coverage. The measurements of Tsubomura et al. and Ogawa and Cook disagree significantly with the other studies at wavelengths >165 nm.

The recommended cross sections given in Table 4D-16 for 165–216 nm were taken from Orkin et al. at 1 nm intervals (higher resolution data are available in Orkin et al.) after rounding to 3 significant figures. For the range 220–230 nm, the recommended values were obtained from a log-linear fit (206–216 nm) and extrapolation of the Orkin et al. data, $\log \sigma(\lambda) = 11.1187 - 0.15069\ \lambda$. Estimated uncertainty factors (2σ) of $F(\lambda) = 1.1 + 6 \times 10^{-23}/\sigma(\lambda)$ are recommended for the 165–216 nm wavelength range.

VUV absorption spectra of CH_3CH_2OH in the Lyman-α (121.567 nm) wavelength region have been reported by Ogawa and Cook,[5] Salahub and Sandorfy,[7] Han et al.,[3] Feng et al.,[2] and Souza Barbosa et al.[8] The agreement among these studies at Lyman-α is reasonably good, although the Ogawa and Cook cross sections are systematically high. The recommended Lyman-α (121.567 nm) cross section is an average of the data of Salahub and Sandorfy and Han et al. with an estimated uncertainty factor (2σ) of 1.2.

Photolysis Quantum Yield and Product Studies: No recommendation.

Table 4D-16. Recommended Absorption Cross Sections of CH_3CH_2OH (ethanol) at 295 K

λ (nm)	10^{20} σ (cm^2)	λ (nm)	10^{20} σ (cm^2)	λ (nm)	10^{20} σ (cm^2)
121.567	2390	183	115	202	4.65
165	80.9	184	114	203	3.35
166	61.9	185	110	204	2.37
167	55.3	186	105	205	1.66
168	53.8	187	99.0	206	1.19
169	55.5	188	91.5	207	0.855
170	59.8	189	83.3	208	0.599
171	65.1	190	74.0	209	0.414
172	71.3	191	64.7	210	0.294
173	77.2	192	55.9	211	0.211
174	83.5	193	47.4	212	0.149
175	90.2	194	39.3	213	0.106
176	96.0	195	31.9	214	0.0742
177	101	196	25.6	215	0.0517
178	106	197	20.0	216	0.0376
179	110	198	15.4	220	*0.00927*
180	113	199	11.7	225	*0.00163*
181	116	200	8.72	230	*0.000288*
182	116	201	6.37		

Note:
121.567 nm: average of Salahub and Sandorfy[7] and Han et al.[3]
165–216 nm: Orkin et al.[6] data at 1 nm intervals
220–230 nm: extrapolation of Orkin et al.[6] data, $\log \sigma(\lambda) = 11.1187 - 0.15069\ \lambda$

(1) Dillon, T. J.; Hölscher, D.; Sivakumaran, V.; Horowitz, A.; Crowley, J. N. Kinetics of the reactions of HO with methanol (210–351 K) and with ethanol (216–368 K). *Phys. Chem. Chem. Phys.* **2005**, *7*, 349-355, doi:10.1039/b413961e.

(2) Feng, R.; Brion, C. E. Absolute photoabsorption cross-sections (oscillator strengths) for ethanol (5–200 eV). *Chem. Phys.* **2002**, *282*, 419-427, doi:10.1016/S0301-0104(02)00722-X.

(3) Han, J. C.; Suto, M.; Lee, L. C. Fluorescence from photoexcitation of C_2H_5OH by vacuum ultraviolet radiation. *J. Quant. Spectrosc. Radiat. Transf.* **1989**, *42*, 557-562, doi:10.1016/0022-4073(89)90046-0.

(4) Harrison, A. J.; Cederholm, B. J.; Terwilliger, M. A. Absorption of acyclic oxygen compounds in the vacuum ultraviolet. I. Alcohols. *J. Chem. Phys.* **1959**, *30*, 355-356, doi:10.1063/1.1729952.

(5) Ogawa, M.; Cook, G. R. Absorption coefficients of methyl, ethyl, *n*-propyl, and *n*-butyl alcohols. *J. Chem. Phys.* **1958**, *28*, 747-748, doi:10.1063/1.1744253.

(6) Orkin, V. L.; Khamaganov, V. G.; Martynova, L. E.; Kurylo, M. J. High-accuracy measurements of $OH^{\bullet}$ reaction rate constants and IR and UV absorption spectra: Ethanol and partially fluorinated ethyl alcohols. *J. Phys. Chem. A* **2011**, *115*, 8656-8668, doi:10.1021/jp202099t.

(7) Salahub, D. R.; Sandorfy, C. The far-ultraviolet spectra of some simple alcohols and fluoroalcohols. *Chem. Phys. Lett.* **1971**, *8*, 71-74, doi:10.1016/0009-2614(71)80578-X.

(8) Souza Barbosa, A.; Mendes, M.; Jones, N. C.; Hoffmann, S. V.; Bettega, M. H. F.; Brunger, M. J.; Limão-Vieira, P. Low-lying electronic states of ethanol investigated by theoretical and synchrotron

radiation methods. *J. Quant. Spectrosc. Radiat. Transf.* **2022**, *285* 108170, doi:10.1016/j.jqsrt.2022.108170.

(9) Tsubomura, H.; Kimura, K.; Kaya, K.; Tanaka, J.; Nagakura, S. Vacuum ultraviolet absorption spectra of saturated organic compounds with non-bonding electrons. *Bull. Chem. Soc. Japan* **1964**, *37*, 417-423, doi:10.1246/bcsj.37.417.

D17. $HOCH_2CHO$ (glycolaldehyde, hydroxyacetaldehyde)

Back to Index

$HOCH_2CHO + h\nu$	$\rightarrow CH_2OH + HCO$	345 kJ mol^{-1}	347 nm	(1)
	$\rightarrow CH_3OH + CO$	6 kJ mol^{-1}	1910 nm	(2)
	$\rightarrow OH + CH_2CHO$	365 kJ mol^{-1}	328 nm	(3)
	$\rightarrow HOCH_2CO + H$	381 kJ mol^{-1}	314 nm	(4)

(Recommendation: 10-6, Note: 25-1, Evaluated: 25-1)

Absorption Cross Sections: The absorption cross sections of $HOCH_2CHO$ (glycolaldehyde, hydroxyacetaldehyde) have been measured at room temperature by Bacher et al.[1] (205–335 nm), Magneron et al.[3] (210–330 nm), Karunanandan et al.[2] (210–335 nm), and Zhu and Zhu[4] (280–340 nm). The spectrum consists of a strong absorption below 220 nm and a weaker absorption band centered near 280 nm with evidence of weak diffuse vibrational progressions. The measurements performed by Magneron et al.[3] were done at two different laboratories and are nearly identical, but reveal significant differences compared to the spectrum measured by Bacher et al.,[1] being about 20% at the maximum. The spectrum measured by Karunanandan et al.[2] is in excellent agreement with Magneron et al.[3] at the maximum near 282 nm and at longer wavelengths. At shorter wavelengths, the cross sections are consistently larger than those measured by Magneron et al.;[3] 15% at 250 nm, 40% at 230 nm and 85% at the minimum near 226 nm. At 184.9 nm, the cross section was measured by Karunanandan et al.[2] to be $(3.85 \pm 0.2) \times 10^{-18}$ cm^2 $molecule^{-1}$. The Zhu and Zhu[4] measurements were performed using cavity ring-down spectroscopy. Their results are consistent with previous studies between 280 and 325 nm, but show a systematic increase at longer wavelengths relative to the other measurements. The average of the cross sections of Magneron et al.[3] and Karunanandan et al.[2] are recommended and listed in Table 4D-17.

Photolysis Quantum Yields and Product Studies: The broad band photolysis (285 ± 25 nm) of glycolaldehyde in air performed by Bacher et al.[1] revealed an overall quantum yield $\Phi > 0.5$, relative to a quantum yield of $\Phi = 0.3$ for the removal of acetone. Product studies with FTIR detection suggests that channel (1) is the major photolysis channel (65–80%), while channel (2) accounts to 15–20%, and channel (3) contributes up to 15%. The formation of channel (4) was suggested to produce $HOCH_2CO$ as a source for OH radicals, whose presence was indirectly invoked due the formation of glyoxal. Magneron et al.[3] also photolysed glycolaldehyde (broadband lamps 275–380 nm) and measured products by FTIR (CO, CO_2, HCHO and CH_3OH). They observed direct evidence for OH production via channel (3) using an OH scavenger and OH tracer species. They performed additional photolysis experiments where glycolaldehyde was used as an OH source to measure rate constants for OH with a series of dienes. The contribution of channel (2) was estimated to be 10% and that of channels (1) + (2) to be 90%. No evidence was found for channel (4). Karunanandan et al.[2] measured a quantum yield of OH formation at 248 nm of $\Phi_3 = (7.0 \pm 1.5) \times 10^{-2}$. Zhu and Zhu used laser photolysis combined with cavity ring-down spectroscopy to measure HCO quantum yields of 0.61, 0.59, 0.61, 0.66, 0.61, 0.65, 0.47, 0.52, and 0.45 at 280, 285, 290, 295, 300, 305, 308, 310, and 315 nm, respectively. The estimated 1σ absolute error in the measurements were in the 35 to 50% range. They also report a OH quantum yield of 0.11 for 308 nm photolysis. On the basis of the combined product studies the following quantum yields are recommended: $\Phi_1 = 0.83$, $\Phi_2 = 0.10$ and $\Phi_3 = 0.07$ in the range 248–328 nm.

Table 4D-17. Recommended Absorption Cross Sections of $HOCH_2CHO$ at 298 K

λ (nm)	10^{20} σ (cm^2)	λ (nm)	10^{20} σ (cm^2)	λ (nm)	10^{20} σ (cm^2)	λ (nm)	10^{20} σ (cm^2)
208	20.6	240	1.39	272	6.74	304	2.65
210	13.1	242	1.63	274	6.98	306	2.26
212	8.15	244	1.77	276	6.98	308	1.88
214	4.93	246	2.25	278	6.93	310	1.57
216	2.94	248	2.57	280	6.91	312	1.28
218	1.72	250	2.94	282	6.92	314	0.94
220	1.00	252	3.37	284	6.60	316	0.70
222	0.64	254	3.76	286	6.38	318	0.53
224	0.45	256	4.15	288	6.09	320	0.40
226	0.39	258	4.61	290	5.88	322	0.31
228	0.42	260	5.03	292	5.43	324	0.21
230	0.53	262	5.33	294	4.87	326	0.14
232	0.63	264	5.68	296	4.50	328	0.10
234	0.79	266	6.10	298	4.10	330	0.07
236	0.97	268	6.35	300	3.74	332	0.04
238	1.15	270	6.49	302	3.19		

Note:
208–332 nm, average of Magneron et al.[3] and Karunanandan et al.[2]

(1) Bacher, C.; Tyndall, G. S.; Orlando, J. J. The atmospheric chemsitry of glycolaldehyde. *J. Atmos. Chem.* **2001**, *39*, 171-189, doi:10.1023/A:1010689706869.

(2) Karunanandan, R.; Hölscher, D.; Dillon, T. J.; Horowitz, A.; Crowley, J. N.; Vereecken, L.; Peeters, J. Reaction of HO with glycolaldehyde, $HOCH_2CHO$: Rate coefficients (240-362 K) and mechanism. *J. Phys. Chem. A* **2007**, *111*, 897-908, doi:10.1021/jp0649504.

(3) Magneron, I.; Mellouki, A.; Le Bras, G.; Moortgat, G. K.; Horowitz, A.; Wirtz, K. Photolysis and OH-initiated oxidation of glycolaldehyde under atmospheric conditions. *J. Phys. Chem. A* **2005**, *109*, 4552-4561, doi:10.1021/jp044346y.

(4) Zhu, C.; Zhu, L. Photolysis of glycolaldehyde in the 280-340nm region. *J. Phys. Chem. A* **2010**, *114*, 8384-8390, doi:10.1021/jp104497d.

D18. $HC(O)OCH_3$ (methyl formate)

Back to Index

$HC(O)OCH_3 + h\nu \rightarrow$ Products (1)

(Recommendation: 25-1, Note: 25-1, Evaluated: 25-1)

Absorption Cross Sections: The UV absorption spectrum of methyl formate, $HC(O)OCH_3$, has been measured at room temperature by Barnes and Simpson[1] (118–242 nm), McMillan[3] (201–260 nm), Suto et al.[7] (106–247 nm), Vésine and Mellouki[8] (211–260 nm), Benayadal and Leila[2] (211–252 nm), Rocha et al.[6] (200–238 nm), Nunes et al.[5] (115–315 nm), and by Doner et al.[4] (128–240 nm) at 323 K. The UV spectrum consists of a continuous absorption band with a maximum near 215 nm and weak diffuse structure. The Suto et al. and Doner et al. spectra are in poor agreement with the other studies and are not considered in the recommendation. For the other studies, the agreement is better than 10%. The recommended cross sections in Table 4D-18 are taken from Calvert[3] for the region 202–210 nm (read from a figure) and Vésine and Mellouki[8] for the region 211–260 nm. The Vésine and Mellouki[8] data given here are obtained from their high resolution (0.04 nm) spectrum over 1 and 2 nm intervals in the ranges 211–230 and 230–260 nm, respectively.

VUV absorption cross sections in the Lyman-α (121.567 nm) wavelength region have been reported by Barnes and Simpson,[1] Suto et al.,[7] and Nunes et al.[5] These studies are in good agreement and a Lyman-α cross section of 2.38×10^{-17} cm^2 $molecule^{-1}$ is recommended.

Photolysis Quantum Yield and Product Studies: No recommendation.

Table 4D-18. Recommended Absorption Cross Sections of $HC(O)OCH_3$ at 298 K

λ (nm)	10^{20} σ (cm^2)	λ (nm)	10^{20} σ (cm^2)	λ (nm)	10^{20} σ (cm^2)	λ (nm)	10^{20} σ (cm^2)
202	16.2	213	20.3	224	16.8	240	3.56
203	17.0	214	21.2	225	15.7	242	2.65
204	17.9	215	21.1	226	14.0	244	1.65
205	18.2	216	20.3	227	12.5	246	1.24
206	18.7	217	19.3	228	12.4	248	0.770
207	18.9	218	19.7	229	12.3	250	0.480
208	19.1	219	20.0	230	11.3	252	0.301
209	19.5	220	19.2	232	8.36	254	0.162
210	20.4	221	17.9	234	7.48	256	0.0717
211	20.4	222	16.7	236	6.11	258	0.0455
212	20.1	223	16.6	238	4.15	260	0.0281

Note:
202–210 nm: Calvert[3] (personal communication from McMillan)
211–260 nm: Vésine and Mellouki[8]

(1) Barnes, E. E.; Simpson, W. T. Correlations among electronic transitions for carbonyl and carboxyl in the vacuum ultraviolet. *J. Chem. Phys.* **1963**, *39*, 670-675, doi:10.1063/1.1734305.
(2) Benayada, B.; Leila, D. O. UV absorption cross sections for acetates. *Desalination* **1999**, *126*, 83-86, doi:10.1016/S0011-9164(99)00157-5.
(3) Calvert, J. G.; Pitts Jr., J. N. In *Photochemistry*; John Wiley & Sons, Inc.: New York, 1966; pp 368.
(4) Doner, A. C.; Moran, H. A.; Webb, A. R.; Christianson, M. G.; Koritzke, A. L.; Dewey, N. S.; Hartness, S. W.; Rotavera, B. Machine learning models for binary molecular classification using VUV absorption spectra. *J. Quant. Spectrosc. Radiat. Transf.* **2023**, *297*, 108438, doi:10.1016/j.jqsrt.2022.108438.
(5) Nunes, Y.; Martins, G.; Mason, N. J.; Duflot, D.; Hoffmann, S. V.; Delwiche, J.; Hubin-Franskin, M.-J.; Limão-Vieira, P. Electronic states spectroscopy of methyl formate probed by high resolution VUV photoabsorption, He(I) photoelectron spectroscopy and ab initio calculations. *Phys. Chem. Chem. Phys.* **2010**, *12*, 15734-15743, doi:10.1039/C0CP00051E.
(6) Rocha, A. B.; Pimentel, A. S.; Bielschowsky, C. E. Direct investigation of the validity of vertical approximation in the calculation of transition moment matrix elements: n → π* transition in methyl formate. *J. Phys. Chem. A* **2002**, *106*, 181-183, doi:10.1021/jp012647r.
(7) Suto, M.; Wang, X.; Lee, L. C. Fluorescence yields from photodissociative excitation of HCOOH, $HCOOCH_3$, and CH_3COOH in the vacuum-ultraviolet region. *J. Phys. Chem.* **1988**, *92*, 3764-3768, doi:10.1021/j100324a015.
(8) Vésine, E.; Mellouki, A. UV absorption cross sections for a series of formates. *J. Chim. Phys.* **1997**, *94*, 1634-1641, doi:10.1051/jcp/1997941634.

D19. CHOCHO (glyoxal)

Back to Index

$CHOCHO + h\nu \rightarrow HCO + HCO$	300 kJ mol^{-1}	399 nm	(1)
$\rightarrow H_2 + 2\ CO$	–8 kJ mol^{-1}	All	(2)
$\rightarrow HCHO + CO$	–7 kJ mol^{-1}	All	(3)
$\rightarrow H + CO + HCO$	364 kJ mol^{-1}	329 nm	(4)

(Recommendation: 10-6, Note: 10-6, Evaluated: 10-6)

Absorption Cross Sections: The UV/vis absorption spectrum of glyoxal, CHOCHO, has been measured in a number of studies. The spectrum has two absorption bands in the wavelength region >220 nm; a weak band with evidence of diffuse vibrational structure in the 220–350 nm region, and a stronger and highly structured band at wavelengths >360 nm with a maximum near 455 nm. The absorption cross sections, particularly in the visible absorption band, are resolution dependent and comparison of results from the various studies need to take this into consideration. The room temperature absorption spectrum of glyoxal has been reported by Plum et al.[11] (230–460 nm), Langford and Moore[6] (308 nm), Zhu et al.[15] (193, 248, 308, and 351 nm), Chen and Zhu[3] (290–420 nm, in 10 nm intervals), Orlando and Tyndall[9] (210–450 nm, 0.6 nm resolution), Horowitz et al.[5] (210–480 nm, 0.25 nm resolution), Zhu and Johnston[14] (436–442 nm), and Volkamer et al.[13] (250–526 nm).

Orlando and Tyndall[9] and Horowitz et al.[5] reported absorption spectra obtained using diode array spectroscopy and their spectra are in good agreement, i.e., to better than 10% between 240 and 440 nm. The absorption cross sections from Chen and Zhu[3] differ from these studies by 10 to 50% depending on the wavelength. However, the absorption cross sections reported by Zhu et al.[15] at 248, 308, and 351 nm agree very well with the data of Horowitz et al.[5] and Orlando and Tyndall.[9] A strong absorption feature at wavelengths <200 nm indicated by the 193 nm measurement of Zhu et al.[15] ($\sigma = 4.8 \times 10^{-19}$ cm^2 molecule^{-1}) was also reported by Orlando and Tyndall.[9] The cross section data from Plum et al.[11] are systematically less, by roughly 10 to 25%, than reported in the more recent studies with larger differences in the region of the absorption minimum near 350 nm and at the shorter wavelengths.

Volkamer et al.[13] reported the highest available resolution absorption spectra of glyoxal to date which were obtained using Fourier transform spectroscopy at 1 cm^{-1} (250–526 nm) and 0.06 cm^{-1} (368–526 nm) resolution. The high-resolution spectrum has more pronounced differential vibrational fine structure in the visible absorption band leading to higher absorption cross sections than reported in the lower resolution studies. The absorption cross sections reported by Volkamer et al.[13] are systematically 10% greater than reported by Horowitz et al.[5] and Orlando and Tyndall[9] (where comparison is possible). The differences in the absorption cross sections are most apparent in the short wavelength band. The UV spectrum reported by Volkamer et al.[13] is consistent with IR spectral parameters which were obtained by simultaneous recording of UV and IR spectra using the same glyoxal sample fillings of the absorption cell. Zhu and Johnston[14] report an absorption cross section at the absorption maximum near 440.7 nm (440.1 nm in the Volkamer et al. spectrum) of 4.6×10^{-19} cm^2 molecule^{-1} that was obtained at high resolution using cavity ring-down spectroscopy. Their cross section value is in poor agreement with the high resolution data of Volkamer et al.[13] which is a factor of two greater. The recommended room temperature absorption cross sections in Table 4D-19-1 are averages over 1 nm intervals of the high resolution spectrum from Volkamer et al.[13] and are appropriate for use in atmospheric photolysis rate calculations. Studies requiring higher resolution data should consult the original literature.

Photolysis Quantum Yield and Product Studies: The photodissociation of CHOCHO as well as the photolysis product channel yields are wavelength and pressure dependent. Calvert and Pitts[2] have summarized the CHOCHO quantum yield data prior to 1966. On the basis of the work by Calvert and Layne[1] and Parmenter[10] it was established that the HCHO + CO photolysis channel (3) was dominant with yields between 0.84 and 0.6 over the wavelength range 254 to 435 nm. There was little experimental evidence for the HCO + HCO radical channel (1) occurring and it was incorrectly concluded to be negligible. Plum et al.[11] has since reported the effective quantum yield for CHOCHO photolysis at wavelengths >290 nm to be 0.029, based on measured photolysis rates in an environmental chamber relative to NO_2 where J_{CHOCHO}/J_{NO2} was found to be 0.008 ± 0.005. An effective atmospheric photolysis rate was measured using solar radiation in the EUPHORE outdoor chamber to be $J_{obs} = 1.04 \pm 0.10 \times 10^{-4}$ s^{-1}, corresponding to an effective quantum yield for glyoxal loss of 0.035 ± 0.007 [7,8] in reasonable agreement with the value reported by Plum et al.[11]

Langford and Moore[6] measured HCO produced in the photolysis of glyoxal in 1000 Torr N_2 at 305 nm by direct HCO resonance absorption and deduced a total HCO yield of 0.8 ± 0.4 at 305 nm. Using cavity ring-down spectroscopy, Zhu et al.[15] reported HCO quantum yields of 1.5 ($\Phi_1 \approx 0.75$) for photolysis at 351 nm, 0.69 at 308 nm, 0.52 at 248 nm and 0.42 at 193 nm. In a later study Chen and Zhu[3] reported zero pressure HCO yields, $\Phi_0(\lambda)$, at 10 nm intervals, that increase from 0.50 ± 0.01 at 290 nm to a maximum of 2.01 ± 0.08 at 390 nm and that decrease to 0.74 ± 0.08 at 400 nm, 0.56 ± 0.04 at 410 nm, and 0.48 ± 0.03 at 420 nm. HCO quantum yields were found to be independent of the N_2 buffer gas pressure (10-400 Torr) for photolysis in the 290–370 nm region. In the wavelength region 380–420 nm the HCO quantum yield decreased with increasing pressure. They reported HCO quantum yields at 760 Torr N_2 to be 0.49 at 380 nm, 0.54 nm at 390 nm, 0.32 at 400 nm, 0.22 at 410 nm and 0.14 at 420 nm. Feierabend et al.[4] measured quantum yields for the production of HCO at 85 discrete wavelengths in the wavelength range 290–420 nm at pressures between 50 and 550 Torr (N_2) at 298 K using pulsed laser photolysis combined with cavity ring-down spectroscopy detection of HCO. $\Phi_0(\lambda)$ varied smoothly with wavelength with a maximum value of ~1.8 in the range 300–385 nm with values decreasing to near 0 at 420 nm and 0.4 at 290 nm. The high precision of the measurements enabled the pressure dependence of the HCO quantum yield to be determined at each wavelength using the Stern-Volmer relationship:

$$\frac{1}{\Phi(\lambda, P)} = \frac{1}{\Phi_0(\lambda)} + \frac{k_q}{k_d}(\lambda)[\mathrm{N_2}]$$

where k_q is the collisional quenching rate coefficient and k_d is the rate coefficient for the dissociation of glyoxal. The wavelength dependence of the rate coefficient ratio was fit to the expression

$$k_q/k_d\ (\lambda) = 2.3 \times 10^{-20} + 1.5 \times 10^{-19} \exp(-0.4\ \Delta E) \qquad (\text{cm}^3\ \text{molecule}^{-1})$$

where ΔE = ((28571/λ) – 72.5) (kcal mol^{-1}), λ is the photolysis wavelength (nm), and 72.5 kcal mol^{-1} is the threshold for glyoxal photodissociation (there is a small barrier to dissociation on the triplet surface). The $\Phi_0(\lambda)$ values from the Feierabend et al.[4] work are in good agreement with the values reported by Chen and Zhu.[3]

Tadić et al.[12] photolysed glyoxal with broadband fluorescent lamps, which selectively overlapped with the two absorption bands, and measured the CO, HCHO and HCOOH end products. Using 275–380 nm irradiation, the quantum yield for glyoxal loss was found to be $\Phi_T = 0.97 \pm 0.05$ and independent of pressure. The absolute quantum yields obtained for 390–470 nm radiation, covering the visible absorption band, were found to be pressure dependent with values ranging from $\Phi_T = 0.12$ at 100 Torr to $\Phi_T = 0.04$ at 700 Torr and was described by the Stern-Volmer expression:

$$\frac{1}{\Phi_T} = 6.80 + [251.8 \times 10^{-4}\ \mathrm{P(Torr)}]$$

The direct HCO quantum yield measurements of Feierabend et al.[4] and Chen and Zhu[3] combined with the end product yield results of Tadić et al.[12] indicate that dissociation into 2 HCO radicals is the most important pathway under atmospheric conditions. On the basis of their HCO quantum yield data, Feierabend et al. reported a set of revised wavelength dependent quantum yields for channels (1), (2) and (3) from those of Tadić et al.,[12] which were recommended in NASA/JPL 06-2. The revised quantum yields are recommended and given in Table 4D-19-2. Although glyoxal has a very low effective quantum yield, photolysis is an important removal path in the atmosphere.

Table 4D-19-1. Recommended Absorption Cross Sections of CHOCHO at 296 K

λ (nm)	10^{20} σ (cm^2)	λ (nm)	10^{20} σ (cm^2)	λ (nm)	10^{20} σ (cm^2)	λ (nm)	10^{20} σ (cm^2)	λ (nm)	10^{20} σ (cm^2)
250	1.73	306	3.22	362	0.706	418	7.87	474	0.108
251	1.52	307	3.20	363	0.639	419	9.13	475	0.159
252	1.48	308	3.15	364	0.680	420	5.60	476	0.155
253	1.55	309	3.12	365	0.665	421	7.19	477	0.181
254	1.60	310	3.10	366	0.743	422	6.99	478	0.255
255	1.67	311	3.22	367	0.860	423	13.0	479	0.142
256	1.62	312	3.34	368	1.01	424	8.24	480	0.074
257	1.81	313	3.39	369	1.06	425	10.4	481	0.070
258	1.82	314	3.23	370	1.14	426	16.4	482	0.065
259	1.85	315	2.80	371	1.18	427	16.1	483	0.053
260	1.83	316	2.65	372	1.14	428	21.4	484	0.071
261	1.96	317	2.46	373	1.21	429	6.50	485	0.050
262	2.03	318	2.21	374	1.35	430	7.03	486	0.041
263	2.14	319	1.93	375	1.33	431	6.52	487	0.056
264	2.18	320	1.85	376	1.38	432	6.08	488	0.070
265	2.26	321	1.89	377	1.47	433	5.66	489	0.042
266	2.33	322	1.77	378	1.61	434	6.81	490	0.045
267	2.37	323	1.72	379	1.53	435	7.66	491	0.041
268	2.36	324	1.68	380	1.93	436	13.2	492	0.039
269	2.48	325	1.60	381	2.46	437	9.19	493	0.040
270	2.51	326	1.61	382	2.02	438	13.8	494	0.041
271	2.61	327	1.70	383	2.07	439	12.1	495	0.042
272	2.72	328	1.94	384	1.94	440	25.9	496	0.045
273	2.81	329	1.86	385	1.89	441	13.1	497	0.033
274	2.92	330	1.69	386	1.83	442	9.01	498	0.035
275	3.00	331	1.13	387	2.29	443	11.1	499	0.032
276	3.06	332	1.05	388	3.00	444	13.5	500	0.033
277	3.09	333	0.966	389	3.21	445	15.1	501	0.038
278	3.08	334	0.919	390	3.48	446	7.82	502	0.031
279	3.09	335	0.737	391	3.92	447	3.73	503	0.042
280	3.13	336	0.630	392	3.80	448	4.14	504	0.034
281	3.22	337	0.589	393	2.85	449	5.53	505	0.035
282	3.32	338	0.647	394	3.15	450	8.68	506	0.046

λ (nm)	10^{20} σ (cm^2)	λ (nm)	10^{20} σ (cm^2)	λ (nm)	10^{20} σ (cm^2)	λ (nm)	10^{20} σ (cm^2)	λ (nm)	10^{20} σ (cm^2)
283	3.45	339	0.585	395	3.86	451	13.8	507	0.042
284	3.57	340	0.553	396	3.68	452	15.9	508	0.037
285	3.67	341	0.563	397	3.36	453	30.4	509	0.030
286	3.80	342	0.510	398	4.32	454	26.9	510	0.023
287	3.79	343	0.499	399	4.35	455	52.0	511	0.023
288	3.81	344	0.649	400	3.87	456	15.7	512	0.030
289	3.80	345	0.624	401	4.46	457	2.66	513	0.023
290	3.73	346	0.733	402	5.84	458	2.20	514	0.030
291	3.64	347	0.631	403	7.16	459	0.902	515	0.053
292	3.65	348	0.604	404	6.24	460	1.20	516	0.035
293	3.68	349	0.415	405	4.49	461	0.883	517	0.051
294	3.73	350	0.391	406	4.48	462	0.588	518	0.102
295	3.81	351	0.395	407	4.07	463	0.322	519	0.065
296	3.82	352	0.423	408	3.44	464	0.339	520	0.100
297	3.92	353	0.415	409	4.01	465	0.330	521	0.169
298	4.07	354	0.403	410	5.66	466	0.416	522	0.037
299	4.12	355	0.422	411	7.22	467	0.522	523	0.011
300	4.04	356	0.443	412	7.41	468	0.149	524	0.007
301	3.91	357	0.431	413	10.8	469	0.091	525	0.004
302	3.78	358	0.471	414	10.1	470	0.076	526	0.000
303	3.57	359	0.503	415	10.2	471	0.086		
304	3.35	360	0.546	416	6.07	472	0.092		
305	3.24	361	0.627	417	6.83	473	0.110		

Note:
Volkamer et al.[13] rounded to three significant figures

Table 4D-19-2. Recommended CHOCHO Photolysis Quantum Yields at 1 Atm and 298 K

λ (nm)	Φ Total	Φ_1 (HCO + HCO)	Φ_2 (H_2 + 2CO)	Φ_3 (H_2CO + CO)
225	1	0.156	0.645	0.199
230	1	0.156	0.625	0.219
235	1	0.156	0.599	0.245
240	1	0.156	0.575	0.269
245	1	0.156	0.553	0.291
250	1	0.156	0.530	0.314
255	1	0.156	0.510	0.334
260	1	0.156	0.492	0.352
265	1	0.156	0.475	0.369
270	1	0.156	0.457	0.387
275	1	0.156	0.440	0.404
280	1	0.156	0.424	0.420
285	1	0.156	0.414	0.430
290	1	0.156	0.404	0.440
295	1	0.167	0.382	0.451
300	1	0.183	0.360	0.457
305	1	0.208	0.332	0.460
310	1	0.242	0.300	0.458
315	1	0.282	0.266	0.452
320	1	0.322	0.245	0.433
325	1	0.358	0.234	0.408
330	1	0.396	0.225	0.379
335	0.95	0.403	0.210	0.337
340	0.879	0.410	0.190	0.279
345	0.782	0.408	0.170	0.204
350	0.691	0.397	0.144	0.150
355	0.54	0.379	0.053	0.108
360	0.429	0.357	0	0.072
365	0.369	0.329	0	0.040
370	0.316	0.294	0	0.022
375	0.267	0.253	0	0.014
380	0.219	0.208	0	0.011
385	0.172	0.164	0	0.008
390	0.132	0.125	0	0.007
395	0.098	0.093	0	0.005
400	0.072	0.068	0	0.004
405	0.052	0.049	0	0.003
410	0.037	0.035	0	0.002
415	0.024	0.023	0	0.001
420	0	0	0	0

(1) Calvert, J. G.; Layne, G. S. The photolysis of glyoxal vapor at wave length 3130 Å. *J. Am. Chem. Soc.* **1953**, *75*, 856-859, doi:10.1021/ja01100a027.

(2) Calvert, J. G.; Pitts, J. N. Photochemistry; John Wiley & Sons, Inc.: New York, 1966; pp 783.

(3) Chen, Y.; Zhu, L. Wavelength-dependent photolysis of glyoxal in the 290-420 nm region. *J. Phys. Chem. A* **2003**, *107*, 4643-4651, doi:10.1021/jp022440d.

(4) Feierabend, K. J.; Flad, J. E.; Brown, S. S.; Burkholder, J. B. HCO quantum yields in the photolysis of HC(O)C(O)H (glyoxal) between 290 and 420 nm. *J. Phys. Chem. A* **2009**, *113*, 7784-7794, doi:10.1021/jp9033003.

(5) Horowitz, A.; Meller, R.; Moortgat, G. K. The UV-VIS absorption cross sections of the a-dicarbonyl compounds: pyruvic acid, biacetyl and glyoxal. *J. Photochem. Photobiol. A: Chem.* **2001**, *146*, 19-27, doi:10.1016/S1010-6030(01)00601-3.

(6) Langford, A. O.; Moore, C. B. Collision complex formation in the reactions of formyl radicals with nitric oxide and oxygen. *J. Chem. Phys.* **1984**, *80*, 4211-4221, doi:10.1063/1.447252.

(7) Moortgat, G. K. Important photochemical processes in the atmosphere. *Pure Appl. Chem.* **2001**, *73*, 487-490, doi:10.1351/pac200173030487.
(8) Moortgat, G. K. RADICAL: Evaluation of Radical Sources in Atmospheric Chemistry through Chamber and Laboratory Studies, ENVA-CT97-0419, EUR 20254 EN, 2002,
(9) Orlando, J. J.; Tyndall, G. S. The atmospheric chemistry of the HC(O)CO radical. *Int. J. Chem. Kinet.* **2001**, *33*, 149-156, doi:10.1002/1097-4601(200103)33:3<149::AID-KIN1008>3.0.CO;2-1.
(10) Parmenter, C. S. Primary photochemical processes in glyoxal at 4358 Å. *J. Chem. Phys.* **1964**, *41*, 658-665, doi:10.1063/1.1725943.
(11) Plum, C. N.; Sanhueza, E.; Atkinson, R.; Carter, W. P. L.; Pitts, J. N., Jr. OH radical rate constant and photolysis rates of α-dicarbonyls. *Environ. Sci. Technol.* **1983**, *17*, 479-484, doi:10.1021/es00114a008.
(12) Tadic, J.; Moortgat, G. K.; Wirtz, K. Photolysis of glyoxal in air. *J. Photochem. Photobiol. A: Chem.* **2005**, *177*, 116-124, doi:10.1016/j.jphotochem.2005.10.010.
(13) Volkamer, R.; Spietz, P.; Burrows, J. P.; Platt, U. High-resolution absorption cross-sections of glyoxal in the UV-vis and IR spectral ranges. *J. Photochem. Photobiol. A: Chem.* **2005**, *172*, 35-36, doi:10.1016/j.jphotochem.2004.11.011.
(14) Zhu, L.; Johnston, G. Kinetics and products of the reaction of the vinoxy radical with O_2. *J. Phys. Chem.* **1995**, *99*, 15114-15119, doi:10.1021/j100041a030.
(15) Zhu, L.; Kellis, D.; Ding, C.-F. Photolysis of glyoxal at 193, 248, 308, and 351 nm. *Chem. Phys. Lett.* **1996**, *257*, 487-491, doi:10.1016/0009-2614(96)00570-2.

D20. $CH_3C(O)OH$ (acetic acid)

Back to Index

$CH_3C(O)OH + h\nu$	$\rightarrow CH_4 + CO_2$	–35 kJ mol^{-1}	All	(1)
	$\rightarrow CH_3 + COOH$	391 kJ mol^{-1}	306 nm	(2)
	$\rightarrow CH_3CO + OH$	459 kJ mol^{-1}	260 nm	(3)
	$\rightarrow CH_3COO + H$	462 kJ mol^{-1}	259 nm	(4)

(Recommendation: 06-2, Note: 10-6, Evaluated: 10-6)

Absorption Cross Sections: The UV absorption spectrum of acetic acid, $CH_3C(O)OH$, and the acetic acid dimer, $(CH_3C(O)OH)_2$, have been measured for a range of sample pressures at 300 K by McMillan[1] (200–241 nm; 12.9, 11.0, 8.3, and 3.6 Torr), at 283, 303 and 338 K by Hintze et al.[2] (195–220 nm), and at 270, 298, 325, and 345 K by Orlando and Tyndall[4] (210–245 nm; 0.12–3.6 Torr). Singleton et al.[5] reported cross sections at 222 nm in connection with quantum yield measurements at 298 and 356.2 K. The monomer spectrum reported by Orlando and Tyndall[4] and Hintze et al.[2] has a broad maximum near 207 nm and a monotonic decrease in intensity with increasing wavelength. The absorption maximum for the dimer appears at shorter wavelength, below 205 nm, and is twice as intense as that of the monomer. The decrease in cross sections with increasing wavelength is more rapid for the dimer than for the monomer resulting in the monomer cross section being greater at 240 nm by a factor 6. Hinze et al.[2] determined the absorption cross section at the maximum for the monomer at 206.1 nm and 297 K to be $(1.27 \pm 0.10) \times 10^{-19}$ cm^2 molecule^{-1} and for the dimer and at 208.1 nm to be $(2.44 \pm 0.08) \times 10^{-19}$ cm^2 molecule^{-1}. The absorption spectra reported by Calvert and Pitts[1] were derived assuming monomers only in spite of undefined amounts of monomer and dimer. The absorption spectrum for the greatest pressure is close to the dimer spectrum reported by Orlando and Tyndall[4], suggesting that the sample was primarily dimer at the higher pressures. The recommended absorption cross sections in Table 4D-20 are taken from Orlando and Tyndall[4] (measured at 0.6 nm resolution).

Photolysis Quantum Yield and Product Studies: Early photolysis studies reported yields of the end products CO, CO_2, CH_4, and C_2H_6 (Calvert and Pitts[1]) and proposed molecular elimination (channel 1) and radical formation (channels 2–4) originating from the monomer. Hunnicutt et al.[3] photolysed acetic acid at 218 nm and used photofragment laser fluorescence to determine channel (2) to be the dominant photochemical path. Singleton et al.[5] determined the OH quantum yield at 222 nm to be 0.546 ± 0.097 at 298 K and 0.692 ± 0.024 at 356.2 K for the monomer and 0.038 ± 0.026 at 298 K for the dimer (a dimer quantum yield of zero was assumed at elevated temperatures).

Table 4D-20. Recommended Absorption Cross Sections of $CH_3C(O)OH$ and $(CH_3C(O)OH)_2$ at 298 K

λ (nm)	10^{20} σ (cm^2) monomer	dimer
210	15.1	23.4
212	14.7	20.9

214	13.5	18.4
216	12.5	15.8
218	11.7	13.2
220	10.5	10.9
222	9.33	8.54
224	8.19	6.68
226	7.17	4.95
228	6.00	3.60
230	5.09	2.45
232	4.20	1.71
234	3.44	1.11
236	2.71	0.65
238	2.11	0.45
240	1.64	0.27
242	1.19	
244	0.89	

Note: Orlando and Tyndall[4]

(1) Calvert, J. G.; Pitts Jr., J. N. In *Photochemistry*; John Wiley & Sons, Inc.: New York, 1966; pp 368.

(2) Hintze, P. E.; Aloisio, S.; Vaida, V. Electronic spectroscopy of organic acid dimers. *Chem. Phys. Lett.* **2001**, *343*, 159-165, doi:10.1016/S0009-2614(01)00664-9.

(3) Hunnicutt, S. S.; Waits, L. D.; Guest, J. A. Energetic constraints in the 218 nm photolysis of acetic acid. *J. Phys. Chem.* **1989**, *93*, 5188-5195, doi:10.1021/j100350a033.

(4) Orlando, J. J.; Tyndall, G. S. Gas phase UV absorption spectra for peracetic acid, and for acetic acid monomers and dimers. *J. Photochem. Photobiol. A: Chem.* **2003**, *157*, 161-166, doi:10.1016/S1010-6030(03)00067-4.

(5) Singleton, D. L.; Paraskevopoulos, G.; Irwin, R. S. Laser photolysis of carboxyclic acids in the gas phase. Direct determination of the OH quantum yield at 222 nm. *J. Phys. Chem.* **1990**, *94*, 695-699, doi:10.1021/j100365a034.

D21. $CH_3C(O)OOH$ (peracetic acid)

Back to Index

$CH_3C(O)OOH + h\nu \rightarrow$ Products (1)

(Recommendation: 06-2, Note: 10-6, Evaluated: 10-6)

Absorption Cross Sections: The UV absorption spectrum of peracetic acid, $CH_3C(O)OOH$, was measured at 248 and 298 K by Orlando and Tyndall[1] (205–340 nm). The absorption cross sections decrease in a monotonic near-exponential fashion with increasing wavelength. The spectrum recorded at 248 K shows a-faster fall-off with increasing wavelength than that recorded at room temperature. The recommended absorption cross sections in Table 4D-21 are taken from Orlando and Tyndall (the only study available) (measured at 0.6 nm resolution).

Photolysis Quantum Yield and Product Studies: No recommendation.

Table 4D-21. Recommended Absorption Cross Sections $CH_3C(O)OOH$ at 298 K

λ (nm)	10^{20} σ (cm^2)	λ (nm)	10^{20} σ (cm^2)	λ (nm)	10^{20} σ (cm^2)	λ (nm)	10^{20} σ (cm^2)
210	38.1	244	4.31	278	0.574	312	*0.045*
212	33.1	246	3.82	280	0.506	314	*0.044*
214	29.5	248	3.41	282	0.444	316	*0.040*
216	25.4	250	3.05	284	0.386	318	*0.035*
218	21.7	252	2.71	286	0.334	320	*0.025*
220	18.9	254	2.42	288	0.297	322	*0.020*
222	16.0	256	2.16	290	0.256	324	*0.020*
224	13.9	258	1.93	292	0.226	326	*0.017*
226	12.0	260	1.71	294	0.193	328	*0.014*
228	10.5	262	1.53	296	0.170	330	*0.009*
230	9.10	264	1.35	298	0.141	332	*0.011*
232	8.01	266	1.21	300	0.123	334	*0.011*
234	7.03	268	1.06	302	0.107	336	*0.009*
236	6.31	270	0.945	304	0.094	338	*0.009*
238	5.61	272	0.835	306	0.078	340	*0.006*
240	5.03	274	0.742	308	0.069		
242	4.83	276	0.651	310	*0.062*		

Note:
Orlando and Tyndall,[1] 310–340 nm region obtained from a linear interpolation of ln(σ)

(1) Orlando, J. J.; Tyndall, G. S. Gas phase UV absorption spectra for peracetic acid, and for acetic acid monomers and dimers. *J. Photochem. Photobiol. A: Chem.* **2003**, *157*, 161-166, doi:10.1016/S1010-6030(03)00067-4.

D22. C_2H_5CHO (propionaldehyde)

Back to Index

$C_2H_5CHO + h\nu \rightarrow C_2H_5 + HCO$	351 kJ mol^{-1}	341 nm	(1)
$\rightarrow C_2H_6 + CO$	–8 kJ mol^{-1}	All	(2)
$\rightarrow C_2H_4 + HCHO$	129 kJ mol^{-1}	926 nm	(3)
$\rightarrow CH_3 + CH_2CHO$	343 kJ mol^{-1}	349 nm	(4)

(Recommendation: 06-2, Note: 10-6, Evaluated: 10-6)

Absorption Cross Sections: The UV absorption spectrum of propionaldehyde (C_2H_5CHO, propanal) has been measured at room temperature by Lucazeau and Sandorfy[5] (118–190 nm), McMillan[2] (220–342 nm), and Martinez et al.[6] (262–365 nm). Absorption cross sections have also been reported for isolated wavelengths by Blacet and Crane[1] (187–313 nm), Heicklen et al.[4] (293–325 nm), and Chen and Zhu[3] (280–330 nm). The spectrum at wavelengths >200 nm consists of an absorption band with structured features (~9 maxima or shoulders) at wavelengths >260 nm and maximum absorption at 285 and 293 nm. The agreement between the results from Martinez et al.[6] and McMillan[2] is excellent, i.e., ≤5% differences, between 238 and 322 nm. At shorter (longer) wavelengths the differences increase to ~30% (~50%). The data points reported by Heicklen et al.[4] fit well to these studies although the value reported at 293 nm is 20% smaller. The cross sections reported at 5 nm intervals by Chen and Zhu[3] agree to within 10% with those reported by Martinez et al.,[6] except the data at 285 and 330 nm which are 20% and 30% larger. The recommended absorption cross sections listed in Table 4D-22 are taken from Martinez et al.[6] and are 4 nm averages of the 0.5 nm resolution data in the region 202–278 nm and 1 nm averages in the region 280–360 nm.

Photolysis Quantum Yield and Product Studies: Quantum yield measurements have been performed by Heicklen et al.[4] and Chen and Zhu.[3] Heicklen et al.[4] measured the quantum yield of HO_2 and $C_2H_5O_2$ radicals (in air bath gas) using laser photolysis at 294, 302, 312, and 325 nm combined with UV absorption to determine Φ_1. Quantum yields of CO and C_2H_6 were obtained in steady-state photolysis (at 254, 312, and 334 nm) experiments in O_2 where $\Phi_1 = \Phi(CO) - \Phi(C_2H_6)$ and $\Phi_2 = \Phi(C_2H_6)$. A Stern-Volmer pressure dependence of the quantum yields was observed at all wavelengths, i.e., lower quantum yields at higher pressures. At atmospheric pressure, values of $\Phi_1 = 0.22$, 0.89, 0.85, 0.50, 0.26, and 0.15 were derived at 254, 294, 302, 313, 325, and 334 nm, respectively. Heicklen et al.[4] reported $\Phi_2 = 0.33$ for 254 nm photolysis and $\Phi_2 = 0$ at longer wavelengths. The contribution of other primary processes (Φ_3 and Φ_4) was found to increase at wavelengths <265 nm from earlier studies as cited in Calvert and Pitts.[2]

Chen and Zhu[3] measured the quantum yield of HCO radicals (Φ_1) over the wavelength range 280–330 nm using time-resolved cavity ring-down spectroscopy with detection of HCO at 613.8 nm. The reported HCO yields are 0.85 ± 0.06 at 280 nm, 1.01 ± 0.07 at 285 nm, 0.95 ± 0.06 at 290 nm, 0.98 ± 0.06 at 295 nm, 0.92 ± 0.06 at 300 nm, 0.95 ± 0.08 at 305 nm, 0.98 ± 0.11 at 310 nm, 0.91 ± 0.05 at 315 nm, 1.08 ± 0.07 at 320 nm, 1.07 ± 0.14 at 325 nm, and 0.84 ± 0.08 at 330 nm. These values are quoted for zero-pressure but no pressure dependence to the HCO quantum yield at any wavelength was observed for pressures over the range 10–400 Torr N_2.

The quantum yield studies by Heicklen et al.[4] and Chen and Zhu[3] are only in agreement in the narrow wavelength range 290–305 nm. At λ >305 nm, the data of Chen and Zhu do not show the decrease of Φ_1 reported by Heicklen et al.[4] Because of the discrepancies between these data sets no quantum yield recommendation is given.

Table 4D-22. Recommended Absorption Cross Sections of C_2H_5CHO at 298 K

λ (nm)	$10^{20}\ \sigma$ (cm^2)	λ (nm)	$10^{20}\ \sigma$ (cm^2)	λ (nm)	$10^{20}\ \sigma$ (cm^2)	λ (nm)	$10^{20}\ \sigma$ (cm^2)
202	0.049	285	5.86	310	3.60	335	0.325
206	0.049	286	5.82	311	3.53	336	0.280
210	0.057	287	5.72	312	3.50	337	0.230
214	0.069	288	5.59	313	3.32	338	0.185
218	0.080	289	5.52	314	3.06	339	0.166
222	0.091	290	5.56	315	2.77	340	0.155
226	0.115	291	5.68	316	2.43	341	0.119
230	0.163	292	5.81	317	2.18	342	0.076
234	0.257	293	5.88	318	2.00	343	0.045
238	0.407	294	5.80	319	1.86	344	0.031
242	0.622	295	5.57	320	1.83	345	0.025
246	0.909	296	5.37	321	1.78	346	0.019
250	1.29	297	5.16	322	1.66	347	0.016
254	1.75	298	5.02	323	1.58	348	0.014
258	2.25	299	5.02	324	1.49	349	0.013
262	2.88	300	5.04	325	1.30	350	0.010
266	3.43	301	5.09	326	1.13	351	0.008
270	4.12	302	5.07	327	0.996	352	0.007
274	4.59	303	4.94	328	0.828	353	0.005
278	5.17	304	4.69	329	0.685	354	0.004
280	5.16	305	4.32	330	0.575	355	0.002
281	5.21	306	4.04	331	0.494	356	0.001
282	5.35	307	3.81	332	0.466	357	0.001
283	5.57	308	3.65	333	0.430		
284	5.78	309	3.62	334	0.373		

Note:
Martinez et al. [6]

(1) Blacet, F. E.; Crane, R. A. The photolysis of the aliphatic aldehydes. XVII. Propionaldehyde, n-butyraldehyde, and isobutyraldehyde at 2380 and 1870 Å. *J. Am. Chem. Soc.* **1954**, *76*, 5337-5340, doi:10.1021/ja01650a020.

(2) Calvert, J. G.; Pitts Jr., J. N. In *Photochemistry*; John Wiley & Sons, Inc.: New York, 1966; pp 368.

(3) Chen, Y.; Zhu, L. The wavelength dependence of the photodissociation of propionaldehyde in the 280-330 nm region. *J. Phys. Chem. A* **2001**, *105*, 9689-9696, doi:10.1021/jp011445s.

(4) Heicklen, J.; Desai, J.; Bahta, A.; Harper, C.; Simonaitis, R. The temperature and wavelength dependence of the photo-oxidation of propionaldehyde. *J. Photochem.* **1986**, *34*, 117-135, doi:10.1016/0047-2670(86)85014-6.

(5) Lucazeau, G.; Sandorfy, C. On the far-ultraviolet spectra of some simple aldehydes. *J. Mol. Spectrosc.* **1970**, *35*, 214-231, doi:10.1016/0022-2852(70)90199-2.

(6) Martinez, R. D.; Buitrago, A. A.; Howell, N. W.; Hearn, C. H.; Joens, J. A. The near UV absorption spectra of several aliphatic aldehydes and ketones. *Atmos. Environ.* **1992**, *26A*, 785-792, doi:10.1016/0960-1686(92)90238-G.

D23. C_2H_5CHOO (propionaldehyde oxide)

Back to Index

$C_2H_5CHOO + h\nu \rightarrow$ Products (1)

(Recommendation: 19-5; Note: 19-5; Evaluated: 19-5)

Absorption Cross Sections: UV absorption cross sections of the Criegee intermediate C_2H_5CHOO (propionaldehyde oxide) have been reported at 298 K by Liu et al.[1] (288–368 nm). The Liu et al. measurements are the only UV absorption spectrum data currently available. Experimental factors in the Liu et al. study, such as inhomogeneity of the UV laser beam, led to large uncertainties in the absolute cross sections (estimated ~100% uncertainty in the original paper). Given the large cross sections reported from this research group for other Criegee intermediates using the UV photodissociation action spectrum technique, it is possible that the reported cross sections for C_2H_5CHOO are also over estimated. No recommendation for the absorption cross sections of C_2H_5CHOO is made at this time.

Photolysis Quantum Yield and Product Studies: No recommendation.

(1) Liu, F.; Beames, J. M.; Green, A. M.; Lester, M. I. UV spectroscopic characterization of dimethyl- and ethyl-substituted carbonyl oxides. *J. Phys. Chem. A* **2014**, *118*, 2298-2306, doi:10.1021/jp412726z.

D24. $(CH_3)_2COO$ (acetone oxide)

Back to Index

$(CH_3)_2COO + h\nu \rightarrow$ Products (1)

(Recommendation: 19-5; Note: 19-5; Evaluated: 19-5)

Absorption Cross Sections: UV absorption cross sections of the Criegee intermediate $(CH_3)_2COO$ (acetone oxide) have been reported at room temperature by Liu et al.[4] (288–368 nm), Huang et al.[3](278.5–390.3 nm), Chang et al.[1] (308.4 nm, 351.8 nm), and Chhantyal-Pun et al.[2](355 nm). The Huang et al. and Chang et al. studies are from the same research group: Huang et al. measured the spectrum wavelength dependence of $(CH_3)_2COO$, and Chang et al. scaled that spectrum to their absolute absorption cross section measured at 308.4 nm. The cross section values of Huang et al. / Chang et al. are in substantial disagreement with the cross sections of Liu et al., as the Liu et al. values are greater by more than a factor of 2 at the spectrum peak, 330 nm. Experimental factors in the Liu et al. study, such as inhomogeneity of the UV photolysis laser beam, led to significant uncertainties in their absolute cross sections.

The cross section value of Chhantyal-Pun et al. at 355 nm ($1.45 \pm 0.24 \times 10^{-17}$ cm^2) is significantly greater than the values from Huang et al. at 355 nm and Chang et al. at 351.8 nm; the uncertainties do not overlap. The reported value of Chhantyal-Pun et al. was not a direct measurement, as it was derived from the fractional loss of $(CH_3)_2CI_2$ following photodissociation. The method used by Chang et al. of laser depletion in a molecular beam was previously used by the same research group to measure cross sections for other Criegee intermediates, CH_2OO and CH_3CHOO.

The recommended cross sections given in Table 4D-24 are from Huang et al., scaled to the cross sections of Chang et al. The recommended values represent 5 nm averages of the Huang et al. data (reported every ~0.6 nm) between 290–390 nm. An estimated uncertainty factor (2σ) of 1.5 is recommended, which is substantially larger than the uncertainty reported by Chang et al. but allows for overlapping error limits with the value of Chhantyal-Pun et al. at 355 nm.

Photolysis Quantum Yield and Product Studies: No recommendation.

Table 4D-24. Recommended Absorption Cross Sections of $(CH_3)_2COO$ (acetone oxide) at 298 K

λ (nm)	10^{20} σ (cm^2)	λ (nm)	10^{20} σ (cm^2)
290	570	345	1410
295	771	350	1110
300	898	355	817
305	1070	360	652
310	1350	365	532
315	1470	370	367
320	1680	375	259
325	1710	380	209
330	1750	385	105
335	1720	390	50.5
340	1630		

Note:
5 nm averages of Huang et al.[3] scaled to Chang et al.[1]

(1) Chang, Y.-P.; Chang, C.-H.; Takahashi, K.; Lin, J. J.-M. Absolute UV absorption cross sections of dimethyl substituted Criegee intermediate $(CH_3)_2COO$. *Chem. Phys. Lett.* **2016**, *653*, 155-160, doi:10.1016/j.cplett.2016.04.082.

(2) Chhantyal-Pun, R.; Welz, O.; Savee, J. D.; Eskola, A. J.; Lee, E. P. F.; Blacker, L.; Hill, H. R.; Ashcroft, M.; Khan, M. A. H.; Lloyd-Jones, G. C.; Evans, L.; Rotavera, B.; Huang, H.; Osborn, D. L.; Mok, D. K. W.; Dyke, J. M.; Shallcross, D. E.; Percival, C. J.; Orr-Ewing, A. J.; Taatjes, C. A. Direct measurements of unimolecular and bimolecular reaction kinetics of the Criegee intermediate $(CH_3)_2COO$. *J. Phys. Chem. A* **2017**, *121*, 4-15, doi:10.1021/acs.jpca.6b07810.

(3) Huang, H.-L.; Chao, W.; Lin, J. J.-M. Kinetics of a Criegee intermediate that would survive high humidity and may oxidize atmospheric SO_2. *Proc. Natl. Acad. Sci.* **2015**, *112*, 10857-10862, doi:10.1073/pnas.1513149112.

(4) Liu, F.; Beames, J. M.; Green, A. M.; Lester, M. I. UV spectroscopic characterization of dimethyl- and ethyl-substituted carbonyl oxides. *J. Phys. Chem. A* **2014**, *118*, 2298-2306, doi:10.1021/jp412726z.

D25. $(CH_3)_2CHOH$ (isopropanol, 2-propanol, isopropyl alcohol)

Back to Index

$(CH_3)_2CHOH + h\nu \rightarrow$ Products (1)

(Recommendation: 19-5; Note: 19-5; Evaluated: 19-5)

Absorption Cross Sections: UV absorption cross sections of $(CH_3)_2CHOH$ (isopropanol) have been measured at room temperature by Harrison et al.[1] (168 nm, 181 nm), Salahub and Sandorfy[3] (120.5–208.3 nm), and Orkin et al.[2] (163–205 nm). At the local absorption maximum of 181 nm, the reported cross section of Harrison et al. is 7% greater than that reported by Orkin et al., while near the local absorption minimum of 168 nm, the value of Harrison et al. is 13% less. The cross sections of Salahub and Sandorfy agree to within 3%, or better, with Orkin et al. from 173 nm to the 181 nm peak, but the discrepancy increases at shorter and longer wavelengths. The recommended cross sections given in Table 4D-25 for the 163–205 nm wavelength range were taken from Orkin et al. at 1 nm intervals (higher resolution data are available in Orkin et al.). For the range 210–220 nm, the recommended values were obtained from a log-linear fit and extrapolation of the Orkin et al. data, $\log \sigma(\lambda) = 12.2226 - 0.15525\ \lambda$. An estimated uncertainty factor of 1.13 (2σ) is recommended for the 163–205 nm wavelength range.

The recommended Lyman-α (121.567 nm) cross section was interpolated from the data of Salahub and Sandorfy[3] with an estimated uncertainty factor (2σ) of 1.3.

Photolysis Quantum Yield and Product Studies: No recommendation.

Table 4D-25. Recommended Absorption Cross Sections of $(CH_3)_2CHOH$ (isopropanol) at 295 K

λ (nm)	10^{20} σ (cm^2)	λ (nm)	10^{20} σ (cm^2)	λ (nm)	10^{20} σ (cm^2)
121.567	5190	178	205	194	63.1
163	506	179	213	195	50.7
164	368	180	218	196	40.3
165	248	181	222	197	31.5
166	170	182	221	198	24.3
167	130	183	219	199	18.3
168	114	184	213	200	13.5
169	111	185	204	201	9.92
170	116	186	193	202	7.14
171	125	187	179	203	5.11
172	136	188	163	204	3.56
173	148	189	145	205	2.49
174	161	190	128	210	*0.417*
175	173	191	110	215	*0.0698*
176	185	192	92.3	220	*0.0117*
177	196	193	77.4		

Note:
121.567 nm: Salahub and Sandorfy[3]
163–205 nm: Orkin et al.[2] data at 1 nm intervals
210–220 nm: Extrapolation of Orkin et al.[2] data, log σ(λ) = 12.2226 – 0.15525 λ

(1) Harrison, A. J.; Cederholm, B. J.; Terwilliger, M. A. Absorption of acyclic oxygen compounds in the vacuum ultraviolet. I. Alcohols. *J. Chem. Phys.* **1959**, *30*, 355-356, doi:10.1063/1.1729952.

(2) Orkin, V. L.; Khamaganov, V. G.; Kurylo, M. J. High accuracy measurements of OH reaction rate constants and IR absorption spectra: Substituted 2-propanols. *J. Phys. Chem. A* **2012**, *116*, 6188-6198, doi:10.1021/jp211534n.

(3) Salahub, D. R.; Sandorfy, C. The far-ultraviolet spectra of some simple alcohols and fluoroalcohols. *Chem. Phys. Lett.* **1971**, *8*, 71-74, doi:10.1016/0009-2614(71)80578-X.

D26. $CH_3C(O)CH_3$ (acetone)

Back to Index

$CH_3C(O)CH_3 + h\nu$	$\rightarrow CH_3C(O) + CH_3$	354 kJ mol^{-1}	338 nm	(1)
	$\rightarrow 2\ CH_3 + CO$	400 kJ mol^{-1}	299 nm	(2)

(Recommendation: 06-2, Note: 10-6; Evaluated: 10-6)

Absorption Cross Sections: The absorption spectrum of acetone, $CH_3C(O)CH_3$, has been measured at room temperature by Lake and Harrison[18] (159–203 nm), Calvert[8] (200–300 nm), Meyrahn et al.[20,21] (220–368 nm), Schneider and Moortgat (196–366 nm) (see Röth et al.[24]), Hynes et al.[14] (253.7 nm and 260–360 nm), Martinez et al.[19] (202–335 nm), Gierczak et al.[12] (215–349 nm), Wollenhaupt et al.[29] (220–346 nm), and Yujing and Mellouki[30] (240–350 nm). Absorption cross sections have also been determined at isolated wavelengths by Braun et al.[6] (193 nm, also for $CD_3C(O)CD_3$), Seki and Okabe[25] (193 nm), Krasnoperov and Mehta[17] (216.51 nm), and Gierczak et al.[13] (184.9 nm, also for $CD_3C(O)CD_3$).

The spectrum below 200 nm is highly structured in the wavelength regions 160–170 nm and 180–195 nm. A broad absorption band was observed between 210 and 340 nm for which higher resolution measurements give evidence for band maxima at ~273 and ~278 nm. The reported absorption cross sections are in excellent agreement with the range of deviations being ≤8% in the 240–320 nm region. The absorption cross section at the spectrum maximum range between 5.2×10^{-20} and 4.8×10^{-20} cm^2 $molecule^{-1}$. In the tails of the absorption band, the various data sets become more divergent with decreasing wavelength with differences of up to ~50% at 220 nm and with increasing wavelength up to more than 100% at 340 nm. The data measured by Meyrahn et al.[20,21] are systematically higher at wavelengths >320 nm than the other studies. The absorption cross sections from Martinez et al.,[19] Gierczak et al.,[12] Wollenhaupt et al.,[29] and Yujing and Mellouki[30] agree to within 2.5% in the region of the absorption maximum and to within 50% in the short and long wavelength tails of the band.

The absorption spectrum temperature dependence has been studied by Hynes et al.[14] (300–340 nm) over the range 261–362 K, Gierczak et al.[12] (215–349 nm) over the range 235–298 K, and Gierczak et al.[13] (184.9 nm, also for $CD_3C(O)CD_3$) over the range 222–296 K. The absorption spectrum has modest temperature dependence at wavelengths >270 nm with the cross sections decreasing with decreasing temperature. At shorter wavelengths the spectrum is essentially independent of temperature, the cross section changes by <5% between 298 and 235 K. Gierczak et al.[12] parameterized the temperature dependent cross sections using the expression:

$$\sigma(\lambda, T) = \sigma(\lambda, 298\ K)[1 + c_1(\lambda)T + c_2(\lambda)T^2]$$

that was later superseded by Burkholder[7] using the expression:

$$\sigma(\lambda, T) = \sigma(\lambda, 298\ K)[1 + A(\lambda)T + B_2(\lambda)T^2 + C(\lambda)T^3]$$

The recommended absorption cross sections at 298 K in Table 4D-26-1 are taken from Gierczak et al.[12] and the temperature coefficients A, B, and C derived by Burkholder.[7]

The absorption cross section of $CH_3C(O)CH_3$ at 184.9 nm was observed to decrease very slightly with decreasing temperature between 296 and 222 K leading to an average value of $(2.98 \pm 0.10) \times 10^{-18}$ cm^2 molecule^{-1}, whereas that of $CD_3C(O)CD_3$ increased noticeably from 3.91×10^{-18} cm^2 molecule^{-1} (average of six results) at 295 K to 4.61×10^{-18} cm^2 molecule^{-1} at 232 K, as reported by Gierczak et al.[13]

Photolysis Quantum Yield and Product Studies: The UV photodissociation of acetone is wavelength, pressure, and temperature dependent. Since NASA/JPL 06-2 there has been a number of acetone photodissociation laboratory studies published [Khamaganov et al.[15] (248 and 266 nm), Khamaganov et al.[16] (248 nm and 266 nm), Nádasdia et al.[22] (248 nm and 308 nm), Rajakumar et al.[23] (248 nm), Somnitz et al.[26,27] (248 nm)]. The focus of these studies has been on the determination of the pressure and temperature dependence of the acetone loss and product (CH_3, CH_3CO, CO, and CO_2) photolysis quantum yields as described further below.

Gardner et al.[11] measured acetone loss (Φ_{AC}) and formation of the products CO_2, CO, CH_3OH and H_2CO following the photolysis of dilute acetone-air mixtures at four wavelengths in the range 279–313 nm as a function of pressure (25–745 Torr) and temperature (271–301 K). At pressures >300 Torr, they observed a near constant quantum yield, $\Phi_{AC} \approx \Phi_{CO2} = \Phi_1 = 0.077$, for photolysis wavelengths in the range 279–313 nm with a slight increase at lower pressures. Meyrahn et al.[20,21] measured the quantum yields of CO and CO_2 in the photolysis of dilute mixtures of acetone in air at nine wavelengths over the range 250–330 nm. At 1 atm, Φ_{CO2} decreased from 1.59 at 250 nm to 0.11 at 310 nm and increased to 0.27 at 330 nm. Φ_{CO} decreased from 0.45 at 250 nm to 0.02 at 310 nm and increased to 0.09 at 330 nm. A CO_2 quantum yield larger than unity was explained to result from secondary reactions. Meyrahn et al.[20,21] measured the quantum yield of peroxyacetyl nitrate, Φ_{PAN}, (which is assumed to be a direct measure of Φ_1) in the photolysis of acetone /air/NO_2 mixtures to decrease from ~0.78 in the region 250–260 nm to 0.03 at 330 nm. Meyrahn et al.[20,21] observed Φ_{CO2} to increase at lower pressures (Stern-Volmer mechanism) at 330 nm. Emrich and Warneck[9,10] also determined Φ_{PAN} following the photolysis of acetone /air/NO_2 mixtures at six wavelengths between 280 and 330 nm at total pressures in the range 10–760 Torr. At 760 Torr, Φ_{PAN} decreased from a value of 1.00 at 280 nm to 0.06 at 320 nm and increased to 0.13 at 330 nm. A Stern-Volmer type pressure dependence was observed at all wavelengths. The results were explained in terms of the rate of photodissociation from the excited singlet $^1[AC]^*$ state of acetone and the competing intersystem crossing to the triplet $^3[AC]^*$, both relative to that of collisional quenching, as a function of energy above the dissociation threshold. It was proposed that:

$$^1[AC]^* \rightarrow 2\ CH_3 + CO$$
$$^3[AC]^* \rightarrow CH_3C(O) + CH_3$$

Gierczak et al.[12] determined Φ_{AC} and Φ_{CO2} in the laser photolysis of acetone at nine wavelengths in the range 248–337 nm as a function of pressure (25–760 Torr, syn. air) and temperature (195–298 K). For photolysis wavelengths >270 nm, Φ followed a Stern-Volmer type pressure dependence and the zero-pressure quantum yield was found to increase with decreasing wavelength to a value of unity near 290 nm. Gierczak et al.[12] observed a temperature dependence for the 308 nm quantum yield except for the lowest temperature included in their study, 195 K, and choose to report a temperature independent quantum yield. The studies of Blitz et al.[4,5] and Nádasdia et al.[22] have since reported temperature dependent quantum yields at 308 nm. The results from these studies are in good agreement. The Gierczak et al.[12] results are also in reasonable agreement. The Gierczak et al.[12] results at 298 K are nearly identical to those of Emrich and Warneck.[9] Gierczak et al.[12] and Warneck[28] have reported parameterizations for the quantum yields for the photodissociation of acetone dependence on wavelength and pressure.

Aloisio and Francisco[1] measured the quantum yield of acetone photodissociation at 248 and 308 nm in the presence and absence of water vapor. The apparent acetone quantum yield decreased from unity to 0.73 ± 0.07 for 248 nm photolysis and from 0.28 ± 0.07 to 0.06 ± 0.04 for 308 nm photolysis with the addition of 9 Torr of H_2O. Nádasdia et al.[22] performed a similar quantum yield study (with and without H_2O) at 298 K and a total pressure of 133 mbar. They studied the effect for the same photolysis wavelengths and report quantum yields for the loss of acetone to be independent of H_2O vapor to within their measurement accuracy; 0.945 ± 0.222 (without H_2O) and 1.021 ± 0.124 (with 12 mbar H_2O) at 248 nm and two sets of measurements at 308 nm using different acetone and H_2O concentrations, 0.342 ± 0.028 (without H_2O) and 0.319 ± 0.018 (with 12 mbar H_2O) and 0.308 ± 0.024 (without) and 0.320 ± 0.024 (with 4 mbar H_2O). There is no explanation for the apparent discrepancy between these studies.

Blitz et al.[4,5] reported the pressure and temperature (218–295 K) dependent quantum yields of acetone for photolysis wavelengths between 279 and 327.5 nm. Blitz et al.[4,5] used a spectroscopic technique to indirectly detect the formation of the CH_3CO radical that is based on the detection of the OH radical formed in the reaction:

$$CH_3CO + O_2 \rightarrow CH_3COO_2^* \rightarrow OH + \text{products}$$

$$\rightarrow CH_3COO_2^* + M \rightarrow CH_3C(O)O_2 + M$$

The time-resolved studies of Blitz et al.[4,5] are more direct and sensitive than earlier studies. They observed "classical" Stern-Volmer behavior at λ <302 nm, but at λ >302 nm an extended form of the Stern-Volmer expression was necessary to fit their data for pressures below 15 Torr; reflecting the dissociation and quenching from both $^1[AC]^*$ and $^3[AC]^*$ excited states as described in Blitz et al.[3] On the basis of the low pressure quantum yield results at wavelengths >300 nm, Blitz et al.[4,5] determined that $\Phi_{CH3CO} = 0.65$ and $\Phi_{CO} = 0.35$ at 248 nm from measurements made relative to this reference photolysis wavelength. Their analysis assumes that the acetone quantum yield in the low-pressure limit is unity in the long wavelength photolysis, the acetone quantum yield at 248 nm is unity, and that the CH_3CO quantum yield at 248 nm is independent of pressure. It has been established that the acetone quantum yield at 248 nm is unity and independent of temperature and pressure [Gierczak et al.,[12] Khamaganov et al.,[16] Aloisio and Francisco,[1] Nádasdia et al.,[22] and Somnitz et al.[27]]. Khamaganov et al.[16] also report that the acetone quantum yield is only weakly pressure dependent (60–760 Torr) at 266 nm. There is strong evidence now that the CH_3CO, CH_3, and CO quantum yields at 248 nm are, however, pressure dependent. For photolysis at 248 nm there is sufficient energy for the nascent energetically excited CH_3CO radical to dissociate via a non-concerted step:

$$CH_3CO^* \rightarrow CH_3 + CO$$

or be collisionally quenched:

$$CH_3CO^* + M \rightarrow CH_3CO + M$$

Khamaganov et al.[15] (5–1500 Torr), Somnitz et al.[26,27] (20–900 mbar), and Rajakumar et al.[23] (60–670 Torr) reported pressure dependent quantum yields for CH_3, CO and CO_2, and CH_3CO, respectively, over the range of pressures indicated. The results from these studies are in reasonable agreement and report low pressure quantum yields of $\Phi(CH_3) = 1.42 \pm 0.15$ (Khamaganov et al.[15]), $\Phi(CO) = 0.51$ (Somnitz et al.[27]), and $\Phi(CH_3CO) = 0.535 \pm 0.09$ (Rajakumar et al.[23]). Somnitz et al.[26,27] have modeled the dissociation process using RRKM theory with a time-dependent master equation approach. The impact of a pressure dependence for the CH_3CO quantum yield at 248 nm on the interpretation of the Blitz et al. quantum yield data at longer wavelengths is at present unclear.

At λ <310 nm and 1 atm, there was very good agreement with the data of Gierczak et al.[12] and Emrich and Warneck[9]; however at λ >310 nm, the measured quantum yields were significantly smaller. The temperature dependence of Φ_{TOTAL} is quite striking at the longer wavelengths: the ratio of the quantum yields at 295 and 218 K reported by Blitz et al.[4,5] are Φ_{TOTAL} (295 K) / Φ_{TOTAL} (218 K) ≈ 4 and ≈ 20 at 310 nm and 322.5 nm, respectively.

A major difference in the study of Blitz et al.,[4,5] from several of the earlier studies is that the OH radicals are detected before undergoing secondary reactions, so that the OH yields represent the CH_3CO radicals produced. The quantum yields reported from the Gierczak et al.[12] and Emrich and Warneck[9] studies were based upon the removal of $CH_3C(O)CH_3$, which may be affected by the additional loss of acetone due to the OH + acetone reaction where OH radicals are produced in the reaction of CH_3CO with O_2. However, the OH yield in the $CH_3CO + O_2$ reaction is a strong function of pressure and measurements made at pressures >50 Torr are expected to have negligible errors.

The quantum yield data of Blitz et al.[4,5] are recommended. The optimized parameterization of the quantum yields for the wavelength range 279–327.5 nm, temperature range 218–295 K and pressure range 0–1000 mbar is as follows:

$$\Phi_{TOTAL}(\lambda, [M], T) = \Phi_{CH3CO}(\lambda, [M], T) + \Phi_{CO}(\lambda, T); \quad \text{all } \lambda$$

For λ = 279-327.5 nm

$$\Phi_{CO}(\lambda, T) = 1 / (1 + A_0)$$

where

$$A_0 = [a_0 / (1 - a_0)] \exp[b_0 (\lambda - 248)]$$

$$a_0 = (0.350 \pm 0.003)\,(T/295)^{(-1.28 \pm 0.03)}$$

$$b_0 = (0.068 \pm 0.002)\,(T/295)^{(-2.65 \pm 0.20)}$$

For λ = 279-302 nm

$$\Phi_{CH3CO}(\lambda, [M], T) = (1 - \Phi_{CO}(\lambda, T)) / (1 + A_1[M])$$

where

$$A_1 = a_1 \exp[-b_1 ((10^7/\lambda) - 33113)]$$

$$a_1 = (1.600 \pm 0.032) \times 10^{-19}\,(T/295)^{(-2.38 \pm 0.08)}$$

$$b_1 = (0.55 \pm 0.02) \times 10^{-3}\,(T/295)^{(-3.19 \pm 0.13)}$$

For λ = 302-327.5 nm

$$\Phi_{CH3CO}(\lambda, [M], T) = ((1 + A_4[M] + A_3) / [(1 + A_2[M] + A_3)(1 + A_4[M])])(1 - \Phi_{CO}(\lambda, T))$$

where

$$A_2 = a_2 \exp[-b_2 ((10^7/\lambda) - 30488)]$$

$$a_2 = (1.62 \pm 0.06) \times 10^{-17}\,(T/295)^{(-10.03 \pm 0.20)}$$

$$b_2 = (1.79 \pm 0.02) \times 10^{-3}\,(T/295)^{(-1.364 \pm 0.036)}$$

$$A_3 = a_3 \exp[-b_3 ((10^7/\lambda) - c_3)^2]$$

$$a_3 = (26.29 \pm 0.88)\,(T/295)^{(-6.59 \pm 0.23)}$$

$$b_3 = (5.72 \pm 0.20) \times 10^{-7}\,(T/295)^{(-2.93 \pm 0.09)}$$

$$c_3 = (30006 \pm 41)\,(T/295)^{(-0.064 \pm 0.004)}$$

$$A_4 = a_4 \exp[-b_4 ((10^7/\lambda) - 30488)]$$

$$a_4 = (1.67 \pm 0.14) \times 10^{-15}\,(T/295)^{(-7.25 \pm 0.54)}$$

$$b_4 = (2.08 \pm 0.02) \times 10^{-3}\,(T/295)^{(-1.16 \pm 0.15)}$$

where [M] is in molecule cm^{-3}, λ in nm and T in K. The equations given above have been used to calculate the quantum yields recommended in Table 4D-26-2**.**

It is well established that acetone photolysis at wavelengths >300 nm has a strong dependence on pressure and temperature but there remains some uncertainty in the absolute quantum yield values in this wavelength region. The effect of the temperature dependent quantum yields of acetone on the chemistry of the upper troposphere has been modeled by Arnold et al.[2] and shown to be significant. Additional quantum yield studies are desired at atmospherically relevant photolysis wavelengths, >290 nm, as a function of pressure and temperature to reduce uncertainties in model calculations.

Table 4D-26-1. Recommended Absorption Cross Sections of $CH_3C(O)CH_3$ at 298 K and Temperature Coefficients

λ (nm)	10^{20} σ (cm^2)	10^3 A (K^{-1})	10^5 B (K^{-2})	10^8 C (K^{-3})	λ (nm)	10^{20} σ (cm^2)	10^3 A (K^{-1})	10^5 B (K^{-2})	10^8 C (K^{-3})
215	0.167	-10.46	8.346	-16.43	283	4.71	1.137	-1.350	3.272
216	0.180	-9.192	7.357	-14.51	284	4.62	0.8530	-1.158	2.943
217	0.196	-6.233	5.039	-10.01	285	4.54	0.6518	-1.023	2.714
218	0.212	-3.190	2.651	-5.359	286	4.44	0.4907	-0.9154	2.531
219	0.228	-1.002	0.9314	-2.003	287	4.36	0.3190	-0.7992	2.332
220	0.246	0.4104	-0.1807	0.1679	288	4.28	0.1109	-0.6586	2.092
221	0.270	1.567	-1.090	1.936	289	4.15	-0.1230	-0.5036	1.833
222	0.294	2.962	-2.183	4.058	290	4.06	-0.3698	-0.3426	1.568
223	0.318	4.839	-3.651	6.909	291	3.95	-0.6430	-0.1615	1.265
224	0.346	6.940	-5.293	10.09	292	3.82	-0.9625	0.05796	0.8847
225	0.380	8.598	-6.588	12.60	293	3.71	-1.316	0.306	0.4472
226	0.419	9.380	-7.200	13.79	294	3.57	-1.650	0.535	0.0477
227	0.456	9.551	-7.336	14.06	295	3.42	-1.905	0.699	-0.2168
228	0.492	9.705	-7.462	14.31	296	3.26	-2.084	0.796	-0.3430
229	0.535	10.08	-7.761	14.89	297	3.11	-2.234	0.867	-0.4086
230	0.584	10.41	-8.023	15.41	298	2.98	-2.391	0.942	-0.4824
231	0.637	10.39	-8.002	15.36	299	2.82	-2.590	1.055	-0.6387
232	0.693	10.01	-7.707	14.79	300	2.67	-2.915	1.277	-1.020
233	0.750	9.534	-7.332	14.06	301	2.58	-3.421	1.649	-1.709
234	0.815	9.138	-7.022	13.46	302	2.45	-4.008	2.091	-2.543
235	0.885	8.851	-6.799	13.02	303	2.30	-4.508	2.465	-3.248
236	0.956	8.638	-6.634	12.70	304	2.18	-4.858	2.715	-3.699
237	1.03	8.471	-6.504	12.45	305	2.05	-5.120	2.880	-3.959
238	1.11	8.318	-6.385	12.22	306	1.89	-5.433	3.062	-4.219
239	1.21	8.125	-6.235	11.93	307	1.75	-6.010	3.429	-4.805
240	1.30	7.861	-6.031	11.53	308	1.61	-6.986	4.096	-5.954
241	1.40	7.554	-5.793	11.07	309	1.49	-8.135	4.899	-7.370
242	1.50	7.268	-5.571	10.64	310	1.36	-8.897	5.415	-8.255
243	1.60	7.035	-5.390	10.29	311	1.24	-8.923	5.378	-8.097
244	1.72	6.838	-5.237	9.994	312	1.14	-8.494	5.001	-7.305
245	1.83	6.649	-5.093	9.718	313	1.06	-8.228	4.754	-6.772
246	1.95	6.472	-4.960	9.464	314	0.944	-8.445	4.881	-6.959
247	2.07	6.326	-4.850	9.256	315	0.837	-8.966	5.240	-7.592
248	2.20	6.210	-4.763	9.091	316	0.760	-9.409	5.528	-8.076
249	2.33	6.099	-4.680	8.936	317	0.684	-9.584	5.588	-8.085
250	2.47	5.972	-4.587	8.763	318	0.598	-9.736	5.596	-7.946
251	2.60	5.832	-4.486	8.576	319	0.523	-10.39	5.958	-8.433
252	2.74	5.697	-4.389	8.399	320	0.455	-11.80	6.869	-9.933
253	2.87	5.581	-4.306	8.249	321	0.411	-13.48	7.962	-11.75
254	3.01	5.483	-4.235	8.120	322	0.348	-14.59	8.600	-12.67
255	3.15	5.385	-4.164	7.989	323	0.294	-14.98	8.670	-12.47
256	3.30	5.261	-4.075	7.825	324	0.248	-15.39	8.743	-12.27
257	3.44	5.101	-3.961	7.620	325	0.210	-16.28	9.187	-12.77
258	3.57	4.932	-3.843	7.410	326	0.174	-17.09	9.588	-13.21
259	3.69	4.802	-3.756	7.262	327	0.141	-17.21	9.471	-12.68
260	3.81	4.746	-3.723	7.215	328	0.113	-16.92	9.048	-11.58
261	3.94	4.744	-3.730	7.239	329	0.0913	-16.66	8.672	-10.62
262	4.07	4.734	-3.729	7.246	330	0.0740	-15.94	7.979	-9.099
263	4.20	4.651	-3.674	7.155	331	0.0586	-13.93	6.340	-5.829
264	4.32	4.482	-3.559	6.956	332	0.0465	-10.93	3.969	-1.214
265	4.41	4.271	-3.416	6.712	333	0.0375	-8.186	1.847	2.840
266	4.49	4.087	-3.296	6.513	334	0.0311	-6.530	0.6289	5.067
267	4.56	3.983	-3.234	6.420	335	0.0248	-5.692	0.1022	5.880

λ (nm)	10^{20} σ (cm^2)	10^3 A (K^{-1})	10^5 B (K^{-2})	10^8 C (K^{-3})	λ (nm)	10^{20} σ (cm^2)	10^3 A (K^{-1})	10^5 B (K^{-2})	10^8 C (K^{-3})
268	4.64	3.969	-3.235	6.440	336	0.0199	-4.656	-0.5382	6.860
269	4.72	4.009	-3.273	6.524	337	0.0162	-2.090	-2.355	10.09
270	4.79	4.025	-3.294	6.577	338	0.0135	3.113	-6.237	17.33
271	4.87	3.935	-3.240	6.494	339	0.0113	11.01	-12.26	28.77
272	4.91	3.704	-3.085	6.231	340	0.0912	20.02	-19.22	42.15
273	4.94	3.378	-2.861	5.845	341	0.0729	27.20	-24.83	53.03
274	4.94	3.061	-2.645	5.473	342	0.0583	29.63	-26.80	56.96
275	4.94	2.854	-2.508	5.243	343	0.0494	25.97	-24.04	51.78
276	4.93	2.790	-2.474	5.201	344	0.0365	16.35	-16.63	37.55
277	4.92	2.816	-2.505	5.276	345	0.00301	3.774	-6.858	18.72
278	4.94	2.820	-2.518	5.316	346	0.00235	-2.414	-1.987	9.304
279	4.92	2.692	-2.433	5.175	347	0.00158	7.880	-9.888	24.53
280	4.91	2.389	-2.222	4.803	348	0.00111	29.52	-26.61	56.78
281	4.86	1.963	-1.922	4.272	349	0.00107	41.03	-35.51	73.95
282	4.79	1.517	-1.612	3.726					

Note:
Gierczak et al.,[12] parameterization of the temperature dependence revised by Burkholder,[7] $\sigma(T, \lambda) = \sigma(298\ K, \lambda)(1 + A\ T + B\ T^2 + C\ T^3)$ for T = 235–298 K

Table 4D-26-2. Recommended Acetone Photolysis Quantum Yields

λ (nm)	Φ(218 K)	Φ(248 K)	Φ(273 K)	Φ(295 K)
279	0.680	0.579	0.571	0.617
280	0.663	0.558	0.551	0.597
281	0.644	0.536	0.530	0.578
282	0.621	0.513	0.509	0.559
283	0.594	0.489	0.489	0.540
284	0.565	0.465	0.468	0.521
285	0.534	0.441	0.448	0.502
286	0.500	0.417	0.427	0.483
287	0.465	0.393	0.407	0.464
288	0.430	0.369	0.388	0.446
289	0.394	0.345	0.368	0.428
290	0.359	0.322	0.350	0.411
291	0.324	0.300	0.331	0.394
292	0.291	0.279	0.314	0.377
293	0.260	0.258	0.297	0.361
294	0.231	0.239	0.280	0.345
295	0.205	0.221	0.264	0.330
296	0.180	0.203	0.249	0.315
297	0.158	0.187	0.235	0.301
298	0.138	0.172	0.221	0.287
299	0.121	0.158	0.208	0.274
300	0.105	0.144	0.195	0.261
301	0.0915	0.132	0.183	0.249
302	0.0794	0.121	0.125	0.237
303	0.0735	0.101	0.105	0.213
304	0.0557	0.0810	0.0873	0.184
305	0.0421	0.0646	0.0728	0.159
306	0.0317	0.0514	0.0608	0.137
307	0.0239	0.0409	0.0508	0.119
308	0.0180	0.0325	0.0426	0.103
309	0.0135	0.0258	0.0358	0.0887
310	0.0101	0.0205	0.0301	0.0769
311	0.00762	0.0164	0.0255	0.0669
312	0.00574	0.0131	0.0216	0.0584
313	0.00433	0.0105	0.0184	0.0511
314	0.00328	0.00842	0.0158	0.0449
315	0.00249	0.00679	0.0136	0.0396
316	0.00190	0.00550	0.0117	0.0350
317	0.00145	0.00447	0.0101	0.0311
318	0.00111	0.00365	0.00882	0.0278
319	0.000858	0.00299	0.00771	0.0248
320	0.000664	0.00246	0.00676	0.0223
321	0.000515	0.00204	0.00595	0.0201
322	0.000400	0.00169	0.00526	0.0181
323	0.000312	0.00141	0.00466	0.0164
324	0.000244	0.00117	0.00414	0.0149
325	0.000191	0.000983	0.00369	0.0135
326	0.000149	0.000826	0.00329	0.0124
327	0.000117	0.000696	0.00295	0.0113

Note:
Blitz et al.[4,5] calculated using the expression given in the text

(1) Aloisio, S.; Francisco, J. S. The photochemistry of acetone in the presence of water. *Chem. Phys. Lett.* **2000**, *329*, 179-184, doi:10.1016/S0009-2614(00)01001-0.
(2) Arnold, S. R.; Chipperfield, M. P.; Blitz, M. A.; Heard, D. E.; Pilling, M. J. Photodissociation of acetone: Atmospheric implications of temperature-dependent quantum yields. *Geophys. Res. Lett.* **2004**, L07110, doi:10.1029/2003GL019099.
(3) Blitz, M. A.; Heard, D. E.; Pilling, M. J. Study of acetone photodissociation over the wavelength range 248-330 nm: Evidence of a mechanism involving both the singlet and triplet excited states. *J. Phys. Chem. A* **2006**, *110*, 6742-6756, doi:10.1021/jp056276g.
(4) Blitz, M. A.; Heard, D. E.; Pilling, M. J.; Arnold, S. R.; Chipperfield, M. P. Correction to ''Pressure and temperature-dependent quantum yields for the photodissociation of acetone between 279 and 327.5 nm''. *Geophys. Res. Lett.* **2004**, *31*, L09104, doi:10.1029/2004GL020182.
(5) Blitz, M. A.; Heard, D. E.; Pilling, M. J.; Arnold, S. R.; Chipperfield, M. P. Pressure and temperature-dependent quantum yields for the photodissociation of acetone between 279 and 327.5 nm. *Geophys. Res. Lett.* **2004**, *31*, L06111, doi:1029/2003GL018793.
(6) Braun, W.; Klein, R.; Fahr, A.; Okabe, H.; Mele, A. Laser photolysis of trimethylgallium at 193 nm: Quantum yields for methyl radical and ethane production. *Chem. Phys. Lett.* **1990**, *166*, 397-403, doi:10.1016/0009-2614(90)85050-M.
(7) Burkholder, J. B., personal communication to the NASA JPL Panel.
(8) Calvert, J. G.; Pitts, J. N. Photochemistry; John Wiley & Sons, Inc.: New York, 1966; pp 783.
(9) Emrich, M.; Warneck, P. Photodissociation of acetone in air: Dependence on pressure and wavelength. Behavior of the excited singlet state. *J. Phys. Chem. A* **2000**, *104*, 9436-9442, doi:10.1021/jp001873i.
(10) Emrich, M.; Warneck, P. Photodissociation of acetone in air: Dependence on pressure and wavelength. Behavior of the excited singlet state. *J. Phys. Chem. A* **2005**, *109*, 1752, doi:10.1021/jp0407627.
(11) Gardner, E. P.; Wijayaratne, R. D.; Calvert, J. G. Primary quantum yields of photodecomposition of acetone in air under tropospheric conditions. *J. Phys. Chem.* **1984**, *88*, 5069-5076, doi:10.1021/j150665a055.
(12) Gierczak, T.; Burkholder, J. B.; Bauerle, S.; Ravishankara, A. R. Photochemisty of acetone under atmospheric conditions. *Chem. Phys.* **1998**, *231*, 229-244, doi:10.1016/S0301-0104(98)00006-8.
(13) Gierczak, T.; Gilles, M. K.; Bauerle, S.; Ravishankara, A. R. Reaction of hydroxyl radical with acetone. 1. Kinetics of the reactions of OH, OD, and ^{18}OH with acetone and acetone-d_6. *J. Phys. Chem. A* **2003**, *107*, 5014-5020, doi:10.1021/jp027301a.
(14) Hynes, A. J.; Kenyon, E. A.; Pounds, A. J.; Wine, P. H. Temperature dependent absorption cross sections for acetone and *n*-butanone - implications for atmospheric lifetimes. *Spectrochim. Acta* **1992**, *48A*, 1235-1242, doi:10.1016/0584-8539(92)80260-4.
(15) Khamaganov, V.; Karunanandan, R.; Rodriguez, A.; Crowley, J. N. Photolysis of $CH_3C(O)CH_3$ (248 nm, 266 nm), $CH_3C(O)C_2H_5$ (248 nm) and $CH_3C(O)Br$ (248 nm): pressure dependent quantum yields of CH_3 formation. *Phys. Chem. Chem. Phys.* **2007**, *9*, 4098-4113, doi:10.1039/b701382e.
(16) Khamaganov, V. G.; Karunanandan, R.; Horowitz, A.; Dillon, T. J.; Crowley, J. N. Photolysis of $CH_3C(O)CH_3$ at 248 and 266 nm: pressure and temperature dependent overall quantum yields. *Phys. Chem. Chem. Phys.* **2009**, *11*, 6173-6181, doi:10.1039/b904130c.
(17) Krasnoperov, L. N.; Mehta, K. Kinetic study of CH_3 + HBr and CH_3 + Br reactions by laser photolysis - transient absorption over 1 - 100 bar pressure range. *J. Phys. Chem. A* **1999**, *103*, 8008-8020, doi:10.1021/jp991183i.
(18) Lake, J. S.; Harrison, A. J. Absorption of acyclic oxygen compounds in the vacuum ultraviolet. III. Acetone and acetaldehyde. *J. Chem. Phys.* **1959**, *30*, 361-362, doi:10.1063/1.1729955.
(19) Martinez, R. D.; Buitrago, A. A.; Howell, N. W.; Hearn, C. H.; Joens, J. A. The near UV absorption spectra of several aliphatic aldehydes and ketones. *Atmos. Environ.* **1992**, *26A*, 785-792, doi:10.1016/0960-1686(92)90238-G.
(20) Meyrahn, H. Bildungswege und Analytik des Peroxyacetylnitrats (PAN) in der Atmosphäre. PhD-Thesis, Johann-Gutenberg-Universität, 1984.
(21) Meyrahn, H.; Pauly, J.; Schneider, W.; Warneck, P. Quantum yields for the photodissociation of acetone in air and an estimate for the life time of acetone in the lower troposphere. *J. Atmos. Chem.* **1986**, *4*, 277-291, doi:10.1007/BF00052006.
(22) Nádasdia, R.; Kovácsa, G.; Szilágyia, I.; Demetera, A.; Dóbé, S. Exciplex laser photolysis study of acetone with relevance to tropospheric chemistry. *Chem. Phys. Lett.* **2007**, *440*, 31-35, doi:10.1016/j.cplett.2007.04.014.
(23) Rajakumar, B.; Gierczak, T.; Flad, J. E.; Ravishankara, A. R.; Burkholder, J. B. The CH_3CO quantum yield in the 248 nm photolysis of acetone, methyl ethyl ketone, and biacetyl. *J. Photochem. Photobiol. A: Chem.* **2008**, *199*, 336-344, doi:10.1016/j.jphotochem.2008.06.015.

(24) Röth, E. P.; Ruhnke, R.; Moortgat, G.; Meller, R.; Schneider, W. UV/VIS-Absorption Cross Sections and Quantum Yields for Use in Photochemistry and Atmospheric Modeling, Forschungszentrum Jülich Publication, Part 1 : Inorganic Substances (jül-3340), Part 2: Organic Substances (jül-3341). **1997**.
(25) Seki, K.; Okabe, H. Photodissociation of methylacetylene at 193 nm. *J. Phys. Chem.* **1992**, *96*, 3345-3349, doi:10.1021/j100187a031.
(26) Somnitz, H.; Fida, M.; Ufer, T.; Zellner, R. Pressure dependence for the CO quantum yield in the photolysis of acetone at 248 nm: A combined experimental and theoretical study. *Phys. Chem. Chem. Phys.* **2005**, *7*, 3342 - 3352, doi:10.1039/b506738c.
(27) Somnitz, H.; Ufer, T.; Zellner, R. Acetone photolysis at 248 nm revisited: pressure dependence of the CO and CO_2 quantum yields. *Phys. Chem. Chem. Phys.* **2009**, *11*, 8522-8531, doi:10.1039/b906751e.
(28) Warneck, P. Photodissociation of acetone in the troposphere: an algorithm for the quantum yield. *Atmos. Environ.* **2001**, *35*, 5773-5777, doi:10.1016/S1352-2310(01)00365-X.
(29) Wollenhaupt, M.; Carl, S. A.; Horowitz, A.; Crowley, J. N. Rate coefficients for reaction of OH with acetone between 202 and 395 K. *J. Phys. Chem. A* **2000**, *104*, 2695-2705, doi:10.1021/jp993738f.
(30) Yujing, M.; Mellouki, A. The near-UV absorption cross sections for several ketones. *J. Photochem. Photobiol. A: Chem.* **2000**, *134*, 31-36, doi:10.1016/S1010-6030(00)00243-4.

D27. $CH_3C(O)CH_2O_2$ (acetonylperoxy radical)

Back to Index

$CH_3C(O)CH_2O_2 + h\nu \rightarrow$ Products (1)

(Recommendation: 10-6, Note: 10-6, Evaluated: 10-6)

Absorption Cross Sections: The UV absorption spectrum of the acetonylperoxy radical, $CH_3C(O)CH_2O_2$, has been measured at room temperature by Cox et al.,[2] Bridier et al.,[1] and Nielsen et al.[3] The spectra from Cox et al.[2] and Nielsen et al.[3] are in good agreement but differ significantly from the spectrum reported by Bridier et al.[1] The spectrum reported by Cox et al.[2] and Nielsen et al.[3] exhibit two absorption features in the 200–340 nm region; a strong band at wavelengths <260 nm and a fairly weak band centered at 300 nm. Nielsen et al.[3] determined the cross section of the acetonylperoxy radical at 240 nm to be $(2.03 \pm 0.22) \times 10^{-18}$ cm^2 molecule^{-1} relative to the well-established absorption cross section of CH_3O_2. The cross sections of Cox et al.,[2] renormalized to the absolute value at 240 nm of Nielsen et al.,[3] are recommended and listed in Table 4D-27.

Photolysis Quantum Yields and Product Studies: No recommendation.

Table 4D-27. Recommended Absorption Cross Sections of $CH_3C(O)CH_2O_2$ at 298 K

λ (nm)	10^{20} σ (cm^2)
225	313
230	254
235	228
240	203
245	186
250	157
255	135
260	111
270	101
280	106
290	111
300	112
310	110
320	104
330	92
340	71
350	51
360	33
370	17
380	7

Note:
Cox et al.,[2] normalized to the 240 nm cross section from Nielsen et al.[3]

(1) Bridier, I.; Veyret, B.; Lesclaux, R.; Jenkin, M. E. Flash photolysis study of the UV spectrum and kinetics of reactions of the acetonylperoxy radical. *J. Chem. Soc. Faraday Trans.* **1993**, *89*, 2993-2997, doi:10.1039/ft9938902993.
(2) Cox, R. A.; Munk, J.; Nielsen, O. J.; Pagsberg, P.; Ratajczak, P. Ultraviolet absorption spectra and kinetics of acetonyl and acetonylperoxy radicals. *Chem. Phys. Lett.* **1990**, *173*, 206-210, doi:10.1016/0009-2614(90)80079-S.
(3) Nielsen, O. J.; Johnson, M. S.; Wallington, T. J.; Christensen, L. K.; Platz, J. UV absorption cross sections of HO_2, CH_3O_2, $C_2H_5O_2$ and $CH_3C(O)CH_2O_2$ radicals and mechanism of the reactions of F and Cl atoms with $CH_3C(O)CH_3$. *Int. J. Chem. Kinet.* **2002**, *34*, 283-291, doi:10.1002/kin.10037.

D28. $CH_3C(O)C(O)H$ (methylglyoxal, MGLY)

Back to Index

$CH_3C(O)C(O)H + h\nu$	$\rightarrow CH_3CO + HCO$	305 kJ mol^{-1}	422 nm	(1)
	$\rightarrow CH_4 + 2CO$	–25 kJ mol^{-1}	All	(2)
	$\rightarrow CH_3CHO + CO$	–6 kJ mol^{-1}	All	(3)

(Recommendation: 06-2, Note: 10-6, Evaluated: 10-6)

Absorption Cross Sections: The UV/vis absorption spectrum of methylglyoxal (MGLY), $CH_3C(O)C(O)H$, has been measured at room temperature by Plum et al.[5] (230–470 nm), Meller et al.[4] (218–494 nm), Chen et al.[1] (290–440 nm), and Staffelbach et al.[7] (205–474 nm). The absorption spectrum exhibits two absorption bands, a slightly structured band between 225 and 335 nm and a stronger band between 335 and 475 nm, which is highly structured in the region above 410 nm. A steep increase of the absorption cross sections was observed at shorter wavelengths going from 225 to 200 nm by Staffelbach et al.[7]

The room temperature values of Meller et al.[4] and Staffelbach et al.[7] are in good agreement at wavelengths >230 nm. In the weaker absorption band the data of Meller et al.[4] are greater by up to 10–15%. In the strong absorption band up to 400 nm, the data of Staffelbach et al.[7] are greater by up to ~10% than the data of Meller et al.,[4] and at higher wavelengths the peak values reported by Meller et al.[4] are higher (due to the higher resolution used in their study) than those measured by Staffelbach et al.[7] The data points of Chen et al.[1] determined at 10 nm intervals fit well to the absorption curves of Meller et al.[4] and Staffelbach et al.[7] except at 380 and 400 nm where the differences are ~20%. The cross sections reported by Plum et al.[5] are approximately only the half of the cross sections reported Meller et al.[4] and Staffelbach et al.[7] The recommended absorption cross sections in Table 4D-28 are from Staffelbach et al.[7] in the region 200–218 nm, the mean of the values from Meller et al.[4] and Staffelbach et al.[7] in the region 219–235 nm, and averages over 1 nm intervals of the data from Meller et al.[4] in the region 236–493 nm.

The temperature dependence of the absorption spectrum is relatively weak with differences on the order of 10% observed in the spectra measured by Staffelbach et al.[7] at 298 and 248 K. The largest changes occur in the structured region between 410 and 450 nm where the fine structure becomes more pronounced at lower temperatures.

Photolysis Quantum Yield and Product Studies: Quantum yields have been measured in several studies. Kyle and Orchard[3] reported products formed in the photolysis of methylglyoxal at 387 K and 436 nm. Staffelbach et al.[7] measured the products after photolysis of dilute mixtures of methylglyoxal in air using a Xe arc equipped with different band pass filters to isolate several regions of the spectrum. The observed products (CO, CO_2, HCHO, CH_3COOH, CH_3COOOH, CH_3OH and HCOOH,) led to the conclusion that only channel (1) is important in the photolysis range 240–480 nm. Quantum yields were derived by modeling the products formed using a number of secondary radical reactions. At 760 Torr, the Φ_1 yields were: 0.005 for the wavelength region 410–418 nm, 0.055 for 355–480 nm, 0.07 for 280–240 nm and 0.14 for 240–420 nm. Raber and Moortgat[6] irradiated methylglyoxal in air at different total pressures using two types of broadband lamps and determined the products (CO, CO_2, HCHO, CH_3OOH, CH_3OH, HCOOH, CH_3CHO, CH_3COOH, CH_3COOOH and $CH_3COCOOH$). The quantum yield derived by modeling the products of the photolysis in the 275-380 nm region varied from 0.94 ± 0.04 at 54 Torr to 0.64 ± 0.03 at 760 Torr, and in the 390–470 nm region from 0.41 ± 0.04 to 0.23 ± 0.02.

Koch and Moortgat[2] determined the quantum yields of CO, HCHO and CH_3CHO formation at 298 K as a function of wavelength (260–440 nm) and pressure of synthetic air (30–900 Torr) using "broad" monochromatic light, with an optical resolution of 8.5 nm. For photolysis in the 260–320 nm band, the overall quantum yield was found to be unity, independent of wavelength and pressure. The analysis of the data gave evidence that channel (1) is the predominant photolysis path. In the 380–440 nm band the quantum yield of CO showed a Stern-Volmer pressure dependence and the quantum yield of H_2CO increased with increasing

methylglyoxal pressure, which was attributed to the reaction of excited methylglyoxal with ground state methylglyoxal.

The quantum yield of channel (1) over the wavelength range 250–500 nm was expressed as:

$$1/\Phi_1(\lambda) = 1/\Phi_0(\lambda) + P(\text{Torr}) / k(\lambda)$$

where

$\Phi_0(\lambda) = 1$ for $\lambda < 380$ nm
$\Phi_0(\lambda) = (8.15 \pm 0.7)\ 10^{-9}\ [\exp(7131 \pm 267) / \lambda]$ for $\lambda > 380$ nm
$k(\lambda) = (7.34 \pm 0.1)\ 10^{-9}\ [\exp(8793 \pm 300) / \lambda]$

Chen et al.[1] used a tunable dye laser to photolysed methylglyoxal at 10 nm intervals over the range 290–440 nm combined with detection of the primary HCO radical photolysis product using cavity ring-down spectroscopy. The HCO quantum yield was calibrated against HCO produced in the photolysis of HCHO or Cl_2/HCHO mixtures. They report the HCO quantum yield to be unity in the wavelength range 320–360 nm, 0.82 ± 0.06 at 290 nm, and to decrease at wavelengths >370 nm to a value of 0.17 ± 0.02 at 440 nm. The HCO quantum yields were reported to be independent of pressure between 290 and 370 nm for the pressure range 10–400 Torr N_2 but to have a Stern-Volmer pressure dependence at wavelengths ≥380 nm given by:

$$1/\Phi_1(\lambda) = 1/\Phi_0(\lambda) + k_Q(\lambda)\ P(\text{Torr})$$

where

$$\Phi_0(\lambda) = (3.63 \pm 0.32) \times 10^{-7}\ [\exp(5693 \pm 533) / \lambda]$$

and

$$k_Q(\lambda) = (1.93 \pm 0.24) \times 10^{4}\ [\exp(-(5639 \pm 497) / \lambda]$$

The zero pressure quantum yields, $\Phi_0(\lambda)$, are in good agreement for wavelengths ≤ 420 nm. However, the quantum yields at 760 Torr from the Chen et al.[1] and Koch and Moortgat[2] expressions deviate by a factor 4 for wavelengths ≥420 nm. The data from the more direct study by Chen et al.[1] are recommended. Additional measurements are needed to establish the quantum yields in the long wavelength tail of the spectrum at atmospherically relevant pressures.

Table 4D-28. Recommended Absorption Cross Sections of $CH_3C(O)C(O)H$ at 298 K

λ (nm)	10^{20} σ (cm^2)	λ (nm)	10^{20} σ (cm^2)	λ (nm)	10^{20} σ (cm^2)	λ (nm)	10^{20} σ (cm^2)	λ (nm)	10^{20} σ (cm^2)
200	33.8	259	3.25	318	1.82	377	2.10	436	11.1
201	30.6	260	3.29	319	1.68	378	2.18	437	10.0
202	27.0	261	3.33	320	1.50	379	2.30	438	10.6
203	23.0	262	3.36	321	1.34	380	2.42	439	11.0
204	18.6	263	3.42	322	1.22	381	2.54	440	9.94
205	15.3	264	3.49	323	1.14	382	2.70	441	10.4
206	12.1	265	3.59	324	1.01	383	2.88	442	10.2
207	10.0	266	3.73	325	0.924	384	3.03	443	10.2
208	8.52	267	3.87	326	0.848	385	3.20	444	11.2
209	7.43	268	4.02	327	0.774	386	3.39	445	9.62
210	6.34	269	4.13	328	0.716	387	3.61	446	8.91
211	5.58	270	4.20	329	0.672	388	3.71	447	9.84
212	4.73	271	4.22	330	0.647	389	3.88	448	9.19
213	4.16	272	4.23	331	0.620	390	4.03	449	10.1
214	3.57	273	4.27	332	0.608	391	4.22	450	8.68
215	3.08	274	4.31	333	0.525	392	4.31	451	6.35
216	2.65	275	4.37	334	0.531	393	4.47	452	6.33
217	2.33	276	4.49	335	0.495	394	4.57	453	6.08
218	2.10	277	4.64	336	0.455	395	4.67	454	4.47
219	1.46	278	4.77	337	0.407	396	4.87	455	3.69
220	1.45	279	4.87	338	0.362	397	5.08	456	3.09
221	1.44	280	4.92	339	0.346	398	5.26	457	2.47
222	1.43	281	4.93	340	0.322	399	5.46	458	1.81
223	1.44	282	4.90	341	0.300	400	5.62	459	1.28
224	1.43	283	4.83	342	0.289	401	5.90	460	0.914
225	1.44	284	4.76	343	0.288	402	6.07	461	0.795

λ (nm)	10^{20} σ (cm^2)	λ (nm)	10^{20} σ (cm^2)	λ (nm)	10^{20} σ (cm^2)	λ (nm)	10^{20} σ (cm^2)	λ (nm)	10^{20} σ (cm^2)
226	1.46	285	4.70	344	0.289	403	6.36	462	0.643
227	1.48	286	4.66	345	0.295	404	6.55	463	0.480
228	1.51	287	4.65	346	0.308	405	6.92	464	0.332
229	1.53	288	4.73	347	0.325	406	7.20	465	0.268
230	1.60	289	4.84	348	0.339	407	7.59	466	0.228
231	1.61	290	4.92	349	0.362	408	7.95	467	0.188
232	1.65	291	4.90	350	0.385	409	8.12	468	0.160
233	1.67	292	4.81	351	0.424	410	8.52	469	0.133
234	1.75	293	4.70	352	0.463	411	8.64	470	0.108
235	1.83	294	4.57	353	0.492	412	9.07	471	0.0998
236	1.86	295	4.37	354	0.523	413	9.38	472	0.0897
237	1.93	296	4.17	355	0.556	414	9.62	473	0.0776
238	1.96	297	4.00	356	0.597	415	9.69	474	0.0680
239	2.00	298	3.88	357	0.635	416	9.72	475	0.0627
240	2.07	299	3.76	358	0.676	417	10.0	476	0.0561
241	2.14	300	3.69	359	0.720	418	10.1	477	0.0515
242	2.19	301	3.70	360	0.765	419	10.1	478	0.0483
243	2.23	302	3.74	361	0.816	420	10.2	479	0.0462
244	2.27	303	3.74	362	0.872	421	10.3	480	0.0392
245	2.30	304	3.62	363	0.933	422	10.5	481	0.0366
246	2.33	305	3.38	364	1.00	423	10.5	482	0.0315
247	2.38	306	3.15	365	1.08	424	10.2	483	0.0278
248	2.46	307	2.92	366	1.15	425	10.3	484	0.0271
249	2.57	308	2.71	367	1.23	426	10.0	485	0.0243
250	2.64	309	2.52	368	1.31	427	9.84	486	0.0217
251	2.68	310	2.34	369	1.40	428	10.0	487	0.0186
252	2.71	311	2.18	370	1.47	429	9.94	488	0.0181
253	2.73	312	2.06	371	1.55	430	10.4	489	0.0170
254	2.76	313	1.97	372	1.64	431	10.5	490	0.0174
255	2.82	314	1.90	373	1.73	432	9.79	491	0.0162
256	2.93	315	1.86	374	1.81	433	10.6	492	0.0161
257	3.06	316	1.86	375	1.90	434	10.5	493	0.0138
258	3.17	317	1.87	376	2.02	435	10.8		

Note:
200–218 nm: Staffelbach et al.[7]
219–235 nm: mean of data from Meller et al.[4] and Staffelbach et al.[7]
219–493 nm: Meller et al.[4]

(1) Chen, Y.; Wang, W.; Zhu, L. Wavelength-dependent photolysis of methylglyoxal in the 290-440 nm region. *J. Phys. Chem. A* **2000**, *104*, 11126-11131, doi:10.1021/jp002262t.

(2) Koch, S.; Moortgat, G. K. Photochemistry of methylglyoxal in the vapor phase. *J. Phys. Chem. A* **1998**, *102*, 9142-9153, doi:10.1021/jp981915r.

(3) Kyle, E.; Orchard, S. W. The photolysis of methyl glyoxal vapour at 436 nm. *J. Photochem.* **1977**, *7*, 305-317, doi:10.1016/0047-2670(77)80012-9.

(4) Meller, R.; Raber, W.; Crowley, J. N.; Jenkin, M. E.; Moortgat, G. K. The UV-visible absorption spectrum of methylglyoxal. *J. Photochem. Photobiol. A: Chem.* **1991**, *62*, 163-171, doi:10.1016/1010-6030(91)87017-P.

(5) Plum, C. N.; Sanhueza, E.; Atkinson, R.; Carter, W. P. L.; Pitts, J. N., Jr. OH radical rate constant and photolysis rates of α-dicarbonyls. *Environ. Sci. Technol.* **1983**, *17*, 479-484, doi:10.1021/es00114a008.

(6) Raber, W. H.; Moortgat, G. K. Photooxidation of selected carbonyl compounds in air: methyl ethyl ketone, methyl vinyl ketone, methacrolein, and methylglyoxal. In *Progress and Problems in Atmospheric Chemistry*; Barker, J., Ed.; World Scientific Publ. Co.: Singapore, 1996; pp 318-373.

(7) Staffelbach, T. A.; Orlando, J. J.; Tyndall, G. S.; Calvert, J. G. The UV-visible absorption spectrum and photolysis quantum yields of methylglyoxal. *J. Geophys. Res.* **1995**, *100*, 14189-14198, doi:10.1029/95JD00541.

D29. $CH_3C(O)CH_2OH$ (hydroxyacetone, acetol)

Back to Index

$CH_3C(O)CH_2OH + h\nu$	$\rightarrow CH_3C(O) + CH_2OH$	376 kJ mol^{-1}	318 nm	(1)
	$\rightarrow HOCH_2C(O) + CH_3$	376 kJ mol^{-1}	318 nm	(2)
	$\rightarrow HOCH_2 + CO + CH_3$	335 kJ mol^{-1}	357 nm	(3)
	$\rightarrow HO + CH_2C(O)CH_3$	335 kJ mol^{-1}	357 nm	(4)

(Recommendation: 25-1, Note: 25-1, Evaluated: 25-1)

Absorption Cross Sections: The absorption cross sections of $CH_3C(O)CH_2OH$ (hydroxyacetone, acetol) have been measured by Meller and Crowley[5] (207–333 nm) at 296 K; by Orlando et al.[7] (235–340 nm) at 298 K by Butkovskaya et al.[2] (240–350 nm) at 294 K using a static method, and at 328 K over the range 250–350 nm using a dynamic method; and by Messaadia et al.[6] (200–360 nm) at 298 K and at 250 and 273 K over the range 200–320 nm. Dillon et al.[4] measured the cross section at 184.9 nm and 358 K to be $(5.4 \pm 0.1) \times 10^{-18}$ cm^2 $molecule^{-1}$, whereas Baasandorj et al.[1] reported a value of $(5.43 \pm 0.08) \times 10^{-18}$ cm^2 $molecule^{-1}$ at 298 K, which implies no cross section temperature dependence at 184.9 nm within the precision of the measurements. The spectrum shows an absorption band with the maximum near 266 nm. The shape of the measured spectra are in excellent agreement except for the spectrum obtained by Butkovskaya et al.[2] using the dynamic method. The maxima cross sections reported by Butkovskaya et al.[2] are 15% and 24% lower for the static and dynamic methods, respectively, than the values obtained by Orlando et al.[7]; the maximum reported by Meller and Crowley[5] is 11% lower than that of Orlando et al.[7] Large discrepancies between the measured spectra exist at $\lambda > 310$ nm.

Table 4D-29 lists the recommended absorption cross sections at 298 K between 200 and 335 nm (see footnote). The spectrum temperature dependence is not well defined by the available data and no recommendation is made.

Photolysis Quantum Yield and Product Studies: Quantum yields for removal of hydroxyacetone were estimated by Orlando et al.[7] to be 0.65 ± 0.25 for the photolysis in the 240–420 nm band. They also suggested that $0.3 \pm 0.2 < \Phi_1 + \Phi_2 < 0.6$ for wavelengths greater than 290 nm. Products detected were CO, CO_2, CH_2O, $CH_3C(O)OH$, $CH_3C(O)O_2H$, HC(O)OH, and CH_3OH. These authors concluded that at most 50% of the photolysis occurred via channel (1). Direct observation of OH radicals, presumably arising from channel (4), was made by Chowdhury et al.[3] at 148 nm. Photolysis of hydroxyacetone at 193 nm was performed by Chowdhury et al.[3] and appears to occur by process (2) with the initial formation of $HOCH_2CO$ yielding OH and ketene.

Table 4D-29. Absorption Cross Sections of $CH_3C(O)CH_2OH$ at 298 K

λ (nm)	10^{20} σ (cm^2)	λ (nm)	10^{20} σ (cm^2)	λ (nm)	10^{20} σ (cm^2)
200	38.7	246	3.57	292	2.17
201	30.5	247	3.76	293	2.00
202	28.0	248	3.91	294	1.82
203	27.9	249	3.93	295	1.65
204	22.6	250	4.33	296	1.48
205	18.1	251	4.51	297	1.34
206	14.7	252	4.69	298	1.19
207	12.0	253	4.87	299	1.05
208	9.37	254	5.01	300	0.936
209	7.24	255	5.17	301	0.846
210	5.73	256	5.34	302	0.748
211	4.43	257	5.48	303	0.655
212	3.42	258	5.61	304	0.575
213	2.69	259	5.71	305	0.500
214	2.11	260	5.81	306	0.444
215	1.72	261	5.90	307	0.393
216	1.37	262	5.98	308	0.368
217	1.14	263	6.05	309	0.332
218	0.990	264	6.09	310	0.294
219	0.880	265	6.11	311	0.249
220	0.760	266	6.12	312	0.219
221	0.800	267	6.12	313	0.192
222	0.710	268	6.11	314	0.177
223	0.740	269	6.08	315	0.157
224	0.760	270	6.01	316	0.142
225	0.800	271	5.93	317	0.133
226	0.840	272	5.84	318	0.117
227	0.900	273	5.74	319	0.104
228	0.980	274	5.63	320	0.095
229	1.04	275	5.51	321	0.087
230	1.12	276	5.39	322	0.078
231	1.25	277	5.22	323	0.072
232	1.38	278	5.06	324	0.067
233	1.47	279	4.88	325	0.063
234	1.60	280	4.68	326	*0.056*
235	1.75	281	4.49	327	*0.053*
236	1.89	282	4.26	328	*0.051*
237	2.04	283	4.08	329	*0.047*
238	2.18	284	3.88	330	*0.044*
239	2.34	285	3.68	331	*0.041*
240	2.46	286	3.48	332	*0.038*
241	2.83	287	3.24	333	*0.036*
242	2.81	288	3.01	334	*0.034*
243	3.01	289	2.80	335	*0.032*
244	3.18	290	2.59		
245	3.37	291	2.38		

Note:
200–239 nm: Messaadia et al.[6]
240–310 nm: average of Orlando et al.,[7] Butkovskaya et al.[2] (static), and Messaadia et al.[6]
311–335 nm: Orlando et al.[7] (at λ >326 nm smoothed)

(1) Baasandorj, M.; Griffith, S.; Dusanter, S.; Stevens, P. S. Experimental and theoretical studies of the OH + hydroxyacetone reaction as a function of temperature. *J. Phys. Chem. A* **2009**, *113*, 10495-10502, doi:10.1021/jp904238w.

(2) Butkovskaya, N. I.; Pouvesle, N.; Kukui, A.; Mu, Y.; Bras, G. L. Mechanism of the OH-initiated oxidation of hydroxyacetone over the temperature range 236-298 K. *J. Phys. Chem. A* **2006**, *110*, 6833-6843, doi:10.1021/jp056345r.
(3) Chowdhury, P. K.; Upadhyaya, H. P.; Naik, P. D.; Mittal, J. P. Direct observation of OH photofragment from triplet hydroxyacetone. *Chem. Phys. Lett.* **2002**, *351*, 201-207, doi:10.1016/S0009-2614(01)01377-X.
(4) Dillon, T. J.; Horowitz, A.; Hölscher, D.; Crowley, J. N.; Vereecken, L.; Peeters, J. Reaction of HO with hydroxyacetone ($HOCH_2C(O)CH_3$): rate coefficients (233-363 K) and mechanism. *Phys. Chem. Chem. Phys.* **2006**, *8*, 236-246, doi:10.1039/B513056E.
(5) Meller, R.; Crowley, J. N. E.-P. Röth, R. Ruhnke, G. Moortgat, R. Meller, and W. Schneider, Berichte des Forschungszentums Jülich, jül-3341 (1997). Data from the CD-ROM of A. Nölle, F. Pätzold, S. Pätzold, R. Meller, G. K. Moortgat, E. P. Röth, R. Ruhnke, H. Keller-Rudek, "UV/VIS Spectra of Atmospheric Constituents, Version 1," ATMOS User Center at Deutsches Fernerkundungsdatenzentrum (DFD). *Personal Communication* **1998**.
(6) Messaadia, L.; El Dib, G.; Ferhati, A.; Roth, E.; Chakir, A. Gas phase UV absorption cross-sections for a series of hydroxycarbonyls. *Chem. Phys. Lett.* **2012**, *529*, 16-22, doi:10.1016/j.cplett.2012.01.044.
(7) Orlando, J. J.; Tyndall, G. S.; Fracheboud, J.-M.; Estupiñan, E. G.; Haberkorn, S.; Zimmer, A. The rate and mechanism of the gas-phase oxidation of hydroxyacetone. *Atmos. Environ.* **1999**, *33*, 1621-1629, doi:10.1016/S1352-2310(98)00386-0.

D30. CH_2=CHCHO (propenal, acrolein)

Back to Index

CH_2=CHCHO + hν	→ CH_2=CH + HCO	–	–	(1)
	→ C_2H_4 + CO	162 kJ mol^{-1}	741 nm	(2)
	→ CH_2=CHCO + H	393 kJ mol^{-1}	305 nm	(3)

(Recommendation: 06-2, Note: 10-6, Evaluated: 10-6)

Absorption Cross Sections: The VUV/UV/vis absorption spectrum of acrolein (CH_2=CHCHO, propenal) has been measured at room temperature by Gardner et al.[1] (227–380 nm), Magneron et al.[3] (192–431 nm), and Lee et al.[2] The UV spectrum displays a broad absorption band between 250 and 400 nm, which is structured at wavelengths above 360 nm. The results of both studies agree to within 10% between 298 and 370 nm (with a few exceptions at 352, 360, 362 and 368 nm). Below 298 nm the differences increase up to ~40% with decreasing wavelength, above 368 nm the differences increase with increasing wavelength up to ~100%. The recommended absorption cross sections in Table 4D-30 are the 2 nm averages from the high resolution data of Magneron et al.[3]

Photolysis Quantum Yield and Product Studies: The photodecomposition of CH_2=CHCHO was studied by Gardner et al.[1] at 313 and 334 nm over the pressure range 26–760 Torr air. They found photolysis at high pressures to be very inefficient at both wavelengths, but the photolysis quantum yield to increase at low pressure. At 313 nm the quantum yield for photodissociation Φ_d of acrolein was 0.0065 at 1 atm and 0.081 at 26 Torr. The pressure dependence was described by:

$$1/(\Phi_d - 0.004) = 0.086 + 1.613 \times 10^{-17}\,[M]$$

for concentrations (M) between 8×10^{17} and 2.6×10^{19} molecule cm^{-3}. The major products observed were CO and C_2H_4. Magneron et al.[3] used broadband photolysis (275–380 nm) of dilute mixtures of acrolein in air to study CH_2=CHCHO photodissociation but did not observe any products using long-path FTIR spectroscopy. An effective quantum yield for photolysis $\Phi_{eff} \leq 0.005$ nm was measured by Magneron et al.[3] in an outdoor smog chamber.

Table 4D-30. Recommended Absorption Cross Sections of CH_2=CHCHO at 298 K

λ (nm)	10^{20} σ (cm^2)	λ (nm)	10^{20} σ (cm^2)	λ (nm)	10^{20} σ (cm^2)	λ (nm)	10^{20} σ (cm^2)
282	0.84	310	3.59	338	5.46	366	3.74
284	0.97	312	3.92	340	5.31	368	3.82
286	1.08	314	4.15	342	5.10	370	2.17
288	1.23	316	4.21	344	5.12	372	1.58
290	1.46	318	4.47	346	5.30	374	1.14
292	1.62	320	4.65	348	5.17	376	1.14
294	1.80	322	5.08	350	5.94	378	1.24
296	1.97	324	5.17	352	5.79	380	1.10
298	2.18	326	5.34	354	4.18	382	0.84
300	2.47	328	5.20	356	3.63	384	0.79
302	2.70	330	5.31	358	3.28	386	1.18
304	2.85	332	5.44	360	3.92	388	0.49
306	3.09	334	5.80	362	3.72	390	0.25
308	3.29	336	6.24	364	2.86		

Note:
Magneron et al.[3]

(1) Gardner, E. P.; Sperry, P. D.; Calvert, J. G. Photodecomposition of acrolein in O_2-N_2 mixtures. *J. Phys. Chem.* **1987**, *91*, 1922-1930, doi:10.1021/j100291a048.

(2) Lee, A. M. D.; Coe, J. D.; Ullrich, S.; Ho, M.-L.; Lee, S.-J.; Cheng, B.-M.; Zgierski, M. Z.; Chen, I.-C.; Martinez, T. J.; Stolow, A. Substituent effects on dynamics at conical intersections: α,β-enones. *J. Phys. Chem. A* **2007**, *111*, 11948–11960, doi:10.1021/jp074622j.

(3) Magneron, I.; Thévenet, R.; Mellouki, A.; Le Bras, G.; Moortgat, G. K.; Wirtz, K. A study of the photolysis and OH-initiated oxidation of acrolein and *trans*-crotonaldehyde. *J. Phys. Chem. A* **2002**, *106*, 2526-2537, doi:10.1021/jp013413a.

D31. $C_2H_5C(O)OH$ (propionic acid)

Back to Index

$C_2H_5C(O)OH + h\nu \rightarrow$ Products (1)

(Recommendation: 06-2, Note: 10-6, Evaluated: 10-6)

Absorption Cross Sections: The absorption spectrum of propionic acid, $C_2H_5C(O)OH$, and the propionic acid dimer, $(C_2H_5C(O)OH)_2$, have been measured by Hintze et al.[1] (195–220 nm) at 283, 303 and 338 K and Vicente et al.[3] (115–257 nm) at 313 K. The spectrum has a strong absorption band in the region 115–192 nm and a weaker band in the region 192–248 nm with a broad maximum near 207 nm. Hinze et al.[1] determined the absorption cross section for the monomer at 206.1 nm and 297 K to be $(1.52 \pm 0.16) \times 10^{-19}$ cm^2 $molecule^{-1}$. The dimer cross section at 208.1 nm was determined to be $(3.24 \pm 0.22) \times 10^{-19}$ cm^2 $molecule^{-1}$. Absorption cross sections have also been measured at 298 and 356.2 K and 222 nm by Singleton et al.[2] These investigators obtained absorption cross sections of 12.2×10^{-20} cm^2 $molecule^{-1}$ at 298 K and 10.6×10^{-20} cm^2 $molecule^{-1}$ at 356.2 K for the monomer and derived absorption cross sections of 10.6×10^{-20} cm^2 $molecule^{-1}$ at 298 K and 25.6×10^{-20} cm^2 $molecule^{-1}$ at 356.2 K for the dimer by an extrapolation procedure.

Photolysis Quantum Yield and Product Studies: Quantum yields for the formation of OH radicals at 222 nm have been measured by Singleton et al.[2] to be 0.148 ± 0.90 and 0.341 ± 0.014 for the monomer at 297.6 and 375.0 K, respectively, and 0.018 ± 0.06 at 297.6 K for the dimer (an OH quantum yield of zero for the dimer was assumed at elevated temperatures).

(1) Hintze, P. E.; Aloisio, S.; Vaida, V. Electronic spectroscopy of organic acid dimers. *Chem. Phys. Lett.* **2001**, *343*, 159-165, doi:10.1016/S0009-2614(01)00664-9.

(2) Singleton, D. L.; Paraskevopoulos, G.; Irwin, R. S. Laser photolysis of carboxyclic acids in the gas phase. Direct determination of the OH quantum yield at 222 nm. *J. Phys. Chem.* **1990**, *94*, 695-699, doi:10.1021/j100365a034.

(3) Vicente, A.; Antunes, R.; Almeida, D.; Franco, I. J. A.; Hoffmann, S. V.; Mason, N. J.; Eden, S.; Duflot, D.; Canneaux, S.; Delwiche, J.; Hubin-Franskin, M.-J.; Limão-Vieira, P. Photoabsorption measurements and theoretical calculations of the electronic state spectroscopy of propionic, butyric, and valeric acids. *Phys. Chem. Chem. Phys.* **2009**, *11*, 5729-5741, doi:10.1039/b823500g.

D32. $CH_3C(O)C(O)OH$ (pyruvic acid)

Back to Index

$$CH_3C(O)C(O)OH + h\nu \rightarrow CH_3CHO + CO_2 \quad (1)$$
$$\rightarrow CH_3CO + COOH \quad (2)$$
$$\rightarrow CH_3COOH + CO \quad (3)$$
$$\rightarrow CH_3CO + CO + OH \quad (4)$$

(Recommendation: 06-2, Note: 10-6, Evaluated: 10-6)

Absorption Cross Sections: The UV absorption spectrum of pyruvic acid, $CH_3C(O)C(O)OH$, has been measured at room temperature by Horowitz et al.[2] (250–410 nm, 0.25 nm resolution) and Mellouki and Mu[3] (290–380 nm). An absorption spectrum of pyruvic acid has also been reported by Yamamoto and Back[7] (250–400 nm) at 358 K. The continuous absorption band between 275–400 nm peaks near 350 nm and contains significant diffuse vibrational band structure. Absolute cross sections for the relative spectrum reported by Yamamoto and Back[7] were given in Horowitz et al.[2] following normalization of the spectrum at 350 nm to 3.82×10^{-20} cm^2 $molecule^{-1}$. The general shapes of the reported spectra are qualitatively similar although the spectrum reported by Yamamoto and Back[7] is red shifted and the cross sections at wavelengths <300 nm are considerably greater. This difference in cross section may in part be ascribed to the effect of temperature on the spectrum. The cross sections measured by Mellouki and Mu[3] are systematically greater than those obtained by Horowitz et al.[2] The difference reaches a factor of two for wavelengths <295 nm and is ~20–30% between 305 and 370 nm. These differences are most likely due to the difficulties in handling the pyruvic acid sample and determining its concentration. The recommended absorption cross sections in Table 4D-32 are 1 nm averages from Horowitz et al.[2] in the range 252–285 nm, the mean of the data from Horowitz et al.[2] and Mellouki and Mu[3] (both 1 nm averages) in the range 290–380 nm, and the data from Horowitz et al.[2] in the range 385–399 nm.

Photolysis Quantum Yield and Product Studies: Moortgat[4] reported an effective quantum yield for pyruvic acid photodissociation under atmospheric conditions from a study in an outdoor photoreactor to be 0.43 ± 0.07. Vesley and Leermakers[5] reported quantum yields of CO_2 of 1.02 ± 0.06 and of CH_3CHO of 0.6 for photolysis at 366 nm. Yamamoto and Back[7] measured quantum yields of CO_2 of 0.9 ± 0.1 and CH_3CHO of 0.45 at 366 nm and 340 K. The CH_3CHO yields obtained for 320 and 345 nm photolysis were more variable. Berges and Warneck[1] measured the quantum yields of CH_3CHO, CO_2 and CH_3COOH at 350 nm to be 0.48 ± 0.01, 1.27 ± 0.18 and 0.14, respectively. In the presence of NO_2, the quantum yield of CH_3CHO was reduced to 0.30 ± 0.04 and PAN was formed with a quantum yield of 0.15 ± 0.02. Berges and Warneck[1] established $\Phi_1 = 0.48 \pm 0.01$ and $\Phi_2 = 0.39 \pm 0.10$. Mellouki and Mu[3] used a laser flash photolysis system at 355 nm and observed the formation of OH originating via channel (4) with a quantum yield of $\Phi_4 = 0.05 \pm 0.03$. The analysis of the products CH_3CHO, CO, CH_3COOH by Winterhalter et al.[6] are consistent with the data of Berges and Warneck[1] and lead to a quantum yield of channel (3) $\Phi_3 = 0.08 \pm 0.03$. For the photolysis of pyruvic acid at 366 nm the following quantum yields are recommended $\Phi_1 = 0.48 \pm 0.01$, $\Phi_2 = 0.39 \pm 0.10$, $\Phi_3 = 0.08 \pm 0.03$ and $\Phi_4 = 0.05 \pm 0.03$.

Table 4D-32. Recommended Absorption Cross Sections of $CH_3C(O)C(O)OH$ at 298 K

λ (nm)	10^{20} σ (cm^2)	λ (nm)	10^{20} σ (cm^2)	λ (nm)	10^{20} σ (cm^2)	λ (nm)	10^{20} σ (cm^2)	λ (nm)	10^{20} σ (cm^2)
252	1.54	280	0.118	312	1.34	340	3.93	368	3.16
253	1.55	281	0.101	313	1.42	341	3.94	369	3.52
254	1.61	282	0.093	314	1.49	342	4.19	370	3.26
255	1.56	283	0.098	315	1.57	343	4.24	371	2.87
256	1.52	284	0.104	316	1.69	344	4.17	372	2.04
257	1.41	285	0.113	317	1.83	345	4.26	373	1.76
258	1.25	290	0.302	318	1.94	346	4.46	374	1.68
259	1.07	291	0.323	319	2.05	347	4.58	375	1.22
260	0.908	292	0.370	320	2.17	348	4.73	376	1.09
261	0.801	293	0.409	321	2.31	349	4.92	377	0.950
262	0.737	294	0.439	322	2.41	350	4.98	378	0.842
263	0.718	295	0.470	323	2.50	351	4.79	379	0.688
264	0.718	296	0.491	324	2.54	352	4.63	380	0.521
265	0.700	297	0.519	325	2.60	353	4.54	385	0.097
266	0.651	298	0.548	326	2.72	354	4.47	386	0.084
267	0.566	299	0.594	327	2.78	355	4.13	387	0.077
268	0.470	300	0.639	328	2.84	356	3.89	388	0.066
269	0.367	301	0.678	329	2.98	357	3.66	389	0.056
270	0.278	302	0.724	330	3.15	358	3.41	390	0.047
271	0.224	303	0.775	331	3.35	359	3.22	391	0.034
272	0.195	304	0.822	332	3.66	360	3.44	392	0.031
273	0.185	305	0.898	333	3.87	361	3.59	393	0.026
274	0.182	306	0.977	334	3.91	362	3.37	394	0.015
275	0.188	307	1.04	335	3.96	363	3.01	395	0.011
276	0.189	308	1.13	336	4.02	364	2.85	396	0.006
277	0.180	309	1.21	337	4.02	365	2.86	397	0.002
278	0.164	310	1.22	338	3.99	366	2.80	398	0.002
279	0.139	311	1.27	339	3.956	367	2.88	399	<0.001

Note:
252–285 nm: Horowitz et al.[2]
290–380 nm: mean of the data from Horowitz et al.[2] and Mellouki and Mu[3]
385–399 nm: Horowitz et al.[2]

(1) Berges, M. G. M.; Warneck, P. Product quantum yields for 350 nm photodecomposition of pyruvic acid in air. *Ber. Bunsenges. Phys. Chem.* **1992**, *96*, 413-416, doi:10.1002/bbpc.19920960334.
(2) Horowitz, A.; Meller, R.; Moortgat, G. K. The UV-VIS absorption cross sections of the a-dicarbonyl compounds: pyruvic acid, biacetyl and glyoxal. *J. Photochem. Photobiol. A: Chem.* **2001**, *146*, 19-27, doi:10.1016/S1010-6030(01)00601-3.
(3) Mellouki, A.; Mu, Y. On the atmospheric degradation of pyruvic acid in the gas phase. *J. Photochem. Photobiol. A: Chem.* **2003**, *157*, 295-300, doi:10.1016/S1010-6030(03)00070-4.
(4) Moortgat, G. K. Important photochemical processes in the atmosphere. *Pure Appl. Chem.* **2001**, *73*, 487-490, doi:10.1351/pac200173030487.
(5) Vesley, G. F.; Leermakers, P. A. The photochemistry of α-keto acids and α-keto esters. III. Photolysis of pyruvic acid in the vapor phase. *J. Phys. Chem.* **1964**, *68*, 2364-2366, doi:10.1021/j100790a507.
(6) Winterhalter, R.; Jensen, N. R.; Magneron, I.; Wirtz, K.; Mellouki, A.; Mu, Y.; Tadic, J.; Horowitz, A.; Moortgat, G. K.; Hjorth, J. "Proceedings of the EUROTRAC-2 Symposium 2000", 2001, Springer, Berlin.
(7) Yamamoto, S.; Back, R. A. The photolysis and thermal decomposition of pyruvic acid in the gas phase. *Can. J. Chem.* **1985**, *63*, 549-554, doi:10.1139/v85-089.

D33. $HC(O)OC_2H_5$ (ethyl formate)

Back to Index

$HC(O)OC_2H_5 + h\nu \rightarrow$ Products (1)

(Recommendation: 25-1, Note: 25-1, Evaluated: 25-1)

Absorption Cross Sections: The UV absorption spectrum of ethyl formate, $HC(O)OC_2H_5$, has been measured at room temperature by McMillan[1] (201–260 nm), Vésine and Mellouki[3] (211–260 nm) and Smialek et al.[2] (114.5–260 nm). The spectrum exhibits a structured absorption band with the maximum near 215 nm. The data sets agree, to within ~15% from 210 to 240 nm, with the data of Vésine and Mellouki being systematically smaller near the spectrum peak. The recommended absorption cross sections in Table 4D-33 are the high resolution (0.04 nm) data of Vésine and Mellouki averaged over 1 and 2 nm intervals in the ranges 211–230 and 230–260 nm, respectively.

A Lyman-α (121.567 nm) cross section of 4×10^{-17} cm^2 molecule^{-1} from Smialek et al., the only study available, is recommended. An uncertainty factor of 1.5 (2σ) is assigned.

Photolysis Quantum Yield and Product Studies: No recommendation.

Table 4D-33. Recommended Absorption Cross Sections of $HC(O)OC_2H_5$ at 297 K

λ (nm)	10^{20} σ (cm^2)	λ (nm)	10^{20} σ (cm^2)	λ (nm)	10^{20} σ (cm^2)	λ (nm)	10^{20} σ (cm^2)
211	18.6	220	17.8	229	11.2	246	1.47
212	18.6	221	17.1	230	11.0	248	1.04
213	18.3	222	15.9	232	9.03	250	0.665
214	18.5	223	15.1	234	7.21	252	0.405
215	19.0	224	15.0	236	6.50	254	0.251
216	18.9	225	14.9	238	4.96	256	0.119
217	18.1	226	14.0	240	3.67	258	0.0611
218	17.5	227	12.6	242	3.00	260	0.0391
219	17.6	228	11.5	244	2.18		

Note:
Vésine and Mellouki[3] averaged over 1 and 2 nm intervals

(1) Calvert, J. G.; Pitts Jr., J. N. In *Photochemistry*; John Wiley & Sons, Inc.: New York, 1966; pp 368.
(2) Smialek, M. A.; Labuda, M.; Guthmuller, J.; Hubin-Franskin, M.-J.; Delwiche, J.; Duflot, D.; Mason, N. J.; Hoffmann, S. V.; Jones, N. C.; Limão-Vieira, P. Valence and ionic lowest-lying electronic states of ethyl formate as studied by high-resolution vacuum ultraviolet photoabsorption, He(I) photoelectron spectroscopy, and ab initio calculations. *J. Chem. Phys.* **2014**, *141*, 104311, doi:10.1063/1.4894762.
(3) Vésine, E.; Mellouki, A. UV absorption cross sections for a series of formates. *J. Chim. Phys.* **1997**, *94*, 1634-1641, doi:10.1051/jcp/1997941634.

D34. $CH_3C(O)CH_2CH_3$ (2-butanone, methyl ethyl ketone, MEK)

Back to Index

$CH_3C(O)CH_2CH_3 + h\nu$	$\rightarrow CH_3 + C_2H_5CO$	339 nm	(1)
	$\rightarrow C_2H_5 + CH_3CO$	342 nm	(2)
	$\rightarrow CH_3 + C_2H_5 + CO$		(3)

(New)

Absorption Cross Sections: UV absorption cross sections of $CH_3C(O)C_2H_5$ (methyl ethyl ketone) have been measured at room temperature by Brewer et al.[2] (200–335 nm), Chen and Venables[3] (335–376 nm), Hynes et al.[5] (253.7, 260–360 nm), Ito et al.[6] (165–200 nm, graphical data), Martinez et al.[7] (202–355 nm), Nádasdi et al.[8] (221–351 nm), Raber and Moorgat[9] (277 nm), Rajakumar et al.[10] (184.9 nm), Schneider and Moortgat[11] (196–365 nm), and Yujing and Mellouki[12] (240–343 nm), and at 323 K by Doner et al.[4] (125–240 nm). Temperature dependent cross sections have been measured over the range 242–320 K by Brewer et al.[2] (200–335 nm), 261–362 K by Hynes et al.[5] (300–340 nm), and 253–363 K by Nádasdi et al.[8] (221–351 nm).

The room temperature values of Brewer et al., Hynes et al., Martinez et al., Nádasdi et al., Raber and Moortgat, Schneider and Moortgat, and Yujing and Mellouki are in excellent agreement between 230–320 nm. The Doner et al. cross sections are higher than these other studies by more than an order of magnitude over most of the overlapping wavelength range from 200–240 nm; however, there is much better agreement between the studies of Doner et al., Ito et al., and Rajakumar et al. at wavelengths <200 nm. At wavelengths >335 nm, the reported cross sections of Chen and Venables, Hynes et al., Martinez et al., Nádasdi et al., Schneider and Moortgat, and Yujing and Mellouki diverge. The recommended cross sections given in Table 4D-34 are 2 nm interval data from Brewer et al. (reported every 1 nm) between 200–334 nm and 2 nm interpolated data of Chen and Venables (reported approximately every 0.12 nm) between 336–340 nm. Estimated uncertainty factors (2σ) of 1.3 for λ = 200–206 nm, 1.08 for λ = 208–328 nm, and 1.2 for λ = 330–340 nm are recommended.

Photolysis Quantum Yield and Product Studies: Raber and Moortgat found the quantum yield for photolysis of $CH_3C(O)C_2H_5$ over the range 275–380 nm to be 0.34 at 1 atm and 0.89 at 51 Torr, with channel (2) being dominant (80–90%). Photodissociation quantum yields of $CH_3C(O)C_2H_5$ at specific wavelengths have been reported by Baeza-Romero et al.[1] (308 and 320 nm), Nádasdi et al.[8] (248 and 308 nm), and Rajakumar et al.[10] (248 nm). There is general agreement between the studies that the photodissociation quantum yield varies with wavelength and has a negative pressure dependence and a positive temperature dependence. All studies agree that channel (2) is the most important. At 308 nm, the quantum yield values as a function of temperature and pressure in Table 2 of Nádasdi et al. are recommended.

Table 4D-34. Recommended Absorption Cross Sections of $CH_3C(O)CH_2CH_3$ (methyl ethyl ketone) at 298 K

λ (nm)	10^{20} σ (cm^2)	λ (nm)	10^{20} σ (cm^2)	λ (nm)	10^{20} σ (cm^2)
200	2.92	248	2.22	296	3.90
202	0.960	250	2.51	298	3.61
204	0.242	252	2.83	300	3.27
206	0.170	254	3.16	302	2.86
208	0.156	256	3.48	304	2.48
210	0.153	258	3.81	306	2.15
212	0.155	260	4.16	308	1.85
214	0.169	262	4.46	310	1.56
216	0.182	264	4.72	312	1.26
218	0.198	266	5.01	314	1.00
220	0.225	268	5.28	316	0.784
222	0.260	270	5.45	318	0.603
224	0.304	272	5.58	320	0.450
226	0.362	274	5.72	322	0.323
228	0.432	276	5.80	324	0.226
230	0.517	278	5.79	326	0.154
232	0.618	280	5.75	328	0.103
234	0.738	282	5.67	330	0.0670
236	0.879	284	5.52	332	0.0425
238	1.04	286	5.33	334	0.0271
240	1.23	288	5.14	336	0.0139
242	1.44	290	4.91	338	0.00919
244	1.68	292	4.58	340	0.00632
246	1.94	294	4.21		

Note:
200–334 nm: 2 nm values from Brewer et al.[2]
336–340 nm: 2 nm interpolated values from Chen and Venables[3]

(1) Baeza-Romero, M. T.; Blitz, M. A.; Heard, D. E.; Pilling, M. J.; Price, B.; Seakins, P. W.; Wanga, L. Photolysis of methylethyl, diethyl and methylvinyl ketones and their role in the atmospheric HO_x budget. *Faraday Discuss.* **2005**, *130*, 73–88, doi:10.1039/b419160a.

(2) Brewer, J. F.; Papanastasiou, D. K.; Burkholder, J. B.; Fischer, E. V.; Ren, Y.; Mellouki, A.; Ravishankara, A. R. Atmospheric photolysis of methyl ethyl, diethyl, and propyl ethyl ketones: Temperature-dependent UV absorption cross sections. *J. Geophys. Res.* **2019**, *124*, 5906-5918, doi:10.1029/2019JD030391.

(3) Chen, J.; Venables, D. S. A broadband optical cavity spectrometer for measuring weak near-ultraviolet absorption spectra of gases. *Atmos. Meas. Tech.* **2011**, *4*, 425-436, doi:10.5194/amt-4-425-2011.

(4) Doner, A. C.; Webb, A. R.; Dewey, N. S.; Christianson, M. G.; Koritzke, A. L.; Larsson, A.; Frandsen, K. M.; Rotavera, B. Vacuum-ultraviolet absorption cross-sections of functionalized four-carbon species. *J. Quant. Spectrosc. Radiat. Transf.* **2022**, *292*, 108346 doi:10.1016/j.jqsrt.2022.108346.

(5) Hynes, A. J.; Kenyon, E. A.; Pounds, A. J.; Wine, P. H. Temperature dependent absorption cross sections for acetone and *n*-butanone - implications for atmospheric lifetimes. *Spectrochim. Acta* **1992**, *48A*, 1235-1242, doi:10.1016/0584-8539(92)80260-4.

(6) Ito, H.; Nogata, Y.; Matsuzaki, S.; Kuboyama, A. Vacuum-ultraviolet absorption spectra of aliphatic ketones. *Bull. Chem. Soc. Japan* **1969**, *42*, 2453-2458, doi:10.1246/bcsj.42.2453.
(7) Martinez, R. D.; Buitrago, A. A.; Howell, N. W.; Hearn, C. H.; Joens, J. A. The near UV absorption spectra of several aliphatic aldehydes and ketones. *Atmos. Environ.* **1992**, *26A*, 785-792, doi:10.1016/0960-1686(92)90238-G.
(8) Nádasdi, R.; Zügner, G. L.; Farkas, M.; Dóbé, S.; Maeda, S.; Morokuma, K. Photochemistry of methyl ethyl ketone: Quantum yields and S_1/S_0-diradical mechanism of photodissociation. *ChemPhysChem* **2010**, *11*, 3883-3895, doi:10.1002/cphc.201000522.
(9) Raber, W. H.; Moortgat, G. K. Photooxidation of selected carbonyl compounds in air: methyl ethyl ketone, methyl vinyl ketone, methacrolein, and methylglyoxal. In *Progress and Problems in Atmospheric Chemistry*; Barker, J., Ed.; World Scientific Publ. Co.: Singapore, 1996; pp 318-373.
(10) Rajakumar, B.; Gierczak, T.; Flad, J. E.; Ravishankara, A. R.; Burkholder, J. B. The CH_3CO quantum yield in the 248 nm photolysis of acetone, methyl ethyl ketone, and biacetyl. *J. Photochem. Photobiol. A: Chem.* **2008**, *199*, 336-344, doi:10.1016/j.jphotochem.2008.06.015.
(11) Schneider, W.; Moortgat, G. K. personal communication to E.-P. Röth, R. Ruhnke, G. Moortgat, R. Meller, and W. Schneider, Berichte des Forschungszentums Jülich, jül-3341 (1997). **1988**.
(12) Yujing, M.; Mellouki, A. The near-UV absorption cross sections for several ketones. *J. Photochem. Photobiol. A: Chem.* **2000**, *134*, 31-36, doi:10.1016/S1010-6030(00)00243-4.

D35. $CH_2=C(CH_3)CHO$ (2-methylpropenal, methacrolein, MACR)

Back to Index

$$CH_2=C(CH_3)CHO + h\nu \rightarrow CH_2=CCH_3 + CHO \quad (1)$$
$$\rightarrow C_3H_6 + CO \quad (2)$$
$$\rightarrow H + CH_2=C(CH_3)CO \quad (3)$$

(Recommendation: 06-2, Note: 10-6, Evaluated: 10-6)

Absorption Cross Sections: The VUV/UV absorption spectrum of methacrolein (2-methylpropenal, MACR), $CH_2=C(CH_3)CHO$, has been measured using diode array spectroscopy at room temperature by Meller (237–391 nm) (see Keller-Rudek et al.[3]), Raber and Moortgat[5] (331 nm), Gierczak et al.[2] (214, 250–395 nm), and Lee et al.[4] The spectrum exhibits a broad absorption band between 250 and 390 nm with vibrational structure above 310 nm. A detailed vibrational-electronic analysis was reported by Birge et al.[1] The reported spectra are in very good agreement in the region 261–351 nm where the agreement is between ~1 and 10%. At shorter wavelengths, <260 nm, the differences increase to nearly 100% at 250 nm and the cross sections from Gierczak et al.[2] are consistently greater than those of Meller[3] and Raber and Moortgat.[5] The cross sections at the peaks in the structured region reported by Meller and Raber and Moortgat are consistently higher than those measured by Gierczak et al. presumably due to the higher resolution used. At the band maximum, Raber and Moortgat reported $\sigma(330.7\text{ nm}) = 7.64 \times 10^{-20}$ cm^2 molecule^{-1} and Gierczak et al. reported $\sigma(331\text{ nm}) = 7.2 \times 10^{-20}$ cm^2 molecule^{-1}. Gierczak et al. also reported $\sigma(213.86\text{ nm}) = (2.21 \pm 0.11) \times 10^{-17}$ cm^2 molecule^{-1} (Zn lamp source). The 1 nm averages of the results from Gierczak et al. and Meller are generally (with a few exceptions) within 20% of each other for wavelengths up to 376 nm. Above 380 nm, the results of Gierczak et al. are larger with increasing wavelength by up to nearly 80% than the results of Meller. A wavelength shift of ~1 nm toward longer wavelengths can be observed above 340 nm in the absorption spectrum of Gierczak et al. when compared to the spectrum reported by Meller. The recommended absorption cross sections listed in Table 4D-35 are from Gierczak et al.[2]

Photolysis Quantum Yield and Product Studies: The photodissociation quantum yield for $CH_2=C(CH_3)CHO$ at atmospherically relevant wavelengths is low. Quantum yields were measured by Raber and Moortgat[5] using broad band photolysis in the wavelength range 275–380 nm, and determination of the stable products (CO, CO_2, HCHO, C_2H_4, C_3H_6, C_2H_2) by FTIR spectroscopy. An upper limit of 0.05 was reported at 760 Torr. Gierczak et al.[2] used GC and GC-MS detection of photolysis end-products to determined $CH_2=C(CH_3)CHO$ quantum yields at 308 nm of 0.008 ± 0.001 and 0.005 ± 0.001 at 25 and 650 Torr total pressure, respectively. At 351 nm they reported quantum yields of 0.005 ± 0.002 and 0.003 ± 0.001 at 25 and 650 Torr, respectively. A value of Φ <0.01 is recommended for wavelengths >308 nm.

Table 4D-35. Recommended Absorption Cross Sections of $CH_2=C(CH_3)CHO$ at 298 K

λ (nm)	10^{20} σ (cm^2)	λ (nm)	10^{20} σ (cm^2)	λ (nm)	10^{20} σ (cm^2)	λ (nm)	10^{20} σ (cm^2)
250	0.207	287	1.67	324	6.58	361	4.28
251	0.194	288	1.79	325	6.74	362	3.61
252	0.187	289	1.90	326	6.73	363	2.86
253	0.180	290	2.03	327	6.68	364	2.68
254	0.179	291	2.16	328	6.83	365	2.33
255	0.177	292	2.28	329	7.07	366	1.92
256	0.180	293	2.39	330	7.15	367	1.62
257	0.180	294	2.52	331	7.16	368	1.40
258	0.186	295	2.68	332	7.03	369	1.31
259	0.193	296	2.85	333	6.69	370	1.42
260	0.201	297	2.99	334	6.41	371	1.67
261	0.211	298	3.13	335	6.08	372	1.53
262	0.224	299	3.26	336	5.97	373	1.43
263	0.241	300	3.44	337	6.25	374	1.08
264	0.263	301	3.61	338	6.38	375	0.977
265	0.283	302	3.76	339	6.37	376	1.00
266	0.305	303	3.91	340	6.24	377	1.07
267	0.333	304	4.04	341	6.02	378	1.35
268	0.363	305	4.19	342	5.98	379	2.18
269	0.398	306	4.40	343	6.58	380	1.30
270	0.436	307	4.58	344	6.79	381	0.984
271	0.479	308	4.71	345	6.53	382	0.555
272	0.520	309	4.81	346	6.11	383	0.456
273	0.567	310	4.92	347	5.63	384	0.364
274	0.616	311	5.13	348	5.22	385	0.331
275	0.673	312	5.35	349	4.55	386	0.246
276	0.732	313	5.50	350	4.16	387	0.205
277	0.793	314	5.61	351	3.85	388	0.181
278	0.863	315	5.70	352	3.89	389	0.161
279	0.936	316	5.87	353	4.35	390	0.147
280	1.01	317	6.04	354	4.31	391	0.156
281	1.09	318	6.19	355	4.14	392	0.159
282	1.18	319	6.28	356	3.62	393	0.153
283	1.26	320	6.27	357	3.53	394	0.149
284	1.35	321	6.18	358	3.46	395	0.123
285	1.45	322	6.21	359	3.81		
286	1.56	323	6.34	360	5.05		

Note:
Gierczak et al.[2]

(1) Birge, R. R.; Pringle, W. C.; Leermakers, P. A. Excited states geometries of the singly substituted methylpropenals. I. Vibrational-electronic analysis of S_1 (n, p*). *J. Am. Chem. Soc.* **1971**, *93*, 6715-6726, doi:10.1021/ja00754a001.

(2) Gierczak, T.; Burkholder, J. B.; Talukdar, R. K.; Mellouki, A.; Barone, S. B.; Ravishankara, A. R. Atmospheric fate of methyl vinyl ketone and methacrolein. *J. Photochem. Photobiol. A: Chem.* **1997**, *110*, 1-10, doi:10.1016/S1010-6030(97)00159-7.

(3) Keller-Rudek, H.; Moortgat, G. K.; Sander, R.; Sörensen, R. The MPI-Mainz UV/Vis spectral atlas of gaseous molecules of atmospheric interest. *Earth Syst. Sci. Data* **2013**, *5*, 365-373, doi:10.5194/essd-5-365-2013.

(4) Lee, A. M. D.; Coe, J. D.; Ullrich, S.; Ho, M.-L.; Lee, S.-J.; Cheng, B.-M.; Zgierski, M. Z.; Chen, I.-C.; Martinez, T. J.; Stolow, A. Substituent effects on dynamics at conical intersections: α,β-enones. *J. Phys. Chem. A* **2007**, *111*, 11948–11960, doi:10.1021/jp074622j.

(5) Raber, W. H.; Moortgat, G. K. Photooxidation of selected carbonyl compounds in air: methyl ethyl ketone, methyl vinyl ketone, methacrolein, and methylglyoxal. In *Progress and Problems in Atmospheric Chemistry*; Barker, J., Ed.; World Scientific Publ. Co.: Singapore, 1996; pp 318-373.

D36. $CH_3C(O)C(O)CH_3$ (biacetyl)

Back to Index

$CH_3C(O)C(O)CH_3 + h\nu$	$\rightarrow CH_3CO + CH_3CO$	390 nm	(1)
	$\rightarrow CH_3CO + CH_3 + CO$	338 nm	(2)
	$\rightarrow 2\ CH_3 + 2\ CO$	300 nm	(3)

(New)

Absorption Cross Sections: UV absorption cross sections of $CH_3C(O)C(O)CH_3$ (biacetyl) have been measured by Horowitz et al.[2] (205.4–494 nm), Plum et al.[3] (230.6–472.5 nm), and Rajakumar et al.[4] (184.9 nm) at room temperature, and by Doner et al.[1] (125–240 nm) at 323 K. The reported values of Horowitz et al. and Plum et al. are generally in good agreement over the wavelength range 230–465 nm with the exception of the Plum et al. values being significantly greater (by as much as a factor of 2) in the 315–350 nm range, where a local minimum between the broad absorption bands occurs. The Doner et al. cross sections are higher than the Horowitz et al. and Plum et al. values by approximately an order of magnitude in the vicinity of 230 nm where the measurement wavelengths overlap. The Doner et al. results are not considered in the recommendation. The recommended cross sections given in Table 4D-36 are from Horowitz et al. and are 4 nm values from their data (reported every 1 nm) between 206–490 nm. Estimated uncertainty factors (2σ) of $F(\lambda) = 1.2 + 5 \times 10^{-23}/\sigma(\lambda)$ are recommended.

Photolysis Quantum Yield and Product Studies: Rajakumar et al.[4] reported the 248 nm quantum yield for CH_3CO formation to be pressure dependent with values of 0.76 at 61 Torr up to 0.96 at 643 Torr. Plum et al.[3] reported an average quantum yield for biacetyl photolysis of 0.16 for wavelengths ≥290 nm. Based on the study of Rajakumar et al., a quantum yield for channels 1 plus 2 of 0.76 is recommended at 248 nm for pressures 61 Torr and below.

Table 4D-36. Recommended Absorption Cross Sections of $CH_3C(O)C(O)CH_3$ (biacetyl) at 298 K

λ (nm)	$10^{20}\ \sigma$ (cm^2)	λ (nm)	$10^{20}\ \sigma$ (cm^2)	λ (nm)	$10^{20}\ \sigma$ (cm^2)
206	10.3	302	1.54	398	4.92
210	6.74	306	1.27	402	5.26
214	4.29	310	0.815	406	6.00
218	2.90	314	0.480	410	6.69
222	1.70	318	0.360	414	7.31
226	1.23	322	0.321	418	7.51
230	1.41	326	0.212	422	7.25
234	1.68	330	0.196	426	6.81
238	2.15	334	0.216	430	6.31
242	2.54	338	0.284	434	6.78
246	2.94	342	0.346	438	6.42
250	3.31	346	0.442	442	6.99
254	3.73	350	0.565	446	5.90
258	3.94	354	0.729	450	4.06
262	4.46	358	0.916	454	2.16
266	4.49	362	1.19	458	0.853
270	4.95	366	1.49	462	0.356
274	4.85	370	1.85	466	0.143
278	4.67	374	2.17	470	0.0686
282	4.65	378	2.50	474	0.0395
286	3.94	382	2.92	478	0.0249
290	3.38	386	3.53	482	0.0179
294	2.96	390	4.17	486	0.0149
298	2.10	394	4.62	490	0.0176

Note: 4 nm values from Horowitz et al.[2]

(1) Doner, A. C.; Webb, A. R.; Dewey, N. S.; Christianson, M. G.; Koritzke, A. L.; Larsson, A.; Frandsen, K. M.; Rotavera, B. Vacuum-ultraviolet absorption cross-sections of functionalized four-carbon species. *J. Quant. Spectrosc. Radiat. Transf.* **2022**, *292*, 108346 doi:10.1016/j.jqsrt.2022.108346.

(2) Horowitz, A.; Meller, R.; Moortgat, G. K. The UV-VIS absorption cross sections of the a-dicarbonyl compounds: pyruvic acid, biacetyl and glyoxal. *J. Photochem. Photobiol. A: Chem.* **2001**, *146*, 19-27, doi:10.1016/S1010-6030(01)00601-3.
(3) Plum, C. N.; Sanhueza, E.; Atkinson, R.; Carter, W. P. L.; Pitts, J. N., Jr. OH radical rate constant and photolysis rates of α-dicarbonyls. *Environ. Sci. Technol.* **1983**, *17*, 479-484, doi:10.1021/es00114a008.
(4) Rajakumar, B.; Gierczak, T.; Flad, J. E.; Ravishankara, A. R.; Burkholder, J. B. The CH_3CO quantum yield in the 248 nm photolysis of acetone, methyl ethyl ketone, and biacetyl. *J. Photochem. Photobiol. A: Chem.* **2008**, *199*, 336-344, doi:10.1016/j.jphotochem.2008.06.015.

D37. $CH_3C(O)CH=CH_2$ (methyl vinyl ketone, MVK)

Back to Index

$$CH_3C(O)CH=CH_2 + h\nu \rightarrow CH_3\text{-}CH=CH_2 + CO \quad (1)$$
$$\rightarrow CH=CH_2 + CH_3C(O) \quad (2)$$
$$\rightarrow CH=CH_2C(O) + CH_3 \quad (3)$$

(Recommendation: 06-2, Note: 10-6, Evaluated: 10-6)

Absorption Cross Sections: The UV absorption spectrum of methyl vinyl ketone (MVK), $CH_3C(O)CH=CH_2$, has been measured at room temperature by Schneider and Moortgat (240–398 nm) (see Keller-Rudek et al.[4]), Raber and Moortgat[5] (235–400 nm), Fahr et al.[2] (160–260 nm), and Gierzcak et al.[3] (216.86 nm and 250–395 nm). The absorption band peaking at ~330 nm displays some weak vibrational band structure, which is superimposed on a continuum envelope. A detailed vibrational-electronic analysis was reported by Birge et al.[1] The cross sections from Schneider and Moortgat are somewhat smaller around the band maximum at 334 nm (agreement within ~10% between 290 and 365 nm), and larger by up to 50% and smaller by up to ~60% in the short- and long-wavelength tails, respectively, than the results of Gierczak et al.[3] Gierczak et al.[3] reported $\sigma(213.86\text{ nm}) = (6.6 \pm 0.04) \times 10^{-17}$ cm^2 molecule^{-1} (Zn lamp source). They also measured the spectrum at reduced temperatures (range 250–298 K), and observed a small increase in the peak cross section of <2% at 250 K. Fahr et al.[2] reported $\sigma(193\text{ nm}) = (3.2 \pm 0.2) \times 10^{-17}$ cm^2 molecule^{-1}. The recommended absorption cross sections in Table 4D-37 are taken from Gierzcak et al.[3]

Photolysis Quantum Yield and Product Studies: Product quantum yields were measured by Raber and Moortgat[5] using broadband photolysis in the range 275–380 nm combined with FTIR monitoring of the stable photolysis products (major CO, C_3H_6 and HCHO; minor CO_2, HCOOH, CH_3OH, CH_3COOH). They report a pressure dependent quantum yield with $\Phi = 0.05$ at 760 Torr and $\Phi = 0.12$ at 54 Torr. Fahr et al.[2] used laser photolysis at 193.3 nm and measured the direct formation of CH_3 radicals at 216.4 nm and final products. They report a quantum yield close to unity for the formation of CH_3 and $CH=CH_2$ radicals. Gierczak et al.[3] measured quantum yields for photolysis at 308, 337, and 351 nm by monitoring the disappearance of MVK. They reported $\Phi = 0.16$ at 25 Torr and $\Phi = 0.04$ at 760 Torr at 308 nm, $\Phi = 0.04$ at 25 Torr and $\Phi = 0.01$ at 760 Torr at 337 nm; and $\Phi = 0.01$ independent of pressure at 351 nm. The quantum yield data were fit to the empirical Stern-Volmer type expression:

$$\Phi(\lambda,P) = \exp[-0.055\ (\lambda - 308)] / (5.5 + 9.2 \times 10^{-19}\ [M])$$

where λ is in nm and [M] in molecule cm^{-3}. This parameterization is recommended.

Table 4D-37. Recommended Absorption Cross Sections of $CH_3C(O)CH=CH_2$ at 298 K

λ (nm)	10^{20} σ (cm^2)	λ (nm)	10^{20} σ (cm^2)	λ (nm)	10^{20} σ (cm^2)	λ (nm)	10^{20} σ (cm^2)
250	0.241	287	2.03	324	6.88	361	3.60
251	0.241	288	2.15	325	6.95	362	3.49
252	0.224	289	2.29	326	7.02	363	3.36
253	0.241	290	2.43	327	7.09	364	3.29
254	0.241	291	2.55	328	7.16	365	3.03
255	0.258	292	2.67	329	7.23	366	2.77
256	0.275	293	2.81	330	7.28	367	2.50
257	0.275	294	2.93	331	7.30	368	2.20
258	0.293	295	3.08	332	7.26	369	2.01
259	0.310	296	3.24	333	7.18	370	1.88
260	0.327	297	3.39	334	7.04	371	1.74
261	0.361	298	3.56	335	6.94	372	1.58
262	0.379	299	3.70	336	6.85	373	1.48
263	0.396	300	3.87	337	6.70	374	1.39
264	0.430	301	4.05	338	6.56	375	1.31
265	0.465	302	4.20	339	6.47	376	1.26
266	0.499	303	4.35	340	6.44	377	1.24
267	0.534	304	4.51	341	6.42	378	1.21
268	0.568	305	4.66	342	6.35	379	1.21
269	0.620	306	4.82	343	6.35	380	1.05
270	0.654	307	4.96	344	6.30	381	0.981
271	0.706	308	5.13	345	6.23	382	0.912
272	0.757	309	5.30	346	6.14	383	0.878
273	0.809	310	5.44	347	6.08	384	0.929
274	0.878	311	5.58	348	5.77	385	0.757
275	0.929	312	5.73	349	5.47	386	0.637
276	0.998	313	5.87	350	5.20	387	0.534
277	1.08	314	6.02	351	4.94	388	0.448
278	1.15	315	6.14	352	4.72	389	0.396
279	1.24	316	6.28	353	4.53	390	0.344
280	1.33	317	6.42	354	4.32	391	0.310
281	1.41	318	6.54	355	4.15	392	0.293
282	1.50	319	6.63	356	4.03	393	0.275
283	1.60	320	6.70	357	3.94	394	0.241
284	1.70	321	6.76	358	3.89	395	0.207
285	1.81	322	6.83	359	3.89		
286	1.91	323	6.85	360	3.68		

Note:
Gierzcak et al.[3]

(1) Birge, R. R.; Pringle, W. C.; Leermakers, P. A. Excited states geometries of the singly substituted methylpropenals. I. Vibrational-electronic analysis of S_1 (n, p*). *J. Am. Chem. Soc.* **1971**, *93*, 6715-6726, doi:10.1021/ja00754a001.

(2) Fahr, A.; Braun, W.; Laufer, A. H. Photolysis of methyl vinyl ketone at 193.3 nm: Quantum yield determination of methyl and vinyl radicals. *J. Phys. Chem.* **1993**, *97*, 1502-1506, doi:10.1021/j100110a007.

(3) Gierczak, T.; Burkholder, J. B.; Talukdar, R. K.; Mellouki, A.; Barone, S. B.; Ravishankara, A. R. Atmospheric fate of methyl vinyl ketone and methacrolein. *J. Photochem. Photobiol. A: Chem.* **1997**, *110*, 1-10, doi:10.1016/S1010-6030(97)00159-7.

(4) Keller-Rudek, H.; Moortgat, G. K.; Sander, R.; Sörensen, R. The MPI-Mainz UV/Vis spectral atlas of gaseous molecules of atmospheric interest. *Earth Syst. Sci. Data* **2013**, *5*, 365-373, doi:10.5194/essd-5-365-2013.

(5) Raber, W. H.; Moortgat, G. K. Photooxidation of selected carbonyl compounds in air: methyl ethyl ketone, methyl vinyl ketone, methacrolein, and methylglyoxal. In *Progress and Problems in Atmospheric Chemistry*; Barker, J., Ed.; World Scientific Publ. Co.: Singapore, 1996; pp 318-373.

D38. $C_2H_2(CO)_2O$ (maleic anhydride, 2,5-furandione) Back to Index

$C_2H_2(CO)_2O + h\nu \rightarrow$ Products

(New)

Absorption Cross Sections: UV absorption cross sections of $C_2H_2(CO)_2O$ (maleic anhydride) have been measured at 420 K by Back and Parsons[1] (250–360 nm, graphical data) and at room temperature by Marshall et al.[2] (200–360 nm). In the overlapping spectral range of 250–330 nm, the spectra from the two studies generally agree to within 15%, with the cross sections of Marshall et al. being consistently larger. At wavelengths longer than 330 nm, the discrepancy between the studies increases, reaching approximately 60% at 360 nm. The recommended cross sections given in Table 4D-38 are from Marshall et al. and are 2 nm values from their data between 200–360 nm (reported every 0.5 nm). An estimated uncertainty factor (2σ) of 1.2 is recommended.

Photolysis Quantum Yield and Product Studies: Marshall et al.[2] found the photodissociation quantum yield of $C_2H_2(CO)_2O$ at 248 nm to be 0.85 ± 0.20 independent of pressure, and the products CO, CO_2, and C_2H_2 to be formed with unit molar yield.

Table 4D-38. Recommended Absorption Cross Sections of $C_2H_2(CO)_2O$ (maleic anhydride) at 298 K

λ (nm)	10^{20} σ (cm^2)	λ (nm)	10^{20} σ (cm^2)	λ (nm)	10^{20} σ (cm^2)
200	3520	254	6.22	308	3.61
202	3470	256	5.90	310	3.54
204	3330	258	5.43	312	3.42
206	3430	260	5.39	314	3.55
208	3050	262	4.92	316	3.16
210	2140	264	5.95	318	2.97
212	1600	266	5.39	320	2.72
214	2140	268	4.90	322	2.55
216	855	270	4.55	324	2.43
218	534	272	4.15	326	2.30
220	388	274	4.86	328	2.21
222	294	276	4.90	330	2.11
224	226	278	4.28	332	1.75
226	174	280	3.86	334	1.57
228	134	282	3.80	336	1.31
230	103	284	3.74	338	1.23
232	78.4	286	4.19	340	0.970
234	59.3	288	4.16	342	0.952
236	44.2	290	3.79	344	0.891
238	33.0	292	3.78	346	0.870
240	24.3	294	3.70	348	0.519
242	18.0	296	3.72	350	0.789
244	13.3	298	3.74	352	0.515
246	10.5	300	3.97	354	0.396
248	8.25	302	3.72	356	0.353
250	7.06	304	3.87	358	0.350
252	6.10	306	3.42	360	0.300

Note:
Taken from Marshall et al.[2]

(1) Back, R. A.; Parsons, J. M. The thermal and photochemical decomposition of maleic anhydride in the gas phase. *Can. J. Chem.* **1981**, *59*, 1342–1346, doi: 10.1139/v81-197.

(2) Marshall, P.; Papadimitriou, V. C.; Papanastasiou, D. K.; Roberts, J. M.; Burkholder, J. B. UV and infrared absorption spectra and 248 nm photolysis of maleic anhydride ($C_4H_2O_3$). *J. Photochem. Photobio. A: Chem.* **2019**, *382*, 111953, doi:10.1016/j.jphotochem.2019.111953.

D39. $CH_2=C(CH_3)CH=CH_2$ (2-methyl-1,3-butadiene, isoprene)

Back to Index

$CH_2=C(CH_3)CH=CH_2 + h\nu \rightarrow$ Products

(New)

Absorption Cross Sections: UV absorption cross sections of $CH_2=C(CH_3)CH=CH_2$ (isoprene) have been measured at room temperature by Campuzano-Jost et al.[1] (203–233 nm), Dillon et al.[2] (184.95, 194–234 nm), Jacobs and Platt[3] (173–231 nm, graphical data), Jones and Taylor[4] (167–228 nm, graphical data), Martins et al.[5] (116–269 nm), Mui and Grunwald[6] (258–268 nm, graphical data), Sahay et al.[7] (261–275 nm), and Wang et al.[8] (197–235 nm). No temperature-dependent UV cross section data are currently available at atmospherically relevant temperatures. The reported room temperature values of Martins et al. and Dillon et al. agree to within <5% at wavelengths below 226 nm. The values of Wang et al., Campuzano-Jost et al., and Jones and Taylor generally agree with Martins et al. and Dillon et al. to within 10% for the overlapping wavelength regions of the studies, with the exception of Jones and Taylor being significantly lower for wavelengths >218 nm. The study of Jacobs and Platt varies significantly relative to the other five studies in the same wavelength range (typically within 30% but as high as 90% deviation). There are substantial differences between the studies of Martins et al., Mui and Grunwald, and Sahay et al. at wavelengths >260 nm.

The recommended cross sections given in Table 4D-39 are 1 nm values from Martins et al. between 170–258 nm. Higher resolution cross section data (0.1 nm) over a broader wavelength range are available from the Martins et al. study. An estimated uncertainty factor (2σ) of 1.1 is recommended.

The recommended Lyman-α (121.567 nm) cross section is taken from Martins et al. with an estimated uncertainty factor (2σ) of 1.2.

Photolysis Quantum Yield and Product Studies: No recommendation.

Table 4D-39. Recommended Absorption Cross Sections of $CH_2=C(CH_3)CH=CH_2$ (isoprene) at 298 K

λ (nm)	10^{20} σ (cm^2)	λ (nm)	10^{20} σ (cm^2)	λ (nm)	10^{20} σ (cm^2)
121.567	5290	199	3028	229	824
170	1250	200	3288	230	551
171	1276	201	3570	231	374
172	1271	202	3974	232	261
173	1276	203	4354	233	172
174	1308	204	4715	234	124
175	1441	205	5094	235	97.9
176	1470	206	5466	236	76.1
177	1290	207	5743	237	60.6
178	1078	208	6298	238	48.3
179	1398	209	6766	239	39.8
180	1815	210	6873	240	34.9
181	2073	211	6747	241	29.6
182	1284	212	6650	242	26.0
183	985	213	6782	243	22.8
184	1468	214	7232	244	19.5
185	1285	215	7809	245	17.6
186	1353	216	7971	246	15.6
187	1146	217	7504	247	13.9
188	1150	218	6606	248	11.8
189	2126	219	5794	249	10.4
190	1788	220	5371	250	8.73
191	2379	221	5325	251	7.39
192	1416	222	5506	252	6.68
193	1459	223	5410	253	5.53
194	1593	224	4761	254	5.28
195	1777	225	3693	255	4.34
196	2006	226	2628	256	3.29
197	2273	227	1813	257	2.43
198	2576	228	1228	258	2.52

Note:
121.567 nm: Martins et al.[5]
170–258 nm: 1 nm values from Martins et al.[5]

(1) Campuzano-Jost, P.; Williams, M. B.; D'Ottone, L.; Hynes, A. J. Kinetics and mechanism of the reaction of the hydroxyl radical with h_8-isoprene and d_8-isoprene: Isoprene absorption cross sections, rate coefficients, and the mechanism of hydroperoxyl radical production. *J. Phys. Chem. A* **2004**, *108*, 1537-1551, doi:10.1021/jp0363601.

(2) Dillon, T. J.; Dulitz, K.; Groß, C. B. M.; Crowley, J. N. Temperature-dependent rate coefficients for the reactions of the hydroxyl radical with the atmospheric biogenics isoprene, alpha-pinene and delta-3-carene. *Atmos. Chem. Phys.* **2017**, *17*, 15137–15150, doi:10.5194/acp-17-15137-2017.

(3) Jacobs, L. E.; Platt, J. R. Does ultraviolet absorption intensity increase in solution? *J. Chem. Phys.* **1948**, *16*, 1137-1145, doi:10.1063/1.1746745.

(4) Jones, L. C.; Taylor, L. W. Far ultraviolet absorption spectra of unsaturated and aromatic hydrocarbons. *Anal. Chem.* **1955**, *27*, 228-237, doi:10.1021/ac60098a015.

(5) Martins, G.; Ferreira-Rodrigues, A. M.; Rodrigues, F. N.; de Souza, G. G.; Mason, N. J.; Eden, S.; Duflot, D.; Flament, J.-P.; Hoffmann, S. V.; Delwiche, J.; et al. Valence shell electronic spectroscopy of isoprene studied by theoretical calculations and by electron scattering, photoelectron, and absolute photoabsorption measurements. *Phys. Chem. Chem. Phys.* **2009**, *11*, 11219-11231, doi:10.1039/B916620C.

(6) Mui, P. W.; Grunwald, E. Enthalpy change for the s-trans to s-cis conformational equilibrium in 2-methyl-1,3-butadiene (isoprene), as studied by high-temperature ultraviolet absorption spectroscopy. *J. Phys. Chem.* **1984**, *88*, 6340-6344, doi:10.1021/j150669a056.

(7) Sahay, P.; Scherrer, S. T.; Wang, C. Measurements of the weak UV absorptions of isoprene and acetone at 261–275 nm using cavity ringdown spectroscopy for evaluation of a potential portable ringdown breath analyzer. *Sensors* **2013**, *13*, 8170-8187, dio:10.3390/s130708170.

(8) Wang, M.; Connolly, S. C.; Venables, D. S. Deep-ultraviolet absorption cross sections of strongly absorbing atmospheric species. *J. Quant. Spectrosc. Radiat. Transf.* **2024**, *323*, 109050, doi:10.1016/j.jqsrt.2024.109050.

D40. CH_3ONO (methylnitrite)

Back to Index

$CH_3ONO + h\nu \rightarrow CH_3O + NO$ 176 kJ mole^{-1} 680 nm (1)

(Recommendation: 10-6, Note: 10-6, Evaluated: 10-6)

Absorption Cross Sections. The UV/vis absorption spectrum of methylnitrite (CH_3ONO) extends over the wavelength range between 190 and 440 nm and has a strong continuous band in the UV (190–300 nm) with a maximum near 214 nm. A sharply banded region exists in the near UV/vis region (300–440 nm) with nine absorption peaks, the strongest at ~339 nm. The spectrum has been measured at room temperature by McMillan,[1] Taylor et al.,[4] and Maricq and Wallington[2] while single wavelength absorption measurements have been reported by Napier and Norrish[3] at 215 and 339 nm at 298 K and by Wiebe and Heicklen[5] at 366 nm for temperatures in the range 298–423 K. Good agreement exists among these studies for the shape of the UV part of the spectrum. However, a slight wavelength shift is apparent (up to 4 nm) in the peak absorptions measured by Taylor et al.[4] and McMillan.[1] Taylor et al.[4] reported the cross section at the short wavelength band maximum near 215 nm to be $(4.59 \pm 0.58) \times 10^{-18}$ compared to 4.97×10^{-18} by Napier and Norrish,[3] 4.2×10^{-18} by McMillan,[1] and 4.47×10^{-18} cm^2 molecule^{-1} by Maricq and Wallington.[2] The cross section of $(3.24 \pm 0.16) \times 10^{-19}$ measured by Taylor et al.[4] at 339 ± 1 nm is in agreement with the values of 3.4×10^{-19} and 3.1×10^{-19} cm^2 molecule^{-1} reported by Napier and Norrish[3] and McMillan,[1] respectively. The spectrum measured by Taylor et al.[4] is recommended and listed in Table 4D-40.

Photolysis Quantum Yields and Product Studies: The quantum yield for the dissociation in the banded region (300–400 nm) was measured by Wiebe et al.[6] to be $\Phi_1 = 0.76$ at 366 nm.

Table 4D-40. Recommended Absorption Cross Sections of CH_3ONO at 298 K

λ (nm)	10^{20} σ (cm^2)	λ (nm)	10^{20} σ (cm^2)	λ (nm)	10^{20} σ (cm^2)
190	180	306	6.2	362	15
195	240	310	9.0	364	17.2
200	300	312	8.0	366	17.4
205	370	314	7.0	368	12.4
210	430	316	10.5	370	12.4
215	455	318	14	372	12.0
220	440	320	10	374	10.0
225	390	322	8.0	376	8.0
230	340	324	10	378	6.0
235	280	326	13	380	5.05
240	230	328	18	382	5.1
245	180	330	23	384	5.4
250	140	332	13	386	5.6
255	105	334	10.2	388	5.2
260	80	339	32.4	390	4.3
265	57	342	19	395	1.4
270	41	345	13	400	0.5
275	29	348	18	405	0.2
280	20	350	29	410	0.1
285	13.5	352	31.5	415	0.045
290	10.0	354	24	420	0.022
295	8.0	356	19	425	0.011
300	6.9	358	15	430	0.006
302	7.1	360	14	440	0.0015

Note:
Taylor et al.[4]

(1) Calvert, J. G.; Pitts, J. N. Photochemistry; John Wiley & Sons, Inc.: New York, 1966; pp 783.
(2) Maricq, M. M.; Wallington, T. J. Absolute ultraviolet cross sections of methyl and ethyl peroxy radicals. *J. Phys. Chem.* **1992**, *96*, 982-986, doi:10.1021/j100181a081.
(3) Napier, I. M.; Norrish, R. G. W. The photolysis and pyrolysis of nitromethane and methyl nitrite. *Proc. Roy. Soc. London A* **1967**, *299*, 317-336, doi:10.1098/rspa.1967.0139.
(4) Taylor, W. D.; Allston, T. D.; Moscato, M. J.; Fazekas, G. B.; Koslowski, R.; Takacs, G. A. Atmospheric photodissociation lifetimes for nitromethane, methyl nitrite, and methyl nitrate. *Int. J. Chem. Kinet.* **1980**, *12*, 231-240, doi:10.1002/kin.550120404.
(5) Wiebe, H. A.; Heicklen, J. Photolysis of methyl nitrite. *J. Am. Chem. Soc.* **1973**, *95*, 1-7, doi:10.1021/ja00782a001.
(6) Wiebe, H. A.; Villa, A.; Hellman, T. M.; Heicklen, J. Photolysis of methyl nitrite in the presenece of nitric oxide, nitrogen dioxide, and oxygen. *J. Am. Chem. Soc.* **1973**, *95*, 7-13, doi:10.1021/ja00782a002.

D41. CH_3ONO_2 (methylnitrate)

Back to Index

$CH_3ONO_2 + h\nu \rightarrow CH_3O + NO_2$	172 kJ mol^{-1}	697 nm	(1)
$\rightarrow HCHO + HONO$		All	(2)
$\rightarrow HCHO + NO + OH$	240 kJ mol^{-1}	497 nm	(3)
$\rightarrow CH_3ONO + O(^3P)$	306 kJ mol^{-1}	391 nm	(4)
$\rightarrow CH_3 + NO_3$	348 kJ mol^{-1}	344 nm	(5)
$\rightarrow CH_2ONO_2 + H$	407 kJ mol^{-1}	294 nm	(6)
$\rightarrow CH_3O + NO + O(^3P)$	479 kJ mol^{-1}	250 nm	(7)
$\rightarrow CH_3ONO + O(^1D)$	496 kJ mol^{-1}	241 nm	(8)

(Recommendation: 10-6, Note: 10-6, Evaluated: 10-6)

Absorption Cross Sections: The UV absorption spectrum of methylnitrate (CH_3ONO_2) displays a strong continuous band in the region (190–250 nm) and a weaker band in the range (250–345 nm). The spectrum was measured at room temperature by McMillan[1] (201–323 nm), Maria et al.[3] (235–305 nm), Taylor et al.[7] (190–330 nm), Roberts and Fajer[5] (270–330 nm), Libuda and Zabel[2] (235–345 nm) and by Rattigan et al.[4] (220–335 nm) over the range 233–294 K, and Talukdar et al.[6] (236–334 nm) over the range 240–360 K. Good agreement exists at wavelengths <240 nm between the absorption cross sections measured by Taylor et al.[7] and Rattigan et al.[4] In the wavelength range 240–340 nm there is good agreement between the measurements of Roberts and Fajer,[5] Libuda and Zabel,[2] Rattigan et al.,[4] and Talukdar et al.[6] The values of Taylor et al.[7] are consistently larger at λ >270 nm. Between 235 and 280 nm the absorption cross sections measured by Talukdar et al.[6] are nearly independent of temperature but for λ >290 nm the cross sections decrease with decreasing temperature. At 330 nm the cross sections decrease by almost a factor of two between 298 and 240 K. Talukdar et al.[6] parameterized the absorption cross section temperature dependence using the expression:

$$\sigma(\lambda, T) = \sigma(\lambda, 298\ K) \times \exp\,[B(\lambda)\,(T - 298)]$$

The absorption cross sections measured at 298 K by Taylor et al.[7] are recommended between 190 and 235 nm and those of Talukdar et al.[6] in the range 236–344 nm, Table 4D-41. The temperature dependence from Talukdar et al.[6] is recommended and the B(λ) coefficients are listed in Table 4D-41.

Photolysis Quantum Yields and Product Studies: The photodissociation quantum yield for CH_3ONO_2 to produce NO_2 and CH_3O was measured by Talukdar et al.[6] to be $\Phi_1 = 0.91 \pm 0.20$ at 248 nm. Upper limits for the other channels at 248 nm were determined to be Φ_2 <0.05, Φ_3 <0.005, Φ_{4+8} <0.1 and Φ_5 <0.015 ± 0.01. It is expected that the quantum yield Φ_1 is unity at wavelengths >248 nm. Oxygen atoms were measured with a quantum yield of 0.65 ± 0.15 at 193 nm and <0.01 at 248 and 308 nm. Yang et al.[8] studied the photodissociation of jet-cooled CH_3ONO_2 at 193 and 248 nm and found channel (1) to be the principal photolysis product channel with relative yields of 0.7 and 1 at 193 and 248 nm, respectively. They also reported an $O(^1D)$ yield of 0.3 at 193 nm.

Table 4D-41. Recommended Absorption Cross Sections of CH_3ONO_2 at 298 K and Temperature Coefficients

λ (nm)	10^{20} σ (cm^2)	10^3 B (K^{-1})	λ (nm)	10^{20} σ (cm^2)	10^3 B (K^{-1})	λ (nm)	10^{20} σ (cm^2)	10^3 B (K^{-1})
190	1800	–	260	3.07	2.81	304	0.241	5.43
195	1500	–	262	2.96	2.84	306	0.194	5.67
200	1180	–	264	2.84	2.89	308	0.154	6.00
205	700	–	266	2.72	2.94	310	0.121	6.27
210	360	–	268	2.57	3.01	312	0.0940	6.68
215	145	–	270	2.42	3.08	314	0.0723	7.13
220	70	–	272	2.27	3.15	316	0.0548	7.54
225	33	–	274	2.10	3.24	318	0.0412	8.00
230	18	–	276	1.94	3.32	320	0.0304	8.88
235	10	–	278	1.77	3.40	322	0.0228	9.32
236	8.27	3.35	280	1.61	3.51	324	0.0164	10.3
238	6.77	3.44	282	1.45	3.61	326	0.01187	10.7
240	5.66	3.49	284	1.29	3.72	328	0.00868	11.5
242	4.88	3.45	286	1.14	3.84	330	0.00618	13.8
244	4.34	3.36	288	1.00	3.96	332	0.00447	15.5
246	3.97	3.24	290	0.871	4.08	334	0.00311	16.1
248	3.72	3.10	292	0.754	4.21	336	0.00216	–
250	3.56	2.97	294	0.642	4.38	338	0.00161	–
252	3.44	2.88	296	0.519	4.56	340	0.00116	–
254	3.34	2.82	298	0.435	4.72	342	0.000812	–
256	3.25	2.79	300	0.364	4.91	344	0.0004687	–
258	3.16	2.80	302	0.298	5.14			

Note:
190–235 nm: Taylor et al.[7]
236–344 nm: Talukdar et al.[6]
B(λ) are the temperature coefficients in the expression $\sigma(\lambda, T) = \sigma(\lambda, 298\ K) \times \exp [B(\lambda) (T - 298)]$, after Talukdar et al.[6]

(1) Calvert, J. G.; Pitts, J. N. Photochemistry; John Wiley & Sons, Inc.: New York, 1966; pp 783.
(2) Libuda, H. G.; Zabel, F. UV absorption cross sections of acetyl peroxynitrate and trifluoroacetyl peroxynitrate at 298 K. *Ber. Bunsenges. Phys. Chem.* **1995**, *99*, 1205-1213, doi:10.1002/bbpc.199500061.
(3) Maria, H. J.; McDonald, J. R.; McGlynn, S. R. Electronic absorption spectrum of nitrate ion and boron trihalides. *J. Am. Chem. Soc.* **1973**, *95*, 1050-1056, doi:10.1021/ja00785a010.
(4) Rattigan, O.; Lutman, R. L.; Jones, R. L.; Cox, R. A. Temperature-dependent absorption cross-sections of gaseous nitric acid and methyl nitrate. *J. Photochem. Photobiol. A: Chem.* **1992**, *66*, 313-326, doi:10.1016/1010-6030(92)80003-E.
(5) Roberts, J. M.; Fajer, R. W. UV absorption cross sections of organic nitrates of potential atmospheric importance and estimation of atmospheric lifetimes. *Environ. Sci. Technol.* **1989**, *23*, 945-951, doi:10.1021/es00066a003.
(6) Talukdar, R. K.; Burkholder, J. B.; Hunter, M.; Gilles, M. K.; Roberts, J. M.; Ravishankara, A. R. Atmospheric fate of several alkyl nitrates. Part 2. UV absorption cross-sections and photodissociation quantum yields. *J. Chem. Soc. Faraday Trans.* **1997**, *93*, 2797-2805, doi:10.1039/a701781b.
(7) Taylor, W. D.; Allston, T. D.; Moscato, M. J.; Fazekas, G. B.; Koslowski, R.; Takacs, G. A. Atmospheric photodissociation lifetimes for nitromethane, methyl nitrite, and methyl nitrate. *Int. J. Chem. Kinet.* **1980**, *12*, 231-240, doi:10.1002/kin.550120404.
(8) Yang, X.; Felder, P.; Huber, J. R. Photodissociation of methyl nitrate in a molecular beam. *J. Phys. Chem.* **1993**, *97*, 10903-10910, doi:10.1021/j100144a002.

D42. $CH_3CH_2ONO_2$ (ethyl nitrate)

Back to Index

$CH_3CH_2ONO_2 + h\nu$	$\rightarrow CH_3CH_2O + NO_2$	697 nm	(1)
	$\rightarrow CH_3CHO + HONO$	All	(2)
	$\rightarrow CH_3CH_2ONO + O(^3P)$	400 nm	(3)

(New)

Absorption Cross Sections: UV absorption cross sections of $C_2H_5ONO_2$ (ethyl nitrate) have been measured at room temperature by Clemitshaw et al.[1] (235–340 nm), Higgins et al.[2] (240–320 nm), Kaya et al.[3] (170.6–227.3 nm, graphical data), Roberts[4] and Roberts and Fajer[5] (270–330 nm), Talukdar et al.[6] (236–350 nm), Turberg et al.[7] (185–330 nm), Wallace-Goodeve[8] (205.2–319.3 nm, graphical data), and Zhu and Ding[9] (265–340 nm).

The reported room temperature values of Talukdar et al., Turberg et al., and Zhu and Ding are in excellent agreement between 240–310 nm, with the studies of Clemitshaw et al., Higgins et al., and Roberts and Fajer also generally in good agreement over this range. Near the long wavelength extremes of each respective study, the reported cross sections can deviate significantly high (e.g., Higgins et al. and Clemitshaw et al.) or low (Roberts and Fajer) relative to the other values. The values of Wallace-Goodeve deviate both higher and lower from the other studies, with differences mostly within 15%, but as large as 60%. The study of Kaya et al. is an outlier with values typically 50–100% greater than other studies.

The recommended cross sections given in Table 4D-42 are from the data of Turberg et al. (typically reported every 5 nm) between 185–235 nm, averages of the data of Turberg et al. and Talukdar et al. (reported every 2 nm and interpolated to 5 nm) between 240–320 nm, and 5 nm interpolated data of Talukdar et al. between 325–340 nm. An estimated uncertainty factor (2σ) of 1.15 over the 185–340 nm range is recommended.

Temperature-dependent cross sections have been measured and parameterized to empirical equations over the range 240–360 K by Talukdar et al.[6] (236–340 nm), over the range 238–298 K by Zhu and Ding[9] (265–340 nm), and over the range 233–298 K by Clemitshaw et al.[1] (235–335 nm). All three studies are in good agreement. Talukdar et al. parameterized the absorption cross section temperature dependence from 240–360 K using the expression:

$$\sigma(\lambda, T) = \sigma(\lambda, 298\ K) \times \exp[B(\lambda)(T - 298)]$$

The temperature dependence from Talukdar et al. is recommended and the $B(\lambda)$ coefficients are listed in Table 4D-42.

Photolysis Quantum Yield and Product Studies: Zhu and Ding[9] found a quantum yield of 1.0 ± 0.1 for channel (1) at 308 nm, independent of temperature over the narrow temperature range 278–298 K.

Table 4D-42. Recommended Absorption Cross Sections of $CH_3CH_2ONO_2$ at 298 K and Temperature Coefficients

λ (nm)	10^{20} σ (cm^2)	10^3 B (K^{-1})	λ (nm)	10^{20} σ (cm^2)	10^3 B (K^{-1})
185	1710	–	265	3.68	2.91
190	1710	–	270	3.27	3.09
195	1490	–	275	2.77	3.31
200	1140	–	280	2.21	3.57
205	738	–	285	1.72	3.87
210	400	–	290	1.28	4.20
215	195	–	295	0.869	4.64
220	91.0	–	300	0.556	5.10
225	45.0	–	305	0.344	5.75
230	24.0	–	310	0.191	6.55
235	13.0	–	315	0.104	7.63
240	8.00	3.28	320	0.0512	9.09
245	5.68	3.24	325	0.0241	10.8
250	4.67	2.98	330	0.0107	13.0
255	4.29	2.79	335	0.00465	14.7
260	4.04	2.78	340	0.00204	17.3

Note:

185–235 nm: 5 nm data of Turberg et al.[7]
240–320 nm: 5 nm averages of Talukdar et al.[6] and Turberg et al.[7]
325–340 nm: 5 nm interpolated data of Talukdar et al.[6]
B(λ) are the temperature coefficients in the expression $\sigma(\lambda, T) = \sigma(\lambda, 298\ K) \times \exp[B(\lambda)(T - 298)]$, interpolated to 5 nm from the 2 nm data of Talukdar et al.[6]

(1) Clemitshaw, K. C.; Williams, J.; Rattigan, O. V.; Shallcross, D. E.; Law, K. S.; Cox, R. A. Gas-phase ultraviolet absorption cross-sections and atmospheric lifetimes of several C_2-C_5 alkyl nitrates. *J. Photochem. Photobiol. A: Chem.* **1996**, *102*, 117-126 doi:10.1016/S1010-6030(96)04458-9.
(2) Higgins, C. M.; Evans, L. A.; Lloyd-Jones, G. C.; Shallcross, D. E.; Tew, D. P.; Orr-Ewing, A. J. Quantum yields for photochemical production of NO_2 from organic nitrates at tropospherically relevant wavelengths. *J. Phys. Chem. A* **2014**, *118*, 2756–2764, doi:10.1021/jp501517t.
(3) Kaya, K.; Kuwata, K.; Nagakura, S. The ultraviolet absorption spectra of nitramide and ethyl nitrate. *Bull. Chem. Soc. Japan* **1964**, *37*, 1055-1061, doi:10.1246/bcsj.37.1055.
(4) Roberts, J. M. Review article: The atmospheric chemistry of organic nitrates. *Atmos. Environ.* **1990**, *24A*, 243-287, doi:10.1016/0960-1686(90)90108-Y.
(5) Roberts, J. M.; Fajer, R. W. UV absorption cross sections of organic nitrates of potential atmospheric importance and estimation of atmospheric lifetimes. *Environ. Sci. Technol.* **1989**, *23*, 945-951, doi:10.1021/es00066a003.
(6) Talukdar, R. K.; Burkholder, J. B.; Hunter, M.; Gilles, M. K.; Roberts, J. M.; Ravishankara, A. R. Atmospheric fate of several alkyl nitrates. Part 2. UV absorption cross-sections and photodissociation quantum yields. *J. Chem. Soc. Faraday Trans.* **1997**, *93*, 2797-2805, doi:10.1039/a701781b.
(7) Turberg, M. P.; Giolando, D. M.; Tilt, C.; Soper, T.; Mason, S.; Davies, M.; Klingensmith, P.; Takacs, G. A. Atmospheric chemistry of alkyl nitrates. *J. Photochem. Photobiol. A* **1990**, *51*, 281-292, doi:10.1016/1010-6030(90)87063-H.
(8) Wallace-Goodeve, J. The absorption spectra of ethyl nitrate, ethyl nitrite, and nitroethane. *Trans. Faraday Soc.* **1934**, *30*, 504-508, doi:10.1039/TF9343000504.
(9) Zhu, L.; Ding, C.-F. Temperature dependence of the near UV absorption spectra and photolysis products of ethyl nitrate. *Chem. Phys. Lett.* **1997**, *265*, 177-184, doi:10.1016/S0009-2614(96)01404-2.

D43. $CH_3O_2NO_2$ (methylperoxynitrate)

Back to Index

$CH_3O_2NO_2 + h\nu$	$\rightarrow CH_3O_2 + NO_2$	86 kJ mol^{-1}	1391 nm	(1)
	$\rightarrow CH_3O + NO_3$	135 kJ mol^{-1}	886 nm	(2)

(Recommendation: 10-6, Note: 10-6, Evaluated: 10-6)

Absorption Cross Sections: The UV absorption spectrum of $CH_3O_2NO_2$ (methylperoxynitrate) has been measured by Cox and Tyndall[2] (200–310 nm) at 275 K, Morel et al.[3] (200–290 nm) at 296 K, Sander and Watson[4] (240–280 nm) at 298 K, and Bridier et al.[1] (200–280 nm) at 298 K. The spectrum has a strong absorption band below 225 nm and a moderate band at longer wavelengths. The reported cross sections are in reasonable agreement in the range 230–250 nm but scatter in the cross section data exists at both shorter and longer wavelengths. The recommended cross sections listed in Table 4D-43 are a smoothed average of the data from the four studies.

Photolysis Quantum Yields and Product Studies: No recommendation.

Table 4D-43. Recommended Absorption Cross Sections of $CH_3O_2NO_2$ at 298 K

λ (nm)	$10^{20}\ \sigma$ (cm^2)
200	525
205	370
210	235
215	150
220	100
225	65
230	60
235	55
240	50
245	46
250	40

255	32
260	26
265	20
270	16
275	13
280	10
285	7
290	4

Note:
200–290 nm: Smoothed average of the data from Cox and Tyndall,[2] Morel et al.,[3] Sander and Watson,[4] and Bridier et al.[1]

(1) Bridier, I.; Lesclaux, R.; Veyret, B. Flash photolysis kinetic study of the equilibrium $CH_3O_2 + NO_2 \leftrightarrow CH_3O_2NO_2$. *Chem. Phys. Lett.* **1992**, *191*, 259-263, doi:10.1016/0009-2614(92)85297-N.

(2) Cox, R. A.; Tyndall, G. Rate constants for reactions of CH_3O_2 in the gas phase. *Chem. Phys. Lett.* **1979**, *65*, 357-360, doi:10.1016/0047-2670(82)80022-1.

(3) Morel, O.; Simonaitis, R.; Heicklen, J. Ultraviolet absorption spectra of HO_2NO_2, $CCl_3O_2NO_2$, $CCl_2FO_2NO_2$, and $CH_3O_2NO_2$. *Chem. Phys. Lett.* **1980**, *73*, 38-41, doi:10.1016/0009-2614(80)85197-9.

(4) Sander, S. P.; Watson, R. T. Kinetic studies of the reactions of CH_3O_2 with NO, NO_2, and CH_3O_2 at 298 K. *J. Phys. Chem.* **1980**, *84*, 1664-1674, doi:10.1021/j100450a002.

D44. $CH_3C(O)O_2NO_2$ (peroxyacetyl nitrate, PAN)

Back to Index

$CH_3C(O)O_2NO_2 + h\nu$	$\rightarrow CH_3C(O)O_2 + NO_2$	119 kJ mol^{-1}	1004 nm	(1)
	$\rightarrow CH_3C(O)O + NO_3$	124 kJ mol^{-1}	963 nm	(2)

(Recommendation: 06-2, Note 10-6, Evaluated 10-6)

Absorption Cross Sections. The absorption cross sections of $CH_3C(O)O_2NO_2$ (peroxyacetyl nitrate, PAN) have been measured at room temperature by Stephens[10] (220–450 nm), Senum et al.[9] (200–300 nm), Basco and Parmar[1] (210–250 nm), and Libuda and Zabel[6] (219–325 nm) and at 250, 273, and 298 K by Talukdar et al.[11] (196–350 nm). The studies are in reasonable agreement. The data of Talukdar et al.[11] and Libuda and Zabel[6] agree within 10% at wavelengths <300 nm. The data of Stephens[10] and Basco and Parmar[1] are greater by up to 20 and 45%, respectively. The Senum et al.[9] cross sections are systematically less than the data of Talukdar et al.[11] Libuda and Zabel[6] carried out simultaneous UV and IR studies that showed that their measured cross sections needed to be corrected for impurities that are transparent in the UV but contribute to the sample pressure in the absorption cell. The corrections were on the order of 20%. The recommended absorption cross sections listed in Table 4D-44 are taken from Talukdar et al.,[11] which are in good agreement with those of Libuda and Zabel[6] but include a wider spectral coverage and temperature range. The uncertainties in the cross sections are estimated to be of the order of a factor of 2 in the long wavelength region but smaller at shorter wavelengths, decreasing to about 10% at 220 nm.

A systematic decrease of the absorption cross sections with decreasing temperature was observed by Talukdar et al.[11] The temperature dependence was parameterized using the expression:

$$\ln \sigma(\lambda, T) = \ln \sigma(\lambda, 298\ K) + B(\lambda)(T - 298)$$

The temperature coefficients $B(\lambda)$ are listed in Table 4D-44.

Photolysis Quantum Yields and Product Studies. Photolysis quantum yields for the production of NO_2 and NO_3 at 248 nm were reported by Mazely et al.[7,8]: $\Phi(NO_2, 248\ nm) = 0.83 \pm 0.09$ and $\Phi(NO_3, 248\ nm) = 0.3 \pm 0.1$. The NO_3 quantum yield was obtained relative to the unity NO_3 quantum yield in the photolysis of N_2O_5 at 248 nm. However, this latter quantum yield was re-measured to be 0.8 ± 0.1 by Harwood et al.,[4] so that the $\Phi(NO_3, 248\ nm)$ should be rescaled to 0.24. Quantum yields for the production of NO_3 in the photolysis of $CH_3C(O)O_2NO_2$ at 248 and 308 nm were also measured by Harwood et al.[5]: $\Phi(NO_3, 248\ nm) = 0.19 \pm 0.04$ and $\Phi(NO_3, 308\ nm) = 0.41 \pm 0.10$. Flowers et al.[2] studied the photolysis of PAN at 289 nm and detected NO_3 using cavity ring-down spectroscopy. They obtained $\Phi(NO_3, 289\ nm) = 0.31 \pm 0.08$ relative to the unity NO_3 quantum yield in the photolysis of N_2O_5 at that wavelength. In a second study, Flowers et al.[3] measured the wavelength dependence of $\Phi(NO_3)$: at 294 nm (0.29 ± 0.07), 299 nm (0.28 ± 0.07), 308 nm (0.28 ± 0.05), and 312 nm (0.39 ± 0.07). These results indicate that between 289 and 308 nm the NO_3 quantum yield is nearly constant with $\Phi(NO_3) = 0.29 \pm 0.07$. An increase of $\Phi(NO_3)$ at longer wavelengths cannot be ruled out. The recommended quantum yields are $\Phi(NO_2) = 0.7$ and $\Phi(NO_3) = 0.3$ for $\lambda > 300$ nm.

Table 4D-44. Recommended Absorption Cross Sections of $CH_3C(O)O_2NO_2$ at 298 K and Temperature Coefficients

λ (nm)	10^{20} σ (cm^2)	10^3 B (K^{-1})	λ (nm)	10^{20} σ (cm^2)	10^3 B (K^{-1})	λ (nm)	10^{20} σ (cm^2)	10^3 B (K^{-1})
196	429	2.02	248	14.6	3.64	300	0.189	8.44
198	398	1.73	250	12.9	3.76	302	0.152	8.61
200	361	1.36	252	11.4	3.87	304	0.125	8.76
202	325	1.07	254	10.0	3.98	306	0.0998	8.87
204	292	0.86	256	8.86	4.10	308	0.0816	9.01
206	261	0.75	258	7.80	4.23	310	0.0666	9.13
208	226	0.71	260	6.85	4.38	312	0.0538	9.30
210	196	0.75	262	6.01	4.53	314	0.0462	9.46
212	168	0.84	264	5.23	4.68	316	0.0363	9.57
214	143	0.97	266	4.54	4.82	318	0.0300	9.75
216	122	1.12	268	3.94	4.97	320	0.0252	10.0
218	104	1.29	270	3.37	5.14	322	0.0199	10.2
220	89.7	1.47	272	2.87	5.34	324	0.0166	10.4
222	77.7	1.64	274	2.45	5.55	326	0.0140	10.6
224	67.6	1.81	276	2.07	5.76	328	0.0117	10.7
226	59.3	1.98	278	1.74	5.98	330	0.0106	10.9
228	52.0	2.14	280	1.46	6.20	332	0.00857	11.2
230	45.8	2.30	282	1.21	6.43	334	*0.0072**	11.5
232	40.4	2.46	284	1.01	6.67	336	*0.0061**	11.7
234	35.5	2.63	286	0.810	6.90	338	*0.0050**	11.9
236	31.4	2.80	288	0.648	7.15	340	*0.0042**	12.2
238	27.9	2.96	290	0.537	7.39	342	*0.0035**	12.4
240	24.4	3.11	292	0.447	7.63	344	*0.0029**	12.5
242	21.5	3.25	294	0.369	7.86	346	*0.0024**	
244	18.8	3.39	296	0.297	8.08	348	*0.0020**	
246	16.6	3.52	298	0.245	8.27	350	*0.0016**	

Note:
Absorption cross sections σ: 196–350 nm, Talukdar et al.[11]
Temperature coefficients B: 250–298 K, Talukdar et al.[11] (ln σ(λ, T) = ln σ(λ, 298 K) + B(T-298))
* Data between 334 and 350 nm were smoothed.

(1) Basco, N.; Parmar, S. S. The reaction of acetylperoxy radicals. *Int. J. Chem. Kinet.* **1987**, *19*, 115-128, doi:10.1002/kin.550190204.

(2) Flowers, B. A.; Angerhofer, M. E.; Simpson, W. R.; Nakayama, T.; Matsumi, Y. Nitrate radical quantum yield from peroxyacetyl nitrate photolysis. *J. Phys. Chem. A* **2005**, *109*, 2252-2558, doi:10.1021/jp045529n.

(3) Flowers, B. A.; Stanton, J. F.; Simpson, W. R. Wavelength dependence of nitrate radical quantum yield from peroxyacetyl nitrate photolysis: Experimental and theoretical studies. *J. Phys. Chem. A* **2007**, *111*, 11602-11607, doi:10.1021/jp0749118.

(4) Harwood, M. H.; Burkholder, J. B.; Ravishankara, A. R. Photodissociation of $BrONO_2$ and N_2O_5: Quantum yields for NO_3 production at 248, 308, and 352.5 nm. *J. Phys. Chem. A* **1998**, *102*, 1309-1317, doi:10.1021/jp9729829.

(5) Harwood, M. H.; Roberts, J. M.; Frost, G. J.; Ravishankara, A. R.; Burkholder, J. B. Photochemical studies of $CH_3C(O)OONO_2$ (PAN) and $CH_3CH_2C(O)OONO_2$ (PPN): NO_3 quantum yields. *J. Phys. Chem. A* **2003**, *107*, 1148-1154, doi:10.1021/jp0264230.

(6) Libuda, H. G.; Zabel, F. UV absorption cross sections of acetyl peroxynitrate and trifluoroacetyl peroxynitrate at 298 K. *Ber. Bunsenges. Phys. Chem.* **1995**, *99*, 1205-1213, doi:10.1002/bbpc.199500061.

(7) Mazely, T. L.; Friedl, R. R.; Sander, S. P. The production of NO_2 from the photolysis of peroxyacetyl nitrate. *J. Phys. Chem.* **1995**, *99*, 8162-8169, doi:10.1021/j100020a044.

(8) Mazely, T. L.; Friedl, R. R.; Sander, S. P. Quantum yield of NO_3 from peroxyacetyl nitrate photolysis. *J. Phys. Chem.* **1997**, *101*, 7090-7097, doi:10.1021/jp971298r.

(9) Senum, G. I.; Lee, Y.-N.; Gaffney, J. S. Ultraviolet absorption spectrum of peroxyacetyl nitrate and peroxypropionyl nitrate. *J. Phys. Chem.* **1984**, *88*, 1269-1270, doi:10.1021/j150651a001.

(10) Stephens, E. R. The formation, reactions, and properties of peroxyacyl nitrates (PANs) in photochemical air pollution. *Adv. Environ. Sci. Technol.* **1969**, *1*, 119-146.
(11) Talukdar, R. K.; Burkholder, J. B.; Schmoltner, A.-M.; Roberts, J. M.; Wilson, R. R.; Ravishankara, A. R. Investigation of the loss processes for peroxyacetyl nitrate in the atmosphere: UV photolysis and reaction with OH. *J. Geophys. Res.* **1995**, *100*, 14163-14173, doi:10.1029/95JD00545.

D45. $C_2H_5C(O)O_2NO_2$ (peroxypropionyl nitrate, PPN)

Back to Index

$$C_2H_5C(O)O_2NO_2 + h\nu \rightarrow C_2H_5C(O)O_2 + NO_2 \quad (1)$$
$$\rightarrow C_2H_5C(O)O + NO_3 \quad (2)$$

(Recommendation: 06-2, Note: 10-6, Evaluated: 10-6)

Absorption Cross Sections: The absorption cross sections of $C_2H_5C(O)O_2NO_2$ (peroxypropionyl nitrate, PPN) have been measured at room temperature by Senum et al.[2] (200–300 nm) and at 253, 273, and 296 K by Harwood et al.[1] (210–340 nm). The absorption spectrum shows monotonically decreasing absorption cross sections with increasing wavelength over the range 200–340 nm. The absorption cross sections reported by Harwood et al.[1] are larger than those reported by Senum et al.[2] over the common wavelength range by ~10% at 210 nm up to ~30% at 300 nm. A wavelength dependent systematic decrease of the absorption cross sections with decreasing temperature was reported by Harwood et al.[1] The temperature dependence was parameterized to the empirical expression:

$$\ln \sigma(\lambda, T) = \ln \sigma(\lambda, 296\ K) + B(\lambda)(T - 296)$$

The recommended absorption cross sections and temperature coefficients in Table 4D-45 are taken from Harwood et al.[1]

Photolysis Quantum Yield and Product Studies: Quantum yields for the production of NO_3 in the photolysis of $C_2H_5C(O)O_2NO_2$ at 248 and 308 nm were measured by Harwood et al.[1] to be $\Phi_2(248\ nm) = 0.22 \pm 0.04$ and $\Phi_2(308\ nm) = 0.39 \pm 0.04$.

Table 4D-45. Recommended Absorption Cross Sections of $C_2H_5C(O)O_2NO_2$ at 296 K and Temperature Coefficients

λ (nm)	10^{20} σ (cm^2)	10^3 B (K^{-1})	λ (nm)	10^{20} σ (cm^2)	10^3 B (K^{-1})	λ (nm)	10^{20} σ (cm^2)	10^3 B (K^{-1})
210	174	1.22	254	9.27	3.25	298	0.325	10.3
212	154	1.20	256	8.23	3.47	300	0.273	10.8
214	135	1.19	258	7.28	3.69	302	0.228	11.2
216	115	1.20	260	6.44	3.92	304	0.192	11.7
218	99.9	1.21	262	5.66	4.17	306	0.162	12.2
220	86.1	1.24	264	4.96	4.42	308	0.136	12.6
222	74.7	1.27	266	4.35	4.69	310	0.114	13.2
224	64.8	1.32	268	3.80	4.96	312	0.0962	13.6
226	56.9	1.37	270	3.31	5.25	314	0.0835	14.2
228	49.6	1.44	272	2.87	5.54	316	0.0689	14.7
230	43.6	1.52	274	2.48	5.85	318	0.0571	15.2
232	38.3	1.60	276	2.14	6.17	320	0.0491	15.8
234	33.6	1.70	278	1.84	6.49	322	0.0443	16.3
236	29.5	1.81	280	1.57	6.83	324	0.0354	16.9
238	25.8	1.93	282	1.33	7.18	326	0.0282	17.5
240	22.6	2.06	284	1.12	7.54	328	0.0242	18.1
242	19.8	2.20	286	0.940	7.91	330	0.0206	18.7
244	17.4	2.35	288	0.790	8.29	332	0.0174	19.3
246	15.3	2.51	290	0.662	8.68	334	0.0146	19.9
248	13.5	2.68	292	0.551	9.08	336	0.0107	20.5
250	11.9	2.86	294	0.462	9.49	338	0.0090	21.2
252	10.5	3.05	296	0.389	9.91	340	0.0066	21.8

Note:
Absorption cross sections
Harwood et al.[1]
Temperature coefficients

Harwood et al.[1] (253–296 K), $\ln \sigma(\lambda, T) = \ln \sigma(\lambda, 298\ K) + B(\lambda)(T - 298)$

(1) Harwood, M. H.; Roberts, J. M.; Frost, G. J.; Ravishankara, A. R.; Burkholder, J. B. Photochemical studies of $CH_3C(O)OONO_2$ (PAN) and $CH_3CH_2C(O)OONO_2$ (PPN): NO_3 quantum yields. *J. Phys. Chem. A* **2003**, *107*, 1148-1154, doi:10.1021/jp0264230.

(2) Senum, G. I.; Lee, Y.-N.; Gaffney, J. S. Ultraviolet absorption spectrum of peroxyacetyl nitrate and peroxypropionyl nitrate. *J. Phys. Chem.* **1984**, *88*, 1269-1270, doi:10.1021/j150651a001.

D46. HCN (hydrogen cyanide)

Back to Index

$HCN + h\nu \rightarrow H + CN$	526 kJ mol^{-1}	228 nm	(1)

(Recommendation 25-1, Note: 25-1, Evaluated: 25-1)

Absorption Cross Sections: The VUV absorption spectrum of hydrogen cyanide, HCN, has been reported by McPherson and Simons[3] (131.22–145.73 nm, graphical data), Lee[2] (105–154.34 nm, graphical data), Nagata et al.[4] (112.39, 80.6–129.63 nm), and Nuth and Glicker[5] (62.66–146.92 nm). The Lyman-α (121.567 nm) cross section data from these studies is in poor agreement. A Lyman-α cross section of 4.5×10^{-17} cm^2 molecule^{-1} is recommended with an uncertainty factor of 1.5 (2σ). Herzberg and Innes[1] have reported a vibrational-rotational spectroscopic analysis of the HCN VUV electronic transitions.

Photolysis Quantum Yield and Product Studies: The solar photodissociation rate for HCN is small, even in the upper stratosphere. The photolysis products are expected to be H + CN.

(1) Herzberg, G.; Innes, K. K. Ultraviolet absorption spectra of HCN and DCN .1. The σ-X and β-X systems. *Can. J. Phys.* **1957**, *35*, 842-879, doi:10.1139/p57-095.

(2) Lee, L. C. CN($A\ ^2\Pi_i \rightarrow X\ ^2\Sigma^+$) and CN($B\ ^2\Sigma^+ \rightarrow X\ ^2\Sigma^+$) yields from HCN photodissociation. *J. Chem. Phys.* **1980**, *72*, 6414-6424, doi:10.1063/1.439140.

(3) Macpherson, M. T.; Simons, J. P. Spectroscopic study of the predissociation H(D)CN ($C\ ^1A'$) → H(D) + CN ($B\ ^2\Sigma^+$). *J. Chem. Soc. Faraday Trans. II* **1978**, *74*, 1965-1977, doi:10.1039/F29787401965.

(4) Nagata, T.; Kondow, T.; Ozaki, Y.; Kuchitsu, K. Absorption spectra of hydrogen cyanide and deuterium cyanide in the 130-80 nm range. *Chem. Phys.* **1981**, *57*, 45-53, doi:10.1016/0301-0104(81)80019-5.

(5) Nuth, J. A.; Glicker, S. The vacuum ultraviolet spectra of HCN, C_2N_2, and CH_3CN. *J. Quant. Spectrosc. Radiat. Transf.* **1982**, *28*, 223-231, doi:10.1016/0022-4073(82)90025-5.

D47. CH_3CN (methyl cyanide)

Back to Index

$CH_3CN + h\nu$	$\rightarrow H + CH_2CN$	397 kJ mol^{-1}	302 nm	(1)
	$\rightarrow CH_3 + CN$	512 kJ mol^{-1}	234 nm	(2)

(Recommendation: 82-57, Note: 10-6, Evaluated: 10-6)

Absorption Cross Sections: Acetonitrile (CH_3CN, methyl cyanide) absorbs weakly at wavelengths >180 nm with absorption cross sections $<10^{-20}$ cm^2 molecule^{-1}. Suto and Lee[3] (114–178 nm), Zetzsch[4] (155–185 nm), and Eden et al.[1] (113–320 nm) have reported cross section data. The agreement among the cross section data sets is, however, poor and no cross section recommendation is given.

Photolysis Quantum Yield and Product Studies: McElcheran et al.[2] studied the photodissociation of CH_3CN at 184.9 nm. On the basis of end-product analysis, channel (1) was identified as the major photolysis pathway.

(1) Eden, S.; Limão-Vieira, P.; Kendall, P.; Mason, N. J.; Hoffmann, S. V.; Spyrou, S. M. High resolution photo-absorption studies of acrylonitrile, C_2H_3CN, and acetonitrile, CH_3CN. *Eur. Phys. J.* **2003**, *D 26*, 201-210, doi:10.1140/epjd/e2003-00223-5.

(2) McElcheran, D. E.; Wijnen, M. H. J.; Steacie, E. W. R. The photolysis of methyl cyanide at 1849 Å. *Can. J. Chem.* **1958**, *36*, 321-339, doi:10.1139/v58-046.

(3) Suto, M.; Lee, L. C. Photoabsorption cross section of CH_3CN: Photodissociation rates by solar flux and interstellar radiation. *J. Geophys. Res.* **1985**, *90*, 13037-13040, doi:10.1029/JD090iD07p13037.

(4) Zetzsch, C. In *Proceedings of the International Ozone Symposium 1988*; Bojkov, R., Fabian, P., Eds.; Deepak: Hampton, VA, 1989.

4.7 Bibliography – Organic Photochemistry

Adachi, H.; Basco, N.; James, D. G. L. The acetyl radical studied by flash photolysis and kinetic spectroscopy. *Chem. Phys. Lett.* **1978**, *59*, 502-505, doi:10.1016/0009-2614(78)85028-3.

Adachi, H.; Basco, N.; James, D. G. L. The ethylperoxy radical spectrum and rate constant for mutual interaction measured by flash photolysis and kinetic spectroscopy. *Int. J. Chem. Kinet.* **1979**, *11*, 1211-1229, doi:10.1002/kin.550111107.

Adachi, H.; Basco, N.; James, D. G. L. Mutual interactions of the methyl and methylperoxy radicals studied by flash photolysis and kinetic spectroscopy. *Int. J. Chem. Kinet.* **1980**, *12*, 949-977, doi:10.1002/kin.550121206.

Adachi, H.; Basco, N.; James, D. G. L. The acetyl radicals CH_3CO and CD_3CO studied by flash photolysis and kinetic spectroscopy. *Int. J. Chem. Kinet.* **1981**, *13*, 1251-1276, doi:10.1002/kin.550131206.

Addison, M. C.; Burrows, J. P.; Cox, R. A.; Patrick, R. Absorption spectrum and kinetics of the acetylperoxy radical. *Chem. Phys. Lett.* **1980**, *73*, 283-287, doi:10.1016/0009-2614(80)80373-3.

Aloisio, S.; Francisco, J. S. The photochemistry of acetone in the presence of water. *Chem. Phys. Lett.* **2000**, *329*, 179-184, doi:10.1016/S0009-2614(00)01001-0.

Anastasi, C.; Maw, P. R. Reaction kinetics in acetyl chemistry over a wide range of temperature and pressure. *J. Chem. Soc. Faraday Trans. 1* **1982**, *78*, 2423-2433, doi:10.1039/f19827802423.

Anastasi, C.; Smith, I. W. M.; Parkes, D. A. Flash photolysis study of the spectra of CH_3O_2 and $C(CH_3)_3O_2$ radicals and the kinetics of their mutual reaction and with NO. *J. Chem. Soc. Faraday Trans. 1* **1978**, *74*, 1693-1701, doi:10.1039/f19787401693.

Anastasi, C.; Waddington, D. J.; Woolley, A. Reactions of oxygenated radicals in the gas phase Part 10.-Self-reactions of ethylperoxy radicals. *J. Chem. Soc. Faraday Trans. 1* **1983**, *79*, 505-516, doi:10.1039/f19837900505.

Arnold, S. R.; Chipperfield, M. P.; Blitz, M. A.; Heard, D. E.; Pilling, M. J. Photodissociation of acetone: Atmospheric implications of temperature-dependent quantum yields. *Geophys. Res. Lett.* **2004**, L07110, doi:10.1029/2003GL019099.

Atkinson, R.; Lloyd, A. C. Evaluation of kinetic and mechanistic data for modeling photochemical smog. *J. Phys. Chem. Ref. Data* **1984**, *13*, 315-444, doi:10.1063/1.555710.

Au, J. W.; Cooper, G.; Burton, G. R.; Olney, T. N.; Brion, C. E. The valence shell photoabsorption of the linear alkanes, C_nH_{2n+2} (n=1-8): Absolute oscillator strengths (7-220 eV). *Chem. Phys.* **1993**, *173*, 209-239, doi:10.1016/0301-0104(93)80142-V.

Baasandorj, M.; Griffith, S.; Dusanter, S.; Stevens, P. S. Experimental and theoretical studies of the OH + hydroxyacetone reaction as a function of temperature. *J. Phys. Chem. A* **2009**, *113*, 10495-10502, doi:10.1021/jp904238w.

Bacher, C.; Tyndall, G. S.; Orlando, J. J. The atmospheric chemsitry of glycolaldehyde. *J. Atmos. Chem.* **2001**, *39*, 171-189, doi:10.1023/A:1010689706869.

Back, R. A.; Parsons, J. M. The thermal and photochemical decomposition of maleic anhydride in the gas phase. *Can. J. Chem.* **1981**, *59*, 1342–1346, doi: 10.1139/v81-197.

Backx, C.; Wight, G. R.; Tol, R. R.; van der Wiel, M. J. Electron-electron coincidence measurements of CH_4. *J. Phys. B: Atom. Mol. Phys.* **1975**, *8*, 3007-3019, doi:10.1088/0022-3700/8/18/020.

Baeza-Romero, M. T.; Blitz, M. A.; Heard, D. E.; Pilling, M. J.; Price, B.; Seakins, P. W.; Wanga, L. Photolysis of methylethyl, diethyl and methylvinyl ketones and their role in the atmospheric HO_x budget. *Faraday Discuss.* **2005**, *130*, 73–88, doi:10.1039/b419160a.

Barnes, E. E.; Simpson, W. T. Correlations among electronic transitions for carbonyl and carboxyl in the vacuum ultraviolet. *J. Chem. Phys.* **1963**, *39*, 670-675, doi:10.1063/1.1734305.

Basco, N.; James, D. G. L.; Suart, R. D. A quantitative study of alkyl radical reactions by kinetic spectroscopy. Part I. Mutual combination of methyl radicals and combination of methyl radicals with nitric acid. *Int. J. Chem. Kinet.* **1970**, *2*, 215-234 doi:10.1002/kin.550020307.

Basco, N.; Parmar, S. S. Spectra and reactions of acetyl and acetylperoxy radicals. *Int. J. Chem. Kinet.* **1985**, *17*, 891-900, doi:10.1002/kin.550170809.

Basco, N.; Parmar, S. S. The reaction of acetylperoxy radicals. *Int. J. Chem. Kinet.* **1987**, *19*, 115-128, doi:10.1002/kin.550190204.

Bass, A. M.; Glasgow, L. C.; Miller, C.; Jesson, J. P.; Filken, S. L. Temperature-dependent absorption cross-sections for formaldehyde (CH_2O) - The effect of formaldehyde on stratospheric chlorine chemistry. *Planet. Space Sci.* **1980**, *28*, 675-679, doi:10.1016/0032-0633(80)90112-9.

Baasandorj, M.; Griffith, S.; Dusanter, S.; Stevens, P. S. Experimental and theoretical studies of the OH + hydroxyacetone reaction as a function of temperature. *J. Phys. Chem. A* **2009**, *113*, 10495-10502, doi:10.1021/jp904238w.

Bauer, D.; Crowley, J. N.; Moortgat, G. K. The UV spectrum of the ethylperoxy radical and its self-reaction kinetics between 218 and 333 K. *J. Photochem. Photobiol. A: Chem.* **1992**, *65*, 329-344, doi:10.1016/1010-6030(92)80015-N.

Bauerle, S.; Moortgat, G. K. Absorption cross-sections of $HOCH_2OOH$ vapor between 205 and 360 nm at 298 K. *Chem. Phys. Lett.* **1999**, *309*, 43-48, doi:10.1016/S0009-2614(99)00652-1.

Beames, J. M.; Liu, F.; Lu, L.; Lester, M. I. Ultraviolet spectrum and photochemistry of the simplest Criegee intermediate CH_2OO. *J. Am. Chem. Soc.* **2012**, *134*, 20045-20048, doi:10.1021/ja310603j.

Beames, J. M.; Liu, F.; Lu, L.; Lester, M. I. UV spectroscopic characterization of an alkyl substituted Criegee intermediate CH_3CHOO. *J. Chem. Phys.* **2013**, *138*, 244307, doi:10.1063/1.4810865.

Benayada, B.; Leila, D. O. UV absorption cross sections for acetates. *Desalination* **1999**, *126*, 83-86, doi:10.1016/S0011-9164(99)00157-5.

Berges, M. G. M.; Warneck, P. Product quantum yields for 350 nm photodecomposition of pyruvic acid in air. *Ber. Bunsenges. Phys. Chem.* **1992**, *96*, 413-416, doi:10.1002/bbpc.19920960334.

Birge, R. R.; Pringle, W. C.; Leermakers, P. A. Excited states geometries of the singly substituted methylpropenals. I. Vibrational-electronic analysis of S_1 (n, p*). *J. Am. Chem. Soc.* **1971**, *93*, 6715-6726, doi:10.1021/ja00754a001.

Blacet, F. E.; Crane, R. A. The photolysis of the aliphatic aldehydes. XVII. Propionaldehyde, n-butyraldehyde, and isobutyraldehyde at 2380 and 1870 Å. *J. Am. Chem. Soc.* **1954**, *76*, 5337-5340, doi:10.1021/ja01650a020.

Blitz, M. A.; Heard, D. E.; Pilling, M. J. Wavelength dependent photodissociation of CH_3OOH. Quantum yields for CH_3O and OH, measurement of the OH + CH_3OOH rate constant. *J. Photochem. Photobiol. A: Chem.* **2005**, *176*, 107-113, doi:10.1016/j.jphotochem.2005.09.017.

Blitz, M. A.; Heard, D. E.; Pilling, M. J. Study of acetone photodissociation over the wavelength range 248-330 nm: Evidence of a mechanism involving both the singlet and triplet excited states. *J. Phys. Chem. A* **2006**, *110*, 6742-6756, doi:10.1021/jp056276g.

Blitz, M. A.; Heard, D. E.; Pilling, M. J.; Arnold, S. R.; Chipperfield, M. P. Correction to ''Pressure and temperature-dependent quantum yields for the photodissociation of acetone between 279 and 327.5 nm''. *Geophys. Res. Lett.* **2004**, *31*, L09104, doi:10.1029/2004GL020182.

Blitz, M. A.; Heard, D. E.; Pilling, M. J.; Arnold, S. R.; Chipperfield, M. P. Pressure and temperature-dependent quantum yields for the photodissociation of acetone between 279 and 327.5 nm. *Geophys. Res. Lett.* **2004**, *31*, L06111, doi:1029/2003GL018793.

Bogumil, K.; Orphal, J.; Homann, T.; Voigt, S.; Spietz, P.; Fleischmann, O. C.; Vogel, A.; Hartmann, M.; Kromminga, H.; Bovensmann, H.; Frerick, J.; Burrows, J. P. Measurements of molecular absorption spectra with the SCIAMACHY pre-flight model: instrument characterization and reference data for atmospheric remote-sensing in the 230-2380 nm region. *J. Photochem. Photobiol. A: Chem.* **2003**, *157*, 167-184, doi:10.1016/S1010-6030(03)00062-5.

Braun, W.; Klein, R.; Fahr, A.; Okabe, H.; Mele, A. Laser photolysis of trimethylgallium at 193 nm: Quantum yields for methyl radical and ethane production. *Chem. Phys. Lett.* **1990**, *166*, 397-403, doi:10.1016/0009-2614(90)85050-M.

Brewer, J. F.; Papanastasiou, D. K.; Burkholder, J. B.; Fischer, E. V.; Ren, Y.; Mellouki, A.; Ravishankara, A. R. Atmospheric photolysis of methyl ethyl, diethyl, and propyl ethyl ketones: Temperature-dependent UV absorption cross sections. *J. Geophys. Res.* **2019**, *124*, 5906-5918, doi:10.1029/2019JD030391.

Bridier, I.; Lesclaux, R.; Veyret, B. Flash photolysis kinetic study of the equilibrium CH_3O_2 + NO_2 ↔ $CH_3O_2NO_2$. *Chem. Phys. Lett.* **1992**, *191*, 259-263.

Bridier, I.; Veyret, B.; Lesclaux, R.; Jenkin, M. E. Flash photolysis study of the UV spectrum and kinetics of reactions of the acetonylperoxy radical. *J. Chem. Soc. Faraday Trans.* **1993**, *89*, 2993-2997, doi:10.1039/ft9938902993.

Brint, P.; O'Toole, L.; Mayhew, C. A.; Dussa, W. Vacuum-ultraviolet absorption spectrum of acetaldehyde, CH_3CHO, and the related deuterides CH_3CDO and CD_3CDO. *J. Chem. Soc. Faraday Trans.* **1990**, *86*, 3349-3354, doi:10.1039/FT9908603349.

Brownsword, R. A.; Hillenkamp, M.; Laurent, T.; Vatsa, R. K.; Volpp, H.-R.; Wolfrum, J. Quantum yield for H atom formation in the methane dissociation after photoexcitation at the Lyman-α (121.6 nm) wavelength. *Chem. Phys. Lett.* **1997**, *266*, 259-266, doi:10.1016/S0009-2614(96)01526-6.

Buras, Z. J.; Elsamra, R. M. I.; Green, W. H. Direct determination of the simplest Criegee intermediate (CH_2OO) self reaction rate. *J. Phys. Chem. Lett.* **2014**, *5*, 2224-2228, doi:10.1021/jz5008406.

Burkholder, J. B., personal communication to the NASA JPL Panel.

Burkholder, J. B.; Mellouki, W.; Fleming, E. L.; George, C.; Heard, D. E.; Jackman, C. H.; Kurylo, M. J.; Orkin, V. L.; Swartz, W. H.; Wallington, T. J. Chapter 3: Evaluation of Atmospheric Loss Processes. In Lifetimes of Stratospheric Ozone-Depleting Substances, Their Replacements, and Related Species; Ko,

M. K. W., Newman, P. A., Reimann, S., Strahan, S. E., Eds., 2013, http://www.sparc-climate.org/publications/sparc-reports/sparc-report-no6/.
Butkovskaya, N. I.; Pouvesle, N.; Kukui, A.; Mu, Y.; Bras, G. L. Mechanism of the OH-initiated oxidation of hydroxyacetone over the temperature range 236-298 K. *J. Phys. Chem. A* **2006**, *110*, 6833-6843, doi:10.1021/jp056345r.
Burton, G. R.; Chan, W. F.; Cooper, G.; Brion, C. E. Absolute oscillator strengths for photoabsorption (6-360 eV) and ionic photofragmentation (10-80 eV) of methanol. *Chem. Phys.* **1992**, *167*, 349-367, doi:10.1016/0301-0104(92)80208-D.
Calvert, J. G.; Atkinson, R.; Kerr, J. A.; Madronich, S.; Moortgat, G. K.; Wallington, T. J.; Yarwood, G. *The Mechanisms of Atmospheric Oxidation of the Alkenes*; Oxford University Press: New York - Oxford, 2000.
Calvert, J. G.; Kerr, J. A.; Demerjian, K. L.; McQuigg, R. D. Photolysis of formaldehyde as a hydrogen atom source in the lower stratosphere. *Science* **1972**, *175*, 751-752, doi:10.1126/science.175.4023.751.
Calvert, J. G.; Layne, G. S. The photolysis of glyoxal vapor at wave length 3130 Å. *J. Am. Chem. Soc.* **1953**, *75*, 856-859, doi:10.1021/ja01100a027.
Calvert, J. G.; Pitts, J. N. Photochemistry; John Wiley & Sons, Inc.: New York, 1966; pp 783.
Calvert, J. G.; Pitts Jr., J. N. In *Photochemistry*; John Wiley & Sons, Inc.: New York, 1966; pp 368.
Cameron, M.; Sivakumaran, V.; Dillon, T. J.; Crowley, J. N. Reaction between OH and CH_3CHO. Part 1. Primary product yields of CH_3 (296 K), CH_3CO (296 K), and H (237-296 K). *Phys. Chem. Chem. Phys.* **2002**, *4*, 3628-3638, doi:10.1039/b202586h.
Campuzano-Jost, P.; Williams, M. B.; D'Ottone, L.; Hynes, A. J. Kinetics and mechanism of the reaction of the hydroxyl radical with h8-isoprene and d8-isoprene: Isoprene absorption cross sections, rate coefficients, and the mechanism of hydroperoxyl radical production. *J. Phys. Chem. A* **2004**, *108*, 1537-1551, doi:10.1021/jp0363601.
Cantrell, C. A.; Davidson, J. A.; McDaniel, A. H.; Shetter, R. E.; Calvert, J. G. Temperature-dependent formaldehyde cross sections in the near-ultraviolet spectral region. *J. Phys. Chem.* **1990**, *94*, 3902-3908, doi:10.1021/j100373a008.
Cattell, F. C.; Cavanagh, J.; Cox, R. A.; Jenkin, M. E. A kinetics study of reactions of HO_2 and $C_2H_5O_2$ using diode laser absorption spectroscopy. *J. Chem. Soc. Faraday Trans. 2* **1986**, *82*, 1999-2018, doi:10.1039/f29868201999.
Chang, Y.-P.; Chang, C.-H.; Takahashi, K.; Lin, J. J.-M. Absolute UV absorption cross sections of dimethyl substituted Criegee intermediate $(CH_3)_2COO$. *Chem. Phys. Lett.* **2016**, *653*, 155-160, doi:10.1016/j.cplett.2016.04.082.
Chen, J.; Venables, D. S. A broadband optical cavity spectrometer for measuring weak near-ultraviolet absorption spectra of gases. *Atmos. Meas. Tech.* **2011**, *4*, 425-436, doi:10.5194/amt-4-425-2011.
Chen, F. Z.; Wu, C. Y. R. Temperature-dependent photoabsorption cross sections in the VUV-UV region. I. Methane and ethane. *J. Quant. Spectrosc. Radiat. Transf.* **2004**, *85*, 195-209, doi:10.1016/S0022-4073(03)00225-5.
Chen, Y.; Wang, W.; Zhu, L. Wavelength-dependent photolysis of methylglyoxal in the 290-440 nm region. *J. Phys. Chem. A* **2000**, *104*, 11126-11131, doi:10.1021/jp002262t.
Chen, Y.; Zhu, L. The wavelength dependence of the photodissociation of propionaldehyde in the 280-330 nm region. *J. Phys. Chem. A* **2001**, *105*, 9689-9696, doi:10.1021/jp011445s.
Chen, Y.; Zhu, L. Wavelength-dependent photolysis of glyoxal in the 290-420 nm region. *J. Phys. Chem. A* **2003**, *107*, 4643-4651, doi:10.1021/jp022440d.
Chen, Y.; Zhu, L.; Francisco, J. S. Wavelength-dependent photolysis of *n*-butyraldehyde and *i*-butyraldehyde in the 280-330-nm region. *J. Phys. Chem. A* **2002**, *106*, 7755-7763, doi:10.1021/jp014544e.
Cheng, B.-M.; Bahou, M.; Lee, Y.-P.; Lee, L. C. Experimental and theoretical studies on VUV absorption cross sections and photodissociation of CH_3OH, CH_3OD, CD_3OH, and CD_3OD. *J. Chem. Phys.* **2002**, *117*, 1633-1640, doi:10.1063/1.1485769.
Chhantyal-Pun, R.; Welz, O.; Savee, J. D.; Eskola, A. J.; Lee, E. P. F.; Blacker, L.; Hill, H. R.; Ashcroft, M.; Khan, M. A. H.; Lloyd-Jones, G. C.; Evans, L.; Rotavera, B.; Huang, H.; Osborn, D. L.; Mok, D. K. W.; Dyke, J. M.; Shallcross, D. E.; Percival, C. J.; Orr-Ewing, A. J.; Taatjes, C. A. Direct measurements of unimolecular and bimolecular reaction kinetics of the Criegee intermediate $(CH_3)_2COO$. *J. Phys. Chem. A* **2017**, *121*, 4-15, doi:10.1021/acs.jpca.6b07810.
Chowdhury, P. K.; Upadhyaya, H. P.; Naik, P. D.; Mittal, J. P. Direct observation of OH photofragment from triplet hydroxyacetone. *Chem. Phys. Lett.* **2002**, *351*, 201-207, doi:10.1016/S0009-2614(01)01377-X.
Clark, J. H.; Moore, C. B.; Nogar, N. S. The photochemistry of formaldehyde: Absolute quantum yields, radical reactions, and NO reactions. *J. Chem. Phys.* **1978**, *68*, 1264-1271, doi:10.1063/1.435848.

Clemitshaw, K. C.; Williams, J.; Rattigan, O. V.; Shallcross, D. E.; Law, K. S.; Cox, R. A. Gas-phase ultraviolet absorption cross-sections and atmospheric lifetimes of several C2-C5 alkyl nitrates. *J. Photochem. Photobiol. A: Chem.* **1996**, *102*, 117-126 doi:10.1016/S1010-6030(96)04458-9.

Co, D.; Hanisco, T. F.; Anderson, J. G.; Keutsch, F. N. Rotationally resolved absorption cross sections of formaldehyde in the 28100-28500 cm^{-1} (351-356 nm) spectral region: Implications for in situ LIF measurements. *J. Phys. Chem. A* **2005**, *109*, 10675-10682, doi:10.1021/jp053466i.

Cooper, G.; Anderson, J. E.; Brion, C. E. Absolute photoabsorption and photoionization of formaldehyde in the VUV and soft X-ray regions (3-200 eV). *Chem. Phys.* **1996**, *209*, 61-77, doi:10.1016/0301-0104(96)00079-1.

Cox, R. A.; Munk, J.; Nielsen, O. J.; Pagsberg, P.; Ratajczak, P. Ultraviolet absorption spectra and kinetics of acetonyl and acetonylperoxy radicals. *Chem. Phys. Lett.* **1990**, *173*, 206-210, doi:10.1016/0009-2614(90)80079-S.

Cox, R. A.; Tyndall, G. Rate constants for reactions of CH_3O_2 in the gas phase. *Chem. Phys. Lett.* **1979**, *65*, 357-360, doi:10.1016/0047-2670(82)80022-1.

Cox, R. A.; Tyndall, G. S. Rate constants for the reactions of CH_3O_2 with HO_2, NO and NO_2 using molecular modulation spectrometry. *J. Chem. Soc. Faraday Trans. II* **1980**, *76*, 153-163, doi:10.1039/f29807600153.

Dagaut, P.; Kurylo, M. J. The gas phase UV absorption spectrum of CH_3O_2 radicals: A reinvestigation. *J. Photochem. Photobiol. A: Chem.* **1990**, *51*, 133-140, doi:10.1016/1010-6030(90)87047-F.

DeMore, W. B.; Sander, S. P.; Golden, D. M.; Hampson, R. F.; Kurylo, M. J.; Howard, C. J.; Ravishankara, A. R.; Kolb, C. E.; Molina, M. J. Chemical Kinetics and Photochemical Data for Use in Stratospheric Modeling, Evaluation Number 12, Jet Propulsion Laboratory, California Institute of Technology Pasadena, CA, JPL Publication 97-4, 1997.

Dillon, T. J.; Dulitz, K.; Groß, C. B. M.; Crowley, J. N. Temperature-dependent rate coefficients for the reactions of the hydroxyl radical with the atmospheric biogenics isoprene, alpha-pinene and delta-3-carene. *Atmos. Chem. Phys.* **2017**, *17*, 15137–15150, doi:10.5194/acp-17-15137-2017.

Dillon, T. J.; Hölscher, D.; Sivakumaran, V.; Horowitz, A.; Crowley, J. N. Kinetics of the reactions of HO with methanol (210–351 K) and with ethanol (216–368 K). *Phys. Chem. Chem. Phys.* **2005**, *7*, 349-355, doi:10.1039/b413961e.

Dillon, T. J.; Horowitz, A.; Hölscher, D.; Crowley, J. N.; Vereecken, L.; Peeters, J. Reaction of HO with hydroxyacetone ($HOCH_2C(O)CH_3$): rate coefficients (233-363 K) and mechanism. *Phys. Chem. Chem. Phys.* **2006**, *8*, 236-246, doi:10.1039/B513056E.

Ditchburn, R. W. Absorption cross-sections in the vacuum ultra-violet III. Methane. *Proc. Roy. Soc. London A* **1955**, *229*, 44-62, doi:10.1098/rspa.1955.0073.

Doner, A. C.; Moran, H. A.; Webb, A. R.; Christianson, M. G.; Koritzke, A. L.; Dewey, N. S.; Hartness, S. W.; Rotavera, B. Machine learning models for binary molecular classification using VUV absorption spectra. *J. Quant. Spectrosc. Radiat. Transf.* **2023**, *297*, 108438, doi:10.1016/j.jqsrt.2022.108438.

Doner, A. C.; Webb, A. R.; Dewey, N. S.; Christianson, M. G.; Koritzke, A. L.; Larsson, A.; Frandsen, K. M.; Rotavera, B. Vacuum-ultraviolet absorption cross-sections of functionalized four-carbon species. *J. Quant. Spectrosc. Radiat. Transf.* **2022**, *292*, 108346 doi:10.1016/j.jqsrt.2022.108346.

Eden, S.; Limão-Vieira, P.; Kendall, P.; Mason, N. J.; Hoffmann, S. V.; Spyrou, S. M. High resolution photo-absorption studies of acrylonitrile, C_2H_3CN, and acetonitrile, CH_3CN. *Eur. Phys. J.* **2003**, *D 26*, 201-210, doi:10.1140/epjd/e2003-00223-5.

Emrich, M.; Warneck, P. Photodissociation of acetone in air: Dependence on pressure and wavelength. Behavior of the excited singlet state. *J. Phys. Chem. A* **2000**, *104*, 9436-9442, doi:10.1021/jp001873i.

Emrich, M.; Warneck, P. Photodissociation of acetone in air: Dependence on pressure and wavelength. Behavior of the excited singlet state. *J. Phys. Chem. A* **2005**, *109*, 1752, doi:10.1021/jp0407627.

Fahr, A.; Braun, W.; Laufer, A. H. Photolysis of methyl vinyl ketone at 193.3 nm: Quantum yield determination of methyl and vinyl radicals. *J. Phys. Chem.* **1993**, *97*, 1502-1506, doi:10.1021/j100110a007.

Fahr, A.; Laufer, A. H.; Kraus, M.; Osman, R. Gas phase absorption spectrum and cross sections of vinylperoxy ($C_2H_3O_2$) radical. *J. Phys. Chem. A* **1997**, *101*, 4879-4886, doi:10.1021/jp964005n.

Fauvet, S.; Ganne, J. P.; Brion, J.; Daumont, D.; Malicet, J.; Chakir, A. Study of $C_2H_5O_2$ using modulated photolysis: Ultra-violet spectrum and self-reaction kinetics in the temperature range 233-363 K. *J. Chim. Phys.* **1997**, *94*, 484-502, doi:10.1051/jcp/1997940484.

Feierabend, K. J.; Flad, J. E.; Brown, S. S.; Burkholder, J. B. HCO quantum yields in the photolysis of HC(O)C(O)H (glyoxal) between 290 and 420 nm. *J. Phys. Chem. A* **2009**, *113*, 7784-7794, doi:10.1021/jp9033003.

Feng, R.; Brion, C. E. Absolute photoabsorption cross-sections (oscillator strengths) for ethanol (5–200 eV). *Chem. Phys.* **2002**, *282*, 419-427, doi:10.1016/S0301-0104(02)00722-X.

Fenter, F. F.; Catoire, V.; Lesclaux, R.; Lightfoot, P. D. The ethylperoxy radical: Its ultraviolet spectrum, self-reaction, and reaction with HO_2, each studied as a function of temperature. *J. Phys. Chem.* **1993**, *97*, 3530-3538, doi:10.1021/j100116a016.

Flowerday, C. E.; Bhardwaj, N.; Thalman, R.; Asplund, M. C.; Sevy, E. T.; Hansen, J. C. Absorption cross-sections for the 5th and 6th vibrational overtones in a series of short chained alcohols using incoherent broadband cavity enhanced-absorption spectroscopy (IBBCEAS). *J. Mol. Spectrosc.* **2023**, *392*, 111746, doi:10.1016/j.jms.2023.111746.

Flowers, B. A.; Angerhofer, M. E.; Simpson, W. R.; Nakayama, T.; Matsumi, Y. Nitrate radical quantum yield from peroxyacetyl nitrate photolysis. *J. Phys. Chem. A* **2005**, *109*, 2252-2558, doi:10.1021/jp045529n.

Flowers, B. A.; Stanton, J. F.; Simpson, W. R. Wavelength dependence of nitrate radical quantum yield from peroxyacetyl nitrate photolysis: Experimental and theoretical studies. *J. Phys. Chem. A* **2007**, *111*, 11602-11607, doi:10.1021/jp0749118.

Foreman, E. S.; Kapnas, K. M.; Jou, Y.; Kalinowski, J.; Feng, D.; Gerber, R. B.; Murray, C. High resolution absolute absorption cross sections of the $B^1A'–X^1A'$ transition of the CH_2OO biradical. *Phys. Chem. Chem. Phys.* **2015**, *17*, 32539-32546, doi:10.1039/c5cp04977f.

Fry, J.; Matthews, L. J.; Lane, J. R.; Sinha, A.; Kjaergaard, H. G.; Wennberg, P. O. OH-Stretch vibrational spectroscopy of hydroxymethyl hydroperoxide. *J. Phys. Chem. A* **2006**, *110*, 7072-7079, doi:10.1021/jp0612127.

Fujimoto, M. M.; Tanaka, H. K.; Marinho, R. R. T.; Medina, A.; Prudente, F. V.; Homem, M. G. P. Cross sections and asymmetry parameters for formic acid in the vacuum-ultraviolet energy range. *J. Phys. Chem. A* **2020**, *124*, 6478-6485, doi:10.1021/acs.jpca.0c03520.

Gardner, E. P.; Sperry, P. D.; Calvert, J. G. Photodecomposition of acrolein in O_2-N_2 mixtures. *J. Phys. Chem.* **1987**, *91*, 1922-1930, doi:10.1021/j100291a048.

Gardner, E. P.; Wijayaratne, R. D.; Calvert, J. G. Primary quantum yields of photodecomposition of acetone in air under tropospheric conditions. *J. Phys. Chem.* **1984**, *88*, 5069-5076, doi:10.1021/j150665a055.

Gentieu, E. P.; Mentall, J. E. Formaldehyde absorption coefficients in the vacuum ultraviolet (650 to 1850 Å). *Science* **1970**, *169*, 681-683, doi:10.1126/science.169.3946.68.

Gierczak, T.; Burkholder, J. B.; Bauerle, S.; Ravishankara, A. R. Photochemisty of acetone under atmospheric conditions. *Chem. Phys.* **1998**, *231*, 229-244, doi:10.1016/S0301-0104(98)00006-8.

Gierczak, T.; Burkholder, J. B.; Talukdar, R. K.; Mellouki, A.; Barone, S. B.; Ravishankara, A. R. Atmospheric fate of methyl vinyl ketone and methacrolein. *J. Photochem. Photobiol. A: Chem.* **1997**, *110*, 1-10, doi:10.1016/S1010-6030(97)00159-7.

Gierczak, T.; Gilles, M. K.; Bauerle, S.; Ravishankara, A. R. Reaction of hydroxyl radical with acetone. 1. Kinetics of the reactions of OH, OD, and ^{18}OH with acetone and acetone-d_6. *J. Phys. Chem. A* **2003**, *107*, 5014-5020, doi:10.1021/jp027301a.

Glicker, S.; Stief, L. J. Photolysis of formaldehyde at 1470 and 1236 Å. *J. Chem. Phys.* **1971**, *54*, 2852-2857, doi:10.1063/1.1675264.

Gorrotxategi Carbajo, P.; Smith, S. C.; Holloway, A.-L.; Smith, C. A.; Pope, F. D.; Shallcross, D. E.; Orr-Ewing, A. J. Ultraviolet photolysis of HCHO: Absolute HCO quantum yields by direct detection of the radical photoproduct. *J. Phys. Chem. A* **2008**, *112*, 12437-12448, doi:10.1021/jp8070508.

Gratien, A.; Nilsson, E.; Doussin, J.-F.; Johnson, M. S.; Nielsen, C. J.; Stenstrøm, Y.; Picquet-Varrault, B. UV and IR absorption cross sections of HCHO, HCDO, and DCDO. *J. Phys. Chem. A* **2007**, *111*, 11506-11513, doi:10.1021/jp074288r.

Gratien, A.; Picquet-Varrault, B.; Orphal, J.; Perraudin, E.; Doussin, J.-F. Laboratory intercomparison of the formaldehyde absorption cross sections in the infrared (1660-1820 cm^{-1}) and ultraviolet (300-360 nm) spectral regions. *J. Geophys. Res.* **2007**, *112*, D053005, doi:10.1029/2006JD007201.

Han, J. C.; Suto, M.; Lee, L. C. Fluorescence from photoexcitation of C_2H_5OH by vacuum ultraviolet radiation. *J. Quant. Spectrosc. Radiat. Transf.* **1989**, *42*, 557-562, doi:10.1016/0022-4073(89)90046-0.

Harrison, A. J.; Cederholm, B. J.; Terwilliger, M. A. Absorption of acyclic oxygen compounds in the vacuum ultraviolet. I. Alcohols. *J. Chem. Phys.* **1959**, *30*, 355-356, doi:10.1063/1.1729952.

Harwood, M. H.; Burkholder, J. B.; Ravishankara, A. R. Photodissociation of $BrONO_2$ and N_2O_5: Quantum yields for NO_3 production at 248, 308, and 352.5 nm. *J. Phys. Chem. A* **1998**, *102*, 1309-1317, doi:10.1021/jp9729829.

Harwood, M. H.; Roberts, J. M.; Frost, G. J.; Ravishankara, A. R.; Burkholder, J. B. Photochemical studies of $CH_3C(O)OONO_2$ (PAN) and $CH_3CH_2C(O)OONO_2$ (PPN): NO_3 quantum yields. *J. Phys. Chem. A* **2003**, *107*, 1148-1154, doi:10.1021/jp0264230.

He, H.-Y.; Fang, W.-H. A CASSCF/MR-CI study toward the understanding of wavelength-dependent and geometrically memorized photodissociation of formic acid. *J. Am. Chem. Soc.* **2003**, *125*, 16139-16147, doi:10.1021/ja0363157.

Heicklen, J.; Desai, J.; Bahta, A.; Harper, C.; Simonaitis, R. The temperature and wavelength dependence of the photo-oxidation of propionaldehyde. *J. Photochem.* **1986**, *34*, 117-135, doi:10.1016/0047-2670(86)85014-6.

Herzberg, G.; Innes, K. K. Ultraviolet absorption spectra of HCN and DCN .1. The alpha-X and beta-X systems. *Can. J. Phys.* **1957**, *35*, 842-879, doi:10.1139/p57-095.

Higgins, C. M.; Evans, L. A.; Lloyd-Jones, G. C.; Shallcross, D. E.; Tew, D. P.; Orr-Ewing, A. J. Quantum yields for photochemical production of NO_2 from organic nitrates at tropospherically relevant wavelengths. *J. Phys. Chem. A* **2014**, *118*, 2756–2764, doi:10.1021/jp501517t.

Hintze, P. E.; Aloisio, S.; Vaida, V. Electronic spectroscopy of organic acid dimers. *Chem. Phys. Lett.* **2001**, *343*, 159-165, doi:10.1016/S0009-2614(01)00664-9.

Hochanadel, C. J.; Ghormley, J. A.; Boyle, J. W.; Ogren, P. J. Absorption spectrum and rates of formation and decay of the CH_3O_2 radical. *J. Phys. Chem.* **1977**, *81*, 3-7, doi:10.1021/j100516a002.

Horowitz, A.; Calvert, J. G. Wavelength dependence of the quantum efficiencies of the primary processes in formaldehyde photolysis at 25°C. *Int. J. Chem. Kinet.* **1978**, *10*, 805-819, doi:10.1002/kin.550100803.

Horowitz, A.; Calvert, J. G. Wavelength dependence of the primary processes in acetaldehyde photolysis. *J. Phys. Chem.* **1982**, *86*, 3105-3114, doi:10.1021/j100213a011.

Horowitz, A.; Kershner, C. J.; Calvert, J. G. Primary processes in the photolysis of acetaldehyde at 3000 Å and 25 °C. *J. Phys. Chem.* **1982**, *86*, 3094-3104, doi:10.1021/j100213a010.

Horowitz, A.; Meller, R.; Moortgat, G. K. The UV-VIS absorption cross sections of the a-dicarbonyl compounds: pyruvic acid, biacetyl and glyoxal. *J. Photochem. Photobiol. A: Chem.* **2001**, *146*, 19-27, doi:10.1016/S1010-6030(01)00601-3.

Huang, H.-L.; Chao, W.; Lin, J. J.-M. Kinetics of a Criegee intermediate that would survive high humidity and may oxidize atmospheric SO_2. *Proc. Natl. Acad. Sci.* **2015**, *112*, 10857-10862, doi:10.1073/pnas.1513149112.

Hunnicutt, S. S.; Waits, L. D.; Guest, J. A. Energetic constraints in the 218 nm photolysis of acetic acid. *J. Phys. Chem.* **1989**, *93*, 5188-5195, doi:10.1021/j100350a033.

Hynes, A. J.; Kenyon, E. A.; Pounds, A. J.; Wine, P. H. Temperature dependent absorption cross sections for acetone and *n*-butanone - implications for atmospheric lifetimes. *Spectrochim. Acta* **1992**, *48A*, 1235-1242, doi:10.1016/0584-8539(92)80260-4.

Indulkar, Y. N.; Louie, M. K.; Sinha, A. UV photochemistry of peroxyformic acid (HC(O)OOH): An experimental and computational study investigating 355 nm photolysis. *J. Phys. Chem. A* **2014**, *118*, 5939-5949, doi:10.1021/jp5039688.

Ito, H.; Nogata, Y.; Matsuzaki, S.; Kuboyama, A. Vacuum-ultraviolet absorption spectra of aliphatic ketones. *Bull. Chem. Soc. Japan* **1969**, *42*, 2453-2458, doi:10.1246/bcsj.42.2453.

Jacobs, L. E.; Platt, J. R. Does ultraviolet absorption intensity increase in solution? *J. Chem. Phys.* **1948**, *16*, 1137-1145, doi:10.1063/1.1746745.

Jenkin, M. E.; Cox, R. A. Kinetics of reactions of CH_3O_2 and $HOCH_2CH_2O_2$ radicals produced by the photolysis of iodomethane and 2-iodoethanol. *J. Phys. Chem.* **1991**, *95*, 3229-3237, doi:10.1021/j100161a049.

Jenkin, M. E.; Cox, R. A.; Hayman, G.; Whyte, L. J. Kinetic study of the reactions CH_3O_2 + CH_3O_2 and CH_3O_2 + HO_2 using molecular modulation spectroscopy. *J. Chem. Soc. Faraday Trans. 2* **1988**, *84*, 913-930, doi:10.1039/f29888400913.

Jiménez, E.; Gilles, M. K.; A.R., R. Kinetics of the reaction of the hydroxyl radical with CH_3OH and C_2H_5OH between 235 and 360 K. *J. Photochem. Photobiol. A: Photochem.* **2003**, *157*, 237-245, doi:10.1016/S1010-6030(03)00073-X.

Jolly, G. S.; Singleton, D. L.; Paraskevopoulos, G. Direct determination of the quantum yield of OH in the laser photolysis of formic acid. *J. Phys. Chem.* **1987**, *91*, 3463-3465, doi:10.1021/j100297a001.

Jones, L. C.; Taylor, L. W. Far ultraviolet absorption spectra of unsaturated and aromatic hydrocarbons. *Anal. Chem.* **1955**, *27*, 228-237, doi:10.1021/ac60098a015.

Kameta, K.; Kouchi, N.; Ukai, M.; Hatano, Y. Photoabsorption, photoionization, and neutral-dissociation cross sections of simple hydrocarbons in the vacuum ultraviolet range. *J. Electron Spectrosc. Related Phenom.* **2002**, *123*, 225-238, doi:10.1016/S0368-2048(02)00022-1.

Kan, C. S.; McQuigg, R. D.; Whitbeck, M. R.; Calvert, J. G. Kinetic flash spectroscopic study of the CH_3O_2-CH_3O_2 and CH_3O_2-SO_2 reactions. *Int. J. Chem. Kinet.* **1979**, *11*, 921-933, doi:10.1002/kin.550110811.

Karunanandan, R.; Hölscher, D.; Dillon, T. J.; Horowitz, A.; Crowley, J. N.; Vereecken, L.; Peeters, J. Reaction of HO with glycolaldehyde, $HOCH_2CHO$: Rate coefficients (240-362 K) and mechanism. *J. Phys. Chem. A* **2007**, *111*, 897-908, doi:10.1021/jp0649504.

Kaya, K.; Kuwata, K.; Nagakura, S. The ultraviolet absorption spectra of nitramide and ethyl nitrate. *Bull. Chem. Soc. Japan* **1964**, *37*, 1055-1061, doi:10.1246/bcsj.37.1055.

Keller-Rudek, H.; Moortgat, G. K.; Sander, R.; Sörensen, R. The MPI-Mainz UV/Vis spectral atlas of gaseous molecules of atmospheric interest. *Earth Syst. Sci. Data* **2013**, *5*, 365-373, doi:10.5194/essd-5-365-2013.

Khamaganov, V.; Karunanandan, R.; Rodriguez, A.; Crowley, J. N. Photolysis of $CH_3C(O)CH_3$ (248 nm, 266 nm), $CH_3C(O)C_2H_5$ (248 nm) and $CH_3C(O)Br$ (248 nm): pressure dependent quantum yields of CH_3 formation. *Phys. Chem. Chem. Phys.* **2007**, *9*, 4098-4113, doi:10.1039/b701382e.

Khamaganov, V. G.; Karunanandan, R.; Horowitz, A.; Dillon, T. J.; Crowley, J. N. Photolysis of $CH_3C(O)CH_3$ at 248 and 266 nm: pressure and temperature dependent overall quantum yields. *Phys. Chem. Chem. Phys.* **2009**, *11*, 6173-6181, doi:10.1039/b904130c.

Ko, M. K. W.; Newman, P. A.; Reimann, S.; Strahan, S. E.; Plumb, R. A.; Stolarski, R. S.; Burkholder, J. B.; Mellouki, W.; Engel, A.; Atlas, E. L.; Chipperfield, M.; Liang, Q. Lifetimes of Stratospheric Ozone-Depleting Substances, Their Replacements, and Related Species, SPARC Report No. 6, WCRP-15/2013, 2013, http://www.sparc-climate.org/publications/sparc-reports/sparc-report-no6/.

Koch, S.; Moortgat, G. K. Photochemistry of methylglyoxal in the vapor phase. *J. Phys. Chem. A* **1998**, *102*, 9142-9153, doi:10.1021/jp981915r.

Krasnoperov, L. N.; Mehta, K. Kinetic study of CH_3 + HBr and CH_3 + Br reactions by laser photolysis - transient absorption over 1 - 100 bar pressure range. *J. Phys. Chem. A* **1999**, *103*, 8008-8020, doi:10.1021/jp991183i.

Kurylo, M. J.; Wallington, T. J.; Ouellette, P. A. Measurements of the UV absorption cross-sections for HO_2 and CH_3O_2 in the gas phase. *J. Photochem.* **1987**, *39*, 201-215, doi:10.1016/0047-2670(87)80032-1.

Kyle, E.; Orchard, S. W. The photolysis of methyl glyoxal vapour at 436 nm. *J. Photochem.* **1977**, *7*, 305-317, doi:10.1016/0047-2670(77)80012-9.

Lake, J. S.; Harrison, A. J. Absorption of acyclic oxygen compounds in the vacuum ultraviolet. III. Acetone and acetaldehyde. *J. Chem. Phys.* **1959**, *30*, 361-362, doi:10.1063/1.1729955.

Lange, E.; Lozano, A. I.; Jones, N. C.; Hoffmann, S. V.; Kumar, S.; Smialek, M. A.; Duflot, D.; Brunger, M. J.; Limão-Vieira, P. Absolute photoabsorption cross-sections of methanol for terrestrial and astrophysical relevance. *J .Phys. Chem. A* **2020**, *124*, 8496-8508, doi:10.1021/acs.jpca.0c06615.

Langford, A. O.; Moore, C. B. Collision complex formation in the reactions of formyl radicals with nitric oxide and oxygen. *J. Chem. Phys.* **1984**, *80*, 4211-4221, doi:10.1063/1.447252.

Laufer, A. H.; McNesby, J. R. Deuterium isotope effect in vacuum-ultraviolet absorption coefficients of water and methane. *Can. J. Chem.* **1965**, *43*, 3487-3490, doi:10.1139/v65-495.

Leach, S.; Schwell, M.; Dulieu, F.; Chotin, J.-L.; Jochims, H.-W.; Baumgärtel, H. Photophysical studies of formic acid in the VUV. Absorption spectrum in the 6-22 eV region. *Phys. Chem. Chem. Phys.* **2002**, *4*, 5025-5039, doi:10.1039/b205729h.

Lee, L. C. $CN(A\ ^2\Pi_i \rightarrow X\ ^2\Sigma^+)$ and $CN(B\ ^2\Sigma^+ \rightarrow X\ ^2\Sigma^+)$ yields from HCN photodissociation. *J. Chem. Phys.* **1980**, *72*, 6414-6424, doi:10.1063/1.439140.

Lee, A. M. D.; Coe, J. D.; Ullrich, S.; Ho, M.-L.; Lee, S.-J.; Cheng, B.-M.; Zgierski, M. Z.; Chen, I.-C.; Martinez, T. J.; Stolow, A. Substituent effects on dynamics at conical intersections: α,β-enones. *J. Phys. Chem. A* **2007**, *111*, 11948–11960, doi:10.1021/jp074622j.

Lee, A. Y. T.; Yung, Y. L.; Cheng, B. M.; Bahou, M.; Chung, C.-Y.; Lee, Y. P. Enhancement of deuterated ethane on Jupiter. *Astrophys. J.* **2001**, *551*, 93-96, doi:10.1086/319827.

Lee, L. C.; Chiang, C. C. Fluorescence yield from photodissociation of CH_4 at 1060-1420 Å. *J. Chem. Phys.* **1983**, *78*, 688-691, doi:10.1063/1.444812.

Lewis, R. S.; Tang, K. Y.; Lee, E. K. C. Photoexcited chemiluminescence spectroscopy: Detection of hydrogen atoms produced from single vibronic level photolysis of formaldehyde. *J. Chem. Phys.* **1976**, *65*, 2910-2911, doi:10.1063/1.433399.

Libuda, H. G. Spektroskopische und kinetische Untersuchungen an halogenierten Carbonylverbindungen von atmosphärischem Interesse. PhD-Thesis, University of Wuppertal, Germany, 1992.

Libuda, H. G.; Zabel, F. UV absorption cross sections of acetyl peroxynitrate and trifluoroacetyl peroxynitrate at 298 K. *Ber. Bunsenges. Phys. Chem.* **1995**, *99*, 1205-1213, doi:10.1002/bbpc.199500061.

Libuda, H. G.; Zabel, F.; Becker, K. H. "UV spectra of some organic chlorine and bromine compounds of atmospheric interest"; Kinetics and Mechanisms for the Reactions of Halogenated Organic Compounds in the Troposphere. STEP-HALOCSIDE/AFEAS WORKSHOP, 1991, Dublin, Ireland.

Lightfoot, P. D.; Cox, R. A.; Crowley, J. N.; Destriau, M.; Hayman, G. D.; Jenkin, M. E.; Moortgat, G. K.; Zabel, F. Organic peroxy radicals: Kinetics, spectroscopy and tropospheric chemistry. *Atmos. Environ.* **1992**, *26A*, 1805-1961, doi:10.1016/0960-1686(92)90423-I.

Lightfoot, P. D.; Jemi-Alade, A. A. The temperature dependence of the UV spectra of the HO_2 and CH_3O_2 radicals. *J. Photochem. Photobiol. A: Chem.* **1991**, *59*, 1-10, doi:10.1016/1010-6030(91)87062-Z.

Limão-Vieira, P.; Eden, S.; Mason, N. J.; Hoffmann, S. V. Electronic state spectroscopy of acetaldehyde, CH_3CHO, by high-resolution VUV photoabsorption. *Chem. Phys. Lett.* **2003**, *376*, 737-747, doi:10.1016/S0009-2614(03)01070-4.

Liu, F.; Beames, J. M.; Green, A. M.; Lester, M. I. UV spectroscopic characterization of dimethyl- and ethyl-substituted carbonyl oxides. *J. Phys. Chem. A* **2014**, *118*, 2298-2306, doi:10.1021/jp412726z.

Lucazeau, G.; Sandorfy, C. On the far-ultraviolet spectra of some simple aldehydes. *J. Mol. Spectrosc.* **1970**, *35*, 214-231, doi:10.1016/0022-2852(70)90199-2.

Macpherson, M. T.; Simons, J. P. Spectroscopic study of the predissociation H(D)CN (C ^{1}A') → H(D) + CN (B $^2\Sigma^+$). *J. Chem. Soc. Faraday Trans. II* **1978**, *74*, 1965-1977, doi:10.1039/F29787401965.

Magneron, I.; Mellouki, A.; Le Bras, G.; Moortgat, G. K.; Horowitz, A.; Wirtz, K. Photolysis and OH-initiated oxidation of glycolaldehyde under atmospheric conditions. *J. Phys. Chem. A* **2005**, *109*, 4552-4561, doi:10.1021/jp044346y.

Magneron, I.; Thévenet, R.; Mellouki, A.; Le Bras, G.; Moortgat, G. K.; Wirtz, K. A study of the photolysis and OH-initiated oxidation of acrolein and *trans*-crotonaldehyde. *J. Phys. Chem. A* **2002**, *106*, 2526-2537, doi:10.1021/jp013413a.

Maria, H. J.; McDonald, J. R.; McGlynn, S. R. Electronic absorption spectrum of nitrate ion and boron trihalides. *J. Am. Chem. Soc.* **1973**, *95*, 1050-1056, doi:10.1021/ja00785a010.

Maric, D.; Crowley, J. N.; Burrows, J. P. Application of a Gaussian distribution function to describe molecular UV-visible absorption continua. 2. The UV spectra of RO_2• radicals. *J. Phys. Chem.* **1997**, *101*, 2561-2567, doi:10.1021/jp961715k.

Maricq, M. M.; Szente, J. J. The $CH_3C(O)O_2$ radical. Its UV spectrum, self-reaction kinetics, and reaction with CH_3O_2. *J. Phys. Chem.* **1996**, *100*, 4507-4513, doi:10.1021/jp9533234.

Maricq, M. M.; Szente, J. J. The UV spectrum of acetyl and the kinetics of the chain reaction between acetaldehyde and chlorine. *Chem. Phys. Lett.* **1996**, *253*, 333-339, doi:10.1016/0009-2614(96)00155-8.

Maricq, M. M.; Wallington, T. J. Absolute ultraviolet cross sections of methyl and ethyl peroxy radicals. *J. Phys. Chem.* **1992**, *96*, 982-986, doi:10.1021/j100181a081.

Marling, L. Isotope separation of oxygen-17, oxygen-18, carbon-13, and deuterium by ion laser induced formaldehyde photopredissociation. *J. Chem. Phys.* **1977**, *66*, 4200-4225, doi:10.1063/1.434496.

Marshall, P.; Papadimitriou, V. C.; Papanastasiou, D. K.; Roberts, J. M.; Burkholder, J. B. UV and infrared absorption spectra and 248 nm photolysis of maleic anhydride ($C_4H_2O_3$). *J. Photochem. Photobio. A: Chem.* **2019**, *382*, 111953, doi:10.1016/j.jphotochem.2019.111953.

Martinez, R. D.; Buitrago, A. A.; Howell, N. W.; Hearn, C. H.; Joens, J. A. The near UV absorption spectra of several aliphatic aldehydes and ketones. *Atmos. Environ.* **1992**, *26A*, 785-792, doi:10.1016/0960-1686(92)90238-G.

Martins, G.; Ferreira-Rodrigues, A. M.; Rodrigues, F. N.; de Souza, G. G.; Mason, N. J.; Eden, S.; Duflot, D.; Flament, J.-P.; Hoffmann, S. V.; Delwiche, J.; et al. Valence shell electronic spectroscopy of isoprene studied by theoretical calculations and by electron scattering, photoelectron, and absolute photoabsorption measurements. *Phys. Chem. Chem. Phys.* **2009**, *11*, 11219-11231, doi:10.1039/B916620C.

Matthews, J.; Sinha, A.; Francisco, J. S. The importance of weak absorption features in promoting tropospheric radical production. *Proc. Natl. Acad. Sci.* **2005**, *102*, 7449-7452, doi:10.1073/pnas.0502687102.

Mazely, T. L.; Friedl, R. R.; Sander, S. P. The production of NO_2 from the photolysis of peroxyacetyl nitrate. *J. Phys. Chem.* **1995**, *99*, 8162-8169, doi:10.1021/j100020a044.

Mazely, T. L.; Friedl, R. R.; Sander, S. P. Quantum yield of NO_3 from peroxyacetyl nitrate photolysis. *J. Phys. Chem.* **1997**, *101*, 7090-7097, doi:10.1021/jp971298r.

McAdam, K.; Veyret, B.; Lesclaux, R. UV absorption spectra of HO_2 and CH_3O_2 radicals and the kinetics of their mutual reactions at 298 K. *Chem. Phys. Lett.* **1987**, *133*, 39-44, doi:10.1016/0009-2614(87)80049-0.

McElcheran, D. E.; Wijnen, M. H. J.; Steacie, E. W. R. The photolysis of methyl cyanide at 1849 Å. *Can. J. Chem.* **1958**, *36*, 321-339, doi:10.1139/v58-046.

Macpherson, M. T.; Pilling, M. J.; Smith, M. J. C. Determination of the absorption cross section for CH_3 at 216.36 nm and the absolute rate constant for methyl radical recombination over the temperature range 296-577 K. *J. Phys. Chem.* **1985**, *89*, 2268-2274, doi:10.1021/j100257a024.

McQuigg, R. D.; Calvert, J. G. The photodecomposition of CH_2O, CD_2O, CHDO, and CH_2O-CD_2O mixtures at xenon flash lamp intensities. *J. Am. Chem. Soc.* **1969**, *91*, 1590-1599, doi:10.1021/ja01035a002.

Meller, R.; Crowley, J. N. E.-P. Röth, R. Ruhnke, G. Moortgat, R. Meller, and W. Schneider, Berichte des Forschungszentums Jülich, jül-3341 (1997). Data from the CD-ROM of A. Nölle, F. Pätzold, S. Pätzold, R. Meller, G. K. Moortgat, E. P. Röth, R. Ruhnke, H. Keller-Rudek, "UV/VIS Spectra of Atmospheric Constituents, Version 1," ATMOS User Center at Deutsches Fernerkundungsdatenzentrum (DFD). *Personal Communication* **1998**.

Meller, R.; Moortgat, G. K. Temperature dependence of the absorption cross sections of formaldehyde between 223 and 323 K in the wavelength range 225-375 nm. *J. Geophys. Res.* **2000**, *105*, 7089-7101, doi:10.1029/1999JD901074.

Meller, R.; Raber, W.; Crowley, J. N.; Jenkin, M. E.; Moortgat, G. K. The UV-visible absorption spectrum of methylglyoxal. *J. Photochem. Photobiol. A: Chem.* **1991**, *62*, 163-171, doi:10.1016/1010-6030(91)87017-P.

Mellouki, A.; Mu, Y. On the atmospheric degradation of pyruvic acid in the gas phase. *J. Photochem. Photobiol. A: Chem.* **2003**, *157*, 295-300, doi:10.1016/S1010-6030(03)00070-4.

Mentall, J. E.; Gentieu, E. P.; Krauss, M.; Neumann, D. Photoionization and absorption spectrum of formaldehyde in the vacuum ultraviolet. *J. Chem. Phys.* **1971**, *55*, 5471-5479, doi:10.1063/1.1675711.

Messaadia, L.; El Dib, G.; Ferhati, A.; Roth, E.; Chakir, A. Gas phase UV absorption cross-sections for a series of hydroxycarbonyls. *Chem. Phys. Lett.* **2012**, *529*, 16-22, doi:10.1016/j.cplett.2012.01.044.

Meyrahn, H. Bildungswege und Analytik des Peroxyacetylnitrats (PAN) in der Atmosphäre. PhD-Thesis, Johann-Gutenberg-Universität, 1984.

Meyrahn, H.; Moortgat, G. K.; Warneck, P. Photolysis of CH_3CHO in the range 250 - 330 nm. *J. Photochem.* **1981**, *17*, 138, doi:10.1016/0047-2670(81)85266-5.

Meyrahn, H.; Pauly, J.; Schneider, W.; Warneck, P. Quantum yields for the photodissociation of acetone in air and an estimate for the life time of acetone in the lower troposphere. *J. Atmos. Chem.* **1986**, *4*, 277-291, doi:10.1007/BF00052006.

Molina, M. J.; Arguello, G. Ultraviolet absorption spectrum of methylhydroperoxide vapor. *Geophys. Res. Lett.* **1979**, *6*, 953-955, doi:10.1029/GL006i012p00953.

Moortgat, G.; Veyret, B.; Lesclaux, R. Absorption spectrum and kinetics of reactions of the acetylperoxy radical. *J. Phys. Chem.* **1989**, *93*, 2362-2368, doi:10.1021/j100343a032.

Moortgat, G. K. Important photochemical processes in the atmosphere. *Pure Appl. Chem.* **2001**, *73*, 487-490.

Moortgat, G. K. RADICAL: Evaluation of Radical Sources in Atmospheric Chemistry through Chamber and Laboratory Studies, ENVA-CT97-0419, EUR 20254 EN, 2002,

Moortgat, G. K.; Klippel, W.; MÖbus, K. H.; Seiler, W.; Warneck, P. Federal Aviation Administration, Washington, DC FAA-EE-80-47, 1980,

Moortgat, G. K.; Seiler, W.; Warneck, P. Photodissociation of HCHO in air: CO and H_2 quantum yields at 220 and 300 K. *J. Chem. Phys.* **1983**, *78*, 1185-1190, doi:10.1063/1.444911.

Moortgat, G. K.; Slemr, F.; Seiler, W.; Warneck, P. Photolysis of formaldehyde: Relative quantum yields of H_2 and CO in the wavelength range 270 - 360 nm. *Chem. Phys. Lett.* **1978**, *54*, 444-447, doi:10.1016/0009-2614(78)85257-9.

Moortgat, G. K.; Warneck, P. CO and H_2 quantum yields in the photodecomposition of formaldehyde in air. *J. Chem. Phys.* **1979**, *70*, 3639-3651, doi:10.1063/1.437956.

Morel, O.; Simonaitis, R.; Heicklen, J. Ultraviolet absorption spectra of HO_2NO_2, $CCl_3O_2NO_2$, $CCl_2FO_2NO_2$, and $CH_3O_2NO_2$. *Chem. Phys. Lett.* **1980**, *73*, 38-41, doi:10.1016/0009-2614(80)85197-9.

Mount, G. H.; Warden, E. S.; Moos, H. W. Photoabsorption cross sections of methane from 1400 to 1850 A. *Astrophys. J.* **1977**, *214*, L47-L49, doi:10.1086/182440.

Mui, P. W.; Grunwald, E. Enthalpy change for the s-trans to s-cis conformational equilibrium in 2-methyl-1,3-butadiene (isoprene), as studied by high-temperature ultraviolet absorption spectroscopy. *J. Phys. Chem.* **1984**, *88*, 6340-6344, doi:10.1021/j150669a056.

Munk, J.; Pagsberg, P.; Ratajczak, E.; Sillesen, A. Spectrokinetic studies of ethyl and ethylperoxy radicals. *J. Phys. Chem.* **1986**, *90*, 2752-2757, doi:10.1021/j100403a038.

Nádasdia, R.; Kovácsa, G.; Szilágyia, I.; Demetera, A.; Dóbé, S. Exciplex laser photolysis study of acetone with relevance to tropospheric chemistry. *Chem. Phys. Lett.* **2007**, *440*, 31-35, doi:10.1016/j.cplett.2007.04.014.

Nádasdi, R.; Zügner, G. L.; Farkas, M.; Dóbé, S.; Maeda, S.; Morokuma, K. Photochemistry of methyl ethyl ketone: Quantum yields and S_1/S_0-diradical mechanism of photodissociation. *ChemPhysChem* **2010**, *11*, 3883-3895, doi:10.1002/cphc.201000522.

Nagakura, S.; Kaya, K.; Tsubomura, H. Vacuum ultraviolet absorption spectra and electronic structures of formic acid, acetic acid and ethyl acetate. *J. Mol. Spectrosc.* **1964**, *13*, 1-8, doi:10.1016/0022-2852(64)90049-9.

Nagata, T.; Kondow, T.; Ozaki, Y.; Kuchitsu, K. Absorption spectra of hydrogen cyanide and deuterium cyanide in the 130-80 nm range. *Chem. Phys.* **1981**, *57*, 45-53, doi:10.1016/0301-0104(81)80019-5.

Napier, I. M.; Norrish, R. G. W. The photolysis and pyrolysis of nitromethane and methyl nitrite. *Proc. Roy. Soc. London A* **1967**, *299*, 317-336, doi:10.1098/rspa.1967.0139.

Nee, J. B.; Suto, M.; Lee, L. C. Photoabsorption cross section of HF at 107-145 nm. *J. Phys. B: At. Mol. Phys.* **1985**, *18*, L293-L294, doi:10.1088/0022-3700/18/10/006.

Nielsen, O. J.; Johnson, M. S.; Wallington, T. J.; Christensen, L. K.; Platz, J. UV absorption cross sections of HO_2, CH_3O_2, $C_2H_5O_2$ and $CH_3C(O)CH_2O_2$ radicals and mechanism of the reactions of F and Cl atoms with $CH_3C(O)CH_3$. *Int. J. Chem. Kinet.* **2002**, *34*, 283-291, doi:10.1002/kin.10037.

Nozière, B.; Lesclaux, R.; Hurley, M. D.; Dearth, M. A.; Wallington, T. J. A kinetic and mechanistic study of the self-reaction and reaction with HO_2 of the benzylperoxy radical. *J. Phys. Chem.* **1994**, *98*, 2864-2873, doi:10.1021/j100062a023.

Nunes, Y.; Martins, G.; Mason, N. J.; Duflot, D.; Hoffmann, S. V.; Delwiche, J.; Hubin-Franskin, M.-J.; Limão-Vieira, P. Electronic states spectroscopy of methyl formate probed by high resolution VUV photoabsorption, He(I) photoelectron spectroscopy and ab initio calculations. *Phys. Chem. Chem. Phys.* **2010**, *12*, 15734-15743, doi:10.1039/C0CP00051E.

Nuth, J. A.; Glicker, S. The vacuum ultraviolet spectra of HCN, C_2N_2, and CH_3CN. *J. Quant. Spectrosc. Radiat. Transf.* **1982**, *28*, 223-231, doi:10.1016/0022-4073(82)90025-5.

Ogawa, M.; Cook, G. R. Absorption coefficients of methyl, ethyl, *n*-propyl, and *n*-butyl alcohols. *J. Chem. Phys.* **1958**, *28*, 747-748, doi:10.1063/1.1744253.

Orkin, V. L.; Khamaganov, V. G.; Kurylo, M. J. High accuracy measurements of OH reaction rate constants and IR absorption spectra: Substituted 2-propanols. *J. Phys. Chem. A* **2012**, *116*, 6188-6198, doi:10.1021/jp211534n.

Orkin, V. L.; Khamaganov, V. G.; Martynova, L. E.; Kurylo, M. J. High-accuracy measurements of $OH^{\bullet}$ reaction rate constants and IR and UV absorption spectra: Ethanol and partially fluorinated ethyl alcohols. *J. Phys. Chem. A* **2011**, *115*, 8656-8668, doi:10.1021/jp202099t.

Orlando, J. J.; Tyndall, G. S. The atmospheric chemistry of the HC(O)CO radical. *Int. J. Chem. Kinet.* **2001**, *33*, 149-156, doi:10.1002/1097-4601(200103)33:3<149::AID-KIN1008>3.0.CO;2-1.

Orlando, J. J.; Tyndall, G. S. Gas phase UV absorption spectra for peracetic acid, and for acetic acid monomers and dimers. *J. Photochem. Photobiol. A: Chem.* **2003**, *157*, 161-166, doi:10.1016/S1010-6030(03)00067-4.

Orlando, J. J.; Tyndall, G. S.; Fracheboud, J.-M.; Estupiñan, E. G.; Haberkorn, S.; Zimmer, A. The rate and mechanism of the gas-phase oxidation of hydroxyacetone. *Atmos. Environ.* **1999**, *33*, 1621-1629, doi:10.1016/S1352-2310(98)00386-0.

Parkes, D. A.; Quinn, C. P. Study of the spectra and recombination kinetics of alkyl radicals by molecular modulation spectrometry. Part 2. - The recombination of ethyl, isopropyl and t-butyl radicals at room temperature and t-butyl radicals between 250 and 450 K. *J. Chem. Soc. Faraday Trans. I* **1976**, *72*, 1952-1971, doi:10.1039/F19767201952.

Parkes, D. A. The oxidation of methyl radicals at room temperature. *Int. J. Chem. Kinet.* **1977**, *9*, 451-469, doi:10.1002/kin.550090313

Parkes, D. A. The ultraviolet absorption spectra of the acetyl radical and the kinetics of the CH_3 + CO reaction at room temperature. *Chem. Phys. Lett.* **1981**, *77*, 527-532, doi:10.1016/0009-2614(81)85201-3.

Parkes, D. A.; Paul, D. M.; Quinn, C. P.; Robson, R. C. The ultraviolet absorption by alkylperoxy radicals and their mutual reactions. *Chem. Phys. Lett.* **1973**, *23*, 425-429, doi:10.1016/0009-2614(73)85115-2.

Parmenter, C. S. Primary photochemical processes in glyoxal at 4358 Å. *J. Chem. Phys.* **1964**, *41*, 658-665, doi:10.1063/1.1725943.

Person, J. C.; Nicole, P. P. Isotope effects in the photoionization yields and in the absorption cross sections for methanol, ethanol, methyl bromide, and ethyl bromide. *J. Chem. Phys.* **1971**, *55*, 3390-3397, doi:10.1063/1.1676590.

Pilling, M. J.; Smith, M. J. C. A laser flash photolysis study of the reaction $CH_3 + O_2 \rightarrow CH_3O_2$ at 298 K. *J. Phys. Chem.* **1985**, *89*, 4713-4720, doi:10.1021/j100268a014.

Plum, C. N.; Sanhueza, E.; Atkinson, R.; Carter, W. P. L.; Pitts, J. N., Jr. OH radical rate constant and photolysis rates of α-dicarbonyls. *Environ. Sci. Technol.* **1983**, *17*, 479-484, doi:10.1021/es00114a008.

Pope, F. D.; Smith, C. A.; Ashfold, N. M. R.; Orr-Ewing, A. J. High-resolution absorption cross sections of formaldehyde at wavelengths from 313 to 320 nm. *Phys. Chem. Chem. Phys.* **2005**, *7*, 79-84, doi:10.1039/b414183k.

Pope, F. D.; Smith, C. A.; Davis, P. R.; Shallcross, D. E.; Ashfold, M. N. R.; Orr-Ewing, A. J. Photochemistry of formaldehyde under troposheric conditions. *J. Chem. Soc., Faraday Disc* **2005**, *130*, 59-73, doi:10.1039/b419227c.

Raber, W. H.; Moortgat, G. K. Photooxidation of selected carbonyl compounds in air: methyl ethyl ketone, methyl vinyl ketone, methacrolein, and methylglyoxal. In *Progress and Problems in Atmospheric Chemistry*; Barker, J., Ed.; World Scientific Publ. Co.: Singapore, 1996; pp 318-373.

Rajakumar, B.; Flad, J. E.; Gierczak, T.; Ravishankara, A. R.; Burkholder, J. B. Visible absorption spectrum of the CH_3CO radical. *J. Phys. Chem. A* **2007**, *111*, 8950-8958, doi:10.1021/jp073339h.

Rajakumar, B.; Gierczak, T.; Flad, J. E.; Ravishankara, A. R.; Burkholder, J. B. The CH_3CO quantum yield in the 248 nm photolysis of acetone, methyl ethyl ketone, and biacetyl. *J. Photochem. Photobiol. A: Chem.* **2008**, *199*, 336-344, doi:10.1016/j.jphotochem.2008.06.015.

Randi, P. A. S.; Pastega, D. F.; Bettega, M. H. F.; Jones, N. C.; Hoffmann, S. V.; Eden, S.; Barbosa, A. S.; Limão-Vieira, P. Electronically excited states of formic acid investigated by theoretical and experimental methods. *Spectrochim. Acta A: Mol. Biomol. Spectrosc.* **2023**, *289*, 122237, doi:10.1016/j.saa.2022.122237.

Rattigan, O.; Lutman, R. L.; Jones, R. L.; Cox, R. A. Temperature-dependent absorption cross-sections of gaseous nitric acid and methyl nitrate. *J. Photochem. Photobiol. A: Chem.* **1992**, *66*, 313-326, doi:10.1016/1010-6030(92)80003-E.

Roberts, J. M.; Fajer, R. W. UV absorption cross sections of organic nitrates of potential atmospheric importance and estimation of atmospheric lifetimes. *Environ. Sci. Technol.* **1989**, *23*, 945-951, doi:10.1021/es00066a003.

Rocha, A. B.; Pimentel, A. S.; Bielschowsky, C. E. Direct investigation of the validity of vertical approximation in the calculation of transition moment matrix elements: n → π* transition in methyl formate. *J. Phys. Chem. A* **2002**, *106*, 181-183, doi:10.1021/jp012647r.

Roehl, C. M.; Bauer, D.; Moortgat, G. K. Absorption spectrum and kinetics of the acetylperoxy radical. *J. Phys. Chem.* **1996**, *100*, 4038-4047, doi:10.1021/jp9526298.

Roehl, C. M.; Marka, Z.; Fry, J. L.; Wennberg, P. O. Near-UV photolysis cross sections of CH_3OOH and $HOCH_2OOH$ determined via action spectroscopy. *Atmos. Chem. Phys.* **2007**, *7*, 713-720, doi:10.5194/acp-7-713-2007.

Rogers, J. D. Ultraviolet absorption cross sections and atmospheric photodissociation rate constants of formaldehyde. *J. Phys. Chem.* **1990**, *94*, 4011-4015, doi:10.1021/j100373a025.

Röth, E. P.; Ruhnke, R.; Moortgat, G.; Meller, R.; Schneider, W. UV/VIS-Absorption Cross Sections and Quantum Yields for Use in Photochemistry and Atmospheric Modeling, Forschungszentrum Jülich Publication, Part 1 : Inorganic Substances (jül-3340), Part 2: Organic Substances (jül-3341). **1997**.

Salahub, D. R.; Sandorfy, C. The far-ultraviolet spectra of some simple alcohols and fluoroalcohols. *Chem. Phys. Lett.* **1971**, *8*, 71-74, doi:10.1016/0009-2614(71)80578-X.

Sander, S. P.; Watson, R. T. Kinetic studies of the reactions of CH_3O_2 with NO, NO_2, and CH_3O_2 at 298 K. *J. Phys. Chem.* **1980**, *84*, 1664-1674, doi:10.1021/j100450a002.

Sander, S. P.; Watson, R. T. Temperature dependence of the self-reaction of CH_3O_2 radicals. *J. Phys. Chem.* **1981**, *85*, 2960-2964, doi:10.1021/j150620a023.

Schneider, W.; Moortgat, G. K. personal communication to E.-P. Röth, R. Ruhnke, G. Moortgat, R. Meller, and W. Schneider, Berichte des Forschungszentums Jülich, jül-3341 (1997). **1988**.

Seki, K.; Okabe, H. Photodissociation of methylacetylene at 193 nm. *J. Phys. Chem.* **1992**, *96*, 3345-3349, doi:10.1021/j100187a031.

Senum, G. I.; Lee, Y.-N.; Gaffney, J. S. Ultraviolet absorption spectrum of peroxyacetyl nitrate and peroxypropionyl nitrate. *J. Phys. Chem.* **1984**, *88*, 1269-1270, doi:10.1021/j150651a001.

Sahay, P.; Scherrer, S. T.; Wang, C. Measurements of the weak UV absorptions of isoprene and acetone at 261–275 nm using cavity ringdown spectroscopy for evaluation of a potential portable ringdown breath analyzer. *Sensors* **2013**, *13*, 8170-8187, dio:10.3390/s130708170.

Sheps, L. Absolute ultraviolet absorption spectrum of a Criegee intermediate CH_2OO. *J. Phys. Chem. Lett.* **2013**, *4*, 4201-4205, doi:10.1021/jz402191w.

Sheps, L.; Scully, A. M.; Au, K. UV absorption probing of the conformer-dependent reactivity of a Criegee intermediate CH_3CHOO. *Phys. Chem. Chem. Phys.* **2014**, *16*, 26701-26706, doi:10.1039/c4cp04408h.

Simon, F.-G.; Schneider, W.; Moortgat, G. K. UV-Absorption spectrum of the methylperoxy radical and the kinetics of its disproportionation reaction at 300 K. *Int. J. Chem. Kinet.* **1990**, *22*, 791-813, doi:10.1002/kin.550220802

Singleton, D. L.; Paraskevopoulos, G.; Irwin, R. S. UV absorption cross-sections of the monomer and dimer of formic acid. *J. Photochem.* **1987**, *37*, 209-216, doi:10.1016/0047-2670(87)85001-3.

Singleton, D. L.; Paraskevopoulos, G.; Irwin, R. S. Laser photolysis of formic acid vapor at 222 nm Quantum yields of stable products. *Res. Chem. Intermediates* **1989**, *12*, 1-12, doi:10.1163/156856789X00131.

Singleton, D. L.; Paraskevopoulos, G.; Irwin, R. S. Laser photolysis of carboxyclic acids in the gas phase. Direct determination of the OH quantum yield at 222 nm. *J. Phys. Chem.* **1990**, *94*, 695-699, doi:10.1021/j100365a034.

Slagle, I. R.; Gutman, D.; Davies, J. W.; Pilling, M. J. Study of the recombination reaction $CH_3 + CH_3 \rightarrow C_2H_6$. 1. Experiment. *J. Phys. Chem.* **1988**, *92*, 2455-2462, doi:10.1021/j100320a015.

Smialek, M. A.; Labuda, M.; Guthmuller, J.; Hubin-Franskin, M.-J.; Delwiche, J.; Duflot, D.; Mason, N. J.; Hoffmann, S. V.; Jones, N. C.; Limão-Vieira, P. Valence and ionic lowest-lying electronic states of ethyl formate as studied by high-resolution vacuum ultraviolet photoabsorption, He(I) photoelectron spectroscopy, and ab initio calculations. *J. Chem. Phys.* **2014**, *141*, 104311, doi:10.1063/1.4894762.

Smith, C. A.; Pope, F. D.; Cronin, B.; Parkes, C. B.; Orr-Ewing, A. J. Absorption cross sections of formaldehyde at wavelengths from 300 to 340 nm and at 294 and 245 K. *J. Phys. Chem. A* **2006**, *110*, 11645-11653, doi:10.1021/jp063713y.

Smith, G. D.; Molina, L. T.; Molina, M. J. Measurement of radical quantum yields from formaldehyde photolysis between 269 and 339 nm. *J. Phys. Chem. A* **2002**, *106*, 1233-1240, doi:10.1021/jp013180n.

Smith, M. C.; Ting, W.-L.; Chang, C.-H.; Takahashi, K.; Boering, K. A.; Lin, J. J.-M. UV absorption spectrum of the C2 Criegee intermediate CH_3CHOO. *J. Chem. Phys.* **2014**, *141*, 074302, doi:10.1063/1.4892582.

Somnitz, H.; Fida, M.; Ufer, T.; Zellner, R. Pressure dependence for the CO quantum yield in the photolysis of acetone at 248 nm: A combined experimental and theoretical study. *Phys. Chem. Chem. Phys.* **2005**, *7*, 3342 - 3352, doi:10.1039/b506738c.

Somnitz, H.; Ufer, T.; Zellner, R. Acetone photolysis at 248 nm revisited: pressure dependence of the CO and CO_2 quantum yields. *Phys. Chem. Chem. Phys.* **2009**, *11*, 8522-8531, doi:10.1039/b906751e.

Souza Barbosa, A.; Mendes, M.; Jones, N. C.; Hoffmann, S. V.; Bettega, M. H. F.; Brunger, M. J.; Limão-Vieira, P. Low-lying electronic states of ethanol investigated by theoretical and synchrotron radiation methods. *J. Quant. Spectrosc. Radiat. Transf.* **2022**, *285* 108170, doi:10.1016/j.jqsrt.2022.108170.

Sršeň, S.; Hollas, D.; Slaviček, P. UV absorption of Criegee intermediates: quantitative cross sections from high-level *ab initio* theory. *Phys. Chem. Chem. Phys.* **2018**, *20*, 6421-6430, doi:10.1039/c8cp00199e.

Staffelbach, T. A.; Orlando, J. J.; Tyndall, G. S.; Calvert, J. G. The UV-visible absorption spectrum and photolysis quantum yields of methylglyoxal. *J. Geophys. Res.* **1995**, *100*, 14189-14198, doi:10.1029/95JD00541.

Stephens, E. R. The formation, reactions, and properties of peroxyacyl nitrates (PANs) in photochemical air pollution. *Adv. Environ. Sci. Technol.* **1969**, *1*, 119-146.

Sun, H.; Weissler, G. L. Absorption cross sections of methane and ammonia in the vacuum ultraviolet. *J. Chem. Phys.* **1955**, *23*, 1160-1164, doi:10.1063/1.1742205.

Suto, M.; Lee, L. C. Photoabsorption cross section of CH_3CN: Photodissociation rates by solar flux and interstellar radiation. *J. Geophys. Res.* **1985**, *90*, 13037-13040, doi:10.1029/JD090iD07p13037.

Suto, M.; Wang, X.; Lee, L. C. Fluorescence yields from photodissociative excitation of HCOOH, $HCOOCH_3$, and CH_3COOH in the vacuum-ultraviolet region. *J. Phys. Chem.* **1988**, *92*, 3764-3768, doi:10.1021/j100324a015.

Tadic, J.; Moortgat, G. K.; Wirtz, K. Photolysis of glyoxal in air. *J. Photochem. Photobiol. A: Chem.* **2005**, *177*, 116-124, doi:10.1016/j.jphotochem.2005.10.010.

Talukdar, R. K.; Burkholder, J. B.; Hunter, M.; Gilles, M. K.; Roberts, J. M.; Ravishankara, A. R. Atmospheric fate of several alkyl nitrates. Part 2. UV absorption cross-sections and photodissociation quantum yields. *J. Chem. Soc. Faraday Trans.* **1997**, *93*, 2797-2805, doi:10.1039/a701781b.

Talukdar, R. K.; Burkholder, J. B.; Schmoltner, A.-M.; Roberts, J. M.; Wilson, R. R.; Ravishankara, A. R. Investigation of the loss processes for peroxyacetyl nitrate in the atmosphere: UV photolysis and reaction with OH. *J. Geophys. Res.* **1995**, *100*, 14163-14173, doi:10.1029/95JD00545.

Tang, K. Y.; Fairchild, P. W.; Lee, E. K. C. Laser-induced photodecomposition of formaldehyde (A^1A_2) from its single vibronic levels. Determination of the quantum yield of H atom by HNO* (A^1A'') chemiluminescence. *J. Phys. Chem.* **1979**, *83*, 569-573, doi:10.1021/j100468a003.

Tatum Ernest, C.; Bauer, D.; Hynes, A. J. High-resolution absorption cross sections of formaldehyde in the 30285−32890 cm^{-1} (304−330 nm) spectral region. *J. Phys. Chem. A* **2012**, *116*, 5910-5922, doi:10.1021/jp210008g.

Tatum Ernest, C.; Bauer, D.; Hynes, A. J. Radical quantum yields from formaldehyde photolysis in the 30 400−32 890 cm^{-1} (304−329 nm) spectral region: Detection of radical photoproducts using pulsed laser photolysis−pulsed laser induced fluorescence. *J. Phys. Chem. A* **2012**, *116*, 6983-6995, doi:10.1021/jp2117399.

Taylor, W. D.; Allston, T. D.; Moscato, M. J.; Fazekas, G. B.; Koslowski, R.; Takacs, G. A. Atmospheric photodissociation lifetimes for nitromethane, methyl nitrite, and methyl nitrate. *Int. J. Chem. Kinet.* **1980**, *12*, 231-240, doi:10.1002/kin.550120404.

Thelen, M.-A.; Felder, P.; Huber, J. R. The photofragmentation of methyl hydroperoxide CH_3OOH at 193 and 248 nm in a cold molecular beam. *Chem. Phys. Lett.* **1993**, *213*, 275-281, doi:10.1016/0009-2614(93)85132-8.

Ting, W.-L.; Chen, Y.-H.; Chao, W.; Smith, M. C.; Lin, J. J.-M. The UV absorption spectrum of the simplest Criegee intermediate CH_2OO. *Phys. Chem. Chem. Phys.* **2014**, *16*, 10438-10443, doi:10.1039/c4cp00877d.

Troe, J. Analysis of quantum yields for the photolysis of formaldehyde at $\lambda > 310$ nm. *J. Phys. Chem. A* **2007**, *111*, 3868-3874, doi:10.1021/jp066886w.

Tsubomura, H.; Kimura, K.; Kaya, K.; Tanaka, J.; Nagakura, S. Vacuum ultraviolet absorption spectra of saturated organic compounds with non-bonding electrons. *Bull. Chem. Soc. Japan* **1964**, *37*, 417-423, doi:10.1246/bcsj.37.417.

Turberg, M. P.; Giolando, D. M.; Tilt, C.; Soper, T.; Mason, S.; Davies, M.; Klingensmith, P.; Takacs, G. A. Atmospheric chemistry of alkyl nitrates. *J. Photochem. Photobiol. A* **1990**, *51*, 281-292, doi:10.1016/1010-6030(90)87063-H.

Tyndall, G. S.; Cox, R. A.; Granier, C.; Lesclaux, R.; Moortgat, G. K.; Pilling, M. J.; Ravishankara, A. R.; Wallington, T. J. Atmospheric chemistry of small organic peroxy radicals. *J. Geophys. Res.* **2001**, *106*, 12157-12182, doi:10.1029/2000JD900746.

Vaghjiani, G. L.; Ravishankara, A. R. Absorption cross sections of CH_3OOH, H_2O_2, and D_2O_2 vapors between 210 and 365 nm at 297 K. *J. Geophys. Res.* **1989**, *94*, 3487-3492, doi:10.1029/JD094iD03p03487.

Vaghjiani, G. L.; Ravishankara, A. R. Photodissociation of H_2O_2 and CH_3OOH at 248 nm and 298 K: Quantum yields for OH, $O(^3P)$ and $H(^2S)$. *J. Chem. Phys.* **1990**, *92*, 996-1003, doi:10.1063/1.458081.

Vatsa, R. K.; Volpp, H.-R. Absorption cross-sections for some atmospherically important molecules at the H atom Lyman-α wavelength (121.567 nm). *Chem. Phys. Lett.* **2001**, *340*, 289-295, doi:10.1016/S0009-2614(01)00373-6.

Vésine, E.; Mellouki, A. UV absorption cross sections for a series of formates. *J. Chim. Phys.* **1997**, *94*, 1634-1641, doi:10.1051/jcp/1997941634.

Vesley, G. F.; Leermakers, P. A. The photochemistry of α-keto acids and α-keto esters. III. Photolysis of pyruvic acid in the vapor phase. *J. Phys. Chem.* **1964**, *68*, 2364-2366, doi:10.1021/j100790a507.

Vicente, A.; Antunes, R.; Almeida, D.; Franco, I. J. A.; Hoffmann, S. V.; Mason, N. J.; Eden, S.; Duflot, D.; Canneaux, S.; Delwiche, J.; Hubin-Franskin, M.-J.; Limão-Vieira, P. Photoabsorption measurements and theoretical calculations of the electronic state spectroscopy of propionic, butyric, and valeric acids. *Phys. Chem. Chem. Phys.* **2009**, *11*, 5729-5741, doi:10.1039/b823500g.

Volkamer, R.; Spietz, P.; Burrows, J. P.; Platt, U. High-resolution absorption cross-sections of glyoxal in the UV-vis and IR spectral ranges. *J. Photochem. Photobiol. A: Chem.* **2005**, *172*, 35-36, doi:10.1016/j.jphotochem.2004.11.011.

Wallace-Goodeve, J. The absorption spectra of ethyl nitrate, ethyl nitrite, and nitroethane. *Trans. Faraday Soc.* **1934**, *30*, 504-508, doi:10.1039/TF9343000504.

Wallington, T. J.; Dagaut, P.; Kurylo, M. J. Measurements of the gas phase UV absorption spectrum of $C_2H_5O_2$• radicals and of the temperature dependence of the rate constant for their self-reaction. *J. Photochem. Photobiol. A: Chem.* **1988**, *42*, 173-185, doi:10.1016/1010-6030(88)80061-3.

Wallington, T. J.; Dagaut, P.; Kurylo, M. J. Ultraviolet absorption cross sections and reaction kinetics and mechanisms for peroxy radicals in the gas phase. *Chem. Rev.* **1992**, *92*, 667-710, doi:10.1021/cr00012a008.

Wallington, T. J.; Mariq, M. M.; Ellerman, T.; Nielsen, O. J. Novel method for the measurement of gas-phase peroxy radical absorption spectra. *J. Phys. Chem.* **1992**, *96*, 982-986, doi:10.1021/j100181a080.

Wang, M.; Connolly, S. C.; Venables, D. S. Deep-ultraviolet absorption cross sections of strongly absorbing atmospheric species. *J. Quant. Spectrosc. Radiat. Transf.* **2024**, *323*, 109050, doi:10.1016/j.jqsrt.2024.109050.

Warneck, P. Photodissociation of acetone in the troposphere: an algorithm for the quantum yield. *Atmos. Environ.* **2001**, *35*, 5773-5777.

Watanabe, K.; Zelikoff, M.; Inn, E. C. I. *Air Force Cambridge Research Center Technical Report* **1953**, *53-23*.

Weaver, J.; Meagher, J.; Heicklen, J. Photo-oxidation of CH_3CHO vapor at 3130 Å. *J. Photochem.* **1976**, *6*, 111-126, doi:10.1016/0047-2670(76)85054-X.

Wiebe, H. A.; Heicklen, J. Photolysis of methyl nitrite. *J. Am. Chem. Soc.* **1973**, *95*, 1-7, doi:10.1021/ja00782a001.

Wiebe, H. A.; Villa, A.; Hellman, T. M.; Heicklen, J. Photolysis of methyl nitrite in the presenece of nitric oxide, nitrogen dioxide, and oxygen. *J. Am. Chem. Soc.* **1973**, *95*, 7-13, doi:10.1021/ja00782a002.

Winterhalter, R.; Jensen, N. R.; Magneron, I.; Wirtz, K.; Mellouki, A.; Mu, Y.; Tadic, J.; Horowitz, A.; Moortgat, G. K.; Hjorth, J. "Proceedings of the EUROTRAC-2 Symposium 2000", 2001, Springer, Berlin.

Wollenhaupt, M.; Carl, S. A.; Horowitz, A.; Crowley, J. N. Rate coefficients for reaction of OH with acetone between 202 and 395 K. *J. Phys. Chem. A* **2000**, *104*, 2695-2705, doi:10.1021/jp993738f.

Yamamoto, S.; Back, R. A. The photolysis and thermal decomposition of pyruvic acid in the gas phase. *Can. J. Chem.* **1985**, *63*, 549-554, doi:10.1139/v85-089.

Yang, X.; Felder, P.; Huber, J. R. Photodissociation of methyl nitrate in a molecular beam. *J. Phys. Chem.* **1993**, *97*, 10903-10910, doi:10.1021/j100144a002.

Yujing, M.; Mellouki, A. The near-UV absorption cross sections for several ketones. *J. Photochem. Photobiol. A: Chem.* **2000**, *134*, 31-36, doi:10.1016/S1010-6030(00)00243-4.

Zetzsch, C. In *Proceedings of the International Ozone Symposium 1988*; Bojkov, R., Fabian, P., Eds.; Deepak: Hampton, VA, 1989.

Zhu, C.; Zhu, L. Photolysis of glycolaldehyde in the 280-340nm region. *J. Phys. Chem. A* **2010**, *114*, 8384-8390, doi:10.1021/jp104497d.

Zhu, L.; Ding, C.-F. Temperature dependence of the near UV absorption spectra and photolysis products of ethyl nitrate. *Chem. Phys. Lett.* **1997**, *265*, 177-184, doi:10.1016/S0009-2614(96)01404-2.
Zhu, L.; Johnston, G. Kinetics and products of the reaction of the vinoxy radical with O_2. *J. Phys. Chem.* **1995**, *99*, 15114-15119, doi:10.1021/j100041a030.
Zhu, L.; Kellis, D.; Ding, C.-F. Photolysis of glyoxal at 193, 248, 308, and 351 nm. *Chem. Phys. Lett.* **1996**, *257*, 487-491, doi:10.1016/0009-2614(96)00570-2.

SECTION 4E. FO_X PHOTOCHEMISTRY

E1. HF (hydrogen fluoride)

Back to Index

$HF + h\nu \rightarrow H + F$ 571 kJ mol^{-1} 210 nm (1)

(Recommendation: 06-2, Note: 15-10 Evaluated: 10-6)

Absorption Cross Sections: The UV absorption spectrum of hydrogen fluoride, HF, has been measured at 289.5, 326, 373, and 438 K by Safary et al.[5] and Safary[4] (153–182 nm) and at room temperature by Nee et al.[3] (107–145 nm), Carnovale et al.[1] (8–155 nm), and Hitchcock et al.[2] (30–200 nm). HF does not absorb significantly at wavelengths >180 nm. On the basis of the Nee et al. VUV spectrum, a Lyman-α (121.567 nm) cross section of 3.1×10^{-18} cm^2 $molecule^{-1}$ is recommended.

Photolysis Quantum Yield and Product Studies: Photodissociation should be an unimportant loss process in the stratosphere.

(1) Carnovale, F.; Tseng, R.; Brion, C. E. Absolute oscillator strengths for the photoabsorption and partial photoionisation of hydrogen fluoride. *J. Phys. B: At. Mol. Phys.* **1981**, *14*, 4771-4785, doi:10.1088/0022-3700/14/24/013.

(2) Hitchcock, A. P.; Williams, G. R. J.; Brion, C. E.; Langhoff, P. W. Experimental and theoretical studies of the valence-shell dipole excitation spectrum and absolute photoabsorption cross section of hydrogen fluoride. *Chem. Phys.* **1984**, *88*, 65-80, doi:10.1016/0301-0104(84)85104-6.

(3) Nee, J. B.; Suto, M.; Lee, L. C. Photoabsorption cross section of HF at 107-145 nm. *J. Phys. B: At. Mol. Phys.* **1985**, *18*, L293-L294, doi:10.1088/0022-3700/18/10/006.

(4) Safary, E. Contribution a l'étude spectrale de l'acide fluorhydrique. *Ann. Phys. (Paris)* **1954**, *9*, 203-254.

(5) Safary, E.; Romand, J.; Vodar, B. Ultraviolet absorption spectrum of gaseous hydrogen fluoride. *J. Chem. Phys.* **1951**, *19*, 379-380, doi:10.1063/1.1748216.

E2. FO_2 (fluoroperoxy radical)

Back to Index

$FO_2 + h\nu \rightarrow F + O_2$ 54 kJ mol^{-1} 2233 nm (1)

(Recommendation: 06-2, Note: 10-6, Evaluated: 10-6)

Absorption Cross Sections: The gas-phase UV absorption spectrum of the fluoroperoxy radical, FO_2, has been measured at room temperature by Pagsberg et al.[6] (206–250 nm; reported in Wayne et al.[7]), Maricq and Szente[4] (186–276 nm), Ellermann et al.[2] (215–254 nm), and at 215 nm by Lyman and Holland.[3] In earlier studies, Chegodaev and Tupikov[1] and Matchuk et al.[5] reported spectra of FO_2 in liquid argon at 87 K. The results from Maricq and Szente,[4] Ellermann et al.,[2] and Lyman and Holland[3] are in excellent agreement. The cross sections measured by Pagsberg et al.[6] are larger by factors of 1.4 to 1.8 between 206 and 245 nm and a factor of 3 at 250 nm. The recommended absorption cross sections in Table 4E-2 are taken from Maricq and Szente.[4]

Photolysis Quantum Yield and Product Studies: No recommendation.

Table 4E-2. Recommended Absorption Cross Sections of FO_2 at 295 K

λ (nm)	10^{20} σ (cm^2)	λ (nm)	10^{20} σ (cm^2)	λ (nm)	10^{20} σ (cm^2)
185.9	950	214.2	1150	242.5	139
188.5	1050	216.8	1050	245.1	112
191.1	1130	219.4	933	247.6	82
193.6	1180	221.9	796	250.2	60
196.2	1200	224.5	677	252.8	51
198.8	1260	227.1	558	255.3	43
201.4	1310	229.6	451	257.9	36
203.9	1330	232.2	368	260.5	32
206.5	1350	234.8	289	263.1	26
209.1	1300	237.4	233	265.6	20
211.6	1240	239.9	173		

Note:
Maricq and Szente[4]

(1) Chegodaev, P. P.; Tubikov, B. I. *Dokl. Akad. Nauk. SSSR* **1973**, *210*, 647-649.

(2) Ellermann, T.; Sehested, J.; Nielson, O. J.; Pagsberg, P.; Wallington, T. J. Kinetics of the reaction of F atoms with O_2 and UV spectrum of FO_2 radicals in the gas phase at 295 K. *Chem. Phys. Lett.* **1994**, *218*, 287-294, doi:10.1016/0009-2614(94)00006-9.
(3) Lyman, J.; Holland, R. Oxygen fluoride chemical kinetics. *J. Phys. Chem.* **1988**, *92*, 7232-7241, doi:10.1021/j100337a015.
(4) Maricq, M. M.; Szente, J. J. Flash photolysis-time-resolved UV absorption study of the reactions $CF_3H + F \rightarrow CF_3 + HF$ and $CF_3O_2 + CF_2O_2 \rightarrow$ products. *J. Phys. Chem.* **1992**, *96*, 4925-4930, doi:10.1021/j100191a037.
(5) Matchuk, N. M.; Tupikov, V. I.; Malkova, A. I.; Pshezhetskii, S. Y. *Opt. Spektrosk. (Opt. Spectrosc.)* **1976**, *40*, 14-18 (17-19).
(6) Pagsberg, P.; Ratajczak, E.; Sillesen, A.; Jodkowski, J. T. Spectrokinetic studies of the gas-phase equilibrium $F + O_2 \rightleftharpoons FO_2$ between 295 and 359 K. *Chem. Phys. Lett.* **1987**, *141*, 88-94, doi:10.1016/0009-2614(87)80097-0.
(7) Wayne, R. P.; Poulet, G.; Biggs, P.; Burrows, J. P.; Cox, R. A.; Crutzen, P. J.; Hayman, G. D.; Jenkin, M. E.; Le Bras, G.; Moorgat, G. K.; et al. Halogen oxides: Radicals, sources and reservoirs in the laboratory and in the atmosphere. *Atmos. Environ.* **1995**, *29*, 2677-2881, doi:10.1016/1352-2310(95)98124-Q.

E3. F_2O (difluorine monoxide)

Back to Index

$F_2O + h\nu \rightarrow F + FO$	164 kJ mol^{-1}	732 nm	(1)
$\rightarrow F_2 + O$	225 kJ mol^{-1}	533 nm	(2)

(Recommendation: 06-2, Note: 10-6, Evaluated: 10-6)

Absorption Cross Sections: The UV absorption spectrum of difluorine monoxide, F_2O, has been measured at 273 K over the wavelength range 210–546 nm by Glissmann and Schuhmacher,[1] the only study available. Their absorption cross section data are recommended and are listed in Table 4E-3.

Photolysis Quantum Yield and Product Studies: No recommendation.

Table 4E-3. Recommended Absorption Cross Sections of F_2O at 273 K

λ (nm)	10^{20} σ (cm^2)	λ (nm)	10^{20} σ (cm^2)	λ (nm)	10^{20} σ (cm^2)	λ (nm)	10^{20} σ (cm^2)
210.2	4.88	239.9	0.65	296.7	0.12	404.0	0.020
211.4	3.39	244.7	0.50	302.7	0.12	421.0	0.023
213.7	3.06	248.2	0.37	313.1	0.11	428.0	0.021
216.5	2.73	253.7	0.27	334.0	0.087	435.8	0.018
218.1	2.60	257.6	0.21	350.0	0.072	445.0	0.017
221.0	2.21	265.5	0.15	365.0	0.064	458.0	0.015
223.6	1.95	270.0	0.13	378.0	0.055	471.5	0.012
225.3	1.76	275.9	0.12	380.0	0.044	491.6	0.0091
229.5	1.30	280.6	0.12	387.0	0.033	513.5	0.0052
234.5	1.14	289.3	0.12	395.0	0.023	546.0	0.0052
237.8	0.78	292.5	0.12	399.0	0.020		

Note:
Glissmann and Schuhmacher[1]

(1) Glissmann, A.; Schumacher, H.-J. Das spektrum des fluoroxyds F_2O. *Z. Phys. Chem. B* **1934**, *24*, 328-334.

E4. F_2O_2 (dioxygen difluoride)

Back to Index

$F_2O_2 + h\nu \rightarrow F + FO_2$	85 kJ mol^{-1}	1402 nm	(1)
$\rightarrow FO + FO$	198 kJ mol^{-1}	604 nm	(2)

(Recommendation: 15-10, Note: 15-10, Evaluated: 10-6)

Absorption Cross Sections: The gas-phase UV/vis absorption spectrum of dioxygen difluoride, F_2O_2, has been measured at 193 K by Chegodaev and Tupikov[2] (197–260 nm), at 195 K by Matchuk et al.[5] (350–600 nm), at 273 K by Brodersen et al.[1] (220–522.5 nm), and at 298 K by Lyman and Holland[4] (215 nm). A measurement of F_2O_2 in liquid freon at 77 K has been reported by Kirshenbaum and Streng[3] (200–480 nm). The absorption

spectrum shows decreasing absorption cross sections with increasing wavelength and evidence for several transitions that appear as shoulders in the spectrum. An absorption feature near 405 nm reported by Brodersen et al.[1] does not appear in the spectra reported by Matchuk et al.[5] and Kirshenbaum and Streng.[3] Although measured at significantly different temperatures, the data from Brodersen et al.[1] and Chegodaev and Tupikov[2] in the wavelength range 220–250 nm agree to within 10-15%, with the Chegodaev and Tupikov data being systematically lower. The recommended absorption cross sections in Table 4E-4 are from Chegodaev and Tupikov[2] in the region 200–210 nm, Brodersen et al.[1] in the region 220–360 nm, and Matchuk et al.[5] for the 370–600 nm region.

Photolysis Quantum Yield and Product Studies: No recommendation.

Table 4E-4. Recommended Absorption Cross Sections of F_2O_2 at 193–273 K

λ (nm)	10^{20} σ (cm^2)	λ (nm)	10^{20} σ (cm^2)	λ (nm)	10^{20} σ (cm^2)
200	700	340	10.9	480	0.34
210	325	350	7.54	490	0.27
220	231	360	5.90	500	0.24
230	163	370	5.15	510	0.22
240	120	380	4.50	520	0.20
250	99.1	390	3.77	530	0.19
260	98.2	400	3.06	540	0.17
270	86.7	410	2.46	550	0.15
280	72.5	420	1.97	560	0.13
290	60.6	430	1.57	570	0.11
300	44.7	440	1.25	580	0.09
310	32.4	450	0.96	590	0.07
320	22.3	460	0.69	600	0.04
330	15.4	470	0.47		

Note:
200–210 nm: Chegodaev and Tupikov[2] (193 K)
220–360 nm: Brodersen et al.[1] (273 K)
370–600 nm: Matchuk et al.[5] (195 K)

(1) Brodersen, P. H.; Frisch, P.; Schumacher, H.-J. Das absorptionsspektrum des F_2O_2. *Z. Phys. Chem. B* **1937**, *37*, 25-29.
(2) Chegodaev, P. P.; Tubikov, B. I. *Dokl. Akad. Nauk. SSSR* **1973**, *210*, 647-649.
(3) Kirshenbaum, A. D.; Streng, A. G. Molar extinction coefficients of liquid O_3F_2, O_2F_2, and O_3 in the visible range. *J. Chem. Phys.* **1961**, *35*, 1440-1442, doi:10.1063/1.1732063.
(4) Lyman, J.; Holland, R. Oxygen fluoride chemical kinetics. *J. Phys. Chem.* **1988**, *92*, 7232-7241, doi:10.1021/j100337a015.
(5) Matchuk, N. M.; Tupikov, V. I.; Malkova, A. I.; Pshezhetskii, S. Y. *Opt. Spektrosk. (Opt. Spectrosc.)* **1976**, *40*, 14-18 (17-19).

E5. FNO (nitrosyl fluoride)

Back to Index

$FNO + h\nu \rightarrow F + NO$ 54 kJ mol^{-1} 2235 nm (1)

(Recommendation: 06-2, Note: 10-6, Evaluated: 10-6)

Absorption Cross Sections: The UV absorption spectrum of nitrosyl fluoride, FNO, has been measured at room temperature by Burley et al.[1] (180–350 nm) and Pagsberg et al.[3] (310.5 nm). Johnston and Bertin[2] report a cross section at 195 K and 310.5 nm. The FNO spectrum has two similar strength bands centered at 180 nm and 310 nm. The 310 nm band has significant vibronic structure at wavelengths >250 nm. The agreement between the single wavelength measurement of Pagsberg et al.[3] and the Burley et al.[1] spectrum is good. The recommended absorption cross sections in Table 4E-5 are at 2 nm intervals for the continuous region of the spectrum (λ <260 nm) and at 1 nm intervals in the structured region (λ >260 nm).

Photolysis Quantum Yield and Product Studies: The quantum yield for decomposition is expected to be unity.

Table 4E-5. Recommended Absorption Cross Sections of FNO at 298 K

λ (nm)	10^{20} σ (cm^2)	λ (nm)	10^{20} σ (cm^2)	λ (nm)	10^{20} σ (cm^2)	λ (nm)	10^{20} σ (cm^2)
180	52.4	246	1.65	286	5.17	319	21.4
182	51.7	248	1.41	287	5.78	320	15.2
184	50.7	250	1.54	288	10.4	321	35.6
186	49.4	252	1.25	289	16.6	322	40.2
188	47.5	254	1.23	290	17.0	323	25.5
190	45.1	256	1.36	291	11.3	324	17.8
192	42.7	258	1.58	292	11.9	325	14.3
194	40.0	260	1.30	293	18.1	326	12.1
196	37.3	261	1.45	294	7.11	327	9.40
198	33.8	262	1.64	295	6.75	328	9.39
200	30.5	263	1.85	296	9.15	329	12.4
202	27.7	264	2.03	297	14.1	330	12.9
204	24.8	265	2.67	298	22.0	331	11.3
206	22.2	266	1.96	299	23.1	332	13.0
208	19.9	267	1.99	300	15.6	333	18.9
210	17.6	268	2.10	301	23.1	334	19.3
212	15.8	269	2.66	302	25.4	335	16.1
214	13.9	270	2.81	303	10.4	336	13.1
216	12.3	271	3.06	304	8.85	337	10.8
218	10.7	272	4.47	305	10.4	338	8.96
220	9.35	273	4.30	306	11.8	339	7.13
222	8.32	274	3.97	307	15.6	340	5.65
224	7.22	275	3.77	308	32.2	341	4.61
226	6.30	276	4.24	309	21.8	342	3.81
228	5.44	277	4.44	310	15.5	343	3.17
230	4.68	278	3.41	311	54.2	344	2.68
232	4.10	279	5.03	312	31.6	345	2.30
234	3.52	280	8.26	313	16.0	346	1.96
236	3.09	281	10.1	314	12.3	347	1.72
238	2.76	282	7.58	315	11.7	348	1.48
240	2.25	283	6.59	316	11.0	349	1.30
242	2.08	284	7.26	317	13.0	350	1.18
244	1.74	285	7.45	318	25.5		

Note:
Burley et al.[1]

(1) Burley, J. D.; Miller, C. E.; Johnston, H. S. Spectroscopy and photoabsorption cross-sections of FNO. *J. Mol. Spectrosc.* **1993**, *158*, 377-391, doi:10.1006/jmsp.1993.1082.

(2) Johnston, H. S.; Bertin, H. J., Jr. Absorption and emission spectra of nitrosyl fluoride. *J. Mol. Spectrosc.* **1959**, *3*, 683-696, doi:10.1016/0022-2852(59)90061-X.

(3) Pagsberg, P.; Sillesen, A.; Jodkowski, J. T.; Ratajczak, E. Kinetics of the reaction F + NO + M → FNO + M studied by pulse radiolysis combined with time-resolved IR and UV spectroscopy. *Chem. Phys. Lett.* **1996**, *249*, 358-364, doi:10.1016/0009-2614(95)01441-1.

E6. CHF_3 (trifluoromethane, HFC-23)

Back to Index

$CHF_3 + h\nu \rightarrow$ Products (1)

(Recommendation: 15-10; Note: 15-10; Evaluated: 15-10)

Absorption Cross Sections: Trifluoromethane, CHF_3 (HFC-23), has negligible absorption at wavelengths >190 nm. The VUV absorption spectrum of HFC-23 was measured at 298 K by Sauvageau et al.[1] (62–122 nm) and Suto and Lee[2] (106–124 nm). The two studies differ by ~50% at Lyman-α (121.567 nm). The recommended Lyman-α cross section is an average of the results from these two studies, 3.5×10^{-19} cm^2 $molecule^{-1}$, where the Sauvageau et al. data were linearly interpolated to 121.567 nm. An uncertainty factor of 2 (2σ) is assigned, which encompasses the results from both studies.

Photolysis Quantum Yield and Product Studies: No recommendation.

(1) Sauvageau, P.; Gilbert, R.; Berlow, P. P.; Sandorfy, C. Vacuum ultraviolet absorption spectra of fluoromethanes. *J. Chem. Phys.* **1973**, *59*, 762-765, doi:10.1063/1.1680086.

(2) Suto, M.; Lee, L. C. Emission spectra of CF_3 radicals. V. Photodissociation of CF_3H, CF_3Cl, and CF_3Br by vacuum ultraviolet. *J. Chem. Phys.* **1983**, *79*, 1127-1133, doi:10.1063/1.445914.

E7. CH_2F_2 (difluoromethane, HFC-32)

Back to Index

$CH_2F_2 + h\nu \rightarrow$ Products (1)

(Recommendation: 15-10; Note: 15-10; Evaluated: 15-10)

Absorption Cross Sections: Difluoromethane, CH_2F_2 (HFC-32), has negligible absorption at wavelengths >190 nm. The VUV absorption spectrum of HFC-32 at 298 K was measured by Sauvageau et al.[1] (60–142 nm; reported in 0.1 to 0.5 nm intervals) and Seccombe et al.[2] (60–152 nm; reported in ~0.015 nm intervals). The cross sections reported in these studies agree at Lyman-α (121.567 nm) to within ~30%. An average Lyman-α cross section from these studies, 5.5×10^{-18} cm^2 molecule^{-1}, is recommended. An uncertainty factor of 1.4 (2σ) is recommended, which covers the range of experimental data.

Photolysis Quantum Yield and Product Studies: No recommendation.

(1) Sauvageau, P.; Gilbert, R.; Berlow, P. P.; Sandorfy, C. Vacuum ultraviolet absorption spectra of fluoromethanes. *J. Chem. Phys.* **1973**, *59*, 762-765, doi:10.1063/1.1680086.

(2) Seccombe, D. P.; Chim, R. Y. L.; Tuckett, R. P.; Jochims, H. W.; Baumgärtel, H. Vacuum–ultraviolet absorption and fluorescence spectroscopy of CF_2H_2, CF_2Cl_2, and CF_2Br_2 in the range 8–22 eV. *J. Chem. Phys.* **2001**, *114*, 4058-4073, doi:10.1063/1.1344888.

E8. CHF_2CF_3 (pentafluoroethane, HFC-125)

Back to Index

$CHF_2CF_3 + h\nu \rightarrow$ Products (1)

(Recommendation: 15-10; Note: 15-10; Evaluated: 15-10)

Absorption Cross Sections: Pentafluoroethane, CHF_2CF_3 (HFC-125), has negligible absorption at wavelengths >190 nm. The VUV absorption spectrum of HFC-125 has not been reported to date. The recommended Lyman-α cross section of HFC-125 is assumed to be similar to that of CHF_3 (HFC-23) with an estimated value of 3.5×10^{-19} cm^2 molecule^{-1}. An uncertainty factor of 3.0 (2σ) is assigned due to the lack of experimental data.

Photolysis Quantum Yield and Product Studies: No recommendation.

E9. CH_2FCF_3 (1,1,1,2-tetrafluoroethane, HFC-134a)

Back to Index

$CH_2FCF_3 + h\nu \rightarrow$ Products (1)

(Recommendation: 15-10; Note: 15-10; Evaluated: 15-10)

Absorption Cross Sections: 1,1,1,2-tetrafluoroethane, CH_2FCF_3 (HFC-134a), has negligible absorption at wavelengths >190 nm. The VUV absorption spectrum of HFC-134a has not been reported to date. The Lyman-α cross section of HFC-134a is expected to be less than that of CH_3CF_3 (HFC-143a) and comparable to that of CH_2F_2 (HFC-32). An estimated value of 5×10^{-18} cm^2 molecule^{-1} is recommended. An uncertainty factor of 2.0 (2σ) is assigned based on the lack of experimental data.

Photolysis Quantum Yield and Product Studies: No recommendation.

E10. CH_3CF_3 (1,1,1-trifluoroethane, HFC-143a)

Back to Index

$CH_3CF_3 + h\nu \rightarrow$ Products (1)

(Recommendation: 15-10; Note: 15-10; Evaluated: 15-10)

Absorption Cross Sections: 1,1,1-trifluoroethane, CH_3CF_3 (HFC-143a), has negligible absorption at wavelengths >190 nm. The VUV absorption spectrum of HFC-143a was measured by Sauvageau et al.[1] between 61 and 132 nm at 298 K with a Lyman-α cross section of 1.75×10^{-17} cm^2 molecule^{-1}, which is

recommended. The uncertainty factor for the Lyman-α cross section is assigned a value of 2.0 (2σ) based primarily on the limited available data.

Photolysis Quantum Yield and Product Studies: No recommendation.

(1) Sauvageau, P.; Doucet, J.; Gilbert, R.; Sandorfy, C. Vacuum ultraviolet and photoelectron spectra of fluoroethanes. *J. Chem. Phys.* **1974**, *61*, 391-395, doi:10.1063/1.1681649.

E11. CH_3CHF_2 (1,1-difluoroethane, HFC-152a)

Back to Index

$CH_3CHF_2 + h\nu \rightarrow$ Products (1)

(Recommendation: 15-10; Note: 15-10; Evaluated: 15-10)

Absorption Cross Sections: 1,1-difluoroethane, CH_3CHF_2 (HFC-152a), has negligible absorption at wavelengths >190 nm. The VUV absorption spectrum of HFC-152a was measured by Sauvageau et al.[1] between 60 and 134 nm at 298 K with a Lyman-α cross section of 3.2×10^{-17} cm^2 molecule^{-1}, which is recommended. The uncertainty factor for the Lyman-α cross section is assigned a value of 2.0 (2σ) based primarily on the limited available data.

Photolysis Quantum Yield and Product Studies: No recommendation.

(1) Sauvageau, P.; Doucet, J.; Gilbert, R.; Sandorfy, C. Vacuum ultraviolet and photoelectron spectra of fluoroethanes. *J. Chem. Phys.* **1974**, *61*, 391-395, doi:10.1063/1.1681649.

E12. CF_4 (carbon tetrafluoride)

Back to Index

$CF_4 + h\nu \rightarrow CF_3 + F$	507 kJ mol^{-1}	236.1 nm	(1)
$\rightarrow CF_2 + 2F$	1030 kJ mol^{-1}	116.1 nm	(2)

(Recommendation: 90-1, Note: 15-10, Evaluated: 10-6)

Absorption Cross Sections: The VUV spectrum of carbon tetrafluoride, CF_4, consists of a strong absorption band between 6 and 120 nm with several broad features assigned to a Rydberg series with maxima near 54, 68, 78, 90 and 99 nm. The spectrum also has discrete vibrational structure in the region 56 to 63 nm. The absolute absorption cross sections have been studied extensively in the VUV by a number of groups as summarized in Table 4E-12. General agreement (to within a factor of 2) exists in the wavelength range 6–100 nm among the data of Rebbert and Ausloos,[10] Sauvageau et al.,[11] Lee et al.,[7] Cole and Dexter,[3] Lee et al.,[8] Au et al.,[1] Cook and Ching,[4] Hatherly and Flaxman,[5] and Chim et al.[2]

The absorption cross section at Lyman-α (121.567 nm) was reported to be $(5.73 \pm 0.97) \times 10^{-21}$ cm^2 molecule^{-1} by Inn,[6] $<1 \times 10^{-20}$ cm^2 molecule^{-1} by Lee et al.,[8] and $<8 \times 10^{-22}$ cm^2 molecule^{-1} by Ravishankara et al.[9] A value of 5.5×10^{-21} cm^2 molecule^{-1} with an uncertainty factor of 2 (2σ) is recommended for the cross section at Lyman-α.

Photolysis Quantum Yield and Product Studies: No recommendation. CF_4 does not absorb strongly at wavelengths >120 nm and therefore it is not expected to photodissociate until it reaches the mesosphere.

Table 4E-12. Summary of CF_4 Absorption Cross Section Studies

Reference	Year	Wavelength Range (nm)	Temperature (K)
Rebbert and Ausloos[10]	1971	73.6–74.4	298
Sauvageau et al.[11]	1973	60–120	298
Lee et al.[7]	1977	17.5–77.0	295
Cole and Dexter[3]	1978	4.6, 10.0	298
Inn[6]	1980	121.567 (Lyman-α)	297
Lee et al.[8]	1986	50–130	298
Zhang et al.[12]	1989	6.2–103.2	298
Ravishankara et al.[9]	1993	121.567 (Lyman-α)	298
Au et al.[1]	1997	6.2–124	298
Cook and Ching[4]	2003	61–100	295
Hatherly and Flaxman[5]	2003	58.4 and 73.6–74.6	298
Chim et al.[2]	2003	30.7–129.5	298

(1) Au, J. W.; Burton, G. R.; Brion, C. E. Quantitative spectroscopic studies of the valence-shell electronic excitations of Freons ($CFCl_3$, CF_2Cl_2, CF_3Cl, and CF_4) in the VUV and soft X-ray regions. *Chem. Phys.* **1997**, *221*, 151-168, doi:10.1016/S0301-0104(97)00146-8.
(2) Chim, R. Y. L.; Kennedy, R. A.; Tuckett, R. P. The vacuum-UV absorption spectrum of SF_5CF_3; implications for its lifetime in the earth's atmosphere. *Chem. Phys. Lett.* **2003**, *367*, 697-703, doi:10.1016/S0009-2614(02)01763-3.
(3) Cole, B. E.; Dexter, R. N. Photoabsorption cross sections for chlorinated methanes and ethanes between 46 and 100 Å. *J. Quant. Spectrosc. Radiat. Transf.* **1978**, *19*, 303-309, doi:10.1016/0022-4073(78)90063-8.
(4) Cook, G. R.; Ching, B. K. Photoionization and absorption cross sections and fluorescence of CF_4. *J. Chem. Phys.* **1965**, *43*, 1794-1797, doi:10.1063/1.1697011.
(5) Hatherly, P. A.; Flaxman, A. J. On the absolute absorption cross-section of SF_5CF_3. *Chem. Phys. Lett.* **2003**, *380*, 512-515, doi:10.1016/j.cplett.2003.09.061.
(6) Inn, E. C. Y. Absorption cross section of CF_4 at H Lyman α (121.57 nm). *J. Geophys. Res.* **1980**, *85*, 7493-7494, doi:10.1029/JC085iC12p07493.
(7) Lee, L. C.; Phillips, E.; Judge, D. L. Photoabsorption cross sections of CH_4, CF_4, CF_3Cl, SF_6, and C_2F_6 from 175 to 770 Å. *J. Chem. Phys.* **1977**, *67*, 1237-1246, doi:10.1063/1.434935.
(8) Lee, L. C.; Wang, X.; Suto, M. Fluorescence from extreme ultraviolet photoexcitation of CF_4. *J. Chem. Phys.* **1986**, *85*, 6294-6300, doi:10.1063/1.451459.
(9) Ravishankara, A. R.; Solomon, S.; Turnipseed, A. A.; Warren, R. F. Atmospheric lifetimes of long-lived halogenated species. *Science* **1993**, *259*, 194-199, doi:10.1126/science.259.5092.194.
(10) Rebbert, R. E.; Ausloos, P. Ionization quantum yields and absorption coefficients of selected compounds at 58.4 and 73.6-74.4 nm. *J. Res. Natl. Bur. Stand.* **1971**, *A 75*, 481-485, doi:10.6028/jres.075A.038.
(11) Sauvageau, P.; Doucet, J.; Gilbert, R.; Sandorfy, C. Vacuum ultraviolet and photoelectron spectra of fluoroethanes. *J. Chem. Phys.* **1974**, *61*, 391-395, doi:10.1063/1.1681649.
(12) Zhang, W.; Cooper, G.; Ibuki, T.; Brion, C. E. Excitation and ionization of freon molecules. I. Absolute oscillator-strengths for the photoabsorption (12-740 eV) and the ionic photofragmentation (15-80 eV) of CF_4. *Chem. Phys.* **1989**, *137*, 391-405, doi:10.1016/0301-0104(89)87122-8.

E13. C_2F_6 (hexafluoroethane)

Back to Index

$C_2F_6 + h\nu \rightarrow$ Products (1)

(Recommendation: 10-6, Note: 10-6, Evaluated: 10-6)

Absorption Cross Sections: The VUV absorption spectrum of hexafluoroethane, C_2F_6, consists of a strong absorption band between 6 and 120 nm with several broad features and maxima near 58, 68, 79, 87 and 93 nm. Absolute absorption cross sections have been reported by Sauvageau et al.[4] (60–117 nm), Lee et al.[2] (18–74 nm), and Cole and Dexter[1] (6.5–10.0 nm). The cross section data from Sauvageau et al. over the range 60 to 75 nm are much smaller than those of Lee et al.

The absorption cross section at Lyman-α (121.567 nm) was determined by Ravishankara et al.[3] to be $(9.87 \pm 0.35) \times 10^{-21}$ cm^2 molecule^{-1}, which is recommended.

Photolysis Quantum Yield and Product Studies: No recommendation. C_2F_6 does not absorb significantly at wavelengths >120 nm and therefore it is not expected to photodissociate until it reaches the mesosphere.

(1) Cole, B. E.; Dexter, R. N. Photoabsorption cross sections for chlorinated methanes and ethanes between 46 and 100 Å. *J. Quant. Spectrosc. Radiat. Transf.* **1978**, *19*, 303-309, doi:10.1016/0022-4073(78)90063-8.
(2) Lee, L. C.; Phillips, E.; Judge, D. L. Photoabsorption cross sections of CH_4, CF_4, CF_3Cl, SF_6, and C_2F_6 from 175 to 770 Å. *J. Chem. Phys.* **1977**, *67*, 1237-1246, doi:10.1063/1.434935.
(3) Ravishankara, A. R.; Solomon, S.; Turnipseed, A. A.; Warren, R. F. Atmospheric lifetimes of long-lived halogenated species. *Science* **1993**, *259*, 194-199, doi:10.1126/science.259.5092.194.
(4) Sauvageau, P.; Doucet, J.; Gilbert, R.; Sandorfy, C. Vacuum ultraviolet and photoelectron spectra of fluoroethanes. *J. Chem. Phys.* **1974**, *61*, 391-395, doi:10.1063/1.1681649.

E14. *c*-C_4F_8 (perfluorocyclobutane)

Back to Index

c-C_4F_8 + hν → Products (1)

(Recommendation: 15-10, Note: 15-10, Evaluated: 15-10)

Absorption Cross Sections: The spectrum of perfluorocyclobutane, *c*-C_4F_8, consists of a strong absorption band in the VUV with a maximum at 117 nm and shows further weak absorption bands at 137 and 174 nm up to about 200 nm. The absolute photoabsorption cross sections have been measured at high resolution in the VUV by Limão-Vieira et al.[1] in the range 115–204 nm, although the data in the wavelength range >190 nm is scattered. They estimated a stratospheric photolysis lifetime of ~400 years at 20 km decreasing to a few days at 40–50 km.

The absorption cross section at Lyman-α (121.567 nm) was determined by Limão-Vieira et al.[1] to be 7.98×10^{-18} cm^2 molecule^{-1} and Ravishankara et al.[2] reported a value of $(8.76 \pm 0.49) \times 10^{-18}$ cm^2 molecule^{-1}. An average of the Lyman-α cross sections from these studies is recommended, 8.37×10^{-18} cm^2 molecule^{-1} with a 1.05 uncertainty factor (2σ), which encompasses the results from both studies.

Photolysis Quantum Yield and Product Studies: No recommendation.

(1) Limão-Vieira, P.; Vasekova, E.; Giuliani, A.; Lourenço, J. M. C.; Santos, P. M.; Duflot, D.; Hoffmann, S. V.; Mason, N. J.; Delwiche, J.; Hubin-Franskin, M.-J. Perfluorocyclobutane electronic state spectroscopy by high-resolution vacuum ultraviolet photoabsorption, electron impact, He I photoelectron spectroscopy, and *ab initio* calculations. *Phys. Rev. A* **2007**, *76*, 032509, doi:10.1103/PhysRevA.76.032509.

(2) Ravishankara, A. R.; Solomon, S.; Turnipseed, A. A.; Warren, R. F. Atmospheric lifetimes of long-lived halogenated species. *Science* **1993**, *259*, 194-199, doi:10.1126/science.259.5092.194.

E15. C_5F_{12} (perfluoropentane)

Back to Index

C_5F_{12} + hν → Products (1)

(Recommendation: 10-6, Note: 10-6, Evaluated: 10-6)

Absorption Cross Sections: No absorption spectrum of perfluoropentane, C_5F_{12}, is known. An absorption cross section at Lyman-α (121.567 nm) was determined by Ravishankara et al.[1] to be $(5.32 \pm 0.30) \times 10^{-18}$ cm^2 molecule^{-1}, which is recommended.

Photolysis Quantum Yield and Product Studies: No recommendation.

(1) Ravishankara, A. R.; Solomon, S.; Turnipseed, A. A.; Warren, R. F. Atmospheric lifetimes of long-lived halogenated species. *Science* **1993**, *259*, 194-199, doi:10.1126/science.259.5092.194.

E16. C_6F_{14} (perfluorohexane)

Back to Index

C_6F_{14} + hν → Products (1)

(Recommendation: 10-6, Note: 10-6, Evaluated: 10-6)

Absorption Cross Sections. No absorption spectrum of C_6F_{14}, perfluorohexane, is known. An absorption cross section at Lyman-α (121.567 nm) was determined by Ravishankara et al.[1] to be $(9.82 \pm 0.53) \times 10^{-18}$ cm^2 molecule^{-1}, which is recommended.

Photolysis Quantum Yield and Product Studies: No recommendation.

(1) Ravishankara, A. R.; Solomon, S.; Turnipseed, A. A.; Warren, R. F. Atmospheric lifetimes of long-lived halogenated species. *Science* **1993**, *259*, 194-199, doi:10.1126/science.259.5092.194.

E17. $(CF_3)_2c$-C_4F_6 (perfluoro-1,2-dimethylcyclobutane)

Back to Index

$(CF_3)_2c$-C_4F_6 + hν → Products (1)

(Recommendation: 10-6, Note: 10-6, Evaluated: 10-6)

Absorption Cross Sections: No absorption spectrum of perfluoro-1,2-dimethylcyclobutane, $(CF_3)_2c$-C_4F_6, is known. An absorption cross section at Lyman-α (121.567 nm) was determined by Ravishankara et al.[1] to be $(1.22 \pm 0.07) \times 10^{-17}$ cm^2 molecule^{-1}, which is recommended. The large cross section implies a local lifetime of only a few days in the mesosphere.

Photolysis Quantum Yield and Product Studies: No recommendation.

(1) Ravishankara, A. R.; Solomon, S.; Turnipseed, A. A.; Warren, R. F. Atmospheric lifetimes of long-lived halogenated species. *Science* **1993**, *259*, 194-199, doi:10.1126/science.259.5092.194.

E18. CF_2O (carbonyl difluoride)

Back to Index

$CF_2O + h\nu$	$\rightarrow CO + F_2$	513 kJ mol^{-1}	233 nm	(1)
	$\rightarrow COF + F$	529 kJ mol^{-1}	226 nm	(2)

(Recommendation: 06-2, Note: 15-10, Evaluated: 10-6)

Absorption Cross Sections: The UV absorption spectrum of carbonyl difluoride (difluorophosgene), CF_2O, has been measured at room temperature by Chou et al.[1] (185–226 nm), Molina and Molina[2] (186–224 nm), and Nölle et al.[3] (199–232 nm). The high resolution spectrum reported by Nölle et al.[3] is highly structured. The cross section data from Nölle et al.[3] are somewhat larger than those from Molina and Molina[2] with differences in the averaged values over 500 cm^{-1} intervals ranging between 1.5 and 22%. The cross section data of Chou et al.[1] are in good agreement with the data from Molina and Molina[2] in the region 186–197 nm. At longer wavelengths the cross sections from these studies diverge with the Chou et al. results being larger, ~200% near 225 nm. The recommended absorption cross sections in Table 4E-18 are the 500 cm^{-1} averages of the data from Molina and Molina[2] in the range 186–199 nm and the data from Nölle et al.[3] at longer wavelengths. The recommended uncertainty factor in the room temperature spectrum is 1.30 (2σ) for all wavelengths included in Table 4E-18.

Photolysis Quantum Yield and Product Studies: The photodissociation of CF_2O has been studied by Nölle et al.[4] at 193, 210, and 220 nm and Molina and Molina[2] at 206 nm. Nölle et al.[4] determined the COF + F quantum yields by combining FTIR detection of products with excimer laser photolysis at 193 nm and Hg lamp photolysis at 210 and 220 nm. The "apparent" quantum yields for CF_2O were 0.47 ± 0.03, 0.57 ± 0.05, and 0.11 ± 0.02 at 193, 210 and 220 nm, respectively. In the case of the laser photolysis at 193 nm, where high concentrations of COF are formed, the self-reaction of the COF photodissociation product regenerates CF_2O via $COF + COF \rightarrow CF_2O + CO$. Assuming that all COF radicals react quantitatively in this way, the actual quantum yield at 193 nm is 0.94 ± 0.06. The quantum yields at 210 and 220 nm obtained using the Hg lamp photolysis generated much lower COF radical concentrations and are reported as the actual quantum yields. Molina and Molina[2] report a quantum yield of 0.26 at 206 nm that is considerably lower than reported by Nölle et al.[4] On the basis of the Nölle et al. study a CF_2O photolysis quantum yield of unity is recommended for wavelengths less than 210 nm.

Table 4E-18. Recommended Absorption Cross Sections of CF_2O at 298 K

λ (nm)	10^{20} σ (cm^2)	λ (nm)	10^{20} σ (cm^2)	λ (nm)	10^{20} σ (cm^2)
186.0	5.5	199.0	1.6	213.9	0.188
187.8	4.8	201.0	1.32	216.2	0.120
189.6	4.2	203.1	0.987	218.6	0.077
191.4	3.7	205.1	0.754	221.0	0.046
193.2	3.1	207.3	0.508	223.5	0.032
195.1	2.6	209.4	0.392	226.0	0.021
197.0	2.1	211.6	0.272	228.6	0.015

Note:
186–199 nm: Molina and Molina[2]
201–229 nm: Nölle et al.[3]

(1) Chou, C. C.; Crescentini, G.; Vera-Ruiz, H.; Smith, W. S.; Rowland, F. S. "Stratospheric photochemistry of CF_2O, CClFO, and CCl_2O"; 173rd American Chemical Society Meeting, 1977, New Orleans, LA.
(2) Molina, L. T.; Molina, M. J. "Chemistry of fluorine in the stratosphere"; 182nd American Chemical Society Meeting, 1982, New York.
(3) Nölle, A.; Heydtmann, H.; Meller, R.; Schneider, W.; Moortgat, G. K. UV absorption spectrum and absorption cross sections of COF_2 at 296 K in the range 200-230 nm. *Geophys. Res. Lett.* **1992**, *19*, 281-284, doi:10.1029/91GL02316.
(4) Nölle, A.; Krumscheid, C.; Heydtmann, H. Determination of quantum yields in the UV photolysis of COF_2 and COFCl. *Chem. Phys. Lett.* **1999**, *299*, 561-565, doi:10.1016/S0009-2614(98)01257-3.

E19. COHF (formyl fluoride)

Back to Index

COHF + hν	→ HF + CO	–27 kJ mol^{-1}	All	(1)
	→ H + FCO	425 kJ mol^{-1}	282 nm	(2)
	→ F + HCO	504 kJ mol^{-1}	237.2 nm	(3)

(Recommendation: 06-2, Note: 10-6, Evaluated: 10-6)

Absorption Cross Sections: The UV absorption spectrum of formyl fluoride, COHF, has been measured at room temperature by Giddings and Innes[1] (195–255 nm), Meller (194–267 nm) (see Röth et al.[3]), and Rattigan et al.[2] (220–267 nm). The high-resolution measurements show the long-wavelength wing of a highly structured absorption band. The absorption cross sections reported by Giddings and Innes[1] are larger by nearly a factor of two than the high resolution (0.016 nm) data reported by Meller using diode array spectrometry. The cross sections measured by Rattigan et al.[2] at a resolution of 1.2 nm lie between the Giddings and Innes[1] and Meller data sets in the range 220–230 nm and are closer to the data of Giddings and Innes[1] in the region 230–245 nm. Rattigan et al.[2] found the absorption cross sections to be independent of temperature over the range 233–318 K. The recommended absorption cross sections in Table 4E-19 are averages over 1 nm intervals of the high-resolution data from Meller.

Photolysis Quantum Yield and Product Studies: No recommendation.

Table 4E-19. Recommended Absorption Cross Sections of COHF at 298 K

λ (nm)	10^{20} σ (cm^2)	λ (nm)	10^{20} σ (cm^2)	λ (nm)	10^{20} σ (cm^2)	λ (nm)	10^{20} σ (cm^2)
200	8.28	217	7.38	234	2.98	251	0.151
201	9.75	218	7.97	235	2.04	252	0.241
202	8.30	219	6.28	236	2.28	253	0.213
203	7.55	220	6.85	237	1.24	254	0.071
204	8.52	221	5.70	238	1.71	255	0.123
205	10.15	222	6.07	239	1.75	256	0.0674
206	8.28	223	6.58	240	1.55	257	0.0520
207	7.41	224	4.94	241	0.967	258	0.0382
208	8.44	225	5.33	242	1.19	259	0.0446
209	9.55	226	4.00	243	0.575	260	0.0427
210	7.76	227	4.65	244	0.765	261	0.0232
211	7.36	228	4.43	245	0.675	262	0.0153
212	7.92	229	4.61	246	0.719	263	0.0156
213	8.56	230	3.57	247	0.412	264	0.0170
214	9.22	231	2.55	248	0.484	265	0.0126
215	7.67	232	3.16	249	0.279	266	0.0118
216	6.51	233	3.09	250	0.210		

Note:
Meller (see Röth et al.[3])

(1) Giddings, L. E., Jr.; Innes, K. K. The near ultraviolet spectra of HCOF and DCOF. *J. Mol. Spectrosc.* **1961**, *6*, 528-549, doi:10.1016/0022-2852(61)90278-8.

(2) Rattigan, O. V.; Rowley, D. M.; Wild, O.; Jones, R. L.; Cox, R. A. Mechanism of atmospheric oxidation of 1,1,1,2-tetrafluoroethane (HFC 134a). *J. Chem. Soc. Faraday Trans.* **1994**, *90*, 1819-1829, doi:10.1039/ft9949001819.

(3) Röth, E. P.; Ruhnke, R.; Moortgat, G.; Meller, R.; Schneider, W. UV/VIS-Absorption Cross Sections and Quantum Yields for Use in Photochemistry and Atmospheric Modeling, Forschungszentrum Jülich Publication, Part 1 : Inorganic Substances (jül-3340), Part 2: Organic Substances (jül-3341). **1997**.

E20. CF_3O_2 (trifluoromethylperoxy radical)

Back to Index

$CF_3O_2 + h\nu \rightarrow$ Products (1)

(Recommendation: 10-6, Note: 10-6, Evaluated: 10-6)

Absorption Cross Sections: The UV absorption cross sections of the trifluoromethylperoxy radical, CF_3O_2, have been measured at room temperature by Maricq and Szente[1] (186–276 nm) and Nielsen et al.[2] (215–270 nm). The absorption spectrum displays a broad absorption band with a maximum at 210 nm. The cross sections reported by Nielsen et al.[2] are in good agreement with those measured by Maricq and Szente[1] in the range 240–270 nm, but are consistently smaller at shorter wavelengths (by 20% at 215 nm). The recommended absorption cross sections listed in Table 4E-20 are taken from Maricq and Szente.[1]

Photolysis Quantum Yield and Product Studies: No recommendation.

Table 4E-20. Recommended Absorption Cross Sections of CF_3O_2 at 295 K

λ (nm)	10^{20} σ (cm^2)	λ (nm)	10^{20} σ (cm^2)	λ (nm)	10^{20} σ (cm^2)
191.1	293	221.9	354	252.8	46
193.6	305	224.5	324	255.3	*37**
196.2	334	227.1	292	257.9	31
198.8	363	229.6	257	260.5	*25**
201.4	388	232.2	222	263.1	21
203.9	407	234.8	192	265.6	17
206.5	426	237.4	156	268.2	15
209.1	429	239.9	131	270.8	13
211.6	430	242.5	107	273.3	10
214.2	419	245.1	89	275.9	8
216.8	404	247.6	68		
219.4	383	250.2	54		

Note:
Maricq and Szente[1]
*smoothed value

(1) Maricq, M. M.; Szente, J. J. Flash photolysis-time-resolved UV absorption study of the reactions $CF_3H + F \rightarrow CF_3 + HF$ and $CF_3O_2 + CF_2O_2 \rightarrow$ products. *J. Phys. Chem.* **1992**, *96*, 4925-4930, doi:10.1021/j100191a037.

(2) Nielsen, O. J.; Ellermann, T.; Sehested, J.; Bartkiewicz, E.; Wallington, T. J.; Hurley, M. D. UV absorption spectra, kinetics, and mechanisms of the self reaction of CF_3O_2 in the gas phase at 298 K. *Int. J. Chem. Kinet.* **1992**, *24*, 1009-1021, doi:10.1002/kin.550241111.

E21. CF_3OH (trifluoromethanol)

Back to Index

$CF_3OH + h\nu$	$\rightarrow CF_3 + OH$	480 kJ mol^{-1}	249 nm	(1)
	$\rightarrow CF_3O + H$	492 kJ mol^{-1}	243.5 nm	(2)

(Recommendation: 97-4, Note: 10-6, Evaluated: 10-6)

Absorption Cross Sections: An upper limit of 10^{-21} cm^2 $molecule^{-1}$ has been determined experimentally by Molina and Molina[1] for the absorption cross sections of trifluoromethanol, CF_3OH, over the wavelength range 185–300 nm. This upper limit is consistent with estimates based on similarities between CF_3OH and CH_3OH, as well as with quantum chemistry calculations reported by Schneider et al.[2]

Photolysis Quantum Yield and Product Studies: No recommendation.

(1) Molina, L. T.; Molina, M. J. Ultraviolet spectrum of CF_3OH: Upper limits to the absorption cross sections. *Geophys. Res. Lett.* **1996**, *23*, 563-565, doi:10.1029/96GL00313.

(2) Schneider, W. F.; Wallington, T. J.; Minschwaner, K.; Stahlberg, E. A. Atmospheric chemistry of CF_3OH: Is photolysis important? *Environ. Sci. Technol.* **1995**, *29*, 247-250, doi:10.1021/es00001a031.

E22. CH_2FCH_2OH (2-fluoroethanol)

Back to Index

$CH_2FCH_2OH + h\nu \rightarrow$ Products (1)

(New Entry)

Absorption Cross Sections: UV absorption cross sections of CH_2FCH_2OH (2-fluoroethanol) have been measured at room temperature by Orkin et al.,[1] in 0.5 nm increments over the wavelength range 163–195.5 nm, and Rajakumar et al.[2] at 184.9 nm. The value of Rajakumar et al. at 184.9 nm is a factor of ~1.8 greater than the corresponding value of Orkin et al. The recommended cross sections given in 1 nm increments in Table 4E-22 for the 163–195 nm range were taken from Orkin et al. after rounding to 3 significant figures. For the range 200–220 nm, the recommended values were obtained from a log-linear fit (185–195 nm) and extrapolation of the Orkin et al. data, $\log \sigma(\lambda) = -1.1939 - 0.09335\ \lambda$. An estimated uncertainty factor of 1.15 (2σ) is recommended for the 163–195 nm wavelength range.

Photolysis Quantum Yield and Product Studies: No recommendation.

Table 4E-22. Recommended Absorption Cross Sections of CH_2FCH_2OH (2-fluoroethanol) at 295 K

λ (nm)	10^{20} σ (cm^2)	λ (nm)	10^{20} σ (cm^2)	λ (nm)	10^{20} σ (cm^2)
163	147	176	147	189	14.7
164	149	177	133	190	11.7
165	153	178	118	191	9.47
166	163	179	102	192	7.54
167	173	180	86.6	193	6.05
168	180	181	73.7	194	4.93
169	187	182	61.1	195	4.12
170	190	183	50.8	200	*1.37*
171	190	184	41.7	205	*0.467*
172	186	185	34.1	210	*0.159*
173	180	186	27.9	215	*0.0544*
174	171	187	22.5	220	*0.0186*
175	159	188	18.2		

Note:
163–195 nm: Orkin et al.[1] data at 1 nm intervals
200–220 nm: extrapolation of Orkin et al.[1] data, $\log \sigma(\lambda) = -1.1939 - 0.09335\ \lambda$

(1) Orkin, V. L.; Khamaganov, V. G.; Martynova, L. E.; Kurylo, M. J. High-accuracy measurements of $OH^{\bullet}$ reaction rate constants and IR and UV absorption spectra: Ethanol and partially fluorinated ethyl alcohols. *J. Phys. Chem. A* **2011**, *115*, 8656-8668, doi:10.1021/jp202099t.

(2) Rajakumar, B.; Burkholder, J. B.; Portmann, R. W.; Ravishankara, A. R. Rate coefficients for the OH + CFH_2CH_2OH reaction between 238 and 355 K. *Phys. Chem. Chem. Phys.* **2005**, *7*, 2498-2505, doi:10.1039/b503332b.

E23. CHF_2CH_2OH (2,2-difluoroethanol)

Back to Index

$CHF_2CH_2OH + h\nu \rightarrow$ Products (1)

(New Entry)

Absorption Cross Sections: UV absorption cross sections of CHF_2CH_2OH (2,2-difluoroethanol) have been measured at 295 K by Orkin et al.[1] in 0.5 nm increments over the wavelength range 163–194 nm. The Orkin et al. measurements are the only UV absorption data currently available for this molecule. The recommended cross sections given in 1 nm increments in Table 4E-23 for the 163–194 nm range were taken from this study. For the range 195–220 nm, the recommended values were obtained from a log-linear fit (185–194 nm) and extrapolation of the Orkin et al. data, $\log \sigma(\lambda) = 1.0683 - 0.10785\ \lambda$. An estimated uncertainty factor of 1.15 (2σ) is recommended for the 163–194 nm wavelength range.

Photolysis Quantum Yield and Product Studies: No recommendation.

Table 4E-23. Recommended Absorption Cross Sections of CHF_2CH_2OH (2,2-difluoroethanol) at 295 K

λ (nm)	10^{20} σ (cm^2)	λ (nm)	10^{20} σ (cm^2)	λ (nm)	10^{20} σ (cm^2)
163	97.3	176	70.3	189	4.83
164	104	177	61.5	190	3.75
165	109	178	53.1	191	2.98
166	113	179	44.9	192	2.36
167	115	180	37.3	193	1.76
168	116	181	30.8	194	1.39
169	116	182	25.0	195	*1.09*
170	113	183	20.3	200	*0.315*
171	109	184	16.3	205	*0.0910*
172	103	185	12.9	210	*0.0263*
173	96.2	186	10.2	215	*0.00760*
174	88.1	187	8.07	220	*0.00219*
175	79.4	188	6.25		

Note:
163–194 nm: Orkin et al.[1] data at 1 nm intervals
195–220 nm: extrapolation of Orkin et al.[1] data, $\log \sigma(\lambda) = 1.0683 - 0.10785\ \lambda$

(1) Orkin, V. L.; Khamaganov, V. G.; Martynova, L. E.; Kurylo, M. J. High-accuracy measurements of $OH^{\bullet}$ reaction rate constants and IR and UV absorption spectra: Ethanol and partially fluorinated ethyl alcohols. *J. Phys. Chem. A* **2011**, *115*, 8656-8668, doi:10.1021/jp202099t.

E24. CF_3CH_2OH (2,2,2-trifluoroethanol)

Back to Index

$CF_3CH_2OH + h\nu \rightarrow$ Products (1)

(New Entry)

Absorption Cross Sections: UV absorption cross sections of CF_3CH_2OH (2,2,2-trifluoroethanol) have been measured at room temperature by Orkin et al.[1] in 0.5 nm increments over the wavelength range 163–201 nm and by Salahub and Sandorfy[2] over the range 119.8–192.3 nm. The cross sections of Salahub and Sandorfy are greater than those of Orkin et al. at all overlapping wavelengths. The discrepancy increases at longer wavelengths, ranging from a 17% difference at 163 nm up to a factor of 6.9 at 192 nm. The Orkin et al. data are considered more reliable at the longer wavelengths, as the Salahub and Sandorfy study was primarily focused on locating absorption features rather than determining absorption cross sections. The recommended cross sections given in 1 nm increments in Table 4E-24 for the 163–201 nm range were taken from Orkin et al. For the range 205–220 nm, the recommended values were obtained from a log-linear fit (191–201 nm) and extrapolation of the Orkin et al. data, $\log \sigma(\lambda) = 4.5910 - 0.12932\ \lambda$. Estimated uncertainty factors (2σ) of $F(\lambda) = 1.15 + 4 \times 10^{-23}/\sigma(\lambda)$ are recommended for the 163–201 nm wavelength range.

The recommended Lyman-α (121.567 nm) cross section was interpolated from the data of Salahub and Sandorfy[2] with an estimated uncertainty factor (2σ) of 1.3.

Photolysis Quantum Yield and Product Studies: No recommendation.

Table 4E-24. Recommended Absorption Cross Sections of CF_3CH_2OH (2,2,2-trifluoroethanol) at 295 K

λ (nm)	10^{20} σ (cm^2)	λ (nm)	10^{20} σ (cm^2)	λ (nm)	10^{20} σ (cm^2)
121.567	1480	177	31.4	192	0.581
163	89.1	178	25.9	193	0.430
164	91.3	179	20.6	194	0.317
165	92.4	180	16.4	195	0.238
166	92.0	181	12.9	196	0.172
167	90.1	182	9.98	197	0.127
168	86.9	183	7.77	198	0.0941
169	82.4	184	5.88	199	0.0705
170	77.1	185	4.48	200	0.0538
171	71.0	186	3.39	201	0.0413
172	64.4	187	2.56	205	*0.0120*
173	57.5	188	1.92	210	*0.00272*
174	50.4	189	1.43	215	*0.000613*
175	43.6	190	1.06	220	*0.000138*
176	37.3	191	0.790		

Note:
121.567 nm: Salahub and Sandorfy[2]
163–201 nm: Orkin et al.[1] data at 1 nm intervals
205–220 nm: extrapolation of Orkin et al.[1] data, $\log \sigma(\lambda) = 4.5910 - 0.12932\ \lambda$

(1) Orkin, V. L.; Khamaganov, V. G.; Martynova, L. E.; Kurylo, M. J. High-accuracy measurements of OH• reaction rate constants and IR and UV absorption spectra: Ethanol and partially fluorinated ethyl alcohols. *J. Phys. Chem. A* **2011**, *115*, 8656-8668, doi:10.1021/jp202099t.

(2) Salahub, D. R.; Sandorfy, C. The far-ultraviolet spectra of some simple alcohols and fluoroalcohols. *Chem. Phys. Lett.* **1971**, *8*, 71-74, doi:10.1016/0009-2614(71)80578-X.

E25. CF_3OOCF_3 (hexafluorodimethyl peroxide)

Back to Index

$CF_3OOCF_3 + h\nu \rightarrow 2\ CF_3O$ 197 kJ mol^{-1} 609 nm (1)

(Recommendation: 06-2, Note: 10-6, Evaluated: 10-6)

Absorption Cross Sections: The UV absorption spectrum of hexafluorodimethyl peroxide, CF_3OOCF_3, has been measured at room temperature over the wavelength range 200–263 nm by Meller and Moortgat.[1] The continuous spectrum shows part of a broad absorption band with monotonically increasing cross sections with decreasing wavelength. The recommended absorption cross sections in Table 4E-25 are values averaged over 1 nm intervals of the 0.2 nm resolution spectrum from Meller and Moortgat.[1]

Photolysis Quantum Yield and Product Studies: No recommendation.

Table 4E-25. Recommended Absorption Cross Sections of CF_3OOCF_3 at 298 K

λ (nm)	10^{20} σ (cm^2)	λ (nm)	10^{20} σ (cm^2)	λ (nm)	10^{20} σ (cm^2)	λ (nm)	10^{20} σ (cm^2)
200	3.61	216	1.25	232	0.501	248	0.204
201	3.37	217	1.18	233	0.462	249	0.195
202	3.13	218	1.10	234	0.433	250	0.183
203	2.92	219	1.04	235	0.408	251	0.174
204	2.73	220	0.983	236	0.380	252	0.166
205	2.53	221	0.926	237	0.361	253	0.157
206	2.35	222	0.869	238	0.339	254	0.147
207	2.20	223	0.822	239	0.323	255	0.138
208	2.06	224	0.778	240	0.303	256	0.132
209	1.94	225	0.737	241	0.288	257	0.125
210	1.80	226	0.693	242	0.274	258	0.119
211	1.69	227	0.654	243	0.263	259	0.112
212	1.61	228	0.614	244	0.246	260	0.107
213	1.51	229	0.584	245	0.240	261	0.101
214	1.42	230	0.555	246	0.227	262	0.096
215	1.33	231	0.525	247	0.214	263	0.091

Note:
Meller and Moortgat[1]

(1) Meller, R.; Moortgat, G. K. Photolysis of $CF_3O_2CF_3$ in the presence of O_3 in oxygen: kinetic study of the reactions of CF_3O and CF_3O_2 radicals with O_3. *J. Photochem. Photobio. A: Chem.* **1995**, *86*, 15-25, doi:10.1016/1010-6030(94)03951-P.

E26. $CF_3O_3CF_3$ (hexafluorodimethyl trioxide)

Back to Index

$CF_3O_3CF_3 + h\nu \rightarrow$ Products (1)

(Recommendation: 06-2, Note: 10-6, Evaluated: 10-6)

Absorption Cross Sections: The UV absorption spectrum of hexafluorodimethyl trioxide, $CF_3O_3CF_3$, has been measured at room temperature over the wavelength range 200–312 nm by Meller and Moortgat.[1] The spectrum shows part of a broad absorption band with monotonically decreasing cross sections with increasing wavelength. The recommended absorption cross sections in Table 4E-26 are from the Meller and Moortgat[1] 0.2 nm resolution data set averaged over 1 nm intervals.

Photolysis Quantum Yield and Product Studies: No recommendation.

Table 4E-26. Recommended Absorption Cross Sections of $CF_3O_3CF_3$ at 298 K

λ (nm)	10^{20} σ (cm^2)	λ (nm)	10^{20} σ (cm^2)	λ (nm)	10^{20} σ (cm^2)	λ (nm)	10^{20} σ (cm^2)
200	46.9	229	20.3	258	4.26	287	0.565
201	45.5	230	19.5	259	3.99	288	0.526
202	44.2	231	18.8	260	3.73	289	0.491
203	42.8	232	18.0	261	3.51	290	0.458
204	41.4	233	17.2	262	3.28	291	0.427
205	40.2	234	16.5	263	3.07	292	0.400
206	39.0	235	15.7	264	2.86	293	0.373
207	37.9	236	15.0	265	2.67	294	0.347
208	37.0	237	14.3	266	2.50	295	0.325
209	36.1	238	13.7	267	2.33	296	0.302
210	35.2	239	13.0	268	2.17	297	0.281
211	34.4	240	12.3	269	2.03	298	0.262
212	33.6	241	11.7	270	1.89	299	0.244
213	32.8	242	11.1	271	1.76	300	0.228
214	32.1	243	10.5	272	1.64	301	0.213
215	31.3	244	10.0	273	1.53	302	0.197
216	30.5	245	9.46	274	1.43	303	0.185
217	29.8	246	8.95	275	1.33	304	0.174
218	29.0	247	8.45	276	1.24	305	0.164
219	28.2	248	7.95	277	1.15	306	0.154
220	27.4	249	7.48	278	1.07	307	0.143
221	26.7	250	7.04	279	0.999	308	0.133
222	25.9	251	6.64	280	0.929	309	0.122
223	25.1	252	6.25	281	0.860	310	0.112
224	24.3	253	5.87	282	0.800	311	0.106
225	23.5	254	5.52	283	0.748	312	0.096
226	22.7	255	5.18	284	0.699		
227	21.9	256	4.86	285	0.653		
228	21.1	257	4.56	286	0.608		

Note:
Meller and Moortgat[1]

(1) Meller, R.; Moortgat, G. K. Photolysis of $CF_3O_2CF_3$ in the presence of O_3 in oxygen: kinetic study of the reactions of CF_3O and CF_3O_2 radicals with O_3. *J. Photochem. Photobio. A: Chem.* **1995**, *86*, 15-25, doi:10.1016/1010-6030(94)03951-P.

E27. CF_3CHO (trifluoroacetaldehyde)

Back to Index

$CF_3CHO + h\nu$	$\rightarrow CF_3 + HCO$	389 kJ mol^{-1}	308 nm	(1)
	$\rightarrow CHF_3 + CO$	7 kJ mol^{-1}	1700 nm	(2)
	$\rightarrow CF_3CO + H$	423 kJ mol^{-1}	283 nm	(3)

(Recommendation: 06-2, Note: 10-6, Evaluated: 10-6)

Absorption Cross Sections: The UV absorption spectrum of trifluoroacetaldehyde, CF_3CHO, has been measured at room temperature by Lucazeau and Sandorfy[6] (118–182 and 250–357 nm), Meller et al.[7] (229–364 nm), Francisco and Williams[4] (230–400 nm), Sellevåg et al.[10] (200–400 nm), Hashikawa et al.[5] (200–500 nm), and Chiappero et al.[2] (230–360 nm). The UV absorption spectrum has an absorption band between 227 and 360 nm with a maximum at 301 nm and weak diffuse structure at wavelengths >250 nm. The absorption cross sections reported by Francisco and Williams,[4] Meller et al.,[7] Sellevåg et al.,[10] Hashikawa et al.,[5] and Chiappero et al.[2] are in reasonable agreement, generally to within 10% or better, in the wavelength region 245–354 nm. There are larger discrepancies in the long and short wavelength wings of the absorption band. In these regions, the cross sections from Sellevåg et al.[10] are smaller than those from Francisco and Williams[4] and larger than those from Meller et al.[7] The data of Lucazeau and Sandorfy,[6] which are reported in graphical form, are appreciably smaller than those reported in the other studies. The recommended absorption cross sections in Table 4E-27 are taken from Sellevåg et al.[10]

The temperature dependence of the absorption spectrum was examined by Chiappero et al.[2] (230–360 nm) between 249 and 297 K. No discernible variation of the absorption spectrum with temperature was observed. Borkowski and Ausloos[1] (313 and 334 nm) reported absorption cross sections at 329 K that are in agreement with the 298 K recommendation.

Photolysis Quantum Yield and Product Studies: The photolysis quantum yield for CF_3CHO and the product branching ratios are wavelength dependent. Sellevåg et al.[10] determined the effective atmospheric photolysis quantum yield for CF_3CHO using an outdoor photoreactor to be <0.02. Dodd and Watson-Smith[3] determined the products following photolysis at 313 nm to be $\Phi_1 = 0.12$ and $\Phi_2 = 0.021$. Pearce and Whytock[8] reported $\Phi_2 = 0$ for 313 nm photolysis. Richer et al.[9] studied the products formed following 254 nm photolysis and reported product yields of CHF_3 (14%), CF_2O (80%), CO (65%), CO_2 (45%) and $\Phi_2 = 0.14$. At 366 nm, Richer et al.[9] observed only a small degree of dissociation after >6 hours of photolysis. Chiappero et al.[2] reported photolysis quantum yields of $\Phi_1 = 0.41 \pm 0.07$ and $\Phi_2 = 0.38 \pm 0.07$ at 254 nm and $\Phi_1 = 0.17 \pm 0.03$ and $\Phi_2 \sim 0$ at 308 nm. Quantum yields of $\Phi_1 = 0.15 \pm 0.03$ and $\Phi_2 < 0.02$ are recommended at 313 nm.

Table 4E-27. Recommended Absorption Cross Sections of CF_3CHO at 298 K

λ (nm)	10^{20} σ (cm^2)	λ (nm)	10^{20} σ (cm^2)	λ (nm)	10^{20} σ (cm^2)	λ (nm)	10^{20} σ (cm^2)
210	0.197	248	0.311	286	2.63	324	2.06
211	0.192	249	0.339	287	2.67	325	1.90
212	0.179	250	0.369	288	2.73	326	1.72
213	0.172	251	0.400	289	2.79	327	1.64
214	0.159	252	0.433	290	2.86	328	1.62
215	0.152	253	0.472	291	2.92	329	1.55
216	0.140	254	0.511	292	2.94	330	1.44
217	0.132	255	0.548	293	3.00	331	1.35
218	0.121	256	0.591	294	3.05	332	1.26
219	0.113	257	0.638	295	3.06	333	1.18
220	0.105	258	0.686	296	3.08	334	1.13
221	0.098	259	0.737	297	3.08	335	1.06
222	0.090	260	0.789	298	3.10	336	1.01
223	0.084	261	0.840	299	3.14	337	0.993
224	0.080	262	0.896	300	3.17	338	0.891
225	0.076	263	0.954	301	3.20	339	0.730
226	0.074	264	1.02	302	3.15	340	0.622
227	0.073	265	1.09	303	3.12	341	0.585
228	0.075	266	1.15	304	3.15	342	0.569
229	0.075	267	1.22	305	3.13	343	0.531
230	0.078	268	1.29	306	3.07	344	0.471
231	0.081	269	1.35	307	3.03	345	0.425
232	0.086	270	1.42	308	2.97	346	0.385
233	0.091	271	1.50	309	2.95	347	0.337
234	0.097	272	1.58	310	2.92	348	0.310
235	0.104	273	1.66	311	2.92	349	0.286
236	0.112	274	1.74	312	2.91	350	0.246
237	0.121	275	1.82	313	2.78	351	0.235
238	0.131	276	1.89	314	2.67	352	0.232
239	0.142	277	1.96	315	2.65	353	0.162
240	0.155	278	2.03	316	2.62	354	0.096
241	0.169	279	2.11	317	2.52	355	0.071
242	0.184	280	2.19	318	2.42	356	0.058
243	0.201	281	2.28	319	2.33	357	0.050
244	0.220	282	2.35	320	2.25	358	0.044
245	0.240	283	2.42	321	2.19	359	0.042
246	0.262	284	2.50	322	2.13	360	0.038
247	0.285	285	2.57	323	2.08		

Note:
Sellevåg et al.[10]

(1) Borkowski, R. P.; Ausloos, P. The vapor phase fluorescence and its relationship to the photolysis of propionaldehyde and the butyraldehydes. *J. Am. Chem. Soc.* **1962**, *84*, 4044-4048, doi:10.1021/ja00880a014.
(2) Chiappero, M. S.; Malanca, F. E.; Argüello, G. A.; Wooldridge, S. T.; Hurley, M. D.; Ball, J. C.; Wallington, T. J.; Waterland, R. L.; Buck, R. C. Atmospheric chemistry of perfluoroaldehydes ($C_xF_{2x+1}CHO$) and fluorotelomer aldehydes ($C_xF_{2x+1}CH_2CHO$): Quantification of the important role of photolysis. *J. Phys. Chem. A* **2006**, *110*, 11944-11953, doi:10.1021/jp064262k.
(3) Dodd, R. E.; Watson-Smith, J. The photolysis of trifluoroacetaldehyde. *J. Chem. Soc.* **1957**, 1465-1473, doi:10.1039/jr9570001465.
(4) Francisco, J. S.; Williams, I. H. Infrared and ultraviolet spectroscopic characterization of trifluoroacetaldehyde. *Mol. Phys.* **1992**, *76*, 1433-1441, doi:10.1080/00268979200102201.
(5) Hashikawa, Y.; Kawasaki, M.; Waterland, R. L.; Hurley, M. D.; Ball, J. C.; Wallington, T. J.; Andersen, M. P. S.; Nielsen, O. J. Gas phase UV and IR absorption spectra of $C_xF_{2x+1}CHO$ (x = 1-4). *J. Fluor. Chem.* **2004**, *125*, 1925-1932, doi:10.1016/j.jfluchem.2004.07.006.
(6) Lucazeau, G.; Sandorfy, C. On the far-ultraviolet spectra of some simple aldehydes. *J. Mol. Spectrosc.* **1970**, *35*, 214-231, doi:10.1016/0022-2852(70)90199-2.
(7) Meller, R.; Boglu, D.; Moortgat, G. K. "UV spectra of several halogenated carbonyl compounds and FTIR studies of the degradation of CF_3COCl, HCFC-123 and HFC-143a"; Kinetics and Mechanisms for the Reactions of Halogenated Organic Compounds in the Troposphere. STEP-HALOCSIDE/AFEAS WORKSHOP, 1991, Dublin, Ireland.
(8) Pearce, C.; Whytock, D. A. Photolysis of trifluoroacetaldehyde at 313 nm *J. Chem. Soc. D: Chem. Commun.* **1971**, 1464-1466, doi:10.1039/c29710001464.
(9) Richer, H. R.; Sodeau, J. R.; Barnes, I. *STEP-HALOCSIDE/AFEAS Workshop, Dublin, 23-25 March* **1993**, 180-188.
(10) Sellevåg, S. R.; Kelly, T.; Sidebottom, H.; Nielsen, C. J. A study of the IR and UV-Vis absorption cross sections, photolysis and OH-initiated oxidation of CF_3CHO and CF_3CH_2CHO. *Phys. Chem. Chem. Phys.* **2004**, *6*, 1243-1252, doi:10.1039/b315941h.

E28. $CF_3C(O)F$ (trifluoroacetyl fluoride)

Back to Index

$CF_3C(O)F + h\nu \rightarrow CF_3 + FCO$ (1)
$\rightarrow CF_3CO + F$ (2)

(Recommendation: 06-2, Note: 15-10, Evaluated: 10-6)

Absorption Cross Sections: The UV absorption spectrum of trifluoroacetyl fluoride, $CF_3C(O)F$, has been measured at room temperature by Meller et al.[3] (200–281 nm), Rattigan et al.[4] (200–295 nm), and Malanca et al.[2] (200–340 nm). The cross sections from Meller et al.[3] and Malanca et al.[2] are in good agreement in the spectral region 200–260 nm. The position of the absorption maximum near 213 nm reported by Rattigan et al.[4] is shifted by ~3 nm to longer wavelengths as compared to that reported by Meller et al.[3] and Malanca et al.[2] The cross sections from these studies differ by 20 to 30% at wavelengths >260 nm.

The temperature dependence of the absorption spectrum has been reported by Rattigan et al.[4] (233–293 K) and Malanca et al.[2] (238–300 K). For wavelengths >210 nm, the absorption cross section decreases with decreasing temperature. The recommended absorption cross sections in Table 4E-28 are taken from Malanca et al.[2] in the region 200–260 nm at 300 and 238 K. In the region 265–280 nm, the data of Meller[3] are recommended at 297 K and those of Rattigan et al.[4] at 238 K. An uncertainty factor of 1.2 (2σ) is recommended for the 297 and 300 K cross section data given in Table 4E-28.

Photolysis Quantum Yield and Product Studies: Bierbrauer et al.[1] measured the quantum yield of disappearance of $CF_3C(O)F$ at 240 and 254 nm to be $\Phi_1 + \Phi_2 = 1.02 \pm 0.05$. It is assumed that this applies over the wavelength region 200–300 nm.

Table 4E-28. Recommended Absorption Cross Sections of $CF_3C(O)F$ at 297/300 K and 238 K

λ (nm)	10^{20} σ (cm^2) 297 and 300 K	10^{20} σ (cm^2) 238 K
200	10.90	10.93
205	12.89	12.89
210	13.94	13.90
215	13.83	13.74
220	12.60	12.48
225	10.57	10.42
230	8.15	7.99
235	5.75	5.61
240	3.69	3.57
245	2.13	2.04
250	1.09	1.03
255	0.47	0.43
260	0.167	0.156
265	0.055	0.047
270	0.013	0.010
275	0.004	0.003
280	0.001	0.001

Note:
200–260 nm, 300 and 238 K: Malanca et al.[2]
265–280 nm, 297 K: Meller et al.[3]; 238 K: Rattigan et al.[4]

(1) Bierbrauer, K. L.; Chiappero, M. S.; Malanca, F. E.; Arguello, G. A. Photochemistry of perfluoroacetyl fluoride kinetics of the reaction between CF_3 and FCO radicals. *J. Photochem. Photobiol. A: Chem.* **1999**, *122*, 73-78, doi:10.1016/S1010-6030(98)00431-6.

(2) Malanca, F. E.; Chiappero, M. S.; Argüello, G. A.; Wallington, T. J. Trifluoro methyl peroxynitrate (CF_3OONO_2): Temperature dependence of the UV absorption spectrum and atmospheric implications. *Atmos. Environ.* **2005**, *39*, 5051-5057, doi:10.1016/j.atmosenv.2005.05.026.

(3) Meller, R., personal communication to NASA Data Panel.

(4) Rattigan, O. V.; Wild, O.; Jones, R. L.; Cox, R. A. Temperature-dependent absorption cross-sections of CF_3COCl, CF_3COF, CH_3COF, CCl_3CHO and CF_3COOH. *J. Photochem. Photobiol. A: Chem.* **1993**, *73*, 1-9, doi:10.1016/1010-6030(93)80026-6.

E29. FC(O)C(O)F (oxalyl fluoride)

Back to Index

$FC(O)C(O)F + h\nu \rightarrow$ Products

(New)

Absorption Cross Sections: UV absorption cross sections of FC(O)C(O)F (oxalyl fluoride) have been measured at room temperature by Balfour[1] (293–309 nm), Cobos et al.[2] (193, 248 nm), and McGillen et al.[3] (190–330 nm). McGillen used two detection methods: a monochromator / photomultiplier tube (PMT) apparatus for wavelengths 190–260 nm and a diode array spectrometer for 210–330 nm; cross sections from both approaches are in good agreement. Relative to McGillen et al., the 248 nm cross section of Cobos et al. agrees within 10%, but the 193 nm value of Cobos et al. is more than 50% larger. The reported values of Balfour were obtained at high resolution and are highly structured, but the general contour agrees with McGillen et al. The recommended cross sections given in Table 4E-29 are from McGillen et al. and are 2 nm values from their data between 190–330 nm (reported every 2 nm for 190–210 nm using their PMT apparatus and every 0.5 nm for 210–330 nm using their diode array spectrometer). An estimated uncertainty factor (2σ) of 1.1 is recommended.

Photolysis Quantum Yield and Product Studies: McGillen et al.[3] conducted product studies of FC(O)C(O)F photolysis at 248 nm by reacting the radical products of photolysis with Br_2 to form stable bromides for detection, e.g., FCO radicals from photolysis were efficiently scavenged by Br_2 to form BrC(O)F. The yield for BrC(O)F was found to be greater than ~90%, indicating that the FCO radical is the dominant photolysis product. CF_2O was found to have a primary photolysis yield of ~10%.

Table 4E-29. Recommended Absorption Cross Sections of FC(O)C(O)F (oxalyl fluoride) at 298 K

λ (nm)	10^{20} σ (cm^2)	λ (nm)	10^{20} σ (cm^2)	λ (nm)	10^{20} σ (cm^2)
190	5.36	238	11.9	286	2.47
192	6.03	240	12.1	288	2.42
194	6.23	242	12.3	290	2.05
196	6.78	244	12.5	292	1.73
198	7.30	246	12.7	294	1.29
200	7.81	248	12.7	296	0.940
202	8.15	250	12.4	298	0.704
204	8.21	252	12.2	300	0.616
206	8.86	254	12.1	302	0.621
208	9.15	256	11.7	304	0.547
210	9.11	258	11.1	306	0.293
212	9.15	260	10.5	308	0.260
214	9.43	262	9.68	310	0.114
216	9.39	264	9.26	312	0.0668
218	9.58	266	8.74	314	0.0558
220	9.81	268	7.81	316	0.0563
222	9.90	270	7.07	318	0.0449
224	9.90	272	6.12	320	0.0336
226	10.1	274	5.62	322	0.0261
228	10.5	276	5.38	324	0.0236
230	10.7	278	4.63	326	0.0222
232	10.8	280	4.17	328	0.0218
234	11.2	282	3.35	330	0.0195
236	11.6	284	2.82		

Note:
Taken from McGillen et al.[3]

(1) Balfour, W. J. The electronic spectra of the oxalyl halides. McMaster University. **1967**.
(2) Cobos, C. J.; Croce, A. E.; Castellano, E. Kinetics of the recombination reaction between F atoms and FCO radicals. *Chem. Phys. Lett.* **1995**, *239*, 320-325, doi:10.1016/0009-2614(95)00483-K.
(3) McGillen, M. R.; Papadimitriou, V. C.; Smith, S. C.; Burkholder, J. B. FC(O)C(O)F, $FC(O)CF_2C(O)F$, and $FC(O)CF_2CF_2C(O)F$: Ultraviolet and infrared absorption spectra and 248 nm photolysis products. *J. Phys. Chem. A* **2020**, *124*, 7123-7133, doi:10.1021/acs.jpca.0c04607.

E30. $FC(O)CF_2C(O)F$ (difluoromalonyl fluoride)

Back to Index

$FC(O)CF_2C(O)F + h\nu \rightarrow$ Products

(New)

Absorption Cross Sections: UV absorption cross sections of $FC(O)CF_2C(O)F$ (difluoromalonyl fluoride) have been measured at room temperature by McGillen et al.[1] (190–270 nm), the only study available. McGillen used two detection methods: a monochromator/photomultiplier tube apparatus for wavelengths 190–260 nm and a diode array spectrometer for 210–270 nm. Cross sections from both approaches are in good agreement overall (typically to within <10%); however, the diode array spectrometer results usually lie outside the small uncertainty range (0.1–1.8%) with which the PMT results were reported. The recommended cross sections given in Table 4E-30 are from McGillen et al. and are 5 nm values from their data between 190–270 nm (reported every 2 nm for 190–210 nm using their PMT apparatus, every 5 nm for 210–260 nm using their PMT apparatus, and every 0.5 nm for 260–270 nm using their diode array spectrometer). An estimated uncertainty factor (2σ) of 1.1 is recommended.

Photolysis Quantum Yield and Product Studies: McGillen et al.[1] conducted product studies of $FC(O)CF_2C(O)F$ photolysis at 248 nm by reacting the radical products of photolysis with Br_2 to form stable bromides for detection, e.g., FCO radicals from photolysis were efficiently scavenged by Br_2 to form BrC(O)F. The yield

for BrC(O)F was found to be greater than ~90%, indicating that the FCO radical is the dominant photolysis product.

Table 4E-30. Recommended Absorption Cross Sections of $FC(O)CF_2C(O)F$ (difluoromalonyl fluoride) at 298 K

λ (nm)	10^{20} σ (cm^2)	λ (nm)	10^{20} σ (cm^2)
190	16.3	235	28.9
195	23.8	240	19.9
200	31.3	245	12.0
205	38.3	250	6.73
210	43.5	255	3.35
215	46.9	260	1.22
220	46.5	265	0.511
225	43.6	270	0.198
230	37.3		

Note:
Taken from McGillen et al.[1]

(1) McGillen, M. R.; Papadimitriou, V. C.; Smith, S. C.; Burkholder, J. B. FC(O)C(O)F, $FC(O)CF_2C(O)F$, and $FC(O)CF_2CF_2C(O)F$: Ultraviolet and infrared absorption spectra and 248 nm photolysis products. *J. Phys. Chem. A* **2020**, *124*, 7123-7133, doi:10.1021/acs.jpca.0c04607.

E31. $FC(O)CF_2CF_2C(O)F$ (tetrafluorosuccinyl fluoride)

Back to Index

$FC(O)CF_2CF_2C(O)F + h\nu \rightarrow$ Products

(New)

Absorption Cross Sections: UV absorption cross sections of $FC(O)CF_2CF_2C(O)F$ (tetrafluorosuccinyl fluoride) have been measured at room temperature by McGillen et al.[1] (190–270 nm), the only study available. McGillen used two detection methods: a monochromator/photomultiplier tube apparatus for wavelengths 190–264 nm and a diode array spectrometer for 210–270 nm. Cross sections from both approaches are in good agreement overall (typically within <10%); however, the diode array spectrometer results usually lie outside the small uncertainty range (0.2–2.5%) with which the PMT results were reported. The recommended cross sections given in Table 4E-31 are from McGillen et al. and are 5 nm values of their data between 190–270 nm (reported every 2 nm for 190–264 nm using their PMT apparatus and every 0.5 nm for 264–270 nm using their diode array spectrometer). An estimated uncertainty factor (2σ) of 1.1 is recommended.

Photolysis Quantum Yield and Product Studies: McGillen et al.[1] conducted product studies of $FC(O)CF_2CF_2C(O)F$ photolysis at 248 nm by reacting the radical products of photolysis with Br_2 to form stable bromides for detection, e.g., FCO radicals from photolysis were efficiently scavenged by Br_2 to form BrC(O)F. The yield for BrC(O)F was found to be greater than ~90%, indicating that the FCO radical is the dominant photolysis product.

Table 4E-31. Recommended Absorption Cross Sections of $FC(O)CF_2CF_2C(O)F$ (tetrafluorosuccinyl fluoride) at 298 K

λ (nm)	10^{20} σ (cm^2)	λ (nm)	10^{20} σ (cm^2)
190	19.9	235	34.2
195	27.9	240	23.1
200	37.7	245	13.3
205	46.7	250	7.54
210	54.1	255	3.92
215	58.6	260	1.79
220	59.5	265	0.886
225	54.6	270	0.422
230	44.5		

Note:
Taken from McGillen et al.[1]

(1) McGillen, M. R.; Papadimitriou, V. C.; Smith, S. C.; Burkholder, J. B. FC(O)C(O)F, $FC(O)CF_2C(O)F$, and $FC(O)CF_2CF_2C(O)F$: Ultraviolet and infrared absorption spectra and 248 nm photolysis products. *J. Phys. Chem. A* **2020**, *124*, 7123-7133, doi:10.1021/acs.jpca.0c04607.

E32. CF_3OONO_2 (trifluoromethyl peroxynitrate)

Back to Index

$CF_3OONO_2 + h\nu \rightarrow CF_3O_2 + NO_2$ (1)

$\rightarrow CF_3O + NO_3$ (2)

(Recommendation: 15-10, Note: 15-10, Evaluated: 15-10)

Absorption Cross Sections: The UV absorption cross sections of trifluoromethyl peroxynitrate, CF_3OONO_2, have been measured at room temperature by Kopitzky et al.[1] (185–340 nm) and over the temperature range 233–300 K by Malanca et al.[2] (200–340 nm). The UV absorption spectrum over this wavelength range consists of at least two overlapping continuous absorption bands with maxima below 185 nm and near 260 nm. The spectrum exhibits continuously decreasing absorption cross sections over the 185–340 nm wavelength range. The absorption spectra measured at room temperature in these studies are in agreement for wavelengths ≤290 nm, to within 10% or better. At longer wavelengths, significant discrepancies in the reported spectra are evident, which is most likely due to differences in measurement precision and the accuracy of corrections applied to account for the NO_2 impurity absorption. The recommended room temperature cross sections given in Table 4E-32-1 are taken from Kopitzky et al.

Table 4E-32-1. Recommended Absorption Cross Sections of CF_3OONO_2 at 301 K

λ (nm)	10^{20} σ (cm^2)	λ (nm)	10^{20} σ (cm^2)
185	430	265	8.2
190	370	270	5.8
195	290	275	4.0
200	220	280	2.6
205	150	285	1.7
210	96	290	1.0
215	74	295	0.69
220	54	300	0.45
225	46	305	0.28
230	38	310	0.20
235	32	315	0.13
240	27	320	0.08
245	22	325	0.050
250	18	330	0.037
255	14.3	335	0.024
260	11.1	340	0.014

Note:

Kopitzky et al.[1]

Malanca et al.[2] reported absorption spectra at 300, 294, 273, 253, and 233 K. The measured spectra were corrected for an unspecified contribution from NO_2 and N_2O_4 impurity absorption, which is particularly important at wavelengths >~260 nm. A decrease in absorption cross section over the wavelength range 260 to 340 nm with decreasing temperature was reported. The temperature dependence was parameterized using the empirical expression:

$$\log_{10}(\sigma) = B \times T + \log_{10} \sigma_0$$

where σ and σ_0 are the cross sections in cm^2 $molecule^{-1}$ at temperatures T and 0 K, respectively. Malanca et al. reported σ(0 K) and B parameters at selected wavelengths as given in Table 4E-32-2.

Table 4E-32-2. Recommended CF_3OONO_2 Absorption Spectrum Temperature Dependence

λ (nm)	10^3 B (K^{-1})	10^{20} σ_0(0 K) (cm^2 $molecule^{-1}$)
290	6.8	1.2×10^{-2}
295	8.3	2.9×10^{-3}
300	10.5	4.4×10^{-4}
305	12	8.4×10^{-5}
310	14	1.9×10^{-5}
315	16.4	2.9×10^{-6}
320	18	6.0×10^{-7}
325	22	3.7×10^{-8}
330	26	1.3×10^{-9}

Note:
Malanca et al.[2]

Photolysis Quantum Yield and Product Studies: No recommendation.

(1) Kopitzky, R.; Willner, H.; Mack, H.-G.; Pfeiffer, A.; Oberhammer, H. IR and UV absorption cross sections, vibrational analysis, and the molecular structure of trifluoromethyl peroxynitrate, CF_3OONO_2. *Inorg. Chem.* **1998**, *37*, 6208-6213, doi:10.1021/ic980776p.

(2) Malanca, F. E.; Chiappero, M. S.; Argüello, G. A.; Wallington, T. J. Trifluoro methyl peroxynitrate (CF_3OONO_2): Temperature dependence of the UV absorption spectrum and atmospheric implications. *Atmos. Environ.* **2005**, *39*, 5051-5057, doi:10.1016/j.atmosenv.2005.05.026.

E33. $CF_3C(O)O_2NO_2$ (trifluoroperoxyacetyl nitrate)

Back to Index

$$CF_3C(O)O_2NO_2 + h\nu \rightarrow CF_3C(O)O_2 + NO_2 \quad (1)$$
$$\rightarrow CF_3C(O)O + NO_3 \quad (2)$$

(Recommendation: 06-2, Note: 15-10, Evaluated: 10-6)

Absorption Cross Sections: The UV absorption spectrum of trifluoroperoxyacetyl nitrate (FPAN), $CF_3C(O)O_2NO_2$, has been measured at room temperature by Libuda and Zabel[2] (227–305 nm) and Kopitzky et al.[1] (190–295 nm). These studies are in agreement for wavelengths >260 nm, but have systematic differences at shorter wavelengths with the Kopitzky et al. cross sections being lower. Over this wavelength range, the $CF_3C(O)O_2NO_2$ spectrum is red shifted by ~5 nm from the $CH_3C(O)O_2NO_2$ spectrum. The recommended absorption cross sections in Table 4E-33 are averages over 5 nm intervals of the 0.6 nm resolution spectrum reported by Libuda and Zabel.[2] As reported by Libuda and Zabel,[2] the estimated cross section uncertainties are ~10% for wavelengths <290 nm and 15 to 45% in the region 295–305 nm.

Photolysis Quantum Yield and Product Studies: No recommendation, although excitation in the UV is expected to break the weak O-ONO_2 bond.

Table 4E-33. Recommended Absorption Cross Sections of $CF_3(O)O_2NO_2$ at 298 K

λ (nm)	10^{20} σ (cm^2)
230	70.0
235	57.5
240	44.9
245	32.5
250	23.9
255	17.0
260	11.8
270	5.46
275	3.56
280	2.21
285	1.40
290	0.87
300	0.33
305	0.20

Note:
Libuda and Zabel[2]

(1) Kopitzky, R.; Beuleke, M.; Balzer, G.; Willner, H. Properties of trifluoroacetyl peroxynitrate, $CF_3C(O)OONO_2$. *Inorg. Chem.* **1997**, *36*, 1994-1997, doi:10.1021/ic9612109.

(2) Libuda, H. G.; Zabel, F. UV absorption cross sections of acetyl peroxynitrate and trifluoroacetyl peroxynitrate at 298 K. *Ber. Bunsenges. Phys. Chem.* **1995**, *99*, 1205-1213, doi:10.1002/bbpc.199500061.

E34. CF_3CH_2CHO (3,3,3-trifluoropropionaldehyde)

Back to Index

$CF_3CH_2CHO + h\nu \rightarrow CF_3CH_2 + HCO$ (1)

$\rightarrow CF_3CH_3 + CO$ (2)

(Recommendation: 06-2, Note: 15-10, Evaluated: 10-6)

Absorption Cross Sections: The UV absorption spectrum of 3,3,3-trifluoropropionaldehyde, CF_3CH_2CHO, has been measured at room temperature by Sellevåg et al.[3] (200–400 nm), Chiappero et al.[2] (230–355 nm), and Antiñolo et al. (230–350 nm).[1] The continuous absorption spectrum has weak diffuse band structure between 270 and 343 nm. The reported spectra are in reasonable agreement, with the cross sections from Sellevåg et al. ~6% greater than the values reported by Chiappero et al. and Antiñolo et al. near the peak of the spectrum. The spectrum reported by Antiñolo et al. is blue shifted by ~1 nm relative to the other two studies. The data reported for the wavelength region above 340 nm are in poor agreement. The recommended 298 K absorption cross sections given in Table 4E-34 were taken from Sellevåg et al.[3]

Chiappero et al.[2] measured the temperature dependence of the absorption spectrum over the range 249–297 K and reported no discernible variation of cross section with temperature. Antiñolo et al. measured the spectrum over the temperature range 269–323 K and reported a decrease in absorption cross sections with decreasing temperature between 260 and 330 nm. No recommendation is given for the spectrum temperature dependence.

Photolysis Quantum Yield and Product Studies: Sellevåg et al.[3] reported the effective atmospheric photolysis quantum yield for CF_3CH_2CHO using an outdoor photoreactor to be <0.02. The quantum yields for channels 1 and 2 were determined by Chiappero et al.[2] to be $\Phi_1 = 0.38 \pm 0.09$ and $\Phi_2 = 0.36 \pm 0.07$ for 254 nm photolysis and $\Phi_1 = 0.04 \pm 0.01$ and $\Phi_2 \sim 0$ at 308 nm in 700 Torr of N_2 bath gas.

Table 4E-34. Recommended Absorption Cross Sections of CF_3CH_2CHO at 298 K

λ (nm)	10^{20} σ (cm^2)	λ (nm)	10^{20} σ (cm^2)	λ (nm)	10^{20} σ (cm^2)	λ (nm)	10^{20} σ (cm^2)
200	0.939	236	0.309	272	2.43	308	3.04
201	0.825	237	0.324	273	2.58	309	3.07
202	0.732	238	0.344	274	2.72	310	3.13
203	0.668	239	0.362	275	2.83	311	3.15
204	0.611	240	0.377	276	2.89	312	3.04
205	0.542	241	0.395	277	2.92	313	2.83
206	0.483	242	0.422	278	2.94	314	2.56
207	0.432	243	0.443	279	2.98	315	2.30
208	0.397	244	0.474	280	3.07	316	2.11
209	0.367	245	0.513	281	3.22	317	1.97
210	0.334	246	0.552	282	3.37	318	1.93
211	0.311	247	0.593	283	3.49	319	1.93
212	0.309	248	0.629	284	3.55	320	1.92
213	0.298	249	0.671	285	3.54	321	1.95
214	0.285	250	0.728	286	3.53	322	1.97
215	0.273	251	0.788	287	3.51	323	1.93
216	0.267	252	0.842	288	3.51	324	1.79
217	0.266	253	0.904	289	3.59	325	1.59
218	0.263	254	0.963	290	3.69	326	1.32
219	0.263	255	1.01	291	3.80	327	1.09
220	0.270	256	1.08	292	3.85	328	0.938
221	0.266	257	1.15	293	3.81	329	0.818
222	0.265	258	1.25	294	3.76	330	0.757
223	0.266	259	1.34	295	3.72	331	0.740
224	0.256	260	1.40	296	3.65	332	0.742
225	0.270	261	1.48	297	3.62	333	0.718
226	0.268	262	1.53	298	3.61	334	0.717
227	0.270	263	1.61	299	3.67	335	0.706
228	0.269	264	1.71	300	3.75	336	0.673
229	0.273	265	1.84	301	3.76	337	0.607
230	0.272	266	1.96	302	3.67	338	0.506
231	0.281	267	2.06	303	3.53	339	0.390
232	0.288	268	2.13	304	3.37	340	0.277
233	0.298	269	2.17	305	3.21	341	0.206
234	0.300	270	2.22	306	3.11	342	0.138
235	0.307	271	2.30	307	3.06	343	0.103

Note:
Sellevåg et al.[3]

(1) Antiñolo, M.; Jiménez, E.; Albaladejo, J. UV absorption cross sections between 230 and 350 nm and pressure dependence of the photolysis quantum yield at 308 nm of CF_3CH_2CHO. *Phys. Chem. Chem. Phys.* **2011**, *13*, 15936-15946, doi:10.1039/c1cp21368g.

(2) Chiappero, M. S.; Malanca, F. E.; Argüello, G. A.; Wooldridge, S. T.; Hurley, M. D.; Ball, J. C.; Wallington, T. J.; Waterland, R. L.; Buck, R. C. Atmospheric chemistry of perfluoroaldehydes ($C_xF_{2x+1}CHO$) and fluorotelomer aldehydes ($C_xF_{2x+1}CH_2CHO$): Quantification of the important role of photolysis. *J. Phys. Chem. A* **2006**, *110*, 11944-11953, doi:10.1021/jp064262k.

(3) Sellevåg, S. R.; Kelly, T.; Sidebottom, H.; Nielsen, C. J. A study of the IR and UV-Vis absorption cross sections, photolysis and OH-initiated oxidation of CF_3CHO and CF_3CH_2CHO. *Phys. Chem. Chem. Phys.* **2004**, *6*, 1243-1252, doi:10.1039/b315941h.

E35. $(CF_3)_2CHOH$ (1,1,1,3,3,3-hexafluoro-2-propanol)

Back to Index

$(CF_3)_2CHOH + h\nu \rightarrow$ Products (1)

(New Entry)

Absorption Cross Sections: UV absorption cross sections of $(CF_3)_2CHOH$ (1,1,1,3,3,3-hexafluoro-2-propanol) have been measured at room temperature by Orkin et al.,[1] in 0.5 nm increments over the wavelength range 163–190 nm, and by Salahub and Sandorfy[2] over the range 121.21–176.99 nm. The cross sections of Salahub and Sandorfy are greater than those of Orkin et al. at all overlapping wavelengths. The discrepancy generally increases at longer wavelengths, ranging from ~20% at 163 nm to ~50% at 177 nm. The Orkin et al. data are considered more reliable, as the Salahub and Sandorfy study was primarily focused on locating absorption features rather than determining absorption cross sections. The recommended cross sections given in 1 nm increments in Table 4E-35 for the 163–190 nm range were taken from Orkin et al. For the range 195–210 nm, the recommended values were obtained from a log-linear fit (180–190 nm) and extrapolation of the Orkin et al. data, $\log \sigma(\lambda) = 2.5762 - 0.12521\ \lambda$. Estimated uncertainty factors (2σ) of $F(\lambda) = 1.15 + 7 \times 10^{-23}/\sigma(\lambda)$ are recommended for the 163–190 nm wavelength range.

The recommended Lyman-α (121.567 nm) cross section was interpolated from the data of Salahub and Sandorfy[2] with an estimated uncertainty factor (2σ) of 1.3.

Photolysis Quantum Yield and Product Studies: No recommendation.

Table 4E-35. Recommended Absorption Cross Sections of $(CF_3)_2CHOH$ (1,1,1,3,3,3-hexafluoro-2-propanol) at 298 K

λ (nm)	10^{20} σ (cm^2)	λ (nm)	10^{20} σ (cm^2)	λ (nm)	10^{20} σ (cm^2)
121.567	1270	173	6.94	184	0.349
163	42.2	174	5.48	185	0.257
164	38.2	175	4.24	186	0.187
165	32.8	176	3.32	187	0.138
166	27.3	177	2.56	188	0.102
167	23.7	178	1.93	189	0.0838
168	19.7	179	1.44	190	0.0653
169	16.2	180	1.10	195	*0.0145*
170	13.2	181	0.821	200	*0.00342*
171	10.8	182	0.617	205	*0.000809*
172	8.69	183	0.468	210	*0.000191*

Note:
121.567 nm: Salahub and Sandorfy[2]
163–190 nm: Orkin et al.[1] data at 1 nm intervals
195–210 nm: extrapolation of Orkin et al.[1] data, $\log \sigma(\lambda) = 2.5762 - 0.12521\ \lambda$

(1) Orkin, V. L.; Khamaganov, V. G.; Kurylo, M. J. High accuracy measurements of OH reaction rate constants and IR absorption spectra: Substituted 2-propanols. *J. Phys. Chem. A* **2012**, *116*, 6188-6198, doi:10.1021/jp211534n.

(2) Salahub, D. R.; Sandorfy, C. The far-ultraviolet spectra of some simple alcohols and fluoroalcohols. *Chem. Phys. Lett.* **1971**, *8*, 71-74, doi:10.1016/0009-2614(71)80578-X.

E36. $CF_3C(O)OH$ (trifluoroacetic acid)

Back to Index

$CF_3C(O)OH + h\nu \rightarrow CF_3CO + OH$ 463 kJ mol^{-1} 258 nm (1)

(Reccommendation: 06-2, Note: 15-10, Evaluated: 10-6)

Absorption Cross Sections: The UV absorption spectrum of trifluoroacetic acid, $CF_3C(O)OH$, was measured at room temperature over the wavelength range 200–280 nm by Rattigan et al.,[1] the only study available, using diode array spectroscopy. The spectrum exhibits an absorption band with a broad maximum near 220 nm. The absorption spectrum of $CF_3C(O)OH$ is red shifted from the $CH_3C(O)OH$ spectrum and has lower absorption cross sections. The recommended absorption cross sections in Table 4E-36 are from Rattigan et al.[1]

Photolysis Quantum Yield and Product Studies: No recommendation.

Table 4E-36. Recommended Absorption Cross Sections of $CF_3C(O)OH$ at 296 K

λ (nm)	10^{20} σ (cm^2)
200	5.20
205	6.48
210	7.23
215	7.59
220	7.76
225	7.21
230	6.03
235	4.46
240	2.89
245	1.69
250	0.870
255	0.390
260	0.155
265	0.050
270	0.013
275	0.006

Note:
Rattigan et al.[1]

(1) Rattigan, O. V.; Wild, O.; Jones, R. L.; Cox, R. A. Temperature-dependent absorption cross-sections of CF_3COCl, CF_3COF, CH_3COF, CCl_3CHO and CF_3COOH. *J. Photochem. Photobiol. A: Chem.* **1993**, *73*, 1-9, doi:10.1016/1010-6030(93)80026-6.

E37. $CH_3C(O)F$ (acetyl fluoride)

Back to Index

$CH_3C(O)F + h\nu \rightarrow CH_3 + FCO$	415 kJ mol^{-1}	288 nm	(1)
$\rightarrow CH_3F + CO$	92.7 kJ mol^{-1}	1292 nm	(2)

(Recommendation: 25-1, Note: 25-1, Evaluated: 25-1)

Absorption Cross Sections: The UV absorption spectrum of acetyl fluoride, $CH_3C(O)F$, has been measured at room temperature by Rattigan et al.[1] (200–310 nm), using diode array spectroscopy, and Song et al.[2] (201–260 nm) using a scanning spectrometer. There is reasonable agreement between the two studies near the peak of the spectrum, around 206 nm, but significant discrepancies in the long-wavelength limit of the Song et al. spectrum. The Rattigan et al. spectrum shows two absorption bands with a maximum cross section near 206 nm and a shoulder near 260 nm. The recommended absorption cross sections in Table 4E-37 are from Rattigan et al.[1]

Photolysis Quantum Yield and Product Studies: Song et al.[2] have reported a $CH_3C(O)F$ photolysis quantum yield of 0.62 for 248 nm photolysis in 655 mbar total pressure.

Table 4E-37. Recommended Absorption Cross Sections of $CH_3C(O)F$ at 296 K

λ (nm)	10^{20} σ (cm^2)
200	11.3
205	12.2
210	12.0
215	10.5
220	8.35
225	5.97
230	3.83
235	2.19
240	1.14
245	0.566
250	0.311
255	0.206
260	0.158
265	0.120
270	0.090
275	0.056
280	0.029
285	0.016
290	0.008
295	0.004
300	0.002
305	0.001

Note:
Rattigan et al.[1]

(1) Rattigan, O. V.; Wild, O.; Jones, R. L.; Cox, R. A. Temperature-dependent absorption cross-sections of CF_3COCl, CF_3COF, CH_3COF, CCl_3CHO and CF_3COOH. *J. Photochem. Photobiol. A: Chem.* **1993**, *73*, 1-9, doi:10.1016/1010-6030(93)80026-6.

(2) Song, X.; Zügner, G. L.; Farkas, M.; Illés, Á.; Sarzynski, D.; Rozgonyi, T.; Wang, B.; Dóbé, S. Experimental and theoretical study on the OH-reaction kinetics and photochemistry of acetyl fluoride (CH_3CO)F), an atmospheric degradation intermediate of HFC-161 (C_2H_5F). *J. Phys. Chem. A* **2015**, *119*, 7753-7786, doi:10.1021/acs.jpca.5b01069.

E38. CH_2=$CHCF_3$ (3,3,3-trifluoro-1-propene)

Back to Index

CH_2=$CHCF_3$ + hν → Products (1)

(Recommendation: 06-2, Note: 10-6, Evaluated: 10-6)

Absorption Cross Sections: The VUV/UV absorption spectrum of 3,3,3-trifluoro-1-propene, CH_2=$CHCF_3$, has been measured at room temperature over the wavelength range 164–205 nm by Orkin et al.,[1] the only study available. The recommended absorption cross sections in Table 4E-38 are from Orkin et al.[1]

Photolysis Quantum Yield and Product Studies: No recommendation.

Table 4E-38. Recommended Absorption Cross Sections of CH_2=$CHCF_3$ at 295 K

λ (nm)	10^{20} σ (cm^2)	λ (nm)	10^{20} σ (cm^2)	λ (nm)	10^{20} σ (cm^2)
164	3569	178	168	192	0.681
165	3377	179	114	193	0.453
166	3146	180	77.7	194	0.298
167	2874	181	53.9	195	0.204
168	2538	182	36.5	196	0.131
169	2184	183	25.0	197	0.0872
170	1814	184	16.8	198	0.0581
171	1481	185	11.3	199	0.0404
172	1165	186	7.74	200	0.0278
173	899	187	5.22	201	0.0185
174	660	188	3.49	202	0.0129
175	475	189	2.32	203	0.00945
176	340	190	1.52	204	0.00669
177	240	191	1.02	205	0.00456

Note:
Orkin et al.[1]

(1) Orkin, V. L.; Huie, R. E.; Kurylo, M. J. Rate constants for the reactions of OH with HFC-245cb ($CH_3CF_2CF_3$) and some fluoroalkenes (CH_2CHCF_3, CH_2CFCF_3, CF_2CFCF_3, and CF_2CF_2). *J. Phys. Chem. A* **1997**, *101*, 9118-9124, doi:10.1021/jp971994r.

E39. CH_2=$CFCF_3$ (2,3,3,3-tetrafluoropropene)

Back to Index

CH_2=$CFCF_3$ + hν → Products (1)

(Recommendation: 06-2, Note: 15-10, Evaluated: 10-6)

Absorption Cross Sections: The VUV/UV absorption spectrum of 2,3,3,3-tetrafluoropropene, CH_2=$CFCF_3$, has been measured at room temperature over the wavelength range 164–186 nm by Orkin et al.[1] and at 184.95 nm by Papadimitriou et al.,[2] $(3.25 \pm 0.10) \times 10^{-19}$ cm^2 $molecule^{-1}$. The recommended absorption cross sections in Table 4E-39 are taken from Orkin et al.[1]

Photolysis Quantum Yield and Product Studies: No recommendation.

Table 4E-39. Recommended Absorption Cross Sections of $CH_2=CFCF_3$ at 295 K

λ (nm)	10^{20} σ (cm^2)
164	3773
165	3732
166	3730
167	3695
168	3594
169	3418
170	3176
171	2877
172	2535
173	2178
174	1802
175	1445
176	1130
177	840
178	600
179	408
180	273
181	185
182	124
183	82.4
184	55.5
185	38.1
186	26.2

Note:
Orkin et al.[1]

(1) Orkin, V. L.; Huie, R. E.; Kurylo, M. J. Rate constants for the reactions of OH with HFC-245cb ($CH_3CF_2CF_3$) and some fluoroalkenes (CH_2CHCF_3, CH_2CFCF_3, CF_2CFCF_3, and CF_2CF_2). *J. Phys. Chem. A* **1997**, *101*, 9118-9124, doi:10.1021/jp971994r.

(2) Papadimitriou, V. C.; Talukdar, R. K.; Portmann, R. W.; Ravishankara, A. R.; Burkholder, J. B. $CF_3CF=CH_2$ and (*Z*)-$CF_3CF=CHF$: temperature dependent OH rate coefficients and global warming potentials. *Phys. Chem. Chem. Phys.* **2008**, *10*, 808-820, doi:10.1039/b714382f.

E40. $CF_2=CF_2$ (tetrafluoroethylene)

Back to Index

$CF_2=CF_2 + h\nu \rightarrow$ Products (1)

(Recommendation: 06-2, Note: 10-6, Evaluated: 10-6)

Absorption Cross Sections: The VUV/UV absorption spectrum of tetrafluoroethylene, $CF_2=CF_2$, has been measured at room temperature by Sharpe et al.[3] (185–209 nm), Orkin et al.[2] (164–220 nm), and Eden et al.[1] (113–330 nm). The spectrum shows a structured absorption band with five maxima between 170 and 200 nm (maximum near 188 nm). The spectra from Orkin et al.[2] and Eden et al.[1] agree to within 10% in the range 164–182 nm, 20% in the range 182–200 nm, and 10% in the range 203–205 nm. Above 195 nm, the absorption cross sections decrease monotonically toward longer wavelengths. The spectrum reported by Eden et al.[1] deviates from that of Orkin et al.[2] at wavelengths >200 nm, but the Eden et al. spectrum is very noisy in this region. The absorption spectrum reported by Sharpe et al.[3] is systematically shifted by 1 to 2 nm to shorter wavelengths relative to the Orkin et al.[2] spectrum. The recommended absorption cross sections given in Table 4E-40 are the mean of the data from Orkin et al.[2] and Eden et al.[1] for the region 164–205 nm and the data from Orkin et al.[2] in the region 206–220 nm.

Photolysis Quantum Yield and Product Studies: No recommendation.

Table 4E-40. Recommended Absorption Cross Sections of $CF_2=CF_2$ at 296 K

λ (nm)	10^{20} σ (cm^2)	λ (nm)	10^{20} σ (cm^2)	λ (nm)	10^{20} σ (cm^2)	λ (nm)	10^{20} σ (cm^2)
164	335	179	341	194	423	209	0.429
165	324	180	362	195	387	210	0.257
166	300	181	432	196	263	211	0.162
167	272	182	521	197	169	212	0.0998
168	243	183	559	198	108	213	0.0633
169	227	184	485	199	64.0	214	0.0392
170	238	185	442	200	39.9	215	0.0249
171	268	186	491	201	23.8	216	0.0160
172	286	187	596	202	14.5	217	0.0105
173	281	188	682	203	8.74	218	0.00668
174	289	189	671	204	5.73	219	0.00443
175	327	190	507	205	3.23	220	0.00288
176	372	191	417	206	1.99		
177	390	192	399	207	1.17		
178	376	193	410	208	0.713		

Note:
164–205 nm: mean of the data from Orkin et al.[2] and Eden et al.[1] (Note: the structure in the spectrum in this wavelength region is not accurately reproduced with the 1 nm resolution given in the table, see the original references.)
206–220 nm: data from Orkin et al.[2]

(1) Eden, S.; Limão-Vieira, P.; Kendall, P. A.; Mason, N. J.; Delwiche, J.; Hubin-Franskin, M.-J.; Tanaka, T.; Kitajima, M.; Tanaka, H.; Cho, H.; Hoffmann, S. V. Electronic excitation of tetrafluoroethylene, C_2F_4. *Chem. Phys.* **2004**, *297*, 257-269, doi:10.1016/j.chemphys.2003.10.031.

(2) Orkin, V. L.; Huie, R. E.; Kurylo, M. J. Rate constants for the reactions of OH with HFC-245cb ($CH_3CF_2CF_3$) and some fluoroalkenes (CH_2CHCF_3, CH_2CFCF_3, CF_2CFCF_3, and CF_2CF_2). *J. Phys. Chem. A* **1997**, *101*, 9118-9124, doi:10.1021/jp971994r.

(3) Sharpe, S.; Hartnett, B.; Sethi, H. S.; Sethi, D. S. Absorption cross-sections of CF_2 in the A $^1B_1$—X $^1A_1$ transition at 0.5 nm intervals and absolute rate constant for $2CF_2 \rightarrow C_2F_4$ at 298 ± 3 K. *J. Photochem.* **1987**, *38*, 1-13, doi:10.1016/0047-2670(87)87001-6.

E41. $CF_2=CFCF_3$ (hexafluoropropene)

Back to Index

$CF_2=CFCF_3 + h\nu \rightarrow$ Products (1)

(Recommendation: 06-2, Note: 10-6, Evaluated: 10-6)

Absorption Cross Sections: The VUV/UV absorption spectrum of hexafluoropropene, $CF_2=CFCF_3$, was measured at room temperature by Sharpe et al.[3] (185–209 nm), Orkin et al.[2] (164–222 nm), and Eden et al.[1] (115–330 nm). The spectrum has overlapping absorption bands between 140 and 220 nm with maxima at 155 and 158.5 nm ($\sigma \approx 3 \times 10^{-17}$ cm^2 $molecule^{-1}$), 166, and 180 nm. In the wavelength region 164–200 nm, the cross sections from Orkin et al.[2] and Eden et al.[1] agree to within 15%. In the region 185–200 nm, the cross sections from Orkin et al.,[2] Eden et al.,[1] and Sharpe et al.[3] agree to within 25%. Above 195 nm, the absorption cross sections decrease toward longer wavelengths. The spectrum reported by Eden et al.[1] deviates from that of Orkin et al.[2] at wavelengths >200 nm, but the Eden et al. spectrum is very noisy in this region. The recommended absorption cross sections given in Table 4E-41 are the mean of the data from Orkin et al.[2] and Eden et al.[1] for the region 164–199 nm and the data from Orkin et al.[2] in the region 200–222 nm.

Photolysis Quantum Yield and Product Studies: No recommendation.

Table 4E-41. Recommended Absorption Cross Sections of CF_2=$CFCF_3$ at 296 K

λ (nm)	10^{20} σ (cm^2)	λ (nm)	10^{20} σ (cm^2)	λ (nm)	10^{20} σ (cm^2)	λ (nm)	10^{20} σ (cm^2)
164	2290	179	929	194	97.8	209	0.585
165	2210	180	912	195	73.3	210	0.396
166	2130	181	880	196	54.7	211	0.269
167	2040	182	835	197	40.4	212	0.184
168	1920	183	779	198	29.7	213	0.125
169	1760	184	708	199	22.3	214	0.0838
170	1570	185	629	200	16.2	215	0.0564
171	1380	186	550	201	11.6	216	0.0381
172	1210	187	472	202	8.17	217	0.0261
173	1080	188	391	203	5.70	218	0.0177
174	995	189	321	204	3.95	219	0.0119
175	946	190	259	205	2.70	220	0.00795
176	930	191	207	206	1.85	221	0.00533
177	928	192	163	207	1.28	222	0.00354
178	931	193	127	208	0.866		

Note:
164–199 nm: mean of the data of Orkin et al.[2] and Eden et al.[1]
200–222 nm: data of Orkin et al.[2]

(1) Eden, S.; Limão-Vieira, P.; Hoffmann, S. V.; Mason, N. J. VUV photoabsorption by hexafluoropropene. *Chem. Phys. Lett.* **2003**, *379*, 170-176, doi:10.1016/j.cplett.2003.08.029.

(2) Orkin, V. L.; Huie, R. E.; Kurylo, M. J. Rate constants for the reactions of OH with HFC-245cb ($CH_3CF_2CF_3$) and some fluoroalkenes (CH_2CHCF_3, CH_2CFCF_3, CF_2CFCF_3, and CF_2CF_2). *J. Phys. Chem. A* **1997**, *101*, 9118-9124, doi:10.1021/jp971994r.

(3) Sharpe, S.; Hartnett, B.; Sethi, H. S.; Sethi, D. S. Absorption cross-sections of CF_2 in the A $^1B_1$—X $^1A_1$ transition at 0.5 nm intervals and absolute rate constant for $2CF_2 \rightarrow C_2F_4$ at 298 ± 3 K. *J. Photochem.* **1987**, *38*, 1-13, doi:10.1016/0047-2670(87)87001-6.

E42. NF_3 (nitrogen trifluoride)

Back to Index

$NF_3 + h\nu \rightarrow$ Products (1)

(Recommendation: 15-10; Note: 15-10; Evaluated: 15-10)

Absorption Cross Sections: The UV absorption spectrum of nitrogen trifluoride, NF_3, has been measured at room temperature by Makeev et al.[4] (210–240 nm), Molina et al.[5] (180–250 nm), and Dillon et al.[1] (184–226 nm), and as a function of temperature by Papadimitriou et al.[6] (184.95–250 nm, 212–296 K). The room temperature spectra reported by Molina et al., Dillon et al., and Papadimitriou et al. are in good agreement over the common wavelength regions. The data from Makeev et al. are significantly greater than the other studies and are not considered in the recommendation. The room temperature spectrum from the Papadimitriou et al. study is given in Table 4E-42-1.

Table 4E-42-1. Recommended Absorption Cross Sections of NF_3 at 296 K

λ (nm)	10^{20} σ (cm^2)
184.95	3.44
190	1.16
195	0.393
200	0.132
205	0.0454
210	0.0168
215	0.00698
220	0.00335
225	0.00154
230	0.000801
235	0.000485
240	0.000287
250	0.000111

Note:
184.95–250 nm: Papadimitriou et al.[6]

Papadimitriou et al. measured the spectrum temperature dependence over the range 212–296 K. They observed a systematic decrease in absorption cross section with decreasing temperature at all wavelengths included in their study. The absorption spectrum was parameterized using the empirical formula:

$$\log_{10}\big(\sigma(\lambda,T)\big) = \sum_i A_i\lambda^i + (296 - \mathrm{T})\sum_i B_i\lambda^i$$

and the parameters are given in Table 4E-42-2. The parameterization is recommended here. The parameterization reproduces the Molina et al. and Dillon et al. datasets to better than ~10% at all wavelengths. An uncertainty factor of 1.1 (2σ) for the room temperature absorption spectrum is assigned, which encompasses the range of the available experimental data.

Table 4E-42-2. Recommended NF_3 UV Absorption Spectrum, σ(λ,T), Parameterization

I	A_i	B_i
0	-218.67	0.9261
1	4.03743	-0.0130187
2	-0.0295605	6.096×10^{-5}
3	9.596×10^{-5}	-9.75×10^{-8}
4	-1.3171×10^{-7}	9.76×10^{-12}
5	4.929×10^{-11}	–

Note:
Papadimitriou et al.[6]

NF_3 VUV absorption cross sections have been measured in the 126.6–178.6 nm wavelength region by La Paglia and Duncan[3] and at 147 nm by Inel.[2] The absorption cross section value reported by Inel is approximately a factor of 2 greater than that reported by La Paglia and Duncan. A recommended Lyman-α cross section of 4.8×10^{-18} cm^2 $molecule^{-1}$ was obtained from an extrapolation of the La Paglia and Duncan data. An uncertainty factor of 1.5 (2σ) is recommended, based primarily on the fact that there are no direct measurements at Lyman-α.

Photolysis Quantum Yield and Product Studies: Dillon et al.[1] measured the F atom quantum yield in the 193 nm photolysis of NF_3 to be 1.03 ± 0.05. A unit photolysis quantum yield for the loss of NF_3 is recommended over the wavelength range most critical for its atmospheric photolysis, i.e., 190–230 nm.

(1) Dillon, T. J.; Horowitz, A.; Crowley, J. N. Cross-sections and quantum yields for the atmospheric photolysis of the potent greenhouse gas nitrogen trifluoride. *Atmos. Environ.* **2010**, *44*, 1186-1191, doi:10.1016/j.atmosenv.2009.12.026.

(2) Inel, Y. Absorption coefficient determination of nitrogen trifluoride at 147 nm. *J. Photochem. Photobiol. A: Chem.* **1993**, *70*, 1-3, doi:10.1016/1010-6030(93)80001-P.

(3) La Paglia, S. R.; Duncan, A. B. F. Vacuum ultraviolet absorption spectrum and dipole moment of nitrogen trifluoride. *J. Chem. Phys.* **1961**, *34*, 1003-1007, doi:10.1063/1.1731623.
(4) Makeev, G. N.; Sinyanskii, V. F.; Smirnov, B. M. Absorption spectra of certain fluorides in the near ultraviolet region. *Doklady Phys. Chem.* **1975**, *222*, 452-455.
(5) Molina, L. T.; Wooldridge, P. J.; Molina, M. J. Atmospheric reactions and ultraviolet and infrared absorptivities of nitrogen trifluoride. *Geophys. Res. Lett.* **1995**, *22*, 1873-1876, doi:10.1029/95GL01669.
(6) Papadimitriou, V. C.; McGillen, M. R.; Fleming, E. L.; Jackman, C. H.; Burkholder, J. B. NF_3: UV absorption spectrum temperature dependence and the atmospheric climate forcing implications. *Geophys. Res. Lett.* **2013**, *40*, 440-445, doi:10.1002/grl.50120.

4.8 Bibliography – FO_x Photochemistry

Antiñolo, M.; Jiménez, E.; Albaladejo, J. UV absorption cross sections between 230 and 350 nm and pressure dependence of the photolysis quantum yield at 308 nm of CF_3CH_2CHO. *Phys. Chem. Chem. Phys.* **2011**, *13*, 15936-15946, doi:10.1039/c1cp21368g.

Au, J. W.; Burton, G. R.; Brion, C. E. Quantitative spectroscopic studies of the valence-shell electronic excitations of Freons ($CFCl_3$, CF_2Cl_2, CF_3Cl, and CF_4) in the VUV and soft X-ray regions. *Chem. Phys.* **1997**, *221*, 151-168, doi:10.1016/S0301-0104(97)00146-8.

Balfour, W. J. The electronic spectra of the oxalyl halides. McMaster University. **1967**.

Bierbrauer, K. L.; Chiappero, M. S.; Malanca, F. E.; Arguello, G. A. Photochemistry of perfluoroacetyl fluoride kinetics of the reaction between CF_3 and FCO radicals. *J. Photochem. Photobiol. A: Chem.* **1999**, *122*, 73-78, doi:10.1016/S1010-6030(98)00431-6.

Borkowski, R. P.; Ausloos, P. The vapor phase fluorescence and its relationship to the photolysis of propionaldehyde and the butyraldehydes. *J. Am. Chem. Soc.* **1962**, *84*, 4044-4048, doi:10.1021/ja00880a014.

Brodersen, P. H.; Frisch, P.; Schumacher, H.-J. Das absorptionsspektrum des F_2O_2. *Z. Phys. Chem. B* **1937**, *37*, 25-29.

Burley, J. D.; Miller, C. E.; Johnston, H. S. Spectroscopy and photoabsorption cross-sections of FNO. *J. Mol. Spectrosc.* **1993**, *158*, 377-391, doi:10.1006/jmsp.1993.1082.

Carnovale, F.; Tseng, R.; Brion, C. E. Absolute oscillator strengths for the photoabsorption and partial photoionisation of hydrogen fluoride. *J. Phys. B: At. Mol. Phys.* **1981**, *14*, 4771-4785, doi:10.1088/0022-3700/14/24/013.

Chegodaev, P. P.; Tubikov, B. I. *Dokl. Akad. Nauk. SSSR* **1973**, *210*, 647-649.

Chiappero, M. S.; Malanca, F. E.; Argüello, G. A.; Wooldridge, S. T.; Hurley, M. D.; Ball, J. C.; Wallington, T. J.; Waterland, R. L.; Buck, R. C. Atmospheric chemistry of perfluoroaldehydes ($C_xF_{2x+1}CHO$) and fluorotelomer aldehydes ($C_xF_{2x+1}CH_2CHO$): Quantification of the important role of photolysis. *J. Phys. Chem. A* **2006**, *110*, 11944-11953, doi:10.1021/jp064262k.

Chim, R. Y. L.; Kennedy, R. A.; Tuckett, R. P. The vacuum-UV absorption spectrum of SF_5CF_3; implications for its lifetime in the earth's atmosphere. *Chem. Phys. Lett.* **2003**, *367*, 697-703, doi:10.1016/S0009-2614(02)01763-3.

Chou, C. C.; Crescentini, G.; Vera-Ruiz, H.; Smith, W. S.; Rowland, F. S. "Stratospheric photochemistry of CF_2O, CClFO, and CCl_2O"; 173rd American Chemical Society Meeting, 1977, New Orleans, LA.

Cobos, C. J.; Croce, A. E.; Castellano, E. Kinetics of the recombination reaction between F atoms and FCO radicals. *Chem. Phys. Lett.* **1995**, *239*, 320-325, doi:10.1016/0009-2614(95)00483-K.

Cole, B. E.; Dexter, R. N. Photoabsorption cross sections for chlorinated methanes and ethanes between 46 and 100 Å. *J. Quant. Spectrosc. Radiat. Transf.* **1978**, *19*, 303-309, doi:10.1016/0022-4073(78)90063-8.

Cook, G. R.; Ching, B. K. Photoionization and absorption cross sections and fluorescence of CF_4. *J. Chem. Phys.* **1965**, *43*, 1794-1797, doi:10.1063/1.1697011.

Dillon, T. J.; Horowitz, A.; Crowley, J. N. Cross-sections and quantum yields for the atmospheric photolysis of the potent greenhouse gas nitrogen trifluoride. *Atmos. Environ.* **2010**, *44*, 1186-1191, doi:10.1016/j.atmosenv.2009.12.026.

Dodd, R. E.; Watson-Smith, J. The photolysis of trifluoroacetaldehyde. *J. Chem. Soc.* **1957**, 1465-1473, doi:10.1039/jr9570001465.

Eden, S.; Limão-Vieira, P.; Hoffmann, S. V.; Mason, N. J. VUV photoabsorption by hexafluoropropene. *Chem. Phys. Lett.* **2003**, *379*, 170-176, doi:10.1016/j.cplett.2003.08.029.

Eden, S.; Limão-Vieira, P.; Kendall, P. A.; Mason, N. J.; Delwiche, J.; Hubin-Franskin, M.-J.; Tanaka, T.; Kitajima, M.; Tanaka, H.; Cho, H.; Hoffmann, S. V. Electronic excitation of tetrafluoroethylene, C_2F_4. *Chem. Phys.* **2004**, *297*, 257-269, doi:10.1016/j.chemphys.2003.10.031.

Ellermann, T.; Sehested, J.; Nielson, O. J.; Pagsberg, P.; Wallington, T. J. Kinetics of the reaction of F atoms with O_2 and UV spectrum of FO_2 radicals in the gas phase at 295 K. *Chem. Phys. Lett.* **1994**, *218*, 287-294, doi:10.1016/0009-2614(94)00006-9.

Francisco, J. S.; Williams, I. H. Infrared and ultraviolet spectroscopic characterization of trifluoroacetaldehyde. *Mol. Phys.* **1992**, *76*, 1433-1441, doi:10.1080/00268979200102201.

Giddings, L. E., Jr.; Innes, K. K. The near ultraviolet spectra of HCOF and DCOF. *J. Mol. Spectrosc.* **1961**, *6*, 528-549, doi:10.1016/0022-2852(61)90278-8.

Glissmann, A.; Schumacher, H.-J. Das spektrum des fluoroxyds F_2O. *Z. Phys. Chem. B* **1934**, *24*, 328-334.

Hashikawa, Y.; Kawasaki, M.; Waterland, R. L.; Hurley, M. D.; Ball, J. C.; Wallington, T. J.; Andersen, M. P. S.; Nielsen, O. J. Gas phase UV and IR absorption spectra of $C_xF_{2x+1}CHO$ (x = 1-4). *J. Fluor. Chem.* **2004**, *125*, 1925-1932, doi:10.1016/j.jfluchem.2004.07.006.

Hatherly, P. A.; Flaxman, A. J. On the absolute absorption cross-section of SF_5CF_3. *Chem. Phys. Lett.* **2003**, *380*, 512-515, doi:10.1016/j.cplett.2003.09.061.
Hitchcock, A. P.; Williams, G. R. J.; Brion, C. E.; Langhoff, P. W. Experimental and theoretical studies of the valence-shell dipole excitation spectrum and absolute photoabsorption cross section of hydrogen fluoride. *Chem. Phys.* **1984**, *88*, 65-80, doi:10.1016/0301-0104(84)85104-6.
Inel, Y. Absorption coefficient determination of nitrogen trifluoride at 147 nm. *J. Photochem. Photobiol. A: Chem.* **1993**, *70*, 1-3, doi:10.1016/1010-6030(93)80001-P.
Inn, E. C. Y. Absorption cross section of CF_4 at H Lyman α (121.57 nm). *J. Geophys. Res.* **1980**, *85*, 7493-7494, doi:10.1029/JC085iC12p07493.
Johnston, H. S.; Bertin, H. J., Jr. Absorption and emission spectra of nitrosyl fluoride. *J. Mol. Spectrosc.* **1959**, *3*, 683-696, doi:10.1016/0022-2852(59)90061-X.
Kirshenbaum, A. D.; Streng, A. G. Molar extinction coefficients of liquid O_3F_2, O_2F_2, and O_3 in the visible range. *J. Chem. Phys.* **1961**, *35*, 1440-1442, doi:10.1063/1.1732063.
Kopitzky, R.; Beuleke, M.; Balzer, G.; Willner, H. Properties of trifluoroacetyl peroxynitrate, $CF_3C(O)OONO_2$. *Inorg. Chem.* **1997**, *36*, 1994-1997, doi:10.1021/ic9612109.
Kopitzky, R.; Willner, H.; Mack, H.-G.; Pfeiffer, A.; Oberhammer, H. IR and UV absorption cross sections, vibrational analysis, and the molecular structure of trifluoromethyl peroxynitrate, CF_3OONO_2. *Inorg. Chem.* **1998**, *37*, 6208-6213, doi:10.1021/ic980776p.
La Paglia, S. R.; Duncan, A. B. F. Vacuum ultraviolet absorption spectrum and dipole moment of nitrogen trifluoride. *J. Chem. Phys.* **1961**, *34*, 1003-1007, doi:10.1063/1.1731623.
Lee, L. C.; Phillips, E.; Judge, D. L. Photoabsorption cross sections of CH_4, CF_4, CF_3Cl, SF_6, and C_2F_6 from 175 to 770 Å. *J. Chem. Phys.* **1977**, *67*, 1237-1246, doi:10.1063/1.434935.
Lee, L. C.; Wang, X.; Suto, M. Fluorescence from extreme ultraviolet photoexcitation of CF_4. *J. Chem. Phys.* **1986**, *85*, 6294-6300, doi:10.1063/1.451459.
Libuda, H. G.; Zabel, F. UV absorption cross sections of acetyl peroxynitrate and trifluoroacetyl peroxynitrate at 298 K. *Ber. Bunsenges. Phys. Chem.* **1995**, *99*, 1205-1213, doi:10.1002/bbpc.199500061.
Limão-Vieira, P.; Vasekova, E.; Giuliani, A.; Lourenço, J. M. C.; Santos, P. M.; Duflot, D.; Hoffmann, S. V.; Mason, N. J.; Delwiche, J.; Hubin-Franskin, M.-J. Perfluorocyclobutane electronic state spectroscopy by high-resolution vacuum ultraviolet photoabsorption, electron impact, He I photoelectron spectroscopy, and *ab initio* calculations. *Phys. Rev. A* **2007**, *76*, 032509, doi:10.1103/PhysRevA.76.032509.
Lucazeau, G.; Sandorfy, C. On the far-ultraviolet spectra of some simple aldehydes. *J. Mol. Spectrosc.* **1970**, *35*, 214-231, doi:10.1016/0022-2852(70)90199-2.
Lyman, J.; Holland, R. Oxygen fluoride chemical kinetics. *J. Phys. Chem.* **1988**, *92*, 7232-7241, doi:10.1021/j100337a015.
Makeev, G. N.; Sinyanskii, V. F.; Smirnov, B. M. Absorption spectra of certain fluorides in the near ultraviolet region. *Doklady Phys. Chem.* **1975**, *222*, 452-455.
Malanca, F. E.; Chiappero, M. S.; Argüello, G. A.; Wallington, T. J. Trifluoro methyl peroxynitrate (CF_3OONO_2): Temperature dependence of the UV absorption spectrum and atmospheric implications. *Atmos. Environ.* **2005**, *39*, 5051-5057, doi:10.1016/j.atmosenv.2005.05.026.
Maricq, M. M.; Szente, J. J. Flash photolysis-time-resolved UV absorption study of the reactions $CF_3H + F \rightarrow CF_3 + HF$ and $CF_3O_2 + CF_2O_2 \rightarrow$ products. *J. Phys. Chem.* **1992**, *96*, 4925-4930, doi:10.1021/j100191a037.
Maricq, M. M.; Szente, J. J. The 193 and 248 nm photodissociation of $CF_3C(O)Cl$. *J. Phys. Chem.* **1995**, *99*, 4554-4557, doi:10.1021/j100013a028.
Matchuk, N. M.; Tupikov, V. I.; Malkova, A. I.; Pshezhetskii, S. Y. *Opt. Spektrosk. (Opt. Spectrosc.)* **1976**, *40*, 14-18 (17-19).
McGillen, M. R.; Papadimitriou, V. C.; Smith, S. C.; Burkholder, J. B. FC(O)C(O)F, $FC(O)CF_2C(O)F$, and $FC(O)CF_2CF_2C(O)F$: Ultraviolet and infrared absorption spectra and 248 nm photolysis products. *J. Phys. Chem. A* **2020**, *124*, 7123-7133, doi:10.1021/acs.jpca.0c04607.
Meller, R., personal communication to NASA Data Panel.
Meller, R.; Boglu, D.; Moortgat, G. K. "UV spectra of several halogenated carbonyl compounds and FTIR studies of the degradation of CF_3COCl, HCFC-123 and HFC-143a"; Kinetics and Mechanisms for the Reactions of Halogenated Organic Compounds in the Troposphere. STEP-HALOCSIDE/AFEAS WORKSHOP, 1991, Dublin, Ireland.
Meller, R.; Moortgat, G. K. Photolysis of $CF_3O_2CF_3$ in the presence of O_3 in oxygen: kinetic study of the reactions of CF_3O and CF_3O_2 radicals with O_3. *J. Photochem. Photobio. A: Chem.* **1995**, *86*, 15-25, doi:10.1016/1010-6030(94)03951-P.
Meller, R.; Moortgat, G. K. $CF_3C(O)Cl$: Temperature-dependent (223-298 K) absorption cross-sections and quantum yields at 254 nm. *J. Photochem. Photobiol. A: Chem.* **1997**, *108*, 105-116, doi:10.1016/S1010-6030(97)00094-4.

Molina, L. T.; Molina, M. J. "Chemistry of fluorine in the stratosphere"; 182nd American Chemical Society Meeting, 1982, New York.
Molina, L. T.; Molina, M. J. Ultraviolet spectrum of CF_3OH: Upper limits to the absorption cross sections. *Geophys. Res. Lett.* **1996**, *23*, 563-565, doi:10.1029/96GL00313.
Molina, L. T.; Wooldridge, P. J.; Molina, M. J. Atmospheric reactions and ultraviolet and infrared absorptivities of nitrogen trifluoride. *Geophys. Res. Lett.* **1995**, *22*, 1873-1876, doi:10.1029/95GL01669.
Nee, J. B.; Suto, M.; Lee, L. C. Photoabsorption cross section of HF at 107-145 nm. *J. Phys. B: At. Mol. Phys.* **1985**, *18*, L293-L294, doi:10.1088/0022-3700/18/10/006.
Nielsen, O. J.; Ellermann, T.; Sehested, J.; Bartkiewicz, E.; Wallington, T. J.; Hurley, M. D. UV absorption spectra, kinetics, and mechanisms of the self reaction of CF_3O_2 in the gas phase at 298 K. *Int. J. Chem. Kinet.* **1992**, *24*, 1009-1021, doi:10.1002/kin.550241111.
Nölle, A.; Heydtmann, H.; Meller, R.; Schneider, W.; Moortgat, G. K. UV absorption spectrum and absorption cross sections of COF_2 at 296 K in the range 200-230 nm. *Geophys. Res. Lett.* **1992**, *19*, 281-284, doi:10.1029/91GL02316.
Nölle, A.; Krumscheid, C.; Heydtmann, H. Determination of quantum yields in the UV photolysis of COF_2 and COFCl. *Chem. Phys. Lett.* **1999**, *299*, 561-565, doi:10.1016/S0009-2614(98)01257-3.
Orkin, V. L.; Huie, R. E.; Kurylo, M. J. Rate constants for the reactions of OH with HFC-245cb ($CH_3CF_2CF_3$) and some fluoroalkenes (CH_2CHCF_3, CH_2CFCF_3, CF_2CFCF_3, and CF_2CF_2). *J. Phys. Chem. A* **1997**, *101*, 9118-9124, doi:10.1021/jp971994r.
Orkin, V. L.; Khamaganov, V. G.; Kurylo, M. J. High accuracy measurements of OH reaction rate constants and IR absorption spectra: Substituted 2-propanols. *J. Phys. Chem. A* **2012**, *116*, 6188-6198, doi:10.1021/jp211534n.
Orkin, V. L.; Khamaganov, V. G.; Martynova, L. E.; Kurylo, M. J. High-accuracy measurements of $OH^{\bullet}$ reaction rate constants and IR and UV absorption spectra: Ethanol and partially fluorinated ethyl alcohols. *J. Phys. Chem. A* **2011**, *115*, 8656-8668, doi:10.1021/jp202099t.
Pagsberg, P.; Ratajczak, E.; Sillesen, A.; Jodkowski, J. T. Spectrokinetic studies of the gas-phase equilibrium $F + O_2 \rightleftharpoons FO_2$ between 295 and 359 K. *Chem. Phys. Lett.* **1987**, *141*, 88-94, doi:10.1016/0009-2614(87)80097-0.
Pagsberg, P.; Sillesen, A.; Jodkowski, J. T.; Ratajczak, E. Kinetics of the reaction $F + NO + M \rightarrow FNO + M$ studied by pulse radiolysis combined with time-resolved IR and UV spectroscopy. *Chem. Phys. Lett.* **1996**, *249*, 358-364, doi:10.1016/0009-2614(95)01441-1.
Papadimitriou, V. C.; McGillen, M. R.; Fleming, E. L.; Jackman, C. H.; Burkholder, J. B. NF_3: UV absorption spectrum temperature dependence and the atmospheric climate forcing implications. *Geophys. Res. Lett.* **2013**, *40*, 440-445, doi:10.1002/grl.50120.
Papadimitriou, V. C.; Talukdar, R. K.; Portmann, R. W.; Ravishankara, A. R.; Burkholder, J. B. $CF_3CF=CH_2$ and (*Z*)-$CF_3CF=CHF$: temperature dependent OH rate coefficients and global warming potentials. *Phys. Chem. Chem. Phys.* **2008**, *10*, 808-820, doi:10.1039/b714382f.
Pearce, C.; Whytock, D. A. Photolysis of trifluoroacetaldehyde at 313 nm *J. Chem. Soc. D: Chem. Commun.* **1971**, 1464-1466, doi:10.1039/c29710001464.
Rajakumar, B.; Burkholder, J. B.; Portmann, R. W.; Ravishankara, A. R. Rate coefficients for the OH + CFH_2CH_2OH reaction between 238 and 355 K. *Phys. Chem. Chem. Phys.* **2005**, *7*, 2498-2505, doi:10.1039/b503332b.
Rattigan, O. V.; Rowley, D. M.; Wild, O.; Jones, R. L.; Cox, R. A. Mechanism of atmospheric oxidation of 1,1,1,2-tetrafluoroethane (HFC 134a). *J. Chem. Soc. Faraday Trans.* **1994**, *90*, 1819-1829, doi:10.1039/ft9949001819.
Rattigan, O. V.; Wild, O.; Jones, R. L.; Cox, R. A. Temperature-dependent absorption cross-sections of CF_3COCl, CF_3COF, CH_3COF, CCl_3CHO and CF_3COOH. *J. Photochem. Photobiol. A: Chem.* **1993**, *73*, 1-9, doi:10.1016/1010-6030(93)80026-6.
Ravishankara, A. R.; Solomon, S.; Turnipseed, A. A.; Warren, R. F. Atmospheric lifetimes of long-lived halogenated species. *Science* **1993**, *259*, 194-199, doi:10.1126/science.259.5092.194.
Rebbert, R. E.; Ausloos, P. Ionization quantum yields and absorption coefficients of selected compounds at 58.4 and 73.6-74.4 nm. *J. Res. Natl. Bur. Stand.* **1971**, *A 75*, 481-485, doi:10.6028/jres.075A.038.
Richer, H. R.; Sodeau, J. R.; Barnes, I. *STEP-HALOCSIDE/AFEAS Workshop, Dublin, 23-25 March* **1993**, 180-188.
Röth, E. P.; Ruhnke, R.; Moortgat, G.; Meller, R.; Schneider, W. UV/VIS-Absorption Cross Sections and Quantum Yields for Use in Photochemistry and Atmospheric Modeling, Forschungszentrum Jülich Publication, Part 1 : Inorganic Substances (jül-3340), Part 2: Organic Substances (jül-3341). **1997**.
Safary, E. Contribution a l'étude spectrale de l'acide fluorhydrique. *Ann. Phys. (Paris)* **1954**, *9*, 203-254.
Safary, E.; Romand, J.; Vodar, B. Ultraviolet absorption spectrum of gaseous hydrogen fluoride. *J. Chem. Phys.* **1951**, *19*, 379-380, doi:10.1063/1.1748216.

Salahub, D. R.; Sandorfy, C. The far-ultraviolet spectra of some simple alcohols and fluoroalcohols. *Chem. Phys. Lett.* **1971**, *8*, 71-74, doi:10.1016/0009-2614(71)80578-X.

Sauvageau, P.; Doucet, J.; Gilbert, R.; Sandorfy, C. Vacuum ultraviolet and photoelectron spectra of fluoroethanes. *J. Chem. Phys.* **1974**, *61*, 391-395, doi:10.1063/1.1681649.

Sauvageau, P.; Gilbert, R.; Berlow, P. P.; Sandorfy, C. Vacuum ultraviolet absorption spectra of fluoromethanes. *J. Chem. Phys.* **1973**, *59*, 762-765, doi:10.1063/1.1680086.

Schneider, W. F.; Wallington, T. J.; Minschwaner, K.; Stahlberg, E. A. Atmospheric chemistry of CF_3OH: Is photolysis important? *Environ. Sci. Technol.* **1995**, *29*, 247-250, doi:10.1021/es00001a031.

Seccombe, D. P.; Chim, R. Y. L.; Tuckett, R. P.; Jochims, H. W.; Baumgärtel, H. Vacuum–ultraviolet absorption and fluorescence spectroscopy of CF_2H_2, CF_2Cl_2, and CF_2Br_2 in the range 8–22 eV. *J. Chem. Phys.* **2001**, *114*, 4058-4073, doi:10.1063/1.1344888.

Sellevåg, S. R.; Kelly, T.; Sidebottom, H.; Nielsen, C. J. A study of the IR and UV-Vis absorption cross sections, photolysis and OH-initiated oxidation of CF_3CHO and CF_3CH_2CHO. *Phys. Chem. Chem. Phys.* **2004**, *6*, 1243-1252, doi:10.1039/b315941h.

Sharpe, S.; Hartnett, B.; Sethi, H. S.; Sethi, D. S. Absorption cross-sections of CF_2 in the A $^1B_1$—X $^1A_1$ transition at 0.5 nm intervals and absolute rate constant for $2CF_2 \rightarrow C_2F_4$ at 298 ± 3 K. *J. Photochem.* **1987**, *38*, 1-13, doi:10.1016/0047-2670(87)87001-6.

Song, X.; Zügner, G. L.; Farkas, M.; Illés, Á.; Sarzynski, D.; Rozgonyi, T.; Wang, B.; Dóbé, S. Experimental and theoretical study on the OH-reaction kinetics and photochemistry of acetyl fluoride (CH_3CO)F), an atmospheric degradation intermediate of HFC-161 (C_2H_5F). *J. Phys. Chem. A* **2015**, *119*, 7753-7786, doi:10.1021/acs.jpca.5b01069.

Suto, M.; Lee, L. C. Emission spectra of CF_3 radicals. V. Photodissociation of CF_3H, CF_3Cl, and CF_3Br by vacuum ultraviolet. *J. Chem. Phys.* **1983**, *79*, 1127-1133, doi:10.1063/1.445914.

Wayne, R. P.; Poulet, G.; Biggs, P.; Burrows, J. P.; Cox, R. A.; Crutzen, P. J.; Hayman, G. D.; Jenkin, M. E.; Le Bras, G.; Moorgat, G. K.; Platt, U.; Schindler, R. N. Halogen oxides: Radicals, sources and reservoirs in the laboratory and in the atmosphere. *Atmos. Environ.* **1995**, *29*, 2677-2881, doi:10.1016/1352-2310(95)98124-Q.

Weibel, D. E.; Argüello, G. A.; de Staricco, E. R.; Staricco, E. H. Quantum yield in the gas phase photolysis of perfluoroacetyl chloride: a comparison with related compounds. *J. Photochem. Photobiol. A: Chem.* **1995**, *86*, 27-31, doi:10.1016/1010-6030(94)03920-P.

Zhang, W.; Cooper, G.; Ibuki, T.; Brion, C. E. Excitation and ionization of freon molecules. I. Absolute oscillator-strengths for the photoabsorption (12-740 eV) and the ionic photofragmentation (15-80 eV) of CF_4. *Chem. Phys.* **1989**, *137*, 391-405, doi:10.1016/0301-0104(89)87122-8.

SECTION 4F. ClO_x PHOTOCHEMISTRY

F1. Cl_2 (molecular chlorine)

Back to Index

$Cl_2 + h\nu$	$\rightarrow Cl(^2P_{3/2}) + Cl(^2P_{3/2})$	243 kJ mol^{-1}	493 nm	(1)
	$\rightarrow Cl(^2P_{3/2}) + Cl(^2P_{1/2})$	253 kJ mol^{-1}	473 nm	(2)

(Recommendation: 25-1, Note: 25-1, Evaluated: 25-1)

Absorption Cross Sections: The recommended absorption cross sections of Cl_2, molecular chlorine, in the range 260–500 nm are taken from the work of Maric et al.,[11] who studied the absorption spectrum in the range 200–550 nm using a spectral resolution of 0.2 nm at 298 K. These authors also measured banded features in the range 476–496 nm at 0.04 nm resolution. The absorption cross sections can be calculated in the range 250–550 nm at various temperatures with the expression derived from their study and previous investigations:

$$\sigma = 10^{-20}\alpha^{0.5}\left\{27.3\exp\left(-99.0\alpha\left(\ln\left(\frac{329.5}{\lambda}\right)\right)^2\right) + 0.932\exp\left(-91.5\alpha\left(\ln\left(\frac{406.5}{\lambda}\right)\right)^2\right)\right\}$$

where $\alpha = \tanh(402.7/T)$; λ in nm, $250 < \lambda < 550$ nm, and T in K; $300\ K > T > 195\ K$. Cross sections calculated at 298 K for 260–500 nm are given in Table 4F-1. Ganske et al.[8] have also measured the cross sections at room temperature and the agreement with the recommended values is excellent. These two sets of data also agree well with earlier recommendations, which were based on the work of Seery and Britton,[14] which is in turn in good agreement with the results reported by Gibson and Bayliss,[9] Fergusson et al.,[7] and Burkholder and Bair.[1] At wavelengths >250 nm, the absorption cross sections measured at room temperature by Hubinger and Nee[10] are in excellent agreement with the values of Maric et al.[11] However, in the range 200–250 nm the cross sections deviate considerably between these groups. Room temperature cross sections have also been obtained by Roxlo and Mandl[13] for the range 170–214 nm. The absorption cross sections reported by Chen and Zhu[3,4] and Chen et al.[5] for the 300–420 nm region at 5 and 10 nm intervals deviate by up to ~30% from those reported by Maric et al.[11] Room temperature cross sections reported by Tellinghuisen[15] (200–600 nm) agree with the recommended values between 260 and 450 nm. Young et al.[16] have reported cross section data in the 509–570 nm region at 197, 233, 273, and 298 K, where the spectrum consists of weak diffuse bands. The Young et al. and Maric et al. experimental measurements at 298 K are in rough agreement between 509 and 550 nm. The Young et al. 298 K cross section data is recommended and included in Table 4F-1.

Photolysis Quantum Yield and Product Studies: The estimated atmospheric photodissociation rate is only weakly affected by the temperature dependence of the spectrum. Chininin[6] measured an upper limit of 5% for the branching ratio for excited atomic $Cl^*(^2P_{1/2})$ at 351 nm in agreement with earlier studies by Busch et al.[2] at 347.1 nm and Park et al.[12] at 308 and 340–355 nm, who determined an upper limit for Cl* formation of 0.01.

Table 4F-1. Recommended Absorption Cross Sections of Cl_2 at 298 K

λ (nm)	10^{20} σ (cm^2)	λ (nm)	10^{20} σ (cm^2)	λ (nm)	10^{20} σ (cm^2)
260	0.198	513	0.01426	542	0.001170
270	0.824	514	0.01283	543	0.002080
280	2.58	515	0.009440	544	0.001720
290	6.22	516	0.01022	545	0.001260
300	11.92	517	0.009980	546	0.000910
310	18.50	518	0.008750	547	0.000860
320	23.71	519	0.006370	548	0.001460
330	25.55	520	0.008960	549	0.001120
340	23.51	521	0.006540	550	0.000840
350	18.77	522	0.006810	551	0.000780
360	13.22	523	0.005430	552	0.000590
370	8.41	524	0.006110	553	0.000660
380	5.00	525	0.005600	554	0.000650
390	2.94	526	0.004270	555	0.000750
400	1.84	527	0.003680	556	0.000570
410	1.28	528	0.005610	557	0.000400
420	0.956	529	0.004170	558	0.000290
430	0.732	530	0.003110	559	0.000480
440	0.546	531	0.003510	560	0.000520
450	0.387	532	0.003960	561	0.000440
460	0.258	533	0.003160	562	0.000310
470	0.162	534	0.002400	563	0.000230
480	0.0957	535	0.00294	564	0.00017
490	0.0534	536	0.00215	565	0.00038
500	0.0283	537	0.00254	566	0.00033
509	0.01600	538	0.00201	567	0.00024
510	0.01561	539	0.00243	568	0.00018
511	0.01468	540	0.00202	569	0.00015
512	0.01150	541	0.00143	570	0.00006

Note:
260–500 nm: Calculated using the Maric et al.[11] parameterization
509–570 nm: Young et al.[16]

(1) Burkholder, J. B.; Bair, E. J. Potential energy parameters and shapes of the vibrational components of the 345-nm system of chlorine. *J. Phys. Chem.* **1983**, *87*, 1859-1863, doi:10.1021/j100234a007.

(2) Busch, G. E.; Mahoney, R. T.; Morse, R. I.; Wilson, K. R. Translational spectroscopy: Cl_2 photodissociation. *J. Chem. Phys.* **1969**, *51*, 449-450, doi:10.1063/1.1671746.

(3) Chen, Y.; Zhu, L. The wavelength dependence of the photodissociation of propionaldehyde in the 280-330 nm region. *J. Phys. Chem. A* **2001**, *105*, 9689-9696, doi:10.1021/jp011445s.

(4) Chen, Y.; Zhu, L. Wavelength-dependent photolysis of glyoxal in the 290-420 nm region. *J. Phys. Chem. A* **2003**, *107*, 4643-4651, doi:10.1021/jp022440d.

(5) Chen, Y.; Zhu, L.; Francisco, J. S. Wavelength-dependent photolysis of *n*-butyraldehyde and *i*-butyraldehyde in the 280-330-nm region. *J. Phys. Chem. A* **2002**, *106*, 7755-7763, doi:10.1021/jp014544e.

(6) Chichinin, A. I. Measurement of $Cl(^2P_{1/2})$ quantum yield for the photodissociaton of NOCl, ICl, PCl_3, Cl_2O and $COCl_2$. *Chem. Phys. Lett.* **1993**, *209*, 459-463, doi:10.1016/0009-2614(93)80117-8.

(7) Fergusson, W. C.; Slotin, L.; Style, D. W. G. The absorption spectrum of aqueous chlorine and hydrogen peroxide vapour. *Trans. Far. Soc.* **1936**, *32*, 956-962, doi:10.1039/tf9363200956.

(8) Ganske, J. A.; Berko, H. N.; Finlayson-Pitts, B. J. Absorption cross sections for gaseous $ClNO_2$ and Cl_2 at 298 K: Potential organic oxidant source in the marine troposphere. *J. Geophys. Res.* **1992**, *97*, 7651-7656, doi:10.1029/92JD00414.

(9) Gibson, G. E.; Bayliss, N. S. Variation with temperature of the continuous absorption spectrum of diatomic molecules: Part I. Experimental,* The absorption spectrum of chlorine. *Phys. Rev.* **1933**, *44*, 188-192, doi:10.1103/PhysRev.44.188.

(10) Hubinger, S.; Nee, J. B. Absorption spectra of Cl_2, Br_2 and BrCl between 190 and 600 nm. *J. Photochem. Photobiol. A: Chem.* **1995**, *86*, 1-7, doi:10.1016/1010-6030(94)03949-U.
(11) Maric, D.; Burrows, J. P.; Meller, R.; Moortgat, G. K. A study of the UV-visible absorption spectrum of molecular chlorine,. *J. Photochem. Photobiol. A: Chem.* **1993**, *70*, 205-214, doi:10.1016/1010-6030(93)85045-A.
(12) Park, J.; Lee, Y.; Flynn, G. W. Tunable diode laser probe of chlorine atoms produced from the photodissociation of a number of molecular precursors. *Chem. Phys. Lett.* **1991**, *186*, 441-449, doi:10.1016/0009-2614(91)90206-O.
(13) Roxlo, C.; Mandl, A. Vacuum ultraviolet absorption cross sections for halogen containing molecules. *J. Appl. Phys.* **1980**, *51*, 2969-2972, doi:10.1063/1.328108.
(14) Seery, D. J.; Britton, D. The continuous absorption spectra of chlorine, bromine, bromine chloride, iodine chloride, and iodine bromide. *J. Phys. Chem.* **1964**, *68*, 2263-2266, doi:10.1021/j100790a039.
(15) Tellinghuisen, J. Precise equilibrium constants from spectrophotometric data: BrCl in Br_2/Cl_2. *J. Phys. Chem. A* **2003**, *107*, 753-757, doi:10.1021/jp027227w.
(16) Young, I. A. K.; Murray, C.; Blaum, C. M.; Cox, R. A.; Jones, R. L.; Pope, F. D. Temperature dependent structured absorption spectra of molecular chlorine. *Phys. Chem. Chem. Phys.* **2011**, *13*, 15318-15325, doi:10.1039/c1cp21337g.

F2. ClO (chlorine monoxide)

Back to Index

$ClO + h\nu \rightarrow Cl + O(^3P)$	269 kJ mol^{-1}	445 nm	(1)
$\rightarrow Cl + O(^1D)$	458 kJ mol^{-1}	262 nm	(2)

(Recommendation: 06-2, Note: 25-1, Evaluated: 10-6)

Absorption Cross Sections: The UV absorption spectrum of chlorine monoxide, ClO, shown in Figure 4F-2-1, is partly composed of a continuum absorption band from 210 nm to the maximum near 265 nm, and a characterized banded structure of a strong A $^2\Pi_{3/2} \leftarrow$ X $^2\Pi_{3/2}$ transition, superposing a weak A $^2\Pi_{1/2} \leftarrow$ X $^2\Pi_{1/2}$ system between 265 nm and 315 nm. Watson[16] has reviewed the cross section measurements prior to 1977. The more recent measurements yield results in reasonable agreement with the earlier studies by Mandelman and Nicholls[9] (250–310 nm), Wine et al.[17] (near 283 nm), Rigaud et al.[11] (272–324 nm), Jourdain et al.[6] (272–320 nm), Barton et al.[1] (274–306 nm) at 315 K, Lang et al.[7] (253.7 and 257.7 nm), Sander and Friedl[12] (244–317 nm, 275.2 nm) at 220, 298, and 400 K, Trolier et al.[15] (220–350 nm, 282.65 nm) over the temperature range 200–263 K, and Simon et al.[14] (240–310 nm). The peak cross section at the maximum of the continuum (near 265 nm) is 5.2×10^{-18} cm^2 molecule^{-1}, based on the average of the results from Jourdain et al., Sander and Friedl, Trolier et al., Simon et al., and Johnston et al.[5] At 257.7 nm an average value of $(4.86 \pm 0.04) \times 10^{-18}$ cm^2 molecule^{-1} was calculated from the data of the Mandelman and Nicholls, Lang et al., Sander and Friedl, Trolier et al., and Simon et al. studies. It should be noted that the cross sections in the structured region of the spectrum are extremely dependent on instrument resolution. Figure 4F-2-1 shows a spectrum of ClO based on the data of Sander and Friedl. The recommended absorption cross sections listed in Table 4F-2-1 are averages over 1 nm intervals of the continuous and banded regions of the spectrum measured at a resolution of 0.3 nm by Sander and Friedl. In Table 4F-2-2 the absorption cross sections for the band heads of the v′,v″ = 1,0 to 21,0 transitions measured at various spectral resolutions are compared.

The cross sections of the continuum are independent of temperature (Trolier et al.[15]), while the structured part of the spectrum is extremely temperature dependent, the bands sharpen and increase in intensity with decreasing temperature. Sander and Friedl[12] measured the temperature dependence at the peak of the 12,0 band (275.2 nm) over the range 220–400 K and Trolier et al.[15] measured the temperature dependence at the peak of the 9,0 band (282.65 nm) over the range 200–298 K. Clyne and Coxon[2] determined the following relationship for the 11,0 sub-band relative to the 294 K value for the temperature range 294–240 K:

$$\sigma_{294} / \sigma_T = 1 + 0.0036 (T - 294)$$

Maric and Burrows[10] performed an analysis of the ClO spectrum and developed an analytical approach that allows the calculation of the UV absorption spectrum as a function of temperature and spectral resolution. Feierabend et al.[4] measured the ClO differential absorption cross section, i.e., peak to valley, $\Delta\sigma_{ClO}$, for the 10,0 band head (~279.6 nm) at 218, 243, 273, and 296 K with a laser bandwidth of 0.005 nm. An empirical temperature dependence parameterization yielded $\Delta\sigma_{ClO}(T)/\Delta\sigma_{ClO}(296\ K) = 3.5234 - 0.014486T + 2.0137 \times 10^{-5}\ T^2$ (T in units of K).

Photolysis Quantum Yield and Product Studies: The calculations of Coxon et al.[3] and Langhoff et al.[8] indicate that photodecomposition of ClO accounts for at most 2 to 3% of the total destruction rate of ClO in the

stratosphere, which occurs predominantly by reaction with oxygen atoms and nitric oxide. The photodissociation of thermal ClO radicals in the wavelength range 237< λ <270 nm was studied by Schmidt et al.[13] using REMPI. Cl($^2P_{3/2,1/2}$) and O(^1D) were formed with unity quantum yield. The threshold wavelength for O(^1D) production was determined to be 263.4 nm. In the structured region of the spectrum oxygen atoms are formed in the triplet ground state.

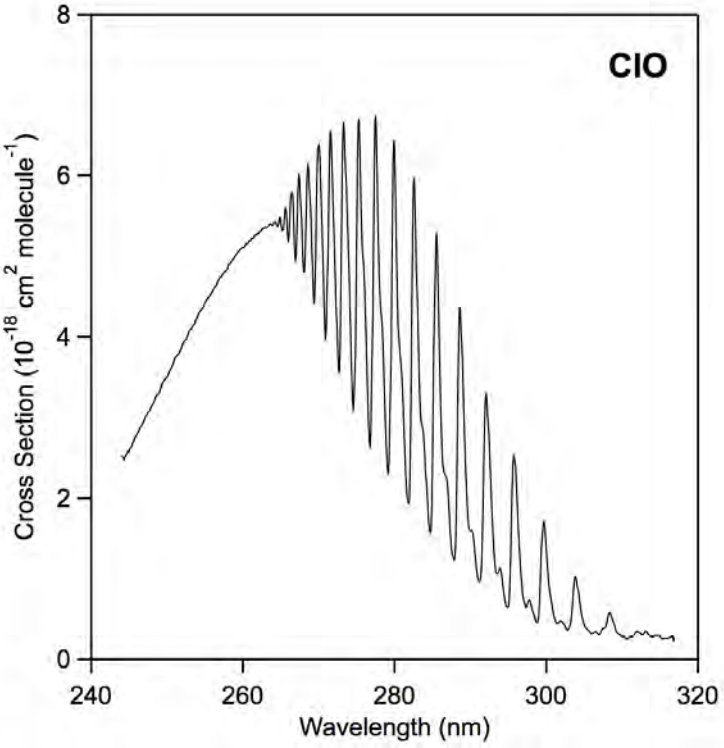


Figure 4F-2-1. Absorption Spectrum of ClO

Table 4F-2-1. Recommended Absorption Cross Sections of ClO at 298 K

λ (nm)	10^{20} σ (cm^2)	λ (nm)	10^{20} σ (cm^2)	λ (nm)	10^{20} σ (cm^2)	λ (nm)	10^{20} σ (cm^2)
245	260	263	536	281	329	299	74.8
246	279	264	540	282	311	300	133
247	297	265	541	283	445	301	56.6
248	315	266	549	284	245	302	45.2
249	333	267	546	285	292	303	44.9
250	352	268	529	286	362	304	87.8
251	371	269	529	287	200	305	45.5
252	388	270	575	288	197	306	33.2
253	407	271	489	289	337	307	33.1
254	425	272	532	290	165	308	47.7
255	442	273	515	291	111	309	41.9
256	457	274	470	292	270	310	28.7
257	473	275	507	293	161	311	27.3
258	486	276	456	294	102	312	33.1
259	500	277	418	295	94.5	313	32.5
260	511	278	501	296	206	314	28.9
261	520	279	283	297	83.1	315	27.8
262	529	280	538	298	65.1	316	26.8

Note:
Sander and Friedl,[12] averages over 1 nm intervals of the continuous and banded spectrum measured at 0.3 nm resolution.

Table 4F-2-2. Summary of Absorption Cross Section Studies of ClO at the band heads of the v′,v″ = 1,0 to 21,0 bands

Band	λ (nm)	10^{20} σ (cm^2)	λ (nm)	10^{20} σ (cm^2)	λ (nm)	10^{20} σ (cm^2)	λ (nm)	10^{20} σ (cm^2)	λ (nm)	10^{20} σ (cm^2)
v′,v″	Trolier et al. res. 0.6 nm		Sander & Friedl res. 0.3(0.18) nm		Simon et al. res. 0.3(0.03) nm		Mandelman res. 0.22 nm		Jourdain et al. res. 0.015 nm	
1,0			312.1	35					312.5	26
2,0	307.7	22	308.3	58	307.9	39	307.8	47	307.9	67
3,0	303.4	64	303.9	103	303.5	86	303.4	104	303.5	133
4,0	299.4	128	299.6	171	299.0	163	299.3	207	299.3	236
5,0	295.4	202	295.7	253	295.4	255	295.4	315	295.4	326
6,0	292.1	286	292.1	330	292.0	338 (400)	292.0	382	291.8	395
7,0	288.7	365	288.6	438	288.4	448 (502)	288.4	516	288.4	504
8,0	286.0	455	285.5	530	285.2	542	285.2	627	285.2	594
9,0	282.6	508	282.6	598	282.3	608	282.2	667	282.2	641
10,0	280.1	555	279.9	645	279.8	655	279.6	688	279.6	686
11,0	277.7	571	277.4	668	277.2	679	277.2	680	277.2	727
12,0	275.5	587	275.3	671 (836)	275.1	681	275.0	634	275.1	733
13,0	273.6	576	273.3	668					272.9	711
14,0	271.8	571	271.5	656						
15,0	269.9	556	270.0	640						
16,0	268.7	545	268.6	615						
17,0			267.4	603						
18,0			266.5	579						
19,0			265.6	562						
20,0			264.9	549						
21,0			264.2	543						

(1) Barton, S. A.; Coxon, J. A.; Roychowdhury, U. K. Absolute absorption cross sections at high-resolution in the $A^2\Pi_i$-$X^2\Pi_i$ band system of ClO. *Can. J. Phys.* **1984**, *62*, 473-486, doi:10.1139/p84-066.

(2) Clyne, M. A. A.; Coxon, J. A. Kinetic studies of oxy-halogen radical systems. *Proc. Roy. Soc. A* **1968**, *303*, 207-231, doi:10.1098/rspa.1968.0048.

(3) Coxon, J. A.; Jones, W. E.; Ramsey, D. A. 12th International Symposium on Free Radicals, 1976, Laguna Beach, California.

(4) Feierabend, K. J.; Papanastasiou, D. K.; Burkholder, J. B. ClO radical yields in the reaction of $O(^1D)$ with Cl_2, HCl, chloromethanes, and chlorofluoromethanes. *J. Phys. Chem. A* **2010**, *114*, 12052-12061, doi:10.1021/jp107761t.

(5) Johnston, H. S.; Morris, E. D., Jr.; Van den Bogaerde, J. Molecular modulation kinetic spectrometry. ClOO and ClO_2 radicals in the photolysis of chlorine in oxygen. *J. Am. Chem. Soc.* **1969**, *91*, 7712-7727, doi:10.1021/ja50001a036.

(6) Jourdain, J. L.; Le Bras, G.; Poulet, G.; Combourieu, J.; Rigaud, P.; LeRoy, B. UV absorption spectrum of ClO($A\ ^2\Pi$-$X^2\Pi$) up to the (1,0) band. *Chem. Phys. Lett.* **1978**, *57*, 109-112, doi:10.1016/0009-2614(78)80361-3.

(7) Lang, V. I.; Sander, S. P.; Friedl, R. R. Absolute infrared band strength measurement of the ClO radical by Fourier transform infrared spectroscopy. *J. Mol. Spectrosc.* **1988**, *132*, 89-103, doi:10.1016/0022-2852(88)90061-6.

(8) Langhoff, S. R.; Jaffe, R. L.; Arnold, J. O. Effective cross sections and rate constants for predissociation of ClO in the Earth's atmosphere. *J. Quant. Spectrosc. Radiat. Transf.* **1977**, *18*, 227-235, doi:10.1016/0022-4073(77)90008-5.

(9) Mandelman, M.; Nicholls, R. W. The absorption cross sections and *f*-values for the v" = 0 progression of bands and associated continuum for the ClO($A^2\Pi_i \leftarrow X^2\Pi_i$) system. *J. Quant. Spectrosc. Radiat. Transf.* **1977**, *17*, 483-491, doi:10.1016/0022-4073(77)90095-4.
(10) Maric, D.; Burrows, J. P. Analysis of the UV absorption spectrum of ClO: a comparative study of four methods for spectral computations. *J. Quant. Spectrosc. Radiat. Transf.* **1999**, *62*, 345-369, doi:10.1016/S0022-4073(98)00108-3.
(11) Rigaud, P.; Leroy, B.; Le Bras, G.; Poulet, G.; Jourdain, J. L.; Combourieu, J. About the identication of some UV atmospheric absorptions: Laboratory study of ClO. *Chem. Phys. Lett.* **1977**, *46*, 161-163, doi:10.1016/0009-2614(77)85186-5.
(12) Sander, S. P.; Friedl, R. R. Kinetics and product studies of the reaction ClO + BrO using flash photolysis-ultraviolet absorption. *J. Phys. Chem.* **1989**, *93*, 4764-4771, doi:10.1021/j100349a017.
(13) Schmidt, S.; Benter, T.; Schindler, R. N. Photodissociation dynamics of ClO radicals in the range ($237 \leq \lambda \leq 270$) nm and at 205 nm and the velocity distribution of $O(^1D)$ atoms. *Chem. Phys. Lett.* **1998**, *282*, 292-298, doi:10.1016/S0009-2614(97)01302-X.
(14) Simon, F. G.; Schneider, W.; Moortgat, G. K.; Burrows, J. P. A study of the ClO absorption cross-section between 240 and 310 nm and the kinetics of the self-reaction at 300 K. *J. Photochem. Photobiol. A: Chem.* **1990**, *55*, 1-23, doi:10.1016/1010-6030(90)80014-O.
(15) Trolier, M.; Mauldin, R. L., III; Ravishankara, A. R. Rate coefficient for the termolecular channel of the self-reaction of ClO. *J. Phys. Chem.* **1990**, *94*, 4896-4907, doi:10.1021/j100375a027.
(16) Watson, R. T. Rate constants for reactions of ClO_x of atmospheric interest. *J. Phys. Chem. Ref. Data* **1977**, *6*, 871-917, doi:10.1063/1.555558.
(17) Wine, P. H.; Ravishankara, A. R.; Philen, D. L.; Davis, D. D.; Watson, R. T. High resolution absorption cross sections for the $A^2\Pi$-$X^2\Pi$ system of ClO. *Chem. Phys. Lett.* **1977**, *50*, 101-106, doi:10.1016/0009-2614(77)80689-1.

F3. ClOO (chlorine superoxide)

Back to Index

$ClOO + h\nu \rightarrow Cl + O_2$ 20 kJ mol^{-1} 6100 nm (1)

(Recommendation: 92-20, Note: 10-6, Evaluated: 10-6)

Absorption Cross Sections: Johnston et al.[2] measured the absorption spectrum of the ClOO radical, chlorine superoxide, using a molecular modulation technique and determined absorption cross sections using a complex kinetic scheme interpretation. More recently, Mauldin et al.[3] (220–280 nm, 191 K) and Baer et al.[1] (240–300 nm, 300 K) have reported cross section measurements. These two studies are in reasonable agreement with cross section values that are more than twice the earlier Johnston et al.[2] values. The recommended cross sections in Table 4F-3 are taken from Mauldin et al.[3]

Photolysis Quantum Yield and Product Studies: The photolysis quantum yield is assumed to be unity over the entire UV absorption band.

Table 4F-3. Absorption Cross Sections of ClOO at 191 K

λ (nm)	10^{20} σ (cm^2)	λ (nm)	10^{20} σ (cm^2)
220	611	252	2630
222	670	254	2370
224	747	256	2120
226	951	258	1890
228	1100	260	1610
230	1400	262	1370
232	1650	264	1120
234	1960	266	905
236	2240	268	725
238	2520	270	596
240	2730	272	435
242	2910	274	344
244	2960	276	282
246	2980	278	210
248	2950	280	200
250	2800		

Note:
Mauldin et al.[3]

(1) Baer, S.; Hippler, H.; Rahn, R.; Siefke, M.; Seitzinger, S.; Troe, J. Thermodynamic and kinetic properties of the reaction Cl + O_2 + M ⇌ ClOO + M in the range 160-300 K and 1-1000 bar. *J. Chem. Phys.* **1991**, *95*, 6463-6468, doi:10.1063/1.461543.

(2) Johnston, H. S.; Morris, E. D., Jr.; Van den Bogaerde, J. Molecular modulation kinetic spectrometry. ClOO and ClO_2 radicals in the photolysis of chlorine in oxygen. *J. Am. Chem. Soc.* **1969**, *91*, 7712-7727, doi:10.1021/ja50001a036.

(3) Mauldin, R. L., III; Burkholder, J. B.; Ravishankara, A. R. A photochemical, thermodynamic, and kinetic study of ClOO. *J. Phys. Chem.* **1992**, *96*, 2582-2588, doi:10.1021/j100185a035.

F4. OClO (chlorine dioxide)

Back to Index

OClO + hν	→ $O(^3P)$ + ClO	251 kJ mol^{-1}	476 nm	(1)
	→ Cl + O_2 ($^3\Sigma_g^-$)	22 kJ mol^{-1}	5500 nm	(2)
	→ Cl + O_2 ($^1\Delta_g$)	116 kJ mol^{-1}	1030 nm	(3)
	→ ClOO	-10 kJ mol^{-1}	All	(4)

(Recommendation: 06-2, Note: 10-6, Evaluated: 10-6)

Absorption Cross Sections: The UV/vis absorption spectrum of chlorine dioxide, OClO, is characterized by a series of well developed progressions of bands extending from ~280 to 480 nm corresponding to the A ($^2A_2$) (i,j,k) ← X ($^2B_1$) (0,0,0) vibronic transitions. The spectroscopy of this molecule has been studied extensively and the quantum yield for photodissociation appears to be unity throughout the above wavelength range. See for example, the review by Watson.[23] Birks et al.[3] have estimated an atmospheric photodissociation half-life of OClO of a few seconds. The measurement of absorption spectra at temperatures between 200 and 378 K has been the subject of many studies as summarized in Table 4F-4-1.

Table 4F-4-1. Summary OClO Cross Section Studies

Study	Year	Type	Temperature (K)	Wavelength Range (nm)	Resolution (nm)
Martin and Gareis[19]	1956		298	263–414	Not given
Knauth et al.[15]	1979	A	333	270–440	0.3–1
Wahner et al.[22]	1987	A	204, 296, 378	242–477	0.25
Hubinger and Nee[14]	1994	R	298	240–477	Not given
Frost et al.[13]	1996	R	200	390–454	0.0015–0.0021
Marston et al.[18]	1998	R	298	275–400	0.05
Kromminga et al.[16]	2003	A	213, 233, 253	312.5–440.5	0.01–0.02
Bogumil et al.[6]	2003	R	293	290–460	0.25

Type:
A: Absolute cross section determination
R: Relative cross section determination

Absorption cross sections at 10 nm intervals for the region 270–440 nm and at 333 K have been reported by Knauth et al.,[15] and for the 351.5 nm maximum at room temperature by Clyne and Coxon [7] and Basco and Dogra.[1] The absorption cross sections of Wahner et al.[22] obtained at a resolution of 0.25 nm, and at 204, 296, and 378 K have been used by Hubinger and Nee,[14] Frost et al.,[13] and Marston et al.[18] for the calibration of their relative spectra. The values at the peaks of the main vibrational bands a(0) to a(26) (i.e., A ($^2A_2$) (i,0,0) ← X ($^2B_1$) (0,0,0), i = 0 to 26) reported by Wahner et al.[22] have been selected as recommended absorption cross sections of OClO in earlier NASA/JPL evaluations. More recently, Kromminga et al.[16] reported high and medium resolution absorption spectra at five temperatures between 213 and 293 K obtained using Fourier transform spectroscopy, which has the advantage of accurate wavelength calibration. There is a clear wavelength shift (~0.2–0.5 nm) between the spectra of Kromminga et al.[16] and Wahner et al.[22] that can't be explained by the shift between measurements in air and in vacuum. The absorption cross sections for the band peaks a(3) to a(26) reported by Kromminga et al. are smaller by 5–10% than those reported by Wahner et al.[22] A decrease of the temperature causes a sharpening of the vibrational bands and an increase of the peak cross sections as observed between 293 and 213 K by Kromminga et al.[16] and between 378 and 200 K by Wahner et al.[22]

The recommended absorption cross sections of OClO in Table 4F-4-2 are averages over 1 nm intervals of the spectrum measured by Wahner et al.[22] (0.25 nm resolution). In Table 4F-4-3 are listed the band peaks at 213, 233, 253, 273, and 293 K recorded in the medium resolution (0.2–0.4 nm) spectra by Kromminga et al.[16] The values for the a(21) to a(16) bands at 293 K are the results of Bogumil et al.,[6] which were measured at medium resolution (0.24–0.44 nm) with the SCIAMACHY pre-flight satellite instrument and scaled to the absorption cross sections measured by Kromminga et al.[16] In addition, the peak cross sections determined by Wahner et al.[22] are listed in Table 4F-4-4. Figure 4F-4-1 shows the spectrum of OClO at 204 K based on the data of Wahner et al.[22]

VUV absorption cross sections have been measured by Basco and Morse,[2] (148–183 nm), Flesch et al.[12] (50–207 nm), Hubinger and Nee[14] (127–183 nm), and Marston et al.[18] (115–191 nm).

Photolysis Quantum Yield and Product Studies: The photochemistry of OClO is extremely complex, with several electronic excited states involved in the photodissociation dynamics. Several channels have been observed at wavelengths important in the stratosphere, including O + ClO, Cl + O_2, and isomerization to ClOO. Colussi[8] measured Φ(Cl) to be <0.01, and Φ(O) =1 (within experimental error) for photolysis at 308 nm. Vaida et al.[21] and Rühl et al.[20] reported Cl atom production at 362 nm and Bishenden et al.[4,5] measured Φ(Cl) to be 0.15 ± 0.10 around the same wavelength. In contrast, Lawrence et al.[17] report Φ(Cl) in the 359–368 nm region to be $<5 \times 10^{-4}$. This conclusion is supported by photofragment studies of Davis and Lee[9] between 350 and 475 nm, who report Φ(Cl) <0.2% in the wavelength range 350–370 nm, rising to a maximum of 3.9 ± 0.8% near 404 nm. In a later study, Davis and Lee[10] report a substantial yield of $O_2(^1\Delta_g)$ and show that the branching ratio between O + ClO and Cl + O_2 depends on the OClO($A\ ^2A_2$) excited state vibrational mode. Delmdahl et al.[11] measured the yield of nascent Cl atoms to be below 3.6% for photolysis in the 365–450 nm range. At λ <365 nm, there was a sharp increase of the Cl yield, which was attributed to the photolysis of vibrationally excited ClO (v ≥4).

The recommendation is to use a quantum yield value of unity for the production of $O(^3P)$ atoms in the range 270–480 nm. An upper limit for the Cl yield can be set at 0.04 for the wavelength range 365–450 nm. While accurate absorption cross section values are valuable for atmospheric measurements of OClO abundance, the identity of the photodissociation products is only of minor importance in the context of atmospheric processes.

Table 4F-4-2. Recommended Absorption Cross Sections of OClO at 204 K (averages over 1 nm intervals)

λ (nm)	10^{20} σ (cm^2)	λ (nm)	10^{20} σ (cm^2)	λ (nm)	10^{20} σ (cm^2)	λ (nm)	10^{20} σ (cm^2)
247	35.6	304	96.1	361	477	418	107
248	34.4	305	276	362	173	419	75.1
249	33.7	306	328	363	179	420	81.4
250	34.6	307	190	364	207	421	323
251	34.3	308	116	365	361	422	151
252	34.6	309	85.4	366	403	423	50.0
253	34.1	310	168	367	625	424	23.8
254	34.9	311	511	368	919	425	23.3
255	34.3	312	338	369	903	426	14.5
256	34.8	313	174	370	268	427	43.8
257	34.8	314	107	371	107	428	99.5
258	35.1	315	94.2	372	180	429	46.9
259	35.0	316	239	373	170	430	44.3
260	35.8	317	686	374	364	431	23.3
261	36.5	318	360	375	376	432	47.0
262	37.5	319	176	376	554	433	173
263	38.2	320	114	377	718	434	69.6
264	38.0	321	125	378	881	435	24.6
265	38.8	322	279	379	278	436	11.2
266	39.9	323	873	380	92.4	437	7.68
267	40.4	324	443	381	135	438	9.09
268	42.3	325	192	382	148	439	5.13
269	44.6	326	121	383	266	440	12.5
270	44.3	327	147	384	298	441	47.8

λ (nm)	10^{20} σ (cm^2)	λ (nm)	10^{20} σ (cm^2)	λ (nm)	10^{20} σ (cm^2)	λ (nm)	10^{20} σ (cm^2)
271	45.7	328	221	385	440	442	23.2
272	49.9	329	838	386	345	443	14.7
273	49.1	330	782	387	762	444	7.59
274	48.1	331	285	388	591	445	3.96
275	54.8	332	155	389	173	446	46.8
276	58.3	333	147	390	71.4	447	55.2
277	52.5	334	208	391	123	448	18.4
278	54.3	335	355	392	109	449	7.17
279	67.4	336	1090	393	203	450	6.96
280	67.2	337	782	394	270	451	4.50
281	58.3	338	266	395	285	452	1.66
282	65.4	339	155	396	275	453	3.57
283	82.4	340	167	397	370	454	0.907
284	77.6	341	250	398	653	455	13.3
285	67.2	342	414	399	225	456	9.70
286	77.7	343	925	400	70.1	457	4.76
287	100	344	1090	401	45.6	458	4.25
288	93.7	345	388	402	96.9	459	3.98
289	79.4	346	176	403	56.3	460	1.84
290	90.5	347	161	404	196	461	17.1
291	127	348	258	405	194	462	17.9
292	116	349	320	406	185	463	11.8
293	90.9	350	581	407	160	464	10.0
294	94.1	351	1100	408	158	465	4.01
295	147	352	993	409	493	466	1.40
296	172	353	330	410	210	467	2.53
297	122	354	164	411	71.6	468	10.1
298	92.0	355	190	412	34.0	469	15.0
299	106	356	276	413	46.8	470	7.69
300	226	357	343	414	44.6	471	6.14
301	222	358	597	415	30.0	472	3.18
302	143	359	830	416	164		
303	94.3	360	1210	417	100		

Note:
Wahner et al.[22]

Table 4F-4-3. Absorption Cross Sections of OClO at the a(21) to a(3) Band Peaks at Temperatures in the Range 213–293 K

Band peak	λ (nm)	10^{20} σ (cm^2)	λ (nm)	10^{20} σ (cm2)	λ (nm)	10^{20} σ (cm^2)	λ (nm)	10^{20} σ (cm^2)	λ (nm)	10^{20} σ (cm^2)
	T = 213 K		T = 233 K		T = 253 K		T = 273 K		T = 293 K	
a(21)									292.05	79.32
a(20)									295.79	107.60
a(19)									300.96	171.03
a(18)									306.12	273.85
a(17)									311.58	391.16
a(16)									316.86	528.84
a(15)	322.96	846.62	322.96	812.45	323.02	786.75	323.02	756.88	323.02	707.16
a(14)	329.49	1054.25	329.49	1011.91	329.55	984.42	329.55	945.36	329.55	892.88
a(13)	336.41	1224.61	336.41	1181.30	336.41	1148.79	336.48	1098.73	336.48	1044.48
a(12)	343.77	1313.77	343.77	1269.99	343.77	1243.47	343.77	1189.35	343.77	1134.36
a(11)	351.53	1328.23	351.53	1289.25	351.53	1265.01	351.53	1212.13	351.53	1164.23
a(10)	359.73	1280.34	359.73	1243.39	359.73	1220.29	359.73	1171.14	359.73	1127.62
a(9)	368.39	1187.04	368.39	1153.33	368.39	1128.23	368.39	1083.63	368.47	1045.41
a(8)	377.56	1048.31	377.56	1019.56	377.56	992.21	377.56	951.69	377.65	916.95
a(7)	387.29	869.95	387.29	849.00	387.29	818.37	387.29	783.53	387.38	750.49
a(6)	397.90	696.60	397.99	683.65	397.90	661.61	397.99	643.31	397.99	619.46
a(5)	408.82	523.40	408.82	518.32	408.82	488.85	408.92	473.08	408.92	452.82
a(4)	420.56	350.83	420.45	350.30	420.45	319.18	420.45	317.13	420.45	301.27
a(3)	432.88	220.71	432.99	197.98	432.99	174.81	432.99	194.21	432.99	189.51

Note: 292–317 nm: Bogumil et al.[6]
323–433 nm: Kromminga et al.[16]

Table 4F-4-4. Absorption Cross Sections of OClO at the Band Peaks

λ (nm)	10^{20} σ (cm^2)		
	204 K	296 K	378 K
475.53		13	
461.15	17	17	16
446.41	94	69	57
432.81	220	166	134
420.58	393	304	250
408.83	578	479	378
397.76	821	670	547
387.37	1046	844	698
377.44	1212	992	808
368.30	1365	1136	920
359.73	1454	1219	984
351.30	1531	1275	989
343.44	1507	1230	938
336.08	1441	1139	864
329.22	1243	974	746
322.78	1009	791	628
317.21	771	618	516
311.53	542	435	390
305.99	393	312	291
300.87	256	219	216
296.42	190	160	167
291.77	138	114	130
287.80	105	86	105
283.51	089	72	90
279.64	073	60	79
275.74	059	46	
272.93	053	33	

Note:
Wahner et al.[22]

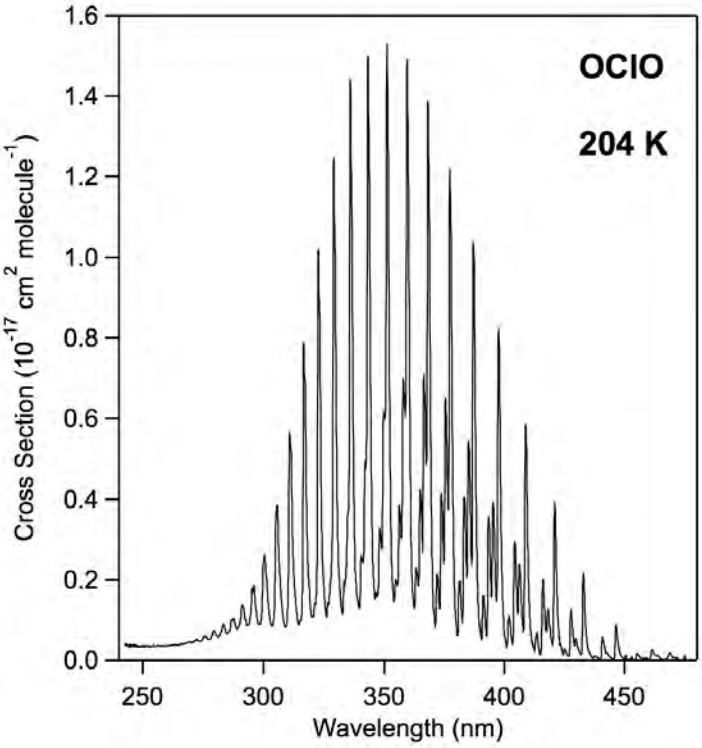


Figure 4F-4-1. Absorption Spectrum of OClO at 204 K

(1) Basco, N.; Dogra, S. K. Reactions of halogen oxides studied by flash photolysis. I. The flash photolysis of chlorine dioxide. *Proc. Roy. Soc. Lond. A.* **1971**, *323*, 29-68, doi:10.1098/rspa.1971.0087.

(2) Basco, N.; Morse, R. D. Reactions of halogen oxides studied by flash photolysis IV. Vacuum ultraviolet kinetic spectroscopy studies on chlorine dioxide. *Proc. Roy. Soc. Lond. A.* **1974**, *336*, 495-505, doi:10.1098/rspa.1974.0032.

(3) Birks, J. W.; Shoemaker, B.; Leck, T. J.; Borders, R. A.; Hart, L. J. Studies of reactions of importance in the stratosphere. II. Reactions involving chlorine nitrate and chlorine dioxide. *J. Chem. Phys.* **1977**, *66*, 4591-4599, doi:10.1063/1.433716.

(4) Bishenden, E.; Haddock, J.; Donaldson, D. J. Resonance-enhanced multiphoton ionization measurement of Cl($^2P_{3/2}$ and $^2P_{1/2}$) produced in the photolysis of OClO from 355 to 370 nm. *J. Phys. Chem.* **1991**, *95*, 2113-2115, doi:10.1021/j100159a006.

(5) Bishenden, E.; Haddock, J.; Donaldson, D. J. Correction. *J. Phys. Chem.* **1992**, *96*, 6513, doi:10.1021/j100194a075.

(6) Bogumil, K.; Orphal, J.; Homann, T.; Voigt, S.; Spietz, P.; Fleischmann, O. C.; Vogel, A.; Hartmann, M.; Kromminga, H.; Bovensmann, H.; Frerick, J.; Burrows, J. P. Measurements of molecular absorption spectra with the SCIAMACHY pre-flight model: instrument characterization and reference data for atmospheric remote-sensing in the 230-2380 nm region. *J. Photochem. Photobiol. A: Chem.* **2003**, *157*, 167-184, doi:10.1016/S1010-6030(03)00062-5.

(7) Clyne, M. A. A.; Coxon, J. A. Kinetic studies of oxy-halogen radical systems. *Proc. Roy. Soc. A* **1968**, *303*, 207-231, doi:10.1098/rspa.1968.0048.

(8) Colussi, A. J. Formation and decay of (^3P_J)O atoms in the laser flash photolysis of chlorine dioxide (OClO) at 308 nm. *J. Phys. Chem.* **1990**, *94*, 8922-8926, doi:10.1021/j100389a014.

(9) Davis, H. F.; Lee, Y. T. Dynamics and mode specificity in OClO photodissociation. *J. Phys. Chem.* **1992**, *96*, 5681-5684, doi:10.1021/j100193a005.

(10) Davis, H. F.; Lee, Y. T. Photodissociation dynamics of OClO. *J. Chem. Phys.* **1996**, *105*, 8142-8163, doi:10.1063/1.472700.

(11) Delmdahl, R. F.; Ullrich, S.; Gericke, K.-H. Photofragmentation of OClO(Ã $^2A_2$ $\nu_1\nu_2\nu_3$) → Cl(^2P_J) + O_2. *J. Phys. Chem. A* **1998**, *102*, 7680-7685, doi:10.1021/jp972111z.

(12) Flesch, R.; Rühl, E.; Hottmann, K.; Baumgärtel, H. Photoabsorption and photoionization of chlorine dioxide. *J. Phys. Chem.* **1993**, *97*, 837-844, doi:10.1021/j100106a007.

(13) Frost, G. J.; Goss, L. M.; Vaida, V. Measurements of high-resolution ultraviolet-visible absorption cross sections at stratospheric temperatures, 2. Chlorine dioxide. *J. Geophys. Res.* **1996**, *101*, 3879-3884, doi:10.1029/95JD03389.
(14) Hubinger, S.; Nee, J. B. Photoabsorption spectrum for OClO between 125 and 470 nm. *Chem. Phys.* **1994**, *181*, 247-257, doi:10.1016/0301-0104(94)85027-5.
(15) Knauth, H.-D.; Alberti, H.; Clausen, H. Equilibrium constant of the gas reaction $Cl_2O + H_2O \rightleftharpoons 2HOCl$ and the ultraviolet spectrum of HOCl. *J. Phys. Chem.* **1979**, *83*, 1604-1612, doi:10.1021/j100475a010.
(16) Kromminga, H.; Orphal, J.; Spietz, P.; Voigt, S.; Burrows, J. P. New measurements of OClO absorption cross-sections in the 325-435 nm region and their temperature dependence between 213 and 293 K. *J. Photochem. Photobiol. A: Chem.* **2003**, *157*, 149-160, doi:10.1016/S1010-6030(03)00071-6.
(17) Lawrence, W. G.; Clemitshaw, K. C.; Apkarian, V. A. On the relevance of OClO photodissociation to the destruction of stratospheric ozone. *J. Geophys. Res.* **1990**, *95*, 18591-18595, doi:10.1029/JD095iD11p18591.
(18) Marston, G.; Walker, I. C.; Mason, N. J.; Gingell, J. M.; Zhao, H.; Brown, K. L.; Motte-Tollet, F.; Delwiche, J.; Siggel, M. R. F. Photoabsorption and near-threshold electron energy-loss spectroscopy of OClO. *J. Phys. B: At. Mol. Phys.* **1998**, *31*, 3387-3405, doi:10.1088/0953-4075/31/15/011.
(19) Martin, H.; Gareis, R. Die kinetik der reaktion von ClO_2 mit NO_2 in der lösungsphase. *Z. Elektrochemie* **1956**, *60*, 959-964.
(20) Rühl, E.; Jefferson, A.; Vaida, V. Photodissociation of OCIO: REMPI study of primary photofragments. *J. Phys. Chem.* **1990**, *94*, 2990-2994, doi:10.1021/j100370a047.
(21) Vaida, V.; Solomon, S.; Richard, E. C.; Rühl, E.; Jefferson, A. Photoisomerization of OClO: a possible mechanism for polar ozone depletion. *Nature* **1989**, *342*, 405-408, doi:10.1038/342405a0.
(22) Wahner, A.; Tyndall, G. S.; Ravishankara, A. R. Absorption cross sections for OClO as a function of temperature in the wavelength range 240-480 nm. *J. Phys. Chem.* **1987**, *91*, 2734-2738, doi:10.1021/j100295a018.
(23) Watson, R. T. Rate constants for reactions of ClO_x of atmospheric interest. *J. Phys. Chem. Ref. Data* **1977**, *6*, 871-917, doi:10.1063/1.555558.

F5. ClO_3 (chlorine trioxide)

Back to Index

$ClO_3 + h\nu \rightarrow$ Products (1)

(Recommendation: 06-2, Note: 10-6, Evaluated: 10-6)

Absorption Cross Sections: The NASA/JPL 83 to NASA/JPL 90 recommendations for the absorption cross sections of the ClO_3 radical, chlorine trioxide, were based on the work of Goodeve and Richardson.[2] Lopez and Sicre[5] have, however, since shown that the spectrum reported by Goodeve and Richardson is most likely that of Cl_2O_6. Thermochemical estimates by Colussi et al.[1] further corroborate this assignment.

Grothe and Willner[3,4] have reported the UV and IR spectra of ClO_3 trapped in a neon matrix following thermal decomposition of Cl_2O_4 or $FOClO_3$. By monitoring the amount of ClO formed as a photolysis product of ClO_3, they determined the absorption cross sections in the range 250–500 nm. The spectrum has a highly structured absorption band around 320 nm ($\sigma \approx 3 \times 10^{-18}$ cm^2 molecule^{-1}) and a second band around 425 nm ($\sigma \approx 2.5 \times 10^{-18}$ cm^2 molecule^{-1}) as depicted in the review article of Wayne et al.[6] A broad absorption spectrum between 280 and 450 nm peaking at ~300 nm ($\sigma \approx 1.8 \times 10^{-17}$ cm^2 molecule^{-1}) was recorded for ClO_3 formed by radiolysis of aqueous solutions of chlorate ions. No recommendation is given for the absorption cross sections of ClO_3 in the gas phase.

Photolysis Quantum Yield and Product Studies: No recommendation.

(1) Colussi, A. J.; Sander, S. P.; Friedl, R. R. Temperature dependence and mechanism of the reaction between $O(^3P)$ and chlorine dioxide. *J. Phys. Chem.* **1992**, *96*, 4442-4445, doi:10.1021/j100190a058.
(2) Goodeve, C. F.; Richardson, F. D. The absorption spectrum of chlorine trioxide and chlorine hexoxide. *Trans. Faraday. Soc.* **1937**, *33*, 453-457, doi:10.1039/tf9373300453.
(3) Grothe, H.; Willner, H. Chlortrioxid: spektroskopische eigenschaften, molekülstruktur und photochemisches verhalten. *Angew. Chem.* **1994**, *106*, 1581-1584, doi:10.1002/anie.199414821
(4) Grothe, H.; Willner, H., personal communication to Wayne et al. (1995).
(5) Lopez, M. I.; Sicre, J. E. Physicochemical properties of chlorine oxides. 1. Composition, ultraviolet spectrum, and kinetics of the thermolysis of gaseous dichlorine hexoxide. *J. Phys. Chem.* **1990**, *94*, 3860-3863, doi:10.1021/j100372a094.
(6) Wayne, R. P.; Poulet, G.; Biggs, P.; Burrows, J. P.; Cox, R. A.; Crutzen, P. J.; Hayman, G. D.; Jenkin, M. E.; Le Bras, G.; Moorgat, G. K.; Platt, U.; Schindler, R. N. Halogen oxides: Radicals, sources and

reservoirs in the laboratory and in the atmosphere. *Atmos. Environ.* **1995**, *29*, 2677-2881, doi:10.1016/1352-2310(95)98124-Q.

F6. Cl_2O (dichlorine monoxide)

Back to Index

$Cl_2O + h\nu \rightarrow Cl + ClO$	142 kJ mol^{-1}	844 nm	(1)
$\rightarrow Cl_2 + O(^3P)$	168 kJ mol^{-1}	712 nm	(2)
$\rightarrow Cl_2 + O(^1D)$	356 kJ mol^{-1}	335 nm	(3)
$\rightarrow O + 2Cl$	411 kJ mol^{-1}	291 nm	(4)

(Recommendation: 15-10, Note: 15-10, Evaluated: 15-10)

Absorption Cross Sections: The UV/vis absorption spectrum of dichlorine monoxide, Cl_2O, has been measured at room temperature by Goodeve and Wallace[4] (230–620 nm), Finkelnburg et al.[3] (220–650 nm), Martin and Gareis[8] (234–331 nm), Lin[7] (180–640 nm), Molina and Molina[9] (200–450 nm), Simon et al.[17] (236–320 nm), Smith et al.[18] (190–399 nm), and Papanastasiou et al.[15] (200–500 nm). The earlier data reported by Goodeve and Wallace,[4] Finkelnburg et al.,[3] and Martin and Gareis[8] deviate substantially from the more recent results and are not considered further in this evaluation. The spectrum measured by Simon et al.[17] was normalized to the data of Lin.[7] The spectrum measured by Papanastasiou et al. was scaled to a cross section value of 1.96×10^{-18} cm^2 $molecule^{-1}$ at 255 nm. The spectrum exhibits three absorption bands in the UV/vis region. An asymmetrical band between ~220–380 nm with the maximum near 255 nm and a shoulder near 290 nm, and two weak bands at ~380–500 nm and ~500–650 nm with maxima near 420 nm and 550 nm, respectively. The absorption cross sections measured by Lin et al.,[7] Molina and Molina,[9] Knauth et al.,[6] Smith et al.,[18] and Papanastasiou et al. are in very good agreement, i.e., to within 10%, for the UV absorption band between 200 and ~350 nm. The values reported by Molina and Molina[9] and Knauth et al.[6] are somewhat larger than those reported by Lin,[7] which are larger than those reported by Smith et al.[18] The discrepancies between the various data sets are larger in the region of the absorption minimum.

The recommended absorption cross sections listed in Table 4F-6 are from Papanastasiou et al. in the region 200–500 nm, which are in good agreement with the Lin cross section data, and the data from Lin[7] in the region 510–640 nm. An uncertainty factor of 1.1 (2σ) is estimated for the 200–500 nm wavelength range. The estimated uncertainty encompasses the majority of the available experimental data.

Measurements at 298 and 333 K have been carried out by Knauth et al.[6] (200–500 nm). Johnsson et al.[5] (210–350 nm) measured the absorption spectrum in Ar matrices and reported a gas-phase absorption cross section at 260 nm. Papanastasiou et al. [15] reported spectra over the temperature range 201–296 K. They parameterized the Cl_2O spectrum temperature dependence as the sum of six Gaussian functions (polynomial fits were also provided). Their parameterization is recommended and the fit expressions and coefficients can be obtained from their paper.

VUV absorption cross sections have been measured by Nee[12] (150–200 nm) and Motte-Tollet et al.[11] (128–190 nm).

Photolysis Quantum Yield and Product Studies: Sander and Friedl[16] have measured the quantum yield for production of O atoms to be 0.25 ± 0.05, using a broadband photolysis source extending from 180 nm to beyond 400 nm. The main photolysis products are Cl and ClO. Using a molecular beam technique, Nelson et al.[13] found Cl + ClO to be the only primary photodissociation channel at 308 nm, a major channel at 248 nm, and a minor channel at 193 nm. At 248 nm a fraction of the photoproduct ClO underwent spontaneous photodissociation. These authors found evidence that the dissociation to three atoms 2 Cl + O takes place at 193 nm and that some $O(^1D)$ atoms are generated as well. Papanastasiou et al.[15] measured a $O(^3P) + O(^1D)$ quantum yield of 0.85 ± 0.15 following 193 nm photolysis of Cl_2O and a $O(^3P)$ quantum yield of 0.20 ± 0.03 for 248 nm photolysis. An analysis presented in Papanastasiou et al. of the Feierabend et al.[2] measured ClO radical yield and its temporal profile following the 248 nm photolysis of Cl_2O yielded a ClO yield of 0.8, a Cl atom yield of 1.2 ± 0.1, a O + 2Cl channel yield of 0.2, and a $O + Cl_2$ channel yield of <0.05. Zou et al.[20] studied the 193 and 248 nm photolysis of Cl_2O using photofragment translational spectroscopy. They report a $O(^3P)$ quantum yield of 0.15 for 248 nm photolysis and that the O + 2Cl channel is a major product at 193 nm.

Nickolaisen et al.[14] reported that broadband photolysis at wavelengths >300 nm results in pressure-dependent ClO quantum yields, which was explained by the rapid intersystem crossing between two metastable states. These states undergo competitive dissociation to ClO + Cl and collisional relaxation to the ground state. Furthermore, these authors detected a transient absorption spectrum, which was assigned to a long-lived metastable triplet state of Cl_2O. However, Moore et al.[10] estimated the lifetime of the metastable excited state to be much shorter. Chichinin[1] and Tanaka et al.[19] found evidence of ground state ($^2P_{3/2}$) and spin-orbit excited

($^2P_{1/2}$) atomic chlorine photoproducts. The implication is that the photodecomposition quantum yield is less than unity at atmospherically relevant wavelengths in spite of the continuous nature of the absorption spectrum.

Table 4F-6. Absorption Cross Sections of Cl_2O at 298 K

λ (nm)	10^{20} σ (cm^2)	λ (nm)	10^{20} σ (cm^2)	λ (nm)	10^{20} σ (cm^2)
200	69.4	350	1.71	500	0.238
210	24.4	360	0.871	510	0.210
220	9.66	370	0.543	520	0.214
230	28.5	380	0.472	530	0.237
240	100	390	0.597	540	0.256
250	183	400	0.853	550	0.256
260	186	410	1.14	560	0.222
270	145	420	1.31	570	0.203
280	121	430	1.30	580	0.176
290	99.9	440	1.14	590	0.149
300	69.3	450	0.891	600	0.122
310	39.4	460	0.642	610	0.0956
320	19.2	470	0.452	620	0.0688
330	8.52	480	0.329	630	0.0344
340	3.73	490	0.262	640	0.0153

Note:
200–500 nm: Papanastasiou et al.[15], higher resolution data are available from this reference.
510–640 nm: Lin[7]

(1) Chichinin, A. I. Measurement of $Cl(^2P_{1/2})$ quantum yield for the photodissociaton of NOCl, ICl, PCl_3, Cl_2O and $COCl_2$. *Chem. Phys. Lett.* **1993**, *209*, 459-463, doi:10.1016/0009-2614(93)80117-8.

(2) Feierabend, K. J.; Papanastasiou, D. K.; Burkholder, J. B. ClO radical yields in the reaction of $O(^1D)$ with Cl_2, HCl, chloromethanes and chlorofluoromethanes. *J. Phys. Chem. A* **2010**, *114*, 12052-12061, doi:10.1021/jp10776lt.

(3) Finkelnburg, W.; Schumacher, H.-J.; Stieger, G. Das spektrum und der photochemische zerfall des chlormonoxyds. *Z. Phys. Chem.* **1931**, *B15*, 127-156, doi.org/10.1515/zpch-1932-1515.

(4) Goodeve, C. F.; Wallace, J. I. The absorption spectrum of chlorine monoxide. *Trans. Faraday Soc.* **1930**, *26*, 254-260, doi:10.1039/tf9302600254.

(5) Johnsson, K.; Engdahl, A.; Nelander, B. The UV and IR spectra of the ClClO molecule. *J. Phys. Chem.* **1995**, *99*, 3965-3968, doi:10.1021/j100012a016.

(6) Knauth, H.-D.; Alberti, H.; Clausen, H. Equilibrium constant of the gas reaction $Cl_2O + H_2O \rightleftharpoons 2HOCl$ and the ultraviolet spectrum of HOCl. *J. Phys. Chem.* **1979**, *83*, 1604-1612, doi:10.1021/j100475a010.

(7) Lin, C. L. Extinction coefficients of chlorine monoxide and chlorine heptoxide. *J. Chem. Eng. Data* **1976**, *21*, 411-413, doi:10.1021/je60071a030.

(8) Martin, H.; Gareis, R. Die kinetik der reaktion von ClO_2 mit NO_2 in der lösungsphase. *Z. Elektrochemie* **1956**, *60*, 959-964.

(9) Molina, L. T.; Molina, M. J. Ultraviolet spectrum of HOCl. *J. Phys. Chem.* **1978**, *82*, 2410-2414, doi:10.1021/j100511a013.

(10) Moore, T. A.; Okumura, M.; Minton, T. K. Photodissociation of Cl_2O at 248 and 308 nm. *J. Chem. Phys.* **1997**, *107*, 3337-3338, doi:10.1063/1.474706.

(11) Motte-Tollet, F.; Ska, M.-P.; Marston, G. M.; Walker, I. C.; Siggel, M. R. F.; Gingell, J. M.; Kaminski, L.; Brown, K.; Mason, N. J. Absolute cross sections for the VUV optical absorption of Cl_2O in the 6.5-9.7 eV energy range. *Chem. Phys. Lett.* **1997**, *275*, 298-306, doi:10.1016/S0009-2614(97)00774-4.

(12) Nee, J. B. Ultraviolet absorption of Cl_2O. *J. Quant. Spectrosc. Radiat. Transf.* **1991**, *46*, 55-58, doi:10.1016/0022-4073(91)90066-Y.

(13) Nelson, C. M.; Moore, T. A.; Okumura, M.; Minton, T. K. Primary and secondary dissociation pathways in the ultraviolet photolysis of Cl_2O. *J. Chem. Phys.* **1994**, *100*, 8055-8064, doi:10.1063/1.466799.

(14) Nickolaisen, S. L.; Miller, C. E.; Sander, S. P.; Hand, M. R.; Williams, I. H.; Francisco, J. S. Pressure dependence and metastable state formation in the photolysis of dichlorine monoxide (Cl_2O). *J. Chem. Phys.* **1996**, *104*, 2857-2868, doi:10.1063/1.471109.

(15) Papanastasiou, D. K.; Feierabend, K. J.; Burkholder, J. B. Cl_2O photochemistry: Ultraviolet/vis absorption spectrum temperature dependence and $O(^3P)$ quantum yield at 193 and 248 nm. *J. Chem. Phys.* **2011**, *134*, 204310, doi:10.1063/1.3592662.
(16) Sander, S. P.; Friedl, R. R. Kinetics and product studies of the reaction ClO + BrO using flash photolysis-ultraviolet absorption. *J. Phys. Chem.* **1989**, *93*, 4764-4771, doi:10.1021/j100349a017.
(17) Simon, F. G.; Schneider, W.; Moortgat, G. K.; Burrows, J. P. A study of the ClO absorption cross-section between 240 and 310 nm and the kinetics of the self-reaction at 300 K. *J. Photochem. Photobiol. A: Chem.* **1990**, *55*, 1-23, doi:10.1016/1010-6030(90)80014-O.
(18) Smith, G. D.; Tablas, F. M. G.; Molina, L. T.; Molina, M. J. Measurement of relative product yields from the photolysis of dichlorine monoxide (Cl_2O). *J. Phys. Chem. A* **2001**, *105*, 8658-8664, doi:10.1021/jp0100957.
(19) Tanaka, Y.; Kawasaki, M.; Matsumi, Y.; Fujiwara, H.; Ishiwata, T.; Rogers, L. J.; Dixon, R. N.; Ashfold, M. N. R. The ultraviolet photodissociation of Cl_2O at 235 nm and of HOCl at 235 and 266 nm. *J. Chem. Phys.* **1998**, *109*, 1315-1325, doi:10.1063/1.476682.
(20) Zou, P.; Shu, J.; North, S. W. The three-body dissociation dynamics of Cl_2O at 248 and 193 nm. *J. Photochem. and Photobiol. A: Chem.* **2010**, *209*, 56-60, doi:10.1016/j.jphotochem.2009.10.009.

F7. ClOOCl (chlorine peroxide, dichlorine dioxide)

Back to Index

$ClOOCl + h\nu \rightarrow ClO + ClO$	16.5 kcal mol^{-1}	1735 nm	(1)
$\rightarrow Cl + ClOO$	20.2 kcal mol^{-1}	1323 nm	(2)

(Recommendation: 15-10, Note: 15-10, Evaluated: 15-10)

Absorption Cross Sections: The gas-phase UV absorption spectrum of ClOOCl is continuous with a maximum near 245 nm, a minimum near 218 nm, and a weak diffuse shoulder in the wavelength region 280–300 nm. There are a number of studies that have reported UV absorption data for ClOOCl over a range of wavelengths or at specific wavelengths. Table 4F-7-1 summarizes the currently available studies. The ClOOCl UV absorption spectra reported by Basco and Hunt[1] and Molina and Molina[18] have been shown to contain systematic errors and are not considered further in this evaluation. In laboratory studies, ClOOCl has been produced in the gas-phase at low temperature as a product of the termolecular ClO radical self-reaction, ClO + ClO + M. Studies, to date, indicate that only one stable isomer of Cl_2O_2 is produced in the ClO self-reaction and that this species is chlorine peroxide, ClOOCl, rather than ClOClO or $ClClO_2$. Using sub-millimeter wave spectroscopy, Birk et al.[2] have further established the structure of the reaction product to be ClOOCl. This is in general agreement with the quantum mechanical calculations of McGrath et al.,[15,16] Jensen and Odershede,[10] and Stanton et al.,[27] although the theoretical study by Matus et al.[14] found the $ClClO_2$ isomer to be more stable than ClOOCl by 3.1 kcal mol^{-1} at 298 K.

Table 4F-7-1. Summary of ClOOCl UV Absorption Spectrum Studies

Study	Year	Temperature (K)	λ (nm)	10^{20} σ(λ) (cm^2)
Cox and Hayman[6]	1988	200–300	220–360	640 ± 60*
Permien et al.[22]	1988	235	211–290	–[$]
Burkholder et al.[4]	1990	205–250	212–410	650 +80/-50*
DeMore and Tschuikow-Roux[7]	1990	206	190–400	680 ± 80*
Vogt and Schindler[30]	1990	230	204–350	–[$]
Huder and DeMore[9]	1995	195	200–310	–[$,@]
Bloss et al.[3]	2001	183–245	210	294 ± 86
McKeachie et al.[17]	2004	223	235–400	–[$]
Pope et al.[25]	2008	193	226–355	–[$]
von Hobe et al.[31]	2009	10	220–400	–[$,#]
Chen et al.[5]	2009	200 250 200 250	308 308 351 351	49.0 ± 2.3[&] 50.9 ± 2.6 11.2 ± 0.5 12.6 ± 0.6
Lien et al.[13]	2009	160 200 260	248.4 248.4 248.4	890 ± 43[&] 885 ± 42 873 ± 39
Wilmouth et al.[32]	2009	240 ± 10	248 308 352	660 ± 100[&&] 39.3 ± 4.9 8.6 ± 1.2
Papanastasiou et al.[21]	2009	200 - 228	200–420	760 +80/-50*
Jin et al.[11]	2010	200 250	330 330	23.1 ± 1.1[&] 24.7 ± 1.2
Young et al.[33]	2014	197	200–350 509–536	[$, @]

* Absorption cross section values at the peak of the spectrum, ~245 nm. Cross section data also given over the reported range of wavelengths. [$] Reported ClOOCl absorption spectrum without absolute cross section determination. [#] Solid-phase ClOOCl absorption spectrum measured in a Ne matrix. [@] ClOOCl absorption spectrum at wavelengths reported at >310 obtained using a log-linear extrapolation. [&] ClOOCl cross section obtained assuming a unit photolysis quantum yield. [&&] Product of absorption cross section and Cl-atom-producing channel: $\sigma \times \varphi_{Cl}$.

Cox and Hayman,[6] Burkholder et al.,[4] DeMore and Tschuikow-Roux,[7] Bloss et al.,[3] and Papanastasiou et al.[21] report absolute ClOOCl cross section, σ(λ), values over a substantial range of wavelengths. The studies of Permien et al.,[22] Vogt and Schindler,[30] Huder and DeMore,[9] McKeachie et al.,[17] and Pope et al.[25] report absorption spectra normalized to 245 nm. von Hobe et al.[31] report a solid-phase ClOOCl UV absorption spectrum measured in a Ne matrix at ~10 K with reported cross sections obtained by normalization using the 245 nm cross section recommended in NASA/JPL 06-2[26] for the gas-phase spectrum.

Discrepancies in the wavelength dependence of the ClOOCl absorption spectrum at wavelengths >300 nm, the region that is most critical for atmospheric photolysis rate calculations, exist and most likely originate from uncertainties in corrections for spectral interferences by reactant precursors (O_3, Cl_2O, and Cl_2) and impurities (OClO, Cl_2, and Cl_2O_3) formed in the ClOOCl source chemistry. Near the peak, the reported spectra are in reasonable agreement. The studies of Cox and Hayman, Burkholder et al., DeMore and Tschuikow-Roux, Vogt and Schindler, and McKeachie et al. show systematic deviations that are possibly consistent with spectral interference due to minor absorption by Cl_2O and, in the cases of Cox and Hayman, Burkholder et al., and McKeachie et al., possibly Cl_2O_3. At λ >300 nm, the ClOOCl spectrum is weaker and more sensitive to spectral interferences from impurities, in particular Cl_2. The studies of Burkholder et al. and DeMore and Tschiukow-Roux are the only pre-2007 gas-phase studies that report cross section data at λ >360 nm. Pope et al. developed a method to isolate bulk samples of ClOOCl in which ClOOCl is produced in the gas-phase and condensed at low temperatures. Pope et al. measured gas-phase UV spectra that are due mostly to Cl_2 and ClOOCl absorption following the warming of the condensate. The spectra were analyzed using a Gaussian fitting procedure and

they report a ClOOCl absorption spectrum that decreases rapidly at λ >320 nm with a cross section at 350 nm that is a factor of 6 lower than recommended in NASA/JPL 2006. The von Hobe et al. matrix study used the Pope et al. method to prepare their ClOOCl samples and Raman spectroscopy to evaluate the spectral contribution from Cl_2 impurities. They report a ClOOCl spectrum with significant absorption at wavelengths out to 400 nm. von Hobe et al. suggest that Pope et al. mistakenly attributed a long-wavelength ClOOCl spectral feature to Cl_2 impurity.

The study of Papanastasiou et al.,[21] which is in generally good agreement with the earlier studies, was carried out using diode array spectroscopy and laser photolysis to generate ClO radicals. The spectral analysis utilized reaction stoichiometry and three observed isosbestic points to account for chemical species, including Cl_2, which appear to represent an interference to a greater or lesser degree in all pre-2009 studies. The isosbestic point observed at 408.5 nm shows that ClOOCl absorbs measurably at wavelengths longer than 350 nm.

The study of Young et al.,[33] which was normalized to the cross section measured by Papanastasiou et al. at 245 nm, is in essentially perfect agreement with the latter from 200 nm to 310 nm and diverges from it somewhat at longer wavelengths. Young et al. prepared and purified ClOOCl using the methods described by Pope et al.[25] and extended the wavelength range into the visible, where their stated errors are relatively small. Young et al. corrected for Cl_2 absorption by using its structured visible absorption spectrum, which they recently reported.[34]

Lower limits to the absolute cross sections have been measured recently at specific wavelengths by a new experimental method involving pulsed laser photolysis of ClOOCl in a molecular beam combined with mass spectrometric detection to determine $\sigma(\lambda)\Phi(\lambda)$, where $\Phi(\lambda)$ is the ClOOCl photolysis quantum yield (see Chen et al.[5]). This new method is not sensitive to spectral interference from Cl_2. It yields the lower-limit for the ClOOCl cross sections, assuming $\Phi(\lambda) = 1$, which is thought be a good assumption. Measurements by Chen et al.[5], Lien et al.,[13] and Jin et al.[11] are slightly higher than, but in good agreement with, the data of Papanastasiou et al.[21] Measurements over limited temperature ranges indicate that the cross sections are only weakly dependent on temperature.

Wilmouth et al.[32] used flow-tube and atomic resonance fluorescence techniques to measure Cl-atom production when ClOOCl is photolyzed at 248, 308, and 352 nm. By scaling their signals to the known Cl-atom yield in the photolysis of Cl_2 or the literature cross section at the peak of the ClOOCl absorption spectrum, they obtained the product of the ClOOCl absorption cross section and the quantum yield for the Cl-atom production channel, $\sigma(\lambda)\varphi_{Cl}(\lambda)$, at the three wavelengths. It is noteworthy that the Cl_2 concentration was monitored in situ using fluorescence excited by the resonance lamp, and appropriate corrections to the Cl-atom yields were made. By assuming $\varphi_{Cl}(\lambda) = 1$, they obtain the lower limit to the absorption cross section. Analyzed in this way, their lower limit cross sections at the three wavelengths are a little lower than the cross sections reported by Papanastasiou et al.,[21] although the agreement is better when quantum yields (see below) are considered.

The recommended ClOOCl absorption cross sections are based on the measurements of Papanastasiou et al.[21] (which were corrected on the basis of the isosbestic analysis), Wilmouth et al.[32] (which were corrected on the basis of in situ monitoring of Cl_2), and Chen et al.,[5] Lien et al.,[13] and Jin et al.[11] (which are not susceptible to interfering species), and Young et al.[34] (which were normalized to the 245 nm value of Papanastasiou et al.[21]). The data of Papanastasiou et al.[21] and Wilmouth et al.[32] tend to be a little higher than the previous measurements, but somewhat lower than the measurements of Chen et al.,[5] Lien et al.,[13] and Jin et al.[11] Bloss et al.[3] measured a value for σ(210 nm) in a pulsed photolysis ClO + ClO + M kinetics study over the temperature range 183–245 K that is similar to the current recommendation. The recommended values (taken from Papanastasiou et al.[21] for 200–310 nm and Young et al.[33] for 510–535 nm) for the temperature range 190–250 K are listed in Table 4F-7-2. Near 310 nm, the measurements of Papanastiou et al. (including an isosbestic point), Wilmouth et al., Chen et al., and Young et al. are in very good agreement; for λ >310 nm, the data of Young et al. begins to diverge from the others and the relative errors grow larger. A log-linear interpolation from 310 to 510 nm gives a good representation of all of the data, including the isosbestic point at 408.5 nm. Data at $310 < \lambda < 510$ nm can be estimated from the formula $\sigma(\lambda) = 4.05 \times 10^{-19} \times \exp[-0.0357\times(\lambda - 310)]$, where λ is in nm and σ is in units of cm^2 $molecule^{-1}$.

Cross Section Uncertainties: The estimated uncertainty factor is 1.35 over the entire wavelength range from 200 to 535 nm.

Photolysis Quantum Yields and Product Studies: Molina et al.[19] reported a quantum yield, Φ, of approximately unity (1.03 ± 0.12) for the Cl + ClOO pathway from a flash photolysis study at 308 nm, in which the yield of Cl atoms was measured using time-resolved atomic resonance fluorescence. These results are in agreement with the steady-state photolysis study of Cox and Hayman.[6] Plenge et al.[24] measured the primary products from

ClOOCl photolysis at 250 and 308 nm using photoionization mass spectrometry. At both wavelengths 2Cl + O_2 was observed as the exclusive product channel corresponding to a primary Cl quantum yield near unity at 250 nm ($\Phi_{Cl} \geq 0.98$) and at 308 nm ($\Phi_{Cl} \geq 0.90$). At both photolysis wavelengths the pathway leading to ClO was not observed corresponding to $\Phi_{ClO} \leq 0.02$ at 250 nm and $\Phi_{ClO} \leq 0.10$ at 308 nm.

In a molecular beam/flash-photolysis study Moore et al.[20] used photofragment translational spectroscopy to measure the relative Cl:ClO product yields from which they derived branching ratios for both photolysis channels ClOO + Cl and ClO + ClO. At 248 nm, they obtained 0.88 ± 0.07 and 0.12 ± 0.07 respectively, and at 308 nm, 0.90 ± 0.1 and 0.10 ± 0.01. Huang et al.[8] also used photofragment translational spectroscopy to re-measure the branching ratios reported by Moore et al. The new results confirm and extend those of Moore et al. Huang et al. identified three product channels: (a) 2 Cl + O_2, (b) 2 ClO, and (c) ClO + Cl + O. The branching ratios among these product channels are 0.82, 0.08, and 0.10 at 248.4 nm, and 0.81, 0.19, and 0.00 at 308.4 nm. These results suggest that the branching ratio of channel-a is only weakly dependent on λ and that of channel-c arises from fragmentation of highly excited ClO radicals; at longer wavelengths, there is not enough available energy to beak the bond.

Recommendations: Quantum yield of channel-a $\Phi_a = 0.8$ (± 0.1) at all λ; $\Phi_b + \Phi_c = 0.2$ (± 0.1) at all λ; $\Phi_c = 0.0$ (±0.1) at $\lambda > 300$ nm. Additional determinations of photolysis quantum yields and product branching ratios at wavelengths longer than 300 nm would be desirable.

Theoretical Studies: Toniolo et al.,[29] Peterson and Francisco,[23] and Matus et al.[14] report theoretical calculations for the electronic transitions of the ClOOCl UV absorption spectrum that include transitions to excited singlet and triplet states. Peterson and Francisco report that the strongest triplet transition is dissociative to Cl + ClOO, centered near 385 nm, and is three orders of magnitude weaker than the strongest singlet transition at shorter wavelengths. Kaledin and Morokuma[12] studied the ClOOCl photodissociation dynamics and predict the synchronous and sequential formation of 2 Cl + O_2 at 308 nm, and three possible fragmentation routes at 248 nm: 2Cl + O_2, Cl + O(^{3}P) + ClO, and 2 Cl + 2O(^{3}P). Similar theoretical calculations performed by Toniolo et al.[28] for excitation at 264, 325, and 406 nm found that 2Cl + O_2 was produced at all wavelengths with only a small yield of 2 ClO at the shortest wavelength.

Table 4F-7-2. Recommended Absorption Cross Sections of ClOOCl

λ (nm)	10^{20} σ (cm^2)	λ (nm)	10^{20} σ (cm^2)	λ (nm)	10^{20} σ (cm^2)
200	423	256	549	510	0.0321
202	395	258	495	515	0.0277
204	362	260	445	520	0.0212
206	331	262	400	525	0.0161
208	303	264	360	530	0.0119
210	277	266	325	535	0.0082
212	255	268	294		
214	238	270	268		
216	228	272	246		
218	225	274	225		
220	232	276	206		
222	249	278	189		
224	277	280	173		
226	316	282	158		
228	366	284	144		
230	424	286	131		
232	488	288	119		
234	555	290	108		
236	618	292	98.2		
238	674	294	88.9		
240	719	296	80.5		
242	747	298	72.9		
244	758	300	66.1		
246	753	302	59.9		
248	732	304	54.4		
250	697	306	49.7		
252	651	308	45.4		
254	601	310	41.6		

Note:
200–310 nm : Papanastasiou et al.[21]
Region between 310 and 510 nm: $4.05 \times 10^{-19} \times \exp[-0.0357\times(\lambda - 310)]$, where λ is in nm
510–535 nm: Young et al.[33]

(1) Basco, N.; Hunt, J. E. Mutual combination of ClO radicals. *Int. J. Chem. Kinet.* **1979**, *11*, 649-664, doi:10.1002/kin.550110611.

(2) Birk, M.; Friedl, R. R.; Cohen, E. A.; Pickett, H. M.; Sander, S. P. The rotational spectrum and structure of chlorine peroxide. *J. Chem. Phys.* **1989**, *91*, 6588-6597, doi:10.1063/1.457377.

(3) Bloss, W. J.; Nickolaisen, S. L.; Salawitch, R. J.; Friedl, R. R.; Sander, S. P. Kinetics of the ClO self-reaction and 210 nm absorption cross section of the ClO dimer. *J. Phys. Chem. A* **2001**, *105*, 11226-11239, doi:10.1021/jp012429y.

(4) Burkholder, J. B.; Orlando, J. J.; Howard, C. J. Ultraviolet absorption cross sections of Cl_2O_2 between 210 and 410 nm. *J. Phys. Chem.* **1990**, *94*, 687-695, doi:10.1021/j100365a033.

(5) Chen, H.-Y., C-Y Lien, W-Y Lin, Y.T. Lee, and J.J. Lin UV absorption cross sections of ClOOCl are consistent with ozone degradation models. *Science* **2009**, *324*, 781-784, doi:10.1126/science.1171305.

(6) Cox, R. A.; Hayman, G. D. The stability and photochemistry of dimers of the ClO radical and implications for Antarctic ozone depletion. *Nature* **1988**, *332*, 796-800, doi:10.1038/332796a0.

(7) DeMore, W. B.; Tschuikow-Roux, E. Ultraviolet spectrum and chemical reactivity of the ClO dimer. *J. Phys. Chem.* **1990**, *94*, 5856-5860, doi:10.1021/j100378a046.

(8) Huang, W.-T.; Chen, A. F.; Chen, I.-C.; Tsai, C.-H.; Lin, J. J.-M. Photodissociation dynamics of ClOOCl at 248.4 and 308.4 nm. *Phys. Chem. Chem. Phys.* **2011**, 8195-8203, doi:10.1039/c0cp02453h.

(9) Huder, K. J.; DeMore, W. B. Absorption cross sections of the ClO dimer. *J. Phys. Chem.* **1995**, *99*, 3905-3908, doi:10.1021/j100012a007.
(10) Jensen, F.; Oddershede, J. Structure and spectra of ClO dimers. *J. Phys. Chem.* **1990**, *94*, 2235-2237, doi:10.1021/j100369a007.
(11) Jin, B.; Chen, I.-C.; Huang, W.-T.; Lien, C.-Y.; Guchhait, N.; Lin, J. J. Photodissociation cross section of ClOOCl at 330 nm. *J. Phys. Chem. A* **2010**, *114*, 4791-4797, doi:10.1021/jp909374k.
(12) Kaledin, A. L.; Morokuma, K. An *ab initio* direct-trajectory study of the photodissociation of ClOOCl. *J. Chem. Phys.* **2000**, *113*, 5750-5762, doi:10.1063/1.1290606.
(13) Lien, C.-Y.; Lin, W.-Y.; Chen, H.-Y.; Huang, W.-T.; Jin, B.; Chen, I.-C.; Lin, J. J. Photodissociation cross sections of ClOOCl at 248.4 and 266 nm. *J. Chem. Phys.* **2009**, *131*, 174301, doi:10.1063/1.3257682.
(14) Matus, M. H.; Nguyen, M. T.; Dixon, D. A.; Peterson, K. A.; Francisco, J. S. $ClClO_2$ is the most stable isomer of Cl_2O_2. Accurate coupled cluster energetics and electronic spectra of Cl_2O_2 isomers. *J. Phys. Chem. A* **2008**, *112*, 9623-9627, doi:10.1021/jp806220r.
(15) McGrath, M. P.; Clemitshaw, K. C.; Rowland, F. S.; Hehre, W. J. Thermochemical stabilities and vibrational spectra of isomers of the chlorine oxide dimer. *Geophys. Res. Lett.* **1988**, *15*, 883-886, doi:10.1029/GL015i008p00883.
(16) McGrath, M. P.; Clemitshaw, K. C.; Rowland, F. S.; Hehre, W. J. Structures, relative stabilities and vibrational spectra of isomers of Cl_2O_2: The role of the chlorine oxide dimer in Antarctic ozone depleting mechanisms. *J. Phys. Chem.* **1990**, *94*, 6126-6132, doi:10.1021/j100378a089.
(17) McKeachie, J. R.; Appel, M. F.; Kirchner, U.; Schindler, R. N.; Benter, T. Observation of a heterogeneous source of OClO from the reaction of ClO radicals on ice. *J. Phys. Chem. B* **2004**, *108*, 16786-16797, doi:10.1021/jp049314p.
(18) Molina, L. T.; Molina, M. J. Production of Cl_2O_2 from the self-reaction of the ClO radical. *J. Phys. Chem.* **1987**, *91*, 433-436, doi:10.1021/j100286a035.
(19) Molina, M. J.; Colussi, A. J.; Molina, L. T.; Schindler, R. N.; Tso, T. L. Quantum yield of chlorine-atom formation in the photodissociation of chlorine peroxide (ClOOCl) at 308 nm. *Chem. Phys. Lett.* **1990**, *173*, 310-315, doi:10.1016/0009-2614(90)85275-H.
(20) Moore, T. A.; Okumura, M.; Seale, J. W.; Minton, T. K. UV photolysis of ClOOCl. *J. Phys. Chem. A* **1999**, *103*, 1691-1695, doi:10.1021/jp984410+.
(21) Papanastasiou, D. K.; Papadimitriou, V. C.; Fahey, D. W.; Burkholder, J. B. UV absorption spectrum of the ClO dimer (Cl_2O_2) between 200 and 420 nm. *J. Phys. Chem. A* **2009**, *113*, 13711-13726, doi:10.1021/jp9065345.
(22) Permien, T.; Vogt, R.; Schindler, R. N. Mechanisms of gas phase-liquid phase chemical transformations. In *Air Pollution Report #17*; Cox, R. A., Ed.; Environmental Research Program of the CEC: Brussels, 1988.
(23) Peterson, K. A.; Francisco, J. S. Does chlorine peroxide absorb below 250 nm? *J. Chem. Phys.* **2004**, *121*, 2611-2616, doi:10.1063/1.1766012.
(24) Plenge, J.; Flesch, R.; Kühl, S.; Vogel, B.; Müller, R.; Stroh, F.; Rühl, E. Ultraviolet photolysis of the ClO dimer. *J. Phys. Chem. A* **2004**, *108*, 4859-4863, doi:10.1021/jp049690+.
(25) Pope, F. D.; Hansen, J. C.; Bayes, K. D.; Friedl, R. R.; Sander, S. P. Ultraviolet absorption spectrum of chlorine peroxide, ClOOCl. *J. Phys. Chem. A* **2007**, *111*, 4322-4332, doi:10.1021/jp067660w.
(26) Sander, S. P.; Finlayson-Pitts, B. J.; Friedl, R. R.; Golden, D. M.; Huie, R. E.; Keller-Rudek, H.; Kolb, C. E.; Kurylo, M. J.; Molina, M. J.; Moortgat, G. K.; Orkin, V. L.; Ravishankara, A. R.; Wine, P. H. Chemical Kinetics and Photochemical Data for Use in Atmospheric Studies, Evaluation Number 15, Jet Propulsion Laboratory Pasadena, JPL Publication 06-2, 2006, http://jpldataeval.jpl.nasa.gov.
(27) Stanton, J. F.; Rittby, C. M. L.; Bartlett, R. J.; Toohey, D. W. Low-lying isomers of the chlorine oxide dimer: A theoretical study. *J. Phys. Chem.* **1991**, *95*, 2107-2110, doi:10.1021/j100159a004.
(28) Toniolo, A.; Granucci, G.; Inglese, S.; Persico, M. Theoretical study of the photodissociation dynamics of ClOOCl. *Phys. Chem. Chem. Phys.* **2001**, *3*, 4266-4279, doi:10.1039/b104044h.
(29) Toniolo, A.; Persico, M.; Pitea, D. Theoretical photoabsorption spectra of ClOOCl and Cl_2O. *J. Phys. Chem. A* **2000**, *104*, 7278-7283, doi:10.1021/jp001142i.
(30) Vogt, R.; Schindler, R. N. Air Pollution Report 34, 1990; pp 167-171.
(31) von Hobe, M.; Stroh, F.; Beckers, H.; Benter, T.; Willner, H. The UV/Vis absorption spectrum of matrix-isolated dichlorine peroxide, ClOOCl. *Phys. Chem. Chem. Phys.* **2009**, *11*, 1571-1580, doi:10.1039/b814373k.
(32) Wilmouth, D. M.; Hanisco, T.; Stimpfle, R. M.; Anderson, J. G. Chlorine-catalyzed ozone destruction: Cl atom production from ClOOCl photolysis. *J. Phys. Chem. A* **2009**, 14099-14108, doi:10.1021/jp9053204.

(33) Young, I. A. K.; Jones, R. L.; Pope, F. D. The UV and visible spectra of chlorine peroxide: Constraining the atmospheric photolysis rate. *Geophys. Res. Lett.* **2014**, *41*, 1781-1788, doi:10.1002/2013GL058626.
(34) Young, I. A. K.; Murray, C.; Blaum, C. M.; Cox, R. A.; Jones, R. L.; Pope, F. D. Temperature dependent structured absorption spectra of molecular chlorine. *Phys. Chem. Chem. Phys.* **2011**, *13*, 15318-15325, doi:10.1039/c1cp21337g.

F8. $ClClO_2$ (chloryl chloride)

Back to Index

$ClClO_2 + h\nu \rightarrow$ Products (1)

(Recommendation: 06-2, Note: 10-6, Evaluated: 10-6)

Absorption Cross Sections: The UV absorption spectrum of chloryl chloride, $ClClO_2$, has been measured in the gas-phase at room temperature and in a noble gas matrix at low temperature by Müller and Willner[2] (220–390 nm). In another study from the same group, Jacobs et al.[1] (180–390 nm) re-investigated the spectrum. The spectrum has two overlapping absorption bands with maxima at 226 nm ($\sigma = 1.38 \times 10^{-17}$ cm^2 molecule^{-1}) and 296 nm ($\sigma = 1.51 \times 10^{-17}$ cm^2 molecule^{-1}). The recommended absorption cross sections in Table 4F-8 are taken from Müller and Willner.[2]

Photolysis Quantum Yield and Product Studies: Photolysis of matrix isolated $ClClO_2$ suggests that it absorbs in the visible between 500 and 800 nm with cross sections estimated to be $<10^{-20}$ cm^2 molecule^{-1}.

Table 4F-8. Recommended Absorption Cross Sections of $ClClO_2$ at 298 K

λ (nm)	10^{20} σ (cm^2)	λ (nm)	10^{20} σ (cm^2)	λ (nm)	10^{20} σ (cm^2)	λ (nm)	10^{20} σ (cm^2)
220	920	265	550	310	1120	355	50
225	1160	270	660	315	870	360	40
230	1270	275	830	320	630	365	40
235	1210	280	1050	325	430	370	30
240	1060	285	1260	330	280	375	30
245	880	290	1430	335	190	380	20
250	720	295	1500	340	120	385	20
255	590	300	1470	345	80	390	20
260	530	305	1330	350	60		

Note:
Müller and Willner[2]

(1) Jacobs, J.; Kronberg, M.; Müller, H. S. P.; Willner, H. An experimental study on the photochemistry and vibrational spectroscopy of three isomers of Cl_2O_2 isolated in cryogenic matrices. *J. Am. Chem. Soc.* **1994**, *116*, 1106-1114, doi:10.1021/ja00082a038.
(2) Müller, H. S. P.; Willner, H. Gas phase studies on chloryl chloride, $ClClO_2$. *Ber. Bunsenges. Phys. Chem.* **1992**, *96*, 427-431, doi:10.1002/bbpc.19920960338.

F9. Cl_2O_3 (dichlorine trioxide, chlorine chlorate)

Back to Index

$Cl_2O_3 + h\nu \rightarrow$ Products (1)

(Recommendation: 06-2, Note: 15-10, Evaluated: 15-10)

Absorption Cross Sections: The UV absorption spectrum of Cl_2O_3 (dichlorine trioxide, chlorine sesquioxide, chlorine chlorate) has been measured by Lipscomb et al.[5] (257.7 nm) at 293 K, Hayman and Cox[4] (220–335 nm) at 233 K, Burkholder et al.[1] (220–320 nm) in the range 200–260 K, Harwood et al.[3] (220–330 nm) at 223 K, and Green et al.[2] (201–320 nm) at 243 K. The spectrum has a strong band centered near 265 nm and evidence for another band at shorter wavelengths. Overall, the agreement among the various studies in terms of the absolute absorption cross sections and the wavelength dependence of the spectrum is poor. Hayman and Cox[3] report the largest peak absorption cross section and Green et al.[2] report the lowest, ~30% lower. The spectra from Green et al.[2] and Burkholder et al.[1] are in reasonable agreement and have significantly lower cross sections in the long wavelength region than reported by Harwood et al.[3] and Hayman and Cox.[4] The recommended absorption cross sections in Table 4F-9 were obtained by averaging the cross section data from Hayman and Cox,[4] Burkholder et al.,[1] Harwood et al.,[3] and Green et al.[2] Uncertainty factors of 1.5 (2σ) for λ <300 nm and 2 (2σ) for λ >300 nm are estimated due primarily to the large spread in the available cross section studies.

Photolysis Quantum Yield and Product Studies: Absorption in the UV is expected to lead to unit photodissociation.

Table 4F-9. Recommended Absorption Cross Sections of Cl_2O_3 at 220–260 K

λ (nm)	10^{20} σ (cm^2)	λ (nm)	10^{20} σ (cm^2)	λ (nm)	10^{20} σ (cm^2)
220	1145	255	1443	290	763
225	1113	260	1596	295	566
230	1060	265	1661	300	417
235	1028	270	1614	305	294
240	1044	275	1464	310	212
245	1127	280	1239	315	159
250	1271	285	995	320	132

Note:
220–320 nm: mean of the data from Hayman and Cox,[4] Burkholder et al.,[1] Harwood et al.,[3] and Green et al.[2]

(1) Burkholder, J. B.; Mauldin, R. L.; Yokelson, R. J.; Solomon, S.; Ravishankara, A. R. Kinetic, thermodynamic, and spectroscopic study of Cl_2O_3. *J. Phys. Chem.* **1993**, *97*, 7597-7605, doi:10.1021/j100131a032.

(2) Green, T. J.; Islam, M.; Guest, P.; Hickson, K.; Canosa-Mas, C. E.; Wayne, R. P. A discharge-flow study of Cl_2O_3. *Phys. Chem. Chem. Phys.* **2003**, *5*, 5409-5418, doi:10.1039/b311005b.

(3) Harwood, M. H.; Rowley, D. M.; Freshwater, R. A.; Cox, R. A.; Jones, R. L. A spectroscopic study of Cl_2O_3. *J. Chem. Soc. Faraday Trans.* **1995**, *91*, 3027-3032, doi:10.1039/ft9959103027.

(4) Hayman, G. D.; Cox, R. A. UV absorption spectrum and thermochemistry of Cl_2O_3 formed in the photolysis of OClO-containing mixtures at low temperatures. *Chem. Phys. Lett.* **1989**, *155*, 1-7, doi:10.1016/S0009-2614(89)87350-6.

(5) Lipscomb, F. J.; Norrish, R. G. W.; Thrush, B. A. The study of energy transfer by kinetic spectroscopy I. The production of vibrationally excited oxygen. *Proc. Roy. Soc. London A* **1956**, *233*, 455-464, doi:10.1098/rspa.1956.0003.

F10. Cl_2O_4 (dichlorine tetraoxide, chlorine perchlorate)

Back to Index

$Cl_2O_4 + h\nu \rightarrow$ Products (1)

(Recommendation: 06-2, Note: 10-6, Evaluated: 10-6)

Absorption Cross Sections: The UV absorption spectrum of Cl_2O_4 (dichlorine tetraoxide, chlorine perchlorate) has been measured at room temperature by Lopez and Sicre[2] (200–310 nm) and Green et al.[1] (200–350 nm). The absorption spectrum has a weak band between 303 and 350 nm with a maximum at 327 nm, a stronger band between 212 and 303 nm with a maximum at 233 nm, and a further increase in cross section below 212 nm. The absorption cross sections reported by Lopez and Sicre[2] and Green et al.,[1] who applied similar methods of preparing Cl_2O_4, are in good agreement in the region ~215–250 nm. Discrepancies in the cross section data are apparent below 215 nm, where the values of Lopez and Sicre[2] are larger by as much as a factor ~1.7 at 200 nm and at wavelengths >260 nm. The recommended absorption cross sections in Table 4F-10 are from Green et al.,[1] which is thought to be the more accurate measurement.

Photolysis Quantum Yield and Product Studies: No recommendation.

Table 4F-10. Recommended Absorption Cross Sections of Cl_2O_4 at 298 K

λ (nm)	10^{20} σ (cm^2)	λ (nm)	10^{20} σ (cm^2)	λ (nm)	10^{20} σ (cm^2)	λ (nm)	10^{20} σ (cm^2)
200	96.81	238	84.94	276	9.95	314	1.35
202	87.88	240	80.97	278	8.38	316	1.49
204	77.84	242	76.05	280	6.98	318	1.62
206	73.24	244	70.95	282	5.76	320	1.74
208	67.51	246	65.17	284	4.70	322	1.83
210	64.62	248	59.53	286	3.79	324	1.91
212	61.79	250	53.84	288	3.03	326	1.96
214	61.74	252	48.55	290	2.40	328	1.98
216	63.46	254	43.30	292	1.89	330	1.96
218	66.58	256	38.52	294	1.50	332	1.92
220	70.82	258	34.33	296	1.21	334	1.85
222	74.95	260	30.28	298	1.01	336	1.75
224	79.70	262	26.63	300	0.88	338	1.63
226	83.84	264	23.55	302	0.83	340	1.50
228	87.21	266	20.58	304	0.83	342	1.36
230	89.19	268	17.97	306	0.88	344	1.23
232	90.06	270	15.81	308	0.97	346	1.11
234	89.67	272	13.62	310	1.08	348	1.02
236	87.86	274	11.77	312	1.21	350	0.98

Note:
Green et al.[1]

(1) Green, T. J.; Islam, M.; Canosa-Mas, C.; Marston, G.; Wayne, R. P. Higher oxides of chlorine: absorption cross-sections of Cl_2O_6 and Cl_2O_4, the decomposition of Cl_2O_6, and the reactions of OClO with O and O_3. *J. Photochem. Photobiol. A: Chem.* **2004**, *162*, 353-370, doi:10.1016/S1010-6030(03)00379-4.

(2) Lopez, M. I.; Sicre, J. E. Ultraviolet spectrum of chlorine perchlorate. *J. Phys. Chem.* **1988**, *92*, 563-564, doi:10.1021/j100313a062.

F11. Cl_2O_6 (dichlorine hexoxide)

Back to Index

$Cl_2O_6 + h\nu \rightarrow$ Products (1)

(Recommendation: 06-2, Note: 10-6, Evaluated: 10-6)

Absorption Cross Sections: The UV/vis absorption spectrum of dichlorine hexoxide, Cl_2O_6, has been measured at room temperature by Lopez and Sicre[4] (200–386 nm), Jansen et al.[3] (268 nm), and Green et al.[2] (200–450 nm). The spectrum reported by Goodeve and Richardson[1] and attributed to ClO_3 was shown by Lopez and Sicre[4] to most likely be that of Cl_2O_6. The cross sections measured by Lopez and Sicre[4] are several times larger than those reported by Goodeve and Richardson[1] but the shape of the spectrum is similar. There is excellent agreement between the data of Lopez and Sicre[4] and Green et al.[2] at wavelengths between 210 and 310 nm. At 200 nm the data from Green et al.[2] are smaller by ~10% than those of Lopez and Sicre.[4] At longer wavelengths the Green et al.[2] cross section data are larger with the difference increasing with increasing wavelength up to a factor ~3 at 380 nm. The recommended absorption cross sections in Table 4F-11 are taken from Green et al.[2]

Photolysis Quantum Yield and Product Studies: No recommendation.

Table 4F-11. Recommended Absorption Cross Sections of Cl_2O_6 at 298 K

λ (nm)	10^{20} σ (cm^2)	λ (nm)	10^{20} σ (cm^2)	λ (nm)	10^{20} σ (cm^2)	λ (nm)	10^{20} σ (cm^2)
200	1104	248	1085	296	1173	344	195
202	1135	250	1111	298	1115	346	180
204	1161	252	1142	300	1056	348	167
206	1208	254	1177	302	997	350	153
208	1233	256	1217	304	939	352	141
210	1254	258	1256	306	880	354	130
212	1261	260	1297	308	822	356	121
214	1266	262	1337	310	767	358	111
216	1260	264	1375	312	714	360	103
218	1245	266	1410	314	664	362	96
220	1230	268	1440	316	615	364	89
222	1207	270	1466	318	569	366	81
224	1182	272	1485	320	526	368	75
226	1156	274	1496	322	485	370	71
228	1132	276	1500	324	447	372	66
230	1108	278	1497	326	412	374	61
232	1086	280	1488	328	380	376	57
234	1066	282	1469	330	350	378	52
236	1052	284	1444	332	322	380	49
238	1042	286	1411	334	296	382	46
240	1039	288	1373	336	271	384	43
242	1041	290	1329	338	251	386	40
244	1049	292	1281	340	231	388	37
246	1065	294	1229	342	212	390	36

Note:
Green et al.[2]

(1) Goodeve, C. F.; Richardson, F. D. The absorption spectrum of chlorine trioxide and chlorine hexoxide. *Trans. Faraday. Soc.* **1937**, *33*, 453-457, doi:10.1039/tf9373300453.

(2) Green, T. J.; Islam, M.; Canosa-Mas, C.; Marston, G.; Wayne, R. P. Higher oxides of chlorine: absorption cross-sections of Cl_2O_6 and Cl_2O_4, the decomposition of Cl_2O_6, and the reactions of OClO with O and O_3. *J. Photochem. Photobiol. A: Chem.* **2004**, *162*, 353-370, doi:10.1016/S1010-6030(03)00379-4.

(3) Jansen, M.; Schatte, G.; Tobias, K. M.; Willner, H. Properties of dichlorine hexoxide in the gas phase and in low-temperature matrices. *Inorg. Chem.* **1988**, *27*, 1703-1706, doi:10.1021/ic00283a009.

(4) Lopez, M. I.; Sicre, J. E. Physicochemical properties of chlorine oxides. 1. Composition, ultraviolet spectrum, and kinetics of the thermolysis of gaseous dichlorine hexoxide. *J. Phys. Chem.* **1990**, *94*, 3860-3863, doi:10.1021/j100372a094.

F12. Cl_2O_7 (dichlorine heptoxide)

Back to Index

$Cl_2O_7 + h\nu \rightarrow$ Products (1)

(Recommendation: 06-2, Note: 10-6, Evaluated: 10-6)

Absorption Cross Sections: The UV absorption spectrum of dichlorine heptoxide, Cl_2O_7, has been measured at room temperature by Goodeve and Windsor[1] (222–302 nm) and Lin[2] (180–310 nm). Although both studies report a spectrum with monotonically decreasing absorption cross sections with increasing wavelength, there is poor agreement between the two data sets. The cross sections reported by Goodeve and Windsor[1] are larger at wavelengths <290 nm than those reported by Lin[2] with a difference of a factor of 4 at 225 nm. At wavelengths >290 nm, the cross sections reported by Goodeve and Windsor[1] are smaller than those of Lin.[2] The recommended absorption cross sections in Table 4F-12 are taken from Lin.[2]

Photolysis Quantum Yield and Product Studies: No recommendation.

Table 4F-12. Recommended Absorption Cross Sections of Cl_2O_7 at 298 K

λ (nm)	10^{20} σ (cm^2)	λ (nm)	10^{20} σ (cm^2)	λ (nm)	10^{20} σ (cm^2)
180	1188	225	79.7	270	3.77
185	908.5	230	61.0	275	2.57
190	674.7	235	45.6	280	1.70
195	475.3	240	34.6	285	1.20
200	322	245	24.7	290	0.705
205	231	250	17.5	295	0.521
210	169	255	12.0	300	0.368
215	132	260	7.74	305	0.203
220	102	265	5.37	310	0.104

Note:
Lin[2]

(1) Goodeve, C. F.; Windsor, B. A. M. The absorption spectrum of chlorine heptoxide. *Trans. Faraday Soc.* **1936**, *32*, 1518-1519, doi:10.1039/tf9363201518.

(2) Lin, C. L. Extinction coefficients of chlorine monoxide and chlorine heptoxide. *J. Chem. Eng. Data* **1976**, *21*, 411-413, doi:10.1021/je60071a030.

F13. HCl (hydrogen chloride)

Back to Index

$HCl + h\nu \rightarrow H + Cl(^2P_{3/2})$	432 kJ mol^{-1}	277 nm	(1)
$\rightarrow H + Cl(^2P_{1/2})$	442 kJ mol^{-1}	271 nm	(2)

(Recommendation: 06-2, Note: 15-10, Evaluated: 15-10)

Absorption Cross Sections: The VUV/UV absorption spectrum of hydrogen chloride, HCl, has been measured at room temperature by Romand and Vodar[18] (139–207 nm), Romand[17] (139–207 nm), Myer and Samson[13] (140–200 nm), Inn[6] (140–220 nm), Roxlo and Mandl[19] (170–215 nm), Nee et al.[14] (132–185 nm), Bahou et al.[2] (120–230 nm), Cheng et al.[3] (120–230 nm), Vatsa and Volpp[21] (121.6 nm), Mo et al.[12] (193 nm), and Hanf et al.[5] (135 nm). Bahou et al.[2] (120–230 nm) and Cheng et al.[3] (120–230 nm) have also measured the absorption spectrum of DCl. VUV absorption cross sections have been obtained by dipole (e,e) spectroscopy in the region 8-40 eV (155–31 nm) by Daviel et al.[4] The absorption spectrum has a broad absorption band between 135 and 230 nm, corresponding to the $A\ ^1\Pi \leftarrow X\ ^1\Sigma^+$ transition, with the maximum at ~154 nm for HCl and ~156 nm for DCl. There is good agreement among the data of Bahou et al.,[2] Cheng et al.,[3] with the data from Nee et al.[14] and Inn.[6] The cross sections of Bahou et al.[2] and Cheng et al.[3] are in general larger than those of Nee et al.[14] by <10% in the region 132–170 nm and by <25% at wavelengths >170 nm. In addition, the cross sections of Bahou et al.[2] and Cheng et al.[3] are slightly smaller, by <10%, than those of Inn[6] except for the region >210 nm. The absorption spectrum of Inn[6] has shoulders near 147.5 nm and 160 nm around the maximum at ~155 nm. This is in contrast to the results of Bahou et al.[2] and Cheng et al.[3] (0.1 nm resolution) and those of Nee et al.[14] (0.05 nm resolution). The recommended absorption cross sections for HCl and DCl in Table 4F-13 are averages over 2.5 nm and 5 nm intervals of the data from Bahou et al.[2] An uncertainty factor of 1.1 (2σ) is estimated for $180 < \lambda < 230$ nm.

Photolysis Quantum Yield and Product Studies: Photodissociation of HCl was studied by Matsumi et al.[9-11] and Tonokura et al.,[20] and the branching fraction $Cl(^2P_{1/2}) / (Cl(^2P_{1/2}) + Cl(^2P_{3/2}))$ was determined to be 0.33 ± 0.05 at 193 nm and 0.45-0.47 (± 0.04) at 157 nm. Lambert et al.[7] measured branching fractions between 0.47 and 0.33 for eight wavelengths between 193 and 235 nm for HCl. Zhang et al.[22] obtained 0.41 ± 0.01 at 193.3 nm. Regan et al.[16] obtained values between 0.42 and 0.48 for 5 wavelengths in the range 201–210 nm, and Regan et al.[15] report values between 0.41 to 0.53 for selected ro-vibrational states at 235 nm. The results from Lambert et al.,[7] Zhang et al.,[22] Regan et al.,[15,16] and Liyanage et al.[8] are in good agreement with the calculations of Alexander et al.[1]

Table 4F-13. Recommended Absorption Cross Sections of HCl and DCl at 298 K

λ (nm)	10^{20} σ (cm^2)		λ (nm)	10^{20} σ (cm^2)	
	HCl	DCl		HCl	DCl
135.0	123	45.5	175.0	106	87.1
137.5	152	75.9	177.5	79.6	58.9
140.0	205	120	180.0	58.9	38.5
142.5	238	184	182.5	42.3	23.9
145.0	279	248	185.0	29.4	14.5
147.5	311	308	187.5	20.3	8.80
150.0	334	364	190.0	13.8	4.93
152.5	342	393	195.0	5.96	1.67
155.0	343	415	200.0	2.39	0.485
157.5	327	407	205.0	0.903	0.136
160.0	306	367	210.0	0.310	0.040
162.5	273	321	215.0	0.101	0.011
165.0	240	267	220.0	0.030	0.0027
167.5	199	211	225.0	0.010	
170.0	163	166	230.0	0.0034	
172.5	136	119			

Note:
Bahou et al.[2]

(1) Alexander, M. H.; Pouilly, B.; Duhoo, T. Spin-orbit branching in the photofragmentation of HCl. *J. Chem. Phys.* **1993**, *99*, 1752-1764, doi:10.1063/1.465292.

(2) Bahou, M.; Chung, C.-Y.; Lee, Y.-P.; Cheng, B. M.; Yung, Y. L.; Lee, L. C. Absorption cross sections of HCl and DCl at 135-232 namometers: Implications for photodissociation on Venus. *Astrophys. J.* **2001**, *559*, L179-L182, doi:10.1086/323753.

(3) Cheng, B. M.; Chung, C.-Y.; Bahou, M.; Lee, Y.-P.; Lee, L. C. Quantitative spectral analysis of HCl and DCl in 120–220 nm: Effects of singlet–triplet mixing. *J. Chem. Phys.* **2002**, *117*, 4293-4298, doi:10.1063/1.1496476.

(4) Daviel, S.; Iida, Y.; Carnovale, F.; Brion, C. E. Absolute oscillator strengths for the partial photoionization, ionic fragmentation and photoabsorption of HCl. *Chem. Phys.* **1984**, *83*, 391-406, doi:10.1016/0301-0104(84)85014-4.

(5) Hanf, A.; Laüter, A.; Volpp, H.-R. Absolute chlorine atom quantum yield measurements in the UV and VUV gas-phase laser photolysis of CCl_4. *Chem. Phys. Lett.* **2003**, *368*, 445-451, doi:10.1016/S0009-2614(02)01896-1.

(6) Inn, E. C. Y. Absorption coefficient of HCl in the region 1400 to 2200 Å. *J. Atmos. Sci.* **1975**, *32*, 2375-2377, doi:10.1175/1520-0469(1975)032<2375:ACOHIT>2.0.CO;2.

(7) Lambert, H. M.; Dagdigian, P. J.; Alexander, M. H. Spin–orbit branching in the photofragmentation of HCl at long wavelength. *J. Chem. Phys.* **1998**, *108*, 4460-4466, doi:10.1063/1.475857.

(8) Liyanage, R.; Yang, Y.-A.; Hashimoto, S.; Gordon, R. J.; Field, R. W. Electronic control of the spin-orbit branching ratio in the photodissociation and predissociation of HCl. *J. Chem. Phys.* **1995**, *103*, 6811-6814, doi:10.1063/1.470360.

(9) Matsumi, Y.; Das, P. K.; Kawasaki, M. Doppler spectroscopy of chlorine atoms generatred from photodissociation of hydrogen chloride and methyl chloride at 157 and 193 nm. *J. Chem. Phys.* **1990**, *92*, 1696-1701, doi:10.1063/1.458051.

(10) Matsumi, Y.; Das, P. K.; Kawasaki, M. Erratum. *J. Chem. Phys.* **1992**, *97*, 5261, doi:10.1063/1.463999.

(11) Matsumi, Y.; Tonokura, K.; Kawasaki, M.; Ibuki, T. Photodissociation of hydrogen chloride and hydrogen bromide. *J. Chem. Phys.* **1990**, *93*, 7981-7985, doi:10.1063/1.459327.

(12) Mo, Y.; Tonokura, K.; Matsumi, Y.; Kawasaki, M.; Sato, T.; Arikawa, T.; Reilly, P. T. A.; Xie, Y.; Yang, Y.; Huang, Y.; et al. Mechanism of the ultraviolet photodissociation of chloroethylenes determined from the Doppler profiles, spatial anisotropy, and power dependence of the photofragments. *J. Chem. Phys.* **1992**, *97*, 4815-4826, doi:10.1063/1.463836.

(13) Myer, J. A.; Samson, J. A. R. Vacuum-ultraviolet absorption cross sections of CO, HCl, and ICN between 1050 and 2100 Å. *J. Chem. Phys.* **1970**, *52*, 266-271, doi:10.1063/1.1672676.

(14) Nee, J. B.; Suto, M.; Lee, L. C. Quantitative photoabsorption and fluorescence study of HCl in vacuum uultraviolet. *J. Chem. Phys.* **1986**, *85*, 719-724, doi:10.1063/1.451278.

(15) Regan, P. M.; Ascenzi, D.; Brown, A.; Balint-Kurti, G. G.; Orr-Ewing, A. J. Ultraviolet photodissociation of HCl in selected rovibrational states: Experiment and theory. *J. Chem. Phys.* **2000**, *112*, 10259-10268, doi:10.1063/1.481707.
(16) Regan, P. M.; Langford, S. R.; Ascenzi, D.; Cook, P. A.; Orr-Ewing, A. J.; Ashfold, M. N. R. Spin–orbit branching in Cl(^{2}P) atoms produced by ultraviolet photodissociation of HCl. *Phys. Chem. Chem. Phys.* **1999**, *1*, 3247-3251, doi:10.1039/a903331i.
(17) Romand, J. Absorption ultraviolette dans la région de Schumann étude de: ClH, BrH et IH gazeux. *Ann. Phys. (Paris)* **1949**, *4*, 529-590, doi:10.1051/anphys/194912040529.
(18) Romand, J.; Vodar, B. Spectre d'absorption de l'acide chlorhydrique gaseux dans la région de Schumann. *Compt. Rend. Acad. Sci. Paris* **1948**, *226*, 238-240.
(19) Roxlo, C.; Mandl, A. Vacuum ultraviolet absorption cross sections for halogen containing molecules. *J. Appl. Phys.* **1980**, *51*, 2969-2972, doi:10.1063/1.328108.
(20) Tonokura, K.; Matsumi, Y.; Kawasaki, M.; Tasaki, S.; Bersohn, R. Photodissociation of hydrogen chloride at 157 and 193 nm: Angular distributions of hydrogen atoms and fine-structure branching ratios of chlorine atoms in the ^2P_j levels. *J. Chem. Phys.* **1992**, *97*, 8210-8215, doi:10.1063/1.463443.
(21) Vatsa, R. K.; Volpp, H.-R. Absorption cross-sections for some atmospherically important molecules at the H atom Lyman-α wavelength (121.567 nm). *Chem. Phys. Lett.* **2001**, *340*, 289-295, doi:10.1016/S0009-2614(01)00373-6.
(22) Zhang, J.; Dulligan, M.; Wittig, C. Photodissociation of HCl at 193.3 nm: Spin-orbit branching ratio. *J. Chem. Phys.* **1997**, *107*, 1403-1405, doi:10.1063/1.474494.

F14. HOCl (hypochlorous acid)

Back to Index

HOCl + hν	→ OH + Cl	234 kJ mol^{-1}	513 nm	(1)
	→ HCl + O(^{3}P)	211 kJ mol^{-1}	568 nm	(2)

(Recommendation: 06-2, Note: 15-10, Evaluated: 15-10)

Absorption Cross Sections: The UV/vis absorption spectrum of hypochlorous acid, HOCl, has an intensive singlet-singlet absorption in the near-UV with a maximum near 240 nm due mostly to the 2 ^{1}A′ ← 1 ^{1}A′ transition and a weaker band arising from the 1 ^{1}A″ ← 1 ^{1}A′ transition that appears as a shoulder near 300 nm. The absorption cross sections of HOCl vapor have been reported by several groups. Molina and Molina[10] and Knauth et al.[7] produced HOCl using equilibrium mixtures with Cl_2O and H_2O. Mishalanie et al.[9] and Permien et al.[12] used a dynamic source to generate the HOCl vapor. The cross section values reported by Molina and Molina,[10] Mishalanie et al.,[9] and Permien et al.[12] are in reasonable agreement between 250 and 330 nm. In this wavelength range, the cross section values reported by Knauth et al.[7] are significantly smaller, e.g. a factor of 4 at 280 nm. At wavelengths >340 nm, the cross sections from Mishalanie et al. are significantly smaller than those obtained by the other three groups with a difference of an order of magnitude at 365 nm.

Burkholder[3] (200–380 nm) measured the HOCl absorption spectrum following photolysis of equilibrium mixtures of Cl_2O–H_2O–HOCl. The HOCl spectrum obtained has two absorption maxima with peaks at 242 and 304 nm in excellent agreement with the work of Knauth et al.[7] The agreement with the spectra reported by Molina and Molina,[10] Mishalanie et al.,[9] and Permien et al.[12] is poor. The discrepancies can most likely be attributed to the methods and uncertainties associated with correcting measured absorption spectra for the presence of Cl_2 and Cl_2O. In the study by Burkholder,[3] several control experiments were carried out in order to check the internal consistency of the data. Barnes et al.[1] examined the near UV HOCl spectrum by monitoring the OH fragments resulting from photodissociation and observed a weak band centered at 387 nm that extends to 480 nm. This transition arises from a weak singlet-triplet transition (Minaev[8]). The recommended cross sections in Table 4F-14 are calculated from an analytical expression provided by Barnes et al.[1] that was based on the cross section values from Burkholder[3] and Barnes et al.[1] The HOCl spectrum reported by Jungkamp et al.[6] is in excellent agreement with this recommendation for wavelengths <350 nm but deviates significantly at longer wavelengths. Uncertainty factors of 1.1 (2σ) and 1.2 (2σ) are estimated for the wavelength regions λ ≤350 nm and λ >350 nm, respectively.

Photolysis Quantum Yield and Product Studies: Molina et al.[11] observed production of OH radicals in the laser photolysis of HOCl around 310 nm. Butler and Phillips [4] found no evidence for O atom production following HOCl photolysis at 308 nm and reported an upper limit for the primary quantum yield for the HCl + O channel of ~0.02. Vogt and Schindler[14] used broadband photolysis in the 290–390 nm wavelength range and report Φ(OH) to be >0.95. Schindler et al.[13] measured Φ(Cl) to be 1.00 ± 0.05 at 308 nm. These authors also determined the probability, P, for production of Cl*($^2P_{1/2}$) relative to Cl ($^2P_{3/2}$) to be 0.035 ± 0.02 at 308 nm, and 0.35 ± 0.02 at 235 nm. These values are in agreement with the value of 0.30 ± 0.07 at 236 nm reported by

Bell et al.[2] Fujiwara and Ishiwata[5] determined the relative yield of OH($^2\Pi_{3/2}$) / OH($^2\Pi_{1/2}$) to be 2.0 at 266 nm and 1.5 at 355 nm. A unit quantum yield for the OH + Cl channel is recommended.

Table 4F-14. Recommended Absorption Cross Sections of HOCl at 298 K

λ (nm)	10^{20} σ (cm^2)	λ (nm)	10^{20} σ (cm^2)	λ (nm)	10^{20} σ (cm^2)
200	7.18	274	5.26	348	1.55
202	6.39	276	4.94	350	1.43
204	5.81	278	4.74	352	1.33
206	5.46	280	4.64	354	1.24
208	5.37	282	4.62	356	1.17
210	5.54	284	4.68	358	1.11
212	5.98	286	4.79	360	1.06
214	6.68	288	4.95	362	1.02
216	7.63	290	5.13	364	0.985
218	8.81	292	5.33	366	0.951
220	10.2	294	5.52	368	0.919
222	11.6	296	5.71	370	0.888
224	13.2	298	5.86	372	0.855
226	14.7	300	5.99	374	0.822
228	16.2	302	6.08	376	0.786
230	17.5	304	6.12	378	0.748
232	18.7	306	6.12	380	0.708
234	19.6	308	6.07	382	0.667
236	20.2	310	5.97	384	0.624
238	20.5	312	5.84	386	0.580
240	20.6	314	5.66	388	0.535
242	20.3	316	5.45	390	0.491
244	19.8	318	5.21	392	0.447
246	19.0	320	4.95	394	0.405
248	18.1	322	4.67	396	0.364
250	17.0	324	4.38	398	0.325
252	15.8	326	4.09	400	0.288
254	14.6	328	3.79	402	0.254
256	13.3	330	3.50	404	0.222
258	12.1	332	3.21	406	0.194
260	10.9	334	2.94	408	0.168
262	9.73	336	2.68	410	0.144
264	8.68	338	2.44	412	0.124
266	7.75	340	2.22	414	0.105
268	6.94	342	2.02	416	0.089
270	6.25	344	1.84	418	0.075
272	5.69	346	1.69	420	0.063

Note:
Barnes et al.[1] (calculated using analytical expression)

(1) Barnes, R. J.; Sinha, A.; Michelsen, H. A. Assessing the contribution of the lowest triplet state to the near-UV absorption spectrum of HOCl. *J. Phys. Chem. A* **1998**, *102*, 8855-8859, doi:10.1021/jp9835869.

(2) Bell, A. J.; Boggis, S. A.; Dyke, J. M.; Frey, J. G.; Richter, R.; Shaw, N.; Tabrizchi, M. Ultraviolet photolysis of HOCl: REMPI measurement of the relative population of chlorine atom (^{2}P) spin-orbit states. *J. Chem. Soc. Faraday Trans.* **1994**, *90*, 17-21, doi:10.1039/ft9949000017.

(3) Burkholder, J. B. Ultraviolet absorption spectrum of HOCl. *J. Geophys. Res.* **1993**, *98*, 2963-2974, doi:10.1029/92JD02522

(4) Butler, P. J. D.; Phillips, L. F. Upper limit for the atomic oxygen yield in the 308-nm photolysis of HOCl. *J. Phys. Chem.* **1983**, *87*, 183-184, doi:10.1021/j100224a040.

(5) Fujiwara, H.; Ishiwata, T. Doppler spectroscopy of OH fragments from the photodissociation of HOCl at 266 and 355 nm. *J. Phys. Chem.* **1998**, *102*, 3856-3859, doi:10.1021/jp980647u.

(6) Jungkamp, T. P. W.; Kirchner, U.; Schmidt, M.; Schindler, R. N. UV absorption cross-section data for the hypochlorites ROCl (R = H, CH_3, C_2H_5, *i*-C_3H_7, *tert*-C_4H_9). *J. Photochem. Photobiol. A: Chem.* **1995**, *99*, 1-6, doi:10.1016/1010-6030(95)04074-P.
(7) Knauth, H.-D.; Alberti, H.; Clausen, H. Equilibrium constant of the gas reaction $Cl_2O + H_2O \rightleftharpoons 2HOCl$ and the ultraviolet spectrum of HOCl. *J. Phys. Chem.* **1979**, *83*, 1604-1612, doi:10.1021/j100475a010.
(8) Minaev, B. F. The singlet-triplet absorption and photodissociation of the HOCl, HOBr, and HOI molecules calculated by the MCSCF quadratic response method. *J. Phys. Chem. A* **1999**, *103*, 7294-7309, doi:10.1021/jp990203d.
(9) Mishalanie, E. A.; Rutkowski, J. C.; Hutte, R. S.; Birks, J. W. Ultraviolet absorption spectrum of gaseous HOCl. *J. Phys. Chem.* **1986**, *90*, 5578-5584, doi:10.1021/j100280a021.
(10) Molina, L. T.; Molina, M. J. Ultraviolet spectrum of HOCl. *J. Phys. Chem.* **1978**, *82*, 2410-2414, doi:10.1021/j100511a013.
(11) Molina, M. J.; Ishiwata, T.; Molina, L. T. Production of OH from photolysis of HOCl at 307-309 nm. *J. Phys. Chem.* **1980**, *84*, 821-826, doi:10.1021/j100445a004.
(12) Permien, T.; Vogt, R.; Schindler, R. N. Mechanisms of gas phase-liquid phase chemical transformations. In *Air Pollution Report #17*; Cox, R. A., Ed.; Environmental Research Program of the CEC: Brussels, 1988.
(13) Schindler, R. N.; Liesner, M.; Schmidt, S.; Kirchner, U.; Benter, T. Identification of nascent products formed in the laser photolysis of CH_3OCl and HOCl at 308 nm and around 235 nm. Total Cl-atom quantum yields and the state and velocity distributions of $Cl(^2P_j)$. *J. Photochem. Photobiol. A: Chem.* **1997**, *107*, 9-19, doi:10.1016/S1010-6030(96)04583-2.
(14) Vogt, R.; Schindler, R. N. Product channels in the photolysis of HOCl. *J. Photochem. Photobiol. A: Chem.* **1992**, *66*, 133-140, doi:10.1016/1010-6030(92)85207-B.

F15. ClNO (nitrosyl chloride)

Back to Index

$ClNO + h\nu \rightarrow Cl + NO$	160 kJ mol^{-1}	749 nm	(1)

(Recommendation: 02-25, Note: 10-6, Evaluated: 10-6)

Absorption Cross Sections: Nitrosyl chloride, ClNO, has a continuous UV/vis absorption spectrum extending beyond 650 nm. There is good agreement between the work of Martin and Gareis[6] (235–400 nm), Ballash and Armstrong[1] (185–540 nm), Illies and Takacs[5] (190–400 nm), and Tyndall et al.[9] (190–350 nm) except around 230 nm where the values of Ballash and Armstrong are larger by almost a factor of two. Roehl et al.[7] (350–650 nm) measured ClNO absorption cross sections at several temperatures between 223 and 343 K. Their room temperature results agree to within 15% with those of Martin and Gareis,[6] Ballash and Amstrong,[1] and Tyndall et al.[9] The recommended absorption cross sections in Table 4F-15 are taken from the work of Tyndall et al.[9] between 190 and 350 nm and from Roehl et al.[7] beyond 350 nm.

Photolysis Quantum Yield and Product Studies: The quantum yield for the primary photolytic process has been reviewed by Calvert and Pitts.[2] The quantum yield is unity over the entire visible and near-ultraviolet bands. Chichinin[3] found evidence of ground state ($^2P_{3/2}$) and excited ($^2P_{1/2}$) atomic chlorine products and measured a relative quantum yield $Cl(^2P_{1/2})/ (Cl(^2P_{1/2}) + Cl(^2P_{3/2}))$ to be 0.88 ± 0.12 at 248 nm and 0.90 ± 0.10 at 351 nm. Felder and Morley[4] obtained 0.80 at 248 nm and Skorokhodov et al.[8] obtained 0.48 ± 0.03 at 212 nm, 0.30 at 235 nm, and 0.52 ± 0.03 at 248 nm.

Table 4F-15. Recommended Absorption Cross Sections of ClNO at 298 K

λ (nm)	10^{20} σ (cm^2)	λ (nm)	10^{20} σ (cm^2)	λ (nm)	10^{20} σ (cm^2)	λ (nm)	10^{20} σ (cm^2)
190	4320	246	45.2	302	10.3	370	11.0
192	5340	248	37.7	304	10.5	375	9.95
194	6150	250	31.7	306	10.8	380	8.86
196	6480	252	27.4	308	11.1	385	7.82
198	6310	254	23.7	310	11.5	390	6.86
200	5860	256	21.3	312	11.9	395	5.97
202	5250	258	19.0	314	12.2	400	5.13
204	4540	260	17.5	316	12.5	405	4.40
206	3840	262	16.5	318	13.0	410	3.83
208	3210	264	15.3	320	13.4	415	3.38
210	2630	266	14.4	322	13.6	420	2.89
212	2180	268	13.6	324	14.0	425	2.45
214	1760	270	12.9	326	14.3	430	2.21
216	1400	272	12.3	328	14.6	435	2.20
218	1110	274	11.8	330	14.7	440	2.20
220	896	276	11.3	332	14.9	445	2.07
222	707	278	10.7	334	15.1	450	1.87
224	552	280	10.6	336	15.3	455	1.79
226	436	282	10.2	338	15.3	460	1.95
228	339	284	9.99	340	15.2	465	2.25
230	266	286	9.84	342	15.3	470	2.50
232	212	288	9.71	344	15.1	475	2.61
234	164	290	9.64	346	15.1	480	2.53
236	120	292	9.63	348	14.9	485	2.33
238	101	294	9.69	350	14.2	490	2.07
240	82.5	296	9.71	355	13.6	495	1.78
242	67.2	298	9.89	360	12.9	500	1.50
244	55.2	300	10.0	365	12.0		

Note:
190–350 nm: Tyndall et al.[9]
355–500 nm: Roehl et al.[7]

(1) Ballash, N. M.; Armstrong, D. A. On the ultraviolet and visible absorption spectrum of ClNO. *Spectrochim. Acta Part A* **1974**, *30*, 941-944, doi:10.1016/0584-8539(74)80009-7.

(2) Calvert, J. G.; Pitts, J. N. In *Photochemistry*; John Wiley & Sons, Inc.: New York, 1966; pp 230-231.

(3) Chichinin, A. I. Measurement of $Cl(^2P_{1/2})$ quantum yield for the photodissociaton of NOCl, ICl, PCl_3, Cl_2O and $COCl_2$. *Chem. Phys. Lett.* **1993**, *209*, 459-463, doi:10.1016/0009-2614(93)80117-8.

(4) Felder, P.; Morley, G. P. Photodissociation of ClNO in the A band. *Chem. Phys.* **1994**, *185*, 145-151, doi:10.1016/0301-0104(94)00120-0.

(5) Illies, A. J.; Takacs, G. A. Gas phase ultra-violet photoabsorption cross-sections for nitrosyl chloride and nitryl chloride. *J. Photochem.* **1976**, *6*, 35-42, doi:10.1016/0047-2670(76)87005-0.

(6) Martin, H.; Gareis, R. Die kinetik der reaktion von ClO_2 mit NO_2 in der lösungsphase. *Z. Elektrochemie* **1956**, *60*, 959-964.

(7) Roehl, C. M.; Orlando, J. J.; Calvert, J. G. The temperature dependence of the UV-visible absorption cross-sections of NOCl,. *J. Photochem. Photobiol. A: Chem.* **1992**, *69*, 1-5, doi:10.1016/1010-6030(92)85253-Q.

(8) Skorokhodov, V.; Sato, Y.; Suto, K.; Matsumi, Y.; Kawasaki, M. Photofragmentation of ClNO in the A-band: Velocity distribution and fine-structure branching ratio of $Cl(^2P_j)$ atoms. *J. Phys. Chem.* **1996**, *100*, 12321-12328, doi:10.1021/jp9535708.

(9) Tyndall, G. S.; Stedman, K. M.; Schneider, W.; Burrows, J. P.; Moortgat, G. K. The absorption spectrum of ClNO between 190 and 350 nm. *J. Photochem.* **1987**, *36*, 133-139, doi:10.1016/0047-2670(87)87070-3.

F16. $ClNO_2$ (nitryl chloride)

Back to Index

$ClNO_2 + h\nu$	$\rightarrow Cl + NO_2$	143 kJ mol^{-1}	839 nm	(1)
	$\rightarrow ClNO + O$	290 kJ mol^{-1}	413 nm	(2)

(Recommendation: 15-10, Note: 15-10, Evaluated: 15-10)

Absorption Cross Sections: The UV absorption spectrum of nitryl chloride, $ClNO_2$, has been measured at room temperature by Martin and Gareis[6] (230–330 nm), Illies and Takacs[5] (185–400 nm), Nelson and Johnston[7] (270–370 nm), Ganske et al.[3] (200–370 nm), Furlan et al.[2] (190–450 nm), and Ghosh et al.[4] (200–475 nm). The absorption spectrum has three broad overlapping bands, a weak band at ~300 nm and two stronger bands at ~215 nm and below 185 nm. In the range 220–280 nm, weak but distinct vibrational structure was observed by Furlan et al.[2] A major source of discrepancies in the data results from the presence of impurities. The recommended absorption cross sections in Table 4F-16 are taken from Ghosh et al. (rounded to 3 significant figures).

Ghosh et al. measured the $ClNO_2$ UV/vis spectrum temperature dependence over the range 210–296 K (the only temperature dependent study available). They parameterized the spectrum temperature dependence using the empirical formula:

$$\sigma(\lambda, T) = \sigma(\lambda, 296\ \mathrm{K}) \times (1 + A(\lambda) \times (\mathrm{T} - 296) + B(\lambda) \times (\mathrm{T} - 296)^2)$$

The recommended fit parameters are included in Table 4F-16.

Photolysis Quantum Yield and Product Studies: Nelson and Johnston[7] report a value of 0.93 ± 0.15 for Φ(Cl) and Φ(O) < 0.02 for photolysis at 350 nm. Carter et al.[1] reported the formation of NO_2 in the electronic ground state (yield 0.15 ± 0.05) and in the excited state (yield 0.85 ± 0.05) for 235 nm photolysis. Ghosh et al.[4] report Φ(O) values of 0.67 ± 0.12 and 0.15 ± 0.03 (2σ) for photolysis at 193 and 248 nm, respectively.

Table 4F-16. Recommended Absorption Cross Sections of $ClNO_2$ at 296 K and Temperature Dependence Coefficients

λ (nm)	10^{20} σ (cm^2)	10^5 $A(\lambda)$ (K^{-1})	10^5 $B(\lambda)$ (K^{-2})	λ (nm)	10^{20} σ (cm^2)	10^5 $A(\lambda)$ (K^{-1})	10^5 $B(\lambda)$ (K^{-2})
200	402	413	2.08	345	2.73	459.8	0.97
205	306	211	1.85	350	2.07	522.1	1.14493
210	326	96	1.50	355	1.56	593	1.46169
215	348	68	1.38	360	1.17	660.3	1.71663
220	332	73	1.29	365	0.870	726.4	2.00104
225	282	105	1.26	370	0.648	792.1	2.33777
230	220	155	1.29	375	0.482	850.9	2.60668
235	170	203	1.36	380	0.358	910.8	2.92818
240	135	229	1.39	385	0.268	974	3.34597
245	111	242	1.48	390	0.201	1024.7	3.65781
250	92.9	239	1.50	395	0.150	1080.8	3.97039
255	75.9	230	1.44	400	0.112	1143.2	4.4706
260	59.6	246	1.54	405	0.0840	1174.7	4.52843
265	45.9	268	1.69	410	0.0642	1236	5.16769
270	34.8	258	1.65	415	0.0486	1231.6	4.89102
275	26.8	236	1.58	420	0.0360	1257	4.91924
280	21.8	194	1.52	425	0.0282	1411.4	7.03785
285	18.8	136	1.36	430	0.0212	1332.4	5.69311
290	17.0	84	1.17	435	0.0169	1528.6	8.564
295	15.8	60	1.04	440	0.0122	1161.9	2.753
300	14.8	58	0.91	445	0.00905	1410	6.785
305	13.5	73	0.82	450	0.007899	1550.1	8.966
310	12.0	99	0.74	455	0.006348	1357.1	5.061
315	10.4	135.6	0.70	460	0.005474	2100.9	17.81
320	8.81	176.8	0.66	465	0.003690	2395.2	21.91
325	7.24	227.6	0.69	470	0.003207	1401.8	6.412
330	5.82	278.8	0.68	475	0.002053	910	2.214
335	4.59	336.4	0.74				
340	3.56	397.9	0.86				

Note:
Ghosh et al.,[4] cross sections rounded to 3 significant figures, higher resolution data available are from this study

(1) Carter, R. T.; Hallou, A.; Huber, J. R. Photodissociation of $ClNO_2$ at 235 nm. *Chem. Phys. Lett.* **1999**, *310*, 166-172, doi:10.1016/S0009-2614(99)00781-2.

(2) Furlan, A.; Haeberli, M. A.; Huber, R. J. The 248 nm photodissociation of $ClNO_2$ studied by photofragment translational energy spectroscopy. *J. Phys. Chem. A* **2000**, *104*, 10392-10397, doi:10.1021/jp000792j.

(3) Ganske, J. A.; Berko, H. N.; Finlayson-Pitts, B. J. Absorption cross sections for gaseous $ClNO_2$ and Cl_2 at 298 K: Potential organic oxidant source in the marine troposphere. *J. Geophys. Res.* **1992**, *97*, 7651-7656, doi:10.1029/92JD00414.

(4) Ghosh, B.; Papanastasiou, D. K.; Talukdar, R. K.; Roberts, J. M.; Burkholder, J. B. Nitryl chloride ($ClNO_2$): UV/Vis absorption spectrum between 210 and 296 K and $O(^3P)$ quantum yield at 193 and 248 nm. *J. Phys. Chem. A* **2011**, *116*, 5796-5805, doi:10.1021/jp207389y.

(5) Illies, A. J.; Takacs, G. A. Gas phase ultra-violet photoabsorption cross-sections for nitrosyl chloride and nitryl chloride. *J. Photochem.* **1976**, *6*, 35-42, doi:10.1016/0047-2670(76)87005-0.

(6) Martin, H.; Gareis, R. Die kinetik der reaktion von ClO_2 mit NO_2 in der lösungsphase. *Z. Elektrochemie* **1956**, *60*, 959-964.

(7) Nelson, H. H.; Johnston, H. S. Kinetics of the reaction of Cl with ClNO and $ClNO_2$ and the photochemistry of $ClNO_2$. *J. Phys. Chem.* **1981**, *85*, 3891-3896, doi:10.1021/j150625a036.

F17. ClONO (chlorine nitrite)

Back to Index

$ClONO + h\nu$	$\rightarrow Cl + NO_2$	80 kJ mol^{-1}	1498 nm	(1)
	$\rightarrow ClO + NO$	227 kJ mol^{-1}	528 nm	(2)

(Recommendation: 78, Note: 10-6, Evaluated: 10-6)

Absorption Cross Sections: The UV absorption spectrum of chlorine nitrite, ClONO, was measured by Molina and Molina.[1] The absorption cross sections were determined by mass balance during the $Cl_2O + ClNO \rightarrow Cl_2 + ClONO$ reaction and isomerization of ClONO to $ClNO_2$. The recommended absorption cross sections in Table 4F-17 are taken from this study.

Photolysis Quantum Yield and Product Studies: It is assumed that the quantum yield for ClONO UV photolysis is unity. The Cl–O bond strength is only ~20 kcal $mole^{-1}$, so that chlorine atoms are likely photolysis products.

Table 4F-17. Recommended Absorption Cross Sections of ClONO at 231 K

λ (nm)	10^{20} σ (cm^2)	λ (nm)	10^{20} σ (cm^2)
235	215.0	320	80.3
240	176.0	325	75.4
245	137.0	330	58.7
250	106.0	335	57.7
255	65.0	340	43.7
260	64.6	345	35.7
265	69.3	350	26.9
270	90.3	355	22.9
275	110.0	360	16.1
280	132.0	365	11.3
285	144.0	370	9.0
290	144.0	375	6.9
295	142.0	380	4.1
300	129.0	385	3.3
305	114.0	390	2.2
310	105.0	395	1.5
315	98.1	400	0.6

Note: Molina and Molina[1]

(1) Molina, L. T.; Molina, M. J. Ultraviolet absorption spectrum of chlorine nitrite, ClONO. *Geophys. Res. Lett.* **1977**, *4*, 83-86, doi:10.1029/GL004i002p00083.

F18. $ClONO_2$ (chlorine nitrate)

Back to Index

$ClONO_2 + h\nu$	$\rightarrow Cl + NO_3$	173 kJ mol^{-1}	692 nm	(1)
	$\rightarrow ClO + NO_2$	113 kJ mol^{-1}	1063 nm	(2)
	$\rightarrow O(^3P) + ClONO$	291 kJ mol^{-1}	412 nm	(3)

(Recommendation: 06-2, Note: 15-10, Evaluated: 15-10)

Absorption Cross Sections: The recommended cross sections of chlorine nitrate, $ClONO_2$, are taken from the work of Burkholder et al. (196–432 nm, 220–296 K).[2] The cross section values are listed in Table 4F-18 together with the parameters needed to compute their temperature dependence. These values are in good agreement with those reported by Molina and Molina,[10] which provided the basis for earlier recommendations and which supersedes the work of Rowland et al.[15] An uncertainty factor in the room temperature cross sections of 1.1 (2σ) is estimated for the wavelength region $196 < \lambda < 432$ nm.

Photolysis Quantum Yield and Product Studies: Several groups have investigated the identity of the primary photolytic fragments. Smith et al.[16] report O + ClONO as the most likely products, using end-product analysis and steady-state photolysis. The results of Chang et al.,[4] which were obtained using the very low-pressure photolysis (VLPPh) technique, indicate that the products are $Cl + NO_3$, with a quantum yield of 1.0 ± 0.2. Adler-Golden and Wiesenfeld,[1] using a flash photolysis atomic absorption technique, find O atoms to be the predominant photolysis product and report a quantum yield for Cl atom production of less than 4%. Marinelli and Johnston[8] report a quantum yield for NO_3 production at 249 nm between 0.45 and 0.85, with a most likely value of 0.55; they monitored NO_3 by tunable dye laser absorption at 662 nm. Margitan[7] used atomic resonance

fluorescence detection of O and Cl atoms and found the quantum yield at 266 nm and at 355 nm to be 0.9 ± 0.1 for Cl atom production and ~0.1 for O atom production, with no discernible difference at the two wavelengths. These results were confirmed by Knauth and Schindler,[6] who used end-product analysis to infer the quantum yields from photolysis studies at 265 and 313 nm. Burrows et al.[3] report also Cl and NO_3 as the photolysis products at 254 nm, with a quantum yield of unity within experimental error, and an O atom quantum yield of 0.24. In contrast, Nikolaisen et al.[13] using broadband photolysis found that at $\lambda > 200$ nm the relative branching ratios are 0.61 ± 0.20 for the channel $ClO + NO_2$ and 0.39 ± 0.20 for the channel $Cl + NO_3$; in the $\lambda > 300$ nm region the quantum yields are found to be 0.44 ± 0.08 for production of ClO and NO_2 and 0.56 ± 0.08 for production of Cl and NO_3. Minton et al.,[9] Nelson et al.,[12] and Moore et al.[11] made the first direct measurements of ClO and obtained comparable yields for the $Cl + NO_3$ and the $ClO + NO_2$ channels, using a molecular beam technique: at 193 nm they obtained respectively 0.64 ± 0.08 and 0.36 ± 0.08, at 248 nm 0.54 ± 0.08 and 0.46 ± 0.08, and at 308 nm 0.67 ± 0.06 and 0.33 ± 0.06. These authors found no evidence for the O + ClONO channel and placed an upper limit for this channel of 0.04. Tyndall et al.[17] observed quantum yields of 0.80 ± 0.08 and 0.28 ± 0.12 for Cl and ClO at 308 nm using resonance fluorescence detection methods and reported a $O(^3P)$ yield of ≤0.05. Ravishankara,[14] Goldfarb et al.,[5] and Yokelson et al.[18] have studied the photodissociation of $ClONO_2$ at 193, 222, 248 and 308 nm using atomic resonance fluorescence and time resolved absorption methods. They found that Cl and ClO are the two major dissociation products at 222, 248 and 308 nm, whereas at 193 nm, the quantum yield of O atoms was larger than the yield of ClO. At 193, 222, 248 and 308 nm, the yield of Cl was 0.53 ± 0.10, 0.46 ± 0.10, 0.41 ± 0.13 and 0.64 ± 0.20, respectively; the O atom yield 0.73 ± 0.08, 0.17 ± 0.08, <0.10 and <0.05; and the ClO yield 0.29 ± 0.20, 0.64 ± 0.20, 0.39 ± 0.19 and 0.37 ± 0.19. The NO_3 yield was determined by Yokelson et al.[18] to be 0.93 ± 0.24 at 352.5 nm, 0.67 ± 0.09 at 308 nm, 0.60 ± 0.09 at 248 nm, and 0.18 ± 0.04 at 193 nm. In addition, Yokelson et al.[18] measured the Cl atom yield as 0.73 ± 0.14 at 308 nm, 0.60 ± 0.12 at 248 nm and 0.45 ± 0.08 at 193 nm, and the O atom yield as <0.4 at 248 nm and <0.9 at 193 nm. Zou et al.[19] determined absolute quantum yields for the Cl and ClO channels at 235 nm to be 0.42 ± 0.1 and 0.58 ± 0.1, respectively, using molecular beam techniques and TOFMS/REMPI.

The recommended quantum yield values for production of $Cl + NO_3$ (Φ_1) and $ClO + NO_2$ (Φ_2) are given at the bottom of Table 4F-18 and are based on the work of Nelson et al.,[12] Moore et al.,[11] Nickolaisen et al.,[13] Goldfarb et al.,[5] and Yokelson et al.[18] For wavelengths shorter than 308 nm the value of Φ_1 is 0.6 and Φ_2 is 0.4. For longer wavelengths Φ_1 increases linearly to 0.9 at 350 nm with the corresponding decrease in Φ_2 to 0.1. There is no evidence for production of O + ClONO in the more recent work; the production of O atoms reported in some of the earlier studies may have resulted from the decomposition of excited NO_3. Zou et al.[19] determined the quantum yield of spontaneous decomposition of NO_3 into $NO_2 + O$ to be 0.20 and into $NO + O_2$ to be 0.006.

Work by Nickolaisen et al.[13] indicates that the photodissociation quantum yield is less than unity at wavelengths longer than ~330 nm because of the formation of a long-lived intermediate that may be quenched under atmospheric conditions (a situation analogous to that of Cl_2O).

Table 4F-18. Recommended Absorption Cross Sections and Temperature Coefficients of $ClONO_2$

$\sigma(\lambda, T) = \sigma(\lambda, 296)\ (1 + A1\ (T–296) + A2\ (T–296)^2)$; T in K

λ (nm)	10^{20} σ(λ, 296) (cm^2)	A1* (K^{-1})	A2* (K^{-2})	λ (nm)	10^{20} σ(λ, 296) (cm^2)	A1* (K^{-1})	A2* (K^{-2})
196	310	9.90 (–5)	–8.38 (–6)	316	1.07	5.07 (–3)	1.56 (–5)
198	294	6.72 (–5)	–8.03 (–6)	318	0.947	5.24 (–3)	1.69 (–5)
200	282	–5.34 (–6)	–7.64 (–6)	320	0.831	5.40 (–3)	1.84 (–5)
202	277	–1.19 (–4)	–7.45 (–6)	322	0.731	5.55 (–3)	2.00 (–5)
204	280	–2.60 (–4)	–7.50 (–6)	324	0.647	5.68 (–3)	2.18 (–5)
206	288	–4.12 (–4)	–7.73 (–6)	326	0.578	5.80 (–3)	2.36 (–5)
208	300	–5.62 (–4)	–8.05 (–6)	328	0.518	5.88 (–3)	2.54 (–5)
210	314	–6.96 (–4)	–8.41 (–6)	330	0.466	5.92 (–3)	2.70 (–5)
212	329	–8.04 (–4)	–8.75 (–6)	332	0.420	5.92 (–3)	2.84 (–5)
214	339	–8.74 (–4)	–9.04 (–6)	334	0.382	5.88 (–3)	2.96 (–5)
216	345	–9.03 (–4)	–9.24 (–6)	336	0.351	5.80 (–3)	3.05 (–5)
218	341	–8.86 (–4)	–9.35 (–6)	338	0.326	5.68 (–3)	3.10 (–5)
220	332	–8.28 (–4)	–9.38 (–6)	340	0.302	5.51 (–3)	3.11 (–5)
222	314	–7.31 (–4)	–9.34 (–6)	342	0.282	5.32 (–3)	3.08 (–5)
224	291	–6.04 (–4)	–9.24 (–6)	344	0.264	5.07 (–3)	2.96 (–5)

λ (nm)	10^{20} σ(λ, 296) (cm^2)	A1* (K^{-1})	A2* (K^{-2})	λ (nm)	10^{20} σ(λ, 296) (cm^2)	A1* (K^{-1})	A2* (K^{-2})
226	264	–4.53 (–4)	–9.06 (–6)	346	0.252	4.76 (–3)	2.74 (–5)
228	235	–2.88 (–4)	–8.77 (–6)	348	0.243	4.39 (–3)	2.42 (–5)
230	208	–1.13 (–4)	–8.33 (–6)	350	0.229	4.02 (–3)	2.07 (–5)
232	182	6.18 (–5)	–7.74 (–6)	352	0.218	3.68 (–3)	1.76 (–5)
234	158	2.27 (–4)	–7.10 (–6)	354	0.212	3.40 (–3)	1.50 (–5)
236	138	3.72 (–4)	–6.52 (–6)	356	0.205	3.15 (–3)	1.27 (–5)
238	120	4.91 (–4)	–6.14 (–6)	358	0.203	2.92 (–3)	1.06 (–5)
240	105	5.86 (–4)	–5.98 (–6)	360	0.200	2.70 (–3)	8.59 (–6)
242	91.9	6.64 (–4)	–6.04 (–6)	362	0.190	2.47 (–3)	6.38 (–6)
244	81.2	7.33 (–4)	–6.27 (–6)	364	0.184	2.22 (–3)	3.66 (–6)
246	71.6	8.03 (–4)	–6.51 (–6)	366	0.175	1.93 (–3)	2.42 (–7)
248	62.4	8.85 (–4)	–6.59 (–6)	368	0.166	1.62 (–3)	–3.62 (–6)
250	56.0	9.84 (–4)	–6.40 (–6)	370	0.159	1.33 (–3)	–7.40 (–6)
252	50.2	1.10 (–3)	–5.93 (–6)	372	0.151	1.07 (–3)	–1.07 (–5)
254	45.3	1.22 (–3)	–5.33 (–6)	374	0.144	8.60 (–4)	–1.33 (–5)
256	41.0	1.33 (–3)	–4.73 (–6)	376	0.138	6.73 (–4)	–1.54 (–5)
258	37.2	1.44 (–3)	–4.22 (–6)	378	0.129	5.01 (–4)	–1.74 (–5)
260	33.8	1.53 (–3)	–3.79 (–6)	380	0.121	3.53 (–4)	–1.91 (–5)
262	30.6	1.62 (–3)	–3.37 (–6)	382	0.115	2.54 (–4)	–2.05 (–5)
264	27.8	1.70 (–3)	–2.94 (–6)	384	0.108	2.25 (–4)	–2.11 (–5)
266	25.2	1.78 (–3)	–2.48 (–6)	386	0.103	2.62 (–4)	–2.11 (–5)
268	22.7	1.86 (–3)	–2.00 (–6)	388	0.0970	3.33 (–4)	–2.08 (–5)
270	20.5	1.94 (–3)	–1.50 (–6)	390	0.0909	4.10 (–4)	–2.05 (–5)
272	18.5	2.02 (–3)	–1.01 (–6)	392	0.0849	5.04 (–4)	–2.02 (–5)
274	16.6	2.11 (–3)	–4.84 (–7)	394	0.0780	6.62 (–4)	–1.94 (–5)
276	14.9	2.20 (–3)**	9.02 (–8)	396	0.0740	8.95 (–4)	–1.79 (–5)
278	13.3	2.29 (–3)	6.72 (–7)	398	0.0710	1.14 (–3)	–1.61 (–5)
280	11.9	2.38 (–3)	1.21 (–6)	400	0.0638	1.38 (–3)	–1.42 (–5)
282	10.5	2.47 (–3)	1.72 (–6)	402	0.0599	1.63 (–3)	–1.20 (–5)
284	9.35	2.56 (–3)	2.21 (–6)	404	0.0568	1.96 (–3)	–8.97 (–6)
286	8.26	2.66 (–3)	2.68 (–6)	406	0.0513	2.36 (–3)	–5.15 (–6)
288	7.24	2.75 (–3)	3.09 (–6)	408	0.0481	2.84 (–3)	–6.64 (–7)
290	6.41	2.84 (–3)	3.41 (–6)	410	0.0444	3.38 (–3)	4.47 (–6)
292	5.50	2.95 (–3)	3.74 (–6)	412	0.0413	3.96 (–3)	1.00 (–5)
294	4.67	3.08 (–3)	4.27 (–6)	414	0.0373	4.56 (–3)	1.60 (–5)
296	4.09	3.25 (–3)	5.13 (–6)	416	0.0356	5.22 (–3)	2.28 (–5)
298	3.57	3.45 (–3)	6.23 (–6)	418	0.0317	5.96 (–3)	3.07 (–5)
300	3.13	3.64 (–3)	7.36 (–6)	420	0.0316	6.70 (–3)	3.87 (–5)
302	2.74	3.83 (–3)	8.38 (–6)	422	0.0275	7.30 (–3)	4.58 (–5)
304	2.39	4.01 (–3)	9.30 (–6)	424	0.0242	7.82 (–3)	5.22 (–5)
306	2.09	4.18 (–3)	1.02 (–5)	426	0.0222	8.41 (–3)	5.95 (–5)
308	1.83	4.36 (–3)	1.11 (–5)	428	0.0207	9.11 (–3)	6.79 (–5)
310	1.60	4.53 (–3)	1.20 (–5)	430	0.0189	9.72 (–3)	7.52 (–5)
312	1.40	4.71 (–3)	1.30 (–5)	432	0.0188	9.96 (–3)	7.81 (–5)
314	1.22	4.89 (–3)	1.42 (–5)				

Notes:
Burkholder et al.[2]
*) (–n) means $\times 10^{-n}$.
**) Value corrected for an obvious misprint.

Quantum yields:

$ClONO_2 + h\nu \rightarrow Cl + NO_3$

$\Phi_1 = 0.6$ ($\lambda < 308$ nm)
$\Phi_1 = 7.143 \times 10^{-3}\ \lambda$ (nm)–1.60 (308 nm < λ < 364 nm)
$\Phi_1 = 1.0$ ($\lambda > 364$ nm)

$ClONO_2 + h\nu \rightarrow ClO + NO_2$

$\Phi_2 = 1–\Phi_1$

(1) Adler-Golden, S. M.; Wiesenfeld, J. R. Production of atomic oxygen following flash photolysis of $ClONO_2$. *Chem. Phys. Lett.* **1981**, *82*, 281-284, doi:10.1016/0009-2614(81)85156-1.

(2) Burkholder, J. B.; Talukdar, R. K.; Ravishankara, A. R. Temperature dependence of the $ClONO_2$ UV absorption spectrum. *Geophys. Res. Lett.* **1994**, *21*, 585-588, doi:10.1029/93GL03303.

(3) Burrows, J. P.; Tyndall, G. S.; Moortgat, G. K. Photolysis of chlorine nitrate at 254 nm. *J. Phys. Chem.* **1988**, *92*, 4340-4348, doi:10.1021/j100326a020.

(4) Chang, J. S.; Barker, J. R.; Davenport, J. E.; Golden, D. M. Chlorine nitrate photolysis by a new technique: Very low pressure photolysis. *Chem. Phys. Lett.* **1979**, *60*, 385-390, doi:10.1016/0009-2614(79)80594-1.

(5) Goldfarb, L.; Schmoltner, A.-M.; Gilles, M. K.; Burkholder, J.; Ravishankara, A. R. Photodissociation of $ClONO_2$: 1. Atomic resonance fluorescence measurements of product quantum yields. *J. Phys. Chem. A* **1997**, *101*, 6658-6666, doi:10.1021/jp970818f.

(6) Knauth, H.-D.; Schindler, R. N. On the photodecomposition of $ClONO_2$ in the middle ultraviolet. *Z. Naturforsch.* **1983**, *38a*, 893-895.

(7) Margitan, J. J. Chlorine nitrate photochemistry. Photolysis products and kinetics of the reaction Cl + $ClONO_2 \rightarrow Cl_2 + NO_3$. *J. Phys. Chem.* **1983**, *87*, 674-679, doi:10.1021/j100227a029.

(8) Marinelli, W. J.; Johnston, H. S. Quantum yield for NO_3 production from photolysis of $ClONO_2$. *Chem. Phys. Lett.* **1982**, *93*, 127-132, doi:10.1016/0009-2614(82)83678-6.

(9) Minton, T. K.; Nelson, C. M.; Moore, T. A.; Okumura, M. Direct observation of ClO from chlorine nitrate photolysis. *Science* **1992**, *258*, 1342-1345, doi:10.1126/science.258.5086.1342.

(10) Molina, L. T.; Molina, M. J. Chlorine nitrate ultraviolet absorption spectrum at stratospheric temperatures. *J. Photochem.* **1979**, *11*, 139-144, doi:10.1016/0047-2670(79)80047-7.

(11) Moore, T. A.; Okumura, M.; Tagawa, M.; Minton, T. K. Dissociation dynamics of $ClONO_2$ and relative Cl and ClO product yields following photoexcitation at 308 nm. *Faraday Discuss.* **1995**, *100*, 295-307, doi:10.1039/fd9950000295.

(12) Nelson, C. M.; Moore, T. A.; Okumura, M.; Minton, T. K. Photodissociation of $ClONO_2$ at 193 and 248 nm. *Chem. Phys.* **1996**, *2248*, 287-307, doi:10.1016/0301-0104(95)00383-5.

(13) Nickolaisen, S. L.; Sander, S. P.; Friedl, R. R. Pressure-dependent yields and product branching ratios in the broadband photolysis of chlorine nitrate. *J. Phys. Chem.* **1996**, *100*, 10165-10178, doi:10.1021/jp953612s.

(14) Ravishankara, A. R. *Faraday Discuss.* **1995**, *100*, 335-336, doi:10.1039/fd9950000333.

(15) Rowland, F. S.; Spencer, J. E.; Molina, M. J. Stratospheric formation and photolysis of chlorine nitrate. *J. Phys. Chem.* **1976**, *80*, 2711-2713, doi:10.1021/j100565a019.

(16) Smith, W. S.; Chou, C. C.; Rowland, F. S. The mechanism for ultraviolet photolysis of gaseous chlorine nitrate at 302.5 nm. *Geophys. Res. Lett.* **1977**, *4*, 517-519, doi:10.1029/GL004i011p00517.

(17) Tyndall, G. S.; Kegley-Owen, C. S.; Orlando, J. J.; Calvert, J. G. Quantum yields for $Cl(^2P_{3/2,1/2})$, ClO and $O(^3P)$ in the photolysis of chlorine nitrate at 308 nm. *J. Chem. Soc. Faraday Trans.* **1997**, *93*, 2675-2682, doi:10.1039/a701585b.

(18) Yokelson, R. J.; Burkholder, J.; Fox, R. W.; Ravishankara, A. R. Photodissociation of $ClONO_2$: 2. Time-resolved absorption studies of product quantum yields. *J. Phys. Chem. A* **1997**, *101*, 6667-6678, doi:10.1021/jp9708198.

(19) Zou, P.; Park, J.; Schmitz, B. A.; Nguyen, T.; North, S. W. Photodissociation of $ClONO_2$ at 235 nm: Final product yields and energy partitioning. *J. Phys. Chem. A* **2002**, *106*, 1004-1010, doi:10.1021/jp013099k.

F19. CCl_4 (carbon tetrachloride)

Back to Index

$CCl_4 + h\nu$	$\rightarrow Cl + CCl_3$	288 kJ mol^{-1}	416 nm	(1)
	$\rightarrow 2Cl + CCl_2$	338 kJ mol^{-1}	354 nm	(2)

(Recommendation: 15-10, Note: 15-10, Evaluated: 15-10)

Absorption Cross Sections: The VUV/UV absorption spectrum of carbon tetrachloride, CCl_4, has been measured at room temperature by Russell et al.[15] (110–200 nm), Causley and Russell[2] (110–200 nm), Gordus and Bernstein[5] (204–250 nm), Rowland and Molina[13] (186–226 nm), Roxlo and Mandl[14] (170–230 nm), Hubrich and Stuhl[8] (160–275 nm), Ibuki et al.[9] (105–210 nm), Hanf et al.[6] (135 and 193 nm), Currie et al.[4] (250 nm), Vanlaethem-Meurée et al.[18] (190–252 nm), Simon et al.[17] (174–250 nm), Prahlad and Kumar[10] (186–240 nm), and Rontu Carlon et al.[12] (184.95, 202.206, 206.200, 213.857, and 228.8 nm atomic lines and 200–235 nm). The room temperature data agree to within 10% between 190 and 235 nm and to within 20% and 40% at 240 and 250 nm, respectively (except the value at 250 nm reported by Currie et al.[4] that is significantly lower). The absorption spectrum of Prahlad and Kumar[10] has irregular structure over the entire wavelength range presumably due to the experimental precision of the measurements. In the range 180–186 nm, the cross section values reported by Hubrich and Stuhl[8] are higher by up to 25% than those reported by Simon et al.,[17] and the value at 186 nm reported by Prahlad and Kumar[10] is lower by 18% than the value of Simon et al. The value at 184.95 nm reported by Rontu Carlon et al. is in good agreement, to within 1.5%, with the NASA/JPL 10-6 recommendation. At the maximum near 176 nm Hubrich and Stuhl[8] and Simon et al.[17] report an absorption cross section of 1.01×10^{-17} cm^2. The peak cross section reported by Roxlo and Mandl[14] is lower, $\sim 7 \times 10^{-18}$ cm^2. Rebbert and Ausloos[11] derived a cross section at 313 nm of $\leq 3.7 \times 10^{-26}$ cm^2 from the C_2H_5Cl yield in the photolysis of CCl_4-C_2H_6 mixtures.

The recommended room temperature absorption cross sections in Table 4F-19 are the mean of the values reported by Hubrich and Stuhl[8] and Simon et al.[17] in the region 174–192 nm, from Simon et al.[17] in the region 194–198 nm, and from the revised cross section parameterization reported by Rontu Carlon et al. (see below) for the $200 \leq \lambda \leq 235$ nm region. Cross sections have been reported at longer wavelengths by Hubrich and Stuhl,[8] although no recommendation is given for this region. For the wavelength region 174–190 nm the estimated uncertainty factor is 1.2 (2σ) and for the region $190 \leq \lambda \leq 235$ nm the estimated uncertainty factor is 1.06 (2σ).

The temperature dependence of the absorption spectrum has been measured by Currie et al.[4] (250 nm) over the range 297–477 K, Vanlaethem-Meurée et al.[18] (190–252 nm) at 279 and 296 K, Simon et al.[17] (174–250 nm) over the range 225–295 K, Prahlad and Kumar[10] (186–240 nm) over the range 220–300 K, and Rontu Carlon et al. (200–235 nm) over the range 210–350 K. The spectrum has a significant temperature dependence at wavelengths >205 nm where the cross sections decrease with decreasing temperature. Simon et al.[17] parameterized the cross section temperature dependence using an empirical polynomial expansion:

$$\log_{10} \sigma(\lambda, T) = \sum A_n \lambda^n + (T-273) \times \sum B_n \lambda^n$$

and reported calculated cross section values for T = 210, 230, 250, 270, and 295 K. The parameters A_n and B_n, are valid for the temperature range 210–300 K and wavelength range 194–250 nm.

$A_0 = -37.104$	$B_0 = 1.0739$
$A_1 = -5.8218 \times 10^{-1}$	$B_1 = -1.6275 \times 10^{-2}$
$A_2 = 9.9974 \times 10^{-3}$	$B_2 = 8.8141 \times 10^{-5}$
$A_3 = -4.6765 \times 10^{-5}$	$B_3 = -1.9811 \times 10^{-7}$
$A_4 = 6.8501 \times 10^{-8}$	$B_4 = 1.5022 \times 10^{-10}$

On the basis of their results, Rontu Carlon et al. used the same empirical formula and reported a revised spectrum parameterization with the coefficients given below. The parameterization is valid for the wavelength range 200–235 nm and temperature range 210–350 K and reproduces their experimental data to within 3%. For the wavelength region 174–200 nm, Simon et al. report a temperature independent spectrum, which is inconsistent with the Rontu Carlon et al. results obtained at 185 and 200 nm. The Rontu Carlon et al. parameterization is recommended.

n	A_n	B_n
0	1112.736208	-1.116511649
1	-22.02146808	0.02447268904
2	0.1596666745	-0.0001954842393
3	-0.0005104078676	$6.775547148 \times 10^{-7}$
4	$6.062440506 \times 10^{-7}$	$-8.621070147 \times 10^{-10}$

The VUV absorption spectrum of CCl_4 has been measured by Russell et al.[15] (112–175 nm), Causley and Russell[2] (111–195 nm), Ibuki et al.[9] (105–210 nm), Ho[7] (4.9–200 nm), and Seccombe et al.[16] (50–200 nm). Burton et al.[1] measured cross sections for the region 6.4–225 nm using dipole (e,e) spectroscopy. The agreement in the σ(Lyman-α, 298 K) values is to within ~15%. The recommended σ(Lyman-α, 298 K) is the average of the interpolated results from Causley and Russell, Ibuki et al., and Ho, 3.7×10^{-17} cm^2 molecule^{-1}, with an uncertainty factor of 1.2 (2σ).

Photolysis Quantum Yield and Product Studies: Quantum yields ≥0.9 and ~0.75 for the photodissociative processes $CCl_4 + h\nu \rightarrow CCl_3 + Cl$ at 213.9 nm and $CCl_4 + h\nu \rightarrow CCl_2 + 2Cl$ at 163.3 nm, respectively, were derived from the gas-phase photolysis of CCl_4 in the presence of HCl, HBr, and C_2H_6 by Rebbert and Ausloos.[11] Clark and Husain[3] report a quantum yield for $Cl^*(^2P_{1/2})$ atom formation in the broadband photolysis of CCl_4 to be 0.78 ± 0.27. Hanf et al.[6] reported Cl atom quantum yields in the photolysis of CCl_4 to be Φ(Cl) = 1.1 ± 0.05 and Φ(Cl*) = 0.4 ± 0.02 (thus Φ(Cl + Cl*) = 1.5 ± 0.1) at 193 nm and Φ(Cl) = 1.5 ± 0.07 and Φ(Cl*) = 0.4 ± 0.02 (thus Φ(Cl + Cl*) = 1.9 ± 0.1) at 135 nm. A quantum yield of unity with Φ(Cl) = 1 is recommended.

Table 4F-19. Recommended Absorption Cross Sections of CCl_4 at 295 K

λ (nm)	10^{20} σ (cm^2)	λ (nm)	10^{20} σ (cm^2)
174	956	206	57.9
176	1010	208	53.0
178	982.5	210	47.4
180	806	212	41.3
182	647	214	35.2
184	478.5	216	29.3
186	338.5	218	23.8
188	227	220	18.9
190	145.5	222	14.7
192	99.6	224	11.3
194	76.7	226	8.53
196	69.5	228	6.63
198	68.0	230	4.71
200	67.8	232	3.48
202	64.8	234	2.57
204	61.9		

Notes:
174–192 nm: mean of data from Hubrich and Stuhl[8] and Simon et al.[17]
194–198 nm: Simon et al.[17]
200–234 nm: Rontu Carlon et al. [12]

(1) Burton, G. R.; Chan, W. F.; Cooper, G.; Brion, C. E. Valence- and inner-shell (Cl 2p, 2s; C 1s) photoabsorption and photoionization of carbon tetrachloride. Absolute oscillator strengths (5-400 eV) and dipole-induced breakdown pathways. *Chem. Phys.* **1994**, *181*, 147-172, doi:10.1016/0301-0104(94)85022-4.

(2) Causley, G. C.; Russell, B. R. The vacuum ultraviolet absorption spectra of the group IVA tetrachlorides. *J. Electron Spectrosc. Relat. Phenom.* **1977**, *11*, 383-397, doi:10.1016/0368-2048(77)80015-7.

(3) Clark, R. H.; Husain, D. Quantum yield measurements of $Cl(3^2P_{1/2})$ and $Cl(3^2P_{3/2})$ in the photolysis of C_1 chlorofluorocarbons determined by atomic resonance absorption spectroscopy in the vacuum UV. *J. Photochem.* **1984**, *24*, 103-115, doi:10.1016/0047-2670(84)80057-X.

(4) Currie, J.; Sidebottom, J. H.; Tedder, J. The reaction of cyclohexyl radicals with carbon tetrachloride. *Int. J. Chem. Kinet.* **1974**, *6*, 481-492, doi:10.1002/kin.550060404.

(5) Gordus, A. A.; Bernstein, R. B. Isotope effect in continuous ultraviolet absorption spectra: Methyl bromide-d_3 and chloroform-d. *J. Chem. Phys.* **1954**, *22*, 790-795, doi:10.1063/1.1740194.
(6) Hanf, A.; Laüter, A.; Volpp, H.-R. Absolute chlorine atom quantum yield measurements in the UV and VUV gas-phase laser photolysis of CCl_4. *Chem. Phys. Lett.* **2003**, *368*, 445-451, doi:10.1016/S0009-2614(02)01896-1.
(7) Ho, G. H. Absolute photabsorption cross section of CCl_4 in the energy range 6-250 eV. *Chem. Phys.* **1998**, *226*, 101-111, doi:10.1016/S0301-0104(97)00259-0.
(8) Hubrich, C.; Stuhl, F. The ultraviolet absorption of some halogenated methanes and ethanes of atmospheric interest. *J. Photochem.* **1980**, *12*, 93-107, doi:10.1016/0047-2670(80)85031-3.
(9) Ibuki, T.; Takahashi, N.; Hiraya, A.; Shobatake, K. $CCl_2(\tilde{A}\ ^1B_1)$ radical formation in VUV photolyses of CCl_4 and $CBrCl_3$. *J. Chem. Phys.* **1986**, *85*, 5717-5722, doi:10.1063/1.451532.
(10) Prahlad, V.; Kumar, V. Temperature dependence of photoabsorption cross sections of carbon tetrachloride at 186-240 nm. *J. Quant. Spectrosc. Radiat. Transf.* **1995**, *54*, 945-955, doi:10.1016/0022-4073(95)00128-8.
(11) Rebbert, R. E.; Ausloos, P. Gas-phase photodecomposition of carbon tetrachloride. *J. Photochem.* **1976/1977**, *6*, 265-276, doi:10.1016/0047-2670(76)85084-8.
(12) Rontu Carlon, N.; Papanastasiou, D. K.; Fleming, E. L.; Jackman, C. H.; Newman, P. A.; Burkholder, J. B. UV absorption cross sections of nitrous oxide (N_2O) and carbon tetrachloride (CCl_4) between 210 and 350 K and the atmospheric implications. *Atmos. Chem. Phys.* **2010**, *10*, 6137-6149, doi:10.5194/acp-10-6137-2010.
(13) Rowland, F. S.; Molina, M. J. Chlorofluoromethanes in the environment. *Rev. Geophys. Space Phys.* **1975**, *13*, 1-35, doi:10.1029/RG013i001p00001.
(14) Roxlo, C.; Mandl, A. Vacuum ultraviolet absorption cross sections for halogen containing molecules. *J. Appl. Phys.* **1980**, *51*, 2969-2972, doi:10.1063/1.328108.
(15) Russell, B. R.; Edwards, L. O.; Raymonda, J. W. Vacuum ultraviolet absorption spectra of the chloromethanes. *J. Am. Chem. Soc.* **1973**, *95*, 2129-2133, doi:10.1021/ja00788a008.
(16) Seccombe, D. P.; Tuckett, R. P.; Baumgärtel, H.; Jochims, H. W. Vacuum-UV fluorescence spectroscopy of CCl_3F, CCl_3H and CCl_3Br in the range 8–30 eV. *Phys. Chem. Chem. Phys.* **1999**, *1*, 773-782, doi:10.1039/a809422e.
(17) Simon, P. C.; Gillotay, D.; Vanlaethem-Meurée, N.; Wisemberg, J. Ultraviolet absorption cross-sections of chloro and chlorofluoro-methanes at stratospheric temperatures. *J. Atmos. Chem.* **1988**, *7*, 107-135, doi:10.1007/BF00048042.
(18) Vanlaethem-Meurée, N.; Wisemberg, J.; Simon, P. C. Absorption des chlorométhanes dans l'ultraviolet: mesures des sections efficaces d'absorption en fonction de la température. *Bull. Acad. Roy. Belgique Cl. Sci.* **1978**, *64*, 31-41, doi:10.3406/barb.1978.58340.

F20. CH_3OCl (methyl hypochorite)

Back to Index

$CH_3OCl + h\nu \rightarrow CH_3O + Cl$	207 kJ mol^{-1}	579 nm	(1)
$\rightarrow CH_2O + HCl$	265 kJ mol^{-1}	451 nm	(2)

(Recommendation: 06-2, Note: 10-6, Evaluated: 10-6)

Absorption Cross Sections: The UV/vis absorption spectrum of methyl hypochorite, CH_3OCl, has been measured by Crowley et al.[1] (200–460 nm) and Jungkamp et al.[2] (230–400 nm). The spectrum has overlapping absorption bands with maxima at 230 and 310 nm. The agreement between the two data sets is good at wavelengths longer than 250 nm. At the maximum near 230 nm the cross sections from Jungkamp et al.[2] are about 15% smaller. The recommended cross sections in Table 4F-20 are the mean of the values reported by these two groups.

Photolysis Quantum Yield and Product Studies: Schindler et al.[4] measured the quantum yield for the product channel Cl + CH_3O to be 0.95 ± 0.05 at 308 nm. They also determined an upper limit of <0.01 for HCl formation at 248 nm and the ratio $Cl^*(^2P_{1/2})/ Cl(^2P_{3/2})$ following photolysis at 235 and 238 nm to be 1.45 ± 0.05. Krisch et al.[3] used photofragment translational spectroscopy to confirm that photodissociation of CH_3OCl at 248 nm resulted in only the cleavage of the O-Cl bond and the formation of Cl and CH_3O.

Table 4F-20. Recommended Absorption Cross Sections of CH_3OCl at 295 K

λ (nm)	10^{20} σ (cm^2)	λ (nm)	10^{20} σ (cm^2)	λ (nm)	10^{20} σ (cm^2)
230	14.9	290	1.32	350	0.662
232	15.4	292	1.34	352	0.611
234	15.7	294	1.35	354	0.574
236	15.9	296	1.37	356	0.529
238	15.8	298	1.40	358	0.482
240	15.5	300	1.43	360	0.445
242	14.9	302	1.45	362	0.411
244	14.2	304	1.47	364	0.389
246	13.2	306	1.48	366	0.356
248	12.2	308	1.49	368	0.331
250	11.1	310	1.49	370	0.298
252	9.96	312	1.48	372	0.273
254	8.86	314	1.47	374	0.246
256	7.77	316	1.46	376	0.225
258	6.80	318	1.43	378	0.209
260	5.87	320	1.41	380	0.202
262	5.05	322	1.37	382	0.186
264	4.31	324	1.33	384	0.17
266	3.69	326	1.30	386	0.16
268	3.16	328	1.24	388	0.15
270	2.71	330	1.20	390	0.13
272	2.35	332	1.14	392	0.14
274	2.06	334	1.09	394	0.13
276	1.83	336	1.04		
278	1.64	338	0.980		
280	1.53	340	0.918		
282	1.42	342	0.875		
284	1.37	344	0.822		
286	1.33	346	0.760		
288	1.32	348	0.709		

Note:
230–394 nm: Mean of the data from Crowley et al.[1] and Jungkamp et al.[2]

(1) Crowley, J. N.; Helleis, F.; Müller, R.; Moortgat, G. K.; Crutzen, P. J.; Orlando, J. J. CH_3OCl: UV/visible absorption cross sections, J values and atmospheric significance. *J. Geophys. Res.* **1994**, *99*, 20683-20688, doi:10.1029/94JD01829.

(2) Jungkamp, T. P. W.; Kirchner, U.; Schmidt, M.; Schindler, R. N. UV absorption cross-section data for the hypochlorites ROCl (R = H, CH_3, C_2H_5, *i*-C_3H_7, *tert*-C_4H_9). *J. Photochem. Photobiol. A: Chem.* **1995**, *99*, 1-6, doi:10.1016/1010-6030(95)04074-P.

(3) Krisch, M. J.; McCunn, L. R.; Takematsu, K.; Butler, L. J.; Blase, F. R.; Shu, J. Photodissociation of CH_3OCl to CH_3O + Cl at 248 nm. *J. Phys. Chem. A* **2004**, *108*, 1650-1656, doi:10.1021/jp0372082.

(4) Schindler, R. N.; Liesner, M.; Schmidt, S.; Kirchner, U.; Benter, T. Identification of nascent products formed in the laser photolysis of CH_3OCl and HOCl at 308 nm and around 235 nm. Total Cl-atom quantum yields and the state and velocity distributions of $Cl(^2P_j)$. *J. Photochem. Photobiol. A: Chem.* **1997**, *107*, 9-19, doi:10.1016/S1010-6030(96)04583-2.

F21. $CHCl_3$ (trichloromethane, chloroform)

Back to Index

$CHCl_3 + h\nu$	$\rightarrow CHCl_2 + Cl$	313 kJ mol^{-1}	382 nm	(1)
	$\rightarrow CCl_3 + H$	392 kJ mol^{-1}	305 nm	(2)

(Recommendation: 25-1, Note: 25-1, Evaluated: 25-1)

Absorption Cross Sections: The VUV/UV absorption spectrum of $CHCl_3$ (trichloromethane, chloroform) has been measured at room temperature by Gordus and Bernstein[3] (222.7 nm), Tsubomura et al.[10] (158–190 , 175.5 nm), Lucazeau and Sandorfy[6] (113–182 nm), Russell et al.[7] (110–200 nm), Vanlaethem-Meurée et al.[11] (190–230 nm), Hubrich and Stuhl[4] (160–255 nm), Lee and Suto[5] (121.567, 105–221 nm), Simon et al.[9] (174–240 nm), Brownsword et al.[2] (121.567 nm), Seccombe et al.[8] (50–150 nm), and Vatsa and Volpp[12] (121.567 nm). The room temperature cross sections from Vanlaethem-Meurée et al. and Simon et al. are nearly identical in the wavelength region 190–210 nm. Differences of ~15% exist at longer wavelengths. The data of Hubrich and Stuhl and Simon et al. agree to within 10% between 180 and 234 nm. Differences of ~25% exist in the long wavelength tail with the values of Hubrich and Stuhl being larger. In the region of the absorption maximum at ~176 nm, the spread in the reported cross section values is the largest. Simon et al. report σ(176 nm) = ~5 × 10^{-18} cm^2 compared to 3.7 × 10^{-18} cm^2 reported by Hubrich and Stuhl and <2 × 10^{-18} cm^2 by Lucazeau and Sandorfy. The recommended absorption cross sections in Table 4F-21 are only for wavelengths >180 nm and are the mean of the values reported by Hubrich and Stuhl and Simon et al. for the wavelength range 180–240 nm. For the wavelength range 242–256 nm the recommended cross sections are obtained by extrapolation, $\log \sigma(\lambda) = -1.2277 - 0.0844\,\lambda$.

The temperature dependence of the absorption spectrum has been measured by Vanlaethem-Meurée et al.[11] (190–230 nm) at 279 and 296 K and Simon et al.[9] (174–240 nm) over the range 225–295 K. The temperature dependence is significant for wavelengths >194 nm where the cross sections decrease with decreasing temperature. Simon et al.[9] parameterized the cross section temperature dependence using an empirical polynomial expansion:

$$\log_{10} \sigma(\lambda, T) = \sum A_n \lambda^n + (T-273) \times \sum B_n \lambda^n$$

and reported calculated cross sections for T = 210, 230, 250, 270, and 295 K. The parameters A_n and B_n, valid for the temperature range 210–300 K and wavelength range 190–240 nm, given below are recommended.

$A_0 = 269.80$	$B_0 = 3.7973$
$A_1 = -6.0908$	$B_1 = -7.0913 \times 10^{-2}$
$A_2 = 4.7830 \times 10^{-2}$	$B_2 = 4.9397 \times 10^{-4}$
$A_3 = -1.6427 \times 10^{-4}$	$B_3 = -1.5226 \times 10^{-6}$
$A_4 = 2.0682 \times 10^{-7}$	$B_4 = 1.7555 \times 10^{-9}$

There are several measurements of the $CHCl_3$ absorption spectrum in the Lyman-α (121.567 nm) region as noted above. The cross section measurements are in good agreement, to within 20%, with the exception of the Lucazeau and Sandorfy[6] value, which is a factor of 2.5 less. The recommended Lyman-α cross section is 3.5 × 10^{-17} cm^2 $molecule^{-1}$ with an uncertainty factor of 1.20 (2σ).

Photolysis Quantum Yield and Product Studies: Quantum yields for H atom formation have been measured by Brownsword et al.[1,2] to be 0.23 ± 0.03 and 0.13 at 121.6 and 157.6 nm, respectively. H atom formation was not detected in the photolysis at 193.3 nm.

Table 4F-21. Recommended Absorption Cross Sections of $CHCl_3$ at 296 K

λ (nm)	10^{20} σ (cm^2)	λ (nm)	10^{20} σ (cm^2)	λ (nm)	10^{20} σ (cm^2)
180	372	206	20.7	232	0.158
182	317	208	15.1	234	0.107
184	248	210	10.7	236	0.0730
186	186	212	7.48	238	0.0503
188	144	214	5.24	240	0.0347
190	113	216	3.60	242	*0.0223*
192	89.9	218	2.48	244	*0.0151*
194	76.1	220	1.69	246	*0.01023*
196	64.2	222	1.13	248	*0.00694*
198	53.0	224	0.750	250	*0.00470*
200	42.6	226	0.503	252	*0.00319*
202	34.4	228	0.342	254	*0.00216*
204	27.2	230	0.234	256	*0.00147*

Note:
180–240 nm: mean of data from Hubrich and Stuhl[4] and Simon et al.[9]
242–256 nm: extrapolation, $\log \sigma(\lambda) = -1.2277 - 0.0844\ \lambda$

(1) Brownsword, R. A.; Hillenkamp, M.; Laurent, T.; Vatsa, R. K.; Volpp, H.-R.; Wolfrum, J. Dynamics of H atom formation in the photodissociation of chloromethanes at 193.3 nm. *J. Phys. Chem. A* **1997**, *101*, 5222-5227, doi:10.1021/jp963811r.

(2) Brownsword, R. A.; Hillenkamp, M.; Laurent, T.; Vatsa, R. K.; Volpp, H.-R.; Wolfrum, J. Photodissociation dynamics of the chloromethanes at the Lyman-α wavelength (121.6 nm). *J. Chem. Phys.* **1997**, *106*, 1359-1366, doi:10.1063/1.473304.

(3) Gordus, A. A.; Bernstein, R. B. Isotope effect in continuous ultraviolet absorption spectra: Methyl bromide-d_3 and chloroform-*d*. *J. Chem. Phys.* **1954**, *22*, 790-795, doi:10.1063/1.1740194.

(4) Hubrich, C.; Stuhl, F. The ultraviolet absorption of some halogenated methanes and ethanes of atmospheric interest. *J. Photochem.* **1980**, *12*, 93-107, doi:10.1016/0047-2670(80)85031-3.

(5) Lee, L. C.; Suto, M. Fluorescence yields from photodissociative excitation of chloromethanes by vacuum ultraviolet radiation. *Chem. Phys.* **1987**, *114*, 423-429 doi:10.1016/0301-0104(87)85056-5.

(6) Lucazeau, G.; Sandorfy, C. On the far-ultraviolet spectra of some simple aldehydes. *J. Mol. Spectrosc.* **1970**, *35*, 214-231, doi:10.1016/0022-2852(70)90199-2.

(7) Russell, B. R.; Edwards, L. O.; Raymonda, J. W. Vacuum ultraviolet absorption spectra of the chloromethanes. *J. Am. Chem. Soc.* **1973**, *95*, 2129-2133, doi:10.1021/ja00788a008.

(8) Seccombe, D. P.; Tuckett, R. P.; Baumgärtel, H.; Jochims, H. W. Vacuum-UV fluorescence spectroscopy of CCl_3F, CCl_3H and CCl_3Br in the range 8–30 eV. *Phys. Chem. Chem. Phys.* **1999**, *1*, 773-782, doi:10.1039/a809422e.

(9) Simon, P. C.; Gillotay, D.; Vanlaethem-Meurée, N.; Wisemberg, J. Ultraviolet absorption cross-sections of chloro and chlorofluoro-methanes at stratospheric temperatures. *J. Atmos. Chem.* **1988**, *7*, 107-135, doi:10.1007/BF00048042.

(10) Tsubomura, H.; Kimura, K.; Kaya, K.; Tanaka, J.; Nagakura, S. Vacuum ultraviolet absorption spectra of saturated organic compounds with non-bonding electrons. *Bull. Chem. Soc. Japan* **1964**, *37*, 417-423, doi:10.1246/bcsj.37.417.

(11) Vanlaethem-Meurée, N.; Wisemberg, J.; Simon, P. C. Absorption des chlorométhanes dans l'ultraviolet: mesures des sections efficaces d'absorption en fonction de la température. *Bull. Acad. Roy. Belgique Cl. Sci.* **1978**, *64*, 31-41, doi:10.3406/barb.1978.58340.

(12) Vatsa, R. K.; Volpp, H.-R. Absorption cross-sections for some atmospherically important molecules at the H atom Lyman-α wavelength (121.567 nm). *Chem. Phys. Lett.* **2001**, *340*, 289-295, doi:10.1016/S0009-2614(01)00373-6.

F22. CH_2Cl_2 (dichloromethane)

Back to Index

$CH_2Cl_2 + h\nu$	$\rightarrow CH_2Cl + Cl$	334 kJ mol^{-1}	358 nm	(1)
	$\rightarrow CHCl_2 + H$	402 kJ mol^{-1}	297 nm	(2)

(Recommendation: 25-1, Note: 25-1, Evaluated: 25-1)

Absorption Cross Sections: The VUV/UV absorption spectrum of dichloromethane, CH_2Cl_2, has been measured at room temperature by Gordus and Bernstein[3] (213 nm), Tsubomura et al.[10] (163–192 nm), Russell et al.[8] (110–200 nm), Vanlaethem-Meurée et al.[11] (176–216 nm), Hubrich and Stuhl[4] (160–255 nm), Lee and Suto[6] (105–204 nm, graphical data), Orkin et al.[7] (164–240 nm), Simon et al.[9] (176–220 nm), Brownsword et al.[2] (Lyman-α, 121.6 nm), Vatsa and Volpp[12] (121.567 nm), and Lange et al.[5] (115–216 nm). The room temperature data of Vanlaethem-Meurée et al. and Simon et al. are nearly identical. The cross sections of Hubrich and Stuhl are as much as 12% greater than those of Simon et al. in the 176–206 nm wavelength range. Differences of ~50% exist in the 185–220 nm range. The recommended absorption cross sections in Table 4F-22 are the mean of the values reported by Hubrich and Stuhl and Simon et al. for the wavelength range 176–220 nm. For wavelengths >220 nm the recommended cross sections are obtained by extrapolation, $\log \sigma(\lambda) = -2.1337 - 0.08439\ \lambda$. The measured cross section values in this wavelength range from Hubrich and Stuhl are smaller by ~7% for wavelengths <230 nm and larger ~50% between 235 and 255 nm than the extrapolated values. The cross sections of Orkin et al. are systematically less than those of Hubrich and Stuhl[4] in the 210–240 nm range.

The temperature dependence of the absorption spectrum has been measured by Vanlaethem-Meurée et al.[11] (176–216 nm) at 279 and 296 K and Simon et al.[9] (176–220 nm) over the range 225–295 K. The temperature dependence is significant for wavelengths >190 nm where the cross sections decrease with decreasing temperature. Simon et al.[9] parameterized the cross section temperature dependence using an empirical polynomial expansion:

$$\log_{10} \sigma(\lambda, T) = \sum A_n \lambda^n + (T-273) \times \sum B_n \lambda^n$$

and reported calculated cross sections for 210, 230, 250, 270, and 295 K. The parameters A_n and B_n, valid for the temperature range 210–300 K and wavelength range 176–220 nm, given below are recommended.

$A_0 = -1431.8$	$B_0 = -3.1171$
$A_1 = 27.395$	$B_1 = 6.7874 \times 10^{-2}$
$A_2 = -1.9807 \times 10^{-1}$	$B_2 = -5.5000 \times 10^{-4}$
$A_3 = 6.3468 \times 10^{-4}$	$B_3 = 1.9649 \times 10^{-6}$
$A_4 = -7.6298 \times 10^{-7}$	$B_4 = -2.6101 \times 10^{-9}$

There are several measurements of the CH_2Cl_2 absorption spectrum in the Lyman-α (121.567 nm) region as noted above. The VUV spectrum in the Lyman-α region consists of diffuse band structure. The cross section measurements are in good agreement, to within 10%, with the exception of the Russell et al.[8] value, which is ~15% less. The recommended Lyman-α cross section is 4×10^{-17} cm^2 $molecule^{-1}$ with an uncertainty factor of 1.10 (2σ).

Photolysis Quantum Yield and Product Studies: Quantum yields for H atom formation have been measured by Brownsword et al.[1,2] to be 0.28 ± 0.03, 0.23, and 0.002 ± 0.001 at 121.6, 157.6, and 193.3 nm, respectively.

Table 4F-22. Recommended Absorption Cross Sections of CH_2Cl_2 at 298 K

λ (nm)	10^{20} σ (cm^2)	λ (nm)	10^{20} σ (cm^2)	λ (nm)	10^{20} σ (cm^2)
176	186	204	4.41	232	*0.0194*
178	182	206	3.07	234	*0.0132*
180	173	208	2.13	236	*0.00892*
182	156	210	1.45	238	*0.00605*
184	135	212	0.978	240	*0.00410*
186	110	214	0.651	242	*0.00278*
188	84.2	216	0.435	244	*0.00188*
190	61.0	218	0.291	246	*0.00128*
192	43.9	220	0.190	248	*0.000866*
194	30.5	222	*0.135*	250	*0.000587*
196	20.6	224	*0.0918*	252	*0.000398*
198	14.1	226	*0.0623*	254	*0.000270*
200	9.48	228	*0.0422*	256	*0.000183*
202	6.40	230	*0.0286*		

Note:
176–220 nm: mean of values from Hubrich and Stuhl[4] and Simon et al.[9]
222–256 nm: extrapolation, $\log \sigma(\lambda) = -2.1337 - 0.08439\ \lambda$

(1) Brownsword, R. A.; Hillenkamp, M.; Laurent, T.; Vatsa, R. K.; Volpp, H.-R.; Wolfrum, J. Dynamics of H atom formation in the photodissociation of chloromethanes at 193.3 nm. *J. Phys. Chem. A* **1997**, *101*, 5222-5227, doi:10.1021/jp963811r.

(2) Brownsword, R. A.; Hillenkamp, M.; Laurent, T.; Vatsa, R. K.; Volpp, H.-R.; Wolfrum, J. Photodissociation dynamics of the chloromethanes at the Lyman-α wavelength (121.6 nm). *J. Chem. Phys.* **1997**, *106*, 1359-1366, doi:10.1063/1.473304.

(3) Gordus, A. A.; Bernstein, R. B. Isotope effect in continuous ultraviolet absorption spectra: Methyl bromide-d_3 and chloroform-*d*. *J. Chem. Phys.* **1954**, *22*, 790-795, doi:10.1063/1.1740194.

(4) Hubrich, C.; Stuhl, F. The ultraviolet absorption of some halogenated methanes and ethanes of atmospheric interest. *J. Photochem.* **1980**, *12*, 93-107, doi:10.1016/0047-2670(80)85031-3.

(5) Lange, E.; Jones, N. C.; Hoffmann, S. V.; Lozanoa, I.; Kumara, S.; Homem, M. G. P.; Smialek, M. A.; Duflot, D.; Brunger, M. J.; Limão-Vieira, P. The electronic excited states of dichloromethane in the 5.8-10.8 eV energy range investigated by experimental and theoretical methods. *J. Quant. Spectrosc. Radiat. Transf.* **2020**, *253*, 107172, doi:10.1016/j.jqsrt.2020.107172.

(6) Lee, L. C.; Suto, M. Fluorescence yields from photodissociative excitation of chloromethanes by vacuum ultraviolet radiation. *Chem. Phys.* **1987**, *114*, 423-429 doi:10.1016/0301-0104(87)85056-5.

(7) Orkin, V. L.; Khamaganov, V. G.; Guschin, A. G.; Huie, R. E.; Kurylo, M. J. Atmospheric fate of chlorobromomethane: Rate constant for the reaction with OH, UV spectrum, and water solubility. *J. Phys. Chem. A* **1997**, *101*, 174-178, doi:10.1021/jp962428j.

(8) Russell, B. R.; Edwards, L. O.; Raymonda, J. W. Vacuum ultraviolet absorption spectra of the chloromethanes. *J. Am. Chem. Soc.* **1973**, *95*, 2129-2133, doi:10.1021/ja00788a008.

(9) Simon, P. C.; Gillotay, D.; Vanlaethem-Meurée, N.; Wisemberg, J. Ultraviolet absorption cross-sections of chloro and chlorofluoro-methanes at stratospheric temperatures. *J. Atmos. Chem.* **1988**, *7*, 107-135, doi:10.1007/BF00048042.

(10) Tsubomura, H.; Kimura, K.; Kaya, K.; Tanaka, J.; Nagakura, S. Vacuum ultraviolet absorption spectra of saturated organic compounds with non-bonding electrons. *Bull. Chem. Soc. Japan* **1964**, *37*, 417-423, doi:10.1246/bcsj.37.417.

(11) Vanlaethem-Meurée, N.; Wisemberg, J.; Simon, P. C. Absorption des chlorométhanes dans l'ultraviolet: mesures des sections efficaces d'absorption en fonction de la température. *Bull. Acad. Roy. Belgique Cl. Sci.* **1978**, *64*, 31-41, doi:10.3406/barb.1978.58340.

(12) Vatsa, R. K.; Volpp, H.-R. Absorption cross-sections for some atmospherically important molecules at the H atom Lyman-α wavelength (121.567 nm). *Chem. Phys. Lett.* **2001**, *340*, 289-295, doi:10.1016/S0009-2614(01)00373-6.

F23. CH_3Cl (chloromethane, methyl chloride)

Back to Index

$CH_3Cl + h\nu$	$\rightarrow CH_3 + Cl$	350 kJ mol^{-1}	342 nm	(1)
	$\rightarrow CH_2Cl + H$	417 kJ mol^{-1}	287 nm	(2)

(Recommendation: 06-2, Note: 25-1, Evaluated: 25-1)

Absorption Cross Sections: The UV absorption spectrum of CH_3Cl (chloromethane, methyl chloride) has been measured at room temperature by Russell et al.[13] (110–200 nm), Robbins[12] (174–220 nm), Hubrich et al.[7] (158–235 nm), Vanlaethem-Meurée et al.[18] (186–216 nm), and Simon et al.[15] (174–216 nm). The room temperature data generally agree to within 10% over the wavelength range 174–216 nm and the data of Vanlaethem-Meurée et al.[18] and Simon et al.[15] are nearly identical. The recommended absorption cross sections in Table 4F-23 are the mean of the values reported by Robbins,[12] Hubrich et al.,[7] and Simon et al.[15] in the range 174–184 nm, the mean of the values reported by Robbins,[12] Hubrich et al.,[7] Vanlaethem-Meurée et al.,[18] and Simon et al.[15] in the range 186–216 nm, and the mean of the values reported by Robbins[12] and Hubrich et al.[7] in the range 218–220 nm. For the wavelength range 222–236 nm the recommended values were obtained from a log-linear fit to the Hubrich et al.[7] data in the range 200–235 nm, $\log \sigma(\lambda) = -0.24164 - 0.09743\ \lambda$. The cross section uncertainty in the 190–230 nm region is estimated to be 1.15 (2σ).

The temperature dependence of the UV absorption spectrum has been measured by Hubrich et al.[7] (158–235 nm) at 208 and 298 K, Vanlaethem-Meurée et al.[18] (186–216 nm) at 255, 279, and 296 K, and Simon et al.[15] (174–216 nm) over the range 225–295 K. The temperature dependence of the absorption cross sections is significant at wavelengths greater than 194 nm where the cross sections decrease with decreasing temperature. There is very good agreement in the values reported by Vanlaethem-Meurée et al.[18] and Simon et al.[15] Simon et al.[15] parameterized the cross section temperature dependence using an empirical polynomial expansion:

$$\log_{10} \sigma(\lambda, T) = \sum A_n \lambda^n + (T-273) \times \sum B_n \lambda^n$$

and reported calculated cross sections for T = 210, 230, 250, 270, and 295 K. The parameters A_n and B_n, valid for the temperature range 210–300 K and wavelength range 174–216 nm, given below are recommended.

$A_0 = -299.80$	$B_0 = -7.1727$
$A_1 = 5.1047$	$B_1 = 1.4837 \times 10^{-1}$
$A_2 = -3.3630 \times 10^{-2}$	$B_2 = -1.1463 \times 10^{-3}$
$A_3 = 9.5805 \times 10^{-5}$	$B_3 = 3.9188 \times 10^{-6}$
$A_4 = -1.0135 \times 10^{-7}$	$B_4 = -4.9994 \times 10^{-9}$

The VUV spectrum in the Lyman-α (121.567 nm) vicinity contains strong diffuse band structure with a maximum nearly coincident with Lyman-α. There is reasonable agreement, to within 30%, in the reported absorption cross sections in the Lyman-α wavelength region by Russell et al.,[13] Lee and Suto,[8] Olney et al.,[10] Brownsword et al.,[2] Locht et al.,[9] Vatsa et al.,[19] Eden et al.[3], and Raymonda et al.[11] and Truch et al.[16] as reported in Locht et al.[9] Several studies have reported the spectrum in other regions of the VUV: Felps et al.[4] (171.2 nm), Gedanken and Rowe[5] (161-197 nm), Herzberg and Scheibe[6] (174-190 nm), Shold and Rebbert[14] (123.6 and 147.0 nm), Tsubomura et al.[17] (160-188 nm), and Wu et al.[20] (18-76 nm). The recommended Lyman-α cross section of 8.8×10^{-17} cm^2 $molecule^{-1}$ is taken from the Brownsword et al.[2] study with an uncertainty factor of 1.15 (2σ).

Photolysis Quantum Yield and Product Studies: Quantum yields for H atom formation have been measured by Brownsword et al.[1,2] to be 0.53 ± 0.05, 0.29, and 0.012 ± 0.006 at 121.6, 157.6, and 193.3 nm, respectively.

Table 4F-23. Recommended Absorption Cross Sections of CH_3Cl at 298 K

λ (nm)	10^{20} σ (cm^2)	λ (nm)	10^{20} σ (cm^2)	λ (nm)	10^{20} σ (cm^2)
174	110	196	3.96	218	0.0345
176	93.9	198	2.68	220	0.0220
178	78.2	200	1.77	222	*0.0135*
180	63.6	202	1.13	224	*0.00859*
182	46.5	204	0.731	226	*0.00549*
184	35.0	206	0.482	228	*0.00350*
186	25.8	208	0.313	230	*0.00224*
188	18.4	210	0.200	232	*0.00143*
190	12.8	212	0.127	234	*0.00091*
192	8.84	214	0.0860	236	*0.00058*
194	5.83	216	0.0534		

Note:
174–184 nm: mean of data from Robbins,[12] Hubrich et al.,[7] and Simon et al.[15]
186–216 nm: mean of data from Robbins,[12] Hubrich et al.,[7] Vanlaethem-Meurée et al.,[18] and Simon et al.[15]
218–220 nm: mean of data from Robbins[12] and Hubrich et al.[7]
222–236 nm: fit to data from Hubrich et al.,[7] $\log \sigma(\lambda) = -0.24164 - 0.09743\ \lambda$

(1) Brownsword, R. A.; Hillenkamp, M.; Laurent, T.; Vatsa, R. K.; Volpp, H.-R.; Wolfrum, J. Dynamics of H atom formation in the photodissociation of chloromethanes at 193.3 nm. *J. Phys. Chem. A* **1997**, *101*, 5222-5227, doi:10.1021/jp963811r.

(2) Brownsword, R. A.; Hillenkamp, M.; Laurent, T.; Vatsa, R. K.; Volpp, H.-R.; Wolfrum, J. Photodissociation dynamics of the chloromethanes at the Lyman-α wavelength (121.6 nm). *J. Chem. Phys.* **1997**, *106*, 1359-1366, doi:10.1063/1.473304.

(3) Eden, S.; Limão-Vieira, P.; Hoffmann, S. V.; Mason, N. J. VUV spectroscopy of CH_3Cl and CH_3I. *Chem. Phys.* **2006**, *331*, 232-244, doi:10.1016/j.chemphys.2006.10.021.

(4) Felps, W. S.; Rupnik, K.; McGlynn, S. P. Electronic spectroscopy of the cyanogen halides. *J. Phys. Chem.* **1991**, *95*, 639-656, doi:10.1021/j100155a028.

(5) Gedanken, A.; Rowe, M. D. Magnetic circular dichroism spectra of the methyl halides. Resolution of the n → σ* continuum. *Chem. Phys. Lett.* **1975**, *34*, 39-43, doi:10.1016/0009-2614(75)80196-5.

(6) Herzberg, G.; Scheibe, G. Über die Absorptionsspektra der dampfförmigen Methylhalogenide und einiger anderer Methylverbindungen im Ultraviolett und im Schumann-Gebiet. *Z. Physik. Chem. [Leipzig]* **1930**, *B 7*, 390-406.

(7) Hubrich, C.; Zetzsch, C.; Stuhl, F. Absorption spectra of halogenated methanes in wavelength region from 275 to 160 nm at temperatures of 298 and 208 K. *Ber. Bunsenges. Phys. Chem.* **1977**, *81*, 437-442, doi:10.1002/bbpc.19770810417.

(8) Lee, L. C.; Suto, M. Fluorescence yields from photodissociative excitation of chloromethanes by vacuum ultraviolet radiation. *Chem. Phys.* **1987**, *114*, 423-429, doi:10.1016/0301-0104(87)85056-5.

(9) Locht, R.; Leyh, B.; Hoxha, A.; Jochims, H. W.; Baumgärtel, H. The vacuum UV absorption spectrum of methyl chloride (CH_3Cl) and its perdeuterated isotopomer CD_3Cl. I. A Rydberg series analysis. *Chem. Phys.* **2001**, *272*, 259-275, doi:10.1016/S0301-0104(01)00464-5.

(10) Olney, T. N.; Cooper, G.; Chan, W. F.; Burton, G. R.; Brion, C. E.; Tan, K. H. Absolute photoabsorption (6-350 eV) and photoionization (11-80 eV) of methyl chloride using dipole electron scattering and synchroton radiation spectroscopies. *Chem. Phys.* **1996**, *205*, 421-439, doi:10.1016/0301-0104(95)00429-7.

(11) Raymonda, J. W.; Edwards, L. O.; Russell, B. R. Vacuum ultraviolet absorption spectra of some chloroalkanes. *J. Am. Chem. Soc.* **1974**, *96*, 1708-1712, doi:10.1021/ja00813a011.

(12) Robbins, D. E. Photodissociation of methyl chloride and methyl bromide in the atmosphere. *Geophys. Res. Lett.* **1976**, *3*, 213-216, doi:10.1029/GL003i004p00213.

(13) Russell, B. R.; Edwards, L. O.; Raymonda, J. W. Vacuum ultraviolet absorption spectra of the chloromethanes. *J. Am. Chem. Soc.* **1973**, *95*, 2129-2133, doi:10.1021/ja00788a008.

(14) Shold, D. M.; Rebbert, R. E. The photochemistry of methyl chloride. *J. Photochem.* **1978**, *9*, 499-517, doi:10.1016/0047-2670(78)80166-X.

(15) Simon, P. C.; Gillotay, D.; Vanlaethem-Meurée, N.; Wisemberg, J. Ultraviolet absorption cross-sections of chloro and chlorofluoro-methanes at stratospheric temperatures. *J. Atmos. Chem.* **1988**, *7*, 107-135, doi:10.1007/BF00048042.

(16) Truch, D. T.; D.R. Salomon; Armstrong, D. A. Rydberg spectroscopy of methyl chloride. *J. Mol. Spectrosc.* **1979**, *78*, 31-39, doi:10.1016/0022-2852(79)90033-X.
(17) Tsubomura, H.; Kimura, K.; Kaya, K.; Tanaka, J.; Nagakura, S. Vacuum ultraviolet absorption spectra of saturated organic compounds with non-bonding electrons. *Bull. Chem. Soc. Japan* **1964**, *37*, 417-423, doi:10.1246/bcsj.37.417.
(18) Vanlaethem-Meurée, N.; Wisemberg, J.; Simon, P. C. Absorption des chlorométhanes dans l'ultraviolet: mesures des sections efficaces d'absorption en fonction de la température. *Bull. Acad. Roy. Belgique Cl. Sci.* **1978**, *64*, 31-41, doi:10.3406/barb.1978.58340.
(19) Vatsa, R. K.; Volpp, H.-R. Absorption cross-sections for some atmospherically important molecules at the H atom Lyman-α wavelength (121.567 nm). *Chem. Phys. Lett.* **2001**, *340*, 289-295, doi:10.1016/S0009-2614(01)00373-6.
(20) Wu, C. Y. R.; Lee, L. C.; Judge, D. L. Photoabsorption cross sections of CH_3F, CHF_3, CH_3Cl, and CF_2Cl_2 from 175 to 760 Å. *J. Chem. Phys.* **1979**, *71*, 5221-5226, doi:10.1063/1.438329.

F24. CH_3CCl_3 (1,1,1-trichloroethane, methylchloroform)

Back to Index

$CH_3CCl_3 + h\nu \rightarrow$ Products (1)

(Recommendation: 15-10, Note: 15-10, Evaluated: 15-10)

Absorption Cross Sections: The VUV/UV absorption spectrum of CH_3CCl_3 (1,1,1-trichloroethane, methylchloroform) has been measured at room temperature by Salomon et al.[4] (147 nm), Hubrich and Stuhl[2] (160–255 nm), Vanlaethem-Meurée et al.[5] (182–240 nm), and Nayak et al.[3] (160–240 nm). Hubrich and Stuhl[2] corrected their measured spectrum between 170 and 190 nm for the presence of a 1,4-dioxane stabilizer, corrections were <10.7%. Nayak et al.[3] also measured the absorption cross sections in the liquid-phase over the range 235–260 nm and used a wavelength shift procedure to derive the gas-phase cross section data in this wavelength range. The agreement of the room temperature data is within 20% in the region 165–205 nm. Between 210 and 240 nm, the data of Vanlaethem-Meurée et al.[5] and Nayak et al.[3] agree to within 15%, whereas the data from Hubrich and Stuhl[2] are 100–150% greater. The recommended absorption cross sections in Table 4F-24 are the mean of the values reported by Hubrich and Stuhl[2] and Nayak et al.[3] in the range 170–180 nm, the mean of the values reported by Vanlaethem-Meurée et al.,[5] Hubrich and Stuhl,[2] and Nayak et al.[3] in the range 185–205 nm, and the mean of the values reported by Vanlaethem-Meurée et al.[5] and Nayak et al.[3] in the range 210–240 nm. For wavelengths >240 nm, the recommended values were obtained by extrapolation of the Nayak et al.[3] data in the range 210–240 nm, $\log \sigma(\lambda) = -1.59792 - 0.08066\,\lambda$. The values measured by Hubrich and Stuhl[2] in this wavelength range are greater by ~140% at 250 nm and less by ~80% at 255 nm than the recommended values. The cross section uncertainty in the 190–230 nm region is estimated to be 1.18 (2σ), which encompasses the available data.

There are no Lyman-α cross section data available. A σ(Lyman-α) value of 7×10^{-17} cm^2 molecule^{-1} is estimated with an uncertainty factor of 1.4 (2σ).

The temperature dependence of the absorption spectrum has been measured by Vanlaethem-Meurée et al.[5] (182–240 nm) over the range 220–295 K and Nayak et al.[3] (160–240 nm) over the range 223–333 K. The temperature dependence of the absorption cross sections is significant at wavelengths >210 nm where the cross sections decrease with decreasing temperature. The studies of Nayak et al.[3] and Vanlaethem-Meurée et al.[5] are in good agreement. Vanlaethem-Meurée et al.[5] parameterized the cross section temperature dependence using an empirical polynomial expansion:

$$\log_{10} \sigma(\lambda, T) = \sum A_n \lambda^n + (T-273) \times \sum B_n \lambda^n$$

and reported calculated cross sections for T = 210, 230, 250, 270, and 295 K. The parameters A_n and B_n, valid for the temperature range 210–300 K and wavelength range 182–240 nm, reported by Gillotay and Simon[1] and given below are recommended.

$A_0 = 341.085191$	$B_0 = -1.660090$
$A_1 = -7.273362$	$B_1 = 3.079969 \times 10^{-2}$
$A_2 = 5.498387 \times 10^{-2}$	$B_2 = -2.106719 \times 10^{-4}$
$A_3 = -1.827552 \times 10^{-4}$	$B_3 = 6.264984 \times 10^{-7}$
$A_4 = 2.238640 \times 10^{-7}$	$B_4 = -6.781342 \times 10^{-10}$

Photolysis Quantum Yield and Product Studies: No recommendation.

Table 4F-24. Recommended Absorption Cross Sections of CH_3CCl_3 at 298 K

λ (nm)	10^{20} σ (cm^2)
170	406
175	424
180	404
185	301
190	212
195	147
200	92.1
205	52.0
210	25.5
215	10.9
220	4.47
225	1.82
230	0.717
235	0.276
240	0.111
245	*0.0437*
250	*0.0173*
255	*0.00682*

Note:
170–180 nm: mean of Hubrich and Stuhl[2] and Nayak et al.[3]
185–205 nm: mean of Vanlaethem-Meurée et al.,[5] Hubrich and Stuhl,[2] and Nayak et al.[3]
210–240 nm: mean of Vanlaethem-Meurée et al.[5] and Nayak et al.[3]
245–255 nm: extrapolation, log σ(λ) = –1.59792–0.08066 λ

(1) Gillotay, D.; Simon, P. C. Ultraviolet absorption cross-sections of photoactive species of stratospheric interest Part 1: The halocarbons. *Aeronomica Acta A* **1990**, *356*, 1-173, doi:10.18758/A_356.

(2) Hubrich, C.; Stuhl, F. The ultraviolet absorption of some halogenated methanes and ethanes of atmospheric interest. *J. Photochem.* **1980**, *12*, 93-107, doi:10.1016/0047-2670(80)85031-3.

(3) Nayak, A. K.; Kurylo, M. J.; Fahr, A. UV absorption cross sections of methylchloroform: Temperature-dependent gas and liquid phase measurements. *J. Geophys. Res.* **1995**, *100*, 11185-11189, doi:10.1029/95JD00695.

(4) Salomon, D.; Kirk, A. W.; Tschuikow-Roux, E. Primary processes in the photochemical decomposition of 1,1,1-trichloroethane at 147 nm. *J. Photochem.* **1977**, *7*, 345-353, doi:10.1016/0047-2670(77)80016-6.

(5) Vanlaethem-Meurée, N.; Wisemberg, J.; Simon, P. C. Ultraviolet absorption spectrum of methylchloroform in the vapor phase. *Geophys. Res. Lett.* **1979**, *6*, 451-454, doi:10.1029/GL006i006p00451.

F25. CH_3CH_2Cl (chloroethane, ethyl chloride)

Back to Index

$CH_3CH_2Cl + h\nu \rightarrow$ Products (1)

(Recommendation: 02-25, Note: 10-6, Evaluated: 10-6)

Absorption Cross Sections: The room temperature VUV/UV absorption spectrum of CH_3CH_2Cl (chloroethane, ethyl chloride) has been measured by Ichimura et al.[2] (147 nm) and Hubrich and Stuhl[1] (160–240 nm). The recommended absorption cross sections in Table 4F-25 are taken from Hubrich and Stuhl.[1]

Photolysis Quantum Yield and Product Studies: No recommendation.

Table 4F-25. Recommended Absorption Cross Sections of CH_3CH_2Cl at 298 K

λ (nm)	10^{20} σ (cm^2)	λ (nm)	10^{20} σ (cm^2)	λ (nm)	10^{20} σ (cm^2)
160	189.0	190	6.85	220	0.0127
165	110.0	195	2.56	225	0.00463
170	70.5	200	1.17	230	0.00117
175	44.4	205	0.375	235	0.000395
180	30.4	210	0.147	240	0.000156
185	13.6	215	0.0433		

Note:
160–240 nm: Hubrich and Stuhl[1]

(1) Hubrich, C.; Stuhl, F. The ultraviolet absorption of some halogenated methanes and ethanes of atmospheric interest. *J. Photochem.* **1980**, *12*, 93-107, doi:10.1016/0047-2670(80)85031-3.

(2) Ichimura, T.; Kirk, A. W.; Kramer, G.; Tschuikow-Roux, E. Photolysis of ethyl chloride (Freon 160) at 147 nm. *J. Photochem.* **1976/1977**, *6*, 77-90, doi:10.1016/0047-2670(76)85050-2.

F26. $CH_3CHClCH_3$ (2-chloropropane)

Back to Index

$CH_3CHClCH_3 + h\nu \rightarrow$ Products (1)

(Recommendation: 02-25, Note: 10-6, Evaluated: 10-6)

Absorption Cross Sections: The VUV/UV absorption spectrum of 2-chloropropane, $CH_3CHClCH_3$, has been measured by Gillotay and Simon.[1] The Gillotay and Simon[1] results are reported (erroneously) as $CH_3CH_2ClCH_3$, which presumably should be $CH_3CHClCH_3$. The recommended data are listed in Table 4F-26.

Photolysis Quantum Yield and Product Studies: No recommendation.

Table 4F-26. Recommended Absorption Cross Sections of $CH_3CHClCH_3$ at 295 K

λ (nm)	10^{20} σ (cm^2)	λ (nm)	10^{20} σ (cm^2)	λ (nm)	10^{20} σ (cm^2)
170	31.7	192	4.67	214	0.0965
172	27.0	194	3.49	216	0.0652
174	24.3	196	2.58	218	0.0444
176	22.1	198	1.88	220	0.0308
178	20.3	200	1.34	222	0.0212
180	18.0	202	0.954	224	0.0144
182	15.0	204	0.671	226	0.0107
184	12.2	206	0.463	228	0.00752
186	9.99	208	0.311	230	0.00580
188	7.93	210	0.214		
190	6.06	212	0.144		

Note:
170–230 nm: Gillotay and Simon[1]

(1) Gillotay, D.; Simon, P. C. Ultraviolet absorption cross-sections of photoactive species of stratospheric interest Part 1: The halocarbons. *Aeronomica Acta A* **1990**, *356*, 1-173, doi:10.18758/A_356.

F27. CH_2ClCH_2Cl (1,2-dichloroethane)

Back to Index

$CH_2ClCH_2Cl + h\nu \rightarrow$ Products (1)

(Recommendation: 02-25, Note: 10-6, Evaluated: 10-6)

Absorption Cross Sections: The VUV/UV absorption spectrum of 1,2-dichloroethane, CH_2ClCH_2Cl, has been measured by Russell et al.[1] (116–192 nm) and Yano and Tschuikow-Roux[2] (147 nm). No recommendation is given.

Photolysis Quantum Yield and Product Studies: No recommendation.

(1) Russell, B. R.; Edwards, L. O.; Raymonda, J. W. Vacuum ultraviolet absorption spectra of the chloromethanes. *J. Am. Chem. Soc.* **1973**, *95*, 2129-2133, doi:10.1021/ja00788a008.
(2) Yano, T.; Tschuikow-Roux, E. A reexamination of the photodissociation of CH_2ClCH_2Cl at 147 nm. Test for chlorine atom reactions. *J. Phys. Chem.* **1980**, *84*, 3372–3377, doi:10.1021/j100462a013.

F28. $CH_2ClCH_2CH_2Cl$ (1,3-dichloropropane)

Back to Index

$CH_2ClCH_2CH_2Cl + h\nu \rightarrow$ Products (1)

(Recommendation: 02-25, Note: 10-6, Evaluated: 10-6)

Absorption Cross Sections: The VUV/UV absorption spectrum of 1,3-dichloropropane, $CH_2ClCH_2CH_2Cl$, has been measured by Russell et al.[1] (116–192 nm). No recommendation is given.

Photolysis Quantum Yield and Product Studies: No recommendation.

(1) Russell, B. R.; Edwards, L. O.; Raymonda, J. W. Vacuum ultraviolet absorption spectra of the chloromethanes. *J. Am. Chem. Soc.* **1973**, *95*, 2129-2133, doi:10.1021/ja00788a008.

F29. $CH_2Cl(CH_2)_2CH_2Cl$ (1,4-dichlorobutane)

Back to Index

$CH_2Cl(CH_2)_2CH_2Cl + h\nu \rightarrow$ Products (1)

(Recommendation: 02-25, Note: 10-6, Evaluated: 10-6)

Absorption Cross Sections: The VUV/UV absorption spectrum of 1,4-dichlorobutane, $CH_2Cl(CH_2)_2CH_2Cl$, has been measured by Russell et al.[1] (129–188 nm). No recommendation is given.

Photolysis Quantum Yield and Product Studies: No recommendation.

(1) Russell, B. R.; Edwards, L. O.; Raymonda, J. W. Vacuum ultraviolet absorption spectra of the chloromethanes. *J. Am. Chem. Soc.* **1973**, *95*, 2129-2133, doi:10.1021/ja00788a008.

F30. CCl_2O (carbonyl dichloride, phosgene)

Back to Index

$CCl_2O + h\nu$	$\rightarrow CO + Cl_2$	110 kJ mol^{-1}	1084 nm	(1)
	$\rightarrow ClCO + Cl$	318 kJ mol^{-1}	377 nm	(2)
	$\rightarrow CO + 2Cl$	353 kJ mol^{-1}	339 nm	(3)
	$\rightarrow CCl_2 + O$	700 kJ mol^{-1}	171 nm	(4)

(Recommendation: 94-26, Note: 25-1, Evaluated: 25-1)

Absorption Cross Sections: The UV absorption spectrum of CCl_2O (carbonyl dichloride, phosgene) has been measured at room temperature by Chou et al.[2] (185–226 nm), Okabe[9] (240–280 nm), Meller et al.[8] (200–315 nm), Jäger et al.[6] (172–220 nm), Okabe[10,11] (147, 184.9, and 253.7 nm), Glicker and Okabe[4] (229 and 254 nm), Gillotay et al.[3] (166–308 nm), and Khamaganov et al.[7] (185 nm). The spectrum shows a weak absorption band between 215 and 310 nm with the maximum at ~235 nm and a strong absorption band below 200 nm with the maximum at ~174 nm. The room temperature values reported in the various studies are in very good agreement, generally within 10%. An exception is in the region of the absorption minimum around 200 nm where the values of Jäger at al.[6] are lower than those of Gillotay et al.[3] by as much as 20%. In this region the values of Chou et al.[2] and Meller et al.[8] are between those of Gillotay et al.[3] and Jäger et al.[6]

The recommended absorption cross sections in Table 4F-30 are averages over 500 cm^{-1} intervals of the values of Gillotay et al.[3] in the region 168.10–173.15 nm, the mean of the values from Gillotay et al.[3] and Jäger et al.[6] in the region 174.65–182.65 nm, the mean of the values from Chou et al.,[2] Gillotay et al.,[3] and Jäger et al.[6] in the region 184.35–199.00 nm, the mean of the values of Chou et al.,[2] Gillotay et al.,[3] Meller et al.,[8] and Jäger et al.[6] in the region 201.01–218.59 nm, the mean of the values from Chou et al.,[2] Gillotay et al.,[3] and Meller et al.[8] in the region 221.00–226.00 nm, and the mean of the values from Gillotay et al.[3] and Meller et al.[8] in the region 228.58–305.36 nm.

The temperature dependence of the absorption spectrum has been measured by Gillotay et al.[3] (166–308 nm) over the range 210–295 K. The temperature dependence is significant only in the region <175 nm and >250 nm. The strong absorption band is shifted slightly to shorter wavelengths with deceasing temperature and a peak cross section increase of ~20% between 295 and 210 K. In the long wavelength region, the absorption cross sections decrease with decreasing temperature with a decrease of ~80% at 305 nm between 295 and 210 K.

Okake et al.[12] (117–159 nm, graphical) is the only available measurement of the CCl_2O absorption spectrum in the Lyman-α (121.567 nm) region. The recommended Lyman-α cross section is 7×10^{-17} cm^2 molecule^{-1} with an estimated uncertainty factor of 1.4 (2σ).

Photolysis Quantum Yield and Product Studies: Phosgene is a useful actinometer in the region 200–280 nm. The photodissociation processes $CCl_2O + h\nu \rightarrow COCl + Cl$ with subsequent decay of the COCl radical, $COCl \rightarrow CO + Cl$, produces CO with unity quantum yield (see Okabe,[9] Wijnen,[13] Heicklen,[5] and Calvert and Pitts[1]).

Table 4F-30. Recommended Absorption Cross Sections of CCl_2O at 298 K

λ (nm)	10^{20} σ (cm^2)	λ (nm)	10^{20} σ (cm^2)	λ (nm)	10^{20} σ (cm^2)	λ (nm)	10^{20} σ (cm^2)
168.10	301	193.25	68.8	223.47	12.6	264.92	2.68
170.95	433	195.15	52.1	226.00	13.0	268.50	1.85
173.15	493	197.05	40.6	228.58	13.2	272.12	1.17
174.65	509	199.00	31.7	231.23	13.4	275.88	0.689
176.20	475	201.01	25.7	233.93	13.5	279.74	0.370
177.80	427	203.05	20.7	236.69	13.0	283.70	0.182
179.40	369	205.14	17.2	239.53	12.4	287.78	0.0771
181.00	313	207.26	14.7	242.43	11.5	291.99	0.0298
182.65	261	209.43	13.0	245.41	10.4	296.32	0.0104
184.35	210	211.65	11.9	248.45	9.07	300.77	0.00323
186.05	178	213.89	11.4	251.59	7.75	305.36	0.00096
187.80	137	216.20	11.3	254.79	6.32		
189.60	112	218.59	11.5	258.08	5.02		
191.40	88.9	221.00	12.2	261.45	3.77		

Note:
168.10–173.15 nm: Gillotay et al.[3]
174.65–182.65 nm: mean of Gillotay et al.[3] and Jäger et al.[6]
184.35–199.00 nm: mean of Chou et al.,[2] Gillotay et al.,[3] and Jäger et al.[6]
201.01–218.59 nm: mean of Chou et al.,[2] Gillotay et al.,[3] Meller et al.,[8] and Jäger et al.[6]
221.00–226.00 nm: mean of Chou et al.,[2] Gillotay et al.,[3] and Meller et al.[8]
228.58–305.36 nm: mean of Gillotay et al.[3] and Meller et al.[8]

(1) Calvert, J. G.; Pitts, J. N. In *Photochemistry*; John Wiley & Sons, Inc.: New York, 1966; pp 230-231.
(2) Chou, C. C.; Crescentini, G.; Vera-Ruiz, H.; Smith, W. S.; Rowland, F. S. "Stratospheric photochemistry of CF_2O, CClFO, and CCl_2O"; 173rd American Chemical Society Meeting, 1977, New Orleans, LA.
(3) Gillotay, D.; Simon, P. C.; Dierickx, L. Ultraviolet absorption cross-sections of some carbonyl compounds and their temperature dependence. *Aeronomica Acta* **1993**, *368*, 1-15, doi:10.18758/A_368.
(4) Glicker, S.; Okabe, H. Photochemistry of diacetylene. *J. Phys. Chem.* **1987**, *91*, 437-440, doi:10.1021/j100286a036.
(5) Heicklen, J. The photolysis of phosgene-ethylene mixtures. *J. Am. Chem. Soc.* **1965**, *87*, 445-453, doi:10.1021/ja01081a010.
(6) Jäger, M.; Heydtmann, H.; Zetzsch, C. Vacuum ultraviolet spectrum and quantum yield of the 193 nm photolysis of phosgene. *Chem. Phys. Lett.* **1996**, *263*, 817-821, doi:10.1016/S0009-2614(96)01278-X.
(7) Khamaganov, V. G.; Karunanandan, R.; Horowitz, A.; Dillon, T. J.; Crowley, J. N. Photolysis of $CH_3C(O)CH_3$ at 248 and 266 nm: pressure and temperature dependent overall quantum yields. *Phys. Chem. Chem. Phys.* **2009**, *11*, 6173-6181, doi:10.1039/b904130c.
(8) Meller, R.; Boglu, D.; Moortgat, G. K. "UV spectra of several halogenated carbonyl compounds and FTIR studies of the degradation of CF_3COCl, HCFC-123 and HFC-143a"; Kinetics and Mechanisms for the Reactions of Halogenated Organic Compounds in the Troposphere. STEP-HALOCSIDE/AFEAS WORKSHOP, 1991, Dublin, Ireland.
(9) Okabe, H. Photodissociation of thiophosgene. *J. Chem. Phys.* **1977**, *66*, 2058-2062, doi:10.1063/1.434166.
(10) Okabe, H. Photochemistry of acetylene at 1470 Å. *J. Chem. Phys.* **1981**, *75*, 2772-2778, doi:10.1063/1.442348.
(11) Okabe, H. Photochemistry of acetylene at 1849 Å. *J. Chem. Phys.* **1983**, *78*, 1312-1317, doi:10.1063/1.444868.

(12) Okabe, H.; Laufer, A. H.; Ball, J. J. Photodissociation of $OCCl_2$ in the vacuum ultraviolet: production and electronic energy of excited Cl_2. *J. Chem. Phys.* **1971**, *55*, 373-378, doi:10.1063/1.1675531.
(13) Wijnen, M. H. Photolysis of phosgene in the presence of ethylene. *J. Am. Chem. Soc.* **1961**, *83*, 3014-3017, doi:10.1021/ja01475a009.

F31. HC(O)Cl (formyl chloride)

Back to Index

$HC(O)Cl + h\nu \rightarrow$ Products (1)

(Recommendation: 06-2, Note: 10-6, Evaluated: 10-6)

Absorption Cross Sections: The UV absorption spectrum of formyl chloride, HC(O)Cl, has been measured at room temperature by Libuda et al.[1] (239–307 nm). The absorption spectrum has a highly structured absorption band with a maximum near 260 nm. The recommended cross sections in Table 4F-31 are the averages over 1 nm intervals of the data from Libuda et al.[1] (0.7 nm resolution).

Photolysis Quantum Yield and Product Studies: No recommendation.

Table 4F-31. Recommended Absorption Cross Sections of HC(O)Cl at 298 K

λ (nm)	10^{20} σ (cm^2)	λ (nm)	10^{20} σ (cm^2)	λ (nm)	10^{20} σ (cm^2)	λ (nm)	10^{20} σ (cm^2)
240	2.76	257	3.92	274	3.53	291	0.624
241	3.36	258	5.03	275	2.30	292	0.605
242	3.41	259	4.45	276	3.28	293	0.342
243	3.32	260	5.46	277	2.38	294	0.431
244	3.03	261	5.09	278	2.09	295	0.303
245	3.53	262	4.66	279	1.89	296	0.275
246	4.01	263	4.54	280	2.22	297	0.184
247	4.64	264	4.03	281	1.06	298	0.165
248	4.44	265	3.83	282	1.98	299	0.178
249	4.27	266	4.72	283	1.36	300	0.0562
250	3.92	267	3.76	284	1.15	301	0.0912
251	4.38	268	4.83	285	1.51	302	0.0805
252	4.57	269	3.79	286	1.00	303	0.0319
253	4.98	270	3.34	287	0.784	304	0.0587
254	5.20	271	3.72	288	0.748	305	0.0275
255	4.59	272	2.68	289	0.880	306	0.0157
256	5.07	273	2.74	290	0.371	307	0.0131

Note:
Libuda et al.[1]

(1) Libuda, H. G.; Zabel, F.; Fink, E. H.; Becker, K. H. Formyl chloride: UV absorption cross sections and rate constants for the reactions with Cl and OH. *J. Phys. Chem.* **1990**, *94*, 5860-5865, doi:10.1021/j100378a047.

F32. ClC(O)F (carbonyl chlorofluoride, fluorochlorophosgene)

Back to Index

$ClC(O)F + h\nu \rightarrow FCO + Cl$ (1)
$\rightarrow ClCO + F$ (2)
$\rightarrow CO + F + Cl$ (3)

(Recommendation: 94-26, Note: 10-6, Evaluated: 10-6)

Absorption Cross Sections: The UV absorption spectrum of ClC(O)F (carbonyl chlorofluoride, fluorochlorophosgene) has been measured at room temperature by Chou et al.[1] (186–226 nm), Hermann et al.[2] (193.4 nm), and Nölle et al.[3,4] (200–262 nm). The spectrum has monotonically decreasing absorptions cross sections with increasing wavelength with a shoulder in the spectrum around 200 nm. The room temperature data are in good agreement in the common wavelength range with differences ≤6%. The recommended absorption cross sections in Table 4F-32-1 are the averages over the 500 cm^{-1} intervals used for atmospheric modeling of the data from Chou et al.[1] and Hermann et al.[2] in the region 186–199 nm, the mean of the data from Chou et al.,[1] and Nölle et al.[3,4] at 201 and 203.1 nm, and the data from Nölle et al.[3,4] at wavelengths >205 nm.

The temperature dependence of the absorption spectrum was measured by Nölle et al.[3,4] (200–262 nm) at 223, 248, 273, and 298 K. The cross sections decrease with decreasing temperature at wavelengths >210 nm with the magnitude of the difference increasing with increasing wavelength. At wavelengths <210 nm the cross sections increase with decreasing temperature with the difference in going from 298 to 223 K is ~18% at 201 nm.

Photolysis Quantum Yield and Product Studies: Photolysis quantum yields of ClC(O)F have been measured by Hermann et al.[2] and Nölle et al.[4] The results are summarized in Table 4F-32-2. The relative distribution of the CO and CF_2O products was shown by Hermann et al.[2] to depend on the total pressure over the range 10 to 900 mbar. The apparent quantum yields were taken as the quantum yields for the decomposition into COF + Cl and CO + F + Cl since the parent molecule cannot be reformed (as in the case of CF_2O) and COCl is known to be unstable.

Table 4F-32-1. Recommended Absorption Cross Sections of ClC(O)F at 298 K

λ (nm)	10^{20} σ (cm^2)	λ (nm)	10^{20} σ (cm^2)	λ (nm)	10^{20} σ (cm^2)	λ (nm)	10^{20} σ (cm^2)
186.0	15.6	201.0	12.2	218.6	5.79	239.5	0.459
187.8	14.0	203.1	11.9	221.0	4.77	242.4	0.292
189.6	13.4	205.1	11.5	223.5	3.81	245.4	0.178
191.4	12.9	207.3	10.8	226.0	2.93	248.5	0.103
193.2	12.7	209.4	9.91	228.6	2.19	251.6	0.0635
195.1	12.5	211.6	8.96	231.2	1.57	254.8	0.0409
197.0	12.4	213.9	7.90	233.9	1.09	258.1	0.0279
199.0	12.3	216.2	6.84	236.7	0.724	261.4	0.0214

Note:
186.0–199.0 nm: Chou et al.[1] and Hermann et al.[2]
201.0 and 203.1 nm: mean of the data from Chou et al.[1] and Nölle et al.[3,4]
205.1–261.4 nm: Nölle et al.[3,4]

Table 4F-32-2. Summary of ClC(O)F Photolysis Quantum Yield Results

Reference	Year	Photolysis Wavelength (nm)	Φ
Hermann et al.[2]	1994	193	0.98 ± 0.09
Nölle et al.[4]	1991	210	0.85 ± 0.25
		210*	0.90 ± 0.05
		222.5	0.77 ± 0.33
		230	0 71 ± 0.30
		248	0.52 ± 0.14

* Hg lamp photolysis source

(1) Chou, C. C.; Crescentini, G.; Vera-Ruiz, H.; Smith, W. S.; Rowland, F. S. "Stratospheric photochemistry of CF_2O, CClFO, and CCl_2O"; 173rd American Chemical Society Meeting, 1977, New Orleans, LA.

(2) Hermann, M.; Nölle, A.; Heydtmann, H. Photolysis and quantum yield of carbonylchlorofluoride at 193 nm. *Chem. Phys. Lett.* **1994**, *226*, 559-562, doi:10.1016/0009-2614(94)00782-9.

(3) Nölle, A.; Heydtmann, H.; Meller, R.; Moortgat, G. K. Temperature dependent UV absorption spectra of carbonyl chloro-fluoride. *Geophys. Res. Lett.* **1993**, *20*, 707-710, doi:10.1029/93GL00248.

(4) Nölle, A.; Krumscheid, C.; Heydtmann, H. Determination of quantum yields in the UV photolysis of COF_2 and COFCl. *Chem. Phys. Lett.* **1999**, *299*, 561-565, doi:10.1016/S0009-2614(98)01257-3.

F33. $CFCl_3$ (fluorotrichloromethane, CFC-11)

Back to Index

$CFCl_3$ (CFC-11) + hν → Products (1)

(Recommendation: 15-10, Note: 15-10, Evaluated: 15-10)

Absorption Cross Sections: The VUV/UV absorption spectrum of fluorotrichloromethane (CFC-11), $CFCl_3$, has been measured at room temperature by Gilbert et al.[4] (60–145 nm), Doucet et al.[3] (120–200 nm), Gordus and Bernstein [5] (225 nm), Rowland and Molina[14] (186–226 nm), Robbins and Stolarski[13] (174–226 nm), Greene and Wayne[6] (186–209 nm), Chou et al.[1] (185–226 nm), Hubrich et al.[8] (158–260 nm), Hubrich and Stuhl[7] (158–

260 nm), Vanlaethem-Meurée et al.[16] (190–220 nm), Simon et al.[15] (174–230 nm), Mérienne et al.[12] (200–238 nm), and McGillen et al.[11] (184.95–230 nm). Absorption cross sections in the region 148–225 nm have also been derived from electron energy loss measurements by Huebner et al.[9], which are up to 30% higher than the values obtained by optical measurements. The room temperature data for wavelengths >180 nm are in good agreement, generally within 10–15%. The recommended absorption cross sections in Table 4F-33 are the values from Simon et al.[15] in the region 174–188 nm, the values from the McGillen et al. parameterization (see below) in the region 190–230 nm, and the data from Hubrich and Stuhl[7] in the region 235–260 nm. An uncertainty factor of 1.04 (2σ) is recommended for the 190–230 nm wavelength region.

A recommended Lyman-α cross section of 9.8×10^{-17} cm^2 molecule^{-1} with an uncertainty factor of 1.20 (2σ) is taken from SPARC.[10]

The temperature dependence of the absorption spectrum was measured by Chou et al.[1] (185–226 nm) over the range 213–296 K, Hubrich et al.[8] (158–260 nm) and Hubrich and Stuhl[7] (158–260 nm) at 208 and 298 K, Vanlaethem-Meurée et al.[16] (190–220 nm) at 255, 279, and 296 K, Simon et al.[15] (174–230 nm) over the range 225–295 K, Mérienne et al.[12] (200–238 nm) at 220, 240, and 296 K, and McGillen et al.[11] (184.95–230 nm) at 5 temperatures between 216 and 296 K. The temperature dependence is significant at wavelengths above 185 nm where the cross sections decrease with decreasing temperature. Simon et al.[15] parameterized their cross section temperature dependence using an empirical polynomial expansion:

$$\log_{10} \sigma(\lambda, T) = \sum A_n \lambda^n + (T–273) \times \sum B_n \lambda^n$$

and reported calculated cross sections for T = 210, 230, 250, 270, and 295 K. The parameters A_n and B_n, valid for the temperature range 210–300 K and wavelength range 174–230 nm are:

$A_0 = –84.611$	$B_0 = –5.7912$
$A_1 = 7.9551 \times 10^{-1}$	$B_1 = 1.1689 \times 10^{-1}$
$A_2 = –2.0550 \times 10^{-3}$	$B_2 = –8.8069 \times 10^{-4}$
$A_3 = –4.4812 \times 10^{-6}$	$B_3 = 2.9335 \times 10^{-6}$
$A_4 = 1.5838 \times 10^{-8}$	$B_4 = –3.6421 \times 10^{-9}$

Mérienne et al.[12] used a similar polynomial expansion to fit their data to:

$$\ln \sigma(\lambda, T) = \Sigma a_n (\lambda–200)^n + (T–296) \times \Sigma b_n (\lambda–200)^n,$$

which is valid for the temperature range 220–296 K and wavelength range 200–238 nm. The reported a_n and b_n parameters are:

$a_0 = –41.925548$	$b_0 = 3.58977 \times 10^{-4}$
$a_1 = –1.142857 \times 10^{-1}$	$b_1 = 3.02973 \times 10^{-4}$
$a_2 = –3.12034 \times 10^{-3}$	$b_2 = –1.13 \times 10^{-8}$
$a_3 = 3.6699 \times 10^{-5}$	

McGillen et al.[11] used the polynomial expansion:

$$\log_{10} \sigma(\lambda, T) = \Sigma A_i (\lambda–200)^i + (T–273) \times \Sigma B_i (\lambda–200)^i$$

to fit their data. The fit is valid for the temperature range 216–296 K and wavelength range 190–230 nm and reproduces their experimental data to within 2%. The reported A_i and B_i parameters are given below. The fit is in good agreement with the Chou et al.[1] data set, to within 5%, in reasonable agreement with the Mérienne et al.[12] data set, differences of 8% or less, but shows systematic differences with the Simon et al. data set, with 15% differences for the data at 230 K. The McGillen et al. parameterization is recommended.

i	A_i	B_i
0	–18.1863	0.0002656
1	–0.0528	4.228×10^{-5}
2	–0.001126	1.4027×10^{-6}
3	$–3.0552 \times 10^{-5}$	6.44645×10^{-7}
4	2.24126×10^{-6}	$–3.8038 \times 10^{-8}$
5	$–3.2064 \times 10^{-8}$	5.99×10^{-10}

Photolysis Quantum Yield and Product Studies: Clark and Husain[2] reported a quantum yield for Cl*($^2P_{1/2}$) atom formation in the broadband photolysis of $CFCl_3$ of 0.79 ± 0.27.

Table 4F-33. Recommended Absorption Cross Sections of $CFCl_3$ at 298 K

λ (nm)	10^{20} σ (cm^2)	λ (nm)	10^{20} σ (cm^2)	λ (nm)	10^{20} σ (cm^2)
174	313.0	198	83.0	222	1.62
176	324.0	200	66.0	224	1.09
178	323.5	202	51.5	226	0.730
180	314.0	204	39.3	228	0.491
182	296.0	206	29.4	230	0.330
184	272.0	208	21.5	235	0.132
186	243.0	210	15.4	240	0.0470
188	213.0	212	10.9	245	0.0174
190	181.9	214	7.57	250	0.0066
192	150.9	216	5.21	255	0.0029
194	124.9	218	3.54	260	0.0015
196	102.6	220	2.40		

Note:
174–188 nm: Simon et al.[15]
190–230 nm: McGillen et al.[11] parameterization
235–260 nm: Hubrich and Stuhl[7]

(1) Chou, C. C.; Smith, W. S.; Ruiz, H. V.; Moe, K.; Crescentini, G.; Molina, M. J.; Rowland, F. S. The temperature dependences of the ultraviolet absorption cross sections of CCl_2F_2 and CCl_3F, and their stratospheric significance. *J. Phys. Chem.* **1977**, *81*, 286-290, doi:10.1021/j100519a002.

(2) Clark, R. H.; Husain, D. Quantum yield measurements of $Cl(3^2P_{1/2})$ and $Cl(3^2P_{3/2})$ in the photolysis of C_1 chlorofluorocarbons determined by atomic resonance absorption spectroscopy in the vacuum UV. *J. Photochem.* **1984**, *24*, 103-115, doi:10.1016/0047-2670(84)80057-X.

(3) Doucet, J.; Sauvageau, P.; Sandorfy, C. Vacuum ultraviolet and photoelectron spectra of fluoro-chloro derivatives of methane. *J. Chem. Phys.* **1973**, *58*, 3708-3716, doi:10.1063/1.1679722.

(4) Gilbert, R.; Sauvageau, P.; Sandorfy, C. Vacuum ultraviolet absorption spectra of chlorofluoromethanes from 120 to 65 nm. *J. Chem. Phys.* **1974**, *60*, 4820-4824, doi:10.1063/1.1680987.

(5) Gordus, A. A.; Bernstein, R. B. Isotope effect in continuous ultraviolet absorption spectra: Methyl bromide-d_3 and chloroform-*d*. *J. Chem. Phys.* **1954**, *22*, 790-795, doi:10.1063/1.1740194.

(6) Green, R. G.; Wayne, R. P. Vacuum ultra-violet absorption spectra of halogenated methanes and ethanes. *J. Photochem.* **1976/77**, *6*, 375-377, doi:10.1016/0047-2670(76)85077-0.

(7) Hubrich, C.; Stuhl, F. The ultraviolet absorption of some halogenated methanes and ethanes of atmospheric interest. *J. Photochem.* **1980**, *12*, 93-107, doi:10.1016/0047-2670(80)85031-3.

(8) Hubrich, C.; Zetzsch, C.; Stuhl, F. Absorption spectra of halogenated methanes in wavelength region from 275 to 160 nm at temperatures of 298 and 208 K. *Ber. Bunsenges. Phys. Chem.* **1977**, *81*, 437-442, doi:10.1002/bbpc.19770810417.

(9) Huebner, R. H.; Bushnell, D. L., Jr.; Celotta, R. J.; Mielczarek, S. R.; Kuyatt, C. E. Ultraviolet photoabsorption by halocarbons 11 and 12 from electron impact measurements. *Nature* **1975**, *257*, 376-378, doi:10.1038/257376a0.

(10) Ko, M. K. W.; Newman, P. A.; Reimann, S.; Strahan, S. E.; Plumb, R. A.; Stolarski, R. S.; Burkholder, J. B.; Mellouki, W.; Engel, A.; Atlas, E. L.; Chipperfield, M.; Liang, Q. Lifetimes of Stratospheric Ozone-Depleting Substances, Their Replacements, and Related Species, SPARC Report No. 6, WCRP-15/2013, 2013, http://www.sparc-climate.org/publications/sparc-reports/sparc-report-no6/.

(11) McGillen, M. R.; Fleming, E. L.; Jackman, C. H.; Burkholder, J. B. $CFCl_3$ (CFC-11): UV absorption spectrum temperature dependence measurements and the impact on its atmospheric lifetime and uncertainty. *Geophys. Res. Lett.* **2013**, *40*, 50915, doi:10.1002/grl.50915.

(12) Mérienne, M. F.; Coquart, B.; Jenouvrier, A. Temperature effect on the ultraviolet-absorption of $CFCl_3$, CF_2Cl_2 and N_2O. *Planet. Space Sci.* **1990**, *38*, 617-625, doi:10.1016/0032-0633(90)90067-Z.

(13) Robbins, D. E.; Stolarski, R. S. Comparison of stratospheric ozone destruction by fluorocarbons 11, 12, 21, and 22. *Geophys. Res. Lett.* **1976**, *3*, 603-606, doi:10.1029/GL003i010p00603.

(14) Rowland, F. S.; Molina, M. J. Chlorofluoromethanes in the environment. *Rev. Geophys. Space Phys.* **1975**, *13*, 1-35, doi:10.1029/RG013i001p00001.

(15) Simon, P. C.; Gillotay, D.; Vanlaethem-Meurée, N.; Wisemberg, J. Ultraviolet absorption cross-sections of chloro and chlorofluoro-methanes at stratospheric temperatures. *J. Atmos. Chem.* **1988**, *7*, 107-135, doi:10.1007/BF00048042.

(16) Vanlaethem-Meurée, N.; Wisemberg, J.; Simon, P. C. Influence de la température sur les sections efficases d'absorption des chlorofluorométhanes dans l'ultraviolet. *Bull. Acad. Roy. Belgique Cl. Sci.* **1978**, *64*, 42-51.

F34. CF_2Cl_2 (difluorodichloromethane, CFC-12)

Back to Index

CF_2Cl_2 (CFC-12) + hν → Products (1)

(Recommendation: 15-10, Note: 15-10, Evaluated: 15-10)

Absorption Cross Sections: The VUV/UV absorption spectrum of difluorodichloromethane (CFC-12), CF_2Cl_2, has been measured at room temperature by Gordus and Bernstein[5] (210 nm), Rowland and Molina[14] (186–216 nm), Robbins and Stolarski[13] (174–216 nm), Greene and Wayne[6] (186–206 nm), Rebbert and Ausloos[12] (213.9 nm), Chou et al.[1] (184–221 nm), Hubrich et al.[7] (159–240 nm), Vanlaethem-Meurée et al.[17] (190–216 nm), Simon et al.[16] (174–230 nm), and Mérienne et al.[11] (200–231 nm). The room temperature data are in good agreement, generally within 10–15%, except for data from Green and Wayne[6] at wavelengths >195 nm and the data from Rowland and Molina[14] near 210 nm. Absorption cross sections have also been derived from electron energy loss measurements by Huebner et al.[8] (148–218 nm), which agree to within 10% with the data obtained by optical measurements around the absorption maximum but are larger than the optical cross section data at wavelengths >196 nm by as much as 100%. The recommended absorption cross sections in Table 4F-34 are values from Hubrich et al.[7] in the region 170–172 nm, the mean of the values reported by Hubrich et al.[7] and Simon et al.[16] in the region 174–178 nm, the values from Simon et al.[16] in the region 180–198 nm, mean of the values reported by Simon et al.[16] and Mérienne et al.[11] in the region 200–226 nm, and the data of Mérienne et al.[11] in the region 228–230 nm. For the range 232–240 nm the recommended values were obtained from a log-linear fit and extrapolation of the Mérienne et al.[11] data, $\log \sigma(\lambda) = 2.1448 – 0.1061\ \lambda$. The measured cross section values from Hubrich et al.[7] over this wavelength range are lower by ~40% at 240 nm than the extrapolated values. An uncertainty factor of 1.08 (2σ) is recommended for the 190–230 nm wavelength region.[9]

High resolution absorption cross section measurements have been carried out by Seccombe et al.[15] (50–150 nm) and Limao-Vieira et al.[10] (113–225 nm) using a synchrotron radiation light source. The results of Limao-Vieira et al.[10] for the absorption band at 170–204 nm are in very good agreement with the recommendation in Table 4F-34. These cross section measurements significantly improve upon the earlier data from Gilbert et al.[4] (60–135 nm) and Doucet et al.[3] (120–200 nm).

The temperature dependence of the absorption spectrum has been measured by Rebbert and Ausloos[12] (213.9 nm) over the range 234–442 K, Chou et al.[1] (184–221 nm) at 212, 252, and 296 K, Hubrich et al.[7] (159–240 nm) at 208 and 298 K, Vanlaethem-Meurée et al.[17] (190–216 nm) at 255, 279, and 296 K, Simon et al.[16] (174–230 nm) at 225–295 K, and Mérienne et al.[11] (200–231 nm) at 220, 240, and 296 K.

The temperature dependence is significant at wavelengths above 186 nm where the cross sections decrease with decreasing temperature. Mérienne et al.[11] parameterized the cross section temperature dependence using an empirical polynomial expansion:

$$\ln \sigma(\lambda, T) = \sum a_n (\lambda – 200)^n + (T – 296) \times \sum b_n (\lambda – 200)^n$$

that is valid for the temperature range 220–296 K and wavelength range 200–231 nm. The a_n and b_n parameters given below are recommended.

$a_0 = –43.8954569$ $\quad b_0 = 4.8438 \times 10^{-3}$
$a_1 = –2.403597 \times 10^{-1}$ $\quad b_1 = 4.96145 \times 10^{-4}$
$a_2 = –4.2619 \times 10^{-4}$ $\quad b_2 = –5.6953 \times 10^{-6}$
$a_3 = 9.8743 \times 10^{-6}$

Simon et al.[16] also parameterized the cross section temperature dependence of their data. However, the parameters reported by Simon et al.[16] contain typographical error(s) that were reproduced in NASA/JPL 02-25. The correct parameters are unknown and therefore not given here.

Photolysis Quantum Yield and Product Studies: Clark and Husain[2] report the quantum yield for $Cl^*(^2P_{1/2})$ atom formation in the broad band photolysis of CF_2Cl_2 to be 0.75 ± 0.26.

Table 4F-34. Recommended Absorption Cross Sections of CF_2Cl_2 at 298 K

λ (nm)	10^{20} σ (cm^2)	λ (nm)	10^{20} σ (cm^2)	λ (nm)	10^{20} σ (cm^2)

170	124.0	194	31.5	218	0.103
172	151.0	196	21.1	220	0.0624
174	168.0	198	13.9	222	0.0381
176	185.5	200	8.71	224	0.0233
178	189.5	202	5.42	226	0.0140
180	179.0	204	3.37	228	0.0090
182	160.0	206	2.06	230	0.0057
184	134.0	208	1.26	232	*0.0034*
186	107.0	210	0.762	234	*0.0021*
188	82.8	212	0.458	236	*0.0013*
190	63.2	214	0.274	238	*0.0008*
192	45.50	216	0.163	240	*0.0005*

Note:
170–172 nm: Hubrich et al.[7]
174–178 nm: the mean of data from Hubrich et al.[7] and Simon et al.[16]
180–198 nm: Simon et al.[16]
200–230 nm: mean of data from Simon et al.[16] and Mérienne et al.[11]
232–240 nm: extrapolation of data from Mérienne et al.[11] data., log $\sigma(\lambda) = 2.1448–0.1061\ \lambda$

(1) Chou, C. C.; Smith, W. S.; Ruiz, H. V.; Moe, K.; Crescentini, G.; Molina, M. J.; Rowland, F. S. The temperature dependences of the ultraviolet absorption cross sections of CCl_2F_2 and CCl_3F, and their stratospheric significance. *J. Phys. Chem.* **1977**, *81*, 286-290, doi:10.1021/j100519a002.

(2) Clark, R. H.; Husain, D. Quantum yield measurements of $Cl(3^2P_{1/2})$ and $Cl(3^2P_{3/2})$ in the photolysis of C_1 chlorofluorocarbons determined by atomic resonance absorption spectroscopy in the vacuum UV. *J. Photochem.* **1984**, *24*, 103-115, doi:10.1016/0047-2670(84)80057-X.

(3) Doucet, J.; Sauvageau, P.; Sandorfy, C. Vacuum ultraviolet and photoelectron spectra of fluoro-chloro derivatives of methane. *J. Chem. Phys.* **1973**, *58*, 3708-3716, doi:10.1063/1.1679722.

(4) Gilbert, R.; Sauvageau, P.; Sandorfy, C. Vacuum ultraviolet absorption spectra of chlorofluoromethanes from 120 to 65 nm. *J. Chem. Phys.* **1974**, *60*, 4820-4824, doi:10.1063/1.1680987.

(5) Gordus, A. A.; Bernstein, R. B. Isotope effect in continuous ultraviolet absorption spectra: Methyl bromide-d_3 and chloroform-*d*. *J. Chem. Phys.* **1954**, *22*, 790-795, doi:10.1063/1.1740194.

(6) Green, R. G.; Wayne, R. P. Vacuum ultra-violet absorption spectra of halogenated methanes and ethanes. *J. Photochem.* **1976/77**, *6*, 375-377, doi:10.1016/0047-2670(76)85077-0.

(7) Hubrich, C.; Zetzsch, C.; Stuhl, F. Absorption spectra of halogenated methanes in wavelength region from 275 to 160 nm at temperatures of 298 and 208 K. *Ber. Bunsenges. Phys. Chem.* **1977**, *81*, 437-442, doi:10.1002/bbpc.19770810417.

(8) Huebner, R. H.; Bushnell, D. L., Jr.; Celotta, R. J.; Mielczarek, S. R.; Kuyatt, C. E. Ultraviolet photoabsorption by halocarbons 11 and 12 from electron impact measurements. *Nature* **1975**, *257*, 376-378, doi:10.1038/257376a0.

(9) Ko, M. K. W.; Newman, P. A.; Reimann, S.; Strahan, S. E.; Plumb, R. A.; Stolarski, R. S.; Burkholder, J. B.; Mellouki, W.; Engel, A.; Atlas, E. L.; Chipperfield, M.; Liang, Q. Lifetimes of Stratospheric Ozone-Depleting Substances, Their Replacements, and Related Species, SPARC Report No. 6, WCRP-15/2013, 2013, http://www.sparc-climate.org/publications/sparc-reports/sparc-report-no6/.

(10) Limão-Vieira, P.; Eden, S.; Kendall, P. A.; Mason, N. J.; Hoffmann, S. V. VUV photo-absorption cross-section for CCl_2F_2. *Chem. Phys. Lett.* **2002**, *364*, 535-541, doi:10.1016/S0009-2614(02)01304-0.

(11) Mérienne, M. F.; Coquart, B.; Jenouvrier, A. Temperature effect on the ultraviolet-absorption of $CFCl_3$, CF_2Cl_2 and N_2O. *Planet. Space Sci.* **1990**, *38*, 617-625, doi:10.1016/0032-0633(90)90067-Z.

(12) Rebbert, R. E.; Ausloos, P. J. Photodecomposition of $CFCl_3$ and CF_2Cl_2. *J. Photochem.* **1975**, *4*, 419-434, doi:10.1016/0047-2670(75)85023-4.

(13) Robbins, D. E.; Stolarski, R. S. Comparison of stratospheric ozone destruction by fluorocarbons 11, 12, 21, and 22. *Geophys. Res. Lett.* **1976**, *3*, 603-606, doi:10.1029/GL003i010p00603.

(14) Rowland, F. S.; Molina, M. J. Chlorofluoromethanes in the environment. *Rev. Geophys. Space Phys.* **1975**, *13*, 1-35, doi:10.1029/RG013i001p00001.

(15) Seccombe, D. P.; Chim, R. Y. L.; Tuckett, R. P.; Jochims, H. W.; Baumgärtel, H. Vacuum–ultraviolet absorption and fluorescence spectroscopy of CF_2H_2, CF_2Cl_2, and CF_2Br_2 in the range 8–22 eV. *J. Chem. Phys.* **2001**, *114*, 4058-4073, doi:10.1063/1.1344888.

(16) Simon, P. C.; Gillotay, D.; Vanlaethem-Meurée, N.; Wisemberg, J. Ultraviolet absorption cross-sections of chloro and chlorofluoro-methanes at stratospheric temperatures. *J. Atmos. Chem.* **1988**, *7*, 107-135, doi:10.1007/BF00048042.

(17) Vanlaethem-Meurée, N.; Wisemberg, J.; Simon, P. C. Influence de la température sur les sections efficases d'absorption des chlorofluorométhanes dans l'ultraviolet. *Bull. Acad. Roy. Belgique Cl. Sci.* **1978**, *64*, 42-51.

F35. CF_3Cl (trifluorochloromethane, CFC-13)

Back to Index

CF_3Cl (CFC-13) + hν → Products (1)

(Recommendation: 02-25, Note: 10-6, Evaluated: 10-6)

Absorption Cross Sections: The VUV/UV absorption spectrum of trifluorochloromethane (CFC-13), CF_3Cl, has been measured at room temperature by Chou et al.[1] (184–203 nm), Vanlaethem-Meurée et al.[8] (172–200 nm), Hubrich and Stuhl[5] (160–220 nm), and Simon et al.[7] (172–200 nm). The cross section values from Vanlaethem-Meurée et al.[8] and Simon et al.[7] are identical. The cross section data from Hubrich and Stuhl[5] deviate from the Vanlaethem-Meurée et al.[8] and Simon et al.[7] values by ±25% and the data from Chou et al.[1] is systematically greater by 15–30% in the region 185–200 nm. The recommended absorption cross sections in Table 4F-35 are taken from Simon et al.[7] for the range 172–200 nm. The recommended cross sections in the range 202–220 nm were obtained by a log-linear extrapolation of the Simon et al.[7] data, $\log \sigma(\lambda) = -5.048 - 0.0834\,\lambda$.

The absorption spectrum has been measured in the far UV by Gilbert et al.[4] (65–130 nm), and Doucet et al.[3] (120–160 nm), and Ravishankara et al.[6] (Lyman-α, 121.6 nm).

The temperature dependence of the absorption spectrum was measured by Vanlaethem-Meurée et al.[8] (172–200 nm) at 255, 279, and 296 K, Hubrich and Stuhl[5] (160–220 nm) at 208 and 298 K, and Simon et al.[7] (172–200 nm) over the range 225–295 K. Vanlaethem-Meurée et al.[8] and Simon et al.[7] reported no measurable temperature dependence. Hubrich and Stuhl[5] report a decrease of the absorption cross sections at 208 K, 4% at 160 nm increasing to 74% at 205 nm. Simon et al.[7] parameterized the cross section wavelength dependence and the temperature dependence using an empirical polynomial expansion:

$$\log_{10} \sigma(\lambda, T) = \sum A_n \lambda^n + (T-273) \times \sum B_n \lambda^n \text{ (with all } B_n = 0)$$

and reported calculated values at 295 K. The A_n parameters, which are valid for the temperature range 210–300 K and wavelength range 172–200 nm, given below are recommended.

$A_0 = -155.88$ $A_1 = 2.0993$
$A_2 = -1.0486 \times 10^{-2}$ $A_3 = 1.6718 \times 10^{-5}$

Photolysis Quantum Yield and Product Studies: Clark and Husain[2] report a quantum yield for $Cl^*(^2P_{1/2})$ atom formation in the broad band photolysis of CF_3Cl to be 0.86 ± 0.29.

Table 4F-35. Recommended Absorption Cross Sections of CF_3Cl at 295 K

λ (nm)	$10^{20}\,\sigma$ (cm^2)	λ (nm)	$10^{20}\,\sigma$ (cm^2)	λ (nm)	$10^{20}\,\sigma$ (cm^2)
172	1.100	190	0.128	208	*0.00406*
174	0.970	192	0.0900	210	*0.00276*
176	0.825	194	0.0610	212	*0.00188*
178	0.681	196	0.0410	214	*0.00128*
180	0.542	198	0.0280	216	*0.000872*
182	0.425	200	0.0190	218	*0.000594*
184	0.326	202	*0.0128*	220	*0.000405*
186	0.244	204	*0.00874*		
188	0.175	206	*0.00595*		

Note:
172–200 nm: Simon et al.[7]
202–220 nm: extrapolation of Simon et al.[7] data

(1) Chou, C. C.; Milstein, R. J.; Smith, W. S.; Vera-Ruiz, H.; Molina, M. J.; Rowland, F. S. Stratospheric photodissociation of several saturated perhalo chlorofluorocarbon compounds in current technological use (fluorocarbons-13, -113, -114, and -115). *J. Phys. Chem.* **1978**, *82*, 1-7, doi:10.1021/j100490a001.

(2) Clark, R. H.; Husain, D. Quantum yield measurements of $Cl(3^2P_{1/2})$ and $Cl(3^2P_{3/2})$ in the photolysis of C_1 chlorofluorocarbons determined by atomic resonance absorption spectroscopy in the vacuum UV. *J. Photochem.* **1984**, *24*, 103-115, doi:10.1016/0047-2670(84)80057-X.
(3) Doucet, J.; Sauvageau, P.; Sandorfy, C. Vacuum ultraviolet and photoelectron spectra of fluoro-chloro derivatives of methane. *J. Chem. Phys.* **1973**, *58*, 3708-3716, doi:10.1063/1.1679722.
(4) Gilbert, R.; Sauvageau, P.; Sandorfy, C. Vacuum ultraviolet absorption spectra of chlorofluoromethanes from 120 to 65 nm. *J. Chem. Phys.* **1974**, *60*, 4820-4824, doi:10.1063/1.1680987.
(5) Hubrich, C.; Stuhl, F. The ultraviolet absorption of some halogenated methanes and ethanes of atmospheric interest. *J. Photochem.* **1980**, *12*, 93-107, doi:10.1016/0047-2670(80)85031-3.
(6) Ravishankara, A. R.; Solomon, S.; Turnipseed, A. A.; Warren, R. F. Atmospheric lifetimes of long-lived halogenated species. *Science* **1993**, *259*, 194-199, doi:10.1126/science.259.5092.194.
(7) Simon, P. C.; Gillotay, D.; Vanlaethem-Meurée, N.; Wisemberg, J. Ultraviolet absorption cross-sections of chloro and chlorofluoro-methanes at stratospheric temperatures. *J. Atmos. Chem.* **1988**, *7*, 107-135, doi:10.1007/BF00048042.
(8) Vanlaethem-Meurée, N.; Wisemberg, J.; Simon, P. C. Influence de la température sur les sections efficases d'absorption des chlorofluorométhanes dans l'ultraviolet. *Bull. Acad. Roy. Belgique Cl. Sci.* **1978**, *64*, 42-51.

F36. CCl_2FCCl_2F (CFC-112)

Back to Index

$CCl_2FCCl_2F + h\nu \rightarrow$ Products (1)

(Recommendation: 19-5, Note: 19-5, Evaluated: 19-5)

Absorption Cross Sections: UV absorption cross sections of CCl_2FCCl_2F (CFC-112, 1,1,2,2-tetrachloro-1,2-difluoroethane) have been measured by Davis et al.[1] (192.5–235 nm, 1 nm resolution). This is the only study of this molecule available at the time of this evaluation. Absorption cross sections were measured at 10 discrete wavelengths and 5 temperatures between 230 and 323 K. The measured spectra were corrected for a minor CFC-112a sample impurity, 4.0%, using the CFC-112a spectrum measured in their study. The UV absorption spectra of CFC-112 are continuous over this wavelength range with a decrease in cross section with increasing wavelength. A decrease in $\sigma(\lambda,T)$ with decreasing temperature was observed at all wavelengths with the temperature dependence greatest at the longer wavelengths.

The CFC-112 spectra were parameterized in Davis et al. using the formula:

$$\ln\left(\sigma(\lambda, T)\right) = \sum_i A_i \lambda_i{}^i + (T - 296) \sum_i B_i \lambda_i{}^i$$

(units: $\sigma(\lambda,T)$ (cm^2 $molecule^{-1}$, base e), λ (nm), and T (K)) which reproduces the experimental data to within 2%, or better, over the wavelength range most critical for atmospheric photolysis, 195–215 nm. The parameterization coefficients from Davis et al. given below are valid for wavelengths from 192.5 to 235 nm and temperatures between 230 and 323 K.

i	A_i	B_i
0	-1488.6207	6.04688
1	18.43604	-0.0801501
2	-0.02897393	0.0001201698
3	-0.00051504703	2.610366×10^{-6}
4	2.644261×10^{-6}	$-1.3959106 \times 10^{-8}$
5	$-3.7258313 \times 10^{-9}$	$2.0719264 \times 10^{-11}$

The CFC-112 absorption cross sections given in Table 4F-36 were calculated using this parameterization. The recommended estimated uncertainty factor ($F(\lambda)$, 2σ) is 1.08 over the temperature and wavelength range of the experimental data.

Photolysis Quantum Yield and Product Studies: No recommendation.

Table 4F-36. Recommended Absorption Cross Sections of CCl_2FCCl_2F (CFC-112) at 296 K

λ (nm)	10^{20} σ (cm^2)
194	107
196	83.4
198	63.3
200	47.3
202	34.9
204	25.6
206	18.7
208	13.7
210	10.1
212	7.54
214	5.68
216	4.35
218	3.38
220	2.67
222	2.15
224	1.76
226	1.47
228	1.25
230	1.08
232	0.940
234	0.828

Note:
Davis et al.[1]

(1) Davis, M. E.; Bernard, F.; McGillen, M. R.; Fleming, E. L.; Burkholder, J. B. UV and infrared absorption spectra, atmospheric lifetimes, and ozone depletion and global warming potentials for CCl_2FCCl_2F (CFC-112), CCl_3CClF_2 (CFC-112a), CCl_3CF_3 (CFC-113a), and CCl_2FCF_3 (CFC-114a). *Atmos. Chem. Phys.* **2016**, *16*, 8043-8052, doi:10.5194/acp-16-8043-2016.

F37. CCl_3CClF_2 (CFC-112a)

Back to Index

$CCl_3CClF_2 + h\nu \rightarrow$ Products (1)

(Recommendation: 19-5, Note: 19-5, Evaluated: 19-5)

Absorption Cross Sections: UV absorption cross sections of CCl_3CClF_2 (CFC-112a, 1,1,1,2-tetrachloro-2,2-difluoroethane) have been measured by Davis et al.[1] (192.5–235 nm, 1 nm resolution). This is the only study of this molecule available at the time of this evaluation. Absorption cross sections were measured at 10 discrete wavelengths and 5 temperatures between 230 and 323 K. The measured spectra were corrected for a minor CFC-112 sample impurity, 3.68%, using the CFC-112 spectrum measured in their study. The UV absorption spectra of CFC-112a are continuous over this wavelength range with a decrease in cross section with increasing wavelength. A decrease in σ(λ,T) with decreasing temperature was observed at all wavelengths with the temperature dependence greatest at the longer wavelengths.

The CFC-112a spectra were parameterized in Davis et al. using the formula:

$$\ln\left(\sigma(\lambda,\mathrm{T})\right) = \sum_i A_i {\lambda_i}^i + (\mathrm{T}-296)\sum_i B_i {\lambda_i}^i$$

(units: σ(λ,T) (cm^2 $molecule^{-1}$, base e), λ (nm), and T (K)) which reproduces the experimental data to within 2%, or better, over the wavelength range most critical for atmospheric photolysis, 195–215 nm. The parameterization coefficients reproduced from Davis et al. given below are valid for wavelengths between 192.5 and 235 nm and temperatures between 230 and 323 K.

i	A_i	B_i
0	-560.3404	10.37492
1	9.534427	-0.182485408
2	-0.06987945	0.0011614979
3	0.0002657157	$-2.9864183 \times 10^{-6}$
4	-5.491224×10^{-7}	1.547878×10^{-9}
5	4.993769×10^{-10}	3.36518×10^{-12}

The CFC-112a absorption cross sections given in Table 4F-37 were calculated using this parameterization. The recommended estimated uncertainty factor (F(λ), 2σ) is 1.08 over the temperature and wavelength range of the experimental data.

Photolysis Quantum Yield and Product Studies: No recommendation.

Table 4F-37. Recommended Absorption Cross Sections of CCl_3CClF_2 (CFC-112a) at 296 K

λ (nm)	10^{20} σ (cm^2)
194	136
196	115
198	95.3
200	77.4
202	61.8
204	48.5
206	37.4
208	28.5
210	21.4
212	15.9
214	11.6
216	8.45
218	6.08
220	4.35
222	3.09
224	2.18
226	1.53
228	1.08
230	0.754
232	0.527
234	0.369

Note:
Davis et al.[1]

(1) Davis, M. E.; Bernard, F.; McGillen, M. R.; Fleming, E. L.; Burkholder, J. B. UV and infrared absorption spectra, atmospheric lifetimes, and ozone depletion and global warming potentials for CCl_2FCCl_2F (CFC-112), CCl_3CClF_2 (CFC-112a), CCl_3CF_3 (CFC-113a), and CCl_2FCF_3 (CFC-114a). *Atmos. Chem. Phys.* **2016**, *16*, 8043-8052, doi:10.5194/acp-16-8043-2016.

F38. $CF_2ClCFCl_2$ (1,1,2-trifluoro-1,2,2-trichloroethane, CFC-113) Back to Index

$CF_2ClCFCl_2$ (CFC-113) + hν → Products (1)

(Recommendation: 06-2, Note: 10-6, Evaluated: 10-6)

Absorption Cross Sections: The UV absorption spectrum of 1,1,2-trifluoro-1,2,2-trichloroethane (CFC-113), $CF_2ClCFCl_2$, has been measured at room temperature by Chou et al.[1] (184–224 nm), Hubrich and Stuhl[3] (160–250 nm), and Simon et al.[4] (184–230 nm). The cross section values agree to within ~10% except in the region near 190 nm where the values of Hubrich and Stuhl[3] are smaller by as much as 20%. The recommended absorption cross sections in Table 4F-38 are the values from Hubrich and Stuhl[3] in the region 175–180 nm, the value at 184 nm was interpolated between those of Hubrich and Stuhl[3] at 180 nm and Simon et al.[4] at 186 nm, and the values from Simon et al.[4] in the region 186–230 nm. The recommended absorption cross sections for

wavelengths >230 nm were obtained from a log-linear extrapolation of the Simon et al.[4] data, log $\sigma(\lambda)= -0.9860–0.0894\ \lambda$. The values measured by Hubrich and Stuhl[3] in the region >230 nm are greater than the extrapolated values by ~20–80% .

The absorption spectrum in the far UV has been measured by Doucet et al.[2] (110–200 nm).

The temperature dependence of the absorption spectrum has been measured by Hubrich and Stuhl[3] (160–250 nm) at 208 and 298 K and Simon et al.[4] (184–230 nm) over the range 225–295 K. The temperature dependence is significant at wavelengths >194 nm and <170 nm where the cross sections decrease with decreasing temperature. Simon et al.[4] parameterized the temperature dependence of the cross sections using an empirical polynomial expansion:

$$\log_{10} \sigma(\lambda, T) = \sum A_n \lambda^n + (T–273) \times \sum B_n \lambda^n$$

and reported calculated values for T = 210, 230, 250, 270, and 295 K. The A_n and B_n parameters, valid over the temperature range 210–300 K and wavelength range 182–230 nm, given below are recommended.

$A_0 = –1087.9$	$B_0 = 12.493$
$A_1 = 20.004$	$B_1 = –2.3937 \times 10^{-1}$
$A_2 = –1.3920 \times 10^{-1}$	$B_2 = 1.7142 \times 10^{-3}$
$A_3 = 4.2828 \times 10^{-4}$	$B_3 = –5.4393 \times 10^{-6}$
$A_4 = –4.9384 \times 10^{-7}$	$B_4 = 6.4548 \times 10^{-9}$.

Photolysis Quantum Yield and Product Studies: No recommendation.

Table 4F-38. Recommended Absorption Cross Sections of $CF_2ClCFCl_2$ at 298 K

λ (nm)	10^{20} σ (cm^2)	λ (nm)	10^{20} σ (cm^2)	λ (nm)	10^{20} σ (cm^2)
175	192	204	5.80	228	0.0410
180	155	206	4.00	230	0.0270
184	*123*	208	2.65	232	*0.0188*
186	104	210	1.80	234	*0.0124*
188	83.5	212	1.15	236	*0.00824*
190	64.5	214	0.760	238	*0.00546*
192	48.8	216	0.505	240	*0.00361*
194	36.0	218	0.318	242	*0.00239*
196	26.0	220	0.220	244	*0.00159*
198	18.3	222	0.145	246	*0.00105*
200	12.5	224	0.0950	248	*0.000696*
202	8.60	226	0.0630	250	*0.000461*

Note:
175–180 nm: Hubrich and Stuhl[3]
184 nm: interpolation of Hubrich and Stuhl[3] and Simon et al.[4] data
186–230 nm: Simon et al.[4]
232–250 nm: extrapolation of Simon et al.[4] data, log $\sigma(\lambda)= –0.9860–0.0894\ \lambda$

(1) Chou, C. C.; Milstein, R. J.; Smith, W. S.; Vera-Ruiz, H.; Molina, M. J.; Rowland, F. S. Stratospheric photodissociation of several saturated perhalo chlorofluorocarbon compounds in current technological use (fluorocarbons-13, -113, -114, and -115). *J. Phys. Chem.* **1978**, *82*, 1-7, doi:10.1021/j100490a001.

(2) Doucet, J.; Sauvageau, P.; Sandorfy, C. Photoelectron and far-ultraviolet absorption spectra of chlorofluoro derivatives of ethane. *J. Chem. Phys.* **1975**, *62*, 355-359, doi:10.1063/1.430493.

(3) Hubrich, C.; Stuhl, F. The ultraviolet absorption of some halogenated methanes and ethanes of atmospheric interest. *J. Photochem.* **1980**, *12*, 93-107, doi:10.1016/0047-2670(80)85031-3.

(4) Simon, P. C.; Gillotay, D.; Vanlaethem-Meurée, N.; Wisemberg, J. Temperature dependence of ultraviolet absorption cross-sections of chlorofluoroethanes. *Ann. Geophys.* **1988**, *6*, 239-248.

F39. CCl_3CF_3 (CFC-113a)

Back to Index

$CCl_3CF_3 + h\nu \rightarrow$ Products (1)

(Recommendation: 19-5, Note: 19-5, Evaluated: 19-5)

Absorption Cross Sections: UV absorption cross sections of CCl_3CF_3 (CFC-113a, 1,1,1-trichloro-2,2,2-trifluoroethane) have been measured by Davis et al.[1] (192.5–235 nm, 1 nm resolution). This is the only study of this molecule available at the time of this evaluation. Absorption cross sections were measured at 10 discrete wavelengths and 6 temperatures between 207 and 323 K. The UV absorption spectra of CFC-113a are continuous over this wavelength range with a decrease in cross section with increasing wavelength. A decrease in $\sigma(\lambda,T)$ with decreasing temperature was observed at nearly all wavelengths with the temperature dependence greatest at the longer wavelengths.

The CFC-113a spectra were parameterized in Davis et al. using the formula:

$$\ln\left(\sigma(\lambda, T)\right) = \sum_i A_i \lambda_i^{\,i} + (T - 296) \sum_i B_i \lambda_i^{\,i}$$

(units: $\sigma(\lambda,T)$ (cm^2 $molecule^{-1}$, base e), λ (nm), and T (K)) which reproduces the experimental data to within ~4%, or better, over the wavelength range most critical for atmospheric photolysis, 195–215 nm. The parameterization coefficients reproduced from Davis et al. below are valid for wavelengths between 192.5 and 235 nm and temperatures between 207 and 323 K.

i	A_i	B_i
0	-319.173	2.89174
1	2.70954	-0.0348043
2	0.00457404	3.6233×10^{-5}
3	-0.0001288147	1.08853×10^{-6}
4	4.71409×10^{-7}	-5.25744×10^{-9}
5	-5.35388×10^{-10}	7.26095×10^{-12}

The CFC-113a absorption cross sections given in Table 4F-39 were calculated using this parameterization. The recommended estimated uncertainty factors ($F(\lambda)$, 2σ) are assigned as $F(\lambda) = 1.05 + 1 \times 10^{-22}/\sigma(\lambda)$.

Photolysis Quantum Yield and Product Studies: No recommendation.

Table 4F-39. Recommended Absorption Cross Sections of CCl_3CF_3 (CFC-113a) at 296 K

λ (nm)	$10^{20}\,\sigma$ (cm^2)	λ (nm)	$10^{20}\,\sigma$ (cm^2)
194	117.5	216	6.13
196	98.2	218	4.36
198	80.2	220	3.08
200	64.1	222	2.17
202	50.3	224	1.52
204	38.8	226	1.07
206	29.4	228	0.748
208	22.0	230	0.523
210	16.2	232	0.367
212	11.8	234	0.258
214	8.56		

Note:
Davis et al.[1]

(1) Davis, M. E.; Bernard, F.; McGillen, M. R.; Fleming, E. L.; Burkholder, J. B. UV and infrared absorption spectra, atmospheric lifetimes, and ozone depletion and global warming potentials for CCl_2FCCl_2F (CFC-112), CCl_3CClF_2 (CFC-112a), CCl_3CF_3 (CFC-113a), and CCl_2FCF_3 (CFC-114a). *Atmos. Chem. Phys.* **2016**, *16*, 8043-8052, doi:10.5194/acp-16-8043-2016.

F40. CF_2ClCF_2Cl (1,1,2,2-tetrafluoro-1,2-dichloroethane, CFC–114)

Back to Index

CF_2ClCF_2Cl (CFC–114) + hν → Products (1)

(Recommendation: 02-25, Note: 10-6, Evaluated: 10-6)

Absorption Cross Sections: The VUV/UV absorption spectrum of 1,1,2,2-tetrafluoro-1,2-dichloroethane (CFC–114), CF_2ClCF_2Cl, has been measured at room temperature by Chou et al.[1] (184–219 nm), Hubrich and Stuhl[3] (160–235 nm), and Simon et al.[5] (172–220 nm). The room temperature values of Simon et al.[5] and Chou et al.[1] agree to within 5% except at 185 and 195 nm. The cross section values from Hubrich and Stuhl[3] are systematically greater than those from Simon et al.[5] The recommended absorption cross sections in Table 4F-40 are the values from Simon et al.[5] in the region 172–220 nm. The recommended cross sections for wavelengths >220 nm were obtained from a log-linear extrapolation of the Simon et al.[5] data, $\log \sigma(\lambda) = -1.8233 - 0.0913\ \lambda$. The values measured by Hubrich et al.[3] are greater by ~40% than the extrapolated values.

The absorption spectrum in the far UV has been measured by Ravishankara et al.[4] (Lyman-α, 121.6 nm) and Doucet et al.[2] (110–190 nm).

The temperature dependence of the absorption spectrum has been measured by Hubrich and Stuhl[3] (160–235 nm) at 208 and 298 K and Simon et al.[5] (182–220 nm) in the range 225–295 K. Simon et al.[5] report decreasing cross sections with decreasing temperature for wavelengths >190 nm . Hubrich and Stuhl[3] report a small decrease of the cross sections (generally <10%) for wavelengths in the range 160–210 nm. Simon et al.[5] parameterized the temperature dependence of the cross sections using an empirical polynomial expansion:

$$\log_{10} \sigma(\lambda, T) = \sum A_n \lambda^n + (T-273) \times \sum B_n \lambda^n$$

and reported calculated values for T = 210, 230, 250, 270, and 295 K. The A_n and B_n parameters, valid for the temperature range 210–300 K and wavelength range 172–220 nm, given below are recommended.

$A_0 = -160.50$	$B_0 = -1.5296$
$A_1 = 2.4807$	$B_1 = 3.5248 \times 10^{-2}$
$A_2 = -1.5202 \times 10^{-2}$	$B_2 = -2.9951 \times 10^{-4}$
$A_3 = 3.8412 \times 10^{-5}$	$B_3 = 1.1129 \times 10^{-6}$
$A_4 = -3.4373 \times 10^{-8}$	$B_4 = -1.5259 \times 10^{-9}$

Photolysis Quantum Yield and Product Studies: No recommendation.

Table 4F-40. Recommended Absorption Cross Sections of CF_2ClCF_2Cl at 295 K

λ (nm)	10^{20} σ (cm^2)	λ (nm)	10^{20} σ (cm^2)	λ (nm)	10^{20} σ (cm^2)
172	69.0	194	2.56	216	0.0290
174	55.0	196	1.75	218	0.0190
176	43.0	198	1.20	220	0.0122
178	34.0	200	0.800	222	*0.00809*
180	26.2	202	0.540	224	*0.00531*
182	19.8	204	0.370	226	*0.00349*
184	15.0	206	0.245	228	*0.00229*
186	11.0	208	0.160	230	*0.00151*
188	7.80	210	0.104	232	*0.00099*
190	5.35	212	0.0680	234	*0.00065*
192	3.70	214	0.0440	235	*0.00053*

Note:
172–220 nm: Simon et al.[5]
222–235 nm: extrapolation of Simon et al.[5] data, $\log \sigma(\lambda) = -1.8233 - 0.0913\ \lambda$

(1) Chou, C. C.; Milstein, R. J.; Smith, W. S.; Vera-Ruiz, H.; Molina, M. J.; Rowland, F. S. Stratospheric photodissociation of several saturated perhalo chlorofluorocarbon compounds in current technological use (fluorocarbons-13, -113, -114, and -115). *J. Phys. Chem.* **1978**, *82*, 1-7, doi:10.1021/j100490a001.

(2) Doucet, J.; Sauvageau, P.; Sandorfy, C. Photoelectron and far-ultraviolet absorption spectra of chlorofluoro derivatives of ethane. *J. Chem. Phys.* **1975**, *62*, 355-359, doi:10.1063/1.430493.

(3) Hubrich, C.; Stuhl, F. The ultraviolet absorption of some halogenated methanes and ethanes of atmospheric interest. *J. Photochem.* **1980**, *12*, 93-107, doi:10.1016/0047-2670(80)85031-3.

(4) Ravishankara, A. R.; Solomon, S.; Turnipseed, A. A.; Warren, R. F. Atmospheric lifetimes of long-lived halogenated species. *Science* **1993**, *259*, 194-199, doi:10.1126/science.259.5092.194.
(5) Simon, P. C.; Gillotay, D.; Vanlaethem-Meurée, N.; Wisemberg, J. Temperature dependence of ultraviolet absorption cross-sections of chlorofluoroethanes. *Ann. Geophys.* **1988**, *6*, 239-248.

F41. CCl_2FCF_3 (CFC-114a)

Back to Index

$CCl_2FCF_3 + h\nu \rightarrow$ Products (1)

(Recommendation: 19-5, Note: 19-5, Evaluated: 19-5)

Absorption Cross Sections: UV absorption cross sections of CCl_2FCF_3 (CFC-114a, 1,2-dichlorotetrafluoroethane) have been measured by Davis et al.[1] (192.5–235 nm, 1 nm resolution). This is the only study of this molecule available at the time of this evaluation. Absorption cross sections were measured at 10 discrete wavelengths and 6 temperatures between 207 and 323 K. The UV absorption spectra of CFC-114a are continuous over this wavelength range with a decrease in cross section with increasing wavelength. A decrease in $\sigma(\lambda,T)$ with decreasing temperature was observed at nearly all wavelengths with the temperature dependence greatest at the longer wavelengths.

The CFC-114a spectra were parameterized in Davis et al. using the formula:

$$\ln\left(\sigma(\lambda, T)\right) = \sum_i A_i \lambda_i^{\,i} + (T - 296) \sum_i B_i \lambda_i^{\,i}$$

(units: $\sigma(\lambda,T)$ (cm^2 $molecule^{-1}$, base e), λ (nm), and T (K)) which reproduces the experimental data to within 5%, or better, over the wavelength range most critical for atmospheric photolysis, 195–215 nm. The parameterization coefficients from Davis et al. given below are valid for wavelengths between 192.5 and 235 nm and temperatures between 207 and 323 K.

i	A_i	B_i
0	-253.6338	0.52031
1	2.899454	-0.005044
2	-0.0081158	1.6142×10^{-6}
3	-3.68328×10^{-5}	7.2259×10^{-8}
4	2.071842×10^{-7}	2.4996×10^{-11}
5	-2.5764×10^{-10}	-5.9642×10^{-13}

The CFC-114a absorption cross sections given in Table 4F-41 were calculated using this parameterization. The recommended estimated uncertainty factors ($F(\lambda)$, 2σ) are assigned as $F(\lambda) = 1.05 + 5 \times 10^{-24}/\sigma(\lambda)$.

Photolysis Quantum Yield and Product Studies: No recommendation.

Table 4F-41. Recommended Absorption Cross Sections of CCl_2FCF_3 (CFC-114a) at 296 K

λ (nm)	$10^{20}\ \sigma$ (cm^2)	λ (nm)	$10^{20}\ \sigma$ (cm^2)
194	24.7	216	0.277
196	17.0	218	0.180
198	11.6	220	0.118
200	7.88	222	0.0770
202	5.28	224	0.0505
204	3.51	226	0.0333
206	2.32	228	0.0221
208	1.52	230	0.0147
210	0.999	232	0.00989
212	0.652	234	0.00669
214	0.425		

Note:
Davis et al.[1]

(1) Davis, M. E.; Bernard, F.; McGillen, M. R.; Fleming, E. L.; Burkholder, J. B. UV and infrared absorption spectra, atmospheric lifetimes, and ozone depletion and global warming potentials for CCl_2FCCl_2F (CFC-112), CCl_3CClF_2 (CFC-112a), CCl_3CF_3 (CFC-113a), and CCl_2FCF_3 (CFC-114a). *Atmos. Chem. Phys.* **2016**, *16*, 8043-8052, doi:10.5194/acp-16-8043-2016.

F42. CF_3CF_2Cl (pentafluorochloroethane, CFC–115)

Back to Index

CF_3CF_2Cl (CFC–115) + hν → Products (1)

(Recommendation: 25-1, Note: 25-1, Evaluated: 25-1)

Absorption Cross Sections: The VUV/UV absorption spectrum of pentafluorochloroethane (CFC–115), CF_3CF_2Cl, has been measured at room temperature by Chou et al.[1] (184–207 nm), Hubrich and Stuhl[3] (160–230 nm), and Simon et al.[5] (172–204 nm). The room temperature cross section data of Simon et al.[5] and Hubrich and Stuhl[3] agree to within ~20% with the Hubrich and Stuhl[3] values being systematically greater over the range 172–204 nm. The data of Chou et al.[1] are greater than those of Simon et al.[5] by as much as 50%. The recommended absorption cross sections in Table 4F-42 are the mean of the values reported by Hubrich and Stuhl[3] and Simon et al.[5] in the region 172–204 nm. The recommended values for wavelengths >204 nm are the mean of the values measured by Hubrich and Stuhl[3] and those obtained by extrapolating the Simon et al.[5] data, $\log \sigma(\lambda) = -6.2191 - 0.0756\,\lambda$, where the extrapolated values are greater than the values measured by Hubrich and Stuhl.[3]

The absorption spectrum has been measured in the VUV by Ravishankara et al.[4] (Lyman-α, 121.6 nm), Doucet et al.[2] (120–175 nm), and Totterdill et al.[6] (121.6 nm). The Ravishankara et al. and Totterdill et al. cross section data are in good agreement and a factor of ~7 less than reported by Doucet et al. An average of the Ravishankara et al. and Totterdill et al. cross section values is recommended, 4.42×10^{-18} cm^2 molecule^{-1} with an estimated uncertainty factor of 1.2 (2σ).

The temperature dependence of the absorption spectrum has been measured by Hubrich and Stuhl[3] (160–230 nm) at 208 and 298 K and Simon et al.[5] (172–204 nm) over the range 225–295 K. No measurable temperature dependence was reported in these studies. Simon et al.[5] parameterized the absorption cross sections using an empirical polynomial expansion:

$$\log_{10} \sigma(\lambda, T) = \sum A_n \lambda^n + (T-273) \times \sum B_n \lambda^n \text{ (with all } B_n = 0)$$

and reported calculated values for 295 K. The A_n parameters, which are valid for the temperature range 210–300 K and wavelength range 172–204 nm, given below are recommended.

$A_0 = 5.8281$ $\quad A_1 = -2.990 \times 10^{-1}$
$A_2 = 1.3525 \times 10^{-3}$ $\quad A_3 = -2.6851 \times 10^{-6}$

Photolysis Quantum Yield and Product Studies: No recommendation.

Table 4F-42. Recommended Absorption Cross Sections of CF_3CF_2Cl at 298 K

λ (nm)	10^{20} σ (cm^2)	λ (nm)	10^{20} σ (cm^2)	λ (nm)	10^{20} σ (cm^2)
172	5.50	188	0.403	204	0.0218
174	4.13	190	0.287	205	*0.0187*
176	3.08	192	0.203	210	*0.00700*
178	2.25	194	0.143	215	*0.00273*
180	1.58	196	0.0985	220	*0.00107*
182	1.13	198	0.0685	225	*0.00046*
184	0.790	200	0.0474	230	*0.00018*
186	0.563	202	0.0325		

Note:
172–204 nm: mean of Hubrich and Stuhl[3] and Simon et al.[5]
205–230 nm: mean of Hubrich and Stuhl[3] and extrapolated Simon et al.[5] data, $\log \sigma(\lambda) = -6.2191 - 0.0756\,\lambda$

(1) Chou, C. C.; Milstein, R. J.; Smith, W. S.; Vera-Ruiz, H.; Molina, M. J.; Rowland, F. S. Stratospheric photodissociation of several saturated perhalo chlorofluorocarbon compounds in current technological use (fluorocarbons-13, -113, -114, and -115). *J. Phys. Chem.* **1978**, *82*, 1-7, doi:10.1021/j100490a001.
(2) Doucet, J.; Sauvageau, P.; Sandorfy, C. Photoelectron and far-ultraviolet absorption spectra of chlorofluoro derivatives of ethane. *J. Chem. Phys.* **1975**, *62*, 355-359, doi:10.1063/1.430493.
(3) Hubrich, C.; Stuhl, F. The ultraviolet absorption of some halogenated methanes and ethanes of atmospheric interest. *J. Photochem.* **1980**, *12*, 93-107, doi:10.1016/0047-2670(80)85031-3.

(4) Ravishankara, A. R.; Solomon, S.; Turnipseed, A. A.; Warren, R. F. Atmospheric lifetimes of long-lived halogenated species. *Science* **1993**, *259*, 194-199, doi:10.1126/science.259.5092.194.
(5) Simon, P. C.; Gillotay, D.; Vanlaethem-Meurée, N.; Wisemberg, J. Temperature dependence of ultraviolet absorption cross-sections of chlorofluoroethanes. *Ann. Geophys.* **1988**, *6*, 239-248.
(6) Totterdill, A.; Kovács, T.; Martín, J. C. G.; Feng, W.; Plane, J. M. C. Mesospheric removal of very long-lived greenhouse gases SF_6 and CFC-115 by metal reactions, Lyman-α photolysis, and electron attachment. *J. Phys. Chem. A* **2015**, *119*, 2016-2025, doi:10.1021/jp5123344.

F43. $CHFCl_2$ (fluorodichloromethane, HCFC–21)

Back to Index

$CHFCl_2$ (HCFC–21) + hν → Products (1)

(Recommendation: 02-25, Note: 10-6, Evaluated: 10-6)

Absorption Cross Sections: The UV absorption spectrum of fluorodichloromethane (HCFC-21), $CHFCl_2$, has been measured at room temperature by Gordus and Bernstein[3] (208 nm), Robbins and Stolarski[7] (174–222 nm), Green and Wayne[4] (184–205 nm), Rebbert et al.[6] (213.9 nm), Hubrich et al.[5] (158–235 nm), and Simon et al.[8] (174–222 nm). The absorption cross section data from these groups are in good agreement, generally to within 15%, except those from Green and Wayne[4] which deviate significantly. The data from Hubrich et al.[5] also contain irregular values around 205 and 220 nm where the agreement is only ~40%. The recommended absorption cross sections in Table 4F-43 are the values of Simon et al.[8] in the region 174–222 nm. The recommended values for wavelengths >222 nm were obtained from a log-linear extrapolation of the Simon et al.[8] data, $\log \sigma(\lambda) = 0.9806 - 0.1013\ \lambda$. The values measured by Hubrich et al.[5] deviate from the extrapolated values significantly.

Measurements in the far UV at 60–120 nm have been reported by Gilbert et al.,[2] measurements at 120–200 nm by Doucet et al.,[1] and a measurement at 147 nm by Rebbert et al.[6]

The temperature dependence of the absorption spectrum has been measured by Hubrich et al.[5] (158–235 nm) at 208 and 298 K and Simon et al.[8] (174–222 nm) over the range 225–295 K. The temperature dependence is significant at wavelengths >190 nm where the cross sections decrease with decreasing temperature. Simon et al.[8] parameterized the temperature dependence of the cross sections using an empirical polynomial expansion:

$$\log_{10} \sigma(\lambda, T) = \sum A_n \lambda^n + (T-273) \times \sum B_n \lambda^n$$

and reported calculated values for T = 210, 230, 250, 270, and 295 K. The A_n and B_n parameters, valid for the temperature range 210–300 K and wavelength range 174–222 nm, given below are recommended.

$A_0 = -514.56$	$B_0 = -3.0577$
$A_1 = 8.7940$	$B_1 = 6.6539 \times 10^{-2}$
$A_2 = -5.6840 \times 10^{-2}$	$B_2 = -5.3964 \times 10^{-4}$
$A_3 = 1.5894 \times 10^{-4}$	$B_3 = 1.9322 \times 10^{-6}$
$A_4 = -1.6345 \times 10^{-7}$	$B_4 = -2.5754 \times 10^{-9}$

Photolysis Quantum Yield and Product Studies: No recommendation.

Table 4F-43. Recommended Absorption Cross Sections of $CHFCl_2$ at 298 K

λ (nm)	10^{20} σ (cm^2)	λ (nm)	10^{20} σ (cm^2)	λ (nm)	10^{20} σ (cm^2)
174	166.0	198	8.10	222	0.0319
176	164.5	200	5.24	224	*0.0195*
178	155.0	202	3.35	225	*0.0154*
180	138.0	204	2.12	226	*0.0122*
182	116.0	206	1.34	228	*0.00766*
184	92.4	208	0.836	230	*0.00480*
186	71.5	210	0.522	232	*0.00301*
188	53.2	212	0.325	234	*0.00189*
190	38.4	214	0.203	235	*0.00150*
192	26.9	216	0.127	236	*0.00119*
194	18.4	218	0.0797		
196	12.3	220	0.0503		

Note:
174–222 nm: Simon et al.[8]

224–236 nm: extrapolation of Simon et al.[8] data, log $\sigma(\lambda) = 0.9806 - 0.1013\ \lambda$

(1) Doucet, J.; Sauvageau, P.; Sandorfy, C. Vacuum ultraviolet and photoelectron spectra of fluoro-chloro derivatives of methane. *J. Chem. Phys.* **1973**, *58*, 3708-3716, doi:10.1063/1.1679722.

(2) Gilbert, R.; Sauvageau, P.; Sandorfy, C. Vacuum ultraviolet absorption spectra of chlorofluoromethanes from 120 to 65 nm. *J. Chem. Phys.* **1974**, *60*, 4820-4824, doi:10.1063/1.1680987.

(3) Gordus, A. A.; Bernstein, R. B. Isotope effect in continuous ultraviolet absorption spectra: Methyl bromide-d_3 and chloroform-*d*. *J. Chem. Phys.* **1954**, *22*, 790-795, doi:10.1063/1.1740194.

(4) Green, R. G.; Wayne, R. P. Vacuum ultra-violet absorption spectra of halogenated methanes and ethanes. *J. Photochem.* **1976/77**, *6*, 375-377, doi:10.1016/0047-2670(76)85077-0.

(5) Hubrich, C.; Zetzsch, C.; Stuhl, F. Absorption spectra of halogenated methanes in wavelength region from 275 to 160 nm at temperatures of 298 and 208 K. *Ber. Bunsenges. Phys. Chem.* **1977**, *81*, 437-442, doi:10.1002/bbpc.19770810417.

(6) Rebbert, R. E.; Lias, S. G.; Ausloos, P. The gas phase photolysis of $CHFCl_2$. *J. Photochem.* **1978**, *8*, 17-27, doi:10.1016/0047-2670(78)80003-3.

(7) Robbins, D. E.; Stolarski, R. S. Comparison of stratospheric ozone destruction by fluorocarbons 11, 12, 21, and 22. *Geophys. Res. Lett.* **1976**, *3*, 603-606, doi:10.1029/GL003i010p00603.

(8) Simon, P. C.; Gillotay, D.; Vanlaethem-Meurée, N.; Wisemberg, J. Ultraviolet absorption cross-sections of chloro and chlorofluoro-methanes at stratospheric temperatures. *J. Atmos. Chem.* **1988**, *7*, 107-135, doi:10.1007/BF00048042.

F44. CHF_2Cl (difluorochloromethane, HCFC–22)

Back to Index

CHF_2Cl (HCFC–22) + hν → Products (1)

(Recommendation: 25-1, Note: 25-1, Evaluated: 25-1)

Absorption Cross Sections: The UV absorption spectrum of difluorochloromethane (CHF_2Cl, HCFC-22) has been measured at room temperature by Robbins and Stolarski[7] (174–202 nm), Green and Wayne[4] (181–194 nm, graphical data), Hubrich et al.[5] (158–220 nm), Simon et al.[8] (174–204 nm), and Cantrell et al.[1] (184.9 nm, 7.46×10^{-21} cm^2 molecule^{-1}). The results of Robbins and Stolarski, [7] Hubrich et al.,[5] and Simon et al.[8] are in agreement, generally to within 15–20%. However, the data from Green and Wayne[4] deviate significantly. The recommended absorption cross sections in Table 4F-44 are the values from Hubrich et al.[5] in the region 170–172 nm and the values from Simon et al.[8] in the region 174–204 nm. The recommended absorption cross sections for wavelengths >204 nm were obtained from a log-linear extrapolation of the Simon et al.[8] data, log $\sigma(\lambda) = -4.1001 - 0.0870\ \lambda$. The measured values of Hubrich et al.[5] deviate from the extrapolated values by as much as 20%.

The absorption spectrum has been measured in the VUV by Gilbert et al.[3] (60–160 nm), Doucet et al.[2] (120–200 nm), Vatsa and Volpp[9] (121.567 nm), and Limão-Vieira et al.[6] (116–225 nm). A Lyman-α (121.567 nm) cross section of 1.75×10^{-17} cm^2 molecule^{-1} is recommended from an average of the Vatsa and Volpp and Limão-Vieira et al. data. An uncertainty factor of 1.2 (2σ) is assigned.

The temperature dependence of the absorption spectrum has been measured by Hubrich et al.[5] (158–220 nm) at 208 and 298 K and Simon et al.[8] (174–204 nm) over the range 225–295 K. A weak temperature dependence was observed for wavelengths >190 nm where the cross sections decrease with decreasing temperature. Simon et al.[8] parameterized the cross sections temperature dependence using an empirical polynomial expansion:

$$\log_{10} \sigma(\lambda, T) = \sum A_n \lambda^n + (T-273) \times \sum B_n \lambda^n$$

and reported calculated cross section values for T = 210, 230, 250, 270, and 295 K. The A_n and B_n parameters, valid for the temperature range 210–300 K and wavelength range 174–204 nm, given below are recommended.

$A_0 = -106.029$	$B_0 = -1.3399 \times 10^{-1}$
$A_1 = 1.5038$	$B_1 = 2.7405 \times 10^{-3}$
$A_2 = -8.2476 \times 10^{-3}$	$B_2 = -1.8028 \times 10^{-5}$
$A_3 = 1.4206 \times 10^{-5}$	$B_3 = 3.8504 \times 10^{-8}$

Photolysis Quantum Yield and Product Studies: No recommendation.

Table 4F-44. Recommended Absorption Cross Sections of CHF_2Cl at 298 K

λ (nm)	10^{20} σ (cm^2)	λ (nm)	10^{20} σ (cm^2)	λ (nm)	10^{20} σ (cm^2)

170	12.9	188	0.372	206	*0.00842*
172	9.79	190	0.245	208	*0.00636*
174	5.72	192	0.156	210	*0.00426*
176	4.04	194	0.103	212	*0.00285*
178	2.76	196	0.072	214	*0.00191*
180	1.91	198	0.048	216	*0.00128*
182	1.28	200	0.032	218	*0.00086*
184	0.842	202	0.0220	220	*0.00057*
186	0.576	204	0.0142		

Note:
170–172 nm: Hubrich et al.[5]
174–204 nm: Simon et al.[8]
206–220 nm: extrapolation of Simon et al.[8] data, log $\sigma(\lambda) = -4.1001 - 0.0870\ \lambda$

(1) Cantrell, C. A.; Zimmer, A.; Tyndall, G. S. Absorption cross sections for water vapor from 183 to 193 nm. *Geophys. Res. Lett.* **1997**, *24*, 2195-2198, 2687 (Erratum), doi:10.1029/97GL02100.

(2) Doucet, J.; Sauvageau, P.; Sandorfy, C. Vacuum ultraviolet and photoelectron spectra of fluoro-chloro derivatives of methane. *J. Chem. Phys.* **1973**, *58*, 3708-3716, doi:10.1063/1.1679722.

(3) Gilbert, R.; Sauvageau, P.; Sandorfy, C. Vacuum ultraviolet absorption spectra of chlorofluoromethanes from 120 to 65 nm. *J. Chem. Phys.* **1974**, *60*, 4820-4824, doi:10.1063/1.1680987.

(4) Green, R. G.; Wayne, R. P. Vacuum ultra-violet absorption spectra of halogenated methanes and ethanes. *J. Photochem.* **1976/77**, *6*, 375-377, doi:10.1016/0047-2670(76)85077-0.

(5) Hubrich, C.; Zetzsch, C.; Stuhl, F. Absorption spectra of halogenated methanes in wavelength region from 275 to 160 nm at temperatures of 298 and 208 K. *Ber. Bunsenges. Phys. Chem.* **1977**, *81*, 437-442, doi:10.1002/bbpc.19770810417.

(6) Limão-Vieira, P.; Vasekova, E.; Sekhar, B. N. R.; Mason, N. J.; Hoffmann, S. V. VUV electronic state spectroscopy of 1,1-difluoroethene and difluorochloromethane by high resolution synchrotron radiation. *Phys. Chem. Chem. Phys.* **2006**, *8*, 4766-4772, doi:10.1039/b610978k.

(7) Robbins, D. E.; Stolarski, R. S. Comparison of stratospheric ozone destruction by fluorocarbons 11, 12, 21, and 22. *Geophys. Res. Lett.* **1976**, *3*, 603-606, doi:10.1029/GL003i010p00603.

(8) Simon, P. C.; Gillotay, D.; Vanlaethem-Meurée, N.; Wisemberg, J. Ultraviolet absorption cross-sections of chloro and chlorofluoro-methanes at stratospheric temperatures. *J. Atmos. Chem.* **1988**, *7*, 107-135, doi:10.1007/BF00048042.

(9) Vatsa, R. K.; Volpp, H.-R. Absorption cross sections for some atmospherically important molecules at the H atom Lyman-α wavelength (121.567 nm). *Chem. Phys. Lett.* **2001**, *340*, 289-295 doi:10.1016/S0009-2614(01)00373-6.

F45. CH_2FCl (fluorochloromethane, HCFC–31)

Back to Index

CH_2FCl (HCFC–31) + hν → Products (1)

(Recommendation: 02-25, Note: 10-6, Evaluated: 10-6)

Absorption Cross Sections: The absorption spectrum of fluorochloromethane (HCFC-31), CH_2FCl, has been measured at 208 and 298 K over the wavelength range 160–230 nm by Hubrich and Stuhl.[3] The recommended room temperature cross sections from this study are listed in Table 4F-45.

The absorption spectrum has been measured in the far UV by Gilbert et al.[2] (60–120 nm) and Doucet et al.[1] (120–200 nm). The cross section values reported by Doucet et al. are significantly greater than those of Hubrich and Stuhl[3] for the common wavelength region.

Photolysis Quantum Yield and Product Studies: No recommendation.

Table 4F-45. Recommended Absorption Cross Sections of CH_2FCl at 298 K

λ (nm)	10^{20} σ (cm^2)
160	47.9
165	55.9
170	43.0
175	23.3
180	12.5
185	4.20
190	1.95
195	0.544
200	0.209
205	0.069
210	0.0188
215	0.00560
220	0.00215
225	0.00049
230	0.00026

Note:
Hubrich and Stuhl[3]

(1) Doucet, J.; Sauvageau, P.; Sandorfy, C. Vacuum ultraviolet and photoelectron spectra of fluoro-chloro derivatives of methane. *J. Chem. Phys.* **1973**, *58*, 3708-3716, doi:10.1063/1.1679722.

(2) Gilbert, R.; Sauvageau, P.; Sandorfy, C. Vacuum ultraviolet absorption spectra of chlorofluoromethanes from 120 to 65 nm. *J. Chem. Phys.* **1974**, *60*, 4820-4824, doi:10.1063/1.1680987.

(3) Hubrich, C.; Stuhl, F. The ultraviolet absorption of some halogenated methanes and ethanes of atmospheric interest. *J. Photochem.* **1980**, *12*, 93-107, doi:10.1016/0047-2670(80)85031-3.

F46. $CHCl_2CClF_2$ (HCFC-122)

Back to Index

$CHCl_2CClF_2 + h\nu \rightarrow$ Products (1)

(Recommendation: 19-5, Note: 19-5, Evaluated: 19-5)

Absorption Cross Sections: UV absorption cross sections of $CHCl_2CClF_2$ (HCFC-122, 1,1-difluoro-1,2,2-trichloroethane) have been measured at room temperature by Minamikawa et al.[1] (298 K, 115–190 nm, 4 nm resolution) and Orkin et al.[2] (295 K, 190–216 nm, 0.5 nm resolution). The agreement between these two studies at 190 nm is good, to within 5%. The 185 nm cross section from the Minamikawa et al. study and the 190–216 nm cross sections at 2 nm intervals from Orkin et al. given in Table 4F-46 are recommended. The recommended estimated uncertainty factors (F(λ), 2σ) are assigned as $F(\lambda) = 1.10 + 2 \times 10^{-21}/\sigma(\lambda)$.

The VUV absorption spectrum has been measured by Minamikawa et al.[1] (115–190 nm, 4 nm resolution). The Lyman–α (121.567 nm) cross section derived from this study, 6.43×10^{-17} cm^2 $molecule^{-1}$, is recommended with an uncertainty factor (2σ) of 1.2.

Photolysis Quantum Yield and Product Studies: No recommendation.

Table 4F-46. Recommended Absorption Cross Sections of $CHCl_2CClF_2$ (HCFC-122) at 295 K

λ (nm)	10^{20} σ (cm^2)
121.567	6430
185	180
190	63.1
192	50.6
194	38.3
196	28.2
198	20.4
200	14.6
202	10.35
204	7.32
206	5.16
208	3.66
210	2.57
212	1.85
214	1.36
216	1.03

Note:
121.567 and 185 nm: Minamikawa et al.[1]
190–216 nm: Orkin et al.[2]

(1) Minamikawa, T.; Sakka, T.; Ogata, Y.; Iwasaki, M. Vacuum ultraviolet spectra of $CClF_2CH_2Cl$ and $CClF_2HCl_2$, and Rydberg assignment based on ab initio molecular orbital calculations. *Spectrochim. Acta A: Mol. Spectrosc.* **1992**, *48*, 849-859, doi:10.1016/0584-8539(92)80081-7.

(2) Orkin, V. L.; Khamaganov, V. G.; Kasimovskaya, E. E.; Guschin, A. G. Photochemical properties of some Cl-containing halogenated alkanes. *J. Phys. Chem. A* **2013**, *117*, 5483-5490, doi:10.1021/jp400408y.

F47. $CHClFCCl_2F$ (HCFC-122a)

Back to Index

$CHClFCCl_2F + h\nu \rightarrow$ Products (1)

(Recommendation: 19-5, Note: 19-5, Evaluated: 19-5)

Absorption Cross Sections: UV absorption cross sections of $CHClFCCl_2F$ (HCFC-122a, 1,2-difluoro-1,1,2-trichloroethane) have been measured at room temperature, 295 K, by Orkin et al.[1] (190–228 nm, 0.5 nm resolution), the only available study at the time of this evaluation. The cross sections from the Orkin et al. study are recommended and given in Table 4F-47 at 2 nm intervals. The recommended estimated uncertainty factors ($F(\lambda)$, 2σ) are assigned as $F(\lambda) = 1.05 + 1 \times 10^{-22}/\sigma(\lambda)$.

Photolysis Quantum Yield and Product Studies: No recommendation.

Table 4F-47. Recommended Absorption Cross Sections of $CHClFCCl_2F$ (HCFC-122a) at 295 K

λ (nm)	10^{20} σ (cm^2)
190	70.5
192	52.7
194	38.3
196	27.2
198	19.06
200	13.12
202	8.93
204	6.04
206	4.05
208	2.72
210	1.82
212	1.21
214	0.806
216	0.536
218	0.356
220	0.237
222	0.157
224	0.105
226	0.070
228	0.047

Note:
Orkin et al.[1]

(1) Orkin, V. L.; Khamaganov, V. G.; Kasimovskaya, E. E.; Guschin, A. G. Photochemical properties of some Cl-containing halogenated alkanes. *J. Phys. Chem. A* **2013**, *117*, 5483-5490, doi:10.1021/jp400408y.

F48. CF_3CHCl_2 (1,1,1-trifluoro-2,2-dichloroethane, HCFC–123)

Back to Index

CF_3CHCl_2 (HCFC–123) + hν → Products (1)

(Recommendation: 25-1, Note: 25-1, Evaluated: 25-1)

Absorption Cross Sections: The absorption spectrum of 1,1,1-trifluoro-2,2-dichloroethane (CF_3CHCl_2, HCFC-123) has been measured at room temperature by Green and Wayne[2] (185–204 nm), Gillotay and Simon[1] (170–250 nm), Orlando et al.[5] (190–230 nm), Nayak et al.[3] (160–230 nm), and Orkin et al.[4] (190–240 nm). The absorption cross sections are within 25% of each other in the region below 220 nm with the exception of the Green and Wayne data that are significantly lower at wavelengths <200 nm. The recommended absorption cross sections in Table 4F-48 are the mean of the values reported by Gillotay and Simon[1] and Nayak et al. in the region 170–188 nm and the mean of the values reported by Gillotay and Simon, Orlando et al., Nayak et al., and Orkin et al. in the region 190–230 nm. The recommended cross sections for wavelengths >230 nm were obtained using a log-linear extrapolation of the Orlando et al. data, $\log \sigma(\lambda) = -3.1097 - 0.0794\,\lambda$.

The temperature dependence of the absorption spectrum has been reported by Gillotay and Simon[1] (170–250 nm) at 225–295 K, Orlando et al.[5] (190–230 nm) over the range 203–295 K, and Nayak et al.[3] (160–230 nm) over the range 223–333 K. These studies report a decrease of the absorption cross sections with decreasing temperature at wavelengths >180 nm and <170 nm. Between 170–180 nm, an increase in the cross section with decreasing temperature was reported by Gillotay and Simon[1] and Nayak et al.[3] An irregular temperature dependence was reported by Orlando et al.[5] for the range 210–230 nm.

Various empirical functional forms have been proposed to parameterize the temperature dependence of the absorption cross sections. Gillotay and Simon[1] parameterized the cross sections and the temperature dependence using the polynomial expansion:

$$\log_{10} \sigma(\lambda, T) = \sum A_n \lambda^n + (T-273) \times \sum B_n \lambda^n$$

and report calculated cross section values for 210, 230, 250, 270, and 295 K. The A_n and B_n parameters, valid for the temperature range 210–300 K and wavelength range 182–250 nm, are given below.

$A_0 = -513.996354$	$B_0 = 1.757133$
$A_1 = 9.089141$	$B_1 = -3.499205 \times 10^{-2}$
$A_2 = -6.136794 \times 10^{-2}$	$B_2 = 2.593563 \times 10^{-4}$
$A_3 = 1.814826 \times 10^{-4}$	$B_3 = -8.489357 \times 10^{-7}$
$A_4 = -1.999514 \times 10^{-7}$	$B_4 = 1.037756 \times 10^{-9}$

Nayak et al.[3] used a sixth-order polynomial of the form:

$$\log_{10}(\sigma_T) = \sum C_n (\lambda - 170)^n$$

for the temperatures measured in their study for the wavelength range 160–230 nm. The C_n parameters are listed below.

	223 K	273 K	295 K	333 K
C_0	-17.6732	-17.6773	-17.6792	-17.6722
C_1	1.70233×10^{-2}	1.3636×10^{-2}	1.19392×10^{-2}	9.07941×10^{-3}
C_2	-7.39366×10^{-4}	-4.98553×10^{-4}	-3.71661×10^{-4}	-1.29566×10^{-4}
C_3	-1.83761×10^{-4}	-1.70566×10^{-4}	-1.61218×10^{-4}	-1.56667×10^{-4}
C_4	7.80778×10^{-6}	6.73373×10^{-6}	6.03101×10^{-6}	5.56409×10^{-6}
C_5	-1.29836×10^{-7}	-1.02726×10^{-7}	-8.76762×10^{-8}	-7.77379×10^{-8}
C_6	8.05415×10^{-10}	5.66688×10^{-10}	4.61745×10^{-10}	3.93859×10^{-10}

Orlando et al.[5] used the expression:

$$\ln \sigma(\lambda, T) = \sum \left(\sum a_{ij} (T - 245.4)^{j-1} \right) (\lambda - 206.214)^{i-1}, \quad i = 1\text{–}4,\ j = 1\text{–}3$$

that is valid for the temperature range 203–295 K and wavelength range 190–230 nm. The coefficients are given below.

$a_{11} = -4.500 \times 10^{1}$	$a_{12} = 3.529 \times 10^{-3}$	$a_{13} = -4.181 \times 10^{-8}$
$a_{21} = -1.985 \times 10^{-1}$	$a_{22} = 6.826 \times 10^{-5}$	$a_{23} = 1.555 \times 10^{-6}$
$a_{31} = -2.802 \times 10^{-4}$	$a_{32} = -1.018 \times 10^{-5}$	$a_{33} = 4.037 \times 10^{-8}$
$a_{41} = 6.312 \times 10^{-5}$	$a_{42} = -3.055 \times 10^{-7}$	$a_{43} = -2.473 \times 10^{-9}$

Photolysis Quantum Yield and Product Studies: No recommendation.

Table 4F-48. Recommended Absorption Cross Sections of CF_3CHCl_2 at 295 K

λ (nm)	10^{20} σ (cm^2)	λ (nm)	10^{20} σ (cm^2)	λ (nm)	10^{20} σ (cm^2)
170	192	198	17.1	226	0.0839
172	207	200	11.6	228	0.0577
174	214	202	8.23	230	0.0412
176	213	204	5.66	232	*0.0295*
178	202	206	3.83	234	*0.0205*
180	184	208	2.66	236	*0.0142*
182	161	210	1.76	238	*0.0098*
184	135	212	1.22	240	*0.0068*
186	109	214	0.824	242	*0.0047*
188	85.5	216	0.557	244	*0.0033*
190	60.8	218	0.378	246	*0.0023*
192	46.0	220	0.252	248	*0.0016*
194	33.6	222	0.176	250	*0.0011*
196	23.9	224	0.120		

Notes:
170–188 nm: mean of the values from Gillotay and Simon[1] and Nayak et al.[3]
190–230 nm: mean of the values from Gillotay and Simon,[1] Orlando et al.,[5] Nayak et al.,[3] and Orkin et al.[4]
232–250 nm: extrapolation of Orlando et al.[5] data, $\log \sigma(\lambda) = -3.1097 - 0.0794\ \lambda$

(1) Gillotay, D.; Simon, P. C. Temperature-dependence of ultraviolet absorption cross-sections of alternative chlorofluoroethanes. *J. Atmos. Chem.* **1991**, *12*, 269-285, doi:10.1007/BF00048076.

(2) Green, R. G.; Wayne, R. P. Vacuum ultra-violet absorption spectra of halogenated methanes and ethanes. *J. Photochem.* **1976/77**, *6*, 375-377, doi:10.1016/0047-2670(76)85077-0.
(3) Nayak, A. K.; Buckley, T. J.; Kurylo, M. J.; Fahr, A. Temperature dependence of the gas and liquid phase ultraviolet absorption cross sections of HCFC-123 (CF_3CHCl_2) and HCFC-142b (CH_3CF_2Cl). *J. Geophys. Res.* **1996**, *101*, 9055-9062, doi:10.1029/96JD00226.
(4) Orkin, V. L.; Khamaganov, V. G.; Kasimovskaya, E. E.; Guschin, A. G. Photochemical properties of some Cl-containing halogenated alkanes. *J. Phys. Chem. A* **2013**, *117*, 5483-5490, doi:10.1021/jp400408y.
(5) Orlando, J. J.; Burkholder, J. B.; McKeen, S. A.; Ravishankara, A. R. Atmospheric fate of several hydrofluoroethanes and hydrochloroethanes: 2. UV absorption cross sections and atmospheric lifetimes. *J. Geophys. Res.* **1991**, *96*, 5013-5023, doi:10.1029/90JD02734.

F49. $CHClFCClF_2$ (HCFC-123a)

Back to Index

$CHClFCClF_2 + h\nu \rightarrow$ Products (1)

(Recommendation: 19-5, Note: 19-5, Evaluated: 19-5)

Absorption Cross Sections: UV absorption cross sections of $CHClFCClF_2$ (HCFC-123a, 1,1,2-trifluoro-1,2-dichloroethane) have been measured at room temperature by Doucet et al.[1] (159–200 nm) and Orkin et al.[2] (190–220 nm, 0.5 nm resolution). The agreement between these studies in the wavelength range 190 to 200 nm is poor with the Doucet et al. study reporting cross sections at 200 nm a factor of 50 greater than obtained in the Orkin et al. study. The spectrum reported in the Orkin et al. study is deemed more reliable because of the consistency with the trends in HCFC absorption spectra and the agreement of spectra measured for other HCFCs (measured in theirs and other laboratories). The recommended cross sections given in Table 4F-49 at 2 nm intervals between 190 and 220 nm are taken from the Orkin et al. study. The recommended estimated uncertainty factors ($F(\lambda), 2\sigma$) are assigned as $F(\lambda) = 1.10 + 2 \times 10^{-23}/\sigma(\lambda)$.

The VUV absorption spectrum of HCFC-123a has been reported over two wavelength ranges by Doucet et al (120–158 nm and 159–200 nm) with a Lyman–α (121.567 nm) cross section of $\sim 3 \times 10^{-17}$ cm^2 molecule^{-1}. Because of the large discrepancy with the Orkin et al. study at longer wavelengths, a Lyman–α cross section is not recommended.

Photolysis Quantum Yield and Product Studies: No recommendation.

Table 4F-49. Recommended Absorption Cross Sections of $CHClFCClF_2$ (HCFC-123a) at 295 K

λ (nm)	$10^{20}\ \sigma$ (cm^2)
190	2.877
192	1.896
194	1.272
196	0.843
198	0.569
200	0.381
202	0.254
204	0.172
206	0.114
208	0.0761
210	0.0519
212	0.0355
214	0.0247
216	0.0173
218	0.0123
220	0.0088

Note:
Orkin et al.[2]

(1) Doucet, J.; Sauvageau, P.; Sandorfy, C. Photoelectron and far-ultraviolet absorption spectra of chlorofluoro derivatives of ethane. *J. Chem. Phys.* **1975**, *62*, 355-359, doi:10.1063/1.430493.
(2) Orkin, V. L.; Khamaganov, V. G.; Kasimovskaya, E. E.; Guschin, A. G. Photochemical properties of some Cl-containing halogenated alkanes. *J. Phys. Chem. A* **2013**, *117*, 5483-5490, doi:10.1021/jp400408y.

F50. CF_3CHFCl (1,1,1,2-tetrafluoro-2-chloroethane, HCFC–124)

Back to Index

CF_3CHFCl (HCFC–124) + hν → Products (1)

(Recommendation: 06-2, Note: 10-6, Evaluated: 10-6)

Absorption Cross Sections: The absorption spectrum of 1,1,1,2-tetrafluoro-2-chloroethane (HCFC-124), CF_3CHFCl, has been measured by Orlando et al.[2] (190–230 nm) over the range 203–295 K and Gillotay and Simon[1] (170–230 nm) over the range 210–295 K. The absorption cross sections from these studies agree to better than 10% between 190 and 220 nm. At wavelengths >220 nm the values of Orlando et al.[2] are greater than those of Gillotay and Simon[1] by as much as 133%. The recommended room temperature cross sections in Table 4F-50 are the values of Gillotay and Simon[1] in the region 170–188 nm and 222–230 nm and the mean of the values reported by Gillotay and Simon[1] and Orlando et al.[2] in the region 190–220 nm.

The absorption cross sections decrease with decreasing temperature. An irregular temperature behavior was reported by Orlando et al.[2] for the range 215–230 nm where the absorption spectra show wiggles. Gillotay and Simon[1] parameterized the cross sections and the temperature dependence using an empirical polynomial expansion:

$$\log_{10} \sigma(\lambda, T) = \sum A_n \lambda^n + (T-273) \times \sum B_n \lambda^n$$

and reported calculated cross section values for T = 210, 230, 250, 270, and 295 K. The A_n and B_n parameters, valid for the temperature range 210–300 K and wavelength range 170–230 nm, are given below.

$A_0 = -101.230250$	$B_0 = -5.795712 \times 10^{-2}$
$A_1 = 1.333519$	$B_1 = 1.053901 \times 10^{-3}$
$A_2 = -6.888672 \times 10^{-3}$	$B_2 = -6.530379 \times 10^{-6}$
$A_3 = 1.114172 \times 10^{-5}$	$B_3 = 1.382056 \times 10^{-8}$

Orlando et al.[2] report a parameterization using the expression:

$$\ln \sigma(\lambda, T) = \sum (\sum a_{ij} (T-251.7)^{j-1}) (\lambda-206.214)^{i-1}, \quad i = 1–4, j = 1–3$$

for the temperature range 203–295 K and wavelength range 190–230 nm. The reported coefficients are given below.

$a_{11} = -4.967 \times 10^{1}$	$a_{12} = 6.562 \times 10^{-3}$	$a_{13} = 1.735 \times 10^{-5}$
$a_{21} = -2.025 \times 10^{-1}$	$a_{22} = 2.788 \times 10^{-4}$	$a_{23} = -3.974 \times 10^{-6}$
$a_{31} = 6.839 \times 10^{-4}$	$a_{32} = 5.523 \times 10^{-6}$	$a_{33} = -3.092 \times 10^{-7}$
$a_{41} = 1.275 \times 10^{-4}$	$a_{42} = -2.959 \times 10^{-7}$	$a_{43} = -1.182 \times 10^{-8}$

Photolysis Quantum Yield and Product Studies: No recommendation.

Table 4F-50. Recommended Absorption Cross Sections of CF_3CHFCl at 295 K

λ (nm)	10^{20} σ (cm^2)	λ (nm)	10^{20} σ (cm^2)	λ (nm)	10^{20} σ (cm^2)
170	13.6	192	0.548	214	0.00859
172	11.1	194	0.387	216	0.00610
174	8.85	196	0.267	218	0.00431
176	6.93	198	0.185	220	0.00312
178	5.33	200	0.128	222	0.00214
180	4.03	202	0.0868	224	0.00153
182	3.00	204	0.0594	226	0.00111
184	2.20	206	0.0401	228	0.00082
186	1.60	208	0.0269	230	0.00061
188	1.14	210	0.0186		
190	0.772	212	0.0126		

Notes:
170–188 nm: Gillotay and Simon[1]
190–220 nm: mean of the values from Gillotay and Simon[1] and Orlando et al.[2]
222–230 nm: Gillotay and Simon[1]

(1) Gillotay, D.; Simon, P. C. Temperature-dependence of ultraviolet absorption cross-sections of alternative chlorofluoroethanes: 2. The 2-chloro-l,1,1,2-tetrafluoro ethane - HCFC-124. *J. Atmos. Chem.* **1991**, *13*, 289-299, doi:10.1007/BF00058136.

(2) Orlando, J. J.; Burkholder, J. B.; McKeen, S. A.; Ravishankara, A. R. Atmospheric fate of several hydrofluoroethanes and hydrochloroethanes: 2. UV absorption cross sections and atmospheric lifetimes. *J. Geophys. Res.* **1991**, *96*, 5013-5023, doi:10.1029/90JD02734.

F51. CH_2FCCl_2F (HCFC-132c)

Back to Index

$CH_2FCCl_2F + h\nu \rightarrow$ Products (1)

(Recommendation: 19-5, Note: 19-5, Evaluated: 19-5)

Absorption Cross Sections: UV absorption cross sections of CH_2FCCl_2F (HCFC-132c, 1,2-difluoro-2,2-dichloroethane) have been measured at room temperature, 295 K, by Orkin et al.[1] (190–240 nm, 0.5 nm resolution), the only study available at the time of this evaluation. The cross sections from the Orkin et al. study are recommended and given in Table 4F-51 at 2 nm intervals. The recommended estimated uncertainty factors (F(λ), 2σ) are assigned as $F(\lambda) = 1.10 + 1 \times 10^{-23}/\sigma(\lambda)$.

Photolysis Quantum Yield and Product Studies: No recommendation.

Table 4F-51. Recommended Absorption Cross Sections of CH_2FCCl_2F (HCFC-132c) at 295 K

λ (nm)	10^{20} σ (cm^2)	λ (nm)	10^{20} σ (cm^2)
190	60.9	216	0.350
192	44.2	218	0.229
194	31.3	220	0.1500
196	21.8	222	0.0980
198	14.8	224	0.0638
200	10.0	226	0.0415
202	6.65	228	0.0268
204	4.40	230	0.0175
206	2.87	232	0.0114
208	1.89	234	0.0074
210	1.238	236	0.0046
212	0.814	238	0.0030
214	0.535	240	0.0019

Note: Orkin et al.[1]

(1) Orkin, V. L.; Khamaganov, V. G.; Kasimovskaya, E. E.; Guschin, A. G. Photochemical properties of some Cl-containing halogenated alkanes. *J. Phys. Chem. A* **2013**, *117*, 5483-5490, doi:10.1021/jp400408y.

F52. CF_3CH_2Cl (1,1,1-trifluoro-2-chloroethane, HCFC–133a)

Back to Index

CF_3CH_2Cl (HCFC–133a) + hν → Products (1)

(Recommendation: 25-1, Note: 25-1, Evaluated: 25-1)

Absorption Cross Sections: The absorption spectrum of 1,1,1-trifluoro-2-chloroethane (CF_3CH_2Cl, HCFC–133a) has been measured at room temperature by Ichimura et al.[3] (147 nm, $\sigma = 1.35 \times 10^{-17}$ cm^2 molecule^{-1}), Green and Wayne[1] (186–203 nm), Hubrich and Stuhl[2] (160–245 nm), and McGillen et al.[4] (185–240 nm). The agreement in the absorption cross sections for wavelengths >180 nm is poor. The recommended absorption cross sections in Table 4F-52 are taken from McGillen et al.

The HCFC-133a UV spectrum temperature dependence has been measured by Hubrich and Stuhl (160–245 nm, 208 K) and McGillen et al. (185–240 nm, 213, 233, 253, 294 and 323 K). McGillen et al. provided a parameterization of the temperature dependence valid over the wavelength range 192.5 to 240 nm for temperatures between 213 and 323 K:

$$\ln(\sigma(\lambda,T)) = \sum A_i (\lambda - 200)^i + (T - 273) \sum B_i (\lambda - 200)^i$$

with the A_i and B_i parameters given below:

i	A_i	B_i
0	-46.3107	0.003221
1	-0.18043	0.0001133
2	-0.000599	2.835×10^{-6}
3	2.4743×10^{-5}	8.007×10^{-7}
4	2.9×10^{-6}	-6.790755×10^{-8}
5	-7.149×10^{-8}	1.2007×10^{-9}

Photolysis Quantum Yield and Product Studies: No recommendation.

Table 4F-52. Recommended Absorption Cross Sections of CF_3CH_2Cl at 298 K

λ (nm)	10^{20} σ (cm^2)	λ (nm)	10^{20} σ (cm^2)
195	2.00	220	0.029
200	0.84	225	0.0015
205	0.34	230	0.0085
210	0.14	235	0.0042
215	0.061	240	0.0014

Note:
Calculated using the McGillen et al.[4] parameterization

(1) Green, R. G.; Wayne, R. P. Vacuum ultra-violet absorption spectra of halogenated methanes and ethanes. *J. Photochem.* **1976/77**, *6*, 375-377, doi:10.1016/0047-2670(76)85077-0.
(2) Hubrich, C.; Stuhl, F. The ultraviolet absorption of some halogenated methanes and ethanes of atmospheric interest. *J. Photochem.* **1980**, *12*, 93-107, doi:10.1016/0047-2670(80)85031-3.
(3) Ichimura, T.; Kirk, A. W.; Tschuikow-Roux, E. Primary processes in the 147- and 123.6-nm photolyses of 1,1,1-trifluoro-2-chloroethane. *J. Phys. Chem.* **1977**, *81*, 1153-1156, doi:10.1021/j100527a006.
(4) McGillen, M. R.; Bernard, F.; Fleming, E. L.; J.B. Burkholder HCFC-133a (CF_3CH_2Cl): OH rate coefficient, UV and infrared absorption spectra, and atmospheric implications. *Geophys. Res. Lett.* **2015**, *42*, 6098- 6105, doi:10.1002/2015GL064939.

F53. CH_3CFCl_2 (1,1,1-fluorodichloroethane, HCFC–141b)

Back to Index

CH_3CFCl_2 (HCFC–141b) + hν → Products (1)

(Recommendation: 25-1, Note: 25-1, Evaluated: 25-1)

Absorption Cross Sections: The UV absorption spectrum of 1,1,1-fluorodichloroethane (CH_3CFCl_2, HCFC–141b) has been measured over the temperature range 210–295 K by Gillotay and Simon[2] (170–240 nm), over the temperature range 203–295 K by Talukdar et al.[4] (190–230 nm), and at room temperature by Fahr et al.[1] (298 K, 190–240 nm), and Orkin et al.[3] (295 K, 190–240 nm). Fahr et al.[1] also measured the absorption spectrum in the liquid-phase and used a wavelength-shift procedure to derive cross sections for the gas-phase. The agreement between the cross section values reported by Gillotay and Simon,[2] Fahr et al.,[1] and Orkin et al. for the 190–240 nm region is good (1–10% up to 236 nm). The agreement of the results from Talukdar et al.[4] are not as good. Their absorption cross sections are smaller at wavelengths <210 nm by as much as ~20% and are greater at wavelengths >210 nm by as much as 70%. The recommended absorption cross sections in Table 4F-53 are the values of Gillotay and Simon in the region 170–188 nm and the mean of the values reported by Gillotay and Simon, Fahr et al., and Orkin et al. in the region 190–240 nm. An estimated cross section uncertainty factor of 1.2 (2σ) is recommended for the data given in Table 4F-53.

A decrease of the absorption cross sections with decreasing temperature for wavelengths >188 nm and <172 nm was reported by Gillotay and Simon.[2] An increase in the cross sections with decreasing temperature was observed between 172 and 188 nm. Gillotay and Simon[2] parameterized the cross sections and the temperature dependence of the absorption cross sections using an empirical polynomial expansion:

$$\log_{10} \sigma(\lambda, T) = \sum A_n \lambda^n + (T–273) \times \sum B_n \lambda^n.$$

and report calculated cross section values for T = 210, 230, 250, 270, and 295 K. The A_n and B_n parameters, valid for the temperature range 210–300 K and wavelength range 172-240 nm, given below are recommended.

$A_0 = –682.913042$	$B_0 = 4.074747$
$A_1 = 12.122290$	$B_1 = –8.053899 \times 10^{–2}$
$A_2 = –8.187699 \times 10^{–2}$	$B_2 = 5.946552 \times 10^{–4}$
$A_3 = 2.437244 \times 10^{–4}$	$B_3 = –1.945048 \times 10^{–6}$
$A_4 = –2.719103 \times 10^{–7}$	$B_4 = 2.380143 \times 10^{–9}$

A Lyman-α (121.567 nm) cross section of 6.6×10^{-17} cm^2 $molecule^{-1}$ from the Vatsa and Volpp[5] study, the only study available, is recommended. An uncertainty factor of 1.25 (2σ) is recommended.

Photolysis Quantum Yield and Product Studies: No recommendation.

Table 4F-53. Recommended Absorption Cross Sections of CH_3CFCl_2 at 298 K

λ (nm)	10^{20} σ (cm^2)	λ (nm)	10^{20} σ (cm^2)	λ (nm)	10^{20} σ (cm^2)
170	143.1	194	48.1	218	0.379
172	145.1	196	34.6	220	0.245
174	154.2	198	24.4	222	0.158
176	162.9	200	16.8	224	0.103
178	172.6	202	11.4	226	0.0665
180	172.3	204	7.60	228	0.0432
182	162.9	206	5.01	230	0.0281
184	146.4	208	3.29	232	0.0183
186	125.7	210	2.15	234	0.0119
188	103.6	212	1.39	236	0.00774
190	84.5	214	0.905	238	0.00499
192	64.9	216	0.585	240	0.00329

Note:
170–188 nm: Gillotay and Simon[2]
190–240 nm: mean of data from Gillotay and Simon,[2] Fahr et al.,[1] and Orkin et al.[3]

(1) Fahr, A.; Braun, W.; Kurylo, M. J. Scattered light and accuracy of the cross-section measurements of weak absorptions: Gas and liquid phase UV absorption cross sections of CH_3CFCl_2. *J. Geophys. Res.* **1993**, *98*, 20467-20472, doi:10.1029/93JD01086.

(2) Gillotay, D.; Simon, P. C. Temperature-dependence of ultraviolet absorption cross-sections of alternative chlorofluoroethanes. *J. Atmos. Chem.* **1991**, *12*, 269-285, doi:10.1007/BF00048076.

(3) Orkin, V. L.; Khamaganov, V. G.; Kasimovskaya, E. E.; Guschin, A. G. Photochemical properties of some Cl-containing halogenated alkanes. *J. Phys. Chem. A* **2013**, *117*, 5483-5490, doi:10.1021/jp400408y.

(4) Talukdar, R.; Mellouki, A.; Gierczak, T.; Burkholder, J. B.; McKeen, S. A.; Ravishankara, A. R. Atmospheric fate of CF_2H_2, CH_3CF_3, CHF_2CF_3, and CH_3CFCl_2: Rate coefficients for reactions with OH and UV absorption cross sections of CH_3CFCl_2. *J. Phys. Chem.* **1991**, *95*, 5815-5821, doi:10.1021/j100168a021.
(5) Vatsa, R. K.; Volpp, H.-R. Absorption cross sections for some atmospherically important molecules at the H atom Lyman-α wavelength (121.567 nm). *Chem. Phys. Lett.* **2001**, *340*, 289-295 doi:10.1016/S0009-2614(01)00373-6.

F54. CH_3CF_2Cl (1,1,1-difluorochloroethane, HCFC–142b)

Back to Index

CH_3CF_2Cl (HCFC–142b) + hν → CH_3CF_2 + Cl 355 kJ mol^{-1} 337 nm (1)

(Recommendation: 25-1, Note: 25-1, Evaluated: 25-1)

Absorption Cross Sections: The absorption spectrum of 1,1,1-difluorochloroethane (CH_3CF_2Cl, HCFC–142b) has been measured at room temperature by Doucet et al.[3] (120–180 nm), Green and Wayne[5] (184–201 nm), Hubrich and Stuhl[6] (160–230 nm), Gillotay and Simon[4] (170–230 nm), Orlando et al.[8] (190–230 nm), and Nayak et al.[7] (160–210 nm). For wavelengths <200 nm, the cross sections reported by Hubrich and Stuhl[6] and Nayak et al.[7] agree to within 15%, while those by Gillotay and Simon[4] and Orlando et al.[8] are systematically smaller by as much as 30%. Over the wavelength range 200–215 nm, the values of Gillotay and Simon,[4] Orlando et al.,[8] and Nayak et al.[7] agree to within 15%. For wavelengths >215 nm, the absorption spectrum reported by Orlando et al.[8] has deviations of up to 100% from the data of Gillotay and Simon.[4] The values reported by Hubrich and Stuhl[6] in the range 205–230 nm have increasingly larger deviations from the values reported by Gillotay and Simon[4] with increasing wavelength. The results of Green and Wayne[5] are significantly different from all the other data sets and are not considered in the recommendation. The recommended room temperature absorption cross sections in Table 4F-54 are the mean of the values reported by Hubrich and Stuhl,[6] Gillotay and Simon,[4] and Nayak et al.[7] in the region 170–185 nm, the mean of the values reported by Gillotay and Simon,[4] Orlando et al.,[8] and Nayak et al.[7] in the region 190–210 nm, and the values reported by Gillotay and Simon[4] in the region 212–230 nm.

The temperature dependence of the absorption spectrum has been measured by Hubrich and Stuhl[6] (160–230 nm) at 298 and 208 K, Gillotay and Simon[4] (170–230 nm) over the range 210–295 K, Orlando et al.[8] (190–230 nm) over the range 203–295 K, and Nayak et al.[7] (160–210 nm) over the range at 223–333 K. A decrease of the absorption cross sections with decreasing temperature was observed by Gillotay and Simon[4] and Nayak et al.[7] over the wavelength range 160–230 nm and by Orlando et al.[8] between 190 and 200 nm. An irregular temperature behavior was reported by Orlando et al.[8] for the range 215–230 nm where the absorption spectrum at various temperatures cross. The absorption cross sections and temperature dependence have been parameterized using several different empirical functional forms. Gillotay and Simon[4] used the polynomial expansion:

$$\log_{10} \sigma(\lambda, T) = \sum A_n \lambda^n + (T-273) \times \sum B_n \lambda^n$$

and reported calculated cross section values for T = 210, 230, 250, 270, and 295 K. The A_n and B_n parameters, valid for the temperature range 210–300 K and wavelength range 172–230 nm, are given below.

$A_0 = -328.092008$	$B_0 = 4.289533 \times 10^{-1}$
$A_1 = 6.342799$	$B_1 = -9.042817 \times 10^{-3}$
$A_2 = -4.810362 \times 10^{-2}$	$B_2 = 7.018009 \times 10^{-5}$
$A_3 = 1.611991 \times 10^{-4}$	$B_3 = -2.389065 \times 10^{-7}$
$A_4 = -2.042613 \times 10^{-7}$	$B_4 = 3.039799 \times 10^{-10}$

Nayak et al.[7] used the expression:

$$\log_{10} (\sigma_T) = \sum C_n (\lambda - 160)^n$$

and reported coefficients for 223, 233, 253, 273, 295, 313, and 333 K and the wavelength range 160–210 nm. The reported C_n parameters are given below.

	223 K	273 K	295 K	333 K
C_0	–18.2361	–18.2441	–18.2406	–18.1777
C_1	-1.26669×10^{-2}	-7.37889×10^{-3}	-6.48269×10^{-3}	-2.39647×10^{-2}
C_2	-2.32945×10^{-3}	-2.66537×10^{-3}	-2.80923×10^{-3}	-7.23910×10^{-4}
C_3	2.81933×10^{-5}	4.19193×10^{-5}	5.01979×10^{-5}	-1.08049×10^{-5}
C_4	-1.37963×10^{-7}	-2.88472×10^{-7}	-3.96860×10^{-7}	1.37618×10^{-7}

Orlando et al.[8] used the expression:

$$\ln \sigma(\lambda, T) = \sum (\sum a_{ij} (T-245.4)^{j-1}) (\lambda-206.214)^{i-1}, \quad i = 1–4, j = 1–3$$

for the temperature range 203–295 K and wavelength range 190–230 nm. The coefficients are given below.

$a_{11} = -4.973 \times 10^{1}$	$a_{12} = 9.077 \times 10^{-3}$	$a_{13} = -4.651 \times 10^{-5}$
$a_{21} = -2.175 \times 10^{-1}$	$a_{22} = 4.712 \times 10^{-4}$	$a_{23} = -1.005 \times 10^{-5}$
$a_{31} = 4.133 \times 10^{-4}$	$a_{32} = -6.432 \times 10^{-5}$	$a_{33} = 1.141 \times 10^{-6}$
$a_{41} = 7.145 \times 10^{-5}$	$a_{42} = -5.396 \times 10^{-6}$	$a_{43} = 1.187 \times 10^{-7}$

Vatsa and Volpp[9] and Doucet et al. have reported cross section data at and near the Lyman-α wavelength (121.567 nm), respectively. The cross sections at 121.567 nm from these studies are in good agreement. The direct measurement from the Vatsa and Volpp study of 3.1×10^{-17} cm^2 molecule^{-1} is recommended with an uncertainty factor of 1.1 (2σ).

Photolysis Quantum Yield and Product Studies: Quantum yields for Cl ($^2P_{3/2}$) and Cl*($^2P_{1/2}$) atom formation in the photolysis of CH_3CF_2Cl at 193.3 nm have been measured by Brownsword et al.[2] to be $\Phi(Cl + Cl^*) = 0.90 \pm 0.17$ with $\Phi(Cl) = 0.65 \pm 0.12$ and $\Phi(Cl^*) = 0.25 \pm 0.05$. Brownsword et al.[1] reported the quantum yields for H atom formation in the photolysis at 121.6 and 193.3 nm to be 0.53 ± 0.12 and 0.06 ± 0.02, respectively.

Table 4F-54. Recommended Absorption Cross Sections of CH_3CF_2Cl at 298 K

λ (nm)	10^{20} σ (cm^2)	λ (nm)	10^{20} σ (cm^2)	λ (nm)	10^{20} σ (cm^2)
170	27.1	200	0.145	218	0.00243
175	14.0	202	0.0949	220	0.00145
180	6.38	204	0.0622	222	0.000845
185	2.73	206	0.0399	224	0.000484
190	1.02	208	0.0256	226	0.000271
192	0.706	210	0.0161	228	0.000148
194	0.482	212	0.0105	230	0.0000783
196	0.324	214	0.00652		
198	0.218	216	0.00401		

Note:
170–185 nm: mean of data from Gillotay and Simon,[4] Hubrich and Stuhl,[6] and Nayak et al.[7]
190–210 nm: mean of data from Gillotay and Simon,[4] Orlando et al.,[8] and Nayak et al.[7]
212–230 nm: Gillotay and Simon[4]

(1) Brownsword, R. A.; Hillenkamp, M.; Laurent, T.; Volpp, H.-R.; Wolfrum, J.; Vatsa, R. K.; Yoo, H.-S. H atom formation dynamics in the dissociation of CH_3–CF_2Cl (HCFC-142b) after UV and VUV laser photoexcitation. *J. Chem. Phys.* **1997**, *107*, 779-785, doi:10.1063/1.474376.

(2) Brownsword, R. A.; Schmiechen, P.; Volpp, H.-R.; Upadhyaya, H. P.; Jung, Y. J.; Jung, K.-H. Chlorine atom formation dynamics in the dissociation of CH_3CF_2Cl(HCFC-142b) after UV laser photoexciation. *J. Chem. Phys.* **1999**, *110*, 11823-11829, doi:10.1063/1.479124.

(3) Doucet, J.; Sauvageau, P.; Sandorfy, C. Photoelectron and far-ultraviolet absorption spectra of chlorofluoro derivatives of ethane. *J. Chem. Phys.* **1975**, *62*, 355-359, doi:10.1063/1.430493.

(4) Gillotay, D.; Simon, P. C. Temperature-dependence of ultraviolet absorption cross-sections of alternative chlorofluoroethanes. *J. Atmos. Chem.* **1991**, *12*, 269-285, doi:10.1007/BF00048076.

(5) Green, R. G.; Wayne, R. P. Vacuum ultra-violet absorption spectra of halogenated methanes and ethanes. *J. Photochem.* **1976/77**, *6*, 375-377, doi:10.1016/0047-2670(76)85077-0.

(6) Hubrich, C.; Stuhl, F. The ultraviolet absorption of some halogenated methanes and ethanes of atmospheric interest. *J. Photochem.* **1980**, *12*, 93-107, doi:10.1016/0047-2670(80)85031-3.

(7) Nayak, A. K.; Buckley, T. J.; Kurylo, M. J.; Fahr, A. Temperature dependence of the gas and liquid phase ultraviolet absorption cross sections of HCFC-123 (CF_3CHCl_2) and HCFC-142b (CH_3CF_2Cl). *J. Geophys. Res.* **1996**, *101*, 9055-9062, doi:10.1029/96JD00226.

(8) Orlando, J. J.; Burkholder, J. B.; McKeen, S. A.; Ravishankara, A. R. Atmospheric fate of several hydrofluoroethanes and hydrochloroethanes: 2. UV absorption cross sections and atmospheric lifetimes. *J. Geophys. Res.* **1991**, *96*, 5013-5023, doi:10.1029/90JD02734.

(9) Vatsa, R. K.; Volpp, H.-R. Absorption cross-sections for some atmospherically important molecules at the H atom Lyman-α wavelength (121.567 nm). *Chem. Phys. Lett.* **2001**, *340*, 289-295, doi:10.1016/S0009-2614(01)00373-6.

F55. CH_2ClCHO (chloroacetaldehyde)

Back to Index

$CH_2ClCHO + h\nu \rightarrow$ Products (1)

(Recommendation: 06-2, Note: 10-6, Evaluated: 10-6)

Absorption Cross Sections: The UV absorption spectrum of chloroacetaldehyde, CH_2ClCHO, has been measured at room temperature by Lucazeau and Sandorfy[2] (118–182 nm) and Libuda[1] (235–360 nm). The absorption band centered at ~290 nm has prominent diffuse band structure at wavelengths >280 nm. The recommended absorption cross sections in Table 4F-55 are the average absorption cross sections over 1 nm intervals of the spectrum reported by Libuda[1] (0.6 nm resolution).

Photolysis Quantum Yield and Product Studies: No recommendation.

Table 4F-55. Recommended Absorption Cross Sections of CH_2ClCHO at 298 K

λ (nm)	10^{20} σ (cm^2)	λ (nm)	10^{20} σ (cm^2)	λ (nm)	10^{20} σ (cm^2)	λ (nm)	10^{20} σ (cm^2)
240	0.952	270	2.46	300	5.57	330	1.64
241	0.887	271	2.65	301	5.10	331	1.52
242	0.885	272	2.85	302	4.92	332	1.68
243	0.881	273	2.98	303	5.01	333	1.42
244	0.845	274	3.04	304	5.30	334	1.36
245	0.814	275	3.13	305	5.27	335	1.06
246	0.815	276	3.29	306	5.48	336	0.747
247	0.841	277	3.38	307	5.34	337	0.622
248	0.857	278	3.57	308	5.44	338	0.502
249	0.864	279	3.82	309	5.37	339	0.411
250	0.875	280	3.99	310	5.03	340	0.340
251	0.884	281	4.23	311	4.61	341	0.281
252	0.926	282	4.09	312	3.92	342	0.247
253	0.959	283	4.15	313	3.71	343	0.213
254	0.977	284	4.31	314	3.73	344	0.190
255	1.01	285	4.55	315	3.96	345	0.159
256	1.08	286	4.64	316	3.85	346	0.136
257	1.18	287	4.80	317	4.16	347	0.0977
258	1.23	288	4.99	318	3.84	348	0.0791
259	1.28	289	5.03	319	3.78	349	0.0623
260	1.33	290	5.20	320	3.84	350	0.0545
261	1.42	291	4.95	321	3.43	351	0.0558
262	1.53	292	4.94	322	3.26	352	0.0603
263	1.68	293	5.14	323	2.49	353	0.0633
264	1.84	294	5.48	324	2.11	354	0.0565
265	1.91	295	5.47	325	1.92	355	0.0377
266	1.98	296	5.64	326	1.87	356	0.0239
267	2.08	297	5.56	327	1.87	357	0.0123
268	2.23	298	5.75	328	1.70		
269	2.33	299	5.63	329	1.92		

Note:
Libuda[1]

(1) Libuda, H. G. Spektroskopische und kinetische Untersuchungen an halogenierten Carbonylverbindungen von atmosphärischem Interesse. PhD-Thesis, University of Wuppertal, Germany, 1992.

(2) Lucazeau, G.; Sandorfy, C. On the far-ultraviolet spectra of some simple aldehydes. *J. Mol. Spectrosc.* **1970**, *35*, 214-231, doi:10.1016/0022-2852(70)90199-2.

F56. $CHCl_2CHO$ (dichloroacetaldehyde)

Back to Index

$CHCl_2CHO + h\nu \rightarrow$ Products (1)

(Recommendation: 06-2, Note: 10-6, Evaluated: 10-6)

Absorption Cross Sections: The UV absorption spectrum of dichloroacetaldehyde, $CHCl_2CHO$, has been measured at room temperature by Lucazeau and Sandorfy[2] (118–182 nm) and Libuda[1] (253–360 nm), who report an absorption band with weak structure around the maximum at ~300 nm. The recommended absorption cross sections in Table 4F-56 are averages over 1 nm intervals of the spectrum reported by Libuda[1] (0.6 nm resolution).

Photolysis Quantum Yield and Product Studies: No recommendation.

Table 4F-56. Recommended Absorption Cross Sections of $CHCl_2CHO$ at 298 K

λ (nm)	10^{20} σ (cm^2)	λ (nm)	10^{20} σ (cm^2)	λ (nm)	10^{20} σ (cm^2)	λ (nm)	10^{20} σ (cm^2)
256	0.0462	281	3.66	306	5.76	331	1.47
257	0.0787	282	3.85	307	5.70	332	1.34
258	0.167	283	4.02	308	5.49	333	1.22
259	0.221	284	4.23	309	5.36	334	1.21
260	0.247	285	4.43	310	5.25	335	1.05
261	0.313	286	4.63	311	4.99	336	0.859
262	0.445	287	4.88	312	4.58	337	0.720
263	0.596	288	4.96	313	4.40	338	0.594
264	0.705	289	5.17	314	4.26	339	0.495
265	0.785	290	5.32	315	4.11	340	0.418
266	0.914	291	5.38	316	3.98	341	0.362
267	1.09	292	5.51	317	3.85	342	0.315
268	1.30	293	5.68	318	3.73	343	0.259
269	1.49	294	5.85	319	3.51	344	0.209
270	1.67	295	5.88	320	3.30	345	0.182
271	1.77	296	6.06	321	3.18	346	0.155
272	1.91	297	5.97	322	3.00	347	0.134
273	2.08	298	6.04	323	2.73	348	0.117
274	2.28	299	6.02	324	2.48	349	0.102
275	2.57	300	6.14	325	2.27	350	0.0844
276	2.74	301	5.94	326	2.14	351	0.0707
277	3.01	302	5.97	327	1.99	352	0.0697
278	3.14	303	5.93	328	1.80	353	0.0638
279	3.26	304	5.90	329	1.67		
280	3.48	305	5.77	330	1.58		

Note:
Libuda[1]

(1) Libuda, H. G. Spektroskopische und kinetische Untersuchungen an halogenierten Carbonylverbindungen von atmosphärischem Interesse. PhD-Thesis, University of Wuppertal, Germany, 1992.

(2) Lucazeau, G.; Sandorfy, C. On the far-ultraviolet spectra of some simple aldehydes. *J. Mol. Spectrosc.* **1970**, *35*, 214-231, doi:10.1016/0022-2852(70)90199-2.

F57. CF_2ClCHO (difluorochloroacetaldehyde)

Back to Index

$CF_2ClCHO + h\nu \rightarrow$ Products (1)

(Recommendation: 06-2, Note: 10-6, Evaluated: 10-6)

Absorption Cross Sections: The UV absorption spectrum of difluorochloroacetaldehyde, CF_2ClCHO, has been measured at room temperature by Libuda[1] (235–355 nm) and Rattigan et al.[2] (235–370 nm). The spectrum displays an absorption band over the wavelength range of the measurements with a maximum at 300 nm. The room temperature cross section data are in good agreement, within 3-10% around the peak, with the data from Rattigan et al.[2] being systematically greater than those of Libuda.[1] At wavelengths away from the peak the data from Rattigan et al.[2] are also greater, by 25% at 340 nm and 15 to 300% between 265 and 235 nm.

Rattigan et al.[2] also reported the temperature dependence of the absorption spectrum over the range 245–298 K. The cross sections increase near the peak and decrease in the long wavelength wing with decreasing temperature. Rattigan et al.[2] fit the measured temperature dependence with the empirical expression:

$$\ln \sigma(\lambda, T) = \ln \sigma(\lambda, 298\ K) + B(\lambda)(T–298)$$

The recommended room temperature absorption cross sections in Table 4F-57 are the mean values of the data from Libuda[1] (using 1 nm averages of spectra recorded with 0.6 nm resolution) and Rattigan et al.[2] (5 nm averages of spectra recorded with 0.6 nm resolution) in the region 235–350 nm and the data from Rattigan et al.[2] in the region 355–370 nm. The temperature coefficients are taken from Rattigan et al.[2]

Photolysis Quantum Yield and Product Studies: No recommendation.

Table 4F-57. Recommended Absorption Cross Sections of CF_2ClCHO at 298 K and Temperature Coefficients

λ (nm)	10^{20} σ (cm^2)	10^4 B (K^{-1})	λ (nm)	10^{20} σ (cm^2)	10^4 B (K^{-1})	λ (nm)	10^{20} σ (cm^2)	10^4 B (K^{-1})
235	0.120	–29.0	285	11.8	–10.2	335	4.64	–2.83
240	0.295	–17.9	290	13.7	–10.6	340	2.66	–2.84
245	0.584	–13.5	295	15.2	–9.54	345	1.46	14.0
250	1.07	–11.8	300	16.0	–10.4	350	0.670	37.3
255	1.78	–10.7	305	15.6	–7.09	355	0.148	68.1
260	2.78	–10.5	310	15.2	–9.73	360	0.036	75.8
265	4.09	–10.4	315	13.0	–8.32	365	0.012	52.9
270	5.75	–10.5	320	11.4	–7.71	370	0.003	63.1
275	7.67	–9.96	325	9.07	–5.02			
280	9.79	–10.6	330	6.38	–3.03			

Note:
Absorption cross-sections:
235–350 nm: mean of data from Libuda[1] and Rattigan et al.[2]
355–370 nm: Rattigan et al.[2]
Temperature coefficients:
Rattigan et al.[2]
$\ln \sigma(\lambda, T) = \ln \sigma(\lambda, 298\ K) + B(\lambda)(T–298)$ for the temperature range 245–298 K

(1) Libuda, H. G. Spektroskopische und kinetische Untersuchungen an halogenierten Carbonylverbindungen von atmosphärischem Interesse. PhD-Thesis, University of Wuppertal, Germany, 1992.

(2) Rattigan, O. V.; Wild, O.; Cox, R. A. UV absorption cross-sections and atmospheric photolysis lifetimes of halogenated aldehydes. *J. Photochem. Photobiol. A: Chem.* **1998**, *112*, 1-7, doi:10.1016/S1010-6030(97)00250-5.

F58. $CFCl_2CHO$ (fluorodichloroacetaldehyde)

Back to Index

$CFCl_2CHO + h\nu \rightarrow$ Products (1)

(Recommendation: 06-2, Note: 10-6, Evaluated: 10-6)

Absorption Cross Sections: The UV absorption spectrum of fluorodichloroacetaldehyde, $CFCl_2CHO$, has been measured at room temperature by Libuda[1] (235–360 nm) and Rattigan et al.[2] (235–370 nm). Over this wavelength range there is an absorption band with a maximum near 296 nm. The cross section data from Libuda[1] are greater by 10-30% than the data from Rattigan et al.[2] over the entire absorption band (except for a few points in the wings).

Rattigan et al.[2] also reported the temperature dependence of the absorption spectrum over the temperature range 253–298 K. The cross sections increase near the peak and decrease in the long wavelength wing with decreasing temperature. Rattigan et al.[2] fit the measured temperature dependence with the empirical expression:

$$\ln \sigma(\lambda, T) = \ln \sigma(\lambda, 298\ K) + B(\lambda)(T–298)$$

The recommended room temperature absorption cross sections in Table 4F-58 are the mean values of the data from Libuda[1] (using 1 nm averages of spectra recorded with 0.6 nm resolution) and Rattigan et al.[2] (5 nm averages of spectra recorded with 0.6 nm resolution) in the region 235–355 nm and the data from Rattigan et al.[2] in the region 360–370 nm. The temperature coefficients are taken from Rattigan et al.[2]

Photolysis Quantum Yield and Product Studies: No recommendation.

Table 4F-58. Recommended Absorption Cross Sections of $CFCl_2CHO$ at 298 K and Temperature Coefficients

λ (nm)	10^{20} σ (cm^2)	10^4 B (K^{-1})	λ (nm)	10^{20} σ (cm^2)	10^4 B (K^{-1})	λ (nm)	10^{20} σ (cm^2)	10^4 B (K^{-1})
235	0.305	136.0	285	14.1	–7.82	335	2.50	24.60
240	0.599	87.0	290	15.3	–6.89	340	1.20	36.50
245	1.22	30.6	295	16.1	–6.41	345	0.616	58.10
250	1.91	6.41	300	15.7	–4.50	350	0.245	84.90
255	2.89	1.24	305	14.9	–2.93	355	0.067	92.80
260	4.21	–6.12	310	13.0	1.73	360	0.017	93.20
265	5.89	–7.55	315	10.9	2.70	365	0.007	103.2
270	7.84	–8.11	320	8.66	6.97	370	0.002	138.3
275	9.95	–8.28	325	5.97	12.2			
280	12.1	–8.04	330	4.11	15.6			

Note:

Absorption cross-sections:

235–355 nm: mean of data from Libuda [1] and Rattigan et al.[2]

360–370 nm: Rattigan et al.[2]

Temperature coefficients:

Rattigan et al.[2]

$\ln \sigma(\lambda, T) = \ln \sigma(\lambda, 298\ K) + B(\lambda)(T–298)$ for the temperature range 253–298 K

(1) Libuda, H. G. Spektroskopische und kinetische Untersuchungen an halogenierten Carbonylverbindungen von atmosphärischem Interesse. PhD-Thesis, University of Wuppertal, Germany, 1992.

(2) Rattigan, O. V.; Wild, O.; Cox, R. A. UV absorption cross-sections and atmospheric photolysis lifetimes of halogenated aldehydes. *J. Photochem. Photobiol. A: Chem.* **1998**, *112*, 1-7, doi:10.1016/S1010-6030(97)00250-5.

F59. CCl_3CHO (trichloroacetaldehyde, chloral)

Back to Index

$CCl_3CHO + h\nu$	$\rightarrow CCl_3 + HCO$	351 kJ mol^{-1}	341 nm	(1)
	$\rightarrow CCl_3CO + H$	391 kJ mol^{-1}	306 nm	(2)
	$\rightarrow CCl_2CHO + Cl$			(3)
	$\rightarrow CCl_3H + CO$	22.6 kJ mol^{-1}	5300 nm	(4)

(Recommendation: 06-2, Note: 10-6, Evaluated: 10-6)

Absorption Cross Sections: The absorption spectrum of trichloroacetaldehyde (chloral), CCl_3CHO, has been measured at room temperature by Lucazeau and Sandorfy [3] (118–182 and 250–357 nm), Libuda[2] (235–350 nm), Rattigan et al.[4,5] (200–360 nm), Gillotay et al.[1] (166–348 nm), and Talukdar et al.[6] (200–344 nm). Overlapping absorption bands were observed with a maximum near 290 nm and a strong band peaking below 180 nm. Except for the data of Lucazeau and Sandorfy,[3] the results for the 290 nm absorption band are in reasonable agreement with a 20% range in cross section values at 290 nm. Gillotay et al.[1] report the largest cross section values and Libuda[2] the smallest. The data sets from Rattigan et al.[4] and Talukdar et al.[6] agree to better than 10% around the absorption maximum. At longer wavelengths, the data sets from Rattigan et al.[4] and Talukdar et al.[6] are nearly identical. The cross sections from Gillotay et al.[1] are appreciably higher at the longer wavelengths and there is no explanation for this discrepancy. The temperature dependence of the absorption spectrum has been measured by Rattigan et al.[4,5] (243–296 K), Gillotay et al.[1] (210–295 K), and Talukdar et al.[6] (240–360 K). These studies are in agreement and found that the absorption cross sections decrease with decreasing temperature below ~260 nm and above ~290 nm. Rattigan et al.[4] and Talukdar et al.[6] parameterized the temperature dependence using the empirical expression:

$$\ln \sigma(\lambda, T) = \ln \sigma(\lambda, 298\ K) + B(\lambda)(T–298)$$

The recommended absorption cross sections and B(λ) temperature coefficients in Table 4F-59 are taken from Talukdar et al.[6].

Photolysis Quantum Yield and Product Studies: Quantum yields for the production of H, $O(^3P)$, and Cl atoms in the photolysis of CCl_3CHO at 193, 248, and 308 nm have been measured by Talukdar et al.[6] The yields of H and O atoms were found to be small or below the detection limit, $\Phi(O(^3P)) < 0.02$ and < 0.01 at 248 and 308

nm, respectively, and Φ(H) = 0.04 ± 0.005, <0.01, and <0.002 at 193, 248, and 308 nm, respectively. Cl atoms were found to be the primary photolysis product at 308 nm with Φ(Cl) = 1.3 ± 0.3.

Table 4F-59. Recommended Absorption Cross Sections of CCl_3CHO at 298 K and Temperature Coefficients

λ (nm)	10^{20} σ (cm^2)	10^4 B (K^{-1})	λ (nm)	10^{20} σ (cm^2)	10^4 B (K^{-1})	λ (nm)	10^{20} σ (cm^2)	10^4 B (K^{-1})
200	187	22.0	250	2.18	3.73	300	9.25	3.07
202	153	23.9	252	2.54	1.50	302	8.77	3.60
204	122	27.2	254	2.92	0.324	304	8.17	4.37
206	95.7	30.6	256	3.36	–0.569	306	7.50	5.25
208	73.8	34.1	258	3.84	–0.877	308	6.86	6.10
210	56.3	37.5	260	4.35	–1.23	310	6.18	6.91
212	42.6	40.9	262	4.90	–1.65	312	5.58	7.90
214	31.8	44.0	264	5.48	–1.62	314	4.98	9.30
216	23.8	47.2	266	6.07	–1.50	316	4.33	11.2
218	17.1	50.2	268	6.68	–1.41	318	3.68	13.2
220	13.1	52.9	270	7.28	–1.22	320	3.09	15.1
222	9.75	55.6	272	7.88	–1.07	322	2.51	16.7
224	7.24	57.6	274	8.46	–0.931	324	2.09	18.5
226	5.39	59.0	276	8.99	–0.584	326	1.76	21.1
228	4.06	60.4	278	9.49	–0.412	328	1.43	25.0
230	3.07	60.5	280	9.94	–0.481	330	1.12	30.3
232	2.39	59.5	282	10.3	–0.235	332	0.849	36.6
234	1.90	55.9	284	10.6	0.242	334	0.590	43.3
236	1.62	49.2	286	10.8	0.475	336	0.373	49.8
238	1.43	41.6	288	10.9	0.750	338	0.261	55.6
240	1.39	33.0	290	10.9	1.09	340	0.188	60.2
242	1.41	24.0	292	10.8	1.51	342	0.136	65.0
244	1.53	16.4	294	10.6	1.96	344	0.100	69.0
246	1.66	10.4	296	10.3	2.38			
248	1.91	6.50	298	9.92	2.71			

Note:

Absorption cross-sections (σ):

Talukdar et al.[6]

Temperature coefficients (B):

Talukdar et al.[6]

$\ln \sigma(\lambda, T) = \ln \sigma(\lambda, 298\ K) + B(\lambda)(T–298)$ (240–360 K range)

(1) Gillotay, D.; Simon, P. C.; Dierickx, L. Ultraviolet absorption cross-sections of some carbonyl compounds and their temperature dependence. *Aeronomica Acta* **1993**, *368*, 1-15, doi:10.18758/A_368.

(2) Libuda, H. G. Spektroskopische und kinetische Untersuchungen an halogenierten Carbonylverbindungen von atmosphärischem Interesse. PhD-Thesis, University of Wuppertal, Germany, 1992.

(3) Lucazeau, G.; Sandorfy, C. On the far-ultraviolet spectra of some simple aldehydes. *J. Mol. Spectrosc.* **1970**, *35*, 214-231, doi:10.1016/0022-2852(70)90199-2.

(4) Rattigan, O. V.; Wild, O.; Cox, R. A. UV absorption cross-sections and atmospheric photolysis lifetimes of halogenated aldehydes. *J. Photochem. Photobiol. A: Chem.* **1998**, *112*, 1-7, doi:10.1016/S1010-6030(97)00250-5.

(5) Rattigan, O. V.; Wild, O.; Jones, R. L.; Cox, R. A. Temperature-dependent absorption cross-sections of CF_3COCl, CF_3COF, CH_3COF, CCl_3CHO and CF_3COOH. *J. Photochem. Photobiol. A: Chem.* **1993**, *73*, 1-9, doi:10.1016/1010-6030(93)80026-6.

(6) Talukdar, R. K.; Mellouki, A.; Burkholder, J. B.; Gilles, M. K.; Le Bras, G.; Ravishankara, A. R. Quantification of the tropospheric removal of chloral (CCl_3CHO): Rate coefficients for the reaction with OH, UV absorption cross sections, and quantum yields. *J. Phys. Chem. A* **2001**, *105*, 5188-5196, doi:10.1021/jp004632j.

F60. $CH_3C(O)Cl$ (acetyl chloride)

Back to Index

$CH_3C(O)Cl + h\nu \rightarrow$ Products (1)

(Recommendation: 06-2, Note: 10-6, Evaluated: 10-6)

Absorption Cross Sections: The UV absorption spectrum of acetyl chloride, $CH_3C(O)Cl$, has been measured at room temperature by Libuda[1] (233–300 nm) and Maricq [2] (190–341 nm). In this wavelength range the spectrum has two overlapping continuous absorption bands, one centered near 240 nm and a stronger band peaking below 190 nm. Both studies report a peak cross section for the 240 nm band of ~1.16×10^{-19} cm^2 $molecule^{-1}$. However, the wavelength dependence of the 240 nm band is significantly different in the two studies. Libuda[1] report a narrower band with a peak shifted to longer wavelength compared to that of Maricq.[2] At wavelengths >280 nm the cross section data reported by Maricq[2] is very noisy making any comparisons difficult. The recommended absorption cross sections in Table 4F-60 are 1 nm averages of data from Maricq[2] (0.5 nm resolution) for the region 191–292 nm and 1 nm averages of the data from Libuda[1] (0.6 nm resolution) for the region 293–302 nm.

Photolysis Quantum Yield and Product Studies: No recommendation.

Table 4F-60. Recommended Absorption Cross Sections of $CH_3C(O)Cl$ at 298 K

λ (nm)	10^{20} σ (cm^2)	λ (nm)	10^{20} σ (cm^2)	λ (nm)	10^{20} σ (cm^2)	λ (nm)	10^{20} σ (cm^2)
191	34.7	219	5.95	247	11.0	275	1.98
192	26.3	220	6.28	248	10.9	276	1.90
193	23.6	221	6.57	249	10.6	277	1.67
194	20.5	222	6.93	250	10.4	278	1.42
195	17.1	223	7.15	251	10.1	279	1.24
196	14.1	224	7.53	252	9.76	280	1.12
197	11.4	225	7.99	253	9.51	281	0.959
198	9.08	226	8.23	254	9.17	282	0.781
199	7.53	227	8.59	255	8.77	283	0.653
200	6.37	228	8.98	256	8.36	284	0.479
201	5.17	229	9.27	257	8.03	285	0.391
202	4.34	230	9.61	258	7.67	286	0.389
203	3.83	231	9.93	259	7.27	287	0.327
204	3.54	232	10.1	260	6.86	288	0.307
205	3.45	233	10.3	261	6.55	289	0.267
206	3.28	234	10.5	262	6.20	290	0.213
207	3.12	235	10.7	263	5.79	291	0.200
208	3.16	236	10.9	264	5.40	292	0.173
209	3.35	237	11.2	265	5.11	293	0.129
210	3.48	238	11.3	266	4.76	294	0.103
211	3.72	239	11.3	267	4.39	295	0.0846
212	3.89	240	11.4	268	4.03	296	0.0716
213	4.06	241	11.5	269	3.70	297	0.0599
214	4.40	242	11.5	270	3.36	298	0.0500
215	4.68	243	11.4	271	3.06	299	0.0404
216	4.88	244	11.3	272	2.77	300	0.0336
217	5.14	245	11.2	273	2.49	301	0.0298
218	5.54	246	11.1	274	2.19	302	0.0265

Note:
191–292 nm: Maricq[2]
293–302 nm: Libuda[1]

(1) Libuda, H. G. Spektroskopische und kinetische Untersuchungen an halogenierten Carbonylverbindungen von atmosphärischem Interesse. PhD-Thesis, University of Wuppertal, Germany, 1992.

(2) Maricq, M. M., personal communication.

F61. $CH_2ClC(O)Cl$ (chloroacetyl chloride)

Back to Index

$CH_2ClC(O)Cl + h\nu \rightarrow$ Products (1)

(Recommendation: 06-2, Note: 10-6, Evaluated: 10-6)

Absorption Cross Sections: The UV absorption spectrum of chloroacetyl chloride, $CH_2ClC(O)Cl$, has been measured at room temperature and 234–342 nm by Libuda.[1] The spectrum has an absorption band with the maximum around 248 nm. Above 315 nm the data shows a somewhat irregular behavior and is considered unreliable. Therefore, the recommended absorption cross sections in Table 4F-61 are the 1 nm averages of the data from Libuda[1] (0.6 nm resolution) excluding this region.

Photolysis Quantum Yield and Product Studies: No recommendation.

Table 4F-61. Recommended Absorption Cross Sections of $CH_2ClC(O)Cl$ at 298 K

λ (nm)	10^{20} σ (cm^2)	λ (nm)	10^{20} σ (cm^2)	λ (nm)	10^{20} σ (cm^2)	λ (nm)	10^{20} σ (cm^2)
235	9.50	256	11.2	277	4.00	298	0.409
236	10.0	257	11.0	278	3.71	299	0.353
237	10.4	258	10.7	279	3.41	300	0.300
238	11.0	259	10.4	280	3.15	301	0.248
239	11.5	260	10.0	281	2.89	302	0.199
240	11.8	261	9.67	282	2.65	303	0.170
241	12.0	262	9.32	283	2.43	304	0.157
242	12.3	263	8.94	284	2.21	305	0.131
243	12.5	264	8.55	285	2.03	306	0.113
244	12.7	265	8.16	286	1.85	307	0.0909
245	12.7	266	7.80	287	1.67	308	0.0809
246	12.7	267	7.41	288	1.50	309	0.0657
247	12.7	268	7.06	289	1.33	310	0.0547
248	12.8	269	6.72	290	1.17	311	0.0522
249	12.7	270	6.30	291	1.04	312	0.0419
250	12.5	271	5.90	292	0.918	313	0.0380
251	12.4	272	5.53	293	0.814	314	0.0311
252	12.3	273	5.23	294	0.717	315	0.0286
253	12.1	274	4.93	295	0.628	316	0.0214
254	11.8	275	4.61	296	0.546		
255	11.5	276	4.33	297	0.473		

Note:
Libuda[1]

(1) Libuda, H. G. Spektroskopische und kinetische Untersuchungen an halogenierten Carbonylverbindungen von atmosphärischem Interesse. PhD-Thesis, University of Wuppertal, Germany, 1992.

F62. $CHCl_2C(O)Cl$ (dichloroacetyl chloride)

Back to Index

$CHCl_2C(O)Cl + h\nu \rightarrow$ Products (1)

(Recommendation: 06-2, Note: 10-6, Evaluated: 10-6)

Absorption Cross Sections: The UV absorption spectrum of dichloroacetyl chloride, $CHCl_2C(O)Cl$, has been measured at room temperature by Libuda[1] (235–338 nm) and Villenave et al.[2] (200–300 nm). The spectrum has an absorption band with the maximum around 258 nm. The reported cross sections are in very good agreement between 242 and 300 nm with the Villenave et al.[2] cross sections being systematically smaller by 1–10%. At shorter wavelengths the absorption cross sections reported by Libuda[1] are smaller by up to ~25% at 235 nm. Villenave et al.[2] observed a minimum near 232 nm and increasing cross sections between 230 and 220 nm. At the longer wavelengths the absorption spectrum reported by Libuda[1] is irregular at wavelengths >316 nm. The recommended absorption cross sections in Table 4F-62 are from Villenave et al.[2]

Photolysis Quantum Yield and Product Studies: No recommendation.

Table 4F-62. Recommended Absorption Cross Sections of $CHCl_2C(O)Cl$ at 298 K

λ (nm)	10^{20} σ (cm^2)
220	21.7
230	13.2
240	15.7
250	20.0
256	20.9
260	20.8
270	17.1
280	10.5
290	4.7
300	1.4

Note:
Villenave et al.[2]

(1) Libuda, H. G. Spektroskopische und kinetische Untersuchungen an halogenierten Carbonylverbindungen von atmosphärischem Interesse. PhD-Thesis, University of Wuppertal, Germany, 1992.

(2) Villenave, E.; Morozov, I.; Lesclaux, R. Kinetics of the self-reactions of peroxy radicals arising from chlorine-initiated oxidation of chloroethenes. *J. Phys. Chem. A* **2000**, *104*, 9933-9940, doi:10.1021/jp001704y.

F63. $CCl_3C(O)Cl$ (trichloroacetyl chloride)

Back to Index

$CCl_3C(O)Cl + h\nu \rightarrow$ Products (1)

(Recommendation: 06-2, Note: 10-6, Evaluated: 10-6)

Absorption Cross Sections: The UV absorption spectrum of trichloroacetyl chloride, $CCl_3C(O)Cl$, has been measured at room temperature by Libuda[2] (235–342 nm), Villenave et al.[3] (220–290 nm), and Gillotay et al.[1] (166–338 nm). The absorption spectrum has two overlapping bands with a peak near 256 nm and a stronger band at shorter wavelengths with a peak at ~176 nm. The spectra reported by Gillotay et al.[1] and Villenave et al.[3] are in good agreement. Although the absolute absorption cross sections are similar, the absorption spectrum reported by Libuda[2] has a significantly different wavelength dependence than reported in the other studies. Although the cross section data from Villenave et al.[3] and Gillotay et al.[1] are in good agreement, the recommended absorption cross sections in Table 4F-63 are from Gillotay et al.[1] (0.015 nm resolution) and are averages over the 500 cm^{-1} and 5 nm intervals generally used in stratospheric photodissociation calculations.

The temperature dependence of the absorption spectrum has been measured by Gillotay et al.[1] over the temperature range 210–295 K. They report an increase in absorption cross section with increasing temperature at all wavelengths.

Photolysis Quantum Yield and Product Studies: No recommendation.

Table 4F-63. Recommended Absorption Cross Sections of $CCl_3C(O)Cl$ at 295 K

λ (nm)	10^{20} σ (cm^2)	λ (nm)	10^{20} σ (cm^2)	λ (nm)	10^{20} σ (cm^2)
166.7–169.5	671	204.1–206.2	231	256.4–259.7	22.6
169.5–172.4	699	206.2–208.3	194	259.7–263.2	22.3
172.4–173.9	712	208.3–210.5	160	263.2–266.7	21.1
173.9–175.4	716	210.5–212.8	129	266.7–270.3	19.1
175.4–177.0	717	212.8–215.0	102	270.3–274.0	16.6
177.0–178.6	714	215.0–217.4	78.9	274.0–277.8	13.7
178.6–180.2	706	217.4–219.8	59.5	277.8–281.7	10.7
180.2–181.8	694	219.8–222.2	44.0	281.7–285.7	8.14
181.8–183.5	677	222.2–224.7	31.8	285.7–289.9	5.86
183.5–185.2	655	224.7–227.3	25.8	289.9–294.1	4.03
185.2–186.9	630	227.3–229.9	21.9	294.1–298.5	2.67
186.9–188.7	599	229.9–232.6	19.5	298.5–303.0	1.68
188.7–190.5	567	232.6–235.3	18.3	303.0–307.7	0.921
190.5–192.3	528	235.3–238.1	17.9	307.7–312.5	0.605
192.3–194.2	487	238.1–241.0	18.1	312.5–317.5	0.339
194.2–196.1	445	241.0–243.9	18.7	317.5–322.5	0.188
196.1–198.0	402	243.9–246.9	19.7	322.5–327.5	0.104
198.0–200.0	358	246.9–250.0	20.9	327.5–332.5	0.0578
200.0–202.0	314	250.0–253.2	21.8	332.5–337.5	0.0326
202.0–204.1	272	253.2–256.4	22.3		

Note:
Gillotay et al.[1]

(1) Gillotay, D.; Simon, P. C.; Dierickx, L. Ultraviolet absorption cross-sections of some carbonyl compounds and their temperature dependence. *Aeronomica Acta* **1993**, *368*, 1-15, doi:10.18758/A_368.

(2) Libuda, H. G. Spektroskopische und kinetische Untersuchungen an halogenierten Carbonylverbindungen von atmosphärischem Interesse. PhD-Thesis, University of Wuppertal, Germany, 1992.

(3) Villenave, E.; Morozov, I.; Lesclaux, R. Kinetics of the self-reactions of peroxy radicals arising from chlorine-initiated oxidation of chloroethenes. *J. Phys. Chem. A* **2000**, *104*, 9933-9940, doi:10.1021/jp001704y.

F64. $CF_3C(O)Cl$ (trifluoroacetyl chloride)

Back to Index

$$CF_3C(O)Cl + h\nu \rightarrow CF_3 + ClCO \quad (1)$$
$$\rightarrow CF_3 + CO + Cl \quad (2)$$
$$\rightarrow CF_3CO + Cl \quad (3)$$
$$\rightarrow CF_3Cl + CO \quad (4)$$

(Recommendation: 06-2, Note: 15-10, Evaluated: 10-6)

Absorption Cross Sections: The UV absorption spectrum of trifluoroacetyl chloride, $CF_3C(O)Cl$, has been measured at room temperature by Maricq and Szente[2] (190–342 nm), Rattigan et al.[4] (220–330 nm), Meller and Moortgat[3] (200–329 nm), and Malanca et al.[1] (200–325 nm). The UV absorption spectrum has a band between 215 and 330 nm with a maximum around 255 nm and the shoulder of a stronger band apparent between 200 and 215 nm. The cross section data from the Rattigan et al.,[4] Meller and Moortgat,[3] and Malanca et al.[1] studies are in agreement for wavelengths >240 nm, with the agreement better than 5% between 240 and 315 nm. The Meller and Moortgat[3] cross sections are greater than those of Rattigan et al.[4] and Malanca et al.[1] by ~65% near the absorption minimum at 215 nm. Maricq and Szente[2] report a very noisy spectrum with an absorption maximum of $(4.6 \pm 0.7) \times 10^{-20}$ cm^2 $molecule^{-1}$ at ~255 nm compared to 6.8×10^{-20} cm^2 $molecule^{-1}$ by Rattigan et al.[4] and Malanca et al.[1] and 6.7×10^{-20} cm^2 $molecule^{-1}$ by Meller and Moortgat.[3]

The temperature dependence of the absorption spectrum has been measured by Rattigan et al.[4] (233, 253 and 296 K), Meller and Moortgat[3] (223, 248, 273 and 298 K), and Malanca et al.[1] (253 and 300 K). These studies show a decrease of the absorption cross sections with decreasing temperature in the wavelength regions below ~215 nm and above 255 nm. For the region between 215 and 255 nm, a very slight decrease in absorption cross

section with decreasing temperature was observed in these studies. The recommended absorption cross sections in Table 4E-64 are taken from Malanca et al.[1]

Photolysis Quantum Yield and Product Studies: Maricq and Szente[2] photolysed $CF_3C(O)Cl$ at 193 and 248 nm in $O_2/N_2/C_2H_6$ mixtures and measured the formation of the products CF_3O_2, HCl, and CO. They report $\Phi_2 + \Phi_3 = 1.01 \pm 0.11$ at 193 nm and $\Phi_2 + \Phi_3 = 0.92 \pm 0.08$ at 248 nm where channel 2 was determined to be the major dissociation pathway at both wavelengths. Meller and Moortgat[3] photolysed $CF_3C(O)Cl$ at 254 nm in N_2 and air/C_2H_6 mixtures over the pressure range 100–760 Torr and measured the formation of the stable end-products CF_3Cl, C_2F_6, Cl_2 and CO. They report the quantum yield for the disappearance of $CF_3C(O)Cl$ to be $\Phi_1 + \Phi_2 = 0.95 \pm 0.05$. Weibel et al.[5] photolysed $CF_3C(O)Cl$ at 254 and 280 nm in N_2 and air/C_2H_6 mixtures in the pressure range 100–600 Torr and measured the formation of the products CF_3Cl, C_2F_6, and CO. A quantum yield for the decomposition of $CF_3C(O)Cl = \Phi[CF_3Cl + 2C_2F_6] = 0.98 \pm 0.13$, $\Phi_1 + \Phi_2 = 0.95 \pm 0.05$ was obtained. The quantum yields measured by Meller and Moortgat[3] and Weibel et al.[5] were independent of total pressure. There are no quantum yield data in the atmospherically important wavelength range >290 nm.

Table 4E-64. Recommended Absorption Cross Sections of $CF_3C(O)Cl$ at 300 and 253 K

λ (nm)	10^{20} σ (cm^2) 300 K	10^{20} σ (cm^2) 253 K
200	36.8	34.0
205	13.3	11.4
210	3.46	2.55
215	1.07	0.83
220	1.17	1.08
225	1.96	1.88
230	2.93	2.76
235	4.02	3.96
240	5.09	4.94
245	5.99	5.91
250	6.57	6.42
255	6.79	6.57
260	6.53	6.31
265	5.90	5.69
270	5.10	4.80
275	4.00	3.79
280	3.12	2.80
285	2.16	2.00
290	1.38	1.21
295	0.80	0.72
300	0.42	0.36
305	0.197	0.164
310	0.079	0.066
315	0.027	0.016
320	0.008	0.006
325	0.002	0.001

Note:
Malanca et al.[1]

(1) Malanca, F. E.; Chiappero, M. S.; Argüello, G. A.; Wallington, T. J. Trifluoro methyl peroxynitrate (CF_3OONO_2): Temperature dependence of the UV absorption spectrum and atmospheric implications. *Atmos. Environ.* **2005**, *39*, 5051-5057, doi:10.1016/j.atmosenv.2005.05.026.

(2) Maricq, M. M.; Szente, J. J. The 193 and 248 nm photodissociation of $CF_3C(O)Cl$. *J. Phys. Chem.* **1995**, *99*, 4554-4557, doi:10.1021/j100013a028.

(3) Meller, R.; Moortgat, G. K. $CF_3C(O)Cl$: Temperature-dependent (223-298 K) absorption cross-sections and quantum yields at 254 nm. *J. Photochem. Photobiol. A: Chem.* **1997**, *108*, 105-116, doi:10.1016/S1010-6030(97)00094-4.

(4) Rattigan, O. V.; Wild, O.; Jones, R. L.; Cox, R. A. Temperature-dependent absorption cross-sections of CF_3COCl, CF_3COF, CH_3COF, CCl_3CHO and CF_3COOH. *J. Photochem. Photobiol. A: Chem.* **1993**, *73*, 1-9, doi:10.1016/1010-6030(93)80026-6.

(5) Weibel, D. E.; Argüello, G. A.; de Staricco, E. R.; Staricco, E. H. Quantum yield in the gas phase photolysis of perfluoroacetyl chloride: a comparison with related compounds. *J. Photochem. Photobiol. A: Chem.* **1995**, *86*, 27-31, doi:10.1016/1010-6030(94)03920-P.

F65. CH_2=CHCl (vinyl chloride)

Back to Index

CH_2=CHCl + hν → Product (1)

(Recommendation: 19-5, Note: 19-5, Evaluated: 19-5)

Absorption Cross Sections: UV absorption cross sections of CH_2=CHCl (vinyl chloride) have been measured at room temperature, 298 K, by Sood and Watanabe[4] (164–200.1 nm), Berry[1] (140–220 nm), Locht et al.[3] (82.65–247.97 nm), and Limão-Vieira et al.[2] (115–340 nm). The spectra reported by Limão-Vieira et al. and Sood and Watanabe are in good agreement, to within 20%, or better, between 185 and 200 nm. The spectrum reported by Locht et al. is ~30% less over the same wavelength range and shows significant scatter at longer wavelengths. The absorption cross sections reported graphically by Berry are significantly greater than in the other studies and not considered further. The recommended UV absorption cross sections given in Table 4F-65 at 1 nm intervals between 185 and 218 nm are taken from Limão-Vieira et al. Higher-resolution data are available from their study. The recommended estimated uncertainty factors ($F(\lambda)$, 2σ) are assigned as $F(\lambda) = 1.20 + 1 \times 10^{-20}/\sigma(\lambda)$.

The VUV absorption spectrum of CH_2=CHCl has been reported by Limão-Vieira et al.[2] (115–340 nm, 298 K) and Locht et al.[3] (82.65–247.97 nm, 298 K). The Lyman–α (121.567 nm) cross section derived from these studies are 5.1×10^{-17} and 4.1×10^{-17} cm^2 molecule^{-1}, respectively. An average value of 4.6×10^{-17} cm^2 molecule^{-1} with an uncertainty factor (2σ) of 1.2 is recommended for the Lyman–α cross section.

Photolysis Quantum Yield and Product Studies: No recommendation.

Table 4F-65. Recommended Absorption Cross Sections of CH_2=CHCl (vinyl chloride) at 298 K

λ (nm)	10^{20} σ (cm^2)	λ (nm)	10^{20} σ (cm^2)
121.567	4600	202	155
185	3110	203	116
186	2780	204	88.8
187	2550	205	66.9
188	2380	206	48.9
189	2210	207	36.7
190	2050	208	27.2
191	1840	209	20.2
192	1640	210	14.6
193	1440	211	10.2
194	1220	212	7.72
195	1000	213	5.72
196	797	214	4.06
197	618	215	3.03
198	476	216	2.30
199	362	217	1.83
200	272	218	1.44
201	206		

Note:
121.567 nm: Average, Limao-Vieira et al.[2] and Locht et al.[3]
185–218 nm: Limao-Vieira et al.[2]

(1) Berry, M. J. Chloroethylene photochemical lasers: Vibrational energy content of the HCl molecular elimination products. *J. Chem. Phys.* **1974**, *61*, 3114-3143, doi:10.1063/1.1682468.
(2) Limão-Vieira, P.; Vasekova, E.; Raja Sekhar, B. N.; Mason, N. J.; Hoffmann, S. V. VUV photoabsorption spectroscopy of vinyl chloride studied by high resolution synchrotron radiation. *Chem. Phys.* **2006**, *330*, 265-274, doi:10.1016/j.chemphys.2006.08.021.

(3) Locht, R.; Leyh, B.; Hottmann, K.; Baumgärtel, H. The photoabsorption spectrum of vinylchloride (C_2H_3Cl) in the 8-12 eV range. *Chem. Phys.* **1997**, *220*, 207-216, doi:10.1016/S0301-0104(97)00127-4.
(4) Sood, S. P.; Watanabe, K. Absorption and ionization coefficients of vinyl chloride. *J. Chem. Phys.* **1966**, *45*, 2913-2915, doi:10.1063/1.1728045.

F66. $CHCl=CCl_2$ (trichloroethene)

Back to Index

$CHCl=CCl_2 + h\nu \rightarrow$ Products (1)

(Recommendation: 19-5, Note: 19-5, Evaluated: 19-5)

Absorption Cross Sections: UV absorption cross sections of $CHCl=CCl_2$ (trichloroethene) have been measured at room temperature by Berry[1] (298 K, 139–244 nm, presented graphically) and Robbins[2] (295 K, 174–270 nm, 0.07 nm resolution). The recommendation is taken from Robbins and given in Table 4F-66. The recommended estimated uncertainty factors ($F(\lambda)$, 2σ) are assigned as $F(\lambda) = 1.20 + 5 \times 10^{-22}/\sigma(\lambda)$.

Photolysis Quantum Yield and Product Studies: No recommendation.

Table 4F-66. Recommended Absorption Cross Sections of $CHCl=CCl_2$ (trichloroethene) at 295 K

λ (nm)	$10^{20}\ \sigma$ (cm^2)
174	545
176	734
178	713
180	826
182	1110
186	1850
192	3020
198	3330
204	2460
210	1780
216	1130
222	731
228	379
234	149
240	42.7
246	9.86
252	1.94
258	0.359
264	0.049

Note:
Robbins[2]

(1) Berry, M. J. Chloroethylene photochemical lasers: Vibrational energy content of the HCl molecular elimination products. *J. Chem. Phys.* **1974**, *61*, 3114-3143, doi:10.1063/1.1682468.
(2) Robbins, D. E. JPL Publication 77-12, International Conference on Problems Related to the Stratosphere. **1976**, 255-257.

F67. $CCl_2=CCl_2$ (tetrachloroethene)

Back to Index

$CCl_2=CCl_2 + h\nu \rightarrow$ Products (1)

(Recommendation: 19-5, Note: 19-5, Evaluated: 19-5)

Absorption Cross Sections: UV absorption cross sections of $CCl_2=CCl_2$ (tetrachloroethene) have been measured at room temperature, 298 K, by Berry[1] (142–254 nm, presented graphically) and Eden et al.[2] (115–328 nm, 0.075 nm resolution). The agreement between these studies is reasonably good, except at the longest wavelengths of the Berry study. The recommended UV cross sections over the wavelength range 184–270 nm were taken from Eden et al. and are given in Table 4F-67 at 2 nm intervals. The recommended estimated uncertainty factors ($F(\lambda)$, 2σ) are assigned as $F(\lambda) = 1.25 + 5 \times 10^{-21}/\sigma(\lambda)$.

The recommended Lyman-α (121.567 nm) absorption cross section of 4.47×10^{-17} cm^2 molecule^{-1} was derived from the VUV spectrum reported in the Eden et al. study. An uncertainty factor (2σ) of 1.2 is recommended.

Photolysis Quantum Yield and Product Studies: No recommendation.

Table 4F-67. Recommended Absorption Cross Sections of $CCl_2=CCl_2$ (tetrachloroethene) at 298 K

λ (nm)	10^{20} σ (cm^2)	λ (nm)	10^{20} σ (cm^2)
121.567	4470	228	832
184	1830	230	759
186	2120	232	688
188	3100	234	612
190	3080	236	532
192	3750	238	449
194	3890	240	367
196	3960	242	289
198	4050	244	220
200	4240	246	163
202	3710	248	117
204	3410	250	82.4
206	3090	252	56.2
208	2700	254	37.8
210	2510	256	24.8
212	2240	258	16.0
214	1980	260	10.0
216	1750	262	6.11
218	1520	264	3.88
220	1310	266	2.33
222	1150	268	1.51
224	1010	270	1.05
226	914		

Note:
Eden et al.[2]

(1) Berry, M. J. Chloroethylene photochemical lasers: Vibrational energy content of the HCl molecular elimination products. *J. Chem. Phys.* **1974**, *61*, 3114-3143, doi:10.1063/1.1682468.

(2) Eden, S.; Barc, B.; Mason, N. J.; Hoffmann, S. V.; Nunes, Y.; Limão-Vieira, P. Electronic state spectroscopy of C_2Cl_4. *Chem. Phys.* **2009**, *365*, 150-157, doi:10.1016/j.chemphys.2009.10.010.

F68. $CF_3CF_2CHCl_2$ (1,1,1,2,2-pentafluoro-3,3-dichloropropane, HCFC–225ca)

Back to Index

$CF_3CF_2CHCl_2$ (HCFC–225ca) + hν → Products (1)

(Recommendation: 02-25, Note: 10-6, Evaluated: 10-6)

Absorption Cross Sections: The UV absorption spectrum of 1,1,1,2,2-pentafluoro-3,3-dichloropropane (HCFC–225ca), $CF_3CF_2CHCl_2$, has been measured in the gas and liquid phase at 298 K by Braun et al.[1] (160–250 nm). The recommended absorption cross sections in Table 4F-68 are taken from this work. Braun et al.[1] give an expression that can be used to calculate the gas-phase absorption cross sections over the wavelength range 170–270 nm:

$$\log_{10} \varepsilon = \sum a_n(\lambda - 160)^n$$

$a_0 = 1.425$ $\quad a_1 = 4.542 \times 10^{-2}$
$a_2 = -2.036 \times 10^{-3}$ $\quad a_3 = 1.042 \times 10^{-5}$

where the absorption coefficients ε are in units of (atm, 298 K)$^{-1}$ cm^{-1} ($\sigma = 4.06 \times 10^{-20}\ \varepsilon$).

Photolysis Quantum Yield and Product Studies: No recommendation.

Table 4F-68. Recommended Absorption Cross Sections of $CF_3CF_2CHCl_2$ (HCFC-225ca) at 298 K

λ (nm)	10^{20} σ (cm^2)	λ (nm)	10^{20} σ (cm^2)
160	268.7	202	11.58
162	236.8	204	8.185
164	207.6	206	5.802
166	189.0	208	4.084
168	181.4	210	2.903
170	182.7	212	2.042
172	182.8	214	1.429
174	189.0	216	1.05
176	190.9	218	0.727
178	187.9	220	0.463
180	177.5	222	0.308
182	161.1	224	0.209
184	140.3	226	0.145
186	118.3	228	0.0987
188	96.51	230	0.0653
190	74.30	232	0.0434
192	57.08	234	0.0299
194	42.83	236	0.0193
196	31.75	238	0.0134
198	23.22	239	0.0119
200	16.24		

Note:
Braun et al.[1]

(1) Braun, M.; Fahr, A.; Klein, R.; Kurylo, M. J.; Huie, R. E. UV gas and liquid phase absorption cross section measurements of hydrochlorofluorocarbons HCFC-225ca and HCFC-225cb. *J. Geophys. Res.* **1991**, *96*, 13009-13015, doi:10.1029/91JD01026.

F69. CF_2ClCF_2CHFCl (1,1,2,2,3-pentafluoro-1,3-dichloropropane, HCFC–225cb)

Back to Index

CF_2ClCF_2CHFCl (HCFC–225cb) + hν → Products (1)

(Recommendation: 02-25, Note: 10-6, Evaluated: 10-6)

Absorption Cross Sections: The UV absorption spectrum of 1,1,2,2,3-pentafluoro-1,3-dichloropropane (HCFC–225cb), CF_2ClCF_2CHFCl, has been measured in the gas and liquid phase at 298 K by Braun et al.[1] (160–250 nm). The recommended absorption cross sections in Table 4F-69 are taken from this work. Braun et al.[1] give an expression that can be used to calculate the gas-phase absorption cross sections over the wavelength range 165–250 nm:

$$\log_{10} \varepsilon = \sum a_n(\lambda - 160)^n$$

$a_0 = 1.677$ $a_1 = -2.175 \times 10^{-2}$
$a_2 = -1.484 \times 10^{-3}$ $a_3 = 1.147 \times 10^{-5}$

where the absorption coefficients ε are in units of $(\text{atm, 298 K})^{-1}\ \text{cm}^{-1}$ ($\sigma = 4.06 \times 10^{-20}\ \varepsilon$).

Photolysis Quantum Yield and Product Studies: No recommendation.

Table 4F-69. Recommended Absorption Cross Sections of CF_2ClCF_2CHFCl (HCFC-225cb) at 298 K

λ (nm)	10^{20} σ (cm^2)	λ (nm)	10^{20} σ (cm^2)
160	187.9	186	7.308
162	173.3	188	5.075
164	154.8	190	3.492
166	135.1	192	2.412
168	113.2	194	1.661
170	91.35	196	1.165
172	70.68	198	0.873
174	54.73	200	0.633
176	40.68	202	0.479
178	30.04	204	0.369
180	21.11	206	0.291
182	14.90	208	0.254
184	10.47	210	0.250

Note:
Braun et al.[1]

(1) Braun, M.; Fahr, A.; Klein, R.; Kurylo, M. J.; Huie, R. E. UV gas and liquid phase absorption cross section measurements of hydrochlorofluorocarbons HCFC-225ca and HCFC-225cb. *J. Geophys. Res.* **1991**, *96*, 13009-13015, doi:10.1029/91JD01026.

F70. $CH_3C(O)CH_2Cl$ (chloroacetone)

Back to Index

$CH_3C(O)CH_2Cl + h\nu \rightarrow$ Products (1)

(Recommendation: 06-2, Note: 10-6, Evaluated: 10-6)

Absorption Cross Sections: The UV absorption cross sections of chloroacetone, $CH_3C(O)CH_2Cl$, have been measured over the temperature range 243–296 K between 210 and 370 nm by Burkholder et al.[1] using diode array spectroscopy (~0.6 nm resolution). The spectrum has two absorption bands, a strong band with the maximum at ~224 nm (3.35×10^{-19} cm^2 $molecule^{-1}$ at 296 K) and a weaker broader band with the maximum at ~292 nm (1.02×10^{-19} cm^2 $molecule^{-1}$ at 296 K). A systematic decrease in the absorption cross section with decreasing temperature was observed at wavelengths >290 nm. A temperature dependence of the absorption cross sections was also reported for the short wavelength absorption band. The reported values at 253 K are larger than those at 273 K below ~240 nm and even larger than those at 296 K below ~230 nm. The recommended absorption cross sections in Table 4F-70 are taken from Burkholder et al.[1]

Photolysis Quantum Yield and Product Studies: Photodissociation quantum yields were measured by Burkholder et al.[1] to be 0.5 ± 0.08 at 308 nm and 351 nm. At both wavelengths, the yields of CO and CO_2 were 0.50 and ~0.25, respectively. The yield of HCOOH and HCl were reported to be 0.25 and 0.5, respectively, at both photolysis wavelengths.

Table 4F-70. Recommended Absorption Cross Sections of $CH_3C(O)CH_2Cl$ at 296 K

λ (nm)	10^{20} σ (cm^2)	λ (nm)	10^{20} σ (cm^2)	λ (nm)	10^{20} σ (cm^2)	λ (nm)	10^{20} σ (cm^2)
210	22.0	248	3.36	286	9.89	324	2.58
211	23.0	249	3.11	287	9.98	325	2.37
212	24.3	250	2.96	288	10.00	326	2.16
213	25.5	251	2.90	289	10.10	327	1.95
214	26.4	252	2.92	290	10.20	328	1.73
215	27.5	253	3.00	291	10.20	329	1.52
216	28.9	254	3.10	292	10.20	330	1.33
217	30.1	255	3.24	293	10.20	331	1.14
218	30.9	256	3.39	294	10.10	332	0.979
219	31.7	257	3.56	295	10.00	333	0.832
220	32.4	258	3.75	296	9.89	334	0.707
221	32.8	259	3.97	297	9.77	335	0.598
222	33.2	260	4.19	298	9.66	336	0.506
223	33.5	261	4.40	299	9.54	337	0.427
224	33.5	262	4.63	300	9.41	338	0.361
225	33.0	263	4.86	301	9.25	339	0.302
226	32.3	264	5.12	302	9.04	340	0.2520
227	31.8	265	5.38	303	8.80	341	0.212
228	31.3	266	5.65	304	8.53	342	0.176
229	30.3	267	5.89	305	8.24	343	0.145
230	28.9	268	6.14	306	7.94	344	0.120
231	27.3	269	6.39	307	7.63	345	0.103
232	25.7	270	6.65	308	7.34	346	0.0887
233	24.0	271	6.93	309	7.06	347	0.0757
234	22.2	272	7.20	310	6.77	348	0.0642
235	20.3	273	7.47	311	6.50	349	0.0547
236	18.4	274	7.71	312	6.22	350	0.0458
237	16.5	275	7.94	313	5.93	351	0.0411
238	14.6	276	8.16	314	5.61	352	0.0328
239	12.7	277	8.37	315	5.28	353	0.0319
240	11.0	278	8.59	316	4.92	354	0.0220
241	9.50	279	8.82	317	4.57	355	0.0193
242	8.15	280	9.03	318	4.22	356	0.0138
243	6.93	281	9.23	319	3.89	357	0.0134
244	5.85	282	9.41	320	3.58	358	0.00917
245	4.95	283	9.56	321	3.30	359	0.0155
246	4.26	284	9.69	322	3.04	360	0.0128
247	3.74	285	9.80	323	2.80		

Note:
Burkholder et al.[1]

(1) Burkholder, J. B.; Gilles, M. K.; Gierczak, T.; Ravishankara, A. R. The atmospheric degradation of 1-bromopropane ($CH_3CH_2CH_2Br$): The photochemistry of bromoacetone. *Geophys. Res. Lett.* **2002**, *29*, 1822, doi:10.1029/2002GL014712.

F71. (*E*)-1,2-*c*-$C_4Cl_2F_6$ ((*E*)-1,2-dichlorohexafluorocyclobutane)

Back to Index

1,2-*c*-$C_4Cl_2F_6$(*E*) + hν → Products (1)

(Recommendation: 15-10; Note: 15-10; Evaluated: 15-10)

Absorption Cross Sections: The UV absorption cross sections of (*E*)-1,2-dichlorohexafluorocyclobutane, 1,2-*c*-$C_4Cl_2F_6$(*E*), have been measured by Papadimitriou et al.[1] (184.95–230 nm) at temperatures between 214 and 296 K. UV absorption spectra of (*E*)- and (*Z*)- isomeric mixtures (0.94:0.06 and 0.475:0.525) were measured experimentally and individual isomer spectra were determined using the measured sample mixing ratios. Over the 185–230 nm wavelength range the spectrum is continuous with a broad peak near 195 nm. The absorption

cross sections decrease nearly exponentially at wavelengths greater than ~200 nm. The (*E*)- isomer was observed to be a stronger absorber than the (*Z*)- isomer over this wavelength range. The 296 K absorption cross section uncertainty was estimated to be ~3% (2σ) at all wavelengths included in their study.

Papadimitriou et al. measured the spectrum temperature dependence over the range 214–296 K. They observed a systematic decrease in absorption cross section with decreasing temperature at all wavelengths included in their study. The absorption spectrum was parameterized using the empirical formula:

$$\log_{10}\big(\sigma(\lambda,T)\big) = \sum_i A_i(\lambda - 200)^i + (296 - \mathrm{T})\sum_i B_i(\lambda - 200)^i$$

and the optimized parameters are given in Table 4F-71. The parameterization reproduces the absorption spectrum to within the estimated measurement precision and is valid over the 190–220 nm wavelength range and 210–296 K temperature range.

Table 4F-71. Recommended (*E*)-1,2-*c*-$C_4Cl_2F_6$ Absorption Spectrum, σ(λ,T), Parameterization

i	A_i	B_i
0	-18.45	-0.000553
1	-0.0876	-8.036×10^{-5}
2	-0.003737	-4.24×10^{-6}
3	0.0001124	-6.01×10^{-7}
4	2.444×10^{-6}	6.00×10^{-8}
5	-9.33×10^{-8}	-1.279×10^{-9}

Photolysis Quantum Yield and Product Studies: Quantum yields for the production of Cl atoms and *c*-C_4F_6 in the photolysis of 1,2-*c*-$C_4Cl_2F_6$(*E*) at 193 nm were measured by Papadimitriou et al.[1] A value of Φ(Cl) = 1.9 ± 0.27 was determined for a 0.475:0.525 isomeric mixture (i.e., quantum yields for the individual isomers were not determined). A value of Φ(Cl) = 2 is recommended. The *c*-C_4F_6 product yield in the photolysis of 1,2-*c*-$C_4Cl_2F_6$(*E*) was found to be 0.7 ± 0.1.

(1) Papadimitriou, V. C.; McGillen, M. R.; Smith, S. C.; Jubb, A. M.; Portmann, R. W.; Hall, B. D.; Fleming, E. L.; Jackman, C. H.; Burkholder, J. B. 1,2-Dichlorohexafluoro-cyclobutane (1,2-*c*-$C_4F_6Cl_2$, R-316c) a potent ozone depleting substance and greenhouse gas: Atmospheric loss processes, lifetimes, and ozone depletion and global warming potentials for the (*E*) and (*Z*) stereoisomers. *J. Phys. Chem. A* **2013**, *117*, 11049-11065, doi:10.1021/jp407823k.

F72. (*Z*)-1,2-*c*-$C_4Cl_2F_6$ ((*Z*)-1,2-dichlorohexafluorocyclobutane)

Back to Index

1,2-*c*-$C_4Cl_2F_6$(*Z*) + hν → Products (1)

(Recommendation: 15-10; Note: 15-10; Evaluated: 15-10)

Absorption Cross Sections: The UV absorption cross sections of (*Z*)-1,2-dichlorohexafluorocyclobutane, 1,2-*c*-$C_4Cl_2F_6$(*Z*), have been measured by Papadimitriou et al.[1] (184.95–230 nm) at temperatures between 214 and 296 K. UV absorption spectra of (*E*)- and (*Z*)- isomeric mixtures (0.94:0.06 and 0.475:0.525) were measured experimentally and individual isomer spectra were determined using the measured mixing ratios. The (*Z*)- isomer was found to be a significantly weaker absorber than the (*E*)- isomer over this wavelength range. The uncertainty in the (*Z*)- isomer 296 K absorption cross sections were estimated to be significantly greater than for the (*E*)- isomer, e.g. ~25% (2σ) at 210 nm.

Papadimitriou et al. measured the spectrum temperature dependence over the range 214–296 K. They observed a systematic decrease in absorption cross section with decreasing temperature at all wavelengths included in their study. The absorption spectrum was parameterized using the empirical formula:

$$\log_{10}\big(\sigma(\lambda,T)\big) = \sum_i A_i(\lambda - 200)^i + (296 - \mathrm{T})\sum_i B_i(\lambda - 200)^i$$

and the optimized parameters are given in Table 4F-72. The parameterization reproduces the absorption spectrum to within the estimated measurement precision and is valid over the 190–220 nm wavelength range and 210–296 K temperature range.

Table 4F-72. Recommended (*Z*)-1,2-*c*-$C_4Cl_2F_6$ Absorption Spectrum, $\sigma(\lambda,T)$, Parameterization

i	A_i	B_i
0	–19.24	–0.00155
1	–0.1037	–0.000761
2	0.00203	-1.22×10^{-5}
3	4.9656×10^{-6}	5.52×10^{-6}
4	-1.65×10^{-5}	-2.365×10^{-7}
5	5.03×10^{-7}	3.33×10^{-9}

Photolysis Quantum Yield and Product Studies: Quantum yields for the production of Cl atoms and *c*-C_4F_6 in the photolysis of 1,2-*c*-$C_4Cl_2F_6$(*Z*) at 193 nm were measured by Papadimitriou et al.[1] A value of $\Phi(Cl) = 1.9 \pm 0.27$ was determined for a 0.475:0.525 isomeric mixture (i.e., quantum yields for the individual isomers were not determined). A value of $\Phi(Cl) = 2$ is recommended. The *c*-C_4F_6 product yield in the photolysis of 1,2-*c*-$C_4Cl_2F_6$(*Z*) was found to be 1.0 ± 0.1.

(1) Papadimitriou, V. C.; McGillen, M. R.; Smith, S. C.; Jubb, A. M.; Portmann, R. W.; Hall, B. D.; Fleming, E. L.; Jackman, C. H.; Burkholder, J. B. 1,2-Dichlorohexafluoro-cyclobutane (1,2-*c*-$C_4F_6Cl_2$, R-316c) a potent ozone depleting substance and greenhouse gas: Atmospheric loss processes, lifetimes, and ozone depletion and global warming potentials for the (*E*) and (*Z*) stereoisomers. *J. Phys. Chem. A* **2013**, *117*, 11049-11065, doi:10.1021/jp407823k.

4.9 Bibliography – ClO_x Photochemistry

Adler-Golden, S. M.; Wiesenfeld, J. R. Production of atomic oxygen following flash photolysis of $ClONO_2$. *Chem. Phys. Lett.* **1981**, *82*, 281-284, doi:10.1016/0009-2614(81)85156-1.

Alexander, M. H.; Pouilly, B.; Duhoo, T. Spin-orbit branching in the photofragmentation of HCl. *J. Chem. Phys.* **1993**, *99*, 1752-1764, doi:10.1063/1.465292.

Baer, S.; Hippler, H.; Rahn, R.; Siefke, M.; Seitzinger, S.; Troe, J. Thermodynamic and kinetic properties of the reaction $Cl + O_2 + M \rightleftharpoons ClOO + M$ in the range 160-300 K and 1-1000 bar. *J. Chem. Phys.* **1991**, *95*, 6463-6468, doi:10.1063/1.461543.

Bahou, M.; Chung, C.-Y.; Lee, Y.-P.; Cheng, B. M.; Yung, Y. L.; Lee, L. C. Absorption cross sections of HCl and DCl at 135-232 namometers: Implications for photodissociation on Venus. *Astrophys. J.* **2001**, *559*, L179-L182, doi:10.1086/323753.

Ballash, N. M.; Armstrong, D. A. On the ultraviolet and visible absorption spectrum of ClNO. *Spectrochim. Acta Part A* **1974**, *30*, 941-944, doi:10.1016/0584-8539(74)80009-7.

Barnes, R. J.; Sinha, A.; Michelsen, H. A. Assessing the contribution of the lowest triplet state to the near-UV absorption spectrum of HOCl. *J. Phys. Chem. A* **1998**, *102*, 8855-8859, doi:10.1021/jp9835869.

Barton, S. A.; Coxon, J. A.; Roychowdhury, U. K. Absolute absorption cross sections at high-resolution in the $A^2\Pi_i$-$X^2\Pi_i$ band system of ClO. *Can. J. Phys.* **1984**, *62*, 473-486, doi:10.1139/p84-066.

Basco, N.; Dogra, S. K. Reactions of halogen oxides studied by flash photolysis. I. The flash photolysis of chlorine dioxide. *Proc. Roy. Soc. Lond. A.* **1971**, *323*, 29-68, doi:10.1098/rspa.1971.0087.

Basco, N.; Hunt, J. E. Mutual combination of ClO radicals. *Int. J. Chem. Kinet.* **1979**, *11*, 649-664, doi:10.1002/kin.550110611.

Basco, N.; Morse, R. D. Reactions of halogen oxides studied by flash photolysis IV. Vacuum ultraviolet kinetic spectroscopy studies on chlorine dioxide. *Proc. Roy. Soc. Lond. A.* **1974**, *336*, 495-505, doi:10.1098/rspa.1974.0032.

Bell, A. J.; Boggis, S. A.; Dyke, J. M.; Frey, J. G.; Richter, R.; Shaw, N.; Tabrizchi, M. Ultraviolet photolysis of HOCl: REMPI measurement of the relative population of chlorine atom (^2P) spin-orbit states. *J. Chem. Soc. Faraday Trans.* **1994**, *90*, 17-21, doi:10.1039/ft9949000017.

Berry, M. J. Chloroethylene photochemical lasers: Vibrational energy content of the HCl molecular elimination products. *J. Chem. Phys.* **1974**, *61*, 3114-3143, doi:10.1063/1.1682468.

Birk, M.; Friedl, R. R.; Cohen, E. A.; Pickett, H. M.; Sander, S. P. The rotational spectrum and structure of chlorine peroxide. *J. Chem. Phys.* **1989**, *91*, 6588-6597, doi:10.1063/1.457377.

Birks, J. W.; Shoemaker, B.; Leck, T. J.; Borders, R. A.; Hart, L. J. Studies of reactions of importance in the stratosphere. II. Reactions involving chlorine nitrate and chlorine dioxide. *J. Chem. Phys.* **1977**, *66*, 4591-4599, doi:10.1063/1.433716.

Bishenden, E.; Haddock, J.; Donaldson, D. J. Resonance-enhanced multiphoton ionization measurement of Cl($^2P_{3/2}$ and $^2P_{1/2}$) produced in the photolysis of OClO from 355 to 370 nm. *J. Phys. Chem.* **1991**, *95*, 2113-2115, doi:10.1021/j100159a006.

Bishenden, E.; Haddock, J.; Donaldson, D. J. Correction. *J. Phys. Chem.* **1992**, *96*, 6513, doi:10.1021/j100194a075.

Bloss, W. J.; Nickolaisen, S. L.; Salawitch, R. J.; Friedl, R. R.; Sander, S. P. Kinetics of the ClO self-reaction and 210 nm absorption cross section of the ClO dimer. *J. Phys. Chem. A* **2001**, *105*, 11226-11239, doi:10.1021/jp012429y.

Bogumil, K.; Orphal, J.; Homann, T.; Voigt, S.; Spietz, P.; Fleischmann, O. C.; Vogel, A.; Hartmann, M.; Kromminga, H.; Bovensmann, H.; Frerick, J.; Burrows, J. P. Measurements of molecular absorption spectra with the SCIAMACHY pre-flight model: instrument characterization and reference data for atmospheric remote-sensing in the 230-2380 nm region. *J. Photochem. Photobiol. A: Chem.* **2003**, *157*, 167-184, doi:10.1016/S1010-6030(03)00062-5.

Braun, M.; Fahr, A.; Klein, R.; Kurylo, M. J.; Huie, R. E. UV gas and liquid phase absorption cross section measurements of hydrochlorofluorocarbons HCFC-225ca and HCFC-225cb. *J. Geophys. Res.* **1991**, *96*, 13009-13015, doi:10.1029/91JD01026.

Brownsword, R. A.; Hillenkamp, M.; Laurent, T.; Vatsa, R. K.; Volpp, H.-R.; Wolfrum, J. Dynamics of H atom formation in the photodissociation of chloromethanes at 193.3 nm. *J. Phys. Chem. A* **1997**, *101*, 5222-5227, doi:10.1021/jp963811r.

Brownsword, R. A.; Hillenkamp, M.; Laurent, T.; Vatsa, R. K.; Volpp, H.-R.; Wolfrum, J. Photodissociation dynamics of the chloromethanes at the Lyman-α wavelength (121.6 nm). *J. Chem. Phys.* **1997**, *106*, 1359-1366, doi:10.1063/1.473304.

Brownsword, R. A.; Hillenkamp, M.; Laurent, T.; Volpp, H.-R.; Wolfrum, J.; Vatsa, R. K.; Yoo, H.-S. H atom formation dynamics in the dissociation of CH_3–CF_2Cl (HCFC-142b) after UV and VUV laser photoexcitation. *J. Chem. Phys.* **1997**, *107*, 779-785, doi:10.1063/1.474376.

Brownsword, R. A.; Schmiechen, P.; Volpp, H.-R.; Upadhyaya, H. P.; Jung, Y. J.; Jung, K.-H. Chlorine atom formation dynamics in the dissociation of CH_3CF_2Cl(HCFC-142b) after UV laser photoexciation. *J. Chem. Phys.* **1999**, *110*, 11823-11829, doi:10.1063/1.479124.

Burkholder, J. B. Ultraviolet absorption spectrum of HOCl. *J. Geophys. Res.* **1993**, *98*, 2963-2974, doi:10.1029/92JD02522.

Burkholder, J. B.; Bair, E. J. Potential energy parameters and shapes of the vibrational components of the 345-nm system of chlorine. *J. Phys. Chem.* **1983**, *87*, 1859-1863, doi:10.1021/j100234a007.

Burkholder, J. B.; Gilles, M. K.; Gierczak, T.; Ravishankara, A. R. The atmospheric degradation of 1-bromopropane ($CH_3CH_2CH_2Br$): The photochemistry of bromoacetone. *Geophys. Res. Lett.* **2002**, *29*, 1822, doi:10.1029/2002GL014712.

Burkholder, J. B.; Mauldin, R. L.; Yokelson, R. J.; Solomon, S.; Ravishankara, A. R. Kinetic, thermodynamic, and spectroscopic study of Cl_2O_3. *J. Phys. Chem.* **1993**, *97*, 7597-7605, doi:10.1021/j100131a032.

Burkholder, J. B.; Orlando, J. J.; Howard, C. J. Ultraviolet absorption cross sections of Cl_2O_2 between 210 and 410 nm. *J. Phys. Chem.* **1990**, *94*, 687-695, doi:10.1021/j100365a033.

Burkholder, J. B.; Talukdar, R. K.; Ravishankara, A. R. Temperature dependence of the $ClONO_2$ UV absorption spectrum. *Geophys. Res. Lett.* **1994**, *21*, 585-588, doi:10.1029/93GL03303.

Burrows, J. P.; Tyndall, G. S.; Moortgat, G. K. Photolysis of chlorine nitrate at 254 nm. *J. Phys. Chem.* **1988**, *92*, 4340-4348, doi:10.1021/j100326a020.

Burton, G. R.; Chan, W. F.; Cooper, G.; Brion, C. E. Valence- and inner-shell (Cl 2p, 2s; C 1s) photoabsorption and photoionization of carbon tetrachloride. Absolute oscillator strengths (5-400 eV) and dipole-induced breakdown pathways. *Chem. Phys.* **1994**, *181*, 147-172, doi:10.1016/0301-0104(94)85022-4.

Busch, G. E.; Mahoney, R. T.; Morse, R. I.; Wilson, K. R. Translational spectroscopy: Cl_2 photodissociation. *J. Chem. Phys.* **1969**, *51*, 449-450, doi:10.1063/1.1671746.

Butler, P. J. D.; Phillips, L. F. Upper limit for the atomic oxygen yield in the 308-nm photolysis of HOCl. *J. Phys. Chem.* **1983**, *87*, 183-184, doi:10.1021/j100224a040.

Calvert, J. G.; Pitts, J. N. In *Photochemistry*; John Wiley & Sons, Inc.: New York, 1966; pp 230-231.

Cantrell, C. A.; Zimmer, A.; Tyndall, G. S. Absorption cross sections for water vapor from 183 to 193 nm. *Geophys. Res. Lett.* **1997**, *24*, 2195-2198, 2687 (Erratum), doi:10.1029/97GL02100.

Carter, R. T.; Hallou, A.; Huber, J. R. Photodissociation of $ClNO_2$ at 235 nm. *Chem. Phys. Lett.* **1999**, *310*, 166-172, doi:10.1016/S0009-2614(99)00781-2.

Causley, G. C.; Russell, B. R. The vacuum ultraviolet absorption spectra of the group IVA tetrachlorides. *J. Electron Spectrosc. Relat. Phenom.* **1977**, *11*, 383-397, doi:10.1016/0368-2048(77)80015-7.

Chang, J. S.; Barker, J. R.; Davenport, J. E.; Golden, D. M. Chlorine nitrate photolysis by a new technique: Very low pressure photolysis. *Chem. Phys. Lett.* **1979**, *60*, 385-390, doi:10.1016/0009-2614(79)80594-1.

Chen, H.-Y., C-Y Lien, W-Y Lin, Y.T. Lee, and J.J. Lin UV absorption cross sections of ClOOCl are consistent with ozone degradation models. *Science* **2009**, *324*, 781-784, doi:10.1126/science.1171305.

Chen, Y.; Zhu, L. The wavelength dependence of the photodissociation of propionaldehyde in the 280-330 nm region. *J. Phys. Chem. A* **2001**, *105*, 9689-9696, doi:10.1021/jp011445s.

Chen, Y.; Zhu, L. Wavelength-dependent photolysis of glyoxal in the 290-420 nm region. *J. Phys. Chem. A* **2003**, *107*, 4643-4651, doi:10.1021/jp022440d.

Chen, Y.; Zhu, L.; Francisco, J. S. Wavelength-dependent photolysis of *n*-butyraldehyde and *i*-butyraldehyde in the 280-330-nm region. *J. Phys. Chem. A* **2002**, *106*, 7755-7763, doi:10.1021/jp014544e.

Cheng, B. M.; Chung, C.-Y.; Bahou, M.; Lee, Y.-P.; Lee, L. C. Quantitative spectral analysis of HCl and DCl in 120–220 nm: Effects of singlet–triplet mixing. *J. Chem. Phys.* **2002**, *117*, 4293-4298, doi:10.1063/1.1496476.

Chichinin, A. I. Measurement of $Cl(^2P_{1/2})$ quantum yield for the photodissociaton of NOCl, ICl, PCl_3, Cl_2O and $COCl_2$. *Chem. Phys. Lett.* **1993**, *209*, 459-463, doi:10.1016/0009-2614(93)80117-8.

Chou, C. C.; Crescentini, G.; Vera-Ruiz, H.; Smith, W. S.; Rowland, F. S. "Stratospheric photochemistry of CF_2O, CClFO, and CCl_2O"; 173rd American Chemical Society Meeting, 1977, New Orleans, LA.

Chou, C. C.; Milstein, R. J.; Smith, W. S.; Vera-Ruiz, H.; Molina, M. J.; Rowland, F. S. Stratospheric photodissociation of several saturated perhalo chlorofluorocarbon compounds in current technological use (fluorocarbons-13, -113, -114, and -115). *J. Phys. Chem.* **1978**, *82*, 1-7, doi:10.1021/j100490a001.

Chou, C. C.; Smith, W. S.; Ruiz, H. V.; Moe, K.; Crescentini, G.; Molina, M. J.; Rowland, F. S. The temperature dependences of the ultraviolet absorption cross sections of CCl_2F_2 and CCl_3F, and their stratospheric significance. *J. Phys. Chem.* **1977**, *81*, 286-290, doi:10.1021/j100519a002.

Clark, R. H.; Husain, D. Quantum yield measurements of $Cl(3^2P_{1/2})$ and $Cl(3^2P_{3/2})$ in the photolysis of C_1 chlorofluorocarbons determined by atomic resonance absorption spectroscopy in the vacuum UV. *J. Photochem.* **1984**, *24*, 103-115, doi:10.1016/0047-2670(84)80057-X.

Clyne, M. A. A.; Coxon, J. A. Kinetic studies of oxy-halogen radical systems. *Proc. Roy. Soc. A* **1968**, *303*, 207-231, doi:10.1098/rspa.1968.0048.

Colussi, A. J. Formation and decay of (^3P_J)O atoms in the laser flash photolysis of chlorine dioxide (OClO) at 308 nm. *J. Phys. Chem.* **1990**, *94*, 8922-8926, doi:10.1021/j100389a014.
Colussi, A. J.; Sander, S. P.; Friedl, R. R. Temperature dependence and mechanism of the reaction between O(^{3}P) and chlorine dioxide. *J. Phys. Chem.* **1992**, *96*, 4442-4445, doi:10.1021/j100190a058.
Cox, R. A.; Hayman, G. D. The stability and photochemistry of dimers of the ClO radical and implications for Antarctic ozone depletion. *Nature* **1988**, *332*, 796-800, doi:10.1038/332796a0.
Coxon, J. A.; Jones, W. E.; Ramsey, D. A. 12th International Symposium on Free Radicals, 1976, Laguna Beach, California.
Crowley, J. N.; Helleis, F.; Müller, R.; Moortgat, G. K.; Crutzen, P. J.; Orlando, J. J. CH_3OCl: UV/visible absorption cross sections, J values and atmospheric significance. *J. Geophys. Res.* **1994**, *99*, 20683-20688, doi:10.1029/94JD01829.
Currie, J.; Sidebottom, J. H.; Tedder, J. The reaction of cyclohexyl radicals with carbon tetrachloride. *Int. J. Chem. Kinet.* **1974**, *6*, 481-492, doi:10.1002/kin.550060404.
Daviel, S.; Iida, Y.; Carnovale, F.; Brion, C. E. Absolute oscillator strengths for the partial photoionization, ionic fragmentation and photoabsorption of HCl. *Chem. Phys.* **1984**, *83*, 391-406, doi:10.1016/0301-0104(84)85014-4.
Davis, H. F.; Lee, Y. T. Dynamics and mode specificity in OClO photodissociation. *J. Phys. Chem.* **1992**, *96*, 5681-5684, doi:10.1021/j100193a005.
Davis, H. F.; Lee, Y. T. Photodissociation dynamics of OClO. *J. Chem. Phys.* **1996**, *105*, 8142-8163, doi:10.1063/1.472700.
Davis, M. E.; Bernard, F.; McGillen, M. R.; Fleming, E. L.; Burkholder, J. B. UV and infrared absorption spectra, atmospheric lifetimes, and ozone depletion and global warming potentials for CCl_2FCCl_2F (CFC-112), CCl_3CClF_2 (CFC-112a), CCl_3CF_3 (CFC-113a), and CCl_2FCF_3 (CFC-114a). *Atmos. Chem. Phys.* **2016**, *16*, 8043-8052, doi:10.5194/acp-16-8043-2016.
Delmdahl, R. F.; Ullrich, S.; Gericke, K.-H. Photofragmentation of OClO($\tilde{A}\ ^2A_2\ \nu_1\nu_2\nu_3$) → Cl($^2P_J$) + O_2. *J. Phys. Chem. A* **1998**, *102*, 7680-7685, doi:10.1021/jp972111z.
DeMore, W. B.; Tschuikow-Roux, E. Ultraviolet spectrum and chemical reactivity of the ClO dimer. *J. Phys. Chem.* **1990**, *94*, 5856-5860, doi:10.1021/j100378a046.
Doucet, J.; Sauvageau, P.; Sandorfy, C. Vacuum ultraviolet and photoelectron spectra of fluoro-chloro derivatives of methane. *J. Chem. Phys.* **1973**, *58*, 3708-3716, doi:10.1063/1.1679722.
Doucet, J.; Sauvageau, P.; Sandorfy, C. Photoelectron and far-ultraviolet absorption spectra of chlorofluoro derivatives of ethane. *J. Chem. Phys.* **1975**, *62*, 355-359, doi:10.1063/1.430493.
Eden, S.; Barc, B.; Mason, N. J.; Hoffmann, S. V.; Nunes, Y.; Limão-Vieira, P. Electronic state spectroscopy of C_2Cl_4. *Chem. Phys.* **2009**, *365*, 150-157, doi:10.1016/j.chemphys.2009.10.010.
Eden, S.; Limão-Vieira, P.; Hoffmann, S. V.; Mason, N. J. VUV spectroscopy of CH_3Cl and CH_3I. *Chem. Phys.* **2006**, *331*, 232-244, doi:10.1016/j.chemphys.2006.10.021.
Fahr, A.; Braun, W.; Kurylo, M. J. Scattered light and accuracy of the cross-section measurements of weak absorptions: Gas and liquid phase UV absorption cross sections of CH_3CFCl_2. *J. Geophys. Res.* **1993**, *98*, 20467-20472, doi:10.1029/93JD01086.
Feierabend, K. J.; Papanastasiou, D. K.; Burkholder, J. B. ClO radical yields in the reaction of O(^{1}D) with Cl_2, HCl, chloromethanes and chlorofluoromethanes. *J. Phys. Chem. A* **2010**, *114*, 12052-12061, doi:10.1021/jp10776lt.
Felder, P.; Morley, G. P. Photodissociation of ClNO in the A band. *Chem. Phys.* **1994**, *185*, 145-151, doi:10.1016/0301-0104(94)00120-0.
Felps, W. S.; Rupnik, K.; McGlynn, S. P. Electronic spectroscopy of the cyanogen halides. *J. Phys. Chem.* **1991**, *95*, 639-656, doi:10.1021/j100155a028.
Fergusson, W. C.; Slotin, L.; Style, D. W. G. The absorption spectrum of aqueous chlorine and hydrogen peroxide vapour. *Trans. Far. Soc.* **1936**, *32*, 956-962, doi:10.1039/tf9363200956.
Finkelnburg, W.; Schumacher, H.-J.; Stieger, G. Das spektrum und der photochemische zerfall des chlormonoxyds. *Z. Phys. Chem.* **1931**, *B15*, 127-156, doi.org/10.1515/zpch-1932-1515.
Flesch, R.; Rühl, E.; Hottmann, K.; Baumgärtel, H. Photoabsorption and photoionization of chlorine dioxide. *J. Phys. Chem.* **1993**, *97*, 837-844, doi:10.1021/j100106a007.
Frost, G. J.; Goss, L. M.; Vaida, V. Measurements of high-resolution ultraviolet-visible absorption cross sections at stratospheric temperatures, 2. Chlorine dioxide. *J. Geophys. Res.* **1996**, *101*, 3879-3884, doi:10.1029/95JD03389.
Fujiwara, H.; Ishiwata, T. Doppler spectroscopy of OH fragments from the photodissociation of HOCl at 266 and 355 nm. *J. Phys. Chem.* **1998**, *102*, 3856-3859, doi:10.1021/jp980647u.
Furlan, A.; Haeberli, M. A.; Huber, R. J. The 248 nm photodissociation of $ClNO_2$ studied by photofragment translational energy spectroscopy. *J. Phys. Chem. A* **2000**, *104*, 10392-10397, doi:10.1021/jp000792j.

Ganske, J. A.; Berko, H. N.; Finlayson-Pitts, B. J. Absorption cross sections for gaseous $ClNO_2$ and Cl_2 at 298 K: Potential organic oxidant source in the marine troposphere. *J. Geophys. Res.* **1992**, *97*, 7651-7656, doi:10.1029/92JD00414.

Gedanken, A.; Rowe, M. D. Magnetic circular dichroism spectra of the methyl halides. Resolution of the n → σ* continuum. *Chem. Phys. Lett.* **1975**, *34*, 39-43, doi:10.1016/0009-2614(75)80196-5.

Ghosh, B.; Papanastasiou, D. K.; Talukdar, R. K.; Roberts, J. M.; Burkholder, J. B. Nitryl chloride ($ClNO_2$): UV/Vis absorption spectrum between 210 and 296 K and $O(^3P)$ quantum yield at 193 and 248 nm. *J. Phys. Chem. A* **2011**, *116*, 5796-5805, doi:10.1021/jp207389y.

Gibson, G. E.; Bayliss, N. S. Variation with temperature of the continuous absorption spectrum of diatomic molecules: Part I. Experimental,* The absorption spectrum of chlorine. *Phys. Rev.* **1933**, *44*, 188-192, doi:10.1103/PhysRev.44.188.

Gilbert, R.; Sauvageau, P.; Sandorfy, C. Vacuum ultraviolet absorption spectra of chlorofluoromethanes from 120 to 65 nm. *J. Chem. Phys.* **1974**, *60*, 4820-4824, doi:10.1063/1.1680987.

Gillotay, D.; Simon, P. C. Ultraviolet absorption cross-sections of photoactive species of stratospheric interest Part 1: The halocarbons. *Aeronomica Acta A* **1990**, *356*, 1-173, doi:10.18758/A_356.

Gillotay, D.; Simon, P. C. Temperature-dependence of ultraviolet absorption cross-sections of alternative chlorofluoroethanes. *J. Atmos. Chem.* **1991**, *12*, 269-285, doi:10.1007/BF00048076.

Gillotay, D.; Simon, P. C. Temperature-dependence of ultraviolet absorption cross-sections of alternative chlorofluoroethanes: 2. The 2-chloro-l,1,1,2-tetrafluoro ethane - HCFC-124. *J. Atmos. Chem.* **1991**, *13*, 289-299, doi:10.1007/BF00058136.

Gillotay, D.; Simon, P. C.; Dierickx, L. Ultraviolet absorption cross-sections of some carbonyl compounds and their temperature dependence. *Aeronomica Acta* **1993**, *368*, 1-15, doi:10.18758/A_368.

Glicker, S.; Okabe, H. Photochemistry of diacetylene. *J. Phys. Chem.* **1987**, *91*, 437-440, doi:10.1021/j100286a036.

Goldfarb, L.; Schmoltner, A.-M.; Gilles, M. K.; Burkholder, J.; Ravishankara, A. R. Photodissociation of $ClONO_2$: 1. Atomic resonance fluorescence measurements of product quantum yields. *J. Phys. Chem. A* **1997**, *101*, 6658-6666, doi:10.1021/jp970818f.

Goodeve, C. F.; Richardson, F. D. The absorption spectrum of chlorine trioxide and chlorine hexoxide. *Trans. Faraday. Soc.* **1937**, *33*, 453-457, doi:10.1039/tf9373300453.

Goodeve, C. F.; Wallace, J. I. The absorption spectrum of chlorine monoxide. *Trans. Faraday Soc.* **1930**, *26*, 254-260, doi:10.1039/tf9302600254.

Goodeve, C. F.; Windsor, B. A. M. The absorption spectrum of chlorine heptoxide. *Trans. Faraday Soc.* **1936**, *32*, 1518-1519, doi:10.1039/tf9363201518.

Gordus, A. A.; Bernstein, R. B. Isotope effect in continuous ultraviolet absorption spectra: Methyl bromide-d_3 and chloroform-*d*. *J. Chem. Phys.* **1954**, *22*, 790-795, doi:10.1063/1.1740194.

Green, R. G.; Wayne, R. P. Vacuum ultra-violet absorption spectra of halogenated methanes and ethanes. *J. Photochem.* **1976/77**, *6*, 375-377, doi:10.1016/0047-2670(76)85077-0.

Green, T. J.; Islam, M.; Canosa-Mas, C.; Marston, G.; Wayne, R. P. Higher oxides of chlorine: absorption cross-sections of Cl_2O_6 and Cl_2O_4, the decomposition of Cl_2O_6, and the reactions of OClO with O and O_3. *J. Photochem. Photobiol. A: Chem.* **2004**, *162*, 353-370, doi:10.1016/S1010-6030(03)00379-4.

Green, T. J.; Islam, M.; Guest, P.; Hickson, K.; Canosa-Mas, C. E.; Wayne, R. P. A discharge-flow study of Cl_2O_3. *Phys. Chem. Chem. Phys.* **2003**, *5*, 5409-5418, doi:10.1039/b311005b.

Green, R. G.; Wayne, R. P. Vacuum ultra-violet absorption spectra of halogenated methanes and ethanes. *J. Photochem.* **1976/77**, *6*, 375-377, doi:10.1016/0047-2670(76)85077-0.

Grothe, H.; Willner, H. Chlortrioxid: spektroskopische eigenschaften, molekülstruktur und photochemisches verhalten. *Angew. Chem.* **1994**, *106*, 1581-1584, doi:10.1002/anie.199414821

Grothe, H.; Willner, H., personal communication to Wayne et al. (1995).

Hanf, A.; Laüter, A.; Volpp, H.-R. Absolute chlorine atom quantum yield measurements in the UV and VUV gas-phase laser photolysis of CCl_4. *Chem. Phys. Lett.* **2003**, *368*, 445-451, doi:10.1016/S0009-2614(02)01896-1.

Harwood, M. H.; Rowley, D. M.; Freshwater, R. A.; Cox, R. A.; Jones, R. L. A spectroscopic study of Cl_2O_3. *J. Chem. Soc. Faraday Trans.* **1995**, *91*, 3027-3032, doi:10.1039/ft9959103027.

Hayman, G. D.; Cox, R. A. UV absorption spectrum and thermochemistry of Cl_2O_3 formed in the photolysis of OClO-containing mixtures at low temperatures. *Chem. Phys. Lett.* **1989**, *155*, 1-7, doi:10.1016/S0009-2614(89)87350-6.

Heicklen, J. The photolysis of phosgene-ethylene mixtures. *J. Am. Chem. Soc.* **1965**, *87*, 445-453, doi:10.1021/ja01081a010.

Hermann, M.; Nölle, A.; Heydtmann, H. Photolysis and quantum yield of carbonylchlorofluoride at 193 nm. *Chem. Phys. Lett.* **1994**, *226*, 559-562, doi:10.1016/0009-2614(94)00782-9.

Herzberg, G.; Scheibe, G. Über die Absorptionsspektra der dampfförmigen Methylhalogenide und einiger anderer Methylverbindungen im Ultraviolett und im Schumann-Gebiet. *Z. Physik. Chem. [Leipzig]* **1930**, *B7*, 390-406

Ho, G. H. Absolute photabsorption cross section of CCl_4 in the energy range 6-250 eV. *Chem. Phys.* **1998**, *226*, 101-111, doi:10.1016/S0301-0104(97)00259-0.

Huang, W.-T.; Chen, A. F.; Chen, I.-C.; Tsai, C.-H.; Lin, J. J.-M. Photodissociation dynamics of ClOOCl at 248.4 and 308.4 nm. *Phys. Chem. Chem. Phys.* **2011**, 8195-8203, doi:10.1039/c0cp02453h.

Hubinger, S.; Nee, J. B. Photoabsorption spectrum for OClO between 125 and 470 nm. *Chem. Phys.* **1994**, *181*, 247-257, doi:10.1016/0301-0104(94)85027-5.

Hubinger, S.; Nee, J. B. Absorption spectra of Cl_2, Br_2 and BrCl between 190 and 600 nm. *J. Photochem. Photobiol. A: Chem.* **1995**, *86*, 1-7, doi:10.1016/1010-6030(94)03949-U.

Hubrich, C.; Stuhl, F. The ultraviolet absorption of some halogenated methanes and ethanes of atmospheric interest. *J. Photochem.* **1980**, *12*, 93-107, doi:10.1016/0047-2670(80)85031-3.

Hubrich, C.; Zetzsch, C.; Stuhl, F. Absorption spectra of halogenated methanes in wavelength region from 275 to 160 nm at temperatures of 298 and 208 K. *Ber. Bunsenges. Phys. Chem.* **1977**, *81*, 437-442, doi:10.1002/bbpc.19770810417.

Huder, K. J.; DeMore, W. B. Absorption cross sections of the ClO dimer. *J. Phys. Chem.* **1995**, *99*, 3905-3908, doi:10.1021/j100012a007.

Huebner, R. H.; Bushnell, D. L., Jr.; Celotta, R. J.; Mielczarek, S. R.; Kuyatt, C. E. Ultraviolet photoabsorption by halocarbons 11 and 12 from electron impact measurements. *Nature* **1975**, *257*, 376-378, doi:10.1038/257376a0.

Ibuki, T.; Takahashi, N.; Hiraya, A.; Shobatake, K. $CCl_2(\tilde{A}\ ^1B_1)$ radical formation in VUV photolyses of CCl_4 and $CBrCl_3$. *J. Chem. Phys.* **1986**, *85*, 5717-5722, doi:10.1063/1.451532.

Ichimura, T.; Kirk, A. W.; Kramer, G.; Tschuikow-Roux, E. Photolysis of ethyl chloride (Freon 160) at 147 nm. *J. Photochem.* **1976/1977**, *6*, 77-90, doi:10.1016/0047-2670(76)85050-2.

Ichimura, T.; Kirk, A. W.; Tschuikow-Roux, E. Primary processes in the 147- and 123.6-nm photolyses of 1,1,1-trifluoro-2-chloroethane. *J. Phys. Chem.* **1977**, *81*, 1153-1156, doi:10.1021/j100527a006.

Illies, A. J.; Takacs, G. A. Gas phase ultra-violet photoabsorption cross-sections for nitrosyl chloride and nitryl chloride. *J. Photochem.* **1976**, *6*, 35-42, doi:10.1016/0047-2670(76)87005-0.

Inn, E. C. Y. Absorption coefficient of HCl in the region 1400 to 2200 Å. *J. Atmos. Sci.* **1975**, *32*, 2375-2377, doi:10.1175/1520-0469(1975)032<2375:ACOHIT>2.0.CO;2.

Jacobs, J.; Kronberg, M.; Müller, H. S. P.; Willner, H. An experimental study on the photochemistry and vibrational spectroscopy of three isomers of Cl_2O_2 isolated in cryogenic matrices. *J. Am. Chem. Soc.* **1994**, *116*, 1106-1114, doi:10.1021/ja00082a038.

Jäger, M.; Heydtmann, H.; Zetzsch, C. Vacuum ultraviolet spectrum and quantum yield of the 193 nm photolysis of phosgene. *Chem. Phys. Lett.* **1996**, *263*, 817-821, doi:10.1016/S0009-2614(96)01278-X.

Jansen, M.; Schatte, G.; Tobias, K. M.; Willner, H. Properties of dichlorine hexoxide in the gas phase and in low-temperature matrices. *Inorg. Chem.* **1988**, *27*, 1703-1706, doi:10.1021/ic00283a009.

Jensen, F.; Oddershede, J. Structure and spectra of ClO dimers. *J. Phys. Chem.* **1990**, *94*, 2235-2237, doi:10.1021/j100369a007.

Jin, B.; Chen, I.-C.; Huang, W.-T.; Lien, C.-Y.; Guchhait, N.; Lin, J. J. Photodissociation cross section of ClOOCl at 330 nm. *J. Phys. Chem. A* **2010**, *114*, 4791-4797, doi:10.1021/jp909374k.

Johnsson, K.; Engdahl, A.; Nelander, B. The UV and IR spectra of the ClClO molecule. *J. Phys. Chem.* **1995**, *99*, 3965-3968, doi:10.1021/j100012a016.

Johnston, H. S.; Morris, E. D., Jr.; Van den Bogaerde, J. Molecular modulation kinetic spectrometry. ClOO and ClO_2 radicals in the photolysis of chlorine in oxygen. *J. Am. Chem. Soc.* **1969**, *91*, 7712-7727, doi:10.1021/ja50001a036.

Jourdain, J. L.; Le Bras, G.; Poulet, G.; Combourieu, J.; Rigaud, P.; LeRoy, B. UV absorption spectrum of ClO($A\ ^2\Pi$-$X^2\Pi$) up to the (1,0) band. *Chem. Phys. Lett.* **1978**, *57*, 109-112, doi:10.1016/0009-2614(78)80361-3.

Jungkamp, T. P. W.; Kirchner, U.; Schmidt, M.; Schindler, R. N. UV absorption cross-section data for the hypochlorites ROCl (R = H, CH_3, C_2H_5, *i*-C_3H_7, *tert*-C_4H_9). *J. Photochem. Photobiol. A: Chem.* **1995**, *99*, 1-6, doi:10.1016/1010-6030(95)04074-P.

Kaledin, A. L.; Morokuma, K. An *ab initio* direct-trajectory study of the photodissociation of ClOOCl. *J. Chem. Phys.* **2000**, *113*, 5750-5762, doi:10.1063/1.1290606.

Khamaganov, V. G.; Karunanandan, R.; Horowitz, A.; Dillon, T. J.; Crowley, J. N. Photolysis of $CH_3C(O)CH_3$ at 248 and 266 nm: pressure and temperature dependent overall quantum yields. *Phys. Chem. Chem. Phys.* **2009**, *11*, 6173-6181, doi:10.1039/b904130c.

Knauth, H.-D.; Alberti, H.; Clausen, H. Equilibrium constant of the gas reaction $Cl_2O + H_2O \rightleftharpoons 2HOCl$ and the ultraviolet spectrum of HOCl. *J. Phys. Chem.* **1979**, *83*, 1604-1612, doi:10.1021/j100475a010.

Knauth, H.-D.; Schindler, R. N. On the photodecomposition of $ClONO_2$ in the middle ultraviolet. *Z. Naturforsch.* **1983**, *38a*, 893-895.

Ko, M. K. W.; Newman, P. A.; Reimann, S.; Strahan, S. E.; Plumb, R. A.; Stolarski, R. S.; Burkholder, J. B.; Mellouki, W.; Engel, A.; Atlas, E. L.; Chipperfield, M.; Liang, Q. Lifetimes of Stratospheric Ozone-Depleting Substances, Their Replacements, and Related Species, SPARC Report No. 6, WCRP-15/2013, 2013, http://www.sparc-climate.org/publications/sparc-reports/sparc-report-no6/.

Krisch, M. J.; McCunn, L. R.; Takematsu, K.; Butler, L. J.; Blase, F. R.; Shu, J. Photodissociation of CH_3OCl to CH_3O + Cl at 248 nm. *J. Phys. Chem. A* **2004**, *108*, 1650-1656, doi:10.1021/jp0372082.

Kromminga, H.; Orphal, J.; Spietz, P.; Voigt, S.; Burrows, J. P. New measurements of OClO absorption cross-sections in the 325-435 nm region and their temperature dependence between 213 and 293 K. *J. Photochem. Photobiol. A: Chem.* **2003**, *157*, 149-160, doi:10.1016/S1010-6030(03)00071-6.

Lambert, H. M.; Dagdigian, P. J.; Alexander, M. H. Spin–orbit branching in the photofragmentation of HCl at long wavelength. *J. Chem. Phys.* **1998**, *108*, 4460-4466, doi:10.1063/1.475857.

Lang, V. I.; Sander, S. P.; Friedl, R. R. Absolute infrared band strength measurement of the ClO radical by Fourier transform infrared spectroscopy. *J. Mol. Spectrosc.* **1988**, *132*, 89-103, doi:10.1016/0022-2852(88)90061-6.

Lange, E.; Jones, N. C.; Hoffmann, S. V.; Lozanoa, I.; Kumara, S.; Homem, M. G. P.; Smialek, M. A.; Duflot, D.; Brunger, M. J.; Limão-Vieira, P. The electronic excited states of dichloromethane in the 5.8-10.8 eV energy range investigated by experimental and theoretical methods. *J. Quant. Spectrosc. Radiat. Transf.* **2020**, *253*, 107172, doi:10.1016/j.jqsrt.2020.107172.

Langhoff, S. R.; Jaffe, R. L.; Arnold, J. O. Effective cross sections and rate constants for predissociation of ClO in the Earth's atmosphere. *J. Quant. Spectrosc. Radiat. Transf.* **1977**, *18*, 227-235, doi:10.1016/0022-4073(77)90008-5.

Lawrence, W. G.; Clemitshaw, K. C.; Apkarian, V. A. On the relevance of OClO photodissociation to the destruction of stratospheric ozone. *J. Geophys. Res.* **1990**, *95*, 18591-18595, doi:10.1029/JD095iD11p18591.

Lee, L. C.; Suto, M. Fluorescence yields from photodissociative excitation of chloromethanes by vacuum ultraviolet radiation. *Chem. Phys.* **1987**, *114*, 423-429 doi:10.1016/0301-0104(87)85056-5.

Libuda, H. G. Spektroskopische und kinetische Untersuchungen an halogenierten Carbonylverbindungen von atmosphärischem Interesse. PhD-Thesis, University of Wuppertal, Germany, 1992.

Libuda, H. G.; Zabel, F.; Fink, E. H.; Becker, K. H. Formyl chloride: UV absorption cross sections and rate constants for the reactions with Cl and OH. *J. Phys. Chem.* **1990**, *94*, 5860-5865, doi:10.1021/j100378a047.

Lien, C.-Y.; Lin, W.-Y.; Chen, H.-Y.; Huang, W.-T.; Jin, B.; Chen, I.-C.; Lin, J. J. Photodissociation cross sections of ClOOCl at 248.4 and 266 nm. *J. Chem. Phys.* **2009**, *131*, 174301, doi:10.1063/1.3257682.

Limão-Vieira, P.; Eden, S.; Kendall, P. A.; Mason, N. J.; Hoffmann, S. V. VUV photo-absorption cross-section for CCl_2F_2. *Chem. Phys. Lett.* **2002**, *364*, 535-541, doi:10.1016/S0009-2614(02)01304-0.

Limão-Vieira, P.; Vasekova, E.; Raja Sekhar, B. N.; Mason, N. J.; Hoffmann, S. V. VUV photoabsorption spectroscopy of vinyl chloride studied by high resolution synchrotron radiation. *Chem. Phys.* **2006**, *330*, 265-274, doi:10.1016/j.chemphys.2006.08.021.

Limão-Vieira, P.; Vasekova, E.; Sekhar, B. N. R.; Mason, N. J.; Hoffmann, S. V. VUV electronic state spectroscopy of 1,1-difluoroethene and difluorochloromethane by high resolution synchrotron radiation. *Phys. Chem. Chem. Phys.* **2006**, *8*, 4766-4772, doi:10.1039/b610978k.

Lin, C. L. Extinction coefficients of chlorine monoxide and chlorine heptoxide. *J. Chem. Eng. Data* **1976**, *21*, 411-413, doi:10.1021/je60071a030.

Lipscomb, F. J.; Norrish, R. G. W.; Thrush, B. A. The study of energy transfer by kinetic spectroscopy I. The production of vibrationally excited oxygen. *Proc. Roy. Soc. London A* **1956**, *233*, 455-464, doi:10.1098/rspa.1956.0003.

Liyanage, R.; Yang, Y.-A.; Hashimoto, S.; Gordon, R. J.; Field, R. W. Electronic control of the spin-orbit branching ratio in the photodissociation and predissociation of HCl. *J. Chem. Phys.* **1995**, *103*, 6811-6814, doi:10.1063/1.470360.

Locht, R.; Leyh, B.; Hottmann, K.; Baumgärtel, H. The photoabsorption spectrum of vinylchloride (C_2H_3Cl) in the 8-12 eV range. *Chem. Phys.* **1997**, *220*, 207-216, doi:10.1016/S0301-0104(97)00127-4.

Locht, R.; Leyh, B.; Hoxha, A.; Jochims, H. W.; Baumgärtel, H. The vacuum UV absorption spectrum of methyl chloride (CH_3Cl) and its perdeuterated isotopomer CD_3Cl. I. A Rydberg series analysis. *Chem. Phys.* **2001**, *272*, 259-275, doi:10.1016/S0301-0104(01)00464-5.

Lopez, M. I.; Sicre, J. E. Ultraviolet spectrum of chlorine perchlorate. *J. Phys. Chem.* **1988**, *92*, 563-564, doi:10.1021/j100313a062.

Lopez, M. I.; Sicre, J. E. Physicochemical properties of chlorine oxides. 1. Composition, ultraviolet spectrum, and kinetics of the thermolysis of gaseous dichlorine hexoxide. *J. Phys. Chem.* **1990**, *94*, 3860-3863, doi:10.1021/j100372a094.

Lucazeau, G.; Sandorfy, C. On the far-ultraviolet spectra of some simple aldehydes. *J. Mol. Spectrosc.* **1970**, *35*, 214-231, doi:10.1016/0022-2852(70)90199-2.

Mandelman, M.; Nicholls, R. W. The absorption cross sections and *f*-values for the v" = 0 progression of bands and associated continuum for the ClO($A^2\Pi_i \leftarrow X^2\Pi_i$) system. *J. Quant. Spectrosc. Radiat. Transf.* **1977**, *17*, 483-491, doi:10.1016/0022-4073(77)90095-4.

Margitan, J. J. Chlorine nitrate photochemistry. Photolysis products and kinetics of the reaction Cl + $ClONO_2$ → Cl_2 + NO_3. *J. Phys. Chem.* **1983**, *87*, 674-679, doi:10.1021/j100227a029.

Maric, D.; Burrows, J. P. Analysis of the UV absorption spectrum of ClO: a comparative study of four methods for spectral computations. *J. Quant. Spectrosc. Radiat. Transf.* **1999**, *62*, 345-369, doi:10.1016/S0022-4073(98)00108-3.

Maric, D.; Burrows, J. P.; Meller, R.; Moortgat, G. K. A study of the UV-visible absorption spectrum of molecular chlorine,. *J. Photochem. Photobiol. A: Chem.* **1993**, *70*, 205-214, doi:10.1016/1010-6030(93)85045-A.

Maricq, M. M., personal communication.

Marinelli, W. J.; Johnston, H. S. Quantum yield for NO_3 production from photolysis of $ClONO_2$. *Chem. Phys. Lett.* **1982**, *93*, 127-132, doi:10.1016/0009-2614(82)83678-6.

Marston, G.; Walker, I. C.; Mason, N. J.; Gingell, J. M.; Zhao, H.; Brown, K. L.; Motte-Tollet, F.; Delwiche, J.; Siggel, M. R. F. Photoabsorption and near-threshold electron energy-loss spectroscopy of OClO. *J. Phys. B: At. Mol. Phys.* **1998**, *31*, 3387-3405, doi:10.1088/0953-4075/31/15/011.

Martin, H.; Gareis, R. Die kinetik der reaktion von ClO_2 mit NO_2 in der lösungsphase. *Z. Elektrochemie* **1956**, *60*, 959-964.

Matsumi, Y.; Das, P. K.; Kawasaki, M. Doppler spectroscopy of chlorine atoms generatred from photodissociation of hydrogen chloride and methyl chloride at 157 and 193 nm. *J. Chem. Phys.* **1990**, *92*, 1696-1701, doi:10.1063/1.458051.

Matsumi, Y.; Das, P. K.; Kawasaki, M. Erratum. *J. Chem. Phys.* **1992**, *97*, 5261, doi:10.1063/1.463999.

Matsumi, Y.; Tonokura, K.; Kawasaki, M.; Ibuki, T. Photodissociation of hydrogen chloride and hydrogen bromide. *J. Chem. Phys.* **1990**, *93*, 7981-7985, doi:10.1063/1.459327.

Matus, M. H.; Nguyen, M. T.; Dixon, D. A.; Peterson, K. A.; Francisco, J. S. $ClClO_2$ is the most stable isomer of Cl_2O_2. Accurate coupled cluster energetics and electronic spectra of Cl_2O_2 isomers. *J. Phys. Chem. A* **2008**, *112*, 9623-9627, doi:10.1021/jp806220r.

Mauldin, R. L., III; Burkholder, J. B.; Ravishankara, A. R. A photochemical, thermodynamic, and kinetic study of ClOO. *J. Phys. Chem.* **1992**, *96*, 2582-2588, doi:10.1021/j100185a035.

McGillen, M. R.; Bernard, F.; Fleming, E. L.; J.B. Burkholder HCFC-133a (CF_3CH_2Cl): OH rate coefficient, UV and infrared absorption spectra, and atmospheric implications. *Geophys. Res. Lett.* **2015**, *42*, 6098-6105, doi:10.1002/2015GL064939.

McGillen, M. R.; Fleming, E. L.; Jackman, C. H.; Burkholder, J. B. $CFCl_3$ (CFC-11): UV absorption spectrum temperature dependence measurements and the impact on its atmospheric lifetime and uncertainty. *Geophys. Res. Lett.* **2013**, *40*, 50915, doi:10.1002/grl.50915.

McGrath, M. P.; Clemitshaw, K. C.; Rowland, F. S.; Hehre, W. J. Thermochemical stabilities and vibrational spectra of isomers of the chlorine oxide dimer. *Geophys. Res. Lett.* **1988**, *15*, 883-886, doi:10.1029/GL015i008p00883.

McGrath, M. P.; Clemitshaw, K. C.; Rowland, F. S.; Hehre, W. J. Structures, relative stabilities and vibrational spectra of isomers of Cl_2O_2: The role of the chlorine oxide dimer in Antarctic ozone depleting mechanisms. *J. Phys. Chem.* **1990**, *94*, 6126-6132, doi:10.1021/j100378a089.

McKeachie, J. R.; Appel, M. F.; Kirchner, U.; Schindler, R. N.; Benter, T. Observation of a heterogeneous source of OClO from the reaction of ClO radicals on ice. *J. Phys. Chem. B* **2004**, *108*, 16786-16797, doi:10.1021/jp049314p.

Meller, R.; Boglu, D.; Moortgat, G. K. "UV spectra of several halogenated carbonyl compounds and FTIR studies of the degradation of CF_3COCl, HCFC-123 and HFC-143a"; Kinetics and Mechanisms for the Reactions of Halogenated Organic Compounds in the Troposphere. STEP-HALOCSIDE/AFEAS WORKSHOP, 1991, Dublin, Ireland.

Mérienne, M. F.; Coquart, B.; Jenouvrier, A. Temperature effect on the ultraviolet-absorption of $CFCl_3$, CF_2Cl_2 and N_2O. *Planet. Space Sci.* **1990**, *38*, 617-625, doi:10.1016/0032-0633(90)90067-Z.

Minaev, B. F. The singlet-triplet absorption and photodissociation of the HOCl, HOBr, and HOI molecules calculated by the MCSCF quadratic response method. *J. Phys. Chem. A* **1999**, *103*, 7294-7309, doi:10.1021/jp990203d.

Minamikawa, T.; Sakka, T.; Ogata, Y.; Iwasaki, M. Vacuum ultraviolet spectra of $CCIF_2CH_2Cl$ and $CClF_2HCl_2$, and Rydberg assignment based on ab initio molecular orbital calculations. *Spectrochim. Acta A: Mol. Spectrosc.* **1992**, *48*, 849-859, doi:10.1016/0584-8539(92)80081-7.

Minton, T. K.; Nelson, C. M.; Moore, T. A.; Okumura, M. Direct observation of ClO from chlorine nitrate photolysis. *Science* **1992**, *258*, 1342-1345, doi:10.1126/science.258.5086.1342.

Mishalanie, E. A.; Rutkowski, J. C.; Hutte, R. S.; Birks, J. W. Ultraviolet absorption spectrum of gaseous HOCl. *J. Phys. Chem.* **1986**, *90*, 5578-5584, doi:10.1021/j100280a021.

Mo, Y.; Tonokura, K.; Matsumi, Y.; Kawasaki, M.; Sato, T.; Arikawa, T.; Reilly, P. T. A.; Xie, Y.; Yang, Y.; Huang, Y.; Gordon, R. J. Mechanism of the ultraviolet photodissociation of chloroethylenes determined from the Doppler profiles, spatial anisotropy, and power dependence of the photofragments. *J. Chem. Phys.* **1992**, *97*, 4815-4826, doi:10.1063/1.463836.

Molina, L. T.; Molina, M. J. Ultraviolet absorption spectrum of chlorine nitrite, ClONO. *Geophys. Res. Lett.* **1977**, *4*, 83-86, doi:10.1029/GL004i002p00083.

Molina, L. T.; Molina, M. J. Ultraviolet spectrum of HOCl. *J. Phys. Chem.* **1978**, *82*, 2410-2414, doi:10.1021/j100511a013.

Molina, L. T.; Molina, M. J. Chlorine nitrate ultraviolet absorption spectrum at stratospheric temperatures. *J. Photochem.* **1979**, *11*, 139-144, doi:10.1016/0047-2670(79)80047-7.

Molina, L. T.; Molina, M. J. Production of Cl_2O_2 from the self-reaction of the ClO radical. *J. Phys. Chem.* **1987**, *91*, 433-436, doi:10.1021/j100286a035.

Molina, M. J.; Colussi, A. J.; Molina, L. T.; Schindler, R. N.; Tso, T. L. Quantum yield of chlorine-atom formation in the photodissociation of chlorine peroxide (ClOOCl) at 308 nm. *Chem. Phys. Lett.* **1990**, *173*, 310-315, doi:10.1016/0009-2614(90)85275-H.

Molina, M. J.; Ishiwata, T.; Molina, L. T. Production of OH from photolysis of HOCl at 307-309 nm. *J. Phys. Chem.* **1980**, *84*, 821-826, doi:10.1021/j100445a004.

Moore, T. A.; Okumura, M.; Minton, T. K. Photodissociation of Cl_2O at 248 and 308 nm. *J. Chem. Phys.* **1997**, *107*, 3337-3338, doi:10.1063/1.474706.

Moore, T. A.; Okumura, M.; Seale, J. W.; Minton, T. K. UV photolysis of ClOOCl. *J. Phys. Chem. A* **1999**, *103*, 1691-1695, doi:10.1021/jp984410+.

Moore, T. A.; Okumura, M.; Tagawa, M.; Minton, T. K. Dissociation dynamics of $ClONO_2$ and relative Cl and ClO product yields following photoexcitation at 308 nm. *Faraday Discuss.* **1995**, *100*, 295-307, doi:10.1039/fd9950000295.

Motte-Tollet, F.; Ska, M.-P.; Marston, G. M.; Walker, I. C.; Siggel, M. R. F.; Gingell, J. M.; Kaminski, L.; Brown, K.; Mason, N. J. Absolute cross sections for the VUV optical absorption of Cl_2O in the 6.5-9.7 eV energy range. *Chem. Phys. Lett.* **1997**, *275*, 298-306, doi:10.1016/S0009-2614(97)00774-4.

Müller, H. S. P.; Willner, H. Gas phase studies on chloryl chloride, $ClClO_2$. *Ber. Bunsenges. Phys. Chem.* **1992**, *96*, 427-431, doi:10.1002/bbpc.19920960338.

Myer, J. A.; Samson, J. A. R. Vacuum-ultraviolet absorption cross sections of CO, HCl, and ICN between 1050 and 2100 Å. *J. Chem. Phys.* **1970**, *52*, 266-271, doi:10.1063/1.1672676.

Nayak, A. K.; Buckley, T. J.; Kurylo, M. J.; Fahr, A. Temperature dependence of the gas and liquid phase ultraviolet absorption cross sections of HCFC-123 (CF_3CHCl_2) and HCFC-142b (CH_3CF_2Cl). *J. Geophys. Res.* **1996**, *101*, 9055-9062, doi:10.1029/96JD00226.

Nayak, A. K.; Kurylo, M. J.; Fahr, A. UV absorption cross sections of methylchloroform: Temperature-dependent gas and liquid phase measurements. *J. Geophys. Res.* **1995**, *100*, 11185-11189, doi:10.1029/95JD00695.

Nee, J. B. Ultraviolet absorption of Cl_2O. *J. Quant. Spectrosc. Radiat. Transf.* **1991**, *46*, 55-58, doi:10.1016/0022-4073(91)90066-Y.

Nee, J. B.; Suto, M.; Lee, L. C. Quantitative photoabsorption and fluorescence study of HCl in vacuum uultraviolet. *J. Chem. Phys.* **1986**, *85*, 719-724, doi:10.1063/1.451278.

Nelson, C. M.; Moore, T. A.; Okumura, M.; Minton, T. K. Primary and secondary dissociation pathways in the ultraviolet photolysis of Cl_2O. *J. Chem. Phys.* **1994**, *100*, 8055-8064, doi:10.1063/1.466799.

Nelson, C. M.; Moore, T. A.; Okumura, M.; Minton, T. K. Photodissociation of $ClONO_2$ at 193 and 248 nm. *Chem. Phys.* **1996**, *2248*, 287-307, doi:10.1016/0301-0104(95)00383-5.

Nelson, H. H.; Johnston, H. S. Kinetics of the reaction of Cl with ClNO and $ClNO_2$ and the photochemistry of $ClNO_2$. *J. Phys. Chem.* **1981**, *85*, 3891-3896, doi:10.1021/j150625a036.

Nickolaisen, S. L.; Miller, C. E.; Sander, S. P.; Hand, M. R.; Williams, I. H.; Francisco, J. S. Pressure dependence and metastable state formation in the photolysis of dichlorine monoxide (Cl_2O). *J. Chem. Phys.* **1996**, *104*, 2857-2868, doi:10.1063/1.471109.

Nickolaisen, S. L.; Sander, S. P.; Friedl, R. R. Pressure-dependent yields and product branching ratios in the broadband photolysis of chlorine nitrate. *J. Phys. Chem.* **1996**, *100*, 10165-10178, doi:10.1021/jp953612s.

Nölle, A.; Heydtmann, H.; Meller, R.; Moortgat, G. K. Temperature dependent UV absorption spectra of carbonyl chloro-fluoride. *Geophys. Res. Lett.* **1993**, *20*, 707-710, doi:10.1029/93GL00248.
Nölle, A.; Krumscheid, C.; Heydtmann, H. Determination of quantum yields in the UV photolysis of COF_2 and COFCl. *Chem. Phys. Lett.* **1999**, *299*, 561-565, doi:10.1016/S0009-2614(98)01257-3.
Okabe, H. Photodissociation of thiophosgene. *J. Chem. Phys.* **1977**, *66*, 2058-2062, doi:10.1063/1.434166.
Okabe, H. Photochemistry of acetylene at 1470 Å. *J. Chem. Phys.* **1981**, *75*, 2772-2778, doi:10.1063/1.442348.
Okabe, H. Photochemistry of acetylene at 1849 Å. *J. Chem. Phys.* **1983**, *78*, 1312-1317, doi:10.1063/1.444868.
Okabe, H.; Laufer, A. H.; Ball, J. J. Photodissociation of $OCCl_2$ in the vacuum ultraviolet: production and electronic energy of excited Cl_2. *J. Chem. Phys.* **1971**, *55*, 373-378, doi:10.1063/1.1675531.
Olney, T. N.; Cooper, G.; Chan, W. F.; Burton, G. R.; Brion, C. E.; Tan, K. H. Absolute photoabsorption (6-350 eV) and photoionization (11-80 eV) of methyl chloride using dipole electron scattering and synchroton radiation spectroscopies. *Chem. Phys.* **1996**, *205*, 421-439, doi:10.1016/0301-0104(95)00429-7.
Orkin, V. L.; Khamaganov, V. G.; Guschin, A. G.; Huie, R. E.; Kurylo, M. J. Atmospheric fate of chlorobromomethane: Rate constant for the reaction with OH, UV spectrum, and water solubility. *J. Phys. Chem. A* **1997**, *101*, 174-178, doi:10.1021/jp962428j.
Orkin, V. L.; Khamaganov, V. G.; Kasimovskaya, E. E.; Guschin, A. G. Photochemical properties of some Cl-containing halogenated alkanes. *J. Phys. Chem. A* **2013**, *117*, 5483-5490, doi:10.1021/jp400408y.
Orlando, J. J.; Burkholder, J. B.; McKeen, S. A.; Ravishankara, A. R. Atmospheric fate of several hydrofluoroethanes and hydrochloroethanes: 2. UV absorption cross sections and atmospheric lifetimes. *J. Geophys. Res.* **1991**, *96*, 5013-5023, doi:10.1029/90JD02734.
Papadimitriou, V. C.; McGillen, M. R.; Smith, S. C.; Jubb, A. M.; Portmann, R. W.; Hall, B. D.; Fleming, E. L.; Jackman, C. H.; Burkholder, J. B. 1,2-Dichlorohexafluoro-cyclobutane (1,2-*c*-$C_4F_6Cl_2$, R-316c) a potent ozone depleting substance and greenhouse gas: Atmospheric loss processes, lifetimes, and ozone depletion and global warming potentials for the (*E*) and (*Z*) stereoisomers. *J. Phys. Chem. A* **2013**, *117*, 11049-11065, doi:10.1021/jp407823k.
Papanastasiou, D. K.; Feierabend, K. J.; Burkholder, J. B. Cl_2O photochemistry: Ultraviolet/vis absorption spectrum temperature dependence and $O(^3P)$ quantum yield at 193 and 248 nm. *J. Chem. Phys.* **2011**, *134*, 204310, doi:10.1063/1.3592662.
Papanastasiou, D. K.; Papadimitriou, V. C.; Fahey, D. W.; Burkholder, J. B. UV absorption spectrum of the ClO dimer (Cl_2O_2) between 200 and 420 nm. *J. Phys. Chem. A* **2009**, *113*, 13711-13726, doi:10.1021/jp9065345.
Park, J.; Lee, Y.; Flynn, G. W. Tunable diode laser probe of chlorine atoms produced from the photodissociation of a number of molecular precursors. *Chem. Phys. Lett.* **1991**, *186*, 441-449, doi:10.1016/0009-2614(91)90206-O.
Permien, T.; Vogt, R.; Schindler, R. N. Mechanisms of gas phase-liquid phase chemical transformations. In *Air Pollution Report #17*; Cox, R. A., Ed.; Environmental Research Program of the CEC: Brussels, 1988.
Peterson, K. A.; Francisco, J. S. Does chlorine peroxide absorb below 250 nm? *J. Chem. Phys.* **2004**, *121*, 2611-2616, doi:10.1063/1.1766012.
Plenge, J.; Flesch, R.; Kühl, S.; Vogel, B.; Müller, R.; Stroh, F.; Rühl, E. Ultraviolet photolysis of the ClO dimer. *J. Phys. Chem. A* **2004**, *108*, 4859-4863, doi:10.1021/jp049690+.
Pope, F. D.; Hansen, J. C.; Bayes, K. D.; Friedl, R. R.; Sander, S. P. Ultraviolet absorption spectrum of chlorine peroxide, ClOOCl. *J. Phys. Chem. A* **2007**, *111*, 4322-4332, doi:10.1021/jp067660w.
Prahlad, V.; Kumar, V. Temperature dependence of photoabsorption cross sections of carbon tetrachloride at 186-240 nm. *J. Quant. Spectrosc. Radiat. Transf.* **1995**, *54*, 945-955, doi:10.1016/0022-4073(95)00128-8.
Rattigan, O. V.; Wild, O.; Cox, R. A. UV absorption cross-sections and atmospheric photolysis lifetimes of halogenated aldehydes. *J. Photochem. Photobiol. A: Chem.* **1998**, *112*, 1-7, doi:10.1016/S1010-6030(97)00250-5.
Rattigan, O. V.; Wild, O.; Jones, R. L.; Cox, R. A. Temperature-dependent absorption cross-sections of CF_3COCl, CF_3COF, CH_3COF, CCl_3CHO and CF_3COOH. *J. Photochem. Photobiol. A: Chem.* **1993**, *73*, 1-9, doi:10.1016/1010-6030(93)80026-6.
Ravishankara, A. R. *Faraday Discuss.* **1995**, *100*, 335-336, doi:10.1039/fd9950000333.
Ravishankara, A. R.; Solomon, S.; Turnipseed, A. A.; Warren, R. F. Atmospheric lifetimes of long-lived halogenated species. *Science* **1993**, *259*, 194-199, doi:10.1126/science.259.5092.194.
Raymonda, J. W.; Edwards, L. O.; Russell, B. R. Vacuum ultraviolet absorption spectra of some chloroalkanes. *J. Am. Chem. Soc.* **1974**, *96*, 1708-1712, doi:10.1021/ja00813a011.
Rebbert, R. E.; Ausloos, P. Gas-phase photodecomposition of carbon tetrachloride. *J. Photochem.* **1976/1977**, *6*, 265-276, doi:10.1016/0047-2670(76)85084-8.
Rebbert, R. E.; Ausloos, P. J. Photodecomposition of $CFCl_3$ and CF_2Cl_2. *J. Photochem.* **1975**, *4*, 419-434, doi:10.1016/0047-2670(75)85023-4.

Rebbert, R. E.; Lias, S. G.; Ausloos, P. The gas phase photolysis of $CHFCl_2$. *J. Photochem.* **1978**, *8*, 17-27, doi:10.1016/0047-2670(78)80003-3.
Regan, P. M.; Ascenzi, D.; Brown, A.; Balint-Kurti, G. G.; Orr-Ewing, A. J. Ultraviolet photodissociation of HCl in selected rovibrational states: Experiment and theory. *J. Chem. Phys.* **2000**, *112*, 10259-10268, doi:10.1063/1.481707.
Regan, P. M.; Langford, S. R.; Ascenzi, D.; Cook, P. A.; Orr-Ewing, A. J.; Ashfold, M. N. R. Spin–orbit branching in $Cl(^2P)$ atoms produced by ultraviolet photodissociation of HCl. *Phys. Chem. Chem. Phys.* **1999**, *1*, 3247-3251, doi:10.1039/a903331i.
Rigaud, P.; Leroy, B.; Le Bras, G.; Poulet, G.; Jourdain, J. L.; Combourieu, J. About the identication of some UV atmospheric absorptions: Laboratory study of ClO. *Chem. Phys. Lett.* **1977**, *46*, 161-163, doi:10.1016/0009-2614(77)85186-5.
Robbins, D. E. JPL Publication 77-12, International Conference on Problems Related to the Stratosphere. **1976**, 255-257.
Robbins, D. E. Photodissociation of methyl chloride and methyl bromide in the atmosphere. *Geophys. Res. Lett.* **1976**, *3*, 213-216, doi:10.1029/GL003i004p00213.
Robbins, D. E.; Stolarski, R. S. Comparison of stratospheric ozone destruction by fluorocarbons 11, 12, 21, and 22. *Geophys. Res. Lett.* **1976**, *3*, 603-606, doi:10.1029/GL003i010p00603.
Roehl, C. M.; Orlando, J. J.; Calvert, J. G. The temperature dependence of the UV-visible absorption cross-sections of NOCl,. *J. Photochem. Photobiol. A: Chem.* **1992**, *69*, 1-5, doi:10.1016/1010-6030(92)85253-Q.
Romand, J. Absorption ultraviolette dans la région de Schumann étude de: ClH, BrH et IH gazeux. *Ann. Phys. (Paris)* **1949**, *4*, 529-590, doi:10.1051/anphys/194912040529.
Romand, J.; Vodar, B. Spectre d'absorption de l'acide chlorhydrique gaseux dans la région de Schumann. *Compt. Rend. Acad. Sci. Paris* **1948**, *226*, 238-240.
Rontu Carlon, N.; Papanastasiou, D. K.; Fleming, E. L.; Jackman, C. H.; Newman, P. A.; Burkholder, J. B. UV absorption cross sections of nitrous oxide (N_2O) and carbon tetrachloride (CCl_4) between 210 and 350 K and the atmospheric implications. *Atmos. Chem. Phys.* **2010**, *10*, 6137-6149, doi:10.5194/acp-10-6137-2010.
Rowland, F. S.; Molina, M. J. Chlorofluoromethanes in the environment. *Rev. Geophys. Space Phys.* **1975**, *13*, 1-35, doi:10.1029/RG013i001p00001.
Rowland, F. S.; Spencer, J. E.; Molina, M. J. Stratospheric formation and photolysis of chlorine nitrate. *J. Phys. Chem.* **1976**, *80*, 2711-2713, doi:10.1021/j100565a019.
Roxlo, C.; Mandl, A. Vacuum ultraviolet absorption cross sections for halogen containing molecules. *J. Appl. Phys.* **1980**, *51*, 2969-2972, doi:10.1063/1.328108.
Rühl, E.; Jefferson, A.; Vaida, V. Photodissociation of OCIO: REMPI study of primary photofragments. *J. Phys. Chem.* **1990**, *94*, 2990-2994, doi:10.1021/j100370a047.
Russell, B. R.; Edwards, L. O.; Raymonda, J. W. Vacuum ultraviolet absorption spectra of the chloromethanes. *J. Am. Chem. Soc.* **1973**, *95*, 2129-2133, doi:10.1021/ja00788a008.
Salomon, D.; Kirk, A. W.; Tschuikow-Roux, E. Primary processes in the photochemical decomposition of 1,1,1-trichloroethane at 147 nm. *J. Photochem.* **1977**, *7*, 345-353, doi:10.1016/0047-2670(77)80016-6.
Sander, S. P.; Finlayson-Pitts, B. J.; Friedl, R. R.; Golden, D. M.; Huie, R. E.; Keller-Rudek, H.; Kolb, C. E.; Kurylo, M. J.; Molina, M. J.; Moortgat, G. K.; Orkin, V. L.; Ravishankara, A. R.; Wine, P. H. Chemical Kinetics and Photochemical Data for Use in Atmospheric Studies, Evaluation Number 15, Jet Propulsion Laboratory Pasadena, JPL Publication 06-2, 2006, http://jpldataeval.jpl.nasa.gov.
Sander, S. P.; Friedl, R. R. Kinetics and product studies of the reaction ClO + BrO using flash photolysis-ultraviolet absorption. *J. Phys. Chem.* **1989**, *93*, 4764-4771, doi:10.1021/j100349a017.
Schindler, R. N.; Liesner, M.; Schmidt, S.; Kirchner, U.; Benter, T. Identification of nascent products formed in the laser photolysis of CH_3OCl and HOCl at 308 nm and around 235 nm. Total Cl-atom quantum yields and the state and velocity distributions of $Cl(^2P_j)$. *J. Photochem. Photobiol. A: Chem.* **1997**, *107*, 9-19, doi:10.1016/S1010-6030(96)04583-2.
Schmidt, S.; Benter, T.; Schindler, R. N. Photodissociation dynamics of ClO radicals in the range ($237 \leq \lambda \leq 270$) nm and at 205 nm and the velocity distribution of $O(^1D)$ atoms. *Chem. Phys. Lett.* **1998**, *282*, 292-298, doi:10.1016/S0009-2614(97)01302-X.
Seccombe, D. P.; Chim, R. Y. L.; Tuckett, R. P.; Jochims, H. W.; Baumgärtel, H. Vacuum–ultraviolet absorption and fluorescence spectroscopy of CF_2H_2, CF_2Cl_2, and CF_2Br_2 in the range 8–22 eV. *J. Chem. Phys.* **2001**, *114*, 4058-4073, doi:10.1063/1.1344888.
Seccombe, D. P.; Tuckett, R. P.; Baumgärtel, H.; Jochims, H. W. Vacuum-UV fluorescence spectroscopy of CCl_3F, CCl_3H and CCl_3Br in the range 8–30 eV. *Phys. Chem. Chem. Phys.* **1999**, *1*, 773-782, doi:10.1039/a809422e.
Seery, D. J.; Britton, D. The continuous absorption spectra of chlorine, bromine, bromine chloride, iodine chloride, and iodine bromide. *J. Phys. Chem.* **1964**, *68*, 2263-2266, doi:10.1021/j100790a039.

Shold, D. M.; Rebbert, R. E. The photochemistry of methyl chloride. *J. Photochem.* **1978**, *9*, 499-517, doi:10.1016/0047-2670(78)80166-X.
Simon, F. G.; Schneider, W.; Moortgat, G. K.; Burrows, J. P. A study of the ClO absorption cross-section between 240 and 310 nm and the kinetics of the self-reaction at 300 K. *J. Photochem. Photobiol. A: Chem.* **1990**, *55*, 1-23, doi:10.1016/1010-6030(90)80014-O.
Simon, P. C.; Gillotay, D.; Vanlaethem-Meurée, N.; Wisemberg, J. Temperature dependence of ultraviolet absorption cross-sections of chlorofluoroethanes. *Ann. Geophys.* **1988**, *6*, 239-248.
Simon, P. C.; Gillotay, D.; Vanlaethem-Meurée, N.; Wisemberg, J. Ultraviolet absorption cross-sections of chloro and chlorofluoro-methanes at stratospheric temperatures. *J. Atmos. Chem.* **1988**, *7*, 107-135, doi:10.1007/BF00048042.
Skorokhodov, V.; Sato, Y.; Suto, K.; Matsumi, Y.; Kawasaki, M. Photofragmentation of ClNO in the A-band: Velocity distribution and fine-structure branching ratio of Cl(^2P_j) atoms. *J. Phys. Chem.* **1996**, *100*, 12321-12328, doi:10.1021/jp9535708.
Smith, G. D.; Tablas, F. M. G.; Molina, L. T.; Molina, M. J. Measurement of relative product yields from the photolysis of dichlorine monoxide (Cl_2O). *J. Phys. Chem. A* **2001**, *105*, 8658-8664, doi:10.1021/jp0100957.
Smith, W. S.; Chou, C. C.; Rowland, F. S. The mechanism for ultraviolet photolysis of gaseous chlorine nitrate at 302.5 nm. *Geophys. Res. Lett.* **1977**, *4*, 517-519, doi:10.1029/GL004i011p00517.
Sood, S. P.; Watanabe, K. Absorption and ionization coefficients of vinyl chloride. *J. Chem. Phys.* **1966**, *45*, 2913-2915, doi:10.1063/1.1728045.
Stanton, J. F.; Rittby, C. M. L.; Bartlett, R. J.; Toohey, D. W. Low-lying isomers of the chlorine oxide dimer: A theoretical study. *J. Phys. Chem.* **1991**, *95*, 2107-2110, doi:10.1021/j100159a004.
Talukdar, R.; Mellouki, A.; Gierczak, T.; Burkholder, J. B.; McKeen, S. A.; Ravishankara, A. R. Atmospheric fate of CF_2H_2, CH_3CF_3, CHF_2CF_3, and CH_3CFCl_2: Rate coefficients for reactions with OH and UV absorption cross sections of CH_3CFCl_2. *J. Phys. Chem.* **1991**, *95*, 5815-5821, doi:10.1021/j100168a021.
Talukdar, R. K.; Mellouki, A.; Burkholder, J. B.; Gilles, M. K.; Le Bras, G.; Ravishankara, A. R. Quantification of the tropospheric removal of chloral (CCl_3CHO): Rate coefficients for the reaction with OH, UV absorption cross sections, and quantum yields. *J. Phys. Chem. A* **2001**, *105*, 5188-5196, doi:10.1021/jp004632j.
Tanaka, Y.; Kawasaki, M.; Matsumi, Y.; Fujiwara, H.; Ishiwata, T.; Rogers, L. J.; Dixon, R. N.; Ashfold, M. N. R. The ultraviolet photodissociation of Cl_2O at 235 nm and of HOCl at 235 and 266 nm. *J. Chem. Phys.* **1998**, *109*, 1315-1325, doi:10.1063/1.476682.
Tellinghuisen, J. Precise equilibrium constants from spectrophotometric data: BrCl in Br_2/Cl_2. *J. Phys. Chem. A* **2003**, *107*, 753-757, doi:10.1021/jp027227w.
Toniolo, A.; Granucci, G.; Inglese, S.; Persico, M. Theoretical study of the photodissociation dynamics of ClOOCl. *Phys. Chem. Chem. Phys.* **2001**, *3*, 4266-4279, doi:10.1039/b104044h.
Toniolo, A.; Persico, M.; Pitea, D. Theoretical photoabsorption spectra of ClOOCl and Cl_2O. *J. Phys. Chem. A* **2000**, *104*, 7278-7283, doi:10.1021/jp001142i.
Tonokura, K.; Matsumi, Y.; Kawasaki, M.; Tasaki, S.; Bersohn, R. Photodissociation of hydrogen chloride at 157 and 193 nm: Angular distributions of hydrogen atoms and fine-structure branching ratios of chlorine atoms in the ^2P_j levels. *J. Chem. Phys.* **1992**, *97*, 8210-8215, doi:10.1063/1.463443.
Totterdill, A.; Kovács, T.; Martín, J. C. G.; Feng, W.; Plane, J. M. C. Mesospheric removal of very long-lived greenhouse gases SF_6 and CFC-115 by metal reactions, Lyman-α photolysis, and electron attachment. *J. Phys. Chem. A* **2015**, *119*, 2016-2025, doi:10.1021/jp5123344.
Trolier, M.; Mauldin, R. L., III; Ravishankara, A. R. Rate coefficient for the termolecular channel of the self-reaction of ClO. *J. Phys. Chem.* **1990**, *94*, 4896-4907, doi:10.1021/j100375a027.
Truch, D. T.; D.R. Salomon; Armstrong, D. A. Rydberg spectroscopy of methyl chloride. *J. Mol. Spectrosc.* **1979**, *78*, 31-39, doi:10.1016/0022-2852(79)90033-X.
Tsubomura, H.; Kimura, K.; Kaya, K.; Tanaka, J.; Nagakura, S. Vacuum ultraviolet absorption spectra of saturated organic compounds with non-bonding electrons. *Bull. Chem. Soc. Japan* **1964**, *37*, 417-423, doi:10.1246/bcsj.37.417.
Tyndall, G. S.; Kegley-Owen, C. S.; Orlando, J. J.; Calvert, J. G. Quantum yields for Cl($^2P_{3/2,1/2}$), ClO and O(^3P) in the photolysis of chlorine nitrate at 308 nm. *J. Chem. Soc. Faraday Trans.* **1997**, *93*, 2675-2682, doi:10.1039/a701585b.
Tyndall, G. S.; Stedman, K. M.; Schneider, W.; Burrows, J. P.; Moortgat, G. K. The absorption spectrum of ClNO between 190 and 350 nm. *J. Photochem.* **1987**, *36*, 133-139, doi:10.1016/0047-2670(87)87070-3.
Vaida, V.; Solomon, S.; Richard, E. C.; Rühl, E.; Jefferson, A. Photoisomerization of OClO: a possible mechanism for polar ozone depletion. *Nature* **1989**, *342*, 405-408, doi:10.1038/342405a0.

Vanlaethem-Meurée, N.; Wisemberg, J.; Simon, P. C. Absorption des chlorométhanes dans l'ultraviolet: mesures des sections efficaces d'absorption en fonction de la température. *Bull. Acad. Roy. Belgique Cl. Sci.* **1978**, *64*, 31-41, doi:10.3406/barb.1978.58340.

Vanlaethem-Meurée, N.; Wisemberg, J.; Simon, P. C. Influence de la température sur les sections efficases d'absorption des chlorofluorométhanes dans l'ultraviolet. *Bull. Acad. Roy. Belgique Cl. Sci.* **1978**, *64*, 42-51.

Vanlaethem-Meurée, N.; Wisemberg, J.; Simon, P. C. Ultraviolet absorption spectrum of methylchloroform in the vapor phase. *Geophys. Res. Lett.* **1979**, *6*, 451-454, doi:10.1029/GL006i006p00451.

Vatsa, R. K.; Volpp, H.-R. Absorption cross-sections for some atmospherically important molecules at the H atom Lyman-α wavelength (121.567 nm). *Chem. Phys. Lett.* **2001**, *340*, 289-295, doi:10.1016/S0009-2614(01)00373-6.

Villenave, E.; Morozov, I.; Lesclaux, R. Kinetics of the self-reactions of peroxy radicals arising from chlorine-initiated oxidation of chloroethenes. *J. Phys. Chem. A* **2000**, *104*, 9933-9940, doi:10.1021/jp001704y.

Vogt, R.; Schindler, R. N. Air Pollution Report 34, 1990; pp 167-171.

Vogt, R.; Schindler, R. N. Product channels in the photolysis of HOCl. *J. Photochem. Photobiol. A: Chem.* **1992**, *66*, 133-140, doi:10.1016/1010-6030(92)85207-B.

von Hobe, M.; Stroh, F.; Beckers, H.; Benter, T.; Willner, H. The UV/Vis absorption spectrum of matrix-isolated dichlorine peroxide, ClOOCl. *Phys. Chem. Chem. Phys.* **2009**, *11*, 1571-1580, doi:10.1039/b814373k.

Wahner, A.; Tyndall, G. S.; Ravishankara, A. R. Absorption cross sections for OClO as a function of temperature in the wavelength range 240-480 nm. *J. Phys. Chem.* **1987**, *91*, 2734-2738, doi:10.1021/j100295a018.

Watson, R. T. Rate constants for reactions of ClO_x of atmospheric interest. *J. Phys. Chem. Ref. Data* **1977**, *6*, 871-917, doi:10.1063/1.555558.

Wayne, R. P.; Poulet, G.; Biggs, P.; Burrows, J. P.; Cox, R. A.; Crutzen, P. J.; Hayman, G. D.; Jenkin, M. E.; Le Bras, G.; Moorgat, G. K.; Platt, U.; Schindler, R. N. Halogen oxides: Radicals, sources and reservoirs in the laboratory and in the atmosphere. *Atmos. Environ.* **1995**, *29*, 2677-2881, doi:10.1016/1352-2310(95)98124-Q.

Wijnen, M. H. Photolysis of phosgene in the presence of ethylene. *J. Am. Chem. Soc.* **1961**, *83*, 3014-3017, doi:10.1021/ja01475a009.

Wilmouth, D. M.; Hanisco, T.; Stimpfle, R. M.; Anderson, J. G. Chlorine-catalyzed ozone destruction: Cl atom production from ClOOCl photolysis. *J. Phys. Chem. A* **2009**, 14099-14108, doi:10.1021/jp9053204.

Wine, P. H.; Ravishankara, A. R.; Philen, D. L.; Davis, D. D.; Watson, R. T. High resolution absorption cross sections for the $A^2\Pi$-$X^2\Pi$ system of ClO. *Chem. Phys. Lett.* **1977**, *50*, 101-106, doi:10.1016/0009-2614(77)80689-1.

Wu, C. Y. R.; Lee, L. C.; Judge, D. L. Photoabsorption cross sections of CH_3F, CHF_3, CH_3Cl, and CF_2Cl_2 from 175 to 760 Å. *J. Chem. Phys.* **1979**, *71*, 5221-5226, doi:10.1063/1.438329.

Yano, T.; Tschuikow-Roux, E. A reexamination of the photodissociation of CH_2ClCH_2Cl at 147 nm. Test for chlorine atom reactions. *J. Phys. Chem.* **1980**, *84*, 3372–3377, doi:10.1021/j100462a013.

Yokelson, R. J.; Burkholder, J.; Fox, R. W.; Ravishankara, A. R. Photodissociation of $ClONO_2$: 2. Time-resolved absorption studies of product quantum yields. *J. Phys. Chem. A* **1997**, *101*, 6667-6678, doi:10.1021/jp9708198.

Young, I. A. K.; Jones, R. L.; Pope, F. D. The UV and visible spectra of chlorine peroxide: Constraining the atmospheric photolysis rate. *Geophys. Res. Lett.* **2014**, *41*, 1781-1788, doi:10.1002/2013GL058626.

Young, I. A. K.; Murray, C.; Blaum, C. M.; Cox, R. A.; Jones, R. L.; Pope, F. D. Temperature dependent structured absorption spectra of molecular chlorine. *Phys. Chem. Chem. Phys.* **2011**, *13*, 15318-15325, doi:10.1039/c1cp21337g.

Zhang, J.; Dulligan, M.; Wittig, C. Photodissociation of HCl at 193.3 nm: Spin-orbit branching ratio. *J. Chem. Phys.* **1997**, *107*, 1403-1405, doi:10.1063/1.474494.

Zou, P.; Park, J.; Schmitz, B. A.; Nguyen, T.; North, S. W. Photodissociation of $ClONO_2$ at 235 nm: Final product yields and energy partitioning. *J. Phys. Chem. A* **2002**, *106*, 1004-1010, doi:10.1021/jp013099k.

Zou, P.; Shu, J.; North, S. W. The three-body dissociation dynamics of Cl_2O at 248 and 193 nm. *J. Photochem. and Photobiol. A: Chem.* **2010**, *209*, 56-60, doi:10.1016/j.jphotochem.2009.10.009.

SECTION 4G. BrO_X PHOTOCHEMISTRY

G1. Br_2 (molecular bromine)

Back to Index

$Br_2 + h\nu \rightarrow 2\ Br$ 193 kJ mol^{-1} 620 nm (1)

(Recommendation: 06-2, Note: 10-6, Evaluated: 10-6)

Absorption Cross Sections: The UV/vis absorption spectrum of Br_2, molecular bromine, has been extensively studied as summarized in Table 4G-1-1.

Table 4G-1-1. Summary of Br_2 Absorption Cross Section Studies

Study	Year	Temperature (K)	Wavelength Range (nm)
Ribaud[14]	1919	289, 593, 893	356–608
Gray and Style[3]	1930	294	240–579
Acton et al.[1]	1936	293, 400, 531, 657, 767, 906	327.4–571.7
Seery and Britton[16]	1964	298	320–590
MacMillan[11]	1966	298	200–599
Passchier et al.[12]	1967	298, 348, 423, 298, 573, 648, 713	200–750
Wen and Noyes[18]	1972	303	220–290
Hemenway et al.[5]	1979	296	556–616.3
Roxlo and Mandl[15]	1980	298	170–230
Maric et al.[10]	1994	298	200–650
Hubinger and Nee[6]	1995	295	190–600
Tellinghuisen[17]	2008	295	190–300

The Br_2 spectrum exhibits an absorption band between 190 and 300 nm with a maximum near 223 nm and another stronger band between 300 and 600 nm, which is composed of three overlapping bands with maxima at ~412, 480, and 549 nm. The reported absorption cross sections are in very good agreement in the region of the UV-visible absorption band. Discrepancies are observed at wavelengths >550 nm, where the data of McMillan[11] and Hemenway et al.[5] are as much as 60% and 100% lower, respectively, than the values measured in the other studies. Large discrepancies arise in the region of the absorption minimum between 230 and 340 nm due to a pressure dependent absorption component of Br_2 vapor, possibly due to a Br_2-Br_2 dimer absorption. A detailed discussion of the available absorption data for Br_2 and an evaluation is given by Maric et al.[10] Maric et al. fit the most reliable data, those of Passchier et al.[12] and Wen and Noyes,[18] to a four-band semi-logarithmic distribution function and derived the following expression for the calculation of the Br_2 absorption spectrum over the wavelength region 200–650 nm:

$$\begin{aligned}\sigma(298\ K) = {} & 1.06 \times 10^{-20} \times \exp(-52.3[\ln(223.3/\lambda)]^2) \\ & + 6.19 \times 10^{-19} \times \exp(-108.5[\ln(411.9/\lambda)]^2) \\ & + 3.39 \times 10^{-19} \times \exp(-106.8[\ln(480.2/\lambda)]^2) \\ & + 3.78 \times 10^{-20} \times \exp(-112.0[\ln(549.3/\lambda)]^2)\end{aligned}$$

where λ is the wavelength in nm (vacuum) and σ is the absorption cross section in $cm^2\ molecule^{-1}$. The recommended absorption cross sections calculated using this expression are listed in Table 4G-1-2. The results of Maric et al.[10] have been confirmed, in general, in a subsequent study by Hubinger and Nee,[6] who reported absorption cross sections for the wavelength range 190–600 nm. The Hubinger and Nee cross sections values that are below 10^{-21} $cm^2\ molecule^{-1}$, i.e., between 260 and 340 nm, differ from the parameterized data of Maric et al.[10] and should be considered as upper limits.

The temperature dependence of the absorption spectrum has been measured by Acton et al.[1] (293–906 K) and Passchier et al.[12] (298–713 K). These studies report a decrease of the cross sections around the absorption maximum, between ~380 and ~500 nm, and an increase in the short and long wavelength tails with increasing temperature.

Photolysis Quantum Yield and Product Studies: Photodissociation of Br_2 leads to the formation of Br atoms in the ground $Br(^2P_{3/2})$ and excited $Br^*(^2P_{1/2})$ states. A few studies have been performed to establish the relative quantum yields of (Br + Br) and (Br + Br*) at various photolysis wavelengths. Petersen and Smith[13] found the

yield of Br* atoms to increase from 0.4 to 0.89 from 444 to 510 nm and decrease at longer wavelengths to a value of ~0.4 at 530 nm. Lindeman and Wiesenfeld[9] observed the relative quantum yield (Br + Br*) to increase from 0.07 at 434 nm to 0.64 at 482 nm and then to decrease to 0.57 at 511 nm. Haugen et al.[4] determined the relative quantum yield (Br + Br*) to increase from 0.44 at 445 nm to 0.87 at 500 nm followed by a decrease to 0.40 at 530 nm. Cooper et al.[2] measured the relative (Br + Br*) yield to be zero in the range 360 to 430 nm and to increase at longer wavelengths to 0.79 at 580 nm; at 260 nm they observed (Br + Br*) to be dominant. Jee at al.[7,8] measured the relative yield of the photodissociation channel into (Br + Br*) at 234 nm to be unity and at 265 nm to be 0.96. Zaraga et al.[19] calculated the zero pressure predissociation quantum yield from high resolution spectroscopic studies in the banded region (B $^3\Pi(0_u^+)$ state) overlapping a continuum at 588 nm to be near unity.

Table 4G-1-2. Recommended Absorption Cross Sections of Br_2 at 298 K

λ (nm)	10^{20} σ (cm^2)	λ (nm)	10^{20} σ (cm^2)	λ (nm)	10^{20} σ (cm^2)	λ (nm)	10^{20} σ (cm^2)
200	0.562	315	0.0274	430	60.1	545	10.1
205	0.723	320	0.0626	435	57.1	550	8.68
210	0.870	325	0.141	440	54.0	555	7.47
215	0.983	330	0.300	445	51.2	560	6.43
220	1.05	335	0.602	450	48.8	565	5.54
225	1.06	340	1.14	455	46.8	570	4.77
230	1.01	345	2.05	460	45.2	575	4.09
235	0.925	350	3.49	465	44.0	580	3.50
240	0.808	355	5.63	470	42.8	585	2.98
245	0.676	360	8.66	475	41.6	590	2.52
250	0.544	365	12.7	480	40.3	595	2.11
255	0.422	370	17.8	485	38.6	600	1.76
260	0.316	375	23.9	490	36.6	605	1.45
265	0.229	380	30.7	495	34.3	610	1.19
270	0.161	385	37.9	500	31.8	615	0.958
275	0.110	390	45.1	505	29.0	620	0.767
280	0.0728	395	51.8	510	26.2	625	0.607
285	0.0472	400	57.4	515	23.4	630	0.475
290	0.0299	405	61.6	520	20.6	635	0.368
295	0.0187	410	64.2	525	18.0	640	0.282
300	0.0122	415	65.1	530	15.7	645	0.214
305	0.0100	420	64.5	535	13.6	650	0.161
310	0.0135	425	62.8	540	11.7		

Note:
Calculated using the expression given by Maric et al.[10] (see text).

(1) Acton, A. P.; Aickin, R. G.; Bayliss, N. S. The continuous absorption spectrum of bromine: A new interpretation. *J. Chem. Phys.* **1936**, *4*, 474-479, doi:10.1063/1.1749887.

(2) Cooper, M. J.; Wrede, E.; Orr-Ewing, A. J.; Ashfold, M. N. R. Ion imaging studies of the Br(^2P_J) atomic products resultings from Br_2 photolysis in the wavelength range 260-580 nm. *J. Chem. Soc. Faraday Trans.* **1998**, *94*, 2901-2907, doi:10.1039/a804112a.

(3) Gray, L. T. M.; Style, D. W. G. The absorption of light by chlorine, bromine and their gaseous mixtures. *Proc. Roy. Soc. London* **1930**, *A 126*, 603-612, doi:10.1098/rspa.1930.0029.

(4) Haugen, H. K.; Weitz, E.; Leone, S. R. Accurate quantum yields by laser gain vs absorption spectroscopy: Investigation of Br/Br* channels in photofragmentation of Br_2 and IBr. *J. Chem. Phys.* **1985**, *83*, 3402-3412, doi:10.1063/1.449145.

(5) Hemenway, C. P.; Lindeman, T. G.; Wiesenfeld, J. R. Measurement of the A $^3\Pi_{1u} \leftarrow$ X $^1\Sigma_g^+$ continuum absorptivity in Br_2. *J. Chem. Phys.* **1979**, *70*, 3560-3561, doi:10.1063/1.437896.

(6) Hubinger, S.; Nee, J. B. Absorption spectra of Cl_2, Br_2 and BrCl between 190 and 600 nm. *J. Photochem. Photobiol. A: Chem.* **1995**, *86*, 1-7, doi:10.1016/1010-6030(94)03949-U.

(7) Jee, Y.-J.; Jung, Y.-J.; Jung, K.-H. Photodissociation of Br_2 at 234 and 265 nm: Imaging studies of one and two photon excitation. *J. Chem. Phys.* **2001**, *115*, 9739-9746, doi:10.1063/1.1410977.

(8) Jee, Y.-J.; Park, M. S.; Kim, Y. S.; Jung, Y.-J.; Jung, K.-H. Photodissociation of bromine molecule near 265 nm. *Chem. Phys. Lett.* **1998**, *287*, 701-708, doi:10.1016/S0009-2614(98)00235-8.

(9) Lindeman, T. G.; Wiesenfeld, J. R. Photodissociation of Br_2 in the visible continuum. *J. Chem. Phys.* **1979**, *70*, 2882-2888, doi:10.1063/1.437824.
(10) Maric, D.; Burrows, J. P.; Moortgat, G. K. A Study of the UV-visible absorption spectra of Br_2 and BrCl. *J. Photochem. Photobiol A: Chem.* **1994**, *83*, 179-192, doi:10.1016/1010-6030(94)03823-6.
(11) McMillan, V. personal communication to J.G. Calvert, J.N. Pitts, Jr., Photochemistry, London, 1966, p. 184. **1966**.
(12) Passchier, A. A.; Christian, J. D.; Gregory, N. W. The ultraviolet-visible absorption spectrum of bromine between room temperature and 440°. *J. Phys. Chem.* **1967**, *71*, 937-942, doi:10.1021/j100863a025.
(13) Petersen, A. B.; Smith, I. W. M. Yields of $Br^*(4^2P_{1/2})$ as a function of wavelength in the photodissociation of Br_2 and IBr. *Chem. Phys.* **1978**, *30*, 407-413, doi:10.1016/0301-0104(78)87012-8.
(14) Ribaud, M. G. Contribution a l'étude de l'absorption de la lumière par les gaz. *Ann. Phys.* **1919**, *12*, 107-226.
(15) Roxlo, C.; Mandl, A. Vacuum ultraviolet absorption cross sections for halogen containing molecules. *J. Appl. Phys.* **1980**, *51*, 2969-2972, doi:10.1063/1.328108.
(16) Seery, D. J.; Britton, D. The continuous absorption spectra of chlorine, bromine, bromine chloride, iodine chloride, and iodine bromide. *J. Phys. Chem.* **1964**, *68*, 2263-2266, doi:10.1021/j100790a039.
(17) Tellinghuisen, J. Equilibrium constants from spectrophotometric data: Dimer formation in gaseous Br_2. *J. Phys. Chem. A* **2008**, *112*, 5902–5907, doi:10.1021/jp8020358.
(18) Wen, W. Y.; Noyes, R. M. Ultraviolet spectra of single and double molecules of gaseous bromine. *J. Phys. Chem.* **1972**, *76*, 1017-1018, doi:10.1021/j100651a012.
(19) Zaraga, F.; Nogar, N. S.; Moore, C. B. Transition moment, radiative lifetime, and quantum yield for dissociation of the $^3\Pi_{0^+_u}$ state of $^{81}Br_2$. *J. Mol. Spectrosc.* **1976**, *63*, 564-571, doi:10.1016/0022-2852(76)90317-9.

G2. HBr (hydrogen bromide)

Back to Index

$HBr + h\nu \rightarrow H + Br$	366 kJ mol^{-1}	327 nm	(1)

(Recommendation: 06-2, Note: 10-6, Evaluated: 10-6)

Absorption Cross Sections: The UV absorption spectrum of HBr, hydrogen bromide, at wavelengths >180 nm consists of a continuous band with a maximum near 178 nm and monotonically decreasing absorption cross sections that have been measured out to 270 nm. At shorter wavelengths the spectrum shows a large number of strong sharp bands that extend to 105 nm.

The room temperature absorption cross sections of HBr have been measured in a number of studies as outlined in Table 4G-2-1. The absorption cross sections near the maximum of the absorption band reported by Nee et al.[7] and Huebert and Martin[6] are in good agreement, 2.4×10^{-18} and 2.7×10^{-18} cm^2 molecule^{-1}, respectively. The values reported by Romand[12] and Roxlo and Mandl[13] are substantially lower, 2×10^{-18} and 1.4×10^{-18} cm^2 molecule^{-1}, respectively. The cross section at 193 nm reported by Vaghjiani[14] and Barone et al.[1] are consistent with the absorption spectra reported by Nee et al.[7] and Huebert and Martin.[6] The cross sections at 184.9 nm measured by Ravishankara et al.[10] and Barone et al.[1] fall between those reported by Nee et al.[7] and Huebert and Martin.[6] The cross section at 184.9 nm measured by Okabe[8] lies between those of Goodeve and Taylor[5] and Romand.[12] The recommended values in Table 4G-2-2 were derived as follows: the spectra of Goodeve and Taylor,[5] Romand,[12] Huebert and Martin,[6] and Nee et al.[7] have been scaled to 2.21×10^{-18} cm^2 molecule^{-1} at 184.9 nm, which is the mean of the values reported by Okabe,[8] Ravishankara et al.,[10] and Barone et al.[1]; the scaled spectra have been averaged, the recommended cross sections for the range 152–168 nm are those of Romand[12] and Nee et al.,[7] for the range 170–180 nm those of Romand,[12] Huebert and Martin,[6] and Nee et al.[7] and for the range 182–230 nm those of Goodeve and Taylor,[5] Romand,[12] Huebert and Martin,[6] and Nee et al.[7]

Table 4G-2-1. Summary of HBr UV Absorption Cross Section Studies

Study	Year	Temperature (K)	Wavelength Range (nm)
Goodeve and Taylor[5]	1935	298	182–286
Romand[12]	1949	298	139–228
Huebert and Martin[6]	1968	297	170–230
Bridges and White[3]	1973	298	214
Okabe[8]	1977	296	240–270
Ravishankara et al.[10]	1979	298	184.9
Roxlo and Mandl[13]	1980	298	170–230
Okabe[9]	1983	296	184.9
Brion et al.[4]	1985	298	30–177
Nee et al.[7]	1986	298	105–238
Vaghjiani[14]	1993	296	193
Barone et al.[1]	1994	298	184.9, 193.0

Photolysis Quantum Yield and Product Studies: The branching fraction for the formation of excited Br*($^2P_{1/2}$) atoms was determined by Regan et al.[11] in the wavelength range 201–253 nm to vary between 0.15 and 0.23. Baumfalk et al.[2] obtained a Br* branching fraction, Br*($^2P_{1/2}$)/(Total Br), of 0.20 ± 0.03 at 243 nm and 0.18 ± 0.03 at 193 nm.

Table 4G-2-2. Recommended Absorption Cross Sections of HBr at 298 K

λ (nm)	10^{20} σ (cm^2)	λ (nm)	10^{20} σ (cm^2)	λ (nm)	10^{20} σ (cm^2)	λ (nm)	10^{20} σ (cm^2)
152	139	172	233	192	181	212	54.8
154	124	174	240	194	168	214	45.7
156	138	176	244	196	154	216	38.8
158	148	178	244	198	140	218	33.0
160	161	180	242	200	125	220	28.0
162	176	182	233	202	111	222	22.9
164	189	184	225	204	98.1	224	18.2
166	201	186	217	206	85.5	226	14.4
168	211	188	206	208	74.7	228	11.7
170	225	190	194	210	64.4	230	9.32

Note:
Goodeve and Taylor,[5] Romand,[12] Huebert and Martin,[6] and Nee et al.[7] data scaled to 2.21×10^{-18} cm^2 $molecule^{-1}$ at 184.9 nm:
152–168 nm: mean of Romand[12] and Nee et al.[7] data
170–180 nm: mean of Romand,[12] Huebert and Martin,[6] and Nee et al.[7] data
182–230 nm: mean of Goodeve and Taylor,[5] Romand,[12] Huebert and Martin,[6] and Nee et al.[7] data

(1) Barone, S. B.; Turnipseed, A. A.; Gierczak, T.; Ravishankara, A. R. Quantum yields of H(^2S) and CH_3S(^2E) from the photolysis of simple organosulfur compounds at 193, 222, and 248 nm. *J. Phys. Chem.* **1994**, *98*, 11969-11977, doi:10.1021/j100097a024.

(2) Baumfalk, R.; Buck, U.; Frischkorn, C.; Nahler, N. H.; Hüwel, L. Photodissociation of HBr molecules and clusters: Anisotropy parameters, branching ratios, and kinetic energy distributions. *J. Chem. Phys.* **1999**, *111*, 2595-2605, doi:10.1063/1.479535.

(3) Bridges, L.; White, J. M. Photochemistry of methanethiol at 254 and 214 nm. *J. Phys. Chem.* **1973**, *77*, 295-298, doi:10.1021/j100621a031.

(4) Brion, C. E.; Iida, Y.; Carnovale, F.; Thomson, J. P. Absolute dipole oscillator strengths for photoabsorption, photoisonization and ionic photofragmentation processes in HBr. *Chem. Phys.* **1985**, *98*, 327-339, doi:10.1016/0301-0104(85)80144-0.

(5) Goodeve, C. F.; Taylor, A. W. C. The continuous absorption spectrum of hydrogen bromide. *Proc. Roy. Soc. London A* **1935**, *152*, 221-230, doi:10.1098/rspa.1935.0187.

(6) Huebert, B. J.; Martin, R. M. Gas-phase far-ultraviolet absorption spectrum of hydrogen bromide and hydrogen iodide. *J. Phys. Chem.* **1968**, *72*, 3046-3048, doi:10.1021/j100854a071.

(7) Nee, J. B.; Suto, M.; Lee, L. C. Quantitative spectroscopy study of HBr in the 105-235 nm region. *J. Chem. Phys.* **1986**, *85*, 4919-4924, doi:10.1063/1.451728.

(8) Okabe, H. Photodissociation of thiophosgene. *J. Chem. Phys.* **1977**, *66*, 2058-2062, doi:10.1063/1.434166.
(9) Okabe, H. Photochemistry of acetylene at 1849 Å. *J. Chem. Phys.* **1983**, *78*, 1312-1317, doi:10.1063/1.444868.
(10) Ravishankara, A. R.; Wine, P. H.; Langford, A. O. Absolute rate constant for the reaction OH + HBr → H_2O + Br. *Chem. Phys. Lett.* **1979**, *63*, 479-484, doi:10.1016/0009-2614(79)80694-6.
(11) Regan, P. M.; Langford, S. R.; Orr-Ewing, A. J.; Ashfold, M. N. R. The ultraviolet photodissociation dynamics of hydrogen bromide. *J. Chem. Phys.* **1999**, *110*, 281-288, doi:10.1063/1.478063.
(12) Romand, J. Absorption ultraviolette dans la région de Schumann étude de: ClH, BrH et IH gazeux. *Ann. Phys. (Paris)* **1949**, *4*, 529-590, doi:10.1051/anphys/194912040529.
(13) Roxlo, C.; Mandl, A. Vacuum ultraviolet absorption cross sections for halogen containing molecules. *J. Appl. Phys.* **1980**, *51*, 2969-2972, doi:10.1063/1.328108.
(14) Vaghjiani, G. CH_3SH ultraviolet absorption cross sections in the region 192.5-309.5 nm and photodecomposition at 222 and 193 nm and 296 K. *J. Chem. Phys.* **1993**, *99*, 5936-5943, doi:10.1063/1.465917.

G3. BrO (bromine monoxide radical)

Back to Index

$BrO + h\nu \rightarrow Br + O$ 238 kJ mol^{-1} 504 nm (1)

(Recommendation: 06-2, Note: 25-1, Evaluated: 10-6)

Absorption Cross Sections: The BrO (bromine monoxide) radical has a UV absorption spectrum in the 290–380 nm range, with vibrational band structure, which is attributed to the A $^2\Pi_{3/2} \leftarrow$ X $^2\Pi_{3/2}$ transition. The spectrum measured by Wilmouth et al.[12] (0.5 nm) is shown in Figure 4G-3-1 and laboratory measurements are summarized in Table 4G-3-1. The absorption spectrum has been measured and cross sections determined for several absorption peaks in the studies listed in Table 4G-3-1, e.g. for the strongest (7,0) band at 338.5 nm and the (11,0) and (12,0) bands at 320.8 nm and 317.3 nm.

Table 4G-3-1. Summary of BrO Absorption Cross Section Studies

Study	Year	Temperature (K)	Wavelength Range (nm)	Resolution (nm)
Clyne and Cruse[2]	1970	293	338.3	0.15
Basco and Dogra[1]	1971	298	320.8, 338.3	not given
Cox et al.[3]	1982	298	296–370	0.22
Wahner et al.[10]	1988	228, 243, 298	312–380	0.4
Sander and Friedl[9]	1989	220, 298	338.5	0.06–1.25
Orlando et al.[8]	1991	298	338.5	0.4
Laszlo et al.[7]	1997	295	338.5	0.6
Gilles et al.[6]	1997	204, 222, 237, 252, 273, 298, 329, 369	338.5	0.5
Wheeler et al.[11]	1998	298	338, 317	4 cm^{-1}
Wilmouth et al.[12]	1999	298	317–388	1.0 cm^{-1}
Wilmouth et al.[12]	1999	228, 298	286–386	10 cm^{-1}
Fleischmann et al.[4] and Fleischmann et al.[5]	2003 2004	203, 223, 243, 273, 298	300–385	~4 cm^{-1}

The cross sections are both temperature and resolution dependent, i.e., the peaks of the vibrational bands become greater and the bands sharper with decreasing temperature and at higher resolution. Wilmouth et al.[12] used their absorption spectrum, recorded at 10 cm^{-1} resolution, in a combined analysis of the results from Cox et al.,[3] Wahner et al.,[10] Orlando et al.,[8] Laszlo et al.,[7] and Gilles et al.[6] at a common resolution of 0.40 nm (details of this procedure are described in Wilmouth et al.[12]). The vibrational band peak absorption cross sections at 298 ± 2 and 228 ± 2 K obtained in their analysis are listed in Table 4G-3-2. Absorption cross sections of the spectrum reported by Wilmouth et al.,[12] averaged over 0.5 nm intervals are listed in Table 4G-3-3.

Absorption cross sections for the rotational peaks of the (7,0) and (12,0) bands were measured at high resolution (1.0 cm^{-1}) by Wilmouth et al.[12] to be 2.17×10^{-17} cm^2 $molecule^{-1}$ for the peak of the (7,0) band and 1.38×10^{-17} cm^2 $molecule^{-1}$ for the peak of the (12,0) band.

The (7,0) absorption maximum (338 nm) temperature dependence was measured by Gilles et al.[6] over the range 204–388 K at a resolution of 0.5 nm and given by the expression:

$$\sigma(T)_{338\ nm} = 3.29 - (5.58 \times 10^{-3}) \times T, \text{ in units of } 10^{-17} \text{ cm}^2 \text{ molecule}^{-1}$$

Photolysis Quantum Yield and Product Studies: Transitions in the A←X system are expected to be dissociative.

Table 4G-3-2. Absorption Cross Sections at the Vibrational Band Peaks in the A←X Spectrum of BrO (0.4 nm resolution)

v′, v″	λ (nm)	10^{20} σ (cm^2 $molecule^{-1}$)	
		298 ± 2 K	228 ± 2 K
26, 0	286.46	107	88.3
25, 0	287.38	132	133
24, 0	288.45	145	175
23, 0	289.83	188	208
22, 0	291.40	188	267
21, 0	292.99	242	284
20, 0	294.88	295	348
19, 0	296.97	356	441
18, 0	299.30	447	541
17, 0	301.81	523	636
16, 0	304.54	601	728
15, 0	307.46	679	819
14, 0	310.54	772	932
13, 0	313.81	904	1090
12, 0	317.29	1190	1480
11, 0	321.20	1360	1670
10, 0	325.37	1260	1510
9, 0	329.56	1210	1430
8, 0	333.89	1250	1510
7, 0	338.69	1580	1970
6, 0	344.04	923	1060
5, 0	349.09	715	828
4, 0	355.02	723	864
3, 0	360.64	267	287
4, 1	364.32	126	95.4
2, 0	367.94	128	129
1, 0	374.69	74.5	77.3
2, 1	377.78	27.5	27.4
0, 0	381.27	22.5	–
1, 1	384.87	9.86	–

Note:
Wilmouth et al.[12], analysis of spectra from Wilmouth et al.[12], Cox et al.,[3] Wahner et al.,[10] Orlando et al.,[8] Laszlo et al.,[7] Gilles et al.[6] at a common resolution of 0.40 nm.

Table 4G-3-3. Recommended Absorption Cross Sections of BrO at 298 K

λ (nm)	10^{20} σ (cm^2)	λ (nm)	10^{20} σ (cm^2)	λ (nm)	10^{20} σ (cm^2)	λ (nm)	10^{20} σ (cm^2)
286.5	104.8	311.5	453.1	336.5	258.7	361.5	226.6
287.0	106.5	312.0	294.8	337.0	222.1	362.0	182.9
287.5	128.8	312.5	203.7	337.5	202.0	362.5	145.2
288.0	95.04	313.0	197.3	338.0	201.8	363.0	119.9
288.5	147.7	313.5	723.9	338.5	1287.0	363.5	103.7
289.0	109.8	314.0	901.3	339.0	1296.0	364.0	113.3
289.5	126.4	314.5	650.8	339.5	734.4	364.5	122.2
290.0	183.8	315.0	443.2	340.0	444.8	365.0	99.15
290.5	133.1	315.5	310.9	340.5	303.1	365.5	87.15
291.0	133.5	316.0	231.7	341.0	243.1	366.0	86.23
291.5	188.6	316.5	173.7	341.5	217.5	366.5	91.26
292.0	157.2	317.0	721.1	342.0	235.0	367.0	105.0
292.5	128.3	317.5	1136.0	342.5	291.6	367.5	123.4
293.0	248.2	318.0	730.7	343.0	423.8	368.0	130.5
293.5	192.5	318.5	482.3	343.5	711.9	368.5	119.5
294.0	140.4	319.0	344.6	344.0	967.8	369.0	100.9
294.5	161.5	319.5	275.1	344.5	814.4	369.5	86.11
295.0	294.4	320.0	251.4	345.0	542.1	370.0	74.79
295.5	216.1	320.5	293.7	345.5	345.0	370.5	64.46
296.0	163.9	321.0	1138.0	346.0	225.9	371.0	53.91
296.5	152.9	321.5	1155.0	346.5	160.3	371.5	46.47
297.0	361.1	322.0	676.9	347.0	146.4	372.0	39.44
297.5	276.5	322.5	419.6	347.5	162.2	372.5	35.13
298.0	193.5	323.0	300.6	348.0	257.8	373.0	34.13
298.5	156.4	323.5	261.7	348.5	529.5	373.5	35.68
299.0	284.0	324.0	288.2	349.0	747.7	374.0	48.08
299.5	421.1	324.5	433.6	349.5	667.4	374.5	74.97
300.0	275.3	325.0	982.6	350.0	499.2	375.0	70.53
300.5	193.5	325.5	1283.0	350.5	363.4	375.5	51.46
301.0	180.1	326.0	837.6	351.0	272.4	376.0	35.44
301.5	350.9	326.5	494.8	351.5	215.3	376.5	30.47
302.0	502.3	327.0	312.0	352.0	181.9	377.0	27.46
302.5	318.4	327.5	231.1	352.5	165.9	377.5	25.66
303.0	217.4	328.0	223.5	353.0	162.8	378.0	25.61
303.5	195.9	328.5	343.1	353.5	163.2	378.5	21.82
304.0	274.0	329.0	789.1	354.0	179.5	379.0	18.60
304.5	609.6	329.5	1261.0	354.5	309.3	379.5	14.96
305.0	466.2	330.0	1058.0	355.0	789.4	380.0	12.28
305.5	298.4	330.5	706.2	355.5	498.6	380.5	13.03
306.0	221.1	331.0	453.4	356.0	276.2	381.0	19.55
306.5	209.7	331.5	295.9	356.5	166.2	381.5	20.93
307.0	407.2	332.0	203.1	357.0	119.9	382.0	16.76
307.5	703.1	332.5	164.7	357.5	111.1	382.5	9.049
308.0	518.3	333.0	259.8	358.0	115.3	383.0	3.059
308.5	343.6	333.5	952.8	358.5	123.6	383.5	4.924
309.0	227.6	334.0	1294.0	359.0	143.6	384.0	3.892
309.5	193.6	334.5	963.3	359.5	182.7	384.5	6.695
310.0	395.5	335.0	652.3	360.0	236.4	385.0	10.93
310.5	798.9	335.5	457.5	360.5	272.3		
311.0	659.2	336.0	338.8	361.0	264.4		

Note:
Wilmouth et al.,[12] averages over 0.5 nm intervals

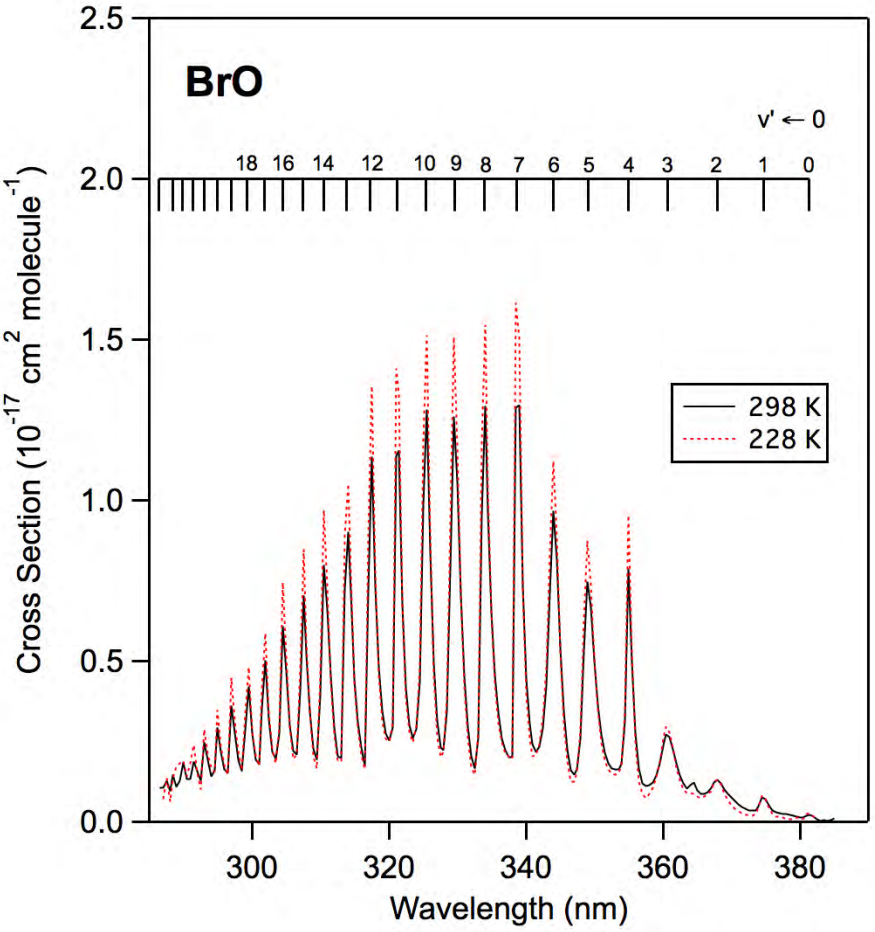


Figure 4G-3-1. Absorption Spectrum of BrO

(1) Basco, N.; Dogra, S. K. Reactions of halogen oxides studied by flash photolysis III. The production and reactions of BrO and ClO radicals in the halogen-sensitized decomposition of chlorine dioxide. *Proc. Roy. Soc. Lond. A.* **1971**, *323*, 417-429, doi:10.1098/rspa.1971.0113.

(2) Clyne, M. A. A.; Cruse, H. W. Rates of elementary reactions involving the BrO ($X^2\Pi$) and IO ($X^2\Pi$) radicals. *Trans. Faraday Soc.* **1970**, *66*, 2214-2226, doi:10.1039/tf9706602214.

(3) Cox, R. A.; Sheppard, D. W.; Stevens, M. P. Absorption coefficients and kinetics of the BrO radical using molecular modulation. *J. Photochem.* **1982**, *19*, 189-207, doi:10.1016/0047-2670(82)80022-1.

(4) Fleischmann, O. C.; Burrows, J. P.; Orphal, J. Time-windowing Fourier transform absorption spectroscopy for flash photolysis investigations. *J. Photochem. Photobiol. A: Chem.* **2003**, *157*, 127-136, doi:10.1016/S1010-6030(03)00069-8.

(5) Fleischmann, O. C.; Hartmann, M.; Burrows, J. P.; Orphal, J. New ultraviolet absorption cross-sections of BrO at atmospheric temperatures measured by a time-windowing Fourier transform spectroscopy. *J. Photochem. Photobiol. A.: Chem.* **2004**, *168*, 117-132, doi:10.1016/j.jphotochem.2004.03.026.

(6) Gilles, M. K.; Turnipseed, A. A.; Burkholder, J. B.; Ravishankara, A. R. Kinetics of the IO radical. 2. Reaction of IO with BrO. *J. Phys. Chem. A* **1997**, *101*, 5526-5534, doi:10.1021/jp9709159.

(7) Laszlo, B.; Huie, R. E.; Kurylo, M. J.; Miziolek, A. W. Kinetic studies of the reactions of BrO and IO radicals. *J. Geophys. Res.* **1997**, *102*, 1523-1532, doi:10.1029/96JD00458.

(8) Orlando, J. J.; Burkholder, J. B.; Bopegedera, A. M. R. P.; Howard, C. J. Infrared measurements of BrO ($X^2\Pi_{3/2}$). *J. Mol. Spectrosc.* **1991**, *145*, 278-289, doi:10.1016/0022-2852(91)90115-Q.

(9) Sander, S. P.; Friedl, R. R. Kinetics and product studies of the reaction ClO + BrO using flash photolysis-ultraviolet absorption. *J. Phys. Chem.* **1989**, *93*, 4764-4771, doi:10.1021/j100349a017.

(10) Wahner, A.; Ravishankara, A. R.; Sander, S. P.; Friedl, R. R. Absorption cross section of BrO between 312 and 385 nm at 298 K and 225 K. *Chem. Phys. Lett.* **1988**, *152*, 507-512, doi:10.1016/0009-2614(88)80450-0.

(11) Wheeler, M. D.; Newman, S. M.; Ishiwata, T.; Kawasaki, M.; Orr-Ewing, A. J. Cavity ring-down spectroscopy of the $A^2\Pi_{3/2}$-$X\ ^2\Pi_{3/2}$ transition of BrO. *Chem. Phys. Lett.* **1998**, *285*, 346-351, doi:10.1016/S0009-2614(98)00082-7.
(12) Wilmouth, D. M.; Hanisco, T. F.; Donahue, N. M.; Anderson, J. G. Fourier transform ultraviolet spectroscopy of the $A\ ^2\Pi_{3/2} \leftarrow X\ ^2\Pi_{3/2}$ trasnsition of BrO. *J. Phys. Chem. A* **1999**, *103*, 8935-8945, doi:10.1021/jp991651o.

G4. OBrO (bromine dioxide)

Back to Index

$OBrO + h\nu$	$\rightarrow Br + O_2$	-52 kJ mol^{-1}	All	(1)
	$\rightarrow BrO + O(^3P)$	209 kJ mol^{-1}	573 nm	(2)

(Recommendation: 06-2, Note: 25-1, Evaluated: 10-6)

Absorption Cross Sections: The visible absorption spectrum of OBrO, bromine dioxide, has been measured in the 400–600 nm region at room temperature by Rowley et al.,[5] Knight et al.,[2] and Fleischmann et al.,[1] at ~250 K by Miller et al.,[3] and at 273, 298, and 338 K by Rattigan et al.[4] The OBrO spectrum measured by Knight et al. is shown in Figure 4G-4-1. The spectrum has a highly structured absorption band consisting of a progression of doublets with a maximum intensity near 500 nm and a progression of less intense bands between the doublets. The spectrum was assigned to the $C\ ^2A_2 \leftarrow X\ ^2B_1$ electronic transition by Miller et al.[3] who combined *ab initio* calculations of the lowest doublet electronic states of OBrO with Franck-Condon simulations. Fleischmann et al. have provided a detailed vibrational analysis of the OBrO spectrum. Knight et al.[2] reported absorption cross section data. The peak positions and cross sections for the vibrational progressions (n,0,0)←(0,0,0) and (n,1,0)←(0,0,0) in Table 4G-4-1 are taken from Knight et al.[2] Table 4G-4-2 gives the absorption cross section averages over 1 nm intervals of the spectrum reported by Knight et al.[2] (0.66 nm resolution).

Photolysis Quantum Yield and Product Studies: No quantum yields are available but theoretical calculations by Vetter et al.[6] indicate that photodissociation occurs via the $BrO + O(^3P)$ channel because of a large transition dipole moment for the $C\ ^2A_2 \leftarrow X\ ^2B_1$ transition. Photodissociation into $Br + O_2$ occurs via the 1^2B_2 state and is less probable.

Table 4G-4-1. Peak Absorption Cross Sections of OBrO at 298 K

n	(n,0,0)←(0,0,0) λ (nm)	10^{20} σ (cm^2)	(n,1,0)←(0,0,0) λ (nm)	10^{20} σ (cm^2)
0	630.4	–	622.0	–
1	606.1	–	598.4	–
2	583.8	–	576.8	–
3	563.4	1080	556.8	1350
4	544.4	1450	538.5	1740
5	527.1	1640	521.6	1910
6	510.7	1770	505.5	1960
7	495.5	1720	490.7	1760
8	481.2	1670	476.9	1510
9	468.2	1440	464.1	1260
10	455.8	1210	452.2	960
11	444.4	1020	440.8	720
12	433.7	790	430.4	490
13	423.5	570	420.6	310
14	414.1	400	411.0	220
15	405.1	260	402.3	130

Note:
Knight et al.[2]

Table 4G-4-2. Recommended Absorption Cross Sections of OBrO at 298 K

λ (nm)	10^{20} σ (cm^2)	λ (nm)	10^{20} σ (cm^2)	λ (nm)	10^{20} σ (cm^2)	λ (nm)	10^{20} σ (cm^2)
401	66.7	443	363	485	301	527	1530
402	112	444	834	486	463	528	1100
403	116	445	777	487	368	529	584
404	153	446	452	488	298	530	326
405	243	447	292	489	425	531	218
406	180	448	254	490	868	532	347
407	131	449	214	491	1580	533	547
408	113	450	180	492	993	534	361
409	105	451	323	493	641	535	344
410	128	452	854	494	583	536	539
411	201	453	672	495	1160	537	434
412	171	454	394	496	1430	538	1200
413	239	455	633	497	826	539	1500
414	380	456	1110	498	458	540	888
415	260	457	729	499	291	541	546
416	180	458	426	500	405	542	442
417	156	459	292	501	512	543	312
418	133	460	314	502	336	544	991
419	147	461	262	503	419	545	1230
420	269	462	213	504	483	546	716
421	274	463	399	505	1230	547	395
422	229	464	1100	506	1650	548	252
423	479	465	868	507	962	549	161
424	481	466	506	508	651	550	302
425	287	467	562	509	556	551	476
426	207	468	1230	510	1030	552	300
427	175	469	1020	511	1570	553	255
428	149	470	568	512	953	554	461
429	194	471	341	513	506	555	349
430	422	472	298	514	307	556	532
431	382	473	362	515	282	557	1250
432	274	474	239	516	532	558	870
433	577	475	286	517	433	559	472
434	661	476	563	518	303	560	350
435	392	477	1390	519	529	561	267
436	251	478	990	520	504	562	204
437	208	479	567	521	1390	563	791
438	179	480	577	522	1610	564	885
439	166	481	1260	523	921	565	504
440	363	482	1310	524	622	566	275
441	651	483	745	525	516	567	170
442	425	484	403	526	654	568	107

Note:
Knight et al.[2], data averages over 1 nm intervals

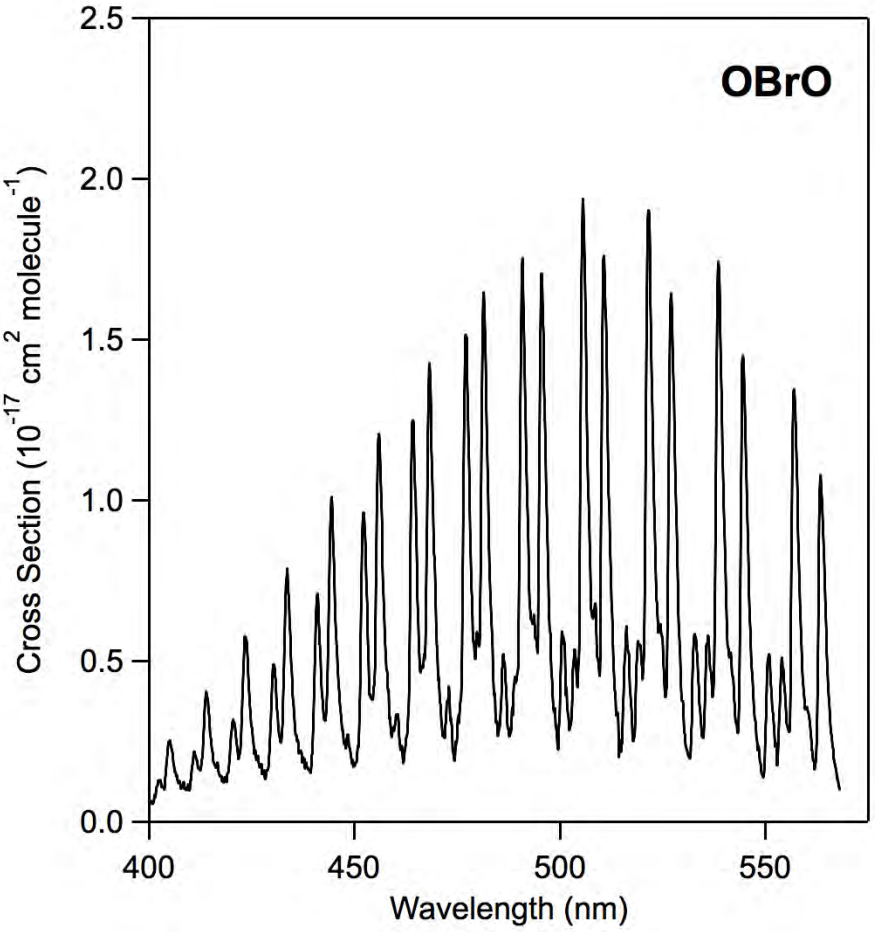


Figure 4G-4-1. Absorption spectrum of OBrO

(1) Fleischmann, O. C.; Meyer-Arnek, J.; Burrows, J. P.; Orphal, J. The visible absorption spectrum of OBrO, investigated by Fourier Transform Spectroscopy. *J. Phys. Chem. A* **2005**, *109*, 5093-5103, doi:10.1021/jp044911x.

(2) Knight, G.; Ravishankara, A. R.; Burkholder, J. B. Laboratory studies of OBrO. *J. Phys. Chem. A* **2000**, *104*, 11121-11125, doi:10.1021/jp002226u.

(3) Miller, C. E.; Nickolaisen, S. L.; Francisco, J. S.; Sander, S. P. The OBrO $C(^2A_2) \leftarrow X(^2B_1)$ absorption spectrum. *J. Chem. Phys.* **1997**, *107*, 2300-2307, doi:10.1063/1.474606.

(4) Rattigan, O. V.; Jones, R. L.; Cox, R. A. The visible spectrum of gaseous OBrO. *Chem. Phys. Lett.* **1994**, *230*, 121-126, doi:10.1016/0009-2614(94)01129-X.

(5) Rowley, D. M.; Harwood, M. H.; Freshwater, R. A.; Jones, R. L. A novel flash photolysis/UV absorption system employing charge-coupled device (CCD) detection: A study of the BrO + BrO reaction at 298 K. *J. Phys. Chem.* **1996**, *100*, 3020-3029, doi:10.1021/jp951825b.

(6) Vetter, R.; Ritschel, T.; Zülicke, L. Theoretical study of the low-lying electronically excited states of OBrO. *J. Phys. Chem. A* **2003**, *107*, 1405-1412, doi:10.1021/jp021952p.

G5. Br_2O (dibromine monoxide)

Back to Index

$Br_2O + h\nu$	$\rightarrow Br + BrO$	128 kJ mol^{-1}	938 nm	(1)
	$\rightarrow Br_2 + O$	173 kJ mol^{-1}	693 nm	(2)
	$\rightarrow Br + Br + O$	366 kJ mol^{-1}	327 nm	(3)

(Recommendation: 06-2, Note: 10-6, Evaluated: 10-6)

Absorption Cross Sections: The UV absorption spectrum of Br_2O, dibromine monoxide, has been measured at room temperature by Orlando and Burkholder[3] (196–432 nm), Rattigan et al.[4] (240–515 nm), and Deters et al.[2] (208–444 nm). The spectrum exhibits a strong narrow band at wavelengths <220 nm with a maximum at 200 nm, a weaker and broader band extending from 250 nm to about 460 nm with a maximum at 313 nm and a shoulder near 350 nm, and two weak bands at 460–580 nm and 580–750 nm with maxima at ~520 nm and ~665

nm. There is good agreement between the various data sets in the wavelength region <380 nm where the data of Orlando and Burkholder[3] and Deters et al.[2] are nearly identical and those of Rattigan et al.[4] are smaller by ~10% below 250 nm and above 290 nm and smaller by up to ~25% in the region of the absorption minimum near 270 nm. Large discrepancies exist between the data sets at wavelengths >380 nm. The absorption cross sections reported by Orlando and Burkholder[3] and Deters et al.[2] decrease at longer wavelengths to values $\leq 1 \times 10^{-20}$ cm^2 molecule^{-1} whereas the values reported by Rattigan et al.[4] show a decrease between 400 and 470 nm and evidence for another absorption band at longer wavelengths. The cutoff at 440 nm of the absorption spectrum reported by Orlando and Burkholder[3] is a result of the assumption that the absorbance of Br_2O is zero at wavelengths >440 nm. The correction procedure used by Rattigan et al.[4] taking the vibrational structure of the Br_2 spectrum into account resulted in appreciable absorption for Br_2O at wavelengths above 440 nm. The recommended cross sections in Table 4G-5 are the data from Orlando and Burkholder[3] at 196 and 200 nm, the mean of the data from Orlando and Burkholder[3] and Deters et al.[2] for the region 210–230 nm, and the mean of the data from Orlando and Burkholder,[3] Deters et al.,[2] and Rattigan et al.[4] for the region 240–400 nm. No recommendation is given for wavelengths >400 nm.

Photolysis Quantum Yield and Product Studies: By analogy to Cl_2O the predominate photodissociation channel is expected to be Br + BrO. Burkholder[1] measured the BrO yield at 308 nm to be near unity.

Table 4G-5. Recommended Absorption Cross Sections of Br_2O at 298 K

λ (nm)	10^{20} σ (cm^2)
196	1740
200	2000
210	1050
220	288
230	140
240	85.8
250	45.4
260	24.6
270	18.8
280	33.5
290	85.5
300	167
310	220
320	212
330	192
340	188
350	186
360	162
370	132
380	99.0
390	74.8
400	54.0

Note:
196, 200 nm: Orlando and Burkholder[3]
210–230 nm: mean of data from Orlando and Burkholder[3] and Deters et al.[2]
240–400 nm: mean of data from Orlando and Burkholder,[3] Deters et al.,[2] and Rattigan et al.[4]

(1) Burkholder, J. B. Rate coefficient for the reaction: Br + Br_2O → Br_2 + BrO. *Int. J. Chem. Kinet.* **1998**, *30*, 571-576, doi:10.1002/(SICI)1097-4601(1998)30:8<571::AID-KIN6>3.0.CO;2-P.

(2) Deters, B.; Burrows, J. P.; Himmelmann, S.; Blindauer, C. Gas phase spectra of HOBr and Br_2O and their atmospheric significance. *Ann. Geophys.* **1996**, *14*, 468-475, doi:10.1007/s00585-996-0468-x.

(3) Orlando, J. J.; Burkholder, J. B. Gas-phase UV/visible absorption spectra of HOBr and Br_2O. *J. Phys. Chem.* **1995**, *99*, 1143-1150, doi:10.1021/j100004a013.

(4) Rattigan, O. V.; Lary, D. J.; Jones, R. L.; Cox, R. A. UV-visible absorption cross sections of gaseous Br_2O and HOBr. *J. Geophys. Res.* **1996**, *101*, 23021-23033, doi:10.1029/96JD02017.

G6. HOBr (hypobromous acid)

Back to Index

$HOBr + h\nu$	$\rightarrow OH + Br$	210 kJ mol^{-1}	571 nm	(1)
	$\rightarrow HBr + O(^3P)$	274 kJ mol^{-1}	437 nm	(2)

(Recommendation: 06-2, Note: 10-6, Evaluated: 10-6)

Absorption Cross Sections: The UV absorption spectrum of HOBr, hypobromous acid, has been measured by Orlando and Burkholder[8] (240–404 nm), Deters et al.[3] (250–400 nm), Benter et al.[2] (234–390 nm), Rattigan et al.[9] (240–510 nm), and Ingham et al.[5] (260–600 nm). Orlando and Burkholder,[8] Deters et al.,[3] and Benter et al.[2] observed two absorption bands with maxima near 284 and 351 nm. The reported spectra agree reasonably well in their wavelength dependence with a sharp decrease in cross section at wavelengths greater than 400 nm. In contrast, the cross sections reported by Rattigan et al.[9] and Ingham et al.[5] are roughly 50% greater between 300 and 400 nm. In addition, the spectrum reported by Rattigan et al.[9] has pronounced long wavelength absorption that extends to 520 nm. Ingham et al.[5] report a similar spectrum to Rattigan et al., but with a more prominent absorption band at long wavelength with a maximum at 457 nm. These two studies are consistent with the observations of Barnes et al.,[1] who showed that laser photolysis of HOBr between 440–600 nm gives rise to OH photofragments. The presence of a weak band beyond 400 nm is attributable to the presence of a forbidden transition from the ground electronic to a triplet state as predicted by the *ab initio* calculations of Francisco et al.[4] and Minaev.[7] The differences in the spectral shapes are probably attributable to impurities such as Br_2O and Br_2, and/or the use of different Br_2O cross sections. However, the presence of impurities alone cannot explain the large difference in cross sections at the peak of the absorption bands.

The recommended absorption cross sections in Table 4G–6 are based on the study by Ingham et al.[5] These authors generated HOBr in situ by laser photolytic production of OH in the presence of Br_2, and determined the HOBr spectrum using a gated diode camera shortly after the pulse, circumventing the problem associated with the presence of the strong absorbing impurity Br_2O, which was present in previous studies. The calibration of the absorption cross sections was made relative to the cross sections of Br_2. No recommendation is given for wavelengths <250 nm where the data are uncertain. On the basis of the level of agreement among the available studies, cross section uncertainty factors (2σ) of 1.25 (250–300 nm), 1.5 (300–400 nm), 3 (400–500 nm), and 10 (>500 nm) are estimated for the wavelength ranges given in parenthesis.

The data presented in Table 4G-6 were computed with the following expression taken from Ingham et al.,[5] which is based on a combination of three Gaussian functions, one for each absorption band:

$$\sigma(\lambda) = 24.77\exp\left\{-109.80\left[\ln\left(\frac{284.01}{\lambda}\right)\right]^2\right\} + 12.22\exp\left\{-93.63\left[\ln\left(\frac{350.57}{\lambda}\right)\right]^2\right\}$$
$$+ 2.283\exp\left\{-242.40\left[\ln\left(\frac{457.38}{\lambda}\right)\right]^2\right\}$$

where $\sigma(\lambda)$ is in units of 10^{-20} cm^2 $molecule^{-1}$ and λ is in nm.

Photolysis Quantum Yield and Product Studies: Benter et al.[2] measured quantum yields for HOBr photolysis at 261 and 363 nm (near the band peaks). The observed quantum yield for Br formation at 363 nm was greater than 0.95 and a unity quantum yield for the OH + Br product channel is recommended. No evidence for the O + HBr product channel was observed. The laser photofragment study of Barnes et al.[1] claimed that OH was the major photolysis product at wavelengths >400 nm. Lock et al.[6] found that at 490 and 510 nm OH and Br photofragments are in their respective vibrational and spin-orbit ground states.

Table 4G-6. Recommended Absorption Cross Sections of HOBr at 298 K

λ (nm)	10^{20} σ (cm^2)	λ (nm)	10^{20} σ (cm^2)	λ (nm)	10^{20} σ (cm^2)
250	4.15	355	12.1	460	2.28
255	6.19	360	11.5	465	2.14
260	10.5	365	10.5	470	1.91
265	14.6	370	9.32	475	1.62
270	18.7	375	7.99	480	1.30
275	22.1	380	6.65	485	0.993
280	24.3	385	5.38	490	0.723
285	25.0	390	4.22	495	0.502
290	24.0	395	3.23	500	0.333
295	21.9	400	2.43	505	0.212
300	19.1	405	1.80	510	0.129
305	16.2	410	1.36	515	0.076
310	13.6	415	1.08	520	0.042
315	11.8	420	0.967	525	0.023
320	10.8	425	0.998	530	0.012
325	10.5	430	1.15	535	0.0059
330	10.8	435	1.40	540	0.0029
335	11.3	440	1.68	545	0.0013
340	11.9	445	1.96	550	0.0006
345	12.3	450	2.18		
350	12.4	455	2.29		

Note:
Ingham et al.[5], calculated using the expression given in the text

(1) Barnes, R. J.; Lock, M.; Coleman, J.; Sinha, A. Observation of a new absorption band of HOBr and its atmospheric implications. *J. Phys. Chem.* **1996**, *100*, 453-457, doi:10.1021/jp952445t.

(2) Benter, T.; Feldmann, C.; Kirchner, U.; Schmidt, M.; Schmidt, S.; Schindler, R. N. UV/VIS-absorption spectra of HOBr and CH_3OBr: $Br(^2P_{3/2})$ atom yields in the photolysis of HOBr. *Ber. Bunsenges. Phys. Chem.* **1995**, *99*, 1144-1147, doi:10.1002/bbpc.199500046.

(3) Deters, B.; Burrows, J. P.; Himmelmann, S.; Blindauer, C. Gas phase spectra of HOBr and Br_2O and their atmospheric significance. *Ann. Geophys.* **1996**, *14*, 468-475, doi:10.1007/s00585-996-0468-x.

(4) Francisco, J. S.; Hand, M. R.; Williams, I. H. *Ab Initio* study of the electronic spectrum of HOBr. *J. Phys. Chem.* **1996**, *100*, 9250-9253, doi:10.1021/jp9529782.

(5) Ingham, T.; Bauer, D.; Landgraf, J.; Crowley, J. N. Ultraviolet-visible absorption cross sections of gaseous HOBr. *J. Phys. Chem. A* **1998**, *102*, 3293-3298, doi:10.1021/jp980272c.

(6) Lock, M.; Barmes, R. J.; Sinha, A. Near-threshold photodissociation dynamics of HOBr: Determination of product state distribution, vector correlation, and heat of formation. *J. Phys. Chem.* **1996**, *100*, 7972-7980, doi:10.1021/jp9532428.

(7) Minaev, B. F. The singlet-triplet absorption and photodissociation of the HOCl, HOBr, and HOI molecules calculated by the MCSCF quadratic response method. *J. Phys. Chem. A* **1999**, *103*, 7294-7309, doi:10.1021/jp990203d.

(8) Orlando, J. J.; Burkholder, J. B. Gas-phase UV/visible absorption spectra of HOBr and Br_2O. *J. Phys. Chem.* **1995**, *99*, 1143-1150, doi:10.1021/j100004a013.

(9) Rattigan, O. V.; Lary, D. J.; Jones, R. L.; Cox, R. A. UV-visible absorption cross sections of gaseous Br_2O and HOBr. *J. Geophys. Res.* **1996**, *101*, 23021-23033, doi:10.1029/96JD02017.

G7. BrNO (nitrosyl bromide)

Back to Index

$BrNO + h\nu \rightarrow Br + NO$ 120.8 kJ mol^{-1} 991 nm (1)

(Recommendation: 06-2, Note: 10-6, Evaluated: 10-6)

Absorption Cross Sections: The absorption spectrum of BrNO, nitrosyl bromide, has been measured at room temperature by Eden et al.[1] (275–550 nm), Houel and van den Bergh[3] (200–800 nm), Uthman et al.[5] (189–300 nm), Hippler et al.[2] (266 nm), and Maloney and Palmer[4] (270 nm). The spectrum exhibits four absorption bands between 200 and 800 nm, a strong band between 190 and 290 nm with the maximum at ~213 nm, a weaker band between 290 and 600 nm with the maximum at 338 nm and a shoulder near 420 nm, and a still weaker band between 600 and 800 nm with the maximum at 708 nm. The absorption cross sections from these studies are in good agreement (after correction of an error in Maloney and Palmer[4]). The recommended absorption cross sections in Table 4G-7 are from Uthman et al.[5] for the region 189–300 nm and the cross sections at 338, 416, and 708 nm reported by Houel and van den Bergh[3].

Photolysis Quantum Yield and Product Studies: No recommendation.

Table 4G-7. Recommended Absorption Cross Sections of BrNO at 298 K

λ (nm)	10^{20} σ (cm^2)	λ (nm)	10^{20} σ (cm^2)
189	18.3	224	4740
193	39.0	230	2990
194	46.2	235	1920
197	166	240	1090
200	566	250	360
201	861	260	117
203	1690	270	40.1
205.5	2950	280	19.5
207	4340	290	16.8
210	6470	300	18.0
211	6910	338	31.0
213	7270	416	20.1
216	7060	708	2.94
220	6070		

Note:
189–300 nm: Uthman et al.[5]
338, 416, 708 nm: Houel and van den Bergh[3]

(1) Eden, C.; Feilchenfeld, H.; Manor, S. Simultaneous spectrophotometric determination of nitrosyl bromide and bromine. *Anal. Chem.* **1969**, *41*, 1150-1151, doi:10.1021/ac60277a042.
(2) Hippler, H.; Luu, S. H.; Teitelbaum, H.; Troe, J. Flash photolysis study of the NO-catalyzed recombination of bromine atoms. *Int. J. Chem. Kinet.* **1978**, *10*, 155-169, doi:10.1002/kin.550100203.
(3) Houel, N.; van den Bergh, H. BrNO—thermodynamic properties, the ultraviolet/vis spectrum, and the kinetics of its formation. *Int. J. Chem. Kinet.* **1977**, *9*, 867-874, doi:10.1002/kin.550090603.
(4) Maloney, K. K.; Palmer, H. B. Low-pressure thermal decomposition of ONBr and ONCl in shock waves. *Int. J. Chem. Kinet.* **1973**, *5*, 1023-1037, doi:10.1002/kin.550050611.
(5) Uthman, A. P.; Demlein, P. J.; Allston, T. D.; Withiam, M. C.; McClements, M. J.; Takacs, G. A. Photoabsorption spectra of gaseous methyl bromide, ethylene dibromide, nitrosyl bromide, thionyl chloride, and sulfuryl chloride. *J. Phys. Chem.* **1978**, *82*, 2252-2257, doi:10.1021/j100509a021.

G8. *cis*-BrONO (bromine nitrite)

Back to Index

cis-$BrONO + h\nu \rightarrow$ Products (1)

(Recommendation: 06-2, Note: 10-6, Evaluated: 10-6)

Absorption Cross Sections: The UV absorption spectrum of *cis*-BrONO, bromine nitrite, has been measured in the temperature range 228–296 K by Burkholder and Orlando[1] (200–365 nm). The spectrum exhibits a strong absorption band between 200 and 270 nm with a maximum at 228 nm and a broader and weaker band between 270 and 364 nm with a maximum at 316 nm. The shape of the *cis*-BrONO spectrum was independent

of temperature over the 228–296 K range to within the uncertainty of the measurements. The results from Burkholder and Orlando[1] are recommended and listed in Table 4G-8.

Photolysis Quantum Yield and Product Studies: No recommendation.

Table 4G-8. Recommended Absorption Cross Sections of BrONO at 253 K

λ (nm)	10^{20} σ (cm^2)	λ (nm)	10^{20} σ (cm^2)	λ (nm)	10^{20} σ (cm^2)	λ (nm)	10^{20} σ (cm^2)
200	–	242	1070	284	247	326	400
202	116	244	874	286	262	328	394
204	221	246	720	288	277	330	387
206	358	248	602	290	293	332	382
208	496	250	514	292	310	334	375
210	687	252	446	294	331	336	364
212	822	254	391	296	350	338	350
214	1070	256	345	298	366	340	332
216	1280	258	306	300	377	342	308
218	1610	260	273	302	386	344	284
220	1940	262	244	304	393	346	263
222	2240	264	221	306	400	348	248
224	2520	266	205	308	407	350	233
226	2630	268	196	310	413	352	214
228	2710	270	192	312	415	354	195
230	2620	272	191	314	413	356	176
232	2390	274	194	316	409	358	157
234	2170	276	200	318	406	360	138
236	1860	278	211	320	406	362	123
238	1550	280	223	322	406	364	117
240	1240	282	235	324	405		

Note:
Burkholder and Orlando[1]

(1) Burkholder, J. B.; Orlando, J. J. UV absorption cross-sections of *cis*-BrONO. *Chem. Phys. Lett.* **2000**, *317*, 603-608, doi:10.1016/S0009-2614(99)01412-8.

G9. $BrNO_2$ (nitryl bromide)

Back to Index

$BrNO_2 + h\nu$	$\rightarrow Br + NO_2$	101 kJ mol^{-1}	1185 nm	(1)
	$\rightarrow BrO + NO$	172 kJ mol^{-1}	693 nm	(2)
	$\rightarrow Br + NO + O$	407 kJ mol^{-1}	294 nm	(3)

(Recommendation: 10-6, Note: 10-6, Evaluated: 10-6)

Absorption Cross Sections: Scheffler et al.[2] measured the room temperature absorption spectrum of $BrNO_2$, nitryl bromide, over the wavelength range 185–530 nm. The spectrum consists of several overlapping electronic transitions with a strong band in the actinic region (>200 nm). The recommended absorption cross sections in Table 4G-9 are taken from Scheffler er al.[2] between 185 and 430 nm while values at λ >430 nm were obtained from a log-linear fit of the data reported by Scheffler et al. The $BrNO_2$ spectrum recorded in the Burkholder and Orlando[1] study of *cis*-BrONO was reported to be in good agreement with the Scheffler et al. spectrum.

Photolysis Quantum Yield and Product Studies: By analogy with $ClNO_2$, the most likely photolysis products are expected to be $Br + NO_2$.

Table 4G-9. Recommended Absorption Cross Sections of $BrNO_2$ at 298 K

λ (nm)	10^{20} σ (cm^2)	λ (nm)	10^{20} σ (cm^2)	λ (nm)	10^{20} σ (cm^2)
185	2048	310	11	435	8.03
190	3601	315	11	440	7.19
195	5013	320	10	445	6.44
200	5386	325	12	450	5.77
205	4499	330	13	455	5.17
210	2521	335	14	460	4.63
215	1170	340	16	465	4.15
220	554	345	15	470	3.71
225	373	350	16	475	3.33
230	343	355	16	480	2.98
235	362	360	18	485	2.67
240	387	365	19	490	2.39
245	390	370	17	495	2.14
250	363	375	18	500	1.92
255	310	380	17	505	1.72
260	251	385	17	510	1.54
265	197	390	16	515	1.38
270	154	395	15	520	1.23
275	116	400	14	525	1.10
280	88	405	14	530	0.99
285	63	410	13	540	*0.79*
290	44	415	12	550	*0.64*
295	30	420	11	560	*0.51*
300	20	425	10	570	*0.41*
305	15	430	9	580	*0.33*

Note:
185–430 nm: Scheffler et al.[2]
435–530 nm: log-linear fit to data reported in Scheffler et al.[2]
540–580 nm: log-linear extrapolation

(1) Burkholder, J. B.; Orlando, J. J. UV absorption cross-sections of *cis*-BrONO. *Chem. Phys. Lett.* **2000**, *317*, 603-608, doi:10.1016/S0009-2614(99)01412-8.

(2) Scheffler, D.; Grothe, H.; Willner, H.; Frenzel, A.; Zetzsch, C. Properties of pure nitryl bromide. Thermal behavior, UV/vis and FTIR spectra, and photoisomerization to *trans*-BrONO in an argon matrix. *Inorg. Chem.* **1997**, *36*, 335-338, doi:10.1021/ic9606946.

G10. $BrONO_2$ (bromine nitrate)

Back to Index

$BrONO_2 + h\nu$	$\rightarrow BrO + NO_2$	115 kJ mol^{-1}	1044 nm	(1)
	$\rightarrow Br + NO_3$	144 kJ mol^{-1}	831 nm	(2)
	$\rightarrow BrO + NO + O(^3P)$	421 kJ mol^{-1}	284 nm	(3)

(Recommendation: 06-2, Note: 10-6, Evaluated: 10-6)

Absorption Cross Sections: The UV/vis absorption spectrum of $BrONO_2$, bromine nitrate, has been measured at room temperature by Spencer and Rowland[5] (186–390 nm), Burkholder et al.[1] (200–500 nm), and Deters et al.[2] (210–500 nm). The absorption cross sections reported by Burkholder et al.[1] and Deters et al.[2] are nearly identical over the range of spectral overlap. The results of Spencer and Rowland[5] agree to within 10% with those of Burkholder et al.[1] and Deters et al.[2] except for the region between 315 and 350 nm where the Spencer data are higher by 10 to 20%.

The temperature dependence of the absorption spectrum has been measured by Burkholder et al.[1] (200–500 nm) at 220, 250, and 298 K and Deters et al.[2] (210–500 nm) at 230 and 298 K. The temperature dependence of the absorption cross sections is in general weak. Burkholder et al.[1] observed decreasing cross sections with decreasing temperature between 200 and 215 nm and between 230 and 500 nm and a slight increase between 215 and 230 nm. The reported ratio σ(220 K)/σ(298 K) has values of ~0.8 to 1.03 between 200 and 235 nm, a minimum of 0.90 at 260 nm, nearly constant values of ~0.95 between 290 and 370 nm, a minimum of ~0.87 at

430 nm, two maxima of ~0.98 around 445 nm, and decreases to ~0.5 at 500 nm. The measurements of Deters et al.[2] show a similar behavior of $\sigma(230\ K)/\sigma(298\ K)$ vs. λ with all values below 1, i.e., a decrease of the cross sections with decreasing temperature is observed over the entire spectrum. Burkholder et al.[1] parameterized the cross section temperature dependence using the expression:

$$\sigma(\lambda,T) = \sigma(\lambda, 296\ K)\ [1 + A_1(\lambda)(T–296) + A_2(\lambda)(T–296)^2]$$

The recommended absorption cross sections and temperature coefficients in Table 4G-10-1 are taken from Burkholder et al.[1] A cross section uncertainty factor of 1.2 (2σ), independent of wavelength, is assigned, which encompasses the results from all the room temperature studies.

Photolysis Quantum Yield and Product Studies: Photodissociation quantum yields have been measured for photolysis wavelengths between 248 and 355 nm as summarized in Table 4G-10-2. The quantum yields for NO_3 production were measured by Harwood et al.[3] to be $\Phi(NO_3) = 0.28 \pm 0.09$ at 248 nm, 1.01 ± 0.35 at 305 nm and 0.92 ± 0.43 at 352.5 nm. The quantum yields for BrO and Br were also estimated at 248 nm to be $\Phi(BrO) \approx 0.5$ and $\Phi(Br) \approx 0.5$. Soller et al.[4] investigated the production of Br, $O(^3P)$, and BrO from the photolysis of $BrONO_2$ in the wavelength range 248–355 nm. The quantum yield for the Br atom are 0.35 ± 0.08, 0.65 ± 0.14, $>0.62 \pm 0.11$, and 0.77 ± 0.19 at 248, 266, 308, and 355 nm, respectively. The values for the $O(^3P)$ atom quantum yields are 0.66 ± 0.15, 0.18 ± 0.04, $<0.13 \pm 0.03$, and <0.02 at 248, 266, 308 and 355 nm, respectively. The measured quantum yields for BrO are 0.37 ± 0.12 at 266 nm and 0.23 ± 0.08 at 355 nm. A total quantum yield Φ_{BrONO2} of unity is recommended for wavelengths >300 nm with $\Phi_{Br+NO_3} = 0.85$ and $\Phi_{BrO+NO_2} = 0.15$. No recommendation is given for wavelengths <300 nm.

Table 4G-10-1. Recommended Absorption Cross Sections of $BrONO_2$ at 296 K and Temperature Coefficients

λ (nm)	10^{20} σ (cm^2)	10^3 A_1 (K^{-1})	10^6 A_2 (K^{-2})	λ (nm)	10^{20} σ (cm^2)	10^3 A_1 (K^{-1})	10^6 A_2 (K^{-2})	λ (nm)	10^{20} σ (cm^2)	10^3 A_1 (K^{-1})	10^6 A_2 (K^{-2})
200	680	0.852	-26.0	302	17.5	0.781	0.784	404	2.04	1.91	3.64
202	616	0.608	-26.1	304	16.6	0.870	1.88	406	1.95	1.86	2.63
204	552	0.308	-26.2	306	15.8	0.872	1.62	408	1.88	1.78	1.52
206	488	0.138	-23.7	308	15.0	0.772	-0.229	410	1.81	1.70	0.316
208	425	0.158	-17.5	310	14.2	0.660	-2.28	412	1.75	1.59	-0.981
210	361	0.184	-9.09	312	13.5	0.652	-1.95	414	1.69	1.49	-2.37
212	334	0.401	-2.61	314	12.8	0.643	-1.58	416	1.63	1.40	-2.60
214	307	0.657	5.03	316	12.1	0.652	-1.42	418	1.56	1.35	-1.54
216	286	0.882	11.2	318	11.6	0.684	-1.48	420	1.50	1.29	-0.381
218	272	1.05	15.3	320	11.0	0.719	-1.56	422	1.45	1.00	-2.34
220	258	1.24	19.7	322	10.5	0.719	-1.06	424	1.40	0.694	-4.43
222	247	1.19	19.7	324	10.1	0.720	-0.508	426	1.36	0.599	-4.31
224	236	1.12	19.6	326	9.64	0.743	0.087	428	1.33	0.734	-1.78
226	226	1.14	20.3	328	9.29	0.791	0.722	430	1.30	0.877	0.880
228	215	1.26	21.8	330	8.94	0.843	1.41	432	1.26	0.747	0.484
230	205	1.40	23.4	332	8.65	0.825	1.33	434	1.22	0.609	0.0625
232	193	1.40	23.1	334	8.36	0.806	1.25	436	1.18	0.519	0.0968
234	180	1.41	22.8	336	8.10	0.800	1.30	438	1.15	0.484	0.632
236	167	1.47	22.8	338	7.87	0.809	1.49	440	1.11	0.447	1.20
238	153	1.59	23.4	340	7.64	0.818	1.70	442	1.08	0.384	-0.388
240	139	1.73	24.0	342	7.45	0.898	2.52	444	1.05	0.318	-2.06
242	126	1.65	20.9	344	7.26	0.982	3.38	446	1.02	0.335	-1.82
244	113	1.56	17.2	346	7.07	0.991	3.48	448	0.974	0.446	0.568
246	101	1.62	15.5	348	6.86	0.918	2.75	450	0.930	0.567	3.18
248	90.0	1.88	16.8	350	6.66	0.842	1.98	452	0.892	0.739	4.40
250	79.5	2.22	18.5	352	6.48	0.942	2.83	454	0.853	0.926	5.74
252	71.7	2.24	17.4	354	6.30	1.05	3.74	456	0.816	1.09	6.94
254	64.0	2.27	16.0	356	6.11	1.08	4.10	458	0.779	1.23	8.00
256	57.5	2.30	14.9	358	5.90	1.03	3.87	460	0.743	1.39	9.16
258	52.3	2.32	14.6	360	5.69	0.969	3.62	462	0.707	1.32	5.99
260	47.1	2.36	14.1	362	5.48	1.02	4.08	464	0.670	1.24	2.46
262	43.8	2.38	14.4	364	5.27	1.08	4.57	466	0.635	1.39	1.87
264	40.5	2.40	14.7	366	5.07	1.13	5.16	468	0.600	1.83	4.74
266	37.9	2.38	14.6	368	4.86	1.18	5.87	470	0.566	2.32	7.95
268	35.8	2.31	14.0	370	4.66	1.24	6.63	472	0.524	2.72	10.9
270	33.8	2.22	13.4	372	4.46	1.29	6.93	474	0.482	3.18	14.4
272	32.5	2.19	13.6	374	4.26	1.35	7.25	476	0.447	3.75	17.9
274	31.2	2.16	13.8	376	4.07	1.44	7.74	478	0.418	4.45	21.4
276	30.0	2.10	13.7	378	3.88	1.54	8.41	480	0.390	5.24	25.4
278	28.9	2.01	13.2	380	3.69	1.66	9.15	482	0.344	5.92	36.6
280	27.9	1.91	12.7	382	3.51	1.60	8.15	484	0.298	6.80	51.2
282	27.0	1.85	12.5	384	3.32	1.54	7.04	486	0.269	7.91	61.2
284	26.1	1.78	12.3	386	3.16	1.62	7.02	488	0.256	9.11	63.1
286	25.1	1.66	11.2	388	3.02	1.85	8.28	490	0.243	10.4	65.2
288	24.2	1.46	9.01	390	2.88	2.11	9.67	492	0.231	11.7	70.6
290	23.2	1.24	6.66	392	2.74	2.16	9.74	494	0.220	13.2	76.5
292	22.2	1.01	4.11	394	2.60	2.22	9.83	496	0.198	14.5	85.0
294	21.2	0.758	1.31	396	2.47	2.21	9.05	498	0.167	16.0	98.6
296	20.2	0.636	-0.188	398	2.36	2.10	7.28	500	0.135	18.2	119
298	19.3	0.666	-0.197	400	2.25	1.98	5.34				
300	18.4	0.699	-0.207	402	2.15	1.95	4.53				

Note: Burkholder et al.,[1] $\sigma(\lambda,T) = \sigma(\lambda, 296\ K)\ [1 + A_1\ (T–296) + A_2\ (T–296)^2]$

Table 4G-10-2. Summary of $BrONO_2$ Photolysis Quantum Yield Results

Wavelength (nm)	Φ(NO_3)	Φ(Br)	Φ(BrO)	Φ($O(^3P)$)
248	0.28 ± 0.09[a]	≈ 0.5[a] 0.35 ± 0.08[b]	≈ 0.5[a]	0.66 ± 0.15[b]
266	–	0.65 ± 0.14[b]	0.37 ± 0.12[b]	0.18 ± 0.04[b]
305	1.01 ± 0.35[a]	–	–	–
308	–	>0.62 ± 0.11[b]	–	<0.13 ± 0.03[b]
352.5	0.92 ± 0.43[a]	–	–	–
355	–	0.77 ± 0.19[b]	0.23 ± 0.08[b]	<0.02[b]

Note:
[a] Harwood et al.[3]
[b] Soller et al.[4]

(1) Burkholder, J. B.; Ravishankara, A. R.; Solomon, S. UV/visible and IR absorption cross sections of $BrONO_2$. *J. Geophys. Res.* **1995**, *100*, 16793-16800, doi:10.1029/95JD01223.

(2) Deters, B.; Burrows, J. P.; Orphal, J. UV-visible absorption cross sections of bromine nitrate determined by photolysis of $BrONO_2/Br_2$ mixtures. *J. Geophys. Res.* **1998**, *103*, 3563-3570, doi:10.1029/97JD02390.

(3) Harwood, M. H.; Burkholder, J. B.; Ravishankara, A. R. Photodissociation of $BrONO_2$ and N_2O_5: Quantum yields for NO_3 production at 248, 308, and 352.5 nm. *J. Phys. Chem. A* **1998**, *102*, 1309-1317, doi:10.1021/jp9729829.

(4) Soller, R.; Nicovich, J. M.; Wine, P. H. Bromine nitrate photochemistry: Quantum yields for O, Br, and BrO over the wavelength range 248-355 nm. *J. Phys. Chem. A* **2002**, *106*, 8378-8385, doi:10.1021/jp020018r.

(5) Spencer, J. E.; Rowland, F. S. Bromine nitrate and its stratospheric significance. *J. Phys. Chem.* **1978**, *82*, 7-10, doi:10.1021/j100490a002.

G11. BrCl (bromine chloride)

Back to Index

$BrCl + h\nu \rightarrow Br + Cl$ 218 kJ mol^{-1} 548 nm (1)

(Recommendation: 06-2, Note: 10-6, Evaluated: 10-6)

Absorption Cross Sections: The UV absorption spectrum of BrCl, bromine chloride, has been measured at room temperature by Gray and Style[1] (240–313 nm and 546 nm), Jost[3] (486–548 nm), Seery and Britton[5] (220–510 nm), Maric et al.[4] (200–600 nm), Hubinger and Nee[2] (190–560 nm), and Tellinghuisen[7] (200–600 nm). The spectrum exhibits an absorption band between 190 and 290 nm with a maximum at 230 nm ($\sigma \approx (6.0\text{-}7.2) \times 10^{-20}$ cm^2 $molecule^{-1}$) and a stronger band between 290 and 600 nm with the maximum at 375 nm ($\sigma \approx (3.9\text{-}4.1) \times 10^{-19}$ cm^2 $molecule^{-1}$ and a shoulder near 470 nm. There is good agreement between the cross section results of the studies except for the values at 289 and 297 nm reported by Gray and Style,[1] which are smaller by a factor of ~2.5 than the rest of the results. The agreement is within 20% for the short wavelength band around 230 nm between the results of Seery and Britton,[5] Maric et al.,[4] and Hubinger and Nee,[2] where Seery and Britton[5] report the highest and Hubinger and Nee[2] the lowest values. There is good agreement, to within ~5-15%, for the stronger band around 375 nm where Seery and Britton[5] and Tellinghuisen[7] report the highest and Hubinger and Nee[2] the lowest cross sections. The discrepancies are larger, up to 50%, in the region of the absorption minimum around 290 nm where Seery and Britton[5] and Hubinger and Nee[2] report the highest cross sections and Tellinghuisen[7] the lowest. Excellent agreement is observed in the long wavelength tail above 450 nm between the data of Maric et al.[4] and Tellinghuisen[7] whereas those from Hubinger and Nee[2] are 50% or more larger and those from Jost [3] are lower by ~20–40%. Maric et al.[4] fit a three-band semi-logarithmic Gaussian distribution function to their 0.2 nm resolution data (200–600 nm) and obtained:

$$\sigma(298\ K) = 6.52 \times 10^{-20} \times \exp(-54.1\ [\ln(227.6/\lambda)]^2) + 3.86 \times 10^{-19} \times \exp(-97.6\ [\ln(372.5/\lambda)]^2) + 9.99 \times 10^{-20} \times \exp(-66.9\ [\ln(442.4/\lambda)]^2)$$

where λ is the wavelength in nm and σ is the absorption cross section in cm^2 $molecule^{-1}$. The recommended absorption cross sections calculated using this expression are listed in Table 4G-11.

A semi-empirical expression based on the theory of Sulzer and Wieland,[6] which describes the temperature and wavelength dependence of an absorption spectrum, was derived by Maric et al.[4] to be

$$\sigma(T, \lambda) = 7.34 \times 10^{-20} \times \tanh^{0.5} \times \exp(-68.6 \times \tanh \times [\ln (227.6/\lambda)]^2) + 4.35 \times 10^{-19} \times \tanh^{0.5} \times \exp(-123.6 \times \tanh \times [\ln (372.5/\lambda)]^2) + 1.12 \times 10^{-19} \times \tanh^{0.5} \times \exp(-84.8 \times \tanh \times [\ln (442.4/\lambda)]^2)$$

where λ is the wavelength in vacuum (200–600 nm), tanh = tanh ($hc\omega_e/2kT$) = tanh(318.8/T) (with ω_e = 443.1 cm^{-1}), and T is the temperature (195–300 K).

Photolysis Quantum Yield and Product Studies: It is expected that BrCl photodissociates with unit quantum yield.

Table 4G-11. Recommended Absorption Cross Sections of BrCl at 298 K

λ (nm)	10^{20} σ (cm^2)	λ (nm)	10^{20} σ (cm^2)	λ (nm)	10^{20} σ (cm^2)	λ (nm)	10^{20} σ (cm^2)
200	2.64	305	0.845	410	22.51	515	2.13
205	3.61	310	1.47	415	19.95	520	1.74
210	4.59	315	2.51	420	17.80	525	1.41
215	5.47	320	4.08	425	16.04	530	1.13
220	6.13	325	6.30	430	14.63	535	0.892
225	6.47	330	9.25	435	13.49	540	0.700
230	6.48	335	12.92	440	12.55	545	0.544
235	6.17	340	17.21	445	11.73	550	0.419
240	5.60	345	21.90	450	10.98	555	0.320
245	4.86	350	26.68	455	10.25	560	0.243
250	4.05	355	31.18	460	9.52	565	0.182
255	3.24	360	35.03	465	8.78	570	0.136
260	2.50	365	37.91	470	8.02	575	0.101
265	1.86	370	39.61	475	7.24	580	0.0739
270	1.35	375	40.04	480	6.47	585	0.0539
275	0.945	380	39.26	485	5.72	590	0.0390
280	0.653	385	37.45	490	4.99	595	0.0281
285	0.458	390	34.87	495	4.31	600	0.0200
290	0.357	395	31.82	500	3.68		
295	0.362	400	28.59	505	3.10		
300	0.504	405	25.43	510	2.59		

Note:
Maric et al.,[4] calculated using the expression given in the text

(1) Gray, L. T. M.; Style, D. W. G. The absorption of light by chlorine, bromine and their gaseous mixtures. *Proc. Roy. Soc. London* **1930**, *A 126*, 603-612, doi:10.1098/rspa.1930.0029.

(2) Hubinger, S.; Nee, J. B. Absorption spectra of Cl_2, Br_2 and BrCl between 190 and 600 nm. *J. Photochem. Photobiol. A: Chem.* **1995**, *86*, 1-7, doi:10.1016/1010-6030(94)03949-U.

(3) Jost, W. Das gleichgewicht zwischen chlor, brom und bromchlorid (BrCl). *Z. Phys. Chem. A* **1931**, *153*, 143-152, doi:10.1515/zpch-1931-15310.

(4) Maric, D.; Burrows, J. P.; Moortgat, G. K. A Study of the UV-visible absorption spectra of Br_2 and BrCl. *J. Photochem. Photobiol A: Chem.* **1994**, *83*, 179-192, doi:10.1016/1010-6030(94)03823-6.

(5) Seery, D. J.; Britton, D. The continuous absorption spectra of chlorine, bromine, bromine chloride, iodine chloride, and iodine bromide. *J. Phys. Chem.* **1964**, *68*, 2263-2266, doi:10.1021/j100790a039.

(6) Sulzer, P.; Wieland, K. Intensitätsverteilung eines kontinuierlichen absorptions-spektrums in abhängigkeit von temperatur und wellenzahl. *Helv. Phys. Acta* **1952**, *25*, 653-676, doi:10.5169/seals-112328.

(7) Tellinghuisen, J. Precise equilibrium constants from spectrophotometric data: BrCl in Br_2/Cl_2 gas mixtures. *J. Phys. Chem. A* **2003**, *107*, 753-775, doi:10.1021/jp027227w.

G12. BrOCl (bromochloromonoxide)

Back to Index

$BrOCl + h\nu \rightarrow$ Products (1)

(Recommendation: 06-2, Note: 10-6, Evaluated: 10-6)

Absorption Cross Sections: The UV absorption spectrum of BrOCl, bromochloromonoxide, was measured at room temperature over the wavelength range 230–390 nm by Burkholder et al.[1] Their results are recommended and given in Table 4G-12.

Photolysis Quantum Yield and Product Studies: No recommendation.

Table 4G-12. Recommended Absorption Cross Sections of BrOCl at 298 K

λ (nm)	10^{20} σ (cm^2)	λ (nm)	10^{20} σ (cm^2)	λ (nm)	10^{20} σ (cm^2)	λ (nm)	10^{20} σ (cm^2)
230	16.8	272	200	314	55.8	338	46.7
232	15.4	274	199	316	56.6	358	22.5
234	15.2	276	191	318	57.2	360	20.2
236	15.5	278	179	320	57.4	362	18.1
238	16.6	280	165	322	57.3	364	16.1
240	18.6	282	149	324	56.9	366	14.2
242	21.7	284	132	326	56.1	368	12.3
244	26.1	286	115	328	55.1	370	10.6
246	31.6	288	100	330	53.8	372	8.66
248	39.1	290	87.2	332	52.3	374	7.34
250	48.1	292	76.3	334	50.6	376	6.12
252	59.9	294	67.9	336	48.7	378	5.01
254	73.8	296	61.6	340	44.5	380	4.00
256	89.4	298	57.0	342	42.3	382	3.10
258	107	300	54.0	344	39.9	384	2.30
260	126	302	52.4	346	37.3	386	1.62
262	145	304	52.1	348	34.7	388	1.03
264	163	306	52.3	350	32.4	390	0.55
266	179	308	53.0	352	29.8		
268	192	310	53.9	354	27.2		
270	198	312	54.7	356	24.8		

Note:
Burkholder et al.[1]

(1) Burkholder, J. B.; Knight, G.; Orlando, J. J. UV absorption spectrum of BrOCl. *J. Photochem. Photobiol. A: Chem.* **2000**, *134*, 133-137, doi:10.1016/S1010-6030(00)00261-6.

G13. CH_3Br (methyl bromide)

Back to Index

$CH_3Br + h\nu$	$\rightarrow CH_3 + Br$	295 kJ mol^{-1}	406 nm	(1)
	$\rightarrow CH_2Br + H$	310 kJ mol^{-1}	387 nm	(2)

(Recommendation: 15-10, Note: 15-10, Evaluated: 15-10)

Absorption Cross Sections: The UV absorption spectrum of CH_3Br, methyl bromide, has been measured at room temperature by Davidson[1] (205–270 nm), Gordus and Bernstein[5] (204–260 nm), Robbins[10] (174–270 nm), Uthman et al.[12] (200–260 nm), Molina et al.[8] (190–290 nm), Felps et al.[3] (201.6 nm), Man et al.[7] (180–264 nm), and over the temperature range 210–295 K by Gillotay and Simon[4] (180–280 nm). At wavelengths >180 nm and <270 nm, the room temperature values of Gordus and Bernstein,[5] Robbins,[10] Uthman et al.,[12] Molina et al.,[8] Gillotay and Simon,[4] and the values of Davidson[1] at wavelengths >210 nm are in very good agreement, to within 10% and within 2% at the absorption maximum ~201 nm. The value from Felps et al.[3] at 202 nm is lower by ~10% than the other studies. The cross section data of Man et al.,[7] reported graphically, are lower by 20–30% over the entire band in comparison with the other data sets. The recommended absorption cross sections in Table 4G-13 are the mean of the values reported by Gillotay and Simon[4] and Robbins[10] for the range 182–188 nm, the mean of the values reported by Gillotay and Simon,[4] Uthman et al.,[12] and Robbins[10] for the range 190–198 nm, the mean of the values reported by Gillotay and Simon,[4] Molina et al.,[8] Uthman et

al.,[12] and Robbins[10] for the range 200–260 nm, the mean of the values reported by Gillotay and Simon,[4] Molina et al.,[8] and Robbins[10] for the range 262–268 nm; the mean of the values reported by Gillotay and Simon[4] and Molina et al.[8] for the range 270–280 nm, and the data from Molina et al.[8] for the range 285–290 nm. A wavelength independent cross section uncertainty factor of 1.2 (2σ) is assigned for the recommended wavelength range.

The VUV absorption spectrum at 298 K was measured by Olney et al.[9] (2.8–199 nm) and Locht et al.[6] (50–207 nm). A Lyman-α cross section of 3.2×10^{-17} cm^2 molecule^{-1} from the Locht et al. study is recommended with an uncertainty factor of 1.3 (2σ), which covers the range in the available experimental data.

Gillotay and Simon[4] report a slight temperature dependence in the absorption cross sections for wavelengths >220 nm where the values decrease with decreasing temperature. Gillotay and Simon[4] parameterized the cross sections and the temperature dependence using an empirical polynomial expansion:

$$\log_{10} \sigma(\lambda, T) = \sum A_n \lambda^n + (T–273) \times \sum B_n \lambda^n$$

and reported calculated values for T = 210, 230, 250, 270, and 295 K. However, the fit parameters given in Gillotay et al. result in a systematic bias in the calculated cross sections at wavelengths greater than 200 nm and a poor fit to their experimental data at shorter wavelengths. A re-fit of their data yielded the A_n and B_n parameters below, which are valid for the wavelength range 210–290 nm and temperature range 210–300 K. The re-fit removes the systematic bias and reproduces the experimental data to within 5%, while improving the short wavelength fit although deviations are still significant. This fit is recommended.

$A_0 = 7.997$	$B_0 = 0.457415$
$A_1 = –0.889724$	$B_1 = –0.00882996$
$A_2 = 0.00838084$	$B_2 = 6.40235 \times 10^{-5}$
$A_3 = –3.03191 \times 10^{-5}$	$B_3 = –2.06827 \times 10^{-7}$
$A_4 = 3.69427 \times 10^{-8}$	$B_4 = 2.51393 \times 10^{-10}$

Photolysis Quantum Yield and Product Studies: Quantum yields for Br and H atom formation in the photodissociation of CH_3Br were measured at 298 K by Talukdar et al.[11] The quantum yields for Br atom formation were found to be close to unity, Φ(Br) = 1.05 ± 0.11, 1.10 ± 0.20, and 1.01 ± 0.16 at 193, 222, and 248 nm, respectively. The quantum yield for H atom formation in the photolysis at 193 nm was measured to be Φ(H) = 0.002 ± 0.001, whereas H atoms could not be detected in the photolysis at 222 and 248 nm. Using broadband flash photolysis of CH_3Br, Ebenstein et al.[2] reported a Br*($^2P_{1/2}$) fractional yield, Br*($^2P_{1/2}$)/(Total Br), of 0.15 ± 0.12.

Table 4G-13. Recommended Absorption Cross Sections of CH_3Br at 296 K

λ (nm)	10^{20} σ (cm^2)	λ (nm)	10^{20} σ (cm^2)	λ (nm)	10^{20} σ (cm^2)
182	19.8	218	42.3	254	0.484
184	21.0	220	36.6	256	0.340
186	27.8	222	31.1	258	0.240
188	35.2	224	26.6	260	0.162
190	44.2	226	22.2	262	0.115
192	53.8	228	18.1	264	0.0795
194	62.6	230	14.7	266	0.0551
196	69.7	232	11.9	268	0.0356
198	76.1	234	9.41	270	0.0246
200	79.0	236	7.38	272	0.0172
202	79.2	238	5.73	274	0.0114
204	78.0	240	4.32	276	0.00808
206	75.2	242	3.27	278	0.00553
208	70.4	244	2.37	280	0.00382
210	65.5	246	1.81	285	0.00110
212	59.9	248	1.31	290	0.00030
214	54.2	250	0.921		
216	47.9	252	0.683		

Note:
182–188 nm: mean of data from Gillotay and Simon[4] and Robbins[10]
190–198 nm: mean of data from Gillotay ad Simon,[4] Uthman et al.,[12] and Robbins[10]

200–260 nm: mean of data from Gillotay and Simon,[4] Molina et al.,[8] Uthman et al.,[12] and Robbins[10]
262–268 nm: mean of data from Gillotay and Simon,[4] Molina et al.,[8] and Robbins[10]
270–280 nm: mean of Gillotay and Simon[4] and Molina et al.[8]
285–290 nm: Molina et al.[8]

(1) Davidson, N. The ultraviolet absorption spectra and the refractive indices of some fluorobromomethanes. *J. Am. Chem. Soc.* **1951**, *73*, 467-468, doi:10.1021/ja01145a506.
(2) Ebenstein, W. L.; Wiesenfeld, J. R.; Wolk, G. L. Photodissociation of alkyl bromides. *Chem. Phys. Lett.* **1978**, *53*, 185-189, doi:10.1016/0009-2614(78)80420-5.
(3) Felps, W. S.; Rupnik, K.; McGlynn, S. P. Electronic spectroscopy of the cyanogen halides. *J. Phys. Chem.* **1991**, *95*, 639-656, doi:10.1021/j100155a028.
(4) Gillotay, D.; Simon, P. C. Ultraviolet absorption cross-sections of methyl bromide at stratospheric temperatures. *Ann. Geophys.* **1988**, *6*, 211-215.
(5) Gordus, A. A.; Bernstein, R. B. Isotope effect in continuous ultraviolet absorption spectra: Methyl bromide-d_3 and chloroform-*d*. *J. Chem. Phys.* **1954**, *22*, 790-795, doi:10.1063/1.1740194.
(6) Locht, R.; Leyh, B.; Jochims, H. W.; Baumgärtel, H. The vacuum UV photoabsorption spectrum of methyl bromide (CH_3Br) and its perdeuterated isotopomer CD_3Br: a Rydberg series analysis. *Chem. Phys.* **2005**, *317*, 73-86, doi:10.1016/j.chemphys.2005.06.002.
(7) Man, S.-Q.; Kwok, W. M.; Phillips, D. L.; Johnson, A. E. Short-time photodissociation dynamics of A-band and B-band bromoiodomethane in solution: An examination of bond selective electronic excitation. *J. Chem. Phys.* **1996**, *105*, 5842-5857, doi:10.1063/1.472426.
(8) Molina, L. T.; Molina, M. J.; Rowland, F. S. Ultraviolet absorption cross sections of several brominated methanes and ethanes of atmospheric interest. *J. Phys. Chem.* **1982**, *86*, 2672-2676, doi:10.1021/j100211a023.
(9) Olney, T. N.; Cooper, G.; Chan, W. F.; Burton, G. R.; Brion, C. E.; Tan, K. H. Absolute photoabsorption and photoionization studies of methyl bromide using dipole electron impact and synchroton radiation PES techniques. *Chem. Phys.* **1997**, *218*, 127-149, doi:10.1016/S0301-0104(97)00066-9.
(10) Robbins, D. E. Photodissociation of methyl chloride and methyl bromide in the atmosphere. *Geophys. Res. Lett.* **1976**, *3*, 213-216, doi:10.1029/GL003i004p00213.
(11) Talukdar, R. K.; Vashjiani, G. L.; Ravishankara, A. R. Photodissociation of bromocarbons at 193, 222, and 248 nm: Quantum yields of Br atom at 298 K. *J. Chem. Phys.* **1992**, *96*, 8194-8201, doi:10.1063/1.462324.
(12) Uthman, A. P.; Demlein, P. J.; Allston, T. D.; Withiam, M. C.; McClements, M. J.; Takacs, G. A. Photoabsorption spectra of gaseous methyl bromide, ethylene dibromide, nitrosyl bromide, thionyl chloride, and sulfuryl chloride. *J. Phys. Chem.* **1978**, *82*, 2252-2257, doi:10.1021/j100509a021.

G14. CH_2Br_2 (dibromomethane)

Back to Index

$CH_2Br_2 + h\nu \rightarrow CH_2Br + Br$	281 kJ mol^{-1}	426 nm	(1)

(Recommendation: 06-2, Note: 10-6, Evaluated: 10-6)

Absorption Cross Sections: The UV absorption spectrum of CH_2Br_2, dibromomethane, has been measured at room temperature by Molina et al.[3] (200–300 nm), Gillotay et al.[1,2] (174–290 nm), and Mössinger et al.[4] (215–300 nm). The absorption cross sections are in good agreement in the range 200–255 nm, to within 10%, and at 275 nm they are within 30%. The recommended absorption cross sections in Table 4G-14 are the values from Gillotay et al.[1,2] in the region 174–198 nm, the mean of the values reported by Molina et al.[3] and Gillotay et al.[1,2] for the range 200–215 nm, the mean of the values reported by the three groups for the range 220–290 nm, and values from Mössinger et al.[4] for the range 295–300 nm. On the basis of the level of agreement among the available studies, cross section uncertainty factors (2σ) of 1.05 (200–250 nm), 1.1 (250–270 nm), and 1.2 (270–300 nm) are estimated for the wavelength ranges given in parenthesis.

The absorption spectrum temperature dependence was measured by Gillotay et al.[1,2] (174–290 nm) over the temperature range 210–295 K and Mössinger et al.[4] (215–300 nm) over the range 250–348 K. The absorption cross sections decrease at wavelength >~235 nm and increase between 235 and 207 nm with decreasing temperature. At shorter wavelengths, Gillotay et al.[1,2] report a slight increase in the cross sections in the range 175–189 nm and a slight decrease around the maximum near 200 nm. Gillotay et al.[1,2] parameterized the cross sections and the temperature dependence using an empirical polynomial expansion:

$$\log_{10} \sigma(\lambda, T) = \sum A_n \lambda^n + (T-273) \times \sum B_n \lambda^n$$

and report calculated values for T = 210, 230, 250, 270, and 295 K. The A_n and B_n parameters, which are valid for the wavelength range 210–290 nm and temperature range 210–300 K are given below.

$A_0 = -70.211776$ $B_0 = 2.899280$
$A_1 = 1.940326 \times 10^{-1}$ $B_1 = -4.327724 \times 10^{-2}$
$A_2 = 2.726152 \times 10^{-3}$ $B_2 = 2.391599 \times 10^{-4}$
$A_3 = -1.695472 \times 10^{-5}$ $B_3 = -5.807506 \times 10^{-7}$
$A_4 = 2.500066 \times 10^{-8}$ $B_4 = 5.244883 \times 10^{-10}$

Mössinger et al.[4] parameterized their cross section data using the expression:

$$\ln \sigma(\lambda, T) = \ln \sigma(\lambda, 298\ K) + B(\lambda)\ (T-298)$$

for the ranges 215–300 nm and 250–348 K. The parameterizations given by Gillotay et al.[1,2] and Mössinger et al.[4] yield cross sections that agree at 250 K to within 5% in the range 215–265 nm and to within 10% in the range 270–285 nm. The B(λ) coefficients from Mössinger et al.[4] are given in Table 4G-14 and recommended for use in model calculations.

Photolysis Quantum Yield and Product Studies: It is expected that photolysis will rupture the C-Br bond with unity quantum yield.

Table 4G-14. Recommended Absorption Cross Sections of CH_2Br_2 at 298 K

λ (nm)	10^{20} σ (cm^2)	λ (nm)	10^{20} σ (cm^2)	10^3 B (K^{-1})	λ (nm)	10^{20} σ (cm^2)	10^3 B (K^{-1})
174	1170.9	198	226.0		255	14.10	3.91
176	662.4	200	225.6		260	6.607	5.16
178	377.2	205	215.3		265	3.037	6.33
180	241.0	210	234.5		270	1.347	7.75
182	178.4	215	263.2	–2.02	275	0.590	8.74
184	154.4	220	272.0	–1.79	280	0.255	11.6
186	153.5	225	247.4	–1.50	285	0.114	13.8
188	166.1	230	195.8	–0.96	290	0.0499	15.3
190	187.0	235	138.9	–0.04	295	0.0210	16.5
192	209.3	240	88.60	0.71	300	0.0090	21.9
194	222.5	245	51.90	1.80			
196	228.3	250	28.03	2.70			

Note:
Absorption cross sections (σ):
174–198 nm: Gillotay et al.[1,2]
200–210 nm: mean of data from Molina et al.[3] and Gillotay et al.[1,2]
215–290 nm: mean of data from Molina et al.[3] Gillotay et al.,[1,2] and Mössinger et al.[4]
295–300 nm: Mössinger et al.[4]
Temperature dependence (B):
Mössinger et al.[4]

(1) Gillotay, D.; Simon, P. C. Ultraviolet absorption cross-sections of photoactive species of stratospheric interest Part 1: The halocarbons. *Aeronomica Acta A* **1990**, *356*, 1-173, doi:10.18758/A_356.
(2) Gillotay, D.; Simon, P. C.; Dierickx, L. Temperature dependence of ultraviolet absorption cross-sections of brominated methanes and ethanes. *Aeronomica Acta* **1988**, *A335*, 1-25.
(3) Molina, L. T.; Molina, M. J.; Rowland, F. S. Ultraviolet absorption cross sections of several brominated methanes and ethanes of atmospheric interest. *J. Phys. Chem.* **1982**, *86*, 2672-2676, doi:10.1021/j100211a023.
(4) Mössinger, J. C.; Shallcross, D. E.; Cox, R. A. UV-Vis absorption cross-sections and atmospheric lifetimes of CH_2Br_2, CH_2I_2 and CH_2BrI. *J. Chem. Soc. Faraday Trans.* **1998**, *94*, 1391-1396, doi:10.1039/a709160e.

G15. $CHBr_3$ (tribromomethane, bromoform)

Back to Index

$CHBr_3 + h\nu$	$\rightarrow CHBr_2 + Br$	245 kJ mol^{-1}	489 nm	(1)
	$\rightarrow CHBr + Br_2$	354 kJ mol^{-1}	338 nm	(2)

(Recommendation: 15-10, Note: 15-10, Evaluated: 15-10)

Absorption Cross Sections: The UV absorption spectrum of $CHBr_3$, tribromomethane (bromoform), has been measured by Gillotay et al.[3] (170–310 nm, 240–295 K), Moortgat et al.[4] (286–362 nm, 256–296 K), and Papanastasiou et al.[5] (300–345 nm, 260–330 K). The agreement in the cross sections reported in these studies at wavelengths less than 310 nm is very good. Moortgat et al. reported possible complications to their measurements at the longer wavelengths due to the possible presence of impurities as well as optical artifacts arising from adsorption of $CHBr_3$ on the cell windows. The Papanastasiou et al. study addressed these potential complications in their cavity ring-down spectroscopy measurements, while also addressing contributions from Rayleigh scattering. The recommended cross sections in Table 4G-15 are the values from Gillotay et al. for the range 170–258 nm and for wavelengths greater than 258 nm from the spectrum parameterization of Papanastasiou et al. given below.

The absorption cross sections increase around the three absorption maxima in the ranges 178–189 nm, 194–208 nm, and 208–234 nm, and decrease at wavelengths <179 nm, over the range 189–194 nm, and >235 nm with decreasing temperature. Gillotay et al.[3] parameterized the cross sections and the temperature dependence using an empirical polynomial expansion:

$$\log_{10}(\sigma(\lambda, T)) = \sum A_n \lambda^n + (T-273) \times \sum B_n \lambda^n$$

and report calculated values for 210, 230, 250, 270, and 295 K. The A_n and B_n parameters, which are valid for the wavelength range 240–310 nm and temperature range 210–300 K are given below.

$A_0 = -110.2782$	$B_0 = -1.5312 \times 10^{-1}$
$A_1 = 1.0281$	$B_1 = 1.6109 \times 10^{-3}$
$A_2 = -3.6626 \times 10^{-3}$	$B_2 = -5.8075 \times 10^{-6}$
$A_3 = 4.1226 \times 10^{-6}$	$B_3 = 7.2893 \times 10^{-9}$

Moortgat et al.[4] parameterized their data using the expression:

$$\sigma(\lambda,T) = \exp[(0.06183 - 0.000241\,\lambda)(273-T) - (2.376 + 0.14757\,\lambda)]$$

for the wavelength range 290–340 nm and temperature range 210–300 K.

Papanastasiou et al. parameterized the $CHBr_3$ spectrum using their experimental data and the data from Gillotay et al. and Moortgat et al. between 260–310 nm using the expression:

$$\log_{10}(\sigma(\lambda,T)) = \sum A_n \lambda^n + (296 - T) \times \sum B_n \lambda^n$$

The obtained parameters are

i	A_i	B_i
0	-32.6067	0.1582
1	0.10308	-0.0014758
2	6.39×10^{-5}	3.8058×10^{-6}
3	-7.7392×10^{-7}	9.187×10^{-10}
4	-2.2513×10^{-9}	-1.0772×10^{-11}
5	6.1376×10^{-12}	–

and the parameterization is valid over the wavelength range 260–345 nm for temperatures in the range 260–330 K. This parameterization is recommended, while the Gillotay et al. parameterization is recommended for wavelengths <260 nm. A cross section uncertainty factor (2σ) of 1.2 (330–345 nm) and 1.1 (240 to <330 nm) is assigned to the room temperature spectrum.

The VUV absorption spectrum was measured by Causley and Russell[2] (112–190 nm) and the absorption cross section at Lyman-α was measured by Vasta and Volpp[7] at 298 K. A Lyman-α cross section of 7.1×10^{-17} cm^2 $molecule^{-1}$ from the direct study of Vasta and Volpp is recommended. There is good agreement between these two studies at Lyman-α and an uncertainty factor of 1.1 (2σ) is assigned.

Photolysis Quantum Yield and Product Studies: The quantum yield for the formation of Br atoms were determined by Bayes et al.[1] between 266 and 324 nm. In the wavelength range 303–306 nm, the Br atom quantum yield is unity within experimental error. At longer wavelengths, the quantum yield decreases to 0.76 at 324 nm. Bayes et al.[1] claim that the lower than unity quantum yield may be due to systematic errors in the recommended absorption cross sections used in their data analysis. Their Br atom quantum yields in the wavelength range 300 to 324 nm would be greater and would encompass unity within their state uncertainty with the cross section data from Papanastasiou et al. Support for a unity quantum yield at λ >300 nm comes from theoretical calculations by Peterson and Francisco.[6] At 266 nm, the Br atom quantum yield is 0.76 ± 0.03, indicating that another photodissociation channel becomes important. Xu et al.[8] measured atomic Br and

molecular Br_2 by TOF mass spectrometry from bromoform photolysis at 234 and 267 nm and report evidence for the formation of CHBr + Br_2. Xu et al.[8] report $\Phi(Br) = 0.74$ and $\Phi(Br_2) = 0.26$ for 234 nm photolysis and $\Phi(Br) = 0.84$ and $\Phi(Br_2) = 0.16$ for 267 nm photolysis. A Br atom quantum yield of unity for wavelengths >300 nm is recommended.

Table 4G-15. Recommended Absorption Cross Sections of $CHBr_3$ at 296 K

λ (nm)	$10^{20}\sigma$ (cm^2)	λ (nm)	$10^{20}\sigma$ (cm^2)	λ (nm)	$10^{20}\sigma$ (cm^2)
170	1603.8	236	323.9	302	0.526
172	1173.2	238	294.7	304	0.392
174	969.6	240	272.8	306	0.292
176	872.0	242	253.3	308	0.216
178	857.6	244	233.7	310	0.160
180	831.3	246	214.4	312	0.118
182	770.3	248	193.9	314	0.0874
184	683.3	250	174.1	316	0.0644
186	570.4	252	157.7	318	0.0475
188	470.8	254	136.1	320	0.0349
190	399.1	256	116.4	322	0.0257
192	360.2	258	98.6	324	0.0189
194	351.3	260	82.9	326	0.0139
196	366.1	262	69.7	328	0.0102
198	393.6	264	58.1	330	0.00754
200	416.4	266	48.0	332	0.00556
202	433.6	268	39.4	334	0.00411
204	440.6	270	32.0	336	0.00304
206	445.0	272	25.9	338	0.00225
208	451.4	274	20.7	340	0.00167
210	468.5	276	16.5	342	0.00124
212	493.4	278	13.1	344	0.000928
214	524.2	280	10.3	346	0.000694
216	553.5	282	8.04	348	0.000521
218	573.9	284	6.25	350	0.000393
220	582.6	286	4.83		
222	578.0	288	3.72		
224	557.8	290	2.85		
226	527.2	292	2.17		
228	486.8	294	1.64		
230	441.2	296	1.24		
232	397.4	298	0.936		
234	361.8	300	0.703		

Note:
170–258 nm: Gillotay et al.[3]
260–350 nm: Papanastasiou et al.[5] parameterization

(1) Bayes, K. D.; Toohey, D. W.; Friedl, R. R.; Sander, S. P. Measurements of quantum yields of bromine atoms in the photolysis of bromoform from 266 to 324 nm. *J. Geophys. Res.* **2003**, *108*, 4095, doi:10.29/2002JD002877.

(2) Causley, G. C.; Russell, B. R. Vacuum ultraviolet absorption spectra of the bromomethanes. *J. Chem. Phys.* **1975**, *62*, 848-857, doi:10.1063/1.430535.

(3) Gillotay, D.; Jenouvrier, A.; Coquart, B.; Mérienne, M. F.; Simon, P. C. Ultraviolet absorption cross-sections of bromoform in the temperature range 295-240K. *Planet. Space Sci.* **1989**, *37*, 1127-1140, doi:10.1016/0032-0633(89)90084-6.

(4) Moortgat, G. K.; Meller, R.; Schneider, W. Temperature dependence (256-296K) of the absorption cross-sections of bromoform in the wavelength range 285-360 nm. In *The Tropospheric Chemistry of Ozone in the Polar Regions*; Niki, H., Becker, K. H., Eds.; Springer-Verlag: Berlin, 1993; pp 359-369.

(5) Papanastasiou, D. K.; McKeen, S. A.; Burkholder, J. B. The very short-lived ozone depleting substance $CHBr_3$ (bromoform): revised UV absorption spectrum, atmospheric lifetime and ozone depletion potential. *Atmos. Chem. Phys.* **2014**, *14*, 3017-3025, doi:10.5194/acp-14-3017-2014.
(6) Peterson, K. A.; Francisco, J. S. Should bromoform absorb at wavelengths longer than 300 nm? *J. Chem. Phys.* **2002**, *117*, 6103-6107, doi:10.1063/1.1502639.
(7) Vatsa, R. K.; Volpp, H.-R. Absorption cross-sections for some atmospherically important molecules at the H atom Lyman-α wavelength (121.567 nm). *Chem. Phys. Lett.* **2001**, *340*, 289-295, doi:10.1016/S0009-2614(01)00373-6.
(8) Xu, D.; Francisco, J. S.; Huang, J.; Jackson, W. M. Ultraviolet photodissociation of bromoform at 234 and 267 nm by means of ion velocity imaging. *J. Chem. Phys.* **2002**, *117*, 2578-2585, doi:10.1063/1.1491877.

G16. CH_2BrCH_2Br (1,2-dibromoethane)

Back to Index

$CH_2BrCH_2Br + h\nu \rightarrow$ Products (1)

(Recommendation: 02-25, Note: 10-6, Evaluated: 10-6)

Absorption Cross Sections: The absorption spectrum of CH_2BrCH_2Br, 1,2-dibromoethane, was measured at room temperature over the wavelength range 190–270 nm by Uthman et al.[1] Their data is recommended and listed in Table 4G-16.

Photolysis Quantum Yield and Product Studies: No recommendation.

Table 4G-16. Recommended Absorption Cross Sections of CH_2BrCH_2Br at 295 K

λ (nm)	10^{20} σ (cm^2)	λ (nm)	10^{20} σ (cm^2)	λ (nm)	10^{20} σ (cm^2)
190	230	218	170	246	9.3
192	250	220	150	248	7.1
194	270	222	130	250	5.9
196	290	224	110	252	4.4
198	300	226	89	254	4.0
200	310	228	75	256	2.8
202	310	230	62	258	2.1
204	300	232	50	260	1.9
206	290	234	41	262	1.7
208	280	236	32	264	1.4
210	260	238	26	266	1.1
212	230	240	20	268	0.9
214	210	242	16	270	0.7
216	190	244	11		

Note:
190–270 nm: Uthman et al.[1]

(1) Uthman, A. P.; Demlein, P. J.; Allston, T. D.; Withiam, M. C.; McClements, M. J.; Takacs, G. A. Photoabsorption spectra of gaseous methyl bromide, ethylene dibromide, nitrosyl bromide, thionyl chloride, and sulfuryl chloride. *J. Phys. Chem.* **1978**, *82*, 2252-2257, doi:10.1021/j100509a021.

G17. C_2H_5Br (bromoethane)

Back to Index

$C_2H_5Br + h\nu \rightarrow$ Products (1)

(Recommendation: 02-25, Note: 10-6, Evaluated: 10-6)

Absorption Cross Sections: The absorption spectrum of C_2H_5Br, bromoethane, was measured at 295 K over the wavelength range 200–260 nm by Zhang et al.[2] In this wavelength range the spectrum shows part of an absorption band with a maximum cross section of ~6×10^{-19} cm^2 at ~200 nm. The cross section at 200 nm reported by Porret and Goodeve[1] is ~10% less than in the Zhang et al. spectrum. The recommended absorption cross sections in Table 4G-17 are estimated from a figure in Zhang et al.[2]

Photolysis Quantum Yield and Product Studies: No recommendation.

Table 4G-17. Recommended Absorption Cross Sections of C_2H_5Br at 295 K

λ (nm)	10^{20} σ (cm^2)
200	61
205	60
210	54
215	45
220	34
225	24
230	15
235	8.3
240	4.3
245	2.3
250	1.1
255	0.5
260	0.2

Note:
Zhang et al.[2], values read from logarithmic plot

(1) Porret, D.; Goodeve, C. F. The continuous absorption spectra of alkyl iodides and alkyl bromides and their quantal interpretation. *Proc. Roy. Soc. Lond. A* **1938**, *165*, 31-42, doi:10.1098/rspa.1938.0042.

(2) Zhang, L.; Fuss, W.; Kompa, K. L. Bond-selective photodissociation of CX (X = Br, I) in $XC_2H_4C_2F_4X$. *Chem. Phys.* **1990**, *144*, 289-297, doi:10.1016/0301-0104(90)80092-C.

G18. CBr_2O (carbonyl dibromide, dibromophosgene)

Back to Index

$CBr_2O + h\nu \rightarrow$ Products (1)

(Recommendation: 06-2, Note: 10-6, Evaluated: 10-6)

Absorption Cross Sections: The absorption spectrum of CBr_2O, carbonyl dibromide (dibromophosgene), was measured at room temperature over the wavelength range 235–353 nm by Libuda et al.[1,2] The spectrum exhibits monotonically decreasing absorption cross sections with increasing wavelength over this range. The recommended absorption cross sections in Table 4G-18 are the averages over 1 nm intervals of the spectrum reported at 0.6 nm intervals.

Photolysis Quantum Yield and Product Studies: No recommendation.

Table 4G-18. Recommended Absorption Cross Sections of CBr_2O at 298 K

λ (nm)	10^{20} σ (cm^2)	λ (nm)	10^{20} σ (cm^2)	λ (nm)	10^{20} σ (cm^2)	λ (nm)	10^{20} σ (cm^2)
240	58.3	263	20.9	286	4.50	309	0.301
241	56.5	264	19.9	287	4.13	310	0.260
242	55.3	265	18.8	288	3.73	311	0.230
243	54.1	266	17.9	289	3.38	312	0.204
244	52.3	267	17.0	290	3.09	313	0.178
245	50.6	268	16.1	291	2.81	314	0.159
246	48.8	269	15.2	292	2.58	315	0.143
247	47.1	270	14.4	293	2.32	316	0.127
248	45.2	271	13.6	294	2.07	317	0.114
249	43.2	272	12.8	295	1.82	318	0.0995
250	41.3	273	12.0	296	1.62	319	0.0892
251	39.5	274	11.4	297	1.42	320	0.0789
252	37.7	275	10.7	298	1.26	321	0.0694
253	35.7	276	9.98	299	1.11	322	0.0633
254	33.7	277	9.24	300	0.971	323	0.0578
255	32.0	278	8.56	301	0.858	324	0.0528
256	30.4	279	7.99	302	0.750	325	0.0499
257	28.9	280	7.44	303	0.661	326	0.0449
258	27.4	281	6.91	304	0.578	327	0.0397
259	26.0	282	6.35	305	0.501	328	0.0336
260	24.5	283	5.81	306	0.437	329	0.0296
261	23.3	284	5.34	307	0.386	330	0.0264
262	22.1	285	4.92	308	0.331	331	0.0229

Note:
Libuda et al.[1,2]

(1) Libuda, H. G. Spektroskopische und kinetische Untersuchungen an halogenierten Carbonylverbindungen von atmosphärischem Interesse. PhD-Thesis, University of Wuppertal, Germany, 1992.

(2) Libuda, H. G.; Zabel, F.; Becker, K. H. "UV spectra of some organic chlorine and bromine compounds of atmospheric interest"; Kinetics and Mechanisms for the Reactions of Halogenated Organic Compounds in the Troposphere. STEP-HALOCSIDE/AFEAS WORKSHOP, 1991, Dublin, Ireland.

G19. HC(O)Br (formyl bromide)

Back to Index

$HC(O)Br + h\nu \rightarrow$ Products (1)

(Recommendation: 06-2, Note: 10-6, Evaluated: 10-6)

Absorption Cross Sections: The absorption spectrum of HC(O)Br, formyl bromide, was measured at room temperature over the wavelength range 240–340 nm by Libuda et al.[1,2] The absorption spectrum exhibits a highly structured absorption band with a maximum near 268 nm. The recommended absorption cross sections in Table 4G-19 are averages over 1 nm intervals of the spectrum reported at 0.6 nm intervals.

Photolysis Quantum Yield and Product Studies: No recommendation.

Table 4G-19. Recommended Absorption Cross Sections of HC(O)Br at 298 K

λ (nm)	10^{20} σ (cm^2)	λ (nm)	10^{20} σ (cm^2)	λ (nm)	10^{20} σ (cm^2)	λ (nm)	10^{20} σ (cm^2)
240	18.7	262	32.4	284	21.7	306	2.77
241	20.1	263	29.9	285	20.1	307	2.43
242	19.4	264	31.1	286	19.1	308	2.12
243	19.8	265	29.9	287	17.5	309	1.90
244	19.1	266	32.5	288	17.3	310	1.65
245	20.0	267	31.6	289	14.9	311	1.51
246	22.6	268	33.8	290	15.5	312	1.34
247	22.6	269	30.9	291	12.7	313	1.13
248	23.6	270	31.9	292	13.3	314	1.01
249	22.5	271	30.9	293	11.1	315	0.801
250	22.3	272	29.6	294	10.8	316	0.687
251	24.0	273	31.4	295	9.79	317	0.613
252	25.0	274	29.3	296	9.08	318	0.611
253	27.1	275	31.5	297	8.03	319	0.576
254	26.9	276	28.5	298	7.35	320	0.522
255	27.5	277	29.1	299	5.97	321	0.476
256	27.5	278	26.8	300	5.86	322	0.424
257	26.9	279	25.6	301	5.25	323	0.363
258	28.8	280	25.1	302	4.47	324	0.308
259	28.9	281	23.2	303	4.38		
260	31.9	282	23.8	304	3.53		
261	30.1	283	22.0	305	3.18		

Note:
Libuda[2]

(1) Libuda, H. G. Spektroskopische und kinetische Untersuchungen an halogenierten Carbonylverbindungen von atmosphärischem Interesse. PhD-Thesis, University of Wuppertal, Germany, 1992.

(2) Libuda, H. G.; Zabel, F.; Becker, K. H. "UV spectra of some organic chlorine and bromine compounds of atmospheric interest"; Kinetics and Mechanisms for the Reactions of Halogenated Organic Compounds in the Troposphere. STEP-HALOCSIDE/AFEAS WORKSHOP, 1991, Dublin, Ireland.

G20. CH_2ClBr (Halon–1011, chlorobromomethane)

Back to Index

CH_2ClBr (Halon–1011) + hν → Products (1)

(Recommendation: 02-25, Note: 10-6, Evaluated: 10-6)

Absorption Cross Sections: The UV absorption spectrum of CH_2ClBr, chlorobromomethane (Halon–1011), has been measured at room temperature by Cadman and Simons[1] (210–260 nm) and Orkin et al.[3] (187–290 nm). The cross section data from Cadman and Simons,[1] reported in graphical form, are up to 20% less than the data from Orkin et al.[3] The recommended absorption cross sections in Table 4G-20 are taken from Orkin et al.[3]

Photolysis Quantum Yield and Product Studies: Quantum yields for Br ($^2P_{3/2}$) and Br*($^2P_{1/2}$) atom formation in the photolysis of CH_2ClBr at 193 and 242 nm and 248, 261.5, and 266.7 nm have been measured by Zou et al.[4] and McGivern et al.,[2] respectively. The reported values are given here.

	193 nm	234 nm	248.5 nm	261.5 nm	266.7 nm
Φ(Br ($^2P_{3/2}$))	0.82 ± 0.10	0.80 ± 0.10	0.86 ± 0.10	0.84 ± 0.10	0.91 ± 0.10
Φ(Br*($^2P_{1/2}$))	0.18 ± 0.10	0.20 ± 0.10	0.14 ± 0.10	0.16 ± 0.10	0.09 ± 0.10

Table 4G-20. Recommended Absorption Cross Sections of CH_2ClBr at 295 K

λ (nm)	10^{20} σ (cm^2)	λ (nm)	10^{20} σ (cm^2)	λ (nm)	10^{20} σ (cm^2)
187	151.1	222	57.4	258	1.45
188	126.4	224	50.5	260	1.09
190	104.6	226	44.1	262	0.807
192	100.5	228	38.2	264	0.596
194	104.7	230	32.8	266	0.440
196	111.8	232	28.0	268	0.322
198	119.4	234	23.6	270	0.235
200	124.7	236	19.7	272	0.170
202	127.1	238	16.3	274	0.123
204	126.3	240	13.4	276	0.089
206	122.5	242	10.8	278	0.064
208	116.3	244	8.73	280	0.046
210	108.4	246	6.94	282	0.033
212	99.6	248	5.46	284	0.024
214	90.5	250	4.24	286	0.0178
216	81.5	252	3.29	288	0.0129
218	72.9	254	2.52	290	0.0098
220	64.8	256	1.92		

Note:
Orkin et al.[3]

(1) Cadman, P.; Simons, J. P. Reactions of hot halomethyl radicals. *Trans. Faraday Soc.* **1966**, *62*, 631-641, doi:10.1039/tf9666200631.

(2) McGivern, W. S.; Li, R.; Zou, P.; North, S. W. Photodissociation dynamics of CH_2BrCl studied using resonance enhanced multiphoton ionization (REMPI) with time-of-flight mass spectrometry. *J. Chem. Phys.* **1999**, *111*, 5771-5779, doi:10.1063/1.479874.

(3) Orkin, V. L.; Khamaganov, V. G.; Guschin, A. G.; Huie, R. E.; Kurylo, M. J. Atmospheric fate of chlorobromomethane: Rate constant for the reaction with OH, UV spectrum, and water solubility. *J. Phys. Chem. A* **1997**, *101*, 174-178, doi:10.1021/jp962428j.

(4) Zou, P.; McGivern, W. S.; North, S. W. Adiabatic and diabatic dynamics in the photodissociation of CH_2BrCl. *Phys. Chem. Chem. Phys.* **2000**, *2*, 3785-3790, doi:10.1039/b004349o.

G21. $CHClBr_2$ (Halon–1012, chlorodibromomethane)

Back to Index

$CHClBr_2$ (Halon–1012) + hν → $CHClBr + Br(^2P_{3/2})$	264 kJ mol^{-1}	454 nm	(1)
→ $CHClBr + Br^*(^2P_{1/2})$	308 kJ mol^{-1}	389 nm	(2)
→ $CHBr_2 + Cl(^2P_{3/2})$	318 kJ mol^{-1}	376 nm	(3)
→ $CHBr_2 + Cl^*(^2P_{1/2})$	329 kJ mol^{-1}	364 nm	(4)

(Recommendation: 06-2, Note: 10-6, Evaluated: 10-6)

Absorption Cross Sections: The UV absorption spectrum of $CHClBr_2$, chlorodibromomethane (Halon–1012), has been measured at room temperature by Ibuki et al.[2] (106–200 nm, presented graphically) and Taketani et al.[5] (193.3 nm) and at 240, 261, and 296 K by Bilde et al.[1] (200–310 nm). Two overlapping absorption bands are apparent at wavelengths >200 nm with maxima near 206 nm and 240 nm. The peak cross sections of these bands at 240 K are approximately 10% greater than at room temperature. In the long wavelength tail of the spectrum, the cross sections decrease with decreasing temperature, the room temperature cross section at 270 nm being ~15% greater than at 240 K. The recommended absorption cross sections in Table 4G-21 are from Bilde et al.[1] (reported at 1 nm intervals). Taketani et al.[5] reported a value of 304×10^{-20} cm^2 $molecule^{-1}$ at 193.3 nm.

Photolysis Quantum Yield and Product Studies: Quantum yields for dissociation have been reported by Tzeng et al.[6] (193 and 248 nm), McGivern et al.[4] (248–268 nm), Zou et al.[7] (193–242 nm), Lee et al.[3] (234 nm), and Taketani et al.[5] (193.3 nm). In the range 248–262 nm, $CHClBr_2$ undergoes C-Br bond rupture exclusively, whereas in the range 193–242 nm it dissociates predominantly via C-Br bond rupture with a minor contribution from C-Cl bond rupture. The relative quantum yield for ground state $Br(^2P_{3/2})$ varies from 0.80 to 0.90 for photolysis in the range 193 to 267 nm.

Table 4G-21. Recommended Absorption Cross Sections of $CHClBr_2$ at 296 K

λ (nm)	10^{20} σ (cm^2)	λ (nm)	10^{20} σ (cm^2)	λ (nm)	10^{20} σ (cm^2)
200	274.6	230	141.4	272	9.415
201	282.8	232	136.4	274	7.552
202	293.9	234	131.4	276	5.950
203	306.7	236	126.8	278	4.687
204	314.2	238	122.2	280	3.691
205	320.6	240	116.0	282	2.884
206	324.9	242	109.2	284	2.261
207	323.7	244	101.2	286	1.734
208	322.9	246	92.70	288	1.331
209	324.6	248	83.52	290	1.016
210	317.8	250	74.04	292	0.7907
211	306.2	252	64.83	294	0.6116
212	297.4	254	55.95	296	0.4583
214	279.4	256	47.67	298	0.3489
216	261.7	258	39.92	300	0.2692
218	234.9	260	33.35	302	0.2076
220	215.1	262	27.50	304	0.1588
222	199.1	264	22.50	306	0.1208
224	184.5	266	18.28	308	0.0945
226	165.3	268	14.78	310	0.0742
228	151.7	270	11.82		

Note:
Bilde et al.[1]

(1) Bilde, M.; Wallington, T. J.; Ferronato, G.; Orlando, J. J.; Tyndall, G. S.; Estupinan, E.; Haberkorn, S. Atmospheric chemistry of CH_2BrCl, $CHBrCl_2$, $CHBr_2Cl$, $CF_3CHBrCl$, and CBr_2Cl_2. *J. Phys. Chem. A* **1998**, *102*, 1976-1986, doi:10.1021/jp9733375.

(2) Ibuki, T. Vacuum ultraviolet absorption spectra and photodissociative excitation of $CHBr_2Cl$ and $CHBrCl_2$. *J. Chem. Phys.* **1992**, *96*, 8793-8798, doi:10.1063/1.462286.

(3) Lee, S.-H.; Jung, Y.-J.; Jung, K.-H. Photodissociation dynamics of CH_2BrCl at 234 nm. *Chem. Phys.* **2000**, *260*, 143-150, doi:10.1016/S0301-0104(00)00216-0.

(4) McGivern, W. S.; Li, R.; Zou, P.; North, S. W. Photodissociation dynamics of CH_2BrCl studied using resonance enhanced multiphoton ionization (REMPI) with time-of-flight mass spectrometry. *J. Chem. Phys.* **1999**, *111*, 5771-5779, doi:10.1063/1.479874.

(5) Taketani, F.; Takahashi, K.; Matsumi, Y. Quantum yields for $Cl(^2P_j)$ atom formation from the photolysis of chlorofluorocarbons and chlorinated hydrocarbons at 193.3 nm. *J. Phys. Chem. A* **2005**, *109*, 2855-2860, doi:10.1021/jp044218+.

(6) Tzeng, W. B.; Lee, Y. R.; Lin, S. M. Photodissociation of CH_2BrCl at 248 and 193 nm investigated by translational spectroscopy. *Chem. Phys. Lett.* **1994**, *227*, 467-471, doi:10.1016/0009-2614(94)00837-X.

(7) Zou, P.; McGivern, W. S.; North, S. W. Adiabatic and diabatic dynamics in the photodissociation of CH_2BrCl. *Phys. Chem. Chem. Phys.* **2000**, *2*, 3785-3790, doi:10.1039/b004349o.

G22. $CHCl_2Br$ (Halon–1021, dichlorobromomethane)

Back to Index

$CHCl_2Br$ (Halon–1021) + hν → Products (1)

(Recommendation: 02-25, Note: 10-6, Evaluated: 10-6)

Absorption Cross Sections: The absorption spectrum of $CHCl_2Br$, dichlorobromomethane (Halon–1021), has been measured at room temperature by Ibuki[3] (106–200 nm, presented graphically), Cadman and Simons[2] (201–270 nm, presented graphically), and Bilde et al.[1] (200–320 nm). Cadman and Simons[2] cross section data agree to within 15% with the room temperature cross section results from Bilde et al.,[1] however, the absorption maximum is shifted to lower wavelengths. The recommended absorption cross sections in Table 4G-22 are taken from Bilde et al.[1]

Bilde et al.[1] (200–320 nm) reported absorption spectrum measurements at 253, 273, and 298 K. A decrease of the absorption cross sections with decreasing temperature was observed over the entire wavelength range of their measurements. The cross section at 220 nm is ~6% lower at 253 K than at room temperature. A stronger temperature dependence was observed at longer wavelengths, the room temperature cross section at 320 nm being about four times larger than at 253 K.

Photolysis Quantum Yield and Product Studies: No recommendation.

Table 4G-22. Recommended Absorption Cross Sections of $CHCl_2Br$ at 298 K

λ (nm)	10^{20} σ (cm^2)	λ (nm)	10^{20} σ (cm^2)	λ (nm)	10^{20} σ (cm^2)
200	115.0	230	58.1	276	1.63
202	93.8	232	54.6	278	1.32
204	81.1	234	50.0	280	1.07
206	73.6	236	45.8	282	0.865
208	69.0	238	41.6	284	0.694
209	69.8	240	37.3	286	0.573
210	68.8	242	33.0	288	0.454
211	67.4	244	29.3	290	0.384
212	68.4	246	25.8	292	0.317
213	70.0	248	22.2	294	0.265
214	70.1	250	19.2	296	0.217
215	70.2	252	16.5	298	0.176
216	71.1	254	13.6	300	0.146
217	71.0	256	11.5	302	0.118
218	70.7	258	9.75	304	0.0962
219	71.3	260	8.19	306	0.0761
220	71.6	262	6.82	308	0.0617
221	70.6	264	5.61	310	0.0496
222	69.3	266	4.68	312	0.0395
223	68.7	268	3.74	314	0.0317
224	68.2	270	3.01	316	0.0259
226	65.2	272	2.48	318	0.0210
228	62.2	274	2.02	320	0.0171

Note:
Bilde et al.[1]

(1) Bilde, M.; Wallington, T. J.; Ferronato, G.; Orlando, J. J.; Tyndall, G. S.; Estupinan, E.; Haberkorn, S. Atmospheric chemistry of CH_2BrCl, $CHBrCl_2$, $CHBr_2Cl$, $CF_3CHBrCl$, and CBr_2Cl_2. *J. Phys. Chem. A* **1998**, *102*, 1976-1986, doi:10.1021/jp9733375.

(2) Cadman, P.; Simons, J. P. Reactions of hot halomethyl radicals. *Trans. Faraday Soc.* **1966**, *62*, 631-641, doi:10.1039/tf9666200631.

(3) Ibuki, T. Vacuum ultraviolet absorption spectra and photodissociative excitation of $CHBr_2Cl$ and $CHBrCl_2$. *J. Chem. Phys.* **1992**, *96*, 8793-8798, doi:10.1063/1.462286.

G23. CCl_3Br (Halon–1031, trichlorobromomethane)

Back to Index

CCl_3Br (Halon–1031) + hν → CCl_3 + $Br(^2P_{3/2})$	224 kJ mol^{-1}	534 nm	(1)
→ CCl_3 + $Br(^2P_{1/2})$	268 kJ mol^{-1}	446 nm	(2)

(Recommendation: 02-25, Note: 10-6, Evaluated: 10-6)

Absorption Cross Sections: The UV absorption spectrum of CCl_3Br, trichlorobromomethane (Halon–1031), has been measured at room temperature by Cadman and Simons[1] (207–305 nm), Sidebottom et al.[6] (365 nm), Roxlo and Mandl[4] (170–230 nm), Ibuki et al.[2] (105–198 nm), and Seccombe et al.[5] (50–200 nm). The absorption spectrum has a strong absorption band between 170 and 220 nm with the maximum near 185 nm and $\sigma \approx (1.1–1.4) \times 10^{-17}$ cm^2 $molecule^{-1}$ with a shoulder in the range 220–305 nm. The recommended absorption cross sections in Table 4G-23 for the wavelength region 235–305 nm have been read at 5 nm intervals from a figure in the paper of Cadman and Simons[1] and the value for 365 nm was reported Sidebottom et al.[6]

Photolysis Quantum Yield and Product Studies: Product quantum yields were studied at 365 nm by Sidebottom et al.[6] They report evidence that Br + CCl_3 are the primary products and the yields are pressure and temperature dependent. Quantum yields for Br*($^2P_{1/2}$) atom formation in the photolysis at 234 and 265 nm were reported to be 0.31 ± 0.01 and 0.68 ± 0.02, respectively, by Jung et al.[3]

Table 4G-23. Recommended Absorption Cross Sections of CCl_3Br at 298 K

λ (nm)	10^{20} σ (cm^2)
235	50
240	50
245	49
250	48
255	46
260	42
265	34
270	19
275	11
280	7.2
285	5.0
290	3.3
295	2.2
300	1.4
305	1.0
365	0.0077

Note:
235–305 nm: Cadman and Simons[1]
365 nm: Sidebottom et al.[6]

(1) Cadman, P.; Simons, J. P. Reactions of hot halomethyl radicals. *Trans. Faraday Soc.* **1966**, *62*, 631-641, doi:10.1039/tf9666200631.

(2) Ibuki, T.; Takahashi, N.; Hiraya, A.; Shobatake, K. $CCl_2(\tilde{A}\ ^1B_1)$ radical formation in VUV photolyses of CCl_4 and $CBrCl_3$. *J. Chem. Phys.* **1986**, *85*, 5717-5722, doi:10.1063/1.451532.

(3) Jung, Y.-J.; Park, M. S.; Kim, Y. S.; Jung, K.-H.; Volpp, H.-R. Photodissociation of $CBrCl_3$ at 234 and 265 nm: Evidence of the curve crossing. *J. Chem. Phys.* **1999**, *111*, 4005-4012, doi:10.1063/1.479182.

(4) Roxlo, C.; Mandl, A. Vacuum ultraviolet absorption cross sections for halogen containing molecules. *J. Appl. Phys.* **1980**, *51*, 2969-2972, doi:10.1063/1.328108.

(5) Seccombe, D. P.; Tuckett, R. P.; Baumgärtel, H.; Jochims, H. W. Vacuum-UV fluorescence spectroscopy of CCl_3F, CCl_3H and CCl_3Br in the range 8–30 eV. *Phys. Chem. Chem. Phys.* **1999**, *1*, 773-782, doi:10.1039/a809422e.

(6) Sidebottom, H. W.; Tedder, J. M.; Walton, J. C. Photolysis of bromotrichloromethane. *Trans. Faraday Soc.* **1969**, *65*, 755-762, doi:10.1039/tf9696500755.

G24. CHF_2Br (Halon–1201, difluorobromomethane)

Back to Index

CHF_2Br (Halon–1201) + hν → Products (1)

(Recommendation: 02-25, Note: 10-6, Evaluated: 10-6)

Absorption Cross Sections: The UV absorption spectrum of CHF_2Br, difluorobromomethane (Halon–1201), has been measured at room temperature by Davidson[1] (207–255 nm), Talukdar et al.[4] (190–280 nm), Gillotay et al.[2] (166–267 nm), and Orkin and Kasimovskaya [3] (190–280 nm). Gillotay et al.[2] carried out measurements at 210–295 K over the wavelength range 166–267 nm and report smoothed calculated cross sections for 210, 230, 250, 270, and 295 K. The results of Davidson,[1] Orkin and Kasimovskaya,[3] and Gillotay et al.[2] are in excellent agreement at wavelengths <240 nm. The values from Gillotay et al.[2] are increasingly smaller (by up to about 40% at 260 nm) and those of Davidson[1] are smaller (by up to about 30% at 250 nm) than the values reported by Orkin and Kasimovskaya.[3] The results of Talukdar et al.,[4] who report a spectrum in graphical form with extrapolated values out to 360 nm, appear to be in agreement with the results of Orkin and Kasimovskaya.[3] The recommended absorption cross sections in Table 4G-24 are the values from Gillotay et al.[2] at the centers of the 500 cm^{-1} intervals between 168 and 188 nm and the values from Orkin and Kasimovskaya[3] in the region 190–280 nm.

An increase in the absorption cross sections around the absorption peak (168–215 nm) and a decrease at wavelengths >215 nm with decreasing temperature (295–210 K) was reported by Gillotay et al.[2]

Photolysis Quantum Yield and Product Studies: No recommendation.

Table 4G-24. Recommended Absorption Cross Sections of CHF_2Br at 298 K

λ (nm)	10^{20} σ (cm^2)	λ (nm)	10^{20} σ (cm^2)	λ (nm)	10^{20} σ (cm^2)
168.10	3.97	206	23.2	246	0.299
170.95	8.21	208	21.2	248	0.220
173.15	12.5	210	19.0	250	0.161
174.65	15.6	212	16.8	252	0.117
176.20	18.8	214	14.6	254	0.0849
177.80	21.9	216	12.6	256	0.0615
179.40	24.5	218	10.6	258	0.0444
181.00	26.6	220	8.85	260	0.0319
182.65	28.3	222	7.25	262	0.0230
184.35	29.6	224	5.88	264	0.0166
186.05	30.6	226	4.71	266	0.0121
187.80	31.4	228	3.73	268	0.0087
190	32.5	230	2.91	270	0.0063
192	32.4	232	2.24	272	0.0046
194	31.8	234	1.71	274	0.0034
196	31.0	236	1.30	276	0.0024
198	29.9	238	0.982	278	0.0018
200	28.6	240	0.735	280	0.0012
202	27.0	242	0.547		
204	25.2	244	0.405		

Note:
168–188 nm: Gillotay et al.[2]
190–280 nm: Orkin and Kasimovskaya[3]

(1) Davidson, N. The ultraviolet absorption spectra and the refractive indices of some fluorobromomethanes. *J. Am. Chem. Soc.* **1951**, *73*, 467-468, doi:10.1021/ja01145a506.
(2) Gillotay, D.; Simon, P. C.; Dierickx, L. Temperature dependence of ultraviolet absorption cross-sections of brominated methanes and ethanes. *Aeronomica Acta* **1988**, *A335*, 1-25.
(3) Orkin, V. L.; Kasimovskaya, E. E. Ultraviolet absorption spectra of some Br-containing haloalkenes. *J. Atmos. Chem.* **1995**, *21*, 1-11, doi:10.1007/BF00712435.
(4) Talukdar, R.; Mellouki, A.; Gierczak, T.; Burkholder, J. B.; McKeen, S. A.; Ravishankara, A. R. Atmospheric lifetime of CHF_2Br, a proposed substitute for halons. *Science* **1991**, *252*, 693-695, doi:10.1126/science.252.5006.693.

G25. CF_2Br_2 (Halon–1202, difluorodibromomethane)

Back to Index

CF_2Br_2 (Halon–1202) + hν → CF_2Br + Br (1)
→ CF_2 + Br + Br (2)
→ CF_2 + Br_2 (3)

(Recommendation: 15-10, Note: 15-10, Evaluated: 15-10)

Absorption Cross Sections: The UV absorption spectrum of CF_2Br_2, difluorodibromomethane (Halon–1202), has been measured at room temperature by Davidson[2] (215–290 nm), Walton[15] (200–310 nm), Molina et al.[8] (190–340 nm), Orkin and Kasimovskaya[9] (190–320 nm), Gillotay and Simon[4] (170–304 nm), Burkholder et al.[1] (190–320 nm), and Papanastasiou et al.[10] (300-350 nm). The study by Papanastasiou et al. reported absorption cross section data in the long wavelength region that were corrected for Rayleigh scattering, which is most important at the longest wavelengths. The room temperature cross section data, except those of Walton,[15] are in good agreement, better than 10%, over the wavelength range 190–300 nm. At the absorption maximum near 226 nm, the data of Davidson[2] and Molina et al.[8] are the highest and lowest, respectively. At wavelengths >300 nm, the values from Orkin and Kasimovskaya,[9] Burkholder et al.,[1] and Papanastasiou et al. agree to within 15%, whereas those of Molina et al.[8] are larger with the difference increasing with increasing wavelength, up to ~200% at 320 nm and ~660% at 340 nm. The recommended absorption cross sections in

Table 4G-25 are the values from Gillotay and Simon[4] in the region 170–188 nm, the mean of the values reported by Gillotay and Simon,[4] Orkin and Kasimovskaya,[9] and Burkholder et al.[1] for the wavelength range 190–264 nm, and for the wavelength range 266–350 nm from the parameterization given by Papanastasiou et al. (see below). Uncertainty factors (2σ) for the room temperature absorption cross sections are estimated to be 1.05 for the wavelength range 180 to 230 nm, 1.1 for the wavelength range 230 to 280 nm, and 1.2 for wavelengths in the range 280 to 350 nm. The uncertainty factors encompass the range of the data used to develop the recommendation.

The VUV absorption spectrum at room temperature has been measured Doucet et al.[3] (60–220 nm) and Seccombe et al.[11] (55–175 nm). The reported spectra show some systematic discrepancies in their wavelength dependence, although the two studies are in reasonable agreement at Lyman-α, 121.567 nm. The high-resolution σ(Lyman-α, 298 K) measurement of Seccombe et al., 10×10^{-17} cm^2 molecule^{-1}, is recommended with an uncertainty factor of 1.5 (2σ).

The absorption spectrum temperature dependence was measured by Gillotay and Simon[4] (170–304 nm) over the range 210–295 K, Burkholder et al.[1] (190–320 nm) over the range 210–296 K, and Papanastasiou et al. (300–325 nm) over the range 210–296 K. The absorption cross sections increase at the absorption peaks, near 190 and 225 nm, and decrease at wavelengths >240 nm and <177 nm with decreasing temperature. Gillotay and Simon[4] observed a systematic temperature behavior with an increase in the peak cross section at ~225 nm of $\sim 9 \times 10^{-20}$ cm^2 molecule^{-1} per 20 K decrease in temperature. Burkholder et al.[1] observed a less pronounced temperature behavior below 250 K with the peak cross section at 210 K that is 5% lower than that observed by Gillotay and Simon[4] (the room temperature cross sections from these two studies are nearly identical). Different empirical parameterizations for the temperature dependence of the absorption cross section were proposed. Gillotay and Simon[4] used a polynomial expansion:

$$\log_{10} \sigma(\lambda, T) = \sum A_n \lambda^n + (T-273) \times \sum B_n \lambda^n$$

and report calculated values for 210, 230, 250, 270, and 295 K. The A_n and B_n parameters, which are valid for the wavelength range 222–304 nm and temperature range 210–300 K are as follows. This parameterization is recommended for wavelengths in the range 222 nm < λ <266 nm.

$A_0 = -206.2$	$B_0 = 1.0460 \times 10^{-1}$
$A_1 = 2.3726$	$B_1 = -1.4124 \times 10^{-3}$
$A_2 = -1.0527 \times 10^{-2}$	$B_2 = 6.9015 \times 10^{-6}$
$A_3 = 1.9239 \times 10^{-5}$	$B_3 = -1.5164 \times 10^{-8}$
$A_4 = -1.2242 \times 10^{-8}$	$B_4 = 1.3990 \times 10^{-11}$

Burkholder et al.[1] used the expression:

$$\ln \sigma(\lambda, T) = (\sum A_i (\lambda - 268.7998)^i) (1 + (296-T) \sum B_i (\lambda - 268.7998)^i)$$

and reported the following A_i and B_i parameters for the wavelength range 235–260 nm and temperature range 210–296 K.

$A_0 = -44.42756$	$B_0 = 1.481886 \times 10^{-4}$
$A_1 = -1.464955 \times 10^{-1}$	$B_1 = 6.77182 \times 10^{-6}$
$A_2 = -5.692188 \times 10^{-4}$	$B_2 = 1.154347 \times 10^{-7}$
$A_3 = 1.155366 \times 10^{-5}$	$B_3 = -2.77145 \times 10^{-11}$
$A_4 = -1.399502 \times 10^{-7}$	$B_4 = -6.619515 \times 10^{-11}$

Burkholder et al.[1] also report a parameterization for cross sections extrapolated out to 400 nm:

$$\ln \sigma(\lambda, T) = (\sum A_i (\lambda - 301.0104)^i) (1 + (296-T) \sum B_i (\lambda - 301.0104)^i)$$

with the following parameters.

$A_0 = -49.50456$	$B_0 = 3.616315 \times 10^{-4}$
$A_1 = -1.633525 \times 10^{-1}$	$B_1 = 5.534952 \times 10^{-6}$
$A_2 = 5.170758 \times 10^{-6}$	$B_2 = -1.997903 \times 10^{-8}$
$A_3 = 4.332654 \times 10^{-6}$	$B_3 = -9.234512 \times 10^{-11}$
$A_4 = -3.899051 \times 10^{-8}$	$B_4 = 1.776346 \times 10^{-12}$

Note: In the Burkholder et al.[1] paper, the parameterization equation is written in terms of $\log_{10}(\sigma(\lambda,T))$ but the correct expression should be given in terms of $\ln(\sigma(\lambda,T))$, as given here.

The recommended spectrum parameterization for wavelengths >264 nm is taken from the Papanastasiou et al. study, which accounted for Rayleigh scattering that was significant for wavelengths >300 nm. They used the same empirical expression used in the Burkholder et al. study

$$\ln\big(\sigma(\lambda,T)\big) = \sum_i A_i\big(\lambda-\bar{\lambda}\big)^i \times \left[1 + (296-T)\sum_i B_i\big(\lambda-\bar{\lambda}\big)^i\right]$$

to parameterize the spectrum for wavelengths ≥260 nm and temperatures between 210 and 298 K using a combination of their cross section data and the data from Burkholder et al. The parameters are given below.

$\bar{\lambda}$ = 287.861		
i	A_i	B_i
0	–47.4178	0.0003173
1	–0.1567273	1.2323×10^{-5}
2	-2.624376×10^{-4}	2.68×10^{-8}
3	-6.78412×10^{-6}	-5.28×10^{-9}
4	1.261478×10^{-7}	6.99×10^{-11}

Photolysis Quantum Yield and Product Studies: The quantum yield for formation of CF_2O and Br_2 in the photolysis of CF_2Br_2 at 206, 248, and 302 nm in the presence of O_2 has been measured to be unity, independent of pressure, by Molina and Molina.[7] This is in contrast to an earlier report by Walton[15] that the quantum yield at 265 nm decreases from unity when the system pressure is raised to 50 Torr of CO_2. Quantum yields for Br atom formation of $\Phi(Br) = 1.96 \pm 0.27$, 1.63 ± 0.19, and 1.01 ± 0.15, in the photodissociation of CF_2Br_2 at 193, 222, and 248 nm, respectively, were reported by Talukdar et al.[13] A quantum yield for CF_2 formation, $\Phi(CF_2) = 1.15 \pm 0.30$, in the 193 nm photolysis was reported by Talukdar et al.[12] The transient CF_2Br radical was detected by molecular beam[6] and spectroscopic studies[5,14] during photolysis at 248 nm and confirm that the C-Br bond is broken.

Table 4G-25. Recommended Absorption Cross Sections of CF_2Br_2 at 296 K

λ (nm)	10^{20} σ (cm^2)	λ (nm)	10^{20} σ (cm^2)	λ (nm)	10^{20} σ (cm^2)
170	124.5	232	230.2	294	0.0964
172	78.1	234	211.9	296	0.0698
174	55.3	236	191.6	298	0.0504
176	49.5	238	169.3	300	0.0363
178	60.3	240	147.3	302	0.0260
180	75.0	242	125.8	304	0.0186
182	86.6	244	106.0	306	0.0133
184	100.9	246	87.8	308	0.00943
186	111.8	248	72.0	310	0.00668
188	118.0	250	58.3	312	0.00472
190	115.9	252	46.5	314	0.00333
192	110.3	254	36.8	316	0.00234
194	101.6	256	28.9	318	0.00164
196	91.4	258	22.4	320	0.00115
198	82.1	260	17.3	322	0.000808
200	74.9	262	13.1	324	0.000565
202	71.7	264	9.90	326	0.000396
204	73.4	266	7.65	328	0.000277
206	80.7	268	5.56	330	0.000194
208	93.0	270	4.06	332	0.000136
210	110.0	272	2.97	334	0.0000960
212	131.0	274	2.18	336	0.0000678
214	154.9	276	1.60	338	0.0000481
216	180.4	278	1.18	340	0.0000343
218	204.7	280	0.864	342	0.0000246
220	226.0	282	0.634	344	0.0000178
222	244.2	284	0.466	346	0.0000129
224	253.3	286	0.341	348	0.00000948
226	256.8	288	0.252	350	0.00000703
228	253.4	290	0.182		
230	244.7	292	0.133		

Note:
170–188 nm: Gillotay and Simon[4]
190–264 nm: mean of data from Gillotay and Simon,[4] Orkin and Kasimovskaya,[9] and Burkholder et al.[1]
266–350 nm: Papanastasiou et al.[10] parameterization

(1) Burkholder, J. B.; Wilson, R. R.; Gierczak, T.; Talukdar, R.; McKeen, S. A.; Orlando, J. J.; Vaghjiani, G. L.; Ravishankara, A. R. Atmospheric fate of CF_3Br, CF_2Br_2, CF_2ClBr, and CF_2BrCF_2Br. *J. Geophys. Res.* **1991**, *96*, 5025-5043, doi:10.1029/90JD02735.

(2) Davidson, N. The ultraviolet absorption spectra and the refractive indices of some fluorobromomethanes. *J. Am. Chem. Soc.* **1951**, *73*, 467-468, doi:10.1021/ja01145a506.

(3) Doucet, J.; Gilbert, R.; Sauvageau, P.; Sandorfy, C. Photoelectron and far-ultraviolet spectra of CF_3Br, CF_2BrCl, and CF_2Br_2. *J. Chem. Phys.* **1975**, *62*, 366-369, doi:10.1063/1.430495.

(4) Gillotay, D.; Simon, P. C. Ultraviolet absorption spectrum of trifluoro-bromo-methane, difluoro-dibromo-methane and difluoro-bromo-chloro-methane in the vapor phase. *J. Atmos. Chem.* **1989**, *8*, 41-62, doi:10.1007/BF00053815.

(5) Gosnell, T. R.; Taylor, A. J.; Lyman, J. L. Ultrafast absorption spectroscopy of photodissociated CF_2Br_2: Details of the reaction mechanism and evidence for anomalously slow intramolecular vibrational redistribution within the CF_2Br intermediate. *J. Chem. Phys.* **1991**, *94*, 5949-5953, doi:10.1063/1.460429.

(6) Krajnovich, D.; Zhang, Z.; Butler, L.; Lee, Y. T. Photodissociation of CF_2Br_2 at 248 nm by the molecular beam method. *J. Phys. Chem.* **1984**, *88*, 4561-4566, doi:10.1021/j150664a023.

(7) Molina, L. T.; Molina, M. J. Quantum yields for the photodissociation of CBr_2F_2 in the 200-300-nm region. *J. Phys. Chem.* **1983**, *87*, 1306-1308, doi:10.1021/j100231a008.

(8) Molina, L. T.; Molina, M. J.; Rowland, F. S. Ultraviolet absorption cross sections of several brominated methanes and ethanes of atmospheric interest. *J. Phys. Chem.* **1982**, *86*, 2672-2676, doi:10.1021/j100211a023.
(9) Orkin, V. L.; Kasimovskaya, E. E. Ultraviolet absorption spectra of some Br-containing haloalkenes. *J. Atmos. Chem.* **1995**, *21*, 1-11, doi:10.1007/BF00712435.
(10) Papanastasiou, D. K.; Rontu Carlon, N.; Neuman, J. A.; Fleming, E. L.; Jackman, C. H.; Burkholder, J. B. Revised UV absorption spectra, ozone depletion potentials, and global warming potentials for the ozone-depleting substances CF_2Br_2, CF_2ClBr, and CF_2BrCF_2Br. *Geophys. Res. Lett.* **2013**, *40*, doi:10.1002/GRL.50121.
(11) Seccombe, D. P.; Chim, R. Y. L.; Tuckett, R. P.; Jochims, H. W.; Baumgärtel, H. Vacuum–ultraviolet absorption and fluorescence spectroscopy of CF_2H_2, CF_2Cl_2, and CF_2Br_2 in the range 8–22 eV. *J. Chem. Phys.* **2001**, *114*, 4058-4073, doi:10.1063/1.1344888.
(12) Talukdar, R. K.; Hunter, M.; Warren, R. F.; Burkholder, J. B.; Ravishankara, A. R. UV laser photodissociation of CF_2ClBr and CF_2Br_2 at 298 K: quantum yields of Cl, Br, and CF_2. *Chem. Phys. Lett.* **1996**, *262*, 669-674, doi:10.1016/S0009-2614(96)01157-8.
(13) Talukdar, R. K.; Vashjiani, G. L.; Ravishankara, A. R. Photodissociation of bromocarbons at 193, 222, and 248 nm: Quantum yields of Br atom at 298 K. *J. Chem. Phys.* **1992**, *96*, 8194-8201, doi:10.1063/1.462324.
(14) Vatsa, R. K.; Kumar, A.; Naik, P. D.; Rama Rao, K. V. S.; Mittal, J. P. UV absorption spectrum and decay kinetics of CF_2Br in CO_2 laser-induced photodissociation of CF_2Br_2. *Chem. Phys. Lett.* **1993**, *207*, 75-80, doi:10.1016/0009-2614(93)85014-F.
(15) Walton, J. C. Photolysis of dibromodifluoromethane at 265 nm. *J. Chem. Soc. Faraday Trans.* **1972**, *68*, 1559-1565, doi:10.1039/f19726801559.

G26. CF_2ClBr (Halon–1211, difluorochlorobromomethane)

Back to Index

CF_2ClBr (Halon–1211) + hν → CF_2Cl + Br	418 kJ mol^{-1}	283 nm	(1)
→ CF_2Br + Cl			(2)
→ CF_2 + Cl + Br			(3)

(Recommendation: 15-10, Note: 15-10, Evaluated: 15-10)

Absorption Cross Sections: The UV absorption spectrum of CF_2ClBr, difluorochlorobromomethane (Halon–1211), has been measured at room temperature by Giolando et al.[4] (191–307 nm), Molina et al.[5] (190–330 nm), Orkin and Kasimovskaya[6] (190–304 nm), Gillotay and Simon[3] (170–302 nm), Burkholder et al.[1] (190–320 nm), and Papanastasiou et al.[7] (300-335 nm). The most recent study by Papanastasiou et al. reported absorption cross section data in the long wavelength region that were corrected for Rayleigh scattering, which is most important at the longest wavelengths. The agreement between the room temperature cross section data of Orkin and Kasimovskaya,[6] Gillotay and Simon,[3] and Burkholder et al.[1] is very good, to within 10%, over the range 190–240 nm and to within 3% at the spectrum maximum near 205 nm. The data from Gillotay and Simon[3] near the absorption maximum differs from the other observations by ~10%. Molina et al.[5] reported values in the range 190–240 nm that are lower by 10–20% than the other data. The few data points of Giolando et al.[4] agree well with the absorption spectra reported by Orkin and Kasimovskaya,[6] Gillotay and Simon,[3] and Burkholder et al.[1] The differences between the various data sets are greatest at the longer wavelengths. The recommended absorption cross sections in Table 4G-26 are the values of Gillotay and Simon[3] in the region 170–188 nm, the mean of the values reported by Molina et al.,[5] Gillotay and Simon,[3] Burkholder et al.,[1] and Orkin and Kasimovskaya[6] in the region 190–298 nm, the spectrum parameterization from Papanastasiou et al. for the region 300 to 350 nm (see below) (values ≥336 nm are an extrapolation beyond the range of the experimental data). The uncertainty factor for the room temperature spectrum is 1.15 (2σ) for the range of data given in Table 4G-26, which encompasses the full range of the experimental data at wavelengths <300 nm as well as the data from Papanastasiou et al. at longer wavelengths.

The VUV absorption spectrum at room temperature was measured by Doucet et al.[2] (60–220 nm). A recommended Lyman-α cross section of 7.75×10^{-17} cm^2 molecule^{-1} was obtained from the two reported spectra by these authors. An uncertainty factor of 1.5 (2σ) is assigned, primarily due to the fact that there is only a single study available.

The temperature dependence of the absorption spectrum has been measured by Gillotay and Simon[3] (210–296 K, 170–302 nm), Burkholder et al.[1] (210–296 K, 190–320 nm), and Papanastasiou et al. (210–296 K, 300-335 nm). The absorption cross sections increase near the peak, 204–206 nm, and decrease at wavelengths >233 nm and <180 nm with decreasing temperature. Gillotay and Simon[3] observed a systematic temperature dependence with an increase in the peak cross section by ~5×10^{-20} cm^2 molecule^{-1} per 20 K decrease in temperature.

Burkholder et al.[1] reported a less pronounced temperature dependence with the peak cross section at 210 K being 15% less than reported Gillotay and Simon[3] (the room temperature cross sections from these two studies agree to within 4%). Different empirical parameterizations for the temperature dependence of the absorption cross section have been used. Gillotay and Simon[3] used a polynomial expansion:

$$\log_{10} \sigma(\lambda, T) = \sum A_n \lambda^n + (T-273) \times \sum B_n \lambda^n$$

and report calculated cross sections for 210, 230, 250, 270, and 295 K. The A_n and B_n parameters, which are valid for the wavelength range 200–302 nm and temperature range 210–300 K, are given below.

$A_0 = -134.80$	$B_0 = 3.3070 \times 10^{-1}$
$A_1 = 1.7084$	$B_1 = -5.0957 \times 10^{-3}$
$A_2 = -9.1540 \times 10^{-3}$	$B_2 = 2.9361 \times 10^{-5}$
$A_3 = 2.1644 \times 10^{-5}$	$B_3 = -7.6198 \times 10^{-8}$
$A_4 = -1.9863 \times 10^{-8}$	$B_4 = 7.6825 \times 10^{-11}$

Burkholder et al.[1] parameterized their data using the expression:

$$\ln \sigma(\lambda, T) = (\sum A_i (\lambda - 259.8989)^i) (1 + (296-T) \sum B_i (\lambda - 259.8989)^i)$$

and report the following A_i and B_i parameters valid for the wavelength range 220–260 nm and temperature range 210–296 K.

$A_0 = -45.4087$	$B_0 = 1.528905 \times 10^{-4}$
$A_1 = -1.304811 \times 10^{-1}$	$B_1 = 6.024833 \times 10^{-6}$
$A_2 = -6.995443 \times 10^{-4}$	$B_2 = 1.030995 \times 10^{-7}$
$A_3 = 6.159709 \times 10^{-6}$	$B_3 = -6.387931 \times 10^{-11}$
$A_4 = -9.384074 \times 10^{-9}$	$B_4 = -3.718503 \times 10^{-11}$

Burkholder et al.[1] also report a parameterization for cross sections extrapolated to 400 nm:

$$\ln \sigma(\lambda, T) = (\sum A_i (\lambda - 292.2083)^i) (1 + (296-T) \sum B_i (\lambda - 292.2083)^i)$$

with the following parameters.

$A_0 = -50.15428$	$B_0 = 3.778659 \times 10^{-4}$
$A_1 = -1.547025 \times 10^{-1}$	$B_1 = 6.338322 \times 10^{-6}$
$A_2 = -9.551083 \times 10^{-5}$	$B_2 = -1.294407 \times 10^{-8}$
$A_3 = 4.076334 \times 10^{-6}$	$B_3 = -2.430137 \times 10^{-10}$
$A_4 = -2.747685 \times 10^{-8}$	$B_4 = 2.234599 \times 10^{-12}$

Note: Errors in the Burkholder et al.[1] paper are corrected here.

The recommended spectrum parameterization for wavelengths >298 nm is taken from the Papanastasiou et al. study, which accounted for Rayleigh scattering that was significant for wavelengths >290 nm. They used the same empirical expression used in the Burkholder et al. study

$$\ln\left(\sigma(\lambda,T)\right) = \sum_i A_i\left(\lambda - \bar{\lambda}\right)^i \times \left[1 + (296 - T)\sum_i B_i\left(\lambda - \bar{\lambda}\right)^i\right]$$

to parameterize the spectrum for wavelengths ≥260 nm and temperatures between 210 and 298 K using a combination of their cross section data and the data from Burkholder et al. The parameters are given below.

$\bar{\lambda} = 280.376$		
i	A_i	B_i
0	–48.3578	0.0002989
1	–0.1547325	8.5306×10^{-6}
2	-4.966942×10^{-4}	4.26×10^{-8}
3	1.56338×10^{-6}	-1.84×10^{-9}
4	3.664034×10^{-8}	1.284×10^{-11}

Photolysis Quantum Yield and Product Studies: Quantum yields for Cl and Br atom formation in the photodissociation of CF_2ClBr at 193, 222, and 248 nm, Φ(Cl) = 1.03 ± 0.14, 0.27 ± 0.04, and 0.18 ± 003, Φ(Br)

= 1.04 ± 0.13, 0.86 ± 0.11, and 0.75 ± 0.13, respectively, and a quantum yield for CF_2 formation in the 193 nm photolysis, $\Phi(CF_2) = 0.91 \pm 0.30$, were reported by Talukdar et al.[8]

Table 4G-26. Recommended Absorption Cross Sections of CF_2ClBr at 298 K

λ (nm)	10^{20} σ (cm^2)	λ (nm)	10^{20} σ (cm^2)	λ (nm)	10^{20} σ (cm^2)
170	323.0	232	33.8	294	0.0106
172	234.2	234	28.8	296	0.00764
174	176.0	236	24.4	298	0.00544
176	120.9	238	20.4	300	0.00402
178	84.7	240	16.9	302	0.00285
180	58.1	242	13.9	304	0.00202
182	41.9	244	11.4	306	0.00142
184	35.0	246	9.28	308	0.00100
186	34.1	248	7.50	310	0.000705
188	38.9	250	5.99	312	0.000495
190	46.1	252	4.76	314	0.000348
192	57.0	254	3.76	316	0.000244
194	69.1	256	2.94	318	0.000171
196	81.4	258	2.29	320	0.000120
198	93.5	260	1.76	322	0.0000840
200	106.0	262	1.36	324	0.0000589
202	113.3	264	1.03	326	0.0000414
204	117.4	266	0.784	328	0.0000291
206	118.7	268	0.593	330	0.0000205
208	117.7	270	0.447	332	0.0000145
210	114.2	272	0.336	334	0.0000103
212	108.5	274	0.250	336	*0.00000728*
214	101.5	276	0.184	338	*0.00000519*
216	93.6	278	0.135	340	*0.00000371*
218	85.3	280	0.0991	342	*0.00000267*
220	76.8	282	0.0724	344	*0.00000193*
222	68.3	284	0.0527	346	*0.00000140*
224	60.4	286	0.0385	348	*0.00000102*
226	52.7	288	0.0282	350	*0.000000754*
228	45.7	290	0.0205		
230	39.2	292	0.0148		

Note:
170–188 nm: Gillotay and Simon[3]
190–298 nm: mean of values from Molina et al.,[5] Gillotay and Simon,[3] Burkholder et al.,[1] and Orkin and Kasimovskaya[6]
300–350 nm: Papanastasiou et al.[7] parameterization with ≥336 nm values based on an extrapolation.

(1) Burkholder, J. B.; Wilson, R. R.; Gierczak, T.; Talukdar, R.; McKeen, S. A.; Orlando, J. J.; Vaghjiani, G. L.; Ravishankara, A. R. Atmospheric fate of CF_3Br, CF_2Br_2, CF_2ClBr, and CF_2BrCF_2Br. *J. Geophys. Res.* **1991**, *96*, 5025-5043, doi:10.1029/90JD02735.

(2) Doucet, J.; Gilbert, R.; Sauvageau, P.; Sandorfy, C. Photoelectron and far-ultraviolet spectra of CF_3Br, CF_2BrCl, and CF_2Br_2. *J. Chem. Phys.* **1975**, *62*, 366-369, doi:10.1063/1.430495.

(3) Gillotay, D.; Simon, P. C. Ultraviolet absorption spectrum of trifluoro-bromo-methane, difluoro-dibromo-methane and difluoro-bromo-chloro-methane in the vapor phase. *J. Atmos. Chem.* **1989**, *8*, 41-62, doi:10.1007/BF00053815.

(4) Giolando, D. M.; Fazekas, G. B.; Taylor, W. D.; Takacs, G. A. Atmospheric photochemistry of CF_2ClBr. *J. Photochem.* **1980**, *14*, 335-339, doi:10.1016/0047-2670(80)85105-7.

(5) Molina, L. T.; Molina, M. J.; Rowland, F. S. Ultraviolet absorption cross sections of several brominated methanes and ethanes of atmospheric interest. *J. Phys. Chem.* **1982**, *86*, 2672-2676, doi:10.1021/j100211a023.

(6) Orkin, V. L.; Kasimovskaya, E. E. Ultraviolet absorption spectra of some Br-containing haloalkenes. *J. Atmos. Chem.* **1995**, *21*, 1-11, doi:10.1007/BF00712435.

(7) Papanastasiou, D. K.; Rontu Carlon, N.; Neuman, J. A.; Fleming, E. L.; Jackman, C. H.; Burkholder, J. B. Revised UV absorption spectra, ozone depletion potentials, and global warming potentials for the ozone-depleting substances CF_2Br_2, CF_2ClBr, and CF_2BrCF_2Br. *Geophys. Res. Lett.* **2013**, *40*, doi:10.1002/GRL.50121.
(8) Talukdar, R. K.; Hunter, M.; Warren, R. F.; Burkholder, J. B.; Ravishankara, A. R. UV laser photodissociation of CF_2ClBr and CF_2Br_2 at 298 K: quantum yields of Cl, Br, and CF_2. *Chem. Phys. Lett.* **1996**, *262*, 669-674, doi:10.1016/S0009-2614(96)01157-8.

G27. CF_3Br (Halon–1301, trifluorobromomethane)

Back to Index

CF_3Br (Halon–1301) + hν → CF_3 + Br 288 kJ mol^{-1} 416 nm (1)

(Recommendation: 25-1, Note: 25-1, Evaluated: 25-1)

Absorption Cross Sections: The UV absorption spectrum of CF_3Br, trifluorobromomethane (Halon–1301), has been measured at room temperature by Davidson[3] (207–255 nm), Roxlo and Mandl[10] (170–230 nm), Pence et al.[9] (180–400 nm, graphical data), Molina et al.[7] (190–300 nm), Orkin and Kasimovskaya[8] (190–270 nm), Gillotay and Simon[6] (168–280 nm), Burkholder et al.[2] (190–285 nm), and Bernard et al.[1] (195–235 nm). The agreement between the room temperature data is generally good in the region between 190 and 230 nm, 10% or better. The exceptions are the data of Davidson[3] below 210 nm and the data set from Roxlo and Mandl.[10] Pence et al.[9] report an absorption cross section at 193 nm that is significantly less than the rest of the data at 193 nm. For wavelengths >250 nm, Burkholder et al.[2] and Orkin and Kasimovskaya[8] report values greater by up to ~35% at 270 nm than reported by Molina et al.[7] and Gillotay and Simon.[6] The recommended absorption cross sections in Table 4G-27 are the values from Gillotay and Simon[6] in the region 168–188 nm, the mean of the values reported by Molina et al.,[7] Gillotay and Simon,[6] Burkholder et al.,[2] and Orkin and Kasimovskaya[8] in the region 190–270 nm, the mean of the values reported by Molina et al.,[7] Gillotay and Simon,[6] and Burkholder et al.[2] in the region 272–280 nm, and the values of Molina et al.[7] in the region 295–300 nm. The recommended uncertainty factors (2σ) are 1.15 (170-190 nm), 1.1 (190-230 nm), and 1.2 (230-280 nm) for the wavelength ranges in parenthesis. Due to the limited available experimental data, the uncertainty factor for wavelengths >280 nm is assigned a value of 2 (2σ).

The VUV absorption spectrum has been measured by Doucet et al.[5] (120-206 nm), Doucet et al.[4] (60–128 nm), Suto and Lee[11] (106–152 nm), and Washida et al.[13] (116–130 nm). The Doucet et al. results near Lyman-α, 121.567 nm, are lower by ~40% than the Suto and Lee and Washida et al. results. The recommended Lyman-α cross section is 2.5×10^{-17} cm^2 molecule^{-1}, which is an average of the four studies, linearly interpolated to 121.567 nm. An uncertainty factor of 1.4 (2σ) that encompasses the available data is assigned.

The temperature dependence of the absorption spectrum has been measured by Gillotay and Simon[6] (168–280 nm) over the range 210–295 K, Burkholder et al.[2] (190–285 nm) over the range 210–296 K, and Bernard et al.[1] (195–235 nm) over the range 210–320 K. The absorption cross sections increase between 174 and 216 nm and decrease at wavelengths >218 nm and <174 nm with decreasing temperature. Gillotay and Simon[6] observed a systematic temperature behavior with an increase of the peak cross section by ~0.6×10^{-20} cm^2 molecule^{-1} per 20 K decrease in temperature. Burkholder et al.[2] reported a less pronounced temperature dependence with the peak cross section at 210 K being ~20% lower than reported by Gillotay and Simon[6] (the cross sections at room temperature are within 6%). Different parameterizations for the temperature dependence of the absorption cross section have been proposed. Gillotay and Simon[6] give the polynomial expansion:

$$\log_{10} \sigma(\lambda, T) = \sum A_n \lambda^n + (T-273) \times \sum B_n \lambda^n$$

and report calculated values for T = 210, 230, 250, 270, and 295 K. The A_n and B_n parameters, which are valid for the wavelength range 178–280 nm and temperature range 210–300 K are as follows.

$A_0 = 62.563$	$B_0 = -9.1755 \times 10^{-1}$
$A_1 = -2.0068$	$B_1 = 1.8575 \times 10^{-2}$
$A_2 = 1.6592 \times 10^{-2}$	$B_2 = -1.3857 \times 10^{-4}$
$A_3 = -5.6465 \times 10^{-5}$	$B_3 = 4.5066 \times 10^{-7}$
$A_4 = 6.7459 \times 10^{-8}$	$B_4 = -5.3803 \times 10^{-10}$

Burkholder et al.[2] parameterized their data using the expression:

$$\ln \sigma(\lambda, T) = (\sum A_i (\lambda - 242.2466)^i) (1 + (296-T) \sum B_i (\lambda - 242.2466)^i)$$

and report the following A_i and B_i parameters valid for the wavelength range 214–285 nm and temperature range 210–296 K.

$A_0 = -46.70542$ $B_0 = 1.694026 \times 10^{-4}$
$A_1 = -1.55047 \times 10^{-1}$ $B_1 = 8.723247 \times 10^{-6}$
$A_2 = -1.020187 \times 10^{-3}$ $B_2 = 5.953165 \times 10^{-9}$
$A_3 = 2.246169 \times 10^{-5}$ $B_3 = -3.872168 \times 10^{-9}$
$A_4 = -1.300982 \times 10^{-7}$ $B_4 = -1.803325 \times 10^{-11}$

Note: In the Burkholder et al.[2] paper, the parameterization equation is written in terms of $\log_{10} \sigma(\lambda, T)$ but the correct expression should be given in terms of $\ln \sigma(\lambda, T)$, as given here.

Bernard et al.[1] parameterized their data using the expression:

$$\ln \sigma(\lambda, T) = \sum A_i \lambda^i) + (T - 296) \sum B_i \lambda^i$$

valid for the wavelength range 195–235 nm and temperature range 210–320 K using the parameters below.

$A_0 = 315.204$ $B_0 = 0.0077$
$A_1 = -8.03836$ $B_1 = -5.6975 \times 10^{-4}$
$A_2 = 0.06362234$ $B_2 = 1.1304 \times 10^{-5}$
$A_3 = -2.1356 \times 10^{-4}$ $B_3 = -7.3977 \times 10^{-8}$
$A_4 = 2.5779 \times 10^{-7}$ $B_4 = 1.5279 \times 10^{-10}$

The parameterization reproduces their experimental data to better than 1% over the specified range of conditions and supercedes the work of Burkholder et al. over the 195–235 nm wavelength range. This parameterization, which covers the most critical wavelength range for atmospheric photolysis rate calculations, is recommended.

Photolysis Quantum Yield and Product Studies: Talukdar et al.[12] reported quantum yields for Br ($Br(^2P_{3/2}$ + $Br^*(^2P_{1/2})$) atom formation in the photodissociation of CF_3Br at 193 and 222 nm to be 1.12 ± 0.16 and 0.92 ± 0.15, respectively. A $Br^*(^2P_{1/2})$ atom fractional yield, $Br^*(^2P_{1/2})$/(Total Br), of 0.56 ± 0.05 was reported by Pence et al.[9] for 193 nm photolysis.

Table 4G-27. Recommended Absorption Cross Sections of CF_3Br at 296 K

λ (nm)	10^{20} σ (cm^2)	λ (nm)	10^{20} σ (cm^2)	λ (nm)	10^{20} σ (cm^2)
168	0.517	210	12.4	252	0.107
170	0.696	212	11.8	254	0.0743
172	0.928	214	10.9	256	0.0516
174	1.22	216	9.91	258	0.0357
176	1.60	218	8.82	260	0.0248
178	2.05	220	7.69	262	0.0171
180	2.61	222	6.57	264	0.0118
182	3.26	224	5.51	266	0.00827
184	4.02	226	4.54	268	0.00580
186	4.88	228	3.67	270	0.00399
188	5.82	230	2.92	272	0.00271
190	6.56	232	2.29	274	0.00188
192	7.58	234	1.77	276	0.00129
194	8.63	236	1.39	278	0.00092
196	9.86	238	1.04	280	0.00064
198	10.9	240	0.766	285	0.00022
200	11.7	242	0.563	290	0.00008
202	12.4	244	0.414	295	0.00003
204	12.8	246	0.296	300	0.00001
206	12.9	248	0.212		
208	12.8	250	0.149		

Note:
168–188 nm: Gillotay and Simon[6]
190–194 nm: mean of Molina et al.,[7] Gillotay and Simon,[6] Burkholder et al.,[2] and Orkin and Kasimovskaya[8]
196–234 nm: Bernard et al.[1]
236–270 nm: mean of Molina et al.,[7] Gillotay and Simon,[6] Burkholder et al.,[2] and Orkin and Kasimovskaya[8]

272–280 nm: mean of Molina et al.[7] and Burkholder et al.[2]
285–300 nm: Molina et al.[7]

(1) Bernard, F.; McGillen, M. R.; Fleming, E. L.; Jackman, C. H.; Burkholder, J. B. $CBrF_3$ (Halon-1301): UV absorption spectrum between 210 and 320 K, atmospheric lifetime, and ozone depletion potential. *J. Photochem. Photobiol. A: Chem.* **2015**, *306*, 13-20, doi:10.1016/j.jphotochem.2015.03.012.

(2) Burkholder, J. B.; Wilson, R. R.; Gierczak, T.; Talukdar, R.; McKeen, S. A.; Orlando, J. J.; Vaghjiani, G. L.; Ravishankara, A. R. Atmospheric fate of CF_3Br, CF_2Br_2, CF_2ClBr, and CF_2BrCF_2Br. *J. Geophys. Res.* **1991**, *96*, 5025-5043, doi:10.1029/90JD02735.

(3) Davidson, N. The ultraviolet absorption spectra and the refractive indices of some fluorobromomethanes. *J. Am. Chem. Soc.* **1951**, *73*, 467-468, doi:10.1021/ja01145a506.

(4) Doucet, J.; Gilbert, R.; Sauvageau, P.; Sandorfy, C. Photoelectron and far-ultraviolet spectra of CF_3Br, CF_2BrCl, and CF_2Br_2. *J. Chem. Phys.* **1975**, *62*, 366-369, doi:10.1063/1.430495.

(5) Doucet, J.; Sauvageau, P.; Sandorfy, C. Vacuum ultraviolet and photoelectron spectra of fluoro-chloro derivatives of methane. *J. Chem. Phys.* **1973**, *58*, 3708-3716, doi:10.1063/1.1679722.

(6) Gillotay, D.; Simon, P. C. Ultraviolet absorption spectrum of trifluoro-bromo-methane, difluoro-dibromo-methane and difluoro-bromo-chloro-methane in the vapor phase. *J. Atmos. Chem.* **1989**, *8*, 41-62, doi:10.1007/BF00053815.

(7) Molina, L. T.; Molina, M. J.; Rowland, F. S. Ultraviolet absorption cross sections of several brominated methanes and ethanes of atmospheric interest. *J. Phys. Chem.* **1982**, *86*, 2672-2676, doi:10.1021/j100211a023.

(8) Orkin, V. L.; Kasimovskaya, E. E. Ultraviolet absorption spectra of some Br-containing haloalkenes. *J. Atmos. Chem.* **1995**, *21*, 1-11, doi:10.1007/BF00712435.

(9) Pence, W. H.; Baughum, S. L.; Leone, S. R. Laser UV photofragmentation of halogenated molecules. Selective bond dissociation and wavelength-specific quantum yields for excited $I(^2P_{1/2})$ and $Br(^2P_{1/2})$ atoms. *J. Phys. Chem.* **1981**, *85*, 3844-3851, doi:10.1021/j150625a027.

(10) Roxlo, C.; Mandl, A. Vacuum ultraviolet absorption cross sections for halogen containing molecules. *J. Appl. Phys.* **1980**, *51*, 2969-2972, doi:10.1063/1.328108.

(11) Suto, M.; Lee, L. C. Emission spectra of CF_3 radicals. V. Photodissociation of CF_3H, CF_3Cl, and CF_3Br by vacuum ultraviolet. *J. Chem. Phys.* **1983**, *79*, 1127-1133, doi:10.1063/1.445914.

(12) Talukdar, R. K.; Vashjiani, G. L.; Ravishankara, A. R. Photodissociation of bromocarbons at 193, 222, and 248 nm: Quantum yields of Br atom at 298 K. *J. Chem. Phys.* **1992**, *96*, 8194-8201, doi:10.1063/1.462324.

(13) Washida, N.; Suto, M.; Nagase, S.; Nagashima, U.; Morokuma, K. Emission spectra of CF_3 radicals. IV. Excitation spectra, quantum yields, and potential enegy surfaces of the CF_3 fluorescences. *J. Chem. Phys.* **1983**, *78*, 1025-1032, doi:10.1063/1.444902.

G28. CH_2=CHBr (bromoethene, vinyl bromide)

Back to Index

CH_2=CHBr + hν → Products (1)

(Recommendation: 06-2, Note: 10-6, Evaluated: 10-6)

Absorption Cross Sections: The UV absorption spectrum of CH_2=CHBr, bromoethene (vinyl bromide), has been measured at room temperature by Schander and Russell[3] (168–208 nm), Hoxha et al.[1] (62–248 nm), and Orkin et al.[2] (164–254 nm). The spectrum has a very strong absorption band with the maximum at 192 nm, characteristic of the CH_2=CBr- group. The absorption cross sections reported in the Orkin et al.[2] study (reported in 0.5 nm increments) are recommended and given in Table 4G-28 for wavelengths ≥184 nm.

Photolysis Quantum Yield and Product Studies: No recommendation.

Table 4G-28. Recommended Absorption Cross Sections of CH_2=CHBr at 295 K

λ (nm)	10^{20} σ (cm^2)	λ (nm)	10^{20} σ (cm^2)	λ (nm)	10^{20} σ (cm^2)
184	1970	208	306	232	18.2
186	2320	210	266	234	12.6
188	2710	212	232	236	8.47
190	3000	214	198	238	5.70
192	3160	216	166	240	3.69
194	2950	218	136	242	2.43
196	2470	220	109	244	1.58
198	1800	222	85.9	246	1.03
200	996	224	65.3	248	0.683
202	605	226	49.1	250	0.454
204	440	228	35.7	252	0.315
206	359	230	25.5	254	0.225

Note:
Orkin et al.[2]

(1) Hoxha, A.; Locht, R.; Leyh, B.; Dehareng, D.; Hottmann, K.; Jochims, H. W.; Baumgärtel, H. The photoabsorption and constant ionic state spectroscopy of vinylbromide. *Chem. Phys.* **2000**, *260*, 237-247, doi:10.1016/S0301-0104(00)00191-9.

(2) Orkin, V. L.; Louis, F.; Huie, R. E.; Kurylo, M. J. Photochemistry of bromine-containing fluorinated alkenes: Reactivity toward OH and UV spectra. *J. Phys. Chem. A* **2002**, *106*, 10195-10199, doi:10.1021/jp014436s.

(3) Schander, J.; Russell, B. R. Vacuum ultraviolet spectra of bromoethylene and dibromoethylenes. *J. Am. Chem. Soc.* **1976**, *98*, 6900-6904, doi:10.1021/ja00438a024.

G29. $CHBr=CF_2$ (1-bromo-2,2-difluoroethene)

Back to Index

$CHBr=CF_2 + h\nu \rightarrow$ Products (1)

(Recommendation: 06-2, Note: 10-6, Evaluated: 10-6)

Absorption Cross Sections: The absorption spectrum of $CHBr=CF_2$, 1-bromo-2,2-difluoroethene, has been measured at room temperature over the wavelength range 164–266 nm by Orkin et al.[1] The spectrum has strong absorption bands between 164 and 190 nm, a weaker and less pronounced band between 190 and 210 nm (maximum 194 nm), and a still weaker band above 210 nm with the maximum near 220 nm. The absorption cross sections reported in the Orkin et al.[1] study (reported in 0.5 nm increments) are recommended and given in Table 4G-29 for wavelengths ≥184 nm.

Photolysis Quantum Yield and Product Studies: No recommendation.

Table 4G-29. Recommended Absorption Cross Sections of $CHBr=CF_2$ at 295 K

λ (nm)	10^{20} σ (cm^2)	λ (nm)	10^{20} σ (cm^2)	λ (nm)	10^{20} σ (cm^2)	λ (nm)	10^{20} σ (cm^2)
184	2160	206	87.6	228	74.0	250	8.81
186	1020	208	70.1	230	68.2	252	6.51
188	670	210	63.4	232	61.3	254	4.75
190	635	212	63.5	234	53.7	256	3.49
192	671	214	66.7	236	45.9	258	2.54
194	703	216	71.1	238	38.8	260	1.86
196	610	218	75.8	240	31.7	262	1.37
198	471	220	79.3	242	25.5	264	1.04
200	306	222	80.7	244	20.1	266	0.796
202	193	224	80.6	246	15.4		
204	124	226	78.4	248	11.7		

Note:
Orkin et al.[1]

(1) Orkin, V. L.; Louis, F.; Huie, R. E.; Kurylo, M. J. Photochemistry of bromine-containing fluorinated alkenes: Reactivity toward OH and UV spectra. *J. Phys. Chem. A* **2002**, *106*, 10195-10199, doi:10.1021/jp014436s.

G30. $CFBr=CF_2$ (trifluorobromoethene)

Back to Index

$CFBr=CF_2 + h\nu \rightarrow$ Products (1)

(Recommendation: 06-2, Note: 10-6, Evaluated: 10-6)

Absorption Cross Sections: The absorption spectrum of $CFBr=CF_2$, trifluorobromoethene, has been measured at room temperature over the wavelength range 164–274 nm by Orkin et al.[1] The spectrum has strong absorption bands between 164 and 188 nm, a weaker and less pronounced band between 188 and 213 nm (maximum 194.5 nm), and a still weaker band above 213 nm with the maximum near 229 nm. The absorption cross sections reported in the Orkin et al.[1] study (reported in 0.5 nm increments) are recommended and given in Table 4G-30 for wavelengths ≥184 nm.

Photolysis Quantum Yield and Product Studies: No recommendation.

Table 4G-30. Recommended Absorption Cross Sections of $CFBr=CF_2$ at 295 K

λ (nm)	10^{20} σ (cm^2)	λ (nm)	10^{20} σ (cm^2)	λ (nm)	10^{20} σ (cm^2)	λ (nm)	10^{20} σ (cm^2)
184	456	208	56.1	232	58.1	256	6.87
186	367	210	39.5	234	54.7	258	5.15
188	350	212	34.1	236	50.4	260	3.77
190	373	214	34.5	238	45.1	262	2.78
192	415	216	37.7	240	39.5	264	2.04
194	439	218	42.2	242	33.9	266	1.49
196	434	220	47.2	244	28.5	268	1.09
198	412	222	52.1	246	23.5	270	0.812
200	354	224	56.2	248	19.2	272	0.613
202	263	226	59.0	250	15.2	274	0.469
204	167	228	60.4	252	11.8		
206	95.1	230	60.0	254	9.03		

Note:
Orkin et al.[1]

(1) Orkin, V. L.; Louis, F.; Huie, R. E.; Kurylo, M. J. Photochemistry of bromine-containing fluorinated alkenes: Reactivity toward OH and UV spectra. *J. Phys. Chem. A* **2002**, *106*, 10195-10199, doi:10.1021/jp014436s.

G31. $CH_2=CBrCF_3$ (2-bromo-3,3,3-trifluoro-1-propene)

Back to Index

$CH_2=CBrCF_3 + h\nu \rightarrow$ Products (1)

(Recommendation: 06-2, Note: 10-6, Evaluated: 10-6)

Absorption Cross Sections: The absorption spectrum of $CH_2=CBrCF_3$, 2-bromo-3,3,3-trifluoro-1-propene, has been measured at room temperature over the wavelength range 164–254 nm by Orkin et al.[1] The spectrum has a very strong absorption band at wavelengths >174 nm with a maximum at 194 nm, similar to the $CH_2=CHBr$ spectrum and characteristic of a $CH_2=CBr-$ group. The recommended absorption cross sections in Table 4G-31 are taken from Orkin et al.[1] (reported in 0.5 nm increments).

Photolysis Quantum Yield and Product Studies: No recommendation.

Table 4G-31. Recommended Absorption Cross Sections of CH_2=$CBrCF_3$ at 295 K

λ (nm)	10^{20} σ (cm^2)	λ (nm)	10^{20} σ (cm^2)	λ (nm)	10^{20} σ (cm^2)	λ (nm)	10^{20} σ (cm^2)
184	1370	202	1520	220	126	238	6.97
186	1700	204	1080	222	97.3	240	4.77
188	2040	206	774	224	73.1	242	3.26
190	2350	208	581	226	54.9	244	2.22
192	2590	210	440	228	40.1	246	1.50
194	2700	212	338	230	28.8	248	1.02
196	2620	214	263	232	20.5	250	0.705
198	2370	216	208	234	14.4	252	0.496
200	1980	218	162	236	10.2		

Note:
Orkin et al.[1]

(1) Orkin, V. L.; Louis, F.; Huie, R. E.; Kurylo, M. J. Photochemistry of bromine-containing fluorinated alkenes: Reactivity toward OH and UV spectra. *J. Phys. Chem. A* **2002**, *106*, 10195-10199, doi:10.1021/jp014436s.

G32. CF_3CH_2Br (Halon–2301, 1,1,1-trifluoro-2-bromoethane) Back to Index

CF_3CH_2Br (Halon–2301) + hν → Products (1)

(Recommendation: 02-25, Note: 10-6, Evaluated: 10-6)

Absorption Cross Sections: The absorption spectrum of CF_3CH_2Br, 1,1,1-trifluoro-2-bromoethane (Halon–2301), has been measured at 295 K over the wavelength range 190–294 nm by Orkin and Kasimovskaya.[1] The recommended absorption cross sections in Table 4G-32 are taken from this study.

Photolysis Quantum Yield and Product Studies: No recommendation.

Table 4G-32. Recommended Absorption Cross Sections of CF_3CH_2Br at 295 K

λ (nm)	10^{20} σ (cm^2)	λ (nm)	10^{20} σ (cm^2)	λ (nm)	10^{20} σ (cm^2)
190	45.4	226	16.6	262	0.190
192	49.5	228	14.1	264	0.137
194	52.5	230	11.9	266	0.0983
196	54.4	232	9.85	268	0.0705
198	55.1	234	8.10	270	0.0504
200	54.7	236	6.58	272	0.0361
202	53.3	238	5.28	274	0.0258
204	51.2	240	4.20	276	0.0184
206	48.6	242	3.31	278	0.0132
208	45.7	244	2.58	280	0.0096
210	42.5	246	2.01	282	0.0069
212	39.1	248	1.53	284	0.0048
214	35.7	250	1.16	286	0.0034
216	32.2	252	0.876	288	0.0025
218	28.8	254	0.653	290	0.0018
220	25.5	256	0.484	292	0.0013
222	22.3	258	0.357	294	0.0011
224	19.4	260	0.261		

Note:
Orkin and Kasimovskaya[1]

(1) Orkin, V. L.; Kasimovskaya, E. E. Ultraviolet absorption spectra of some Br-containing haloalkenes. *J. Atmos. Chem.* **1995**, *21*, 1-11, doi:10.1007/BF00712435.
(2) Orkin, V. L.; Louis, F.; Huie, R. E.; Kurylo, M. J. Photochemistry of bromine-containing fluorinated alkenes: Reactivity toward OH and UV spectra. *J. Phys. Chem. A* **2002**, *106*, 10195-10199, doi:10.1021/jp014436s.

G33. $CF_3CHClBr$ (Halon–2311, 1,1,1-trifluoro-2,2-chlorobromoethane)

Back to Index

$$CF_3CHClBr \text{ (Halon–2311)} + h\nu \rightarrow CF_3CHCl + Br \quad (1)$$
$$\rightarrow CF_3CHBr + Cl \quad (2)$$

(Recommendation: 06-2, Note: 10-6, Evaluated: 10-6)

Absorption Cross Sections: The absorption spectrum of $CF_3CHClBr$, 1,1,1-trifluoro-2,2-chlorobromoethane (Halon–2311), has been measured at room temperature by Orkin and Kasimovskaya[4] (190–310 nm), Gillotay et al.[2,3] (170–290 nm), Bilde et al.[1] (200–310 nm), and Taketani et al.[5] (193.3 nm). The room temperature cross section values are in good agreement, to within 5–15%, at wavelengths <280 nm. In this region, Gillotay et al.[2,3] report the lowest cross section values and Orkin and Kasimovskaya the greatest values. At wavelengths >280 nm, the data from Bilde et al. are greater than those of Orkin and Kasimovskaya[4] with the difference increasing with increasing wavelength, up to a factor of two at 310 nm. The recommended absorption cross sections in Table 4G-33 are the values from Gillotay et al.[3] in the region 170–188 nm, the mean of the values reported by Gillotay et al.[3] and Orkin and Kasimovskaya[4] in the region 190–198 nm, the mean of the values reported by the three groups in the region 200–290 nm, and the mean of the values reported by Orkin and Kasimovskaya[4] and Bilde et al.[1] in the region 292–310 nm.

The absorption spectrum temperature dependence has been measured by Gillotay et al.[3] (170–290 nm) over the range 210–295 K and Bilde et al.[1] (200–310 nm) over the range 223–298 K. Gillotay et al.[3] report an increase of the absorption cross sections near the maximum of the absorption band between 192 and 238 nm with decreasing temperature and the opposite effect at wavelengths >238 nm and <192 nm. The increase at ~202 nm is ~2.4×10^{-20} cm^2 $molecule^{-1}$ per 20 K decrease in temperature, i.e., an increase of ~10% between 295 and 210 K. Bilde et al.[1] observed a less pronounced temperature behavior in the absorption band and a decrease of the absorption cross sections with decreasing temperature at wavelengths above 214 nm.

Gillotay et al.[3] parameterized the cross sections and the temperature dependence using an empirical polynomial expansion:

$$\log_{10} \sigma(\lambda, T) = \sum A_n \lambda^n + (T-273) \times \sum B_n \lambda^n$$

and report calculated values for 210, 230, 250, 270, and 295 K. The A_n and B_n parameters, which are valid for the wavelength range 190–290 nm and temperature range 210–300 K, are given below and are recommended.

$A_0 = -127.157358$	$B_0 = -7.959828 \times 10^{-2}$
$A_1 = 1.635435$	$B_1 = 1.978026 \times 10^{-3}$
$A_2 = -9.002683 \times 10^{-3}$	$B_2 = -1.627866 \times 10^{-5}$
$A_3 = 2.190678 \times 10^{-5}$	$B_3 = 5.480744 \times 10^{-8}$
$A_4 = -2.062651 \times 10^{-8}$	$B_4 = -6.480935 \times 10^{-11}$

Photolysis Quantum Yield and Product Studies: Taketani et al.[5] reported the total yield of Cl atoms to be 0.28 ± 0.02 in the photodissociation of $CF_3CHClBr$ at 193.3 nm. Assuming a unit quantum yield for photodissociation this implies that the rupture of the C-Br bond should be dominant photodissociation channel.

Table 4G-33. Recommended Absorption Cross Sections of $CF_3CHClBr$ at 298 K

λ (nm)	10^{20} σ (cm^2)	λ (nm)	10^{20} σ (cm^2)	λ (nm)	10^{20} σ (cm^2)
170	702.6	218	78.7	266	0.980
172	614.6	220	71.0	268	0.765
174	496.8	222	63.3	270	0.575
176	379.8	224	56.3	272	0.444
178	281.1	226	49.5	274	0.339
180	206.1	228	43.3	276	0.258
182	153.3	230	37.3	278	0.196
184	118.4	232	32.2	280	0.149
186	97.1	234	27.6	282	0.111
188	86.6	236	23.6	284	0.0818
190	93.4	238	20.0	286	0.0606
192	99.8	240	16.8	288	0.0448
194	107.1	242	14.0	290	0.0331
196	114.3	244	11.7	292	0.0263
198	119.7	246	9.51	294	0.0198
200	121.5	248	7.79	296	0.0147
202	123.0	250	6.38	298	0.0109
204	122.3	252	5.15	300	0.00808
206	119.7	254	4.13	302	0.00583
208	115.1	256	3.31	304	0.00450
210	109.0	258	2.63	306	0.00313
212	102.0	260	2.06	308	0.00235
214	94.6	262	1.61	310	0.00180
216	86.7	264	1.26		

Note:
170–188 nm: Gillotay et al.[2,3]
190–198 nm: mean of values from Gillotay et al.[2,3] and Orkin and Kasimovskaya[4]
200–290 nm: mean of values from Gillotay et al.,[2,3] Orkin and Kasimovskaya,[4] and Bilde et al.[1]
292–310 nm: mean of values from Orkin and Kasimovskaya[4] and Bilde et al.[1]

(1) Bilde, M.; Wallington, T. J.; Ferronato, G.; Orlando, J. J.; Tyndall, G. S.; Estupinan, E.; Haberkorn, S. Atmospheric chemistry of CH_2BrCl, $CHBrCl_2$, $CHBr_2Cl$, $CF_3CHBrCl$, and CBr_2Cl_2. *J. Phys. Chem. A* **1998**, *102*, 1976-1986, doi:10.1021/jp9733375.

(2) Gillotay, D.; Simon, P. C. Ultraviolet absorption cross-sections of photoactive species of stratospheric interest Part 1: The halocarbons. *Aeronomica Acta A* **1990**, *356*, 1-173, doi:10.18758/A_356.

(3) Gillotay, D.; Simon, P. C.; Dierickx, L. Temperature dependence of ultraviolet absorption cross-sections of brominated methanes and ethanes. *Aeronomica Acta* **1988**, *A335*, 1-25.

(4) Orkin, V. L.; Kasimovskaya, E. E. Ultraviolet absorption spectra of some Br-containing haloalkenes. *J. Atmos. Chem.* **1995**, *21*, 1-11, doi:10.1007/BF00712435.

(5) Taketani, F.; Takahashi, K.; Matsumi, Y. Quantum yields for $Cl(^2P_j)$ atom formation from the photolysis of chlorofluorocarbons and chlorinated hydrocarbons at 193.3 nm. *J. Phys. Chem. A* **2005**, *109*, 2855-2860, doi:10.1021/jp044218+.

G34. CF_3CHFBr (Halon–2401, 1,1,1,2-tetrafluoro-2-bromoethane)

Back to Index

CF_3CHFBr (Halon–2401) + hν → Products (1)

(Recommendation: 25-1, Note: 25-1, Evaluated: 25-1)

Absorption Cross Sections: The absorption spectrum of CF_3CHFBr, 1,1,1,2-tetrafluoro-2-bromoethane (Halon–2401), has been measured at room temperature (295–298 K) by Brown et al.[1] (190–240 nm, graphical data) and Orkin and Kasimovskaya[2] (190–280 nm). The Brown et al. cross sections are systematically less than reported by Orkin and Kasimovskaya, by ~10% at 200 nm. The Orkin and Kasimovskaya results are recommended and given in Table 4G-34.

Cross section measurements for CF_3CHFBr in the Lyman-α wavelength (121.567 nm) range are not presently available.

Photolysis Quantum Yield and Product Studies: No recommendation.

Table 4G-34. Recommended Absorption Cross Sections of CF_3CHFBr at 295 K

λ (nm)	10^{20} σ (cm^2)	λ (nm)	10^{20} σ (cm^2)	λ (nm)	10^{20} σ (cm^2)
190	24.9	222	11.0	254	0.226
192	26.1	224	9.38	256	0.166
194	27.0	226	7.91	258	0.121
196	27.5	228	6.58	260	0.0873
198	27.7	230	5.42	262	0.0628
200	27.4	232	4.42	264	0.0450
202	26.9	234	3.53	266	0.0325
204	26.0	236	2.79	268	0.0235
206	24.8	238	2.19	270	0.0171
208	23.4	240	1.69	272	0.0124
210	21.9	242	1.30	274	0.0093
212	20.2	244	0.991	276	0.0069
214	18.3	246	0.736	278	0.0053
216	16.5	248	0.556	280	0.0040
218	14.6	250	0.416		
220	12.8	252	0.308		

Note:
Orkin and Kasimovskaya[2]

(1) Brown, A. C.; Canosa-Mas, C. E.; Parr, A. D.; Rothwell, K.; Wayne, R. P. Tropospheric lifetimes of three compounds for possible replacement of CFC and halons. *Nature* **1990**, *347*, 541-543, doi.org/10.1038/347541a0.

(2) Orkin, V. L.; Kasimovskaya, E. E. Ultraviolet absorption spectra of some Br-containing haloalkenes. *J. Atmos. Chem.* **1995**, *21*, 1-11, doi:10.1007/BF00712435.

G35. CF_2BrCF_2Br (Halon–2402, 1,1,2,2-tetrafluoro-1,2-dibromoethane)

Back to Index

$$CF_2BrCF_2Br \text{ (Halon–2402)} + h\nu \rightarrow CF_2BrCF_2 + Br \quad (1)$$
$$\rightarrow CF_2CF_2 + Br + Br \quad (2)$$

(Recommendation: 15-10, Note: 15-10, Evaluated: 15-10)

Absorption Cross Sections: The absorption cross sections of CF_2BrCF_2Br, 1,1,2,2-tetrafluoro-1,2-dibromoethane (Halon–2402), has been measured at room temperature by Molina et al.[3] (195–320 nm), Orkin and Kasimovskaya[4] (190–300 nm), Gillotay et al.[2] (170–280 nm), Burkholder et al.[1] (190–320 nm), and Papanastasiou et al.[5] (300–320 nm). The most recent study by Papanastasiou et al. reported absorption cross section data in the long wavelength region that were corrected for Rayleigh scattering, which is most important at the longest wavelengths. The room temperature absorption cross sections are in good agreement in the region180–290 nm, generally to within 10%. The agreement at the absorption maximum near 200 nm is to within 5% and in the long wavelength tail out to 310 nm it is to within 15%. The recommended absorption cross sections in Table 4G-35 are the values from Gillotay et al.[2] in the region 170–186 nm, the mean of the values reported by Molina et al.,[3] Gillotay et al.,[2] Burkholder et al.,[1] and Orkin and Kasimovskaya[4] in the region 196–264 nm, and the parameterization from Papanastasiou et al.[5] in the region >264 nm (see below). In the region 186 and 196 nm, a smoothed absorption spectrum was used to estimate values at 188, 190, 192, and 194 nm. An uncertainty factor of 1.15 (2σ) is recommended for the room temperature spectrum over the wavelength range where experimental data are available.

There are no VUV spectrum measurements available for Halon-2402. The Lyman-α, 121.567 nm, cross section is expected to be greater than that for CF_3Br (Halon-1301) and less than that for CF_2Br_2 (Halon-1202). A Lyman-α cross section of 5×10^{-17} cm^2 $molecule^{-1}$ is estimated and an uncertainty factor of 2 assigned.

The temperature dependence of the absorption spectrum has been measured by Gillotay et al.[2] (170–280 nm) over the range 210–295 K, Burkholder et al.[1] (190–320 nm) over the range 210–296 K, and Papanastasiou et al. over the range 250–296 K. The Gillotay et al. and Burkholder et al. studies do not agree on the spectrum temperature dependence with the Burkholder et al. spectrum having a systematically greater temperature dependence at wavelengths <230 nm and weaker dependence at longer wavelengths. Gillotay et al. report a

decrease in the absorption maximum at 200 nm of ~1.0×10^{-20} cm^2 molecule^{-1} per 20 K temperature decrease, i.e., a decrease of ~4% between 295 and 210 K. Burkholder et al.[1] report an increase in the peak absorption cross section of ~20% with decreasing temperature over the full temperature range studied. Gillotay et al.[2] parameterized the cross section temperature dependence using an empirical polynomial expansion:

$$\log_{10} \sigma(\lambda, T) = \sum A_n \lambda^n + (T-273) \times \sum B_n \lambda^n$$

and report calculated values for 210, 230, 250, 270, and 295 K. The A_n and B_n parameters, which are valid for the wavelength range 190–290 nm and temperature range 210–300 K are given below.

$A_0 = 34.026000$	$B_0 = 4.010664 \times 10^{-1}$
$A_1 = -1.152616$	$B_1 = -8.358968 \times 10^{-3}$
$A_2 = 8.959798 \times 10^{-3}$	$B_2 = 6.415741 \times 10^{-5}$
$A_3 = -2.9089 \times 10^{-5}$	$B_3 = -2.157554 \times 10^{-7}$
$A_4 = 3.307212 \times 10^{-8}$	$B_4 = 2.691871 \times 10^{-10}$

Burkholder et al.[1] parameterized the temperature dependence using the empirical expression:

$$\ln \sigma(\lambda, T) = (\sum A_i (\lambda - 242.4015)^i) (1 + (296 - T) \sum B_i (\lambda - 242.4015)^i)$$

and report the following A_i and B_i parameters for the wavelength range 190–320 nm and temperature range 210–296 K.

$A_0 = -43.69218$	$B_0 = 3.301341 \times 10^{-5}$
$A_1 = -1.124704 \times 10^{-1}$	$B_1 = 4.695917 \times 10^{-6}$
$A_2 = -1.213301 \times 10^{-3}$	$B_2 = 6.128629 \times 10^{-8}$
$A_3 = 5.275007 \times 10^{-6}$	$B_3 = -5.443107 \times 10^{-10}$
$A_4 = 6.936195 \times 10^{-8}$	$B_4 = -1.035596 \times 10^{-11}$

Note: In the original Burkholder et al.[1] paper, the parameterization equation is written in terms of $\log_{10} \sigma(\lambda, T)$ but the correct expression should be given in terms of $\ln \sigma(\lambda, T)$, as given here.

The recommended spectrum parameterization for wavelengths >264 nm is taken from the Papanastasiou et al. study, which accounted for Rayleigh scattering that was significant for wavelengths >290 nm. They used the empirical expression used in the Burkholder et al. study:

$$\ln\left(\sigma(\lambda, T)\right) = \sum_i A_i \left(\lambda - \bar{\lambda}\right)^i \times \left[1 + (296 - T) \sum_i B_i \left(\lambda - \bar{\lambda}\right)^i\right]$$

to parameterize the spectrum for wavelengths ≥260 nm and temperatures between 210 and 298 K using a combination of their cross section data and data from Burkholder et al. The parameters are given below.

$\bar{\lambda} = 274.64$		
i	A_i	B_i
0	–48.3611	0.0001877
1	–0.1595	7.252×10^{-6}
2	-1.026×10^{-4}	2.917×10^{-7}
3	-1.334×10^{-5}	-1.725×10^{-9}
4	1.458×10^{-7}	-2.675×10^{-11}

For wavelengths <266 nm, there is no apparent reason to prefer the spectrum temperature dependence reported by either Gillotay et al. or Burkholder et al.

Photolysis Quantum Yield and Product Studies: Zou et al.[6] report quantum yields for Br atom formation in the photodissociation of CF_2BrCF_2Br at 193, 233, and 266 nm to be 1.9 ± 0.1, 1.9 ± 0.1, and 1.4 ± 0.1, respectively. These results indicate bond breaking of both C–Br bonds for photolysis at 193 and 233 nm and at an appreciable fraction at 266 nm.

Table 4G-35. Recommended Absorption Cross Sections of CF_2BrCF_2Br at 296 K

λ (nm)	10^{20} σ (cm^2)	λ (nm)	10^{20} σ (cm^2)	λ (nm)	10^{20} σ (cm^2)
170	50.9	232	28.8	294	0.00404
172	56.4	234	24.1	296	0.00284
174	62.3	236	19.9	298	0.00199
176	68.5	238	16.4	300	0.00139
178	75.1	240	13.2	302	0.000967
180	81.8	242	10.6	304	0.000669
182	88.6	244	8.45	306	0.000461
184	95.3	246	6.68	308	0.000316
186	101.8	248	5.25	310	0.000216
188	107.0	250	4.03	312	0.000147
190	112.0	252	3.12	314	0.000100
192	116.5	254	2.37	316	0.0000678
194	120.0	256	1.78	318	0.0000458
196	122.3	258	1.34	320	0.0000309
198	123.7	260	0.973	322	*0.0000209*
200	124.3	262	0.718	324	*0.0000141*
202	123.6	264	0.529	326	*0.00000949*
204	120.3	266	0.395	328	*0.00000641*
206	115.9	268	0.286	330	*0.00000434*
208	110.4	270	0.208	332	*0.00000295*
210	104.2	272	0.151	334	*0.00000201*
212	97.4	274	0.110	336	*0.00000137*
214	90.1	276	0.0799	338	*0.000000946*
216	82.4	278	0.0580	340	*0.000000656*
218	74.8	280	0.0420	342	*0.000000459*
220	67.0	282	0.0304	344	*0.000000324*
222	59.6	284	0.0219	346	*0.000000231*
224	52.6	286	0.0157	348	*0.000000167*
226	45.9	288	0.0113	350	*0.000000122*
228	39.7	290	0.00804		
230	33.9	292	0.00571		

Notes:
170–186 nm: Gillotay et al.[2]
188–194 nm: values estimated by smoothing the absorption curve
196–264 nm: mean of data from Molina et al.,[3] Gillotay et al.,[2] Burkholder et al.,[1] and Orkin and Kasimovskaya[4]
>264 nm: Papanastasiou et al.[5] parameterization with values at ≥322 obtained by an extrapolation.

(1) Burkholder, J. B.; Wilson, R. R.; Gierczak, T.; Talukdar, R.; McKeen, S. A.; Orlando, J. J.; Vaghjiani, G. L.; Ravishankara, A. R. Atmospheric fate of CF_3Br, CF_2Br_2, CF_2ClBr, and CF_2BrCF_2Br. *J. Geophys. Res.* **1991**, *96*, 5025-5043, doi:10.1029/90JD02735.

(2) Gillotay, D.; Simon, P. C.; Dierickx, L. Temperature dependence of ultraviolet absorption cross-sections of brominated methanes and ethanes. *Aeronomica Acta* **1988**, *A335*, 1-25.

(3) Molina, L. T.; Molina, M. J.; Rowland, F. S. Ultraviolet absorption cross sections of several brominated methanes and ethanes of atmospheric interest. *J. Phys. Chem.* **1982**, *86*, 2672-2676, doi:10.1021/j100211a023.

(4) Orkin, V. L.; Kasimovskaya, E. E. Ultraviolet absorption spectra of some Br-containing haloalkenes. *J. Atmos. Chem.* **1995**, *21*, 1-11, doi:10.1007/BF00712435.

(5) Papanastasiou, D. K.; Rontu Carlon, N.; Neuman, J. A.; Fleming, E. L.; Jackman, C. H.; Burkholder, J. B. Revised UV absorption spectra, ozone depletion potentials, and global warming potentials for the ozone-depleting substances CF_2Br_2, CF_2ClBr, and CF_2BrCF_2Br. *Geophys. Res. Lett.* **2013**, *40*, doi:10.1002/GRL.50121.

(6) Zou, P.; McGivern, W. S.; Sokhabi, O.; Suits, A. G.; North, S. W. Quantum yields and energy partitioning in the ultraviolet photodissociation of 1,2 dibromo-tetrafluoroethane (Halon-2402). *J. Chem. Phys.* **2000**, *113*, 7149-7157, doi:10.1063/1.1313545.

G36. CF_3CF_2Br (Halon–2501, pentafluorobromoethane)

Back to Index

CF_3CF_2Br (Halon–2501) + hν → CF_3CF_2 + Br 284 kJ mol^{-1} 420 nm (1)

(Recommendation: 02-25, Note: 10-6, Evaluated: 10-6)

Absorption Cross Sections: The UV absorption spectrum of CF_3CF_2Br, pentafluorobromoethane (Halon–2501), has been measured at room temperature by Molina et al.[2] (190–300 nm), Zhang et al.[4] (200–250 nm), and Pence et al.[3] (180–400 nm, 193 nm). The absorption cross sections from Zhang et al.,[4] reported graphically, are ~30% greater than the results from Molina et al.[2] Pence et al.[3] report a spectrum graphically over the range 180–400 nm and a 193 nm cross section that is ~ 40% less than reported by Molina et al.[2] The recommended absorption cross sections in Table 4G-36 are taken from Molina et al.[2]

Photolysis Quantum Yield and Product Studies: Ebenstein et al.[1] used broadband flash photolysis of CF_3CF_2Br and reported a $Br^*(^2P_{1/2})$ fractional yield, $Br^*(^2P_{1/2})$/(Total Br), of 0.48 ± 0.02. A $Br^*(^2P_{1/2})$ fractional yield of 0.16 ± 0.08 was reported by Pence et al.[3] for 193 nm photolysis.

Table 4G-36. Recommended Absorption Cross Sections of CF_3CF_2Br at 298 K

λ (nm)	10^{20} σ (cm^2)	λ (nm)	10^{20} σ (cm^2)	λ (nm)	10^{20} σ (cm^2)
190	18.1	230	3.83	270	0.0112
195	18.4	235	2.22	275	0.00505
200	18.1	240	1.20	280	0.00218
205	16.9	245	0.620	285	0.00100
210	14.8	250	0.305	290	0.00045
215	12.0	255	0.135	295	0.00020
220	8.94	260	0.0590	300	0.00009
225	6.13	265	0.0260		

Note:
190–300 nm: Molina et al.[2]

(1) Ebenstein, W. L.; Wiesenfeld, J. R.; Wolk, G. L. Photodissociation of alkyl bromides. *Chem. Phys. Lett.* **1978**, *53*, 185-189, doi:10.1016/0009-2614(78)80420-5.

(2) Molina, L. T.; Molina, M. J.; Rowland, F. S. Ultraviolet absorption cross sections of several brominated methanes and ethanes of atmospheric interest. *J. Phys. Chem.* **1982**, *86*, 2672-2676, doi:10.1021/j100211a023.

(3) Pence, W. H.; Baughum, S. L.; Leone, S. R. Laser UV photofragmentation of halogenated molecules. Selective bond dissociation and wavelength-specific quantum yields for excited $I(^2P_{1/2})$ and $Br(^2P_{1/2})$ atoms. *J. Phys. Chem.* **1981**, *85*, 3844-3851, doi:10.1021/j150625a027.

(4) Zhang, L.; Fuss, W.; Kompa, K. L. Bond-selective photodissociation of CX (X = Br, I) in $XC_2H_4C_2F_4X$. *Chem. Phys.* **1990**, *144*, 289-297, doi:10.1016/0301-0104(90)80092-C.

G37. $CH_3CH_2CH_2Br$ (1-bromopropane, n-propyl bromide)

Back to Index

$CH_3CH_2CH_2Br + h\nu \rightarrow$ Products (1)

(Recommendation: 06-2, Note: 10-6, Evaluated: 10-6)

Absorption Cross Sections: The absorption spectrum of $CH_3CH_2CH_2Br$, 1-bromopropane (n-propyl bromide), has been measured at room temperature by Kozlov et al.[1] (164–270 nm). The spectrum has an absorption band above 180 nm with maxima at ~201 nm and structured features at wavelengths <180 nm similar to those in the CH_3Br spectrum, i.e., characteristic of the C-Br band absorptions in bromoalkanes. The recommended absorption cross sections in Table 4G-37 are taken from Kozlov et al.[1]

Photolysis Quantum Yield and Product Studies: No recommendation.

Table 4G-37. Recommended Absorption Cross Sections of $CH_3CH_2CH_2Br$ and $CH_3CHBrCH_3$ at 295 K

λ (nm)	10^{20} σ (cm^2)		λ (nm)	10^{20} σ (cm^2)	
	$CH_3CH_2CH_2Br$	$CH_3CHBrCH_3$		$CH_3CH_2CH_2Br$	$CH_3CHBrCH_3$
180	108.5	220.2	206	68.8	43.5
182	29.9	36.5	208	65.2	44.2
184	29.5	18.2	210	61.0	44.2
186	35.6	17.6	212	56.5	43.6
188	42.7	19.4	214	51.5	42.2
190	49.8	22.1	216	46.6	40.1
192	56.5	24.8	218	41.4	37.4
194	62.5	28.0	220	35.8	34.1
196	67.0	31.3	222	30.8	30.7
198	70.2	34.3	224	26.0	27.1
200	71.8	37.3	226	21.8	23.6
202	72.6	39.9	228	17.8	20.2
204	71.2	42.0	230	14.4	16.8

Note:
Kozlov et al.[1]

(1) Kozlov, S. N.; Orkin, V. L.; Huie, R. E.; Kurylo, M. J. OH reactivity and UV spectra of propane, n-propyl bromide, and isopropyl bromide. *J. Phys. Chem. A* **2003**, *107*, 1333-1338, doi:10.1021/jp021806j.

G38. $CH_3CHBrCH_3$ (2-bromopropane, isopropyl bromide)

Back to Index

$CH_3CHBrCH_3 + h\nu \rightarrow$ Products (1)

(Recommendation: 06-2, Note: 10-6, Evaluated: 10-6)

Absorption Cross Sections: The absorption spectrum of $CH_3CHBrCH_3$, 2-bromopropane (isopropyl bromide), was measured at room temperature by Kozlov et al.[1] (164–270 nm). The spectrum has an absorption band above 180 nm with maxima at ~209 nm and structured features at wavelengths <180 nm similar to those in the CH_3Br and $CH_3CH_2CH_3Br$ spectra, i.e., characteristic of the C-Br band absorptions in bromoalkanes. The recommended absorption cross sections in Table 4G-37 are taken from Kozlov et al.[1]

Photolysis Quantum Yield and Product Studies: No recommendation.

(1) Kozlov, S. N.; Orkin, V. L.; Huie, R. E.; Kurylo, M. J. OH reactivity and UV spectra of propane, n-propyl bromide, and isopropyl bromide. *J. Phys. Chem. A* **2003**, *107*, 1333-1338, doi:10.1021/jp021806j.

G39. $CH_3C(O)CH_2Br$ (bromoacetone)

Back to Index

$CH_3C(O)CH_2Br + h\nu \rightarrow$ Products (1)

(Recommendation: 06-2, Note: 10-6, Evaluated: 10-6)

Absorption Cross Sections: The absorption spectrum of $CH_3C(O)CH_2Br$, bromoacetone, has been measured by Burkholder et al.[1] (210-370 nm) over the temperature range 238–296 K using a diode array spectrometer (0.6 nm resolution). The spectrum has overlapping absorption bands with a maximum at 299 nm ($\sigma = 1.15 \times 10^{-19}$ cm^2 molecule^{-1} at room temperature) and increasing absorption cross sections below 255 nm to a second stronger band peaking below 210 nm. The recommended absorption cross sections in Table 4G-39 are taken from Burkholder et al.[1] A slight, but not systematic, decrease of the absorption cross sections with decreasing temperature was observed around the absorption minimum at 255 nm and in the long wavelength wings of both absorption bands.

Photolysis Quantum Yield and Product Studies: The photodissociation quantum yield was measured by Burkholder et al.[1] to be 1.6 ± 0.25 at 308 nm and 1.0 ± 0.15 at 351 nm. At both wavelengths, the yields of CO and CO_2 were unity and ~0.5, respectively, whereas the yield of HC(O)OH was measured to be 0.15 and that of HBr to be ~0.15.

Table 4G-39. Recommended Absorption Cross Sections of $CH_3C(O)CH_2Br$ at 296 K

λ (nm)	10^{20} σ (cm^2)	λ (nm)	10^{20} σ (cm^2)	λ (nm)	10^{20} σ (cm^2)	λ (nm)	10^{20} σ (cm^2)
210	59.2	248	6.40	286	9.78	324	5.55
211	58.0	249	6.07	287	9.98	325	5.20
212	57.5	250	5.77	288	10.2	326	4.87
213	56.2	251	5.49	289	10.4	327	4.55
214	53.2	252	5.25	290	10.6	328	4.24
215	50.7	253	5.14	291	10.8	329	3.94
216	48.4	254	4.98	292	11.0	330	3.64
217	46.2	255	4.88	293	11.1	331	3.35
218	43.9	256	4.76	294	11.2	332	3.06
219	41.8	257	4.68	295	11.3	333	2.77
220	39.7	258	4.62	296	11.4	334	2.51
221	37.5	259	4.66	297	11.4	335	2.26
222	35.6	260	4.70	298	11.5	336	2.02
223	33.9	261	4.76	299	11.5	337	1.80
224	32.0	262	4.72	300	11.5	338	1.60
225	30.1	263	4.79	301	11.4	339	1.41
226	28.5	264	4.91	302	11.4	340	1.24
227	26.8	265	5.01	303	11.3	341	1.09
228	25.2	266	5.12	304	11.2	342	0.955
229	23.7	267	5.39	305	11.1	343	0.831
230	22.1	268	5.44	306	11.1	344	0.724
231	20.7	269	5.57	307	10.9	345	0.627
232	19.4	270	5.77	308	10.7	346	0.545
233	18.1	271	6.03	309	10.4	347	0.473
234	16.9	272	6.25	310	10.2	348	0.408
235	15.7	273	6.48	311	9.89	349	0.351
236	14.7	274	6.68	312	9.62	350	0.303
237	13.6	275	6.90	313	9.36	351	0.259
238	12.6	276	7.16	314	9.10	352	0.223
239	11.7	277	7.45	315	8.82	353	0.190
240	10.9	278	7.74	316	8.52	354	0.164
241	10.2	279	8.00	317	8.19	355	0.140
242	9.47	280	8.25	318	7.83	356	0.120
243	8.80	281	8.50	319	7.45	357	0.108
244	8.18	282	8.75	320	7.06	358	0.0952
245	7.68	283	9.04	321	6.66	359	0.0838
246	7.22	284	9.29	322	6.28	360	0.0784
247	6.79	285	9.58	323	5.89		

Note:
Burkholder et al.[1]

(1) Burkholder, J. B.; Gilles, M. K.; Gierczak, T.; Ravishankara, A. R. The atmospheric degradation of 1-bromopropane ($CH_3CH_2CH_2Br$): The photochemistry of bromoacetone. *Geophys. Res. Lett.* **2002**, *29*, 1822, doi:10.1029/2002GL014712.

G40. CH_2=$CBrCF_2CF_3$ (2-bromo-3,3,4,4,4-pentafluoro-1-butene)

Back to Index

CH_2=$CBrCF_2CF_3$ + hν → Products (1)

(Recommendation: 19-5, Note: 19-5, Evaluated: 19-5)

Absorption Cross Sections: UV absorption cross sections of CH_2=$CBrCF_2CF_3$ (2-bromo-3,3,4,4,4-pentafluoro-1-butene) have been measured at 295 K by Orkin et al.[1] and reported in 0.5 nm increments over the wavelength range 164–250 nm, the only data available for this molecule at the time of this evaluation. The recommended cross sections at 2 nm intervals given in Table 4G-40 were taken from Orkin et al. The recommended estimated uncertainty factors (F(λ), 2σ) are assigned as $F(\lambda) = 1.05 + 1 \times 10^{-20}/\sigma(\lambda)$.

Photolysis Quantum Yield and Product Studies: No recommendation.

Table 4G-40. Recommended Absorption Cross Sections of CH_2=$CBrCF_2CF_3$ (2-bromo-3,3,4,4,4-pentafluoro-1-butene) at 295 K

λ (nm)	10^{20} σ (cm^2)	λ (nm)	10^{20} σ (cm^2)
164	352.2	208	983.2
166	304.4	210	709.1
168	306.3	212	532.9
170	264.9	214	408.2
172	226.3	216	312.3
174	186.1	218	244.9
176	214.7	220	191.6
178	303.0	222	147.9
180	441.5	224	113.7
182	616.2	226	87.20
184	847.9	228	66.92
186	1090	230	49.34
188	1365	232	36.32
190	1681	234	26.43
192	1955	236	19.29
194	2184	238	14.02
196	2323	240	10.05
198	2367	242	7.327
200	2262	244	5.191
202	2031	246	3.687
204	1724	248	2.642
206	1338	250	1.966

Note:
Orkin et al.[1]

(1) Orkin, V. L.; Louis, F.; Huie, R. E.; Kurylo, M. J. Photochemistry of bromine-containing fluorinated alkenes: Reactivity toward OH and UV spectra. *J. Phys. Chem. A* **2002**, *106*, 10195-10199, doi:10.1021/jp014436s.

G41. CH_2=$CHCF_2CF_2Br$ (3,3,4,4-tetrafluoro-4-bromo-1-butene)

Back to Index

CH_2=$CHCF_2CF_2Br$ + hν → Products (1)

(Recommendation: 19-5, Note: 19-5, Evaluated: 19-5)

Absorption Cross Sections: UV absorption cross sections of CH_2=$CHCF_2CF_2Br$ (3,3,4,4-tetrafluoro-4-bromo-1-butene) have been measured at 295 K by Orkin et al.[1] and reported in 0.5 nm increments over the wavelength range 164–255 nm, the only data available for this molecule at the time of this evaluation. The recommended

cross sections at 2 nm intervals given in Table 4G-41 were taken from Orkin et al. The recommended estimated uncertainty factors (F(λ), 2σ) are assigned as $F(\lambda) = 1.05 + 2 \times 10^{-21}/\sigma(\lambda)$.

Photolysis Quantum Yield and Product Studies: No recommendation.

Table 4G-41. Recommended Absorption Cross Sections of CH_2=$CHCF_2CF_2Br$ (3,3,4,4-tetrafluoro-4-bromo-1-butene) at 295 K

λ (nm)	10^{20} σ (cm^2)	λ (nm)	10^{20} σ (cm^2)
164	4101	210	47.97
166	4325	212	42.41
168	4482	214	36.81
170	4346	216	31.90
172	3888	218	27.54
174	3190	220	23.47
176	2372	222	19.99
178	1563	224	16.75
180	948.7	226	13.99
182	571.0	228	11.52
184	362.6	230	9.381
186	257.1	232	7.590
188	197.5	234	6.049
190	162.3	236	4.826
192	140.2	238	3.816
194	123.7	240	2.952
196	111.1	242	2.292
198	99.56	244	1.764
200	88.31	246	1.348
202	78.74	248	1.035
204	69.83	250	0.782
206	61.65	252	0.594
208	54.57	254	0.449

Note:
Orkin et al.[1]

(1) Orkin, V. L.; Louis, F.; Huie, R. E.; Kurylo, M. J. Photochemistry of bromine-containing fluorinated alkenes: Reactivity toward OH and UV spectra. *J. Phys. Chem. A* **2002**, *106*, 10195-10199, doi:10.1021/jp014436s.

G42. CH_2=$CHCFClCF_2Br$ (4-bromo-3-chloro-3,4,4-trifluoro-1-butene)

Back to Index

CH_2=$CHCFClCF_2Br$ + hν → Products (1)

(Recommendation: 19-5, Note: 19-5, Evaluated: 19-5)

Absorption Cross Sections: UV absorption cross sections of CH_2=$CHCFClCF_2Br$ (4-bromo-3-chloro-3,4,4-trifluoro-1-butene) have been measured at 295 K by Orkin et al.[1] over the wavelength range 164–260 nm, the only data available for this molecule at the time of this evaluation. The recommended cross sections at 2 nm intervals given in Table 4G-42 were taken from Orkin et al. The recommended estimated uncertainty factors (F(λ), 2σ) are assigned as $F(\lambda) = 1.05 + 2 \times 10^{-21}/\sigma(\lambda)$.

Photolysis Quantum Yield and Product Studies: No recommendation.

Table 4G-42. Recommended Absorption Cross Sections of CH_2=CHCFClCF$_2$Br (4-bromo-3-chloro-3,4,4-trifluoro-1-butene) at 295 K

λ (nm)	10^{20} σ (cm^2)	λ (nm)	10^{20} σ (cm^2)
164	3800	214	68.2
166	4070	216	56.9
168	4280	218	47.5
170	4340	220	39.4
172	4250	222	32.7
174	4010	224	27.1
176	3620	226	22.5
178	3160	228	18.46
180	2660	230	15.18
182	2180	232	12.44
184	1750	234	10.04
186	1390	236	8.08
188	1100	238	6.51
190	860	240	5.18
192	678	242	4.11
194	537	244	3.22
196	423	246	2.54
198	339	248	1.99
200	275	250	1.54
202	223	252	1.21
204	180.1	254	0.94
206	148.0	256	0.73
208	121.0	258	0.58
210	99.3	260	0.45
212	82.4		

Note:
Orkin et al.[1]

(1) Orkin, V. L.; Martynova, L. E.; Kurylo, M. J. Photochemical properties of CH_2=CH-CFCl-CF_2Br (4-bromo-3-chloro-3,4,4-trifluoro-1-butene) and CH_3-O-$CH(CF_3)_2$ (methyl hexafluoroisopropyl ether): OH reaction rate constants and UV and IR absorption spectra. *J. Phys. Chem. A* **2017**, *121*, 5675-5680, doi:10.1021/acs.jpca.7b04256.

4.10 Bibliography – BrO_x Photochemistry

Acton, A. P.; Aickin, R. G.; Bayliss, N. S. The continuous absorption spectrum of bromine: A new interpretation. *J. Chem. Phys.* **1936**, *4*, 474-479, doi:10.1063/1.1749887.

Barnes, R. J.; Lock, M.; Coleman, J.; Sinha, A. Observation of a new absorption band of HOBr and its atmospheric implications. *J. Phys. Chem.* **1996**, *100*, 453-457, doi:10.1021/jp952445t.

Barone, S. B.; Turnipseed, A. A.; Gierczak, T.; Ravishankara, A. R. Quantum yields of $H(^2S)$ and $CH_3S(^2E)$ from the photolysis of simple organosulfur compounds at 193, 222, and 248 nm. *J. Phys. Chem.* **1994**, *98*, 11969-11977, doi:10.1021/j100097a024.

Basco, N.; Dogra, S. K. Reactions of halogen oxides studied by flash photolysis III. The production and reactions of BrO and ClO radicals in the halogen-sensitized decomposition of chlorine dioxide. *Proc. Roy. Soc. Lond. A.* **1971**, *323*, 417-429, doi:10.1098/rspa.1971.0113.

Baumfalk, R.; Buck, U.; Frischkorn, C.; Nahler, N. H.; Hüwel, L. Photodissociation of HBr molecules and clusters: Anisotropy parameters, branching ratios, and kinetic energy distributions. *J. Chem. Phys.* **1999**, *111*, 2595-2605, doi:10.1063/1.479535.

Bayes, K. D.; Toohey, D. W.; Friedl, R. R.; Sander, S. P. Measurements of quantum yields of bromine atoms in the photolysis of bromoform from 266 to 324 nm. *J. Geophys. Res.* **2003**, *108*, 4095, doi:10.29/2002JD002877.

Benter, T.; Feldmann, C.; Kirchner, U.; Schmidt, M.; Schmidt, S.; Schindler, R. N. UV/VIS-absorption spectra of HOBr and CH_3OBr: $Br(^2P_{3/2})$ atom yields in the photolysis of HOBr. *Ber. Bunsenges. Phys. Chem.* **1995**, *99*, 1144-1147, doi:10.1002/bbpc.199500046.

Bernard, F.; McGillen, M. R.; Fleming, E. L.; Jackman, C. H.; Burkholder, J. B. $CBrF_3$ (Halon-1301): UV absorption spectrum between 210 and 320 K, atmospheric lifetime, and ozone depletion potential. *J. Photochem. Photobiol. A: Chem.* **2015**, *306*, 13-20, doi:10.1016/j.jphotochem.2015.03.012.

Bilde, M.; Wallington, T. J.; Ferronato, G.; Orlando, J. J.; Tyndall, G. S.; Estupinan, E.; Haberkorn, S. Atmospheric chemistry of CH_2BrCl, $CHBrCl_2$, $CHBr_2Cl$, $CF_3CHBrCl$, and CBr_2Cl_2. *J. Phys. Chem. A* **1998**, *102*, 1976-1986, doi:10.1021/jp9733375.

Bridges, L.; White, J. M. Photochemistry of methanethiol at 254 and 214 nm. *J. Phys. Chem.* **1973**, *77*, 295-298, doi:10.1021/j100621a031.

Brion, C. E.; Iida, Y.; Carnovale, F.; Thomson, J. P. Absolute dipole oscillator strengths for photoabsorption, photoisonization and ionic photofragmentation processes in HBr. *Chem. Phys.* **1985**, *98*, 327-339, doi:10.1016/0301-0104(85)80144-0.

Brown, A. C.; Canosa-Mas, C. E.; Parr, A. D.; Rothwell, K.; Wayne, R. P. Tropospheric lifetimes of three compounds for possible replacement of CFC and halons. *Nature* **1990**, *347*, 541-543, doi.org/10.1038/347541a0.

Burkholder, J. B. Rate coefficient for the reaction: $Br + Br_2O \rightarrow Br_2 + BrO$. *Int. J. Chem. Kinet.* **1998**, *30*, 571-576, doi:10.1002/(SICI)1097-4601(1998)30:8<571::AID-KIN6>3.0.CO;2-P.

Burkholder, J. B.; Gilles, M. K.; Gierczak, T.; Ravishankara, A. R. The atmospheric degradation of 1-bromopropane ($CH_3CH_2CH_2Br$): The photochemistry of bromoacetone. *Geophys. Res. Lett.* **2002**, *29*, 1822, doi:10.1029/2002GL014712.

Burkholder, J. B.; Knight, G.; Orlando, J. J. UV absorption spectrum of BrOCl. *J. Photochem. Photobiol. A: Chem.* **2000**, *134*, 133-137, doi:10.1016/S1010-6030(00)00261-6.

Burkholder, J. B.; Orlando, J. J. UV absorption cross-sections of *cis*-BrONO. *Chem. Phys. Lett.* **2000**, *317*, 603-608, doi:10.1016/S0009-2614(99)01412-8.

Burkholder, J. B.; Ravishankara, A. R.; Solomon, S. UV/visible and IR absorption cross sections of $BrONO_2$. *J. Geophys. Res.* **1995**, *100*, 16793-16800, doi:10.1029/95JD01223.

Burkholder, J. B.; Wilson, R. R.; Gierczak, T.; Talukdar, R.; McKeen, S. A.; Orlando, J. J.; Vaghjiani, G. L.; Ravishankara, A. R. Atmospheric fate of CF_3Br, CF_2Br_2, CF_2ClBr, and CF_2BrCF_2Br. *J. Geophys. Res.* **1991**, *96*, 5025-5043, doi:10.1029/90JD02735.

Cadman, P.; Simons, J. P. Reactions of hot halomethyl radicals. *Trans. Faraday Soc.* **1966**, *62*, 631-641, doi:10.1039/tf9666200631.

Causley, G. C.; Russell, B. R. Vacuum ultraviolet absorption spectra of the bromomethanes. *J. Chem. Phys.* **1975**, *62*, 848-857, doi:10.1063/1.430535.

Clyne, M. A. A.; Cruse, H. W. Rates of elementary reactions involving the BrO ($X^2\Pi$) and IO ($X^2\Pi$) radicals. *Trans. Faraday Soc.* **1970**, *66*, 2214-2226, doi:10.1039/tf9706602214.

Cooper, M. J.; Wrede, E.; Orr-Ewing, A. J.; Ashfold, M. N. R. Ion imaging studies of the $Br(^2P_J)$ atomic products resultings from Br_2 photolysis in the wavelength range 260-580 nm. *J. Chem. Soc. Faraday Trans.* **1998**, *94*, 2901-2907, doi:10.1039/a804112a.

Cox, R. A.; Sheppard, D. W.; Stevens, M. P. Absorption coefficients and kinetics of the BrO radical using molecular modulation. *J. Photochem.* **1982**, *19*, 189-207, doi:10.1016/0047-2670(82)80022-1.

Davidson, N. The ultraviolet absorption spectra and the refractive indices of some fluorobromomethanes. *J. Am. Chem. Soc.* **1951**, *73*, 467-468, doi:10.1021/ja01145a506.
Deters, B.; Burrows, J. P.; Himmelmann, S.; Blindauer, C. Gas phase spectra of HOBr and Br_2O and their atmospheric significance. *Ann. Geophys.* **1996**, *14*, 468-475.
Deters, B.; Burrows, J. P.; Orphal, J. UV-visible absorption cross sections of bromine nitrate determined by photolysis of $BrONO_2/Br_2$ mixtures. *J. Geophys. Res.* **1998**, *103*, 3563-3570, doi:10.1029/97JD02390.
Doucet, J.; Gilbert, R.; Sauvageau, P.; Sandorfy, C. Photoelectron and far-ultraviolet spectra of CF_3Br, CF_2BrCl, and CF_2Br_2. *J. Chem. Phys.* **1975**, *62*, 366-369, doi:10.1063/1.430495.
Doucet, J.; Sauvageau, P.; Sandorfy, C. Vacuum ultraviolet and photoelectron spectra of fluoro-chloro derivatives of methane. *J. Chem. Phys.* **1973**, *58*, 3708-3716, doi:10.1063/1.1679722.
Ebenstein, W. L.; Wiesenfeld, J. R.; Wolk, G. L. Photodissociation of alkyl bromides. *Chem. Phys. Lett.* **1978**, *53*, 185-189, doi:10.1016/0009-2614(78)80420-5.
Eden, C.; Feilchenfeld, H.; Manor, S. Simultaneous spectrophotometric determination of nitrosyl bromide and bromine. *Anal. Chem.* **1969**, *41*, 1150-1151, doi:10.1021/ac60277a042.
Felps, W. S.; Rupnik, K.; McGlynn, S. P. Electronic spectroscopy of the cyanogen halides. *J. Phys. Chem.* **1991**, *95*, 639-656, doi:10.1021/j100155a028.
Fleischmann, O. C.; Burrows, J. P.; Orphal, J. Time-windowing Fourier transform absorption spectroscopy for flash photolysis investigations. *J. Photochem. Photobiol. A: Chem.* **2003**, *157*, 127-136, doi:10.1016/S1010-6030(03)00069-8.
Fleischmann, O. C.; Hartmann, M.; Burrows, J. P.; Orphal, J. New ultraviolet absorption cross-sections of BrO at atmospheric temperatures measured by a time-windowing Fourier transform spectroscopy. *J. Photochem. Photobiol. A.: Chem.* **2004**, *168*, 117-132, doi:10.1016/j.jphotochem.2004.03.026.
Fleischmann, O. C.; Meyer-Arnek, J.; Burrows, J. P.; Orphal, J. The visible absorption spectrum of OBrO, investigated by Fourier transform spectroscopy. *J. Phys. Chem. A* **2005**, *109*, 5093-5103, doi:10.1021/jp044911x.
Francisco, J. S.; Hand, M. R.; Williams, I. H. *Ab Initio* study of the electronic spectrum of HOBr. *J. Phys. Chem.* **1996**, *100*, 9250-9253, doi:10.1021/jp9529782.
Gilles, M. K.; Turnipseed, A. A.; Burkholder, J. B.; Ravishankara, A. R. Kinetics of the IO radical. 2. Reaction of IO with BrO. *J. Phys. Chem. A* **1997**, *101*, 5526-5534, doi:10.1021/jp9709159.
Gillotay, D.; Jenouvrier, A.; Coquart, B.; Mérienne, M. F.; Simon, P. C. Ultraviolet absorption cross-sections of bromoform in the temperature range 295-240K. *Planet. Space Sci.* **1989**, *37*, 1127-1140, doi:10.1016/0032-0633(89)90084-6.
Gillotay, D.; Simon, P. C. Ultraviolet absorption cross-sections of methyl bromide at stratospheric temperatures. *Ann. Geophys.* **1988**, *6*, 211-215.
Gillotay, D.; Simon, P. C. Ultraviolet absorption spectrum of trifluoro-bromo-methane, difluoro-dibromo-methane and difluoro-bromo-chloro-methane in the vapor phase. *J. Atmos. Chem.* **1989**, *8*, 41-62, doi:10.1007/BF00053815.
Gillotay, D.; Simon, P. C. Ultraviolet absorption cross-sections of photoactive species of stratospheric interest Part 1: The halocarbons. *Aeronomica Acta A* **1990**, *356*, 1-173, doi:10.18758/A_356.
Gillotay, D.; Simon, P. C.; Dierickx, L. Temperature dependence of ultraviolet absorption cross-sections of brominated methanes and ethanes. *Aeronomica Acta* **1988**, *A335*, 1-25.
Giolando, D. M.; Fazekas, G. B.; Taylor, W. D.; Takacs, G. A. Atmospheric photochemistry of CF_2ClBr. *J. Photochem.* **1980**, *14*, 335-339, doi:10.1016/0047-2670(80)85105-7.
Goodeve, C. F.; Taylor, A. W. C. The continuous absorption spectrum of hydrogen bromide. *Proc. Roy. Soc. London A* **1935**, *152*, 221-230.
Gordus, A. A.; Bernstein, R. B. Isotope effect in continuous ultraviolet absorption spectra: Methyl bromide-d_3 and chloroform-*d*. *J. Chem. Phys.* **1954**, *22*, 790-795, doi:10.1063/1.1740194.
Gosnell, T. R.; Taylor, A. J.; Lyman, J. L. Ultrafast absorption spectroscopy of photodissociated CF_2Br_2: Details of the reaction mechanism and evidence for anomalously slow intramolecular vibrational redistribution within the CF_2Br intermediate. *J. Chem. Phys.* **1991**, *94*, 5949-5953, doi:10.1063/1.460429.
Gray, L. T. M.; Style, D. W. G. The absorption of light by chlorine, bromine and their gaseous mixtures. *Proc. Roy. Soc. London* **1930**, *A 126*, 603-612, doi:10.1098/rspa.1930.0029.
Harwood, M. H.; Burkholder, J. B.; Ravishankara, A. R. Photodissociation of $BrONO_2$ and N_2O_5: Quantum yields for NO_3 production at 248, 308, and 352.5 nm. *J. Phys. Chem. A* **1998**, *102*, 1309-1317, doi:10.1021/jp9729829.
Haugen, H. K.; Weitz, E.; Leone, S. R. Accurate quantum yields by laser gain vs absorption spectroscopy: Investigation of Br/Br* channels in photofragmentation of Br_2 and IBr. *J. Chem. Phys.* **1985**, *83*, 3402-3412, doi:10.1063/1.449145.
Hemenway, C. P.; Lindeman, T. G.; Wiesenfeld, J. R. Measurement of the $A\ ^3\Pi_{1u} \leftarrow X\ ^1\Sigma_g^+$ continuum absorptivity in Br_2. *J. Chem. Phys.* **1979**, *70*, 3560-3561, doi:10.1063/1.437896.

Hippler, H.; Luu, S. H.; Teitelbaum, H.; Troe, J. Flash photolysis study of the NO-catalyzed recombination of bromine atoms. *Int. J. Chem. Kinet.* **1978**, *10*, 155-169, doi:10.1002/kin.550100203.
Houel, N.; van den Bergh, H. BrNO—thermodynamic properties, the ultraviolet/vis spectrum, and the kinetics of its formation. *Int. J. Chem. Kinet.* **1977**, *9*, 867-874, doi:10.1002/kin.550090603.
Hoxha, A.; Locht, R.; Leyh, B.; Dehareng, D.; Hottmann, K.; Jochims, H. W.; Baumgärtel, H. The photoabsorption and constant ionic state spectroscopy of vinylbromide. *Chem. Phys.* **2000**, *260*, 237-247, doi:10.1016/S0301-0104(00)00191-9.
Hubinger, S.; Nee, J. B. Absorption spectra of Cl_2, Br_2 and BrCl between 190 and 600 nm. *J. Photochem. Photobiol. A: Chem.* **1995**, *86*, 1-7, doi:10.1016/1010-6030(94)03949-U.
Huebert, B. J.; Martin, R. M. Gas-phase far-ultraviolet absorption spectrum of hydrogen bromide and hydrogen iodide. *J. Phys. Chem.* **1968**, *72*, 3046-3048, doi:10.1021/j100854a071.
Ibuki, T. Vacuum ultraviolet absorption spectra and photodissociative excitation of $CHBr_2Cl$ and $CHBrCl_2$. *J. Chem. Phys.* **1992**, *96*, 8793-8798, doi:10.1063/1.462286.
Ibuki, T.; Takahashi, N.; Hiraya, A.; Shobatake, K. $CCl_2(\tilde{A}\ ^1B_1)$ radical formation in VUV photolyses of CCl_4 and $CBrCl_3$. *J. Chem. Phys.* **1986**, *85*, 5717-5722, doi:10.1063/1.451532.
Ingham, T.; Bauer, D.; Landgraf, J.; Crowley, J. N. Ultraviolet-visible absorption cross sections of gaseous HOBr. *J. Phys. Chem. A* **1998**, *102*, 3293-3298, doi:10.1021/jp980272c.
Jee, Y.-J.; Jung, Y.-J.; Jung, K.-H. Photodissociation of Br_2 at 234 and 265 nm: Imaging studies of one and two photon excitation. *J. Chem. Phys.* **2001**, *115*, 9739-9746, doi:10.1063/1.1410977.
Jee, Y.-J.; Park, M. S.; Kim, Y. S.; Jung, Y.-J.; Jung, K.-H. Photodissociation of bromine molecule near 265 nm. *Chem. Phys. Lett.* **1998**, *287*, 701-708, doi:10.1016/S0009-2614(98)00235-8.
Jost, W. Das gleichgewicht zwischen chlor, brom und bromchlorid (BrCl). *Z. Phys. Chem. A* **1931**, *153*, 143-152.
Jung, Y.-J.; Park, M. S.; Kim, Y. S.; Jung, K.-H.; Volpp, H.-R. Photodissociation of $CBrCl_3$ at 234 and 265 nm: Evidence of the curve crossing. *J. Chem. Phys.* **1999**, *111*, 4005-4012, doi:10.1063/1.479182.
Knight, G.; Ravishankara, A. R.; Burkholder, J. B. Laboratory studies of OBrO. *J. Phys. Chem. A* **2000**, *104*, 11121-11125, doi:10.1021/jp002226u.
Ko, M. K. W.; Newman, P. A.; Reimann, S.; Strahan, S. E.; Plumb, R. A.; Stolarski, R. S.; Burkholder, J. B.; Mellouki, W.; Engel, A.; Atlas, E. L.; Chipperfield, M.; Liang, Q. Lifetimes of Stratospheric Ozone-Depleting Substances, Their Replacements, and Related Species, SPARC Report No. 6, WCRP-15/2013, 2013, http://www.sparc-climate.org/publications/sparc-reports/sparc-report-no6/.
Kozlov, S. N.; Orkin, V. L.; Huie, R. E.; Kurylo, M. J. OH reactivity and UV spectra of propane, n-propyl bromide, and isopropyl bromide. *J. Phys. Chem. A* **2003**, *107*, 1333-1338, doi:10.1021/jp021806j.
Krajnovich, D.; Zhang, Z.; Butler, L.; Lee, Y. T. Photodissociation of CF_2Br_2 at 248 nm by the molecular beam method. *J. Phys. Chem.* **1984**, *88*, 4561-4566, doi:10.1021/j150664a023.
Laszlo, B.; Huie, R. E.; Kurylo, M. J.; Miziolek, A. W. Kinetic studies of the reactions of BrO and IO radicals. *J. Geophys. Res.* **1997**, *102*, 1523-1532, doi:10.1029/96JD00458.
Lee, S.-H.; Jung, Y.-J.; Jung, K.-H. Photodissociation dynamics of CH_2BrCl at 234 nm. *Chem. Phys.* **2000**, *260*, 143-150, doi:10.1016/S0301-0104(00)00216-0.
Libuda, H. G. Spektroskopische und kinetische Untersuchungen an halogenierten Carbonylverbindungen von atmosphärischem Interesse. PhD-Thesis, University of Wuppertal, Germany, 1992.
Libuda, H. G.; Zabel, F.; Becker, K. H. "UV spectra of some organic chlorine and bromine compounds of atmospheric interest"; Kinetics and Mechanisms for the Reactions of Halogenated Organic Compounds in the Troposphere. STEP-HALOCSIDE/AFEAS WORKSHOP, 1991, Dublin, Ireland.
Lindeman, T. G.; Wiesenfeld, J. R. Photodissociation of Br_2 in the visible continuum. *J. Chem. Phys.* **1979**, *70*, 2882-2888, doi:10.1063/1.437824.
Locht, R.; Leyh, B.; Jochims, H. W.; Baumgärtel, H. The vacuum UV photoabsorption spectrum of methyl bromide (CH_3Br) and its perdeuterated isotopomer CD_3Br: a Rydberg series analysis. *Chem. Phys.* **2005**, *317*, 73-86, doi:10.1016/j.chemphys.2005.06.002.
Lock, M.; Barmes, R. J.; Sinha, A. Near-threshold photodissociation dynamics of HOBr: Determination of product state distribution, vector correlation, and heat of formation. *J. Phys. Chem.* **1996**, *100*, 7972-7980, doi:10.1021/jp9532428.
Maloney, K. K.; Palmer, H. B. Low-pressure thermal decomposition of ONBr and ONCl in shock waves. *Int. J. Chem. Kinet.* **1973**, *5*, 1023-1037, doi:10.1002/kin.550050611.
Man, S.-Q.; Kwok, W. M.; Phillips, D. L.; Johnson, A. E. Short-time photodissociation dynamics of A-band and B-band bromoiodomethane in solution: An examination of bond selective electronic excitation. *J. Chem. Phys.* **1996**, *105*, 5842-5857, doi:10.1063/1.472426.
Maric, D.; Burrows, J. P.; Moortgat, G. K. A Study of the UV-visible absorption spectra of Br_2 and BrCl. *J. Photochem. Photobiol A: Chem.* **1994**, *83*, 179-192, doi:10.1016/1010-6030(94)03823-6.

McGivern, W. S.; Li, R.; Zou, P.; North, S. W. Photodissociation dynamics of CH_2BrCl studied using resonance enhanced multiphoton ionization (REMPI) with time-of-flight mass spectrometry. *J. Chem. Phys.* **1999**, *111*, 5771-5779, doi:10.1063/1.479874.
McMillan, V. personal communication to J.G. Calvert, J.N. Pitts, Jr., Photochemistry, London, 1966, p. 184. **1966**.
Miller, C. E.; Nickolaisen, S. L.; Francisco, J. S.; Sander, S. P. The OBrO $C(^2A_2) \leftarrow X(^2B_1)$ absorption spectrum. *J. Chem. Phys.* **1997**, *107*, 2300-2307, doi:10.1063/1.474606.
Minaev, B. F. The singlet-triplet absorption and photodissociation of the HOCl, HOBr, and HOI molecules calculated by the MCSCF quadratic response method. *J. Phys. Chem. A* **1999**, *103*, 7294-7309, doi:10.1021/jp990203d.
Molina, L. T.; Molina, M. J. Quantum yields for the photodissociation of CBr_2F_2 in the 200-300-nm region. *J. Phys. Chem.* **1983**, *87*, 1306-1308, doi:10.1021/j100231a008.
Molina, L. T.; Molina, M. J.; Rowland, F. S. Ultraviolet absorption cross sections of several brominated methanes and ethanes of atmospheric interest. *J. Phys. Chem.* **1982**, *86*, 2672-2676, doi:10.1021/j100211a023.
Moortgat, G. K.; Meller, R.; Schneider, W. Temperature dependence (256-296K) of the absorption cross-sections of bromoform in the wavelength range 285-360 nm. In *The Tropospheric Chemistry of Ozone in the Polar Regions*; Niki, H., Becker, K. H., Eds.; Springer-Verlag: Berlin, 1993; pp 359-369.
Mössinger, J. C.; Shallcross, D. E.; Cox, R. A. UV-Vis absorption cross-sections and atmospheric lifetimes of CH_2Br_2, CH_2I_2 and CH_2BrI. *J. Chem. Soc. Faraday Trans.* **1998**, *94*, 1391-1396, doi:10.1039/a709160e.
Nee, J. B.; Suto, M.; Lee, L. C. Quantitative spectroscopy study of HBr in the 105-235 nm region. *J. Chem. Phys.* **1986**, *85*, 4919-4924, doi:10.1063/1.451728.
Okabe, H. Photodissociation of thiophosgene. *J. Chem. Phys.* **1977**, *66*, 2058-2062, doi:10.1063/1.434166.
Okabe, H. Photochemistry of acetylene at 1849 Å. *J. Chem. Phys.* **1983**, *78*, 1312-1317, doi:10.1063/1.444868.
Olney, T. N.; Cooper, G.; Chan, W. F.; Burton, G. R.; Brion, C. E.; Tan, K. H. Absolute photoabsorption and photoionization studies of methyl bromide using dipole electron impact and synchroton radiation PES techniques. *Chem. Phys.* **1997**, *218*, 127-149, doi:10.1016/S0301-0104(97)00066-9.
Orkin, V. L.; Kasimovskaya, E. E. Ultraviolet absorption spectra of some Br-containing haloalkenes. *J. Atmos. Chem.* **1995**, *21*, 1-11, doi:10.1007/BF00712435.
Orkin, V. L.; Khamaganov, V. G.; Guschin, A. G.; Huie, R. E.; Kurylo, M. J. Atmospheric fate of chlorobromomethane: Rate constant for the reaction with OH, UV spectrum, and water solubility. *J. Phys. Chem. A* **1997**, *101*, 174-178, doi:10.1021/jp962428j.
Orkin, V. L.; Louis, F.; Huie, R. E.; Kurylo, M. J. Photochemistry of bromine-containing fluorinated alkenes: Reactivity toward OH and UV spectra. *J. Phys. Chem. A* **2002**, *106*, 10195-10199, doi:10.1021/jp014436s.
Orkin, V. L.; Martynova, L. E.; Kurylo, M. J. Photochemical properties of CH_2=CH-CFCl-CF_2Br (4-bromo-3-chloro-3,4,4-trifluoro-1-butene) and CH_3-O-CH$(CF_3)_2$ (methyl hexafluoroisopropyl ether): OH reaction rate constants and UV and IR absorption spectra. *J. Phys. Chem. A* **2017**, *121*, 5675-5680, doi:10.1021/acs.jpca.7b04256.
Orlando, J. J.; Burkholder, J. B. Gas-phase UV/visible absorption spectra of HOBr and Br_2O. *J. Phys. Chem.* **1995**, *99*, 1143-1150, doi:10.1021/j100004a013.
Orlando, J. J.; Burkholder, J. B.; Bopegedera, A. M. R. P.; Howard, C. J. Infrared measurements of BrO ($X^2\Pi_{3/2}$). *J. Mol. Spectrosc.* **1991**, *145*, 278-289, doi:10.1016/0022-2852(91)90115-Q.
Papanastasiou, D. K.; McKeen, S. A.; Burkholder, J. B. The very short-lived ozone depleting substance $CHBr_3$ (bromoform): revised UV absorption spectrum, atmospheric lifetime and ozone depletion potential. *Atmos. Chem. Phys.* **2014**, *14*, 3017-3025, doi:10.5194/acp-14-3017-2014.
Papanastasiou, D. K.; Rontu Carlon, N.; Neuman, J. A.; Fleming, E. L.; Jackman, C. H.; Burkholder, J. B. Revised UV absorption spectra, ozone depletion potentials, and global warming potentials for the ozone-depleting substances CF_2Br_2, CF_2ClBr, and CF_2BrCF_2Br. *Geophys. Res. Lett.* **2013**, *40*, doi:10.1002/GRL.50121.
Passchier, A. A.; Christian, J. D.; Gregory, N. W. The ultraviolet-visible absorption spectrum of bromine between room temperature and 440°. *J. Phys. Chem.* **1967**, *71*, 937-942, doi:10.1021/j100863a025.
Pence, W. H.; Baughum, S. L.; Leone, S. R. Laser UV photofragmentation of halogenated molecules. Selective bond dissociation and wavelength-specific quantum yields for excited I($^2P_{1/2}$) and Br($^2P_{1/2}$) atoms. *J. Phys. Chem.* **1981**, *85*, 3844-3851, doi:10.1021/j150625a027.
Petersen, A. B.; Smith, I. W. M. Yields of Br*($4^2P_{1/2}$) as a function of wavelength in the photodissociation of Br_2 and IBr. *Chem. Phys.* **1978**, *30*, 407-413, doi:10.1016/0301-0104(78)87012-8.
Peterson, K. A.; Francisco, J. S. Should bromoform absorb at wavelengths longer than 300 nm? *J. Chem. Phys.* **2002**, *117*, 6103-6107, doi:10.1063/1.1502639.
Porret, D.; Goodeve, C. F. The continuous absorption spectra of alkyl iodides and alkyl bromides and their quantal interpretation. *Proc. Roy. Soc. Lond. A* **1938**, *165*, 31-42, doi:10.1098/rspa.1938.0042.

Rattigan, O. V.; Jones, R. L.; Cox, R. A. The visible spectrum of gaseous OBrO. *Chem. Phys. Lett.* **1994**, *230*, 121-126, doi:10.1016/0009-2614(94)01129-X.
Rattigan, O. V.; Lary, D. J.; Jones, R. L.; Cox, R. A. UV-visible absorption cross sections of gaseous Br_2O and HOBr. *J. Geophys. Res.* **1996**, *101*, 23021-23033, doi:10.1029/96JD02017.
Ravishankara, A. R.; Wine, P. H.; Langford, A. O. Absolute rate constant for the reaction OH + HBr → H_2O + Br. *Chem. Phys. Lett.* **1979**, *63*, 479-484, doi:10.1016/0009-2614(79)80694-6.
Regan, P. M.; Langford, S. R.; Orr-Ewing, A. J.; Ashfold, M. N. R. The ultraviolet photodissociation dynamics of hydrogen bromide. *J. Chem. Phys.* **1999**, *110*, 281-288, doi:10.1063/1.478063.
Ribaud, M. G. Contribution a l'étude de l'absorption de la lumière par les gaz. *Ann. Phys.* **1919**, *12*, 107-226.
Robbins, D. E. Photodissociation of methyl chloride and methyl bromide in the atmosphere. *Geophys. Res. Lett.* **1976**, *3*, 213-216, doi:10.1029/GL003i004p00213.
Romand, J. Absorption ultraviolette dans la région de Schumann étude de: ClH, BrH et IH gazeux. *Ann. Phys. (Paris)* **1949**, *4*, 529-590.
Rowley, D. M.; Harwood, M. H.; Freshwater, R. A.; Jones, R. L. A novel flash photolysis/UV absorption system employing charge-coupled device (CCD) detection: A study of the BrO + BrO reaction at 298 K. *J. Phys. Chem.* **1996**, *100*, 3020-3029, doi:10.1021/jp951825b.
Roxlo, C.; Mandl, A. Vacuum ultraviolet absorption cross sections for halogen containing molecules. *J. Appl. Phys.* **1980**, *51*, 2969-2972, doi:10.1063/1.328108.
Sander, S. P.; Friedl, R. R. Kinetics and product studies of the reaction ClO + BrO using flash photolysis-ultraviolet absorption. *J. Phys. Chem.* **1989**, *93*, 4764-4771, doi:10.1021/j100349a017.
Schander, J.; Russell, B. R. Vacuum ultraviolet spectra of bromoethylene and dibromoethylenes. *J. Am. Chem. Soc.* **1976**, *98*, 6900-6904, doi:10.1021/ja00438a024.
Scheffler, D.; Grothe, H.; Willner, H.; Frenzel, A.; Zetzsch, C. Properties of pure nitryl bromide. Thermal behavior, UV/vis and FTIR spectra, and photoisomerization to *trans*-BrONO in an argon matrix. *Inorg. Chem.* **1997**, *36*, 335-338, doi:10.1021/ic9606946.
Seccombe, D. P.; Chim, R. Y. L.; Tuckett, R. P.; Jochims, H. W.; Baumgärtel, H. Vacuum–ultraviolet absorption and fluorescence spectroscopy of CF_2H_2, CF_2Cl_2, and CF_2Br_2 in the range 8–22 eV. *J. Chem. Phys.* **2001**, *114*, 4058-4073, doi:10.1063/1.1344888.
Seccombe, D. P.; Tuckett, R. P.; Baumgärtel, H.; Jochims, H. W. Vacuum-UV fluorescence spectroscopy of CCl_3F, CCl_3H and CCl_3Br in the range 8–30 eV. *Phys. Chem. Chem. Phys.* **1999**, *1*, 773-782, doi:10.1039/a809422e.
Seery, D. J.; Britton, D. The continuous absorption spectra of chlorine, bromine, bromine chloride, iodine chloride, and iodine bromide. *J. Phys. Chem.* **1964**, *68*, 2263-2266, doi:10.1021/j100790a039.
Sidebottom, H. W.; Tedder, J. M.; Walton, J. C. Photolysis of bromotrichloromethane. *Trans. Faraday Soc.* **1969**, *65*, 755-762, doi:10.1039/tf9696500755.
Soller, R.; Nicovich, J. M.; Wine, P. H. Bromine nitrate photochemistry: Quantum yields for O, Br, and BrO over the wavelength range 248-355 nm. *J. Phys. Chem. A* **2002**, *106*, 8378-8385, doi:10.1021/jp020018r.
Spencer, J. E.; Rowland, F. S. Bromine nitrate and its stratospheric significance. *J. Phys. Chem.* **1978**, *82*, 7-10, doi:10.1021/j100490a002.
Sulzer, P.; Wieland, K. Intensitätsverteilung eines kontinuierlichen absorptions-spektrums in abhängigkeit von temperatur und wellenzahl. *Helv. Phys. Acta* **1952**, *25*, 653-676, doi:10.5169/seals-112328.
Suto, M.; Lee, L. C. Emission spectra of CF_3 radicals. V. Photodissociation of CF_3H, CF_3Cl, and CF_3Br by vacuum ultraviolet. *J. Chem. Phys.* **1983**, *79*, 1127-1133, doi:10.1063/1.445914.
Taketani, F.; Takahashi, K.; Matsumi, Y. Quantum yields for Cl(^2P_J) atom formation from the photolysis of chlorofluorocarbons and chlorinated hydrocarbons at 193.3 nm. *J. Phys. Chem. A* **2005**, *109*, 2855-2860, doi:10.1021/jp044218+.
Talukdar, R.; Mellouki, A.; Gierczak, T.; Burkholder, J. B.; McKeen, S. A.; Ravishankara, A. R. Atmospheric lifetime of CHF_2Br, a proposed substitute for halons. *Science* **1991**, *252*, 693-695, doi:10.1126/science.252.5006.693.
Talukdar, R. K.; Hunter, M.; Warren, R. F.; Burkholder, J. B.; Ravishankara, A. R. UV laser photodissociation of CF_2ClBr and CF_2Br_2 at 298 K: quantum yields of Cl, Br, and CF_2. *Chem. Phys. Lett.* **1996**, *262*, 669-674, doi:10.1016/S0009-2614(96)01157-8.
Talukdar, R. K.; Vashjiani, G. L.; Ravishankara, A. R. Photodissociation of bromocarbons at 193, 222, and 248 nm: Quantum yields of Br atom at 298 K. *J. Chem. Phys.* **1992**, *96*, 8194-8201, doi:10.1063/1.462324.
Tellinghuisen, J. Precise equilibrium constants from spectrophotometric data: BrCl in Br_2/Cl_2 gas mixtures. *J. Phys. Chem. A* **2003**, *107*, 753-775, doi:10.1021/jp027227w.
Tellinghuisen, J. Equilibrium constants from spectrophotometric data: Dimer formation in gaseous Br_2. *J. Phys. Chem. A* **2008**, *112*, 5902–5907, doi:10.1021/jp8020358.
Tzeng, W. B.; Lee, Y. R.; Lin, S. M. Photodissociation of CH_2BrCl at 248 and 193 nm investigated by translational spectroscopy. *Chem. Phys. Lett.* **1994**, *227*, 467-471, doi:10.1016/0009-2614(94)00837-X.

Uthman, A. P.; Demlein, P. J.; Allston, T. D.; Withiam, M. C.; McClements, M. J.; Takacs, G. A. Photoabsorption spectra of gaseous methyl bromide, ethylene dibromide, nitrosyl bromide, thionyl chloride, and sulfuryl chloride. *J. Phys. Chem.* **1978**, *82*, 2252-2257, doi:10.1021/j100509a021.

Vaghjiani, G. CH_3SH ultraviolet absorption cross sections in the region 192.5-309.5 nm and photodecomposition at 222 and 193 nm and 296 K. *J. Chem. Phys.* **1993**, *99*, 5936-5943, doi:10.1063/1.465917.

Vatsa, R. K.; Kumar, A.; Naik, P. D.; Rama Rao, K. V. S.; Mittal, J. P. UV absorption spectrum and decay kinetics of CF_2Br in CO_2 laser-induced photodissociation of CF_2Br_2. *Chem. Phys. Lett.* **1993**, *207*, 75-80, doi:10.1016/0009-2614(93)85014-F.

Vatsa, R. K.; Volpp, H.-R. Absorption cross-sections for some atmospherically important molecules at the H atom Lyman-α wavelength (121.567 nm). *Chem. Phys. Lett.* **2001**, *340*, 289-295, doi:10.1016/S0009-2614(01)00373-6.

Vetter, R.; Ritschel, T.; Zülicke, L. Theoretical study of the low-lying electronically excited states of OBrO. *J. Phys. Chem. A* **2003**, *107*, 1405-1412, doi:10.1021/jp021952p.

Wahner, A.; Ravishankara, A. R.; Sander, S. P.; Friedl, R. R. Absorption cross section of BrO between 312 and 385 nm at 298 K and 225 K. *Chem. Phys. Lett.* **1988**, *152*, 507-512, doi:10.1016/0009-2614(88)80450-0.

Walton, J. C. Photolysis of dibromodifluoromethane at 265 nm. *J. Chem. Soc. Faraday Trans.* **1972**, *68*, 1559-1565, doi:10.1039/f19726801559.

Washida, N.; Suto, M.; Nagase, S.; Nagashima, U.; Morokuma, K. Emission spectra of CF_3 radicals. IV. Excitation spectra, quantum yields, and potential enegy surfaces of the CF_3 fluorescences. *J. Chem. Phys.* **1983**, *78*, 1025-1032, doi:10.1063/1.444902.

Wen, W. Y.; Noyes, R. M. Ultraviolet spectra of single and double molecules of gaseous bromine. *J. Phys. Chem.* **1972**, *76*, 1017-1018, doi:10.1021/j100651a012.

Wheeler, M. D.; Newman, S. M.; Ishiwata, T.; Kawasaki, M.; Orr-Ewing, A. J. Cavity ring-down spectroscopy of the $A^2\Pi_{3/2}$-$X\ ^2\Pi_{3/2}$ transition of BrO. *Chem. Phys. Lett.* **1998**, *285*, 346-351, doi:10.1016/S0009-2614(98)00082-7.

Wilmouth, D. M.; Hanisco, T. F.; Donahue, N. M.; Anderson, J. G. Fourier transform ultraviolet spectroscopy of the $A\ ^2\Pi_{3/2} \leftarrow X\ ^2\Pi_{3/2}$ trasnsition of BrO. *J. Phys. Chem. A* **1999**, *103*, 8935-8945, doi:10.1021/jp991651o.

Xu, D.; Francisco, J. S.; Huang, J.; Jackson, W. M. Ultraviolet photodissociation of bromoform at 234 and 267 nm by means of ion velocity imaging. *J. Chem. Phys.* **2002**, *117*, 2578-2585, doi:10.1063/1.1491877.

Zaraga, F.; Nogar, N. S.; Moore, C. B. Transition moment, radiative lifetime, and quantum yield for dissociation of the $^3\Pi_{0^+_u}$ state of $^{81}Br_2$. *J. Mol. Spectrosc.* **1976**, *63*, 564-571, doi:10.1016/0022-2852(76)90317-9.

Zhang, L.; Fuss, W.; Kompa, K. L. Bond-selective photodissociation of CX (X = Br, I) in $XC_2H_4C_2F_4X$. *Chem. Phys.* **1990**, *144*, 289-297, doi:10.1016/0301-0104(90)80092-C.

Zou, P.; McGivern, W. S.; North, S. W. Adiabatic and diabatic dynamics in the photodissociation of CH_2BrCl. *Phys. Chem. Chem. Phys.* **2000**, *2*, 3785-3790, doi:10.1039/b004349o.

Zou, P.; McGivern, W. S.; Sokhabi, O.; Suits, A. G.; North, S. W. Quantum yields and energy partitioning in the ultraviolet photodissociation of 1,2 dibromo-tetrafluoroethane (Halon-2402). *J. Chem. Phys.* **2000**, *113*, 7149-7157, doi:10.1063/1.1313545.

SECTION 4H. IO_X PHOTOCHEMISTRY

H1. I_2 (molecular iodine)

Back to Index

$I_2 + h\nu$	$\rightarrow 2\ I(^2P_{3/2})$	151 kJ mol^{-1}	792 nm	(1)
	$\rightarrow I(^2P_{3/2}) + I^*(^2P_{1/2})$	241.8 kJ mol^{-1}	495 nm	(2)

(Recommendation: 06-2, Note: 15-10, Evaluated: 10-6)

Absorption Cross Sections: The UV/vis absorption spectrum of I_2, molecular iodine, between 180 and 750 nm consists of several overlapping electronic transitions. The spectrum has a strong absorption band below 210 nm that peaks at ~181 nm and contains some diffuse band structure. Between 210 and 380 nm the spectrum is continuous with decreasing absorption cross sections toward longer wavelength and a minimum cross section of ~1×10^{-20} cm^2 molecule^{-1} at 380 nm. The visible region of the spectrum shows a strong broad band between 400 and 650 nm that is continuous below 500 nm but shows pronounced rovibrational structure between 500 and 630 nm. The structure is due to the transition from the $X^1\Sigma$ ground state to the bound $B^3\Pi$ upper state. There is also a weaker underlying continuum in the structured region with a maximum near 533 nm that is due to a transition to a $^1\Pi$ repulsive state. At wavelengths >650 nm there is evidence for another weak absorption band. There have been numerous studies of the I_2 absorption spectrum as summarized in Table 4H-1-1.

Table 4H-1-1. Summary of I_2 Absorption Cross Sections Studies

Study	Year	Temperature (K)	Wavelength (nm)	10^{20} σ(500 nm) (cm^2)
Vogt and Koenigsberger[15]	1923	321–673	400–600	–
Rabinowitch and Wood[7]	1936	298	440–650	~291
Kortüm and Friedheim[3]	1947	353	450–580	~160 ± 30
Kortüm and Friedheim[3]	1947	613	230–600	~170 ± 30
Sulzer and Wieland[12]	1952	423–1323	360–740	*
Mathieson and Rees[4]	1956	393	600–850	–
McMillan[5]	1966	348	400–650	218
Myer and Samson[6]	1970	298	105–220	–
Tellinghuisen[13]	1973	298	420–800	219
Roxlo and Mandl[8]	1980	298	170–230	–
Bauer et al.[1]	1998	298	436, 500	225 ± 9
Saiz-Lopez et al.[9]	2004	298	182–750	229 ± 27
Spietz[10]	2005	298	428–588	–
Spietz et al.[11]	2006	298	500	219 ± 2
Tellinghuisen[14]	2011	273–337	520–640	–

Note:
Uncertainties as reported
* Cross section values at 488 nm are in the range (176–113) × 10^{-20} cm^2 molecule^{-1} over the temperature range 423–1323 K

The cross section data sets from Tellinghuisen,[13] Saiz-Lopez et al.,[9] and Spietz et al.[10,11] are the primary focus of this evaluation. Tellinghuisen[13] reported room temperature cross sections obtained with a continuum light source at moderate resolution (~2.5 nm). Saiz-Lopez et al.[9] used a Fourier transform spectrometer to record spectra at a resolution of 4 cm^{-1} (0.1 nm at 500 nm). Spietz[10,11] used a grating/CCD spectrometer with a resolution of 0.25 nm. The reported spectra show the largest differences in the structured and long wavelength regions of the spectrum. A direct comparison of cross section data in the structured region is, however, difficult due to the differences in measurement resolution. Saiz-Lopez et al.[9] examined the cross section dependence on absolute I_2 concentration and bath gas pressure. Their final cross section data were obtained at high bath gas pressure and high resolution. The cross section data sets agree in the structured region to within ~15% when averages over 5 nm intervals are compared. There are significant discrepancies between the Tellinghuisen[13] and Saiz-Lopez et al.[9] spectra at wavelengths >~600 nm with differences increasing from 35% at 600 nm to factors of ~2 and ~20 at 710 and 740 nm, respectively. The cross sections reported by Bauer et al.[1] at 436 and 500 nm, (1.41 ± 0.05) × 10^{-18} and (2.25 ± 0.09) × 10^{-18} cm^2 molecule^{-1}, respectively, are in agreement with the Saiz-Lopez et al.[9] values. Tellinghuisen[14] used his I_2 spectrum measured at 0.1 nm resolution to determine the *B-X* transition moment.

The absorption cross sections listed in Table 4H-1-2 are averages over 5 nm intervals (+2 to -2 nm of the center wavelength) of the data reported by Saiz-Lopez et al.[9] The average values in Table 4H-1-2 removes the

vibrational band structure in the spectrum and smoothes the data elsewhere. The data in Table 4H-1-2 are appropriate for atmospheric photolysis rate calculations. Higher resolution cross section data should be obtained from the original studies. Table 4H-1-3 lists the absorption cross sections at the maxima and minima in the banded region reported by Saiz-Lopez et al.[9]

Photolysis Quantum Yield and Product Studies: Photodissociation quantum yields for I_2 in the structured region of the spectrum were measured by Brewer and Tellinghuisen[2] using atomic fluorescence under conditions of steady-state irradiation of I_2 at 12 wavelengths in the region 501–624 nm. The quantum yields were determined relative to the purely dissociative continuum at 492 nm, where a unity quantum yield is assumed. The quantum yields were found to be wavelength dependent with values ranging from 0.9 to 0.33.

Table 4H-1-2. Absorption Cross Sections of I_2 at 295 K

λ (nm)	10^{20} σ (cm^2)	λ (nm)	10^{20} σ (cm^2)	λ (nm)	10^{20} σ (cm^2)	λ (nm)	10^{20} σ (cm^2)
185	1853	315	15.1	445	25.8	575	96.6
190	2012	320	12.2	450	33.3	580	92.7
195	1226	325	10.5	455	44.0	585	74.1
200	732	330	7.79	460	57.1	590	65.8
205	519	335	6.18	465	72.2	595	59.4
210	418	340	4.71	470	89.7	600	47.4
215	352	345	4.08	475	109	605	43.3
220	302	350	2.58	480	131	610	40.8
225	260	355	1.94	485	155	615	34.4
230	225	360	1.24	490	179	620	30.5
235	197	365	1.02	495	204	625	28.2
240	169	370	0.659	500	228	630	28.0
245	147	375	0.823	505	254	635	22.6
250	128	380	1.14	510	277	640	23.6
255	110	385	1.01	515	297	645	22.8
260	97.1	390	0.925	520	309	650	21.6
265	84.2	395	1.11	525	319	655	20.7
270	72.9	400	2.93	530	326	660	19.0
275	63.1	405	3.89	535	320	665	17.3
280	54.4	410	4.43	540	306	670	17.7
285	45.9	415	5.44	545	281	675	15.9
290	38.9	420	5.96	550	265	680	14.9
295	32.4	425	8.32	555	237	685	13.9
300	27.4	430	13.5	560	191	690	12.8
305	23.1	435	15.7	565	155	695	10.9
310	18.1	440	20.3	570	130	700	10.3

Note:
Saiz-Lopez et al.,[9] averaged (see text).

Table 4H-1-3. Cross Sections at the Maxima and Minima of I_2 at 295 K

λ (nm) Maximum	10^{20} σ (cm^2)	λ (nm) minimum	10^{20} σ (cm^2)	λ (nm) maximum	10^{20} σ (cm^2)	λ (nm) minimum	10^{20} σ (cm^2)
500.6	232.5	500.7	231.5	543.6	406.7	545.1	225.3
500.8	233.9	501.0	231.0	545.4	240.5	545.6	219.9
501.1	235.9	501.2	233.7	545.8	371.9	547.4	231.3
501.4	236.6	501.6	234.8	547.6	246.7	548.1	208.0
501.8	239.6	501.9	236.3	548.4	372.2	549.7	226.5
502.1	240.5	502.4	238.8	550.0	251.7	550.6	197.1
502.6	246.5	502.8	240.6	550.8	347.6	552.1	220.6
503.0	247.8	503.3	240.6	552.4	256.8	553.2	187.0
503.5	252.3	503.8	241.0	553.5	321.4	554.6	211.2
504.0	254.4	504.4	243.7	554.8	257.7	555.8	176.3
504.5	255.6	504.9	245.1	556.2	299.4	557.1	200.3
505.2	263.2	505.6	252.0	557.5	254.2	558.6	161.2
505.8	268.7	506.2	252.7	559.0	263.9	559.8	186.1
506.5	271.6	507.0	252.3	560.1	250.0	561.5	126.8
507.2	275.4	507.7	253.7	561.9	203.1	562.7	153.9
507.9	281.7	508.5	254.6	562.9	216.0	564.5	103.7
508.7	284.4	509.3	255.0	564.9	175.0	565.4	143.7
509.6	291.1	510.3	262.8	565.8	208.0	567.5	96.9
510.5	301.6	511.2	264.1	568.1	142.9	568.4	115.4
511.5	308.1	512.2	266.0	568.7	203.5	569.5	131.4
512.5	309.9	513.3	263.0	569.9	139.8	570.7	70.3
513.6	323.1	514.4	266.1	571.0	127.5	571.4	113.9
514.7	325.9	515.6	266.4	571.7	147.2	573.9	76.1
515.9	334.3	516.8	265.0	574.9	131.8	577.3	68.8
517.1	345.9	518.1	269.2	578.1	122.6	580.7	62.7
518.3	353.6	519.4	266.0	581.4	109.7	584.3	51.8
519.8	356.6	520.9	267.1	585.1	105.4	587.8	48.6
521.1	371.0	522.3	267.3	588.7	95.9	591.7	42.4
522.7	379.3	523.9	259.8	592.1	85.7	595.4	42.8
524.2	384.5	525.4	261.4	596.0	80.5	599.1	34.3
525.8	393.7	527.2	252.8	599.6	76.0	603.0	31.6
527.4	398.8	528.9	258.7	603.5	64.3	606.8	28.8
529.2	407.8	530.8	252.2	607.6	53.8	610.8	30.3
531.0	415.9	532.7	242.1	611.8	49.1	614.6	26.4
533.0	423.8	534.7	242.8	615.5	42.5	618.8	26.7
534.9	416.4	536.7	232.6	620.0	37.4	622.2	22.3
537.0	414.8	538.8	224.4	623.6	35.8	627.0	23.1
539.1	409.3	541.0	216.5	628.2	31.8	629.8	24.0
541.4	406.1	543.0	218.5				

Note:
Saiz-Lopez et al.[9]

(1) Bauer, D.; Ingham, T.; Carl, S. A.; Moortgat, G. K.; Crowley, J. N. Ultraviolet-visible absorption cross sections of gaseous HOI and its photolysis at 355 nm. *J. Phys. Chem.* **1998**, *102*, 2857-2864, doi:10.1021/jp9804300.

(2) Brewer, L.; Tellinghuisen, J. Quantum yield for unimolecular dissociation of I_2 in visible absorption. *J. Chem. Phys.* **1972**, *56*, 3929-3938, doi:10.1063/1.1677797.

(3) Kortüm, G.; Friedheim, G. Lichtabsorption und molekularzustand des jods in dampf und lösung. *Z. Naturforsch.* **1947**, *2a*, 20-27, doi:10.1515/zna-1947-0107.

(4) Mathieson, L.; Rees, A. L. G. Electronic states and potential energy diagram of the iodine molecule. *J. Chem. Phys.* **1956**, *25*, 753-761, doi:10.1063/1.1743043.

(5) McMillan, V. personal communication to J.G. Calvert, J.N. Pitts, Jr., Photochemistry, London, 1966, p. 184. **1966**.
(6) Myer, J. A.; Samson, J. A. R. Absorption cross section and photoionization yield of I_2 between 1050 and 2200 Å. *J. Chem. Phys.* **1970**, *52*, 716-718, doi:10.1063/1.1673044.
(7) Rabinowitch, E.; Wood, W. C. The extinction coefficient of iodine and other halogens. *Trans. Faraday Soc.* **1936**, *32*, 540-546, doi:10.1039/tf9363200540.
(8) Roxlo, C.; Mandl, A. Vacuum ultraviolet absorption cross sections for halogen containing molecules. *J. Appl. Phys.* **1980**, *51*, 2969-2972, doi:10.1063/1.328108.
(9) Saiz-Lopez, A.; Saunders, R. W.; Joseph, D. M.; Ashworth, S. H.; Plane, J. M. C. Absolute absorption cross-section and photolysis rate of I_2. *Atmos. Chem. Phys.* **2004**, *4*, 1443-1450, doi:10.5194/acp-4-1443-2004.
(10) Spietz, P. Absorption cross sections for iodine species of relevance to the photolysis of mixtures of I_2 and O_3 and for the atmosphere. *PhD-Thesis, Univ. of Bremen, Germany* **2005**.
(11) Spietz, P.; Gómez Martín, J.; Burrows, J. P. Effects of column density on I_2 spectroscopy and a determination of I_2 absorption cross section at 500 nm. *Atmos. Chem. Phys.* **2006**, *6*, 2177-2191, doi:10.5194/acp-6-2177-2006.
(12) Sulzer, P.; Wieland, K. Intensitätsverteilung eines kontinuierlichen absorptions-spektrums in abhängigkeit von temperatur und wellenzahl. *Helv. Phys. Acta* **1952**, *25*, 653-676, doi:10.5169/seals-112328.
(13) Tellinghuisen, J. Resolution of the visible-infrared absorption spectrum of I_2 into three contributing transitions. *J. Chem. Phys.* **1973**, *58*, 2821-2834, doi:10.1063/1.1679584.
(14) Tellinghuisen, J. Intensity analysis of overlapped discrete and continuous absorption by spectral simulation: The electronic transition moment for the *B-X* system in I_2. *J. Chem. Phys.* **2011**, *134*, 084301, doi:10.1063/1.3555623.
(15) Vogt, K.; Koenigsberger, J. Beobachtungen über Absorption in Joddampf and anderen Dämpfen. *Z. Physik* **1923**, *13*, 292-310, doi:10.1007/BF01328221.

H2. IO (iodine monoxide)

Back to Index

$IO + h\nu$	$\rightarrow I + O(^3P)$	240.2 kJ mol^{-1}	498 nm	(1)
	$\rightarrow I + O(^1D)$	428.9 kJ mol^{-1}	279 nm	(2)

(Recommendation: 06-2, Note: 10-6, Evaluated: 10-6)

Absorption Cross Sections: The A $^2\Pi_{3/2} \leftarrow$ X $^2\Pi_{3/2}$ electronic transition for IO, iodine monoxide, yields a UV/vis absorption spectrum between 338 and 488 nm. The A –X band consists of a continuous absorption band with a maximum near 400 nm with a broad progression of vibrational bands superimposed on the continuum at wavelengths >400 nm. The pronounced vibrational band structure has been assigned to progressions in v', 7-0←0 and 3-1←1. Of particular interest (e.g. for the study of the reaction kinetics of IO) is the peak absorption cross section of the strongest vibrational band (4,0) at 427.2 nm. A summary of the available studies (which utilized photolysis of N_2O/I_2, N_2O/CF_3I, and O_3/I_2 mixtures to produce IO) and the corresponding (4,0) peak cross sections at room temperature is given in Table 4H-2-1.

Table 4H-2-1. Summary of IO Absorption Cross Section Studies

Study	Year	Temperature (K)	Wavelength Range (nm)	Resolution (nm)	σ(427.2 nm) 10^{-17} cm^2
Cox and Coker[3]	1983	303	415–470	0.27	$3.1^{+2.0}_{-1.5}$
Jenkin and Cox[8]	1985	303	426.9	0.27	2.2 ± 0.5
Sander[10]	1986	250, 273, 298, 317, 341, 373	427.2	0.17	3.1 ± 0.3
Stickel et al.[12]	1988	300	420–455 444.8–446.4	0.3 0.025	3.1 ± 0.6
Laszlo et al.[9]	1995	295	340–447	0.3	2.8 ± 0.5
Harwood et al.[6]	1997	203, 220, 250, 298, 323, 353, 373	427.2	0.14	3.6 ± 0.5*
		203, 213, 233, 253, 273, 298	338–488	0.44	3.0 ± 0.4
Atkinson et al.[1]	1999	295	444.48–447.83 454.98–457.88	0.0013	–
			445.04, 455.17	0.7	
Bloss et al.[2]	2001	220, 250, 273, 295, 325	342–455	1.13	1.9 ± 0.17
Dillon et al.[4]	2005	298	427.08, 427.2	0.08	3.55 ± 0.35
Gómez Martín et al.[5]	2005	298	427.7, 449.3, 484.9	0.12	3.5 ± 0.3
Spietz et al.[11]	2005	298	320.26–480.09	1.3	3.2

* Average value between 203 and 373 K (see text)

The shape of the 298 K spectra reported by Laszlo et al., Harwood et al., and Bloss et al. are similar but with notable differences in the magnitude of the vibrational features due to the dependence on the resolution of the measurement. The absorption cross sections reported by Harwood et al. with a resolution of 0.44 nm and scaled to 0.83 of the value obtained for the (4,0) peak cross section at higher resolution, 0.14 nm, are generally (with exceptions in the region 350–415 nm) higher than those reported by Lazlo et al. (0.3 nm resolution) and Bloss et al. (1.13 nm resolution). The Bloss et al. cross section data are the lowest throughout the spectral region 340–465 nm. The Bloss et al. cross section data are lower than the values reported by Harwood et al. by a factor of ~1.5 in the continuous region of the spectrum and at the peaks of the vibrational bands and up to factor of 5 at the minima between the vibrational bands. Bloss et al. attributed the differences in the spectra to an underlying absorption due to the absorbing species I_2O_2 that is considered to be a product of the IO self-reaction. The absorption spectrum of I_2O_2 is currently not known.

The absorption spectrum reported by Laszlo et al. is higher by a factor of ~1.2–1.5 in the wavelength region 350–370 nm and at the maxima in the 395–405 nm region than the values reported by Harwood et al. However, the spectra are similar in the region of the (6,0) to (4,0) maxima. The absorption cross section measured by Atkinson et al. at high resolution (0.0013 nm) for the (2,0) peak is higher by a factor of ~5 than that reported by Harwood et al., whereas the cross sections reported by Atkinson et al. and Harwood et al. for the (1,0) maximum are nearly the same.

The recommended cross sections in Table 4H-2-2 were obtained as follows: (1) the spectra of Harwood et al. and Laszlo et al. were degraded to the resolution of the spectrum of Bloss et al. (1.13 nm), (2) the degraded spectra of Harwood et al. were normalized to the (4,0) peak value of Bloss et al., (3) the mean of the degraded and normalized spectra of Harwood et al. and Laszlo et al. and that of Bloss et al. were calculated and averaged over 1 nm intervals. The studies of Dillon et al.,[4] Gómez Martin et al.,[5] and Spietz et al.[11] are noted but not considered in the present evaluation.

The temperature dependence of the absorption cross section of the (4,0) peak has been studied by Sander (250 –373 K), Harwood et al. (203 –373 K), and Bloss et al. (220 –325 K). The results from these studies are significantly different. Sander report a significant increase in σ(427 nm) from a value of $(2.1 \pm 0.1) \times 10^{-17}$

cm^2 $molecule^{-1}$ at 373 K to $(5.3 \pm 0.5) \times 10^{-17}$ cm^2 $molecule^{-1}$ at 250 K. Bloss et al. report a smaller increase in the absorption cross sections with the ratio $\sigma(T)/\sigma(295\ K)$ being 0.85 and 1.23 at 325 K and 220 K, respectively. Harwood et al. used several pulsed laser photolysis sources of IO (N_2O/CF_3I, O_3/I_2, and N_2O/I_2) in their experiments and reported absorption cross sections between $(3.1 \pm 0.4) \times 10^{-17}$ and $(3.9 \pm 0.1) \times 10^{-17}$ cm^2 $molecule^{-1}$ independent of temperature (203–373 K) and report an average value of $(3.6 \pm 0.5) \times 10^{-17}$ cm^2 $molecule^{-1}$.

Photolysis Quantum Yield and Product Studies: The quantum yield for $O(^3P)$ formation following photolysis of IO at 355 nm was measured relative to NO_2 photolysis at the same wavelength to be 0.91 ($^{+0.19}_{-0.26}$) by Ingham et al.[7] The lifetime of the A $^2\Pi_{3/2}$ was measured to be < 20 ns by Turnipseed et al.,[13] which indicates that electronic collisional quenching does not compete with the dissociation into $O(^3P)$ + I. This is consistent with the results of Ingham et al.

Table 4H-2-2. Recommended Absorption Cross Sections of IO at 298 K

λ (nm)	10^{20} σ (cm^2)	λ (nm)	10^{20} σ (cm^2)	λ (nm)	10^{20} σ (cm^2)	λ (nm)	10^{20} σ (cm^2)
339	81.2	373	381	407	606	441	219
340	118	374	413	408	578	442	168
341	100	375	422	409	643	443	183
342	107	376	402	410	813	444	195
343	89	377	413	411	1010	445	957
344	96.2	378	435	412	976	446	805
345	86.2	379	463	413	786	447	392
346	126	380	504	414	589	448	214
347	112	381	548	415	568	449	269
348	108	382	472	416	414	450	156
349	142	383	435	417	460	451	96.9
350	160	384	523	418	734	452	102
351	154	385	560	419	1380	453	87.3
352	165	386	591	420	1200	454	100
353	163	387	603	421	681	455	457
354	181	388	580	422	365	456	441
355	185	389	598	423	253	457	213
356	194	390	622	424	204	458	132
357	207	391	620	425	205	459	183
358	223	392	617	426	302	460	123
359	230	393	642	427	2050	461	82.3
360	242	394	684	428	1370	462	51.9
361	247	395	694	429	543	463	53.6
362	242	396	709	430	309	464	38.2
363	241	397	701	431	208	465	43.4
364	268	398	654	432	173	466	118
365	273	399	671	433	166	467	134
366	291	400	671	434	177	468	67.2
367	313	401	700	435	653	469	24.2
368	326	402	765	436	1880	470	125
369	343	403	859	437	807	471	76.4
370	346	404	864	438	381		
371	339	405	787	439	249		
372	360	406	667	440	256		

Note:
See text

(1) Atkinson, D. B.; Hudgens, J. W.; Orr-Ewing, A. J. Kinetic studies of the reactions of IO radicals determined by cavity ring-down spectroscopy. *J. Phys. Chem. A* **1999**, *103*, 6173-6180, doi:10.1021/jp9902497.

(2) Bloss, W. J.; Rowley, D. M.; Cox, R. A.; Jones, R. L. Kinetics and products of the IO self-reaction. *J. Phys. Chem. A* **2001**, *105*, 7840-7854, doi:10.1021/jp0044936.

(3) Cox, R. A.; Coker, G. B. Absorption cross sections and kinetics of IO in the photolysis of CH_3I in the presence of ozone. *J. Phys. Chem.* **1983**, *87*, 4478-4484, doi:10.1021/j100245a030.
(4) Dillon, T. J.; Tucceri, M. E.; Hölscher, D.; Crowley, J. N. Absorption cross-section of IO at 427.2 nm and 298 K. *J. Photochem. Photobiol. A: Chem.* **2005**, *176*, 3-14, doi:10.1016/j.jphotochem.2005.09.025.
(5) Gómez Martín, J. C.; Spietz, P.; Burrows, J. P. Spectroscopic studies of the I_2/O_3 photochemistry Part 1: Determination of the absolute absorption cross sections of iodine oxides of atmospheric relevance. *J. Photochem. Photobiol. A: Chem.* **2005**, *176*, 15-38, doi:10.1016/j.jphotochem.2005.09.024.
(6) Harwood, M. H.; Burkholder, J. B.; Hunter, M.; Fox, R. W.; Ravishankara, A. R. Absorption cross sections and self-reaction kinetics of the IO radical. *J. Phys. Chem. A* **1997**, *101*, 853-863, doi:10.1021/jp962429b.
(7) Ingham, T.; Cameron, M.; Crowley, J. N. Photodissociation of IO (355 nm) and OIO (532 nm): Quantum yields for $O(^3P)$ and $I(^2P_J)$ production. *J. Phys. Chem. A* **2000**, *104*, 8001-8010, doi:10.1021/jp001166p.
(8) Jenkin, M. E.; Cox, R. A. Kinetics study of the reactions IO + NO_2 + M → $IONO_2$ + M, IO + IO → products, and I + O_3 → IO + O_2. *J. Phys. Chem.* **1985**, *89*, 192-199, doi:10.1021/j100247a040.
(9) Laszlo, B.; Kurylo, M. J.; Huie, R. E. Absorption cross sections, kinetics of formation, and self-reaction of the IO radical produced via the laser photolysis of $N_2O/I_2/N_2$ Mixtures. *J. Phys. Chem.* **1995**, *99*, 11701-11707, doi:10.1021/j100030a013.
(10) Sander, S. P. Kinetics and mechanism of the IO + IO reaction. *J. Phys. Chem.* **1986**, *90*, 2194-2199, doi:10.1021/j100401a039.
(11) Spietz, P.; Gómez Martín, J. C.; Burrows, J. P. Spectroscopic studies of the I_2/O_3 photochemistry Part 2. Improved spectra of iodine oxides and analysis of the IO absorption spectrum. *J. Photochem. Photobiol. A: Chem.* **2005**, *176*, 50-67, doi:10.1016/j.jphotochem.2005.08.023.
(12) Stickel, R. E.; Hynes, A. J.; Bradshaw, J. D.; Chameides, W. L.; Davis, D. D. Absorption cross sections and kinetic considerations of the IO radical as determined by laser flash photolysis/laser absorption spectroscopy. *J. Phys. Chem.* **1988**, *92*, 1862-1864, doi:10.1021/j100318a600.
(13) Turnipseed, A. A.; Gilles, M. K.; Burkholder, J. B.; Ravishankara, A. R. LIF detection of IO and the rate coefficients for I + O_3 and IO + NO reactions. *Chem. Phys. Lett.* **1995**, *242*, 427-434, doi:10.1016/0009-2614(95)00774-X.

H3. OIO (iodine dioxide)

Back to Index

OIO + hν → $I(^2P_{3/2}) + O_2$	–25 kJ mol^{-1}	All	(1)
→ $IO(^2\Pi) + O(^3P)$	242.7 kJ mol^{-1}	493 nm	(2)

(Recommendation: 06-2, Note: 10-6, Evaluated: 10-6)

Absorption Cross Sections: A qualitative absorption spectrum of OIO, iodine dioxide, was first reported by Himmelmann et al.[7] at 298 K over the wavelength range 476–667 nm. The absorption spectrum is highly structured due to transitions in the A ($^2A_2$) (i,j,k) ← X ($^2B_1$) (0,0,0) band with vibrational progressions in the upper state of the symmetric I-O stretch (i = 0-9) and O-I-O bend (j = 0, 1, 2). Absorption cross sections have been measured at room temperature by Cox et al.[3] (400–600 nm) and Bloss et al.[2] (514–573 nm) at a resolution of 1.13 nm, by Spietz et al.[10] (392–660 nm) and Gómez Martín et al.[6] at a resolution of 1.3 nm who report a cross section of $(1.3 \pm 0.3) \times 10^{-17}$ cm^2 molecule^{-1} at 549.1 nm, and at high resolution (<0.006 nm) using cavity ring-down spectroscopy by Ashworth et al.[1] and Joseph et al.[9] (558–578 nm). Joseph et al.[9] report a cross section of $(1.5 \pm 0.18) \times 10^{-17}$ cm^2 molecule^{-1} at 567.93 nm.

The peak cross sections at 562 and 568 nm obtained at high resolution are higher by a factor ~1.7 than those reported for a resolution of 1.13 nm. The recommended cross sections listed in Table 4H-3 were obtained by averaging the data reported by Bloss et al.[2] over 1 nm intervals (reported at intervals of 0.22 nm). The estimated uncertainty in the absolute absorption cross sections is a factor of 3.

Photolysis Quantum Yield and Product Studies: Ingham et al.[8] studied the photodissociation of OIO at 532 nm. $O(^3P)$ atom formation was not detected and an upper limit for the O atom quantum yield of <0.012 was reported (based on an OIO absorption cross section of 2.4×10^{-17} cm^2 molecule^{-1} at 532 nm). Subsequently, Ashworth et al.[1] inferred that OIO predissociates to I + O_2 via the upper $^2B_2$ state. Ingham et al.[8] detected $I(^2P_J)$ atoms at high photolysis laser fluence, presumably in a sequential two-photon process, and an upper limit for the I atom quantum yield of < 0.15 was reported. Joseph et al.[9] report the photolysis quantum yield of OIO at 562 nm to be <0.10. Tucceri et al.[11] used pulsed laser photolysis combined with transient absorption spectroscopy/resonance fluorescence detection techniques and reported I atom quantum yields of <0.05 in the wavelength range 560–580 nm and <0.24 at 532 nm. A study by Gómez Martín et al.[5] contradicts the results

from Joseph et al.,[9] Ingham et al.,[8] and Tucceri et al.[11] Gómez Martín et al.[5] used a tunable pulsed laser photolysis source combined with cavity ring-down spectroscopy detection of OIO and atomic resonance fluorescence detection of I atoms. They report an I atom quantum yield of (1.07 ± 0.15) over the wavelength range 480–650 nm. In an additional study from the same group, Gómez Martín et al.[4] report the IO quantum yield to be unity at wavelengths <480 nm. No quantum yield recommendation is given.

Table 4H-3. Recommended Absorption Cross Sections of OIO at 295 K

λ (nm)	10^{20} σ (cm^2)	λ (nm)	10^{20} σ (cm^2)	λ (nm)	10^{20} σ (cm^2)	λ (nm)	10^{20} σ (cm^2)
516	833	531	989	546	582	561	476
517	696	532	1012	547	513	562	769
518	565	533	779	548	665	563	709
519	599	534	636	549	1030	564	524
520	719	535	519	550	842	565	442
521	626	536	643	551	575	566	384
522	573	537	709	552	429	567	613
523	517	538	640	553	377	568	937
524	496	539	548	554	609	569	699
525	534	540	470	555	661	570	475
526	754	541	451	556	604	571	322
527	840	542	494	557	474	572	224
528	697	543	715	558	393		
529	626	544	817	559	373		
530	651	545	676	560	350		

Note:
Bloss et al.,[2] averaged (see text).

(1) Ashworth, S. H.; Allan, B. J.; Plane, J. M. C. High resolution spectroscopy of the OIO radical: Implications for the ozone-depleting potential of iodine. *Geophys. Res. Lett.* **2002**, *29*, 1-4, doi:10.1029/2001GL13851.

(2) Bloss, W. J.; Rowley, D. M.; Cox, R. A.; Jones, R. L. Kinetics and products of the IO self-reaction. *J. Phys. Chem. A* **2001**, *105*, 7840-7854, doi:10.1021/jp0044936.

(3) Cox, R. A.; Bloss, W. J.; Jones, R. L.; Rowley, D. M. OIO and the atmospheric cycle of iodine. *Geophys. Res. Lett.* **1999**, *26*, 1857-1860, doi:10.1029/1999GL900439.

(4) Gómez Martín, J. C.; Ashworth, S. H.; Mahajan, A. S.; Plane, J. M. C. Photochemistry of OIO: Laboratory study and atmospheric implications. *Geophys. Res. Lett.* **2009**, *36*, L09802, doi:10.1029/2009GL037642.

(5) Gómez Martín, J. C.; Plane, J. M. C. Determination of the O–IO bond dissociation energy by photofragment excitation spectroscopy. *Chem. Phys. Lett.* **2009**, *474*, 79-83, doi:10.1016/j.cplett.2009.04.052.

(6) Gómez Martín, J. C.; Spietz, P.; Burrows, J. P. Spectroscopic studies of the I_2/O_3 photochemistry Part 1: Determination of the absolute absorption cross sections of iodine oxides of atmospheric relevance. *J. Photochem. Photobiol. A: Chem.* **2005**, *176*, 15-38, doi:10.1016/j.jphotochem.2005.09.024.

(7) Himmelmann, S.; Orphal, J.; Bovensmann, H.; Richter, A.; Ladstätter-Weissenmayer, A.; Burrows, J. P. First observation of the OIO molecule by time-resolved flash photolysis absorption spectroscopy. *Chem. Phys. Lett.* **1996**, *251*, 330-334, doi:10.1016/0009-2614(96)00114-5.

(8) Ingham, T.; Cameron, M.; Crowley, J. N. Photodissociation of IO (355 nm) and OIO (532 nm): Quantum yields for $O(^3P)$ and $I(^2P_J)$ production. *J. Phys. Chem. A* **2000**, *104*, 8001-8010, doi:10.1021/jp001166p.

(9) Joseph, D. M.; Ashworth, S. H.; Plane, J. M. C. The absorption cross-section and photochemistry of OIO. *J. Photochem. Photobiol. A: Chem.* **2005**, *176*, 68-77, doi:10.1016/j.jphotochem.2005.09.003.

(10) Spietz, P.; Gómez Martín, J. C.; Burrows, J. P. Spectroscopic studies of the I_2/O_3 photochemistry Part 2. Improved spectra of iodine oxides and analysis of the IO absorption spectrum. *J. Photochem. Photobiol. A: Chem.* **2005**, *176*, 50-67, doi:10.1016/j.jphotochem.2005.08.023.

(11) Tucceri, M. E.; Hölscher, D.; Rodriguez, A.; Dillon, T. J.; Crowley, J. N. Absorption cross section and photolysis of OIO. *Phys. Chem. Chem. Phys.* **2006**, *8*, 834-846, doi:10.1039/b512702e.

H4. HI (hydrogen iodide)

Back to Index

HI + hν	$\rightarrow$ H + I($^2P_{3/2}$)	298 kJ mol^{-1}	401 nm	(1)
	$\rightarrow$ H + I*($^2P_{1/2}$)	389 kJ mol^{-1}	308 nm	(2)

(Recommendation: 06-2, Note: 10-6, Evaluated: 10-6)

Absorption Cross Sections: The UV absorption spectrum of HI, hydrogen iodide, at wavelengths >180 nm has a continuous absorption band with a maximum near 222 nm. At wavelengths <180 nm the spectrum shows strong diffuse band structure. The available studies are summarized in Table 4H-4-1. For wavelengths >180 nm, there is good agreement between the room temperature absorption cross sections reported by Campuzano-Jost and Crowley,[3] Ogilvie,[9] and Huebert and Martin.[6] The data reported by Huebert and Martin[6] and Campuzano-Jost and Crowley[3] are nearly identical around the absorption maximum and out to ~275 nm. The cross sections reported by Ogilvie[9] are slightly greater. At wavelengths >280 nm, the absorption spectra from these three studies diverge somewhat with the cross sections reported by Huebert and Martin[6] being greater and those of Ogilvie[9] being smaller than the cross sections reported by Campuzano-Jost and Crowley.[3] The recommended cross sections listed in Table 4H-4-2 are average values over 1 nm intervals of the high resolution (0.08 nm) data from Campuzano-Jost and Crowley.[3]

Table 4H-4-1. Summary of HI Absorption Cross Sections Studies

Study	Year	Temperature (K)	Wavelength (nm)	10^{20} σ(222 nm) (cm^2)
Goodeve and Taylor[5]	1936	298	200–368	69
Romand[11]	1949	298	149 –159, 164–175, 178–244	62
Huebert and Martin[6]	1968	195 296	180–200 180–300	– 81
Ogilvie[9]	1971	298	192–313	84
Roxlo and Mandl[12]	1980	298	170–230	62
Bridges and White[2]	1973	298	254	–
Rebbert et al.[10]	1973	298	147	–
Campuzano-Jost and Crowley[3]	1999	298	198–341	81

Table 4H-4-2. Recommended Absorption Cross Sections of HI at 298 K

λ (nm)	10^{20} σ (cm^2)	λ (nm)	10^{20} σ (cm^2)	λ (nm)	10^{20} σ (cm^2)	λ (nm)	10^{20} σ (cm^2)
199	59.7	235	71.9	271	16.1	307	1.29
200	61.1	236	70.6	272	15.1	308	1.19
201	62.4	237	69.2	273	14.2	309	1.10
202	63.7	238	67.6	274	13.3	310	1.01
203	65.0	239	66.2	275	12.5	311	0.929
204	66.4	240	64.6	276	11.7	312	0.852
205	67.7	241	62.9	277	10.9	313	0.781
206	69.0	242	61.3	278	10.2	314	0.715
207	70.3	243	59.6	279	9.57	315	0.653
208	71.5	244	57.9	280	8.94	316	0.596
209	72.7	245	56.1	281	8.36	317	0.544
210	73.8	246	54.2	282	7.81	318	0.495
211	74.8	247	52.5	283	7.30	319	0.450
212	75.9	248	50.7	284	6.82	320	0.409
213	76.9	249	48.8	285	6.37	321	0.371
214	77.7	250	47.0	286	5.94	322	0.336
215	78.4	251	45.2	287	5.55	323	0.303
216	79.1	252	43.5	288	5.18	324	0.274
217	79.7	253	41.7	289	4.83	325	0.247
218	80.2	254	39.9	290	4.51	326	0.223
219	80.5	255	38.2	291	4.21	327	0.200
220	80.8	256	36.5	292	3.92	328	0.180
221	80.9	257	34.8	293	3.66	329	0.162
222	81.0	258	33.2	294	3.41	330	0.145
223	80.9	259	31.6	295	3.18	331	0.130
224	80.7	260	30.0	296	2.96	332	0.116
225	80.4	261	28.5	297	2.76	333	0.104
226	80.0	262	27.1	298	2.57	334	0.0928
227	79.5	263	25.7	299	2.40	335	0.0828
228	78.9	264	24.3	300	2.23	336	0.0740
229	78.2	265	23.0	301	2.07	337	0.0660
230	77.4	266	21.7	302	1.92	338	0.0591
231	76.5	267	20.5	303	1.77	339	0.0528
232	75.5	268	19.4	304	1.64	340	0.0470
233	74.4	269	18.3	305	1.52		
234	73.2	270	17.2	306	1.40		

Note:
Campuzano-Jost and Crowley,[3] averaged (see text).

Photolysis Quantum Yield and Product Studies: Martin and Willard[8] measured the quantum yield for H and I atoms in the photolysis of HI at 184.9 and 253.7 nm to be near unity. A quantum yield for the loss of HI of unity is recommended for wavelengths >180 nm. Brewer et al.[1] reported the relative quantum yield for the formation of $I^*(^2P_{1/2})$ to be 0.47 ± 0.03 at 248 nm. Using broadband flash photolysis, Donohue and Wiesenfeld[4] obtained an $I^*(^2P_{1/2})$ yield of 0.10 ± 0.05. Langford et al.[7] measured the branching ratio $I^*(^2P_{1/2})$ /$I(^2P_{3/2})$ in a detailed study at 24 different wavelengths in the range 200–303 nm. They reported a wavelength dependence of the ratio with a value of 0.2 near 208 nm, a maximum value of 1.7 near 252 nm, and a value of 0.1 at 303 nm. These authors review several similar earlier studies and should be consulted for more detailed information.

(1) Brewer, P.; Das, P.; Ondrey, G.; Bersohn, R. Measurement of the relative populations of I($^2P_{1/2}^0$) and I($^2P_{3/2}^0$) by laser induced vacuum ultraviolet fluorescence. *J. Chem. Phys.* **1983**, *79*, 720-723, doi:10.1063/1.445820.
(2) Bridges, L.; White, J. M. Photochemistry of methanethiol at 254 and 214 nm. *J. Phys. Chem.* **1973**, *77*, 295-298, doi:10.1021/j100621a031.
(3) Campuzano-Jost, P.; Crowley, J. N. Kinetics of the reaction of OH with HI between 246 and 353 K. *J. Phys. Chem. A* **1999**, *103*, 2712-2719, doi:10.1021/jp984321x.
(4) Donohue, T.; Wiesenfeld, J. R. Photodissociation of alkyl iodides. *J. Chem. Phys.* **1975**, *63*, 3130-3135, doi:10.1063/1.431741.
(5) Goodeve, C. F.; Taylor, A. W. C. The continuous absorption spectrum of hydrogen iodide. *Proc. Roy. Soc. London* **1936**, *A 154*, 181-187, doi:10.1098/rspa.1936.0044.
(6) Huebert, B. J.; Martin, R. M. Gas-phase far-ultraviolet absorption spectrum of hydrogen bromide and hydrogen iodide. *J. Phys. Chem.* **1968**, *72*, 3046-3048, doi:10.1021/j100854a071.
(7) Langford, S. R.; Regan, P. M.; Orr-Ewing, A. J.; Ashfold, M. N. R. On the UV photodissociation dynamics of hydrogen iodide. *Chem. Phys.* **1998**, *231*, 245-260, doi:10.1016/S0301-0104(98)00013-5.
(8) Martin, R. M.; Willard, J. E. Reactions of photochemically produced hot hydrogen atoms. I. Photolysis of HI at 1849 Å. *J. Chem. Phys.* **1964**, *40*, 2999-3007, doi:10.1063/1.1724940.
(9) Ogilvie, J. F. Semi-experimental determination of a repulsive potential curve for hydrogen iodide. *Trans. Faraday Soc.* **1971**, *67*, 2205-2215, doi:10.1039/tf9716702205.
(10) Rebbert, R. E.; Lias, S. G.; Ausloos, P. Photolysis of alkyl iodides at 147.0 nm. The reaction H + $C_nH_{2n+1}I \rightarrow HI + C_nH_{2n+1}$. *Int. J. Chem. Kinet.* **1973**, *5*, 893-908, doi:10.1002/kin.550050515.
(11) Romand, J. Absorption ultraviolette dans la région de Schumann étude de: ClH, BrH et IH gazeux. *Ann. Phys. (Paris)* **1949**, *4*, 529-590.
(12) Roxlo, C.; Mandl, A. Vacuum ultraviolet absorption cross sections for halogen containing molecules. *J. Appl. Phys.* **1980**, *51*, 2969-2972, doi:10.1063/1.328108.

H5. HOI (hypoiodous acid)

Back to Index

$HOI + h\nu \rightarrow OH + I$	213 kJ mol^{-1}	561 nm	(1)

(Recommendation: 06-2, Note: 10-6, Evaluated: 10-6)

Absorption Cross Sections: The absorption spectrum of HOI, hypoiodous acid, has been measured at room temperature by Bauer et al.[1] (280–500 nm) and Rowley et al.[2] (280–450 nm). In these studies HOI was produced by reacting OH, which was generated by pulsed laser photolysis, with I_2. Absorption cross sections were determined assuming iodine mass balance and the measured loss of I_2. Two absorption bands of comparable intensity were observed, one between 280 and ~375 nm with a maximum near 340 nm and the other between ~375 and 500 nm with a maximum near 408 nm. The spectra of Bauer et al.[1] and Rowley et al.[2] are in reasonable agreement with slight differences in the wavelength of the absorption maxima, 2–3 nm, and absolute cross sections, less than ~15% difference. The recommended cross sections listed in Table 4H-5 are the mean of the values reported by Rowley et al.[2] and Bauer et al.[1]

Photolysis Quantum Yield and Product Studies: The OH quantum yield in the photolysis of HOI at 355 nm was measured by Bauer et al. to be close to unity.

Table 4H-5. Recommended Absorption Cross Sections of HOI at 298 K

λ (nm)	10^{20} σ (cm^2)	λ (nm)	10^{20} σ (cm^2)	λ (nm)	10^{20} σ (cm^2)	λ (nm)	10^{20} σ (cm^2)
280	0.077	332	36.1	384	20.8	436	11.9
282	0.121	334	37.6	386	22.1	438	10.6
284	0.186	336	38.5	388	23.4	440	9.30
286	0.281	338	39.1	390	24.8	442	8.10
288	0.417	340	39.2	392	26.1	444	7.03
290	0.608	342	38.9	394	27.3	446	6.05
292	0.867	344	38.2	396	28.4	448	5.17
294	1.22	346	37.1	398	29.4	450	4.40
296	1.68	348	35.6	400	30.1	452	3.72
298	2.27	350	33.9	402	30.6	454	3.13
300	3.02	352	32.0	404	30.9	456	2.61
302	3.95	354	30.1	406	30.9	458	2.17
304	5.09	356	28.0	408	30.7	460	1.79
306	6.44	358	26.0	410	30.2	462	1.47
308	8.03	360	24.1	412	29.5	464	1.20
310	9.85	362	22.4	414	28.5	466	0.973
312	11.9	364	20.8	416	27.4	468	0.785
314	14.2	366	19.5	418	26.1	470	0.632
316	16.6	368	18.5	420	24.7	472	0.505
318	19.2	370	17.8	422	23.1	474	0.402
320	21.9	372	17.4	424	21.5	476	0.318
322	24.6	374	17.3	426	19.9	478	0.250
324	27.3	376	17.5	428	18.2	480	0.196
326	29.9	378	18.0	430	16.6		
328	32.2	380	18.8	432	15.0		
330	34.3	382	19.7	434	13.4		

Note:
mean of the data from Bauer et al.[1] and Rowley et al.[2]

(1) Bauer, D.; Ingham, T.; Carl, S. A.; Moortgat, G. K.; Crowley, J. N. Ultraviolet-visible absorption cross sections of gaseous HOI and its photolysis at 355 nm. *J. Phys. Chem.* **1998**, *102*, 2857-2864, doi:10.1021/jp9804300.

(2) Rowley, D. M.; Mössinger, J. C.; Cox, R. A.; Jones, R. L. The UV-visible absorption cross-sections and atmospheric photolysis rate of HOI. *J. Atmos. Chem.* **1999**, *34*, 137-151, doi:10.1023/A:1006210322389.

H6. ICl (iodine chloride)

Back to Index

ICl + hν	→ $I(^3P_{3/2}) + Cl(^3P_{3/2})$	210 kJ mol^{-1}	569 nm	(1)
	→ $I(^3P_{3/2}) + Cl^*(^3P_{1/2})$	221 kJ mol^{-1}	542 nm	(2)
	→ $I^*(^3P_{1/2}) + Cl(^3P_{3/2})$	301 kJ mol^{-1}	397 nm	(3)
	→ $I^*(^3P_{1/2}) + Cl^*(^3P_{1/2})$	312 kJ mol^{-1}	384 nm	(4)

(Recommendation: 10-6, Note: 10-6, Evaluated: 10-6)

Absorption Cross Sections: The absorption spectrum of ICl, iodine chloride, has been measured at room temperature by Gibson and Ramsperger[4] (380–570 nm), Seery and Britton[9] (220–600 nm), Binder[1] (216.5–310 nm), and Jenkin et al.[5] (210–690 nm). Spectra measured at elevated temperatures have been reported by Binder[1] (293, 387, 489, and 685 K). The spectrum shows two absorption bands of nearly equal peak height, one between 220 and 350 nm with the maximum at ~244 nm and one between 350 and 600 nm with the maximum near 470 nm. The latter band is asymmetric due to the overlap of the B $^3\Pi_{0+} \leftarrow X\ ^1\Sigma_{0+}$, $^1\Pi \leftarrow X\ ^1\Sigma_{0+}$, and A $^3\Pi_i \leftarrow X\ ^1\Sigma_{0+}$ transitions, as discussed by Seery and Britton[9] and Mashnin et al.[7] The experimental data of Seery and Britton[9] and Jenkin et al.[5] are in excellent agreement in the region of the visible absorption band but are appreciably higher (by ~35% at the maximum) than the earlier data from Gibson and Ramsperger.[4] The cross section at the 242 nm maximum reported by Jenkin et al.[5] is greater by ~14% than those observed by Gibson and Ramsperger[4] and Seery and Britton.[9] The larger absorption cross sections reported by Seery and Britton[9] over the wavelength range 290–360 nm are most likely due to Cl_2 impurities as argued by Jenkin et al.,[5] who subtracted Cl_2 contributions in their spectral analysis. Jenkin et al.[5] report their absorption spectrum in graphical form along with cross section values of 5.00×10^{-19} cm^2 molecule^{-1} and 4.20×10^{-19} cm^2 molecule^{-1} at 244 nm and 467 nm, respectively. The recommended cross sections in Table 4H-6 use these values combined with the absorption cross sections read from a figure given in Jenkin et al.[5]

Binder[1] report a decrease in the 244 nm peak absorption cross section with increasing temperature from 4.40×10^{-19} cm^2 molecule^{-1} at 293 K to 3.53×10^{-19} cm^2 molecule^{-1} at 685 K.

Photolysis Quantum Yield and Product Studies: The ratio of the Cl atom spin-state quantum yields, $\Phi(Cl^*)/(\Phi(Cl^*) + \Phi(Cl))$, has been reported by several groups. Mashnin et al.[7] showed that for wavelengths in the range 437–532 nm the ratio varied between 0.41 ± 0.02 and 0.79 ± 0.02. The ratio has been reported by Ni and Flynn[8] to be 0.17 ± 0.04 at 237 nm, 0.67 ± 0.05 at 248 nm by Chichinin,[2] and 0.55 ± 0.05 at 530 nm by Chichinin et al.[3] Tonokura et al.[10] reported $\Phi(I + Cl)$, $\Phi(I + Cl^*)$, and $\Phi(I^* + Cl)$ to be 0.2, 0.4 and 0.4, respectively, for the wavelength range 235–248 nm. The ratio of I* to I, I*/I, has been reported by Tonokura et al.[10] to be 0.71 ± 0.27 and Jung et al.[6] to be 0.43 at 304 nm.

Table 4H-6. Recommended Absorption Cross Sections of ICl at 298 K

λ (nm)	10^{20} σ (cm^2)	λ (nm)	10^{20} σ (cm^2)
210	7.4	410	25.0
220	21.3	420	28.5
230	40.0	430	32.0
240	49.0	440	35.4
244	50.0	450	38.8
250	47.8	460	41.7
260	36.8	467	42.0
270	24.4	470	41.8
280	12.9	480	40.0
290	6.4	490	35.4
300	3.2	500	29.0
310	<1	510	21.1
320	<1	520	15.6
330	<1	530	11.0
340	<1	540	7.3
350	<1	550	5.5
360	2.3	560	4.2
370	4.6	570	3.4
380	8.74	580	2.9
390	13.8	590	2.1
400	19.0	600	1.9

Note:
Jenkin et al.[5]

(1) Binder, J. L. The continuous absorption spectrum of iodine monochloride in the ultraviolet. *Phys. Rev.* **1938**, *54*, 114-117, doi:10.1103/PhysRev.54.114.

(2) Chichinin, A. I. Measurement of $Cl(^2P_{1/2})$ quantum yield for the photodissociaton of NOCl, ICl, PCl_3, Cl_2O and $COCl_2$. *Chem. Phys. Lett.* **1993**, *209*, 459-463, doi:10.1016/0009-2614(93)80117-8.

(3) Chichinin, A. I.; Chasovnikov, S. A.; Krasnoperov, L. N. The laser photolysis of ICl at 530 nm: A time-resolved LMR study. *Chem. Phys. Lett.* **1987**, *138*, 371-376, doi:10.1016/0009-2614(87)80401-3.

(4) Gibson, G. E.; Ramsperger, H. C. Band spectra and dissociation of iodine monochloride. *Phys. Rev.* **1927**, *30*, 598-600, doi:10.1103/PhysRev.30.598.

(5) Jenkin, M. E.; Cox, R. A.; Mellouki, A.; Le Bras, G.; Poulet, G. Kinetics of the reaction of iodine atoms with HO_2 radicals. *J. Phys. Chem.* **1990**, *94*, 2927-2934, doi:10.1021/j100370a036.

(6) Jung, K.-W.; Ahmadi, T. S.; El-Sayed, M. A. Photofragment translational spectroscopy of ICl at 304 nm. *J. Phys. Chem. A* **1997**, *101*, 6562-6567, doi:10.1021/jp970837p.

(7) Mashnin, T. S.; Cheryshev, A. V.; Krasnoperov, L. N. Laser photolysis of ICl. A time-resolved LMR measurement of $Cl(^2P_{1/2})$ relative yield. *Chem. Phys. Lett.* **1993**, *207*, 105-109, doi:10.1016/0009-2614(93)85019-K.

(8) Ni, C.-K.; Flynn, G. W. State and velocity distributions of Cl atoms produced in the photodissociation of ICl at 237 nm. *Chem. Phys. Lett.* **1993**, *210*, 333-339, doi:10.1016/0009-2614(93)87032-X.

(9) Seery, D. J.; Britton, D. The continuous absorption spectra of chlorine, bromine, bromine chloride, iodine chloride, and iodine bromide. *J. Phys. Chem.* **1964**, *68*, 2263-2266, doi:10.1021/j100790a039.

(10) Tonokura, K.; Matsumi, Y.; Kawasaki, M.; Kim, H. L.; Yabushita, S.; Fujimura, S.; Saito, K. Photodissociation of ICl at 235-248 nm. *J. Chem. Phys.* **1993**, *99*, 3461-3467, doi:10.1063/1.466169.

H7. IBr (iodine bromide)

Back to Index

IBr + hν	$\rightarrow I(^3P_{3/2}) + Br(^3P_{3/2})$	178 kJ mol^{-1}	673 nm	(1)
	$\rightarrow I(^3P_{3/2}) + Br^*(^3P_{1/2})$	222 kJ mol^{-1}	539 nm	(2)
	$\rightarrow I^*(^3P_{1/2}) + Br(^3P_{3/2})$	269 kJ mol^{-1}	446 nm	(3)
	$\rightarrow I^*(^3P_{1/2}) + Br^*(^3P_{1/2})$	312 kJ mol^{-1}	383 nm	(4)

(Recommendation: 06-2, Note: 10-6, Evaluated: 10-6)

Absorption Cross Sections: The absorption spectrum of IBr, iodine bromide, has been measured at room temperature by Seery and Britton[4] over the wavelength range 220–600 nm. The spectrum consists of two

absorption bands, a weak band between 220 and 350 nm with the maximum at ~270 nm and a stronger band between 350 and 600 nm with the maximum at ~500 nm. The recommended absorption cross sections in Table 4H-7 are taken from Seery and Britton.[4]

Photolysis Quantum Yield and Product Studies: Absolute quantum yields for Br* formation, Φ(Br*), were measured by Haugen et al.[1] over the wavelength range 450–530 nm. Φ(Br*) increases from a value of 0.28 at 450 nm to a maximum of 0.73 near 500 nm. Peterson and Smith[3] reported the ratio of the Br atom spin-state quantum yields, Φ(Br*)/(Φ(Br*) + Φ(Br)), to vary from ~0.3 at 444 nm to a maximum of unity near 520 nm followed by a decline to ~0.1 at 670 nm. Wrede et al.[5] reported a similar trend over the wavelength range 440–544 nm. Kim et al.[2] measured the relative quantum yields for the photolysis channels Φ(I + Br), Φ(I + Br*) and Φ(I* + Br) to be 0.23, 0.35 and 0.42, respectively, at 267 nm.

Table 4H-7. Recommended Absorption Cross Sections of IBr at 298 K

λ (nm)	10^{20} σ (cm^2)	λ (nm)	10^{20} σ (cm^2)
220	3.59	420	31.7
230	5.70	430	44.8
240	10.2	440	58.7
250	16.7	450	71.9
260	21.4	460	85.2
270	23.1	470	98.5
280	21.1	480	111
290	16.8	490	120
300	12.4	500	122
310	7.95	510	116
320	5.39	520	103
330	3.36	530	85.8
340	2.14	540	67.5
350	1.45	550	52.3
360	1.52	560	36.6
370	2.37	570	27.2
380	4.17	580	19.9
390	6.96	590	14.6
400	12.0	600	11.3
410	20.5		

Note:
Seery and Britton[4]

(1) Haugen, H. K.; Weitz, E.; Leone, S. R. Accurate quantum yields by laser gain vs absorption spectroscopy: Investigation of Br/Br* channels in photofragmentation of Br_2 and IBr. *J. Chem. Phys.* **1964**, *83*, 3402-3412, doi:10.1063/1.449145.

(2) Kim, Y. S.; Jung, Y.-J.; Jung, K.-H. Photodissociation of IBr near 267 nm by center-stripe analysis of two-dimensional image. *J. Chem. Phys.* **1997**, *107*, 3805-3812, doi:10.1063/1.474739.

(3) Petersen, A. B.; Smith, I. W. M. Yields of Br*($4^2P_{1/2}$) as a function of wavelength in the photodissociation of Br_2 and IBr. *Chem. Phys.* **1978**, *30*, 407-413, doi:10.1016/0301-0104(78)87012-8.

(4) Seery, D. J.; Britton, D. The continuous absorption spectra of chlorine, bromine, bromine chloride, iodine chloride, and iodine bromide. *J. Phys. Chem.* **1964**, *68*, 2263-2266, doi:10.1021/j100790a039.

(5) Wrede, E.; Laubach, S.; Schulenburg, S.; Brown, A.; Wouters, E. R.; Orr-Ewing, A. J.; Ashfold, M. N. R. Continuum state spectroscopy: A high resolution ion imaging study of IBr in the wavelength range 440-685 nm. *J. Chem. Phys.* **2001**, *114*, 2629-2646, doi:10.1063/1.1337049#.

H8. INO (nitrosyl iodide)

Back to Index

$INO + h\nu \rightarrow I + NO$	77 kJ mol^{-1}	1563 nm	(1)

(Recommendation: 06-2, Note: 10-6, Evaluated: 10-6)

Absorption Cross Sections: The absorption cross sections of INO, nitrosyl iodide, have been measured at room temperature by Porter et al.[3] (390–470 nm), van den Bergh and Troe[4] (around 265 and 410 nm), Basco and Hunt[1] (220–460 nm), and Forte et al.[2] (223–300 nm and around 410 nm). The spectrum shows two absorption

bands, a strong and asymmetric band in the UV between 220 and 300 nm with the maximum at 238 nm, and a second weaker band, weaker by two orders of magnitude, between 355 and 470 nm with a maximum near 410 nm. The results for the UV band are in good agreement except for the region around 250 nm, where the absorption spectrum reported by Basco and Hunt[1] shows a hump and an absorption cross section larger by a factor of ~1.5 than that reported by Forte et al.[2] The absorption curve in the near UV and visible reported by Porter et al.[3] is shifted to longer wavelengths by ~20 nm and the absorption cross sections are smaller by 50-30% at 400–430 nm compared to the results of Basco and Hunt.[1]

The recommended absorption cross sections in Table 4H-8 are the mean of the data from Basco and Hunt[1] and Forte et al.[2] for the wavelength range 223–290 nm and the data from Basco and Hunt[1] at 300, 310, and 360 nm. For the wavelength range 360< λ <400 nm, the recommended cross sections are smoothed values from Basco and Hunt.[1] For wavelengths >400 nm, the recommendation is based on the data from van den Berg and Troe,[4] Basco and Hunt,[1] and Forte et al.[2]

Photolysis Quantum Yield and Product Studies: The photolysis quantum yield is expected to be unity at wavelengths above the dissociation threshold.

Table 4H-8. Recommended Absorption Cross Sections of INO at 298 K

λ (nm)	10^{20} σ (cm^2)	λ (nm)	10^{20} σ (cm^2)
223	225	360	45
230	1690	370	59
235	5640	380	65
238	6850	390	78
245	6000	400	92
251	4880	410	110
260	2270	420	100
270	1040	430	94
280	500	440	80
290	187	450	60
300	92	460	40
310	41		

Note:
223–290 nm: mean of data from Basco and Hunt[1] and Forte et al.[2]
300, 310, 360 nm: Basco and Hunt[1]
370–400 nm: smoothed data from Basco and Hunt[1]
>400 nm: based on the data from van den Berg and Troe,[4] Basco and Hunt,[1] and Forte et al.[2]

(1) Basco, N.; Hunt, J. E. The recombination of iodine atoms in the presence of nitric oxide. *Int. J. Chem. Kinet.* **1978**, *10*, 733-743, doi:10.1002/kin.550100707.
(2) Forte, E.; Hippler, H.; van den Bergh, H. INO thermodynamic properties and ultraviolet spectrum. *Int. J. Chem. Kinet.* **1981**, *13*, 1227-1233, doi:10.1002/kin.550131203.
(3) Porter, G., F.R.S.; Szabó, Z. G.; Townsend, M. G. The recombination of atoms V. Iodine atom recombination in nitric oxide. *Proc. Roy. Soc. Lond. A* **1962**, *A 270*, 493-500, doi:10.1098/rspa.1962.0239.
(4) van den Bergh, H.; Troe, J. Kinetic and thermodynamic properties of INO and INO_2 intermediate complexes in iodine recombination. *J. Chem. Phys.* **1976**, *64*, 736-742, doi:10.1063/1.432220.

H9. INO_2 (nitryl iodide)

Back to Index

$INO_2 + h\nu \rightarrow I + NO_2$ (1)
$\rightarrow IO + NO$ (2)

(Recommendation: 15-10, Note: 15-10, Evaluated: 15-10)

Absorption Cross Sections: The UV absorption spectrum of INO_2, nitryl iodide, has been measured at room temperature by Bröske[2] over the wavelength range 210–390 nm. The spectrum consists of three broad absorption bands with cross sections of 4.20×10^{-18}, 9.6×10^{-19}, and 3.9×10^{-19} cm^2 $molecule^{-1}$ at 240, 282, and 342 nm, respectively. These values were obtained assuming the stoichiometric conversion of NO_2 to INO_2 in the photolysis of I_2–NO_2 mixtures. The recommended absorption cross section values in Table 4H-9 were

taken from the evaluation by Atkinson et al.[1] Note the cross section values from Bröske[2] quoted in the Mainz spectral atlas[3] differ significantly. On the basis of the mass balance uncertainty in the Bröske study an uncertainty factor of 4 (2σ) is recommended.

Photolysis Quantum Yield and Product Studies: No recommendation.

Table 4H-9. Recommended Absorption Cross Sections of INO_2 at 298 K

λ (nm)	10^{20} σ (cm^2)	λ (nm)	10^{20} σ (cm^2)
210	236	300	37.3
215	187	305	30.8
220	196	310	24.7
225	279	315	25.1
230	347	320	27.5
235	399	325	32.5
240	422	330	31.2
245	400	335	34.9
250	330	340	37.3
255	234	345	37.3
260	162	350	29.8
265	99.6	355	29.5
270	87.1	360	27.1
275	89.8	365	20.7
280	99.6	370	14.9
285	92.2	375	7.40
290	81.0	380	2.40
295	62.0		

Note:
Bröske[2] from Atkinson et al.[1]

(1) Atkinson, R.; Baulch, D. L.; Cox, R. A.; Hampson, R. F., Jr.; Kerr, J. A.; Rossi, M. J.; Troe, J. Evaluated kinetic and photochemical data for atmospheric chemistry: Supplement VIII, Halogen species. IUPAC subcommittee on gas kinetic data evaluation for atmospheric chemistry. *J. Phys. Chem. Ref. Data* **2000**, *29*, 167-266, doi:10.1063/1.556058.

(2) Broske, R. Ph.D. Thesis, University of Wuppertal, Germany, 1999.

(3) Keller-Rudek, H.; Moortgat, G. K.; Sander, R.; Sörensen, R. The MPI-Mainz UV/Vis spectral atlas of gaseous molecules of atmospheric interest. *Earth Syst. Sci. Data* **2013**, *5*, 365-373, doi:10.5194/essd-5-365-2013.

H10. $IONO_2$ (iodine nitrate)

Back to Index

$IONO_2 + h\nu$	$\rightarrow IO + NO_2$	118 kJ mol^{-1}	1018 nm	(1)
	$\rightarrow I + NO_3$	148 kJ mol^{-1}	808 nm	(2)
	$\rightarrow I + NO_2 + O$	358 kJ mol^{-1}	299 nm	(3)

(Recommendation: 06-2, Note: 10-6, Evaluated: 10-6)

Absorption Cross Sections: The UV absorption spectrum of $IONO_2$, iodine nitrate, has been reported by Mössinger et al.[2] (245–415 nm) and Joseph et al.[1] (240–370 nm) using 351 and 248 nm pulsed laser photolysis of $NO_2/CF_3I/N_2$ mixtures, respectively, to produce $IONO_2$ in the gas-phase. The $IONO_2$ spectrum consists of a broad continuous absorption band over this wavelength range. There are, however, significant discrepancies between the two studies for the wavelength dependence and absolute absorption cross sections. The reason for the discrepancies in these very similar studies is not known. The recommended cross section values given in Table 4H-10 are taken from Mössinger et al.,[2] however, the uncertainty in the $IONO_2$ spectrum is large and the lower cross sections reported in the Joseph et al. study can't be ruled out.

Photolysis Quantum Yield and Product Studies: The photoproducts of $IONO_2$ are not well characterized. In the only quantum yield study to date, Joseph et al.[1] report IO and NO_3 quantum yields of $\Phi(IO) \leq 0.02$ and $\Phi(NO_3) = 0.21 \pm 0.09$ at 248 nm, based on a modeled $IONO_2$ concentration and their measured cross section at 248 nm. Photolysis is most likely the major daytime loss process for $IONO_2$ even considering the current large uncertainty in the UV absorption cross sections.

Table 4H-10. Recommended Absorption Cross Sections of $IONO_2$ at 298 K

λ (nm)	10^{20} σ (cm^2)	λ (nm)	10^{20} σ (cm^2)
245	1210	335	374
250	1170	340	360
255	1060	345	348
260	946	350	334
265	880	355	316
270	797	360	294
275	772	365	270
280	741	370	242
285	691	375	213
290	631	380	184
295	577	385	153
300	525	390	130
305	495	395	103
310	462	400	78.0
315	441	405	60.5
320	404	410	49.6
325	396	415	41.6
330	380		

Note:
Mössinger et al.,[2] values in the range 335–385 nm were obtained from an interpolation of the experimental data.

(1) Joseph, D. M.; Ashworth, S. H.; Plane, J. M. C. On the photochemistry of $IONO_2$: absorption cross section (240–370 nm) and photolysis product yields at 248 nm. *Phys. Chem. Chem. Phys.* **2007**, *9*, 5599-5607, doi:10.1039/b709465e.

(2) Mössinger, J. C.; Rowley, D. M.; Cox, R. A. The UV-visible absorption cross-sections of $IONO_2$. *Atmos. Chem. Phys.* **2002**, *2*, 227-234, doi:10.5194/acp-2-227-2002.

H11. CH_3I (methyl iodide)

Back to Index

$CH_3I + h\nu \rightarrow CH_3 + I(^2P_{3/2})$	240 kJ mol^{-1}	498 nm	(1)
$\rightarrow CH_3 + I^*(^2P_{1/2})$	331 kJ mol^{-1}	362 nm	(2)

(Recommendation: 25-1, Note: 25-1, Evaluated: 25-1)

Absorption Cross Sections: The VUV and UV absorption spectrum of CH_3I, methyl iodide, has been measured at room temperature by Porret and Goodeve[16] (200–360 nm, graphical data), Boschi and Salahub[2] (117–299 nm, graphical data), Rebbert et al.[18] (147 nm), Gedanken and Rowe[7] (232–310 mm, graphical data), Baughcum and Leone[1] (200–310 nm, graphical data), Pence et al.[15] (180–400 nm), Felps et al.[6] (257.7 nm), Jenkin et al.[8] (205–335 nm), Fahr et al.[5] (160–330 nm), Man et al.[13] (205–360 nm, graphical data), Waschewsky et al.[23] (196–304 nm, graphical data), Kwok and Phillips[10] (192–225 nm, graphical data), Rattigan et al.[17] (235–365 nm), Roehl et al.[19] (200–350 nm), Eden et al.[4] (115–315 nm), and Locht et al.[12] (61–248 nm). Kwok and Phillips[10] also measured the CH_3I spectrum in cyclohexane solution. Fahr et al.[5] also measured the absorption cross sections in the range 330–400 nm in the liquid phase and used a wavelength-shift procedure to derive gas-phase cross section values. The temperature dependence of the absorption spectrum has been reported by Fahr et al.[5] (223–333 K), Rattigan et al.[17] (243–333 K), and Roehl et al.[19] (210–298 K). The room temperature cross section data for the wavelength range 210–305 nm are in reasonable to good agreement with Rattigan et al.[17] reporting the smallest and Fahr et al.[5] the largest values. The agreement is generally better than 15% except for the region around the absorption maximum, where the spread is ~30%. Rattigan et al.[17] and Fahr et al.[5] report values of 1.07×10^{-18} cm^2 $molecule^{-1}$ and 1.4×10^{-18} cm^2 $molecule^{-1}$, respectively, for the maximum at ~260 nm. The peak cross section values from the other studies range from 1.15×10^{-18} cm^2 $molecule^{-1}$ to 1.22×10^{-18} cm^2 $molecule^{-1}$. In the wavelength range 305–330 nm, the agreement is within 20%. At wavelengths below 210 nm, the data reported by Jenkin et al.,[8] Roehl et al.,[19] and Kwok and Phillips[11] fit into the strong and highly structured band system reported by Fahr et al.[5] and Eden et al.[4] However, the absorption cross sections reported by Eden et al.[4] in this wavelength range are significantly larger, ~×10. The recommended room temperature absorption cross sections for the wavelength range above 210 nm in Table 4H-11 are the mean of the values reported by Jenkin et al.,[8] Fahr et al.,[5] and Roehl et al.[19] for the range 210–230 nm, the mean of the

values reported by Jenkin et al.,[8] Fahr et al.,[5] Rattigan et al.,[17] and Roehl et al.[19] for the range 235–330 nm; the mean of the values reported by Fahr et al.,[5] Rattigan et al.,[17] and Roehl et al.[19] for the range 335–350 nm, and the values of Rattigan et al.[17] for the range 355–365 nm.

Studies of the UV spectrum temperature dependence are in qualitative agreement with an increase in the peak absorption cross section and decrease in the long wavelength tail cross sections with decreasing temperature. Roehl et al.[19] and Rattigan et al.[17] parameterized the cross section temperature dependence using the empirical expressions:

$$\sigma(\lambda, T) = \sigma(298\ K)\ [1 + a_1(\lambda)(T–298) + a_2(\lambda)(T–298)^2] \quad \text{(Roehl et al.[19])}$$

$$\ln \sigma(\lambda, T) = \ln \sigma(\lambda, 298\ K) + B(\lambda)(T–298) \quad \text{(Rattigan et al.[17])}$$

Both expressions reproduce the experimental data well and the $a_1(\lambda)$, $a_2(\lambda)$, and $B(\lambda)$ parameters are included in Table 4H-11.

The Lyman-α (121.567 nm) absorption cross section recommendation of 6.1×10^{-17} cm^2 molecule^{-1} is an average of the results from the Eden et al.[4] and Locht et al.[12] studies. An estimated cross section uncertainty factor of 1.25 (2σ) is recommended.

Photolysis Quantum Yield and Product Studies: The photolysis quantum yield for CH_3I is expected to be unity for wavelengths above the dissociation threshold. Quantum yields for I*($^2P_{1/2}$) atom formation, Φ(I*), have been reported by several groups for photolysis between 222 and 333.5 nm. Uma and Das[20-22] reported Φ(I*) values of 0.63 ± 0.02, 0.79 ± 0.02, 0.69 ± 0.02, and 0.43 ± 0.02 for 222, 266, 280, and ~305 nm, respectively. Gedanken[22] reported Φ(I*) = 0.72 ± 0.08 at 248 nm. Pence et al.[15] reported Φ(I*) = 0.81 ± 0.03 and ~0.05 at 248 and 308 nm, respectively. Kang et al.[9] reported Φ(I*) = 0.30 at 304 nm. Ogorzalek Loo et al.[14] reported Φ(I*) = 0.47, 0.77, and 0.92 at 325.8, 329.4, and 333.5, respectively. Ogorzalek Loo et al.[14] and Brewer et al.[3] have also reported I* quantum yields for the photolysis of CD_3I. Quantum yields for I($^2P_{3/2}$) atom formation, Φ(I), can be derived from $\Phi(I) = 1–\Phi(I^*)$.

Table 4H-11. Recommended Absorption Cross Sections of CH_3I at 298 K and Temperature Coefficients

λ (nm)	10^{20} σ (cm^2)	10^3 a_1 (K^{-1})	10^5 a_2 (K^{-2})	10^3 B (K^{-1})
210	3.62	3.07	2.42	–
215	5.08	2.61	2.28	–
220	6.90	1.06	1.22	–
225	9.11	1.74	1.96	–
230	12.6	1.47	1.67	–
235	20.5	1.91	2.04	0.67
240	38.1	1.74	2.06	0.61
245	65.6	1.52	2.15	0.34
250	96.3	1.20	2.11	0.08
255	117.7	0.890	1.95	–0.10
260	119.7	0.882	1.93	–0.12
265	102.9	1.21	2.00	0.10
270	75.9	1.77	2.11	0.54
275	49.6	2.52	2.12	1.33
280	29.2	3.62	2.24	2.43
285	15.6	4.84	2.38	3.74
290	8.04	6.14	2.57	4.98
295	4.00	7.27	2.91	6.38
300	2.06	7.82	3.53	6.97
305	1.10	7.82	3.85	6.84
310	0.621	7.37	3.71	6.78
315	0.359	6.98	3.47	6.75
320	0.221	7.39	3.54	6.53
325	0.126	7.23	2.82	6.79
330	0.0684	8.93	3.74	7.82
335	0.0388	10.88	4.88	9.34
340	0.0212	11.30	4.46	10.95
345	0.0114	15.68	8.44	13.58
350	0.00609	15.94	8.22	16.83
355	0.00320	–	–	18.91
360	0.00190	–	–	17.28
365	0.00090	–	–	23.63

Note:

Absorption cross sections (σ)

210–230 nm: mean of data from Jenkin et al.,[8] Fahr et al.,[5] and Roehl et al.[19]

235–330 nm: mean of data from Jenkin et al.,[8] Fahr et al.,[5] Rattigan et al.,[17] and Roehl et al.[19]

335–350 nm: mean of data from Fahr et al.,[5] Rattigan et al.,[17] and Roehl et al.[19]

355–365 nm: Rattigan et al.[17]

Temperature coefficients

$a_1(\lambda)$ and $a_2(\lambda)$: Roehl et al.[19] (210–298 K), $\sigma(\lambda, T) = \sigma(298\ K)\ [1 + a_1(T–298) + a_2(T–298)^2]$

$B(\lambda)$: Rattigan et al.[17] (243–333 K), $\ln \sigma(\lambda, T) = \ln \sigma(\lambda, 298\ K) + B(\lambda)(T–298)$

(1) Baughum, S. L.; Leone, S. R. Photofragmentation infrared emission studies of vibrationally excited free radicals CH_3 and CH_2I. *J. Chem. Phys.* **1980**, *72*, 6531-6545, doi:10.1063/1.439111.

(2) Boschi, R. A.; Salahub, D. R. The far ultra-violet spectra of some 1-iodoalkanes. *Mol. Phys.* **1972**, *24*, 289-299, doi:10.1080/00268977200101451.

(3) Brewer, P.; Das, P.; Ondrey, G.; Bersohn, R. Measurement of the relative populations of $I(^2P_{1/2}{}^0)$ and $I(^2P_{3/2}{}^0)$ by laser induced vacuum ultraviolet fluorescence. *J. Chem. Phys.* **1983**, *79*, 720-723, doi:10.1063/1.445820.

(4) Eden, S.; Limão-Vieira, P.; Hoffmann, S. V.; Mason, N. J. VUV spectroscopy of CH_3Cl and CH_3I. *Chem. Phys.* **2006**, *331*, 232-244, doi:10.1016/j.chemphys.2006.10.021.

(5) Fahr, A.; Nayak, A. K.; Kurylo, M. J. The ultraviolet absorption cross sections of CH_3I temperature dependent gas and liquid phase measurements. *Chem. Phys.* **1995**, *197*, 195-203, doi:10.1016/0301-0104(95)00172-K.

(6) Felps, W. S.; Rupnik, K.; McGlynn, S. P. Electronic spectroscopy of the cyanogen halides. *J. Phys. Chem.* **1991**, *95*, 639-656, doi:10.1021/j100155a028.
(7) Gedanken, A.; Rowe, M. D. Magnetic circular dichroism spectra of the methyl halides. Resolution of the n → σ* continuum. *Chem. Phys. Lett.* **1975**, *34*, 39-43, doi:10.1016/0009-2614(75)80196-5.
(8) Jenkin, M. E.; Murrells, T. P.; Shalliker, S. J.; Hayman, G. D. Kinetics and product study of the self-reactions of allyl and allyl peroxy radicals at 296 K. *J. Chem. Soc. Faraday Trans.* **1993**, *89*, 433-446, doi:10.1039/ft9938900433.
(9) Kang, W. K.; Jung, K. W.; Kim, D.-C.; Jung, K.-H. Photodissociation of alkyl iodides and CF_3I at 304 nm: Relative populations of I($^2P_{1/2}$) and I($^2P_{3/2}$) and dynamics of curve crossing. *J. Chem. Phys.* **1996**, *104*, 5815-5820, doi:10.1063/1.471313.
(10) Kwok, W. M.; Phillips, D. L. Gas and solution phase chloroiodomethane short-time photodissociation dynamics in the B-band absorption. *Chem. Phys. Lett.* **1997**, *270*, 506-516, doi:10.1016/S0009-2614(97)00400-4.
(11) Kwok, W. M.; Phillips, D. L. Gas-phase chloroiodomethane short-time photodissociation dynamics of the A-band absorption and a comparison with the solution phase short-time photodissociation dynamics. *Mol. Phys.* **1997**, *90*, 315-326, doi:10.1080/002689797172444.
(12) Locht, R.; Leyh, B.; Jochims, H. W.; Baumgärtel, H. Medium and high resolution vacuum UV photoabsorption spectroscopy of methyl iodide (CH_3I) and its deuterated isotopomers CD_3I and CH_2DI. A Rydberg series analysis. *Chem. Phys.* **2009**, *365*, 109-128, doi:10.1016/j.chemphys.2009.09.025.
(13) Man, S.-Q.; Kwok, W. M.; Phillips, D. L.; Johnson, A. E. Short-time photodissociation dynamics of A-band and B-band bromoiodomethane in solution: An examination of bond selective electronic excitation. *J. Chem. Phys.* **1996**, *105*, 5842-5857, doi:10.1063/1.472426.
(14) Ogorzalek Loo, R.; Haerri, H.-P.; Hall, G. E.; Houston, P. L. Methyl rotation, vibration, and alignment from a multiphoton ionization study of the 266 nm photodissociation of methyl iodide. *J. Chem. Phys.* **1989**, *90*, 4222-4236, doi:10.1063/1.455779.
(15) Pence, W. H.; Baughum, S. L.; Leone, S. R. Laser UV photofragmentation of halogenated molecules. Selective bond dissociation and wavelength-specific quantum yields for excited I($^2P_{1/2}$) and Br($^2P_{1/2}$) atoms. *J. Phys. Chem.* **1981**, *85*, 3844-3851, doi:10.1021/j150625a027.
(16) Porret, D.; Goodeve, C. F. The continuous absorption spectrum of methyl iodide. *Trans. Faraday Soc.* **1937**, *33*, 690-693, doi:10.1039/tf9373300690.
(17) Rattigan, O. V.; Shallcross, D. E.; Cox, R. A. UV absorption cross sections and atmospheric photolysis rates of CF_3I, CH_3I, C_2H_5I and CH_2ICl. *J. Chem. Soc. Faraday Trans.* **1997**, *93*, 2839-2846, doi:10.1039/a701529a.
(18) Rebbert, R. E.; Lias, S. G.; Ausloos, P. Photolysis of alkyl iodides at 147.0 nm. The reaction H + $C_nH_{2n+1}I$ → HI + C_nH_{2n+1}. *Int. J. Chem. Kinet.* **1973**, *5*, 893-908, doi:10.1002/kin.550050515.
(19) Roehl, C. M.; Burkholder, J. B.; Moortgat, G. K.; Ravishankara, A. R.; Crutzen, P. J. Temperature dependence of UV absorption cross sections and atmospheric implications of several alkyl iodides. *J. Geophys. Res.* **1997**, *102*, 12819-12829, doi:10.1029/97JD00530.
(20) Uma, S.; Das, P. K. Dynamics of I*($^2P_{1/2}$) production in the ultraviolet photodissociation of alkyl iodides. *Can. J. Chem.* **1994**, *72*, 865-869, doi:10.1139/v94-113.
(21) Uma, S.; Das, P. K. I* production from *n*-alkyl iodides at 222 nm. *Chem. Phys. Lett.* **1995**, *241*, 335-338, doi:10.1016/0009-2614(95)00661-M.
(22) Uma, S.; Das, P. K. Production of I*($^2P_{1/2}$) in the ultraviolet photodissociation of α-branched alkyl iodides. *J. Chem. Phys.* **1996**, *104*, 4470-4474, doi:10.1063/1.471199.
(23) Waschewsky, G. C. G.; Horansky, R.; V. Vaida Effect of dimers on the temperature-dependent absorption cross section of methyl iodide. *J. Phys. Chem. A* **1996**, *100*, 11559-11565, doi:10.1021/jp960809r.

H12. CH_2I_2 (diiodomethane)

Back to Index

$CH_2I_2 + h\nu$	$\rightarrow CH_2I + I(^2P_{3/2})$	216 kJ mol^{-1}	554 nm	(1)
	$\rightarrow CH_2I + I^*(^2P_{1/2})$	307 kJ mol^{-1}	390 nm	(2)

(Recommendation: 02-25, Note: 10-6, Evaluated: 10-6)

Absorption Cross Sections: The UV absorption spectrum of CH_2I_2, diiodomethane, has been measured at room temperature by Pence et al.[5] (180–400 nm), Schmitt and Comes[7] (220–360 nm), Baughcum and Leone[1] (200–360 nm), Koffend and Leone[2] (265–341 nm), Kwok and Phillips[3] (220–400 nm), Roehl et al.[6] (215–385 nm), and Mössinger et al.[4] (215–385 nm). Kwok and Phillips[3] also measured the CH_2I_2 spectrum in methanol and cyclohexane solvents. The temperature dependence of the absorption spectrum has been reported by Roehl et al.[6] (273 and 298 K) and Mössinger et al.[4] (273, 298, and 348 K).

The absorption spectrum shows clear evidence for multiple transitions in the wavelength range 200–400 nm with absorption maxima at ~215, 250, and 290 nm. The room temperature cross section data from the various groups are in good agreement with the exception of Kwok and Phillips;[3] the reported cross sections are within 5 to 10% between 230 and 380 nm. The data from Schmitt and Comes[7] and Koffend and Leone[2] near the 290 nm peak are higher than those of Roehl et al.[6] and Mössinger et al.[4] The values of Kwok and Phillips[3] are lower by 15–20% near 290 nm. The recommended room temperature absorption cross sections in Table 4H-12 are the values from Roehl et al.[6] for the range 205–215 nm, the mean of the values reported by Roehl et al.[6] and Mössinger et al.[4] for the range 220–380 nm, and the value of Mössinger et al.[4] at 385 nm.

The studies of the spectrum temperature dependence are in good agreement with a slight increase in the peak absorption cross section and decrease in the long wavelength tail cross section with decreasing temperature. Mössinger et al.[4] parameterized the cross section temperature dependence between 273 and 348 K using the expression:

$$\ln \sigma(\lambda, T) = \ln \sigma(\lambda, 298K) + B(\lambda)(T–298)$$

The B(λ) coefficients are listed in Table 4H-12. (Note: an erroneous B value at 305 nm was corrected via a personal communication with Dr. Mössinger).

Photolysis Quantum Yield and Product Studies: The photolysis quantum yield for CH_2I_2 is expected to be unity for wavelengths above the dissociation threshold. Pence et al.[5] have reported quantum yields for $I^*(^2P_{1/2})$ atom formation, Φ(I*), at 193, 248, and 308 nm of ~0.05, 0.46 ± 0.04, and 0.25 ± 0.02, respectively. Quantum yields for $I(^2P_{3/2})$ atom formation, Φ(I), can be derived from Φ(I) = 1–Φ(I*).

Table 4H-12. Recommended Absorption Cross Sections of CH_2I_2 at 298 K and Temperature Coefficients

λ (nm)	10^{20} σ (cm^2)	10^3 B (K^{-1})	λ (nm)	10^{20} σ (cm^2)	10^3 B (K^{-1})
205	407.0	–	300	357.0	–0.37
210	404.0	–	305	338.5	–0.16
215	366.0	0.15	310	313.5	0.07
220	260.0	0.14	315	280.0	0.15
225	197.5	0.19	320	244.0	0.27
230	133.0	0.51	325	203.0	0.27
235	109.0	0.56	330	161.5	0.51
240	122.5	0.15	335	120.5	0.55
245	150.0	0.18	340	83.3	1.36
250	157.0	0.67	345	53.7	1.99
255	139.5	1.58	350	32.6	3.19
260	120.5	2.04	355	19.2	4.09
265	130.0	1.30	360	10.9	5.39
270	178.5	0.00	365	6.05	6.77
275	255.0	–0.71	370	3.45	8.25
280	328.5	–1.24	375	1.93	11.3
285	371.5	–1.21	380	1.17	–
290	380.5	–0.94	385	0.769	–
295	371.5	–0.58			

Note:

Absorption cross sections
205–215 nm: Roehl et al.[6]
220–380 nm: mean of data from Roehl et al.[6] and Mössinger et al.[4]
385 nm: Mössinger et al.[4]
Temperature coefficients
B(λ): Mössinger et al.[4] (273–348 K), $\ln \sigma(\lambda, T) = \ln \sigma(\lambda, 298\ K) + B(\lambda)(T–298)$

(1) Baughum, S. L.; Leone, S. R. Photofragmentation infrared emission studies of vibrationally excited free radicals CH_3 and CH_2I. *J. Chem. Phys.* **1980**, *72*, 6531-6545, doi:10.1063/1.439111.
(2) Koffend, J. B.; Leone, S. R. Tunable laser photodissociation: Quantum yield of $I^*(^2P_{1/2})$ from CH_2I_2. *Chem. Phys. Lett.* **1981**, *81*, 136-141, doi:10.1016/0009-2614(81)85344-4.
(3) Kwok, W. M.; Phillips, D. L. Solvation and solvent effects on the short-time photodissociation dynamics of CH_2I_2 from resonance Raman spectroscopy. *J. Chem. Phys.* **1996**, *104*, 2529-2540, doi:10.1063/1.471001.
(4) Mössinger, J. C.; Shallcross, D. E.; Cox, R. A. UV-Vis absorption cross-sections and atmospheric lifetimes of CH_2Br_2, CH_2I_2 and CH_2BrI. *J. Chem. Soc. Faraday Trans.* **1998**, *94*, 1391-1396, doi:10.1039/a709160e.
(5) Pence, W. H.; Baughum, S. L.; Leone, S. R. Laser UV photofragmentation of halogenated molecules. Selective bond dissociation and wavelength-specific quantum yields for excited $I(^2P_{1/2})$ and $Br(^2P_{1/2})$ atoms. *J. Phys. Chem.* **1981**, *85*, 3844-3851, doi:10.1021/j150625a027.
(6) Roehl, C. M.; Burkholder, J. B.; Moortgat, G. K.; Ravishankara, A. R.; Crutzen, P. J. Temperature dependence of UV absorption cross sections and atmospheric implications of several alkyl iodides. *J. Geophys. Res.* **1997**, *102*, 12819-12829, doi:10.1029/97JD00530.
(7) Schmitt, G.; Comes, F. J. Photolysis of CH_2I_2 and 1,1-$C_2H_4I_2$ at 300 nm. *J. Photochem.* **1980**, *14*, 107-123, doi:10.1016/0047-2670(80)80002-5.

H13. C_2H_5I (iodoethane)

Back to Index

$C_2H_5I + h\nu$	$\rightarrow C_2H_5 + I(^2P_{3/2})$	235 kJ mol^{-1}	509 nm	(1)
	$\rightarrow C_2H_5 + I^*(^2P_{1/2})$	326 kJ mol^{-1}	367 nm	(2)

(Recommendation: 02-25, Note: 25-1, Evaluated: 10-6)

Absorption Cross Sections: The UV absorption spectrum of C_2H_5I, iodoethane, has been measured at room temperature by Rebbert et al.[6] (147 nm, $\sigma = 1.48 \times 10^{-17}$ cm^2 molecule^{-1}), Porret and Goodeve[4] (205–360 nm), Roehl et al.[7] (205–365 nm), Rattigan et al.[5] (235–355 nm), and Young et al.[11] (200–319 nm). The temperature dependence of the absorption spectrum has been reported by Roehl et al.[7] (223–298 K), Rattigan et al.[5] (243–333 K), and Zhang et al.[12] (323 K, 220–320 nm). The room temperature data are in good agreement with the values of Roehl et al.[7] larger than the values of Rattigan et al.[5] by 5–15% over the wavelength range 235–325 nm and 125% at 355 nm. The Young et al. data is in general agreement with the Roehl et al. and Rattigan et al. studies, but the data has considerable scatter and is not considered in the recommendation. The Rattigan et al.[5] values agree to within 10–15% with the values from Porret and Goodeve.[4] The recommended absorption cross sections in Table 4H-13 are the mean of the values reported by Roehl et al.[7] and Rattigan et al.[5] for the wavelength range 235–355 nm and the data from Roehl et al.[7] in the range 205–230 nm.

Studies of the spectrum temperature dependence by Roehl et al.[7] and Rattigan et al.[5] show that the peak absorption cross section increases with decreasing temperature. The absorption cross sections in the long wavelength tail of the spectrum decrease with decreasing temperature. The data reported by Zhang et al.[12] for 323 K are 10–40% larger around the absorption maximum and as much as 200% larger in the long wavelength tail than the data for 313 and 333 K reported by Rattigan et al.[5] Roehl et al.[7] and Rattigan et al.[5] parameterized the cross section temperature dependence using the empirical expressions:

$$\sigma(\lambda, T) = \sigma(298\ K)\ [(1 + a_1(\lambda)(T–298) + a_2(\lambda)(T–298)^2)] \quad \text{(Roehl et al.[7])}$$

$$\ln \sigma(\lambda, T) = \ln \sigma(\lambda, 298\ K) + B(\lambda)(T–298) \quad \text{(Rattigan et al.[5])}$$

Both expressions reproduce the experimental data well and the $a_1(\lambda)$, $a_2(\lambda)$, and $B(\lambda)$ parameters are included in Table 4H-13.

Photolysis Quantum Yield and Product Studies: The photolysis quantum yield for C_2H_5I is expected to be unity for wavelengths above the dissociation threshold. Uma and Das[8-10] have reported quantum yields for $I^*(^2P_{1/2})$ atom formation, $\Phi(I^*)$, at wavelengths between 222 and 305 nm to be 0.57 ± 0.02, 0.72 ± 0.02, 060 ± 0.02, and 0.39 ± 0.02 at 222, 266, 280, and ~305 nm, respectively. Gedanken[2] report $\Phi(I^*) = 0.78 \pm 0.07$ at 248 nm.

Brewer et al.[1] report $\Phi(I^*) = 0.68 \pm 0.02$ at 248 nm. Kang et al.[3] report $\Phi(I^*) = 0.22$ at 304 nm. Quantum yields for $I(^2P_{3/2})$ atom formation, $\Phi(I)$, can be derived from $\Phi(I) = 1 - \Phi(I^*)$. Rebbert et al.[6] report that the quantum yield at 147 nm for the overall process $C_2H_5I + h\nu \rightarrow C_2H_4 + H + I$ to be 0.75.

Table 4H-13. Recommended Absorption Cross Sections of C_2H_5I at 298 K and Temperature Coefficients

λ (nm)	$10^{20}\,\sigma$ (cm^2)	$10^3\,a_1$ (K^{-1})	$10^5\,a_2$ (K^{-2})	$10^3\,B$ (K^{-1})
205	11.9	6.38	3.15	–
210	4.22	4.07	6.28	–
215	4.56	4.93	6.57	–
220	6.18	4.06	5.70	–
225	9.09	2.81	3.81	–
230	14.3	2.62	3.83	–
235	23.2	1.28	2.17	–0.27
240	41.7	0.876	1.96	–0.40
245	69.3	0.233	1.62	–0.62
250	99.3	–0.111	1.58	–0.79
255	119.7	–1.03	0.606	–0.82
260	121.8	–1.48	–0.0332	–0.75
265	105.9	–1.09	1.2×10^{-6}	–0.44
270	80.6	–0.538	–0.257	0.36
275	54.4	0.770	0.0299	1.23
280	33.5	2.01	0.110	2.36
285	19.1	3.85	0.962	3.61
290	10.3	5.47	1.65	4.83
295	5.38	7.00	2.52	6.33
300	2.78	8.56	4.11	7.48
305	1.44	9.31	4.89	8.08
310	0.777	10.56	6.87	7.55
315	0.416	10.83	6.81	7.92
320	0.227	11.98	9.76	8.27
325	0.127	12.98	11.3	8.81
330	0.0743	14.56	17.5	9.30
335	0.0403	18.81	24.6	10.20
340	0.0246	13.90	9.08	11.16
345	0.0133	18.86	22.1	12.41
350	0.00840	20.19	20.1	11.28
355	0.00488	–7.04	–40.5	12.20

Note:

Absorption cross sections

205–230 nm: Roehl et al.[7]

235–355 nm: mean of data from Roehl et al.[7] and Rattigan et al.[5]

Temperature coefficients

$a_1(\lambda)$ and $a_2(\lambda)$: Roehl et al.[7] (223–298 K), $\sigma(\lambda, T) = \sigma(298\text{ K})\,[1 + a_1(\lambda)(T–298) + a_2(\lambda)(T–298)^2]$

$B(\lambda)$: Rattigan et al.[5] (243–333 K), $\ln \sigma(\lambda, T) = \ln \sigma(\lambda, 298\text{ K}) + B(\lambda)(T–298)$

(1) Brewer, P.; Das, P.; Ondrey, G.; Bersohn, R. Measurement of the relative populations of $I(^2P_{1/2}{}^0)$ and $I(^2P_{3/2}{}^0)$ by laser induced vacuum ultraviolet fluorescence. *J. Chem. Phys.* **1983**, *79*, 720-723, doi:10.1063/1.445820.

(2) Gedanken, A. The magnetic circular dichroism of the *A* band in CF_3I, C_2H_5I and *t*-BuI. *Chem. Phys. Lett.* **1987**, *137*, 462-466, doi:10.1016/0009-2614(87)80234-8.

(3) Kang, W. K.; Jung, K. W.; Kim, D.-C.; Jung, K.-H. Photodissociation of alkyl iodides and CF_3I at 304 nm: Relative populations of $I(^2P_{1/2})$ and $I(^2P_{3/2})$ and dynamics of curve crossing. *J. Chem. Phys.* **1996**, *104*, 5815-5820, doi:10.1063/1.471313.

(4) Porret, D.; Goodeve, C. F. The continuous absorption spectra of alkyl iodides and alkyl bromides and their quantal interpretation. *Proc. Roy. Soc. Lond. A* **1938**, *165*, 31-42, doi:10.1098/rspa.1938.0042.

(5) Rattigan, O. V.; Shallcross, D. E.; Cox, R. A. UV absorption cross sections and atmospheric photolysis rates of CF_3I, CH_3I, C_2H_5I and CH_2ICl. *J. Chem. Soc. Faraday Trans.* **1997**, *93*, 2839-2846, doi:10.1039/a701529a.
(6) Rebbert, R. E.; Lias, S. G.; Ausloos, P. Photolysis of alkyl iodides at 147.0 nm. The reaction $H + C_nH_{2n+1}I \rightarrow HI + C_nH_{2n+1}$. *Int. J. Chem. Kinet.* **1973**, *5*, 893-908, doi:10.1002/kin.550050515.
(7) Roehl, C. M.; Burkholder, J. B.; Moortgat, G. K.; Ravishankara, A. R.; Crutzen, P. J. Temperature dependence of UV absorption cross sections and atmospheric implications of several alkyl iodides. *J. Geophys. Res.* **1997**, *102*, 12819-12829, doi:10.1029/97JD00530.
(8) Uma, S.; Das, P. K. Dynamics of $I^*(^2P_{1/2})$ production in the ultraviolet photodissociation of alkyl iodides. *Can. J. Chem.* **1994**, *72*, 865-869, doi:10.1139/v94-113.
(9) Uma, S.; Das, P. K. I* production from *n*-alkyl iodides at 222 nm. *Chem. Phys. Lett.* **1995**, *241*, 335-338, doi:10.1016/0009-2614(95)00661-M.
(10) Uma, S.; Das, P. K. Production of $I^*(^2P_{1/2})$ in the ultraviolet photodissociation of α-branched alkyl iodides. *J. Chem. Phys.* **1996**, *104*, 4470-4474, doi:10.1063/1.471199.
(11) Young, C. J.; Hurley, M. D.; Wallington, T. J.; Mabury, S. A. Atmospheric chemistry of 4:2 fluorotelomer iodide ($n\text{-}C_4F_9CH_2CH_2I$): Kinetics and products of photolysis and reaction with OH radicals and Cl atoms. *J. Phys. Chem. A* **2008**, *112*, 13542-13558, doi:10.1021/jp807322x.
(12) Zhang, L.; Fuss, W.; Kompa, K. L. Bond-selective photodissociation of CX (X = Br, I) in $XC_2H_4C_2F_4X$. *Chem. Phys.* **1990**, *144*, 289-297, doi:10.1016/0301-0104(90)80092-C.

H14. CH_3CHI_2 (1,1-diiodoethane)

Back to Index

$CH_3CHI_2 + h\nu \rightarrow$ Products (1)

(Recommendation: 02-25, Note: 10-6, Evaluated: 10-6)

Absorption Cross Sections: The UV absorption spectrum of CH_3CHI_2, 1,1-diiodoethane, has been measured at 298 K by Schmitt and Comes[1] over the wavelength range 220–360 nm. The continuous spectrum consists of several overlapping transitions with maxima at <220 nm and peaks at 250 and 290 nm. A weaker band appears as a shoulder in the spectrum near 320 nm. The recommended cross sections in Table 4H-14 are taken from Schmitt and Comes.[1]

Photolysis Quantum Yield and Product Studies: The photolysis quantum yield for CH_3CHI_2 is expected to be unity for wavelengths above the dissociation threshold.

Table 4H-14. Recommended Absorption Cross Sections of CH_3CHI_2 at 298 K

λ (nm)	10^{20} σ (cm^2)	λ (nm)	10^{20} σ (cm^2)
220	304	295	366
225	240	300	339
230	181	305	305
235	144	310	273
240	138	315	247
245	151	320	222
250	157	325	201
255	143	330	175
260	133	335	138
265	145	340	107
270	183	345	75.7
275	243	350	49.3
280	304	355	31.7
285	352	360	19.1
290	374		

Note:
Schmitt and Comes[1]

(1) Schmitt, G.; Comes, F. J. Photolysis of CH_2I_2 and $1,1\text{-}C_2H_4I_2$ at 300 nm. *J. Photochem.* **1980**, *14*, 107-123, doi:10.1016/0047-2670(80)80002-5.

H15. $CH_3CH_2CH_2I$ (1-iodopropane)

Back to Index

$CH_3CH_2CH_2I + h\nu \rightarrow C_3H_7 + I(^2P_{3/2})$ (1)

$\rightarrow C_3H_7 + I^*(^2P_{1/2})$ (2)

(Recommendation: 25-1, Note: 25-1, Evaluated: 25-1)

Absorption Cross Sections: The UV/VUV absorption spectrum of 1-C_3H_7I, 1-iodopropane, has been measured by Boschi and Salahub[1] (120.7–299.5 nm, graphical data) at 298 K and over the wavelength range 205–335 nm by Roehl et al.[5] at 223, 248, 273, and 298 K. The continuous absorption spectrum peaks at 255 nm with evidence for another absorption band at wavelengths <205 nm. A VUV absorption cross section of 7×10^{-18} cm^2 $molecule^{-1}$ at 147 nm has been reported by Rebbert et al.[4] The Boschi and Salahub UV cross sections are systematically lower than those of Roehl et al. The recommended room temperature cross sections for 1-C_3H_7I in Table 4H-15 are taken from Roehl et al.[5]

The absorption cross section near the peak increases with decreasing temperature. The cross sections in the long wavelength tail decrease with decreasing temperature. Roehl et al.[5] parameterized the temperature dependence using the empirical expression:

$$\sigma(\lambda, T) = \sigma(298\ K)\ [1 + a_1(\lambda)(T–298) + a_2(\lambda)(T–298)^2]$$

The $a_1(\lambda)$ and $a_2(\lambda)$ parameters are included in Table 4H-15.

Boschi and Salahub[1] reported the 1-C_3H_7I spectrum in the Lyman-α wavelength region. On the basis of this single study, a Lyman-α cross section of 7.1×10^{-17} cm^2 $molecule^{-1}$ is recommended.

Photolysis Quantum Yield and Product Studies: The photolysis quantum yield for 1-C_3H_7I is expected to be unity for wavelengths above the dissociation threshold. Uma and Das[6,7] report quantum yields for $I^*(^2P_{1/2})$ atom formation, $\Phi(I^*)$, at several photolysis wavelengths to be 0.54 ± 0.02, 0.66 ± 002, 0.56 ± 0.02, and 0.35 ± 0.02 at 222, 266, 280, and ~305 nm, respectively. Brewer et al.[2] report $\Phi(I^*) = 0.60 \pm 0.02$ at 248 nm. Kang et al.[3] report $\Phi(I^*) = 0.20$ at 304 nm. Quantum yields for $I(^2P_{3/2})$ atom formation, $\Phi(I)$, can be derived from $\Phi(I) = 1–\Phi(I^*)$. At 147 nm, Rebbert et al.[4] report quantum yields for the overall processes 1-$C_3H_7I + h\nu \rightarrow C_3H_6 + H + I$ and 1-$C_3H_7I + h\nu \rightarrow CH_3 + C_2H_4 + I$ to be 0.38 and 0.47, respectively.

Table 4H-15. Recommended Absorption Cross Sections of C_3H_7I at 298 K and Temperature Coefficients

λ (nm)	1-C_3H_7I			2-C_3H_7I		
	10^{20} σ (cm^2)	10^3 a_1 (K^{-1})	10^5 a_2 (K^{-2})	10^{20} σ (cm^2)	10^3 a_1 (K^{-1})	10^5 a_2 (K^{-2})
205	15.6	7.60	4.37	44.9	15.14	8.46
210	5.05	0.283	1.57	4.53	7.84	7.23
215	5.14	–1.49	–2.46	3.57	4.96	5.08
220	6.84	–1.59	–2.97	4.20	1.55	1.27
225	10.4	–0.891	–2.14	6.45	2.21	1.99
230	17.7	–0.375	–1.26	11.0	1.60	1.80
235	32.8	–0.311	–1.04	20.4	0.480	0.681
240	58.1	–0.611	–0.804	38.2	–0.333	0.121
245	91.9	–0.849	–0.609	66.7	–0.680	0.0947
250	124	–1.22	–0.611	102	–0.795	0.289
255	141	–1.55	–0.776	133	–0.966	0.570
260	136	–1.44	–0.867	148	–1.14	0.512
265	113	–1.02	–1.04	143	–0.589	0.824
270	82.2	–0.306	–1.16	120	–0.439	0.281
275	53.4	0.524	–1.50	90.2	0.792	0.873
280	32.0	1.68	–1.66	61.4	1.65	0.466
285	18.1	3.08	–1.44	38.6	2.88	0.534
290	9.96	5.56	0.812	22.6	4.13	0.559
295	5.42	6.76	2.05	12.8	5.71	1.04
300	2.96	7.16	2.90	6.94	7.20	1.93
305	1.63	6.90	3.20	3.73	8.19	2.33
310	0.945	7.10	4.01	2.04	8.75	2.81
315	0.532	5.59	2.78	1.09	8.49	2.25
320	0.301	3.68	0.0140	0.627	10.79	4.36
325	0.177	4.23	0.0238	0.348	9.54	2.76
330	0.110	11.40	12.3	0.202	10.99	5.94
335	0.0627	15.76	25.8	0.115	12.37	7.58
340	–	–	–	0.0688	13.69	12.2
345	–	–	–	0.0402	16.32	17.1
350	–	–	–	0.0253	18.50	24.7
355	–	–	–	0.0150	19.41	24.3
360	–	–	–	0.0105	18.61	13.9
365	–	–	–	0.00666	29.85	50.9
370	–	–	–	0.00479	37.24	76.8
375	–	–	–	0.00535	36.71	80.7
380	–	–	–	0.00530	22.00	40.0

Note:
Roehl et al.[5]

(1) Boschi, R. A.; Salahub, D. R. The far ultra-violet spectra of some 1-iodoalkanes. *Mol. Phys.* **1972**, *24*, 289-299, doi:10.1080/00268977200101451.

(2) Brewer, P.; Das, P.; Ondrey, G.; Bersohn, R. Measurement of the relative populations of $I(^2P_{1/2}{}^0)$ and $I(^2P_{3/2}{}^0)$ by laser induced vacuum ultraviolet fluorescence. *J. Chem. Phys.* **1983**, *79*, 720-723, doi:10.1063/1.445820.

(3) Kang, W. K.; Jung, K. W.; Kim, D.-C.; Jung, K.-H. Photodissociation of alkyl iodides and CF_3I at 304 nm: Relative populations of $I(^2P_{1/2})$ and $I(^2P_{3/2})$ and dynamics of curve crossing. *J. Chem. Phys.* **1996**, *104*, 5815-5820, doi:10.1063/1.471313.

(4) Rebbert, R. E.; Lias, S. G.; Ausloos, P. Photolysis of alkyl iodides at 147.0 nm. The reaction $H + C_nH_{2n+1}I \rightarrow HI + C_nH_{2n+1}$. *Int. J. Chem. Kinet.* **1973**, *5*, 893-908, doi:10.1002/kin.550050515.

(5) Roehl, C. M.; Burkholder, J. B.; Moortgat, G. K.; Ravishankara, A. R.; Crutzen, P. J. Temperature dependence of UV absorption cross sections and atmospheric implications of several alkyl iodides. *J. Geophys. Res.* **1997**, *102*, 12819-12829, doi:10.1029/97JD00530.

(6) Uma, S.; Das, P. K. Dynamics of I*($^2P_{1/2}$) production in the ultraviolet photodissociation of alkyl iodides. *Can. J. Chem.* **1994**, *72*, 865-869, doi:10.1139/v94-113.
(7) Uma, S.; Das, P. K. Production of I*($^2P_{1/2}$) in the ultraviolet photodissociation of α-branched alkyl iodides. *J. Chem. Phys.* **1996**, *104*, 4470-4474, doi:10.1063/1.471199.

H16. CH_3CHICH_3 (2-iodopropane)

Back to Index

$CH_3CHICH_3 + h\nu \rightarrow C_3H_7 + I(^2P_{3/2})$ (1)
$\rightarrow C_3H_7 + I^*(^2P_{1/2})$ (2)

(Recommendation: 02-25, Note: 10-6, Evaluated: 10-6)

Absorption Cross Sections: The UV absorption spectrum of 2-C_3H_7I, 2-iodopropane, has been measured by Roehl et al.[4] (223–298 K and 205–380 nm) and Phillips et al.[2] (298 K, 235–305 nm). Phillips et al.[2] also report an absorption spectrum of 2-C_3H_7I in a cyclohexane solution. The continuous absorption spectrum peaks at 260 nm with evidence for another absorption band at wavelengths <205 nm. The gas-phase data reported by Phillips et al.[2] are larger by 30–70% over the entire absorption band than the data from Roehl et al.[4] A room temperature cross section of 7.59×10^{-17} cm^2 molecule^{-1} at 147 nm has been reported by Rebbert et al.[3] The recommended room temperature values for 2-C_3H_7I in Table 4H-15 are taken from Roehl et al.[4]

The absorption cross section near the peak increases with decreasing temperature. The cross sections in the long-wavelength tail decrease with decreasing temperature. Roehl et al.[4] parameterized the temperature dependence using the empirical expression:

$$\sigma(\lambda, T) = \sigma(298\ K)\ [1 + a_1(\lambda)(T–298) + a_2(\lambda)(T–298)^2]$$

The $a_1(\lambda)$ and $a_2(\lambda)$ parameters are included in Table 4H-15.

Photolysis Quantum Yield and Product Studies: The photolysis quantum yield for 2-C_3H_7I is expected to be unity for wavelengths above the dissociation threshold. Uma and Das[5] report quantum yields for I*($^2P_{1/2}$) atom formation, Φ(I*), at several wavelengths to be 0.40 ± 0.02, 0.44 ± 0.03, and 0.19 ± 0.02 at 222, 266, and ~305 nm, respectively. Brewer et al.[1] report Φ(I*) = 0.26 ± 0.02 at 248 nm. Quantum yields for I($^2P_{3/2}$) atom formation, Φ(I), can be derived from Φ(I) = 1–Φ(I*). At 147 nm, Rebbert et al.[3] report quantum yields for the overall processes 2-$C_3H_7I + h\nu \rightarrow C_3H_6 + H + I$ and 2-$C_3H_7I + h\nu \rightarrow CH_3 + C_2H_4 + I$ to be 0.80 and 0.07.

(1) Brewer, P.; Das, P.; Ondrey, G.; Bersohn, R. Measurement of the relative populations of I($^2P_{1/2}^0$) and I($^2P_{3/2}^0$) by laser induced vacuum ultraviolet fluorescence. *J. Chem. Phys.* **1983**, *79*, 720-723, doi:10.1063/1.445820.
(2) Phillips, D. L.; Myers, A. B.; Valentini, J. J. Investigation of solvation effects on short-time photodissociation dynamics of alkyl iodides. *J. Phys. Chem.* **1992**, *96*, 2039-2044, doi:10.1021/j100184a006.
(3) Rebbert, R. E.; Lias, S. G.; Ausloos, P. Photolysis of alkyl iodides at 147.0 nm. The reaction H + $C_nH_{2n+1}I \rightarrow HI + C_nH_{2n+1}$. *Int. J. Chem. Kinet.* **1973**, *5*, 893-908, doi:10.1002/kin.550050515.
(4) Roehl, C. M.; Burkholder, J. B.; Moortgat, G. K.; Ravishankara, A. R.; Crutzen, P. J. Temperature dependence of UV absorption cross sections and atmospheric implications of several alkyl iodides. *J. Geophys. Res.* **1997**, *102*, 12819-12829, doi:10.1029/97JD00530.
(5) Uma, S.; Das, P. K. I* production from *n*-alkyl iodides at 222 nm. *Chem. Phys. Lett.* **1995**, *241*, 335-338, doi:10.1016/0009-2614(95)00661-M.

H17. *n*-C_4H_9I (*n*-butyl iodide)

Back to Index

n-$C_4H_9I + h\nu \rightarrow C_4H_9 + I(^2P_{3/2})$ (1)
$\rightarrow C_4H_9 + I^*(^2P_{1/2})$ (2)

(Recommendation: 25-1, Note: 25-1, Evaluated: 25-1)

Absorption Cross Sections: UV/VUV absorption cross sections for *n*-C_4H_9I, *n*-butyl iodide, have been reported by Boschi and Salahub[1] (120–301 nm, graphical data), which is the only study available.. Further spectrum measurements are needed before a recommendation is given.

Photolysis Quantum Yield and Product Studies: The quantum yield of *n*-C_4H_9I for UV photolysis is expected to be unity. Quantum yields for I*($^2P_{1/2}$) atom formation has been reported by Uma and Das[4,5] to be 0.51 ± 0.02, 0.64 ± 0.03, 0.50 ± 0.03, and 0.30 ± 0.02 at 222, 266, 280, and ~305 nm, respectively. Brewer et al.[2] and

Kang et al.[3] have reported quantum yields for I*($^2P_{1/2}$) of 0.53 ± 0.03 and = 0.14 at 248 nm and 304 nm, respectively.

(1) Boschi, R. A.; Salahub, D. R. The far ultra-violet spectra of some 1-iodoalkanes. *Mol. Phys.* **1972**, *24*, 289-299, doi:10.1080/00268977200101451.

(2) Brewer, P.; Das, P.; Ondrey, G.; Bersohn, R. Measurement of the relative populations of I($^2P_{1/2}^0$) and I($^2P_{3/2}^0$) by laser induced vacuum ultraviolet fluorescence. *J. Chem. Phys.* **1983**, *79*, 720-723, doi:10.1063/1.445820.

(3) Kang, W. K.; Jung, K. W.; Kim, D.-C.; Jung, K.-H. Photodissociation of alkyl iodides and CF_3I at 304 nm: Relative populations of I($^2P_{1/2}$) and I($^2P_{3/2}$) and dynamics of curve crossing. *J. Chem. Phys.* **1996**, *104*, 5815-5820, doi:10.1063/1.471313.

(4) Uma, S.; Das, P. K. Dynamics of I*($^2P_{1/2}$) production in the ultraviolet photodissociation of alkyl iodides. *Can. J. Chem.* **1994**, *72*, 865-869, doi:10.1139/v94-113.

(5) Uma, S.; Das, P. K. Production of I*($^2P_{1/2}$) in the ultraviolet photodissociation of α-branched alkyl iodides. *J. Chem. Phys.* **1996**, *104*, 4470-4474, doi:10.1063/1.471199.

H18. $(CH_3)_2CHCH_2I$ (*iso*-butyl iodide)

Back to Index

$$(CH_3)_2CHCH_2I + h\nu \rightarrow (CH_3)_2CHCH_2 + I(^2P_{3/2}) \quad (1)$$
$$\rightarrow (CH_3)_2CHCH_2 + I^*(^2P_{1/2}) \quad (2)$$

(Recommendation: 02-25, Note: 25-1, Evaluated: 10-6)

Absorption Cross Sections: UV/VUV absorption cross sections for $(CH_3)_2CHCH_2I$, *iso*-butyl iodide, have been reported by Boschi and Salahub[1] (~120–300 nm, graphical data), which is the only study available. Further spectrum measurements are needed before a recommendation is given.

Photolysis Quantum Yield and Product Studies: The quantum yield of *iso*-C_4H_9I for UV photolysis is expected to be unity. The I*($^2P_{1/2}$) atom quantum yield, Φ(I*($^2P_{1/2}$), has been shown to be wavelength dependent with lower yields at longer photolysis wavelengths. Uma and Das[3] reported Φ(I*($^2P_{1/2}$) values of 0.71 ± 0.01, 0.56 ± 0.03, and 0.35 ± 0.02, at 266, 280, and ~305 nm, respectively. Brewer et al.[2], however, reported a significantly lower value of Φ(I*($^2P_{1/2}$)) at 248 nm, 0.20 ± 0.02.

(1) Boschi, R. A.; Salahub, D. R. The far ultraviolet spectra of some branched chain iodo-alkanes, iodo-cyclo-alkanes, fluoro-iodo-alkanes and iodoalkenes. *Mol. Phys.* **1972**, *24*, 735-752, doi:10.1080/00268977200101871.

(2) Brewer, P.; Das, P.; Ondrey, G.; Bersohn, R. Measurement of the relative populations of I($^2P_{1/2}^0$) and I($^2P_{3/2}^0$) by laser induced vacuum ultraviolet fluorescence. *J. Chem. Phys.* **1983**, *79*, 720-723, doi:10.1063/1.445820.

(3) Uma, S.; Das, P. K. Production of I*($^2P_{1/2}$) in the ultraviolet photodissociation of α-branched alkyl iodides. *J. Chem. Phys.* **1996**, *104*, 4470-4474, doi:10.1063/1.471199.

H19. $(CH_3)_3CI$ (*tert*-butyl iodide)

Back to Index

$$(CH_3)_3CI + h\nu \rightarrow (CH_3)_3C + I(^2P_{3/2}) \quad (1)$$
$$\rightarrow (CH_3)_3C + I^*(^2P_{1/2}) \quad (2)$$

(Recommendation: 02-25, Note: 10-6, Evaluated: 10-6)

Absorption Cross Sections: The UV absorption spectrum of *tert*-C_4H_9I, *tert*-butyl iodide, at 323 K has been reported by Phillips et al.[5] (230–310 nm). The spectrum is continuous and shows a single absorption band with a peak cross section of ~2.1×10^{-18} cm^2 molecule^{-1} at ~268 nm. The recommended absorption cross sections in Table 4H-19 were taken from a figure given in Phillips et al.,[5] as reported in the Mainz spectral atlas.[3]

Photolysis Quantum Yield and Product Studies: Quantum yields for I atom formation in the photolysis of *tert*-C_4H_9I have been reported by Kim et al.[4] to be Φ(I($^2P_{3/2}$)+I*($^2P_{1/2}$)) = 0.93 and 0.92 at 277 and 304 nm, respectively. On the basis of this study a *tert*-C_4H_9I photolysis quantum yield of unity is recommended for wavelengths <310 nm. The I*($^2P_{1/2}$) atom quantum yield, Φ(I*($^2P_{1/2}$)), has been shown to be wavelength dependent with lower yields for photolysis at the longer wavelengths. Uma and Das[6] reported values for Φ(I*($^2P_{1/2}$)) of 0.33 ± 0.03, 0.20 ± 0.03, and 0.12 ± 0.03 at 222, 266, and ~305 nm, respectively. Gedanken[2] reported Φ(I*($^2P_{1/2}$)) = 0.41 ± 0.10 for 248 nm photolysis. Brewer et al.[1] reported a much lower value, 0.03 ± 0.02, for photolysis at 248 nm in disagreement with the other studies.

Table 4H-19. Recommended Absorption Cross Sections of $(CH_3)_3CI$ at 323 K

λ (nm)	10^{20} σ (cm^2)
235	28.5
240	42.5
245	64.8
250	98.0
255	140
260	180
265	209
270	211
275	186
280	150
285	116
290	83.0
295	54.0
300	34.0
305	21.5
310	14.0

Note:
Phillips et al.[5]

(1) Brewer, P.; Das, P.; Ondrey, G.; Bersohn, R. Measurement of the relative populations of $I(^2P_{1/2}{}^0)$ and $I(^2P_{3/2}{}^0)$ by laser induced vacuum ultraviolet fluorescence. *J. Chem. Phys.* **1983**, *79*, 720-723, doi:10.1063/1.445820.

(2) Gedanken, A. The magnetic circular dichroism of the *A* band in CF_3I, C_2H_5I and *t*-BuI. *Chem. Phys. Lett.* **1987**, *137*, 462-466, doi:10.1016/0009-2614(87)80234-8.

(3) Keller-Rudek, H.; Moortgat, G. K.; Sander, R.; Sörensen, R. The MPI-Mainz UV/Vis spectral atlas of gaseous molecules of atmospheric interest. *Earth Syst. Sci. Data* **2013**, *5*, 365-373, doi:10.5194/essd-5-365-2013.

(4) Kim, Y. S.; Kang, W. K.; Kim, D.-C.; Jung, K.-H. Photodissociation of *tert*-butyl iodide at 277 and 304 nm: Evidence for direct and indirect dissociation in A-band photolysis of alkyl iodide. *J. Phys. Chem. A* **1997**, *101*, 7576-7581, doi:10.1021/jp970574z.

(5) Phillips, D. L.; Myers, A. B.; Valentini, J. J. Investigation of solvation effects on short-time photodissociation dynamics of alkyl iodides. *J. Phys. Chem.* **1992**, *96*, 2039-2044, doi:10.1021/j100184a006.

(6) Uma, S.; Das, P. K. I* production from *n*-alkyl iodides at 222 nm. *Chem. Phys. Lett.* **1995**, *241*, 335-338, doi:10.1016/0009-2614(95)00661-M.

H20. *n*-$C_5H_{11}I$ (1-iodopentane)

Back to Index

$n\text{-}C_5H_{11}I + h\nu \rightarrow C_5H_{11} + I(^2P_{3/2})$ (1)

$\rightarrow C_5H_{11} + I^*(^2P_{1/2})$ (2)

(Recommendation: 02-25, Note: 25-1, Evaluated: 10-6)

Absorption Cross Sections: UV/VUV absorption cross sections for *n*-$C_5H_{11}I$, 1-iodopentane, have been reported by Boschi and Salahub[1] (~120–300 nm, graphical data), which is the only study available. Further spectrum measurements are needed before a recommendation is given.

Photolysis Quantum Yield and Product Studies: By analogy with other alkyl iodides the photolysis quantum yield of *n*-$C_5H_{11}I$ in the UV is expected to be unity. A quantum yield for $I^*(^2P_{1/2})$ atom formation in the photolysis of *n*-$C_5H_{11}I$ at 222 nm, $\Phi(I^*(^2P_{1/2}))$ of 0.50 ± 0.03 has been reported by Uma and Das.[2]

(1) Boschi, R. A.; Salahub, D. R. The far ultra-violet spectra of some 1-iodoalkanes. *Mol. Phys.* **1972**, *24*, 289-299, doi:10.1080/00268977200101451.

(2) Uma, S.; Das, P. K. Dynamics of $I^*(^2P_{1/2})$ production in the ultraviolet photodissociation of alkyl iodides. *Can. J. Chem.* **1994**, *72*, 865-869, doi:10.1139/v94-113.

H21. CF_3I (trifluoroiodomethane)

Back to Index

$CF_3I + h\nu \rightarrow CF_3 + I(^2P_{3/2})$	227 kJ mol^{-1}	527 nm	(1)
$\rightarrow CF_3 + I^*(^2P_{1/2})$	318 kJ mol^{-1}	376 nm	(2)

(Recommendation: 02-25, Note: 10-6, Evaluated: 10-6)

Absorption Cross Sections: The UV absorption spectrum of CF_3I, trifluoroiodomethane, has been reported in a number of studies as summarized in Table 4H-21-1. The spectrum is continuous between 180 and 400 nm with a strong band centered at 267 nm with a long wavelength tail and a strong band evident at wavelengths <200 nm. The agreement among the room temperature cross section values at wavelengths >200 nm is better than 20% near the absorption maximum. At wavelengths <255 nm and in the range 280–350 nm the agreement is better than 15%. Fahr et al.[6] report the largest peak cross section and Rattigan et al.[14] the smallest. The cross section data from Solomon et al.[16] become increasingly greater than those of Rattigan et al.[14] at the longer wavelengths. The cross section data from Limão-Vieira et al.[13] lie between the data of Solomon et al.[16] and Fahr et al.[6] For wavelengths <230 nm and >310 nm the Limão-Vieira et al.[13] data shows systematic deviations from the other studies. The recommended absorption cross sections in Table 4H-21-2 are taken from the data of Fahr et al.[6] in the range 180–215 nm, the mean of the values reported by Brouwer and Troe,[5] Solomon et al.,[16] and Fahr et al.[6] in the range 220–230 nm, the mean of the values reported by Brouwer and Troe,[5] Solomon et al.,[16] Fahr et al.,[6] and Rattigan et al.[14] in the range 235–310 nm, the mean of the values reported by Solomon et al.,[16] Fahr et al.,[6] and Rattigan et al.[14] in the range 315–350 nm, and the values from Rattigan et al.[14] in the range 355–385 nm.

Table 4H-21-1. Summary of CF_3I Absorption Cross Section Studies

Study	Year	Temperature (K)	Wavelength (nm)	10^{20} σ(267 nm) (cm^2)
Roxlo and Mandl[15]	1980	298	170–230	–
Brouwer and Troe[5]	1981	298, 625, 1050	220–360	~60.5
Bagratashvili et al.[3] and Abel et al.[1,2]	1985	~4000 *	450	–
Solomon et al.[16]	1994	200–298	216–370	64.4
Fahr et al.[6]	1995	218–333	160–350	~70
Rattigan et al.[14]	1997	243–333	235–390	59.5
Limão-Vieira et al.[13]	2003	298	205–325 113–181	66.9

* CF_3I molecules excited by infrared laser absorption

Fahr et al.[6] (160–350 nm) and Limão-Vieira et al.[13] (113–181 nm) reported spectra with pronounced band structure and large absorption cross sections in the short wavelength region. The maximum absorption cross section reported was ~1 × 10^{-16} cm^2 molecule^{-1} at ~160 nm. The spectrum reported by Roxlo and Mandl[15] (170–230 nm) is in poor agreement with the results of Fahr et al.[6] and Limão-Vieira et al.[13]

Studies of the spectrum temperature dependence by Solomon et al.,[16] Fahr et al.,[6] and Rattigan et al.[14] are in qualitative agreement with an increase in the peak absorption cross section and decrease in the long wavelength tail cross sections (>280 nm) with decreasing temperature. The ratio σ(298 K)/σ(~240 K) at 267 nm is ~0.9 and the ratio σ(333 K)/σ(298 K) is ~1. Solomon et al.[16] report a further increase of the peak cross section down to 200 K, whereas Fahr at al.[6] report a slight decrease between 253 and 218 K. The ratio σ(298 K)/σ(~240 K) increases from ~1.0 to ~1.9 between 280 and 340 nm and the ratio σ(333 K)/σ(298 K) is nearly constant at ~1.3. In the wavelength region 160–180 nm, Fahr et al.[6] report a decrease in the absorption cross sections with decreasing temperature. Solomon et al.[16] and Rattigan et al.[14] parameterized the cross section temperature dependence using the empirical expression:

$$\ln \sigma(\lambda, T) = \ln \sigma(\lambda, 298\ K) + B(\lambda)(T–298)$$

which reproduces the experimental data reasonably well. Fahr et al.[6] parameterized their measured cross section wavelength dependence using the empirical expression:

$$\sigma(\lambda) = \sigma_0(\lambda) \exp(–L/\lambda) \text{ for } \lambda > 320 \text{ nm}$$

and the temperature dependence at 300, 310, 320, 330, 340, and 350 nm using:

$$\sigma(T) = \sigma_0(T) \exp(–\theta/T)$$

Their paper should be consulted for the optimized $\sigma_0(\lambda)$, L, $\sigma_0(T)$ and θ parameters. There are some systematic differences in the $B(\lambda)$ coefficients reported by Solomon et al.[16] and Rattigan et al.[14] The $B(\lambda)$ coefficients reported by Rattigan et al.[14] are recommended and listed in Table 4H-21-2.

Photolysis Quantum Yield and Product Studies: The photolysis quantum yield for CF_3I is expected to be unity for wavelengths above the dissociation threshold. CF_3I serves as a model system for the study of the photodynamics of $I^*(^2P_{1/2})$ atom production following UV photolysis of iodine containing molecules. There are a number of studies reporting iodine spin-state quantum yields, $\Phi(I^*(^2P_{1/2}))$ and $\Phi(I(^2P_{3/2}))$. A summary of the quantum yield studies for photolysis in the wavelength range 248–308 nm is given in Table 4H-21-3. Quantum yields for $I(^2P_{3/2})$ atom formation, $\Phi(I)$, can be derived from $\Phi(I) = 1–\Phi(I^*)$.

Table 4H-21-2. Recommended Absorption Cross Sections of CF_3I at 298 K and Temperature Coefficients

λ (nm)	$10^{20}\ \sigma$ (cm^2)	10^3 B (K^{-1})	λ (nm)	$10^{20}\ \sigma$ (cm^2)	10^3 B (K^{-1})
180	3.11	–	285	33.4	0.55
185	0.75	–	290	22.7	1.65
190	0.28	–	295	14.3	2.98
195	0.16	–	300	8.6	4.22
200	0.15	–	305	5.06	5.61
205	0.19	–	310	2.82	6.84
210	0.34	–	315	1.62	7.68
215	0.68	–	320	0.905	8.27
220	1.52	–	325	0.485	8.74
225	2.88	–	330	0.262	9.25
230	5.03	–	335	0.142	9.92
235	8.21	0.16	340	0.0750	10.27
240	13.6	–0.16	345	0.0407	11.71
245	21.8	–0.52	350	0.0210	12.85
250	32.4	–0.86	355	0.0115	13.26
255	45.2	–1.17	360	0.0064	14.65
260	56.9	–1.37	365	0.0036	14.63
265	63.4	–1.43	370	0.002	15.49
270	63.1	–1.30	375	0.0011	17.14
275	56.1	–0.94	380	0.0007	17.66
280	45.1	–0.62	385	0.0004	19.71

Note:

Absorption cross sections

180–215 nm: Fahr et al.[6]

220–230 nm: mean of data from Brouwer and Troe,[5] Solomon et al.,[16] and Fahr et al.[6]

235–310 nm: mean of data from Brouwer and Troe,[5] Solomon et al.,[16] Fahr et al.,[6] and Rattigan et al.[14]

315–350 nm: mean of data from Solomon et al.,[16] Fahr et al.,[6] and Rattigan et al.[14]

355–385 nm: Rattigan et al.[14]

Temperature coefficients

$B(\lambda)$: Rattigan et al.[14] (243–333 K); $\ln \sigma(\lambda, T) = \ln \sigma(\lambda, 298\ K) + B(\lambda)(T–298)$

Table 4H-21-3. Summary of CF_3I Quantum Yield Studies

Study	Year	Photolysis Wavelength (nm)	$\Phi(I^*(^2P_{1/2}))$
Brewer et al.[4]	1983	248	0.89 ± 0.01
Gedanken et al.[10]	1987	248	0.87 ± 0.04
Felder[7]	1991	248	0.88
Furlan et al.[9]	1996	275	0.99 ± 0.01
Kim et al.[12]	1996	277	0.87
Furlan et al.[9]	1996	279	0.91 ± 0.01
		283	0.89 ± 0.01
		290	0.84 ± 0.01
		293	0.81 ± 0.01
		295	0.69 ± 0.01
		296	0.68 ± 0.01
		297	0.63 ±0.02
		298	0.61 ± 0.02
		300	0.47 ± 0.01
		302	0.41 ± 0.01
		303	0.37 ± 0.01
Kang et al.[11]	1996	304	0.69
Felder[8]	1992	308	0.21

(1) Abel, B.; Herzog, B.; Hippler, H.; Troe, J. Infrared multiphoton excitation of CF_3I. I. Transient ultraviolet absorption study of after-pulse dissociation and excited state populations. *J. Chem. Phys.* **1989**, *91*, 890-899, doi:10.1063/1.457140.

(2) Abel, B.; Hippler, H.; Troe, J. Infrared multiphoton excitation dynamics of CF_3I. I. Populations and dissociation rates of highly excited rovibrational states. *J. Chem. Phys.* **1992**, *96*, 8863-8871, doi:10.1063/1.462243.

(3) Bagratashvili, V. N.; Ionov, S. I.; Mishakov, G. V.; Semchishen, V. A. Photolysis of highly vibrationally excited CF_3I molecules by visible laser light. *Chem. Phys. Lett.* **1985**, *115*, 144-148, doi:10.1016/0009-2614(85)80667-9.

(4) Brewer, P.; Das, P.; Ondrey, G.; Bersohn, R. Measurement of the relative populations of $I(^2P_{1/2}{}^0)$ and $I(^2P_{3/2}{}^0)$ by laser induced vacuum ultraviolet fluorescence. *J. Chem. Phys.* **1983**, *79*, 720-723, doi:10.1063/1.445820.

(5) Brouwer, L.; Troe, J. Shock wave study of the UV spectrum of CF_3I. *Chem. Phys. Lett.* **1981**, *82*, 1-4, doi:10.1016/0009-2614(81)85094-4.

(6) Fahr, A.; Nayak, A. K.; Huie, R. E. Temperature dependence of the ultraviolet absorption cross section of CF_3I. *Chem. Phys.* **1995**, *199*, 275-284, doi:10.1016/0301-0104(95)00193-R.

(7) Felder, P. Photodissociation of CF_3I at 248 nm: kinetic energy dependence of the recoil anisotropy. *Chem. Phys.* **1991**, *155*, 435-445, doi:10.1016/0301-0104(91)80119-3.

(8) Felder, P. The influence of the molecular beam temperature on the photodissociation of CF_3I at 308 nm. *Chem. Phys. Lett.* **1992**, *197*, 425-432, doi:10.1016/0009-2614(92)85795-C.

(9) Furlan, A.; Gejo, T.; Huber, J. R. Probing curve crossing by wavelength-dependent recoil anisotropy: The photodissociation of CF_3I at 275-303 nm studied by photofragment translational spectroscopy. *J. Phys. Chem.* **1996**, *100*, 7956-7961, doi:10.1021/jp953130g.

(10) Gedanken, A. The magnetic circular dichroism of the *A* band in CF_3I, C_2H_5I and *t*-BuI. *Chem. Phys. Lett.* **1987**, *137*, 462-466, doi:10.1016/0009-2614(87)80234-8.

(11) Kang, W. K.; Jung, K. W.; Kim, D.-C.; Jung, K.-H. Photodissociation of alkyl iodides and CF_3I at 304 nm: Relative populations of $I(^2P_{1/2})$ and $I(^2P_{3/2})$ and dynamics of curve crossing. *J. Chem. Phys.* **1996**, *104*, 5815-5820, doi:10.1063/1.471313.

(12) Kim, Y. S.; Kang, W. K.; Jung, K.-H. State-selective photofragment imaging of iodine atoms via photodissociation of CF_3I at 277 nm. *J. Chem. Phys.* **1996**, *105*, 551-557, doi:10.1063/1.471908.

(13) Limão-Vieira, P.; Eden, S.; Mason, N. J. Absolute photo-absorption cross sections and electronic state spectroscopy of selected fluorinated hydrocarbons relevant to the plasma processing industry. *Radiation Phys. Chem.* **2003**, *68*, 187-192, doi:10.1016/S0969-806X(03)00278-0.

(14) Rattigan, O. V.; Shallcross, D. E.; Cox, R. A. UV absorption cross sections and atmospheric photolysis rates of CF_3I, CH_3I, C_2H_5I and CH_2ICl. *J. Chem. Soc. Faraday Trans.* **1997**, *93*, 2839-2846, doi:10.1039/a701529a.

(15) Roxlo, C.; Mandl, A. Vacuum ultraviolet absorption cross sections for halogen containing molecules. *J. Appl. Phys.* **1980**, *51*, 2969-2972, doi:10.1063/1.328108.
(16) Solomon, S.; Burkholder, J. B.; Ravishankara, A. R.; Garcia, R. R. Ozone depletion and global warming potentials of CF_3I. *J. Geophys. Res.* **1994**, *99*, 20929-20935, doi:10.1029/94JD01833.

H22. CF_2I_2 (difluorodiiodomethane)

Back to Index

$CF_2I_2 + h\nu \rightarrow CF_2I + I(^2P_{3/2})$			(1)
$\rightarrow CF_2I + I^*(^2P_{1/2})$			(2)
$\rightarrow CF_2 + I(^2P_{3/2}) + I(^2P_{3/2})$	297 kJ mol^{-1}	402 nm	(3)
$\rightarrow CF_2 + I(^2P_{3/2}) + I^*(^2P_{1/2})$	388 kJ mol^{-1}	308 nm	(4)

(Recommendation: 02-25, Note: 10-6, Evaluated: 10-6)

Absorption Cross Sections: The room temperature UV absorption spectrum of CF_2I_2, difluorodiiodomethane, has been measured by Wannenmacher et al.[3] and Baum et al.[1] over the wavelength range 190–420 nm. The spectrum consists of a strong band that peaks at ~195 nm and several weaker overlapping absorption bands between 230 and 400 nm. The overlapping bands suggest transitions corresponding to the different dissociation processes. Numerical cross section data was obtained from the Mainz spectral atlas.[2] The recommended absorption cross sections in Table 4H-22 are from Wannenmacher et al.[3] and were normalized to a peak value of 2.929×10^{-18} cm^2 molecule^{-1} at 300 nm. The peak cross section was derived from five different spectra and has an uncertainty of ±16%.

Photolysis Quantum Yield and Product Studies: The photodissociation of CF_2I_2 has been studied at room temperature and wavelengths 248, 308, 337, and 351 nm by Wannenmacher et al.[3] and Baum et al.[1] These studies report a competition between the radical channel, $CF_2I + I$, and a three body dissociation channel to form $CF_2 + I + I$. The spin-orbit branching ratio, $I^*(^2P_{1/2})/ I(^2P_{3/2})$ was observed to increase at shorter photolysis wavelengths.

Table 4H-22. Recommended Absorption Cross Sections of CF_2I_2 at 294 K

λ (nm)	10^{20} σ (cm^2)	λ (nm)	10^{20} σ (cm^2)
190	3163	310	266.7
195	4616	315	235.6
200	4070	320	198.6
205	2285	325	163.9
210	837.0	330	135.5
215	238.1	335	111.6
220	75.78	340	91.33
225	36.39	345	78.25
230	29.50	350	66.24
235	35.51	355	57.76
240	47.34	360	49.81
245	66.07	365	41.51
250	89.21	370	33.92
255	118.0	375	26.85
260	150.1	380	18.90
265	180.5	385	13.60
270	203.1	390	9.892
275	215.7	395	6.713
280	224.3	400	4.240
285	236.4	405	3.356
290	259.5	410	1.943
295	281.9	415	1.413
300	292.9	420	0.7066
305	288.5		

Note:
Wannenmacher et al.,[3] taken from the Mainz spectral atlas.[2]

(1) Baum, G.; Felder, P.; Huber, J. R. Photofragmentation of CF_2I_2. Competition between radical and three-body dissociation. *J. Chem. Phys.* **1993**, *98*, 1999-2010, doi:10.1063/1.464233.

(2) Keller-Rudek, H.; Moortgat, G. K.; Sander, R.; Sörensen, R. The MPI-Mainz UV/Vis spectral atlas of gaseous molecules of atmospheric interest. *Earth Syst. Sci. Data* **2013**, *5*, 365-373, doi:10.5194/essd-5-365-2013.

(3) Wannenmacher, E. A. J.; Felder, P.; Huber, J. R. The simultaneous three-body dissociation of CF_2I_2. *J. Chem. Phys.* **1991**, *95*, 986-997, doi:10.1063/1.461054.

H23. C_2F_5I (pentafluoroiodoethane)

Back to Index

$C_2F_5I + h\nu$	$\rightarrow C_2F_5 + I(^2P_{3/2})$	207 kJ mol^{-1}	578 nm	(1)
	$\rightarrow C_2F_5 + I^*(^2P_{1/2})$	298 kJ mol^{-1}	402 nm	(2)

(Recommendation: 02-25, Note: 10-6, Evaluated: 10-6)

Absorption Cross Sections: The UV absorption spectrum of C_2F_5I, pentafluoroiodoethane, was measured at 323 K by Zhang et al.[4] over the wavelength range 220–320 nm. The continuous absorption band has a maximum at ~269 nm with a cross section of ~6.7×10^{-19} cm^2 $molecule^{-1}$. Pence et al.[3] report a slightly smaller cross section of 6.39×10^{-19} cm^2 $molecule^{-1}$ at 268 nm and 295 K. The recommended values in Table 4H-23 were obtained from a figure in Zhang et al.,[4] as reported in the Mainz spectral atlas.[2]

Photolysis Quantum Yield and Product Studies: The photolysis quantum yield for C_2H_5I is expected to be unity for wavelengths above the dissociation threshold. Kavita and Das[1] reported quantum yields for $I^*(^2P_{1/2})$ atom formation, Φ(I*), at 266, 288, and ~305 nm to be 0.97 ± 0.03, 0.75 ± 0.03, and 0.83 ± 0.05, respectively. Quantum yields for $I(^2P_{3/2})$ atom formation, Φ(I), can be derived from Φ(I) = 1–Φ(I*).

Table 4H-23. Recommended Absorption Cross Sections of C_2F_5I at 323 K

λ (nm)	10^{20} σ (cm^2)
220	1.95
225	3.27
230	5.60
235	9.40
240	16.0
245	25.3
250	37.5
255	49.8
260	60.0
265	65.5
270	66.8
275	63.2
280	56.1
285	46.5
290	35.3
295	25.0
300	16.3
305	10.4
310	6.4
315	3.9
320	2.3

Note:
Zhang et al.,[4] taken from the Mainz spectral atlas.[2]

(1) Kavita, K.; Das, P. K. Dynamics of I*($^2P_{1/2}$) production from fluorinated alkyl iodides at 266, 280, and ~305 nm. *J. Chem. Phys.* **2000**, *112*, 8426-8431, doi:10.1063/1.481445.

(2) Keller-Rudek, H.; Moortgat, G. K.; Sander, R.; Sörensen, R. The MPI-Mainz UV/Vis spectral atlas of gaseous molecules of atmospheric interest. *Earth Syst. Sci. Data* **2013**, *5*, 365-373, doi:10.5194/essd-5-365-2013.

(3) Pence, W. H.; Baughum, S. L.; Leone, S. R. Laser UV photofragmentation of halogenated molecules. Selective bond dissociation and wavelength-specific quantum yields for excited I($^2P_{1/2}$) and Br($^2P_{1/2}$) atoms. *J. Phys. Chem.* **1981**, *85*, 3844-3851, doi:10.1021/j150625a027.

(4) Zhang, L.; Fuss, W.; Kompa, K. L. Bond-selective photodissociation of CX (X = Br, I) in $XC_2H_4C_2F_4X$. *Chem. Phys.* **1990**, *144*, 289-297, doi:10.1016/0301-0104(90)80092-C.

H24. *n*-C_3F_7I (*n*-heptafluoropropyl iodide)

Back to Index

n-$C_3F_7I + h\nu \rightarrow C_3F_7 + I(^2P_{3/2})$ (1)

$\rightarrow C_3F_7 + I^*(^2P_{1/2})$ (2)

(Recommendation: 25-1, Note: 25-1, Evaluated: 25-1)

Absorption Cross Sections: The UV absorption spectrum of n-C_3F_7I, *n*-heptafluoropropyl iodide, has been measured at room temperature by Haszeldine[2] (229 and 271 nm), Boschi and Salahub[1] (116–315 nm, graphical), Koffend and Leone[4] (265–341 nm), and Pence et al.[5] (180–400 nm). The graphical UV data from Boschi and Salahub are not considered in this recommendation. Pence et al.[5] report a plot (in arbitrary units) that shows an absorption band between ~220 and 340 nm with the maximum at ~268 nm. They report absolute absorption cross sections at 248, 268, and 308 nm. The data for 268 and 308 nm are in good agreement with the corresponding data reported by Koffend and Leone. The 271 nm cross section from Haszeldine is in good agreement with the data of Koffend and Leone, while the 229 value is greater. The recommended absorption cross sections in Table 4H-24 include the value at 248 nm reported by Pence et al.,[5] the mean of the values from Pence et al. and Koffend and Leone at 268 nm, and values from Koffend and Leone for the wavelength range 270–340 nm (values obtained by interpolation and extrapolation).

Boschi and Salahub[1] have reported the n-C_3F_7I spectrum in the Lyman-α wavelength region. On the basis of this single study, a Lyman-α cross section of 8×10^{-17} cm^2 $molecule^{-1}$ is recommended.

Photolysis Quantum Yield and Product Studies: The quantum yield for n-C_3F_7I at wavelengths above the dissociation threshold is expected to be unity. Kavita and Das[3] reported quantum yields for I*($^2P_{1/2}$) atom formation , Φ(I*), of 0.83 ± 0.02, 0.89 ± 0.03, and 0.90 ± 0.05 at 266, 288, and ~305 nm, respectively. They also report Φ(I*) = 0.83 ± 0.01, 0.80 ± 0.03, and 0.89 ± 0.02 for 2-C_3F_7I at 266, 288, and ~305 nm, respectively. Quantum yields for I($^2P_{3/2}$) atom formation, Φ(I), can be derived from Φ(I) = 1–Φ(I*).

Table 4H-24. Recommended Absorption Cross Sections of *n*-C_3F_7I at 298 K

λ (nm)	10^{20} σ (cm^2)
248	31.0
268	77.3
270	77.0
275	74.0
280	66.5
285	56.2
290	43.7
295	31.8
300	21.3
305	14.2
310	9.2
315	5.5
320	3.3
325	2.0
330	1.2
335	0.70
340	0.42

Note:
248 nm: Pence et al.[5]
268 nm: mean of data from Pence et al.[5] and Koffend and Leone[4]
270–340 nm: Koffend and Leone[4] (interpolation and extrapolation)

(1) Boschi, R. A.; Salahub, D. R. The far ultraviolet spectra of some branched chain iodo-alkanes, iodo-cyclo-alkanes, fluoro-iodo-alkanes and iodoalkenes. *Mol. Phys.* **1972**, *24*, 735-752, doi:10.1080/00268977200101871.

(2) Haszeldine, R. N. Studies in spectroscopy, III. The ultraviolet absorption spectra of halogen-containing aliphatic iodo-compounds, and the relative stability of free halogen-containig alkyl radicals. *J. Chem. Soc.* **1953**, 1764-1771, doi:10.1039/JR9530001764.

(3) Kavita, K.; Das, P. K. Dynamics of I*($^2P_{1/2}$) production from fluorinated alkyl iodides at 266, 280, and ~305 nm. *J. Chem. Phys.* **2000**, *112*, 8426-8431, doi:10.1063/1.481445.

(4) Koffend, J. B.; Leone, S. R. Tunable laser photodissociation: Quantum yield of I*($^2P_{1/2}$) from CH_2I_2. *Chem. Phys. Lett.* **1981**, *81*, 136-141, doi:10.1016/0009-2614(81)85344-4.

(5) Pence, W. H.; Baughum, S. L.; Leone, S. R. Laser UV photofragmentation of halogenated molecules. Selective bond dissociation and wavelength-specific quantum yields for excited I($^2P_{1/2}$) and Br($^2P_{1/2}$) atoms. *J. Phys. Chem.* **1981**, *85*, 3844-3851, doi:10.1021/j150625a027.

H25. *n*-C_4F_9I (perfluorobutyl iodide)

Back to Index

n-$C_4F_9I + h\nu \rightarrow C_4F_9 + I(^2P_{3/2})$ (1)

$\rightarrow C_4F_9 + I^*(^2P_{1/2})$ (2)

(Recommendation: 02-25, Note: 10-6, Evaluated: 10-6)

Absorption Cross Sections: Absorption cross sections for n-C_4F_9I, perfluorobutyl iodide, are not available.

Photolysis Quantum Yield and Product Studies: The quantum yield for n-C_4F_9I at wavelengths above the dissociation threshold is expected to be unity. Kavita and Das[1] report quantum yields for I*($^2P_{1/2}$) atom formation, Φ(I*), of 0.75 ± 0.03, 0.80 ± 0.03, and 0.87 ± 0.02 at 266, 288, and ~305 nm, respectively. Quantum yields for I($^2P_{3/2}$) atom formation, Φ(I), can be derived from Φ(I) = 1–Φ(I*).

(1) Kavita, K.; Das, P. K. Dynamics of I*($^2P_{1/2}$) production from fluorinated alkyl iodides at 266, 280, and ~305 nm. *J. Chem. Phys.* **2000**, *112*, 8426-8431, doi:10.1063/1.481445.

H26. *n*-$C_6F_{13}I$ (perfluorohexyl iodide)

Back to Index

n-$C_6F_{13}I + h\nu$	$\rightarrow C_6F_{13} + I(^2P_{3/2})$	(1)
	$\rightarrow C_6F_{13} + I^*(^2P_{1/2})$	(2)

(Recommendation: 02-25, Note: 10-6, Evaluated: 10-6)

Absorption Cross Sections: Absorption cross sections for *n*-$C_6F_{13}I$, perfluorohexyl iodide, are not available.

Photolysis Quantum Yield and Product Studies: The quantum yield for *n*-$C_6F_{13}I$ at wavelengths above the dissociation threshold is expected to be unity. Kavita and Das[1] report quantum yields for I*($^2P_{1/2}$) atom formation, $\Phi(I^*)$, of 0.82 ± 0.02, 0.74 ± 0.03, and 0.82 ± 0.01 at 266, 288, and ~305 nm, respectively. Quantum yields for I($^2P_{3/2}$) atom formation, $\Phi(I)$, can be derived from $\Phi(I) = 1–\Phi(I^*)$.

(1) Kavita, K.; Das, P. K. Dynamics of I*($^2P_{1/2}$) production from fluorinated alkyl iodides at 266, 280, and ~305 nm. *J. Chem. Phys.* **2000**, *112*, 8426-8431, doi:10.1063/1.481445.

H27. CH_2ICl (chloroiodomethane)

Back to Index

$CH_2ICl + h\nu$	$\rightarrow CH_2Cl + I$	213 kJ mol^{-1}	562 nm	(1)
	$\rightarrow CH_2I + Cl$	327 kJ mol^{-1}	366 nm	(2)

(Recommendation: 02-25, Note: 10-6, Evaluated: 10-6)

Absorption Cross Sections: The UV absorption spectrum of CH_2ICl, chloroiodomethane, at room temperature has been reported by Schmitt and Comes[5] (205–330 nm), Kwok and Phillips[1,2] (192–225 nm and 215–400 nm), Roehl et al.[4] (205–355 nm), and Rattigan et al.[3] (235–390 nm). Kwok and Phillips also measured the CH_2ICl spectrum in cyclohexane solution. Schmitt and Comes[5] and Kwok and Phillips[1,2] have only given their data as plots and are not considered further in this evaluation. Roehl et al.[4] (223–298 K) and Rattigan et al.[3] (243–333 K) have also reported cross section data over a range of temperatures. The room temperature data of Roehl et al. and Rattigan et al. are in good agreement with the values from Rattigan et al. being lower by ≤10% between 240 and 345 nm. The recommended absorption cross sections in Table 4H-27 are from Roehl et al. for the wavelength range 205–230 nm, the mean of the values reported by Roehl et al. and Rattigan et al. for the range 235–355 nm, and from Rattigan et al.[3] for the range 360–390 nm.

The cross section data from Roehl et al. and Rattigan et al. show an increase in absorption cross sections around the absorption peak (~250–285 nm) with decreasing temperature. An opposite effect was reported for wavelengths >285 nm. The peak cross section at ~250 K reported in the two studies agree to within 15%. Roehl et al. and Rattigan et al. parameterized the cross section temperature dependence using different empirical expressions:

$$\sigma(\lambda, T) = \sigma(298\ K)\ [1 + a_1(\lambda)(T–298) + a_2(\lambda)(T–298)^2]\ \text{(Roehl et al.)}$$

$$\ln \sigma(\lambda, T) = \ln \sigma(\lambda, 298\ K) + B(\lambda)(T–298)\ \text{(Rattigan et al.)}$$

Both expressions reproduce the experimental data well and the $a_1(\lambda)$, $a_2(\lambda)$, and $B(\lambda)$ coefficients are given in Table 4H-27.

Photolysis Quantum Yield and Product Studies: The photolysis quantum yield for CH_2ICl is expected to be unity for wavelengths above the dissociation threshold. The quantum yield branching ratio I*($^2P_{1/2}$)/(I($^2P_{3/2}$)+ I*($^2P_{1/2}$)) has been reported by Senapati et al.[7] at 5 wavelengths to be 0.47 ± 0.02 at 222 nm, 0.51 ± 0.01 at 236 nm, 0.51 ± 0.02 at 266 nm, 0.55 ± 0.03 at 280 nm, and 0.38 ± 0.01 at 304 nm. The quantum yield branching ratio Cl*($^2P_{1/2}$)/(Cl($^2P_{3/2}$) + Cl*($^2P_{1/2}$)) was reported by Senapati and Das[6] at 4 wavelengths to be 0.44 at 222 nm, 0.44 at 266 nm, 0.30 at 280 nm, and 0.22 at 304 nm.

Table 4H-27. Recommended Absorption Cross Sections of CH_2ICl at 298 K and Temperature Coefficients

λ (nm)	10^{20} σ (cm^2)	10^3 a_1 (K^{-1})	10^5 a_2 (K^{-2})	10^3 B (K^{-1})
205	132	–1.59	–3.83	–
210	42.1	8.47	3.76	–
215	11.1	6.12	4.30	–
220	7.50	0.232	0.129	–
225	9.76	–0.0938	0.660	–
230	14.9	–0.268	-1.4×10^{-6}	–
235	21.2	–0.512	–0.388	0.24
240	32.1	–0.793	–0.664	0.12
245	45.9	–0.929	–0.758	–0.02
250	63.3	–1.22	–1.13	–0.11
255	84.5	–1.25	–0.998	–0.28
260	106	–1.56	–1.14	–0.44
265	122	–1.05	–0.294	–0.55
270	128	–1.33	–0.593	–0.59
275	121	–1.07	–0.298	–0.47
280	104	–0.618	–0.309	–0.18
285	81.1	–0.326	–0.554	0.32
290	58.5	0.300	–0.711	0.99
295	39.9	1.55	–0.245	1.73
300	25.9	2.38	–0.0473	2.56
305	16.7	3.13	0.394	3.08
310	10.9	3.13	0.303	3.50
315	7.16	2.74	–0.317	3.56
320	4.79	2.44	–0.533	3.46
325	3.23	2.87	0.140	3.44
330	2.14	8.52	–4.21	3.72
335	1.40	2.02	–2.25	4.09
340	0.906	5.20	4.54	4.87
345	0.569	7.05	6.88	5.69
350	0.350	9.12	11.7	6.88
355	0.225	12.27	18.9	8.16
360	0.133	–	–	9.01
365	0.081	–	–	11.06
370	0.048	–	–	11.47
375	0.027	–	–	12.77
380	0.017	–	–	15.14
385	0.008	–	–	19.12
390	0.006	–	–	20.48

Note:

Absorption cross sections (σ)

205–230 nm: Roehl et al.[4]

235–355 nm: mean of data from Roehl et al.[4] and Rattigan et al.[3]

360–390 nm: Rattigan et al.[3]

Temperature coefficients

$a_1(\lambda)$and $a_2(\lambda)$: Roehl et al.[4] (223–298 K); $\sigma(\lambda, T) = \sigma(298\ K)\ [1 + a_1(\lambda)(T–298) + a_2(\lambda)(T–298)^2]$

$B(\lambda)$: Rattigan et al.[3] (243–333 K); $\ln \sigma(\lambda, T) = \ln \sigma(\lambda, 298\ K) + B(\lambda)(T–298)$

(1) Kwok, W. M.; Phillips, D. L. Gas and solution phase chloroiodomethane short-time photodissociation dynamics in the B-band absorption. *Chem. Phys. Lett.* **1997**, *270*, 506-516, doi:10.1016/S0009-2614(97)00400-4.

(2) Kwok, W. M.; Phillips, D. L. Gas-phase chloroiodomethane short-time photodissociation dynamics of the A-band absorption and a comparison with the solution phase short-time photodissociation dynamics. *Mol. Phys.* **1997**, *90*, 315-326, doi:10.1080/002689797172444.

(3) Rattigan, O. V.; Shallcross, D. E.; Cox, R. A. UV absorption cross sections and atmospheric photolysis rates of CF_3I, CH_3I, C_2H_5I and CH_2ICl. *J. Chem. Soc. Faraday Trans.* **1997**, *93*, 2839-2846, doi:10.1039/a701529a.
(4) Roehl, C. M.; Burkholder, J. B.; Moortgat, G. K.; Ravishankara, A. R.; Crutzen, P. J. Temperature dependence of UV absorption cross sections and atmospheric implications of several alkyl iodides. *J. Geophys. Res.* **1997**, *102*, 12819-12829, doi:10.1029/97JD00530.
(5) Schmitt, G.; Comes, F. J. Competitive photodecomposition reactions of chloroiodomethane. *J. Photochem. Photobiol. A: Chem.* **1987**, *41*, 13-30, doi:10.1016/1010-6030(87)80002-3.
(6) Senapati, D.; Das, P. K. $Cl^*(^2P_{1/2})$ production dynamics from chloroiodomethane (CH_2ICl) in the ultraviolet. *Chem. Phys. Lett.* **2004**, *393*, 535-538, doi:10.1016/j.cplett.2004.06.095.
(7) Senapati, D.; Kavita, K.; Das, P. K. Photodissociation dynamics of CH_2ICl at 222, 236, 266, 280, and ~304 nm. *J. Phys. Chem. A* **2002**, *106*, 8479-8482, doi:10.1021/jp026021s.

H28. CH_2BrI (bromoiodomethane)

Back to Index

$CH_2BrI + h\nu$	$\rightarrow CH_2Br + I$	224 kJ mol^{-1}	534 nm	(1)
	$\rightarrow CH_2I + Br$	274 kJ mol^{-1}	437 nm	(2)

(Recommendation: 02-25, Note: 10-6, Evaluated: 10-6)

Absorption Cross Sections: The UV absorption cross sections of CH_2BrI, bromoiodomethane, have been measured at room temperature by Man et al.[1] (180–360 nm) and at 273, 298, and 348 K by Mössinger et al.[2] (215–390 nm). The spectrum exhibits two absorption bands with maxima near 210 and 267 nm that can be assigned to electronic transitions to repulsive states anti-bonding in C–Br and C–I, respectively. The results from the two studies are not in quantitative agreement. Mössinger et al. report room temperature absorption cross sections of 5.7×10^{-18} and 2.3×10^{-18} cm^2 $molecule^{-1}$ at 215 and 270 nm, whereas Man et al. give larger values of ~1×10^{-17} and 3.5×10^{-18} cm^2 $molecule^{-1}$ at these wavelengths (values extracted from a figure in their paper), respectively. The recommended room temperature cross sections in Table 4H-28 are taken from Mössinger et al. The absorption cross sections increase with decreasing temperature around the band maxima and decrease in the long wavelength tail, in the region 220–240 nm, and above 290 nm. Mössinger et al. parameterized the temperature dependence using the empirical relation:

$$\ln \sigma(\lambda, T) = \ln \sigma(\lambda, 298\ K) + B(\lambda)(T–298)$$

The $B(\lambda)$ coefficients are listed in Table 4H-28 (an erroneous B value at 280 nm has been corrected).

Photolysis Quantum Yield and Product Studies: The photolysis quantum yield for wavelengths above the dissociation threshold is expected to be unity.

Table 4H-28. Recommended Absorption Cross Sections of CH_2BrI at 298 K and Temperature Coefficients

λ (nm)	10^{20} σ (cm^2)	10^3 B (K^{-1})
215	567	–2.16
220	423	–0.12
225	269	1.34
230	155	2.06
235	97.9	2.05
240	80.9	1.01
245	93.7	0.00
250	125	–0.58
255	170	–1.16
260	207	–1.29
265	228	–1.45
270	229	–1.73
275	214	–1.22
280	184	–0.94
285	150	–0.53
290	110	0.10
295	82.5	0.63
300	60.6	1.03
305	42.9	1.13
310	31.4	1.41
315	23.1	1.52
320	16.8	1.71
325	11.5	2.36
330	8.02	2.99
335	5.52	3.89
340	3.50	4.79
345	2.24	5.74
350	1.41	6.73
355	0.817	9.47
360	0.498	11.5
365	0.303	11.6
370	0.165	14.3
375	0.098	17.4
380	0.070	–
385	0.039	–
390	0.025	–

Note:
Mössinger et al.[2]
B(λ) values valid for the range 273–348 K; $\ln \sigma(\lambda, T) = \ln \sigma(\lambda, 298\ K) + B(\lambda)(T–298)$

(1) Man, S.-Q.; Kwok, W. M.; Phillips, D. L.; Johnson, A. E. Short-time photodissociation dynamics of A-band and B-band bromoiodomethane in solution: An examination of bond selective electronic excitation. *J. Chem. Phys.* **1996**, *105*, 5842-5857, doi:10.1063/1.472426.

(2) Mössinger, J. C.; Shallcross, D. E.; Cox, R. A. UV-Vis absorption cross-sections and atmospheric lifetimes of CH_2Br_2, CH_2I_2 and CH_2BrI. *J. Chem. Soc. Faraday Trans.* **1998**, *94*, 1391-1396, doi:10.1039/a709160e.

H29. $CHClI_2$ (chlorodiiodomethane)

Back to Index

$CHClI_2 + h\nu \rightarrow$ Products

(New)

Absorption Cross Sections: UV absorption cross sections of $CHClI_2$ (chlorodiiodomethane) have been measured at room temperature by Kapnas et al.[1] (200–450 nm). This is the only data set available. The recommended cross sections given in Table 4H-29 are from Kapnas et al. at 2 nm intervals from their data (reported every 1 nm) between 200–410 nm. An estimated uncertainty factor (2σ) of 1.3 is recommended.

Photolysis Quantum Yield and Product Studies: No recommendation.

Table 4H-29. Recommended Absorption Cross Sections of $CHClI_2$ (chlorodiiodomethane) at 298 K

λ (nm)	10^{20} σ (cm^2)	λ (nm)	10^{20} σ (cm^2)	λ (nm)	10^{20} σ (cm^2)	λ (nm)	10^{20} σ (cm^2)
200	1162	254	149	308	233	362	49.1
202	1453	256	148	310	225	364	47.3
204	1715	258	150	312	219	366	39.7
206	1962	260	150	314	208	368	40.5
208	2085	262	153	316	201	370	36.8
210	2080	264	157	318	190	372	33.0
212	1942	266	156	320	178	374	30.3
214	1744	268	154	322	165	376	28.8
216	1482	270	153	324	157	378	23.5
218	1208	272	150	326	141	380	24.0
220	970	274	147	328	134	382	20.3
222	745	276	150	330	121	384	20.3
224	596	278	147	332	111	386	17.2
226	471	280	151	334	105	388	14.8
228	396	282	158	336	97.0	390	13.1
230	334	284	166	338	91.0	392	11.9
232	300	286	178	340	87.0	394	12.1
234	283	288	191	342	81.0	396	9.02
236	259	290	202	344	74.1	398	9.46
238	242	292	215	346	72.6	400	9.51
240	227	294	221	348	67.8	402	7.45
242	205	296	231	350	64.2	404	8.03
244	190	298	235	352	63.4	406	6.47
246	177	300	238	354	60.6	408	5.44
248	164	302	240	356	58.3	410	5.11
250	153	304	237	358	59.2		
252	149	306	237	360	55.6		

Note:
Taken from Kapnas et al.[1]

(1) Kapnas, K. M.; Toulson, B. W.; Foreman, E. S.; Block, S. A.; Hill, J. G.; Murray, C. UV photodissociation dynamics of CHI_2Cl and its role as a photolytic precursor for a chlorinated Criegee intermediate. *Phys. Chem. Chem. Phys.* **2017**, *19*, 31039-31053, doi:10.1039/c7cp06532a.

H30. CF_2BrCF_2I (1,1,2,2-tetrafluoro-1,2-bromoiodoethane)

Back to Index

$CF_2BrCF_2I + h\nu \rightarrow CF_2BrCF_2 + I$ (1)

$\rightarrow CF_2ICF_2 + Br$ (2)

(Recommendation: 02-25, Note: 10-6, Evaluated: 10-6)

Absorption Cross Sections: The absorption spectrum of CF_2BrCF_2I, 1,1,2,2-tetrafluoro-1,2-bromoiodoethane, has been measured at room temperature over the wavelength range 190–350 nm by Pence et al.[1] The absorption spectrum shows two distinct bands with a maxima near 268 nm that corresponds to excitation in the C–I bond and below 193 nm that corresponds to excitation in the C–Br bond. An absorption cross section of 2.36×10^{-18} cm^2 $molecule^{-1}$ at 193 nm was reported. The recommended cross sections in Table 4H-30 were taken from a figure in Pence et al.[1] and normalized to the quoted 193 nm cross section value.

Photolysis Quantum Yield and Product Studies: The quantum yield for CF_2BrCF_2I photolysis is assumed to be unity for wavelengths <350 nm. A quantum yield for Br atom formation in the excited ($^2P_{1/2}$) spin state of 0.07 ± 0.05 at 193 nm was reported by Pence et al.[1]

Table 4H-30. Recommended Absorption Cross Sections of CF_2BrCF_2I at 298 K

λ (nm)	10^{20} σ (cm^2)
190	256
195	219
200	181
205	138
210	105
215	72.7
220	53.4
225	42.5
230	37.3
235	37.3
240	42.9
245	50.2
250	63.2
255	80.3
260	98.0
265	114
270	119
275	117
280	107
285	92.0
290	73.0
295	54.6
300	39.5
305	27.8
310	18.4
315	11.4
320	5.77
325	3.61
330	1.34

Note:
Pence et al.[1]

(1) Pence, W. H.; Baughum, S. L.; Leone, S. R. Laser UV photofragmentation of halogenated molecules. Selective bond dissociation and wavelength-specific quantum yields for excited I($^2P_{1/2}$) and Br($^2P_{1/2}$) atoms. *J. Phys. Chem.* **1981**, *85*, 3844-3851, doi:10.1021/j150625a027.

4.11 Bibliography – IO_x Photochemistry

Abel, B.; Herzog, B.; Hippler, H.; Troe, J. Infrared multiphoton excitation of CF_3I. I. Transient ultraviolet absorption study of after-pulse dissociation and excited state populations. *J. Chem. Phys.* **1989**, *91*, 890-899, doi:10.1063/1.457140.

Abel, B.; Hippler, H.; Troe, J. Infrared multiphoton excitation dynamics of CF_3I. I. Populations and dissociation rates of highly excited rovibrational states. *J. Chem. Phys.* **1992**, *96*, 8863-8871, doi:10.1063/1.462243.

Ashworth, S. H.; Allan, B. J.; Plane, J. M. C. High resolution spectroscopy of the OIO radical: Implications for the ozone-depleting potential of iodine. *Geophys. Res. Lett.* **2002**, *29*, 1-4, doi:10.1029/2001GL13851.

Atkinson, D. B.; Hudgens, J. W.; Orr-Ewing, A. J. Kinetic studies of the reactions of IO radicals determined by cavity ring-down spectroscopy. *J. Phys. Chem. A* **1999**, *103*, 6173-6180, doi:10.1021/jp9902497.

Atkinson, R.; Baulch, D. L.; Cox, R. A.; Hampson, R. F., Jr.; Kerr, J. A.; Rossi, M. J.; Troe, J. Evaluated kinetic and photochemical data for atmospheric chemistry: Supplement VIII, Halogen species. IUPAC subcommittee on gas kinetic data evaluation for atmospheric chemistry. *J. Phys. Chem. Ref. Data* **2000**, *29*, 167-266, doi:10.1063/1.556058.

Bagratashvili, V. N.; Ionov, S. I.; Mishakov, G. V.; Semchishen, V. A. Photolysis of highly vibrationally excited CF_3I molecules by visible laser light. *Chem. Phys. Lett.* **1985**, *115*, 144-148, doi:10.1016/0009-2614(85)80667-9.

Basco, N.; Hunt, J. E. The recombination of iodine atoms in the presence of nitric oxide. *Int. J. Chem. Kinet.* **1978**, *10*, 733-743, doi:10.1002/kin.550100707.

Bauer, D.; Ingham, T.; Carl, S. A.; Moortgat, G. K.; Crowley, J. N. Ultraviolet-visible absorption cross sections of gaseous HOI and its photolysis at 355 nm. *J. Phys. Chem.* **1998**, *102*, 2857-2864, doi:10.1021/jp9804300.

Baughum, S. L.; Leone, S. R. Photofragmentation infrared emission studies of vibrationally excited free radicals CH_3 and CH_2I. *J. Chem. Phys.* **1980**, *72*, 6531-6545, doi:10.1063/1.439111.

Baum, G.; Felder, P.; Huber, J. R. Photofragmentation of CF_2I_2. Competition between radical and three-body dissociation. *J. Chem. Phys.* **1993**, *98*, 1999-2010, doi:10.1063/1.464233.

Binder, J. L. The continuous absorption spectrum of iodine monochloride in the ultraviolet. *Phys. Rev.* **1938**, *54*, 114-117, doi:10.1103/PhysRev.54.114.

Bloss, W. J.; Rowley, D. M.; Cox, R. A.; Jones, R. L. Kinetics and products of the IO self-reaction. *J. Phys. Chem. A* **2001**, *105*, 7840-7854, doi:10.1021/jp0044936.

Boschi, R. A.; Salahub, D. R. The far ultra-violet spectra of some 1-iodoalkanes. *Mol. Phys.* **1972**, *24*, 289-299, doi:10.1080/00268977200101451.

Boschi, R. A.; Salahub, D. R. The far ultraviolet spectra of some branched chain iodo-alkanes, iodo-cyclo-alkanes, fluoro-iodo-alkanes and iodoalkenes. *Mol. Phys.* **1972**, *24*, 735-752, doi:10.1080/00268977200101871.

Brewer, L.; Tellinghuisen, J. Quantum yield for unimolecular dissociation of I_2 in visible absorption. *J. Chem. Phys.* **1972**, *56*, 3929-3938, doi:10.1063/1.1677797.

Brewer, P.; Das, P.; Ondrey, G.; Bersohn, R. Measurement of the relative populations of $I(^2P_{1/2}{}^0)$ and $I(^2P_{3/2}{}^0)$ by laser induced vacuum ultraviolet fluorescence. *J. Chem. Phys.* **1983**, *79*, 720-723, doi:10.1063/1.445820.

Bridges, L.; White, J. M. Photochemistry of methanethiol at 254 and 214 nm. *J. Phys. Chem.* **1973**, *77*, 295-298, doi:10.1021/j100621a031.

Broske, R. Ph.D. Thesis, University of Wuppertal, Germany, 1999.

Brouwer, L.; Troe, J. Shock wave study of the UV spectrum of CF_3I. *Chem. Phys. Lett.* **1981**, *82*, 1-4, doi:10.1016/0009-2614(81)85094-4.

Campuzano-Jost, P.; Crowley, J. N. Kinetics of the reaction of OH with HI between 246 and 353 K. *J. Phys. Chem. A* **1999**, *103*, 2712-2719, doi:10.1021/jp984321x.

Chichinin, A. I. Measurement of $Cl(^2P_{1/2})$ quantum yield for the photodissociaton of NOCl, ICl, PCl_3, Cl_2O and $COCl_2$. *Chem. Phys. Lett.* **1993**, *209*, 459-463, doi:10.1016/0009-2614(93)80117-8.

Chichinin, A. I.; Chasovnikov, S. A.; Krasnoperov, L. N. The laser photolysis of ICl at 530 nm: A time-resolved LMR study. *Chem. Phys. Lett.* **1987**, *138*, 371-376, doi:10.1016/0009-2614(87)80401-3.

Cox, R. A.; Bloss, W. J.; Jones, R. L.; Rowley, D. M. OIO and the atmospheric cycle of iodine. *Geophys. Res. Lett.* **1999**, *26*, 1857-1860, doi:10.1029/1999GL900439.

Cox, R. A.; Coker, G. B. Absorption cross sections and kinetics of IO in the photolysis of CH_3I in the presence of ozone. *J. Phys. Chem.* **1983**, *87*, 4478-4484, doi:10.1021/j100245a030.

Dillon, T. J.; Tucceri, M. E.; Hölscher, D.; Crowley, J. N. Absorption cross-section of IO at 427.2 nm and 298 K. *J. Photochem. Photobiol. A: Chem.* **2005**, *176*, 3-14, doi:10.1016/j.jphotochem.2005.09.025.

Donohue, T.; Wiesenfeld, J. R. Photodissociation of alkyl iodides. *J. Chem. Phys.* **1975**, *63*, 3130-3135, doi:10.1063/1.431741.

Eden, S.; Limão-Vieira, P.; Hoffmann, S. V.; Mason, N. J. VUV spectroscopy of CH_3Cl and CH_3I. *Chem. Phys.* **2006**, *331*, 232-244, doi:10.1016/j.chemphys.2006.10.021.

Fahr, A.; Nayak, A. K.; Huie, R. E. Temperature dependence of the ultraviolet absorption cross section of CF_3I. *Chem. Phys.* **1995**, *199*, 275-284, doi:10.1016/0301-0104(95)00193-R.

Fahr, A.; Nayak, A. K.; Kurylo, M. J. The ultraviolet absorption cross sections of CH_3I temperature dependent gas and liquid phase measurements. *Chem. Phys.* **1995**, *197*, 195-203, doi:10.1016/0301-0104(95)00172-K.

Felder, P. Photodissociation of CF_3I at 248 nm: kinetic energy dependence of the recoil anisotropy. *Chem. Phys.* **1991**, *155*, 435-445, doi:10.1016/0301-0104(91)80119-3.

Felder, P. The influence of the molecular beam temperature on the photodissociation of CF_3I at 308 nm. *Chem. Phys. Lett.* **1992**, *197*, 425-432, doi:10.1016/0009-2614(92)85795-C.

Felps, W. S.; Rupnik, K.; McGlynn, S. P. Electronic spectroscopy of the cyanogen halides. *J. Phys. Chem.* **1991**, *95*, 639-656, doi:10.1021/j100155a028.

Forte, E.; Hippler, H.; van den Bergh, H. INO thermodynamic properties and ultraviolet spectrum. *Int. J. Chem. Kinet.* **1981**, *13*, 1227-1233, doi:10.1002/kin.550131203.

Furlan, A.; Gejo, T.; Huber, J. R. Probing curve crossing by wavelength-dependent recoil anisotropy: The photodissociation of CF_3I at 275-303 nm studied by photofragment translational spectroscopy. *J. Phys. Chem.* **1996**, *100*, 7956-7961, doi:10.1021/jp953130g.

Gedanken, A. The magnetic circular dichroism of the *A* band in CF_3I, C_2H_5I and *t*-BuI. *Chem. Phys. Lett.* **1987**, *137*, 462-466, doi:10.1016/0009-2614(87)80234-8.

Gedanken, A.; Rowe, M. D. Magnetic circular dichroism spectra of the methyl halides. Resolution of the $n \rightarrow \sigma^*$ continuum. *Chem. Phys. Lett.* **1975**, *34*, 39-43, doi:10.1016/0009-2614(75)80196-5.

Gibson, G. E.; Ramsperger, H. C. Band spectra and dissociation of iodine monochloride. *Phys. Rev.* **1927**, *30*, 598-600, doi:10.1103/PhysRev.30.598.

Gómez Martín, J. C.; Ashworth, S. H.; Mahajan, A. S.; Plane, J. M. C. Photochemistry of OIO: Laboratory study and atmospheric implications. *Geophys. Res. Lett.* **2009**, *36*, L09802, doi:10.1029/2009GL037642.

Gómez Martín, J. C.; Plane, J. M. C. Determination of the O–IO bond dissociation energy by photofragment excitation spectroscopy. *Chem. Phys. Lett.* **2009**, *474*, 79-83, doi:10.1016/j.cplett.2009.04.052.

Gómez Martín, J. C.; Spietz, P.; Burrows, J. P. Spectroscopic studies of the I_2/O_3 photochemistry Part 1: Determination of the absolute absorption cross sections of iodine oxides of atmospheric relevance. *J. Photochem. Photobiol. A: Chem.* **2005**, *176*, 15-38, doi:10.1016/j.jphotochem.2005.09.024.

Goodeve, C. F.; Taylor, A. W. C. The continuous absorption spectrum of hydrogen iodide. *Proc. Roy. Soc. London* **1936**, *A 154*, 181-187, doi:10.1098/rspa.1936.0044.

Harwood, M. H.; Burkholder, J. B.; Hunter, M.; Fox, R. W.; Ravishankara, A. R. Absorption cross sections and self-reaction kinetics of the IO radical. *J. Phys. Chem. A* **1997**, *101*, 853-863, doi:10.1021/jp962429b.

Haszeldine, R. N. Studies in spectroscopy, III. The ultraviolet absorption spectra of halogen-containing aliphatic iodo-compounds, and the relative stability of free halogen-containig alkyl radicals. *J. Chem. Soc.* **1953**, 1764-1771, doi:10.1039/JR9530001764.

Haugen, H. K.; Weitz, E.; Leone, S. R. Accurate quantum yields by laser gain vs absorption spectroscopy: Investigation of Br/Br* channels in photofragmentation of Br_2 and IBr. *J. Chem. Phys.* **1964**, *83*, 3402-3412, doi:10.1063/1.449145.

Himmelmann, S.; Orphal, J.; Bovensmann, H.; Richter, A.; Ladstätter-Weissenmayer, A.; Burrows, J. P. First observation of the OIO molecule by time-resolved flash photolysis absorption spectroscopy. *Chem. Phys. Lett.* **1996**, *251*, 330-334, doi:10.1016/0009-2614(96)00114-5.

Huebert, B. J.; Martin, R. M. Gas-phase far-ultraviolet absorption spectrum of hydrogen bromide and hydrogen iodide. *J. Phys. Chem.* **1968**, *72*, 3046-3048, doi:10.1021/j100854a071.

Ingham, T.; Cameron, M.; Crowley, J. N. Photodissociation of IO (355 nm) and OIO (532 nm): Quantum yields for $O(^3P)$ and $I(^2P_J)$ production. *J. Phys. Chem. A* **2000**, *104*, 8001-8010, doi:10.1021/jp001166p.

Jenkin, M. E.; Cox, R. A. Kinetics study of the reactions $IO + NO_2 + M \rightarrow IONO_2 + M$, $IO + IO \rightarrow$ products, and $I + O_3 \rightarrow IO + O_2$. *J. Phys. Chem.* **1985**, *89*, 192-199, doi:10.1021/j100247a040.

Jenkin, M. E.; Cox, R. A.; Mellouki, A.; Le Bras, G.; Poulet, G. Kinetics of the reaction of iodine atoms with HO_2 radicals. *J. Phys. Chem.* **1990**, *94*, 2927-2934, doi:10.1021/j100370a036.

Jenkin, M. E.; Murrells, T. P.; Shalliker, S. J.; Hayman, G. D. Kinetics and product study of the self-reactions of allyl and allyl peroxy radicals at 296 K. *J. Chem. Soc. Faraday Trans.* **1993**, *89*, 433-446, doi:10.1039/ft9938900433.

Joseph, D. M.; Ashworth, S. H.; Plane, J. M. C. The absorption cross-section and photochemistry of OIO. *J. Photochem. Photobiol. A: Chem.* **2005**, *176*, 68-77, doi:10.1016/j.jphotochem.2005.09.003.

Joseph, D. M.; Ashworth, S. H.; Plane, J. M. C. On the photochemistry of $IONO_2$: absorption cross section (240–370 nm) and photolysis product yields at 248 nm. *Phys. Chem. Chem. Phys.* **2007**, *9*, 5599-5607, doi:10.1039/b709465e.

Jung, K.-W.; Ahmadi, T. S.; El-Sayed, M. A. Photofragment translational spectroscopy of ICl at 304 nm. *J. Phys. Chem. A* **1997**, *101*, 6562-6567, doi:10.1021/jp970837p.

Kang, W. K.; Jung, K. W.; Kim, D.-C.; Jung, K.-H. Photodissociation of alkyl iodides and CF_3I at 304 nm: Relative populations of I($^2P_{1/2}$) and I($^2P_{3/2}$) and dynamics of curve crossing. *J. Chem. Phys.* **1996**, *104*, 5815-5820, doi:10.1063/1.471313.

Kapnas, K. M.; Toulson, B. W.; Foreman, E. S.; Block, S. A.; Hill, J. G.; Murray, C. UV photodissociation dynamics of CHI_2Cl and its role as a photolytic precursor for a chlorinated Criegee intermediate. *Phys. Chem. Chem. Phys.* **2017**, *19*, 31039-31053, doi:10.1039/c7cp06532a.

Kavita, K.; Das, P. K. Dynamics of I*($^2P_{1/2}$) production from fluorinated alkyl iodides at 266, 280, and ~305 nm. *J. Chem. Phys.* **2000**, *112*, 8426-8431, doi:10.1063/1.481445.

Keller-Rudek, H.; Moortgat, G. K.; Sander, R.; Sörensen, R. The MPI-Mainz UV/Vis spectral atlas of gaseous molecules of atmospheric interest. *Earth Syst. Sci. Data* **2013**, *5*, 365-373, doi:10.5194/essd-5-365-2013.

Kim, Y. S.; Jung, Y.-J.; Jung, K.-H. Photodissociation of IBr near 267 nm by center-stripe analysis of two-dimensional image. *J. Chem. Phys.* **1997**, *107*, 3805-3812, doi:10.1063/1.474739.

Kim, Y. S.; Kang, W. K.; Jung, K.-H. State-selective photofragment imaging of iodine atoms via photodissociation of CF_3I at 277 nm. *J. Chem. Phys.* **1996**, *105*, 551-557, doi:10.1063/1.471908.

Kim, Y. S.; Kang, W. K.; Kim, D.-C.; Jung, K.-H. Photodissociation of *tert*-butyl iodide at 277 and 304 nm: Evidence for direct and indirect dissociation in A-band photolysis of alkyl iodide. *J. Phys. Chem. A* **1997**, *101*, 7576-7581, doi:10.1021/jp970574z.

Koffend, J. B.; Leone, S. R. Tunable laser photodissociation: Quantum yield of I*($^2P_{1/2}$) from CH_2I_2. *Chem. Phys. Lett.* **1981**, *81*, 136-141, doi:10.1016/0009-2614(81)85344-4.

Kortüm, G.; Friedheim, G. Lichtabsorption und molekularzustand des jods in dampf und lösung. *Z. Naturforsch.* **1947**, *2a*, 20-27.

Kwok, W. M.; Phillips, D. L. Solvation and solvent effects on the short-time photodissociation dynamics of CH_2I_2 from resonance Raman spectroscopy. *J. Chem. Phys.* **1996**, *104*, 2529-2540, doi:10.1063/1.471001.

Kwok, W. M.; Phillips, D. L. Gas and solution phase chloroiodomethane short-time photodissociation dynamics in the B-band absorption. *Chem. Phys. Lett.* **1997**, *270*, 506-516, doi:10.1016/S0009-2614(97)00400-4.

Kwok, W. M.; Phillips, D. L. Gas-phase chloroiodomethane short-time photodissociation dynamics of the A-band absorption and a comparison with the solution phase short-time photodissociation dynamics. *Mol. Phys.* **1997**, *90*, 315-326, doi:10.1080/002689797172444.

Langford, S. R.; Regan, P. M.; Orr-Ewing, A. J.; Ashfold, M. N. R. On the UV photodissociation dynamics of hydrogen iodide. *Chem. Phys.* **1998**, *231*, 245-260, doi:10.1016/S0301-0104(98)00013-5.

Laszlo, B.; Kurylo, M. J.; Huie, R. E. Absorption cross sections, kinetics of formation, and self-reaction of the IO radical produced via the laser photolysis of $N_2O/I_2/N_2$ Mixtures. *J. Phys. Chem.* **1995**, *99*, 11701-11707, doi:10.1021/j100030a013.

Limão-Vieira, P.; Eden, S.; Mason, N. J. Absolute photo-absorption cross sections and electronic state spectroscopy of selected fluorinated hydrocarbons relevant to the plasma processing industry. *Radiation Phys. Chem.* **2003**, *68*, 187-192, doi:10.1016/S0969-806X(03)00278-0.

Locht, R.; Leyh, B.; Jochims, H. W.; Baumgärtel, H. Medium and high resolution vacuum UV photoabsorption spectroscopy of methyl iodide (CH_3I) and its deuterated isotopomers CD_3I and CH_2DI. A Rydberg series analysis. *Chem. Phys.* **2009**, *365*, 109-128, doi:10.1016/j.chemphys.2009.09.025.

Man, S.-Q.; Kwok, W. M.; Phillips, D. L.; Johnson, A. E. Short-time photodissociation dynamics of A-band and B-band bromoiodomethane in solution: An examination of bond selective electronic excitation. *J. Chem. Phys.* **1996**, *105*, 5842-5857, doi:10.1063/1.472426.

Martin, R. M.; Willard, J. E. Reactions of photochemically produced hot hydrogen atoms. I. Photolysis of HI at 1849 Å. *J. Chem. Phys.* **1964**, *40*, 2999-3007, doi:10.1063/1.1724940.

Mashnin, T. S.; Cheryshev, A. V.; Krasnoperov, L. N. Laser photolysis of ICl. A time-resolved LMR measurement of Cl($^2P_{1/2}$) relative yield. *Chem. Phys. Lett.* **1993**, *207*, 105-109, doi:10.1016/0009-2614(93)85019-K.

Mathieson, L.; Rees, A. L. G. Electronic states and potential energy diagram of the iodine molecule. *J. Chem. Phys.* **1956**, *25*, 753-761, doi:10.1063/1.1743043.

McMillan, V. personal communication to J.G. Calvert, J.N. Pitts, Jr., Photochemistry, London, 1966, p. 184. **1966**.

Mössinger, J. C.; Rowley, D. M.; Cox, R. A. The UV-visible absorption cross-sections of $IONO_2$. *Atmos. Chem. Phys.* **2002**, *2*, 227-234, doi:10.5194/acp-2-227-2002.

Mössinger, J. C.; Shallcross, D. E.; Cox, R. A. UV-Vis absorption cross-sections and atmospheric lifetimes of CH_2Br_2, CH_2I_2 and CH_2BrI. *J. Chem. Soc. Faraday Trans.* **1998**, *94*, 1391-1396, doi:10.1039/a709160e.

Myer, J. A.; Samson, J. A. R. Absorption cross section and photoionization yield of I_2 between 1050 and 2200 Å. *J. Chem. Phys.* **1970**, *52*, 716-718, doi:10.1063/1.1673044.

Ni, C.-K.; Flynn, G. W. State and velocity distributions of Cl atoms produced in the photodissociation of ICl at 237 nm. *Chem. Phys. Lett.* **1993**, *210*, 333-339, doi:10.1016/0009-2614(93)87032-X.
Ogilvie, J. F. Semi-experimental determination of a repulsive potential curve for hydrogen iodide. *Trans. Faraday Soc.* **1971**, *67*, 2205-2215, doi:10.1039/tf9716702205.
Ogorzalek Loo, R.; Haerri, H.-P.; Hall, G. E.; Houston, P. L. Methyl rotation, vibration, and alignment from a multiphoton ionization study of the 266 nm photodissociation of methyl iodide. *J. Chem. Phys.* **1989**, *90*, 4222-4236, doi:10.1063/1.455779.
Pence, W. H.; Baughum, S. L.; Leone, S. R. Laser UV photofragmentation of halogenated molecules. Selective bond dissociation and wavelength-specific quantum yields for excited I($^2P_{1/2}$) and Br($^2P_{1/2}$) atoms. *J. Phys. Chem.* **1981**, *85*, 3844-3851, doi:10.1021/j150625a027.
Petersen, A. B.; Smith, I. W. M. Yields of Br*($4^2P_{1/2}$) as a function of wavelength in the photodissociation of Br_2 and IBr. *Chem. Phys.* **1978**, *30*, 407-413, doi:10.1016/0301-0104(78)87012-8.
Phillips, D. L.; Myers, A. B.; Valentini, J. J. Investigation of solvation effects on short-time photodissociation dynamics of alkyl iodides. *J. Phys. Chem.* **1992**, *96*, 2039-2044, doi:10.1021/j100184a006.
Porret, D.; Goodeve, C. F. The continuous absorption spectrum of methyl iodide. *Trans. Faraday Soc.* **1937**, *33*, 690-693, doi:10.1039/tf9373300690.
Porret, D.; Goodeve, C. F. The continuous absorption spectra of alkyl iodides and alkyl bromides and their quantal interpretation. *Proc. Roy. Soc. Lond. A* **1938**, *165*, 31-42, doi:10.1098/rspa.1938.0042.
Porter, G., F.R.S.; Szabó, Z. G.; Townsend, M. G. The recombination of atoms V. Iodine atom recombination in nitric oxide. *Proc. Roy. Soc. Lond. A* **1962**, *A 270*, 493-500, doi:10.1098/rspa.1962.0239.
Rabinowitch, E.; Wood, W. C. The extinction coefficient of iodine and other halogens. *Trans. Faraday Soc.* **1936**, *32*, 540-546, doi:10.1039/tf9363200540.
Rattigan, O. V.; Shallcross, D. E.; Cox, R. A. UV absorption cross sections and atmospheric photolysis rates of CF_3I, CH_3I, C_2H_5I and CH_2ICl. *J. Chem. Soc. Faraday Trans.* **1997**, *93*, 2839-2846, doi:10.1039/a701529a.
Rebbert, R. E.; Lias, S. G.; Ausloos, P. Photolysis of alkyl iodides at 147.0 nm. The reaction H + $C_nH_{2n+1}I \rightarrow HI + C_nH_{2n+1}$. *Int. J. Chem. Kinet.* **1973**, *5*, 893-908, doi:10.1002/kin.550050515.
Roehl, C. M.; Burkholder, J. B.; Moortgat, G. K.; Ravishankara, A. R.; Crutzen, P. J. Temperature dependence of UV absorption cross sections and atmospheric implications of several alkyl iodides. *J. Geophys. Res.* **1997**, *102*, 12819-12829, doi:10.1029/97JD00530.
Romand, J. Absorption ultraviolette dans la région de Schumann étude de: ClH, BrH et IH gazeux. *Ann. Phys. (Paris)* **1949**, *4*, 529-590.
Rowley, D. M.; Mössinger, J. C.; Cox, R. A.; Jones, R. L. The UV-visible absorption cross-sections and atmospheric photolysis rate of HOI. *J. Atmos. Chem.* **1999**, *34*, 137-151, doi:10.1023/A:1006210322389.
Roxlo, C.; Mandl, A. Vacuum ultraviolet absorption cross sections for halogen containing molecules. *J. Appl. Phys.* **1980**, *51*, 2969-2972, doi:10.1063/1.328108.
Saiz-Lopez, A.; Saunders, R. W.; Joseph, D. M.; Ashworth, S. H.; Plane, J. M. C. Absolute absorption cross-section and photolysis rate of I_2. *Atmos. Chem. Phys.* **2004**, *4*, 1443-1450, doi:10.5194/acp-4-1443-2004.
Sander, S. P. Kinetics and mechanism of the IO + IO reaction. *J. Phys. Chem.* **1986**, *90*, 2194-2199, doi:10.1021/j100401a039.
Schmitt, G.; Comes, F. J. Photolysis of CH_2I_2 and 1,1-$C_2H_4I_2$ at 300 nm. *J. Photochem.* **1980**, *14*, 107-123, doi:10.1016/0047-2670(80)80002-5.
Schmitt, G.; Comes, F. J. Competitive photodecomposition reactions of chloroiodomethane. *J. Photochem. Photobiol. A: Chem.* **1987**, *41*, 13-30, doi:10.1016/1010-6030(87)80002-3.
Seery, D. J.; Britton, D. The continuous absorption spectra of chlorine, bromine, bromine chloride, iodine chloride, and iodine bromide. *J. Phys. Chem.* **1964**, *68*, 2263-2266, doi:10.1021/j100790a039.
Senapati, D.; Das, P. K. Cl*($^2P_{1/2}$) production dynamics from chloroiodomethane (CH_2ICl) in the ultraviolet. *Chem. Phys. Lett.* **2004**, *393*, 535-538, doi:10.1016/j.cplett.2004.06.095.
Senapati, D.; Kavita, K.; Das, P. K. Photodissociation dynamics of CH_2ICl at 222, 236, 266, 280, and ~304 nm. *J. Phys. Chem. A* **2002**, *106*, 8479-8482, doi:10.1021/jp026021s.
Solomon, S.; Burkholder, J. B.; Ravishankara, A. R.; Garcia, R. R. Ozone depletion and global warming potentials of CF_3I. *J. Geophys. Res.* **1994**, *99*, 20929-20935, doi:10.1029/94JD01833.
Spietz, P. Absorption cross sections for iodine species of relevance to the photolysis of mixtures of I_2 and O_3 and for the atmosphere. *PhD-Thesis, Univ. of Bremen, Germany* **2005**.
Spietz, P.; Gómez Martín, J.; Burrows, J. P. Effects of column density on I_2 spectroscopy and a determination of I_2 absorption cross section at 500 nm. *Atmos. Chem. Phys.* **2006**, *6*, 2177-2191, doi:10.5194/acp-6-2177-2006.

Spietz, P.; Gómez Martín, J. C.; Burrows, J. P. Spectroscopic studies of the I_2/O_3 photochemistry Part 2. Improved spectra of iodine oxides and analysis of the IO absorption spectrum. *J. Photochem. Photobiol. A: Chem.* **2005**, *176*, 50-67, doi:10.1016/j.jphotochem.2005.08.023.

Stickel, R. E.; Hynes, A. J.; Bradshaw, J. D.; Chameides, W. L.; Davis, D. D. Absorption cross sections and kinetic considerations of the IO radical as determined by laser flash photolysis/laser absorption spectroscopy. *J. Phys. Chem.* **1988**, *92*, 1862-1864, doi:10.1021/j100318a600.

Sulzer, P.; Wieland, K. Intensitätsverteilung eines kontinuierlichen absorptions-spektrums in abhängigkeit von temperatur und wellenzahl. *Helv. Phys. Acta* **1952**, *25*, 653-676, doi:10.5169/seals-112328.

Tellinghuisen, J. Resolution of the visible-infrared absorption spectrum of I_2 into three contributing transitions. *J. Chem. Phys.* **1973**, *58*, 2821-2834, doi:10.1063/1.1679584.

Tellinghuisen, J. Intensity analysis of overlapped discrete and continuous absorption by spectral simulation: The electronic transition moment for the *B*-*X* system in I_2. *J. Chem. Phys.* **2011**, *134*, 084301, doi:10.1063/1.3555623.

Tonokura, K.; Matsumi, Y.; Kawasaki, M.; Kim, H. L.; Yabushita, S.; Fujimura, S.; Saito, K. Photodissociation of ICl at 235-248 nm. *J. Chem. Phys.* **1993**, *99*, 3461-3467, doi:10.1063/1.466169.

Tucceri, M. E.; Hölscher, D.; Rodriguez, A.; Dillon, T. J.; Crowley, J. N. Absorption cross section and photolysis of OIO. *Phys. Chem. Chem. Phys.* **2006**, *8*, 834-846, doi:10.1039/b512702e.

Turnipseed, A. A.; Gilles, M. K.; Burkholder, J. B.; Ravishankara, A. R. LIF detection of IO and the rate coefficients for I + O_3 and IO + NO reactions. *Chem. Phys. Lett.* **1995**, *242*, 427-434, doi:10.1016/0009-2614(95)00774-X.

Uma, S.; Das, P. K. Dynamics of I*($^2P_{1/2}$) production in the ultraviolet photodissociation of alkyl iodides. *Can. J. Chem.* **1994**, *72*, 865-869, doi:10.1139/v94-113.

Uma, S.; Das, P. K. I* production from *n*-alkyl iodides at 222 nm. *Chem. Phys. Lett.* **1995**, *241*, 335-338, doi:10.1016/0009-2614(95)00661-M.

Uma, S.; Das, P. K. Production of I*($^2P_{1/2}$) in the ultraviolet photodissociation of α-branched alkyl iodides. *J. Chem. Phys.* **1996**, *104*, 4470-4474, doi:10.1063/1.471199.

van den Bergh, H.; Troe, J. Kinetic and thermodynamic properties of INO and INO_2 intermediate complexes in iodine recombination. *J. Chem. Phys.* **1976**, *64*, 736-742, doi:10.1063/1.432220.

Vogt, K.; Koenigsberger, J. Beobachtungen über Absorption in Joddampf and anderen Dämpfen. *Z. Physik* **1923**, *13*, 292-310, doi:10.1007/BF01328221.

Wannenmacher, E. A. J.; Felder, P.; Huber, J. R. The simultaneous three-body dissociation of CF_2I_2. *J. Chem. Phys.* **1991**, *95*, 986-997, doi:10.1063/1.461054.

Waschewsky, G. C. G.; Horansky, R.; V. Vaida Effect of dimers on the temperature-dependent absorption cross section of methyl iodide. *J. Phys. Chem. A* **1996**, *100*, 11559-11565, doi:10.1021/jp960809r.

Wrede, E.; Laubach, S.; Schulenburg, S.; Brown, A.; Wouters, E. R.; Orr-Ewing, A. J.; Ashfold, M. N. R. Continuum state spectroscopy: A high resolution ion imaging study of IBr in the wavelength range 440-685 nm. *J. Chem. Phys.* **2001**, *114*, 2629-2646, doi:10.1063/1.1337049#.

Young, C. J.; Hurley, M. D.; Wallington, T. J.; Mabury, S. A. Atmospheric chemistry of 4:2 fluorotelomer iodide (n-$C_4F_9CH_2CH_2I$): Kinetics and products of photolysis and reaction with OH radicals and Cl atoms. *J. Phys. Chem. A* **2008**, *112*, 13542-13558, doi:10.1021/jp807322x.

Zhang, L.; Fuss, W.; Kompa, K. L. Bond-selective photodissociation of CX (X = Br, I) in $XC_2H_4C_2F_4X$. *Chem. Phys.* **1990**, *144*, 289-297, doi:10.1016/0301-0104(90)80092-C.

SECTION 4I. SO_X PHOTOCHEMISTRY

I1. SO_2 (sulfur dioxide)

Back to Index

$SO_2 + h\nu \rightarrow SO + O(^3P)$ 552.3 kJ mol^{-1} 217 nm (1)

(Note: 25-1, Evaluated: 25-1)

Absorption Cross Sections: The UV absorption spectrum of sulfur dioxide, SO_2, is highly structured with a very weak absorption band in the 340–390 nm region, an absorption band in the 260–340 nm region, and a strong absorption band extending from 180 to 235 nm. Table 4I-1 provides a summary of the literature studies of the UV and VUV SO_2 absorption spectrum studies. Endo et al.[12] and Danielache et al.[11] have reported spectra for the sulfur isotopologues. Absorption cross sections are not recommended due to the highly structured and resolution dependent nature of the spectrum and should be obtained from the original literature.

Table 4I-1: SO_2 UV/VUV Absorption Spectrum Measurements [1]

Reference	Year	Resolving Power	Approximate Spectral Range (nm)	Temperature (K)
Endo et al.[12]	2015	–	189.5–225	293
Olive[32]	2015	–	190–306	298
Blackie et al.[3]	2011	≈450,000	212–326	198
Chen and Venables[8]	2011	–	336–376	296
Hermans et al. [20]	2009	13,250	227–345	345–420
Rufus et al. [35]	2009	≈420,000	199.6–220	160
Vandaele et al.[42]	2009	–	227.2–416.6	298, 318, 338, 358
Danielache et al.[11]	2008	2,000	183–350	293
Zhang[51]	2008	–	195–303	298, 373, 415
Olive[31]	2007	–	205–320	298
Holand et al.[23]	2005	–	40.0–100.4	298
Rufus et al.[34]	2003	≈450,000	220–325	295
Bogumil et al.[4]	2003	1,040	239–395	203, 223, 243, 273, 293
Wu et al.[50]	2000	5,200	208–295	200, 295, 400
Feng et al.[14]	1999	–	4.77–248	298
Stark et al.[38]	1999	450,000	198–220	295
Koplow et al.[25]	1998	1.5×10^8	215.21–215.23	295
Prahlad and Kumar[33]	1997	–	188–220	220, 240, 260, 280, 300
Vattulainen et al.[44]	1997	600	195–350	293, 873, 1073
Prahlad et al.[33]	1996	3,000	281–313	220, 240, 260, 280, 300
Wu[48]	1996	–	228–238	200, 295, 300, 400
Sprague and Joens[37]	1995	–	352.7–396	298
Vandaele et al.[43]	1994	16,600	250–370	295
Manatt and Lane[27]	1993	2,500	106–404	293
Ahmed and Kumar[1]	1992	1,250	188–231 279–320	298
Martinez and Joens[28]	1992	2,200	197–240	300
Cooper et al.[10]	1991	–	4.77–7.75 7.7–248	298
Hamdy et al.[17]	1991	–	14.7–101.7	298
Hearn and Joens[18]	1991	4,725	228–339	300
Hippler et al.[22]	1988	–	190–436	300, 1500, 2000, 3000
McGee and Burris[30]	1987	10,400	300–320	210, 295
Freeman et al.[15]	1984	200,000	171–240	213
Brassington et al.[6]	1984	600,000	299.2–300.12	295
Woods et al.[47]	1984	1.5×10^5	297–301	295
Leroy et al.[26]	1983	–	281–312	218, 263, 292, 296
Suto et al.[39]	1982	–	106–120 119–133	295
Wu and Judge[49]	1981	4,560	17.6–83.9	294, 298

			70.5–78.8 208–218.4 319.1–329.9	
Wu and Judge [49]	1981	4,560	299–340	295
Brassington [5]	1981	6,000	290–317	294
Marx et al. [29]	1980	1.5×10^6	300–300.27	298
Woods et al.[46]	1980	–	297–300	293, 373
Hicks et al.[21]	1979	–	281–314	199, 223, 253, 273, 300
Bertrand et al.[2]	1975	–	123.6	298
Chung et al.[9]	1975	–	235–334 337–400	298
Thompson et al.[41]	1975	–	296–301	298
Sidebottom et al.[36]	1972	–	217.9–330 338.5–403	298
Warneck et al.[45]	1964	–	135–230 200–315	298
Thompson et al.[40]	1963	–	185–330	298
Golomb et al.[16]	1962	–	106–217	298
Fajans and Goodeve[13]	1936	–	204–311	291

Note

[1] Data taken from Blackie et al.[3] and the Mainz spectral atlas.[24]

Photolysis Quantum Yield and Product Studies: The atmospheric photochemistry of SO_2 has been reviewed by Heicklen et al.[19] and Calvert and Stockwell.[7] Photo-oxidation at λ >~300 nm by way of the electronically excited states of SO_2 appears to be relatively unimportant.

(1) Ahmed, S. M.; Kumar, V. Quantitative photoabsorption and fluorescence spectroscopy of SO_2 at 188–231 and 278.7–320 nm. *J. Quant. Spectrosc. Radiat. Transf.* **1992**, *47*, 359–373, doi:10.1016/0022-4073(92)90038-6.

(2) Bertrand, C.; Collin, G. J.; Gagnon, H. Coefficients d'absorption et rendements quantiques ioniques de composés inorganiques et d'hydrocarbones insaturés. *J. Chim. Phys.* **1975**, *72*, 719-723, doi:10.1051/jcp/1975720719.

(3) Blackie, D.; Blackwell-Whitehead, R.; Stark, G.; Pickering, J. C.; Smith, P. L.; Rufus, J.; Thorne, A. P. High-resolution photoabsorption cross-section measurements of SO_2 at 198 K from 213 to 325 nm. *J. Geophys. Res.* **2011**, *116*, E03006, doi:10.1029/2010JE003707.

(4) Bogumil, K.; Orphal, J.; Homann, T.; Voigt, S.; Spietz, P.; Fleischmann, O. C.; Vogel, A.; Hartmann, M.; Kromminga, H.; Bovensmann, H.; et al. Measurements of molecular absorption spectra with the SCIAMACHY pre-flight model: instrument characterization and reference data for atmospheric remote sensing in the 230-2380 nm region. *J. Photochem. Photobiol. A: Chem.* **2003**, *157*, 167-184, doi:10.1016/S1010-6030(03)00062-5.

(5) Brassington, D. J. Sulfur dioxide absorption cross-section measurements from 290 nm to 317 nm. *Appl. Opt.* **1981**, *20*, 3774–3779, doi:10.1364/AO.20.003774.

(6) Brassington, D. J.; Felton, R. C.; Jolliffe, B. W.; Marx, B. R.; Moncrieff, J. T. M.; Rowley, W. R. C.; Woods, P. T. Errors in spectroscopic measurements of SO_2 due to nonexponential absorption of laser radiation, with application to the remote monitoring of atmospheric pollutants. *Appl. Opt.* **1984**, *23*, 469–475, doi:10.1364/AO.23.000469.

(7) Calvert, J. G.; Stockwell, W. R. In *Acid Precipitation: SO_2, NO, NO_2 Oxidation Mechanisms: Atmospheric Considerations*; Ann Arbor Sci. Publishers: Ann Arbor, Michigan, 1983.

(8) Chen, J.; Venables, D. S. A broadband optical cavity spectrometer for measuring weak near-ultraviolet absorption spectra of gases. *Atmos. Meas. Tech.* **2011**, *4*, 425-436, doi:10.5194/amt-4-425-2011.

(9) Chung, K.; Calvert, J. G.; Bottenheim, J. W. The photochemistry of sulfur dioxide excited within its first allowed band (3130 Å) and the "forbidden" band (3700-4000 Å). *Int. J. Chem. Kinet.* **1975**, *7*, 161-182 doi:10.1002/kin.550070202.

(10) Cooper, G.; Zarate, E. B.; Jones, R. K.; Brion, C. E. Absolute oscillator strengths for photoabsorption, photoionization and ionic photofragmentation of sulfur dioxide. I. The valence shell. *Chem. Phys.* **1991**, *150*, 237-250, doi:10.1016/0301-0104(91)80132-2.

(11) Danielache, S. O.; Eskebjerg, C.; Johnson, M. S.; Ueno, Y.; Yoshida, N. High-precision spectroscopy of ^{32}S, ^{33}S, and ^{34}S sulfur dioxide: Ultraviolet absorption cross sections and isotope effects. *J. Geophys. Res. D* **2008**, *113*, D17314, doi:10.1029/2007JD009695.

(12) Endo, Y.; Danielache, S. O.; Ueno, Y.; Hattori, S.; Johnson, M. S.; Yoshida, N.; Kjaergaard, H. G. Photoabsorption cross-section measurements of ^{32}S, ^{33}S, ^{34}S, and ^{36}S sulfur dioxide from 190 to 220 nm. *J. Geophys. Res. D* **2015**, *120*, 2546-2557, doi:10.1002/2014JD021671.

(13) Fajans, E.; Goodeve, C. F. The absorption spectrum of sulphur trioxide. *Trans. Faraday Soc.* **1936**, *32*, 511-514, doi:10.1039/TF9363200511.

(14) Feng, R.; Cooper, G.; Burton, G. R.; Brion, C. E.; Avaldi, L. Absolute photoabsorption oscillator strengths by electron energy loss methods: the valence and S 2p and 2s inner shells of sulphur dioxide in the discrete and continuum regions (3.5−260 eV). *Chem. Phys.* **1999**, *240*, 371-386, doi:10.1016/S0301-0104(98)00364-4.

(15) Freeman, D. E.; Yoshino, K.; Esmond, J. R.; Parkinson, W. H. High resolution absorption cross section measurements of SO_2 at 213 K in the wavelength region 172–240 nm. *Planet. Space Sci.* **1984**, *32*, 1125–1134, doi:10.1016/0032-0633(84)90139-9.

(16) Golomb, D.; Watanabe, K.; Marmo, F. F. Absorption coefficients of sulfur dioxide in the vacuum ultraviolet. *J. Chem. Phys.* **1962**, *36*, 958-960, doi:10.1063/1.1732695.

(17) Hamdy, H.; He, Z. X.; Samson, J. A. R. Precision photoabsorption cross section measurements of SO_2 from 147 to 1017 Å. *J. Phys. B: At. Mol. Opt. Phys.* **1991**, *24*, 4803-4807, doi:10.1088/0953-4075/24/22/017.

(18) Hearn, C. H.; Joens, J. A. The near U.V. absorption spectrum of CS_2 and SO_2 at 300 K. *J. Quant. Spectrosc. Radiat. Transf.* **1991**, *45*, 69–75, doi:10.1016/0022-4073(91)90101-U.

(19) Heicklen, J.; Kelly, N.; Partymiller, K. The photophysics and photochemistry of SO_2. *Rev. Chem. Intermediates* **1980**, *3*, 315-404.

(20) Hermans, C.; Vandaele, A. C.; Fally, S. Fourier transform measurements of SO_2 absorption cross sections: I. Temperature dependence in the 24000-29000 cm^{-1} (345-420 nm) region. *J. Quant. Spectrosc. Radiat. Transf.* **2009**, *110*, 756-765, doi:10.1016/j.jqsrt.2009.01.031.

(21) Hicks, E.; Leroy, B.; Rigaud, P.; Joudain, J.-L.; Le Bras, G. Near ultraviolet and visible absorption spectra of minor atmospheric components NO_2 and SO_2 between 200 and 300 K. *J. Chim. Phys.* **1979**, *76*, 693-698, doi:10.1051/jcp/1979760693.

(22) Hippler, H.; Nahr, D.; Plach, H. J.; Troe, J. Excitation dependence of the ultraviolet absorption spectrum of SO_2. *J. Phys. Chem.* **1988**, *92*, 5503-5506, doi:10.1021/j100330a034.

(23) Holland, D. M. P.; Shaw, D. A.; Walker, I. C.; McEwen, J.; Aprà, E.; Guest, M. F. A study of the valence shell photoelectron and photoabsorption spectra of CF_3SF_5. *J. Phys. B: At. Mol. Opt. Phys.* **2005**, *38*, 2047–2067, doi:10.1088/0953-4075/38/12/017.

(24) Keller-Rudek, H.; Moortgat, G. K.; Sander, R.; Sörensen, R. The MPI-Mainz UV/VIS spectral atlas of gaseous molecules of atmospheric interest. *Earth Syst. Sci. Data* **2013**, *5*, 365-373, doi:10.5194/essd-5-365-2013.

(25) Koplow, J. P.; Kliner, D. A. V.; Goldberg, L. Development of a narrow-band, tunable, frequency-quadrupled diode laser for UV absorption spectroscopy. *Appl. Opt.* **1998**, *37*, 3954–3960, doi:10.1364/AO.37.003954.

(26) Leroy, B.; Rigaud, P.; Jourdain, J. L.; Le Bras, G. Spectres d'absorption dans le proche ultraviolet de CS_2 et SO_2 entre 200 et 300 K. *Moon Planets* **1983**, *29*, 177-183, doi:10.1007/BF00928323.

(27) Manatt, S. L.; Lane, A. L. A compilation of the absorption cross-sections of SO_2 from 106 to 403 nm. *J. Quant. Spectrosc. Radiat. Transf.* **1993**, *50*, 267-276, doi:10.1016/0022-4073(93)90077-U.

(28) Martinez, R. D.; Joens, J. A. SO_2 absorption cross-section measurements from 197 nm to 240 nm. *Geophys. Res. Lett.* **1992**, *19*, 277–279, doi:10.1029/91GL03165.

(29) Marx, B. R.; Birch, K. P.; Felton, R. C.; Jolliffe, B. W.; Rowley, W. R. C.; Woods, P. T. High-resolution spectroscopy of SO_2 using a frequency-doubled, continuous-wave dye laser. *Opt. Commun.* **1980**, *33*, 287–291, doi:10.1016/0030-4018(80)90245-X.

(30) McGee, T. J.; Burris, J. SO_2 absorption cross sections in the near U.V. *J. Quant. Spectrosc. Radiat. Transf.* **1987**, *37*, 165-182, doi:10.1016/0022-4073(87)90020-3.

(31) Olive, B. S. "Absorption spectrum of sulfur dioxide", Results from measurements at the Department of Chemistry and Industrial Hygiene, University of North Alabama, Florence, AL, 2007. In *MPI-Mainz UV/VIS Spectral Atlas*; The Max-Planck Institute of Chemistry, Mainz, Germany, http://satellite.mpic.de/spectral_atlas, 2007.

(32) Olive, B. S. “Absorption spectra of benzene, toluene, and sulfur dioxide", Results from measurements at the Department of Chemistry and Industrial Hygiene, University of North Alabama, Florence, AL, 2015. In *MPI-Mainz UV/VIS Spectral Atlas*; The Max-Planck Institute of Chemistry, Mainz, Germany, http://satellite.mpic.de/spectral_atlas, 2015.

(33) Prahlad, V.; Kumar, V. Temperature dependence of photoabsorption cross-sections of sulfur dioxide at 188-220 nm. *J. Quant. Spectrosc. Radiat. Transf.* **1997**, *57*, 719-723, doi:10.1016/S0022-4073(97)00008-3.

(34) Rufus, J.; Stark, G.; Smith, P. L.; Pickering, J. C.; Thorne, A. P. High-resolution photoabsorption cross section measurements of SO_2, 2: 220 to 325 nm at 295 K. *J. Geophys. Res. Planets* **2003**, *108*, 5011, doi:10.1029/2002JE001931.

(35) Rufus, J.; Stark, G.; Thorne, A. P.; Pickering, J. C.; Blackwell-Whitehead, R. J.; Blackie, D.; Smith, P. L. High-resolution photoabsorption cross-section measurements of SO_2 at 160 K between 199 and 220 nm. *J. Geophys. Res.* **2009**, *114*, E06003, doi:10.1029/2008JE003319.

(36) Sidebottom, W. H.; Badcock, C. C.; Jackson, G. E.; Calvert, J. G.; Reinhardt, G. W.; Damon, E. K. Photooxidation of sulfur dioxide in the vacuum ultraviolet. *Environ. Sci. Technol.* **1972**, *6*, 72-79, doi:10.1021/es60060a001.

(37) Sprague, K. E.; Joens, J. A. SO_2 absorption cross-section measurements from 320 to 305 nm. *J. Quant. Spectrosc. Radiat. Transf.* **1995**, *53*, 349-352, doi:10.1029/94JD02187.

(38) Stark, G.; Smith, P. L.; Rufus, J.; Thorne, A. P.; Pickering, J. C.; Cox, G. High-resolution photoabsorption cross-section measurements of SO_2 at 295 K between 198 and 220 nm. *J. Geophys. Res.* **1999**, *104(E7)*, 16585-16590, doi:10.1029/1999JE001022.

(39) Suto, M.; Day, R. L.; Lee, L. C. Fluorescence yields from photodissociation of SO_2 at 1060-1330 Å. *J. Phys. B: At. Mol. Phys.* **1982**, *15*, 4165-4174, doi:10.1088/0022-3700/15/22/017.

(40) Thompson, B. A.; Harteck, P.; Reeves Jr., R. R. Ultraviolet absorption coefficients of CO_2, CO, O_2, H_2O, N_2O, NH_3, NO, SO_2, and CH_4 between 1850 and 4000 Å. *J. Geophys. Res.* **1963**, *68*, 6431-6436, doi:10.1029/JZ068i024p06431.

(41) Thompson Jr., R. T.; Hoell Jr., J. M.; Wade, W. R. Measurements of SO_2 absorption coefficients using a tunable dye laser. *J. Appl. Phys.* **1975**, *46*, 3040-3043, doi:10.1063/1.321995.

(42) Vandaele, A. C.; Hermans, C.; Fally, S. Fourier transform measurements of SO_2 absorption cross sections: II. Temperature dependence in the 29000-44000 cm^{-1} (227-345 nm) region. *J. Quant. Spectrosc. Radiat. Transf.* **2009**, *110*, 2115-2126, doi:10.1016/j.jqsrt.2009.05.006.

(43) Vandaele, A. C.; Simon, P. C.; Guilmot, J. M.; Carleer, M.; Colin, R. SO_2 absorption cross section measurement in the UV using a Fourier transform spectrometer. *J. Geophys. Res.* **1994**, *99*, 25599-25605, doi:10.1029/94JD02187.

(44) Vattulainen, J.; Wallenius, L.; Stenberg, J.; Hernberg, R.; Linna, V. Experimental determination of SO_2, C_2H_2, and O_2 UV absorption cross sections at elevated temperatures and pressures. *Appl. Spectrosc.* **1997**, *57*, 1311-1315, doi:10.1366/0003702971942.

(45) Warneck, P.; Marmo, F. F.; Sullivan, J. O. Ultraviolet absorption of SO_2: Dissociation energies of SO_2 and SO. *J. Chem. Phys.* **1964**, *40*, 1132-1136, doi:10.1063/1.1725260.

(46) Woods, P. T.; Jollife, B. W.; Marx, B. R. High resolution spectroscopy of SO_2 using a frequency-doubled pulsed dye laser, with application to the remote sensing of atmospheric pollutants. *Opt. Commun.* **1980**, *33*, 281-285, doi:10.1016/0030-4018(80)90244-8.

(47) Woods, P. T.; Jolliffe, B. W.; Marx, B. R. High-resolution spectroscopy of SO_2 using a frequency-doubled pulsed dye laser, with application to the remote sensing of atmospheric pollutants. *Opt. Commun.* **1984**, *33*, 281–286, doi:10.1016/0030-4018(80)90244-8.

(48) Wu, C. Y. R.; Chen, F. Z.; Judge, D. L. Temperature-dependent photoabsorption cross sections of selected molecular systems. *J. Electron Spectrosc. Relat. Phenom.* **1996**, *79*, 453-456, doi:10.1016/0368-2048(96)02893-9.

(49) Wu, C. Y. R.; Judge, D. L. SO_2 and CS_2 cross section data in the ultraviolet region. *Geophys. Res. Lett.* **1981**, *8*, 769–771, doi:10.1029/GL008i007p00769.

(50) Wu, C. Y. R.; Yang, B. W.; Chen, F. Z.; Judge, D. L.; Caldwell, J.; Trafton, L. M. Measurements of high-, room-, and low-temperature photoabsorption cross sections of SO_2 in the 2080- to 2950-Å region, with application to Io. *Icarus* **2000**, *145*, 289-296, doi:10.1006/icar.1999.6322.

(51) Zhang, S.; Zhou, J.; Chen, X. Experimental study on the temperature dependence of ultraviolet absorption cross-sections of sulfur dioxide. *Front. Energy Power Eng. China* **2008**, *2*, 183-186, doi:10.1007/s11708-008-0025-2.

I2. SO_3 (sulfur trioxide)

Back to Index

$SO_3 + h\nu$	$\rightarrow SO_2 + O(^3P)$	348.1 kJ mol^{-1}	343 nm	(1)
	$\rightarrow SO + O_2$	400.8 kJ mol^{-1}	298 nm	(2)
	$\rightarrow SO_2 + O(^1D)$	536.8 kJ mol^{-1}	223 nm	(3)

(Recommendation: 15-10, Note: 15-10, Evaluated: 10-6)

Absorption Cross Sections: The VUV/UV absorption spectrum of sulfur trioxide, SO_3, is continuous between 140 and 330 nm with weak vibrational band structure superimposed between 222 and 285 nm. Absorption cross sections have been reported by Leroy et al.[3] (240–264 nm), Burkholder and McKeen[1] (196–330 nm), and Hintze et al.[2] (140–194 nm). The cross section values are in good agreement in the regions of overlap and the recommended cross sections between 180 and 330 nm in Table 4I-2 are taken from Burkholder et al.[1] and Hintze et al.[2]

Photolysis Quantum Yield and Product Studies: No recommendation.

Table 4I-2. Recommended Absorption Cross Sections of SO_3 at 298 K

λ (nm)	10^{20} σ (cm^2)	λ (nm)	10^{20} σ (cm^2)	λ (nm)	10^{20} σ (cm^2)	λ (nm)	10^{20} σ (cm^2)
180	114	220	19.1	260	0.867	300	0.0424
182	108	222	15.6	262	0.75	302	0.0361
184	102	224	12.8	264	0.648	304	0.0308
186	97.3	226	10.6	266	0.559	306	0.0263
188	91.4	228	8.88	268	0.482	308	0.0224
190	87.8	230	7.49	270	0.416	310	0.0192
192	85 *	232	6.51	272	0.358	312	0.0163
194	82 *	234	5.62	274	0.308	314	0.014
196	79.4	236	4.87	276	0.265	316	0.0119
198	76.8	238	4.24	278	0.228	318	0.00976
200	73.2	240	3.69	280	0.195	320	0.00809
202	69.1	242	3.21	282	0.167	322	0.00693
204	64.5	244	2.79	284	0.143	324	0.0059
206	58.8	246	2.41	286	0.123	326	0.00502
208	52.6	248	2.09	288	0.106	328	0.00427
210	46.4	250	1.8	290	0.0907	330	0.00363
212	40	252	1.56	292	0.0774		
214	33.9	254	1.34	294	0.0664		
216	28.3	256	1.16	296	0.0574		
218	23.3	258	1.00	298	0.0496		

Note:
140–190 nm: Hintze et al.[2]
* 192–194 nm: Values adjusted for smooth interpolation.
196–330 nm: Burkholder et al.[1]

(1) Burkholder, J. B.; McKeen, S. A. UV absorption cross sections for SO_3. *Geophys. Res. Lett.* **1997**, *24*, 3201-3204, doi:10.1029/97GL03255.

(2) Hintze, P. E.; Kjaergaard, H. G.; Vaida, V.; Burkholder, J. B. Vibrational and electronic spectroscopy of sulfuric acid vapor. *J. Phys. Chem. A* **2003**, *107*, 1112-1118, doi:10.1021/jp0263626.

(3) Leroy, B.; Le Bras, G.; Rigaud, P. Ultraviolet-absorption spectra of sulfured compounds of aeronomic interest (COS, CS_2, SO_3). *Ann. Geophys.* **1981**, *37*, 297-302.

I3. H_2S (hydrogen sulfide)

Back to Index

$H_2S + h\nu \rightarrow H_2 + S(^3P)$	297.5 kJ mol^{-1}	401.7 nm	(1)
$\rightarrow HS + H$	381.6 kJ mol^{-1}	313 nm	(2)

(Recommendation: 02-25, Note: 10-6, Evaluated: 10-6)

Absorption Cross Sections: The UV absorption spectrum of hydrogen sulfide, H_2S, is weak at wavelengths >250 nm. H_2S has a strong absorption band with diffuse structure centered near 200 nm and a broad VUV spectrum. The H_2S absorption cross section at 184.9 nm has been measured by Wine et al.[3] to be 3.82×10^{-18} cm^2 molecule^{-1} and at 121.6 nm by Watanabe and Jursa[2] and Vatsa and Volpp[1] to be 2.65×10^{-17} cm^2 molecule^{-1} (average value). The recommended absorption cross sections in Table 4I-3 are taken from Wu and Chen.[4] Note that the values given here do not reproduce the full detail of the diffuse band structure.

Photolysis Quantum Yield and Product Studies: Photolysis is a minor atmospheric loss process for H_2S throughout the troposphere and stratosphere.

Table 4I-3. Recommended Absorption Cross Sections of H_2S at 298 K

λ (nm)	10^{20} σ (cm^2)	λ (nm)	10^{20} σ (cm^2)
180	189	216	187
182	242	218	155
184	302	220	129
186	382	222	106
188	452	224	86.4
190	534	226	69.6
192	616	228	55.3
194	636	230	43.2
196	724	232	33.3
198	667	234	25.5
200	670	236	19.3
202	623	238	14.3
204	512	240	10.4
206	423	242	7.55
208	359	244	5.38
210	307	246	3.75
212	260	248	2.55
214	223	250	1.69

Note:
Wu and Chen[4]

(1) Vatsa, R. K.; Volpp, H.-R. Absorption cross-sections for some atmospherically important molecules at the H atom Lyman-α wavelength (121.567 nm). *Chem. Phys. Lett.* **2001**, *340*, 289-295, doi:10.1016/S0009-2614(01)00373-6.

(2) Watanabe, K.; Jursa, A. S. Absorption and photoionization cross sections of H_2O and H_2S. *J. Chem. Phys.* **1964**, *41*, 1650-1653, doi:10.1063/1.1726138.

(3) Wine, P. H.; Kreutter, N. M.; Gump, C. A.; Ravishankara, A. R. Kinetics of OH reactions with the atmospheric sulfur compounds H_2S, CH_3SH, CH_3SCH_3, and CH_3SSCH_3. *J. Phys. Chem.* **1981**, *85*, 2660-2665, doi:10.1021/j150618a019.

(4) Wu, C. Y. R.; Chen, F. Z. Temperature-dependent photoabsorption cross sections of H_2S in the 1600-2600 Å region. *J. Quant. Spectrosc. Radiat. Transf.* **1998**, *60*, 17-23, doi:10.1016/S0022-4073(97)00163-5.

I4. H_2SO_4 (sulfuric acid)

Back to Index

$H_2SO_4 + h\nu \rightarrow OH + HSO_3$	397.1 kJ mol^{-1}	301 nm	(1)
$\rightarrow 2OH + SO_2$	510.6 kJ mol^{-1}	234 nm	(2)

(Recommendation: 10-6, Note: 10-6, Evaluated: 10-6)

Absorption Cross Sections: The gas–phase absorption spectrum of sulfuric acid, H_2SO_4, was reported by Burkholder et al.[1] (195–330 nm) at 473 K, using diode array spectroscopy, to have cross sections $<1 \times 10^{-21}$

cm^2 $molecule^{-1}$. Hintze et al.[2] studied the spectrum of H_2SO_4 vapor at 403–423 K and reported an upper limit of 1×10^{-18} cm^2 $molecule^{-1}$ for the absorption cross sections between 140 and 170 nm and an upper limit of 1×10^{-19} cm^2 $molecule^{-1}$ in the wavelength range 170-195 nm.

Photolysis Quantum Yield and Product Studies: No recommendation.

(1) Burkholder, J. B.; Mills, M.; McKeen, S. Upper limit for the UV absorption cross sections of H_2SO_4. *Geophys. Res. Lett.* **2000**, *27*, 2493-2496, doi:10.1029/1999GL011271.

(2) Hintze, P. E.; Kjaergaard, H. G.; Vaida, V.; Burkholder, J. B. Vibrational and electronic spectroscopy of sulfuric acid vapor. *J. Phys. Chem. A* **2003**, *107*, 1112-1118, doi:10.1021/jp0263626.

I5. CS_2 (carbon disulfide)

Back to Index

$CS_2 + h\nu \rightarrow CS + S(^3P)$	440.2 kJ mol^{-1}	272 nm	(1)
$\rightarrow CS + S(^1D)$	550.6 kJ mol^{-1}	217 nm	(2)

(Recommendation: 10-6, Note: 15-10, Evaluated: 10-6)

Absorption Cross Sections: The UV absorption spectrum of carbon disulfide, CS_2, has two distinct highly structured bands with a strong absorption extending from 185 to 230 nm and a weaker band in the 290–380 nm range. The absorption cross sections have been measured in a number of studies (Cook and Ogawa[4] (60– 96.5 nm, 298 K), Carnovale et al.[2] (31–248 nm, 298 K), Leroy et al.[8] (314–330 nm, 294 K), Leroy et al.[9] (314–330 nm, 197–288 K), Wine et al.[12] (280–360 nm, 298 K), Wu and Judge[13] (319–330 nm, 294 K), Dove et al.[5] (190–500 nm, 300–4000 K), Hearn and Joens[7] (296–334 nm, 300 K), Ahmed and Kumar[1] (188–340 nm, 300 K), Xu and Joens[14] (187–220 nm, 300 K), Chen and Wu[3] (180–228 nm, 295 K), Grosch et al.[6] (195–370 nm, 295–773 K), and Sunanda et al.[11] (105–226 nm, 298 K)), which are in reasonable agreement. Due to the high degree of structure in the absorption spectrum, absorption cross sections at specific wavelengths should be obtained from the original literature. The absorption cross sections in Table 4I-5 were obtained by averaging the data from Hearn and Joens[7] over 1 nm intervals.

Photolysis Quantum Yield and Product Studies: The photochemistry of CS_2 has been reviewed by Okabe[10] and discussed by Wine et al.[12] Wine et al. report that electronically excited CS_2 may react with O_2 to yield OCS.

Table 4I-5. Recommended Absorption Cross Sections of CS_2 at 298 K

λ (nm)	10^{20} σ (cm^2)	λ (nm)	10^{20} σ (cm^2)	λ (nm)	10^{20} σ (cm^2)	λ (nm)	10^{20} σ (cm^2)
275	0.017	299	2.017	323	5.180	347	0.328
276	0.020	300	1.879	324	3.517	348	0.109
277	0.027	301	3.269	325	8.628	349	0.368
278	0.043	302	3.166	326	5.023	350	0.239
279	0.050	303	3.131	327	3.481	351	0.127
280	0.053	304	4.438	328	2.849	352	0.255
281	0.062	305	4.461	329	2.848	353	0.066
282	0.080	306	3.658	330	3.802	354	0.172
283	0.103	307	5.122	331	1.301	355	0.247
284	0.122	308	7.101	332	3.057	356	0.052
285	0.158	309	4.930	333	1.552	357	0.133
286	0.209	310	8.838	334	1.506	358	0.055
287	0.254	311	5.611	335	1.375	359	0.059
288	0.309	312	6.692	336	0.861	360	0.119
289	0.445	313	8.148	337	1.377	361	0.042
290	0.438	314	7.842	338	0.591	362	0.048
291	0.635	315	9.440	339	1.121	363	0.021
292	0.640	316	7.039	340	0.489	364	0.037
293	0.878	317	9.462	341	0.386	365	0.012
294	0.801	318	7.159	342	0.573	366	0.036
295	1.137	319	9.803	343	0.387	367	0.023
296	1.134	320	4.518	344	0.556	368	0.020
297	1.861	321	6.122	345	0.353	369	0.011
298	2.287	322	4.221	346	0.350	370	0.018

Note: Hearn and Joens[7] average values

(1) Ahmed, S. M.; Kumar, V. Measurement of photoabsorption and fluorescence cross sections for carbon disulfide at 188-213 and 287.5-339.5 nm. *Pramana - J. Phys.* **1992**, *39*, 367-380, doi:10.1007/BF02845821.
(2) Carnovale, F.; White, M. G.; Brion, C. E. Absolute dipole oscillator strengths for photoabsorption and photoionization of carbon disulfide. *J. Electron Spectrosc. Relat. Phenom.* **1981**, *24*, 63-76, doi:10.1016/0368-2048(81)80046-1.
(3) Chen, F. Z.; Wu, C. Y. R. High, room and low temperature photoabsorption cross sections of CS_2 in the 1800 - 2300 Å region. *Geophys. Res. Lett.* **1995**, *22*, 2131-2134, doi:10.1029/95GL01898.
(4) Cook, G. R.; Ogawa, M. Photoionization, absorption, and fluorescence of CS_2. *J. Chem. Phys.* **1969**, *51*, 2419-2424, doi:10.1063/1.1672361.
(5) Dove, J. E.; Hippler, H.; Plach, J.; Troe, J. Ultraviolet spectra of vibrationally highly excited CS_2 molecules. *J. Chem. Phys.* **1984**, *81*, 1209-1214, doi:10.1063/1.447797.
(6) Grosch, H.; Fateev, A.; Clausen, S. UV absorption cross-sections of selected sulfur-containing compounds at temperatures up to 500 °C. *J. Quant. Spectrosc. Radiat. Transf.* **2015**, *154*, 28-34, doi:10.1016/j.jqsrt.2014.11.020.
(7) Hearn, C. H.; Joens, J. A. The near U.V. absorption spectrum of CS_2 and SO_2 at 300 K. *J. Quant. Spectrosc. Radiat. Transf.* **1991**, *45*, 69-75, doi:10.1016/0022-4073(91)90101-U.
(8) Leroy, B.; Le Bras, G.; Rigaud, P. Ultraviolet-absorption spectra of sulfured compounds of aeronomic interest (COS, CS_2, SO_3). *Ann. Geophys.* **1981**, *37*, 297-302.
(9) Leroy, B.; Rigaud, P.; Jourdain, J. L.; Le Bras, G. Spectres d'absorption dans le proche ultraviolet de CS_2 et SO_2 entre 200 et 300 K. *Moon Planets* **1983**, *29*, 177-183, doi:10.1007/BF00928323.
(10) Okabe, H. *Photochemistry of Small Molecules*; John Wiley and Sons Inc.: New York, 1978.
(11) Sunanda, K.; Shastri, A.; Das, A. K.; Sekhar, B. N. R. Electronic states of carbon disulphide in the 5.5–11.8 eV region by VUV photo absorption spectroscopy. *J. Quant. Spectrosc. Radiat. Transf.* **2015**, *151*, 76-87, doi:10.1016/j.jqsrt.2014.08.020.
(12) Wine, P. H.; Chameides, W. L.; Ravishankara, A. R. Potential role of CS_2 photooxidation in tropospheric sulfur chemistry. *Geophys. Res. Lett.* **1981**, *8*, 543-546, doi:10.1029/GL008i005p00543.
(13) Wu, C. Y. R.; Judge, D. L. SO_2 and CS_2 cross section data in the ultraviolet region. *Geophys. Res. Lett.* **1981**, *8*, 769-771, doi:10.1029/GL008i007p00769.
(14) Xu, H.; Joens, J. A. CS_2 absorption cross-section measurements from 187 nm to 230 nm. *Geophys. Res. Lett.* **1993**, *20*, 1035-1037, doi:10.1029/93GL00809

I6. $CH_3S(O)CH_3$ (dimethyl sulfoxide, DMSO)

Back to Index

$CH_3S(O)CH_3 + h\nu \rightarrow$ Products

(New)

Absorption Cross Sections: VUV/UV absorption cross sections of $CH_3S(O)CH_3$ (dimethyl sulfoxide) have been measured at room temperature by Clark and Simpson[1] (125.2–241.3 nm, graphical data), Drage et al.[2] (115–340 nm), Gollnick and Stracke[3] (140–240 nm, graphical data), Hynes and Wine[4] (190.4–245.0 nm, graphical data), and Li et al.[5] (185–250 nm). The reported values of Drage et al. and Li et al. agree within 5% over the 185–237 nm wavelength range. The data of Clark and Simpson are also in excellent agreement with both studies from 190–222 nm. Relative to the studies of Drage et al., Li et al., and Clark and Simpson, the UV cross sections (>200 nm) of Hynes and Wine are lower by ~10–40%, and the values of Gollnick and Stracke are lower by ~50–60%. The recommended cross sections given in Table 4I-6 are from Drage et al. and represent 1 nm values from their data between 190–260 nm (reported every 0.1 nm <246 nm, every 1 nm >246 nm). An estimated uncertainty factor (2σ) of 1.1 is recommended.

In the VUV, the reported cross sections of Drage et al. and Clark and Simpson agree to within ~10–20% over the 125–190 nm wavelength range, with the values of Clark and Simpson being consistently lower. The values of Gollnick and Stracke are ~45–60% lower than those of Drage et al. from 140–190 nm. The recommended Lyman-α (121.567 nm) cross section given in Table 4I-6 is from Drage et al. with an estimated uncertainty factor (2σ) of 1.2.

Photolysis Quantum Yield and Product Studies: No recommendation.

Table 4I-6. Recommended Absorption Cross Sections of CH_3SOCH_3 (dimethyl sulfoxide) at 298 K

λ (nm)	10^{20} σ (cm^2)	λ (nm)	10^{20} σ (cm^2)	λ (nm)	10^{20} σ (cm^2)
121.567	4277	213	765	237	33.6
190	2483	214	669	238	26.8
191	2005	215	594	239	21.4
192	1526	216	528	240	16.8
193	1166	217	480	241	13.3
194	939	218	439	242	10.3
195	840	219	404	243	8.45
196	832	220	373	244	6.18
197	879	221	345	245	5.08
198	971	222	317	246	4.23
199	1080	223	291	247	3.03
200	1201	224	264	248	2.41
201	1317	225	238	249	1.91
202	1420	226	214	250	1.57
203	1514	227	189	251	1.35
204	1557	228	165	252	1.31
205	1576	229	143	253	1.03
206	1549	230	123	254	0.954
207	1490	231	104	255	0.717
208	1385	232	88.3	256	0.688
209	1258	233	73.4	257	0.424
210	1128	234	60.4	258	0.461
211	998	235	49.7	259	0.223
212	869	236	40.9	260	0.276

Note:
Taken from Drage et al.[2]

(1) Clark, L. B.; Simpson, W. T. Vacuum-ultraviolet studies of sulfides. I. Spectral correlations and assignment of the NV transitions. *J. Chem. Phys.* **1965**, *43*, 3666-3672, doi:10.1063/1.1696534.

(2) Drage, E. A.; Cahillane, P.; Hoffmann, S. V.; Mason, N. J.; Limão-Vieira, P. High resolution VUV photoabsorption cross section of dimethyl sulphoxide $(CH_3)_2SO$. *Chem. Phys.* **2006**, *331*, 447-452, doi:10.1016/j.chemphys.2006.11.017.

(3) Gollnick, K.; Stracke, H.-U. Direct and sensitized photolysis of dimethyl sulphoxide in solution. *Pure Appl. Chem.* **1973**, *33*, 217-245, doi:10.1351/pac197333020217.

(4) Hynes, A. J.; Wine, P. H. The atmospheric chemistry of dimethylsulfoxide (DMSO) kinetics and mechanism of the OH+DMSO reaction. *J. Atmos. Chem.* **1996**, *24*, 23–37, doi:10.1007/BF00053821.

(5) Li, Y.-L.; Lin, C.-Y.; Lin, Y.-H.; Lin, J. J.-M. Temperature-dependent kinetics of the simplest Criegee intermediate reaction with dimethyl sulfoxide. *J. Chin. Chem. Soc.* **2020**, *67*, 1563-1570, doi:10.1002/jccs.202000206.

I7. CH_3SCH_2Cl (monochlorodimethyl sulfide, MCDMS)

Back to Index

$CH_3SCH_2Cl + h\nu \rightarrow$ Products

(New)

Absorption Cross Sections: UV absorption cross sections of CH_3SCH_2Cl (monochlorodimethyl sulfide) have been measured at room temperature by Chattopadhyay et al.[1] (200–330 nm) and Copeland et al.[2] (200–357 nm). At wavelengths below 250 nm, discrepancies in reported cross sections from the two studies are typically in the range of 0–30%, but at longer wavelengths, particularly >270 nm, the disagreement is extremely large, with the Copeland et al. values at times more than two orders of magnitude greater than the Chattopadhyay et al. values. An absorbing impurity in the Copeland et al. samples is most likely responsible for the discrepancy. The recommended cross sections given in Table 4I-7 are from Chattopadhyay et al. and are 4 nm values from their data between 200–330 nm (reported every 1 nm). An estimated uncertainty factor (2σ) of 1.2 is recommended.

Photolysis Quantum Yield and Product Studies: No recommendation.

Table 4I-7. Recommended Absorption Cross Sections of CH_3SCH_2Cl (monochlorodimethyl sulfide) at 298 K

λ (nm)	10^{20} σ (cm^2)	λ (nm)	10^{20} σ (cm^2)
200	307	268	0.283
204	241	272	0.103
208	261	276	0.0407
212	95.6	280	0.0214
216	65.6	284	0.0165
220	81.2	288	0.0167
224	114	292	0.0185
228	151	296	0.0204
232	174	300	0.0203
236	169	304	0.0182
240	134	308	0.0150
244	86.5	312	0.0103
248	45.2	316	0.00880
252	19.6	320	0.00597
256	7.24	324	0.00386
260	2.37	328	0.00280
264	0.810		

Note:
Taken from Chattopadhyay et al.[1]

(1) Chattopadhyay, A.; Assaf, E.; Finewax, Z.; Burkholder, J. B. UV absorption spectrum of monochlorodimethyl sulfide (CH_3SCH_2Cl). *J. Photochem. Photobio. A: Chem.* **2022**, *433*, 114214, doi:10.1016/j.jphotochem.2022.114214.

(2) Copeland, G.; Lee, E. P. F.; Williams, R. G.; Archibald, A. T.; Shallcross, D. E.; Dyke, J. M. Determination of the photolysis rate coefficient of monochlorodimethyl sulfide (MClDMS) in the atmosphere and its implications for the enhancement of SO_2 production from the DMS + Cl_2 reaction. *Environ. Sci. Technol.* **2014**, *48*, 1557-1565, doi:10.1021/es402956r.

I8. CH_3SSCH_3 (dimethyl disulfide, DMDS)

Back to Index

$CH_3SSCH_3 + h\nu \rightarrow$ Products (1)

(Recommendation: 19-5, Note: 19-5, Evaluated: 19-5)

Absorption Cross Sections: UV absorption cross sections of CH_3SSCH_3 (dimethyl disulfide) have been measured at room temperature by McMillan.[3] (200–312 nm), Wine et al.[5] (184.9 nm), Tokue et al.[4] (108–220 nm), Hearn et al.[2] (201–360 nm), and Barone et al.[1] (184.9 and 193 nm). The more atmospherically relevant values of Hearn et al. and McMillan agree to within less than 15% over most of the overlapping wavelength range. The recommended cross sections given in Table 4I-8 are from Hearn et al. and represent 5 nm averages of their data (reported every 1 nm) between 205–350 nm. Estimated uncertainty factors (2σ) of $F(\lambda) = 1.15 + 3 \times 10^{-22}/\sigma(\lambda)$ are recommended, which increase rapidly as the cross sections decrease at wavelengths >325 nm, consistent with the reported uncertainties of Hearn et al.

Photolysis Quantum Yield and Product Studies: Barone et al.[1] measured the quantum yield for the formation of CH_3S from DMDS to be 1.20 ± 0.14 at 193 nm and 1.65 ± 0.38 at 248 nm. In the same study, they measured the quantum yield for the formation of H from DMDS to be <0.08 at 193 nm and <0.06 at 222 nm; no H atom production was observed from photolysis of DMDS at 248 nm. The primary products of DMDS photolysis at wavelengths relevant to atmospheric photodissociation are $CH_3S + CH_3S$.

Table 4I-8. Recommended Absorption Cross Sections of CH_3SSCH_3 (dimethyl disulfide) at 300 K

λ (nm)	10^{20} σ (cm^2)	λ (nm)	10^{20} σ (cm^2)	λ (nm)	10^{20} σ (cm^2)
205	884	255	123	305	7.30
210	620	260	114	310	4.61
215	320	265	99.3	315	2.88
220	143	270	82.7	320	1.78
225	87.7	275	65.6	325	1.10
230	84.7	280	49.8	330	0.67
235	96.3	285	36.1	335	0.388
240	110	290	25.2	340	0.226
245	120	295	17.1	345	0.128
250	125	300	11.3	350	0.0720

Note:
5 nm averages of Hearn et al.[2]

(1) Barone, S. B.; Turnipseed, A. A.; Gierczak, T.; Ravishankara, A. R. Quantum yields of H(^{2}S) and $CH_3S(^2E)$ from the photolysis of simple organosulfur compounds at 193, 222, and 248 nm. *J. Phys. Chem. A* **1994**, *98*, 11969-11977, doi:10.1021/j100097a024.

(2) Hearn, C. H.; Turcu, E.; Joens, J. A. The near UV absorption spectra of dimethyl sulfide, diethyl sulfide, and dimethyl disulfide at T = 300 K. *Atmos. Environ.* **1990**, *24A*, 1939-1944, doi:10.1016/0960-1686(90)90527-T.

(3) McMillan, V. personal communication to J. G. Calvert, J. N. Pitts, Jr., Photochemistry, John Wiley & Sons, New York, 1966, p. 490.

(4) Tokue, I.; Hiraya, A.; Shobatake, K. Photoexcitation of dimethyl sulfide and dimethyl disulfide in the vacuum ultraviolet region: Rydberg states and photofragment emissions. *Chem. Phys.* **1989**, *130*, 401-408, doi:10.1016/0301-0104(89)87069-7.

(5) Wine, P. H.; Kreutter, N. M.; Gump, C. A.; Ravishankara, A. R. Kinetics of OH reactions with the atmospheric sulfur compounds H_2S, CH_3SH, CH_3SCH_3, and CH_3SSCH_3. *J. Phys. Chem.* **1981**, *85*, 2660-2665, doi:10.1021/j150618a019.

I9. OCS (carbonyl sulfide)

Back to Index

$OCS + h\nu \rightarrow CO + S(^3P)$	308.4 kJ mol^{-1}	388 nm	(1)
$\rightarrow CO + S(^1D)$	418.4 kJ mol^{-1}	285 nm	(2)
$\rightarrow CO + S(^1S)$	573.2 kJ mol^{-1}	209 nm	(3)

(Recommendation: 25-1, Note: 25-1, Evaluated: 25-1)

Absorption Cross Sections: The UV absorption spectrum of carbonyl sulfide, OCS, peaks near 222 nm with weak diffuse structure near the peak and in the long wavelength tail that is superimposed on a stronger continuum. The absorption cross sections of OCS have been measured at room temperature by Breckenridge and Taube[1] (200–260 nm), Rudolph and Inn[9] (200–270 nm), Leroy et al.[6] (210–260 nm), Ferro and Ruben[3] (210–250 nm), Wu[12] (200–252 nm), Molina et al.[8] (185–300 nm), White et al.[11] (12.4–206.6 nm), Feng et al.[2] (3.44–248 nm), Hattori et al.[5] (195–260 nm), Grosch et al.[4] (205–315 nm), and Limão-Vieira et al.[7] (115–320 nm). The reported peak absorption cross sections agree to within 15%. The absorption spectrum temperature dependence has been measured by Wu[12] (170–370 K), Rudolph and Inn[9] (195 K), Molina et al. (295, 225 K), and Grosch et al. (294–773 K). The OCS spectrum shows a decrease in absolute cross section with decreasing temperature at all wavelengths between 210–300 nm. The recommended cross sections in Table 4I-9 are the values averaged over the wavelength intervals used in solar photolysis calculations taken from Molina et al. Hattori et al. reported UV absorption spectra for the isotopologues $OC^{32}S$, $OC^{33}S$, $OC^{34}S$, and $O^{13}CS$.

Limão-Vieira et al.[7] measured the VUV spectrum of OCS. The recommended Lyman-α (121.567 nm) cross section of 6.6×10^{-18} cm^2 $molecule^{-1}$ is taken from this study.

Photolysis Quantum Yield and Product Studies: Rudolph and Inn[9] measured the CO quantum yield following the photolysis of OCS at 220, 225.8, 230, 253.7 nm (Hg lines) and 214 nm (Zn line). The CO quantum yield was found to be independent of the photolysis wavelength, within the precision of the measurement, with an average value of 0.72 ± 0.08. In a more direct CO quantum yield study using 248 nm pulsed laser photolysis

of OCS coupled with time resolved tunable diode laser absorption of CO, Zhao et al.[13] reported a CO quantum yield of >0.95. A unity CO quantum yield is recommended. Toulson and Murray[10]used photofragment excitation action spectroscopy of OCS to probe the S(^{1}D) and S(^{3}P) products over the wavelength range 212–260 nm via 2 + 1 REMPI. S(^{1}D) is the major product. See Toulson and Murray for the detailed analysis.

Table 4I-9. Recommended Absorption Cross Sections of OCS at 225 and 295 K

λ (nm)	10^{20} σ (cm^2)		λ (nm)	10^{20} σ (cm^2)	
	295 K	225 K		295 K	225 K
186.1	18.9	13.0	231.2	22.1	18.8
187.8	8.33	5.63	233.9	17.1	14.0
189.6	3.75	2.50	236.7	12.5	9.72
191.4	2.21	1.61	239.5	8.54	6.24
193.2	1.79	1.53	242.5	5.61	3.89
195.1	1.94	1.84	245.4	3.51	2.29
197.0	2.48	2.44	248.5	2.11	1.29
199.0	3.30	3.30	251.6	1.21	0.679
201.0	4.48	4.50	254.6	0.674	0.353
203.1	6.12	6.17	258.1	0.361	0.178
205.1	8.19	8.27	261.4	0.193	0.0900
207.3	10.8	10.9	264.9	0.0941	0.0419
209.4	14.1	14.2	268.5	0.0486	0.0199
211.6	17.6	17.6	272.1	0.0248	0.0101
213.9	21.8	21.8	275.9	0.0119	0.0048
216.2	25.5	25.3	279.7	0.0584	0.0021
218.6	28.2	27.7	283.7	0.0264	0.0009
221.5	30.5	29.4	287.8	0.0012	0.0005
223.5	31.9	29.5	292.0	0.0005	0.0002
226.0	30.2	27.4	296.3	0.0002	–
228.6	26.8	23.7			

Note:
Molina et al.[8]

(1) Breckenridge, W. H.; Taube, H. Ultraviolet absorption spectrum of carbonyl sulfide. *J. Chem. Phys.* **1970**, *52*, 1713-1715, doi:10.1063/1.1673209.

(2) Feng, R.; Cooper, G.; Brion, C. E. Quantitative studies of the photoabsorption of carbonyl sulphide in the valence-shell, S 2p, 2s and C1s inner-shell regions (4-360 eV) by dipole electron impact spectroscopies. *Chem. Phys. Lett.* **2000**, *252*, 359-378, doi:10.1016/S0301-0104(99)00363-8.

(3) Ferro, B. M.; Reuben, B. G. Temperature dependence of the absorption spectrum of carbonyl sulfide in quartz ultra-violet. *Trans. Faraday Soc.* **1971**, *67*, 2847-2851, doi:/10.1039/TF9716702847.

(4) Grosch, H.; Fateev, A.; Clausen, S. UV absorption cross-sections of selected sulfur-containing compounds at temperatures up to 500 °C. *J. Quant. Spectrosc. Radiat. Transf.* **2015**, *154*, 28–34, doi:10.1016/j.jqsrt.2014.11.020.

(5) Hattori, S.; Danielache, S. O.; Johnson, M. S.; Schmidt, J. A.; Kjaergaard, H. G.; Toyoda, S.; Ueno, Y.; Yoshida, N. Ultraviolet absorption cross sections of carbonyl sulfide isotopologues $OC^{32}S$, $OC^{33}S$, $OC^{34}S$ and $O^{13}CS$: isotopic fractionation in photolysis and atmospheric implications. *Atmos. Chem. Phys.* **2011**, *11*, 10293-10303 doi.org/10.5194/acp-11-10293-2011.

(6) Leroy, B.; Le Bras, G.; Rigaud, P. Ultraviolet-absorption spectra of sulfured compounds of aeronomic interest (COS, CS_2, SO_3). *Ann. Geophys.* **1981**, *37*, 297-302.

(7) Limão-Vieira, P.; Silva, P. F. F. d.; Almeida, D.; Hoshino, M.; Tanaka, H.; Mogi, D.; Tanioka, T.; Mason, N. J.; Hoffmann, S. V.; Hubin-Franskin, M.-J.; et al. Electronic excitation of carbonyl sulphide (COS) by high-resolution vacuum ultraviolet photoabsorption and electron-impact spectroscopy in the energy region from 4 to 11 eV. *J. Chem. Phys.* **2015**, *142*, 064303, doi:10.1063/1.4907200.

(8) Molina, L. T.; Lamb, J. J.; Molina, M. J. Temperature dependent UV absorption cross sections for carbonyl sulfide. *Geophys. Res. Lett.* **1981**, *8*, 1008-1011, doi:10.1029/GL008i009p01008.

(9) Rudolph, R. N.; Inn, E. C. Y. OCS photolysis and absorption in the 200- to 300-nm region. *J. Geophys. Res.* **1981**, *86*, 9891-9894, doi:10.1029/JC086iC10p09891.

(10) Toulson, B.; Murray, C. Decomposing the first absorption band of OCS using photofragment excitation spectroscopy. *J. Phys. Chem. A* **2016**, *120*, 6745–6752, doi:10.1021/acs.jpca.6b06060.
(11) White, M. G.; Leung, K. T.; Brion, C. E. Absolute dipole oscillator strengths for the photoionization and photoabsorption of COS (5-50 eV). *J. Electron Spectrosc. Relat. Phenom.* **1981**, *23*, 127-145, doi:10.1016/0368-2048(81)80030-8.
(12) Wu, C. Y. R.; Chen, F. Z.; Judge, D. L. Temperature-dependent photoabsorption cross sections of OCS in the 2000-2600 Å region. *J. Quant. Spectrosc. Radiat. Transf.* **1999**, *61*, 265-271, doi:10.1016/S0022-4073(97)00220-3.
(13) Zhao, Z.; Stickel, R. E.; Wine, P. H. Quantum yield for carbon monoxide production in the 248 nm photodissociation of carbonyl sulfide (OCS). *Geophys. Res. Lett.* **1995**, *22*, 615–618, doi:10.1029/95GL00170.

I10. SF_6 (sulfur hexafluoride)

Back to Index

$SF_6 + h\nu \rightarrow SF_5 + F$	391.6 kJ mol^{-1}	305 nm	(1)
$\rightarrow SF_4 + F_2$	458.1 kJ mol^{-1}	261 nm	(2)

(Recommendation: 25-1, Note: 25-1, Evaluated: 25-1)

Absorption Cross Sections: Sulfur hexafluoride, SF_6, has weak absorption at wavelengths >130 nm and its atmospheric photolysis occurs primarily at Lyman-α (121.567 nm). The absorption cross section at Lyman-α has been reported by Ravishankara et al.[4] (1.76×10^{-18} cm^2 molecule^{-1}) and Totterdill et al.[5] (1.37×10^{-18} cm^2 molecule^{-1}). Bertrand et al.,[1] Hitchcock and Van der Weil,[2] Zetzsch,[6] and Pradayrol et al.[3] have reported cross sections near Lyman-α that are within a factor of two of the Ravishankara et al. and Totterdill et al. values. The recommended Lyman-α cross section of 1.56×10^{-18} cm^2 molecule^{-1} is an average of the Ravishankara et al.[4] and Totterdill et al. values. The estimated Lyman-α cross section uncertainty factor is 1.2 (2σ).

Photolysis Quantum Yield and Product Studies: No recommendation.

(1) Bertrand, C.; Collin, G. J.; Gagnon, H. Coefficients d'absorption et rendements quantiques ioniques de composés inorganiques et d'hydrocarbones insaturés. *J. Chim. Phys.* **1975**, *72*, 719-723, doi:10.1051/jcp/1975720719.
(2) Hitchcock, A. P.; Van der Wiel, M. J. Absolute oscillator strengths (5-63 eV) for photoabsorption and ionic fragmentation of SF_6. *J. Phys. B: At. Mol. Phys.* **1979**, *12*, 2153-2169, doi:10.1088/0022-3700/12/13/012.
(3) Pradayrol, C.; Casanovas, A. M.; Deharo, I.; Guelfucci, J. P.; Casanovas, J. Absorption coefficients of SF_6, SF_4, SOF_2, and SO_2F_2 in the vacuum ultraviolet. *J. Phys. III France* **1996**, *6*, 603-612 doi:10.1051/jp3:1996143.
(4) Ravishankara, A. R.; Solomon, S.; Turnipseed, A. A.; Warren, R. F. Atmospheric lifetimes of long-lived halogenated species. *Science* **1993**, *259*, 194-199, doi:10.1126/science.259.5092.194.
(5) Totterdill, A.; Kovács, T.; Martín, J. C. G.; Feng, W.; Plane, J. M. C. Mesospheric removal of very long-lived greenhouse gases SF_6 and CFC-115 by metal reactions, Lyman-α photolysis, and electron attachment. *J. Phys. Chem. A* **2015**, *119*, 2016-2025, doi:10.1021/jp5123344.
(6) Zetzsch, C. UV absorption cross sections of sulfur hexafluoride and acetonitrile. In *Ozone in the Atmosphere*; Boikov, R. D., Fabian, P., Eds.; DEEPAK, 1989; pp 685-689.

I11. SF_5CF_3 (trifluoromethyl sulfur pentafluoride)

Back to Index

$SF_5CF_3 + h\nu \rightarrow SF_5 + CF_3$	347.3 kJ mol^{-1}	344 nm	(1)

(Recommendation: 25-1, Note: 25-1, Evaluated: 25-1)

Absorption Cross Sections: Trifluoromethyl sulfur pentafluoride, SF_5CF_3, does not absorb significantly at wavelengths >160 nm. The VUV absorption cross sections have been measured in several studies,[1-6] and photodissociation at Lyman-α (121.567 nm) accounts for the majority of the SF_5CF_3 atmospheric photolysis rate. Chim et al.[1] reported σ(121.567 nm) = 1.33×10^{-17} cm^2 molecule^{-1}. The absorption cross sections reported by Takahashi et al.,[6] Limão-Vieira et al.[4,5] and Holland et al.[3] are significantly smaller. The values of Limão-Vieira et al.[4,5] and Holland et al. agree to within 2% with each other and provide the basis for the recommended Lyman-α cross section, 6.45×10^{-18} cm^2 molecule^{-1}. The estimated Lyman-α cross section uncertainty factor is 1.05 (2σ).

Photolysis Quantum Yield and Product Studies: No recommendation.

(1) Chim, R. Y. L.; Kennedy, R. A.; Tuckett, R. P. The vacuum-UV absorption spectrum of SF_5CF_3; implications for its lifetime in the earth's atmosphere. *Chem. Phys. Lett.* **2003**, *367*, 697-703, doi:10.1016/S0009-2614(02)01763-3.
(2) Hatherly, P. A.; Flaxman, A. J. On the absolute absorption cross-section of SF_5CF_3. *Chem. Phys. Lett.* **2003**, *380*, 512-515, doi:10.1016/j.cplett.2003.09.061.
(3) Holland, D. M. P.; Shaw, D. A.; Walker, I. C.; McEwen, J.; Aprà, E.; Guest, M. F. A study of the valence shell photoelectron and photoabsorption spectra of CF_3SF_5. *J. Phys. B: At. Mol. Opt. Phys.* **2005**, *38*, 2047–2067, doi:10.1088/0953-4075/38/12/017.
(4) Limão-Vieira, P.; Eden, S.; Kendall, P. A.; Mason, N. J.; Giuliani, A.; Heinesch, J.; Hubin-Franskin, M.-J.; Delwiche, J.; Hoffmann, S. V. An experimental study of SF_5CF_3 by electron energy loss spectroscopy, VUV photo-absorption and photoelectron spectroscopy. *Int. J. Mass Spectrom.* **2004**, *233*, 335–341, doi:10.1016/j.ijms.2004.01.008.
(5) Limão-Vieira, P.; Kendall, P. A.; Eden, S.; Mason, N. J.; Heinesch, J.; Hubin-Franskin, M. J.; Delwiche, J.; Giuliani, A. Electron and photon induced processes in SF_5CF_3. *Radiation Phys. Chem.* **2003**, *68*, 193-197, doi:10.1016/S0969-806X(03)00279-2.
(6) Takahashi, K.; Nakayama, T.; Matsumi, Y.; Solomon, S.; Gejo, T.; Shigemasa, E.; Wallington, T. J. Atmospheric lifetime of SF_5CF_3. *Geophys. Res. Lett.* **2002**, *29*, doi:10.1029/2002GL015356.

I12. SO_2F_2 (sulfuryl fluoride)

Back to Index

$SO_2F_2 + h\nu$	$\rightarrow SO_2F + F$	452.7 kJ mol^{-1}	264 nm	(1)
	$\rightarrow SO_2 + F_2$	462.3 kJ mol^{-1}	258 nm	(2)

(Recommendation: 10-6, Note: 10-6, Evaluated: 10-6)

Absorption Cross Sections: The UV and VUV absorption spectrum of sulfuryl fluoride, SO_2F_2, has been measured at room temperature by Pradayrol et al.[2] over the wavelength range 120–210 nm and by Papadimitriou et al.[1] at 184.9, 193, and 213.9 nm, Table 4I-12. The agreement between these two studies is ~10% at 184.9 nm, but large deviations exist at longer wavelengths. Due to the large discrepancy between these studies at wavelengths >185 nm no cross section recommendation is given.

Photolysis Quantum Yield and Product Studies: Papadimitriou et al.[1] reported the photodissociation quantum yield of SO_2F_2 at 193 nm to be <0.02. This upper limit is recommended for wavelengths >193 nm. No photolysis product studies are currently available.

Table 4I-12. Absorption Cross Sections of SO_2F_2 at 298 K

λ (nm)	10^{20} σ (cm^2)
184.9	0.717
193	0.40
213.9	0.0208

Note: Papadimitriou et al.[1]

(1) Papadimitriou, V. C.; Portmann, R. W.; Fahey, D. W.; Muhle, J.; Weiss, R. F.; Burkholder, J. B. Experimental and theoretical study of the atmospheric chemistry and global warming potential of SO_2F_2. *J. Phys. Chem. A* **2008**, *112*, 12657-12666, doi:10.1021/jp806368u.
(2) Pradayrol, C.; Casanovas, A. M.; Deharo, I.; Geuelfucci, J. P.; Casanovas, J. Absorption coefficients of SF_6, SF_4, SOF_2 and SO_2F_2 in the vacuum ultraviolet. *J. Phys. III France* **1996**, *6*, 603-612, doi:10.1051/jp3:1996143.

4.12 Bibliography – SO_x Photochemistry

Ahmed, S. M.; Kumar, V. Measurement of photoabsorption and fluorescence cross sections for carbon disulfide at 188-213 and 287.5-339.5 nm. *Pramana - J. Phys.* **1992**, *39*, 367-380, doi:10.1007/BF02845821.

Ahmed, S. M.; Kumar, V. Quantitative photoabsorption and fluorescence spectroscopy of SO_2 at 188–231 and 278.7–320 nm. *J. Quant. Spectrosc. Radiat. Transf.* **1992**, *47*, 359–373, doi:10.1016/0022-4073(92)90038-6.

Barone, S. B.; Turnipseed, A. A.; Gierczak, T.; Ravishankara, A. R. Quantum yields of $H(^2S)$ and $CH_3S(^2E)$ from the photolysis of simple organosulfur compounds at 193, 222, and 248 nm. *J. Phys. Chem. A* **1994**, *98*, 11969-11977, doi:10.1021/j100097a024.

Bertrand, C.; Collin, G. J.; Gagnon, H. Coefficients d'absorption et rendements quantiques ioniques de composés inorganiques et d'hydrocarbones insaturés. *J. Chim. Phys.* **1975**, *72*, 719-723, doi:10.1051/jcp/1975720719.

Blackie, D.; Blackwell-Whitehead, R.; Stark, G.; Pickering, J. C.; Smith, P. L.; Rufus, J.; Thorne, A. P. High-resolution photoabsorption cross-section measurements of SO_2 at 198 K from 213 to 325 nm. *J. Geophys. Res.* **2011**, *116*, E03006, doi:10.1029/2010JE003707.

Bogumil, K.; Orphal, J.; Homann, T.; Voigt, S.; Spietz, P.; Fleischmann, O. C.; Vogel, A.; Hartmann, M.; Kromminga, H.; Bovensmann, H.; Frerick, J.; Burrows, J. P. Measurements of molecular absorption spectra with the SCIAMACHY pre-flight model: instrument characterization and reference data for atmospheric remote sensing in the 230-2380 nm region. *J. Photochem. Photobiol. A: Chem.* **2003**, *157*, 167-184, doi:10.1016/S1010-6030(03)00062-5.

Brassington, D. J. Sulfur dioxide absorption cross-section measurements from 290 nm to 317 nm. *Appl. Opt.* **1981**, *20*, 3774–3779, doi:10.1364/AO.20.003774.

Brassington, D. J.; Felton, R. C.; Jolliffe, B. W.; Marx, B. R.; Moncrieff, J. T. M.; Rowley, W. R. C.; Woods, P. T. Errors in spectroscopic measurements of SO_2 due to nonexponential absorption of laser radiation, with application to the remote monitoring of atmospheric pollutants. *Appl. Opt.* **1984**, *23*, 469–475, doi:10.1364/AO.23.000469.

Breckenridge, W. H.; Taube, H. Ultraviolet absorption spectrum of carbonyl sulfide. *J. Chem. Phys.* **1970**, *52*, 1713-1715, doi:10.1063/1.1673209.

Burkholder, J. B.; McKeen, S. A. UV absorption cross sections for SO_3. *Geophys. Res. Lett.* **1997**, *24*, 3201-3204, doi:10.1029/97GL03255.

Burkholder, J. B.; Mills, M.; McKeen, S. Upper limit for the UV absorption cross sections of H_2SO_4. *Geophys. Res. Lett.* **2000**, *27*, 2493-2496, doi:10.1029/1999GL011271.

Calvert, J. G.; Stockwell, W. R. In *Acid Precipitation: SO_2, NO, NO_2 Oxidation Mechanisms: Atmospheric Considerations*; Ann Arbor Sci. Publishers: Ann Arbor, Michigan, 1983.

Carnovale, F.; White, M. G.; Brion, C. E. Absolute dipole oscillator strengths for photoabsorption and photoionization of carbon disulfide. *J. Electron Spectrosc. Relat. Phenom.* **1981**, *24*, 63-76, doi:10.1016/0368-2048(81)80046-1.

Chattopadhyay, A.; Assaf, E.; Finewax, Z.; Burkholder, J. B. UV absorption spectrum of monochlorodimethyl sulfide (CH_3SCH_2Cl). *J. Photochem. Photobio. A: Chem.* **2022**, *433*, 114214, doi:10.1016/j.jphotochem.2022.114214.

Chen, J.; Venables, D. S. A broadband optical cavity spectrometer for measuring weak near-ultraviolet absorption spectra of gases. *Atmos. Meas. Tech.* **2011**, *4*, 425-436, doi:10.5194/amt-4-425-2011.

Chen, F. Z.; Wu, C. Y. R. High, room and low temperature photoabsorption cross sections of CS_2 in the 1800 - 2300 Å region. *Geophys. Res. Lett.* **1995**, *22*, 2131-2134, doi:10.1029/95GL01898.

Chim, R. Y. L.; Kennedy, R. A.; Tuckett, R. P. The vacuum-UV absorption spectrum of SF_5CF_3; implications for its lifetime in the earth's atmosphere. *Chem. Phys. Lett.* **2003**, *367*, 697-703, doi:10.1016/S0009-2614(02)01763-3.

Chung, K.; Calvert, J. G.; Bottenheim, J. W. The photochemistry of sulfur dioxide excited within its first allowed band (3130 Å) and the "forbidden" band (3700-4000 Å). *Int. J. Chem. Kinet.* **1975**, *7*, 161-182 doi:10.1002/kin.550070202.

Clark, L. B.; Simpson, W. T. Vacuum-ultraviolet studies of sulfides. I. Spectral correlations and assignment of the NV transitions. *J. Chem. Phys.* **1965**, *43*, 3666-3672, doi:10.1063/1.1696534.

Cooper, G.; Zarate, E. B.; Jones, R. K.; Brion, C. E. Absolute oscillator strengths for photoabsorption, photoionization and ionic photofragmentation of sulfur dioxide. I. The valence shell. *Chem. Phys.* **1991**, *150*, 237-250, doi:10.1016/0301-0104(91)80132-2.

Cook, G. R.; Ogawa, M. Photoionization, absorption, and fluorescence of CS_2. *J. Chem. Phys.* **1969**, *51*, 2419-2424, doi:10.1063/1.1672361.

Copeland, G.; Lee, E. P. F.; Williams, R. G.; Archibald, A. T.; Shallcross, D. E.; Dyke, J. M. Determination of the photolysis rate coefficient of monochlorodimethyl sulfide (MClDMS) in the atmosphere and its

implications for the enhancement of SO_2 production from the DMS + Cl_2 reaction. *Environ. Sci. Technol.* **2014**, *48*, 1557-1565, doi:10.1021/es402956r.

Danielache, S. O.; Eskebjerg, C.; Johnson, M. S.; Ueno, Y.; Yoshida, N. High-precision spectroscopy of ^{32}S, ^{33}S, and ^{34}S sulfur dioxide: Ultraviolet absorption cross sections and isotope effects. *J. Geophys. Res. D* **2008**, *113*, D17314, doi:10.1029/2007JD009695.

Dove, J. E.; Hippler, H.; Plach, J.; Troe, J. Ultraviolet spectra of vibrationally highly excited CS_2 molecules. *J. Chem. Phys.* **1984**, *81*, 1209-1214, doi:10.1063/1.447797.

Drage, E. A.; Cahillane, P.; Hoffmann, S. V.; Mason, N. J.; Limão-Vieira, P. High resolution VUV photoabsorption cross section of dimethyl sulphoxide $(CH_3)_2SO$. *Chem. Phys.* **2006**, *331*, 447-452, doi:10.1016/j.chemphys.2006.11.017.

Endo, Y.; Danielache, S. O.; Ueno, Y.; Hattori, S.; Johnson, M. S.; Yoshida, N.; Kjaergaard, H. G. Photoabsorption cross-section measurements of ^{32}S, ^{33}S, ^{34}S, and ^{36}S sulfur dioxide from 190 to 220 nm. *J. Geophys. Res. D* **2015**, *120*, 2546-2557, doi:10.1002/2014JD021671.

Fajans, E.; Goodeve, C. F. The absorption spectrum of sulphur trioxide. *Trans. Faraday Soc.* **1936**, *32*, 511-514, doi:10.1039/TF9363200511.

Feng, R.; Cooper, G.; Brion, C. E. Quantitative studies of the photoabsorption of carbonyl sulphide in the valence-shell, S 2p, 2s and C1s inner-shell regions (4-360 eV) by dipole electron impact spectroscopies. *Chem. Phys. Lett.* **2000**, *252*, 359-378, doi:10.1016/S0301-0104(99)00363-8.

Feng, R.; Cooper, G.; Burton, G. R.; Brion, C. E.; Avaldi, L. Absolute photoabsorption oscillator strengths by electron energy loss methods: the valence and S 2p and 2s inner shells of sulphur dioxide in the discrete and continuum regions (3.5−260 eV). *Chem. Phys.* **1999**, *240*, 371-386, doi:10.1016/S0301-0104(98)00364-4.

Ferro, B. M.; Reuben, B. G. Temperature dependence of the absorption spectrum of carbonyl sulfide in quartz ultra-violet. *Trans. Faraday Soc.* **1971**, *67*, 2847-2851, doi:/10.1039/TF9716702847.

Freeman, D. E.; Yoshino, K.; Esmond, J. R.; Parkinson, W. H. High resolution absorption cross section measurements of SO_2 at 213 K in the wavelength region 172–240 nm. *Planet. Space Sci.* **1984**, *32*, 1125–1134, doi:10.1016/0032-0633(84)90139-9.

Gollnick, K.; Stracke, H.-U. Direct and sensitized photolysis of dimethyl sulphoxide in solution. *Pure Appl. Chem.* **1973**, *33*, 217-245, doi:10.1351/pac197333020217.

Golomb, D.; Watanabe, K.; Marmo, F. F. Absorption coefficients of sulfur dioxide in the vacuum ultraviolet. *J. Chem. Phys.* **1962**, *36*, 958-960, doi:10.1063/1.1732695.

Grosch, H.; Fateev, A.; Clausen, S. UV absorption cross-sections of selected sulfur-containing compounds at temperatures up to 500 °C. *J. Quant. Spec. Rad. Transf.* **2015**, *154*, 28-34, doi:10.1016/j.jqsrt.2014.11.020.

Hamdy, H.; He, Z. X.; Samson, J. A. R. Precision photoabsorption cross section measurements of SO_2 from 147 to 1017 Å. *J. Phys. B: At. Mol. Opt. Phys.* **1991**, *24*, 4803-4807, doi:10.1088/0953-4075/24/22/017.

Hatherly, P. A.; Flaxman, A. J. On the absolute absorption cross-section of SF_5CF_3. *Chem. Phys. Lett.* **2003**, *380*, 512-515, doi:10.1016/j.cplett.2003.09.061.

Hattori, S.; Danielache, S. O.; Johnson, M. S.; Schmidt, J. A.; Kjaergaard, H. G.; Toyoda, S.; Ueno, Y.; Yoshida, N. Ultraviolet absorption cross sections of carbonyl sulfide isotopologues $OC^{32}S$, $OC^{33}S$, $OC^{34}S$ and $O^{13}CS$: isotopic fractionation in photolysis and atmospheric implications. *Atmos. Chem. Phys.* **2011**, *11*, 10293-10303 doi.org/10.5194/acp-11-10293-2011.

Hearn, C. H.; Joens, J. A. The near U.V. absorption spectrum of CS_2 and SO_2 at 300 K. *J. Quant. Spectrosc. Radiat. Transf.* **1991**, *45*, 69-75.

Hearn, C. H.; Turcu, E.; Joens, J. A. The near UV absorption spectra of dimethyl sulfide, diethyl sulfide, and dimethyl disulfide at T = 300 K. *Atmos. Environ.* **1990**, *24A*, 1939-1944, doi:10.1016/0960-1686(90)90527-T, doi:10.1016/0022-4073(91)90101-U.

Heicklen, J.; Kelly, N.; Partymiller, K. The photophysics and photochemistry of SO_2. *Rev. Chem. Intermediates* **1980**, *3*, 315-404.

Hermans, C.; Vandaele, A. C.; Fally, S. Fourier transform measurements of SO_2 absorption cross sections: I. Temperature dependence in the 24000-29000 cm^{-1} (345-420 nm) region. *J. Quant. Spectrosc. Radiat. Transf.* **2009**, *110*, 756-765, doi:10.1016/j.jqsrt.2009.01.031.

Hicks, E.; Leroy, B.; Rigaud, P.; Joudain, J.-L.; Le Bras, G. Near ultraviolet and visible absorption-spectra of minor atmospheric components NO_2 and SO_2 between 200 and 300 K. *J. Chim. Phys.* **1979**, *76*, 693-698, doi:10.1051/jcp/1979760693.

Hintze, P. E.; Kjaergaard, H. G.; Vaida, V.; Burkholder, J. B. Vibrational and electronic spectroscopy of sulfuric acid vapor. *J. Phys. Chem. A* **2003**, *107*, 1112-1118, doi:10.1021/jp0263626.

Hippler, H.; Nahr, D.; Plach, H. J.; Troe, J. Excitation dependence of the ultraviolet absorption spectrum of SO_2. *J. Phys. Chem.* **1988**, *92*, 5503-5506, doi:10.1021/j100330a034.

Hitchcock, A. P.; Van der Wiel, M. J. Absolute oscillator strengths (5-63 eV) for photoabsorption and ionic fragmentation of SF_6. *J. Phys. B: At. Mol. Phys.* **1979**, *12*, 2153-2169, doi:10.1088/0022-3700/12/13/012.

Holland, D. M. P.; Shaw, D. A.; Walker, I. C.; McEwen, J.; Aprà, E.; Guest, M. F. A study of the valence shell photoelectron and photoabsorption spectra of CF_3SF_5. *J. Phys. B: At. Mol. Opt. Phys.* **2005**, *38*, 2047–2067, doi:10.1088/0953-4075/38/12/017.

Hynes, A. J.; Wine, P. H. The atmospheric chemistry of dimethylsulfoxide (DMSO) kinetics and mechanism of the OH+DMSO reaction. *J. Atmos. Chem.* **1996**, *24*, 23–37, doi:10.1007/BF00053821.

Keller-Rudek, H.; Moortgat, G. K.; Sander, R.; Sörensen, R. The MPI-Mainz UV/VIS spectral atlas of gaseous molecules of atmospheric interest. *Earth Syst. Sci. Data* **2013**, *5*, 365-373, doi:10.5194/essd-5-365-2013.

Koplow, J. P.; Kliner, D. A. V.; Goldberg, L. Development of a narrow-band, tunable, frequency-quadrupled diode laser for UV absorption spectroscopy. *Appl. Opt.* **1998**, *37*, 3954–3960, doi:10.1364/AO.37.003954.

Leroy, B.; Le Bras, G.; Rigaud, P. Ultraviolet-absorption spectra of sulfured compounds of aeronomic interest (COS, CS_2, SO_3). *Ann. Geophys.* **1981**, *37*, 297-302.

Leroy, B.; Rigaud, P.; Jourdain, J. L.; Le Bras, G. Spectres d'absorption dans le proche ultraviolet de CS_2 et SO_2 entre 200 et 300 K. *Moon Planets* **1983**, *29*, 177-183, doi:10.1007/BF00928323.

Li, Y.-L.; Lin, C.-Y.; Lin, Y.-H.; Lin, J. J.-M. Temperature-dependent kinetics of the simplest Criegee intermediate reaction with dimethyl sulfoxide. *J. Chin. Chem. Soc.* **2020**, *67*, 1563-1570, doi:10.1002/jccs.202000206.

Limão-Vieira, P.; Eden, S.; Kendall, P. A.; Mason, N. J.; Giuliani, A.; Heinesch, J.; Hubin-Franskin, M.-J.; Delwiche, J.; Hoffmann, S. V. An experimental study of SF_5CF_3 by electron energy loss spectroscopy, VUV photo-absorption and photoelectron spectroscopy. *Int. J. Mass Spectrom.* **2004**, *233*, 335–341, doi:10.1016/j.ijms.2004.01.008.

Limão-Vieira, P.; Kendall, P. A.; Eden, S.; Mason, N. J.; Heinesch, J.; Hubin-Franskin, M. J.; Delwiche, J.; Giuliani, A. Electron and photon induced processes in SF_5CF_3. *Radiation Phys. Chem.* **2003**, *68*, 193-197, doi:10.1016/S0969-806X(03)00279-2.

Limão-Vieira, P.; Silva, P. F. F. d.; Almeida, D.; Hoshino, M.; Tanaka, H.; Mogi, D.; Tanioka, T.; Mason, N. J.; Hoffmann, S. V.; Hubin-Franskin, M.-J.; et al. Electronic excitation of carbonyl sulphide (COS) by high-resolution vacuum ultraviolet photoabsorption and electron-impact spectroscopy in the energy region from 4 to 11 eV. *J. Chem. Phys.* **2015**, *142*, 064303, doi:10.1063/1.4907200.

Manatt, S. L.; Lane, A. L. A compilation of the absorption cross-sections of SO_2 from 106 to 403 nm,. *J. Quant. Spectrosc. Radiat. Transf.* **1993**, *50*, 267-276, doi:10.1016/0022-4073(93)90077-U.

Martinez, R. D.; Joens, J. A. SO_2 absorption cross-section measurements from 197 nm to 240 nm. *Geophys. Res. Lett.* **1992**, *19*, 277–279, doi:10.1029/91GL03165.

Marx, B. R.; Birch, K. P.; Felton, R. C.; Jolliffe, B. W.; Rowley, W. R. C.; Woods, P. T. High-resolution spectroscopy of SO_2 using a frequency-doubled, continuous-wave dye laser. *Opt. Commun.* **1980**, *33*, 287–291, doi:10.1016/0030-4018(80)90245-X.

McGee, T. J.; Burris, J. SO_2 absorption cross sections in the near U.V. *J. Quant. Spectrosc. Radiat. Transf.* **1987**, *37*, 165-182, doi:10.1016/0022-4073(87)90020-3.

McMillan, V. personal communication to J. G. Calvert, J. N. Pitts, Jr., Photochemistry, John Wiley & Sons, New York, 1966, p. 490.

Molina, L. T.; Lamb, J. J.; Molina, M. J. Temperature dependent UV absorption cross sections for carbonyl sulfide. *Geophys. Res. Lett.* **1981**, *8*, 1008-1011, doi:10.1029/GL008i009p01008.

Okabe, H. *Photochemistry of Small Molecules*; John Wiley and Sons Inc.: New York, 1978.

Olive, B. S. "Absorption spectrum of sulfur dioxide", Results from measurements at the Department of Chemistry and Industrial Hygiene, University of North Alabama, Florence, AL, 2007. In *MPI-Mainz UV/VIS Spectral Atlas*; The Max-Planck Institute of Chemistry, Mainz, Germany, http://satellite.mpic.de/spectral_atlas, 2007.

Papadimitriou, V. C.; Portmann, R. W.; Fahey, D. W.; Muhle, J.; Weiss, R. F.; Burkholder, J. B. Experimental and theoretical study of the atmospheric chemistry and global warming potential of SO_2F_2. *J. Phys. Chem. A* **2008**, *112*, 12657-12666, doi:10.1021/jp806368u.

Pradayrol, C.; Casanovas, A. M.; Deharo, I.; Geuelfucci, J. P.; Casanovas, J. Absorption coefficients of SF_6, SF_4, SOF_2 and SO_2F_2 in the vacuum ultraviolet. *J. Phys. III France* **1996**, *6*, 603-612, doi:10.1051/jp3:1996143.

Prahlad, V.; Kumar, V. Temperature dependence of photoabsorption cross-sections of sulfur dioxide at 188-220 nm. *J. Quant. Spectrosc. Radiat. Transf.* **1997**, *57*, 719-723, doi:10.1016/S0022-4073(97)00008-3.

Ravishankara, A. R.; Solomon, S.; Turnipseed, A. A.; Warren, R. F. Atmospheric lifetimes of long-lived halogenated species. *Science* **1993**, *259*, 194-199, doi:10.1126/science.259.5092.194.

Rudolph, R. N.; Inn, E. C. Y. OCS photolysis and absorption in the 200- to 300-nm region. *J. Geophys. Res.* **1981**, *86*, 9891-9894, doi:10.1029/JC086iC10p09891.

Rufus, J.; Stark, G.; Smith, P. L.; Pickering, J. C.; Thorne, A. P. High-resolution photoabsorption cross section measurements of SO_2, 2: 220 to 325 nm at 295 K. *J. Geophys. Res. Planets* **2003**, *108*, 5011, doi:10.1029/2002JE001931.

Rufus, J.; Stark, G.; Thorne, A. P.; Pickering, J. C.; Blackwell-Whitehead, R. J.; Blackie, D.; Smith, P. L. High-resolution photoabsorption cross-section measurements of SO_2 at 160 K between 199 and 220 nm. *J. Geophys. Res.* **2009**, *114*, E06003, doi:10.1029/2008JE003319.

Sidebottom, W. H.; Badcock, C. C.; Jackson, G. E.; Calvert, J. G.; Reinhardt, G. W.; Damon, E. K. Photooxidation of sulfur dioxide in the vacuum ultraviolet. *Environ. Sci. Technol.* **1972**, *6*, 72-79, doi:10.1021/es60060a001.

Sprague, K. E.; Joens, J. A. SO_2 absorption cross-section measurements from 320 to 305 nm. *J. Quant. Spectrosc. Radiat. Transf.* **1995**, *53*, 349-352, doi:10.1029/94JD02187.

Stark, G.; Smith, P. L.; Rufus, J.; Thorne, A. P.; Pickering, J. C.; Cox, G. High-resolution photoabsorption cross-section measurements of SO_2 at 295 K between 198 and 220 nm. *J. Geophys. Res.* **1999**, *104(E7)*, 16585-16590, doi:10.1029/1999JE001022.

Sunanda, K.; Shastri, A.; Das, A. K.; Sekhar, B. N. R. Electronic states of carbon disulphide in the 5.5–11.8 eV region by VUV photo absorption spectroscopy. *J. Quant. Spec. Rad. Transf.* **2015**, *151*, 76-87, doi:10.1016/j.jqsrt.2014.08.020.

Suto, M.; Day, R. L.; Lee, L. C. Fluorescence yields from photodissociation of SO_2 at 1060-1330 Å. *J. Phys. B: At. Mol. Phys.* **1982**, *15*, 4165-4174, doi:10.1088/0022-3700/15/22/017.

Takahashi, K.; Nakayama, T.; Matsumi, Y.; Solomon, S.; Gejo, T.; Shigemasa, E.; Wallington, T. J. Atmospheric lifetime of SF_5CF_3. *Geophys. Res. Lett.* **2002**, *29*, doi:10.1029/2002GL015356.

Thompson, B. A.; Harteck, P.; Reeves, J., R. R. Ultraviolet absorption coefficients of CO_2, CO, O_2, H_2O, N_2O, NH_3, NO, SO_2, and CH_4 between 1850 and 4000 Å. *J. Geophys. Res.* **1963**, *68*, 6431-6436, doi:10.1029/JZ068i024p06431.

Thompson Jr., R. T.; Hoell Jr., J. M.; Wade, W. R. Measurements of SO_2 absorption coefficients using a tunable dye laser. *J. Appl. Phys.* **1975**, *46*, 3040-3043, doi:10.1063/1.321995.

Tokue, I.; Hiraya, A.; Shobatake, K. Photoexcitation of dimethyl sulfide and dimethyl disulfide in the vacuum ultraviolet region: Rydberg states and photofragment emissions. *Chem. Phys.* **1989**, *130*, 401-408, doi:10.1016/0301-0104(89)87069-7.

Totterdill, A.; Kovács, T.; Martín, J. C. G.; Feng, W.; Plane, J. M. C. Mesospheric removal of very long-lived greenhouse gases SF_6 and CFC-115 by metal reactions, Lyman-α photolysis, and electron attachment. *J. Phys. Chem. A* **2015**, *119*, 2016-2025, doi:10.1021/jp5123344.

Toulson, B.; Murray, C. Decomposing the first absorption band of OCS using photofragment excitation spectroscopy. *J. Phys. Chem. A* **2016**, *120*, 6745–6752, doi:10.1021/acs.jpca.6b06060.

Vandaele, A. C.; Simon, P. C.; Guilmot, J. M.; Carleer, M.; Colin, R. SO_2 absorption cross section measurement in the UV using a Fourier transform spectrometer. *J. Geophys. Res.* **1994**, *99*, 25599-25605, doi:10.1029/94JD02187.

Vatsa, R. K.; Volpp, H.-R. Absorption cross-sections for some atmospherically important molecules at the H atom Lyman-α wavelength (121.567 nm). *Chem. Phys. Lett.* **2001**, *340*, 289-295, doi:10.1016/S0009-2614(01)00373-6.

Vattulainen, J.; Wallenius, L.; Stenberg, J.; Hernberg, R.; Linna, V. Experimental determination of SO_2, C_2H_2, and O_2 UV absorption cross sections at elevated temperatures and pressures. *Appl. Spectrosc.* **1997**, *57*, 1311-1315, doi:10.1366/0003702971942.

Warneck, P.; Marmo, F. F.; Sullivan, J. O. Ultraviolet absorption of SO_2: Dissociation energies of SO_2 and SO. *J. Chem. Phys.* **1964**, *40*, 1132-1136, doi:10.1063/1.1725260.

Watanabe, K.; Jursa, A. S. Absorption and photoionization cross sections of H_2O and H_2S. *J. Chem. Phys.* **1964**, *41*, 1650-1653, doi:10.1063/1.1726138.

White, M. G.; Leung, K. T.; Brion, C. E. Absolute dipole oscillator strengths for the photoionization and photoabsorption of COS (5-50 eV). *J. Electron Spectrosc. Relat. Phenom.* **1981**, *23*, 127-145, doi:10.1016/0368-2048(81)80030-8.

Wine, P. H.; Chameides, W. L.; Ravishankara, A. R. Potential role of CS_2 photooxidation in tropospheric sulfur chemistry. *Geophys. Res. Lett.* **1981**, *8*, 543-546, doi:10.1029/GL008i005p00543.

Wine, P. H.; Kreutter, N. M.; Gump, C. A.; Ravishankara, A. R. Kinetics of OH reactions with the atmospheric sulfur compounds H_2S, CH_3SH, CH_3SCH_3, and CH_3SSCH_3. *J. Phys. Chem.* **1981**, *85*, 2660-2665, doi:10.1021/j150618a019.

Woods, P. T.; Jollife, B. W.; Marx, B. R. High resolution spectroscopy of SO_2 using a frequency-doubled pulsed dye laser, with application to the remote sensing of atmospheric pollutants. *Opt. Commun.* **1980**, *33*, 281-285, doi:10.1016/0030-4018(80)90244-8.

Wu, C. Y. R.; Chen, F. Z. Temperature-dependent photoabsorption cross sections of H_2S in the 1600-2600 Å region. *J. Quant. Spectrosc. Radiat. Transf.* **1998**, *60*, 17-23, doi:10.1016/S0022-4073(97)00163-5.

Wu, C. Y. R.; Chen, F. Z.; Judge, D. L. Temperature-dependent photoabsorption cross sections of selected molecular systems. *J. Electron Spectrosc. Relat. Phenom.* **1996**, *79*, 453-456, doi:10.1016/0368-2048(96)02893-9.

Wu, C. Y. R.; Chen, F. Z.; Judge, D. L. Temperature-dependent photoabsorption cross sections of OCS in the 2000-2600 Å region. *J. Quant. Spectrosc. Radiat. Transf.* **1999**, *61*, 265-271, doi:10.1016/S0022-4073(97)00220-3.

Wu, C. Y. R.; Judge, D. L. SO_2 and CS_2 cross section data in the ultraviolet region. *Geophys. Res. Lett.* **1981**, *8*, 769-771, doi:10.1029/GL008i007p00769.

Wu, C. Y. R.; Yang, B. W.; Chen, F. Z.; Judge, D. L.; Caldwell, J.; Trafton, L. M. Measurements of high-, room-, and low-temperature photoabsorption cross sections of SO_2 in the 2080- to 2950-Å region, with application to Io. *Icarus* **2000**, *145*, 289-296, doi:10.1006/icar.1999.6322.

Xu, H.; Joens, J. A. CS_2 absorption cross-section measurements from 187 nm to 230 nm. *Geophys. Res. Lett.* **1993**, *20*, 1035-1037, doi:10.1029/93GL00809

Zetzsch, C. UV absorption cross sections of sulfur hexafluoride and acetonitrile. In *Ozone in the Atmosphere*; Boikov, R. D., Fabian, P., Eds.; DEEPAK, 1989; pp 685-689.

Zhang, S.; Zhou, J.; Chen, X. Experimental study on the temperature dependence of ultraviolet absorption cross-sections of sulfur dioxide. *Front. Energy Power Eng. China* **2008**, *2*, 183-186, doi:10.1007/s11708-008-0025-2.

Zhao, Z.; Stickel, R. E.; Wine, P. H. Quantum yield for carbon monoxide production in the 248 nm photodissociation of carbonyl sulfide (OCS). *Geophys. Res. Lett.* **1995**, *22*, 615–618, doi:10.1029/95GL00170.

SECTION 4J. METAL PHOTOCHEMISTRY

J1. NaOH (sodium hydroxide)

Back to Index

$NaOH + h\nu$	$\rightarrow Na(^2S) + OH$	345.6 kJ mol^{-1}	346 nm	(1)
	$\rightarrow NaO + H$	518.8 kJ mol^{-1}	230 nm	(2)
	$\rightarrow Na(^2P) + OH$	548.1 kJ mol^{-1}	218 nm	(3)

(Recommendation: 10-6, Note: 10-6, Evaluated: 10-6)

Absorption Cross Sections: The spectrum of NaOH, sodium hydroxide, has been reported by Rowland and Makide[2] (200–400 nm) and Self and Plane[3] (193–395 nm). Rowland and Makide inferred absorption cross section values and the average solar photodissociation rate from the flame measurements of Daidoji.[1] Self and Plane[3] used laser photofragment spectroscopy to measure absorption cross sections at 200 and 300 K from the production of Na atoms. The reported cross sections at the lower temperature are systematically smaller at all wavelengths, but fall within the limits of the measurement precision for the room temperature values. The results from the Rowland and Makide[2] and Self and Plane[3] studies are in reasonable agreement. The recommended cross sections in Table 4J-1 are taken from Self and Plane.[3]

Photolysis Quantum Yield and Product Studies: The quantum yield for photodissociation at wavelengths <346 nm is expected to be unity.

Table 4J-1. Recommended Absorption Cross Sections of NaOH at 298 K

λ (nm)	10^{20} σ (cm^2)
193.4	551
205.7	867
205.9	563
210.3	185
216.3	489
218.7	696
225.2	1430
230.6	1820
234.0	1680
248.4	173
254.8	115
265.9	48
268.3	41.8
277.0	19.1
285.0	7.1
291.8	43.8
313.0	585
319.6	510
353.4	53.9
354.6	57
359.8	41.4
395.2	51.2

Note:
Self and Plane,[3] reported negative values are not included

(1) Daidoji, H. Molecular absorption spectra of some sodium salts in flames. Spectral interference in atomic absorption spectrometry. III. *Bunseki Kagaku* **1979**, *28*, 77-82.

(2) Rowland, F. S.; Makide, Y. Upper stratospheric photolysis of NaOH. *Geophys. Res. Lett.* **1982**, *9*, 473-475, doi:10.1029/GL009i004p00473.

(3) Self, D. E.; Plane, J. M. C. Absolute photolysis cross-sections for $NaHCO_3$, NaOH, NaO, NaO_2 and NaO_3: implications for sodium chemistry in the upper mesosphere. *Phys. Chem. Chem. Phys.* **2002**, *4*, 16-23, doi:10.1039/b107078a.

J2. NaCl (sodium chloride)

Back to Index

$NaCl + h\nu \rightarrow Na + Cl$ 410 kJ mol^{-1} 292 nm (1)

(Recommendation: 87-41; Note: 10-6; Evaluated: 10-6)

Absorption Cross Sections: There are several studies of the UV absorption spectra of NaCl, sodium chloride, vapor. For a review of work prior to 1982, which was carried out at high temperatures, see Rowland and Rogers.[2] The study of Davidovitz and Brodhead[1] is particularly noteworthy. They report a NaCl absorption spectrum over the wavelength range 200–300 nm for temperatures between 1123–1223 K with a cross section of $(3.5 \pm 0.3) \times 10^{-17}$ cm^2 molecule^{-1} at 238 nm. The recommended cross sections in Table 4J-2 are taken from the work of Silver et al.,[3] who measured a spectrum of gas-phase NaCl at room temperature over the wavelength range 189–360 nm by directly monitoring Na atoms produced in the photolysis of NaCl.

Photolysis Quantum Yield and Product Studies: The photolysis quantum yield for NaCl is expected to be unity for absorption above the dissociation threshold.

Table 4J-2. Recommended Absorption Cross Sections of NaCl at 300 K

λ (nm)	10^{20} σ (cm^2)
189.7	612
193.4	556
203.1	148
205.3	90.6
205.9	89.6
210.3	73.6
216.3	151
218.7	46.3
225.2	146
230.4	512
231.2	947
234.0	1300
237.6	638
241.4	674
248.4	129
251.6	251
254.8	424
260.2	433
268.3	174
277.0	40
291.8	0.8

Note:
Silver et al.[3]

(1) Davidovits, P.; Brodhead, D. C. Ultraviolet absorption cross sections for the alkali halide vapors. *J. Chem. Phys.* **1967**, *46*, 2968-2973, doi:10.1063/1.1841164.

(2) Rowland, F. S.; Rogers, P. J. Upper stratospheric photolysis of NaCl and KCl. *Proc. Natl. Acad. Sci. USA* **1982**, *79*, 2737-2739, doi:10.1073/pnas.79.8.2737.

(3) Silver, J. A.; Worsnop, D. R.; Freedman, A.; Kolb, C. E. Absolute photodissociation cross sections of gas phase sodium chloride at room temperature. *J. Chem. Phys.* **1986**, *84*, 4378-4384, doi:10.1063/1.450060.

J3. NaO (sodium oxide)

Back to Index

$NaO + h\nu \rightarrow Na + O$ 266.5 kJ mol^{-1} 449 nm (1)

(Recommendation: 10-6, Note: 10-6, Evaluated: 10-6)

Absorption Cross Sections: The UV absorption spectrum of NaO, sodium oxide, has been reported by Self and Plane[1] at 200 and 300 K at wavelengths between 193 and 423 nm. Absorption cross sections were determined using pulsed laser photolysis of NaO combined with detection of Na atoms using laser induced fluorescence. A systematic decrease in absorption cross section at lower temperature was reported for all wavelengths

included in their study. The recommended absorption cross sections in Table 4J-3 are taken from Self and Plane,[1] which is the only study available.

Photolysis Quantum Yield and Product Studies: The photolysis quantum yield for NaO is expected to be unity for absorption above the dissociation threshold.

Table 4J-3. Recommended Absorption Cross Sections of NaO at 200 and 300 K

λ (nm)	10^{20} σ (cm^2) 300 K	10^{20} σ (cm^2) 200 K
193.4	501	–
216.3	1490	515
225.2	1100	–
231.2	1170	353
248.4	206	93.7
265.9	180	–
268.3	160	24.6
277.0	46.3	–
291.8	102	95.5
313.0	1250	–
319.6	1070	703
353.4	276	119
354.6	280	–
359.8	174	–
395.2	244	155
423.0	52.2	–

Note:
Self and Plane[1]

(1) Self, D. E.; Plane, J. M. C. Absolute photolysis cross-sections for $NaHCO_3$, NaOH, NaO, NaO_2 and NaO_3: implications for sodium chemistry in the upper mesosphere. *Phys. Chem. Chem. Phys.* **2002**, *4*, 16-23, doi:10.1039/b107078a.

J4. NaO_2 (sodium superoxide)

Back to Index

$NaO_2 + h\nu$	$\rightarrow Na + O_2(^3\Sigma)$	155 kJ mol^{-1}	771 nm	(1)
	$\rightarrow Na + O_2(^1\Delta)$	249.4 kJ mol^{-1}	480 nm	(2)
	$\rightarrow NaO + O$	387.4 kJ mol^{-1}	309 nm	(3)

(Recommendation: 10-6, Note: 10-6, Evaluated: 10-6)

Absorption Cross Sections: The UV absorption spectrum of NaO_2, sodium superoxide, has been reported by Rajasekhar et al.[1] at 193, 248, and 308 nm (230 K) and Self and Plane[2] at wavelengths between 193 and 423 nm (200, 230, and 300 K). Absorption cross sections were determined using pulsed laser photolysis of NaO_2 combined with detection of Na atoms using laser induced fluorescence. The results from these studies are in good agreement. At most wavelengths, the temperature dependence of the NaO_2 absorption cross sections falls within the estimated measurement uncertainty. The recommended absorption cross sections in Table 4J-4 are taken from Self and Plane.[2]

Photolysis Quantum Yield and Product Studies: The photolysis quantum yield for NaO_2 is expected to be unity for absorption above the dissociation threshold.

Table 4J-4. Recommended Absorption Cross Sections of NaO_2 at 300 K

λ (nm)	10^{20} σ (cm^2)
193.4	383
205.9	146
210.3	542
216.3	511
225.2	235
230.8	935
248.4	414
254.8	550
268.3	458
277.0	181
285.0	73.4
291.8	168
313.0	127
319.6	12.1
353.4	16.2
354.6	35
359.8	61
395.2	108
423.0	42.8

Note:
Self and Plane[2]

(1) Rajasekhar, B.; Plane, J. M. C.; Bartolotti, L. Determination of the absolute photolysis cross section of sodium superoxide at 230 K: Evidence for the formation of sodium tetroxide in the gas phase. *J. Phys. Chem.* **1989**, *93*, 7399-7404, doi:10.1021/j100358a030.

(2) Self, D. E.; Plane, J. M. C. Absolute photolysis cross-sections for $NaHCO_3$, NaOH, NaO, NaO_2 and NaO_3: implications for sodium chemistry in the upper mesosphere. *Phys. Chem. Chem. Phys.* **2002**, *4*, 16-23, doi:10.1039/b107078a.

J5. NaO_3 (sodium trioxide)

Back to Index

$NaO_3 + h\nu$	$\rightarrow NaO + O_2$	141 kJ mol^{-1}	849 nm	(1)
	$\rightarrow NaO_2 + O$	252 kJ mol^{-1}	474 nm	(2)

(Recommendation: 10-6, Note: 10-6, Evaluated: 10-6)

Absorption Cross Sections: The UV absorption spectrum of NaO_3, sodium trioxide, at 300 K has been reported by Self and Plane[1] for wavelengths between 216 and 396 nm. The recommended absorption cross sections in Table 4J-5 are taken from Self and Plane,[1] which is the only study available.

Photolysis Quantum Yield and Product Studies: The photolysis quantum yield for NaO_3 is expected to be unity for absorption above the dissociation threshold.

Table 4J-5. Recommended Absorption Cross Sections of NaO_3 at 300 K

λ (nm)	10^{20} σ (cm^2)
216.3	1310
231.2	228
248.4	119
268.3	94.9
291.8	145
319.6	345
353.4	55.6
395.2	71.7

Note:
Self and Plane[1]

(1) Self, D. E.; Plane, J. M. C. Absolute photolysis cross-sections for $NaHCO_3$, NaOH, NaO, NaO_2 and NaO_3: implications for sodium chemistry in the upper mesosphere. *Phys. Chem. Chem. Phys.* **2002**, *4*, 16-23, doi:10.1039/b107078a.

J6. $NaHCO_3$ (sodium bicarbonate)

Back to Index

$NaHCO_3 + h\nu \rightarrow$ Products (1)

(Recommendation: 10-6, Note: 10-6, Evaluated: 10-6)

Absorption Cross Sections: The UV absorption spectrum of $NaHCO_3$, sodium bicarbonate, at 200 and 300 K has been reported by Self and Plane[1] for wavelengths between 193 and 277 nm. Absorption cross sections were determined using pulsed laser photolysis of $NaHCO_3$ combined with detection of Na atoms using laser induced fluorescence. No significant difference in absorption cross section with temperature was reported. The recommended absorption cross sections in Table 4J-6 are taken from Self and Plane,[1] which is the only study available.

Photolysis Quantum Yield and Product Studies: The photolysis quantum yield for $NaHCO_3$ is expected to be unity for absorption above the dissociation threshold.

Table 4J-6. Recommended Absorption Cross Sections of $NaHCO_3$ at 200 and 300 K

λ (nm)	10^{20} σ (cm^2) 300 K	10^{20} σ (cm^2) 200 K
193.4	113	73.5
205.9	48.7	–
210.3	116	94.7
216.3	120	–
225.2	77.3	98.7
230.9	54.7	57.8
248.4	4.01	3.55
268.3	0.95	–
277.0	1.09	5.49

Note:
Self and Plane,[1] reported negative values are not included

(1) Self, D. E.; Plane, J. M. C. Absolute photolysis cross-sections for $NaHCO_3$, NaOH, NaO, NaO_2 and NaO_3: implications for sodium chemistry in the upper mesosphere. *Phys. Chem. Chem. Phys.* **2002**, *4*, 16-23, doi:10.1039/b107078a.

4.13 Bibliography – Metal Photochemistry

Daidoji, H. Molecular absorption spectra of some sodium salts in flames. Spectral interference in atomic absorption spectrometry. III. *Bunseki Kagaku* **1979**, *28*, 77-82.

Davidovits, P.; Brodhead, D. C. Ultraviolet absorption cross sections for the alkali halide vapors. *J. Chem. Phys.* **1967**, *46*, 2968-2973, doi:10.1063/1.1841164.

Rajasekhar, B.; Plane, J. M. C.; Bartolotti, L. Determination of the absolute photolysis cross section of sodium superoxide at 230 K: Evidence for the formation of sodium tetroxide in the gas phase. *J. Phys. Chem.* **1989**, *93*, 7399-7404, doi:10.1021/j100358a030.

Rowland, F. S.; Makide, Y. Upper stratospheric photolysis of NaOH. *Geophys. Res. Lett.* **1982**, *9*, 473-475, doi:10.1029/GL009i004p00473.

Rowland, F. S.; Rogers, P. J. Upper stratospheric photolysis of NaCl and KCl. *Proc. Natl. Acad. Sci. USA* **1982**, *79*, 2737-2739, doi:10.1073/pnas.79.8.2737.

Self, D. E.; Plane, J. M. C. Absolute photolysis cross-sections for $NaHCO_3$, NaOH, NaO, NaO_2 and NaO_3: implications for sodium chemistry in the upper mesosphere. *Phys. Chem. Chem. Phys.* **2002**, *4*, 16-23, doi:10.1039/b107078a.

Silver, J. A.; Worsnop, D. R.; Freedman, A.; Kolb, C. E. Absolute photodissociation cross sections of gas phase sodium chloride at room temperature. *J. Chem. Phys.* **1986**, *84*, 4378-4384, doi:10.1063/1.450060.

SECTION 4K. RAYLEIGH SCATTERING CROSS SECTIONS

Table 4-2 lists the atom and molecule recommendations for the Rayleigh scattering cross sections included in this evaluation. The linked Notes contain a summary of the available studies and the basis for the scattering cross section recommendation and estimated uncertainty.

4.14 Introduction

Rayleigh scattering is the dispersion of electromagnetic radiation by molecules and particles of size much smaller than the wavelength of the incident light.[7,9,10,13] Accurate (<±2%), wavelength-dependent Rayleigh scattering cross sections for molecules are needed for modeling the propagation of electromagnetic radiation in planetary atmospheres and, in recent years, for calibrating mirror reflectivity in high finesse optical cavities. Because Rayleigh scattering is proportional to the inverse of the wavelength of light to the fourth power, it increases dramatically with decreasing wavelength. A well-known example of the manifestation of this wavelength dependence is the Earth's sky appearing blue due to Rayleigh scattering of solar radiation in our nitrogen-rich atmosphere.

In the past, determinations of Rayleigh scattering cross sections were typically performed at a single visible wavelength. The first direct measurement of Rayleigh scattering cross sections as a function of wavelength for atmospheric gases was reported by Shardanand and Rao.[11] The study used nephelometry to measure the scattering at four laser wavelengths in the visible and one in the ultraviolet, and the results were reported with relatively large uncertainties of ±11%. More recently, experimental measurements of Rayleigh scattering cross sections were made using cavity-ringdown spectroscopy (CRDS).[4,5,8,12] At each discrete observational wavelength, the CRDS detection method involved obtaining a series of pressure ramp measurements of the gas to distinguish signal loss due to Rayleigh scattering, which varies with pressure, from signal loss due to mirror reflectivity, which is constant. The scattering cross section uncertainties using CRDS were generally improved from the early nephelometry work but were often still too large for the scattering cross sections to be used as accurate reference values for mirror reflectivity calibrations.

Following the early CRDS studies,[4,5,8,12] Thalman et al.[14,15] used Broadband Cavity Enhanced Spectroscopy (BBCES) in combination with CRDS to accurately determine Rayleigh scattering cross sections for several gases. Other BBCES studies have since significantly expanded the wavelength range and number of gases for which accurate Rayleigh scattering cross sections are now available.[1-3,6,16,17] The BBCES technique enables the acquisition of data with long pathlengths over a range of wavelengths simultaneously, providing improved precision, faster data collection, and greater wavelength coverage relative to other methods. The past studies where Rayleigh scattering cross sections were reported with the highest accuracy typically used the BBCES technique.

An alternative, in principle highly accurate, approach to determining Rayleigh scattering cross sections is to calculate the scattering cross sections using a refractive index-based, or *n*-based method. The wavelength-dependent Rayleigh scattering cross section (σ, expressed in cm^2 molecule^{-1}) is calculated as:[9,12]

$$\sigma(\nu) = \frac{24\pi^3\nu^4}{N^2}\left(\frac{n_{(\nu)}^2 - 1}{n_{(\nu)}^2 + 2}\right)^2 F_k(\nu) \quad (1)$$

where ν is the radiation wavenumber (cm^{-1}), N is the density of the gas (molecules cm^{-3}), $n_{(\nu)}$ is the wavenumber-dependent refractive index, and $F_k(\nu)$ is the wavenumber-dependent dimensionless King correction factor, which accounts for the effect of depolarization for non-spherical molecules.[7,10,13] Despite the appearance of the Rayleigh scattering cross section depending on density in Eq. (1), it actually does not because the refractive index is defined at density N. Provided the index of refraction and King correction factor are known at the relevant wavenumbers, the *n*-based method enables a straightforward determination of the Rayleigh scattering cross sections of a gas at a given temperature and pressure.

The BBCES and CRDS experimental methods for directly measuring Rayleigh scattering cross sections have shown that the calculation of Rayleigh scattering cross sections from the index of refraction of the gas is a very accurate approach. The *n*-based method has been at times referred to as *theory* in the literature to distinguish it from Rayleigh scattering cross sections determined from empirical fit expressions, but the *n*-based method is not truly theory, because it relies on experimentally-determined indices of refraction and King correction factors.[16] Rayleigh scattering cross sections calculated using the *n*-based method must be experimentally verified, particularly in the ultraviolet region due to the $1/\lambda^4$ scattering dependence and because most refractive indices in the literature were measured at visible or infrared wavelengths. The Rayleigh scattering cross section values recommended here are presented as *n*-based expressions that have been determined from direct measurements of the cross sections or experimentally verified by direct measurements, most often with BBCES.

The recommended refractive indices and King correction factors for Ar, CH_4, CO_2, He, N_2, N_2O, O_2, and SF_6 are given in Table 4-2. These values should be used in Eq (1) to calculate the recommended wavelength-dependent

Rayleigh scattering cross sections. The King correction factor is taken as 1.0 for mono-atomic gases and spherical molecules but deviates from unity for non-spherical molecules. The $F_k(\nu)$ values typically have uncertainty of less than 1%. The density values at which the listed dispersion formulas are defined and the wavelength range over which the Rayleigh scattering cross sections are recommended are given in the Table 4-2 footnote.

(1) He, Q.; Bluvshtein, N.; Segev, L.; Meidan, D.; Flores, J. M.; Brown, S. S.; Brune, W.; Rudich, Y. Evolution of the complex refractive index of secondary organic aerosols during atmospheric aging. *Environ. Sci. Technol.* **2018**, *52*, 3456–3465, doi:10.1021/acs.est.7b05742.

(2) He, Q.; Fang, Z.; Shoshanim, O.; Brown, S. S.; Rudich, Y. Scattering and absorption cross sections of atmospheric gases in the ultraviolet–visible wavelength range (307–725 nm). *Atmos. Chem. Phys.* **2021**, *21*, 14927–14940, doi:10.5194/acp-21-14927-2021.

(3) Issac, S. I.; Suhail, K.; Arun, R.; Varma, R. Scattering cross-sections of common calibration gases measured by IBBCEAS technique. *Results Phys.* **2016**, *6*, 84–85, doi:10.1016/j.rinp.2016.01.014.

(4) Ityaksov, D.; Linnartz, H.; Ubachs, W. Deep-UV absorption and Rayleigh scattering of carbon dioxide. *Chem. Phys. Lett.* **2008**, *462*, 31–34, doi:10.1016/j.cplett.2008.07.049.

(5) Ityaksov, D.; Linnartz, H.; Ubachs, W. Deep-UV Rayleigh scattering of N_2, CH_4 and SF_6. *Mol. Phys.* **2008**, *106*, 2471–2479, doi:10.1080/00268970802570334.

(6) Jordan, N.; Ye, C. Z.; Ghosh, S.; Washenfelder, R. A.; Brown, S. S.; Osthoff, H. D. A broadband cavity-enhanced spectrometer for atmospheric trace gas measurements and Rayleigh scattering cross sections in the cyan region (470–540 nm). *Atmos. Meas. Tech.* **2019**, *12*, 1277–1293, doi:10.5194/amt-12-1277-2019.

(7) King, L. V. On the complex anisotropic molecule in relation to the dispersion and scattering of light. *Proc. R. Soc. A* **1923**, *104*, 333–357, doi:10.1098/rspa.1923.0113.

(8) Naus, H.; Ubachs, W. Experimental verification of Rayleigh scattering cross sections. *Opt. Lett.* **2000**, *25*, 347–349, doi:10.1364/OL.25.000347.

(9) Rayleigh, L. On the transmission of light through an atmosphere containing small particles in suspension, and on the origin of the blue of the sky. *Philos. Mag.* **1899**, *47*, 375–384, doi:10.1080/14786449908621276.

(10) Rayleigh, L. A re-examination of the light scattered by gases in respect of polarisation. I. Experiments on the common gases. *Proc. R. Soc. A* **1920**, *97*, 435–450, doi:10.1098/rspa.1920.0044.

(11) Shardanand, R. A. Absolute Rayleigh scattering cross sections of gases and freons of stratospheric interest in the visible and ultraviolet regions. *NASA Technical Note TN-D-8442* **1977**.

(12) Sneep, M.; Ubachs, W. Direct measurement of the Rayleigh scattering cross section in various gases. *J. Quant. Spectrosc. Radiat. Transf.* **2005**, *92*, 293–310, doi:10.1016/j.jqsrt.2004.07.025.

(13) Strutt, R. J. The light scattered by gases: its polarization and intensity. *Proc. R. Soc. A* **1918**, *95*, 155–176, doi:10.1098/rspa.1918.0057.

(14) Thalman, R.; Zarzana, K. J.; Tolbert, M. A.; Volkamer, R. Rayleigh scattering cross-section measurements of nitrogen, argon, oxygen and air. *J. Quant. Spectrosc. Radiat. Transf.* **2014**, *147*, 171–177, doi:10.1016/j.jqsrt.2014.05.030.

(15) Thalman, R.; Zarzana, K. J.; Tolbert, M. A.; Volkamer, R. Erratum to "Rayleigh scattering cross-section measurements of nitrogen, argon, oxygen and air". *J. Quant. Spectrosc. Radiat. Transf.* **2017**, *189*, 281–282, doi:10.1016/j.jqsrt.2016.12.014.

(16) Wilmouth, D.; Sayres, D. Rayleigh scattering cross sections of argon, carbon dioxide, sulfur hexafluoride, and methane in the UV-A region using Broadband Cavity Enhanced Spectroscopy. *J. Quant. Spectrosc. Radiat. Transf.* **2019**, *234*, 32–39, doi:10.1016/j.jqsrt.2019.05.031.

(17) Wilmouth, D.; Sayres, D. Determination of Rayleigh scattering cross sections and indices of refraction for Ar, CO_2, SF_6, and CH_4 using BBCES in the ultraviolet. *J. Quant. Spectrosc. Radiat. Transf.* **2020**, *255*, 107224, doi:10.1016/j.jqsrt.2020.107224.

Table 4-2. Refractive Indices and King Correction Factors for Calculating Recommended Rayleigh Scattering Cross Sections [a] Return to Photochem Index

Gas	$(n_{(\nu)}-1)\times10^8$	$F_k(\nu)$	Note
Ar	$6432.135 + \frac{2.8606021 \times 10^{14}}{(1.44 \times 10^{10} - \nu^2)}$	1.0	K1
CH_4	$4869.8 + \frac{4.1023 \times 10^{14}}{(1.133 \times 10^{10} - \nu^2)}$	1.0	K2
CO_2	$1.1427 \times 10^{11} \left(\frac{5799.25}{(128908.9)^2 - \nu^2} + \frac{120.05}{(89223.8)^2 - \nu^2} + \frac{5.3334}{(75037.5)^2 - \nu^2} + \frac{4.3244}{(67837.7)^2 - \nu^2} + \frac{1.218145 \times 10^{-5}}{(2418.136)^2 - \nu^2} \right)$	$1.1364 + 2.53 \times 10^{-11}\ \nu^2$	K3
He	$2283 + \frac{1.8102 \times 10^{13}}{(1.5342 \times 10^{10} - \nu^2)}$	1.0	K4
N_2	$5677.465 + \frac{3.1881874 \times 10^{14}}{(1.44 \times 10^{10} - \nu^2)}$	$1.034 + 3.17 \times 10^{-12}\ \nu^2$	K5
N_2O	$22095 + \frac{1.66291 \times 10^{14}}{(6.75226 \times 10^{9} - \nu^2)}$	$\frac{3.3462 + 7.08 \times 10^{-11}\ \nu^2}{2.7692 - 4.72 \times 10^{-11}\ \nu^2}$	K6
O_2	$20564.8 + \frac{2.480899 \times 10^{13}}{(4.09 \times 10^{9} - \nu^2)}$	$1.09 + 1.385 \times 10^{-11}\ \nu^2 + 1.448 \times 10^{-20}\ \nu^4$	K7
SF_6	$18611.4 + \frac{8.9566 \times 10^{14}}{(1.680 \times 10^{10} - \nu^2)}$	1.0	K8

[a] Rayleigh scattering cross sections are calculated using the following equation (see intro text):

$$\sigma(\nu) = \frac{24\pi^3\nu^4}{N^2}\left(\frac{n_{(\nu)}^2 - 1}{n_{(\nu)}^2 + 2}\right)^2 F_k(\nu)$$

Units of ν are cm^{-1}. For all gases except O_2, $N = 2.5469\times10^{19}$ molecules cm^{-3} (i.e., refractive indices are scaled to 288.15 K and 101325 Pa). For O_2, $N = 2.68678\times10^{19}$ molecules cm^{-3} (i.e., refractive indices are scaled to 273.15 K and 101325 Pa).

The recommended wavelength ranges for using the Rayleigh scattering cross sections determined from Table 1 are:
250–700 nm (wavenumbers 40,000 > ν > 14,286 cm^{-1}) for Ar, CH_4, CO_2, He, N_2, and SF_6
310–700 nm (wavenumbers 32,258 > ν > 14,286 cm^{-1}) for N_2O
350–700 nm (wavenumbers 28,571 > ν > 14,286 cm^{-1}) for O_2

Figure 1 shows the Rayleigh scattering cross sections calculated from the values in Table 4-2. The range of Rayleigh scattering cross sections shown spans more than two orders of magnitude from the smallest (He) to largest (SF_6).

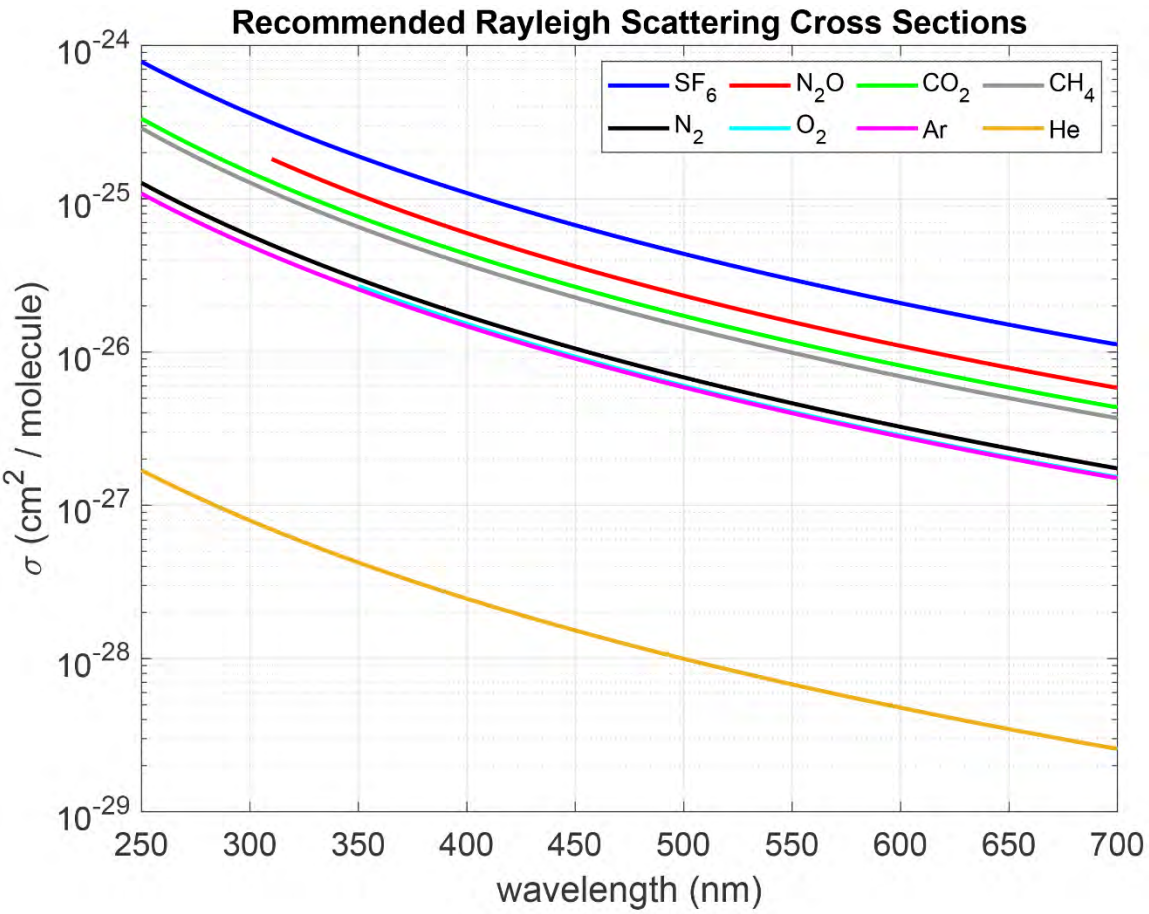


Figure 1. Recommended Rayleigh scattering cross sections calculated using values from Table 4-2.

4.15 Notes

K1. Ar (argon) Back to Table

The recommended values for Ar in Table 4-2 are from Sneep and Ubachs,[5] based on the refractive index data of Peck and Fisher.[4] The recommended Rayleigh scattering cross sections for Ar agree with the BBCES studies of Thalman et al.[6,7] (350–660 nm) to within 1%, Isaac et al.[1] (650–670 nm) to within 1%, Jordan et al.[2] (480–535 nm) generally to within 2%, and Wilmouth and Sayres[8,9] (264–363 nm) to within 1%. The CRDS studies of Naus and Ubachs[3] (560–650 nm) and Sneep and Ubachs (467–649 nm) agree with the recommended values to within 1%, while Sneep and Ubachs (532.2 nm) is lower by 2.5%. Note that extrapolation of the experimentally-derived, parameterized expressions from Naus and Ubachs and Sneep and Ubachs to wavelengths beyond those at which the data were acquired results in substantial errors in the Rayleigh scattering cross sections, particularly in the ultraviolet.

The Rayleigh scattering cross sections for Ar calculated from Table 4-2 are recommended for the 250–700 nm wavelength range and have a recommended uncertainty factor of 1.01 (2σ).

(1) Issac, S. I.; Suhail, K.; Arun, R.; Varma, R. Scattering cross-sections of common calibration gases measured by IBBCEAS technique. *Results Phys.* **2016**, *6*, 84–85, doi:10.1016/j.rinp.2016.01.014.

(2) Jordan, N.; Ye, C. Z.; Ghosh, S.; Washenfelder, R. A.; Brown, S. S.; Osthoff, H. D. A broadband cavity-enhanced spectrometer for atmospheric trace gas measurements and Rayleigh scattering cross sections in the cyan region (470–540 nm). *Atmos. Meas. Tech.* **2019**, *12*, 1277–1293, doi:10.5194/amt-12-1277-2019.

(3) Naus, H.; Ubachs, W. Experimental verification of Rayleigh scattering cross sections. *Opt. Lett.* **2000**, *25*, 347–349, doi:10.1364/OL.25.000347.

(4) Peck, E. R.; Fisher, D. J. Dispersion of argon. *J. Opt. Soc. Am.* **1964**, *54*, 1362–1364, doi:10.1364/JOSA.54.001362.

(5) Sneep, M.; Ubachs, W. Direct measurement of the Rayleigh scattering cross section in various gases. *J. Quant. Spectrosc. Radiat. Transf.* **2005**, *92*, 293–310, doi:10.1016/j.jqsrt.2004.07.025.

(6) Thalman, R.; Zarzana, K. J.; Tolbert, M. A.; Volkamer, R. Rayleigh scattering cross-section measurements of nitrogen, argon, oxygen and air. *J. Quant. Spectrosc. Radiat. Transf.* **2014**, *147*, 171–177, doi:10.1016/j.jqsrt.2014.05.030.

(7) Thalman, R.; Zarzana, K. J.; Tolbert, M. A.; Volkamer, R. Erratum to "Rayleigh scattering cross-section measurements of nitrogen, argon, oxygen and air". *J. Quant. Spectrosc. Radiat. Transf.* **2017**, *189*, 281–282, doi:10.1016/j.jqsrt.2016.12.014.

(8) Wilmouth, D.; Sayres, D. Rayleigh scattering cross sections of argon, carbon dioxide, sulfur hexafluoride, and methane in the UV-A region using Broadband Cavity Enhanced Spectroscopy. *J. Quant. Spectrosc. Radiat. Transf.* **2019**, *234*, 32–39, doi:10.1016/j.jqsrt.2019.05.031.

(9) Wilmouth, D.; Sayres, D. Determination of Rayleigh scattering cross sections and indices of refraction for Ar, CO_2, SF_6, and CH_4 using BBCES in the ultraviolet. *J. Quant. Spectrosc. Radiat. Transf.* **2020**, *255*, 107224, doi:10.1016/j.jqsrt.2020.107224.

K2. CH_4 (methane) Back to Table

The recommended values for CH_4 are from Wilmouth and Sayres[9] based on the Rayleigh scattering cross section data from their two BBCES studies[8,9] in the ultraviolet and the index of refraction data of Cuthbertson and Cuthbertson[1] and Watson and Ramaswamy[7] in the visible, as detailed in Wilmouth and Sayres.[9] The recommended Rayleigh scattering cross sections for CH_4 agree with the BBCES studies of He et al.[2] (307–400 nm) to within 1.2% on average and Jordan et al.[5] (480–535 nm) generally to within 4%, although the sampling region of Jordan et al. contained absorption bands that complicated the measurement. The Wilmouth and Sayres[8,9] work corrects an earlier nearly 30% high bias in the Rayleigh scattering cross sections of CH_4 from Sneep and Ubachs[6] determined using the polarizability data of Hohm.[3] The CRDS study of Ityaksov et al.[4] (198–270 nm) is higher than the recommended values by approximately 37% in the overlapping wavelength region of 250–270 nm. He et al. report two dispersion relations for CH_4 in their BBCES study: the first approach used only their own data (307–400 nm), and the Rayleigh scattering cross sections are on average 1.2% higher than the Wilmouth and Sayres[9] values (1.6% higher when extrapolated to 700 nm). The second, preferred approach of He et al. was to essentially replicate the method of Wilmouth and Sayres,[9] with the He et al. data added in but weighted so lightly that the inclusion of their data had a negligible impact on the previously published Wilmouth and Sayres[9]

expression (agreement to within 0.1% over the entire wavelength range). The original dispersion formula from Wilmouth and Sayres[9] is recommended.

The Rayleigh scattering cross sections for CH_4 calculated from Table 4-2 are recommended for the 250–700 nm wavelength range and have a recommended uncertainty factor of 1.015 (2σ). Note that CH_4 also absorbs at many wavelengths over the recommended range.

(1) Cuthbertson, C.; Cuthbertson, M. On the refraction and dispersion of carbon dioxide, carbon monoxide, and methane. *Proc. R. Soc. A* **1920**, *97*, 152–159, doi:10.1098/rspa.1920.0020.

(2) He, Q.; Fang, Z.; Shoshanim, O.; Brown, S. S.; Rudich, Y. Scattering and absorption cross sections of atmospheric gases in the ultraviolet–visible wavelength range (307–725 nm). *Atmos. Chem. Phys.* **2021**, *21*, 14927–14940, doi:10.5194/acp-21-14927-2021.

(3) Hohm, U. Experimental determination of the dispersion in the mean linear dipole polarizability α(ω) of small hydrocarbons and evaluation of Cauchy moments between 325 nm and 633 nm. *Mol. Phys.* **1993**, *78*, 929–941, doi:10.1080/00268979300100621.

(4) Ityaksov, D.; Linnartz, H.; Ubachs, W. Deep-UV Rayleigh scattering of N_2, CH_4 and SF_6. *Mol. Phys.* **2008**, *106*, 2471–2479, doi:10.1080/00268970802570334.

(5) Jordan, N.; Ye, C. Z.; Ghosh, S.; Washenfelder, R. A.; Brown, S. S.; Osthoff, H. D. A broadband cavity-enhanced spectrometer for atmospheric trace gas measurements and Rayleigh scattering cross sections in the cyan region (470–540 nm). *Atmos. Meas. Tech.* **2019**, *12*, 1277–1293, doi:10.5194/amt-12-1277-2019.

(6) Sneep, M.; Ubachs, W. Direct measurement of the Rayleigh scattering cross section in various gases. *J. Quant. Spectrosc. Radiat. Transf.* **2005**, *92*, 293–310, doi:10.1016/j.jqsrt.2004.07.025.

(7) Watson, H. E.; Ramaswamy, K. L. The refractive index dispersion and polarization of gases. *Proc. R. Soc. A* **1936**, *156*, 144–157, doi:10.1098/rspa.1936.0140.

(8) Wilmouth, D.; Sayres, D. Rayleigh scattering cross sections of argon, carbon dioxide, sulfur hexafluoride, and methane in the UV-A region using Broadband Cavity Enhanced Spectroscopy. *J. Quant. Spectrosc. Radiat. Transf.* **2019**, *234*, 32–39, doi:10.1016/j.jqsrt.2019.05.031.

(9) Wilmouth, D.; Sayres, D. Determination of Rayleigh scattering cross sections and indices of refraction for Ar, CO_2, SF_6, and CH_4 using BBCES in the ultraviolet. *J. Quant. Spectrosc. Radiat. Transf.* **2020**, *255*, 107224, doi:10.1016/j.jqsrt.2020.107224.

K3. CO_2 (carbon dioxide)

Back to Table

The recommended values for CO_2 in Table 4-2 are from Bideau-Mehu et al.,[2] Alms et al.,[1] and Sneep and Ubachs;[8] the original dispersion formulas had typographical errors in Bideau-Mehu et al. and Sneep and Ubachs, which were corrected in Wilmouth and Sayres.[9] The recommended Rayleigh scattering cross sections for CO_2 agree with the BBCES studies of Isaac et al.[5] (650–670 nm) to within 4%, He et al.[3] (400–700 nm) to within 4.5%, Jordan et al.[7] (480–535 nm) generally to within 5%, Wilmouth and Sayres[9,10] (264–363 nm) to within 1% on average, and He et al.[4] (307–700 nm) to within 1% on average. The CRDS studies of Ityaksov et al.[6] (198–270 nm) and Sneep and Ubachs (467–575 nm) agree with the recommended values to within 3% and 4%, respectively, while the Sneep and Ubachs value at 532.2 nm is lower by 7%. Note that extrapolation of the experimentally-derived, parameterized expressions from Sneep and Ubachs and Ityaksov et al.[6] to wavelengths beyond those at which the data were acquired results in large errors in the Rayleigh scattering cross sections.

The Rayleigh scattering cross sections for CO_2 calculated from Table 4-2 are recommended for the 250–700 nm wavelength range and have a recommended uncertainty factor of 1.015 (2σ).

(1) Alms, G. R.; Burnham, A. K.; Flygare, W. H. Measurement of the dispersion in polarizability anisotropies. *J. Chem. Phys.* **1975**, *63*, 3321–3326, doi:10.1063/1.431821.

(2) Bideau-Mehu, A.; Guern, Y.; Abjean, R.; Johannin-Gilles, A. Interferometric determination of the refractive index of carbon dioxide in the ultraviolet region. *Opt. Commun.* **1973**, *9*, 432–434, doi:10.1016/0030-4018(73)90289-7.

(3) He, Q.; Bluvshtein, N.; Segev, L.; Meidan, D.; Flores, J. M.; Brown, S. S.; Brune, W.; Rudich, Y. Evolution of the complex refractive index of secondary organic aerosols during atmospheric aging. *Environ. Sci. Technol.* **2018**, *52*, 3456–3465, doi:10.1021/acs.est.7b05742.

(4) He, Q.; Fang, Z.; Shoshanim, O.; Brown, S. S.; Rudich, Y. Scattering and absorption cross sections of atmospheric gases in the ultraviolet–visible wavelength range (307–725 nm). *Atmos. Chem. Phys.* **2021**, *21*, 14927–14940, doi:10.5194/acp-21-14927-2021.

(5) Issac, S. I.; Suhail, K.; Arun, R.; Varma, R. Scattering cross-sections of common calibration gases measured by IBBCEAS technique. *Results Phys.* **2016**, *6*, 84–85, doi:10.1016/j.rinp.2016.01.014.
(6) Ityaksov, D.; Linnartz, H.; Ubachs, W. Deep-UV absorption and Rayleigh scattering of carbon dioxide. *Chem. Phys. Lett.* **2008**, *462*, 31–34, doi:10.1016/j.cplett.2008.07.049.
(7) Jordan, N.; Ye, C. Z.; Ghosh, S.; Washenfelder, R. A.; Brown, S. S.; Osthoff, H. D. A broadband cavity-enhanced spectrometer for atmospheric trace gas measurements and Rayleigh scattering cross sections in the cyan region (470–540 nm). *Atmos. Meas. Tech.* **2019**, *12*, 1277–1293, doi:10.5194/amt-12-1277-2019.
(8) Sneep, M.; Ubachs, W. Direct measurement of the Rayleigh scattering cross section in various gases. *J. Quant. Spectrosc. Radiat. Transf.* **2005**, *92*, 293–310, doi:10.1016/j.jqsrt.2004.07.025.
(9) Wilmouth, D.; Sayres, D. Rayleigh scattering cross sections of argon, carbon dioxide, sulfur hexafluoride, and methane in the UV-A region using Broadband Cavity Enhanced Spectroscopy. *J. Quant. Spectrosc. Radiat. Transf.* **2019**, *234*, 32–39, doi:10.1016/j.jqsrt.2019.05.031.
(10) Wilmouth, D.; Sayres, D. Determination of Rayleigh scattering cross sections and indices of refraction for Ar, CO_2, SF_6, and CH_4 using BBCES in the ultraviolet. *J. Quant. Spectrosc. Radiat. Transf.* **2020**, *255*, 107224, doi:10.1016/j.jqsrt.2020.107224.

K4. He (helium) Back to Table

The recommended values for He in Table 4-2 are from Thalman et al.,[7,8] Abjean et al.,[1] Leonard,[6] and Cuthbertson and Cuthbertson.[2] The Rayleigh scattering cross sections for He as recommended here have been used in many BBCES studies as reference values, e.g., Thalman et al.[7] (350–660 nm), He et al.[3] (400–700 nm), Jordan et al.[5] (480–535 nm), Wilmouth and Sayres[9,10] (264–363 nm), and He et al.[4] (307–725 nm). Because the Rayleigh scattering cross sections of He are much smaller than the other gases typically used in BBCES studies, e.g., a factor of ~70 less than N_2, uncertainty in the He cross sections is both less important and harder to quantify.[9] Thalman et al.[7] have highlighted that additional Rayleigh scattering cross section measurements of He using CRDS would be a valuable addition to the literature.

The Rayleigh scattering cross sections for He calculated from Table 4-2 are recommended for the 250–700 nm wavelength range and have a recommended uncertainty factor of 1.05 (2σ).

(1) Abjean, R.; Mehu, A.; Johannin-Gilles, A. Interferometric measurement of refraction indices of helium and neon in ultraviolet. *C. R. Acad. Sci. B* **1970**, *271*, 835–838.
(2) Cuthbertson, C.; Cuthbertson, M. The refraction and dispersion of neon and helium. *Proc. R. Soc. A* **1932**, *135*, 40–47, doi:10.1098/rspa.1932.0019.
(3) He, Q.; Bluvshtein, N.; Segev, L.; Meidan, D.; Flores, J. M.; Brown, S. S.; Brune, W.; Rudich, Y. Evolution of the complex refractive index of secondary organic aerosols during atmospheric aging. *Environ. Sci. Technol.* **2018**, *52*, 3456–3465, doi:10.1021/acs.est.7b05742.
(4) He, Q.; Fang, Z.; Shoshanim, O.; Brown, S. S.; Rudich, Y. Scattering and absorption cross sections of atmospheric gases in the ultraviolet–visible wavelength range (307–725 nm). *Atmos. Chem. Phys.* **2021**, *21*, 14927–14940, doi:10.5194/acp-21-14927-2021.
(5) Jordan, N.; Ye, C. Z.; Ghosh, S.; Washenfelder, R. A.; Brown, S. S.; Osthoff, H. D. A broadband cavity-enhanced spectrometer for atmospheric trace gas measurements and Rayleigh scattering cross sections in the cyan region (470–540 nm). *Atmos. Meas. Tech.* **2019**, *12*, 1277–1293, doi:10.5194/amt-12-1277-2019.
(6) Leonard, P. J. Refractive indices, Verdet constants, and polarizabilities of the inert gases. *Atom Data Nucl. Data Tables* **1974**, *14*, 21–37, doi:10.1016/S0092-640X(74)80028-8.
(7) Thalman, R.; Zarzana, K. J.; Tolbert, M. A.; Volkamer, R. Rayleigh scattering cross-section measurements of nitrogen, argon, oxygen and air. *J. Quant. Spectrosc. Radiat. Transf.* **2014**, *147*, 171–177, doi:10.1016/j.jqsrt.2014.05.030.
(8) Thalman, R.; Zarzana, K. J.; Tolbert, M. A.; Volkamer, R. Erratum to "Rayleigh scattering cross-section measurements of nitrogen, argon, oxygen and air". *J. Quant. Spectrosc. Radiat. Transf.* **2017**, *189*, 281–282, doi:10.1016/j.jqsrt.2016.12.014.
(9) Wilmouth, D.; Sayres, D. Rayleigh scattering cross sections of argon, carbon dioxide, sulfur hexafluoride, and methane in the UV-A region using Broadband Cavity Enhanced Spectroscopy. *J. Quant. Spectrosc. Radiat. Transf.* **2019**, *234*, 32–39, doi:10.1016/j.jqsrt.2019.05.031.

(10) Wilmouth, D.; Sayres, D. Determination of Rayleigh scattering cross sections and indices of refraction for Ar, CO_2, SF_6, and CH_4 using BBCES in the ultraviolet. *J. Quant. Spectrosc. Radiat. Transf.* **2020**, *255*, 107224, doi:10.1016/j.jqsrt.2020.107224.

K5. N_2 (nitrogen) Back to Table

The recommended values for N_2 in Table 4-2 are from Sneep and Ubachs[10] based on data from Peck and Khanna[9] and Abjean et al.[1] and the dispersion relation of Bates.[2] The Rayleigh scattering cross sections for N_2 as recommended here have been tested and used in many BBCES studies as reference values, e.g., Thalman et al.[11,12] (350–660 nm), He et al.[3] (400–700 nm), Jordan et al.[7] (480–535 nm), Wilmouth and Sayres[13,14] (264–363 nm), and He et al.[4] (307–725 nm). Because N_2 was used as the reference gas for determining mirror reflectivity in many BBCES studies that found agreement to within 1% between experimental and *n*-based methods for other gases, it provides confidence that the Rayleigh scattering cross sections of N_2 are accurate to within 1%. The CRDS studies of Thalman et al.[11] (405.8 and 532.2 nm), Sneep and Ubachs[10] (467–649 nm), and Naus and Ubachs[8] (560–650 nm) agree with the recommended values to within 0.5%, 1%, and 0.2%, respectively, while the Sneep and Ubachs value at 532.2 nm is lower by 4% and Ityaksov et al.[6] (198–270 nm) is higher by 4%. Note that extrapolation of the experimentally-derived, parameterized expressions from Naus and Ubachs, Sneep and Ubachs, and especially Ityaksov et al.[5] to wavelengths beyond those at which the data were acquired results in large errors in the Rayleigh scattering cross sections.

The Rayleigh scattering cross sections for N_2 calculated from Table 4-2 are recommended for the 250–700 nm wavelength range and have a recommended uncertainty factor of 1.01 (2σ).

(1) Abjean, R.; Mehu, A.; Johannin-Gilles, A. Interferometric measurement of refraction indices of nitrogen and argon in ultraviolet. *C. R. Acad. Sci. B* **1970**, *271*, 411–414.
(2) Bates, D. R. Rayleigh scattering by air. *Planet Space Sci.* **1984**, *32*, 785–790, doi:10.1016/0032-0633(84)90102-8.
(3) He, Q.; Bluvshtein, N.; Segev, L.; Meidan, D.; Flores, J. M.; Brown, S. S.; Brune, W.; Rudich, Y. Evolution of the complex refractive index of secondary organic aerosols during atmospheric aging. *Environ. Sci. Technol.* **2018**, *52*, 3456–3465, doi:10.1021/acs.est.7b05742.
(4) He, Q.; Fang, Z.; Shoshanim, O.; Brown, S. S.; Rudich, Y. Scattering and absorption cross sections of atmospheric gases in the ultraviolet–visible wavelength range (307–725 nm). *Atmos. Chem. Phys.* **2021**, *21*, 14927–14940, doi:10.5194/acp-21-14927-2021.
(5) Ityaksov, D.; Linnartz, H.; Ubachs, W. Deep-UV absorption and Rayleigh scattering of carbon dioxide. *Chem. Phys. Lett.* **2008**, *462*, 31–34, doi:10.1016/j.cplett.2008.07.049.
(6) Ityaksov, D.; Linnartz, H.; Ubachs, W. Deep-UV Rayleigh scattering of N_2, CH_4 and SF_6. *Mol. Phys.* **2008**, *106*, 2471–2479, doi:10.1080/00268970802570334.
(7) Jordan, N.; Ye, C. Z.; Ghosh, S.; Washenfelder, R. A.; Brown, S. S.; Osthoff, H. D. A broadband cavity-enhanced spectrometer for atmospheric trace gas measurements and Rayleigh scattering cross sections in the cyan region (470–540 nm). *Atmos. Meas. Tech.* **2019**, *12*, 1277–1293, doi:10.5194/amt-12-1277-2019.
(8) Naus, H.; Ubachs, W. Experimental verification of Rayleigh scattering cross sections. *Opt. Lett.* **2000**, *25*, 347–349, doi:10.1364/OL.25.000347.
(9) Peck, E. R.; Khanna, B. N. Dispersion of nitrogen. *J. Opt. Soc. Am.* **1966**, *56*, 1059–1063, doi:10.1364/JOSA.56.001059.
(10) Sneep, M.; Ubachs, W. Direct measurement of the Rayleigh scattering cross section in various gases. *J. Quant. Spectrosc. Radiat. Transf.* **2005**, *92*, 293–310, doi:10.1016/j.jqsrt.2004.07.025.
(11) Thalman, R.; Zarzana, K. J.; Tolbert, M. A.; Volkamer, R. Rayleigh scattering cross-section measurements of nitrogen, argon, oxygen and air. *J. Quant. Spectrosc. Radiat. Transf.* **2014**, *147*, 171–177, doi:10.1016/j.jqsrt.2014.05.030.
(12) Thalman, R.; Zarzana, K. J.; Tolbert, M. A.; Volkamer, R. Erratum to "Rayleigh scattering cross-section measurements of nitrogen, argon, oxygen and air". *J. Quant. Spectrosc. Radiat. Transf.* **2017**, *189*, 281–282, doi:10.1016/j.jqsrt.2016.12.014.
(13) Wilmouth, D.; Sayres, D. Rayleigh scattering cross sections of argon, carbon dioxide, sulfur hexafluoride, and methane in the UV-A region using Broadband Cavity Enhanced Spectroscopy. *J. Quant. Spectrosc. Radiat. Transf.* **2019**, *234*, 32–39, doi:10.1016/j.jqsrt.2019.05.031.

(14) Wilmouth, D.; Sayres, D. Determination of Rayleigh scattering cross sections and indices of refraction for Ar, CO_2, SF_6, and CH_4 using BBCES in the ultraviolet. *J. Quant. Spectrosc. Radiat. Transf.* **2020**, *255*, 107224, doi:10.1016/j.jqsrt.2020.107224.

K6. N_2O (nitrous oxide) Back to Table

The recommended values for N_2O in Table 1 are from He et al.[2] There are relatively few studies of the Rayleigh scattering cross sections for N_2O. The He et al. study used BBCES to determine Rayleigh scattering cross sections over the wavelength range 307–725 nm. Rayleigh scattering cross sections determined using the dispersion formula of Sneep and Ubachs[3] from the polarizability data of Alms et al.[1] (458–647 nm) are within 1.1% of the recommended values in the overlapping wavelength range. The CRDS study of Sneep and Ubachs (532.2 nm) is 12% lower than the recommended value.

The Rayleigh scattering cross sections for N_2O calculated from Table 4-2 are recommended for the 310–700 nm wavelength range and have a recommended uncertainty factor of 1.02 (2σ). We do not recommend extrapolating the dispersion formula in Table 1 deeper into the ultraviolet, as our relative cross section analysis indicates a high bias in the calculated N_2O Rayleigh scattering cross sections below 310 nm that increases with decreasing wavelength.

(1) Alms, G. R.; Burnham, A. K.; Flygare, W. H. Measurement of the dispersion in polarizability anisotropies. *J. Chem. Phys.* **1975**, *63*, 3321–3326, doi:10.1063/1.431821.
(2) He, Q.; Fang, Z.; Shoshanim, O.; Brown, S. S.; Rudich, Y. Scattering and absorption cross sections of atmospheric gases in the ultraviolet–visible wavelength range (307–725 nm). *Atmos. Chem. Phys.* **2021**, *21*, 14927–14940, doi:10.5194/acp-21-14927-2021.
(3) Sneep, M.; Ubachs, W. Direct measurement of the Rayleigh scattering cross section in various gases. *J. Quant. Spectrosc. Radiat. Transf.* **2005**, *92*, 293–310, doi:10.1016/j.jqsrt.2004.07.025.

K7. O_2 (oxygen) Back to Table

The recommended values for O_2 in Table 4-2 are from Sneep and Ubachs[5] based on Bates.[1] The determination of Rayleigh scattering cross sections of O_2 at visible wavelengths is complicated by a number of overlapping absorption bands, particularly due to O_2–O_2 collision-induced absorption (CIA), also called O_4 bands. The recommended Rayleigh scattering cross sections for O_2 agree with the BBCES studies of Thalman et al.[6,7] (350–660 nm) to within 1% in the wavelength regions with no O_4 bands (370–420 nm, 660 nm), Isaac et al.[3] (650–670 nm) to within 4%, and He et al.[2] (307–700 nm) to within 3% in regions with no absorption. Jordan et al.[4] used BBCES to determine O_2 Rayleigh scattering cross sections in the 490–515 nm region, where absorption is small but not zero, and reported values generally 3–9% higher than the recommendation.

The Rayleigh scattering cross sections for O_2 calculated from Table 4-2 are recommended for the 350–700 nm wavelength range and have a recommended uncertainty factor of 1.02 (2σ). We do not recommend extrapolating the dispersion formula in Table 4-2 deeper into the ultraviolet, as our relative cross section analysis indicates a high bias in the calculated O_2 Rayleigh scattering cross sections below 350 nm that increases with decreasing wavelength.

(1) Bates, D. R. Rayleigh scattering by air. *Planet Space Sci.* **1984**, *32*, 785–790, doi:10.1016/0032-0633(84)90102-8.
(2) He, Q.; Fang, Z.; Shoshanim, O.; Brown, S. S.; Rudich, Y. Scattering and absorption cross sections of atmospheric gases in the ultraviolet–visible wavelength range (307–725 nm). *Atmos. Chem. Phys.* **2021**, *21*, 14927–14940, doi:10.5194/acp-21-14927-2021.
(3) Issac, S. I.; Suhail, K.; Arun, R.; Varma, R. Scattering cross-sections of common calibration gases measured by IBBCEAS technique. *Results Phys.* **2016**, *6*, 84–85, doi:10.1016/j.rinp.2016.01.014.
(4) Jordan, N.; Ye, C. Z.; Ghosh, S.; Washenfelder, R. A.; Brown, S. S.; Osthoff, H. D. A broadband cavity-enhanced spectrometer for atmospheric trace gas measurements and Rayleigh scattering cross sections in the cyan region (470–540 nm). *Atmos. Meas. Tech.* **2019**, *12*, 1277–1293, doi:10.5194/amt-12-1277-2019.
(5) Sneep, M.; Ubachs, W. Direct measurement of the Rayleigh scattering cross section in various gases. *J. Quant. Spectrosc. Radiat. Transf.* **2005**, *92*, 293–310, doi:10.1016/j.jqsrt.2004.07.025.
(6) Thalman, R.; Zarzana, K. J.; Tolbert, M. A.; Volkamer, R. Rayleigh scattering cross-section measurements of nitrogen, argon, oxygen and air. *J. Quant. Spectrosc. Radiat. Transf.* **2014**, *147*, 171–177, doi:10.1016/j.jqsrt.2014.05.030.

(7) Thalman, R.; Zarzana, K. J.; Tolbert, M. A.; Volkamer, R. Erratum to "Rayleigh scattering cross-section measurements of nitrogen, argon, oxygen and air". *J. Quant. Spectrosc. Radiat. Transf.* **2017**, *189*, 281–282, doi:10.1016/j.jqsrt.2016.12.014.

K8. SF_6 (sulfur hexafluoride) Back to Table

The recommended values for SF_6 are from Wilmouth and Sayres[7] based on the Rayleigh scattering cross section data from their two BBCES studies[6,7] in the ultraviolet and the index of refraction data of Vukovic et al.[5] in the visible, as detailed in Wilmouth and Sayres.[7] The recommended Rayleigh scattering cross sections for SF_6 agree with the fit data from the BBCES study of He et al.[1] (307–700 nm) to within 0.9% on average. Although He et al. obtained data over a very broad wavelength range (307–725 nm), they did not produce a dispersion formula for SF_6 using their own data. Instead, He et al. produced their dispersion relation by essentially replicating the method of Wilmouth and Sayres,[7] with the He et al. data added in but weighted such that the inclusion of their data had a negligible impact on the previously published Wilmouth and Sayres[7] expression (agreement to within 0.1% on average). The CRDS study of Naus and Ubachs[3] (560–650 nm) is in agreement with the recommended values to within 0.5%, while Ityaksov et al.[2] (198–270 nm) is higher than the recommended values by 4–5% in the overlapping wavelength region of 250–270 nm, and Sneep and Ubachs[4] (532.2 nm) is lower by 5%. The dispersion formula of Sneep and Ubachs, determined from the visible and infrared index of refraction data of Vukovic et al., produces Rayleigh scattering cross sections for SF_6 in excellent agreement with the recommended values at longer wavelengths (within 0.5% for 540–700 nm) but have an increasing high bias towards shorter wavelengths (5% at 254 nm). Note that extrapolation of the experimentally-derived, parameterized expression of Ityaksov et al. to wavelengths beyond those at which the data were acquired results in large errors in the Rayleigh scattering cross sections.

The Rayleigh scattering cross sections for SF_6 calculated from Table 4-2 are recommended for the 250–700 nm wavelength range and have a recommended uncertainty factor of 1.015 (2σ).

(1) He, Q.; Fang, Z.; Shoshanim, O.; Brown, S. S.; Rudich, Y. Scattering and absorption cross sections of atmospheric gases in the ultraviolet–visible wavelength range (307–725 nm). *Atmos. Chem. Phys.* **2021**, *21*, 14927–14940, doi:10.5194/acp-21-14927-2021.
(2) Ityaksov, D.; Linnartz, H.; Ubachs, W. Deep-UV Rayleigh scattering of N_2, CH_4 and SF_6. *Mol. Phys.* **2008**, *106*, 2471–2479, doi:10.1080/00268970802570334.
(3) Naus, H.; Ubachs, W. Experimental verification of Rayleigh scattering cross sections. *Opt. Lett.* **2000**, *25*, 347–349, doi:10.1364/OL.25.000347.
(4) Sneep, M.; Ubachs, W. Direct measurement of the Rayleigh scattering cross section in various gases. *J. Quant. Spectrosc. Radiat. Transf.* **2005**, *92*, 293–310, doi:10.1016/j.jqsrt.2004.07.025.
(5) Vukovic, D.; Woolsey, G. A.; Scelsi, G. B. Refractivities of SF_6 and SOF_2 at wavelengths of 632.99 and 1300 nm. *J. Phys. D: Appl. Phys.* **1996**, *29*, 634–637, doi:10.1088/0022-3727/29/3/023.
(6) Wilmouth, D.; Sayres, D. Rayleigh scattering cross sections of argon, carbon dioxide, sulfur hexafluoride, and methane in the UV-A region using Broadband Cavity Enhanced Spectroscopy. *J. Quant. Spectrosc. Radiat. Transf.* **2019**, *234*, 32–39, doi:10.1016/j.jqsrt.2019.05.031.
(7) Wilmouth, D.; Sayres, D. Determination of Rayleigh scattering cross sections and indices of refraction for Ar, CO_2, SF_6, and CH_4 using BBCES in the ultraviolet. *J. Quant. Spectrosc. Radiat. Transf.* **2020**, *255*, 107224, doi:10.1016/j.jqsrt.2020.107224.

SECTION 5: HETEROGENEOUS PROCESSES

Table of Contents

SECTION 5: HETEROGENEOUS PROCESSES 1

5.1 OVERVIEW 2
5.2 NON-EQUILBRIUM PROCESSES 2
5.2.1 Introduction 2
5.2.1.1 Surface Types—Acid/Water, Liquids and Solids 2
5.2.1.2 Surface Types—Soot and Alumina 3
5.2.1.3 Surface Types—Solid Alkali Halide Salts and Aqueous Salt Solutions 5
5.2.1.4 Surface Composition and Morphology 6
5.2.1.5 Surface Porosity 6
5.2.1.6 Temperature Dependences of Parameters 8
5.2.1.7 Solubility Limitations 8
5.2.1.8 Parameter Definitions 8
5.2.1.9 Bibliography – Introduction 13
5.2.2 Table NEq1. Mass Accommodation Coefficients (α) and Reversible Uptake Data for non-Soot Surfaces 16
5.2.2.1 Notes for Table NEq1 19
5.2.2.2 Bibliography – Table NEq1 50
5.2.3 Table NEq2. Gas/Surface Reaction Probabilities (γ) for Surfaces Other Than Soot 59
5.2.3.1 Notes for Table NEq2 66
5.2.3.2 Bibliography – Table NEq2 133
5.2.4 Table NEq3. Soot Surface Uptake Coefficients 150
5.2.4.1 Notes for Table NEq3 150
5.2.4.2 Bibliography – Table NEq3 157
5.3 EQUILBRIUM PROCESSES 160
5.3.1 Introduction 160
5.3.1.1 Henry's Law Constants 160
5.3.1.2 Temperature dependence 160
5.3.1.3 Thermodynamics 160
5.3.1.4 Effective Henry's law constants 162
5.3.1.5 Sechenov parameters 162
5.3.1.6 Schumpe parameters 162
5.3.2 Table Eq1. Henry's Law Constants for Pure Water 163
5.3.2.1 Notes for Table Eq1 169
5.3.2.2 Bibliography – Table Eq1 196
5.3.3 Schumpe Parameters 203
5.3.3.1 Table Eq2: Gas-specific Schumpe Parameters 203
5.3.3.2 Notes for Table Eq2 203
5.3.3.3 Table Eq3. Ion-Specific Schumpe Parameters 206
5.3.3.4 Notes for Table Eq3 206
5.3.4 Table Eq4. Henry's Law Constants for Acids as Solvent 207
5.3.4.1 Notes for Table Eq4 208
5.3.4.2 Bibliography – Table Eq4 217
5.3.5 Table Eq5. Henry's Law Constants for Sea Water as Solvent 220
5.3.5.1 Notes for Table Eq5 221
5.3.5.2 Bibliography – Table Eq5 229
5.4 PARTICULATE OPTICAL PROPERTIES 231
5.4.1 Table P1. Recommended complex refractive indices for ammonium sulfate 231
5.4.2 Table P2. Ammonium sulfate complex refractive indices uncertainty estimates 233
5.4.3 Table P3. Summary of ammonium sulfate complex refractive index studies across the infrared range 235
5.4.4 Table P4. Results from single wavelength or narrow range studies 236
5.4.4.1 Notes for Optical Properties 237
5.4.4.2 Bibliography 238

5.1 Overview

Historically this section has presented evaluated and tabulated published information on stratospheric heterogeneous processes. The scope of this section has expanded over the years to include tropospheric processes, due to the role tropospheric processes affect the flux of reactive species into the stratosphere, as well as heterogeneous contrail and cloud processing of exhaust species from aircraft and solar radiation management (SRM) research, i.e., stratospheric aerosol injection and marine cloud brightening. In addition, to support NASA's interest in the climate impact of tropospheric heterogeneous processes that influence greenhouse gas concentrations and the formation and chemical evolution of tropospheric fine aerosol particles, selected heterogeneous interactions relevant to modeling cloud droplet and aqueous aerosol chemistry in the free troposphere are included in the evaluation. For instance, recent evaluations have built on reviews[1,2] of relevant inorganic and volatile organic species (VOCs) uptake on water ice surfaces relevant to aircraft contrails and cirrus clouds.

It should be noted, however, that both stratospheric and tropospheric heterogeneous chemistry are rapidly evolving research fields, and future results are expected to change our quantitative and even our qualitative understanding. The complexity is compounded by the difficulty of characterizing the chemical and physical properties of atmospheric heterogeneous surfaces and then reproducing suitable simulations in the laboratory.[3,4]

The heterogeneous processes section is presented in three sub-sections: Non-Equilibrium Processes, Equilibrium Processes, and Particulate Optical Properties. The **Non-Equilibrium Processes** sub-section includes evaluations of heterogeneous uptake processes focused on the kinetics of several highly reactive gaseous atmospheric species including for example: OH on ice and liquid water; O_3 on aqueous bromide solutions; N_2O_5 on liquid water, aqueous nitrate and halide solutions and mineral dust; and HO_2 on aqueous salt solutions, mineral dust and organic surfaces. In the case of N_2O_5, uptake coefficients measured in laboratories were compared with those occurring on ambient particles during field measurements. The **Equilibrium Processes** sub-section includes an evaluation of Henry's Law constants. The **Particulate Opitcal Properties** sub-section includes a review and evaluation of aerosol optical properties for atmospherically relevant ambient aerosol components; presently limited to an evaluation of the complex refractive index of ammonium sulfate over wavelengths from the far infrared to the near ultraviolet.

(1) Abbatt, J. P. D. Interactions of atmospheric trace gases with ice surfaces: Adsorption and reaction. *Chem. Rev.* **2003**, *103*, 4783-4800, doi:10.1021/cr0206418.

(2) Huthwelker, T.; Ammann, M.; Peter, T. The uptake of acidic gases on ice. *Chem. Rev.* **2006**, *106*, 1375-1444, doi:10.1021/cr020506v.

(3) Kolb, C. E.; Cox, R. A.; Abbatt, J. P. D.; Ammann, M.; Davis, E. J.; Donaldson, D. J.; Garrett, B. C.; George, C.; Griffiths, P. T.; Hanson, D. R.; Kulmala, M.; McFiggans, G.; Pöschl, U.; Riipinen, I.; Rossi, M. J.; Rudich, Y.; Wagner, P. E.; Winkler, P. M.; Worsnop, D. R.; O' Dowd, C. D. An overview of current issues in the uptake of atmospheric trace gases by aerosols and clouds. *Atmos. Chem. Phys.* **2010**, *10*, 10561-10605, doi:10.5194/acp-10-10561-2010.

(4) Kolb, C. E.; Worsnop, D. R.; Zahniser, M. S.; Davidovits, P.; Keyser, L. F.; Leu, M.-T.; Molina, M. J.; Hanson, D. R.; Ravishankara, A. R.; Williams, L. R.; Tolbert, M. A. Progress and Problems in Atmospheric Chemistry. In *Adv. Phys. Chem. Series, 3*; Barker, J. R., Ed., 1994; pp 771-875.

5.2 Non-Equilbrium Processes

5.2.1 Introduction

5.2.1.1 Surface Types—Acid/Water, Liquids and Solids

To a first approximation there are three major types of water containing surfaces believed to be present at significant levels in the stratosphere. They are: (1) Type I polar stratospheric clouds (PSCs), nominally composed of nitric acid trihydrate (NAT, $HNO_3 \cdot 3H_2O$); (2) crystals of relatively pure water ice, designated as Type II PSCs because they form at lower temperatures than Type I and are believed to be nucleated by Type I (similar surfaces may form as contrails behind high-altitude aircraft under some stratospheric conditions); and (3) sulfuric acid aerosol, which is nominally a liquid phase surface generally composed of 60–80 weight percent H_2SO_4 and, concomitantly, 40–20 weight percent H_2O. While PSCs, as their name suggests, are formed primarily in the cold winter stratosphere at high latitudes, sulfuric acid aerosol is present year round at all latitudes and may influence stratospheric chemistry on a global basis, particularly after large injections of volcanic sulfur episodically increase their abundance and surface area. There is also evidence that ternary $H_2SO_4/HNO_3/H_2O$ liquid solutions may play a significant role in PSC formation.

In addition to the major stratospheric surface types noted above, several other types of heterogeneous surfaces are found in the stratosphere and may play a significant role in some stratospheric processes. For instance, laboratory

work has indicated that nitric acid dihydrate (NAD) may play an important role in the nucleation of Type I PSCs (Worsnop et al.,[7] Fox et al.[1]) and that mixtures of solid nitric acid hydrates and sulfuric acid tetrahydrate (SAT) (Molina et al.,[4] Zhang et al.[8]) and/or a more complex sulfuric acid/nitric acid hydrate (Fox et al.[1]) may also be key to understanding Type I PSC nucleation and evolution. Analyses of the range of atmospheric conditions possible in the polar stratosphere have also led to interest in solid SAT surfaces and possibly other forms of frozen sulfuric acid aerosols (Toon et al.,[5] Middlebrook et al.[3]), as well as liquid sulfuric acid aerosols significantly more dilute than the 60–80 weight percent normally present at lower latitudes (Wolff and Mulvaney,[6] Hofmann and Oltmans,[2] Toon et al.[5]).

In the free troposphere the heterogeneous surfaces of interest include liquid or solid water (cloud droplets and crystals, contrails), and sulfate particles. Uptake data are compiled for liquid water for several reasons. First this surface is one asymptote of the aqueous acid aerosol continuum; second, the interactions of some trace species with liquid water and water ice (Type II PSC) surfaces are often similar, and third, the uptake of some trace species by liquid water surfaces in the troposphere can play a key role in understanding their tropospheric chemical lifetimes and thus, the fraction that may be transported into the stratosphere. The nature of the sulfate-bearing aerosol is complex. Field measurements by single-particle mass spectrometry show that the particles contain organic species to some degree. The chemical nature of the organics has not been quantified, although it is likely that they are highly oxidized having had long residence times in the atmosphere. Similarly, the inorganic composition is not clear. Most particles of continental origin are neutralized with ammonium, and there is some evidence from the free troposphere that this remains true far above the ground. However, in regions away from ammonia sources, there is the potential for the aerosol to be acidic. The phase of the particles may be either solid, or supercooled liquid. Low relative humidities and full neutralization with ammonia promotes crystallization, whereas higher relative humidities and acidic content are more frequently associated with liquid particles. The phase of the organics is not known but is unlikely to be crystalline and more likely to be an amorphous liquid or solid.

(1) Fox, L. E.; Worsnop, D. R.; Zahniser, M. S.; Wofsy, S. C. Metastable phases in polar stratospheric aerosols. *Science* **1994**, *267*, 351-355, doi:10.1126/science.267.5196.351.

(2) Hofmann, D. J.; Oltmans, S. J. The effect of stratospheric water vapor on the heterogeneous reaction rate of $ClONO_2$ and H_2O for sulfuric acid aerosol. *Geophys. Res. Lett.* **1992**, *22*, 2211-2214, doi:10.1029/92GL02493

(3) Middlebrook, A. M.; Iraci, L. T.; McNeil, L. S.; Koehler, B. G.; Wilson, M. A.; Saastad, O. W.; Tolbert, M. A. Fourier transform-infrared studies of thin H_2SO_4/H_2O films: Formation, water uptake, and solid-liquid phase changes. *J. Geophys. Res.* **1993**, *98*, 20473-20481, doi:10.1029/93JD02454.

(4) Molina, M. J.; Zhang, R.; Woolridge, P. J.; McMahon, J. R.; Kim, J. E.; Chang, H. Y.; Beyer, K. D. Physical chemistry of the $H_2SO_4/HNO_3/H_2O$ system: Implicaitons for polar stratospheric clouds. *Science* **1993**, *261*, 1418-1423, doi:10.1126/science.261.5127.1418.

(5) Toon, O.; Browell, E.; Gray, B.; Lait, L.; Livingston, J.; Newman, P.; Russell, R.; P., P.; Schoeberl, M.; Toon, G.; Traub, W.; Valero, F. P. J.; Selkirk, H.; Jordan, J. Heterogeneous reaction probabilities, solubilities, and the physical state of cold volcanic aerosols. *Science* **1993**, *261*, 1136-1140, doi:10.1126/science.261.5125.1136.

(6) Wolff, E. W.; Mulvaney, R. Reactions on sulphuric acid aerosol and on polar stratospheric clouds in the Antarctic stratosphere. *Geophys. Res. Lett.* **1991**, *18*, 1007-1010, doi:10.1029/91GL01158.

(7) Worsnop, D. R.; Fox, L. E.; Zahniser, M. S.; Wofsy, S. C. Vapor pressures of solid hydrates of nitric acid: Implications for polar stratospheric clouds. *Science* **1993**, *259*, 71-74, doi:10.1126/science.259.5091.71.

(8) Zhang, R.; Wooldridge, P. J.; Molina, M. J. Vapor pressure measurements for the $H_2SO_4/HNO_3/H_2O$ and $H_2SO_4/HCl/H_2O$ systems: Incorporation of stratospheric acids into background sulfate aerosols. *J. Phys. Chem.* **1993**, *97*, 8541-8548, doi:10.1021/j100134a026.

5.2.1.2 Surface Types—Soot and Alumina

Aircraft at cruise altitudes and rocket exhausts contribute small but measurable amounts of carbonaceous “soot” (Pueschel et al.[14]) and aluminized solid propellant rocket exhausts and spacecraft debris produce increasing levels of alumina (Al_2O_3) and similar metal oxide particles (Zolensky et al.[17]) in the stratosphere and upper troposphere. Soot lofted above from surface combustion sources may also be present in the upper troposphere, and to a lesser extent in the lower stratosphere. Alumina from rocket exhausts is generally emitted as liquid droplets from the rocket nozzle and crystalizes as the alpha or metastable gamma phases as it solidifies in the exhaust plume. “Soot” refers to a material that is a combination of elemental and organic carbon, with proportions varying depending on

the source material and the combustion conditions. In studies of soot directed to understanding the interaction with atmospheric gases, two types of soot have been used: carbon blacks having relatively small hydrogen and oxygen contents (e.g. Degussa FW2, Cabot Monarch 1000, ground charcoal and spark-generated soot) and organic combustion soots having higher hydrogen, oxygen and nitrogen content (e.g. soot from the combustion of *n*-hexane, methane, propane, decane, ethylene, acetylene, toluene and stearic candles). In the case of organic combustion soot, even different fuels used to generate the soot have been reported to affect the chemistry; for example, the yields of HONO from the reaction of NO_2 with acetylene, toluene, ethylene and decane soot were observed to vary with the fuel used.[4,10]

Polycyclic aromatic hydrocarbons (PAH) and oxygenated polycyclic aromatic compounds (O-PAC) are major constituents of soot formed from the combustion of liquid fuels.[1-3,5,9,11,15] The bulk composition of soot can have varying amounts of C, H, and O. For example, Chughtai et al. [6] report that the composition (in weight %) of *n*-hexane soot varies from 87 to 92 % C, 1.2 to 1.6 % H, and 11 to 6% oxygen. Stadler and Rossi[16] showed that the elemental composition of the soot as well as its surface area depended on whether the flame was rich or lean; in the case of the rich flame giving a grey-colored soot, the composition (weight %) was 97.3% C, 0.83% H, 1.65% O, and 0.20% N while the lean flame produced a black soot comprised of 96.4% C, 0.19% H, 3.2% O, and 0.27% N.

The functional groups on the soot surface are expected to be important in terms of the uptake and reaction of gases on the surface. X-ray photoelectron spectroscopy (XPS) studies of *n*-hexane soot show surface carbon and oxygen, although the specific nature of the bonding could not be determined (Akhter et al.[3]). The surface functional groups on soot vary, depending on the fuel composition, method of generation and the post-treatment of the soot. For example, Degussa FW2 carbon black, which has been used in a number of studies of uptake and reactions of gases on soot, is post-treated with NO_2 by the manufacturer and Cabot Monarch 1000 is post-treated with aqueous HNO_3. There may be sufficient NO and NO_2 concentrations generated under some conditions during the formation of soot by spark generators that these may also have been reacted with these gases prior to collection and uptake studies. Studies of a number of gases interacting with soot surfaces suggest there are at least two and likely more, types of reactive surface sites; one type reacts very rapidly, e.g. with O_3, while others react more slowly. The first type may be most relevant to the reactions of soot particles in exhaust plumes from combustion sources, while the latter is most relevant to soot diluted in air.

Fourier transform infrared (FTIR), Raman and electron paramagnetic resonance (EPR) spectroscopic studies of *n*-hexane soot show C–O functionalities assigned to anhydrides and aryl ethers, alkyl ketones; they also detected -C=C–H, highly substituted aromatics and conjugated carbonyl-aromatic groups.[2,15] Kirchner et al.[13] measured the FTIR spectra of soot from the combustion of diesel fuel and *n*-hexane (described as "flame deposited") and soot collected from a commercial spark generator in Ar, and from the emissions of a diesel automobile as well as Degussa FW2 soot (described as "filter deposited"). In all cases, absorption peaks characteristic of --C–C–, –C=C–, –C–O, aromatic –C=O, and carboxylic –C=O groups (both aromatic and aliphatic) were observed. However, the flame-deposited soot showed bands due to substituted aromatics while the filter-collected samples did not. The filter-deposited samples had bands due to aliphatic –C–H groups that were not observed for the flame-deposited soot. Only the spark-generated soot showed bands due to both –C=C–H and to –O–H.

For soot formed from the combustion of liquid fuels, the location in the flame at which the soot is collected also changes the surface enough to alter its reactions. For example, Akhter et al. [2] showed that the functional groups as well as particle size depend on the height of collection of soot from the base of the flame. Such changes appear to also alter the reactions of soot; for example, Gerecke et al.[10] measured HONO and NO yields from the reaction of NO_2 with ethylene soot and found that the HONO yield decreased with distance from the bottom of the flame that the soot was collected from, while the yield of NO increased. Kirchner et al.[13] reported much stronger infrared absorption bands due to substituted aromatics in soot samples collected from the combustion of *n*-hexane near the bottom of the flame compared to the top; in addition, absorption bands due to the –O–H group were only observed in samples collected at the bottom of the flame.

Not only can the surface groups directly affect its interaction with gases, but they determine the hygroscopic properties of the soot surface. Chughtai et al.[7,8] have shown that the hydration of soot surfaces depends on the fuel composition (particularly sulfur and trace metal content) and combustion conditions, as well as the extent of surface oxidation. A highly hygroscopic surface holding significant amounts of water may behave differently than a "dry" surface with respect to the interaction with gases; for example, black carbon suspended in aqueous solutions with ozone and irradiated to generate OH has been shown to help assist in the initiation of bulk solution phase OH chemistry.[12] There are also free radical sites on soot surfaces whose EPR signals are strongly affected by the adsorption of paramagnetic species such as NO_2 (e.g. see Chughtai et al.[6]). These unpaired electrons in soot may contribute to the surface reactivity.

The *International Steering Committee for Black Carbon Reference Materials* (http: //www.du.edu/~dwismith/bcsteer.html) has issued preliminary recommendations for representative black carbon reference materials. They recommend that soot formed from the combustion of saturated hydrocarbons, preferably *n*-hexane, be used for soot black carbon. For aerosol black carbon, they recommend the use of Urban Dust Reference Material (SRM) 1649a, which is a sample collected in Washington, D.C. in a baghouse in 1976–1977. However, for studies of the uptake and reactions of gases in the atmosphere with combustion-generated soots, organic combustion generated soots, particularly *n*-hexane soot, appear to be the most reasonable surrogate.

(1) Akhter, M. S.; Chughtai, A. R.; Smith, D. M. The structure of hexance soot II: Extraction studies. *Appl. Spectrosc.* **1985**, *39*, 154-167, doi:10.1366/0003702854249204.

(2) Akhter, M. S.; Chughtai, A. R.; Smith, D. M. The structure of hexane soot I: Spectroscopic studies. *Appl. Spectrosc.* **1985**, *39*, 143-153, doi:10.1366/0003702854249114.

(3) Akhter, M. S.; Chughtai, A. R.; Smith, D. M. Spectroscopic studies of oxidized soots. *Appl. Spectrosc.* **1991**, *45*, 653-665, doi:10.1366/0003702914336750.

(4) Alcala-Jornod, C.; Van den Bergh, H.; Rossi, M. J. Reactivity of NO_2 and H_2O on soot generated in the laboratory : a diffusion tube study at ambient temperature. *Phys. Chem. Chem. Phys.* **2000**, *2*, 5584-5593, doi:10.1039/b007235o.

(5) Cachier, H. Carbonaceous Combustion Aerosols. In *Atmospheric Particles*; Harrison, R. M., VanGrieken, R., Eds.; Wiley: New York, 1998.

(6) Chughtai, A. R.; Atteya, M. M. O.; Kim, J.; Konowalchuck, B. K.; Smith, D. M. Adsorption and adsorbate interaction at soot particle surfaces. *Carbon* **1998**, *36*, 1573-1589.

(7) Chughtai, A. R.; Miller, N. J.; Smith, D. M.; Pitts, J. R. Carbonaceous particle hydration III. *J. Atmos. Chem.* **1999**, *34*, 259-279, doi:10.1023/A:1006221326060.

(8) Chughtai, A. R.; Williams, G. R.; Atteya, M. M. O.; Miller, N. J.; Smith, D. M. Carbonaceous particle hydration. *Atmos. Environ.* **1999**, *33*, 2679-2687, doi:10.1016/S1352-2310(98)00329-X.

(9) Finlayson-Pitts, B. J.; Pitts, J. N. *Chemistry of the Upper and Lower Atmosphere: Theory, Experiments and Applications*; Academic: San Diego, 2000.

(10) Gerecke, A.; Thielmann, A.; Gutzwiller, L.; Rossi, M. J. The chemical kinetics of HONO formation resulting from heterogeneous interaction of NO_2 with flame soot. *Geophys. Res. Lett.* **1998**, *25*, 2453-2456, doi:10.1029/98GL01796.

(11) Goldberg, E. D. *Black Carbon in the Environment*; Wiley: New York, 1985.

(12) Jans, U.; Hoigne, J. Atmospheric water: transformation of ozone into OH-radical by sensitized photoreactions or black carbon. *Atmos. Environ.* **2000**, *34*, 1069-1085, doi:10.1016/S1352-2310(99)00361-1.

(13) Kirchner, U.; Scheer, V.; Vogt, R. FTIR spectroscopic investigation of the mechanism and kinetics of the heterogeneous reactions of NO_2 and HNO_3 with soot. *J. Phys. Chem. A* **2000**, *104*, 8908-8915, doi:10.1021/jp0005322.

(14) Pueschel, R. F.; Blake, D. F.; Suetsinger, A. G.; Hansen, A. D. A.; Verma, S.; Kato, K. Black carbon (soot) aerosol in the low stratosphere and upper troposphere. *Geophys. Res. Lett.* **1992**, *19*, 1659-1662, doi:10.1029/92GL01801.

(15) Smith, D. M.; Chughtai, A. R. The surface structure and reactivity of black carbon. *Colloids and Surfaces* **1995**, *105*, 47-77, doi:10.1016/0927-7757(95)03337-1.

(16) Stadler, D.; Rossi, M. J. The reactivity of NO_2 and HONO on Ñame soot at ambient temperature: The influence of combustion conditions. *Phys. Chem. Chem. Phys.* **2000**, *2*, 5420-5429, doi:10.1039/b005680o.

(17) Zolensky, M. E.; McKay, D. S.; Kaczor, L. A. A tenfold increase in the abundance of large solid particles in the stratosphere, as measured over the period 1976-1984. *J. Geophys. Res.* **1989**, *94*, 1047-1056, doi:10.1029/JD094iD01p01047.

5.2.1.3 Surface Types—Solid Alkali Halide Salts and Aqueous Salt Solutions

Some modeling studies also suggest that certain types of major volcanic eruptions transport significant levels of sodium chloride and associated alkali halide salts into the stratosphere (Michelangeli et al.[2]), so studies of stratospheric trace species interacting with solid NaCl or similar alkali halide salts, as well as salt solutions, have also been included. Sea salt aerosols are, of course, much more abundant in the troposphere, and have their largest influence on the chemistry of the marine boundary layer.

The heterogeneous chemistry of salt surfaces is very complex. For example; the uptake and reaction of gases with NaCl and NaBr have been shown to be very sensitive to the presence of small amounts of strongly adsorbed water (SAW) on the salt surface. Because water is not taken up on the 100 crystal surface of NaCl at room temperature, the SAW is thought to be concentrated at steps and edges where one water molecule can interact with two ions, resulting in a larger enthalpy of adsorption. This means that powders of salt, which have a larger surface-to-volume than single crystals, also have more SAW because of the relatively larger numbers of steps and edges. In addition, the amount of SAW on sprayed films is affected by the solvent used, with more SAW when water is used as the solvent. This SAW plays a key role in facilitating the reorganization of the surface during the reaction; thus, it appears to mobilize the product ions and allow them to recrystallize into 3-D microcrystallites of product on the surface, exposing fresh salt and allowing the reaction to continue well beyond the point that the surface would normally passivate. While the overall features of this process are reasonably well understood, the exact nature of the SAW and the molecular level interactions and processes are not. The overall effect, however, is time-dependent trace gas uptake coefficients.

Salt particles may also exist as aqueous solutions, if the relative humidities are sufficiently high. Chemistry may then occur both on the surface of the liquid droplets and in the bulk. The surface composition is not necessarily the same as the bulk. In particular, it is believed that the more polarizable anions (such as bromide and iodide) partition to the surface of such particles, perhaps affecting their reactivity. When salt aerosols freeze, the resulting particle will be composed of ice and the vast majority of the solutes will be excluded into a brine that will exist on the surface of the particles and at any grain boundaries and crystal-crystal interfaces that exist. At sufficiently low temperatures, the sodium chloride component will crystallize but other components, such as bromide, are expected to remain in an increasingly concentrated brine.[1] It is also likely that marine organics are mixed with sea-salt inorganics, via the bubble bursting mechanism occurring at the sea surface when an organic microlayer exists on the sea surface. These organics may affect the surface reactivity of salt particles.

(1) Koop, T.; Kapilashrami, A.; Molina, L. T.; Molina, M. J. Phase transitions of sea-salt/water mixtures at low temperatures: Implications for ozone chemistry in the polar marine boundary layer. *J. Geophys. Res.* **2000**, *105*, 26393-26402, doi:10.1029/2000JD900413.

(2) Michelangeli, D. V.; Allen, M.; Yung, Y. L. Heterogeneous reactions with NaCl in the El Chichon volcanic aerosols. *Geophys. Res. Lett.* **1991**, *18*, 673-676, doi:10.1029/91GL00547.

5.2.1.4 Surface Composition and Morphology

The detailed composition and morphology of each surface type are uncertain and probably subject to a significant range of natural variability. Certain chemical and physical properties of these surfaces, such as their ability to absorb and/or solvate HCl and HNO_3, are known to be strongly dependent on their detailed chemical composition. Moreover, most heterogeneous processes studied under laboratory conditions (and in some cases proceeding under atmospheric conditions) can change the chemical composition of the surface in ways that significantly affect the kinetic or thermodynamic processes of interest. Thus, a careful analysis of the time-dependent nature of the active surface is required in the evaluation of measured uptake kinetics experiments. Experimental techniques which allow the measurement of mass accommodation or surface reaction kinetics with high time resolution and/or with low trace gas fluxes are often more credible in establishing that measured kinetic parameters are not seriously compromised by surface saturation or changing surface chemical composition.

The relevant kinetic uptake parameters: mass accommodation coefficients and surface reaction probabilities, are separately documented for relevant atmospheric trace gas species for the major and, where available, the minor stratospheric and upper tropospheric surfaces noted above. Since these parameters can vary significantly with surface composition (e.g., the H_2SO_4/H_2O ratio for sulfate aerosol or the HNO_3/H_2O ratio for Type I PSC) the dependence of these parameters on surface composition is reviewed where sufficient data are available. In addition, in the notes to Table NEq1, we summarize the thermodynamic information that is now available to describe the non-reactive partitioning of species to a variety of surfaces, especially ice. Due to its chemical and morphological complexity, uptake values for soot are documented in a separate table.

5.2.1.5 Surface Porosity

The experimental techniques utilized to measure mass accommodation, heterogeneous reaction, and other uptake coefficients generally require knowledge of the surface area under study. For solid surfaces, and most particularly for water and acid ice surfaces formed *in situ*, the determination of how the molecular scale ice surface differs from the geometrical surface of the supporting substrate is not easy. Keyser, Leu, and coworkers have investigated the

structure of water and nitric acid ice films prepared under conditions similar to those used in their flow reactor for uptake studies.[6,7,9] They have demonstrated that ice films grown *in situ* from the vapor can have a considerably larger available surface than that represented by the geometry of the substrate; they have also developed a simple model to attempt to correct measured uptake rates for this effect.[8,9] This model predicts that correction factors are largest for small uptake coefficients and thick films. The application of the model to experimental uptake data remains controversial (Keyser et al.,[8] Hanson and Ravishakara,[4] Kolb et al.[10]). Some experimenters prefer to attempt growing ice surfaces as smooth as possible and to demonstrate that their measured uptake coefficients are only weakly dependent on surface thickness (Hanson and Ravishankara[5]). For the case of ice surfaces, it has been demonstrated that freezing thin films of liquid water leads to ice films that are smooth at the molecular level.[1]

Similar issues arise for uptake experiments performed on powered, fused and single crystal salt or oxide surfaces (Fenter et al.,[2] Hanning-Lee et al.[3]). There are two issues here. First, the molecular level Brunauer, Emmett, Teller (BET) surface area that is commonly measured by determining the mass of a gas such as N_2 adsorbed by a given sample mass is, for many atmospheric solids, larger than the geometric surface area. However, determining the BET surface area of porous materials does not necessarily reflect the available surface area for molecules larger than that used in the BET measurement. Second, many experimental studies have used samples consisting of multiple layers of particles in order to increase the amount of gas that is taken up and hence improve the accuracy of the measurement. However, there is considerable uncertainty in how to accurately assess the fraction of the total sample that is available for reaction. When recommendations are made for uptake coefficients on solid alkali salts in this assessment, the values have generally been obtained using at least two different sample types (e.g., powders, single crystals and spray-deposited films) and/or two different techniques (e.g., flow tubes and Knudsen cells).

The issue of surface area available for uptake is also important for interpreting uptake measurements on soot and soot surrogate surfaces. The degree to which measured uptake parameters must be corrected for porosity effects will remain in some doubt until a method is devised for accurately determining the effective surface area for the surfaces actually used in uptake studies.

Some studies evaluated in this review assume that the effective ice or salt surface area is the geometrical area, but more recent studies on solid surfaces generally attempt to assess the available surface area by employing BET measurements and porosity models. However, uncertainty in true reactive surface area for heterogeneous uptake on solids is often the dominate systematic error in reporting uptake coefficient values for these systems and makes evaluation of these data across laboratories and techniques difficult.

(1) Abbatt, J. P. D.; Bartels-Rausch, T.; Ullerstam, M.; Ye, T. J. Uptake of acetone, ethanol and benzene to snow and ice: effects of surface area and temperature. *Environ. Res. Lett.* **2008**, *3*, 045008, doi:10.1088/1748-9326/3/4/045008.

(2) Fenter, F. F.; Rossi, M. J. The heterogeneous kinetics of HONO on H_2SO_4 and on ice: activation of HCl. *J. Phys. Chem.* **1996**, *100*, 13765-13775, doi:10.1021/jp960797+.

(3) Hanning-Lee, M. A.; Brady, B. B.; Martin, L. R.; Syage, J. A. Ozone decomposition on alumina: Implications for solid rocket motor exhaust. *Geophys. Res. Lett.* **1996**, *23*, 1961-1964, doi:10.1029/96GL01808

(4) Hanson, D. R.; Ravishankara, A. R. Reaction of $ClONO_2$ with HCl on NAT, NAD, and frozen sulfuric acid and hydrolysis of N_2O_5 and $ClONO_2$ on frozen sulfuric acid. *J. Geophys. Res.* **1993**, *98*, 22931-22936, doi:10.1029/93JD01929

(5) Hanson, D. R.; Ravishankara, A. R. Response to "Comment on porosities of ice films used to simulate stratospheric cloud surfaces". *J. Phys. Chem.* **1993**, *97*, 2802-2803, doi:10.1021/j100113a054.

(6) Keyser, L. F.; Leu, M.-T. Morphology of nitric acid and water ice films. *Micros. Res. Technol.* **1993**, *25*, 434-438, doi:10.1002/jemt.1070250514.

(7) Keyser, L. F.; Leu, M.-T. Surface areas and porosities of ices used to simulate stratospheric clouds. *J. Colloid Interface Sci.* **1993**, *155*, 137-145, doi:10.1006/jcis.1993.1018.

(8) Keyser, L. F.; Leu, M.-T.; Moore, S. B. Comment on porosities of ice films used to simulate stratospheric cloud surfaces. *J. Phys. Chem.* **1993**, *97*, 2800-2801, doi:10.1021/j100113a053.

(9) Keyser, L. F.; Moore, S. B.; Leu, M. T. Surface reaction and pore diffusion in flow tube reactors. *J. Phys. Chem.* **1991**, *95*, 5496-5502, doi:10.1021/j100167a026.

(10) Kolb, C. E.; Worsnop, D. R.; Zahniser, M. S.; Davidovits, P.; Keyser, L. F.; Leu, M.-T.; Molina, M. J.; Hanson, D. R.; Ravishankara, A. R.; Williams, L. R.; Tolbert, M. A. Progress and Problems in Atmospheric Chemistry. In *Adv. Phys. Chem. Series, 3*; Barker, J. R., Ed., 1994; pp 771-875.

5.2.1.6 Temperature Dependences of Parameters

A number of laboratory studies have shown that mass accommodation coefficients and, to some extent, surface reaction probabilities can be temperature dependent. While these dependencies have not been characterized for many systems of interest, temperature effects on kinetic data are noted where available. More work that fully separates heterogeneous kinetic temperature effects from temperature-controlled surface composition is obviously needed.

5.2.1.7 Solubility Limitations

The uptake of certain trace gases by atmospherically relevant surfaces is often governed by solubility limitations rather than kinetic processes. In these cases properly analyzed data can yield measurements of trace gas solubility parameters relevant to stratospheric conditions. In general, such parameters can be strongly dependent on both condensed phase composition and temperature. Such parameters may be very important in stratospheric models, since they can govern the availability of a reactant for a bimolecular heterogeneous process (e.g., the concentration of HCl available for the HCl + $ClONO_2$ reaction on sulfuric acid aerosols) or the gas/condensed phase partitioning of a heterogeneous reaction product (e.g. the HNO_3 formed by the reaction of N_2O_5 on sulfuric acid aerosols). Surface saturation limitations have also been observed in experimental uptake studies on solid surfaces, including liquid water and water/acid ice surfaces.

5.2.1.8 Parameter Definitions

Mass accommodation coefficients (α), represent the probability of reversible uptake of a gaseous species colliding with the condensed surface of interest. For liquid surfaces this process is associated with interfacial (gas-to-liquid) transport and is generally followed by bulk liquid phase solvation. Examples include: simple surface absorption, absorption followed by ionic dissociation and solvation (e.g., $HCl + nH_2O \leftrightarrow H^+(aq) + Cl^-(aq)$), and absorption followed by a reversible chemical reaction with a condensed phase substituent (e.g., $SO_2 + H_2O \leftrightarrow H^+ + HSO_3^-$ or $CH_2O + H_2O \leftrightarrow CH_2(OH)_2$).

The term "sticking coefficient" is often used for mass accommodation on solid surfaces where physisorption or chemisorption takes the place of true interfacial mass transport.

Also included in the specific notes are parameters relating to the non-reactive uptake of gases to solid atmospheric surfaces, such as ice. These quantities are useful for determining the likelihood that gas-phase species will be scavenged to the condensed phase, and to interpret the rates of surface-phase reactions. Many experimental approaches that can measure reactive uptake or mass accommodation coefficients can also assess the degree of non-reactive uptake, so these data are reported in the same table. Experimental studies usually measure a total uptake (i.e. molecules or moles of adsorbate per unit surface area) at a specific temperature and gas-phase partial pressure or concentration.

By varying the gas-phase amounts, an adsorption isotherm is measured. For surfaces such as ice, simple isotherms such as the Langmuir form have been utilized. While this isotherm neglects adsorbate-adsorbate interactions and assumes that all adsorption sites are equivalent, these may be reasonable assumptions for ice surfaces, which are highly dynamic and where adsorbate molecules are likely to be strongly hydrated. From the isotherm, the saturated surface coverage at high gas-phase concentrations and the gas-surface partition coefficient can be assessed:

$$\theta \equiv \text{fractional surface coverage} = K_{conc}[gas] / (1 + K_{conc}[gas]) = K_p P_{gas} / (1 + K_P P_{gas})$$

where K_{conc} and K_P are the adsorption coefficients, depending on whether concentration or pressure units are used for the gas phase. For consistency with the rest of the evaluation and to match the approach typically used in the literature, surface uptakes will be reported in units of molecules/cm^2. Correspondingly, adsorption coefficients will be converted into K_{conc} units, i.e. cm^3 $molecules^{-1}$. Note that a partitioning coefficient (K_{part}, units molecules cm^{-2} / molecules cm^{-3}) can also be derived by taking the slope of a plot of uptake to gas-phase concentration in the surface-unsaturated regime. The relationship between a K_{conc} value derived from a Langmuir adsorption isotherm to a partition coefficient (K_{part}) is:

$$K_{part} = K_{conc} N_{sat}$$

where N_{sat} is the saturated surface coverage in units of molecules cm^{-2}.

By varying the temperature in uptake studies, the heat of adsorption can be derived in a van't Hoff analysis from the temperature dependence of the partition or adsorption coefficients. This approach is most accurate at low surface coverages where adsorbate-adsorbate interactions are likely to be fewest. While we report such values from the literature, care should be taken in their interpretation because an assumption of this approach is that the surface structure and the strength of the adsorbate-surface interactions remain constant as a function of temperature. Also, as the temperature changes, the degree of adsorbate-adsorbate interactions may change as well. Surface reaction probabilities (γ) are kinetic values for generally irreversible reactive uptake of trace gas species on condensed surfaces. The rates of such processes may not be limited by Henry's law constraints; however, the fate of the uptake reaction products may be subject to saturation limitations. For example, N_2O_5 has been shown to react with sulfuric acid aerosol surfaces. However, if the H_2SO_4/H_2O ratio is too high, the product HNO_3 will be insoluble, and a large fraction will be expelled back into the gas phase. Surface reaction probabilities for substantially irreversible processes are presented in Table NEq2. Reaction products are identified where known.

Surface reaction probabilities on crystalline and non-ice amorphous solid surfaces, such as alumina and alkali salts are particularly susceptible to surface saturation effects, especially when exposed to the relatively high trace gas concentrations sometimes employed in laboratory experiments. In the case of gaseous HNO_3 reacting with NaCl for example, there is a rapid initial uptake of HNO_3 and formation of nitrate on the surface, followed by a decrease to a relatively constant (but slowly declining) value. When they are available, we tabulate the initial uptake coefficient, γ_0, in Table NEq2, since that value often sets the upper limit for atmospheric uptake. In the corresponding note we may also site the reactive uptake coefficient appropriate to longer time exposure when the uptake appears to have reached an approximate steady-state, γ_{ss}.

The total experimental uptake coefficient measured in laboratory heterogeneous kinetic experiments are also often represented by the symbol γ. In those cases where surface and/or bulk reaction dominate the uptake, the total uptake coefficient (γ_{total}) and reactive uptake coefficient (γ_{rxn}) may well be identical. More formally, for cases where bulk liquid phase reaction is facile and there are no gas phase diffusion constraints, the total uptake coefficient for aerosol or cloud droplets can be approximated in terms of γ_{rxn} and γ_{sol} as:[4]

$$\frac{1}{\gamma_{total}} = \frac{1}{\alpha} + \frac{1}{\gamma_{sol} + \gamma_{rxn}}$$

where

$$\gamma_{sol} = \frac{8HRT}{\pi^{1/2}\bar{c}} \left(\frac{D}{t}\right)^{1/2}$$

and

$$\gamma_{rxn} = \frac{4HRT}{\bar{c}} \ (Dk_{rxn})^{1/2}$$

where t is the time integrated exposure of the trace gas to the liquid surface, R is the gas constant, D is the liquid phase diffusion coefficient, and $\bar{c}$ is the mean trace gas molecular speed. In the limit of low solubility or long exposure time γ_{sol} becomes negligible and

$$\frac{1}{\gamma_{total}} = \frac{1}{\alpha} + \frac{1}{\gamma_{rxn}}$$

Discussion of how to use this approach to model chemical reactions in liquid stratospheric aerosols can be found in Hanson et al.[1] and Kolb et al.[4] Note that these formulations are approximate. In cases where separate terms are competitive, more rigorous solution of the kinetic differential equations may be appropriate.

For solid surfaces, bulk diffusion is generally too slow to allow bulk solubility or bulk kinetic processes to dominate uptake. For solids, reactive uptake is driven by chemisorption/chemical reaction at the interface, a process that can also influence trace gas uptake on liquids. For liquids, surface reaction (γ_{surf}) occurs in parallel, rather than in series with mass accommodation, thus:

$$\gamma_{total} = \gamma_{surf} + \left[\frac{1}{\alpha} + \frac{1}{\gamma_{sol} + \gamma_{rxn}}\right]^{-1}$$

Examples where this more complex situation holds for liquid surfaces can be found in Hu et al.[2] and Jayne et al.[3] In such cases γ may be significantly larger than α.

Uptake of gases on soot may occur due to three different processes: (1) physisorption (e.g. SO_2 or HNO_3 at room temperature and low nitric acid pressures); (2) reaction with the surface (e.g. NO_2), and (3) catalytic decomposition/reactions of the gas on the surface. All three processes may occur in parallel, and the relative contributions of each of these three may vary during the course of the reaction as the surface "ages." As discussed above, there are different types of reactive sites on soot, leading in some cases to a rapid initial uptake followed by a slower uptake; these are often characterized as reactions on "fresh" and "aged" surfaces respectively. Another complexity is that in some cases the geometric surface areas were used to calculate the uptake coefficients from the experimental data while in others, the available reactive surface area was estimated and used.

Because of these complexities with soot heterogeneous chemistry, uptake coefficients for soot interactions with gases have been broken out into a separate Table NEq3 rather than being included with the other surfaces in Tables NEq1 and NEq2. When the uncertainty is more than an order of magnitude, a recommendation is not given in Table NEq3 and the range of reported values is given in the Notes. In most cases, the available reactive surface area rather than the geometric areas have been used in obtaining the uptake coefficients; in those cases where the geometric area was used but a higher available surface area was involved in the measured uptake, the uptake coefficient is given as an upper limit. Data are most commonly available for room temperature or there are very limited data at lower temperatures characteristic of the upper troposphere.

The data in Tables NEq1 and NEq2 for uptake on non-soot surfaces are organized by trace gas species, since some systematic variation may be expected for surface accommodation or reaction as the surface composition and/or phase is varied. Data presented for one surface may be judged for "reasonableness" by comparing with data for a "similar" surface. In some cases it is not yet clear if surface uptake is truly reversible (accommodation) or irreversibly reactive in nature. In such cases the available uptake coefficients are generally tabulated in Table NEq1 as mass accommodation coefficients, a judgment that will be subject to change if more definitive data become available.

Where a specific evaluated value for an accommodation coefficient or reaction probability has been obtained, an estimated uncertainty factor is also tabulated. However, when the data evaluation yielded only a lower or upper limit, no uncertainty factor can be reliably estimated and none is presented.

Description of and reference citations to many of the laboratory techniques used to obtain the data in the following tables can be found in Kolb et al.[4] Reactions of N_2O_5, $ClONO_2$, HOCl and $BrONO_2$ on/in sulfuric acid are generally dependent on the species' Henry's law solubility and liquid phase diffusion coefficient in the liquid acid as well as the surface and/or liquid phase reaction rate parameters. All of these processes are generally functions of the acid composition and temperature (Hanson et al.,[1] Robinson et al.,[5] Shi et al.[6]). Thus, these reactions' reactive uptake coefficients must be represented by a complex phenomenological or empirical models that defy simple entry into Table NEq2. The notes in Table NEq2 for these reactions discuss and present the models adopted.

To aid in visualizing the resulting reactive uptake parameters the results for several reactions have been plotted in Figure 5.1 as a function of temperature for a background pressure of 50 mbar and background water vapor and HCl mixing ratios of 5 ppmv and 2 ppbv, respectively. These calculations are presented for monodisperse background sulfate aerosol particles with a radius of 1×10^{-5} cm (0.1 μm).

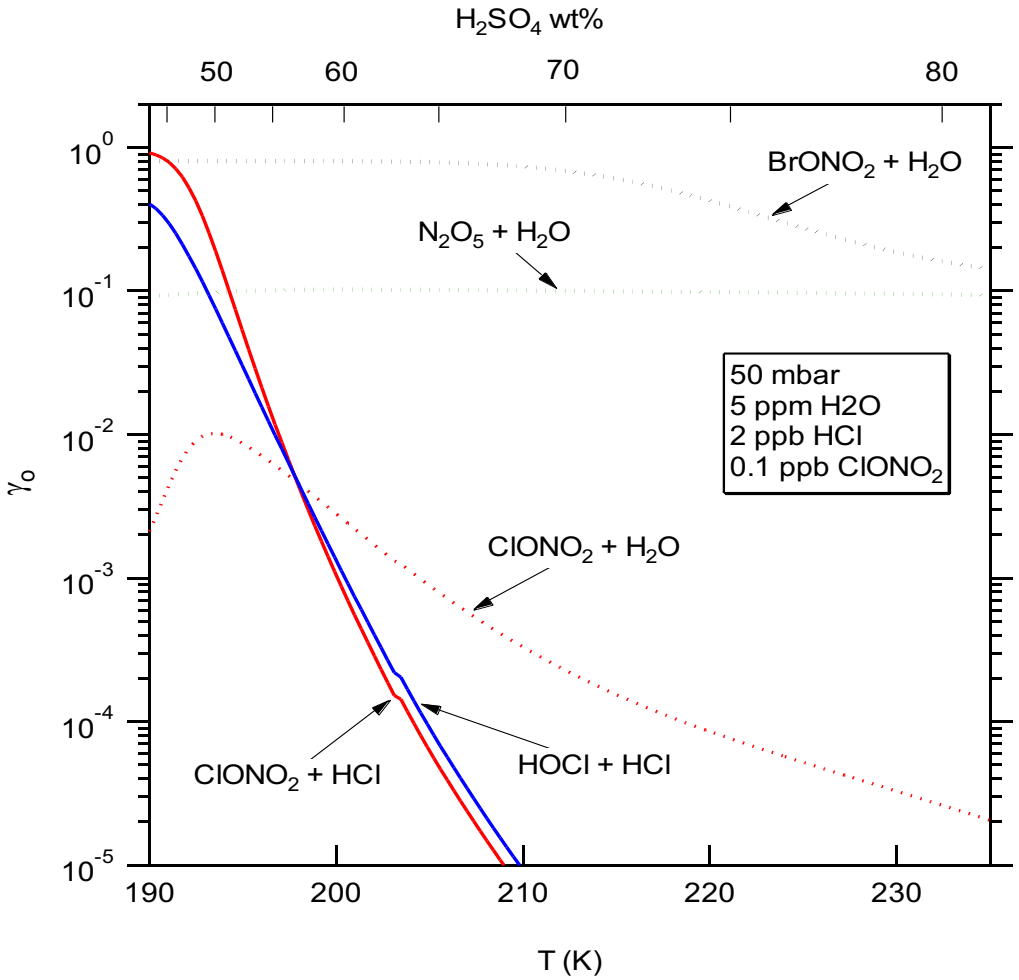


Figure 5.1. Recommended reactive uptake coefficients as a function of temperature for key stratospheric heterogeneous processes on sulfuric acid aerosols. For $ClONO_2$ and HOCl species, the aerosol radius used in the calculation is 10^{-5} cm, a typical value in the stratosphere. Because the current uptake models for N_2O_5 and $BrONO_2$ hydrolysis do not provide the information about the reacto-diffusive length (ℓ), the aerosol radius used in the calculation is assumed to be much larger than their reacto-diffusive length (i.e. ℓ for N_2O_5 and $BrONO_2$ are set to zero.)

(1) Hanson, D. R.; Ravishankara, A. R.; Solomon, S. Heterogeneous reactions in sulfuric acid aerosols: A framework for model calculations. *J. Geophys. Res.* **1994**, *99*, 3615-3629, doi:10.1029/93JD02932.

(2) Hu, J. H.; Shi, Q.; Davidovits, P.; Worsnop, D. R.; Zahniser, M. S.; Kolb, C. E. Reative uptake of Cl_2(g) and Br_2(g) by aqueous surfaces as a function of Br^- and I^- ion concentration: The effect of chemical reaction at the interface. *J. Phys. Chem.* **1995**, *99*, 8768-8776, doi:10.1021/j100021a050.

(3) Jayne, J. T.; Worsnop, D. R.; Kolb, C. E.; Swartz, E.; Davidovits, P. Uptake of gas-phase formaldehyde by aqueous acid surfaces. *J. Phys. Chem.* **1996**, *100*, 8015-8022, doi:10.1021/jp953196b.

(4) Kolb, C. E.; Cox, R. A.; Abbatt, J. P. D.; Ammann, M.; Davis, E. J.; Donaldson, D. J.; Garrett, B. C.; George, C.; Griffiths, P. T.; Hanson, D. R.; Kulmala, M.; McFiggans, G.; Pöschl, U.; Riipinen, I.; Rossi, M. J.; Rudich, Y.; Wagner, P. E.; Winkler, P. M.; Worsnop, D. R.; O' Dowd, C. D. An overview of current issues in the uptake of atmospheric trace gases by aerosols and clouds. *Atmos. Chem. Phys.* **2010**, *10*, 10561-10605, doi:10.5194/acp-10-10561-2010.

(5) Robinson, G. N.; Worsnop, D. R.; Jayne, J. T.; Kolb, C. E.; Davidovits, P. Heterogeneous uptake of $ClONO_2$ and N_2O_5 by sulfuric acid solutions. *J. Geophys. Res.* **1997**, *102*, 3583-3601, doi:10.1029/96JD03457.

(6) Shi, Q.; Davidovits, P.; Jayne, J. T.; Kolb, C. E.; Worsnop, D. R. Kinetic model for reaction of $ClONO_2$ with H_2O and HCl and HOCl with HCl in sulfuric acid solutions. *J. Geophys. Res.* **2001**, *106*, 24259-24274, doi:10.1029/2000JD000181.

5.2.1.9 Bibliography – Introduction

Abbatt, J. P. D. Interactions of atmospheric trace gases with ice surfaces: Adsorption and reaction. *Chem. Rev.* **2003**, *103*, 4783-4800, doi:10.1021/cr0206418.

Abbatt, J. P. D.; Bartels-Rausch, T.; Ullerstam, M.; Ye, T. J. Uptake of acetone, ethanol and benzene to snow and ice: effects of surface area and temperature. *Environ. Res. Lett.* **2008**, *3*, 045008, doi:10.1088/1748-9326/3/4/045008.

Akhter, M. S.; Chughtai, A. R.; Smith, D. M. The structure of hexance soot II: Extraction studies. *Appl. Spectrosc.* **1985**, *39*, 154-167, doi:10.1366/0003702854249204.

Akhter, M. S.; Chughtai, A. R.; Smith, D. M. The structure of hexane soot I: Spectroscopic studies. *Appl. Spectrosc.* **1985**, *39*, 143-153, doi:10.1366/0003702854249114.

Akhter, M. S.; Chughtai, A. R.; Smith, D. M. Spectroscopic studies of oxidized soots. *Appl. Spectrosc.* **1991**, *45*, 653-665, doi:10.1366/0003702914336750.

Alcala-Jornod, C.; Van den Bergh, H.; Rossi, M. J. Reactivity of NO_2 and H_2O on soot generated in the laboratory : a diffusion tube study at ambient temperature. *Phys. Chem. Chem. Phys.* **2000**, *2*, 5584-5593, doi:10.1039/b007235o.

Cachier, H. Carbonaceous Combustion Aerosols. In *Atmospheric Particles*; Harrison, R. M., VanGrieken, R., Eds.; Wiley: New York, 1998.

Chughtai, A. R.; Atteya, M. M. O.; Kim, J.; Konowalchuck, B. K.; Smith, D. M. Adsorption and adsorbate interaction at soot particle surfaces. *Carbon* **1998**, *36*, 1573-1589, doi:10.1016/S0008-6223(98)00116-X.

Chughtai, A. R.; Miller, N. J.; Smith, D. M.; Pitts, J. R. Carbonaceous particle hydration III. *J. Atmos. Chem.* **1999**, *34*, 259-279, doi:10.1023/A:1006221326060.

Chughtai, A. R.; Williams, G. R.; Atteya, M. M. O.; Miller, N. J.; Smith, D. M. Carbonaceous particle hydration. *Atmos. Environ.* **1999**, *33*, 2679-2687, doi:10.1016/S1352-2310(98)00329-X.

Clegg, S. L.; Brimblecombe, P. The dissociation constant and Henry's law constant of HCl in queous solution. *Atmos. Environ.* **1986**, *20*, 2483-2485, doi:10.1016/0004-6981(86)90079-X.

Fenter, F. F.; Rossi, M. J. The heterogeneous kinetics of HONO on H_2SO_4 and on ice: activation of HCl. *J. Phys. Chem.* **1996**, *100*, 13765-13775, doi:10.1021/jp960797+.

Finlayson-Pitts, B. J.; Pitts, J. N. *Chemistry of the Upper and Lower Atmosphere: Theory, Experiments and Applications*; Academic: San Diego, 2000.

Fox, L. E.; Worsnop, D. R.; Zahniser, M. S.; Wofsy, S. C. Metastable phases in polar stratospheric aerosols. *Science* **1994**, *267*, 351-355, doi:10.1126/science.267.5196.351.

Gerecke, A.; Thielmann, A.; Gutzwiller, L.; Rossi, M. J. The chemical kinetics of HONO formation resulting from heterogeneous interaction of NO_2 with flame soot. *Geophys. Res. Lett.* **1998**, *25*, 2453-2456, doi:10.1029/98GL01796.

Goldberg, E. D. *Black Carbon in the Environment*; Wiley: New York, 1985.

Hanning-Lee, M. A.; Brady, B. B.; Martin, L. R.; Syage, J. A. Ozone decomposition on alumina: Implications for solid rocket motor exhaust. *Geophys. Res. Lett.* **1996**, *23*, 1961-1964, doi:10.1029/96GL01808.

Hanson, D. R.; Ravishankara, A. R. Reaction of $ClONO_2$ with HCl on NAT, NAD, and frozen sulfuric acid and hydrolysis of N_2O_5 and $ClONO_2$ on frozen sulfuric acid. *J. Geophys. Res.* **1993**, *98*, 22931-22936, doi:10.1029/93JD01929.

Hanson, D. R.; Ravishankara, A. R. Response to "Comment on porosities of ice films used to simulate stratospheric cloud surfaces". *J. Phys. Chem.* **1993**, *97*, 2802-2803, doi:10.1021/j100113a054.

Hanson, D. R.; Ravishankara, A. R.; Solomon, S. Heterogeneous reactions in sulfuric acid aerosols: A framework for model calculations. *J. Geophys. Res.* **1994**, *99*, 3615-3629, doi:10.1029/93JD02932.

Hofmann, D. J.; Oltmans, S. J. The effect of stratospheric water vapor on the heterogeneous reaction rate of $ClONO_2$ and H_2O for sulfuric acid aerosol. *Geophys. Res. Lett.* **1992**, *22*, 2211-2214, doi:10.1029/92GL02493

Hu, J. H.; Shi, Q.; Davidovits, P.; Worsnop, D. R.; Zahniser, M. S.; Kolb, C. E. Reative uptake of Cl_2(g) and Br_2(g) by aqueous surfaces as a function of Br^- and I^- ion concentration: The effect of chemical reaction at the interface. *J. Phys. Chem.* **1995**, *99*, 8768-8776, doi:10.1021/j100021a050.

Huthwelker, T.; Ammann, M.; Peter, T. The uptake of acidic gases on ice. *Chem. Rev.* **2006**, *106*, 1375-1444, doi:10.1021/cr020506v.

Huthwelker, T.; Peter, T.; Juo, B. P.; Clegg, S. L.; Carshlaw, K. S.; Brimblecombe, P. Solubility of HOCl in water and aqueous H_2SO_4 to stratospheric temperatures. *J. Atmos. Chem.* **1995**, *21*, 81-95, doi:10.1007/BF00712439.

Jans, U.; Hoigne, J. Atmospheric water: transformation of ozone into OH-radical by sensitized photoreactions or black carbon. *Atmos. Environ.* **2000**, *34*, 1069-1085, doi:10.1016/S1352-2310(99)00361-1.

Jayne, J. T.; Worsnop, D. R.; Kolb, C. E.; Swartz, E.; Davidovits, P. Uptake of gas-phase formaldehyde by aqueous acid surfaces. *J. Phys. Chem.* **1996**, *100*, 8015-8022, doi:10.1021/jp953196b.

Keyser, L. F.; Leu, M.-T. Morphology of nitric acid and water ice films. *Micros. Res. Technol.* **1993**, *25*, 434-438, doi:10.1002/jemt.1070250514.

Keyser, L. F.; Leu, M.-T. Surface areas and porosities of ices used to simulate stratospheric clouds. *J. Colloid Interface Sci.* **1993**, *155*, 137-145, doi:10.1006/jcis.1993.1018.

Keyser, L. F.; Leu, M.-T.; Moore, S. B. Comment on porosities of ice films used to simulate stratospheric cloud surfaces. *J. Phys. Chem.* **1993**, *97*, 2800-2801, doi:10.1021/j100113a053.

Keyser, L. F.; Moore, S. B.; Leu, M. T. Surface reaction and pore diffusion in flow tube reactors. *J. Phys. Chem.* **1991**, *95*, 5496-5502, doi:10.1021/j100167a026.

Kirchner, U.; Scheer, V.; Vogt, R. FTIR spectroscopic investigation of the mechanism and kinetics of the heterogeneous reactions of NO_2 and HNO_3 with soot. *J. Phys. Chem. A* **2000**, *104*, 8908-8915, doi:10.1021/jp0005322.

Kolb, C. E.; Cox, R. A.; Abbatt, J. P. D.; Ammann, M.; Davis, E. J.; Donaldson, D. J.; Garrett, B. C.; George, C.; Griffiths, P. T.; Hanson, D. R.; Kulmala, M.; McFiggans, G.; Pöschl, U.; Riipinen, I.; Rossi, M. J.; Rudich, Y.; Wagner, P. E.; Winkler, P. M.; Worsnop, D. R.; O' Dowd, C. D. An overview of current issues in the uptake of atmospheric trace gases by aerosols and clouds. *Atmos. Chem. Phys.* **2010**, *10*, 10561-10605, doi:10.5194/acp-10-10561-2010.

Kolb, C. E.; Worsnop, D. R.; Zahniser, M. S.; Davidovits, P.; Keyser, L. F.; Leu, M.-T.; Molina, M. J.; Hanson, D. R.; Ravishankara, A. R.; Williams, L. R.; Tolbert, M. A. Progress and Problems in Atmospheric Chemistry. In *Adv. Phys. Chem. Series, 3*; Barker, J. R., Ed., 1994; pp 771-875.

Koop, T.; Kapilashrami, A.; Molina, L. T.; Molina, M. J. Phase transitions of sea-salt/water mixtures at low temperatures: Implications for ozone chemistry in the polar marine boundary layer. *J. Geophys. Res.* **2000**, *105*, 26393-26402, doi:10.1029/2000JD900413.

Michelangeli, D. V.; Allen, M.; Yung, Y. L. Heterogeneous reactions with NaCl in the El Chichon volcanic aerosols. *Geophys. Res. Lett.* **1991**, *18*, 673-676, doi:10.1029/91GL00547.

Middlebrook, A. M.; Iraci, L. T.; McNeil, L. S.; Koehler, B. G.; Wilson, M. A.; Saastad, O. W.; Tolbert, M. A. Fourier transform-infrared studies of thin H_2SO_4/H_2O films: Formation, water uptake, and solid-liquid phase changes. *J. Geophys. Res.* **1993**, *98*, 20473-20481, doi:10.1029/93JD02454.

Molina, M. J.; Zhang, R.; Woolridge, P. J.; McMahon, J. R.; Kim, J. E.; Chang, H. Y.; Beyer, K. D. Physical chemistry of the $H_2SO_4/HNO_3/H_2O$ system: Implicaitons for polar stratospheric clouds. *Science* **1993**, *261*, 1418-1423, doi:10.1126/science.261.5127.1418.

Pueschel, R. F.; Blake, D. F.; Suetsinger, A. G.; Hansen, A. D. A.; Verma, S.; Kato, K. Black carbon (soot) aerosol in the low stratosphere and upper troposphere. *Geophys. Res. Lett.* **1992**, *19*, 1659-1662, doi:10.1029/92GL01801.

Robinson, G. N.; Worsnop, D. R.; Jayne, J. T.; Kolb, C. E.; Davidovits, P. Heterogeneous uptake of $ClONO_2$ and N_2O_5 by sulfuric acid solutions. *J. Geophys. Res.* **1997**, *102*, 3583-3601, doi:10.1029/96JD03457.

Schumpe, A. The estimation of gas solubilities in salt-solutions. *Chem. Engineer. Sci.* **1993**, *48*, 153-158, doi:10.1016/0009-2509(93)80291-W.

Schwartz, S. E. Henry's law and sheep's tails. *Atmos. Environ.* **1988**, *22*, 2331-2332, doi:10.1016/0004-6981(88)90145-X.

Shi, Q.; Davidovits, P.; Jayne, J. T.; Kolb, C. E.; Worsnop, D. R. Kinetic model for reaction of $ClONO_2$ with H_2O and HCl and HOCl with HCl in sulfuric acid solutions. *J. Geophys. Res.* **2001**, *106*, 24259-24274, doi:10.1029/2000JD000181.

Sieg, K.; Starokozhev, E.; Schmidt, M. U.; Puttmann, W. Inverse temperature dependence of Henry's law coefficients for volatile organic compounds in supercooled water. *Chemosphere* **2009**, *77*, 8-14, doi:10.1016/j.chemosphere.2009.06.028.

Smith, D. M.; Chughtai, A. R. The surface structure and reactivity of black carbon. *Colloids and Surfaces* **1995**, *105*, 47-77, doi:10.1016/0927-7757(95)03337-1.

Stadler, D.; Rossi, M. J. The reactivity of NO_2 and HONO on Ñame soot at ambient temperature: The influence of combustion conditions. *Phys. Chem. Chem. Phys.* **2000**, *2*, 5420-5429, doi:10.1039/b005680o.

Toon, O.; Browell, E.; Gray, B.; Lait, L.; Livingston, J.; Newman, P.; Russell, R.; P., P.; Schoeberl, M.; Toon, G.; Traub, W.; Valero, F. P. J.; Selkirk, H.; Jordan, J. Heterogeneous reaction probabilities, solubilities, and the physical state of cold volcanic aerosols. *Science* **1993**, *261*, 1136-1140, doi:10.1126/science.261.5125.1136.

Watson, L. R.; Doren, J. M. V.; Davidovits, P.; Worsnop, D. R.; Zahniser, M. S.; Kolb, C. E. Uptake of HCl molecules by aqueous sulfuric acid droplets as a function of acid concentration. *J. Geophys. Res.* **1990**, *95*, 5631-5638, doi:10.1029/JD095iD05p05631.

Weisenberger, S.; Schumpe, A. Estimation of gas solubilities in salt solutions at temperatures from 273 K to 363 K. *AIChE Journal* **1996**, *42*, 298-300, doi:10.1002/aic.690420130.

Wolff, E. W.; Mulvaney, R. Reactions on sulphuric acid aerosol and on polar stratospheric clouds in the Antarctic stratosphere. *Geophys. Res. Lett.* **1991**, *18*, 1007-1010, doi:10.1029/91GL01158.

Worsnop, D. R.; Fox, L. E.; Zahniser, M. S.; Wofsy, S. C. Vapor pressures of solid hydrates of nitric acid: Implications for polar stratospheric clouds. *Science* **1993**, *259*, 71-74, doi:10.1126/science.259.5091.71.

Zhang, R.; Wooldridge, P. J.; Molina, M. J. Vapor pressure measurements for the $H_2SO_4/HNO_3/H_2O$ and $H_2SO_4/HCl/H_2O$ systems: Incorporation of stratospheric acids into background sulfate aerosols. *J. Phys. Chem.* **1993**, *97*, 8541-8548, doi:10.1021/j100134a026.

Zolensky, M. E.; McKay, D. S.; Kaczor, L. A. A tenfold increase in the abundance of large solid particles in the stratosphere, as measured over the period 1976-1984. *J. Geophys. Res.* **1989**, *94*, 1047-1056, doi:10.1029/JD094iD01p01047.

5.2.2 Table NEq1. Mass Accommodation Coefficients (α) and Reversible Uptake Data for non-Soot Surfaces

Gaseous Species	Surface Type	Surface Composition	T(K)	α	Uncertainty Factor	Notes
O	Water Ice	H_2O(s)	See Note	See Note		1
	Sulfuric Acid	H_2SO_4•nH_2O(l) (97 wt% H_2SO_4)	298	See Note		2
O_3	Water Ice	H_2O(s)	195–262	>0.04		3
	Liquid Water	H_2O(l)	275–300	≥1 × 10^{-2}*		4
	Nitric Acid Ice	HNO_3•3H_2O(s)	195	2.5 × 10^{-4}‡	3	3
	Sulfuric Acid	H_2SO_4•nH_2O(l) (50–98 wt% H_2SO_4)	193–295	See Note		5
OH	Water Ice	H_2O(s)	205–253	>0.1		6
	Liquid Water	H_2O(l)	275–300	≥1 × 10^{-2}*		7
HO_2	Liquid Water	H_2O(l)	275	> 0.02		8
	Aqueous Salts and Sulfuric Acid	NH_4HSO_4(aq), $LiNO_3$(aq), H_2SO_4•nH_2O, NaCl (aq), $(NH_4)_2SO_4$(aq), KCl(aq)	293–298	> 0.4		8
H_2O	Water Ice	H_2O(s)	<235	>0.2		9
	Liquid Water	H_2O(l)	250–290	≥0.1*		10
	Liquid Nitric Acid	HNO_3•nH_2O(l)	278	>0.3		11
	Nitric Acid Ice	HNO_3•3H_2O(s)	197	See Note	1.3	12
	Sulfuric Acid	H_2SO_4•nH_2O (96 wt% H_2SO_4)	298	> 2 × 10^{-3}‡	1.3	13
		(50 wt.% H_2SO_4)	250–280	0.5	1.3	13
		(70 wt.% H_2SO_4)	250–295	0.6		13
	Sodium Chloride	(82 wt.% H_2SO_4)	270–300	0.85		13
		NaCl(s)	~298	See Note		14
		NaCl(aq)	~299	See Note		15
H_2O_2	Water Ice	H_2O(s)	213–238	See Note		16
	Liquid Water	H_2O(l)	273	0.18*	2	17
	Sulfuric Acid	H_2SO_4•nH_2O(l) (96 wt% H_2SO_4)	298	> 8 × 10^{-4}‡		18
NO	Water Ice	H_2O(s)	195	See Note		19
	Sulfuric Acid	H_2SO_4•nH_2O		See Note		
		(70 wt% H_2SO_4)	193–243	See Note		20
		(97 wt% H_2SO_4)	298	See Note		20
NO_2	Water Ice	H_2O(s)	195	See Note		21
NO_3	Liquid Water	H_2O(l)	273–293	≥ 2 × 10^{-3}		22
HONO	Water Ice	H_2O(s)	180–200	See Note		23
HNO_3	Water Ice	H_2O(s)	<200	>0.1		24
	Liquid Water	H_2O(l)	250–300	≥0.05*		25
	Nitric Acid Ice	HNO_3•3H_2O(s)	191–200	0.4	2	26
	Liquid Nitric Acid	HNO_3•nH_2O(l)	278	0.6	2	27
	Sulfuric Acid	H_2SO_4•nH_2O(l)				
		(57.7 wt% H_2SO_4)	191–200	>0.3	2	28
		(73 wt% H_2SO_4)	283	0.1		28
		(75 wt% H_2SO_4)	230	>2 × 10^{-3}		28
	Sulfuric Acid	(97 wt% H_2SO_4)	295	>2.4 × 10^{-3}		28
	Tetrahydrate	H_2SO_4•4 H_2O(s)	~192	>0.02*		28
N_2O_5	Liquid Water	H_2O(l)	295	>0.4		29
HO_2NO_2	Water Ice	H_2O(s)	200	0.1‡	3	30
	Sulfuric Acid	H_2SO_4•nH_2O(l) (97 wt% H_2SO_4)	298	See Note		31
NH_3	Water Ice	H_2O(s)	190	See Note		32
	Liquid Water	H_2O(l)	260–300	≥0.05*		33
CO_2	Water Ice	H_2O(s)	209–263	See Note		34
	Liquid Water	H_2O(l)	290–300	≥5 × 10^{-5}		35
CH_3OH	Water Ice	H_2O(s)	150–213	See Note		36
	Liquid Water	H_2O(l)	260–291	0.12–0.02*	2	37
CH_3CH_2OH	Water Ice	H_2O(s)	193–243	See Note		38
	Liquid Water	H_2O(l)	260–292	≥2 × 10^{-2}*		39
$CH_3CH_2CH_2OH$	Water Ice	H_2O(s)	228	See Note		40
	Liquid Water	H_2O(l)	260–291	0.08–0.02*	2	41
$CH_3CH(OH)CH_3$	Liquid Water	H_2O(l)	260–291	0.10–0.02*	2	41
$HOCH_2CH_2OH$	Liquid Water	H_2O(l)	260–291	0.13–0.04*	2	42

Gaseous Species	Surface Type	Surface Composition	T(K)	α	Uncertainty Factor	Notes
CH_3O_2	Sodium Chloride	NaCl(s)	296	$>4 \times 10^{-3}$		43
CH_3OOH	Liquid Water	H_2O(l)	260–282	$\geq 7 \times 10^{-3}$*		44
CH_2O	Water Ice	H_2O(s)	198–268	See Note		45
	Liquid Water	H_2O(l)	260–270	0.04	3	46
	Sulfuric Acid	H_2O•mHNO_3•nH_2O(l)	235–300	0.04	3	46
CH_3CHO	Water Ice	H_2O(s)	120–233	See Note		47
	Liquid Water	H_2O(l)	267	>0.03*		48
CH(O)CH(O)	Liquid Water	H_2O(l)	260–285	$\geq 1 \times 10^{-2}$*		49
$CH_3C(O)CH_3$	Water Ice	H_2O(s)	217–243	See Note		50
	Liquid Water	H_2O(l)	260–292	$\geq 2 \times 10^{-2}$*		51
$CH_2(OH)C(O)CH_3$	Water Ice	H_2O(s)	233–253	See Note		52
$CH_3C(O)CHO$	Liquid Water	H_2O(l)	260–293	$\geq 1 \times 10^{-4}$*		53
$CH_3OC(O)OCH_3$	Liquid Water	H_2O(l)	270–278	$\geq 2 \times 10^{-2}$*		54
HC(O)OH	Water Ice	H_2O(s)	187–221	See Note		55
	Liquid Water	H_2O(l)	260–291	0.10–0.02*	2	56
$CH_3C(O)OH$	Water Ice	H_2O(s)	193–245	See Note		57
	Liquid Water	H_2O(l)	258–292	$\geq 2 \times 10^{-2}$*		58
$CH_3CO(O_2)NO_2$	Water Ice	H_2O(s)	80–250	See Note		59
Cl_2	Water Ice	H_2O(s)	200	See Note		60
OClO	Water Ice	H_2O(s)	100,189, 200	See Note		61
HCl	Water Ice	H_2O(s)	<205	>0.1		62
	Liquid Water	H_2O(l)	260–295	≥0.05*		63
	Nitric Acid Ice	HNO_3•3H_2O(s)	191–211	>0.3		64
	Sulfuric Acid	H_2SO_4•nH_2O(l)			2	
		(n≥8, ≤40 wt% H_2SO_4)	284	0.15*		65
	Sulfuric Acid	(n<8, >40 wt% H_2SO_4)	<243	>0.1		65
	Tetrahydrate	H_2SO_4•4H_2O(s)	192–201	See Note		66
$ClONO_2$	Liquid Water	H_2O(l)	260–280	≥0.05*		67
CCl_3CHO	Water Ice	H_2O(s)	208–228	See Note		68
CCl_2O	Liquid Water	H_2O(l)	260–290	See Note		69
CCl_3CClO	Liquid Water	H_2O(l)	260–290	See Note		69
HBr	Water Ice	H_2O(s)	200	>0.2		70
	Liquid Water	H_2O(l)	260–295	≥0.05*		71
	Nitric Acid Ice	HNO_3•3H_2O(s)	200	>0.3		70
	Sulfuric Acid	H_2SO_4•nH_2O(l)(55-70wt% H_2SO_4)	213	≥0.1		72
HOBr	Water Ice	H_2O(s)	190–239	See Note		73
	Liquid Water	H_2O(l)	298	0.6	1.5	74
	Sulfuric Acid	H_2SO_4 in H_2O(l) (58 wt% H_2SO_4)	228	>0.05‡		75
$BrONO_2$	Liquid Water	H_2O(l)	260–280	≥0.03*		76
	Sulfuric Acid	H_2SO_4 in H_2O(l) (45-83 wt% H_2SO_4)	230–300	0.8	1.5	77
$CHBr_3$	Water Ice	H_2O(l)	220	See Note		78
	Sulfuric Acid	H_2SO_4•nH_2O(l) (97 wt% H_2SO_4)	220	$>3 \times 10^{-3}$‡		78
BrCl	Liquid Water	H_2O(l)	270–285	≥0.15*		79
I_2	Liquid Water	H_2O(l)	270–293	≥0.01*		80
HI	Water Ice	H_2O(s)	188–233	See Note		81
	Liquid Water	H_2O(l)	260–280	≥0.05*		82
HOI	Sulfuric Acid	H_2SO_4•nH_2O(l)				83
		(40 wt% H_2SO_4)	195	0.07	3	
		(40 wt% H_2SO_4)	205	0.03	3	
		(40 wt% H_2SO_4)	212	0.04	3	
		(50 wt% H_2SO_4)	222–224	0.02	3	
		(70 wt% H_2SO_4)	230–232	0.02	3	
		(70 wt% H_2SO_4)	252	0.02	3	
HF	Water Ice	H_2O(s)	200	See Note		84
	Nitric Acid Ice	HNO_3•3H_2O(s)	200	See Note		84
CF_3CH_2OH	Water Ice	H_2O(s)	208–228	See Note		85
$CF_3CF_2CH_2OH$	Water Ice	H_2O(s)	203–223	See Note		86
$CF_3CF_2CF_2CH_2OH$	Water Ice	H_2O(s)	203–223	See Note		87
CF_3CHO	Water Ice	H_2O(s)	208–228	See Note		88

Gaseous Species	Surface Type	Surface Composition	T(K)	α	Uncertainty Factor	Notes
CF_2O	Water Ice	$H_2O(s)$	192	See Note		89
	Liquid Water	$H_2O(l)$	260–290	See Note		69
	Nitric Acid Ice	$HNO_3•3H_2O(s)$	192	See Note		89
	Sulfuric Acid	$H_2SO_4•nH_2O(l)$	215–230			
		(40 wt% H_2SO_4)		>3 × 10^{-6}‡		89
		(60 wt% H_2SO_4)		>6 × 10^{-5}‡		89
CF_3CFO	Liquid Water	$H_2O(l)$	260–290	See Note		69
$CF_3C(O)OH$	Water Ice	$H_2O(s)$	208–238	See Note		90
CF_3COOH	Liquid Water	$H_2O(l)$	263–288	0.2–0.1*	2	91
CF_3CClO	Liquid Water	$H_2O(l)$	260–290	See Note		69
SO_2	Water Ice	$H_2O(s)$	190–238	See Note		92
	Liquid Water	$H_2O(l)$	260–298	≥0.12*	2	93
	Sulfuric Acid	$H_2SO_4•nH_2O(l)$ (97 wt% H_2SO_4)	298	See Note		94
H_2S	Liquid Water	$H_2O(l)$	260–298	≥0.05*		95
H_2SO_4	Sulfuric Acid	$H_2SO_4•nH_2O(l)$ (50–98 wt% H_2SO_4)	200–300	0.7	1.4	96
$CH_3S(O)CH_3$	Liquid Water	$H_2O(l)$	262–281	0.16–0.08*	2	97
$CH_3S(O_2)CH_3$	Liquid Water	$H_2O(l)$	262–281	0.27–0.08*	2	97
$CH_3S(O_2)OH$	Liquid Water	$H_2O(l)$	260–283	≥0.1*		97

* Varies with T, see Notes

‡ May be affected by surface saturation

5.2.2.1 Notes for Table NEq1

1. **O on H_2O(s).** Murray and Plane[1] measured the uptake of O atoms on water ice at temperatures relevant to the upper mesosphere (112–151 K), where noctilucent clouds are present. Their results indicate that in the absence of oxygen molecules the uptake coefficient α is small (7×10^{-6}). They recommend the following expression: $\alpha = 7 \times 10^{-6} + 1.5 \times 10^{-10}$ exp (11.4 kJ/mol/RT), with an uncertainty of ± 24%.
Back to Table

   (1) Murray, B. J.; Plane, M. C. The uptake of atomic oxygen on ice films: Implications for noctilucent clouds. *Phys. Chem. Chem. Phys.* **2003**, *107*, 4129-4138, doi:10.1039/b305555h.

2. **O on H_2SO_4•nH_2O.** Knudsen cell experiment of Baldwin and Golden[1] measured an uptake coefficient limit of $<10^{-6}$, this result probably cannot be equated with an accommodation coefficient due to surface saturation.
Back to Table

   (1) Baldwin, A. C.; Golden, D. M. Heterogeneous atmospheric reactions 2. Atom and radical reactions with sulfuric acid. *J. Geophys. Res.* **1980**, *85*, 2888-2889, doi:10.1029/JC085iC05p02888.

3. **O_3 on H_2O(s) and HNO_3•nH_2O.** Undoped ice surfaces saturate too quickly for reliable measurements. When ice is doped with Na_2SO_3 to chemically remove absorbed O_3 the apparent α increases to 1×10^{-2} (0.1 M) or up to 4×10^{-2} (1 M) (Dlugokencky and Ravishankara[1]). Limit of $\gamma < 10^{-6}$ for undoped ice is consistent with earlier measurement by Leu[3] of $\geq 1 \times 10^{-4}$ and with $< 6 \times 10^{-5}$ obtained by Kenner et al.[2] Dlugokencky and Ravishankara also measured the tabulated value of an uptake coefficient for O_3 on a NAT "like" surface, but the data were difficult to reproduce and the surfaces were not well characterized. Kenner et al. also measured a lower limit for an uptake coefficient of 8×10^{-5} on NAT at 183 K, but this measurement is also certainly limited by surface saturation.
Back to Table

   (1) Dlugokencky, E. J.; Ravishankara, A. R. Laboratory measurements of direct ozone loss on ice and doped-ice surfaces. *Geophys. Res. Lett.* **1992**, *19*, 41-44, doi:10.1029/91GL02092.
   (2) Kenner, R. D.; Plumb, I. C.; Ryan, K. R. Laboratory measurements of the loss of ClO on Pyrex, ice and NAT at 183 K. *Geophys. Res. Lett.* **1993**, *20*, 193-196, doi:10.1029/93GL00238.
   (3) Leu, M.-T. Heterogeneous reaction of N_2O_5 with H_2O and HCl on ice surfaces: implications for Antarctic ozone depletion. *Geophys. Res. Lett.* **1988**, *15*, 851-854, doi:10.1029/GL015i008p00851.

4. **O_3 on H_2O(l).** Utter et al.[9] used a wetted wall flow tube technique with various chemical scavengers to measure a lower limit for α of 2×10^{-3}. The stopped flow measurement technique using an SO_3^{2-} scavenger (Tang and Lee[8]) is subject to saturation effects, so their quoted α of 5.3×10^{-4} is also taken as a lower limit. Using a droplet train flow reactor Hu et al.[1] measured a value of ~0.1 at 277 K with I^- as a reactive scavenger, consistent with a more extensive droplet train flow reactor measurement by Magi et al.[2] yielding a value of ≥0.1 also using I^- as a reactive scavenger and with the aerosol flow tube work of Rouviere at al.[5] that also obtained a value of >0.1 at room temperature. Schurath et al.[6] used a coaxial flow liquid jet to obtain a value of 4.5×10^{-3} at 298 K, probably limited by surface saturation although they also used I^- as a reactive scavenger. Müller and Heal[3] obtained a value of 4×10^{-2} at 293 K in a wetted wall flow tube with $S_2O_3^{2-}$ as a reactive scavenger. Schütze and Herrmann[7] measured a lower limit of 2×10^{-2} at 298 K using a suspended droplet flow reactor method that also employed I^- as a reactive scavenger. It is highly likely that the mass accommodation coefficient for ozone on liquid water is ≥0.01 between ~275 and 300 K and may be significantly higher, although it is possible that interfacial reactions with near surface I^- bias some mass accommodation evaluations high because surface reactive uptake occurs in parallel with mass accommodation. Molecular dynamic simulations of O_3 uptake on water by Roeselováet al.[4] indicate a mass accommodation coefficient of order 0.1.
Back to Table

   (1) Hu, J. H.; Shi, Q.; Davidovits, P.; Worsnop, D. R.; Zahniser, M. S.; Kolb, C. E. Reative uptake of Cl_2(g) and Br_2(g) by aqueous surfaces as a function of Br^- and I^- ion concentration: The effect of chemical reaction at the interface. *J. Phys. Chem.* **1995**, *99*, 8768-8776, doi:10.1021/j100021a050.

(2) Magi, L.; Schweitzer, F.; Pallares, C.; Cherif, S.; Mirabel, P.; George, C. Investigation of the uptake rate of ozone and methyl hydroperoxide by water surfaces. *J. Phys. Chem. A* **1997**, *4*, 4943-4948, doi:10.1021/jp970646m.
(3) Müller, B.; Heal, M. R. The mass accommodation coefficient of ozone on an aqueous surface. *Phys. Chem. Chem. Phys.* **2002**, *4*, 3365-3369, doi:10.1039/b202491h.
(4) Roeselová, M.; Jungwirth, P.; Tobias, D. J.; Gerber, R. B. Impact, trapping, and accommodation of hydroxyl radical and ozone at aqueous salt aerosol surfaces. A molecular dynamics study. *J. Phys. Chem. B* **2003**, *107*, 12690-12699, doi:10.1021/jp030592i.
(5) Rouvière, A.; Sosedova, Y.; Ammann, M. Uptake of ozone to deliquesced KI and mixed KI/NaCl aerosol particles. *J. Phys. Chem. A* **2010**, *114*, 7085-7093, doi:10.1021/jp103257d.
(6) Schurath, U.; Bongartz, A.; Kames, J.; Wunderlich, C.; Carstens, T. In *Heterogeneous and Liquid Phase Processes. Transport and Chemical Transformation of Pollutants in the Troposphere*; Warneck, P., Ed.; Springer-Verlag: Berlin, 1996; Vol. 2; pp 182-189.
(7) Schütze, M.; Herrmann, H. Determination of phase transfer parameters for the uptake of HNO_3, N_2O_5 and O_3 on single aqueous drops. *Phys. Chem. Chem. Phys.* **2002**, *4*, 60-67, doi:10.1039/b106078n.
(8) Tang, I. N.; Lee, J. H. In *The Chemistry of Acid Rain*; Gordon, G. E., Johnson, R. W., Eds.; Am. Chem. Soc. Symp. Series, 1987; pp 109-117.
(9) Utter, R. G.; Burkholder, J. B.; Howard, C. J.; Ravishankara, A. R. Measurement of the mass accommodation coefficient of ozone on aqueous surfaces. *J. Phys. Chem.* **1992**, *96*, 4973-4979, doi:10.1021/j100191a045.

5. **O_3 on H_2SO_4•nH_2O.** Flow tube measurements (Dlugokencky and Ravishankara[2]) of an uptake coefficient limit of $<10^{-6}$ on both 50 and 97 wt% H_2SO_4 surfaces are consistent with earlier, but probably less quantitative, static systems measurements of Olszyna et al.[5] and aerosol chamber measurements of Harker and Ho,[3] who report uptake coefficients of the order 10^{-8} or less for a variety of sulfuric acid concentrations and temperatures. In these earlier experiments, doping the H_2SO_4 with Ni^{2+}, Cr^{2+}, Al^{3+}, Fe^{3+}, and NH_4^+ (Olszyna et al.[5]) or Al_2O_3 or Fe_2O_3 (Harker and Ho[3]) did not significantly increase measured O_3 loss. An upper limit of 1×10^{-6} was also reported by Baldwin and Golden[1] for 97 wt% H_2SO_4 at 295 K. Il'in et al.[4] performed static tube reactor measurements on 98 wt.% sulfuric acid at 239, 258, 273 K measuring uptake coefficients between 1.2 and 1.75×10^{-6}. Although these measurements are slightly larger than the limits in the other studies, uptake values this small are extremely hard to quantify and these measurements are not seen to be in serious disagreement with other studies finding slightly lower upper limits. All measurements are subject to solubility limitations and probably do not reflect true limits on mass accommodation.
Back to Table

(1) Baldwin, A. C.; Golden, D. M. Heterogeneous atmospheric reactions: Sulfuric acid aerosols as tropospheric sinks. *Science* **1979**, *206*, 562-563, doi:10.1126/science.206.4418.562.
(2) Dlugokencky, E. J.; Ravishankara, A. R. Laboratory measurements of direct ozone loss on ice and doped-ice surfaces. *Geophys. Res. Lett.* **1992**, *19*, 41-44, doi:10.1029/91GL02092.
(3) Harker, A. B.; Ho, W. W. Heterogeneous ozone decomposition on sulfuric acid surfaces at stratospheric temperatures. *Atmos. Environ.* **1979**, *13*, 1005-1010, doi:10.1016/0004-6981(79)90011-8.
(4) Il'in, S. D.; Selikhonovich, V. V.; Gershenson, Y. M.; Rozenshtein, V. B. Study of heterogeneous ozone loss on materials typical of atmospheric aerosol species. *Sov. J. Chem. Phys.* **1991**, *8*, 1858-1880.
(5) Olszyna, K.; Cadle, R. D.; dePena, R. G. Stratospheric heterogeneous decomposition of ozone. *J. Geophys. Res.* **1979**, *84*, 1771-1775, doi:10.1029/JC084iC04p01771.

6. **OH on H_2O(s).** Cooper and Abbatt[1] analyzed uptake rates in a wall-coated flow tube to determine an initial γ ~0.1 over the temperature range of 205–230 K. Uptake coefficients decreased at longer exposure times, indicating surface saturation. These data indicate that α is at least 0.1 and possibly much larger. This is confirmed by an earlier experiment using a coated insert/flow tube technique by Gershenzon et al.,[2] which yielded α >0.4 at 253 K.
Back to Table

(1) Cooper, P. L.; Abbatt, J. P. D. Heterogeneous interactions of OH and HO_2 radicals with surfaces characertistic of atmospheric particulate matter. *J. Phys. Chem.* **1996**, *100*, 2249-2254, doi:10.1021/jp952142z.
(2) Gershenzon, Y. M.; Ivanov, A. V.; Kucheryavyi, S. I.; Rozenshtein, V. B. Anihilation of OH radicals on the surfaces of subtances chemically similar to atmospheric aerosol particles. *Kinet. Katal.* **1986**, *27*, 1069-1074.

7. **OH on H_2O(l).** A lower limit of α on pure water of 3.5×10^{-3} at 275 K was determined by Hanson et al.[1] using a liquid-wall flow tube. Takami et al.[4] using a gas/liquid impinging flow technique obtained a pure water value near pH 7 at 293 K of $(4.2 \pm 2.8) \times 10^{-3}$ while values 2 to 3 times higher where obtained for acid (pH=1) and basic (pH=10–13) aqueous solutions; a value of $(1.1 \pm 0.4) \times 10^{-2}$ was obtained when benzoic acid was added as a radical scavenger. Takami et al. also observed that uptake for pure water solutions decreased with gas/liquid contact times, indicating a saturation limitation and explaining the higher uptake values observed for solutions with H^+, OH^-, or benzoic acid reactive scavengers. Based on these experimental results a value of $\alpha \geq 0.1$ is suggested. This recommendation is consistent with molecular dynamics calculations by Roeselová et al.[2,3] who first published simulation values at room temperature 0.2 to 0.3, but later reported a value of 0.83 at 300 K using revised intermolecular potentials.
Back to Table

(1) Hanson, D. R.; Burkholder, J. B.; Howard, C. J.; Ravishankara, A. R. Measurement of OH and HO_2 radical uptake coefficients on water and sulfuric acid surfaces. *J. Phys. Chem.* **1992**, *96*, 4979-4985, doi:10.1021/j100191a046.
(2) Roeselová, M.; Jungwirth, P.; Tobias, D. J.; Gerber, R. B. Impact, trapping, and accommodation of hydroxyl radical and ozone at aqueous salt aerosol surfaces. A molecular dynamics study. *J. Phys. Chem. B* **2003**, *107*, 12690-12699, doi:10.1021/jp030592i.
(3) Roeselová, M.; Vieceli, J.; Dang, L. X.; Garrett, B. C.; Tobias, D. J. Hydroxyl radical at the air-water interface. *J. Am. Chem. Soc.* **2004**, *126*, 16308-16309, doi:10.1021/ja045552m.
(4) Takami, A.; Kato, S.; Shimono, A.; Koda, S. Uptake coefficient of OH radical on aqueous surface. *Chem. Phys.* **1998**, *231*, 215-227, doi:10.1016/S0301-0104(98)00004-4.

8. **HO_2 on H_2O(l), aqueous salt solutions and $H_2SO_4 \cdot nH_2O$.** Determination of α in liquid-wall flow tube (Hanson et al.[2]) is dependent on gas-phase diffusion corrections; measured limit ($\alpha > 0.02$) is consistent with $\alpha = 1$. In the aqueous salt aerosol measurements of Mozurkewich et al.,[3] HO_2 was chemically scavenged by Cu^{++} from added $CuSO_4$ to avoid Henry's law constraints; the measured limit of >0.2 is also consistent with $\alpha = 1$. Thornton and Abbatt[6] and Taketani et al.[4,5] have raised the upper limit to the mass accommodation coefficient to >0.4 for Cu^{++} doped aqueous particles composed of sulfuric acid, ammonium sulfate, sodium chloride and potassium chloride, for relative humidities between 35 and 75% at room temperature. George et al.[1] report a value of >0.1 for copper-doped salt solutions as measured at low HO_2 gas phase concentrations in an aerosol flow tube reactor. This is consistent with the mass accommodation coefficient inferred by prior studies.
Back to Table

(1) George, I. J.; Matthews, P. S. J.; Whalley, L. K.; Brooks, B.; Goddard, A.; Baeza-Romero, M. T.; Heard, D. E. Measurements of uptake coefficients for heterogeneous loss of HO_2 onto submicron inorganic salt aerosols. *Phys. Chem. Chem. Phys.* **2013**, *15*, 12829-12845, doi:10.1039/c3cp51831k.
(2) Hanson, D. R.; Burkholder, J. B.; Howard, C. J.; Ravishankara, A. R. Measurement of OH and HO_2 radical uptake coefficients on water and sulfuric acid surfaces. *J. Phys. Chem.* **1992**, *96*, 4979-4985, doi:10.1021/j100191a046.
(3) Mozurkewich, M.; McMurray, P. H.; Gupta, A.; Calvert, J. G. Mass accommodation coefficient for HO_2 radicals on aqueous particles. *J. Geophys. Res.* **1987**, *92*, 4163-4170, doi:10.1029/JD092iD04p04163.
(4) Taketani, F.; Kanaya, Y.; Akimoto, H. Kinetics of heterogeneous reactions of HO_2 radical at ambient concentration levels with $(NH_4)_2SO_4$ and NaCl aerosol particles. *J. Phys. Chem. A* **2008**, *112*, 2370-2377, doi:10.1021/jp0769936.
(5) Taketani, F.; Kanaya, Y.; Akimoto, H. Heterogeneous loss of HO_2 by KCl, synthetic sea salt, and natural seawater aerosol particles. *Atmos. Environ.* **2009**, *43*, 1660-1665, doi:10.1016/j.atmosenv.2008.12.010.

(6) Thornton, J. A.; Abbatt, J. P. D. Measurements of HO_2 uptake to aqueous aerosol: Mass accommodation coefficients and net reactive loss. *J. Geophys. Res.* **2005**, *110*, D08309, doi:10.1029/2004JD005402.

9. **H_2O on H_2O(s).** Uptake coefficient measurements are available from Leu[5] (0.3 (+0.7, –0.1)) at 200 K, Haynes et al.[4] (1.06 ± 0.1 to 0.65 ± 0.08 from 20 to 185 K), Brown et al.[1] (0.99 ± 0.03 between 85 and 150 K and 0.97 ± 0.10 between 97 and 145 K), Fluckiger et al.[3] (0.43 at 200 K using D_2O^{18}), and Magee et al.[6] (0.006 at 223 K using levitated particles, in a wind tunnel). Uptake coefficients measured by Delval et al.[2] and Pratte et al.,[8] that should be viewed as lower limits to the mass accommodation coefficient, show a strong negative temperature dependence consistent with a precursor adsorption model; values are about 0.1 at 200 K. The sticking coefficient of D_2O on ice at a translational energy of 69 kJ/mole has been measured under ultrahigh vacuum conditions to be close to unity, consistent with other measurements (Hundt et al.[7]). At higher temperatures, Skrotzki et al.[9] have measured the growth of ice particles formed by deposition nucleation from 190 to 235 K in a large, cooled cloud chamber where supersaturations are generated by pressure expansion. Ice crystal number density and size, and ice water content are monitored. By comparing microphysical models to measured ice properties, the mass accommodation coefficient has been inferred to be 0.7(+0.3/–0.5), independent of temperature and particle size indicating that there is not a significant kinetic barrier to the uptake of water over these temperatures. The lower value measured by Magee et al. at elevated temperatures is not consistent with this report.
Back to Table

(1) Brown, D. E.; George, S. M.; Huang, C.; Wong, E. K. L.; Rider, K. B.; Smith, R. S.; Kay, B. D. H_2O condensation coefficient and refractive index for vapor-deposited ice from molecular beam and optical interference measurements. *J. Phys. Chem.* **1996**, *100*, 4988-4995, doi:10.1021/jp952547j.
(2) Delval, C.; Rossi, M. J. The kinetics of condensation and evaporation of H_2O from pure ice in the range 173-223 K: a quartz crystal microbalance study. *Phys. Chem. Chem. Phys.* **2004**, *6*, 4665-4676, doi:10.1039/b409995h.
(3) Fluckiger, B.; Rossi, M. J. Common precursor mechanism for the heterogeneous reaction of D_2O, HCl, HBr, and HOBr with water ice in the range 170-230 K: Mass accommodation coefficients on ice. *J. Phys. Chem. A* **2003**, *107*, 4103-4115, doi:10.1021/jp021956u.
(4) Haynes, D. R.; Tro, N. J.; George, S. M. Condensation and evaporation of H_2O on ice surfaces. *J. Phys. Chem.* **1992**, *96*, 8502-8509, doi:10.1021/j100200a055.
(5) Leu, M.-T. Laboratory studies of sticking coefficients and heterogeneous reactions important in the Antarctic stratosphere. *Geophys. Res. Lett.* **1988**, *15*, 17-20, doi:10.1029/GL015i001p00017.
(6) Magee, N.; Moyle, A. M.; Lamb, D. Experimental determination of the deposition coefficient of small cirrus-like ice crystals near-50 °C. *Geophys. Res. Lett.* **2006**, *33*, L17813, doi:10.1029/2006GL026665.
(7) Morten Hundt, P.; Bisson, R.; Beck, R. D. The sticking probability of D_2O-water on ice: Isotope effects and the influence of vibrational excitation. *J. Chem. Phys.* **2012**, *137*, 074701, doi:10.1063/1.4742914.
(8) Pratte, P.; van den Bergh, H.; Rossi, M. J. The kinetics of H_2O vapor condensation and evaporation on different types of ice in the range 130-210 K. *J. Phys. Chem. A* **2006**, *110*, 3042-3058, doi:10.1021/jp053974s.
(9) Skrotzki, J.; Connolly, P.; Schnaiter, M.; Saathoff, H.; Möhler, O.; Wagner, R.; Niemand, M.; Ebert, V.; Leisner, T. The accommodation coefficient of water molecules on ice – cirrus cloud studies at the AIDA simulation chamber. *Atmos. Chem. Phys.* **2013**, *13*, 4451-4466, doi:10.5194/acp-13-4451-2013.

10. **H_2O on H_2O(l).** Because the uptake of water vapor on and evaporation of water from liquid water are fundamental processes that are linked by microscopic reversibility and play extremely important roles in cloud physics, they have been the subject of over 75 published experimental studies spanning over eight decades. Many of these studies were reviewed by Marek and Staub,[7] who note values of α deduced from these experiments range from ~0.001 to 1.0, with experiments involving growing water drops tending to higher values. Recently published experiments support values near the higher end of the range. Shaw and Lamb[8] used an electrodynamic droplet levitation cell to make simultaneous ice nucleation/water droplet evaporation rate observations to deduce a range of $0.04 < \alpha < 0.1$ at 237 K. Li et al.[5] used a droplet train flow reactor to measure the uptake of small excesses of $H_2{}^{17}O$ on water droplets that were in equilibrium with the surrounding normal water vapor, deducing a value of 0.17 ± 0.03 at 280 K that increased to 0.32 ± 0.04 at

258 K. Winkler et al.[11] used Mie scattering analyses of the growth of freshly nucleated droplets in an expansion chamber to deduce $0.4 < \alpha < 1.0$ over a temperature range of 270 to 290 K and $0.8 < \alpha < 1.0$ for 250–270 K. Voigtländer et al.[10] analyzed droplet growth in a laminar diffusion flow reactor to estimate $0.3 < \alpha < 1.0$ at 275–277 K. Saykally, Cohen, and co-workers[1,3,9] performed a series of evaporation experiments from liquid jets and jet breakup droplet trains in very low-pressure reactors that approximate free evaporation conditions. Their studies of H/D isotope fraction in vapor from D_2O doped water jets yielded estimates of $\sim 0.15 < \alpha < \sim 0.3$ for the temperature range of 255–295 K.[1] Further experiments with jet break-up droplet trains produced an estimate of $\alpha = 0.62 \pm 0.09$ for H_2O between 245 and 298 K[9] and $\alpha = 0.57 \pm 0.06$ for D_2O between 255 and 295 K.[3] Maerefat and coworkers used a unique shock tube method to study the time resolved evolution of water film thickness on a window surface to estimate that $\alpha = 0.35$ over the temperature range 297.1–299.1 K.[6] Jakubczyk and co-workers applied an atmospheric pressure single droplet evaporation electrodynamic trap technique[4,13,14] and a continuum vapor diffusion and heat transfer model, which they argue is more complete than that employed by Winkler et al.[12] and Voigtländer et al.[10] When applied to temperature dependent data Jakubczyk and co-workers report $\alpha = 0.13 \pm 0.01$ at 293.1 K increasing to 0.18 ± 0.05 at 273.1 K,[14] in close agreement with magnitude and temperature dependence reported by Li et al.[5] Given the results from this wide range of experiments, it seems clear that mass accommodation values of water vapor on liquid water for temperatures below 295 K must exceed 0.1. The Li et al. and Winkler et al. experiments are further discussed in Davidovits et al.,[2] which notes that reasons for the differences in their deduced values are not yet understood.

Back to Table

(1) Cappa, C. D.; Drisdell, W. S.; Smith, J. D.; Saykally, R. J.; Cohen, R. C. Isotope fractionation of water during evaporation without condensation. *J. Phys. Chem. B* **2005**, *109*, 24391-24400, doi:10.1021/jp0539066.

(2) Davidovits, P.; Worsnop, D. R.; Jayne, J. T.; Kolb, C. E.; Winkler, P.; Vrtala, A.; Wagner, P. E.; Kulmula, M.; Lehtinen, K. E. J.; Vessala, T.; Mozurkewich, M. Mass accommodation coefficient of water vapor on liquid water. *Geophys. Res. Lett.* **2004**, *31*, L22111, doi:10.1029/2004GRL020835.

(3) Drisdell, W. S.; Cappa, C. D.; Smith, J. D.; Saykally, R. J.; Cohen, R. C. Determination of the evaporation coefficient of D_2O. *Atmos. Chem. Phys.* **2008**, *8*, 6699-6706, doi:10.5194/acp-8-6699-2008.

(4) Jakubcyzk, D.; Zientara, M.; Kolwas, K.; Kolwas, M. Temperature dependence of evaporation coefficient for water measured in droplets in nitrogen under atmospheric pressure. *J. Atmos. Sci.* **2007**, *64*, 996-1004, doi:10.1175/JAS3860.1.

(5) Li, Y. Q.; Davidovits, P.; Shi, Q.; Jayne, J. T.; Kolb, C. E.; Worsnop, D. R. Mass and thermal accommodation coefficients of $H_2O(g)$ on liquid water as a function of temperature. *J. Phys. Chem. A* **2001**, *105*, 10627-10634, doi:10.1021/jp012758q.

(6) Maerefat, M.; Akamatsu, T.; Fujikawa, S. Non-equilibrium condensation of water and carbontetrachloride vapor in a shock tube. *Experiments in Fluids* **1990**, *9*, 345-351.

(7) Marek, R.; Straub, J. Analysis of the evaporation coefficient and the condensation coefficient of water. *Int. J. Heat Mass Transfer* **2001**, *44*, 39-53, doi:10.1016/S0017-9310(00)00086-7.

(8) Shaw, R. A.; Lamb, D. Experimental determination of the thermal accommodation and condensation coefficients of water. *J. Chem. Phys.* **1999**, *111*, 10659-10663, doi:10.1063/1.480419.

(9) Smith, J. D.; Cappa, C. D.; Drisdell, W. S.; Cohen, R. C.; Saykally, R. J. Raman thermometry measurements of free evaporation from liquid water droplets. *J. Am. Chem. Soc.* **2006**, *128*, 12892 - 12898, doi:10.1021/ja063579v.

(10) Voigtländer, J.; Stratmann, F.; Niedermeier, D.; Wex, H.; Kiselev, A. Mass accommodation coefficient of water: A combined computational fluid dynamics and experimental data analysis. *J. Geophys. Res.* **2007**, *112*, D20208, doi:10.1029/2007JD008604.

(11) Winkler, P.; Vrtala, A.; Wagner, P. E.; Kulmula, M.; Lehtinen, K. E. J.; Vesala, T. Mass and thermal accommodation during gas-liquid condensation of water. *Phys. Rev. Lett.* **2004**, *93*, 075701, doi: 10.1103/Phys.Rev.Lett93.075701.

(12) Winkler, P. M.; Vrtala, A.; Rudolf, R.; Wagner, P. E.; Riipinen, I.; Vesala, T.; Lehtinen, K. E. J.; Viisanen, Y.; Kulmala, M. Condensation of water vapor: Experimental determination of mass and thermal accommodation coefficients. *J. Geophys. Res.* **2006**, *111*, D19202, doi:10.1029/2006JD007194.

(13) Zientara, M.; Jakubcyzk, D.; Derkachov, G.; Kolwas, K.; Kolwas, M. Simultaneous determination of mass and thermal accommodation coefficients from temporal evolution of an evaporating water microdroplet. *J. Phys. D: Applied Phys.* **2005**, *38*, 1978-1983, doi:10.1088/0022-3727/38/12/018.

(14) Zientara, M.; Jakubczyk, D.; Kolwas, K.; Kolwas, M. Temperature dependence of the evaporation coefficient of water in air and nitrogen under atmospheric pressure: Study in water droplets. *J. Phys. Chem. A* **2008**, *112*, 5152-5158, doi:10.1021/jp7114324.

11. **H_2O on HNO_3/H_2O(l).** Rudolf and Wagner[1] used aerosol expansion chamber techniques to illustrate that α on liquid water/nitric acid aerosols is greater than 0.3 and is consistent with 1.0 at 278 K. Experiments are similar to those at Winkler et al.;[2] supersaturated vapor may lead to a larger value of α than found for near equilibrium conditions.
Back to Table

(1) Rudolf, R.; Wagner, P. E. Experimental study of condensational particle growth in nitric acid-water vapor mixtures at nearly ambient pressures and temperatures. *J. Aerosol Sci.* **1994**, *25*, 97-98, doi:10.1016/0021-8502(94)90279-8.
(2) Winkler, P.; Vrtala, A.; Wagner, P. E.; Kulmula, M.; Lehtinen, K. E. J.; Vesala, T. Mass and thermal accommodation during gas-liquid condensation of water. *Phys. Rev. Lett.* **2004**, *93*, 075701, doi: 10.1103/Phys.Rev.Lett93.075701.

12. **H_2O on HNO_3•nH_2O(s).** Middlebrook et al.[1] measured an uptake coefficient of 0.002 for water vapor co-depositing with nitric acid over NAT at 197 K.
Back to Table

(1) Middlebrook, A. M.; Koehler, B. G.; McNeill, L. S.; Tolbert, M. A. Formation of model polar stratospheric cloud films. *Geophys. Res. Lett.* **1992**, *19*, 2417-2420, doi:10.1029/92GL02635.

13. **H_2O on H_2SO_4•nH_2O.** Baldwin and Golden[1] using a Knudsen cell measured ~2×10^{-3} at 96 wt%, which is strongly affected by surface saturation (see Note for H_2O_2 on H_2SO_4•nH_2O). Gershenzon et al.[2] used a droplet train flow reactor to measure the uptake of $H_2{}^{17}O$ on 50 wt% sulfuric acid from 250 to 278 K, on 70 wt% from 250 to 295 K, and on 82 wt% from 272 to 298 K. Measured mass accommodation coefficients range from 0.4 to 0.9, increasing with acid wt% and decreasing temperature.
Back to Table

(1) Baldwin, A. C.; Golden, D. M. Heterogeneous atmospheric reactions: Sulfuric acid aerosols as tropospheric sinks. *Science* **1979**, *206*, 562-563, doi:10.1126/science.206.4418.562.
(2) Gershenzon, M.; Davidovits, P.; Williams, L. R.; Shi, Q.; Jayne, J. T.; Kolb, C. E.; Worsnop, D. Uptake of $H_2{}^{17}O$(g) and D_2O(g) by aqueous sulfuric acid droplets. *J. Phys. Chem. A* **2004**, *106*, 1567-1573, doi:10.1021/jp036402l.

14. **H_2O on NaCl(s).** Fenter et al.[3] used Knudsen cell/mass spectrometry methods to measure $\gamma < 2 \times 10^{4}$ for H_2O(g) uptake on NaCl powders, an observation confirmed by Beichert and Finlayson-Pitts,[1] who found $\gamma < 1 \times 10^{-5}$. However, Dai et al.[2] used FTIR spectroscopy on NaCl crystallite films at 240 and 296 K to determine that a water adlayer does adhere to dry salt and that a small fraction of surface sites (<1%) cause H_2O dissociation. It is likely that the measurements of Fenter et al. and Beichert and Finlayson-Pitts were affected by surface saturation.
Back to Table

(1) Beichert, P.; Finlayson-Pitts, B. J. Knudson cell studies of the uptake of gaseous HNO_3 and other oxides of nitrogen on solid NaCl. The role of surface absorbed water. *J. Phys. Chem.* **1996**, *100*, 15218-15228, doi:10.1021/jp960925u.
(2) Dai, D. J.; Peters, S. J.; Ewing, G. E. Water absorption and dissociation on NaCl surfaces. *J. Phys. Chem.* **1995**, *99*, 10299-10304, doi:10.1021/j100025a035.
(3) Fenter, F. F.; Caloz, F.; Rossi, M. J. Kinetics of nitric acid uptake by salt. *J. Phys. Chem.* **1994**, *98*, 9801-9810, doi:10.1021/j100090a014.

15. **H_2O on NaCl(aq).** Fung et al.[1] used Mie resonance scattering techniques to quantify aqueous NaCl droplet growth (5.8 to 7.8 μm), yielding fitted values of $\alpha > 0.5$ and consistent with 1.0. Such droplet growth measurements require modeling of heat and mass transfer and may not correspond to atmospheric conditions near vapor/liquid equilibrium.
Back to Table

(1) Fung, K. N.; Tang, I. N.; Munkelwitz, H. R. Study of condensational growth of water droplets by Mie resonance spectroscopy. *Appl. Opt.* **1987**, *26*, 1282-1287, doi:10.1364/AO.26.001282.

16. **H_2O_2 on H_2O(s).** The uptake of H_2O_2 on ice surfaces has been studied by Clegg and Abbatt[1] who measured relatively small, reversible uptake between 213 and 238 K in a coated-wall flow tube experiment. The uptake scaled linearly with partial pressure and there was a weak temperature dependence, increasing with increasing temperature. By contrast, using the same flow tube technique but with a more direct H_2O_2 detection technique, values reported by Crowley and co-workers[2] are several orders of magnitude higher. A value of $K_{part} = 2.1 \times 10^{-5}$ exp(3800/T) cm is reported. Although the source of discrepancy between these studies is not clear, the later study by Crowley and co-workers is preferred by virtue of the more direct detection technique.
Back to Table

(1) Clegg, S. M.; Abbatt, J. P. D. Uptake of SO_2, H_2O_2 and oxygenated organics by ice surfaces under conditions of the free troposphere. *J. Phys. Chem. A* **2001**, *105*, 6630-6636, doi:10.1021/jp010062r.
(2) Pouvesle, N.; Kippenberger, M.; Schuster, G.; Crowley, J. N. The interaction of H_2O_2 with ice surfaces between 203 and 233 K. *Phys. Chem. Chem. Phys.* **2010**, *12*, 15544-15550, doi:10.1039/c0cp01656j.

17. **H_2O_2 on H_2O(l).** Measured accommodation coefficient (Worsnop et al.[1]) has a strong negative temperature dependence over the measured range of 260–292 K, with $\alpha = 0.3$ at 260 K decreasing to 0.1 at 292 K.
Back to Table

(1) Worsnop, D. R.; Zahniser, M. S.; Kolb, C. E.; Gardner, J. A.; Watson, L. R.; Doren, J. M. V.; Jayne, J. T.; Davidovits, P. Temperature dependence of mass accommodation of SO_2 and H_2O_2 on aqueous surfaces. *J. Phys. Chem.* **1989**, *93*, 1159-1172, doi:10.1021/j100340a027.

18. **H_2O_2 on H_2SO_4•nH_2O.** Knudsen cell uptake measurements are subject to surface saturation, thus uptake coefficient value of 7.8×10^{-4} quoted by Baldwin and Golden[1] is almost certainly a lower limit for α. This effect is probably also responsible for the lack of measured uptake ($\gamma < 10^{-6}$) for NO, NO_2, SO_2, Cl_2, and other species reported in this reference and Baldwin and Golden.[2]
Back to Table

(1) Baldwin, A. C.; Golden, D. M. Heterogeneous atmospheric reactions: Sulfuric acid aerosols as tropospheric sinks. *Science* **1979**, *206*, 562-563, doi:10.1126/science.206.4418.562.
(2) Baldwin, A. C.; Golden, D. M. Heterogeneous atmospheric reactions 2. Atom and radical reactions with sulfuric acid. *J. Geophys. Res.* **1980**, *85*, 2888-2889, doi:10.1029/JC085iC05p02888.

19. **NO on H_2O(s).** NO data (Leu[2] and Saastad et al.[3]) are subject to the same concerns as NO_2. See Note for NO_2 on H_2O(s). Using a radioactive tracer in a chromatographic technique, the adsorption enthalpy has been measured to be –20 kJ/mole by Bartels-Rausch et al.[1]
Back to Table

(1) Bartels-Rausch, T.; Eichler, B.; Zimmermann, P.; Gaggeler, H. W.; Ammann, M. The adsorption enthalpy of nitrogen oxides on crystalline ice. *Atmos. Chem. Phys.* **2002**, *2*, 235-247, doi:10.5194/acp-2-235-2002.
(2) Leu, M.-T. Heterogeneous reaction of N_2O_5 with H_2O and HCl on ice surfaces: implications for Antarctic ozone depletion. *Geophys. Res. Lett.* **1988**, *15*, 851-854, doi:10.1029/GL015i008p00851.
(3) Saastad, O. W.; Ellerman, T.; Nielson, C. J. On the adsorption of NO and NO_2 on cold H_2O/H_2SO_4 surfaces. *Geophys. Res. Lett.* **1993**, *20*, 1191-1193, doi:10.1029/93GL01621.

20. **NO on H_2SO_4•nH_2O.** See Notes for H_2O_2 on H_2SO_4•nH_2SO_4 and NO_2 on H_2SO_4•nH_2O. NO is subject to the same concerns as NO_2 for both reported measurements (Saastad et al.[2] and Baldwin and Golden[1]).
Back to Table

(1) Baldwin, A. C.; Golden, D. M. Heterogeneous atmospheric reactions: Sulfuric acid aerosols as tropospheric sinks. *Science* **1979**, *206*, 562-563, doi:10.1126/science.206.4418.562.
(2) Saastad, O. W.; Ellerman, T.; Nielson, C. J. On the adsorption of NO and NO_2 on cold H_2O/H_2SO_4 surfaces. *Geophys. Res. Lett.* **1993**, *20*, 1191-1193, doi:10.1029/93GL01621.

21. **NO_2 on H_2O(s).** In the absence of a chemical sink, Leu[2] measured no sustained uptake of NO_2 on ice yielding an apparent $\alpha < 1 \times 10^{-4}$. Saastad et al.[3] measured a lower limit of 5×10^{-5} for temperatures between 193 and 243 K. However these values are probably influenced by surface saturation. Using a radioactive tracer in a chromatographic technique, the adsorption enthalpy has been measured to be –22 kJ/mole by Bartels-Rausch et al.[1]

Back to Table

(1) Bartels-Rausch, T.; Eichler, B.; Zimmermann, P.; Gaggeler, H. W.; Ammann, M. The adsorption enthalpy of nitrogen oxides on crystalline ice. *Atmos. Chem. Phys.* **2002**, *2*, 235-247, doi:10.5194/acp-2-235-2002.

(2) Leu, M.-T. Heterogeneous reaction of N_2O_5 with H_2O and HCl on ice surfaces: implications for Antarctic ozone depletion. *Geophys. Res. Lett.* **1988**, *15*, 851-854, doi:10.1029/GL015i008p00851.

(3) Saastad, O. W.; Ellerman, T.; Nielson, C. J. On the adsorption of NO and NO_2 on cold H_2O/H_2SO_4 surfaces. *Geophys. Res. Lett.* **1993**, *20*, 1191-1193, doi:10.1029/93GL01621.

22. **NO_3 on H_2O(l).** Rudich et al.[2] analyzed uptake on KI solutions as a function of $[I^-]$ at 273 K. This work suggested that $\alpha > 0.04$, but this result may be biased due to reactive uptake by interfacial I^-. Potentially smaller estimates of α were suggested by the work of Thomas et al. as quoted in Mihelcic et al.[1] at 293 K on pure water and Thomas et al.,[4] on 293 K 0.1 M NaCl solutions, which reported uptake coefficients of 2.5×10^{-3} and 2×10^{-3}, respectively. Schütze and Herrman[3] used a single suspended droplet flow reactor technique and the resistor model to analyze uptake data on aqueous Alizarin Red S dye and NaCl solutions to estimate a 293 K value of $\alpha = 4.2\ (+2.2, -1.7) \times 10^{-3}$, consistent with the limits suggested by Thomas and co-workers. However, their data do not rule out possible surface reactions with either interfacial Cl^- or Alizarin Red S. A lower limit of 2×10^{-3} for 273–293 K is recommended.

Back to Table

(1) Mihelcic, D.; Klemp, D.; Müsgen, P.; Pätz, H. W.; Volz-Thomas, A. Simultaneous measurements of peroxy and nitrate radicals at Schauinsland. *J. Atmos. Chem.* **1993**, *16*, 313-335, doi:10.1007/BF01032628.

(2) Rudich, Y.; Talukdar, R. K.; Imamura, T.; Fox, R. W.; Ravishankara, A. R. Uptake of NO_3 on KI solutions: Rate coefficient for the $NO_3 + I^-$ reaction and gas-phase diffusion coefficient for NO_3. *Chem. Phys. Lett.* **1996**, *261*, 467-473, doi:10.1016/0009-2614(96)00980-3.

(3) Schütze, M.; Herrmann, H. Uptake of the NO_3 radical on aqueous surfaces. *J. Atmos. Chem.* **2005**, *52*, 1-18, doi:10.1007/s10874-005-6153-8.

(4) Thomas, K.; Volz-Thomas, A.; Mihelcic, D.; Smit, H. G. J.; Kley, D. On the exchange of NO_3 radicals with aqueous solutions: Solubility and sticking coefficient. *J. Atmos. Chem.* **1998**, *29*, 17-43, doi:10.1023/A:1005860312363.

23. **HONO on H_2O(s).** Fenter and Rossi[3] measured reversible uptake on water ice between 180 and 200 K using a Knudsen cell technique. An initial uptake coefficient of 1×10^{-3} suggests that α equals or exceeds this value. Chu et al.[2] used a cylindrical flow reactor to measure the uptake coefficient as a function of temperature, obtaining values ranging from 3.7×10^{-3} at 178 K to 6.4×10^{-4} at 200 K, in good agreement with the results of Fenter and Rossi. On the other hand, Chu et al. report significantly lower values after correction for the effects of surface porosity, i.e. 1.4×10^{-4} at 178 K and 1.3×10^{-5} at 200 K (see Keyser et al.[6]). The adsorption enthalpy has been measured to be –32 kJ/mole by Bartels-Rausch et al.[1] Using radioactively labeled HONO uptake on ice was studied in a packed ice bed between 213 and 253 K by Kerbrat et al.,[5] who attempted to disentangle surface adsorption and bulk diffusion. A partition coefficient to the ice surface is reported ($K_{Part} = 7.4 \times 10^{-9} \exp(5.4 \times 10^3/T)$ cm) with an enthalpy of adsorption of -45 ± 20 kJ/mole. The kinetics of the diffusion into the bulk ice were studied. In another study from the same group, nitrous acid and acetic acid simultaneous uptake measurements to packed ice beds were found to be well described by a competitive Langmuir adsorption isotherm between 213 and 243 K. Labeled nitrous acid was monitored by radioactive methods, and acetic acid by CIMS (Kerbrat et al.[4]).

Back to Table

(1) Bartels-Rausch, T.; Eichler, B.; Zimmermann, P.; Gaggeler, H. W.; Ammann, M. The adsorption enthalpy of nitrogen oxides on crystalline ice. *Atmos. Chem. Phys.* **2002**, *2*, 235-247, doi:10.5194/acp-2-235-2002.

(2) Chu, L.; Diao, G.; Chu, L. T. Heterogeneous interaction and reaction of HONO on ice films between 173 and 230 K. *J. Phys. Chem. A* **2000**, *104*, 3150-3158, doi:10.1021/jp9937151.
(3) Fenter, F. F.; Rossi, M. J. The heterogeneous kinetics of HONO on H_2SO_4 and on ice: activation of HCl. *J. Phys. Chem.* **1996**, *100*, 13765-13775, doi:10.1021/jp960797+.
(4) Kerbrat, M.; Huthwelker, T.; Bartels-Rausch, T.; Gäggeler, H. W.; Ammann, M. Co-adsorption of acetic acid and nitrous acid on ice. *Phys. Chem. Chem. Phys.* **2010**, *12*, 7194-7202, doi:10.1039/b924782c.
(5) Kerbrat, M.; Huthwelker, T.; Gäggeler, H. W.; Ammann, M. Interaction of nitrous acid with polycrystalline ice: Adsorption on the surface and diffusion into the bulk. *J. Phys. Chem. C* **2010**, *114*, 2208-2219, doi:10.1021/jp909535c.
(6) Keyser, L. F.; Moore, S. B.; Leu, M. T. Surface reaction and pore diffusion in flow tube reactors. *J. Phys. Chem.* **1991**, *95*, 5496-5502, doi:10.1021/j100167a026.

24. **HNO_3 on H_2O(s).** Leu[10] report a lower limit of 0.2 at 195 K, Hanson[5] measured an uptake coefficient of greater than 0.3 at 191.5 and 200 K, and Aguzzi and Rossi[2] measured an uptake coefficient of 0.3 over the temperature range from 180 to 190 K with the value decreasing at T >195 with an exponential temperature dependence of $-(3400 \pm 500)/T$. Aguzzi and Rossi attributed this change to an increasing evaporation rate, concluding that the accommodation coefficient most likely remains large. In a higher temperature regime, Hynes et al.[7] measured uptake coefficients as a function of temperature decreasing from 0.03 at 215 K to 0.006 at 235 K and Hudson et al.[6] report initial uptake coefficients ranging from 0.007 at 209 K to 0.003 at 220 K. On the other hand, Ullerstam et al.[14] report a temperature independent lower limit to the uptake coefficient of 0.1 from 200 K up to 239 K. It is unclear the extent to which the work of Aguzzi and Rossi, Hudson et al., and Hynes et al. are affected by outgassing of nitric acid from wall surfaces during uptake experiments at high temperatures, which would lead to apparently low uptake coefficients. Also, uptakes on surfaces that have already been exposed to nitric acid are smaller than on those that are freshly exposed. Additional uncertainty is introduced by the effective ice surface area in the older fast-flow measurements (see Keyser et al.[8]) but these effects should be absent in the work of Hynes et al. and Ullerstam et al., which used smooth ice surfaces.

25. For low partial pressure experiments and temperatures above about 190 K, the uptake of nitric acid displays both reversible and irreversible components in amounts that do not exceed monolayer coverage.[1,14,15] For high partial pressures and/or low temperatures, a different uptake regime is encountered where much larger uptakes can occur that are not necessarily atmospherically relevant. In particular, the ice surfaces may melt to form a thermodynamically stable nitric acid solution on the surface, or nitric acid hydrate layers may form. Focusing only on the sub-monolayer, atmospherically-relevant uptake regime, it is believed that the uptake proceeds initially via adsorption to the ice surface, with some degree of diffusion along grain boundaries and into the underlying ice bulk then proceeding. The relative fractions of adsorbed molecular nitric acid and dissociated nitric acid are not fully known, although it is likely that nitrate is present to a large degree.[15] Indeed, XPS and NEXAFS spectra of ice at 230 K which contains surface nitrate, formed from NO_2 hydrolysis, indicate that the nitrate is similar in character to that of ions present in a concentrated solution (Křepelová et al.[9]). The implication is that the chemical environment on the surface of ice of adsorbed nitric acid is similar to that of pure ice and concentrated nitrate solutions. For initial exposures, uptakes are saturated at between 1 to 3×10^{14} molecules cm^{-2} [1,7,14,15] when the gas phase concentrations are high (roughly 10^9 to 10^{10} molecules/cm^3) for temperatures between roughly 200 and 230 K. At lower concentrations, the surface is unsaturated and the uptakes obey temperature-dependent Langmuir adsorption curves, with enhanced uptake at low temperatures.[14] In this regime, for temperatures between 214 to 239 K, the adsorption coefficient (converted to concentration units) for the initial uptake is $K_{conc} = -8.2 \times 10^{-12} T + 2.01 \times 10^{-9}$ cm^3/molecule. The temperature dependence is qualitatively consistent with observations of nitric acid uptake to cirrus cloud particles, with more uptake at low temperature.[14] For repeated exposures, the amounts of nitric acid decrease relative to the initial uptake value. Cox et al.[4] have used a numerical model of the Ullerstam et al.[14] data to decouple adsorptive uptake from uptake arising by nitric acid diffusing into the upper layers of the ice. As a result, an effective temperature-dependent adsorption equilibrium constant has been deduced, which shows that roughly 85% of the uptake measured by Ullerstam et al. is adsorptive. The related enthalpy of adsorption is –31 kJ/mole. Using a radioactive tracer, chromatographic technique Bartels-Rausch et al.[3] have measured the adsorption enthalpy to be –44 kJ/mole, and Hynes et al.[7] report a value of –54 kJ/mole from a Van't Hoff analysis.

Note that uptake may be affected by co-adsorbed species. Studies by Hynes et al.[7] and Sokolov and Abbatt[11] involving co-adsorption of HCl indicate that HNO_3 binds more strongly than HCl, but that the presence of HCl does lead to suppressed HNO_3 uptake relative to behavior on bare ice surfaces. Also, enhanced uptake is observed if the ice surfaces are growing and not at equilibrium,[13] probably arising through the formation of a metastable solution of HNO_3 in ice. The uptakes are larger under burial conditions than the amounts of nitric acid that are thermodynamically stable.[12]
Back to Table

(1) Abbatt, J. P. D. Interaction of HNO_3 with water-ice surfaces at temperatures of the free troposphere. *Geophys. Res. Lett.* **1997**, *24*, 1479-1482, doi:10.1029/97GL01403.

(2) Aguzzi, A.; Rossi, M. J. The kinetics of the uptake of HNO_3 on ice, solid H_2SO_4-H_2O and solid ternary solutions of H_2SO_4-HNO_3-H_2O in the temperature range 180-211 K. *Phys. Chem. Chem. Phys.* **2001**, *3*, 3707-3716, doi:10.1039/b100546o.

(3) Bartels-Rausch, T.; Eichler, B.; Zimmermann, P.; Gaggeler, H. W.; Ammann, M. The adsorption enthalpy of nitrogen oxides on crystalline ice. *Atmos. Chem. Phys.* **2002**, *2*, 235-247, doi:10.5194/acp-2-235-2002.

(4) Cox, R. A.; Fernandez, M. A.; Symington, A.; Ullerstam, M.; Abbatt, J. P. D. A kinetic model for uptake of HNO_3 and HCl on ice in a coated wall flow system. *Phys. Chem. Chem. Phys.* **2005**, *7*, 3434-3442, doi:10/1039/b506683b.

(5) Hanson, D. R. The uptake of HNO_3 onto ice, NAT, and frozen sulfuric acid. *Geophys. Res. Lett.* **1992**, *19*, 2063-2066, doi:10.1029/92GL02182.

(6) Hudson, P. K.; Shilling, J. E.; Tolbert, M. A.; Toon, O. B. Uptake of nitric acid on ice at tropospheric temperatures: Implications for cirrus clouds. *J. Phys. Chem. A* **2002**, *106*, 9874-9882, doi:10.1021/jp020508j.

(7) Hynes, A. J.; Fernandez, M. A.; Cox, R. A. Uptake of HNO_3 on water-ice and coadsorption of HNO_3 and HCl in the temperature range 210–235 K. *J. Geophys. Res.* **2002**, *107*, 4797, doi:10.1029/2001JD001557.

(8) Keyser, L. F.; Moore, S. B.; Leu, M. T. Surface reaction and pore diffusion in flow tube reactors. *J. Phys. Chem.* **1991**, *95*, 5496-5502, doi:10.1021/j100167a026.

(9) Křepelová, A.; Newberg, J.; Huthwelker, T.; Bluhm, H.; Ammann, M. The nature of nitrate at the ice surface studied by XPS and NEXAFS. *Phys. Chem. Chem. Phys.* **2010**, *12*, 8870-8880, doi:10.1039/c0cp00359j.

(10) Leu, M.-T. Laboratory studies of sticking coefficients and heterogeneous reactions important in the Antarctic stratosphere. *Geophys. Res. Lett.* **1988**, *15*, 17-20, doi:10.1029/GL015i001p00017.

(11) Sokolov, O.; Abbatt, J. P. D. Competitive adsorption of atmospheric trace gases onto ice at 228 K: HNO_3/HCl, 1-butanol/acetic acid and 1-butanol/HCl. *Geophys. Res. Lett.* **2002**, *29*, 1851, doi:10.1029/2002GL014843.

(12) Thibert, E.; Domine, F. Thermodynamics and kinetics of the solid solution of HNO_3 in ice. *J. Phys. Chem. B* **1998**, *102*, 4432-4439, doi:10.1021/jp980569a.

(13) Ullerstam, M.; Abbatt, J. P. D. Burial of gas-phase HNO_3 by growing ice surfaces under tropospheric conditions. *Phys. Chem. Chem. Phys.* **2005**, *7*, 3596-3600, doi:10.1039/b507797d.

(14) Ullerstam, M.; Thornberry, T.; Abbatt, J. P. D. Uptake of gas-phase nitric acid to ice at low partial pressures: evidence for unsaturated surface coverage. *Faraday Discuss.* **2005**, *130*, 211-226, doi:10.1039/b417418f.

(15) Zondlo, M. A.; Barone, S. B.; Tolbert, M. A. Uptake of HNO_3 on ice under upper tropospheric conditions. *Geophys. Res. Lett.* **1997**, *24*, 1391-1394, doi:10.1029/97GL01287.

25. HNO_3 on H_2O(l). Measurements using a droplet train flow reactor show that α has a strong negative temperature dependence varying from 0.19 ± 0.02 at 268 K to 0.07 ± 0.02 at 293 K (Van Doren et al.[3]). Ponche et al.[1] measured a very consistent mass accommodation coefficient of 0.05 ± 0.01 at 297 K using the same technique. Schütze and Herrmann[2] measured a lower limit of 3×10^{-2} at 298 K using a suspended droplet flow reactor method, consistent with the droplet train flow reactor measurements.
Back to Table

(1) Ponche, J. L.; George, C.; Mirabel, P. Mass transfer at the air/water interface: Mass accommodation coefficients of SO_2, HNO_3, NO_2 and NH_3. *J. Atmos. Chem.* **1993**, *16*, 1-21, doi:10.1007/BF00696620.

(2) Schütze, M.; Herrmann, H. Determination of phase transfer parameters for the uptake of HNO_3, N_2O_5 and O_3 on single aqueous drops. *Phys. Chem. Chem. Phys.* **2002**, *4*, 60-67, doi:10.1039/b106078n.
(3) Van Doren, J. M.; Watson, L. R.; Davidovits, P.; Worsnop, D. R.; Zahniser, M. S.; Kolb, C. E. Uptake of N_2O_5 and HNO_3 by aqueous sulfuric acid droplets. *J. Phys. Chem.* **1991**, *95*, 1684-1689, doi:10.1021/j100157a037.

26. **HNO_3 on HNO_3•nH_2O(s).** Hanson[1] measured uptake coefficients of >0.3 and >0.2 on NAT surfaces at 191 K and 200 K, respectively. Middlebrook et al.[2] measured an uptake coefficient of 0.7 on NAT at 197 K under conditions where both nitric acid and water vapor were co-depositing.
Back to Table

(1) Hanson, D. R. The uptake of HNO_3 onto ice, NAT, and frozen sulfuric acid. *Geophys. Res. Lett.* **1992**, *19*, 2063-2066, doi:10.1029/92GL02182.
(2) Middlebrook, A. M.; Koehler, B. G.; McNeill, L. S.; Tolbert, M. A. Formation of model polar stratospheric cloud films. *Geophys. Res. Lett.* **1992**, *19*, 2417-2420, doi:10.1029/92GL02635.

27. **HNO_3 on HNO_3•nH_2O(l).** Rudolf and Wagner[1] used an aerosol expansion chamber techniques to deduce that α for HNO_3 on 278 K H_2O/HNO_3 droplets is >0.3 and probably close to 1. The consistency of this value with smaller (~0.2) values measured for uptake on pure water by Van Doren et al.[2] is unclear, since the mechanism of co-condensation is unknown and the composition of the surface in the aerosol expansion chamber experiments may be kinetically controlled and has not been well determined.
Back to Table

(1) Rudolf, R.; Wagner, P. E. Experimental study of condensational particle growth in nitric acid-water vapor mixtures at nearly ambient pressures and temperatures. *J. Aerosol Sci.* **1994**, *25*, 97-98, doi:10.1016/0021-8502(94)90279-8.
(2) Van Doren, J. M.; Watson, L. R.; Davidovits, P.; Worsnop, D. R.; Zahniser, M. S.; Kolb, C. E. Uptake of N_2O_5 and HNO_3 by aqueous sulfuric acid droplets. *J. Phys. Chem.* **1991**, *95*, 1684-1689, doi:10.1021/j100157a037.

28. **HNO_3 on H_2SO_4•nH_2O and H_2SO_4•4H_2O(s).** Initial uptake at 73 wt% H_2SO_4 allows a measurement of α = 0.11 ± 0.01 at 283 K (Van Doren et al. [7]). This value is expected to increase at lower temperatures, in a manner similar to H_2O(1) uptake (Van Doren et al.[6]). Total HNO_3 uptake is subject to Henry's law solubility constraints, even at stratospheric temperatures (Reihs et al.[4]). Solubility limitations also affected the earlier "sticking coefficient" measurements of Tolbert et al.[5] for 75 wt% H_2SO_4 at 230 K. Hanson[2] measured an uptake coefficient of >0.3 for frozen 57.7 wt% sulfuric acid at 191.5 and 200 K. Baldwin and Golden[1] reported a lower limit of 2.4×10^{-4} on 97 wt% H_2SO_4 at 295 K, also reflecting solubility limits. Iraci et al.[3] monitored nitric acid trihydrate growth on sulfuric acid tetrahydrate with infrared techniques, measuring HNO_3 uptake coefficient limits of >0.03 at 192.5 K and >0.08 at 192 K. These measurements involved co-deposition of water vapor.
Back to Table

(1) Baldwin, A. C.; Golden, D. M. Heterogeneous atmospheric reactions: Sulfuric acid aerosols as tropospheric sinks. *Science* **1979**, *206*, 562-563, doi:10.1126/science.206.4418.562.
(2) Hanson, D. R. The uptake of HNO_3 onto ice, NAT, and frozen sulfuric acid. *Geophys. Res. Lett.* **1992**, *19*, 2063-2066, doi:10.1029/92GL02182.
(3) Iraci, L. T.; Middlebrook, A. M.; Wilson, M. A.; Tolbert, M. A. Growth of nitric acid hydrates on thin sulfuric acid films. *Geophys. Res. Lett.* **1994**, *21*, 867-870, doi:10.1029/94GL00916.
(4) Reihs, C. M.; Golden, D. M.; Tolbert, M. A. Nitric acid uptake by sulfuric acid solutions under stratospheric conditions: Determination of Henry's law solubility. *J. Geophys. Res.* **1990**, *95*, 16545-16550, doi:10.1029/JD095iD10p16545.
(5) Tolbert, M. A.; Rossi, M. J.; Golden, D. M. Heterogeneous interactions of chlorine nitrate, hydrogen chloride and nitric acid with sulfuric acid surfaces at stratospheric temperatures. *Geophys. Res. Lett.* **1988**, *15*, 847-850, doi:10.1029/GL015i008p00847.
(6) Van Doren, J. M.; Watson, L. R.; Davidovits, P.; Worsnop, D. R.; Zahniser, M. S.; Kolb, C. E. Temperature dependence of the uptake coefficients of HNO_3, HCl, and N_2O_5 by water droplets. *J. Phys. Chem.* **1990**, *94*, 3265-3269, doi:10.1021/j100371a009.

(7) Van Doren, J. M.; Watson, L. R.; Davidovits, P.; Worsnop, D. R.; Zahniser, M. S.; Kolb, C. E. Uptake of N_2O_5 and HNO_3 by aqueous sulfuric acid droplets. *J. Phys. Chem.* **1991**, *95*, 1684-1689, doi:10.1021/j100157a037.

29. **N_2O_5 on Aqueous Aerosol.** Gržinić et al.[1] have demonstrated that the bulk mass accommodation coefficient for N_2O_5 into nitrate water solutions is larger than 0.4 at room temperature. The experiments were performed with an isotopically labelled gas phase reactant. The data are consistent with rapid N_2O_5 dissociation in solution into NO_2^+ and NO_3^-, with the isotopically labelled nitrate undergoing significant dilution into the non-isotopically labelled pool of nitrate. This is indirect confirmation of the dissociation pathway that has been invoked previously as the first step of the mechanism by which N_2O_5 undergoes hydrolysis in aqueous solutions.
Back to Table

(1) Gržinić, G.; Bartels-Rausch, T.; Türler, A.; Ammann, M. Efficient bulk mass accommodation and dissociation of N_2O_5 in neutral aqueous aerosol. *Atmos. Chem. Phys.* **2017**, *17*, 6493-6502, doi:10.5194/acp-17-6493-2017.

30. **HO_2NO_2 on H_2O(s).** Li et al.[1] measured an uptake coefficient of 0.15 ± 0.10 at 200 K, where the uptake may be limited by surface saturation and appears to be reversible with no decomposition. Consistent with this, adsorption of $HOONO_2$ to ice was studied in a coated wall flow tube using CIMS for gas phase detection (Ulrich et al.[2]) at temperatures between 230 and 253 K. Only reversible uptake was observed, with a partition coefficient, K_{Part}, of $3.74 \times 10^{-12} \times \exp(7098/T)$ cm. Uptake is much smaller than for stronger acids, such as HNO_3.
Back to Table

(1) Li, Z.; Friedl, R. R.; Moore, S. B.; Sander, S. P. Interaction of peroxynitric acid with solid H_2O-ice. *J. Geophys. Res.* **1996**, *101*, 6795-6802, doi:10.1029/96JD00065.
(2) Ulrich, T.; Ammann, M.; Leutwyler, S.; Bartels-Rausch, T. The adsorption of peroxynitric acid on ice between 230 K and 253 K. *Atmos. Chem. Phys.* **2012**, *12*, 1833-1845, doi:10.5194/acp-12-1833-2012.

31. **HO_2NO_2 on H_2SO_4•nH_2O(l).** Baldwin and Golden[1] measured $\gamma = 2.7 \times 10^{-5}$, which is probably solubility limited; see Note for H_2O_2 on H_2SO_4•nH_2O.
Back to Table

(1) Baldwin, A. C.; Golden, D. M. Heterogeneous atmospheric reactions: Sulfuric acid aerosols as tropospheric sinks. *Science* **1979**, *206*, 562-563, doi:10.1126/science.206.4418.562.

32. **NH_3 on H_2O(s).** NH_3 interacts somewhat efficiently with ice surfaces according to the coated-wall flow tube results of Jin and Chu[1] at 190 K. The porosity-corrected uptake coefficients are 4×10^{-4}, with no evidence for surface saturation when partial pressures of 10^{-6} Torr are used over hours of exposure time. This suggests that the surface is being substantially modified by the NH_3 exposure.
Back to Table

(1) Jin, R. H.; Chu, L. T. Uptake of NH_3 and NH_3 + HOBr reaction on ice surfaces at 190 K. *J. Phys. Chem. A* **2007**, *111*, 7833-7840, doi:10.1021/jp073233m.

33. **NH_3 on H_2O(l).** Ponche et al.[3] used a droplet train technique to obtain $\alpha = (9.7 \pm 0.9) \times 10^{-2}$ at 290 K, and Bongartz et al.[1] used a liquid jet technique to obtain $\alpha = 4.0\ (+3.0, -0.05) \times 10^{-2}$ at the same temperature. These experiments where extended to other temperatures by Carstens et al.,[2] demonstrating a negative temperature dependence. Ammonia uptake on liquid water as a function of both pH and temperature was investigated by Shi et al.[4] using a droplet train apparatus, yielding values that also demonstrated negative temperature dependence, varying between 0.08 at 290 K to 0.35 at 260 K. The data from these four studies are all in reasonable agreement and a temperature dependent data plot with a non-linear least squares fit to all of these measurements has been published by Worsnop et al.[6] Earlier levitated droplet evaporation experiments[5] on NH_4Cl obtained a larger evaporation coefficient of $\alpha = 0.29 \pm 0.03$, which is discounted because of the indirect nature of the experiment.
Back to Table

(1) Bongartz, A.; Schweighoefer, S.; Roose, C.; Schurath, U. The mass accommodation coefficient of ammonia on water. *J. Atmos. Chem.* **1995**, *20*, 35-58, doi:10.1007/BF01099917.
(2) Carstens, T.; Wunderlich, C.; Schurath, U. "*Proceedings EUROTRAC Symposium ' 96*", 1996, Southhampton, U. K.
(3) Ponche, J. L.; George, C.; Mirabel, P. Mass transfer at the air/water interface: Mass accommodation coefficients of SO_2, HNO_3, NO_2 and NH_3. *J. Atmos. Chem.* **1993**, *16*, 1-21, doi:10.1007/BF00696620.
(4) Shi, Q.; Davidovits, P.; Jayne, J. T.; Worsnop, D. R.; Kolb, C. E. Uptake of gas-phase ammonia. 1. Uptake by aqueous surfaces as a function of pH. *J. Phys. Chem. A* **1999**, *103*, 8812-8823, doi:10.1021/jp991696p.
(5) Tang, I. N.; Munkelwitz, H. R. Evaporation kinetics of ammonium chloride solution droplets in water vapor. *J. Colloid Interface Sci.* **1989**, *128*, 289-295, doi:10.1016/0021-9797(89)90406-2.
(6) Worsnop, D. R.; Williams, L. R.; Kolb, C. E.; Mozurkewich, M.; Gershenzon, M.; Davidovits, P. Comment on "The NH_3 mass accommodation coefficient for uptake onto sulfuric acid solution". *J. Phys. Chem. A* **2004**, *108*, 8546-8548, doi:10.1021/jp036519+.

34. **CO_2 on H_2O(s).** The uptake of carbon dioxide on ice has been studied in a classical BET adsorption experiment from 209 to 263 K by Ocampo and Klinger.[1] The system is unusual in that the measured uptakes are higher at higher temperatures, unlike the behavior displayed by most gases that physically adsorb to ice surfaces. Similar to SO_2, the uptake may occur via formation and decomposition of H_2CO_3 in which case the ice surfaces may be somewhat acidified by this process.
Back to Table

(1) Ocampo, J.; Klinger, J. Adsorption of N_2 and CO_2 on ice. *J. Colloid Interface Sci.* **1982**, *86*, 377-383, doi:10.1016/0021-9797(82)90083-2.

35. **CO_2 on H_2O(l).** Noyes et al.[2] used a dynamic stirring technique to monitor pressure decreases in a closed cylinder. They inferred $\alpha = (5.5 \pm 0.5) \times 10^{-8}$ at 293 K. This technique is uncalibrated against more widely used procedures and probably suffers from severe surface saturation effects. Schurath et al.[3] employed a coaxial jet flow technique to measure a 298 K value of α of $1–2 \times 10^{-4}$, noting that its low Henry's law solubility in water made the measurement very difficult. For this reason, the measurement probably also suffered from surface saturation even at their shortest gas/liquid contact times, so this value is most likely a lower limit. Boniface et al.[1] used a bubble train reactor to study the uptake by water as a function of pH. At high pH the reaction of CO_2 with OH^- partially relieves surface saturation allowing determination that the uptake coefficient, and therefore α, is $\geq 1 \times 10^{-5}$, consistent with the value measured by Schurath et al. and completely inconsistent with the much lower value obtained by Noyes et al.[2]
Back to Table

(1) Boniface, J.; Shi, Q.; Li, Y. Q.; Chueng, J. L.; Rattigan, O. V.; Davidovits, P.; Worsnop, D. R.; Jayne, J. T.; Kolb, C. E. Uptake of gas-phase SO_2, H_2S, and CO_2 by aqueous solutions. *J. Phys. Chem. A* **2000**, *104*, 7502-7510, doi:10.1021/jp000479h.
(2) Noyes, R. M.; Rubin, M. B.; Bowers, P. G. Transport of carbon dioxide between the gas phase and water under well-stirred conditions: Rate constants and mass accommodation coefficient. *J. Phys. Chem.* **1996**, *100*, 4167-4172, doi:10.1021/jp952382e.
(3) Schurath, U.; Bongartz, A.; Kames, J.; Wunderlich, C.; Carstens, T. In *Heterogeneous and Liquid Phase Processes. Transport and Chemical Transformation of Pollutants in the Troposphere*; Warneck, P., Ed.; Springer-Verlag: Berlin, 1996; Vol. 2; pp 182-189.

36. **CH_3OH on H_2O(s).** The uptake of methanol on ice has been measured in a coated-wall flow tube from 198 to 213 K[2,3] and in a Knudsen cell from 150 to 180 K.[1] Reversible uptakes are observed. Winkler et al. fit their data to a Langmuir adsorption isotherm and report $K_{part} = 6.24 \times 10^{-12} \exp(6178/T)$ cm and $N_{sat} = 3.2 \times 10^{14}$ molecules/cm^2. Hudson et al. measure the initial uptake coefficient and find it to be strongly temperature dependent, decreasing with increasing temperature to less than 0.01 at 180 K.
Back to Table

(1) Hudson, P. K.; Shilling, J. E.; Tolbert, M. A.; Toon, O. B. Uptake of nitric acid on ice at tropospheric temperatures: Implications for cirrus clouds. *J. Phys. Chem. A* **2002**, *106*, 9874-9882, doi:10.1021/jp020508j.

(2) Jedlovszky, P.; Partay, L.; Hoang, P. N. M.; Picaud, S.; von Hessberg, P.; Crowley, J. N. Determination of the adsorption isotherm of methanol on the surface of ice. An experimental and grand canonical Monte Carlo simulation study. *J. Am. Chem. Soc.* **2006**, *128*, 15300-15309, doi:10.1021/ja065553+.
(3) Winkler, A. K.; Holmes, N. S.; Crowley, J. N. Interaction of methanol, acetone and formaldehyde with ice surfaces between 198 and 223 K. *Phys. Chem. Chem. Phys.* **2002**, *4*, 5270-5275, doi:10.1039/b206258e.

37. **CH_3OH on H_2O(l).** Jayne et al.[1] measured uptake from 260–291 K and derived accommodation coefficients fitting $\alpha/(1-\alpha) = \exp(-\Delta G^{\ddagger}_{obs}/RT)$, where $\Delta G^{\ddagger}_{obs} = -8.0$ kcal/mol + 34.9 cal mol^{-1} K^{-1} T(K).
Back to Table

(1) Jayne, J. T.; Duan, S. X.; Davidovits, P.; Worsnop, D. R.; Zahniser, M. S.; Kolb, C. E. Uptake of gas-phase alcohol and organic acid molecules by water surfaces. *J. Phys. Chem.* **1991**, *95*, 6329-6336, doi:10.1021/j100169a047.

38. **CH_3CH_2OH on H_2O(s).** The uptake of ethanol on ice has been measured in coated-wall flow tubes by Sokolov and Abbatt[3] from 217 to 236 K, by Peybernes et al.[2] from 193 to 223 K, by Kerbrat et al.[1] from 213 to 243 K, and by Symington et al.[4] from 208 to 228 K. In all cases, either BET or Langmuir adsorption isotherms are obeyed and saturated surface coverage is observed at 2 to 3 × 10^{14} molecules/cm^2, with reversible adsorption and desorption of ethanol displayed. Similar adsorption enthalpies are reported: –62 kJ/mole (Sokolov and Abbatt), –57 kJ/mole (Peybernes et al.), –68 kJ/mole (Kerbrat et al.), and –54 kJ/mole (Symington et al.). Symington et al. report a partition coefficient, K_{Part}, of 1.36 × 10^{-11} exp(5573/T) cm.
Back to Table

(1) Kerbrat, M.; Le Calve, S.; Mirabel, P. Uptake measurements of ethanol on ice surfaces and on supercooled aqueous solutions doped with nitric acid between 213 and 243 k. *J. Phys. Chem. A* **2007**, *111*, 925-931, doi:10.1021/jp0635011.
(2) Peybernes, N.; Le Calve, S.; Mirabel, P.; Picaud, S.; Hoang, P. N. M. Experimental and theoretical adsorption study of ethanol on ice surfaces. *J. Phys. Chem. B* **2004**, *108*, 17425-17432, doi:10.1021/jp046983u.
(3) Sokolov, O.; Abbatt, J. P. D. Adsorption to ice of n-alcohols (ethanol to 1-hexanol), acetic acid, and hexanal. *J. Phys. Chem. A* **2002**, *106*, 775-782, doi:10.1021/jp013291m.
(4) Symington, A.; Leow, L. M.; Griffiths, P. T.; Cox, R. A. Adsorption and hydrolysis of alcohols and carbonyls on ice at temperatures of the upper troposphere. *J. Phys. Chem. A* **2012**, *116*, 5990-6002, doi:10.1021/jp210935b.

39. **CH_3CH_2OH on H_2O(l).** Jayne et al.[1] measured uptake from 260–291 K with a droplet train flow reactor and derived mass accommodation coefficients fitting $\alpha/(1-\alpha) = \exp(-\Delta G^{\ddagger}_{obs}/RT)$, where $\Delta G^{\ddagger}_{obs} = -11.0$ kcal/mol + 46.2 cal mol^{-1} K^{-1} T(K). Similar, but somewhat larger values were reported for chloro-, bromo-, and iodo-ethanols. Shi et al.[3] used the same technique to measure the uptake of both normal and deuterated ethanol over the temperature range of 263–291 K as a function of pH. Normal ethanol uptake was not dependent on pH, while the uptake of the deuterated species was enhanced by surface isotopic exchange, especially at high and low pH. The mass accommodation values obtained for normal ethanol obtained by Shi et al. ranged from 0.128 ± 0.023 at 263 K to 0.057 ± 0.005 are consistent, within experimental error, with the lowest temperature value measured by Jayne et al., but are significantly higher above ~275 K. Katrib et al.[2] also used the droplet train technique to measure the ethanol mass accommodation coefficient between ~266 and 281 K, obtaining lower values than those measured by Shi et al.,[3] but agreeing with the higher temperature data of Jayne et al.[1] Katrib et al. obtained mass accommodation coefficients fitting $\alpha/(1-\alpha) = \exp(-\Delta G^{\ddagger}_{obs}/RT)$, where $\Delta G^{\ddagger}_{obs} = -(5.6 \pm 1.5)$ kcal/mol + (27.4 ± 5.5) cal mol^{-1} K^{-1} T(K). While the data of Shi et al. and Katrib et al. are off-set by about a factor of three, the negative temperature dependencies measure by the two groups are very similar. The differences among the three data sets are difficult to explain, given that all three used essentially the experimental same technique; the recommended lower limit is consistent with the lower values measured by Katrib et al.[2]
Back to Table

(1) Jayne, J. T.; Duan, S. X.; Davidovits, P.; Worsnop, D. R.; Zahniser, M. S.; Kolb, C. E. Uptake of gas-phase alcohol and organic acid molecules by water surfaces. *J. Phys. Chem.* **1991**, *95*, 6329-6336, doi:10.1021/j100169a047.
(2) Katrib, Y.; Mirabel, P.; Le Calve, S.; Weck, G.; Kochanski, E. Experimental uptake study of ethanol by water droplets and its theoretical modeling of cluster formation at the interface. *J. Phys. Chem. B* **2002**, *106*, 7237-7245, doi:10.1021/jp015558n.
(3) Shi, Q.; Li, Y. Q.; Davidovits, P.; Jayne, J. T.; Worsnop, D. R.; Mozurkewich, M.; Kolb, C. E. Isotope exchange for gas-phase acetic acid and ethanol at aqueous interfaces: A study of surface reactions. *J. Phys. Chem. B* **1999**, *103*, 2417-2430, doi:10.1021/jp983525a.

40. **$CH_3CH_2CH_2OH$ on $H_2O(s)$.** The uptake of propanol by ice surfaces was studied in a coated-wall flow tube by Sokolov and Abbatt.[1] Uptake was well described by a Langmuir adsorption isotherm at 228 K, with a saturated surface coverage of 3.1×10^{14} molecules/cm^2 and an adsorption coefficient $K_{conc} = 8.3 \times 10^{-14}$ cm^3/molecule.
Back to Table

(1) Sokolov, O.; Abbatt, J. P. D. Adsorption to ice of n-alcohols (ethanol to 1-hexanol), acetic acid, and hexanal. *J. Phys. Chem. A* **2002**, *106*, 775-782, doi:10.1021/jp013291m.

41. **$CH_3CH_2CH_2OH$ and $CH_3CH(OH)CH_3$ on $H_2O(l)$.** Jayne et al.[1] measured uptake coefficients between 260 and 291 K and derived accommodation coefficients fitting $\alpha/(1-\alpha) = \exp(-\Delta G^{\ddagger}_{obs}/RT)$, where $\Delta G^{\ddagger}_{obs} = -9.2$ kcal mol^{-1} + 40.9 cal mol^{-1} K^{-1} T(K) for 1-propanol and –9.1 kcal mol^{-1} + 43.0 cal mol^{-1} K^{-1} T(K) for 2-propanol. Similar data for t-butanol were also reported.
Back to Table

(1) Jayne, J. T.; Duan, S. X.; Davidovits, P.; Worsnop, D. R.; Zahniser, M. S.; Kolb, C. E. Uptake of gas-phase alcohol and organic acid molecules by water surfaces. *J. Phys. Chem.* **1991**, *95*, 6329-6336, doi:10.1021/j100169a047.

42. **$HOCH_2CH_2OH$ on $H_2O(l)$.** Jayne et al.[1] measured uptake coefficients for ethylene glycol between 260 and 291 K and derived accommodation coefficients fitting $\alpha/(1-\alpha) = \exp(-\Delta G^{\ddagger}_{obs}/RT)$, where $\Delta G^{\ddagger}_{obs} = -5.3$ kcal mol^{-1} + 24.5 cal mol^{-1} K^{-1} T(K).
Back to Table

(1) Jayne, J. T.; Duan, S. X.; Davidovits, P.; Worsnop, D. R.; Zahniser, M. S.; Kolb, C. E. Uptake of gas-phase alcohol and organic acid molecules by water surfaces. *J. Phys. Chem.* **1991**, *95*, 6329-6336, doi:10.1021/j100169a047.

43. **CH_3O_2 on NaCl(s).** Gershenzon et al.[1] measured the uptake of CH_3O_2 on crystalline NaCl(s) in a central rod flow apparatus. They determined a value of $\gamma = (4 \pm 1) \times 10^{-3}$ at 296 K, suggesting that $\alpha \geq 4 \times 10^{-3}$.
Back to Table

(1) Gershenzon, Y. M.; Grigorieva, V. M.; Ivanov, A. V.; Remorov, R. G. O_3 and OH sensitivity to heterogeneous sinks of HO_x and CH_3O_2 on aerosol particles. *Faraday Discuss.* **1995**, *100*, 83-100.

44. **CH_3OOH on $H_2O(l)$.** Magi et al.[1] used a droplet train flow reactor to measure α over a temperature range of 261–281 K, showing a negative temperature dependence with values ranging from 9.2×10^{-3} at 281 to 20.8×10^{-3} at 261 K. Allowing for measurement uncertainty produces a recommendation that $\alpha \geq 7 \times 10^{-3}$ from 260 to 282 K.
Back to Table

(1) Magi, L.; Schweitzer, F.; Pallares, C.; Cherif, S.; Mirabel, P.; George, C. Investigation of the uptake rate of ozone and methyl hydroperoxide by water surfaces. *J. Phys. Chem. A* **1997**, *4*, 4943-4948, doi:10.1021/jp970646m.

45. **CH_2O on $H_2O(s)$.** The uptake of formaldehyde on ice in a coated-wall flow tube has been measured by Winkler et al.[2] They report reversible uptake behavior with a partition coefficient of $K_{part} = 0.7$ cm, temperature independent between 198 and 208 K. At much higher temperatures (238 to 268 K), the

partitioning to ice was studied by Burkhart et al.[1] using artificial snow. It was found that the partitioning increased at lower temperatures, in accord with Winkler et al. Although there is also likely to be a significant surface component, the partition coefficients in this work are expressed in bulk solubility format, ranging from 56 to 245 M/atm from 268 to 238 K.
Back to Table

(1) Burkhart, J. F.; Hutterli, M. A.; Bales, R. C. Partitioning of formaldehyde between air and ice at-35°C to-5°C. *Atmos. Environ.* **2002**, *36*, 2157-2163, doi:10.1016/S1352-2310(02)00221-2.
(2) Winkler, A. K.; Holmes, N. S.; Crowley, J. N. Interaction of methanol, acetone and formaldehyde with ice surfaces between 198 and 223 K. *Phys. Chem. Chem. Phys.* **2002**, *4*, 5270-5275, doi:10.1039/b206258e.

46. CH_2O on H_2O(l) and H_2SO_4•mHNO_3•nH_2O(l). Jayne et al.[4] report uptake measurements for 0–85 wt% H_2SO_4 and 0–54 wt% HNO_3 over a temperature range of 241–300 K. Measured uptake coefficients vary from 0.0027–0.027, increasing with H^+ activity (Jayne et al.[4] and Tolbert et al.[5]), and with increasing pH above 7 (Jayne et al.[3]). Reversible uptake is solubility limited through reactions to form $H_2C(OH)_2$ and CH_3O^+. A model of uptake kinetics (Jayne et al.[4]) is consistent with $\gamma = 0.04 \pm 0.01$ for all compositions. A chemisorbed surface complex dominates uptake at 10–20 wt% H_2SO_4, and CH_3O^+ formation dominates above 20 wt% (Tolbert et al.,[5] Jayne et al.,[4] and Iraci and Tolbert[2]). Low temperature (197–214 K) uptake studies by Iraci and Tolbert[2] confirm that uptake is solubility limited for uptake coefficients in the 10^{-3} to 10^{-2} range even at low temperatures. These chemical mechanisms allow γ to greatly exceed α for strong acidic and basic solutions. A full uptake model for acid solutions is presented in Jayne et al.,[4] and for basic solutions in Jayne et al.[3] XPS surface analysis by Fairbrother and Somorjai[1] failed to see CH_3O^+ surface species reported by Jayne et al.; however, their sensitivity of 1% of surface coverage is too poor to see the predicted amounts of the surface species.
Back to Table

(1) Fairbrother, D. H.; Somorjai, G. Equilibrium surface composition of sulfuric acid films in contact with various atmospheric gases (HNO_3, CO_2, CH_2O, Cl_2, NO, NO_2). *J. Phys. Chem. B* **2000**, *104*, 4649-4652, doi:10.1021/jp992889f.
(2) Iraci, L. T.; Tolbert, M. A. Heterogeneous interaction of formaldehyde with cold sulfuric acid: Implications for the upper troposphere and lower stratosphere. *J. Geophys. Res.* **1997**, *102*, 16099-16107, doi:10.1029/97JD01259.
(3) Jayne, J. T.; Duan, S. X.; Davidovits, P.; Worsnop, D. R.; Zahniser, M. S.; Kolb, C. E. Uptake of gas-phase aldehydes by water surfaces. *J. Phys. Chem.* **1992**, *96*, 5452-5460, doi:10.1021/j100192a049.
(4) Jayne, J. T.; Worsnop, D. R.; Kolb, C. E.; Swartz, E.; Davidovits, P. Uptake of gas-phase formaldehyde by aqueous acid surfaces. *J. Phys. Chem.* **1996**, *100*, 8015-8022, doi:10.1021/jp953196b.
(5) Tolbert, M. A.; Praff, J.; Jayaweera, I.; Prather, M. J. Uptake of formaldehyde by sulfuric acid solutions: Impact on stratospheric ozone. *J. Geophys. Res.* **1993**, *98*, 2957-2962, doi:10.1029/92JD02386.

47. CH_3CHO on H_2O(s). The uptake of acetaldehyde to ice surfaces was measured in a Knudsen cell from 120 to 160 K by Hudson et al.[1] finding the uptake to decrease with increasing temperature. Fitting the results to a Langmuir adsorption model and extrapolating to 210 K, the authors conclude that there will be low surface coverages under upper tropospheric conditions of $<5 \times 10^9$ molecules/cm^2. Hudson et al. report the initial uptake coefficient and find it to be strongly temperature dependent, decreasing with increasing temperature to less than 0.01 at 160 K. Petitjean et al.[2] have used a coated-wall flow tube to measure relatively small reversible uptakes. They report saturated surface coverages of between 1 and 2×10^{14} molecules/cm^2 and a heat of adsorption of –16 kJ/mole from 203 to 233 K. A higher heat of adsorption is calculated if the entropy of adsorption is fixed according to Trouton's rule. Larger uptakes are observed on mixed ice and nitric acid solution surfaces.
Back to Table

(1) Hudson, P. K.; Shilling, J. E.; Tolbert, M. A.; Toon, O. B. Uptake of nitric acid on ice at tropospheric temperatures: Implications for cirrus clouds. *J. Phys. Chem. A* **2002**, *106*, 9874-9882, doi:10.1021/jp020508j.

(2) Petitjean, M.; Mirabel, P.; Le Calve, S. Uptake measurements of acetaldehyde on solid ice surfaces and on solid/liquid supercooled mixtures doped with HNO_3 in the temperature range 203-253 K. *J. Phys. Chem. A* **2009**, *113*, 5091-5098, doi:10.1021/jp810131f.

48. **CH_3CHO on $H_2O(l)$.** Jayne et al.[1] measured a lower accommodation coefficient limit of >0.03 at 267 K. Uptake can be limited by Henry's law and hydrolysis kinetics effects–see reference.
Back to Table

(1) Jayne, J. T.; Duan, S. X.; Davidovits, P.; Worsnop, D. R.; Zahniser, M. S.; Kolb, C. E. Uptake of gas-phase aldehydes by water surfaces. *J. Phys. Chem.* **1992**, *96*, 5452-5460, doi:10.1021/j100192a049.

49. **CH(O)CH(O) on $H_2O(l)$.** Schweitzer et al.[1] used a droplet train flow reactor to investigate the uptake of glyoxyl by water droplets over a temperature range of 263–283 K; measured uptake was near their detection limit. They reported an average α over their experimental temperature range of $2.3\ (+1.1/-0.7) \times 10^{-2}$.
Back to Table

(1) Schweitzer, F.; Magi, L.; Mirabel, P.; George, C. Uptake rate measurements of methanesulfonic acid and glyoxal by aqueous droplets. *J. Phys. Chem. A* **1998**, *102*, 593-600, doi:10.1021/jp972451k.

50. **$CH_3C(O)CH_3$ on $H_2O(s)$.** The uptake of acetone to ice surfaces has been measured in both coated-wall flow tubes[1,2,4-6] and in a Knudsen cell.[3] Reversible uptake that is described by the simple Langmuir adsorption isotherm is demonstrated. Winkler et al. report a partition coefficient $K_{part} = 1.25 \times 10^{-10} \exp(5575/T)$ cm, an enthalpy of adsorption of –46 kJ/mole, and a saturated surface coverage of 3×10^{14} molecules/cm^2, for temperatures between 198 and 218 K. Symington et al.[5] report a partition coefficient $K_{part} = 3.04 \times 10^{-9} \exp(4625/T)$ cm, an enthalpy of adsorption of –39 kJ/mole, and a saturated surface coverage of 3×10^{14} molecules/cm^2, for temperatures between 208 and 228 K. Between 193 to 223 K, Peybernes et al.[4] report an adsorption enthalpy of –49 kJ/mole with a smaller saturated surface coverage of 1.3×10^{14} molecules/cm^2. By fitting observed adsorption and desorption profiles at 190 to 220 K, Behr et al. conclude that a two-site model best represents their observations. Total adsorbed species are close to 3×10^{14} molecules/cm^2 at saturation but the modeling suggests the presence of two crystallographic surfaces, one which binds acetone more strongly than the other. The relative proportion of the sites changes with ice film age, and adsorption energies are between –32 and –49 kJ/mole. Bartels-Rausch et al. report very similar adsorption enthalpies (–51 ± 2 kJ/mole) on a range of ice surfaces, including single and polycrystalline laboratory crystal ice, and snow from the field, at 198 to 223 K. Hudson et al. report somewhat smaller adsorption enthalpies at low temperatures (140 to 170 K) ranging from –28 to –39 kJ/mole. They also measure the initial uptake coefficient and find it to be strongly temperature dependent, decreasing with increasing temperature to less than 0.1 at 170 K.
Back to Table

(1) Bartels-Rausch, T.; Guimbaud, C.; Gaggeler, H. W.; Ammann, M. The partitioning of acetone to different types of ice and snow between 198 and 223 K. *Geophys. Res. Lett.* **2004**, *31*, 4432, doi:10.1029/2004GL020070.
(2) Behr, P.; Terziyski, A.; Zellner, R. Acetone adsorption on ice surfaces in the temperature range T=190-220 K: Evidence for aging effects due to crystallographic changes of the adsorption sites. *J. Phys. Chem. A* **2006**, *110*, 8098-8107, doi:10.1021/jp0563742.
(3) Hudson, P. K.; Shilling, J. E.; Tolbert, M. A.; Toon, O. B. Uptake of nitric acid on ice at tropospheric temperatures: Implications for cirrus clouds. *J. Phys. Chem. A* **2002**, *106*, 9874-9882, doi:10.1021/jp020508j.
(4) Peybernes, N.; Marchand, C.; Le Calve, S.; Mirabel, P. Adsorption studies of acetone and 2,3-butanedione on ice surfaces between 193 and 223 K. *Phys. Chem. Chem. Phys.* **2004**, *6*, 1277-1284, doi:10.1039/b315064j.
(5) Symington, A.; Leow, L. M.; Griffiths, P. T.; Cox, R. A. Adsorption and hydrolysis of alcohols and carbonyls on ice at temperatures of the upper troposphere. *J. Phys. Chem. A* **2012**, *116*, 5990-6002, doi:10.1021/jp210935b.
(6) Winkler, A. K.; Holmes, N. S.; Crowley, J. N. Interaction of methanol, acetone and formaldehyde with ice surfaces between 198 and 223 K. *Phys. Chem. Chem. Phys.* **2002**, *4*, 5270-5275, doi:10.1039/b206258e.

51. **$CH_3C(O)CH_3$ on $H_2O(l)$.** Duan et al.[1] measured uptake between 260 and 285 K, deriving $\alpha = 0.066$ at the lower temperature and 0.013 at the higher, with several values measured in between. Measured values fit $\alpha/(1-\alpha) = \exp(-\Delta G^{\ddagger}_{obs}/RT)$, where $\Delta G^{\ddagger}_{obs} = -12.7$ kcal/mol + 53.6 cal mol^{-1} K^{-1} T(K). Schütze and Herrmann[2] used a single suspended droplet flow reactor to measure the uptake of acetone and several larger carbonyl compounds at 293 K; their value for acetone of $\alpha = 5.4(+4.5/-2.6) \times 10^{-3}$ agrees well with the values of Duan et al. extrapolated to 293 K.
Back to Table

(1) Duan, S. X.; Jayne, J. T.; Davidovits, P.; Worsnop, D. R.; Zahniser, M. S.; Kolb, C. E. Uptake of gas-phase acetone by water surfaces. *J. Phys. Chem.* **1993**, *97*, 2284-2288, doi:10.1021/j100112a033.
(2) Schütze, M.; Herrmann, H. Uptake of acetone, 2-butanone, 2,3-butanedione and 2-oxopropanal on a water surface. *Phys. Chem. Chem. Phys.* **2004**, *6*, 965-971, doi:10.1039/b313474a.

52. **$CH_2(OH)C(O)CH_3 + H_2O(s)$.** The uptake of hydroxyacetone was studied by Petitjean et al.[1] in a coated wall flow tube from 233 to 253 K. The uptake was reversible and obeyed a Langmuir adsorption isotherm. Heat of adsorption was reported to be –62 kJ/mole.
Back to Table

(1) Petitjean, M.; Darvas, M.; Picaud, S.; Jedlovszky, P.; Le Calvé, S. Adsorption of hydroxyacetone on pure ice surfaces. *ChemPhysChem* **2010**, *11*, 3921-3927, doi:10.1002/cphc.201000629.

53. **$CH_3C(O)CHO$ on $H_2O(l)$.** Schütze and Herrmann[1] used a single suspended droplet flow reactor to measure the uptake of 2-oxypropynal at 293 K, their value of $\alpha = (1.5 \pm 0.5) \times 10^{-4}$ is lower than those measured for acetone and acetaldehyde.
Back to Table

(1) Schütze, M.; Herrmann, H. Uptake of acetone, 2-butanone, 2,3-butanedione and 2-oxopropanal on a water surface. *Phys. Chem. Chem. Phys.* **2004**, *6*, 965-971, doi:10.1039/b313474a.

54. **$CH_3OC(O)OCH_3$ on $H_2O(l)$.** Katrib et al.[1] measured the uptake of dimethyl carbonate on pure water and 0.1 M aqueous NaOH over a temperature range of 270–278 K using a droplet train flow reactor. Uptake was not obviously dependent on [OH^-] and displayed a negative temperature dependence with individual measurements varying from $(11 \pm 2) \times 10^{-2}$ at 270 K to $(1.2 \pm 0.9) \times 10^{-2}$ at 276 K. Although the data are fairly noisy the authors derived a mass accommodation coefficient fitting of $\alpha/(1-\alpha) = \exp(-\Delta G^{\ddagger}_{obs}/RT)$, where $\Delta G^{\ddagger}_{obs} = -(26 \pm 9)$kcal mol^{-1} + (99 ± 35) cal mol^{-1} K^{-1} T(K). Similar mass accommodation data for diethyl carbonate are also presented.
Back to Table

(1) Katrib, Y.; Deiber, Y.; Mirabel, P.; Le Calve, S.; George, C.; Mellouki, A.; Le Bras, G. Atmospheric loss processes of dimethyl and diethyl carbonate. *J. Atmos. Chem.* **2002**, *43*, 151-174, doi:10.1023/A:1020605807298.

55. **$HC(O)OH$ on $H_2O(s)$.** The uptake of formic acid on ice has been measured in coated-wall flow tube from 187 to 221 K by von Hessberg et al.[3] and Jedlovsky et al.[1] Reversible uptakes are observed. Von Hessberg et al. fit their data to the Langmuir adsorption isotherm and report the adsorption constant to be $K_{conc} = 1.54 \times 10^{-24} \exp(6150/T)$ cm^3/molecule, for a saturated surface coverage of 2.2×10^{14} molecules/cm^2. Using a coated-wall flow tube coupled to a mass spectrometer, Symington et al.[2] report partition coefficients from 208 to 238 K. The uptake was reversible with partition coefficients, K_{Part}, of $1.5 \times 10^{-8} \exp(5143/T)$ cm.
Back to Table

(1) Jedlovszky, P.; Hantal, G.; Neurohr, K.; Picaud, S.; Hoang, P. N. M.; von Hessberg, P.; Crowley, J. N. Adsorption isotherm of formic acid on the surface of ice, as seen from experiments and grand canonical Monte Carlo simulation. *J. Phys. Chem. C* **2008**, *112*, 8976-8987, doi:10.1021/jp8012915.
(2) Symington, A.; Cox, R. A.; Fernandez, M. A. Uptake of organic acids on ice surfaces: Evidence for surface modification and hydrate formation. *Z. Phys. Chem.* **2010**, *224*, 1219-1245, doi:10.1524/zpch.2010.6149.

(3) von Hessberg, P.; Pouvesle, N.; Winkler, A. K.; Schuster, G.; Crowley, J. N. Interaction of formic and acetic acid with ice surfaces between 187 and 227 K. Investigation of single species- and competitive adsorption. *Phys. Chem. Chem. Phys.* **2008**, *10*, 2345-2355, doi:10.1039/b800831k.

56. HC(O)OH on H_2O(l). Jayne et al.[1] measured uptake coefficients for formic acid between 260 and 291 K and derived accommodation coefficients fitting $\alpha/(1-\alpha) = \exp(-\Delta G^{\ddagger}_{obs}/RT)$, where $\Delta G^{\ddagger}_{obs} = -7.9$ kcal mol^{-1} + 34.9 cal mol^{-1} K^{-1} T(K).
Back to Table

(1) Jayne, J. T.; Duan, S. X.; Davidovits, P.; Worsnop, D. R.; Zahniser, M. S.; Kolb, C. E. Uptake of gas-phase alcohol and organic acid molecules by water surfaces. *J. Phys. Chem.* **1991**, *95*, 6329-6336, doi:10.1021/j100169a047.

57. $CH_3C(O)OH$ on H_2O(s). The uptake of acetic acid on ice has been measured in coated-wall flow tubes by Sokolov and Abbatt[3] from 222 to 245 K, by Picaud et al.[2] from 193 to 223 K, by von Hessberg et al.[5] from 197 to 227 K, and Symington et al.[4] from 208 to 238 K. In all cases, either BET or Langmuir adsorption isotherms are demonstrated and saturated surface coverage is observed with between 2 to 3 × 10^{14} molecules/cm^2. The values of the partition coefficients between the Sokolov and Abbatt, von Hessberg et al. and Symington et al. studies agree to within roughly a factor of two, whereas the Picaud et al. results are one to two orders of magnitude smaller at low temperatures. The overall adsorption coefficient expressions from the Sokolov and Abbatt data, von Hessberg et al. and Symington et al. are $K_{conc} = 8.3 \times 10^{-28} \exp(7825/T)$, $6.55 \times 10^{-25} \exp(6610/T)$, and $2.2 \times 10^{-23} \exp(5703/T)$ cm^3/molecule (assuming a saturated surface coverage of 2.5 × 10^{14} molecules/cm^2), respectively. Nitrous acid and acetic acid simultaneous uptake measurements to packed ice beds were found to be well described by a competitive Langmuir adsorption isotherm between 213 and 243 K. Labeled nitrous acid was monitored by radioactive methods, and acetic acid by CIMS (Kerbrat et al.[1]).
Back to Table

(1) Kerbrat, M.; Huthwelker, T.; Bartels-Rausch, T.; Gäggeler, H. W.; Ammann, M. Co-adsorption of acetic acid and nitrous acid on ice. *Phys. Chem. Chem. Phys.* **2010**, *12*, 7194-7202, doi:10.1039/b924782c.
(2) Picaud, S.; Hoang, P. N. M.; Peybernes, N.; Le Calve, S.; Mirabel, P. Adsorption of acetic acid on ice: Experiments and molecular dynamics simulations. *J. Chem. Phys.* **2005**, *122*, 194707, doi:10.1063/1.1888368.
(3) Sokolov, O.; Abbatt, J. P. D. Adsorption to ice of n-alcohols (ethanol to 1-hexanol), acetic acid, and hexanal. *J. Phys. Chem. A* **2002**, *106*, 775-782, doi:10.1021/jp013291m.
(4) Symington, A.; Cox, R. A.; Fernandez, M. A. Uptake of organic acids on ice surfaces: Evidence for surface modification and hydrate formation. *Z. Phys. Chem.* **2010**, *224*, 1219-1245, doi:10.1524/zpch.2010.6149.
(5) von Hessberg, P.; Pouvesle, N.; Winkler, A. K.; Schuster, G.; Crowley, J. N. Interaction of formic and acetic acid with ice surfaces between 187 and 227 K. Investigation of single species- and competitive adsorption. *Phys. Chem. Chem. Phys.* **2008**, *10*, 2345-2355, doi:10.1039/b800831k.

58. $CH_3C(O)OH$ on H_2O(l). Jayne et al.[1] using a droplet train flow reactor measured uptake coefficients for acetic acid between 260 and 291 K and derived a mass accommodation coefficient fitting $\alpha/(1-\alpha) = \exp(-\Delta G^{\ddagger}_{obs}/RT)$, where $\Delta G^{\ddagger}_{obs} = -8.1$ kcal mol^{-1} + 34.9 cal mol^{-1} K^{-1} T(K). Shi et al.[2] used the same technique to measure the uptake of both normal and deuterated acetic acid at 258 K and pH = 7. They obtained α = 0.19 (± 0.03) for normal acetic acid, while the uptake coefficient of the deuterated species was enhanced by surface isotopic exchange, equaling 0.96 (± 0.21).
Back to Table

(1) Jayne, J. T.; Duan, S. X.; Davidovits, P.; Worsnop, D. R.; Zahniser, M. S.; Kolb, C. E. Uptake of gas-phase alcohol and organic acid molecules by water surfaces. *J. Phys. Chem.* **1991**, *95*, 6329-6336, doi:10.1021/j100169a047.
(2) Shi, Q.; Li, Y. Q.; Davidovits, P.; Jayne, J. T.; Worsnop, D. R.; Mozurkewich, M.; Kolb, C. E. Isotope exchange for gas-phase acetic acid and ethanol at aqueous interfaces: A study of surface reactions. *J. Phys. Chem. B* **1999**, *103*, 2417-2430, doi:10.1021/jp983525a.

59. **$CH_3CO(O_2)NO_2$ on $H_2O(s)$.** The adsorption enthalpy has been measured to be –30 kJ/mole by Bartels-Rausch et al.[1]
Back to Table

(1) Bartels-Rausch, T.; Eichler, B.; Zimmermann, P.; Gaggeler, H. W.; Ammann, M. The adsorption enthalpy of nitrogen oxides on crystalline ice. *Atmos. Chem. Phys.* **2002**, *2*, 235-247, doi:10.5194/acp-2-235-2002.

60. **Cl_2 on $H_2O(s)$.** Measurement of Leu[2] yielded a limit of $<1 \times 10^{-4}$ for Cl_2 and is subject to same concern as NO_2 (see note). A similar limit of $<5 \times 10^{-5}$ has been measured by Kenner et al.,[1] which is also probably limited by surface saturation.
Back to Table

(1) Kenner, R. D.; Plumb, I. C.; Ryan, K. R. Laboratory measurements of the loss of ClO on Pyrex, ice and NAT at 183 K. *Geophys. Res. Lett.* **1993**, *20*, 193-196, doi:10.1029/93GL00238.
(2) Leu, M.-T. Laboratory studies of sticking coefficients and heterogeneous reactions important in the Antarctic stratosphere. *Geophys. Res. Lett.* **1988**, *15*, 17-20, doi:10.1029/GL015i001p00017.

61. **OClO + $H_2O(s)$.** Brown et al.[1] and Graham et al.[2] used complementary ultra high-vacuum (UHV) and coated-wall flow tube techniques to show sub-monolayer reversible absorption of OClO on water ice at 100 K (UHV) and 189 and 200 K (flow tube). No kinetic data are available at stratospheric temperatures but the mass accommodation coefficient for 100 K ice surfaces is near unity, with values of 0.8 ± 0.2 reported for amorphous ice and 0.6 ± 0.2 for crystalline ice.[2]
Back to Table

(1) Brown, L. A.; Vaida, V.; Hanson, D. R.; Graham, J. D.; Roberts, J. T. Uptake of chlorine dioxide by model PSCs under stratospheric conditions. *J. Phys. Chem.* **1996**, *100*, 3121-3125, doi:10.1021/jp951664b.
(2) Graham, J. D.; Roberts, J. T.; Brown, L. A.; Vaida, V. Uptake of chlorine dioxide by model polar stratospheric cloud surfaces: Ultra high-vacuum studies. *J. Phys. Chem.* **1996**, *100*, 3115-3120, doi:10.1021/jp9516654.

62. **HCl on $H_2O(s)$.** The uptake coefficients of Leu[17] (0.4; +0.6, –0.2) and Hanson and Ravishankara[10] (≥0.3) are in reasonable agreement at stratospheric ice temperatures. At somewhat higher temperatures (205 K), Hynes et al.[13] measured slightly lower values (0.1) which decreased at higher temperatures. At very low temperatures (80 to 120 K), Rieley et al.[22] measured $\alpha = 0.95 \pm 0.05$.

A great deal of experimental effort (Abbatt et al.;[1,2] Barone et al.;[3] Koehler et al.;[14] Chu et al.;[4] Foster et al.;[6] Graham and Roberts ;[8] Graham and Roberts;[9] Hanson and Ravishankara;[10] Henson et al.;[11] Hynes et al.;[13] Leu et al.;[18] Marti et al.;[19] McNeil et al.;[21] and McNeil et al.[20], Kong et al.,[15] Zimmerman et al.[25]) has gone into understanding the magnitude and nature of the uptake of HCl by ice surfaces under stratospheric and upper tropospheric conditions. A general observation is that water ice at stratospheric temperatures can take up a significant, but sub-monolayer, amount of HCl even at HCl partial pressures typical of the stratosphere. However, quantitative agreement in the size of the uptake is lacking, with a range of close to three orders of magnitude for partial pressures of 10^{-7} Torr at roughly 200 K. One issue is that the specific surface area of the ice was not measured in a number of early studies. Because the ice surface may have some roughness, depending on how it is prepared, a number of these uptakes may be biased high, if the surfaces were assumed to be smooth. Another issue is the partial pressure dependence of the uptake. In accord with a number of uptake measurements of other species on ice, saturated surface coverages are observed at about 2 to 3×10^{14} molecules/cm^2 in experiments where the specific surface area of the ice is well known (e.g. Henson et al.,[11] Hynes et al.,[13] McNeil et al.[20] and Zimmerman et al.[25]). The drop-off into the unsaturated part of the adsorption isotherm appears to vary from experiment to experiment, as the HCl partial pressure is lowered. For example, Hanson and Ravishankara,[10] do not observe a drop off down to partial pressures well below 10^{-7} Torr, whereas others (e.g. Henson et al.[11] and McNeil et al.[20]) see a significant drop-off at higher partial pressures. And so, at the very low partial pressures of the upper troposphere, the surface coverage may be quite unsaturated; even in the stratospheric regime, there may not exist a full monolayer coverage.

A number of studies have been particularly thorough. For example, in a coated-wall flow tube study on a variety of ice surfaces at close to 200 K McNeill et al.[20] show that uptakes obeyed conventional Langmuir

adsorption isotherms, and that they did not scale as well with the dissociative Langmuir isotherm. A weak adsorption enthalpy of –15 kJ/mole was derived. Langmuir adsorption constants, $K_{conc} = 3.1 \times 10^{-11}$, 8.4×10^{-11}, and 3.9×10^{-11} cm^3/molecule, were obtained at 213, 203, and 196 K, respectively. There is good agreement between McNeill et al. and the work of Zimmerman et al.[25] which used a similar experimental approach, and obtained a temperature independent K_{conc} value of 3.7×10^{-11} cm^3/molecule over the temperature range from 190 to 220 K. By contrast the work of Henson et al.[11] using a static adsorption technique yields a much lower (one to two orders of magnitude) surface coverage for the same HCl partial pressures and temperatures.

Note that for the same experimental conditions, the uptake may be affected by co-adsorbed species. Studies by Hynes et al.[12] and Sokolov and Abbatt[23] involving co-adsorption of HNO_3 indicate that HNO_3 binds more strongly than HCl, but that the presence of HCl does lead to suppressed HNO_3 uptake relative to behavior on bare ice surfaces. Fernandez et al.[5] also show that HCl uptake is significantly suppressed on a surface that has been exposed to HNO_3.

Both the thermodynamic and spectroscopic properties of adsorbed HCl suggest that a large fraction dissociates to ions, forms ionic hydrates (especially at low temperatures), and is highly reactive (with $ClONO_2$, HOBr and HOCl). Also, adsorption and desorption profiles in flow tubes suggest that uptake occurs via both reversible and irreversible processes, probably related to partitioning to different surface sites such as the ice faces or grain boundaries. Measurements using x-ray photoelectron spectroscopy at high pressure have directly observed both dissociated and undissociated states at the surface of ice at 253 K (Kong et al.[15]). The physisorbed molecular state is closer to the surface than the dissociated molecules. These experimental results contrast with initial theoretical calculations that predicted undissociated HCl hydrogen bonded to the ice surface and a very small adsorption probability at stratospheric temperatures (Kroes and Clary[16]); more recent simulations result in higher adsorption energies and theoretical accommodation coefficients of one for 190-K surfaces (Wang and Clary[24]). Molecular dynamics calculations by Gertner and Hynes[7] also show that ionic absorption is thermodynamically favorable by about 5 kcal/mole, facilitated by the role of mobile water molecules on the ice surface that can hydrate the ions. Using ellipsometry McNeil et al.[21] have experimentally shown the presence of a disordered layer on the ice surface, sometimes referred to as the quasi liquid layer, arising from HCl adsorption at low temperatures and partial pressures. The work of Kong et al.[15] confirms the disruption of the hydrogen bonding network. By contrast, at HCl partial pressures significantly above those typical of the stratosphere, a thermodynamically stable liquid surface layer forms on the ice, greatly enhancing the total amount of HCl that the surface can absorb (Abbatt et al.[2]). These conditions should be avoided for lab studies as they are not atmospherically appropriate.

Back to Table

(1) Abbatt, J. P. D. Interaction of HNO_3 with water-ice surfaces at temperatures of the free troposphere. *Geophys. Res. Lett.* **1997**, *24*, 1479-1482, doi:10.1029/97GL01403.

(2) Abbatt, J. P. D.; Beyer, K. D.; Fucaloro, A. F.; McMahon, J. R.; Wooldridge, P. J.; Zhong, R.; Molina, M. J. Interaction of HCl vapor with water-ice: Implications for the stratosphere. *J. Geophys. Res.* **1992**, *97*, 15819-15826, doi:10.1029/92JD01220.

(3) Barone, S. B.; Zondlo, M. A.; Tolbert, M. A. Investigation of the heterogeneous reactivity of HCl, HBr, and HI on ice surfaces. *J. Phys. Chem. A* **1999**, *103*, 9717-9730, doi:10.1021/jp990400c.

(4) Chu, L. T.; Leu, M.-T.; Keyser, L. F. Uptake of HCl in water ice and nitric acid ice films. *J. Phys. Chem.* **1993**, *97*, 7779-7785, doi:10.1021/j100131a057.

(5) Fernandez, M. A.; Hynes, R. G.; Cox, R. A. Kinetics of $ClONO_2$ reactive uptake on ice surfaces at temperatures of the upper troposphere. *J. Phys. Chem. A* **2005**, *109*, 9986-9996, doi:10.1021/jp053477b.

(6) Foster, K. L.; Tolbert, M. A.; George, S. M. Interaction of HCl with ice: Investigation of the predicted trihydrate, hexahydrate, and monolayer regimes. *J. Phys. Chem. A* **1997**, *101*, 4979-4986, doi:10.1021/jp970772q.

(7) Gertner, B. J.; Hynes, J. T. Molecular dynamics simulation of hydrochloric acid ionization at the surface of srtatospheric ice. *Science* **1996**, *271*, 1563-1566, doi:10.1126/science.271.5255.1563.

(8) Graham, J. D.; Roberts, J. T. Interaction of hydrogen chloride with an ultrathin ice film: Observation of adsorbed and absorbed states. *J. Phys. Chem.* **1994**, *98*, 5974-5983, doi:10.1021/j100074a026.

(9) Graham, J. D.; Roberts, J. T. Interactions of HCl with crystalline and amorphous ice: Implications for the mechanisms of ice-catalyzed reactions. *Geophys. Res. Lett.* **1995**, *22*, 251-254, doi:10.1029/94GL03022

(10) Hanson, D. R.; Ravishankara, A. R. Investigation of the reactive and nonreactlve processes involving $ClONO_2$ and HCl on water and nitric acid doped ice. *J. Phys. Chem.* **1992**, *96*, 2682-2691, doi:10.1021/j100185a052.
(11) Henson, B. F.; Wilson, K. R.; Robinson, J. M.; Noble, C. A.; Casson, J. L.; Worsnop, D. R. Experimental isotherms of HCl on H_2O ice under stratospheric conditions: Connections between bulk and interfacial thermodynamics. *J. Chem. Phys.* **2004**, *121*, 8486-8499, doi:10.1063/1.1803542.
(12) Hynes, A. J.; Fernandez, M. A.; Cox, R. A. Uptake of HNO_3 on water-ice and coadsorption of HNO_3 and HCl in the temperature range 210–235 K. *J. Geophys. Res.* **2002**, *107*, 4797, doi:10.1029/2001JD001557.
(13) Hynes, R. G.; Mossinger, J. C.; Cox, R. A. The interaction of HCl with water-ice at tropospheric temperatures. *Geophys. Res. Lett.* **2001**, *28*, 2827-2830, doi:10.1029/2000GL012706.
(14) Koehler, B. G.; McNeill, L. S.; Middlebrook, A. M.; Tolbert, M. A. Fourier transform infrared studies of the interaction of HCl with model polar stratospheric cloud films. *J. Geophys. Res.* **1993**, *98*, 10563-10571, doi:10.1029/93JD00586.
(15) Kong, X.; Waldner, A.; Orlando, F.; Artiglia, L.; Huthwelker, T.; Ammann, M.; Bartels-Rausch, T. Coexistence of physisorbed and solvated HCI at warm ice surfaces. *J. Phys. Chem. Lett.* **2017**, *8*, 4757-4762, doi:10.1021/acs.jpclett.7b01573.
(16) Kroes, G.-J.; Clary, D. C. Sticking of HCl and ClOH to ice: A computational study. *J. Phys. Chem.* **1992**, *96*, 7079-7088, doi:10.1021/j100196a044.
(17) Leu, M.-T. Laboratory studies of sticking coefficients and heterogeneous reactions important in the Antarctic stratosphere. *Geophys. Res. Lett.* **1988**, *15*, 17-20, doi:10.1029/GL015i001p00017.
(18) Leu, M.-T.; Timonen, R. S.; Keyser, L. F. Kinetics of the heterogeneous reaction $HNO_3(g)$ + $NaBr(s) \leftrightarrow HBr(g) + NaNO_3(s)$. *J. Phys. Chem. A* **1997**, *101*, 278-282, doi:10.1021/jp9626069.
(19) Marti, J.; Mauersberger, K.; Hanson, D. HCl dissolved in solid mixtures of nitric acid and ice: Implications for the polar stratosphere. *Geophys. Res. Lett.* **1991**, *18*, 1861-1864, doi:10.1029/91GL02313.
(20) McNeill, V. F.; Geiger, F. M.; Loerting, T.; Trout, B. L.; Molina, L. T.; Molina, M. J. Interaction of hydrogen chloride with ice surfaces: The effects of grain size, surface roughness, and surface disorder. *J. Phys. Chem. A* **2007**, *111*, 6274-6284, doi:10.1021/jp068914g.
(21) McNeill, V. F.; Loerting, T.; Geiger, F. M.; Trout, B. L.; Molina, M. J. Hydrogen chloride-induced surface disordering on ice. *Proc. Nat. Acad. Sci.* **2006**, *103*, 9422-9427, doi:10.1073/pnas.0603494103.
(22) Rieley, H.; Aslin, H. D.; Haq, S. Sticking of HCl on a type-II polar stratospheric cloud minic. *J. Chem. Soc. Faraday Trans.* **1995**, *91*, 2349-2351, doi:10.1039/ft9959102349.
(23) Sokolov, O.; Abbatt, J. P. D. Competitive adsorption of atmospheric trace gases onto ice at 228 K: HNO_3/HCl, 1-butanol/acetic acid and 1-butanol/HCl. *Geophys. Res. Lett.* **2002**, *29*, 1851, doi:10.1029/2002GL014843.
(24) Wang, L.; Clary, D. C. Time-dependent wave packet studies on the sticking of HCl to an ice surface. *J. Chem. Phys.* **1996**, *104*, 5663-5673, doi:10.1063/1.471772.
(25) Zimmermann, S.; Kippenberger, M.; Schuster, G.; Crowley, J. N. Adsorption isotherms for hydrogen chloride (HCl) on ice surfaces between 190 and 220 K. *Phys. Chem. Chem. Phys.* **2016**, *18*, 13799-13810, doi:10.1039/c6cp01962e.

63. HCl on H_2O(1). Recommendation is based on Van Doren et al.[4] and Schweitzer et al.[2] Using a droplet train flow reactor, Van Doren et al.[4] measured α's decrease from 0.18 ± 0.02 at 274 K to 0.064 ± 0.01 at 294 K, demonstrating strong negative temperature dependence. Schweitzer et al.[2] used the same technique over a temperature range of 262 to 281 K obtaining values decreasing from 0.24 to 0.13 that agree very well with the Van Doren et al. data. Tang and Munkelwitz[3] have measured a larger (0.45 ± 0.4) HCl evaporation coefficient for an aqueous NH_4Cl droplet at 299 K. In accord with large mass accommodation coefficients, dynamical studies by Faust et al.[1] with a liquid microjet of lithium halide solutions at 238 K indicate that HCl is efficiently ionized and taken up into solution, rather than experiencing efficient desorption to the gas phase. Back to Table

(1) Faust, J. A.; Sobyra, T. B.; Nathanson, G. M. Gas-microjet reactive scattering: Collisions of HCl and DCl with cool salty water. *J. Phys. Chem. Lett.* **2016**, *7*, 730-735, doi:10.1021/acs.jpclett.5b02848.
(2) Schweitzer, F.; Mirabel, P.; George, C. Uptake of hydrogen halides by water droplets. *J. Phys. Chem. A* **2000**, *104*, 72-76, doi:10.1021/jp992621o.

(3) Tang, I. N.; Munkelwitz, H. R. Evaporation kinetics of ammonium chloride solution droplets in water vapor. *J. Colloid Interface Sci.* **1989**, *128*, 289-295, doi:10.1016/0021-9797(89)90406-2.
(4) Van Doren, J. M.; Watson, L. R.; Davidovits, P.; Worsnop, D. R.; Zahniser, M. S.; Kolb, C. E. Temperature dependence of the uptake coefficients of HNO_3, HCl, and N_2O_5 by water droplets. *J. Phys. Chem.* **1990**, *94*, 3265-3269, doi:10.1021/j100371a009.

64. HCl on HNO_3•nH_2O. There was previously severe disagreement between Hanson and Ravishankara[3] ($\alpha \geq 0.3$) for NAT (54 wt% HNO_3), and Leu and coworkers (Moore et al.[5] and Leu et al.[4]). However, subsequent experiments at lower HCl concentrations by Leu and coworkers[2] as well as Abbatt and Molina[1] are generally consistent with Hanson and Ravishankara. The measurements of Hanson and Ravishankara are consistent with $\alpha = 1$. The experiments at stratospherically representative HCl concentrations show that HNO_3-rich NAT surfaces adsorb significantly less HCl than H_2O-rich surfaces, with the uptake at a fixed temperature determined by the partial pressure of water.[1]
Back to Table

(1) Abbatt, J. P. D.; Molina, M. J. The heterogeneous reaction of HOCl + HCl → Cl_2 + H_2O on ice and nitric acid trihydrate: Reaction probabilities and stratospheric implications. *Geophys. Res. Lett.* **1992**, *19*, 461-464, doi:10.1029/92GL00373.
(2) Chu, L. T.; Leu, M.-T.; Keyser, L. F. Uptake of HCl in water ice and nitric acid ice films. *J. Phys. Chem.* **1993**, *97*, 7779-7785, doi:10.1021/j100131a057.
(3) Hanson, D. R.; Ravishankara, A. R. Investigation of the reactive and nonreactlve processes involving $ClONO_2$ and HCl on water and nitric acid doped ice. *J. Phys. Chem.* **1992**, *96*, 2682-2691, doi:10.1021/j100185a052.
(4) Leu, M.-T.; Moore, S. B.; Keyser, L. F. Heterogeneous reactions of chlorine nitrate and hydrogen chloride on Type I polar stratospheric clouds. *J. Phys. Chem.* **1991**, *95*, 7763-7771, doi:10.1021/j100173a040.
(5) Moore, S. B.; Keyser, L. F.; Leu, M. T.; Turco, R. P.; Smith, R. H. Heterogeneous reactions on nitric acid trihydrate. *Nature* **1990**, *345*, 333-335, doi:10.1038/345333a0.

65. HCl on H_2SO_4•nH_2O. Measurements by Watson et al.[9] at 284 K show $\alpha = 0.15 \pm 0.01$ independent of n for $n \geq 8$. Experimental uptake and, therefore, apparent α falls off for $n \leq 8$ (≥40 wt% H_2SO_4). This behavior is also observed at a stratospheric temperature (218 K) by Hanson and Ravishankara.[4] Hanson and Lovejoy[3] reported a value of 0.75 ± 0.2 for 26 wt% H_2SO_4 at 272 K. More extensive measurements performed by Robinson et al.[7] at lower temperatures, also yielded higher values, reaching 1.03 ± 0.10 for 39 wt% H_2SO_4 at 230 K; they also observed enhanced uptake for 69 wt% H_2SO_4 that was attributed to the formation of chlorosulfonic acid. Solubility constraints also controlled earlier low temperature uptake measurements of Tolbert et al.[8] A review of the most recent solubility data is presented in Table 5-6.

Molecular beam measurements of HCl impingement on liquid deuterated sulfuric acid surfaces determine the fraction of HCl scattered with no reaction and the fraction that is reactively converted and emitted as DCl. The fraction converted to DCl is assumed to have undergone interfacial transport, representing a lower limit to the mass accommodation coefficient, which varies from ~0.7 at 53–55 wt% D_2SO_4 to ~0.1 near 70 wt.% Behr et al.[1] More recent measurements indicate that the conversion fraction is relatively insensitive to HCl kinetic energy over the range of 6 to 140 kJ mol^{-1}, and that the conversion fraction for 72 wt% D_2SO_4 varies less dramatically, from~0.33 at 213 K to ~0.47 at 243 K Behr et al.[2] The basic technique and analysis rationale are reviewed by Nathanson.[5] The impact of organic surfactants on mass accommodation sulfuric acid, including the surprising fact that a surface layer of butanol actually significantly enhances HCl uptake in 213 K, 56–68 wt% D_2SO_4 is reviewed in Park et al.[6] These studies strongly indicate that the mass accommodation coefficient for 50–72 wt% sulfuric acid surfaces for temperatures below 243 K is >0.1.
Back to Table

(1) Behr, P.; Morris, J. R.; Antman, M. D.; Ringeisen, B. R.; Splan, J. R.; Nathanson, G. M. Reaction and desorption of HC1 and HBr following collisions with supercooled sulfuric acid. *Geophys. Res. Lett.* **2001**, *28*, 1961-1964, doi:10.1029/2000GL012716
(2) Behr, P.; Scharfenort, U.; Ataya, K.; Zellner, R. Dynamics and mass accommodation of HCl molecules on sulfuric acid-water surfaces. *Phys. Chem. Chem. Phys.* **2009**, *11*, 8048-8055, doi:10.1039/b904629a.

(3) Hanson, D. R.; Lovejoy, E. R. Heterogeneous reactions in liquid sulfuric Acid: HOCl + HCl as a model system. *J. Phys. Chem.* **1996**, *100*, 6397-6405, doi:10.1021/jp953250o.
(4) Hanson, D. R.; Ravishankara, A. R. Investigation of the reactive and nonreactlve processes involving $ClONO_2$ and HCl on water and nitric acid doped ice. *J. Phys. Chem.* **1992**, *96*, 2682-2691, doi:10.1021/j100185a052.
(5) Nathanson, G. M. Molecular beam studies of gas-liquid interfaces. *Ann. Rev. Phys. Chem.* **2004**, *55*, 231-255, doi:10.1146/annurev.physchem.55.091602.094357.
(6) Park, S.-C.; Burden, D. K.; Nathanson, G. M. Surfactant control of gas transport and reactions at the surface of sulfuric acid. *Acc. Chem. Res.* **2009**, *42*, 379-387, doi:10.1021/ar800172m.
(7) Robinson, G. N.; Worsnop, D. R.; Jayne, J. T.; Kolb, C. E.; Swartz, E.; Davidovits, P. Heterogeneous uptake of HCl by sulfuric acid solutions. *J. Geophys. Res.* **1998**, *103*, 25371-25381, doi:10.1029/98JD02085
(8) Tolbert, M. A.; Rossi, M. J.; Golden, D. M. Heterogeneous interactions of chlorine nitrate, hydrogen chloride and nitric acid with sulfuric acid surfaces at stratospheric temperatures. *Geophys. Res. Lett.* **1988**, *15*, 847-850, doi:10.1029/GL015i008p00847
(9) Watson, L. R.; Doren, J. M. V.; Davidovits, P.; Worsnop, D. R.; Zahniser, M. S.; Kolb, C. E. Uptake of HCl molecules by aqueous sulfuric acid droplets as a function of acid concentration. *J. Geophys. Res.* **1990**, *95*, 5631-5638, doi:10.1029/JD095iD05p05631

66. HCl on H_2SO_4•$4H_2O$(s). Uptake is a strong function of temperature and water vapor partial pressure (relative humidity) (Zhang et al.[1]), both of which affect adsorbed surface water.
Back to Table

(1) Zhang, R.; Wooldridge, P. J.; Molina, M. J. Vapor pressure measurements for the $H_2SO_4/HNO_3/H_2O$ and $H_2SO_4/HCl/H_2O$ systems: Incorporation of stratospheric acids into background sulfate aerosols. *J. Phys. Chem.* **1993**, *97*, 8541-8548, doi:10.1021/j100134a026.

67. $ClONO_2$ on H_2O(1). Deiber et al.[1] used a droplet train apparatus to measure the uptake of $ClONO_2$ on NaBr aqueous solutions to deduce the mass accommodation coefficient of 0.108 ± 0.011 at 274.5 K. This value may be affected by the reaction with interfacial Br^-.
Back to Table

(1) Deiber, G.; George, C.; Le Calve, S.; Schweitzer, F.; Mirabel, P. Uptake study of $ClONO_2$ and $BrONO_2$ by halide containing droplets. *Atmos. Chem. Phys.* **2004**, *4*, 1291-1299, doi:10.5194/acp-4-1291-2004.

68. $CCl_3CHO + H_2O$(s). The uptake of CCl_3CHO to ice was studied by Symington et al.[1] from 208 to 228 K in a coated-wall flow reactor coupled to a mass spectrometer. There was an irreversible component to the uptake, which was attributed to hydrolysis. The partition coefficient is reported to be 7.52×10^{-4} exp(2069/T) cm.
Back to Table

(1) Symington, A.; Leow, L. M.; Griffiths, P. T.; Cox, R. A. Adsorption and hydrolysis of alcohols and carbonyls on ice at temperatures of the upper troposphere. *J. Phys. Chem. A* **2012**, *116*, 5990-6002, doi:10.1021/jp210935b.

69. Halocarbonyls on H_2O(l). Uptake is limited by Henry's law solubility and hydrolysis rate constants (De Bruyn et al.[1,2] and George et al.[3,4]).
Back to Table (CCl_2O) Back to Table (CCl_3CClO) Back to Table (CF_2O) Back to Table (CF_3CFO) Back to Table (CF_3CClO)

(1) De Bruyn, W. J.; Duan, S. X.; Shi, X. Q.; Davidovits, P.; Worsnop, D. R.; Zahniser, M. S.; Kolb, C. E. Tropospheric heterogeneous chemistry of haloacetyl and carbonyl halides. *Geophys. Res. Lett.* **1992**, *19*, 1939-1942, doi:10.1029/92GL02199.
(2) De Bruyn, W. J.; Shorter, J. A.; Davidovits, P.; Worsnop, D. R.; Zahniser, M. S.; Kolb, C. E. Uptake of haloacetyl and carbonyl halides by water surfaces. *Environ. Sci. Technol.* **1995**, *29*, 1179-1185, doi:10.1021/es00005a007.

(3) George, C.; Lagrange, J.; Lagrange, P.; Mirabel, P.; Pallares, C.; Ponche, J. L. Heterogeneous chemistry of trichloroacetyl choride in the atmosphere. *J. Geophys. Res.* **1994**, *99*, 1255-1262, doi:10.1029/93JD02915

(4) George, C.; Saison, J. Y.; Ponche, J. L.; Mirabel, P. Kinetics of mass transfer of carbonyl fluoride, trifluoroacetyl fluoride, and trifluoroacetyl chloride at the air/water interface. *J. Phys. Chem.* **1994**, *98*, 10857-10862, doi:10.1021/j100093a029.

70. HBr on H_2O(s) and $HNO_3 \cdot nH_2O$. Hanson and Ravishankara[5,6] have reported large uptake coefficients for HBr on 200-K ice and NAT. Lower limits of >0.3 and >0.2 for ice are reported in the two referenced publications, respectively, and a limit of >0.3 is reported for NAT. No surface saturation was observed, leading to the supposition that HBr, like HCl, dissociates to ions on ice surfaces at stratospheric temperatures. Abbatt[1] measured an uptake coefficient lower limit of >0.03 on water ice at 228 K consistent with Hanson and Ravishankara. Rieley et al.[9] measured an α of 1.0 ± 0.05 for water ice at 80–120 K. Flückiger et al.[4] report α values of ~0.2 at 210 K, increasing to ~0.3 at 190 K, while Percival et al.[8] measured an α of 0.03 ± 0.005 for water ice at T >212 K, and α > 0.1 at T <212 K, attributing the apparent increase in the uptake coefficient to an increase in the surface area of the ice. Hudson et al.[7] report $\alpha = 0.61 \pm 0.06$ at 140 K, and $\alpha = 0.24 \pm 0.05$ at 100 K, for HBr pressures ranging from 3×10^{-8} to 1.4×10^{-7} Torr. Equilibrium HBr coverages for ice are reported by Chu and Heron[3] at 188 and 195 K, and by Chu and Chu[2] at 180–220 K. The latter authors also report the formation of various solid HBr hydrates. Given that no surface saturation is observed in the kinetics experiments leads to the supposition that HBr, like HCl, dissociates to ions. In addition to hydrate formation, it is likely that bulk melting of the ice surfaces may occur at stratospheric temperatures and the partial pressures used in the lab, to form thermodynamically stable HBr-H_2O solutions. Such behavior may not occur in the atmosphere where partial pressures of HBr are typically much lower than those used in the lab.

Back to Table

(1) Abbatt, J. P. D. Heterogeneous reaction of HOBr with HBr and HCl on ice surfaces at 228 K. *Geophys. Res. Lett.* **1994**, *21*, 665-668, doi:10.1029/94GL00775.

(2) Chu, L.; Chu, L. T. Heterogeneous interaction and reaction of HOBr on ice films. *J. Phys. Chem. A* **1999**, *103*, 8640-8649, doi:10.1021/jp991136q.

(3) Chu, L. T.; Heron, J. W. Uptake of HBr on ice at polar atmospheric conditions. *Geophys. Res. Lett.* **1995**, *22*, 3211-3214, doi:10.1029/95GL03290.

(4) Flückiger, B.; Thielmann, A.; Gutzwiller, L.; Rossi, M. J. Real time kinetics and thermochemistry of the uptake of HCl, HBr, and HI on water cce in the temperature range of 190 to 210 K. *Ber. Bunsenges. Phys. Chem.* **1998**, *102*, 915-928, doi:10.1002/bbpc.19981020704.

(5) Hanson, D. R.; Ravishankara, A. R. Heterogeneous chemistry of HBr and HF. *J. Phys. Chem.* **1992**, *96*, 9441-9446, doi:10.1021/j100202a069.

(6) Hanson, D. R.; Ravishankara, A. R. In *The Tropospheric Chemistry of Ozone in the Polar Regions*; Niki, H., Becker, K. H., Eds.; NATO, 1993; pp 17281-17290.

(7) Hudson, P. K.; Foster, K. L.; Tolbert, M. A.; George, S. M.; Carlo, S. R.; Grassian, V. H. HBr uptake on ice: Uptake coefficient, H_2O/HBr hydrate formation, and H_2O desorption kinetics. *J. Phys. Chem. A* **2001**, *105*, 694-702, doi:10.1021/jp002700w.

(8) Percival, C. J.; Mossinger, J. C.; Cox, R. A. The uptake of HI and HBr on ice. *Phys. Chem. Chem. Phys.* **1999**, *1*, 4565-4570, doi:10.1039/a904651h.

(9) Rieley, H.; Aslin, H. D.; Haq, S. Sticking of HCl on a type-II polar stratospheric cloud minic. *J. Chem. Soc. Faraday Trans.* **1995**, *91*, 2349-2351, doi:10.1039/ft9959102349.

71. HBr on H_2O(1). Schweitzer et al.[2] used the droplet train flow reactor technique over a temperature range of 262 to 281 K obtaining values decreasing from 0.16 to 0.0.68. Li et al.[1] and Zhang et al.[3] used the same technique to measure higher values of 0.14 ± 0.02 at 283 K and 0.21 ± 0.3 at 273 K, respectively. Given the good agreement between the two groups for HCl mass accommodation coefficients on water, there is no obvious reason for the discrepancy of a factor of 2-3 for HBr.

Back to Table

(1) Li, Y. Q.; Zhang, H. Z.; Davidovits, P.; Jayne, J. T.; Kolb, C. E.; Worsnop, D. R. Uptake of HCl(g) and HBr(g) on ethylene glycol surfaces as a function of relative humidity and temperature. *J. Phys. Chem. A* **2002**, *106*, 1220-1227, doi:10.1021/jp012861f.

(2) Schweitzer, F.; Mirabel, P.; George, C. Uptake of hydrogen halides by water droplets. *J. Phys. Chem. A* **2000**, *104*, 72-76, doi:10.1021/jp992621o.
(3) Zhang, H. Z.; Li, Y. Q.; Davidovits, P.; R., W. L.; Jayne, J. T.; Kolb, C. E.; Worsnop, D. R. Uptake of gas-phase species by 1-octanol. 2. Uptake of hydrogen halides and acetic acid as a function of relative humidity and temperature. *J. Phys. Chem. A* **2003**, *107*, 6398-6407, doi:10.1021/jp034254t.

72. **HBr on H_2SO_4•nH_2O.** Molecular beam measurements of HBr impingement on liquid deuterated sulfuric acid surfaces determine the fraction of HBr scattered with no reaction and the fraction that reacts, exchanging H for D, and is emitted as DBr. The fraction converted to DBr is assumed to have undergone interfacial transport, representing a lower limit to the mass accommodation coefficient, which varies from ~0.7 at 55 wt% D_2SO_4 to ~0.2 near 70 wt% Behr et al.[1] This strongly indicates that the mass accommodation coefficient for HBr is >0.1 for 55–72 wt% H_2SO_4 at 213 K.
Back to Table

(1) Behr, P.; Morris, J. R.; Antman, M. D.; Ringeisen, B. R.; Splan, J. R.; Nathanson, G. M. Reaction and desorption of HC1 and HBr following collisions with supercooled sulfuric acid. *Geophys. Res. Lett.* **2001**, *28*, 1961-1964, doi:10.1029/2000GL012716

73. **HOBr on H_2O(s).** Abbatt[1] measured an uptake coefficient for water ice of 2×10^{-3} at 228 K. Chu and Chu[3] report an uptake coefficient corrected for porosity effects in the range 0.11 to 0.007 at 190–218 K, with an exponential temperature dependence of (3809 ± 76)/T, and in the range 2×10^{-3} to 6×10^{-4} at 223–239 K, with an exponential temperature dependence of (4658 ± 456)/T. Chaix et al.[2] measured the uptake coefficient as a function of temperature on three different types of water-ice, obtaining values ranging from ~0.3 at 185 K to ~0.03 at 205 K, with an exponential temperature dependence of (4900 ± 500)/T. Mössinger et al.[5] report an uptake coefficient value of 0.003 at 227 K increasing to 0.040 at 205 K. The four sets of results are in reasonable agreement with each other, and the temperature dependence of the uptake coefficient is attributed predominantly to changes in the evaporation rate. The results indicate that the uptake of HOBr on ice cannot be explained with Langmuir-type adsorption isotherms and that the process is not reversible, probably proceeding via the self-reaction of HOBr to form Br_2O, or possibly by formation of hydrates. Using a common precursor model, Flückiger and Rossi[4] have estimated accommodation coefficients α which are considerably larger than the measured uptake coefficients, with α values ranging from 0.18 at 215 K to 0.46 at 190 K.
Back to Table

(1) Abbatt, J. P. D. Heterogeneous reaction of HOBr with HBr and HCl on ice surfaces at 228 K. *Geophys. Res. Lett.* **1994**, *21*, 665-668, doi:10.1029/94GL00775.
(2) Chaix, L.; Allanic, A.; Rossi, M. J. Heterogeneous chemistry of HOBr on different types of ice and on ice doped with HC1, HBr, and HNO_3 at 175 K < T < 125 K. *J. Phys. Chem. A* **2000**, *104*, 7268-7277, doi:10.1021/jp001018z.
(3) Chu, L.; Chu, L. T. Heterogeneous interaction and reaction of HOBr on ice films. *J. Phys. Chem. A* **1999**, *103*, 8640-8649, doi:10.1021/jp991136q.
(4) Flückiger, B.; Rossi, M. J. Common precursor mechanism for the heterogeneous reaction of D_2O, HCl, HBr, and HOBr with water ice in the range 170-230 K: Mass accommodation coefficients on ice. *J. Phys. Chem. A* **2003**, *107*, 4103-4115, doi:10.1021/jp021956u.
(5) Mössinger, J. C.; Hynes, R. G.; Cox, R. A. Interaction of HOBr and HCl on ice surfaces in the temperature range 205–227 K. *J. Geophys. Res.* **2002**, *107*, 4740, doi:10.1029/2002JD002151.

74. **HOBr on H_2O(l).** See Note on HOBr + KBr and NaBr in reactive uptake table.
Back to Table

75. **HOBr on H_2SO_4•nH_2O(l).** Abbatt[1] measured an uptake coefficient of 0.06 ± 0.02 by measuring HOBr gas phase loss at 228 K. This result may well be a lower limit due to surface saturation effects and the uptake may have been due to Br_2O formation.
Back to Table

(1) Abbatt, J. P. D. Heterogeneous reaction of HOBr with HBr and HCl on ice surfaces at 228 K. *Geophys. Res. Lett.* **1994**, *21*, 665-668, doi:10.1029/94GL00775.

76. **$BrONO_2$ on H_2O(1).** Deiber et al.[1] used a droplet train apparatus to measure the uptake of $BrONO_2$ on NaBr aqueous solutions to deduce the mass accommodation coefficient of 0.063 ± 0.021 at 274.5 K. This value may be affected by the reaction with interfacial Br^-.
Back to Table

(1) Deiber, G.; George, C.; Le Calve, S.; Schweitzer, F.; Mirabel, P. Uptake study of $ClONO_2$ and $BrONO_2$ by halide containing droplets. *Atmos. Chem. Phys.* **2004**, *4*, 1291-1299, doi:10.5194/acp-4-1291-2004.

77. **$BrONO_2$ on H_2SO_4•nH_2O.** Hanson[1] modeled wetted-wall flow reactor data and aerosol flow reactor data to estimate $\alpha = 0.80$ over a wide range of temperatures and acid concentrations.
Back to Table

(1) Hanson, D. Reactivity of $BrONO_2$ and HOBr on sulfuric acid solutions at low temperatures. *J. Geophys. Res.* **2003**, *108*, 4239, doi:10.1029/2002JD002519.

78. **$CHBr_3$ on H_2O(s) and H_2SO_4•nH_2O(l).** Hanson and Ravishankara[1] investigated the uptake of bromoform on ice and 58 wt% sulfuric acid at 220 K. No uptake on ice was observed, with a measured uptake coefficient of $<6 \times 10^{-5}$. Reversible uptake by the sulfuric acid surface was observed with an initial uptake coefficient of $>3 \times 10^{-3}$; both measurements are probably limited by surface saturation.
Back to Table

(1) Hanson, D. R.; Ravishankara, A. R. In *The Tropospheric Chemistry of Ozone in the Polar Regions*; Niki, H., Becker, K. H., Eds.; NATO, 1993; pp 17281-17290.

79. **BrCl on H_2O(1).** Katrib et al.[1] used a droplet train flow reactor to measure the uptake of BrCl as a function of NaOH concentration over the temperature range of 270–285 K. Data were too noisy to assign a clear temperature dependence, but an average over measurements at 270, 274, 280, and 285 K for higher [NaOH] where reactive scavenging relieved solubility constraints yielded $\alpha = 0.33 \pm 0.18$. The recommended lower limit is consistent with this value.
Back to Table

(1) Katrib, Y.; Deiber, G.; Schweitzer, F.; Mirabel, P.; George, C. Chemical transformation of bromine chloride at the air/water interface. *J. Aerosol Sci.* **2001**, *32*, 893-911, doi:10.1016/S0021-8502(00)00114-2.

80. **I_2 on H_2O(1).** Takami et al.[1] used the impinging flow technique to investigate the uptake of I_2 at 293 K as a function of pH. While solubility constraints prevented a clear measure of mass accommodation, they modeled high pH data where solubility constraints were relaxed by reactive scavenging by OH^- to determine that $\alpha \geq 0.1$.
Back to Table

(1) Takami, A.; Kondo, T.; Kado, A.; Koda, S. The uptake coefficient of I_2 on various aqueous surfaces. *J. Atmos. Chem.* **2001**, *39*, 139-153, doi:10.1023/A:1010657818117.

81. **HI on H_2O(s).** The uptake of HI has been studied by Chu and Chu[1] in a coated-wall flow tube to be large between 188 and 195 K, in the multi-layer coverage regime. Under their experimental conditions, it is likely that the surface is melting to form a bulk solution and/or hydrates are forming. Percival et al.[2] also report efficient uptake with the same technique between 200 and 233 K, with the uptake coefficient of 0.02 ± 0.004 above 212 K and larger than 0.1 for temperatures below 212 K.
Back to Table

(1) Chu, L. T.; Chu, L. Uptake and interaction of HI on ice films. *J. Phys. Chem. B* **1997**, *101*, 6271-6275, doi:10.1021/jp963185y.
(2) Percival, C. J.; Mossinger, J. C.; Cox, R. A. The uptake of HI and HBr on ice. *Phys. Chem. Chem. Phys.* **1999**, *1*, 4565-4570, doi:10.1039/a904651h.

82. **HI on H_2O(1).** Schweitzer et al.[1] used the droplet train flow reactor technique over a temperature range of 262 to 281 K, obtaining values decreasing from 0.19 to 0.079. Zhang et al.[2] used the same technique to

obtain a value of 0.17 ± 0.02 at 273 K, which is a little less than a factor of two higher than indicated by the Schweitzer et al. measurements for that temperature.
Back to Table

(1) Schweitzer, F.; Mirabel, P.; George, C. Uptake of hydrogen halides by water droplets. *J. Phys. Chem. A* **2000**, *104*, 72-76, doi:10.1021/jp992621o.
(2) Zhang, H. Z.; Li, Y. Q.; Davidovits, P.; R., W. L.; Jayne, J. T.; Kolb, C. E.; Worsnop, D. R. Uptake of gas-phase species by 1-octanol. 2. Uptake of hydrogen halides and acetic acid as a function of relative humidity and temperature. *J. Phys. Chem. A* **2003**, *107*, 6398-6407, doi:10.1021/jp034254t.

83. HOI on H_2SO_4•nH_2O. Knudsen cell studies by Allanic and Rossi[1] measured uptake at several temperatures for 40, 50, and 70 acid wt%. Time dependent studies show no sign of saturation, so uptake coefficients should correspond to mass accommodation coefficients. Some acid concentration data in the table have been averaged for similar temperatures and rounded to one significant figure. An uncertainty factor of three has been assigned due to the relatively small number of temperature/concentration points studied and a lack of confirming studies from other laboratories. The authors note evidence of HOI disproportionation to form I_2, however, this second order reaction is unlikely to occur under atmospheric conditions.
Back to Table

(1) Allanic, A.; Rossi, M. J. Heterogeneous reactions of HOI on substrates of atmospheric importance. *J. Geophys. Res.* **1999**, *104*, 18689-18696, doi:10.1029/1999JD900285.

84. HF on H_2O(s) and HNO_3•nH_2O(s). Hanson and Ravishankara[1] attempted to measure the uptake of HF by 200 K water ice and NAT surfaces but were unable to observe measurable adsorption. They surmise that, unlike HCl and HBr, HF does not dissociate to ions on ice or NAT surfaces at 200 K. Lack of measurable uptake is probably due to surface saturation.
Back to Table

(1) Hanson, D. R.; Ravishankara, A. R. Heterogeneous chemistry of HBr and HF. *J. Phys. Chem.* **1992**, *96*, 9441-9446, doi:10.1021/j100202a069.

85. CF_3CH_2OH + H_2O(s). The uptake of 1,1,1-trifluoroethanol to ice was studied by Symington et al.[1] from 208 to 228 K in a coated-wall flow reactor coupled to a mass spectrometer. Uptakes were observed to be reversible and exhibited Langmuir-type behavior. The partition coefficient is reported to be 3.74×10^{-12} exp(6427/T) cm.
Back to Table

(1) Symington, A.; Leow, L. M.; Griffiths, P. T.; Cox, R. A. Adsorption and hydrolysis of alcohols and carbonyls on ice at temperatures of the upper troposphere. *J. Phys. Chem. A* **2012**, *116*, 5990-6002, doi:10.1021/jp210935b.

86. $CF_3CF_2CH_2OH$ + H_2O(s). The uptake of $CF_3CF_2CH_2OH$ was studied in a coated wall flow tube from 203 to 223 K by Moreno et al.[1] The uptakes were reversible and obeyed a Langmuir adsorption isotherm. Heat of adsorption was reported to be –45 kJ/mole.
Back to Table

(1) Moreno, E.; Aranda, A.; Díaz-de-Mera, Y.; Notario, A.; Rodríguez, D.; Bravo, I. Uptake of partially fluorinated alcohols on atmospheric ice surfaces. *Atmos. Environ.* **2012**, *60*, 76-81, doi:10.1016/j.atmosenv.2012.06.028.

87. $CF_3CF_2CF_2CH_2OH$ + H_2O(s). The uptake of $CF_3CF_2CF_2CH_2OH$ was studied in a coated wall flow tube from 203 to 223 K.[1] The uptakes were reversible and obeyed a Langmuir adsorption isotherm. Heat of adsorption was reported to be –46 kJ/mole.
Back to Table

(1) Moreno, E.; Aranda, A.; Díaz-de-Mera, Y.; Notario, A.; Rodríguez, D.; Bravo, I. Uptake of partially fluorinated alcohols on atmospheric ice surfaces. *Atmos. Environ.* **2012**, *60*, 76-81, doi:10.1016/j.atmosenv.2012.06.028.

88. **$CF_3CHO + H_2O(s)$.** The uptake of CF_3CHO to ice was studied by Symington et al.[1] from 208 to 228 K in a coated-wall flow reactor coupled to a mass spectrometer. There was an irreversible component to the uptake which was attributed to hydrolysis. The partition coefficient is reported to be 1.06×10^{-2} exp(904/T) cm.
Back to Table

(1) Symington, A.; Leow, L. M.; Griffiths, P. T.; Cox, R. A. Adsorption and hydrolysis of alcohols and carbonyls on ice at temperatures of the upper troposphere. *J. Phys. Chem. A* **2012**, *116*, 5990-6002, doi:10.1021/jp210935b.

89. **CF_2O on $H_2O(s)$, $HNO_3 \bullet nH_2O$ and $H_2SO_4 \bullet nH_2O$.** Uptake coefficient measurements by Hanson and Ravishankara[1] on stratospheric surfaces are probably subject to surface and/or bulk saturation effects and may not represent accommodation coefficient measurements, particularly the lower limits of $>3 \times 10^{-6}$ reported for water and nitric acid ices.
Back to Table

(1) Hanson, D. R.; Ravishankara, A. R. The loss of CF_2O on ice, NAT, and sulfuric acid solutions. *Geophys. Res. Lett.* **1991**, *18*, 1699-1701, doi:10.1029/91GL02093

90. **$CF_3C(O)OH + H_2O(s)$.** Using a coated-wall flow tube coupled to a mass spectrometer, Symington et al.[1] measured the uptake to ice of CF_3COOH from 208 to 238 K. There is some evidence for non-reversible uptake due to hydrate formation. The partition coefficient is reported to be 5.12×10^{-6} exp(309/T) cm.
Back to Table

(1) Symington, A.; Cox, R. A.; Fernandez, M. A. Uptake of organic acids on ice surfaces: Evidence for surface modification and hydrate formation. *Z. Phys. Chem.* **2010**, *224*, 1219-1245, doi:10.1524/zpch.2010.6149.

91. **$CF_3C(O)OH$ on $H_2O(l)$.** Hu et al.[1] measured mass accommodation coefficients for five haloacetic acids, including trifluoroacetic acid (TFA); the others were mono-, di-, trichloro-, and chlorodifluoro-acetic acids. All displayed negative temperature dependence and values for α of about 0.1 at 273 K.
Back to Table

(1) Hu, J. H.; Shorter, J. A.; Davidovits, P.; Worsnop, D. R.; Zahniser, M. S.; Kolb, C. E. Uptake of gas-phase halogenated acetic acid molecules by water surfaces. *J. Phys. Chem.* **1993**, *97*, 11037-11042, doi:10.1021/j100144a022.

92. **SO_2 on $H_2O(s)$.** Uptake experiments in coated–wall flow tubes have been conducted by Chu et al.[1] and by Clegg and Abbatt[3] who observe sub-monolayer reversible uptakes for temperatures between 190–211 K and 213–233 K, respectively. Chu et al. report an uptake coefficient of 1×10^{-5} at 191 K. Earlier studies from Clappsaddle and Lamb[2] using chromatographic-like uptake experiments with small ice spheres packed into a column, are in good quantitative agreement with those of Clegg and Abbatt. Both studies report that uptake increases with increasing temperature, unlike most other species that demonstrate more adsorption at lower temperatures. From the partial pressure dependence of the uptake and from the behavior on basic and acidic surfaces, Clegg and Abbatt infer the uptake occurs by formation of bisulfite on the surface, in the quasi-liquid layer on the surface of ice.
Back to Table

(1) Chu, L.; Diao, G. W.; Chu, L. T. Heterogeneous interaction of SO_2 on H_2O_2-ice films at 190-210 K. *J. Phys. Chem. A* **2000**, *104*, 7565-7573, doi:10.1021/jp001323k.
(2) Clappsaddle, C.; Lamb, D. The sorption behavior of SO_2 on ice at temperatures between -30 °C and -5 °C. *Geophys. Res. Lett.* **1989**, *16*, 1173-1176, doi:10.1029/GL016i010p01173
(3) Clegg, S. M.; Abbatt, J. P. D. Uptake of SO_2, H_2O_2 and oxygenated organics by ice surfaces under conditions of the free troposphere. *J. Phys. Chem. A* **2001**, *105*, 6630-6636, doi:10.1021/jp010062r.

93. **SO_2 on $H_2O(1)$.** Using a droplet train flow reactor Worsnop et al.[7] measured an α of 0.11 ± 0.02 with no significant temperature variation over a temperature range of 260–292 K. Ponche et al.[4] measured 0.13 ± 0.01 at 298 K, in agreement with the earlier measurement. Shimono and Koda[6] estimated an α of 0.2 at 293.5 K from analysis of pH-dependent uptake coefficients in a liquid impingement technique. Schurath et al.[5]

used a coaxial flow liquid jet to obtain a value of 0.1 at 298 K. Boniface et al.[1] performed more extensive droplet train flow reactor measurements at high pH to relieve solubility constraints, obtaining a negative temperature dependence with α values ranging from 0.43 ± 0.4 at 264 K to 0.175 ± 0.015 at 291 K, their data can be fit to $\alpha/(1-\alpha) = \exp(-\Delta G^{\ddagger}_{obs}/RT)$, where $\Delta G^{\ddagger}_{obs} = -(7.6 \pm 0.6)$ kcal/mol + (29.2 ± 2.1) cal mol^{-1} K^{-1} T(K). Donaldson et al.[2] have used second harmonic generation spectroscopy to detect a chemisorbed SO_2 surface species which was predicted from earlier uptake measurements by Jayne et al.;[3] this surface complex may play a role in SO_2 heterogeneous reactions on aqueous surfaces.
Back to Table

(1) Boniface, J.; Shi, Q.; Li, Y. Q.; Chueng, J. L.; Rattigan, O. V.; Davidovits, P.; Worsnop, D. R.; Jayne, J. T.; Kolb, C. E. Uptake of gas-phase SO_2, H_2S, and CO_2 by aqueous solutions. *J. Phys. Chem. A* **2000**, *104*, 7502-7510, doi:10.1021/jp000479h.

(2) Donaldson, D. J.; Guest, J. A.; Goh, M. C. Evidence for absorbed SO_2 at the aqueous-air interface. *J. Phys. Chem.* **1995**, *99*, 9313-9315, doi:10.1021/j100023a002.

(3) Jayne, J. T.; Davidovits, P.; Worsnop, D. R.; Zahniser, M. S.; Kolb, C. E. Uptake of SO_2(g) by aqueous surfaces as a function of pH: The effect of chemical reaction at the interface. *J. Phys. Chem.* **1990**, *94*, 6041-6048, doi:10.1021/j100378a076.

(4) Ponche, J. L.; George, C.; Mirabel, P. Mass transfer at the air/water interface: Mass accommodation coefficients of SO_2, HNO_3, NO_2 and NH_3. *J. Atmos. Chem.* **1993**, *16*, 1-21.

(5) Schurath, U.; Bongartz, A.; Kames, J.; Wunderlich, C.; Carstens, T. In *Heterogeneous and Liquid Phase Processes. Transport and Chemical Transformation of Pollutants in the Troposphere*; Warneck, P., Ed.; Springer-Verlag: Berlin, 1996; Vol. 2; pp 182-189.

(6) Shimono, A.; Koda, S. Laser-spectroscopic measurements of uptake coefficients of SO_2 on aqueous surfaces. *J. Phys. Chem.* **1996**, *100*, 10269-10276, doi:10.1021/jp9537670.

(7) Worsnop, D. R.; Zahniser, M. S.; Kolb, C. E.; Gardner, J. A.; Watson, L. R.; Doren, J. M. V.; Jayne, J. T.; Davidovits, P. Temperature dependence of mass accommodation of SO_2 and H_2O_2 on aqueous surfaces. *J. Phys. Chem.* **1989**, *93*, 1159-1172, doi:10.1021/j100340a027.

94. **SO_2 on H_2SO_4•nH_2O.** See Note for H_2O_2 on H_2SO_4•nH_2O.
Back to Table

95. **H_2S on H_2O(1).** Boniface et al.[1] performed droplet train flow reactor measurements over at 260–298 K at high pH to relieve solubility constraints, measured uptake coefficients were consistent with $\alpha \geq 0.05$.
Back to Table

(1) Boniface, J.; Shi, Q.; Li, Y. Q.; Chueng, J. L.; Rattigan, O. V.; Davidovits, P.; Worsnop, D. R.; Jayne, J. T.; Kolb, C. E. Uptake of gas-phase SO_2, H_2S, and CO_2 by aqueous solutions. *J. Phys. Chem. A* **2000**, *104*, 7502-7510, doi:10.1021/jp000479h.

96. **H_2SO_4 on H_2SO_4•nH_2O.** Pöschl et al.[2] measured $0.43 < \alpha < 1.0$ for 73–98 wt% H_2SO_4 at 303 K in a wetted wall flow tube. Lower temperatures and acid concentrations would be expected to lead to larger values of a. As discussed in Pöschl et al.[2] this contradicts an indirect measurement of $0.02 < \alpha < 0.09$ at 42.5 wt% at 298 K by Van Dingenen and Raes[3] in a photochemical aerosol reactor. The Pöschl et al.[2] result is consistent with room temperature α values very near that measured for $(NH_4)_2SO_4$ particles in an aerosol flow reactor by Jefferson et al.[1]
Back to Table

(1) Jefferson, A.; Eisele, F. L.; Ziemann, P. J.; Weber, R. J.; Marti, J. J.; McMurry, P. H. Measurements of the H_2SO_4 mass accommodation coefficient onto polydisperse aerosol. *J. Geophys. Res.* **1997**, *102*, 19021-19028, doi:10.1029/97JD01152

(2) Pöschl, U.; Canagaratna, M.; Jayne, J. T.; Molina, L. T.; Worsnop, D. R.; Kolb, C. E.; Molina, M. J. Mass accommodation coefficient of H_2SO_4 vapor on aqueous sulfuric acid surfaces and gaseous diffusion coefficient of H_2SO_4 in N_2/H_2O. *J. Phys. Chem. A* **1998**, *102*, 10082-10089, doi:10.1021/jp982809s.

(3) Van Dingenen, R.; Raes, F. Determination of the condensation accomodation coefficient of sulfuric acid on water-sulfuric acid aerosol. *Aerosol Sci. Technol.* **1991**, *15*, 93-106, doi:10.1080/02786829108959516.

97. $CH_3S(O)CH_3$, $CH_3S(O_2)CH_3$ and $CH_3S(O_2)OH$ on $H_2O(l)$. De Bruyn et al.[1] measured uptake over the temperature range ~262–281 K and derived accommodation coefficients fitting $\alpha / (1 - \alpha) = \exp(-\Delta G^{\ddagger}_{obs}/RT)$, where $\Delta G^{\ddagger}_{obs}$ =

- -0.12 kcal mole^{-1} + 23.1 cal mole^{-1} K^{-1} T(K) for dimethylsulfoxide
- -10.7 kcal mole^{-1} + 43.0 cal mole^{-1} K^{-1} T(K) for dimethylsulfone
- -3.50 kcal mole^{-1} + 16.7 cal mole^{-1} K^{-1} T(K) for methanesulfonic acid.

Schweitzer et al.[2] used a droplet train flow reactor to investigate the uptake of $CH_3S(O_2)OH$ by water over a temperature range of 262–281 K, obtaining mass accommodation coefficient values decreasing from 0.17 to 0.11, in excellent agreement with those obtained by De Bruyn et al.[1]

Back to Table

(1) De Bruyn, W. J.; Shorter, J. A.; Davidovits, P.; Worsnop, D. R.; Zahniser, M. S.; Kolb, C. E. Uptake of gas phase sulfur species methanesulfonic acid, dimethylsulfoxide, and dimethyl sulfone by aqueous surfaces. *J. Geophys. Res.* **1994**, *99*, 16927-16932, doi:10.1029/94JD00684.

(2) Schweitzer, F.; Magi, L.; Mirabel, P.; George, C. Uptake rate measurements of methanesulfonic acid and glyoxal by aqueous droplets. *J. Phys. Chem. A* **1998**, *102*, 593-600, doi:10.1021/jp972451k.

5.2.2.2 Bibliography – Table NEq1

Abbatt, J. P. D. Heterogeneous reaction of HOBr with HBr and HCl on ice surfaces at 228 K. *Geophys. Res. Lett.* **1994**, *21*, 665-668, doi:10.1029/94GL00775.

Abbatt, J. P. D. Interaction of HNO_3 with water-ice surfaces at temperatures of the free troposphere. *Geophys. Res. Lett.* **1997**, *24*, 1479-1482, doi:10.1029/97GL01403.

Abbatt, J. P. D.; Beyer, K. D.; Fucaloro, A. F.; McMahon, J. R.; Wooldridge, P. J.; Zhong, R.; Molina, M. J. Interaction of HCl vapor with water-ice: Implications for the stratosphere. *J. Geophys. Res.* **1992**, *97*, 15819-15826, doi:10.1029/92JD01220.

Abbatt, J. P. D.; Molina, M. J. The heterogeneous reaction of HOCl + HCl → Cl_2 + H_2O on ice and nitric acid trihydrate: Reaction probabilities and stratospheric implications. *Geophys. Res. Lett.* **1992**, *19*, 461-464, doi:10.1029/92GL00373.

Aguzzi, A.; Rossi, M. J. The kinetics of the uptake of HNO_3 on ice, solid H_2SO_4-H_2O and solid ternary solutions of H_2SO_4-HNO_3-H_2O in the temperature range 180-211 K. *Phys. Chem. Chem. Phys.* **2001**, *3*, 3707-3716, doi:10.1039/b100546o.

Allanic, A.; Rossi, M. J. Heterogeneous reactions of HOI on substrates of atmospheric importance. *J. Geophys. Res.* **1999**, *104*, 18689-18696, doi:10.1029/1999JD900285.

Baldwin, A. C.; Golden, D. M. Heterogeneous atmospheric reactions: Sulfuric acid aerosols as tropospheric sinks. *Science* **1979**, *206*, 562-563, doi:10.1126/science.206.4418.562.

Baldwin, A. C.; Golden, D. M. Heterogeneous atmospheric reactions 2. Atom and radical reactions with sulfuric acid. *J. Geophys. Res.* **1980**, *85*, 2888-2889, doi:10.1029/JC085iC05p02888.

Barone, S. B.; Zondlo, M. A.; Tolbert, M. A. Investigation of the heterogeneous reactivity of HCl, HBr, and HI on ice surfaces. *J. Phys. Chem. A* **1999**, *103*, 9717-9730, doi:10.1021/jp990400c.

Bartels-Rausch, T.; Eichler, B.; Zimmermann, P.; Gaggeler, H. W.; Ammann, M. The adsorption enthalpy of nitrogen oxides on crystalline ice. *Atmos. Chem. Phys.* **2002**, *2*, 235-247, doi:10.5194/acp-2-235-2002.

Bartels-Rausch, T.; Guimbaud, C.; Gaggeler, H. W.; Ammann, M. The partitioning of acetone to different types of ice and snow between 198 and 223 K. *Geophys. Res. Lett.* **2004**, *31*, 4432, doi:10.1029/2004GL020070.

Behr, P.; Morris, J. R.; Antman, M. D.; Ringeisen, B. R.; Splan, J. R.; Nathanson, G. M. Reaction and desorption of HC1 and HBr following collisions with supercooled sulfuric acid. *Geophys. Res. Lett.* **2001**, *28*, 1961-1964, doi:10.1029/2000GL012716.

Behr, P.; Scharfenort, U.; Ataya, K.; Zellner, R. Dynamics and mass accommodation of HCl molecules on sulfuric acid-water surfaces. *Phys. Chem. Chem. Phys.* **2009**, *11*, 8048-8055, doi:10.1039/b904629a.

Behr, P.; Terziyski, A.; Zellner, R. Acetone adsorption on ice surfaces in the temperature range T=190-220 K: Evidence for aging effects due to crystallographic changes of the adsorption sites. *J. Phys. Chem. A* **2006**, *110*, 8098-8107, doi:10.1021/jp0563742.

Beichert, P.; Finlayson-Pitts, B. J. Knudson cell studies of the uptake of gaseous HNO_3 and other oxides of nitrogen on solid NaCl. The role of surface absorbed water. *J. Phys. Chem.* **1996**, *100*, 15218-15228, doi:10.1021/jp960925u.

Bongartz, A.; Schweighoefer, S.; Roose, C.; Schurath, U. The mass accommodation coefficient of ammonia on water. *J. Atmos. Chem.* **1995**, *20*, 35-58, doi:10.1007/BF01099917.

Boniface, J.; Shi, Q.; Li, Y. Q.; Chueng, J. L.; Rattigan, O. V.; Davidovits, P.; Worsnop, D. R.; Jayne, J. T.; Kolb, C. E. Uptake of gas-phase SO_2, H_2S, and CO_2 by aqueous solutions. *J. Phys. Chem. A* **2000**, *104*, 7502-7510, doi:10.1021/jp000479h.

Brown, D. E.; George, S. M.; Huang, C.; Wong, E. K. L.; Rider, K. B.; Smith, R. S.; Kay, B. D. H_2O condensation coefficient and refractive index for vapor-deposited ice from molecular beam and optical interference measurements. *J. Phys. Chem.* **1996**, *100*, 4988-4995, doi:10.1021/jp952547j.

Brown, L. A.; Vaida, V.; Hanson, D. R.; Graham, J. D.; Roberts, J. T. Uptake of chlorine dioxide by model PSCs under stratospheric conditions. *J. Phys. Chem.* **1996**, *100*, 3121-3125, doi:10.1021/jp951664b.

Burkhart, J. F.; Hutterli, M. A.; Bales, R. C. Partitioning of formaldehyde between air and ice at-35°C to-5°C. *Atmos. Environ.* **2002**, *36*, 2157-2163, doi:10.1016/S1352-2310(02)00221-2.

Cappa, C. D.; Drisdell, W. S.; Smith, J. D.; Saykally, R. J.; Cohen, R. C. Isotope fractionation of water during evaporation without condensation. *J. Phys. Chem. B* **2005**, *109*, 24391-24400, doi:10.1021/jp0539066.

Carstens, T.; Wunderlich, C.; Schurath, U. "*Proceedings EUROTRAC Symposium ' 96*", 1996, Southhampton, U. K.

Chaix, L.; Allanic, A.; Rossi, M. J. Heterogeneous chemistry of HOBr on different types of ice and on ice doped with HC1, HBr, and HNO_3 at 175 K < T < 125 K. *J. Phys. Chem. A* **2000**, *104*, 7268-7277, doi:10.1021/jp001018z.

Chu, L.; Chu, L. T. Heterogeneous interaction and reaction of HOBr on ice films. *J. Phys. Chem. A* **1999**, *103*, 8640-8649, doi:10.1021/jp991136q.

Chu, L.; Diao, G.; Chu, L. T. Heterogeneous interaction and reaction of HONO on ice films between 173 and 230 K. *J. Phys. Chem. A* **2000**, *104*, 3150-3158, doi:10.1021/jp9937151.

Chu, L.; Diao, G. W.; Chu, L. T. Heterogeneous interaction of SO_2 on H_2O_2-ice films at 190-210 K. *J. Phys. Chem. A* **2000**, *104*, 7565-7573, doi:10.1021/jp001323k.

Chu, L. T.; Chu, L. Uptake and interaction of HI on ice films. *J. Phys. Chem. B* **1997**, *101*, 6271-6275, doi:10.1021/jp963185y.

Chu, L. T.; Heron, J. W. Uptake of HBr on ice at polar atmospheric conditions. *Geophys. Res. Lett.* **1995**, *22*, 3211-3214, doi:10.1029/95GL03290.

Chu, L. T.; Leu, M.-T.; Keyser, L. F. Uptake of HCl in water ice and nitric acid ice films. *J. Phys. Chem.* **1993**, *97*, 7779-7785, doi:10.1021/j100131a057.

Clappsaddle, C.; Lamb, D. The sorption behavior of SO_2 on ice at temperatures between -30 °C and -5 °C. *Geophys. Res. Lett.* **1989**, *16*, 1173-1176, doi:10.1029/GL016i010p01173

Clegg, S. M.; Abbatt, J. P. D. Uptake of SO_2, H_2O_2 and oxygenated organics by ice surfaces under conditions of the free troposphere. *J. Phys. Chem. A* **2001**, *105*, 6630-6636, doi:10.1021/jp010062r.

Cooper, P. L.; Abbatt, J. P. D. Heterogeneous interactions of OH and HO_2 radicals with surfaces characertistic of atmospheric particulate matter. *J. Phys. Chem.* **1996**, *100*, 2249-2254, doi:10.1021/jp952142z.

Cox, R. A.; Fernandez, M. A.; Symington, A.; Ullerstam, M.; Abbatt, J. P. D. A kinetic model for uptake of HNO_3 and HCl on ice in a coated wall flow system. *Phys. Chem. Chem. Phys.* **2005**, *7*, 3434-3442, doi:10/1039/b506683b.

Dai, D. J.; Peters, S. J.; Ewing, G. E. Water absorption and dissociation on NaCl surfaces. *J. Phys. Chem.* **1995**, *99*, 10299-10304, doi:10.1021/j100025a035.

Davidovits, P.; Worsnop, D. R.; Jayne, J. T.; Kolb, C. E.; Winkler, P.; Vrtala, A.; Wagner, P. E.; Kulmula, M.; Lehtinen, K. E. J.; Vessala, T.; Mozurkewich, M. Mass accommodation coefficient of water vapor on liquid water. *Geophys. Res. Lett.* **2004**, *31*, L22111, doi:10.1029/2004GRL020835.

De Bruyn, W. J.; Duan, S. X.; Shi, X. Q.; Davidovits, P.; Worsnop, D. R.; Zahniser, M. S.; Kolb, C. E. Tropospheric heterogeneous chemistry of haloacetyl and carbonyl halides. *Geophys. Res. Lett.* **1992**, *19*, 1939-1942, doi:10.1029/92GL02199.

De Bruyn, W. J.; Shorter, J. A.; Davidovits, P.; Worsnop, D. R.; Zahniser, M. S.; Kolb, C. E. Uptake of gas phase sulfur species methanesulfonic acid, dimethylsulfoxide, and dimethyl sulfone by aqueous surfaces. *J. Geophys. Res.* **1994**, *99*, 16927-16932, doi:10.1029/94JD00684.

De Bruyn, W. J.; Shorter, J. A.; Davidovits, P.; Worsnop, D. R.; Zahniser, M. S.; Kolb, C. E. Uptake of haloacetyl and carbonyl halides by water surfaces. *Environ. Sci. Technol.* **1995**, *29*, 1179-1185, doi:10.1021/es00005a007.

Deiber, G.; George, C.; Le Calve, S.; Schweitzer, F.; Mirabel, P. Uptake study of $ClONO_2$ and $BrONO_2$ by halide containing droplets. *Atmos. Chem. Phys.* **2004**, *4*, 1291-1299, doi:10.5194/acp-4-1291-2004.

Delval, C.; Rossi, M. J. The kinetics of condensation and evaporation of H_2O from pure ice in the range 173-223 K: a quartz crystal microbalance study. *Phys. Chem. Chem. Phys.* **2004**, *6*, 4665-4676, doi:10.1039/b409995h.

Dlugokencky, E. J.; Ravishankara, A. R. Laboratory measurements of direct ozone loss on ice and doped-ice surfaces. *Geophys. Res. Lett.* **1992**, *19*, 41-44, doi:10.1029/91GL02092.

Donaldson, D. J.; Guest, J. A.; Goh, M. C. Evidence for absorbed SO_2 at the aqueous-air interface. *J. Phys. Chem.* **1995**, *99*, 9313-9315, doi:10.1021/j100023a002.

Drisdell, W. S.; Cappa, C. D.; Smith, J. D.; Saykally, R. J.; Cohen, R. C. Determination of the evaporation coefficient of D_2O. *Atmos. Chem. Phys.* **2008**, *8*, 6699-6706, doi:10.5194/acp-8-6699-2008.

Duan, S. X.; Jayne, J. T.; Davidovits, P.; Worsnop, D. R.; Zahniser, M. S.; Kolb, C. E. Uptake of gas-phase acetone by water surfaces. *J. Phys. Chem.* **1993**, *97*, 2284-2288, doi:10.1021/j100112a033.

Fairbrother, D. H.; Somorjai, G. Equilibrium surface composition of sulfuric acid films in contact with various atmospheric gases (HNO_3, CO_2, CH_2O, Cl_2, NO, NO_2). *J. Phys. Chem. B* **2000**, *104*, 4649-4652, doi:10.1021/jp992889f.

Faust, J. A.; Sobyra, T. B.; Nathanson, G. M. Gas-microjet reactive scattering: Collisions of HCl and DCl with cool salty water. *J. Phys. Chem. Lett.* **2016**, *7*, 730-735, doi:10.1021/acs.jpclett.5b02848.

Fenter, F. F.; Caloz, F.; Rossi, M. J. Kinetics of nitric acid uptake by salt. *J. Phys. Chem.* **1994**, *98*, 9801-9810, doi:10.1021/j100090a014.

Fenter, F. F.; Rossi, M. J. The heterogeneous kinetics of HONO on H_2SO_4 and on ice: activation of HCl. *J. Phys. Chem.* **1996**, *100*, 13765-13775, doi:10.1021/jp960797+.

Fernandez, M. A.; Hynes, R. G.; Cox, R. A. Kinetics of $ClONO_2$ reactive uptake on ice surfaces at temperatures of the upper troposphere. *J. Phys. Chem. A* **2005**, *109*, 9986-9996, doi:10.1021/jp053477b.

Fluckiger, B.; Rossi, M. J. Common precursor mechanism for the heterogeneous reaction of D_2O, HCl, HBr, and HOBr with water ice in the range 170-230 K: Mass accommodation coefficients on ice. *J. Phys. Chem. A* **2003**, *107*, 4103-4115, doi:10.1021/jp021956u.

Flückiger, B.; Thielmann, A.; Gutzwiller, L.; Rossi, M. J. Real time kinetics and thermochemistry of the uptake of HCl, HBr, and HI on water cce in the temperature range of 190 to 210 K. *Ber. Bunsenges. Phys. Chem.* **1998**, *102*, 915-928, doi:10.1002/bbpc.19981020704.

Foster, K. L.; Tolbert, M. A.; George, S. M. Interaction of HCl with ice: Investigation of the predicted trihydrate, hexahydrate, and monolayer regimes. *J. Phys. Chem. A* **1997**, *101*, 4979-4986, doi:10.1021/jp970772q.

Fung, K. N.; Tang, I. N.; Munkelwitz, H. R. Study of condensational growth of water droplets by Mie resonance spectroscopy. *Appl. Opt.* **1987**, *26*, 1282-1287, doi:10.1364/AO.26.001282.

George, C.; Lagrange, J.; Lagrange, P.; Mirabel, P.; Pallares, C.; Ponche, J. L. Heterogeneous chemistry of trichloroacetyl choride in the atmosphere. *J. Geophys. Res.* **1994**, *99*, 1255-1262, doi:10.1029/93JD02915.

George, C.; Saison, J. Y.; Ponche, J. L.; Mirabel, P. Kinetics of mass transfer of carbonyl fluoride, trifluoroacetyl fluoride, and trifluoroacetyl chloride at the air/water interface. *J. Phys. Chem.* **1994**, *98*, 10857-10862, doi:10.1021/j100093a029.

George, I. J.; Matthews, P. S. J.; Whalley, L. K.; Brooks, B.; Goddard, A.; Baeza-Romero, M. T.; Heard, D. E. Measurements of uptake coefficients for heterogeneous loss of HO_2 onto submicron inorganic salt aerosols. *Phys. Chem. Chem. Phys.* **2013**, *15*, 12829-12845, doi:10.1039/c3cp51831k.

Gershenzon, M.; Davidovits, P.; Williams, L. R.; Shi, Q.; Jayne, J. T.; Kolb, C. E.; Worsnop, D. Uptake of $H_2{}^{17}O(g)$ and $D_2O(g)$ by aqueous sulfuric acid droplets. *J. Phys. Chem. A* **2004**, *106*, 1567-1573, doi:10.1021/jp036402l.

Gershenzon, Y. M.; Grigorieva, V. M.; Ivanov, A. V.; Remorov, R. G. O_3 and OH sensitivity to heterogeneous sinks of HO_x and CH_3O_2 on aerosol particles. *Faraday Discuss.* **1995**, *100*, 83-100, doi:10.1039/fd9950000083.

Gershenzon, Y. M.; Ivanov, A. V.; Kucheryavyi, S. I.; Rozenshtein, V. B. Anihilation of OH radicals on the surfaces of subtances chemically similar to atmospheric aerosol particles. *Kinet. Katal.* **1986**, *27*, 1069-1074.

Gertner, B. J.; Hynes, J. T. Molecular dynamics simulation of hydrochloric acid ionization at the surface of srtatospheric ice. *Science* **1996**, *271*, 1563-1566, doi:10.1126/science.271.5255.1563.

Graham, J. D.; Roberts, J. T. Interaction of hydrogen chloride with an ultrathin ice film: Observation of adsorbed and absorbed states. *J. Phys. Chem.* **1994**, *98*, 5974-5983, doi:10.1021/j100074a026.

Graham, J. D.; Roberts, J. T. Interactions of HCl with crystalline and amorphous ice: Implications for the mechanisms of ice-catalyzed reactions. *Geophys. Res. Lett.* **1995**, *22*, 251-254, doi:10.1029/94GL03022.

Graham, J. D.; Roberts, J. T.; Brown, L. A.; Vaida, V. Uptake of chlorine dioxide by model polar stratospheric cloud surfaces: Ultra high-vacuum studies. *J. Phys. Chem.* **1996**, *100*, 3115-3120, doi:10.1021/jp9516654.

Gržinić, G.; Bartels-Rausch, T.; Türler, A.; Ammann, M. Efficient bulk mass accommodation and dissociation of N_2O_5 in neutral aqueous aerosol. *Atmos. Chem. Phys.* **2017**, *17*, 6493-6502, doi:10.5194/acp-17-6493-2017.

Hanson, D. Reactivity of $BrONO_2$ and HOBr on sulfuric acid solutions at low temperatures. *J. Geophys. Res.* **2003**, *108*, 4239, doi:10.1029/2002JD002519.

Hanson, D. R. The uptake of HNO_3 onto ice, NAT, and frozen sulfuric acid. *Geophys. Res. Lett.* **1992**, *19*, 2063-2066, doi:10.1029/92GL02182.

Hanson, D. R.; Burkholder, J. B.; Howard, C. J.; Ravishankara, A. R. Measurement of OH and HO_2 radical uptake coefficients on water and sulfuric acid surfaces. *J. Phys. Chem.* **1992**, *96*, 4979-4985, doi:10.1021/j100191a046.

Hanson, D. R.; Lovejoy, E. R. Heterogeneous reactions in liquid sulfuric Acid: HOCl + HCl as a model system. *J. Phys. Chem.* **1996**, *100*, 6397-6405, doi:10.1021/jp953250o.

Hanson, D. R.; Ravishankara, A. R. The loss of CF_2O on ice, NAT, and sulfuric acid solutions. *Geophys. Res. Lett.* **1991**, *18*, 1699-1701, doi:10.1029/91GL02093.
Hanson, D. R.; Ravishankara, A. R. Heterogeneous chemistry of HBr and HF. *J. Phys. Chem.* **1992**, *96*, 9441-9446, doi:10.1021/j100202a069.
Hanson, D. R.; Ravishankara, A. R. Investigation of the reactive and nonreactlve processes involving $ClONO_2$ and HCl on water and nitric acid doped ice. *J. Phys. Chem.* **1992**, *96*, 2682-2691, doi:10.1021/j100185a052.
Hanson, D. R.; Ravishankara, A. R. In *The Tropospheric Chemistry of Ozone in the Polar Regions*; Niki, H., Becker, K. H., Eds.; NATO, 1993; pp 17281-17290.
Harker, A. B.; Ho, W. W. Heterogeneous ozone decomposition on sulfuric acid surfaces at stratospheric temperatures. *Atmos. Environ.* **1979**, *13*, 1005-1010, doi:10.1016/0004-6981(79)90011-8.
Haynes, D. R.; Tro, N. J.; George, S. M. Condensation and evaporation of H_2O on ice surfaces. *J. Phys. Chem.* **1992**, *96*, 8502-8509, doi:10.1021/j100200a055.
Henson, B. F.; Wilson, K. R.; Robinson, J. M.; Noble, C. A.; Casson, J. L.; Worsnop, D. R. Experimental isotherms of HCl on H_2O ice under stratospheric conditions: Connections between bulk and interfacial thermodynamics. *J. Chem. Phys.* **2004**, *121*, 8486-8499, doi:10.1063/1.1803542.
Hu, J. H.; Shi, Q.; Davidovits, P.; Worsnop, D. R.; Zahniser, M. S.; Kolb, C. E. Reative uptake of Cl_2(g) and Br_2(g) by aqueous surfaces as a function of Br^- and I^- ion concentration: The effect of chemical reaction at the interface. *J. Phys. Chem.* **1995**, *99*, 8768-8776, doi:10.1021/j100021a050.
Hu, J. H.; Shorter, J. A.; Davidovits, P.; Worsnop, D. R.; Zahniser, M. S.; Kolb, C. E. Uptake of gas-phase halogenated acetic acid molecules by water surfaces. *J. Phys. Chem.* **1993**, *97*, 11037-11042, doi:10.1021/j100144a022.
Hudson, P. K.; Foster, K. L.; Tolbert, M. A.; George, S. M.; Carlo, S. R.; Grassian, V. H. HBr uptake on ice: Uptake coefficient, H_2O/HBr hydrate formation, and H_2O desorption kinetics. *J. Phys. Chem. A* **2001**, *105*, 694-702, doi:10.1021/jp002700w.
Hudson, P. K.; Shilling, J. E.; Tolbert, M. A.; Toon, O. B. Uptake of nitric acid on ice at tropospheric temperatures: Implications for cirrus clouds. *J. Phys. Chem. A* **2002**, *106*, 9874-9882, doi:10.1021/jp020508j.
Hynes, A. J.; Fernandez, M. A.; Cox, R. A. Uptake of HNO_3 on water-ice and coadsorption of HNO_3 and HCl in the temperature range 210–235 K. *J. Geophys. Res.* **2002**, *107*, 4797, doi:10.1029/2001JD001557.
Hynes, R. G.; Mossinger, J. C.; Cox, R. A. The interaction of HCl with water-ice at tropospheric temperatures. *Geophys. Res. Lett.* **2001**, *28*, 2827-2830, doi:10.1029/2000GL012706.
Il'in, S. D.; Selikhonovich, V. V.; Gershenson, Y. M.; Rozenshtein, V. B. Study of heterogeneous ozone loss on materials typical of atmospheric aerosol species. *Sov. J. Chem. Phys.* **1991**, *8*, 1858-1880.
Iraci, L. T.; Middlebrook, A. M.; Wilson, M. A.; Tolbert, M. A. Growth of nitric acid hydrates on thin sulfuric acid films. *Geophys. Res. Lett.* **1994**, *21*, 867-870, doi:10.1029/94GL00916.
Iraci, L. T.; Tolbert, M. A. Heterogeneous interaction of formaldehyde with cold sulfuric acid: Implications for the upper troposphere and lower stratosphere. *J. Geophys. Res.* **1997**, *102*, 16099-16107, doi:10.1029/97JD01259.
Jakubcyzk, D.; Zientara, M.; Kolwas, K.; Kolwas, M. Temperature dependence of evaporation coefficient for water measured in droplets in nitrogen under atmospheric pressure. *J. Atmos. Sci.* **2007**, *64*, 996-1004, doi:10.1175/JAS3860.1.
Jayne, J. T.; Davidovits, P.; Worsnop, D. R.; Zahniser, M. S.; Kolb, C. E. Uptake of SO_2(g) by aqueous surfaces as a function of pH: The effect of chemical reaction at the interface. *J. Phys. Chem.* **1990**, *94*, 6041-6048, doi:10.1021/j100378a076.
Jayne, J. T.; Duan, S. X.; Davidovits, P.; Worsnop, D. R.; Zahniser, M. S.; Kolb, C. E. Uptake of gas-phase alcohol and organic acid molecules by water surfaces. *J. Phys. Chem.* **1991**, *95*, 6329-6336, doi:10.1021/j100169a047.
Jayne, J. T.; Duan, S. X.; Davidovits, P.; Worsnop, D. R.; Zahniser, M. S.; Kolb, C. E. Uptake of gas-phase aldehydes by water surfaces. *J. Phys. Chem.* **1992**, *96*, 5452-5460, doi:10.1021/j100192a049.
Jayne, J. T.; Worsnop, D. R.; Kolb, C. E.; Swartz, E.; Davidovits, P. Uptake of gas-phase formaldehyde by aqueous acid surfaces. *J. Phys. Chem.* **1996**, *100*, 8015-8022, doi:10.1021/jp953196b.
Jedlovszky, P.; Hantal, G.; Neurohr, K.; Picaud, S.; Hoang, P. N. M.; von Hessberg, P.; Crowley, J. N. Adsorption isotherm of formic acid on the surface of ice, as seen from experiments and grand canonical Monte Carlo simulation. *J. Phys. Chem. C* **2008**, *112*, 8976-8987, doi:10.1021/jp8012915.

Jedlovszky, P.; Partay, L.; Hoang, P. N. M.; Picaud, S.; von Hessberg, P.; Crowley, J. N. Determination of the adsorption isotherm of methanol on the surface of ice. An experimental and grand canonical Monte Carlo simulation study. *J. Am. Chem. Soc.* **2006**, *128*, 15300-15309, doi:10.1021/ja065553+.

Jefferson, A.; Eisele, F. L.; Ziemann, P. J.; Weber, R. J.; Marti, J. J.; McMurry, P. H. Measurements of the H_2SO_4 mass accommodation coefficient onto polydisperse aerosol. *J. Geophys. Res.* **1997**, *102*, 19021-19028, doi:10.1029/97JD01152.

Jin, R. H.; Chu, L. T. Uptake of NH_3 and NH_3 + HOBr reaction on ice surfaces at 190 K. *J. Phys. Chem. A* **2007**, *111*, 7833-7840, doi:10.1021/jp073233m.

Katrib, Y.; Deiber, G.; Schweitzer, F.; Mirabel, P.; George, C. Chemical transformation of bromine chloride at the air/water interface. *J. Aerosol Sci.* **2001**, *32*, 893-911, doi:10.1016/S0021-8502(00)00114-2.

Katrib, Y.; Deiber, Y.; Mirabel, P.; Le Calve, S.; George, C.; Mellouki, A.; Le Bras, G. Atmospheric loss processes of dimethyl and diethyl carbonate. *J. Atmos. Chem.* **2002**, *43*, 151-174, doi:10.1023/A:1020605807298.

Katrib, Y.; Mirabel, P.; Le Calve, S.; Weck, G.; Kochanski, E. Experimental uptake study of ethanol by water droplets and its theoretical modeling of cluster formation at the interface. *J. Phys. Chem. B* **2002**, *106*, 7237-7245, doi:10.1021/jp015558n.

Kenner, R. D.; Plumb, I. C.; Ryan, K. R. Laboratory measurements of the loss of ClO on Pyrex, ice and NAT at 183 K. *Geophys. Res. Lett.* **1993**, *20*, 193-196, doi:10.1029/93GL00238.

Kerbrat, M.; Huthwelker, T.; Bartels-Rausch, T.; Gäggeler, H. W.; Ammann, M. Co-adsorption of acetic acid and nitrous acid on ice. *Phys. Chem. Chem. Phys.* **2010**, *12*, 7194-7202, doi:10.1039/b924782c.

Kerbrat, M.; Huthwelker, T.; Gäggeler, H. W.; Ammann, M. Interaction of nitrous acid with polycrystalline ice: Adsorption on the surface and diffusion into the bulk. *J. Phys. Chem. C* **2010**, *114*, 2208-2219, doi:10.1021/jp909535c.

Kerbrat, M.; Le Calve, S.; Mirabel, P. Uptake measurements of ethanol on ice surfaces and on supercooled aqueous solutions doped with nitric acid between 213 and 243 k. *J. Phys. Chem. A* **2007**, *111*, 925-931, doi:10.1021/jp0635011.

Keyser, L. F.; Moore, S. B.; Leu, M. T. Surface reaction and pore diffusion in flow tube reactors. *J. Phys. Chem.* **1991**, *95*, 5496-5502, doi:10.1021/j100167a026.

Koehler, B. G.; McNeill, L. S.; Middlebrook, A. M.; Tolbert, M. A. Fourier transform infrared studies of the interaction of HCl with model polar stratospheric cloud films. *J. Geophys. Res.* **1993**, *98*, 10563-10571, doi:10.1029/93JD00586.

Kong, X.; Waldner, A.; Orlando, F.; Artiglia, L.; Huthwelker, T.; Ammann, M.; Bartels-Rausch, T. Coexistence of physisorbed and solvated HCI at warm ice surfaces. *J. Phys. Chem. Lett.* **2017**, *8*, 4757-4762, doi:10.1021/acs.jpclett.7b01573.

Křepelová, A.; Newberg, J.; Huthwelker, T.; Bluhm, H.; Ammann, M. The nature of nitrate at the ice surface studied by XPS and NEXAFS. *Phys. Chem. Chem. Phys.* **2010**, *12*, 8870-8880, doi:10.1039/c0cp00359j.

Kroes, G.-J.; Clary, D. C. Sticking of HCl and ClOH to ice: A computational study. *J. Phys. Chem.* **1992**, *96*, 7079-7088, doi:10.1021/j100196a044.

Leu, M.-T. Heterogeneous reaction of N_2O_5 with H_2O and HCl on ice surfaces: implications for Antarctic ozone depletion. *Geophys. Res. Lett.* **1988**, *15*, 851-854, doi:10.1029/GL015i008p00851.

Leu, M.-T. Laboratory studies of sticking coefficients and heterogeneous reactions important in the Antarctic stratosphere. *Geophys. Res. Lett.* **1988**, *15*, 17-20, doi:10.1029/GL015i001p00017.

Leu, M.-T.; Moore, S. B.; Keyser, L. F. Heterogeneous reactions of chlorine nitrate and hydrogen chloride on Type I polar stratospheric clouds. *J. Phys. Chem.* **1991**, *95*, 7763-7771, doi:10.1021/j100173a040.

Leu, M.-T.; Timonen, R. S.; Keyser, L. F. Kinetics of the heterogeneous reaction $HNO_3(g)$ + NaBr(s) ↔ HBr(g) + $NaNO_3$(s). *J. Phys. Chem. A* **1997**, *101*, 278-282, doi:10.1021/jp9626069.

Li, Y. Q.; Davidovits, P.; Shi, Q.; Jayne, J. T.; Kolb, C. E.; Worsnop, D. R. Mass and thermal accommodation coefficients of H_2O(g) on liquid water as a function of temperature. *J. Phys. Chem. A* **2001**, *105*, 10627-10634, doi:10.1021/jp012758q.

Li, Y. Q.; Zhang, H. Z.; Davidovits, P.; Jayne, J. T.; Kolb, C. E.; Worsnop, D. R. Uptake of HCl(g) and HBr(g) on ethylene glycol surfaces as a function of relative humidity and temperature. *J. Phys. Chem. A* **2002**, *106*, 1220-1227, doi:10.1021/jp012861f.

Li, Z.; Friedl, R. R.; Moore, S. B.; Sander, S. P. Interaction of peroxynitric acid with solid H_2O-ice. *J. Geophys. Res.* **1996**, *101*, 6795-6802, doi:10.1029/96JD00065.

Maerefat, M.; Akamatsu, T.; Fujikawa, S. Non-equilibrium condensation of water and carbontetrachloride vapor in a shock tube. *Experiments in Fluids* **1990**, *9*, 345-351.

Magee, N.; Moyle, A. M.; Lamb, D. Experimental determination of the deposition coefficient of small cirrus-like ice crystals near-50 °C. *Geophys. Res. Lett.* **2006**, *33*, L17813, doi:10.1029/2006GL026665.
Magi, L.; Schweitzer, F.; Pallares, C.; Cherif, S.; Mirabel, P.; George, C. Investigation of the uptake rate of ozone and methyl hydroperoxide by water surfaces. *J. Phys. Chem. A* **1997**, *4*, 4943-4948, doi:10.1021/jp970646m.
Marek, R.; Straub, J. Analysis of the evaporation coefficient and the condensation coefficient of water. *Int. J. Heat Mass Transfer* **2001**, *44*, 39-53, doi:10.1016/S0017-9310(00)00086-7.
Marti, J.; Mauersberger, K.; Hanson, D. HCl dissolved in solid mixtures of nitric acid and ice: Implications for the polar stratosphere. *Geophys. Res. Lett.* **1991**, *18*, 1861-1864, doi:10.1029/91GL02313.
McNeill, V. F.; Geiger, F. M.; Loerting, T.; Trout, B. L.; Molina, L. T.; Molina, M. J. Interaction of hydrogen chloride with ice surfaces: The effects of grain size, surface roughness, and surface disorder. *J. Phys. Chem. A* **2007**, *111*, 6274-6284, doi:10.1021/jp068914g.
McNeill, V. F.; Loerting, T.; Geiger, F. M.; Trout, B. L.; Molina, M. J. Hydrogen chloride-induced surface disordering on ice. *Proc. Nat. Acad. Sci.* **2006**, *103*, 9422-9427, doi:10.1073/pnas.0603494103.
Middlebrook, A. M.; Koehler, B. G.; McNeill, L. S.; Tolbert, M. A. Formation of model polar stratospheric cloud films. *Geophys. Res. Lett.* **1992**, *19*, 2417-2420, doi:10.1029/92GL02635.
Mihelcic, D.; Klemp, D.; Müsgen, P.; Pätz, H. W.; Volz-Thomas, A. Simultaneous measurements of peroxy and nitrate radicals at Schauinsland. *J. Atmos. Chem.* **1993**, *16*, 313-335, doi:10.1007/BF01032628.
Moore, S. B.; Keyser, L. F.; Leu, M. T.; Turco, R. P.; Smith, R. H. Heterogeneous reactions on nitric acid trihydrate. *Nature* **1990**, *345*, 333-335, doi:10.1038/345333a0.
Moreno, E.; Aranda, A.; Díaz-de-Mera, Y.; Notario, A.; Rodríguez, D.; Bravo, I. Uptake of partially fluorinated alcohols on atmospheric ice surfaces. *Atmos. Environ.* **2012**, *60*, 76-81, doi:10.1016/j.atmosenv.2012.06.028.
Morten Hundt, P.; Bisson, R.; Beck, R. D. The sticking probability of D_2O-water on ice: Isotope effects and the influence of vibrational excitation. *J. Chem. Phys.* **2012**, *137*, 074701, doi:10.1063/1.4742914.
Mössinger, J. C.; Hynes, R. G.; Cox, R. A. Interaction of HOBr and HCl on ice surfaces in the temperature range 205–227 K. *J. Geophys. Res.* **2002**, *107*, 4740, doi:10.1029/2002JD002151.
Mozurkewich, M.; McMurray, P. H.; Gupta, A.; Calvert, J. G. Mass accommodation coefficient for HO_2 radicals on aqueous particles. *J. Geophys. Res.* **1987**, *92*, 4163-4170, doi:10.1029/JD092iD04p04163.
Müller, B.; Heal, M. R. The mass accommodation coefficient of ozone on an aqueous surface. *Phys. Chem. Chem. Phys.* **2002**, *4*, 3365-3369, doi:10.1039/b202491h.
Murray, B. J.; Plane, M. C. The uptake of atomic oxygen on ice films: Implications for noctilucent clouds. *Phys. Chem. Chem. Phys.* **2003**, *107*, 4129-4138, doi:10.1039/b305555h.
Nathanson, G. M. Molecular beam studies of gas-liquid interfaces. *Ann. Rev. Phys. Chem.* **2004**, *55*, 231-255, doi:10.1146/annurev.physchem.55.091602.094357.
Noyes, R. M.; Rubin, M. B.; Bowers, P. G. Transport of carbon dioxide between the gas phase and water under well-stirred conditions: Rate constants and mass accommodation coefficient. *J. Phys. Chem.* **1996**, *100*, 4167-4172, doi:10.1021/jp952382e.
Ocampo, J.; Klinger, J. Adsorption of N_2 and CO_2 on ice. *J. Colloid Interface Sci.* **1982**, *86*, 377-383, doi:10.1016/0021-9797(82)90083-2.
Olszyna, K.; Cadle, R. D.; dePena, R. G. Stratospheric heterogeneous decomposition of ozone. *J. Geophys. Res.* **1979**, *84*, 1771-1775, doi:10.1029/JC084iC04p01771.
Park, S.-C.; Burden, D. K.; Nathanson, G. M. Surfactant control of gas transport and reactions at the surface of sulfuric acid. *Acc. Chem. Res.* **2009**, *42*, 379-387, doi:10.1021/ar800172m.
Percival, C. J.; Mossinger, J. C.; Cox, R. A. The uptake of HI and HBr on ice. *Phys. Chem. Chem. Phys.* **1999**, *1*, 4565-4570, doi:10.1039/a904651h.
Petitjean, M.; Darvas, M.; Picaud, S.; Jedlovszky, P.; Le Calvé, S. Adsorption of hydroxyacetone on pure ice surfaces. *ChemPhysChem* **2010**, *11*, 3921-3927, doi:10.1002/cphc.201000629.
Petitjean, M.; Mirabel, P.; Le Calve, S. Uptake measurements of acetaldehyde on solid ice surfaces and on solid/liquid supercooled mixtures doped with HNO_3 in the temperature range 203-253 K. *J. Phys. Chem. A* **2009**, *113*, 5091-5098, doi:10.1021/jp810131f.
Peybernes, N.; Le Calve, S.; Mirabel, P.; Picaud, S.; Hoang, P. N. M. Experimental and theoretical adsorption study of ethanol on ice surfaces. *J. Phys. Chem. B* **2004**, *108*, 17425-17432, doi:10.1021/jp046983u.
Peybernes, N.; Marchand, C.; Le Calve, S.; Mirabel, P. Adsorption studies of acetone and 2,3-butanedione on ice surfaces between 193 and 223 K. *Phys. Chem. Chem. Phys.* **2004**, *6*, 1277-1284, doi:10.1039/b315064j.

Picaud, S.; Hoang, P. N. M.; Peybernes, N.; Le Calve, S.; Mirabel, P. Adsorption of acetic acid on ice: Experiments and molecular dynamics simulations. *J. Chem. Phys.* **2005**, *122*, 194707, doi:10.1063/1.1888368.

Ponche, J. L.; George, C.; Mirabel, P. Mass transfer at the air/water interface: Mass accommodation coefficients of SO_2, HNO_3, NO_2 and NH_3. *J. Atmos. Chem.* **1993**, *16*, 1-21, doi:10.1007/BF00696620.

Pöschl, U.; Canagaratna, M.; Jayne, J. T.; Molina, L. T.; Worsnop, D. R.; Kolb, C. E.; Molina, M. J. Mass accommodation coefficient of H_2SO_4 vapor on aqueous sulfuric acid surfaces and gaseous diffusion coefficient of H_2SO_4 in N_2/H_2O. *J. Phys. Chem. A* **1998**, *102*, 10082-10089, doi:10.1021/jp982809s.

Pouvesle, N.; Kippenberger, M.; Schuster, G.; Crowley, J. N. The interaction of H_2O_2 with ice surfaces between 203 and 233 K. *Phys. Chem. Chem. Phys.* **2010**, *12*, 15544-15550, doi:10.1039/c0cp01656j.

Pratte, P.; van den Bergh, H.; Rossi, M. J. The kinetics of H_2O vapor condensation and evaporation on different types of ice in the range 130-210 K. *J. Phys. Chem. A* **2006**, *110*, 3042-3058, doi:10.1021/jp053974s.

Reihs, C. M.; Golden, D. M.; Tolbert, M. A. Nitric acid uptake by sulfuric acid solutions under stratospheric conditions: Determination of Henry's law solubility. *J. Geophys. Res.* **1990**, *95*, 16545-16550, doi:10.1029/JD095iD10p16545.

Rieley, H.; Aslin, H. D.; Haq, S. Sticking of HCl on a type-II polar stratospheric cloud minic. *J. Chem. Soc. Faraday Trans.* **1995**, *91*, 2349-2351, doi:10.1039/ft9959102349.

Robinson, G. N.; Worsnop, D. R.; Jayne, J. T.; Kolb, C. E.; Swartz, E.; Davidovits, P. Heterogeneous uptake of HCl by sulfuric acid solutions. *J. Geophys. Res.* **1998**, *103*, 25371-25381, doi:10.1029/98JD02085.

Roeselová, M.; Jungwirth, P.; Tobias, D. J.; Gerber, R. B. Impact, trapping, and accommodation of hydroxyl radical and ozone at aqueous salt aerosol surfaces. A molecular dynamics study. *J. Phys. Chem. B* **2003**, *107*, 12690-12699, doi:10.1021/jp030592i.

Roeselová, M.; Vieceli, J.; Dang, L. X.; Garrett, B. C.; Tobias, D. J. Hydroxyl radical at the air-water interface. *J. Am. Chem. Soc.* **2004**, *126*, 16308-16309, doi:10.1021/ja045552m.

Rouvière, A.; Sosedova, Y.; Ammann, M. Uptake of ozone to deliquesced KI and mixed KI/NaCl aerosol particles. *J. Phys. Chem. A* **2010**, *114*, 7085-7093, doi:10.1021/jp103257d.

Rudich, Y.; Talukdar, R. K.; Imamura, T.; Fox, R. W.; Ravishankara, A. R. Uptake of NO_3 on KI solutions: Rate coefficient for the $NO_3 + I^-$ reaction and gas-phase diffusion coefficient for NO_3. *Chem. Phys. Lett.* **1996**, *261*, 467-473, doi:10.1016/0009-2614(96)00980-3.

Rudolf, R.; Wagner, P. E. Experimental study of condensational particle growth in nitric acid-water vapor mixtures at nearly ambient pressures and temperatures. *J. Aerosol Sci.* **1994**, *25*, 97-98, doi:10.1016/0021-8502(94)90279-8.

Saastad, O. W.; Ellerman, T.; Nielson, C. J. On the adsorption of NO and NO_2 on cold H_2O/H_2SO_4 surfaces. *Geophys. Res. Lett.* **1993**, *20*, 1191-1193, doi:10.1029/93GL01621.

Schurath, U.; Bongartz, A.; Kames, J.; Wunderlich, C.; Carstens, T. In *Heterogeneous and Liquid Phase Processes. Transport and Chemical Transformation of Pollutants in the Troposphere*; Warneck, P., Ed.; Springer-Verlag: Berlin, 1996; Vol. 2; pp 182-189.

Schütze, M.; Herrmann, H. Determination of phase transfer parameters for the uptake of HNO_3, N_2O_5 and O_3 on single aqueous drops. *Phys. Chem. Chem. Phys.* **2002**, *4*, 60-67, doi:10.1039/b106078n.

Schütze, M.; Herrmann, H. Uptake of acetone, 2-butanone, 2,3-butanedione and 2-oxopropanal on a water surface. *Phys. Chem. Chem. Phys.* **2004**, *6*, 965-971, doi:10.1039/b313474a.

Schütze, M.; Herrmann, H. Uptake of the NO_3 radical on aqueous surfaces. *J. Atmos. Chem.* **2005**, *52*, 1-18, doi:10.1007/s10874-005-6153-8.

Schweitzer, F.; Magi, L.; Mirabel, P.; George, C. Uptake rate measurements of methanesulfonic acid and glyoxal by aqueous droplets. *J. Phys. Chem. A* **1998**, *102*, 593-600, doi:10.1021/jp972451k.

Schweitzer, F.; Mirabel, P.; George, C. Uptake of hydrogen halides by water droplets. *J. Phys. Chem. A* **2000**, *104*, 72-76, doi:10.1021/jp992621o.

Shaw, R. A.; Lamb, D. Experimental determination of the thermal accommodation and condensation coefficients of water. *J. Chem. Phys.* **1999**, *111*, 10659-10663, doi:10.1063/1.480419.

Shi, Q.; Davidovits, P.; Jayne, J. T.; Worsnop, D. R.; Kolb, C. E. Uptake of gas-phase ammonia. 1. Uptake by aqueous surfaces as a function of pH. *J. Phys. Chem. A* **1999**, *103*, 8812-8823, doi:10.1021/jp991696p.

Shi, Q.; Li, Y. Q.; Davidovits, P.; Jayne, J. T.; Worsnop, D. R.; Mozurkewich, M.; Kolb, C. E. Isotope exchange for gas-phase acetic acid and ethanol at aqueous interfaces: A study of surface reactions. *J. Phys. Chem. B* **1999**, *103*, 2417-2430, doi:10.1021/jp983525a.

Shimono, A.; Koda, S. Laser-spectroscopic measurements of uptake coefficients of SO_2 on aqueous surfaces. *J. Phys. Chem.* **1996**, *100*, 10269-10276, doi:10.1021/jp9537670.
Skrotzki, J.; Connolly, P.; Schnaiter, M.; Saathoff, H.; Möhler, O.; Wagner, R.; Niemand, M.; Ebert, V.; Leisner, T. The accommodation coefficient of water molecules on ice – cirrus cloud studies at the AIDA simulation chamber. *Atmos. Chem. Phys.* **2013**, *13*, 4451-4466, doi:10.5194/acp-13-4451-2013.
Smith, J. D.; Cappa, C. D.; Drisdell, W. S.; Cohen, R. C.; Saykally, R. J. Raman thermometry measurements of free evaporation from liquid water droplets. *J. Am. Chem. Soc.* **2006**, *128*, 12892 - 12898, doi:10.1021/ja063579v.
Sokolov, O.; Abbatt, J. P. D. Adsorption to ice of n-alcohols (ethanol to 1-hexanol), acetic acid, and hexanal. *J. Phys. Chem. A* **2002**, *106*, 775-782, doi:10.1021/jp013291m.
Sokolov, O.; Abbatt, J. P. D. Competitive adsorption of atmospheric trace gases onto ice at 228 K: HNO_3/HCl, 1-butanol/acetic acid and 1-butanol/HCl. *Geophys. Res. Lett.* **2002**, *29*, 1851, doi:10.1029/2002GL014843.
Symington, A.; Cox, R. A.; Fernandez, M. A. Uptake of organic acids on ice surfaces: Evidence for surface modification and hydrate formation. *Z. Phys. Chem.* **2010**, *224*, 1219-1245, doi:10.1524/zpch.2010.6149.
Symington, A.; Leow, L. M.; Griffiths, P. T.; Cox, R. A. Adsorption and hydrolysis of alcohols and carbonyls on ice at temperatures of the upper troposphere. *J. Phys. Chem. A* **2012**, *116*, 5990-6002, doi:10.1021/jp210935b.
Takami, A.; Kato, S.; Shimono, A.; Koda, S. Uptake coefficient of OH radical on aqueous surface. *Chem. Phys.* **1998**, *231*, 215-227, doi:10.1016/S0301-0104(98)00004-4.
Takami, A.; Kondo, T.; Kado, A.; Koda, S. The uptake coefficient of I_2 on various aqueous surfaces. *J. Atmos. Chem.* **2001**, *39*, 139-153, doi:10.1023/A:1010657818117.
Taketani, F.; Kanaya, Y.; Akimoto, H. Kinetics of heterogeneous reactions of HO_2 radical at ambient concentration levels with $(NH_4)_2SO_4$ and NaCl aerosol particles. *J. Phys. Chem. A* **2008**, *112*, 2370-2377, doi:10.1021/jp0769936.
Taketani, F.; Kanaya, Y.; Akimoto, H. Heterogeneous loss of HO_2 by KCl, synthetic sea salt, and natural seawater aerosol particles. *Atmos. Environ.* **2009**, *43*, 1660-1665, doi:10.1016/j.atmosenv.2008.12.010.
Tang, I. N.; Lee, J. H. In *The Chemistry of Acid Rain*; Gordon, G. E., Johnson, R. W., Eds.; Am. Chem. Soc. Symp. Series, 1987; pp 109-117.
Tang, I. N.; Munkelwitz, H. R. Evaporation kinetics of ammonium chloride solution droplets in water vapor. *J. Colloid Interface Sci.* **1989**, *128*, 289-295, doi:10.1016/0021-9797(89)90406-2.
Thibert, E.; Domine, F. Thermodynamics and kinetics of the solid solution of HNO_3 in ice. *J. Phys. Chem. B* **1998**, *102*, 4432-4439, doi:10.1021/jp980569a.
Thomas, K.; Volz-Thomas, A.; Mihelcic, D.; Smit, H. G. J.; Kley, D. On the exchange of NO_3 radicals with aqueous solutions: Solubility and sticking coefficient. *J. Atmos. Chem.* **1998**, *29*, 17-43, doi:10.1023/A:1005860312363.
Thornton, J. A.; Abbatt, J. P. D. Measurements of HO_2 uptake to aqueous aerosol: Mass accommodation coefficients and net reactive loss. *J. Geophys. Res.* **2005**, *110*, D08309, doi:10.1029/2004JD005402.
Tolbert, M. A.; Praff, J.; Jayaweera, I.; Prather, M. J. Uptake of formaldehyde by sulfuric acid solutions: Impact on stratospheric ozone. *J. Geophys. Res.* **1993**, *98*, 2957-2962, doi:10.1029/92JD02386.
Tolbert, M. A.; Rossi, M. J.; Golden, D. M. Heterogeneous interactions of chlorine nitrate, hydrogen chloride and nitric acid with sulfuric acid surfaces at stratospheric temperatures. *Geophys. Res. Lett.* **1988**, *15*, 847-850, doi:10.1029/GL015i008p00847.
Ullerstam, M.; Abbatt, J. P. D. Burial of gas-phase HNO_3 by growing ice surfaces under tropospheric conditions. *Phys. Chem. Chem. Phys.* **2005**, *7*, 3596-3600, doi:10.1039/b507797d.
Ullerstam, M.; Thornberry, T.; Abbatt, J. P. D. Uptake of gas-phase nitric acid to ice at low partial pressures: evidence for unsaturated surface coverage. *Faraday Discuss.* **2005**, *130*, 211-226, doi:10.1039/b417418f.
Ulrich, T.; Ammann, M.; Leutwyler, S.; Bartels-Rausch, T. The adsorption of peroxynitric acid on ice between 230 K and 253 K. *Atmos. Chem. Phys.* **2012**, *12*, 1833-1845, doi:10.5194/acp-12-1833-2012.
Utter, R. G.; Burkholder, J. B.; Howard, C. J.; Ravishankara, A. R. Measurement of the mass accommodation coefficient of ozone on aqueous surfaces. *J. Phys. Chem.* **1992**, *96*, 4973-4979, doi:10.1021/j100191a045.
Van Dingenen, R.; Raes, F. Determination of the condensation accomodation coefficient of sulfuric acid on water-sulfuric acid aerosol. *Aerosol Sci. Technol.* **1991**, *15*, 93-106, doi:10.1080/02786829108959516.

Van Doren, J. M.; Watson, L. R.; Davidovits, P.; Worsnop, D. R.; Zahniser, M. S.; Kolb, C. E. Temperature dependence of the uptake coefficients of HNO_3, HCl, and N_2O_5 by water droplets. *J. Phys. Chem.* **1990**, *94*, 3265-3269, doi:10.1021/j100371a009.

Van Doren, J. M.; Watson, L. R.; Davidovits, P.; Worsnop, D. R.; Zahniser, M. S.; Kolb, C. E. Uptake of N_2O_5 and HNO_3 by aqueous sulfuric acid droplets. *J. Phys. Chem.* **1991**, *95*, 1684-1689, doi:10.1021/j100157a037.

Voigtländer, J.; Stratmann, F.; Niedermeier, D.; Wex, H.; Kiselev, A. Mass accommodation coefficient of water: A combined computational fluid dynamics and experimental data analysis. *J. Geophys. Res.* **2007**, *112*, D20208, doi:10.1029/2007JD008604.

von Hessberg, P.; Pouvesle, N.; Winkler, A. K.; Schuster, G.; Crowley, J. N. Interaction of formic and acetic acid with ice surfaces between 187 and 227 K. Investigation of single species- and competitive adsorption. *Phys. Chem. Chem. Phys.* **2008**, *10*, 2345-2355, doi:10.1039/b800831k.

Wang, L.; Clary, D. C. Time-dependent wave packet studies on the sticking of HCl to an ice surface. *J. Chem. Phys.* **1996**, *104*, 5663-5673, doi:10.1063/1.471772.

Watson, L. R.; Doren, J. M. V.; Davidovits, P.; Worsnop, D. R.; Zahniser, M. S.; Kolb, C. E. Uptake of HCl molecules by aqueous sulfuric acid droplets as a function of acid concentration. *J. Geophys. Res.* **1990**, *95*, 5631-5638, doi:10.1029/JD095iD05p05631.

Winkler, A. K.; Holmes, N. S.; Crowley, J. N. Interaction of methanol, acetone and formaldehyde with ice surfaces between 198 and 223 K. *Phys. Chem. Chem. Phys.* **2002**, *4*, 5270-5275, doi:10.1039/b206258e.

Winkler, P.; Vrtala, A.; Wagner, P. E.; Kulmula, M.; Lehtinen, K. E. J.; Vesala, T. Mass and thermal accommodation during gas-liquid condensation of water. *Phys. Rev. Lett.* **2004**, *93*, 075701, doi: 10.1103/Phys.Rev.Lett93.075701.

Winkler, P. M.; Vrtala, A.; Rudolf, R.; Wagner, P. E.; Riipinen, I.; Vesala, T.; Lehtinen, K. E. J.; Viisanen, Y.; Kulmala, M. Condensation of water vapor: Experimental determination of mass and thermal accommodation coefficients. *J. Geophys. Res.* **2006**, *111*, D19202, doi:10.1029/2006JD007194.

Worsnop, D. R.; Williams, L. R.; Kolb, C. E.; Mozurkewich, M.; Gershenzon, M.; Davidovits, P. Comment on "The NH_3 mass accommodation coefficient for uptake onto sulfuric acid solution". *J. Phys. Chem. A* **2004**, *108*, 8546-8548, doi:10.1021/jp036519+.

Worsnop, D. R.; Zahniser, M. S.; Kolb, C. E.; Gardner, J. A.; Watson, L. R.; Doren, J. M. V.; Jayne, J. T.; Davidovits, P. Temperature dependence of mass accommodation of SO_2 and H_2O_2 on aqueous surfaces. *J. Phys. Chem.* **1989**, *93*, 1159-1172, doi:10.1021/j100340a027.

Zhang, H. Z.; Li, Y. Q.; Davidovits, P.; R., W. L.; Jayne, J. T.; Kolb, C. E.; Worsnop, D. R. Uptake of gas-phase species by 1-octanol. 2. Uptake of hydrogen halides and acetic acid as a function of relative humidity and temperature. *J. Phys. Chem. A* **2003**, *107*, 6398-6407, doi:10.1021/jp034254t.

Zhang, R.; Wooldridge, P. J.; Molina, M. J. Vapor pressure measurements for the $H_2SO_4/HNO_3/H_2O$ and $H_2SO_4/HCl/H_2O$ systems: Incorporation of stratospheric acids into background sulfate aerosols. *J. Phys. Chem.* **1993**, *97*, 8541-8548, doi:10.1021/j100134a026.

Zientara, M.; Jakubcyzk, D.; Derkachov, G.; Kolwas, K.; Kolwas, M. Simultaneous determination of mass and thermal accommodation coefficients from temporal evolution of an evaporating water microdroplet. *J. Phys. D: Applied Phys.* **2005**, *38*, 1978-1983, doi:10.1088/0022-3727/38/12/018.

Zientara, M.; Jakubczyk, D.; Kolwas, K.; Kolwas, M. Temperature dependence of the evaporation coefficient of water in air and nitrogen under atmospheric pressure: Study in water droplets. *J. Phys. Chem. A* **2008**, *112*, 5152-5158, doi:10.1021/jp7114324.

Zimmermann, S.; Kippenberger, M.; Schuster, G.; Crowley, J. N. Adsorption isotherms for hydrogen chloride (HCl) on ice surfaces between 190 and 220 K. *Phys. Chem. Chem. Phys.* **2016**, *18*, 13799-13810, doi:10.1039/c6cp01962e.

Zondlo, M. A.; Barone, S. B.; Tolbert, M. A. Uptake of HNO_3 on ice under upper tropospheric conditions. *Geophys. Res. Lett.* **1997**, *24*, 1391-1394, doi:10.1029/97GL01287.

5.2.3 Table NEq2. Gas/Surface Reaction Probabilities (γ) for Surfaces Other Than Soot

Gaseous Species	Surface Type	Surface Composition	T (K)	γ	Uncertainty Factor	Note
O_3 + Surface → Products						
O_3	Water Ice	H_2O(s)	223–258	$<10^{-8}$		1
	Alumina	α-Al_2O_3(s), γ-Al_2O_3(s)	210–300	$\gamma_o<2\times10^{-4}$		2
	Sodium Chloride	NaCl(s)	223–300	$\gamma_o<10^{-4}$		3
		NaCl(aq)	298	$\gamma_o<10^{-4}$		3
	Sodium Bromide	NaBr(s)	300	$\gamma_o<10^{-4}$		4
		NaBr(aq)	298	See Note		4
	Potassium Bromide	KBr(s)	300	$\gamma_o<10^{-4}$		4
	Potassium Iodide	KI(s)	~298	See Note		5
	Sea Salt	See Note	300	$\gamma_o<2\times10^{-2}$		6
	Organic Surfaces	See Note	298	See Note		7
OH + Surface → Products						
OH	Water Ice	H_2O(s)	205–230	>0.01		8
	Hydrochloric Acid	HCl•nH_2O(l)	220	>0.2		9
	Nitric Acid Ice	HNO_3•3H_2O(s)	200–228	>0.2		10
	Sulfuric Acid	H_2SO_4•nH_2O(l)	200–298	>0.2	3	11
	Sodium Chloride	NaCl(s)	245–300	$\gamma_o\sim10^{-2}$		12
		NaCl(aq)	298	≥0.1		12
	Alumina	Al_2O_3(s)	250–300	$\gamma_o<0.1$		13
	Organic Surfaces	See Note	298	$\gamma_o>0.1$		14
HO_2 + Surface → Products						
HO_2	Water Ice	H_2O(s)	223	0.025	3	15
	Sulfuric Acid	H_2SO_4•nH_2O(l)		See Note		15
		(28 wt%)	275			
		(47–50 wt%)	293			
		(55 wt%)	223			
		(80–96 wt%)	243	≤0.1		15
	Aqueous Salt	$(NH_4)_2SO_4$(aq) and NaCl(aq)	298	See Note		16
	Sodium Chloride	NaCl(s)	245–300	See Note		17
	Potassium Chloride	KCl(s)	295			
	Ammonium Sulfate	$(NH_4)_2SO_4$(s)	298	See Note		18
	Organic Aerosol	Organic	298	See Note		19
	Mineral Dust	See Note	298	See Note		20
H_2O + Surface → Products						
H_2O	Alumina	α-Al_2O_3(s)	295–300	$\gamma_o<0.2$		21
H_2O_2 + Surface → Products						
H_2O_2	Alumina	α-Al_2O_3(s), γ-Al_2O_3(s)	268-320	$\gamma_o<5\times10^{-3}$		22
$2NO_2 + H_2O(l) \rightarrow HONO + HNO_3$						
NO_2	Liquid Water	H_2O(l)	270–295	$<1\times10^{-2}$		23
	Sulfuric Acid	H_2SO_4•nH_2O (40–98 wt%)	250–325	5×10^{-7}	3	24
	Alumina	γ-Al_2O_3(s)	298	$\gamma_o<1\times10^{-7}$		25
		α-Al_2O_3(s)	298	$\gamma_o<5\times10^{-5}$		25
$2NO_2$ (N_2O_4) + MX → Products						
NO_2/N_2O_4	Sodium Chloride	NaCl(s)	298	See Note		26
		NaCl(aq)	298	$<1\times10^{-4}$		26
	Sodium Bromide	NaBr(s)	298	See Note		27
	Sea Salt	See Note for O_3 + Sea Salt	298	See Note		28
$NO_3 + H_2O \rightarrow HNO_3 + OH$						
NO_3	Water Ice	H_2O(s)	170–200	$<10^{-3}$		29
	Liquid Water	H_2O(l)	273	$\geq2\times10^{-3}$		30

Gaseous Species	Surface Type	Surface Composition	T (K)	γ	Uncertainty Factor	Note
NO_3 + NaX → Products						
NO_3	Sodium Chloride	NaCl(s)	293	γ_o <6×10^{-2}		31
		NaCl(aq)	273–293	See Note		31
	Sodium Bromide	NaBr(s)	293	γ_o=0.2±0.1	2	32
		NaBr(aq)	273	See Note		32
	Sodium Iodide	NaI(aq)	273	See Note		32
NO_3 + Organic Surfaces → Products						
NO_3	Organic Surfaces	See Note	298	See Note		33
N_2O_5 + H_2O → $2HNO_3$						
N_2O_5	Water Ice	H_2O(s)	188–195	0.02	2	34
	Liquid Water/Solutions	H_2O(l)/$(NH_4)_2SO_4$(aq)	260–295	See Note	See Note	35
	Nitric Acid Ice	HNO_3•$3H_2O$(s)	200	4×10^{-4}	3	36
	Sulfuric Acid	H_2SO_4•nH_2O(l)	195–300	See Note*	See Note	37
	Ternary Acid	H_2SO_4•$nHNO_3$ •nH_2O(l)	195–218	See Note		37
	Sulfuric Acid Monohydrate	H_2SO_4•H_2O(s)	200–300	See Note	3	38
	Sulfuric Acid Tetrahydrate	H_2SO_4•$4H_2O$(s)	195–207	0.006	2	39
	Mineral Dust	See Note	298	See Note		40
N_2O_5 + HCl → $ClNO_2$ + HNO_3						
N_2O_5	Water Ice	H_2O(s)•HCl(s)	190–220	0.03	See Note	41
	Nitric Acid Ice	HNO_3•$3H_2O$(s)•HCl(s)	200	0.003	2	42
	Sulfuric Acid Monohydrate	H_2SO_4•H_2O(s)	195	<1×10^{-4}		43
N_2O_5 + HBr → $BrNO_2$ + HNO_3						
N_2O_5	Water Ice	H_2O	180–200	See Note		44
	Nitric Acid Ice	HNO_3•$3H_2O$(s)	200	0.005	10	45
N_2O_5 + MX → Products						
N_2O_5	Sodium Chloride	NaCl(s)	295	γ_o <5×10^{-3}		46
		NaCl(aq)	262–291	γ_o <0.05		46
	Potassium Bromide	KBr(s)	298	γ_o <5×10^{-3}		47
	Sodium Bromide	NaBr(aq)	270–277	γ_o <0.05		47
	Sodium Iodide	NaI(aq)	262–278	γ_o <0.05		47
	Sea Salt	See Note for O_3 + Sea Salt	295	See Note		48
HONO + H_2O → Products						
HONO	Liquid Water	H_2O(l)	245–295	0.03	5	49
HONO + H_2SO_4 → Products						
HONO	Sulfuric Acid	H_2SO_4•nH_2O(l)	180–200	See Note		50
HONO + HCl → ClNO + H_2O						
HONO	Water Ice	H_2O(s)	180–200	0.05	3	51
	Sulfuric Acid	H_2SO_4•nH_2O(l)		See Note	See Note	52
HONO + HBr → BrNO + H_2O						
HONO	Water Ice	H_2O(s)	180–200	See Note		53
HONO + NaCl → Products						
HONO	Sodium Chloride	NaCl(s)	~300	<1×10^{-4}		54
HONO + Al_2O_3(s) → Products						
HONO	Alumina	γ-Al_2O_3(s)	274-320	See Note		55
HNO_3 + NaX(s) → HX + $NaNO_3$						
HNO_3	Sodium Chloride	NaCl(s)	295–298	γ_o = 2×10^{-3}	2	56
		NaCl(aq)	298	γ_o >0.2		56
	Sodium Bromide	NaBr(s)	298	γ_o <3×10^{-2}		57
	Potassium Bromide	KBr(s)	298	γ_o <3×10^{-2}		57
	Sea Salt	See Note for O_3 + Sea Salt	298	γ_o = 0.5	3	58

Gaseous Species	Surface Type	Surface Composition	T (K)	γ	Uncertainty Factor	Note
$HNO_3 + Al_2O_3(s) \rightarrow$ Products						
HNO_3	Alumina	α-$Al_2O_3(s)$	295–300	γ_o <0.2		59
$HO_2NO_2 + HCl \rightarrow$ Products						
HO_2NO_2	Sulfuric Acid	$H_2SO_4 \cdot nH_2O$ (50–75 wt%)	200–225	$<1\times10^{-4}$		60
$NH_3 + H_2SO_4 \rightarrow NH_4HSO_4$						
NH_3	Sulfuric Acid	$H_2SO_4 \cdot nH_2O$ <50 wt% 50-70 wt%	 260–300 260–300	 See Note 1.0	 1.2	61
$CO_2 + Al_2O_3(s) \rightarrow$ Products						
CO_2	Alumina	γ-$Al_2O_3(s)$	290-300	See Note		62
$H_2CO + Al_2O_3 \rightarrow$ Products						
H_2CO	Alumina	α-$Al_2O_3(s)$, γ-$Al_2O_3(s)$	270–300	γ_o $<5\times10^{-4}$		63
$CH_3OH + H_2SO_4$ and $H_2SO_4 + HNO_3 \rightarrow$ Products						
CH_3OH	Sulfuric Acid Ternary Acid	$H_2SO_4 \cdot nH_2O$ $H_2SO_4 \cdot mHNO_3 \cdot nH_2O$	293 283–329	See Note See Note		64 64
$CH_3OH + Al_2O_3 \rightarrow$ Products						
CH_3OH	Alumina	γ-$Al_2O_3(s)$	290–300	γ_o $<3\times10^{-4}$		65
$HC(O)OH + Al_2O_3 \rightarrow$ Products						
$HC(O)OH$	Alumina	α-$Al_2O_3(s)$ γ-$Al_2O_3(s)$	240-298 298	γ_o <0.01 See Note		66 66
$CH_3CH_2OH + H_2SO_4 \cdot nH_2O \rightarrow$ Products						
CH_3CH_2OH	Sulfuric Acid	$H_2SO_4 \cdot nH_2O(l)$	193–273	See Note		67
$CH_3C(O)OH + Al_2O_3 \rightarrow$ Products						
$CH_3C(O)OH$	Alumina	α-$Al_2O_3(s)$	290–310	γ_o <0.02		68
$CH_3CHO + H_2SO_4 \cdot nH_2O \rightarrow$ Products						
CH_3CHO	Sulfuric Acid	$H_2SO_4 \cdot nH_2O(l)$	211–298	See Note		69
$CH_3CHO + Al_2O_3 \rightarrow$ Products						
CH_3CHO	Alumina	α-$Al_2O_3(s)$	290–300	γ_o $>1.5\times10^{-5}$		70
$CH_3CH_2CHO + Al_2O_3 \rightarrow$ Products						
CH_3CH_2CHO	Alumina	α-$Al_2O_3(s)$	290–300	γ_o $>2.5\times10^{-5}$		70
$CH_3C(O)CH_3 + H_2SO_4 \cdot nH_2O \rightarrow$ Products						
$CH_3C(O)CH_3$	Sulfuric Acid	$H_2SO_4 \cdot nH_2O$	198–298	See Note		71
$CH_3C(O)CH_3 + Al_2O_3 \rightarrow$ Products						
$CH_3C(O)CH_3$	Alumina	α-$Al_2O_3(s)$	290–300	γ_o $>1.5\times10^{-5}$		70
$CH_3C(O)O_2 + H_2O \rightarrow CH_3C(O)OH + HO_2$						
$CH_3C(O)O_2$	Liquid Water Sulfuric Acid (84 wt% H_2SO_4) (51 wt% H_2SO_4) (71 wt% H_2SO_4)	$H_2O(l)$ $H_2SO_4 \cdot nH_2O$ 	225 246 223 298	4×10^{-3} 3×10^{-3} 1×10^{-3} 1×10^{-3}	3 3 3 3	72 72
$H_2C=C(CH_3)CHO$ and $H_2C=CHC(O)CH_3 + Al_2O_3 \rightarrow$ Products						
$H_2C=C(CH_3)CHO$	Alumina	α-$Al_2O_3(s)$	~300	See Note		73
$H_2C=CHC(O)CH_3$	Alumina	α-$Al_2O_3(s)$	~300	See Note		73
$CH_3C(O)O_2NO_2$ + (HCl, Cl, ClO, and OClO) + $H_2SO_4 \cdot nH_2O \rightarrow$ Products						
$CH_3C(O)O_2NO_2$	Sulfuric Acid	$H_2SO_4 \cdot nH_2O$ (40–70 wt%)	200–225	$<1\times10^{-4}$		74

Gaseous Species	Surface Type	Surface Composition	T (K)	γ	Uncertainty Factor	Note
Trans-β-isoprene epoxydiol						
	Sulfate Aerosol	NH3HSO4(aq)	298	See Note		75
Cl + Surface →Products						
Cl	Sulfuric Acid	H_2SO_4•nH_2O(l)	221–296	2×10^{-4}	10	76
	Sodium Chloride	NaCl(s)	298	See Note		77
Cl_2 + HBr → BrCl + HCl						
Cl_2/HBr	Water Ice	H_2O(s)	200	>0.2		78
Cl_2 + MX → Products						
Cl_2	Sodium Chloride	NaCl(s)	298	$\gamma_o < 1\times10^{-3}$		79
	Sodium Bromide	NaBr(s)	298	$0.02 < \gamma_o < 0.2$		80
		NaBr(aq)	263–293	$\gamma_o < 0.3$		80
	Sodium Iodide	NaI(aq)	263–293	$\gamma_o < 0.3$		80
	Potassium Bromide	KBr(s)	298	$0.02 < \gamma_o < 0.2$		81
	Sea Salt	See Note for O_3 + Sea Salt	298	See Note		82
ClO + Surface → Products						
ClO	Water Ice	H_2O(s)	183–213	$<10^{-4}$		83
	Nitric Acid Ice	HNO_3•3H_2O(s)	183	See Note		83
	Sulfuric Acid	H_2SO_4•nH_2O(l) (60 to 95 wt% H_2SO_4)	221–296	See Note		84
HCl + HNO_3 → Products						
HCl + HNO_3	Sulfuric Acid	H_2SO_4•mHNO_3•nH_2O(l)		See Note	See Note	85
HOCl + HCl → Cl_2 + H_2O						
HOCl/HCl	Water Ice	H_2O(s)•HCl(s)	195–200	0.2	2	86
	Nitric Acid Ice	HNO_3•3H_2O(s)•HCl(s)	195–200	0.1	2	86
	Sulfuric Acid	H_2SO_4•nH_2O(l)	198–209	See Note	See Note	87
HOCl + HBr → BrCl + H_2O						
HOCl/HBr	Water Ice	H_2O(s)	189–220	See Note		88
	Sulfuric Acid	H_2SO_4•nH_2O(l)	228	See Note	See Note	89
HOCl + NaBr and KBr → Products						
HOCl	Sodium Bromide	NaBr(aq) Ice	233	0.03	3	90
	Potassium Bromide	KBr(s)	300	$\gamma_o > 5\times10^{-3}$		90
ClNO + Surface → Products						
ClNO	Liquid Water	H_2O(l)	270–295	$\geq 4\times10^{-3}$*		91
	Sodium Chloride	NaCl(s)	298	$<1\times10^{-5}$		92
$ClNO_2$ + H_2O → Products						
$ClNO_2$	Liquid Water	H_2O(l)	275–295	4×10^{-6}	2	93
$ClNO_2$ + MX → Products						
$ClNO_2$	Potassium Bromide	KBr(s)	300	1×10^{-4}	2	94
	Sodium Chloride	NaCl(aq)	291	See Note		94
	Sodium Bromide	NaBr(aq)	275–293	See Note		94
	Sodium Iodide	NaI(aq)	275–293	See Note		94
$ClONO_2$ + H_2O → HOCl + HNO_3						
$ClONO_2$	Water Ice	H_2O(s)	180–200	0.3	3	95
	Liquid Water	H_2O(l)	270-290	2.5×10^{-2}	4	96
	Nitric Acid Ice	HNO_3•3H_2O(s)	200–202	0.004	3	97
	Sulfuric Acid	H_2SO_4•nH_2O(l)	200–265	See Note*	See Note	98
	Sulfuric Acid Monohydrate	H_2SO_4•H_2O(s)	195	$<1\times10^{-3}$		99
	Sulfuric Acid Tetrahydrate	H_2SO_4•4H_2O(s)	196–206	See Note*		99

Gaseous Species	Surface Type	Surface Composition	T (K)	γ	Uncertainty Factor	Note
$ClONO_2 + HCl \rightarrow Cl_2 + HNO_3$						
$ClONO_2$/HCl	Water Ice	H_2O(s)	180–200	0.3	2	100
	Nitric Acid Ice	$HNO_3 \cdot 3H_2O \cdot HCl$	185–210	0.2	2	101
	Sulfuric Acid	$H_2SO_4 \cdot nH_2O$(l)•HCl(l)	195–235	See Note	See Note	102
	Sulfuric Acid Monohydrate	$H_2SO_4 \cdot H_2O$(s)	195	$<1\times10^{-4}$		103
	Sulfuric Acid Tetrahydrate	$H_2SO_4 \cdot 4H_2O$(s)	195–206	See Note		103
	Alumina	α-Al_2O_3(s)	195–230	0.02	3	104
$ClONO_2 + MX \rightarrow$ Products						
$ClONO_2$	Sodium Chloride	NaCl(s)	295	$0.005<\gamma_o<0.2$		105
		NaCl(aq)	272–280	See Note		105
	Potassium Bromide	KBr(s)	298	>0.1		106
	Sodium Bromide	NaBr(aq)	272–280	See Note		106
	Sea Salt	See Note for O_3 + Sea Salt	298	>0.1		107
$ClONO_2 + HBr \rightarrow BrCl + HNO_3$						
$ClONO_2$/HBr	Water Ice	H_2O(s)•HBr(s)	200	>0.3		108
	Nitric Acid Ice	$HNO_3 \cdot 3H_2O$(s)•HBr(s)	200	>0.3		108
$ClONO_2 + HF \rightarrow$ Products						
$ClONO_2$/HF	Water Ice	H_2O(s)•HF(s)	200	See Note		109
	Nitric Acid Ice	H_2O(s)•HNO_3(s)•HF(s)	200	See Note		109
$CF_xCl_y + Al_2O_3 \rightarrow$ Products						
CCl_4	Alumina	γ-Al_2O_3(s)	120–300	1×10^{-5}	10	110
$CFCl_3$	Alumina	γ-Al_2O_3(s)	120–300	1×10^{-5}	10	110
CF_2Cl_2	Alumina	α-Al_2O_3(s), γ-Al_2O_3(s)	120–300	1×10^{-5}	10	110
CF_3Cl	Alumina	γ-Al_2O_3(s)	120–300	1×10^{-5}	10	110
BrCl + MX → Products						
BrCl	Sodium Chloride	NaCl(s)	298	See Note		111
	Potassium Bromide	KBr(s)	298	See Note		111
	Sodium Iodide	NaI(aq)	273–288	See Note		111
	Alkali Bromides	MBr(aq) Ice	233	0.03	3	111
$Br_2 + MX \rightarrow$ Products						
Br_2	Sodium Chloride	NaCl(s)	298	See Note		112
	Potassium Bromide	KBr(s)	298	See Note		112
	Sodium Iodide	NaI(aq)	263–293	γ_o <0.5		112
$2BrO \rightarrow Br_2 + O_2$						
BrO	Water Ice	H_2O(s)	213	$<1\times10^{-3}$	3	113
	Sulfuric Acid	$H_2SO_4 \cdot nH_2O$				
		(60 wt% H_2SO_4)	213	7×10^{-4}	3	113
		(70 wt% H_2SO_4)	213	5×10^{-4}	3	113
	Aqueous Sodium Chloride	NaCl(aq) (23 wt% NaCl)	253	$<10^{-3}$		113
$HOBr + H_2SO_4 \cdot nH_2O \rightarrow$ Products						
HOBr	Sulfuric Acid	$H_2SO_4 \cdot nH_2O$	201–270	See Note		114
$HOBr + HCl \rightarrow BrCl + H_2O$						
HOBr/HCl	Water Ice	H_2O(s)•HCl(s)	180–228	0.3	3	115
	Sulfuric Acid	$H_2SO_4 \cdot nH_2O$ (60–69 wt% H_2SO_4)	198–218	See Note		116
$HOBr + HBr \rightarrow Br_2 + H_2O$						
HOBr/HBr	Water Ice	H_2O(s)•HBr(s)	180–228	>0.1		117
	Sulfuric Acid	$H_2SO_4 \cdot nH_2O$	228	See Note		117

Gaseous Species	Surface Type	Surface Composition	T (K)	γ	Uncertainty Factor	Note
HOBr + MX → Products						
HOBr	Sodium Chloride	NaCl(s)	298	γ_o <10^{-2}		118
		NaCl(aq)	298	γ_o >0.2		118
		NaCl → NaCl(aq) Ice	~238	See Note		119
	Alkali Bromides	KBr(s)	298	γ_o ≤0.2		119
		NaBr(s)	250	See Note		119
		NaBr(aq)	298	γ_o = 0.6	1.5	119
		NaBr → NaBr(aq) Ice	~233	See Note		119
$BrNO_2$ + H_2O → Products						
$BrNO_2$	Liquid Water	H_2O(l)	275–300	2×10^{-6}	2	120
$BrNO_2$ + MX → Products						
$BrNO_2$	Potassium Chloride	KCl(s)	298	See Note		121
	Sodium Chloride	NaCl(aq)	277–293	γ_o >10^{-6}		121
	Potassium Bromide	KBr(s)	298	γ_o >0.1		122
	Sodium Bromide	NaBr(aq)	277–293	See Note		122
	Sodium Iodide	NaI(aq)	262–278	See Note		122
$BrONO_2$ + H_2O → HOBr + HNO_3						
$BrONO_2$	Water Ice	H_2O(s)	190–200	>0.2		123
	Liquid Water	H_2O(l)	270–280	3×10^{-2}	4	124
	Sulfuric Acid	H_2SO_4•nH_2O	210–300	See Note		125
$BrONO_2$ + HCl → BrCl + HNO_3						
$BrONO_2$/HCl	Water Ice	H_2O(s)	200	See Note		123
	Sulfuric Acid	H_2SO_4•nH_2O	229	0.9	2	125
$BrONO_2$ + HBr						
$BrONO_2$/HBr	Water Ice	H_2O(s)	180–210	γ_o >0.1		126
$BrONO_2$ + MX → Products						
$BrONO_2$	Sodium Chloride	NaCl(s)	298	γ_o >0.2		127
		NaCl(aq)	278–280	See Note		127
	Potassium Bromide	KBr(s)	298	γ_o >0.2		128
	Sodium Bromide	NaBr(aq)	272–280	See Note		128
ICl + NaCl and NaBr → Products						
	Sodium Chloride	NaCl(aq)	274–298	See Note		129
	Sodium Bromide	NaBr(aq)	274–298	See Note		129
HOI + NaCl and NaBr → Products						
HOI	Sodium Chloride	NaCl(s)	243–298	>0.01		130
		NaCl(aq)	274	>2×10^{-3}		130
	Sodium Bromide	NaBr(s)	243–298	>0.01		130
		NaBr(aq)	274	>2×10^{-3}		130
CF_2Br_2 + Al_2O_3 → Products						
CF_2Br_2	Alumina	α-Al_2O_3(s)	210, 315	2×10^{-5}	10	110
CF_3OH + H_2O → Products						
CF_3OH	Water Ice	H_2O(l)	274	>0.01		131
	Sulfuric Acid	H_2SO_4•nH_2O				
		(40 wt% H_2SO_4)	210–250	0.07	3	131
		(45 wt% H_2SO_4)	210–250	0.04	3	131
		(50 wt% H_2SO_4)	210–250	0.01	3	131
		(50 wt% H_2SO_4)	210–250	0.001	3	131
SO_2 + O_3 → Products						
SO_2/O_3		α-Al_2O_3(s), Al_2O_3(s)	See Note	See Note		132

Gaseous Species	Surface Type	Surface Composition	T (K)	γ	Uncertainty Factor	Note
$SO_2 + H_2O(s) \rightarrow$ Products						
SO_2	Water Ice	$HOOH/H_2O(s)$	200–228	See Note		133
$SO_2 + H_2O_2, O_3, HONO, NO_2$ and $HNO_3 \rightarrow$ Products						
SO_2/H_2O_2, etc.	Sulfuric Acid	$H_2SO_4 \cdot nH_2O$ (20–60 wt% H_2SO_4)	293	See Note		134
$SO_2 + Al_2O_3 \rightarrow$ Products						
SO_2	Alumina	α-$Al_2O_3(s)$, γ-$Al_2O_3(s)$	295–300	$\gamma_o > 5\times10^{-5}$ (α-alumina) $\gamma_o > 1\times10^{-3}$ (γ-alumina)		135 135
$SO_2 + MX \rightarrow$ Products						
SO_2	Sodium Chloride	NaCl(s)	298	$\gamma_o < 1\times10^{-4}$		136
	Sea Salt	See Note for O_3 + Sea Salt	298	$\gamma_o < 0.1$		136
$SO_3 + H_2O \rightarrow$ Products						
SO_3	Sulfuric Acid	$H_2SO_4 \cdot nH_2O$ (78–92 wt% H_2SO_4)	300	1.0	+0.0, –0.3	137
$OCS + Al_2O_3 \rightarrow$ Products						
OCS	Alumina	α-$Al_2O_3(s)$, γ-$Al_2O_3(s)$	298	See Note		138

*γ is temperature dependent

5.2.3.1 Notes for Table NEq2

1. **O_3 on H_2O(s).** Ozone loss on pure ice is highly inefficient, with uptake coefficients in the range of 10^{-8} to 10^{-9} for partial pressures between 2×10^{-8} and 10^{-6} atm at 223 and 258 K, as measured in an ice-coated column. The uptake coefficients are dependent on the ozone partial pressure, increasing at low partial pressures Langenberg et al.[1]
Back to Table

(1) Langenberg, S.; Schurath, U. Ozone destruction on ice. *Geophys. Res. Lett.* **1999**, *26*, 1695-1698, doi:10.1029/1999GL900325.

2. **O_3 + Al_2O_3(s).** Very low ozone decomposition efficiencies for reaction on coarse (3 μm dia.) and fine (0.1 μm dia., partially hydroxylated) γ-alumina and coarse (3 μm dia.) α-alumina were measured in flowing and static systems by Hanning-Lee et al.[3] at temperatures ranging between 212 and 473 K. Based on measured BET surface areas, γs ranged from 2×10^{-11} to 4×10^{-10} over the 212 to 298 K temperature range. γs for γ-alumina at lower temperatures exceeded those for α-alumina. Results are roughly consistent with earlier, unpublished flow tube data from L. F. Keyser and from fluidized bed reactor studies of Alebić-Juretić et al.[1] Note that γs based on geometric surface particle surface areas would be significantly (10^4–10^7) larger. Additional fluidized bed reactor studies by Alebić-Juretić et al.[2] demonstrated that room temperature uptake are initially first order in O_3, but change to a slower second order reaction at longer exposure times. Klimovskii et al.[4] reported an initial uptake coefficient (γ_o) of 1×10^{-4} on a γ-alumina surface at 293 K assuming a geometric surface area, BET surface correction presumably would have yielded a lower value. Michel et al.[5,6] reported Knudsen cell uptake studies at 296 K on α-alumina particles that yielded γ_o values of $(8 \pm 5) \times 10^{-5}$ and $(1.4 \pm 0.3) \times 10^{-4}$ after BET surface area corrections. Sullivan et al.[9] used a coated wall flow reactor to obtain 298 K γ_o values of 7×10^{-6} to 1.6×10^{-5} for α-alumina powder films exposed to no more than [O_3] of 10^{13} cm^{-3} after BET surface area correction. Higher [O_3] yielded lower apparent γ_os. Usher et al.[10] demonstrated the pretreatment of α-alumina with HNO_3 vapor reduced O_3 Knudsen cell γ_o values by ~70%. Mogili et al.[7]measured O_3 uptake on α-alumina particles in a room temperature environmental chamber obtaining an uptake coefficient of $(3.5 \pm 0.9) \times 10^{-8}$ for dry (RH ≤1%) particles that fell to $(4.5 \pm 1.1) \times 10^{-9}$ for measurements at 19% RH. Roscoe and Abbatt[8] demonstrated spectroscopically that there is a competition for surface sites when gas phase ozone and water vapor are exposed to the alumina surface.
Back to Table

(1) Alebić-Juretić, A.; Cvitas, T.; Klasinc, L. Ozone destruction on powders. *Ber. Bunsenges Phys. Chem.* **1992**, *96*, 493-495, doi:10.1002/bbpc.19920960352.
(2) Alebić-Juretić, A.; Cvitas, T.; Klasinc, L. Kinetics of heterogeneous ozone reactions. *Chemosphere* **2000**, *41*, 667-670, doi:10.1016/S0045-6535(99)00485-3.
(3) Hanning-Lee, M. A.; Brady, B. B.; Martin, L. R.; Syage, J. A. Ozone decomposition on alumina: Implications for solid rocket motor exhaust. *Geophys. Res. Lett.* **1996**, *23*, 1961-1964, doi:10.1029/96GL01808.
(4) Klimovskii, A. O.; Bavin, A. V.; Tkalich, V. S.; Lisachenko, A. A. Interaction of ozone with γ-Al_2O_3 surface. *React. Kinet. Catal. Lett.* **1983**, *23*, 95-98, doi:10.1007/BF02065670.
(5) Michel, A. E.; Usher, C. R.; Grassian, V. H. Heterogeneous and catalytic uptake of ozone on mineral oxides and dusts: A Knudsen cell investigation. *Geophys. Res. Lett.* **2002**, *29*, 1665, doi:1029/2002/GL014896.
(6) Michel, A. E.; Usher, C. R.; Grassian, V. H. Reactive uptake of ozone on mineral oxides and mineral dusts. *Atmos. Environ.* **2003**, *37*, 3201-3211, doi:10.1016/S1352-2310(03)00319-4.
(7) Mogili, P. K.; Kleiber, P. D.; Young, M. A.; Grassian, V. H. Heterogeneous uptake of ozone on reactive components of mineral dust aerosol: An environmental aerosol reaction chamber study. *J. Phys. Chem. A* **2006**, *110*, 13799-13807, doi:10.1021/jp063620g.
(8) Roscoe, J. M.; Abbatt, J. P. D. Diffuse reflectance FTIR study of the interaction of alumina surfaces with ozone and water vapor. *J. Phys. Chem. A* **2005**, *109*, 9028-9034, doi:10.1021/jp050766r.
(9) Sullivan, R. C.; Thornberry, T.; Abbatt, J. P. D. Ozone decomposition kinetics on alumina: effects of ozone partial pressure, relative humidity and repeated oxidation cycles. *Atmos. Chem. Phys.* **2004**, *4*, 1301-1310, doi:10.5194/acp-4-1301-2004.
(10) Usher, C. R.; Michel, A. E.; Stec, D.; Grassian, V. H. Laboratory studies of ozone uptake on processed mineral dust. *Atmos. Environ.* **2003**, *37*, 5337-5347, doi:10.1016/j.atmosenv.2003.09.014.

3. **O_3 + NaCl.** The reaction of O_3 with NaCl is slow. Il'in et al.[3] measured the loss of O_3 in a coated reactor over the temperature range 223–305 K, and found the same uptake coefficients, $\gamma \sim 10^{-6}$, independent of temperature, for NaCl and NH_4NO_3 and $(NH_4)_2SO_4$, suggesting that even the small uptake is not due to reaction with the chloride. Alebić-Juretić[2] did not observe any uptake on NaCl powders using a fluidized bed reactor but did not report an upper limit to the uptake coefficient. Akimoto and coworkers[6,7] reported an upper limit of $\gamma_o < 1 \times 10^{-5}$ on NaCl. When the NaCl was mixed with 0.5–1% w:w $FeCl_3$, γ_0 increased to 3×10^{-2} and production of gaseous Cl_2 was observed with yields from 25–50% of the ozone taken up. With 0.1% $FeCl_3$, no production of Cl_2 was observed but the initial uptake coefficient was still 3×10^{-2}. These experiments were carried out with a Knudsen cell using multiple salt layers and the measured initial uptake coefficients were converted to the reported values using the pore diffusion model of Keyser et al.[4,5]
Abbatt and Waschewsky[1] followed O_3 in a flow tube containing deliquesced 1–5 μm NaCl particles (75% RH); no significant loss was observed on unbuffered particles or particles buffered at pH of 7.2. An upper limit of $\gamma_o < 1 \times 10^{-4}$ was derived from these measurements.
Back to Table

(1) Abbatt, J. P. D.; Waschewsky, G. C. G. Heterogeneous interactions of HOBr, HNO_3, O_3, and NO_2 with deliquescent NaCl aerosols at room temperature. *J. Phys. Chem. A* **1998**, *102*, 3719-3725, doi:10.1021/jp980932d.

(2) Alebić-Juretić, A.; Cvitas, T.; Klasinc, L. Ozone destruction on powders. *Ber. Bunsenges Phys. Chem.* **1992**, *96*, 493-495, doi:10.1002/bbpc.19920960352.

(3) Il'in, S. D.; Selikhonovich, V. V.; Gershenson, Y. M.; Rozenshtein, V. B. Study of heterogeneous ozone loss on materials typical of atmospheric aerosol species. *Sov. J. Chem. Phys.* **1991**, *8*, 1858-1880.

(4) Keyser, L. F.; Leu, M.-T.; Moore, S. B. Comment on porosities of ice films used to simulate stratospheric cloud surfaces. *J. Phys. Chem.* **1993**, *97*, 2800-2801, doi:10.1021/j100113a053.

(5) Keyser, L. F.; Moore, S. B.; Leu, M. T. Surface reaction and pore diffusion in flow tube reactors. *J. Phys. Chem.* **1991**, *95*, 5496-5502, doi:10.1021/j100167a026.

(6) Mochida, M.; Hirokawa, J.; Akimoto, H. Unexpected large uptake of O_3 on sea salts and the observed Br_2 formation. *Geophys. Res. Lett.* **2000**, *27*, 2629-2632, doi:10.1029/1999GL010927.

(7) Sandanaga, Y.; Hirokawa, J.; Akimoto, H. Formation of molecular chlorine in dark condition: Heterogeneous reaction of ozone with sea salt in the presence of ferric ion. *Geophys. Res. Lett.* **2001**, *28*, 4433-4436, doi:10.1029/2001GL013722.

4. **O_3 + NaBr and KBr.** Mochida et al.[6] did not observe any uptake of O_3 on NaBr or KBr powders, from which they derived an upper limit of $\gamma < 1 \times 10^{-5}$. Hirokawa et al.[3] reported production of gas phase Br_2 from the reaction of O_3 with NaBr only when water vapor was added so that the salt was near deliquescence.

Uptake of O_3 and production of gas phase Br_2 has been observed for deliquesced NaBr salt on a glass surface.[1] Production of Br_2 has also been measured by Hunt et al.[4] in the reaction of O_3 with deliquesced NaBr particles in the dark in an aerosol chamber; the production of Br_2 exceeded that from known aqueous phase chemistry by about an order of magnitude, suggesting that a surface reaction of O_3 with bromide at the air-solution interface was occurring with a reaction probability of $\gamma_0 = (1.9 \pm 0.8) \times 10^{-6}$ (2σ).

The uptake of O_3 by frozen salt solutions and cold liquid solutions containing bromide have been studied in a coated wall flow tube from 233 to 273 K by Oldridge and Abbatt.[7] Br_2 was the sole product formed. Reaction kinetics were well described by a combination of a bulk reaction in the associated solution and a surface reaction component, so that the overall ozone uptake coefficients increased with decreasing ozone concentrations. The similarity between the results on both liquid solutions and frozen solutions implied the reaction was occurring only with the liquid component of the substrates. The simultaneous occurrence of significant reactivity within sodium bromide solutions and at their surfaces has been confirmed by Artiglia et al.[2] As well, this study identified for the first time the presence of an ozonide reaction intermediate that is formed at the gas-aqueous interface at the first stage of the reaction between ozone and bromide ions. The efficiency of this oxidation reaction was shown by Lee et al.[5] to be increased by the presence of dissolved citric acid, perhaps due to the stronger partitioning of ozone into an organic substrate than to water.

Using glancing angle LIF and Raman spectroscopy, Wren et al.[8] have studied the reactions of ozone with both frozen and unfrozen bromide solutions with sea water concentrations. They demonstrate that the kinetics proceed one to two orders of magnitude faster on the frozen substrates than on the corresponding unfrozen solutions.

Back to Table

(1) Anastasio, C.; Mozurkewich, M. Laboratory studies of bromide oxidation in the presence of ozone: Evidence for a glass-surface mediated reaction. *J. Atmos. Chem.* **2002**, *41*, 135-162, doi:10.1023/A:1014286326984.
(2) Artiglia, L.; Edebeli, J.; Orlando, F.; Chen, S.; Lee, M.-T.; Arroyo, P. C.; Gilgen, A.; Bartels-Rausch, T.; Kleibert, A.; Vazdar, M.; Carignano, M. A.; Francisco, J. S.; Shepson, P. B.; Gladich, I.; Ammann, M. A surface-stabilized ozonide triggers bromide oxidation at the aqueous solution-vapour interface. *Nat. Commun.* **2017**, *8*, 700, doi:10.1038/s41467-017-00823-x.
(3) Hirokawa, J.; Onaka, K.; Kajii, Y.; Akimoto, H. Heterogeneous processes involving sodium halide particles and ozone: Molecular bromine release in the marine boundary layer in the absence of nitrogen oxides. *Geophys. Res. Lett.* **1998**, *25*, 2449-2452, doi:10.1029/98GL01815.
(4) Hunt, S. W.; Roesolová, M.; Wang, W.; Wingen, L. M.; Knipping, E. M.; Tobias, D. J.; Dabdub, D.; Finlayson-Pitts, B. J. Formation of molecular bromine from the reaction of ozone with deliquesced NaBr aerosol: Evidence for interface chemistry. *J. Phys. Chem. A* **2004**, *108*, 11559-11572, doi:10.1021/jp0467346.
(5) Lee, M.-T.; Brown, M. A.; Kato, S.; Kleibert, A.; Türler, A.; Ammann, M. Competition between organics and bromide at the aqueous solution-air interface as seen from ozone uptake kinetics and X-ray photoelectron spectroscopy. *J. Phys. Chem. A.* **2015**, *119*, 4600-4608, doi:10.1021/jp510707s.
(6) Mochida, M.; Hirokawa, J.; Akimoto, H. Unexpected large uptake of O_3 on sea salts and the observed Br_2 formation. *Geophys. Res. Lett.* **2000**, *27*, 2629-2632, doi:10.1029/1999GL010927.
(7) Oldridge, N. W.; Abbatt, J. P. D. Formation of gas-phase bromine from interaction of ozone with frozen and liquid NaCl/NaBr solutions: Quantitative separation of surficial chemistry from bulk-phase reaction. *J. Phys. Chem. A* **2010**, *115*, 2590-2598, doi:10.1021/jp200074u.
(8) Wren, S. N.; Kahan, T. F.; Jumaa, K. B.; Donaldson, D. J. Spectroscopic studies of the heterogeneous reaction between O_3(g) and halides at the surface of frozen salt solutions. *J. Geophys. Res.* **2010**, *115*, D16309, doi:10.1029/2010JD013929.

5. **O_3 + KI.** Brown et al.[1,2] report that KIO_3 forms on single crystal, water-free KI surfaces with a reaction probability of 1.4×10^{-4}. On room temperature KI solutions, Sakamoto et al.[8] report that ozone exposure yields gas-phase I_2 and small amounts of IO (ratio of I_2 to IO >100). The reaction kinetics are indicative of a Langmuir-Hinshelwood mechanism, exhibiting saturation in the gas-phase yields as both ozone and iodide concentrations are increased. The reaction forming I_2 proceeds more rapidly with increasing acidity for pH <4, but there is a pH-independent pathway operative to pH 11.

Complex chemistry for ozone reacting at the surface of solutions containing iodide and other reactants is illustrated from studies of solution microdroplet analysis by electrospray ionization (Pillar et al.,[5] Enami et al.,[3] and Hayase et al.[4]). In particular, a number of researchers have shown that surfactants and/or dissolved organic species can affect the rate of iodide oxidation by ozone (Hayase et al.,[4] Shaw and Carpenter,[9] Reeser et al.,[6] and Rouvière et al.[7]).

Back to Table

(1) Brown, M. A.; Ashby, P. D.; Ogletree, D. F.; Salmeron, M.; Hemminger, J. C. Reactivity of ozone with solid potassium iodide investigated by atomic force microscopy. *J. Phys. Chem. C* **2008**, *112*, 8110-8113, doi:10.1021/jp801620w.
(2) Brown, M. A.; Newberg, J. T.; Krisch, M. J.; Mun, B. S.; Hemminger, J. C. Reactive uptake of ozone on solid potassium iodide. *J. Phys. Chem. C* **2008**, *112*, 5520-5525, doi:10.1021/jp077225h.
(3) Enami, S.; Vecitis, C. D.; Cheng, J.; Hoffmann, M. R.; Colussi, A. J. Mass spectrometry of interfacial layers during fast aqueous aerosol/ozone gas reactions of atmospheric interest. *Chem. Phys. Lett.* **2008**, *455*, 316-320, doi:10.1016/j.cplett.2008.02.075.
(4) Hayase, S.; Yabushita, A.; Kawasaki, M.; Enami, S.; Hoffmann, M. R.; Colussi, A. J. Heterogeneous reaction of gaseous ozone with aqueous iodide in the presence of aqueous organic species. *J. Phys. Chem. A* **2010**, *114*, 6016-6021, doi:10.1021/jp101985f.
(5) Pillar, E. A.; Guzman, M. I.; Rodriguez, J. M. Conversion of iodide to hypoiodous acid and iodine in aqueous microdroplets exposed to ozone. *Environ. Sci. Technol.* **2013**, *47*, 10971-10979, doi:10.1021/es401700h.
(6) Reeser, D. I.; Donaldson, D. J. Influence of water surface properties on the heterogeneous reaction between $O_{3(g)}$ and $I^-_{(aq)}$. *Atmos. Environ.* **2011**, *45*, 6116-6120, doi:10.1016/j.atmosenv.2011.08.042.

(7) Rouvière, A.; Ammann, M. The effect of fatty acid surfactants on the uptake of ozone to aqueous halogenide particles. *Atmos. Chem. Phys.* **2010**, *10*, 11489-11500, doi:10.5194/acp-10-11489-2010.
(8) Sakamoto, Y.; Yabushita, A.; Kawasaki, M.; Enami, S. Direct emission of I_2 molecule and IO radical from the heterogeneous reactions of gaseous ozone with aqueous potassium iodide Solution. *J. Phys. Chem. A* **2009**, *113*, 7707-7713, doi:10.1021/jp903486u.
(9) Shaw, M. D.; Carpenter, L. J. Modification of ozone deposition and I_2 emissions at the air—aqueous interface by dissolved organic carbon of marine origin. *Environ. Sci. Technol.* **2013**, *47*, 10947-10954, doi:10.1021/es4011459.

6. **O_3 + sea salt.** Akimoto and coworkers[11,14] reported uptake coefficients for O_3 on synthetic and natural sea salt powders of ~1×10^{-3} using a Knudsen cell with multiple salt layers. Similar uptake coefficients were reported for the hydrates of $MgBr_2$ and $CaBr_2$. These are the initial uptake coefficients after correction for the available surface area using the pore diffusion model of Keyser et al.[9,10] The measured values before this correction was applied were about a factor of 20 larger. Given the uncertainty associated with these corrections, the final values derived have a large uncertainty associated with them as well. When $FeCl_3$ was added to synthetic sea salt (Fe/Na weight ratio of 1%), the uptake coefficient increased by an order of magnitude to $(3.2 \pm 1.1) \times 10^{-2}$. Br_2 was the gas phase product, with variable yields up to 100% of the O_3 lost. The enhanced reactivity of sea salt compared to NaCl and NaBr is due to the significant amounts of surface-adsorbed water (SAW) present on sea salt; the component of sea salt present in the second highest concentration is magnesium chloride which forms a stable hydrate and is quite hygroscopic. Reactions with powders of $MgCl_2 \cdot 6H_2O$ and sea salt are often observed to be similar to reaction with aqueous salt solutions (see note on SO_2 uptake). The formation of Br_2 is favored over Cl_2 by a number of factors: (1) surface segregation of bromide ions[3,4,15] in mixed solid crystals of NaCl and NaBr, (2) higher solubility of NaBr which increases its concentration in the surface layer as a mixture of NaCl and NaBr crystallizes, (3) faster oxidation of Br^- compared to Cl^-,[2,5,6,13] (4) solution phase chemistry of chloride and bromide ion mixtures that favors the production of gas phase bromine compounds,[2,13] (5) enhanced interfacial bromide ion concentrations compared to chloride ions at the air-water interface of aqueous solutions of mixed salts.[7,8] The yields of I_2 from exposure of sea water to ozone have been studied by Carpenter et al.[1] under ambient ozone concentrations. I_2 was quantified by conversion to small particles, which were sized and counted. On frozen sea-salt solutions, gas phase Br_2 was formed by exposure of O_3 (44 ppbv to 2.9 ppmv) to frozen sea salt solutions, at temperatures below 272 K.[12] No other products were reported and the production of Br_2 scaled with increasing O_3.
Back to Table

(1) Carpenter, L. J.; MacDonald, S. M.; Shaw, M. D.; Kumar, R.; Saunders, R. W.; Parthipan, R.; Wilson, J.; Plane, J. M. C. Atmospheric iodine levels influenced by sea surface emissions of inorganic iodine. *Nature Geosci.* **2013**, *6*, 108-111, doi:10.1038/NGEO1687.
(2) Finlayson-Pitts, B. J. The tropospheric chemistry of sea salt: A molecular level view of the chemistry of NaCl and NaBr. *Chem. Rev.* **2003**, *103*, 4801-4822, doi:10.1021/cr0206420.
(3) Ghosal, S.; Hemminger, J. C. Surface adsorbed water on NaCl and its effect on nitric acid reactivity with NaCl powders. *J. Phys. Chem. B* **2004**, *108*, 14102-14108, doi:10.1021/jp047774c.
(4) Ghosal, S.; Shbeeb, A.; Hemminger, J. C. Surface segragation of bromine in bromide doped NaCl: Implications for the seasonal variations in Arctic ozone. *Geophys. Res. Lett.* **2000**, *27*, 1879-1882, doi:10.1029/2000GL011381.
(5) Haag, W. R.; Hoigné, J. Ozonation of bromide-containing waters: Kinetics of formation of hypobromous acid and bromate. *Environ. Sci. Technol.* **1983**, *17*, 261-267, doi:10.1021/es00111a004.
(6) Haag, W. R.; Hoigné, J. Ozonation of water containing chlorine or chloramines. Reaction products and kinetics. *Water Research* **1983**, *17*, 1397-1402, doi:10.1016/0043-1354(83)90270-1.
(7) Jungwirth, P.; Tobias, D. Molecular structure of salt solutions: A new view of the interface with implications for heterogeneous atmospheric chemistry. *J. Phys. Chem. B* **2001**, *105*, 10468-10472, doi:10.1021/jp012750g.
(8) Jungwirth, P.; Tobias, D. J. Ions at the air/water interface. *J. Phys. Chem. B* **2002**, *106*, 6361-6373, doi:10.1021/jp020242g.
(9) Keyser, L. F.; Leu, M.-T.; Moore, S. B. Comment on porosities of ice films used to simulate stratospheric cloud surfaces. *J. Phys. Chem.* **1993**, *97*, 2800-2801, doi:10.1021/j100113a053.
(10) Keyser, L. F.; Moore, S. B.; Leu, M. T. Surface reaction and pore diffusion in flow tube reactors. *J. Phys. Chem.* **1991**, *95*, 5496-5502, doi:10.1021/j100167a026.

(11) Mochida, M.; Hirokawa, J.; Akimoto, H. Unexpected large uptake of O_3 on sea salts and the observed Br_2 formation. *Geophys. Res. Lett.* **2000**, *27*, 2629-2632, doi:10.1029/1999GL010927.
(12) Oum, K. W.; Lakin, M. J.; Finlayson-Pitts, B. J. Bromine activation in the troposphere by the dark reaction of O_3 with seawater ice. *Geophys. Res. Lett.* **1998**, *25*, 3923-3926, doi:10.1029/1998GL900078.
(13) Rossi, M. J. Heterogeneous reactions on salts. *Chem. Rev.* **2003**, *103*, 4823-4882, doi:10.1021/cr020507n.
(14) Sandanaga, Y.; Hirokawa, J.; Akimoto, H. Formation of molecular chlorine in dark condition: Heterogeneous reaction of ozone with sea salt in the presence of ferric ion. *Geophys. Res. Lett.* **2001**, *28*, 4433-4436, doi:10.1029/2001GL013722.
(15) Zangmeister, C. D.; Turner, J. A.; Pemberton, J. E. Segregation of NaBr in NaBr/NaCl crystals grown from aqueous solutions: Implications for sea salt surface chemistry. *Geophys. Res. Lett.* **2001**, *28*, 995-998, doi:10.1029/2000GL012539.

7. **O_3 + organic surfaces.** Reactive initial uptake of ozone occurs on organic substrates that contain unsaturated carbon-carbon bonds, whereas uptake to substrates that are fully saturated is minimal. This reaction occurs not only with simple alkenes, but with electron-rich conjugated systems such as PAHs as well. Ozone adds across carbon-carbon double bonds forming an ozonide, which then falls apart into more reactive intermediates. The product distributions are complex. Initial uptake coefficients are highly dependent upon the chemical nature of the substrate, ranging from values of roughly 10^{-3} on pure alkene aerosol particles such as oleic acid, to much lower values of 10^{-6} or below with PAH-coated particles. A more detailed discussion of this complex chemistry is given in two review articles: Kolb et al.[3] and Abbatt et al.[1] Note that the ozone uptake can be photochemically enhanced on some organic substrates, via a photosensitization process as described in a review article by George et al.[2]
Back to Table

(1) Abbatt, J. P. D.; Lee, A. K. Y.; Thornton, J. A. Quantifying trace gas uptake to tropospheric aerosol: recent advances and remaining challenges. *Chem. Soc. Rev.* **2012**, *41*, 6555-6581, doi:10.1039/C2CS35052A.
(2) George, C.; Ammann, M.; D'Anna, B.; Donaldson, D. J.; Nizkorodov, S. A. Heterogeneous photochemistry in the atmosphere. *Chem. Rev.,* **2015**, *115*, 4218-4258, doi:10.1021/cr500648z.
(3) Kolb, C. E.; Cox, R. A.; Abbatt, J. P. D.; Ammann, M.; Davis, E. J.; Donaldson, D. J.; Garrett, B. C.; George, C.; Griffiths, P. T.; Hanson, D. R.; Kulmala, M.; McFiggans, G.; Pöschl, U.; Riipinen, I.; Rossi, M. J.; Rudich, Y.; Wagner, P. E.; Winkler, P. M.; Worsnop, D. R.; O' Dowd, C. D. An overview of current issues in the uptake of atmospheric trace gases by aerosols and clouds. *Atmos. Chem. Phys.* **2010**, *10*, 10561-10605, doi:10.5194/acp-10-10561-2010.

8. **OH + H_2O(s).** Cooper and Abbatt[1] measured initial irreversible OH uptake coefficients of ~0.1 for water ice between 205–230 K; these decayed to $\gamma = 0.03 \pm 0.02$ after repeated exposure to OH. Self-reaction to form H_2O or H_2O_2 was indicated by the lack of observable gas phase products despite observation of first-order OH loss**.** It can not be ruled out that contamination of the ice surface drove the initial reactivity.
Back to Table

(1) Cooper, P. L.; Abbatt, J. P. D. Heterogeneous interactions of OH and HO_2 radicals with surfaces characertistic of atmospheric particulate matter. *J. Phys. Chem.* **1996**, *100*, 2249-2254, doi:10.1021/jp952142z.

9. **OH + HCl•nH_2O(l).** Cooper and Abbatt[1] demonstrated significant enhancement of OH uptake (to $\gamma > 0.2$) after HCl doping of 220 K ice surfaces sufficient to melt the surface layer. It is unclear whether OH is lost to self-reaction or reaction with hydrated Cl^- ions.
Back to Table

(1) Cooper, P. L.; Abbatt, J. P. D. Heterogeneous interactions of OH and HO_2 radicals with surfaces characertistic of atmospheric particulate matter. *J. Phys. Chem.* **1996**, *100*, 2249-2254, doi:10.1021/jp952142z.

10. **OH + HNO_3•$3H_2O$.** Cooper and Abbatt[1] measured $\gamma > 0.2$ for nitric acid-doped ice surfaces under conditions suitable for NAT formation at 200 and 228 K. Increase over pure ice uptake rates is probably due to $HNO_3 + OH \rightarrow H_2O + NO_3$ reaction.
Back to Table

(1) Cooper, P. L.; Abbatt, J. P. D. Heterogeneous interactions of OH and HO_2 radicals with surfaces characertistic of atmospheric particulate matter. *J. Phys. Chem.* **1996**, *100*, 2249-2254, doi:10.1021/jp952142z.

11. **OH + H_2SO_4•nH_2O.** Lower limits of 0.2 for uptake coefficients on 45–65 wt% H_2SO_4 between 220 and 230 K and for 96 wt% H_2SO_4 at 230 and 298 K by Cooper and Abbatt[2] are consistent with a lower limit of 0.07 on 28 wt% H_2SO_4 at 275 K in similar experiments by Hanson et al.[4] and a probable surface saturated value of $(4.9 \pm 0.5) \times 10^{-4}$ from Knudsen cell measurements by Baldwin and Golden[1] and an estimate of $\gamma = 1$ on ~96 wt% H_2SO_4 at 298 K by Gershenzon et al.[3] using a coated insert flow tube technique. Uptake is probably reactive with $OH + HSO_4^- \rightarrow H_2O + SO_4^-$ the hypothesized process.
Back to Table

(1) Baldwin, A. C.; Golden, D. M. Heterogeneous atmospheric reactions 2. Atom and radical reactions with sulfuric acid. *J. Geophys. Res.* **1980**, *85*, 2888-2889, doi:10.1029/JC085iC05p02888.
(2) Cooper, P. L.; Abbatt, J. P. D. Heterogeneous interactions of OH and HO_2 radicals with surfaces characertistic of atmospheric particulate matter. *J. Phys. Chem.* **1996**, *100*, 2249-2254, doi:10.1021/jp952142z.
(3) Gershenzon, Y. M.; Ivanov, A. V.; Kucheryavyi, S. I.; Rozenshtein, V. B. Anihilation of OH radicals on the surfaces of subtances chemically similar to atmospheric aerosol particles. *Kinet. Katal.* **1986**, *27*, 1069-1074.
(4) Hanson, D. R.; Burkholder, J. B.; Howard, C. J.; Ravishankara, A. R. Measurement of OH and HO_2 radical uptake coefficients on water and sulfuric acid surfaces. *J. Phys. Chem.* **1992**, *96*, 4979-4985, doi:10.1021/j100191a046.

12. **OH + NaCl.** Ivanov et al.[2] measured the uptake of OH on solid NaCl and on NH_4NO_3 over the temperature range from 245–340 K using a fast flow discharge reactor with a coated rod along the axis and EPR detection of OH. The initial values of the uptake coefficient approached 10^{-2}. The OH was generated from the reaction of H atoms with excess NO_2; it is not clear whether NO_2 might have also reacted with the salt surface. Given that the uptake coefficients were similar for NaCl and NH_4NO_3, the uptake likely does not reflect oxidation of the chloride. The pseudo-steady state value, γ_{ss}, was measured to be 4×10^{-3} at 298 K and the temperature dependence was described by $\gamma_{ss} = (1.2 \pm 0.7) \times 10^{-5} \exp[(1750 \pm 200)/T]$. This value is quite close to later measurements by Park et al.[6] who see little dependence of the uptake coefficient on relative humidity, up to 38% at room temperature. Product studies have been performed by Sjostedt and Abbatt[8] who have exposed dessicated NaCl salts to gas-phase OH in a coated-wall flow tube at 298 and 253 K. Gas-phase Br_2 is formed with a yield of 0.6, relative to the loss of OH. The source of the Br_2 is the trace Br^- impurity in commercial, high purity $NaCl_{(s)}$. BrCl was formed at a considerably smaller yield, 0.008. Humidification of the salt surface led to more sustained production but somewhat smaller yields.
Aerosol chamber studies by Finlayson-Pitts and coworkers showed that there was no Cl_2 production from NaCl particles when OH was generated by reaction of $O(^1D)$ from photolysis of O_3 at relative humidities below the deliquescence point of NaCl; above the deliquescence point, however, a rapid reaction of OH with Cl^- at the interface to generate gas phase Cl_2 is observed.[3,5] Because the mechanism is uncertain, and clearly must involve multiple steps, a unique value of the reaction probability for this interface reaction could not be obtained. At 269 K Frinak and Abbatt[1] have exposed acidic solutions containing molar levels of NaCl to gas-phase OH. The gas-phase product observed is Br_2, unless considerable OH exposure has reduced Br^-levels in the solution, in which case the product is Cl_2. The source of the Br_2 is the trace Br^- impurity in commercial, high purity $NaCl_{(s)}$. At neutral pH, the products were below detection limit. Shaka et al.[7] and Laskin et al.[4] have both exposed chloride solutions to gas-phase OH, observing changes in solution alkalinity and chloride concentrations, respectively. This is another indication that chloride ions in solution are readily heterogeneously oxidized by OH. Laskin et al. report an uptake coefficient of ≥ 0.1 at room temperature. However, the OH concentrations were not measured which may lead to uncertainty in this value.
Back to Table

(1) Frinak, E. K.; Abbatt, J. P. D. Br_2 production from the heterogeneous reaction of gas-phase OH with aqueous salt solutions: Impacts of acidity, halide concentration, and organic surfactants. *J. Phys. Chem. A* **2006**, *110*, 10456-10464, doi:10.1021/jp063165o.
(2) Ivanov, A. V.; Gershenzon, Y. M.; Gratpanche, F.; Devolder, P.; Saverysyn, J.-P. Heterogeneous loss of OH on NaCl and NH_4NO_3 at tropospheric temperatures. *Ann. Geophys.* **1996**, *14*, 659-664, doi:10.1007/s00585-996-0659-5.
(3) Knipping, E. M.; Lakin, M. J.; Foster, K. L.; Jungwirth, P.; Tobias, D. J.; Gerber, R. B.; Dabdub, D.; Finlayson-Pitts, B. J. Experiments and simulations of ion-enhanced interfacial chemistry on aqueous NaCl aerosols. *Science* **2000**, *288*, 301-306, doi:10.1126/science.288.5464.301.
(4) Laskin, A.; Wang, H.; Robertson, W. H.; Cowin, J. P.; Ezell, M. J.; Finlayson-Pitts, B. J. A new approach to determining gas-particle reaction probabilities and application to the heterogeneous reaction of deliquesced sodium chloride particles with gas-phase hydroxyl radicals. *J. Phys. Chem. A* **2006**, *110*, 10619-10627, doi:10.1021/jp063263+.
(5) Oum, K. W.; Lakin, M. J.; DeHaan, D. O.; Brauers, T.; Finlayson-Pitts, B. J. Formation of molecular chlorine from the photolysis of ozone and aqueous sea-salf particles. *Science* **1998**, *297*, 74-76, doi:10.1126/science.279.5347.74.
(6) Park, J. H.; Ivanov, A. V.; Molina, M. J. Effect of relative humidity on OH uptake by surfaces of atmospheric importance. *J. Phys. Chem. A* **2008**, *112*, 6968-6977, doi:10.1021/jp8012317.
(7) Shaka, H.; Robertson, W. H.; Finlayson-Pitts, B. J. A new approach to studying aqueous reactions using diffuse reflectance infrared Fourier transform spectrometry: application to the uptake and oxidation of SO_2 on OH-processed model sea salt aerosol. *Phys. Chem. Chem. Phys.* **2007**, *9*, 1980-1990, doi:10.1039/b612624c.
(8) Sjostedt, S. J.; Abbatt, J. P. D. Release of gas-phase halogens from sodium halide substrates: heterogeneous oxidation of frozen solutions and desiccated salts by hydroxyl radicals. *Environ. Res. Lett.* **2008**, *3*, 045007, doi:10.1088/1748-9326/3/4/045007.

13. **OH + Al_2O_3(s).** Measured value is from flow tube experiment with native oxide on aluminum as the active surface. An uptake coefficient of 0.04 ± 0.02 independent of temperature over the range of 253–348 K was recommended by (Gershenzon et al.[1] based on three measured values ranging unsystematically from 0.02 to 0.06 at 253, 298 and 348 K).
Back to Table

(1) Gershenzon, Y. M.; Ivanov, A. V.; Kucheryavyi, S. I.; Rozenshtein, V. B. Anihilation of OH radicals on the surfaces of subtances chemically similar to atmospheric aerosol particles. *Kinet. Katal.* **1986**, *27*, 1069-1074.

14. **OH + organic surfaces.** It has been shown through a large number of studies that the OH radical is efficiently lost on organic surfaces via condensed phase reactions that add oxygenated functional groups to the organics, and lead to some carbon-carbon bond breakage as well. The uptake coefficient for OH loss has been studied at room temperature on both chemically reduced and oxidized surfaces, and found to be larger than 0.1, as determined both by monitoring loss of OH directly and by monitoring loss of specific organics within the aerosol. A more detailed discussion of this complex chemistry is given in three review articles: Kolb et al.,[3] George and Abbatt,[2] and Abbatt et al.[1]
Back to Table

(1) Abbatt, J. P. D.; Lee, A. K. Y.; Thornton, J. A. Quantifying trace gas uptake to tropospheric aerosol: recent advances and remaining challenges. *Chem. Soc. Rev.* **2012**, *41*, 6555-6581, doi:10.1039/C2CS35052A.
(2) George, I. J.; Abbatt, J. P. D. Heterogeneous oxidation of atmospheric aerosol particles by gas-phase radicals. *Nature Chem.* **2010**, *2*, 713-722, doi:10.1038/nchem.806.
(3) Kolb, C. E.; Cox, R. A.; Abbatt, J. P. D.; Ammann, M.; Davis, E. J.; Donaldson, D. J.; Garrett, B. C.; George, C.; Griffiths, P. T.; Hanson, D. R.; Kulmala, M.; McFiggans, G.; Pöschl, U.; Riipinen, I.; Rossi, M. J.; Rudich, Y.; Wagner, P. E.; Winkler, P. M.; Worsnop, D. R.; O' Dowd, C. D. An overview of current issues in the uptake of atmospheric trace gases by aerosols and clouds. *Atmos. Chem. Phys.* **2010**, *10*, 10561-10605, doi:10.5194/acp-10-10561-2010.

15. **HO_2 + H_2O(s) and H_2SO_4•nH_2O(l).** Uptake of HO_2 on ice and super–cooled 55 wt.% sulfuric acid at 223 K has been demonstrated to be limited by HO_2 surface saturation by Cooper and Abbatt.[1] They argue that self-

reaction, presumably $2HO_2 \rightarrow H_2O_2 + O_2$ is controlling measured uptake coefficients of 0.025 ± 0.005 for ice and 0.055 ± 0.020 for 55 wt.% H_2SO_4. Thornton and Abbatt[4] report room temperature aerosol flow reactor submicron droplet measurements on 47–50 wt% H_2SO_4, without HO_2 scavenger species, yielding $\gamma < 0.01$. Gershenzon et al.[2] measured $\gamma > 0.2$ for 80 and 96 wt.% H_2SO_4 at 243 K and Hanson et al.[3] measured a lower limit for 28 wt% H_2SO_4 at 275 K of 0.07. However, large gas phase diffusion corrections mean these values are consistent with $\gamma = 1$. Thornton et al.[5] have used available experimental data to develop a parameterized HO_2 self-reaction uptake model valid for pH <6 aqueous droplets and gas phase HO_2 generation rates exceeding 1×10^5 cm^{-3} s^{-1}. They also assess the relative role of Cu^{++} catalyzed oxidation of HO_2 in aqueous aerosols.

Back to Table

(1) Cooper, P. L.; Abbatt, J. P. D. Heterogeneous interactions of OH and HO_2 radicals with surfaces characertistic of atmospheric particulate matter. *J. Phys. Chem.* **1996**, *100*, 2249-2254, doi:10.1021/jp952142z.

(2) Gershenzon, Y. M.; Grigorieva, V. M.; Ivanov, A. V.; Remorov, R. G. O_3 and OH sensitivity to heterogeneous sinks of HO_x and CH_3O_2 on aerosol particles. *Faraday Discuss.* **1995**, *100*, 83-100, doi:10.1039/fd9950000083.

(3) Hanson, D. R.; Burkholder, J. B.; Howard, C. J.; Ravishankara, A. R. Measurement of OH and HO_2 radical uptake coefficients on water and sulfuric acid surfaces. *J. Phys. Chem.* **1992**, *96*, 4979-4985, doi:10.1021/j100191a046.

(4) Thornton, J. A.; Abbatt, J. P. D. Measurements of HO_2 uptake to aqueous aerosol: Mass accommodation coefficients and net reactive loss. *J. Geophys. Res.* **2005**, *110*, D08309, doi:10.1029/2004JD005402.

(5) Thornton, J. A.; Jaeglé, L.; McNeil, V. F. Assessing known pathways for HO_2 loss in aqueous atmospheric aerosols: Regional and global impacts on tropospheric oxidants. *J. Geophys. Res.* **2008**, *113*, D05303, doi:10.1029/2007JD009236.

16. HO_2 + $(NH_4)_2SO_4$(aq) and NaCl(aq). HO_2 uptake on aerosol particles has been studied in aerosol flow tubes. At high HO_2 concentrations detected by CIMS, Thornton and Abbatt[6] observed loss of HO_2 on aqueous ammonium sulfate particles, buffered to pH 5.1 at RH 42% and room temperature. An uptake coefficient of 0.1 could describe the kinetics, but the HO_2 decays were best fit by second-order kinetics consistent with a bulk-phase reaction between dissolved HO_2 species, when using literature HO_2 solubility and bulk liquid-phase rate constants. Because of the second-order kinetics, it was inferred that the uptake coefficient would be substantially smaller at lower (atmospheric) HO_2 gas-phase concentrations.[7] This prediction is confirmed by the detailed study of George et al.[1] which examined HO_2 uptake at gas phase concentrations between 10^8 and 10^9 molecules/cm^3 in an aerosol flow tube using LIF detection methods. The uptake coefficients measured were between 0.003 and 0.02 on deliquesced particles of $(NH_4)_2SO_4$, NaCl and NH_4NO_3. These results are not in agreement with the work performed using LIF by Taketani et al.[3,4] who reported much larger uptake coefficients on ammonium sulphate (0.11 to 0.19, 45 to 75% RH), sodium chloride (0.1, 50 to 75% RH) and sea salt (0.1, 35 to 75% RH) at atmospheric HO_2 concentrations about two orders of magnitude lower (<10^8 molecules/cm^3) than those of Thornton and Abbatt, but similar to those of George et al. George et al. observed much more efficient loss when transition metals were present in solution, highlighting the importance of working with clean aerosol samples. As well, there are complex dependencies of the kinetics on HO_2 concentration and on reaction time. However, these dependencies do not appear to explain the large discrepancy between the results from the Taketani et al. and George et al. experiments, performed under nominally similar conditions. In the absence of transition metal impurities such as iron or copper ions, there is no known reactive chemistry that will deplete HO_2 as rapidly as observed in the Taketani et al. experiments.

Using the technique described above, Taketani et al.[5] have separately measured the HO_2 uptake coefficients at 75% relative humidity on ambient aerosol material that has been collected on a filter, extracted and then re-atomized to produce suspended particles. The uptake coefficients measured (between 0.1 and 0.4) are large, consistent with the large uptake coefficients measured by this group previously on laboratory-prepared aerosol systems. Such large values are likely arising from the presence of transition metal ions that catalyze the HO_2 self reaction in the aqueous phase. In the ambient environment these transition metals may only be present in a subset of particles but in these experiments they will have been mixed into all the particles. The composition of the atomized ambient material was analyzed, indicating large iron and significant copper abundances, along with sulfate, nitrate, organics etc. The acidity was largely neutralized by high levels of

ammonium. Note that studies by Lakey et al.[2] have shown that the presence of some organic constituents can reduce this catalytic role, if present in the same particles. This inhibition effect does not appear to be important for the results of Taketani et al.[5]

Back to Table

(1) George, I. J.; Matthews, P. S. J.; Whalley, L. K.; Brooks, B.; Goddard, A.; Baeza-Romero, M. T.; Heard, D. E. Measurements of uptake coefficients for heterogeneous loss of HO_2 onto submicron inorganic salt aerosols. *Phys. Chem. Chem. Phys.* **2013**, *15*, 12829-12845, doi:10.1039/c3cp51831k.

(2) Lakey, P. S. J.; George, I. J.; Baeza-Romero, M. T.; Whalley, L. K.; Heard, D. E. Organics substantially reduce HO_2 uptake onto aerosols containing transition metal ions. *J. Phys. Chem. A.* **2016**, *120*, 1421-1430, doi:10.1021/acs.jpca.5b06316.

(3) Taketani, F.; Kanaya, Y.; Akimoto, H. Kinetics of heterogeneous reactions of HO_2 radical at ambient concentration levels with $(NH_4)_2SO_4$ and NaCl aerosol particles. *J. Phys. Chem. A* **2008**, *112*, 2370-2377, doi:10.1021/jp0769936.

(4) Taketani, F.; Kanaya, Y.; Akimoto, H. Heterogeneous loss of HO_2 by KCl, synthetic sea salt, and natural seawater aerosol particles. *Atmos. Environ.* **2009**, *43*, 1660-1665, doi:10.1016/j.atmosenv.2008.12.010.

(5) Taketani, F.; Kanaya, Y.; Pochanart, P.; Liu, Y.; Li, J.; Okuzawa, K.; Kawamura, K.; Wang, Z.; Akimoto, H. Measurement of overall uptake coefficients for HO_2 radicals by aerosol particles sampled from ambient air at Mts. Tai and Mang (China). *Atmos. Chem. Phys.* **2012**, *12*, 11907-11916, doi:10.5194/acp-12-11907-2012.

(6) Thornton, J. A.; Abbatt, J. P. D. Measurements of HO_2 uptake to aqueous aerosol: Mass accommodation coefficients and net reactive loss. *J. Geophys. Res.* **2005**, *110*, D08309, doi:10.1029/2004JD005402.

(7) Thornton, J. A.; Jaeglé, L.; McNeil, V. F. Assessing known pathways for HO_2 loss in aqueous atmospheric aerosols: Regional and global impacts on tropospheric oxidants. *J. Geophys. Res.* **2008**, *113*, D05303, doi:10.1029/2007JD009236.

17. HO_2 + NaCl(s) and KCl(s). Gershenzon and coworkers[2,5] used a combination of matrix isolation EPR and gas phase EPR with a fast flow tube to measure the uptake of HO_2 on NaCl from 245–335 K. Early studies by Gershenzon et al.[2] measured values of $\gamma = 1.8 \times 10^{-2}$ for KCl and 1.6×10^{-2} for NaCl, both at 295 K, supplementing an even earlier value of $\gamma \sim 8 \times 10^{-3}$ measured by Gershenzon and Purmal.[3] In later studies on NaCl[5] the uptake was reported to remain constant for at least 30 min, so this is likely to be a steady-state value, $\gamma_{ss} = 1.2 \times 10^{-2}$ at 295 K. The temperature dependence is given by $\gamma_{ss} = (5.7 \pm 3.6) \times 10^{-5} \exp[(1560 \pm 140)/T]$. Above 330 K, the uptake coefficient was significantly smaller than expected from this temperature dependence. The data are indistinguishable, within experimental error, from the uptake of HO_2 on NH_4NO_3, suggesting that the uptake of HO_2 likely involves recombination on the surface rather than oxidation of the chloride. The surface recombination was interpreted in terms of a combined Eley-Rideal and Langmuir-Hinshelwood mechanism. The addition of small amounts of water vapor decreased the uptake coefficient for HO_2; the authors attributed this to water adsorption on the active sites. Another possibility is formation of HO_2-H_2O complexes whose uptake and recombination on the surface is not as fast as for uncomplexed HO_2. A study by Loukhovitskaya et al.[4] using a coated-wall flow tube finds temperature dependent uptake coefficients on salt surfaces, reporting uptake coefficient between 10^{-3} and 10^{-2} at room temperature. They report that gas-phase H_2O_2 was observed as a product, indicative of self-reaction. George et al.[1] and Taketani et al.[6] report uptake coefficients of less than 0.0004 and 0.01, respectively, on dry NaCl aerosol in aerosol flow tubes using HO_2 concentrations of 10^8 to 10^9 molecules/cm^3. The small upper limit for this process from George et al., measured at low concentrations of HO_2, suggests that the earlier measurements may have been dominated by radical recombination on salt surfaces.

Back to Table

(1) George, I. J.; Matthews, P. S. J.; Whalley, L. K.; Brooks, B.; Goddard, A.; Baeza-Romero, M. T.; Heard, D. E. Measurements of uptake coefficients for heterogeneous loss of HO_2 onto submicron inorganic salt aerosols. *Phys. Chem. Chem. Phys.* **2013**, *15*, 12829-12845, doi:10.1039/c3cp51831k.

(2) Gershenzon, Y. M.; Grigorieva, V. M.; Ivanov, A. V.; Remorov, R. G. O_3 and OH sensitivity to heterogeneous sinks of HO_x and CH_3O_2 on aerosol particles. *Faraday Discuss.* **1995**, *100*, 83-100, doi:10.1039/fd9950000083.

(3) Gershenzon, Y. M.; Purmal, A. P. Heterogeneous processes in the Earth's atmosphere and their ecological consequences. *Russ. Chem. Rev.* **1990**, *59*, 1007-1023.

(4) Loukhovitskaya, E.; Bedjanian, Y.; Morozov, I.; Le Bras, G. Laboratory study of the interaction of HO_2 radicals with the NaCl, NaBr, $MgCl_2 \cdot 6H_2O$ and sea salt surfaces. *Phys. Chem. Chem. Phys.* **2009**, *11*, 7896-7905, doi:10.1039/b906300e.
(5) Remorov, R. G.; Gershenzon, Y. M.; Molina, L. T.; Molina, M. J. Kinetics and mechanism of HO_2 uptake on solid NaCl. *J. Phys. Chem. A* **2002**, *106*, 4558-4565, doi:10.1021/jp013179o.
(6) Taketani, F.; Kanaya, Y.; Akimoto, H. Kinetics of heterogeneous reactions of HO_2 radical at ambient concentration levels with $(NH_4)_2SO_4$ and NaCl aerosol particles. *J. Phys. Chem. A* **2008**, *112*, 2370-2377, doi:10.1021/jp0769936.

18. **HO_2 + $(NH_4)_2SO_4$(s).** George et al.[1] report uptake coefficients of less than 0.0004 on dry $(NH_4)_2SO_4$ aerosol in an aerosol flow tube using HO_2 concentrations of 10^8–10^9 molecules/cm^3. Taketani et al.[2] report a considerably larger value, 0.04, measured with the same experimental approach. The discrepancy between these measurements is mirrored by an equivalent disagreement between these groups' measurements of HO_2 loss on aqueous salt solutions. The source of the disagreement is not clear but trace metal impurities have the potential to drive very efficient uptake and might be the cause of the higher values by Taketani et al.
Back to Table

(1) George, I. J.; Matthews, P. S. J.; Whalley, L. K.; Brooks, B.; Goddard, A.; Baeza-Romero, M. T.; Heard, D. E. Measurements of uptake coefficients for heterogeneous loss of HO_2 onto submicron inorganic salt aerosols. *Phys. Chem. Chem. Phys.* **2013**, *15*, 12829-12845, doi:10.1039/c3cp51831k.
(2) Taketani, F.; Kanaya, Y.; Akimoto, H. Kinetics of heterogeneous reactions of HO_2 radical at ambient concentration levels with $(NH_4)_2SO_4$ and NaCl aerosol particles. *J. Phys. Chem. A* **2008**, *112*, 2370-2377, doi:10.1021/jp0769936.

19. **HO_2 + Organic Aerosol.** The uptake coefficients of HO_2 to organic-containing aerosol particles have been measured by two groups, both using nominally the same approach of an aerosol flow tube coupled to chemical conversion/laser induced fluorescence for the detection of HO_2. Just as described in the note for HO_2 uptake to inorganic aqueous aerosol, these two groups likewise disagree on the magnitude of the uptake coefficients measured with organic substrates. For example, Taketani et al.[4] report values of 0.02 to 0.07 for a range of small di-carboxylic acids at 28% relative humidity, increasing to values of 0.06 to 0.18 at 68% RH. On the other hand, Lakey et al.[3] report values of 0.008 or below for a range of organic species, including di-carboxylic acids across a wide range of RH values. This group measured higher values on humic acid aerosol, but this behavior could be explained by high dissolved copper and iron concentrations in those particles, with the transition metal ions able to catalyze the self-reaction of HO_2 in the condensed phase. As in the case of the aqueous inorganic aerosols, the source of this discrepancy is not understood. Lakey et al.[2] show that the addition of specific organics, such as oxalic acid, to an aqueous inorganic aerosol that contains dissolved copper can lead to a significant inhibition of the reactive uptake, likely because of complexation of the transition metal ion thus making it unavailable for catalysis. This effect could significantly impact the importance of reactive HO_2 loss on aerosol, if transition metals and oxidized organics are present in the same particles. Likewise, Lakey et al.[1] demonstrate that the viscosity of the organic material may also be important, with the uptake coefficients measured on sucrose particles being larger on less viscous particles at RH=65% versus a more viscous, solid-like substrate at 17% RH.
Back to Table

(1) Lakey, P. S. J.; Berkemeier, T.; Krapf, M.; Dommen, J.; Steimer, S. S.; Whalley, L. K.; Ingham, T.; Baeza-Romero, M. T.; Pőschl, U.; Shiraiwa, M.; Ammann, M.; Heard, D. E. The effect of viscosity and diffusion on the HO_2 uptake by sucrose and secondary organic aerosol particles. *Atmos. Chem. Phys.* **2016**, *16*, 13035-13047, doi:10.5194/acp-16-13035-2016.
(2) Lakey, P. S. J.; George, I. J.; Baeza-Romero, M. T.; Whalley, L. K.; Heard, D. E. Organics substantially reduce HO_2 uptake onto aerosols containing transition metal ions. *J. Phys. Chem. A.* **2016**, *120*, 1421-1430, doi:10.1021/acs.jpca.5b06316.
(3) Lakey, P. S. J.; George, I. J.; Whalley, L. K.; Baeza-Romero, M. T.; Heard, D. E. Measurements of the HO_2 uptake coefficients onto single component organic aerosols. *Environ. Sci. Technol.* **2015**, *49*, 4878-4885, doi:10.1021/acs.est.5b00948.
(4) Taketani, F.; Kanaya, Y.; Akimoto, H. Kinetic studies of heterogeneous reaction of HO_2 radical by dicarboxylic acid particles. *Int. J. Chem. Kinet.* **2013**, *45*, 560-565, doi:10.1002/kin.20783.

20. **HO_2 + Mineral Dust.** Uptake coefficients for the interaction of HO_2 with Arizona Test Dust (ATD) from 5 to 76% relative humidity at room temperature have been reported by Matthews et al.[2] who used LIF to detect HO_2 in an aerosol flow tube. The HO_2 concentrations are quite low, on the order of 10^8 to 10^9 molecules/cm^3. The uptake coefficients are between 0.02 and 0.03, with larger values measured at short reaction times. The decrease of the uptake coefficient with longer reaction times may be due to some degree of surface modification or perhaps because the reaction is not first order, i.e. some self-reaction of HO_2 on the surface is occurring. Thus, these uptake coefficients may be upper limits to values that will prevail in the atmosphere. For comparison, James et al.[1] have reported uptake coefficients using the same technique on igneous-type dusts, such as synthetic olivine ($MgFeSiO_4$, uptake coefficient = 0.069), forsterite (Mg_2SiO_4, 0.0043) and fayalite (Fe_2SiO_4, 0.073).

Back to Table

(1) James, A. D.; Moon, D. R.; Feng, W.; Lakey, P. S. J.; Frankland, V. L.; Heard, D. E.; Plane, J. M. C. The uptake of HO_2 on meteoric smoke analogues. *J. Geophys. Res.* **2017**, *122*, 554-565, doi:10.1002/2016JD025882.

(2) Matthews, P. S. J.; Baeza-Romero, M. T.; Whalley, L. K.; Heard, D. E. Uptake of HO_2 radicals onto Arizona test dust particles using an aerosol flow tube. *Atmos. Chem. Phys.* **2014**, *14*, 7397-7408, doi:10.5194/acp-14-7397-2014.

21. **H_2O (g) + Al_2O_3 (s).** Isotopic thermal programmed desorption studies at 300 K by Elam et al.[2] show that H_2O dissociatively absorbs on α-alumina surfaces and that initial uptake coefficient (γ_o) is ~0.1. Pre-hydroxylation or long term exposure to water vapor decreases the H_2O uptake coefficient nearly exponentially. Al-Abadleh et al.[1] used FTIR techniques to study water vapor uptake at 296 K on α-alumina crystal 0001 surfaces as a function of relative humidity (RH). Below 10% RH uptake is dissociative, but molecular absorption dominates uptake between 10 and 70% RH. FTIR spectra of water absorbed on both α-alumina and γ-alumina powder surfaces are similar to those on 0001 crystal surfaces. Goodman et al.[3] used FTIR to show that α-alumina surfaces saturated with HNO_3 vapor has the same water absorption isotherm as untreated samples at 296 K.

Back to Table

(1) Al-Abadleh, H. A.; Grassian, V. H. FT-IR study of water adsorption on aluminum oxide surfaces. *Langmuir* **2003**, *19*, 341-347, doi:10.1021/la026208a.

(2) Elam, J. W.; Nelson, C. E.; Cameron, M. A.; Tolbert, M. A.; George, S. M. Adsorption of H_2O on a single-crystal α-Al_2O_3(0001) surface. *J. Phys. Chem. B* **1998**, *102*, 7008-7015, doi:10.1021/jp981070j.

(3) Goodman, A. L.; Bernard, E. T.; Grassian, V. H. Spectroscopic study of nitric acid and water adsorption on oxide particles: Enhanced nitric acid uptake kinetics in the presence of adsorbed water. *J. Phys. Chem. A* **2001**, *105*, 6443-6457, doi:10.1021/jp003722l.

22. **H_2O_2 + Al_2O_3(s).** Zhao et al.[3] measured H_2O_2 uptake on a bed of ~35nm α-alumina particles in a solid sample flow reactor as a function of relative humidity at room temperature and ambient pressure. BET surface area was used in analyzing uptake coefficients. Uptake was RH dependent, which was varied over a wide range (2–76%). Gas phase hydrogen peroxide leaving the reactor was scrubbed and quantified using liquid chromatography. Uptake was largely irreversible with reactive uptake ~75% at low RH rising to ~85% at high RH. Reported uptake coefficients (γ) were lower at higher RHs: $\gamma(\text{RH-2\%}) = (1.21 \pm 0.04) \times 10^{-7}$**;** $\gamma(\text{RH-21\%}) = (0.84 \pm 0.07) \times 10^{-7}$ and $\gamma(\text{RH} \geq 42\%) = (0.72 \pm 0.04) \times 10^{-7}$. Use of BET surface areas probably led to underestimated γ values. Uptake experiments were performed for 30 minutes; larger uptake coefficients may have characterized shorter uptake times. The authors also reported largely reversible H_2O_2 uptake coefficients on SiO_2 submicron particles that were about an order of magnitude lower than those measured for alumina.[3]

Wang et al.[2] report Knudsen cell studies, also on α-alumina and other mineral oxide surfaces at room temperature and very low RH. For α-alumina the measured gas phase products also indicate catalytic decomposition. Measured γ_o values using BET surface areas were $(1.00 \pm 0.11) \times 10^{-4}$ for α-Al_2O_3, $(1.66 \pm 0.23) \times 10^{-5}$ for MgO, $(9.70 \pm 1.05) \times 10^{-5}$ for Fe_2O_3 and $(5.22 \pm 0.9) \times 10^{-5}$ for SiO_2. Their γ_o value for α-Al_2O_3 is roughly a factor of a thousand higher than the steady-state γ values reported by Zhao et al.[3]

Romanias et al.[1] used a coated wall flow reactor with solid films of ~20 nm γ-alumina particles to measure H_2O_2 uptake coefficients over a RH range of 0.003 to 73% and a temperature range of 268–329 K. Near

ultraviolet (315-400 nm) illumination had no effect on uptake. BET surface area measurements were also used to calculate uptake coefficients. They observed that longer exposure times lead to saturated surfaces, so initial γ_o uptake coefficients as well as steady-state γ values were reported. Desorption measurements showed reversible H_2O_2 uptake was 5% or less of total uptake. Initial uptake values were dependant on both RH and T; for instance, γ_o (for 0.003% RH and 300 K) = $(9.0 \pm 2.7) \times 10^{-4}$, is nearly constant for (0.003–0.02% RH) then falls off to $\sim 2 \times 10^{-5}$ at 73% RH. The steady-state uptake coefficient also decreases at higher RH values, γ(280 K) falls from about 2.5×10^{-5} at about 0.005% RH to $\sim 5 \times 10^{-7}$ at RH of 73%. Clearly adsorbed water vapor competes with irreversible H_2O_2 chemisorption. At fixed RH the initial uptake of H_2O_2 increases with falling temperature, $\gamma_o(0.03\%\ RH) = 8.7 \times 10^{-4}/(1 + 5.0 \times 10^{13} \exp(-9700/T)$ rising from 2.0×10^{-4} at 320 K to 8.8×10^{-4} at 268 K.[1] Note that the low RH γ_o values reported in this work are the same order of magnitude as the dry α-Al_2O_3 value reported by Wang et al.[2]

Given that there is little reason to expect that α-alumina and γ-alumina have the same initial uptake coefficients, not to mention similar RH or temperature dependencies, the available data will support only a conservative upper limit estimate of $\gamma_o < 5 \times 10^{-3}$.
Back to Table

(1) Romanias, M. N.; El Zein, A.; Bedjanian, Y. Uptake of hydrogen peroxide on the surface of Al_2O_3 and Fe_2O_3. *Atmos. Environ.* **2013**, *77*, 1-8, doi:10.1016/j.atmosenv.2013.04.065.
(2) Wang, W.-g.; Ge, M.-f.; Sun, Q. Heterogeneous uptake of hydrogen peroxide on mineral oxides. *Chin. J. Chem. Phys.* **2011**, *24*, 515-520, doi:10.1088/1674-0068/24/05/515-520.
(3) Zhao, Y.; Chen, Z.; Shen, X.; Zhang, X. Kinetics and mechanisms of heterogeneous reaction of gaseous hydrogen peroxide on mineral oxide particles. *Environ. Sci. Technol.* **2011**, *45*, 3317-3324, doi:10.1021/es104107c.

23. **NO_2 + H_2O(l).** Value for γ of $(6.3 \pm 0.7) \times 10^{-4}$ at 273 K (Tang and Lee[9]) was achieved by chemical consumption of NO_2 by SO_3^{2-}; their stopped-flow measurement was probably still affected by surface saturation, leading to the measurement of a lower limit. Ponche et al.[7] measured an uptake coefficient of $(1.5 \pm 0.6) \times 10^{-3}$ at 298 K, which was also probably subject to saturation limitations. Mertes and Wahner[5] used a liquid jet technique to measure a lower limit of $\gamma \geq 2 \times 10^{-4}$ at 278 K, and they observed partial conversion of the absorbed NO_2 to HONO. Msibi et al.[6] used a cylindrical/annular flow reactor to derive $\gamma = (8.7 \pm 0.6) \times 10^{-5}$ on pH = 7 deionized water surfaces and $(4.2 \pm 0.9) \times 10^{-4}$ on pH = 9.3 wet ascorbate surfaces; it seems likely that these results are also subject to surface saturation given the gas/surface interaction times involved in the experiment. Harrison and Collins[3] performed aerosol flow reactor experiments on deliquescent sodium chloride and ammonium sulfate droplets at 279 K obtaining reactive uptake coefficients in the range of (2.8–10) $\times 10^{-4}$, probably with some surface saturation constraints. Cheung et al.[1] used a droplet train flow reactor to show that the reactive uptake coefficient for NO_2 at number densities between 10^{13} and 10^{16} on pure water at 273 K is $< 5 \times 10^{-4}$, contradicting many of the earlier experiments. Cheung et al. also used a bubble train reactor to demonstrate that the reactive uptake of NO_2 is second order, so that experimental uptake coefficients will be dependent on gas phase NO_2 concentrations.

Colussi and co-workers[2,4,10] measured the adsorption/reaction of gaseous NO_2 on ~293 K aqueous microstreams by measuring the nitrate ion content by electrospray mass spectrometry after the microstreams break up into small charged droplets. In Yabushita et al.[10] the aqueous microstreams were doped with alkali salts (NaCl, NaBr and NaI), in Kinugawa et al.[4] doping agents were cationic and anionic surfactants (tetrabutylammonium bromide, tetradecyltrimethylammonium bromide and potassium perfluorooctanesulfonate) as well as NaBr, and in Colussi et al.[2] the additives were dicarboxylic acids representing components of secondary organic aerosol (SOA) including malonic, glutaric and glutamic acids with low enough pK1 values to dissociate to monoanions. The nitrate detected is assumed to be produced by the surface reaction: $2\ NO_2 + H_2O \rightarrow HONO + HNO_3$. This experimental process is semi-quantitative, Colussi et al. estimate that the non-detectable nitrate levels in undoped water microstreams indicate a $\gamma_o < 2 \times 10^{-7}$ for pure water. However, when the aqueous microstreams are doped with gas/liquid interface active anions or cations, the apparent NO_2 γ_o values increase nonmonotonically with electrolyte concentrations peaking at $\gamma_o \sim 10^{-4}$ for [NaX] concentrations of ~1 mM.[10] Colussi et al.[2] also present theoretical models of NO_2 interactions with water clusters containing Cl^- in a aqueous interfacial environment that identify electrostatic interactions strong enough to potentially enhance the reactivity of adsorbed NO_2.

Sosedova et al.[8] measured the uptake of radioactive $^{13}NO_2$ (half-life 10 min.), which can be detected at extremely low concentrations, by deliquesced sodium salts of hydroquinone (1,4-dihydroxybenzene) and

gentisic acid (2,5-dihydroxybenzoic acid) in a flow tube reactor at 296 K and 40% RH. Reactant $^{13}NO_2$ and product $HO^{13}NO$ are trapped on chemically selective denuder surfaces and quantified by counting ^{13}N decay gamma rays. Observed reactive uptake coefficients (γs) ranged from ~5×10^{-4} to ~ 6×10^{-3}. The measured time dependence of NO_2 reactive uptake was fitted to a kinetic model of reactant consumption in the droplet phase using the NO_2 mass accommodation coefficient and the rate constants for dissolved NO_2 with the deprotonated phenolic compounds as variables, yielding an estimated room temperature bulk liquid mass accommodation coefficient: $\alpha = 0.024$ (+0.018/-0.003). If accurate for pure water, it indicates that the lower reactive uptake coefficients measurements above are subject to some degree of surface saturation.

Data are consistent with reactive uptake coefficients less than 1×10^{-2} for 270–295 K and a liquid-phase second-order hydrolysis of NO_2 to HONO and HNO_3, which depends on temperature and pH. However, the interplay between mass accommodation, possible surface reaction, and bulk reaction may be complex.
Back to Table

(1) Cheung, J. L.; Li, Y. Q.; Boniface, J.; Shi, Q.; Davidovits, P.; Worsnop, D.; Jayne, J. T.; Kolb, C. E. Heterogeneous interactions of NO_2 with aqueous surfaces. *J. Phys. Chem. A* **2000**, *104*, 2655-2662, doi:10.1021/jp992929f.

(2) Colussi, A. J.; Enami, S.; Yabushita, A.; Hoffmann, M. R.; Liu, W.-G.; Mishra, H.; Goddard, W. A., III Tropospheric aerosol as a reactive intermediate. *Faraday Discuss.* **2013**, *165*, 407-420, doi:10.1039/c3fd00040k.

(3) Harrison, R. M.; Collins, G. M. Measurements of reaction coefficients of NO_2 and HONO on aerosol particles. *J. Atmos. Chem.* **1998**, *30*, 397-406, doi:10.1023/A:1006094304069.

(4) Kinugawa, T.; Enami, S.; Yabushita, A.; Kawasaki, M.; Hoffmann, M. R.; Colussi, A. J. Conversion of gaseous nitrogen dioxide to nitrate and nitrite on aqueous surfactants. *Phys. Chem. Chem. Phys.* **2011**, *13*, 5144-5149, doi:10.1039/c0cp01497d.

(5) Mertes, S.; Wahner, A. Uptake of nitrogen dioxide and nitrous acid on aqueous surfaces. *J. Phys. Chem.* **1995**, *99*, 14000-14006, doi:10.1021/j100038a035.

(6) Msibi, I. M.; Shi, J. P.; Harrison, R. M. Accommodation coefficient for trace gas uptake using deposition profile measurement in an annular reactor. *J. Atmos. Chem.* **1993**, *17*, 339-351, doi:10.1007/BF00696853.

(7) Ponche, J. L.; George, C.; Mirabel, P. Mass transfer at the air/water interface: Mass accommodation coefficients of SO_2, HNO_3, NO_2 and NH_3. *J. Atmos. Chem.* **1993**, *16*, 1-21, doi:10.1007/BF00696620.

(8) Sosedova, Y.; Rouviére, A.; Gäggeler, H. W.; Ammann, M. Uptake of NO_2 to deliquesced dihydroxybenzoate aerosol particles. *J. Phys. Chem. A* **2009**, *113*, 10979-10987, doi:10.1021/jp9050462.

(9) Tang, I. N.; Lee, J. H. In *The Chemistry of Acid Rain*; Gordon, G. E., Johnson, R. W., Eds.; Am. Chem. Soc. Symp. Series, 1987; pp 109-117.

(10) Yabushita, A.; Enami, S.; Sakamoto, Y.; Kawasaki, M.; Hoffmann, M. R.; Colussi, A. J. Anion-catalyzed dissolution of NO_2 on aqueous microdroplets. *J. Phys. Chem. A* **2009**, *113*, 4844-4848, doi:10.1021/jp900685f.

24. **$NO_2 + H_2SO_4 \bullet nH_2O$.** Kleffmann et al.[2] performed bubble tube reactor uptake measurements for 0–98 wt% acid at 298 K and for 44.6 and 56.1 wt% from 250–325 K. At 298 K, measured uptake coefficients varied between 6 and 3×10^{-7} with a minimum near 70 wt%. Most measurements at 44.6 and 56.1 wt% overlapped within their error limits and showed little temperature dependence although there is evidence that uptake increases at the lowest temperatures. The data can all be captured with a recommended value of 5×10^{-7} with an uncertainty factor of three.

This recommendation is consistent with earlier upper limits of 1×10^{-6} by Baldwin and Golden[1] for 96 wt% at 295 K and 5×10^{-6} for 70 wt% between 193 and 243 K by Saastad et al.[3] Kleffmann et al.[2] conclude that their uptake measurements are mass accommodation limited; however, it is not clear that their values are not influenced by bulk or surface reaction of two NO_2 with H_2O to form HONO and HNO_3 at lower acid wt%values and the formation of nitrosyl sulfuric acid at higher acid concentrations. Kleffmann et. al.[2] did perform separate static wetted wall reactor studies showing the formation of gas phase HONO at acid concentrations below 60 wt%. It is more likely that reactive uptake is a controlling factor and the measured uptakes are solubility and/or reaction rate limited. Thus, the mass accommodation coefficient may be much larger than the recommended uptake values.
Back to Table

(1) Baldwin, A. C.; Golden, D. M. Heterogeneous atmospheric reactions: Sulfuric acid aerosols as tropospheric sinks. *Science* **1979**, *206*, 562-563, doi:10.1126/science.206.4418.562.
(2) Kleffmann, J.; Becker, K. H.; Wiesen, P. Heterogeneous NO_2 conversion processes on acid surfaces: Possible atmospheric implications. *Atmos. Environ.* **1998**, *32*, 2721-2729, doi:10.1016/S1352-2310(98)00065-X.
(3) Saastad, O. W.; Ellerman, T.; Nielson, C. J. On the adsorption of NO and NO_2 on cold H_2O/H_2SO_4 surfaces. *Geophys. Res. Lett.* **1993**, *20*, 1191-1193, doi:10.1029/93GL01621.

25. **NO_2 + Al_2O_3.** Miller and Grassian[5] observed NO_2 adsorbed reactively on γ-alumina using FTIR and UV spectroscopy to observe surface nitrite and nitrate. Szanyi et al.[7] used FTIR and thermal programmed desorption/mass spectrometry to determine products formed on γ-alumina surfaces at 300 K, observing nitrites and nitrates (at higher NO_2 only nitrate). Exposure to water vapor converted most bridging nitrates to bidentate and monodentate nitrates. Baltrusaitis et al.[1] also used FTIR to observe monodentate, bidentate and bridging nitrates products on both α-alumina and γ-alumina particles at 296 K. They also observed that co-absorbed water solvates surface nitrates. Underwood et al.[8-10] report Knudsen cell studies measuring γ_o values on γ-alumina particles of 2×10^{-8}, 2.0×10^{-8}, and 2.2×10^{-8} at 298 K based on BET surface area corrections and either Keyser, Moore, Leu (KLM) formulation[4] or linear mass dependent (LMD) corrections for porosity, with the KML and LMD corrections leading to very similar values.[8] They also report larger γ_o values for α-alumina of 9.3×10^{-6} and 9.1×10^{-6}.[8,10] Underwood et al.[10] also suggest a final "multiple collision" that would raise the γ_o values for γ-alumina by factor of 1.1 and α-alumina by 9.4. This proposed correction is not included in the recommended upper limits. Börensen et al.[2] report diffuse reflectance FTIR measurements of uptake on γ-alumina showing that the reaction order is 1.86 ± 0.1 in NO_2. They report BET corrected γ_o values varying linearly from 7.3×10^{-10} to 1.3×10^{-8} as $[NO_2]$ was increased from 2.5×10^{13} to 8.5×10^{14}. Rubasinghege and Grassian[6] irradiated nitrate absorbed on γ-alumina particles with broad band light (>300 nm) as a function of RH (at ~1, 20, 45 and 80% and with and without gas phase O_2) observing photolytic production of gas phase NO (primary product), NO_2 and N_2O.
Guan et al.[3] report α-Al_2O_3 BET uptake coefficients at 298 K for both dark measurements ($9.9 \pm 4.8 \times 10^{-10}$) and simulated sunlight (350–700 nm) conditions ranging from 2.55 to 3.33×10^{-9} for light fluxes of 0.45–2.25 mW/cm^2. They also showed that NO_2 uptake was independent of its gas phase concentration between 2.7 and 53.8×10^{14} molecules/cm^3, so surface saturation was probably not an issue.[3] However, they assumed that all NO_2 uptake resulted in surface NO_3^- production and integrated the observed nitrate bands to estimate nitrate surface concentrations. For gaseous mixtures of NO_2 and O_2 they determined that the nitrate production rate reaction order was 0.960 ± 0.111 for NO_2 and 0.620 ± 0.083 for O_2.[3] Note, that they cite Börensen et al. (2000), but do not discuss the fact that Zellner's group measured a NO_2 uptake order on γ-alumina of 1.86 ± 0.1. Wu et al.[11] report the effect of temperature (250–318 K) on "dry air" NO_2 uptake and nitrate production on γ-alumina surfaces using a DRIFTS set-up. They obtained geometrical γ_o values increasing from $(7.42 \pm 0.77) \times 10^{-4}$ at 318 K to $(23.0 \pm 2.58) \times 10^{-4}$ at 250 K, corresponding to γ_o(BET) values of $(2.58 \pm 0.27) \times 10^{-10}$ and $(8.17 \pm 0.92) \times 10^{-10}$. There is no discussion of the very large (>10^6) differences between γ_o(BET) and γ_o(GEO).
Given the currently available data and the extremely low uptake coefficients reported for BET estimated surface areas, only upper limits for γ_o's on α-alumina and γ-alumina are listed.
Back to Table

(1) Baltrusaitis, J.; Schuttlefield, J.; Jensen, J. H.; Grassian, V. H. FTIR spectroscopy combined with quantum chemical calculations to investigate adsorbed nitrate on aluminium oxide surfaces in the presence and absence of co-adsorbed water. *Phys. Chem. Chem. Phys.* **2007**, *9*, 4970-4980, doi:10.1039/b705189a.
(2) Börensen, C.; Kirchner, U.; Scheer, V.; Vogt, R.; Zellner, R. Mechanism and kinetics of the reactions of NO_2 or HNO_3 with alumina as a mineral dust model compound. *J. Phys. Chem. A* **2000**, *104*, 5036-5045, doi:10.1021/jp994170d.
(3) Guan, C.; Li, X.; Luo, Y.; Huang, Z. Heterogeneous reaction of NO_2 on α-Al_2O_3 in the dark and simulated sunlight. *J. Phys. Chem. A* **2014**, *118*, 6999-7006, doi:10.1021/jp503017k.
(4) Keyser, L. F.; Moore, S. B.; Leu, M. T. Surface reaction and pore diffusion in flow tube reactors. *J. Phys. Chem.* **1991**, *95*, 5496-5502, doi:10.1021/j100167a026.

(5) Miller, T. M.; Grassian, V. H. Heterogeneous chemistry of NO_2 on mineral oxide particles: Spectroscopic evidence for oxide-coordinated and water-solvated surface nitrate. *Geophys. Res. Lett.* **1998**, *25*, 3835-3838, doi:10.1029/1998GL900011.
(6) Rubasinghege, G.; Grassian, V. H. Photochemistry of adsorbed nitrate on aluminum oxide particle surfaces. *J. Phys. Chem. A* **2009**, *113*, 7818-7825, doi:10.1021/jp902252s.
(7) Szanyi, J.; Kwak, J. H.; Chimentao, R. J.; Peden, C. H. F. Effect of H_2O on the adsorption of NO_2 on γ-Al_2O_3: an in situ FTIR/MS study. *J. Phys. Chem. C* **2007**, *111*, 2661-2669, doi:10.1021/jp066326x.
(8) Underwood, G. M.; Li, P.; Usher, C. R.; Grassian, V. H. Determining accurate kinetic parameters of potentially important heterogeneous atmospheric reactions on solid particle surfaces with a Knudsen cell reactor. *J. Phys. Chem. A* **2000**, *104*, 819-829, doi:10.1021/jp9930292.
(9) Underwood, G. M.; Miller, T. M.; Grassian, V. H. Transmission FT-IR and Knudsen cell study of the heterogeneous reactivity of gaseous nitrogen dioxide on mineral oxide particles. *J. Phys. Chem. A* **1999**, *103*, 6184-6190, doi:10.1021/jp991586i.
(10) Underwood, G. M.; Song, C. H.; Phadnis, M.; Carmichael, G. R.; Grassian, V. H. Heterogeneous reactions of NO_2 and HNO_3 on oxides and mineral dust: A combined laboratory and modeling study. *J. Geophys. Res.* **2001**, *106*, 18055-18066, doi:10.1029/2000JD900552
(11) Wu, L.; Tong, S.; Ge, M. Heterogeneous reaction of NO_2 on Al_2O_3: The effect of temperature on the nitrite and nitrate formation. *J. Phys. Chem. A* **2013**, *117*, 4937-4944, doi:10.1021/jp402773c.

26. **NO_2/N_2O_4 + NaCl.** Schroeder and Urone reported that NO_2 at Torr concentrations reacted with NaCl to form ClNO.[7] Subsequently, Finlayson-Pitts[4] showed that the reaction continued at ppm concentrations of NO_2 and estimated a lower limit to the uptake coefficient for NO_2 of 5×10^{-8}, assuming the reaction was first order in NO_2. Winkler et al.[11] used XPS to follow the increase in nitrate during the reaction of NO_2 with NaCl and reported that the rate was proportional to the square of the NaCl surface sites and the square root of NO_2. Vogt and Finlayson-Pitts[8-10] used diffuse reflectance Fourier transform infrared spectrometry (DRIFTS) to follow the formation of nitrate and showed that the reaction was second order in NO_2; assuming that N_2O_4 was the reactant, the uptake coefficient was measured to be $(1.3 \pm 0.6) \times 10^{-4}$ (1σ). Peters and Ewing[6] followed the formation of nitrate on single crystal NaCl(100) and also found the reaction was second order in NO_2. Assuming that N_2O_4 is the reactant, the uptake coefficient was $(1.3 \pm 0.3) \times 10^{-6}$, two orders of magnitude less than reported by Vogt and Finlayson-Pitts. However, in the presence of 9.5 mbar water vapor, the uptake coefficient increased by a factor of about 100. It is likely that the difference is that their single crystals did not hold significant amounts of surface adsorbed water, whereas the powders used by Vogt and Finlayson-Pitts are known to hold significant amounts of SAW[2] which enhances the reactivity through mobilization of the nitrate ions and exposure of fresh NaCl during the reaction. Caloz et al.[3] measured using a Knudsen cell an upper limit of $<10^{-7}$ for uptake of NO_2 on NaCl and $<2 \times 10^{-7}$ for uptake on KBr, with the reaction being first order in NO_2. Yoshitake[13] also used DRIFTS to study this reaction and reported that for "dry" NaCl, the reaction was second order in NO_2 with an uptake coefficient assuming the reactant is N_2O_4 of $(4 \pm 2) \times 10^{-5}$. However, if the NaCl had been pretreated with water vapor, the uptake was first order in NO_2 with $\gamma = (1.5 \pm 0.2) \times 10^{-8}$. Karlsson and Ljungstrom[5] generated NaCl particles and measured the loss of chloride and formation of nitrate using ion chromatography on particles collected on filters; they obtained a lower limit for the reaction probability of 3×10^{-4}. Surprisingly, the conversion of NO_2 to nitrate decreased as the relative humidity increased from 9 to 79%. These reactions are sufficiently slow that they are unlikely to be important in the atmosphere.

Abbatt and Waschewsky[1] measured the loss of NO_2 in a flow tube containing deliquesced 1–5 μm NaCl particles (75% RH); no significant loss was observed on unbuffered particles or particles buffered at pH of 7.2 or having pH of 0.3 using HCl. An upper limit of $\gamma_o < 1 \times 10^{-4}$ for the uptake of NO_2 was derived from these measurements. Yabushita et al.[12] have recently shown using ESI-MS that uptake of NO_2 to aqueous droplets, yielding the nitrate anion, is facilitated by the presence of halide anions, perhaps through the formation of a complex with NO_2 on the surface.
Back to Table

(1) Abbatt, J. P. D.; Waschewsky, G. C. G. Heterogeneous interactions of HOBr, HNO_3, O_3, and NO_2 with deliquescent NaCl aerosols at room temperature. *J. Phys. Chem. A* **1998**, *102*, 3719-3725, doi:10.1021/jp980932d.

(2) Beichert, P.; Finlayson-Pitts, B. J. Knudson cell studies of the uptake of gaseous HNO_3 and other oxides of nitrogen on solid NaCl. The role of surface absorbed water. *J. Phys. Chem.* **1996**, *100*, 15218-15228, doi:10.1021/jp960925u.
(3) Caloz, F.; Fenter, F. F.; Tabor, K. D.; Rossi, M. J. Paper I: Design and construction of a Knudsen-cell reactor for the study of heterogeneous reactions over the temperature range 130-750 K: Performances and limitations. *Rev. Sci. Instrum.* **1997**, *68*, 3172-3179, doi:10.1063/1.1148263.
(4) Finlayson-Pitts, B. J. Reaction of NO_2 with NaCl and atmospheric implications of NOCl formation. *Nature* **1983**, *306*, 676-677, doi:10.1038/306676a0.
(5) Karlsson, R.; Ljungstrom, E. Nitrogen dioxide and sea salt particles - A laboratory study. *J. Aerosol Sci.* **1995**, *26*, 39-50, doi:10.1016/0021-8502(94)00098-J.
(6) Peters, S. J.; Ewing, G. E. Reaction of NO_2(g) with NaCl(100). *J. Phys. Chem.* **1996**, *100*, 14093-14102, doi:10.1021/jp9603694.
(7) Schroeder, W. H.; Urone, P. Formation of nitrosyl chloride from salt particles in air. *Environ. Sci. Technol.* **1974**, *8*, 756-758, doi:10.1021/es60093a015.
(8) Vogt, R.; Finlayson-Pitts, B. A diffuse reflectance infrared Fourier transform spectroscopic (DRIFTS) study of the surface reaction of NaCl with gaseous NO_2 and HNO_3. *J. Phys. Chem.* **1994**, *98*, 3747-3755, doi:10.1021/j100065a033.
(9) Vogt, R.; Finlayson-Pitts, B. F. Tropospheric HONO and reactions of oxides of nitrogen with NaCl. *Geophys. Res. Lett.* **1994**, *21*, 2291-2294, doi:10.1029/94GL02238.
(10) Vogt, R.; Finlayson-Pitts, B. J. Errata. *J. Phys. Chem.* **1995**, *99*, 13052, doi:10.1021/j100034a057.
(11) Winkler, T.; Goschnick, J.; Ache, H. J. Reactions of nitrogen oxides with NaCl as a model of sea salt aerosol. *J. Aerosol Sci.* **1991**, *22*, S605-S608, doi:10.1016/S0021-8502(05)80174-0.
(12) Yabushita, A.; Enami, S.; Sakamoto, Y.; Kawasaki, M.; Hoffmann, M. R.; Colussi, A. J. Anion-catalyzed dissolution of NO_2 on aqueous microdroplets. *J. Phys. Chem. A* **2009**, *113*, 4844-4848, doi:10.1021/jp900685f.
(13) Yoshitake, H. Effects of surface water on NO_2-NaCl reaction studied by diffuse reflectance infrared spectroscopy (DRIRS). *Atmos. Environ.* **2000**, *34*, 2571-2580, doi:10.1016/S1352-2310(99)00494-X.

27. **NO_2 + NaBr(s).** Vogt et al.[1] used diffuse reflectance infrared spectroscopy to study NO_2 + NaBr(s) at 298 K. The reaction was determined to be approximately second order in NO_2. Assuming that adsorbed N_2O_4 is the reactant leads to $\gamma = 2\ (+4, -1.3) \times 10^{-4}$.
Back to Table

(1) Vogt, R.; Elliott, C.; Allen, H. C.; Laux, J. M.; Hemminger, J. C.; Finlayson-Pitts, B. J. Some new laboratory approaches to studying tropospheric heterogeneous reactions. *Atmos. Environ.* **1996**, *30*, 1729-1737, doi:10.1016/1352-2310(95)00392-4.

28. **NO_2/N_2O_4 + sea salt.** Sverdrup and Kuhlman[2] measured the uptake of NO_2 on artificial sea salt using the NO_2 loss measured in a flow tube lined with the salt. The uptake coefficient was reported to increase from 10^{-7} to 10^{-6} as the relative humidity increased from 44% to 88%. Langer et al.[1] used diffuse reflectance Fourier transform infrared spectrometry to follow nitrate formation on synthetic sea salt and found the reaction was approximately second order (1.8 ± 0.2) in NO_2 in He carrier gas but approximately first order (1.2 ± 0.2) in NO_2 in air. Assuming that N_2O_4 was the reactant in He, $\gamma_{ss} = 1 \times 10^{-4}$, and assuming NO_2 is the reactant in air, $\gamma_{ss} = 1 \times 10^{-8}$. These reactions are sufficiently slow that they are unlikely to be important in the atmosphere.
Back to Table

(1) Langer, S.; Pemberton, R. S.; Finlayson-Pitts, B. J. Diffuse reflectance infrared studies of the reaction of synthetic sea salt mixtures with NO_2: A key role for hydrates in the kinetics and mechanism. *J. Phys. Chem. A* **1997**, *101*, 1277-1286, doi:10.1021/jp962122c.
(2) Sverdrup, G. M.; Kuhlman, M. R. "Heterogeneous Nitrogen Oxide-Particle Reactions"; 14th International Colloquium on Atmospheric Pollution, 1980, Paris.

29. **NO_3 + H_2O(s).** Fenter and Rossi[1] measured an upper limit for γ of 10^{-3} over the range from 170 to 200 K.
Back to Table

(1) Fenter, F. F.; Rossi, M. J. Heterogeneous reaction of NO_3 with ice and sulfuric acid solutions: Upper limits for the uptake coefficients. *J. Phys. Chem. A* **1997**, *101*, 4110-4113, doi:10.1021/jp970162q.

30. **NO_3 + H_2O(l).** Rudich et al.[3,4] used wetted-wall flow tube techniques to measure uptake coefficients for NO_3 on pure water and aqueous NaCl, NaBr, NaI, and $NaNO_2$ solutions. These studies were extended to other aqueous solutions by Imamura et al.[1] Uptake on pure water was consistent with reaction of NO_3 to produce HNO_3 and OH. Uptake coefficients with solutions containing I^-, Cl^-, Br^-, NO_2^-, and other anions were larger and scaled with anion concentration, indicating electron transfer reactions to produce NO_3^-. Reactions with these anions and/or adsorbed organic contaminants may well dominate the reactive uptake of NO_3 by real atmospheric aqueous surfaces. The γ of $(2.0 \pm 1.0 \times 10^{-4})$ at 273 K determined for pure water by Rudich et al. is significantly lower than the lower limit of 2.5×10^{-3} from Thomas and co-workers as quoted by Mihelcic et al.[2] and further discussed in Thomas et al.,[6] who also dispute that reactive uptake coefficient on pure water reported by Rudich et al. is due to nitric acid production. A detailed analysis of uptake coefficients for KI aqueous solutions by Rudich et al.[3] indicated that the NO_3 mass accommodation coefficient is >0.04,[3] but this result may be biased due to reactive uptake by interfacial I^-. Single droplet uptake results on Alizarin Red S dye and NaCl solutions at 293 K by Schütze and Herrman[5] suggest a value an order of magnitude smaller (see Table 5–1).
Back to Table

(1) Imamura, T.; Rudich, Y.; Talukdar, R. K.; Fox, R. W.; Ravishankara, A. R. Uptake of NO_3 onto water-solutions: Rate coefficient for reaction of NO_3 with cloud water constituents. *J. Phys. Chem.* **1997**, *101*, 2316-2322, doi:10.1021/jp962787e.
(2) Mihelcic, D.; Klemp, D.; Müsgen, P.; Pätz, H. W.; Volz-Thomas, A. Simultaneous measurements of peroxy and nitrate radicals at Schauinsland. *J. Atmos. Chem.* **1993**, *16*, 313-335, doi:10.1007/BF01032628.
(3) Rudich, Y.; Talukdar, R. K.; Imamura, T.; Fox, R. W.; Ravishankara, A. R. Uptake of NO_3 on KI solutions: Rate coefficient for the $NO_3 + I^-$ reaction and gas-phase diffusion coefficient for NO_3. *Chem. Phys. Lett.* **1996**, *261*, 467-473, doi:10.1016/0009-2614(96)00980-3.
(4) Rudich, Y.; Talukdar, R. K.; Ravishankara, A. R.; Fox, R. W. Reactive uptake of NO_3 on pure water and ionic solutions. *J. Geophys. Res.* **1996**, *101*, 21023-21031, doi:10.1029/96JD01844.
(5) Schütze, M.; Herrmann, H. Uptake of the NO_3 radical on aqueous surfaces. *J. Atmos. Chem.* **2005**, *52*, 1-18, doi:10.1007/s10874-005-6153-8.
(6) Thomas, K.; Volz-Thomas, A.; Mihelcic, D.; Smit, H. G. J.; Kley, D. On the exchange of NO_3 radicals with aqueous solutions: Solubility and sticking coefficient. *J. Atmos. Chem.* **1998**, *29*, 17-43, doi:10.1023/A:1005860312363.

31. **NO_3 + NaCl.** Also see note for $NO_3 + H_2O$(l). Recommended value for the initial uptake coefficient on solid NaCl is based on work of Seisel et al.,[4,5] Gershenzon and coworkers,[1] and Gratpanche and Sawerysyn[2]. Seisel et al.[4,5] used a Knudsen cell with mass spectrometric and laser-induced fluorescence detection of the NO_3. Salt powders from 60–630 μm in size were used, as well as spray-deposited samples; no dependence on the sample mass for powders or between powders and the spray-deposited samples was observed so no corrections for diffusion into underlying layers were applied. They obtained values for γ_0 of $(4.9 \pm 3) \times 10^{-2}$ and $(4.6 \pm 4) \times 10^{-2}$ (1σ), respectively. Gershenzon and coworkers used flow reactors with ESR and MS detection and measured the loss of NO_3 on an axially located rod coated with salt; they interpret their results, and the associated value of γ_0 derived from their data based on a multi-step mechanism involving adsorption and then reaction of NO_3 on the salt. The value for γ_0 is sensitive to several unknown parameters in the model, and they give a range from $(0.2–3.9) \times 10^{-2}$. Gratpanche and Sawerysyn[2] used a flow tube coated with NaCl and ESR detection of NO_3, and reported a value of $(1.7 \pm 1.2) \times 10^{-2}$ (1σ); on very dry NaCl, no uptake was observed, again indicating the importance of small amounts of water for the reaction. Gershenzon et al.[1] reported that the uptake coefficient decreased by about a factor of 20 over about half an hour, suggesting that the steady state value of γ_{ss} is approximately 1.5×10^{-3}. Zelenov et al. reported that the uptake coefficient for NO_3 on NaCl (and NaBr; see next note)[7,8] could be fit by a time-dependent term and a time-independent term: $\gamma(t) = \gamma_0 \exp(-t/\tau) + \gamma_{ss}$. They observed that γ_{ss} depends on the type of salt, as well as the NO_3 and water concentrations, while γ_0 depended only on the type of salt and NO_3 concentration. They concluded that the products are chemisorbed Cl atoms. No temperature dependence has been observed over

the temperature range 258–301 K by Gratpanche and Sawerysyn,[2] consistent with only an ~10% change in the uptake coefficient from 293 to 373 K observed by Gershenzon et al.[1]

The uptake of NO_3 on aqueous solutions of NaCl has been measured at 273 K by Rudich et al.[3] and at 293 K by Thomas et al.[6] NO_3 reacts in solutions with the halide ions. The measured uptake coefficients varied from (0.8–6) × 10^{-3} for solutions of activity ranging from 0.008 to 0.45 at 273 K[3] and was reported to be >2 × 10^{-3} on 0.1 M NaCl at 293 K.[6]

Back to Table

(1) Gershenzon, M. Y.; Il'in, S.; Fedotov, N. G.; Gershenzon, Y. M.; Aparina, E. V.; Zelenov, V. V. The mechanism of reactive NO_3 uptake on dry NaX (X = Cl, Br). *J. Atmos. Chem.* **1999**, *34*, 119-135, doi:10.1023/A:1006258205551.

(2) Gratpanche, F.; Sawerysyn, J.-P. Uptake coefficients of NO_3 radicals on solid surfaces of sea-salts. *J. Chim. Phys.* **1999**, *96*, 213-231, doi:10.1051/jcp:1999132.

(3) Rudich, Y.; Talukdar, R. K.; Ravishankara, A. R.; Fox, R. W. Reactive uptake of NO_3 on pure water and ionic solutions. *J. Geophys. Res.* **1996**, *101*, 21023-21031, doi:10.1029/96JD01844.

(4) Seisel, S.; Caloz, F.; Fenter, F. F.; vandenBergh, H.; Rossi, M. J. The heterogeneous reaction of NO_3 with NaCl and KBr: A nonphotolytic source of halogen atoms. *Geophys. Res. Lett.* **1997**, *24*, 2757-2760, doi:10.1029/97GL02857

(5) Seisel, S.; Fluckiger, B.; Caloz, F.; Rossi, M. J. Heterogeneous reactivity of the nitrate radical: Reactions on halogen salt at ambient temperature and on ice in the presence of HX (X = Cl, Br, I) at 190 K. *Phys. Chem. Chem. Phys.* **1999**, *1*, 2257-2266, doi:10.1039/A809355E.

(6) Thomas, K.; Volz-Thomas, A.; Mihelcic, D.; Smit, H. G. J.; Kley, D. On the exchange of NO_3 radicals with aqueous solutions: Solubility and sticking coefficient. *J. Atmos. Chem.* **1998**, *29*, 17-43, doi:10.1023/A:1005860312363.

(7) Zelenov, V. V.; Aparina, E. V.; Gershenzon, M. Y.; Il'in, S. D.; Gershenzon, Y. M. Kinetic mechanisms of atmospheric gases uptake on sea salt surfaces. 3. Reactive NO_3 uptake on humidified sea salts NaX (X=Cl, Br) under steady state conditions. *Khim. Fiz.* **2003**, *22*, 58-70.

(8) Zelenov, V. V.; Aparina, E. V.; Gershenzon, M. Y.; Il'in, S. D.; Gershenzon, Y. M. Kinetic mechanisms of atmospheric gases uptake on sea salt surfaces. 4. Initial step of NO_3 uptake on salts NaCl and NaBr. *Khim. Fiz.* **2003**, *22*, 37-48.

32. NO_3 + NaBr and NaI. Also see notes for NO_3 + NaCl and NO_3 + H_2O(l). Recommended value of γ_0 for the reaction with solid NaBr is based on reported values of 0.16 ± 0.08,[4] 0.20 ± 0.10,[5] a range of 0.1 to 0.3 [1] and 0.11 ± 0.06 [2] (all errors cited are 1σ). Gershenzon et al.[1] observed a decrease of about a factor of two with time, suggesting that γ_{ss} ~0.05. Gratpanche and Sawerysyn[2] found a slight negative temperature dependence, $\gamma_0 = (1.6^{+1.8}_{-0.9} \times 10^{-3}) \exp[(1210 \pm 200)/T]$ over the range from 243–293 K. Gershenzon et al.[1] also reported a small (30%) decrease in γ_0 from 293 to 373 K. Zelenov et al.[6,7] reported that the uptake coefficient for NO_3 on NaBr (and NaCl; see preceding note) could be fit by a time-dependent term and a time-independent term: $\gamma(t) = \gamma_0 \exp(-t/\tau) + \gamma_{ss}$. They observed that γ_{ss} depends on the type of salt, as well as the NO_3 and water concentrations, while γ_0 depended only on the type of salt and NO_3 concentration. They concluded that the products are bromine atoms in agreement with the observations of the branching ratio as well as the mass balance by Seisel et al.[4,5]

Rudich et al.[3] measured the uptake of NO_3 on aqueous KI solutions; NO_3 is taken up and reacts with I^- in solution. Uptake coefficients increased with the concentration of I^-, ranging from $\gamma = 0.9 \times 10^{-3}$ at 5×10^{-6} M KaI to 3.2×10^{-3} at a concentration of 8×10^{-5} M.

Back to Table

(1) Gershenzon, M. Y.; Il'in, S.; Fedotov, N. G.; Gershenzon, Y. M.; Aparina, E. V.; Zelenov, V. V. The mechanism of reactive NO_3 uptake on dry NaX (X = Cl, Br). *J. Atmos. Chem.* **1999**, *34*, 119-135, doi:10.1023/A:1006258205551.

(2) Gratpanche, F.; Sawerysyn, J.-P. Uptake coefficients of NO_3 radicals on solid surfaces of sea-salts. *J. Chim. Phys.* **1999**, *96*, 213-231, doi:10.1051/jcp:1999132.

(3) Rudich, Y.; Talukdar, R. K.; Imamura, T.; Fox, R. W.; Ravishankara, A. R. Uptake of NO_3 on KI solutions: Rate coefficient for the $NO_3 + I^-$ reaction and gas-phase diffusion coefficient for NO_3. *Chem. Phys. Lett.* **1996**, *261*, 467-473, doi:10.1016/0009-2614(96)00980-3.

(4) Seisel, S.; Caloz, F.; Fenter, F. F.; vandenBergh, H.; Rossi, M. J. The heterogeneous reaction of NO_3 with NaCl and KBr: A nonphotolytic source of halogen atoms. *Geophys. Res. Lett.* **1997**, *24*, 2757-2760, doi:10.1029/97GL02857.
(5) Seisel, S.; Fluckiger, B.; Caloz, F.; Rossi, M. J. Heterogeneous reactivity of the nitrate radical: Reactions on halogen salt at ambient temperature and on ice in the presence of HX (X = Cl, Br, I) at 190 K. *Phys. Chem. Chem. Phys.* **1999**, *1*, 2257-2266, doi:10.1039/A809355E.
(6) Zelenov, V. V.; Aparina, E. V.; Gershenzon, M. Y.; Il'in, S. D.; Gershenzon, Y. M. Kinetic mechanisms of atmospheric gases uptake on sea salt surfaces. 3. Reactive NO_3 uptake on humidified sea salts NaX (X=Cl, Br) under steady state conditions. *Khim. Fiz.* **2003**, *22*, 58-70.
(7) Zelenov, V. V.; Aparina, E. V.; Gershenzon, M. Y.; Il'in, S. D.; Gershenzon, Y. M. Kinetic mechanisms of atmospheric gases uptake on sea salt surfaces. 4. Initial step of NO_3 uptake on salts NaCl and NaBr. *Khim. Fiz.* **2003**, *22*, 37-48.

33. **NO_3 + organic surfaces.** Initial uptake of the nitrate radical occurs on organic surfaces that contain both unsaturated carbon-carbon bonds and saturated carbon-carbon bonds. The former reactions occur with large initial uptake coefficients (as large as 0.1) whereas smaller uptake coefficients describe uptake to saturated organic surfaces. The product distributions are highly complex. A more detailed discussion of this complex chemistry is given in two review articles: Kolb et al.[2] and Abbatt et al.[1]
Back to Table

(1) Abbatt, J. P. D.; Lee, A. K. Y.; Thornton, J. A. Quantifying trace gas uptake to tropospheric aerosol: recent advances and remaining challenges. *Chem. Soc. Rev.* **2012**, *41*, 6555-6581, doi:10.1039/C2CS35052A.
(2) Kolb, C. E.; Cox, R. A.; Abbatt, J. P. D.; Ammann, M.; Davis, E. J.; Donaldson, D. J.; Garrett, B. C.; George, C.; Griffiths, P. T.; Hanson, D. R.; Kulmala, M.; McFiggans, G.; Pöschl, U.; Riipinen, I.; Rossi, M. J.; Rudich, Y.; Wagner, P. E.; Winkler, P. M.; Worsnop, D. R.; O' Dowd, C. D. An overview of current issues in the uptake of atmospheric trace gases by aerosols and clouds. *Atmos. Chem. Phys.* **2010**, *10*, 10561-10605, doi:10.5194/acp-10-10561-2010.

34. **N_2O_5 + H_2O(s).** Leu[4] and Hanson and Ravishankara[1] measured nearly identical values of 0.028 (±0.011) and 0.024 (±30%) in the 195–202 K range on relatively thick ice films in coated wall flow tubes. Quinlan et al.[5] measured a maximum value for γ on ice surfaces at 188 K of 0.03 in a Knudsen cell reactor. The average of these three studies is 0.027 with a standard deviation of 0.003. Hanson and Ravishankara[2,3] presented new and re-analyzed data as a function of ice thickness, with a value of ~0.008 for the thinnest ice sample, rising to 0.024 for the thickest. From these data there would appear to be no strong dependence on temperature, at least over the 188–195 K range. It is unclear whether the measured dependence on ice film thickness is due to added porosity surface area in the thicker films or decreased ice film integrity in thinner films. The error estimate in the table is driven by the possible systematic error due to unresolved film thickness effects rather than the small statistical error among the "thick film" values from the three groups.

Zondlo et al.[6] report the formation of a supercooled H_2O/HNO_3 liquid layer at 185 K as a reaction product, forming NAT or NAD only after decreasing the relative humidity below the ice frost point. This effect is similar to that resulting from the interaction of gaseous HNO_3 or $ClONO_2$ with the ice surface. These authors measured $\gamma = (7 \pm 3) \times 10^{-4}$ at 185 K for the reaction of N_2O_5 with this supercooled liquid layer.
Back to Table

(1) Hanson, D. R.; Ravishankara, A. R. The reaction probabilities of $ClONO_2$ and N_2O_5 on 40 to 75% sulfuric acid solutions. *J. Geophys. Res.* **1991**, *96*, 17307-17314, doi:10.1029/91JD01750.
(2) Hanson, D. R.; Ravishankara, A. R. Investigation of the reactive and nonreactlve processes involving $ClONO_2$ and HCl on water and nitric acid doped ice. *J. Phys. Chem.* **1992**, *96*, 2682-2691, doi:10.1021/j100185a052.
(3) Hanson, D. R.; Ravishankara, A. R. Response to "Comment on porosities of ice films used to simulate stratospheric cloud surfaces". *J. Phys. Chem.* **1993**, *97*, 2802-2803, doi:10.1021/j100113a054.
(4) Leu, M.-T. Laboratory studies of sticking coefficients and heterogeneous reactions important in the Antarctic stratosphere. *Geophys. Res. Lett.* **1988**, *15*, 17-20, doi:10.1029/GL015i001p00017.

(5) Quinlan, M. A.; Reihs, C. M.; Golden, D. M.; Tolbert, M. A. Heterogeneous reactions on model polar stratospheric cloud surfaces: Reaction of N_2O_5 on ice and nitric acid trihydrate. *J. Phys. Chem.* **1990**, *94*, 3255-3260, doi:10.1021/j100371a007.
(6) Zondlo, M. A.; Barone, S. B.; Tolbert, M. A. Condensed-phase products in heterogeneous reactions: N_2O_5, $ClONO_2$ and HNO_3 reacting on ice films at 185 K. *J. Phys. Chem. A* **1998**, *102*, 5735-5748, doi:10.1021/jp980131a.

35. N_2O_5 + H_2O(l). This reaction has now been studied widely on both pure water and on aqueous surfaces. The kinetics of the reaction are dependent on a number of conditions, as described below.

On pure water, Van Doren et al.[26] measured γs of 0.057 ± 0.003 at 271 K and 0.036 ± 0.004 at 282 K using a droplet train uptake technique, indicating that the reaction has a negative temperature dependence. George et al.[8] also used a droplet train technique to measure γs of $(3.0 \pm 0.2) \times 10^{-2}$ (262 K), $(2.9 \pm 1.2) \times 10^{-2}$ (267 K), $(2.0 \pm 0.2) \times 10^{-2}$ (273 K), $(1.6 \pm 0.8) \times 10^{-2}$ (276 K), and $(1.3 \pm 0.8) \times 10^{-2}$ (277 K) on pure water, while Schweitzer et al.[23] used the same approach for pure water and salt solutions between 262 and 278 K, obtaining similar results. Msibi et al.[17] measured a smaller γ of 2.5×10^{-3} for water adsorbed on a denuder flow tube well under 66–96% relative humidity conditions at room temperature, making the nature of the surface unclear. After correction for gas-phase diffusion effects, Schütze and Herrmann[22] measured a γ of 1.1×10^{-2} at 293 K using a single suspended droplet flow reactor method that was probably constrained by nitrate build-up in the droplet's surface layer.

A number of other groups have measured the uptake coefficients of N_2O_5 on aqueous solutions where, in the absence of halide ions, the reactivity of the N_2O_5 is with the water solvent molecules. These studies include: Mozurkewich and Calvert[16] on $NH_3/H_2SO_4/H_2O$ aerosols in an aerosol flow tube, Hu and Abbatt[13] on $(NH_4)_2SO_4$ aerosols at 297 K in an aerosol flow tube, Mentel and co-workers[15,28] on sodium sulfate and sodium nitrate particles in a large aerosol chamber, Thornton et al.[25] for uptake on malonic acid aerosols in an aerosol flow tube, Hallquist et al.[12] studied ammonium sulfate and sodium nitrate particles, and Griffiths et al.[9] measured uptake on a variety of soluble organic acids with and without ammonium sulfate present. Note that the studies conducted with sodium chloride or sea salt as the solute are listed in the N_2O_5 + NaCl note below.

Overall, the γ values measured at high relative humidity by Van Doren et al., Mozurkewhich and Calvert, Hu and Abbatt, Thornton et al., Hallquist et al., Griffiths et al., Gaston et al.[7] and Gaston and Thornton,[6] and those from experiments with NaCl at high relative humidity (Behnke et al.[2] and Thornton and Abbatt[24]) are quite consistent when temperature and RH effects are factored in, yielding uptake coefficients in the 0.02 to 0.04 range at room temperature. The lower values from the Louis Pasteur (George et al. and Schweitzer et al.) and Birmingham (Msibi et al.) groups appear to have much less pronounced temperature dependence and are inconsistent with the other measurements. The same function used to fit the N_2O_5 uptake on sulfuric acid as a function of temperature and concentration, discussed below, has been extended to the Van Doren et al. and Hu and Abbatt data for pure water and very high RH aerosols. See note on N_2O_5 + H_2SO_4•nH_2O(l) for the functional fit and its error discussion.

However, other factors that affect the uptake coefficient include: 1. At low relative humidities, the γ values are reduced from the values close to water saturation, with the uptake coefficient scaling linearly with the water content of the aerosol below a specific relative humidity (roughly 50% RH). This is indicative of a competition for water of a reactive intermediate formed via N_2O_5 initial uptake (see in particular Thornton et al.,[25] Thornton and Abbatt,[24] Hallquist et al.,[12] and Griffiths et al.[9]). 2. At high aerosol nitrate concentrations the kinetics are slower, falling below 0.001 in some cases, indicative that a reactive intermediate along the reaction pathway is less stable under such conditions (see Mentel and co-workers[15,28] and Hallquist et al.[12]). Note that high nitrate levels may develop in laboratory experiments where high N_2O_5 concentrations are used, potentially biasing the uptake coefficients to lower values than are atmospherically significant. This may be manifest as an uptake coefficient that is dependent on the concentration of N_2O_5 used.[25] 3. By varying particle diameters, the reacto-diffusive length has been measured to be 48 nm at 50% RH on malonic acid aqueous particles, indicating that this process is not fully occurring at the surface of the particle and that there might be a particle-size dependence to the uptake coefficient.[25] Likewise, studies by Gaston and Thornton[6] have indicated the reacto-diffusive length to be 32 nm in the case of uptake to aqueous ammonium sulfate and bisulfate particles. 4. The uptake coefficients can be substantially suppressed when large organic molecules, such as those formed by the reaction of ozone with alpha-pinene or those present in humic-like materials are present in/on aqueous inorganic aerosol.[1,5] The uptake coefficients in these systems can be

substantially below 0.01, with only a few weight percent of organic present. Also, monolayers of surfactant organics on aqueous particles can have the same effect (Thornton and Abbatt[24] and McNeill et al.[14]). Gaston et al.[7] have further explored the role of organics, showing that the chemical nature of the organic material (as described by its O/C ratio) and the relative humidity need to be taken into consideration. Low O/C substances generally depress the uptake coefficient more effectively, but not universally, than high O/C substances. The picture that arises is that core-shell morphologies arise in many mixed organic-inorganic particles, with the solubility and/or diffusivity of N_2O_5 in the organic shell driving the reduction of the uptake coefficient relative to its value for the pure inorganic system. Consistent with this model is the work of Grzinic et al.,[11] which demonstrated the viscosity of the organic material (in particular, citric acid at different relative humidities) has a strong role in affecting the uptake. Higher viscosity presumably sets the diffusion of either water or N_2O_5 as the rate determining step in the reaction, sometimes confining the reactive uptake to the surface of the particle. Finally, as observed with pure water by Van Doren et al.,[26] there is a negative temperature dependence to the uptake coefficient over the small temperature range that has been studied.[9,12] For example, the most recent measurements by Griffiths et al.[10] show the uptake coefficient changing from 0.035 to 0.005 from 263 to 303 K at 50% RH with ammonium sulfate particles. A parameterization of laboratory kinetics that takes into account the water, nitrate, dissolved organic, and chloride concentrations has been published by Bertram and Thornton.[3]

Beyond the laboratory, the uptake coefficient of N_2O_5 has been measured from decays on ambient (outdoor air) particles in an aerosol flow tube. It has been observed that the uptake coefficients are smallest (<0.005) when the organic content of the particles is high. Uptake coefficients of 0.03 were measured, but only on some occasions and when the sulphate/organic content of the particles was highest.[4] Additional studies with ambient particles have confirmed the wide range of uptake coefficients under ambient conditions with a wide range of relative humidities, observing a substantial amount of day-to-day variability that may be due to variable particle phase and/or organic composition.[18-21,27] As examples, Phillips et al.[18] observed uptake coefficients that varied from 0.004 to 0.11 at a semi-rural, non-coastal, mountain site. Yields of $ClNO_2$ were also variable from 0.035 to 1.38, dependent on the amount of chloride in the particles. Wagner et al.[27] illustrate the importance of the nitrate inhibition of uptake, via measurements in wintertime in Colorado. Ryder et al.[20] show that marine sea spray aerosol does not exhibit much uptake inhibition arising from organic components in the particles, relative to a purely inorganic aqueous particle.
Back to Table

(1) Badger, C. L.; Griffiths, P. T.; George, I.; Abbatt, J. P. D.; Cox, R. A. Reactive uptake of N_2O_5 by aerosol particles containing mixtures of humic acid and ammonium sulfate. *J. Phys. Chem. A* **2006**, *110*, 6986-6994, doi:10.1021/jp0562678.

(2) Behnke, W.; George, C.; Scheer, V.; Zetsch, C. Production and decay of $ClNO_2$ from the reaction of gaseous N_2O_5 with NaCl solution: Bulk and aerosol experiments. *J. Geophys. Res.* **1997**, *102*, 3795-3804, doi:10.1029/96JD03057.

(3) Bertram, T. H.; Thornton, J. A. Toward a general parameterization of N_2O_5 reactivity on aqueous particles: the competing effects of particle liquid water, nitrate and chloride. *Atmos. Chem. Phys.* **2009**, *9*, 8351-8363, doi:10.5194/acp-9-8351-2009.

(4) Bertram, T. H.; Thornton, J. A.; Riedel, T. P.; Middlebrook, A. M.; Bahreini, R.; Bates, T. S.; Quinn, P. K.; Coffman, D. J. Direct observations of N_2O_5 reactivity on ambient aerosol particles. *Geophys. Res. Lett.* **2009**, *36*, L19803, doi:10.1029/2009gl040248.

(5) Folkers, M.; Mentel, T. F.; Wahner, A. Influence of an organic coating on the reactivity of aqueous aerosols probed by the heterogeneous hydrolysis of N_2O_5. *Geophys. Res. Lett.* **2003**, *30*, 1644, doi:10.1029/2003GL017168.

(6) Gaston, C. J.; Thornton, J. A. Reacto-diffusive length of N_2O_5 in aqueous sulfate- and chloride-containing aerosol particles. *J. Phys. Chem. A.* **2016**, *120*, 1039-1045, doi:10.1021/acs.jpca.5b11914.

(7) Gaston, C. J.; Thornton, J. A.; Ng, N. L. Reactive uptake of N_2O_5 to internally mixed inorganic and organic particles: the role of organic carbon oxidation state and inferred organic phase separations. *Atmos. Chem. Phys.* **2014**, *14*, 5693-5707, doi:10.5194/acp-14-5693-2014.

(8) George, C.; Ponche, J. L.; Mirabel, P.; Behnke, W.; Sheer, V.; Zetzsch, C. Study of the uptake of N_2O_5 by water and NaCl solutions. *J. Phys. Chem.* **1994**, *98*, 8780-8784, doi:10.1021/j100086a031.

(9) Griffiths, P. T.; Badger, C. L.; Cox, R. A.; Folkers, M.; Henk, H. H.; Mentel, T. F. Reactive uptake of N_2O_5 by aerosols containing dicarboxylic acids. effect of particle phase, composition, and nitrate content. *J. Phys. Chem. A* **2009**, *113*, 5082-5090, doi:10.1021/jp8096814.

(10) Griffiths, P. T.; Cox, R. A. Temperature dependence of heterogeneous uptake of N_2O_5 by ammonium sulfate aerosol. *Atmos. Sci. Lett.* **2009**, *10*, 159-163, doi:10.1002/asl.225.
(11) Gržinić, G.; Bartels-Rausch, T.; Berkemeier, T.; Türler, A.; Ammann, M. Viscosity controls humidity dependence of N_2O_5 uptake to citric acid aerosol. *Atmos. Chem. Phys.* **2015**, *15*, 13615-13625, doi:10.5194/acp-15-13615-2015.
(12) Hallquist, M.; Stewart, D. J.; Stephenson, S. K.; Cox, R. A. Hydrolysis of N_2O_5 on sub-micron sulfate aerosols. *Phys. Chem. Chem. Phys.* **2003**, *5*, 3453-3463, doi:10.1039/b301827j.
(13) Hu, J. H.; Abbatt, J. P. D. Reaction probabilities for N_2O_5 hydrolysis on sulfuric acid and ammonium sulfate aerosols at room temperature. *J. Phys. Chem. A* **1997**, *101*, 871-878, doi:10.1021/jp9627436.
(14) McNeill, V. F.; Patterson, J.; Wolfe, G. M.; Thornton, J. A. The effect of varying levels of surfactant on the reactive uptake of N_2O_5 to aqueous aerosol. *Atmos. Chem. Phys.* **2006**, *6*, 1635-1644, doi:10.5194/acp-6-1635-2006.
(15) Mentel, T. F.; Sohn, M.; Wahner, A. Nitrate effect in the heterogeneous hydrolysis of dinitrogen pentoxide on aqueous aerosols. *Phys. Chem. Chem. Phys.* **1999**, *1*, 5451-5457, doi:10.1039/A905338G.
(16) Mozurkewich, M.; Calvert, J. Reaction probability of N_2O_5 on aqueous aerosols. *J. Geophys. Res.* **1988**, *93*, 15882-15896, doi:10.1029/JD093iD12p15889.
(17) Msibi, I. M.; Li, Y.; Shi, J. P.; Harrison, R. M. Determination of heterogeneous reaction probability using deposition profile measurement in an annular reactor: application to the N_2O_5/H_2O reaction. *J. Atmos. Chem.* **1994**, *18*, 291-300, doi:10.1007/BF00696784.
(18) Phillips, G. J.; Thieser, J.; Tang, M.; Sobanski, N.; Schuster, G.; Fachinger, J.; Drewnick, F.; Borrmann, S.; Bingemer, H.; Lelieveld, J.; Crowley, J. N. Estimating N_2O_5 uptake coefficients using ambient measurements of NO_3, N_2O_5, $ClNO_2$ and particle-phase nitrate. *Atmos. Chem. Phys.* **2016**, *16*, 13231-13249, doi:10.5194/acp-16-13231-2016.
(19) Riedel, T. P.; Bertram, T. H.; Ryder, O. S.; Liu, S.; Day, D. A.; Russell, L. M.; Gaston, C. J.; Prather, K. A.; Thornton, J. A. Direct N_2O_5 reactivity measurements at a polluted coastal site. *Atmos. Chem. Phys.* **2012**, *12*, 2959-2968, doi:10.5194/acp-12-2959-2012.
(20) Ryder, O. S.; Ault, A. P.; Cahill, J. F.; Guasco, T. L.; Riedel, T. P.; Cuadra-Rodriguez, L. A.; Gaston, C. J.; Fitzgerald, E.; Lee, C.; Prather, K. A.; Bertram, T. H. On the role of particle inorganic mixing atate in the reactive uptake of N_2O_5 to ambient aerosol particles. *Environ. Sci. Technol.* **2014**, *48*, 1618-1627, doi:10.1021/es4042622.
(21) Ryder, O. S.; Ault, A. P.; Cahill, J. F.; Guasco, T. L.; Riedel, T. P.; Cuadra-Rodriguez, L. A.; Gaston, C. J.; Fitzgerald, E.; Lee, C.; Prather, K. A.; Bertram, T. H. On the role of particle inorganic mixing state in the reactive uptake of N_2O_5 to ambient aerosol particles. *Environ. Sci. Technol.* **2014**, *48*, 1618-1627, doi:10.1021/es4042622.
(22) Schütze, M.; Herrmann, H. Determination of phase transfer parameters for the uptake of HNO_3, N_2O_5 and O_3 on single aqueous drops. *Phys. Chem. Chem. Phys.* **2002**, *4*, 60-67, doi:10.1039/b106078n.
(23) Schweitzer, F.; Mirabel, P.; George, C. Multiphase chemistry of N_2O_5, $ClNO_2$ and $BrNO_2$. *J. Phys. Chem. A* **1998**, *102*, 3942-3952, doi:10.1021/jp980748s.
(24) Thornton, J. A.; Abbatt, J. P. D. N_2O_5 reaction on submicron sea salt aerosol: Kinetics, products, and the effect of surface active organics. *J. Phys. Chem. A* **2005**, *109*, 10004-10012, doi:10.1021/Jp054183t.
(25) Thornton, J. A.; Braban, C. F.; Abbatt, J. P. D. N_2O_5 hydrolysis on sub-micron organic aerosols: the effect of relative humidity, particle phase, and particle size. *Phys. Chem. Chem. Phys.* **2003**, *5*, 4593-4603, doi:10.1039/b307498f.
(26) Van Doren, J. M.; Watson, L. R.; Davidovits, P.; Worsnop, D. R.; Zahniser, M. S.; Kolb, C. E. Temperature dependence of the uptake coefficients of HNO_3, HCl, and N_2O_5 by water droplets. *J. Phys. Chem.* **1990**, *94*, 3265-3269, doi:10.1021/j100371a009.
(27) Wagner, N. L.; Riedel, T. P.; Young, C. J.; Bahreini, R.; Brock, C. A.; Dubé, W. P.; Kim, S.; Middlebrook, A. M.; Oztürk, F.; Roberts, J. M.; Russo, R.; Sive, B.; Swarthout, R.; Thornton, J. A.; VandenBoer, T. C.; Zhou, Y.; Brown, S. S. N_2O_5 uptake coefficients and nocturnal NO_2 removal rates determined from ambient wintertime measurements. *J. Geophys. Res.* **2013**, *118*, 9331-9350, doi:10.1002/jgrd.50653.
(28) Wahner, A.; Mentel, T. F.; Sohn, M.; Stier, J. Heterogeneous reaction of N_2O_5 on sodium nitrate aerosol. *J. Geophys. Res.* **1998**, *103*, 31103-31112, doi:10.1029/1998JD100022.

36. **$N_2O_5 + HNO_3 \cdot 3H_2O(s)$.** Hanson and Ravishankara[1] have measured $\gamma = 0.0006$ (± 30%) near 200 K. They re-analyzed their results and give additional data as a function of ice thickness (Hanson and Ravishankara[2,3]), deriving a value of 3×10^{-4} for the thinnest nitric acid trihydrate (NAT) covered ice layer, with values up to three times higher for thicker NAT-covered ice layers. As in the case of uptake on water ice this may be due to increased surface area from porosity in the thicker films, or less integrity in the thinner films. The uncertainty listed in the Table is driven by this observed effect. All of the Hanson et al. data are in poor agreement with the $\gamma = 0.015 \pm 0.006$ reported by Quinlan et al.[4] from their Knudsen cell measurements; this measurement may have been biased by formation of a super-cooled aqueous nitric acid surface and is judged to be unreliable. It is possible that the uptake coefficients will be affected by whether the NAT surfaces are water-rich or poor.
Back to Table

(1) Hanson, D. R.; Ravishankara, A. R. The reaction probabilities of $ClONO_2$ and N_2O_5 on polar stratospheric cloud materials. *J. Geophys. Res.* **1991**, *96*, 5081-5090, doi:10.1029/90JD02613.
(2) Hanson, D. R.; Ravishankara, A. R. Investigation of the reactive and nonreactlve processes involving $ClONO_2$ and HCl on water and nitric acid doped ice. *J. Phys. Chem.* **1992**, *96*, 2682-2691, doi:10.1021/j100185a052.
(3) Hanson, D. R.; Ravishankara, A. R. Response to "Comment on porosities of ice films used to simulate stratospheric cloud surfaces". *J. Phys. Chem.* **1993**, *97*, 2802-2803, doi:10.1021/j100113a054.
(4) Quinlan, M. A.; Reihs, C. M.; Golden, D. M.; Tolbert, M. A. Heterogeneous reactions on model polar stratospheric cloud surfaces: Reaction of N_2O_5 on ice and nitric acid trihydrate. *J. Phys. Chem.* **1990**, *94*, 3255-3260, doi:10.1021/j100371a007.

37. **$N_2O_5 + H_2SO_4 \cdot nH_2O(l)$.** This reaction has been intensively studied between 195 and 296 K for a wide range of H_2SO_4 wt.% values using four complementary experimental techniques. Data are available from aerosol flow tube studies (Fried et al.,[3] Hanson and Lovejoy,[5] Hu and Abbatt,[7] and Hallquist et al.[4]), coated wall flow tube studies (Hanson and Ravishankara[6] and Zhang et al.[14]), a stirred Knudsen cell (Manion et al.[9]) and droplet train studies (Van Doren et al.[12] and Robinson et al.[11]). All studies have yielded γs between ~0.05 and 0.20 with modest dependence on surface H_2SO_4 wt.% and temperature. The Knudsen cell studies, aerosol flow tube studies at higher N_2O_5 exposure and the ternary $H_2SO_4/HNO_3/H_2O$ studies of Zhang et al.[14] all illustrate that significant levels of HNO_3 in the H_2SO_4/H_2O solutions will reduce γ measurably; this fact explains some of the scatter in aerosol flow tube studies and the surface saturation evident in the Knudsen cell studies. The "nitrate effect" reduction of γ was also studied in extensive aerosol chamber studies at 193.6 K by Wagner et al.[13] The effect of 5.0×10^{-7} Torr HNO_3 on γ as a function of temperature at two water vapor concentrations are plotted in Zhang et al.;[14] the decrease in γ is greatest at low temperatures, approaching a factor of 2–5 between 200 and 195 K.

Experimental data on sulfuric acid surfaces between 40 and 80 wt% sulfuric acid deemed to be free of saturation effects, plus the pure water uptake data of Van Doren et al.[12] and high relative humidity ammonium sulfate aerosol uptake data of Hu and Abbatt[7] were all fit to a polynomial expression to yield a single model describing γ for N_2O_5 uptake valid between 0 and 80 wt% H_2SO_4 and 180 to 300 K (Robinson et al.[11]). The form of this function is: $\gamma_o = \exp(k_o + k_1/T + k_2/T^2)$, where T is the temperature in K. The parameters k_o, k_1, and k_2 obtained from the best-fit are:

$$k_o = -25.5265 - 0.133188wt + 0.00930846wt^2 - 9.0194 \times 10^{-5}wt^3$$

$$k_1 = 9283.76 + 115.345wt - 5.19258wt^2 + 0.0483464wt^3$$

$$k_2 = -851801 - 22191.2wt + 766.916\ wt^2 - 6.85427wt^3$$

where wt is the weight percentage of H_2SO_4.

The overall error of applying the uptake function provided here consists of two components. One is the standard deviation of the model-calculated value with respect to measured data, σ_m, which is given by

$$\sigma_m = \sqrt{\frac{\sum_{i=1}^{N}\left(1-\frac{\gamma_i}{\gamma_{model}}\right)^2}{N-1}}.$$

The other is the standard deviation of relative experimental measurement error from the mean, σ_d, which is given by

$$\sigma_d = \sqrt{\frac{\sum_{i=1}^{N}\left(\frac{\Delta\gamma_i}{\gamma_i}\right)^2}{N(N-1)}}.$$

The overall error is

$$\sigma = \sqrt{\sigma_m^2 + \sigma_d^2}\,.$$

(These formulations are also applied below in the error estimation for the $ClONO_2 + H_2O$ and HCl, $BrONO_2 + H_2O$, and HOCl + HCl reaction system. For N_2O_5, the error is estimated to be 15% (1σ), with σ_m = 14.7% and σ_d = 2.9%).

Liquid trough flow reactor studies on 60–80 wt%H_2SO_4 at 273–280 K by Bertram and co-workers demonstrated that adsorbed single and dual component coatings of organics like 1-hexadeconal, 1-octadeconal and stearic acid could reduce γ by well over a factor of 10, while coatings of phytanic acid had little effect. Even 0.75 monolayer coatings of 1-octadeconal reduced γ by a factor of 10.[1,2,8] Park et al.[10] impinged a molecular beam of N_2O_5 on 72 wt% H_2SO_4 at 216 K, observing that sub-monolayer coverage of 1-butanol and 1-hexanol reduced bare acid reactive uptake coefficients from ~0.15 to ~0.10 and 0.06, respectively.

Back to Table

(1) Cosman, L. M.; Bertram, A. K. Reactive uptake of N_2O_5 on aqueous H_2SO_4 solutions coated with 1-component and 2-component monolayers. *J. Phys. Chem. A* **2008**, *112*, 4625-4635, doi:10.1021/jp8005469.

(2) Cosman, L. M.; Knopf, D. A.; Bertram, A. K. N_2O_5 reactive uptake on aqueous sulfuric acid solutions coated with branched and straight-chain insoluble organic surfactants. *J. Phys. Chem. A* **2008**, *112*, 2386-2396, doi:10.1021/jp710685r.

(3) Fried, A.; Henry, B. E.; Calvert, J. G.; Mozukewich, M. The reaction probability of N_2O_5 with sulfuric acid aerosols at stratospheric temperatures and compositions. *J. Geophys. Res.* **1994**, *99*, 3517-3532, doi:10.1029/93JD01907.

(4) Hallquist, M.; Stewart, D. J.; Baker, J.; Cox, R. A. Hydrolysis of N_2O_5 on submicron sulfuric acid aerosols. *J. Phys. Chem. A* **2000**, *104*, 3984-3990, doi:10.1021/jp9939625.

(5) Hanson, D. R.; Lovejoy, E. R. The uptake of N_2O_5 onto small sulfuric acid particles. *Geophys. Res. Lett.* **1994**, *21*, 2401-2404, doi:10.1029/94GL02288.

(6) Hanson, D. R.; Ravishankara, A. R. The reaction probabilities of $ClONO_2$ and N_2O_5 on polar stratospheric cloud materials. *J. Geophys. Res.* **1991**, *96*, 5081-5090, doi:10.1029/90JD02613.

(7) Hu, J. H.; Abbatt, J. P. D. Reaction probabilities for N_2O_5 hydrolysis on sulfuric acid and ammonium sulfate aerosols at room temperature. *J. Phys. Chem. A* **1997**, *101*, 871-878, doi:10.1021/jp9627436.

(8) Knopf, D. A.; Cosman, L. M.; Mousavi, P.; Mokamati, S.; Bertram, A. K. A novel flow reactor for studying reactions on liquid surfaces coated by organic monolayers: Methods, validation, and initial results. *J. Phys. Chem. A* **2007**, *111*, 11021-11032, doi:10.1021/jp075724c.

(9) Manion, J. A.; Fittschen, C. M.; Golden, D. M.; Williams, L. R.; Tolbert, M. A. Heterogeneous reactions of chlorine nitrate and dinitrogen pentoxide on sulfuric acid surfaces representative of global stratospheric aerosol particles. *Israel J. Chem.* **1994**, *34*, 355-363.

(10) Park, S.-C.; Burden, D. K.; Nathanson, G. M. The inhibition of N_2O_5 hydrolysis in sulfuric acid by 1-butanol and 1-hexanol surfactant coatings. *J. Phys. Chem. A* **2007**, *111*, 2921-2929, doi:10.1021/jp068228h.

(11) Robinson, G. N.; Worsnop, D. R.; Jayne, J. T.; Kolb, C. E.; Davidovits, P. Heterogeneous uptake of $ClONO_2$ and N_2O_5 by sulfuric acid solutions. *J. Geophys. Res.* **1997**, *102*, 3583-3601, doi:10.1029/96JD03457.

(12) Van Doren, J. M.; Watson, L. R.; Davidovits, P.; Worsnop, D. R.; Zahniser, M. S.; Kolb, C. E. Temperature dependence of the uptake coefficients of HNO_3, HCl, and N_2O_5 by water droplets. *J. Phys. Chem.* **1990**, *94*, 3265-3269, doi:10.1021/j100371a009.

(13) Wagner, R.; Naumann, K.-H.; Mangold, A.; Möhler, O.; Saathoff, H.; Schurath, U. Aerosol chamber study of optical constants and N_2O_5 uptake on supercooled $H_2SO_4/H_2O/HNO_3$ solution droplets at

polar stratospheric cloud temperatures. *J. Phys. Chem. A* **2005**, *109*, 8140-8148, doi:10.1021/jp0513364.
(14) Zhang, R.; Leu, M.-T.; Keyser, L. F. Heterogeneous reactions of $ClONO_2$, HCl and HOCl on liquid sulfuric acid surfaces. *J. Phys. Chem.* **1994**, *98*, 13563-13574, doi:10.1021/j100102a022.

38. **N_2O_5 + H_2SO_4•H_2O(s).** Zhang et al.[1] used coated flow tube techniques to measure the uptake of N_2O_5 on solid sulfuric acid monohydrate over a temperature range of 200 to 225 K. The measurement values of γ were significantly higher at 200 K ($\gamma \sim 1 \times 10^{-3}$) than at 225 K ($\gamma \sim 10^{-4}$) and were well fit by $\log \gamma = [4.78 - 0.0386T(K)]$. Acid-rich H_2SO_4•H_2O surfaces had a lower γ than water rich surfaces ($\log \gamma = [0.162 - 0.789 \times \log p_{H2O}]$ where p_{H2O} is their experimental water vapor partial pressure in Torr).
Back to Table

(1) Zhang, R.; Leu, M.-T.; Keyser, L. F. Hydrolysis of N_2O_5 and $ClONO_2$ on the $H_2SO_4/HNO_3/H_2O$ ternary solutions under stratospheric conditions. *Geophys. Res. Lett.* **1995**, *22*, 1493-1496, doi:10.1029/95GL01177.

39. **N_2O_5 + H_2SO_4•4H_2O(s).** Hanson and Ravishankara[1] studied N_2O_5 uptake by frozen 57.5 and 60 wt.% H_2SO_4 as a function of temperature and relative humidity. The 57.5 wt% surface was not sensitive to relative humidity and was slightly more reactive (γ = 0.008 vs 0.005) at 205 K than at 195 K. Reaction probabilities on the 60 wt% surface dropped off with temperature and relative humidity.
Back to Table

(1) Hanson, D. R.; Ravishankara, A. R. Reaction of $ClONO_2$ with HCl on NAT, NAD, and frozen sulfuric acid and hydrolysis of N_2O_5 and $ClONO_2$ on frozen sulfuric acid. *J. Geophys. Res.* **1993**, *98*, 22931-22936, doi:10.1029/93JD01929.

40. **N_2O_5 + Mineral Dust.** Tang et al.[1] have studied the room temperature reactive uptake of N_2O_5 to two different mineral dust aerosol types using an aerosol flow tube coupled to a thermal-dissociation cavity ring-down detection technique. It is notable that the reactive uptake of N_2O_5 to illite clay particles is large, on the order of 0.09 under dry conditions. This value is larger than values commonly measured for N_2O_5 uptake to aqueous substrates, such as ammonium sulfate or sodium chloride salts. Clays take up water at elevated relative humidity and so it is interesting that the uptake coefficient drops to 0.04 at an RH of 67%. The value of 0.04 is much closer to the values for gamma on deliquesced salt solutions. Given that there is a drop of the uptake coefficient with increasing relative humidity, it is possible that there is a change in uptake mechanism occurring. By contrast, the uptake coefficient of N_2O_5 to Arizona Test Dust (ATD), a multicomponent dust mixture, is much smaller, about 0.006, and it does not show a strong relative humidity dependence.
Back to Table

(1) Tang, M. J.; Schuster, G.; Crowley, J. N. Heterogeneous reaction of N_2O_5 with illite and Arizona test dust particles. *Atmos. Chem. Phys.* **2014**, *14*, 245-254, doi:10.5194/acp-14-245-2014.

41. **N_2O_5 + HCl on H_2O(s).** Leu[3] measured $\gamma = 0.028 \pm 0.011$ at 195 K, while Tolbert et al.[5] measured a lower limit of 1×10^{-3} at 185 K. Seisel et al.[4] measured $\gamma \sim 0.03$ at 200 K using a Knudsen flow reactor with a range of HCl flows. The uptake coefficient at low HCl flows is only slightly enhanced compared to the uptake on a pure ice surface. $ClNO_2$ was observed as the product in these studies. These experiments were done at high HCl levels probably leading to a liquid water/acid surface solution (Abbatt et al.[1]). Indeed, Hanson and Ravishankara[2] point out that a pure ice surface is readily converted to one with a thin NAT coating even with low N_2O_5 partial pressures, making this reaction difficult to study on pure ice surfaces.
Back to Table

(1) Abbatt, J. P. D.; Beyer, K. D.; Fucaloro, A. F.; McMahon, J. R.; Wooldridge, P. J.; Zhong, R.; Molina, M. J. Interaction of HCl vapor with water-ice: Implications for the stratosphere. *J. Geophys. Res.* **1992**, *97*, 15819-15826, doi:10.1029/92JD01220.
(2) Hanson, D. R.; Ravishankara, A. R. The reaction probabilities of $ClONO_2$ and N_2O_5 on polar stratospheric cloud materials. *J. Geophys. Res.* **1991**, *96*, 5081-5090, doi:10.1029/90JD02613.
(3) Leu, M.-T. Heterogeneous reaction of N_2O_5 with H_2O and HCl on ice surfaces: implications for Antarctic ozone depletion. *Geophys. Res. Lett.* **1988**, *15*, 851-854, doi:10.1029/GL015i008p00851.

(4) Seisel, S.; Fluckiger, B.; Rossi, M. J. The heterogeneous reaction of N_2O_5 with HBr on ice: Comparison with N_2O_5 + HC1. *Ber. Bunsenges. Phys. Chem.* **1998**, *102*, 811-820, doi:10.1002/bbpc.19981020604.
(5) Tolbert, M. A.; Rossi, M. J.; Golden, D. M. Antarctic ozone depletion chemistry: Reactions of N_2O_5 with H_2O and HCl on ice surfaces. *Science* **1988**, *240*, 1018-1021, doi:10.1126/science.240.4855.1018.

42. **N_2O_5 + HCl on HNO_3•3H_2O(s).** Hanson and Ravishankara[1] measured $\gamma = 0.0032$ (±30%) near 200 K.
Back to Table

(1) Hanson, D. R.; Ravishankara, A. R. The reaction probabilities of $ClONO_2$ and N_2O_5 on polar stratospheric cloud materials. *J. Geophys. Res.* **1991**, *96*, 5081-5090, doi:10.1029/90JD02613.

43. **N_2O_5 + HCl on H_2SO_4•H_2O(s).** Zhang et al.[1] saw no increase in N_2O_5 uptake on sulfuric acid monohydrate at 195 K upon exposure to HCl, setting $\gamma < 10^{-4}$.
Back to Table

(1) Zhang, R.; Leu, M.-T.; Keyser, L. F. Hydrolysis of N_2O_5 and $ClONO_2$ on the $H_2SO_4/HNO_3/H_2O$ ternary solutions under stratospheric conditions. *Geophys. Res. Lett.* **1995**, *22*, 1493-1496, doi:10.1029/95GL01177.

44. **N_2O_5 + HBr on H_2O(s).** Seisel et al.[1] report γ values ranging from ~3×10^{-3} to 0.1, depending on the HBr concentrations employed; the measurements were conducted at 180 and 200 K. These authors report Br_2 and HONO in 80% yield as products with respect to N_2O_5 taken up, generated presumably by the secondary reaction of the primary product $BrNO_2$ with HBr.
Back to Table

(1) Seisel, S.; Fluckiger, B.; Rossi, M. J. The heterogeneous reaction of N_2O_5 with HBr on ice: Comparison with N_2O_5 + HC1. *Ber. Bunsenges. Phys. Chem.* **1998**, *102*, 811-820, doi:10.1002/bbpc.19981020604.

45. **N_2O_5 + HBr on HNO_3•3H_2O(s).** This reaction, yielding γ ~0.005, was investigated on NAT surfaces near 200 K by Hanson and Ravishankara.[1] Under some conditions a much higher reaction coefficient of ~0.04 was observed.
Back to Table

(1) Hanson, D. R.; Ravishankara, A. R. Heterogeneous chemistry of HBr and HF. *J. Phys. Chem.* **1992**, *96*, 9441-9446, doi:10.1021/j100202a069.

46. **N_2O_5 + NaCl.** This reaction has been studied on both solid NaCl and on aqueous solutions. The uptake of N_2O_5 on solid NaCl has been studied using Knudsen cells,[3,6] flow reactors,[8,9] annular reactors[11] and diffusion tubes.[7] The reaction has two possible channels if there is water available on the surface: $N_2O_5 + NaCl \rightarrow ClNO_2 + NaNO_3$ (1) and $N_2O_5 + H_2O/NaCl \rightarrow 2\ HNO_3$ (2). The presence of the two channels is supported by measured yields of $ClNO_2$ (relative to N_2O_5 lost) that vary from 60–100% [3,6,7,9] and by the observation of gaseous HCl as a reaction product.[6] Because hydrolysis on the surface occurs in addition to the reaction with Cl^-, the net uptake coefficient for N_2O_5 is particularly sensitive to the presence of surface-adsorbed water (SAW), with higher values for powders where there are more steps and edges that hold SAW. For example, Leu et al.[8] measured an upper limit of $\gamma < 1.0 \times 10^{-4}$ for salt powders that had been heated overnight in a vacuum, but ~4.5×10^{-4} for samples that were only pumped on for about an hour. Fenter et al.[3] reported a preferred value for the uptake coefficient of $(5 \pm 2) \times 10^{-4}$; however, the measured values varied from 2×10^{-3} for monodisperse powders (after correction for pore diffusion by factors of ~5 to 30) to $< 1.0 \times 10^{-4}$ for a polished window face. Hoffman et al.[6] report a steady state value of $\gamma_{ss} = 3 \times 10^{-3}$ based on Knudsen cell studies of powders using less than a layer of salt where corrections to the available surface area due to diffusion into the salt are not necessary; the branching ratio for reaction (1) was measured to be 0.73 ± 0.28 (2σ).

The uptake of N_2O_5 on NaCl solutions or aqueous particles has been measured by a number of techniques.[1,2,4,5,12,16-18] Overall, the reported values of γ for relative humidities between 45 and 100% are

between 1.5×10^{-2} to 5.0×10^{-2} and temperatures between 263 K and room temperature. Zetzsch and coworkers[1,2] used an aerosol chamber to measure the uptake of N_2O_5 on deliquesced NaCl particles from 71–94% RH, and obtained a value of $\gamma = 3.2 \times 10^{-2}$. Behnke et al.[1] measured $ClNO_2$ in a yield of 66 ± 7% from aerosol particle experiments. In a wetted wall flow tube, the yield was observed to increase to 100% at concentrations of NaCl of 1 M and above. Thornton and Abbatt[17] report a yield of at least 50% $ClNO_2$ at 50% RH, using an aerosol flow tube technique. It is proposed by both groups that a mechanism involving a competition between the reaction of NO_2^+ (or $H_2ONO_2^+$) with water to form HNO_3 or with Cl^- to form $ClNO_2$ determines the product yield. George et al.[5] used a droplet train and measured the formation of NO_3^- in the droplets; the value of γ decreased from 0.039 ± 0.013 at 263 K to 0.014 ± 0.008 at 278 K. Stewart et al.[16] measured the uptake of N_2O_5 on NaCl particles in a flow tube; after correction for diffusion/particle size effects, an uptake coefficient of 3×10^{-2} was derived at relative humidities 30% and above. The work of Gaston and Thornton[4] in which the uptake coefficients were independent of particle size indicates that the reactive process is occurring with a short reacto-diffusive length, close to the surface. This is consistent with facile reaction of the NO_2^+ intermediate with aqueous chloride. Shaloski et al.[15] have explored the surficial interactions of N_2O_5 with bromide, in the presence of a range of surfactants, finding that the nature of the intermolecular interactions can have a strong effect of the efficiency of bromide oxidation. Schweitzer et al.[14] used a droplet train apparatus to measure the uptake of N_2O_5 on water and on solutions of NaCl, NaBr and NaI with concentrations ranging from 0.1 to 1 M over a temperature range from 262 to 278 K. Within experimental error, all of the uptake coefficients were the same, with an average value of $\gamma = 0.018 \pm 0.003$. For 1 M NaCl, the $ClNO_2$ yield was 100%.

Note that the uptake kinetics can be suppressed by the presence of an organic monolayer on the aqueous particles.[10,17] Also, the product yield can change to Cl_2, when the acidity of the surface is taken below 2 and for chloride concentrations as low as 0.05 M (Roberts et al.[13]).

Back to Table

(1) Behnke, W.; George, C.; Scheer, V.; Zetsch, C. Production and decay of $ClNO_2$ from the reaction of gaseous N_2O_5 with NaCl solution: Bulk and aerosol experiments. *J. Geophys. Res.* **1997**, *102*, 3795-3804, doi:10.1029/96JD03057.

(2) Behnke, W.; Kruger, H.-U.; Scheer, V.; Zetzsch, C. Formation of atomic Cl from sea spray via photolysis of nitryl chloride: Determination of the sticking coefficient of N_2O_5 on NaCl aerosol. *J. Aerosol Sci.* **1991**, *22*, S609-S612, doi:10.1016/S0021-8502(05)80175-2.

(3) Fenter, F. F.; Caloz, F.; Rossi, M. J. Heterogeneous kinetics of N_2O_5 uptake on salt, with a systematic study of the role of surface presentation (for N_2O_5 and HNO_3). *J. Phys. Chem.* **1996**, *100*, 1008-1019, doi:10.1021/jp9503829.

(4) Gaston, C. J.; Thornton, J. A. Reacto-diffusive length of N_2O_5 in aqueous sulfate- and chloride-containing aerosol particles. *J. Phys. Chem. A.* **2016**, *120*, 1039-1045, doi:10.1021/acs.jpca.5b11914.

(5) George, C.; Behnke, W.; Scheer, V.; Zetsch, C.; Magi, L.; Ponche, J. L.; Mirabel, P. Fate of $ClNO_2$ over aqueous solutions containing iodide. *Geophys. Res. Lett.* **1995**, *22*, 1505-1508, doi:10.1029/95GL01417.

(6) Hoffman, R. C.; Gebel, M. E.; Fox, B. S.; Finlayson-Pitts, B. J. Knudsen cell studies of the reactions of N_2O_5 and $ClONO_2$ with NaCl: Development and application of a model for estimating available surface areas and corrected uptake coefficients. *Phys. Chem. Chem. Phys.* **2003**, *5*, 1780-1789, doi:10.1039/b301126g.

(7) Koch, T. G.; vandenBergh, H.; Rossi, M. J. A molecular diffusion tube study of N_2O_5 and $HONO_2$ interacting with NaCl and KBr at ambient temperature. *Phys. Chem. Chem. Phys.* **1999**, *1*, 2687-2694, doi:10.1039/A901894H.

(8) Leu, M.-T.; Timonen, R. S.; Keyser, L. F.; Yung, Y. L. Heterogeneous reactions of HNO_3(g) + NaCl(s) HCl(g) + $NaNO_3$(s) and N_2O_5(g) + NaCl(s) $ClNO_2$(g) + $NaNO_3$(s). *J. Phys. Chem.* **1995**, *99*, 13203-13212, doi:10.1021/j100035a026.

(9) Livingston, F. E.; Finlayson-Pitts, B. J. The reaction of gaseous N_2O_5 with solid NaCl at 298 K: Estimated lower limit to the reaction probability and its potential role in tropospheric and stratospheric chemistry. *Geophys. Res. Lett.* **1991**, *18*, 17-21, doi:10.1029/90GL02595.

(10) McNeill, V. F.; Patterson, J.; Wolfe, G. M.; Thornton, J. A. The effect of varying levels of surfactant on the reactive uptake of N_2O_5 to aqueous aerosol. *Atmos. Chem. Phys.* **2006**, *6*, 1635-1644, doi:10.5194/acp-6-1635-2006.

(11) Msibi, I. M.; Li, Y.; Shi, J. P.; Harrison, R. M. Determination of heterogeneous reaction probability using deposition profile measurement in an annular reactor: application to the N_2O_5/H_2O reaction. *J. Atmos. Chem.* **1994**, *18*, 291-300, doi:10.1007/BF00696784.
(12) Msibi, I. M.; Shi, J. P.; Harrison, R. M. Accommodation coefficient for trace gas uptake using deposition profile measurement in an annular reactor. *J. Atmos. Chem.* **1993**, *17*, 339-351, doi:10.1007/BF00696853.
(13) Roberts, J. M.; Osthoff, H. D.; Brown, S. S.; Ravishankara, A. R. N_2O_5 oxidizes chloride to Cl_2 in acidic atmospheric aerosol. *Science* **2008**, *321*, 1059-1059, doi:10.1126/science.1158777.
(14) Schweitzer, F.; Mirabel, P.; George, C. Multiphase chemistry of N_2O_5, $ClNO_2$ and $BrNO_2$. *J. Phys. Chem. A* **1998**, *102*, 3942-3952, doi:10.1021/jp980748s.
(15) Shaloski, M. A.; Gord, J. R.; Staudt, S.; Quinn, S. L.; Bertram, T. H.; Nathanson, G. M. Reactions of N_2O_5 with salty and surfactant-coated glycerol: Interfacial conversion of Br- to Br_2 mediated by alkylammonium cations. *J. Phys. Chem. A.* **2017**, *121*, 3708-3719, doi:10.1021/acs.jpca.7b02040.
(16) Stewart, D. J.; Griffiths, P. T.; Cox, R. A. Reactive uptake coefficients for heterogeneous reacton of N_2O_5 with submicron aerosols of NaCl and natural sea salt. *Atmos. Chem. Phys.* **2004**, *4*, 1381-1388, doi:10.5194/acp-4-1381-2004.
(17) Thornton, J. A.; Abbatt, J. P. D. N_2O_5 reaction on submicron sea salt aerosol: Kinetics, products, and the effect of surface active organics. *J. Phys. Chem. A* **2005**, *109*, 10004-10012, doi:10.1021/Jp054183t.
(18) Zetzsch, C.; Behnke, W. Heterogeneous photochemical sources of atomic chlorine in the troposphere. *Ber. Bunsenges. Phys. Chem.* **1992**, *96*, 488-493, doi:10.1002/bbpc.19920960351.

47. **N_2O_5 + KBr, NaBr, NaI.** Fenter et al.[1] and Koch et al.[3] measured the uptake coefficient for N_2O_5 on KBr at ambient temperature using a Knudsen cell and molecular diffusion tube respectively. The Knudsen cell experiments gave a value of $(4 \pm 2) \times 10^{-3}$ after correction (by factors of 6–16) for pore diffusion, and the molecular diffusion tube a value of $(2.5 \pm 1) \times 10^{-3}$. In the Knudsen cell studies, the uptake coefficient was larger for powders and a depolished window face (both 4×10^{-3}) than for a polished window face ($<1 \times 10^{-4}$), similar to the observations for the NaCl reaction (N_2O_5 + NaCl); this again suggests the importance of surface-adsorbed water and possibly surface defects created by roughening (which, however, also hold water) for the reaction. The initial product of the reaction is $BrNO_2$, identified by Finlayson-Pitts et al.[2] by FTIR but this can react further with the salt to generate Br_2, the product observed by Fenter et al.[1]

Schweitzer et al.[4] used a droplet train apparatus to measure the uptake of N_2O_5 on water and on solutions of NaBr and NaI, as well as NaCl, with concentrations ranging from 0.1 to 1 M over a temperature range from 262 to 278 K. Within experimental error, all of the uptake coefficients were the same, with an average value of $\gamma = 0.018 \pm 0.003$. For the NaBr reaction, the gas phase products were $BrNO_2$, Br_2, and HONO. For the NaI reaction, the only gas phase product observed was I_2.
Back to Table

(1) Fenter, F. F.; Caloz, F.; Rossi, M. J. Heterogeneous kinetics of N_2O_5 uptake on salt, with a systematic study of the role of surface presentation (for N_2O_5 and HNO_3). *J. Phys. Chem.* **1996**, *100*, 1008-1019, doi:10.1021/jp9503829.
(2) Finlayson-Pitts, B. J.; Livingston, F. E.; Berko, H. N. Synthesis and identification by infrared spectroscopy of gaseous nitryl bromide, $BrNO_2$. *J. Phys. Chem.* **1989**, *93*, 4397-4400, doi:10.1021/j100348a005.
(3) Koch, T. G.; vandenBergh, H.; Rossi, M. J. A molecular diffusion tube study of N_2O_5 and $HONO_2$ interacting with NaCl and KBr at ambient temperature. *Phys. Chem. Chem. Phys.* **1999**, *1*, 2687-2694, doi:10.1039/A901894H.
(4) Schweitzer, F.; Mirabel, P.; George, C. Multiphase chemistry of N_2O_5, $ClNO_2$ and $BrNO_2$. *J. Phys. Chem. A* **1998**, *102*, 3942-3952, doi:10.1021/jp980748s.

48. **N_2O_5 + sea salt.** The uptake of N_2O_5 on solid synthetic sea salt was measured to be $\gamma = (3.4 \pm 0.8) \times 10^{-2}$ (2σ) by Hoffman et al.[1] This will be an upper limit as 1–2 layers of salt were used and no correction was made for diffusion into the bottom layer. However, it is clear that the reaction is at least an order of magnitude faster than that for NaCl; the yield of $ClNO_2$ is 100%.

Stewart and Cox[4] measured the uptake of N_2O_5 on submicron synthetic sea salt aerosols in a flow tube; after correction for diffusion/particle size effects, a value of $\gamma = 2.5 \times 10^{-2}$ was derived, independent of relative

humidity above 30%. Similar results are reported for the same substrate by Thornton and Abbatt,[5] with the uptake coefficient changing from 0.02 to 0.03 from 43 to 70% RH. For partially crystallized artificial sea salt, the uptake coefficient was 0.005 at 30% RH. Employing sea spray particles generated using a process that mimics that which proceeds in the environment, and using either genuine seawater or artificial seawater, the uptake coefficient was measured by Ryder et al.[3] to be between 0.01 and 0.03 for relative humidities between 50 and 65%. Addition of trace organics to the artificial seawater, such as a sterol, sugar or polysaccharide, did not affect the overall update of N_2O_5. Thus, the organic constituents on the surfaces of these particles appear to not inhibit the reaction relative to the values measured on pure aqueous sodium chloride aerosol.

Experiments were conducted by Lopez-Hilfiker et al.[2] in a coated-wall flow tube on the uptake of N_2O_5 to frozen salt solutions containing variable ratios of Cl to Br, from temperatures of 258 to about 240 K. Br_2 and $ClNO_2$ products were observed with a total yield of unity, with their ratios dependent upon both temperature and the Cl/Br ratio of the frozen solution.

Back to Table

(1) Hoffman, R. C.; Gebel, M. E.; Fox, B. S.; Finlayson-Pitts, B. J. Knudsen cell studies of the reactions of N_2O_5 and $ClONO_2$ with NaCl: Development and application of a model for estimating available surface areas and corrected uptake coefficients. *Phys. Chem. Chem. Phys.* **2003**, *5*, 1780-1789, doi:10.1039/b301126g.

(2) Lopez-Hilfiker, F. D.; Constantin, K.; Kercher, J. P.; Thornton, J. A. Temperature dependent halogen activation by N_2O_5 reactions on halide-doped ice surfaces. *Atmos. Chem. Phys.* **2012**, *12*, 5237-5247, doi:10.5194/acp-12-5237-2012.

(3) Ryder, O. S.; Campbell, N. R.; Morris, H.; Forestieri, S.; Ruppel, M. J.; Cappa, C.; Tivanski, A.; Prather, K.; Bertram, T. H. Role of organic coatings in regulating N_2O_5 reactive uptake to sea spray aerosol. *J. Phys. Chem. A.* **2015**, *119*, 11683-11692, doi:10.1021/acs.jpca.5b08892.

(4) Stewart, D. J.; Griffiths, P. T.; Cox, R. A. Reactive uptake coefficients for heterogeneous reacton of N_2O_5 with submicron aerosols of NaCl and natural sea salt. *Atmos. Chem. Phys.* **2004**, *4*, 1381-1388, doi:10.5194/acp-4-1381-2004.

(5) Thornton, J. A.; Abbatt, J. P. D. N_2O_5 reaction on submicron sea salt aerosol: Kinetics, products, and the effect of surface active organics. *J. Phys. Chem. A* **2005**, *109*, 10004-10012, doi:10.1021/Jp054183t.

49. HONO + H_2O(l). Bongartz et al.[1] present uptake measurements by two independent techniques, the liquid jet technique of Schurath and co-workers and the droplet train/flow tube technique of Mirabel and co-workers (Ponche et al.[4]). With a surface temperature of ~245 K the droplet train techniques yielded $0.045 < \gamma < 0.09$, while the liquid jet operating with a surface temperature of 297 K obtained $0.03 < \gamma < 0.15$. Mertes and Wahner[3] used a liquid jet technique to measure $4 \times 10^{-3} < \gamma < 4 \times 10^{-2}$ at 278 K. Harrison and Collins[2] performed aerosol flow reactor experiments on deliquescent sodium chloride and ammonium sulfate droplets at 279 K obtaining reactive uptake coefficients of 0.0028 ± 0.0015 and 0.0028 ± 0.0006, for 85% relative humidity conditions, respectively; these measurements are probably subject to significant surface saturation. Since HONO uptake by liquid water probably involves hydrolysis, an increase in Henry's law solubility with decreasing temperature may be offset by a decreasing hydrolysis rate constant, leaving the uptake coefficient's temperature trend uncertain. Measured uptake coefficients will not correspond to the mass accommodation coefficient.

Back to Table

(1) Bongartz, A.; Kames, J.; Schurath, U.; George, C.; Mirabel, P.; Ponche, J. L. Experimental determination of HONO mass accommodation coefficients using two different techniques. *J. Atmos. Chem.* **1994**, *18*, 149-169, doi:10.1007/BF00696812.

(2) Harrison, R. M.; Collins, G. M. Measurements of reaction coefficients of NO_2 and HONO on aerosol particles. *J. Atmos. Chem.* **1998**, *30*, 397-406, doi:10.1023/A:1006094304069.

(3) Mertes, S.; Wahner, A. Uptake of nitrogen dioxide and nitrous acid on aqueous surfaces. *J. Phys. Chem.* **1995**, *99*, 14000-14006, doi:10.1021/j100038a035.

(4) Ponche, J. L.; George, C.; Mirabel, P. Mass transfer at the air/water interface: Mass accommodation coefficients of SO_2, HNO_3, NO_2 and NH_3. *J. Atmos. Chem.* **1993**, *16*, 1-21, doi:10.1007/BF00696620.

50. HONO + H_2SO_4•nH_2O(l). Zhang et al.[4] measured uptake coefficients for HONO on sulfuric acid that increased from $(1.6 \pm 0.1) \times 10^{-2}$ for 65.3 wt% H_2SO_4 (214 K) to $(9.1 \pm 1.6) \times 10^{-2}$ for 73 wt% H_2SO_4 (226 K). Fenter and Rossi[3] measured uptake coefficients rising from 1.8×10^{-4} for 55 wt% H_2SO_4 (220 K) to 3.1×10^{-1} for 95 wt% H_2SO_4 (220 K and 273 K). Baker et al.[1] measured much smaller uptake coefficients for 60 wt% at 298 K. In general, the values measured by Zhang et al.[4] are a factor of 2 to 5 higher than those of Fenter et al.[3] for comparable acid concentrations. Since the reaction probably depends on both temperature and acid concentration and since the data scatter is high in both experiments, further independent data will be required to define γ as a function of acid concentration and temperature. These data are generally consistent with the effective Henry's law constant measurements of Becker et al.[2] who illustrate that HONO solubility decreases exponentially with H_2SO_4 concentration until ~53 wt%, at which point reaction to form nitrosyl sulfuric acid increases H* dramatically as H_2SO_4 concentration increases. Baker et al.[1] invoke surface decomposition of HONO to explain their room temperature data, since they separately determine that the bulk second-order disproportionation rate for HONO is too slow to account for even their small uptake coefficients. It is possible that surface formation of nitrosyl sulfuric acid and not HONO disproportionation is responsible for much of their measured uptake. The Zhang et al.[4] and Fenter and Rossi[3] data have been combined and fit with a four-term polynomial as a function of acid wt% (these data did not show an obvious temperature dependence):

$$\ln \gamma = a + b\ wt + c\ wt^2 + d\ wt^3$$

where wt is the H_2SO_4 wt%, and

$$a = -155.7 \pm 29.7$$

$$b = 5.663 \pm 1.232$$

$$c = -0.07061 \pm 0.01679$$

$$d = 0.000297 \pm 0.000076$$

This parameterization should be used only within the 55–95-wt% H_2SO_4 range and the 214 to 273 K temperature range.

Back to Table

(1) Baker, J.; Ashbourn, S. F. M.; Cox, R. A. Heterogeneous reactivity of nitrous acid on submicron sulfuric acid aerosol. *Phys. Chem. Chem. Phys.* **1999**, *1*, 683-690, doi:10.1039/a808702d.

(2) Becker, K. H.; Kleffman, J.; Kurtenbach, R.; Wiesen, P. Solubility of nitrous acid (HONO) in sulfuric acid solutions. *J. Phys. Chem.* **1996**, *100*, 14984-14990, doi:10.1021/jp961140r.

(3) Fenter, F. F.; Rossi, M. J. The heterogeneous kinetics of HONO on H_2SO_4 and on ice: activation of HCl. *J. Phys. Chem.* **1996**, *100*, 13765-13775, doi:10.1021/jp960797+.

(4) Zhang, R.; Leu, M.-T.; Keyser, L. F. Heterogeneous chemistry of HONO on liquid sulfuric acid: A new mechanism of chlorine activation on stratospheric sulfate aerosol. *J. Phys. Chem.* **1996**, *100*, 339-345, doi:10.1021/jp952060a.

51. HONO + HCl + H_2O(s). Knudsen cell uptake studies for HONO/HCl co-deposited on ice (180–200 K) and for HONO on 0.1 to 10 M HCl frozen solutions (~190 K) by Fenter and Rossi[3] showed HONO uptake coefficients in the 0.02 to 0.12 range as long as surface HCl concentrations significantly exceed HONO concentrations. ClNO was evolved quantitatively with HONO consumption. In a coated wall flow tube Diao and Chu[2] observed orders of magnitude lower uptake coefficients, even though low partial pressures of HONO were used. Some of the HCl partial pressures will have been large enough to melt the ice surface (Abbatt et al.[1]).

Back to Table

(1) Abbatt, J. P. D.; Beyer, K. D.; Fucaloro, A. F.; McMahon, J. R.; Wooldridge, P. J.; Zhong, R.; Molina, M. J. Interaction of HCl vapor with water-ice: Implications for the stratosphere. *J. Geophys. Res.* **1992**, *97*, 15819-15826, doi:10.1029/92JD01220.

(2) Diao, G. W.; Chu, L. T. Heterogeneous reactions of HX plus HONO and I_2 on ice surfaces: Kinetics and linear correlations. *J. Phys. Chem. A* **2005**, *109*, 1364-1373, doi:10.1021/jp045965+.

(3) Fenter, F. F.; Rossi, M. J. The heterogeneous kinetics of HONO on H_2SO_4 and on ice: activation of HCl. *J. Phys. Chem.* **1996**, *100*, 13765-13775, doi:10.1021/jp960797+.

52. HONO + HCl on H_2SO_4•nH_2O(l). Fenter and Rossi[1] saw no reaction for acid wt% >65. They measured $\gamma = 2.0 \pm 0.7 \times 10^{-3}$ for 60 wt% acid saturated with HONO at 230 K. Zhang et al.[3] also measured the uptake of HCl after exposure to HONO, they observed HCl uptake with γs between 0.01–0.02 over an acid wt.% range of 60.8–71.3 (T = 207.9–222.6 K). The reaction was also studied by Longfellow et al.[2] using both HCl doped and HONO doped sulfuric acid aerosols. Their uptake measurements confirmed reaction at higher acid wt%, but by using lower HONO partial pressures they measured smaller γs. The reverse reaction, ClNO hydrolysis, was also studied in a wetted wall flow reactor and in the aerosol flow reactor by Longfellow et al.[2] and in a Knudsen cell reactor by Fenter and Rossi.[1] Data show clear evidence of both surface and bulk kinetics for the forward reaction. Longfellow et al.[2] report k^{II} values for the bulk reaction (in units of 10^4 M^{-1} s^{-1}) for 50 wt%: 81 at 250 K and 15 at 205 K; for 60 wt%: 9.4 at 250 K, 6.9 at 230 K and 5.0 at 219 K; for 67 wt%: 3.9 at 250 K; and for 70 wt%: 5.8 at 269 K and 0.35 at 215 K. The reaction is clearly complex and will require a comprehensive model of both the surface and bulk processes to arrive at an appropriate parameterization for γ.
Back to Table

(1) Fenter, F. F.; Rossi, M. J. The heterogeneous kinetics of HONO on H_2SO_4 and on ice: activation of HCl. *J. Phys. Chem.* **1996**, *100*, 13765-13775, doi:10.1021/jp960797+.
(2) Longfellow, C. A.; Imamura, T.; Ravishankara, A. R.; Hanson, D. R. HONO solubility and heterogeneous reactivity on sulfuric acid surfaces. *J. Phys. Chem. A* **1998**, *102*, 3323-3332, doi:10.1021/jp9807120.
(3) Zhang, R.; Leu, M.-T.; Keyser, L. F. Heterogeneous chemistry of HONO on liquid sulfuric acid: A new mechanism of chlorine activation on stratospheric sulfate aerosol. *J. Phys. Chem.* **1996**, *100*, 339-345, doi:10.1021/jp952060a.

53. HONO + HBr + H_2O(s). HONO reacts with HBr on ice films (Seisel and Rossi[2] and Diao and Chu[1]), but note that the HBr partial pressures used are generally higher than those prevalent in the atmosphere and so melting of the ice film may have occurred in these experiments. Diao and Chu observe BrNO as a product in a coated-wall flow tube.
Back to Table

(1) Diao, G. W.; Chu, L. T. Heterogeneous reactions of HX plus HONO and I_2 on ice surfaces: Kinetics and linear correlations. *J. Phys. Chem. A* **2005**, *109*, 1364-1373, doi:10.1021/jp045965+.
(2) Seisel, S.; Rossi, M. J. The heterogeneous reaction of HONO and HBr on ice and on sulfuric acid. *Ber. Bunsenges. Phys. Chem.* **1997**, *101*, 943-955, doi:10.1002/bbpc.19971010609.

54. HONO + NaCl(s). Diffuse reflectance experiments by Vogt and Finlayson-Pitt[3] on room temperature NaCl(s) and Knudsen cell uptake experiments by Fenter and Rossi on room temperature NaCl(s) and frozen 0.1 M NaCl aqueous solutions, all failed to show HONO uptake.[1] The latter results yield $\gamma < 1 \times 10^{-4}$. HONO + NaCl. Junkermann and Ibusuki[2] reported that HONO reacts with NaCl to form nitrite on the surface. However, subsequent studies[3] showed that the infrared bands assigned to NO_2^- were due to nitrate, likely from the reaction of gas phase NO_2 and perhaps HNO_3 present in the HONO. There is no evidence at the present time for a reaction between HONO and NaCl.
Back to Table

(1) Fenter, F. F.; Rossi, M. J. The heterogeneous kinetics of HONO on H_2SO_4 and on ice: activation of HCl. *J. Phys. Chem.* **1996**, *100*, 13765-13775, doi:10.1021/jp960797+.
(2) Junkermann, W.; Ibusuki, T. FTIR spectroscopic measurements of surface bond products of nitrogen oxides on aerosol surfaces—Implications for heterogeneous HNO_2 production. *Atmos. Environ.* **1992**, *26A*, 3099-3103, doi:10.1016/0960-1686(92)90466-X.
(3) Vogt, R.; Finlayson-Pitts, B. F. Tropospheric HONO and reactions of oxides of nitrogen with NaCl. *Geophys. Res. Lett.* **1994**, *21*, 2291-2294, doi:10.1029/94GL02238.

55. HONO + Al_2O_3(s). Romanias et al.[2] used a coated wall flow reactor with solid films of ~20 nm γ-alumina particles to measure HONO uptake coefficients over a RH range of 1.4×10^{-4} to 35.4% and a temperature range of 274–320 K, implementing mass spectrometric detection of HONO and its gaseous reaction products NO and NO_2.

The effect of near ultraviolet radiation (315–400 nm, $J_{NO2} = 0.002–0.012\ s^{-1}$) on uptake was also investigated. Reactive uptake was confirmed by a lack of HONO desorption and direct NOx product detection. Measured uptake coefficients are independent of [HONO] and T, but strongly dependent on RH. A moderate UV dependence that increased with RH and was linear in J_{NO2} was observed; neither significantly affected measured product branching ratios of (0.40 ± 0.06) for NO and (0.60 ± 0.09) for NO_2. Uptake coefficients were determined as a function of RH without and with UV radiation (J_{NO2} ~0.012 s^{-1}). The results were parameterized (estimated uncertainty of ± 30%):

$$\gamma(\text{dark}) = 4.8 \times 10^{-6}\,(\text{RH})^{-0.61} \quad (\text{RH} = 1.4 \times 10^{-4}\text{ to }10.5\%)$$
$$\gamma(\text{UV}) = 1.7 \times 10^{-5}\,(\text{RH})^{-0.44} \quad (\text{RH} = 1.4 \times 10^{-4}\text{ to }35.4\%)$$

The same authors published similar results for HONO reactive uptake on Fe_2O_3 and Arizona Test Dust.[1]

Given results from only one laboratory and no information on α-alumina surfaces, no uptake coefficient values are recommended.
Back to Table

(1) El Zein, A.; Romanias, M. N.; Bedjanian, Y. Kinetics and products of heterogeneous reactions of HONO with Fe_2O_3 and Arizona test dust. *Environ. Sci. Technol.* **2013**, *47*, 6325-6331, doi:10.1021/es400794c.
(2) Romanias, M. N.; El Zein, A.; Bedjanian, Y. Reactive uptake of HONO on aluminum oxide surface. *J. Photochem. Photobiol. A: Chem.* **2012**, *250*, 50-57, doi:10.1016/j.photochem.2012.09.018.

56. HNO_3 + NaCl(s) and NaCl(aq). Recommendation is based on an average of the values of Hoffman et al.,[8] Ghosal and Hemminger,[6] the data of Davies and Cox[3] as revised by Ghosal and Hemminger[6] using their model for surface reactivation, and the single crystal data of Leu et al.[12] Hoffman et al.[8] used less than a single layer of particles so that diffusion into the underlying layers is not a factor to obtain an initial value of $\gamma_0 = (2.3 \pm 1.9) \times 10^{-3}$ (2σ). This is consistent within the combined experimental errors with a value of $(1.3 \pm 0.6) \times 10^{-3}$ determined from the formation of nitrate on the surface of single crystal (100) NaCl by Ghosal and Hemminger,[6] and with a value of 1.1×10^{-3} from application of the Ghosal and Hemminger model to the Davis and Cox data.[3] Ghosal and Hemminger suggest that the value could be as high as 5×10^{-3} for NaCl powders that have more steps and edges that hold SAW.[7] At longer reaction times, the steady-state value[8] is a factor of two smaller, $\gamma = 1 \times 10^{-3}$. The reaction is hypothesized to occur both on dry terraces, which saturate rapidly, and on steps and edges that hold surface-adsorbed water. The water acts to recrystallize the product $NaNO_3$ so that the surface does not passivate during the reaction at atmospherically relevant HNO_3 pressures. This model, developed and modified by several research groups[2,3,6,8] brings together most of the seemingly disparate measurements of the reaction probability made using a variety of techniques including flow tubes,[3] Knudsen cells,[2,4,5,8] and XPS studies of nitrate formation on single crystals.[6,7,17] The only gas phase product observed is HCl, with a yield that is within experimental error of 100%. The higher value of $(1.3 \pm 0.4) \times 10^{-2}$ of Leu et al.[12] was obtained by correcting even larger measured values using a pore diffusion model;[9,10] the corrections were typically in the range of a factor of 4–6. On single crystal NaCl where such corrections were not necessary, Leu et al.[12] measured a value of $(2.4 \pm 0.6) \times 10^{-3}$. A value of $(4 \pm 1) \times 10^{-2}$ was measured using a molecular diffusion tube technique by Koch et al.[11] The corrected value of $(8.7 \pm 1.4) \times 10^{-5}$ reported by Zangmeister and Pemberton[18,19] using Raman spectroscopy to follow the nitrate formed on the surface is lower than the other values likely because a much higher HNO_3 concentration was used (~ 10^{18} cm^{-3}), which would lead to a larger coverage of the surface by the recrystallized $NaNO_3$ product and passivation of much of the NaCl surface.

Abbatt and Waschewsky[1] measured the loss of gas-phase HNO_3 in a flow tube containing deliquesced 1–5 μm NaCl particles (75% RH) and obtained a lower limit to the uptake coefficient for HNO_3 of 0.2 on unbuffered NaCl. Stemmler et al.[15] report a value of 0.5 ± 0.2 for the initial uptake coefficient on deliquesced particles at 60% RH. Tolocka et al.[16] followed the reaction of HNO_3 with 100–220 nm NaCl particles at 80% RH using single particle MS to measure the Cl^-/NO_3^- ratio; the uptake coefficient for 100 nm particles was $(4.9 \pm 2.7) \times 10^{-3}$ and increased with droplet size. Saul et al.[14] have extended the Tolocka et al. work, by studying the reaction over a wide range of relative humidities, both above and below the efflorescence point. Uptake coefficients on the mixed nitrate-chloride particles reach a maximum of 0.12 or so at 50% RH, decreasing at both higher and lower RHs. The presence of hygroscopic $MgCl_2$ increases the uptake coefficient at low RHs, where the particles may remain liquid. Liu et al.[13] using static particles probed spectroscopically determine the maximum uptake coefficients to be 0.2 (uncertainty a factor of three), also

close to 50% RH, decreasing at higher and lower RHs. The combination of these studies shows that the initial uptake of HNO_3 into solution is fast, with $\gamma_0 > 0.2$; as the solution becomes acidified, HCl is expelled as the gaseous product. The uptake coefficient may decrease when the reaction proceeds on processed particles, where a large amount of nitrate has built up. In such cases, the maximum reactivity is at close to 50% RH. Note that the Stemmler et al.[15] study illustrated that monolayer coverages of long-chain surfactants can reduce the initial uptake coefficient by over an order of magnitude.

Back to Table

(1) Abbatt, J. P. D.; Waschewsky, G. C. G. Heterogeneous interactions of HOBr, HNO_3, O_3, and NO_2 with deliquescent NaCl aerosols at room temperature. *J. Phys. Chem. A* **1998**, *102*, 3719-3725, doi:10.1021/jp980932d.

(2) Beichert, P.; Finlayson-Pitts, B. J. Knudson cell studies of the uptake of gaseous HNO_3 and other oxides of nitrogen on solid NaCl. The role of surface absorbed water. *J. Phys. Chem.* **1996**, *100*, 15218-15228, doi:10.1021/jp960925u.

(3) Davies, J. A.; Cox, R. A. Kinetics of the heterogeneous reaction of HNO_3 with NaCl: Effect of water vapor. *J. Phys. Chem. A* **1998**, *102*, 7631-7642, doi:10.1021/jp982134t.

(4) Fenter, F. F.; Caloz, F.; Rossi, M. J. Kinetics of nitric acid uptake by salt. *J. Phys. Chem.* **1994**, *98*, 9801-9810, doi:10.1021/j100090a014.

(5) Fenter, F. F.; Caloz, F.; Rossi, M. J. Heterogeneous kinetics of N_2O_5 uptake on salt, with a systematic study of the role of surface presentation (for N_2O_5 and HNO_3). *J. Phys. Chem.* **1996**, *100*, 1008-1019, doi:10.1021/jp9503829.

(6) Ghosal, S.; Hemminger, J. C. Effect of water on the HNO_3 pressure dependence of the reaction between gas-phase HNO_3 and NaCl surfaces. *J. Phys. Chem. A* **1999**, *103*, 4777-4781, doi:10.1021/jp991142m.

(7) Ghosal, S.; Hemminger, J. C. Surface adsorbed water on NaCl and its effect on nitric acid reactivity with NaCl powders. *J. Phys. Chem. B* **2004**, *108*, 14102-14108, doi:10.1021/jp047774c.

(8) Hoffman, R. C.; Kaleuati, M.; Finlayson-Pitts, B. J. Knudsen cell studies of the reaction of gaseous HNO_3 with NaCl using less than a single layer of particles at 298 K: A modified mechanism. *J. Phys. Chem. A* **2003**, *107*, 7818-7826, doi:10.1021/jp030611o.

(9) Keyser, L. F.; Leu, M.-T.; Moore, S. B. Comment on porosities of ice films used to simulate stratospheric cloud surfaces. *J. Phys. Chem.* **1993**, *97*, 2800-2801, doi:10.1021/j100113a053.

(10) Keyser, L. F.; Moore, S. B.; Leu, M. T. Surface reaction and pore diffusion in flow tube reactors. *J. Phys. Chem.* **1991**, *95*, 5496-5502, doi:10.1021/j100167a026.

(11) Koch, T. G.; vandenBergh, H.; Rossi, M. J. A molecular diffusion tube study of N_2O_5 and $HONO_2$ interacting with NaCl and KBr at ambient temperature. *Phys. Chem. Chem. Phys.* **1999**, *1*, 2687-2694, doi:10.1039/A901894H.

(12) Leu, M.-T.; Timonen, R. S.; Keyser, L. F.; Yung, Y. L. Heterogeneous reactions of HNO_3(g) + NaCl(s) HCl(g) + $NaNO_3$(s) and N_2O_5(g) + NaCl(s) $ClNO_2$(g) + $NaNO_3$(s). *J. Phys. Chem.* **1995**, *99*, 13203-13212, doi:10.1021/j100035a026.

(13) Liu, Y.; Cain, J. P.; Wang, H.; Laskin, A. Kinetic study of heterogeneous reaction of deliquesced NaCl particles with gaseous HNO_3 using particle-on-substrate stagnation flow reactor approach. *J. Phys. Chem. A* **2007**, *111*, 10026-10043, doi:10.1021/jp072978p.

(14) Saul, T. D.; Tolocka, M. P.; Johnston, M. V. Reactive uptake of nitric acid onto sodium chloride aerosols across a wide range of relative humidities. *J. Phys. Chem. A* **2006**, *110*, 7614-7620, doi:10.1021/jp060639a.

(15) Stemmler, K.; Vlasenko, A.; Guimbaud, C.; Ammann, M. The effect of fatty acid surfactants on the uptake of nitric acid to deliquesced NaCl aerosol. *Atmos. Chem. Phys.* **2008**, *8*, 5127-5141, doi:10.5194/acp-8-5127-2008.

(16) Tolocka, M.; Saul, T. D.; Johnston, M. V. Reactive uptake of nitric acid into aqueous sodium chloride droplets using real-time single-particle mass spectrometry. *J. Phys. Chem. A* **2004**, *108*, 2659-2665, doi:10.1021/jp036612y.

(17) Vogt, R.; Finlayson-Pitts, B. F. Tropospheric HONO and reactions of oxides of nitrogen with NaCl. *Geophys. Res. Lett.* **1994**, *21*, 2291-2294, doi:10.1029/94GL02238.

(18) Zangmeister, C. D.; Pemberton, J. E. Raman spectroscopy of the reaction of sodium chloride with nitric acid: Sodium nitrate growth and the effect of water exposure. *J. Phys. Chem. A* **2001**, *105*, 3788-3795, doi:10.1021/jp003374n.

(19) Zangmeister, C. D.; Pemberton, J. E. Raman spectroscopy of the reaction of sodium chloride with nitric acid: Sodium nitrate growth and effect of water exposure. *J. Phys. Chem. A* **2004**, *108*, 236, doi:10.1021/jp0214357.

57. **HNO_3 + NaBr and KBr.** Fenter et al.[1] reported that the value of γ for uptake of HNO_3 on NaCl, NaBr, KBr and KCl was the same, $(2.8 \pm 0.3) \times 10^{-2}$, independent of sample mass. Koch et al.[2] reported an uptake coefficient of HNO_3 on KBr of $(2 \pm 1) \times 10^{-2}$ using a molecular diffusion tube technique. As discussed in Note 7, integration of the results of an extensive series of studies in different laboratories using different techniques, uptake coefficients for HNO_3 on NaCl give a value for the HNO_3-NaCl reaction that is smaller than measured in the Fenter et al.[1] and Koch et al.[2] studies. These values for KBr may therefore be upper limits. Leu et al.[3] reported a value that is an order of magnitude smaller, $(2.8 \pm 0.5) \times 10^{-3}$ after applying large corrections (about an order of magnitude) for pore diffusion; the average uncorrected value using the geometric area was 0.027.
Back to Table

(1) Fenter, F. F.; Caloz, F.; Rossi, M. J. Kinetics of nitric acid uptake by salt. *J. Phys. Chem.* **1994**, *98*, 9801-9810, doi:10.1021/j100090a014.
(2) Koch, T. G.; vandenBergh, H.; Rossi, M. J. A molecular diffusion tube study of N_2O_5 and $HONO_2$ interacting with NaCl and KBr at ambient temperature. *Phys. Chem. Chem. Phys.* **1999**, *1*, 2687-2694, doi:10.1039/A901894H.
(3) Leu, M.-T.; Timonen, R. S.; Keyser, L. F. Kinetics of the heterogeneous reaction $HNO_3(g)$ + $NaBr(s) \leftrightarrow HBr(g) + NaNO_3(s)$. *J. Phys. Chem. A* **1997**, *101*, 278-282, doi:10.1021/jp9626069.

58. **HNO_3 + sea salt.** The uptake coefficient for HNO_3 on synthetic sea salt[1] is much larger than that on NaCl, which is attributed to the very hygroscopic nature of sea salt due to such components as the magnesium chloride and its hydrates (see Note on O_3 + sea salt). De Haan and Finlayson-Pitts[1] reported initial uptake coefficients of γ_0 in the range of 0.07 to 0.75 and steady state values in the range of 0.03 to 0.25; these were measured using salt layers from 2 layers to 10^3 layers. The initial uptake coefficient on $MgCl_2 \cdot 6H_2O$ was $\geq$0.4 and the steady-state value >0.1. At these high uptake values, the correction for diffusion into underlying layers is expected to be small. The large uptake coefficient on sea salt is consistent with the values measured for uptake on concentrated aqueous solutions of NaCl and the high water content of the surface of sea salt (see O_3 + seasalt Note above). The yield of HCl was within experimental error of 100%.

Guimbaud et al.[2] measured the uptake coefficient of HNO_3 on 70 nm supersaturated sea salt particles (deliquesced particles held at 55% RH) to be 0.50 ± 0.20; they concluded that this was the mass accommodation coefficient.
Back to Table

(1) De Haan, D. O.; Finlayson-Pitts, B. J. Knudsen cell studies of the reaction of gaseous nitric acid with synthetic sea salt at 298 K. *J. Phys. Chem. A* **1997**, *101*, 9993-9999, doi:10.1021/jp972450s.
(2) Guimbaud, C.; Arens, F.; Gutzwiller, L.; Gäggeler, H. W.; Ammann, M. Uptake of HNO_3 to deliquescent sea-salt particles: a study using short-lived radioactive isotope tracer ^{13}N. *Atmos. Chem. Phys.* **2002**, *2*, 249-257, doi:10.5194/acp-2-249-2002.

59. **HNO_3 + Al_2O_3.** Börensen et al.[1] used diffuse reflectance FTIR observations to show that HNO_3 reacts with surface hydroxyl groups on γ-alumina at 299 K to produce surface bonded nitrate, while Goodman et al. reported similar observations for α-alumina at 296 K.[2] Goodman et al.[2] also observed that higher relative humidity lead to higher HNO_3 uptake. They integrated their nitrate absorbance feature to yield a time averaged uptake coefficient of $(4 \pm 1) \times 10^{-8}$.[2] Underwood et al.[5] report a linear mass dependent, BET corrected γ_o for α-alumina at 295 K of $(9.7 \pm 0.5) \times 10^{-5}$. Hanisch and Crowley also measured liner mass dependent γ_os on α-alumina (at 298 K) for four particle sizes, which yielded an average value of 0.133 ± 0.033.[3] They argue that the lack of variance of γ_os on a large range of particle sizes and masses indicate that the BET correction to the geometrical surface area is not required. They also measured γ_o for an unpolished single crystal of $(1.6 \pm 1.4) \times 10^{-3}$ and smaller values on polished single crystals, showing the higher density of surface defect sites on small amorphous particle are critical for their high reactive active uptake coefficients. The recommendation is based on the Hanisch and Crowley data and analyses for particulate samples.[3] Seisel et al.,[4] used Knudsen cell uptake experiments at 298 K to measure an initial uptake (γ_o) value of 0.13 ± 0.02 for γ–alumina with HNO_3 vapor concentrations of ~10^{11} cm^{-3}. Lower values of γ were

observed for higher nitric acid partial pressures; water vapor was observed as a product. They also performed DRIFTS experiments that yielded a mean uptake coefficient for surface nitrate formation of $(7.7 \pm 0.8) \times 10^{-3}$ at 298 K.
Back to Table

(1) Börensen, C.; Kirchner, U.; Scheer, V.; Vogt, R.; Zellner, R. Mechanism and kinetics of the reactions of NO_2 or HNO_3 with alumina as a mineral dust model compound. *J. Phys. Chem. A* **2000**, *104*, 5036-5045, doi:10.1021/jp994170d.

(2) Goodman, A. L.; Bernard, E. T.; Grassian, V. H. Spectroscopic study of nitric acid and water adsorption on oxide particles: Enhanced nitric acid uptake kinetics in the presence of adsorbed water. *J. Phys. Chem. A* **2001**, *105*, 6443-6457, doi:10.1021/jp003722l.

(3) Hanisch, F.; Crowley, J. N. Heterogeneous reactivity of gaseous nitric acid on Al_2O_3, $CaCO_3$, and atmospheric dust samples: A Knudsen cell study. *J. Phys. Chem. A* **2001**, *105*, 3096-3106, doi:10.1021/jp001254+.

(4) Seisel, S.; Börensen, C.; Vogt, R.; Zellner, R. The heterogeneous reaction of HNO_3 on mineral dust and γ-alumina surfaces: a combined Knudsen cell and DRIFTS study. *Phys. Chem. Chem. Phys.* **2004**, *6*, 5498-5508, doi:10.1039/b410793d.

(5) Underwood, G. M.; Li, P.; Al-Abadleh, H. A.; Grassian, V. H. A Knudsen cell study of the heterogeneous reactivity of nitric acid on oxide and mineral dust particles. *J. Phys. Chem. A* **2001**, *105*, 6609-6620, doi:10.1021/jp002223h.

60. HO_2NO_2 + HCl on H_2SO_4•nH_2O(l). Zhang et al.[1] performed wetted-wall flow-reactor studies with HCl and HO_2NO_2 partial pressures in the 10^{-6} to 10^{-7} Torr range. Using chemical ionization mass spectrometry (CIMS) to detect expected reaction products, no Cl_2 (using SF_4^- as an analyte ion) or HOCl (using F^-) was detected over a temperature range of 200–225 K and an acid concentration range of 50–70 wt% H_2SO_4. An upper limit for the reactive uptake coefficient for HO_2NO_2 reacting with HCl of $\gamma < 1 \times 10^{-4}$ was deduced.
Back to Table

(1) Zhang, R.; Leu, M.-T.; Keyser, L. F. Heterogeneous chemistry of HO_2NO_2 in liquid sulfuric acid. *J. Phys. Chem. A* **1997**, *101*, 3324-3330, doi:10.1021/jp963321z.

61. NH_3 + H_2SO_4•nH_2O. Robbins and Cadle,[6] Huntzicker et al.,[4] McMurry et al.,[5] and Däumer et al.[1] all studied NH_3 uptake by sulfuric acid aerosols in near room temperature flow reactors (T = 281–300 K). Uptake coefficients varied between 0.1 and 0.5. Rubel and Gentry[7] used levitated H_3PO_4 acid droplets to show that heterogeneous reaction does control the initial NH_3 uptake on strong acid solutions. Both Rubel and Gentry and Däumer et al. also explored the effect of organic surface coatings. Swartz et al.[8] used a droplet train flow reactor to measure reactive uptake coefficients on 20 to 70 wt% acid over a temperature range from 248 to 288 K. Measured uptake coefficients varied from 1.0 at 55 wt% and above to 0.3 at 20 wt% and drop off smoothly to the pure water results reported by the same group, as well as other droplet train flow reactor and coaxial jet uptake studies.[9] Hanson and Kosciuch[2] used an aerosol flow reactor to measure reactive uptake coefficients at room temperature (287 to 297 K) from 15 to 65 wt%. While the data have a fair amount of scatter, taken as a whole they are consistent with $\gamma = 1$ over the whole range of acid concentrations. There is no obvious reason for the discrepancy between the 15 to ~45 wt% results from Swartz et al.[8] and Hanson and Kosciuch,[2] the two groups have discussed conceivable issues at length in print[9] and Hanson and Kosciuch.[3]
Back to Table

(1) Däumer, B.; Nissner, R.; Klockow, D. Laboratory studies of the influence of their organic films on the neutralization reaction of H_2SO_4 aerosol with ammonia. *J. Aerosol Sci.* **1992**, *23*, 315-325, doi:10.1016/0021-8502(92)90001-C.

(2) Hanson, D.; Kosciuch, E. The NH_3 mass accommodation coefficient for uptake onto sulfuric acid solutions. *J. Phys. Chem. A* **2003**, *107*, 2199-2208, doi:10.1021/jp021570j.

(3) Hanson, D.; Kosciuch, E. Reply to "Comment on "The NH_3 mass accommodation coefficient for uptake onto sulfuric acid solutions". *J. Phys. Chem. A* **2004**, *108*, 8549-8551, doi:10.1021/jp0311761.

(4) Huntzicker, J. J.; Cary, R. A.; Ling, C.-S. Neutralization of sulfuric acid aerosols by ammonia. *Environ. Sci. Technol.* **1980**, *14*, 819-824, doi:10.1021/es60167a009.

(5) McMurry, P. H.; Takano, H.; Anderson, G. R. Study of the ammonia (gas) - sulfuric acid (aerosol) reaction rate. *Environ. Sci. Technol.* **1983**, *17*, 347-357, doi:10.1021/es00112a008.

(6) Robbins, R. C.; Cadle, R. D. Kinetics of the reaction between gaseous ammonia and sulfuric acid droplets in an aerosol. *J. Phys. Chem.* **1958**, *62*, 469-471, doi:10.1021/j150562a025.
(7) Rubel, G. O.; Gentry, J. W. Investigation of the reaction between single aerosol acid droplets and ammonia gas. *J. Aerosol Sci.* **1984**, *15*, 661-671, doi:10.1016/0021-8502(84)90004-1.
(8) Swartz, E.; Shi, Q.; Davidovits, P.; Jayne, J. T.; Worsnop, D.; Kolb, C. E. Uptake of gas-phase ammonia. 2. Uptake by sulfuric acid surfaces. *J. Phys. Chem. A* **1999**, *103*, 8824-8833, doi:10.1021/jp991697h.
(9) Worsnop, D. R.; Williams, L. R.; Kolb, C. E.; Mozurkewich, M.; Gershenzon, M.; Davidovits, P. Comment on "The NH_3 mass accommodation coefficient for uptake onto sulfuric acid solution". *J. Phys. Chem. A* **2004**, *108*, 8546-8548, doi:10.1021/jp036519+.

62. CO_2 + Al_2O_3(s). Parkyns[1] and Szanyi and Kwak[2] each report FTIR studies of CO_2 chemisorbed on γ-alumina surfaces annealed at temperatures up to ~800 K. They report that CO_2 can react with the HO-Al surface sites of γ-alumina at room temperature to form adsorbed bicarbonate structures. They also show that the surface OH on γ-alumina can be eliminated by calcination of the alumina surfaces at temperatures near 800 K. Adsorbed CO_2 on the dehydroxylated γ-alumina forms weakly bound carbonate species. No kinetic uptake data are available for CO_2 uptake.
Back to Table

(1) Parkyns, N. D. The influence of thermal pretreatment on the infrared spectrum of carbon dioxide adsorbed on alumina. *J. Phys. Chem.* **1971**, *75*, 526-531, doi:10.1021/j100674a014.
(2) Szanyi, J.; Kwak, J. H. Dissecting the steps of CO_2 reduction: 1. The interaction of CO and CO_2 with γ-Al_2O_3: an *in situ FTIR* study. *Phys. Chem. Chem. Phys.* **2014**, *16*, 15117-15125, doi:10.1039/c4cp00616j.

63. H_2CO + Al_2O_3(s). Carlos-Cueller et al.[1] reported Knudsen cell studies that determined γ_o values for oxygenated volatile organic compounds (VOCs) at 295 K. They measured a γ_o on α-alumina for formaldehyde of $(7.7 \pm 0.3) \times 10^{-5}$, based on BET surface areas and the KML[2] correction for porosity; relatively "sticky" formaldehyde may not access the full BET surface and thus γ_o may be underestimated. Xu et al.[3] used a DRIFTS Reactor with γ-Al_2O_3 surfaces over a temperature range of 84–573 K and a RH range of 0–80%. BET and geometric surface areas were used to calculate initial uptake coefficients. Formaldehyde uptake was independent of gas phase O_2 over the studied range ($0.18–730 \times 10^{13}$ cm^{-3}); uptake was negatively correlated with RH. Surface analyses included FTIR, X-ray Diffraction and SEM. The initial surface product is dioxymethylene that is oxidized to formate, with reaction order of 0.74 ± 0.05. Polyoxymethylene is a secondary adsorbed product. Reactive uptake saturates active surface sites so initial γ_o values are reported for both geometric and BET surface areas. For T = 298 K, γ_o(Geo) = $(3.6 \pm 0.8) \times 10^{-4}$ and γ_o(BET) = $(1.4 \pm 0.31) \times 10^{-8}$ (T = 298 K, RH = 0); γ_o(BET, 298 K) deceases approximately a factor of 2 as RH increases from 0 to 80%; γ_o(BET, 0 RH) increases irregularly by approximately a factor of 3 as T increases from 273 to 373 K. The Xu et al. room temperature BET value for γ-Al_2O_3 is ~5000 lower than the Carlos-Cueller et al. value for α-alumina. It is unclear how much of this is due to systematic error in one or both experiments and how much is due to different surface properties for the two alumina phases. Given the available data an upper limit of $\gamma_o < 5 \times 10^{-4}$ over the temperature range of 270–300 K is estimated for both phases.
Back to Table

(1) Carlos-Cuellar, S.; Li, P.; Christensen, A. P.; Krueger, B. J.; Burrichter, C.; Grassian, V. H. Heterogeneous uptake kinetics of volatile organic compounds on oxide surfaces using a Knudsen cell reactor: Adsorption of acetic acid, formaldehyde, and methanol on α-Fe_2O_3, α-Al_2O_3, and SiO_2. *J. Phys. Chem. A* **2003**, *107*, 4250-4261, doi:10.1021/jp0267609.
(2) Keyser, L. F.; Leu, M.-T. Surface areas and porosities of ices used to simulate stratospheric clouds. *J. Colloid Interface Sci.* **1993**, *155*, 137-145, doi:10.1006/jcis.1993.1018.
(3) Xu, B.; Shang, J.; Zhu, T.; Tang, X. Heterogeneous reaction of formaldehyde on the surface of γ-Al_2O_3 particles. *Atmos. Environ.* **2011**, *45*, 3569-3575, doi:10.1016/j.atmosenv.2011.03.067.

64. CH_3OH + H_2SO_4•nH_2O(l) and H_2SO_4•mHNO_3•nH_2O(l). Van Loon and Allen[2] report spectroscopic observations at 293 K for 0 to 96.5 wt% H_2SO_4 exposed to methanol vapor. They observed rapid surface adsorption and saturation, followed by slower bulk absorption. For acid concentrations between 47.1 and 63.3 wt% they observed surface reaction between methanol and sulfuric acid that formed methyl hydrogen

sulfate, CH_3SO_4H. Iraci et al.[1] used infrared spectroscopy to monitor the production of gas phase methyl nitrate, CH_3ONO_2, from the bulk reaction of ternary sulfuric acid/nitric acid/water solutions with 0.00005–0.005 M CH_3OH in 50.5 to 63.6 wt% H_2SO_4 with 0.03–0.21 M HNO_3 between 278.2 and 328.6 K. Within this range methyl nitrate production increased linearly with methanol and nitric acid concentration and exponentially with sulfuric acid concentration. At high acid concentrations nitric acid reacts with protons to form water and the nitronium ion, NO_2^+; methyl nitrate production was observed to be proportional to the NO_2^+ concentration indicating it was the nitrating agent.

Back to Table

(1) Iraci, L. T.; Riffel, B. G.; Robinson, C. B.; Michelsen, R. R.; Stephenson, R. M. The acid catalyzed nitration of methanol: formation of methyl nitrate via aerosol chemistry. *J. Atmos. Chem.* **2007**, *58*, 253-266, doi:10.1007/s10874-007-9091-9.

(2) Van Loon, L.; Allen, H. C. Uptake and surface reaction of methanol by sulfuric acid solutions investigated by vibrational sum frequency generation and Raman spectroscopies. *J. Phys. Chem. A* **2008**, *112*, 7873 (7878), doi:10.1021/jp712134s.

65. CH_3OH + Al_2O_3(s). Carlos-Cueller et al.[1] reported Knudsen cell studies that determined γ_o values for oxygenated volatile organic compounds (VOCs) at 295 K. They measured γ_o on α-alumina for methanol of $(1.0 \pm 0.7) \times 10^{-4}$, based on BET surface areas and the KML[2] correction for porosity. Since data is only available from a single laboratory using only a single method, an upper limit of $\gamma_o < 3 \times 10^{-4}$ is recommended for α-Al_2O_3.

Back to Table

(1) Carlos-Cuellar, S.; Li, P.; Christensen, A. P.; Krueger, B. J.; Burrichter, C.; Grassian, V. H. Heterogeneous uptake kinetics of volatile organic compounds on oxide surfaces using a Knudsen cell reactor: Adsorption of acetic acid, formaldehyde, and methanol on α-Fe_2O_3, α-Al_2O_3, and SiO_2. *J. Phys. Chem. A* **2003**, *107*, 4250-4261, doi:10.1021/jp0267609.

(2) Keyser, L. F.; Leu, M.-T. Surface areas and porosities of ices used to simulate stratospheric clouds. *J. Colloid Interface Sci.* **1993**, *155*, 137-145, doi:10.1006/jcis.1993.1018.

66. HC(O)OH + Al_2O_3(s). Tong and co-workers[3,4] used a DRIFTS reactor to investigate the uptake of formic acid on beds of α-Al_2O_3 particles; surface areas were estimated with BET measurements as well by geometric sample area. Their initial study[3] reported γ(BET) and γ(Geo) for formic, acetic and propionic acids on α-Al_2O_3 at 300 K over a RH range (0–90%). For RH(0) they reported:

Acid	γ (BET)	γ (Geo)
HC(O)OH	$(2.37 \pm 0.30) \times 10^{-7}$	$(2.07 \pm 0.26) \times 10^{-3}$
$CH_3C(O)OH$	$(5.99 \pm 0.78) \times 10^{-7}$	$(5.00 \pm 0.69) \times 10^{-3}$
$CH_3CH_2C(O)OH$	$(3.03 \pm 0.52) \times 10^{-7}$	$(3.04 \pm 0.63) \times 10^{-3}$

It is likely that γ(BET) underestimates the true uptake coefficient since organic acids adsorb and react before penetrating some pores and that γ(Geo) overestimates uptake rates. The effect of relative humidity on the HC(O)OH uptake co-efficients is modest, with a slight (~10%) rise between RH(0) and RH(20%) and then a gradual fall off (~33%) between RH(20%) and RH(95%). A second publication by Tong and co-workers[4] focused on the effects of temperature on uptake rate. For RH(0) they measured a modest increase (less than a factor of two) as T decreases from 298 to 240 K:

T (K)	γ(BET)	γ(Geo)
298	$(1.34 \pm 0.02) \times 10^{-6}$	$(2.35 \pm 0.03) \times 10^{-3}$
285	$(1.52 \pm 0.04) \times 10^{-6}$	$(2.65 \pm 0.07) \times 10^{-3}$
277	$(1.70 \pm 0.03) \times 10^{-6}$	$(2.98 \pm 0.03) \times 10^{-3}$
273	$(1.77 \pm 0.01) \times 10^{-6}$	$(3.09 \pm 0.03) \times 10^{-3}$
263	$(1.96 \pm 0.02) \times 10^{-6}$	$(3.43 \pm 0.04) \times 10^{-3}$
250	$(2.22 \pm 0.02) \times 10^{-6}$	$(3.89 \pm 0.03) \times 10^{-3}$
240	$(2.39 \pm 0.03) \times 10^{-6}$	$(4.18 \pm 0.05) \times 10^{-3}$

Note that their earlier γ(Geo) for room temperature and RH(0) of $(2.07 \pm 0.26) \times 10^{-3}$ [3] is in good agreement with the value of $(2.35 \pm 0.03) \times 10^{-3}$ reported in Wu et al.;[4] however, their later room temperature γ(BET) value is more than a factor of five larger than their earlier value, calling into question the reliability of BET surface area determinations. Infrared spectra indicated surface enhanced crystallization of HCOOH at lower

temperatures as well reaction with surface hydroxyl groups to form formate. Based on these data only an upper limit of $\gamma_o < 0.01$ is recommended for α-Al_2O_3.

Rubasinghege et al.[2] used a Quartz Crystal Microbalance (QCM) and Attenuated Total Reflectance FTIR (ATR-FTIR) to characterize total HC(O)OH uptake and surface reactions on γ-Al_2O_3, SiO_2 and kaolinite surfaces at T (298 K) and RH (<1%); no kinetic data was presented. They observed both reversible and irreversible adsorption of HC(O)OH on γ-Al_2O_3. Adsorbed water, controlled by RH, increases the irreversible uptake of HC(O)OH. The resulting layer of adsorbed formate decreases the surface hydrophilicity, decreasing the amount of water uptake. Ruan et al.[1] report a density functional simulation of HC(O)OH interacting with an α-Al_2O_3 (0001) surface, presenting adsorbate dissociation pathways and estimating the energy barrier for dehydration reactions.

Back to Table

(1) Ruan, M.; Hou, H.; Li, W.; Wang, B. Theoretical study of the adsorptive/dissociation reactions of formic acid on the α-Al_2O_3 (0001) surface. *J. Phys. Chem. C* **2014**, *118*, 20889-20898, doi:10.1021/jp504542n.

(2) Rubasinghege, G.; Ogden, S.; Baltrusaitis, J.; Grassian, V. H. Heterogeneous uptake and adsorption of gas-phase formic acid on oxide and clay particle surfaces: The roles of surface hydroxyl groups and adsorbed water in formic acid adsorption and the impact of formic acid adsorption on water uptake. *J. Phys. Chem. A* **2013**, *112*, 11316-11327, doi:10.1021/jp408169w.

(3) Tong, S. R.; Wu, L. Y.; Ge, M. F.; Wang, W. G.; Pu, Z. F. Heterogeneous chemistry of monocarboxylic acids on α-Al_2O_3 at different relative humidities. *Atmos. Chem. Phys.* **2010**, *10*, 7561-7574, doi:10.5194/acp-10-7561-2010.

(4) Wu, L.-Y.; Tong, S.-R.; Hou, S.-Q.; Ge, M.-F. Influence of temperature on the heterogeneous reaction of formic acid on α-Al_2O_3. *J. Phys. Chem. A* **2012**, *116*, 10390-10396, doi:10.1021/jp3073393.

67. **$CH_3CH_2OH + H_2SO_4 \bullet nH_2O$.** Timonen and Leu[2] used a trough flow reactor to measure uptake coefficients for ethanol on 41.1 to 79.3 wt% H_2SO_4, for selected temperatures between 193 to 273 K, but primarily for temperatures from 203 to 258 K. Uptake coefficients for 70.3–79.3 wt% acid showed little temperature variation, starting at ~0.07 for 203 K and falling to 0.05 to 0.06 above 250 K, while uptake coefficients for 41.1 to 64.1 wt% started at ~0.07 at 203 K and decreased to about 0.02 at 233 K for 41.1 wt% 1, to ~0.03 at 243 K for 54.4 wt% and ~0.035 at 253 K for 64.1 wt%. Uptake was only partially reversible, so it was attributed to both physical and reactive processes, making the reported uptake coefficients as upper limits for γ. The authors attributed the reactive portion of the uptake to esterification reactions, forming ethyl hydrogen sulfate and diethyl sulfate, and saw some mass spectral evidence for these products when they mixed ethanol with 80 wt% acid in their reactor at 296 K. Michelsen et al.[1] found no evidence for ethyl hydrogen sulfate in Knudsen cell ethanol uptake experiments for 39–76 wt% H_2SO_4 over a 209–237K temperature range, so the extent of reaction for low temperature acid solutions remains uncertain. Timonen and Leu suggest that at low ethanol vapor fluxes surface reactivity may be important.

Back to Table

(1) Michelsen, R. R.; Staton, S. J. R.; Iraci, L. T. Uptake and dissolution of gaseous ethanol in sulfuric acid. *J. Phys. Chem. A* **2006**, *110*, 6711-6717, doi:10.1021/jp056234s.

(2) Timonen, R. S.; Leu, M.-T. Interaction of ethyl alcohol vapor with sulfuric acid solutions. *J. Phys. Chem. A* **2006**, *110*, 6660-6666, doi:10.1021/jp055810h.

68. **$CH_3C(O)OH + Al_2O_3(s)$.** Carlos-Cueller et al.[1] reported γ_o values for oxygenated volatile organic compounds (VOCs) at 295 K. They measured a γ_o on α-alumina for acetic acid of $(2 \pm 1) \times 10^{-3}$, based on BET surface areas and the KML[2] correction for porosity; "sticky" acetic acid may not access the full BET surface and thus γ_o may be underestimated. Tong et al.[3] used a DRIFTS reactor to investigate the uptake of acetic acid on beds of α-Al_2O_3 particles at 300 K; surface areas were estimated with BET measurements as well by geometric sample area. For RH(0) they reported $\gamma(BET) = (5.99 \pm 0.78) \times 10^{-7}$ and $\gamma(Geo) = (5.00 \pm 0.69) \times 10^{-3}$; this $\gamma(BET)$ is over 3000 times smaller than that reported by Carlos-Cueller et al.[1] Given the disparity between the two values only an upper limit of $\gamma_o < 0.02$ for α-Al_2O_3 is recommended.

Back to Table

(1) Carlos-Cuellar, S.; Li, P.; Christensen, A. P.; Krueger, B. J.; Burrichter, C.; Grassian, V. H. Heterogeneous uptake kinetics of volatile organic compounds on oxide surfaces using a Knudsen cell reactor: Adsorption of acetic acid, formaldehyde, and methanol on α-Fe_2O_3, α-Al_2O_3, and SiO_2. *J. Phys. Chem. A* **2003**, *107*, 4250-4261, doi:10.1021/jp0267609.
(2) Keyser, L. F.; Leu, M.-T. Surface areas and porosities of ices used to simulate stratospheric clouds. *J. Colloid Interface Sci.* **1993**, *155*, 137-145, doi:10.1006/jcis.1993.1018.
(3) Tong, S. R.; Wu, L. Y.; Ge, M. F.; Wang, W. G.; Pu, Z. F. Heterogeneous chemistry of monocarboxylic acids on α-Al_2O_3 at different relative humidities. *Atmos. Chem. Phys.* **2010**, *10*, 7561-7574, doi:10.5194/acp-10-7561-2010.

69. **CH_3CHO + H_2SO_4•nH_2O.** Knudsen cell uptake measurements are reported by Michelsen et al.[3] for 38.5–76.2 wt% H_2SO_4 over a temperature range of 211–241 K, with evidence of reactive uptake for some temperatures in the 38.5–66.3 wt% H_2SO_4 range. Using a rotating wetted-wall flow reactor Esteve and Nozière[2] measured small, probably solubility constrained, uptake coefficients at 298 ± 3 K for 96 wt% and 89.4 wt% of 9.4×10^{-6} and 4.2×10^{-7}, respectively. Michelsen et al. found uptake over the 211–241 K temperature range was controlled by Henry's law solubility, and had a complex dependence on acid concentration due to competition among the reversible bulk phase processes of physical dissolution, hydration to form the gem diol, protonation and enolization, all of which affect H*. They also saw evidence for aldol condensation at some temperatures for acid concentrations of 66.3 wt% and below. Drawing on the complex aldol condensation mechanism presented to explain the bulk kinetic studies of Baigrie et al.,[1] Michelsen et al. present plausible arguments why non-reversible condensation reactions might have the complex dependence on acid concentrations and temperature that they observed. Given its relatively small rate constant, they suggest that aldol condensation bulk reactions will play a negligible role for typical aldehyde concentrations in the atmosphere.
Back to Table

(1) Baigrie, L. M.; Cox, R. A.; Slebocka-Tilk, H.; Tencer, M.; Tidwell, T. T. Acid-catalyze enolization and aldol condensation of acetaldehyde. *J. Am. Chem. Soc.* **1985**, *107*, 3640-3645, doi:10.1021/ja00298a039.
(2) Esteve, W.; Nozière, B. Uptake and reaction kinetics of acetone, 2-butanone, 2,4-pentanedione, and acetaldehyde in sulfuric acid solutions. *J. Phys. Chem. A* **2005**, *109*, 10920-10928, doi:10.1021/jp051199a.
(3) Michelsen, R. R.; Ashbourn, S. F. M.; Iraci, L. T. Dissolution, speciation, and reaction of acetaldehyde in cold sulfuric acid. *J. Geophys. Res.* **2004**, *109*, D23205, doi:10.1029/2004JD005041.

70. **CH_3CHO, CH_3CH_2CHO and $CH_3C(O)CH_3$ + Al_2O_3(s).** Li et al.[1] reported Knudsen cell studies that determined γ_o values for oxygenated volatile organic compounds (VOCs) at 298 K. They reported very similar BET corrected γ_os values on α-alumina for acetaldehyde (3.2×10^{-5}), propionaldehyde (4.7×10^{-5}), and acetone (2.0×10^{-5}). For molecules this large BET surface area may not be assessable and derived γ_os may be underestimated. Since data are from a single laboratory using only one technique, only conservative lower limits are recommended.
Back to Table

(1) Li, P.; Perreau, K. A.; Covington, E.; Song, C. H.; Carmichael, G. R.; Grassian, V. H. Heterogeneous reactions of volatile organic compounds on oxide particles of the most abundant crustal elements: Surface reactions of acetaldehyde, acetone, and propionaldehyde on SiO_2, Al_2O_3, Fe_2O_3, TiO_2, and CaO. *J. Geophys. Res.* **2001**, *106*, 5517-5529, doi:10.1029/2000JD900573.

71. **$CH_3C(O)CH_3$ + H_2SO_4•nH_2O.** Duncan et al.[1,2] used IR spectra of thin sulfuric acid films to establish that acetone is absorbed as the protonated species. Above 70 wt.% protonated acetone undergoes a self condensation/dehydration reaction to form protonated mesityl oxide, which can, in turn, react with an additional protonated acetone to form trimethyl benzene. Kane et al.[4] Henry's law uptake measurements diverged above 80 wt%, which they attribute to reactive uptake as suggested by Duncan et al. Using a rotating wetted-wall flow reactor Esteve and Nozière[3] measured small, probably solubility constrained, uptake coefficients at 298 ± 3 K for 89.4, 85, 80.8 and 73.9 wt% H_2SO_4 of 5.2×10^{-5}, 5.6×10^{-6}, 4.7×10^{-6} and 1.6×10^{-6}, respectively.
Back to Table

(1) Duncan, J. L.; Schindler, L. R.; Roberts, J. T. A new sulfate-mediated reaction: Conversion of acetone to trimethylbenzene in the presence of liquid sulfuric acid. *Geophys. Res. Lett.* **1998**, *25*, 631-634, doi:10.1029/98GL00250

(2) Duncan, J. L.; Schindler, L. R.; Roberts, J. T. Chemistry at and near the surface of liquid sulfuric acid: A kinetic, thermodynamic, and mechanistic analysis of heterogeneous reactions of acetone. *J. Phys. Chem. B* **1999**, *103*, 7247-7259, doi:10.1021/jp991322w.

(3) Esteve, W.; Nozière, B. Uptake and reaction kinetics of acetone, 2-butanone, 2,4-pentanedione, and acetaldehyde in sulfuric acid solutions. *J. Phys. Chem. A* **2005**, *109*, 10920-10928, doi:10.1021/jp051199a.

(4) Kane, S. M.; Timonen, R. S.; Leu, M. T. Heterogeneous chemistry of acetone in sulfuric acid solutions: Implications for the upper troposphere. *J. Phys. Chem. A* **1999**, *103*, 9259-9265, doi:10.1021/jp9926692.

72. **$CH_3C(O)O_2$ + H_2O(l) and H_2SO_4•nH_2O.** Villalta et al.[1] used wetted-wall flow tube techniques to measure $\gamma = 4.3$ (+ 2.4 /–1.5) × 10^{-3} for water at 274 ± 3K. They also measured uptake for 34 wt% H_2SO_4 at 246 K ($\gamma = (2.7 \pm 1.5) \times 10^{-3}$), 51 wt% at 273 K ($\gamma = (0.9 \pm 0.5) \times 10^{-3}$), and 71 wt% at 298 K ($\gamma = (1.4 \pm 0.7) \times 10^{-3}$). They suggest that products subsequent to hydrolysis are HO_2 and $CH_3C(O)OH$.
Back to Table

(1) Villalta, P. W.; Lovejoy, E. R.; Hanson, D. R. Reaction probability of peroxyacetyl radical on aqueous surfaces. *Geophys. Res. Lett.* **1996**, *23*, 1765-1768, doi:10.1029/96GL01286.

73. **$H_2C=C(CH_3)CHO$** and **$H_2C=CHC(O)CH_3$ + Al_2O_3(s).** Zhao et al.[1] report a coated wall flow reactor study with Transmission FTIR measurements of adsorption and reaction of both methacrolein (MAC) and methyl vinyl ketone **(**MVK) on α-Al_2O_3 at T~300 K and relative humidity values of RH <1%, 20% and 60%. They reported RH = 0 γ_o values based on BET surface areas of: γ_o(MAC) = (2.0 ± 0.5) × 10^{-8} and γ_o(MVK) = (3.8 ± 0.8) × 10^{-8}. They measured significantly lower γ_os for RH = 20 and 60% indicating that water vapor blocks reactive surface sites. Major products (>0.03) were CH_3CH_2CHO, HCHO and HCOOH for MAC and isomerization of MVK to $CH_3CH=CHCHO$ (crotonaldehyde) that then reacted to produce CHOCHO, CH_3CHO and $CH_3C(O)OH$**.** For molecules this large some BET surface area may not be accessible and derived γ_os may be underestimated. Given the strong impact of relative humidity and uncertainty in effective surface area no recommendations for γ_os are made.
Back to Table

(1) Zhao, Y.; Chen, Z.; Zhao, J. Heterogeneous reactions of methacrolein and methyl vinyl ketone on α-Al_2O_3 particles. *Environ. Sci. Technol.* **2010**, *44*, 2035-2041, doi:10.1021/es9037275.

74. **$CH_3C(O)O_2NO_2$ + HCl, Cl, ClO, and OClO on H_2SO_4•nH_2O(l).** Zhang and Leu[1] performed wetted wall flow reactor studies with Cl species partial pressures in the 10^{-6} to 10^{-7} Torr range and $CH_3C(O)O_2NO_2$ at 3 × 10^{-6} Torr after equilibrating the acid surfaces (42, 51, and 69 wt% at 202 and 224 K) with $CH_3C(O)O_2NO_2$. Also uptake studies with 5 × 10^{-7} Torr $CH_3C(O)O_2NO_2$ were performed after exposing the acid surface to the Cl species. No Cl species or $CH_3C(O)O_2NO_2$ uptake enhancements were observed under either condition and an upper limit for the reactive uptake coefficient of γ <1 × 10^{-4} of $CH_3C(O)O_2NO_2$ was deduced. No gas phase reaction products were observed using CIMS after 42 wt% H_2SO_4 at 210 K was exposed to $CH_3C(O)O_2NO_2$ and each Cl species for 20 minutes.
Back to Table

(1) Zhang, R.; Leu, M.-T. Heterogeneous interaction of peroxyacetyl nitrate with liquid sulfuric acid. *J. Geophys. Res.* **1997**, *102*, 8837-8843, doi:10.1029/97JD00131.

75. **IEPOX + Sulfate Aerosol.** Isoprene-derived epoxides (IEPOX) are important oxidation products of isoprene that are involved in the formation of secondary organic aerosol. Specifically, the reactive uptake of trans-beta-isoprene epoxydiol to aerosol particles was studied by Riedel et al.[2] and Gaston et al.[1] in an aerosol flow tube at room temperature using chemical ionization monitoring of the gas phase reactant. The uptake coefficient was studied as a function of aerosol acidity, composition and relative humidity. It was found that acidic particles (i.e. ammonium bisulfate vs. ammonium sulfate) were much more reactive, consistent with an acid-catalyzed nucleophilic attack mechanism. For example, the uptake coefficient varied between

roughly 0.01 to 0.1 on ammonium bisulfate to values two orders of magnitude lower on ammonium sulfate, at 50% relative humidity. There was a weak negative dependence of the uptake coefficient on relative humidity with ammonium sulfate particles.
Back to Table

(1) Gaston, C. J.; Riedel, T. P.; Zhang, Z. F.; Gold, A.; Surratt, J. D.; Thornton, J. A. Reactive uptake of an isoprene-derived epoxydiol to submicron aerosol particles. *Environ. Sci. Technol.* **2014**, *48*, 11178-11186, doi:10.1021/es5034266.
(2) Riedel, T. P.; Lin, Y.-H.; Budisulistiorini, S. H.; Gaston, C. J.; Thornton, J. A.; Zhang, Z.; Vizuete, W.; Gold, A.; Surratt, J. D. Heterogeneous reactions of isoprene-derived epoxides: Reaction probabilities and molar secondary organic aerosol yield estimates. *Environ. Sci. Technol. Lett.* **2015**, *2*, 38-42, doi:10.1021/ez500406f.

76. **Cl + H_2SO_4•nH_2O(l).** Measured reaction probability (Martin et al.[1]) varies between 3×10^{-5} and 7×10^{-4} as H_2O and T co-vary. Reaction product is claimed to be HCl.
Back to Table

(1) Martin, L. R.; Judeikis, H. S.; Wun, M. Heterogeneous reactions of Cl and ClO in the stratosphere. *J. Geophys. Res.* **1980**, *85*, 5511-5518, doi:10.1029/JC085iC10p05511.

77. **Cl + NaCl(s).** Ciuraru et al.[1] have measured the uptake coefficients for Cl atoms onto pure NaCl and artificial sea-salt in a coated-wall flow tube. The surface area of the substrates is not easily estimated. Uptake coefficients are on the order of 10^{-2} for dry NaCl, with evidence for Cl_2 as a reaction product probably arising from surface recombination.
Back to Table

(1) Ciuraru, R.; Gosselin, S.; Visez, N.; Petitprez, D. Heterogeneous reactivity of chlorine atoms with sodium chloride and synthetic sea salt particles. *Phys. Chem. Chem. Phys.* **2011**, *13*, 19460-19470, doi:10.1039/c1cp22170a.

78. **Cl_2+HBr + H_2O(s).** Hanson and Ravishankara[1] measured a reaction probability of >0.2 on water ice near 200 K. BrCl was not detected, presumably due to rapid reaction with excess HBr.
Back to Table

(1) Hanson, D. R.; Ravishankara, A. R. Heterogeneous chemistry of HBr and HF. *J. Phys. Chem.* **1992**, *96*, 9441-9446, doi:10.1021/j100202a069.

79. **Cl_2 + NaCl.** Mochida et al.[2] used salt powders and spray-deposited films of NaCl and reported an initial uptake coefficient of 1.0×10^{-3}. Aguzzi and Rossi[1] reported no measurable uptake of Cl_2 on NaCl.
Back to Table

(1) Aguzzi, A.; Rossi, M. J. The kinetics of the heterogeneous reaction of $BrONO_2$ with solid alkali halides at ambient temperature. A comparison with the interaction of $ClONO_2$ on NaCl and KBr. *Phys. Chem. Chem. Phys.* **1999**, *1*, 4337-4346, doi:10.1039/a904611i.
(2) Mochida, M.; Akimoto, H.; van den Bergh, H.; Rossi, M. J. Heterogeneous kinetics of the uptake of HOBr on solid alkali metal halides at ambient temperature. *J. Phys. Chem. A* **1998**, *102*, 4819-4828, doi:10.1021/jp980849q.

80. **Cl_2 + NaBr and NaI.** Mochida et al.[5] used salt powders and spray-deposited films to obtain a value for the initial uptake coefficient of 2×10^{-2}. The measured uptake coefficients for the salt powders were a factor of six larger, but application of the pore diffusion model of Keyser et al.[3,4] gave this value, which is in agreement with that for a spray-deposited film. Br_2 was generated in a yield of 100%, within experimental error.

Hu et al.[1] measured the uptake of Cl_2 on aqueous solutions of NaBr and NaI over the temperature range of 263–293 K using a droplet train flow reactor. Measured values of the uptake coefficients on NaBr solutions ranged from 0.16 at 263 K to 0.05 at 293 K, and there was evidence of a surface reaction between Cl_2 and Br^- at the air-particle interface. Similarly, the uptake coefficients for Cl_2 on NaI solutions ranged from 0.20 to 0.07 over the same temperature range, again with evidence for a contribution from an interface reaction. Huff and Abbatt[2] have studied the reaction of Cl_2 with films formed by freezing NaBr solutions at 233 K,

observing Br_2 as the reaction product and that the maximum reaction probability is 0.1 when the surface is saturated with bromide ions.
Back to Table

(1) Hu, J. H.; Shi, Q.; Davidovits, P.; Worsnop, D. R.; Zahniser, M. S.; Kolb, C. E. Reative uptake of Cl_2(g) and Br_2(g) by aqueous surfaces as a function of Br^- and I^- ion concentration: The effect of chemical reaction at the interface. *J. Phys. Chem.* **1995**, *99*, 8768-8776, doi:10.1021/j100021a050.
(2) Huff, A. K.; Abbatt, J. P. D. Gas-phase Br_2 production in heterogeneous reactions of Cl_2, HOCl, and BrCl with halide-ice surfaces. *J. Phys. Chem. A* **2000**, *104*, 7284-7293, doi:10.1021/jp001155w.
(3) Keyser, L. F.; Leu, M.-T.; Moore, S. B. Comment on porosities of ice films used to simulate stratospheric cloud surfaces. *J. Phys. Chem.* **1993**, *97*, 2800-2801, doi:10.1021/j100113a053.
(4) Keyser, L. F.; Moore, S. B.; Leu, M. T. Surface reaction and pore diffusion in flow tube reactors. *J. Phys. Chem.* **1991**, *95*, 5496-5502, doi:10.1021/j100167a026.
(5) Mochida, M.; Akimoto, H.; van den Bergh, H.; Rossi, M. J. Heterogeneous kinetics of the uptake of HOBr on solid alkali metal halides at ambient temperature. *J. Phys. Chem. A* **1998**, *102*, 4819-4828, doi:10.1021/jp980849q.

81. Cl_2 + KBr. Mochida et al.[2] used salt powders and spray-deposited films to obtain a value for the initial uptake coefficients. The value measured for salt powders was 0.176, but after correction for pore diffusion, this became 3.7×10^{-2}, similar to a value of 2.3×10^{-2} measured for spray-deposited films. Br_2 was generated in a yield of 100%, within experimental error. Aguzzi and Rossi[1] measured a similar value, 2.7×10^{-2}, using a Knudsen cell. Santschi and Rossi[3] reported an initial value of $\gamma_0 = 0.11$ for the uptake of Cl_2 on thin spray-deposited films of KBr that had not been extensively pumped on; this initial value was 4×10^{-2} for films that had been pumped on for hours. They attributed the difference to the removal of surface-adsorbed water (SAW) by extensive pumping.
Back to Table

(1) Aguzzi, A.; Rossi, M. J. The kinetics of the heterogeneous reaction of $BrONO_2$ with solid alkali halides at ambient temperature. A comparison with the interaction of $ClONO_2$ on NaCl and KBr. *Phys. Chem. Chem. Phys.* **1999**, *1*, 4337-4346, doi:10.1039/a904611i.
(2) Mochida, M.; Akimoto, H.; van den Bergh, H.; Rossi, M. J. Heterogeneous kinetics of the uptake of HOBr on solid alkali metal halides at ambient temperature. *J. Phys. Chem. A* **1998**, *102*, 4819-4828, doi:10.1021/jp980849q.
(3) Santschi, C.; Rossi, M. J. The heterogeneous interaction of Br_2, Cl_2 and Cl_2O with solid KBr and NaCl substrates: The role of adsorbed H_2O and halogens. *Phys. Chem. Chem. Phys.* **2004**, *6*, 3447-3460, doi:10.1039/b404415k.

82. Cl_2 + sea salt. Mochida et al.[1] used a synthetic sea salt and a "natural" seasoning sea salt in Knudsen cell studies of the uptake of Cl_2. The synthetic sea salt value of $(2.2 \pm 0.3) \times 10^{-2}$ is the value reported after correction of the measured value of 0.138 using the pore diffusion model. For the "natural" seasoning salt, the measured value was 0.11 which after correction for diffusion into the underlying layers became $(3.1 \pm 1.1) \times 10^{-2}$. Br_2 was the major gas phase product, with small mass spectrometric signals also seen for BrCl.
Back to Table

(1) Mochida, M.; Akimoto, H.; van den Bergh, H.; Rossi, M. J. Heterogeneous kinetics of the uptake of HOBr on solid alkali metal halides at ambient temperature. *J. Phys. Chem. A* **1998**, *102*, 4819-4828, doi:10.1021/jp980849q.

83. ClO + H_2O(s) and HNO_3•nH_2O(s). Proposed reaction (Leu[3]) is 2 ClO → Cl_2 + O_2; reactive uptake may depend on ClO surface coverage, which in turn may depend on gas phase ClO concentrations. Kenner et al.[2] measured reaction probabilities of $(8 \pm 2) \times 10^{-5}$ for ice at 183 K which is far lower than the limit of $>1 \times 10^{-3}$ obtained by Leu.[3] Abbatt,[1] using nearly the same low levels of ClO as Kenner et al., obtained $\gamma < 1 \times 10^{-5}$ at 213 K. The difference may lie in the level of ClO or other adsorbable reactive species present. The lower value of Abbatt is probably closer to the expected reactivity under stratospheric conditions. Using high concentrations of ClO radicals ($>10^{12}$ molecules/cm^3) exposed to ice surfaces at 225 K, McKeachie et al.[4] infer an uptake coefficient of 0.001, which increases with ClO exposure. Formation of higher chlorine oxides, notably OClO, is observed mass spectrometrically and by UV-VIS spectroscopy, upon warming the

ice. It is likely that the high ClO concentrations drive self-reactions on the ice surface. Kenner et al. also measured a reaction probability limit of $< (8 \pm 4) \times 10^{-5}$ for NAT at 183 K.
Back to Table

(1) Abbatt, J. P. D. Heterogeneous interactions of BrO and ClO: Evidence for BrO surface recombination and reaction with HSO_3^-/SO_3^{2-}. *Geophys. Res. Lett.* **1996**, *23*, 1681-1684, doi:10.1029/96GL01430.
(2) Kenner, R. D.; Plumb, I. C.; Ryan, K. R. Laboratory measurements of the loss of ClO on Pyrex, ice and NAT at 183 K. *Geophys. Res. Lett.* **1993**, *20*, 193-196, doi:10.1029/93GL00238.
(3) Leu, M.-T. Heterogeneous reaction of N_2O_5 with H_2O and HCl on ice surfaces: implications for Antarctic ozone depletion. *Geophys. Res. Lett.* **1988**, *15*, 851-854, doi:10.1029/GL015i008p00851.
(4) McKeachie, J. R.; Appel, M. F.; Kirchner, U.; Schindler, R. N.; Benter, T. Observation of a heterogeneous source of OClO from the reaction of ClO radicals on ice. *J. Phys. Chem. B* **2004**, *108*, 16786-16797, doi:10.1021/jp049314p.

84. **ClO + H_2SO_4•nH_2O.** Measured reaction probability (Martin et al.[2]) varies between 2×10^{-5} and 2×10^{-4} as H_2O content is varied by changing wall temperature. Reaction product is claimed to be HCl, not Cl_2. Abbatt[1] measured $\gamma < 1 \times 10^{-5}$ for 60 and 70 wt% H_2SO_4 at 213 K.
Back to Table

(1) Abbatt, J. P. D. Heterogeneous interactions of BrO and ClO: Evidence for BrO surface recombination and reaction with HSO_3^-/SO_3^{2-}. *Geophys. Res. Lett.* **1996**, *23*, 1681-1684, doi:10.1029/96GL01430.
(2) Martin, L. R.; Judeikis, H. S.; Wun, M. Heterogeneous reactions of Cl and ClO in the stratosphere. *J. Geophys. Res.* **1980**, *85*, 5511-5518, doi:10.1029/JC085iC10p05511.

85. **HCl + HNO_3 on H_2SO_4•mHNO_3•nH_2O(l).** Two studies have noted HCl activation in concentrated ternary $H_2SO_4/HNO_3/H_2O$ solutions or ice slurries. Luick et al.[2] saw only gas phase HCl in 64.6 wt% H_2SO_4/ 4.8 wt% HNO_3 at 200 K, but saw a vapor phase Cl partitioning of 50% HCl and 50% $ClNO/ClNO_2$ for a 76.6/20.1 wt% solution (an ice slurry) at 200 K. Cappa et al.[1] saw substantial yields of ClNO, $ClNO_2$, and Cl_2 at 273 K for a range of solution compositions; e.g. 32.6%, 9.8%, and 44.4% respectively for a total HCl conversion of 86.9% in a 35% H_2SO_4 /45% HNO_3 solution and 20.2%, 6.9%, 27.9% for a 60/25 wt% solution. While no kinetic coefficients or detailed mechanisms are available, these studies do show the potential for HCl activation in strong $H_2SO_4/HNO_3/H_2O$ solutions.
Back to Table

(1) Cappa, C. D.; Kuipers, S. E.; Roberts, J. M.; Gilbert, A. S.; Elrod, M. J. Product identification and kinetics of reactions of HCl with $HNO_3/H_2SO_4/H_2O$ solutions. *J. Phys. Chem. A* **2000**, *104*, 4449-4457, doi:10.1021/jp992666p.
(2) Luick, T. J.; Heckbert, R. W.; Schultz, K.; Disselkamp, R. S. Nitrosyl and nitryl chloride formation in $H_2SO_4/HNO_3/H_2O$/HCl solutions at 200 K. *J. Atmos. Chem.* **1999**, *32*, 315-325, doi:10.1023/A:1006152517987.

86. **HOCl + HCl + H_2O(s) and HNO_3•3H_2O(s).** Hanson and Ravishankara[5] and Abbatt and Molina[1] have investigated the HOCl + HCl reaction on water ice and NAT-like surfaces, and Chu et al.[3,4] studied the reaction on water ice. Product yield measurements support the identification of Cl_2 and H_2O as the sole products. The measured yield of product Cl_2 is 0.87 ± 0.20 and was stated to be similar on both surfaces according to Abbatt and Molina. Within the accuracy of the experiments, the reaction probability does not depend on the gas phase HCl and HOCl densities. Only Abbatt and Molina investigated at more than one temperature, their data indicates that γ increases at lower temperatures. A plot of data from the three studies does show a weak temperature trend, with γ increasing about a factor of two as the temperature drops from 202 to 188 K. However, the data are too sparse to assign a definitive temperature dependence. The average of all three studies yields $\gamma = 0.26 \pm 0.08$ for data based on the geometrical area of the flow tube surfaces. Chu et al.[3] indicate that a porosity correction for their data would reduce their value by a factor of 3 to 4. The real uncertainty would appear to be dominated by systematic uncertainties in porosity corrections and a potential temperature dependence. Given the fact that any porosity correction must reduce the value, a central value of 0.2 is adopted with an uncertainty factor of 2. The high reaction probabilities measured for water ice indicate that this reaction may play a significant role in release of reactive chlorine from the HCl reservoir.

Two studies (Hanson and Ravishankara[5] and Abbatt and Molina[1]) have measured the reaction probability of HOCl + HCl on NAT surfaces. These data show γ increases as the ambient water pressure increases and then reaches a plateau. At relatively high water pressure, the two studies averaged γ = 0.135 ± 0.049, with no porosity correction. The reaction probability on water-poor NAT-like surfaces falls off dramatically (a factor of 10). A recommendation of 0.1 with an uncertainty factor of 2 is shown in Table 5-2. Carslaw and Peter[2] have published a model of this reaction and its dependence on HCl uptake.
Back to Table

(1) Abbatt, J. P. D.; Molina, M. J. The heterogeneous reaction of HOCl + HCl → Cl_2 + H_2O on ice and nitric acid trihydrate: Reaction probabilities and stratospheric implications. *Geophys. Res. Lett.* **1992**, *19*, 461-464, doi:10.1029/92GL00373.

(2) Carslaw, K. S.; Peter, T. Uncertainties in reactive uptake coefficients for solid stratospheric particles-1. Surface chemistry. *Geophys. Res. Lett.* **1997**, *24*, 1743-1746, doi:10.1029/97GL01683.

(3) Chu, L.; Chu, L. T. Heterogeneous reaction HOCl + HBr → BrCl + H_2O on ice films. *J. Phys. Chem. A* **1999**, *103*, 691-699, doi:10.1021/jp983407n.

(4) Chu, L. T.; Leu, M.-T.; Keyser, L. F. Heterogeneous reactions of HOCl + HCl → Cl_2 + H_2O and $ClONO_2$ + HCl → Cl_2 + HNO_3 on ice surfaces at polar stratospheric conditions. *J. Phys. Chem.* **1993**, *97*, 12798-12804, doi:10.1021/j100151a028.

(5) Hanson, D. R.; Ravishankara, A. R. Investigation of the reactive and nonreactlve processes involving $ClONO_2$ and HCl on water and nitric acid doped ice. *J. Phys. Chem.* **1992**, *96*, 2682-2691, doi:10.1021/j100185a052.

87. HOCl + HCl + H_2SO_4•nH_2O(l). This process has been studied in coated flow tubes over ~200–260 K by Zhang et al.,[7] Hanson and Ravishankara,[3] Donaldson et al.,[1] and Hanson and Lovejoy.[2] Hanson and Lovejoy also made measurements in an aerosol flow tube from 251 to 276 K. A model of this and related sulfuric acid aerosol reactions tailored to stratospheric conditions has been published by Hanson et al.[4] Zhang et al. held the water vapor partial pressure at 3.8×10^{-4} Torr and showed γ increased by a factor of 50 as the temperature was lowered from 209 to 198 K increasing the water mole fraction, showing that the reaction rate is strongly dependent on water activity.
A detailed kinetic uptake model has been developed to fit the experimental data.[6] The formulation for γ is given as:

$$\frac{1}{\gamma} = \frac{1}{\alpha} + \frac{1}{\Gamma_{HOCl}^{rxn}}$$

where

$$\Gamma_{HOCl}^{rxn} = \frac{4H_{HOCl}RT}{\bar{c}} \left(D_{HOCl} k_{HOCl_HCl}\right)^{1/2}$$

At the low temperatures of interest, α for HOCl was assumed to be unity consistent with the value for HCl measured at 240 K and below (Robinson et al.[5]). The individual formulations for H_{HOCl}, D_{HOCl} and $k_{HOCl\text{-}HCl}$ are given in Table A-4 in Shi et al.[6] Reaction of HOCl with HCl is considered to be acid catalyzed. It is known that the reaction rate for HOCl + HCl in pure water is low (Donaldson et al.[1]). Experimental data noted above indicated that the reaction rate of HOCl + HCl increases with acidity of H_2SO_4 solution. The data from the experimental studies noted above were fit to the model without bias. Using the same error analysis discussed in the note for N_2O_5 uptake on sulfuric acid, a detailed kinetic model yields a 33.4% error (one sigma fit to the available data set, with σ_m = 33.3% and σ_d = 3.0%).

In the cold stratosphere where T<190 K, the reaction of $ClONO_2$ + HCl is so fast that HCl is depleted which slows down the reaction of HOCl + HCl. As shown in Table A-4 in Shi et al., the effect of HCl depletion on the HOCl reactive uptake coefficient (due to reaction with $ClONO_2$ inside/on the surface of particles) is taken into account via the factor F_{HCl} (also see the note on chlorine nitrate/hydrochloric acid reactive uptake on sulfuric acid surfaces).
Back to Table

(1) Donaldson, D. J.; Ravishankara, A. R.; Hanson, D. R. Detailed study of HOCl + HCl → Cl_2 + H_2O in sulfuric acid. *J. Phys. Chem. A* **1997**, *101*, 4717-4725, doi:10.1021/jp9633153.

(2) Hanson, D. R.; Lovejoy, E. R. Heterogeneous reactions in liquid sulfuric Acid: HOCl + HCl as a model system. *J. Phys. Chem.* **1996**, *100*, 6397-6405, doi:10.1021/jp953250o.

(3) Hanson, D. R.; Ravishankara, A. R. Uptake of HCl and HOCl onto sulphuric acid: Solubilities, diffusivities and reaction. *J. Phys. Chem.* **1993**, *97*, 12309-12319, doi:10.1021/j100149a035.
(4) Hanson, D. R.; Ravishankara, A. R.; Solomon, S. Heterogeneous reactions in sulfuric acid aerosols: A framework for model calculations. *J. Geophys. Res.* **1994**, *99*, 3615-3629, doi:10.1029/93JD02932
(5) Robinson, G. N.; Worsnop, D. R.; Jayne, J. T.; Kolb, C. E.; Swartz, E.; Davidovits, P. Heterogeneous uptake of HCl by sulfuric acid solutions. *J. Geophys. Res.* **1998**, *103*, 25371-25381, doi:10.1029/98JD02085
(6) Shi, Q.; Davidovits, P.; Jayne, J. T.; Kolb, C. E.; Worsnop, D. R. Kinetic model for reaction of $ClONO_2$ with H_2O and HCl and HOCl with HCl in sulfuric acid solutions. *J. Geophys. Res.* **2001**, *106*, 24259-24274, doi:10.1029/2000JD000181
(7) Zhang, R.; Jayne, J. T.; Molina, M. J. Heterogeneous interactions of $ClONO_2$ and HCl with sulfuric acid tetrahydrate: Implications for the stratosphere. *J. Phys. Chem.* **1994**, *98*, 867-874, doi:10.1021/j100054a022.

88. **HOCl + HBr on H_2O(s).** Chu and Chu[1] measured γ at 189 K to be in the range from 0.06 to 0.38 for HBr partial pressures ranging from 1.1×10^{-7} to 6.6×10^{-5} Torr. At 220 K they measured γ in the range from 0.01 to 0.07 for HBr partial pressures in the range from 7.2×10^{-7} to 1.3×10^{-5} Torr. These γ values were estimated assuming the area of the ice surface to be equal to the geometric area of the cylindrical flow reactor; corrections for surface porosity effects range from a factor of 3 to 10 lower.
Back to Table

(1) Chu, L.; Chu, L. T. Heterogeneous reaction HOCl + HBr → BrCl + H_2O on ice films. *J. Phys. Chem. A* **1999**, *103*, 691-699, doi:10.1021/jp983407n.

89. **HOCl + HBr on H_2SO_4•nH_2O(l).** Abbatt and Nowak[1] measured uptake of HOCl in the presence of excess HBr on a 69.3 wt% sulfuric acid solution in a wetted wall flow reactor at 228 K. A second order bulk reaction rate constant, k^{II}, of 2×10^6 M^{-1} s^{-1} was derived; this is a factor of ~10 faster than HOBr + HCl under the same conditions. Since HOCl and HBr have variable solubilities under stratospheric conditions, characterizing this reaction with a simple uptake coefficient is not appropriate. A full reaction/solubility/liquid phase diffusion model will require further data.
Back to Table

(1) Abbatt, J. P. D.; Nowak, J. B. Heterogeneous interactions of HBr and HOCl with cold sulfuric acid solutions: Implications for Arctic boundary layer bromine chemistry. *J. Phys. Chem. A* **1997**, *101*, 2131-2137, doi:10.1021/jp963117b.

90. **HOCl + NaBr and KBr.** Rossi[2] reported studies of the uptake of HOCl in a Knudsen cell using KBr powders and spray-deposited thin films. Values for the initial uptake coefficients covered a wide range, from 5×10^{-3} to 0.2, due to changes in the surface from adsorbed reaction products. The major product initially was Br_2, and subsequently BrCl and HOBr, with much smaller amounts of BrOCl and Br_2O. The mechanism was interpreted as the formation of small amounts of HBr on the surface from hydrolysis of KBr, followed by the reaction of HOCl with adsorbed HBr to form BrCl which then reacts with KBr to form Br_2. On frozen solutions of NaBr, Huff and Abbatt[1]observe reactivity of HOCl with uptake coefficients between 0.02 and 0.04 at 233 K in a coated-wall flow tube. Br_2 is the gas-phase product, thought to arise from the intermediate BrCl reacting with the bromide film. Although the kinetics are faster on the most acidic films (pH 2), there is no dependence of the acidity of the solution from pH 4 to 10.
Back to Table

(1) Huff, A. K.; Abbatt, J. P. D. Gas-phase Br_2 production in heterogeneous reactions of Cl_2, HOCl, and BrCl with halide-ice surfaces. *J. Phys. Chem. A* **2000**, *104*, 7284-7293, doi:10.1021/jp001155w.
(2) Rossi, M. J. Heterogeneous reactions on salts. *Chem. Rev.* **2003**, *103*, 4823-4882, doi:10.1021/cr020507n.

91. **ClNO + H_2O(l).** Scheer et al.[1] used droplet train and wetted wall flow reactor measurements to determine reactive uptake coefficients for ClNO over a temperature range of 273–293 K. Measured values show a weak negative temperature dependence ranging from 0.12 at 273 K to 0.0058 at 293 K. The reaction was shown to be base catalyzed producing HONO.
Back to Table

(1) Scheer, V.; Frenzel, A.; Behnke, W.; Zetsch, C.; Magi, L.; George, C.; Mirabel, P. Uptake of nitrosyl chloride (NOCl) by aqueous solutions. *J. Phys. Chem. A* **1997**, *101*, 9359-9366, doi:10.1021/jp972143m.

92. **ClNO + NaCl(s).** Using a Knudsen cell technique Beichart and Finlayson-Pitts[1] set upper limits of $\gamma <\sim 10^{-5}$ for reactive uptake of ClNO on NaCl(s) powders at 298 K.
Back to Table

(1) Beichert, P.; Finlayson-Pitts, B. J. Knudson cell studies of the uptake of gaseous HNO_3 and other oxides of nitrogen on solid NaCl. The role of surface absorbed water. *J. Phys. Chem.* **1996**, *100*, 15218-15228, doi:10.1021/jp960925u.

93. **$ClNO_2$ + H_2O(l).** Behnke, George and co-workers have used droplet train and wetted wall flow reactor techniques to investigate the reactive uptake of $ClNO_2$ on aqueous solutions.[1-4] Droplet train flow reactor experiments from 268–279 K demonstrated that the reactive uptake coefficient on pure water is $<1 \times 10^{-5}$.[3] Wetted wall flow reactor studies from 279 to 292 K on pure water and very low concentration sodium halide solutions all yielded reactive uptake coefficients in the 10^{-6} range, with typical values of $(4.84 \pm 0.13) \times 10^{-6}$ at 291 K,[1] and 3.41×10^{-6} at 276.6 K, 4.27×10^{-6} at 282.2 K, and 4.48×10^{-6} at 287.4 K.[2] There is apparently no significant temperature dependence.
Back to Table

(1) Behnke, W.; George, C.; Scheer, V.; Zetsch, C. Production and decay of $ClNO_2$ from the reaction of gaseous N_2O_5 with NaCl solution: Bulk and aerosol experiments. *J. Geophys. Res.* **1997**, *102*, 3795-3804, doi:10.1029/96JD03057.
(2) Frenzel, A.; Scheer, V.; Sikorski, R.; George, C.; Behnke, W.; Zetsch, C. Heterogeneous interconversion reactions of $BrNO_2$, $ClNO_2$, Br_2, and Cl_2. *J. Phys. Chem. A* **1998**, *102*, 1329-1337, doi:10.1021/jp973044b.
(3) George, C.; Behnke, W.; Scheer, V.; Zetsch, C.; Magi, L.; Ponche, J. L.; Mirabel, P. Fate of $ClNO_2$ over aqueous solutions containing iodide. *Geophys. Res. Lett.* **1995**, *22*, 1505-1508, doi:10.1029/95GL01417
(4) Schweitzer, F.; Mirabel, P.; George, C. Multiphase chemistry of N_2O_5, $ClNO_2$ and $BrNO_2$. *J. Phys. Chem. A* **1998**, *102*, 3942-3952, doi:10.1021/jp980748s.

94. **$ClNO_2$ + KBr, NaBr, NaI and NaCl.** Caloz et al.[3] measured the uptake of $ClNO_2$ on solid KBr at room temperature using a Knudsen cell and salt samples in the form of powders, spray-deposited films, polished windows and depolished windows. The uptake coefficient increased with the number of layers of salt powders; correction of the uptake coefficients using the pore diffusion model gave initial uptake coefficients of $(1.0–1.3) \times 10^{-4}$, in agreement with values measured for the spray-deposited film (1.0×10^{-4}) and depolished window (1.0×10^{-4}). The value for the polished window was an order of magnitude smaller, as expected since this has much less surface-adsorbed water (SAW) that assists in keeping the surface from becoming passivated. The yield of Br_2 relative to $ClNO_2$ lost was 0.55 ± 0.2. Using a diffusion tube method, Koch and Rossi[7] measured an uptake coefficient of 2.0×10^{-4}, in reasonable agreement with the Knudsen cell results.
The uptake of $ClNO_2$ on aqueous solutions of NaBr has been shown to increase with the concentration of NaBr. Frenzel et al.[5] measured the uptake of $ClNO_2$ on $(0.5–5) \times 10^{-3}$ M NaBr solutions from 275–291 K using a wetted wall flow tube apparatus; the values of γ increased from 1.2×10^{-5} to 4.0×10^{-5} over this range of NaBr concentrations. Schweitzer et al.[9] used a droplet train apparatus from 275–288 K; γ increased from 8.6×10^{-6} to 9.4×10^{-4} as the NaBr concentration increased from 10^{-4} to 1.0 M. The main product was Br_2, with traces of $BrNO_2$ and BrCl. In a subsequent study,[10] they applied a wetted wall flow tube method from 275–293 K and reported uptake coefficients that were independent of temperature over this range, but again increased with the concentration of NaBr: γ increased from 7.1×10^{-6} at 10^{-4} M NaBr to 9.2×10^{-4} at 1.0 M. Fickert et al.[4] used a wetted wall flow tube at 274 K and measured an uptake coefficient of 1.1×10^{-5} for 10^{-4} M NaBr, increasing to 1.1×10^{-4} for 10^{-2} M NaBr. The major gas phase products were Br_2 and $BrNO_2$, with the yield of $BrNO_2$ decreasing as the initial bromide ion concentration in solution increased. The mass accommodation coefficient for $ClNO_2$ on aqueous solutions at 275 K was measured to be $(9 \pm 4) \times 10^{-3}$. A Knudsen cell study by Beichart and Finlayson-Pitts[2] found $\gamma <\sim 10^{-5}$ on NaCl powders at 298 K.

The uptake of $ClNO_2$ on solutions of NaI was studied by George et al.[6] and by Schweitzer et al.[9,10] The uptake coefficient increases with the concentration of NaI. For example, George et al.[6] reported that γ_0 increased from 1.1×10^{-3} to 6.6×10^{-3} as the iodide concentration increased from 10^{-3} M to 10^{-2} M at 280 K. This is consistent with the results of Schweitzer et al.[9,10] who reported that γ_0 increased from 3.1×10^{-5} to 4.5×10^{-3} as the iodide concentration increased from 10^{-4} M to 10^{-2} M at 275 K.

The uptake of $ClNO_2$ on solutions of NaCl is much slower than on NaBr or NaI solutions. Behnke et al.[1] reported uptake of $ClNO_2$ at 291 K using a wetted wall flow tube, with uptake coefficients decreasing as the NaCl concentration increased. At 0.1 M NaCl, $\gamma_0 = (3.1 \pm 0.3) \times 10^{-6}$ but at 4.6 M NaCl, the value was about an order of magnitude smaller, $\gamma_0 = (0.27 \pm 0.02) \times 10^{-6}$. They proposed that this was due to the common ion effect owing to the reversible hydrolysis of $ClNO_2$ to $Cl^- + NO_2^+$.

Roberts et al.[8] report that $ClNO_2$ produces Cl_2 when exposed to solutions of chloride with concentrations as low as 0.05 M, when the pH is less than 2.
Back to Table

(1) Behnke, W.; George, C.; Scheer, V.; Zetsch, C. Production and decay of $ClNO_2$ from the reaction of gaseous N_2O_5 with NaCl solution: Bulk and aerosol experiments. *J. Geophys. Res.* **1997**, *102*, 3795-3804, doi:10.1029/96JD03057.

(2) Beichert, P.; Finlayson-Pitts, B. J. Knudson cell studies of the uptake of gaseous HNO_3 and other oxides of nitrogen on solid NaCl. The role of surface absorbed water. *J. Phys. Chem.* **1996**, *100*, 15218-15228, doi:10.1021/jp960925u.

(3) Caloz, F.; Seisel, S.; Fenter, F. F.; Rossi, M. J. Reactivity of $BrNO_2$ and $ClNO_2$ with solid alkali salt substrates. *J. Phys. Chem. A* **1998**, *102*, 7470-7479, doi:10.1021/jp982000f.

(4) Fickert, S.; Helleis, F.; Adams, J. W.; Moortgat, G. K.; Crowley, J. N. Reactive uptake of $ClNO_2$ on aqueous bromide solutions. *J. Phys. Chem. A* **1998**, *102*, 10689-10696, doi:10.1021/jp983004n.

(5) Frenzel, A.; Scheer, V.; Sikorski, R.; George, C.; Behnke, W.; Zetzsch, C. Heterogeneous interconversion reactions of $BrNO_2$, $ClNO_2$, Br_2, and Cl_2. *J. Phys. Chem. A* **1998**, *102*, 1329-1337, doi:10.1021/jp973044b.

(6) George, C.; Behnke, W.; Scheer, V.; Zetsch, C.; Magi, L.; Ponche, J. L.; Mirabel, P. Fate of $ClNO_2$ over aqueous solutions containing iodide. *Geophys. Res. Lett.* **1995**, *22*, 1505-1508, doi:10.1029/95GL01417.

(7) Koch, T. G.; Rossi, M. J. Direct measurement of surface residence times: Nitryl chloride and chlorine nitrate on alkali halides at room temperature. *J. Phys. Chem. A* **1998**, *102*, 9193-9201, doi:10.1021/jp982539d.

(8) Roberts, J. M.; Osthoff, H. D.; Brown, S. S.; Ravishankara, A. R. N_2O_5 oxidizes chloride to Cl_2 in acidic atmospheric aerosol. *Science* **2008**, *321*, 1059-1059, doi:10.1126/science.1158777.

(9) Schweitzer, F.; Mirabel, P.; George, C. Multiphase chemistry of N_2O_5, $ClNO_2$ and $BrNO_2$. *J. Phys. Chem. A* **1998**, *102*, 3942-3952, doi:10.1021/jp980748s.

(10) Schweitzer, F.; Mirabel, P.; George, C. Heterogeneous chemistry of nitryl halides in relation to tropospheric halogen activation. *J. Atmos. Chem.* **1999**, *34*, 101-117, doi:10.1023/A:1006249921480.

95. **$ClONO_2 + H_2O(s)$.** Measurement of $\gamma = 0.3$ (+0.7, –0.1) (Hanson and Ravishankara[5]) significantly exceeds early measurements of Molina et al.,[11] Tolbert et al.,[14] Leu,[9] and Moore et al.[12] but agrees reasonably well with subsequent measurements by Chu et al.,[2] Zhang et al.,[15] and Fernandez et al.[3] when geometrical surface areas are assumed for analysis. Previous measurements were probably complicated by NAT formation on the surface (Hanson and Ravishankara[6] and Chu et al.[2]). Lower levels of $ClONO_2$(g) used by Hanson and Ravishankara[5] minimized this surface saturation problem. Also, using lower $ClONO_2$ concentrations, Zhang et al. obtained a reaction probability of 0.08 ± 0.02 at 195 K, Fernandez et al. measured 0.1, and values were 0.03 to 0.13 from Chu et al. Subsequent Knudsen cell measurements at 180 and 200 K by Oppliger et al.[13] showed initial uptake γs in the 0.2 to 0.4 range. Measured reaction products were HNO_3 and HOCl. All of the HNO_3 and much of the HOCl is retained on the surface under polar stratospheric conditions (Hanson and Ravishankara[5,6]). Hanson[4] deposited $ClONO_2$ on $H_2{}^{18}O$ enriched ice and detected $H^{18}OCl$ showing the Cl–ONO_2 bond is broken at 191 K.

Data plots confirm a trend showing that at a high density of $ClONO_2$, the product HNO_3 covers the ice surface preventing the further reaction of $ClONO_2$ with H_2O molecules on the surface. Therefore, data obtained at high $ClONO_2$ densities (>10^{14} molecules/cm^3) are excluded from further evaluation. An experiment (Berland

et al.[1]) using a laser-induced thermal desorption technique yielded a much lower value of $ClONO_2$ reaction probability at 190 K (about 3 orders of magnitude lower) after extrapolating the results obtained at temperatures of 140 K and below. We also exclude this point in the averaging of data since the physical characteristics of ice surfaces at these very low temperatures may not be very representative of those found at stratospheric temperatures. Selected data show no temperature dependence between T = 180 and 200 K and averaged $\gamma_o = 0.28 \pm 0.25$. Again, within the experimental accuracy, the Hanson and Ravishankara[6,7] and Chu et al.[2] data show that uptake measurements are nearly independent of ice substrate thickness. See Henson et al.[8] for discussion of a model which accounts for the effect of HNO_3 on the reaction $ClONO_2$ on water and nitric acid ice surfaces. The reactivity of $ClONO_2$ on ice, as modeled with high level ab initio methods and simulations with four water molecules is consistent with the above laboratory results, i.e., the uptake coefficient is modeled to be close to 0.1 at 180 K with a strong negative temperature dependence (Loerting et al.[10]).

Zondlo et al.[16] report the formation of a supercooled H_2O/HNO_3 liquid layer at 185 K as a reaction product, forming NAT or NAD only after decreasing the relative humidity below the ice frost point. This effect is similar to that resulting from the interaction of gaseous HNO_3 or N_2O_5 with the ice surface. These authors measured $\gamma = (3 \pm 2) \times 10^{-3}$ at 185 K for the reaction of $ClONO_2$ with this supercooled liquid layer.
Back to Table

(1) Berland, B. S.; Tolbert, M. A.; George, S. M. Surface sensitive studies of the reactive uptake of chlorine nitrate on ice. *J. Phys. Chem. A* **1997**, *101*, 9954-9963, doi:10.1021/jp971121x.

(2) Chu, L. T.; Leu, M.-T.; Keyser, L. F. Heterogeneous reactions of HOCl + HCl → Cl_2 + H_2O and $ClONO_2$ + HCl → Cl_2 + HNO_3 on ice surfaces at polar stratospheric conditions. *J. Phys. Chem.* **1993**, *97*, 12798-12804, doi:10.1021/j100151a028.

(3) Fernandez, M. A.; Hynes, R. G.; Cox, R. A. Kinetics of $ClONO_2$ reactive uptake on ice surfaces at temperatures of the upper troposphere. *J. Phys. Chem. A* **2005**, *109*, 9986-9996, doi:10.1021/jp053477b.

(4) Hanson, D. R. Reactivity of $ClONO_2$ on $H_2{}^{18}O$ ice and organic liquids. *J. Phys. Chem.* **1995**, *99*, 13059-13061, doi:10.1021/j100035a003.

(5) Hanson, D. R.; Ravishankara, A. R. The reaction probabilities of $ClONO_2$ and N_2O_5 on polar stratospheric cloud materials. *J. Geophys. Res.* **1991**, *96*, 5081-5090, doi:10.1029/90JD02613.

(6) Hanson, D. R.; Ravishankara, A. R. Investigation of the reactive and nonreactlve processes involving $ClONO_2$ and HCl on water and nitric acid doped ice. *J. Phys. Chem.* **1992**, *96*, 2682-2691, doi:10.1021/j100185a052.

(7) Hanson, D. R.; Ravishankara, A. R. Response to "Comment on porosities of ice films used to simulate stratospheric cloud surfaces". *J. Phys. Chem.* **1993**, *97*, 2802-2803, doi:10.1021/j100113a054.

(8) Henson, B. F.; Wilson, K. R.; Robinson, J. M. A physical absorption model of the dependence of $ClONO_2$ heterogeneous reactions on relative humidity. *Geophys. Res. Lett.* **1996**, *23*, 1021-1024, doi:10.1029/96GL00871.

(9) Leu, M.-T. Laboratory studies of sticking coefficients and heterogeneous reactions important in the Antarctic stratosphere. *Geophys. Res. Lett.* **1988**, *15*, 17-20, doi:10.1029/GL015i001p00017.

(10) Loerting, T.; Voegele, A. F.; Tautermann, C. S.; Liedl, K. R.; Molina, L. T.; Molina, M. J. Modeling the heterogeneous reaction probability for chlorine nitrate hydrolysis on ice. *J. Geophys. Res.* **2006**, *111*, D14307, doi:10.1029/2006JD007065.

(11) Molina, M. J.; Tso, T. L.; Molina, L. T.; Wang, F. C. Antarctic stratosheric chemistry of chlorine nitrate, hydrogen chloride, and ice: Release of active chlorine. *Science* **1987**, *238*, 1253-1259, doi:10.1126/science.238.4831.1253.

(12) Moore, S. B.; Keyser, L. F.; Leu, M. T.; Turco, R. P.; Smith, R. H. Heterogeneous reactions on nitric acid trihydrate. *Nature* **1990**, *345*, 333-335, doi:10.1038/345333a0.

(13) Oppliger, R.; Allanic, A.; Rossi, M. J. Real-time kinetics of the uptake of $ClONO_2$ on ice and in the presence of HCl in the temperature range 160 K ≤ T ≤ 200 K. *J. Phys. Chem. A* **1997**, *101*, 1903-1911, doi:10.1021/jp963065q.

(14) Tolbert, M. A.; Rossi, M. J.; Malhotra, R.; Golden, D. M. Reaction of chlorine nitrate with hydrogen chloride and water at Antarctic stratospheric temperatures. *Science* **1987**, *238*, 1258-1260, doi:10.1126/science.238.4831.1258.

(15) Zhang, R.; Leu, M.-T.; Keyser, L. F. Heterogeneous reactions of $ClONO_2$, HCl and HOCl on liquid sulfuric acid surfaces. *J. Phys. Chem.* **1994**, *98*, 13563-13574, doi:10.1021/j100102a022.

(16) Zondlo, M. A.; Barone, S. B.; Tolbert, M. A. Condensed-phase products in heterogeneous reactions: N_2O_5, $ClONO_2$ and HNO_3 reacting on ice films at 185 K. *J. Phys. Chem. A* **1998**, *102*, 5735-5748, doi:10.1021/jp980131a.

96. **$ClONO_2$ + H_2O(l).** Deiber et al.[1] used a droplet train rector to measure to uptake of $ClONO_2$ on pure water between 274 and 285 K. No apparent temperature dependence was observed with all three temperatures measured resulting in reactive uptake measurements near 0.025.
Back to Table

(1) Deiber, G.; George, C.; Le Calve, S.; Schweitzer, F.; Mirabel, P. Uptake study of $ClONO_2$ and $BrONO_2$ by halide containing droplets. *Atmos. Chem. Phys.* **2004**, *4*, 1291-1299, doi:10.5194/acp-4-1291-2004.

97. **$ClONO_2$ + HNO_3•nH_2O(s).** Hanson and Ravishankara[3] report a γ value of 0.006 at 201 K for the $ClONO_2$ reaction with the water on NAT (HNO_3•nH_2O). However, these authors present re-analyzed and additional data with $\gamma \approx 0.001$ at 191 K in Hanson and Ravishankara.[4,5] Similar experiments (Moore et al.[8] and Leu et al.[7]) report a larger value of 0.02 ± 0.01 which falls very rapidly as slight excesses of H_2O above the 3/1 H_2O/HNO_3 ratio for NAT are removed. In general, it is difficult to know that only NAT is formed when freezing from solution; it is likely that the high value reflects the reactivity on water ice that will form when the solution stoichiometry is water rich. They measured γ of less than 1×10^{-6} for slightly water-poor NAT surfaces. Abbatt and Molina[1] report γ values reaching 0.002 at 202 K and high RH. Hanson and Ravishankara[4] reported that γ for this reaction increases by a factor of 4 as the surface temperature increases from 191 to 211 K. However, Knudsen cell measurements at 185 K by Barone et al.[2] reported $\gamma = 0.004$ at a relative humidity (RH) of 100%, rising to 0.007 near RH = 120%, indicating a possible mild negative temperature dependence when high RH values from this and other studies are compared. Excluding the JPL data,[7,8] the other data obtained at high RH (~90%) were averaged, assuming no temperature dependence, to yield $\gamma = 0.0043 \pm 0.0021$. The strong dependence on RH and the possible temperature dependence suggest that systematic error probably exceeds the calculated statistical error. Within the experimental accuracy, the data of Hanson and Ravishankara[4,5] show that measured uptake coefficients are independent of ice substrate thickness. Barone et al. report very similar uptake coefficients for nitric acid dihydrate (NAD) as for NAT as a function of RH at 202 K. See Henson et al.[6] for discussion of a model which accounts for the effect of HNO_3 on the reaction of $ClONO_2$ on water and nitric acid ice surfaces.
Back to Table

(1) Abbatt, J. P. D.; Molina, M. J. Heterogeneous interactions of $ClONO_2$ and HCl on nitric acid trihydrate at 202 K. *J. Phys. Chem.* **1992**, *96*, 7674-7679, doi:10.1021/j100198a036.
(2) Barone, S. B.; Zondlo, M. A.; Tolbert, M. A. A kinetic and product study of the hydrolysis of $ClONO_2$ on type Ia polar stratospheric cloud materials at 185 K. *J. Phys. Chem. A* **1997**, *101*, 8643-8652, doi:10.1021/jp971107k.
(3) Hanson, D. R.; Ravishankara, A. R. The reaction probabilities of $ClONO_2$ and N_2O_5 on polar stratospheric cloud materials. *J. Geophys. Res.* **1991**, *96*, 5081-5090, doi:10.1029/90JD02613
(4) Hanson, D. R.; Ravishankara, A. R. Investigation of the reactive and nonreactlve processes involving $ClONO_2$ and HCl on water and nitric acid doped ice. *J. Phys. Chem.* **1992**, *96*, 2682-2691, doi:10.1021/j100185a052.
(5) Hanson, D. R.; Ravishankara, A. R. Response to "Comment on porosities of ice films used to simulate stratospheric cloud surfaces". *J. Phys. Chem.* **1993**, *97*, 2802-2803, doi:10.1021/j100113a054.
(6) Henson, B. F.; Wilson, K. R.; Robinson, J. M. A physical absorption model of the dependence of $ClONO_2$ heterogeneous reactions on relative humidity. *Geophys. Res. Lett.* **1996**, *23*, 1021-1024, doi:10.1029/96GL00871.
(7) Leu, M.-T.; Moore, S. B.; Keyser, L. F. Heterogeneous reactions of chlorine nitrate and hydrogen chloride on Type I polar stratospheric clouds. *J. Phys. Chem.* **1991**, *95*, 7763-7771, doi:10.1021/j100173a040.
(8) Moore, S. B.; Keyser, L. F.; Leu, M. T.; Turco, R. P.; Smith, R. H. Heterogeneous reactions on nitric acid trihydrate. *Nature* **1990**, *345*, 333-335, doi:10.1038/345333a0.

98. **$ClONO_2$ + H_2SO_4•nH_2O(l).** Results from wetted-wall flow tube (Hanson and Ravishankara[5]) Knudsen cell reactor (Manion et al.[6]), aerosol flow tube (Hanson and Lovejoy[3]), and droplet train uptake (Robinson et al.[7])

experiments supplement older wetted-wall flow tube (Hanson and Ravishankara[4]) and Knudsen cell measurements (Rossi et al.[8] and Tolbert et al.[10]). Although earlier Knudsen cell measurements probably suffered from surface saturation, more recent results compare well with those from other techniques. Saturation free results, available over a temperature range of 200–265 K and a H_2SO_4 concentration range of 39 to 75 wt%, were fit to a phenomenological model developed by Robinson et al.[7] Measured γ values depend strongly on H_2SO_4 concentration and vary modestly with temperature, with a trend to somewhat higher values for the 210–220 K temperature range. The temperature-dependent uptake model takes into account the temperature and composition dependence of the effective Henry's Law constant, liquid phase diffusion coefficient, and the liquid phase hydrolysis rate constant. The hydrolysis reaction was treated by modeling two reaction channels, a direct hydrolysis process dominating reaction at low H_2SO_4 concentrations with a reaction rate proportional to water activity and a proton-catalyzed reaction with a rate proportional to H^+ activity, which dominates at higher acid concentrations.

The data fit to the original Robinson et al. model have been supplemented by additional wetted-wall flow tube and aerosol flow tube data from Hanson[2] and aerosol flow tube data from Ball et al.[1] A revised kinetic model (Shi et al.[9]) incorporating these data has been developed that is based on the earlier work of Robinson et al.[7] In this model, γ is calculated using the expression

$$\frac{1}{\gamma} = \frac{1}{\alpha} + \frac{1}{\Gamma_b^{H_2O}}$$

where,

$$\Gamma_b^{H_2O} = \frac{4H_{ClONO_2}RT}{\bar{c}}\left(D_{ClONO_2}k_{hydr}\right)^{1/2}$$

The detailed parameterizations for H_{ClONO_2}, D_{ClONO_2}, and k_{hydr} are given in the Appendix in Shi et al.[9] As was the case for N_2O_5 hydrolysis k_{hydr} is seen to have a direct and an acid catalyzed channel. Using the same error analysis approach as in the note on N_2O_5 uptake, the model error is about 32.4% (1σ), with σ_m = 32.2% and σ_d = 4.0%.

In the calculation of the chlorine activation (Cl_2 production) rate under stratospheric conditions, one needs to take into account the competition between the reactions of $ClONO_2$ + H_2O and $ClONO_2$ + HCl. The presence of HCl will depress the reaction probability of $ClONO_2$ with H_2O.
Back to Table

(1) Ball, S. M.; Fried, A.; Henry, B. E.; Mozurkewich, M. The hydrolysis of $ClONO_2$ on sub-micron liquid sulfuric acid aerosols. *Geophys. Res. Lett.* **1998**, *25*, 3339-3342, doi:10.1029/98GL02566.

(2) Hanson, D. R. Reaction of $ClONO_2$ with H_2O and HCl in sulfuric acid and $HNO_3/H_2SO_4/H_2O$ mixtures. *J. Phys. Chem. A* **1998**, *102*, 4794-4807, doi:10.1021/jp972767s.

(3) Hanson, D. R.; Lovejoy, E. R. The reaction of $ClONO_2$ with submicrometer sulfuric acid aerosol. *Science* **1995**, *267*, 1326-1329, doi:10.1126/science.267.5202.1326.

(4) Hanson, D. R.; Ravishankara, A. R. The reaction probabilities of $ClONO_2$ and N_2O_5 on 40 to 75% sulfuric acid solutions. *J. Geophys. Res.* **1991**, *96*, 17307-17314, doi:10.1029/91JD01750.

(5) Hanson, D. R.; Ravishankara, A. R. Reactive uptake of $ClONO_2$ onto sulfuric acid due to reaction with HCl and H_2O. *J. Phys. Chem.* **1994**, *98*, 5728-5735, doi:10.1021/j100073a026.

(6) Manion, J. A.; Fittschen, C. M.; Golden, D. M.; Williams, L. R.; Tolbert, M. A. Heterogeneous reactions of chlorine nitrate and dinitrogen pentoxide on sulfuric acid surfaces representative of global stratospheric aerosol particles. *Israel J. Chem.* **1994**, *34*, 355-363.

(7) Robinson, G. N.; Worsnop, D. R.; Jayne, J. T.; Kolb, C. E.; Davidovits, P. Heterogeneous uptake of $ClONO_2$ and N_2O_5 by sulfuric acid solutions. *J. Geophys. Res.* **1997**, *102*, 3583-3601, doi:10.1029/96JD03457.

(8) Rossi, M. J.; Malhotra, R.; Golden, D. M. Heterogeneous chemical reaction of chlorine nitrate and water on sulfuric-acid surfaces at room temperature. *Geophys. Res. Lett.* **1987**, *14*, 127-130, doi:10.1029/GL014i002p00127.

(9) Shi, Q.; Davidovits, P.; Jayne, J. T.; Kolb, C. E.; Worsnop, D. R. Kinetic model for reaction of $ClONO_2$ with H_2O and HCl and HOCl with HCl in sulfuric acid solutions. *J. Geophys. Res.* **2001**, *106*, 24259-24274, doi:10.1029/2000JD000181.

(10) Tolbert, M. A.; Rossi, M. J.; Golden, D. M. Heterogeneous interactions of chlorine nitrate, hydrogen chloride and nitric acid with sulfuric acid surfaces at stratospheric temperatures. *Geophys. Res. Lett.* **1988**, *15*, 847-850, doi:10.1029/GL015i008p00847.

99. **$ClONO_2$ + H_2SO_4•H_2O(s) and H_2SO_4•$4H_2O$(s).** Measurements by Hanson and Ravishankara[1] and Zhang et al.[2] demonstrate that the reaction probability on the tetrahydrate is a strong function of both temperature and relative humidity, both of which affect the level of adsorbed H_2O. Both groups covered the temperature range of 192–205 K. The reaction is slowest at higher temperatures and lower relative humidities. Zhang et al.[2] have parameterized their data in the form of $\log \gamma = a_1 + a_2 \log x + a_3 \log^2 x$; for 195 K and x = water partial pressure in Torr: $a_1 = 10.12$, $a_2 = 5.75$ and $a_3 = 0.62$; for a water partial pressure of 3.4×10^{-4} Torr and x = T(K) between 182 and 206: $a_1 = 318.67$, $a_2 = -3.13$ and $a_3 = 0.0076$. Zhang et al.[3] have also measured a low value of $\gamma \sim 2 \times 10^{-4}$ on sulfuric acid monohydrate at 195 K.
Back to Table

(1) Hanson, D. R.; Ravishankara, A. R. Reaction of $ClONO_2$ with HCl on NAT, NAD, and frozen sulfuric acid and hydrolysis of N_2O_5 and $ClONO_2$ on frozen sulfuric acid. *J. Geophys. Res.* **1993**, *98*, 22931-22936, doi:10.1029/93JD01929.
(2) Zhang, R.; Jayne, J. T.; Molina, M. J. Heterogeneous interactions of $ClONO_2$ and HCl with sulfuric acid tetrahydrate: Implications for the stratosphere. *J. Phys. Chem.* **1994**, *98*, 867-874, doi:10.1021/j100054a022.
(3) Zhang, R.; Leu, M.-T.; Keyser, L. F. Sulfuric acid monohydrate: Formation and heterogeneous chemistry in the stratosphere. *J. Geophys. Res.* **1995**, *100*, 18845-18854, doi:10.1029/95JD01876.

100. **$ClONO_2$ + HCl + H_2O(s).** Reaction probabilities of 0.27 (+0.73, –0.13) (Leu [6]) and 0.05 to 0.1 (Molina et al.[8]) were reported at 195 and 185 K, respectively. Abbatt and Molina[1] and Hanson and Ravishankara[4] report that a portion of the reaction may be due to $HOCl + HCl \rightarrow Cl_2 + H_2O$, with HOCl formed from $ClONO_2 + H_2O(s) \rightarrow HOCl + HNO_3(s)$. Hanson and Ravishankara[5] saw no enhancement of the $ClONO_2$ reaction probability when H_2O(s) is doped with HCl. Their preferred value at 192 K is $\gamma = 0.3$, but this is consistent with $\gamma = 1$. Chu et al.[2] also report a value of 0.27 (±0.19) at 188 K, assuming no correction for porosity, but suggest the true value is 0.10 (±0.08). Using a Knudsen cell technique and looking at initial uptake, Oppliger et al.[9] measured $\gamma = 0.7$ at 180 K and 0.2 at 200 K with HCl in excess, and both Fernandez et al.[3] and McNeil et al.[7] report a value of >0.1 at close to 200 K. McNeil et al. report that this value is substantially smaller at 218 K. Eliminating the Molina et al. points, which were taken at much higher $ClONO_2$ concentrations than the others, plots of the remaining data show no obvious bias when plotted as a function of reactant concentration or temperature (180–200 K). Their average value $\gamma = 0.26 \pm 0.06$. The Oppliger et al. data were presented for two HCl concentrations, differing by a factor of three. All points from both HCl concentrations were included since all the data were generally consistent with previous measurements, although the higher HCl concentrations did tend to produce modestly higher uptake coefficients. Until a fuller model is available, a single temperature independent value with a moderate uncertainty due to surface porosity seems appropriate.
Back to Table

(1) Abbatt, J. P. D.; Molina, M. J. Heterogeneous interactions of $ClONO_2$ and HCl on nitric acid trihydrate at 202 K. *J. Phys. Chem.* **1992**, *96*, 7674-7679, doi:10.1021/j100198a036.
(2) Chu, L. T.; Leu, M.-T.; Keyser, L. F. Heterogeneous reactions of $HOCl + HCl \rightarrow Cl_2 + H_2O$ and $ClONO_2 + HCl \rightarrow Cl_2 + HNO_3$ on ice surfaces at polar stratospheric conditions. *J. Phys. Chem.* **1993**, *97*, 12798-12804, doi:10.1021/j100151a028.
(3) Fernandez, M. A.; Hynes, R. G.; Cox, R. A. Kinetics of $ClONO_2$ reactive uptake on ice surfaces at temperatures of the upper troposphere. *J. Phys. Chem. A* **2005**, *109*, 9986-9996, doi:10.1021/jp053477b.
(4) Hanson, D. R.; Ravishankara, A. R. The reaction probabilities of $ClONO_2$ and N_2O_5 on 40 to 75% sulfuric acid solutions. *J. Geophys. Res.* **1991**, *96*, 17307-17314, doi:10.1029/91JD01750.
(5) Hanson, D. R.; Ravishankara, A. R. The reaction probabilities of $ClONO_2$ and N_2O_5 on polar stratospheric cloud materials. *J. Geophys. Res.* **1991**, *96*, 5081-5090, doi:10.1029/90JD02613.
(6) Leu, M.-T. Laboratory studies of sticking coefficients and heterogeneous reactions important in the Antarctic stratosphere. *Geophys. Res. Lett.* **1988**, *15*, 17-20, doi:10.1029/GL015i001p00017.

(7) McNeill, V. F.; Loerting, T.; Geiger, F. M.; Trout, B. L.; Molina, M. J. Hydrogen chloride-induced surface disordering on ice. *Proc. Nat. Acad. Sci.* **2006**, *103*, 9422-9427, doi:10.1073/pnas.0603494103.
(8) Molina, M. J.; Tso, T. L.; Molina, L. T.; Wang, F. C. Antarctic stratosheric chemistry of chlorine nitrate, hydrogen chloride, and ice: Release of active chlorine. *Science* **1987**, *238*, 1253-1259, doi:10.1126/science.238.4831.1253.
(9) Oppliger, R.; Allanic, A.; Rossi, M. J. Real-time kinetics of the uptake of $ClONO_2$ on ice and in the presence of HCl in the temperature range 160 K ≤ T ≤ 200 K. *J. Phys. Chem. A* **1997**, *101*, 1903-1911, doi:10.1021/jp963065q.

101. $ClONO_2$ + HCl + HNO_3•3H_2O. Measurements by Hanson and Ravishankara,[3,4] Leu and co-workers in Moore et al.[6] and Leu et al.,[5] and Abbatt and Molina[1] all report high γ values (>0.1) on NAT for temperatures between 192 and 202 K on water-rich NAT. Hanson and Ravishankara indicate that reaction probabilities on NAD are similar to those on NAT. The most recent NAT studies (Abbatt and Molina[1]) show a strong fall-off with relative humidity from γ >0.2 at 90% RH to 0.002 at 20% RH, indicating the necessity of sufficient water to solvate reactants. Within the limited measurements, data plots show no indication that the reaction probability of $ClONO_2$ + HCl depends on HCl and $ClONO_2$ gas phase concentrations or temperature between 191 and 202 K for water-rich NAT, but for nitric acid-rich NAT, there is a strong dependence on the partial pressure of HCl indicating that HCl is a limiting reagent on the surface under those conditions (Abbatt and Molina[1]). Averaged data yield γ = 0.23 ± 0.10 for the water-rich case. Carslaw and Peter[2] have published a model of this reaction and its dependence on HCl uptake.
Back to Table

(1) Abbatt, J. P. D.; Molina, M. J. Heterogeneous interactions of $ClONO_2$ and HCl on nitric acid trihydrate at 202 K. *J. Phys. Chem.* **1992**, *96*, 7674-7679, doi:10.1021/j100198a036.
(2) Carslaw, K. S.; Peter, T. Uncertainties in reactive uptake coefficients for solid stratospheric particles-1. Surface chemistry. *Geophys. Res. Lett.* **1997**, *24*, 1743-1746, doi:10.1029/97GL01683.
(3) Hanson, D. R.; Ravishankara, A. R. The reaction probabilities of $ClONO_2$ and N_2O_5 on polar stratospheric cloud materials. *J. Geophys. Res.* **1991**, *96*, 5081-5090, doi:10.1029/90JD02613.
(4) Hanson, D. R.; Ravishankara, A. R. Investigation of the reactive and nonreactlve processes involving $ClONO_2$ and HCl on water and nitric acid doped ice. *J. Phys. Chem.* **1992**, *96*, 2682-2691, doi:10.1021/j100185a052.
(5) Leu, M.-T.; Moore, S. B.; Keyser, L. F. Heterogeneous reactions of chlorine nitrate and hydrogen chloride on Type I polar stratospheric clouds. *J. Phys. Chem.* **1991**, *95*, 7763-7771, doi:10.1021/j100173a040.
(6) Moore, S. B.; Keyser, L. F.; Leu, M. T.; Turco, R. P.; Smith, R. H. Heterogeneous reactions on nitric acid trihydrate. *Nature* **1990**, *345*, 333-335, doi:10.1038/345333a0.

102. $ClONO_2$ + HCl + H_2SO_4•nH_2O(l). Early work by Tolbert et al.[10] and Hanson and Ravishankara[4] indicated that the presence of HCl had little effect on the reaction of $ClONO_2$ with concentrated sulfuric acid (>65 wt% H_2SO_4). Subsequent realization that HCl would be more soluble, and therefore a more potent reactant, in the colder, more dilute sulfuric acid aerosols characteristic of the polar stratosphere led to additional investigations by Hanson and Ravishankara,[5] Zhang et al.,[11] Elrod et al.,[1] and Hanson.[2] All these measurements show a strong dependence of reactivity on HCl solubility, which in turn depends on water activity. The solubility of HCl in a wide range of sulfuric acid solutions has been experimentally determined by a range of techniques that agree well with current thermodynamic models. See Robinson et al.[8] for a review. Hanson and Lovejoy[3] measured a reacto-diffusive length, ℓ, of only 0.009 ± 0.005 μm for 60 wt% H_2SO_4 in an aerosol flow reactor. (See Hanson et al.[6] for a definition of ℓ) This is a factor of four lower than the value for the hydrolysis reaction of $ClONO_2$ showing the significant enhancement of $ClONO_2$ uptake due to HCl.

The $ClONO_2$ + HCl reaction on/in sulfuric acid has been modeled in Shi et al.[9] using the same phenomenological model for $ClONO_2$ hydrolysis driven uptake by sulfuric acid. Since the effect of HCl on the $ClONO_2$ uptake is to increase the $ClONO_2$ pseudo-first-order reaction rate, the model of $ClONO_2$ uptake (see note on $ClONO_2$ uptake on sulfuric acid) should include the pseudo first order reaction rate, k_{HCl}. The formulation of k_{HCl} is found in the appendix in Shi et al.[9] It is likely that the $ClONO_2$ reaction with HCl, like the $ClONO_2$ hydrolysis reaction, is acid catalyzed via protonated $HClONO_2^+$, where Cl^+ is activated as in the case of HOCl + HCl. For the $ClONO_2$ + HCl reaction, there is also a surface reaction (Hanson[2]). Hanson

proposed that Γ_s, the effective uptake rate due to surface reactions, is linearly proportional to water activity; however, the calculated value of γ_o at 250 K and 60 wt% H_2SO_4 using his formulation is 0.02 (here $\gamma_o \sim \Gamma_s$), which is contradictory to his aerosol flow reactor result, which yielded $\gamma_o = 0.0079$ (here $\gamma_o \sim \Gamma_b$) (Hanson and Lovejoy[3]). In the model presented in the Shi et al. appendix, it is assumed that that Γ_s is linearly proportional to Henry's law constant of $ClONO_2$, rather than the water activity. The temperature dependence of Γ_s is determined, based on two measured values of Γ_s at 203 K (Hanson[2]) and 250 K (Hanson and Lovejoy[3]). The model yields a value of $\gamma_o \sim 0.011$ (here $\gamma_o \sim \Gamma_s$), which is close to the measured value.

In the stratosphere, when the reaction rate of $ClONO_2$ with HCl exceeds the flux of HCl to the particle surface, HCl is depleted. This, in turn, will depress the rate of both the $ClONO_2$ and HOCl + HCl reactions, and increase the $ClONO_2$ hydrolysis rate. Shi et al.[9] have proposed a model in which this effect is taken into account by including a factor F_{HCl} (see Table A–3 in Shi et al.). The formulation of F_{HCl} is based on scaling HCl reaction and accommodation fluxes. This flux correction is not exact (i.e., it does not rigorously calculate the HCl surface or bulk concentration) but provides a good approximation to the expected reduction in HCl + $ClONO_2$/HOCl reactivity and, just as importantly, the effective increase in $ClONO_2$ + H_2O reactivity when $p_{ClONO_2} > p_{HCl}$. This is particularly relevant during cold Cl activation events when HCl can be removed almost completely (i.e., see Jaegle et al.[7]).

Using the same error analysis approach as in the note on N_2O_5 uptake by sulfuric acid, the error of using the model in the Appendix is about 40.0% (one sigma), with $\sigma_m = 39.8\%$ and $\sigma_d = 4.0\%$.
Back to Table

(1) Elrod, M. J.; Koch, R. E.; Kim, J. E.; Molina, M. S. HCl vapour pressures and reaction probablilities of $ClONO_2$ + HCl on liquid H_2SO_4-HNO_3-HCl-H_2O solutions. *Faraday Discuss.* **1995**, *100*, 269-278, doi:10.1039/fd9950000269.

(2) Hanson, D. R. Reaction of $ClONO_2$ with H_2O and HCl in sulfuric acid and HNO_3/H_2SO_4/H_2O mixtures. *J. Phys. Chem. A* **1998**, *102*, 4794-4807, doi:10.1021/jp972767s.

(3) Hanson, D. R.; Lovejoy, E. R. The reaction of $ClONO_2$ with submicrometer sulfuric acid aerosol. *Science* **1995**, *267*, 1326-1329, doi:10.1126/science.267.5202.1326.

(4) Hanson, D. R.; Ravishankara, A. R. The reaction probabilities of $ClONO_2$ and N_2O_5 on 40 to 75% sulfuric acid solutions. *J. Geophys. Res.* **1991**, *96*, 17307-17314, doi:10.1029/91JD01750.

(5) Hanson, D. R.; Ravishankara, A. R. Reactive uptake of $ClONO_2$ onto sulfuric acid due to reaction with HCl and H_2O. *J. Phys. Chem.* **1994**, *98*, 5728-5735, doi:10.1021/j100073a026.

(6) Hanson, D. R.; Ravishankara, A. R.; Solomon, S. Heterogeneous reactions in sulfuric acid aerosols: A framework for model calculations. *J. Geophys. Res.* **1994**, *99*, 3615-3629, doi:10.1029/93JD02932.

(7) Jaegle, L.; Webster, C. R.; May, R. D.; Scott, D. C.; Stimpfle, R. M.; Kohn, D. W.; Wennberg, P. O.; Hansico, T. F.; Cohen, R. C.; Proffitt, M. H.; Kelly, K. K.; Elkins, J.; Baumgardner, D.; Dye, J. E.; Wilson, J. C.; Pueschel, R. F.; Chan, K. R.; Salawitch, R. J.; Tuck, A. F.; Hovde, S. J.; Yung, Y. L. Evolution and stoichiometry of heterogeneous processing in the Antarctic stratosphere. *J. Geophys. Res.* **1997**, *102*, 13235-13253, doi:10.1029/97JD00935.

(8) Robinson, G. N.; Worsnop, D. R.; Jayne, J. T.; Kolb, C. E.; Swartz, E.; Davidovits, P. Heterogeneous uptake of HCl by sulfuric acid solutions. *J. Geophys. Res.* **1998**, *103*, 25371-25381, doi:10.1029/98JD02085.

(9) Shi, Q.; Davidovits, P.; Jayne, J. T.; Kolb, C. E.; Worsnop, D. R. Kinetic model for reaction of $ClONO_2$ with H_2O and HCl and HOCl with HCl in sulfuric acid solutions. *J. Geophys. Res.* **2001**, *106*, 24259-24274, doi:10.1029/2000JD000181.

(10) Tolbert, M. A.; Rossi, M. J.; Golden, D. M. Heterogeneous interactions of chlorine nitrate, hydrogen chloride and nitric acid with sulfuric acid surfaces at stratospheric temperatures. *Geophys. Res. Lett.* **1988**, *15*, 847-850, doi:10.1029/GL015i008p00847.

(11) Zhang, R.; Jayne, J. T.; Molina, M. J. Heterogeneous interactions of $ClONO_2$ and HCl with sulfuric acid tetrahydrate: Implications for the stratosphere. *J. Phys. Chem.* **1994**, *98*, 867-874, doi:10.1021/j100054a022.

103. $ClONO_2$+HCl + H_2SO_4•H_2O(s) and H_2SO_4•$4H_2O$(s). This reaction has been studied by Hanson and Ravishankara[1] and Zhang et al.[2] The reaction probability is strongly dependent on the thermodynamic state of the SAT surface, which is controlled by the temperature and the water vapor partial pressure. At a water vapor pressure of 5.6×10^{-4} Torr the measured γ drops by over two orders of magnitude as the SAT surface temperature rises from 195 to 206 K. The results from the two groups are in qualitative agreement, but

sample different H_2O and HCl partial pressures. Zhang et al. have parameterized their data as a function of water partial pressure (at 195 K) and temperature (both at an HCl partial pressure of 4 to 8 × 10^{-7} Torr) in the form $\log \gamma = a_1 + a_2 \log x + a_3 (\log x)^2$. For H_2O partial pressure, $a_1 = 5.25$, $a_2 = 1.91$, and $a_3 = 0.0$; for T(K), $a_1 = 175.74$, $a_2 = -1.59$, and $a_3 = 0.0035$. Care must be taken in extrapolating either data set to lower HCl concentrations. Zhang et al.[3] measured no enhancement of $ClONO_2$ uptake on sulfuric acid monohydrate at 195 K with (2–8) × 10^{-7} Torr of HCl present, implying $\gamma < 1 \times 10^{-4}$.
Back to Table

(1) Hanson, D. R.; Ravishankara, A. R. Reaction of $ClONO_2$ with HCl on NAT, NAD, and frozen sulfuric acid and hydrolysis of N_2O_5 and $ClONO_2$ on frozen sulfuric acid. *J. Geophys. Res.* **1993**, *98*, 22931-22936, doi:10.1029/93JD01929.
(2) Zhang, R.; Jayne, J. T.; Molina, M. J. Heterogeneous interactions of $ClONO_2$ and HCl with sulfuric acid tetrahydrate: Implications for the stratosphere. *J. Phys. Chem.* **1994**, *98*, 867-874, doi:10.1021/j100054a022.
(3) Zhang, R.; Leu, M.-T.; Keyser, L. F. Sulfuric acid monohydrate: Formation and heterogeneous chemistry in the stratosphere. *J. Geophys. Res.* **1995**, *100*, 18845-18854, doi:10.1029/95JD01876.

104. $ClONO_2$ + HCl + Al_2O_3(s). Molina et al.[1] used flow tube techniques to measure $\gamma = 0.020 \pm 0.005$ on α–alumina at 195–230 K with stratospheric (5 ppmV) water vapor levels. Measured γ was independent of T and was affected very little by 5 ppbv HNO_3 vapor. The same γ was measured for a Pyrex surface, indicating the absorbed water and not the inorganic substrate hosted the reaction.
Back to Table

(1) Molina, M. J.; Meads, R. F.; Spencer, D. D.; Molina, L. T. The reaction of $ClONO_2$ with HCl on aluminum oxide. *Geophys. Res. Lett.* **1997**, *24*, 1619-1622, doi:10.1029/97GL01560.

105. $ClONO_2$ + NaCl. Timonen et al.[10] studied the uptake of $ClONO_2$ on NaCl powders at 296 K and 225 K using a flow tube. Complete deactivation of the surface was observed at 225 K but not at 296 K. The uptake coefficients, after correction (typically by an order of magnitude) using the pore diffusion model of Keyser et al.[7,8] were $\gamma_0 = (4.6 \pm 3.1) \times 10^{-3}$ (1σ) at 296 K and $\gamma_0 = (6.7 \pm 3.2) \times 10^{-3}$ (1σ) at 225 K. Similarly low values for the uptake coefficient are reported by Zelenov et al.[11] using a flow tube approach. On the other hand, Caloz et al.[2] used a Knudsen cell and found that the initial uptake coefficient was 0.23 ± 0.06, independent of the type of salt used (powders, single crystals, deposited salt films) and without applying a correction for pore diffusion since no mass dependence for γ was observed; in similar studies. Aguzzi and Rossi[1] measured a value of $\gamma_0 = 0.10 \pm 0.05$ for the uptake of $ClONO_2$ on NaCl and 0.27 ± 0.10 for uptake on the unreactive $NaNO_3$ and Na_2SO_4 salts. The Cl_2 yield was 100% for NaCl, in agreement with the earlier studies[2,10] but 27 ± 7 % on the unreactive salts. Koch and Rossi[9] used a diffusion tube technique to measure a value of 0.1 for the uptake coefficient. Gebel and Finlayson-Pitts[5] used a Knudsen cell and measured an initial value of $\gamma_0 = 0.14 \pm 0.11$ (2σ) and a steady-state value of $\gamma = (3.9 \pm 1.8) \times 10^{-2}$, but concluded that approximately two layers of salt were sampled in these multi-layer experiments. The use of a single or sub-single layer of NaCl gave a steady state value corrected using the model of Hoffman et al. of $\gamma = (2.4 \pm 1.2) \times 10^{-2}$.[6] The source of the very disparate results from the different groups and techniques is not clear. All studies agree that the yield of Cl_2 is 100%, consistent with $ClONO_2 + NaCl \rightarrow Cl_2 + NaNO_3$ as observed earlier,[4] with small amounts of HOCl from hydrolysis of $ClONO_2$ on the surface being observed in the presence of water.

Deiber et al.[3] studied the uptake of $ClONO_2$ on water, NaCl and NaBr solutions using a droplet train flow reactor. The uptake coefficient was the same on water and 0.1 M NaCl, and Cl_2 was observed as the gas phase product.
Back to Table

(1) Aguzzi, A.; Rossi, M. J. The kinetics of the heterogeneous reaction of $BrONO_2$ with solid alkali halides at ambient temperature. A comparison with the interaction of $ClONO_2$ on NaCl and KBr. *Phys. Chem. Chem. Phys.* **1999**, *1*, 4337-4346, doi:10.1039/a904611i.
(2) Caloz, F.; Fentner, F. F.; Rossi, M. J. Heterogeneous kinetics of the uptake of $ClONO_2$ on NaCl and NaBr. *J. Phys. Chem.* **1996**, *100*, 7494-7501, doi:10.1021/jp953099i.

(3) Deiber, G.; George, C.; Le Calve, S.; Schweitzer, F.; Mirabel, P. Uptake study of $ClONO_2$ and $BrONO_2$ by halide containing droplets. *Atmos. Chem. Phys.* **2004**, *4*, 1291-1299, doi:10.5194/acp-4-1291-2004.
(4) Finlayson-Pitts, B. J.; Ezell, M. J.; Pitts, J. N., Jr. Formation of chemically active chlorine compounds by reactions of atmospheric NaCl particles with gaseous N_2O_5 and $ClONO_2$. *Nature* **1989**, *337*, 241-244, doi:10.1038/337241a0.
(5) Gebel, M. E.; Finlayson-Pitts, B. J. Uptake and reaction of $ClONO_2$ on NaCl and synthetic sea salt. *J. Phys. Chem. A* **2001**, *105*, 5178-5187, doi:10.1021/jp0046290.
(6) Hoffman, R. C.; Gebel, M. E.; Fox, B. S.; Finlayson-Pitts, B. J. Knudsen cell studies of the reactions of N_2O_5 and $ClONO_2$ with NaCl: Development and application of a model for estimating available surface areas and corrected uptake coefficients. *Phys. Chem. Chem. Phys.* **2003**, *5*, 1780-1789, doi:10.1039/b301126g.
(7) Keyser, L. F.; Leu, M.-T.; Moore, S. B. Comment on porosities of ice films used to simulate stratospheric cloud surfaces. *J. Phys. Chem.* **1993**, *97*, 2800-2801, doi:10.1021/j100113a053.
(8) Keyser, L. F.; Moore, S. B.; Leu, M. T. Surface reaction and pore diffusion in flow tube reactors. *J. Phys. Chem.* **1991**, *95*, 5496-5502, doi:10.1021/j100167a026.
(9) Koch, T. G.; Rossi, M. J. Direct measurement of surface residence times: Nitryl chloride and chlorine nitrate on alkali halides at room temperature. *J. Phys. Chem. A* **1998**, *102*, 9193-9201, doi:10.1021/jp982539d.
(10) Timonen, R. S.; Chu, L. T.; Leu, M.-T.; Keyser, L. F. Heterogeneous reaction of $ClONO_2(g)$ + $NaCl(s) \rightarrow Cl_2(g) + NaNO_3(s)$. *J. Phys. Chem.* **1994**, *98*, 9509-9517, doi:10.1021/j100089a025.
(11) Zelenov, V. V.; Aparina, E. V.; Kashtanov, S. A.; Shestakov, D. V.; Gershenzon, Y. M. Kinetic mechanism of $ClONO_2$ uptake on polycrystalline film of NaCl. *J. Phys. Chem. A* **2006**, *110*, 6771-6780, doi:10.1021/jp056272b.

106. $ClONO_2$ + KBr and NaBr. Caloz et al.[2] and Aguzzi and Rossi[1] report a rapid uptake of $ClONO_2$ on KBr solid salts at room temperature, $\gamma_0 = 0.35 \pm 0.06$ and $\gamma_0 = 0.18 \pm 0.07$ respectively; corrections for pore diffusion were not applied but are not expected to be large at these high uptake coefficients (see Introduction). This is consistent with a value of 0.1 measured by Koch and Rossi[4] using a diffusion tube technique. The reaction products are BrCl, Br_2 and Cl_2. BrCl is the initial reaction product formed from $ClONO_2 + KBr \rightarrow BrCl + KNO_3$. Br_2 is generated in a secondary reaction of BrCl with KBr: $BrCl + KBr \rightarrow Br_2 + KCl$. Cl_2 is then formed as the surface KBr is converted to KCl, which then reacts with $ClONO_2$.

Deiber et al.[3] studied the uptake of $ClONO_2$ on water, NaCl and NaBr solutions using a droplet train flow reactor. On NaBr, the uptake increased from 0.041 at 0.01 M NaBr to 0.073 at 1 M NaBr. From the dependence on the NaBr concentration, a value for the mass accommodation coefficient for $ClONO_2$ of 0.108 $\pm$ 0.033 (2σ) was obtained. The gas phase products were BrCl and Br_2, the latter formed by secondary reactions of BrCl with Br^-.
Back to Table

(1) Aguzzi, A.; Rossi, M. J. The kinetics of the heterogeneous reaction of $BrONO_2$ with solid alkali halides at ambient temperature. A comparison with the interaction of $ClONO_2$ on NaCl and KBr. *Phys. Chem. Chem. Phys.* **1999**, *1*, 4337-4346, doi:10.1039/a904611i.
(2) Caloz, F.; Fentner, F. F.; Rossi, M. J. Heterogeneous kinetics of the uptake of $ClONO_2$ on NaCl and NaBr. *J. Phys. Chem.* **1996**, *100*, 7494-7501, doi:10.1021/jp953099i.
(3) Deiber, G.; George, C.; Le Calve, S.; Schweitzer, F.; Mirabel, P. Uptake study of $ClONO_2$ and $BrONO_2$ by halide containing droplets. *Atmos. Chem. Phys.* **2004**, *4*, 1291-1299, doi:10.5194/acp-4-1291-2004.
(4) Koch, T. G.; Rossi, M. J. Direct measurement of surface residence times: Nitryl chloride and chlorine nitrate on alkali halides at room temperature. *J. Phys. Chem. A* **1998**, *102*, 9193-9201, doi:10.1021/jp982539d.

107. $ClONO_2$ + sea salt. Gebel and Finlayson-Pitts[1] reported a rapid reaction between $ClONO_2$ and synthetic sea salt, with initial values based on the geometric sample area of $\gamma_0 = 0.42$ and steady-state values of $\gamma = 0.16$ (2σ). These were measured with multiple salt layers (3–236) but corrections for diffusion into underlying layers for such high uptake coefficients are relatively small, less than a factor of three. The yield of Cl_2 was 78 $\pm$ 13%; small amounts of HCl and HOCl were also observed as products. The recommended lower limit is based on these studies and the rapid uptake of other reactive species such as HNO_3 and N_2O_5.

Back to Table

(1) Gebel, M. E.; Finlayson-Pitts, B. J. Uptake and reaction of $ClONO_2$ on NaCl and synthetic sea salt. *J. Phys. Chem. A* **2001**, *105*, 5178-5187, doi:10.1021/jp0046290.

108. $ClONO_2$ + HBr + H_2O(s) and HNO_3•nH_2O(s). This reaction was studied by Hanson and Ravishankara[2] on water ice and NAT near 200 K. A diffusion-limited reaction probability of >0.3 was observed. Allanic et al.[1] measured $\gamma = 0.56 \pm 0.11$ at 200 K on water ice, observing Cl_2 and Br_2 to be formed in yields of 100% and 66 to 80%, respectively, in the range 180 to 200 K.
Back to Table

(1) Allanic, A.; Oppliger, R.; van den Bergh, H.; Rossi, M. J. The heterogeneous kinetics of the reactions $ClONO_2$ + HX/ice (X = Cl, Br, I), $BrONO_2$ + HI/ice and the reactivity of the interhalogens BrCl, ICl and IBr with HX/ice (X = Cl, Br, I) in the temperature range 180 to 205 K. *Z. Phys. Chem.* **2000**, *214*, 1479-1500, doi:10.1524/zpch.2000.214.11.1479.
(2) Hanson, D. R.; Ravishankara, A. R. Heterogeneous chemistry of HBr and HF. *J. Phys. Chem.* **1992**, *96*, 9441-9446, doi:10.1021/j100202a069.

109. $ClONO_2$ + HF + H_2O(s) and HNO_3•nH_2O(s). Hanson and Ravishankara[1] were not able to observe this reaction on water ice and NAT surfaces near 200 K.
Back to Table

(1) Hanson, D. R.; Ravishankara, A. R. Heterogeneous chemistry of HBr and HF. *J. Phys. Chem.* **1992**, *96*, 9441-9446, doi:10.1021/j100202a069.

110. $CF_xCl_{(4-x)}$ (x=0–3) and CF_2Br_2 + Al_2O_3(s). Robinson et al.[3] reported steady-state dissociative uptake of CF_2Cl_2 and CF_2Br_2 on α-alumina surfaces at 210 and 315 K. Reaction probabilities of about 1×10^{-3} at 210 K were measured by monitoring the amounts of surface species bonded to the Al_2O_3 substrate. A re-analysis (Robinson et al.[4]) lowered this value by about a factor of 50. Moderate surface dosage with water vapor did not quench the reaction. In addition, Dai et al.[1] and Robinson et al.[2] studied dissociative chemisorption of CF_3Cl, CF_2Cl_2, $CFCl_3$, and CCl_4 on dehydroxylated γ-alumina powders. The obtained reactive uptake probabilities ranging from 0.4×10^{-5} for $CFCl_3$ to 1.0×10^{-5} for $CFCl_3$ over a temperature range of 120 to 300 K. HCl and halomethyl radicals were observed as desorption products. Loss of these products may point to somewhat higher γs, since they were measured by integrating halogen bound to Al_2O_3 substrates.
Back to Table $CF_xCl_{(4-x)}$ Back to Table CF_2Br_2

(1) Dai, Q.; Robinson, G. N.; Freedman, A. Reactions of halomethanes with γ-alumina surfaces. I: An infrared spectroscopic study. *J. Phys. Chem. B* **1997**, *101*, 4940-4946, doi:10.1021/jp9630151.
(2) Robinson, G. N.; Dai, Q.; Freedman, A. Reaction of halomethanes on y-alumina surfaces. II: X-ray photoelectron and temperature programmed reaction spectroscopy studies. *J. Phys. Chem. B* **1997**, *101*, 4947-4953, doi:10.1021/jp963016d.
(3) Robinson, G. N.; Freedman, A.; Kolb, C. E.; Worsnop, D. R. Decomposition of halomethanes on α-alumina at stratospheric temperatures. *Geophys. Res. Lett.* **1994**, *21*, 377-380, doi:10.1029/94GL00034.
(4) Robinson, G. N.; Freedman, A.; Kolb, C. E.; Worsnop, D. R. Correction to decomposition of halomethanes on α-alumina at stratospheric temperatures. *Geophys. Res. Lett.* **1996**, *23*, 317, doi:10.1029/95GL03809.

111. BrCl + NaCl, NaBr, KBr and NaI. The uptake of BrCl on solid NaCl and KBr using a Knudsen cell has been reported by Aguzzi and Rossi,[1] yielding 298 K values of 6×10^{-2} for NaCl and 0.14 on KBr. An earlier preliminary study from the same group reported a value at $\gamma > 0.1$ on KBr.[2] Insufficient data are available to make a recommendation.
Katrib et al.[4] measured the uptake of BrCl on aqueous solutions of NaI over the temperature range from 273 to 288 K; the uptake coefficient increased from 0.37×10^{-2} to 0.7 as the I^- concentration increased from 1×10^{-4} to 0.5 M NaI. The complex dependence on the I^- concentration indicated that a surface reaction was occurring at the air-solution interface.

Huff and Abbatt[3] studied the loss of BrCl on frozen bromide salt solutions at 233 K, finding that the uptake coefficients vary between 0.02 and 0.04 depending on the bromide concentration, independent of solution acidity.
Back to Table

(1) Aguzzi, A.; Rossi, M. J. The kinetics of the heterogeneous reaction of $BrONO_2$ with solid alkali halides at ambient temperature. A comparison with the interaction of $ClONO_2$ on NaCl and KBr. *Phys. Chem. Chem. Phys.* **1999**, *1*, 4337-4346, doi:10.1039/a904611i.
(2) Caloz, F.; Fentner, F. F.; Rossi, M. J. Heterogeneous kinetics of the uptake of $ClONO_2$ on NaCl and NaBr. *J. Phys. Chem.* **1996**, *100*, 7494-7501, doi:10.1021/jp953099i.
(3) Huff, A. K.; Abbatt, J. P. D. Gas-phase Br_2 production in heterogeneous reactions of Cl_2, HOCl, and BrCl with halide-ice surfaces. *J. Phys. Chem. A* **2000**, *104*, 7284-7293, doi:10.1021/jp001155w.
(4) Katrib, Y.; Deiber, G.; Schweitzer, F.; Mirabel, P.; George, C. Chemical transformation of bromine chloride at the air/water interface. *J. Aerosol Sci.* **2001**, *32*, 893-911, doi:10.1016/S0021-8502(00)00114-2.

112. Br_2 + NaCl, KBr and NaI. Only one report of the uptake of Br_2 on solid NaCl and KBr using a Knudsen cell is available[1] as part of a study of $BrONO_2$ uptake on salts. The uptake coefficient for Br_2 was 4×10^{-3} on NaCl and 3×10^{-3} on KBr. Insufficient data are available to make a recommendation.
Hu et al.[2] measured the uptake of Br_2 on aqueous solutions of NaI using a droplet train flow reactor over the temperature range of 263 to 293 K. The measured uptake coefficients decreased from 0.33 at 263 K to 0.08 at 293 K, with evidence for a significant contribution from a reaction at the interface between Br_2 and I^-.
Back to Table

(1) Aguzzi, A.; Rossi, M. J. The kinetics of the heterogeneous reaction of $BrONO_2$ with solid alkali halides at ambient temperature. A comparison with the interaction of $ClONO_2$ on NaCl and KBr. *Phys. Chem. Chem. Phys.* **1999**, *1*, 4337-4346, doi:10.1039/a904611i.
(2) Hu, J. H.; Shi, Q.; Davidovits, P.; Worsnop, D. R.; Zahniser, M. S.; Kolb, C. E. Reative uptake of Cl_2(g) and Br_2(g) by aqueous surfaces as a function of Br^- and I^- ion concentration: The effect of chemical reaction at the interface. *J. Phys. Chem.* **1995**, *99*, 8768-8776, doi:10.1021/j100021a050.

113. BrO + H_2O(s), $H_2SO_4 \cdot nH_2O$(l) and NaCl(aq). Abbatt[1] used a coated flow tube technique to measure heterogeneous uptake on water ice, 60 and 70 wt% H_2SO_4 at 213 K, and 23 wt% aqueous NaCl at 253 K. He obtained γ(ice) = $(1.0 \pm 0.4) \times 10^{-3}$, γ (60 wt% H_2SO_4) = $(7 \pm 2) \times 10^{-4}$, γ (70 wt% H_2SO_4) = $(5 \pm 2) \times 10^{-4}$ and γ (23 wt% NaCl) $< 3 \times 10^{-3}$. He observed product Br_2, indicating BrO self-reaction on both water ice and sulfuric acid solutions. Since reaction rate will depend on BrO concentrations, no recommendation is made for an atmospheric rate.
Back to Table

(1) Abbatt, J. P. D. Heterogeneous interactions of BrO and ClO: Evidence for BrO surface recombination and reaction with HSO_3^-/SO_3^{2-}. *Geophys. Res. Lett.* **1996**, *23*, 1681-1684, doi:10.1029/96GL01430.

114. HOBr + $H_2SO_4 \cdot nH_2O$. Hanson[1] reported that uptake of HOBr on 80 wt.% H_2SO_4, producing Br_2. Br_2 and Br_2O production was also observed by Iraci et al.[2] during Knudsen cell studied of HOBr uptake on 70 wt% uptake for temperatures below 228 K. These products probably arise from HOBr self-reaction, although impurities in the acid solution might also play a role. Iraci et al. discuss methods to correct HOBr uptake data for the effects of self-reaction and secondary reactions with its products. The bulk phase self-reaction of HOBr noted above is not likely to be significant over the expected range of atmospheric concentrations.
Back to Table

(1) Hanson, D. Reactivity of $BrONO_2$ and HOBr on sulfuric acid solutions at low temperatures. *J. Geophys. Res.* **2003**, *108*, 4239, doi: 10.1029/2002JD002519.
(2) Iraci, L. T.; Michelsen, R. R.; Ashbourn, S. F. M.; Rammer, T. A.; Golden, D. M. Uptake of hypobromous acid (HOBr) by aqueous sulfuric acid solutions: low-temperature solubility and reaction. *Atmos. Chem. Phys.* **2005**, *5*, 1577-1587, doi:10.5194/acp-5-1577-2005.

115. HOBr + HCl + H_2O(s). Abbatt[1] measured $\gamma = 0.25$ (+0.10/-0.05) for this reaction on ice at 228 K. Chaix et al.[3] measured $\gamma = 0.3$ on ice from 180 to 195 K, dropping to ~0.15 at 205 K. The BrCl product was observed by mass spectrometry. Allanic et al.[2] report a faster rate for this reaction than for HOBr uptake on pure ice (which had an uptake coefficient of 0.15 at 200 K). Mössinger et al.[4] report a lower limit for γ of 0.1, under conditions with HCl concentration in excess of the HOBr concentration. No data on NAT surfaces is available.

Back to Table

(1) Abbatt, J. P. D. Heterogeneous reaction of HOBr with HBr and HCl on ice surfaces at 228 K. *Geophys. Res. Lett.* **1994**, *21*, 665-668, doi:10.1029/94GL00775.

(2) Allanic, A.; Oppliger, R.; Rossi, M. J. Real-time kinetics of the uptake of HOBr and $BrONO_2$ on ice and in the presence of HCl in the temperature range 190-200 K. *J. Geophys. Res.* **1997**, *102*, 23529-23541, doi:10.1029/97JD01833.

(3) Chaix, L.; Allanic, A.; Rossi, M. J. Heterogeneous chemistry of HOBr on different types of ice and on ice doped with HC1, HBr, and HNO_3 at 175 K < T < 125 K. *J. Phys. Chem. A* **2000**, *104*, 7268-7277, doi:10.1021/jp001018z.

(4) Mössinger, J. C.; Hynes, R. G.; Cox, R. A. Interaction of HOBr and HCl on ice surfaces in the temperature range 205–227 K. *J. Geophys. Res.* **2002**, *107*, 4740, doi:10.1029/2002JD002151.

116. HOBr + HCl + $H_2SO_4 \bullet nH_2O$. For the sulfuric acid reaction, Abbatt[1] measured γs of ~ 0.1 to 0.2 for [HCl] $>1 \times 10^{12}$ cm^{-3} over 68.8 wt% H_2SO_4 at 228 K; yielding an estimated $k^{II}_{HCl+HOBr} = 1.4 \times 10^5$ M^{-1} s^{-1} with a factor of 2 uncertainty. Hanson and Ravishankara[3] also measured $\gamma \leq 0.2$ (+0.2, – 0.1) for 60 wt% H_2SO_4 at 210 K. However, both of these measurements were based on significant underestimation of the solubility of HOBr in the relevant sulfuric acid solutions. More recent measurements by Waschewsky and Abbatt[5] indicate that the Henry's law constant for HOBr varies slightly with acidity between 60 to 70 wt% H_2SO_4 and more strongly with temperature between 208 and 238 K. (For 59.7 wt% H_2SO_4, H (M atm^{-1}) = 1.2×10^6 at 208 K and and 2.2×10^5 at 228 K.) The HOBr + HCl second order liquid phase rate constant, $k^{II}_{HCl+HOBr}$, varies between 2×10^5 and 3×10^8 (M^{-1} s^{-1}) between 213 and 238 K over the same composition range (60–70 wt% H_2SO_4). Such a strong dependence on acid composition for the reaction rate of HOBr + HCl and the very small acid composition dependence for HOBr solubility in H_2SO_4 solution might be partially due to the formation of H_2OBr^+ in the acidic solution as discussed in their paper. However, this acid catalyzed reaction, i.e. H_2OBr^+ + HCl, alone does not completely account for measured reaction rates over the acid composition range studied.

Using the Henry's Law data for HOBr reported by Waschewsky and Abbatt,[5] the limiting reagent will vary depending on atmospheric temperature (H_2SO_4 wt%) and the concentrations of HOBr and HCl. For stratospheric conditions where [HOBr] is 10 pptv and [HCl] 1 ppbv, they predict dissolved HOBr will be in excess above 204 K and HCl in excess below 204 K for a H_2O vapor partial pressure of 3×10^{-7} atm. From their coated wall flow reactor uptake measurements, Waschewsky and Abbatt[5] derived expressions for $k^{II}_{HCl+HOBr}$ and predicted uptake coefficients. For temperature between 204 and 218 K where HOBr is likely to be in excess, they calculated HCl uptake coefficients, γ_{HCl}, which range between 7×10^{-5} and 9×10^{-5}. For temperatures in the 202–198 K range, where dissolved HCl is likely to be excess, the calculated uptake coefficients for HOBr, γ_{HOBr}, of ~1×10^{-2}. Hanson has reported Henry's law solubility data for 58–70 wt.% sulfuric acid and reactive uptake coefficients for HCl on HOBr doped sulfuric acid surfaces using a wetted wall flow reactor.[2] Hanson's reported that H_{HOBr} was independent of acid concentration at 250 K, however, the heat of solvation for HOBr derived is significantly lower (-12.5 ± 3.7 versus -9 ± 1 kcal/mol reported at lower temperatures by Waschewsky and Abbatt) that the values of H* based on Hanson's data, taken from 250 to 270 K, are much higher than the prior study's when extrapolated to their lower temperatures. Hanson's reported γ_{HCl} are strongly dependent on HOBr partial pressure and drop almost three orders of magnitude as the sulfuric acid concentration is raised from 58 to 95 wt%, possibly because HCl may be reacting with sulfuric acid at higher acid concentrations. The higher temperature $k^{II}_{HCl+HOBr}$ values computed by Hanson for his data disagree, when extrapolated to lower temperatures with the values reported by Waschewsky and Abbatt as well as a prior lower temperature value reported by Hanson and Ravishankara.[3] Better agreement can be obtained if the solvation enthalpy reported by Hanson is used to adjust the H_{HOBr} values used in the earlier, lower temperature studies. Clearly, the HOBr + HCl reaction will be difficult to parameterize in a simple manner. Potential inconsistencies in their $k^{II}_{HCl+HOBr}$ values, as discussed by Waschewsky and Abbatt[5] and Hanson[2] indicate that further measurements are required before this reaction can be definitively modeled. Iraci et al.[4] subsequently measured HOBr uptake over both of the temperature ranges covered in the prior

experiments. Their derived H* values agreed well with data from Waschewsky and Abbatt[5] at lower temperatures but fell far below Hanson's higher temperature measurements. Thus, it appears that HOBr + HCl kinetic parameters developed from analyses based on the Hanson[2] data may need to be reanalyzed.
Back to Table

(1) Abbatt, J. P. D. Interactions of HBr, HCl, and HOBr with supercooled sulfuric acid solutions of stratospheric composition. *J. Geophys. Res.* **1995**, *100*, 14009-14017, doi:10.1029/95JD01367.
(2) Hanson, D. Reactivity of $BrONO_2$ and HOBr on sulfuric acid solutions at low temperatures. *J. Geophys. Res.* **2003**, *108*, 4239, doi:10.1029/2002JD002519.
(3) Hanson, D. R.; Ravishankara, A. R. Heterogeneous chemistry of bromine species in sulfuric acid under stratospheric conditions. *Geophys. Res. Lett.* **1995**, *22*, 385-388, doi:10.1029/94GL03379.
(4) Iraci, L. T.; Michelsen, R. R.; Ashbourn, S. F. M.; Rammer, T. A.; Golden, D. M. Uptake of hypobromous acid (HOBr) by aqueous sulfuric acid solutions: low-temperature solubility and reaction. *Atmos. Chem. Phys.* **2005**, *5*, 1577-1587, doi:10.5194/acp-5-1577-2005.
(5) Waschewsky, G. C. G.; Abbatt, J. P. D. HOBr in sulfuric acid solution: solubility and reaction as a function of temperature and concentration. *J. Phys. Chem. A* **1999**, *103*, 5312-5320, doi:10.1021/jp984489i.

117. HOBr + HBr + H_2O(s) and H_2SO_4•nH_2O. Abbatt[1] measured $\gamma = 0.12 \pm (0.03)$ on ice at 228 K. Chaix et al.[3] measured γ_o values ranging from 0.44 at 180 K to 0.15 at 205 K. The Br_2 product was observed by mass spectrometry. The HBr concentrations were such that the ice surface had probably melted. Abbatt[2] measured $\gamma = 0.25$ for [HBr] = 1×10^{12} cm^{-3} over 68.8 wt% H_2SO_4 at 228 K; yielding an estimated $k_{II} > 5 \times 10^4$ M^{-1} s^{-1}.
Back to Table

(1) Abbatt, J. P. D. Heterogeneous reaction of HOBr with HBr and HCl on ice surfaces at 228 K. *Geophys. Res. Lett.* **1994**, *21*, 665-668, doi:10.1029/94GL00775.
(2) Abbatt, J. P. D. Interactions of HBr, HCl, and HOBr with supercooled sulfuric acid solutions of stratospheric composition. *J. Geophys. Res.* **1995**, *100*, 14009-14017, doi:10.1029/95JD01367.
(3) Chaix, L.; Allanic, A.; Rossi, M. J. Heterogeneous chemistry of HOBr on different types of ice and on ice doped with HC1, HBr, and HNO_3 at 175 K < T < 125 K. *J. Phys. Chem. A* **2000**, *104*, 7268-7277, doi:10.1021/jp001018z.

118. HOBr + NaCl. Studies have been done on solid salts and aqueous surfaces. On solids, Mochida et al.[4] studied the uptake of HOBr on NaCl using multi-layer powders (10–500 μm) in a Knudsen cell at room temperature. After correction (by about an order of magnitude) for diffusion into the underlying layers, they obtained values for the initial uptake coefficient in the range of $(0.97–6.5) \times 10^{-3}$, with the corrected values decreasing with increasing concentrations of HOBr. They attributed this to competition between the reaction of HOBr with NaCl and a self-reaction of HOBr on the surface: $2\ HOBr \rightarrow Br_2 + H_2O + ½\ O_2$. Their final value of $\leq 6.5 \times 10^{-3}$ is based on their extrapolation back to very low HOBr concentrations. Both Br_2 and BrCl were observed as products. Chu et al.[2] measured the uptake of HOBr on NaCl at 250 K over a range of RH from 1.5 to 22.5%. After correcting the measured loss of HOBr by a factor of ~30 for diffusion into the underlying salt layers using the pore diffusion model, they obtained a value $\gamma_o = 5 \times 10^{-5}$. The smaller value compared to the Knudsen cell results of Mochida et al.[4] may be due to the much lower temperature they used; BrCl was the only gas phase product observed. Huff and Abbatt[3] report reactivity with frozen NaCl solutions in a coated-wall flow tube at 233 K. Uptake coefficients were dependent on the chloride concentration of the solution and on the acidity, with faster kinetics on the more acidic surfaces. BrCl was the only product observed.

Abbatt and Waschewsky[1] measured the uptake of HOBr on deliquesced 1–5 μm NaCl particles (75% RH); for particles at pH values of 0.3 and 7.2, a lower limit to the uptake coefficient of $\gamma_o > 0.2$ was measured. On unbuffered particles, the upper limit for the uptake coefficient was $\gamma_o < 1.5 \times 10^{-3}$ due to the limited availability of H^+ for the reaction between HOBr and Cl^- to form BrCl. Somewhat smaller values have been measured by Pratte and Rossi[5] in another aerosol flow tube experiment, using acidified NaCl particles. Acidification was necessary for the reaction to be observable. In general, the uptake coefficients varied from 1 to 10×10^{-3} from 70 to 90% relative humidity. The particles were acidified with quite large amounts of H_2SO_4, and the authors show that the reactivity on pure H_2SO_4 is less than that on the acidified salts. This could be a reason for the disagreement between the lower limit of Abbatt and Waschewsky and the Pratte and Rossi results.
Back to Table

(1) Abbatt, J. P. D.; Waschewsky, G. C. G. Heterogeneous interactions of HOBr, HNO_3, O_3, and NO_2 with deliquescent NaCl aerosols at room temperature. *J. Phys. Chem. A* **1998**, *102*, 3719-3725, doi:10.1021/jp980932d.
(2) Chu, L. T.; Diao, G.; Chu, L. Kinetics of HOBr uptake on NaBr and NaCl surfaces at varying relative humidity. *J. Phys. Chem. B* **2002**, *106*, 5679-5688, doi:10.1021/jp013594g.
(3) Huff, A. K.; Abbatt, J. P. D. Kinetics and product yields in the heterogeneous reactions of HOBr with ice surfaces containing NaBr and NaCl. *J. Phys. Chem. A* **2002**, *106*, 5279-5287, doi:10.1021/jp014296m.
(4) Mochida, M.; Hirokawa, J.; Kajii, Y.; Akimoto, H. Heterogeneous reactions of Cl_2 with sea salts at ambient temperature: Implications for halogen exchange in the atmosphere. *Geophys. Res. Lett.* **1998**, *25*, 3927-3930, doi:10.1029/1998GL900100.
(5) Pratte, P.; Rossi, M. J. The heterogeneous kinetics of HOBr and HOCl on acidified sea salt and model aerosol at 40-90% relative humidity and ambient temperature. *Phys. Chem. Chem. Phys.* **2006**, *8*, 3988-4001, doi:10.1039/b604321f.

119. HOBr + NaBr and KBr. Mochida et al.[6] studied the uptake of HOBr on solid KBr using multi-layer powders and spray-deposited films in a Knudsen cell. After correction (by factors of ~4–5) for diffusion into the underlying layers for the powders, they obtained values for the initial uptake coefficient in the range of $(1.3–8.4) \times 10^{-2}$, with the corrected values again decreasing with increasing concentrations of HOBr due to the self-reaction of HOBr on the surface: $2\ HOBr \rightarrow Br_2 + H_2O + ½\ O_2$. On spray-deposited films where correction for diffusion into the underlying layers is not necessary, a value of 0.18 ± 0.04 was measured. The recommended upper limit is based on their extrapolation back to very low HOBr concentrations for the powders, and the spray-deposited film results. Br_2 was the only product observed.

Chu et al.[2] measured the uptake of HOBr on NaBr at 250 K in a flow tube at RH from 0.5 to 12 %. After correction by approximately an order of magnitude for diffusion of HOBr into the underlying salt layers using a pore diffusion model, a value for γ_0 of 2.5×10^{-3} was obtained; the smaller value may be due to the much lower temperature at which these studies were carried out. Again, Br_2 was the only product observed.

The uptake of HOBr on aqueous solutions of NaBr has been measured by Wachsmuth et al.[7] and by Fickert et al.[3] Wachsmuth et al.[7] report a rapid rate of uptake that is limited by mass accommodation; the mass accommodation coefficient was calculated to be 0.6 ± 0.2. This is consistent with the studies of Fickert et al.[3] who reported a lower limit for the mass accommodation coefficient of 1×10^{-2} at 274 K and observed that Br_2 was released at 100% yield at pH <6.5. The yield of Br_2 decreased rapidly with pH at higher pH values due to the declining ratio of HOBr to BrO^-. Fickert et al.[3] also measured the uptake of HOBr on aqueous solutions containing mixtures of NaCl and NaBr. BrCl was the major product at small Br^- concentrations while Br_2 dominated as the bromide ion concentration in solution increased.

Finally, there have been a number of coated-wall flow tube studies of HOBr reactivity on frozen salt solutions containing both NaCl and NaBr (Kirchner et al.,[5] Huff and Abbatt,[4] and Adams et al.[1]). HOBr uptake coefficients are in the 10^{-2} to 10^{-3} range at roughly 233 K. A general finding is that if the HOBr concentrations are too high, then only BrCl is seen as a gas-phase product from films composed of the (low) seawater ratios of bromide to chloride. The reason for this is that the small concentrations of bromide at the surface are rapidly depleted, leaving only chloride available for reaction. However, for low HOBr concentrations (10^9 to 10^{10} molecules/cm^3), as used by Adams et al., Br_2 is observed as the initial product.
Back to Table

(1) Adams, J. W.; Holmes, N. S.; Crowley, J. N. Uptake and reaction of HOBr on frozen and dry NaCl/NaBr surfaces between 253 and 233 K. *Atmos. Chem. Phys.* **2002**, *2*, 79-91, doi:10.5194/acp-2-79-2002.
(2) Chu, L. T.; Diao, G.; Chu, L. Kinetics of HOBr uptake on NaBr and NaCl surfaces at varying relative humidity. *J. Phys. Chem. B* **2002**, *106*, 5679-5688, doi:10.1021/jp013594g.
(3) Fickert, S.; Adams, J. W.; Crowley, J. N. Activation of Br_2 and BrCl via Uptake of HOBr onto Aqueous Salt Solutions. *J. Geophys. Res.* **1999**, *104*, 23719-23727, doi:10.1029/1999JD900359
(4) Huff, A. K.; Abbatt, J. P. D. Kinetics and product yields in the heterogeneous reactions of HOBr with ice surfaces containing NaBr and NaCl. *J. Phys. Chem. A* **2002**, *106*, 5279-5287, doi:10.1021/jp014296m.

(5) Kirchner, U.; Benter, T.; Schindler, R. N. Experimental verification of gas phase bromine enrichment in reactions of HOBr with sea salt doped ice surfaces. *Phys. Chem. Chem. Phys.* **1997**, *101*, 975-977, doi:10.1002/bbpc.19971010614.
(6) Mochida, M.; Hirokawa, J.; Kajii, Y.; Akimoto, H. Heterogeneous reactions of Cl_2 with sea salts at ambient temperature: Implications for halogen exchange in the atmosphere. *Geophys. Res. Lett.* **1998**, *25*, 3927-3930, doi:10.1029/1998GL900100.
(7) Wachsmuth, M.; Gäggeler, H. W.; von Glasow, R.; Ammann, M. Accommodation coefficient of HOBr on deliquescent sodium bromide aerosol particles. *Atmos. Chem. Phys.* **2002**, *2*, 121-131, doi:10.5194/acp-2-121-2002.

120. **$BrNO_2$ + H_2O(l).** Behnke, George and co-workers have used wetted wall flow reactor techniques to investigate the reactive uptake of $BrNO_2$ on aqueous solutions from 276 to 298 K.[1,2] Measured reactive uptake coefficients range from 1 to 3.5×10^{-6} with a small positive temperature dependence.
Back to Table

(1) Frenzel, A.; Scheer, V.; Sikorski, R.; George, C.; Behnke, W.; Zetsch, C. Heterogeneous interconversion reactions of $BrNO_2$, $ClNO_2$, Br_2, and Cl_2. *J. Phys. Chem. A* **1998**, *102*, 1329-1337, doi:10.1021/jp973044b.
(2) Schweitzer, F.; Mirabel, P.; George, C. Multiphase chemistry of N_2O_5, $ClNO_2$ and $BrNO_2$. *J. Phys. Chem. A* **1998**, *102*, 3942-3952, doi:10.1021/jp980748s.

121. **$BrNO_2$ + KCl and NaCl.** Caloz et al.[1] measured an uptake coefficient for $BrNO_2$ on KCl of 5×10^{-2}, but concluded that it was due only to reaction with a small bromide impurity in the KCl; as expected if this is the case, only Br_2 was generated in the reaction.
The uptake of $BrNO_2$ on aqueous solutions of 0.5 M NaCl has been measured using a droplet train flow reactor by Schweitzer et al.[3] from 277–293 K yielding $\gamma_0 \sim 1 \times 10^{-5}$. Frenzel et al.[2] used a wetted wall flow tube to obtain a lower limit for the uptake coefficient of 3.8×10^{-5} at 291 K.
Back to Table

(1) Caloz, F.; Seisel, S.; Fenter, F. F.; Rossi, M. J. Reactivity of $BrNO_2$ and $ClNO_2$ with solid alkali salt substrates. *J. Phys. Chem. A* **1998**, *102*, 7470-7479, doi:10.1021/jp982000f.
(2) Frenzel, A.; Scheer, V.; Sikorski, R.; George, C.; Behnke, W.; Zetzsch, C. Heterogeneous interconversion reactions of $BrNO_2$, $ClNO_2$, Br_2, and Cl_2. *J. Phys. Chem. A* **1998**, *102*, 1329-1337, doi:10.1021/jp973044b.
(3) Schweitzer, F.; Mirabel, P.; George, C. Multiphase chemistry of N_2O_5, $ClNO_2$ and $BrNO_2$. *J. Phys. Chem. A* **1998**, *102*, 3942-3952, doi:10.1021/jp980748s.

122. **$BrNO_2$ + KBr, NaBr and NaI.** Caloz et al.[1] used a Knudsen cell to study the uptake of $BrNO_2$ on solid KBr powders. The uptake was fast, $\gamma_0 \geq 0.3$, with production of Br_2 as the gas phase product.
On aqueous solutions of NaBr, the uptake coefficient increases as the concentration of NaBr increases.[2-4] For example, at 278 K, γ_0 increased from 8.6×10^{-6} to 1.1×10^{-4} as the NaBr concentration increased from 5×10^{-4} to 5×10^{-2}, but was independent of temperature over the range from 275–293 K.[4] The major gas phase product is Br_2, with smaller amounts of $BrNO_2$ and only at the smaller concentrations of NaBr.[3,4] The uptake of $BrNO_2$ on aqueous NaI solutions has been determined using a droplet train flow reactor[3] and a wetted wall flow tube;[4] the uptake coefficient from 4.4×10^{-5} to 4.4×10^{-4} as the iodide concentration increased from 10^{-4} M to 5×10^{-3} M.[4]
Back to Table

(1) Caloz, F.; Seisel, S.; Fenter, F. F.; Rossi, M. J. Reactivity of $BrNO_2$ and $ClNO_2$ with solid alkali salt substrates. *J. Phys. Chem. A* **1998**, *102*, 7470-7479, doi:10.1021/jp982000f.
(2) Frenzel, A.; Scheer, V.; Sikorski, R.; George, C.; Behnke, W.; Zetzsch, C. Heterogeneous interconversion reactions of $BrNO_2$, $ClNO_2$, Br_2, and Cl_2. *J. Phys. Chem. A* **1998**, *102*, 1329-1337, doi:10.1021/jp973044b.
(3) Schweitzer, F.; Mirabel, P.; George, C. Multiphase chemistry of N_2O_5, $ClNO_2$ and $BrNO_2$. *J. Phys. Chem. A* **1998**, *102*, 3942-3952, doi:10.1021/jp980748s.

(4) Schweitzer, F.; Mirabel, P.; George, C. Heterogeneous chemistry of nitryl halides in relation to tropospheric halogen activation. *J. Atmos. Chem.* **1999**, *34*, 101-117, doi:10.1023/A:1006249921480.

123. $BrONO_2$ and $BrONO_2$ + HCl + H_2O(s). Hanson and Ravishankara[3] investigated these reactions in an ice-coated flow reactor at 200 (±10) K. The reaction of $BrONO_2$ with H_2O(s) proceeded at a rate indistinguishable from the gas phase diffusion limit, implying that the reaction probability may be as high as one; the product BrNO(g) was observed. Allanic et al.[2] used a Knudsen cell reactor to measure $BrONO_2$ uptake between 190–200 K. Values of initial γ's in the 0.2–0.3 range were observed. An average γ = 0.26 ± 0.05 was obtained from all of the appropriate data from both experiments**.** Aguzzi and Rossi[1] studied the hydrolysis reaction on various types of ices, obtaining γ = 0.34 ± 0.03 at 180 K and γ = 0.15 ± 0.01 at 210 K. They observed HOBr as the main product and Br_2O as a secondary product. Hanson and Ravishankara[3] also codeposited HCl with $BrONO_2$ observing rapid production of BrCl. It is unclear whether BrCl is produced directly from $BrONO_2$ + HCl or via HOBr (from $BrONO_2$ hydrolysis) reacting with HCl.
Back to Table ($BrONO_2$ + H_2O) Back to Table ($BrONO_2$ + HCl)

(1) Aguzzi, A.; Rossi, M. J. Heterogeneous hydrolysis and reaction of $BrONO_2$ and Br_2O on pure ice and ice doped with HBr. *J. Phys. Chem. A* **2002**, *106*, 5891-5901, doi:10.1021/jp014383e.
(2) Allanic, A.; Oppliger, R.; Rossi, M. J. Real-time kinetics of the uptake of HOBr and $BrONO_2$ on ice and in the presence of HCl in the temperature range 190-200 K. *J. Geophys. Res.* **1997**, *102*, 23529-23541, doi:10.1029/97JD01833.
(3) Hanson, D. R.; Ravishankara, A. R. Response to "Comment on porosities of ice films used to simulate stratospheric cloud surfaces". *J. Phys. Chem.* **1993**, *97*, 2802-2803, doi:10.1021/j100113a054.

124. $BrONO_2$ + H_2O(l). Deiber et al.[1] used a droplet train rector to measure to uptake of $BrONO_2$ on pure water between 272 and 280 K. An apparent positive temperature dependence was observed with measured reactive uptake measurements ranging from 0.024 ± 0.0008 at 272.5 K to 0.039 ± 0.0012 at 279.7 K.
Back to Table

(1) Deiber, G.; George, C.; Le Calve, S.; Schweitzer, F.; Mirabel, P. Uptake study of $ClONO_2$ and $BrONO_2$ by halide containing droplets. *Atmos. Chem. Phys.* **2004**, *4*, 1291-1299, doi:10.5194/acp-4-1291-2004.

125. $BrONO_2$ and $BrONO_2$ + HCl + H_2SO_4•nH_2O(l). Hanson and co-workers used both coated flow tube and aerosol flow tube techniques to show that the reaction of $BrONO_2$ with 45–70 wt% H_2SO_4 is extremely facile at temperatures from 210 to 298 K. Hanson and Ravishankara[2] measured γs of 0.5 (+0.5, –0.25) (45 wt% H_2SO_4, 210 K, 0.4 (+0.6, –0.2) (60 wt%, 210 K), and 0.3 (+0.7, –0.1) (70 wt%, 220 K) in a coated-wall flow tube experiment. Hanson et al.,[3] measured γ ~0.8 (20 to 40% error) for submicron aerosols at temperatures between 249 and 298 K and H_2SO_4 concentrations of 45 to 70 wt%; there was a sharp fall off in γ for H_2SO_4 concentrations between 73 and 83 wt%. Hanson also reported additional temperature dependent (230–295 K) coated flow reactor and room temperature (295–300 K) aerosol flow reactor studies extending measurements to higher acid wt% values.[1] Hanson has analyzed these combined data sets, the data indicated that γ is a function of sulfuric acid concentration, but independent of temperature. After eliminating one previously reported anomalously low 83 wt% data point Hanson has fit an empirical expression for measured γs for $BrONO_2$ + H_2O in the form of: $1/\gamma = 1/\alpha + 1/\gamma_{rxn}$, where $\gamma_{rxn} = \exp(a+b*wt.)$ and α = 0.80, and a = 29.2, b = –0.40.[1] Using the same approach as detailed in the note for N_2O_5 uptake on sulfuric acid, the error for $BrONO_2$ + H_2O is 27.3% (1σ), with γ_m = 26.6% and γ_d = 6.3%. Addition of excess HCl to 229 K, 40 and 60 wt% H_2SO_4 aerosols caused an increase in γ to 1.0 and 0.9, respectively.[3]
Back to Table ($BrONO_2$ + H_2O) Back to Table ($BrONO_2$ + HCl)

(1) Hanson, D. Reactivity of $BrONO_2$ and HOBr on sulfuric acid solutions at low temperatures. *J. Geophys. Res.* **2003**, *108*, 4239, doi:10.1029/2002JD002519.
(2) Hanson, D. R.; Ravishankara, A. R. Heterogeneous chemistry of bromine species in sulfuric acid under stratospheric conditions. *Geophys. Res. Lett.* **1995**, *22*, 385-388, doi:10.1029/94GL03379.
(3) Hanson, D. R.; Ravishankara, A. R.; Lovejoy, E. R. Reaction of $BrONO_2$ with H_2O on submicron sulfuric acid aerosol and the implications for the lower stratosphere. *J. Geophys. Res.* **1996**, *101*, 9063-9069, doi:10.1029/96JD00347.

126. $BrONO_2$ + HBr. Aguzzi and Rossi[1] measured γ over the 180–210 K temperature range, with γ = 0.3 at 180 K and an activation energy of –1.2 ± 0.2 kcal/mol.
Back to Table

(1) Aguzzi, A.; Rossi, M. J. Heterogeneous hydrolysis and reaction of $BrONO_2$ and Br_2O on pure ice and ice doped with HBr. *J. Phys. Chem. A* **2002**, *106*, 5891-5901, doi:10.1021/jp014383e.

127. $BrONO_2$ + NaCl. Aguzzi and Rossi[1] used a Knudsen cell and three types of NaCl samples (powders, spray-deposited and single crystal) to measure the uptake of $BrONO_2$ and obtained consistent results with $\gamma_0 = 0.31 \pm 0.12$. No correction for diffusion into the powders was made because of the high uptake coefficient (see Subsection 5.6). BrCl was the major product, 80 ± 20%, with smaller amounts (~10%) of Br_2 and some HCl. Rapid uptake of $BrONO_2$ of the same magnitude was observed on the unreactive salts $NaNO_3$ and Na_2SO_4, with a Br_2 yield of 45 ± 10%; this uptake and reaction was attributed to the self-reaction of $BrONO_2$ on the surface to generate Br_2O which decomposed to Br_2.

Deiber et al.[2] studied the uptake of $BrONO_2$ on water, NaCl and NaBr solutions using a droplet train apparatus from 272–280 K. The uptake coefficient was the same on water and 0.1 M NaCl, where BrCl was observed as the gas phase product. On NaBr, the uptake increased with the square root of the NaBr concentration, from which a value for the mass accommodation coefficient for $BrONO_2$ of 0.063 ± 0.021 (2σ) was obtained.
Back to Table

(1) Aguzzi, A.; Rossi, M. J. The kinetics of the heterogeneous reaction of $BrONO_2$ with solid alkali halides at ambient temperature. A comparison with the interaction of $ClONO_2$ on NaCl and KBr. *Phys. Chem. Chem. Phys.* **1999**, *1*, 4337-4346, doi:10.1039/a904611i.
(2) Deiber, G.; George, C.; Le Calve, S.; Schweitzer, F.; Mirabel, P. Uptake study of $ClONO_2$ and $BrONO_2$ by halide containing droplets. *Atmos. Chem. Phys.* **2004**, *4*, 1291-1299, doi:10.5194/acp-4-1291-2004.

128. $BrONO_2$ + KBr and NaBr. Aguzzi and Rossi[1] used a Knudsen cell and three types of KBr samples (powders, spray-deposited and single crystal) to measure the uptake of $BrONO_2$ and obtained consistent results with $\gamma_0 = 0.33 \pm 0.12$. No correction for diffusion into the powders was made because of the high uptake coefficient (see Subsection 5.6). Br_2 was the major product, with its yield decreasing as the concentration of $BrONO_2$ increased; this was attributed to a competition between the reaction of $BrONO_2$ with KBr and the self-reaction of $BrONO_2$ on the surface.

Deiber et al.[2] studied the uptake of $BrONO_2$ on water, NaCl and NaBr solutions using a droplet train flow reactor from 272–280 K. The uptake coefficient was the same on water and 0.1 M NaCl. On NaBr, the uptake increased with the square root of the NaBr concentration, from which a value for the mass accommodation coefficient for $BrONO_2$ of 0.063 ± 0.021 (2σ) was obtained. The gas phase product on the NaBr solution was Br_2.
Back to Table

(1) Aguzzi, A.; Rossi, M. J. The kinetics of the heterogeneous reaction of $BrONO_2$ with solid alkali halides at ambient temperature. A comparison with the interaction of $ClONO_2$ on NaCl and KBr. *Phys. Chem. Chem. Phys.* **1999**, *1*, 4337-4346, doi:10.1039/a904611i.
(2) Deiber, G.; George, C.; Le Calve, S.; Schweitzer, F.; Mirabel, P. Uptake study of $ClONO_2$ and $BrONO_2$ by halide containing droplets. *Atmos. Chem. Phys.* **2004**, *4*, 1291-1299, doi:10.5194/acp-4-1291-2004.

129. ICl on NaCl/NaBr. ICl uptake onto acidified and neutral NaCl/NaBr solutions at 274 to 298 K was studied in coated–wall flow tubes. The initial uptake coefficients were in the 0.6 to 3×10^{-3} range depending on the experimental system used, for solutions containing bromide; IBr was the gas-phase product observed. In an aerosol flow tube, uptake of ICl onto concentrated NaBr solutions showed uptake coefficients of 1 to 2×10^{-2}, which dropped to values of 10^{-4} on sea-salt solution aerosols. IBr was the product of the reaction on NaBr particles, with a yield of 0.6 (Braban et al.[1]).
Back to Table

(1) Braban, C. F.; Adams, J. W.; Rodriguez, D.; Cox, R. A.; Crowley, J. N.; Schuster, G. Heterogeneous reactions of HOI, ICl and IBr on sea salt and sea salt proxies. *Phys. Chem. Chem. Phys.* **2007**, *9*, 3136-3148, doi:10.1039/b700829e.

130. HOI on NaCl/NaBr. HOI uptake on acidified and neutral NaCl/NaBr solutions at 274 K in a wetted-wall flow tube indicate a lower limit for the uptake coefficient of 2.2×10^{-3} (Braban et al.[1]). IBr is identified as the major gas-phase product when the solutions contain bromide to chloride ratios of 1:200, whereas ICl is the product from pure NaCl solutions. HOI uptake on dry and frozen solutions of NaCl and NaBr with chloride to bromide ratios equal to that of seawater were also studied in a coated wall-flow tube. The product ICl is only formed when the surface is depleted of bromide, otherwise IBr forms. Uptake coefficients measured in a flow reactor by Holmes et al.[2] are >0.01 at 243 K on the frozen films and >0.01 at 243 K and 298 K on dry salts. Mössinger and Cox[3] report uptake of HOI onto dry films of NaCl, NaBr and sea salt from 278 to 298 K and measured uptake coefficients of 0.016, 0.034 and 0.061 respectively. The products are ICl, IBr and IC//IBr, respectively.
Back to Table

(1) Braban, C. F.; Adams, J. W.; Rodriguez, D.; Cox, R. A.; Crowley, J. N.; Schuster, G. Heterogeneous reactions of HOI, ICl and IBr on sea salt and sea salt proxies. *Phys. Chem. Chem. Phys.* **2007**, *9*, 3136-3148, doi:10.1039/b700829e.
(2) Holmes, N. S.; Adams, J. W.; Crowley, J. N. Uptake and reaction of HOI and $IONO_2$ on frozen and dry NaCl/NaBr surfaces and H_2SO_4. *Phys. Chem. Chem. Phys.* **2001**, *3*, 1679-1687, doi:10.1039/b100247n.
(3) Mössinger, J. C.; Cox, R. A. Heterogeneous reaction of HOI with sodium halide salts. *J. Phys. Chem. A* **2001**, *105*, 5165-5177, doi:10.1021/jp0044678.

131. $CF_3OH + H_2O + H_2O(l)$ and $H_2SO_4 \bullet nH_2O(l)$. Lovejoy et al.[1] used both wetted-wall and aerosol flow tube techniques to measure reactive uptake of CF_3OH on water at 274 K and 39–60 wt% H_2SO_4 at various temperatures between 206 and 250 K. γ's showed a strong dependence on water activity. Aerosol uptake studies yielded reacto-diffusive lengths of >0.4 μm for 40 wt% H_2SO_4 and 1.0 μm for 50 wt% H_2SO_4, both at 250 K. Recommended γ's were estimated by averaging bulk uptake measurements at similar H_2SO_4 concentrations and ignoring temperature effects on water activity.
Back to Table

(1) Lovejoy, E. R.; Huey, L. G.; Hanson, D. R. Atmospheric fate of CF_3OH 2: Heterogeneous reaction. *J. Geophys. Res.* **1995**, *100*, 18775-18780, doi:10.1029/95JD01843.

132. $SO_2 + O_3 + Al_2O_3(s)$. Usher et al.[1] present Knudsen cell data showing that pretreatment of α-alumina with SO_2 increases γ_o values for O_3 uptake by 30%; FTIR observations by the same group show that O_3 oxidized surface sulfite and bisulfite formed by SO_2 absorption to sulfate and bisulfate.
Back to Table

(1) Usher, C. R.; Michel, A. E.; Stec, D.; Grassian, V. H. Laboratory studies of ozone uptake on processed mineral dust. *Atmos. Environ.* **2003**, *37*, 5337-5347, doi:10.1016/j.atmosenv.2003.09.014.

133. SO_2 on H_2O_2/ice. SO_2 loss on ice surfaces has been observed to proceed when H_2O_2 is present, making the reaction of potential significance in ice clouds. Clegg and Abbatt[2] have observed this reaction when both SO_2 and H_2O_2 are delivered from the gas phase in a coated-wall flow tube at 228 K, with H_2O_2 in excess. For both SO_2 and H_2O_2 only small fractions of a monolayer are present on the surface during the reaction. It is inferred that the reaction proceeds through the HSO_3^- intermediate because the reaction rate declines as acidity builds up on the surface from the sulphuric acid product, i.e., because dissociation of adsorbed SO_2 to form HSO_3^- is becoming inhibited. At about 200 K, relative to the uptake on pure ice, Chu et al.[1] observe enhanced loss of SO_2 on ice films that have been doped with 3% H_2O_2 and they detect sulphate as a product. Uptake coefficients are reported in Clegg and Abbatt that are dependent on both the H_2O_2 and SO_2 partial pressure, so no single value prevails for atmospheric conditions.
Back to Table

(1) Chu, L.; Diao, G. W.; Chu, L. T. Heterogeneous interaction of SO_2 on H_2O_2-ice films at 190-210 K. *J. Phys. Chem. A* **2000**, *104*, 7565-7573, doi:10.1021/jp001323k.

(2) Clegg, S. M.; Abbatt, J. P. D. Oxidation of SO_2 by H_2O_2 on ice surfaces at 228 K: A sink for SO_2 in ice clouds. *Atmos. Chem. Phys.* **2001**, *1*, 73-78, doi:10.5194/acp-1-73-2001.

134. $SO_2 + H_2O_2$, O_3, HONO, NO_2, $HNO_3 + H_2SO_4 \bullet nH_2O$(l). Rattigan et al.[2] used a bubble train reactor to measure the uptake of SO_2 in the presence of solvated oxidants at 293 K. For H_2O_2 the second order rate constant at 1 wt% H_2SO_4 agreed well with previous bulk kinetics measurements and with previous droplet train/flow reactor measurements. Measurements at 20, 40, and 60 wt% H_2SO_4 are the first reported for concentrated acid. Reaction rate data were fit to a two term (acid catalyzed and water catalyzed) bulk second order rate expression, which, in the limit of high acid activity ($a_{H^+} = \alpha_{H+}[H^+]$, where α_{H+} is the H^+ activity coefficient) reduces to: $k^{II}_{H_2O_2} = 8.3 \times 10^4$ (α_{H_2O}/ a_{H^+}), where α_{H_2O} is the water activity coefficient. Both α_{H+} and α_{H_2O} can be obtained from the sulfuric acid thermodynamic model of Carslaw et al.[1] The high a_{H^+} approximation for $k^{II}_{H_2O_2}$ should be accurate to a factor of two between 40 and 70 wt%.

Uptake of SO_2 in the presence of solvated O_3 was measured for 1–70 wt% acid; the Henry's law expression for O_3 was determined in separate experiments. Measured second order rates agree reasonably well with previous results measured below 18 wt%. A three-term fit for reaction with SO_2(aq), HSO_3^-, and $SO_4^=$ was fit to the data: $k^{ii}_{O_3} = 6.6 \times 10^3$ [SO_2(aq)] + 3.2×10^5 [HSO_3^-] + 1×10^9 [$SO_4^=$]. This expression should be accurate to a factor of two between 20 and 70 wt.%.

The HONO reaction was studied by adding nitrosyl sulfuric acid to 20, 40, 60, and 70 wt% acid. Measured second order rate constants were moderately consistent with previous measurements below 10 wt%. A $k^{II}_{HONO} = 142[H^+]$ was fit to the full data set; it should be accurate to a factor of two for acid concentrations between 10 and 70 wt%.

No enhanced SO_2 uptake was observed with added gas phase NO, NO_2, or with 20 wt% HNO_3 added to 50–60 wt% sulfuric acid.
Back to Table

(1) Carslaw, K. S.; Clegg, S. L.; Brimblecombe, P. A thermodynamic model of the system HCl-HNO_3-H_2SO_4-H_2O, including solubilities of HBr, from <200 to 328 K. *J. Phys. Chem.* **1995**, *99*, 11557-11574, doi:10.1021/j100029a039.
(2) Rattigan, O. V.; Boniface, J.; Swartz, E.; Davidovits, P.; Jayne, J. T.; Kolb, C. E.; Worsnop, D. R. Uptake of gas-phase SO_2 in aqueous sulfuric acid: Oxidation by H_2O_2, O_3, and HONO. *J. Geophys. Res.* **2000**, *105*, 29065-29078, doi:10.1029/2000JD900372.

135. $SO_2 + Al_2O_3$. Goodman et al.[2] used FTIR observations of SO_2 absorption on α-alumina to show that surface bound sulfite and bisulfite products are produced, they integrated these surface feature absorbencies to estimate a γ_o of $(9.5 \pm 0.3) \times 10^{-5}$. Usher et al.[8] performed BET corrected room temperature studies on four α-alumina samples reporting an average γ_o of $(1.6 \pm 0.5) \times 10^{-4}$. Seisel et al.[7] measured $\gamma_0 = (7.4 \pm 0.9) \times 10^{-3}$ on γ-alumina at 298 K using a pulsed Knudsen cell method. FTIR studies of SO_2 uptake on commercial γ-alumina catalyst samples also show sulfite formation on non-hydroxylated surfaces.[1,3] Ma et al.[6] co-deposited SO_2 and NO_2 on γ-alumina surfaces, using FTIR to observe that rather than forming adsorbed nitrite or nitrate, NO_2 dimerized and the dimer oxidized SO_2 to sulfate. Ma and coworkers[4] extended their studies of NO_2/N_2O_4 interactions with adsorbed SO_2 on α-Al_2O_3, CaO, α-Fe_2O_3, ZNO_3, MgO, TiO_2 and SiO_2. Lo et al.[5] published a density functional theory study of SO_2 interactions with hydrated and dehydrated γ-alumina surfaces calculating the theromochemistry of SO_2 adsorption and conversion to SO_3/HSO_3.
Back to Table

(1) Datta, A.; Cavell, R. G.; Tower, R. W.; George, Z. M. Claus catalysis. 1. Adsorption on the alumina catalyst studied by FTIR and EPR spectroscopy. *J. Phys. Chem.* **1985**, *89*, 443-449, doi:10.1021/j100249a014.
(2) Goodman, A. L.; Li, P.; Usher, C. R.; Grassian, V. H. Heterogeneous uptake of sulfur dioxide on aluminum and magnesium oxide particles. *J. Phys. Chem. A* **2002**, *105*, 6109-6120, doi:10.1021/jp004423z.
(3) Karge, H. G.; Dalla Lana, I. G. Infrared studies of SO_2 adsorption on a Claus catalyst by selective poisoning of sites. *J. Phys. Chem.* **1984**, *88*, 1538-1543, doi:10.1021/j150652a019.
(4) Liu, C.; Ma, Q.; Liu, Y.; Ma, J.; He, H. Synergistic reaction between SO_2 and NO_2 on mineral oxides: a potential formation pathway of sulfate aerosol. *Phys. Chem. Chem. Phys* **2012**, *14*, 1668-1676, doi:10.1039/c1cp22217a.

(5) Lo, J. M. H.; Ziegler, T.; Clark, P. D. SO_2 adsorption and transformations on γ-Al_2O_3 surfaces: A density functional theory study. *J. Phys. Chem. C* **2010**, *114*, 10444-10454, doi:10.1021/jp910895g.
(6) Ma, Q.; Liu, Y.; He, H. Synergistic effect between NO_2 and SO_2 in their adsorption and reaction on γ-alumina. *J. Phys. Chem. A* **2008**, *112*, 6630-6635, doi:10.1021/jp802025z.
(7) Seisel, S.; Keil, T.; Lian, Y.; Zellner, R. Kinetics of the uptake of SO_2 on mineral oxides: Improved initial uptake coefficients at 298 K from pulsed Knudsen cell experiments. *Int. J. Chem. Kinet.* **2006**, *38*, 242-249, doi:10.1002/kin.20148.
(8) Usher, C. R.; Al-Hosney, H.; Carlos-Cuellar, S.; Grassian, V. H. A laboratory study of the heterogeneous uptake and oxidation of sulfur dioxide on mineral dust particles. *J. Geophys. Res.* **2002**, *107*, 4713, doi:10.1029/2002JD002051.

136. SO_2 + NaCl and sea salt. Gebel et al.[1] reported no measurable uptake of SO_2 on NaCl, yielding an upper limit of 1×10^{-4} for the uptake coefficient. The same was true for synthetic sea salt that had been heated while pumping. However, sea salt that had not been heated or pumped on extensively had a rapid uptake of SO_2, with initial uptake coefficients as large as 0.09. The time dependence of the uptake coefficient was consistent with uptake of SO_2 into a liquid layer, likely due to large amounts of water adsorbed on the hygroscopic components of sea salt such as magnesium hydrate. No gas phase products were observed but sulfite formation in the salt was seen by FTIR, indicating that uptake was due to dissolution of SO_2 into the water film on the salt surface.
Back to Table

(1) Gebel, M. E.; Finlayson-Pitts, B. J.; Ganske, J. S. The uptake of SO_2 on synthetic sea salt and some of its components. *Geophys. Res. Lett.* **2000**, *27*, 887-890, doi:10.1029/1999GL011152.

137. SO_3 + H_2SO_4•nH_2O(l). Jayne et al.[1] measured the uptake coefficient in a wetted wall-flow reactor at 300 K over a composition range of 78–92 H_2SO_4 wt%. The measured γ was indistinguishable from 1.0. Higher water concentrations and lower temperatures probably tend to increase γ, so a value near 1.0 probably holds for all atmospheric conditions.
Back to Table

(1) Jayne, J. T.; Poschl, U.; Chen, Y.; Dai, D.; Molina, L. T.; Worsnop, D. R.; Kolb, C. E.; Molina, M. J. Pressure and temperature dependence of the gas-phase reaction of SO_3 with H_2O and the heterogeneous reaction of SO_3 with H_2O/H_2SO_4 surfaces. *J. Phys. Chem. A* **1997**, *101*, 10000-10011, doi:10.1021/jp972549z.

138. OCS + Al_2O_3. Liu and co-workers have measured OCS uptake on both α-alumina and γ-alumina surfaces at 298 K using Knudsen cell techniques[3] and on α-alumina surfaces with controlled water vapor levels using both a Knudsen cell and a reaction chamber equipped with diffuse reflectance infrared Fourier transform spectroscopy (DRIFTS).[4] The DRIFTS technique was also used to investigate heterogeneous reaction mechanisms, revealing that surface Al-OH plays a major role in oxidizing adsorbed OCS to CO_2 and that a number of surface adsorbed reactive intermediate anions, including $HSCO_2^-$, are formed. The overall reaction is essentially a surface catalyzed hydrolysis reaction producing both CO_2 and H_2S.[1,2,4] Liu et al.[3] report uptake of relatively dry OCS yielding rather small $\gamma_0 = (4.9 \pm 0.5) \times 10^{-7}$ and $\gamma_{ss} = (6.5 \pm 2.4) \times 10^{-8}$ values for α-alumina and $\gamma_0 = (1.0 \pm 0.2) \times 10^{-7}$ and $\gamma_{ss} = (1.8 \pm 0.4) \times 10^{-8}$ values for γ-alumina at 298 K. The low steady-state uptake coefficients are probably due to consumption of most of the surface Al-OH sites and a low regeneration rate due to limited water vapor. OCS uptake experiments that provide controlled water vapor fluxes to α-alumina surfaces produce somewhat higher γ_{ss} values in the Knudsen apparatus, and the values obtained by integrating the DRIFTS spectra for RH values between 7 and 47% fall in the range of 7.4×10^{-6} to 3.3×10^{-6}.[4] Interestingly, the highest uptake values are not obtained for the highest RH values because water vapor can also occupy reactive alumina surface sites and block OCS adsorption.
Back to Table

(1) He, H.; Liu, J.; Mu, Y.; Yu, Y.; Chen, M. Heterogeneous oxidation of carbonyl sulfide on atmospheric particles and alumina. *Environ. Sci. Technol.* **2005**, *39*, 9637-9642, doi:10.1021/es048865q.
(2) Liu, J.; Yu, Y.; Mu, Y.; He, H. Mechanism of heterogeneous oxidation ofcarbonyl sulfide on Al_2O_3: an *in situ* diffuse reflectance infrared fourier transform spectroscopy investigation *J. Phys. Chem. B* **2006**, *110*, 3225-3230, doi:10.1021/jp055646y.

(3) Liu, Y.; He, H.; Mu, Y. Heterogeneous reactivity of carbonyl sulfide on α-Al_2O_3 and γ-Al_2O_3. *Atmos. Environ.* **2008**, *42*, 960-969, doi:10.1016/j.atmosenv.2007.10.007.
(4) Liu, Y.; Ma, Q.; He, H. Comparative study of the effect of water on the heterogeneous reactions of carbonyl sulfide on the surface of α-Al_2O_3 and MgO. *Atmos. Chem. Phys.* **2009**, *9*, 6273-6286, doi:10.5194/acp-9-6273-2009.

5.2.3.2 Bibliography – Table NEq2

Abbatt, J. P. D. Heterogeneous reaction of HOBr with HBr and HCl on ice surfaces at 228 K. *Geophys. Res. Lett.* **1994**, *21*, 665-668, doi:10.1029/94GL00775.

Abbatt, J. P. D. Interactions of HBr, HCl, and HOBr with supercooled sulfuric acid solutions of stratospheric composition. *J. Geophys. Res.* **1995**, *100*, 14009-14017, doi:10.1029/95JD01367.

Abbatt, J. P. D. Heterogeneous interactions of BrO and ClO: Evidence for BrO surface recombination and reaction with HSO_3^-/SO_3^{2-}. *Geophys. Res. Lett.* **1996**, *23*, 1681-1684, doi:10.1029/96GL01430.

Abbatt, J. P. D.; Beyer, K. D.; Fucaloro, A. F.; McMahon, J. R.; Wooldridge, P. J.; Zhong, R.; Molina, M. J. Interaction of HCl vapor with water-ice: Implications for the stratosphere. *J. Geophys. Res.* **1992**, *97*, 15819-15826, doi:10.1029/92JD01220.

Abbatt, J. P. D.; Lee, A. K. Y.; Thornton, J. A. Quantifying trace gas uptake to tropospheric aerosol: recent advances and remaining challenges. *Chem. Soc. Rev.* **2012**, *41*, 6555-6581, doi:10.1039/C2CS35052A.

Abbatt, J. P. D.; Molina, M. J. Heterogeneous interactions of $ClONO_2$ and HCl on nitric acid trihydrate at 202 K. *J. Phys. Chem.* **1992**, *96*, 7674-7679, doi:10.1021/j100198a036.

Abbatt, J. P. D.; Molina, M. J. The heterogeneous reaction of HOCl + HCl → Cl_2 + H_2O on ice and nitric acid trihydrate: Reaction probabilities and stratospheric implications. *Geophys. Res. Lett.* **1992**, *19*, 461-464, doi:10.1029/92GL00373.

Abbatt, J. P. D.; Nowak, J. B. Heterogeneous interactions of HBr and HOCl with cold sulfuric acid solutions: Implications for Arctic boundary layer bromine chemistry. *J. Phys. Chem. A* **1997**, *101*, 2131-2137, doi:10.1021/jp963117b.

Abbatt, J. P. D.; Waschewsky, G. C. G. Heterogeneous interactions of HOBr, HNO_3, O_3, and NO_2 with deliquescent NaCl aerosols at room temperature. *J. Phys. Chem. A* **1998**, *102*, 3719-3725, doi:10.1021/jp980932d.

Adams, J. W.; Holmes, N. S.; Crowley, J. N. Uptake and reaction of HOBr on frozen and dry NaCl/NaBr surfaces between 253 and 233 K. *Atmos. Chem. Phys.* **2002**, *2*, 79-91, doi:10.5194/acp-2-79-2002.

Aguzzi, A.; Rossi, M. J. The kinetics of the heterogeneous reaction of $BrONO_2$ with solid alkali halides at ambient temperature. A comparison with the interaction of $ClONO_2$ on NaCl and KBr. *Phys. Chem. Chem. Phys.* **1999**, *1*, 4337-4346, doi:10.1039/a904611i.

Aguzzi, A.; Rossi, M. J. Heterogeneous hydrolysis and reaction of $BrONO_2$ and Br_2O on pure ice and ice doped with HBr. *J. Phys. Chem. A* **2002**, *106*, 5891-5901, doi:10.1021/jp014383e.

Al-Abadleh, H. A.; Grassian, V. H. FT-IR study of water adsorption on aluminum oxide surfaces. *Langmuir* **2003**, *19*, 341-347, doi:10.1021/la026208a.

Alebić-Juretić, A.; Cvitas, T.; Klasinc, L. Ozone destruction on powders. *Ber. Bunsenges Phys. Chem.* **1992**, *96*, 493-495, doi:10.1002/bbpc.19920960352.

Alebić-Juretić, A.; Cvitas, T.; Klasinc, L. Kinetics of heterogeneous ozone reactions. *Chemosphere* **2000**, *41*, 667-670, doi:10.1016/S0045-6535(99)00485-3.

Allanic, A.; Oppliger, R.; Rossi, M. J. Real-time kinetics of the uptake of HOBr and $BrONO_2$ on ice and in the presence of HCl in the temperature range 190-200 K. *J. Geophys. Res.* **1997**, *102*, 23529-23541, doi:10.1029/97JD01833.

Allanic, A.; Oppliger, R.; van den Bergh, H.; Rossi, M. J. The heterogeneous kinetics of the reactions $ClONO_2$ + HX/ice (X = Cl, Br, I), $BrONO_2$ + HI/ice and the reactivity of the interhalogens BrCl, ICl and IBr with HX/ice (X = Cl, Br, I) in the temperature range 180 to 205 K. *Z. Phys. Chem.* **2000**, *214*, 1479-1500, doi:10.1524/zpch.2000.214.11.1479.

Anastasio, C.; Mozurkewich, M. Laboratory studies of bromide oxidation in the presence of ozone: Evidence for a glass-surface mediated reaction. *J. Atmos. Chem.* **2002**, *41*, 135-162, doi:10.1023/A:1014286326984.

Artiglia, L.; Edebeli, J.; Orlando, F.; Chen, S.; Lee, M.-T.; Arroyo, P. C.; Gilgen, A.; Bartels-Rausch, T.; Kleibert, A.; Vazdar, M.; Carignano, M. A.; Francisco, J. S.; Shepson, P. B.; Gladich, I.; Ammann, M. A surface-stabilized ozonide triggers bromide oxidation at the aqueous solution-vapour interface. *Nat. Commun.* **2017**, *8*, 700, doi:10.1038/s41467-017-00823-x.

Badger, C. L.; Griffiths, P. T.; George, I.; Abbatt, J. P. D.; Cox, R. A. Reactive uptake of N_2O_5 by aerosol particles containing mixtures of humic acid and ammonium sulfate. *J. Phys. Chem. A* **2006**, *110*, 6986-6994, doi:10.1021/jp0562678.

Baigrie, L. M.; Cox, R. A.; Slebocka-Tilk, H.; Tencer, M.; Tidwell, T. T. Acid-catalyze enolization and aldol condensation of acetaldehyde. *J. Am. Chem. Soc.* **1985**, *107*, 3640-3645, doi:10.1021/ja00298a039.

Baker, J.; Ashbourn, S. F. M.; Cox, R. A. Heterogeneous reactivity of nitrous acid on submicron sulfuric acid aerosol. *Phys. Chem. Chem. Phys.* **1999**, *1*, 683-690, doi:10.1039/a808702d.

Baldwin, A. C.; Golden, D. M. Heterogeneous atmospheric reactions: Sulfuric acid aerosols as tropospheric sinks. *Science* **1979**, *206*, 562-563, doi:10.1126/science.206.4418.562.

Baldwin, A. C.; Golden, D. M. Heterogeneous atmospheric reactions 2. Atom and radical reactions with sulfuric acid. *J. Geophys. Res.* **1980**, *85*, 2888-2889, doi:10.1029/JC085iC05p02888.

Ball, S. M.; Fried, A.; Henry, B. E.; Mozurkewich, M. The hydrolysis of $ClONO_2$ on sub-micron liquid sulfuric acid aerosols. *Geophys. Res. Lett.* **1998**, *25*, 3339-3342, doi:10.1029/98GL02566.

Baltrusaitis, J.; Schuttlefield, J.; Jensen, J. H.; Grassian, V. H. FTIR spectroscopy combined with quantum chemical calculations to investigate adsorbed nitrate on aluminium oxide surfaces in the presence and absence of co-adsorbed water. *Phys. Chem. Chem. Phys.* **2007**, *9*, 4970-4980, doi:10.1039/b705189a.

Barone, S. B.; Zondlo, M. A.; Tolbert, M. A. A kinetic and product study of the hydrolysis of $ClONO_2$ on type Ia polar stratospheric cloud materials at 185 K. *J. Phys. Chem. A* **1997**, *101*, 8643-8652, doi:10.1021/jp971107k.

Becker, K. H.; Kleffman, J.; Kurtenbach, R.; Wiesen, P. Solubility of nitrous acid (HONO) in sulfuric acid solutions. *J. Phys. Chem.* **1996**, *100*, 14984-14990, doi:10.1021/jp961140r.

Behnke, W.; George, C.; Scheer, V.; Zetsch, C. Production and decay of $ClNO_2$ from the reaction of gaseous N_2O_5 with NaCl solution: Bulk and aerosol experiments. *J. Geophys. Res.* **1997**, *102*, 3795-3804, doi:10.1029/96JD03057.

Behnke, W.; Kruger, H.-U.; Scheer, V.; Zetzsch, C. Formation of atomic Cl from sea spray via photolysis of nitryl chloride: Determination of the sticking coefficient of N_2O_5 on NaCl aerosol. *J. Aerosol Sci.* **1991**, *22*, S609-S612, doi:10.1016/S0021-8502(05)80175-2.

Beichert, P.; Finlayson-Pitts, B. J. Knudson cell studies of the uptake of gaseous HNO_3 and other oxides of nitrogen on solid NaCl. The role of surface absorbed water. *J. Phys. Chem.* **1996**, *100*, 15218-15228, doi:10.1021/jp960925u.

Berland, B. S.; Tolbert, M. A.; George, S. M. Surface sensitive studies of the reactive uptake of chlorine nitrate on ice. *J. Phys. Chem. A* **1997**, *101*, 9954-9963, doi:10.1021/jp971121x.

Bertram, T. H.; Thornton, J. A. Toward a general parameterization of N_2O_5 reactivity on aqueous particles: the competing effects of particle liquid water, nitrate and chloride. *Atmos. Chem. Phys.* **2009**, *9*, 8351-8363, doi:10.5194/acp-9-8351-2009.

Bertram, T. H.; Thornton, J. A.; Riedel, T. P.; Middlebrook, A. M.; Bahreini, R.; Bates, T. S.; Quinn, P. K.; Coffman, D. J. Direct observations of N_2O_5 reactivity on ambient aerosol particles. *Geophys. Res. Lett.* **2009**, *36*, L19803, doi:10.1029/2009gl040248.

Bongartz, A.; Kames, J.; Schurath, U.; George, C.; Mirabel, P.; Ponche, J. L. Experimental determination of HONO mass accommodation coefficients using two different techniques. *J. Atmos. Chem.* **1994**, *18*, 149-169, doi:10.1007/BF00696812.

Borensen, C.; Kirchner, U.; Scheer, V.; Vogt, R.; Zellner, R. Mechanism and kinetics of the reactions of NO_2 or HNO_3 with alumina as a mineral dust model compound. *J. Phys. Chem. A* **2000**, *104*, 5036-5045, doi:10.1021/jp994170d.

Braban, C. F.; Adams, J. W.; Rodriguez, D.; Cox, R. A.; Crowley, J. N.; Schuster, G. Heterogeneous reactions of HOI, ICl and IBr on sea salt and sea salt proxies. *Phys. Chem. Chem. Phys.* **2007**, *9*, 3136-3148, doi:10.1039/b700829e.

Brown, M. A.; Ashby, P. D.; Ogletree, D. F.; Salmeron, M.; Hemminger, J. C. Reactivity of ozone with solid potassium iodide investigated by atomic force microscopy. *J. Phys. Chem. C* **2008**, *112*, 8110-8113, doi:10.1021/jp801620w.

Brown, M. A.; Newberg, J. T.; Krisch, M. J.; Mun, B. S.; Hemminger, J. C. Reactive uptake of ozone on solid potassium iodide. *J. Phys. Chem. C* **2008**, *112*, 5520-5525, doi:10.1021/jp077225h.

Caloz, F.; Fenter, F. F.; Tabor, K. D.; Rossi, M. J. Paper I: Design and construction of a Knudsen-cell reactor for the study of heterogeneous reactions over the temperature range 130-750 K: Performances and limitations. *Rev. Sci. Instrum.* **1997**, *68*, 3172-3179, doi:10.1063/1.1148263.

Caloz, F.; Fentner, F. F.; Rossi, M. J. Heterogeneous kinetics of the uptake of $ClONO_2$ on NaCl and NaBr. *J. Phys. Chem.* **1996**, *100*, 7494-7501, doi:10.1021/jp953099i.

Caloz, F.; Seisel, S.; Fenter, F. F.; Rossi, M. J. Reactivity of $BrNO_2$ and $ClNO_2$ with solid alkali salt substrates. *J. Phys. Chem. A* **1998**, *102*, 7470-7479, doi:10.1021/jp982000f.

Cappa, C. D.; Kuipers, S. E.; Roberts, J. M.; Gilbert, A. S.; Elrod, M. J. Product identification and kinetics of reactions of HCl with $HNO_3/H_2SO_4/H_2O$ solutions. *J. Phys. Chem. A* **2000**, *104*, 4449-4457, doi:10.1021/jp992666p.

Carlos-Cuellar, S.; Li, P.; Christensen, A. P.; Krueger, B. J.; Burrichter, C.; Grassian, V. H. Heterogeneous uptake kinetics of volatile organic compounds on oxide surfaces using a Knudsen cell reactor: Adsorption of acetic acid, formaldehyde, and methanol on α-Fe_2O_3, α-Al_2O_3, and SiO_2. *J. Phys. Chem. A* **2003**, *107*, 4250-4261, doi:10.1021/jp0267609.

Carpenter, L. J.; MacDonald, S. M.; Shaw, M. D.; Kumar, R.; Saunders, R. W.; Parthipan, R.; Wilson, J.; Plane, J. M. C. Atmospheric iodine levels influenced by sea surface emissions of inorganic iodine. *Nature Geosci.* **2013**, *6*, 108-111, doi:10.1038/NGEO1687.

Carslaw, K. S.; Clegg, S. L.; Brimblecombe, P. A thermodynamic model of the system HCl-HNO_3-H_2SO_4-H_2O, including solubilities of HBr, from <200 to 328 K. *J. Phys. Chem.* **1995**, *99*, 11557-11574, doi:10.1021/j100029a039.

Carslaw, K. S.; Peter, T. Uncertainties in reactive uptake coefficients for solid stratospheric particles-1. Surface chemistry. *Geophys. Res. Lett.* **1997**, *24*, 1743-1746, doi:10.1029/97GL01683.

Chaix, L.; Allanic, A.; Rossi, M. J. Heterogeneous chemistry of HOBr on different types of ice and on ice doped with HC1, HBr, and HNO_3 at 175 K < T < 125 K. *J. Phys. Chem. A* **2000**, *104*, 7268-7277, doi:10.1021/jp001018z.

Cheung, J. L.; Li, Y. Q.; Boniface, J.; Shi, Q.; Davidovits, P.; Worsnop, D.; Jayne, J. T.; Kolb, C. E. Heterogeneous interactions of NO_2 with aqueous surfaces. *J. Phys. Chem. A* **2000**, *104*, 2655-2662, doi:10.1021/jp992929f.

Chu, L.; Chu, L. T. Heterogeneous reaction HOCl + HBr → BrCl + H_2O on ice films. *J. Phys. Chem. A* **1999**, *103*, 691-699, doi:10.1021/jp983407n.

Chu, L.; Diao, G. W.; Chu, L. T. Heterogeneous interaction of SO_2 on H_2O_2-ice films at 190-210 K. *J. Phys. Chem. A* **2000**, *104*, 7565-7573, doi:10.1021/jp001323k.

Chu, L. T.; Diao, G.; Chu, L. Kinetics of HOBr uptake on NaBr and NaCl surfaces at varying relative humidity. *J. Phys. Chem. B* **2002**, *106*, 5679-5688, doi:10.1021/jp013594g.

Chu, L. T.; Leu, M.-T.; Keyser, L. F. Heterogeneous reactions of HOCl + HCl → Cl_2 + H_2O and $ClONO_2$ + HCl → Cl_2 + HNO_3 on ice surfaces at polar stratospheric conditions. *J. Phys. Chem.* **1993**, *97*, 12798-12804, doi:10.1021/j100151a028.

Ciuraru, R.; Gosselin, S.; Visez, N.; Petitprez, D. Heterogeneous reactivity of chlorine atoms with sodium chloride and synthetic sea salt particles. *Phys. Chem. Chem. Phys.* **2011**, *13*, 19460-19470, doi:10.1039/c1cp22170a.

Clegg, S. M.; Abbatt, J. P. D. Oxidation of SO_2 by H_2O_2 on ice surfaces at 228 K: A sink for SO_2 in ice clouds. *Atmos. Chem. Phys.* **2001**, *1*, 73-78, doi:10.5194/acp-1-73-2001.

Colussi, A. J.; Enami, S.; Yabushita, A.; Hoffmann, M. R.; Liu, W.-G.; Mishra, H.; Goddard, W. A., III Tropospheric aerosol as a reactive intermediate. *Faraday Discuss.* **2013**, *165*, 407-420, doi:10.1039/c3fd00040k.

Cooper, P. L.; Abbatt, J. P. D. Heterogeneous interactions of OH and HO_2 radicals with surfaces characertistic of atmospheric particulate matter. *J. Phys. Chem.* **1996**, *100*, 2249-2254, doi:10.1021/jp952142z.

Cosman, L. M.; Bertram, A. K. Reactive uptake of N_2O_5 on aqueous H_2SO_4 solutions coated with 1-component and 2-component monolayers. *J. Phys. Chem. A* **2008**, *112*, 4625-4635, doi:10.1021/jp8005469.

Cosman, L. M.; Knopf, D. A.; Bertram, A. K. N_2O_5 reactive uptake on aqueous sulfuric acid solutions coated with branched and straight-chain insoluble organic surfactants. *J. Phys. Chem. A* **2008**, *112*, 2386-2396, doi:10.1021/jp710685r.

Dai, Q.; Robinson, G. N.; Freedman, A. Reactions of halomethanes with γ-alumina surfaces. I: An infrared spectroscopic study. *J. Phys. Chem. B* **1997**, *101*, 4940-4946, doi:10.1021/jp963015l.

Datta, A.; Cavell, R. G.; Tower, R. W.; George, Z. M. Claus catalysis. 1. Adsorption on the alumina catalyst studied by FTIR and EPR spectroscopy. *J. Phys. Chem.* **1985**, *89*, 443-449, doi:10.1021/j100249a014.

Daumer, B.; Nissner, R.; Klockow, D. Laboratory studies of the influence of their organic films on the neutralization reaction of H_2SO_4 aerosol with ammonia. *J. Aerosol Sci.* **1992**, *23*, 315-325, doi:10.1016/0021-8502(92)90001-C.

Davies, J. A.; Cox, R. A. Kinetics of the heterogeneous reaction of HNO_3 with NaCl: Effect of water vapor. *J. Phys. Chem. A* **1998**, *102*, 7631-7642, doi:10.1021/jp982134t.

De Haan, D. O.; Finlayson-Pitts, B. J. Knudsen cell studies of the reaction of gaseous nitric acid with synthetic sea salt at 298 K. *J. Phys. Chem. A* **1997**, *101*, 9993-9999, doi:10.1021/jp972450s.

Deiber, G.; George, C.; Le Calve, S.; Schweitzer, F.; Mirabel, P. Uptake study of $ClONO_2$ and $BrONO_2$ by halide containing droplets. *Atmos. Chem. Phys.* **2004**, *4*, 1291-1299, doi:10.5194/acp-4-1291-2004.

Diao, G. W.; Chu, L. T. Heterogeneous reactions of HX plus HONO and I_2 on ice surfaces: Kinetics and linear correlations. *J. Phys. Chem. A* **2005**, *109*, 1364-1373, doi:10.1021/jp045965+.

Donaldson, D. J.; Ravishankara, A. R.; Hanson, D. R. Detailed study of HOCl + HCl → Cl_2 + H_2O in sulfuric acid. *J. Phys. Chem. A* **1997**, *101*, 4717-4725, doi:10.1021/jp9633153.

Duncan, J. L.; Schindler, L. R.; Roberts, J. T. A new sulfate-mediated reaction: Conversion of acetone to trimethylbenzene in the presence of liquid sulfuric acid. *Geophys. Res. Lett.* **1998**, *25*, 631-634, doi:10.1029/98GL00250.

Duncan, J. L.; Schindler, L. R.; Roberts, J. T. Chemistry at and near the surface of liquid sulfuric acid: A kinetic, thermodynamic, and mechanistic analysis of heterogeneous reactions of acetone. *J. Phys. Chem. B* **1999**, *103*, 7247-7259, doi:10.1021/jp991322w.

El Zein, A.; Romanias, M. N.; Bedjanian, Y. Kinetics and products of heterogeneous reactions of HONO with Fe_2O_3 and Arizona test dust. *Environ. Sci. Technol.* **2013**, *47*, 6325-6331, doi:10.1021/es400794c.

Elam, J. W.; Nelson, C. E.; Cameron, M. A.; Tolbert, M. A.; George, S. M. Adsorption of H_2O on a single-crystal α-Al_2O_3(0001) surface. *J. Phys. Chem. B* **1998**, *102*, 7008-7015, doi:10.1021/jp981070j.

Elrod, M. J.; Koch, R. E.; Kim, J. E.; Molina, M. S. HCl vapour pressures and reaction probablilities of $ClONO_2$ + HCl on liquid H_2SO_4-HNO_3-HCl-H_2O solutions. *Faraday Discuss.* **1995**, *100*, 269-278, doi:10.1039/fd9950000269.

Enami, S.; Vecitis, C. D.; Cheng, J.; Hoffmann, M. R.; Colussi, A. J. Mass spectrometry of interfacial layers during fast aqueous aerosol/ozone gas reactions of atmospheric interest. *Chem. Phys. Lett.* **2008**, *455*, 316-320, doi:10.1016/j.cplett.2008.02.075.

Esteve, W.; Nozière, B. Uptake and reaction kinetics of acetone, 2-butanone, 2,4-pentanedione, and acetaldehyde in sulfuric acid solutions. *J. Phys. Chem. A* **2005**, *109*, 10920-10928, doi:10.1021/jp051199a.

Fenter, F. F.; Caloz, F.; Rossi, M. J. Kinetics of nitric acid uptake by salt. *J. Phys. Chem.* **1994**, *98*, 9801-9810, doi:10.1021/j100090a014.

Fenter, F. F.; Caloz, F.; Rossi, M. J. Heterogeneous kinetics of N_2O_5 uptake on salt, with a systematic study of the role of surface presentation (for N_2O_5 and HNO_3). *J. Phys. Chem.* **1996**, *100*, 1008-1019, doi:10.1021/jp9503829.

Fenter, F. F.; Rossi, M. J. The heterogeneous kinetics of HONO on H_2SO_4 and on ice: activation of HCl. *J. Phys. Chem.* **1996**, *100*, 13765-13775, doi:10.1021/jp960797+.

Fenter, F. F.; Rossi, M. J. Heterogeneous reaction of NO_3 with ice and sulfuric acid solutions: Upper limits for the uptake coefficients. *J. Phys. Chem. A* **1997**, *101*, 4110-4113, doi:10.1021/jp970162q.

Fernandez, M. A.; Hynes, R. G.; Cox, R. A. Kinetics of $ClONO_2$ reactive uptake on ice surfaces at temperatures of the upper troposphere. *J. Phys. Chem. A* **2005**, *109*, 9986-9996, doi:10.1021/jp053477b.

Fickert, S.; Adams, J. W.; Crowley, J. N. Activation of Br_2 and BrCl via Uptake of HOBr onto Aqueous Salt Solutions. *J. Geophys. Res.* **1999**, *104*, 23719-23727, doi:10.1029/1999JD900359.

Fickert, S.; Helleis, F.; Adams, J. W.; Moortgat, G. K.; Crowley, J. N. Reactive uptake of $ClNO_2$ on aqueous bromide solutions. *J. Phys. Chem. A* **1998**, *102*, 10689-10696, doi:10.1021/jp983004n.

Finlayson-Pitts, B. J. Reaction of NO_2 with NaCl and atmospheric implications of NOCl formation. *Nature* **1983**, *306*, 676-677, doi:10.1038/306676a0.

Finlayson-Pitts, B. J. The tropospheric chemistry of sea salt: A molecular level view of the chemistry of NaCl and NaBr. *Chem. Rev.* **2003**, *103*, 4801-4822, doi:10.1021/cr0206420.

Finlayson-Pitts, B. J.; Ezell, M. J.; Pitts, J. N., Jr. Formation of chemically active chlorine compounds by reactions of atmospheric NaCl particles with gaseous N_2O_5 and $ClONO_2$. *Nature* **1989**, *337*, 241-244, doi:10.1038/337241a0.

Finlayson-Pitts, B. J.; Livingston, F. E.; Berko, H. N. Synthesis and identification by infrared spectroscopy of gaseous nitryl bromide, $BrNO_2$. *J. Phys. Chem.* **1989**, *93*, 4397-4400, doi:10.1021/j100348a005.

Folkers, M.; Mentel, T. F.; Wahner, A. Influence of an organic coating on the reactivity of aqueous aerosols probed by the heterogeneous hydrolysis of N_2O_5. *Geophys. Res. Lett.* **2003**, *30*, 1644, doi:10.1029/2003GL017168.

Frenzel, A.; Scheer, V.; Sikorski, R.; George, C.; Behnke, W.; Zetsch, C. Heterogeneous interconversion reactions of $BrNO_2$, $ClNO_2$, Br_2, and Cl_2. *J. Phys. Chem. A* **1998**, *102*, 1329-1337, doi:10.1021/jp973044b.

Frenzel, A.; Scheer, V.; Sikorski, R.; George, C.; Behnke, W.; Zetzsch, C. Heterogeneous interconversion reactions of $BrNO_2$, $ClNO_2$, Br_2, and Cl_2. *J. Phys. Chem. A* **1998**, *102*, 1329-1337, doi:10.1021/jp973044b.

Fried, A.; Henry, B. E.; Calvert, J. G.; Mozukewich, M. The reaction probability of N_2O_5 with sulfuric acid aerosols at stratospheric temperatures and compositions. *J. Geophys. Res.* **1994**, *99*, 3517-3532, doi:10.1029/93JD01907.

Frinak, E. K.; Abbatt, J. P. D. Br_2 production from the heterogeneous reaction of gas-phase OH with aqueous salt solutions: Impacts of acidity, halide concentration, and organic surfactants. *J. Phys. Chem. A* **2006**, *110*, 10456-10464, doi:10.1021/jp063165o.

Gaston, C. J.; Riedel, T. P.; Zhang, Z. F.; Gold, A.; Surratt, J. D.; Thornton, J. A. Reactive uptake of an isoprene-derived epoxydiol to submicron aerosol particles. *Environ. Sci. Technol.* **2014**, *48*, 11178-11186, doi:10.1021/es5034266.

Gaston, C. J.; Thornton, J. A. Reacto-diffusive length of N_2O_5 in aqueous sulfate- and chloride-containing aerosol particles. *J. Phys. Chem. A.* **2016**, *120*, 1039-1045, doi:10.1021/acs.jpca.5b11914.

Gaston, C. J.; Thornton, J. A.; Ng, N. L. Reactive uptake of N_2O_5 to internally mixed inorganic and organic particles: the role of organic carbon oxidation state and inferred organic phase separations. *Atmos. Chem. Phys.* **2014**, *14*, 5693-5707, doi:10.5194/acp-14-5693-2014.

Gebel, M. E.; Finlayson-Pitts, B. J. Uptake and reaction of $ClONO_2$ on NaCl and synthetic sea salt. *J. Phys. Chem. A* **2001**, *105*, 5178-5187, doi:10.1021/jp0046290.

Gebel, M. E.; Finlayson-Pitts, B. J.; Ganske, J. S. The uptake of SO_2 on synthetic sea salt and some of its components. *Geophys. Res. Lett.* **2000**, *27*, 887-890, doi:10.1029/1999GL011152.

George, C.; Ammann, M.; D'Anna, B.; Donaldson, D. J.; Nizkorodov, S. A. Heterogeneous photochemistry in the atmosphere. *Chem. Rev.,* **2015**, *115*, 4218-4258, doi:10.1021/cr500648z.

George, C.; Behnke, W.; Scheer, V.; Zetsch, C.; Magi, L.; Ponche, J. L.; Mirabel, P. Fate of $ClNO_2$ over aqueous solutions containing iodide. *Geophys. Res. Lett.* **1995**, *22*, 1505-1508, doi:10.1029/95GL01417.

George, C.; Ponche, J. L.; Mirabel, P.; Behnke, W.; Sheer, V.; Zetzsch, C. Study of the uptake of N_2O_5 by water and NaCl solutions. *J. Phys. Chem.* **1994**, *98*, 8780-8784, doi:10.1021/j100086a031.

George, I. J.; Abbatt, J. P. D. Heterogeneous oxidation of atmospheric aerosol particles by gas-phase radicals. *Nature Chem.* **2010**, *2*, 713-722, doi:10.1038/nchem.806.

George, I. J.; Matthews, P. S. J.; Whalley, L. K.; Brooks, B.; Goddard, A.; Baeza-Romero, M. T.; Heard, D. E. Measurements of uptake coefficients for heterogeneous loss of HO_2 onto submicron inorganic salt aerosols. *Phys. Chem. Chem. Phys.* **2013**, *15*, 12829-12845, doi:10.1039/c3cp51831k.

Gershenzon, M. Y.; Il'in, S.; Fedotov, N. G.; Gershenzon, Y. M.; Aparina, E. V.; Zelenov, V. V. The mechanism of reactive NO_3 uptake on dry NaX (X = Cl, Br). *J. Atmos. Chem.* **1999**, *34*, 119-135, doi:10.1023/A:1006258205551.

Gershenzon, Y. M.; Grigorieva, V. M.; Ivanov, A. V.; Remorov, R. G. O_3 and OH sensitivity to heterogeneous sinks of HO_x and CH_3O_2 on aerosol particles. *Faraday Discuss.* **1995**, *100*, 83-100, doi:10.1039/fd9950000083.

Gershenzon, Y. M.; Ivanov, A. V.; Kucheryavyi, S. I.; Rozenshtein, V. B. Anihilation of OH radicals on the surfaces of subtances chemically similar to atmospheric aerosol particles. *Kinet. Katal.* **1986**, *27*, 1069-1074.

Gershenzon, Y. M.; Purmal, A. P. Heterogeneous processes in the Earth's atmosphere and their ecological consequences. *Russ. Chem. Rev.* **1990**, *59*, 1007-1023.

Ghosal, S.; Hemminger, J. C. Effect of water on the HNO_3 pressure dependence of the reaction between gas-phase HNO_3 and NaCl surfaces. *J. Phys. Chem. A* **1999**, *103*, 4777-4781, doi:10.1021/jp991142m.

Ghosal, S.; Hemminger, J. C. Surface adsorbed water on NaCl and its effect on nitric acid reactivity with NaCl powders. *J. Phys. Chem. B* **2004**, *108*, 14102-14108, doi:10.1021/jp047774c.

Ghosal, S.; Shbeeb, A.; Hemminger, J. C. Surface segragation of bromine in bromide doped NaCl: Implications for the seasonal variations in Arctic ozone. *Geophys. Res. Lett.* **2000**, *27*, 1879-1882, doi:10.1029/2000GL011381.

Goodman, A. L.; Bernard, E. T.; Grassian, V. H. Spectroscopic study of nitric acid and water adsorption on oxide particles: Enhanced nitric acid uptake kinetics in the presence of adsorbed water. *J. Phys. Chem. A* **2001**, *105*, 6443-6457, doi:10.1021/jp003722l.

Goodman, A. L.; Li, P.; Usher, C. R.; Grassian, V. H. Heterogeneous uptake of sulfur dioxide on aluminum and magnesium oxide particles. *J. Phys. Chem. A* **2002**, *105*, 6109-6120, doi:10.1021/jp004423z.

Gratpanche, F.; Sawerysyn, J.-P. Uptake coefficients of NO_3 radicals on solid surfaces of sea-salts. *J. Chim. Phys.* **1999**, *96*, 213-231, doi:10.1051/jcp:1999132.

Griffiths, P. T.; Badger, C. L.; Cox, R. A.; Folkers, M.; Henk, H. H.; Mentel, T. F. Reactive uptake of N_2O_5 by aerosols containing dicarboxylic acids. effect of particle phase, composition, and nitrate content. *J. Phys. Chem. A* **2009**, *113*, 5082-5090, doi:10.1021/jp8096814.

Griffiths, P. T.; Cox, R. A. Temperature dependence of heterogeneous uptake of N_2O_5 by ammonium sulfate aerosol. *Atmos. Sci. Lett.* **2009**, *10*, 159-163, doi:10.1002/asl.225.
Gržinić, G.; Bartels-Rausch, T.; Berkemeier, T.; Türler, A.; Ammann, M. Viscosity controls humidity dependence of N_2O_5 uptake to citric acid aerosol. *Atmos. Chem. Phys.* **2015**, *15*, 13615-13625, doi:10.5194/acp-15-13615-2015.
Guan, C.; Li, X.; Luo, Y.; Huang, Z. Heterogeneous reaction of NO_2 on α-Al_2O_3 in the dark and simulated sunlight. *J. Phys. Chem. A* **2014**, *118*, 6999-7006, doi:10.1021/jp503017k.
Guimbaud, C.; Arens, F.; Gutzwiller, L.; Gäggeler, H. W.; Ammann, M. Uptake of HNO_3 to deliquescent sea-salt particles: a study using short-lived radioactive isotope tracer ^{13}N. *Atmos. Chem. Phys.* **2002**, *2*, 249-257, doi:10.5194/acp-2-249-2002.
Haag, W. R.; Hoigné, J. Ozonation of bromide-containing waters: Kinetics of formation of hypobromous acid and bromate. *Environ. Sci. Technol.* **1983**, *17*, 261-267, doi:10.1021/es00111a004.
Haag, W. R.; Hoigné, J. Ozonation of water containing chlorine or chloramines. Reaction products and kinetics. *Water Research* **1983**, *17*, 1397-1402, doi:10.1016/0043-1354(83)90270-1.
Hallquist, M.; Stewart, D. J.; Baker, J.; Cox, R. A. Hydrolysis of N_2O_5 on submicron sulfuric acid aerosols. *J. Phys. Chem. A* **2000**, *104*, 3984-3990, doi:10.1021/jp9939625.
Hallquist, M.; Stewart, D. J.; Stephenson, S. K.; Cox, R. A. Hydrolysis of N_2O_5 on sub-micron sulfate aerosols. *Phys. Chem. Chem. Phys.* **2003**, *5*, 3453-3463, doi:10.1039/b301827j.
Hanisch, F.; Crowley, J. N. Heterogeneous reactivity of gaseous nitric acid on Al_2O_3, $CaCO_3$, and atmospheric dust samples: A Knudsen cell study. *J. Phys. Chem. A* **2001**, *105*, 3096-3106, doi:10.1021/jp001254+.
Hanning-Lee, M. A.; Brady, B. B.; Martin, L. R.; Syage, J. A. Ozone decomposition on alumina: Implications for solid rocket motor exhaust. *Geophys. Res. Lett.* **1996**, *23*, 1961-1964, doi:10.1029/96GL01808.
Hanson, D. Reactivity of $BrONO_2$ and HOBr on sulfuric acid solutions at low temperatures. *J. Geophys. Res.* **2003**, *108*, 4239, doi:10.1029/2002JD002519.
Hanson, D.; Kosciuch, E. The NH_3 mass accommodation coefficient for uptake onto sulfuric acid solutions. *J. Phys. Chem. A* **2003**, *107*, 2199-2208, doi:10.1021/jp021570j.
Hanson, D.; Kosciuch, E. Reply to "Comment on "The NH_3 mass accommodation coefficient for uptake onto sulfuric acid solutions". *J. Phys. Chem. A* **2004**, *108*, 8549-8551, doi:10.1021/jp0311761.
Hanson, D. R. Reactivity of $ClONO_2$ on $H_2{}^{18}O$ ice and organic liquids. *J. Phys. Chem.* **1995**, *99*, 13059-13061, doi:10.1021/j100035a003.
Hanson, D. R. Reaction of $ClONO_2$ with H_2O and HCl in sulfuric acid and $HNO_3/H_2SO_4/H_2O$ mixtures. *J. Phys. Chem. A* **1998**, *102*, 4794-4807, doi:10.1021/jp972767s.
Hanson, D. R.; Burkholder, J. B.; Howard, C. J.; Ravishankara, A. R. Measurement of OH and HO_2 radical uptake coefficients on water and sulfuric acid surfaces. *J. Phys. Chem.* **1992**, *96*, 4979-4985, doi:10.1021/j100191a046.
Hanson, D. R.; Lovejoy, E. R. The uptake of N_2O_5 onto small sulfuric acid particles. *Geophys. Res. Lett.* **1994**, *21*, 2401-2404, doi:10.1029/94GL02288.
Hanson, D. R.; Lovejoy, E. R. The reaction of $ClONO_2$ with submicrometer sulfuric acid aerosol. *Science* **1995**, *267*, 1326-1329, doi:10.1126/science.267.5202.1326.
Hanson, D. R.; Lovejoy, E. R. Heterogeneous reactions in liquid sulfuric Acid: HOCl + HCl as a model system. *J. Phys. Chem.* **1996**, *100*, 6397-6405, doi:10.1021/jp953250o.
Hanson, D. R.; Ravishankara, A. R. The reaction probabilities of $ClONO_2$ and N_2O_5 on 40 to 75% sulfuric acid solutions. *J. Geophys. Res.* **1991**, *96*, 17307-17314, doi:10.1029/91JD01750.
Hanson, D. R.; Ravishankara, A. R. The reaction probabilities of $ClONO_2$ and N_2O_5 on polar stratospheric cloud materials. *J. Geophys. Res.* **1991**, *96*, 5081-5090, doi:10.1029/90JD02613.
Hanson, D. R.; Ravishankara, A. R. Heterogeneous chemistry of HBr and HF. *J. Phys. Chem.* **1992**, *96*, 9441-9446, doi:10.1021/j100202a069.
Hanson, D. R.; Ravishankara, A. R. Investigation of the reactive and nonreactlve processes involving $ClONO_2$ and HCl on water and nitric acid doped ice. *J. Phys. Chem.* **1992**, *96*, 2682-2691, doi:10.1021/j100185a052.
Hanson, D. R.; Ravishankara, A. R. Reaction of $ClONO_2$ with HCl on NAT, NAD, and frozen sulfuric acid and hydrolysis of N_2O_5 and $ClONO_2$ on frozen sulfuric acid. *J. Geophys. Res.* **1993**, *98*, 22931-22936, doi:10.1029/93JD01929.
Hanson, D. R.; Ravishankara, A. R. Response to "Comment on porosities of ice films used to simulate stratospheric cloud surfaces". *J. Phys. Chem.* **1993**, *97*, 2802-2803, doi:10.1021/j100113a054.

Hanson, D. R.; Ravishankara, A. R. Uptake of HCl and HOCl onto sulphuric acid: Solubilities, diffusivities and reaction. *J. Phys. Chem.* **1993**, *97*, 12309-12319, doi:10.1021/j100149a035.

Hanson, D. R.; Ravishankara, A. R. Reactive uptake of $ClONO_2$ onto sulfuric acid due to reaction with HCl and H_2O. *J. Phys. Chem.* **1994**, *98*, 5728-5735, doi:10.1021/j100073a026.

Hanson, D. R.; Ravishankara, A. R. Heterogeneous chemistry of bromine species in sulfuric acid under stratospheric conditions. *Geophys. Res. Lett.* **1995**, *22*, 385-388, doi:10.1029/94GL03379.

Hanson, D. R.; Ravishankara, A. R.; Lovejoy, E. R. Reaction of $BrONO_2$ with H_2O on submicron sulfuric acid aerosol and the implications for the lower stratosphere. *J. Geophys. Res.* **1996**, *101*, 9063-9069, doi:10.1029/96JD00347.

Hanson, D. R.; Ravishankara, A. R.; Solomon, S. Heterogeneous reactions in sulfuric acid aerosols: A framework for model calculations. *J. Geophys. Res.* **1994**, *99*, 3615-3629, doi:10.1029/93JD02932.

Harrison, R. M.; Collins, G. M. Measurements of reaction coefficients of NO_2 and HONO on aerosol particles. *J. Atmos. Chem.* **1998**, *30*, 397-406, doi:10.1023/A:1006094304069.

Hayase, S.; Yabushita, A.; Kawasaki, M.; Enami, S.; Hoffmann, M. R.; Colussi, A. J. Heterogeneous reaction of gaseous ozone with aqueous iodide in the presence of aqueous organic species. *J. Phys. Chem. A* **2010**, *114*, 6016-6021, doi:10.1021/jp101985f.

He, H.; Liu, J.; Mu, Y.; Yu, Y.; Chen, M. Heterogeneous oxidation of carbonyl sulfide on atmospheric particles and alumina. *Environ. Sci. Technol.* **2005**, *39*, 9637-9642, doi:10.1021/es048865q.

Henson, B. F.; Wilson, K. R.; Robinson, J. M. A physical absorption model of the dependence of $ClONO_2$ heterogeneous reactions on relative humidity. *Geophys. Res. Lett.* **1996**, *23*, 1021-1024, doi:10.1029/96GL00871.

Hirokawa, J.; Onaka, K.; Kajii, Y.; Akimoto, H. Heterogeneous processes involving sodium halide particles and ozone: Molecular bromine release in the marine boundary layer in the absence of nitrogen oxides. *Geophys. Res. Lett.* **1998**, *25*, 2449-2452, doi:10.1029/98GL01815.

Hoffman, R. C.; Gebel, M. E.; Fox, B. S.; Finlayson-Pitts, B. J. Knudsen cell studies of the reactions of N_2O_5 and $ClONO_2$ with NaCl: Development and application of a model for estimating available surface areas and corrected uptake coefficients. *Phys. Chem. Chem. Phys.* **2003**, *5*, 1780-1789, doi:10.1039/b301126g.

Hoffman, R. C.; Kaleuati, M.; Finlayson-Pitts, B. J. Knudsen cell studies of the reaction of gaseous HNO_3 with NaCl using less than a single layer of particles at 298 K: A modified mechanism. *J. Phys. Chem. A* **2003**, *107*, 7818-7826, doi:10.1021/jp030611o.

Holmes, N. S.; Adams, J. W.; Crowley, J. N. Uptake and reaction of HOI and $IONO_2$ on frozen and dry NaCl/NaBr surfaces and H_2SO_4. *Phys. Chem. Chem. Phys.* **2001**, *3*, 1679-1687, doi:10.1039/b100247n.

Hu, J. H.; Abbatt, J. P. D. Reaction probabilities for N_2O_5 hydrolysis on sulfuric acid and ammonium sulfate aerosols at room temperature. *J. Phys. Chem. A* **1997**, *101*, 871-878, doi:10.1021/jp9627436.

Hu, J. H.; Shi, Q.; Davidovits, P.; Worsnop, D. R.; Zahniser, M. S.; Kolb, C. E. Reative uptake of Cl_2(g) and Br_2(g) by aqueous surfaces as a function of Br^- and I^- ion concentration: The effect of chemical reaction at the interface. *J. Phys. Chem.* **1995**, *99*, 8768-8776, doi:10.1021/j100021a050.

Huff, A. K.; Abbatt, J. P. D. Gas-phase Br_2 production in heterogeneous reactions of Cl_2, HOCl, and BrCl with halide-ice surfaces. *J. Phys. Chem. A* **2000**, *104*, 7284-7293, doi:10.1021/jp001155w.

Huff, A. K.; Abbatt, J. P. D. Kinetics and product yields in the heterogeneous reactions of HOBr with ice surfaces containing NaBr and NaCl. *J. Phys. Chem. A* **2002**, *106*, 5279-5287, doi:10.1021/jp014296m.

Hunt, S. W.; Roesolová, M.; Wang, W.; Wingen, L. M.; Knipping, E. M.; Tobias, D. J.; Dabdub, D.; Finlayson-Pitts, B. J. Formation of molecular bromine from the reaction of ozone with deliquesced NaBr aerosol: Evidence for interface chemistry. *J. Phys. Chem. A* **2004**, *108*, 11559-11572, doi:10.1021/jp0467346.

Huntzicker, J. J.; Cary, R. A.; Ling, C.-S. Neutralization of sulfuric acid aerosols by ammonia. *Environ. Sci. Technol.* **1980**, *14*, 819-824, doi:10.1021/es60167a009.

Il'in, S. D.; Selikhonovich, V. V.; Gershenson, Y. M.; Rozenshtein, V. B. Study of heterogeneous ozone loss on materials typical of atmospheric aerosol species. *Sov. J. Chem. Phys.* **1991**, *8*, 1858-1880.

Imamura, T.; Rudich, Y.; Talukdar, R. K.; Fox, R. W.; Ravishankara, A. R. Uptake of NO_3 onto water-solutions: Rate coefficient for reaction of NO_3 with cloud water constituents. *J. Phys. Chem.* **1997**, *101*, 2316-2322, doi:10.1021/jp962787e.

Iraci, L. T.; Michelsen, R. R.; Ashbourn, S. F. M.; Rammer, T. A.; Golden, D. M. Uptake of hypobromous acid (HOBr) by aqueous sulfuric acid solutions: low-temperature solubility and reaction. *Atmos. Chem. Phys.* **2005**, *5*, 1577-1587, doi:10.5194/acp-5-1577-2005.

Iraci, L. T.; Riffel, B. G.; Robinson, C. B.; Michelsen, R. R.; Stephenson, R. M. The acid catalyzed nitration of methanol: formation of methyl nitrate via aerosol chemistry. *J. Atmos. Chem.* **2007**, *58*, 253-266, doi:10.1007/s10874-007-9091-9.

Ivanov, A. V.; Gershenzon, Y. M.; Gratpanche, F.; Devolder, P.; Saverysyn, J.-P. Heterogeneous loss of OH on NaCl and NH_4NO_3 at tropospheric temperatures. *Ann. Geophys.* **1996**, *14*, 659-664, doi:10.1007/s00585-996-0659-5.

Jaegle, L.; Webster, C. R.; May, R. D.; Scott, D. C.; Stimpfle, R. M.; Kohn, D. W.; Wennberg, P. O.; Hansico, T. F.; Cohen, R. C.; Proffitt, M. H.; Kelly, K. K.; Elkins, J.; Baumgardner, D.; Dye, J. E.; Wilson, J. C.; Pueschel, R. F.; Chan, K. R.; Salawitch, R. J.; Tuck, A. F.; Hovde, S. J.; Yung, Y. L. Evolution and stoichiometry of heterogeneous processing in the Antarctic stratosphere. *J. Geophys. Res.* **1997**, *102*, 13235-13253, doi:10.1029/97JD00935.

James, A. D.; Moon, D. R.; Feng, W.; Lakey, P. S. J.; Frankland, V. L.; Heard, D. E.; Plane, J. M. C. The uptake of HO_2 on meteoric smoke analogues. *J. Geophys. Res.* **2017**, *122*, 554-565, doi:10.1002/2016JD025882.

Jayne, J. T.; Poschl, U.; Chen, Y.; Dai, D.; Molina, L. T.; Worsnop, D. R.; Kolb, C. E.; Molina, M. J. Pressure and temperature dependence of the gas-phase reaction of SO_3 with H_2O and the heterogeneous reaction of SO_3 with H_2O/H_2SO_4 surfaces. *J. Phys. Chem. A* **1997**, *101*, 10000-10011, doi:10.1021/jp972549z.

Jungwirth, P.; Tobias, D. Molecular structure of salt solutions: A new view of the interface with implications for heterogeneous atmospheric chemistry. *J. Phys. Chem. B* **2001**, *105*, 10468-10472, doi:10.1021/jp012750g.

Jungwirth, P.; Tobias, D. J. Ions at the air/water interface. *J. Phys. Chem. B* **2002**, *106*, 6361-6373, doi:10.1021/jp020242g.

Junkermann, W.; Ibusuki, T. FTIR spectroscopic measurements of surface bond products of nitrogen oxides on aerosol surfaces—Implications for heterogeneous HNO_2 production. *Atmos. Environ.* **1992**, *26A*, 3099-3103, doi:10.1016/0960-1686(92)90466-X.

Kane, S. M.; Timonen, R. S.; Leu, M. T. Heterogeneous chemistry of acetone in sulfuric acid solutions: Implications for the upper troposphere. *J. Phys. Chem. A* **1999**, *103*, 9259-9265, doi:10.1021/jp9926692.

Karge, H. G.; Dalla Lana, I. G. Infrared studies of SO_2 adsorption on a Claus catalyst by selective poisoning of sites. *J. Phys. Chem.* **1984**, *88*, 1538-1543, doi:10.1021/j150652a019.

Karlsson, R.; Ljungstrom, E. Nitrogen dioxide and sea salt particles - A laboratory study. *J. Aerosol Sci.* **1995**, *26*, 39-50, doi:10.1016/0021-8502(94)00098-J.

Katrib, Y.; Deiber, G.; Schweitzer, F.; Mirabel, P.; George, C. Chemical transformation of bromine chloride at the air/water interface. *J. Aerosol Sci.* **2001**, *32*, 893-911, doi:10.1016/S0021-8502(00)00114-2.

Kenner, R. D.; Plumb, I. C.; Ryan, K. R. Laboratory measurements of the loss of ClO on Pyrex, ice and NAT at 183 K. *Geophys. Res. Lett.* **1993**, *20*, 193-196, doi:10.1029/93GL00238.

Keyser, L. F.; Leu, M.-T. Surface areas and porosities of ices used to simulate stratospheric clouds. *J. Colloid Interface Sci.* **1993**, *155*, 137-145, doi:10.1006/jcis.1993.1018.

Keyser, L. F.; Leu, M.-T.; Moore, S. B. Comment on porosities of ice films used to simulate stratospheric cloud surfaces. *J. Phys. Chem.* **1993**, *97*, 2800-2801, doi:10.1021/j100113a053.

Keyser, L. F.; Moore, S. B.; Leu, M. T. Surface reaction and pore diffusion in flow tube reactors. *J. Phys. Chem.* **1991**, *95*, 5496-5502, doi:10.1021/j100167a026.

Kinugawa, T.; Enami, S.; Yabushita, A.; Kawasaki, M.; Hoffmann, M. R.; Colussi, A. J. Conversion of gaseous nitrogen dioxide to nitrate and nitrite on aqueous surfactants. *Phys. Chem. Chem. Phys.* **2011**, *13*, 5144-5149, doi:10.1039/c0cp01497d.

Kirchner, U.; Benter, T.; Schindler, R. N. Experimental verification of gas phase bromine enrichment in reactions of HOBr with sea salt doped ice surfaces. *Phys. Chem. Chem. Phys.* **1997**, *101*, 975-977, doi:10.1002/bbpc.19971010614.

Kleffmann, J.; Becker, K. H.; Wiesen, P. Heterogeneous NO_2 conversion processes on acid surfaces: Possible atmospheric implications. *Atmos. Environ.* **1998**, *32*, 2721-2729, doi:10.1016/S1352-2310(98)00065-X.

Klimovskii, A. O.; Bavin, A. V.; Tkalich, V. S.; Lisachenko, A. A. Interaction of ozone with γ-Al_2O_3 surface. *React. Kinet. Catal. Lett.* **1983**, *23*, 95-98, doi:10.1007/BF02065670.

Knipping, E. M.; Lakin, M. J.; Foster, K. L.; Jungwirth, P.; Tobias, D. J.; Gerber, R. B.; Dabdub, D.; Finlayson-Pitts, B. J. Experiments and simulations of ion-enhanced interfacial chemistry on aqueous NaCl aerosols. *Science* **2000**, *288*, 301-306, doi:10.1126/science.288.5464.301.

Knopf, D. A.; Cosman, L. M.; Mousavi, P.; Mokamati, S.; Bertram, A. K. A novel flow reactor for studying reactions on liquid surfaces coated by organic monolayers: Methods, validation, and initial results. *J. Phys. Chem. A* **2007**, *111*, 11021-11032, doi:10.1021/jp075724c.

Koch, T. G.; Rossi, M. J. Direct measurement of surface residence times: Nitryl chloride and chlorine nitrate on alkali halides at room temperature. *J. Phys. Chem. A* **1998**, *102*, 9193-9201, doi:10.1021/jp982539d.

Koch, T. G.; vandenBergh, H.; Rossi, M. J. A molecular diffusion tube study of N_2O_5 and $HONO_2$ interacting with NaCl and KBr at ambient temperature. *Phys. Chem. Chem. Phys.* **1999**, *1*, 2687-2694, doi:10.1039/A901894H.

Kolb, C. E.; Cox, R. A.; Abbatt, J. P. D.; Ammann, M.; Davis, E. J.; Donaldson, D. J.; Garrett, B. C.; George, C.; Griffiths, P. T.; Hanson, D. R.; Kulmala, M.; McFiggans, G.; Pöschl, U.; Riipinen, I.; Rossi, M. J.; Rudich, Y.; Wagner, P. E.; Winkler, P. M.; Worsnop, D. R.; O' Dowd, C. D. An overview of current issues in the uptake of atmospheric trace gases by aerosols and clouds. *Atmos. Chem. Phys.* **2010**, *10*, 10561-10605, doi:10.5194/acp-10-10561-2010.

Lakey, P. S. J.; Berkemeier, T.; Krapf, M.; Dommen, J.; Steimer, S. S.; Whalley, L. K.; Ingham, T.; Baeza-Romero, M. T.; Pŏschl, U.; Shiraiwa, M.; Ammann, M.; Heard, D. E. The effect of viscosity and diffusion on the HO_2 uptake by sucrose and secondary organic aerosol particles. *Atmos. Chem. Phys.* **2016**, *16*, 13035-13047, doi:10.5194/acp-16-13035-2016.

Lakey, P. S. J.; George, I. J.; Baeza-Romero, M. T.; Whalley, L. K.; Heard, D. E. Organics substantially reduce HO_2 uptake onto aerosols containing transition metal ions. *J. Phys. Chem. A.* **2016**, *120*, 1421-1430, doi:10.1021/acs.jpca.5b06316.

Lakey, P. S. J.; George, I. J.; Whalley, L. K.; Baeza-Romero, M. T.; Heard, D. E. Measurements of the HO_2 uptake coefficients onto single component organic aerosols. *Environ. Sci. Technol.* **2015**, *49*, 4878-4885, doi:10.1021/acs.est.5b00948.

Langenberg, S.; Schurath, U. Ozone destruction on ice. *Geophys. Res. Lett.* **1999**, *26*, 1695-1698, doi:10.1029/1999GL900325.

Langer, S.; Pemberton, R. S.; Finlayson-Pitts, B. J. Diffuse reflectance infrared studies of the reaction of synthetic sea salt mixtures with NO_2. A key role for hydrates in the kinetics and mechanism. *J. Phys. Chem. A* **1997**, *101*, 1277-1286, doi:10.1021/jp962122c.

Laskin, A.; Wang, H.; Robertson, W. H.; Cowin, J. P.; Ezell, M. J.; Finlayson-Pitts, B. J. A new approach to determining gas-particle reaction probabilities and application to the heterogeneous reaction of deliquesced sodium chloride particles with gas-phase hydroxyl radicals. *J. Phys. Chem. A* **2006**, *110*, 10619-10627, doi:10.1021/jp063263+.

Lee, M.-T.; Brown, M. A.; Kato, S.; Kleibert, A.; Türler, A.; Ammann, M. Competition between organics and bromide at the aqueous solution-air interface as seen from ozone uptake kinetics and X-ray photoelectron spectroscopy. *J. Phys. Chem. A.* **2015**, *119*, 4600-4608, doi:10.1021/jp510707s.

Leu, M.-T. Heterogeneous reaction of N_2O_5 with H_2O and HCl on ice surfaces: implications for Antarctic ozone depletion. *Geophys. Res. Lett.* **1988**, *15*, 851-854, doi:10.1029/GL015i008p00851.

Leu, M.-T. Laboratory studies of sticking coefficients and heterogeneous reactions important in the Antarctic stratosphere. *Geophys. Res. Lett.* **1988**, *15*, 17-20, doi:10.1029/GL015i001p00017.

Leu, M.-T.; Moore, S. B.; Keyser, L. F. Heterogeneous reactions of chlorine nitrate and hydrogen chloride on Type I polar stratospheric clouds. *J. Phys. Chem.* **1991**, *95*, 7763-7771, doi:10.1021/j100173a040.

Leu, M.-T.; Timonen, R. S.; Keyser, L. F. Kinetics of the heterogeneous reaction $HNO_3(g) + NaBr(s) \leftrightarrow HBr(g) + NaNO_3(s)$. *J. Phys. Chem. A* **1997**, *101*, 278-282, doi:10.1021/jp9626069.

Leu, M.-T.; Timonen, R. S.; Keyser, L. F.; Yung, Y. L. Heterogeneous reactions of $HNO_3(g) + NaCl(s)$ $HCl(g) + NaNO_3(s)$ and $N_2O_5(g) + NaCl(s)$ $ClNO_2(g) + NaNO_3(s)$. *J. Phys. Chem.* **1995**, *99*, 13203-13212, doi:10.1021/j100035a026.

Li, P.; Perreau, K. A.; Covington, E.; Song, C. H.; Carmichael, G. R.; Grassian, V. H. Heterogeneous reactions of volatile organic compounds on oxide particles of the most abundant crustal elements: Surface reactions of acetaldehyde, acetone, and propionaldehyde on SiO_2, Al_2O_3, Fe_2O_3, TiO_2, and CaO. *J. Geophys. Res.* **2001**, *106*, 5517-5529, doi:10.1029/2000JD900573.

Liu, C.; Ma, Q.; Liu, Y.; Ma, J.; He, H. Synergistic reaction between SO_2 and NO_2 on mineral oxides: a potential formation pathway of sulfate aerosol. *Phys. Chem. Chem. Phys* **2012**, *14*, 1668-1676, doi:10.1039/c1cp22217a.

Liu, J.; Yu, Y.; Mu, Y.; He, H. Mechanism of heterogeneous oxidation ofcarbonyl sulfide on Al_2O_3: an *in situ* diffuse reflectance infrared fourier transform spectroscopy investigation *J. Phys. Chem. B* **2006**, *110*, 3225-3230, doi:10.1021/jp055646y.

Liu, Y.; Cain, J. P.; Wang, H.; Laskin, A. Kinetic study of heterogeneous reaction of deliquesced NaCl particles with gaseous HNO_3 using particle-on-substrate stagnation flow reactor approach. *J. Phys. Chem. A* **2007**, *111*, 10026-10043, doi:10.1021/jp072978p.

Liu, Y.; He, H.; Mu, Y. Heterogeneous reactivity of carbonyl sulfide on α-Al_2O_3 and γ-Al_2O_3. *Atmos. Environ.* **2008**, *42*, 960-969, doi:10.1016/j.atmosenv.2007.10.007.

Liu, Y.; Ma, Q.; He, H. Comparative study of the effect of water on the heterogeneous reactions of carbonyl sulfide on the surface of α-Al_2O_3 and MgO. *Atmos. Chem. Phys.* **2009**, *9*, 6273-6286, doi:10.5194/acp-9-6273-2009.

Livingston, F. E.; Finlayson-Pitts, B. J. The reaction of gaseous N_2O_5 with solid NaCl at 298 K: Estimated lower limit to the reaction probability and its potential role in tropospheric and stratospheric chemistry. *Geophys. Res. Lett.* **1991**, *18*, 17-21, doi:10.1029/90GL02595.

Lo, J. M. H.; Ziegler, T.; Clark, P. D. SO_2 adsorption and transformations on γ-Al_2O_3 surfaces: A density functional theory study. *J. Phys. Chem. C* **2010**, *114*, 10444-10454, doi:10.1021/jp910895g.

Loerting, T.; Voegele, A. F.; Tautermann, C. S.; Liedl, K. R.; Molina, L. T.; Molina, M. J. Modeling the heterogeneous reaction probability for chlorine nitrate hydrolysis on ice. *J. Geophys. Res.* **2006**, *111*, D14307, doi:10.1029/2006JD007065.

Longfellow, C. A.; Imamura, T.; Ravishankara, A. R.; Hanson, D. R. HONO solubility and heterogeneous reactivity on sulfuric acid surfaces. *J. Phys. Chem. A* **1998**, *102*, 3323-3332, doi:10.1021/jp9807120.

Lopez-Hilfiker, F. D.; Constantin, K.; Kercher, J. P.; Thornton, J. A. Temperature dependent halogen activation by N_2O_5 reactions on halide-doped ice surfaces. *Atmos. Chem. Phys.* **2012**, *12*, 5237-5247, doi:10.5194/acp-12-5237-2012.

Loukhovitskaya, E.; Bedjanian, Y.; Morozov, I.; Le Bras, G. Laboratory study of the interaction of HO_2 radicals with the NaCl, NaBr, $MgCl_2$•$6H_2O$ and sea salt surfaces. *Phys. Chem. Chem. Phys.* **2009**, *11*, 7896-7905, doi:10.1039/b906300e.

Lovejoy, E. R.; Huey, L. G.; Hanson, D. R. Atmospheric fate of CF_3OH 2: Heterogeneous reaction. *J. Geophys. Res.* **1995**, *100*, 18775-18780, doi:10.1029/95JD01843.

Luick, T. J.; Heckbert, R. W.; Schultz, K.; Disselkamp, R. S. Nitrosyl and nitryl chloride formation in H_2SO_4/HNO_3/H_2O/HCl solutions at 200 K. *J. Atmos. Chem.* **1999**, *32*, 315-325, doi:10.1023/A:1006152517987.

Ma, Q.; Liu, Y.; He, H. Synergistic effect between NO_2 and SO_2 in their adsorption and reaction on γ-alumina. *J. Phys. Chem. A* **2008**, *112*, 6630-6635, doi:10.1021/jp802025z.

Manion, J. A.; Fittschen, C. M.; Golden, D. M.; Williams, L. R.; Tolbert, M. A. Heterogeneous reactions of chlorine nitrate and dinitrogen pentoxide on sulfuric acid surfaces representative of global stratospheric aerosol particles. *Israel J. Chem.* **1994**, *34*, 355-363.

Martin, L. R.; Judeikis, H. S.; Wun, M. Heterogeneous reactions of Cl and ClO in the stratosphere. *J. Geophys. Res.* **1980**, *85*, 5511-5518, doi:10.1029/JC085iC10p05511.

Matthews, P. S. J.; Baeza-Romero, M. T.; Whalley, L. K.; Heard, D. E. Uptake of HO_2 radicals onto Arizona test dust particles using an aerosol flow tube. *Atmos. Chem. Phys.* **2014**, *14*, 7397-7408, doi:10.5194/acp-14-7397-2014.

McKeachie, J. R.; Appel, M. F.; Kirchner, U.; Schindler, R. N.; Benter, T. Observation of a heterogeneous source of OClO from the reaction of ClO radicals on ice. *J. Phys. Chem. B* **2004**, *108*, 16786-16797, doi:10.1021/jp049314p.

McMurry, P. H.; Takano, H.; Anderson, G. R. Study of the ammonia (gas) - sulfuric acid (aerosol) reaction rate. *Environ. Sci. Technol.* **1983**, *17*, 347-357, doi:10.1021/es00112a008.

McNeill, V. F.; Loerting, T.; Geiger, F. M.; Trout, B. L.; Molina, M. J. Hydrogen chloride-induced surface disordering on ice. *Proc. Nat. Acad. Sci.* **2006**, *103*, 9422-9427, doi:10.1073/pnas.0603494103.

McNeill, V. F.; Patterson, J.; Wolfe, G. M.; Thornton, J. A. The effect of varying levels of surfactant on the reactive uptake of N_2O_5 to aqueous aerosol. *Atmos. Chem. Phys.* **2006**, *6*, 1635-1644, doi:10.5194/acp-6-1635-2006.

Mentel, T. F.; Sohn, M.; Wahner, A. Nitrate effect in the heterogeneous hydrolysis of dinitrogen pentoxide on aqueous aerosols. *Phys. Chem. Chem. Phys.* **1999**, *1*, 5451-5457, doi:10.1039/A905338G.

Mertes, S.; Wahner, A. Uptake of nitrogen dioxide and nitrous acid on aqueous surfaces. *J. Phys. Chem.* **1995**, *99*, 14000-14006, doi:10.1021/j100038a035.

Michel, A. E.; Usher, C. R.; Grassian, V. H. Heterogeneous and catalytic uptake of ozone on mineral oxides and dusts: A Knudsen cell investigation. *Geophys. Res. Lett.* **2002**, *29*, 1665, doi:1029/2002/GL014896.

Michel, A. E.; Usher, C. R.; Grassian, V. H. Reactive uptake of ozone on mineral oxides and mineral dusts. *Atmos. Environ.* **2003**, *37*, 3201-3211, doi:10.1016/S1352-2310(03)00319-4.

Michelsen, R. R.; Ashbourn, S. F. M.; Iraci, L. T. Dissolution, speciation, and reaction of acetaldehyde in cold sulfuric acid. *J. Geophys. Res.* **2004**, *109*, D23205, doi:10.1029/2004JD005041.
Michelsen, R. R.; Staton, S. J. R.; Iraci, L. T. Uptake and dissolution of gaseous ethanol in sulfuric acid. *J. Phys. Chem. A* **2006**, *110*, 6711-6717, doi:10.1021/jp056234s.
Mihelcic, D.; Klemp, D.; Müsgen, P.; Pätz, H. W.; Volz-Thomas, A. Simultaneous measurements of peroxy and nitrate radicals at Schauinsland. *J. Atmos. Chem.* **1993**, *16*, 313-335, doi:10.1007/BF01032628.
Miller, T. M.; Grassian, V. H. Heterogeneous chemistry of NO_2 on mineral oxide particles: Spectroscopic evidence for oxide-coordinated and water-solvated surface nitrate. *Geophys. Res. Lett.* **1998**, *25*, 3835-3838, doi:10.1029/1998GL900011.
Mochida, M.; Akimoto, H.; van den Bergh, H.; Rossi, M. J. Heterogeneous kinetics of the uptake of HOBr on solid alkali metal halides at ambient temperature. *J. Phys. Chem. A* **1998**, *102*, 4819-4828, doi:10.1021/jp980849q.
Mochida, M.; Hirokawa, J.; Akimoto, H. Unexpected large uptake of O_3 on sea salts and the observed Br_2 formation. *Geophys. Res. Lett.* **2000**, *27*, 2629-2632, doi:10.1029/1999GL010927.
Mochida, M.; Hirokawa, J.; Kajii, Y.; Akimoto, H. Heterogeneous reactions of Cl_2 with sea salts at ambient temperature: Implications for halogen exchange in the atmosphere. *Geophys. Res. Lett.* **1998**, *25*, 3927-3930, doi:10.1029/1998GL900100.
Mogili, P. K.; Kleiber, P. D.; Young, M. A.; Grassian, V. H. Heterogeneous uptake of ozone on reactive components of mineral dust aerosol: An environmental aerosol reaction chamber study. *J. Phys. Chem. A* **2006**, *110*, 13799-13807, doi:10.1021/jp063620g.
Molina, M. J.; Meads, R. F.; Spencer, D. D.; Molina, L. T. The reaction of $ClONO_2$ with HCl on aluminum oxide. *Geophys. Res. Lett.* **1997**, *24*, 1619-1622, doi:10.1029/97GL01560.
Molina, M. J.; Tso, T. L.; Molina, L. T.; Wang, F. C. Antarctic stratosheric chemistry of chlorine nitrate, hydrogen chloride, and ice: Release of active chlorine. *Science* **1987**, *238*, 1253-1259, doi:10.1126/science.238.4831.1253.
Moore, S. B.; Keyser, L. F.; Leu, M. T.; Turco, R. P.; Smith, R. H. Heterogeneous reactions on nitric acid trihydrate. *Nature* **1990**, *345*, 333-335, doi:10.1038/345333a0.
Mössinger, J. C.; Cox, R. A. Heterogeneous reaction of HOI with sodium halide salts. *J. Phys. Chem. A* **2001**, *105*, 5165-5177, doi:10.1021/jp0044678.
Mössinger, J. C.; Hynes, R. G.; Cox, R. A. Interaction of HOBr and HCl on ice surfaces in the temperature range 205–227 K. *J. Geophys. Res.* **2002**, *107*, 4740, doi:10.1029/2002JD002151.
Mozurkewich, M.; Calvert, J. Reaction probability of N_2O_5 on aqueous aerosols. *J. Geophys. Res.* **1988**, *93*, 15882-15896, doi:10.1029/JD093iD12p15889.
Msibi, I. M.; Li, Y.; Shi, J. P.; Harrison, R. M. Determination of heterogeneous reaction probability using deposition profile measurement in an annular reactor: application to the N_2O_5/H_2O reaction. *J. Atmos. Chem.* **1994**, *18*, 291-300, doi:10.1007/BF00696784.
Msibi, I. M.; Shi, J. P.; Harrison, R. M. Accommodation coefficient for trace gas uptake using deposition profile measurement in an annular reactor. *J. Atmos. Chem.* **1993**, *17*, 339-351, doi:10.1007/BF00696853.
Oldridge, N. W.; Abbatt, J. P. D. Formation of gas-phase bromine from interaction of ozone with frozen and liquid NaCl/NaBr solutions: Quantitative separation of surficial chemistry from bulk-phase reaction. *J. Phys. Chem. A* **2010**, *115*, 2590-2598, doi:10.1021/jp200074u.
Oppliger, R.; Allanic, A.; Rossi, M. J. Real-time kinetics of the uptake of $ClONO_2$ on ice and in the presence of HCl in the temperature range 160 K ≤ T ≤ 200 K. *J. Phys. Chem. A* **1997**, *101*, 1903-1911, doi:10.1021/jp963065q.
Oum, K. W.; Lakin, M. J.; DeHaan, D. O.; Brauers, T.; Finlayson-Pitts, B. J. Formation of molecular chlorine from the photolysis of ozone and aqueous sea-salf particles. *Science* **1998**, *297*, 74-76, doi:10.1126/science.279.5347.74.
Oum, K. W.; Lakin, M. J.; Finlayson-Pitts, B. J. Bromine activation in the troposphere by the dark reaction of O_3 with seawater ice. *Geophys. Res. Lett.* **1998**, *25*, 3923-3926, doi:10.1029/1998GL900078.
Park, J. H.; Ivanov, A. V.; Molina, M. J. Effect of relative humidity on OH uptake by surfaces of atmospheric importance. *J. Phys. Chem. A* **2008**, *112*, 6968-6977, doi:10.1021/jp8012317.
Park, S.-C.; Burden, D. K.; Nathanson, G. M. The inhibition of N_2O_5 hydrolysis in sulfuric acid by 1-butanol and 1-hexanol surfactant coatings. *J. Phys. Chem. A* **2007**, *111*, 2921-2929, doi:10.1021/jp068228h.
Parkyns, N. D. The influence of thermal pretreatment on the infrared spectrum of carbon dioxide adsorbed on alumina. *J. Phys. Chem.* **1971**, *75*, 526-531, doi:10.1021/j100674a014.
Peters, S. J.; Ewing, G. E. Reaction of NO_2(g) with NaCl(100). *J. Phys. Chem.* **1996**, *100*, 14093-14102, doi:10.1021/jp9603694.

Phillips, G. J.; Thieser, J.; Tang, M.; Sobanski, N.; Schuster, G.; Fachinger, J.; Drewnick, F.; Borrmann, S.; Bingemer, H.; Lelieveld, J.; Crowley, J. N. Estimating N_2O_5 uptake coefficients using ambient measurements of NO_3, N_2O_5, $ClNO_2$ and particle-phase nitrate. *Atmos. Chem. Phys.* **2016**, *16*, 13231-13249, doi:10.5194/acp-16-13231-2016.

Pillar, E. A.; Guzman, M. I.; Rodriguez, J. M. Conversion of iodide to hypoiodous acid and iodine in aqueous microdroplets exposed to ozone. *Environ. Sci. Technol.* **2013**, *47*, 10971-10979, doi:10.1021/es401700h.

Ponche, J. L.; George, C.; Mirabel, P. Mass transfer at the air/water interface: Mass accommodation coefficients of SO_2, HNO_3, NO_2 and NH_3. *J. Atmos. Chem.* **1993**, *16*, 1-21, doi:10.1007/BF00696620.

Pratte, P.; Rossi, M. J. The heterogeneous kinetics of HOBr and HOCl on acidified sea salt and model aerosol at 40-90% relative humidity and ambient temperature. *Phys. Chem. Chem. Phys.* **2006**, *8*, 3988-4001, doi:10.1039/b604321f.

Quinlan, M. A.; Reihs, C. M.; Golden, D. M.; Tolbert, M. A. Heterogeneous reactions on model polar stratospheric cloud surfaces: Reaction of N_2O_5 on ice and nitric acid trihydrate. *J. Phys. Chem.* **1990**, *94*, 3255-3260, doi:10.1021/j100371a007.

Rattigan, O. V.; Boniface, J.; Swartz, E.; Davidovits, P.; Jayne, J. T.; Kolb, C. E.; Worsnop, D. R. Uptake of gas-phase SO_2 in aqueous sulfuric acid: Oxidation by H_2O_2, O_3, and HONO. *J. Geophys. Res.* **2000**, *105*, 29065-29078, doi:10.1029/2000JD900372.

Reeser, D. I.; Donaldson, D. J. Influence of water surface properties on the heterogeneous reaction between $O_{3(g)}$ and $I^-_{(aq)}$. *Atmos. Environ.* **2011**, *45*, 6116-6120, doi:10.1016/j.atmosenv.2011.08.042.

Remorov, R. G.; Gershenzon, Y. M.; Molina, L. T.; Molina, M. J. Kinetics and mechanism of HO_2 uptake on solid NaCl. *J. Phys. Chem. A* **2002**, *106*, 4558-4565, doi:10.1021/jp013179o.

Riedel, T. P.; Bertram, T. H.; Ryder, O. S.; Liu, S.; Day, D. A.; Russell, L. M.; Gaston, C. J.; Prather, K. A.; Thornton, J. A. Direct N_2O_5 reactivity measurements at a polluted coastal site. *Atmos. Chem. Phys.* **2012**, *12*, 2959-2968, doi:10.5194/acp-12-2959-2012.

Riedel, T. P.; Lin, Y.-H.; Budisulistiorini, S. H.; Gaston, C. J.; Thornton, J. A.; Zhang, Z.; Vizuete, W.; Gold, A.; Surratt, J. D. Heterogeneous reactions of isoprene-derived epoxides: Reaction probabilities and molar secondary organic aerosol yield estimates. *Environ. Sci. Technol. Lett.* **2015**, *2*, 38-42, doi:10.1021/ez500406f.

Robbins, R. C.; Cadle, R. D. Kinetics of the reaction between gaseous ammonia and sulfuric acid droplets in an aerosol. *J. Phys. Chem.* **1958**, *62*, 469-471, doi:10.1021/j150562a025.

Roberts, J. M.; Osthoff, H. D.; Brown, S. S.; Ravishankara, A. R. N_2O_5 oxidizes chloride to Cl_2 in acidic atmospheric aerosol. *Science* **2008**, *321*, 1059-1059, doi:10.1126/science.1158777.

Robinson, G. N.; Dai, Q.; Freedman, A. Reaction of halomethanes on y-alumina surfaces. II: X-ray photoelectron and temperature programmed reaction spectroscopy studies. *J. Phys. Chem. B* **1997**, *101*, 4947-4953, doi:10.1021/jp963016d.

Robinson, G. N.; Freedman, A.; Kolb, C. E.; Worsnop, D. R. Decomposition of halomethanes on α-alumina at stratospheric temperatures. *Geophys. Res. Lett.* **1994**, *21*, 377-380, doi:10.1029/94GL00034.

Robinson, G. N.; Freedman, A.; Kolb, C. E.; Worsnop, D. R. Correction to decomposition of halomethanes on α-alumina at stratospheric temperatures. *Geophys. Res. Lett.* **1996**, *23*, 317, doi:10.1029/95GL03809.

Robinson, G. N.; Worsnop, D. R.; Jayne, J. T.; Kolb, C. E.; Davidovits, P. Heterogeneous uptake of $ClONO_2$ and N_2O_5 by sulfuric acid solutions. *J. Geophys. Res.* **1997**, *102*, 3583-3601, doi:10.1029/96JD03457.

Robinson, G. N.; Worsnop, D. R.; Jayne, J. T.; Kolb, C. E.; Swartz, E.; Davidovits, P. Heterogeneous uptake of HCl by sulfuric acid solutions. *J. Geophys. Res.* **1998**, *103*, 25371-25381, doi:10.1029/98JD02085.

Romanias, M. N.; El Zein, A.; Bedjanian, Y. Reactive uptake of HONO on aluminum oxide surface. *J. Photochem. Photobiol. A: Chem.* **2012**, *250*, 50-57, doi:10.1016/j.photochem.2012.09.018.

Romanias, M. N.; El Zein, A.; Bedjanian, Y. Uptake of hydrogen peroxide on the surface of Al_2O_3 and Fe_2O_3. *Atmos. Environ.* **2013**, *77*, 1-8, doi:10.1016/j.atmosenv.2013.04.065.

Roscoe, J. M.; Abbatt, J. P. D. Diffuse reflectance FTIR study of the interaction of alumina surfaces with ozone and water vapor. *J. Phys. Chem. A* **2005**, *109*, 9028-9034, doi:10.1021/jp050766r.

Rossi, M. J. Heterogeneous reactions on salts. *Chem. Rev.* **2003**, *103*, 4823-4882, doi:10.1021/cr020507n.

Rossi, M. J.; Malhotra, R.; Golden, D. M. Heterogeneous chemical reaction of chlorine nitrate and water on sulfuric-acid surfaces at room temperature. *Geophys. Res. Lett.* **1987**, *14*, 127-130, doi:10.1029/GL014i002p00127.

Rouvière, A.; Ammann, M. The effect of fatty acid surfactants on the uptake of ozone to aqueous halogenide particles. *Atmos. Chem. Phys.* **2010**, *10*, 11489-11500, doi:10.5194/acp-10-11489-2010.

Ruan, M.; Hou, H.; Li, W.; Wang, B. Theoretical study of the adsorptive/dissociation reactions of formic acid on the α-Al_2O_3 (0001) surface. *J. Phys. Chem. C* **2014**, *118*, 20889-20898, doi:10.1021/jp504542n.

Rubasinghege, G.; Grassian, V. H. Photochemistry of adsorbed nitrate on aluminum oxide particle surfaces. *J. Phys. Chem. A* **2009**, *113*, 7818-7825, doi:10.1021/jp902252s.

Rubasinghege, G.; Ogden, S.; Baltrusaitis, J.; Grassian, V. H. Heterogeneous uptake and adsorption of gas-phase formic acid on oxide and clay particle surfaces: The roles of surface hydroxyl groups and adsorbed water in formic acid adsorption and the impact of formic acid adsorption on water uptake. *J. Phys. Chem. A* **2013**, *112*, 11316-11327, doi:10.1021/jp408169w.

Rubel, G. O.; Gentry, J. W. Investigation of the reaction between single aerosol acid droplets and ammonia gas. *J. Aerosol Sci.* **1984**, *15*, 661-671, doi:10.1016/0021-8502(84)90004-1.

Rudich, Y.; Talukdar, R. K.; Imamura, T.; Fox, R. W.; Ravishankara, A. R. Uptake of NO_3 on KI solutions: Rate coefficient for the $NO_3 + I^-$ reaction and gas-phase diffusion coefficient for NO_3. *Chem. Phys. Lett.* **1996**, *261*, 467-473, doi:10.1016/0009-2614(96)00980-3.

Rudich, Y.; Talukdar, R. K.; Ravishankara, A. R.; Fox, R. W. Reactive uptake of NO_3 on pure water and ionic solutions. *J. Geophys. Res.* **1996**, *101*, 21023-21031, doi:10.1029/96JD01844.

Ryder, O. S.; Ault, A. P.; Cahill, J. F.; Guasco, T. L.; Riedel, T. P.; Cuadra-Rodriguez, L. A.; Gaston, C. J.; Fitzgerald, E.; Lee, C.; Prather, K. A.; Bertram, T. H. On the role of particle inorganic mixing atate in the reactive uptake of N_2O_5 to ambient aerosol particles. *Environ. Sci. Technol.* **2014**, *48*, 1618-1627, doi:10.1021/es4042622.

Ryder, O. S.; Campbell, N. R.; Morris, H.; Forestieri, S.; Ruppel, M. J.; Cappa, C.; Tivanski, A.; Prather, K.; Bertram, T. H. Role of organic coatings in regulating N_2O_5 reactive uptake to sea spray aerosol. *J. Phys. Chem. A.* **2015**, *119*, 11683-11692, doi:10.1021/acs.jpca.5b08892.

Saastad, O. W.; Ellerman, T.; Nielson, C. J. On the adsorption of NO and NO_2 on cold H_2O/H_2SO_4 surfaces. *Geophys. Res. Lett.* **1993**, *20*, 1191-1193, doi:10.1029/93GL01621.

Sakamoto, Y.; Yabushita, A.; Kawasaki, M.; Enami, S. Direct emission of I_2 molecule and IO radical from the heterogeneous reactions of gaseous ozone with aqueous potassium iodide Solution. *J. Phys. Chem. A* **2009**, *113*, 7707-7713, doi:10.1021/jp903486u.

Sandanaga, Y.; Hirokawa, J.; Akimoto, H. Formation of molecular chlorine in dark condition: Heterogeneous reaction of ozone with sea salt in the presence of ferric ion. *Geophys. Res. Lett.* **2001**, *28*, 4433-4436, doi:10.1029/2001GL013722.

Santschi, C.; Rossi, M. J. The heterogeneous interaction of Br_2, Cl_2 and Cl_2O with solid KBr and NaCl substrates: The role of adsorbed H_2O and halogens. *Phys. Chem. Chem. Phys.* **2004**, *6*, 3447-3460, doi:10.1039/b404415k.

Saul, T. D.; Tolocka, M. P.; Johnston, M. V. Reactive uptake of nitric acid onto sodium chloride aerosols across a wide range of relative humidities. *J. Phys. Chem. A* **2006**, *110*, 7614-7620, doi:10.1021/jp060639a.

Scheer, V.; Frenzel, A.; Behnke, W.; Zetsch, C.; Magi, L.; George, C.; Mirabel, P. Uptake of nitrosyl chloride (NOCl) by aqueous solutions. *J. Phys. Chem. A* **1997**, *101*, 9359-9366, doi:10.1021/jp972143m.

Schroeder, W. H.; Urone, P. Formation of nitrosyl chloride from salt particles in air. *Environ. Sci. Technol.* **1974**, *8*, 756-758, doi:10.1021/es60093a015.

Schütze, M.; Herrmann, H. Determination of phase transfer parameters for the uptake of HNO_3, N_2O_5 and O_3 on single aqueous drops. *Phys. Chem. Chem. Phys.* **2002**, *4*, 60-67, doi:10.1039/b106078n.

Schütze, M.; Herrmann, H. Uptake of the NO_3 radical on aqueous surfaces. *J. Atmos. Chem.* **2005**, *52*, 1-18, doi:10.1007/s10874-005-6153-8.

Schweitzer, F.; Mirabel, P.; George, C. Multiphase chemistry of N_2O_5, $ClNO_2$ and $BrNO_2$. *J. Phys. Chem. A* **1998**, *102*, 3942-3952, doi:10.1021/jp980748s.

Schweitzer, F.; Mirabel, P.; George, C. Heterogeneous chemistry of nitryl halides in relation to tropospheric halogen activation. *J. Atmos. Chem.* **1999**, *34*, 101-117, doi:10.1023/A:1006249921480.

Seisel, S.; Börensen, C.; Vogt, R.; Zellner, R. The heterogeneous reaction of HNO_3 on mineral dust and γ-alumina surfaces: a combined Knudsen cell and DRIFTS study. *Phys. Chem. Chem. Phys.* **2004**, *6*, 5498-5508, doi:10.1039/b410793d.

Seisel, S.; Caloz, F.; Fenter, F. F.; vandenBergh, H.; Rossi, M. J. The heterogeneous reaction of NO_3 with NaCl and KBr: A nonphotolytic source of halogen atoms. *Geophys. Res. Lett.* **1997**, *24*, 2757-2760, doi:10.1029/97GL02857.

Seisel, S.; Fluckiger, B.; Caloz, F.; Rossi, M. J. Heterogeneous reactivity of the nitrate radical: Reactions on halogen salt at ambient temperature and on ice in the presence of HX (X = Cl, Br, I) at 190 K. *Phys. Chem. Chem. Phys.* **1999**, *1*, 2257-2266, doi:10.1039/A809355E.

Seisel, S.; Fluckiger, B.; Rossi, M. J. The heterogeneous reaction of N_2O_5 with HBr on ice: Comparison with N_2O_5 + HC1. *Ber. Bunsenges. Phys. Chem.* **1998**, *102*, 811-820, doi:10.1002/bbpc.19981020604.

Seisel, S.; Keil, T.; Lian, Y.; Zellner, R. Kinetics of the uptake of SO_2 on mineral oxides: Improved initial uptake coefficients at 298 K from pulsed Knudsen cell experiments. *Int. J. Chem. Kinet.* **2006**, *38*, 242-249, doi:10.1002/kin.20148.

Seisel, S.; Rossi, M. J. The heterogeneous reaction of HONO and HBr on ice and on sulfuric acid. *Ber. Bunsenges. Phys. Chem.* **1997**, *101*, 943-955, doi:10.1002/bbpc.19971010609.

Shaka, H.; Robertson, W. H.; Finlayson-Pitts, B. J. A new approach to studying aqueous reactions using diffuse reflectance infrared Fourier transform spectrometry: application to the uptake and oxidation of SO_2 on OH-processed model sea salt aerosol. *Phys. Chem. Chem. Phys.* **2007**, *9*, 1980-1990, doi:10.1039/b612624c.

Shaloski, M. A.; Gord, J. R.; Staudt, S.; Quinn, S. L.; Bertram, T. H.; Nathanson, G. M. Reactions of N_2O_5 with salty and surfactant-coated glycerol: Interfacial conversion of Br- to Br_2 mediated by alkylammonium cations. *J. Phys. Chem. A.* **2017**, *121*, 3708-3719, doi:10.1021/acs.jpca.7b02040.

Shaw, M. D.; Carpenter, L. J. Modification of ozone deposition and I_2 emissions at the air—aqueous interface by dissolved organic carbon of marine origin. *Environ. Sci. Technol.* **2013**, *47*, 10947-10954, doi:10.1021/es4011459.

Shi, Q.; Davidovits, P.; Jayne, J. T.; Kolb, C. E.; Worsnop, D. R. Kinetic model for reaction of $ClONO_2$ with H_2O and HCl and HOCl with HCl in sulfuric acid solutions. *J. Geophys. Res.* **2001**, *106*, 24259-24274, doi:10.1029/2000JD000181.

Sjostedt, S. J.; Abbatt, J. P. D. Release of gas-phase halogens from sodium halide substrates: heterogeneous oxidation of frozen solutions and desiccated salts by hydroxyl radicals. *Environ. Res. Lett.* **2008**, *3*, 045007, doi:10.1088/1748-9326/3/4/045007.

Sosedova, Y.; Rouviére, A.; Gäggeler, H. W.; Ammann, M. Uptake of NO_2 to deliquesced dihydroxybenzoate aerosol particles. *J. Phys. Chem. A* **2009**, *113*, 10979-10987, doi:10.1021/jp9050462.

Stemmler, K.; Vlasenko, A.; Guimbaud, C.; Ammann, M. The effect of fatty acid surfactants on the uptake of nitric acid to deliquesced NaCl aerosol. *Atmos. Chem. Phys.* **2008**, *8*, 5127-5141, doi:10.5194/acp-8-5127-2008.

Stewart, D. J.; Griffiths, P. T.; Cox, R. A. Reactive uptake coefficients for heterogeneous reacton of N_2O_5 with submicron aerosols of NaCl and natural sea salt. *Atmos. Chem. Phys.* **2004**, *4*, 1381-1388, doi:10.5194/acp-4-1381-2004.

Sullivan, R. C.; Thornberry, T.; Abbatt, J. P. D. Ozone decomposition kinetics on alumina: effects of ozone partial pressure, relative humidity and repeated oxidation cycles. *Atmos. Chem. Phys.* **2004**, *4*, 1301-1310, doi:10.5194/acp-4-1301-2004.

Sverdrup, G. M.; Kuhlman, M. R. "Heterogeneous Nitrogen Oxide-Particle Reactions"; 14th International Colloquium on Atmospheric Pollution, 1980, Paris.

Swartz, E.; Shi, Q.; Davidovits, P.; Jayne, J. T.; Worsnop, D.; Kolb, C. E. Uptake of gas-phase ammonia. 2. Uptake by sulfuric acid surfaces. *J. Phys. Chem. A* **1999**, *103*, 8824-8833, doi:10.1021/jp991697h.

Szanyi, J.; Kwak, J. H. Dissecting the steps of CO_2 reduction: 1. The interaction of CO and CO_2 with γ-Al_2O_3: an *in situ FTIR* study. *Phys. Chem. Chem. Phys.* **2014**, *16*, 15117-15125, doi:10.1039/c4cp00616j.

Szanyi, J.; Kwak, J. H.; Chimentao, R. J.; Peden, C. H. F. Effect of H_2O on the adsorption of NO_2 on γ-Al_2O_3: an in situ FTIR/MS study. *J. Phys. Chem. C* **2007**, *111*, 2661-2669, doi:10.1021/jp066326x.

Taketani, F.; Kanaya, Y.; Akimoto, H. Kinetics of heterogeneous reactions of HO_2 radical at ambient concentration levels with $(NH_4)_2SO_4$ and NaCl aerosol particles. *J. Phys. Chem. A* **2008**, *112*, 2370-2377, doi:10.1021/jp0769936.

Taketani, F.; Kanaya, Y.; Akimoto, H. Heterogeneous loss of HO_2 by KCl, synthetic sea salt, and natural seawater aerosol particles. *Atmos. Environ.* **2009**, *43*, 1660-1665, doi:10.1016/j.atmosenv.2008.12.010.

Taketani, F.; Kanaya, Y.; Akimoto, H. Kinetic studies of heterogeneous reaction of HO_2 radical by dicarboxylic acid particles. *Int. J. Chem. Kinet.* **2013**, *45*, 560-565, doi:10.1002/kin.20783.

Taketani, F.; Kanaya, Y.; Pochanart, P.; Liu, Y.; Li, J.; Okuzawa, K.; Kawamura, K.; Wang, Z.; Akimoto, H. Measurement of overall uptake coefficients for HO_2 radicals by aerosol particles sampled from ambient air at Mts. Tai and Mang (China). *Atmos. Chem. Phys.* **2012**, *12*, 11907-11916, doi:10.5194/acp-12-11907-2012.

Tang, I. N.; Lee, J. H. In *The Chemistry of Acid Rain*; Gordon, G. E., Johnson, R. W., Eds.; Am. Chem. Soc. Symp. Series, 1987; pp 109-117.

Tang, M. J.; Schuster, G.; Crowley, J. N. Heterogeneous reaction of N_2O_5 with illite and Arizona test dust particles. *Atmos. Chem. Phys.* **2014**, *14*, 245-254, doi:10.5194/acp-14-245-2014.

Thomas, K.; Volz-Thomas, A.; Mihelcic, D.; Smit, H. G. J.; Kley, D. On the exchange of NO_3 radicals with aqueous solutions: Solubility and sticking coefficient. *J. Atmos. Chem.* **1998**, *29*, 17-43, doi:10.1023/A:1005860312363.

Thornton, J. A.; Abbatt, J. P. D. Measurements of HO_2 uptake to aqueous aerosol: Mass accommodation coefficients and net reactive loss. *J. Geophys. Res.* **2005**, *110*, D08309, doi:10.1029/2004JD005402.

Thornton, J. A.; Abbatt, J. P. D. N_2O_5 reaction on submicron sea salt aerosol: Kinetics, products, and the effect of surface active organics. *J. Phys. Chem. A* **2005**, *109*, 10004-10012, doi:10.1021/Jp054183t.

Thornton, J. A.; Braban, C. F.; Abbatt, J. P. D. N_2O_5 hydrolysis on sub-micron organic aerosols: the effect of relative humidity, particle phase, and particle size. *Phys. Chem. Chem. Phys.* **2003**, *5*, 4593-4603, doi:10.1039/b307498f.

Thornton, J. A.; Jaeglé, L.; McNeil, V. F. Assessing known pathways for HO_2 loss in aqueous atmospheric aerosols: Regional and global impacts on tropospheric oxidants. *J. Geophys. Res.* **2008**, *113*, D05303, doi:10.1029/2007JD009236.

Timonen, R. S.; Chu, L. T.; Leu, M.-T.; Keyser, L. F. Heterogeneous reaction of $ClONO_2(g) + NaCl(s) \rightarrow Cl_2(g) + NaNO_3(s)$. *J. Phys. Chem.* **1994**, *98*, 9509-9517, doi:10.1021/j100089a025.

Timonen, R. S.; Leu, M.-T. Interaction of ethyl alcohol vapor with sulfuric acid solutions. *J. Phys. Chem. A* **2006**, *110*, 6660-6666, doi:10.1021/jp055810h.

Tolbert, M. A.; Rossi, M. J.; Golden, D. M. Antarctic ozone depletion chemistry: Reactions of N_2O_5 with H_2O and HCl on ice surfaces. *Science* **1988**, *240*, 1018-1021, doi:10.1126/science.240.4855.1018.

Tolbert, M. A.; Rossi, M. J.; Golden, D. M. Heterogeneous interactions of chlorine nitrate, hydrogen chloride and nitric acid with sulfuric acid surfaces at stratospheric temperatures. *Geophys. Res. Lett.* **1988**, *15*, 847-850, doi:10.1029/GL015i008p00847.

Tolbert, M. A.; Rossi, M. J.; Malhotra, R.; Golden, D. M. Reaction of chlorine nitrate with hydrogen chloride and water at Antarctic stratospheric temperatures. *Science* **1987**, *238*, 1258-1260, doi:10.1126/science.238.4831.1258.

Tolocka, M.; Saul, T. D.; Johnston, M. V. Reactive uptake of nitric acid into aqueous sodium chloride droplets using real-time single-particle mass spectrometry. *J. Phys. Chem. A* **2004**, *108*, 2659-2665, doi:10.1021/jp036612y.

Tong, S. R.; Wu, L. Y.; Ge, M. F.; Wang, W. G.; Pu, Z. F. Heterogeneous chemistry of monocarboxylic acids on α-Al_2O_3 at different relative humidities. *Atmos. Chem. Phys.* **2010**, *10*, 7561-7574, doi:10.5194/acp-10-7561-2010.

Underwood, G. M.; Li, P.; Al-Abadleh, H. A.; Grassian, V. H. A Knudsen cell study of the heterogeneous reactivity of nitric acid on oxide and mineral dust particles. *J. Phys. Chem. A* **2001**, *105*, 6609-6620, doi:10.1021/jp002223h.

Underwood, G. M.; Li, P.; Usher, C. R.; Grassian, V. H. Determining accurate kinetic parameters of potentially important heterogeneous atmospheric reactions on solid particle surfaces with a Knudsen cell reactor. *J. Phys. Chem. A* **2000**, *104*, 819-829, doi:10.1021/jp9930292.

Underwood, G. M.; Miller, T. M.; Grassian, V. H. Transmission FT-IR and Knudsen cell study of the heterogeneous reactivity of gaseous nitrogen dioxide on mineral oxide particles. *J. Phys. Chem. A* **1999**, *103*, 6184-6190, doi:10.1021/jp991586i.

Underwood, G. M.; Song, C. H.; Phadnis, M.; Carmichael, G. R.; Grassian, V. H. Heterogeneous reactions of NO_2 and HNO_3 on oxides and mineral dust: A combined laboratory and modeling study. *J. Geophys. Res.* **2001**, *106*, 18055-18066, doi:10.1029/2000JD900552.

Usher, C. R.; Al-Hosney, H.; Carlos-Cuellar, S.; Grassian, V. H. A laboratory study of the heterogeneous uptake and oxidation of sulfur dioxide on mineral dust particles. *J. Geophys. Res.* **2002**, *107*, 4713, doi:10.1029/2002JD002051.

Usher, C. R.; Michel, A. E.; Stec, D.; Grassian, V. H. Laboratory studies of ozone uptake on processed mineral dust. *Atmos. Environ.* **2003**, *37*, 5337-5347, doi:10.1016/j.atmosenv.2003.09.014.

Van Doren, J. M.; Watson, L. R.; Davidovits, P.; Worsnop, D. R.; Zahniser, M. S.; Kolb, C. E. Temperature dependence of the uptake coefficients of HNO_3, HCl, and N_2O_5 by water droplets. *J. Phys. Chem.* **1990**, *94*, 3265-3269, doi:10.1021/j100371a009.

Van Loon, L.; Allen, H. C. Uptake and surface reaction of methanol by sulfuric acid solutions investigated by vibrational sum frequency generation and Raman spectroscopies. *J. Phys. Chem. A* **2008**, *112*, 7873 (7878), doi:10.1021/jp712134s.

Villalta, P. W.; Lovejoy, E. R.; Hanson, D. R. Reaction probability of peroxyacetyl radical on aqueous surfaces. *Geophys. Res. Lett.* **1996**, *23*, 1765-1768, doi:10.1029/96GL01286.

Vogt, R.; Elliott, C.; Allen, H. C.; Laux, J. M.; Hemminger, J. C.; Finlayson-Pitts, B. J. Some new laboratory approaches to studying tropospheric heterogeneous reactions. *Atmos. Environ.* **1996**, *30*, 1729-1737, doi:10.1016/1352-2310(95)00392-4.

Vogt, R.; Finlayson-Pitts, B. A diffuse reflectance infrared Fourier transform spectroscopic (DRIFTS) study of the surface reaction of NaCl with gaseous NO_2 and HNO_3. *J. Phys. Chem.* **1994**, *98*, 3747-3755, doi:10.1021/j100065a033.

Vogt, R.; Finlayson-Pitts, B. F. Tropospheric HONO and reactions of oxides of nitrogen with NaCl. *Geophys. Res. Lett.* **1994**, *21*, 2291-2294, doi:10.1029/94GL02238.

Vogt, R.; Finlayson-Pitts, B. J. Errata. *J. Phys. Chem.* **1995**, *99*, 13052, doi:10.1021/j100034a057.

Wachsmuth, M.; Gäggeler, H. W.; von Glasow, R.; Ammann, M. Accommodation coefficient of HOBr on deliquescent sodium bromide aerosol particles. *Atmos. Chem. Phys.* **2002**, *2*, 121-131, doi:10.5194/acp-2-121-2002.

Wagner, N. L.; Riedel, T. P.; Young, C. J.; Bahreini, R.; Brock, C. A.; Dubé, W. P.; Kim, S.; Middlebrook, A. M.; Oztürk, F.; Roberts, J. M.; Russo, R.; Sive, B.; Swarthout, R.; Thornton, J. A.; VandenBoer, T. C.; Zhou, Y.; Brown, S. S. N_2O_5 uptake coefficients and nocturnal NO_2 removal rates determined from ambient wintertime measurements. *J. Geophys. Res.* **2013**, *118*, 9331-9350, doi:10.1002/jgrd.50653.

Wagner, R.; Naumann, K.-H.; Mangold, A.; Möhler, O.; Saathoff, H.; Schurath, U. Aerosol chamber study of optical constants and N_2O_5 uptake on supercooled $H_2SO_4/H_2O/HNO_3$ solution droplets at polar stratospheric cloud temperatures. *J. Phys. Chem. A* **2005**, *109*, 8140-8148, doi:10.1021/jp0513364.

Wahner, A.; Mentel, T. F.; Sohn, M.; Stier, J. Heterogeneous reaction of N_2O_5 on sodium nitrate aerosol. *J. Geophys. Res.* **1998**, *103*, 31103-31112, doi:10.1029/1998JD100022.

Wang, W.-g.; Ge, M.-f.; Sun, Q. Heterogeneous uptake of hydrogen peroxide on mineral oxides. *Chin. J. Chem. Phys.* **2011**, *24*, 515-520, doi:10.1088/1674-0068/24/05/515-520.

Waschewsky, G. C. G.; Abbatt, J. P. D. HOBr in sulfuric acid solution: solubility and reaction as a function of temperature and concentration. *J. Phys. Chem. A* **1999**, *103*, 5312-5320, doi:10.1021/jp984489i.

Winkler, T.; Goschnick, J.; Ache, H. J. Reactions of nitrogen oxides with NaCl as a model of sea salt aerosol. *J. Aerosol Sci.* **1991**, *22*, S605-S608, doi:10.1016/S0021-8502(05)80174-0.

Worsnop, D. R.; Williams, L. R.; Kolb, C. E.; Mozurkewich, M.; Gershenzon, M.; Davidovits, P. Comment on "The NH_3 mass accommodation coefficient for uptake onto sulfuric acid solution". *J. Phys. Chem. A* **2004**, *108*, 8546-8548, doi:10.1021/jp036519+.

Wren, S. N.; Kahan, T. F.; Jumaa, K. B.; Donaldson, D. J. Spectroscopic studies of the heterogeneous reaction between O_3(g) and halides at the surface of frozen salt solutions. *J. Geophys. Res.* **2010**, *115*, D16309, doi:10.1029/2010JD013929.

Wu, L.; Tong, S.; Ge, M. Heterogeneous reaction of NO_2 on Al_2O_3: The effect of temperature on the nitrite and nitrate formation. *J. Phys. Chem. A* **2013**, *117*, 4937-4944, doi:10.1021/jp402773c.

Wu, L.-Y.; Tong, S.-R.; Hou, S.-Q.; Ge, M.-F. Influence of temperature on the heterogeneous reaction of formic acid on α-Al_2O_3. *J. Phys. Chem. A* **2012**, *116*, 10390-10396, doi:10.1021/jp3073393.

Xu, B.; Shang, J.; Zhu, T.; Tang, X. Heterogeneous reaction of formaldehyde on the surface of γ-Al_2O_3 particles. *Atmos. Environ.* **2011**, *45*, 3569-3575, doi:10.1016/j.atmosenv.2011.03.067.

Yabushita, A.; Enami, S.; Sakamoto, Y.; Kawasaki, M.; Hoffmann, M. R.; Colussi, A. J. Anion-catalyzed dissolution of NO_2 on aqueous microdroplets. *J. Phys. Chem. A* **2009**, *113*, 4844-4848, doi:10.1021/jp900685f.

Yoshitake, H. Effects of surface water on NO_2-NaCl reaction studied by diffuse reflectance infrared spectroscopy (DRIRS). *Atmos. Environ.* **2000**, *34*, 2571-2580, doi:10.1016/S1352-2310(99)00494-X.

Zangmeister, C. D.; Pemberton, J. E. Raman spectroscopy of the reaction of sodium chloride with nitric acid: Sodium nitrate growth and the effect of water exposure. *J. Phys. Chem. A* **2001**, *105*, 3788-3795, doi:10.1021/jp003374n.

Zangmeister, C. D.; Pemberton, J. E. Raman spectroscopy of the reaction of sodium chloride with nitric acid: Sodium nitrate growth and effect of water exposure. *J. Phys. Chem. A* **2004**, *108*, 236, doi:10.1021/jp0214357.

Zangmeister, C. D.; Turner, J. A.; Pemberton, J. E. Segregation of NaBr in NaBr/NaCl crystals grown from aqueous solutions: Implications for sea salt surface chemistry. *Geophys. Res. Lett.* **2001**, *28*, 995-998, doi:10.1029/2000GL012539.

Zelenov, V. V.; Aparina, E. V.; Gershenzon, M. Y.; Il'in, S. D.; Gershenzon, Y. M. Kinetic mechanisms of atmospheric gases uptake on sea salt surfaces. 3. Reactive NO_3 uptake on humidified sea salts NaX (X=Cl, Br) under steady state conditions. *Khim. Fiz.* **2003**, *22*, 58-70.

Zelenov, V. V.; Aparina, E. V.; Gershenzon, M. Y.; Il'in, S. D.; Gershenzon, Y. M. Kinetic mechanisms of atmospheric gases uptake on sea salt surfaces. 4. Initial step of NO_3 uptake on salts NaCl and NaBr. *Khim. Fiz.* **2003**, *22*, 37-48.

Zelenov, V. V.; Aparina, E. V.; Kashtanov, S. A.; Shestakov, D. V.; Gershenzon, Y. M. Kinetic mechanism of $ClONO_2$ uptake on polycrystalline film of NaCl. *J. Phys. Chem. A* **2006**, *110*, 6771-6780, doi:10.1021/jp056272b.

Zetzsch, C.; Behnke, W. Heterogeneous photochemical sources of atomic chlorine in the troposphere. *Ber. Bunsenges. Phys. Chem.* **1992**, *96*, 488-493, doi:10.1002/bbpc.19920960351.

Zhang, R.; Jayne, J. T.; Molina, M. J. Heterogeneous interactions of $ClONO_2$ and HCl with sulfuric acid tetrahydrate: Implications for the stratosphere. *J. Phys. Chem.* **1994**, *98*, 867-874, doi:10.1021/j100054a022.

Zhang, R.; Leu, M.-T. Heterogeneous interaction of peroxyacetyl nitrate with liquid sulfuric acid. *J. Geophys. Res.* **1997**, *102*, 8837-8843, doi:10.1029/97JD00131.

Zhang, R.; Leu, M.-T.; Keyser, L. F. Heterogeneous reactions of $ClONO_2$, HCl and HOCl on liquid sulfuric acid surfaces. *J. Phys. Chem.* **1994**, *98*, 13563-13574, doi:10.1021/j100102a022.

Zhang, R.; Leu, M.-T.; Keyser, L. F. Hydrolysis of N_2O_5 and $ClONO_2$ on the $H_2SO_4/HNO_3/H_2O$ ternary solutions under stratospheric conditions. *Geophys. Res. Lett.* **1995**, *22*, 1493-1496, doi:10.1029/95GL01177.

Zhang, R.; Leu, M.-T.; Keyser, L. F. Sulfuric acid monohydrate: Formation and heterogeneous chemistry in the stratosphere. *J. Geophys. Res.* **1995**, *100*, 18845-18854, doi:10.1029/95JD01876.

Zhang, R.; Leu, M.-T.; Keyser, L. F. Heterogeneous chemistry of HONO on liquid sulfuric acid: A new mechanism of chlorine activation on stratospheric sulfate aerosol. *J. Phys. Chem.* **1996**, *100*, 339-345, doi:10.1021/jp952060a.

Zhang, R.; Leu, M.-T.; Keyser, L. F. Heterogeneous chemistry of HO_2NO_2 in liquid sulfuric acid. *J. Phys. Chem. A* **1997**, *101*, 3324-3330, doi:10.1021/jp963321z.

Zhao, Y.; Chen, Z.; Shen, X.; Zhang, X. Kinetics and mechanisms of heterogeneous reaction of gaseous hydrogen peroxide on mineral oxide particles. *Environ. Sci. Technol.* **2011**, *45*, 3317-3324, doi:10.1021/es104107c.

Zhao, Y.; Chen, Z.; Zhao, J. Heterogeneous reactions of methacrolein and methyl vinyl ketone on α-Al_2O_3 particles. *Environ. Sci. Technol.* **2010**, *44*, 2035-2041, doi:10.1021/es9037275.

Zondlo, M. A.; Barone, S. B.; Tolbert, M. A. Condensed-phase products in heterogeneous reactions: N_2O_5, $ClONO_2$ and HNO_3 reacting on ice films at 185 K. *J. Phys. Chem. A* **1998**, *102*, 5735-5748, doi:10.1021/jp980131a.

5.2.4 Table NEq3. Soot Surface Uptake Coefficients

Gaseous Species	Uptake Coefficient (γ)	Notes
SO_2	See Note	1, 2
NH_3	0, See Note	1, 3
O_3	See Note	1, 4
HNO_3	See Note	1, 5
N_2O_5	See Note	1, 6
NO_2	See Note	1, 7
NO_3	See Note	1, 8
HO_2	See Note	1, 9
HO_2NO_2	See Note	1, 10
H_2O	See Note	1, 11

5.2.4.1 Notes for Table NEq3

1. See the discussions on soot presented in the introductory discussions of "Surface Types" and "Parameter Definitions" for descriptions of some of the factors affecting the uptake and reaction of gases on soot surfaces. In most cases, the available reactive surface area rather than the geometric areas have been used in obtaining the uptake coefficients; in those cases where the geometric area was used but a higher available surface area was involved in the measured uptake, the uptake coefficient is given as an upper limit. Most data are available at room temperature or there are very limited data at lower temperatures characteristic of the upper troposphere.
Back to Table

2. **SO_2 + soot.** $\gamma \leq 3 \times 10^{-3}$ measured using Degussa FW2 carbon black by Rogaski et al.[7] This is an upper limit since it is based on the geometric surface area. Koehler et al.[5] measured an average value of $(2 \pm 1) \times 10^{-3}$ over the first 10–30 s on n-hexane soot at –100° C (the initial uptake may be larger), but indicate that taking into account surface roughness would reduce this value. A number of studies[1-7] suggest that uptake is primarily due to physisorption on the surface; oxidation occurs in the presence of water, oxidants and metals.
Back to Table

(1) Baldwin, A. C. Heterogeneous reactions of sulfur dioxide with carbonaceous particles. *Int. J. Chem. Kinet.* **1982**, *14*, 269-277, doi:10.1002/kin.550140307.

(2) Chughtai, A. R.; Atteya, M. M. O.; Kim, J.; Konowalchuck, B. K.; Smith, D. M. Adsorption and adsorbate interaction at soot particle surfaces. *Carbon* **1998**, *36*, 1573-1589, doi:10.1016/S0008-6223(98)00116-X.

(3) Chughtai, A. R.; Brooks, M. E.; Smith, D. M. Effect of metal oxides and black carbon (soot) on $SO_2/O_2/H_2O$ reaction systems. *Aerosol Sci. Technol.* **1993**, *19*, 121-132, doi:10.1080/02786829308959626.

(4) Cofer, W. R., III; Schryer, D. R.; Rogowski, R. S. The oxidation of SO_2 on carbon particles in the presence of O_3, NO_2 and N_2O. *Atmos. Environ.* **1981**, *15*, 1281-1286, doi:10.1016/0004-6981(81)90321-8.

(5) Koehler, B. G.; Nicholson, V. T.; Roe, H. G.; Whitney, E. S. A Fourier transform infrared study of the adsorption of SO_2 on n-hexane soot from -130° to -40°C. *J. Geophys. Res.* **1999**, *104*, 5507-5514, doi:10.1029/1998JD100081.

(6) Liberti, A.; Brocco, D.; Possanzini, M. Adsorption and oxidation of sulfur dioxide on particles. *Atmos. Environ.* **1978**, *12*, 255-261, doi:10.1016/B978-0-08-022932-4.50027-6.

(7) Rogaski, C. A.; Golden, D. M.; Williams, L. R. Reactive uptake and hydration experiments on amorphous carbon treated with NO_2, SO_2, O_3, HNO_3, and H_2SO_4. *Geophys. Res. Lett.* **1997**, *24*, 381-384, doi:10.1029/97GL00093.

3. **NH_3 + soot.** Chughtai et al.[1] and Muenter and Koehler[2] measured the uptake of NH_3 on soot. Based on Muenter and Koehler[2] where conditions are closest to atmospheric, NH_3 is not taken up by soot particles at temperatures above 173 K.
Back to Table

(1) Chughtai, A. R.; Atteya, M. M. O.; Kim, J.; Konowalchuck, B. K.; Smith, D. M. Adsorption and adsorbate interaction at soot particle surfaces. *Carbon* **1998**, *36*, 1573-1589.
(2) Muenter, A. H.; Koehler, B. G. Adsorption of ammonia on soot at low temperatures. *J. Phys. Chem. A* **2000**, *104*, 8527-8534, doi:10.1021/jp0017339.

4. **O_3 + soot.** Many studies report a rapid, initial loss of O_3 followed by a slower loss that also occurs on aged soot or soot pre-exposed to ozone[2,4-10,13,14,17,18]. Initial, rapid O_3 loss may be most applicable for soot as it comes out of aircraft exhaust, with $\gamma^{init} \sim 10^{-3}$ from most studies using both carbon black and organic combustion soots.[6-8,13,18] The second stage of the reaction is probably more applicable to soot dispersed in air; $\gamma^{aged} \sim 10^{-4}$–$10^{-6}$ using both carbon black and organic combustion soots,[6-10,12,18] but in the range of 10^{-4} to 10^{-5} based on organic combustion soot data alone.[8,10] A few studies have been carried out at temperatures below room temperature;[2,8-10] given the wide ranges measured even at room temperature, these values generally fall in the same range. Il'in et al.[8] report a temperature dependence for the initial uptake on fresh soot of $\gamma^{fresh} = 1.9 \times 10^{-3}\exp(-780/T)$ and for aged soots, $\gamma^{aged} = 1.8 \times 10^{-4}\exp(-1000/T)$. Both physisorption and reaction of ozone with the surface appear to take place. The studies of Fendel et al.[6] suggest that lower particle growth in size below 40 ppb O_3 is due to less than a monolayer of O_3 on the surface. Stephens et al.[18] proposed a Langmuir-type reversible adsorption of O_3, followed by a slower reaction with the surface. Pöschl et al.[12] proposed a similar scheme for uptake of ozone on spark-generated graphite soot coated with benzo[*a*]pyrene. Initial reversible physisorption occurred with $\gamma \sim 10^{-3}$, and "apparent reaction probabilities" for O_3 with BaP on soot of $\gamma \sim 10^{-5}$–10^{-6} were reported. The presence of water inhibited the reaction, which was postulated to be due to competitive adsorption between water and ozone on the surface; this is in contrast to the report of Chughtai et al.[1] in which the rate of ozone loss increased with RH. Pöschl et al.[12] report Langmuir adsorption equilibrium constants for O_3 and H_2O, and a second order surface reaction rate constant for the O_3-BaP reaction of $(2.6 \pm 0.8) \times 10^{-17}$ cm^{-2} s^{-1}. Three possible paths have been proposed: (1) chemisorption of O_3; (2) catalytic decomposition of O_3: $2O_3 \rightarrow 3O_2$; (3) surface oxidation and formation of gas-phase carbon oxides. The studies of Fendel et al.[6] suggest that lower particle growth in size below 40 ppb O_3 is due to less than a monolayer of O_3. Studies of Smith et al.[17] and Smith and Chughtai[14] suggest that catalytic decomposition occurs to some extent over the entire reaction sequence. CO_2 and H_2O are the major gas phase and surface oxidized functional groups on the surface such as carboxylic acids are observed.[1-3,5,6,9,11,14-16,18]

Back to Table

(1) Chughtai, A. R.; Kim, J. M.; Smith, D. M. The effect of air/fuel ratio on properties and reactivity of combustion soots. *J. Atmos. Chem.* **2002**, *43*, 21-43, doi:10.1023/A:1016131112199.
(2) Chughtai, A. R.; Kim, J. M.; Smith, D. M. The effect of temperature and humidity on the reaction of ozone with combustion soot: Implications for reactivity near the tropopause. *J. Atmos. Chem.* **2003**, *45*, 231-243, doi:10.1023/A:1024250505886.
(3) Chughtai, A. R.; Miller, N. J.; Smith, D. M.; Pitts, J. R. Carbonaceous particle hydration III. *J. Atmos. Chem.* **1999**, *34*, 259-279, doi:10.1023/A:1006221326060.
(4) Chughtai, A. R.; Williams, G. R.; Atteya, M. M. O.; Miller, N. J.; Smith, D. M. Carbonaceous particle hydration. *Atmos. Environ.* **1999**, *33*, 2679-2687, doi:10.1016/S1352-2310(98)00329-X.
(5) Disselkamp, R. S.; Carpenter, M. A.; Cowin, J. P.; Berkowitz, C. M.; Chapman, E. G.; Zaveri, R. A.; Laulainen, N. S. Ozone loss in soot aerosols. *J. Geophys. Res.* **2000**, *105*, 9767-9771, doi:10.1029/1999JD901189.
(6) Fendel, W.; Matter, D.; Burtscher, H.; Schimdt-Ott, A. Interaction between carbon or iron aerosol particle and ozone. *Atmos. Environ.* **1995**, *29*, 967-973, doi:10.1016/1352-2310(95)00038-Z.
(7) Fendel, W.; Schmidt-Ott, A. Ozone depletion potential of carbon aerosol particles. *J. Aerosol Sci.* **1993**, *24*, S317-S318, doi:10.1016/0021-8502(93)90251-4.
(8) Il'in, S. D.; Selikhonovich, V. V.; Gershenson, Y. M.; Rozenshtein, V. B. Study of heterogeneous ozone loss on materials typical of atmospheric aerosol species. *Sov. J. Chem. Phys.* **1991**, *8*, 1858-1880.
(9) Kamm, S.; Mohler, O.; Naumann, K.-H.; Saathoff, H.; Schurath, U. The heterogeneous reaction of ozone with soot aerosol. *Atmos. Environ.* **1999**, *33*, 4651-4661, doi:10.1016/S1352-2310(99)00235-6.
(10) Longfellow, C. A.; Ravishankara, A. R.; Hanson, D. R. Reactive and nonreactive uptake on hydrocarbon soot: HNO_3, O_3, and N_2O_5. *J. Geophys. Res.* **2000**, *105*, 24345-24350, doi:10.1029/2000JD900297.

(11) Mawhinney, D. B.; Yates, J. J. T. FTIR study of the oxidation of amorphous carbon by ozone at 300 K - Direct COOH formation. *Carbon* **2001**, *39*, 1167-1173, doi:10.1016/S0008-6223(00)00238-4.
(12) Pöschl, U.; Letzel, T.; Schauer, C.; Niessner, R. Interaction of ozone and water vapor with spark discharge soot aerosol particles coated with benzo[*a*]pyrene: O_3 and H_2O adsorption, benzo[a]pyrene degradation, and atmospheric implications. *J. Phys. Chem. A* **2001**, *105*, 4029-4041, doi:10.1021/jp004137n.
(13) Rogaski, C. A.; Golden, D. M.; Williams, L. R. Reactive uptake and hydration experiments on amorphous carbon treated with NO_2, SO_2, O_3, HNO_3, and H_2SO_4. *Geophys. Res. Lett.* **1997**, *24*, 381-384, doi:10.1029/97GL00093.
(14) Smith, D. M.; Chughtai, A. R. Reaction kinetics of ozone at low concentrations with *n*-hexane soot. *J. Geophys. Res.* **1996**, *101*, 19607-19620, doi:10.1029/95JD03032.
(15) Smith, D. M.; Chughtai, A. R. Photochemical effects in the heterogeneous reaction of soot with ozone at low concentrations. *J. Atmos. Chem.* **1997**, *26*, 77-91, doi:10.1023/A:1005702818675.
(16) Smith, D. M.; Welch, W. F.; Graham, S. M.; Chughtai, A. R.; Wicke, B. G.; Grady, K. A. Reaction of nitrogen oxides with black carbon: An FT-IR study. *Appl. Spectrosc.* **1988**, *42*, 674-680, doi:10.1366/0003702884429247.
(17) Smith, D. M.; Welch, W. F.; Jassim, J. A.; Chughtai, A. R.; Stedman, D. H. Soot-ozone reaction kinetics: Spectroscopic and gravimetric studies. *Appl. Spectrosc.* **1988**, *42*, 1473-1482, doi:10.1366/0003702884429779.
(18) Stephens, S.; Rossi, M. J.; Golden, D. M. The Heterogeneous Reaction of Ozone on Carbonaceous Surfaces. *Int. J. Chem. Kinet.* **1986**, *18*, 1133-1149, doi:10.1002/kin.550181004.

5. **HNO_3 + soot.** Studies of the uptake of HNO_3 on soot have been carried out over a range of nitric acid pressures.[1-8] Measured values of γ at room temperature are typically in the range 10^{-1}–10^{-5}, with smaller uptake coefficients measured at longer reaction times. Saatthoff et al.[7] report an upper limit of 3×10^{-7} as a time-averaged value over two days. At lower concentrations characteristic of the atmosphere, uptake appears to be primarily due to physisorption while at higher concentrations, $>2 \times 10^{12}$ molecule cm^{-3}, a surface reaction occurs. At 220 K, γ ~0.1 with irreversible uptake attributed to reaction with surface groups.[1] Reaction of HNO_3 at concentrations from (1–9) $\times 10^{12}$ molecule cm^{-3} with "grey" soot from a rich flame using hexane has been reported[8] to generate HONO as the major gaseous product with initial and steady-state reaction probabilities of $\gamma_o = 4.6 \times 10^{-3}$ and $\gamma_{ss} = 5.2 \times 10^{-4}$, respectively; reaction with "black" soot from a lean flame gave NO as the major gaseous product, with initial and steady-state reaction probabilities of $\gamma_o = 2.0 \times 10^{-2}$ and $\gamma_{ss} = 4.6 \times 10^{-3}$, respectively (based on geometric surface area of sample holder). The NO was hypothesized to result from secondary reactions of an initial HONO product.
Back to Table

(1) Choi, W.; Leu, M. T. Nitric acid uptake and decomposition on black carbon (soot) surfaces: Its implications for the upper troposphere and lower stratosphere. *J. Phys. Chem. A* **1998**, *102*, 7618-7630, doi:10.1021/jp981647x.
(2) Disselkamp, R. S.; Carpenter, M. A.; Cowin, J. P. A chamber investigation of nitric acid-soot aerosol chemistry at 298 K. *J. Atmos. Chem.* **2000**, *37*, 113-123, doi:10.1023/A:1006304724241.
(3) Kirchner, U.; Scheer, V.; Vogt, R. FTIR spectroscopic investigation of the mechanism and kinetics of the heterogeneous reactions of NO_2 and HNO_3 with soot. *J. Phys. Chem. A* **2000**, *104*, 8908-8915, doi:10.1021/jp0005322.
(4) Longfellow, C. A.; Ravishankara, A. R.; Hanson, D. R. Reactive and nonreactive uptake on hydrocarbon soot: HNO_3, O_3, and N_2O_5. *J. Geophys. Res.* **2000**, *105*, 24345-24350, doi:10.1029/2000JD900297.
(5) Rogaski, C. A.; Golden, D. M.; Williams, L. R. Reactive uptake and hydration experiments on amorphous carbon treated with NO_2, SO_2, O_3, HNO_3, and H_2SO_4. *Geophys. Res. Lett.* **1997**, *24*, 381-384, doi:10.1029/97GL00093.
(6) Rossi, M. J.; Fenter, F. F.; Tabor, K.; Caloz, F.; Gutzwiller, L. In *Heterogeneous and Liquid Phase Processes. Transport and Chemical Transformation of Pollutants in the Troposphere*; Warneck, P., Ed.; Springer-Verlag: Berlin, 1996; pp 213-220.
(7) Saathoff, H.; Naumann, K.-H.; Riemer, N.; Kamm, S.; Möhler, O.; Schurath, U.; Vogel, H.; Vogel, B. The loss of NO_2, HNO_3, NO_3/N_2O_5, and $HO_2/HOONO_2$ on soot aerosol: A chamber and modeling study. *Geophys. Res. Lett.* **2001**, *28*, 1957-1960, doi:10.1029/2000GL012619.

(8) Salgado-Muñoz, M. S.; Rossi, M. J. Heterogeneous reactions of HNO_3 with flame soot generated under different combustion conditions. Reaction mechanism and kinetics. *Phys. Chem. Chem. Phys.* **2002**, *4*, 5110-5118, doi:10.1039/b203912p.

6. **N_2O_5 + soot.** Brouwer et al.,[1] Longfellow et al.,[2] and Saathoff et al.[3] studied the uptake of N_2O_5 at room temperature on a ground charcoal (carbon black) sample, on propane soot and on spark-generated graphite soot, respectively. Brouwer et al. and Longfellow et al. report uptake coefficients based on the geometric sample surface area, and therefore give upper limits. An upper limit of $\gamma \leq 0.02$ can be derived based on the larger value of 0.016 reported by Longfellow et al. As discussed below, much smaller values are reported by Saathoff et al.: 4×10^{-5} under dry conditions and 2×10^{-4} at 50% RH. Three possible reactions may occur: (1) decomposition of N_2O_5 on the surface to generate $NO_2 + NO_3$; (2) reaction of N_2O_5 with the soot; (3) hydrolysis of N_2O_5 with water on the surface to generate HNO_3. The studies of Longfellow et al. support the decomposition reaction, with yields of NO_2 within experimental error of 100%; the generation of NO_3 on the surface followed by its decomposition to NO_2, may contribute to the observed production of NO_2. The studies of Brouwer et al. suggest that a redox reaction with the soot surface to generate NO occurs in parallel with hydrolysis of N_2O_5 to generate HNO_3. Saathoff et al. propose two independent, parallel reactions: (1) hydrolysis generating HNO_3, N_2O_5 + soot $\rightarrow$ 2 HNO_3 with $\gamma = (4 \pm 2) \times 10^{-5}$ under dry conditions (<10 ppm H_2O) which increases to $(2 \pm 1) \times 10^{-4}$ at 50% RH. (2) decomposition to NO and NO_2: N_2O_5 + soot $\rightarrow$ NO + NO_2 + products, with $\gamma = (4 \pm 2) \times 10^{-6}$ under dry conditions.
Back to Table

(1) Brouwer, L.; Rossi, M. J.; Golden, D. M. Reaction of N_2O_5 with H_2O on carbonaceous surfaces. *J. Phys. Chem.* **1986**, *90*, 4599-4603, doi:10.1021/j100410a025.
(2) Longfellow, C. A.; Ravishankara, A. R.; Hanson, D. R. Reactive and nonreactive uptake on hydrocarbon soot: HNO_3, O_3, and N_2O_5. *J. Geophys. Res.* **2000**, *105*, 24345-24350, doi:10.1029/2000JD900297.
(3) Saathoff, H.; Naumann, K.-H.; Riemer, N.; Kamm, S.; Möhler, O.; Schurath, U.; Vogel, H.; Vogel, B. The loss of NO_2, HNO_3, NO_3/N_2O_5, and $HO_2/HOONO_2$ on soot aerosol: A chamber and modeling study. *Geophys. Res. Lett.* **2001**, *28*, 1957-1960, doi:10.1029/2000GL012619.

7. **NO_2 + soot.** A fast initial uptake of NO_2 is observed on fresh soots[1-3,8-12,15,17,19,20,24-26] with the initial uptake coefficient in studies involving both carbon blacks and organic combustion soots in the range of $\gamma^{init} \cong 10^{-1}$ to 10^{-4}. For longer reaction times on carbon black soots, $\gamma^{aged} \sim 10^{-4}$ based on studies by Kalberer et al.[16] and Ammann et al.[3,4] However, Kleffmann et al.[18] report a lower uptake coefficient of $\sim 10^{-7}$ on carbon black over the first 5 minutes of reaction and and Saathoff et al.[21] report an upper limit of $< 4 \times 10^{-8}$ averaged over 5 days under dry conditions (<10 ppm H_2O) on spark-generated graphite. On organic combustion soots, γ^{aged} has been reported to be in the range of $\sim 10^{-4}$–10^{-6}.[1,4,5,19,22,24] All studies were done at room temperature except those of Longfellow et al.[19] which were carried out at 262 K. The surface deactivates on continued exposure to NO_2, suggesting a maximum amount of HONO that can be formed per cm^2 of soot area or mg of soot; this has been reported to be in the range of 10^{16} to 10^{18} HONO per mg of soot.[5,12,14,15,18,24] However, reactivation on heating of the surface, exposure to water vapor and/or with time after the exposure is stopped has been observed.[12,19,24-26] A small portion (~10–20%) of the NO_2 taken up appears to be chemisorbed to the surface.[1,5,9,14,15,17,18,24-26] Infrared studies[1,17,23] show that surface C–ONO, C–N–NO_2, and C–NO_2 groups are formed. The remainder of NO_2 reacted appears as gaseous HONO and NO; Salgado and Rossi[22] report HONO as the major product for hexane soot from a flame at near stoichiometric ratio but NO as the major product for soot from an extremely lean flame. In addition, N_2O, CO, and CO_2 have been observed as products at higher temperatures.[6,7] At lower NO_2 concentrations, the HONO yield can approach 100%; production of NO may be due to the bimolecular reaction of HONO on the surface at higher concentrations to give NO + NO_2 + H_2O. The HONO yield at 262 K appears to be smaller than at room temperature.[19] Formation of HONO is due to reaction with a reduced surface site and not to NO_2 surface-catalyzed hydrolysis. The formation of HONO from the reaction of NO_2 with unspecified semi-volatile organics in diesel exhaust has been reported [13] and proposed to be a much larger source of HONO than the reaction with the soot itself.
Back to Table

(1) Al-Abadleh, H. A.; Grassian, V. H. Heterogeneous reaction of NO_2 on hexane soot: A Knudsen cell and FT-IR study. *J. Phys. Chem. A* **2000**, *104*, 11926-11933, doi:10.1021/jp002918i.

(2) Alcala-Jornod, C.; Van den Bergh, H.; Rossi, M. J. Reactivity of NO_2 and H_2O on soot generated in the laboratory : a diffusion tube study at ambient temperature. *Phys. Chem. Chem. Phys.* **2000**, *2*, 5584-5593, doi:10.1039/b007235o.

(3) Ammann, M.; Kalberer, M.; Jost, D. T.; Tobler, L.; Rossler, E.; Piguet, D.; Gaggeler, H. W.; Baltensperger, U. Heterogeneous production of nitrous acid on soot in polluted air masses. *Nature* **1998**, *395*, 157-160, doi:10.1038/25965.

(4) Ammann, M.; Kalberer, M.; Tabor, K.; Tobler, K.; Zellweger, C.; Weingartner, E.; Nyeki, S.; Parrat, Y.; Li, F.; Piguet, D.; Rossler, E.; Jost, D. T.; Gaggeler, H. W.; Baltensperger, U. "Proc. 7th Euro. Symp. on Physico-Chem. Behav. of Atmos. Poll.", 1996.

(5) Arens, F.; Gutzwiller, L.; Baltensperger, U.; Gaggeler, H.; Ammann, M. Heterogeneous reaction of NO_2 on diesel soot particles. *Environ. Sci. Technol.* **2001**, *35*, 2191-2199, doi:10.1021/es000207s.

(6) Battino, R. Nitrogen in water. In *Nitrogen and Air*; Battino, R., Ed.; Pergamon: Oxford, 1982; Vol. 10; pp 1-29.

(7) Battino, R. Chlorine dioxide in water. In *Sulfur Dioxide, Chlorine, Fluorine and Chlorine Oxides*; Young, C. L., Ed.; Pergamon: Oxford, 1983; Vol. 12; pp 454-456.

(8) Chughtai, A. R.; Atteya, M. M. O.; Kim, J.; Konowalchuck, B. K.; Smith, D. M. Adsorption and adsorbate interaction at soot particle surfaces. *Carbon* **1998**, *36*, 1573-1589, doi:10.1016/S0008-6223(98)00116-X.

(9) Chughtai, A. R.; Gordon, S. A.; Smith, D. M. Kinetics of the hexane soot reaction with NO_2/N_2O_4 at low concentration. *Carbon* **1994**, *32*, 405-416, doi:10.1016/0008-6223(94)90160-0.

(10) Chughtai, A. R.; Welch, W. F.; Akhter, M. S.; Smith, D. M. A spectroscopic study of gaseous products of soot-oxides of nitrogen/water reactions. *Appl. Spectrosc.* **1990**, *44*, 294-298, doi:10.1366/0003702904085598.

(11) Chughtai, A. R.; Welch, W. F.; Smith, D. M. A spectroscopic and gravimetric study of the soot-NO_2/N_2O_4 reaction at various temperatures. *Carbon* **1990**, *28*, 411-421, doi:10.1016/0008-6223(90)90015-Q.

(12) Gerecke, A.; Thielmann, A.; Gutzwiller, L.; Rossi, M. J. The chemical kinetics of HONO formation resulting from heterogeneous interaction of NO_2 with flame soot. *Geophys. Res. Lett.* **1998**, *25*, 2453-2456, doi:10.1029/98GL01796.

(13) Gutzwiller, L.; Arens, F.; Baltensperger, U.; Gäggeler, H. W.; Ammann, M. significance of semivolatile diesel exhaust organics for secondary HONO formation. *Environ. Sci. Technol.* **2002**, *36*, 677-682, doi:10.1021/es015673b.

(14) Kalberer, M.; Ammann, M.; Arens, F.; Gaggeler, H. W.; Baltensperger, U. Heterogeneous formation of nitrous acid (HONO) on soot aerosol particles. *J. Geophys. Res.* **1999**, *104*, 13825-13832, doi:10.1029/1999JD900141.

(15) Kalberer, M.; Ammann, M.; Gaggeler, H. W.; Baltensperger, U. Adsorption of NO_2 on carbon aerosol particles in the low ppb range. *Atmos. Environ.* **1999**, *33*, 2815-2822, doi:10.1016/S1352-2310(98)00390-2.

(16) Kalberer, M.; Tabor, K.; Ammann, M.; Parrat, Y.; Weingartner, E.; Piguet, D.; Rossler, E.; Jost, D. T.; Turler, A.; Gaggeler, H. W.; Baltensperger, U. Heterogeneous chemical processing of $^{13}NO_2$ by monodisperse carbon aerosols at very low concentrations. *J. Phys. Chem.* **1996**, *100*, 15487-15493, doi:10.1021/jp9606974.

(17) Kirchner, U.; Scheer, V.; Vogt, R. FTIR spectroscopic investigation of the mechanism and kinetics of the heterogeneous reactions of NO_2 and HNO_3 with soot. *J. Phys. Chem. A* **2000**, *104*, 8908-8915, doi:10.1021/jp0005322.

(18) Kleffmann, J.; Becker, K. H.; Lackhoff, M.; Wiesen, P. Heterogeneous conversion of NO_2 on carbonaceous surfaces. *Phys. Chem. Chem. Phys.* **1999**, *1*, 5443-5450, doi:10.1039/a905545b.

(19) Longfellow, C. A.; Ravishankara, A. R.; Hanson, D. R. Reactive uptake on hydrocarbon soot: Focus on NO_2. *J. Geophys. Res.* **1999**, *104*, 13833-13840, doi:10.1029/1999JD900145.

(20) Rogaski, C. A.; Golden, D. M.; Williams, L. R. Reactive uptake and hydration experiments on amorphous carbon treated with NO_2, SO_2, O_3, HNO_3, and H_2SO_4. *Geophys. Res. Lett.* **1997**, *24*, 381-384, doi:10.1029/97GL00093.

(21) Saathoff, H.; Naumann, K.-H.; Riemer, N.; Kamm, S.; Möhler, O.; Schurath, U.; Vogel, H.; Vogel, B. The loss of NO_2, HNO_3, NO_3/N_2O_5, and $HO_2/HOONO_2$ on soot aerosol: A chamber and modeling study. *Geophys. Res. Lett.* **2001**, *28*, 1957-1960, doi:10.1029/2000GL012619.

(22) Salgado-Muñoz, M. S.; Rossi, M. J. Heterogeneous reactions of HNO_3 with flame soot generated under different combustion conditions. Reaction mechanism and kinetics. *Phys. Chem. Chem. Phys.* **2002**, *4*, 5110-5118, doi:10.1039/b203912p.
(23) Smith, D. M.; Welch, W. F.; Graham, S. M.; Chughtai, A. R.; Wicke, B. G.; Grady, K. A. Reaction of nitrogen oxides with black carbon: An FT-IR study. *Appl. Spectrosc.* **1988**, *42*, 674-680, doi:10.1366/0003702884429247.
(24) Stadler, D.; Rossi, M. J. The reactivity of NO_2 and HONO on Ñame soot at ambient temperature: The influence of combustion conditions. *Phys. Chem. Chem. Phys.* **2000**, *2*, 5420-5429, doi:10.1039/b005680o.
(25) Tabor, K.; Gutzwiller, L.; Rossi, M. J. The heterogeneous interaction of NO_2 with amorphous carbon. *Geophys. Res. Lett.* **1993**, *20*, 1431-1434, doi:10.1029/93GL01434.
(26) Tabor, K.; Gutzwiller, L.; Rossi, M. J. Heterogeneous chemical kinetics of NO_2 on amorphous carbon at ambient temperature. *J. Phys. Chem.* **1994**, *98*, 6172-7186, doi:10.1021/j100075a021.

8. **NO_3 + soot.** Saathoff et al.[1] report an upper limit of $\gamma < 3 \times 10^{-4}$ on dry soot (<10 ppm H_2O) and $\leq 10^{-3}$ at 50% RH based on measurements of NO_3 and N_2O_5.
Back to Table

(1) Saathoff, H.; Naumann, K.-H.; Riemer, N.; Kamm, S.; Möhler, O.; Schurath, U.; Vogel, H.; Vogel, B. The loss of NO_2, HNO_3, NO_3/N_2O_5, and $HO_2/HOONO_2$ on soot aerosol: A chamber and modeling study. *Geophys. Res. Lett.* **2001**, *28*, 1957-1960, doi:10.1029/2000GL012619.

9. **HO_2 + soot.** Saathoff et al.[1] report an upper limit of $\gamma < 10^{-2}$ on dry soot (<10 ppm H_2O) based on the decay of HO_2NO_2 (in equilibrium with HO_2 and NO_2) in the presence and absence of soot.
Back to Table

(1) Saathoff, H.; Naumann, K.-H.; Riemer, N.; Kamm, S.; Möhler, O.; Schurath, U.; Vogel, H.; Vogel, B. The loss of NO_2, HNO_3, NO_3/N_2O_5, and $HO_2/HOONO_2$ on soot aerosol: A chamber and modeling study. *Geophys. Res. Lett.* **2001**, *28*, 1957-1960, doi:10.1029/2000GL012619.

10. **HO_2NO_2 + soot.** Saathoff et al.[1] report an upper limit of $\gamma < 10^{-5}$ on dry soot (<10 ppm H_2O) based on the decay of HO_2NO_2 in the presence and absence of soot.
Back to Table

(1) Saathoff, H.; Naumann, K.-H.; Riemer, N.; Kamm, S.; Möhler, O.; Schurath, U.; Vogel, H.; Vogel, B. The loss of NO_2, HNO_3, NO_3/N_2O_5, and $HO_2/HOONO_2$ on soot aerosol: A chamber and modeling study. *Geophys. Res. Lett.* **2001**, *28*, 1957-1960, doi:10.1029/2000GL012619.

11. **H_2O + soot.** Alcala–Jornod et al.[1] report an upper limit to the initial uptake coefficient of $\gamma < 2 \times 10^{-3}$, consistent with the earlier measurements of Rogaski et al.[8] The uptake is most likely a reversible physisorption[1,7] although based on water uptake isotherms, Chughtai et al.[2,3,5,6] propose that at low relative humidities (<25%) chemisorption occurs. While prior exposure of Degussa FW-2 to NO_2 and SO_2 was not found to increase the uptake coefficient for water, treatment with HNO_3 increased the measured uptake coefficient by a factor of 28 and with H_2SO_4 by a factor of 68.[8] Water adsorption isotherms on soot have been measured in a number of studies, e.g.[2-6] and the amount of water taken up found to increase with the air/fuel ratio used to generate the soot, with the sulfur content, with aging and oxidation of the surface (e.g. by O_3) and with the presence of metals.[2-6,9]
Back to Table

(1) Alcala-Jornod, C.; Van den Bergh, H.; Rossi, M. J. Reactivity of NO_2 and H_2O on soot generated in the laboratory : a diffusion tube study at ambient temperature. *Phys. Chem. Chem. Phys.* **2000**, *2*, 5584-5593, doi:10.1039/b007235o.
(2) Chughtai, A. R.; Atteya, M. M. O.; Kim, J.; Konowalchuck, B. K.; Smith, D. M. Adsorption and adsorbate interaction at soot particle surfaces. *Carbon* **1998**, *36*, 1573-1589, doi:10.1016/S0008-6223(98)00116-X.
(3) Chughtai, A. R.; Brooks, M. E.; Smith, D. M. Hydration of black carbon. *J. Geophys. Res.* **1996**, *101*, 19505-19514, doi:10.1029/95JD01882.

(4) Chughtai, A. R.; Kim, J. M.; Smith, D. M. The effect of air/fuel ratio on properties and reactivity of combustion soots. *J. Atmos. Chem.* **2002**, *43*, 21-43, doi:10.1023/A:1016131112199.
(5) Chughtai, A. R.; Miller, N. J.; Smith, D. M.; Pitts, J. R. Carbonaceous particle hydration III. *J. Atmos. Chem.* **1999**, *34*, 259-279, doi:10.1023/A:1006221326060.
(6) Chughtai, A. R.; Williams, G. R.; Atteya, M. M. O.; Miller, N. J.; Smith, D. M. Carbonaceous particle hydration. *Atmos. Environ.* **1999**, *33*, 2679-2687, doi:10.1016/S1352-2310(98)00329-X.
(7) Pöschl, U.; Canagaratna, M.; Jayne, J. T.; Molina, L. T.; Worsnop, D. R.; Kolb, C. E.; Molina, M. J. Mass accommodation coefficient of H_2SO_4 vapor on aqueous sulfuric acid surfaces and gaseous diffusion coefficient of H_2SO_4 in N_2/H_2O. *J. Phys. Chem. A* **1998**, *102*, 10082-10089, doi:10.1021/jp982809s.
(8) Rogaski, C. A.; Golden, D. M.; Williams, L. R. Reactive uptake and hydration experiments on amorphous carbon treated with NO_2, SO_2, O_3, HNO_3, and H_2SO_4. *Geophys. Res. Lett.* **1997**, *24*, 381-384, doi:10.1029/97GL00093.
(9) Weingartner, E.; Burtscher, H.; Baltensperger, U. Hygroscopic properties of carbon and diesel soot particles. *Atmos. Environ.* **1997**, *31*, 2311-2327, doi:10.1016/S1352-2310(97)00023-X.

5.2.4.2 Bibliography – Table NEq3

Al-Abadleh, H. A.; Grassian, V. H. Heterogeneous reaction of NO_2 on hexane soot: A Knudsen cell and FT-IR study. *J. Phys. Chem. A* **2000**, *104*, 11926-11933, doi:10.1021/jp002918i.

Alcala-Jornod, C.; Van den Bergh, H.; Rossi, M. J. Reactivity of NO_2 and H_2O on soot generated in the laboratory : a diffusion tube study at ambient temperature. *Phys. Chem. Chem. Phys.* **2000**, *2*, 5584-5593, doi:10.1039/b007235o.

Ammann, M.; Kalberer, M.; Jost, D. T.; Tobler, L.; Rossler, E.; Piguet, D.; Gaggeler, H. W.; Baltensperger, U. Heterogeneous production of nitrous acid on soot in polluted air masses. *Nature* **1998**, *395*, 157-160, doi:10.1038/25965.

Ammann, M.; Kalberer, M.; Tabor, K.; Tobler, K.; Zellweger, C.; Weingartner, E.; Nyeki, S.; Parrat, Y.; Li, F.; Piguet, D.; Rossler, E.; Jost, D. T.; Gaggeler, H. W.; Baltensperger, U. "Proc. 7th Euro. Symp. on Physico-Chem. Behav. of Atmos. Poll.", 1996.

Arens, F.; Gutzwiller, L.; Baltensperger, U.; Gaggeler, H.; Ammann, M. Heterogeneous reaction of NO_2 on diesel soot particles. *Environ. Sci. Technol.* **2001**, *35*, 2191-2199, doi:10.1021/es000207s.

Baldwin, A. C. Heterogeneous reactions of sulfur dioxide with carbonaceous particles. *Int. J. Chem. Kinet.* **1982**, *14*, 269-277, doi:10.1002/kin.550140307.

Battino, R. Nitrogen in water. In *Nitrogen and Air*; Battino, R., Ed.; Pergamon: Oxford, 1982; Vol. 10; pp 1-29.

Battino, R. Chlorine dioxide in water. In *Sulfur Dioxide, Chlorine, Fluorine and Chlorine Oxides*; Young, C. L., Ed.; Pergamon: Oxford, 1983; Vol. 12; pp 454-456.

Brouwer, L.; Rossi, M. J.; Golden, D. M. Reaction of N_2O_5 with H_2O on carbonaceous surfaces. *J. Phys. Chem.* **1986**, *90*, 4599-4603, doi:10.1021/j100410a025.

Choi, W.; Leu, M. T. Nitric acid uptake and decomposition on black carbon (soot) surfaces: Its implications for the upper troposphere and lower stratosphere. *J. Phys. Chem. A* **1998**, *102*, 7618-7630, doi:10.1021/jp981647x.

Chughtai, A. R.; Atteya, M. M. O.; Kim, J.; Konowalchuck, B. K.; Smith, D. M. Adsorption and adsorbate interaction at soot particle surfaces. *Carbon* **1998**, *36*, 1573-1589, doi:10.1016/S0008-6223(98)00116-X.

Chughtai, A. R.; Brooks, M. E.; Smith, D. M. Effect of metal oxides and black carbon (soot) on $SO_2/O_2/H_2O$ reaction systems. *Aerosol Sci. Technol.* **1993**, *19*, 121-132, doi:10.1080/02786829308959626.

Chughtai, A. R.; Brooks, M. E.; Smith, D. M. Hydration of black carbon. *J. Geophys. Res.* **1996**, *101*, 19505-19514, doi:10.1029/95JD01882.

Chughtai, A. R.; Gordon, S. A.; Smith, D. M. Kinetics of the hexane soot reaction with NO_2/N_2O_4 at low concentration. *Carbon* **1994**, *32*, 405-416, doi:10.1016/0008-6223(94)90160-0.

Chughtai, A. R.; Kim, J. M.; Smith, D. M. The effect of air/fuel ratio on properties and reactivity of combustion soots. *J. Atmos. Chem.* **2002**, *43*, 21-43, doi:10.1023/A:1016131112199.

Chughtai, A. R.; Kim, J. M.; Smith, D. M. The effect of temperature and humidity on the reaction of ozone with combustion soot: Implications for reactivity near the tropopause. *J. Atmos. Chem.* **2003**, *45*, 231-243, doi:10.1023/A:1024250505886.

Chughtai, A. R.; Miller, N. J.; Smith, D. M.; Pitts, J. R. Carbonaceous particle hydration III. *J. Atmos. Chem.* **1999**, *34*, 259-279, doi:10.1023/A:1006221326060.

Chughtai, A. R.; Welch, W. F.; Akhter, M. S.; Smith, D. M. A spectroscopic study of gaseous products of soot-oxides of nitrogen/water reactions. *Appl. Spectrosc.* **1990**, *44*, 294-298, doi:10.1366/0003702904085598.

Chughtai, A. R.; Welch, W. F.; Smith, D. M. A spectroscopic and gravimetric study of the soot-NO_2/N_2O_4 reaction at various temperatures. *Carbon* **1990**, *28*, 411-421, doi:10.1016/0008-6223(90)90015-Q.

Chughtai, A. R.; Williams, G. R.; Atteya, M. M. O.; Miller, N. J.; Smith, D. M. Carbonaceous particle hydration. *Atmos. Environ.* **1999**, *33*, 2679-2687, doi:10.1016/S1352-2310(98)00329-X.

Cofer, W. R., III; Schryer, D. R.; Rogowski, R. S. The oxidation of SO_2 on carbon particles in the presence of O_3, NO_2 and N_2O. *Atmos. Environ.* **1981**, *15*, 1281-1286, doi:10.1016/0004-6981(81)90321-8.

Disselkamp, R. S.; Carpenter, M. A.; Cowin, J. P. A chamber investigation of nitric acid-soot aerosol chemistry at 298 K. *J. Atmos. Chem.* **2000**, *37*, 113-123, doi:10.1023/A:1006304724241.

Disselkamp, R. S.; Carpenter, M. A.; Cowin, J. P.; Berkowitz, C. M.; Chapman, E. G.; Zaveri, R. A.; Laulainen, N. S. Ozone loss in soot aerosols. *J. Geophys. Res.* **2000**, *105*, 9767-9771, doi:10.1029/1999JD901189.

Fendel, W.; Matter, D.; Burtscher, H.; Schimdt-Ott, A. Interaction between carbon or iron aerosol particle and ozone. *Atmos. Environ.* **1995**, *29*, 967-973, doi:10.1016/1352-2310(95)00038-Z.

Fendel, W.; Schmidt-Ott, A. Ozone depletion potential of carbon aerosol particles. *J. Aerosol Sci.* **1993**, *24*, S317-S318, doi:10.1016/0021-8502(93)90251-4.

Gerecke, A.; Thielmann, A.; Gutzwiller, L.; Rossi, M. J. The chemical kinetics of HONO formation resulting from heterogeneous interaction of NO_2 with flame soot. *Geophys. Res. Lett.* **1998**, *25*, 2453-2456, doi:10.1029/98GL01796.

Gutzwiller, L.; Arens, F.; Baltensperger, U.; Gäggeler, H. W.; Ammann, M. significance of semivolatile diesel exhaust organics for secondary HONO formation. *Environ. Sci. Technol.* **2002**, *36*, 677-682, doi:10.1021/es015673b.

Il'in, S. D.; Selikhonovich, V. V.; Gershenson, Y. M.; Rozenshtein, V. B. Study of heterogeneous ozone loss on materials typical of atmospheric aerosol species. *Sov. J. Chem. Phys.* **1991**, *8*, 1858-1880.

Kalberer, M.; Ammann, M.; Arens, F.; Gaggeler, H. W.; Baltensperger, U. Heterogeneous formation of nitrous acid (HONO) on soot aerosol particles. *J. Geophys. Res.* **1999**, *104*, 13825-13832, doi:10.1029/1999JD900141.

Kalberer, M.; Ammann, M.; Gaggeler, H. W.; Baltensperger, U. Adsorption of NO_2 on carbon aerosol particles in the low ppb range. *Atmos. Environ.* **1999**, *33*, 2815-2822, doi:10.1016/S1352-2310(98)00390-2.

Kalberer, M.; Tabor, K.; Ammann, M.; Parrat, Y.; Weingartner, E.; Piguet, D.; Rossler, E.; Jost, D. T.; Turler, A.; Gaggeler, H. W.; Baltensperger, U. Heterogeneous chemical processing of $^{13}NO_2$ by monodisperse carbon aerosols at very low concentrations. *J. Phys. Chem.* **1996**, *100*, 15487-15493, doi:10.1021/jp9606974.

Kamm, S.; Mohler, O.; Naumann, K.-H.; Saathoff, H.; Schurath, U. The heterogeneous reaction of ozone with soot aerosol. *Atmos. Environ.* **1999**, *33*, 4651-4661, doi:10.1016/S1352-2310(99)00235-6.

Kirchner, U.; Scheer, V.; Vogt, R. FTIR spectroscopic investigation of the mechanism and kinetics of the heterogeneous reactions of NO_2 and HNO_3 with soot. *J. Phys. Chem. A* **2000**, *104*, 8908-8915, doi:10.1021/jp0005322.

Kleffmann, J.; Becker, K. H.; Lackhoff, M.; Wiesen, P. Heterogeneous conversion of NO_2 on carbonaceous surfaces. *Phys. Chem. Chem. Phys.* **1999**, *1*, 5443-5450, doi:10.1039/a905545b.

Koehler, B. G.; Nicholson, V. T.; Roe, H. G.; Whitney, E. S. A Fourier transform infrared study of the adsorption of SO_2 on n-hexane soot from -130° to -40°C. *J. Geophys. Res.* **1999**, *104*, 5507-5514, doi:10.1029/1998JD100081.

Liberti, A.; Brocco, D.; Possanzini, M. Adsorption and oxidation of sulfur dioxide on particles. *Atmos. Environ.* **1978**, *12*, 255-261, doi:10.1016/B978-0-08-022932-4.50027-6.

Longfellow, C. A.; Ravishankara, A. R.; Hanson, D. R. Reactive uptake on hydrocarbon soot: Focus on NO_2. *J. Geophys. Res.* **1999**, *104*, 13833-13840, doi:10.1029/1999JD900145.

Longfellow, C. A.; Ravishankara, A. R.; Hanson, D. R. Reactive and nonreactive uptake on hydrocarbon soot: HNO_3, O_3, and N_2O_5. *J. Geophys. Res.* **2000**, *105*, 24345-24350, doi:10.1029/2000JD900297.

Mawhinney, D. B.; Yates, J. J. T. FTIR study of the oxidation of amorphous carbon by ozone at 300 K - Direct COOH formation. *Carbon* **2001**, *39*, 1167-1173, doi:10.1016/S0008-6223(00)00238-4.

Muenter, A. H.; Koehler, B. G. Adsorption of ammonia on soot at low temperatures. *J. Phys. Chem. A* **2000**, *104*, 8527-8534, doi:10.1021/jp0017339.

Pöschl, U.; Canagaratna, M.; Jayne, J. T.; Molina, L. T.; Worsnop, D. R.; Kolb, C. E.; Molina, M. J. Mass accommodation coefficient of H_2SO_4 vapor on aqueous sulfuric acid surfaces and gaseous diffusion coefficient of H_2SO_4 in N_2/H_2O. *J. Phys. Chem. A* **1998**, *102*, 10082-10089, doi:10.1021/jp982809s.

Pöschl, U.; Letzel, T.; Schauer, C.; Niessner, R. Interaction of ozone and water vapor with spark discharge soot aerosol particles coated with benzo[*a*]pyrene: O_3 and H_2O adsorption, benzo[a]pyrene degradation, and atmospheric implications. *J. Phys. Chem. A* **2001**, *105*, 4029-4041, doi:10.1021/jp004137n.

Rogaski, C. A.; Golden, D. M.; Williams, L. R. Reactive uptake and hydration experiments on amorphous carbon treated with NO_2, SO_2, O_3, HNO_3, and H_2SO_4. *Geophys. Res. Lett.* **1997**, *24*, 381-384, doi:10.1029/97GL00093.

Rossi, M. J.; Fenter, F. F.; Tabor, K.; Caloz, F.; Gutzwiller, L. In *Heterogeneous and Liquid Phase Processes. Transport and Chemical Transformation of Pollutants in the Troposphere*; Warneck, P., Ed.; Springer-Verlag: Berlin, 1996; pp 213-220.

Saathoff, H.; Naumann, K.-H.; Riemer, N.; Kamm, S.; Möhler, O.; Schurath, U.; Vogel, H.; Vogel, B. The loss of NO_2, HNO_3, NO_3/N_2O_5, and $HO_2/HOONO_2$ on soot aerosol: A chamber and modeling study. *Geophys. Res. Lett.* **2001**, *28*, 1957-1960, doi:10.1029/2000GL012619.

Salgado-Muñoz, M. S.; Rossi, M. J. Heterogeneous reactions of HNO_3 with flame soot generated under different combustion conditions. Reaction mechanism and kinetics. *Phys. Chem. Chem. Phys.* **2002**, *4*, 5110-5118, doi:10.1039/b203912p.

Smith, D. M.; Chughtai, A. R. Reaction kinetics of ozone at low concentrations with *n*-hexane soot. *J. Geophys. Res.* **1996**, *101*, 19607-19620, doi:10.1029/95JD03032.
Smith, D. M.; Chughtai, A. R. Photochemical effects in the heterogeneous reaction of soot with ozone at low concentrations. *J. Atmos. Chem.* **1997**, *26*, 77-91, doi:10.1023/A:1005702818675.
Smith, D. M.; Welch, W. F.; Graham, S. M.; Chughtai, A. R.; Wicke, B. G.; Grady, K. A. Reaction of nitrogen oxides with black carbon: An FT-IR study. *Appl. Spectrosc.* **1988**, *42*, 674-680, doi:10.1366/0003702884429247.
Smith, D. M.; Welch, W. F.; Jassim, J. A.; Chughtai, A. R.; Stedman, D. H. Soot-ozone reaction kinetics: Spectroscopic and gravimetric studies. *Appl. Spectrosc.* **1988**, *42*, 1473-1482, doi:10.1366/0003702884429779.
Stadler, D.; Rossi, M. J. The reactivity of NO_2 and HONO on Ñame soot at ambient temperature: The influence of combustion conditions. *Phys. Chem. Chem. Phys.* **2000**, *2*, 5420-5429, doi:10.1039/b005680o.
Stephens, S.; Rossi, M. J.; Golden, D. M. The Heterogeneous Reaction of Ozone on Carbonaceous Surfaces. *Int. J. Chem. Kinet.* **1986**, *18*, 1133-1149, doi:10.1002/kin.550181004.
Tabor, K.; Gutzwiller, L.; Rossi, M. J. The heterogeneous interaction of NO_2 with amorphous carbon. *Geophys. Res. Lett.* **1993**, *20*, 1431-1434, doi:10.1029/93GL01434.
Tabor, K.; Gutzwiller, L.; Rossi, M. J. Heterogeneous chemical kinetics of NO_2 on amorphous carbon at ambient temperature. *J. Phys. Chem.* **1994**, *98*, 6172-7186, doi:10.1021/j100075a021.
Weingartner, E.; Burtscher, H.; Baltensperger, U. Hygroscopic properties of carbon and diesel soot particles. *Atmos. Environ.* **1997**, *31*, 2311-2327, doi:10.1016/S1352-2310(97)00023-X.

5.3 Equilbrium Processes

5.3.1 Introduction

5.3.1.1 Henry's Law Constants

The equilibrium distribution of a substance between the gas and the liquid phase is controlled by Henry's law. It relates the concentration of the substance in solution to its partial pressure in the gas phase. The Henry's law solubility constant H_s is defined as:

$$H_s = c/p$$

We use the unit mol L^{-1} (M) for the aqueous-phase concentration c and atm (101325 Pa) for the partial pressure p in the gas phase. In many studies and other compilations, Henry's law volatility constants H_v are presented, which are the inverse of H_s. Sometimes, other variants are used, for example dimensionless constants with no indication from the units if it pertains to solubility or to volatility.

Henry's law is a limiting law, strictly valid only at the limit of zero concentration. For typical concentrations of most atmospheric gases, deviations from this law are not significant.

5.3.1.2 Temperature dependence

The value of the Henry's law constant H_s depends strongly upon temperature. For a typical gas, it increases with decreasing temperature at lower temperatures, at least down to 273 K. At higher temperatures, typically well above 298 K, the value will increase with temperature. Over limited temperature ranges, there is a linear correlation between the logarithm of H_s and the reciprocal of temperature. This can be written as:

$$H_s = \exp(A + B/T)\ \text{M atm}^{-1}$$

For a number of gases, the experimental data are sufficient to display the expected curvature in a plot of $\ln(H_s)$ vs. 1/T. Here, we have represented these results by the three-parameter equation:

$$H_s = \exp(A + B/T + C \ln(T/\text{K}))\ \text{M atm}^{-1}$$

Below 273 K, measurements in strong acid solutions have suggested that the Henry's law constant for a substrate would continue to increase as the temperature is lowered. A study on the solubilities of benzene, alkyl benzenes, and methyl and ethyl *tert*-butyl ethers, however, indicates that this is not the case.[4] In this study, the values were found to decrease with temperature in supercooled water. Indeed, the results from 298 to 248 K are almost symmetrical around 273 K. Additional studies on this phenomenon are clearly needed, particularly for smaller solutes.

Table 5.2 presents Henry's law constants and their temperature dependence for pure water as the solvent.

5.3.1.3 Thermodynamics

Like all equilibrium constants, Henry's law constants are closely related to thermodynamic properties. The Gibbs energy of solution $\Delta_{sol}G$ is the difference between the Gibbs energies of formation $\Delta_{f,g}G$ in the gas phase and $\Delta_{f,aq}G$ in the aqueous phase:

$$\Delta_{sol}G = \Delta_{f,g}G - \Delta_{f,aq}G$$

A large compilation of $\Delta_f G$ values has been published by Wagman et al.[5] From $\Delta_{sol}G$, the Henry's law constant H_s can be calculated as:

$$\frac{H_s^{bp}}{\text{mol kg}^{-1}\ \text{bar}^{-1}} = \exp\left(\frac{\Delta_{sol}G}{RT}\right)$$

where R = 8.314 J mol^{-1} K^{-1} is the gas constant and T is the thermodynamic temperature. The exponential expression on the right-hand side of the equation is just a dimensionless number, and the unit of the Henry's law constant results from the standard states on which $\Delta_{sol}G$ is based. When using a standard pressure of 10^5 Pa = 1 bar and a standard molality of 1 mol/kg, the equation above yields the molality-based Henry's law constant H_s^{bp} with the unit mol kg^{-1} bar^{-1}.

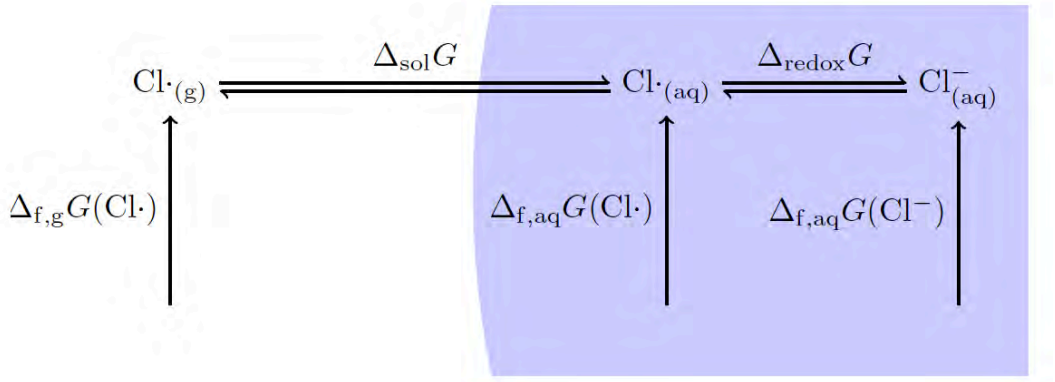
As an example, the Gibbs energies of formation for HOCl are $\Delta_{f,g}G$ = –66.1 kJ/mol and $\Delta_{f,aq}G$ = –79.9 kJ/mol for the gas- and aqueous-phase, respectively. From this, a Henry's law constant of H_s^{bp} = 262 mol kg^{-1} bar^{-1} can be calculated:

$$\frac{H_s^{bp}(\text{HOCl})}{\text{mol kg}^{-1}\ \text{bar}^{-1}} = \exp\left(\frac{(-66100) - (-79900)}{8.314 \times 298.15}\right) = 262$$

Inserting the density of water, this can be converted further to H_s^{cp} in M atm^{-1}:

$$H_s^{cp}(\mathrm{HOCl}) = 262\ \mathrm{mol\ kg^{-1}\ bar^{-1}} \times 0.9970\ \mathrm{kg\ L^{-1}} \times 1.01325\ \mathrm{bar\ atm^{-1}} = 265\ \mathrm{M\ atm^{-1}}$$

If the Gibbs energy of formation is not directly available for the aqueous phase, it may be possible to obtain it via a thermodynamic cycle. Many radicals can be reduced to a stable anion, e.g., chlorine can be reduced to chloride.



The Gibbs energy for the redox reaction is the difference between the Gibbs energies of formation of the anion and the radical:

$$\Delta_{\mathrm{redox}}G = \Delta_{\mathrm{f,aq}}G(\mathrm{Cl^-}) - \Delta_{\mathrm{f,aq}}G(\mathrm{Cl\cdot})$$

It can be obtained from the standard reduction potential E^0:

$$\Delta_{\mathrm{redox}}G = -zFE^0(\mathrm{Cl\cdot}\ /\ \mathrm{Cl^-})$$

where F = 96485 J mol^{-1} V^{-1} is the Faraday constant and z = 1 for a one-electron transfer. A compilation of standard reduction potentials has been published by Armstrong et al.[1] The Gibbs energy of formation of the aqueous chlorine radical can be calculated as:

$$\Delta_{\mathrm{f,aq}}G(\mathrm{Cl\cdot}) = \Delta_{\mathrm{f,aq}}G(\mathrm{Cl^-}) + FE^0(\mathrm{Cl\cdot}\ /\ \mathrm{Cl^-})$$

and the Gibbs energy of solution $\Delta_{\mathrm{sol}}G$ is:

$$\Delta_{\mathrm{sol}}G = \Delta_{\mathrm{f,aq}}G(\mathrm{Cl\cdot}) - \Delta_{\mathrm{f,aq}}G(\mathrm{Cl^-}) - FE^0(\mathrm{Cl\cdot}\ /\ \mathrm{Cl^-})$$

Using $E^0(\mathrm{Cl\cdot}\ /\ \mathrm{Cl^-})$ = 2.432 V from Armstrong et al.[1] and the Gibbs energies $\Delta_{\mathrm{f,aq}}G(\mathrm{Cl\cdot})$ = 105.680 kJ/mol and $\Delta_{\mathrm{f,aq}}G(\mathrm{Cl^-})$ = -131.228 kJ/mol from Wagman et al.,[5] the Henry's law constant of the chlorine radical can be calculated as:

$$\frac{H_s^{bp}(\mathrm{Cl})}{\mathrm{mol\ kg^{-1}\ bar^{-1}}} = \exp\left(\frac{105680 - (-131228) - (96485 \times 2.432)}{8.314 \times 298.15}\right) = 2.5$$

It should be noted that the Henry's law constant depends exponentially on the values of the reduction potentials and the Gibbs energies. Therefore, even small uncertainties in E^0 and ΔG will result in large uncertainties in the calculated Henry's law constants. For example, the stated uncertainty in $E^0(\mathrm{Cl\cdot}\ /\ \mathrm{Cl^-})$ of ±0.018 V leads to an uncertainty of a factor of two in the calculated value of H_s. This does not include the uncertainties in any of the other Gibbs energies.

List of Symbols

Symbol	quantity	unit*
A	parameter for the temperature dependence of H_s	dimensionless
m	molality	mol kg^{-1}
B	parameter for the temperature dependence of H_s	K
c	concentration	M = mol L^{-1}
C	parameter for the temperature dependence of H_s	dimensionless
E^0	standard reduction potential	V
h_G	gas-specific Schumpe parameter	M^{-1}
$h_{G,0}$	h_G at T$^{\ominus}$	M^{-1}
h_i	ion-specific Schumpe parameter	M^{-1}

h_T	temperature dependence of h_G	M^{-1} K^{-1}
H_s	Henry's law solubility constant	M atm^{-1}
H_{s0}	Henry's law solubility constant in pure water, i.e., in the absence of any salts in the solution	M atm^{-1}
$H_{s,eff}$	effective Henry solubility	M atm^{-1}
K_a	acidity constant	M
K_s	Sechenov parameter	M^{-1}
p	partial pressure	atm = 101325 Pa
R	gas constant	8.314 J mol^{-1} K^{-1}
T	temperature	K
$T^{\ominus}$	reference temperature	298.15 K
μ	ionic strength	M

* The units listed here are those used in this document. In some cases, the coherent derived SI units are different.

5.3.1.4 Effective Henry's law constants

If the gas-phase species is simply dissolved, the equilibrium is described with an ``intrinsic" (or ``physical") Henry's law constant. If the dissolved species is involved in fast equilibria in the condensed phase, an ``effective Henry's law constant" $H_{s,eff}$ can be defined. For example, HCHO is in equilibrium with its hydrated form in aqueous solutions:

$$HCHO + H_2O \leftrightarrows H_2C(OH)_2$$

An effective Henry's law constant $H_{s,eff}$ can be defined as:

$$H_{s,eff} = \frac{c_{tot}}{p(\mathrm{HCHO})}$$

where c_{tot} refers to the sum of HCHO and $H_2C(OH)_2$.

5.3.1.5 Sechenov parameters

The solubility of a gas also depends upon the presence of other substances in the solution. The best known effect is that of an added salt. In most cases, the addition of a salt to the solution results in a lowering of the solubility of the gas. This effect is usually described with the Sechenov equation:

$$\log_{10}\left(\frac{H_{s0}}{H_s}\right) = K_s c_s$$

which describes the ratio of the Henry's law constants in the absence, H_{s0}, and presence, H_s, of a given concentration of salt, c_s. The proportionality constant is the Sechenov parameter, K_s.

5.3.1.6 Schumpe parameters

The Sechenov parameter is specific to both the gas and the salt. Thus, in general, an individual value is needed for any particular gas-salt combination. Several models have been developed to predict K_s for systems where no measurements have been made. Here, we have adopted the procedure developed by Schumpe[3] and Weisenberger and Schumpe.[6] It assumes that K_s is composed of an ion-specific constant h_i and a gas-specific constant h_G. For a mixed electrolyte solution with more than one salt, it is necessary to sum over the individual salt concentrations c_i (instead of using the total concentration c_s):

$$\log_{10}\left(\frac{H_{s0}}{H_s}\right) = \sum_i (h_i + h_G)\, c_i$$

The small temperature dependence is assumed to lie completely in h_G:

$$h_G = h_{G,0} + h_T(T - 298.15\ \mathrm{K})$$

where $h_{G,0}$ is the value of h_G at 298.15 K. Weisenberger and Schumpe[6] analyzed 892 Sechenov parameters for various gases in salt solutions over the temperature range 273 to 363 K. They derived an optimum set of h_i, $h_{G,0}$, and h_T parameters for a diverse set of ions and gases. Values for O_2 and H^+ were arbitrarily set to zero to make the set unique. The standard deviation in the predicted Sechenov parameters is 0.026.

In Tables Eq2 and Eq3, we present the parameters $h_{G,0}$, h_T, and h_i from Weisenberger and Schumpe,[6] along with some parameters derived from other studies. In the latter cases, the ion-specific parameters h_i are considered fixed and we have solved for the gas-specific parameters.

Note that in the previous recommendation, $h_{G,0}$ and h_T were listed in Table Eq1.

As an example, the solubility of ozone in a solution of 0.8 M HCl and 1.2 M Na_2SO_4 at 273 K is calculated:

First, the Henry's law constant for pure water, H_{s0}^{273} = 0.024 M atm^{-1} at 273 K is calculated from Table Eq1. The gas-specific parameters from Table Eq2 for ozone are $h_{G,0}$ = 0.00396 M^{-1} and h_T = 1.79 × 10^{-3} M^{-1} K^{-1}, thus:

$$h_G = 0.00396\ \mathrm{M^{-1}} + 1.79 \times 10^{-3}\ \mathrm{M^{-1}\ K^{-1}} \times (273 - 298)\ \mathrm{K} = -0.0408\ \mathrm{M^{-1}}$$

The ion-specific parameters from Table Eq3 are corrected by this value to calculate the change in the logarithm of the Henry's law constant:

$$\log_{10}\left({H_{s0}^{273}}/{H_s^{273}}\right) = 2 \times (0.1143 - 0.0408)\ \mathrm{M^{-1}} + 1.2\ M \times (0.1117 - 0.0408)\ \mathrm{M^{-1}} + 0.8\ \mathrm{M} \times (0 - 0.0408)\ \mathrm{M^{-1}} + 0.8\ M \times (0.0318 - 0.0408)\ \mathrm{M^{-1}} = 0.181$$

Thus, ${H_{s0}^{273}}/{H_s^{273}} = 10^{0.181} = 1.517$, and the solubility of O_3 in this salt solution at 273 K is:

$$H_s^{273} = {0.024\ \mathrm{M\ atm^{-1}}}/{1.517} = 0.016\ \mathrm{M\ atm^{-1}}$$

A new expression for the solubility model has been proposed by Gordeev and Ershov.[2] It is, however, currently not used in our work.

(1) Armstrong, D., A.; Huie, R., E.; Koppenol, W., H.; Lymar Sergei, V.; Merényi, G.; Neta, P.; Ruscic, B.; Stanbury David, M.; Steenken, S.; Wardman, P. Standard electrode potentials involving radicals in aqueous solution: inorganic radicals (IUPAC Technical Report). *Pure Appl. Chem.* **2015**, *87*, 1139-1150, doi:10.1515/pac-2014-0502.

(2) Gordeev, A. V.; Ershov, B. G. Development and validation of the successor to the Weisenberger–Schumpe solubility model of gas in aqueous electrolytes: Solubilities of Ar, He, Xe, and O_3 in electrolyte solutions at 25 °C. *Ind. Eng. Chem. Res.* **2021**, *60*, 16509–16521, doi:10.1021/acs.iecr.1c02883.

(3) Schumpe, A. The estimation of gas solubilities in salt-solutions. *Chem. Engineer. Sci.* **1993**, *48*, 153-158, doi:10.1016/0009-2509(93)80291-W.

(4) Sieg, K.; Starokozhev, E.; Schmidt, M. U.; Puttmann, W. Inverse temperature dependence of Henry's law coefficients for volatile organic compounds in supercooled water. *Chemosphere* **2009**, *77*, 8-14, doi:10.1016/j.chemosphere.2009.06.028.

(5) Wagman, D. D.; Evans, W. H.; Parker, V. B.; Schumm, R. H.; Halow, I.; Bailey, S. M.; Churney, K. L.; Nutall, R. L. The NBS tables of chemical thermodynamic properties. Selected values for inorganic and C_1 and C_2 organic substances in SI unites. *J. Phys. Chem. Ref. Data* **1982**, *11*, Suppl. No. 2.

(6) Weisenberger, S.; Schumpe, A. Estimation of gas solubilities in salt solutions at temperatures from 273 K to 363 K. *AIChE Journal* **1996**, *42*, 298-300, doi:10.1002/aic.690420130.

5.3.2 Table Eq1. Henry's Law Constants for Pure Water

Substance	Temperature Range, K	H_s (298 K)[a] (M atm^{-1})	*A*	*B*	*C*	Uncertainty Range[b]	Note
Simple O and H Compounds							
O_2	273–348	1.27 × 10^{-3}	–161.6	8160	22.39	I	1
O_3	273–333	1.03 × 10^{-2}	–14.08	2830		II	1
H	298	3.1 × 10^{-4}				IV	1
OH	298	25				IV	1
HO_2	298	690				IV	1
H_2O_2	278–303	8.70 × 10^{4}	–13.08	7290		III	1
Simple Inorganic Nitrogen Compounds							
N_2	273–348	6.52 × 10^{-4}	–177.1	8640	24.71	I	2
NH_3	273–348	60.2	–9.84	4160		III	2
NF_3	283–323	7.96 × 10^{-4}	–242.8	12100	34.236	II	2
N_2F_4	288–318	8.53 × 10^{-4}	–332.7	16610	47.370	III	2
NH_2Cl	293–313	93	-11.57	4800		IV	2

Substance	Temperature Range, K	H_s (298 K)[a] ($M\ atm^{-1}$)	*A*	*B*	*C*	Uncertainty Range[b]	Note
$NHCl_2$	293–313	29	-10.68	4180		IV	2
NCl_3	293–313	0.10	-16.17	4130		IV	2
NO	273–358	1.92×10^{-3}	–163.86	8234	22.816	II	2
NO_2	276–293	1.2×10^{-2}	–12.32	2360		III	2
NO_3	298	3.0×10^{-2}				IV	2
N_2O	273–313	2.42×10^{-2}	–148.1	8610	20.266	I	2
NOCl	273–293	>0.05					2
HN_3	277–309	12.0	–10.19	3780		III	2
HNCO	273–298	23	−11.62	4400		III	2
Simple Inorganic Carbon Compounds							
CO	278–323	9.81×10^{-4}	–178.0	8750	24.875	I	3
CO_2	273–353	3.44×10^{-2}	–123.3	7335	16.739	I	3
Hydrocarbons							
CH_4	273–328	1.41×10^{-3}	–194.7	9750	27.274	I	4
C_2H_6	273–323	1.88×10^{-3}	–240.2	12420	33.744	I	4
C_3H_8	273–348	1.51×10^{-3}	–281.1	14510	39.652	I	4
n–C_4H_{10}	273–348	1.49×10^{-3}	–269.9	14330	37.734	I	4
$CH_3CH(CH_3)CH_3$	278–318	9.18×10^{-4}	–360.6	18020	51.444	II	4
C_2H_4	288–348	5.96×10^{-3}	–154.6	8540	21.202	II	4
C_2H_2	273–343	4.14×10^{-2}	–145.8	7880	20.384	II	4
C_2H_5CCH	298	5.67×10^{-2}				III	4
C1 Haloalkanes							
CH_3F	273–353	0.0619	–98.98	6070	13.31	III	5
CH_3Cl	273–366	0.101	–162.02	9544	22.42	II	5
CH_3Br	273–313	0.166	–12.90	3310		III	5
CH_3I	273–313	0.198	–297.36	15870	42.56	III	5
CH_2Cl_2	283–313	0.393	–13.23	3665		III	5
CH_2Br_2	283–363	1.23	–108.37	8524	14.04	III	5
$CHCl_3$	275–323	0.261	–15.63	4261		II	5
$CHCl_2Br$	273–313	0.409	–18.32	5200		III	5
$CHClBr_2$	273–313	0.868	–18.67	5530		III	5
$CHBr_3$	273–313	1.76	–16.79	5170		III	5
CF_2Cl_2	273–313	3.09×10^{-3}	–17.41	3470		III	5
$CFCl_3$	273–313	1.07×10^{-2}	–15.74	3340		III	5
CCl_4	283–320	3.61×10^{-2}	–17.69	4284		II	5
CHF_3	278–348	1.34×10^{-2}	–12.84	2540		III	5
$CHClF_2$	278–363	3.58×10^{-2}	–11.90	2555		II	5
$CClF_3$	298–348	1.0×10^{-3}	–12.53	1660		IV	5
CF_4	276–323	2.11×10^{-4}	–313.47	15140	44.62	III	5
C2 Haloalkanes							
C_2H_5Cl	281–366	8.25×10^{-2}	–178.12	10274	24.78	III	6
$CHCl_2CH_3$	273–366	0.177	–243.22	14160	34.05	III	6
CH_2ClCH_2Cl	275–323	0.906	–14.65	4340		III	6
CCl_3CH_3	273–333	6.12×10^{-2}	–15.19	3697		II	6
$CHCl_2CH_2Cl$	276–323	1.14	–13.48	4060		III	6
CCl_3CH_2Cl	293–313	0.43	–16.36	4626		IV	6
$CHCl_2CHCl_2$	284–323	2.38	–15.18	4784		IV	6
C_2HCl_5	293–298	0.60	–18.62	5400		III	6
CCl_2FCClF_2	283–303	3.4×10^{-3}	−16.55	3241		III	6
C_2Cl_6	283–313	0.27	–20.53	5730		IV	6
CH_2=CHCl	283–308	3.90×10^{-2}	–13.79	3144		III	6
CCl_2=CH_2	283–313	3.74×10^{-2}	–14.82	3439		III	6
Z-CHCl=CHCl	283–343	0.259	–13.76	3701		III	6
E-CHCl=CHCl	275–343	0.103	–14.18	3550		III	6
CCl_2=CHCl	274–343	0.111	–16.64	4307		III	6
CCl_2=CCl_2	274–343	5.58×10^{-2}	–17.84	4459		III	6
C_2H_5Br	273–303	0.136	–15.14	3918		IV	6

Substance	Temperature Range, K	H_s (298 K)[a] ($M\ atm^{-1}$)	*A*	*B*	*C*	Uncertainty Range[b]	Note
CH_2BrCH_2Br	283–303	1.38	−13.96	4257		IV	6
$CHBr_2CHBr_2$	298–323	1.0	–2.82	840		IV	6
C3 Haloalkanes							
$CH_2ClCHClCH_3$	274–303	0.343	−15.41	4275		IV	7
$CH_2ClCH_2CH_2Cl$	274–300	1.03	−13.13	3923		IV	7
$CH_2ClCHClCH_2Cl$	274–318	3.60	−11.25	3736		IV	7
Alcohols							
CH_3OH	273–373	203	–97.53	9240	12.61	II	8
CH_3CH_2OH	273–373	190	–162.9	12900	21.91	II	8
$CH_3CH_2CH_2OH$	273–373	142	–217.7	15800	29.76	III	8
$CH_3CH(OH)CH_3$	283–358	124	–225.2	16260	30.8	III	8
$CH_3CH_2CH_2CH_2OH$	273–373	123	–265.7	18400	36.64	III	8
$CH_3CH(CH_3)CH_2OH$	273–373	84	−263.6	18080	36.40	III	8
$CH_3CH(OH)CH_2CH_3$	273–343	111	–283.3	19280	39.2	III	8
$(CH_3)_3COH$	298–372	79	–275.9	19045	37.98	III	8
Diols							
HOC_2H_4OH	298	6.6×10^5				V	9
$HOCH_2CH(OH)CH_3$	298	2.7×10^5				V	9
HOC_3H_6OH	298	1.6×10^6				V	9
$HOCH(OH)C_2H_5$	298	2.1×10^5				V	9
$HOCH_2CH_2CH(OH)CH_3$	298	7.1×10^5				V	9
HOC_4H_8OH	298	3.5×10^6				V	9
$CH_3CH(OH)CH(OH)CH_3$	298	1.1×10^5				V	9
Polyols							
$HOCH_2CH(OH)CH_2OH$	298	4.8×10^8				V	10
$HOCH2(CH(OH))_2CH_2OH$	298	1.1×10^{12}				V	10
$C_5H_8(OH)_4$	298	7.4×10^{12}				V	10
$C_5H_7(OH)_5$	298	5.2×10^{13}				V	10
$C_6H_8(OH)_6$	298	1.1×10^{17}				V	10
Ethers							
$(C_2H_5)_2O$	273–333	1.0	−269.99	16990	37.39	IV	11
Hydroperoxides							
CH_3OOH	277–293	300	–11.99	5280		IV	12
$HOCH_2OOH$	278–293	1.7×10^6	–18.79	9870		V	12
$CH_3C(O)OOH$	278–301	837	–11.07	5310		V	12
C_2H_5OOH	278–301	336	–14.28	5995		V	12
Aldehydes							
HCHO ($H_{s,eff}$)	288–318	3.23×10^3	–15.73	7100		IV	13
CH_3CHO ($H_{s,eff}$)	273–313	12.9	–17.19	5890		IV	13
C_2H_5CHO	273–313	13	–16.55	5700		V	13
C_3H_7CHO	283–318	9.6	–18.59	6220		V	13
$CH_3CH(CH_3)CHO$	298	5.13				V	13
CHOCHO ($H_{s,eff}$)	278–308	4.19×10^5	–12.15	7480		IV	13
$HOCH_2CHO$ ($H_{s,eff}$)	298–313	4.14×10^4	–4.80	4600		V	13
$CH_3C(O)CHO$ ($H_{s,eff}$)	288–318	3.5×10^3	–17.15	7545		IV	13
CH_2CHCHO	298	7.3	–15.12	5100		V	13
$CH_2C(CH_3)CHO$	273–333	4.55	–14.02	4630		IV	13
$CH_3CHCHCHO$	273–363	54.7	–177.34	12585	24.42	IV	13
Ketones							
$CH_3C(O)CH_3$	273–311	27.8	–15.23	5530		III	14
$C_2H_5C(O)CH_3$	273–298	18	–16.40	5740		IV	14
$CH_3C(O)C(O)CH_3$	288–318	74	–14.66	5650			14
$CH_2CHC(O)CH_3$	298	41				V	14
C1 and C2 Organic Acids							
HC(O)OH	275–308	8.9×10^3	–11.40	6100		IV	15

Substance	Temperature Range, K	H_s (298 K)[a] (M atm^{-1})	*A*	*B*	*C*	Uncertainty Range[b]	Note
$CH_3C(O)OH$	275–308	4.1×10^3	–12.50	6200		IV	15
$HC(OH)C(O)OH$ ($H_{s,eff}$)	278–308	2.83×10^4	–3.26	4030		IV	15
$HC(O)C(O)OH$ ($H_{s,eff}$)	278–308	1.09×10^4	–6.84	4810		IV	15
$HOC(O)C(O)OH$	298	6.2×10^8				V	15
C3 and Higher Organic Acids							
$CH_3C(O)C(O)OH$	278–308	3.11×10^5	–4.417	5090		V	15
$HOC(O)CH_2C(O)OH$	298	2.4×10^{10}				V	16
$HOC(O)CH_2CH_2C(O)OH$	298	3.1×10^9				V	16
$HOC(O)(CHOH)_2C(O)OH$	298	5×10^{17}				V	16
$HOC(O)C_3H_6C(O)OH$	298	3.8×10^9				V	16
$HOC(O)C_4H_8C(O)OH$	298	6.7×10^9				V	16
$(CH_2C(O)OH)_2C(OH)C(O)OH$	298	3.1×10^{17}				V	16
Formates and Acetates							
$CH_3OC(O)H$	278–298	4.2	–11.88	3970		V	17
$C_2H_5OC(O)H$	278–298	3.4	–14.11	4570		V	17
n-$C_3H_7OC(O)H$	278–298	2.6	–15.99	5050		V	17
$CH_3C(O)OCH_3$	293–343	8.58	–442.6	24800	63.45	V	17
$CH_3C(O)OC_2H_5$	293–353	6.55	–226.3	14950	31.26	IV	17
$CH_3C(O)OC_3H_7$	293–343	4.46	–275.9	17500	38.38	V	17
Carbonates and Other Esters							
$(CH_3O)_2CO$	288–318	16.4	–13.765	4940		III	18
$(C_2H_5O)_2CO$	288–318	10.3	–17.72	5980		III	18
$CH_2CHOC(O)CH_3$	288–318	2.04	–14.42	4510		III	18
$CH_2C(CH_3)C(O)OCH_3$	288–318	3.1	–16.64	5300		III	18
Peroxyacyl Compounds							
$CH_3C(O)O_2$	274	<0.1				III	19
Amines							
CH_3NH_2	298	90				V	20
$C_2H_5NH_2$	298	81				V	20
$C_3H_7NH_2$	298	67				V	20
$C_4H_9NH_2$	298	57				V	20
$(CH_3)_2NH$	298	56				V	20
$(C_2H_5)_2NH$	298	39				V	20
$(C_3H_7)_2NH$	298	20				V	20
$(CH_3)_3N$	298	10				V	20
$(C_2H_5)_3N$	298	6.7				V	20
CH_3NCl_2	278–318	0.333	–15.55	4308		V	20
$(CH_3)_2NNO$	293	400				V	20
Amides							
$CH_3NHC(O)H$	333–373	1.4×10^5	–12.43	7240		IV	21
$CH_3C(O)NHCH_3$	333–353	3.3×10^5	–17.14	8900		IV	21
$(CH_3)_2NC(O)H$	343–372	1.7×10^4	–15.41	7500		IV	21
$(CH_3)_2NC(O)CH_3$	343–272	4.4×10^3	–18.15	8600		IV	21
Cyano Compounds							
HCN	287–311	9.02	–25.323	8206		III	22
CH_3CN	273–303	52.8	–9.35	3970		III	22
Nitro Compounds							
CH_3NO_2	293–323	34.6	–9.92	4010		IV	23
$C_2H_5NO_2$	293–323	21.7	–11.80	4430		IV	23
$C_3H_7NO_2$	293–323	13.1	–13.22	4710		IV	23
$CH_3CH(NO_2)CH_3$	293–323	8.42	–13.02	4520		IV	23
CH_3ONO_2	273–298	2.0	–15.20	4740		IV	23
$C_2H_5ONO_2$	273–298	1.45	–16.20	4940		III	23
CH_3ONO_2	273–298	2.0	–15.20	4740		IV	23
$CH_3CH_2CH_2ONO_2$	273–298	1.10	–18.31	5490		IV	23
$CH_3CH(ONO_2)CH_3$	273–298	0.791	–18.20	5360		IV	23

Substance	Temperature Range, K	H_s (298 K)[a] ($M\ atm^{-1}$)	*A*	*B*	*C*	Uncertainty Range[b]	Note
$CH_3CH_2CH_2CH_2ONO_2$	273–298	1.01	–19.40	5790		IV	23
$CH_3CH(ONO_2)CH_2CH_3$	273–298	0.648	–18.59	5410		IV	23
$CH_3C(O)O_2NO_2$	274–297	2.8	–18.15	5730		IV	23
$O_2NOC_2H_4ONO_2$	293	640				IV	23
$HOC_2H_4ONO_2$	293	3.99×10^4				IV	23
$HOCH_2CH(ONO_2)CH_3$	293	7.3×10^3				IV	23
$CH_3CH(OH)CH_2ONO_2$	293	6.7×10^3				IV	23
$CH_3C(O)CH_2ONO_2$	293	1.01×10^3				IV	23
$CH_3CH(ONO_2)CH_2ONO_2$	293	175				IV	23
$O_2NO_2CH_2CH_2CH_2ONO_2$	298	160				V	23
CCl_3NO_2	298	0.48				III	23
Haloacetones							
$CH_2FC(O)CH_3$	293	47				V	24
$CH_2ClC(O)CH_3$	288–318	59	–14.08	5410		IV	24
$CHCl_2C(O)CH_3$	293	33				V	24
$CF_3C(O)CH_3$	288–318	138	–24.92	8900		IV	24
Haloalcohols							
CH_2FCH_2OH	293	47				V	25
CHF_2CH_2OH	293	94				V	25
CF_3CH_2OH	276–299	47.7	–17.00	6220		III	25
$CHF_2CF_2CH_2OH$	275–299	141	–18.53	7000		III	25
$CF_3CF_2CH_2OH$	275–299	14.6	–11.71	4290		III	25
$CHCl_2CH_2OH$	293	37				V	25
Haloaldehydes							
CCl_3CHO ($H_{s,eff}$)	288–318	3.4×10^5	1.16	3450		IV	26
Haloacids							
$CH_2FC(O)OH$	298	8.1×10^4				V	27
$CHF_2C(O)OH$	278–308	3.0×10^4	–12.71	6870		IV	27
$CF_3C(O)OH$	278–298	5.78×10^3	–5.16	4120		IV	27
$CH_2ClC(O)OH$	278–308	1.1×10^5	–21.08	9740		IV	27
$CHCl_2C(O)OH$	298-308	1.2×10^5	–15.18	8010		IV	27
$CCl_3C(O)OH$	298-308	7.4×10^4	–17.83	8660		IV	27
$CClF_2C(O)OH$	278–308	2.5×10^4	–24.26	10250		IV	27
$CH_2BrC(O)OH$	278–308	1.5×10^5	–19.12	9260		IV	27
$CHBr_2C(O)OH$	298–308	2.3×10^5	–17.64	8940		IV	27
$CBr_3C(O)OH$	298–308	3.0×10^5	–17.6	9000		V	27
Halogenated Esters							
$CF_3C(O)OCH_3$	278–298	0.12	–18.55	4900		IV	28
$CF_3CH_2OC(O)H$	278–298	0.55	–16.33	4690		IV	28
$CH_3C(O)OCH_2CF_3$	278–298	0.58	–18.32	5300		IV	28
$C_2H_5OC(O)CF_3$	278–298	0.09	–18.95	4930		IV	28
Halogens							
Cl	298	2.5				IV	29
Cl_2	283–383	6.2×10^{-2}	–13.51	3200		II	29
Br	298	0.33					29
Br_2	273–308	0.725	–15.05	4390		II	29
BrCl	279–299	0.94	–18.94	5630		III	29
I	298	0.34				IV	29
Inorganic Halogen Compounds							
ClO	298	1.4				V	30
Cl_2O	273–293	7.1				IV	30
ClO_2	283–333	1.01	–11.65	3470		III	30
HOCl	293–313	660	–13.2	5880		IV	30
HOBr	298	$>1.3 \times 10^3$				V	30
Inorganic Sulfur Compounds							
SO_2	278–383	1.36	–39.72	4250	4.525	II	31

Substance	Temperature Range, K	H_s (298 K)[a] ($M\ atm^{-1}$)	*A*	*B*	*C*	Uncertainty Range[b]	Note
H_2S	273–323	0.102	–145.2	8120	20.296	III	31
Organic Sulfur Compounds							
CS_2	274–305	0.062	–17.05	4250		II	32
COS	273–288	2.02×10^{-2}	–15.68	3510		III	32
CH_3SH	298–368	0.39	–12.42	3420		III	32
C_2H_5SH	298–368	0.28	–13.82	3740		II	32
CH_3SCH_3	272–305	0.54	–12.19	3460		III	32
$CH_3SC_2H_5$	298	0.43				I	32
$C_2H_5SC_2H_5$	298	0.35				I	32
$CH_2CHCH_2SCH_3$	298	0.43				I	32
$CH_3S(O)CH_3$	280–308	9.5×10^4	7.10	1300		I	32
CH_3NCS	298	17				IV	32
CH_3SSCH_3	298	0.59				I	32
$C_2H_5SSC_2H_5$	298	0.37				I	32
Mercury Compounds							
Hg	278–308	0.13	−10.74	2590		IV	33

[a] $H_s = \exp(A + B/T + C \ln(T))\ M\ atm^{-1}$

[b] Uncertainty Classes:

I—Better than 10%
II—10% to 50%
III—50% to 100%
IV—Factor of 2 to factor of 10
V—Factor of 10 to factor of 100
VI—Greater than a factor of 100

5.3.2.1 Notes for Table Eq1

Note 1: *Simple O, H Compounds* Back to Table

O_2 (Oxygen, CAS RN: 7782-44-7)

The recommendation was taken from the studies of Benson et al.[2] and Rettich et al.[9] The data show clear curvature in a plot of ln (H_s) vs. 1/T. A two-parameter fit gives A = –13.26 and B = 1950 K for the temperature range 273–285 K.

O_3 (Ozone, CAS RN: 10028-15-6)

The recommendation of Rischbieter et al.[10] was accepted and refitted.

H (Hydrogen atom, CAS RN: 12385-13-6)

Calculated from the IUPAC-recommended value of the Gibbs energy of solution $\Delta_{sol}G$ = 20 kJ mol^{-1}, based on the similarity of H to He and H_2.[1] The previous recommendation was $H_s = 2.6 \times 10^{-4}$ M atm^{-1}.

OH (Hydroxyl radical CAS RN: 3352-57-6)

Calculated using the standard reduction potential $E^0(OH\cdot/OH^-)$ = 1.902 V from Armstrong et al.[1] and the Gibbs energies of formation $\Delta_{f,g}G(OH\cdot)$ = 34.23 kJ mol^{-1} and $\Delta_{f,aq}G(OH^-)$ = −157.244 kJ mol^{-1} from Wagman et al.[13] The previous recommendation was H_s = 39 M atm^{-1}.

HO_2 (Hydroperoxy radical, CAS RN: 3170-83-0)

The recommendation was based on a calculation by Schwartz[11] based on the gas phase constituents HO_2, H^+, and O_2^-. Thermodynamic values were updated to those in our Thermodynamic tables, to pK_a = (4.8 ± 0.1) and to a standard reduction potential $E^o(O_2/O_2^-)$ = −(0.35 ± 0.01) V. The standard reduction potential, referenced to one atmosphere O_2, is based primarily on equilibria reported by Meisel and Czapski,[7] corrected for a revised duroquinone potential.[14]

H_2O_2 (Hydrogen peroxide, CAS RN: 7722-84-1)

The data of Lind and Kok[5] and Lind and Kok[6] (corrected), Hwang and Dasgupta,[4] Yoshizumi et al.,[15] Staffelback and Kok,[12] O'Sullivan et al.,[8] and Huang and Chen[3] are all in good agreement. The recommendation is from a two-parameter fit to all the results (Lind and Kok and Hwang and Dasgupta are represented by calculated endpoints; Huang and Chen by calculated points at the experimental temperatures).

(1) Armstrong, D., A.; Huie, R., E.; Koppenol, W., H.; Lymar Sergei, V.; Merényi, G.; Neta, P.; Ruscic, B.; Stanbury David, M.; Steenken, S.; Wardman, P. Standard electrode potentials involving radicals in aqueous solution: inorganic radicals (IUPAC Technical Report). *Pure Appl. Chem.* **2015**, *87*, 1139-1150, doi:10.1515/pac-2014-0502.

(2) Benson, B. B.; Krause, D.; Peterson, M. A. The solubility and isotope fractionation of gases in dilute aqueous solution. 1. Oxygen. *J. Sol. Chem.* **1979**, *8*, 655-690, doi:10.1007/BF01033696.

(3) Huang, D.; Chen, Z. Reinvestigation of the Henry's law constant for hydrogen peroxide with temperature and acidity variation. *J. Environ. Sci.* **2010**, *22*, 570-574, doi:10.1016/S1001-0742(09)60147-9.

(4) Hwang, H.; Dasgupta, P. K. Thermodynamics of the hydrogen peroxide-water system. *Environ. Sci. Technol.* **1985**, *19*, 255-258, doi:10.1021/es00133a006.

(5) Lind, J. A.; Kok, G. L. Henry's law determinations for aqueous solutions of hydrogen peroxide, methylhydroperoxide, and peroxyacetic acid. *J. Geophys. Res.* **1986**, *91*, 7889-7895, doi:10.1029/JD091iD07p07889.

(6) Lind, J. A.; Kok, G. L. Correction to "Henry's law determinations for aqueous solutions of hydrogen peroxide, methylhydroperoxide, and peroxyacetic acid". *J. Geophys. Res.* **1994**, *99*, 21119, doi:10.1029/94JD01155.

(7) Meisel, D.; Czapski, G. One-electron transfer equilibria and redox potentials of radicals studied by pulse radiolysis. *J. Phys. Chem.* **1975**, *79*, 1503-1509, doi:10.1021/j100582a004.

(8) O'Sullivan, D. W.; Lee, M.; Noone, B. C.; Heikes, B. G. Henry's law constant determinations for hydrogen peroxide, methyl hydroperoxide, hydroxymethyl hydroperoxide, ethyl

hydroperoxide, and peroxyavetic acid. *J. Phys. Chem.* **1996**, *100*, 3241-3247, doi:10.1021/jp951168n.
(9) Rettich, T. R.; Battino, R.; Wilhelm, E. Solubility of gases in liquids. 22. High-precision determination of Henry's law constants of oxygen in liquid water from T = 274 K to T = 328 K. *J. Chem. Themo.* **2000**, *32*, 1145-1156, doi:10.1006/jcht.1999.0581.
(10) Rischbieter, E.; Stein, H.; Schumpe, A. Ozone solubilities in water and aqueous salt solutions. *J. Chem. Eng. Data* **2000**, *45*, 338-340, doi:10.1021/je990263c.
(11) Schwartz, S. E. Gas- and aqueous phase chemistry of HO_2 in liquid water clouds. *J. Geophys. Res.* **1984**, *89*, 11589-11598, doi:10.1029/JD089iD07p11589.
(12) Staffelbach, T. A.; Kok, G. L. Henry's law constants for aqueous solutions of hydrogen peroxide and hydroxymethyl hydroperoxide. *J. Geophys. Res.* **1993**, *98*, 12713-12717, doi:10.1029/93JD01022.
(13) Wagman, D. D.; Evans, W. H.; Parker, V. B.; Schumm, R. H.; Halow, I.; Bailey, S. M.; Churney, K. L.; Nutall, R. L. The NBS tables of chemical thermodynamic properties. Selected values for inorganic and C_1 and C_2 organic substances in SI unites. *J. Phys. Chem. Ref. Data* **1982**, *11*, Suppl. No. 2.
(14) Wardman, P. The reduction potential of benzyl viologen: An important reference compound for oxidant/radical redox couples. *Free Rad. Res. Comm.* **1991**, *14*, 57-67, doi:10.3109/10715769109088942.
(15) Yoshizumi, K.; Aoki, K.; Nouchi, I.; Okita, T.; Kobayashi, T.; Kamakura, S.; Tajima, M. Measurements of the concentrations in rainwater and of the Henry's Law constant of hydrogen peroxide. *Atmos. Environ.* **1984**, *18*, 395-401, doi:10.1016/0004-6981(84)90114-8.

Note 2: *Simple Inorganic Nitrogen Species*

Back to Table

N_2 (Nitrogen, CAS RN: 7727-37-9)
The recommendation of Battino[2] was accepted and refitted to three-parameter equations. A two-parameter fit gives A = 12.81 and B = 1625 K for the temperature range 273–293 K.

NH_3 (Ammonia, CAS RN: 7664-41-7)
Based on the recommendation by Edwards et al.,[9] refit to a two-parameter equation. Over the temperature range 273–348 K, there appears to be little curvature in the data. The more recent work of Dasgupta and Dong[8] are in quite good agreement with this recommendation, whereas the results of Hales and Drewes[10] are somewhat higher and those of Shi et al.[15] (an uptake study) are significantly lower. The Hales and Drewes paper also included studies of the effect of dissolved CO_2 on the solubility of NH_3. The solubility of NH_3 in solutions containing a wide variety of ions is discussed by Clegg and Brimblecombe.[7]

NF_3 (Nitrogen trifluoride, CAS RN: 7783-54-2)
N_2F_4 (Tetrafluorohydrazine, CAS RN: 10036-47-2)
Refit to three-parameter equation from the recommendation of Wilhelm et al.[18]

NH_2Cl (Chloramide, CAS RN: 10599-90-3)
$NHCl_2$ (Dichloroamine, CAS RN: 3400-09-7)
NCl_3 (Nitrogen trichloride, CAS RN: 10025-85-1)
Derived from flashoff studies with glass sparging columns at 293 and 313 K.[11] The previous recommendation for NH_2Cl was H_s = 87 M atm^{-1} at 298 K.

NO (Nitric oxide, CAS RN: 10102-43-9)
Three-parameter refit from the recommendation of Young.[19] The previous recommendation contained an error in the temperature-dependence parameters A, B, and C.

NO_2 (Nitrogen dioxide, CAS RN: 10102-44-0)
Based on NO_2 uptake studies and an analysis of literature values.[6]

NO_3 (Nitrate radical, CAS RN: 12033-49-7)
Calculated using the standard reduction potential $E^0(NO_3\cdot/NO_3^-)$ = 2.466 V (Armstrong et al.[1]) and the Gibbs energies of formation $\Delta_{f,g}G(NO_3\cdot)$ = 117.971 kJ mol^{-1} (from our table of gas-phase entropy

and enthalpy values) and $\Delta_{f,g}G(NO_3^-)$ = −111.25 kJ mol^{-1} from Wagman et al.[17] The derived solubility value is in good agreement with that calculated by Berdnikov and Bazhin.[3] It is, however, much lower than the values from the uptake of NO_3 into a wetted-wall flow reactor containing Cl^- (Rudich et al.[13]) and a study of the uptake of NO_3 by a series of wetted denuders (Thomas et al.[16]). The previous recommendation was $H_s = 3.8 \times 10^{-2}$ M atm^{-1}.

N_2O (Nitrous oxide, CAS RN: 10024-97-2)

Three-parameter refit to the recommendation of Young.[20] Two parameter fit gives A = 13.40 and B = 2880 K for the temperature range 273–293 K.

NOCl (Nitrosyl chloride, CAS RN: 2696-92-6)

Uptake kinetics measured as function of temperature into water and solutions containing HCl, NaCl, and NaOH. Only the latter had an effect. The kinetics were consistent with an uptake coefficient of 0.03.[14]

HN_3 (Hydrogen azide, CAS RN: 7782-79-8)

Measured using a packed column technique at pH 1.8 (μ = 0.02 M). The effective Henry's law constant can be calculated using $H_{s,eff} = H_s(1 + K_a/[H^+])$, with pK_a = 4.65.[4] The previous recommendation contained a sign error in the parameter A.

HNCO (Isocyanic acid, CAS RN: 75-13-8)

The recommendation is the average of the values obtained by Borduas et al.[5] and Roberts and Liu.[12] The value at T⊖ is the intrinsic Henry's law constant but the temperature dependence refers to the effective Henry's law constant at pH 3. The previously recommended values were erroneous.

(1) Armstrong, D., A.; Huie, R., E.; Koppenol, W., H.; Lymar Sergei, V.; Merényi, G.; Neta, P.; Ruscic, B.; Stanbury David, M.; Steenken, S.; Wardman, P. Standard electrode potentials involving radicals in aqueous solution: inorganic radicals (IUPAC Technical Report). *Pure Appl. Chem.* **2015**, *87*, 1139-1150, doi:10.1515/pac-2014-0502.

(2) Battino, R. Nitrogen in water. In *Nitrogen and Air*; Battino, R., Ed.; Pergamon: Oxford, 1982; Vol. 10; pp 1-29.

(3) Berdnikov, V. M.; Bazhin, N. M. Oxidation-reduction potentials of certain inorganic radicals in aqueous solutions. *Russ. J. Phys. Chem.* **1970**, *44*, 395–398.

(4) Betterton, E. A.; Robinson, J. L. Henry's law coefficient of hydrazoic acid. *J. Air Waste Manage. Assoc.* **1997**, *47*, 1216-1219, doi:10.1080/10473289.

(5) Borduas, N.; Place, B.; Wentworth, G. R.; Abbatt, J. P. D.; Murphy, J. G. Solubility and reactivity of HNCO in water: insights into HNCO's fate in the atmosphere. *Atmos. Chem. Phys.* **2016**, *16*, 703-714, doi:10.5194/acp-16-703-2016.

(6) Cheung, J. L.; Li, Y. Q.; Boniface, J.; Shi, Q.; Davidovits, P.; Worsnop, D.; Jayne, J. T.; Kolb, C. E. Heterogeneous interactions of NO_2 with aqueous surfaces. *J. Phys. Chem. A* **2000**, *104*, 2655-2662, doi:10.1021/jp992929f.

(7) Clegg, S. L.; Brimblecombe, P. Solubility of ammonia in pure aqueous and multicomponent solutions. *J. Phys. Chem.* **1989**, *93*, 7237-7248, doi:10.1021/j100357a041.

(8) Dasgupta, P. K.; Dong, S. Solubility of ammonia in liquid water and generation of trace levels of standard gaseous ammonia. *Atmos. Environ.* **1986**, *20*, 565-570, doi:10.1016/0004-6981(86)90099-5.

(9) Edwards, T. J.; Maurer, G.; Newman, J.; Prausnitz, J. M. Vapor-liquid equilibria in multicomponent aqueous solutions of volatile weak electrolytes. *AIChE Journal* **1978**, *24*, 966-976, doi:10.1002/aic.690240605.

(10) Hales, J. M.; Drewes, D. R. Solubility of ammonia in water at low concentrations. *Atmos. Environ.* **1979**, *13*, 1133-1147, doi:10.1016/0004-6981(79)90037-4.

(11) Holzwarth, G.; Balmer, R. G.; Soni, L. The fate of chorine and chloramines in cooling towers. *Water Research* **1984**, *18*, 1421-1427, doi:10.1016/0043-1354(84)90012-5.

(12) Roberts, J. M.; Liu, Y. Solubility and solution-phase chemistry of isocyanic acid, methyl isocyanate, and cyanogen halides. *Atmos. Chem. Phys.* **2019**, *19*, 4419–4437, doi:10.5194/ACP-19-4419-2019.

(13) Rudich, Y.; Talukdar, R. K.; Ravishankara, A. R.; Fox, R. W. Reactive uptake of NO_3 on pure water and ionic solutions. *J. Geophys. Res.* **1996**, *101*, 21023-21031, doi:10.1029/96JD01844.

(14) Scheer, V.; Frenzel, A.; Behnke, W.; Zetsch, C.; Magi, L.; George, C.; Mirabel, P. Uptake of nitrosyl chloride (NOCl) by aqueous solutions. *J. Phys. Chem. A* **1997**, *101*, 9359-9366, doi:10.1021/jp972143m.
(15) Shi, Q.; Davidovits, P.; Jayne, J. T.; Worsnop, D. R.; Kolb, C. E. Uptake of gas-phase ammonia. 1. Uptake by aqueous surfaces as a function of pH. *J. Phys. Chem. A* **1999**, *103*, 8812-8823, doi:10.1021/jp991696p.
(16) Thomas, K.; Volz-Thomas, A.; Mihelcic, D.; Smit, H. G. J.; Kley, D. On the exchange of NO_3 radicals with aqueous solutions: Solubility and sticking coefficient. *J. Atmos. Chem.* **1998**, *29*, 17-43, doi:10.1023/A:1005860312363.
(17) Wagman, D. D.; Evans, W. H.; Parker, V. B.; Schumm, R. H.; Halow, I.; Bailey, S. M.; Churney, K. L.; Nuttall, R. L. Erratum: The NBS tables of chemical thermodynamic properties; Selected values for inorganic and C1 and C2 organic substances in SI units. *J. Phys. Chem. Ref. Data* **1989**, *18*, 1807–1812, doi:10.1063/1.555845.
(18) Wilhelm, E.; Battino, R.; Wilcock, R. J. Low-pressure solubility of gases in liquid water. *Chem. Rev.* **1977**, *77*, 219-262, doi:10.1021/cr60306a003.
(19) Young, C. L. IUPAC Solubility Data Series, Volume 8, Oxides of Nitrogen, Pergamon Press, Oxford. **1981**, doi:10.1016/C2009-0-00222-0.
(20) Young, C. L. Nitrous oxide in water. In *Oxides of Nitrogen*; Young, C. L., Ed.; Pergamon: Oxford, 1981; Vol. 8; pp 1-22.

Note 3: *Simple Inorganic Carbon Species*

Back to Table

CO (Carbon monoxide, CAS RN: 630-08-0)

The recommendation is based on smoothed data from Rettich et al.[2] and refit to three-parameter equation. A two-parameter fit gives $A = -12.72$ and $B = 1720$ K for the temperature range 273–293 K.

CO_2 (Carbon dioxide, CAS RN: 124-38-9)

Refit to three-parameter equation from the recommendation of Carroll et al.[1] Two-parameter fit gives $A = -11.92$ and $B = 2550$ K for the temperature range 273–293 K.

(1) Carroll, J. J.; Slupsky, J. D.; Mather, A. E. The solubility of carbon dioxide in water at low pressure. *J. Phys. Chem. Ref. Data* **1991**, *20*, 1201-1209, doi:10.1063/1.555900.
(2) Rettich, T. R.; Battino, R.; Wilhelm, E. Solubility of gases in liquids. 15. High-presion determination of Henry coefficients for carbon-monoxide in liquid water at 278 K to 323 K. *Ber. Bunsenges. Phys. Chem.* **1982**, *86*, 1128-1132, doi:10.1002/bbpc.198200051.

Note 4: *Hydrocarbons*

Back to Table

CH_4 (Methane, CAS RN: 74-82-8)

The recommendation is a three-parameter fit to the smoothed recommendation of Clever and Young.[4] There is very good agreement with the more recent data of Ben-Naim and Battino.[2] A two-parameter fit gives $A = -13.45$ and $B = 2040$ K for the temperature range 273–293 K.

C_2H_6 (Ethane, CAS RN: 74-84-0)

The recommendation is a three-parameter fit to the smoothed recommendation of Hayduk.[6] There is very good agreement with the more recent data of Ben-Naim and Battino.[2] Two parameter fit gives $A = -15.95$ and $B = 2875$ K for the temperature range 273−293 K.

C_3H_8 (Propane, CAS RN: 74-98-6)

The recommendation is a three-parameter fit to the smoothed recommendation of Hayduk (1986). There is very good agreement with the more recent data of Ben-Naim and Battino.[2] A two parameter fit gives $A = 17.52$ and $B = 3275$ K for the temperature range 273–293 K.

***n*-C_4H_{10}** (Butane, CAS RN: 106-97-8)

The recommendation is a three-parameter fit to the smoothed recommendation of Hayduk.[7] There is very good agreement with the more recent data of Ben-Naim and Battino.[2] A two parameter fit

gives A = –19.28 and B = 3740 K for the temperature range 273–288 K. The previous recommendation was $H_s = 1.49 \times 10^{-3}$ M atm^{-1} at 298 K.

$CH_3CH(CH_3)CH_3$ (Isobutane, CAS RN: 75-28-5)
The recommendation is from a three-parameter fit to the smoothed recommendation of Battino.[1] A two-parameter fit gives A = 18.22 and B = 3340 K for the temperature range 278–293 K.

C_2H_4 (Ethylene, CAS RN: 74-85-1)
The recommendation is from a three-parameter fit to the smoothed recommendation of Wilhelm.[8] A two parameter fit gives A = –12.40 and B = 2170 K for the temperature range 288–313 K.

C_2H_2 (Acetylene, CAS RN: 74-86-2)
Converted from the evaluation of Fogg et al.[5] A two parameter fit gives A = –10.70 and B = 2230 for the temperature range 272–298 K.

C_2H_5CCH (1-Butyne, ethylacetylene; CAS RN: 107-00-6)
Adopted from Brockbank.[3] The previously recommended value was erroneous.

(1) Battino, R. Methane in water. In *Methane*; Clever, H. L., Young, C. L., Eds.; Pergamon: Oxford, 1987; Vol. 27/28; pp 1-44.
(2) Ben-Naim, A.; Battino, R. Solubilization of methane, ethane, propane and n-butane in aqueous solutions of sodium dodecylsulfate. *J. Sol. Chem.* **1985**, *14*, 245-253, doi:10.1007/BF00644456.
(3) Brockbank, S. A. Aqueous Henry's law constants, infinite dilution activity coefficients, and water solubility: Critically evaluated database, experimental analysis, and prediction methods, Brigham Young, 2013.
(4) Clever, H. L.; Young, C. L. IUPAC Solubility Data Series, Volume 27/28, Methane, Pergamon Press, Oxford. **1987**, doi:10.1016/C2009-0-00752-1.
(5) Fogg, P. G. T.; Bligh, S. A.; Derrick, M. E.; Yampol'skii, Y. P.; Clever, H. L.; Skrzecz, A.; Young, C. L. IUPAC-NIST solubility data series. 76. Solubility of ethyne in liquids. *J. Phys. Chem. Ref. Data* **2002**, *30*, 1693-1876, doi:10.1063/1.1397768.
(6) Hayduk, W. IUPAC Solubility Data Series, Volume 9, Ethane, Pergamon Press, Oxford. **1982**.
(7) Hayduk, W. IUPAC Solubility Data Series, Volume 24, Propane, Butane and 2-Methylpropane, Pergamon Press, Oxford. **1986**.
(8) Wilhelm, E.; Battino, R.; Wilcock, R. J. Low-pressure solubility of gases in liquid water. *Chem. Rev.* **1977**, *77*, 219-262, doi:10.1021/cr60306a003.

Note 5: *C1 Haloalkanes*

Back to Table

CH_3F (Methyl fluoride, CAS RN: 593-53-3)
A fit to the transformed recommended values of Staudinger and Roberts[6] and Brockbank.[2] The values are very close at lower temperatures, but diverge 16% at 273 K. A two-parameter fit yields: $H_s = \exp(-10.08 + 2180\ \text{K/T})$ M atm^{-1}.

CH_3Cl (Chloromethane, CAS RN: 74-87-3)
A refit to the recommendation of Brockbank.[2] A two-parameter fit over the temperature range 293−318 K results in $H_s = \exp(-12.13 + 2942\ \text{K/T})$ M atm^{-1}.

CH_3Br (Bromomethane, CAS RN: 74-83-9)
A fit to the transformed recommended values of Staudinger and Roberts[6] and Brockbank.[2] The values are very close at lower temperatures, but diverge up to 20% at 303 K. The previously recommended value was erroneous. $H_s = \exp(-12.16 + 3100\ \text{K/T})$ M atm^{-1} from Staudinger and Roberts.[6]

CH_3I (iodomethane, CAS RN: 74-88-4)
A fit to the transformed recommended values of Staudinger and Roberts[6] and Brockbank.[2] The values are very close at lower temperatures, but diverge 12% at 313 K. A two-parameter fit yields: $H_s = \exp(-13.51 + 3550\ \text{K/T})$ M atm^{-1}.

CH_2Cl_2 (Methylene chloride, CAS RN: 75-09-2)
From the review of Warneck.[7] The uncertainties quoted are ±0.78 in *A* and ±231 K in *B*. A more recent study over the temperature range 281–364 K is also in close agreement, with H_s = 0.401 vs. 0.485 M atm^{-1} at 293 K.[4]

CH_2Br_2 (Dibromomethane, CAS RN: 74-95-3)
A refit to the recommendation of Brockbank.[2] A two-parameter fit over the temperature range 293−313 K results in $H_s = \exp(-14.50 + 4389\ K/T)$ M atm^{-1}.

$CHCl_3$ (Trichloromethane, chloroform; CAS RN: 67-66-3)
From the review of Warneck.[7] The uncertainties quoted are ±0.38 in *A* and ±112 K in *B*. A more recent study over the temperature range 281–364 K is also in close agreement, with H_s = 0.313 vs. 0.334 M atm^{-1} at 293 K.[4] A more recent review by Brockbank[2] results in $H_s = \exp(-213.32 + 12980\ K/T + 29.53\ \ln(T/K))$ M atm^{-1} for the temperature range 273–366 K or $H_s = \exp(-13.51 + 3550\ K/T)$ M atm^{-1} for the temperature range 273–323 K, falling about 20% below these other values.

$CHBrCl_2$ (Bromodichloromethane, CAS RN: 75-27-4)
A refit to the evaluation of Staudinger and Roberts.[6]

$CHBr_2Cl$ (Dibromochloromethane, CAS RN: 124-48-1)
A refit to the evaluation of Staudinger and Roberts.[6]

$CHBr_3$ (Tribromomethane, CAS RN: 75-25-2)
A refit to the evaluation of Staudinger and Roberts.[6]

CCl_2F_2 (Dichlorodifluoromethane, CFC-12; CAS RN: 75-71-8)
A refit to the evaluation of Staudinger and Roberts.[6]

CCl_3F (Trichloromonofluoromethane, CFC-11; CAS RN: 75-69-4)
A refit to the evaluation of Staudinger and Roberts.[6]

CCl_4 (Carbon tetrachloride, CAS RN: 56-23-5)
From the review of Warneck.[7] The uncertainties quoted are ±0.40 in *A* and ±119 K in *B*. A more recent study over the temperature range 281–364 K is also in close agreement, with H_s = 0.040 vs. 0.046 M atm^{-1} at 293 K.[4] A more recent review by Brockbank[2] results in $H_s = \exp(-359.12 + 19390\ K/T + 29.53\ \ln(T/K))$ M atm^{-1} for the temperature range 273−366 K or $H_s = \exp(-16.73 + 4020\ K/T)$ M atm^{-1} for the temperature range 273–323 K, in close agreement.[2]

CHF_3 (Fluoroform, HFC-23; CAS RN: 75-46-7)
Calculated values from the evaluation of Wilhelm[8] were combined with results from Zheng et al.,[9] double weighted. In the latter study, gas solubilities measured at 278, 308, and 338 K in solutions containing 0 to 0.0564 mole/mole NaCl (0 to 174‰) with a gas absorption unit. Calculated values for 0‰ NaCl taken at each temperature and fitted to a two-parameter equation.

$CHClF_2$ (Difluorochloromethane, HFC-22; CAS RN: 75-45-6)
A linear fit to the data of Zheng et al.,[9] Boggs and Buck,[1] and Kutsuna and Hori.[5] The data of Chang and Criddle[3] were significantly lower than these results and not included in the fit. The review by Wilhelm, et al.[8] gave a three-parameter fit that indicated curvature, but this does not appear to be supported by these more recent data.

$CClF_3$ (Chlorotrifluoromethane, CFC-13; CAS RN: 75-72-9)
A refit to the evaluation of Wilhelm et al.[8]

CF_4 (Tetrafluoromethane, CFC-14; CAS RN: 75-73-0)
A refit to the evaluation of Wilhelm et al.[8]

(1) Boggs, J. E.; Buck, A. E., Jr. The solubility of some chloromethanes in water. *J. Phys. Chem.* **1958**, *62*, 1459-1461, doi:10.1021/j150569a031.

(2) Brockbank, S. A. Aqueous Henry's law constants, infinite dilution activity coefficients, and water solubility: Critically evaluated database, experimental analysis, and prediction methods, Brigham Young, 2013.

(3) Chang, W.-K.; Criddle, C. S. Biotransformation of HCFC-22, HCFC-142b, HCFC-123, and HFC-134a by methanotropic mixed culture MM1. *Biodegradation* **1995**, *6*, 2-9, doi:10.1007/BF00702293.
(4) Chen, F.; Freedman, D. L.; Falta, R. W.; Murdoch, L. C. Henry's law constants of chlorinated solvents at elevated temperatures. *Chemosphere* **2012**, *86*, 156-165, doi:10.1016/j.chemosphere.2011.10.004.
(5) Kutsuna, S.; Hori, H. Experimental determination of Henry's law constants of trifluoroacetic acid at 278–298 K. *Atmos. Environ.* **2008**, *42*, 1399-1412, doi:10.1016/j.atmosenv.2007.11.009.
(6) Staudinger, J.; Roberts, P. V. A critical compilation of Henry's law constant temperature dependence relations for organic compounds in dilute aqueous solutions. *Chemosphere* **2001**, *44*, 561-576, doi:10.1016/S0045-6535(00)00505-1.
(7) Warneck, P. A review of Henry's law coefficients for chlorine-containing C_1 and C_2 hydrocarbons. *Chemosphere* **2007**, *69*, 347-361, doi:10.1016/j.chemosphere.2007.04.088.
(8) Wilhelm, E.; Battino, R.; Wilcock, R. J. Low-pressure solubility of gases in liquid water. *Chem. Rev.* **1977**, *77*, 219-262, doi:10.1021/cr60306a003.
(9) Zheng, D.-Q.; Guo, T.-M.; Knapp, H. Experimental and modeling studies on the solubility of CO_2, $CHClF_2$, CHF_3, $C_2H_2F_4$ and $C_2H_4F_2$ in water and aqueous NaCl solutions under low pressures *Fluid Phase Equilibria* **1997**, *129*, 197-209, doi:10.1016/S0378-3812(96)03177-9.

Note 6: *C2 Haloalkanes*

Back to Table

C_2H_5Cl (Ethyl chloride, CAS RN: 75-00-3)

A refit to the recommendation of Brockbank.[2] A two-parameter fit over the temperature range 283−318 K results in $H_s = \exp(-12.21 + 2900\ K/T)$ M atm^{-1}. The results are essentially identical to the previous recommendation taken from Warneck,[8] but cover a wider temperature range, showing slight curvature. The uncertainties quoted by Warneck are ±1.04 in *A* and ±305 K in *B*.

$CHCl_2CH_3$ (1,1-dichloroethane, CAS RN: 75-34-3)

A refit to the recommendation of Brockbank.[2] A two-parameter fit over the temperature range 283−318 K results in $H_s = \exp(-15.84 + 4214\ K/T)$ M atm^{-1}. The results are essentially identical to the previous recommendation taken from Warneck, with a slight deviation above 310 K. This probably reflects the more recent study of Chen, et al.[3] over the temperature range 281–364 K. Note that the lowest temperature point of Chen, et al., is above both recommendations.

CH_2ClCH_2Cl (1,2-dichloroethane, CAS RN: 107-06-2)

Recommended values taken from the review of Warneck.[8] The uncertainties quoted are ±0.56 in *A* and ±165 K in *B*. A more recent study over the temperature range 281–364 K is also in close agreement, with H_s = 1.33 vs. 1.16 M atm^{-1} at 293 K.[3]

CCl_3CH_3 (1,1,1-trichloroethane, CAS RN: 71-55-6)

Recommended values taken from the review of Warneck.[8] The uncertainties quoted are ±0.32 in *A* and ±96 K in *B*. A more recent study over the temperature range 281–364 K is also in close agreement, with H_s = 0.070 vs. 0.076 M atm^{-1} at 293 K.[3]

$CHCl_2CH_2Cl$ (1,1,2-trichloroethane, CAS RN: 79-00-5)

Recommended values taken from the review of Warneck.[8] The uncertainties quoted are ±0.40 in *A* and ±118 K in *B*.

CCl_3CH_2Cl (1,1,1,2-tetrachloroethane, CAS RN: 630-20-6)

Recommended values taken from the review of Warneck.[8] The uncertainties quoted are ±1.30 in *A* and ±394 K in *B*.

$CHCl_2CHCl_2$ 1,1,2,2-tetrachloroethane, CAS RN: 79-34-5)

Recommended values taken from the review of Warneck.[8] The uncertainties quoted are ±0.94 in *A* and ±281 K in *B*.

$CHCl_2CCl_3$ (Pentachloroethane, CAS RN: 76-01-7)

Adopted from the experimental determination by Hiatt.[4] The previous recommendation was H_s = 0.42 M atm^{-1} at 298 K from Brockbank.[2]

CCl_2FCClF_2 (1,1,2-trichloro-1,2,2-trifluoroethane, CFC-113; CAS RN: 76-13-1)
Adopted from Ashworth et al.[1]

CCl_3CCl_3 (Hexachloroethane, CAS RN: 67-72-1)
A refit to the evaluation of Staudinger and Roberts.[7] Warneck[8] did not make a recommendation for this substance.

Chloroethenes

$CHCl=CH_2$ (Chloroethene, CAS RN: 75-01-4)
Adopted from the review of Warneck.[8] The uncertainties quoted are ±0.66 in *A* and ±194 K in *B*. A more recent study over the temperature range 281–364 K is also in close agreement, with H_s = 0.048 vs. 0.047 M atm^{-1} at 293 K.[7]

$CCl_2=CH_2$ (1,1-dichloroethene, CAS RN: 75-35-4)
Adopted from the review of Warneck.[8] The uncertainties quoted are ±0.61 in *A* and ±182 K in *B*.

***Z*-CHCl=CHCl** (1,2-dichloroethylene-*Z*, CAS RN: 156-59-2)
Adopted from the review of Warneck.[8] The uncertainties quoted are ±0.34 in *A* and ±104 K in *B*. A more recent study over the temperature range 281–364 K is also in close agreement, with H_s = 0.313 vs. 0.320 M atm^{-1} at 293 K.[3]

***E*-CHCl=CHCl** (1,2-dichloroethylene-*E*, CAS RN: 156-60-5)
Adopted from the review of Warneck.[8] The uncertainties quoted are ±0.28 in *A* and ±86 K in *B*.

$CHCl=CCl_2$ (Trichloroethylene, CAS RN: 79-01-6)
Adopted from the review of Warneck.[8] The uncertainties quoted are ±0.40 in *A* and ±120 K in *B*. A more recent study over the temperature range 281–364 K is also in close agreement, with H_s = 0.131 vs. 0.142 M atm^{-1} at 293 K.[3]

$CCl_2=CCl_2$ (Tetrachloroethylene, CAS RN: 127-18-4)
Adopted from the review of Warneck.[8] The uncertainties quoted are ±0.25 in *A* and ±74 K in *B*. A more recent study over the temperature range 281–364 K is also in close agreement, with H_s = 0.080 vs. 0.081 M atm^{-1} at 293 K.[3]

CH_3CH_2Br (Ethyl bromide, CAS RN: 74-96-4)
Adopted from Rex.[6]

CH_2BrCH_2Br (1,2-dibromoethane, CAS RN: 106-93-4)
A refit to the recommendation of Brockbank.[2] The previous value, H_s = exp(−17.97 + 5890 K/T) M atm^{-1} (H_S^{298} = 3.4 M atm^{-1}), was a refit to the evaluation of Staudinger and Roberts[7] for T = 283–303 K.

$CHBr_2CHBr_2$ (1,1,2,2-tetrabromoethane, CAS RN: 79-27-6)
Adopted from Khalfaoui and Newsham.[5] The previous recommendation was H_s = 1.44 M atm^{-1} at 298 K from Brockbank.[2]

(1) Ashworth, R. A.; Howe, G. B.; Mullins, M. E.; Rogers, T. N. Air–water partitioning coefficients of organics in dilute aqueous solutions. *J. Hazard. Mater.* **1988**, *18*, 25–36, doi:10.1016/0304-3894(88)85057-X.

(2) Brockbank, S. A. Aqueous Henry's law constants, infinite dilution activity coefficients, and water solubility: Critically evaluated database, experimental analysis, and prediction methods, Brigham Young, 2013.

(3) Chen, F.; Freedman, D. L.; Falta, R. W.; Murdoch, L. C. Henry's law constants of chlorinated solvents at elevated temperatures. *Chemosphere* **2012**, *86*, 156-165, doi:10.1016/j.chemosphere.2011.10.004.

(4) Hiatt, M. H. Determination of Henry's law constants using internal standards with benchmark values. *J. Chem. Eng. Data* **2013**, *58*, 902–908, doi:10.1021/JE3010535.

(5) Khalfaoui, B.; Newsham, D. M. T. Phase equilibria in very dilute mixtures of water and brominated hydrocarbons. *Fluid Phase Equilib.* **1994**, *98*, 213–223, doi:10.1016/0378-3812(94)80120-7.
(6) Rex, A. Über die Löslichkeit der Halogenderivate der Kohlenwasserstoffe in Wasser. *Z. Phys. Chem.* **1906**, *55*, 355–370, doi:10.1515/ZPCH-1906-5519.
(7) Staudinger, J.; Roberts, P. V. A critical compilation of Henry's law constant temperature dependence relations for organic compounds in dilute aqueous solutions. *Chemosphere* **2001**, *44*, 561-576, doi:10.1016/S0045-6535(00)00505-1.
(8) Warneck, P. A review of Henry's law coefficients for chlorine-containing C_1 and C_2 hydrocarbons. *Chemosphere* **2007**, *69*, 347-361, doi:10.1016/j.chemosphere.2007.04.088.

Note 7: *C3 Haloalkanes*

Back to Table

$CH_2ClCHClCH_3$ (1,2-dichloropropane, CAS RN: 78-87-5)
A refit to the evaluation of Staudinger and Roberts.[1]

$CH_2ClCH_2CH_2Cl$ (1,3-dichloropropane, CAS RN: 142-28-9)
A refit to the evaluation of Staudinger and Roberts.[1]

$CH_2ClCHClCH_2Cl$ (1,2,3-trichloropropane, CAS RN: 96-18-4)
A refit to the evaluation of Staudinger and Roberts.[1]

(1) Staudinger, J.; Roberts, P. V. A critical compilation of Henry's law constant temperature dependence relations for organic compounds in dilute aqueous solutions. *Chemosphere* **2001**, *44*, 561-576, doi:10.1016/S0045-6535(00)00505-1.

Note 8: *Alcohols*

Back to Table

CH_3OH (Methanol, CAS RN: 67-56-1)
The recommendation is from a three-parameter fit to the values derived through a comprehensive analysis of limiting activity coefficients, infinite-dilution partial molar excess enthalpies and heat capacities, and measured Henry's law constants.[4] A two-parameter fit up to 298 K gives $A = -13.61$ and $B = 5640$ K, whereas a two-parameter fit up to 373 K gave $A = -12.16$ and $B = 5215$ K. An evaluation by Warneck[9] for the temperature range 273−353 K resulted in recommended parameters of $A = -12.45$ and $B = 5310$. The previous recommendation was $A = -12.08$ and $B = 5210$ K. The 298 K result of Butler et al.[3] and a calculation based on the NBS Thermodynamic tables,[8] are in very good agreement. The 298 K result of Altschuh et al.[1] is about 40% lower.

CH_3CH_2OH (Ethanol, CAS RN: 64-17-5)
The recommendation is from a three-parameter fit to the values derived through a comprehensive analysis of limiting activity coefficients, infinite-dilution partial molar excess enthalpies and heat capacities, and measured Henry's law constants.[4] A two-parameter fit up to 298 K gives $A = -17.14$ and $B = 6660$ K, whereas a two-parameter fit up to 373 K gave $A = -14.57$ and $B = 5908$ K. An evaluation by Warneck[9] for the temperature range 273−353 K resulted in recommended parameters of $A = -15.87$ and $B = 6274$ K. The 298 K result of Altschuh, et al.[1] is about 50% lower.

$CH_3CH_2CH_2OH$ (1-propanol, CAS RN: 71-23-8)
The recommendation is from a three-parameter fit to the values derived through a comprehensive analysis of limiting activity coefficients, infinite-dilution partial molar excess enthalpies and heat capacities, and measured Henry's law constants.[4] A two-parameter fit up to 298 K gives $A = -19.80$ and $B = 7370$. The previous recommendation was $A = -20.16$ and $B = 7470$, which was based on two data points from Snider and Dawson.[7] Room temperature data from other studies[1-3] support these results.

$CH_3CH(OH)CH_3$ (2-propanol, CAS RN: 67-63-0)
The recommendation is from a three-parameter fit to the values derived through a comprehensive analysis of limiting activity coefficients, infinite-dilution partial molar excess enthalpies and heat capacities, and measured Henry's law constants.[5] A two-parameter fit up to 298 K gives $A = -18.95$ and $B = 7100$ K.

$CH_3CH_2CH_2CH_2OH$ (1-butanol, CAS RN: 71-36-3)

The recommendation is from a three-parameter fit to the values derived through a comprehensive analysis of limiting activity coefficients, infinite-dilution partial molar excess enthalpies and heat capacities, and measured Henry's law constants.[4] A two-parameter fit up to 298 K gives $A = -17.68$ and $B = 6725$ K.

$CH_3CH(CH_3)CH_2OH$ (2-methyl-1-propanol, CAS RN: 78-83-1)

The recommendation is from a three-parameter fit to the values derived through a comprehensive analysis of limiting activity coefficients, infinite-dilution partial molar excess enthalpies and heat capacities, and measured Henry's law constants, over the temperature range 298−372 K.[5] A two-parameter fit up to 298 K gives $A = -21.56$ and $B = 7720$ K. Extrapolated values are in very good agreement with the results of Snider and Dawson[7] at 273 and 298 K and room temperature data from other studies.[3,1] A room temperature value of 22.2 M atm^{-1} from a thermal desorption-GC/MS study is about 40% lower than this recommendation.[6]

$CH_3CH(OH)CH_2CH_3$ (2-butanol, CAS RN: 78-92-2)

The recommendation is from a three-parameter fit to the values derived through a comprehensive analysis of limiting activity coefficients, infinite-dilution partial molar excess enthalpies and heat capacities, and measured Henry's law constants, over the temperature range 298−372 K.[5] A two-parameter fit up to 298 K gives $A = -22.60$ and $B = 7095$ K. Extrapolated values are in very good agreement with the results of Snider and Dawson[7] at 273 and 298 K and room temperature data from Butler et al.[3]

$CH_3C(CH_3)(OH)CH_3$ (2-methyl-2-propanol, CAS RN: 75-65-0)

The recommendation is from a three-parameter fit to the values derived through a comprehensive analysis of limiting activity coefficients, infinite-dilution partial molar excess enthalpies and heat capacities, and measured Henry's law constants, over the temperature range 298−372 K.[5] Extrapolated values are in very good agreement with the results of Snider and Dawson[7] at 273 and 298 K and room temperature data from Butler et al.[3] The two data points of Snider and Dawson yield $A = -23.63$ and $B = 8310$ K. The previous recommendation contained an error in the temperature-dependence parameter C.

(1) Altschuh, J.; Bruggemann, R.; Santl, H.; Eichinger, G.; Piringer, O. G. Henry's law constants for a diverse set of organic chemicals: Experimental determination and comparison of estimation methods. *Chemosphere* **1999**, *39*, 1871-1887, doi:10.1016/S0045-6535(99)00082-X.

(2) Burnett, M. G. Determination of partition coefficients at infinite dilution by the gas chromatographic analysis of the vapor above dilute solutions. *Anal. Chem.* **1963**, *35*, 1567-1570, doi:10.1021/ac60204a007.

(3) Butler, J. V. A.; Ramchandani, C. N.; Thomson, D. W. The solubility of non-electrolytes. Part 1. The free energy of hydration of some aliphatic alcohols. *J. Chem. Soc.* **1935**, 280-285, doi:10.1039/jr9350000280.

(4) Dohnal, V.; Fenclova, D.; Vrbka, P. Temperature dependences of limiting activety coefficients, Henry's law constants, and derivative infinite dilution properties of lower (C_1 - C_5) 1-alkanols in water. Critical compilation, correlation, and recommended data. *J. Phys. Chem. Ref. Data* **2006**, *35*, 1621-1651, doi:10.1063/1.220335.

(5) Fenclová, D.; Dohnal, V.; Vrbka, P.; Laštovka, V. Temperature dependence of limiting activity coefficients, Henry's Law constants, and related infinite dilution properties of branched (C3 and C4) alkanols in water. Measurement, critical compilation, correlation, and recommended data. *J. Chem. Eng. Data* **2007**, *52*, 989-1002, doi:10.1021/je600567z.

(6) Kim, Y.-H.; Kim, K.-Y. Recent advances in thermal desorption-gas chromatography-mass spectrometery method to eliminate the matrix effect between air and water samples: Application to the accurate determination of Henry's law constant. *J. Chromatog. A* **2014**, *1342*, 78-85, doi:10.1016/j.chroma.2014.03.040.

(7) Snider, J. R.; Dawson, G. A. Tropospheric light alcohols, carbonyls,, and acetonitrile: Concentrations in the southwest United States and Henry's law data. *J. Geophys. Res.* **1985**, *90*, 3797-3805, doi:10.1029/JD090iD02p03797.

(8) Wagman, D. D.; Evans, W. H.; Parker, V. B.; Schumm, R. H.; Halow, I.; Bailey, S. M.; Churney, K. L.; Nutall, R. L. The NBS tables of chemical thermodynamic properties. Selected values for inorganic and C_1 and C_2 organic substances in SI unites. *J. Phys. Chem. Ref. Data* **1982**, *11*, Suppl. No. 2.
(9) Warneck, P. A note on the temperature dependence of Henry's Law coefficients for methanol and ethanol. *Atmos. Environ.* **2006**, *40*, 7146-7151, doi:10.1016/j.atmosenv.2006.06.024.

Note 9: *Diols*

Back to Table

HOC_2H_4OH (1,2-ethanediol, CAS RN: 107-21-1)
$HOCH_2CH(OH)CH_3$ (Propylene glycol, CAS RN: 57-55-6)
HOC_3H_6OH (1,3-propanediol, CAS RN: 504-63-2)
$HOCH_2CH(OH)C_2H_5$ (1,2-butanediol, CAS RN: 584-03-2)
$HOCH_2CH_2CH(OH)CH_3$ (1,3-butanediol, CAS RN: 107-88-0)
HOC_4H_8OH (1,4-butanediol, CAS RN: 110-63-4)
$CH_3CH(OH)CH(OH)CH_3$ (2,3-butanediol, CAS RN: 513-85-9)

The vapor pressure of the pure liquid and the activity coefficient of the dilute solution were determined from an analysis of literature data. These were then used to obtain the Henry's law values.[1]

(1) Compernolle, S.; Müller, J. F. Henry's law constants of polyols. *Atmos. Chem. Phys.* **2014**, *14*, 12815-12837, doi:10.5194/acpd-14-13529-2014.

Note 10: *Polyols*

Back to Table

$HOCH_2CH(OH)CH_2OH$ (Glycerol, CAS RN: 56-81-5)

The vapor pressure of the pure liquid and the activity coefficient of the dilute solution were determined from an analysis of literature data. These were then used to obtain the Henry's law value.[1]

$HOCH_2(CH(OH))_2CH_2OH$ (Erythritol, CAS RN: 149-32-6)

Determined from the solubility, water activity, obtained by a review of the literature, and solid vapor pressure of the polyol.[1]

$C(CH_2OH)_4$ (Pentaerythritol, CAS RN: 115-77-5)

Determined from the solubility, water activity, obtained by a review of the literature, and solid vapor pressure of the polyol.[1]

$HOCH_2CH(OH)CH(OH)CH(OH)CH_2(OH)$ (Xylitol, Adonitol, Arabitol; CAS RN: 7643-75-6)

Determined from the solubility, water activity, obtained by a review of the literature, and solid vapor pressure of the polyols steroisomers.[1] These values, xylitol (4.0×10^{13} M atm^{-1}), adonitol (4.7×10^{13} M atm^{-1}), and arabitol (6.8×10^{13} M atm^{-1}) were averaged to get the value in the Table.

$C_6H_8(OH)_6$ (Sorbitol, Mannitol, Galactitol; CAS RN: 45007-61-2)

Determined from the solubility, water activity, obtained by a review of the literature, and solid vapor pressure of the polyols steroisomers.[1] These values, sorbitol (6.7×10^{16} M atm^{-1}), mannitol (1.8×10^{17} M atm^{-1}), and galactitol (9.1×10^{16} M atm^{-1}) were averaged to get the value in the Table.

(1) Compernolle, S.; Müller, J. F. Henry's law constants of polyols. *Atmos. Chem. Phys.* **2014**, *14*, 12815-12837, doi:10.5194/acpd-14-13529-2014.

Note 11: *Ethers*

Back to Table

$CH_2CH_2OCH_2CH_3$ (Diethyl ether, CAS RN: 60-29-7)

A refit to the recommendation of Brockbank.[1] A two-parameter fit over the temperature range 293−313 K results in H_s = exp(−20.91 + 6234 K/T) M atm^{-1}. The previous value, H_s = exp(−1867 + 5774 K/T) M atm^{-1} (H_s^{298} = 2.0 M atm^{-1}), was from a refit to the recommendation of Staudinger and Roberts.[2]

(1) Brockbank, S. A. Aqueous Henry's law constants, infinite dilution activity coefficients, and water solubility: Critically evaluated database, experimental analysis, and prediction methods, Brigham Young, 2013.
(2) Staudinger, J.; Roberts, P. V. A critical compilation of Henry's law constant temperature dependence relations for organic compounds in dilute aqueous solutions. *Chemosphere* **2001**, *44*, 561-576, doi:10.1016/S0045-6535(00)00505-1.

Note 12: *Hydroperoxides*

Back to Table

CH_3OOH (Methyl peroxide, CAS RN: 3031-73-0)

The data of Lind and Kok[1,2] and O'Sullivan et al.[4] are in excellent agreement and were fit to a two-parameter expression. A lower limit value of 700 M atm^{-1} at 281 K was estimated from an uptake study, in agreement with the present recommendation.[3]

$HOCH_2OOH$ (Hydroperoxymethanol, CAS RN: 15932-89-5)

The results of O'Sullivan et al.[4] and Staffelback and Kok[5] are very close and were fit to obtain the recommended values. The results of Zhou and Lee[6] are much lower and were not included.

$CH_3C(O)OOH$ (Peracetic acid, CAS RN: 79-21-0)

Experimental results of O'Sullivan et al.[4]

CH_3CH_2OOH (Ethyl hydroperoxide, CAS RN: 3031-74-1)

Experimental results of O'Sullivan et al.[4]

(1) Lind, J. A.; Kok, G. L. Henry's law determinations for aqueous solutions of hydrogen peroxide, methylhydroperoxide, and peroxyacetic acid. *J. Geophys. Res.* **1986**, *91*, 7889-7895, doi:10.1029/JD091iD07p07889.
(2) Lind, J. A.; Kok, G. L. Correction to "Henry's law determinations for aqueous solutions of hydrogen peroxide, methylhydroperoxide, and peroxyacetic acid". *J. Geophys. Res.* **1994**, *99*, 21119, doi:10.1029/94JD01155.
(3) Magi, L.; Schweitzer, F.; Pallares, C.; Cherif, S.; Mirabel, P.; George, C. Investigation of the uptake rate of ozone and methyl hydroperoxide by water surfaces. *J. Phys. Chem. A* **1997**, *4*, 4943-4948, doi:10.1021/jp970646m.
(4) O'Sullivan, D. W.; Lee, M.; Noone, B. C.; Heikes, B. G. Henry's law constant determinations for hydrogen peroxide, methyl hydroperoxide, hydroxymethyl hydroperoxide, ethyl hydroperoxide, and peroxyacetic acid. *J. Phys. Chem.* **1996**, *100*, 3241-3247, doi:10.1021/jp951168n.
(5) Staffelbach, T. A.; Kok, G. L. Henry's law constants for aqueous solutions of hydrogen peroxide and hydroxymethyl hydroperoxide. *J. Geophys. Res.* **1993**, *98*, 12713-12717, doi:10.1029/93JD01022.
(6) Zhou, X.; Lee, Y. N. Aqueous solubility and reaction kinetics of hydroxymethyl hydroperoxide. *J. Phys. Chem.* **1992**, *96*, 265-272, doi:10.1021/j100180a051.

Note 13: *Aldehydes*

Back to Table

HCHO (Formaldehyde, CAS RN: 50-00-0)

The recommended value is the effective Henry's law constant and includes a contribution due to hydration $H_{s,eff} = H_s(1 + K_{hyd})$. Data from Betterton and Hoffmann[3] and Zhou and Mopper[10] are in substantial agreement and were fit to a two-parameter expression. The more recent results of Allou et al.[1] are in complete agreement. Betterton and Hoffmann have calculated $H_s = 2.5$ M atm^{-1} at 298 K for the physical solubility. A gas-stripping study over the temperature range 278–323 K agreed at room temperature, but was lower below and higher above room temperature (Seyfioglu and Odabasi[8]).

CH_3CHO (Acetaldehyde, CAS RN: 75-07-0)

The recommended value is the effective Henry's law constant and includes a contribution due to hydration $H_{s,eff} = H_s(1 + K_{hyd})$. The results of Snider and Dawson,[9] Benkelberg et al.,[2] and Betterton and Hoffmann[3] are in excellent agreement and have been fit to a two-parameter expression for the

recommendation. The results of Zhou and Mopper[10] curve off at higher temperatures and were not included in the fit (note the similar situation for acetone). Betterton and Hoffmann[3] have calculated H_s = 4.8 M atm^{-1} at 298 K for the physical solubility. Brockbank[4] recommends H_s = exp(−16.761 + 5560 K/T) M atm^{-1} over 293 to 318 K (H_s^{298} = 14.8 M atm^{-1}).

CH_3CH_2CHO (Propanal, CAS RN: 123-38-6)

Adopted from Zhou and Mopper.[10] A room temperature value of 9.26 M atm^{-1} from a thermal desorption-GC/MS study is in good agreement with this recommendation (Kim and Kim[7]). The previous recommendation was taken from Brockbank.[4]

$CH_3CH_2CH_2CHO$ (Butanal, CAS RN: 123-72-8)

The results from Zhou and Mopper[10] were fit to a two-parameter expression. A room temperature value of 6.19 M atm^{-1} from a thermal desorption-GC/MS study is about 40% lower than this recommendation.[7] Brockbank[4] recommends H_s = exp(−18.1085 + 6060 K/T) M atm^{-1} over 293−318 K (H_s^{298} = 9.24 M atm^{-1}).

$CH_3CH(CH_3)CHO$ (2-Methyl propanal, isobutyraldehyde; CAS RN: 78-84-2)

Taken from the recommendation of Brockbank.[4]

CHOCHO (Glyoxal, CAS RN: 107-22-2)

Measured using a bubble-column method.[5] Validation measurements on formaldehyde and acetic acid gave results of 4.8 × 10^3 M atm^{-1} and 5.0 × 10^3 M atm^{-1}, slightly higher than the recommendations here. The recommended value is the effective Henry's law constant and includes a contribution due to hydration $H_{s,\mathrm{eff}} = H_s(1 + K_{hyd})$. An intrinsic H_s = 1.90 M atm^{-1} was calculated at 298 K. The solubility increased by about a factor of three at 0.05 M NaCl, but dropped by ~50% when the concentration was increased to 5 M. Na_2SO_3 concentrations of 0.0003 M to 0.03 M increased the solubility, up to a factor of ~50. Even higher sulfate concentrations led to values too high to measure. An earlier study reported only limiting values of ≥3 × 10^5.[3]

$HOCH_2CHO$ (Hydroxyacetaldehyde, CAS RN: 141-46-8)

Effective Henry's law constant measured by a bubble-column technique at 298 and 318 K.[3] An intrinsic Henry's law constant of 4.1 × 10^3 M atm^{-1} at 298 K was calculated. The previous recommendation was essentially identical.

$CH_3C(O)CHO$ (Methyl glyoxal, CAS RN: 78-98-8)

Effective Henry's law constant measured by a bubble-column technique.[3] An intrinsic Henry's law constant of 1.4 M atm^{-1} at 298 K was calculated.

CH_2=CHCHO (2-Propenal, acrolein, CAS RN: 107-02-8)

Taken from Snider and Dawson.[9] The previous recommendation was incorrectly cited from Brockbank.[4]

$CH_2C(CH_3)CHO$ (Methacrolein, CAS RN: 78-85-3)

Taken from the recommendation of Brockbank.[4] Previous value, H_s(298 K) = 6.5 M atm^{-1}, was measured using a static technique with daily instrument calibrations and absolute determinations of partial pressures.[6] An uncertainty of ±0.7 M atm^{-1} was reported.

CH_3CH=CHCHO (Crotonaldehyde, 2-butenal; CAS RN: 4170-30-3)

A refit to the recommendation of Brockbank.[4] Two-parameter fit over the temperature range 273–308 K results in H_s = exp(−14.452 + 5505 K/T) M atm^{-1}.

(1) Allou, L.; El Maimouni, L.; Le Calvé, S. Henry's law constant measurements for formaldehyde and benzaldehyde as a function of temperature and water composition. *Atmos. Environ.* **2011**, *45*, 2991-2998, doi:10.1016/j.atmosenv.2010.05.044.

(2) Benkelberg, H. J.; Hamm, S.; Warneck, P. Henry's law coefficients for aqueous solutions of acetone, acetaldehyde and acetonitrile and equilibrium constants for the addition compounds of acetone and acetaldehyde with bisulfite. *J. Atmos. Chem.* **1995**, *20*, 17-34, doi:10.1007/BF01099916.

(3) Betterton, E. A.; Hoffmann, M. R. Henry's law constants of some environmentally important aldehydes. *Environ. Sci. Technol.* **1988**, *22*, 1415-1418, doi:10.1021/es00177a004.

(4) Brockbank, S. A. Aqueous Henry's law constants, infinite dilution activity coefficients, and water solubility: Critically evaluated database, experimental analysis, and prediction methods, Brigham Young, 2013.
(5) Ip, H. S. S.; Huang, X. H. H.; Yu, J. Z. Effective Henry's law constants of glyoxal, glyoxylic acid, and glycolic acid. *Geophys. Res. Lett.* **2009**, *36*, L01802, doi:10.1029/2008GL036212.
(6) Iraci, L. T.; Baker, B. M.; Tyndall, G. S.; Orlando, J. J. Measurements of the Henry's law coefficients of 2-methyl-3-buten-2-ol, methacrolein, and methylvinyl ketone. *J. Atmos. Chem.* **1999**, *33*, 321-330, doi:10.1023/A:1006169029230.
(7) Kim, Y.-H.; Kim, K.-Y. Recent advances in thermal desorption-gas chromatography-mass spectrometery method to eliminate the matrix effect between air and water samples: Application to the accurate determination of Henry's law constant. *J. Chromatog. A* **2014**, *1342*, 78-85, doi:10.1016/j.chroma.2014.03.040.
(8) Seyfioglu, R.; Odabasi, M. Determination of Henry's Law constant of formaldehyde as a function of temperature: Application to air-water exchange in Tahtali Lake in Izmir, Turkey. *Environ. Monit. Assess.* **2007**, *128*, 343-349, doi:10.1007/s10661-006-9317-3.
(9) Snider, J. R.; Dawson, G. A. Tropospheric light alcohols, carbonyls,, and acetonitrile: Concentrations in the southwest United States and Henry's law data. *J. Geophys. Res.* **1985**, *90*, 3797-3805, doi:10.1029/JD090iD02p03797.
(10) Zhou, X.; Mopper, K. Apparent partition coefficients of 15 carbonyl compounds between air and seawater and between air and freshwater; Implications for air-sea exchange. *Environ. Sci. Technol.* **1990**, *24*, 1864-1869, doi:10.1021/es00082a013.

Note 14: *Ketones*

Back to Table

$CH_3C(O)CH_3$ (Acetone, CAS RN: 67-64-1)

The recommendation is from a fit to the data of Snider and Dawson,[10] Benkelberg et al.,[1] Betterton,[2] and Strekowski and George.[11] Room temperature data points of Nozière and Riemer,[8] Hoff et al.,[5] Burnett,[3] and Vitenberg et al.[12] are in very good agreement. Results of Zhou and Mopper[13] are somewhat higher, particularly at room temperature and above. The situation is similar for acetaldehyde.

$CH_3CH_2C(O)CH_3$ (Butanone, methyl ethyl ketone, CAS RN: 78-93-3)

The recommendation is from the two points of Snider and Dawson.[10] The room temperature points of Vitenberg et al.[12] and Rohrschneider[9] are in good agreement, while a room temperature value of 10.5 M atm^{-1} from a thermal desorption-GC/MS study[7] is about 80% lower. The higher temperature data of Zhou and Mopper[13] are somewhat higher and those of Friant and Suffet[4] are lower than the recommendation.

$CH_3C(O)C(O)CH_3$ (2,3-butanedione, CAS RN: 431-03-8)

Measured by a bubble-column technique.[2]

$CH_2CHC(O)CH_3$ (Methyl vinyl ketone, CAS RN: 78-94-4)

Measured using a static technique with daily instrument calibrations and absolute determinations of partial pressures.[6] An uncertainty of ±7 M atm^{-1} was reported.

(1) Benkelberg, H. J.; Hamm, S.; Warneck, P. Henry's law coefficients for aqueous solutions of acetone, acetaldehyde and acetonitrile and equilibrium constants for the addition compounds of acetone and acetaldehyde with bisulfite. *J. Atmos. Chem.* **1995**, *20*, 17-34, doi:10.1007/BF01099916.
(2) Betterton, E. A. The partitioning of ketones between the gas and aqueous phases. *Atmos. Environ.* **1991**, *25*, 1473-1477, doi:10.1016/0960-1686(91)90006-S.
(3) Burnett, M. G. Determination of partition coefficients at infinite dilution by the gas chromatographic analysis of the vapor above dilute solutions. *Anal. Chem.* **1963**, *35*, 1567-1570, doi:10.1021/ac60204a007.
(4) Friant, S. L.; Suffet, I. H. Interactive effects of temperature, salt concentration, and pH on head space analysis for isolating volitile trace organics in aqueous environmental samples. *Anal. Chem.* **1979**, *51*, 2167-2176, doi:10.1021/ac50049a027.

(5) Hoff, J. T.; Mackay, D.; Gillham, R.; Shiu, W. Y. Partitioning of organic chemicals at the air-water interface in environmental systems. *Environ. Sci. Technol.* **1993**, *27*, 2174-2180, doi:10.1021/es00047a026.
(6) Iraci, L. T.; Baker, B. M.; Tyndall, G. S.; Orlando, J. J. Measurements of the Henry's law coefficients of 2-methyl-3-buten-2-ol, methacrolein, and methylvinyl ketone. *J. Atmos. Chem.* **1999**, *33*, 321-330, doi:10.1023/A:1006169029230.
(7) Kim, Y.-H.; Kim, K.-Y. Recent advances in thermal desorption-gas chromatography-mass spectrometery method to eliminate the matrix effect between air and water samples: Application to the accurate determination of Henry's law constant. *J. Chromatog. A* **2014**, *1342*, 78-85, doi:10.1016/j.chroma.2014.03.040.
(8) Nozière, B.; Riemer, D. D. The chemical processing of gas-phase carbonyl compounds by sulfuric acid aerosols: 2,4-pentanedione. *Atmos. Environ.* **2003**, *37*, 841-851, doi:10.1016/S1352-2310(02)00934-2.
(9) Rohrschneider, L. Solvent characterization by gas-liquid partition coefficients of selected solvents. *Anal. Chem.* **1973**, *45*, 1241-1247, doi:10.1021/ac60329a023.
(10) Snider, J. R.; Dawson, G. A. Tropospheric light alcohols, carbonyls,, and acetonitrile: Concentrations in the southwest United States and Henry's law data. *J. Geophys. Res.* **1985**, *90*, 3797-3805, doi:10.1029/JD090iD02p03797.
(11) Strekowski, R. S.; George, C. Measurement of Henry's Law constants for acetone, 2-butanone, 2,3-butanedione, and isobutyraldehyde using a horizontal flow reactor. *J. Chem. Eng. Data* **2005**, *50*, 804-810, doi:10.1021/je034137r.
(12) Vitenberg, A. G.; Ioffe, B. V.; Dimitrova, Z. S.; Butaeva, I. L. Determination of gas-liquid partition coefficients by means of gas chromatographic analysis. *J. Chromatog.* **1975**, *112*, 319-327, doi:10.1016/S0021-9673(00)99964-3.
(13) Zhou, X.; Mopper, K. Apparent partition coefficients of 15 carbonyl compounds between air and seawater and between air and freshwater; Implications for air-sea exchange. *Environ. Sci. Technol.* **1990**, *24*, 1864-1869, doi:10.1021/es00082a013.

Note 15: *C1 and C2 Organic Acids*

Back to Table

HC(O)OH (Formic acid, CAS RN: 64-18-6)
The results of Johnson et al.[3] are accepted. The 298 K result of Khan et al.[4] is about 75% lower.

$CH_3C(O)OH$ (Acetic acid, CAS RN: 64-19-7)
The results of Johnson et al.[3] are accepted. A value calculated from the NBS Thermodynamic tables[6] is about a factor of two higher.

$H_2C(OH)C(O)OH$ (Glycolic acid, CAS RN: 79-14-1)
Measured using a bubble-column method with no pH control (measured ~3–3.1).[2] Validation measurements on formaldehyde and acetic acid gave results of 4.8×10^3 M atm^{-1} and 5.0×10^3 M atm^{-1}, slightly higher than the recommendations in the Table. An intrinsic $H_s = 2.37 \times 10^4$ M atm^{-1} was calculated at 298 K.

HC(O)C(O)OH Glyoxylic acid, CAS RN: 298-12-4)
Measured using a bubble-column method with no pH control (measured ~2.6–2.8).[2] Validation measurements on formaldehyde and acetic acid gave results of 4.8×10^3 M atm^{-1} and 5.0×10^3 M atm^{-1}, slightly higher than the recommendations in the Table. An intrinsic $H_s = 28.67$ M atm^{-1} was calculated at 298 K.

HOC(O)C(O)OH (Oxalic acid, CAS RN: 144-62-7)
Determined from the solubility, water activity, obtained by a review of the literature, and solution vapor pressure of the acid.[1] The first two were obtained by a review of the literature; the vapor pressure was from evaporation measurements on levitated particles.[5]

(1) Compernolle, S.; Müller, J. F. Henry's law constants of diacids and hydroxy polyacids: recommended values. *Atmos. Chem. Phys.* **2014**, *14*, 2699-2712, doi:10.5194/acp-14-2699-2014.

(2) Ip, H. S. S.; Huang, X. H. H.; Yu, J. Z. Effective Henry's law constants of glyoxal, glyoxylic acid, and glycolic acid. *Geophys. Res. Lett.* **2009**, *36*, L01802, doi:10.1029/2008GL036212.
(3) Johnson, B. J.; Betterton, E. A.; Craig, D. Henry's law coefficients of formic and acetic acids. *J. Atmos. Chem.* **1996**, *24*, 113-119, doi:10.1007/BF00162406.
(4) Khan, I.; Brimblecombe, P.; Clegg, S. L. Solubilities of pyruvic acid and the lower(C_1 -C_6) carboxylic acids. Experimental determinatoin of equilibrium vapour pressures above pure aqueous and salt solutions. *J. Atmos. Chem.* **1995**, *22*, 285-302, doi:10.1007/BF00696639.
(5) Soonsin, V.; Zardini, A. A.; Marcolli, C.; Zuend, A.; Krieger, U. K. The vapor pressures and activities of dicarboxylic acids reconsidered: the impact of the physical state of the aerosol. *Atmos. Chem. Phys.* **2010**, *10*, 11753-11767, doi:10.5194/acp-10-11753-2010.
(6) Wagman, D. D.; Evans, W. H.; Parker, V. B.; Schumm, R. H.; Halow, I.; Bailey, S. M.; Churney, K. L.; Nutall, R. L. The NBS tables of chemical thermodynamic properties. Selected values for inorganic and C_1 and C_2 organic substances in SI unites. *J. Phys. Chem. Ref. Data* **1982**, *11*, Suppl. No. 2.

Note 16: *C3 and Higher Organic Acids*

Back to Table

$CH_3C(O)C(O)OH$ (Pyruvic acid, CAS RN: 127-17-3)
Taken from Khan et al.[4]

$HOC(O)CH_2C(O)OH$ (Malonic acid, CAS RN: 141-82-2)
The solubility and water activity for the acid were obtained through a review of the literature. These were combined with solid vapor pressure[1] or solution vapor pressure[5] data to derive Henry's law values of 0.94×10^{10} M atm^{-1} and 3.9×10^{10} M atm^{-1}.[2]

$HOC(O)CH_2CH_2C(O)OH$ (Succinic acid, CAS RN: 110-15-6)
The solubility and water activity for the acid were obtained through a review of the literature. These were combined with solid vapor pressure[1] or solution vapor pressure[5] data to derive Henry's law values of 2.0×10^9 M atm^{-1} and 4.2×10^9 M atm^{-1}.[2]

$HOC(O)(CHOH)_2C(O)OH$ (Tartaric acid, CAS RN: 87-69-4)
Determined from the solubility, water activity, obtained by a review of the literature, and liquid vapor pressure of the acid.[2] The first two were obtained by a review of the literature; the vapor pressure was obtained from the evaporation rate of levitated, supersaturated liquid particles.[3] The value listed is the midpoint of the range ($0.7–9.3 \times 10^{17}$ M atm^{-1}) from the uncertainty in the vapor pressure data.

$HOC(O)C_3H_6C(O)OH$ (Glutaric acid, CAS RN: 110-94-1)
The solubility and water activity for the acid were obtained through a review of the literature. These were combined with solid vapor pressure[1] or solution vapor pressure[5] data to derive Henry's law values of 2.4×10^9 M atm^{-1} and 5.2×10^9 M atm^{-1}.[2]

$HOC(O)C_4H_8C(O)OH$ (Adipic acid, CAS RN: 124-04-9)
Determined from the solubility, water activity, obtained by a review of the literature, and solid vapor pressure of the acid.[2] The first two were obtained by a review of the literature; the vapor pressure was from evaporation rates of aerosol samples.[1]

$(CH_2C(O)OH)_2C(OH)C(O)OH$ (Citric acid, CAS RN: 77-92-9)
Determined from the solubility, water activity, obtained by a review of the literature, and liquid vapor pressure of the acid.[2] The first two were obtained by a review of the literature; the vapor pressure was obtained from the evaporation rate of levitated, supersaturated liquid particles.[3] The value listed is the midpoint of the range ($0.2–6 \times 10^{17}$ M atm^{-1}) from the uncertainty in the vapor pressure data.

(1) Cappa, C. D.; Lovejoy, E. R.; Ravishankara, A. R. Evidence for liquid-like and nonideal behavior of a mixture of organic aerosol components. *Proc. Nat. Acad. Sci.* **2008**, *105*, 18687-18691, doi:o10.1073/pnas.0802144105.

(2) Compernolle, S.; Müller, J. F. Henry's law constants of diacids and hydroxy polyacids: recommended values. *Atmos. Chem. Phys.* **2014**, *14*, 2699-2712, doi:10.5194/acp-14-2699-2014.
(3) Huisman, A. J.; Krieger, U. K.; Zuend, A.; Marcolli, C.; Peter, T. Vapor pressures of substituted polycarboxylic acids are much lower than previously reported. *Atmos. Chem. Phys.* **2013**, *13*, 6647-6662, doi:10.5194/acp-13-6647-2013.
(4) Khan, I.; Brimblecombe, P.; Clegg, S. L. Solubilities of pyruvic acid and the lower(C_1 -C_6) carboxylic acids. Experimental determinatoin of equilibrium vapour pressures above pure aqueous and salt solutions. *J. Atmos. Chem.* **1995**, *22*, 285-302, doi:10.1007/BF00696639.
(5) Soonsin, V.; Zardini, A. A.; Marcolli, C.; Zuend, A.; Krieger, U. K. The vapor pressures and activities of dicarboxylic acids reconsidered: the impact of the physical state of the aerosol. *Atmos. Chem. Phys.* **2010**, *10*, 11753-11767, doi:10.5194/acp-10-11753-2010.

Note 17: *Formates and Acetates*

Back to Table

$CH_3OC(O)H$ (Methyl formate, CAS RN: 107-31-3)
Measured using a column-stripping method.[2]

$CH_3CH_2OC(O)H$ (Ethyl formate, CAS RN: 109-94-4)
Measured using a column-stripping method.[2]

$CH_3CH_2CH_2OC(O)H$ (n-propyl formate, CAS RN: 110-74-7)
Measured using a column-stripping method.[2]

$CH_3C(O)OCH_3$ (Methyl acetate, CAS RN: 79-20-9)
A refit to the recommendation of Brockbank.[1] A two-parameter fit over the temperature range 293−313 K results in H_s = exp(−16.596 + 5590 K/T) M atm^{-1}. The previous value, H_s = exp(−14.745 + 5008 K/T) M atm^{-1} (H_s^{298} = 4.2 M atm^{-1}), was a refit to the evaluation of Staudinger and Roberts.[3]

$CH_3C(O)OC_2H_5$ (Ethyl acetate, CAS RN: 141-78-6)
A refit to the recommendation of Brockbank.[1] A two-parameter fit over the temperature range 293−308 K results in H_s = exp(−16.761 + 5560 K/T) M atm^{-1}. The previous value, H_s = exp(−17.97 + 5890 K/T) M atm^{-1} (H_s^{298} = 3.4 M atm^{-1}), was from a study utilizing a column-stripping method over temperature range 272−298 K.[2]

$CH_3C(O)OC_3H_7$ (n-propyl acetate, CAS RN: 109-60-4)
A refit to the recommendation of Brockbank.[1] A two-parameter fit over the temperature range 293−308 K results in H_s = exp(−18.418 + 5970 K/T) M atm^{-1}.

(1) Brockbank, S. A. Aqueous Henry's law constants, infinite dilution activity coefficients, and water solubility: Critically evaluated database, experimental analysis, and prediction methods, Brigham Young, 2013.
(2) Kutsuna, S.; Chen, L.; Abe, T.; Mizukado, J.; Uchimaru, T.; Tokuhashi, K.; Sekiya, A. Henry's Law constant of 2,2,2-trifluoroethyl formate, ethyl trifluoroacetate, and non-fluroinated analogous esters. *Atmos. Environ.* **2005**, *39*, 5884-5892, doi:10.1016/j.atmosenv.2005.06.021.
(3) Staudinger, J.; Roberts, P. V. A critical compilation of Henry's law constant temperature dependence relations for organic compounds in dilute aqueous solutions. *Chemosphere* **2001**, *44*, 561-576, doi:10.1016/S0045-6535(00)00505-1.

Note 18: *Carbonates and other Esters*

Back to Table

$(CH_3O)_2CO$ (Dimethyl carbonate, CAS RN: 616-38-6)
$(C_2H_5O)_2CO$ (Diethyl carbonate, CAS RN: 105-58-8)
$CH_2CHOC(O)CH_3$, (Vinyl acetate, CAS RN: 108-05-4)
$CH_2C(CH_3)C(O)OCH_3$ (Methyl methacrylate, CAS RN: 80-62-6)
Infinite dilution activity coefficients were determined and combined with vapor pressure values to yield Henry's law constants. These were presented as a three-parameter equation. The values

showed only slight curvature and are given here as fit to a two-parameter equation.[1] The previously recommended value for methyl methacrylate was erroneous.

(1) Dohnal, V.; Vrbka, P.; Řehák, K.; Böhme, A.; Paschke, A. Activity coefficients and partial molar excess enthalpies at infinite dilution for four esters in water. *Fluid Phase Equilibria* **2010**, *295*, 194-200, doi:10.1016/j.fluid.2010.05.010.

Note 19: *Peroxyacyl Species*

Back to Table

$CH_3C(O)O_2$ (Peroxyacetyl radical, CAS RN: 36709-10-1)

Villalta et al.[1] measured an upper limit for $H_s \leq 0.1$ M atm^{-1} in a coated-wall flow tube uptake experiment on aqueous sodium ascorbate solutions.

(1) Villalta, P. W.; Lovejoy, E. R.; Hanson, D. R. Reaction probability of peroxyacetyl radical on aqueous surfaces. *Geophys. Res. Lett.* **1996**, *23*, 1765-1768, doi:10.1029/96GL01286.

Note 20: *Amines*

Back to Table

CH_3NH_2 (Methylamine, CAS RN: 74-89-5)
$CH_3CH_2NH_2$ (Ethylamine, CAS RN: 75-04-7)
$CH_3CH_2CH_2NH$ (Propylamine, CAS RN: 107-10-8)
$C_4H_9NH_2$ (1-butanamine, CAS RN: 109-73-9)
$(CH_3)_2NH$ (Dimethylamine, CAS RN: 124-40-3)
$(C_2H_5)_2NH$ (Diethylamine, CAS RN: 109-89-7)
$(C_3H_7)NH_2$ (Di-n-propylamine, CAS RN: 142-84-7)
$(CH_3)_3N$ (Trimethylamine, CAS RN: 75-50-3)
$(C_2H_5)_3)N$ (Triethylamine, CAS RN: 121-44-8)

Water-saturated air was bubbled through a 0.01 N NaOH solutions containing the amines and the amine removed from the air stream by passing through a 0.01 N HCl solution. The concentration of the uncharged amine in the original solution was adjusted for the percentage of ionized amine.[1]

CH_3NCl_2 (N,N-dichloromethylamine, CAS RN: 7651-91-4)

Determined by using a static method with a variable headspace and measuring the dichloromethylamine concentration in the liquid phase by UV spectroscopy.[2]

$(CH_3)_2NNO$ (N-nitrosodimethylamine, CAS RN: 62-75-9)

Determined from the rate of loss of ^{14}C labeled N-nitrosodimethylanime from a stirred aqueous solution.[3]

(1) Christie, A. O.; Crisp, D. J. Activity coefficients of the n-primary, secondary, and tertiary amines in aqueous solution. *J. Appl. Chem.* **1967**, *17*, 11-14, doi:10.1002/JCTB.5010170103.
(2) Cimetiere, N.; De Laat, J. Henry's law constant of N,N-dichloromethylamine: application to the contamination of the atmosphere of indoor swimming pools. *Chemosphere* **2009**, *77*, 465-470, doi:10.1016/j.chemosphere.2009.07.056.
(3) Haruta, A.; Jiao, W.; Chen, W.; Chang, A. C.; Gan, J. Evaluating Henry's law constant of N-nitrosodimethylamine (NDMA). *Water Sci. Tech.* **2011**, *64*, 1636-1641, doi:10.2166/wst.2011.742.

Note 21: *Amides*

Back to Table

$CH_3NHC(O)H$ (N-methylformamide, CAS RN: 123-39-7)

Measured by circulating still and differential distillation methods.[1]

$CH_3C(O)NHCH_3$ (N-methylacetamide, CAS RN: 79-16-3)

Measured by a differential distillation method.[1] The temperature dependence was recalculated, yielding different results than in the previous recommendation.

$(CH_3)_2NC(O)H$ (N,N-dimethylformamide, CAS RN: 68-12-2)

Measured by comparative ebulliometry.[1] The temperature dependence was recalculated, yielding different results than in the previous recommendation.

$(CH_3)_2NC(O)CH_3$ (N,N-dimethylacetamide**,** CAS RN: 127-19-5)
Measured by comparative ebulliometry, circulating still, and differential distillation methods.[1] The temperature dependence was recalculated, yielding different results than in the previous recommendation.

(1) Bernauer, M.; Dohnal, V. Temperature dependence of air−water partitioning of N-methylated (C1 and C2) fatty acid amides. *J. Chem. Eng. Data* **2008**, *53*, 2622-2631, doi:10.1021/je800517r.

Note 22: *Cyano compounds*

Back to Table

HCN (Hydrogen cyanide, CAS RN: 74-90-8)
Determined in a 0.1 mol L^{-1} sodium phosphate buffer (pH = 9.00 ± 0.03) by air equilibrium of aqueous cyanide partitioned by a microporous membrane. The error limits were estimated to be ±1.44 on *A* and ±342 K on *B*.[3]

CH_3CN (Acetonitrile, CAS RN: 75-05-8)
The values reported by Benkelberg et al.,[1] Snider and Dawson,[4] Hamm et al.[2] are all in good agreement and have been fit to a two-parameter expression for the recommendation.

(1) Benkelberg, H. J.; Hamm, S.; Warneck, P. Henry's law coefficients for aqueous solutions of acetone, acetaldehyde and acetonitrile and equilibrium constants for the addition compounds of acetone and acetaldehyde with bisulfite. *J. Atmos. Chem.* **1995**, *20*, 17-34, doi:10.1007/BF01099916.
(2) Hamm, S.; Hahn, J.; Helas, G.; Warneck, P. Acetonitrile in the troposphere: Residence time due to rainout and uptake by ocean. *Geophys. Res. Lett.* **1984**, *11*, 1207-1210, doi:10.1029/GL011i012p01207
(3) Ma, J.; Dasgupta, P. K.; Blackledge, W.; Boss, G. R. Temperature dependence of Henry's law constant for hydrogen cyanide. Generation of trace standard gaseous hydrogen cyanide. *Environ. Sci. Technol.* **2010**, *44*, 3028-3034, doi:10.1021/es1001192.
(4) Snider, J. R.; Dawson, G. A. Tropospheric light alcohols, carbonyls,, and acetonitrile: Concentrations in the southwest United States and Henry's law data. *J. Geophys. Res.* **1985**, *90*, 3797-3805, doi:10.1029/JD090iD02p03797.

Note 23: *Nitro compounds*

Back to Table

CH_3NO_2 (Nitromethane, CAS RN: 75-52-5)
$CH_3CH_2NO_2$ (Nitroethane, CAS RN: 79-24-3)
$CH_3CH_2CH_2NO_2$ (1-nitropropane, CAS RN: 108-03-2)
$CH_3CH(NO_2)CH_3$ (2-nitropropane, CAS RN: 79-46-9)
The recommended values are all taken from the work of Benes and Dohnal.[1] For nitromethane, the 298 K value from Rohrschneider[10] is about 30% higher.

$CH_3CH_2ONO_2$ (Ethyl nitrate, CAS RN: 625-58-1)
The recommendation from Easterbrook et al.[2] has been adopted. It is a combined fit of their data with those of Kames and Schurath.[8] The previous recommendation was taken only from Kames and Schurath.

CH_3ONO_2 (Methyl nitrate, CAS RN: 598-58-3)
$CH_3CH_2CH_2ONO_2$ (*n*-propyl nitrate, CAS RN: 627-13-4)
$CH_3CH(ONO_2)CH_3$ (*iso*-propyl nitrate, CAS RN: 1712-64-7)
$1\text{-}C_4H_9ONO_2$ (Butyl nitrate, CAS RN: 928-45-0)
$CH_3CH(ONO_2)CH_2CH_3$ (2-butyl nitrate, CAS RN: 924-52-7)
The recommended values are all taken from the work of Kames and Schurath.[8] The results of Luke et al.[9] are in very good agreement for 1-butyl and 2-butyl nitrates, but the values reported by Hauff[5] for 1- and 2-propyl and butyl nitrates by head-space chromatography are significantly (~50%) lower.

$CH_3C(O)O_2NO_2$ (Peroxyacetyl nitrate (PAN), CAS RN: 2278-22-0)

The results of Kames and Schurath[8] and Frenzel et al.[4] are close and were used for the recommendation. They are somewhat higher (~60%) than the single temperature point of Holdren et al.[6] Kames and Schurath[8] and Holdren et al.[6] also measured hydrolysis rate constants.

$ONO_2C_2H_4ONO_2$ (Ethylene dinitrate, CAS RN: 628-96-6)

The recommended values (at 293 K) are taken from the work of Kames and Schurath.[7]

$HOC_2H_4ONO_2$ (2-hydroxyethyl nitrate, CAS RN: 16051-48-2)
$HOCH_2CH(ONO_2)CH_3$ (2-(nitrooxy)propan-1-ol, CAS RN: 20266-74-4)
$CH_3CH(OH)CH_2ONO_2$ (2-hydroypropyl nitrate, CAS RN: 20266-65-3)
$CH_3C(O)CH_2ONO_2$ (2-propanone, 1-(nitrooxy)-, CAS RN: 6745-71-7)

The recommended values (at 293 K) are taken from the work of Kames and Schurath.[7]

$CH_3CH(ONO_2)CH_2ONO_2$ (1,2-propane dinitrate, CAS RN: 6423-43-4)

Direct measurement at 293 K.[7] A much lower value of 33 M atm^{-1} was calculated from vapor pressure and solubility measurements.[3]

$O_2NO_2CH_2CH_2CH_2ONO_2$ (1,3-propane dinitrate, CAS RN: 3457-90-7)

Calculated from vapor pressure and solubility measurements.[3] Note that the value for 1,2-propane dinitrate was much lower than that directly measured.

CCl_3NO_2 (Trichloromethylnitrate (chloropicrin), CAS RN: 76-06-2)

Measured by a stripping technique in water, 0.1 M and 0.2 M NaCl, and at pH 4.0 and 8.0 (buffered). All values were within the stated margin of error (±0.3).[11]

(1) Benes, M.; Dohnal, V. Limiting activity coefficients of some aromatic and aliphatic nitro compounds in water. *J. Chem. Eng. Data* **1999**, *44*, 1097-1102, doi:10.1021/je9900326.

(2) Easterbrook, K. D.; Vona, M. A.; Osthoff, H. D. Measurement of Henry's law constants of ethyl nitrate in deionized water, synthetic sea salt solutions, and n-octanol. *Chemosphere* **2024**, *346*, 140482, doi:10.1016/J.CHEMOSPHERE.2023.

(3) Fischer, R. G.; Ballschmiter, K. Prediction of the environmental distribution of alkyl dinitrates - Chromatographic determination of vapor pressure p(0), water solubility SH_2O, gas-water partition coefficient K-GW (Henry's law constant) and octanol-water partition coefficient K-OW. *Fresenius J. Anal. Chem.* **1998**, *360*, 769-776, doi:10.1007/s002160050803.

(4) Frenzel, A.; Kutsuna, S.; Takeuchi, K.; Ibusuki, T. Solubility and reactivity of peroxyacetyl nitrate (PAN) in dilute aqueous salt solutions and in sulphuric acid. *Atmos. Environ.* **2000**, *34*, 3641-3544, doi:10.1016/S1352-2310(00)00132-1.

(5) Hauff, K.; Fischer, R. G.; Ballschmiter, K. Determination of C_1 - C_5 alkyl nitrates in rain, smow, white frost, lake, and tap water by a combined codistillation head-space gas chromatography technique. Determination of Henry's law constants by head-space gc. *Chemosphere* **1998**, *37*, 2599-2615, doi:10.1016/S0045-6535(98)00159-3.

(6) Holdren, M. W.; Spicer, C. W.; Hales, J. M. Peroxyacetyl nitrate solubility and decomposition rate in acedic water. *Atmos. Environ.* **1984**, *18*, 1171-1173, doi:10.1016/0004-6981(84)90148-3.

(7) Kames, J.; Schurath, U. Alkyl nitrates and bifunctional nitrates of atmospheric interest: Henry's law constants and their temperature dependencies. *J. Atmos. Chem.* **1992**, *15*, 79-95, doi:10.1007/BF00053611.

(8) Kames, J.; Schurath, U. Henry's law and hydrolysis-rate constants for peroxyacyl nitrates (PANs) using a homogeneous gas-phase source. *J. Atmos. Chem.* **1995**, *21*, 151-164, doi:10.1007/BF00696578.

(9) Luke, W. T.; Dickerson, R. R.; Nunnermacker, L. J. Direct measurements of the photolysis rate coefficients and Henry's law constants of several alkyl nitrates. *J. Geophys. Res.* **1989**, *94*, 14905-14921, doi:10.1029/JD094iD12p14905.

(10) Rohrschneider, L. Solvent characterization by gas-liquid partition coefficients of selected solvents. *Anal. Chem.* **1973**, *45*, 1241-1247, doi:10.1021/ac60329a023.

(11) Worthington, E. K.; Wade, E. A. Henry's law coefficients of chloropicrin and methyl isothiocyanate. *Atmos. Environ.* **2007**, *41*, 5510-5515, doi:10.1016/j.atmosenv.2007.02.019.

Note 24: *Haloacetones*

Back to Table

$CH_2FC(O)CH_3$ (Fluoroacetone, CAS RN: 430-51-3)
Measured by a static approach.[2] The stated uncertainty was ±0.08%.

$CH_2ClC(O)CH_3$ (Chloroacetone CAS RN: 78-95-5)
Measured by a bubble-column technique.[1]

$CHCl_2C(O)CH_3$ (1,1-dichloroacetone, CAS RN: 513-88-2)
Measured by a static approach.[2] The stated uncertainty was ±0.06%.

$CF_3C(O)CH_3$ (1,1,1-trifluoroacetone, CAS RN: 421-50-1)
Measured by a bubble-column technique.[1]

(1) Betterton, E. A. The partitioning of ketones between the gas and aqueous phases. *Atmos. Environ.* **1991**, *25*, 1473-1477, doi:10.1016/0960-1686(91)90006-S.
(2) O'Farrell, C. E.; Waghorne, W. E. Henry's law constants of organic compounds in water and *n*-octane at $T = 293.2$ K. *J. Chem. Eng. Data* **2010**, *55*, 1655-1658, doi:10.1021/je900711h.

Note 25: *Haloalcohols*

Back to Table

CH_2FCH_2OH (2-fluoroethanol, CAS RN: 371-62-0)
Measured by a static approach.[2] The stated uncertainty was ±0.17%.

CHF_2CH_2OH (2,2-difluoroethanol, CAS RN: 359-13-7)
Measured by a static approach.[2] The stated uncertainty was ±0.33%.

CF_3CH_2OH (2,2,2-trifluoroethanol, CAS RN: 75-89-8)
$CHF_2CF_2CH_2OH$ (2,2,3,3-tetrafluoro-1-propanol, CAS RN: 76-37-9)
$CF_3CF_2CH_2OH$ (2,2,3,3,3-Pentafluoro-1-propanol, CAS RN: 422-05-9)
Measured using the equilibrium headspace technique.[1] Parameters derived through a linear fit to the reported data.

$CHCl_2CH_2OH$ (2,2-dichloroethanol, CAS RN: 598-38-9)
Measured by a static approach.[2] The stated uncertainty was ±0.67%.

(1) Chen, L.; Takenaka, N.; Bandow, H.; Maeda, Y. Henry's law constants for C_2-C_3 fluorinated alcohols and their wet deposition in the atmosphere. *Atmos. Environ.* **2003**, *37*, 4817-4822, doi:10.1016/j.atmosenv.2003.08.002.
(2) O'Farrell, C. E.; Waghorne, W. E. Henry's law constants of organic compounds in water and *n*-octane at $T = 293.2$ K. *J. Chem. Eng. Data* **2010**, *55*, 1655-1658, doi:10.1021/je900711h.

Note 26: *Haloaldehydes*

Back to Table

CCl_3CHO (1,1,1-trichloroacetaldehyde, Chloral, CAS RN: 75-87-6)
Effective Henry's law constant measured by head-space analysis.[1] An intrinsic Henry's law constant of 14 M atm^{-1} at 298 K was derived. Listed parameters from a refit to the data.

(1) Betterton, E. A.; Hoffmann, M. R. Henry's law constants of some environmentally important aldehydes. *Environ. Sci. Technol.* **1988**, *22*, 1415-1418, doi:10.1021/es00177a004.

Note 27: *Haloacids*

Back to Table

$CFH_2C(O)OH$ (Fluoroacetic acid, CAS RN: 144-49-0)
Equilibrium partial pressure of the acid obtained using a stripping technique over a solution containing 0.15 to 6.0 mol kg^{-1} HBr to suppress dissociation.[1] Reported values corrected for the effect on the activity of the solution. Due to the high toxicity, only a single determination was made for this acid.

$CF_2HC(O)OH$ (Difluoroacetic acid, CAS RN: 381-73-7)

Equilibrium partial pressure of the acid obtained using a stripping technique over a solution containing 0.15 to 6.0 mol kg^{-1} HBr to suppress dissociation.[1] Reported values corrected for the effect on the activity of the solution.

$CF_3C(O)OH$ (Trifluoroacetic acid, CAS RN: 76-05-1)
Values derived at 178, 288, and 298 K from the simultaneous measurement of the equilibrium partial pressures of TFA over aqueous solutions and the concentration of undissociated TFA in solution using total reflection IR spectroscopy.[2]

$CClH_2C(O)OH$ (Chloroacetic acid, CAS RN: 79-11-8)
$CCl_2HC(O)OH$ (Dichloroacetic acid, CAS RN: 79-43-6)
Equilibrium partial pressure of the acid obtained using a stripping technique over a solution containing 0.15 to 6.0 mol kg^{-1} HBr to suppress dissociation. Reported values corrected for the effect on the activity of the solution.[1]

$CCl_3C(O)OH$ (Trichloroacetic acid, CAS RN: 76-03-9)
Equilibrium partial pressure of the acid obtained using a stripping technique over a solution containing 0.25 to 6.0 mol kg^{-1} HBr to suppress dissociation. Reported values corrected for the effect on the activity of the solution.[1]

$CClF_2C(O)OH$ (Chlorodifluoroacetic acid, CAS RN: 76-04-0)
$CH_2BrC(O)OH$ (Bromoacetic acid, CAS RN: 79-08-3)
$CHBr_2C(O)OH$ (Dibromoacetic acid, CAS RN: 631-64-1)
Equilibrium partial pressure of the acid obtained using a stripping technique over a solution containing 0.15 to 6.0 mol kg^{-1} HBr to suppress dissociation. Reported values corrected for the effect on the activity of the solution.[1]

$CBr_3C(O)OH$ (Tribromoacetic acid, CAS RN: 75-96-7)
Equilibrium partial pressure of the acid obtained using a stripping technique over a solution containing 0.15 to 6.0 mol kg^{-1} HBr to suppress dissociation. Reported values corrected for the effect on the activity of the solution.[1] Only a few measurements at 308 K and one at 298 K were made. The reported value of *B* is the mean of those for $CF_3C(O)OOH$ and $CCl_3C(O)OOH$.[1]

(1) Bowden, D. J.; Clegg, S. L.; Brimblecombe, P. The Henry's law constants of the haloacetic acids. *J. Atmos. Chem.* **1998**, *29*, 85-107, doi:10.1023/A:1005899813756.
(2) Kutsuna, S.; Hori, H. Experimental determination of Henry's law constants of trifluoroacetic acid at 278–298 K. *Atmos. Environ.* **2008**, *42*, 1399-1412, doi:10.1016/j.atmosenv.2007.11.009.

Note 28: *Halogenated esters*

Back to Table

$CF_3C(O)OCH_3$ (Methyl trifluoroacetate CAS RN: 431-47-0)
Parameters derived from a linear fit to the reported data from a column-stripping study. A hydrolysis rate constant of $10^{5.3\pm2.0}$ exp[-(5.07 ± 1.27) × 10^3 K/T] s^{-1} was also obtained.[2] The temperature dependence was recalculated, yielding different results than in the previous recommendation.

$CF_3CH_2OC(O)H$ (2,2,2-trifluoroethyl formate, CAS RN: 32042-38-9)
Value measured using a column-stripping method.[1]

$CH_3C(O)OCH_2CF_3$ (2,2,2-trifluoroethyl acetate, CAS RN: 406-95-1)
Parameters derived from a linear fit to the reported data from a column-stripping study. The hydrolysis rate constant was too slow to measure.[2] The temperature dependence was recalculated, yielding different results than in the previous recommendation.

$C_2H_5OC(O)CF_3$ (Ethyl trifluoroacetate, CAS RN: 383-63-1)
Value measured using a column-stripping method.[1]

(1) Kutsuna, S.; Chen, L.; Abe, T.; Mizukado, J.; Uchimaru, T.; Tokuhashi, K.; Sekiya, A. Henry's Law constant of 2,2,2-trifluoroethyl formate, ethyl trifluoroacetate, and non-fluroinated analogous esters. *Atmos. Environ.* **2005**, *39*, 5884-5892, doi:10.1016/j.atmosenv.2005.06.021.

(2) Kutsuna, S.; Chen, L.; Ohno, K.; Tokuhashi, K.; Sekiya, A. Henry's Law constants and hydrolysis rate constants of 2,2,2-trifluoroethyl acetate and methyl trifluoroacetate. *Atmos. Environ.* **2004**, *38*, 725-732, doi:10.1016/j.atmosenv.2003.10.019.

Note 29: *Halogens*

Back to Table

Cl (Chlorine atom, CAS RN: 22537-15-1)

Calculated using the standard reduction potential $E^0(Cl\cdot/Cl^-) = 2.432$ V from Armstrong et al.[2] and the Gibbs energies of formation $\Delta_{f,g}G(Cl\cdot) = 105.680$ kJ mol^{-1} and $\Delta_{f,aq}G(Cl^-) = -131.228$ kJ mol^{-1} from Wagman et al.[8] Using these updated electrochemical and thermodynamic data resulted in different values than in the previous recommendation.

Cl_2 (Chlorine, CAS RN: 7782-50-5)

The value recommended here has been adopted from Aieta and Roberts,[1] in good agreement with older measurements by Whitney and Vivian[9] and Yakovkin.[10] It represents the intrinsic Henry's law constant of Cl_2. The value that was presented in previous recommendations described the total dissolved chlorine ($HOCl + Cl_2$) at a partial pressure of $p(Cl_2) = 1$ atm. This is different, for details see Sect. 2.5.3 of Sander.[7]

Br (Bromine atom, CAS RN: 10097-32-2)

Calculated using the standard reduction potential $E^0(Br\cdot/Br^-) = 1.96$ V from Armstrong et al.[2] and the Gibbs energies of formation $\Delta_{f,g}G(Br\cdot) = 82.396$ kJ mol^{-1} and $\Delta_{f,aq}G(Br^-) = -103.96$ kJ mol^{-1} from Wagman et al.[8] Using these updated electrochemical and thermodynamic data resulted in different values than in the previous recommendation.

Br_2 (Bromine, CAS RN: 7726-95-6)

The results of Kelley and Tartar[6] and Jenkins and King[5] agree well below about 313 K, and with the 298 K point of Hill et al.[4] Recommendation based on a two-parameter fit to all data at and below 308 K.

BrCl (Bromine chloride, CAS RN: 13863-41-7)

The recommendation is from the work of Barlett and Margerum.[3] The previous recommendation was essentially identical.

I (Iodine atom, CAS RN: 14362-44-8)

Calculated using the standard reduction potential $E^0(I\cdot/I^-) = 1.35$ V from Armstrong et al.[2] and the Gibbs energies of formation $\Delta_{f,g}G(I\cdot) = 70.250$ kJ mol^{-1} and $\Delta_{f,aq}G(I^-) = -51.57$ kJ mol^{-1} from Wagman et al.[8] Using these updated electrochemical and thermodynamic data resulted in different values than in the previous recommendation.

(1) Aieta, E. M.; Roberts, P. V. Henry constant of molecular chlorine in aqueous solution. *J. Chem. Eng. Data* **1986**, *31*, 51–53, doi:10.1021/JE00043A017.
(2) Armstrong, D., A.; Huie, R., E.; Koppenol, W., H.; Lymar Sergei, V.; Merényi, G.; Neta, P.; Ruscic, B.; Stanbury David, M.; Steenken, S.; Wardman, P. Standard electrode potentials involving radicals in aqueous solution: inorganic radicals (IUPAC Technical Report). *Pure Appl. Chem.* **2015**, *87*, 1139-1150, doi:10.1515/pac-2014-0502.
(3) Barlett, W. P.; Margerum, D. W. Temperature dependencies of the Henry's law constant and the aqueous phase dissociation constant of bromine chloride. *Environ. Sci. Technol.* **1999**, *33*, 3410-3414, doi:10.1021/es990300k.
(4) Hill, J. O.; Worsley, I. G.; Helper, L. G. Calorimetric determination of the distribution coefficient and thermodynamic properties of bromine in water and carbon dioxide. *J. Phys. Chem.* **1968**, *72*, 3695-3697, doi:10.1021/j100856a066.
(5) Jenkins, J.; King, M. B. Vapour-liquid equilibria for the system bromine/water at low bromine concentraions. *Chem. Engin. Sci.* **1965**, *20*, 921-922, doi:10.1016/0009-2509(65)80089-6.
(6) Kelley, C. M.; Tartar, H. V. On the system: bromine-water. *J. Am. Chem. Soc.* **1956**, *78*, 5752-5756, doi:10.1021/ja01603a010.
(7) Sander, R. Compilation of Henry's law constants (version 5.0.0) for water as solvent. *Atmos. Chem. Phys.* **2023**, *23*, 10 901–912 440, doi:10.5194/ACP-23-10901-2023.

(8) Wagman, D. D.; Evans, W. H.; Parker, V. B.; Schumm, R. H.; Halow, I.; Bailey, S. M.; Churney, K. L.; Nutall, R. L. The NBS tables of chemical thermodynamic properties. Selected values for inorganic and C_1 and C_2 organic substances in SI unites. *J. Phys. Chem. Ref. Data* **1982**, *11*, Suppl. No. 2.
(9) Whitney, R. P.; Vivian, J. E. Solubility of chlorine in water. *Ind. Eng. Chem.* **1941**, *33*, 741–744, doi:10.1021/IE50378A014.
(10) Yakovkin, A. A. About the hydrolysis of chlorine. *J. Russ. Phys. Chem. Soc. (in Russian)* **1900**, *32*, 673–721.

Note 30: *Inorganic Halogen Species*

Back to Table

ClO (Chlorine monoxide radical, CAS RN: 14989-30-1)
Calculated using the standard reduction potential $E^0(ClO\cdot/ClO^-)$ = 1.39 V from Armstrong et al.[1] and the Gibbs energies of formation $\Delta_{f,g}G(ClO\cdot)$ = 98.11 kJ mol^{-1} and $\Delta_{f,aq}G(ClO^-)$ = –36.8 kJ mol^{-1} from Wagman et al.[7] Using these updated electrochemical and thermodynamic data resulted in different values than in the previous recommendation.

Cl_2O (Dichloromonoxide, CAS RN: 7791-21-1)
Value at 277 K adopted from Roth.[6] The previously cited value from Wilhelm et al.[8] appears to be erroneous.

OClO (Chlorine dioxide, CAS RN: 10049-04-4)
Two-parameter fit to the recommendation of Young.[9]

HOCl (Hypochlorous acid, CAS RN: 7790-92-3)
Huthwelker et al.[5] analyzed the limited data for pure water from Blatchley et al.,[2] Holzwarth et al.,[4] and the more extensive data for uptake by sulfuric acid from Hanson and Ravishankara,[3] along with thermodynamic information, and obtained a consistent expression for the solubility of HOCl.

HOBr (Hypobromous acid, CAS RN: 13517-11-8)
The Henry solubility was estimated to be more than twice that of HOCl based on a study of the effective Henry's law constant for free bromine from a stripping column.[2]

(1) Armstrong, D., A.; Huie, R., E.; Koppenol, W., H.; Lymar Sergei, V.; Merényi, G.; Neta, P.; Ruscic, B.; Stanbury David, M.; Steenken, S.; Wardman, P. Standard electrode potentials involving radicals in aqueous solution: inorganic radicals (IUPAC Technical Report). *Pure Appl. Chem.* **2015**, *87*, 1139-1150, doi:10.1515/pac-2014-0502.
(2) Blatchley, E. R.; Johnson, R. W.; Alleman, J. E.; McCoy, W. F. Effective Henry's law constants for free chlorine and free bromine. *Water Research* **1992**, *26*, 99-106, doi:10.1016/0043-1354(92)90117-M.
(3) Hanson, D. R.; Ravishankara, A. R. Uptake of HCl and HOCl onto sulphuric acid: Solubilities, diffusivities and reaction. *J. Phys. Chem.* **1993**, *97*, 12309-12319, doi:10.1021/j100149a035.
(4) Holzwarth, G.; Balmer, R. G.; Soni, L. The fate of chorine and chloramines in cooling towers. *Water Research* **1984**, *18*, 1421-1427, doi:10.1016/0043-1354(84)90012-5.
(5) Huthwelker, T.; Peter, T.; Juo, B. P.; Clegg, S. L.; Carshlaw, K. S.; Brimblecombe, P. Solubility of HOCl in water and aqueous H_2SO_4 to stratospheric temperatures. *J. Atmos. Chem.* **1995**, *21*, 81-95, doi:10.1007/BF00712439.
(6) Roth, W. A. Notiz zur Thermochemie des Chlormonoxydes. *Z. Phys. Chem.* **1942**, *A191*, 248–250, doi:10.1515/ZPCH-1942-19117, 1942.
(7) Wagman, D. D.; Evans, W. H.; Parker, V. B.; Schumm, R. H.; Halow, I.; Bailey, S. M.; Churney, K. L.; Nutall, R. L. The NBS tables of chemical thermodynamic properties. Selected values for inorganic and C_1 and C_2 organic substances in SI unites. *J. Phys. Chem. Ref. Data* **1982**, *11*, Suppl. No. 2.
(8) Wilhelm, E.; Battino, R.; Wilcock, R. J. Low-pressure solubility of gases in liquid water. *Chem. Rev.* **1977**, *77*, 219-262, doi:10.1021/cr60306a003.
(9) Young, C. L. IUPAC Solubility Data Series, Volume 12, Sulfur Dioxide, Chlorine, Fluorine and Chlorine Oxides, Pergamon Press, Oxford. **1983**, doi:10.1016/C2013-0-03419-6.

Note 31: *Inorganic Sulfur Species*

Back to Table

SO_2 (Sulfur dioxide, CAS RN: 7446-09-5)

The recommendation of Young[8] was accepted and refit to a three-parameter equation. The earlier recommendation of Edwards et al.[2] is slightly lower. A two-parameter fit gives A = –9.53 and B = 2930 K for the temperature range 278–298 K.

H_2S (Hydrogen sulfide, CAS RN: 7783-06-4)

In the recommendation of Fogg and Young[3] two expressions were given, representing the results above and below 283 K. The predicted values from these expressions were calculated, with the points at 283 K averaged, converted to the desired units, and then fit with the two- and three-parameter expressions. These are the recommended values. More recent results of Rinker and Sandall[5] and Munder et al.[4] are slightly lower. In these studies, the physical solubility of H_2S was determined through measurements involving aqueous solutions of glycols or amines, neutralized with HCl. The reported values of De Bruyn et al.[1] are significantly (~30%) lower. The earlier recommendation of Edwards et al.[2] is very close to the recommendation of Fogg and Young[3] as is the recommendation of Yaws et al.[7] The room temperature point calculated from the NBS Thermodynamic tables Wagman et al.[6] is also slightly lower. The work of De Bruyn et al.[1] covered also a wide range of NaCl and $(NH_4)_2SO_4$ concentration and of pH.

(1) De Bruyn, W. J.; Swartz, E.; Hu, J. H.; Shorter, J. A.; Davidovits, P.; Worsnop, D. R.; Zahniser, M. S.; Kolb, C. E. Henry's law solubilities and Śetchenow coefficients of biogenic reduced sulfur species obtained from gas-liquid uptake measurements. *J. Geophys. Res.* **1995**, *100*, 7245-7251, doi:10.1029/95JD00217.

(2) Edwards, T. J.; Maurer, G.; Newman, J.; Prausnitz, J. M. Vapor-liquid equilibria in multicomponent aqueous solutions of volatile weak electrolytes. *AIChE Journal* **1978**, *24*, 966-976, doi:10.1002/aic.690240605.

(3) Fogg, P. G. T.; Young, C. L. IUPAC Solubility Data Series, Volume 32, Hydrogen Sulfide, Deuterium Sulfide and Hydrogen Selenide, Pergamon Press, Oxford. **1988**, doi:10.1016/C2009-0-00348-1.

(4) Munder, B.; Lidal, H.; Sandall, O. C. Physical solubility of hydrogen sulfide in aqueous solutions of 2-(*tert*-butylamino)ethanol. *J. Chem. Eng. Data* **2000**, *45*, 1201-1204, doi:10.1021/je000166f.

(5) Rinker, E. B.; Sandall, O. C. Physical solubility of hydrogen sulfide in several aqueous solvents. *Can. J. Chem. Eng.* **2000**, *78*, 232-236, doi:10.1002/cjce.5450780130.

(6) Wagman, D. D.; Evans, W. H.; Parker, V. B.; Schumm, R. H.; Halow, I.; Bailey, S. M.; Churney, K. L.; Nutall, R. L. The NBS tables of chemical thermodynamic properties. Selected values for inorganic and C_1 and C_2 organic substances in SI unites. *J. Phys. Chem. Ref. Data* **1982**, *11*, Suppl. No. 2.

(7) Yaws, C. L.; Hopper, J. R.; Wang, X.; Rathinsamy, A. K. Calculating solubility & Henry's Law constants for gases in water. *Chem. Eng.* **1999**, 102-105.

(8) Young, C. L. IUPAC Solubility Data Series, Volume 12, Sulfur Dioxide, Chlorine, Fluorine and Chlorine Oxides, Pergamon Press, Oxford. **1983**, doi:10.1016/C2013-0-03419-6.

Note 32: *Organic Sulfur Species*

Back to Table

CS_2 (Carbon disulfide, CAS RN: 75-15-0)

The recommendation is from a fit to data of Elliott,[3] who also present data in 0.5 M NaCl. The work of De Bruyn et al.[2] covered also a wide range of NaCl and $(NH_4)_2SO_4$ concentration and of pH.

COS (Carbonyl sulfide, CAS RN: 463-58-1)

The reviews by Wilhelm et al.[8] and Yaws et al[11] result in identical values over the low temperature range (<303 K) and are combined to generate the recommendation. The work of De Bruyn et al[2] covered also a wide range of NaCl and $(NH_4)_2SO_4$ concentration and of pH.

CH_3SH (Methyl mercaptan, CAS RN: 74-93-1)

The recommendation is based on the data of Przyjazny et al.[4] Results of De Bruyn et al.[2] are about half the recommended value at 298 K.

CH_3CH_2SH (Ethyl mercaptan, CAS RN: 75-08-1)

The recommendation is based on the data of Przyjazny et al.[4] The results of Vitenberg[6] are slightly lower.

CH_3SCH_3 (Dimethyl sulfide, CAS RN: 75-18-3)

The recommendation is based on the values of Dacey et al.[1] The single temperature point of Wong and Wang[9] and the higher temperature results of Przyjazny et al.[4] are in good agreement. The results of De Bruyn et al.[2] are about 30% lower. A more recent value, obtained by Schuhfried et al.[5] with a dynamic gas stripping approach coupled to a mass spectrometer, is in good agreement. The studies of Dacey et al.[1] and Wong and Wang[9] were also carried out with seawater. The work of De Bruyn et al.[2] covered also a wide range of NaCl and $(NH_4)_2SO_4$ concentration and of pH.

$CH_3SC_2H_5$ (Ethyl methyl sulfide, CAS RN: 624-89-5)
$C_2H_5SC_2H_5$ (Diethyl sulfide, CAS RN: 352-93-2)
$CH_2CHCH_2SCH_3$ (Allyl methyl sulfide, CAS RN: 10152-76-8)

Obtained by a dynamic gas stripping approach coupled to a mass spectrometer.[5] An uncertainty of ±0.03 M atm^{-1} was estimated for $CH_3SC_2H_5$, of ±0.01 M atm^{-1} for $C_2H_5SC_2H_5$, and ±0.02 M atm^{-1} for $CH_2CHCH_2SCH_3$.

$CH_3S(O)CH_3$ (Dimethyl sulfoxide, CAS RN: 67-68-5)

The recommendation is taken directly from Watts and Brimblecombe.[7] The previous recommendation was based on an indirect citation.

CH_3NCS (Methyl isothiocyanate CAS RN: 556-61-6)

Measured by stripping technique in pure water.[10] Measurements in NaCl and buffer solutions tended to be lower (0.1 M NaCl, 9 M atm^{-1}; 0.2 M, 7 M atm^{-1}).

CH_3SSCH_3 (Dimethyl disulfide, CAS RN: 624-92-0)
$C_2H_5SSC_2H_5$ (Diethyl disulfide, CAS RN: 110-81-6)

Obtained by a dynamic gas stripping approach coupled to a mass spectrometer.[5] An uncertainty of ±0.04 M atm^{-1} was estimated for CH_3SSCH_3 and ±0.03 M atm^{-1} for $C_2H_5SSC_2H_5$.

(1) Dacey, J. W. H.; Wakeham, S. G.; Howes, B. L. Henry's law constants for dimethylsulfide in freshwater and seawater. *Geophys. Res. Lett.* **1984**, *11*, 991-994, doi:10.1029/GL011i010p00991.

(2) De Bruyn, W. J.; Swartz, E.; Hu, J. H.; Shorter, J. A.; Davidovits, P.; Worsnop, D. R.; Zahniser, M. S.; Kolb, C. E. Henry's law solubilities and Śetchenow coefficients of biogenic reduced sulfur species obtained from gas-liquid uptake measurements. *J. Geophys. Res.* **1995**, *100*, 7245-7251, doi:10.1029/95JD00217.

(3) Elliott, S. The solubility of carbon disulfide vapor in natural aqueous systems. *Atmos. Environ.* **1989**, *23*, 1977-1980, doi:10.1016/0004-6981(89)90523-4.

(4) Przyjazny, A.; Janicki, W.; Chrzanowski, W.; Staszewski, R. Headspace gas chromatographic determination of distribution coefficients of selected organosulfur compounds and their dependence on some parameters. *J. Chromatogr.* **1983**, *280*, 249-260, doi:10.1016/S0021-9673(00)91567-X.

(5) Schuhfried, E.; Biasioli, F.; Aprea, E.; Cappellin, L.; Soukoulis, C.; Ferrigno, A.; Märk, T. D.; Gasperi, F. PTR-MS measurements and analysis of models for the calculation of Henry's law constants of monosulfides and disulfides. *Chemosphere* **2011**, *83*, 311-317, doi:10.1016/j.chemosphere.2010.12.051.

(6) Vitenberg, A. G.; Ioffe, B. V.; Dimitrova, Z. S.; Butaeva, I. L. Determination of gas-liquid partition coefficients by means of gas chromatographic analysis. *J. Chromatog.* **1975**, *112*, 319-327, doi:10.1016/S0021-9673(00)99964-3.

(7) Watts, S. F.; Brimblecombe, P. The Henry's law constant of dimethylsulfoxide. *Environ. Technol. Lett.* **1987**, *8*, 483-486, doi:10.1080/09593338709384509.

(8) Wilhelm, E.; Battino, R.; Wilcock, R. J. Low-pressure solubility of gases in liquid water. *Chem. Rev.* **1977**, *77*, 219-262, doi:10.1021/cr60306a003.

(9) Wong, P. K.; Wang, Y. H. Determination of the Henry's law constant for dimethyl sulfide in seawater. *Chemosphere* **1997**, *35*, 535-544, doi:10.1016/S0045-6535(97)00118-5.
(10) Worthington, E. K.; Wade, E. A. Henry's law coefficients of chloropicrin and methyl isothiocyanate. *Atmos. Environ.* **2007**, *41*, 5510-5515, doi:10.1016/j.atmosenv.2007.02.019.
(11) Yaws, C. L.; Hopper, J. R.; Wang, X.; Rathinsamy, A. K. Calculating solubility & Henry's Law constants for gases in water. *Chem. Eng.* **1999**, 102-105.

Note 33: *Mercury Compounds*

Back to Table

Hg (Mercury, CAS RN: 7439-97-6)

A direct measurement of the partitioning between the gas and aqueous phases, carried out in the presence of added $SnCl_2$ as a reducing agent.[1]

(1) Andersson, M. E.; Gårdfeldt, K.; Wängberg, I.; Strömberg, D. Determination of Henry's law constant for elemental mercury. *Chemosphere* **2008**, *73*, 587-592, doi:10.1016/j.chemosphere.2008.05.067.

5.3.2.2 Bibliography – Table Eq1

Aleta, E. M.; Roberts, P. V. Henry constant of molecular chlorine in aqueous solution *J. Chem. Eng. Data* **1986**, *31*, 51-53, doi:10.1021/je00043a017.

Allen, H. C.; Gragson, D. E.; Richmond, G. L. Molecular structure and adsorption of dimethyl sulfoxide at the surface of aqueous solutions. *J. Phys. Chem. B* **1999**, *103*, 660-666, doi:10.1021/jp9820323.

Allou, L.; El Maimouni, L.; Le Calvé, S. Henry's law constant measurements for formaldehyde and benzaldehyde as a function of temperature and water composition. *Atmos. Environ.* **2011**, *45*, 2991-2998, doi:10.1016/j.atmosenv.2010.05.044.

Altschuh, J.; Bruggemann, R.; Santl, H.; Eichinger, G.; Piringer, O. G. Henry's law constants for a diverse set of organic chemicals: Experimental determination and comparison of estimation methods. *Chemosphere* **1999**, *39*, 1871-1887, doi:10.1016/S0045-6535(99)00082-X.

Andersson, M. E.; Gårdfeldt, K.; Wängberg, I.; Strömberg, D. Determination of Henry's law constant for elemental mercury. *Chemosphere* **2008**, *73*, 587-592, doi:10.1016/j.chemosphere.2008.05.067.

Armstrong, D., A.; Huie, R., E.; Koppenol, W., H.; Lymar Sergei, V.; Merényi, G.; Neta, P.; Ruscic, B.; Stanbury David, M.; Steenken, S.; Wardman, P. Standard electrode potentials involving radicals in aqueous solution: inorganic radicals (IUPAC Technical Report). *Pure Appl. Chem.* **2015**, *87*, 1139-1150, doi:10.1515/pac-2014-0502.

Ashworth, R. A.; Howe, G. B.; Mullins, M. E.; Rogers, T. N. Air–water partitioning coefficients of organics in dilute aqueous solutions. *J. Hazard. Mater.* **1988**, *18*, 25–36, doi:10.1016/0304-3894(88)85057-X.

Barlett, W. P.; Margerum, D. W. Temperature dependencies of the Henry's law constant and the aqueous phase dissociation constant of bromine chloride. *Environ. Sci. Technol.* **1999**, *33*, 3410-3414, doi:10.1021/es990300k.

Battino, R. Nitrous oxide in water. In *Oxides of Nitrogen*; Young, C. L., Ed.; Pergamon: Oxford, 1981; Vol. 8; pp 1-22.

Battino, R. Oxygen in water. In *Oxygen and Ozone*; Battino, R., Ed.; Pergamon: Oxford, 1981; Vol. 7; pp 1-5.

Battino, R. Nitrogen in water. In *Nitrogen and Air*; Battino, R., Ed.; Pergamon: Oxford, 1982; Vol. 10; pp 1-29.

Battino, R. Chlorine dioxide in water. In *Sulfur Dioxide, Chlorine, Fluorine and Chlorine Oxides*; Young, C. L., Ed.; Pergamon: Oxford, 1983; Vol. 12; pp 454-456.

Battino, R. Chlorine in water. In *Sulfur Dioxide, Chlorine, Fluorine and Chlorine Oxides*; Young, C. L., Ed.; Pergamon: Oxford, 1983; Vol. 12; pp 333-347.

Battino, R. Sulfur dioxide in water. In *Sulfur Dioxide, Chlorine, Fluorine and Chlorine Oxides*; Young, C. L., Ed.; Pergamon: Oxford, 1983; Vol. 12; pp 3-33.

Battino, R. Methane in water. In *Methane*; Clever, H. L., Young, C. L., Eds.; Pergamon: Oxford, 1987; Vol. 27/28; pp 1-44.

Ben-Naim, A.; Battino, R. Solubilization of methane, ethane, propane and n-butane in aqueous solutions of sodium dodecylsulfate. *J. Sol. Chem.* **1985**, *14*, 245-253.

Benes, M.; Dohnal, V. Limiting activity coefficients of some aromatic and aliphatic nitro compounds in water. *J. Chem. Eng. Data* **1999**, *44*, 1097-1102, doi:10.1021/je9900326.

Benkelberg, H. J.; Hamm, S.; Warneck, P. Henry's law coefficients for aqueous solutions of acetone, acetaldehyde and acetonitrile and equilibrium constants for the addition compounds of acetone and acetaldehyde with bisulfite. *J. Atmos. Chem.* **1995**, *20*, 17-34, doi:10.1007/BF01099916.

Benson, B. B.; Krause, D.; Peterson, M. A. The solubility and isotope fractionation of gases in dilute aqueous solution. 1. Oxygen. *J. Sol. Chem.* **1979**, *8*, 655-690.

Berdnikov, V. M.; Bazhin, N. M. Oxidation-reduction potentials of certain inorganic radicals in aqueous solutions. *Russ. J. Phys. Chem.* **1970**, *44*, 395–398.

Bernauer, M.; Dohnal, V. Temperature dependence of air−water partitioning of N-methylated (C1 and C2) fatty acid amides. *J. Chem. Eng. Data* **2008**, *53*, 2622-2631, doi:10.1021/je800517r.

Betterton, E. A. The partitioning of ketones between the gas and aqueous phases. *Atmos. Environ.* **1991**, *25*, 1473-1477, doi:10.1016/0960-1686(91)90006-S.

Betterton, E. A.; Hoffmann, M. R. Henry's law constants of some environmentally important aldehydes. *Environ. Sci. Technol.* **1988**, *22*, 1415-1418, doi:10.1021/es00177a004.

Betterton, E. A.; Robinson, J. L. Henry's law coefficient of hydrazoic acid. *J. Air Waste Manage. Assoc.* **1997**, *47*, 1216-1219.

Blatchley, E. R.; Johnson, R. W.; Alleman, J. E.; McCoy, W. F. Effective Henry's law constants for free chlorine and free bromine. *Water Research* **1992**, *26*, 99-106.

Boggs, J. E.; Buck, A. E., Jr. The solubility of some chloromethanes in water. *J. Phys. Chem.* **1958**, *62*, 1459-1461, doi:10.1021/j150569a031.

Borduas, N.; Place, B.; Wentworth, G. R.; Abbatt, J. P. D.; Murphy, J. G. Solubility and reactivity of HNCO in water: insights into HNCO's fate in the atmosphere. *Atmos. Chem. Phys.* **2016**, *16*, 703-714, doi:10.5194/acp-16-703-2016.

Bowden, D. J.; Clegg, S. L.; Brimblecombe, P. The Henry's law constants of the haloacetic acids. *J. Atmos. Chem.* **1998**, *29*, 85-107, doi:10.1023/A:1005899813756.

Brockbank, S. A. Aqueous Henry's law constants, infinite dilution activity coefficients, and water solubility: Critically evaluated database, experimental analysis, and prediction methods, Brigham Young, 2013.

Burnett, M. G. Determination of partition coefficients at infinite dilution by the gas chromatographic analysis of the vapor above dilute solutions. *Anal. Chem.* **1963**, *35*, 1567-1570, doi:10.1021/ac60204a007.

Butler, J. V. A.; Ramchandani, C. N.; Thomson, D. W. The solubility of non-electrolytes. Part 1. The free energy of hydration of some aliphatic alcohols. *J. Chem. Soc.* **1935**, 280-285, doi:10.1039/jr9350000280.

Buxton, G. V.; Salmon, G. A.; Wang, J. The equilibrium $NO_3 + Cl^- \rightleftharpoons NO_3^- + Cl$: A laser flash photolysis and pulse radiolysis study of the reactivity of NO_3 with chloride ion in aqueous solution. *Phys. Chem. Chem. Phys.* **1999**, *1*, 3589-3593, doi:10.1039/a903286j.

Cappa, C. D.; Lovejoy, E. R.; Ravishankara, A. R. Evidence for liquid-like and nonideal behavior of a mixture of organic aerosol components. *Proc. Nat. Acad. Sci.* **2008**, *105*, 18687-18691, doi:o10.1073pnas.0802144105.

Carroll, J. J.; Slupsky, J. D.; Mather, A. E. The solubility of carbon dioxide in water at low pressure. *J. Phys. Chem. Ref. Data* **1991**, *20*, 1201-1209, doi:10.1063/1.555900.

Chang, W.-K.; Criddle, C. S. Biotransformation of HCFC-22, HCFC-142b, HCFC-123, and HFC-134a by methanotropic mixed culture MM1. *Biodegradation* **1995**, *6*, 2-9.

Chen, F.; Freedman, D. L.; Falta, R. W.; Murdoch, L. C. Henry's law constants of chlorinated solvents at elevated temperatures. *Chemosphere* **2012**, *86*, 156-165, doi:10.1016/j.chemosphere.2011.10.004.

Chen, L.; Takenaka, N.; Bandow, H.; Maeda, Y. Henry's law constants for C_2-C_3 fluorinated alcohols and their wet deposition in the atmosphere. *Atmos. Environ.* **2003**, *37*, 4817-4822, doi:10.1016/j.atmosenv.2003.08.002.

Cheung, J. L.; Li, Y. Q.; Boniface, J.; Shi, Q.; Davidovits, P.; Worsnop, D.; Jayne, J. T.; Kolb, C. E. Heterogeneous interactions of NO_2 with aqueous surfaces. *J. Phys. Chem. A* **2000**, *104*, 2655-2662, doi:10.1021/jp992929f.

Christie, A. O.; Crisp, D. J. Activity coefficients of the n-primary, secondary, and tertiary amines in aqueous solution. *J. Appl. Chem.* **1967**, *17*, 11-14.

Cimetiere, N.; De Laat, J. Henry's law constant of N,N-dichloromethylamine: application to the contamination of the atmosphere of indoor swimming pools. *Chemosphere* **2009**, *77*, 465-470, doi:10.1016/j.chemosphere.2009.07.056.

Clegg, S. L.; Brimblecombe, P. Solubility of ammonia in pure aqueous and multicomponent solutions. *J. Phys. Chem.* **1989**, *93*, 7237-7248, doi:10.1021/j100357a041.

Clever, H. L.; Young, C. L. IUPAC Solubility Data Series, Volume 27/28, Methane, Pergamon Press, Oxford. **1987**, doi:10.1016/C2009-0-00752-1.

Compernolle, S.; Müller, J. F. Henry's law constants of diacids and hydroxy polyacids: recommended values. *Atmos. Chem. Phys.* **2014**, *14*, 2699-2712, doi:10.5194/acp-14-2699-2014.

Compernolle, S.; Müller, J. F. Henry's law constants of polyols. *Atmos. Chem. Phys.* **2014**, *14*, 12815-12837, doi:10.5194/acpd-14-13529-2014.

Dacey, J. W. H.; Wakeham, S. G.; Howes, B. L. Henry's law constants for dimethylsulfide in freshwater and seawater. *Geophys. Res. Lett.* **1984**, *11*, 991-994, doi:10.1029/GL011i010p00991.

Dasgupta, P. K.; Dong, S. Solubility of ammonia in liquid water and generation of trace levels of standard gaseous ammonia. *Atmos. Environ.* **1986**, *20*, 565-570, doi:10.1016/0004-6981(86)90099-5.

De Bruyn, W. J.; Swartz, E.; Hu, J. H.; Shorter, J. A.; Davidovits, P.; Worsnop, D. R.; Zahniser, M. S.; Kolb, C. E. Henry's law solubilities and Śetchenow coefficients of biogenic reduced sulfur species obtained from gas-liquid uptake measurements. *J. Geophys. Res.* **1995**, *100*, 7245-7251, doi:10.1029/95JD00217.

Dohnal, V.; Fenclova, D.; Vrbka, P. Temperature dependences of limiting activety coefficients, Henry's law constants, and derivative infinite dilution properties of lower (C_1 - C_5) 1-alkanols in water. Critical compilation, correlation, and recommended data. *J. Phys. Chem. Ref. Data* **2006**, *35*, 1621-1651, doi:10.1063/1.220335.

Dohnal, V.; Vrbka, P.; Řehák, K.; Böhme, A.; Paschke, A. Activity coefficients and partial molar excess enthalpies at infinite dilution for four esters in water. *Fluid Phase Equilibria* **2010**, *295*, 194-200, doi:10.1016/j.fluid.2010.05.010.

Edwards, T. J.; Maurer, G.; Newman, J.; Prausnitz, J. M. Vapor-liquid equilibria in multicomponent aqueous solutions of volatile weak electrolytes. *AIChE Journal* **1978**, *24*, 966-976, doi:10.1002/aic.690240605.

Elliott, S. The solubility of carbon disulfide vapor in natural aqueous systems. *Atmos. Environ.* **1989**, *23*, 1977-1980, doi:10.1016/0004-6981(89)90523-4.

Easterbrook, K. D.; Vona, M. A.; Osthoff, H. D. Measurement of Henry's law constants of ethyl nitrate in deionized water, synthetic sea salt solutions, and n-octanol. *Chemosphere* **2024**, *346*, 140482, doi:10.1016/J.CHEMOSPHERE.2023.

Fenclová, D.; Dohnal, V.; Vrbka, P.; Laštovka, V. Temperature dependence of limiting activity coefficients, Henry's Law constants, and related infinite dilution properties of branched (C3 and C4) alkanols in water. Measurement, critical compilation, correlation, and recommended data. *J. Chem. Eng. Data* **2007**, *52*, 989-1002, doi:10.1021/je600567z.

Fischer, R. G.; Ballschmiter, K. Prediction of the environmental distribution of alkyl dinitrates - Chromatographic determination of vapor pressure p(0), water solubility SH_2O, gas-water partition coefficient K-GW (Henry's law constant) and octanol-water partition coefficient K-OW. *Fresenius J. Anal. Chem.* **1998**, *360*, 769-776, doi:10.1007/s002160050803.

Fogg, P. G. T. Hydrogen sulfide in water. In *Hydrogen Sulfide, Deuterium Sulfide and Hydrogen Selenide*; Fogg, P. G. T., Young, C. L., Eds.; Pergamon: Oxford, 1988; Vol. 32; pp 1-19.

Fogg, P. G. T.; Bligh, S. A.; Derrick, M. E.; Yampol'skii, Y. P.; Clever, H. L.; Skrzecz, A.; Young, C. L. IUPAC-NIST solubility data series. 76. Solubility of ethyne in liquids. *J. Phys. Chem. Ref. Data* **2002**, *30*, 1693-1876, doi:10.1063/1.1397768.

Fogg, P. G. T.; Young, C. L. IUPAC Solubility Data Series, Volume 32, Hydrogen Sulfide, Deuterium Sulfide and Hydrogen Selenide, Pergamon Press, Oxford. **1988**, doi:10.1016/C2009-0-00348-1.

Frenzel, A.; Kutsuna, S.; Takeuchi, K.; Ibusuki, T. Solubility and reactivity of peroxyacetyl nitrate (PAN) in dilute aqueous salt solutions and in sulphuric acid. *Atmos. Environ.* **2000**, *34*, 3641-3544, doi:10.1016/S1352-2310(00)00132-1.

Friant, S. L.; Suffet, I. H. Interactive effects of temperature, salt concentration, and pH on head space analysis for isolating volitile trace organics in aqueous environmental samples. *Anal. Chem.* **1979**, *51*, 2167-2176, doi:10.1021/ac50049a027.

Hales, J. M.; Drewes, D. R. Solubility of ammonia in water at low concentrations. *Atmos. Environ.* **1979**, *13*, 1133-1147, doi:10.1016/0004-6981(79)90037-4.

Hamm, S.; Hahn, J.; Helas, G.; Warneck, P. Acetonitrile in the troposphere: Residence time due to rainout and uptake by ocean. *Geophys. Res. Lett.* **1984**, *11*, 1207-1210, doi:10.1029/GL011i012p01207

Hanson, D. R.; Ravishankara, A. R. Uptake of HCl and HOCl onto sulphuric acid: Solubilities, diffusivities and reaction. *J. Phys. Chem.* **1993**, *97*, 12309-12319, doi:10.1021/j100149a035.

Haruta, A.; Jiao, W.; Chen, W.; Chang, A. C.; Gan, J. Evaluating Henry's law constant of N-nitrosodimethylamine (NDMA). *Water Sci. Tech.* **2011**, *64*, 1636-1641, doi:10.2166/wst.2011.742.

Hauff, K.; Fischer, R. G.; Ballschmiter, K. Determination of C_1 - C_5 alkyl nitrates in rain, smow, white frost, lake, and tap water by a combined codistillation head-space gas chromatography technique. Determination of Henry's law constants by head-space gc. *Chemosphere* **1998**, *37*, 2599-2615, doi:10.1016/S0045-6535(98)00159-3.

Hayduk, W. IUPAC Solubility Data Series, Volume 9, Ethane, Pergamon Press, Oxford. **1982**.

Hayduk, W. IUPAC Solubility Data Series, Volume 24, Propane, Butane and 2-Methylpropane, Pergamon Press, Oxford. **1986**.

Hiatt, M. H. Determination of Henry's law constants using internal standards with benchmark values. *J. Chem. Eng. Data* **2013**, *58*, 902–908, doi:10.1021/JE3010535.

Hill, J. O.; Worsley, I. G.; Helper, L. G. Calorimetric determination of the distribution coefficient and thermodynamic properties of bromine in water and carbon dioxide. *J. Phys. Chem.* **1968**, *72*, 3695-3697, doi:10.1021/j100856a066.

Hoff, J. T.; Mackay, D.; Gillham, R.; Shiu, W. Y. Partitioning of organic chemicals at the air-water interface in environmental systems. *Environ. Sci. Technol.* **1993**, *27*, 2174-2180, doi:10.1021/es00047a026.

Holdren, M. W.; Spicer, C. W.; Hales, J. M. Peroxyacetyl nitrate solubility and decomposition rate in acedic water. *Atmos. Environ.* **1984**, *18*, 1171-1173, doi:10.1016/0004-6981(84)90148-3.

Holzwarth, G.; Balmer, R. G.; Soni, L. The fate of chorine and chloramines in cooling towers. *Water Research* **1984**, *18*, 1421-1427, doi:10.1016/0043-1354(84)90012-5.

Huang, D.; Chen, Z. Reinvestigation of the Henry's law constant for hydrogen peroxide with temperature and acidity variation. *J. Environ. Sci.* **2010**, *22*, 570-574, doi:10.1016/S1001-0742(09)60147-9.

Huie, R. E.; Clifton, C. L.; Neta, P. Electron transfer reaction rates and equilibria of the carbonate and sulfate radical anions. *Radiation Phys. Chem.* **1991**, *38*, 477-481.

Huisman, A. J.; Krieger, U. K.; Zuend, A.; Marcolli, C.; Peter, T. Vapor pressures of substituted polycarboxylic acids are much lower than previously reported. *Atmos. Chem. Phys.* **2013**, *13*, 6647-6662, doi:10.5194/acp-13-6647-2013.

Huthwelker, T.; Peter, T.; Juo, B. P.; Clegg, S. L.; Carshlaw, K. S.; Brimblecombe, P. Solubility of HOCl in water and aqueous H_2SO_4 to stratospheric temperatures. *J. Atmos. Chem.* **1995**, *21*, 81-95, doi:10.1007/BF00712439.

Hwang, H.; Dasgupta, P. K. Thermodynamics of the hydrogen peroxide-water system. *Environ. Sci. Technol.* **1985**, *19*, 255-258, doi:10.1021/es00133a006.

Ip, H. S. S.; Huang, X. H. H.; Yu, J. Z. Effective Henry's law constants of glyoxal, glyoxylic acid, and glycolic acid. *Geophys. Res. Lett.* **2009**, *36*, L01802, doi:10.1029/2008GL036212.

Iraci, L. T.; Baker, B. M.; Tyndall, G. S.; Orlando, J. J. Measurements of the Henry's law coefficients of 2-methyl-3-buten-2-ol, methacrolein, and methylvinyl ketone. *J. Atmos. Chem.* **1999**, *33*, 321-330, doi:10.1023/A:1006169029230.

Jenkins, J.; King, M. B. Vapour-liquid equilibria for the system bromine/water at low bromine concentraions. *Chem. Engin. Sci.* **1965**, *20*, 921-922, doi:10.1016/0009-2509(65)80089-6.

Johnson, B. J.; Betterton, E. A.; Craig, D. Henry's law coefficients of formic and acetic acids. *J. Atmos. Chem.* **1996**, *24*, 113-119, doi:10.1007/BF00162406.

Khalfaoui, B.; Newsham, D. M. T. Phase equilibria in very dilute mixtures of water and brominated hydrocarbons. *Fluid Phase Equilib.* **1994**, *98*, 213–223, doi:10.1016/0378-3812(94)80120-7.

Kames, J.; Schurath, U. Alkyl nitrates and bifunctional nitrates of atmospheric interest: Henry's law constants and their temperature dependencies. *J. Atmos. Chem.* **1992**, *15*, 79-95, doi:10.1007/BF00053611.

Kames, J.; Schurath, U. Henry's law and hydrolysis-rate constants for peroxyacyl nitrates (PANs) using a homogeneous gas-phase source. *J. Atmos. Chem.* **1995**, *21*, 151-164, doi:10.1007/BF00696578.

Kelley, C. M.; Tartar, H. V. On the system: bromine-water. *J. Am. Chem. Soc.* **1956**, *78*, 5752-5756, doi:10.1021/ja01603a010.

Khan, I.; Brimblecombe, P.; Clegg, S. L. Solubilities of pyruvic acid and the lower(C_1 -C_6) carboxylic acids. Experimental determinatoin of equilibrium vapour pressures above pure aqueous and salt solutions. *J. Atmos. Chem.* **1995**, *22*, 285-302, doi:10.1007/BF00696639.

Kim, Y.-H.; Kim, K.-Y. Recent advances in thermal desorption-gas chromatography-mass spectrometery method to eliminate the matrix effect between air and water samples: Application to the accurate determination of Henry's law constant. *J. Chromatog. A* **2014**, *1342*, 78-85, doi:10.1016/j.chroma.2014.03.040.

Kutsuna, S.; Chen, L.; Abe, T.; Mizukado, J.; Uchimaru, T.; Tokuhashi, K.; Sekiya, A. Henry's Law constant of 2,2,2-trifluoroethyl formate, ethyl trifluoroacetate, and non-fluroinated analogous esters. *Atmos. Environ.* **2005**, *39*, 5884-5892, doi:10.1016/j.atmosenv.2005.06.021.

Kutsuna, S.; Chen, L.; Ohno, K.; Tokuhashi, K.; Sekiya, A. Henry's Law constants and hydrolysis rate constants of 2,2,2-trifluoroethyl acetate and methyl trifluoroacetate. *Atmos. Environ.* **2004**, *38*, 725-732, doi:10.1016/j.atmosenv.2003.10.019.

Kutsuna, S.; Hori, H. Experimental determination of Henry's law constants of trifluoroacetic acid at 278–298 K. *Atmos. Environ.* **2008**, *42*, 1399-1412, doi:10.1016/j.atmosenv.2007.11.009.

Lind, J. A.; Kok, G. L. Henry's law determinations for aqueous solutions of hydrogen peroxide, methylhydroperoxide, and peroxyacetic acid. *J. Geophys. Res.* **1986**, *91*, 7889-7895, doi:10.1029/JD091iD07p07889.

Lind, J. A.; Kok, G. L. Correction to "Henry's law determinations for aqueous solutions of hydrogen peroxide, methylhydroperoxide, and peroxyacetic acid". *J. Geophys. Res.* **1994**, *99*, 21119, doi:10.1029/94JD01155.

Luke, W. T.; Dickerson, R. R.; Nunnermacker, L. J. Direct measurements of the photolysis rate coefficients and Henry's law constants of several alkyl nitrates. *J. Geophys. Res.* **1989**, *94*, 14905-14921, doi:10.1029/JD094iD12p14905.

Ma, J.; Dasgupta, P. K.; Blackledge, W.; Boss, G. R. Temperature dependence of Henry's law constant for hydrogen cyanide. Generation of trace standard gaseous hydrogen cyanide. *Environ. Sci. Technol.* **2010**, *44*, 3028-3034, doi:10.1021/es1001192.

Magi, L.; Schweitzer, F.; Pallares, C.; Cherif, S.; Mirabel, P.; George, C. Investigation of the uptake rate of ozone and methyl hydroperoxide by water surfaces. *J. Phys. Chem. A* **1997**, *4*, 4943-4948, doi:10.1021/jp970646m.

Meisel, D.; Czapski, G. One-electron transfer equilibria and redox potentials of radicals studied by pulse radiolysis. *J. Phys. Chem.* **1975**, *79*, 1503-1509, doi:10.1021/j100582a004.

Milne, J. B. Trifluoroacetic acid. In *Acidic and Aprotic Solvents*; Lagowski, J. J., Ed.; Academic Press: New York, 1978; Vol. VB; pp 1.

Munder, B.; Lidal, H.; Sandall, O. C. Physical solubility of hydrogen sulfide in aqueous solutions of 2-(*tert*-butylamino)ethanol. *J. Chem. Eng. Data* **2000**, *45*, 1201-1204, doi:10.1021/je000166f.

Nozière, B.; Riemer, D. D. The chemical processing of gas-phase carbonyl compounds by sulfuric acid aerosols: 2,4-pentanedione. *Atmos. Environ.* **2003**, *37*, 841-851, doi:10.1016/S1352-2310(02)00934-2.

O'Farrell, C. E.; Waghorne, W. E. Henry's law constants of organic compounds in water and *n*-octane at T = 293.2 K. *J. Chem. Eng. Data* **2010**, *55*, 1655-1658, doi:10.1021/je900711h.

O'Sullivan, D. W.; Lee, M.; Noone, B. C.; Heikes, B. G. Henry's law constant determinations for hydrogen peroxide, methyl hydroperoxide, hydroxymethyl hydroperoxide, ethyl hydroperoxide, and peroxyavetic acid. *J. Phys. Chem.* **1996**, *100*, 3241-3247, doi:10.1021/jp951168n.

Parker, V. D. The reversible reduction potential of the proton in water and in non-aqueous solvents. *Acta Chem. Scand.* **1992**, *46*, 692-694, doi:10.3891/acta.chem.scand.46-0692.

Poskrebyshev, G. A.; Huie, R. E.; Neta, P. The rate and equilibrium constants for the reaction $NO_3 + Cl^- \rightleftarrows NO_3^- +$ Cl in aqueous solution. *J. Phys. Chem. A* **2003**, *107*, 1964-1970, doi:10.1021/jp0215724.

Przyjazny, A.; Janicki, W.; Chrzanowski, W.; Staszewski, R. Headspace gas chromatographic determination of distribution coefficients of selected organosulfur compounds and their dependence on some parameters. *J. Chromatogr.* **1983**, *280*, 249-260, doi:10.1016/S0021-9673(00)91567-X.

Rettich, T. R.; Battino, R.; Wilhelm, E. Solubility of gases in liquids. 15. High-presion determination of Henry coefficients for carbon-monoxide in liquid water at 278 K to 323 K. *Ber. Bunsenges. Phys. Chem.* **1982**, *86*, 1128-1132, doi:10.1002/bbpc.198200051.

Rettich, T. R.; Battino, R.; Wilhelm, E. Solubility of gases in liquids. 22. High-precision determination of Henry's law constants of oxygen in liquid water from T = 274 K to T = 328 K. *J. Chem. Themo.* **2000**, *32*, 1145-1156, doi:10.1006/jcht.1999.0581.

Rex, A. Über die Löslichkeit der Halogenderivate der Kohlenwasserstoffe in Wasser. *Z. Phys. Chem.* **1906**, *55*, 355–370, doi:10.1515/ZPCH-1906-5519.

Rinker, E. B.; Sandall, O. C. Physical solubility of hydrogen sulfide in several aqueous solvents. *Can. J. Chem. Eng.* **2000**, *78*, 232-236, doi:10.1002/cjce.5450780130.

Rischbieter, E.; Stein, H.; Schumpe, A. Ozone solubilities in water and aqueous salt solutions. *J. Chem. Eng. Data* **2000**, *45*, 338-340, doi:10.1021/je990263c.

Roberts, J. M.; Liu, Y. Solubility and solution-phase chemistry of isocyanic acid, methyl isocyanate, and cyanogen halides. *Atmos. Chem. Phys.* **2019**, *19*, 4419–4437, doi:10.5194/ACP-19-4419-2019.

Roberts, J. M.; Veres, P. R.; Cochran, A. K.; Warneke, C.; Burling, I. R.; Yokelson, R. J.; Lerner, B.; Gilman, J. B.; Kuster, W. C.; Fall, R.; de Gouw, J. Isocyanic acid in the atmosphere and its possible link to smoke-related health effects. *Proc. Nat. Acad. Sci.* **2011**, *108*, 8966-8971, doi:10.1073/pnas.1103352108.

Rodriguez-Sevilla, J.; Alvarez, M.; Liminana, G.; Diaz, M. C. Dilute SO_2 absorption equilibria in aqueous HCl and NaCl solutions at 298.15 K. *J. Chem. Eng. Data* **2002**, *47*, 1339-1345, doi:10.1021/je015538e.

Roduner, E.; Bartels, D. M. Solvent and isotope effects on addition of atomic hydrogen to benzene in aqueous solution. *Ber. Bunsenges. Phys. Chem.* **1992**, *96*, 1037-1042, doi:10.1002/bbpc.19920960813.

Rohrschneider, L. Solvent characterization by gas-liquid partition coefficients of selected solvents. *Anal. Chem.* **1973**, *45*, 1241-1247, doi:10.1021/ac60329a023.

Roth, W. A. Notiz zur Thermochemie des Chlormonoxydes. *Z. Phys. Chem.* **1942**, *A191*, 248–250, doi:10.1515/ZPCH-1942-19117, 1942.

Rudich, Y.; Talukdar, R. K.; Ravishankara, A. R.; Fox, R. W. Reactive uptake of NO_3 on pure water and ionic solutions. *J. Geophys. Res.* **1996**, *101*, 21023-21031, doi:10.1029/96JD01844.

Sander, R. Compilation of Henry's law constants (version 5.0.0) for water as solvent. *Atmos. Chem. Phys.* **2023**, *23*, 10 901–912 440, doi:10.5194/ACP-23-10901-2023.

Scheer, V.; Frenzel, A.; Behnke, W.; Zetsch, C.; Magi, L.; George, C.; Mirabel, P. Uptake of nitrosyl chloride (NOCl) by aqueous solutions. *J. Phys. Chem. A* **1997**, *101*, 9359-9366, doi:10.1021/jp972143m.

Schuhfried, E.; Biasioli, F.; Aprea, E.; Cappellin, L.; Soukoulis, C.; Ferrigno, A.; Märk, T. D.; Gasperi, F. PTR-MS measurements and analysis of models for the calculation of Henry's law constants of monosulfides and disulfides. *Chemosphere* **2011**, *83*, 311-317, doi:10.1016/j.chemosphere.2010.12.051.

Schwartz, S. E. Gas- and aqueous phase chemistry of HO_2 in liquid water clouds. *J. Geophys. Res.* **1984**, *89*, 11589-11598, doi:10.1029/JD089iD07p11589.
Schwartz, S. E.; White, W. H. In *Trace Atmospheric Species. Properties, Transformations and Fates*; Schwartz, S. E., Ed.; John Wiley & Sons: New York, 1983; Vol. 12; pp 1-116.
Schwarz, H. A.; Dodson, R. W. Equilibrium between hydroxyl radicals and thallium(II) and the oxidation potential of OH(aq). *J. Phys. Chem.* **1984**, *88*, 3643-3647, doi:10.1021/j150660a053.
Seyfioglu, R.; Odabasi, M. Determination of Henry's Law constant of formaldehyde as a function of temperature: Application to air-water exchange in Tahtali Lake in Izmir, Turkey. *Environ. Monit. Assess.* **2007**, *128*, 343-349, doi:10.1007/s10661-006-9317-3.
Shi, Q.; Davidovits, P.; Jayne, J. T.; Worsnop, D. R.; Kolb, C. E. Uptake of gas-phase ammonia. 1. Uptake by aqueous surfaces as a function of pH. *J. Phys. Chem. A* **1999**, *103*, 8812-8823, doi:10.1021/jp991696p.
Snider, J. R.; Dawson, G. A. Tropospheric light alcohols, carbonyls,, and acetonitrile: Concentrations in the southwest United States and Henry's law data. *J. Geophys. Res.* **1985**, *90*, 3797-3805, doi:10.1029/JD090iD02p03797.
Soonsin, V.; Zardini, A. A.; Marcolli, C.; Zuend, A.; Krieger, U. K. The vapor pressures and activities of dicarboxylic acids reconsidered: the impact of the physical state of the aerosol. *Atmos. Chem. Phys.* **2010**, *10*, 11753-11767, doi:10.5194/acp-10-11753-2010.
Staffelbach, T. A.; Kok, G. L. Henry's law constants for aqueous solutions of hydrogen peroxide and hydroxymethyl hydroperoxide. *J. Geophys. Res.* **1993**, *98*, 12713-12717, doi:10.1029/93JD01022.
Staudinger, J.; Roberts, P. V. A critical compilation of Henry's law constant temperature dependence relations for organic compounds in dilute aqueous solutions. *Chemosphere* **2001**, *44*, 561-576, doi:10.1016/S0045-6535(00)00505-1.
Strekowski, R. S.; George, C. Measurement of Henry's Law constants for acetone, 2-butanone, 2,3-butanedione, and isobutyraldehyde using a horizontal flow reactor. *J. Chem. Eng. Data* **2005**, *50*, 804-810, doi:10.1021/je034137r.
Thomas, K.; Volz-Thomas, A.; Mihelcic, D.; Smit, H. G. J.; Kley, D. On the exchange of NO_3 radicals with aqueous solutions: Solubility and sticking coefficient. *J. Atmos. Chem.* **1998**, *29*, 17-43, doi:10.1023/A:1005860312363.
Villalta, P. W.; Lovejoy, E. R.; Hanson, D. R. Reaction probability of peroxyacetyl radical on aqueous surfaces. *Geophys. Res. Lett.* **1996**, *23*, 1765-1768, doi:10.1029/96GL01286.
Vitenberg, A. G.; Ioffe, B. V.; Dimitrova, Z. S.; Butaeva, I. L. Determination of gas-liquid partition coefficients by means of gas chromatographic analysis. *J. Chromatog.* **1975**, *112*, 319-327, doi:10.1016/S0021-9673(00)99964-3.
Wagman, D. D.; Evans, W. H.; Parker, V. B.; Schumm, R. H.; Halow, I.; Bailey, S. M.; Churney, K. L.; Nutall, R. L. The NBS tables of chemical thermodynamic properties. Selected values for inorganic and C_1 and C_2 organic substances in SI unites. *J. Phys. Chem. Ref. Data* **1982**, *11*, Suppl. No. 1.
Wagman, D. D.; Evans, W. H.; Parker, V. B.; Schumm, R. H.; Halow, I.; Bailey, S. M.; Churney, K. L.; Nuttall, R. L. Erratum: The NBS tables of chemical thermodynamic properties; Selected values for inorganic and C1 and C2 organic substances in SI units. *J. Phys. Chem. Ref. Data* **1989**, *18*, 1807–1812, doi:10.1063/1.555845.
Wardman, P. The reduction potential of benzyl viologen: An important reference compound for oxidant/radical redox couples. *Free Rad. Res. Comm.* **1991**, *14*, 57-67, doi:10.3109/10715769109088942.
Warneck, P. A note on the temperature dependence of Henry's Law coefficients for methanol and ethanol. *Atmos. Environ.* **2006**, *40*, 7146-7151, doi:10.1016/j.atmosenv.2006.06.024.
Warneck, P. A review of Henry's law coefficients for chlorine-containing C_1 and C_2 hydrocarbons. *Chemosphere* **2007**, *69*, 347-361, doi:10.1016/j.chemosphere.2007.04.088.
Watts, S. F.; Brimblecombe, P. The Henry's law constant of dimethylsulfoxide. *Environ. Technol. Lett.* **1987**, *8*, 483-486, doi:10.1080/09593338709384509.
Weisenberger, S.; Schumpe, A. Estimation of gas solubilities in salt solutions at temperatures from 273 K to 363 K. *AIChE Journal* **1996**, *42*, 298-300, doi:10.1002/aic.690420130.
Whitney, R. P.; Vivian, J. E. Solubility of chlorine in water. *Ind. Eng. Chem.* **1941**, *33*, 741–744, doi:10.1021/IE50378A014.
Wilhelm, E.; Battino, R.; Wilcock, R. J. Low-pressure solubility of gases in liquid water. *Chem. Rev.* **1977**, *77*, 219-262, doi:10.1021/cr60306a003.
Wong, P. K.; Wang, Y. H. Determination of the Henry's law constant for dimethyl sulfide in seawater. *Chemosphere* **1997**, *35*, 535-544, doi:10.1016/S0045-6535(97)00118-5.

Worthington, E. K.; Wade, E. A. Henry's law coefficients of chloropicrin and methyl isothiocyanate. *Atmos. Environ.* **2007**, *41*, 5510-5515, doi:10.1016/j.atmosenv.2007.02.019.
Yakovkin, A. A. About the hydrolysis of chlorine. *J. Russ. Phys. Chem. Soc. (in Russian)* **1900**, *32*, 673–721.
Yaws, C. L.; Hopper, J. R.; Wang, X.; Rathinsamy, A. K. Calculating solubility & Henry's Law constants for gases in water. *Chem. Eng.* **1999**, 102-105.
Yoshizumi, K.; Aoki, K.; Nouchi, I.; Okita, T.; Kobayashi, T.; Kamakura, S.; Tajima, M. Measurements of the concentrations in rainwater and of the Henry's Law constant of hydrogen peroxide. *Atmos. Environ.* **1984**, *18*, 395-401, doi:10.1016/0004-6981(84)90114-8.
Young, C. L. IUPAC Solubility Data Series, Volume 8, Oxides of Nitrogen, Pergamon Press, Oxford. **1981**, doi:10.1016/C2009-0-00222-0.
Young, C. L. Nitrous oxide in water. In *Oxides of Nitrogen*; Young, C. L., Ed.; Pergamon: Oxford, 1981; Vol. 8; pp 1-22.
Young, C. L. IUPAC Solubility Data Series, Volume 12, Sulfur Dioxide, Chlorine, Fluorine and Chlorine Oxides, Pergamon Press, Oxford. **1983**, doi:10.1016/C2013-0-03419-6.
Yu, X. Y.; Barker, J. R. Hydrogen peroxide photolysis in acidic aqueous solutions containing chloride ions. I. Chemical mechanism. *J. Phys. Chem. A* **2003**, 1325-1332, doi:10.1021/jp026666s.
Zheng, D.-Q.; Guo, T.-M.; Knapp, H. Experimental and modeling studies on the solubility of CO_2, $CHClF_2$, CHF_3, $C_2H_2F_4$ and $C_2H_4F_2$ in water and aqueous NaCl solutions under low pressures *Fluid Phase Equilibria* **1997**, *129*, 197-209, doi:10.1016/S0378-3812(96)03177-9.
Zhou, X.; Lee, Y. N. Aqueous solubility and reaction kinetics of hydroxymethyl hydroperoxide. *J. Phys. Chem.* **1992**, *96*, 265-272, doi:10.1021/j100180a051.
Zhou, X.; Mopper, K. Apparent partition coefficients of 15 carbonyl compounds between air and seawater and between air and freshwater; Implications for air-sea exchange. *Environ. Sci. Technol.* **1990**, *24*, 1864-1869, doi:10.1021/es00082a013.

5.3.3 Schumpe Parameters

5.3.3.1 Table Eq2: Gas-specific Schumpe Parameters

Substance	$h_{G,o}$ [M^{-1}]	1000 h_T [M^{-1} K^{-1}]
O_2	0	–0.334
O_3	0.00396	1.79
N_2	–0.0010	–0.605
NH_3	–0.0481	
NO	0.0060	
N_2O	–0.0085	–0.479
CO_2	–0.0172	–0.338
CH_4	0.0022	–0.524
C_2H_6	0.0120	–0.601
C_3H_8	0.0240	–0.702
n-C_4H_{10}	0.0297	–0.726
C_2H_4	0.0037	
C_2H_2	–0.0159	
HCHO	–2.40	69.
CH_3CHO	–0.030	–5.5
C_2H_5CHO	0.022	–4.0
C_3H_7CHO	0.087	–0.06
$CH_3C(O)CH_3$	–0.052	–2.9
$C_2H_5C(O)CH_3$	0.011	–0.9
$CH_3C(O)C(O)OH$	0.090	
CH_3CN	–0.00049	
$CH_3C(O)O_2NO_2$	–0.065	
SO_2	–0.0607	0.275
H_2S	–0.0333	
CS_2	0.0549	–4.65
CH_3SH	0.003	
CH_3SCH_3	–0.031	–0.26

5.3.3.2 Notes for Table Eq2

All values are taken from the optimization of Weisenberger and Schumpe[10] unless noted otherwise.

O_2 (Oxygen, CAS RN: 7782-44-7)
The parameter $h_{G,o}$ is set to zero for oxygen (see discussion in the introduction).

O_3 (Ozone, CAS RN: 10028-15-6)
Adopted from Rischbieter et al.[8] Ershov and Gordeev[5] proposed a value of $h_{G,o}$ = –0.0152 M^{-1} for ozone.

HCHO (Formaldehyde, CAS RN: 50-00-0)
Salt effect parameters derived from data on the effect of seawater on the measured H_s (Zhou and Mopper[13]). For these calculations, the seawater was assumed to be a solution of pure NaCl, with 35‰ salinity equal to 0.6 M. Additional studies of the effect of NaCl as a function of temperature have been carried out by Allou et al.[1]

CH_3CHO (Acetaldehyde, CAS RN: 75-07-0)
Salt effect parameters derived from data on the effect of seawater on the measured H_s (Zhou and Mopper[13]). For these calculations, the seawater was assumed to be a solution of pure NaCl, with 35‰ salinity equal to 0.6 M.

C_2H_5CHO (Propanal, CAS RN: 123-38-6)
Salt effect parameters derived from data on the effect of seawater on the measured H_s (Zhou and Mopper[13]). For these calculations, the seawater was assumed to be a solution of pure NaCl, with 35‰ salinity equal to 0.6 M.

C_3H_7CHO (Butanal, CAS RN: 123-72-8)

Salt effect parameters derived from data on the effect of seawater on the measured H_s (Zhou and Mopper[13]). For these calculations, the seawater was assumed to be a solution of pure NaCl, with 35‰ salinity equal to 0.6 M.

$CH_3C(O)CH_3$ (Acetone, CAS RN: 67-64-1)

Salt effect parameters derived from data on the effect of seawater on the measured H_s (Zhou and Mopper[13]). For these calculations, the seawater was assumed to be a solution of pure NaCl, with 35‰ salinity equal to 0.6 M. The K_S values from this work are somewhat different than those obtained by Benkelberg et al.,[2] 0.089 M^{-1} vs. 0.17 M^{-1} at 298 K and 0.17 M^{-1} vs. 0.085 M^{-1} at 273 K. The magnitude of this difference is not too great, but the two studies predict a different sign for h_T.

$C_2H_5C(O)CH_3$ ((2-Butanone, CAS RN: 78-93-3)

Salt effect parameters derived from data on the effect of seawater on the measured H_s (Zhou and Mopper[13]). For these calculations, the seawater was assumed to be a solution of pure NaCl, with 35‰ salinity equal to 0.6 M.

$CH_3C(O)C(O)OH$ (Pyruvic acid, CAS RN: 127-17-3)

Salt effect derived from effect of NaCl (K_S = 0.236 M^{-1}) and KCl (K_S = 0.235 M^{-1}) on the partial pressure over 1.5 M solution of pyruvic acid at various salt concentrations. Much different values derived when other salts were used, suggesting complications due to specific interactions and, possibly, to the weakly buffered nature of the solution.

CH_3CN (Acetonitrile, CAS RN: 75-05-8)

Hamm et al.[6] includes a measurement with artificial seawater at 293 K. Salt effect derived from the effect of 0.6 M NaCl on solubility at 293 K (Benkelberg et al.[2]).

$CH_3C(O)O_2NO_2$ (Peroxyacetyl nitrate, CAS RN: 2278-22-0)

K_S = 0.0807 M^{-1} for NaCl at 293.2 K based on solubility in artificial sea water (about 0.7 M) (Kames and Schurath[7]).

SO_2 (Sulphur dioxide, CAS RN: 7446-09-5)

Value of $h_{G,o}$ is from absorption equilibria studies in aqueous HCl and NaCl solutions (Rodríguez-Sevilla et al.[9]).

CS_2 (Carbon disulphide, CAS RN: 75-15-0)

Salt effect parameters derived from the ratio of the solubility of CS_2 in water and 0.5 M NaCl (Young[12]). At 278 K, k_s = 0.184 M^{-1}, compared to 0.150 M^{-1} from the results of De Bruyn et al. Note also De Bruyn et al.[4]) obtained K_S = 0.410 M^{-1} for $(NH_4)_2SO_4$, whereas these parameters would predict 0.261 M^{-1}.

CH_3SH (Methyl mercaptan, CAS RN: 74-93-1)

The work of De Bruyn et al.[4]) covered a wide range of pH and NaCl and $(NH_4)_2SO_4$ concentrations. At 298 K, they obtained K_S = 0.314 M^{-1} for $(NH_4)_2SO_4$ and K_S = 0.143 M^{-1} for NaCl. From the latter, we calculate h_G = 0.003 M^{-1}. The values for $(NH_4)_2SO_4$ from this work have tended to be high.

CH_3SCH_3 (Dimethyl sulfide, CAS RN: 75-18-3)

Salt effect parameters based on the values of Dacey et al.[3] for Sargasso sea water from 273 to 302 K. The values for H_s obtained by Wong and Wang[11] for sea water from 291 to 317 K are in good agreement. Dacey et al.[3] also measured KH_s at 291 K for NaCl solutions up to 32%. For the 10–32% data, a value of K_s = 0.117 M^{-1} can be derived, in good agreement with the predicted value of 0.113 M^{-1}. The 278 K value of K_s = 0.180 M^{-1} obtained by De Bruyn et al.[4]) is somewhat larger. Note also the De Bruyn et al.[4]) obtained K_s = 0.332 M^{-1} for $(NH_4)_2SO_4$, whereas these values would predict 0.223.

(1) Allou, L.; El Maimouni, L.; Le Calvé, S. Henry's law constant measurements for formaldehyde and benzaldehyde as a function of temperature and water composition. *Atmos. Environ.* **2011**, *45*, 2991-2998, doi:10.1016/j.atmosenv.2010.05.044.

(2) Benkelberg, H. J.; Hamm, S.; Warneck, P. Henry's law coefficients for aqueous solutions of acetone, acetaldehyde and acetonitrile and equilibrium constants for the addition compounds of acetone and acetaldehyde with bisulfite. *J. Atmos. Chem.* **1995**, *20*, 17-34, doi:10.1007/BF01099916.

(3) Dacey, J. W. H.; Wakeham, S. G.; Howes, B. L. Henry's law constants for dimethylsulfide in freshwater and seawater. *Geophys. Res. Lett.* **1984**, *11*, 991-994, doi:10.1029/GL011i010p00991.

(4) De Bruyn, W. J.; Swartz, E.; Hu, J. H.; Shorter, J. A.; Davidovits, P.; Worsnop, D. R.; Zahniser, M. S.; Kolb, C. E. Henry's law solubilities and Śetchenow coefficients of biogenic reduced sulfur species obtained from gas-liquid uptake measurements. *J. Geophys. Res.* **1995**, *100*, 7245-7251, doi:10.1029/95JD00217.
(5) Ershov, B. G.; Gordeev, A. V. Ozone solubility in aqueous solutions of perchlorates and other electrolytes: Correction of the Weisenberger-Schumpe model parameters for the ClO_4^- and O_3. *Ozone: Sci. Eng.* **2019**, *41*, 207–220, doi:10.1080/01919512.2018.1525278.
(6) Hamm, S.; Hahn, J.; Helas, G.; Warneck, P. Acetonitrile in the troposphere: Residence time due to rainout and uptake by ocean. *Geophys. Res. Lett.* **1984**, *11*, 1207-1210, doi:10.1029/GL011i012p01207
(7) Kames, J.; Schurath, U. Henry's law and hydrolysis-rate constants for peroxyacyl nitrates (PANs) using a homogeneous gas-phase source. *J. Atmos. Chem.* **1995**, *21*, 151-164, doi:10.1007/BF00696578.
(8) Rischbieter, E.; Stein, H.; Schumpe, A. Ozone solubilities in water and aqueous salt solutions. *J. Chem. Eng. Data* **2000**, *45*, 338-340, doi:10.1021/je990263c.
(9) Rodríguez-Sevilla, J.; Álvarez, M.; Limiñana, G.; Díaz, M. C. Dilute SO_2 absorption equilibria in aqueous HCl and NaCl solutions at 298.15 K. *J. Chem. Eng. Data* **2002**, *47*, 1339-1345, doi:10.1021/je015538e.
(10) Weisenberger, S.; Schumpe, A. Estimation of gas solubilities in salt solutions at temperatures from 273 K to 363 K. *AIChE Journal* **1996**, *42*, 298-300, doi:10.1002/aic.690420130.
(11) Wong, P. K.; Wang, Y. H. Determination of the Henry's law constant for dimethyl sulfide in seawater. *Chemosphere* **1997**, *35*, 535-544, doi:10.1016/S0045-6535(97)00118-5.
(12) Young, C. L. IUPAC Solubility Data Series, Volume 12, Sulfur Dioxide, Chlorine, Fluorine and Chlorine Oxides, Pergamon Press, Oxford. **1983**, doi:10.1016/C2013-0-03419-6.
(13) Zhou, X.; Mopper, K. Apparent partition coefficients of 15 carbonyl compounds between air and seawater and between air and freshwater; Implications for air-sea exchange. *Environ. Sci. Technol.* **1990**, *24*, 1864-1869, doi:10.1021/es00082a013.

5.3.3.3 Table Eq3. Ion-Specific Schumpe Parameters

Cation	h_i (M^{-1})		Anion	h_i (M^{-1})
H^+	0		OH^-	0.0839
Li^+	0.0754		HS^-	0.0851
Na^+	0.1143		F^-	0.092
K^+	0.0922		Cl^-	0.0318
Rb^+	0.0839		Br^-	0.0269
Cs^+	0.0759		I^-	0.0039
NH_4^+	0.0556		NO_2^-	0.0795
Mg^{2+}	0.1694		NO_3^-	0.0128
Ca^{2+}	0.1762		ClO_3^-	0.1348
Sr^{2+}	0.1881		BrO_3^-	0.1116
Ba^{2+}	0.2168		IO_3^-	0.0913
Mn^{2+}	0.1463		ClO_4^-	0.0492
Fe^{2+}	0.1523		IO_4^-	0.1464
Co^{2+}	0.168		CN^-	0.0679
Ni^{2+}	0.1654		SCN^-	0.0627
Cu^{2+}	0.1675		$HCrO_4^-$	0.0401
Zn^{2+}	0.1537		HCO_3^-	0.0967
Cd^{2+}	0.1869		CO_3^{2-}	0.1423
Al^{3+}	0.2174		HPO_4^{2-}	0.1499
Cr^{3+}	0.0648		HSO_3^-	0.0549
Fe^{3+}	0.1161		SO_3^{2-}	0.127
La^{3+}	0.2297		SO_4^{2-}	0.1117
Ce^{3+}	0.2406		$S_2O_3^{2-}$	0.1149
Th^{4+}	0.2709		$C_2O_4^{2-}$	0.1266
			PO_4^{3-}	0.2119
			$Fe(CN)_6^{4-}$	0.3574

5.3.3.4 Notes for Table Eq3

All values in this table are adopted from Weisenberger and Schumpe[3] unless noted otherwise.

H^+ The parameter h_i is set to zero for H^+ (see discussion in the introduction).

HCO_3^- The value in our previous recommendation was wrong.

$C_2O_4^{2-}$ Adopted from Gordeev et al.[2]

ClO_4^- Ershov and Gordeev[1] proposed a value of $h_i = 0.0391$ M^{-1}.

(1) Ershov, B. G.; Gordeev, A. V. Ozone solubility in aqueous solutions of perchlorates and other electrolytes: Correction of the Weisenberger-Schumpe model parameters for the ClO_4^- and O_3. *Ozone: Sci. Eng.* **2019**, *41*, 207–220, doi:10.1080/01919512.2018.1525278.

(2) Gordeev, A. V.; Seliverstov, A. F.; Ershov, B. G. Solubility of ozone in aqueous solutions of oxalic acid and potassium and sodium nitrates: Determination of the anion-specific parameter for the oxalate ion in a model for the solubility of gases in electrolyte solutions. *Theor. Found. Chem. Eng.* **2019**, *53*, 1067–1077, doi:10.1134/S0040579519050282.

(3) Weisenberger, S.; Schumpe, A. Estimation of gas solubilities in salt solutions at temperatures from 273 K to 363 K. *AIChE Journal* **1996**, *42*, 298-300, doi:10.1002/aic.690420130.

5.3.4 Table Eq4. Henry's Law Constants for Acids as Solvent

	T(K)	Wt.% H_2SO_4	H_s or $H_{s,eff}$ ($M\ atm^{-1}$)	Notes
O_3 in $H_2SO_4 \cdot nH_2O$(l)	293	1–70	$\ln(H_{s0}/H_s) = (4.08 \pm 0.2) \times 10^{-3} \times wt$ $H_{s0} = 0.012\ M\ atm^{-1}$ wt is the H_2SO_4 wt%	1
NO_2 in $H_2SO \cdot nH_2O$(l)	203–343	39–68	See Note	2
HONO in $H_2SO_4 \cdot nH_2O$(l)	248–298	>60	$\ln(H_{s,eff}) = a_1 + a_2\,wt + a_3\,wt^2 + (b_1 + b_2\,wt)/T$ $a_1 = 26.1 \pm 9.4$, $a_2 = -1.095 \pm 0.21$, $a_3 = 0.00732 \pm 0.00121$ $b_1 = -5792 \pm 1610$, $b_2 = 181.3 \pm 24$	3
HNO_3 in $H_2SO_4 \cdot nH_2O$(l)	~195–300	0–80	See Note	4
HNO_3 and HCl in $H_2SO_4 \cdot nHNO_3 \cdot mH_2O$(l)	~195–300	0–80	See Note	4
HO_2NO_2 in $H_2SO_4 \cdot nH_2O$(l)	201–230	50–75	$\ln(H_s) = 3.69 - m H_2SO_4 \times (-0.25 + 65\ K/T) - 8400 \times (1/298.15\ K - 1/T)$ $m(H_2SO_4)$ = molality of H_2SO_4	5
CH_2O in $H_2SO_4 \cdot mHNO_3 \cdot nH_2O$(l)	240–300	10–85 also 8–40 wt.% HNO_3	See Note	6
CH_3OH in $H_2SO_4 \cdot nH_2O$(l)	197–223	40–85	See Note	7
CH_3CH_2OH in $H_2SO_4 \cdot nH_2O$(l)	209–237	39–76	See Note	8
CH_3CHO in $H_2SO_4 \cdot nH_2O$	211–241	30–76	See Note	9
$CH_3C(O)CH_3$ in $H_2SO_4 \cdot nH_2O$(l)	198–298	10–80	$\ln(H_{s,eff}) = a_1 + a_2\,wt + a_3\,wt^2 + (b_1 + b_2\,wt + b_3\,wt^2)/T$ wt is the H_2SO_4 wt%, $a_1 = -21.438 \pm 4.31$, $a_2 = -0.32163 \pm 0.207$, $a_3 = 0.0072935 \pm 0.00235$ $b_1 = 7292 \pm 1220$, $b_2 = 33.524 \pm 53.42$, $b_3 = -0.975 \pm 0.571$	10
$CH_3C(O)O_2NO_2$ in H_2O(l), $H_2SO_4 \cdot nH_2O$(l)	199–295	0–75	$\ln(H_{s,eff}) = 1.07 - m H_2SO_4 \times (0.69 - 152\ K/T) - 5810\ K \times (1/298.15\ K - 1/T)$, $m(H_2SO_4)$ = molality of the H_2SO_4 solution	11
CF_2O in $H_2SO_4 \cdot nH_2O$(l)	215–230	60	<5	12
CF_3OH in $H_2SO_4 \cdot nH_2O$(l)	250	40 50	>240 210	13
HOCl in $H_2SO_4 \cdot nH_2O$(l)	200–300	46–80	$1.91 \times 10^{-6} \times \exp(5862.4\ K/T) \times \exp(-S_{HOCl} \times C)$ where: $S_{HOCl} = 0.0776 + 59.18\ K/T\ M^{-1}$, C = H_2SO_4 molar conc.	14
$ClONO_2$ in $H_2SO_4 \cdot nH_2O$(l)	200–265	40–75	$1.6 \times 10^{-6} \times \exp(4710\ K/T) \times \exp(-S_{ClNO2} \times C)$ where: $S_{ClONO2} = 0.306 + 24.0\ K/T\ M^{-1}$, C = H_2SO_4 molar conc.	15
HBr in $H_2SO_4 \cdot nH_2O \cdot H_2O$(l) and $H_2SO_4 \cdot nHNO_3 \cdot mH_2O$(l)	200–240	40–72	$\ln(H_{s,eff}) = a_1 + (b_1 + b_2\,wt)/T$ $a_1 = -11.695 \pm 0.537$, $b_1 = 11{,}101 \pm 163$, $b_2 = -90.7 \pm 1.2$	16
HOBr in $H_2SO_4 \cdot nH_2O$(l)	201–252	45–252	See Note	17
SO_2 in H_2O(l), $H_2SO_4 \cdot nH_2O$(l)	193–242	0–97	$\ln(H_{s,eff}) = a_1 + a_2\,wt + a_3\,wt^2 + (b_1 + b_2\,wt + b_3\,wt^2)/T$, where: wt is the H_2SO_4 wt%, $a_1 = -10.778 \pm 2.07$, $a_2 = -0.11541 \pm 0.0827$, $a_3 = 0.0012506 \pm 0.000811$ $b_1 = 3310 \pm 578$, $b_2 = 30.581 \pm 22.2$, $b_3 = -0.35469 \pm 0.209$	18

5.3.4.1 Notes for Table Eq4

1. O_3 in H_2SO_4•nH_2O(l)

Bubble train uptake measurements where performed by Rattigan et al.[1] at 293 K for 1–70 wt% H_2SO_4. Recommended expression is a Sechenov coefficient formulation where H_{s0} = 0.012 M atm^{-1} is the 293 K value of H_S for pure water from Wilhelm et al.[2] In the measurement, account was taken of the loss of O_3 due to reaction with H^+.

Back to Table

(1) Rattigan, O. V.; Boniface, J.; Swartz, E.; Davidovits, P.; Jayne, J. T.; Kolb, C. E.; Worsnop, D. R. Uptake of gas-phase SO_2 in aqueous sulfuric acid: Oxidation by H_2O_2, O_3, and HONO. *J. Geophys. Res.* **2000**, *105*, 29065-29078, doi:10.1029/2000JD900372.

(2) Wilhelm, E.; Battino, R.; Wilcock, R. J. Low-pressure solubility of gases in liquid water. *Chem. Rev.* **1977**, *77*, 219-262, doi:10.1021/cr60306a003.

2. NO_2 in H_2SO_4•nH_2O(l)

Langenberg et al.[1] present novel capillary gas chromatography measurements for 39, 59, and 68 wt% H_2SO_4 over the temperature range 203–243 K. However, NO_2 solubility must be derived from chromatographic waveforms, which are contorted by much higher N_2O_4 solubility. The resulting values for $H_S(NO_2)$ are in the 1 M atm^{-1} to 10^2 M atm^{-1} range, but show inconsistent trends with temperature and concentration, indicating possibly large systematic error.

Back to Table

(1) Langenberg, S.; Proksch, V.; Schurath, U. Solubilities and diffusion of trace gases in cold sulfuric acid films. *Atmos. Environ.* **1998**, *32*, 3129-3137, doi:10.1016/S1352-2310(97)00490-1.

3. HONO in H_2SO_4•nH_2O(l)

Becker et al.[1] measured HONO partial pressure, p(HONO), over bulk solutions in a temperature range 248–298 K and a H_2SO_4 concentration range of 0–67 wt%. Longfellow et al.[2] measured p(HONO) in a wetted wall flow reactor over the temperature range 218–295 K and an acid concentration range of 60–83 wt%. Agreement between these two data sets is excellent. $H_{s,eff}$ decreases from 0 wt% to 53 wt% due to physical solubility, then increases above 53 wt% due to protonation and/or association with H_2SO_4 to make nitrosyl sulfuric acid. Becker et al. parameterized their data as a function of sulfuric acid wt% and temperature. However, the Becker et al. parameterization is not able to fit the combined sets of Becker et al.[1] and Longfellow et al.[2] data, particularly at the lower temperatures and higher wt% most relevant to the stratosphere. Therefore, the recommended functional form was used to fit the data for >60 wt%. This function fits both sets of data very well. It is important to note that this function is only valid for H_2SO_4 concentrations near 60 wt% and above. The parameterization in Becker et al.[1] should be used to calculate H_S for H_2SO_4 concentrations <60 wt%. (Note that the units for H_S are mol/(kg bar) in Becker et al.[1] The density parameterization of Myhre et al.[3] was used to convert to M atm^{-1}).

Back to Table

(1) Becker, K. H.; Kleffman, J.; Kurtenbach, R.; Wiesen, P. Solubility of nitrous acid (HONO) in sulfuric acid solutions. *J. Phys. Chem.* **1996**, *100*, 14984-14990, doi:10.1021/jp961140r.

(2) Longfellow, C. A.; Imamura, T.; Ravishankara, A. R.; Hanson, D. R. HONO solubility and heterogeneous reactivity on sulfuric acid surfaces. *J. Phys. Chem. A* **1998**, *102*, 3323-3332, doi:10.1021/jp9807120.

(3) Myhre, C. E. L.; Nielsen, C. J.; Saastad, O. W. Density and surface tension of aqueous H_2SO_4 at low temperature. *J. Chem. Eng. Data* **1998**, *43*, 617-622, doi:10.1021/je980013g.

4. HNO_3 and HCl in H_2SO_4•nH_2O(l) and H_2SO_4•nHNO_3•mH_2O(l)

Effective Henry's law constants, $H_{s,eff}$, for HNO_3, and HCl in binary H_2SO_4/H_2O and ternary $H_2SO_4/HNO_3/H_2O$ solutions over the temperature range 195 to 300 K are required to model the composition and heterogeneous chemistry of stratospheric and upper tropospheric aerosols. Solubility data can be obtained from analysis of heterogeneous uptake experiments with the liquid phase diffusion coefficient estimated from acid solution viscosity (Williams and Long[15]). Solubilities can also be obtained from equilibrium or from vapor pressure data.

Experimental solubility data for HNO_3 is provided by Van Doren et al.,[12] Reihs et al.,[9] and Zhang et al.[16] Data for HCl solubility is provided by Watson et al.,[13] Hanson and Ravishankara,[5,6] Zhang et al.,[16] Williams and Golden,[14] Abbatt,[1] Elrod et al.,[4] and Robinson et al.[10]

These studies all show that trace species solubility in H_2SO_4/H_2O and $H_2SO_4/HNO_3/H_2O$ solutions is a strong function of water activity, which, in turn, depends on both temperature and acid concentrations. Prediction of HNO_3 and HCl $H_{s,eff}$ values for atmospheric compositions requires a sophisticated model. Comprehensive thermodynamic models of acid solutions for a range of atmospheric conditions have been published by Carslaw et al.,[2] Tabazadeh et al.,[11] and Luo et al.[7] and reviewed by Carslaw et al.[3] These models do an excellent job of reproducing the available experimental data, even for ternary $H_2SO_4/HNO_3/H_2O$ solutions (Elrod et al.[4]). These models and the Carslaw et al.[3] review should be consulted for plots/predictions of $H_{s,eff}$ for HNO_3 and HCl in strong acid solutions over the atmospheric temperature range. The most widely used model of Carslaw et al.[2] was revised in Massucci et al.[8]

Back to Table

(1) Abbatt, J. P. D. Interactions of HBr, HCl, and HOBr with supercooled sulfuric acid solutions of stratospheric composition. *J. Geophys. Res.* **1995**, *100*, 14009-14017, doi:10.1029/95JD01367.

(2) Carslaw, K. S.; Clegg, S. L.; Brimblecombe, P. A thermodynamic model of the system HCl-HNO_3-H_2SO_4-H_2O, including solubilities of HBr, from <200 to 328 K. *J. Phys. Chem.* **1995**, *99*, 11557-11574, doi:10.1021/j100029a039.

(3) Carslaw, K. S.; Peter, T.; Clegg, S. L. Modeling the composition of liquid stratospheric aerosols. *Rev. Geophys.* **1997**, *35*, 125-154, doi:10.1029/97RG00078.

(4) Elrod, M. J.; Koch, R. E.; Kim, J. E.; Molina, M. S. HCl vapour pressures and reaction probablilities of $ClONO_2$ + HCl on liquid H_2SO_4-HNO_3-HCl-H_2O solutions. *Faraday Discuss.* **1995**, *100*, 269-278, doi:10.1039/fd9950000269.

(5) Hanson, D. R.; Ravishankara, A. R. Investigation of the reactive and nonreactlve processes involving $ClONO_2$ and HCl on water and nitric acid doped ice. *J. Phys. Chem.* **1992**, *96*, 2682-2691, doi:10.1021/j100185a052.

(6) Hanson, D. R.; Ravishankara, A. R. Uptake of HCl and HOCl onto sulphuric acid: Solubilities, diffusivities and reaction. *J. Phys. Chem.* **1993**, *97*, 12309-12319, doi:10.1021/j100149a035.

(7) Luo, B.; Carslaw, K. S.; Peter, T.; Clegg, S. L. Vapor pressures of $H_2SO_4/HNO_3/HCl/HBr/H_2O$ solutions to low stratospheric temperatures. *Geophys. Res. Lett.* **1995**, *22*, 247-250, doi:10.1029/94GL02988.

(8) Massucci, M.; Clegg, S. L.; Brimblecombe, P. Equilibrium partial pressures, thermodynamic properties of aqueous and solid phases, and Cl_2 production from aqueous HCl and HNO_3 and their mixtures. *J. Phys. Chem. A* **1999**, *103*, 4209-4226, doi:10.1021/jp9847179.

(9) Reihs, C. M.; Golden, D. M.; Tolbert, M. A. Nitric acid uptake by sulfuric acid solutions under stratospheric conditions: Determination of Henry's law solubility. *J. Geophys. Res.* **1990**, *95*, 16545-16550, doi:10.1029/JD095iD10p16545.

(10) Robinson, G. N.; Worsnop, D. R.; Jayne, J. T.; Kolb, C. E.; Swartz, E.; Davidovits, P. Heterogeneous uptake of HCl by sulfuric acid solutions. *J. Geophys. Res.* **1998**, *103*, 25371-25381, doi:10.1029/98JD02085.

(11) Tabazadeh, A.; Turco, R. P.; Jacobson, M. Z. A model for studying the composition and chemical effects of stratospheric aerosols. *J. Geophys. Res.* **1994**, *99*, 12897-12914, doi:10.1029/94JD00820.

(12) Van Doren, J. M.; Watson, L. R.; Davidovits, P.; Worsnop, D. R.; Zahniser, M. S.; Kolb, C. E. Uptake of N_2O_5 and HNO_3 by aqueous sulfuric acid droplets. *J. Phys. Chem.* **1991**, *95*, 1684-1689, doi:10.1021/j100157a037.

(13) Watson, L. R.; Doren, J. M. V.; Davidovits, P.; Worsnop, D. R.; Zahniser, M. S.; Kolb, C. E. Uptake of HCl molecules by aqueous sulfuric acid droplets as a function of acid concentration. *J. Geophys. Res.* **1990**, *95*, 5631-5638, doi:10.1029/JD095iD05p05631.

(14) Williams, L. R.; Golden, D. M. Solubility of HCl in sulfuric acid at stratospheric temperatures. *Geophys. Res. Lett.* **1993**, *20*, 2227-2230, doi:10.1029/93GL02607.

(15) Williams, L. R.; Long, F. S. Viscosity of supercooled sulfuric acid solutions. *J. Phys. Chem.* **1995**, *99*, 3748-3751, doi:10.1021/j100011a050.

(16) Zhang, R.; Wooldridge, P. J.; Molina, M. J. Vapor pressure measurements for the $H_2SO_4/HNO_3/H_2O$ and $H_2SO_4/HCl/H_2O$ systems: Incorporation of stratospheric acids into background sulfate aerosols. *J. Phys. Chem.* **1993**, *97*, 8541-8548, doi:10.1021/j100134a026.

5. HO_2NO_2 in H_2SO_4•nH_2O(l)

Zhang et al.[3] performed wetted wall flow reactor studies using CIMS to detect HO_2NO_2 uptake over the temperature range 201–230 K and an acid concentration range of 52.9–74 wt% H_2SO_4. $HD_l^{1/2}$ values where determined for 52.9, 58.3/59.1, 66.4 and 73.8/74 wt%, with 5 to 15 data points per temperature or temperature pair. All uptake appeared to be reversible with the variation in H_S strongly temperature dependent, but only moderately dependent on H_2SO_4 wt%. D_l values were calculated from a cubic cell model to derive H_S. Uncertainties in measured H_S values were estimated by authors to be 25% for H_S <1 × 10^6 M atm^{-1} and 50% for H_S >1 × 10^6 M atm^{-1}. These data were parameterized by Leu and Zhang [2] in the Sechenov coefficient form adopted by Huthwelker et al.[1] for HOCl, and their formulation is recommended.

Back to Table

(1) Huthwelker, T.; Peter, T.; Juo, B. P.; Clegg, S. L.; Carshlaw, K. S.; Brimblecombe, P. Solubility of HOCl in water and aqueous H_2SO_4 to stratospheric temperatures. *J. Atmos. Chem.* **1995**, *21*, 81-95, doi:10.1007/BF00712439.

(2) Leu, M.-T.; Zhang, R. Solubilities of $CH_3C(O)O_2NO_2$ and HO_2NO_2 in water and liquid H_2SO_4. *Geophys. Res. Lett.* **1999**, *26*, 1129-1132, doi:10.1029/1999GL900158.

(3) Zhang, R.; Leu, M.-T.; Keyser, L. F. Heterogeneous chemistry of HO_2NO_2 in liquid sulfuric acid. *J. Phys. Chem. A* **1997**, *101*, 3324-3330, doi:10.1021/jp963321z.

6. CH_2O in H_2SO_4•mHNO_3•nH_2O(l)

The recommended Henry's Law relationship is:

$$H_{s,\mathrm{eff}} = H_S\left(1 + K_2 a_{H_2O} + K_3 a_{H^+}\right)$$

where: H_s = 3.4 × 10^{-5} exp –[(–0.0456 + 55.5 K/T) (0.46 $m(H_2SO_4)$ + 0.13 $m(HNO_3)$)] M atm^{-1}, T is the temperature in K, and $m(H_2SO_4)$ and $m(HNO_3)$ are the respective acid molalities; K_2 = exp (4020 K/T–5.83) M^{-1}, K_3 = 0.56 exp [8.84 × (T–260 K)/T)] M^{-1}, and a_{H_2O} and a_{H^+} are the water and H^+ activities which are obtained from a thermodynamic model of the solution, e.g. Carslaw et al.[1] Valid for 10–85 wt% H_2SO_4, 8–40 wt% HNO_3.

Knudsen cell studies by Tolbert et al.[4] and Iraci and Tolbert[2] and droplet train/flow reactor studies by Jayne et al.[3] all yield data showing that CH_2O is strongly absorbed by sulfuric acid solutions, and Jayne et al. also provide data for ternary acid solutions. The Jayne et al.[3] study included H_2SO_4 concentrations from 10 to 85 wt% and HNO_3 concentration between 8 and 40 wt% with temperature variations from 241 to 300 K. These data were parameterized with three terms, representing physical CH_2O solubility, reversible hydration to $CH_2(OH)_2$, important in more dilute solutions, and reversible formation of CH_3O^+, dominant at high acidities. The Jayne et al.[3] parameterization is recommended above. The $H_{s,\mathrm{eff}}$ data from Iraci and Tolbert[2] cover 49 to 95 wt% H_2SO_4 and a temperature range of 197 to 214.5 K and are in fair agreement with extrapolation of $H_{s,\mathrm{eff}}$ expression from Jayne et al.[3] for concentrations below ~75 wt%. However, the Iraci and Tolbert data are taken on such thin acid films that initial uptake slopes are difficult to determine accurately and the data scatter is large. While the Iraci and Tolbert data do indicate significantly larger $H_{s,\mathrm{eff}}$ values for H_2SO_4 concentrations above 75 wt%, the data do not compel a reformulation of the Jayne et al. parameterization.

Back to Table

(1) Carslaw, K. S.; Clegg, S. L.; Brimblecombe, P. A thermodynamic model of the system HCl-HNO_3-H_2SO_4-H_2O, including solubilities of HBr, from <200 to 328 K. *J. Phys. Chem.* **1995**, *99*, 11557-11574, doi:10.1021/j100029a039.

(2) Iraci, L. T.; Tolbert, M. A. Heterogeneous interaction of formaldehyde with cold sulfuric acid: Implications for the upper troposphere and lower stratosphere. *J. Geophys. Res.* **1997**, *102*, 16099-16107, doi:10.1029/97JD01259.

(3) Jayne, J. T.; Worsnop, D. R.; Kolb, C. E.; Swartz, E.; Davidovits, P. Uptake of gas-phase formaldehyde by aqueous acid surfaces. *J. Phys. Chem.* **1996**, *100*, 8015-8022, doi:10.1021/jp953196b.

(4) Tolbert, M. A.; Praff, J.; Jayaweera, I.; Prather, M. J. Uptake of formaldehyde by sulfuric acid solutions: Impact on stratospheric ozone. *J. Geophys. Res.* **1993**, *98*, 2957-2962, doi:10.1029/92JD02386.

7. CH_3OH in H_2SO_4•nH_2O(l)

$H_{s,eff}$ data from Kane and Leu,[3] taken over 40–85 wt% H_2SO_4 and from 210–235 K, indicate soluble uptake below 65 wt% and predominately reactive uptake to form methanesulfonic acid and dimethysulfate above 65 wt%. Uptake decreased slightly with temperature below 65 wt% and increases slightly with temperature above. Data yield $H_{s,eff}k^{1/2}$ at high acid concentrations. Weakly temperature dependent $\gamma \approx 0.15$ were measured for 65, 75, and 80 wt%. However, Knudsen cell studies by Iraci et al.[1] at 45, 61 and 72 wt% over a 197–223 K temperature range show only well behaved reversible uptake. They argue that low vapor pressures explain the lack of CH_3OH recovery for the short observation times used by Kane and Leu. They also cite three older literature studies on the reaction of methanol and ethanol at room temperature in sulfuric acid which report reaction rate constants much lower than those deduced by Kane and Leu.[1] Iraci et al. present the following parameterization of their data plus data for water:

$$\log H_{s,eff} = A + 1000B/T$$

where $A = 7.00 + \log c_{H2O}$, $B = (0.000619\ m^2 + 0.00544\ m + 2.267)$ K, c_{H2O} is the molarity of water in the solution (mol L^{-1}) and m is the molality of the H_2SO_4 (mol kg^{-1}).

Note that this parameterization is based only on the Iraci et al. data. A reanalysis of the Kane and Leu[3] results to provide additional data in the 40–72 wt% range, and $H_{s,eff}$ values for higher wt% should be undertaken to validate and extend the Iraci et al. data.

Iraci et al.[2] used infrared spectroscopy to monitor the production of gas phase methyl nitrate, CH_3ONO_2, from the bulk reaction of ternary sulfuric acid/nitric acid/water solutions with 0.00005–0.005 M CH_3OH in 50.5 to 63.6 wt% H_2SO_4 with 0.03–0.21 M HNO_3 between 278.2 and 328.6 K. This reaction may complicate determinations of Henry's law solubility of methanol in ternary acid solutions when sulfuric acid concentrations are high enough (probably >70 wt%) to produce high levels of NO_2^+, the assumed nitrating agent.
Back to Table

(1) Iraci, L. T.; Essin, A. M.; Golden, D. M. Solubility of methanol in low-temperature aqueous sulfuric acid and implications for atmospheric particle composition. *J. Phys. Chem. A* **2002**, *106*, 4054-4060, doi:10.1021/jp012332b.
(2) Iraci, L. T.; Riffel, B. G.; Robinson, C. B.; Michelsen, R. R.; Stephenson, R. M. The acid catalyzed nitration of methanol: formation of methyl nitrate via aerosol chemistry. *J. Atmos. Chem.* **2007**, *58*, 253-266, doi:10.1007/s10874-007-9091-9.
(3) Kane, S. M.; Leu, M.-T. Uptake of methanol vapor in sulfuric acid solutions. *J. Phys. Chem. A* **2001**, *105*, 1411-1415, doi:10.1021/jp001707a.

8. CH_3CH_2OH in $H_2SO_4 \bullet nH_2O$ (l)

Michelsen et al.[1] reported Knudsen cell ethanol uptake experiments for 36–76 wt% H_2SO_4 over a 209–237 K temperature range as well as equilibrium ethanol vapor pressure measurements for 0.5 M ethanol in 59.1 wt% acid between 214.3 and 230.8 K and 0.1 M ethanol in 38.5 wt% acid between 214.0 and 223.9 K. Henry's law solubility parameters from the two methods agreed well. Solubility increased dramatically with increasing acid wt% and decreasing temperature. Michelsen et al. present the following parameterization of their data:

$$\log H_{s,eff} = A + 1000B/T$$

where $A = \Delta S^o/(2.303R) + \log c_{H2O}$, $B = (5.319\ (\chi_{acid})^2 + 0.812\ (\chi_{acid}) + 2.647)$ K, and ΔS^o is –174 J mol^{-1} K^{-1}, c_{H2O} is the molarity of water in the solution calculated at 220K (mol L^{-1}) and χ_{acid} is the mole fraction of sulfuric acid in the solution. Representative values of these parameters are presented in Table 2 of Michelsen et al.[1] Williams et al.[3] performed Knudsen cell $H_{s,eff}$ measurements on the effect of 0.1M acetone on the uptake of ethanol by 38.4 wt% H_2SO_4 at 219.1 K yielding $H_{s,eff} = (2.2 \pm 0.1) \times 10^5$ M atm^{-1} in good agreement with values without added acetone reported by Michelsen et al.[1] and Timonen and Leu;[2] indicating no effect of added acetone.

Timonen and Leu[2] calculated $H_{s,eff}$ values from their uptake coefficients on 41.1 wt% H_2SO_4 that are in moderate agreement with the Michelsen et al. parameterization.
Back to Table

(1) Michelsen, R. R.; Staton, S. J. R.; Iraci, L. T. Uptake and dissolution of gaseous ethanol in sulfuric acid. *J. Phys. Chem. A* **2006**, *110*, 6711-6717, doi:10.1021/jp056234s.
(2) Timonen, R. S.; Leu, M.-T. Interaction of ethyl alcohol vapor with sulfuric acid solutions. *J. Phys. Chem. A* **2006**, *110*, 6660-6666, doi:10.1021/jp055810h.

(3) Williams, M. B.; Michelsen, R. R. H.; Axson, J. L.; Iraci, L. T. Uptake of acetone, acetaldehyde and ethanol in cold sulfuric acid solutions containing organic material: Carbon accretion mechanisms. *Atmos. Environ.* **2010**, *44*, 1145-1151, doi:10.1016/j.atmosenv.2009.12.036.

9. CH_3CHO in $H_2SO_4 \bullet nH_2O$(l)

Michelsen et al.[1] reported Knudsen cell acetaldehyde uptake experiments for 39–76 wt% H_2SO_4 over a 211–241 K temperature range. Tabulated $H_{s,eff}$ values for 37 experiments covering four acid concentrations ranged from 2×10^2 to 1.5×10^5 M atm^{-1}; with highest values at highest acid concentration and lowest temperatures. Data for the highest acid concentrations (~76 wt% H_2SO_4) generally indicated simple solubility behavior, while some measurements at lower acid concentrations (39–66 wt%) showed indications of reactive uptake.

Williams et al.[2] performed Knudsen cell $H_{s,eff}$ measurements on the effect of 0.1M ethanol or acetone on the uptake of acetaldehyde, reproducing a few temperatures and acid concentrations used for the data reported in Michelsen et al.[1] The solubility of acetaldehyde in acid with 0.1 M ethanol or 0.1 M acetone was nearly an order of magnitude higher than the corresponding organic free measurements. Two measurements at 216.1 and 226.8 K with 0.0016 M formaldehyde added to 38.5 wt% H_2SO_4 showed no $H_{s,eff}$ enhancement over organic free measurements but time resolved uptake measurements showed evidence for enhanced reactive uptake.
Back to Table

(1) Michelsen, R. R.; Ashbourn, S. F. M.; Iraci, L. T. Dissolution, speciation, and reaction of acetaldehyde in cold sulfuric acid. *J. Geophys. Res.* **2004**, *109*, D23205, doi:10.1029/2004JD005041.
(2) Williams, M. B.; Michelsen, R. R. H.; Axson, J. L.; Iraci, L. T. Uptake of acetone, acetaldehyde and ethanol in cold sulfuric acid solutions containing organic material: Carbon accretion mechanisms. *Atmos. Environ.* **2010**, *44*, 1145-1151, doi:10.1016/j.atmosenv.2009.12.036.

10. $CH_3C(O)CH_3$ in $H_2SO_4 \bullet nH_2O$(l)

Duncan et al.[2,3] used IR spectra of thin sulfuric acid films to establish that acetone is absorbed as the protonated species. Above 70 wt% protonated acetone undergoes a self-condensation/dehydration reaction to form protonated mesityl oxide, which, in turn, reacts with an additional protonated acetone to form trimethyl benzene. Duncan et al.[3] measured reversible uptake and derived Henry's law constants for 70 wt% H_2SO_4 at 180, 187 and 195 K and a value at 201 K for 76 wt%. Kane et al.[6] measured uptake in a wetted wall flow reactor and derived $H_{s,eff}$ parameters for 40, 50, 65, and 75 wt% over a much wider temperature range than Duncan et al.[3] Their data diverge above 80 wt% which they attribute to reactive uptake as suggested by Duncan et al.[2,3] Klassen et al.[7] provide Knudsen cell uptake derived data for 48.7 to 78.3 H_2SO_4 wt% between 210 and 240 K that are generally consistent with that of Kane et al.[6] Imamura and Akiyoshi[5] report wetted wall flow reactor $H_{s,eff}$ measurements at 230 K for 50 and 60 wt%, 250 K for 60, 69 and 76 wt%, and 270 K for 76 and 79 wt%; their data diverge a factor of 2 to 4 from that of Kane et al.[6] and Klassen et al.[7]

Equally weighted data sets from Kane et al.[6] and Klassen et al.[7] were combined and fit to generate the recommended parameterization. Two points for the solubility of acetone in water at 298 K and 273 K (Benkelberg et al.[1]) were included to improve the extrapolation to low wt% solutions. The data points from Imamura and Akiyoshi[5] were not included because they were inconsistent with the other data and have a very different temperature dependence. The few data points from Duncan et al.[2,3] are also inconsistent with the other data and were not included in the parameterization. Using a rotating wetted-wall flow reactor Esteve and Nozière[4] measured $H_{s,eff}$ coefficients at 298 ± 3K for 89.4, 85, 80.8 73.9 and 70 wt% H_2SO_4, reporting values of 840, 650, 500, and 320 M atm^{-1}, respectively. These data are not included in the recommended parameterization since the temperature/wt% ranges they cover are unlikely to occur in the atmosphere.

Williams et al.[8] performed Knudsen cell $H_{s,eff}$ measurements on the effect of 0.1 M ethanol on the uptake of acetone by 38.4 to 75.0 wt% H_2SO_4 at temperatures between 217.6 and 238.5 K, corresponding to data points previously reported by Kane et al. and Klassen et al. Their data indicated that the added ethanol had "no significant effect" on the solubility of acetone for comparable ethanol free measurements.
Back to Table

(1) Benkelberg, H. J.; Hamm, S.; Warneck, P. Henry's law coefficients for aqueous solutions of acetone, acetaldehyde and acetonitrile and equilibrium constants for the addition compounds of acetone and acetaldehyde with bisulfite. *J. Atmos. Chem.* **1995**, *20*, 17-34, doi:10.1007/BF01099916.

(2) Duncan, J. L.; Schindler, L. R.; Roberts, J. T. A new sulfate-mediated reaction: Conversion of acetone to trimethylbenzene in the presence of liquid sulfuric acid. *Geophys. Res. Lett.* **1998**, *25*, 631-634, doi:10.1029/98GL00250.
(3) Duncan, J. L.; Schindler, L. R.; Roberts, J. T. Chemistry at and near the surface of liquid sulfuric acid: A kinetic, thermodynamic, and mechanistic analysis of heterogeneous reactions of acetone. *J. Phys. Chem. B* **1999**, *103*, 7247-7259, doi:10.1021/jp991322w.
(4) Esteve, W.; Nozière, B. Uptake and reaction kinetics of acetone, 2-butanone, 2,4-pentanedione, and acetaldehyde in sulfuric acid solutions. *J. Phys. Chem. A* **2005**, *109*, 10920-10928, doi:10.1021/jp051199a.
(5) Imamura, T.; Akiyoshi, H. Uptake of acetone into sulfuric-acid solutions. *Geophys. Res. Lett.* **2000**, *27*, 1419-1422, doi:10.1029/1999GL011137.
(6) Kane, S. M.; Timonen, R. S.; Leu, M. T. Heterogeneous chemistry of acetone in sulfuric acid solutions: Implications for the upper troposphere. *J. Phys. Chem. A* **1999**, *103*, 9259-9265, doi:10.1021/jp9926692.
(7) Klassen, J. K.; Lynton, J.; Golden, D. M.; Williams, L. R. Solubility of acetone in low-temperature (210-240 K) sulfuric acid solutions. *J. Geophys. Res.* **1999**, *104*, 26355-26361, doi:10.1029/1999JD900751.
(8) Williams, M. B.; Michelsen, R. R. H.; Axson, J. L.; Iraci, L. T. Uptake of acetone, acetaldehyde and ethanol in cold sulfuric acid solutions containing organic material: Carbon accretion mechanisms. *Atmos. Environ.* **2010**, *44*, 1145-1151, doi:10.1016/j.atmosenv.2009.12.036.

11. $CH_3C(O)O_2NO_2$ in H_2O and H_2SO_4•nH_2O(l)

Zhang and Leu[5] performed wetted wall flow reactor studies using CIMS to detect $CH_3C(O)O_2NO_2$ uptake over the temperature range 199–226 K. Uptake studies were performed at 46, 54, 59, and 72 wt% H_2SO_4 to yield $H_{s,eff}D_l^{1/2}$ values. D_l values were calculated from a cubic cell model to derive $H_{s,eff}$. Leu and Zhang[4] fit their data from Zhang and Leu,[5] including water data from Kames and Schurath[2] and Kames et al.,[3] using the Sechenov coefficient form adopted by Huthwelker for HOCl.[1] This formulation is recommended for both water and sulfuric acid solutions.

Back to Table

(1) Huthwelker, T.; Peter, T.; Juo, B. P.; Clegg, S. L.; Carshlaw, K. S.; Brimblecombe, P. Solubility of HOCl in water and aqueous H_2SO_4 to stratospheric temperatures. *J. Atmos. Chem.* **1995**, *21*, 81-95, doi:10.1007/BF00712439.
(2) Kames, J.; Schurath, U. Henry's law and hydrolysis-rate constants for peroxyacyl nitrates (PANs) using a homogeneous gas-phase source. *J. Atmos. Chem.* **1995**, *21*, 151-164, doi:10.1007/BF00696578.
(3) Kames, J.; Schweighoefer, S.; Schurath, U. Henry's law constant and hydrolysis of peroyacetylnitrate (PAN). *J. Atmos. Chem.* **1991**, *12*, 169-180, doi:10.1007/BF00115778.
(4) Leu, M.-T.; Zhang, R. Solubilities of $CH_3C(O)O_2NO_2$ and HO_2NO_2 in water and liquid H_2SO_4. *Geophys. Res. Lett.* **1999**, *26*, 1129-1132, doi:10.1029/1999GL900158.
(5) Zhang, R.; Leu, M.-T. Heterogeneous interaction of peroxyacetyl nitrate with liquid sulfuric acid. *J. Geophys. Res.* **1997**, *102*, 8837-8843, doi:10.1029/97JD00131.

12. CF_2O in H_2SO_4•nH_2O(l)

Hanson and Ravishankara[1] calculate an upper limit for H_S of CF_2O based on assumed solubility limit resulting in lack of measurable uptake into 60 wt% H_2SO_4.

Back to Table

(1) Hanson, D. R.; Ravishankara, A. R. The loss of CF_2O on ice, NAT, and sulfuric acid solutions. *Geophys. Res. Lett.* **1991**, *18*, 1699-1701, doi:10.1029/91GL02093.

13. CF_3OH in H_2SO_4•nH_2O(l)

Lovejoy et al.[1] determined reacto-diffusive lengths of >0.4 μm and 1.0 μm for CF_3OH uptake at 250 K on 40 and 50 wt% H_2SO_4 aerosols, respectively. This leads to $H_{s,eff}$ estimates of >240 M atm^{-1} and 210 M atm^{-1}, respectively.

Back to Table

(1) Lovejoy, E. R.; Huey, L. G.; Hanson, D. R. Atmospheric fate of CF_3OH 2: Heterogeneous reaction. *J. Geophys. Res.* **1995**, *100*, 18775-18780, doi:10.1029/95JD01843.

14. HOCl in H_2SO_4•nH_2O(l)

Recommendation is from the model of Shi et al.[5] which is based on wetted wall flow tube data from Hanson and Ravishankara[3] and Hanson and Lovejoy,[2] and uptake by stirred and static solutions by Donaldson et al.[1] This model incorporates newer, higher temperature data and replaces earlier recommended formulation by Huthwelker et al.[4]

Back to Table

(1) Donaldson, D. J.; Ravishankara, A. R.; Hanson, D. R. Detailed study of HOCl + HCl → Cl_2 + H_2O in sulfuric acid. *J. Phys. Chem. A* **1997**, *101*, 4717-4725, doi:10.1021/jp9633153.
(2) Hanson, D. R.; Lovejoy, E. R. Heterogeneous reactions in liquid sulfuric Acid: HOCl + HCl as a model system. *J. Phys. Chem.* **1996**, *100*, 6397-6405, doi:10.1021/jp953250o.
(3) Hanson, D. R.; Ravishankara, A. R. Reaction of $ClONO_2$ with HCl on NAT, NAD, and frozen sulfuric acid and hydrolysis of N_2O_5 and $ClONO_2$ on frozen sulfuric acid. *J. Geophys. Res.* **1993**, *98*, 22931-22936, doi:10.1029/93JD01929.
(4) Huthwelker, T.; Peter, T.; Juo, B. P.; Clegg, S. L.; Carshlaw, K. S.; Brimblecombe, P. Solubility of HOCl in water and aqueous H_2SO_4 to stratospheric temperatures. *J. Atmos. Chem.* **1995**, *21*, 81-95, doi:10.1007/BF00712439.
(5) Shi, Q.; Davidovits, P.; Jayne, J. T.; Kolb, C. E.; Worsnop, D. R. Kinetic model for reaction of $ClONO_2$ with H_2O and HCl and HOCl with HCl in sulfuric acid solutions. *J. Geophys. Res.* **2001**, *106*, 24259-24274, doi:10.1029/2000JD000181.

15. $ClONO_2$ in H_2SO_4•nH_2O(l)

Recommendation is from the model of Shi et al.[2] who used a measurement of the hydrolysis reaction's reacto-diffusive length by Hanson and Lovejoy[1] on 60 wt% H_2SO_4 at 250 K to derive the hydrolysis rate constant, k_{hyd}, and constrain $H_S(ClONO_2)$ at 250 K. Shi et al. fit the $Hk^{1/2}$ dependence of the $ClONO_2$ uptake coefficients for a variety of $ClONO_2$ hydrolysis and $ClONO_2$ + HCl data to derive a parameterization for H_S as a function of wt% and T.

Back to Table

(1) Hanson, D. R.; Lovejoy, E. R. The reaction of $ClONO_2$ with submicrometer sulfuric acid aerosol. *Science* **1995**, *267*, 1326-1329, doi:10.1126/science.267.5202.1326.
(2) Shi, Q.; Davidovits, P.; Jayne, J. T.; Kolb, C. E.; Worsnop, D. R. Kinetic model for reaction of $ClONO_2$ with H_2O and HCl and HOCl with HCl in sulfuric acid solutions. *J. Geophys. Res.* **2001**, *106*, 24259-24274, doi:10.1029/2000JD000181.

16. HBr in H_2SO_4•mHNO_3•nH_2O(l)

Experimental data for HBr solubility is provided by Williams et al.,[7] Abbatt,[1] Abbatt and Nowak,[2] Kleffman et al.,[4] and Behr et al.[3] Data from time-dependent uptake measurements and from vapor pressure measurements are in good agreement after correcting for the fact that for some of the vapor pressure measurements the HBr concentration in solution was high enough to increase the acidity and thereby decrease the HBr solubility. By comparing pairs of data points with different HBr concentrations (from the same experiment), an average correction factor was obtained. The correction factor was used to correct the vapor pressure data of Williams et al.,[7] Abbatt and Nowak,[2] and Kleffmann et al. to zero effective HBr concentration. (This is different than the approach taken in Kleffmann et al. of using a "corrected" H_2SO_4 wt%. However, the resulting parameterization is very similar to the one in Kleffmann et al.[4]) The time-dependent uptake data of Williams et al.[7] and Abbatt,[1] and the molecular beam uptake data of Behr et al.[3] did not require correction. All of the experimental data have been fit to obtain the recommended parameterization as a function of H_2SO_4 wt% and temperature.

Agreement between this parameterization and the updated activity coefficient model of Massucci et al.[6] (http://www.aim.env.uea.ac.uk/aim/aim.php) is good for >60 wt%, but not very good at lower H_2SO_4 wt%, particularly at low temperatures. Therefore, this parameterization is recommended for calculating HBr Henry's law solubilities.

The only data for HBr solubilities in ternary solutions is from Kleffmann et al.[4] The data do not agree well with the updated activity coefficient in Massucci et al.[4] or with the older activity coefficient model in Luo et al.[5] Until further information becomes available, the recommendation is to use the parameterization for ternary solutions given in Kleffmann et al.[4]

Back to Table

(1) Abbatt, J. P. D. Interactions of HBr, HCl, and HOBr with supercooled sulfuric acid solutions of stratospheric composition. *J. Geophys. Res.* **1995**, *100*, 14009-14017, doi:10.1029/95JD01367.

(2) Abbatt, J. P. D.; Nowak, J. B. Heterogeneous interactions of HBr and HOCl with cold sulfuric acid solutions: Implications for Arctic boundary layer bromine chemistry. *J. Phys. Chem. A* **1997**, *101*, 2131-2137, doi:10.1021/jp963117b.

(3) Behr, P.; Morris, J. R.; Antman, M. D.; Ringeisen, B. R.; Splan, J.; Nathanson, G. M. Reaction and desorption of HCl and HBr following collisions with supercoolded sulfuric acid. *Geophys. Res. Lett.* **2001**, *28*, 1961-1964, doi:10.1029/2000GL012716.

(4) Kleffman, J.; Becker, K. H.; Broske, R.; Rothe, D.; Wiesen, P. Solubility of HBr in H_2SO_4/H_2O and $HNO_3/H_2SO_4/H_2O$ solutions. *J. Phys. Chem. A* **2000**, *104*, 8489-8495, doi:10.1021/jp000815u.

(5) Luo, B.; Carslaw, K. S.; Peter, T.; Clegg, S. L. Vapor pressures of $H_2SO_4/HNO_3/HCl/HBr/H_2O$ solutions to low stratospheric temperatures. *Geophys. Res. Lett.* **1995**, *22*, 247-250, doi:10.1029/94GL02988.

(6) Massucci, M.; Clegg, S. L.; Brimblecombe, P. Equilibrium partial pressures, thermodynamic properties of aqueous and solid phases, and Cl_2 production from aqueous HCl and HNO_3 and their mixtures. *J. Phys. Chem. A* **1999**, *103*, 4209-4226, doi:10.1021/jp9847179.

(7) Williams, L. R.; Golden, D. M.; Huestis, D. L. Solubility of HBr in sulfuric acid at stratospheric temperatures. *J. Geophys. Res.* **1995**, *100*, 7329-7335, doi:10.1029/95JD00218.

17. HOBr in $H_2SO_4 \cdot nH_2O$(l)

HOBr solubility measurements have been reported from coated wall flow reactor uptake studies by Waschewsky and Abbatt[3] and Hanson[1] and from Knudsen cell uptake studies from Iraci et al.[2] Although they were performed in different temperature ranges, extrapolations of Hanson's higher temperature data to the temperature range investigated by Waschewsky and Abbatt predicted much higher HOBr solubility than they measured. Iraci et al. subsequently measured HOBr uptake over both of the temperature ranges covered in the prior experiments. Their data agreed well with data from Waschewsky and Abbatt[3] at lower temperatures (213–238 K) but fall far below Hanson's higher (250–270 K) temperature measurements. The Iraci et al. measurements were performed at ≈ 45, 55, 61 and 70 wt% H_2SO_4 and investigated over the temperature range from 201 to 252 K. Their results, like the earlier studies, indicate that the dependence of $H_{s,eff}$ on acid concentration is relatively weak. For H_2SO_4 acid wt% from 55 to 75, $H_{s,eff}$ is well described by: $\log H_{s,eff} = (2349 \pm 280)\ K/T - (5.27 \pm 1.24)$. Their ≈ 45 wt% data are fit by: $\log H_{s,eff} = (3665 \pm 270)\ K/T - (10.63 \pm 1.23)$.

Back to Table

(1) Hanson, D. Reactivity of $BrONO_2$ and HOBr on sulfuric acid solutions at low temperatures. *J. Geophys. Res.* **2003**, *108*, 4239, doi: 10.1029/2002JD002519.

(2) Iraci, L. T.; Michelsen, R. R.; Ashbourn, S. F. M.; Rammer, T. A.; Golden, D. M. Uptake of hypobromous acid (HOBr) by aqueous sulfuric acid solutions: low-temperature solubility and reaction. *Atmos. Chem. Phys.* **2005**, *5*, 1577-1587, doi:10.5194/acp-5-1577-2005.

(3) Waschewsky, G. C. G.; Abbatt, J. P. D. HOBr in sulfuric acid solution: solubility and reaction as a function of temperature and concentration. *J. Phys. Chem. A* **1999**, *103*, 5312-5320, doi:10.1021/jp984489i.

18. SO_2 in $H_2SO_4 \cdot nH_2O$(l)

Room temperature vapor pressure measurements reviewed by Hayduk et al.[1] and bubble train reactor uptake measurements by Rattigan et al.[4] for 0–70 wt% H_2SO_4 agree very well. Langenberg et al.[2] used a novel capillary gas chromatography technique to deduce $H_{s,eff}$ values for 41–83 wt% H_2SO_4 over the temperature range 193–242 K. The recommended parameterization is a fair fit to the Rattigan et al. and Langenberg et al. data sets and allows reasonable extrapolation over the full range of atmospheric temperatures. Note that the Langenberg et al.[2] data is in mol/(kgbar) and was converted to mol L^{-1} using the density parameterization of Myhre et al.[3]

Back to Table

(1) Hayduk, W.; Asatani, H.; Lu, B. C. Y. Solubility of sulfur dioxide in aqueous sulfuric acid solutions. *J. Chem. Eng. Data* **1988**, *33*, 506-509, doi:10.1021/je00054a033.
(2) Langenberg, S.; Proksch, V.; Schurath, U. Solubilities and diffusion of trace gases in cold sulfuric acid films. *Atmos. Environ.* **1998**, *32*, 3129-3137, doi:10.1016/S1352-2310(97)00490-1.
(3) Myhre, C. E. L.; Nielsen, C. J.; Saastad, O. W. Density and surface tension of aqueous H_2SO_4 at low temperature. *J. Chem. Eng. Data* **1998**, *43*, 617-622, doi:10.1021/je980013g.
(4) Rattigan, O. V.; Boniface, J.; Swartz, E.; Davidovits, P.; Jayne, J. T.; Kolb, C. E.; Worsnop, D. R. Uptake of gas-phase SO_2 in aqueous sulfuric acid: Oxidation by H_2O_2, O_3, and HONO. *J. Geophys. Res.* **2000**, *105*, 29065-29078, doi:10.1029/2000JD900372.

5.3.4.2 Bibliography – Table Eq4

Abbatt, J. P. D. Interactions of HBr, HCl, and HOBr with supercooled sulfuric acid solutions of stratospheric composition. *J. Geophys. Res.* **1995**, *100*, 14009-14017, doi:10.1029/95JD01367.

Abbatt, J. P. D.; Nowak, J. B. Heterogeneous interactions of HBr and HOCl with cold sulfuric acid solutions: Implications for Arctic boundary layer bromine chemistry. *J. Phys. Chem. A* **1997**, *101*, 2131-2137, doi:10.1021/jp963117b.

Becker, K. H.; Kleffman, J.; Kurtenbach, R.; Wiesen, P. Solubility of nitrous acid (HONO) in sulfuric acid solutions. *J. Phys. Chem.* **1996**, *100*, 14984-14990, doi:10.1021/jp961140r.

Behr, P.; Morris, J. R.; Antman, M. D.; Ringeisen, B. R.; Splan, J.; Nathanson, G. M. Reaction and desorption of HCl and HBr following collisions with supercoolded sulfuric acid. *Geophys. Res. Lett.* **2001**, *28*, 1961-1964, doi:10.1029/2000GL012716.

Benkelberg, H. J.; Hamm, S.; Warneck, P. Henry's law coefficients for aqueous solutions of acetone, acetaldehyde and acetonitrile and equilibrium constants for the addition compounds of acetone and acetaldehyde with bisulfite. *J. Atmos. Chem.* **1995**, *20*, 17-34, doi:10.1007/BF01099916.

Carslaw, K. S.; Clegg, S. L.; Brimblecombe, P. A thermodynamic model of the system HCl-HNO_3-H_2SO_4-H_2O, including solubilities of HBr, from <200 to 328 K. *J. Phys. Chem.* **1995**, *99*, 11557-11574, doi:10.1021/j100029a039.

Carslaw, K. S.; Peter, T.; Clegg, S. L. Modeling the composition of liquid stratospheric aerosols. *Rev. Geophys.* **1997**, *35*, 125-154, doi:10.1029/97RG00078.

Donaldson, D. J.; Ravishankara, A. R.; Hanson, D. R. Detailed study of HOCl + HCl → Cl_2 + H_2O in sulfuric acid. *J. Phys. Chem. A* **1997**, *101*, 4717-4725, doi:10.1021/jp9633153.

Duncan, J. L.; Schindler, L. R.; Roberts, J. T. A new sulfate-mediated reaction: Conversion of acetone to trimethylbenzene in the presence of liquid sulfuric acid. *Geophys. Res. Lett.* **1998**, *25*, 631-634, doi:10.1029/98GL00250.

Duncan, J. L.; Schindler, L. R.; Roberts, J. T. Chemistry at and near the surface of liquid sulfuric acid: A kinetic, thermodynamic, and mechanistic analysis of heterogeneous reactions of acetone. *J. Phys. Chem. B* **1999**, *103*, 7247-7259, doi:10.1021/jp991322w.

Elrod, M. J.; Koch, R. E.; Kim, J. E.; Molina, M. S. HCl vapour pressures and reaction probablilities of $ClONO_2$ + HCl on liquid H_2SO_4-HNO_3-HCl-H_2O solutions. *Faraday Discuss.* **1995**, *100*, 269-278, doi:10.1039/fd9950000269.

Esteve, W.; Nozière, B. Uptake and reaction kinetics of acetone, 2-butanone, 2,4-pentanedione, and acetaldehyde in sulfuric acid solutions. *J. Phys. Chem. A* **2005**, *109*, 10920-10928, doi:10.1021/jp051199a.

Hanson, D. Reactivity of $BrONO_2$ and HOBr on sulfuric acid solutions at low temperatures. *J. Geophys. Res.* **2003**, *108*, 4239, doi:10.1029/2002JD002519.

Hanson, D. R.; Lovejoy, E. R. The reaction of $ClONO_2$ with submicrometer sulfuric acid aerosol. *Science* **1995**, *267*, 1326-1329, doi:10.1126/science.267.5202.1326.

Hanson, D. R.; Lovejoy, E. R. Heterogeneous reactions in liquid sulfuric Acid: HOCl + HCl as a model system. *J. Phys. Chem.* **1996**, *100*, 6397-6405, doi:10.1021/jp953250o.

Hanson, D. R.; Ravishankara, A. R. The loss of CF_2O on ice, NAT, and sulfuric acid solutions. *Geophys. Res. Lett.* **1991**, *18*, 1699-1701, doi:10.1029/91GL02093.

Hanson, D. R.; Ravishankara, A. R. Investigation of the reactive and nonreactlve processes involving $ClONO_2$ and HCl on water and nitric acid doped ice. *J. Phys. Chem.* **1992**, *96*, 2682-2691, doi:10.1021/j100185a052.

Hanson, D. R.; Ravishankara, A. R. Reaction of $ClONO_2$ with HCl on NAT, NAD, and frozen sulfuric acid and hydrolysis of N_2O_5 and $ClONO_2$ on frozen sulfuric acid. *J. Geophys. Res.* **1993**, *98*, 22931-22936, doi:10.1029/93JD01929.

Hanson, D. R.; Ravishankara, A. R. Uptake of HCl and HOCl onto sulphuric acid: Solubilities, diffusivities and reaction. *J. Phys. Chem.* **1993**, *97*, 12309-12319, doi:10.1021/j100149a035.

Hayduk, W.; Asatani, H.; Lu, B. C. Y. Solubility of sulfur dioxide in aqueous sulfuric acid solutions. *J. Chem. Eng. Data* **1988**, *33*, 506-509, doi:10.1021/je00054a033.

Huthwelker, T.; Peter, T.; Juo, B. P.; Clegg, S. L.; Carshlaw, K. S.; Brimblecombe, P. Solubility of HOCl in water and aqueous H_2SO_4 to stratospheric temperatures. *J. Atmos. Chem.* **1995**, *21*, 81-95, doi:10.1007/BF00712439.

Imamura, T.; Akiyoshi, H. Uptake of acetone into sulfuric-acid solutions. *Geophys. Res. Lett.* **2000**, *27*, 1419-1422, doi:10.1029/1999GL011137.

Iraci, L. T.; Essin, A. M.; Golden, D. M. Solubility of methanol in low-temperature aqueous sulfuric acid and implications for atmospheric particle composition. *J. Phys. Chem. A* **2002**, *106*, 4054-4060, doi:10.1021/jp012332b.

Iraci, L. T.; Michelsen, R. R.; Ashbourn, S. F. M.; Rammer, T. A.; Golden, D. M. Uptake of hypobromous acid (HOBr) by aqueous sulfuric acid solutions: low-temperature solubility and reaction. *Atmos. Chem. Phys.* **2005**, *5*, 1577-1587, doi:10.5194/acp-5-1577-2005.

Iraci, L. T.; Riffel, B. G.; Robinson, C. B.; Michelsen, R. R.; Stephenson, R. M. The acid catalyzed nitration of methanol: formation of methyl nitrate via aerosol chemistry. *J. Atmos. Chem.* **2007**, *58*, 253-266, doi:10.1007/s10874-007-9091-9.

Iraci, L. T.; Tolbert, M. A. Heterogeneous interaction of formaldehyde with cold sulfuric acid: Implications for the upper troposphere and lower stratosphere. *J. Geophys. Res.* **1997**, *102*, 16099-16107, doi:10.1029/97JD01259.

Jayne, J. T.; Worsnop, D. R.; Kolb, C. E.; Swartz, E.; Davidovits, P. Uptake of gas-phase formaldehyde by aqueous acid surfaces. *J. Phys. Chem.* **1996**, *100*, 8015-8022, doi:10.1021/jp953196b.

Kames, J.; Schurath, U. Henry's law and hydrolysis-rate constants for peroxyacyl nitrates (PANs) using a homogeneous gas-phase source. *J. Atmos. Chem.* **1995**, *21*, 151-164, doi:10.1007/BF00696578.

Kames, J.; Schweighoefer, S.; Schurath, U. Henry's law constant and hydrolysis of peroyacetylnitrate (PAN). *J. Atmos. Chem.* **1991**, *12*, 169-180, doi:10.1007/BF00115778.

Kane, S. M.; Leu, M.-T. Uptake of methanol vapor in sulfuric acid solutions. *J. Phys. Chem. A* **2001**, *105*, 1411-1415, doi:10.1021/jp001707a.

Kane, S. M.; Timonen, R. S.; Leu, M. T. Heterogeneous chemistry of acetone in sulfuric acid solutions: Implications for the upper troposphere. *J. Phys. Chem. A* **1999**, *103*, 9259-9265, doi:10.1021/jp9926692.

Klassen, J. K.; Lynton, J.; Golden, D. M.; Williams, L. R. Solubility of acetone in low-temperature (210-240 K) sulfuric acid solutions. *J. Geophys. Res.* **1999**, *104*, 26355-26361, doi:10.1029/1999JD900751.

Kleffman, J.; Becker, K. H.; Broske, R.; Rothe, D.; Wiesen, P. Solubility of HBr in H_2SO_4/H_2O and $HNO_3/H_2SO_4/H_2O$ solutions. *J. Phys. Chem. A* **2000**, *104*, 8489-8495, doi:10.1021/jp000815u.

Langenberg, S.; Proksch, V.; Schurath, U. Solubilities and diffusion of trace gases in cold sulfuric acid films. *Atmos. Environ.* **1998**, *32*, 3129-3137, doi:10.1016/S1352-2310(97)00490-1.

Leu, M.-T.; Zhang, R. Solubilities of $CH_3C(O)O_2NO_2$ and HO_2NO_2 in water and liquid H_2SO_4. *Geophys. Res. Lett.* **1999**, *26*, 1129-1132, doi:10.1029/1999GL900158.

Longfellow, C. A.; Imamura, T.; Ravishankara, A. R.; Hanson, D. R. HONO solubility and heterogeneous reactivity on sulfuric acid surfaces. *J. Phys. Chem. A* **1998**, *102*, 3323-3332, doi:10.1021/jp9807120.

Lovejoy, E. R.; Huey, L. G.; Hanson, D. R. Atmospheric fate of CF_3OH 2: Heterogeneous reaction. *J. Geophys. Res.* **1995**, *100*, 18775-18780, doi:10.1029/95JD01843.

Luo, B.; Carslaw, K. S.; Peter, T.; Clegg, S. L. Vapor pressures of $H_2SO_4/HNO_3/HCl/HBr/H_2O$ solutions to low stratospheric temperatures. *Geophys. Res. Lett.* **1995**, *22*, 247-250, doi:10.1029/94GL02988.

Massucci, M.; Clegg, S. L.; Brimblecombe, P. Equilibrium partial pressures, thermodynamic properties of aqueous and solid phases, and Cl_2 production from aqueous HCl and HNO_3 and their mixtures. *J. Phys. Chem. A* **1999**, *103*, 4209-4226, doi:10.1021/jp9847179.

Michelsen, R. R.; Ashbourn, S. F. M.; Iraci, L. T. Dissolution, speciation, and reaction of acetaldehyde in cold sulfuric acid. *J. Geophys. Res.* **2004**, *109*, D23205, doi:10.1029/2004JD005041.

Michelsen, R. R.; Staton, S. J. R.; Iraci, L. T. Uptake and dissolution of gaseous ethanol in sulfuric acid. *J. Phys. Chem. A* **2006**, *110*, 6711-6717, doi:10.1021/jp056234s.

Myhre, C. E. L.; Nielsen, C. J.; Saastad, O. W. Density and surface tension of aqueous H_2SO_4 at low temperature. *J. Chem. Eng. Data* **1998**, *43*, 617-622, doi:10.1021/je980013g.

Rattigan, O. V.; Boniface, J.; Swartz, E.; Davidovits, P.; Jayne, J. T.; Kolb, C. E.; Worsnop, D. R. Uptake of gas-phase SO_2 in aqueous sulfuric acid: Oxidation by H_2O_2, O_3, and HONO. *J. Geophys. Res.* **2000**, *105*, 29065-29078, doi:10.1029/2000JD900372.

Reihs, C. M.; Golden, D. M.; Tolbert, M. A. Nitric acid uptake by sulfuric acid solutions under stratospheric conditions: Determination of Henry's law solubility. *J. Geophys. Res.* **1990**, *95*, 16545-16550, doi:10.1029/JD095iD10p16545.

Robinson, G. N.; Worsnop, D. R.; Jayne, J. T.; Kolb, C. E.; Swartz, E.; Davidovits, P. Heterogeneous uptake of HCl by sulfuric acid solutions. *J. Geophys. Res.* **1998**, *103*, 25371-25381, doi:10.1029/98JD02085.

Shi, Q.; Davidovits, P.; Jayne, J. T.; Kolb, C. E.; Worsnop, D. R. Kinetic model for reaction of $ClONO_2$ with H_2O and HCl and HOCl with HCl in sulfuric acid solutions. *J. Geophys. Res.* **2001**, *106*, 24259-24274, doi:10.1029/2000JD000181.

Tabazadeh, A.; Turco, R. P.; Jacobson, M. Z. A model for studying the composition and chemical effects of stratospheric aerosols. *J. Geophys. Res.* **1994**, *99*, 12897-12914, doi:10.1029/94JD00820.

Timonen, R. S.; Leu, M.-T. Interaction of ethyl alcohol vapor with sulfuric acid solutions. *J. Phys. Chem. A* **2006**, *110*, 6660-6666, doi:10.1021/jp055810h.

Tolbert, M. A.; Praff, J.; Jayaweera, I.; Prather, M. J. Uptake of formaldehyde by sulfuric acid solutions: Impact on stratospheric ozone. *J. Geophys. Res.* **1993**, *98*, 2957-2962, doi:10.1029/92JD02386.

Van Doren, J. M.; Watson, L. R.; Davidovits, P.; Worsnop, D. R.; Zahniser, M. S.; Kolb, C. E. Uptake of N_2O_5 and HNO_3 by aqueous sulfuric acid droplets. *J. Phys. Chem.* **1991**, *95*, 1684-1689, doi:10.1021/j100157a037.

Waschewsky, G. C. G.; Abbatt, J. P. D. HOBr in sulfuric acid solution: solubility and reaction as a function of temperature and concentration. *J. Phys. Chem. A* **1999**, *103*, 5312-5320, doi:10.1021/jp984489i.

Watson, L. R.; Doren, J. M. V.; Davidovits, P.; Worsnop, D. R.; Zahniser, M. S.; Kolb, C. E. Uptake of HCl molecules by aqueous sulfuric acid droplets as a function of acid concentration. *J. Geophys. Res.* **1990**, *95*, 5631-5638, doi:10.1029/JD095iD05p05631.

Wilhelm, E.; Battino, R.; Wilcock, R. J. Low-pressure solubility of gases in liquid water. *Chem. Rev.* **1977**, *77*, 219-262, doi:10.1021/cr60306a003.

Williams, L. R.; Golden, D. M. Solubility of HCl in sulfuric acid at stratospheric temperatures. *Geophys. Res. Lett.* **1993**, *20*, 2227-2230, doi:10.1029/93GL02607.

Williams, L. R.; Golden, D. M.; Huestis, D. L. Solubility of HBr in sulfuric acid at stratospheric temperatures. *J. Geophys. Res.* **1995**, *100*, 7329-7335, doi:10.1029/95JD00218.

Williams, L. R.; Long, F. S. Viscosity of supercooled sulfuric acid solutions. *J. Phys. Chem.* **1995**, *99*, 3748-3751, doi:10.1021/j100011a050.

Williams, M. B.; Michelsen, R. R. H.; Axson, J. L.; Iraci, L. T. Uptake of acetone, acetaldehyde and ethanol in cold sulfuric acid solutions containing organic material: Carbon accretion mechanisms. *Atmos. Environ.* **2010**, *44*, 1145-1151, doi:10.1016/j.atmosenv.2009.12.036.

Zhang, R.; Leu, M.-T. Heterogeneous interaction of peroxyacetyl nitrate with liquid sulfuric acid. *J. Geophys. Res.* **1997**, *102*, 8837-8843, doi:10.1029/97JD00131.

Zhang, R.; Leu, M.-T.; Keyser, L. F. Heterogeneous chemistry of HO_2NO_2 in liquid sulfuric acid. *J. Phys. Chem. A* **1997**, *101*, 3324-3330, doi:10.1021/jp963321z.

Zhang, R.; Wooldridge, P. J.; Molina, M. J. Vapor pressure measurements for the $H_2SO_4/HNO_3/H_2O$ and $H_2SO_4/HCl/H_2O$ systems: Incorporation of stratospheric acids into background sulfate aerosols. *J. Phys. Chem.* **1993**, *97*, 8541-8548, doi:10.1021/j100134a026.

5.3.5 Table Eq5. Henry's Law Constants for Sea Water as Solvent

Substance	Temperature Range (K)	H_s(298 K) [a] (M atm^{-1})	A	B (K)	C	Uncertainty Range [b]	Note
Inorganic Gases							
N_2O	272–313	0.021	-12.65	2620		II	1
CO	273–297	8.1×10^{-4}	-11.89	1420		III	1
CO_2	272–297	0.028	-12.21	2580		II	1
Alkanes							
CH_4	288–308	0.0012	-10.26	1050		III	2
Fluoromethanes							
CH_2F_2	276–313	0.050	-9.91	2060		III	3
CHF_3	278–348	0.010	-260.24	14510	36.33	III	3
CF_4	288–303	1.7×10^{-4}	-16.57	2340		IV	3
Chlorofluoromethanes							
CHF_2Cl	273–353	0.027	-190.74	10990	26.38	III	4
$CFCl_3$	273–306	0.0074	-17.86	3860		IV	4
CF_2Cl_2	288–348	0.0021	-322.70	17000	45.55	III	4
CF_3Cl	288–303	8.1×10^{-4}	-12.20	1520		IV	4
Chloromethanes							
CH_3Cl	273–298	0.088	-13.97	3440		III	5
CH_2Cl_2	273–303	0.35	-13.97	3860		III	5
$CHCl_3$	273–298	0.20	-16.19	4350		II	5
CCl_4	273–313	0.026	-17.67	4180		II	5
Bromomethanes							
CH_3Br	274–304	0.15	-11.91	2990		III	6
CH_2Br_2	273–303	0.91	-15.40	4560		III	6
$CHBr_3$	273–303	1.07	-20.57	6150		III	6
Bromochloromethanes							
$CHBrCl_2$	273–293	0.40	-17.51	4940		IV	7
$CHBr_2Cl$	273–293	0.73	-17.69	5180		IV	7
Iodomethanes							
CH_3I	273–295	0.15	-15.14	3940		II	8
CH_2I_2	273–293	2.31	-16.84	5270		IV	8
Chloroiodomethanes							
CH_2ClI	273–303	0.85	-17.34	5120		III	9
Fluoroethanes							
CHF_2CH_3	278–338	0.050	-11.80	2600		IV	10
CF_3CH_2F	273–353	0.012	-261.44	14260	36.71	III	10
C_2F_6	278–328	4.18×10^{-5}	-328.3	16420	46.18	V	10
Chloroethanes and Chloroethenes							
$CHCl_2CH_3$	275–298	0.15	-14.93	3890		IV	11
CH_2ClCH_2Cl	279–298	0.77	-12.75	3725		IV	11
CH_3CCl_3	275–298	0.043	-17.27	4210		III	11
C_2HCl_3	275–318	0.087	-16.58	4215		II	11
C_2Cl_4	275–318	0.047	-17.635	4350		II	11
Chlorofluoroethanes							
CH_3CClF_2	273–353	0.011	-261.30	14280	36.66	IV	12
CH_3CCl_2F	278–353	0.022	-247.77	13810	34.69	IV	12
Iodoethanes							
C_2H_5I	274–303	0.14	-18.06	4800		IV	13

[a] $H_s = \exp(A + B/T + C\ln(T/K))$ M atm^{-1}

[b] Uncertainty Classes:

I—Better than 10%
II—10% to 50%
III—50% to 100%
IV—Factor of 2 to factor of 10
V—Factor of 10 to factor of 100
VI—Greater than a factor of 100

5.3.5.1 Notes for Table Eq5

Note 1: *Inorganic Gases* Back to Table

N_2O (Nitrous oxide, CAS RN: 10024-97-2)

Measurements at 36.13‰ NaCl using a microgasometric technique.[5] Data taken from the IUPAC evaluation.[7]

CO (Carbon monoxide, CAS RN: 630-08-0)

The two published reports on the solubility of CO into salt water were evaluated by Wiesenburg,[6] who concluded that the data of Douglas[1] were significantly more reliable than those of Schmidt.[3] Those data were fit to a function of temperature and salinity. The present recommendation takes this function, calculates the values for 35‰ salinity, and fits those results to a two-parameter equation. A three parameter fit over the temperature range 274–303 K yields $H_S = \exp(-179.224 + 8620\ \mathrm{K}/T + 25.13\ln(\mathrm{T/K}))$ M atm^{-1}.

CO_2 (Carbon dioxide, CAS RN: 124-38-9)

Published data on the solubility of CO_2 into salt water were evaluated by Weiss,[4] who also carried out some confirmatory measurements. The extensive results of Murray and Riley[2] were accepted and fit as a function of temperature and salinity. The present recommendation for seawater takes the calculated values for 35‰ salinity and the newer values for 35.33‰ and fits them to a two-parameter equation over the indicated temperature range. A three-parameter fit over the temperature range 272–313 K yields $H_S = \exp(-157.779 + 8810\ \mathrm{K}/T + 21.88\ln(T/\mathrm{K}))$ M atm^{-1}.

(1) Douglas, E. Carbon monoxide solubilities in sea water. *J. Phys. Chem.* **1967**, *71*, 1931-1933, doi:10.1021/j100865a064.
(2) Murray, C. N.; Riley, J. P. The solubility of gases in distilled water and sea water—IV. Carbon dioxide. *Deep Sea Research* **1971**, *18*, 533-541, doi:10.1016/0011-7471(71)90077-5.
(3) Schmidt, U. The solubility of carbon monoxide and hydrogen in water and sea-water at partial pressures of about 10^{-5} atmospheres. *Tellus* **1979**, *31*, 68-74, doi:10.1111/j.2153-3490.1979.tb00883.x.
(4) Weiss, R. F. Carbon dioxide in water and seawater: The solubility of a non-ideal gas. *Marine Chem.* **1974**, *2*, 203-215, doi:10.1016/0304-4203.
(5) Weiss, R. F.; Price, B. A. Nitrous oxide solubility in water and seawater. *Marine Chem.* **1980**, *8*, 347-359, doi:10.1016/0304-4203.
(6) Wiesenburg, D. A. Carbon Monoxide in Seawater. In *Carbon Monoxide*; Cargill, R. W., Ed.; Pergamon Press: Oxford, 1990; Vol. 43.
(7) Young, C. L. Nitrous oxide in water. In *Oxides of Nitrogen*; Young, C. L., Ed.; Pergamon: Oxford, 1981; Vol. 8; pp 1-22.

Note 2: *Alkanes* Back to Table

CH_4 (Methane, CAS RN: 74-82-8)

Ostwald coefficients determined in filtered seawater with a salinity of 35‰.[1] Results expressed as a two-parameter fit.

(1) Scharlin, P.; Battino, R. Solubility of CCl_2F_2, $CClF_3$, CF_4, and CH_4 in water and seawater at 288.15-303.15 K and 101.325 kPa. *J. Chem. Eng. Data* **1995**, *40*, 167-169, doi:10.1021/je00017a036.

Note 3: *Fluoromethanes*

Back to Table

CH_2F_2 (HFC-32, Difluoromethane; CAS RN: 75-10-5)

Henry's Law constants were determined by Kutsuna[3] for a salinity S up to 51.5‰ and temperature from 276.15 to 312.65 K. The table reports a linear fit to the values derived at 35‰. The complete equation reported as a function of salinity is $H_S = \exp(-137.85 + (7770 - 13.4 \times S^{0.5})\ \mathrm{K}/T + 19.14\ln(T/\mathrm{K}))$ M atm^{-1}.

CHF_3 (HCFC-23, Trifluoromethane; CAS RN: 75-46-7)

A refit to the evaluation of Li et al.[4] over the temperature range 278–348 K. A two-parameter fit over the temperature range 278–318 K results in $H_s = \exp(-13.73 + 2720\ \mathrm{K}/T)$ M atm^{-1} at a salinity of 35‰. The salinity dependence of the solubility was estimated at 298 K using a poly-parameter-linear free-energy relationship (pp-LFER) based on the work of Abraham et al.[1] and modified by Goss.[2] It was assumed that the temperature dependence of this parameter was small and could be ignored. The descriptors were obtained from Abraham et al.[1] The resulting Sechenov parameter, K_s, is expressed in molar units and $H_s =$ $H_{s0} \times 10^{-Ks \times S}$, where S is the molar salinity and $K_s = 0.168 \pm 0.21$ M^{-1}. Calculated values for 35‰ NaCl taken at each temperature and fitted to a two-parameter equation. The previous recommendation provided only a two-parameter fit.

CF_4 (PFC-14, Carbon tetrafluoride; CAS RN: 75-73-0)

A refit to the evaluation of Li et al.[4] over the temperature range 278–328 K. A two-parameter fit over the temperature range 278–308 K results in $H_s = \exp(-15.77 + 2100\ \mathrm{K}/T)$ M atm^{-1} at a salinity of 35‰. The salinity dependence of the solubility was estimated at 298 K using a poly-parameter-linear free-energy relationship (pp-LFER) based on the work of Abraham et al.[1] and modified by Goss.[2] It was assumed that the temperature dependence of this parameter was small and could be ignored. The descriptors were obtained from Abraham et al.[1] The resulting Sechenov parameter, K_s, is expressed in molar units and $H_s =$ $H_{s0} \times 10^{-Ks \times S}$, where S is the molar salinity and $K_s = 0.202 \pm 0.022$ M^{-1}. Calculated values for 35‰ NaCl taken at each temperature and fitted to a two-parameter equation. The previous recommendation provided only a two-parameter fit.

(1) Abraham, M. H.; Gola, J. M. R.; Cometto-Mu˜niz, J. E.; Cain, W. S. Solvation properties of refrigerants, and the estimation of their water-solvent and gas-solvent partitions. *Fluid Phase Equilib.* **2001**, *180*, 41–58, doi:10.1016/S0378-3812(00)00511-2.

(2) Goss, K.-U. Prediction of the temperature dependency of Henry's law constant using poly-parameter linear free energy relationships. *Chemosphere* **2006**, *64*, 1369–1374, doi:10.1016/J.CHEMOSPHERE.2005.12.049.

(3) Kutsuna, S. Experimental determination of Henry's law constants of difluoromethane (HFC-32) and the salting-out effects in aqueous salt solutions relevant to seawater. *Atmos. Chem. Phys.* **2017**, *17*, 7495–7507, doi:10.5194/ACP-17-7495-2017.

(4) Li, P.; Mühle, J.; Montzka, S. A.; Oram, D. E.; Miller, B. R.; Weiss, R. F.; Fraser, P. J.; Tanhua, T. Atmospheric histories, growth rates and solubilities in seawater and other natural waters of the potential transient tracers HCFC-22, HCFC-141b, HCFC-142b, HFC-134a, HFC-125, HFC-23, PFC-14 and PFC-116. *Ocean Sci.* **2019**, *15*, 33–60, doi:10.5194/OS-15-33-2019.

Note 4: *Fluorochloromethanes*

Back to Table

$CHClF_2$ (HCFC-22, Chlorodifluoromethane; CAS RN: 75-45-6)

A refit to the evaluation of Li et al.[4] over the temperature range 278–353 K. A two-parameter fit over the temperature range 278–318 K results in $H_s = \exp(-14.13 + 3150\ \mathrm{K}/T)$ M atm^{-1} at a salinity of 35‰. The salinity dependence of the solubility was estimated at 298 K using a poly-parameter-

linear free-energy relationship (pp-LFER) based on the work of Abraham et al.[1] and modified by Goss.[2] It was assumed that the temperature dependence of this parameter was small and could be ignored. The descriptors were obtained from Abraham et al.[1] The resulting Sechenov parameter, K_s, is expressed in molar units and $H_s = H_{s0} \times 10^{-Ks \times S}$, where S is the molar salinity and $K_s = 0.169 \pm 0.022$ M^{-1}. Previous recommendation, $H_s = \exp(-12.56 + 2720\ \text{K}/T)$ M atm^{-1} and $H_s^{298} = 0.032$ M atm^{-1} was from gas solubilities measured at 278, 308, and 338 K and at NaCl fraction from 0 to 0.0564 mol/mol (0 to 174‰) with a gas absorption unit.[7] Calculated values for 35‰ NaCl taken at each temperature and fitted to a two-parameter equation. These values were double-weighted and fit together with the values measured in seawater by a purge-and-trap technique.[5]

$CFCl_3$ (CFC-11, Trichlorofluoromethane; CAS RN: 75-69-4)
A two-parameter fit to the results of Hunter-Smith, et al.[3] and Ooki and Yokouchi[5] in seawater. The results are in good agreement at low temperatures (<293 K) but diverge at room temperature and above.

CF_2Cl_2 (CFC-12, Dichlorodifluoromethane; CAS RN: 75-71-8)
A refit to the evaluation of Li et al.[4] over the temperature range 273–348 K. A two-parameter fit over the temperature range 273–308 K results in $H_s = \exp(-18.10 + 3570\ \text{K}/T)$ M atm^{-1} at a salinity of 35‰. The salinity dependence of the solubility was estimated at 298 K using a poly-parameter-linear free-energy relationship (pp-LFER) based on the work of Abraham et al.[1] and modified by Goss.[2] It was assumed that the temperature dependence of this parameter was small and could be ignored. The descriptors were obtained from Abraham et al.[1] The resulting Sechenov parameter, K_s, is expressed in molar units and $H_s = H_{s0} \times 10^{-Ks \times S}$, where S is the molar salinity and $K_s = 0.204 \pm 0.021$ M^{-1}. Previous recommendation, $H_s = \exp(-12.93 + 2080\ \text{K}/T)$ M atm^{-1} and $H_s^{298} = 0.0026$ M atm^{-1} was from Ostwald coefficients determined in filtered seawater with a salinity of 35‰.[6] Results expressed as a two-parameter fit.

CF_3Cl (CFC-13, Chlorotrifluoromethane; CAS RN: 75-72-9)
Ostwald coefficients determined in filtered seawater with a salinity of 35‰.[6] Results expressed as a two-parameter fit.

(1) Abraham, M. H.; Gola, J. M. R.; Cometto-Mu˜niz, J. E.; Cain, W. S. Solvation properties of refrigerants, and the estimation of their water-solvent and gas-solvent partitions. *Fluid Phase Equilib.* **2001**, *180*, 41–58, doi:10.1016/S0378-3812(00)00511-2.

(2) Goss, K.-U. Prediction of the temperature dependency of Henry's law constant using poly-parameter linear free energy relationships. *Chemosphere* **2006**, *64*, 1369–1374, doi:10.1016/J.CHEMOSPHERE.2005.12.049.

(3) Hunter-Smith, R. J.; Balls, P. W.; Liss, P. S. Henry's law constants and the air-sea exchange of various low molecular weight halocarbon gases. *Tellus* **1983**, *35B*, 170-176, doi:10.1111/j.1600-0889.1983.tb00021.x.

(4) Li, P.; Mühle, J.; Montzka, S. A.; Oram, D. E.; Miller, B. R.; Weiss, R. F.; Fraser, P. J.; Tanhua, T. Atmospheric histories, growth rates and solubilities in seawater and other natural waters of the potential transient tracers HCFC-22, HCFC-141b, HCFC-142b, HFC-134a, HFC-125, HFC-23, PFC-14 and PFC-116. *Ocean Sci.* **2019**, *15*, 33–60, doi:10.5194/OS-15-33-2019.

(5) Ooki, A.; Yokouchi, Y. Determination of Henry's law constant of halocarbons in seawater and analysis of sea-to-air flux of iodoethane (C_2H_5I) in the Indian and Southern oceans based on partial pressure measurements. *Geochem. J.* **2011**, *45*, e1-e7, doi:10.2343/geochemj.1.0122.

(6) Scharlin, P.; Battino, R. Solubility of CCl_2F_2, $CClF_3$, CF_4, and CH_4 in water and seawater at 288.15-303.15 K and 101.325 kPa. *J. Chem. Eng. Data* **1995**, *40*, 167-169, doi:10.1021/je00017a036.

(7) Zheng, D.-Q.; Guo, T.-M.; Knapp, H. Experimental and modeling studies on the solubility of CO_2, $CHClF_2$, CHF_3, $C_2H_2F_4$ and $C_2H_4F_2$ in water and aqueous NaCl solutions under low pressures. *Fluid Phase Equilib.* **1997**, *129*, 197–209, doi:10.1016/S0378-3812(96)03177-9.

Note 5: *Chloromethanes* Back to Table

CH_3Cl (Chloromethane, CAS RN: 74-87-3)

From a measurement of the concentration in seawater at 30.4 or 34.34‰ salinity as a stream of nitrogen is bubbled through.[5,6] Similar results were reported by Elliott and Rowland at 273 and 295 K.[3]

CH_2Cl_2 (Dichloromethane, CAS RN: 75-09-2)

From a measurement of the concentration in seawater at 34.34‰ salinity as a stream of nitrogen is bubbled through[5] combined with values determined in seawater of salinities of 33.1‰ to 36.1‰ by using a purge-and-trap method and an equilibrator.[7]

$CHCl_3$ (Trichloromethane, CAS RN: 67-66-3)

Taken from a two-parameter fit to the results of Moore, et al.,[5,6] Hunter-Smith et al.,[4] and Dewulf, et al.[2] The latter were from a study as a function of salinity and the calculated value at 35‰ was used. These data were double-weighted in the fit. A measurement at 298 K with a purge-and-trap/GC method gave a result in close agreement.[8]

CCl_4 (Carbon tetrachloride, CAS RN: 56-23-5)

A two-parameter fit to the results of Hunter-Smith, et al.,[4] Bullister and Wisegarver,[1] and Dewulf, et al.[2] The latter were from a study as a function of salinity and the calculated value at 35‰ was used. These data were double-weighted in the fit. The Bullister and Wisgarver[1] data were from a study of the solubility as a function of temperature and salinity. Calculated values for 35‰ from a complex expression were used.

(1) Bullister, J. L.; Wisegarver, D. P. The solubility of carbon tetrachloride in water and seawater. *Deep-Sea Research Part I-Oceanographic Research Papers* **1998**, *45*, 1285-1302, doi:10.1016/S0967-0637(98)00017-X.

(2) Dewulf, J.; Drijvers, D.; Van Langenhove, H. Measurement of Henry's law constant as function of temperature and salinity for the low temperature range. *Atmos. Environ.* **1995**, *29*, 323-331, doi:10.1016/1352-2310(94)00256-K.

(3) Elliott, S.; Rowland, F. S. Nucleophilic substitution rates and solubilities for methyl halides in seawater. *Geophys. Res. Lett.* **1993**, *20*, 1043-1046, doi:10.1029/93GL01081.

(4) Hunter-Smith, R. J.; Balls, P. W.; Liss, P. S. Henry's law constants and the air-sea exchange of various low molecular weight halocarbon gases. *Tellus* **1983**, *35B*, 170-176, doi:10.1111/j.1600-0889.1983.tb00021.x.

(5) Moore, R. M. The solubility of a suite of low molecular weight organochlorine compounds in seawater and implications for estimating the marine source of methyl chloride to the atmosphere. *Chemosphere - Global Change Science* **2000**, *2*, 95-99, doi:10.1016/S1465-9972(99)00045-8.

(6) Moore, R. M.; Geen, C. E.; Tait, V. K. Determination of Henry law constants for a suite of naturally-occurring halogenated methanes in seawater. *Chemosphere* **1995**, *30*, 1183-1191, doi:10.1016/0045-6535(95)00009-W.

(7) Ooki, A.; Yokouchi, Y. Determination of Henry's law constant of halocarbons in seawater and analysis of sea-to-air flux of iodoethane (C_2H_5I) in the Indian and Southern oceans based on partial pressure measurements. *Geochem. J.* **2011**, *45*, e1-e7, doi:10.2343/geochemj.1.0122.

(8) Ruiz-Bevia, F.; Fernandez-Torres, M. J. Determining the Henry's law constants of THMs in seawater by means of purge-and-trap gas chromatography (PT-GC): The influence of seawater as sample matrix. *Anal. Sci.* **2010**, *26*, 723-726, doi:10.2116/analsci.26.723.

Note 6: *Bromomethanes*

Back to Table

CH_3Br (Bromomethane, CAS RN: 74-83-9)

Solubility determined with a gas-liquid membrane equilibrator with a 35‰ NaCl solution.[1] An approximately 5% correction was applied for non-ideality and to express the result in terms of fugacities. Very similar values were measured for filtered seawater. The results of Elliott and Rowland at 273 and 295 K are very close to these.[2]

CH_2Br_2 (Dibromomethane, CAS RN: 74-95-3)

From a measurement of the concentration in seawater at 34.34‰ salinity as a stream of nitrogen is bubbled through[3] combined with values determined in seawater of salinities of 33.1‰ to 36.1‰ by using a purge-and-trap method and an equilibrator.[5]

$CHBr_3$ (Tribromomethane, CAS RN: 75-25-2)
A two-parameter fit to the results from a purge-and-trap method,[5] calculated from the expression presented, and with a stripping technique with mass spectrometric detection.[4] Another measurement at 298 K with a purge-and-trap/GC method gave a result about 50% higher.[6]

(1) De Bruyn, W. J.; Saltzman, E. S. The solubility of methyl bromide in pure water, 35‰ sodium chloride and seawater. *Marine Chem.* **1997**, *56*, 51-57, doi:10.1016/S0304-4203(96)00089-8.
(2) Elliott, S.; Rowland, F. S. Nucleophilic substitution rates and solubilities for methyl halides in seawater. *Geophys. Res. Lett.* **1993**, *20*, 1043-1046, doi:10.1029/93GL01081.
(3) Moore, R. M. The solubility of a suite of low molecular weight organochlorine compounds in seawater and implications for estimating the marine source of methyl chloride to the atmosphere. *Chemosphere - Global Change Science* **2000**, *2*, 95-99, doi:10.1016/S1465-9972(99)00045-8.
(4) Moore, R. M.; Geen, C. E.; Tait, V. K. Determination of Henry law constants for a suite of naturally-occurring halogenated methanes in seawater. *Chemosphere* **1995**, *30*, 1183-1191, doi:10.1016/0045-6535(95)00009-W.
(5) Ooki, A.; Yokouchi, Y. Determination of Henry's law constant of halocarbons in seawater and analysis of sea-to-air flux of iodoethane (C_2H_5I) in the Indian and Southern oceans based on partial pressure measurements. *Geochem. J.* **2011**, *45*, e1-e7, doi:10.2343/geochemj.1.0122.
(6) Ruiz-Bevia, F.; Fernandez-Torres, M. J. Determining the Henry's law constants of THMs in seawater by means of purge-and-trap gas chromatography (PT-GC): The influence of seawater as sample matrix. *Anal. Sci.* **2010**, *26*, 723-726, doi:10.2116/analsci.26.723.

Note 7: *Chlorobromomethanes*

Back to Table

$CHBrCl_2$ (Bromodichloromethane, CAS RN: 75-27-4)
A two-parameter fit to the results measured by a stripping technique at a salinity of 30.4‰.[1] A measurement at 298 K with a purge-and-trap/GC method gave a bit higher result.[2]

$CHBr_2Cl$ (Dibromochloromethane, CAS RN: 124-48-1)
A two-parameter fit to the results from a stripping technique at a salinity of 30.4‰.[1] A measurement at 298 K with a purge-and-trap/GC method gave a result about 20% higher.[2]

(1) Moore, R. M.; Geen, C. E.; Tait, V. K. Determination of Henry law constants for a suite of naturally-occurring halogenated methanes in seawater. *Chemosphere* **1995**, *30*, 1183-1191, doi:10.1016/0045-6535(95)00009-W.
(2) Ruiz-Bevia, F.; Fernandez-Torres, M. J. Determining the Henry's law constants of THMs in seawater by means of purge-and-trap gas chromatography (PT-GC): The influence of seawater as sample matrix. *Anal. Sci.* **2010**, *26*, 723-726, doi:10.2116/analsci.26.723.

Note 8: *Iodomethanes*

Back to Table

CH_3I (Iodomethane, CAS RN: 74-88-4)
A two-parameter fit to the results from a stripping technique at a salinity of 30.4‰ by Moore, et al.,[2] Elliott and Rowland,[1] who also found similar results in 0.5 M NaCl, and Ooki and Yokouchi at salinities of 33.1‰ to 36.1‰.[3]

CH_2I_2 (Diiodomethane, CAS RN: 75-11-6)
A two-parameter fit to the results from a stripping technique at a salinity of 30.4‰.[2]

(1) Elliott, S.; Rowland, F. S. Nucleophilic substitution rates and solubilities for methyl halides in seawater. *Geophys. Res. Lett.* **1993**, *20*, 1043-1046, doi:10.1029/93GL01081.

(2) Moore, R. M.; Geen, C. E.; Tait, V. K. Determination of Henry law constants for a suite of naturally-occurring halogenated methanes in seawater. *Chemosphere* **1995**, *30*, 1183-1191, doi:10.1016/0045-6535(95)00009-W.
(3) Ooki, A.; Yokouchi, Y. Determination of Henry's law constant of halocarbons in seawater and analysis of sea-to-air flux of iodoethane (C_2H_5I) in the Indian and Southern oceans based on partial pressure measurements. *Geochem. J.* **2011**, *45*, e1-e7, doi:10.2343/geochemj.1.0122.

Note 9: *Chloroiodomethanes*

Back to Table

CH_2ClI (Chloroiodomethane, CAS RN: 593-71-5)
From a measurement of the concentration in seawater at 34.34‰ salinity as a stream of nitrogen is bubbled through[1] combined with values determined in seawater of salinities of 33.1‰ to 36.1‰ by using a purge-and-trap method and an equilibrator.[2]

(1) Moore, R. M. The solubility of a suite of low molecular weight organochlorine compounds in seawater and implications for estimating the marine source of methyl chloride to the atmosphere. *Chemosphere - Global Change Science* **2000**, *2*, 95-99, doi:10.1016/S1465-9972(99)00045-8.
(2) Ooki, A.; Yokouchi, Y. Determination of Henry's law constant of halocarbons in seawater and analysis of sea-to-air flux of iodoethane (C_2H_5I) in the Indian and Southern oceans based on partial pressure measurements. *Geochem. J.* **2011**, *45*, e1-e7, doi:10.2343/geochemj.1.0122.

Note 10: *Fluoroethanes*

Back to Table

CH_3CHF_2 (HFC-152a, 1,1-Difluoroethane; CAS RN: 75-37-6)
Gas solubilities measured at 278, 308, and 338 K and at NaCl fractions from 0 to 0.0564 mol/mol (0 to 174‰) with a gas absorption unit.[5] Calculated values for 35‰ NaCl taken at each temperature and fitted to a two-parameter equation.

CH_2FCF_3 (HFC-134a, 1,1,1,2-Tetrafluoroethane; CAS RN: 811-97-2)
A refit to the evaluation of Li et al.[3] over the temperature range 278 to 353 K. A two-parameter fit over the temperature range 278 to 318 K results in $H_s = \exp(-14.97 + 3160/T)$ M atm^{-1} at a salinity of 35‰. The salinity dependence of the solubility was estimated at 298 K using a poly-parameter-linear free-energy relationship (pp-LFER) based on the work of Abraham et al.[1] and modified by Goss.[2] It was assumed that the temperature dependence of this parameter was small and could be ignored. The descriptors were obtained from Abraham et al.[1] The resulting Sechenov parameter, K_s, is expressed in molar units and $H_s = H_{s0} \times 10^{-Ks \times S}$, where S is the molar salinity and $K_s = 0.193 \pm 0.022$ M^{-1}. Previous recommendation, $H_s = \exp(-13.13 + 2680$ K/T) M atm^{-1} and $H_S^{298} = 0.016$ M atm^{-1} was from gas solubilities measured at 278, 308, and 338 K and at NaCl fractions from 0 to 0.0564 mol/mol (0 to 174‰) with a gas absorption unit.[5] Calculated values for 35‰ NaCl taken at each temperature and fitted to a two-parameter equation. These values were double-weighted and fit together with values determined in seawater of salinities of 33.1 to 36.1‰ by using a purge-and-trap method and an equilibrator (Ooki and Yokouchi[4]).

C_2F_6 (PFC-116, Hexaflluoroethane; CAS RN: 76-16-4)
A refit to the evaluation of Li et al.[3] over the temperature range 278 to 328 K. A two-parameter fit over the temperature range 273 to 308 K results in $H_s = \exp(-19.44 + 2798$ K/T) M atm^{-1} at a salinity of 35‰. The salinity dependence of the solubility was estimated at 298 K using a poly-parameter-linear free-energy relationship (pp-LFER) based on the work of Abraham et al.[1] and modified by Goss.[2] It was assumed that the temperature dependence of this parameter was small and could be ignored. The descriptors were obtained from Abraham et al.[1] The resulting Sechenov parameter, K_s, is expressed in molar units and $H_s = H_{s0} \times 10^{-Ks \times S}$, where S is the molar salinity and $K_s = 0.244 \pm 0.022$ M^{-1}.

(1) Abraham, M. H.; Gola, J. M. R.; Cometto-Mu˜niz, J. E.; Cain, W. S. Solvation properties of refrigerants, and the estimation of their water-solvent and gas-solvent partitions. *Fluid Phase Equilib.* **2001**, *180*, 41–58, doi:10.1016/S0378-3812(00)00511-2.
(2) Goss, K.-U. Prediction of the temperature dependency of Henry's law constant using poly-parameter linear free energy relationships. *Chemosphere* **2006**, *64*, 1369–1374, doi:10.1016/J.CHEMOSPHERE.2005.12.049.
(3) Li, P.; Mühle, J.; Montzka, S. A.; Oram, D. E.; Miller, B. R.; Weiss, R. F.; Fraser, P. J.; Tanhua, T. Atmospheric histories, growth rates and solubilities in seawater and other natural waters of the potential transient tracers HCFC-22, HCFC-141b, HCFC-142b, HFC-134a, HFC-125, HFC-23, PFC-14 and PFC-116. *Ocean Sci.* **2019**, *15*, 33–60, doi:10.5194/OS-15-33-2019.
(4) Ooki, A.; Yokouchi, Y. Determination of Henry's law constant of halocarbons in seawater and analysis of sea-to-air flux of iodoethane (C_2H_5I) in the Indian and Southern oceans based on partial pressure measurements. *Geochem. J.* **2011**, *45*, e1-e7, doi:10.2343/geochemj.1.0122.
(5) Zheng, D.-Q.; Guo, T.-M.; Knapp, H. Experimental and modeling studies on the solubility of CO_2, $CHClF_2$, CHF_3, $C_2H_2F_4$ and $C_2H_4F_2$ in water and aqueous NaCl solutions under low pressures *Fluid Phase Equilibria* **1997**, *129*, 197-209, doi:10.1016/S0378-3812(96)03177-9.

Note 11: *Chloroethanes, Chloroethenes*

Back to Table

CH_3CHCl_2 (1,1-Dichloroethane, CAS RN: 75-34-3)

Derived from an equilibrium partitioning study as a function of salinity and temperature.[1] The derived value at 35‰ at each temperature was used.

$CH_2ClCHCl$ (1,2-Dichloroethane, CAS RN: 107-06-2)

Derived from an equilibrium partitioning study as a function of salinity and temperature.[1] The derived value at 35‰ at each temperature was used. The data at 275 K were rejected due to a high reported standard deviation and a poor fit to the other results.

CH_3CCl_3 (1,1,1-Trichloroethane, CAS RN: 71-55-6)

The results from a multiple equilibration technique,[2] were combined with the derived values at 35‰ at each temperature from an equilibrium partitioning study as a function of salinity and temperature.[1] The highest temperature point from this latter study was not included in the fit.

$CHCl_2CCl_3$ (Pentachloroethane, CAS RN: 76-01-7)
C_2Cl_4 (Tetrachloroethene, CAS RN: 127-18-4)

A fit to results from measurements of the concentration in seawater at 34.34‰ salinity as a stream of nitrogen is bubbled through,[3] from an equilibrium partitioning study as a function of salinity and temperature,[1] and from a GC/headspace method with seawater of 35‰ salinity.[4] The derived value at 35‰ at each temperature from Dewulf et al.[1] was used and double-weighted.

(1) Dewulf, J.; Drijvers, D.; Van Langenhove, H. Measurement of Henry's law constant as function of temperature and salinity for the low temperature range. *Atmos. Environ.* **1995**, *29*, 323-331, doi:10.1016/1352-2310(94)00256-K.
(2) Hunter-Smith, R. J.; Balls, P. W.; Liss, P. S. Henry's law constants and the air-sea exchange of various low molecular weight halocarbon gases. *Tellus* **1983**, *35B*, 170-176, doi:10.1111/j.1600-0889.1983.tb00021.x.
(3) Moore, R. M. The solubility of a suite of low molecular weight organochlorine compounds in seawater and implications for estimating the marine source of methyl chloride to the atmosphere. *Chemosphere - Global Change Science* **2000**, *2*, 95-99, doi:10.1016/S1465-9972(99)00045-8.
(4) Peng, J.; Wan, A. M. Effect of ionic strength on Henry's constants of volatile organic compounds. *Chemosphere* **1998**, *36*, 2731-2740, doi:10.1016/S0045-6535(97)10232-6.

Note 12: *Chlorofluoroethanes*

Back to Table

CH_3CClF_2 (HCFC-142b, 1-chloro-1,1-difluoroethane; CAS RN: 75-68-3)

A refit to the evaluation of Li et al.[3] over the temperature range 278 to 353 K. A two-parameter fit over the temperature range 273 to 318 K results in $H_s = \exp(-15.38 + 3250\ K/T)$ M atm^{-1} at a salinity of 35‰. The salinity dependence of the solubility was estimated at 298 K using a poly-parameter-linear free-energy relationship (pp-LFER) based on the work of Abraham et al.[1] and modified by Goss.[2] It was assumed that the temperature dependence of this parameter was small and could be ignored. The descriptors were obtained from Abraham et al.[1] The resulting Sechenov parameter, K_s, is expressed in molar units and $H_s = H_{s0} \times 10^{-Ks \times S}$, where S is the molar salinity and $K_s = 0.198 \pm 0.022$ M^{-1}.

CH_3CCl_2F (HCFC-141b, 1,1-dichloro-1-fluoroethane; CAS RN: 1717-00-6)

A refit to the evaluation of Li et al.[3] over the temperature range 278 to 353 K. A two-parameter fit over the temperature range 273−318 K results in $H_s = \exp(-15.53 + 3500\ K/T)$ M^{-1} at a salinity of 35‰. The salinity dependence of the solubility was estimated at 298 K using a poly-parameter-linear free-energy relationship (pp-LFER) based on the work of Abraham et al.[1] and modified by Goss.[2] It was assumed that the temperature dependence of this parameter was small and could be ignored. The descriptors were obtained from Abraham et al.[1] The resulting Sechenov parameter, K_s, is expressed in molar units and $H_s = H_{s0} \times 10^{-Ks \times S}$, where S is the molar salinity and $K_s = 0.204 \pm 0.023$ M^{-1}.

(1) Abraham, M. H.; Gola, J. M. R.; Cometto-Mu˜niz, J. E.; Cain, W. S. Solvation properties of refrigerants, and the estimation of their water-solvent and gas-solvent partitions. *Fluid Phase Equilib.* **2001**, *180*, 41–58, doi:10.1016/S0378-3812(00)00511-2.

(2) Goss, K.-U. Prediction of the temperature dependency of Henry's law constant using poly-parameter linear free energy relationships. *Chemosphere* **2006**, *64*, 1369–1374, doi:10.1016/J.CHEMOSPHERE.2005.12.049.

(3) Li, P.; M¨uhle, J.; Montzka, S. A.; Oram, D. E.; Miller, B. R.; Weiss, R. F.; Fraser, P. J.; Tanhua, T. Atmospheric histories, growth rates and solubilities in seawater and other natural waters of the potential transient tracers HCFC-22, HCFC-141b, HCFC-142b, HFC-134a, HFC-125, HFC-23, PFC-14 and PFC-116. *Ocean Sci.* **2019**, *15*, 33–60, doi:10.5194/OS-15-33-2019.

Note 13: *Iodoethanes*

Back to Table

C_2H_5I (Iodoethane, CAS RN: 75-03-6)

Values determined in seawater of salinities of 33.1‰ to 36.1‰ by using a purge-and-trap method and an equilibrator.[1]

(1) Ooki, A.; Yokouchi, Y. Determination of Henry's law constant of halocarbons in seawater and analysis of sea-to-air flux of iodoethane (C_2H_5I) in the Indian and Southern oceans based on partial pressure measurements. *Geochem. J.* **2011**, *45*, e1-e7.

5.3.5.2 Bibliography – Table Eq5

Abraham, M. H.; Gola, J. M. R.; Cometto-Mu˜niz, J. E.; Cain, W. S. Solvation properties of refrigerants, and the estimation of their water-solvent and gas-solvent partitions. *Fluid Phase Equilib.* **2001**, *180*, 41–58, doi:10.1016/S0378-3812(00)00511-2.

Bullister, J. L.; Wisegarver, D. P. The solubility of carbon tetrachloride in water and seawater. *Deep-Sea Research Part I-Oceanographic Research Papers* **1998**, *45*, 1285-1302, doi:10.1016/S0967-0637(98)00017-X.

De Bruyn, W. J.; Saltzman, E. S. The solubility of methyl bromide in pure water, 35‰ sodium chloride and seawater. *Marine Chem.* **1997**, *56*, 51-57, doi:10.1016/S0304-4203(96)00089-8.

Dewulf, J.; Drijvers, D.; Van Langenhove, H. Measurement of Henry's law constant as function of temperature and salinity for the low temperature range. *Atmos. Environ.* **1995**, *29*, 323-331, doi:10.1016/1352-2310(94)00256-K.

Douglas, E. Carbon monoxide solubilities in sea water. *J. Phys. Chem.* **1967**, *71*, 1931-1933, doi:10.1021/j100865a064.

Elliott, S.; Rowland, F. S. Nucleophilic substitution rates and solubilities for methyl halides in seawater. *Geophys. Res. Lett.* **1993**, *20*, 1043-1046, doi:10.1029/93GL01081.

Goss, K.-U. Prediction of the temperature dependency of Henry's law constant using poly-parameter linear free energy relationships. *Chemosphere* **2006**, *64*, 1369–1374, doi:10.1016/J.CHEMOSPHERE.2005.12.049.

Hunter-Smith, R. J.; Balls, P. W.; Liss, P. S. Henry's law constants and the air-sea exchange of various low molecular weight halocarbon gases. *Tellus* **1983**, *35B*, 170-176, doi:10.1111/j.1600-0889.1983.tb00021.x.

Kutsuna, S. Experimental determination of Henry's law constants of difluoromethane (HFC-32) and the salting-out effects in aqueous salt solutions relevant to seawater. *Atmos. Chem. Phys.* **2017**, *17*, 7495–7507, doi:10.5194/ACP-17-7495-2017.

Moore, R. M. The solubility of a suite of low molecular weight organochlorine compounds in seawater and implications for estimating the marine source of methyl chloride to the atmosphere. *Chemosphere - Global Change Science* **2000**, *2*, 95-99, doi:10.1016/S1465-9972(99)00045-8.

Li, P.; Mühle, J.; Montzka, S. A.; Oram, D. E.; Miller, B. R.; Weiss, R. F.; Fraser, P. J.; Tanhua, T. Atmospheric histories, growth rates and solubilities in seawater and other natural waters of the potential transient tracers HCFC-22, HCFC-141b, HCFC-142b, HFC-134a, HFC-125, HFC-23, PFC-14 and PFC-116. *Ocean Sci.* **2019**, *15*, 33–60, doi:10.5194/OS-15-33-2019.

Moore, R. M. The solubility of a suite of low molecular weight organochlorine compounds in seawater and implications for estimating the marine source of methyl chloride to the atmosphere. *Chemosphere - Global Change Science* **2000**, *2*, 95-99, doi:10.1016/S1465-9972(99)00045-8.

Moore, R. M.; Geen, C. E.; Tait, V. K. Determination of Henry law constants for a suite of naturally-occurring halogenated methanes in seawater. *Chemosphere* **1995**, *30*, 1183-1191, doi:10.1016/0045-6535(95)00009-W.

Murray, C. N.; Riley, J. P. The solubility of gases in distilled water and sea water—IV. Carbon dioxide. *Deep Sea Research* **1971**, *18*, 533-541, doi:10.1016/0011-7471(71)90077-5.

Ooki, A.; Yokouchi, Y. Determination of Henry's law constant of halocarbons in seawater and analysis of sea-to-air flux of iodoethane (C_2H_5I) in the Indian and Southern oceans based on partial pressure measurements. *Geochem. J.* **2011**, *45*, e1-e7.

Peng, J.; Wan, A. M. Effect of ionic strength on Henry's constants of volatile organic compounds. *Chemosphere* **1998**, *36*, 2731-2740, doi:10.1016/S0045-6535(97)10232-6.

Ruiz-Bevia, F.; Fernandez-Torres, M. J. Determining the Henry's law constants of THMs in seawater by means of purge-and-trap gas chromatography (PT-GC): The influence of seawater as sample matrix. *Anal. Sci.* **2010**, *26*, 723-726, doi:10.2116/analsci.26.723.

Scharlin, P.; Battino, R. Solubility of CCl_2F_2, $CClF_3$, CF_4, and CH_4 in water and seawater at 288.15-303.15 K and 101.325 kPa. *J. Chem. Eng. Data* **1995**, *40*, 167-169, doi:10.1021/je00017a036.

Schmidt, U. The solubility of carbon monoxide and hydrogen in water and sea-water at partial pressures of about 10^{-5} atmospheres. *Tellus* **1979**, *31*, 68-74, doi:10.1111/j.2153-3490.1979.tb00883.x.

Weiss, R. F. Carbon dioxide in water and seawater: The solubility of a non-ideal gas. *Marine Chem.* **1974**, *2*, 203-215.

Weiss, R. F.; Price, B. A. Nitrous oxide solubility in water and seawater. *Marine Chem.* **1980**, *8*, 347-359.

Wiesenburg, D. A. Carbon Monoxide in Seawater. In *Carbon Monoxide*; Cargill, R. W., Ed.; Pergamon Press: Oxford, 1990; Vol. 43.

Young, C. L. Nitrous oxide in water. In *Oxides of Nitrogen*; Young, C. L., Ed.; Pergamon: Oxford, 1981; Vol. 8; pp 1-22.

Zheng, D.-Q.; Guo, T.-M.; Knapp, H. Experimental and modeling studies on the solubility of CO_2, $CHClF_2$, CHF_3, $C_2H_2F_4$ and $C_2H_4F_2$ in water and aqueous NaCl solutions under low pressures *Fluid Phase Equilibria* **1997**, *129*, 197-209, doi:10.1016/S0378-3812(96)03177-9.

5.4 Particulate Optical Properties

This section includes an evaluation of optical properties of atmospherically relevant aerosol components (presently limited to an evaluation of ammonium sulfate, a common component of submicron particulate matter). Atmospheric particles are composed of one or more components, the relative abundance of which varies dramatically throughout the atmosphere.

Scattering and absorption by aerosol particles depends on both the size and composition of the particles, and on the wavelength of light. Further, scattering and absorption depend on particle shape. This assessment focuses on the complex refractive index (CRI). The CRI = $n - ki$, where n is the real part and k is the imaginary part, can be used to calculate scattering and absorption by particles of a given shape. A commonly made assumption is that the particle average CRI can be calculated using a volume-weighted method:

$$\bar{n}(\lambda) = \sum_j X_j n_j(\lambda)$$

and

$$\bar{k}(\lambda) = \sum_j X_j k_j(\lambda)$$

where X_j is the volume fraction of component j and n_j and k_j are the real and imaginary components of the CRI for component j, respectively.

It is necessary to know how n and k for a given component vary with wavelength. For Earth's atmosphere, most important are the values for wavelengths between ca. 0.3 μm and 2 μm and between ca. 5 μm and 40 μm, corresponding to solar radiation and Earth's emitted radiation, respectively.

5.4.1 Table P1. Recommended complex refractive indices for ammonium sulfate

Wavelength (μm)	k	n	Uncertainty Class [a]	Note	Wavelength (μm)	k	n	Uncertainty Class [a]	Note
0.3	1.00×10^{-7}		I	3	6.74	1.08×10^{-1}	1.15	VI	4
0.405	1.00×10^{-7}	1.54	I	2,3	6.79	1.71×10^{-1}	1.11	VI	4
0.535	1.00×10^{-7}	1.53	I	3	6.83	2.64×10^{-1}	1.09	VI	4
0.53	1.00×10^{-7}	1.524 ± 0.004	II	2,3	6.88	3.75×10^{-1}	1.1	VI	4
0.656	1.00×10^{-7}	1.525	I	1,3	6.93	4.70×10^{-1}	1.15	VI	4
0.706	1.00×10^{-7}	1.525	I	1,3	6.98	5.82×10^{-1}	1.2	VI	4
0.8	1.00×10^{-7}		I	1,3	7.03	7.48×10^{-1}	1.33	VI	4
1.0	1.50×10^{-7}	1.51	I	1,3	7.07	8.05×10^{-1}	1.64	VI	4
1.07	2.40×10^{-6}		III	4	7.12	6.00×10^{-1}	1.91	VI	4
1.15	9.50×10^{-7}		III	4	7.17	3.35×10^{-1}	1.94	VI	4
1.2	3.40×10^{-6}	1.5	III	4	7.22	1.85×10^{-1}	1.86	VI	4
1.3	1.70×10^{-5}		III	4	7.27	1.16×10^{-1}	1.79	VII	4
1.4	1.10×10^{-5}		III	4	7.32	7.73×10^{-2}	1.74	VII	4
1.5	3.40×10^{-5}	1.49	III	4	7.37	5.24×10^{-2}	1.69	VII	4
1.58	2.10×10^{-4}		III	4	7.42	3.69×10^{-2}	1.65	VII	4
1.6	1.90×10^{-4}		III	4	7.48	2.84×10^{-2}	1.62	VII	4
1.7	9.00×10^{-5}		III	4	7.53	1.93×10^{-2}	1.59	VII	4
1.8	7.60×10^{-5}	1.48	III	4	7.79	1.82×10^{-3}	1.47	VII	4
1.9	1.50×10^{-4}		III	4	8.07	6.38×10^{-3}	1.36	VII	4
2.0	1.00×10^{-3}	1.47	III	4	8.12	1.21×10^{-2}	1.33	VII	4
2.05	1.50×10^{-3}		III	4	8.18	2.16×10^{-2}	1.3	VII	4
2.14	3.40×10^{-3}		III	4	8.23	2.67×10^{-2}	1.28	VII	4
2.2	1.70×10^{-3}	1.46	III	4	8.29	3.27×10^{-2}	1.24	VII	4
2.3	7.70×10^{-4}		III	4	8.35	4.59×10^{-2}	1.2	VII	4
2.4	4.50×10^{-4}	1.45	III	4	8.41	5.93×10^{-2}	1.16	VII	4
2.5	3.50×10^{-4}	1.44	III	4	8.47	8.08×10^{-2}	1.1	VII	4
2.63	9.00×10^{-4}	1.42	III	4	8.52	1.07×10^{-1}	1.04	VII	4
2.78	5.00×10^{-3}	1.4	III	4	8.58	1.47×10^{-1}	0.96	VII	4
2.94	7.52×10^{-3}	1.37	IV	4	8.64	2.24×10^{-1}	0.87	VIII	4
2.96	2.16×10^{-2}	1.34	IV	4	8.7	3.53×10^{-1}	0.77	VIII	4
2.98	4.75×10^{-2}	1.32	IV	4	8.76	5.23×10^{-1}	0.72	VIII	4

Wavelength (μm)	*k*	*n*	Uncertainty Class [a]	Note	Wavelength (μm)	*k*	*n*	Uncertainty Class [a]	Note
3.0	8.83×10^{-2}	1.3	IV	4	8.82	7.11×10^{-1}	0.70	VIII	4
3.02	1.43×10^{-1}	1.3	IV	4	8.88	9.38×10^{-1}	0.71	VIII	4
3.05	1.80×10^{-1}	1.32	IV	4	8.95	1.21E+00	0.77	VIII	4
3.07	2.22×10^{-1}	1.34	IV	4	9.01	1.52E+00	0.94	VIII	4
3.09	2.59×10^{-1}	1.38	IV	4	9.07	1.76E+00	1.33	VIII	4
3.11	2.66×10^{-1}	1.43	IV	4	9.13	1.73E+00	1.85	VIII	4
3.13	2.59×10^{-1}	1.48	IV	4	9.2	1.48E+00	2.21	VIII	4
3.15	2.38×10^{-1}	1.5	IV	4	9.26	1.24E+00	2.38	VIII	4
3.17	2.18×10^{-1}	1.52	IV	4	9.32	1.02E+00	2.46	VIII	4
3.20	2.04×10^{-1}	1.52	IV	4	9.39	8.12×10^{-1}	2.52	VIII	4
3.22	2.03×10^{-1}	1.52	IV	4	9.45	6.19×10^{-1}	2.54	VIII	4
3.24	2.14×10^{-1}	1.52	IV	4	9.52	4.43×10^{-1}	2.50	VIII	4
3.26	2.24×10^{-1}	1.54	IV	4	9.59	2.95×10^{-1}	2.41	VIII	4
3.29	2.25×10^{-1}	1.57	IV	4	9.65	2.10×10^{-1}	2.34	VIII	4
3.31	2.17×10^{-1}	1.59	IV	4	9.72	1.55×10^{-1}	2.26	VIII	4
3.33	1.99×10^{-1}	1.62	IV	4	9.79	1.16×10^{-1}	2.21	VIII	4
3.35	1.76×10^{-1}	1.63	IV	4	9.85	7.85×10^{-2}	2.15	IX	4
3.38	1.51×10^{-1}	1.64	IV	4	9.92	5.74×10^{-2}	2.10	IX	4
3.40	1.34×10^{-1}	1.63	IV	4	9.99	4.52×10^{-2}	2.05	IX	4
3.42	1.24×10^{-1}	1.63	IV	4	10.06	3.94×10^{-2}	2.02	IX	4
3.45	1.15×10^{-1}	1.62	IV	4	10.13	3.23×10^{-2}	1.99	IX	4
3.47	1.14×10^{-1}	1.62	IV	4	10.2	3.36×10^{-2}	1.96	IX	4
3.50	1.12×10^{-1}	1.63	IV	4	10.27	3.21×10^{-2}	1.95	IX	4
3.52	1.03×10^{-1}	1.63	IV	4	10.34	2.17×10^{-2}	1.93	IX	4
3.55	9.41×10^{-2}	1.64	IV	4	10.71	4.88×10^{-3}	1.85	IX	4
3.57	7.98×10^{-2}	1.64	IV	4	11.08	2.18×10^{-3}	1.80	IX	4
3.59	6.64×10^{-2}	1.64	IV	4	11.47	2.44×10^{-3}	1.76	IX	4
3.62	5.23×10^{-2}	1.64	IV	4	11.88	2.28×10^{-3}	1.74	IX	4
3.64	4.21×10^{-2}	1.63	IV	4	12.29	9.00×10^{-4}	1.71	IX	4
3.67	4.02×10^{-2}	1.62	IV	4	12.72	8.62×10^{-4}	1.69	IX	4
3.70	3.31×10^{-2}	1.62	IV	4	13.17	1.30×10^{-3}	1.67	IX	4
3.72	2.69×10^{-2}	1.62	IV	4	13.63	1.19×10^{-3}	1.65	IX	4
3.75	2.46×10^{-2}	1.61	IV	4	14.11	1.29×10^{-3}	1.63	IX	4
3.88	1.25×10^{-2}	1.59	IV	4	14.61	3.33×10^{-3}	1.59	IX	4
4.01	6.31×10^{-3}	1.57	V	4	15.12	8.83×10^{-3}	1.51	IX	4
4.16	3.68×10^{-3}	1.56	V	4	15.23	1.70×10^{-2}	1.49	X	4
4.18	1.87×10^{-3}	1.56	V	4	15.33	2.66×10^{-2}	1.47	X	4
4.21	[b]	1.56	V	4	15.44	2.15×10^{-2}	1.43	X	4
4.24	[b]	1.55	V	4	15.55	3.06×10^{-2}	1.38	X	4
4.27	[b]	1.55	V	4	15.65	5.61×10^{-2}	1.32	X	4
4.30	[b]	1.55	V	4	15.76	9.14×10^{-2}	1.22	X	4
4.33	[b]	1.55	V	4	15.87	2.58×10^{-1}	1.06	X	4
4.36	[b]	1.54	V	4	15.98	6.08×10^{-1}	1.02	X	4
4.39	[b]	1.54	V	4	16.09	9.16×10^{-1}	1.14	X	4
4.55	6.17×10^{-4}	1.53	V	4	16.21	1.20	1.50	X	4
4.71	8.80×10^{-4}	1.52	V	4	16.32	1.24	1.97	X	4
4.74	1.40×10^{-3}	1.52	V	4	16.43	8.40×10^{-1}	2.57	X	4
4.91	3.31×10^{-3}	1.51	V	4	16.54	3.16×10^{-1}	2.45	X	4
5.08	2.51×10^{-3}	1.51	V	4	16.66	1.32×10^{-1}	2.25	X	4
5.11	2.35×10^{-3}	1.5	V	4	16.77	7.34×10^{-2}	2.12	X	4
5.29	2.98×10^{-3}	1.49	V	4	16.89	7.66×10^{-2}	2.12	X	4
5.48	9.06×10^{-3}	1.48	V	4	18.2	2.00×10^{-2}	1.77	XI	4
5.52	1.03×10^{-2}	1.47	V	4	20	2.00×10^{-2}	1.69	XI	4
5.55	1.16×10^{-2}	1.48	V	4	22.2	3.00×10^{-2}	1.62	XI	4
5.59	1.34×10^{-2}	1.47	V	4	25	5.00×10^{-2}	1.55	XI	4
5.63	1.24×10^{-2}	1.48	V	4	28.6	1.10×10^{-1}	1.42	XI	4
5.67	1.03×10^{-2}	1.47	V	4	33.3	4.60×10^{-1}	1.18	XI	4
5.71	1.21×10^{-2}	1.47	V	4	40	1.12E+00	2.14	XI	4
5.75	1.13×10^{-2}	1.47	V	4					
5.95	5.87×10^{-3}	1.45	V	4					
6.16	5.18×10^{-3}	1.42	V	4					
6.38	6.00×10^{-3}	1.37	V	4					
6.42	6.14×10^{-3}	1.36	V	4					
6.47	7.64×10^{-3}	1.34	V	4					

Wavelength (μm)	*k*	*n*	Uncertainty Class [a]	Note	Wavelength (μm)	*k*	*n*	Uncertainty Class [a]	Note
6.51	1.49×10^{-2}	1.32	V	4					
6.56	1.97×10^{-2}	1.30	V	4					
6.60	2.77×10^{-2}	1.27	V	4					
6.65	4.46×10^{-2}	1.24	V	4					
6.69	6.39×10^{-2}	1.20	V	4					

[a] Uncertainty classes and uncertainties (1σ) in *k* (σ_k) and *n* (σ_n):

I: λ = 0.3–1.0 μm: *k* is an upper limit; σ_n is ±0.01

II: λ = 0.532 μm: σ_n(532 nm) is ±0.004

III: λ = 1.07–2.78 μm: σ_k is ±10%; σ_n is ±0.02; From Toon et al.[18]

IV: λ = 2.94–3.88 μm: σ_k is ±10%; σ_n is ±2%

V: λ = 4.01–6.69 μm: σ_k is factor of 3, *k* is likely a lower limit; σ_n is ±3%

VI: λ = 6.74–7.22 μm: σ_k is ±10%; σ_n is ±5%; Estimated from measurement spread

VII: λ = 7.27–8.58 μm: σ_k is factor of 15, *k* is likely a lower limit; σ_n is ±5%

VIII: λ = 8.64–9.79 μm: σ_k is ±10%; σ_n is ±5%

IX: λ = 9.85–15.12 μm: σ_k is factor of 30, *k* is likely a lower limit; σ_n is ±5%

X: λ = 15.23–16.89 μm: σ_k is ±10%; σ_n is ±7%

XI: λ = 16.9–40 μm: σ_k is factor of 5; σ_n is ±15%; Measurements strongly impacted by unmeasured mode at >40 μm

[b] Values reported as zero by Earle et al.,[9] see Note 4

5.4.2 Table P2. Ammonium sulfate complex refractive indices uncertainty estimates

Wavelength Range (μm)	*k*	*n*	Comments
0.3–1.0	Upper limit	±0.01	Estimated uncertainty in *n* at 532 nm is ±0.004
1.07–2.78	±10%	±0.02	From Toon et al.[18]
2.94–3.88	±10%	±2%	Estimated from measurement spread
4.01–6.69	Factor of 3; likely lower limit	±3%	
6.74–7.22	±10%	±5%	
7.27–8.58	Factor of 15; likely lower limit	±10%	
8.64–9.79	±10%	±5%	
9.85–15.12	Factor of 30; likely lower limit	±5%	
15.23–16.89	±10%	±7%	
>16.89–40	Factor of 5	±15%	Measurements strongly impacted by unmeasured mode at >40 μm

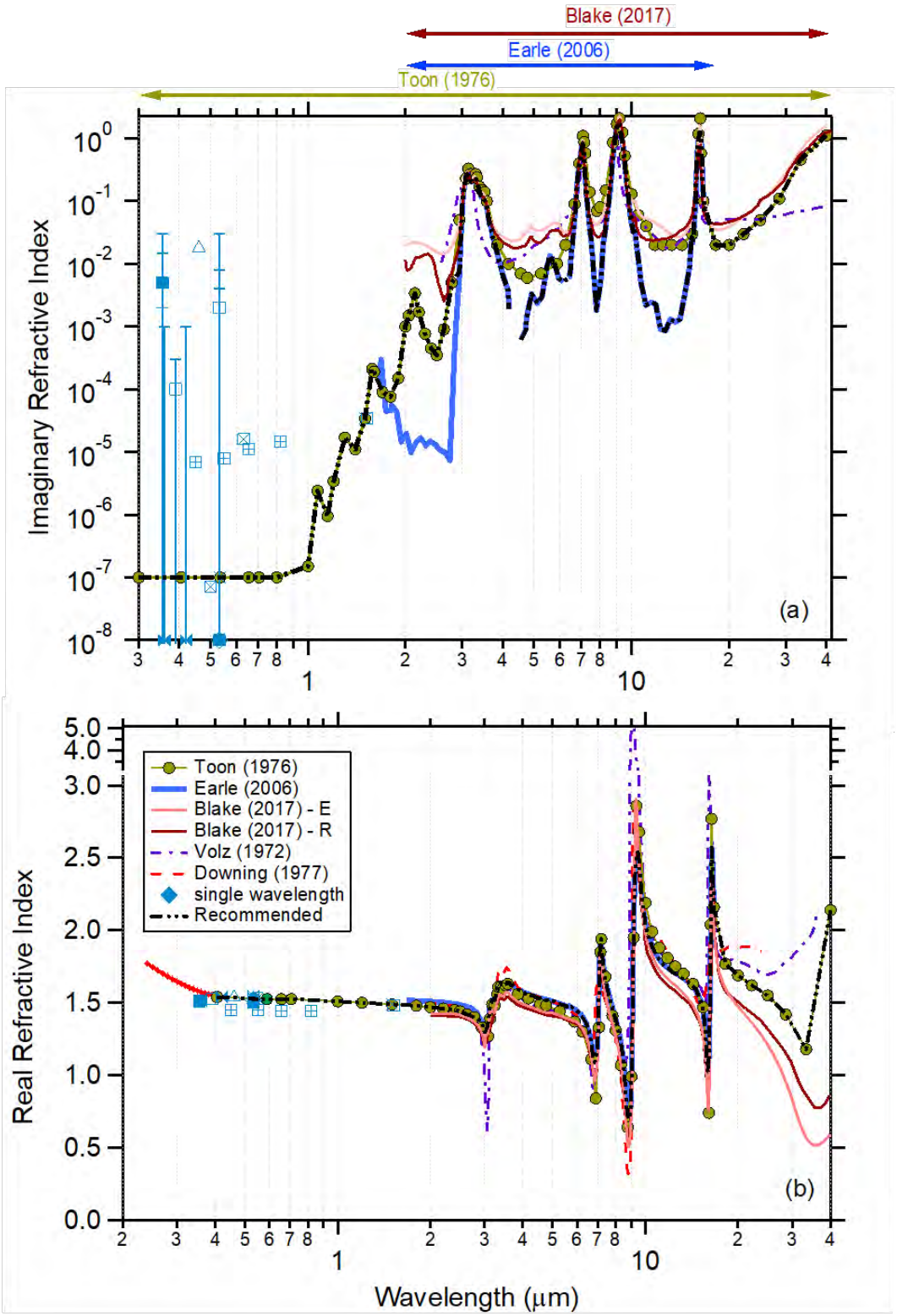


Figure P1: Wavelength dependent (a) imaginary and (b) real refractive indices for ammonium sulfate. For the single wavelength measurements, if a value of zero was reported for the imaginary RI it is shown as 10^{-8}. For (b), note the break and change in scale at $n = 3$. Recommended values are reported in Table P1 and discussed in Notes 3 and 4.

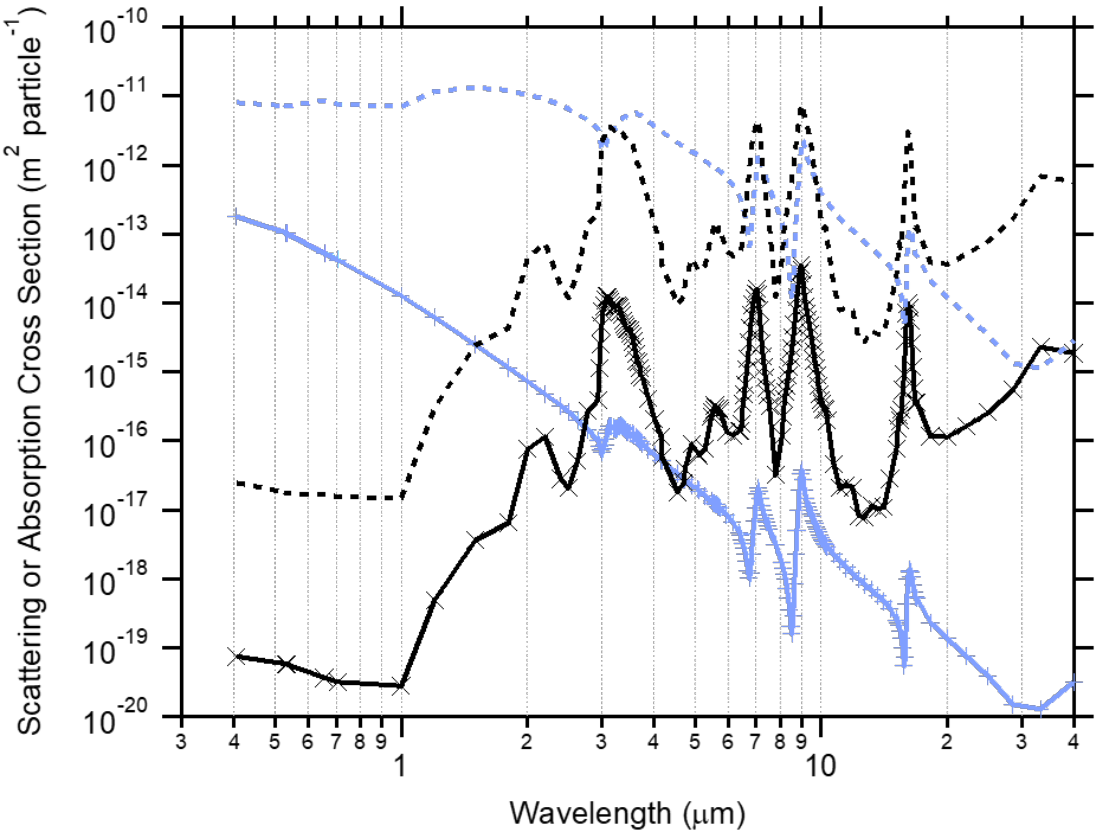


Figure P2: Wavelength dependent scattering (blue) and absorption (black) cross sections calculated from spherical particle Mie theory using the recommended complex refractive index (CRI) values assuming either 300 nm (solid lines, with symbols) or 2 μm (dashed lines) diameter particles. See Note 5.

5.4.3 Table P3. Summary of ammonium sulfate complex refractive index studies across the infrared range

Study	Wavelength Range (μm)	Method
Chermack[5]	1.2–2.5	Transmission and Reflection
	2.5–40	Reflection at 25° and 75°
Volz[20]	2.5–40	Transmission and Reflectivity Using KBr method
Toon et al.[18]	0.2–2.5	Transmission
	2.5–40	Reflectivity with dispersion analysis
Downing et al.[8]	2.8–25	Spectral reflectance of aqueous solutions
Earle et al.[9]	1.67–17	Aerosol Extinction
Blake et al.[3]	2–40	Reflectivity or Ellipsometry

(see Note 1)

5.4.4 Table P4. Results from single wavelength or narrow range studies

Reference	Wavelength (nm)	*n*	*k*	Method [a]
Beyer and Ebeling[2]	240–400	1.77–1.55		Aqueous $(NH_4)_2SO_4$ solutions, estimated for pure $(NH_4)_2SO_4$
Trainic et al.[19]	355	1.553 ± 0.005	0.002 ± 0.013	P-CRDS + size-selected particles
Flores et al. [11]	355	1.507 ± 0.024	0.005 ± 0.025	P-CRDS + size-selected particles
Washenfelder et al.[21]	360	1.513 ± 0.004	0.000 ± 0.001	BBCEAS + size-selected particles (360-420 nm)
Dinar et al.[7]	390	1.525 ± 0.0019	$1\times10^{-4} \pm 2\times10^{-4}$	P-CRDS + size-selected particles
Washenfelder et al.[21]	420	1.540 ± 0.007	0.000 ± 0.001	BBCEAS + size-selected particles
Zhao et al.[22]	445–470	1.538	0.018	IBBCEAS + particle distribution
Egan[10]	450	1.45	6.92×10^{-6}	Diffuse reflectance
Toon et al.[18]	535	1.53	10^{-7}	Transmission + reflectance; crystals
Abo Riziq et al.[1]	532	1.52	0	P-CRDS + size-selected particles; exclude small particles
Dinar et al.[7]	532	1.521 ± 0.0026	0.002 ± 0.002	P-CRDS + size-selected particles
Freedman et al.[12]	532	1.546		P-CRDS + size-selected particles
Lang-Yona et al.[14]	532	1.52 ± 0.01	0.00 ± 0.03	CW-CRDS + size-selected particles
Flores et al.[11]	532	1.504	0.0	P-CRDS + size-selected particles
Bluvshtein et al.[4]	532	1.521 ± 0.004	0.000 ± 0.008	P-CRDS + size-selected particles
Clarke and Waggoner[6]	550	1.53		Integrating plate on collected particles; report Single Scatter Albedo = 0.9999
Stadnyk et al.[17]	550	1.525–1.535		Spectral polarization optical method; range from dispersion; crystals
Egan[10]	550	1.448	7.94×10^{-6}	Diffuse reflectance
Patterson and Marshall[16]	500–700		7×10^{-8}	Diffuse reflectance + bulk sample (with Kubelka-Munk transformation)
Patterson and Marshall[16]	633		1.6×10^{-5}	Laser transmission + aerosol samples
Egan[10]	655	1.445	1.12×10^{-5}	Diffuse reflectance
Egan[10]	820	1.442	1.45×10^{-5}	
Toon et al.[18]	1500	1.49	3.4×10^{-5}	Transmission + reflectance; crystals
Mellon et al.[15]	1520	1.48 ± 0.02	3.4×10^{-5}	P-CRDS + size-selected particles

[a] Acronym definitions: P-CRDS = pulsed cavity ringdown spectroscopy; CW-CRDS = continuous wave cavity ringdown spectroscopy; BBCEAS = broadband cavity enhanced absorption spectroscopy; IBBCEAS = integrated broadband cavity enhanced absorption spectroscopy (see Note 2)

5.4.4.1 Notes for Optical Properties

Note 1: *Summary of Broadband Visible-IR Measurements:* Studies reporting the infrared wavelength-dependent CRI of ammonium sulfate are summarized in Table 5-8-2. Many of the studies determine *n* and *k* from measurement of transmission through a sample of the substance and/or reflectivity measurements. Volz[20] measured IR transmittance using the KBr disk technique to determine *k* and near-normal reflectance of disks made by compressing a power of $(NH_4)_2SO_4$ to determine *n*. Toon et al.[18] made transmission and reflectivity (at 11° from normal) measurements on slowly grown pure crystals of $(NH_4)_2SO_4$ to determine *n* and *k* over different wavelength ranges based on dispersion analysis. Their measurements were made along each of the three crystallographic axes, with minor differences between them. Chermack[5] reported *n* and *k* values based on transmissivity and reflectivity measurements; for the range 2.5–40 μm, the reflectivity was measured at 25° and 75°, rather than at near-normal, and Toon et al.[18] argues that the Chermack[5] values contain some unreported errors. We thus exclude the Chermack[5] values. Downing et al.[8] measured spectral reflectance from aqueous solutions of $(NH_4)_2SO_4$, and derived *n* and *k* values from a Kramers-Kronig phase-shift analysis. They determined *k* for the $(NH_4)_2SO_4$ solute specifically by subtracting the absorption of pure water, and then extrapolated these to match the number densities of the ions in crystalline $(NH_4)_2SO_4$. They report *n* values only for a 3.4 M aqueous solution, not for ammonium sulfate specifically. Given the assumptions involved in the Downing et al.[8] analysis, their reported *n* and *k* values should be considered only for general comparison with direct measurements of crystalline $(NH_4)_2SO_4$ and not used in a quantitative manner. More recently, Blake et al.[3] made independent measurements of *n* and *k* using single-angle reflectance and ellipsometry with pellets pressed from ammonium sulfate powder. The *n* and *k* were determined from the reflectance measurements using the Kramers-Kronig relationship and from the ellipsometry measurements using an oscillator model. Earle et al.[9] used a different approach, making measurements of the light extinction by suspended polydisperse aerosol particles. They derived *n* and *k* values using a combination of Mie theory and the Kramers-Kronig relationship, and anchoring their values to a value of $n = 1.528$ in the visible wavelength range.

Note 2: *Summary of Narrowband or Single-Wavelength Measurements in the near UV to near IR range:* There have been numerous individual measurements of *n* and *k* for $(NH_4)_2SO_4$ at discrete wavelengths or over narrow wavelength ranges in the near UV, visible and near-IR, which are summarized in Table 5-8-3. Most of these measurements have been made using cavity ringdown spectroscopy (CRDS), with a few using broadband cavity enhanced absorption spectroscopy (BBCEAS), with all of these occurring since 2007. With these studies, the *n* and *k* are determined from minimization of the difference between the observed extinction coefficients and that calculated from Mie theory. There is a group of measurements from the early 1980's that are all derived from the First International Workshop on light absorption by aerosol particles (Clarke and Waggoner;[6] Egan;[10] Patterson and Marshall[16]). Not all of the studies clearly indicate the uncertainties in the derived values.

Note 3: *Assessment of Near-UV and Visible Studies:* The spectral dependence of *n* and *k* is featureless across the near UV and visible spectrum, up to 1 μm. Based on the discrete-wavelength and narrowband measurements, we conclude that $n(532\text{ nm}) = 1.524 \pm 0.004$, where the uncertainty is the standard error of the mean across the measurements reported at 532 nm and 550 nm. (These wavelengths have been combined given the negligible wavelength dependence of *n* in this range.) The *n* values reported by Egan[10] are excluded as they are clearly outliers. There is little evidence to indicate that the *n* values change appreciably from $n(532\text{ nm})$ as the wavelength decreases.

All of the CRDS and BBCEAS studies indicate that the *k* for ammonium sulfate is zero to within the uncertainty of the measurements from 355-532 nm; these methods are not suitable for determining *k* values smaller than about 0.001. The other measurements in this wavelength range, and up to 820 nm, indicate an upper-limit of $k = 10^{-5}$. However, the measurements of Toon et al.[18] and Chermack[5] clearly indicate that *k* increases rapidly starting at 1 μm, and both Toon et al.[18] and Mellon et al.[15] report that $k = 3.4 \times 10^{-5}$ around 1500 nm. As such, the upper-limit of $k = 10^{-7}$ for $\lambda < 1$ μm from Toon et al.[18] is recommended. From the standpoint of calculation of aerosol optical properties, the calculated extinction, scatting and absorption are insensitive to differences in *k* for all $k < 10^{-4}$.

Note 4: *Assessment of Infrared Studies:* At wavelengths greater than 1 μm, absorption by ammonium sulfate increases appreciably. A series of resonances occur at 3 μm, 7 μm, 9 μm, and 16 μm. Only Toon et al.[18] reports wavelength-dependent *n* and *k* between 1 and 1.7 μm, and those values are recommended. Between 1.7 μm and 9 μm, there is good agreement between all of the studies on crystalline or powder samples in terms of *n*, although differences are larger at the resonances where *n* changes rapidly with λ. In these resonance regions, the *n* from Volz[20] differs most notably from the other studies. The estimated uncertainty outside of the resonance regions, characterized as σ_n/n, is 0.03 between 1.7 μm and 9 μm. Between 9 and 17 μm the two measurements from Blake et al.[3] differ from

the other studies, with overall lower n values. The estimated uncertainty in this range increases to σ_n/n, = 0.05. At λ >20 μm, the n values differ substantially between studies. The difference increases with λ to the longest wavelengths considered (λ = 40 μm). Most likely, these differences result largely from the existence of a strong absorption band at 50 μm, which contributes substantial uncertainty to the n values at λ >20 μm from limitations of either the Kramers-Kronig or dispersion analysis. Differences in n between the three crystallographic axes may also contribute to the greater differences between studies above λ = 20 μm. The estimated uncertainty at λ = 20 μm is 0.08, which increases monotonically to 0.6 at 40 μm.

There are substantial differences in the k values among studies across the IR. The k values vary over many orders of magnitude. The differences among studies is best characterized by the logarithmic difference. The logarithmic differences are generally largest when the k values are smallest. In the low k regions (k <~0.02), the aerosol extinction measurements (Earle et al.[9]) consistently yield the lowest k values, while the transmission/reflection measurements and ellipsometry measurements that used pressed pellets Blake et al.[3] tend to yield the largest k values. That the pellet-based measurements yield the largest k values is consistent with unaccounted for scattering. Differences between studies in the high k regions (k >~0.02) are reasonably small, and the normalized error (σ_k/k) generally decreases with increasing k.

In all analyses, the values of n and k are not independent, but linked through various mathematical relationships that depend on the interpretation method used. In general, in wavelength regions where only reflectivity is measured (common for λ >3 μm) the uncertainties in n and k are anti-correlated; when k is small the uncertainty in n is smaller and when k is large the uncertainty in n is larger, and vice versa. The direct transmission measurements of Toon et al.[18] up to 2.5 μm are likely the most robust, as they are least dependent on interpretation; we recommend the Toon et al.[18] values be used up to 2.78 μm as this limits the occurrence of obvious discontinuities in the observations. In the major resonance regions (k >0.1) we recommend that Earle et al.[9] values are adopted, as these are available at the highest resolution and there are only minor differences between studies. The measurements are available at much higher resolution (2 cm^{-1}) than is necessary for robust aerosol optical property calculations. For simplicity we recommend binning these into smaller wavelength bands, with $\Delta\log(\lambda)$ = 0.001 providing sufficient resolution. Between the resonance at 3 and 7 μm we recommend the Earle et al.[9] values be adopted; there is a clear feature at 5.5 μm in the IR spectrum measured by Earle et al.[9] and, separately by Garland et al.[13] , that is not evident in the Toon et al.[18] measurements. This feature is also somewhat apparent in the Blake et al.[3] measurements, but their estimate of k is likely an overestimate in this low k region. In the other between-resonance regions, we also recommend the Earle et al.[9] values be adopted for consistency. However, the Earle et al.[9] k values should not be used at the reported resolution in these low k regions, as the individual values are subject to substantial uncertainties from instrument noise. We recommend that the reported n and k values are averaged into $\Delta\log(\lambda)$ = 0.015 bins for regions where k <0.01. Above 17 μm we recommend the Toon et al.[18] measurements are adopted as they were made on ammonium sulfate crystals, as opposed to pressed pellets. Values of both n and k above 17 μm have large uncertainties.

Note 5: The wavelength-dependent scattering and absorption cross sections were calculated using spherical particle Mie theory. Values were calculated for each of the wavelengths reported in Table 5-8-1 using the reported recommended n and k. Calculations were performed assuming that the particle diameters were either 300 nm or 2 μm to illustrate how the calculated cross-sections depend on particle size.

5.4.4.2 Bibliography

(1) Abo Riziq, A.; Erlick, C.; Dinar, E.; Rudich, Y. Optical properties of absorbing and non-absorbing aerosols retrieved by cavity ring down (CRD) spectroscopy. *Atmos. Chem. Phys.* **2007**, *7*, 1523-1536, doi:10.5194/acp-7-1523-2007.

(2) Beyer, K. D.; Ebeling, D. D. UV refractive indices of aqueous ammonium sulfate solutions. *Geophys. Res. Lett.* **1998**, *25*, 3147-3150, doi:10.1029/98GL02333.

(3) Blake, T. A.; Brauer, C. S.; Kelly-Gorham, M. R.; Burton, S. D.; Bliss, M.; Myers, T. L.; Johnson, T. J.; Tiwald, T. E. "Measurement of the infrared optical constants for spectral modeling: n and k values for $(NH_4)_2SO_4$ via single-angle reflectance and ellipsometric methods"; Proc. SPIE 10198, Algorithms and Technologies for Multispectral, Hyperspectral, and Ultraspectral Imagery XXIII, 101980J, 2017.

(4) Bluvshtein, N.; Flores, J. M.; Abo Riziq, A.; Rudich, Y. An approach for faster retrieval of aerosols' complex refractive index using cavity ring-down spectroscopy. *Aerosol Sci. Technol.* **2012**, *46*, 1140-1150, doi:10.1080/02786826.2012.700141.

(5) Chermack, E. A. The optical constants (n, k) of ammonium sulfate in the infrared, New York University, 1970.
(6) Clarke, A. D.; Waggoner, A. P. Measurement of particle optical absorption, imaginary refractive index, mass concentration, and size at first international LAAP workshop. *Appl. Opt.* **1982**, *21*, 398-402, doi:10.1364/AO.21.000398.
(7) Dinar, E.; Abo Riziq, A., C., S.; Erlick, C.; Kiss, G.; Rudich, Y. The complex refractive index of atmospheric and model humic-like substances (HULIS) retrieved by a cavity ring down aerosol spectrometer (CRD-AS). *Faraday Discuss.* **2008**, *137*, 279-295, doi:10.1039/B703111D.
(8) Downing, H. D.; Pinkley, L. W.; Sethna, P. P.; Williams, D. Optical-constants of ammonium sulfate in the infrared. *J. Opt. Soc. Am.* **1977**, *67*, 186-190, doi:10.1364/josa.67.000186.
(9) Earle, M. E.; Pancescu, R. G.; Cosic, B.; Zasetsky, A. Y.; Sloan, J. J. Temperature-dependent complex indices of refraction for crystalline $(NH_4)_2SO_4$. *J. Phys. Chem. A* **2006**, *110*, 13022-13028, doi:10.1021/jp064704s.
(10) Egan, W. G. Volumetric scattering and absorption by aerosols: parametric sensitivity in Mie modeling and comparisons to observations. *Appl. Opt.* **1982**, *21*, 1445-1453, doi:10.1364/AO.21.001445.
(11) Flores, J. M.; Bar-Or, R. Z.; Bluvshtein, N.; Abo-Riziq, A.; Kostinski, A.; Borrmann, S.; Koren, I.; Koren, I.; Rudich, Y. Absorbing aerosols at high relative humidity: linking hygroscopic growth to optical properties. *Atmos. Chem. Phys.* **2012**, *12*, 5511-5521, doi:10.5194/acp-12-5511-2012.
(12) Freedman, M. A.; Hasenkopf, C. A.; Beaver, M. R.; Tolbert, M. A. Optical properties of internally mixed aerosol particles composed of dicarboxylic acids and ammonium sulfate. *J. Phys. Chem. A* **2009**, *113*, 13584-13592, doi:10.1021/jp906240y.
(13) Garland, R. M.; Wise, M. E.; Beaver, M. R.; DeWitt, H. L.; Aiken, A. C.; Jimenez, J. L.; Tolbert, M. A. Impact of palmitic acid coating on the water uptake and loss of ammonium sulfate particles. *Atmos. Chem. Phys.* **2005**, *5*, 1951-1961, doi:10.5194/acp-5-1951-2005.
(14) Lang-Yona, N.; Rudich, Y.; Segre, E.; Dinar, E.; Abo-Riziq, A. Complex refractive indices of aerosols retrieved by continuous wave-cavity ring down aerosol spectrometer. *Anal. Chem.* **2009**, *81*, 1762-1769, doi:10.1021/ac8017789.
(15) Mellon, D.; King, S. J.; Kim, J.; Reid, J. P.; Orr-Ewing, A. J. Measurements of extinction by aerosol particles in the near-infrared using continuous wave cavity ring-down spectroscopy. *J. Phys. Chem. A* **2011**, *115*, 774-783, doi:10.1021/jp109894x.
(16) Patterson, E. M.; Marshall, B. T. Diffuse reflectance and diffuse transmission measurements of aerosol absorption at the first international workshop on light absorption by aerosol particles. *Appl. Opt.* **1982**, *21*, 387-393, doi:10.1364/AO.21.000387.
(17) Stadnyk, V. Y.; Romanyuk, M. O.; Andrievskii, B. V.; Tuzyak, N. R. Refractive indices of $(NH_4)_2SO_4$ crystals under uniaxial pressure. *Crystallogr. Rep.* **2009**, *54*, 313-319, doi:10.1134/s1063774509020229.
(18) Toon, O. B.; Pollack, J. B.; Khare, B. N. Optical-constants of several atmospheric aerosol species - Ammonium-sulfate, aluminum-oxide, and sodium-chloride. *J. Geophys. Res.* **1976**, *81*, 5733-5748, doi:10.1029/JC081i033p05733.
(19) Trainic, M.; Abo Riziq, A.; Lavi, A.; Flores, J. M.; Rudich, Y. The optical, physical and chemical properties of the products of glyoxal uptake on ammonium sulfate seed aerosols. *Atmos. Chem. Phys.* **2011**, *11*, 9697-9707, doi:10.5194/acp-11-9697-2011.
(20) Volz, F. E. Infrared optical constants of ammonium sulfate, Sahara dust, volcanic pumice, and flyash. *Appl. Opt.* **1973**, *12*, 564-568, doi:10.1364/AO.12.000564.
(21) Washenfelder, R. A.; Flores, J. M.; Brock, C. A.; Brown, S. S.; Rudich, Y. Broadband measurements of aerosol extinction in the ultraviolet spectral region *Atmos. Meas. Tech.* **2013**, *6*, 861-877, doi:10.5194/amt-6-861-2013.
(22) Zhao, W.; Dong, M.; Chen, W.; Gu, X.; Hu, C.; Gao, X.; Huang, W.; Zhang, W. Wavelength-resolved optical extinction measurements of aerosols using broad-band cavity-enhanced absorption spectroscopy over the spectral range of 445–480 nm. *Anal. Chem.* **2013**, *85*, 2260-2268, doi:10.1021/ac303174n.

SECTION 6: HOMOGENEOUS AQUEOUS-PHASE CHEMISTRY

Table of Contents

SECTION 6: HOMOGENEOUS AQUEOUS-PHASE CHEMISTRY 1
6.1 Introduction 2
6.2 Reactions Leading to and Consuming OH 5
6.2.1 Notes: Reactions Leading to and Consuming OH 6
6.2.2 References 9
6.3 Reactions of Oxygen Species with Halogen Species 13
6.3.1 Notes: Reactions of Oxygen Species with Halogen Species 15
6.3.2 References 20
6.4 Formation and Dissociation of Dihalo Radicals 25
6.4.1 Notes: Formation of Dihalo Radicals 26
6.4.2 References 26
6.5 Formation and Loss of Halogen Molecules and Dihalo Radicals 28
6.5.1 Notes: Formation and Loss of Halogen Molecules and Dihalo Radicals 28
6.5.2 References 30
6.6 Halogen Interconversion Reactions 31
6.6.1 Notes: Halogen Interconversion Reactions 32
6.6.2 References 36
6.7 Other Reactions of Possible Importance 40
6.7.1 Notes: Other Reactions of Possible Importance 40
6.7.2 References 40
6.8 Reactions of other Oxidants with Halides 41
6.8.1 Notes: Reactions of other Oxidants with Halides 41
6.8.2 References 42
6.9 Reactions of Reductants with Halides 44
6.9.1 Notes: Reactions of Reductants with Halides 44
6.9.2 References 47
6.10 Tri-halo Compounds 49
6.10.1 Notes: Tri-halo compounds 49
6.10.2 References 50
6.11 Bibliography 51

6.1 Introduction

The scope of the data evaluation has evolved over the years to include heterogeneous processes, including reactions on surfaces and uptake of molecules into aerosols and liquid droplets. The scope also includes chemistry in the troposphere which may have an impact on the stratosphere by, for example, removing halogen-containing molecules which may transport to the stratosphere and contribute to chemical processes there. This obviously includes homogeneous gas-phase chemistry. In addition, however, some of the chemistry may take place on or in atmospheric particles, aerosols, or droplets. These processes are often referred to as heterogeneous and this characterization is certainly the case for those involving gas-surface interactions. Chemical transformations which take place within the atmospheric aqueous phase, however, are more properly considered homogeneous aqueous-phase reactions. This includes reactions taking place in clouds, fogs, aqueous aerosols, and raindrops.

For many atmospheric species, the aqueous environment is quite different than the gas phase. In water, molecules can hydrate, protonate, deprotonate, or dissociate. In addition to participating in similar reactions as in the gas phase, such as abstraction or addition, species may also react by electron transfer. Sometimes, reactions that appear to be simple reactions between neutrals can actually involve concerted protonation or deprotonation, or even electron transfer. An important example is proton transfer-assisted electron transfer, which appears to be a simple hydrogen abstraction, but the features of which can only be explained by assuming a proton transfer mediated by the solvent coupled to an electron transfer.[162,176] Other examples of liquid water having a strong impact on the course of a reaction can be found in the reactions of NH_2 with O_2 and SH with O_2. These reactions are vanishingly slow in the gas phase, but proceed rapidly in the aqueous phase, probably due to the ability of water to interact with the hydrogen atoms.[50,176]

Many of the important reactions in the atmospheric aqueous phase involve charged species. Thus, their reactivity depends on the activity of the solution, which is essentially its deviation from ideality. It is similar to an "effective concentration". This difference is expressed as the activity coefficient. The activity coefficient of an ion can be estimated for dilute solutions by use of the extended Debye-Hückel equation:[93]

$$log\,\gamma_{\pm} = \frac{-Az_a z_b I}{1 + Ba\sqrt{I}}$$

where A and B are collections of fundamental constants which depend on temperature and the solution dielectric constant, a is the mean ionic radius, I is the ionic strength of the solution, and z_a and z_b are the charges on the two reactants.[158] If the ionic strength is in mol $L^{-1}$and the mean effective diameter of the ions, a, is in nm, $A = 1.82455 \times 10^6/(DT)^{3/2}$ and $B = 502.904/(DT)^{1/2}$ for any solvent, where D is the dielectric constant. We have recalculated these values of A and B at various temperatures using a more recent recommendation for the dielectric constant of water[182] and present these in the Table below.

Temperature (ºC)	A	B $(nm)^{-1}$
0	0.49020	3.24507
5	0.49385	3.25312
10	0.49774	3.26164
15	0.50186	3.27061
20	0.50621	3.28003
25	0.51079	3.28989
30	0.51560	3.30018
35	0.52064	3.31089

For a = 0.3 nm, the product Ba is very close to unity.

By inserting the activity into the transition-state expression for the rate constant, we obtain[45]

$$log\ k = log\ k_0 + \frac{2Az_a z_b I}{1 + Ba\sqrt{I}}$$

At very low ionic strength, this becomes

$$log\ k = log\ k_0 + 2Az_a z_b I$$

Rate constants for reactions in aqueous solutions are often pH dependent, sometimes strongly. This is typically a consequence of a pH dependence of the reduction potential of one or both of the reactants. A dramatic example is the HO_2/O_2^- radical. HO_2 behaves as an oxidant, with a standard potential for the half-reaction $HO_2 + e^- + H^+ \rightarrow H_2O_2$ of $E^\circ = +1.46 \pm 0.01$ V.[7] O_2^-, on the other hand, behaves as a reductant, with $O_2(aq) + e^- \rightarrow O_2^-$ having $E^\circ = -0.18 \pm 0.02$ V. A pH dependence can also result from the protonation of the product. An important example is OH, for which $OH + e^- \rightarrow OH^-$ has $E^\circ = +1.902 \pm 0.017$ V and $OH + e^- + H^+ \rightarrow H_2O$ has $E^\circ = +2.730 \pm 0.017$ V.[7]

The standard potentials of non-radical species have been measured extensively over the years. These results were reviewed by a team under the auspices of IUPAC in 1985.[10] More recently, in another IUPAC-sponsored effort, recommended values for the standard potentials for inorganic free radicals were reported, with extensive background information as supplementary material.[7] Also, in 1989 Wardman published an extensive review of organic free radical standard potentials, including a thorough discussion of the methodology used in obtaining these data and on the practical application of this information.[236] This latter review is recommended as a very useful tutorial on the use of standard potentials.

This section of the report focuses on reactions that lead to the activation of halides in atmospheric droplets. That is, reactions that transform halides, X^-, into a volatile halogen molecule, X_2. These reactions are listed in the Tables along with a rate constant or rate expression. Unless otherwise indicated in the Table or the note, the rate constants are at 25 ºC, or room temperature, and have units of L mol^{-1} s^{-1}. The reactions are grouped according to some defining characteristic.

The first grouping is reactions leading to and consuming the hydroxyl radical, the major atmospheric oxidant, but not including its reactions with halogen species. The next

grouping is reactions of oxygen species with halogen species, including reactions of OH with halides. Particularly important here in addition to OH are reaction of O_3, H_2O_2, and HO_2. Subsequent groupings involve further reactions of halogen species, including interconversion reactions, reactions of other oxidants that might be formed in atmospheric droplets with halides, reactions of reductants with oxidized halogen species, and reactions that can generate volatile halogens.

At present, this section covers only a small fraction of the chemistry of the atmospheric aqueous phase: those reactions directly involved in the activation of halides. There is, for example, a rich chemistry involving organic compounds which is just beginning to be understood (see: Herkes, et al., McNeill, Ervens, and Shen, et al.)[70,102,163,209] Nor does this section cover photolysis,[88,89] which also can lead directly to reactive halogen species.[103] It is important to point out that some of the chemistry discussed here is also mentioned in other reviews, often as a part of larger picture of halogens and their role in atmospheric chemistry.[77,105,212] This includes tying together the chemistry of the gas phase with the homogeneous aqueous phase, and even with the surface of the drops. In an earlier discussion of halogen chemistry, Finlayson-Pitts presents evidence for halogen activation involving the atmospheric aqueous phase and its importance in atmospheric gas-phase chemistry.[76]

6.2 Reactions Leading to and Consuming OH

Reaction			k (L mol^{-1} s^{-1}) *	Note
$O_3 + OH^-$	→	$HO_2 + O_2^-$	52 ± 20	A1
$O_3 + H_2O$	→	chain initiation	See Note	A2
$O_3 + HO_2^-$	→	$OH + O_2^- + O_2$ $OH^- + 2O_2$	$(2.8 \pm 0.5) \times 10^6$	A3
$O_3 + H_2O_2$	→	products	<0.06	A3
$O_3 + O_2^-$	→	$O_3^- + O_2$	$(1.6 \pm 0.2) \times 10^9$	A4
$H_2O + O(^1D)$	→	H_2O_2 2OH	0.9 (yield) 0.1	A5
O_3^-	→	$O_2 + O^-$	$9 \times 10^{10} \exp(-5170/T)$ s^{-1}	A6
$O_3^- + H^+$	→	$O_2 + OH$	$(9 \pm 1) \times 10^{10}$	A7
$O_3^- + OH$ $(+OH^-)$	→ →	$O_3 + OH^-$ $2O_2^- + (H_2O)$	2.6×10^9 5.9×10^9	A8
$O_3 + OH$	→	$HO_2 + O_2$	$(1 \pm 0.2) \times 10^8$	A9
$OH + CO_3^{2-}$	→	$OH^- + CO_3^-$	$6.68 \times 10^{12} \exp(-2840/T)$	A10
$OH + HCO_3^-$	→	$H_2O + CO_3^-$	$6.21 \times 10^{10} \exp(-2550/T)$	A10
$CO_3^- + O_3$	→	products	$<1 \times 10^5$	A11
$CO_3^- + O_2^-$	→	$O_2 + CO_3^{2-}$	$(5 \pm 2) \times 10^8$	A12
$CO_3^- + O_3^-$	→	$O_3 + CO_3^{2-}$	$(5.5 \pm 0.5) \times 10^7$	A13
$OH + O_2$	→	HO_3	$<10^4$	A14
$OH + H_2O_2$	→	$H_2O + HO_2$	$8.47 \times 10^9 \exp(-1680/T)$	A15
$OH + HO_2^-$	→	$H_2O + O_2^-$	7.5×10^9	A15
$OH + HO_2$	→	$H_2O + O_2$	1×10^{10}	A16
$OH + O_2^-$	→	$HO^- + O_2$	$1.4 \times 10^{13} \exp(-2120/T)$	A17
$HO_2 + HO_2$	→	$H_2O_2 + O_2$	$3.98 \times 10^9 \exp(-2480/T)$	A18
$HO_2 + O_2^-$ $(+H_2O)$	→	$H_2O_2 + O_2$ $(+OH^-)$	9.7×10^7	A19
$O_2^- + O_2^-$ $(+2H_2O)$	→	$H_2O_2 + O_2$ $(+2OH^-)$	Negligible, See Note	A19
$O_2^- + H_2O_2$	→	$O_2 + OH + OH^-$	0.13	A20
$HO_2 + H_2O_2$	→	$O_2 + OH + H_2O$	0.5	A20
$OH + HSO_4^-$	→	$H_2O + SO_4^-$	4.7×10^5	A21
$OH + H_2SO_4$	→	$H_2O + H^+ + SO_4^-$	1.4×10^7	A21
$OH + NO_2^-$	→	$OH^- + NO_2$	$(1 \pm 0.5) \times 10^{10}$	A22
OH + HONO	→	$H_2O + NO_2$	3×10^9	A23
$OH + HNO_3$	→	$H_2O + NO_3$	$(8.6 \pm 1.3) \times 10^7$	A24
$NO_3 + OH^-$	→	$NO_3^- + OH$	8.2×10^7	A25
$H + N_2O$	→	$N_2 + OH$	$(9 \pm 2) \times 10^4$	A26
$H + H_2O$	→	$H_2 + OH$	7×10^{-5}	A27
$H + O_2$	→	HO_2	1.3×10^{10}	A28
$H + H_2O_2$	→	$H_2O + OH$	3.4×10^7	A29
OH + OH	→	H_2O_2	5.5×10^9	A30
$SO_4^- + OH^-$	→	$SO_4^{2-} + OH$	5.6×10^7	A31

* Unless units noted otherwise

6.2.1 Notes: Reactions Leading to and Consuming OH

A1. **$O_3 + OH^-$.** There have been three pathways proposed for the reaction of OH^- with O_3:

(a) $\rightarrow HO_2^- + O_2$
(b) $\rightarrow HO_2 + O_2^-$
(c) $\rightarrow OH + O_3^-$

Reaction (a) generates no free radicals in the initial step, whereas reaction (b) generates two HO_2/O_2^- radicals and reaction (c) produces (after protonation and decomposition of O_3^-) two OH radicals. Under typical experimental conditions, secondary chain reactions make the exact identity of the initial step seem not too important. But from the perspective of chemistry induced by ozone in an atmospheric droplet, these differences are likely to be critical. Reaction (c) has been discounted based on apparent OH yields of 0.55±0.08[44] or 0.78[21]. An induction period in the formation of O_3^- was interpreted as indicating reaction (b) was not as important as reaction (a)[47]. But Merényi et al.,[28] have argued, based on thermokinetic and quantum chemical calculations, that the reaction between OH^- and O_3 leads to the formation of an adduct, HO_4^- (ΔG = 3.5 kJ mol^{-1}), which decays rapidly (k ~10^7 s^{-1}). Although the direct decay route to HO_2^- and O_2 is exoergonic (ΔG = −73.3 kJ mol^{-1}), it is spin forbidden; the spin-allowed route to HO_2^- and $O_2(^1\Delta_g)$ is endergonic (ΔG = 23.2 kJ mol^{-1}), whereas the route to HO_2 and O_2^- is spin allowed and less endergonic (ΔG = 14.8 kJ mol^{-1}).

The rate constant for this reaction has been measured at 20 ± 1 ºC in alkali (pH>11) solutions containing carbonate by monitoring ozone decay (38 ± 14 L mol^{-1} s^{-1}, assuming a stoichiometry of 3) or carbonate radical formation (57.5 ± 10 L mol^{-1} s^{-1} assuming a stoichiometry of 2).[21] An upper limit to the rate constant of 80 ± 10 L mol^{-1} s^{-1} from the formation of ozonide was also reported. The authors recommend the average of the first two results of 48 ± 12 L mol^{-1} s^{-1}.

A second study at 20 ± 1 ºC over the pH range 8-10 was carried out using either carbonate or methyl mercury as radical scavengers at 20 ºC.[44] Again taking a stoichiometry of 3, this study resulted in a rate constant of 70 ± 7 L mol^{-1} s^{-1}.

In a stopped-flow study at 20 ºC in slightly basic ([OH] = 0.0117 M) and basic ([OH] = 0.126 M) solutions containing carbonate at 20 ºC, rate constants of 37 and 43 L mol^{-1} s^{-1}, respectively, were reported.[47]

An extensive study of ozone decomposition at 25 ºC by following O_3 (260 nm), O_3^- (430 nm), and CO_3^- (600 nm), followed by a simultaneous fit of 60 kinetic traces, led to a value of 170 ± 2 L mol^{-1} s^{-1}.[18] Six additional critical rate constants were also fitted, which may make this less reliable than the stated error limits would suggest.

Several other studies of ozone decomposition without the use of radical scavengers have also been carried out (see Sotelo[43] and references within). Due to the high reactivity of radicals toward ozone, it does not seem possible to extract useful rate constants from these studies. Therefore, the value reported in the Table is an average of the values from the three studies which employed scavengers.

An investigation of the decomposition of O_3 in phosphate-buffer solutions at pH 4.5, 6.1, and 9 resulted in an apparent value of the mean value over the temperature range 20 to 30 °C for the rate constant for OH^- + O_3 of 71.4 L mol^{-1} s^{-1}, in good agreement with the chosen value.[19] The simplified model used, however, did not include the fast reaction $O_3 + O_2^- \rightarrow O_3^- + O_2$. This may be compensated for somewhat by the fact that the subsequent reactions, $O_3^- + H^+ \rightarrow OH + O_2$ and $OH + O_3 \rightarrow HO_2 + O_2$ are very fast. Back to Table

A2. **$O_3 + H_2O$.** Several studies have been carried out on the decomposition of ozone in water at low pH values. The chain nature of the reaction makes the extraction of absolute rate constants problematic; the temperature dependent studies all result in quite high activation energies, 40–110 kJ mol^{-1} (Sotelo, et al.[43] and references within). Indeed, not only is the magnitude of the measured decomposition rate constants highly scattered, so is the order of the reaction.[22] A careful study of the thermal decomposition found a retarding effect of O_2 on the rate, along with an increase in isotopic scrambling in $^{18,18}O_2$ with temperature(0–46 ºC).[36] In this study, an activation energy of 79.5 ± 8.0 kJ mol^{-1} was reported. These authors used this information to suggest that the decomposition in pure water arose from the thermal decomposition of ozone, followed by reaction with water

$O_3 \rightarrow O + O_2$

$O + H_2O \rightarrow 2OH$

A similar activation energy of 82.5 ± 8.0 kJ mol^{-1} was found in an acetate solution.[37]

A more recent investigation of the decomposition of O_3, based on solubility measurements, in the presence of added H_2SO_4 suggested a significantly enhanced rate below pH 2.[13] The possibility of trace amounts of metal ions, however, makes this result uncertain.

It is very unlikely that these reactions would be important in atmospheric chemistry. Back to Table

A3. **O_3 + H_2O_2.** The reaction of hydrogen peroxide with ozone has generally been accepted to be an electron transfer from the HO_2^- anion.[44]

$O_3 + HO_2^- \rightarrow OH + O_2^- + O_2$ (or $O_3^- + HO_2$)

More recently, however, this conclusion has been called into question in a study of the deuterium-isotope effect on the reaction.[25] The large effect was interpreted as due to a hydride-transfer reaction:

$O_3 + HO_2^- \rightarrow HO_3^- + O_2$

A subsequent study, however, involving the use of radical scavengers, found very little kinetic isotope effect.[42] These authors suggested that the earlier work was compromised by the presence of trace impurities in the D_2O.

Merényi, et al.[28] have argued, based on thermokinetic and quantum chemical calculations, that the reaction between HO_2^- and O_3 leads to the formation of an adduct, HO_5^- ($\Delta G° = -39.8$ kJ mol^{-1}), which decays to HO_2 and O_3^- ($\Delta G° = 13.2$ kJ mol^{-1}) and to $2O_2 + OH^-$. The latter decay pathway accounts for the peroxone process, which is based upon this chemistry, being only ~50% efficient. This reduced yield of OH has been confirmed by Fischbacher, et al.,[20] who found an average yield of slightly over 0.5 by following trace reactants in the presence of excess *t*-butanol. This approach was confirmed by generating OH by γ-radiolysis under the same conditions.

The kinetics of the reaction of ozone with hydrogen peroxide were measured over the pH range 5 to 6 at 20°C in the presence of methyl mercury as a free radical scavenger.[44] The rate was found to increase by one order a magnitude per pH unit, supporting the contention that only the anion reacts. The reported rate constant, $(2.8 \pm 0.5) \times 10^6$ L mol^{-1} s^{-1}, for the reaction of O_3 with HO_2^- includes a stoichiometric factor of 2. Another stopped-flow measurement, without radical scavenger but fitting only the initial rate, led to 2.2×10^6 L mol^{-1} s^{-1}.[47] A kinetic spectrophotometric measurement with a *t*-butanol scavenger, also at 20 °C, led to a slightly higher value of $(4.8 \pm 1) \times 10^6$ L mol^{-1} s^{-1}.[42] A simultaneous fit to a complex system involving ten rate constants (See Note A1) led to $k = (3.1 \pm 0.1) \times 10^6$ L mol^{-1} s^{-1}, in remarkable agreement.[18]

The rate constant for the reaction of ozone with hydrogen peroxide has also been studied by the reactive-absorption method.[4] At 20°C, this approach led to rate constants of 2.40 or 1.91×10^6 L mol^{-1} s^{-1}, depending on the value chosen for the Henry's Law constant; at 35°C, these values were 5.68 and 7.31×10^6 L mol^{-1} s^{-1}. These suggest an activation energy for the reaction of between 45 and 69 kJ mol^{-1}.

The rate of loss of ozone at pH 2 in the presence of H_2O_2 was determined in acetic acid solutions. At 31 °C, a rate constant of 0.065 L mol^{-1} s^{-1} was determined.[37] But measurements over the temperature range 18−46 °C suggested an activation energy, 73.5 ± 8.0 kJ mol^{-1}, only slightly lower than in the absence of peroxide, so it is probably best to consider this an upper limit. Indeed, results from this group suggest considerable complications associated with the formation and loss of H_2O_2 in ozone decomposition at low pH.[38] A measurement, also following ozone loss, at 20 °C led to a reported rate constant of (0.023 ± 0.002) L mol^{-1} s^{-1}.[33] The pH in this study was not completely clear, but seemed to be about 6.2.

An investigation of the decomposition of O_3 in phosphate-buffer solutions at pH 4.5, 6.1, and 9 resulted in an calculated value of the value over at pH 7 for the rate constant for $HO_2^-/H_2O_2 + O_3$ of 251 L mol^{-1} s^{-1}.[19] This leads to approximately 1×10^6 L mol^{-1} s^{-1} for the anion. The simplified model used, however, did not include the fast reaction $O_3 + O_2^- \rightarrow O_3^- + O_2$. This may be compensated for somewhat by the fact that the subsequent reactions, $O_3^- + H^+ \rightarrow OH + O_2$ and $OH + O_3 \rightarrow HO_2 + O_2$ are very fast. Back to Table

A4. **$O_3 + O_2^-$.** Two independent pulse radiolysis measurements, both following the build-up of O_3^- at 430 nm, give 1.5 and 1.6×10^9 L mol^{-1} s^{-1}.[6,7,41] A simultaneous fit involving ten rate constants (see Note A1) led to $k = (7 \pm 0.6) \times 10^7$ L mol^{-1} s^{-1}, in very poor agreement.[18] A calculation at the B3LYP/LACV3P** level of theory, with solvent interactions calculated using Jaguar's Poisson-Boltzmann solver, led to a free energy for this reaction of $\Delta G° = -176$ kJ mol^{-1}.[30] There was no evidence for the formation of an adduct as a minimum on the potential energy surface. Back to Table

A5. **$H_2O + O(^1D)$.** Quantum yields were derived from a study of the photolysis of solutions containing ~3×10^{-4} mol L^{-1} O_3 in the presence of varying amounts of *t*-butanol over a wavelength range of 245–300 nm. The direct product of photolysis at these wavelengths is $O(^1D)$. The quantum yield for ozone loss was $\Phi(-O_3)$ ~0.5, based on a measurement of 0.64 coupled with corrections for loss to organic radicals.[34] See also work on the photochemical oxidation of chloride by ozone.[26] Back to Table

A6. **O_3^-.** Obtained from a pulse radiolysis study over 298–343 K.[15] (E_a = 43.0 kJ mol^{-1}) Derived from decay kinetics of O_3^- as a function of O_2, methanol, and 2-propanol in 1 molar KOH. At 298 K, $k = 2.6 \times 10^3$ s^{-1}, in agreement with earlier pulse radiolysis and flash photolysis studies, which ranged from 3.3–6.2×10^3 s^{-1}.[35] HO_3 is a very strong acid, with p$K_a = -2.1$.[29] Back to Table

A7. **$O_3^- + H^+$.** From a pulse radiolysis study following the temporal behavior of the absorption at 260 and 430 nm at pH 10–13.[39] The use of this rate constant leads to a "satisfactory" fit. Another report from the same laboratory gave $k = 5.2 \times 10^{10}$ L mol^{-1} s^{-1} at pH 5.[6,7] Back to Table

A8. **O_3^- + OH.** From a high-pressure pulse radiolysis study (40 atm. N_2O) following the decay of O_3^- at 430 nm and formation of O_2^- at 260 nm and ~20 ºC.[39] Total rate constant is 8.5×10^9 L mol^{-1} s^{-1}. Back to Table

A9. **O_3 + OH.** From a pulse radiolysis study using product formation kinetics at pH 9-10, following O_3^- from the subsequent reaction of O_2^- with O_3, along with decay kinetics at pH 1 following O_3 at 280-310 nm. This value is supported by a relative rate measurement at pH 10.3 against OH + CO_3^{2-}.[40] A calculation at the B3LYP/LACV3P** level of theory, with solvent interactions calculated using Jaguar's Poisson-Boltzmann solver, led to a free energy for this reaction of $\Delta G° = -229$ kJ mol^{-1}.[30] There was no evidence for the formation of an adduct on the potential energy surface. Back to Table

A10. **OH + CO_3^{2-}/HCO_3^-.** From a pulse radiolysis study using product formation kinetics over a range of carbonate concentrations and four different hydroxide ion concentrations between 20 and 200 °C.[9] (E_a = 23.6 kJ mol^{-1} for carbonate and 21.2 kJ mol^{-1} for bicarbonate) Other reported values range from 3.2×10^8 to 4.2×10^8 L mol^{-1} s^{-1} at ~298 K, in good agreement.[35] Back to Table

A11. **$CO_3^- + O_3$.** Obtained by following decay kinetics of CO_3^- after pulse radiolysis in a 0.1 mol L^{-1} bicarbonate solution containing 90 µmol L^{-1} ozone.[41] Back to Table

A12. **$CO_3^- + O_2^-$.** A pulse radiolysis study,[16] following the decay of CO_3^- at 600 nm gave 6.5×10^8 L mol^{-1} s^{-1} and a flash photolysis study[3] monitoring both the decay of CO_3^- and of O_2^- at 260 nm gave 4.0×10^8 L mol^{-1} s^{-1}. A simultaneous fit involving ten rate constants (see reaction 1) led to $k = (6.8 \pm 0.4) \times 10^9$ L mol^{-1} s^{-1}, in poor agreement.[18] Back to Table

A13. **$CO_3^- + O_3^-$.** Derived from an investigation of the effect of carbonate on ozone decomposition at pH 10.7–12.8. The ozone concentration was about 10^{-4} mol L^{-1} and 1×10^{-5} to 4×10^{-3} mol L^{-1} carbonate at an ionic strength of 0.5 mol L^{-1}. The temporal dependence of the absorption at 260, 430, and 600 nm was monitored and fit to a complex mechanism.[31] Back to Table

A14. **OH + O_2.** A Gibbs energy change of +47 kJ mol^{-1} was calculated for this reaction at the B3LYP/LACV3P** level of theory, with solvent interactions calculated using Jaguar's Poisson-Boltzmann solver.[29] That, together with kinetic and acidity information on OH and HO_3, leads to this upper limit. HO_3 is a very strong acid, with p$K_a = -2.1$.[29] Back to Table

A15. **OH + H_2O_2/HO_2^-.** From a pulse radiolysis study following product formation at 250–270 nm (O_2^-) over 287–433 K at pH 7.8.[12] (E_a = 14.0 kJ mol^{-1}) Several other studies at room temperature agree with the 298 K value (2.7×10^7 L mol^{-1} s^{-1}). Yu recommends $(3.2 \pm 1.5) \times 10^7$.[49] From the pH dependence over the range

6.8–13.8, the rate constant for the reaction with HO_2^- was derived. Other published values are in basic agreement.[35] Back to Table

A16. **OH + HO_2.** From a pulse radiolysis study in 0.01 M $HClO_4$. The rate constant is about twice as high at 200 °C.[14] Back to Table

A17. **OH + O_2^-.** From a pulse radiolysis study of solutions containing 0.3 MPa O_2 and 0–10 MPa H_2 over 293–558 K.[11] (E_a = 17.6 kJ mol^{-1}) Back to Table

A18. **HO_2 + HO_2.** From a pulse radiolysis study of solutions containing 0.2 MPa O_2 and 10 MPa H_2 over 293–373 K.[10] (E_a = 20.6 kJ mol^{-1}) A recommended value at 298 K of 8.3×10^5 L mol^{-1} s^{-1} in good agreement.[5] Back to Table

A19. **O_2^- + HO_2/O_2^-.** Recommended value from the evaluation of Bielski, et al. based on the pH dependence of the measured decay rate.[5] Back to Table

A20. **H_2O_2 + HO_2/O_2^-.** Based on the observed O_2 yield in the gamma radiolysis of H_2O_2 solutions over the pH ranges 7–9.9 and 0.5–3.5.[48] Other studies report both higher and lower rate constants.[35] Back to Table

A21. **OH + HSO_4^-/H_2SO_4.** From the pulse radiolysis of concentrated sulfuric acid solutions, 0.4 to 7.5 mol L^{-1}, following the build-up of the product SO_4^- at 450 nm.[23] Back to Table

A22. **OH + NO_2^-.** There have been several pulse radiolysis and flash photolysis determinations of this reaction, with results ranging from 0.6 to 1.4×10^{10} L mol^{-1} s^{-1}. The listed value represents this range. Due to the very weak optical absorption by NO_2, the studies were usually competition kinetics or, in one case, the analysis of a complex system involving the formation of peroxynitrate.[35] Back to Table

A23. **OH + HONO.** The rate constant for this reaction is assumed to be equal to that for the gas-phase reaction. Note that this is the case for the gas and aqueous phase reactions of OH with $HONO_2$. Back to Table

A24. **OH + HNO_3.** From a pulse radiolysis study of the behavior of the optical absorbance due to NO_3 as the concentration of HNO_3 was varied at a total ionic strength of 1 mol L^{-1} and pH values from 0 to 1. The reverse rate constant of $(3 \pm 1) \times 10^2$ L mol^{-1} s^{-1} was also derived.[32] These values lead to a reduction potential for the NO_3 radical of 2.58 V, significantly higher than the recommended value of 2.466 ± 0.019 V.[1] Back to Table

A25. **NO_3 + OH^-.** From a study of the flash photolysis of persulfate solutions containing 0.1 mol L^{-1} nitrate and 1.9–10 µmol L^{-1} OH^-.[17] Decay of the NO_3 absorption at 633 nm was followed. Back to Table

A26. **H + N_2O.** Derived from a pulse-radiolysis study on N_2O-saturated, 0.1 mol L^{-1} HCl solutions at room temperature.[24] The decay of the Cl_2^- absorbance at 340 nm was monitored and fit to a multi-step mechanism. Back to Table

A27. **H +H_2O.** The Gibbs energy change for this reaction was derived from thermodynamic arguments utilizing a non-symmetric standard state convention. The resulting equilibrium constant was then combined with experimental values of the reverse reaction.[46] See also the original paper by these authors[45] and the comment on that article by Bartels.[2] Back to Table

A28. **H + O_2.** The value given is an average of a large number of experimental determinations.[27] Back to Table

A29. **H + H_2O_2.** Recommendation based on averaging selected values.[27] Note that the reaction probably involves H-atom addition followed by dissociation of the adduct. A rate constant of 1.4×10^9 L mol^{-1} s^{-1} was recommended for H + HO_2^-. Back to Table

A30. **OH + OH.** Recommended value from an extensive review of the literature.[8] Back to Table

A31. **SO_4^- + OH^-.** The value listed is the average of five investigations reporting results for this reaction. The range is $(1.4–8.3) \times 10^7$ L mol^{-1} s^{-1}.[35] Back to Table

6.2.2 References

(1) Armstrong, D. A.; Huie, R. E.; Koppenol, W. H.; Lymar, S. V.; Merenyi, G.; Neta, P.; Ruscic, B.; Stanbury, D. M.; Steenken, S.; Wardman, P. Standard electrode potentials involving radicals

in aqueous solution: inorganic radicals (IUPAC Technical Report). *Pure Appl. Chem.* **2015**, *87*, 1139-1150, doi:10.1515/pac-2014-0502.

(2) Bartels, D. M. Comment on the possible role of the reaction $H^{\bullet} + H_2O \rightarrow H_2 + {}^{\bullet}OH$ in the radiolysis of water at high temperatures. *Rad. Phys. Chem.* **2009**, *78*, 191-194, doi:10.1016/j.radphyschem.2008.09.005.

(3) Behar, D.; Czapski, G.; Duchovny, I. Carbonate radical in flash photolysis and pulse radiolysis of aqueous carbonate solutions. *J. Phys. Chem.* **1970**, *74*, 2206-2210, doi:10.1021/j100909a029.

(4) Biard, P.-F.; Dang, T. T.; Couvert, A. Determination by reactive absorption of the rate constant of the ozone reaction with the hydroperoxide anion. *Chem. Eng. Res. Des.* **2017**, 62-71, doi:10.1016/j.cherd.2017.09.004.

(5) Bielski, B. H. J.; Cabelli, D. E.; Arudi, R. L.; Ross, A. B. Reactivity of HO_2/O_2^- radicals in aqueous solution. *J. Phys. Chem. Ref. Data* **1985**, *14*, 1041-1100, doi:10.1063/1.555739.

(6) Buhler, R.; Staehelin, J.; Hoigne, J. Ozone decomposition in water studied by pulse radiolysis 1. HO_2/O_2^- and HO_3/O_3^- as intermediates - Correction. *J. Phys. Chem.* **1984**, *88*, 5450-5450, doi:10.1021/j150666a600.

(7) Bühler, R. E.; Staehelin, J.; Hoigné, J. Ozone decomposition in water studied by pulse radiolysis. 1. HO_2/O_2^- and HO_3/O_3^- as intermediates. *J. Phys. Chem.* **1984**, *88*, 2560-2564, doi:10.1021/j150656a026.

(8) Buxton, G. V.; Greenstock, C. L.; Helman, W. P.; Ross, A. B. Critical review of rate constants for reactions of hydrated electrons, hydrogen atoms and hydroxyl radicals (•OH/•O–) in aqueous solution. *J. Phys. Chem. Ref. Data* **1988**, *17*, 1-21, doi:10.1063/1.555805.

(9) Buxton, G. V.; Wood, N. D.; Dyster, S. Ionisation constants of ${}^{\bullet}OH$ and $HO_2^{\bullet}$ in aqueous solution up to 200 ºC. A pulse radiolysis study. *J. Chem. Soc. Faraday Trans. I* **1988**, *84*, 1113-1121, doi:10.1039/F19888401113.

(10) Christensen, H.; Sehested, K. HO_2 and O_2^- radicals at elevated temperatures. *J. Phys. Chem.* **1988**, *92*, 3007-3011, doi:10.1021/j100321a060.

(11) Christensen, H.; Sehested, K.; Bjergbakke, E. Radiolysis of reactor water: Reactions of hydroxyl radicals with superxide (O_2^-). *Water Chem. Nucl. React. Syst.* **1989**, *5*, 141-144.

(12) Christensen, H.; Sehested, K.; Corfitzen, H. Reactions of hydroxyl radicals with hydrogen peroxide at ambient and elevated temperatures. *J. Phys. Chem.* **1982**, *86*, 1588-1590, doi:10.1021/j100206a023.

(13) Egorova, G. V.; Voblikova, V. A.; Sabitova, L. V.; Tkachenko, I. S.; Tkachenko, S. N.; Lunin, V. V. Ozone solubility in water. *Moscow University Chemistry Bulletin* **2015**, *70*, 207-210, doi:10.3103/s0027131415050053.

(14) Elliot, A. J.; Buxton, G. V. Temperature dependence of the reactions $OH + O_2^-$ and $OH + HO_2$ in water up to 200 C. *J. Chem. Soc. Faraday Trans.* **1992**, *88*, 2465-2470, doi:10.1039/FT9928802465.

(15) Elliot, A. J.; McCracken, D. R. Effect of temperature on O^- reactions and equilibria: A pulse radiolysis study. *Int. J. Radiat. Appl. Inst. Part C. Radiat. Phys. Chem.* **1989**, *33*, 69-74.

(16) Eriksen, T. E.; Lind, J.; Merenyi, G. On the acid-base equilibrium of the carbonate radical. *Radiat. Phys. Chem. (1977)* **1985**, *26*, 197-199, doi:10.1016/0146-5724(85)90185-2.

(17) Exner, M.; Herrmann, H.; Zellner, R. Laser-based studies of reactions of the nitrate radical in aqueous solution. *Ber. Bunsenges. Phys. Chem.* **1992**, *96*, 470-477, doi:10.1002/bbpc.19920960347.

(18) Fábián, I. Reactive intermediates in aqueous ozone decomposition: A mechanistic approach. *Pure Appl. Chem.* **2006**, *78*, 1559-1570, doi:10.1351/pac200678081559.

(19) Ferre-Aracil, J.; Cardona, S. C.; Navarro-Laboulais, J. Kinetic study of ozone decay in homogeneous phosphate-buffered medium. *Ozone: Sci. Eng.* **2015**, *37*, 330-342, doi:10.1080/01919512.2014.998756.

(20) Fischbacher, A.; von Sonntag, J.; von Sonntag, C.; Schmidt, T. C. The •OH radical yield in the $H_2O_2 + O_3$ (peroxone) reaction. *Environ. Sci. Technol.* **2013**, *47*, 9959-9964, doi:10.1021/es402305r.

(21) Forni, L.; Bahnemann, D.; Hart, E. J. Mechanism of the hydroxide ion initated decomposition of ozone in aqueous solution. *J. Phys. Chem.* **1982**, *86*, 255-259, doi:10.1021/j100391a025.

(22) Gardoni, D.; Vailati, A.; Canziani, R. Decay of ozone in water: A review. *Ozone Sci. Eng.* **2012**, *34*, 233-242, doi:10.1080/01919512.2012.686354.
(23) Jiang, P. Y.; Katsumura, Y.; Nagaishi, R.; Domae, M.; Ishikawa, K.; Ishigure, K.; Yoshida, Y. Pulse radiolysis studies of concentrated sulfuric acid solutions. Formation mechanism, yield and reactivity of sulfate radicals. *J. Chem. Soc. Faraday Trans.* **1992**, *88*, 1653-1658, doi:10.1039/FT9928801653.
(24) Kazmierczak, L.; Swiatla-Wojcik, D.; Szala-Bilnik, J.; Wolszczak, M. Rate of reaction of the hydrogen atom with nitrous oxide in ambient water. *Radiat. Phys. Chem.* **2016**, *125*, 156-159, doi:10.1016/j.radphyschem.2016.04.007.
(25) Lesko, T. M.; Colussi, A. J.; Hoffmann, M. J. Hydrogen isotope effects and mechanism of aqueous ozone and peroxone decomposition. *J. Am. Chem. Soc.* **2004**, *126*, 4432-4436, doi:10.1021/ja038907v.
(26) Levanov, A. V.; Isaykina, O. Y.; Amirova, N. K.; Antipenko, E. E.; Lunin, V. V. Photochemical oxidation of chloride ion by ozone in acid aqueous solution. *Environ. Sci. Pollut. Res.* **2015**, *22*, 16554-16569, doi:10.1007/s11356-015-4832-9.
(27) Madden, K. P.; Mezyk, S. P. Critical review of aqueous solution reaction rate constants for hydrogen atoms. *J. Phys. Chem. Ref. Data* **2011**, *40*, 023103, doi:10.1063/1.3578343.
(28) Merényi, G.; Lind, J.; Naumov, S.; von Sonntag, C. The reaction of ozone with the hydroxide ion: mechanistic considerations based on thermokinetic and quantum chemical calculations and the role of HO_4^- in superoxide dismutation. *Chem. Eur. J.* **2010**, *16*, 1372-1377, doi:10.1002/chem.200802539.
(29) Naumov, S.; Von Sonntag, C. The reaction of •OH with O_2, the decay of O_3^- and the pKa of HO_3^- interrelated questions in aqueous free-radical chemistry. *J. Phys. Org. Chem.* **2010**.
(30) Naumov, S.; von Sonntag, C. Standard Gibbs free energies of reactions of ozone with free radicals in aqueous solution: Quantum-chemical calculations. *Environ. Sci. Technol.* **2011**, *45*, 9195-9204, doi:10.1021/es2018658.
(31) Nemes, A.; Fábián, I.; van Eldik, R. Kinetics and mechanism of the carbonate ion inhibited aqueous ozone decomposition. *J. Phys. Chem. A* **2000**, *104*, 7995-8000, doi:10.1021/jp000972t.
(32) Poskrebyshev, G. A.; Neta, P.; Huie, R. E. Equilibrium constant of the reaction -OH + HNO_3 → H_2O^+ NO_3 in aqueous solution *J. Geophys. Res.* **2001**, *106*, 4995-5004, doi:10.1029/2000JD900702.
(33) Razumovskii, S. D.; Grinevich, T. V.; Korovina, G. V. Reactivity of hydrogen peroxide with respect to ozone. *Russ. J. Phys. Chem.* **2011**, *5*, 797-799, doi:10.1134/S1990793111090211.
(34) Reisz, E.; Schmidt, W.; Schuchmann, H. P.; von Sonntag, C. Photolysis of ozone in aqueous solutions in the presence of tertiary butanol. *Environ. Sci. Technol.* **2003**, *37*, 1941-1948, doi:10.1021/es0113100.
(35) Ross, A. B.; Mallard, W. G.; Hellman, W. P.; Bielski, B. H. J.; Buxton, G. V.; Cabelli, D. E.; Greenstock, C. L.; Huie, R. E.; Neta, P. *NDRL/NIST Solution Kinetics Database*, 1997; Vol. 40.
(36) Sehested, K.; Corfitzen, H.; Holcman, J.; Fisher, C. H.; Hart, E. J. The primary reaction in the decomposition of ozone in acidic aqueous solutions. *Environ. Sci. Technol.* **1991**, *25*, 1589-1596, doi:10.1021/es00021a010.
(37) Sehested, K.; Corfitzen, H.; Holcman, J.; Hart, E. J. Decomposition of ozone in aqueous acetic acid solutions (pH 0-4). *J. Phys. Chem.* **1992**, *96*, 1005-1009, doi:10.1021/j100181a084.
(38) Sehested, K.; Corfitzen, H.; Holcman, J.; Hart, E. J. On the mechanism of the decomposition of acidic O_3 solutions, thermally or H_2O_2-initiated. *J. Phys. Chem. A* **1998**, *102*, 2667-2672, doi:10.1021/jp9721053.
(39) Sehested, K.; Holcman, J.; Bjergbakke, E.; Hart, E. J. Formation of ozone in the reaction of OH with O_3^- and the decay of the ozonide ion radical at pH 10-13 *J. Phys. Chem.* **1984**, *88*, 269-273, doi:10.1021/j150646a021.
(40) Sehested, K.; Holcman, J.; Bjergbakke, E.; Hart, E. J. A pulse radiolytic study of the reaction OH + O_3 in aqueous medium. *J. Phys. Chem.* **1984**, *88*, 4144-4147, doi:10.1021/j150662a058.
(41) Sehested, K.; Holcman, J.; Hart, E. J. Rate constants and products of the reactions of e_{aq}^-, O_2^-, and H with ozone in aqueous solution. *J. Phys. Chem.* **1983**, *87*, 1951-1954, doi:10.1021/j100234a024.

(42) Sein, M. M.; Golloch, A.; Schmidt, T. C.; Sonntag, C. v. No marked kinetic isotope effect in the peroxone ($H_2O_2/D_2O_2 + O_3$) reaction: mechanistic consequences. *ChemPhysChem* **2007**, *8*, 2065-2067, doi:10.1002/cphc.200700493.
(43) Sotelo, J. L.; Beltrán, F. J.; Benítez, F. J.; Beltrán-Heredia, J. Ozone decomposition in water: Kinetic study. *Ind. Eng. Chem. Res.* **1987**, *26*, 39-43, doi:10.1021/ie00061a008.
(44) Staehelin, J.; Hoigné, J. Decomposition of ozone in water: Rate of initiation by hydroxide ions and hydrogen peroxide. *Environ. Sci. Technol.* **1982**, *16*, 676-681, doi:10.1021/es00104a009.
(45) Swiatla-Wojcik, D.; Buxton, G. V. On the possible role of the reaction $H + H_2O \rightarrow H_2 + OH$ in the radiolysis of water at high temperatures. *Rad. Phys. Chem.* **2005**, *74*, 210-219, doi:10.1016/j.radphyschem.2005.04.014.
(46) Swiatla-Wojcik, D.; Buxton, G. V. Reply to comment on the possible role of the reaction $H + H_2O \rightarrow H_2 + OH$ in the radiolysis of water at high temperatures. *Rad. Phys. Chem.* **2010**, *79*, 52-56, doi:10.1016/j.radphyschem.2009.07.024.
(47) Tomiyasu, H.; Fukutomi, H.; Gordon, G. Kinetics and mechanism of ozone decomposition in basic aqueous solution. *Inorg. Chem.* **1985**, *24*, 2962-2966, doi:10.1021/ic00213a018.
(48) Weinstein, J.; Bielski, B. H. J. Kinetics of the interaction of HO_2 and O_2^- radicals with hydrogen peroxide. The Haber-Weiss reaction. *J. Am. Chem. Soc.* **1979**, *101*, 58-62, doi:10.1021/ja00495a010.
(49) Yu, X. Y. Critical evaluation of rate constants and equilibrium constants of hydrogen peroxide photolysis in acidic aqueous solutions containing chloride ions. *J. Phys. Chem. Ref. Data* **2004**, *33*, 747-763, doi:10.1063/1.1695414.

6.3 Reactions of Oxygen Species with Halogen Species

Reaction	k (L mol^{-1} s^{-1}) *	Note
$O_3 + Cl^- \rightarrow ClO^- + O_2$	$1.57 \times 10^{11} \exp(-9470/T)$	B1
$O_3 + Cl^- + H^+ \leftrightarrow HO_3Cl$	$4.41 \times 10^8 \exp(-6580/T)$ L^2 mol^{-1}s^{-1}	B1
$HO_3Cl \rightarrow HOCl + O_2$	$2.79 \times 10^2 \exp(-2180/T)$ s^{-1}	B1
$O_3 + Cl \rightarrow ClO + O_2$	See Note	B2
$O_3 + Cl_2^- \rightarrow ClO + O_2 + Cl^-$	$(9.0 \pm 0.3) \times 10^7$	B3
$O_3 + Br^- \rightarrow BrO^- + O_2$	$2.11 \times 10^8 \exp(-4050$ kJ/RT)	B4
$O_3 + I^- \rightarrow IO^- + O_2$	$(1.2 \pm 0.1) \times 10^9$	B5
$O_3 + ClO^- \rightarrow$ products	$1.7 \times 10^{12} \exp(-6860$ kJ/RT)	B6
$O_3 + BrO^- \rightarrow$ products	$2.7 \times 10^{13} \exp(-7220$ kJ/RT)	B7
$O_3 + HOI \rightarrow$ products	$(3.6 \pm 1.0) \times 10^4$	B8
$O_3 + IO^- \rightarrow$ products	$(1.6 \pm 0.5) \times 10^6$	B8
$O_3 + ClO \rightarrow OClO + O_2$ $\rightarrow Cl + 2O_2$	See Note	B9
$O_3 + BrO \rightarrow OBrO + O_2$ $\rightarrow BrOO + O_2$	See Note	B10
$BrOO \rightarrow Br + O_2$	See Note	B11
$O_3 + OClO^- \rightarrow O_3^- + OClO$	$2.9 \times 10^{12} \exp(-3790/T)$	B12
$O_3 + OBrO^- \rightarrow O_3^- + OBrO$	1.0 $10^{15} \exp(-6900/T)$	B12
$O_3 + ClO_2 \rightarrow O_2 + ClO_3$	1.3×10^3	B13
$O_3 + OBrO \rightarrow O_2 + BrO_3$	See Note	B14
$O_3 + ClO_3^- \rightarrow$ products	See Note	B15
$OH + Cl^- \rightarrow ClOH^-$	$(4.3 \pm 0.4) \times 10^9$	B16
$ClOH^- \rightarrow OH + Cl^-$	$(6.1 \pm 0.8) \times 10^9$ s^{-1}	B16
$ClOH^- + H^+ \rightarrow Cl + H_2O$	$(2.4 \pm 0.4) \times 10^{10}$	B17
$Cl + H_2O \rightarrow ClOH^- + H^+$	$(1.8 \pm 0.6) \times 10^5$ s^{-1}	B17
$ClOH^- + Cl^- \rightarrow OH^- + Cl_2^-$	1×10^4	B18
$OH + Br^- \rightarrow BrOH^-$	8.7×10^9	B19
$BrOH^- \rightarrow Br^- + OH$	3×10^7 s^{-1}	B19
$BrOH^- \rightarrow Br + OH^-$	4.5×10^6 s^{-1}	B19
$Br + OH^- \rightarrow BrOH^-$	1.3×10^{10}	B19
$BrOH^- + H^+ \rightarrow Br + H_2O$	4.4×10^{10}	B19
$BrOH^- + Br^- \rightarrow Br_2^- + OH^-$	1.9×10^8	B19
$OH + I^- \rightarrow IOH^-$	$2.1 \times 10^{12} \exp(-1440/T)$	B20
$IOH^- \rightarrow I + OH^-$	3.5×10^7 s^{-1}	B21
$OH^- + Cl_2 \rightarrow HOCl + Cl^-$	$1 \times 10^{17} \exp(-5610/T)$	B22
$OH + HOCl \rightarrow H_2O + ClO$	2.3×10^8	B23
$OH + ClO^- + H^+ \rightarrow H_2O + ClO$	2.7×10^9	B24
$OH + HOBr \rightarrow H_2O + BrO$	2.0×10^9	B25
$OH + BrO^- + H^+ \rightarrow H_2O + BrO$	4.2×10^9	B26
$OH + HOI \rightarrow H_2O + IO$	7×10^9	B27
$OH + OClO \rightarrow H^+ + ClO_3^-$	3.75×10^9	B28
$OH + OClO^- + H^+ \rightarrow H_2O + OClO$	7.0×10^9	B29
$O^- + IO^- + H^+ \rightarrow HO^- + IO$	1.7×10^9	B30
$O_2^- + Cl^- \rightarrow$ products	$<1.4 \times 10^2$	B31
$O_2^- + HOCl \rightarrow O_2 + OH + Cl^-$	7.5×10^6	B32
$O_2^- + HOBr \rightarrow O_2 + OH^- + Br$	3.5×10^9	B33
$O_2^- + BrO^- + H^+ \rightarrow O_2 + OH^- + Br$	$<2 \times 10^8$	B33
$O_2^- + HOI \rightarrow O_2 + OH^- + I$	$<1 \times 10^7$	B34
$O_2^- + IO^- + H^+ \rightarrow O_2 + OH^- + I$	$<5 \times 10^5$	B34

Reaction			k (L mol^{-1} s^{-1}) *	Note
$HO_2 + Cl_2$	→	$Cl_2^- + O_2 + H^+$	1×10^9	B35
$O_2^- + Br_2$	→	$Br_2^- + O_2$	5×10^9	B36
$HO_2 + Br_2$	→	$Br_2^- + O_2 + H^+$	1.3×10^8	B36
$O_2^- + Br_3^-$	→	$Br_2^- + Br^- + O_2$	1.5×10^9	B36
$HO_2 + I^-$	→	products	<100	B37
$O_2^- + I_2$	→	$I_2^- + O_2$	$1.6 \times 10^{12} \exp(-1660/T)$	B38
$HO_2 + I_2$	→	$I_2^- + O_2 + H^+$	1.8×10^7	B38
$O_2^- + I_3^-$	→	$I_2^- + I^- + O_2$	$1.0 \times 10^{12} \exp(-2470/T)$	B38
$H_2O_2 + Cl^-$	→	$H_2O + ClO^-$	$2.18 \times 10^{10} \exp(-11{,}870/T)$	B39
$H_2O_2 + Cl^- + H^+$	→	$H_2O + HOCl$	$7.91 \times 10^{10} \exp(-10{,}440/T)$	B39
$H_2O_2 + Br^-$	→	$H_2O + BrO^-$	$6.63 \times 10^{10} \exp(-10620/T)$	B39
$H_2O_2 + Br^- + H^+$	→	$H_2O + HOBr$	$2.42 \times 10^{10} \exp(-8410/T)$	B39
$H_2O_2 + I^-$	→	$H_2O + IO^-$	$4.91 \times 10^9 \exp(-6750/T)$	B40
$H_2O_2 + I^- + H^+$	→	$H_2O + HOI$	$4.58 \times 10^8 \exp(-5270/T)$	B40
$HO_2^- + HOCl$	→	$H_2O + Cl^- + O_2(^1\Delta_g)$	4.4×10^7	B41
$HO_2^- + HOBr$	→	$H_2O + Br^- + O_2(^1\Delta_g)$	$(7.6 \pm 1.3) \times 10^8$	B42
$H_2O_2 + IO^-$	→	$H_2O + I^- + O_2$	5.8×10^7	B43
$H_2O_2 + I_2OH^-$	→	$H_2O + H^+ + 2I^- + O_2$	1.3×10^4	B43
$O_2 + I$	→	products	$<10^7$	B44
$HO_2^- + OClO$	→	$H^+ + O_2^- + OClO^-$	$(6.5 \pm 2.0) \times 10^4$	B45
$H_2O_2 + OClO$	→	products	<0.1	B45
$OH + I_2$	→	$I + HOI$	$(9.5 \pm 1.0) \times 10^9$	B46
$O_2(^1\Delta_g) + Cl^-$	→	products	1×10^3	B47
$O_2(^1\Delta_g) + I^-$	→	IO_2^-	$(8.7 \pm 0.2) \times 10^5$	B48

* Unless units noted otherwise

6.3.1 Notes: Reactions of Oxygen Species with Halogen Species

B1. **$O_3 + Cl^-$.** The reaction between ozone and chloride was investigated using a bubble-column reactor over the temperature range 7 to 60 °C and with HCl concentrations ranging from 0.01 to 1 mol L^{-1}, typically at a total ionic strength of 1 mol L^{-1}.[48] The reaction was followed by monitoring the concentration of Cl_2 at the reactor outlet and the O_3 concentration in the reaction solution. The observed rate showed a significant dependence on proton concentration, leading to the proposed mechanism and the rate and equilibrium constants. Values were reported at 7, 24, 41.5, and 60 °C, but for the second and third steps, these rates were only upper and lower limits, respectively. The fits to these values were not presented in this paper, but are taken from a subsequent paper from the same group.[43] The results are in good agreement with an earlier report from the same group,[52] an upper limit of 0.018 L mol^{-1} s^{-1} for the uncatalyzed reaction,[35] and measurements made at 0 and 9.5 °C over a somewhat lower range of acid concentrations.[72]

The authors reported a small positive effect of ionic strength when going from 0.5 to 3 mol L^{-1} using $NaClO_4$ or KNO_3, but a slight negative effect when using NaCl. A positive ionic strength effect may, at these high salt concentrations, simply reflect an impurity effect. There is also some evidence for a slow reaction between ozone and nitrate.[61]

Since the earliest work, this reaction has been assumed to involve oxygen-atom transfer to generate hypochlorite or chlorite, HClO/ClO^- and molecular oxygen, as shown in the Table. An alternate mechanism, however, has been proposed in which an electron transfer takes place:[63]

$$O_3 + Cl^- \rightarrow O_3^- + Cl$$

followed by

$$Cl + O_3 \rightarrow ClO + O_2$$

$$ClO + O_3 \rightarrow Cl + 2O_2$$

This mechanism was proposed to account for the lack of spectral evidence for the formation of ClO^- and some spectral indication of H_2O_2. Further, the authors argued that a gravimetric analysis of the products was not consistent with a mass increase that should be associated with the formation of chlorine oxides, such as sodium chlorite. The possibility that the reaction might proceed by electron transfer is quite important since the reaction would generate two free radicals, OH (from the decomposition of O_3^-) and Cl. The arguments presented in this paper are not particularly compelling, however, and have been thoroughly critiqued by Levanov et al.[42] The earlier observation that chlorine gas is generated in the reaction,[48] means that the residue of the reaction would not be expected to weigh much more than the starting materials. It is also not surprising that no absorption due to ClO^- is observed, since the rate constant for the reaction of this species with ozone is much faster than the reaction of chloride with ozone, so its steady-state concentration would be low. The expected final product, ClO_3^-, has an absorption maximum at 197 nm and is unlikely to be observed in the presence of the other reactants. Beyond this, Levanov, et al. have analyzed this reaction thermodynamically and concluded that the electron-transfer mechanism would be highly endothermic, in agreement with the well-known gas-phase electron affinities of O_3 and Cl. In a companion paper, Levanov et al.[43] have summarized and expanded on the arguments in favor of an oxygen-atom transfer mechanism, concluding that the reaction likely goes through an adduct to circumvent spin restrictions. In an investigation of the stoichiometry of the reaction, Levanov et al.[45] found that, in a 1 mol L^{-1} Cl^- solution at low pH, the consumption of one ozone molecule results in the formation of one chlorine molecule. This is consistent with the atom-transfer mechanism, since the product hypochlorous acid is driven to chlorine under those conditions.

In alkali solutions, the main product of the reaction is chlorite, $OClO^-$, formed from the subsequent reaction of ClO^- with O_3.[44] The effective rate constant for the production of chlorite is 7.7×10^{-4} L mol^{-1} s^{-1} (pH 8.4–9.6 at 20 °C).

The reaction of O_3 with Cl^- in acid solutions of increasing concentrations has been investigated and shown to lead to increasing evolution of Cl_2.[46,47] In the same study, a significant effect of added metal ion catalysts was observed.

Note that ClO_4^- is produced in very small yields from the overall reaction system.[38,62] This is probably due to subsequent reactions of oxyradicals with ozone and other secondary reactions. Back to Table

B2. **O_3 + Cl.** No rate constant has been reported for this reaction, but a calculation at the B3LYP/LACV3P** level of theory, with solvent interactions calculated using Jaguar's Poisson-Boltzmann solver, led to a free energy change of $\Delta G° = -204$ kJ mol^{-1}.[59] There was no evidence for the formation of an adduct as a minimum on the potential energy surface. Back to Table

B3. **O_3 + Cl_2^-.** Rate constant obtained from decay kinetics at 340 nm in solutions containing NaCl, $HClO_4$ and ozone following pulse radiolysis.[6] The products were not determined, but were assumed to be ClO + O_2 + Cl^-. A calculation at the B3LYP/LACV3P** level of theory, with solvent interactions calculated using Jaguar's Poisson-Boltzmann solver, led to a free energy change of $\Delta G° = -133$ kJ mol^{-1}.[59] There was no evidence for the formation of an adduct as a minimum on the potential energy surface. Back to Table

B4. **O_3 + Br^-.** Kinetics obtained from a stopped-flow spectrophotometric study following both the rate of loss of O_3 and the rate of formation of Br_3^- over T = 1–25 ºC.[50] (E_a = 33.7 kJ mol^{-1} presented in paper) The rate constant was found to be pH dependent and was resolved through a mechanism involving the formation of an intermediate $BrOOO^-$ and its subsequent reaction with either H^+ or H_2O to give O_2 and HOBr. Quoted value in Table is for the H^+-independent path at μ = 1.0 mol L^{-1}. The H^+-dependent pathway gives $k = 3.27 \times 10^{11}$ exp(-45.6 kJ/RT) L mol^{-1} s^{-1}. Arrhenius parameters were calculated by the reviewer and agree with the activation enthalpies presented in the paper. In earlier work, activation energies of 37 kJ mol^{-1} and 24 kJ mol^{-1} were reported by Haag and Hoigné (1–30 ºC) and by Haruta and Takeyama (5 –30 ºC), respectively.[29,32] The energetics of the reaction have been calculated at the B3LYP/6-311+G(d) level of theory, with solvent interactions calculated using Jaguar's Poisson-Boltzmann solver, supporting adduct formation and subsequent decay into BrO^- and $O_2(^1\Delta_g)$.[58] The formation of $BrOOO^-$ at a water surface was confirmed in an X-ray photoelectron experiment.[3] Computational studies also showed that the singlet pre-complex is stabilized by water.[3] Back to Table

B5. **O_3 + I^-.** A pulsed-accelerated-flow spectrophotometric study at μ = 0.1 M and 25 ± 0.1 ºC following the loss of O_3 at 260 nm was used to obtain the kinetics of this reaction. Adduct formation prior to O-atom transfer is proposed,[50] which is supported by a computational study which revealed three conformers of $IOOO^-$.[26] An investigation of the uptake kinetics of O_3 into aqueous solutions of I^- led to estimated rate constants in the range 3.2×10^8 to 2.4×10^9 L mol^{-1} s^{-1} between 275 and 293 K.[54] High concentrations (0.5 to 3 mol L^{-1}) were employed, so activities were used in calculating the rate constants. A fit to the data gave $k = 1.4 \times 10^{22}$ exp(-73.08 kJ/RT) L mol^{-1} s^{-1}. Back to Table

B6. **O_3 + ClO^-.** The decay of O_3 was followed at 258 nm over the temperature range 11–34 C.[30] (E_a = 57 ± 6 kJ mol^{-1} presented in paper) Product measurements were carried out by ion chromatography, iodometric titration, and uv absorption. The overall rate constant corresponds to two basic reactions:

$$ClO^- + O_3 \rightarrow 2O_2 + Cl^- \qquad k = 1.1 \times 10^2 \text{ L mol}^{-1} \text{ s}^{-1} \text{ (25 ºC)}$$

$$ClO^- + O_3 \rightarrow O_2 + OClO^- \qquad k = 3.0 \times 10^1 \text{ L mol}^{-1} \text{ s}^{-1} \text{ (25 ºC)}$$

followed by

$$OClO^- + O_3 \rightarrow ClO_3^- + O_2.$$

The reaction of O_3 with HOCl was too slow to measure. Back to Table

B7. **O_3 + BrO^-.** The decay of O_3 was followed at 258 nm over the temperature range 10–30 ºC.[29] (E_a = 60 ± 10 kJ mol^{-1} presented in paper) Product analysis was carried by a bromide-selective electrode, iodometric titration, UV absorption, and by GC analysis after solvent extraction. This overall rate constant corresponds to two basic reactions:

$$BrO^- + O_3 \rightarrow 2O_2 + Br^- \qquad k = 3.3 \times 10^2 \text{ L mol}^{-1} \text{ s}^{-1} \text{ (20 ºC)}$$

$$BrO^- + O_3 \rightarrow O_2 + OBrO^- \qquad k = 1.0 \times 10^2 \text{ L mol}^{-1} \text{ s}^{-1} \text{ (20 ºC)}$$

followed by

$$BrO_2^- + O_3 \rightarrow BrO_3^- + O_2 \qquad k > 10^5$$

The reaction of O_3 with HOBr was too slow to measure. The energetics of the reaction, including possible adduct formation, have been calculated at the B3LYP/6-311+G(d) level of theory, but suffered from spin contamination.[58] Back to Table

B8. **O_3 + IO^-/HOI.** The kinetics of oxidation of HOI/IO^- was determined over pH 6.0–9.7 by measuring O_3 depletion in a flow apparatus at 25 ± 2 ºC.[5] Back to Table

B9. **O_3 + ClO.** There have been no reported experimental measurements on this reaction in the aqueous phase. A calculation at the B3LYP/LACV3P** level of theory, with solvent interactions calculated using Jaguar's Poisson-Boltzmann solver, led to a free energy change of $\Delta G° = -119$ kJ mol^{-1} for the path leading to OClO and $\Delta G° = -229$ kJ mol^{-1} for the path to ClOO.[59] The species that was observed as a minimum on the potential energy surface had a Cl-OO bond length of 1.888 Å, indicating that ClOO is probably a van der Waals complex with $\Delta G° = +5$ kJ mol^{-1} for dissociation. Back to Table

B10. **O_3 + BrO.** There have been no reported experimental measurements on this reaction in the aqueous phase. A calculation at the B3LYP/LACV3P** level of theory, with interactions between water and the molecules were calculated using Jaguar's Poisson-Boltzmann solver, led to a free energy change of $\Delta G° = -47$ kJ mol^{-1} for the path leading to OBrO and $\Delta G° = -268$ kJ mol^{-1} for the path to BrOO.[59] There was no evidence for the formation of an adduct as a minimum on the potential energy surface. Back to Table

B11. **BrOO →.** There have been no reported experimental measurements on this reaction in the aqueous phase. A calculation at the B3LYP/LACV3P** level of theory, with interactions between water and the molecules were calculated using Jaguar's Poisson-Boltzmann solver, led to a free energy change of $\Delta G° = -11$ kJ mol^{-1}.[59] Back to Table

B12. **O_3 + $OClO^-$/$OBrO^-$.** Kinetics of the reaction were determined by stopped-flow kinetic spectrophotometry, following the loss of O_3 at 260 nm at a pH 6 and an ionic strength of 1 mol L^{-1}.[60] The reported Eyring parameters are $\Delta H^‡ = 29 \pm 2$ kJ mol^{-1} and $\Delta S^‡ = -14.6 \pm 0.7$ J $mol^{-1}K^{-1}$ for chlorite and $\Delta H^‡ = 54.9 \pm 0.8$ kJ mol^{-1} and $\Delta S^‡ = 34 \pm 3$ J $mol^{-1}K^{-1}$ for bromite. The reported rate constants at 298 K for chlorite is $(8.2 \pm 4) \times 10^8$ L mol^{-1} s^{-1} and for bromite, $(8.9 \pm 3) \times 10^4$ L mol^{-1} s^{-1}. The rate constant at room temperature is about twice that reported by Kläning et al.[39] In the chlorite reaction, as the ratio of $[ClO_2^-]/[O_3]$ is increased to greater than 200, the stoichiometry of ClO_2 production becomes 2, supporting a mechanism in which the product O_3^- yields OH, which in turn reacts with ClO_2^- by electron transfer. On the other hand, in the bromite reaction, the products are found to be O_2 and BrO_3^-. Although this could suggest an atom-transfer reaction, the observation of BrO_2 as an intermediate supports an electron-transfer mechanism. Bromate, then, is formed in the disproportionation of BrO_2 which, unlike the comparable ClO_2 reaction, is fast. The electron-transfer mechanism has been supported in a study of the ozonation of bromide in the presence of methanol or *t*–butanol.[25] Back to Table

B13. **O_3 + OClO.** There have been several stopped-flow determinations of this reaction, all in close agreement.[64] The path leading to ClO_3 and O_2 has a calculated free energy of $\Delta G° = +6$ kJ mol^{-1} while that leading to ClO + $2O_2$ has $\Delta G° = -311$ kJ mol^{-1} at the B3LYP/LACV3P** level of theory, with interactions between water and the molecules calculated using Jaguar's Poisson-Boltzmann solver.[59] The generation of ClO_3 in the reaction of O_3 with OClO has been suggested as a possible step in the formation of ClO_4^-.[62] The fact that perchlorate production is a minor process in the oxidation of OClO, however, suggests this is not a very fast reaction. Back to Table

B14. **O_3 + OBrO.** No rate constants have been reported for this reaction. The path leading to BrO_3 and O_2 has a calculated free energy of $\Delta G° = +81$ kJ mol^{-1} while that leading to BrO + $2O_2$ has $\Delta G° = -380$ kJ mol^{-1}.[59] Unlike OClO, OBrO is unstable in water, lessening the chance of other secondary reactions. Back to Table

B15. **O_3 + ClO_3^-.** In a study of the production of perchlorate from the oxidation of chloride, a solution of chlorate was exposed to ozone for seven days. No reaction was observed.[62] Back to Table

B16. **OH + Cl^-.** Derived from a pulse radiolysis determination of the rise in Cl_2^- absorption with pH, with a steady-state analysis.[37] An equilibrium constant of 0.7 ± 0.13 M^{-1} was derived, leading to the rate constant for the reverse reaction. Other direct and indirect measurements are discussed in the review of Yu,[73] who recommends $k_f = (4.2 \pm 0.2) \times 10^9$ L mol^{-1} s^{-1} and $k_r = 6.1 \pm 0.8$ s^{-1} and by Ershov,[24], who also provides a thorough discussion of the effect of ionic strength on the overall system. The binding in the $ClOH^-$ complex has been investigated by *ab intio* quantum mechanical/molecular mechanics calculations for the aqueous

phase at the CCSD(T) level. The calculations indicate a hemibonded (HO−Cl$^-$) structure,[68] contrary to earlier calculations at lower levels of theory[17] and contrary to gas-phase observations,[18] which indicated a hydrogen-bonded structure. This difference is due to the greater solvation stabilization of the hemibonded complex. The energy difference appears small, so that the hydrogen-bonded structure might still be important at the interface, as indicated by earlier studies.[40] Back to Table

B17. **ClOH$^-$ + H$^+$ and Cl + H$_2$O.** Recommendation of Yu based on an analysis of the reported studies.[73] Back to Table

B18. **ClOH$^-$ + Cl$^-$.** Obtained from a pulse radiolysis study of a concentrated chloride solution following product Cl_2^- formation at 340 nm.[28] The rate constant was derived through a complex analysis. Back to Table

B19. **OH + Br$^-$.** Rate constant obtained from a pulse-radiolysis study of N_2O and Ar saturated solutions containing 0.9 to 900 mmol L^{-1} NaBr by Yamashita, et al.[71] The results were improved by using a spur-diffusion model for very short times after the pulse. The kinetic model was optimized and the experimental observations were reproduced with the addition of one reaction to the set commonly employed: the self-reaction of BrOH$^-$ to produce Br_2, with a rate constant of 3.8×10^9 L mol^{-1}s^{-1}. For most of these individual reactions, similar results were reported earlier by Zehavi and Rabani,[74] the largest difference being for OH + Br$^-$, $k = 1.06 \times 10^{10}$ L mol^{-1}s^{-1}. A value for BrOH$^-$ + H$^+$ was not reported by Yamashita, et al. and the listed value is from Zehavi and Rabani. The spectrum of the intermediate BrOH$^-$ has been characterized using picosecond pulse radiolysis, augmented by quantum chemical calculations that suggest the importance of different water-BrOH$^-$ complexes.[41] Back to Table

B20. **OH + I$^-$.** Absolute value at 297 K derived from the growth in optical absorbance at 380 nm following pulse radiolysis.[57] Temperature dependence obtained from rate constants measured relative to OH + HCO_2^- by pulse radiolysis.[21] (E_a = 12 kJ mol^{-1} presented in paper) Back to Table

B21. **IOH$^-$.** Taken from an optical study with modeling of reaction system at 22 ± 2 ºC following pulse radiolysis of an alkaline solution.[57] $k = (1.2 \pm 1.0) \times 10^8$ s^{-1} was reported in an older pulse radiolysis measurement of the formation of I_2^-.[22] Back to Table

B22. **OH$^-$ + Cl$_2$.** Derived from measurements of the uptake of Cl_2 gas into water in a bubble-train flow reactor.[27] Measurements were made from 275 to 303 K and pH 6 to 10.4. Rate constants of 1.3 ± 0.5 (275 K), 6 ± 2 (293 K) and 8 ± 3 (303 K) × 10^8 L mol^{-1} s^{-1} were reported. Back to Table

B23. **OH + HOCl.** OH generated by pulse radiolysis with the rate constant measured in competition with HSO_4^- (1.4×10^8) and HNO_3 (1.1×10^8).[75] A later study by continuous photolysis (primarily 254 nm) of HOCl and competition with OH + nitrobenzene, resulted in $k = 8.5 \times 10^4$ L mol^{-1} s^{-1}.[70] In this latter study, there appeared to be no allowance for any complication from ClO + nitrobenzene, which would tend to lower the apparent rate constant. A density-functional calculation on this reaction at the B3LYP/6-31(2df,p) level of theory, including the implicit polarizable continuum model SMD, has been reported.[55] Values of ΔG^{react} = –87.0 kJ mol^{-1} and ΔG^{act} = 49.4 kJ mol^{-1} were obtained. This high activation energy leads Minakata, et al. to argue in favor of this lower rate constant. But this argument only holds for a simple hydrogen-abstraction reaction. This is more likely to be a proton-transfer assisted electron-transfer reaction. This would make the reaction more similar to the Cl-atom reaction with HOCl, which is even faster and that is generally agreed to be an electron transfer reaction. Back to Table

B24. **OH + ClO$^-$.** Pulse radiolysis at pH 10.3, measured relative to the reaction of OH with CO_3^{2-}.[75] An earlier pulse radiolysis study at pH 11, also relative to CO_3^{2-}, resulted in a rate constant of 8.8×10^9 L mol^{-1} s^{-1} and a rate constant for oxidation by O$^-$ of 2.3×10^8 L mol^{-1} s^{-1}.[13] Back to Table

B25. **OH + HOBr.** Kinetics derived from a flash photolysis study of HOBr solutions.[39] Back to Table

B26. **OH + BrO$^-$.** Rate constant obtained through a pulse radiolysis study of HOBr solutions containing carbonate at pH 11–13,[10] relative to OH + CO_3^{2-} (3.9×10^8 L mol^{-1} s^{-1}).[11] Also assuming p*K*a(OH) = 11.9. The rate constant for O$^-$ + BrO$^-$ was determined to be also 4.2×10^9 L mol^{-1} s^{-1}. Back to Table

B27. **OH + HOI.** Pulse radiolysis of HOI solution containing a borax buffer, with product formation kinetics at 350–550 nm, pH 9.[9] Back to Table

B28. **OH + OClO.** The average of two reported values, both by pulse radiolysis following the absorption of ClO_2, 4.0×10^9 L mol^{-1} s^{-1} [39] and 3.5×10^9 L mol^{-1} s^{-1}.[75] The reaction is probably electron transfer, with subsequent hydration of the ClO_2^+ product to yield ClO_3^-. Back to Table

B29. **OH + OClO$^-$ (+ H$^+$).** An average of three reported values, 6.1×10^9 L mol^{-1} s^{-1} by pulse radiolysis and competition with carbonate;[13] 7.0×10^9 L mol^{-1} s^{-1} following the production of ClO_2 after pulse radiolysis;[23] and 7.9×10^9 L mol^{-1} s^{-1} following ClO_2 after the flash photolysis of H_2O_2.[75] Back to Table

B30. **O$^-$ + IO$^-$.** Rate constant obtained by formation kinetics of IO at 490 nm after pulse radiolysis of HOI solution containing 0.4 mol L^{-1} OH$^-$.[12] Back to Table

B31. **O_2^- + Cl$^-$.** Decay kinetics at 240 nm following the pulse radiolysis of a O_2-saturated formate solution.[51] Back to Table

B32. **O_2^- + HOCl.** Derived from the effect of pH on the decay kinetics at 240 nm in an O_2-saturated formate solution, using pulse radiolysis. K(HOCl) taken as 3.8×10^8 mol L^{-1}.[51] The formation of free OH radicals was confirmed by the hydroxylation of benzoate.[14] The reaction of HO_2 with HOCl is likely to be considerably slower, since it is a much weaker reductant than O_2^-.[2] Back to Table

B33. **O_2^- + HOBr/OBr$^-$.** Derived from a pH dependence study of the pulse radiolysis of bromine solutions containing formate.[66] The reaction of HO_2 with HOBr is likely to be considerably slower, since it is a much weaker reductant than O_2^-. Back to Table

B34. **O_2^- + HOI/OI$^-$.** Derived from a pH dependence study of the pulse radiolysis of iodine solutions containing formate.[66] The reaction of HO_2 with HOI is likely to be considerably slower, since it is a much weaker reductant than O_2^-. Back to Table

B35. **HO_2 + Cl_2.** Obtained from a pulse radiolysis study, following the decay of HO_2 and the formation of Cl_2^- at pH 2.[7] The rate constant for Cl_3^- was taken to be the same. Back to Table

B36. **O_2^-/HO_2 + Br_2.** Kinetics obtained by following the decay of HO_2 and the formation of Br_2^- as a function of pH and Br$^-$ concentration, after pulse radiolysis.[66] Back to Table

B37. **HO_2 + I$^-$.** Limiting value from a pulse radiolysis study cited in a paper primarily about sonolysis. No reaction observed.[31] Back to Table

B38. **O_2^-/HO_2 + I_2.** Pulse radiolysis of an oxygen-saturated solution containing at least 10^{-4} mol L^{-1} iodide at 25 ºC.[66] The pH dependence and dependence on total iodine determined, allowing the determination of rate constants for individual species. For the $HO_2 + I_2^-$ reaction, the equilibrium constant for was also obtained, $K_{eq} = 30$ mol L^{-1}. Kinetics were also measured at 3, 45, and 60 °C, leading to activation energies of 3.3 ± 0.4 kcal mol^{-1} for $O_2^- + I_2$ and 4.9 ± 0.4 kcal mol^{-1} for $O_2^- + I_3^-$. Back to Table

B39. **H_2O_2 + X$^-$.** Rates determined by following the evolution of oxygen from reaction mixtures containing hydrogen peroxide and the halide at temperatures from 0 to 50 °C (40 °C with added acid). Third-order rate constants listed for [H$^+$]-dependent pathway.[56] Activation energies of 23.6 ± 0.57 and 20.74 kcal mol^{-1} were reported for the Cl$^-$ reactions; 21.1 ± 0.45 and 16.7 ± 0.18 kcal mol^{-1} for the Br$^-$ reactions. Back to Table

B40. **H_2O_2 + I$^-$.** Reaction followed by monitoring the formation of triiodide by thiosulfate titration in solutions containing hydrogen peroxide and iodide at temperatures from 0 to 40 °C. Third-order rate also constants listed for a [H$^+$]-dependent pathway.[49] Activation energies of 13.4 ± 0.15 and 10.45 ± 0.12 kcal mol^{-1} were reported for the I$^-$ reactions. Back to Table

B41. **HO_2^- + HOCl.** Reaction monitored at 25 ºC by spectrophotometry and O_2-evolution over the pH range 5–13, building on earlier work by Connick.[16] Measured rate constants reach a peak at about pH 9.5. Arguments based on the nucleophilic character of HO_2^- used to justify the preferred mechanism. The alternate mechanism, $H_2O_2 + OCl^- \rightarrow H_2O + Cl^- + O_2$ would have a derived rate constant of 3.4×10^3.[33] Studies from 8–25 ºC indicate weak temperature dependence with scattered results ($\Delta H^{\#}$ ~3 kcal mol^{-1}). Chemical trapping by 2,5-dimethylfuran indicated an essentially 100% yield of singlet oxygen. See also discussion by Hurst.[36] Maetzke and Jensen and Storch, et al. have investigated the generation of singlet oxygen in the reaction with quantum chemical calculations, finding three possible pathways for the reaction[53] and predict close to a 100% yield.[67]

Castagna, et al.[15] observed OH from the reaction by using spin traps and electron-spin resonance spectroscopy. They ascribed this to the mechanism:

$$ClO^- + H_2O_2 \rightarrow ClO + OH + OH^-$$

This paper did not cite the earlier work by Held et al.,[33] or the various papers indicating singlet oxygen production. Also, no particular care to prevent exogenous transition-metal ions was indicated. This is particularly troublesome since both reagents, HOCl and H_2O_2, participate in Fenton chemistry, leading to OH production. Some arguments were presented based on reduction potentials, but used a very low value of the ClO/ClO- potential (0.64V) vs. the recommended value (1.39 ± 0.03 V).[2] DFT calculations also indicated that the direct reaction was about 10 kcal/mol endothermic. Much stronger evidence is needed to conclude that ClO and OH are generated directly in this reaction. Back to Table

B42. **HO_2^- + HOBr.** Measurements were performed using a stopped-flow spectrometer at 265 and 340 nm over the pH range 6–12 at 25 ºC. Arguments based on the nucleophilic character of HO_2^- were employed to justify the preferred mechanism. The alternate mechanism, $H_2O_2 + OBr^- \rightarrow H_2O + Br^- + O_2$ would have a derived rate constant of $(1.2 \pm 0.2) \times 10^6$.[69] Back to Table

B43. **H_2O_2 + IO^-.** Based on a re-analysis of several studies of the reduction of I_2 by H_2O_2 by Schmitz.[65] Contradictions among the results were resolved by assuming the equilibria for HOI in the presence of I^-:

$$HOI \leftrightarrow IO^- + H^+$$
$$HOI + I^- \leftrightarrow I_2OH^-$$

Both reactions are thought to proceed through an IOOH intermediate, which is assumed to react rapidly with OH^-. There are significant differences between this mechanism and that proposed earlier by Ball and Hnatiw.[4] Back to Table

B44. **O_2 + I.** In a study involving the flash photolysis aryl iodides to generate I atoms, no effect of O_2 was observed on the subsequent reaction of I with I^-.[1] Back to Table

B45. **HO_2^-/H_2O_2 + OClO.** Rate constant obtained from a stopped-flow study over the pH range 5 to 11 and 22–24 ºC, correcting for the stoichiometry of 2.[34] Back to Table

B46. **OH + I_2.** Pulse radiolysis of acidic iodine solutions, following the decrease in iodine absorption at 460 nm and modeling a complex mechanism, led to the rate constant.[20] A product formation study, monitoring the I atom at 280 nm, found $k = 1.1 \times 10^{10}$.[66] Back to Table

B47. **$O_2(^1\Delta_g)$ + Cl^-.** Rate from a flash-photolysis study in the presence of a photosensitizer. No information to indicate that this is a chemical reaction as opposed to physical quenching.[19,64] Back to Table

B48. **$O_2(^1\Delta_g)$ + I^-.** Rate obtained by following the $O_2(^1\Delta_g) \rightarrow O_2(^3\Sigma)$ emission at 1.3 μm. Evidence for the oxidation of I^- instead of quenching was obtained by observing I_3^- formation. The mechanism was postulated to involve the formation of $HOOI/IO_2^-$ followed by subsequent reaction with I^- to give I_3^- and H_2O_2.[8] Earlier studies, primarily by chemical analysis of sensitized systems, support these conclusions.[64] Back to Table

6.3.2 References

(1) Alfassi, Z.; Huie, R.; Marguet, S.; Natarajan, E.; Neta, P. Rate constants for reactions of iodine atoms in solution. *Int. J. Chem. Kinet.* **1995**, *27*, 181-188, doi:10.1002/kin.550270208.

(2) Armstrong, D. A.; Huie, R. E.; Koppenol, W. H.; Lymar, S. V.; Merenyi, G.; Neta, P.; Ruscic, B.; Stanbury, D. M.; Steenken, S.; Wardman, P. Standard electrode potentials involving radicals in aqueous solution: inorganic radicals (IUPAC Technical Report). *Pure Appl. Chem.* **2015**, *87*, 1139-1150, doi:10.1515/pac-2014-0502.

(3) Artiglia, L.; Edebeli, J.; Orlando, F.; Chen, S.; Lee, M.-T.; Arroyo, P. C.; Gilgen, A.; Bartels-Rausch, T.; Kleibert, A.; Vazdar, M.; et al. A surface-stabilized ozonide triggers bromide oxidation at the aqueous solution-vapour interface. *Nature Comm.* **2017**, *8*, 700, doi:10.1038/s41467-017-00823-x.

(4) Ball, J. M.; Hnatiw, J. B. The reduction of I_2 by H_2O_2 in aqueous solutions. *Can. J. Chem.* **2001**, *79*, 304-311, doi:10.1139/cjc-79-3-304.

(5) Bichsel, Y.; von Gunten, U. Oxidation of iodide and hypoiodous acid in the disinfection of natural waters. *Environ. Sci. Technol.* **1999**, *33*, 4040-4045, doi:10.1021/es990336c.
(6) Bielski, B. H. J. A pulse radiolysis study of the reaction of ozone with Cl_2^- in aqueous solutions. *Radiat. Phys. Chem.* **1993**, *41*, 527-530, doi:10.1016/0969-806X(93)90015-M.
(7) Bjergbakke, E.; Navaratnam, S.; Parsons, B. J. Reaction between HO_2• and chlorine in aqueous solution. *J. Am. Chem. Soc.* **1981**, *103*, 5926-5928, doi:10.1021/ja00409a059.
(8) Braathen, G.; Chou, P.-T.; Frei, H. Time-resolved reaction of oxygen($^1\Delta$) with iodide in aqueous solution. *J. Phys. Chem.* **1988**, *92*, 6610-6615, doi:10.1021/j100334a026.
(9) Buxton, G. V. Pulse radiolysis of HOI and IO- in aqueous solution. Formation and characterisation of I(II). *Proc. Tihany Symp. Radiat. Chem.* **1987**, *6*, 155-159.
(10) Buxton, G. V.; Dainton, F. S. The radiolysis of aqueous solutions of oxybromine compounds; the spectra and reactions of BrO and BrO_2. *Proc. Roy. Soc. (London)* **1968**, *304*, 427-439.
(11) Buxton, G. V.; Greenstock, C. L.; Helman, W. P.; Ross, A. B. Critical review of rate constants for reactions of hydrated electrons, hydrogen atoms and hydroxyl radicals (•OH/•O–) in aqueous solution. *J. Phys. Chem. Ref. Data* **1988**, *17*, 1-21, doi:10.1063/1.555805.
(12) Buxton, G. V.; Kilner, C.; Sellers, R. M. Pulse radiolysis of HOI and IO- in aqueous solution. Formation and characterisation of I(II). *Proc. Tihany Symp. Radiat. Chem.* **1986**, *6*, 155-159.
(13) Buxton, G. V.; Subhani, M. S. Ratiation-chemistry and photochemistry of oxychlorine ions. I. Radiolysis of aqueous solutions of hypochlorite and chlorite ions. *J. Chem. Soc. Faraday Transactions I* **1972**, *68*, 947-957, doi:10.1039/F19726800947.
(14) Candeias, L. P.; Patel, K. B.; Stratford, M. R. L.; Wardman, P. Free hydroxyl radicals are formed on reaction between the neutrophil-derived species superoxide anion and hypochlorous acid. *FEBS Lett.* **1993**, *333*, 151-153, doi:10.1016/0014-5793(93)80394-a.
(15) Castagna, R.; Eiserich, J. P.; Budamagunta, M. S.; Stipa, P.; Cross, C. E.; Proietti, E.; Voss, J. C.; Greci, L. Hydroxyl radical from the reaction between hypochlorite and hydrogen peroxide. *Atmos. Environ.* **2008**, *42*, 6551-6554, doi:10.1016/j.atmosenv.2008.04.029.
(16) Connick, R. E. The interaction of hydrogen peroxide and hypochlorous acid in acidic solutions containing chloride ion *J. Am. Chem. Soc.* **1947**, *69*, 1509-1514, doi:10.1021/ja01198a074.
(17) D'Auria; Kuo, I. F. W.; Tobias, D. J. Ab initio molecular dynamics study of the solvated $OHCl^-$ complex: Implications for the atmospheric oxidation of chloride anion to molecular chlorine. *J. Phys. Chem. A* **2008**, *112*, 4644-4650, doi:10.1021/jp077669d.
(18) Davis, M.; Koizumi, H.; Schatz, G. C.; Bradforth, S. E.; Neumark, D. M. Experimental and theoretical study of the O + HCl transition state region by photodetachment of $OHCl^-$. *J. Chem. Phys.* **1994**, *101*, 4708-4721, doi:10.1063/1.468463.
(19) Egorov, S. Y.; Krasnovsky, A. A. Quenching of singlet molecular oxygen by components of media used for isolating chloroplasts and studying photosynthetic activity. *Sov. Plant Physiol.* **1986**, *33*, 5-8.
(20) Elliot, A. J. A pulse radiolysis study of the reaction of OH with I_2 and the decay of I_2^-. *Can. J. Chem.* **1992**, *70*, 1658-1666, doi:10.1139/v92-207.
(21) Elliot, A. J.; Simsons, A. S. Rate constants for reactions of hydroxyl radicals as a function of temperature. *Radiat. Phys. Chem. (1977)* **1984**, *24*, 229-231, doi:10.1016/0146-5724(84)90056-6.
(22) Ellison, D. H.; Salmon, G. A.; Wilkinson, F. Nanosecond pulse radiolysis of methanolic and aqueous solutions of readily oxidizable solutes. *Proc. Roy. Soc. (London)* **1972**, 23-36, doi:10.1098/rspa.1972.0066.
(23) Eriksen, T. E.; Lind, J.; Merenyi, G. Generation of chlorine dioxide from ClO by pulse radiolysis. *J. Chem. Soc., Faraday Trans. 1* **1981**, *77*, 2115-2123, doi:10.1039/f19817702115.
(24) Ershov, B. G. Kinetics, mechanism and intermediates of some radiation-induced reactions in aqueous solutions. *Russ. Chem. Rev.* **2004**, *73*, 101-113, doi:10.1070/RC2004v073n01ABEH000865.
(25) Fischbacher, A.; Löppenberg, K.; Von Sonntag, C.; Schmidt, T. C. A new reaction pathway for bromite to bromate in the ozonation of bromide. *Environ. Sci. Technol.* **2015**, *49*, 11714-11720, doi:10.1021/acs.est.5b02634.

(26) Gálvez, O.; Teresa Baeza-Romero, M.; Sanz, M.; Pacios, L. F. A theoretical study on the reaction of ozone with aqueous iodide. *Phys. Chem. Chem. Phys.* **2016**, *18*, 7651-7660, doi:10.1039/c5cp06440f.
(27) Gershenzon, M.; Davidovits, P.; Jayne, J. T.; Kolb, C. E.; Worsnop, D. R. Rate constant for the reaction of Cl_2(aq) with OH^-. *J. Phys. Chem. A* **2002**, *106*, 7748-7754, doi:10.1021/jp014146b.
(28) Grigor'ev, A. E.; Makarov, I. E.; Pikaev, A. K. Formation of Cl_2^- in the bulk solution during the radiolysis of concentrated aqueous solutions of chlorides. *High Energy Chem.* **1987**, *21*, 99-102.
(29) Haag, W. R.; Hoigné, J. Ozonation of bromide-containing waters: Kinetics of formation of hypobromous acid and bromate. *Environ. Sci. Technol.* **1983**, *17*, 261-267, doi:10.1021/es00111a004.
(30) Haag, W. R.; Hoigné, J. Ozonation of water containing chlorine or chloramines. Reaction products and kinetics. *Water Res.* **1983**, *17*, 1397-1402, doi:10.1016/0043-1354(83)90270-1.
(31) Hart, E. J.; Henglein, A. Free radical and free atom reactions in the sonolysis of aqueous iodide and formate solutions. *J. Phys. Chem.* **1985**, *89*, 4342-4347, doi:10.1021/j100266a038.
(32) Haruta, K.; Takeyama, T. Kinetics of oxidation of aqueous bromide ion by ozone. *J. Phys. Chem.* **1981**, *85*, 2383-2388, doi:10.1021/j150616a018.
(33) Held, A. M.; Halko, D. J.; Hurst, J. K. Mechanisms of chlorine oxidation of hydrogen peroxide. *J. Am. Chem. Soc.* **1978**, *100*, 5732-5740, doi:10.1021/ja00486a025.
(34) Hoigné, J.; Bader, H. Kinetics of reactions of chlorine dioxide (OClO) in water. - 1. Rate constants for inorganic and organic compounds. *Water Research* **1994**, *28*, 45-55, doi:10.1016/0043-1354(94)90118-X.
(35) Hoigné, J.; Bader, H.; Haag, W. R.; Staehelin, J. Rate constants of reactions of ozone with organic and inorganic compounds in water—III. Inorganic compounds and radicals *Water Research* **1985**, *19*, 993-1004, doi:10.1016/0043-1354(85)90368-9.
(36) Hurst, J. K. The role of inorganic chemistry in cellular mechanisms of host resistance to desease. *Adv. Chem. Series* **1997**, *253*, 399-421.
(37) Jayson, G. C.; Parson, B. J.; Swallow, A. J. Some simple, highly reactive, inorganic chlorine derivatives in aqueous solution. *J. Chem. Soc. Faraday Trans.* **1973**, *69*, 1597-1607, doi:10.1039/F19736901597.
(38) Kang, N.; Jackson, W. A.; Dasgupta, P. K.; Anderson, T. A. Perchlorate production by ozone oxidation of chloride in aqueous and dry systems. *Sci. Total Environ.* **2008**, *405*, 301-309, doi:10.1016/j.scitotenv.2008.07.010.
(39) Kläning, U. K.; Sehested, K.; Holcman, J. Standard Gibbs energy of formation of the hydroxyl radical in aqueous solution. Rate constants for the reaction $ClO_2^- + O_3 \rightleftarrows O_3^- + ClO_2$. *J. Phys. Chem.* **1985**, *89*, 760-763, doi:10.1021/j100251a008.
(40) Knipping, E. M.; Lakin, M. J.; Foster, K. L.; Jungwirth, P.; Tobias, D. J.; Gerber, R. B.; Dabdub, D.; Finlayson-Pitts, B. J. Experiments and simulations of ion-enhanced interfacial chemistry on aqueous NaCl aerosols. *Science* **2000**, *288*, 301-306, doi:10.1126/science.288.5464.301.
(41) Lampre, I.; Marignier, J.-L.; Mirdamadi-Esfahani, M.; Pernot, P.; Archirel, P.; Mostafavi, M. Oxidation of bromide ions by hydroxyl radicals: Spectral characterization of the intermediate $BrOH^{\bullet-}$. *J. Phys. Chem. A* **2013**, *117*, 877-887, doi:10.1021/jp310759u.
(42) Levanov, A. V.; Antipenko, E. E.; Lunin, V. V. Primary stage of the reaction between ozone and chloride ions in aqueous solution: Can chloride ion oxidation by ozone proceed via electron transfer mechanism? *Russ. J. Phys. Chem.* **2012**, *86*, 584-589, doi:10.1134/S0036024412040164.
(43) Levanov, A. V.; Antipenko, E. E.; Lunin, V. V. Primary stage of the reaction between ozone and chloride ions in aqueous solution: Oxidation of chloride ions with ozone through the mechanism of oxygen atom transfer. *Russ. J. Phys. Chem.* **2012**, *85*, 519-522, doi:10.1134/S0036024412030193.
(44) Levanov, A. V.; Kuskov, I. V.; Antipenko, E. E.; Lunin, V. V. The solubility of ozone and kinetics of its chemical reactions in aqueous solutions of sodium chloride. *Russ. J. Phys. Chem. A* **2008**, *82*, 2045-2050, doi:10.1134/s0036024408120133.
(45) Levanov, A. V.; Kuskov, I. V.; Antipenko, E. E.; Lunin, V. V. Stoichiometry and products of ozone reaction with chloride ion in an acidic medium. *Russ. J. Phys. Chem.* **2012**, *86*, 757-762.

(46) Levanov, A. V.; Kuskov, I. V.; Koiaidarova, K. B.; Antipenko, E. E.; Lunin, V. V. Interaction between ozone and the chloride ion in sulfuric acid solutions up to 6-M concentration. *Kin. Cat.* **2006**, *47*, 682-685, doi:10.1134/S0023158406050053.

(47) Levanov, A. V.; Kuskov, I. V.; Koiaidarova, K. B.; Zosimov, A. V.; Antipenko, E. E.; Lunin, V. V. Catalysis of the reaction of ozone with chloride ions by metal ions in an acidic medium. *Kin. Cat.* **2005**, *46*, 138-143, doi:10.1007/s10975-005-0021-z.

(48) Levanov, A. V.; Kuskov, I. V.; Zosimov, A. V.; Antipenko, E. E.; Lunin, V. V. Acid catalysis in reaction of ozone with chloride ions. *Kin. Cat.* **2003**, *44*, 740-746, doi:10.1023/B:KICA.0000009047.90252.2d.

(49) Liebhafsky, H. A.; Mohammad, A. The kinetics of the reduction, in acid solution, of hydrogen peroxide by iodide ion. *J. Am. Chem. Soc.* **1933**, *55*, 3977-3986, doi:10.1021/ja01337a010.

(50) Liu, Q.; Schurter, L. M.; Muller, C. E.; Aloisio, S.; Franscisco, J. S.; Margerum, D. W. Kinetics and mechanisms of aqueous ozone reactions with bromide, sulfite, hydrogen sulfite, and nitrite ions. *Inorg. Chem.* **2001**, *40*, 4436-4442, doi:10.1021/ic000919j.

(51) Long, C. A.; Bielski, B. H. J. Rate of reaction of superoxide radical with chlorine-containing species. *J. Phys. Chem.* **1980**, *84*, 555-557, doi:10.1021/j100442a023.

(52) Lunin, V. V.; Levanov, A. V.; Kuskov, I. V.; Zosimov, A. V.; Antipenko, E. E. Chlorine evolution in the interaction between ozone and a solution of sodium chloride in the presence of carbon dioxide. *Russ. J. Phys. Chem.* **2003**, *77*, 580-585.

(53) Maetzke, A.; Jensen, S. J. K. Reaction paths for production of singlet oxygen from hydrogen peroxide and hypochlorite. *Chem. Phys. Lett.* **2006**, *425*, 40-43, doi:10.1016/j.cplett.2006.04.097.

(54) Magi, L.; Schweitzer, F.; Pallares, C.; Cherif, S.; Mirabel, P.; George, C. Investigation of the uptake rate of ozone and methyl hydroperoxide by water surfaces. *J. Phys. Chem. A* **1997**, *101*, 4943-4949, doi:10.1021/jp970646m.

(55) Minakata, D.; Kamath, D.; Maetzold, S. Mechanistic insight into the reactivity of chlorine-derived radicals in the aqueous-phase UV–chlorine advanced oxidation process: Quantum mechanical calculations. *Environ. Sci. Technol.* **2017**, *51*, 6918-6926, doi:10.1021/acs.est.7b00507.

(56) Mohammad, A.; Liebhafsky, H. A. The kinetics of the reduction of hydrogen peroxide by the halides. *J. Am. Chem. Soc.* **1934**, *56*, 1680-1685, doi:10.1021/ja01323a009.

(57) Mulazzani, Q. G.; Buxton, G. V. On the kinetics and mechanism of the oxidation of I^- by (OH)-O-center dot/O center dot- in alkaline aqueous solution. *Chem. Phys. Lett.* **2006**, *421*, 261-265, doi:10.1016/j.cplett.2006.01.088.

(58) Naumov, S.; von Sonntag, C. The reactions of bromide with ozone towards bromate and the hypobromite puzzle: A density functional theory study. *Ozone: Science and Engineering* **2008**, *30*, 339-343, doi:10.1080/01919510802326120.

(59) Naumov, S.; von Sonntag, C. Standard Gibbs free energies of reactions of ozone with free radicals in aqueous solution: Quantum-chemical calculations. *Environ. Sci. Technol.* **2011**, *45*, 9195-9204, doi:10.1021/es2018658.

(60) Nicoson, J. S.; Margerum, D. W. Kinetics and mechanisms of aqueous chlorine reactions with chlorite ion in the presence of chloride ion and acetic acid/acetate buffer. *Inorg. Chem.* **2002**, *41*, 342-347, doi:10.1021/ic010762a.

(61) Panich, N. M.; Ershov, B. G. The solubility and kinetics of decomposition of ozone in aqueous solutions of nitrates. *Russ. J. Phys. Chem. A* **2008**, *82*, 1262-1265, doi:10.1134/S0036024408080049.

(62) Rao, B.; Anderson, T. A.; Redder, A.; Jackson, W. A. Perchlorate formation by ozone oxidation of aqueous chlorine/oxy-chlorine species: Role of Cl_xO_y radicals. *Environ. Sci. Technol.* **2010**, *44*, 2961-1967, doi:10.1021/es903065f.

(63) Razumovskii, S. D.; Korovina, G. V.; Grinevich, T. V. Mechanism of the first step of ozone decomposition in aqueous solutions of sodium chloride in view of new data on the composition of reaction products. *Doklady Phys. Chem.* **2010**, *424*, 163-165, doi:10.1134/S0012501610100027.

(64) Ross, A. B.; Mallard, W. G.; Hellman, W. P.; Bielski, B. H. J.; Buxton, G. V.; Cabelli, D. E.; Greenstock, C. L.; Huie, R. E.; Neta, P. *NDRL/NIST Solution Kinetics Database*, 1997; Vol. 40.

(65) Schmitz, G. Iodine(+1) reduction by hydrogen peroxide. *Russ. J. Phys. Chem. A* **2009**, *83*, 1447-1451, doi:10.1134/s0036024409090052.
(66) Schwarz, H. A.; Bielski, B. H. J. Reactions of HO_2 and O_2^- with iodine and bromine and I_2^- and I atom reduction potentials. *J. Phys. Chem.* **1986**, *90*, 1445-1448, doi:10.1021/j100398a045.
(67) Storch, D. M.; Dymek, C. J.; Davis, L. P. MNDO study of the mechanismm of $O_2(^1\Delta)$ formation in the reaction of Cl_2 with basic H_2O_2. *J. Am. Chem. Soc.* **1983**, *105*, 1765-1768, doi:10.1021/ja00345a011.
(68) Valiev, M.; D'Auria; Tobias, D. J.; Garrett, B. C. Interactions of Cl^- and OH radical in aqueous solution. *J. Phys. Chem. A Lett.* **2009**, *113*, 8823-8825, doi:10.1021/jp903625k.
(69) von Gunten, U.; Oliveras, Y. Kinetics of the reaction between hydrogen peroxide and hypobromous acid: Implication on water treatment and natural systems. *Water Research* **1997**, *31*, 900-906, doi:10.1016/S0043-1354(96)00368-5.
(70) Watts, M. J.; Rosenfeldt, E. J.; Linden, K. G. Comparative OH radical oxidation using UV-Cl_2 and UV-H_2O_2 processes. *J. Water Supply Res. Technol.-Aqua* **2007**, *56*, 469-477, doi:10.2166/aqua.2007.028.
(71) Yamashita, S.; Iwamatsu, K.; Maehashi, Y.; Taguchi, M.; Hata, K.; Muroya, Y.; Katsumura, Y. Sequential radiation chemical reactions in aqueous bromide solutions: pulse radiolysis experiment and spur model simulation. *RSC Adv.* **2015**, *5*, 25877-25886, doi:10.1039/C5RA03101J.
(72) Yeatts, L. R. B.; Taube, H. The kinetics of the reaction of ozone and chloride ion in acid aqueous solution. *J. Am. Chem. Soc.* **1949**, *71*, 4100-4105, doi:10.1021/ja01180a063.
(73) Yu, X. Y. Critical evaluation of rate constants and equilibrium constants of hydrogen peroxide photolysis in acidic aqueous solutions containing chloride ions. *J. Phys. Chem. Ref. Data* **2004**, *33*, 747-763, doi:10.1063/1.1695414.
(74) Zehavi, D.; Rabani, J. The oxidation of aqueous bromide ions by hydroxyl radicals. A pulse radiolytic investigation. *J. Phys. Chem.* **1972**, *76*, 312-319, doi:10.1021/j100647a006.
(75) Zuo, Z.; Katsumura, Y.; Ueda, K.; Ishigure, K. Reactions between some inorganic radicals and oxychlorides studied by pulse radiolysis and laser photolysis. *J. Chem. Soc. Faraday Trans.* **1997**, *93*, 1885-1891, doi:10.1039/A700256D.

6.4 Formation and Dissociation of Dihalo Radicals

Reaction	k (L mol^{-1} s^{-1}) *	Note
$Cl + Cl^- \rightarrow Cl_2^-$	$(7.8 \pm 0.8) \times 10^9$	C1
$Cl_2^- \rightarrow Cl + Cl^-$	$(5.7 \pm 0.4) \times 10^4$ s^{-1}	C1
$Br + Br^- \rightarrow Br_2^-$	$(5.11 \pm 0.98) \times 10^{12} \exp(-1812 \pm 60/T)$	C2
$Br_2^- \rightarrow Br + Br^-$	$(2.54 \pm 2.03) \times 10^{10} \exp(-4068 \pm 255/T)$ s^{-1}	C2
$I + I^- \rightarrow I_2^-$	$(2.4 \pm 0.1) \times 10^{13} \exp(-2324 \pm 77/T)$	C3
$I_2^- \rightarrow I + I^-$	$(2.6 \pm 0.4) \times 10^{12} \exp(-5157 \pm 198/T)$ s^{-1}	C3
$Br + Cl^- \rightarrow ClBr^-$	1.0×10^{10}	C4
$ClBr^- \rightarrow Br + Cl^-$	8.5×10^7 s^{-1}	C4
$Cl_2^- + Br^- \rightarrow ClBr^- + Cl^-$	4×10^9	C4
$ClBr^- + Cl^- \rightarrow Cl_2^- + Br^-$	1.1×10^2	C4
$ClBr^- + Br^- \rightarrow Br_2^- + Cl^-$	8.0×10^9	C4
$Br_2^- + Cl^- \rightarrow ClBr^- + Br^-$	4.3×10^6	C4
$I + Br^- \rightarrow BrI^-$	1.0×10^{10}	C5
$BrI^- \rightarrow I + Br^-$	5.7×10^8 s^{-1}	C5
$Br_2^- + I^- \rightarrow BrI^- + Br^-$	4.3×10^9	C5
$BrI^- + Br^- \rightarrow Br_2^- + I^-$	$<1 \times 10^5$	C5
$BrI^- + I^- \rightarrow I_2^- + Br^-$	5.8×10^9	C5
$I_2^- + Br^- \rightarrow BrI^- + I^-$	4.3×10^6	C5
$Cl_2^- + I^- \rightarrow 2\ Cl^- + I$	4.5×10^9	C6
$ICl + Br^- \rightarrow IBr + Cl^-$	See Note	C7
$ICl + I^- \rightarrow I_2 + Cl^-$	$(1.1 \pm 0.1) \times 10^9$	C8
$HOI + Cl^- + H^+ \rightarrow ICl + H_2O$	fast	C9
$HOI + Br^- + H^+ \rightarrow IBr + H_2O$	fast	C10
$HOI + I^- (+ H^+) \rightarrow I_2 + H_2O$	$(0.3–3) \times 10^9$	C11

* Unless units noted otherwise

6.4.1 Notes: Formation of Dihalo Radicals

C1. **$Cl + Cl^- \leftrightarrow Cl_2^-$.** Selected values from review of the extensive literature on these reactions and the equilibrium constant.[10] Back to Table

C2. **$Br + Br^- \leftrightarrow Br_2^-$.** Bromine atoms produced by flash photolysis of 1,2-dibromoethane in solutions containing Br^-, monitoring Br_2^- at 365 nm by optical absorption, over the temperature range 10.5−50 ºC.[6] Room temperature value for forward reaction in agreement with the several earlier flash photolysis and pulse radiolysis studies.[9] Back to Table

C3. **$I + I^- \leftrightarrow I_2^-$.** Flash photolysis of iodide solutions following the temporal behavior of the absorption due to I_2^- over the temperature range 286–320 K. Forward reaction shows some ionic strength dependence; somewhat greater was observed for the reverse reaction.[7] Back to Table

C4. **$Br + Cl^- \leftrightarrow ClBr^-$.** Rate constant derived in a pulse radiolysis investigation of the oxidation of Br^- by Cl_2^-.[5] The kinetics was determined by following the absorbance at 700 nm, where Br_2^- and $BrCl^-$ absorb, but not Cl_2^-, and then modeling a complex mechanism. Back to Table

C5. **$I + Br^- \leftrightarrow BrI_2^-$.** Pulse radiolysis of a 0.1 mol L^{-1} NaBr solution (pH 3.3) containing 5×10^{-5} mol L^{-1} NaI and modeling a complex mechanism led to the rate constant. Data obtained by absorption spectroscopy at 725, 340, and 400 nm.[4] Back to Table

C6. **$Cl_2 + I^-$.** Pulse radiolysis of a 1 mol L^{-1} NaCl solution (pH 3.3) containing 5×10^{-5} mol L^{-1} NaI. Rate constant derived from a fit to a complex model.[3] Back to Table

C7. **$ICl + Br^-$.** The uptake of ICl into droplets containing Br^- showed a rapid production of ICl suggesting a fast reaction.[1] No rate constant was derived, however. Back to Table

C8. **$ICl + I^-$.** Rate constants were measured at an ionic strength of 1.0 mol L^{-1} by investigating the reaction of ICl_2^- with I^- using a pulsed-accelerated flow system at 25 ºC, monitoring at 350 nm.[8] Back to Table

C9. **$HOI + Cl^- + H^+$.** A study of the uptake of HOI on solutions containing Cl^- suggested that this reaction is fast.[1] No rate constant was derived, however. Back to Table

C10. **$HOI + Br^- + H^+$.** By analogy with the reaction of HOI with Cl^- and with I^-, this reaction is expected to be fast. Back to Table

C11. **$HOI + I^-$ (+ H^+).** Results from a pulse radiolysis study of N_2O- saturated solutions of iodide at pH 9.5–11.1 were combined with earlier studies of the γ-radiolysis of unbuffered solutions, to derive this rate constant.[2] Back to Table

6.4.2 References

(1) Braban, C. F.; Adams, J. W.; Rodriguez, D.; Cox, R. A.; Crowley, J. N.; Schuster, G. Heterogeneous reactions of HOI, ICl, and IBr on sea salt and sea sale proxies. *Phys. Chem. Chem. Phys.* **2007**, *9*, 3136-3148, doi:10.1039/b700829e.

(2) Buxton, G. V.; Mulazzani, Q. G. On the hydrolysis of iodine in alkaline solution: A radiation chemical study. *Radiat. Phys. Chem.* **2007**, *76*, 932-940, doi:10.1016/j.radphyschem.2006.06.009.

(3) Ershov, B. G.; Janata, E.; Gordeev, A. V. Pulse radiolysis study of I^- oxidation with radical anions Cl_2^- in an aqueous solution. *Russ. Chem. Bull.* **2005**, *54*, 1378-1382, doi:10.1007/s11172-005-0413-2.

(4) Ershov, B. G.; Janata, E.; Gordeev, A. V. Pulse radiolysis study of the oxidation of the I^- ions with the radical anions Br_2^- in an aqueous solution: formation and properties of the radical anion BrI^-. *Russ. Chem. Bull.* **2008**, *57*, 1821-1826, doi:10.1007/s11172-008-0245-y.

(5) Ershov, B. G.; Janata, E.; Kelm, M.; Gordeev, A. V. Formation and absorption spectra of X_3^- ions upon the radiation-chemical oxidation of Cl^- in the presence of Br^- (Cl, Br = X) in aqueous solution. *Mendeleev Comm.* **2002**, 55-57, doi:10.1070/MC2002v012n02ABEH001561.

(6) Liu, Y.; Pimentel, A. S.; Antoku, Y.; Giles, B. J.; Barker, J. R. Temperature-dependent rate and equilibrium constants for Br(aq) + Br^-(aq) ↔ Br_2^-(aq). *J. Phys. Chem. A* **2002**, *106*, 11075-11082, doi:10.1021/jp0255536.

(7) Liu, Y.; Sheaffer, R. L.; Barker, J. R. Effects of temperature and ionic strength on the rate and equilibrium constants for the reaction $I^{\bullet}_{aq}$ + I^-_{aq} ↔ $I_2^{\bullet -}{}_{aq}$. *J. Phys. Chem. A* **2003**, *107*, 10296-10302, doi:10.1021/jp036126a.

(8) Margerum, D. W.; Dickson, P. N.; Nagy, J. C.; Kumar, K.; Bowers, C. P.; Fogelman, K. D. Kinetics of the iodine monochloride reaction with iodide measured by the pulsed-accelerated-flow method. *Inorg. Chem.* **1986**, *25*, 4900-4904, doi:10.1021/ic00247a025.

(9) Ross, A. B.; Mallard, W. G.; Hellman, W. P.; Bielski, B. H. J.; Buxton, G. V.; Cabelli, D. E.; Greenstock, C. L.; Huie, R. E.; Neta, P. *NDRL/NIST Solution Kinetics Database*, 1997; Vol. 40.

(10) Yu, X. Y. Critical evaluation of rate constants and equilibrium constants of hydrogen peroxide photolysis in acidic aqueous solutions containing chloride ions. *J. Phys. Chem. Ref. Data* **2004**, *33*, 747-763, doi:10.1063/1.1695414.

6.5 Formation and Loss of Halogen Molecules and Dihalo Radicals

Reaction	k (L mol^{-1} s^{-1})	Note
$Cl_2^- + Cl_2^- \rightarrow Cl^- + Cl_3^-$	$(3.5 \pm 2.7) \times 10^9$	D1
$Br_2^- + Br_2^- \rightarrow Br^- + Br_3^-$	1.9×10^9	D2
$I_2^- + I_2^- \rightarrow I^- + I_3^-$	$1 \times 10^{12} \exp(-1800/T)$	D3
$Cl + Cl_2^- \rightarrow Cl^- + Cl_2$	$(1.4 \pm 1.0) \times 10^9$	D4
$Br + Br_2^- \rightarrow Br^- + Br_2$	5×10^9	D5
$I + I_2^- \rightarrow I_3^-$	6.5×10^9	D6
$OH^- + Cl_2^- \rightarrow ClOH^- + Cl^-$	4.5×10^7	D7
$HO_2 + Cl_2^- \rightarrow O_2 + 2Cl^- + H^+$	$(3.1 \pm 1.5) \times 10^9$	D8
$O_2^- + Cl_2^- \rightarrow O_2 + 2Cl^-$	$<2 \times 10^8$	D9
$HO_2 + Br_2^- \rightarrow Br_2 + HO_2^-$	9.1×10^7	D10
$HO_2 + Br_2^- \rightarrow O_2 + 2Br^- + H^+$	1.0×10^8	D10
$O_2^- + Br_2^- \rightarrow O_2 + 2Br^-$	1.7×10^8	D10
$HO_2 + I_2^- \rightarrow I_2 + HO_2^-$	$(4.0 \pm 0.5) \times 10^9$	D11
$O_2^- + I_2^- \rightarrow O_2 + 2I^-$	$(0.5\text{-}1) \times 10^9$	D11
$H_2O_2 + Cl \rightarrow H^+ + Cl^- + HO_2$	$(2.0 \pm 0.1) \times 10^9$	D12
$H_2O_2 + Cl_2^- \rightarrow H^+ + 2Cl^- + HO_2$	$(6.2 \pm 6.8) \times 10^5$	D13
$ClO^- + Cl_2^- \rightarrow ClO + 2Cl^-$	1.1×10^8	D14
$ClO_2^- + Cl_2^- \rightarrow ClO_2 + 2Cl^-$	2×10^8	D15
$ClO_2^- + Br_2^- \rightarrow ClO_2 + 2Br^-$	$6.3 \times 10^{10} \exp(-2410/T)$	D16
$ClO_2^- + Cl_2 \rightarrow ClOClO + Cl^-$	$(5.7 \pm 0.2) \times 10^5$	D17
$ClO_2^- + Br_2 \rightarrow ClO_2 + Br_2^-$	$(1.3 \pm 0.2) \times 10^3$	D18
$HCO_3^- + Cl \rightarrow Cl^- + CO_3^- + H^+$	2.2×10^8	D19
$CO_3^{2-} + Cl \rightarrow Cl^- + CO_3^-$	5.0×10^8	D19

6.5.1 Notes: Formation and Loss of Halogen Molecules and Dihalo Radicals

D1. **$Cl_2^- + Cl_2^-$.** The value given is an unweighted average taken from an extensive literature review.[16] Back to Table

D2. **$Br_2^- + Br_2^-$.** In a pulse radiolysis study of decay kinetics at 360 nm at an ionic strength of 0.01 mol L^{-1} and pH 2–7 and taking ε = 9,900 L mol^{-1} cm^{-1}, rate constants of 2.2 and 2.5 × 10^9 L mol^{-1} s^{-1} were measured at ionic strengths of 0.1 and 1.0 mol L^{-1}.[2] These values are in agreement with a number of other reports.[11] Back to Table

D3. **$I_2^- + I_2^-$.** Pulse radiolysis study of decay kinetics at 725 nm at an ionic strength of 0.1 mol L^{-1}, T = 15−90 ºC, and pH 7 and taking ε = 2,650 L mol^{-1} cm^{-1}.[4] E_a = 15 kJ mol^{-1}. Room temperature value slightly below some earlier reports, but in agreement with more recent measurements.[11] Back to Table

D4. **$Cl + Cl_2^-$.** Selected value, which is an unweighted average of two reports, from review of the literature.[16] Back to Table

D5. **$Br + Br_2^-$.** An assumed value that was used in modeling hydrogen abstraction reactions of bromine atoms generated from the one-electron reduction of 1,2-dibromoethane. [8] This reaction would be followed by the rapid reaction $Br^- + Br_2 \rightarrow Br_3^-$. Back to Table

D6. **$I + I_2^-$.** Value is an unweighted average of results from Elliot[3] and Ishigure, et al. (See Note on $O_2^-/HO_2 + I_2^-$)[6], both of which were obtained in pulse radiolysis studies. Back to Table

D7. **$OH^- + Cl_2^-$.** Rate constant taken from a study involving the pulse radiolysis of concentrated chloride solutions, following the decay of Cl_2^- at 340 nm.[5] Back to Table

D8. **$HO_2 + Cl_2^-$.** An unweighted average of three values taken from a review of the literature.[16] The possibility that the reaction might yield Cl_2 and H_2O_2 was considered in a pulse radiolysis study of the HO_2/Cl_2 reaction. It was concluded that this path was not important and an upper limit of of 5×10^7 L mol^{-1} s^{-1} was suggested.[1] Back to Table

D9. **$O_2^- + Cl_2^-$.** From an analysis of the decay kinetics of Cl_2^- in an O_2-saturated solution compared with a deaerated solution.[18] By comparison with the other dihalide radicals, this rate constant seems too low. Back to Table

D10. **$O_2^-/HO_2 + Br_2^-$.** Results from the flash photolysis of bromide solutions following conductivity changes. Computer simulation utilized to extract rate constants and branching ratios.[15] Earlier studies assumed only Br^- was formed. A more recent study with continuous illumination at 313 nm and following Br_2(g) production, led to the conclusion that the rate constants for Br_2 and Br^- production in the $HO_2 + Br_2^-$ reaction were equal at 4.4×10^9 L mol^{-1} s^{-1}.[7] Back to Table

D11. **$O_2^-/HO_2 + I_2^-$.** Data obtained in an investigation on the radiolysis of aqueous iodine solutions.[6] The main study utilized continuous radiation and a flow system to investigate the mechanism of the overall reaction. Pulse radiolysis was then utilized to obtain kinetic data. Results were presented, but there was no detailed analysis. An earlier study, fitting to a complex mechanism and assuming a concentration of $\sim 7 \times 10^{-8}$ mol L^{-1} for the radicals, resulted in $k \sim 1 \times 10^{10}$ L mol^{-1} s^{-1} for the HO_2 reaction.[12] Back to Table

D12. **$H_2O_2 + Cl$.** Rate constant obtained from a study of the photolysis of H_2O_2 in acid solutions.[17] Derived value depends on $K_{eq}(Cl + Cl^- \leftrightarrow Cl_2^-) = 1.4 \times 10^5$ L mol^{-1}. Back to Table

D13. **$H_2O_2 + Cl_2^-$.** Preferred value from a review of the literature. [16] The large spread in the reported values is reflected in the error limit. Back to Table

D14. **$ClO^- + Cl_2^-$.** Rate constant extrapolated to zero ionic strength. From the pulse radiolysis of a 5 mol^{-1} L^{-1} LiCl solution containing HClO.[19] Back to Table

D15. **$OClO^- + Cl_2^-$.** Average of two rate constants extrapolated to zero ionic strength at ~20 ºC. One from the pulse radiolysis of a 5 mol^{-1} L^{-1} LiCl solution containing $HClO^-$; the other from the flash photolysis of a persulfate solution at an ionic strength of 0.25 mol^{-1} L^{-1}.[19] Back to Table

D16. **$OClO^- + Br_2^-$.** Radicals generated by the pulse radiolysis of an 0.1 mol L^{-1} solution of NaBr, saturated with N_2O, at pH 6.8, over the temperature range 5-79 ºC and rate constants derived by following the decay of the optical absorption at 360 nm.[13] $E_a = 20 \pm 2.7$ kJ mol^{-1}. At 298 K, the rate constant is 1.9×10^7 L mol^{-1} s^{-1}, which is significantly greater than the value obtained from fitting a multi-step mechanism to observations on the chlorite - bromine system, $k = (4.0 \pm 0.1) \times 10^6$ L mol^{-1} s^{-1}.[14] Back to Table

D17. **$OClO^- + Cl_2$.** The formation of ClO_2 was followed in the reaction of Cl_2 with ClO_2^- at 359 nm with stopped-flow spectrophotometry over the pH range 3.6 to 6.0, at 25 ºC and at an ionic strength of 1 mol L^{-1}.[10] The possibility of an electron-transfer reaction leading to the direct formation of ClO_2 was ruled out by the lack of suppression by added ClO_2. The results indicated that the rate constant for the reaction of ClOClO with ClO_2^- must be $>> 6 \times 10^5$ L mol^{-1} s^{-1}. Back to Table

D18. **$OClO^- + Br_2$.** Rate constant obtained by fitting observations at 25 ºC on the chlorite-bromine system to a multi-step model.[14] The rate constant for the reverse reaction was reported to be $k = 1.1 \times 10^9$ L mol^{-1} s^{-1}. See also Note on $ClO_2^- + Br_2^-$. Back to Table

D19. **$HCO_3^-/CO_3^{2-} + Cl$.** Rate constants were determined relative to the reaction of chlorine atoms with tetrachlorethene during its 254 nm photolysis in the presence of added carbonate/bicarbonate.[9] Back to Table

6.5.2 References

(1) Bjergbakke, E.; Navaratnam, S.; Parsons, B. J. Reaction between HO_2• and chlorine in aqueous solution. *J. Am. Chem. Soc.* **1981**, *103*, 5926-5928, doi:10.1021/ja00409a059.

(2) D`Angelantonio, M.; Venturi, M.; Mulazzani, Q. G. A re-examination of the decay kinetics of pulse radiolytically generated Br_2^- radicals in aqueous solution. *Int. J. Radiat. Appl. Inst. Part C. Radiat. Phys. Chem.* **1988**, *32*, 319-324, doi:10.1016/1359-0197(88)90028-8.

(3) Elliot, A. J. A pulse radiolysis study of the reaction of OH with I_2 and the decay of I_2^-. *Can. J. Chem.* **1992**, *70*, 1658-1666, doi:10.1139/v92-207.

(4) Elliot, A. J.; Sopchyshyn, C. F. A pulse radiolysis study of I_2^- and $(SCN)_2^-$ in aqueous solutions over the temperature range 15 - 90 C. *Int. J. Chem. Kinet.* **1984**, *16*, 1247-1256, doi:10.1002/kin.550161007.

(5) Grigor'ev, A. E.; Makarov, I. E.; Pikaev, A. K. Formation of Cl_2^- in the bulk solution during the radiolysis of concentrated aqueous solutions of chlorides. *High Energy Chem.* **1987**, *21*, 99-102.

(6) Ishigure, K.; Shiraishi, H.; Okuda, H. Radiation chemistry of aqueous iodine systems under nuclear reactor accident conditions. *Int. J. Radiat. Appl. Inst. Part C. Radiat. Phys. Chem.* **1988**, *32*, 593-597, doi:10.1016/1359-0197(88)90070-7.

(7) Matthew, B. M.; George, I.; Anastasio, C. Hydroperoxyl radical (HO_2) oxidizes dibromide radical anion (Br_2^-) to bromine (Br_2) in aqueous solution: Implicatins for the formation of Br_2 in the marine boundary layer. *Geophys. Res. Lett.* **2003**, *30*, 2297, doi:10.1029/2003GL018572.

(8) Merényi, G.; Lind, J. Reaction-mechanism of hydrogen abstraction by the bromine atom in water. *J. Am. Chem. Soc* **1994**, *116*, 7872-7876, doi:10.1021/ja00096a050.

(9) Mertens, R.; Von Sonntag, C. Photolysis (λ = 254 nm) of tetrachloroethene in aqueous solutions. *J. Photochem. Photobiol.* **1995**, *85*, 1-9, doi:10.1016/1010-6030(94)03903-8.

(10) Nicoson, J. S.; Margerum, D. W. Kinetics and mechanisms of aqueous chlorine reactions with chlorite ion in the presence of chloride ion and acetic acid/acetate buffer. *Inorg. Chem.* **2002**, *41*, 342-347, doi:10.1021/ic010762a.

(11) Ross, A. B.; Mallard, W. G.; Hellman, W. P.; Bielski, B. H. J.; Buxton, G. V.; Cabelli, D. E.; Greenstock, C. L.; Huie, R. E.; Neta, P. *NDRL/NIST Solution Kinetics Database*, 1997; Vol. 40.

(12) Schwarz, H. A.; Bielski, B. H. J. Reactions of HO_2 and O_2^- with iodine and bromine and I_2^- and I atom reduction potentials. *J. Phys. Chem.* **1986**, *90*, 1445-1448, doi:10.1021/j100398a045.

(13) Shoute, L. C. T.; Alfassi, Z. B.; Neta, P.; Huie, R. E. Temperature dependence of the rate constants for reaction of dihalide and azide radicals with inorganic reductants. *J. Phys. Chem.* **1991**, *95*, 3238-3242, doi:10.1021/j100161a050.

(14) Tóth, Z.; Fábián, I. Kinetics and mechanism of the initial phase of the bromine-chlorite ion reaction in aqueous solution. *Inorg. Chem.* **2000**, *39*, 4608-4614, doi:10.1021/ic990329p.

(15) Wagner, I.; Strehlow, H. On the flash photolysis of bromide ions in aqueous solutions. *Ber. Bunsenges. Phys. Chem.* **1987**, *91*, 1317-1321, doi:10.1002/bbpc.19870911203.

(16) Yu, X. Y. Critical evaluation of rate constants and equilibrium constants of hydrogen peroxide photolysis in acidic aqueous solutions containing chloride ions. *J. Phys. Chem. Ref. Data* **2004**, *33*, 747-763, doi:10.1063/1.1695414.

(17) Yu, X. Y.; Barker, J. R. Hydrogen peroxide photolysis in acidic aqueous solutions containing chloride ions. I. Chemical mechanism. *J. Phys. Chem. A* **2003**, *107*, 1313-1324.

(18) Zhestkova, T. P.; Pikaev, A. K. Destruction rate of Cl_2^- anion-radicals during pulse radiolysis of concentrated aqueous lithium chloride solutions. *Izv. Akad. Nauk SSSR, Ser. Chem. Sci.* **1974**, *23*, 877-878.

(19) Zuo, Z.; Katsumura, Y.; Ueda, K.; Ishigure, K. Reactions between some inorganic radicals and oxychlorides studied by pulse radiolysis and laser photolysis. *J. Chem. Soc. Faraday Trans.* **1997**, *93*, 1885-1891, doi:10.1039/A700256D.

6.6 Halogen Interconversion Reactions

Reaction	k (L mol^{-1} s^{-1}) *	Note
$OCl^- + Br^-$ → products	9×10^{-4}	E1
$HOCl + Br^-$ → $HOBr + Cl^-$	1.55×10^3	E1
$OCl^- + I^-$ → products	<30	E2
$HOCl + I^-$ → $HOClI^-$	$(4.3 \pm 0.3) \times 10^8$	E3
$HOClI^-$ → $OH^- + ICl$	$(9 \pm 3) \times 10^5$ s^{-1}	E3
$OBr^- + I^-$ (+ H^+) → $OH^- + IBr$	$(6.8 \pm 0.4) \times 10^5$	E4
$HOBr + I^-$ → $OH^- + IBr$	$(5.0 \pm 0.3) \times 10^9$	E4
$IO^- + I^-$ (+ H_2O) ↔ $I_2OH^- + OH^-$	$K_{eq} = 0.15 \pm 0.01$	E5
$IO^- + I_2OH^-$ → $IO_2^- + 2\ I^- + H^+$	6.0 ± 0.2	E5
$IO_2^- + I_2OH^-$ → $IO_3^- + 2I^- + H^+$	26 ± 2	E5
$HOCl + HOCl$ → $Cl_2O + H_2O$	0.12	E6
$HOCl + HOCl$ → $O_2 + 2Cl^- + 2H^+$	See Note	E6
$ClO^- + ClO^-$ → $ClO_2^- + Cl^-$	7.7×10^{-9}	E6
$ClO^- + ClO_2^-$ → $ClO_3^- + Cl^-$	1.5×10^{-6}	E6
$BrCl + ClO^-$ → $BrOCl + Cl^-$	$>10^6$	E7
$BrOCl + ClO^-$(+ H_2O) → $ClO_2^- + Br^- + H^+ + HOCl$	$>10^3$	E7
$BrCl + BrO^-$ → $BrOBr + Cl^-$	$>10^6$	E7
$BrOCl + BrO^-$(+ H_2O) → $BrO_2^- + Br^- + H^+ + HOBr$	$>10^3$	E7
$BrOBr + ClO^-$(+ H_2O) → $ClO_2^- + Br^- + H^+ + HOBr$	$>10^3$	E7
$BrOBr + BrO^-$(+ H_2O) → $BrO_2^- + Br^- + H^+ + HOCl$	$>10^3$	E7
$HOCl + HOBr$ → $BrOCl + H_2O$	Slow, See Note	E8
$HOBr + HOBr$ → $BrO_2^- + Br^- + 2H^+$	$(2.3 \pm 1.7) \times 10^{-3}$	E9
$HOBr + BrO^-$ → $BrO_2^- + Br^- + H^+$	2.3×10^{-4}	E9
$BrO^- + BrO^-$ → $BrO_2^- + Br^-$	$(6 \pm 4) \times 10^{-7}$	E9
$HOCl + HOI$ → $IO_2^- + Cl^- + 2H^+$	8.2 ± 0.8	E10
$OCl^- + HOI$ → $IO_2^- + Cl^- + H^+$	52 ± 5	E10
$HOI + HOI$ → $OIO^- + 2H^+ + I^-$	0.3 ± 0.2	E11
$HOI + IO^-$ → $OIO^- + H^+ + I^-$	15 ± 1	E10
$IO^- + IO^-$ → products	$<7.2 \times 10^{-2}$	E12
$IO^- + IO_2^-$ → $IO_3^- + I^-$	0.5 ± 0.1	E13
$HOI + IO_2^-$ → $IO_3^- + H^+ + I^-$	Fast, See Note	E13
$Cl_2 + I^-$ → ICl_2^-	3.5×10^9	E14
$Cl + ClO^-$ → $ClO + Cl^-$	8.2×10^9	E15
$Cl + HOCl$ → $ClO + H^+ + Cl^-$	3×10^9	E15
$Br + BrO^-$ → $BrO + Br^-$	4.1×10^9	E15
$ClO + ClO$ → Cl_2O_2	2.5×10^9	E15
$BrO + BrO$ → Br_2O_2	2.8×10^9	E15
$IO + IO$ → products	1.5×10^9	E16
$BrO_2 + ClO_2^-$ → $BrO_2^- + ClO_2$	3.6×10^7	E17
$HOCl + OClO^-$ → $HOClOClO^-$	1.6 ± 0.1	E18
$HOCl + BrO_2^-$ → ClO_3^- + HOBr (85%) ClO_2 + HOBr (8%) $BrO_3^- + Cl^-$ (7%)	See Note	E19
$ClO^- + ClO_2$ → $ClO + ClO_2^-$	$9.6 \times 10^{10} \exp(-7630/T)$	E20
$ClO + ClO_2^-$ → $ClO^- + ClO_2$	9.4×10^8	E21

Reaction			k (L mol^{-1} s^{-1}) *	Note
$HOBr + ClO_2^-$	→	$HOBrOClO^-$	96 ± 6	E22
$BrO^- + ClO_2$	→	$BrO + ClO_2^-$	$4.7 \times 10^{10} \exp(-6910/T)$	E23
$BrO + ClO_2^-$	→	$BrO^- + ClO_2$	1.6×10^7	E23
$ClO + ClO_2$	→	$ClOClO_2$	7×10^9	E23
$BrO + ClO_2$	→	$BrOClO_2$	1.0×10^8	E23
$ClO_2 + Cl^-$	→	products	See Note	E24
$ClO_2 + Br^-$	→	products	$<10^{-4}$	E25
$ClO_2 + I^-$	→	$ClO_2^- + I$	$8.1 \times 10^9 \exp(-4560/T)$	E26

* Unless units noted otherwise

6.6.1 Notes: Halogen Interconversion Reactions

E1. **$OCl/ClO^- + Br^-$.** The reaction was studied by the stopped-flow method and appears to take place by two mechanisms, both a general-acid catalyzed reaction:

$$HA + HOCl + Br^- \rightarrow A^- + H_2O + BrCl$$

and a direct reaction

$$HOCl + Br^- \rightarrow OH^- + BrCl$$

followed, in both cases, by the rapid hydrolysis reaction

$$BrCl + H_2O \rightarrow HOBr + H^+ + Cl^-$$

Kumar and Margerum[27] measured the rate constant for direct reaction in acid by stopped-flow kinetic spectrophotometry to be $k = 1.55 \times 10^3$ L mol^{-1} s^{-1}. The acid-catalyzed reaction has a rate constant of $(1.32 \pm 0.03) \times 10^6$ L^2 mol^{-2} s^{-1} for HA = H^+ and $(6.11 \pm 0.34) \times 10^4$ L^2 mol^{-2} s^{-1} and $(2.09 \pm 0.01) \times 10^4$ L^2 mol^{-2} s^{-1} for chloroacetic acid and acetic acid, respectively. No values were reported for the inorganic acids of importance in atmospheric aerosols. All rate constants are at 25 °C.

Farkas, et al.[15] carried out rate measurements over the pH range 10–14 by using batch reactors and titrating aliquots. The rate constant was proportional to [H^+], indicating HOCl is the only oxidant. At 25 °C, a value of 2.95×10^3 L mol^{-1} s^{-1}was determined, in good agreement with the value of Kumar, et al. From measurement at 15 to 40 °C, a temperature dependence of ~2300 K was estimated.

Bousher, et al.[9] determined rate constants both with and without the addition of alkali and alkaline-metal ions. Measurements over the pH range 8.1–11.4 confirmed that HOCl was the reactive species. There was a small dependence on ionic strength above $\mu = 0.3$ mol L^{-1}, which was suggested to be due to the formation of NaOCl ion-pairs. Rate constants measured over the temperature range 3.3–37.0 °C led to the rate expression $k = 1.57 \times 10^6 \exp(-1.62 \times 10^3/T)$ L mol^{-1} s^{-1} (k(298 K) = 6.8×10^3 L mol^{-1} s^{-1}). Third-order rate constants were derived to express the effect of alkali and alkaline-metal ions: Na^+, 11.6; K^+, 2.9; Mg^{2+}, 4.2×10^3; Ca^{2+}, 1.7×10^4, all in units of L^2 mol^{-2} s^{-1}. Transition-metal ions were found to have no effect on the reaction, other than to be oxidized themselves. Back to Table

E2. **$ClO^- + I^-$.** This value was estimated by Gerritsen and Margerum [18] from a study of the oxidation of iodide by hypochlorite reported earlier from the same laboratory.[26] Back to Table

E3. **$HOCl + I^-$.** In the reaction of HOCl with I^-, there is kinetic evidence from the pulsed-accelerated flow method for the formation of an intermediate addition product.[32]

$$HOCl + I^- \leftrightarrow HOClI^-$$

This is followed by the dissociation of this complex, either directly or acid-assisted

$$HOClI^- \rightarrow OH^- + ICl$$
$$HOClI^- + H^+ \rightarrow H_2O + ICl$$
$$HOClI^- + HA \rightarrow A^- + H_2O + ICl$$

At 298 K and I = 0.1 mol L^{-1}, the equilibrium constant for the formation of the intermediate is $K_{eq} = (2.2 \pm 0.5) \times 10^2$ L mol^{-1}. The forward and reverse rate constants are $(4.3 \pm 0.3) \times 10^8$ L mol^{-1} s^{-1} and (1.9 ± 0.7)

$\times 10^6$ s^{-1}, respectively. Rate constants for the direct dissociation of the complex is $(9 \pm 3) \times 10^5$ s^{-1}; for the proton-assisted dissociation $k = (2.3 \pm 0.5) \times 10^9$ L mol^{-1} s^{-1}; and for the dissociation assisted by $H_2PO_4^-$, $k = (1.7 \pm 0.6) \times 10^8$ L mol^{-1} s^{-1}.

It is expected that any similar complexes for the other halides are too short lived to be important.

The rate constant for the overall reaction

$$HOCl + I^- + H^+ \rightarrow H_2O + ICl$$

can be calculated to be 3.5×10^{11} L^2 mol^{-1} s^{-1}.

For the overall reaction assisted by phosphorous acid

$$HOCl + I^- + H_2PO_4^- \rightarrow H_2O + ICl + HPO_4^{2-}$$

$k = 2.6 \times 10^{10}$ L^2 mol^{-1} s^{-1}.

An earlier study using a rapid-flow technique at 17.3, 25, and 34.3 °C at [NaOH] = 0.3 mol L^{-1} and an ionic strength of 1.0 mol L^{-1} resulted in a rate expression of $k = 1.6 \times 10^9 \exp(-0.9 \text{ kcal/RT})$ L mol^{-1} s^{-1} ($1.6 \times 10^9 \exp(-450/T)$).[30] An earlier study demonstrated that the reaction showed an inverse dependence on $[OH^-]$ and derived a rate constant at 25 °C of 61 s^{-1}.[11] Back to Table

E4. **BrO^-/HOBr + I^-.** The reaction was studied by the accelerated-pulsed flow method at 25 °C and an ionic strength of 0.5 mol L^{-1} by following the loss of BrO^- at 329 nm. $[OH^-]$ was varied from 0.10 to 0.50 mol L^{-1}, leading to the individual rate constants.[42] (As part of this study, the pK_a value for HOBr was determined under these conditions to be 8.8 ± 0.1.) The formation of an intermediate $HOBrI^-$ was suggested, but its lifetime was too short for observation. Back to Table

E5 **IO^- + I^-.** The rate constant was derived during a study of the I_2/I^- system under strongly basic conditions (25 ºC,1 mol L^{-1}, and pH 10.5 and 12). UV/VIS and Raman spectroscopy were used to monitor IO^-, I_2OH^-, and IO_2^-.[46] Back to Table

E6. **HOCl + HOCl.** The decomposition of HOCl/ClO^- has been studied extensively over the past century. In general, the final products have been reported to be chlorate, ClO_3^-, and chloride, with a ratio of HOCl to ClO_3^- of 2.91 ± 0.09.[1] The overall rate is proportional to $[OCl^-]$ and to $[HOCl]^2$, with a maximum at pH 6.9. The observation of both HOCl and Cl_2O in the vapor above HOCl solutions, with the latter predominating at high concentrations,[35] along with the kinetic observations, has led to the accepted mechanism for the system:[1]

$$2\ HOCl \leftrightarrow Cl_2O{\cdot}H_2O \quad (1)$$

$$OCl^- + Cl_2O{\cdot}H_2O \rightarrow HCl_2O_2^- + HOCl \quad (2)$$

$$HCl_2O_2^- \rightarrow HClO_2 + Cl^- \quad (3)$$

$$ClO_2^- + Cl_2O{\cdot}H_2O \rightarrow HCl_2O_3^- + HOCl \quad (4)$$

$$HCl_2O_3^- \rightarrow HClO_3 + Cl^- \quad (5)$$

The equilibrium constant for reaction (1) is uncertain, but has been estimated to be 1.15×10^{-2} at 298 K.[5] A value of 1.5×10^{-2} has also been theoretically calculated (see Note on HOCl + HOBr).[37] A rate constant of $k_1 = 0.12$ L mol^{-1} s^{-1} for the reaction was determined by monitoring the oxidation of $Ni^{II}(CN)_4^{2-}$ by the Cl_2O generated in HOCl solutions at pH 5–6 and $\mu = 0.1$ mol L^{-1}.[5] An acetic acid catalyzed pathway with a rate constant of 280 L^2 mol^{-2} s^{-1} was also reported. A rate constant at $\mu = 0.6$ mol L^{-1} of 0.124 L mol^{-1} s^{-1} for the direct reaction and 3.1 L^2 mol^{-2} s^{-1} for the general acid catalyzed reaction were reported from a study of the chlorination of anisole.[40] The acid-catalyzed pathway is expected to be negligible above pH 4.

At higher pH values (>9), the decomposition reaction is very slow and seems to involve only a second-order interaction of OCl^-

$$2\ OCl^- \rightarrow OClO^- + Cl^- \quad (6)$$

$$OCl^- + OClO^- \rightarrow ClO_3^- + Cl^- \quad (7)$$

where reaction (6) is rate limiting.[2] The rate constant was determined by following the decomposition of 2.15 mol L^{-1} ClO^- at $[OH^-] = 0.10$ mol L^{-1}.[2] A fit of kinetic data taken as a function of temperature (25–50

°C) and ionic strength, μ = (2.5–5.7 mol L^{-1}) led to the complex rate constant expression: log k = 0.149μ + log[2.083 × 10^{10} T exp(–1.018 × 10^5/RT) exp(–56.5/R)]. The enthalpies and entropies of activation range from $\Delta H^{\neq}$ = 101.0 kJ mol^{-1} and $\Delta S^{\neq}$ = –56.2 J $mol^{-1}K^{-1}$ at μ = 1 mol L^{-1} to $\Delta H^{\neq}$ = 97.1 kJ mol^{-1} $\Delta S^{\neq}$ = –54.8 J mol^{-1} K^{-1} at μ = 6 mol L^{-1}. The rate constant for reaction (7) was from the formation and decay of ClO_2^-.

There is also a less important pathway leading to O_2:[29,36]

$$HOCl + HOCl \rightarrow O_2 + 2Cl^- + 2H^+$$

Subsequent work demonstrated that some significant fraction of the oxygen was formed in the excited state, $O_2(^1\Delta_g)$.[24] Mechanistic details for the generation of singlet oxygen in this system have been investigated theoretically.[22] Back to Table

E7. **BrCl + ClO^-/BrO^- and subsequent reactions.** Rate constants for individual steps were obtained in a study of the effect of the bromide ion on solutions of HOCl, by following the evolution of the system spectrophotometrically.[31] This set of reactions, along with others previously reported, was proposed to explain the observations. Back to Table

E8. **HOCl + HOBr.** In a spectrophotometric study of the effect of the bromide ion on solutions of HOCl, no direct reaction of HOCl with HOBr was observed.[31]

$$K_{eq}(HOCl + HOBr) = 0.35$$

Sivey, et al.[37] have carried out quantum chemical calculations on the reaction

$$HOCl + HOBr \rightarrow BrOCl + H_2O$$

Geometric parameters were optimized at the CCSD(T) level of theory using the acg-cc-pVTZ basis set. Energies were computed extrapolating to infinite basis set and corrected for higher order excitations. Additional correction for core/valence correlation and scalar relativistic effects were applied. These gas-phase Gibbs energies were then transferred to the aqueous phase by using a variant of the cluster continuum approach. They obtained a value of K_{eq} = 0.35, with a suggested uncertainty of a factor of two. Taking the same approach, K_{eq}(HOCl + HOCl) = 0.015 was also calculated. Back to Table

E9. ***K_{eq}*(HOBr + HOBr) = 6.31** Beckwith and Margerum measured the rate of hydrobromous acid decomposition at 25 ºC from pH 0.2 to 10.2 spectrophotometrically at 260 nm (310 nm for pH <2).[6] They combined their measurements with literature results, primarily at higher pH, to derive the listed values. A value of K_{eq} = 6.3 for 2HOBr → Br_2O + H_2O has also been theoretically calculated (see Note on HOCl + HOBr).[37] Back to Table

E10. **HOCl/ClO^- + HOI.** The kinetics of the reaction of HOCl/ClO^- with HOI + IO^- was investigated over pH 5.3–8.9 by following the formation of IO_3^-. The rate constant for the HOCl reaction decreased to 5.6 ± 1.0 at 10 ºC. The reaction involved both second-order and a third order paths (second-order in HOCl). The derived third-order rate constant was k^{3d} = (8.3 ± 0.8) × 10^4 $M^{-2}s^{-1}$.[7] For the ClO^-, the rate constant decreased to 33 ± 4 at 10 ºC. Back to Table

E11. **HOI + HOI/IO^-.** The overall disproportionation of HOI involves the self-reaction of HOI to generate IO_2^- in the rate-limiting step, followed by the rapid reaction of IO_2^- with HOI to yield IO_3^- and I^-. The reaction was followed over the pH range 7.6–11.1 by Bichsel and von Gunten[8] at 25 ºC in a batch reactor containing borate or carbonate buffer solutions. Aliquots were withdrawn and an excess of KI added to convert the HOI to I_3^-, which was then measured spectrophotometrically. The measured rates were found to be proportional to $[HOI]^2$, [HOI][OI^-], and [base]$[HOI]^2$, where "base" is the basic form of the buffer. The rate constants obtained for HCO_3^-, CO_3^{2-}, and $B(OH)_4^-$ were 50 ± 20, 5000 ± 500, and 1700 ± 600 L^2 mol^{-2} s^{-1}, respectively.

As part of this study, the acid dissociation constant of HOI was determined to be pK_a = 10.4 ± 0.1 at 25 °C and μ = 0.05 mol L^{-1}.

In an earlier study by Urbansky, et al.,[43] an upper limit of 2 L mol^{-1} s^{-1} for the uncatalyzed reaction at 25 ºC was determined. Both catalysis and inhibition by acetate were observed.

In an earlier work, a rate constant for the reaction at 25 ºC of k = 25 ± 5 L mol^{-1} s^{-1} was reported for a system in which a significant concentration of sulfate/bisulfate was present.[17]

In a study of the I_2/I^- system under strongly basic conditions (25 ºC, 1 mol L^{-1}, and pH 10.5 and 12), using both uv/vis and Raman spectroscopy,[46] a rate constant for HOI + IO^- was reported to be $k = 40 \pm 5$ L mol^{-1} s^{-1}. Back to Table

E12. **IO^- + IO^-.** In a study of the I_2/I^- system under strongly basic conditions (25 ºC, 1 mol L^{-1}, and pH 10.5 and 12), using both uv/vis and Raman spectroscopy,[46] this upper limit was reported for the IO^- + IO^- reaction. Back to Table

E13. **IO^-/HOI + IO_2^-.** The rate constant for the reaction of IO^- + IO_2^- was reported under strongly basic conditions.[46] From a study over the pH range 7.6–11.1, the reaction HOI + IO_2^- was simply reported as "fast".[8] Back to Table

E14. **Cl_2 + I^-.** Pulse radiolysis of a 1 mol L^{-1} NaCl solution pH 3.3) containing 5×10^{-5} mol L^{-1} NaI. The absorption increase at 725 nm was followed and fit to a complex model.[13] Back to Table

E15. Reactions of Cl and Br with HOCl and HOBr and subsequent reactions. Rate constants derived from a laser-flash photolysis study at 248 nm and 308 nm of hypochlorous and hypobromous acid.[25] The X_2O_2 products of the XO self-reactions are expected to convert to XO^- and XO_2^-, primarily through hydrolysis. Back to Table

E16. **IO + IO.** Pulse radiolysis of an N_2O-saturated borate-buffer solution (pH 9) containing HOI.[10] Similar values found using flash photolysis at pH 12.8 (2.1×10^9 [39]) and pulse radiolysis at pH 13.6 (2.0×10^9 [4]) Back to Table

E17. **BrO_2 + $OClO^-$.** Pulse radiolysis at pH 9.2, following both the decay of BrO_2 at 475 nm and the formation of ClO_2^- at 360 nm.[21] In a study of the bromite ion catalysis of ClO_2 disproportionation, the rate constant for the reverse reaction was determined to be 36 L mol^{-1} s^{-1}.[45] Back to Table

E18. **HOCl + $OClO^-$.** The reaction was studied by following the absorption due to OClO at 360 nm using kinetic spectrophotometry.[23] The mechanism is complex and involves the formation of $HOClOClO^-$:

$$HOCl + OClO^- \rightarrow HOClOClO^- \qquad (1)$$

This intermediate reacts with a general base to form the ClO dimer:

$$HOClOClO^- + HA \rightarrow ClOClO + A^- + H_2O \qquad (2)$$

Followed by the rapid reaction:

$$ClOClO + OClO \rightarrow 2OClO + Cl^- \qquad (3)$$

The rate constant $k_1 = 1.6 \pm 0.1$ L mol^{-1} s^{-1} was derived by varying $[H^+]$ and $[H_2PO_4^-]$ by fitting to a complex equation. This also led to $k_2/k_{-1} = 8.5 \pm 0.9$ L mol^{-1} for the phosphate monoanion. For acetic acid, the ratio is 20 L mol^{-1}. From the study in acetic acid, the value k_2/k_{-1} was calculated to be $(1.6 \pm 0.5) \times 10^4$ L mol^{-1} for $[H^+]$.

The ClO dimer reacts with $OClO^-$, OH^-, or a general base catalyst, A^-, all in rapid reactions. The first yields two molecules of ClO_2; the other two generate ClO_3^-.

The work of Jai, et al.[23] built upon and expanded the earlier work of Taube and Dodgen,[41] Peintler, et al.,[34] and Gordon and Tachiyashiki.[19]

In a kinetic spectrophotometric experiment, Yin and Ni determined that the generation or addition of chloride positively influenced the generation of OClO.[47] The mechanism for this effect is not clear. Back to Table

E19 **HOCl + $OBrO^-$.** The reaction was studied by kinetic spectrophotometry.[33] The mechanism is complex and the products of the over-all reaction are given. The loss of BrO_2^- and formation of ClO_2 were both monitored, and ion chromatography was used to determine the end products. The rate-determining steps are:

(1) $HOCl + OBrO^- \leftrightarrow HOClOBrO^-$ $\quad k_1 = 1.6 \times 10^2$ L mol^{-1} s^{-1}

(2) $HOClOBrO^- + H^+ \rightarrow {}^-OClOBrOH + H^+$ $\quad k_2/k_{-1} = 2.8 \times 10^5$ M^{-1}

These are followed by:

(3) $^{-}OClOBrOH \rightarrow ClO_2^{-} + HOBr$ k_3 = fast

(4) $^{-}OClOBrOH + H^{+} \rightarrow ClOBrO + H_2O$ k_4 = fast

The ClO_3^{-} and BrO_3^{-} are formed thru subsequent reactions of HOCl with the ClOBrO intermediate. Cl_2O, formed in the self-reaction on HOCl, $2HOCl \leftrightarrow Cl_2O + H_2O$, $K_{eq} = 0.0115\ M^{-1}$, also reacts with BrO_2^{-}

(5) $Cl_2O + OBrO^{-} \leftrightarrow HOClOBrO^{-}$ $k_5 = 1.8 \times 10^5\ L\ mol^{-1}\ s^{-1}$ Back to Table

E20. ClO⁻ + OClO. From a spectrophotometric study of the effect of hypochlorite on the decomposition of chlorine dioxide.[44] The suppression of the reaction by the addition of ClO_2^{-} led to the conclusion that the reaction is electron transfer, unlike the addition reaction proposed in an earlier study.[12] Activation parameters were determined from measurements over 5−25 °C to be $\Delta H^{\neq} = 61 \pm 3$ kJ mol^{-1} and $\Delta S^{\neq} = -43 \pm 2$ J mol^{-1} K^{-1}. Back to Table

E21. ClO + OClO⁻. Pulse radiolysis of a N_2O-saturated solution of 0.01 mol L^{-1} sodium hypochlorite containing $3. \times 10^{-5}$ to 2.5×10^{-4} mol L^{-1} added sodium chlorite at pH 10.[3] Wang and Margerum estimated $k = 7 \times 10^9$ L mol^{-1} s^{-1}.[44] Back to Table

E22. HOBr + OClO⁻. A study of the formation of ClO_2 and ClO_3^{-} from the action of HOBr with ClO_2^{-} that the intermediate $HOBrOClO^{-}$ (or $HOBrClO_2^{-}$) is formed in a reversible reaction with the listed rate constant.[16] This intermediate then either reacts with a general acid to yield BrOClO or reverts to the original reactants. The ratios of the acid-assisted rate constant to the decomposition rate constant were: $(3.1 \pm 0.5) \times 10^5$ (H_3O^{+}); 8.3 ± 0.6 ($H_2PO_4^{-}$); 0.064 ± 0.004 (HCO_3^{-}); and $\sim 3.5 \times 10^{-6}$ (H_2O), all in units of L mol^{-1}. The intermediate BrOClO then reacts rapidly with either ClO_2^{-} to generate 2 molecules of ClO_2, or with OH^{-} to generate ClO_3^{-}. Back to Table

E23. BrO/BrO⁻ + ClO₂/ClO₂⁻. From a spectrophotometric study of the effect of hypohalites on the decomposition of chlorine dioxide.[44] The suppression of the reaction by the addition of ClO_2^{-} led to the conclusion that the reaction is electron transfer. The equilibrium constant for the reaction was estimated from the reduction potentials, leading to the calculated value for the reverse reaction. The rate constant for the addition of BrO to ClO_2 was evaluated from the effect of excess ClO_2^{-} on the reaction, which leads to a second-order dependence. For the reaction of BrO^{-} with ClO_2, activation parameters of $\Delta H^{\neq} = 55 \pm 1$ kJ mol^{-1} and $\Delta S^{\neq} = -49 \pm 2$ J mol^{-1} K^{-1} for T = 5–25 °C were determined. Back to Table

E24. ClO₂ + Cl⁻. In a careful study of this reaction, either as expressed as a bimolecular reaction or as a termolecular reaction, $2ClO_2 + Cl^{-}$, it was concluded that what little reaction observed was probably due to photolysis by the light source used to monitor the reaction.[38] Back to Table

E25. ClO₂ + Br⁻. The absorbance of ClO_2 at 358 nm was monitored and no reaction observed.[20] Back to Table

E26. ClO₂ + I⁻. The reaction was monitored in a stopped-flow study over the temperature range 3 to 46 °C by following the generation of I_3^{-} in the 350–470 nm range.[14] The 298 K value, $(1.87 \pm 1.02) \times 10^3$ L mol^{-1} s^{-1} is slightly higher than the earlier value of $(1.4 \pm 0.2) \times 10^3$ L mol^{-1} s^{-1},[20] but less than the value of 6×10^3 L mol^{-1} s^{-1} derived from fitting a complex mechanism for the complete chlorine dioxide/chlorite - iodide system.[28] A reaction component second-order in I^{-} was also observed, with $k = 9.4 \times 10^{10} \exp(-4710/T)$ $M^{-2}s^{-1}$ ($(1.25 \pm 0.2) \times 10^4$ $M^{-2}s^{-1}$ at 298 K). Back to Table

6.6.2 References

(1) Adam, L. C.; Fábián, I.; Suzuki, K.; Gordon, G. Hypochlorous acid decomposition in the pH 5-8 region. *Inorg. Chem.* **1992**, *31*, 3534-3541, doi:10.1021/ic00043a011.

(2) Adam, L. C.; Gordon, G. Hypochlorinte ion decomposition: Effects of temperature, ionic strength, and chloride ion. *Inorg. Chem.* **1999**, *38*, 1299-1304, doi:10.1021/ic980020q.

(3) Alfassi, Z. B.; Huie, R. E.; Mosseri, S.; Neta, P. Kinetics of one-electron oxidation by the ClO radical. *Int. J. Radiat. Appl. Inst. Part C. Radiat. Phys. Chem.* **1988**, *32*, 85-88, doi:10.1016/1359-0197(88)90018-5.

(4) Amichai, O.; Treinin, A. On the oxyiodine radicals in aqueous solution. *J. Phys. Chem.* **1970**, *74*, 830-835.

(5) Beach, M. W.; Margerum, D. W. Kinetics of oxidation of tetracyanonickelate(Ii) by chlorine monoxide, chlorine, and hypochlorous acid and kinetics of chlorine monoxide formation. *Inorg. Chem.* **1990**, *29*, 1225-1232, doi:10.1021/ic00331a023.
(6) Beckwith, R. C.; Margerum, D. W. Kinetics of hypobromous acid disproportionation. *Inorg. Chem.* **1997**, *17*, 3754-3760, doi:10.1021/ic970155g.
(7) Bichsel, Y.; von Gunten, U. Oxidation of iodide and hypoiodous acid in the disinfection of natural waters. *Environ. Sci. Technol.* **1999**, *33*, 4040-4045, doi:10.1021/es990336c.
(8) Bichsel, Y.; Von Gunten, U. Hypoiodous acid: kinetics of the buffer-catalyzed disproportionation *Water Research* **2000**, *34*, 3197-3203, doi:10.1016/S0043-1354(00)00077-4.
(9) Bousher, A.; Brimblecombe, P.; Midgley, D. Kinetics of reactions in solutions containing monochloramine and bromide *Water Res.* **1989**, *23*, 1049-1058, doi:10.1016/0043-1354(89)90180-2.
(10) Buxton, G. V.; Kilner, C.; Sellers, R. M. Pulse radiolysis of HOI and IO- in aqueous solution. Formation and characterisation of I(II). *Proc. Tihany Symp. Radiat. Chem.* **1986**, *6*, 155-159.
(11) Chia, Y. T.; Connick, R. E. The rate of oxidation of I^- to hypoiodite ion by hypochlorite ion. *J. Phys. Chem.* **1959**, *63*, 1518-1519, doi:10.1021/j150579a051.
(12) Csordas, V.; Bubnis, B.; Fabian, I.; Gordon, G. Kinetics and mechanism of catalytic decomposition and oxidation of chlorine dioxide by the hypochlorite ion. *Inorg. Chem.* **2001**, *40*, 1833-1836, doi:10.1021/ic001106y.
(13) Ershov, B. G.; Janata, E.; Gordeev, A. V. Pulse radiolysis study of I^- oxidation with radical anions $Cl_2^{\bullet-}$ in an aqueous solution. *Russ. Chem. Bull.* **2005**, *54*, 1378-1382, doi:10.1007/s11172-005-0413-2.
(14) Fábián, I.; Gordon, G. The kinetics and mechanism of the chlorine dioxide-iodine ion reaction. *Inorg. Chem.* **1997**, *36*, 2494-2497, doi:10.1021/ic961279g.
(15) Farkas, L.; Lewin, M.; Bloch, R. The reaction between hypochlorities and bromides. *J. Am. Chem. Soc.* **1949**, *71*, 1988-1991, doi:10.1021/ja01174a025.
(16) Furman, C. S.; Margerum, D. W. Mechanism of chlorine dioxide and chlorate ion formation from the reaction of hypobromous acid and chlorite ion. *Inorg. Chem.* **1998**, *37*, 4321-4327, doi:10.1021/ic980262q.
(17) Furrow, S. Reactions of iodine intermediates in iodate-hydrogen peroxide oscillators. *J. Phys. Chem.* **1987**, *91*, 2129-2135, doi:10.1021/j100292a031.
(18) Gerritsen, C. M.; Margerum, D. W. Nonmetal redox kinetics - hypochlorite and hypochlorous acid reactions with cyanide. *Inorg. Chem.* **1990**, *29*, 2757-2762, doi:10.1021/ic00340a010.
(19) Gordon, G.; Tachiyashiki, S. Kinetics and mechanism of formation of chlorate ion from the hypochlorous acid/chlorite ion reaction at pH 6-10. *Environ. Sci. Technol.* **1991**, *25*, 468-474, doi:10.1021/es00015a014.
(20) Hoigné, J.; Bader, H. Kinetics of reactions of chlorine dioxide (OClO) in water. - 1. Rate constants for inorganic and organic compounds. *Water Research* **1994**, *28*, 45-55, doi:10.1016/0043-1354(94)90118-X.
(21) Huie, R. E.; Neta, P. Kinetics of one-electron transfer-reactions involving ClO_2 and NO_2. *J. Phys. Chem.* **1986**, *90*, 1193-1198, doi:10.1021/j100278a046.
(22) Jacobsen, J.; Jensen, S. J. K. A mechanism for production of singlet oxygen by acidification of hypochlorite. *Chem. Phys. Lett.* **2007**, *449*, 135-137, doi:10.1016/j.cplett.2007.10.056.
(23) Jia, Z. J.; Margerum, D. W.; Francisco, J. S. General-acid-catalyzed reactions of hypochlorous acid and acetyl hypochlorite with chlorite ion. *Inorg. Chem.* **2000**, *39*, 2614-2620, doi:10.1021/ic991486r.
(24) Khan, A. U.; Kasha, M. Singlet molecular oxygen evolution upon simple acidification of aqueous hypochlorite: Application to studies on the deleterious health effects of chlorinated drinking water. *Proc. Natl. Acad. Sci. USA* **1994**, *91*, 12362-12364.
(25) Kläning, U. K.; Sehested, K.; Holcman, J. Standard Gibbs energy of formation of the hydroxyl radical in aqueous solution. Rate constants for the reaction $ClO_2^- + O_3 \rightleftarrows O_3^- + ClO_2$. *J. Phys. Chem.* **1985**, *89*, 760-763, doi:10.1021/j100251a008.
(26) Kumar, K.; Day, R. A.; Margerum, D. W. Atom-transfer redox kinetics - general-acid-assisted oxidation of iodide by chloramines and hypochlorite. *Inorg. Chem.* **1986**, *25*, 4344-4350, doi:10.1021/ic00244a012.

(27) Kumar, K.; Margerum, D. W. Kinetics and mechanism of general-acid-assisted oxidation of bromide by hypochlorite and hypochlorous acid. *Inorg. Chem.* **1987**, *26*, 2706-2711, doi:10.1021/ic00263a030.
(28) Lengyel, I.; Li, J.; Kustin, K.; Epstein, I. R. Rate constants for reactions between iodine- and chlorine-containing species: A detailed mechanism of the chlorine dioxide/ chlorite-iodide reaction. *J. Am. Chem. Soc.* **1996**, *118*, 3708-3719, doi:10.1021/ja953938e.
(29) Lister, M. W.; Petterson, R. C. Oxygen evolution from sodium hypochlorite solutions. *Can. J. Chem.* **1962**, *40*, 729-733, doi:10.1139/v62-109.
(30) Lister, M. W.; Rosenblum, P. Rates of reaction of hypochlorite ions with sulphite and iodide ions. *Can. J. Chem.* **1963**, *41*, 3013-3020, doi:10.1139/v63-442.
(31) Margerum, D. W.; Hartz, K. E. H. Role of halogen(I) cation-transfer mechanisms in water chlorination in the presence of bromide ion. *J. Environ. Monit.* **2002**, *4*, 20-26, doi:10.1039/b105541k.
(32) Nagy, J. C.; Kumar, K.; Margerum, D. W. Non-metal redox kinetics: Oxidation of iodide by hypochlorous acid and by nitrogen trichloride measured by the pulsed-accelerated-flow method. *Inorg. Chem.* **1988**, *27*, 2773-2780, doi:10.1021/ic00289a007.
(33) Nicoson, J. S.; Perrone, T. F.; Hartz, K. E. H.; Margerum, D. W. Kinetics and mechanisms of the reactions of hypochlorous acid, chlorine, and chlorine monoxide with bromite ion. *Inorg. Chem.* **2003**, *42*, 5818-5824, doi:10.1021/ic0301223.
(34) Peintler, G.; Nagypál, I.; Epstein, I. R. Kinetics and mechanism of the reactions between chlorite and hypochlorous acid. *J. Phys. Chem.* **1990**, *94*, 2954-2958, doi:10.1021/j100370a040.
(35) Renard, J. J.; Bolker, H. I. The chemistry of chlorine monoxide (dochlorine monoxide). *Chem. Rev.* **1976**, *76*, 487-508, doi:10.1021/cr60302a004.
(36) Sandin, S.; Karlsson, R. K. B.; Cornell, A. Catalyzed and uncatalyzed decomposition of hypochlorite in dilute solutions. *Ind. Eng. Chem. Res.* **2015**, *54*, 3767-3774, doi:10.1021/ie504890a.
(37) Sivey, J. D.; Arey, J. S.; Tentscher, P. R.; Roberts, A. L. Reactivity of BrCl, Br_2, BrOCl, Br_2O, and HOBr toward dimethenamid in solutions of bromide + aqueous free chlorine. *Environ. Sci. Technol.* **2013**, *47*, 1330-1338, doi:10.1021/es302730h.
(38) Stanbury, D. M.; Figlar, J. N. Vanishingly small kinetics of the ClO_2/Cl^- reaction: its questionable significance in nonlinear chlorite reactions. *Coord. Chem. Revs.* **1999**, *187*,
223-232.
(39) Subhani, M. S. Photodecomposition of hypoiodite ion in aqueous solution. *Rev. Roum. Chim.* **1983**, *28*, 397-403.
(40) Swain, C. G.; Crist, D. R. Mechanisms of chlorination by hypochlorous acid. The last of chlorinium ion, Cl^{+1}. *J. Am. Chem. Soc.* **1972**, *94*, 3195-3200, doi:10.1021/ ja00764a050.
(41) Taube, H.; Dodgen, H. Applications of radioactive chlorine to the study of the mechanisms of reactions involving changes in the oxidation state of chlorine. *J. Am. Chem. Soc.* **1949**, *71*, 3330-3336, doi:10.1021/ja01178a016.
(42) Troy, R. C.; Margerum, D. W. Nonmetal redox kinetics - Hypobromite and hypobromous acid reactions with iodide and with sulfite and the hydrolysis of bromosulfate. *Inorg. Chem.* **1991**, *30*, 3538-3543, doi:10.1021/ic00018a028.
(43) Urbansky, E. T.; Cooper, B. T.; Margerum, D. W. Disproportionation kinetics of hypoiodous acid as catalyzed and supressed by acetic acid-acetate buffer. *Inorg. Chem.* **1997**, *36*, 1338-1344, doi:10.1021/ic960745z.
(44) Wang, L.; Margerum, D. W. Hypohalite ion catalysis of the disproportionation of chlorine dioxide. *Inorg. Chem.* **2002**, *41*, 6099-6105, doi:10.1021/ic020440m.
(45) Wang, L.; Nicoson, J. S.; Hartz, K. E. H.; Francisco, J. S.; Margerum, D. W. Bromite ion catalysis of the disproportionation of chlorine dioxide with nucleophile assistance of electron-transfer reactions between ClO_2 and BrO_2 in basic solution. *Inorg. Chem.* **2002**, *41*, 108-113, doi:10.1021/ic010849w.
(46) Wren, J. C.; Paquette, J.; Sunder, S.; Ford, B. L. Iodine chemistry in the +1 oxidation state. II. A Raman and uv–visible spectroscopic study of the disproportionation of hypoiodite in basic solutions. *Can. J. Chem.* **1986**, *64*, 2284-2296, doi:10.1139/v86-375.

(47) Yin, G. H.; Ni, Y. G. Quantitative description of the chloride effect on chlorine dioxide generation from the ClO_2^- -HOCl reaction *Can. J. Chem. Eng.* **1998**, *76*, 921-926, doi:10.1002/cjce.5450760509

6.7 Other Reactions of Possible Importance

Reaction			k (L mol^{-1} s^{-1})	Note
$OH + NO$	→	$HONO$	1.0×10^{10}	F1
$OH + NO_2$	→	$HONO_2$	4.5×10^{9}	F2
$HO_2/O_2^- + NO$	→	$HOONO/^-OONO$	$>7.5 \times 10^{9}$	F3
$HO_2 + NO_2$	→	HO_2NO_2	1.8×10^{9}	F4
$CO_3^- + H_2O_2$	→	$HCO_3^- + HO_2$	8×10^{5}	F5
$SO_4^- + CO_3^{2-}$	→	$SO_4^{2-} + CO_3^-$	$2 \times 10^{11} \exp(-6410/T)$	F6

6.7.1 Notes: Other Reactions of Possible Importance

F1. **OH + NO.** Rate constant determined in a complex reaction system by the pulse radiolysis of NO solutions at pH 7, monitoring NO_2^- at 220 nm.[6] Back to Table

F2. **OH + NO_2.** Rate constant determined by monitoring the formation of $OONO^-$ at 300 nm in N_2O-saturated solutions containing (0.05-1.0) × 10^{-3} mol L^{-1} $NaNO_2$.[4] Back to Table

F3. **O_2^-/HO_2 + NO.** A limiting rate constant obtained from the flash photolysis investigation of $OONO^-$ solutions at 37 ºC and pH >12.[2] It was obtained by extrapolating values obtained from the equilibrium constant and the measured dissociation rate constant, to $[OONO^-] \rightarrow 0$. This rate constant is essentially at the diffusion rate and shows a small negative temperature dependence. This value agrees with $k = 6.7 \times 10^9$ L mol^{-1} s^{-1} at room temperature obtained from the flash photolysis of nitrate ion in the presence of formate.[3] In this study, no dependence of the rate constant on pH was found.

Computer fit to yield of ONO_2^- at 300 nm 8 ms after the pulse in N_2O-saturated solution containing (0.05-1.0) × 10^{-3} mol L^{-1} $NaNO_2$; pK_a (HO_2NO) = 6.5. Back to Table

F4. **HO_2 + NO_2.** Product buildup kinetics after the pulse radiolysis of a 1 mmol L^{-1} nitrate solution at 10 atm O_2.[4] Back to Table

F5. **CO_3^- + H_2O_2.** Pulse radiolysis of aqueous carbonate solutions at pH 8-9 following the decay of the absorption at 600 nm.[1] A rate constant of 5.6×10^7 L mol^{-1} s^{-1} for the reaction of CO_3^- with HO_2^- was also obtained. Back to Table

F6. **SO_4^- + CO_3^{2-}.** Laser-flash photolysis of a persulfate solution containing various amounts of carbonate over the temperature range 11-58 ºC,[5] $E_a = -26.8 \pm 0.5$ kJ mol^{-1}. Back to Table

6.7.2 References

(1) Behar, D.; Czapski, G.; Duchovny, I. Carbonate radical in flash photolysis and pulse radiolysis of aqueous carbonate solutions. *J. Phys. Chem.* **1970**, *74*, 2206-2210, doi:10.1021/j100909a029.

(2) Botti, H.; Möller, M. N.; Steinmann, D.; Nauser, T.; Koppenol, W. H.; Denicola, A.; Radi, R. Distance-dependent diffusion-controlled reaction of •NO and O_2•- at chemical equilibrium with $ONOO^-$. *J. Phys. Chem. B* **2010**, *114*, 16584-16593, doi:10.1021/jp105606b.

(3) Huie, R. E.; Padmaja, S. The reaction of NO with superoxide. *Free Rad. Res. Comm.* **1993**, *18*, 195-199, doi:10.3109/10715769309145868.

(4) Løgager, T.; Sehested, K. Formation and decay of peroxynitric acid: A pulse radiolysis study. *J. Phys. Chem.* **1993**, *97*, 10047-10052, doi:10.1021/j100141a025.

(5) Padmaja, S.; Neta, P.; Huie, R. E. Rate constants for some reactions of inorganic radicals with inorganic ions. Temperature and solvent dependence. *Int. J. Chem. Kinet.* **1993**, *25*, 445-455, doi:10.1002/kin.550250604.

(6) Seddon, W. A.; Fletcher, J. W.; Sopchyshyn, F. C. Pulse radiolysis of nitric oxide in aqueous solution. *Can. J. Chem.* **1973**, *51*, 1123-1130, doi:10.1139/v73-166.

6.8 Reactions of other Oxidants with Halides

Reaction	k (L mol^{-1} s^{-1}) *	Note
$NO_3 + Cl^- \rightarrow Cl + NO_3^-$	$(3.5 \pm 0.5) \times 10^8$	G1
$NO_3 + Br^- \rightarrow Br + NO_3^-$	4×10^9	G2
$NO_3 + I^- \rightarrow I + NO_3^-$	$(4.6 \pm 0.5) \times 10^9$	G3
$NO_3 + HOCl \rightarrow ClO + HNO_3$	4.3×10^7	G4
$NO_3 + ClO^- \rightarrow ClO + NO_3^-$	3.6×10^9	G5
$NO_2 + I^- \rightarrow NO_2^- + I$	1.1×10^5	G6
$HOONO_2 + Cl^- \rightarrow HOCl + NO_3^-$	1.4×10^{-3}	G7
$HOONO_2 + Br^- \rightarrow HOBr + NO_3^-$	0.54	G7
$HOONO_2 + I^- \rightarrow HOI + NO_3^-$	890	G7
$CO_3^- + 2Br^- \rightarrow CO_3^{2-} + Br_2^-$	$(3.4 \pm 0.5) \times 10^4$ L^2 mol^{-2} s^{-1}	G8
$CO_3^- + I^- \rightarrow$ products	$2.5 \times 10^6 \exp(2720/T)$	G9
$CO_3^- + ClO^- \rightarrow CO_3^{2-} + ClO$	$(5.7 \pm 0.7) \times 10^7$	G10
$SO_4^- + Cl^- \rightarrow Cl + SO_4^{2-}$	$(2.47 \pm 0.09) \times 10^8$	G11
$SO_4^- + Br^- \rightarrow Br + SO_4^{2-}$	3.5×10^9	G12
$SO_4^- + I^- \rightarrow I + SO_4^{2-}$	See Note	G13
$SO_4^- + HOCl \rightarrow HSO_4^- + ClO$	1.1×10^7	G14
$SO_4^- + ClO^- \rightarrow SO_4^{2-} + ClO$	6.6×10^9	G15
$HSO_5^- + Cl^- \rightarrow HSO_4^- + ClO^-$	$(2.06 \pm 0.03) \times 10^{-3}$	G16
$HSO_5^- + Br^- \rightarrow HSO_4^- + BrO^-$	$(2.8 \pm 0.5) \times 10^{-4}$	G16
$HSO_5^- + I^- \rightarrow HSO_4^- + IO^-$	$(7.0 \pm 0.1) \times 10^{-1}$	G16
$SO_5^{2-} + Cl^- \rightarrow SO_4^{2-} + ClO^-$	$(1.7 \pm 0.3) \times 10^{-1}$	G16
$SO_5^{2-} + Br^- \rightarrow SO_4^{2-} + BrO^-$	$(1.41 \pm 0.03) \times 10^3$	G16
$SO_5^{2-} + I^- \rightarrow SO_4^{2-} + IO^-$	$(3.0 \pm 0.2) \times 10^2$	G16

* Unless units noted otherwise

6.8.1 Notes: Reactions of other Oxidants with Halides

G1. **$NO_3 + Cl^-$.** Derived from a study at room temperature, 20 ± 2 ºC, of the pulse radiolysis of deoxygenated solutions containing nitric acid and sodium chloride, monitoring NO_3 at 641 nm and Cl_2^- at 340 nm. The equilibrium constant, $K_{eq} = 3.5 \pm 0.5$, and the forward rate constant were derived from modeling a complex mechanism.[12] The rate constant for the reverse reaction, $(1.02 \pm 0.04) \times 10^8$, was taken from a study in which chlorine atoms were generated through the flash photolysis of chloroacetone.[2] In this latter work, there was some apparent dependence of the forward rate constant on ionic strength, with an almost identical rate constant when extrapolated to zero ionic strength, to that listed here. A measurement using flash photolysis of cerium nitrate in nitric acid resulted in $k = 9.1 \times 10^6$ L mol^{-1} s^{-1}, considerably lower than other reported measurements.[16] This is similar to values reported earlier from persulfate flash photolysis, when extrapolated to zero ionic strength.[3] Back to Table

G2. **$NO_3 + Br^-$.** Pulse radiolysis in a 5 mol L^{-1} $NaNO_3$ solution monitoring the decay of NO_3 at 640 nm.[11] Back to Table

G3. **$NO_3 + I^-$.** Derived from studies of the uptake of NO_3 into KI solutions at 273 ± 1 K.[15] Back to Table

G4. **$NO_3 + HClO$.** Pulse radiolysis of a 0.015 mol^{-1} L^{-1} HNO_3 solution, following the decay of NO_3 at 635 nm.[16] Back to Table

G5. **$NO_3 + ClO^-$.** Pulse radiolysis of a 5 mol^{-1} L^{-1} $NaNO_3$ solution, following the decay of NO_3 at 635 nm.[16] Back to Table

G6. **$NO_2 + I^-$.** Pulse radiolysis study. Actual data unpublished, but cited.[4] Rate constant for the reverse reaction was measured to be $k = 8.8 \times 10^8$ in an investigation of the laser-flash photolysis of triiodide solutions.[1] Back to Table

G7. **$HOONO_2 + X^-$.** Decay of peroxynitric acid at 298.2 K was followed by spectroidometry, in which a small aliquot of the dilute reaction mixture was added to a solution containing a great excess of KI and the I_3^- generated monitored at 352 nm.[14] Back to Table

G8. **$CO_3^- + 2Br^-$.** Derived from a pulse radiolysis study of the equilibrium reaction at an ionic strength of 3 mol L^{-1}.[7] The rate constant for the reverse reaction is $(1.05 \pm 0.1) \times 10^5$ L $mol^{-1}s^{-1}$. Back to Table

G9. **$CO_3^- + I^-$.** Pulse radiolysis of a carbonate solution at pH 11.4 over the temperature range 4 to 79 °C. The negative temperature dependence of E_a = 11.4 kJ mol^{-1} suggests that this reaction involves the formation of an intermediate adduct.[8] Back to Table

G10. **$CO_3^- + ClO^-$.** From a pulse radiolysis study of the approach to equilibrium, monitoring CO_3^- at 600 nm.[7] The rate constant for the reverse reaction is $(6 \pm 2) \times 10^2$ L $mol^{-1}s^{-1}$. Back to Table

G11. **$SO_4^- + Cl^-$.** Rate constants measured by laser-flash photolysis over the temperature range 11 to 35 °C and corrected to zero ionic strength gave a constant value within experimental error.[6] The absorption due to SO_4^- was followed at 500 nm to avoid interference from absorption due to Cl_2^-. The rate constant for the reverse reaction was determined by modeling the system to be 2.5×10^8 L $mol^{-1}s^{-1}$.[7] Back to Table

G12. **$SO_4^- + Br^-$.** Rate constant measured through the pulse radiolysis of a $S_2O_8^{2-}$ solution containing 0.5 mol L^{-1} *tert*-BuOH.[13] Back to Table

G13. **$SO_4^- + I^-$.** A rate constant for this reaction of $(1.8 \pm 0.1) \times 10^8$ L $mol^{-1}s^{-1}$ was calculated from fitting a complex mechanism for the photoinitiated autoxidation of S(IV) in the presence of iodide ion.[9] Based on the values for the reactions of SO_4^- with Cl^- and Br^-, this value seems much too low. Back to Table

G14. **$SO_4^- + HOCl$.** Pulse radiolysis of a 1 mol^{-1} L^{-1} H_2SO_4 solution containing HOCl, following the decay of SO_4^-.[16] Back to Table

G15. **$SO_4^- + ClO^-$.** Pulse radiolysis of a 2 mol^{-1} L^{-1} Li_2SO_4 solution containing ClO^-, following the decay of SO_4^-.[16] A rate constant of 1.3×10^9 L mol^{-1} s^{-1} at zero ionic strength was calculated. Back to Table

G16. **$HSO_5^-/SO_5^{2-} + X^-$.** Rate constants determined by kinetic spectrophotometry, both regular and stopped-flow.[10] At a halide excess, for Cl^-, Cl_2 is the dominate product; for I^-, it is I_3^-, but for Br^-, the final product depends upon pH. Kinetics were measured over the pH range 0 to 10, with the results independent of pH in the acid region, but dropping rapidly from pH 7 to 10, reflecting the deprotonation of HSO_5^-. For the reactions of HSO_5^- with the halides, measurements over the temperature range of ~10–30 ºC resulted in $\Delta H^{\#} = 58.9 \pm 0.5$ k J mol^{-1} and $\Delta S^{\#} = -100 \pm 2$ J K^{-1} mol^{-1} for Cl^-; $\Delta H^{\#} = 44.8 \pm 1.6$ k J mol^{-1} and $\Delta S^{\#} = -97 \pm 5$ J K^{-1} mol^{-1} for Br^-; $\Delta H^{\#} = 27.7 \pm 0.7$ k J mol^{-1} and $\Delta S^{\#} = -91 \pm 2$ J K^{-1} mol^{-1} for I^-. These rate constants are in good agreement with those reported earlier by Fortnum, et al.[5] Back to Table

6.8.2 References

(1) Barkatt, A.; Ottolenghi, M. Laser flash photolysis of aqueous triiodide solutions. *Mol. Photochem.* **1974**, *6*, 253-261.

(2) Buxton, G. V.; Salmon, G. A.; Wang, J. The equilibrium $NO_3^{\bullet} + Cl^- \rightleftarrows NO_3^- + Cl^{\bullet}$: A laser flash photolysis and pulse radiolysis study of the reactivity of NO_3 with chloride ion in aqueous solution. *Phys. Chem. Chem. Phys.* **1999**, *1*, 3589-3593, doi:10.1039/A903286J.

(3) Exner, M.; Herrmann, H.; Zellner, R. Laser-based studies of reactions of the nitrate radical in aqueous solution. *Ber. Bunsenges. Phys. Chem.* **1992**, *96*, 470-477, doi:10.1002/bbpc.19920960347.

(4) Forni , G. L.; Mora-Arellano , V. O.; Packer , J. E.; Willson , R. L. Nitrogen dioxide and related free radicals: Electron-transferreactions with organic compounds in solutions containing nitrite or nitrate. *J. Chem. Soc. Perkin Trans. II* **1986**, 1-6 doi:10.1039/P29860000001.

(5) Fortnum, D. H.; Battaglia, C. J.; Cohen, S. R.; Edwards, J. O. The kinetics of the oxidation of halide ions by monosubstituted peroxides. *J. Am. Chem. Soc.* **1960**, *82*, 778-782, doi:10.1021/ja01489a004.

(6) Huie, R. E.; Clifton, C. L. Temperature dependence of the rate constants for reactions of the sulfate radical, SO_4^-, with anions. *J. Phys. Chem.* **1990**, *94*, 8561-8567, doi:10.1021/j100386a015.

(7) Huie, R. E.; Clifton, C. L.; Neta, P. Electron transfer reaction rates and equilibria of the carbonate and sulfate radical anions. *Int. J. Radiat. Appl. Inst. Part C. Radiat. Phys. Chem.* **1991**, *38*, 477-481, doi:10.1016/1359-0197(91)90065-A.

(8) Huie, R. E.; Shoute, L. C. T.; Neta, P. Temperature dependence of the rate constants for reactions of the carbonate radical with organic and inorganic reductants. *Int. J. Chem. Kinet.* **1991**, *23*, 541-552, doi:10.1002/kin.550230606.

(9) Kerezsi, I.; Lente, G.; Fábián, I. Kinetics and mechanism of the photoinitiated autoxidation of sulfur(IV) in the presence of iodide ion. *Inorg. Chem.* **2007**, *46*, 4230-4238, doi:10.1021/ic061521b.

(10) Lente, G.; Kalmár, J.; Baranyai, Z.; Kun, A.; Kék, I.; Bajusz, D.; Takács, M.; Veres, L.; Fábián, I. One- versus two-electron oxidation with peroxomonosulfate ion: Reactions with iron(II), vanadium(IV), halide ions, and photoreaction with cerium(III). *Inorg. Chem.* **2009**, *48*, 1763, doi:10.1021/ic801569k.

(11) Neta, P.; Huie, R. E. Rate constants for reactions of NO_3 radicals in aqueous-solutions. *J. Phys. Chem.* **1986**, *90*, 4644-4648, doi:10.1021/j100410a035.

(12) Poskrebyshev, G. A.; Huie, R. E.; Neta, P. The rate and equilibrium constants for the reaction $NO_3\cdot + Cl^- \leftrightarrow NO_3^- + Cl\cdot$ in aqueous solutions. *J. Phys. Chem. A* **2003**, *107*, 1964-1970, doi:10.1021/jp0215724.

(13) Redpath, J. L.; Willson, R. L. Chain reactions and radiosensitization: Model enzyme studies. *Int. J. Radiat. Biol.* **1975**, *27*, 389-398, doi:10.1080/09553007514550361.

(14) Régimbal , J. M.; Mozurkewich, M. Kinetics of peroxynitric acid reactions with halides at low pH. *J. Phys. Chem. A* **2000**, *104*, 6580-6589, doi:10.1021/jp971908n.

(15) Rudich, Y.; Talukdar, R. K.; Imamura, T.; Fox, R. W.; Ravishankara, A. R. Uptake of NO_3 on KI solutions: rate coefficient fo the $NO_3 + I^-$ reaction and gas-phase difussion coefficients for NO_3. *Chem. Phys. Lett.* **1996**, *261*, 467-473, doi:10.1016/0009-2614(96)00980-3.

(16) Zuo, Z.; Katsumura, Y.; Ueda, K.; Ishigure, K. Reactions between some inorganic radicals and oxychlorides studied by pulse radiolysis and laser photolysis. *J. Chem. Soc. Faraday Trans.* **1997**, *93*, 1885-1891, doi:10.1039/A700256D.

6.9 Reactions of Reductants with Halides

Reaction			k (L mol^{-1} s^{-1})	Note
$NO + HOCl$	$\rightarrow$	products	Fast, See Note	H1
$NO_2 + HOCl$	$\rightarrow$	products	Slow, See Note	H1
$NO_2^- + HOCl$	$\leftrightarrow$	$ClNO_2 + OH^-$	$K_{eq} = (2.2 \pm 0.2) \times 10^{-4}$	H2
$ClNO_2 + NO_2^-$	$\rightarrow$	$N_2O_4 + Cl^-$	See Note	H2
$ClNO_2 + H_2O$	$\rightarrow$	$NO_3^- + Cl^- + 2H^+$	See Note	H2
$NO_2^- + HOBr$	$\leftrightarrow$	$BrNO_2 + OH^-$	$K_{eq} = (10 \pm 2) \times 10^{-6}$	H3
$BrNO_2 + NO_2^-$	$\rightarrow$	$N_2O_4 + Br^-$	$(5.5 \pm 1.1) \times 10^3$	H3
$NO_2^- + Br_2^-$	$\rightarrow$	$NO_2 + 2Br^-$	$5.0 \times 10^9 \exp(-1720/T)$	H4
$HSO_3^- + Cl_2^-$	$\rightarrow$	$SO_3^- + H^+ + 2Cl^-$	$2.0 \times 10^{10} \exp(-1080/T)$	H5
$HSO_3^- + Br_2^-$	$\rightarrow$	$SO_3^- + H^+ + 2Br^-$	$7.9 \times 10^8 \exp(-780/T)$	H6
$HSO_3^- + I_2^-$	$\rightarrow$	$SO_3^- + H^+ + 2I^-$	$2.0 \times 10^9 \exp(-2980/T)$	H7
$SO_3^{2-} + Cl_2^-$	$\rightarrow$	$SO_3^- + 2Cl^-$	6.2×10^7	H8
$SO_3^{2-} + Br_2^-$	$\rightarrow$	$SO_3^- + 2Br^-$	$8.1 \times 10^9 \exp(-650/T)$	H9
$SO_3^{2-} + I_2^-$	$\rightarrow$	$SO_3^- + 2I^-$	$2.0 \times 10^{10} \exp(-1420/T)$	H10
$NH_3 + HOCl$	$\rightarrow$	$NH_2Cl + H_2O$	$5.40 \times 10^9 \exp(-2237/T)$	H11
$NH_3 + HOBr$	$\rightarrow$	$NH_2Br + H_2O$	5.5×10^7	H12
$NH_3 + BrO^- (+ H^+)$	$\rightarrow$	$NH_2Br + H_2O$	8.8×10^4	H12

6.9.1 Notes: Reactions of Reductants with Halides

H1. **HOCl + NO.** This reaction was investigated by Ghibaudi, et al. by bubbling a gas stream containing NO through solutions of HOCl. A rapid uptake was observed, along with the evolution of NO_2.[7] The uptake lessened at higher pH, leading to the conclusion that ClO^- is 30 times less reactive toward NO than HOCl. Based upon their observations, the authors suggested that the reaction involved a OH transfer, followed by a short chain:

$$NO + HOCl \leftrightarrow HONO + Cl$$

$$Cl + HOCl \rightarrow HCl + ClO$$

$$ClO + NO \rightarrow Cl + NO_2$$

The initial reaction is endothermic, necessitating the subsequent chain.

Subsequent studies have demonstrated that Cl^+ transfer is the predominant mode of HOCl oxidations[10] and, thus, the following reaction scheme seems more likely:

$$NO + HOCl \leftrightarrow NOCl^+ + OH^-$$

$$NOCl^+ + H_2O \rightarrow NOClOH + H^+$$

$$NOClOH \rightarrow NO_2 + HCl$$

Regardless of the mechanism, the observation that NO_2 bubbles out of the solution as NO is bubbled in suggests that any reaction of HOCl with NO_2 must be slow. Back to Table

H2. **HOCl + NO_2^-.** Although there have been a number of measurements, discussed below, we report here only an equilibrium constant along with rate constants for the two subsequent reactions, all in a NaCl solution at $\mu = 0.01$M.

There have been a large number of studies of the reaction of hypochlorous acid with nitrous acid. There is essential agreement on the overall behavior of the reaction system, but some differences in the details of how the data are interpreted. The earliest studies identified nitrate and chloride as products, leading to the suggestion that this was an O-atom transfer reaction from the hypochlorite ion.[1,15] Pendelbury and Smith[17] suggested the reaction instead involved the reversible formation of nitryl chloride, NO_2Cl, with subsequent

reactions leading to the final products. This was supported in kinetic studies at 25 ºC by Cachaza, et al.[3] and Johnson and Margerum.[10] Other studies of the reaction have further supported this basic mechanism. For example, it has been observed that when hypochlorous acid reacts with nitrite, a reactive species capable of nitrating and chlorinating organic compounds is generated.[5,11] Further, a transient species with the spectral characteristics of nitryl chloride, NO_2Cl, has been observed directly in the reaction.[5] One of the proposed mechanistic steps, the reaction of nitryl chloride with nitrite, has been confirmed by observing the release of NO_2 into the gas phase in a wetted-wall flow tube.[6] The uptake is suppressed by Cl^-, suggesting that the hydrolysis reaction is reversible (probably in an initial step involving the formation of NO_2^+) and that the reaction of nitryl chloride with chloride is slow.

The generally-agreed upon mechanism for the reaction is:

(1) $ClO^- + H^+ \leftrightarrow HOCl$

(2) $HOCl + NO_2^- \leftrightarrow NO_2Cl + OH^-$

(3) $NO_2Cl + NO_2^- \rightarrow N_2O_4 + Cl^-$

(4) $N_2O_4 + OH^- \rightarrow NO_2^- + NO_3^- + H^+$

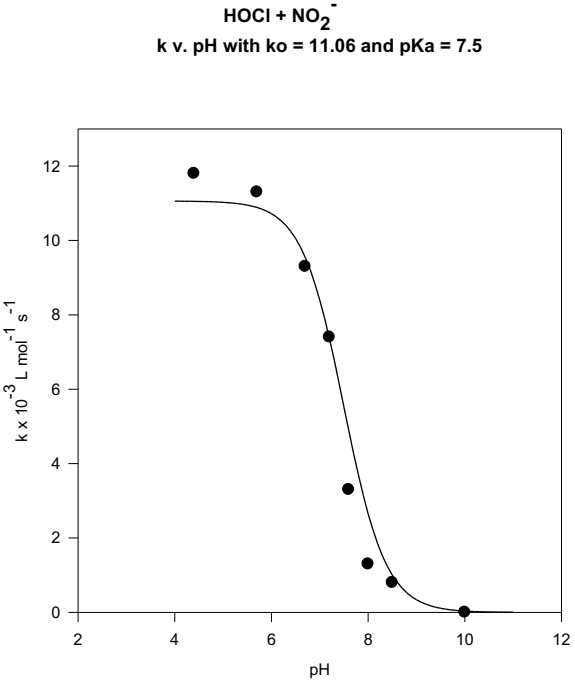
(5) $NO_2Cl + H_2O \rightarrow NO_3^- + Cl^- + 2H^+$

or

($NO_2Cl \rightarrow NO_2^+ + Cl^-$

$NO_2^+ + OH^- \rightarrow NO_3^- + H^+$)

Stopped-flow spectrophotometric studies at high (0.05 mol L^{-1}) nitrite concentration support the unreactivity of ClO^-.[16] An unweighted fit to these data at 25 ºC,[20] taking pK_a(HOCl) = 7.5, results in a rate constant of about 1.1×10^4 L mol^{-1} s^{-1} for the reaction of HOCl with NO_2^-.



In this study, there was not a systematic variation of the nitrite concentration. Therefore, the reaction could just as well have involved the equilibrium formation of nitryl chloride, with rate-limiting secondary reactions.

A study of the reaction in acid, $[H^+]$ = 0.174 to 0.979 mol L^{-1}, and high chloride concentration, $[Cl^-]$ = 1.875 mol L^{-1}, revealed an inverse acid dependence.[17] This was interpreted to indicate that NO_2^- was much more reactive than HONO (pK_a (HONO) = 3.20). An alternate explanation, however, would be that HOCl is more reactive that Cl_2, particularly since an inverse dependence on $[Cl^-]^2$ was also observed. On the other hand,

the data of Panasenko[20] does suggest a slight additional positive dependence on acid concentration below pH 6.

The reaction was also studied by bubbling chlorine through a nitrite solution over the pH range 3.4 to 11.5.[4] The reaction was too fast to follow in acid or neutral conditions, but was sufficiently slow over the pH range 9.5 to 11.6. Based on the pH behavior, it was concluded the reaction takes place predominantly between the neutral molecules. Experiments over the temperature range 17.5 to 21.2 ºC indicated some positive temperature dependence, but not sufficient to derive a meaningful activation energy. An earlier study by Lister and Rosenblum at pH 13.1 to 13.6 and a temperature range of 50 to 70 ºC was interpreted to support the conclusion that the reactions takes place between the nitrite ion and the hypochlorous acid molecule.[15] These results suggest a temperature dependence of about 3200 K, including a correction for the heat of hydrolysis of hypochlorite.

The most extensive kinetic measurements on this reaction were done by Lahoutifard, et al.,[12] at 298 K, who measured rate constants over the pH range 5–11, varying nitrite, hypochlorite, ionic strength, and supporting electrolyte. Their results support the contention that the initial reaction between hypochlorite and nitrite involves the reversible formation of nitryl chloride and that the kinetics are controlled by its subsequent fate. Because of this, they were unable to derive a rate constant for the initial reaction, only an equilibrium constant, but they did report rate constants for the two subsequent reactions of nitryl chloride. As a separate part of the study, Lahoutifard, et al. measured the hypochlorous acid hydrolysis constant, K_a, and the water constant, K_w, as a function of ionic strength in both NaCl and Na_2SO_4 solutions. These results are presented in the table below.

	Na_2SO_4 (μ = 1.0 M)	NaCl (μ = 1.0 M)	NaCl (μ = 0.01 M)
K_{eq}	$(1.1 \pm 0.1) \times 10^{-4}$	$(8.8 \pm 0.8) \times 10^{-4}$	$(2.0 \pm 0.2) \times 10^{-4}$
$k(ClNO_2 + NO_2^-)$	$(13 \pm 1) \times 10^3$	$(8 \pm 0.7) \times 10^3$	$(2.9 \pm 0.2) \times 10^3$
$k(ClNO_2 + H_2O)$, s^{-1}	81 ± 7	4.8 ± 0.4	79 ± 7
$K_{eq}(ClO^- + H^+ \leftrightarrow HOCl)$, M	1.28×10^7	1.99×10^7	0.89×10^7
pK_w	12.95	13.68	13.75

Back to Table

H3. **NO_2^- + HOBr.** The reactions of hypobromide solutions with nitrite were followed spectrophotometrically after either conventional or stopped-flow mixing by Lahoutifard, et al.[13] Both HOBr solutions free of additional bromide or in its presence were used. The ionic strength was adjusted with either Na_2SO_4 or NaCl. In the presence of 1.0 mol L^{-1} Na_2SO_4, 1.0 mol L^{-1} NaCl, and 0.1 mol L^{-1} NaCl, respectively, the equilibrium constants, $K_{eq}(NO_2^- + HOBr \leftrightarrow BrNO_2 + OH^-) = (5.6 \pm 1.1) \times 10^{-6}$, $(14 \pm 3) \times 10^{-6}$, and $(10 \pm 2) \times 10^{-6}$ and the rate constants, $k(BrNO_2 + NO_2^- \rightarrow N_2O_4 + Br^-) = (14 \pm 3) \times 10^3$, $(3.8 \pm 0.8) \times 10^3$, and $(5.5 \pm 1.1) \times 10^3$ L mol^{-1} s^{-1}.

This study has been criticized by Becker, et al.,[2] who point out that large concentrations of chloride will lead to a much more complicated system containing, for example, BrCl and HOCl. Lahoutifard and Scott[14] have replied to these comments, arguing that the bromide concentrations in most of their kinetic studies were sufficient to prevent this problem. Certainly, at this point these results need to be viewed with some suspicion, particularly those at higher Cl^- concentration.

In a stopped-flow study of the reaction between bromine and nitrous acid at high acidity (pH <2.4), a quadratic dependence on HONO was observed.[21] Also, both H^+ and and added Br^- showed a retarding effect and the effect of Br_2 on the rate demonstrated saturation. It was suggested that concurring reactions involving either N_2O_3 (formed by $2HONO \leftrightarrow N_2O_3 + H_2O$) or NO_2^- reacting with Br_2

$$Br_2 + N_2O_3 \rightarrow BrN_2O_3^+ + Br^-$$

$$Br_2 + NO_2^- \rightarrow BrNO_2 + Br^-.$$

An alternate explanation would be that HOBr is more reactive than Br_2 and is the more important reactant in this system. Back to Table

H4. **Br_2^- + NO_2^-.** Pulse radiolysis of N_2O-saturated 0.1 mol^{-1} L^{-1} Br^- solution containing NO_2^- following the decay of Br_2^- at 360 nm.[19] Temperature was varied from 5–79 ºC. $E_a = 14.3 \pm 0.4$ kJ mol^{-1}. Back to Table

H5. **$Cl_2^- + HSO_3^-$.** Pulse radiolysis of N_2O-saturated 0.1 mol^{-1} L^{-1} Cl^- solution containing HSO_3^- following the decay of Cl_2^- at 350 nm.[19] Temperature was varied from 5–80 ºC. E_a = 9.0 ± 0.3 kJ mol^{-1}. A 298 K value of $k = 1.7 \times 10^8$ L mol^{-1} s^{-1} at zero ionic strength was reported from the flash photolysis of persulfate solutions containing Cl^-.[9] Back to Table

H6. **$Br_2^- + HSO_3^-$.** Pulse radiolysis of N_2O-saturated 0.1 mol^{-1} L^{-1} Br^- solution containing HSO_3^- following the decay of Br_2^- at 360 nm.[19] Temperature was varied from 5–75 ºC. E_a = 6.5 ± 0.8 kJ mol^{-1}. Back to Table

H7. **$I_2^- + HSO_3^-$.** Pulse radiolysis of N_2O-saturated 0.1 mol^{-1} L^{-1} I^- solution containing HSO_3^- following the decay of I_2^- at 380 nm.[19] Temperature was varied from 5–79 ºC. E_a = 24.8 ± 2.1 kJ mol^{-1}. Back to Table

H8. **$Cl_2^- + SO_3^{2-}$.** Flash photolysis at 279 K of a persulfate solution containing Cl^-.[9] Rate constant corrected to zero ionic strength. Back to Table

H9. **$Br_2^- + SO_3^{2-}$.** Pulse radiolysis of N_2O-saturated 0.1 mol^{-1} L^{-1} Br^- solution containing SO_3^{2-} following the decay of Br_2^- at 360 nm.[19] Temperature was varied from 1–76 ºC. E_a = 5.4 ± 1.0 kJ mol^{-1}. Back to Table

H10. **$I_2^- + SO_3^{2-}$.** Pulse radiolysis of N_2O-saturated 0.1 mol^{-1} L^{-1} I^- solution containing SO_3^{2-} following the decay of I_2^- at 380 nm.[19] Temperature was varied from 4–79 ºC. E_a = 11.8 ± 0.4 kJ mol^{-1}. Back to Table

H11. **$NH_3 + HOCl$.** Rate constant measured over the temperature range 5–35 ºC and pH 6–12 by stopped-flow spectrophotometry, monitoring ClO^- at 294 nm and NH_2Cl at 243 nm.[18] The observed reaction is strongly pH dependent, with a maximum rate at pH 8.5, where the product $[HOCl]\cdot[NH_3]$ is also maximum. This points to these two as the reactive species, but the ions NH_4^+ and ClO^- can not be excluded by kinetic considerations, alone. Qiang and Adams argue, however, that the observed unreactivity of NH_4^+ toward O_3, as opposed to NH_3, supports the conclusion that the neutral species are correct. Another stopped-flow study resulted in $k = 1.9 \times 10^6$ L mol^{-1} s^{-1}, in good agreement.[8] Back to Table

H12. **$NH_3 + HOBr/BrO^-$.** Calculated from a stopped-flow study at various pH values from 6.5 to 13 and 24 ± 2 ºC.[8] Back to Table

6.9.2 References

(1) Anbar, M.; Taube, H. The exchange of hypochlorite and of hypobromite ions with water. *J. Am. Chem. Soc.* **1958**, *82*, 1073-1077, doi:10.1021/ja01538a015.

(2) Becker, R. H.; Hartz, K. E. H.; Margerum, D. W. Comment on "Kinetics and mechanism of nitrite oxidation by HOBr/BrO- in atmospheric water and comparison with oxidation by HOCl/ClO-" *J. Phys. Chem. A* **2004**, *108*, 10615-10616, doi:10.1021/jp036101b.

(3) Cachaza, J. M.; Casado, J.; Castro, A.; Lopez Quintela, M. A. Kinetics of oxidation of nitrite by hypochlorite ions in aqueous basic solution. *Can. J. Chem.* **1976**, *54*, 3401-3406, doi:10.1139/v76-488.

(4) Diyamandoglu, V.; Marinas, B. J.; Selleck, R. E. Stoichiometry and nitrite kinetics of the reaction of nitrite with free chlorine in aqueous solutions. *Environ. Sci. Technol.* **1990**, *24*, 1711-1716, doi:10.1021/es00081a014.

(5) Eiserich, J. P.; Cross, C. E.; Jones, A. D.; Halliwell, B.; van der Vliet, A. Formation of nitrating and chlorinating species by reaction of nitrite with hypochlorous acid. *J. Biol. Chem.* **1996**, *271*, 19199-19208, doi:10.1074/jbc.271.32.19199.

(6) Frenzel, A.; Scheer, V.; Sikorski, R.; George, C.; Behnke, W.; Zetzsch, C. Heterogeneous interconversion reactions of $BrNO_2$, $ClNO_2$, Br_2, and Cl_2. *J. Phys. Chem. A* **1998**, *102*, 1329-1337, doi:10.1021/jp973044b.

(7) Ghibaudi, E.; Barker, J. R.; Benson, S. W. Reaction of NO with hypochlorous acid. *Int. J. Chem. Kinet.* **1979**, *11*, 843-851, doi:10.1002/kin.550110804.

(8) Heeb, M. B.; Kristiana, I.; Trogolo, D.; Arey, J. S.; von Gunten, U. Formation and reactivity of inorganic and organic chloramines and bromamines during oxidative water treatment. *Water Res.* **2017**, *110*, 91-101, doi:10.1016/j.watres.2016.11.065.

(9) Herrmann, H.; Jacobi, H.-W.; Raabe, G.; Reese, A.; Zellner, R. Laser-spectroscopic laboratory studies of atmospheric aqueous phase free radical chemistry. *Fresenius' J. Anal. Chem.* **1996**, *355*, 343-344, doi:10.1007/s0021663550343.

(10) Johnson, D. W.; Margerum, D. W. Non-metal redox kinetics: A reexamination of the mechansim of the reaction between hypochlorite and nitrite ions. *Inorg. Chem.* **1991**, *30*, 4845-4851, doi:10.1021/ic00025a031.
(11) Kono, Y. The production of nitrating species by the reaction between nitrite and hypochlorous acid. *Biochem. Mol. Biol. Int.* **1995**, *36*, 275-283.
(12) Lahoutifard, N.; Lagrange, P.; Lagrange, J. Kinetics and mechanism of nitrite oxidation by hypochlorous acid in the aqueous phase. *Chemosphere* **2003**, *50*, 1349-1357, doi:10.1016/S0045-6535(02)00765-8.
(13) Lahoutifard, N.; Lagrange, P.; Lagrange, J.; Scott, S. L. Kinetics and mechanism of nitrite oxidation by HOBr/BrO^- in atmospheric water and comparison with oxidation by HOCl/ClO^-. *J. Phys. Chem. A* **2002**, *106*, 11891-11896, doi:10.1021/jp021185u.
(14) Lahoutifard, N.; Scott, S. L. Reply to "Comment on 'Kinetics and mechanism of nitrite oxidation by HOBr/BrO^- in atmospheric water and comparison with oxidation by HOCI/ClO^-' ". *J. Phys. Chem. A* **2004**, *108*, 10617-10618, doi:10.1021/jp0311456.
(15) Lister, M. W.; Rosenblum, P. The oxidation of nitrite and iodate ions by hypochlorite ions. *Can. J. Chem.* **1961**, *39*, 1645-1651, doi:10.1139/v61-211.
(16) Panasenko, O. M.; Briviba, K.; Klotz, L. O.; Sies, H. Oxidative modification and nitration of human low-density lipoproteins by the reaction of hypochlorous acid with nitrite. *Arch. Biochem. Biophys.* **1997**, *343*, 254-259, doi:10.1006/abbi.1997.0171.
(17) Pendlebury, J. N.; Smith, R. H. Kinetics of oxidation of nitrite by aqueous chlorine. *Aust. J. Chem.* **1973**, *26*, 1857-1861, doi:10.1071/CH9731857.
(18) Qiang, Z.; Adams, C. D. Determination of monochloramine formation rate constants with stopped-flow spectrophotometry. *Environ. Sci. Technol.* **2004**, *38*, 1435-1444, doi:10.1021/es0347484.
(19) Shoute, L. C. T.; Alfassi, Z. B.; Neta, P.; Huie, R. E. Temperature dependence of the rate constants for reaction of dihalide and azide radicals with inorganic reductants. *J. Phys. Chem.* **1991**, *95*, 3238-3242, doi:10.1021/j100161a050.
(20) Sies, H., Data for the reaction of HOCl with NO_2^-.
(21) Valent, I.; Schreiber, I.; Marek, M. Kinetics and mechanism of the oxidation of nitrous acid by bromine in aqueous sulfuric acid. *Int. J. Chem. Kinet.* **2000**, *32*, 279-285, doi:10.1002/(SICI)1097-4601.

6.10 Tri-halo Compounds

Reaction	k (L mol^{-1} s^{-1}) *	Note
$Cl_2 + Cl^- \rightarrow Cl_3^-$	2.0×10^4	I1
$Cl_3^- \rightarrow Cl_2 + Cl^-$	1.1×10^5 s^{-1}	I1
$Br_2 + Br^- \rightarrow Br_3^-$	9.6×10^8	I2
$Br_3^- \rightarrow Br_2 + Br^-$	5.5×10^7 s^{-1}	I2
$Cl_2 + Br^- \rightarrow Cl_2Br^-$	6.0×10^9	I3
$Cl_2Br^- \rightarrow Cl_2 + Br^-$	9.0×10^3 s^{-1}	I3
$ClBr^- + Cl^- \rightarrow Cl_2Br^-$	1.0×10^6	I4
$Cl_2Br^- \rightarrow ClBr + Cl^-$	1.7×10^5 s^{-1}	I4
$Cl_2Br^- + Br^- \rightarrow ClBr_2^- + Cl^-$	3.0×10^8	I5
$ClBr + Br^- \rightarrow ClBr_2^-$	See Note	I6
$Br_2 + Cl^- \rightarrow ClBr_2^-$	See Note	I6
$ClI + Cl^- \rightarrow Cl_2I^-$	See Note	I7
$BrI + Br^- \rightarrow Br_2I^-$	See Note	I8
$BrI + I^- \rightarrow BrI_2^-$	$(2.0 \pm 0.3) \times 10^9$	I9
$BrI_2^- \rightarrow BrI + I^-$	800 ± 300 s^{-1}	I9
$I_2 + Cl^- \rightarrow ClI_2^-$	1.58	I10
$I_2 + Br^- \rightarrow BrI_2^-$	See Note	I10
$I_2 + I^- \rightarrow I_3^-$	See Note	I11

* Unless units noted otherwise

6.10.1 Notes: Tri-halo compounds

I1. **$Cl_2 + Cl^- \leftrightarrow Cl_3^-$.** From a pulse radiolysis study of the disappearance of Cl_2^- and formation of Cl_3^-, monitored spectroscopically.[3] The mechanism included the self-reaction of Cl_2^-, for which a rate constant of 1.5×10^9 L mol^{-1} s^{-1} at 5 mol L^{-1} NaCl was calculated, which is in the range of other reported values.[10] An equilibrium constant of $K_{eq} = 0.18$ M^{-1} was reported, the same as the average of values determined earlier at 25.0 ± 0.1 ºC.[8] Back to Table

I2. **$Br_2 + Br^- \leftrightarrow Br_3^-$.** From a pulse radiolysis study of the disappearance of Br_2^- and formation of Br_3^-, monitored spectroscopically.[2] Results lead to $K_{eq} = 17.5$ M^{-1}, close to the value reported by Wang, et al. for 25.0 ± 0.1 ºC, $K_{eq} = 16.1 \pm 0.3$ M^{-1}.[8] Back to Table

I3. **$Cl_2 + Br^- \leftrightarrow Cl_2Br^-$ $K_{eq} = 6.7 \pm 1.3 \times 10^5$ M^{-1}.** From a spectroscopic measurement of the pulse radiolysis-induced oxidation of chloride in the presence of added bromide.[4] In a pulsed-accelerated flow determination, a forward rate constant $k_f = (7.7 \pm 1.3) \times 10^9$ L mol^{-1} s^{-1} was reported at 25 ± 0.1 ºC and $\mu = 1.0$ M, in good agreement.[8] Back to Table

I4. **$Br + Cl^- \leftrightarrow Cl_2Br^-$.** The equilibrium constant $K_{eq} = 6.0 \pm 0.3$ M^{-1} was derived in a spectrophotometric investigation of solutions of BrCl in the presence of added chloride ions at 25 ± 0.1º C and $\mu = 1.0$ M.[8] The value was used in a simulation of the pulse radiolysis-induced oxidation of chloride in the presence of added bromide to derive the forward and reverse rate constants.[4] Back to Table

I5. **$Cl_2Br + Br^- \rightarrow ClBr_2^- + Cl^-$.** From a spectroscopic measurement of the pulse radiolysis-induced oxidation of chloride in the presence of added bromide.[4] Back to Table

I6. A spectrophotometric investigation of solutions of BrCl in the presence of added chloride ions yielded the following equilibrium constants at 25 ± 0.1 ºC and $\mu = 1.0$ M:[8]

$ClBr + Br^- \leftrightarrow ClBr_2^-$ $\quad K_{eq} = (1.8 \pm 0.2) \times 10^4$ M^{-1}

$Br_2 + Cl^- \leftrightarrow ClBr_2^-$ $\quad K_{eq} = 1.3 \pm 0.3$ M^{-1} Back to Table

I7. **$ClI + Cl^- \leftrightarrow Cl_2I^-$.** Equilibrium constant determined by a spectrophotometric titration of a Cl_2I^- solution by HCl.[9] $K_{eq} = 77 \pm 6$ M^{-1}at 25 ± 0.1 ºC and $\mu = 0.5$ and 1.0 M. For $HOI + 2Cl^- \leftrightarrow Cl_2I^-$, $K_{eq} = 9.4 \times 10^5$ M^{-1}at 25 °C and $\mu = 0.5$. Back to Table

I8. **$BrI + Br^- \leftrightarrow Br_2I^-$.** Equilibrium constant determined by a spectrophotometric titration of a Br_2I^- solution by HBr.[7] $K_{eq} = 286 \pm 50\ M^{-1}$ at 25 °C and $\mu = 1.0$ M. Back to Table

I9. **$BrI + I^- \leftrightarrow BrI_2^-$.** The rate constants for this reaction were determined as the rate-limiting step in the overall reaction $Br_2I^- + I^- \leftrightarrow BrI_2^- + Br^-$ using the pulse-accelerated flow method in 1 M H^+ and at 25 °C. The rate was proportional to I^- and inversely to Br^-, indicating that I^- does not react directly with Br_2I^-, but through a multi-step mechanism involving BrI.[7] Back to Table

I10. **$I_2 + Cl^- \rightarrow ClI_2^-$; $K_{eq} = 1.59\ M^{-1}$ $I_2 + Br^- \rightarrow BrI_2^-$; $K_{eq} = 12.2\ M^{-1}$.** Equilibrium constants determined from measurements of the solubility of I_2 in solution containing the halide ion.[5] For $I_2 + I^- \rightarrow I_3^-$, $K_{eq} = 740\ M^{-1}$, in good agreement with the value recommended here. Back to Table

I11. **$I_2 + I^- \rightarrow I_3^-$** $\log K_{eq} = 2.8580 - 1.170 \times 10^{-2}(T - 25) - 3.77 \times 10^{-5}(T - 25)^2\ M^{-1}$ or, at 25 ºC, $K_{eq} = 721\ M^{-1}$. Taken from a spectrophotometric measurements from 15 to 35º C by Daniele,[1] reported by Ramette and Sanford,[6] who also discussed other earlier studies. Back to Table

6.10.2 References

(1) Daniele, G. Spectrophotometric measurement of the equilibrium constant of potassium triiodide. *Gazz. Chim. Ital.* **1960**, *90*.

(2) Ershov, B. G.; Gordeev, A. V.; Janata, E.; Kelm, M. Radiation-chemical oxidation of bromide ions and formation of tribromide ions in weakly acidic aqueous solutions *Mendeleev Comm.* **2001**, *11*, 149-150.

(3) Ershov, B. G.; Janata, E.; Kelm, M.; Gordeev, A. V. Formation and absorption spectra of X_3^- ions upon the radiation-chemical oxidation of Cl^- in the presence of Br^- (Cl, Br = X) in aqueous solution. *Mendeleev Comm.* **2002**, 55-57, doi:10.1070/MC2002v012n02ABEH001561.

(4) Ershov, B. G.; Kelm, M.; Janata, E.; Gordeev, A. V.; Bohnert, E. Radiation-chemical effects in the near-field of a final disposal site: role of bromine on the radiolytic processes in NaCl-solutions. *Radiochem. Acta* **2002**, *90*, 617-622, doi:10.1524/ract.2002.90.9-11_2002.617.

(5) LaMer, V. K. L.; Lewinsohn, M. H. Halide–iodine equilibria in neutral salt solvents. *J. Phys. Chem.* **1934**, *38*, 171-195, doi:10.1021/j150353a004.

(6) Ramette, R. W.; Sandford, R. W. Thermodynamics of iodine solubility and triiodide ion formation in water and in deuterium oxide. *J. Am. Chem. Soc.* **1965**, *87*, 5001-5005, doi:10.1021/ja00950a005.

(7) Troy, R. C.; Kelley, M. D.; Nagy, J. C.; Margerum, D. W. Nonmetal redox kinetics - iodine monobromide reaction with iodide-ion and the hydrolysis of IBr. *Inorg. Chem.* **1991**, *30*, 4838-4845, doi:10.1021/ic00025a030.

(8) Wang, T. X.; Kelley, M. D.; Cooper, J. N.; Beckwith, R. C.; Margerum, D. W. Equilibrium, kinetic, and UV-spectral characteristics of aqueous bromine chloride, bromine, and chlorine species. *Inorg. Chem.* **1994**, *33*, 5872-5878, doi:10.1021/ic00103a040.

(9) Wang, Y. L.; Nagy, J. C.; Margerum, D. W. Kinetics of hydrolysis of iodine monochloride measured by the pulsed-accelerated-flow method. *J. Am. Chem. Soc.* **1989**, *111*, 7838-7844, doi:10.1021/ja00202a026.

(10) Yu, X. Y. Critical evaluation of rate constants and equilibrium constants of hydrogen peroxide photolysis in acidic aqueous solutions containing chloride ions. *J. Phys. Chem. Ref. Data* **2004**, *33*, 747-763, doi:10.1063/1.1695414.

6.11 Bibliography

Adam, L. C.; Fábián, I.; Suzuki, K.; Gordon, G. Hypochlorous acid decomposition in the pH 5-8 region. *Inorg. Chem.* **1992**, *31*, 3534-3541, doi:10.1021/ic00043a011.

Adam, L. C.; Gordon, G. Hypochlorinte ion decomposition: Effects of temperature, ionic strength, and chloride ion. *Inorg. Chem.* **1999**, *38*, 1299-1304, doi:10.1021/ic980020q.

Alfassi, Z.; Huie, R.; Marguet, S.; Natarajan, E.; Neta, P. Rate constants for reactions of iodine atoms in solution. *Int. J. Chem. Kinet.* **1995**, *27*, 181-188, doi:10.1002/kin.550270208.

Alfassi, Z. B.; Huie, R. E.; Mosseri, S.; Neta, P. Kinetics of one-electron oxidation by the ClO radical. *Int. J. Radiat. Appl. Inst. Part C. Radiat. Phys. Chem.* **1988**, *32*, 85-88, doi:10.1016/1359-0197(88)90018-5.

Amichai, O.; Treinin, A. On the oxyiodine radicals in aqueous solution. *J. Phys. Chem.* **1970**, *74*, 830-835.

Anbar, M.; Taube, H. The exchange of hypochlorite and of hypobromite ions with water. *J. Am. Chem. Soc.* **1958**, *82*, 1073-1077, doi:10.1021/ja01538a015.

Armstrong, D. A.; Huie, R. E.; Koppenol, W. H.; Lymar, S. V.; Merenyi, G.; Neta, P.; Ruscic, B.; Stanbury, D. M.; Steenken, S.; Wardman, P. Standard electrode potentials involving radicals in aqueous solution: inorganic radicals (IUPAC Technical Report). *Pure Appl. Chem.* **2015**, *87*, 1139-1150, doi:10.1515/pac-2014-0502.

Artiglia, L.; Edebeli, J.; Orlando, F.; Chen, S.; Lee, M.-T.; Arroyo, P. C.; Gilgen, A.; Bartels-Rausch, T.; Kleibert, A.; Vazdar, M.; Carignano, M. A.; Francisco, J. S.; Shepson, P. B.; Gladich, I.; Amm, M. A surface-stabilized ozonide triggers bromide oxidation at the aqueous solution-vapour interface. *Nature Comm.* **2017**, *8*, 700, doi:10.1038/s41467-017-00823-x.

Ball, J. M.; Hnatiw, J. B. The reduction of I_2 by H_2O_2 in aqueous solutions. *Can. J. Chem.* **2001**, *79*, 304-311, doi:10.1139/cjc-79-3-304.

Standard Potentials in Aqueous Solution; Bard, A. J.; Parsons, R.; Jordan, J., Eds.; Marcel Dekker, Inc: New York and Basel, 1985.

Barkatt, A.; Ottolenghi, M. Laser flash photolysis of aqueous triiodide solutions. *Mol. Photochem.* **1974**, *6*, 253-261.

Bartels, D. M. Comment on the possible role of the reaction $H^{\bullet} + H_2O \rightarrow H_2 + {}^{\bullet}OH$ in the radiolysis of water at high temperatures. *Rad. Phys. Chem.* **2009**, *78*, 191-194, doi:10.1016/j.radphyschem.2008.09.005.

Beach, M. W.; Margerum, D. W. Kinetics of oxidation of tetracyanonickelate(Ii) by chlorine monoxide, chlorine, and hypochlorous acid and kinetics of chlorine monoxide formation. *Inorg. Chem.* **1990**, *29*, 1225-1232, doi:10.1021/ic00331a023.

Becker, R. H.; Hartz, K. E. H.; Margerum, D. W. Comment on "Kinetics and mechanism of nitrite oxidation by $HOBr/BrO^-$ in atmospheric water and comparison with oxidation by $HOCl/ClO^-$" *J. Phys. Chem. A* **2004**, *108*, 10615-10616, doi:10.1021/jp036101b.

Beckwith, R. C.; Margerum, D. W. Kinetics of hypobromous acid disproportionation. *Inorg. Chem.* **1997**, *17*, 3754-3760, doi:10.1021/ic970155g.

Behar, D.; Czapski, G.; Duchovny, I. Carbonate radical in flash photolysis and pulse radiolysis of aqueous carbonate solutions. *J. Phys. Chem.* **1970**, *74*, 2206-2210, doi:10.1021/j100909a029.

Biard, P.-F.; Dang, T. T.; Couvert, A. Determination by reactive absorption of the rate constant of the ozone reaction with the hydroperoxide anion. *Chem. Eng. Res. Des.* **2017**, 62-71, doi:10.1016/j.cherd.2017.09.004.

Bichsel, Y.; von Gunten, U. Oxidation of iodide and hypoiodous acid in the disinfection of natural waters. *Environ. Sci. Technol.* **1999**, *33*, 4040-4045, doi:10.1021/es990336c.

Bichsel, Y.; Von Gunten, U. Hypoiodous acid: kinetics of the buffer-catalyzed disproportionation *Water Research* **2000**, *34*, 3197-3203, doi:10.1016/S0043-1354(00)00077-4.

Bielski, B. H. J. A pulse radiolysis study of the reaction of ozone with Cl_2^- in aqueous solutions. *Radiat. Phys. Chem.* **1993**, *41*, 527-530, doi:10.1016/0969-806X(93)90015-M.

Bielski, B. H. J.; Cabelli, D. E.; Arudi, R. L.; Ross, A. B. Reactivity of HO_2/O_2^- radicals in aqueous solution. *J. Phys. Chem. Ref. Data* **1985**, *14*, 1041-1100, doi:10.1063/1.555739.

Bjergbakke, E.; Navaratnam, S.; Parsons, B. J. Reaction between $HO_2\bullet$ and chlorine in aqueous solution. *J. Am. Chem. Soc.* **1981**, *103*, 5926-5928, doi:10.1021/ja00409a059.

Botti, H.; Möller, M. N.; Steinmann, D.; Nauser, T.; Koppenol, W. H.; Denicola, A.; Radi, R. Distance-dependent diffusion-controlled reaction of •NO and O_2•- at chemical equilibrium with $ONOO^-$. *J. Phys. Chem. B* **2010**, *114*, 16584-16593, doi:10.1021/jp105606b.

Bousher, A.; Brimblecombe, P.; Midgley, D. Kinetics of reactions in solutions containing monochloramine and bromide *Water Res.* **1989**, *23*, 1049-1058, doi:10.1016/0043-1354(89)90180-2.

Braathen, G.; Chou, P.-T.; Frei, H. Time-resolved reaction of oxygen($^1\Delta$) with iodide in aqueous solution. *J. Phys. Chem.* **1988**, *92*, 6610-6615, doi:10.1021/j100334a026.

Braban, C. F.; Adams, J. W.; Rodriguez, D.; Cox, R. A.; Crowley, J. N.; Schuster, G. Heterogeneous reactions of HOI, ICl, and IBr on sea salt and sea sale proxies. *Phys. Chem. Chem. Phys.* **2007**, *9*, 3136-3148, doi:10.1039/b700829e.

Buhler, R.; Staehelin, J.; Hoigne, J. Ozone decomposition in water studied by pulse radiolysis 1. HO_2/O_2^- and HO_3/O_3^- as intermediates - Correction. *J. Phys. Chem.* **1984**, *88*, 5450-5450, doi:10.1021/j150666a600.

Bühler, R. E.; Staehelin, J.; Hoigné, J. Ozone decomposition in water studied by pulse radiolysis. 1. HO_2/O_2^- and HO_3/O_3^- as intermediates. *J. Phys. Chem.* **1984**, *88*, 2560-2564, doi:10.1021/j150656a026.

Buxton, G. V. Pulse radiolysis of HOI and IO- in aqueous solution. Formation and characterisation of I(II). *Proc. Tihany Symp. Radiat. Chem.* **1987**, *6*, 155-159.

Buxton, G. V.; Dainton, F. S. The radiolysis of aqueous solutions of oxybromine compounds; the spectra and reactions of BrO and BrO_2. *Proc. Roy. Soc. (London)* **1968**, *304*, 427-439.

Buxton, G. V.; Greenstock, C. L.; Helman, W. P.; Ross, A. B. Critical review of rate constants for reactions of hydrated electrons, hydrogen atoms and hydroxyl radicals (•OH/•O–) in aqueous solution. *J. Phys. Chem. Ref. Data* **1988**, *17*, 1-21, doi:10.1063/1.555805.

Buxton, G. V.; Kilner, C.; Sellers, R. M. Pulse radiolysis of HOI and IO- in aqueous solution. Formation and characterisation of I(II). *Proc. Tihany Symp. Radiat. Chem.* **1986**, *6*, 155-159.

Buxton, G. V.; Mulazzani, Q. G. On the hydrolysis of iodine in alkaline solution: A radiation chemical study. *Radiat. Phys. Chem.* **2007**, *76*, 932-940, doi:10.1016/j.radphyschem.2006.06.009.

Buxton, G. V.; Salmon, G. A.; Wang, J. The equilibrium $NO_3^\bullet + Cl^- \rightleftarrows NO_3^- + Cl^\bullet$: A laser flash photolysis and pulse radiolysis study of the reactivity of NO_3 with chloride ion in aqueous solution. *Phys. Chem. Chem. Phys.* **1999**, *1*, 3589-3593, doi:10.1039/A903286J.

Buxton, G. V.; Subhani, M. S. Ratiation-chemistry and photochemistry of oxychlorine ions. I. Radiolysis of aqueous solutions of hypochlorite and chlorite ions. *J. Chem. Soc. Faraday Transactions I* **1972**, *68*, 947-957, doi:10.1039/F19726800947.

Buxton, G. V.; Wood, N. D.; Dyster, S. Ionisation constants of $^{\cdot}OH$ and $HO_2^{\cdot}$ in aqueous solution up to 200 ^oC. A pulse radiolysis study. *J. Chem. Soc. Faraday Trans. I* **1988**, *84*, 1113-1121, doi:10.1039/F19888401113.

Cachaza, J. M.; Casado, J.; Castro, A.; Lopez Quintela, M. A. Kinetics of oxidation of nitrite by hypochlorite ions in aqueous basic solution. *Can. J. Chem.* **1976**, *54*, 3401-3406, doi:10.1139/v76-488.

Candeias, L. P.; Patel, K. B.; Stratford, M. R. L.; Wardman, P. Free hydroxyl radicals are formed on reaction between the neutrophil-derived species superoxide anion and hypochlorous acid. *FEBS Lett.* **1993**, *333*, 151-153, doi:10.1016/0014-5793(93)80394-a.

Castagna, R.; Eiserich, J. P.; Budamagunta, M. S.; Stipa, P.; Cross, C. E.; Proietti, E.; Voss, J. C.; Greci, L. Hydroxyl radical from the reaction between hypochlorite and hydrogen peroxide. *Atmos. Environ.* **2008**, *42*, 6551-6554, doi:10.1016/j.atmosenv.2008.04.029.

Chia, Y. T.; Connick, R. E. The rate of oxidation of I^- to hypoiodite ion by hypochlorite ion. *J. Phys. Chem.* **1959**, *63*, 1518-1519, doi:10.1021/j150579a051.

Christensen, H.; Sehested, K. HO_2 and O_2^- radicals at elevated temperatures. *J. Phys. Chem.* **1988**, *92*, 3007-3011, doi:10.1021/j100321a060.

Christensen, H.; Sehested, K.; Bjergbakke, E. Radiolysis of reactor water: Reactions of hydroxyl radicals with superxide (O_2^-). *Water Chem. Nucl. React. Syst.* **1989**, *5*, 141-144.

Christensen, H.; Sehested, K.; Corfitzen, H. Reactions of hydroxyl radicals with hydrogen peroxide at ambient and elevated temperatures. *J. Phys. Chem.* **1982**, *86*, 1588-1590, doi:10.1021/j100206a023.

Connick, R. E. The interaction of hydrogen peroxide and hypochlorous acid in acidic solutions containing chloride ion *J. Am. Chem. Soc.* **1947**, *69*, 1509-1514, doi:10.1021/ja01198a074.

Connors, K. A. *Chemical Kinetics*; VCH Publishers, Inc.: New York, 1990.

Csordas, V.; Bubnis, B.; Fabian, I.; Gordon, G. Kinetics and mechanism of catalytic decomposition and oxidation of chlorine dioxide by the hypochlorite ion. *Inorg. Chem.* **2001**, *40*, 1833-1836, doi:10.1021/ic001106y.

D'Auria; Kuo, I. F. W.; Tobias, D. J. Ab initio molecular dynamics study of the solvated OHCl− complex: Implications for the atmospheric oxidation of chloride anion to molecular chlorine. *J. Phys. Chem. A* **2008**, *112*, 4644-4650, doi:10.1021/jp077669d.

D`Angelantonio, M.; Venturi, M.; Mulazzani, Q. G. A re-examination of the decay kinetics of pulse radiolytically generated Br_2^- radicals in aqueous solution. *Int. J. Radiat. Appl. Inst. Part C. Radiat. Phys. Chem.* **1988**, *32*, 319-324, doi:10.1016/1359-0197(88)90028-8.

Daniele, G. Spectrophotometric measurement of the equilibrium constant of potassium triiodide. *Gazz. Chim. Ital.* **1960**, *90*.

Das, T. N.; Huie, R. E.; Neta, P.; Padmaja, S. Reduction potential of the sulfhydryl radical: Pulse radiolysis and laser flash photolysis studies of the formation and reactions of ·SH and $HSSH^{\cdot -}$ in aqueous solutions. *J. Phys. Chem. A* **1999**, *103*, 5221-5226, doi:10.1021/jp9907544.

Davis, M.; Koizumi, H.; Schatz, G. C.; Bradforth, S. E.; Neumark, D. M. Experimental and theoretical study of the O + HCl transition state region by photodetachment of $OHCl^-$. *J. Chem. Phys.* **1994**, *101*, 4708-4721, doi:10.1063/1.468463.

Diyamandoglu, V.; Marinas, B. J.; Selleck, R. E. Stoichiometry and nitrite kinetics of the reaction of nitrite with free chlorine in aqueous solutions. *Environ. Sci. Technol.* **1990**, *24*, 1711-1716, doi:10.1021/es00081a014.

Egorov, S. Y.; Krasnovsky, A. A. Quenching of singlet molecular oxygen by components of media used for isolating chloroplasts and studying photosynthetic activity. *Sov. Plant Physiol.* **1986**, *33*, 5-8.

Egorova, G. V.; Voblikova, V. A.; Sabitova, L. V.; Tkachenko, I. S.; Tkachenko, S. N.; Lunin, V. V. Ozone solubility in water. *Moscow University Chemistry Bulletin* **2015**, *70*, 207-210, doi:10.3103/s0027131415050053.

Eiserich, J. P.; Cross, C. E.; Jones, A. D.; Halliwell, B.; van der Vliet, A. Formation of nitrating and chlorinating species by reaction of nitrite with hypochlorous acid. *J. Biol. Chem.* **1996**, *271*, 19199-19208, doi:10.1074/jbc.271.32.19199.

Elliot, A. J. A pulse radiolysis study of the reaction of OH with I_2 and the decay of I_2^-. *Can. J. Chem.* **1992**, *70*, 1658-1666, doi:10.1139/v92-207.

Elliot, A. J.; Buxton, G. V. Temperature dependence of the reactions OH + O_2^- and OH + HO_2 in water up to 200 C. *J. Chem. Soc. Faraday Trans.* **1992**, *88*, 2465-2470, doi:10.1039/FT9928802465.

Elliot, A. J.; McCracken, D. R. Effect of temperature on O^- reactions and equilibria: A pulse radiolysis study. *Int. J. Radiat. Appl. Inst. Part C. Radiat. Phys. Chem.* **1989**, *33*, 69-74.

Elliot, A. J.; Simsons, A. S. Rate constants for reactions of hydroxyl radicals as a function of temperature. *Radiat. Phys. Chem. (1977)* **1984**, *24*, 229-231, doi:10.1016/0146-5724(84)90056-6.

Elliot, A. J.; Sopchyshyn, C. F. A pulse radiolysis study of I_2^- and $(SCN)_2^-$ in aqueous solutions over the temperature range 15 - 90 C. *Int. J. Chem. Kinet.* **1984**, *16*, 1247-1256, doi:10.1002/kin.550161007.

Ellison, D. H.; Salmon, G. A.; Wilkinson, F. Nanosecond pulse radiolysis of methanolic and aqueous solutions of readily oxidizable solutes. *Proc. Roy. Soc. (London)* **1972**, 23-36, doi:10.1098/rspa.1972.0066.

Eriksen, T. E.; Lind, J.; Merenyi, G. Generation of chlorine dioxide from ClO by pulse radiolysis. *J. Chem. Soc., Faraday Trans. 1* **1981**, *77*, 2115-2123, doi:10.1039/f19817702115.

Eriksen, T. E.; Lind, J.; Merenyi, G. On the acid-base equilibrium of the carbonate radical. *Radiat. Phys. Chem. (1977)* **1985**, *26*, 197-199, doi:10.1016/0146-5724(85)90185-2.

Ershov, B. G. Kinetics, mechanism and intermediates of some radiation-induced reactions in aqueous solutions. *Russ. Chem. Rev.* **2004**, *73*, 101-113, doi:10.1070/RC2004v073n01ABEH000865.

Ershov, B. G.; Gordeev, A. V.; Janata, E.; Kelm, M. Radiation-chemical oxidation of bromide ions and formation of tribromide ions in weakly acidic aqueous solutions *Mendeleev Comm.* **2001**, *11*, 149-150.

Ershov, B. G.; Janata, E.; Gordeev, A. V. Pulse radiolysis study of I^- oxidation with radical anions $Cl_2^{\cdot -}$ in an aqueous solution. *Russ. Chem. Bull.* **2005**, *54*, 1378-1382, doi:10.1007/s11172-005-0413-2.

Ershov, B. G.; Janata, E.; Gordeev, A. V. Pulse radiolysis study of the oxidation of the I^- ions with the radical anions Br_2^- in an aqueous solution: formation and properties of the radical anion BrI^-. *Russ. Chem. Bull.* **2008**, *57*, 1821-1826, doi:10.1007/s11172-008-0245-y.

Ershov, B. G.; Janata, E.; Kelm, M.; Gordeev, A. V. Formation and absorption spectra of X_3^- ions upon the radiation-chemical oxidation of Cl^- in the presence of Br^- (Cl, Br = X) in aqueous solution. *Mendeleev Comm.* **2002**, 55-57, doi:10.1070/MC2002v012n02ABEH001561.

Ershov, B. G.; Kelm, M.; Janata, E.; Gordeev, A. V.; Bohnert, E. Radiation-chemical effects in the near-field of a final disposal site: role of bromine on the radiolytic processes in NaCl-solutions. *Radiochem. Acta* **2002**, *90*, 617-622, doi:10.1524/ract.2002.90.9-11_2002.617.

Ervens, B. Modeling the processing of aerosol and trace gases in clouds and fogs. *Chem. Rev.* **2015**, *115*, 4157-4198, doi:10.1021/cr5005887.

Exner, M.; Herrmann, H.; Zellner, R. Laser-based studies of reactions of the nitrate radical in aqueous solution. *Ber. Bunsenges. Phys. Chem.* **1992**, *96*, 470-477, doi:10.1002/bbpc.19920960347.

Fábián, I. Reactive intermediates in aqueous ozone decomposition: A mechanistic approach. *Pure Appl. Chem.* **2006**, *78*, 1559-1570, doi:10.1351/pac200678081559.

Fábián, I.; Gordon, G. The kinetics and mechanism of the chlorine dioxide-iodine ion reaction. *Inorg. Chem.* **1997**, *36*, 2494-2497, doi:10.1021/ic961279g.

Farkas, L.; Lewin, M.; Bloch, R. The reaction between hypochlorities and bromides. *J. Am. Chem. Soc.* **1949**, *71*, 1988-1991, doi:10.1021/ja01174a025.

Ferre-Aracil, J.; Cardona, S. C.; Navarro-Laboulais, J. Kinetic study of ozone decay in homogeneous phosphate-buffered medium. *Ozone: Sci. Eng.* **2015**, *37*, 330-342, doi:10.1080/01919512.2014.998756.

Finlayson-Pitts, B. J. The tropospheric chemistry of sea salt: A molecular-level view of the chemistry of NaCl and NaBr *Chem. Rev.* **2003**, *103*, 4801-4822, doi:10.1021/cr020653t.

Finlayson-Pitts, B. J. Halogens in the troposphere. *Anal. Chem.* **2010**, *82*, 770-776, doi:10.1021/ac901478p.

Fischbacher, A.; Löppenberg, K.; Von Sonntag, C.; Schmidt, T. C. A new reaction pathway for bromite to bromate in the ozonation of bromide. *Environ. Sci. Technol.* **2015**, *49*, 11714-11720, doi:10.1021/acs.est.5b02634.

Fischbacher, A.; von Sonntag, J.; von Sonntag, C.; Schmidt, T. C. The •OH radical yield in the $H_2O_2 + O_3$ (peroxone) reaction. *Environ. Sci. Technol.* **2013**, *47*, 9959-9964, doi:10.1021/es402305r.

Forni , G. L.; Mora-Arellano , V. O.; Packer , J. E.; Willson , R. L. Nitrogen dioxide and related free radicals: Electron-transferreactions with organic compounds in solutions containing nitrite or nitrate. *J. Chem. Soc. Perkin Trans. II* **1986**, 1-6 doi:10.1039/P29860000001.

Forni, L.; Bahnemann, D.; Hart, E. J. Mechanism of the hydroxide ion initated decomposition of ozone in aqueous solution. *J. Phys. Chem.* **1982**, *86*, 255-259, doi:10.1021/j100391a025.

Fortnum, D. H.; Battaglia, C. J.; Cohen, S. R.; Edwards, J. O. The kinetics of the oxidation of halide ions by monosubstituted peroxides. *J. Am. Chem. Soc.* **1960**, *82*, 778-782, doi:10.1021/ja01489a004.

Frenzel, A.; Scheer, V.; Sikorski, R.; George, C.; Behnke, W.; Zetzsch, C. Heterogeneous interconversion reactions of $BrNO_2$, $ClNO_2$, Br_2, and Cl_2. *J. Phys. Chem. A* **1998**, *102*, 1329-1337, doi:10.1021/jp973044b.

Furman, C. S.; Margerum, D. W. Mechanism of chlorine dioxide and chlorate ion formation from the reaction of hypobromous acid and chlorite ion. *Inorg. Chem.* **1998**, *37*, 4321-4327, doi:10.1021/ic980262q.

Furrow, S. Reactions of iodine intermediates in iodate-hydrogen peroxide oscillators. *J. Phys. Chem.* **1987**, *91*, 2129-2135, doi:10.1021/j100292a031.

Gálvez, O.; Teresa Baeza-Romero, M.; Sanz, M.; Pacios, L. F. A theoretical study on the reaction of ozone with aqueous iodide. *Phys. Chem. Chem. Phys.* **2016**, *18*, 7651-7660, doi:10.1039/c5cp06440f.

Gardoni, D.; Vailati, A.; Canziani, R. Decay of ozone in water: A review. *Ozone Sci. Eng.* **2012**, *34*, 233-242, doi:10.1080/01919512.2012.686354.

George, C.; Ammann, M.; D'Anna, B.; Donaldson, D. J.; Nizkorodov, S. A. Heterogeneous photochemistry in the atmosphere. *Chem. Rev.* **2015**, *115*, 4218-4258, doi:10.1021/cr500648z.

George, C.; D'Anna, B.; Herrmann, H.; Weller, C.; Vaida, V.; Donaldson, D. J.; Bartels-Rausch, T.; Ammann, M. Emerging Areas in Atmospheric Photochemistry. In *Atmospheric and Aerosol Chemistry*; McNeill, V. F., Ariya, P. A., Eds.; Springer Berlin Heidelberg: Berlin, Heidelberg, 2014; pp 1-53.

Gerritsen, C. M.; Margerum, D. W. Nonmetal redox kinetics - hypochlorite and hypochlorous acid reactions with cyanide. *Inorg. Chem.* **1990**, *29*, 2757-2762, doi:10.1021/ic00340a010.

Gershenzon, M.; Davidovits, P.; Jayne, J. T.; Kolb, C. E.; Worsnop, D. R. Rate constant for the reaction of Cl_2(aq) with OH^-. *J. Phys. Chem. A* **2002**, *106*, 7748-7754, doi:10.1021/jp014146b.

Ghibaudi, E.; Barker, J. R.; Benson, S. W. Reaction of NO with hypochlorous acid. *Int. J. Chem. Kinet.* **1979**, *11*, 843-851, doi:10.1002/kin.550110804.
Glasstone, S. Textbook of Physical Chemistry, Institution; D. van Nostrand Company, Inc., 1946.
Gordon, G.; Tachiyashiki, S. Kinetics and mechanism of formation of chlorate ion from the hypochlorous acid/chlorite ion reaction at pH 6-10. *Environ. Sci. Technol.* **1991**, *25*, 468-474, doi:10.1021/es00015a014.
Grigor'ev, A. E.; Makarov, I. E.; Pikaev, A. K. Formation of Cl_2^- in the bulk solution during the radiolysis of concentrated aqueous solutions of chlorides. *High Energy Chem.* **1987**, *21*, 99-102.
Haag, W. R.; Hoigné, J. Ozonation of bromide-containing waters: Kinetics of formation of hypobromous acid and bromate. *Environ. Sci. Technol.* **1983**, *17*, 261-267, doi:10.1021/es00111a004.
Haag, W. R.; Hoigné, J. Ozonation of water containing chlorine or chloramines. Reaction products and kinetics. *Water Res.* **1983**, *17*, 1397-1402, doi:10.1016/0043-1354(83)90270-1.
Hart, E. J.; Henglein, A. Free radical and free atom reactions in the sonolysis of aqueous iodide and formate solutions. *J. Phys. Chem.* **1985**, *89*, 4342-4347, doi:10.1021/j100266a038.
Haruta, K.; Takeyama, T. Kinetics of oxidation of aqueous bromide ion by ozone. *J. Phys. Chem.* **1981**, *85*, 2383-2388, doi:10.1021/j150616a018.
Heeb, M. B.; Kristiana, I.; Trogolo, D.; Arey, J. S.; von Gunten, U. Formation and reactivity of inorganic and organic chloramines and bromamines during oxidative water treatment. *Water Res.* **2017**, *110*, 91-101, doi:10.1016/j.watres.2016.11.065.
Held, A. M.; Halko, D. J.; Hurst, J. K. Mechanisms of chlorine oxidation of hydrogen peroxide. *J. Am. Chem. Soc.* **1978**, *100*, 5732-5740, doi:10.1021/ja00486a025.
Herckes, P.; Valsaraj, K. T.; Collett, J., L. A review of observations of organic matter in fogs and clouds: Origin, processing and fate. *Atmos. Res.* **2013**, *132-133*, 434-449, doi:10.1016/j.atmosres.2013.06.005.
Herrmann, H. On the photolysis of simple anions and neutral molecules as sources of O-/OH, SO_x^- and Cl in aqueous solution. *Phys. Chem. Chem. Phys.* **2007**, *9*, 3935-3964, doi:10.1039/b618565g.
Herrmann, H.; Jacobi, H.-W.; Raabe, G.; Reese, A.; Zellner, R. Laser-spectroscopic laboratory studies of atmospheric aqueous phase free radical chemistry. *Fresenius' J. Anal. Chem.* **1996**, *355*, 343-344, doi:10.1007/s0021663550343.
Herrmann, H.; Schaefer, T.; Tilgner, A.; Styler, S. A.; Weller, C.; Teich, M.; Otto, T. Tropospheric aqueous-phase chemistry: Kinetics, mechanisms, and its coupling to a changing gas phase. *Chem. Rev.* **2015**, *115*, 4259-4334, doi:10.1021/cr500447k.
Hoigné, J.; Bader, H. Kinetics of reactions of chlorine dioxide (OClO) in water. - 1. Rate constants for inorganic and organic compounds. *Water Research* **1994**, *28*, 45-55, doi:10.1016/0043-1354(94)90118-X.
Hoigné, J.; Bader, H.; Haag, W. R.; Staehelin, J. Rate constants of reactions of ozone with organic and inorganic compounds in water—III. Inorganic compounds and radicals *Water Research* **1985**, *19*, 993-1004, doi:10.1016/0043-1354(85)90368-9.
Huie, R. E.; Clifton, C. L. Temperature dependence of the rate constants for reactions of the sulfate radical, SO_4^-, with anions. *J. Phys. Chem.* **1990**, *94*, 8561-8567, doi:10.1021/j100386a015.
Huie, R. E.; Clifton, C. L.; Neta, P. Electron transfer reaction rates and equilibria of the carbonate and sulfate radical anions. *Int. J. Radiat. Appl. Inst. Part C. Radiat. Phys. Chem.* **1991**, *38*, 477-481, doi:10.1016/1359-0197(91)90065-A.
Huie, R. E.; Neta, P. Kinetics of one-electron transfer-reactions involving ClO_2 and NO_2. *J. Phys. Chem.* **1986**, *90*, 1193-1198, doi:10.1021/j100278a046.
Huie, R. E.; Padmaja, S. The reaction of NO with superoxide. *Free Rad. Res. Comm.* **1993**, *18*, 195-199, doi:10.3109/10715769309145868.
Huie, R. E.; Shoute, L. C. T.; Neta, P. Temperature dependence of the rate constants for reactions of the carbonate radical with organic and inorganic reductants. *Int. J. Chem. Kinet.* **1991**, *23*, 541-552, doi:10.1002/kin.550230606.
Hurst, J. K. The role of inorganic chemistry in cellular mechanisms of host resistance to desease. *Adv. Chem. Series* **1997**, *253*, 399-421.
Ishigure, K.; Shiraishi, H.; Okuda, H. Radiation chemistry of aqueous iodine systems under nuclear reactor accident conditions. *Int. J. Radiat. Appl. Inst. Part C. Radiat. Phys. Chem.* **1988**, *32*, 593-597, doi:10.1016/1359-0197(88)90070-7.

Jacobsen, J.; Jensen, S. J. K. A mechanism for production of singlet oxygen by acidification of hypochlorite. *Chem. Phys. Lett.* **2007**, *449*, 135-137, doi:10.1016/j.cplett.2007.10.056.

Jayson, G. C.; Parson, B. J.; Swallow, A. J. Some simple, highly reactive, inorganic chlorine derivatives in aqueous solution. *J. Chem. Soc. Faraday Trans.* **1973**, *69*, 1597-1607, doi:10.1039/F19736901597.

Jia, Z. J.; Margerum, D. W.; Francisco, J. S. General-acid-catalyzed reactions of hypochlorous acid and acetyl hypochlorite with chlorite ion. *Inorg. Chem.* **2000**, *39*, 2614-2620, doi:10.1021/ic991486r.

Jiang, P. Y.; Katsumura, Y.; Nagaishi, R.; Domae, M.; Ishikawa, K.; Ishigure, K.; Yoshida, Y. Pulse radiolysis studies of concentrated sulfuric acid solutions. Formation mechanism, yield and reactivity of sulfate radicals. *J. Chem. Soc. Faraday Trans.* **1992**, *88*, 1653-1658, doi:10.1039/FT9928801653.

Johnson, D. W.; Margerum, D. W. Non-metal redox kinetics: A reexamination of the mechansim of the reaction between hypochlorite and nitrite ions. *Inorg. Chem.* **1991**, *30*, 4845-4851, doi:10.1021/ic00025a031.

Kang, N.; Jackson, W. A.; Dasgupta, P. K.; Anderson, T. A. Perchlorate production by ozone oxidation of chloride in aqueous and dry systems. *Sci. Total Environ.* **2008**, *405*, 301-309, doi:10.1016/j.scitotenv.2008.07.010.

Kazmierczak, L.; Swiatla-Wojcik, D.; Szala-Bilnik, J.; Wolszczak, M. Rate of reaction of the hydrogen atom with nitrous oxide in ambient water. *Radiat. Phys. Chem.* **2016**, *125*, 156-159, doi:10.1016/j.radphyschem.2016.04.007.

Kerezsi, I.; Lente, G.; Fábián, I. Kinetics and mechanism of the photoinitiated autoxidation of sulfur(IV) in the presence of iodide ion. *Inorg. Chem.* **2007**, *46*, 4230-4238, doi:10.1021/ic061521b.

Khan, A. U.; Kasha, M. Singlet molecular oxygen evolution upon simple acidification of aqueous hypochlorite: Application to studies on the deleterious health effects of chlorinated drinking water. *Proc. Natl. Acad. Sci. USA* **1994**, *91*, 12362-12364.

Kläning, U. K.; Sehested, K.; Holcman, J. Standard Gibbs energy of formation of the hydroxyl radical in aqueous solution. Rate constants for the reaction $ClO_2^- + O_3 \rightleftarrows O_3^- + ClO_2$. *J. Phys. Chem.* **1985**, *89*, 760-763, doi:10.1021/j100251a008.

Knipping, E. M.; Lakin, M. J.; Foster, K. L.; Jungwirth, P.; Tobias, D. J.; Gerber, R. B.; Dabdub, D.; Finlayson-Pitts, B. J. Experiments and simulations of ion-enhanced interfacial chemistry on aqueous NaCl aerosols. *Science* **2000**, *288*, 301-306, doi:10.1126/science.288.5464.301.

Kono, Y. The production of nitrating species by the reaction between nitrite and hypochlorous acid. *Biochem. Mol. Biol. Int.* **1995**, *36*, 275-283.

Kumar, K.; Day, R. A.; Margerum, D. W. Atom-transfer redox kinetics - general-acid-assisted oxidation of iodide by chloramines and hypochlorite. *Inorg. Chem.* **1986**, *25*, 4344-4350, doi:10.1021/ic00244a012.

Kumar, K.; Margerum, D. W. Kinetics and mechanism of general-acid-assisted oxidation of bromide by hypochlorite and hypochlorous acid. *Inorg. Chem.* **1987**, *26*, 2706-2711, doi:10.1021/ic00263a030.

Lahoutifard, N.; Lagrange, P.; Lagrange, J. Kinetics and mechanism of nitrite oxidation by hypochlorous acid in the aqueous phase. *Chemosphere* **2003**, *50*, 1349-1357, doi:10.1016/S0045-6535(02)00765-8.

Lahoutifard, N.; Lagrange, P.; Lagrange, J.; Scott, S. L. Kinetics and mechanism of nitrite oxidation by $HOBr/BrO^-$ in atmospheric water and comparison with oxidation by $HOCl/ClO^-$. *J. Phys. Chem. A* **2002**, *106*, 11891-11896, doi:10.1021/jp021185u.

Lahoutifard, N.; Scott, S. L. Reply to "Comment on 'Kinetics and mechanism of nitrite oxidation by $HOBr/BrO^-$ in atmospheric water and comparison with oxidation by $HOCl/ClO^-$' ". *J. Phys. Chem. A* **2004**, *108*, 10617-10618, doi:10.1021/jp0311456.

LaMer, V. K. L.; Lewinsohn, M. H. Halide–iodine equilibria in neutral salt solvents. *J. Phys. Chem.* **1934**, *38*, 171-195, doi:10.1021/j150353a004.

Lampre, I.; Marignier, J.-L.; Mirdamadi-Esfahani, M.; Pernot, P.; Archirel, P.; Mostafavi, M. Oxidation of bromide ions by hydroxyl radicals: Spectral characterization of the intermediate $BrOH^{\bullet-}$. *J. Phys. Chem. A* **2013**, *117*, 877-887, doi:10.1021/jp310759u.

Lengyel, I.; Li, J.; Kustin, K.; Epstein, I. R. Rate constants for reactions between iodine- and chlorine-containing species: A detailed mechanism of the chlorine dioxide/chlorite-iodide reaction. *J. Am. Chem. Soc.* **1996**, *118*, 3708-3719, doi:10.1021/ja953938e.

Lente, G.; Kalmár, J.; Baranyai, Z.; Kun, A.; Kék, I.; Bajusz, D.; Takács, M.; Veres, L.; Fábián, I. One- versus two-electron oxidation with peroxomonosulfate ion: Reactions with iron(II), vanadium(IV), halide ions, and photoreaction with cerium(III). *Inorg. Chem.* **2009**, *48*, 1763, doi:10.1021/ic801569k.

Lesko, T. M.; Colussi, A. J.; Hoffmann, M. J. Hydrogen isotope effects and mechanism of aqueous ozone and peroxone decomposition. *J. Am. Chem. Soc.* **2004**, *126*, 4432-4436, doi:10.1021/ja038907v.

Levanov, A. V.; Antipenko, E. E.; Lunin, V. V. Primary stage of the reaction between ozone and chloride ions in aqueous solution: Can chloride ion oxidation by ozone proceed via electron transfer mechanism? *Russ. J. Phys. Chem.* **2012**, *86*, 584-589, doi:10.1134/S0036024412040164.

Levanov, A. V.; Antipenko, E. E.; Lunin, V. V. Primary stage of the reaction between ozone and chloride ions in aqueous solution: Oxidation of chloride ions with ozone through the mechanism of oxygen atom transfer. *Russ. J. Phys. Chem.* **2012**, *85*, 519-522, doi:10.1134/S0036024412030193.

Levanov, A. V.; Isaykina, O. Y.; Amirova, N. K.; Antipenko, E. E.; Lunin, V. V. Photochemical oxidation of chloride ion by ozone in acid aqueous solution. *Environ. Sci. Pollut. Res.* **2015**, *22*, 16554-16569, doi:10.1007/s11356-015-4832-9.

Levanov, A. V.; Kuskov, I. V.; Antipenko, E. E.; Lunin, V. V. The solubility of ozone and kinetics of its chemical reactions in aqueous solutions of sodium chloride. *Russ. J. Phys. Chem. A* **2008**, *82*, 2045-2050, doi:10.1134/s0036024408120133.

Levanov, A. V.; Kuskov, I. V.; Antipenko, E. E.; Lunin, V. V. Stoichiometry and products of ozone reaction with chloride ion in an acidic medium. *Russ. J. Phys. Chem.* **2012**, *86*, 757-762.

Levanov, A. V.; Kuskov, I. V.; Koiaidarova, K. B.; Antipenko, E. E.; Lunin, V. V. Interaction between ozone and the chloride ion in sulfuric acid solutions up to 6-M concentration. *Kin. Cat.* **2006**, *47*, 682-685, doi:10.1134/S0023158406050053.

Levanov, A. V.; Kuskov, I. V.; Koiaidarova, K. B.; Zosimov, A. V.; Antipenko, E. E.; Lunin, V. V. Catalysis of the reaction of ozone with chloride ions by metal ions in an acidic medium. *Kin. Cat.* **2005**, *46*, 138-143, doi:10.1007/s10975-005-0021-z.

Levanov, A. V.; Kuskov, I. V.; Zosimov, A. V.; Antipenko, E. E.; Lunin, V. V. Acid catalysis in reaction of ozone with chloride ions. *Kin. Cat.* **2003**, *44*, 740-746, doi:10.1023/B:KICA.0000009047.90252.2d.

Liebhafsky, H. A.; Mohammad, A. The kinetics of the reduction, in acid solution, of hydrogen peroxide by iodide ion. *J. Am. Chem. Soc.* **1933**, *55*, 3977-3986, doi:10.1021/ja01337a010.

Lister, M. W.; Petterson, R. C. Oxygen evolution from sodium hypochlorite solutions. *Can. J. Chem.* **1962**, *40*, 729-733, doi:10.1139/v62-109.

Lister, M. W.; Rosenblum, P. The oxidation of nitrite and iodate ions by hypochlorite ions. *Can. J. Chem.* **1961**, *39*, 1645-1651, doi:10.1139/v61-211.

Lister, M. W.; Rosenblum, P. Rates of reaction of hypochlorite ions with sulphite and iodide ions. *Can. J. Chem.* **1963**, *41*, 3013-3020, doi:10.1139/v63-442.

Liu, Q.; Schurter, L. M.; Muller, C. E.; Aloisio, S.; Franscisco, J. S.; Margerum, D. W. Kinetics and mechanisms of aqueous ozone reactions with bromide, sulfite, hydrogen sulfite, and nitrite ions. *Inorg. Chem.* **2001**, *40*, 4436-4442, doi:10.1021/ic000919j.

Liu, Y.; Pimentel, A. S.; Antoku, Y.; Giles, B. J.; Barker, J. R. Temperature-dependent rate and equilibrium constants for Br(aq) + Br^-(aq) ↔ $Br_2^{\bullet-}$(aq). *J. Phys. Chem. A* **2002**, *106*, 11075-11082, doi:10.1021/jp0255536.

Liu, Y.; Sheaffer, R. L.; Barker, J. R. Effects of temperature and ionic strength on the rate and equilibrium constants for the reaction $I^{\bullet}_{aq}$ + I^-_{aq} ↔ $I_2^{\bullet-}{}_{aq}$. *J. Phys. Chem. A* **2003**, *107*, 10296-10302, doi:10.1021/jp036126a.

Løgager, T.; Sehested, K. Formation and decay of peroxynitric acid: A pulse radiolysis study. *J. Phys. Chem.* **1993**, *97*, 10047-10052, doi:10.1021/j100141a025.

Long, C. A.; Bielski, B. H. J. Rate of reaction of superoxide radical with chlorine-containing species. *J. Phys. Chem.* **1980**, *84*, 555-557, doi:10.1021/j100442a023.

Lunin, V. V.; Levanov, A. V.; Kuskov, I. V.; Zosimov, A. V.; Antipenko, E. E. Chlorine evolution in the interaction between ozone and a solution of sodium chloride in the presence of carbon dioxide. *Russ. J. Phys. Chem.* **2003**, *77*, 580-585.

Madden, K. P.; Mezyk, S. P. Critical review of aqueous solution reaction rate constants for hydrogen atoms. *J. Phys. Chem. Ref. Data* **2011**, *40*, 023103, doi:10.1063/1.3578343.

Maetzke, A.; Jensen, S. J. K. Reaction paths for production of singlet oxygen from hydrogen peroxide and hypochlorite. *Chem. Phys. Lett.* **2006**, *425*, 40-43, doi:10.1016/j.cplett.2006.04.097.

Magi, L.; Schweitzer, F.; Pallares, C.; Cherif, S.; Mirabel, P.; George, C. Investigation of the uptake rate of ozone and methyl hydroperoxide by water surfaces. *J. Phys. Chem. A* **1997**, *101*, 4943-4949, doi:10.1021/jp970646m.

Manov, G. G.; Bates, R. G.; Hamer, W. J.; Acree, S. F. Values of the constants in the Debye-Huckel equation for activity coefficients. *J. Am. Chem. Soc.* **1943**, *65*, 1765-1767, doi:10.1021/ja01249a028.

Margerum D. W.; Hartz, K. E. H. Role of halogen(I) cation-transfer mechanisms in water chlorination in the presence of bromide ion. *J. Environ. Monit.* **2002**, *4*, 20-26, doi:10.1039/b105541k.

Margerum, D. W.; Dickson, P. N.; Nagy, J. C.; Kumar, K.; Bowers, C. P.; Fogelman, K. D. Kinetics of the iodine monochloride reaction with iodide measured by the pulsed-accelerated-flow method. *Inorg. Chem.* **1986**, *25*, 4900-4904, doi:10.1021/ic00247a025.

Matthew, B. M.; George, I.; Anastasio, C. Hydroperoxyl radical (HO_2) oxidizes dibromide radical anion (Br_2^-) to bromine (Br_2) in aqueous solution: Implicatins for the formation of Br_2 in the marine boundary layer. *Geophys. Res. Lett.* **2003**, *30*, 2297, doi:10.1029/2003GL018572.

Mayer, J. M. Proton-coupled electron transfer: A reaction chemist's view. *Annu. Rev. Phys. Chem.* **2004**, *55*, 363-390, doi:10.1146/annurev.physchem.55.091602.094446.

McNeill, V. F. Aqueous organic chemistry in the atmosphere: Sources and chemical processing of organic aerosols. *Environ. Sci. Technol.* **2015**, *49*, 1237-1244, doi:10.1021/es5043707.

Merényi, G.; Lind, J. Reaction-mechanism of hydrogen abstraction by the bromine atom in water. *J. Am. Chem. Soc* **1994**, *116*, 7872-7876, doi:10.1021/ja00096a050.

Merényi, G.; Lind, J.; Naumov, S.; von Sonntag, C. The reaction of ozone with the hydroxide ion: mechanistic considerations based on thermokinetic and quantum chemical calculations and the role of HO_4^- in superoxide dismutation. *Chem. Eur. J.* **2010**, *16*, 1372-1377, doi:10.1002/chem.200802539.

Mertens, R.; Von Sonntag, C. Photolysis (λ = 254 nm) of tetrachloroethene in aqueous solutions. *J. Photochem. Photobiol.* **1995**, *85*, 1-9, doi:10.1016/1010-6030(94)03903-8.

Minakata, D.; Kamath, D.; Maetzold, S. Mechanistic insight into the reactivity of chlorine-derived radicals in the aqueous-phase UV–chlorine advanced oxidation process: Quantum mechanical calculations. *Environ. Sci. Technol.* **2017**, *51*, 6918-6926, doi:10.1021/acs.est.7b00507.

Mohammad, A.; Liebhafsky, H. A. The kinetics of the reduction of hydrogen peroxide by the halides. *J. Am. Chem. Soc.* **1934**, *56*, 1680-1685, doi:10.1021/ja01323a009.

Mulazzani, Q. G.; Buxton, G. V. On the kinetics and mechanism of the oxidation of I^- by (OH)-O-center dot/O center dot- in alkaline aqueous solution. *Chem. Phys. Lett.* **2006**, *421*, 261-265, doi:10.1016/j.cplett.2006.01.088.

Nagy, J. C.; Kumar, K.; Margerum, D. W. Non-metal redox kinetics: Oxidation of iodide by hypochlorous acid and by nitrogen trichloride measured by the pulsed-accelerated-flow method. *Inorg. Chem.* **1988**, *27*, 2773-2780, doi:10.1021/ic00289a007.

Naumov, S.; von Sonntag, C. The reactions of bromide with ozone towards bromate and the hypobromite puzzle: A density functional theory study. *Ozone: Science and Engineering* **2008**, *30*, 339-343, doi:10.1080/01919510802326120.

Naumov, S.; Von Sonntag, C. The reaction of •OH with O_2, the decay of O_3^- and the pKa of HO_3^- interrelated questions in aqueous free-radical chemistry. *J. Phys. Org. Chem.* **2010**.

Naumov, S.; von Sonntag, C. Standard Gibbs free energies of reactions of ozone with free radicals in aqueous solution: Quantum-chemical calculations. *Environ. Sci. Technol.* **2011**, *45*, 9195-9204, doi:10.1021/es2018658.

Nemes, A.; Fábián, I.; van Eldik, R. Kinetics and mechanism of the carbonate ion inhibited aqueous ozone decomposition. *J. Phys. Chem. A* **2000**, *104*, 7995-8000, doi:10.1021/jp000972t.

Neta, P.; Huie, R. E. Rate constants for reactions of NO_3 radicals in aqueous-solutions. *J. Phys. Chem.* **1986**, *90*, 4644-4648, doi:10.1021/j100410a035.

Neta, P.; Huie, R. E.; Maruthamuthu, P.; Steenken, S. Solvent effects in the reactions of peroxyl radicals with organic reductants: evidence for proton-transfer-mediated electron transfer. *J. Phys. Chem.* **1989**, *93*, 7654-7659, doi:10.1021/j100359a025.

Nicoson, J. S.; Margarum, D. W. Kinetics and mechanisms of aqueous chlorine reactions with chlorite ion in the presence of chloride ion and acetic acid/acetate buffer. *Inorg. Chem.* **2002**, *41*, 342-347, doi:10.1021/ic010762a.

Nicoson, J. S.; Perrone, T. F.; Hartz, K. E. H.; Margarum, D. W. Kinetics and mechanisms of the reactions of hypochlorous acid, chlorine, and chlorine monoxide with bromite ion. *Inorg. Chem.* **2003**, *42*, 5818-5824, doi:10.1021/ic0301223.

Padmaja, S.; Neta, P.; Huie, R. E. Rate constants for some reactions of inorganic radicals with inorganic ions. Temperature and solvent dependence. *Int. J. Chem. Kinet.* **1993**, *25*, 445-455, doi:10.1002/kin.550250604.

Panasenko, O. M.; Briviba, K.; Klotz, L. O.; Sies, H. Oxidative modification and nitration of human low-density lipoproteins by the reaction of hypochlorous acid with nitrite. *Arch. Biochem. Biophys.* **1997**, *343*, 254-259, doi:10.1006/abbi.1997.0171.

Panich, N. M.; Ershov, B. G. The solubility and kinetics of decomposition of ozone in aqueous solutions of nitrates. *Russ. J. Phys. Chem. A* **2008**, *82*, 1262-1265, doi:10.1134/S0036024408080049.

Pátek, J.; Hrubý, J.; Klomfar, J.; Součková, M.; Harvey, A. H. Reference correlations for thermophysical properties of liquid water at 0.1 MPa. *J. Phys. Chem. Ref. Data* **2009**, *38*, 21-29, doi:10.1063/1.3043575.

Peintler, G.; Nagypál, I.; Epstein, I. R. Kinetics and mechanism of the reactions between chlorite and hypochlorous acid. *J. Phys. Chem.* **1990**, *94*, 2954-2958, doi:10.1021/j100370a040.

Pendlebury, J. N.; Smith, R. H. Kinetics of oxidation of nitrite by aqueous chlorine. *Aust. J. Chem.* **1973**, *26*, 1857-1861, doi:10.1071/CH9731857.

Poskrebyshev, G. A.; Huie, R. E.; Neta, P. The rate and equilibrium constants for the reaction $NO_3\cdot + Cl^- \leftrightarrow NO_3^- + Cl\cdot$ in aqueous solutions. *J. Phys. Chem. A* **2003**, *107*, 1964-1970, doi:10.1021/jp0215724.

Poskrebyshev, G. A.; Neta, P.; Huie, R. E. Equilibrium constant of the reaction -OH + $HNO_3 \rightarrow H_2O^+ NO_3$ in aqueous solution *J. Geophys. Res.* **2001**, *106*, 4995-5004, doi:10.1029/2000JD900702.

Qiang, Z.; Adams, C. D. Determination of monochloramine formation rate constants with stopped-flow spectrophotometry. *Environ. Sci. Technol.* **2004**, *38*, 1435-1444, doi:10.1021/es0347484.

Ramette, R. W.; Sandford, R. W. Thermodynamics of iodine solubility and triiodide ion formation in water and in deuterium oxide. *J. Am. Chem. Soc.* **1965**, *87*, 5001-5005, doi:10.1021/ja00950a005.

Rao, B.; Anderson, T. A.; Redder, A.; Jackson, W. A. Perchlorate formation by ozone oxidation of aqueous chlorine/oxy-chlorine species: Role of Cl_xO_y radicals. *Environ. Sci. Technol.* **2010**, *44*, 2961-1967, doi:10.1021/es903065f.

Razumovskii, S. D.; Grinevich, T. V.; Korovina, G. V. Reactivity of hydrogen peroxide with respect to ozone. *Russ. J. Phys. Chem.* **2011**, *5*, 797-799, doi:10.1134/S1990793111090211.

Razumovskii, S. D.; Korovina, G. V.; Grinevich, T. V. Mechanism of the first step of ozone decomposition in aqueous solutions of sodium chloride in view of new data on the composition of reaction products. *Doklady Phys. Chem.* **2010**, *424*, 163-165, doi:10.1134/S0012501610100027.

Redpath, J. L.; Willson, R. L. Chain reactions and radiosensitization: Model enzyme studies. *Int. J. Radiat. Biol.* **1975**, *27*, 389-398, doi:10.1080/09553007514550361.

Régimbal , J. M.; Mozurkewich, M. Kinetics of peroxynitric acid reactions with halides at low pH. *J. Phys. Chem. A* **2000**, *104*, 6580-6589, doi:10.1021/jp971908n.

Reisz, E.; Schmidt, W.; Schuchmann, H. P.; von Sonntag, C. Photolysis of ozone in aqueous solutions in the presence of tertiary butanol. *Environ. Sci. Technol.* **2003**, *37*, 1941-1948, doi:10.1021/es0113100.

Renard, J. J.; Bolker, H. I. The chemistry of chlorine monoxide (dochlorine monoxide). *Chem. Rev.* **1976**, *76*, 487-508, doi:10.1021/cr60302a004.

Ross, A. B.; Mallard, W. G.; Hellman, W. P.; Bielski, B. H. J.; Buxton, G. V.; Cabelli, D. E.; Greenstock, C. L.; Huie, R. E.; Neta, P. *NDRL/NIST Solution Kinetics Database*, 1997; Vol. 40.

Rudich, Y.; Talukdar, R. K.; Imamura, T.; Fox, R. W.; Ravishankara, A. R. Uptake of NO_3 on KI solutions: rate coefficient fo the $NO_3 + I^-$ reaction and gas-phase difussion coefficients for NO_3. *Chem. Phys. Lett.* **1996**, *261*, 467-473, doi:10.1016/0009-2614(96)00980-3.

Sandin, S.; Karlsson, R. K. B.; Cornell, A. Catalyzed and uncatalyzed decomposition of hypochlorite in dilute solutions. *Ind. Eng. Chem. Res.* **2015**, *54*, 3767-3774, doi:10.1021/ie504890a.

Schmitz, G. Iodine(+1) reduction by hydrogen peroxide. *Russ. J. Phys. Chem. A* **2009**, *83*, 1447-1451, doi:10.1134/s0036024409090052.

Schwarz, H. A.; Bielski, B. H. J. Reactions of HO_2 and O_2^- with iodine and bromine and I_2^- and I atom reduction potentials. *J. Phys. Chem.* **1986**, *90*, 1445-1448, doi:10.1021/j100398a045.

Seddon, W. A.; Fletcher, J. W.; Sopchyshyn, F. C. Pulse radiolysis of nitric oxide in aqueous solution. *Can. J. Chem.* **1973**, *51*, 1123-1130, doi:10.1139/v73-166.

Sehested, K.; Corfitzen, H.; Holcman, J.; Fisher, C. H.; Hart, E. J. The primary reaction in the decomposition of ozone in acidic aqueous solutions. *Environ. Sci. Technol.* **1991**, *25*, 1589-1596, doi:10.1021/es00021a010.

Sehested, K.; Corfitzen, H.; Holcman, J.; Hart, E. J. Decomposition of ozone in aqueous acetic acid solutions (pH 0-4). *J. Phys. Chem.* **1992**, *96*, 1005-1009, doi:10.1021/j100181a084.

Sehested, K.; Corfitzen, H.; Holcman, J.; Hart, E. J. On the mechanism of the decomposition of acidic O_3 solutions, thermally or H_2O_2-initiated. *J. Phys. Chem. A* **1998**, *102*, 2667-2672, doi:10.1021/jp9721053.

Sehested, K.; Holcman, J.; Bjergbakke, E.; Hart, E. J. Formation of ozone in the reaction of OH with O_3^- and the decay of the ozonide ion radical at pH 10-13 *J. Phys. Chem.* **1984**, *88*, 269-273, doi:10.1021/j150646a021.

Sehested, K.; Holcman, J.; Bjergbakke, E.; Hart, E. J. A pulse radiolytic study of the reaction OH + O_3 in aqueous medium. *J. Phys. Chem.* **1984**, *88*, 4144-4147, doi:10.1021/j150662a058.

Sehested, K.; Holcman, J.; Hart, E. J. Rate constants and products of the reactions of e_{aq}^-, O_2^-, and H with ozone in aqueous solution. *J. Phys. Chem.* **1983**, *87*, 1951-1954, doi:10.1021/j100234a024.

Sein, M. M.; Golloch, A.; Schmidt, T. C.; Sonntag, C. v. No marked kinetic isotope effect in the peroxone (H_2O_2/D_2O_2 + O_3) reaction: mechanistic consequences. *ChemPhysChem* **2007**, *8*, 2065-2067, doi:10.1002/cphc.200700493.

Shen, X.; Zhao, Y.; Chen, Z. M.; Huang, D. Heterogeneous reactions of volatile organic compounds in the atmosphere. *Atmos. Environ.* **2013**, *68*, 297-314, doi:10.1016/j.atmosenv.2012.11.027.

Shoute, L. C. T.; Alfassi, Z. B.; Neta, P.; Huie, R. E. Temperature dependence of the rate constants for reaction of dihalide and azide radicals with inorganic reductants. *J. Phys. Chem.* **1991**, *95*, 3238-3242, doi:10.1021/j100161a050.

Sies, H., Data for the reaction of HOCl with NO_2^-.

Simon, H.; Bhave, P. V. Simulating the degree of oxidation in atmospheric organic particles. *Environ. Sci. Technol.* **2012**, *46*, 331-339, doi:10.1021/es202361w.

Sivey, J. D.; Arey, J. S.; Tentscher, P. R.; Roberts, A. L. Reactivity of BrCl, Br_2, BrOCl, Br_2O, and HOBr toward dimethenamid in solutions of bromide + aqueous free chlorine. *Environ. Sci. Technol.* **2013**, *47*, 1330-1338, doi:10.1021/es302730h.

Sotelo, J. L.; Beltrán, F. J.; Benítez, F. J.; Beltrán-Heredia, J. Ozone decomposition in water: Kinetic study. *Ind. Eng. Chem. Res.* **1987**, *26*, 39-43, doi:10.1021/ie00061a008.

Staehelin, J.; Hoigné, J. Decomposition of ozone in water: Rate of initiation by hydroxide ions and hydrogen peroxide. *Environ. Sci. Technol.* **1982**, *16*, 676-681, doi:10.1021/es00104a009.

Stanbury, D. M.; Figlar, J. N. Vanishingly small kinetics of the ClO_2/Cl^- reaction: its questionable significance in nonlinear chlorite reactions. *Coord. Chem. Revs.* **1999**, *187*, 223-232.

Storch, D. M.; Dymek, C. J.; Davis, L. P. MNDO study of the mechanismm of $O_2(^1\Delta)$ formation in the reaction of Cl_2 with basic H_2O_2. *J. Am. Chem. Soc.* **1983**, *105*, 1765-1768, doi:10.1021/ja00345a011.

Subhani, M. S. Photodecomposition of hypoiodite ion in aqueous solution. *Rev. Roum. Chim.* **1983**, *28*, 397-403.

Swain, C. G.; Crist, D. R. Mechanisms of chlorination by hypochlorous acid. The last of chlorinium ion, Cl^{+1}. *J. Am. Chem. Soc.* **1972**, *94*, 3195-3200, doi:10.1021/ja00764a050.

Swiatla-Wojcik, D.; Buxton, G. V. On the possible role of the reaction H + H_2O → H_2 + OH in the radiolysis of water at high temperatures. *Rad. Phys. Chem.* **2005**, *74*, 210-219, doi:10.1016/j.radphyschem.2005.04.014.

Swiatla-Wojcik, D.; Buxton, G. V. Reply to comment on the possible role of the reaction H + H_2O → H_2 + OH in the radiolysis of water at high temperatures. *Rad. Phys. Chem.* **2010**, *79*, 52-56, doi:10.1016/j.radphyschem.2009.07.024.

Taube, H.; Dodgen, H. Applications of radioactive chlorine to the study of the mechanisms of reactions involving changes in the oxidation state of chlorine. *J. Am. Chem. Soc.* **1949**, *71*, 3330-3336, doi:10.1021/ja01178a016.

Tomiyasu, H.; Fukutomi, H.; Gordon, G. Kinetics and mechanism of ozone decomposition in basic aqueous solution. *Inorg. Chem.* **1985**, *24*, 2962-2966, doi:10.1021/ic00213a018.

Tóth, Z.; Fábián, I. Kinetics and mechanism of the initial phase of the bromine-chlorite ion reaction in aqueous solution. *Inorg. Chem.* **2000**, *39*, 4608-4614, doi:10.1021/ic990329p.

Troy, R. C.; Kelley, M. D.; Nagy, J. C.; Margerum, D. W. Nonmetal redox kinetics - iodine monobromide reaction with iodide-ion and the hydrolysis of IBr. *Inorg. Chem.* **1991**, *30*, 4838-4845, doi:10.1021/ic00025a030.

Troy, R. C.; Margerum, D. W. Nonmetal redox kinetics - Hypobromite and hypobromous acid reactions with iodide and with sulfite and the hydrolysis of bromosulfate. *Inorg. Chem.* **1991**, *30*, 3538-3543, doi:10.1021/ic00018a028.

Urbansky, E. T.; Cooper, B. T.; Margerum, D. W. Disproportionation kinetics of hypoiodous acid as catalyzed and supressed by acetic acid-acetate buffer. *Inorg. Chem.* **1997**, *36*, 1338-1344, doi:10.1021/ic960745z.

Valent, I.; Schreiber, I.; Marek, M. Kinetics and mechanism of the oxidation of nitrous acid by bromine in aqueous sulfuric acid. *Int. J. Chem. Kinet.* **2000**, *32*, 279-285, doi:10.1002/(SICI)1097-4601.

Valiev, M.; D'Auria; Tobias, D. J.; Garrett, B. C. Interactions of Cl^- and OH radical in aqueous solution. *J. Phys. Chem. A Lett.* **2009**, *113*, 8823-8825, doi:10.1021/jp903625k.

von Gunten, U.; Oliveras, Y. Kinetics of the reaction between hydrogen peroxide and hypobromous acid: Implication on water treatment and natural systems. *Water Research* **1997**, *31*, 900-906, doi:10.1016/S0043-1354(96)00368-5.

Wagner, I.; Strehlow, H. On the flash photolysis of bromide ions in aqueous solutions. *Ber. Bunsenges. Phys. Chem.* **1987**, *91*, 1317-1321, doi:10.1002/bbpc.19870911203.

Wang, L.; Margerum, D. W. Hypohalite ion catalysis of the disproportionation of chlorine dioxide. *Inorg. Chem.* **2002**, *41*, 6099-6105, doi:10.1021/ic020440m.

Wang, L.; Nicoson, J. S.; Hartz, K. E. H.; Francisco, J. S.; Margerum, D. W. Bromite ion catalysis of the disproportionation of chlorine dioxide with nucleophile assistance of electron-transfer reactions between ClO_2 and BrO_2 in basic solution. *Inorg. Chem.* **2002**, *41*, 108-113, doi:10.1021/ic010849w.

Wang, T. X.; Kelley, M. D.; Cooper, J. N.; Beckwith, R. C.; Margerum, D. W. Equilibrium, kinetic, and UV-spectral characteristics of aqueous bromine chloride, bromine, and chlorine species. *Inorg. Chem.* **1994**, *33*, 5872-5878, doi:10.1021/ic00103a040.

Wang, Y. L.; Nagy, J. C.; Margerum, D. W. Kinetics of hydrolysis of iodine monochloride measured by the pulsed-accelerated-flow method. *J. Am. Chem. Soc.* **1989**, *111*, 7838-7844, doi:10.1021/ja00202a026.

Wardman, P. Reduction potentials of one-electron couples involving free radicals in aqueous solution. *J. Phys. Chem. Ref. Data* **1989**, *18*, 1637-1755, doi:10.1063/1.555843.

Watts, M. J.; Rosenfeldt, E. J.; Linden, K. G. Comparative OH radical oxidation using UV-Cl_2 and UV-H_2O_2 processes. *J. Water Supply Res. Technol.-Aqua* **2007**, *56*, 469-477, doi:10.2166/aqua.2007.028.

Weinstein, J.; Bielski, B. H. J. Kinetics of the interaction of HO_2 and O_2^- radicals with hydrogen peroxide. The Haber-Weiss reaction. *J. Am. Chem. Soc.* **1979**, *101*, 58-62, doi:10.1021/ja00495a010.

Wren, J. C.; Paquette, J.; Sunder, S.; Ford, B. L. Iodine chemistry in the +1 oxidation state. II. A Raman and uv–visible spectroscopic study of the disproportionation of hypoiodite in basic solutions. *Can. J. Chem.* **1986**, *64*, 2284-2296, doi:10.1139/v86-375.

Yamashita, S.; Iwamatsu, K.; Maehashi, Y.; Taguchi, M.; Hata, K.; Muroya, Y.; Katsumura, Y. Sequential radiation chemical reactions in aqueous bromide solutions: pulse radiolysis experiment and spur model simulation. *RSC Adv.* **2015**, *5*, 25877-25886, doi:10.1039/C5RA03101J.

Yeatts, L. R. B.; Taube, H. The kinetics of the reaction of ozone and chloride ion in acid aqueous solution. *J. Am. Chem. Soc.* **1949**, *71*, 4100-4105, doi:10.1021/ja01180a063.

Yin, G. H.; Ni, Y. G. Quantitative description of the chloride effect on chlorine dioxide generation from the ClO_2^- -HOCl reaction *Can. J. Chem. Eng.* **1998**, *76*, 921-926, doi:10.1002/cjce.5450760509

Yu, X. Y. Critical evaluation of rate constants and equilibrium constants of hydrogen peroxide photolysis in acidic aqueous solutions containing chloride ions. *J. Phys. Chem. Ref. Data* **2004**, *33*, 747-763, doi:10.1063/1.1695414.

Yu, X. Y.; Barker, J. R. Hydrogen peroxide photolysis in acidic aqueous solutions containing chloride ions. I. Chemical mechanism. *J. Phys. Chem. A* **2003**, *107*, 1313-1324.

Zehavi, D.; Rabani, J. The oxidation of aqueous bromide ions by hydroxyl radicals. A pulse radiolytic investigation. *J. Phys. Chem.* **1972**, *76*, 312-319, doi:10.1021/j100647a006.

Zhestkova, T. P.; Pikaev, A. K. Destruction rate of Cl_2^- anion-radicals during pulse radiolysis of concentrated aqueous lithium chloride solutions. *Izv. Akad. Nauk SSSR, Ser. Chem. Sci.* **1974**, *23*, 877-878.

Zuo, Z.; Katsumura, Y.; Ueda, K.; Ishigure, K. Reactions between some inorganic radicals and oxychlorides studied by pulse radiolysis and laser photolysis. *J. Chem. Soc. Faraday Trans.* **1997**, *93*, 1885-1891, doi:10.1039/A700256D.

SECTION 7: THERMODYNAMIC PARAMETERS

Table of Contents

SECTION 7: THERMODYNAMIC PARAMETERS 1
7.1 Introduction 1
7.2 Table 7-1. Glossary of Groupings 2
7.3 Table 7-2. Gas-Phase Entropy and Enthalpy Values at 100 kPa 3
7.4 Notes for Table 7-2 22
7.5 Bibliography – Thermodynamic Parameters 126

7.1 Introduction

Table 7-2 lists selected entropy and enthalpy of formation values at 298 K for a number of atmospheric species. As much as possible, the values were taken from primary evaluations that develop a recommended value from the original studies. Otherwise, the values were selected from the original literature, which is referenced in the table. Often, the enthalpy of formation and the entropy values are taken from different sources, usually due to a more recent value for the enthalpy of formation. The cited error limits are from the original references and therefore reflect often widely varying criteria. Some enthalpy values have been adjusted to reflect the value of a reference compound selected for this table; these are mentioned in the Notes. Values that are calculated or estimated are also indicated in the Notes, along with information on the level of theory. Results other than those recommended are also often mentioned in the Notes, including recommendations from previous versions of this Table. These should provide a better perspective on the selected value. All values in the Table are in SI (Joule) units. In the notes, some values are reported in calorie units (1 cal = 4.184 J).

In order to make the utilization of Table 7-2 more convenient, the species are grouped according to some defining characteristic. Each of these groupings has a number linked to that group in the Table. Each group, in turn, has a linked Note associated with it, in which the group's species are listed sequentially, followed by comments. At the end of each Note, the applicable references are given. Table 7-1 is a list of these various groups, group numbers, and links to the notes. Formulas are presented in the order: C H O N F Cl Br I S Hg.

7.2 Table 7-1. Glossary of Groupings

$H_{0-2}\ O_{0-3}$	1	$C_1\ H_1\ Br_{1-3}\ Cl_{1-3}$	46
H_2O complexes	2	$C_1\ H_1\ Br_{1,2}\ Cl_{1,2}\ F_{1,2}$	47
$H_{0-4}\ N_{1-2}$	3	$C_1\ H_{0,1}\ Br_{1-4}\ Cl_{0,1}\ F_{0,1}\ O_{1,2}$	48
$N_{1-2}\ O_{1-5}$	4	$C_2\ H_{0-5}\ Br_{1-6}$	49
$H_{1-4}\ N_{1-2}\ O_{1-3}$	5	$C_2\ H_{0-2}\ Br_{1,2}\ Cl_{0-2}\ F_{0-4}$	50
$C_1\ H_{0-4}$	6	$C_2\ H_{0-2}\ Br_1\ O_{1,2}$	51
$C_1\ H_{0-4}\ O_{1-4}$	7	$C_3\ H_7\ Br$	52
$C_1\ H_n\ N_m$	8	$H_{0,1}\ I_{1,2}$	53
$C_1\ H_n\ N_m\ O_1$	9	$I_{1,2}\ O_{1-5}$	54
$C_1\ H_n\ N_m\ O_r$ containing NO_2 moiety	10	$H_1\ I_1\ O_{1,2}$	55
$C_2\ H_{0-6}$	11	$Br_{0,1}\ Cl_{0,1}\ F_{0,1}\ I_1$	56
$C_2\ H_{1-6}\ O_1$	12	$F_1\ I_1\ O_{1,2}$	57
$C_2\ H_{1-6}\ O_2$	13	$Cl_1\ I_1\ O_{1,2}$	58
$C_{0-4}\ H_n$ OC(O)O (carbonate) radicals	14	$Br_1\ I_1\ O_{1,2}$	59
$C_2\ H_n\ O_{3,4}$	15	$I_1\ N_1\ O_{1-3}$	60
$C_2\ H_n\ N_{1-2}\ O_{0-5}$	16	$C_1\ H_{0-3}\ I_{1-4}$	61
$C_3\ H_n$	17	$C_1\ H_{2,3}\ I_{1,2}\ O_2$	62
$C_3\ H_{1-8}\ O$	18	$C_1\ F_{1-3}\ I_{1,2}$	63
$C_3\ H_{1-8}\ O_2$	19	$C_1\ H_{0-2}\ Cl_{1-3}\ I_1$	64
$C_3\ H_{1-8}\ N\ O_{0-2}$	20	$C_1\ H_{0-2}\ Br_{1,2}\ I_{1,2}$	65
$C_4\ H_{6-10}\ O_{0-4}$	21	$C_2\ H_{2-5}\ I_1$	66
$F_{1-3}\ H_{0,1}\ N_{0-1}\ O_{0-3}$	22	$C_2\ H_{0-2}\ F_{3-5}\ I_1$	67
$C_1\ H_{0-3}\ F_{1-4}$	23	$C_2\ H_{3-5}\ I_1\ O_1$	68
$C_1\ H_{0-n}\ F_{1-3}\ O_{1,2}$	24	$C_2\ H_2\ I_1\ N_1$	69
$CF_3O_2NO_2$ and CF_2CN	25	$C_3\ H_7\ I_1$	70
$C_2\ H_{0-n}\ F_{1-6}$	26	$H_{0-2}\ S_{1-3}$	71
$C_2\ H_{0-n}\ F_{1-6}\ O_{1-3}$	27	$O_{1-3}\ S_{1-2}$	72
$C_{3,4}\ H_{0-n}\ F_{1-3}\ O_{0-2}$	28	$H_{1,2}\ O_{1-4}\ S_{1,2}$	73
$Cl_{1,2}\ F_{0,1}\ H_{0,1}\ O_{0-4}$	29	$H_1\ N_1\ O_1\ S_1$	74
$Cl_{1-3}\ H_{0-2}\ N_1\ O_{0-5}$	30	$Cl_{0,1}\ H_{0,1}\ F_{1,2}\ O_{1,2}\ S_1$	75
$C_1\ H_{0-3}\ Cl_{1-4}$	31	NS and PS	76
$C_1\ H_{0-3}\ Cl_{1-4}\ O_{1,2}$	32	$C_1\ H_{0,1}\ S_{1,2}$	77
$C_1\ H_{0-2}\ Cl_{1-3}\ F_{1-3}$	33	$C_1\ H_{1-3}\ O_{1,2}\ S_{1,2}$	78
$C_1\ H_{0-2}\ Cl_{1-3}\ F_{1-3}\ O_{1,2}$	34	$C_2\ H_{5,6}\ S_{1,2}$	79
$C_2\ H_{0-5}\ Cl_{1-6}$	35	$C_2\ H_{4-6}\ O_{1,2}\ S_1$	80
$C_2\ H_{0-3}Cl_{1-3}\ F_{1-5}$	36	Li compounds	81
$C_2\ H_{0-4}\ Cl_{1-3}\ O_{1,2}$	37	Na compounds	82
$C_3\ H_{2-6}\ Cl_1\ F_{0-2}$	38	K compounds	83
$Br_{1,2}\ H_{0,1}\ O_{0-2}$	39	$H_{0-2}\ Hg_1\ O_{0,1}$	84
$Br_1\ F_1\ O_{0-2}$	40	Hg mono-and di-halides	85
$Br_1\ Cl_1\ O_{0-2}$	41	Hg mixed di-halides	86
$Br_1\ N_1\ O_{1-3}$	42	$Hg_1\ I_1\ O_1$	87
$Br_{1-3}\ Cl_{0-2}\ H_{0-2}\ N_1$	43	$Br_{0-2}\ Cl_{0-2}\ H_{0,1}\ Hg_1\ N_{0,1}\ O_{1,2}$	88
$C_1\ H_{0-3}\ Br_{1-4}$	44	$C_{1-4}\ H_{3-10}\ Hg_1$	89
$C_1\ H_{0-2}\ Br_{1-3}\ F_{1-3}$	45	$C_{1,2}\ H_{3,5}\ Br_{0,1}\ Cl_{0,1}\ Hg_1$	90

7.3 Table 7-2. Gas-Phase Entropy and Enthalpy Values at 100 kPa

SPECIES	$\Delta_f H(298\ K)$ kJ mol^{-1}	$\Delta_f H(0\ K)$ kJ mol^{-1}	S(298 K) J K^{-1} mol^{-1}
(1) *Simple compounds of H and O*			Back
H	217.997 ± 0.001	216.034 ± 0.0001	114.717 ± 0.001
H_2	0.00	0.00	130.680 ± 0.003
$O(^3P)$	249.229 ± 0.002	246.844 ± 0.002	161.059 ± 0.003
$O(^1D)$	438.05 ± 0.1		
O_2	0.00		205.152 ± 0.005
$O_2(^1\Delta_g)$	94.29 ± 0.01		
$O_2(^1\Sigma_g^+)$	156.96 ± 0.01		
O_3	141.732 ± 0.039	144.386 ± 0.039	239.01
OH	37.492 ± 0.026	37.253 ± 0.026	183.737
H_2O	–241.831 ± 0.026	–238.928 ± 0.026	188.832
HO_2	12.30 ± 0.35	15.21 ± 0.35	229.1
H_2O_2	–135.51 ± 0.16	–129.50 ± 0.16	234.5 ± 0.1
HO_3	22.0 ± 0.6	25.3 ± 0.6	
HOOOH	–88.1	–79.8	
HOOOOH	–44.4	-33.5	
(2) *Water complexes*			Back
$H_2O•H_2O$	–491.115 ± 0.052	–491.075 ± 0.080	300.946
$OH•H_2O$	−226		
$HO_2•H_2O$	–268.0 ± 3	–259.6 ± 3	308.9
$O_3•H_2O$	−107		
$CH_2O•H_2O$	–380		
$OCl•OH_2$	–130		
ClO•HOH	–125		
$OBr•OH_2$	–133		
BrO•HOH	–126		
(3) *Simple compounds of N and H*			Back
$N(^4S)$	472.435 ± 0.023	470.573 ± 0.023	153.301 ± 0.003
N_2	0.00	0.00	191.609 ± 0.004
NH	357 ± 1	357 ± 1	181.25 ± 0.04
NH_2	186.2 ± 1.0	189.1 ± 1.0	194.868
NH_3	–45.94 ± 0.35	–38.95 ± 0.35	192.77 ± 0.05
N_2H	251	254	156.77
NNH_2	299		218
trans-N_2H_2	201	209	218.20
cis-N_2H_2	223	230	218.45
N_2H_3	225	235	237.27
NH_3NH	281		227.7
N_2H_4	97.42 ± 0.47	111.57 ± 0.47	238.165
(4) *Simple compounds containing N and O*			Back
NO	91.090 ± 0.062	90.586 ± 0.062	210.76
N_2O	81.6 ± 0.5	85.3 ± 0.5	220.01
NO_2	33.97 ± 0.08	36.78 ± 0.08	240.17
NO_3	74.7 ± 1.1	79.9 ± 1.1	258.4 ± 1.0
N_2O_3	86.6 ± 1	91.2 ± 1	314.74
N_2O_4	11.1 ± 1	20.4 ± 1	304.45
N_2O_5	14.4	24.0	353.45
(5) *Compounds containing N, H, and O*			Back

SPECIES	$\Delta_f H$(298 K) kJ mol^{-1}	$\Delta_f H$(0 K) kJ mol^{-1}	S(298 K) J K^{-1} mol^{-1}
HNO	109.2 ± 2.1	112.1 ± 2.1	220.914
HON	217.1 ± 2.1	220.0 ± 2.1	
NH_2O	66.9 ± 3.3	72.4 ± 3.3	
NH_2OH	–47.7 ± 2.5		236.18
NH_3O	61.8 ± 4.2	72.5 ± 4.1	
HNOH	96.7 ± 3.3	103.8 ± 3.3	
NH_2NO_2	4.9 ± 2.4	18.3 ± 2.4	268.0 ± 1.5
HONO	–78.45 ± 0.8	–72.80 ± 0.8	254.07
trans-HONO	–78.94 ± 0.6	–72.80 ± 0.6	249.109
cis-HONO	–77.45 ± 0.7	–71.1 ± 0.7	266.876
trans-HOON	95.1		
HNO_2	–45.61 ± 0.2		232.46
$HONO_2$	–134.3 ± 0.5	–124.6 ± 0.5	266.88 ± 0.7
cis,cis-HOONO	–15.0	–7.8	279
trans,perp-HOONO	–0.5	6.1	285
HO_2NO_2	–52.7 ± 4.1	–41.6 ± 4.1	297±4
NH_4NO_3	–259 ± 21		342.3
(6) *Compounds with one C and 0-4 H*			Back
C	716.68 ± 0.45	711.19 ± 0.45	158.100 ± 0.001
CH	595.8 ± 0.6	592.5 ± 0.6	183.04
$CH_2(^3B_1)$	391.52 ± 0.12	390.96 ± 0.12	194.436
$CH_2(^1A_1)$	429.03 ± 0.13	428.62 ± 0.13	189.220
CH_3	146.374 ± 0.080	149.788 ± 0.080	194.008
CH_4	–74.520 ± 0.056	–66.550 ± 0.056	186.38
(7) *Compounds containing one C, 0-4 H, and one or more O*			Back
CO	–110.523 ± 0.026	–113.803 ± 0.026	197.660 ± 0.004
CO_2	–393.51 ± 0.13	–393.14 ± 0.13	213.785 ± 0.010
HCO	41.80 ± 0.10	41.43 ± 0.10	224.34
COH	217.69 ± 0.67	217.31 ± 0.67	
HCOH	108.64 ± 0.33	112.40 ± 0.33	
CH_2O	–109.19 ± 0.10	–105.35 ± 0.10	218.76
trans-HOCO	–184.5 ± 1.2	–181.3 ± 1.2	251.4
cis-HOCO	–177.8 ± 1.2	–174.6 ± 1.2	251.7
HC(O)O	–126.6 ± 1.7	–123.0 ± 1.7	244.7
C(O)OH	–193		251.6
HC(O)OH	–378.6 ± 0.7		248.2
trans-HC(O)OO	–95.4 ± 14.6		
cis-HC(O)OO	–85.8 ± 14.6		
trans-HC(O)OOH	–289.1 ± 3.8	–279.5 ± 3.8	
cis-HC(O)OOH	–274.9 ± 3.8	–265.3 ± 3.8	
CH_2OO	110	118	
CH_2O_2	5.0	12.6	
CH_3O	21.53 ± 0.34	28.90 ± 0.34	234.278
CH_3O_2	9.0 ± 5.1		279.74
CH_2OH	–16.57 ± 0.33	–10.26 ± 0.33	244.170 ± 0.018
CH_3OH	–200.71 ± 0.16	–189.83 ± 0.16	239.865
$CH_3OH•HO_2$	179.3		381
CH_2OOH	67.20		270.4
CH_3OOH	–136.8	–124.0	276.5 ± 3.0
CH_3O_3	24.3		317.52

SPECIES	$\Delta_f H$(298 K) kJ mol^{-1}	$\Delta_f H$(0 K) kJ mol^{-1}	S(298 K) J K^{-1} mol^{-1}
CH_3O_4	5.9		404.83
(8) *Compounds containing one C and H and N*			Back
CN	436.715 ± 0.145	440.001 ± 0.145	202.64
HCN	129.28 ± 0.10	129.66 ± 0.10	201.82
HNC	192.39 ± 0.38	192.00 ± 0.38	
NCN	450.8 ± 0.8		225.6
CH_2NH	89.5 ± 1.2	97.1 ± 1.2	
CH_3NH	176.7		250.0
CH_2NH_2	149 ± 8		
CH_3NH_2	–23.4 ± 1.0		242.89
CH_2CN	252.6 ± 4	255.2 ± 4	
CH_3CN	74.0 ± 0.4	81.0 ± 0.4	245.12 ± 0.8
CH_2N_2	273.2	279.1	
(9) *Compounds containing one C and H, N, and O*			Back
CH_2NO	157 ± 4		
NH_2CO	–13.1 ± 1.5	–7.2 ± 1.5	256.5
NCO	151 ± 14		232.38
HCNO	166.5 ± 2.1	167.8 ± 2.9	
HONC	231.7 ± 2.4	232.5 ± 2.4	
HOCN	–14.4 ± 2.0	–12.6 ± 2.0	
HNCO	–119.2 ± 1.4	–116.2 ± 1.4	237.97 ± 0.8
$HCONH_2$	–193.9 ± 2.0		
CH_2NO_2	147.3		272.48
CH_3NO_2	–74.3 ± 0.6		275.2
CH_3ONO	–64.0		284.3
CH_3ONO_2	–122.2 ± 4.3		301.9
$CH_3O_2NO_2$	–62.8		
$C(NO_2)_4$	82.0		
$(NH_2)_2CO$	–235.7 ± 1.4	–218.9 ± 1.4	
(10) *A series of nitroalkanes, their isomers, and radical products*			Back
$CH_2N(O)OH$	–13.0		
$CH(NO_2)_2$	169		
$CH_2(NO_2)_2$	–42.7		
$CH_2(NO_2)ONO$	–75.7		
$CH(NO_2)N(O)OH$	–1.26		
$CH(NO_2)_3$	7.1		
$CH(NO_2)_2ONO$	–50.2		
$C(NO_2)_2(NOOH)$	68.6		
(11) *Compounds containing two C and 0 - 6 H*			Back
C_2	828.68 ± 0.27	820.21 ± 0.27	199.382
C_2H	567.99 ± 0.15	563.87 ± .0.15	209.73
C_2H_2	228.27 ± 0.13	228.84 ± 0.13	200.93
H_2CC	412.20 ± 0.33	411.29 ± 0.33	
CH_3C	504.88 ± 0.87	508.58 ± 0.87	
CH_2CH	296.91 ± 0.33	301.11 ± 0.33	233.0
CH_3CH	354.47 ± 0.82	361.45 ± 0.82	
C_2H_4	52.45 ± 0.13	60.96 ± 0.13	219.316
C_2H_5	119.86 ± 0.28	130.92 ± 0.28	250.52
C_2H_6	–83.91 ± 0.14	–68.29 ± 0.14	229.162
(12) *Compounds containing two C, one O, and 1-6 H*			Back

SPECIES	$\Delta_f H$(298 K) kJ mol^{-1}	$\Delta_f H$(0 K) kJ mol^{-1}	S(298 K) J K^{-1} mol^{-1}
CHCO	173.0 ± 9.6		
CH_2CO	–49.58 ± 0.88	–46.44 ± 0.88	
CH_3CO	–10.3 ± 1.8	–3.6 ± 1.8	267.448
C_2H_2OH	121 ± 11		
$CH_2C(O)H$	16.1 ± 1.5	23.4 ± 1.5	259.52
$CH_3C(O)H$	–166.1 ± 0.5		263.95
syn-CHCHOH	130.9 ± 2		267.6
anti-CHCHOH	140.2 ± 2		267.2
anti-CH_2COH	113.2 ± 2		264.1
syn-CH_2CHOH	−125.4 ± 2		258.4
anti-CH_2CHOH	−120.8 ± 2		258.3
CH_3CH_2O	–13.6 ± 4.0	–0.2 ± 4.0	277.642
CH_2CH_2OH	–31 ± 7		
CH_3CHOH	–53.22		282.2
C_2H_5OH	–234.8 ± 0.5	–217.08 ± 0.5	281.622
CH_3OCH_2	3.8		278.2
CH_3OCH_3	–184.1 ± 0.5		267.34
(13) *Compounds containing two C, two O, and 1-6 H*			Back
$(CHO)_2$	–212 ± 0.8	-206.4 ± 0.5	
cy-$(C_2H_2O)O$	–190 ± 10		
CH_3CHOOH	26.40		314.8
$C_2H_5O_2$	–27.4 ± 9.9		
C_2H_5OOH	–166.9		311.5
CH_3OCO	–173.8 ± 2.4		290.1
$CH_2OC(O)H$	–155.2		289.7
$CH_3OC(O)H$	–357.6 ± 1.8		287.1
CH_3COO	–190		284.9
$CH_2(OH)C(O)$	–154		
$CH(OH)C(O)H$	–207		
$CH_2(OH)C(O)H$	–318		
$CH_2C(O)OH$	–253 ± 13		283.4
$CH_3C(O)O$	–192.5		
$CH_3C(O)OH$	–432.8 ± 0.5		332.67
$CH_2C(OH)_2$	–309.2 ± 1.3		
$CH_2(OH)CH_2OH$	–392.2 ± 4.0		303.81
$C(OH)_2C(O)H$	–400 ± 1		
$CH(OH)_2C(O)H$	–496 ± 0.4		
$C(O)HC(O)H$	–212.0 ± 0.7		
CH_2OOCH_3	71.42		303.8
CH_3OOCH_3	–125.5 ± 5.0	–106.5 ± 5.0	308.4 ± 3.0
(14) *Alkylcarbonate radicals*			Back
HOC(O)O	−360.0		
$CH_3OC(O)O$	−347.9		
$C_2H_5OC(O)O$	−379.3		
i-$C_3H_7OC(O)O$	−419.7		
t-$C_4H_9OC(O)O$	−457.7		
(15) *Compounds with two C and more than 2 O*			Back
$CH_3C(O)O_2$	–154.4		
$CH_2(OH)C(O)OH$	–583 ± 10	–568 ± 10	318.6 ± 5.0
$CH_2(OH)OOCH_2OH$	–571.7 ± 6.6		

SPECIES	$\Delta_f H$(298 K) kJ mol^{-1}	$\Delta_f H$(0 K) kJ mol^{-1}	S(298 K) J K^{-1} mol^{-1}
$(HOCO)_2$	–731.8 ± 2.0	–721.2 ± 2.0	320.6 ± 5.0
$CH_3O_4CH_3$	−41.0		368.74
$C(OH)_2C(O)H$	–400 ± 1		
$CH(OH)_2C(O)H$	–496 ± 0.4		
(16) *Compounds with two C, 1-2 N, and 0-5 O*			Back
NCCN	309.1 ± 0.8	307.15 ± 0.8	242.20
CNCN	412.3 ± 3.0	409.6 ± 3.9	
CNNC	612.8 ± 4.2	609.3 ± 4.1	
$C_2H_5NO_2$	–105.56 ± 0.29		
C_2H_5ONO	–99.37 ± 0.50		
$C_2H_5O_2NO_2$	–96.7		
$CH_3C(O)O_2NO_2$	–240.1		
$CH_3CHN(O)OH$	–54.4		
$C_2H_5NH_2$	–47.5 ± 0.6		
$(CH_3)_2N$	156.3		281.8
CH_3NHCH_2	150.7		272.0
$(CH_3)_2NH$	–18.8 ± 1.5		273.3
CH_3CONH_2	–238.3 ± 0.8		
(17) *C3 hydrocarbons*			Back
C_3H_4	190.5 ± 1.1		
C_3H_4	185.4 ± 1.7		
cy-C_3H_3		497.5 ± 16.7	
cy-C_3H_4	277.1 ± 2.5		
C_3H_5	166.1 ± 4.3	177.8 ± 4.3	248 ± 15
C_3H_6	18.6 ± 2.5		266.6
n–C_3H_7	101.3 ± 1.0	119.1 ± 1.0	
i–C_3H_7	86.6 ± 2.0		281 ± 5
C_3H_8	–104.5 ± 1.1		270.20
(18) *Compounds containing 3 C 1-8 H, and 1 O*			Back
1-C_3H_7OH	–256.2 ± 2.3		322.58
2-C_3H_7OH	–272.6 ± 0.5		309.20
C_2H_5CO	–36.4 ± 2.9		298.3
$C_2H_5C(O)H$	–191.8 ± 0.8		304.51
syn- CH_2CHOCH_2	88.9 ± 2		316.14
anti- CH_2CHOCH_2	92.2 ± 2		316.85
syn- $CHCHOCH_3$	148.8 ± 2		300.62
anti- $CHCHOCH_3$	164.2 ± 2		307.40
syn- CH_2COCH_3	140.3 ± 2		312.50
anti- CH_2COCH_3	134.8 ± 2		319.49
syn- CH_2CHOCH_3	–107.0 ± 2		273.80
anti-CH_2CHOCH_3	–100.0 ± 2		299.37
$CH_3C(O)CH_2$	–34 ± 3		303.99
$CH_3C(O)CH_3$	–217.1 ± 0.7		295.46
CH_3CHOCH_3	–37.2		313.7
$CH_3CH_2OCH_2$	–31.3		315.1
$CH_3CH_2OCH_3$	–216.4 ± 0.6		305.9
$CH_2CC(O)H$	177.8 ± 1.7		
CH_2CHCO	100 ± 13		279.5
CH_3CHCO	−64.9		
$CH_2CHC(O)H$	–69.9 ± 4.1	–59.6 ± 4.1	279.16

SPECIES	$\Delta_f H$(298 K) kJ mol^{-1}	$\Delta_f H$(0 K) kJ mol^{-1}	S(298 K) J K^{-1} mol^{-1}
(19) *Compounds containing 3 C 1-8 H, and 2 O*			Back
$C_3H_5O_2$	90.5 ± 6.6		
$CH_2CHOOCH_3$	−42.0		344.2
$C_2H_5C(O)OH$	−456.3 ± 0.7		
$CH_3CH(OH)CH_2OH$	–429.8 ± 4.1		
C_3H_5OOH	–183.4 ± 1.1		
$CH_2OC(O)CH_3$	–210.6		323.5
$CH_3OC(O)CH_3$	–413.0		320.9
$CH_3OCH_2OCH_3$	–348.5 ± 0.8		
$CH_3CH_2OC(O)$	–194.6		325.8
$CH_3CHOC(O)H$	–197.2		327.6
$CH_3CH_2OC(O)H$	–392.8		323.5
$CH_2(OH)C(O)CH_3$	–373		
$CH_3CHOOCH_3$	31.5		347.52
$CH_3CH_2OOCH_3$	–154.5		344.4
$(CH_3)_2CHOO$	–65.4 ± 11.3		
$(CH_3)_2COOH$	–14.2		349.9
$(CH_3)_2CHOOH$	–204.2		340.0
$CH_3C(OH)_2C(O)H$	–550.8 ± 7.1		
$CH_2(OH)CH(OH)CH_2OH$	–577.9 ± 1.1		
$CH_2CHOOCH_3$	−42.0		344.2
(20) *Compounds containing 3 C, H, N, and O*			Back
$C_3H_7NH_2$	–70.8 ± 1.5	-43.3 ± 1.5	
$(CH_3)_2NCH_2$	140.4		308.9
$(CH_3)_3N$	–23.6 ± 1.3		299.2
$(CH_3)_3NO$	80 ± 5		
$C_3H_7O_2NO_2$	–111		
NCC(O)CN	247.5 ± 6.4	246.5 ± 6.4	310.0 ± 1.0
(21) *Compounds containing 4 C, H, and O*			Back
1-C_4H_6	165.2 ± 0.9		
2-C_4H_6	145.1 ± 1.0		
1-C_4H_8	−0.6 ± 0.9		
cis-2-C_4H_8	−7.6 ±1.3		
trans-2-C_4H_8	−10.7 ± 1.0		
$CH_3C(CH_3)CH_2$	−17.9 ± 1.0		
$CH_3CH(CH_3)CH_3$	−134.9 ± 1.4		
n-C_4H_{10}	–126.2 ± 1.4		309.91
$CH_3CH(CH_3)C(O)OH$	–476.6 ± 0.6		
$C_3H_7C(O)OH$	–475.6 ± 1.3		
$C_2H_5OC(O)CH_3$	−443.3 ± 0.6		
$(CH_3)_2CCO$	−90.8		
$CH_3C(CH_3)_2O$	–91.3 ± 1.5		
$(CH_3)_3COO$	–101.5 ± 9.2		
$(CH_3)_3COOH$	–239 ± 18		
$(CH_3COO)_2$	–500 ± 10	–477 ± 10	390.7 ± 6.0
trans-$CH_3CHCHOOCH_3$	−83.5		381.7
cis-$CH_3CHCHOOCH_3$	−89.0		382.8
$CH_2C(CH_3)OOCH_3$	−87.0		366.9
$CH_2CHCH_2OOCH_3$	−50.5		394.3
(22) *Inorganic compounds containing F*			Back

SPECIES	$\Delta_f H$(298 K) kJ mol^{-1}	$\Delta_f H$(0 K) kJ mol^{-1}	S(298 K) J K^{-1} mol^{-1}
F	79.38 ± 0.05	77.29 ± 0.05	158.751 ± 0.004
F_2	0.00	0.00	202.791 ± 0.005
HF	–273.30 ± 0.70	273.25 ± 0.70	173.799 ± 0.003
HOF	–86.7 ± 1.0	–83.8 ± 1.0	226.77 ± 0.21
FO	110.7 ± 0.5	110.0 ± 0.5	216.40 ± 0.3
FOF	24.5 ± 2	26.8 ± 2	247.46 ± 0.4
OFO	523.0 ± 1.3	523.8 ± 1.3	251 ± 1
FOO	25.6 ± 2		259.5 ± 0.2
HOOF	–42.7 ± 4	–36.8 ± 4	
FOOF	19.2 ± 2.0	22.9 ± 2.0	277.2 ± 0.2
FOOOF	110.3 ± 4		209.7
FNO	–87.2 ± 1.2	–84.7 ± 1.2	247.7 ± 1.5
cis-FONO	42.6 ± 1.6	47.1 ± 1.6	274.0 ± 1.5
trans-FONO	54.2 ± 1.6	58.4 ± 1.6	275.5 ± 1.5
FNO_2	–114.9 ± 1.6	–108.7 ± 1.6	258.5 ± 1.5
$FONO_2$	12.3 ± 2.0	19.8 ± 2.0	291.3 ± 1.5
NF_2	35.6 ± 8		
NF_3	–132.8 ± 0.8		
(23) *Compounds containing one C, H, and one or more F*			Back
CF	244.1 ± 10	240.5 ± 10	213.03
CHF	149.8 ± 2.1	149.8 ± 2.1	223.09
CH_2F	–32 ± 8	–29 ± 8	236.52
CH_3F	–238.9 ± 0.8	–230.5 ± 0.8	222.78
CF_2	–192.0 ± 3.3	–192.5 ± 3.3	240.66
CHF_2	–239 ± 4	–235 ± 4	258.50
CH_2F_2	–452.7 ± 0.8	–444.8 ± 0.8	246.59
CF_3	–465.7 ± 2.1	–462.8 ± 2.1	264.56
CHF_3	–692.9 ± 2.1	–685.8 ± 2.1	259.67
CF_4	–933.20 ± 0.75	–927.20 ± 0.75	261.454
(24) *Compounds containing one C and one or more F and O*			Back
CFH_2O	–210		
CFH_2OH	–433		
FCO	–176.7 ± 0.9	–177.2 ± 0.9	248.78
FCO_2	–362.8 ± 2.5		
CHFO	–382.5 ± 1.2	–378.8 ± 1.2	246.69
CF_2HO	–417		
CF_2HOH	–682		
CF_2O	–606.5 ± 1.2	–603.4 ± 1.2	258.97
CF_3O	–635 ± 7		
CF_2O_2	–427 ± 6		
CF_3O_2	-614 ± 15		
CF_3OH	–923.4 ± 13.4		
CF_3OF	–740.1 ± 7.5		
CH_2FOOH	–352		
CHF_2OOH	–575		
CF_3OOH	–807		
(25) *$CF_3O_2NO_2$ and CF_2CN*			Back
$CF_3O_2NO_2$	102.7 ± 2.0		163 ± 7
CF_3CN	–495.4 ± 1.7	–491.6 ± 1.7	
(26) *Compounds containing two C and one or more F*			Back

SPECIES	$\Delta_f H$(298 K) kJ mol^{-1}	$\Delta_f H$(0 K) kJ mol^{-1}	S(298 K) J K^{-1} mol^{-1}
CH_2CHF	–138.8 ± 1.7		
CH_2CH_2F	–59.9 ± 2.8	–49.1 ± 2.8	278.5
CH_3CHF	–74.5 ± 2.8	–64.0 ± 2.8	272.4
CH_3CH_2F	–272.5 ± 3.2	–257.03 ± 3.2	264.6 ± 1.5
C_2F_2	5.9 ± 1.3	2.9 ± 1.3	
CH_2CF_2	–335.0 ± 4.5		
cis-CHFCHF	–309.2 ± 2.5	–302.5 ± 2.5	
trans-CHFCHF	–305.9 ± 2.5	–299.6 ± 2.5	
CH_3CF_2	–297.6 ± 2.8	–287.7 ± 2.8	289.0
CH_3CHF_2	–503.0 ± 3.2	–488.6 ± 3.2	282.0 ± 1.5
anti-CH_2FCH_2F	–443.4 ± 3.2	–429.8 ± 3.2	289.5 ± 1.4
gauche-CH_2FCH_2F	–447.3 ± 3.2	–433.5 ± 3.2	288.8 ± 1.4
CH_2FCHF	248.0 ± 2.8	239.5 ± 2.8	296.0
CHF_2CH_2	–282.1 ± 2.8	–272.1 ± 2.8	295.9
CH_3CF_2	–302.5 ± 8.4		290.3
CH_3CHF_2	–500.8 ± 6.3	–486.9 ± 6.3	282.4
anti-CH_2FCHF_2	–666.4 ± 3.2	–653.7 ± 3.2	309.8 ± 1.5
gauche-CH_2FCHF_2	–661.0 ± 3.2	–648.3 ± 3.2	309.2 ± 1.5
CH_2CF_3	–526.0 ± 2.8	–517.3 ± 2.8	300.9
CH_3CF_3	–751.5 ± 3.2	–738.3 ± 1.7	286.8 ± 1.5
CF_2CF_2	–658.9 ± 4.9		
anti-CHF_2CHF_2	–878.4 ± 3.2	–867.9 ± 3.2	319.0 ± 1.5
gauche-CHF_2CHF_2	–872.2 ± 3.2	–861.7 ± 3.2	318.9 ± 1.5
$CHFCF_3$	–695.1 ± 2.8	–688.6 ± 2.8	325.7
CH_2FCF_3	–906.2 ± 3.2	–894.6 ± 3.2	316.0 ± 1.5
CF_2CF_3	–894.4 ± 2.8	–888.9 ± 2.8	340.6
CHF_2CF_3	–1110.6 ± 3.2	–1100.6 ± 3.2	332.9 ± 1.5
C_2F_6	–1344.3 ± 3.4	–1335.9 ± 3.4	331.8
(27) *Compounds containing two C and one or more F and O*			Back
CH_2FCH_2OH	–423.6 ± 5		
CH_2FCOOH	–594.0 ± 5		
CF_3CO	–605 ± 2		325.5
$CF_3C(O)H$	–810.4		317.6
$CH_3C(O)F$	–442.1 ± 3.3		
$CF_3C(O)F$	–1038 ± 4		
$CF_3C(O)OH$	–1031 ± 1.7		
CF_3OCO_2	–958 ± 16		
CF_3OOCF_3	–1471 ± 21		
(28) *Compounds containing more than two C and one or more F*			Back
iso-C_3H_7F	–315.5 ± 2.1		
tert-C_4H_9F	–360 ± 8		
$CF_3C(O)OCH_3$	–993		402
(29) *Inorganic compounds containing Cl*			Back
Cl	121.303 ± 0.002	119.622 ± 0.0002	165.190 ± 0.004
Cl_2	0.0		223.081 ± 0.010
HCl	–92.31 ± 0.10	–92.13 ± 0.10	186.902 ± 0.005
ClO	101.681 ± 0.040	101.086 ± 0.040	224.96 ± 0.1
ClOO	98.3 ± 2.1		270.3
ClOOH	0.8 ± 4		

SPECIES	$\Delta_f H$(298 K) kJ mol^{-1}	$\Delta_f H$(0 K) kJ mol^{-1}	S(298 K) J K^{-1} mol^{-1}
OClO	98.1 ± 0.6	100.6 ± 0.6	256.84
ClO_3	185.4 ± 1.7	191.2 ± 1.7	270.75 ± 0.5
ClClO	133.5	134.7	277.6
ClOCl	81.3 ± 1.8	83.1 ± 1.8	
ClOOCl	130.1 ± 1	133.3 ± 1	302.9
$ClClO_2$	114.6 ± 5	118.7 ± 5	294.4 ± 6
ClOClO	164.0 ± 5	166.5 ± 5	312.6
Cl_2O_3	140 ± 5	144 ± 5	337.8 ± 6
HOCl	–74.8 ± 1.2	–71.8 ± 1.2	236.50 ± 0.42
HOClO	20.9 ± 1.7	25.9 ± 1.7	
$HOClO_2$	–10.9 ± 1.3	–3.8 ± 1.3	
$HOClO_3$	–0.4 ± 4.2	12.1 ± 4.2	
ClF	–55.70 ± 0.31	–55.605 ± 0.31	217.94
ClOF	19.7		264.0
ClO_2F	−41.0		279.7
(30) *Inorganic compounds containing Cl, O, and N*			Back
ClNO	54.3 ± 1.4	56.2 ± 1.4	261.0 ± 1.5
$ClNO_2$	12.5 ± 1.0	17.9 ± 1	272.23
cis–ClONO	55.2 ± 2.7	59.6 ± 2.7	282.8 ± 1.5
trans–ClONO	68.4 ± 2.7	72.4 ± 2.7	286.1 ± 1.5
cis, perp-ClO_2NO	102		315.9
trans, perp-ClO_2NO	108		318.8
$ClONO_2$	26.7 ± 3.1	33.8 ± 2.7	301.9 ± 1.5
cis,perp-ClOONO	130.0 ± 3.1	135.5 ± 3.1	312.2 ± 1.5
trans,perp-ClOONO	136.4 ± 3.1	143.0 ± 3.1	315.1 ± 1.5
trans,perp-OClONO	179	183	
O_2ClONO_2	92 ± 17		
NH_2Cl	50.4	57.5	
$NHCl_2$	140.0	145.9	
NCl_3	227.4	230.9	
(31) *Compounds containing one C and one or more Cl and H*			Back
CCl	433.7 ± 1.1	430.0 ± 1.1	224.3 ± 1.1
CHCl	319.4 ± 0.8	319.2 ± 0.8	234.88
CH_2Cl	117.3 ± 3.1	120.7 ± 3.1	271 ± 7
CH_3Cl	–81.9 ± 0.6	−73.6 ± 0.6	227.15
CCl_2	229.4 ± 0.8	228.3 ± 0.8	265.03
$CHCl_2$	89.0 ± 3.0	91.4 ± 3.0	280 ± 7
CH_2Cl_2	–95.1 ± 2.5	−89.7 ± 2.5	270.31
CCl_3	71.1 ± 2.5	71.7 ± 2.5	303.24
$CHCl_3$	–102.9 ± 2.5	–97.8 ± 2.5	295.51
CCl_4	–95.6 ± 2.5	–93.3 ± 2.5	309.90
(32) *Compounds containing one C and one or more Cl, H, and O*			Back
$CClH_2O$	–18.4		
$CClH_2OH$	–246		
CClO	−21.8 ± 2.5		265.3 ± 1.3
CHClO	–184.2 ± 1.7	–180.8 ± 1.7	259.07
CH_2OCl	135.5		279.7
CH_3OCl	–64.5		272.8
CH_2ClO_2	–5.1 ± 13.6		
CH_2ClOOH	–173.3 ± 6.1		303.09

SPECIES	$\Delta_f H$(298 K) kJ mol^{-1}	$\Delta_f H$(0 K) kJ mol^{-1}	S(298 K) J K^{-1} mol^{-1}
CCl_2O	–220.9		283.8
CCl_2HO	–27.6		
CCl_2HOH	–277		
$CHCl_2O_2$	–19.2 ± 11.2		
CH_2ClOCl	–92.3		311.8
$CHCl_2OOH$	–187.2 ± 13.6		330.75
$CHCl_2OCl$	–109.4		339.1
CCl_3O	–43.5 ± 20		
CCl_3OH	–293		
CCl_3O_2	–20.9 ± 8.9		
CCl_3OOH	–190.9 ± 13.1		346.64
CCl_3OCl	–111.8		357.2
(33) *Compounds containing one C and one or more Cl and F*			Back
CHFCl	–61 ± 10	–57.8 ± 10	273.5 ± 1.5
CH_2FCl	–263.9 ± 3.1	–256.3 ± 3.1	263.8 ± 1.5
CFCl	31 ± 13	30.2 ± 13	259.03
CF_2Cl	–274.4 ± 2.7	–272.2 ± 2.7	285.5 ± 1.5
$CFCl_2$	–93.3 ± 3.8	–91.8 ± 3.8	297.4 ± 1.5
$CHFCl_2$	–283.1 ± 4.2	–277.3 ± 4.2	292.4 ± 1.5
CHF_2Cl	–482.6 ± 3.2	–476.1 ± 3.2	280.8
$CFCl_3$	–285.3	–282	309.9
CF_2Cl_2	–494.1	–489.9	300.7
CF_3Cl	–709.2 ± 2.9	–704.2 ± 2.9	285.2
(34) *Compounds containing one C and one or more Cl, F, and O*			Back
CFClO	–410.9 ± 1.7	–408.4 ± 1.7	276.70
CF_3OCl	–734.7 ± 4.2		
CCl_3OF	–158.1		
cis-FC(O)OCl	–418	–414	
trans-FC(O)OCl	–429	–425	
CHClFOOH	–345		
CCl_2FOOH	–390		
(35) *Compounds containing two C and one or more Cl*			Back
C_2HCl	226 ± 10		
C_2H_3Cl	22 ± 3		
CH_2CH_2Cl	93.0 ± 2.4		271 ± 7
CH_3CHCl	76.5 ± 1.6		279 ± 6
CH_3CH_2Cl	–112.1 ± 0.7		275.78
C_2Cl_2	227 ± 14		
CH_2CCl_2	2.4 ± 2.0		
cis–CHClCHCl	–3 ± 2		
trans–CHClCHCl	–0.5 ± 2.0		
CH_3CCl_2	42.5 ± 1.7		288 ± 5
CH_3CHCl_2	–132.5 ± 3.5		305.05
$CHCl_2CH_2$	90.1		
CH_2ClCH_2Cl	–132.0 ± 3.5		
C_2HCl_3	–17.5 ± 3.0		325.20
$CH_2ClCHCl_2$	–148.0 ± 4.0		
CH_2CCl_3	71.5 ± 8		
CH_3CCl_3	–144.6 ± 2.0		320.03
C_2Cl_4	–24.2 ± 4		341.03

SPECIES	$\Delta_f H$(298 K) kJ mol^{-1}	$\Delta_f H$(0 K) kJ mol^{-1}	S(298 K) J K^{-1} mol^{-1}
$CHCl_2CHCl_2$	–156.7 ± 3.5		
CH_2ClCCl_3	–152.3 ± 2.4		
C_2Cl_5	–21.3 ± 5.4		
C_2HCl_5	–155.9 ± 4.3		
C_2Cl_6	–148.2 ± 5.7		398.62
(36) *Compounds containing two C and one or more F and Cl*			Back
CH_3CHFCl	–313.4 ± 2.6		
CH_2CF_2Cl	–316.2		322.08
CH_3CF_2Cl	–536.2 ± 5.2		307.1
CH_3CFCl_2	–347.0		
CF_2CFCl	–505.5 ± 4.7		
CF_3CHFCl	–690.4 ± 4.9		
CF_3CH_2Cl	–746.4		
CF_3CHCl_2	–749.7		
CF_3CCl_3	–754.0		
CF_2ClCF_2Cl	–937.0 ± 7.3		
$CF_2ClCFCl_2$	–716.8 ± 4.3		
C_2F_5Cl	–1118.8 ± 4.1		
(37) *Compounds containing two C and one or more Cl and O*			Back
$ClCH_2CH_2OH$	–267.2 ± 0.8		
CH_3CHClO_2	–54.7 ± 3.4		
$CH_3C(O)Cl$	–242.8 ± 0.8		
$CH_2ClC(O)OH$	–427.6 ± 1.0	–416.0 ± 1.0	325.9 ± 5.0
CH_2ClCH_2OOH	–191 ± 5		373.38
$CH_3CHClOOH$	–226		331
CH_3CCl_2OOH	–244		362
$CH_2ClC(O)Cl$	–244.8 ± 8.6		
$Cl(O)CC(O)Cl$	–335.8 ± 6.2		
$CHCl_2C(O)Cl$	–241.0 ± 8.6		
CCl_3CH_2OOH	–210 ± 6		405.26
CCl_3CO	–62.8		359.4
$CCl_3C(O)H$	–236		346.4
$CCl_3C(O)Cl$	–240 ± 9		
$CH_3CCl_2O_2$	–69.7 ± 4		
$CHCl_2CH_2OOH$	–205 ± 6		386.31
(38) *Compounds containing three C and, possibly, F, Cl, and O*			Back
$CH_3CHClCH_3$	–145.7 ± 0.7	–124.9 ± 0.7	
$CF_2ClC(O)OCH_3$	–819		
$CF_2ClC(O)OCH_2$	–610		
(39) *Inorganic compounds containing Br*			Back
Br	111.87 ± 0.12	117.93 ± 0.12	175.018 ± 0.004
Br_2(g)	30.91 ± 0.11	45.71 ± 0.11	245.468 ± 0.005
HBr	–36.29 ± 0.16	–28.44 ± 0.16	198.700 ± 0.004
BrO	123.4 ± 0.4	131.0 ± 0.4	232.97 ± 0.1
OBrO	163.9 ± 4.4	171.1 ± 4.3	271 ± 2
BrOO	119.8 ± 6	128.2 ± 6	289 ± 3
BrO_3	221 ± 50	233 ± 50	285 ± 2
BrOBr	107.6 ± 3.5	124.1 ± 3.5	290.8 ± 2
BrBrO	168.2 ± 6	184.1 ± 6	313 ± 2
BrOOBr	166.1 ± 6	184.5 ± 6	

SPECIES	$\Delta_f H$(298 K) kJ mol^{-1}	$\Delta_f H$(0 K) kJ mol^{-1}	S(298 K) J K^{-1} mol^{-1}
BrOBrO	205.0 ± 6	222.2 ± 6	
OBrBrO	303		
$BrBrO_2$	201.7 ± 6	219.7 ± 6	
HOBr	–60.5 ± 1.1	–50.0 ± 1.1	248.0
BrOOH	24.3 ± 4		
HOBrO	42.3		
$HBrO_2$	249		
(40) *Inorganic compounds containing Br and F*			Back
BrF	–58.85 ± 1.0	–51.2 ± 1.0	228.985
BrOF	28.0		
BrO_2F	12.6		
(41) *Inorganic compounds containing Br and Cl*			Back
BrCl	14.79 ± 0.16	22.23 ± 0.16	240.046
ClOBr	94.1 ± 6	103.3 ± 6	
ClBrO	145.2 ± 6	154.0 ± 6	
BrClO	159.4 ± 6	168.2 ± 6	
ClOOBr	151.5 ± 6	162.3 ± 6	
ClOBrO	192.5 ± 6	202.5 ± 6	
BrOClO	186.2 ± 6	196.2 ± 6	
$ClBrO_2$	171.1 ± 6	182.0 ± 6	
$BrClO_2$	158.2 ± 6	169.5 ± 6	
(42) *Inorganic compounds containing Br, N, and O*			Back
BrNO	82.17 ± 0.8	91.46 ± 0.8	273.66 ± 0.8
cis–BrONO	71.9		
trans–BrONO	88.3		
$BrNO_2$	45.2		
$BrONO_2$	42.7 ± 8		
$OBrONO_2$	153.6 ± 8		
O_2BrONO_2	161.9 ± 8		
(43) *Bromoamines and Mixed Chlorobromoamines*			Back
NH_2Br	79.4	93.9	
$NHBr_2$	200.9	221.3	
NBr_3	308.9	333.5	
NHBrCl	166.5	179.7	
$NBrCl_2$	258.2	268.8	
NBr_2Cl	380.7	398.4	
(44) *Compounds containing one C and one or more Br*			Back
CBr	498.3 ± 2.1	501.7 ± 2.1	230.9
CHBr	378.7 ± 2.9	386.4 ± 2.9	252.9
CH_2Br	172.8 ± 2.7		260.465
CH_3Br	–36.36 ± 0.4		245.85 ± 0.25
CBr_2	350.2 ± 0.4	363.7 ± 0.4	288.7
$CHBr_2$	188.9 ± 9		298.6
CH_2Br_2	3.6 ± 3.4	24.9 ± 3.4	294
CBr_3	224 ± 9		334.57
$CHBr_3$	55.4 ± 3.3		330.67
CBr_4	83.9 ± 3.4		358.06

SPECIES	$\Delta_f H$(298 K) kJ mol^{-1}	$\Delta_f H$(0 K) kJ mol^{-1}	S(298 K) J K^{-1} mol^{-1}
(45) *Compounds containing one C and one or more F and Br*			Back
CFBr	89.1		
CH_2FBr	–214.2		276.19
CHF_2Br	–424.9 ± 1.0		295.17
CF_3Br	–641.4 ± 2.3	–637.6 ± 2.3	297.49
$CHFBr_2$	–191.6	–171.8	316.98
CF_2Br_2	–386.6	–368.4	325.24
$CFBr_3$	–143.5	–119.5	345.87
(46) *Compounds containing one C and one or more Cl and Br*			Back
CClBr	285		
CHClBr	143 ± 6		
CH_2ClBr	–43.7 ± 1.9	–43.3 ± 1.9	
CCl_2Br	124		
$CHCl_2Br$	–48.8	–36.8	316.18
CCl_3Br	–41.1 ± 2.0	–32.0 ± 2.0	332.92
$CClBr_2$	163		
$CHClBr_2$	–9.0	10.1	327.79
CCl_2Br_2	9.3	25.5	348.30
$CClBr_3$	48.7	71.6	357.69
(47) *Compounds containing one C and one or more Cl and Br*			Back
CHFClBr	–229.8		304.74
CF_2ClBr	–446.6 ± 2.7		318.70
$CFCl_2Br$	–230.1		330.48
$CFClBr_2$	–183.0	–165.9	342.82
(48) *Compounds containing one C, one or more O, and Br*			Back
CBr_2O	–27.1 ± 0.6		
CBr_3O	93.4		
CBr_3OH	–125.0		
CBr_3OF	11.5		
CBr_3OCl	24.7		
CBr_3OBr	38.7		
CF_3OBr	–755.6		
CCl_3OBr	–132.6		
CH_2BrOOH	–112		
CHFBrOOH	–330		
CHClBrOOH	–143		
CH_2BrOOH	–112		
(49) *Compounds containing two C and Br*			Back
C_2Br	623.7		295.0
C_2HBr	296 ± 6	298 ± 6	252.7
CH_2CHBr	79.2 ± 1.9		
CH_2CH_2Br	135.6 ± 6.7		
CH_3CHBr	125.8 ± 8	149.9 ± 8	
CH_3CH_2Br	−62.9 ± 1.5	−40.8 ± 1.5	287.3 ± 0.4
C_2Br_2	335.3		294.5
trans-CHBrCBr	333.6		326.7

SPECIES	$\Delta_f H$(298 K) kJ mol^{-1}	$\Delta_f H$(0 K) kJ mol^{-1}	S(298 K) J K^{-1} mol^{-1}
CH_3CBr_2	140.2 ± 5.4		
CH_3CBr_2H	–26.7 ± 1.9		
$CHBrCBr_2$	144.2		360.0
CH_2BrCH_2Br	–71.6 ± 1.1		
C_2Br_3	385.4		369.9
$CH_2BrCHBr_2$	53.5 ± 4.3		
CH_3CBr_3	–4.6	27.2	354.1
C_2Br_4	190.1		387.4
$CHBr_2CBr_2$	218.8		419.0
CBr_3CHBr	243.6		416.9
C_2Br_5	183.3		444.7
C_2HBr_5	113.1		439.2
C_2Br_6	165.5		459.1
(50) *Compounds containing two C and Br and F and/or Cl*			Back
CF_3CH_2Br	–694.5 ± 2.0		
CF_2HCF_2Br	–833.4 ± 4.9		
CF_3CF_2Br	–1064.4 ± 4.1		
CF_2BrCF_2Br	–789.1 ± 5.7		
$CHFClCF_2Br$	–644.8 ± 6.4		
$CHClBrCHClBr$	–36.9 ± 8.4		
$CF_2BrCFClBr$	–656.6 ± 20.7		
(51) *Compounds containing two C, O and Br*			Back
$CH_3C(O)Br$	–190.4 ± 0.6		
$CH_2BrCOOH$	–383.5 ± 3.1	–364.6 ± 4	337.0 ± 5.0
$BrCH_2CH_2OH$	–221.7 ± 0.7		
(52) *Compounds containing three C and Br*			Back
$CH_3CHBrCH_3$	–95.6 ± 0.9	–67.6 ± 0.9	
(53) *Compounds containing I and 0 or 1 H*			Back
I	106.760 ± 0.04	107.161 ± 0.04	180.787 ± 0.004
I_2	62.42 ± 0.08	65.50 ± 0.08	260.687 ± 0.005
HI	26.50 ± 0.10	28.676 ± 0.10	206.589 ± 0.005
(54) *Compounds containing I and O*			Back
IO	122.2 ± 1.3	124.3 ± 1.3	239.6 ± 0.1
OIO	118.5 ± 2.0	122.1 ± 2.0	279.9
IOO	86.3 ± 6	87.6 ± 6	308.4
IO_3	147.8	153.9	293 ± 4
IOI	107.5 ± 6	114.2 ± 6	306.5
IIO	158.2 ± 6	164.0 ± 6	317.8
IOOI	177.8 ± 6	186.2 ± 6	337.0
IIO_2	138.5 ± 6	147.7 ± 6	339.9
IOIO	152.3 ± 6	161.5 ± 6	349.7
OIIO	259.4 ± 6	263.2 ± 6	356.3
I_2O_3	64.0	77.6	
I_2O_4	111.3	131.5	
I_2O_5	33.0	54.6	
(55) *Compounds containing I, H and O*			Back
HOI	–70.7 ± 3.7	–66.1 ± 3.7	255.0 ± 0.1

SPECIES	$\Delta_f H$(298 K) kJ mol^{-1}	$\Delta_f H$(0 K) kJ mol^{-1}	S(298 K) J K^{-1} mol^{-1}
HIO	143.3	148.0	
HOIO	−24.8 ± 0.9		290.40
HOOI	18.7 ± 0.4		287.09
(56) *Di-halo compounds containing I*			Back
IF	−81.2		
ICl	17.393 ± 0.040	19.026 ± 0.040	247.572
IBr	40.807 ± 0.14	49.754 ± 0.14	258.809
(57) *Compounds containing I, O, and F*			Back
IOF	−32.6		
IO_2F	−109.6		
(58) *Compounds containing I, O, and Cl*			Back
ClOI	94.1 ± 6	97.5 ± 6	
ClIO	95.0 ± 6	97.5 ± 6	
IClO	180.7 ± 6	183.3 ± 6	
$ClIO_2$	56.9 ± 6	61.5 ± 6	
ClOIO	143.1 ± 6	149.0 ± 6	
ClOOI	154.4 ± 6	161.1 ± 6	
IOClO	182.4 ± 6	188.7 ± 6	
$IClO_2$	191.6 ± 6	196.6 ± 6	
(59) *Compounds containing I, O, and Br*			Back
BrOI	107.1 ± 6	118.0 ± 6	
BrIO	122.2 ± 6	133.9 ± 6	
IBrO	192.5 ± 6	204.2 ± 6	
BrOOI	169.9 ± 6	184.1 ± 6	
BrOIO	152.3 ± 6	166.9 ± 6	
IOBrO	202.5 ± 6	216.3 ± 6	
$BrIO_2$	92.5 ± 6	105.9 ± 6	
$IBrO_2$	239.7 ± 6	253.1 ± 6	
OIBrO	273.6 ± 6	292.5 ± 6	
(60) *Compounds containing I, O, and N*			Back
INO	121 ± 4		282.8 ± 4
INO_2	60.2 ± 4		294±6
IOONO	141	144	
$IONO_2$	36.8	45.3	320.95
(61) *Compounds containing one C and I and H*			Back
CI	559 ± 4	556 ± 4	
CHI	425 ± 4	430 ± 4	
CHI	425		
CH_2I	217.2 ± 3	221.6 ± 3	
CH_3I	15.23 ± 0.3	24.76 ± 0.3	253.70 ± 0.25
CI_2	457 ± 4	456 ± 4	
CHI_2	290.4 ± 6	295.8 ± 6	
CH_2I_2	107.9 ± 4.5	117.4 ± 4.5	309.39
CHI_3	208.5 ± 9	216.4 ± 9	355.5
CI_3	369 ± 20	366 ± 20	
CI_4	321 ± 60	326 ± 60	391.6
(62) *Compounds containing one C and I, H and O*			Back
CH_2IOOH	−247		
CHI_2OOH	−157		

SPECIES	$\Delta_f H$(298 K) kJ mol^{-1}	$\Delta_f H$(0 K) kJ mol^{-1}	S(298 K) J K^{-1} mol^{-1}
(63) *Compounds containing one C, F, and I*			Back
CFI	159.4 ± 4	159.4 ± 4	
CF_3I	–586.2 ± 2.1	–580.3 ± 2.1	307.78
CF_2I_2	–274.8	–269.3	346.34
(64) *Compounds containing one C, Cl, and I*			Back
CClI	344.3 ± 4	345.6 ± 4	
CH_2ClI	11.1 ± 1.9	19.2 ± 1.9	
CCl_3I	9.0	12.1	340.31
(65) *Compounds containing one C, Br, and I*			Back
CHBrI	242 ± 6	232 ± 6	
CH_2BrI	55.4 ± 3.4	70.8 ± 3.4	
CBr_2I	272 ± 9		
$CHBr_2I$	105 ± 9		
CBrI	400.4 ± 4	407.5 ± 4	
$CBrI_2$	321 ± 9		
$CHBrI_2$	158 ± 9		
(66) *Compounds containing two C and I*			Back
cis-CHICHI	207.4 ± 0.8		
trans-CHICHI	207.4 ± 0.8		
CH_3CH_2I	–9.8 ± 1.5	6.3 ± 1.5	295.52 ± 0.42
CH_2ICH_2I	64.5 ± 2.5	80.0 ± 2.5	
(67) *Compounds containing two C, F and I*			Back
CF_3CH_2I	–644.5 ± 2.8		
CF_3CF_2I	–1000.2 ± 4.1		
(68) *Compounds containing two C, O and I*			Back
$CH_3C(O)I$	–126.4 ± 2.7		
ICH_2CH_2OH	–150.3 ± 0.7		
(69) *Compounds containing two C, N and I*			Back
CH_2ICN	172.5 ± 4.0		
(70) *Compounds containing three C and I*			Back
CH_3CHICH_3	–38.5 ± 0.9	–16.4 ± 0.9	
(71) *Compounds containing S and H*			Back
S	277.17 ± 0.15	274.92 ± 0.15	167.829 ± 0.006
S_2	128.60 ± 0.3	128.29 ± 0.3	228.167 ± 0.010
HS	142.92 ± 0.78	142.47 ± 0.78	195.552
H_2S	–20.60 ± 0.5	–17.68 ± 0.5	205.81 ± 0.05
HSS	105 ± 4		
HSSH	15.5		252.40
HSSS	110 ± 4	129 ± 4	
HSSSH	22 ± 4	28.9 ± 4	
(72) *Compounds containing S and O*			Back
SO	4.78 ± 0.25	4.73 ± 0.25	221.94
SOO	205 ± 4	207 ± 4	
SO_2	–296.81 ± 0.20	–294.30 ± 0.20	248.223 ± 0.050
SO_3	–395.9 ± 0.7	–390.16 ± 0.7	256.541
SSO	–55.39 ± 1.10	–53.35 ± 1.10	266.961
SOS	224 ± 4	226 ± 4	
(73) *Compounds containing S, H and O*			Back
HSO	–24.7 ± 4.2	–21.8 ± 4.2	241.4

SPECIES	$\Delta_f H$(298 K) kJ mol^{-1}	$\Delta_f H$(0 K) kJ mol^{-1}	S(298 K) J K^{-1} mol^{-1}
HOS	–7.5 ± 4.2	–4.6 ± 4.2	240.0
HSO_2	–178 ± 8		
HOSO	–247 ± 4	–243 ± 4	
HSOO	113 ± 6	118 ± 6	
HOSH	–117 ± 4	–111 ± 4	
HOOS	59 ± 6	64 ± 6	
HOOSH	–31.0 ± 4	–23.4 ± 4	
HOSOH	–285 ± 4	–276 ± 4	
$HOSO_2$	–375.7 ± 4.4	–367.5 ± 4.4	294.1
H_2SO_4	–732.7 ± 2	-720.8 ± 2.0	311.3 ± 1.5
HOSS	–67 ± 4	–63 ± 4	
HSSO	–40 ± 4	–36 ± 4	
HSOS	105 ± 6	109 ± 6	
HOSSH	–128 ± 4	–120 ± 4	
HSOSH	–0.4 ± 4	6.3 ± 4	
(74) *Compounds containing S, H, N and O*			Back
trans-HSNO	107.3 ± 2.7	112.4 ± 2.7	266.4
cis-HSNO	110.7 ± 2.7	115.8 ± 2.7	266.1
(75) *Compounds containing halogens, S and O or H*			Back
FSH	–128.2		
F_2SO	–588	–584	
F_2SO_2	–758	–750	
FClSO	–387	–384	
$FClSO_2$	–554	–547	
(76) *NS and PS*			Back
NS	283 ± 24	283 ± 24	222.093
PS	152 ± 10	153 ± 10	234.065
(77) *Compounds containing one C and S, H*			Back
CS	279.775 ± 0.75	276.529 ± 0.75	210.55
CS_2	116.70 ± 1.0	115.91 ± 1.0	237.882
HCS	300.4 ± 8.4	300.0 ± 8.4	
CH_2S	114.6 ± 8.4	118.4 ± 8.4	
CH_3S	124.7 ± 1.8		
CH_2SH	151.9 ± 9.2	158.2 ± 9.2	270.0
CH_3SH	–22.9 ± 0.7		255.14
(78) *Compounds containing one C and S, H, O*			Back
CS_2OH	108.4 ± 5.4		321 ± 20
CH_2SO	–35.1 ± 3.1	–28.3 ± 3.1	261.4
$CH_2S(O)O$	–144.7		
CH_3SO	–70.3		
$CH_3S(O)O$	–219		290.9
CH_3OSO	–230		
CH_3SOO	75.7 ± 5.4		
CH_3SO_3	–318 ± 10		315
$CH_2S(O)OH$	–107		317.0
$CH_3S(O)OH$	–324		302.6
OCS	–141.7 ± 2	–141.8 ± 2	231.644
SCSOH	108.9 ± 5.0	111.4 ± 5.0	321.8
S_2COH	60.3 ± 4.6	65.4 ± 4.6	296.9
(79) *Compounds containing two C and S, H*			Back

SPECIES	$\Delta_f H$(298 K) kJ mol^{-1}	$\Delta_f H$(0 K) kJ mol^{-1}	S(298 K) J K^{-1} mol^{-1}
CH_3SCH_2	136.3 ± 8.2		
CH_3SCH_3	–37.4 ± 0.6		285.96
CH_3SSCH_3	–24.7 ± 1.0		336.80
C_2H_5S	96.15		
C_2H_5SH	–46.1 ± 0.6		
$HSCH_2CH_2SH$	–9.7 ± 1.2		
(80) *Compounds containing two C and S, H,O*			Back
$CH_3S(O)CH_3$	–151.3 ± 0.8		
$CH_3S(O)OCH_3$	–304		342.8
CH3C(O)SH	–175.1 ± 8.4		
(81) *Compounds containing Li*			Back
Li	159.3 ± 1	157.7 ± 1	138.78
Li_2	215.9 ± 3.0	215.5 ± 3.0	197.00
LiH	140.624 ± 0.04	140.794 ± 0.04	170.909
LiF	–341 ± 4	–341 ± 8	200.278 ± 0.008
LiCl	–196 ± 4	–196 ± 12	212.92
LiBr	–154 ± 13	–146 ± 13	224.35
LiOH	–229.0 ± 5	–227.1 ± 5	214.66
LiO	53.1 ± 4	53.6 ± 4	210.96
LiO_2	–94.6 ± 4	–92.5 ± 4	
LiO_3	–77.8 ± 4	–73.6 ± 4	
Li_2O	–158.6 ± 4	–157.7 ± 4	229.11
Li_2SO_4	–1042 ± 84	–1030 ± 84	332.82 ± 42
(82) *Compounds containing Na*			Back
Na	107.5 ± 0.7	107.8 ± 0.7	153.72
Na_2	142.07 ± 1.2	144.56 ± 1.2	230.243 ± 0.030
NaH	124.3 ± 19	126.2 ± 19	188.39
NaF	–290 ± 2	–289 ± 2	217.61
NaCl	–181 ± 2	–180 ± 2	229.79
NaBr	–143.9 ± 2.1	–135.0 ± 2.2	241.22
NaOH	–191.0 ± 8	–187.4 ± 8	229.27
NaO	90.4 ± 4	92.0 ± 4	229.13 ± 2.1
NaO_2	–47.7 ± 4	–44.4 ± 4	
NaO_3	–51.5 ± 4	–46.0 ± 4	
Na_2O	–21.8 ± 4	–18.8 ± 4	260.66 ± 6.24
Na_2SO_4	–1034 ± 25	–1020 ± 25	346.85 ± 16.7
(83) *Compounds containing K*			Back
K	89.0 ± 0.8	89.9 ± 0.8	160.22
KH	123.0 ± 15	125.5 ± 15	198.02
KF	–326.8 ± 2	–324.7 ± 2	226.612 ± 0.04
KCl	–214.7 ± 0.4	–212.9 ± 0.4	239.09
KBr	–180.1 ± 2.1	–170.9 ± 2.1	250.53
KOH	–232 ± 3	–228 ± 3	238.59
KO	62.3 ± 4	64.0 ± 4	238.027 ± 2.1
KO_2	–86.6 ± 4	–83.3 ± 4	
KO_3	–77.0 ± 4	–72.0 ± 4	
K_2O	–61.0 ± 4	–57.3 ± 4	284.11 ± 6.24
K_2SO_4	–1094 ± 17	–1081 ± 17	366.15 ± 17
(84) *Compounds containing Hg and H or O*			Back

SPECIES	$\Delta_f H$(298 K) kJ mol^{-1}	$\Delta_f H$(0 K) kJ mol^{-1}	S(298 K) J K^{-1} mol^{-1}
Hg^0	61.380 ± 0.04	64.526 ± 0.04	174.971 ± 0.005
HgH	238.5 ± 16.7	243.4 ± 16.7	219.705
HgH_2	153	132	
HgO	295 ± 20	297 ± 20	
(85) *Mono- and di-halides of Hg*			Back
HgF	2.9 ± 20	7.4 ± 20	248.373
HgCl	78.45 ± 9.6	82.5 ± 9.6	260.005
HgBr	104 ± 10	115.5 ± 10	271.538
HgI	133.5 ± 4.6	138.8 ± 4.6	280.752
HgF_2	−295 ± 10	−290 ± 10	271.74
$HgCl_2$	−146.3 ± 6.3	−142.3 ± 6.3	294.793
$HgBr_2$	−85.45 ± 8.4	−67.3 ± 6.3	320.223
HgI_2	−16.1 ± 2.1	−9.8 ± 2.1	336.206
(86) *Mixed di-halides of Hg*			Back
ClHgBr			299.37
ClHgI		−83.5	176
BrHgI		−46.9	320.45
(87) *Compounds containing Hg, a halogen, and O*			Back
IHgO		140	
(88) *Addition compounds formed by HgCl, HgBr and free radicals*			Back
ClHgNO		119	
BrHgNO		157	
ClHgONO		−46	
BrHgONO		−8	
$ClHgNO_2$		−34	
$BrHgNO_2$		3	
ClHgOO		50	
BrHgOO		88	
ClHgOOH		−85	
BrHgOOH		−47	
ClHgOCl		−42	
BrHgOCl		−4	
ClHgOBr		−24	
BrHgOBr		14	
(89) *Organo-mercury compounds*			Back
$HgCH_3$	188 ± 8	201 ± 8	
$Hg(CH_3)_2$	93.3 ± 4.1		305
$Hg(C_2H_5)_2$	72.0 ± 4.1		
(90) *Halo-organo-mercury compounds*			Back
$ClHgCH_3$	−51.5 ± 2.9		
$BrHgCH_3$	−18.4 ± 2.9		
$IHgCH_3$	22.0 ± 2.9		
$ClHgC_2H_5$	−66.1 ± 4.1		
$BrHgC_2H_5$	−32.0 ± 4.1		
$IHgC_2H_5$	12.8 ± 4.6		

7.4 Notes for Table 7-2

Note 1: *Simple compounds of H and O* Back to Table

H Enthalpy value is from the optimization of Ruscic et al.[19] and is almost the same as the CODATA Key Value,[3] but with a smaller error limit. Entropy value from CODATA.[3]

H_2 CODATA Key Value.[3]

O(^{3}P) Enthalpy value is from the optimization of Ruscic et al.[19] CODATA Key Value[3] of $\Delta_f H^\circ_{298}$ = 249.18 ± 0.10 kJ mol^{-1} was used in previous evaluation. Entropy value is from CODATA.

O(^{1}D) Based on a transition to the weighted midpoint of the O(^{3}P) J-levels.[15]

O_2 CODATA Key Value.[3]

$O_2(^1\Delta_g)$ Spectroscopic value from Huber and Herzberg.[12]

$O_2(^1\Sigma_g^+)$ Spectroscopic value from Huber and Herzberg.[12]

O_3 Enthalpy value is from the optimization of Ruscic, et al.[21] Entropy from Gurvich et al. review, which also gave the previously-listed enthalpy of 141.8 ± 2 kJ mol^{-1}.[10]

OH Enthalpy value is an update[19] to the recommendation of the IUPAC Task Group.[20] It is an optimization, based on photoionization measurements. Values based on Birge-Sponer extrapolations of OH vibrational levels are 2.1 kJ mol^{-1} higher. The entropy is taken from Gurvich et al.[10] A network optimization of *ab initio* reaction enthalpies results in a value of $\Delta_f H_0^\circ$ = 36.90 ± 0.16 kJ mol^{-1}.[4] Uncertainty corresponds to the 95% confidence limit. The reference atomic values were taken from the Active Thermochemical Tables ver. 1.20.

H_2O The enthalpy and entropy values are the result of an optimization in the Active Thermochemical Tables (ATcT).[18] Previous values of –241.826 ± 0.040 kJ mol^{-1} and 188.835 ± 0.010 J mol^{-1} K^{-1} are CODATA Key Values.[3] A network optimization of *ab initio* reaction enthalpies results in a value of $\Delta_f H_0^\circ$ = –239.18 ± 0.23 kJ mol^{-1}.[4] The uncertainty corresponds to the 95% confidence limit. The reference atomic values were taken from the Active Thermochemical Tables, ver. 1.20.

HO_2 The enthalpy and entropy values are the result of an optimization by Ruscic, et al. as part of the Active Thermochemical Tables project (ATcT).[20] We accept the larger uncertainty recommended by Burgess, however.[1] The previous Table values, $\Delta_f H^\circ_{298}$ = 11.92 ± 0.22 kJ mol^{-1} and $\Delta_f H_0^\circ$ = 14.85 ± 0.22 kJ mol^{-1}, were from an optimization of a local thermochemical network consisting of 14 experimental and 7 theoretical reaction enthalpies, and grounded in very well established reference enthalpies.[8] Most theoretical values from the literature were rejected in favor of determinations at a higher level of theory. In this study, computed values of $\Delta_f H^\circ_{298}$ = 11.88 ± 0.33 kJ mol^{-1} and $\Delta_f H_0^\circ$ = 14.81 ± 0.33 kJ mol^{-1} were obtained from a composite quantum chemical method discussed in the study, roughly 0.5 kJ mol^{-1} lower than earlier values. An earlier Table enthalpy value at 298 K of 13.4 ± 2.1 kJ mol^{-1} was based upon a negative ion thermodynamic cycle,[17] which was in good agreement with the photoionization result of 13.8 ± 3.3 kJ mol^{-1}.[14] An earlier network optimization of *ab initio* reaction enthalpies resulted in a value of $\Delta_f H_0^\circ$ = 15.09 ± 0.23 kJ mol^{-1}.[4] The uncertainty corresponds to the 95% confidence limit.

H_2O_2 Taken from the review of Burgess.[1] Previous enthalpy values, $\Delta_f H^\circ_{298}$ = –135.9 ± 0.2 kJ mol^{-1} and $\Delta_f H_0^\circ$ = –129.9 ± 0.2 kJ mol^{-1}, were based on the enthalpy of formation of liquid H_2O_2 and the enthalpy of vaporization.[7] The entropy is also from the Dorofeeva, et al., review. A CCSD(T) calculation of the atomization energy, employing the cc-pVnZ basis sets (n=T,Q,5,6) led to $\Delta_f H^\circ_{298}$ = -32.28 kcal mol^{-1} and $\Delta_f H_0^\circ$ = -30.83 kcal mol^{-1}.[6]

HO_3 Taken from the review of Burgess.[1] Previous enthalpy values, $\Delta_f H^\circ_{298}$ = 18.1 ± 6.2 kJ mol^{-1} and $\Delta_f H_0^\circ$ = 21.8 ± 6.3 kJ mol^{-1}, were based on the enthalpy for the reaction HOOOH + FOO → HOOF + HOOO at the CCSD(T)/CBS(Q5) level of theory is 9.50 kcal mol^{-1}. Adjusted for the Table reference values, this gives the cited enthalpy of formation. The minimum was found to be the *trans* configuration at the CCSD(T)/CBS(Q5) level of theory, with the *cis* configuration 0.5 kcal mol^{-1} higher in energy.[9] Note that the enthalpy values obtained from the atomization energy were higher, due, apparently, to higher order correlation effects.[9] A more recent calculation employing the 2-electron reduced density

matrix method suggests that the *cis* isomer is 1.84 kcal mol^{-1} higher in energy than the trans isomer with a aug-cc-pVQZ basis set.[11] The selected value is supported by another analysis using the isodesmic reaction $HO_2 + FOO \rightarrow HO_3 + FO$ which leads to a value of $\Delta_f H_{298}^o$ = 6.3 kcal mol^{-1}.[6] An older theoretical study, using both atomization energies and the reaction $HOOO + HOH \rightarrow HOOOH + OH$, resulted in $\Delta_f H_{298}^o$ = 7.1 ± 2 kcal mol^{-1} (not adjusted).[5] The enthalpy of formation derived from an estimate of the ionization energy of HO_3, which comes from a study of the electron transfer reactions between HO_3^+ and a series of neutral substrates, was $\Delta_f H_{298}^o$ = -1 ± 5 kcal mol^{-1}.[22] The stability of HO_3 has been supported by a neutralization-reionization mass spectrometry experiment, which led to a lifetime of >1 μs,[2] and an infrared action spectrum, which leads to an upper limit for the HO-O_2 bond strength of 6.12 kcal mol^{-1}.[16]

HO_3H Enthalpy value based on the atomization energy calculated by CCSD(T) extrapolated to the CBS limit, with geometry optimized at the CCSD(T)/aV(n+d)Z (n = D,T,Q,5) level.[9] The listed value and uncertainty are those given by Burgess, who corrected the ZPE slightly.[1] Previous enthalpy values, $\Delta_f H^{\circ}_{298}$ = −90.0 kJ mol^{-1} and $\Delta_f H_0^o$ = −81.10 kJ mol^{-1}, were based on a CCSD(T) calculation of the atomization energy, employing the cc-pVnZ basis sets (n=T,Q,5,6).[6] Reaction enthalpy for the reaction 2 HOOH → HOOOH + HOH was calculated to be −15.5 kcal mol^{-1} using the G2 method, leading to $\Delta_f H^{\circ}_{298}$ = -22.7 kcal mol^{-1}.[13]

HO_4H CCSD(T) calculation of the atomization energy, employing the cc-pVnZ basis sets (n = T,Q,5,6).[6]

(1) Burgess, D. R. An evaluation of gas phase enthalpies of formation for hydrogen-oxygen (H_xO_y) species. *J. Res. Natl. Inst. Sci. Technol.* **2016**, *121*, 108-138, doi:10.6028/jres.121.005.

(2) Cacace, F.; de Petris, G.; Pepi, F.; Troiani, A. Experimental detection of hydrogen trioxide. *Science* **1999**, *285*, 81-82, doi:10.1126/science.285.5424.81.

(3) Cox, J. D.; Wagman, D. D.; Medvedev, V. A. *CODATA Key Values for Thermodynamics*; Hemisphere Publishing Corp.: New York, 1989.

(4) Császár, A. G.; Furtenbacher, T. From a network of computed reaction enthalpies to atom-based thermochemistry (NEAT). *Chem. Eur. J.* **2010**, *16*, 4826-4835, doi:10.1002/chem.200903252.

(5) Denis, P. A.; Kieniger, M.; Ventura, O. N.; Cachau, R. E.; Diercksen, G. H. F. Complete basis set and density functional determination of the enthalpy of formation of the controversial HO_3 radical: a discrepancy between theory and experiment. *Chem. Phys. Lett.* **2002**, *365*, 440-449, doi:10.1016/S0009-2614(02)01432-X.

(6) Denis, P. A.; Ornellas, F. R. Theoretical characterization of hydrogen polyoxides: HOOH, HOOOH, HOOOOH, and HOOO. *J. Phys. Chem. A* **2009**, *113*, 199-506, doi:10.1021/jp808795e.

(7) Dorofeeva, O.; Iorish, V. S.; Novikov, V. P.; Neumann, D. B. NIST-JANAF thermochemical tables. II. Three molecules related to atmospheric chemistry: HNO_3, H_2SO_4, and H_2O_2. *J. Phys. Chem. Ref. Data* **2003**, *32*, 879-901, doi:10.1063/1.1547435.

(8) Ganyecz, Á.; Csontos, J.; Nagy, B.; Kállay, M. Theoretical and thermochemical network approaches to determine the heats of formation for HO_2 and its ionic counterparts. *J. Phys. Chem. A* **2015**, *119*, 1164-1176, doi:10.1021/jp5104643.

(9) Grant, D. J.; Dixon, D. A.; Francisco, J. S.; Feller, D.; Peterson, K. A. Heats of formation of the $H_{1,2}O_mS_n$ (m,n = 0-3) molecules from electronic structure calculations. *J. Phys. Chem. A* **2009**, *113*, 11343-11353, doi:10.1021/jp905847e.

(10) Gurvich, L. V.; Veyts, I. V.; Alcock, C. B. *Thermodynamic Properties of Individual Substances,*, Fourth ed.; Hemisphere Publishing Corp.: New York, 1991; Vol. 2.

(11) Hoy, E. P.; Schwerdtfeger, C. A.; Mazziotti, D. A. Relative energies and geometries of the *cis*- and *trans*-HO_3 radicals from the parametric 2-electron density matrix method. *J. Phys. Chem A* **2013**, *117*, 1817-1825, doi:10.1021/jp3105562.

(12) Huber, K. P.; Herzberg, G. *Constants of Diatomic Molecules*; National Institute of Standards and Technology, 1998.

(13) Lay, T. H.; Bozzelli, J. W. Enthalpies of formation and group additivity of alkyl peroxides and trioxides. *J. Phys. Chem. A* **1997**, *101*, 9505-9510, doi:10.1021/jp972103i.

(14) Litorja, M.; Ruscic, B. A photoionization study of the hydroperoxyl radical, HO_2, and hydrogen peroxide, H_2O_2. *J. Electron.Spec. Rel. Phenom.* **1998**, *97*, 131-146, doi:10.1016/S0368-2048(98)00264-3

(15) Moore, C. E. *Atomic Energy Levels*; NSRDS: Washington. DC, 1971; Vol. 1.

(16) Murray, C.; Derro, E. L.; Sechler, T. D.; Lester, M. I. Stability of the hydrogen trioxide radical via infrared action spectroscopy. *J. Phys. Chem. A* **2007**, *111*, 4727-4730, doi:10.1021/jp071473w.
(17) Ramond, T. M.; Blanksby, S. J.; Kato, S.; Bierbaum, V. M.; Davico, G. E.; Schwartz, R. L.; Lineberger, W. C.; Ellison, G. B. Heat of formation of the hydroperoxyl radical HOO via negative ion studies. *J. Phys. Chem. A* **2002**, *106*, 9641-9647, doi:10.1021/jp014614h.
(18) Ruscic, B. Active thermochemical tables: Water and water dimer. *J. Phys. Chem. A* **2013**, *117*, 11940-11953, doi:10.1021/jp403197t.
(19) Ruscic, B.; Feller, D.; Peterson, K. Active Thermochemical Tables: dissociation energies of several homonuclear first-row diatomics and related thermochemical values. *Theor. Chem. Acc.* **2014**, *133*, 1415, doi:10.1007/s00214-013-1415-z.
(20) Ruscic, B.; Pinzon, R. E.; Morton, M. L.; Srinivasan, N. K.; Su, M.-C.; Sutherland, J. W.; Michael, J. V. Active thermochemical tables: Accurate enthalpy of formation of hydroperoxyl radical, HO_2. *J. Phys. Chem. A* **2006**, *110*, 6592–6601, doi:10.1021/jp056311j.
(21) Ruscic, B.; Pinzon, R. E.; Morton, M. L.; von Laszevski, G.; Bittner, S. J.; Nijsure, S. G.; Amin, K. A.; Minkoff, M.; Wagner, A. F. Introduction to active thermochemical tables: Several "key" enthalpies of formation revisited. *J. Phys. Chem. A* **2004**, *108*, 9979-9997, doi:10.1021/jp047912y.
(22) Speranza, M. Structure, stability, and reactivity of cationic hydrogen trioxides and thermochemistry of their neutral analogs. A Fourier-transform ion cyclotron resonance study. *Inorg. Chem.* **1996**, *35*, 6140-6151, doi:10.1021/ic960549s.

Note 2: *Water complexes*

Back to Table

$H_2O•H_2O$ The enthalpy and entropy values are the result of an optimization in the Active Thermochemical Tables (ATcT).[7]

$OH•H_2O$ The structure was optimized with A' symmetry at the CCSD(T(/aug-cc-pVTZ level and a binding energy of 5.88 kcal mol^{-1} calculated, resulting in the listed formation enthalpy.[4] In another calculation, the binding energy for the hydrogen-bonded complex was calculated by optimizing the structure using the PM3 method followed by HF/6-31G* self-consistent field optimization. A G3 calculation leads to a reaction enthalpy of −4.49 kcal mol^{-1} for the formation of the complex.[1]

$HO_2•H_2O$ Derived from the recommended equilibrium constant for the formation of the complex (Table 3-1, Note 4).

$O_3•H_2O$ Structures were optimized using the QCISD approach, using the 6-311G(2df,2p) and G+ with aug-cc-pVDZ and aug-cc-pVTZ basis sets. Single point calculations were carried out using the CCSD(T) method with the same basis sets. The lowest energy complexes have van der Waals structures, not hydrogen-bonding, with the two terminal oxygens of ozone interacting with the oxygen atom of water. The calculated bond dissociation enthalpy is 1.58 kcal mol^{-1}. The structure involving the central oxygen atom of ozone has a slightly weaker bond, but, due to ZPE corrections, a slightly lower enthalpy.[3]

$CH_2O•H_2O$ Obtained from a binding energy of 3.5 kcal mol^{-1} calculated using B3LYP and the 6-311++G(3df,2pd) basis set.[2]

$OCl•OH_2$ Obtained from a dissociation energy of 2.70 kcal mol^{-1}, calculated at the MP2//aug-cc-pVTZ level of theory with a quadruple-ζ basic set. Values of 1.70–1.79 kcal mol^{-1} were calculated using B3LYP with triple to quintuple-ζ bases sets. B3LYP//aug-cc-pVTZ was also used to calculate BDEs for hydrates with up to six water molecules.[5]

ClO•HOH Obtained from a dissociation energy of 1.55 kcal mol^{-1}, calculated at the MP2//aug-cc-pVTZ level of theory with a quadruple-ζ basic set. Value of 1.06–1.23 kcal mol^{-1} were calculated using B3LYP with triple to quintuple-ζ bases sets. B3LYP//aug-cc-pVTZ was also used to calculate BDEs for hydrates with up to six water molecules.[5]

$OBr•OH_2$ Obtained from a dissociation energy of 3.48 kcal mol^{-1}, calculated at the MP2//aug-cc-pVTZ level of theory. A value of 2.54 kcal mol^{-1} was calculated using B3LYP, which was also used to calculate BDEs for hydrates with up to four water molecules.[6]

BrO•HOH Obtained from dissociation energy of 1.70 kcal mol^{-1}, calculated at the MP2//aug-cc-pVTZ level of theory. A value of 1.58 kcal mol^{-1} was calculated using B3LYP, which was also used to calculate BDEs for hydrates with up to four water molecules.[6]

(1) Allodi, M. A.; Dunn, M. E.; Livada, J.; Kirschner, K. N.; Shields, G. C. Do hydroxyl radical-water clusters, $OH(H_2O)_n$, n = 1-5, exist in the atmosphere? *J. Phys. Chem. A* **2006**, *110*, 13283-13289, doi:10.1021/jp064468l.

(2) Aloisio, S.; Francisco, J. S. The role of complexes of water and carbonyl containing molecules in the atmosphere. *Phys. Chem. Earth Pt. C* **2000**, *25*, 245-253, doi:10.1016/S1464-1917(00)00012-X.

(3) Anglada, J. M.; Hoffman, G. J.; Slipchenko, L. V.; Costa, M. M.; Ruiz-López, M. F.; Francisco, J. S. Atmospheric significance of water clusters and ozone−water complexes. *J. Phys. Chem. A* **2013**, *117*, 10381-10396, doi:10.1021/jp407282c.

(4) Du, S.; Francisco, J. S.; Schenter, G. K.; Iordanov, T. D.; Garrett, B. C.; Dupris, M.; Li, J. The OH radical-H_2O molecular interaction potential. *J. Chem. Phys.* **2006**, *124*, 224318, doi:10.1063/1.2200701.

(5) Gálvez, O.; Gómez, P. C. An ab initio study on the structure and energetics of the ClO hydrates. *Chem. Phys. Lett.* **2007**, *448*, 16-23, doi:10.1016/j.cplett.2007.09.072.

(6) Gálvez, O.; Zoermer, A.; Grothe, H. Theoretical study on the structure of the BrO hydrates. *J. Phys. Chem. A* **2006**, *110*, 8818-8825, doi:10.1021/jp062048q.

(7) Ruscic, B. Active thermochemical tables: Water and water dimer. *J. Phys. Chem. A* **2013**, *117*, 11940-11953, doi:10.1021/jp403197t.

Note 3: *Simple compounds of N and H*

Back to Table

N(^{4}S) The enthalpy value is the result of an optimization in the Active Thermochemical Tables (ATcT).[12] Previous value of 472.420 ± 0.050 kJ mol^{-1} derived from a PFI-PEPICO TOF study.[14] Entropy from CODATA Key Values.[4]

N_2 CODATA Key Values.[4]

NH Enthalpy from review of Anderson.[1] Entropy and enthalpy difference (0.05 kJ mol^{-1}) from JANAF.[3] A network optimization of *ab initio* reaction enthalpies results in a value of $\Delta_f H_0^\circ$ = 359.17 ± 0.17 kJ mol^{-1}.[5] The uncertainty corresponds to the 95% confidence limit. The reference atomic values were taken from the Active Thermochemical Tables, ver. 1.20.[12] A value of $\Delta_f H_{298}^\circ$ = 361 kJ mol^{-1} was calculated for triplet NH by an atomization procedure at the CBS-QB3 level of theory and for singlet NH, a value of 531 kJ mol^{-1} was calculated.[2]

NH_2 Recommended values from the IUPAC Task Group.[11] Enthalpy is a weighted average of four measurements since 1982. Previous recommendation was 186 ± 1 kJ mol^{-1}.[1] Entropy was taken from a computed anharmonic potential surface,[9] and is close to the JANAF value of 194.71 ± 0.05 kJ mol^{-1}.[3] A value of $\Delta_f H_{298}^\circ$ = 188 kJ mol^{-1} was calculated for NH_2 by an atomization procedure at the CBS-QB3 level of theory.[2]

NH_3 CODATA Key Value.[4] The JANAF Tables give $\Delta_f H_0^\circ$ = –38.91 kJ mol^{-1}, $\Delta_f H_{298}^\circ$ = –45.90 kJ mol^{-1}, and S° = 192.774 J K^{-1}mol^{-1}.[3] A network optimization of *ab initio* reaction enthalpies results in a value of $\Delta_f H_0^\circ$ = –38.52 ± 0.26 kJ mol^{-1}.[5] The uncertainty corresponds to the 95% confidence limit. The reference atomic values were taken from the Active Thermochemical Tables, ver. 1.20.

N_2H Geometry optimized at the frozen core CCSD(T) level of theory with aug-cc-pVDZ and aug-cc-pVTZ basis sets; the CCSD(T) energy extrapolated to the CBS limit.[10] A value of $\Delta_f H_{298}^\circ$ = 249 kJ mol^{-1} was calculated for NH_2 by an atomization procedure at the CBS-QB3 level of theory.[2]

NNH_2 Isodiazene. Enthalpy calculated by an atomization procedure at the CBS-QB3 level of theory. B3LYP geometries were verified by MP2/6-311++G(3df,3dp) calculations.[2] A computational

study involving the use of several composite models, CBS-QB3, CBS-APNO, G3, and G4, led to values of $\Delta_f H_0^\circ$ = 309.0 ± 3.5 kJ mol^{-1} and $\Delta_f H_{298}^\circ$= 301.9 ± 3.6 kJ mol^{-1}.[13]

***trans*-N_2H_2** Geometry optimized at the frozen core CCSD(T) level of theory with aug-cc-pVDZ and aug-cc-pVTZ basis sets; the CCSD(T) energy extrapolated to the CBS limit.[10] Previous value, 212 ± 10 kJ mol^{-1}, taken from the Gurvich et al. review.[8] (The same value was used for the equilibrium mixture.) A value of $\Delta_f H_{298}^\circ$ = 202 kJ mol^{-1} was calculated for *trans*-N_2H_2 by an atomization procedure at the CBS-QB3 level of theory.[2] A computational study involving the use of several composite models, CBS-QB3, CBS-APNO, G3, and G4, led to values of $\Delta_f H_0^\circ$ = 210.0 ± 2.9 kJ mol^{-1} and $\Delta_f H_{298}^\circ$= 202.8 ± 2.9 kJ mol^{-1}.[13]

***cis*-N_2H_2** Geometry optimized at the frozen core CCSD(T) level of theory with aug-cc-pVDZ and aug-cc-pVTZ basis sets; the CCSD(T) energy extrapolated to the CBS limit.[10] Previous enthalpy value, 248 ± 12 kJ mol^{-1}, based on enthalpy of conversion of the *trans* to *cis* isomers, 36±12 kJ mol^{-1}.[8] A value of $\Delta_f H_{298}^\circ$ = 223 kJ mol^{-1} was calculated for *cis*-N_2H_2 by an atomization procedure at the CBS-QB3 level of theory.[2] A computational study involving the use of several composite models, CBS-QB3, CBS-APNO, G3, and G4, led to values of $\Delta_f H_0^\circ$ = 231.7 ± 3.2 kJ mol^{-1} and $\Delta_f H_{298}^\circ$= 224.6 ± 3.2 kJ mol^{-1}.[13]

N_2H_3 Geometry optimized at the frozen core CCSD(T) level of theory with aug-cc-pVDZ and aug-cc-pVTZ basis sets; the CCSD(T) energy extrapolated to the CBS limit.[10] A value of $\Delta_f H_{298}^\circ$ = 226 kJ mol^{-1} was calculated for N_2H_3 by an atomization procedure at the CBS-QB3 level of theory.[2]

NH_3NH, iminoammonium ylide

Enthalpy calculated by an atomization procedure at the CBS-QB3 level of theory. B3LYP geometries were verified by MP2/6-311++G(3df,3dp) calculations.[2]

N_2H_4, hydrazine

Enthalpy values taken from a re-evaluation of the Active Thermochemical Tables.[7] A computational study in which four composite methods were used on 45 isogyric reactions, led to a recommended value of $\Delta_f H_{298}^\circ$ = 97.7 ± 2.0 kJ mol^{-1}.[6] An enthalpy value of 23.1 kcal mol^{-1} (96.7 kJ mol^{-1}) was obtained using a geometry optimized at the frozen core CCSD(T) level of theory with aug-cc-pVDZ and aug-cc-pVTZ basis sets; the CCSD(T) energy extrapolated to the CBS limit.[10] The previous recommendation and the entropy value, $\Delta_f H_{298}^\circ$ = 95.2 ± 0.5 kJ mol−1, were taken from the review of Gurvich et al.[8] A computational study involving the use of several composite models, CBS-QB3, CBS-APNO, G3, and G4, led to values of $\Delta_f H_0^\circ$ = 115.4 ± 2.0 kJ mol^{-1} and $\Delta_f H_{298}^\circ$= 100.8 ± 2.0 kJ mol^{-1}.[13]

(1) Anderson, W. R. Oscillator strengths of NH_2 and the heats of formation of NH and NH_2. *J. Phys. Chem.* **1989**, *93*, 530-536, doi:10.1021/j100339a009.

(2) Asatryan, R.; Bozzelli, J. W.; da Silva, G.; Swinnen, S.; Nguyen, M. T. Formation and decomposition of chemically activated and stabilized hydrazine. *J. Phys. Chem. A* **2010**, *114*, 6235-6249, doi:10.1021/jp101640p.

(3) Chase, M. W. NIST-JANAF thermochemical tables. *J. Phys. Chem. Ref. Data* **1998**, *Monograph 9*.

(4) Cox, J. D.; Wagman, D. D.; Medvedev, V. A. *CODATA Key Values for Thermodynamics*; Hemisphere Publishing Corp.: New York, 1989.

(5) Császár, A. G.; Furtenbacher, T. From a network of computed reaction enthalpies to atom-based thermochemistry (NEAT). *Chem. Eur. J.* **2010**, *16*, 4826-4835, doi:10.1002/chem.200903252.

(6) Dorofeeva, O. V.; Osina, E. L. Performance of DFT, MP2, and composite ab initio methods for the prediction of enthalpies of formations of CHON compounds using isodesmic reactions. *Comput. Theor. Chem.* **2017**, *1106*, 28-35, doi:10.1016/j.comptc.2017.03.006.

(7) Feller, D. F.; Bross, D.; Ruscic, B. Enthalpy of formation of N_2H_4 (hydrazine) revisited. *J. Phys. Chem. A* **2017**, doi:10.1021/acs.jpca.7b06017.

(8) Gurvich, L. V.; Veyts, I. V.; Alcock, C. B. *Thermodynamic Properties of Individual Substances,*, Fourth ed.; Hemisphere Publishing Corp.: New York, 1991; Vol. 2.
(9) Martin, J. M. L.; François, J. P.; Gijbels, R. First principles computation of thermochemical properties beyond the harmonic approximation. II. Application to the amino radical NH_2. *J. Chem. Phys.* **1992**, *97*, 3530, doi:10.1063/1.462987.
(10) Matus, M. H.; Arduengo, A. J.; Dixon, D. A. The heats of formation of diazene, hydrazine, $N_2H_3^+$, $N_2H_5^+$, N_2H, and N_2H_3 and the methyl derivatives CH_3NNH, CH_3NNCH_3, and $CH_3HNNHCH_3$. *J. Phys. Chem. A* **2006**, *110*, 10116-10121, doi:10.1021/jp064086f.
(11) Ruscic, B.; Boggs, J. E.; Burcat, A.; Csaszar, A. G.; Demaison, J.; Janoschek, R.; Martin, J. M. L.; Morton, M. L.; Rossi, M. J.; Stanton, J. F.; Szalay, P. G.; Westmoreland, P. R.; Zabel, F.; Berces, T. IUPAC critical evaluation of thermochemical properties of selected radicals. Part I. *J. Phys. Chem. Ref. Data* **2005**, *34*, 573-656, doi:10.1063/1.1724828.
(12) Ruscic, B.; Feller, D.; Peterson, K. Active Thermochemical Tables: dissociation energies of several homonuclear first-row diatomics and related thermochemical values. *Theor. Chem. Acc.* **2014**, *133*, 1415, doi:10.1007/s00214-013-1415-z.
(13) Simmie, J. M. A database of formation enthalpies of nitrogen species by compound methods (CBS-QB3, CBS-APNO, G3, G4). *J. Phys. Chem. A* **2015**, *119*, 10511-10526, doi:10.1021/acs.jpca.5b06054.
(14) Tang, X.; Hou, Y.; Ng, C. Y.; Ruscic, B. Pulsed field-ionization photoelectron-photoion coincidence study of the process $N_2 + h\nu \rightarrow N^+ + B + e^-$: Bond dissociation energies of N_2 anad N_2^+. *J. Chem. Phys.* **2005**, *123*, 074330, doi:10.1063/1.1995699.

Note 4: *Simple compounds containing N and O*

Back to Table

NO Enthalpy value is an update[7] to the recommendation of the IUPAC Task Group, which is from an optimization based on experimental data.[8] Previous enthalpy value, 91.29 ± 0.17 kJ mol^{-1} from review of Anderson.[3] Much of the difference can be ascribed to the change in the enthalpy for N. Entropy from JANAF.[4]

N_2O Taken from review of Gurvich et al.[6] The JANAF Tables give $\Delta_f H_0^o$ = 85.48 kJ mol^{-1}, $\Delta_f H_{298}^o$ = 82.05 kJ mol^{-1}, and S^o = 219.957 J $K^{-1}mol^{-1}$.[4]

NO_2 The enthalpy value is from an optimization based on experimental data.[8] Entropy from Gurvich et al.[6]

NO_3 Enthalpy derived from a molecular beam photofragmentation translational spectroscopic study, adjusted to Table values for O and NO_2.[5] Entropy from review of Abramowitz, et al.[1]

N_2O_3 Taken from review of Gurvich et al.[6] The JANAF Tables give $\Delta_f H_0^o$ = 89.6 kJ mol^{-1}, $\Delta_f H_{298}^o$ = 82.8 kJ mol^{-1}, and S^o = 308.539 J $K^{-1}mol^{-1}$.[4]

N_2O_4 Taken from review of Gurvich et al.[6] The JANAF Tables give $\Delta_f H_0^o$ = 18.7 kJ mol^{-1}, $\Delta_f H_{298}^o$ = 9.1 kJ mol^{-1}, and S^o = 304.376 J $K^{-1}mol^{-1}$.[4]

N_2O_5 Selected enthalpy value derived from a third-law calculation on the equilibrium constant for the reaction, $NO_2 + NO_3 \leftrightarrow N_2O_5$, presented in Table 3-1, note 11. Entropy value was calculated by Alecu and Marshall,[2] as discussed in Table 3-1. Previous values ($\Delta_f H_{298}^o$ = 13.3 kJ mol^{-1}, and S^o = 355.7 J mol^{-1}) and enthalpy difference taken from review of Gurvich et al.[6] The JANAF Tables give $\Delta_f H_0^o$ = 12.7 kJ mol^{-1}, $\Delta_f H_{298}^o$ = 11.3 kJ mol^{-1}, and S^o = 346.548 J $K^{-1}mol^{-1}$.[4]

(1) Abramowitz, S.; Chase, M. W. Thermodynamic properties of gas phase species of importance to ozone depletion. *Pure App. Chem.* **1991**, *63*, 1449-1454, doi:10.1351/pac199163101449.
(2) Alecu, I. M.; Marshall, P. Computational study of the thermochemistry of N_2O_5 and the kinetics of the reaction $N_2O_5 + H_2O \rightarrow 2\ HNO_3$. *J. Phys. Chem A* **2014**, *118*, 11405-11416, doi:10.1021/jp509301t.
(3) Anderson, W. R. Oscillator strengths of NH_2 and the heats of formation of NH and NH_2. *J. Phys. Chem.* **1989**, *93*, 530-536, doi:10.1021/j100339a009.

(4) Chase, M. W. NIST-JANAF thermochemical tables. *J. Phys. Chem. Ref. Data* **1998**, *Monograph 9*.
(5) Davis, H. F.; Kim, B.; Johnston, H. S.; Lee, Y. T. Dissociation energy and photochemistry of NO_3. *J. Phys. Chem.* **1993**, *97*, 2172-2180, doi:10.1021/j100112a018.
(6) Gurvich, L. V.; Veyts, I. V.; Alcock, C. B. *Thermodynamic Properties of Individual Substances,*, Fourth ed.; Hemisphere Publishing Corp.: New York, 1991; Vol. 2.
(7) Ruscic, B.; Feller, D.; Peterson, K. Active Thermochemical Tables: dissociation energies of several homonuclear first-row diatomics and related thermochemical values. *Theor. Chem. Acc.* **2014**, *133*, 1415, doi:10.1007/s00214-013-1415-z.
(8) Ruscic, B.; Pinzon, R. E.; Morton, M. L.; Srinivasan, N. K.; Su, M.-C.; Sutherland, J. W.; Michael, J. V. Active thermochemical tables: Accurate enthalpy of formation of hydroperoxyl radical, HO_2. *J. Phys. Chem. A* **2006**, *110*, 6592–6601, doi:10.1021/jp056311j.

Note 5: *Compounds containing N, H, and O*

Back to Table

HNO Geometry optimized at the frozen core CCSD(T) level of theory with aug-cc-pVDZ and aug-cc-pVTZ basis sets; the CCSD(T) energy extrapolated to the CBS limit.[4] Previous enthalpy, 107.1 ± 2.5 kJ mol^{-1}, from review of Anderson.[1] Entropy from Gurvich et al., who cites an enthalpy of 102 kJ mol^{-1}.[7] A computational study involving the use of several composite models, CBS-QB3, CBS-APNO, G3, and G4, led to values of $\Delta_f H_0^\circ$ = 109.7 ± 3.6 kJ mol^{-1} and $\Delta_f H^\circ_{298}$= 107.2 ± 3.6 kJ mol^{-1}.[13]

HON Geometry optimized at the frozen core CCSD(T) level of theory with aug-cc-pVDZ and aug-cc-pVTZ basis sets; the CCSD(T) energy extrapolated to the CBS limit.[4]

NH_2O Geometry optimized at the frozen core CCSD(T) level of theory with aug-cc-pVDZ and aug-cc-pVTZ basis sets; the CCSD(T) energy extrapolated to the CBS limit.[4]

NH_2OH Calculated using isodesmic reactions at several levels of theory and several basis sets.[12] Previous value of –9.6±2.2 kcal mol^{-1} based on average of theoretical and experimental values.[1] Entropy from Gurvich et al.[7] A computational study involving the use of several composite models, CBS-QB3, CBS-APNO, G3, and G4, led to values of $\Delta_f H_0^\circ$ = −32.0 ± 3.0 kJ mol^{-1} and $\Delta_f H^\circ_{298}$= −41.9 ± 3.1 kJ mol^{-1} for *trans*-hydroxylamine and $\Delta_f H_0^\circ$ = −14.2 ± 3.0 kJ mol^{-1} and $\Delta_f H^\circ_{298}$ = −24.2 ± 3.0 kJ mol^{-1} for *cis*-hydroxylamine.[13]

NH_3O Ammonia oxide. Enthalpy values for this isomer of hydroxylamine were calculated by using several composite models, CBS-QB3, CBS-APNO, G3, and G4.[13]

HNOH Geometry optimized at the frozen core CCSD(T) level of theory with aug-cc-pVDZ and aug-cc-pVTZ basis sets; the CCSD(T) energy extrapolated to the CBS limit.[4]

NH_2NO_2 The equilibrium geometry was calculated at the CCSD(T)/cc-pVQZ level of theory, while the energy was calculated by summing various contributions calculated at the CCSC(T) level with the use of various basis sets.[14] The previous value, $\Delta_f H^\circ_{298}$ = −26 ± 10 kJ mol^{-1}, was based on measurements of the enthalpy of formation of the crystalline substance and an estimated value of the enthalpy of sublimation, 60.7±10 kJ mol^{-1}.[7]

HONO Thermodynamic properties for the equilibrium mixtures of isomers from Gurvich et al. review.[7]

***trans*-HONO**
Taken from review of Gurvich et al.[7] Values calculated using G3, CBS-QB3, and CBS-APNO methods applied to atomization, isomerization, and work reactions are $\Delta_f H_{298}^\circ$ = −18.90 ± 0.05 kcal mol^{-1} and S° = 57.89 cal K^{-1} mol^{-1}.[2] A computational study involving the use of several composite models, CBS-QB3, CBS-APNO, G3, and G4, led to values of $\Delta_f H_0^\circ$ = −73.2 ± 4.0 kJ mol^{-1} and $\Delta_f H^\circ_{298}$= −78.5 ± 3.9 kJ mol^{-1}.[13]

***cis*-HONO** Enthalpy value obtained on basis of enthalpy of conversion of trans-HONO into cis-HONO, 1.7 ± 0.4 kJ mol^{-1}.[7] Values calculated using G3, CBS-QB3, and CBS-APNO methods applied to atomization, isomerization, and work reactions are $\Delta_f H_{298}^\circ$ = −18.40 ± 0.05 kcal mol^{-1} and S°

= 57.64 cal K^{-1} mol^{-1}.[2] A computational study involving the use of several composite models, CBS-QB3, CBS-APNO, G3, and G4, led to values of $\Delta_f H_0^\circ$ = −70.9 ± 4.3 kJ mol^{-1} and $\Delta_f H_{298}^\circ$ = −76.4 ± 4.3 kJ mol^{-1}.[13]

***trans*-HOON, hydroperoxynitrene or nitrosyl O-oxide**

The O-O dissociation energy was calculated at the CCSDTQ/aug-cc-pVTZ level of theory as 39.0 kJ mol^{-1}. This was corrected to 298 K by −5.7 kJ mol^{-1} to give the selected enthalpy value. The *cis* isomer was calculated to be 6.4–8.5 kJ mol^{-1} less stable.[15]

HNO_2, nitryl hydride

Calculated using G3, CBS-QB3, and CBS-APNO methods applied to atomization, isomerization, and work reactions.[2]

$HONO_2$ Nitric acid. Taken from the updated NIST-JANAF Tables.[5] A computational study involving the use of several composite models, CBS-QB3, CBS-APNO, G3, and G4, led to values of $\Delta_f H_0^\circ$ = −137.4 ± 6.2 kJ mol^{-1} and $\Delta_f H_{298}^\circ$ = −129.0 ± 6.3 kJ mol^{-1}.[13]

***cis,cis*-HOONO**

Derived from a third-law analysis of the equilibrium constant for HO + NO_2 ↔ *c,c*-HOONO (Table 3-1, Note 1). Previous enthalpy value of –5.7 kcal mol^{-1} and values for the *cis,perp*- and *trans,perp*-HOONO calculated at the MP2 level of theory.[10] A computational study with geometry optimization carried out at the CCSD(T) level of theory with the cc-pZQZ basis set, followed by an enthalpy calculated by summing various contributions calculated at the CCSC(T) level with the use of various basis sets, led to $\Delta_f H_0^\circ$ = −6.4 ± 2.0 kJ mol^{-1}, $\Delta_f H_{298}^\circ$ = −15.5 ± 2.0 kJ mol^{-1}, and S = 271.0 ± 2.0 J K^{-1} mol^{-1}.[14] A computational study involving the use of several composite models, CBS-QB3, CBS-APNO, G3, and G4, led to values of $\Delta_f H_0^\circ$ = 6.2 ± 6.1 kJ mol^{-1} and $\Delta_f H_{298}^\circ$ = 0.3 ± 5.9 kJ mol^{-1} for peroxynitrous acid.[13] It was noted that the two lowest energy conformations did not converge, however.

***trans, perp*-HOONO**

Derived from the dissociation energy for *t,p*-HOONO and reported molecular constants (Table 3-1, Note 1). Enthalpy values for the *cis,cis*-, *cis,perp*-, and *trans,perp*-HOONO have also been calculated at the MP2 level of theory.[10]

HO_2NO_2 Derived from a third-law analysis of the equilibrium constant for HO_2NO_2 ↔ HO_2 + NO_2.[6] Previous recommended enthalpy value of –12.7 ± 0.6 kcal mol^{-1} from Regimbal and Mozurkewich.[11] A value of $\Delta_f H_{298}^\circ$ = –52.3 kJ mol^{-1} was obtained from a computational study in which equilibrium structures optimized at the MP2 level with the 6-311G(d,p) basis set and enthalpy values calculated by both atomization energies and through use of isodesmic reactions at the G3, G3B3, and G4 methods.[3] A computational study with geometry optimization carried out at the CCSD(T) level of theory with the cc-pZQZ basis set, followed by an enthalpy calculated by summing various contributions calculated at the CCSC(T) level with the use of various basis sets, led to $\Delta_f H_0^\circ$ = −41.3 ± 2.4 kJ mol^{-1}, $\Delta_f H_{298}^\circ$ = −52.4 ± 2.4 kJ mol^{-1}, and S = 296.2 ± 2.0 J K^{-1} mol^{-1}.[14] The enthalpy difference was used to calculate the 0 K value in the Table.

NH_4NO_3 Enthalpy obtained from a third-law analysis of the sublimation pressure of NH_4NO_3 over the range 321−360 K. The entropy was calculated from molecular constants taken from the literature.[8] A high-level theoretical calculation, CCSD(T) extrapolated to the aug-cc-pV∞Z basis set, gives $\Delta_f H_0^\circ$ = −221.1 ± 3 kJ mol^{-1}, $\Delta_f H_{298}^\circ$ = −230.6 ± 3 kJ mol^{-1}, and S = 342.4 J $K^{-1}mol^{-1}$.[9]

(1) Anderson, W. R. Heats of formation of HNO and some related species. *Comb. Flame* **1999**, *117*, 394-403, doi:10.1016/S0010-2180(98)00077-7.

(2) Asatryan, R.; Bozzelli, J. W.; Simmie, J. M. Thermochemistry for enthalpies and reaction paths of nitrous acid isomers. *Int. J. Chem. Kinet.* **2007**, *39*, 378-398, doi:10.1002/kin.20247.

(3) Buendía-Atencio, C.; Leyva, V.; González, L. Thermochemistry and UV spectroscopy of alkyl peroxynitrates. *J. Phys. Chem. A* **2010**, *114*, 9537-9544, doi:10.1021/jp103854y.

(4) Dixon, D. A.; Francisco, J. S.; Alexeev, Y. Thermochemical properties of H_xNO molecules and ions from ab initio electronic structure theory. *J. Phys. Chem. A* **2006**, *110*, 185-191, doi:10.1021/jp054642q.
(5) Dorofeeva, O.; Iorish, V. S.; Novikov, V. P.; Neumann, D. B. NIST-JANAF thermochemical tables. II. Three molecules related to atmospheric chemistry: HNO_3, H_2SO_4, and H_2O_2. *J. Phys. Chem. Ref. Data* **2003**, *32*, 879-901, doi:10.1063/1.1547435.
(6) Gierczak, T.; Jimenez, E.; Riffault, V.; Burkholder, J. B.; Ravishankara, A. R. Thermal decomposition of HO_2NO_2 (peroxynitric acid, PNA): Rate coefficient and determination of the enthalpy of formation. *J. Phys. Chem. A* **2005**, *109*, 586-596, doi:10.1021/jp046632f.
(7) Gurvich, L. V.; Veyts, I. V.; Alcock, C. B. *Thermodynamic Properties of Individual Substances,*, Fourth ed.; Hemisphere Publishing Corp.: New York, 1991; Vol. 2.
(8) Hildenbrand, D. L.; Lau, K. H.; Chandra, D. Revised thermochemistry of gaseous ammonium nitrate, NH_4NO_3(g). *J. Phys. Chem. A* **2010**, *114*, 11654-11655, doi:10.1021/jp105773q.
(9) Irikura, K. K. Thermochemistry of ammonium nitrate, NH_4NO_3, in the gas phase. *J. Phys. Chem. A* **2010**, *114*, 11651-11653, doi:10.1021/jp105770d.
(10) McGrath, M. P.; Rowland, F. S. Determination of the barriers to interneal rotatoin in ONOOX (X = H, Cl) and characterization of the minimum energy conformers. *J. Phys. Chem.* **1994**, *98*, 1061-1067, doi:10.1021/j100055a004.
(11) Regimbal, J. M.; Mozurkewich, M. Peroxynitric acid decay mechanisms and kinetics at low pH. *J. Phys. Chem. A* **1997**, *101*, 8822-8829, doi:10.1021/jp971908n.
(12) Saraf, S. R.; Rogers, W. J.; Mannan, M. S.; Hall, M. B.; Thomson, L. M. Theoretical thermochemistry: Ab initio heat of formation for hydroxylamine. *J. Phys. Chem. A* **2003**, *107*, 1077-1081, doi:10.1021/jp026027h.
(13) Simmie, J. M. A database of formation enthalpies of nitrogen species by compound methods (CBS-QB3, CBS-APNO, G3, G4). *J. Phys. Chem. A* **2015**, *119*, 10511-10526, doi:10.1021/acs.jpca.5b06054.
(14) Szakács, P.; Csontos, J.; Das, S.; Kállay, M. High-accuracy theoretical thermochemistry of atmospherically important nitrogen oxide derivatives. *J. Phys. Chem. A* **2011**, *115*, 3144-3153, doi:10.1021/jp112116x.
(15) Talipov, M. R.; Timerghazin, Q. K.; Safiullin, R. L.; Khursan, S. L. No longer a complex, not yet a molecule: A challenging case of nitrosyl O-hydroxide, HOON. *J. Phys. Chem. A* **2013**, *117*, 679-685, doi:10.1021/jp3110858.

Note 6: *Compounds with one C and 0-4 H*

Back to Table

C Enthalpy from an active thermochemical tables optimization.[9] The previous enthalpy of ΔH_f(298 K) = 716.68 ± 0.45 kJ mol^{-1} and ΔH_f(0 K) = 711.19 ± 0.45 kJ mol^{-1} and the entropy are CODATA Key Values.[2] The JANAF Tables give $\Delta_f H_0^\circ$ = 711.2 kJ mol^{-1}, $\Delta_f H_{298}^\circ$ = 716.7 kJ mol^{-1}, and S° = 158.100 J K^{-1} mol^{-1}.[1] The cited enthalpy is identical to that for the triplet carbon atom, ^{3}C. The singlet carbon atom, ^{1}C, is higher at ΔH_f(298 K) = 838.478 ± 0.050 kJ mol^{-1},[9] and is completely unimportant under atmospheric conditions.

CH Enthalpy from an active thermochemical tables optimization,[9] which is very slightly different from the recommendation, ΔH_f(298 K) = 595.8 ± 0.6 kJ mol^{-1}, from an IUPAC Task Group, used previously.[10] An earlier recommendation of ΔH_f(298 K) = 597.37 ± 1.3 kJ mol^{-1} was from Gurvich et al.[6] The preferred value corresponds to the theoretical value of Császár et al.,[4] which is in agreement with the experimental values but is considered to be of higher accuracy. The entropy was taken from Gurvich et al.[6] A network optimization of *ab initio* reaction enthalpies results in a value of $\Delta_f H_0^\circ$ = 592.62 ± 0.24 kJ mol^{-1}.[3] The uncertainty corresponds to the 95% confidence limit. The reference atomic values were taken from the Active Thermochemical Tables, ver. 1.20. The cited enthalpy is identical to that for doublet methyidyne, ^{2}CH. Quartet methylidyne, ^{4}CH, is higher at ΔH_f(298 K) = 667.88 ± 0.59 kJ mol^{-1},[9] and is completely unimportant under atmospheric conditions.

$CH_2(^3B_1)$ Enthalpy from an active thermochemical tables optimization,[9] which is very slightly different from the recommendation from IUPAC Task Group[10] and its update.[11] Entropy value from the

ICPAC Task Group.[10] Previous recommendations of $\Delta H_f(298\ K) = 390.4 \pm 0.8$ kJ mol^{-1} and $S(298\ K) = 194.90$ J K^{-1} mol^{-1} were from experiments of Ruscic et al.[12] A network optimization of *ab initio* reaction enthalpies results in a value of $\Delta_f H_0^\circ = 390.86 \pm 0.29$ kJ mol^{-1}.[3] The uncertainty corresponds to the 95% confidence limit. The reference atomic values were taken from the Active Thermochemical Tables, ver. 1.20. Ruscic. et al.,[9] also include information on "regular methylene", or methylene thermally equilibrated over all available electronic states. At atmospheric temperatures, this is essentially equal to the value for triplet methylene.

$CH_2(^1A_1)$ Enthalpy from an active thermochemical tables optimization,[9] which is very slightly different from the recommendation from IUPAC Task Group[10] and its update.[11] Entropy value from the ICPAC Task Group.[10] Previous recommendation of $\Delta H_f(298\ K) = 428.0 \pm 0.8$ kJ mol^{-1} was from Jacox.[7] The preferred value is based on the enthalpy of formation of triplet methylene and a separation between the singlet and triplet sates of 3147 ± 5 cm^{-1}.

CH_3 Enthalpy from an active thermochemical tables optimization,[9] which is slightly different, but with a much smaller error limit, than the earlier recommendation, $\Delta H_f(298\ K) = 146.7 \pm 0.3$ kJ mol^{-1}, taken from IUPAC Task Group.[10] Entropy value differs only slightly from an earlier recommended value of 193.96 J K^{-1} mol^{-1} from Gurvich et al.[6] A network optimization of *ab initio* reaction enthalpies results in a value of $\Delta_f H_0^\circ = 149.66 \pm 0.34$ kJ mol^{-1}.[3] The uncertainty corresponds to the 95% confidence limit. The reference atomic values were taken from the Active Thermochemical Tables, ver. 1.20.

CH_4 Enthalpy from an active thermochemical tables optimization, [9] which is slightly different from the earlier optimization value of $\Delta H_f(298\ K) = -74.549 \pm 0.060$ kJ mol^{-1}.[13] Enthalpy from flame calorimetry -74.48 ± 0.41 kJ mol^{-1} used previously.[8] Entropy from Frenkel et al.[5] A network optimization of *ab initio* reaction enthalpies results in a value of $\Delta_f H_0^\circ = -66.35 \pm 0.46$ kJ mol^{-1}.[3] The uncertainty corresponds to the 95% confidence limit. The reference atomic values were taken from the Active Thermochemical Tables, ver. 1.20.

(1) Chase, M. W. NIST-JANAF thermochemical tables. *J. Phys. Chem. Ref. Data* **1998**, *Monograph 9*.

(2) Cox, J. D.; Wagman, D. D.; Medvedev, V. A. *CODATA Key Values for Thermodynamics*; Hemisphere Publishing Corp.: New York, 1989.

(3) Császár, A. G.; Furtenbacher, T. From a network of computed reaction enthalpies to atom-based thermochemistry (NEAT). *Chem. Eur. J.* **2010**, *16*, 4826-4835, doi:10.1002/chem.200903252.

(4) Császár, A. G.; Szalay, P. G.; Leininger, M. L. The enthalpy of formation of $^2\Pi$ CH. *Mol. Phys.* **2002**, *100*, 3879-3883, doi:10.1080/0026897021000016684.

(5) Frenkel, M.; Kabo, G. J.; Marsh, K. N.; Roganov, G. N.; Wilhoit, R. C. *Thermodynamics of Organic Compounds in the Gas State*; Thermodynamics Research Center: College Station, TX, 1994; Vol. I.

(6) Gurvich, L. V.; Veyts, I. V.; Alcock, C. B. *Thermodynamic Properties of Individual Substances,*, Fourth ed.; Hemisphere Publishing Corp.: New York, 1991; Vol. 2.

(7) Jacox, M. E. *Vibrational and Electronic Energy Levels of Polyatomic Transient Molecules*; National Institute of Standards and Technology, 1998.

(8) Pittam, D. A.; Pilcher, G. Measurements of heats of combustion by flame calorimetry. Part 8. Methane, ethane, propane, n-butane and 2-methylpropane. *J. Chem. Soc. Faraday Trans. 1* **1972**, *68*, 2224-2229, doi:10.1039/F19726802224.

(9) Ruscic, B. Active thermochemical tables: Sequential bond dissociation enthalpies of methane, ethane, and methanol and the related thermochemistry. *J. Phys. Chem. A* **2015**, *119*, 7810-7837, doi:10.1021/acs.jpca.5b01346.

(10) Ruscic, B.; Boggs, J. E.; Burcat, A.; Csaszar, A. G.; Demaison, J.; Janoschek, R.; Martin, J. M. L.; Morton, M. L.; Rossi, M. J.; Stanton, J. F.; Szalay, P. G.; Westmoreland, P. R.; Zabel, F.; Berces, T. IUPAC critical evaluation of thermochemical properties of selected radicals. Part I. *J. Phys. Chem. Ref. Data* **2005**, *34*, 573-656, doi:10.1063/1.1724828.

(11) Ruscic, B.; Feller, D.; Peterson, K. Active Thermochemical Tables: dissociation energies of several homonuclear first-row diatomics and related thermochemical values. *Theor. Chem. Acc.* **2014**, *133*, 1415, doi:10.1007/s00214-013-1415-z.
(12) Ruscic, B.; Litorja, M.; Asher, R. L. Ionization energy of methylene revisited: Improved values for the enthalpy of formation of CH_2 and the bond dissociation energy of CH_3 via simultaneous solution of the local thermochemical network. *J. Phys. Chem. A* **1999**, *103*, 8625-8633, doi:10.1021/jp992403v.
(13) Ruscic, B.; Pinzon, R. E.; Morton, M. L.; von Laszevski, G.; Bittner, S. J.; Nijsure, S. G.; Amin, K. A.; Minkoff, M.; Wagner, A. F. Introduction to active thermochemical tables: Several "key" enthalpies of formation revisited. *J. Phys. Chem. A* **2004**, *108*, 9979-9997, doi:10.1021/jp047912y.

Note 7: *Compounds containing one C, 0-4 H, and one or more O*

Back to Table

CO Enthalpy from an active thermochemical tables optimization,[23] which is slightly different than the CODATA Key Value, $\Delta_f H^\circ_{298} = -110.53 \pm 0.17$ kJ mol^{-1}, previously recommended.[3] The entropy value is still from CODATA. Atomization energies calculated using CCSD(T) with aug cc-pVnZ (n = D − 7) basis sets, using frozen-core CCSD(T) optimized geometries and extrapolated to the complete basis set limit, led to enthalpies of $\Delta_f H_0^\circ = -27.0 \pm 0.2$ kcal mol^{-1} and $\Delta_f H^\circ_{298} = -26.2 \pm 0.2$ kcal mol^{-1}.[12] A network optimization of *ab initio* reaction enthalpies results in a value of $\Delta_f H_0^\circ = -114.09 \pm 0.32$ kJ mol^{-1}.[4] The uncertainty corresponds to the 95% confidence limit. The reference atomic values were taken from the Active Thermochemical Tables, ver. 1.20.

CO_2 CODATA Key Value.[3] The active thermochemical tables optimization gives $\Delta_f H^\circ_{298} = -393.474 \pm 0.014$ kJ mol^{-1} and $\Delta_f H_0^\circ = -393.108 \pm 0.014$ kJ mol^{-1}.[25] Atomization energies calculated using CCSD(T) with aug cc-pVnZ (n=D − 7) basis sets, using frozen-core CCSD(T) optimized geometries and extrapolated to the complete basis set limit, led to enthalpies of $\Delta_f H_0^\circ = -93.7 \pm 0.2$ kcal mol^{-1} and $\Delta_f H^\circ_{298} = -93.8 \pm 0.2$ kcal mol^{-1}.[12] A network optimization of *ab initio* reaction enthalpies results in a value of $\Delta_f H_0^\circ = -392.98 \pm 0.40$ kJ mol^{-1}.[4] The uncertainty corresponds to the 95% confidence limit. The reference atomic values were taken from the Active Thermochemical Tables, ver. 1.20.

HCO, formyl

Enthalpy from an active thermochemical tables optimization.[23]The previous recommendation, $\Delta_f H_{298}^\circ = 44.15 \pm 0.43$ kJ mol^{-1}, was from reversible reactions of I and Br with CH_2O,[1] using present values for HI and HBr. Entropy taken from Gurvich et al.[13] Atomization energies calculated using CCSD(T) with aug cc-pVnZ (n=D − 7) basis sets, using frozen-core CCSD(T) optimized geometries and extrapolated to the complete basis set limit, led to enthalpies of $\Delta_f H_0^\circ = 10.4 \pm 0.2$ kcal mol^{-1} and $\Delta_f H^\circ_{298} = 10.5 \pm 0.2$ kcal mol^{-1}.[12]

COH, isoformyl

Enthalpy from an active thermochemical tables optimization.[23]

HCOH Enthalpy from an active thermochemical tables optimization.[23] The cited enthalpy is almost identical to that for the *trans* singlet hydroxymethylene, *t*-^{1}HCOH, $\Delta H_f(298\text{ K}) = 108.64 \pm 0.33$ kJ mol^{-1}. The *cis* singlet, *c*-^{1}HCOH, is higher at $\Delta H_f(298\text{ K}) = 127.11 \pm 0.33$ kJ mol^{-1}.[23] The triplet, which is in a gauche configuration, is much higher at $\Delta H_f(298\text{ K}) = 216.1 \pm 1.1$ kJ mol^{-1}.

CH_2O Enthalpy from an active thermochemical tables optimization.[23] The previous recommendation, $\Delta_f H_{298}^\circ = -108.99 \pm 1.76$ kJ mol^{-1}, was obtained by using experimental reaction enthalpies taken from the literature.[7] This value was confirmed by three computational approaches involving enthalpies of the same reaction, isodesmic reaction enthalpies, and atomization energies, using a range of high-level computational techniques. An earlier recommended value, $\Delta_f H_{298}^\circ = -108.7 \pm 0.50$ kJ mol^{-1}, was taken from review of Gurvich et al., as is the present

entropy value.[13] A CCSD(T) calculation with the aug-cc-pVnZ (n = D,T,Q,5) basis set extrapolated to the CBS limit gave $\Delta_f H_0^\circ$ = –104.2 ± 2.1 kJ mol^{-1}, $\Delta_f H_{298}^\circ$ = −107.95 ± 2.1 kJ mol^{-1}, and S = 218.57 J K^{-1} mol^{-1}.[20] A computation using the focal-point analysis approach resulted in $\Delta_f H_0^\circ$ = –105.42 ± 0.33 kJ mol^{-1}, $\Delta_f H_{298}^\circ$ = −109.23 ± 0.33 kJ mol^{-1}.[5]

***trans*-HOCO**

The enthalpy and entropy values are taken from a CCSDT(Q) calculation, with structure optimized using the cc-pVQZ basis set.[21] The previous $\Delta_f H_{298}^\circ$ = –187.9 ± 2.1 was obtained from atomization energies calculated using CCSD(T) with aug cc-pVnZ (n=D – 7) basis sets, using frozen-core CCSD(T) optimized geometries and extrapolated to the complete basis set limit.[12] An earlier computational study using G3 and CBS-QB3 methods gave $\Delta_f H_{298}^?$ = –43.3 ± 2 kcal mol^{-1}.[10] These results are in agreement with photoionization lower limit of –46.5 kcal mol^{-1}.[26]

cis-HOCO The enthalpy and entropy values are taken from a CCSDT(Q) calculation, with structure optimized using the cc-pVQZ basis set.[21] The previous $\Delta_f H_{298}^\circ$ = –175.7 ± 2.1 was obtained from atomization energies calculated using CCSD(T) with aug cc-pVnZ (n=D – 7) basis sets, using frozen-core CCSD(T) optimized geometries and extrapolated to the complete basis set limit; $\Delta_f H_0^\circ$ = –41.0 ± 0.5 kcal mol^{-1}. (Result presented in text as an energy difference of 2.9 kcal mol^{-1} over the t*rans* form.)[12] An earlier computational study using G3 and CBS-Qb3 methods gave $\Delta_f H_{298}^?$ = –41.4 ± 2 kcal mol^{-1}.[10]

HC(O)O Enthalpy obtained from atomization energies calculated using CCSD(T) with aug cc-pVnZ (n = D – 7) basis sets, using frozen-core CCSD(T) optimized geometries and extrapolated to the complete basis set limit.[12] An earlier study using vibrational frequencies calculated at the HF/6-31G(D) level and total energies evaluated at the G2(MP2) level, also making use of isodesmic reactions, gave $\Delta_f H_{298}^?$ = –30 kcal mol^{-1} and the quoted entropy value.[31] A CCSD(T)-CBS (W1U) calculation gives $\Delta_f H_{298}^?$ = –129.4 ± 12.6 kJ mol^{-1}.[11]

C(O)OH Vibrational frequencies calculated at the HF/6-31G(D) level and total energies evaluated at the G2(MP2) level, also making use of isodesmic reactions.[31] Enthalpy calculated using the atomization energy method at the CBS-Q level gave –41.62 kcal mol^{-1}.[28]

HC(O)OH Enthalpy taken from NBS Tables;[30] entropy calculated based on structure optimized at MP2/6-31G(D) and frequencies calculated at HF6/31G(D) level.[31] See also discussion of enthalpy in Yu et al.[31] $\Delta_f H_{298}^\circ$ = –90.5 kcal mol^{-1} also obtained by calculating optimized geometry at the CCSD(T)/aVTZ level with the aug-cc-pVTZ basis set; CCSD(T) energy extrapolated to the CBS limit.[22] Atomization energies calculated using CCSD(T) with aug cc-pVnZ (n = D – 7) basis sets, using frozen-core CCSD(T) optimized geometries and extrapolated to the complete basis set limit, led to enthalpies of $\Delta_f H_0^\circ$ = –88.9 ± 0.4 kcal mol^{-1} and $\Delta_f H_{298}^?$ = –90.7 ± 0.4 kcal mol^{-1}.[12] Microwave intensity measurements have determined that the *cis* rotamer of HC(O)OH to be 16.3 ± 0.4 kJ mol^{-1} higher in energy than the *trans* rotamer.[14]

***trans*-and *cis*-HC(O)OO**

Photoelectron spectroscopy of the peroxyformate anion was used to obtain the electron affinity of the peroxyformate radical. Through a thermochemical cycle, this leads to the O-H bond dissociation energy, which combined with the calculated enthalpy of the acid, yields the enthalpy of formation. BDEs for both the *cis* and *trans* conformers of the acid could be determined, both leading to the lower-energy *trans* conformer of the radical.[29]

***trans*-HC(O)OOH**

Enthalpy obtained from the calculated heat of an isodesmic reaction, at the G3B3MP2 level of theory.[29] This value is slightly lower than $\Delta_f H_{298}^?$ = –285.3 ± 2.5 kJ mol^{-1} ($\Delta_f H_0^\circ$ = –275.7 kJ mol^{-1}) obtained from atomization energies calculated using CCSD(T) with aug cc-pVnZ (n = D – 7) basis sets, using frozen-core CCSD(T) optimized geometries and extrapolated to the complete basis set limit.[12] The present value was chosen as it is conformer specific; the 0 K value is based on the Feller et al.[12] enthalpy difference.

***cis*-HC(O)OOH**

The enthalpy value is derived from the value for the *trans* conformer, which is calculated at the G3B3MP2 level of theory, to be 14.2 kJ mol^{-1} lower in energy than the *cis* conformer.[29]

CH_2OO, formaldehyde carbonyl oxide (Criegee intermediate)

Optimized geometry calculated at the CCSD(T)/aVTZ level with the aug-cc-pVTZ basis set; CCSD(T) energy extrapolated to the CBS limit.[22]

CH_2O_2, dioxirane

Optimized geometry calculated at the CCSD(T)/aVTZ level with the aug-cc-pVTZ basis set; CCSD(T) energy extrapolated to the CBS limit.[22]

CH_3O Enthalpy from an active thermochemical tables optimization,[23] which is slightly different than the previous recommendation taken from IUPAC Task Group, ΔH_f(298 K) = 21.0±2.1 kJ mol^{-1}.[24] The recommendation is supported by one recent high-level theoretical study. This value is significantly higher than that recommended here earlier, 17.15 ± 3.8 kJ mol^{-1} from the evaluation of Berkowitz et al.,[2] and most other previous recommendations. The recommended entropy is also somewhat different that the previously recommended value of 232.86 J K^{-1} mol^{-1}.[13] Atomization energies calculated using CCSD(T) with cc-pVnZ (n = D, T, and Q) basis sets, using (U)MP2/aug-cc-pVTZ optimized geometries and extrapolated to the complete basis set limit, led to enthalpies of $\Delta_f H_0^\circ$ = 7.4 kcal mol^{-1} and $\Delta_f H^\circ_{298}$ = 5.5 kcal mol^{-1}.[19] The entropy value is taken from the IUPAC Task Group.[24]

CH_3O_2 Based on a re-analysis of previous equilibrium data on R + O_2 ↔ RO_2 from the same laboratory.[16] In a computational study, $\Delta_f H^\circ_{298}$ = 8.8 kJ mol^{-1} was determined using G3B3 and CBS-APNO methods with isodesmic reactions to minimize systematic errors, where the geometry was optimized at the B3LYP/cc-pVTZ+d level of theory. This work also provided the recommended entropy.[6]

CH_2OH Enthalpy from an active thermochemical tables optimization,[23] which is slightly different from the recommendation taken from IUPAC Task Group, ΔH_f(298 K) = −17.0 ± 0.7 kJ mol^{-1}.[24] (Note that an earlier value listed in this Table, $\Delta_f H_{298}^\circ$ = −11.5±1.3 kJ mol^{-1}, inadvertently was actually $\Delta_f H_0^\circ$ for 0 K.) The entropy value reported by Johnson and Hudgens was accepted and is included here with their error limits.[15] Results of Dóbé, et al.[8] give –16.6 ± 1.3 kJ mol^{-1}. Atomization energies calculated using CCSD(T) with cc-pVnZ (n=D, T, and Q) basis sets, using (U)MP2/aug-cc-pVTZ optimized geometries and extrapolated to the complete basis set limit, led to enthalpies of $\Delta_f H_0^\circ$ = –2.3 kcal mol^{-1} and $\Delta_f H^\circ_{298}$ = –3.8 kcal mol^{-1}.[19]

CH_3OH Enthalpy from an active thermochemical tables optimization.[23] The previous enthalpy of ΔH_f(298 K) = –201.0 ± 0.6 kJ mol^{-1} was taken from review of Gurvich et al.,[13] as is the entropy value. Atomization energies calculated using CCSD(T) with cc-pVnZ (n = D, T, and Q) basis sets, using (U)MP2/aug-cc-pVTZ optimized geometries and extrapolated to the complete basis set limit, led to enthalpies of $\Delta_f H_0^\circ$ = –45.7 kcal mol^{-1} and $\Delta_f H^\circ_{298}$ = –48.3 kcal mol^{-1}.[19]

$CH_3OH{\bullet}HO_2$

Estimated from studies on the decay of HO_2 in the presence of CH_3OH, with supporting *ab initio* calculations (Table 3-1, Note 5).

CH_2OOH Calculated using the complete basis set method, CBS-Q. Enthalpies calculated using the atomization energy method. Entropy based on geometric properties optimized at the MP2/6-31G(d') level and vibrational frequencies at the HF/6-31G(d') level.[28] This radical is unstable to decomposition to CH_2O + OH.

CH_3OOH Geometry optimization and frequency calculations were performed at the MP2/6-31G(d) and the B3LYP/6-311++G(d,p) levels of theory, with a single-point energy calculation at the CCSD(T)/6-311++G(d,p//B3LYP/6-311++G(d,p) level. The dissociation energy into HO_2 and the alkyl radical was then evaluated and used, after thermal correction, to calculate the enthalpy of formation at 298 K.[17] This was adjusted to the radical values from the present Table. Reaction enthalpies determined using the G2 method indicated ΔH°_{298}(CH_3OO–H) is 1.6 kcal mol^{-1} lower than ΔH°_{298}(HOO–H), or 85.9 kcal mol^{-1} (359.4 kJ mol^{-1}), leading to the previous

enthalpy value of –132.2 kJ mol^{-1}.[18] An earlier recommended enthalpy value (–139.0 ± 8.1 kJ mol^{-1}) was computed on the assumption that the dissociation energy for ROO–H is 366±3 kJ mol^{-1} (Stocker and Pilling, unpublished work).[16] Enthalpy calculated using the atomization energy method at the CBS-Q level gave –30.75 kcal mol^{-1} (−128.7 kJ mol^{-1}).[28] The entropy and enthalpy difference is from the updated JANAF Table.[9] An entropy value of 273.4 J K^{-1} mol^{-1} was calculated based on geometric properties optimized at the MP2/6-31G(d') level and vibrational frequencies at the HF/6-31G(d') level.[28] Calculations using the CBS-QB3 and CBS-APNO model chemistries on three isodesmic reactions led to $\Delta_f H^{\circ}_{298} = -129.5 \pm 0.9$ kJ mol^{-1}.[27]

CH_3O_3 and CH_3O_4

Bond dissociation energies were calculated for $CH_3OOOOCH_3$ at the G3B3 and CBS-APNO levels of theory, using isodesmic and bond dissociation work reactions. The molecular geometry was optimized at the B3LYP/cc-pVTZ+d level of theory.[6]

(1) Becerra, R.; Carpenter, I. W.; Walsh, R. Time-resolved studies of the kinetics of the reactions of CHO with HI and HBr: Thermochemistry of the CHO radical and the H-C bond strengths in CH_2O and CHO. *J. Phys. Chem.* **1997**, *101*, 4185-4190, doi:10.1021/jp970443y.

(2) Berkowitz, J.; Ellison, G. B.; Gutman, D. Three methods to measure RH bond energies. *J. Phys. Chem.* **1994**, *98*, 2744-2765, doi:10.1021/j100062a009.

(3) Cox, J. D.; Wagman, D. D.; Medvedev, V. A. *CODATA Key Values for Thermodynamics*; Hemisphere Publishing Corp.: New York, 1989.

(4) Császár, A. G.; Furtenbacher, T. From a network of computed reaction enthalpies to atom-based thermochemistry (NEAT). *Chem. Eur. J.* **2010**, *16*, 4826-4835, doi:10.1002/chem.200903252.

(5) Czakó, G.; Nagy, B.; Tasi, G.; Somogyi, A.; Šimunek, J.; Noga, J.; Braams, B. J.; Bowman, J. M.; Császár, A. Proton affinity and enthalpy of formation of formaldehyde. *Int. J. Quantum Chem.* **2009**, *109*, 2393-2409, doi:10.1002/qua.22009.

(6) da Silva, G.; Bozzelli, J. W. Thermochemistry, bond energies, and internal rotor potentials of dimethyl tetraoxide. *J. Phys. Chem A* **2007**, *111*, 12026-12036, doi:10.1021/jp075144f.

(7) da Silva, G.; Kim, C. H.; Bozzelli, J. W. Thermodynamic properties (enthalpy, bond energy, entropy, and heat capacity) and internal rotor potentials of vinyl alcohol, methyl vinyl ether, and their corresponding radicals. *J. Phys. Chem. A* **2006**, *110*, 7925-7934, doi:10.1021/jp0602878.

(8) Dóbé, S.; Bérces, T.; Turányi, T.; Márta, F.; Grussdorf, J.; Temps, F.; Wagner, H. G. Direct kinetic studies of the reactions Br + CH_3OH and CH_2OH + HBr: The heat of formation of CH_2OH. *J. Phys. Chem.* **1996**, *100*, 19864-19873, doi:10.1021/jp961398h.

(9) Dorofeeva, O.; Novikov, V. P.; Neumann, D. B. NIST-JANAF thermochemical tables. 1. Ten organic molecules related to atmospheric chemistry. *J. Phys. Chem. Ref. Data* **2001**, *30*, 475-513, doi:10.1063/1.1364518.

(10) Duncan, T. V.; Miller, C. E. The HCO_2 potential energy surface: Stationary point energetics and the HOCO heat of formation. *J. Chem. Phys.* **2000**, *113*, 5138-5140, doi:10.1063/1.1312824.

(11) Fabian, W. M. F.; Janoschek, R. Thermochemical properties of the hydroxy-formyl radical HO-CO, and the formyloxy radical, HC(O)O, and their role in the reaction OH + CO → H + CO_2. Computational G3MP2B3 and CCSD(T)-CBS studies. *J. Mol. Struct. - Theochem* **2005**, *713*, 227-234, doi:10.1016/j.theochem.2004.08.065.

(12) Feller, D.; Dixon, D. A.; Francisco, J. S. Coupled cluster theory determination of the heats of formation of combustion-related compounds: CO, HCO, CO_2, HCO_2, HOCO, HC(O)OH, and HC(O)OOH. *J. Phys. Chem. A* **2003**, *107*, 1604-1617, doi:10.1021/jp030267v.

(13) Gurvich, L. V.; Veyts, I. V.; Alcock, C. B. *Thermodynamic Properties of Individual Substances,*, Fourth ed.; Hemisphere Publishing Corp.: New York, 1991; Vol. 2.

(14) Hocking, W. H. The other rotamer of formic acid, *cis*-HCOOH. *Z. Naturforsch.* **1976**, *31a*, 1113-1121, doi:10.1515/zna-1976-0919

(15) Johnson, R. D.; Hudgens, J. W. Structural and thermochemical properties of hydroxymethyl (CH_2OH) radicals and cations derived from observations of $B^2A'(3p) \leftarrow X^2A''$ electronic spectra and from ab initio calculations. *J. Phys. Chem.* **1996**, *100*, 19874-19890, doi:10.1021/jp961399+.

(16) Knyazev, V. D.; Slagle, I. R. Thermochemistry of the R-O_2 bond in alkyl and chloroalkyl peroxy radicals. *J. Phys. Chem. A* **1998**, *102*, 1770-1778, doi:10.1021/jp9726091.
(17) Kosmas, A. M.; Mpellos, C.; Salta, Z.; Drougas, E. Structural and heat of formation studies of halogenated methyl hydro-peroxides. *Chem. Phys.* **2010**, *371*, 36-42, doi:10.1016/j.chemphys.2010.03.026.
(18) Lay, T. H.; Bozzelli, J. W. Enthalpies of formation and group additivity of alkyl peroxides and trioxides. *J. Phys. Chem. A* **1997**, *101*, 9505-9510, doi:10.1021/jp972103i.
(19) Matus, M. H.; Nguyen, M. T.; Dixon, D. A. Theoretical prediction of the heats of formation of C_2H_5O radicals derived from ethanol and of the kinetics of β-C-C scission in the ethoxy radical. *J. Phys. Chem. A* **2007**, *111*, 113-126, doi:10.1021/jp064086f.
(20) Matus, M. H.; Nguyen, M. T.; Dixon, D. A.; Christe, K. O. Thermochemical properties of CHFO and CF_2O. *J. Phys. Chem. A* **2008**, *112*, 4973-4981, doi:10.1021/jp800103y.
(21) Nagy, B.; Csontos, J.; Kállay, M.; Tasi, G. High-accuracy theoretical study on the thermochemistry of several formaldehyde derivatives. *J. Phys. Chem. A* **2010**, *114*, 13213-13221, doi:10.1021/jp1085203.
(22) Nguyen, M. T.; Nguyen, T. L.; Ngan, V. T.; Nguyen, H. M. T. Heats of formation of the Criegee formaldehyde oxide and dioxirane. *Chem. Phys. Lett.* **2007**, *448*, 183-188, doi:10.1016/j.cplett.2007.10.033.
(23) Ruscic, B. Active thermochemical tables: Sequential bond dissociation enthalpies of methane, ethane, and methanol and the related thermochemistry. *J. Phys. Chem. A* **2015**, *119*, 7810-7837, doi:10.1021/acs.jpca.5b01346.
(24) Ruscic, B.; Boggs, J. E.; Burcat, A.; Csaszar, A. G.; Demaison, J.; Janoschek, R.; Martin, J. M. L.; Morton, M. L.; Rossi, M. J.; Stanton, J. F.; et al. IUPAC critical evaluation of thermochemical properties of selected radicals. Part I. *J. Phys. Chem. Ref. Data* **2005**, *34*, 573-656, doi:10.1063/1.1724828.
(25) Ruscic, B.; Feller, D.; Peterson, K. Active Thermochemical Tables: dissociation energies of several homonuclear first-row diatomics and related thermochemical values. *Theor. Chem. Acc.* **2014**, *133*, 1415, doi:10.1007/s00214-013-1415-z.
(26) Ruscic, B.; Litorja, M. Photoionization of HOCO revisited: a new upper limit to the adiabatic ionization energy and lower limit to the enthalpy of formation. *Chem. Phys. Lett.* **2000**, *316*, 45-50, doi:10.1016/S0009-2614(99)01267-1.
(27) Simmie, J. M.; Black, G.; Curran, H. J.; Hinde, J. P. Enthalpies of formation and bond dissociation energies of lower alkyl hydroperoxides and related hydroperoxy and alkoxy radicals. *J. Phys. Chem. A* **2008**, *112*, 5010-5016, doi:10.1021/jp711360z.
(28) Sumathi, R.; Green, W. H. Oxygenate, oxyalkyl and alkoxcarbonyl thermochemistry and rates for hydrogen abstraction from oxygenates. *Phys. Chem. Chem. Phys.* **2003**, *5*, 3402-3417, doi:10.1039/b307050f.
(29) Villano, S. M.; Eyet, N.; Wren, S. W.; Ellison, G. B.; Bierbaum, V. M.; Lineberger, W. C. Photoelectron spectroscopy and thermochemistry of the peroxyformate anion. *J. Phys. Chem. A* **2010**, *114*, 191-200, doi:10.1021/jp907569w.
(30) Wagman, D. D.; Evans, W. H.; Parker, V. B.; Schumm, R. H.; Halow, I.; Bailey, S. M.; Churney, K. L.; Nutall, R. L. The NBS tables of chemical thermodynamic properties. Selected values for inorganic and C_1 and C_2 organic substances in SI unites. *J. Phys. Chem. Ref. Data* **1982**, *11*, Suppl. No. 1, Erratum doi:10.1063/1.555845.
(31) Yu, D.; Rauk, A.; Armstrong, D. A. Radicals and ions of formic and acetic acids: An ab initio study of the structures and gas and solution phase thermochemistry. *J. Chem. Soc. Perkin Trans 2* **1994**, 2207-2215, doi:10.1039/p29940002207.

Note 8: *Compounds containing one C and H and N*

Back to Table

CN Enthalpy from an active thermochemical tables optimization.[12]The previous recommendation, $\Delta_f H_{298}^o$ = 440 ± 5 kJ mol^{-1}, and the entropy value, were from the review of Gurvich, et al.[6]

HCN Enthalpy from an active thermochemical tables optimization, augmented by HEAT-456QP calculations using the aug-cc-pCVXZ basis sets, X+Q,6, and 6.[10]The previous recommendation, $\Delta_f H_{298}^o$ = 132 ± 4 kJ mol^{-1}, and the entropy value, were from the review of Gurvich, et al.[6] A

computational study involving the use of several composite models, CBS-QB3, CBS-APNO, G3, and G4, led to values of $\Delta_f H_0^\circ$ = 131.8 ± 2.4 kJ mol^{-1} and $\Delta_f H^\circ_{298}$= 131.7 ± 2.4 kJ mol^{-1}.[14]

HNC Enthalpy from an active thermochemical tables optimization, augmented by HEAT-456QP calculations using the aug-cc-pCVXZ basis sets, X+Q,6, and 6.[10] A computational study involving the use of several composite models, CBS-QB3, CBS-APNO, G3, and G4, led to values of $\Delta_f H_0^\circ$ = 192.1 ± 1.5 kJ mol^{-1} and $\Delta_f H^\circ_{298}$= 192.7 ± 1.5 kJ mol^{-1}.[14]

NCN Enthalpy from an active thermochemical tables optimization.[5] Entropy value also listed in a summary table.

C_2N_2 From the review of Gurvich et al.[6]

CH_2NH, Methylenimine
Enthalpy values obtained from computational study of atomization involving the use of several composite models, CBS-QB3, CBS-APNO, G3, and G4.[14]

CH_3NH Obtained from a computational analysis involving B3LYP/6-31G(2df,p) for geometric factors and G4 for atomization energies.[13]

CH_2NH_2 Based on recommendation of McMillen et al.,[9] adjusted for enthalpy for CH_3NH_2 used here (–5.6 kcal mol^{-1} vs. –5.5 kcal mol^{-1}). Calculations at the G2(MP2) level lead to an enthalpy of 147 kJ mol^{-1}.[16] A computational analysis involving B3LYP/6-31G(2df,p) for geometric factors and G4 for atomization energies resulting in $\Delta_f H^\circ_{298}$ = 150.2 kJ mol^{-1} and S_{298} = 236.2 J K^{-1}mol^{-1}.[13]

CH_3NH_2 Enthalpy from review of Pedley;[11] entropy value from the Thermodynamics Research Center Data Series.[4] Values of $\Delta_f H^\circ_{298}$ = −21.8 ± 1.5 kJ mol^{-1} and $\Delta_f H_0^\circ$ = –7.0 ± 1.5 kJ mol^{-1} have been derived from a threshold PEPICO study of alkyl amines and the use of two isodesmic reaction networks, connected through the TPEPICO dissociation energies, and with reaction heats calculated at the CBS-APNO and W1U levels of theory.[2] A computational analysis involving B3LYP/6-31G(2df,p) for geometric factors and G4 for atomization energies resulted in $\Delta_f H^\circ_{298}$ = –19.7 kJ mol^{-1} and S_{298} = 242.0 J K^{-1}mol^{-1}.[13] A computational study involving the use of several composite models, CBS-QB3, CBS-APNO, G3, and G4, led to values of $\Delta_f H_0^\circ$ = −5.4 ± 2.0 kJ mol^{-1} and $\Delta_f H^\circ_{298}$= −20.2 ± 2.0 kJ mol^{-1}.[14]

CH_2CN Based on an analysis of the negative ion cycle.[8]

CH_3CN Enthalpy at 298 K by combustion calorimetry;[1] 0 K value based on measured vibrational frequencies.[8] Entropy from NBS Tables.[15]

CH_2N_2 Enthalpy value calculated from the atomization energy at the G3 level of theory. Calculations also carried out at the G2, G2M(CC5), B3LYP, MW1B95, and MPWB1K levels.[7]

CH_2N_2 Enthalpy from a CCSD(T) calculation of the atomization energy.[3]

(1) An, X. W.; Mansson, M. Enthalpies of combustion and formation of acetonitrile. *J. Chem. Thermo.* **1983**, *15*, 287-293, doi:10.1016/0021-9614(83)90121-0.

(2) Bodi, A.; Kercher, J. P.; Bond, C.; Meteesatien, P.; Sztaray, B.; Baer, T. Photoion photoelectron coincidence spectroscopy of primary amines RCH_2NH_2 (R=H, CH_3, C_2H_5, C_3H_7, *i*-C_3H_7): Alkylamine and alkyl radical heats of formation by isodesmic reaction networks *J. Phys. Chem. A* **2006**, *110*, 13425-13433, doi:10.1021/jp064739s.

(3) Dixon, D. A.; de Jong, W. A.; Peterson, K. A.; McMahon, T. B. Methyl cation affinities of rare gases and nitrogen and the heat of formation of diazomethane. *J. Phys. Chem. A* **2005**, *109*, 4073-4080, doi:10.1021/jp044561e.

(4) Frenkel, M.; Kabo, G. J.; Marsh, K. N.; Roganov, G. N.; Wilhoit, R. C. *Thermodynamics of Organic Compounds in the Gas State*; Thermodynamics Research Center: College Station, TX, 1994; Vol. I.

(5) Glarborg, P.; Miller, J. A.; Ruscic, B.; Klippenstein, S. J. Modeling nitrogen chemistry in combustion. *Progress in Energy and Combustion Science* **2018**, *67*, 31-68, doi:10.1016/j.pecs.2018.01.002.

(6) Gurvich, L. V.; Veyts, I. V.; Alcock, C. B. *Thermodynamic Properties of Individual Substances,*, Fourth ed.; Hemisphere Publishing Corp.: New York, 1991; Vol. 2.
(7) Kiselev, V. G.; Gritsan, N. P. Theoretical study of the nitroalkane thermolysis. 1. Computation of the formation enthalpy of the nitroalkanes, their isomers and radical products. *J. Phys. Chem. A* **2008**, *112*, 4458-4464, doi:10.1021/jp077391p.
(8) Lafleur, R. D.; Szatary, B.; Baer, T. A photoelectron-photoion coincidence study of the ICH_2CN ion dissociation: Thermochemistry of CH_2CN, $^+CH_2CN$, and ICH_2CN. *J. Phys. Chem. A* **2000**, *104*, 1450-1455, doi:10.1021/jp993569z.
(9) McMillen, D. F.; Golden, D. M. Hydrocarbon bond dissociation energies. *Ann. Rev. Phys. Chem.* **1982**, *33*, 493-532.
(10) Nguyen, T. L.; Baraban, J. H.; Ruscic, B.; Stanton, J. F. On the HCN – HNC energy difference. *J. Phys. Chem. A* **2015**, *119*, 10929-10934, doi:10.1021/acs.jpca.5b08406.
(11) Pedley, J. B. *Thermochemical Data and Structures of Organic Compounds*; Thermodynamics Data Center: College Station, TX, 1994.
(12) Ruscic, B.; Feller, D.; Peterson, K. Active Thermochemical Tables: dissociation energies of several homonuclear first-row diatomics and related thermochemical values. *Theor. Chem. Acc.* **2014**, *133*, 1415, doi:10.1007/s00214-013-1415-z.
(13) Shi, J. C.; Shang, Y. L.; Du, S. Y.; Luo, S. N. Hydrogen abstraction from CH_3NH_2, $(CH_3)_2NH$, and $(CH_3)_3N$ by $H\dot{O}_2$ radicals: A theoretical study. *Chem. Phys. Lett.* **2018**, *691*, 307-313, doi:10.1016/j.cplett.2017.11.034.
(14) Simmie, J. M. A database of formation enthalpies of nitrogen species by compound methods (CBS-QB3, CBS-APNO, G3, G4). *J. Phys. Chem. A* **2015**, *119*, 10511-10526, doi:10.1021/acs.jpca.5b06054.
(15) Wagman, D. D.; Evans, W. H.; Parker, V. B.; Schumm, R. H.; Halow, I.; Bailey, S. M.; Churney, K. L.; Nutall, R. L. The NBS tables of chemical thermodynamic properties. Selected values for inorganic and C_1 and C_2 organic substances in SI unites. *J. Phys. Chem. Ref. Data* **1982**, *11*, Suppl. No. 1, Erratum doi:10.1063/1.555845.
(16) Wayner, D. D. M.; Clark, K. B.; Rauk, A.; Yu, D.; Armstrong, D. A. C-H bond dissociation energies of alkyl amines: Radical structures and stabilization energies. *J. Am. Chem. Soc.* **1997**, *119*, 8925-8932, doi:10.1021/ja971365v.

Note 9: *Compounds containing one C and H, N, and O*

Back to Table

CH_2NO From computed G2 heats of reaction.[11]

NH_2CO This is the more stable isomer of CH_2NO (above), which is formed by the association of CH_2 with NO. The enthalpy and entropy values are taken from a CCSDT(Q) calculation, with structure optimized using the cc-pVQZ basis set.[8] The previous $\Delta_f H_{298}^\circ = -15.1 \pm 4$ was from computed G2 heats of reaction.[11]

NCO Enthalpy from D(H-NCO) = 4.9±0.01 eV,[9] using present value for HNCO. Entropy from Gurvich et al.[6]

HCNO, Fulmic acid

Enthalpy values obtained from a computational study of atomization involving the use of several composite models, CBS-QB3, CBS-APNO, G3, and G4.[12]

HONC, Isofulmic acid

Enthalpy values obtained from a computational study of atomization involving the use of several composite models, CBS-QB3, CBS-APNO, G3, and G4.[12]

HOCN, Cyanic acid

Enthalpy values obtained from a computational study of atomization involving the use of several composite models, CBS-QB3, CBS-APNO, G3, and G4.[12]

HNCO, isocyanic acid

The dissociative photoionization of urea was investigated by iPEPICO.[2] The lowest energy channel, $CO(NH_2)_2 + h\nu \rightarrow NH_3^+ + HNCO + e^-$, was measured accurately and the appearance

energy of the second channel, $CO(NH_2)_2 + h\nu \rightarrow NH_2 + H_2NCO^+ + e^-$, was measured with somewhat lower precision. These were used together with W1 and CBS-APNO calculations on three isodesmic reactions for $CO(NH_2)_2$ and two isoelectonic reactions for HNCO to determine the enthalpy values for both HNCO and $CO(NH_2)_2$. The previous value, $\Delta_f H_{298}^o = -104 \pm 12$ kJ mol^{-1} from threshold photodissociation of HNCO by measuring NH($a^1\Delta$) threshold and fragment energy, adjusted for the present enthalpy of NH.[13] Entropy from NBS Tables.[15] A computational study involving the use of several composite models, CBS-QB3, CBS-APNO, G3, and G4, led to values of $\Delta_f H_0^o = -117.6 \pm 0.8$ kJ mol^{-1} and $\Delta_f H_{298}^o = -119.7 \pm 0.8$ kJ mol^{-1}.[12]

$HCONH_2$, Formamide

From review of Pedley et al.[10]

CH_2NO_2 Recommendation from the Thermodynamics Research Center Data Series.[5] A calculation of the atomization energy at the G3 level of theory leads to $\Delta_f H_{298}^o = 31.5$ kcal mol^{-1}. Calculations also carried out at the G2, G2M(CC5), B3LYP, MW1B95, and MPWB1K levels.[7]

CH_3NO_2 Enthalpy from Pedley,[10] entropy from Frenkel et al.[5] Enthalpy value calculated using G3, CBS-QB3, and CBS-APNO methods applied to atomization, isomerization, and work reactions is $\Delta_f H_{298}^o = -17.67 \pm 0.27$ kcal mol^{-1}, which becomes -17.73 ± 0.27 kcal mol^{-1} using the reference enthalpy for *cis*-HONO from this Table.[1] A calculation of the atomization energy at the G3 level of theory leads to $\Delta_f H_{298}^o = -17.5$ kcal mol^{-1}. Calculations also carried out at the G2, G2M(CC5), B3LYP, MW1B95, and MPWB1K levels.[7] A value of $\Delta_f H_{298}^o = -73.2$ kJ mol^{-1} was calculated at the G4 level of theory, making use of isodesmic reactions.[4]

CH_3ONO Taken from review of Stull et al.[14] Enthalpy value calculated using G3, CBS-QB3, and CBS-APNO methods applied to atomization, isomerization, and work reactions is $\Delta_f H_{298}^o = -15.64 \pm 0.10$ kcal mol^{-1}, which becomes -15.81 ± 0.10 kcal mol^{-1} using the reference enthalpy for *cis*-HONO from this Table.[1] A calculation of the atomization energy at the G3 level of theory leads to $\Delta_f H_{298}^o = -15.4$ kcal mol^{-1}. Calculations also carried out at the G2, G2M(CC5), B3LYP, MW1B95, and MPWB1K levels.[7]

CH_3ONO_2 Enthalpy from Pedley,[10] entropy from Stull et al.[14]

$CH_3O_2NO_2$ Equilibrium structures optimized at the MP2 level with the 6-311G(d,p) basis set and enthalpy values calculated by both atomization energies and through use of isodesmic reactions at the G3, G3B3, and G4 methods.[3]

$C(NO_2)_4$ Enthalpy value calculated from the atomization energy at the G3 level of theory. Calculations also carried out at the G2, G2M(CC5), B3LYP, MW1B95, and MPWB1K levels.[7] (see addition and corrections)

$(NH_2)_2CO$, Urea

The dissociative photoionization of urea was investigated by iPEPICO.[2] The lowest energy channel, $CO(NH_2)_2 + h\nu \rightarrow NH_3^+ + HNCO + e^-$, was measured accurately and the appearance energy of the second channel, $CO(NH_2)_2 + h\nu \rightarrow NH_2 + H_2NCO^+ + e^-$, was measured with somewhat lower precision. These were used together with W1 and CBS-APNO calculations on three isodesmic reactions for $CO(NH_2)_2$ and two isoelectonic reactions for HNCO to determine the enthalpy values for both HNCO and $CO(NH_2)_2$. The previous value, $\Delta_f H_{298}^o = -245.8 \pm 2.0$ kJ mol^{-1} from Pedley et al.,[10] depended on a value of the sublimation energy that appears to be too low.[2]

(1) Asatryan, R.; Bozzelli, J. W.; Simmie, J. M. Thermochemistry of methyl and ethyl nitro, RNO_2, and nitrite, RONO, organic compounds. *J. Phys. Chem. A* **2008**, *112*, 3172-3185, doi:10.1021/jp710960u.

(2) Bodi, A.; Hemberger, P.; Gerber, T. A robust link between the thermochemistry of urea and isocyanic acid by dissociative photoionization. *J. Chem. Thermo.* **2013**, *58*, 292-299, doi:10.1016/j.jct.2012.11.013.

(3) Buendía-Atencio, C.; Leyva, V.; González, L. Thermochemistry and UV spectroscopy of alkyl peroxynitrates. *J. Phys. Chem. A* **2010**, *114*, 9537-9544, doi:10.1021/jp103854y.

(4) Dorofeeva, O. V.; Suntsova, M. A. Enthalpies of formation of nitromethane and nitrobenzene: Theory *vs* experiment. *J. Chem. Thermo.* **2013**, *58*, 221-225, doi:10.1016/j.jct.2012.11.008.
(5) Frenkel, M.; Kabo, G. J.; Marsh, K. N.; Roganov, G. N.; Wilhoit, R. C. *Thermodynamics of Organic Compounds in the Gas State*; Thermodynamics Research Center: College Station, TX, 1994; Vol. I.
(6) Gurvich, L. V.; Veyts, I. V.; Alcock, C. B. *Thermodynamic Properties of Individual Substances,*, Fourth ed.; Hemisphere Publishing Corp.: New York, 1991; Vol. 2.
(7) Kiselev, V. G.; Gritsan, N. P. Theoretical study of the nitroalkane thermolysis. 1. Computation of the formation enthalpy of the nitroalkanes, their isomers and radical products. *J. Phys. Chem. A* **2008**, *112*, 4458-4464, doi:10.1021/jp077391p.
(8) Nagy, B.; Csontos, J.; Kállay, M.; Tasi, G. High-accuracy theoretical study on the thermochemistry of several formaldehyde derivatives. *J. Phys. Chem. A* **2010**, *114*, 13213-13221, doi:10.1021/jp1085203.
(9) Okabe, H. Photodissociation of HNCO in the vacuum ultraviolet; Production of NCO $A^2\Sigma$ and NH($A^3\pi$, πC^1). *J. Chem. Phys.* **1970**, *53*, 3507-3515, doi:10.1063/1.1674525.
(10) Pedley, J. B. *Thermochemical Data and Structures of Organic Compounds*; Thermodynamics Data Center: College Station, TX, 1994.
(11) Shapley, W. A.; Bacskay, G. B. Ab initio quantum chemical studies of the formaldiminoxt (CH_2NO) radical: 1. Isomerization reactions. *J. Phys. Chem. A* **1999**, *103*, 4505-4513, doi:10.1021/jp984817e.
(12) Simmie, J. M. A database of formation enthalpies of nitrogen species by compound methods (CBS-QB3, CBS-APNO, G3, G4). *J. Phys. Chem. A* **2015**, *119*, 10511-10526, doi:10.1021/acs.jpca.5b06054.
(13) Spiglanin, T. A.; Pery, R. A.; Chandler, D. W. Photodissociation studies of HNCO: Heat of formation and product branching ratios. *J. Phys. Chem.* **1986**, *90*, 6184-6189, doi:10.1021/j100281a025.
(14) Stull, D. R.; Westrum, E. F.; Sinke, G. C. *The Chemical Thermodynamics of Organic Compounds*; John Wiley & Sons: New York, 1969.
(15) Wagman, D. D.; Evans, W. H.; Parker, V. B.; Schumm, R. H.; Halow, I.; Bailey, S. M.; Churney, K. L.; Nutall, R. L. The NBS tables of chemical thermodynamic properties. Selected values for inorganic and C_1 and C_2 organic substances in SI unites. *J. Phys. Chem. Ref. Data* **1982**, *11*, Suppl. No. 1, Erratum doi:10.1063/1.555845.

Note 10: *A series of nitroalkanes, their isomers, and radical products* Back to Table

For all these species, the enthalpy value was calculated from the atomization energy at the G3 level of theory. Calculations also carried out at the G2, G2M(CC5), B3LYP, MW1B95, and MPWB1K levels.[1]

(1) Kiselev, V. G.; Gritsan, N. P. Theoretical study of the nitroalkane thermolysis. 1. Computation of the formation enthalpy of the nitroalkanes, their isomers and radical products. *J. Phys. Chem. A* **2008**, *112*, 4458-4464, doi:10.1021/jp077391p.

Note 11: *Compounds containing two C and 0 - 4 H* Back to Table

C_2, ethynylene

Enthalpy from an active thermochemical tables optimization.[14] The slightly-different previous enthalpy value of $\Delta H_f(298\ K) = 828.73 \pm 0.29$ kJ mol^{-1} was from an earlier optimization in the Active Thermochemical Tables (ATcT).[15] The entropy value is from JANAF.[4] The cited enthalpy is close to the value for singlet ethynylene, $^1C_2$, $\Delta H_f(298\ K) = 826.78 \pm 0.27$ kJ mol^{-1}. The triplet ethynylene, $^3C_2$, is higher at $\Delta H_f(298\ K) = 864.08 \pm 0.27$ kJ mol^{-1}.[14]

C_2H Enthalpy from an active thermochemical tables optimization.[14] The previous enthalpy of $\Delta H_f(298\ K) = 565.3 \pm 3.9$ kJ mol^{-1} was from the review of Berkowitz, Ellison, and Gutman.[1] $\Delta_f H_0^o = 134.1 \pm 0.7$ kcal mol^{-1}. Entropy from Gurvich et al.[7] High level *ab initio* calculations result in an enthalpy value of 567.4 ± 1.5 kJ mol^{-1}.[17]

C_2H_2 Enthalpy from an active thermochemical tables optimization.[14] The previous enthalpy of $\Delta H_f(298\ K) = 227.4 \pm 0.8$ kJ mol^{-1} was from the review of Gurvich et al.[7] Pedley gives the enthalpy as 228.2 ± 0.7 kJ mol^{-1}.[12] The JANAF Tables give $\Delta_f H_0^o = 227.3$ kJ mol^{-1}, $\Delta_f H_{298}^o = 226.7$ kJ mol^{-1}, and $S^o = 200.958$ J K^{-1} mol^{-1}.[4] The critical evaluation by the Thermodynamic Research Center at NIST recommends $\Delta_f H^o_{298} = 226.4$ kJ mol^{-1}.[20] A network optimization of *ab initio* reaction enthalpies results in a value of $\Delta_f H_0^o = 228.67 \pm 0.35$ kJ mol^{-1}.[5] The reference atomic values were taken from the Active Thermochemical Tables, ver. 1.20.

H_2CC, vinylidene

Enthalpy from an active thermochemical tables optimization.[14] The previous enthalpy of $\Delta H_f(298\ K) = 428 \pm 17$ kJ mol^{-1} was based on a series of negative ion photoelectron spectroscopic measurements combined with proton-transfer kinetics.[6] CCSD(T) calculations, extrapolated to the CBS level, lead to $\Delta_f H_0^o = 98.6$ kcal mol^{-1} and $\Delta_f H^o_{298} = 98.8$ kcal mol^{-1}.[11]

CH_3C, ethylidyne

Enthalpy from an active thermochemical tables optimization.[14] The cited enthalpy is identical to that for doublet ethylidyne, $^2CH_3C$. Quartet ethylidyne, $^4CH_3C$, is higher at $\Delta H_f(298\ K) = 636.07 \pm 1.20$ kJ mol^{-1},[14] and is completely unimportant under atmospheric conditions.

C_2H_3, CH_2CH, vinyl

Enthalpy from an active thermochemical tables optimization.[14] The previous enthalpy of $\Delta H_f(298\ K) = 295.4 \pm 1.7$ kJ mol^{-1} was derived from a third-law analysis of the reaction $Cl + C_2H_4 \leftrightarrow HCl + C_2H_3$.[8] A second-law analysis gives 69.1±1.6 kcal mol^{-1}. The recommendation of Tsang is 71.5±1 kcal mol^{-1}.[19] See also discussion by Lago and Baer.[9] Negative ion photoelectron spectroscopy combined with proton-transfer kinetics leads to a value of $\Delta_f H^o_{298} = 71.6 \pm 0.8$ kcal mol^{-1}.[6] A calculation at the HEAT345-Q level of theory gives recommended values of $\Delta_f H_0^o = 301.5 \pm 1.3$ kJ mol^{-1} and $\Delta_f H_{298}^o = 297.3 \pm 1.3$ kJ mol^{-1}.[18] This enthalpy difference provides the 0 K value in the Table. The entropy value was taken from the evaluation of Tsang.[19]

CH_3CH, ethylidene

Enthalpy from an active thermochemical tables optimization.[14] The cited enthalpy is very close to the value for triplet ethylidene, $^3CH_3CH$, $\Delta H_f(298\ K) = 354.45 \pm 0.82$ kJ mol^{-1}. The singlet ethylidene, $^1CH_3CH$, is higher at $\Delta_f H^o_{298} = 366.70 \pm 0.86$ kJ mol^{-1}.[14]

C_2H_4 Enthalpy from an active thermochemical tables optimization,[14] which is slightly different, but with a smaller error limit, than the earlier recommendation, $\Delta_f H^o_{298} = 52.4 \pm 0.5$ kJ mol^{-1} from the review of Gurvich et al.[7] The JANAF Tables give $\Delta_f H_0^o = 60.0$ kJ mol^{-1}, $\Delta_f H_{298}^o = 52.5$ kJ mol^{-1}, and $S^o = 219.330$ J K^{-1} mol^{-1}.[4] The critical evaluation by the Thermodynamic Research Center at NIST recommends $\Delta_f H^o_{298} = 52.5 \pm 0.5$ kJ mol^{-1}, where the uncertainty represents the 95% confidence level.[20]

C_2H_5 Enthalpy from an active thermochemical tables optimization.[14] The previous enthalpy of $\Delta_f H^o_{298} = 120.9 \pm 1.7$ kJ mol^{-1} and $\Delta H_f(0\ K) = 131.8 \pm 1.7$ kJ mol^{-1} are from the review of Berkowitz, Ellison, and Gutman.[1] A recent evaluation recommended $\Delta_f H^o_{298} = 119.9 \pm 3.1$ kJ mol^{-1}, where the error limit is a standard deviation of the results considered.[3] Entropy from Gurvich et al.[7] Enthalpy of 120.7 ± 1.0 kJ mol^{-1} has been derived from a threshold PEPICO study of alkyl amines and the use of two isodesmic reaction networks, connected through the TPEPICO dissociation energies, and with reaction heats calculated at the CBS-APNO and W1U levels of theory. $\Delta_f H_0^o = 132.3 \pm 1.0$ kJ mol^{-1}.[2] A re-analysis of the thermal decomposition of C_2H_5I, making use of calculated molecular parameters, led to a value of $\Delta_f H_{298}^o = 124 \pm 3$ kJ mol^{-1}.[16] The reaction enthalpy for $C_2H_5 + HI \rightarrow C_2H_6 + I$ was calculated using CCSD optimizations and CCSD(T) single-point energies, with small energetic corrections.[10] A value of $\Delta_r H^o_{298} = -125.45$ kJ mol^{-1} vs. the value of −124.45 kJ mol^{-1} calculated using the formation enthalpies in this Table.

C_2H_6 Enthalpy from an active thermochemical tables optimization,[14] which is slightly different and with a smaller error limit, than the earlier recommendation, $\Delta_f H^o_{298} = -83.85 \pm 0.29$ kJ mol^{-1}

from a flame calorimetry measurement.[13] A recent evaluation recommended $\Delta_f H^\circ_{298}$ = −80.41 ± 1.26 kJ mol^{-1}, where the error limit is a standard deviation of the results considered.[3] The critical evaluation by the Thermodynamic Research Center at NIST recommends $\Delta_f H^\circ_{298}$ = −84.0 ± 0.9 kJ mol^{-1}, where the uncertainty represents the 95% confidence level.[20] Entropy from Gurvich et al.,[7] who gives $\Delta_f H_{298}^\circ$ = -84.00 ± 0.40 kJ mol^{-1} and $\Delta_f H_0^\circ$ = -68.38 ± 0.40 kJ mol^{-1}.

(1) Berkowitz, J.; Ellison, G. B.; Gutman, D. Three methods to measure RH bond energies. *J. Phys. Chem.* **1994**, *98*, 2744-2765, doi:10.1021/j100062a009.

(2) Bodi, A.; Kercher, J. P.; Bond, C.; Meteesatien, P.; Sztaray, B.; Baer, T. Photoion photoelectron coincidence spectroscopy of primary amines RCH_2NH_2 (R=H, CH_3, C_2H_5, C_3H_7, *i*-C_3H_7): Alkylamine and alkyl radical heats of formation by isodesmic reaction networks *J. Phys. Chem. A* **2006**, *110*, 13425-13433, doi:10.1021/jp064739s.

(3) Burke, S. M.; Simmie, J. M.; Curran, H. J. Critical evaluation of thermochemical properties of C1–C4 species: Updated group-contributions to estimate thermochemical properties. *J. Phys. Chem. Ref. Data* **2015**, *44*, 013101, doi:10.1063/1.4902535.

(4) Chase, M. W. NIST-JANAF thermochemical tables. *J. Phys. Chem. Ref. Data* **1998**, *Monograph 9*.

(5) Császár, A. G.; Furtenbacher, T. From a network of computed reaction enthalpies to atom-based thermochemistry (NEAT). *Chem. Eur. J.* **2010**, *16*, 4826-4835, doi:10.1002/chem.200903252.

(6) Ervin, K. M.; Gronert, S.; Barlow, E. E.; Gilles, M. K.; Harrison, A. G.; Bierbaum, V. M.; DePuy, C. H.; Lineberger, W. C.; Ellison, G. B. Bond strengths of ethylene and avetylene. *J. Am. Chem. Soc.* **1990**, *112*, 5750-5759, doi:10.1021/JA00171A013.

(7) Gurvich, L. V.; Veyts, I. V.; Alcock, C. B. *Thermodynamic Properties of Individual Substances,*, Fourth ed.; Hemisphere Publishing Corp.: New York, 1991; Vol. 2.

(8) Kaiser, E. W.; Wallington, T. J. Kinetics of the reactions of chlorine atoms with C_2H_4 (k_1) and C_2H_2 (k_2): A determination of $\Delta H_{f,298}^\circ$ for C_2H_3. *J. Phys. Chem.* **1996**, *100*, 4111-4119, doi:10.1021/jp953178u.

(9) Lago, A. F.; Baer, T. A photoelectron photoion coincidence study of the vinyl bromide and tribromoethane ion dissociation dynamics: Heats of formation of $C_2H_3^+$, C_2H_3Br, $C_2H_3Br^+$, $C_2H_3Br_2^+$, and $C_2H_3Br_3$ *J. Phys. Chem. A* **2006**, *110*, 3036-3041, doi:10.1021/jp053943x.

(10) Leplat, N.; Federič, J.; Šulková, K.; Sudolská, M.; Louis, F.; Černušák, I.; Rossi, M. J. The Kinetics of the reaction C_2H_5• + HI → C_2H_6 + I• over an extended temperature range (213–623 K): Experiment and modeling. *Z. Phys. Chem.* **2015**, *229*, 1475, doi:10.1515/zpch-2015-0607.

(11) Nguyen, M. T.; Matus, M. H.; Lester, W. A., Jr.; Dixon, D. A. Heats of formation of triplet ethylene, ethylidene, and acetylene. *J. Phys. Chem. A* **2008**, *112*, 2082-2087, doi:10.1021/jp074769a.

(12) Pedley, J. B. *Thermochemical Data and Structures of Organic Compounds*; Thermodynamics Data Center: College Station, TX, 1994.

(13) Pittam, D. A.; Pilcher, G. Measurements of heats of combustion by flame calorimetry. Part 8. Methane, ethane, propane, n-butane and 2-methylpropane. *J. Chem. Soc. Faraday Trans. 1* **1972**, *68*, 2224-2229, doi:10.1039/F19726802224.

(14) Ruscic, B. Active thermochemical tables: Sequential bond dissociation enthalpies of methane, ethane, and methanol and the related thermochemistry. *J. Phys. Chem. A* **2015**, *119*, 7810-7837, doi:10.1021/acs.jpca.5b01346.

(15) Ruscic, B.; Feller, D.; Peterson, K. Active Thermochemical Tables: dissociation energies of several homonuclear first-row diatomics and related thermochemical values. *Theor. Chem. Acc.* **2014**, *133*, 1415, doi:10.1007/s00214-013-1415-z.

(16) Skorobogatov, G. A.; Dymov, B. P.; Pogosyan, Y. I.; Khripun, V. K.; Tschuikow-Roux, E. Molecular, thermodynamic, and kinetic parameters of the free radical C_2H_5· in the gas phase. *Russ. J. General Chem.* **2003**, *73*, 75-84.

(17) Szalay, P. G.; Tajti, A.; Stanton, J. F. Ab initio determination of the heat of formation of ketenyl (HCCO) and ethynyl (CCH) radicals. *Mol. Phys.* **2005**, *103*, 2159-2168, doi:10.1080/00268970500131124.

(18) Tabor, D. P.; Harding, M. E.; Ichino, T.; Stanton, J. F. High-accuracy extrapolated ab initio thermochemistry of the vinyl, allyl, and vinoxy radicals. *J. Phys. Chem. A* **2012**, *116*, 7668-7676, doi:10.1021/jp302527n.
(19) Tsang, W. Heats of formation of organic free radicals by kinetic methods. In *Energetics of Free Radicals*; Simoes, J. A. M., Greenberg, A., Liebman, J. F., Eds.; Blackie Academic & Professional: London, 1996; pp 22-58.
(20) Verevkin, S. P.; Emel'yanenko, V. N.; Diky, V.; Muzny, C. D.; Chirico, R. D.; Frenkel, M. New group-contribution approach to thermochemical properties of organic compounds: Hydrocarbons and oxygen-containing compounds. *J. Phys. Chem. Ref. Data* **2013**, *42*, 033102, doi:10.1063/1.4815957.

Note 12: *Compounds containing two C, one O, and 1-6 H* Back to Table

CHCO Based on the recommended dissociation energy for CH_2CO of 105.3 ± 2.1 kcal mol^{-1}.[1] High level *ab initio* calculations result in an enthalpy of 173.8 ± 1.5 kJ mol^{-1}.[20]

CH_2CO From photoionization or CH_2CO and a subsequent optimization of a local thermochemical network.[17] Calculations on several isodesmic reactions using CBS-QB3, CBS-APNO, and G3 methods led to a value of $\Delta_f H_{298}^\circ = -48.2 \pm 2.6$ kJ mol^{-1}.[18]

CH_3CO Recommendation taken from IUPAC Task Group.[16] Enthalpy is a weighted average of the experimental results, with amplified uncertainties assigned to the most negative values. This recommendation is only slightly lower that the value –10.0 ± 1.2 kJ mol^{-1} previously recommended here.[1]

C_2H_2OH Calculated from the heat of reactions for OH + C_2H_2 of −146 ± 10 kJ mol^{-1}.[7]

$CH_2C(O)H$, vinoxy radical

Enthalpy values calculated at the HEAT345-Q level of theory.[21] Previous enthalpy value an average of the a value obtained from the gas-phase basicity and proton affinity determined by a kinetic method (9.9 ± 3.9 kJ mol^{-1}) and a reexamination of the results of Holmes, et al.[11] on the dissociation of ethyl acetate after electron ionization (15.9 ± 5.6 kJ mol^{-1}).[3] This value is supported by several computational studies.[5,9,10,12] Previous recommendation, 10.5 ± 9.2 kJ mol^{-1}, was from an analysis of gas-phase acidity and electron affinity studies.[1] A G3MP2B3 calculation led to $\Delta_f H_{298}^\circ$ = 13.45 kJ mol^{-1} and the selected entropy value.[12]

$CH_3C(O)H$

Enthalpy from Pedley,[15] entropy from Frenkel et al.[6] A critical evaluation by the Thermodynamics Research Center at NIST resulted in $\Delta_f H^\circ_{298} = -165.3$ kJ mol^{-1}.[22]

Vinyl alcohol and corresponding radicals (CH_2CHOH, CH_2COH, $CHCHOH$)

Molecular geometry optimized at the B3LYP/6-31G(d,p) level of theory. The enthalpy was determined using CBS-Q, CBS-APNO, and G3 methods with isodesmic reactions to minimize systematic errors. Entropies calculated by using the SMCPS program. The enthalpy values for both conformers of vinyl alcohol are within about 5 kJ mol^{-1} the average of the experimental values, which are based on ionization techniques.[4]

CH_3CH_2O Recommendation taken from IUPAC Task Group.[16] Enthalpy is based on a collision-induced dissociation measurement, which lies between the theoretical results and most of the previous recommendations, including that previously included here, $\Delta_f H_{298}^\circ$ = –15.5 ± 3.3 kJ mol^{-1}.[1] Ruscic et al. note that their new preferred value corresponds to an O–H bond dissociation energy for ethanol more in line with that in methanol. Atomization energies calculated using CCSD(T) with cc-pVnZ (n = D, T, and Q) basis sets, using (U)MP2/aug-cc-pVTZ optimized geometries and extrapolated to the complete basis set limit, led to enthalpies of $\Delta_f H_0^\circ$ = 0.8 kcal mol^{-1} and $\Delta_f H^\circ_{298}$ = –2.7 kcal mol^{-1}.[13]

CH_2CH_2OH

Calculated from the heat of reaction for the addition of OH to C_2H_4 of −123±6 kJ mol^{-1}.[7] Atomization energies calculated using CCSD(T) with cc-pVnZ (n = D, T, and Q) basis sets,

using (U)MP2/aug-cc-pVTZ optimized geometries and extrapolated to the complete basis set limit, led to enthalpies of $\Delta_f H_0^\circ$ = –3.1 kcal mol^{-1} and $\Delta_f H^\circ_{298}$ = –6.2 kcal mol^{-1}.[13] The enthalpy of formation was also calculated from a set of isodesmic and isogyric reactions at the CBS-QB3 level of theory to be $\Delta_f H^\circ_{298}$ = –28.7 ± 2.2 kJ mol^{-1}. Calculations with B3LYP/cc-pVTZ were about 6 kJ mol^{-1} more negative.[2]

CH_3CHOH

Calculated using the complete basis set method, CBS-Q. Enthalpies calculated using the atomization energy method. Entropy based on geometric properties optimized at the MP2/6-31G(d') level and vibrational frequencies at the HF/6-31G(d') level.[19] Enthalpy recommended in the review of McMillen and Golden is –15.2 ± 1 kcal mol^{-1}.[14] Atomization energies calculated using CCSD(T) with cc-pVnZ (n = D, T, and Q) basis sets, using (U)MP2/aug-cc-pVTZ optimized geometries and extrapolated to the complete basis set limit, led to enthalpies of $\Delta_f H_0^\circ$ = –9.8 kcal mol^{-1} and $\Delta_f H^\circ_{298}$ = –13.1 kcal mol^{-1}.[13]

C_2H_5OH Taken from review of Gurvich, et al.[8] Atomization energies calculated using CCSD(T) with cc-pVnZ (n = D, T, and Q) basis sets, using (U)MP2/aug-cc-pVTZ optimized geometries and extrapolated to the complete basis set limit, led to enthalpies of $\Delta_f H_0^\circ$ = −52.1 kcal mol^{-1} and $\Delta_f H^\circ_{298}$ = −56.4 kcal mol^{-1}.[13] A critical evaluation by the Thermodynamics Research Center at NIST resulted in $\Delta_f H^\circ_{298}$ = −235.3 kJ mol^{-1}.[22]

CH_3OCH_2 Calculated using the complete basis set method, CBS-Q. Enthalpies calculated using the atomization energy method. Entropy based on geometric properties optimized at the MP2/6-31G(d') level and vibrational frequencies at the HF/6-31G(d') level.[19] Recommendation in the review of McMillen and Golden, adjusted to allow for present enthalpy of CH_3COCH_3, is –3 ± 1 kcal mol^{-1}.[14]

CH_3OCH_3 Enthalpy from Pedley,[15] entropy from Frenkel et al.[6] Enthalpy calculated using the atomization energy method at the CBS-Q level gave –43.98 kcal mol^{-1}.[19] A critical evaluation by the Thermodynamics Research Center at NIST resulted in $\Delta_f H^\circ_{298}$ = −184.0 kJ mol^{-1}.[22]

(1) Berkowitz, J.; Ellison, G. B.; Gutman, D. Three methods to measure RH bond energies. *J. Phys. Chem.* **1994**, *98*, 2744-2765, doi:10.1021/j100062a009.

(2) Bernardes, C. E. S.; Minas da Piedade, M. E.; Amaral, L. M. P. F.; Ferreira, A. I. M. C. L.; Ribeiro da Silva, M. A. V.; Diogo, H. P.; Costa Cabral, B. J. Energetics of C−F, C−Cl, C−Br, and C−I bonds in 2-haloethanols. Enthalpies of formation of XCH_2CH_2OH (X = F, Cl, Br, I) compounds and of the 2-hydroxyethyl radical. *J. Phys. Chem. A* **2007**, *111*, 1713-1720, doi:10.1021/jp0675678.

(3) Bouchoux, G.; Chamot-Rooke, J.; Leblanc, D.; Mourgues, P.; Sablier, M. Proton affinity and heat of formation of vinyloxy [CH_2CHO]. and acetonyl [CH_2COCH_3]. radicals. *ChemPhysChem* **2001**, *2*, 235-241, doi:10.1002/1439-7641(20010417)2:4<235::AID-CPHC235>3.0.CO;2-S.

(4) da Silva, G.; Kim, C. H.; Bozzelli, J. W. Thermodynamic properties (enthalpy, bond energy, entropy, and heat capacity) and internal rotor potentials of vinyl alcohol, methyl vinyl ether, and their corresponding radicals. *J. Phys. Chem. A* **2006**, *110*, 7925-7934, doi:10.1021/jp0602878.

(5) El-Nahas, A. M.; Bozzelli, J. W.; Simmie, J. M.; Navarro, M. V.; Black, G.; Curran, H. J. Thermochemistry of acetonyl and related radicals. *J. Phys. Chem. A* **2006**, *110*, 13618-13623, doi:10.1021/jp065003y.

(6) Frenkel, M.; Kabo, G. J.; Marsh, K. N.; Roganov, G. N.; Wilhoit, R. C. *Thermodynamics of Organic Compounds in the Gas State*; Thermodynamics Research Center: College Station, TX, 1994; Vol. I.

(7) Fulle, D.; Hamann, H. F.; Hippler, H.; Jänsch, C. P. The high pressure range of the addition of OH to C_2H_2 and C_2H_4. *Ber. Bunsenges. Phys. Chem.* **1997**, *101*, 1433-1442, doi:10.1002/bbpc.199700004.

(8) Gurvich, L. V.; Veyts, I. V.; Alcock, C. B. *Thermodynamic Properties of Individual Substances,*, Fourth ed.; Hemisphere Publishing Corp.: New York, 1991; Vol. 2.

(9) Hassouna, M.; Delbos, E.; Devolder, P.; Viskolcz, B.; Fittschen, C. Rate and equilibrium constant of the reaction of 1-methylvinoxy radicals with O_2: $CH_3COCH_2 + O_2 \leftrightarrow CH_3COCH_2O_2$. *J. Phys. Chem. A* **2006**, *110*, 6667-6672, doi:10.1021/jp0558270.
(10) Henry, D. J.; Parkinson, C. J.; Mayer, P. M.; Radom, L. Bond dissociation energies and radical stabilization energies associated with substituted methyl radicals. *J. Phys. Chem. A* **2001**, *105*, 6750-6756, doi:10.1021/jp010442c.
(11) Holmes, J. L.; Lossing, F. P.; Terlouw, J. K. Heats of formation and homolytic bond dissociation energies in the keto-enol tautomers C_2H_4O, C_3H_6O. *J. Am. Chem. Soc.* **1986**, *108*, 1086-1087, doi:10.1021/ja00265a042.
(12) Janoschek, R.; Rossi, M. J. Thermochemical properties of free radicals from G3MP2B3 calculations. *Int. J. Chem. Kinet.* **2002**, *34*, 550-560, doi:10.1002/kin.20035.
(13) Matus, M. H.; Nguyen, M. T.; Dixon, D. A. Theoretical prediction of the heats of formation of C_2H_5O radicals derived from ethanol and of the kinetics of β-C-C scission in the ethoxy radical. *J. Phys. Chem. A* **2007**, *111*, 113-126, doi:10.1021/jp064086f.
(14) McMillen, D. F.; Golden, D. M. Hydrocarbon bond dissociation energies. *Ann. Rev. Phys. Chem.* **1982**, *33*, 493-532.
(15) Pedley, J. B. *Thermochemical Data and Structures of Organic Compounds*; Thermodynamics Data Center: College Station, TX, 1994.
(16) Ruscic, B.; Boggs, J. E.; Burcat, A.; Csaszar, A. G.; Demaison, J.; Janoschek, R.; Martin, J. M. L.; Morton, M. L.; Rossi, M. J.; Stanton, J. F.; et al. IUPAC critical evaluation of thermochemical properties of selected radicals. Part I. *J. Phys. Chem. Ref. Data* **2005**, *34*, 573-656, doi:10.1063/1.1724828.
(17) Ruscic, B.; Litorja, M.; Asher, R. L. Ionization energy of methylene revisited: Improved values for the enthalpy of formation of CH_2 and the bond dissociation energy of CH_3 via simultaneous solution of the local thermochemical network. *J. Phys. Chem. A* **1999**, *103*, 8625-8633, doi:10.1021/jp992403v.
(18) Simmie, J. M.; Metcalfe, W. K.; Curran, H. J. Ketene thermochemistry. *ChemPhysChem* **2005**, *9*, 700-702, doi:10.1002/cphc.200800003.
(19) Sumathi, R.; Green, W. H. Oxygenate, oxyalkyl and alkoxcarbonyl thermochemistry and rates for hydrogen abstraction from oxygenates. *Phys. Chem. Chem. Phys.* **2003**, *5*, 3402-3417, doi:10.1039/b307050f.
(20) Szalay, P. G.; Tajti, A.; Stanton, J. F. Ab initio determination of the heat of formation of ketenyl (HCCO) and ethynyl (CCH) radicals. *Mol. Phys.* **2005**, *103*, 2159-2168, doi:10.1080/00268970500131124.
(21) Tabor, D. P.; Harding, M. E.; Ichino, T.; Stanton, J. F. High-accuracy extrapolated ab initio thermochemistry of the vinyl, allyl, and vinoxy radicals. *J. Phys. Chem. A* **2012**, *116*, 7668-7676, doi:10.1021/jp302527n.
(22) Verevkin, S. P.; Emel'yanenko, V. N.; Diky, V.; Muzny, C. D.; Chirico, R. D.; Frenkel, M. New group-contribution approach to thermochemical properties of organic compounds: Hydrocarbons and oxygen-containing compounds. *J. Phys. Chem. Ref. Data* **2013**, *42*, 033102, doi:10.1063/1.4815957.

Note 13: *Compounds containing two C, two O, and 1-6 H*

Back to Table

$(CHO)_2$, glyoxal

The lowest energy conformer is the *trans* isomer. From the updated JANAF Tables, based on measurements of the heat of combustion.[2]

***cy*-$(C_2H_2O)O$, oxiranone (an α-lactone of ethylene oxide)**

Ab initio calculations utilizing isodesmic reactions.[9]

CH_3CHOOH

Calculated using the complete basis set method, CBS-Q. Enthalpies calculated using the atomization energy method. Entropy based on geometric properties optimized at the MP2/6-31G(d') level and vibrational frequencies at the HF/6-31G(d') level.[12] This radical is unstable towards dissociation.

$C_2H_5O_2$ Based on a re-analysis of previous equilibrium data on $R + O_2 \leftrightarrow RO_2$ from the same laboratory.[5]

C_2H_5OOH Reaction enthalpy for the reaction $CH_3CH_2OO + CH_3OOH \rightarrow CH_3CH_2OOH + CH_3OO$ calculated to be 0.5 kcal mol^{-1} using the QCISD(T)/6-31G**// MP2/6-31G* method.[6] Previous enthalpy value (−175.4 ± 12.9 kJ mol^{-1}) was computed on the assumption that the dissociation energy for ROO-H is 366 ± 3 kJ mol^{-1} (Stocker and Pilling, unpublished work).[5] Pedley gives a value of –198.9 ± 58.7 kJ mol^{-1}.[8] Enthalpy calculated using the atomization energy method at the CBS-Q level gave –38.78 kcal mol^{-1}.[12] Calculations using the CBS-QB3 and CBS-APNO model chemistries on three isodesmic reactions led to $\Delta_f H^{\circ}_{98} = -163.7 \pm 0.9$ kJ mol^{-1}.[11] Entropy based on geometric properties optimized at the MP2/6-31G(d') level and vibrational frequencies at the HF/6-31G(d') level.[12]

CH_3OCO, radical from methyl formate

An average of two isodesmic reactions calculated at the G3MP2//B3LYP/6-31G(d) level.[10] Enthalpy calculated using the atomization energy method at the CBS-Q level gave $\Delta_f H_{298}^{\circ}$ = –37.87 kcal mol^{-1}.[12] Entropy based on geometric properties optimized at the MP2/6-31G(d') level and vibrational frequencies at the HF/6-31G(d') level.[12]

$CH_2OC(O)H$

Calculated using the complete basis set method, CBS-Q. Enthalpies calculated using the atomization energy method. Entropy based on geometric properties optimized at the MP2/6-31G(d') level and vibrational frequencies at the HF/6-31G(d') level.[12]

$CH_3OC(O)H$, methyl formate

Taken from a critical evaluation by the Thermodynamics Research Center at NIST, where the uncertainty represents the 95% confidence level.[13] Previous enthalpy value of −357.4 ± 0.7 kJ mol^{-1} taken from review of Pedley.[8] An average of three isodesmic reactions calculated at the G3MP2//B3LYP/6-31G(d) level, supported by G3 and B3LYP calculations gives $\Delta_f H_{298}^{\circ}$ = –82.3 ± 0.49 kcal mol^{-1}.[10] Enthalpy calculated using the atomization energy method at the CBS-Q level gave $\Delta_f H_{298}^{\circ}$ = –85.87 kcal mol^{-1}.[12] Entropy based on geometric properties optimized at the MP2/6-31G(d') level and vibrational frequencies at the HF/6-31G(d') level.[12]

CH_3COO Vibrational frequencies calculated at the HF/6-31G(D) level and total energies evaluated at the G2(MP2) level, also making use of isodesmic reactions.[15]

$CH_2(OH)CO$ and $CH(OH)C(O)H$

Enthalpy derived from isodesmic reactions calculated by the B3LYP/6-31G(d,p) and G3 methods. Reported results were adjusted for enthalpy values of reference compounds in this Table.[3]

$CH_2(OH)C(O)H$, glycoaldehyde

Enthalpy derived from isodesmic reactions calculated by the B3LYP/6-31G(d,p) and G3 methods. Reported results were adjusted for enthalpy values of reference compounds in this Table.[3]

$CH_2C(O)OH$

Enthalpy based on CID studies of the acetate radical anion yielding D(H-CH2COOH) = 95.3 ± 2.9 kcal mol^{-1}.[14] Entropy based on vibrational frequencies calculated at the HF/6-31G(D) level.[15] Isodesmic reactions at the G2(MP2) level give –243 kJ mol^{-1}.

$CH_3C(O)O$

Derived from a hybrid experimental/CBS-Q approach.[7]

$CH_3C(O)OH$, acetic acid

Enthalpy from Pedley[8], entropy from Chao.[1]

$CH_2C(OH)_2$, ethene, 1-diol

Enthalpy obtained from three isodesmic reactions at the G3MP2//B3LYP/6-31G(d) level of theory.[10]

$CH_2(OH)CH_2OH$, 1,2-ethanediol

Enthalpy from Pedley,[8] entropy from Frenkel et al.[4]

$C(OH)_2C(O)H$, radical from ethanal, 2-diol

Calculated from two isodesmic reactions at the G3MP2//B3LYP/6-31G(d) level of theory.[10]

$CH(OH)_2C(O)H$, ethanal, 2-diol

Calculated from two isodesmic reactions at the G3MP2//B3LYP/6-31G(d) level of theory.[10]

C(O)HC(O)H, ethanedial (glyoxal)

From the review of Pedley.[8]

CH_2OOCH_3

Calculated using the complete basis set method, CBS-Q. Enthalpies calculated using the atomization energy method. Entropy based on geometric properties optimized at the MP2/6-31G(d') level and vibrational frequencies at the HF/6-31G(d') level.[12] This radical is unstable towards decomposition.

CH_3OOCH_3

Enthalpy from updated JANAF Tables, based on calorimetric measurements.[2] Enthalpy calculated using the atomization energy method at the CBS-Q level gave $\Delta_f H_{298}^{\circ} = -29.17$ kcal mol^{-1}.[12] Entropy based on geometric properties optimized at the MP2/6-31G(d') level and vibrational frequencies at the HF/6-31G(d') level.[12]

(1) Chao, J.; Zwolinski, B. J. Ideal gas thermodynamic properties of methanoic and ethanoic acids. *J. Phys. Chem. Ref. Data* **1978**, *7*, 363-377, doi:10.1063/1.555571.

(2) Dorofeeva, O.; Novikov, V. P.; Neumann, D. B. NIST-JANAF thermochemical tables. 1. Ten organic molecules related to atmospheric chemistry. *J. Phys. Chem. Ref. Data* **2001**, *30*, 475-513, doi:10.1063/1.1364518.

(3) Espinosa-Garcia, J.; Dóbé, S. Theoretical enthalpies of formation for atmospheric hydroxycarbonyls. *J. Mol. Struct. - Theochem* **2005**, *713*, 119-125, doi:10.1016/j.theochem.2004.11.002.

(4) Frenkel, M.; Kabo, G. J.; Marsh, K. N.; Roganov, G. N.; Wilhoit, R. C. *Thermodynamics of Organic Compounds in the Gas State*; Thermodynamics Research Center: College Station, TX, 1994; Vol. I.

(5) Knyazev, V. D.; Slagle, I. R. Thermochemistry of the R-O_2 bond in alkyl and chloroalkyl peroxy radicals. *J. Phys. Chem. A* **1998**, *102*, 1770-1778, doi:10.1021/jp9726091.

(6) Lay, T. H.; Bozzelli, J. W. Enthalpies of formation and group additivity of alkyl peroxides and trioxides. *J. Phys. Chem. A* **1997**, *101*, 9505-9510, doi:10.1021/jp972103i.

(7) Miller, C. E.; Lynton, J. I.; Keevil, D. M.; Franscisco, J. S. Dissociation pathways of peroxyacetyl nitrate (PAN). *J. Phys. Chem. A* **1999**, *103*, 11451-11459, doi:10.1021/jp992667h.

(8) Pedley, J. B. *Thermochemical Data and Structures of Organic Compounds*; Thermodynamics Data Center: College Station, TX, 1994.

(9) Rodriquez, C. F.; Williams, I. H. Ring strain energy and enthalpy of formation of oxiranone: an ab initio theoretical determination. *J. Chem. Soc.-Perkin Trans. 2* **1997**, 953-957, doi:10.1039/A606820K

(10) Sebbar, N.; Bozzelli, J. W.; Bockhorn, H. Enthalpy of formation and bond energies on unsaturated oxygenated hydrocarbons using G3MP2B3 calculation methods. *Int. J. Chem. Kinet.* **2005**, *37*, 633-648, doi:10.1002/kin.20086.

(11) Simmie, J. M.; Black, G.; Curran, H. J.; Hinde, J. P. Enthalpies of formation and bond dissociation energies of lower alkyl hydroperoxides and related hydroperoxy and alkoxy radicals. *J. Phys. Chem. A* **2008**, *112*, 5010-5016, doi:10.1021/jp711360z.

(12) Sumathi, R.; Green, W. H. Oxygenate, oxyalkyl and alkoxcarbonyl thermochemistry and rates for hydrogen abstraction from oxygenates. *Phys. Chem. Chem. Phys.* **2003**, *5*, 3402-3417, doi:10.1039/b307050f.

(13) Verevkin, S. P.; Emel'yanenko, V. N.; Diky, V.; Muzny, C. D.; Chirico, R. D.; Frenkel, M. New group-contribution approach to thermochemical properties of organic compounds: Hydrocarbons and oxygen-containing compounds. *J. Phys. Chem. Ref. Data* **2013**, *42*, 033102, doi:10.1063/1.4815957.

(14) Wenthold, P. G.; Squires, R. R. Gas-phase properties and reactivity of the acetate radical anion. Determination of the C-H bond strengths in acetic acid and acetate ion. *J. Am. Chem. Soc.* **1994**, *116*, 11890-11897, doi:10.1021/ja00105a032.
(15) Yu, D.; Rauk, A.; Armstrong, D. A. Radicals and ions of formic and acetic acids: An ab initio study of the structures and gas and solution phase thermochemistry. *J. Chem. Soc. Perkin Trans 2* **1994**, 2207-2215, doi:10.1039/p29940002207.

Note 14: *Alkylcarbonate radicals*

Back to Table

Alkylcarbonate radials

Formation enthalpies for these short-lived radicals were studied by the CBS-Q method, with geometry optimization at the MP2/6-31G(d) level. Enthalpies from both atomization and bond-separation reactions were calculated. The differences were 4 kJ mol^{-1} or less, so the values were averaged for inclusion in the Table. The decomposition of the radicals was investigated by charge-reversal and neutralization-reionization mass spectrometry. For these ROC(O)O radicals, hydrogen-atom migration was important for R = CH_3 and C_2H_5, whereas decarboxylation was more important for R = H, *i*-C_3H_7, and *t*-C_4H_9.[1]

(1) Soldi-Lose, H.; Schröder, D.; Schwarz, H. Gas-phase chemistry of alkylcarbonate anions and radicals. *Int. J. Mass Spec.* **2008**, *270*, 68-80, doi:10.1016/j.ijms.2007.12.007.

Note 15: *Compounds with two C and more than 2 O*

Back to Table

$CH_3C(O)O_2$

Derived from a hybrid experimental/CBS-Q approach.[3]

$CH_2(OH)C(O)OH$, glycolic acid

From the updated JANAF Tables, estimated based on additivity methods.[2]

$CH_2(OH)OOCH_2OH$, dioxybismethanol

Taken from the review of Pedley[4]

$(HOCO)_2$, oxalic acid

Updated JANAF Tables, based on the enthalpy of combustion of the solid and the enthalpy of vaporization.[2]

$CH_3O_4CH_3$, dimethyl tetroxide

Molecular geometry optimized at the B3LYP/cc-pVTZ+d level of theory. The enthalpy was determined using G3B3 and CBS-APNO methods with isodesmic reactions to minimize systematic errors. Several bond dissociation energies were also reported.[1]

$C(OH)_2C(O)H$, radical from ethanal, 2-diol

Calculated from two isodesmic reactions at the G3MP2//B3LYP/6-31G(d) level of theory.[5]

$CH(OH)_2C(O)H$, ethanal, 2-diol

Calculated from two isodesmic reactions at the G3MP2//B3LYP/6-31G(d) level of theory.[5]

(1) da Silva, G.; Bozzelli, J. W. Thermochemistry, bond energies, and internal rotor potentials of dimethyl tetraoxide. *J. Phys. Chem A* **2007**, *111*, 12026-12036, doi:10.1021/jp075144f.
(2) Dorofeeva, O.; Novikov, V. P.; Neumann, D. B. NIST-JANAF thermochemical tables. 1. Ten organic molecules related to atmospheric chemistry. *J. Phys. Chem. Ref. Data* **2001**, *30*, 475-513, doi:10.1063/1.1364518.
(3) Miller, C. E.; Lynton, J. I.; Keevil, D. M.; Franscisco, J. S. Dissociation pathways of peroxyacetyl nitrate (PAN). *J. Phys. Chem. A* **1999**, *103*, 11451-11459, doi:10.1021/jp992667h.
(4) Pedley, J. B. *Thermochemical Data and Structures of Organic Compounds*; Thermodynamics Data Center: College Station, TX, 1994.

(5) Sebbar, N.; Bozzelli, J. W.; Bockhorn, H. Enthalpy of formation and bond energies on unsaturated oxygenated hydrocarbons using G3MP2B3 calculation methods. *Int. J. Chem. Kinet.* **2005**, *37*, 633-648, doi:10.1002/kin.20086.

Note 16: *Compounds with two C, one N, and 0-5 O*

Back to Table

NCCN, Cyanogen

Enthalpy and entropy values taken from the review of Gurvich.[4] A computational study involving the use of several composite models, CBS-QB3, CBS-APNO, G3, and G4, led to values of $\Delta_f H_0^\circ$ = 307.8 ± 4.2 kJ mol^{-1} and $\Delta_f H_{298}^\circ$= 310.0 ± 4.2 kJ mol^{-1}.[9]

CNCN, Isocyanogen

Enthalpy values obtained from a computational study of atomization involving the use of several composite models, CBS-QB3, CBS-APNO, G3, and G4.[9]

CNNC, Diisocyanogen

Enthalpy values obtained from a computational study of atomization involving the use of several composite models, CBS-QB3, CBS-APNO, G3, and G4.[9]

$C_2H_5NO_2$ Calculated using G3, CBS-QB3, and CBS-APNO methods applied to atomization, isomerization, and work reactions. Value reported is $\Delta_f H_{298}^\circ$ = –25.06 ± 0.07 kcal mol^{-1}, which is adjusted using the reference enthalpy for *cis*-HONO from this Table.[1] A calculation of the atomization energy at the G3 level of theory leads to $\Delta_f H_{298}^\circ$ = –24.7 kcal mol^{-1}. Calculations also carried out at the G2, G2M(CC5), B3LYP, MW1B95, and MPWB1K levels.[5]

C_2H_5ONO Calculated using G3, CBS-QB3, and CBS-APNO methods applied to atomization, isomerization, and work reactions. Value reported is $\Delta_f H_{298}^\circ$ = –23.58±0.12 kcal mol^{-1}, which is adjusted using the reference enthalpy for *cis*-HONO from this Table.[1] A calculation of the atomization energy at the G3 level of theory leads to $\Delta_f H_{298}^\circ$ = –22.9 kcal mol^{-1}. Calculations also carried out at the G2, G2M(CC5), B3LYP, MW1B95, and MPWB1K levels.[5]

$C_2H_5O_2NO_2$

Equilibrium structures optimized at the MP2 level with the 6-311G(d,p) basis set and enthalpy values calculated by both atomization energies and through use of isodesmic reactions at the G3, G3B3, and G4 methods.[3]

$CH_3C(O)O_2NO_2$

Derived from a hybrid experimental/CBS-Q approach.[6]

$CH_3CHN(O)OH$

Enthalpy value calculated from the atomization energy at the G3 level of theory. Calculations also carried out at the G2, G2M(CC5), B3LYP, MW1B95, and MPWB1K levels.[5]

$C_2H_5NH_2$, ethylamine

From the review of Pedley.[7] Values of $\Delta_f H_{298}^\circ$ = –50.1 ± 1.5 kJ mol^{-1} and $\Delta_f H_0^\circ$ = –28.6 ± 1.5 kJ mol^{-1} have been derived from a threshold PEPICO study of alkyl amines and the use of two isodesmic reaction networks, connected through the TPEPICO dissociation energies, and with reaction heats calculated at the CBS-APNO and W1U levels of theory.[2]

$(CH_3)_2N$ Obtained from a computational analysis involving B3LYP/6-31G(2df,p) for geometric factors and G4 for atomization energies.[8]

CH_3NHCH_2

Obtained from a computational analysis involving B3LYP/6-31G(2df,p) for geometric factors and G4 for atomization energies.[8]

CH_3NHCH_3, dimethylamine

From the review of Pedley.[7] A computational analysis involving B3LYP/6-31G(2df,p) for geometric factors and G4 for atomization energies resulted in $\Delta_f H_{298}^\circ$ = −16.0 kJ mol^{-1} and the listed entropy value.[8] A computational study involving the use of several composite models,

CBS-QB3, CBS-APNO, G3, and G4, led to values of $\Delta_f H_0^\circ$ = 5.1 ± 3.0 kJ mol^{-1} and $\Delta_f H^\circ_{298}$= −16.1 ± 3.0 kJ mol^{-1}.[9]

CH_3CONH_2, acetamide

From the review of Pedley.[7]

(1) Asatryan, R.; Bozzelli, J. W.; Simmie, J. M. Thermochemistry of methyl and ethyl nitro, RNO_2, and nitrite, RONO, organic compounds. *J. Phys. Chem. A* **2008**, *112*, 3172-3185, doi:10.1021/jp710960u.

(2) Bodi, A.; Kercher, J. P.; Bond, C.; Meteesatien, P.; Sztaray, B.; Baer, T. Photoion photoelectron coincidence spectroscopy of primary amines RCH_2NH_2 (R=H, CH_3, C_2H_5, C_3H_7, *i*-C_3H_7): Alkylamine and alkyl radical heats of formation by isodesmic reaction networks *J. Phys. Chem. A* **2006**, *110*, 13425-13433, doi:10.1021/jp064739s.

(3) Buendía-Atencio, C.; Leyva, V.; González, L. Thermochemistry and UV spectroscopy of alkyl peroxynitrates. *J. Phys. Chem. A* **2010**, *114*, 9537-9544, doi:10.1021/jp103854y.

(4) Gurvich, L. V.; Veyts, I. V.; Alcock, C. B. *Thermodynamic Properties of Individual Substances,*, Fourth ed.; Hemisphere Publishing Corp.: New York, 1991; Vol. 2.

(5) Kiselev, V. G.; Gritsan, N. P. Theoretical study of the nitroalkane thermolysis. 1. Computation of the formation enthalpy of the nitroalkanes, their isomers and radical products. *J. Phys. Chem. A* **2008**, *112*, 4458-4464, doi:10.1021/jp077391p.

(6) Miller, C. E.; Lynton, J. I.; Keevil, D. M.; Franscisco, J. S. Dissociation pathways of peroxyacetyl nitrate (PAN). *J. Phys. Chem. A* **1999**, *103*, 11451-11459, doi:10.1021/jp992667h.

(7) Pedley, J. B. *Thermochemical Data and Structures of Organic Compounds*; Thermodynamics Data Center: College Station, TX, 1994.

(8) Shi, J. C.; Shang, Y. L.; Du, S. Y.; Luo, S. N. Hydrogen abstraction from CH_3NH_2, $(CH_3)_2NH$, and $(CH_3)_3N$ by HO_2 radicals: A theoretical study. *Chem. Phys. Lett.* **2018**, *691*, 307-313, doi:10.1016/j.cplett.2017.11.034.

(9) Simmie, J. M. A database of formation enthalpies of nitrogen species by compound methods (CBS-QB3, CBS-APNO, G3, G4). *J. Phys. Chem. A* **2015**, *119*, 10511-10526, doi:10.1021/acs.jpca.5b06054.

Note 17: *C3 hydrocarbons*

Back to Table

C_3H_4, propadiene

Enthalpy from Pedley.[4]

C_3H_4, propyne

Taken from a critical evaluation by the Thermodynamics Research Center at NIST, where the uncertainty represents the 95% confidence level.[11] The previous enthalpy value, $\Delta_f H^\circ_{298}$ = 184.9 ± 0.7 kJ mol^{-1}, from Pedley.[4]

***cy*-C_3H_3, 3-cyclopropenyl radical**

The 3-cyclopropenium cation was reacted with a series of reagents to establish the ionization energy of the radical as 6.00 ± 0.17 eV or 578.9 ± 16.4 kJ mol^{-1}.[9] This, combined with the enthalpy of formation of the reaction of 1076.5±3.3 kJ mol^{-1}, leads to the reported value. High level G3 and W1 calculation lead to similar values.

***cy*-C_3H_4, cyclopropene**

Enthalpy from Pedley.[4]

C_3H_5 From a second-law analysis of C_3H_5 + HBr ↔ C_3H_6 + Br.[6] A calculation at the HEAT345-Q level of theory gives recommended values of $\Delta_f H_0^\circ$ = 180.3 ± 1.8 kJ mol^{-1} and $\Delta_f H_{298}^\circ$ = 168.6 ± 1.8 kJ mol^{-1}.[8] This enthalpy difference provides the 0 K value in the Table.

C_3H_6 Taken from a critical evaluation by the Thermodynamics Research Center at NIST, where the uncertainty represents the 95% confidence level.[11] The previous enthalpy value, $\Delta_f H^\circ_{298}$ = 20.0 ± 0.7 kJ mol^{-1}, from Pedley[4]. Entropy value from Chao.[3]

***n*-C_3H_7** Enthalpy derived from a threshold PEPICO study of alkyl amines and the use of two isodesmic reaction networks, connected through the TPEPICO dissociation energies, and with reaction heats calculated at the CBS-APNO and W1U levels of theory.[1] Previous value of $\Delta_f H_{298}^o$ = 100 ± 2 kJ mol^{-1} estimated by Tsang.[10]

***i*-C_3H_7** From a second-law analysis of iso-C_3H_7 + HBr ↔ iso-C_3H_8 + Br.[7] An enthalpy of $\Delta_f H_{298}^o$ = 88.5 ± 1.0 kJ mol^{-1} and $\Delta_f H_0^o$ = 106.2 ± 1.0 kJ mol^{-1} has been derived from a threshold PEPICO study of alkyl amines and the use of two isodesmic reaction networks, connected through the TPEPICO dissociation energies, and with reaction heats calculated at the CBS-APNO and W1U levels of theory.[1]

C_3H_8 Taken from a critical evaluation by the Thermodynamics Research Center at NIST, where the uncertainty represents the 95% confidence level.[11] The previous enthalpy value, $\Delta_f H_{298}^o$ = –104.68 ± 0.50 kJ mol^{-1}, from a combustion calorimetry study.[5] Entropy from ideal gas properties calculations.[2]

(1) Bodi, A.; Kercher, J. P.; Bond, C.; Meteesatien, P.; Sztaray, B.; Baer, T. Photoion photoelectron coincidence spectroscopy of primary amines RCH_2NH_2 (R=H, CH_3, C_2H_5, C_3H_7, *i*-C_3H_7): Alkylamine and alkyl radical heats of formation by isodesmic reaction networks *J. Phys. Chem. A* **2006**, *110*, 13425-13433, doi:10.1021/jp064739s.

(2) Chao, J.; Wilhoit, R. C.; Zwolinski, B. J. Ideal gas thermodynamic properties of ethane and propane. *J. Phys. Chem. Ref. Data* **1973**, *2*, 427-437, doi:10.1063/1.3253123.

(3) Chao, J.; Zwolinski, B. J. Ideal gas thermodynamic properties of ethylene and propylene. *J. Phys. Chem. Ref. Data* **1975**, *4*, 251-261, doi:10.1063/1.555518.

(4) Pedley, J. B. *Thermochemical Data and Structures of Organic Compounds*; Thermodynamics Data Center: College Station, TX, 1994.

(5) Pittam, D. A.; Pilcher, G. Measurements of heats of combustion by flame calorimetry. Part 8. Methane, ethane, propane, n-butane and 2-methylpropane. *J. Chem. Soc. Faraday Trans. 1* **1972**, *68*, 2224-2229, doi:10.1039/F19726802224.

(6) Seetula, J. A. Kinetics and thermochemistry of the C_3H_5 + HBr ⇌ C_3H_6 + Br equilibrium. *Phys. Chem. Chem. Phys.* **1999**, *1*, 4727-4731, doi:10.1039/A905347F.

(7) Seetula, J. A.; Slagel, I. R. Kinetics and thermochemistry of the R + HBr ⇄ RH + Br (R = n-C_3H_7, isoC_3H_7, isoC_4H_9, sec-C_4H_9, or tert-C_4H_9) equilibrium. *J. Chem. Soc. Faraday Trans.* **1997**, *93*, 1709-1719, doi:10.1039/a608224f.

(8) Tabor, D. P.; Harding, M. E.; Ichino, T.; Stanton, J. F. High-accuracy extrapolated ab initio thermochemistry of the vinyl, allyl, and vinoxy radicals. *J. Phys. Chem. A* **2012**, *116*, 7668-7676, doi:10.1021/jp302527n.

(9) Tian, Z.; Lis, L.; Kass, S. R. Carbon−hydrogen bond dissociation energies: The curious case of cyclopropene. *J. Org. Chem.* **2013**, *78*, 12650-12653, doi:10.1021/jo402263v.

(10) Tsang, W. Heats of formation of organic free radicals by kinetic methods. In *Energetics of Free Radicals*; Simoes, J. A. M., Greenberg, A., Liebman, J. F., Eds.; Blackie Academic & Professional: London, 1996; pp 22-58.

(11) Verevkin, S. P.; Emel'yanenko, V. N.; Diky, V.; Muzny, C. D.; Chirico, R. D.; Frenkel, M. New group-contribution approach to thermochemical properties of organic compounds: Hydrocarbons and oxygen-containing compounds. *J. Phys. Chem. Ref. Data* **2013**, *42*, 033102, doi:10.1063/1.4815957.

Note 18: *Compounds containing 3 C 1-8 H, and 1 O*

Back to Table

1-C_3H_7OH Enthalpy taken from a critical evaluation by the Thermodynamics Research Center at NIST, where the uncertainty represents the 95% confidence level.[16] Previous value, $\Delta_f H_{298}^o$ = −255.1 ± 0.4 kJ mol^{-1}, from review of Pedely et al.[12] Entropy value from evaluation of Chao, et al.[3]

2-C_3H_7OH Enthalpy taken from a critical evaluation by the Thermodynamics Research Center at NIST, where the uncertainty represents the 95% confidence level.[16] Previous value, $\Delta_f H_{298}^o$ = −272.6 ± 0.5 kJ mol^{-1}, from review of Pedely et al.[12] Entropy value from evaluation of Chao, et al.[3]

C_2H_5CO CBS-4 and G2(MP2,SVP) methods used to obtain thermodynamic properties. Value listed is recommendation based on theoretical and experimental results. Entropy at the G2(MP2(full)//MP2(full)/6-31G(d) level treating internal rotations as harmonic oscillators.[17]

$C_2H_5C(O)H$

Enthalpy taken from a critical evaluation by the Thermodynamics Research Center at NIST, where the uncertainty represents the 95% confidence level.[16] The previous enthalpy value, $\Delta_f H^\circ_{298} = -185.6 \pm 0.8$ kJ mol^{-1}, from Pedley.[12] Entropy from Frenkel et al.[7]

CH_2CHOCH_3 and C_3H_5O

Methyl vinyl ether and corresponding radicals. Molecular geometry optimized at the B3LYP/6-31G(d,p) level of theory. The enthalpy was determined using CBS-Q, CBS-APNO, and G3 methods with isodesmic reactions to minimize systematic errors. Entropies calculated by using the SMCPS program.[4]

$CH_3C(O)CH_2$

Enthalpy value an average of the a value obtained from the gas-phase basicity and proton affinity determined by a kinetic method (-34.6 ± 8.4 kJ mol^{-1}) and a reexamination of the results of Holmes et al.[9] on the dissociation of 2-propenyl acetate and acetylacetone after electron ionization (-33.1 and -30.3 kJ mol^{-1}).[2] This value is supported by several computational studies.[5,8,10] The previous recommendation, -28.1 ± 3.1 kJ mol^{-1}, was derived from forward and reverse rate constants for the reaction $CH_3C(O)CH_2 + HBr \leftrightarrow CH_3C(O)CH_3 + Br$.[6] The reverse rate constant requires an extrapolation from high temperatue for the reference reaction. An earlier photobromination determination of the reverse reaction results in an enthalpy value of -24.3 ± 5.8 kJ mol^{-1}.[11] Density functional and ab initio calculations at the CBS-QB3 level of theory, using a series of isodesmic reactions, led to $\Delta_f H^\circ_{298} = -24.3 \pm 5.8$ kJ mol^{-1}.[5] The entropy value is from G3MP2B3 calculation.[10]

$CH_3C(O)CH_3$

Enthalpy from review of Pedley;[12] entropy value from Frenkel.[7]

CH_3CHOCH_3 and $CH_3CH_2OCH_2$

Calculated using the complete basis set method, CBS-Q. Enthalpies calculated using the atomization energy method. Entropy based on geometric properties optimized at the MP2/6-31G(d') level and vibrational frequencies at the HF/6-31G(d') level.[15]

$CH_3CH_2OCH_3$, methoxyethane (methyl ethyl ether)

Enthalpy from Pedley et al.[12] An identical value was recommended by the Thermodynamics Research Center at NIST.[16] Enthalpy calculated using the atomization energy method at the CBS-Q level gave -52.20 kcal mol^{-1}.[15] Entropy based on geometric properties optimized at the MP2/6-31G(d') level and vibrational frequencies at the HF/6-31G(d') level.[15]

$CH_2CC(O)H$, radical from propenal

Enthalpy obtained from four isodesmic reactions at the G3MP2//B3LYP/6-31G(d) level of theory.[13]

CH_2CHCO, radical from propenal

CBS-4 and G2(MP2,SVP) methods used to obtain thermodynamic properties. Value listed is recommendation based on theoretical and experimental results. Entropy at the G2(MP2(full)//MP2(full)/6-31G(d) level treating internal rotations as harmonic oscillators.[17]

CH_3CHCO, methyl ketene

Reaction enthalpies for two isodesmic reactions were calculated at the CBS-QB3, CBS-APNO, and G3 levels.[14] Preferred values for the reference compounds from this Table were employed.

$CH_2CHC(O)H$, propenal, acrolein

Enthalpy obtained from W1 atomization energy calculations. Geometric properties evaluated at the B3LYP/cc-pVTZ+d level of theory, with the rotation about the C-C bond treated as a hindered rotation.[1] The previous enthalpy value, $\Delta_f H^\circ_{298} = -74.3 \pm 1.7$ kJ mol^{-1}, was determined

in the same laboratory from two isodesmic reactions at the G3MP2//B3LYP/6-31G(d) level of theory.[13]

(1) Asatryan, R.; Silva, G. d.; Bozzelli, J. W. Quantum chemical study of the acrolein (CH_2CHCHO) + OH + O_2 reactions. *J. Phys. Chem. A* **2010**, *114*, 8302-8311, doi:10.1021/jp104828a.

(2) Bouchoux, G.; Chamot-Rooke, J.; Leblanc, D.; Mourgues, P.; Sablier, M. Proton affinity and heat of formation of vinyloxy [CH_2CHO]. and acetonyl [CH_2COCH_3]. radicals. *ChemPhysChem* **2001**, *2*, 235-241, doi:10.1002/1439-7641(20010417)2:4<235::AID-CPHC235>3.0.CO;2-S.

(3) Chao, J.; Hall, K. R.; Marsh, K. N.; Wilhoit, R. C. Thermodynamic properties of key organic oxygen compounds in the carbon range C1 to C4. Part 2. Ideal gas properties. *J. Phys. Chem. Ref. Data* **1986**, *15*, 1369-1436, doi:10.1063/1.555769.

(4) da Silva, G.; Kim, C. H.; Bozzelli, J. W. Thermodynamic properties (enthalpy, bond energy, entropy, and heat capacity) and internal rotor potentials of vinyl alcohol, methyl vinyl ether, and their corresponding radicals. *J. Phys. Chem. A* **2006**, *110*, 7925-7934, doi:10.1021/jp0602878.

(5) El-Nahas, A. M.; Bozzelli, J. W.; Simmie, J. M.; Navarro, M. V.; Black, G.; Curran, H. J. Thermochemistry of acetonyl and related radicals. *J. Phys. Chem. A* **2006**, *110*, 13618-13623, doi:10.1021/jp065003y.

(6) Farkas, E.; Kovács, G.; Szilágyi, I.; Dóbé, S.; Bérces, T.; Márta, F. Rate constant for the reaction of $CH_3C(O)CH_2$ radical with HBr and its thermochemical implication. *Int. J. Chem. Kinet.* **2006**, *38*, 32-37, doi:10.1002/kin.20135.

(7) Frenkel, M.; Kabo, G. J.; Marsh, K. N.; Roganov, G. N.; Wilhoit, R. C. *Thermodynamics of Organic Compounds in the Gas State*; Thermodynamics Research Center: College Station, TX, 1994; Vol. I.

(8) Hassouna, M.; Delbos, E.; Devolder, P.; Viskolcz, B.; Fittschen, C. Rate and equilibrium constant of the reaction of 1-methylvinoxy radicals with O_2: $CH_3COCH_2 + O_2 \leftrightarrow CH_3COCH_2O_2$. *J. Phys. Chem. A* **2006**, *110*, 6667-6672, doi:10.1021/jp0558270.

(9) Holmes, J. L.; Lossing, F. P.; Terlouw, J. K. Heats of formation and homolytic bond dissociation energies in the keto-enol tautomers C_2H_4O, C_3H_6O. *J. Am. Chem. Soc.* **1986**, *108*, 1086-1087, doi:10.1021/ja00265a042.

(10) Janoschek, R.; Rossi, M. J. Thermochemical properties from G3MP2B3 calculations, set 2: Free radicals with special consideration of CH_2=CH-C$^{\bullet}$=CH_2, cyclo-$^{\bullet}C_5H_5$, $^{\bullet}CH_2OOH$, HO-$^{\bullet}$CO, and HC(O)O$^{\bullet}$. *Int. J. Chem. Kinet.* **2004**, *36*, 661-686, doi:10.1002/kin.20035.

(11) King, K. D.; Golden, D. M.; Benson, S. W. Kinetics of the gas-phase thermal bromination of acetone. Heat of formation and stabilization energy of the acetonyl radical. *J. Am. Chem. Soc.* **1970**, *92*, 5541-5546, doi:10.1021/ja00722a001.

(12) Pedley, J. B. *Thermochemical Data and Structures of Organic Compounds*; Thermodynamics Data Center: College Station, TX, 1994.

(13) Sebbar, N.; Bozzelli, J. W.; Bockhorn, H. Enthalpy of formation and bond energies on unsaturated oxygenated hydrocarbons using G3MP2B3 calculation methods. *Int. J. Chem. Kinet.* **2005**, *37*, 633-648, doi:10.1002/kin.20086.

(14) Simmie, J. M.; Metcalfe, W. K.; Curran, H. J. Ketene thermochemistry. *ChemPhysChem* **2005**, *9*, 700-702, doi:10.1002/cphc.200800003.

(15) Sumathi, R.; Green, W. H. Oxygenate, oxyalkyl and alkoxcarbonyl thermochemistry and rates for hydrogen abstraction from oxygenates. *Phys. Chem. Chem. Phys.* **2003**, *5*, 3402-3417, doi:10.1039/b307050f.

(16) Verevkin, S. P.; Emel'yanenko, V. N.; Diky, V.; Muzny, C. D.; Chirico, R. D.; Frenkel, M. New group-contribution approach to thermochemical properties of organic compounds: Hydrocarbons and oxygen-containing compounds. *J. Phys. Chem. Ref. Data* **2013**, *42*, 033102, doi:10.1063/1.4815957.

(17) Viskolcz, B.; Berces, T. Enthalpy of formation of selected carbonyl radicals from theory and comparison with experiment. *Phys. Chem. Chem. Phys.* **2000**, *2*, 5430-6436, doi:10.1039/b004548i.

Note 19: *Compounds containing 3 C 1-8 H, and 2 O* Back to Table

$C_3H_5O_2$ Equilibrium constants for the reaction $C_3H_5 + O_2 \leftrightarrow C_3H_5O_2$ were determined over the temperature range 320–420 K and fit to a van't Hoff plot. Combining the results with previous results led to $\Delta_r H^{\circ}_{298} = -75.6 \pm 2.3$ kJ mol^{-1} and $\Delta_r S = -129.9 \pm 3.1$ J K^{-1}mol^{-1}.[5]

$CH_2CHOOCH_3$
Thermodynamic parameters were determined at the B3LYP/6-311G(d,p) level of theory, with the enthalpy the average of 4-6 isodesmic reactions. The standard deviation of the enthalpy from the average of the isodesmic reactions was ±2.8 kJ mol^{-1}, but the estimated error limits for the individual isodesmic reactions, which take into account the uncertainty in each reactant and an estimated uncertainty due to thermal energy of 0.46 kJ mol^{-1}, ranged from ±6.7 to 14 kJ mol^{-1}.[6]

$C_2H_5C(O)OH$
Enthalpy taken from a critical evaluation by the Thermodynamics Research Center at NIST, where the uncertainty represents the 95% confidence level.[10]

$CH_3CH(OH)CH_2OH$, 1,2-propanediol
From review of Pedley et al.[4]

C_3H_5OOH Enthalpy based on calculations made using the CBS-QB3 and CBS-APNO model chemistries on two isodesmic reactions.[8]

$CH_2OC(O)CH_3$ and $CH_3OC(O)CH_3$
Calculated using the complete basis set method, CBS-Q. Enthalpies calculated using the atomization energy method. Entropy based on geometric properties optimized at the MP2/6-31G(d') level and vibrational frequencies at the HF/6-31G(d') level.[9] An enthalpy value of $\Delta_r H^{\circ}_{298} = -413.5$ kJ mol^{-1} for methyl ethanoate, $CH_3CH_2OC(O)H$, was recommended by the Thermodynamics Research Center at NIST.[10]

$CH_3OCH_2OCH_3$, dimethoxymethane
From the review of Pedley et al.[4]

$CH_3CH_2OC(O)$, $CH_3CHOC(O)H$, $CH_3CH_2OC(O)H$
Calculated using the complete basis set method, CBS-Q. Enthalpies calculated using the atomization energy method. Entropy based on geometric properties optimized at the MP2/6-31G(d') level and vibrational frequencies at the HF/6-31G(d') level.[9] An enthalpy value of $\Delta_r H^{\circ}_{298} = -398.5 \pm 8.5$ kJ mol^{-1} for ethyl methanoate, $CH_3CH_2OC(O)H$, was recommended by the Thermodynamics Research Center at NIST, where the uncertainty represents the 95% confidence level.[10]

$CH_2(OH)C(O)CH_3$, hydroxyacetone
Enthalpy derived from isodesmic reactions calculated by the B3LYP/6-31G(d,p) and G3 methods. Reported results were adjusted for enthalpy values of reference compounds in this Table.[1]

$CH_3CHOOCH_3$
Calculated using the complete basis set method, CBS-Q. Enthalpies calculated using the atomization energy method. Entropy based on geometric properties optimized at the MP2/6-31G(d') level and vibrational frequencies at the HF/6-31G(d') level.[9] This radical is unstable towards dissociation

$CH_3CH_2OOCH_3$
Calculated using the complete basis set method, CBS-Q. Enthalpies calculated using the atomization energy method. Entropy based on geometric properties optimized at the MP2/6-31G(d') level and vibrational frequencies at the HF/6-31G(d') level.[9]

$(CH_3)_2CHOO$
Based on a re-analysis of previous equilibrium data on $R + O_2 \leftrightarrow RO_2$ from the same laboratory.[2]

$(CH_3)_2COOH$

Calculated using the complete basis set method, CBS-Q. Enthalpies calculated using the atomization energy method. Entropy based on geometric properties optimized at the MP2/6-31G(d') level and vibrational frequencies at the HF/6-31G(d') level.[9]

$(CH_3)_2CHOOH$

Reaction enthalpy for the reaction $(CH_3)_2CHOO + CH_3OOH \rightarrow (CH_3)_2CHOOH + CH_3OO$ calculated to be 0.6 kcal mol^{-1} using the QCISD(T)/6-31G**// MP2/6-31G* method.[3] Enthalpy calculated using the atomization energy method at the CBS-Q level gave –48.1 kcal mol^{-1}.[9] Entropy based on geometric properties optimized at the MP2/6-31G(d') level and vibrational frequencies at the HF/6-31G(d') level.[9]

$CH_3C(OH)_2C(O)OH$

Enthalpy obtained from three isodesmic reactions at the G3MP2//B3LYP/6-31G(d) level of theory.[7]

$CH_2(OH)CH(OH)CH_2OH$, 1,2,3-propanetriol

Taken from the review of Pedley et al.[4]

$CH_2CHOOCH_3$

Thermodynamic parameters were determined at the B3LYP/6-311G(d,p) level of theory, with the enthalpy the average of 4–6 isodesmic reactions. The standard deviation of the enthalpy from the average of the isodesmic reactions was ±2.8 kJ mol^{-1}, but the estimated error limits for the individual isodesmic reactions, which take into account the uncertainty in each reactant and an estimated uncertainty due to thermal energy of 0.46 kJ mol–1, ranged from ±6.7 to 14 kJ mol^{-1}.[6]

(1) Espinosa-Garcia, J.; Dóbé, S. Theoretical enthalpies of formation for atmospheric hydroxycarbonyls. *J. Mol. Struct. - Theochem* **2005**, *713*, 119-125, doi:10.1016/j.theochem.2004.11.002.

(2) Knyazev, V. D.; Slagle, I. R. Thermochemistry of the R-O_2 bond in alkyl and chloroalkyl peroxy radicals. *J. Phys. Chem. A* **1998**, *102*, 1770-1778, doi:10.1021/jp9726091.

(3) Lay, T. H.; Bozzelli, J. W. Enthalpies of formation and group additivity of alkyl peroxides and trioxides. *J. Phys. Chem. A* **1997**, *101*, 9505-9510, doi:10.1021/jp972103i.

(4) Pedley, J. B. *Thermochemical Data and Structures of Organic Compounds*; Thermodynamics Data Center: College Station, TX, 1994.

(5) Rissanen, M. P.; Amedro, D.; Eskola, A. J.; Kurten, T.; Timonen, R. S. Kinetic (T = 201−298 K) and equilibrium (T = 320−420 K) measurements of the $C_3H_5 + O_2 \leftrightharpoons C_3H_5O_2$ reaction. *J. Phys. Chem. A* **2012**, *116*, 3969-3978, doi:10.1021/jp209977h.

(6) Sebbar, N.; Bozzelli, J. W.; Bockhorn, H. Thermochemical properties, rotation barriers, bond energies, and group additivity for vinyl, phenyl, ethynyl, and allyl peroxides *J. Phys. Chem. A* **2004**, *2004*, 8353-8366, doi:10.1021/jp031067m.

(7) Sebbar, N.; Bozzelli, J. W.; Bockhorn, H. Enthalpy of formation and bond energies on unsaturated oxygenated hydrocarbons using G3MP2B3 calculation methods. *Int. J. Chem. Kinet.* **2005**, *37*, 633-648, doi:10.1002/kin.20086.

(8) Simmie, J. M.; Black, G.; Curran, H. J.; Hinde, J. P. Enthalpies of formation and bond dissociation energies of lower alkyl hydroperoxides and related hydroperoxy and alkoxy radicals. *J. Phys. Chem. A* **2008**, *112*, 5010-5016, doi:10.1021/jp711360z.

(9) Sumathi, R.; Green, W. H. Oxygenate, oxyalkyl and alkoxcarbonyl thermochemistry and rates for hydrogen abstraction from oxygenates. *Phys. Chem. Chem. Phys.* **2003**, *5*, 3402-3417, doi:10.1039/b307050f.

(10) Verevkin, S. P.; Emel'yanenko, V. N.; Diky, V.; Muzny, C. D.; Chirico, R. D.; Frenkel, M. New group-contribution approach to thermochemical properties of organic compounds: Hydrocarbons and oxygen-containing compounds. *J. Phys. Chem. Ref. Data* **2013**, *42*, 033102, doi:10.1063/1.4815957.

Note 20: *Compounds containing 3 C, H, N, and O* Back to Table

$C_3H_7NH_2$ Enthalpy derived from a threshold PEPICO study of alkyl amines and the use of two isodesmic reaction networks, connected through the TPEPICO dissociation energies, and with reaction heats calculated at the CBS-APNO and W1U levels of theory.[2]

$(CH_3)_2NCH_2$

Obtained from a computational analysis involving B3LYP/6-31G(2df,p) for geometric factors and G4 for atomization energies.[6]

$(CH_3)_3N$, trimethylamine

From the review of Pedley et al.[5] A computational analysis involving B3LYP/6-31G(2df,p) for geometric factors and G4 for atomization energies resulted in $\Delta_f H^\circ_{298} = -25.56$ kJ mol^{-1} and the listed entropy value.[6] A computational study involving the use of several composite models, CBS-QB3, CBS-APNO, G3, and G4, led to values of $\Delta_f H_0^\circ = 1.5 \pm 4.2$ kJ mol^{-1} and $\Delta_f H^\circ_{298} = -26.1 \pm 4.3$ kJ mol^{-1}.[7]

$(CH_3)_3NO$, trimethylene-*N*-oxide

Enthalpy from heat of combustion of solid and estimated sublimation enthalpy.[1]

$C_3H_7O_2NO_2$

Equilibrium structures optimized at the MP2 level with the 6-311G(d,p) basis set and enthalpy values calculated by both atomization energies and through use of isodesmic reactions at the G3, G3B3, and G4 methods.[3]

NCC(O)CN, oxopropanedinitrile

From the updated JANAF Tables, based on calorimetric measurements.[4]

(1) Acree, W. E.; Pilcher, G.; da Silva, M. The dissociation enthalpies of terminal (N-O) bonds in organic compounds. *J. Phys. Chem. Ref. Data* **2005**, *34*, 553-572, doi:10.1063/1.1851531.

(2) Bodi, A.; Kercher, J. P.; Bond, C.; Meteesatien, P.; Sztaray, B.; Baer, T. Photoion photoelectron coincidence spectroscopy of primary amines RCH_2NH_2 (R=H, CH_3, C_2H_5, C_3H_7, *i*-C_3H_7): Alkylamine and alkyl radical heats of formation by isodesmic reaction networks *J. Phys. Chem. A* **2006**, *110*, 13425-13433, doi:10.1021/jp064739s.

(3) Buendía-Atencio, C.; Leyva, V.; González, L. Thermochemistry and UV spectroscopy of alkyl peroxynitrates. *J. Phys. Chem. A* **2010**, *114*, 9537-9544, doi:10.1021/jp103854y.

(4) Dorofeeva, O.; Novikov, V. P.; Neumann, D. B. NIST-JANAF thermochemical tables. 1. Ten organic molecules related to atmospheric chemistry. *J. Phys. Chem. Ref. Data* **2001**, *30*, 475-513, doi:10.1063/1.1364518.

(5) Pedley, J. B. *Thermochemical Data and Structures of Organic Compounds*; Thermodynamics Data Center: College Station, TX, 1994.

(6) Shi, J. C.; Shang, Y. L.; Du, S. Y.; Luo, S. N. Hydrogen abstraction from CH_3NH_2, $(CH_3)_2NH$, and $(CH_3)_3N$ by $H\dot{O}_2$ radicals: A theoretical study. *Chem. Phys. Lett.* **2018**, *691*, 307-313, doi:10.1016/j.cplett.2017.11.034.

(7) Simmie, J. M. A database of formation enthalpies of nitrogen species by compound methods (CBS-QB3, CBS-APNO, G3, G4). *J. Phys. Chem. A* **2015**, *119*, 10511-10526, doi:10.1021/acs.jpca.5b06054.

Note 21: *Compounds containing 4 C, H, and O*

Back to Table

1-C_4H_6, *1*-butyne

Taken from a critical evaluation by the Thermodynamics Research Center at NIST, where the uncertainty represents the 95% confidence level.[10]

2-C_4H_6, 2-butyne

Taken from a critical evaluation by the Thermodynamics Research Center at NIST, where the uncertainty represents the 95% confidence level.[10]

1-C_4H_8, *1*-butene

Taken from a critical evaluation by the Thermodynamics Research Center at NIST, where the uncertainty represents the 95% confidence level.[10]

***cis*-2-C_4H_8, *cis*-2-butene**

Taken from a critical evaluation by the Thermodynamics Research Center at NIST, where the uncertainty represents the 95% confidence level.[10]

***trans*-C_4H_8, *trans*-2-butene**

Taken from a critical evaluation by the Thermodynamics Research Center at NIST, where the uncertainty represents the 95% confidence level.[10]

$CH_3C(CH_3)CH_2$, *2*-methylpropene

Taken from a critical evaluation by the Thermodynamics Research Center at NIST, where the uncertainty represents the 95% confidence level.[10]

$CH_3CH(CH_3)CH_3$, *2*-methylpropane

Taken from a critical evaluation by the Thermodynamics Research Center at NIST, where the uncertainty represents the 95% confidence level.[10]

***n*-C_4H_{10}** Taken from a critical evaluation by the Thermodynamics Research Center at NIST, where the uncertainty represents the 95% confidence level.[10] The previous enthalpy value, $\Delta_f H^\circ_{298} = -125.65 \pm 0.67$ kJ mol^{-1}, from a combustion calorimetry study.[7] Entropy by ideal gas properties calculations.[4]

$CH_3CH(CH_3)C(O)OH$, $C_3H_7C(O)OH$

Taken from a critical evaluation by the Thermodynamics Research Center at NIST, where the uncertainty represents the 95% confidence level.[10]

$C_2H_5OC(O)CH_3$, ethyl acetate

Taken from a critical evaluation by the Thermodynamics Research Center at NIST, where the uncertainty represents the 95% confidence level.[10]

$(CH_3)_2CCO$, dimethyl ketene

Reaction enthalpies for three isodesmic reactions were calculated at the CBS-QB3, CBS-APNO, and G3 levels.[9] The preferred value for ketene from this Table was employed.

$(CH_3)_3CO$, *tert*-Butoxyl

Earlier photoacoustic calorimetry results were combined with redetermined values of the enthalpy of formation and vaporization of di-1,1-dimethylethyl peroxide (using combustion calorimetry, ebulliometry, and heat capacity measurements) to derive this improved enthalpy of formation.[2]

$(CH_3)_3COO$

Based on a re-analysis of previous equilibrium data on $R + O_2 \leftrightarrow RO_2$ from the same laboratory.[5]

$(CH_3)_3COOH$

Enthalpy based on the gas-phase acidity and electron affinity from a negative ion photoelectron spectral study, leading to a BDE(O-H) of 85±2 kcal mol^{-1} (83±2 kcal mol^{-1} at 0 K).[1] Reaction enthalpy for the reaction $(CH_3)_3COO + CH_3OOH \rightarrow (CH_3)_3COOH + CH_3OO$ was calculated to be 1.3 kcal mol^{-1} using the QCISD(T)/6-31G**// MP2/6-31G* method, leading to $\Delta_f H^\circ_{298} = -56.8$ kcal mol^{-1}.[6]

$(CH_3COO)_2$, diacetyl peroxide

From updated JANAF Tables, based on a calorimetric measurement on the liquid and an assumed enthalpy of vaporization.[3]

***trans*-$CH_3CHCHOOCH_3$**

Thermodynamic parameters were determined at the B3LYP/6-311G(d,p) level of theory, with the enthalpy the average of 4-6 isodesmic reactions. The standard deviation of the enthalpy from the average of the isodesmic reactions was ±2.8 kJ mol^{-1}, but the estimated error limits for the individual isodesmic reactions, which take into account the uncertainty in each reactant and an estimated uncertainty due to thermal energy of 0.46 kJ mol^{-1}, ranged from ±4.2 to 10.3 kJ mol^{-1}.[8]

***cis*-$CH_3CHCHOOCH_3$**

Thermodynamic parameters were determined at the B3LYP/6-311G(d,p) level of theory, with the enthalpy the average of 4-6 isodesmic reactions. The standard deviation of the enthalpy from the average of the isodesmic reactions was ±2.0 kJ mol^{-1}, but the estimated error limits for the individual isodesmic reactions, which take into account the uncertainty in each reactant and an estimated uncertainty due to thermal energy of 0.46 kJ mol^{-1}, ranged from ±4.0 to 8.0 kJ mol^{-1}.[8]

$CH_2C(CH_3)OOCH_3$

Thermodynamic parameters were determined at the B3LYP/6-311G(d,p) level of theory, with the enthalpy the average of 4-6 isodesmic reactions. The standard deviation of the enthalpy from the average of the isodesmic reactions was ±1.8 kJ mol^{-1}, but the estimated error limits for the individual isodesmic reactions, which take into account the uncertainty in each reactant and an estimated uncertainty due to thermal energy of 0.46 kJ mol^{-1}, ranged from ±3.8 to 7.8 kJ mol^{-1}.[8]

$CH_2CHCH_2OOCH_3$

Thermodynamic parameters were determined at the B3LYP/6-311G(d,p) level of theory, with the enthalpy the average of 4-6 isodesmic reactions. The standard deviation of the enthalpy from the average of the isodesmic reactions was ±1.1 kJ mol^{-1}, but the estimated error limits for the individual isodesmic reactions, which take into account the uncertainty in each reactant and an estimated uncertainty due to thermal energy of 0.46 kJ mol^{-1}, ranged from ±3.2 to 7.4 kJ mol^{-1}.[8]

(1) Clifford, E. P.; Wenthold, P. G.; Gareyev, R.; Lineberger, W. C.; DePuy, C. H.; Bierbaum, V. M.; Ellison, G. B. Photoelectron spectroscopy, gas phase acidity, and thermochemistry of tert-butyl hydroperoxide: Mechanism for the rearrangement of peroxyl radicals. *J. Chem. Phys.* **1998**, *109*, 10293-10310, doi:10.1063/1.477725.

(2) Diogo, H. P.; Minas de Piedada, M. E.; Simões, J. A. M.; Nagano, Y. Standard enthalpy of formation and enthalpy of vaporization of di-1,1-dimethylethyl peroxide: Re-evaluation of the standard enthalpy of formation of the di-1,1-dimethylethoxy radical *J. Chem. Thermo.* **1995**, *27*, 597-604, doi:10.1006/jcht.1995.0061.

(3) Dorofeeva, O.; Novikov, V. P.; Neumann, D. B. NIST-JANAF thermochemical tables. 1. Ten organic molecules related to atmospheric chemistry. *J. Phys. Chem. Ref. Data* **2001**, *30*, 475-513, doi:10.1063/1.1364518.

(4) Frenkel, M.; Kabo, G. J.; Marsh, K. N.; Roganov, G. N.; Wilhoit, R. C. *Thermodynamics of Organic Compounds in the Gas State*; Thermodynamics Research Center: College Station, TX, 1994; Vol. I.

(5) Knyazev, V. D.; Slagle, I. R. Thermochemistry of the R-O_2 bond in alkyl and chloroalkyl peroxy radicals. *J. Phys. Chem. A* **1998**, *102*, 1770-1778, doi:10.1021/jp9726091.

(6) Lay, T. H.; Bozzelli, J. W. Enthalpies of formation and group additivity of alkyl peroxides and trioxides. *J. Phys. Chem. A* **1997**, *101*, 9505-9510, doi:10.1021/jp972103i.

(7) Pittam, D. A.; Pilcher, G. Measurements of heats of combustion by flame calorimetry. Part 8. Methane, ethane, propane, n-butane and 2-methylpropane. *J. Chem. Soc. Faraday Trans. 1* **1972**, *68*, 2224-2229, doi:10.1039/F19726802224.

(8) Sebbar, N.; Bozzelli, J. W.; Bockhorn, H. Thermochemical properties, rotation barriers, bond energies, and group additivity for vinyl, phenyl, ethynyl, and allyl peroxides *J. Phys. Chem. A* **2004**, *2004*, 8353-8366, doi:10.1021/jp031067m.

(9) Simmie, J. M.; Metcalfe, W. K.; Curran, H. J. Ketene thermochemistry. *ChemPhysChem* **2005**, *9*, 700-702, doi:10.1002/cphc.200800003.

(10) Verevkin, S. P.; Emel'yanenko, V. N.; Diky, V.; Muzny, C. D.; Chirico, R. D.; Frenkel, M. New group-contribution approach to thermochemical properties of organic compounds: Hydrocarbons and oxygen-containing compounds. *J. Phys. Chem. Ref. Data* **2013**, *42*, 033102, doi:10.1063/1.4815957.

Note 22: *Inorganic compounds containing F*

Back to Table

F Enthalpy value is from the optimization in the Active Thermochemical Tables (ATcT).[16] CODATA Key Value[4] of $\Delta_f H^\circ_{298}$ = 79.38 ± 0.30 kJ mol^{-1} was used in previous evaluation. Entropy value is from CODATA.

F_2 CODATA Key Value.[4]

HF CODATA Key Value.[4] The active thermochemical tables optimization gives an enthalpy value of –272.775 ± 0.24 kJ mol^{-1}.[17] The most recent NIST-JANAF review gives and enthalpy of –273.3000 ± 0.70 kJ mol^{-1} and an entropy of 173.778 ± 0.005 J K^{-1} mol^{-1}.[18] A network optimization of *ab initio* reaction enthalpies results in a value of $\Delta_f H_0^\circ$ = –272.82 ± 0.35 kJ mol^{-1}.[5] The uncertainty corresponds to the 95% confidence limit. The reference atomic values were taken from the Active Thermochemical Tables, ver. 1.20.

HOF Enthalpy value at 0 K from a re-evaluation of the photoionization studies, along with the newer enthalpy for OH and a more recent ionization energy for OH.[15] Previous values of $\Delta_f H^\circ_{298}$ = −98.3 ± 4.2 kJ mol^{-1} and $\Delta_f H_0^\circ$ = −95.4 ± 4.2 kJ mol^{-1} from JANAF review from 1972.[3] A calculation of the isodesmic reaction HOF + OH → FO + H_2O at the W4.2 level of theory leads to $\Delta_f H^\circ_{298}$ = −87.2 ± 0.6 kJ mol^{-1} and $\Delta_f H_0^\circ$ = −84.3 ± 0.6 kJ mol^{-1}, in good agreement.[13]

FO Atomization energy was calculated using the Wn family of computational methods. Small increases in the atomization energy were found going from W2.2 to W4.4. These results led to $\Delta_f H^\circ_{298}$ = 110.58 ± 0.46 kJ mol^{-1} and $\Delta_f H_0^\circ$ = 109.96 ± 0.46 kJ mol^{-1}.[13] Atomization energy calculated at the CCSD(T)(FC) level through aug-cc-PV7Z basis sets led to $\Delta_f H^\circ_{298}$ = 110.88 ± 0.84 kJ mol^{-1} and $\Delta_f H_0^\circ$ = 110.04 ± 0.84 kJ mol^{-1}.[9] These were averaged to give the Table values. The previous table values of $\Delta_f H^\circ_{298}$ = 109 ± 10 kJ mol^{-1} and $\Delta_f H_0^\circ$ = 108 ± 10 kJ mol^{-1} were from the NIST-JANAF thermochemical tables for the oxygen fluorides[2] and were based on mass spectrometric and thermal decomposition studies of FOF. The atomization energy calculated with CCSD(T) using aug-cc-pVnZ (n=D-6) basis sets, approaching the complete basis set limit, resulted in $\Delta_f H^\circ_{298}$ = 27.9 ± 0.4 kcal mol^{-1} and $\Delta_f H_0^\circ$ = 27.6 ± 0.4 kcal mol^{-1}.[7] The entropy value is from JANAF.[2]

FOF NIST-JANAF thermochemical tables for the oxygen fluorides.[2] Enthalpy based on a series of calorimetric studies. Atomization energy calculated at the CCSD(T)(FC) level through aug-cc-PV7Z basis sets led to $\Delta_f H^\circ_{298}$ = 24.7 ± 1.3 kJ mol^{-1} and $\Delta_f H_0^\circ$ = 26.8 ± 1.3 kJ mol^{-1}.[9] The atomization energy calculated with CCSD(T) using aug-cc-pVnZ (n=D-6) basis sets, approaching the complete basis set limit, resulted in $\Delta_f H^\circ_{298}$ = 6.6 ± 0.5 kcal mol^{-1} and $\Delta_f H_0^\circ$ = 7.1 ± 0.5 kcal mol^{-1}.[7] An extrapolation of a CCSD(T) calculation with aug-cc-pVTZ and aug-cc-pVQZ basis sets lead to $\Delta_f H^\circ_{298}$ = 24.4 ± 4 kJ mol^{-1}.[12]

OFO Atomization energy calculated at the CCSD(T)(FC) level through aug-cc-PV7Z basis sets led to the listed enthalpy.[9] The previous Table values of $\Delta_f H^\circ_{298}$ = 380 ± 20 kJ mol^{-1} and $\Delta_f H_0^\circ$ = 381 ± 20 kJ mol^{-1} were from the NIST-JANAF thermochemical tables for the oxygen fluorides and was based on a calculated value of enthalpy difference between OFO and FOO at 0 K of 356 kJ mol^{-1}.[2] The entropy value is also from the JANAF Table and is based on the earlier computational results.

FOO From an analysis of studies of the equilibrium F + O_2 ↔ FOO (Table 3-1, Note 10). NIST-JANAF thermochemical tables for the oxygen fluorides, based on several experimental values, primarily from kinetic studies recommends $\Delta_f H^\circ_{298}$ = 25.4 ± 2 kJ mol^{-1} and $\Delta_f H_0^\circ$ = 27.2 ± 2 kJ mol^{-1}.[2] This is also the source of the entropy value. A determination of the atomization energy gave $\Delta_f H^\circ_{298}$= 5.8 ± 0.3 kcal mol^{-1},[8] whereas a UCCSDT calculation led to $\Delta_f H^\circ_{298}$= 6.5 ± 1 kcal mol^{-1}.[6] Atomization energy was calculated using the Wn family of computational methods. Significant increases in the atomization energy were found going from W2.2 to W4.4. These results led to $\Delta_f H^\circ_{298}$ = 24.6 ± 0.7 kJ mol^{-1} and $\Delta_f H_0^\circ$ = 26.4 ± 0.7 kJ mol^{-1}.[13] Atomization energy calculated at the CCSD(T)(FC) level through aug-cc-PV7Z basis sets led to $\Delta_f H^\circ_{298}$ = 26.8 ± 2.9 kJ mol^{-1} and $\Delta_f H_0^\circ$ = 28.9 ± 2.9 kJ mol^{-1}.[9]

HOOF Atomization energy calculated by the CCSD(T) extrapolated to the CBS limit, with geometry optimized through the CCSD(T)/aV(T+d)Z level.[10]

FOOF NIST-JANAF thermochemical tables for the oxygen fluorides.[2] Value adopted for enthalpy is that recommended by Lyman[14] based on a calorimetric measurement on the decomposition into O_2 and F_2. The atomization energy calculated with CCSD(T) using aug-cc-pVnZ (n=D-6) basis sets, approaching the complete basis set limit, resulted in $\Delta_f H^\circ_{298}$ = 40.2 ± 3.8 kJ mol^{-1} and $\Delta_f H_0^\circ$ = 43.9 ± 3.8 kJ mol^{-1}.[7] Atomization energy was calculated using the Wn family of computational methods. Significant increases in the atomization energy were found going from W2.2 to W4.4. These results led to $\Delta_f H^\circ_{298}$ = 32.8 ± 0.75 kJ mol^{-1} and $\Delta_f H_0^\circ$ = 37.24 ± 0.75 kJ mol^{-1}.[13] Atomization energy calculated at the CCSD(T)(FC) level through aug-cc-PV7Z basis sets led to $\Delta_f H^\circ_{298}$ = 26.8 ± 2.9 kJ mol^{-1} and $\Delta_f H_0^\circ$ = 31.0 ± 2.9 kJ mol^{-1}.[9] An extrapolation of a CCSD(T) calculation with aug-cc-pVTZ and aug-cc-pVQZ basis sets lead to $\Delta_f H^\circ_{298}$ = 34.8 ± 4 kJ mol^{-1}.[12]

FOOOF, for the C_2 conformer
Based on an extrapolation of a CCSD(T) calculation with aug-cc-pVTZ and aug-cc-pVQZ basis sets. For the C_s conformer, $\Delta_f H^\circ_{298}$ = 111.3 ± 4 kJ mol^{-1} and S = 204.3 J K mol^{-1} K^{-1}.[12]

FNO The equilibrium geometry was calculated at the CCSD(T)/cc-pVQZ level of theory, while the energy was calculated by summing various contributions calculated at the CCSC(T) level with the use of various basis sets.[20] The previous value, $\Delta_f H^\circ_{298}$ = −65.7 kJ mol^{-1}, was taken from review of Stull, et al.[19] The JANAF Tables give $\Delta_f H_0^\circ$ = −63.3 kJ mol^{-1}, $\Delta_f H_{298}^\circ$ = −65.7 kJ mol^{-1}, and S° = 248.082 J mol^{-1} K^{-1}.[3]

***cis, trans*-FONO**
The equilibrium geometry was calculated at the CCSD(T)/cc-pVQZ level of theory, while the energy was calculated by summing various contributions calculated at the CCSC(T) level with the use of various basis sets.[20] The previous value, $\Delta_f H^\circ_{298}$ = 67 kJ mol^{-1}, was estimated.[1]

FNO_2 The equilibrium geometry was calculated at the CCSD(T)/cc-pVQZ level of theory, while the energy was calculated by summing various contributions calculated at the CCSC(T) level with the use of various basis sets.[20] The previous value, $\Delta_f H^\circ_{298}$ = −79 kJ mol^{-1}, was taken from review of Stull et al.[19]

$FONO_2$ The equilibrium geometry was calculated at the CCSD(T)/cc-pVQZ level of theory, while the energy was calculated by summing various contributions calculated at the CCSC(T) level with the use of various basis sets.[20] The previous value, $\Delta_f H^\circ_{298}$ = 15 ± 3 kJ mol^{-1}, was taken from review of Gurvich et al.[11] The JANAF estimate from 1963 gave an enthalpy of 10 ± 2 kJ mol^{-1}.[3]

NF_2 Enthalpy value from a reanalysis of the data used by JANAF, combined with the newer enthalpy value for NF_3.[21]

NF_3 A study of the combustion of rhombic sulfur in NF_3 to generate SF_6 and N_2 using $\Delta_f H^\circ_{298}(SF_6)$ = −1220.8 ± 0.8 kJ mol^{-1} results in the enthalpy of NF_3.[21]

(1) Atkinson, R.; Baulch, D. L.; Cox, R. A.; Hampson, R. F.; Kerr, J. A.; Rossi, M. J.; Troe, J. Evaluated kinetic, photochemical, and heterogeneous data for atmospheric chemistry: Supplement V, IUPAC subcommittee on gas kinetic data evaluation for atmospheric chemistry. *J. Phys. Chem. Ref. Data* **1997**, *26*, 521-1011, doi:10.1063/1.556011.

(2) Chase, M. W. NIST-JANAF thermochemical tables for the oxygen fluorides. *J. Phys. Chem. Ref. Data* **1996**, *25*, 551-603, doi:10.1063/1.555992.

(3) Chase, M. W. NIST-JANAF thermochemical tables. *J. Phys. Chem. Ref. Data* **1998**, *Monograph 9*.

(4) Cox, J. D.; Wagman, D. D.; Medvedev, V. A. *CODATA Key Values for Thermodynamics*; Hemisphere Publishing Corp.: New York, 1989.

(5) Császár, A. G.; Furtenbacher, T. From a network of computed reaction enthalpies to atom-based thermochemistry (NEAT). *Chem. Eur. J.* **2010**, *16*, 4826-4835, doi:10.1002/chem.200903252.

(6) Denis, P. A., and O. N. Ventura CCSDT study of the fluoroperoxyl radical, FOO. *Chem. Phys. Lett.* **2004**, *385*, 292-297, doi:10.1016/j.cplett.2003.12.081.
(7) Feller, D.; Dixon, D. A. Coupled cluster theory and multireference configuration interaction study of FO, F_2O, FO_2, and FOOF. *J. Phys. Chem. A* **2003**, *107*, 9641-9651, doi:10.1021/jp030267v.
(8) Feller, D.; Peterson, K. A.; Dixon, D. A. A survey of factors contributing to accurate theoretical predictions of atomization energies and molecular structures. *J. Chem. Phys.* **2008**, *129*, 204105, doi:10.1063/1.3008061.
(9) Feller, D.; Peterson, K. A.; Dixon, D. A. Refined theoretical estimates of the atomization energies and molecular structures of selected small oxygen fluorides. *J. Phys. Chem. A* **2010**, *114*, 613-623, doi:10.1021/jp908128g.
(10) Grant, D. J.; Dixon, D. A.; Francisco, J. S.; Feller, D.; Peterson, K. A. Heats of formation of the $H_{1,2}O_mS_n$ (m,n = 0-3) molecules from electronic structure calculations. *J. Phys. Chem. A* **2009**, *113*, 11343-11353, doi:10.1021/jp905847e.
(11) Gurvich, L. V.; Veyts, I. V.; Alcock, C. B. *Thermodynamic Properties of Individual Substances,*, Fourth ed.; Hemisphere Publishing Corp.: New York, 1991; Vol. 2.
(12) Huang, M.-J.; Watts, J. D. Theoretical characterization of the F_2O_3 molecule by coupled-cluster methods. *J. Phys. Chem. A* **2010**, *114*, 10197-10201, doi:10.1021/jp101106n.
(13) Karton, A.; Parthiban, S.; Martin, J. M. L. Post-CCSD(T) ab initio thermochemistry of halogen oxides and related hydrides XOX, XOOX, HOX, XO_n, and HXO_n (X = F, Cl), and evaluation of DFT methods for these systems. *J. Phys. Chem. A* **2009**, *113*, 4802-4816, doi:10.1021/jp8087435.
(14) Lyman, J. Thermodynamic properties of dioxygen difluoride (O_2F_2) and dioxygen fluoride (O_2F). *J. Phys. Chem. Ref. Data* **1989**, *18*, 799-807, doi:10.1063/1.555830.
(15) Ramachandran, R.; Vegesna, N. S.; Peterson, K. A. Effects of electron correlation and scalar relativistic corrections on the thermochemical and spectroscopic properties of HOF. *J. Phys. Chem. A* **2003**, *107*, 7938-7944, doi:10.1021/jp035266h.
(16) Ruscic, B.; Feller, D.; Peterson, K. Active Thermochemical Tables: dissociation energies of several homonuclear first-row diatomics and related thermochemical values. *Theor. Chem. Acc.* **2014**, *133*, 1415, doi:10.1007/s00214-013-1415-z.
(17) Ruscic, B.; Pinzon, R. E.; Morton, M. L.; von Laszevski, G.; Bittner, S. J.; Nijsure, S. G.; Amin, K. A.; Minkoff, M.; Wagner, A. F. Introduction to active thermochemical tables: Several "key" enthalpies of formation revisited. *J. Phys. Chem. A* **2004**, *108*, 9979-9997, doi:10.1021/jp047912y.
(18) Shenyavskaya, E. A.; Yungman, V. S. NIST-JANAF thermochemical tables. III. Diatomic hydrogen halide gases. *J. Phys. Chem. Ref. Data* **2004**, *33*, 923-957, doi:10.1063/1.1638781.
(19) Stull, D. R.; Westrum, E. F.; Sinke, G. C. *The Chemical Thermodynamics of Organic Compounds*; John Wiley & Sons: New York, 1969.
(20) Szakács, P.; Csontos, J.; Das, S.; Kállay, M. High-accuracy theoretical thermochemistry of atmospherically important nitrogen oxide derivatives. *J. Phys. Chem. A* **2011**, *115*, 3144-3153, doi:10.1021/jp112116x.
(21) Walker, L. C. The enthalpy of reaction of sulfur and nitrogen trifluoride. *J. Phys. Chem.* **1967**, *71*, 361-363, doi:10.1021/j100861a023.

Note 23: *Compounds containing one C and one or more F* Back to Table

CF Thermodynamic properties from Gurvich et al. review.[6] A computational study with geometry optimization carried out at the CCSD(T) level of theory with the cc-pZQZ basis set, followed by an enthalpy calculation using the HEAT protocols, led to $\Delta_f H_0^\circ$ =243.3 ± 0.8 kJ mol^{-1}, $\Delta_f H_{298}^\circ$ =247.0 ± 0.8 kJ mol^{-1}, and S = 212.9 ± 1.5 J K^{-1} mol^{-1}.[5] A simulation of the atomization reaction using the CCSD(T) method with the vTz-F12 and vQz-F12 basis sets led to $\Delta_f H_0^\circ$ = 243.8 ± 1.0 kJ mol^{-1} and $\Delta_f H_{298}^\circ$= 247.9 ± 1.0 kJ mol^{-1}.[1]

CHF Calculated for the X^1A' state. Enthalpy from a CCSD(T) calculation with the aug-cc-pVnZ (n=D,T,Q,5) basis set extrapolated to the CBS limit and entropy from a MP2/aVTZ calculation.[9] Enthalpy obtained using the computed enthalpy of a reaction of the type: $CH_2(^1A_1)$ + CH_2F_2 +

$2CH_3Y \rightarrow CFY(^1A_1) + 3CH_4$ results in $\Delta_f H^\circ_{298}$ = 146 kJ mol^{-1} at the QCISD(T)/6-311+G(3df,2p)//QCISD/6-311G(d,p) level of theory. Calculations also done at the G2 level.[15] Previous recommendation, $\Delta_f H^\circ_{298}$ = 143 ± 13.0 kJ mol^{-1}, based on combining experimental chloride dissociation energies from the parent anion, prior experimental measurements, and G2 calculations.[12] A computational study with geometry optimization carried out at the CCSD(T) level of theory with the cc-pZQZ basis set, followed by an enthalpy calculation using the HEAT protocols, led to $\Delta_f H_0^\circ$ =148.9 ± 1.2 kJ mol^{-1}, $\Delta_f H^\circ_{298}$ = 149.0 ± 1.2 kJ mol^{-1}, and S = 223.1 ± 1.5 J K^{-1} mol^{-1}.[5]

CH_2F Derived from the kinetics and equilibria of the iodination reaction $CH_3F + I_2 \leftrightarrow CH_2FI + HI$.[11] A QCISD(T)/6-311+G(3df,2p) isodesmic study resulted in an enthalpy of –29.0±4.1 kJ mol^{-1}.[16] A computational study with geometry optimization carried out at the CCSD(T) level of theory with the cc-pZQZ basis set, followed by an enthalpy calculation using the HEAT protocols, led to $\Delta_f H_0^\circ$ = −27.9 ± 1.6 kJ mol^{-1}, $\Delta_f H^\circ_{298}$ = −31.2 ± 1.6 kJ mol^{-1}, and S = 232.5 ± 1.5 J K^{-1} mol^{-1}.[5] This enthalpy difference was used to calculate the 0 K value in the Table.

CH_3F Enthalpies of reaction calculated (and averaged) at the MCG3//MCQCISD level of theory (up to 6-311++G(3d2f,2df,2p) basis set) for the homolytic fragmentation to the alkyl radical and fluoride atom, and for the atomization reaction. Enthalpy also calculated for the heterolytic fragmentation into the alkyl cation and fluoride anion for support.[7] Previous value, $\Delta_f H^\circ_{298}$ = -238 ± 8 kJ mol^{-1}, estimated in review of Rodgers et al.[13] Luo and Benson recommend -55.9 ± 1 kcal/mol.[8] A computational study with geometry optimization carried out at the CCSD(T) level of theory with the cc-pZQZ basis set, followed by an enthalpy calculation using the HEAT protocols, led to $\Delta_f H_0^\circ$ = −228.5 ± 2.0 kJ mol^{-1}, $\Delta_f H^\circ_{298}$= −236.9 ± 2.0 kJ mol^{-1}, and S = 222.5 ± 1.5 J K^{-1} mol^{-1}.[5] This enthalpy difference was used to calculate the 0 K value in the Table.

CF_2 Calculated for the X^1A' state. Enthalpy from a CCSD(T) calculation with the aug-cc-pVnZ (n=D,T,Q,5) basis set extrapolated to the CBS limit and entropy from a MP2/aVTZ calculation.[9] $\Delta_f H_0^\circ$ = –46.0±0.8 kcal mol^{-1}. Enthalpy obtained using the computed enthalpy of a reaction of the type: $CH_2(^1A_1) + CH_2F_2 + 2CH_3Y \rightarrow CFY(^1A_1) + 3CH_4$ results in $\Delta_f H^\circ_{298}$ = -196 kJ mol^{-1} at the QCISD(T)/6-311+G(3df,2p)//QCISD/6-311G(d,p) level of theory. Calculations also done at the G2 level.[15] Previous recommendation, –44.0±2 kcal mol^{-1}, based on combining experimental chloride dissociation energies from the parent anion, prior experimental measurements, and G2 calculations.[12] A computational study with geometry optimization carried out at the CCSD(T) level of theory with the cc-pZQZ basis set, followed by an enthalpy calculation using the HEAT protocols, led to $\Delta_f H_0^\circ$ = −193.6 ± 1.2 kJ mol^{-1}, $\Delta_f H^\circ_{298}$= −193.2 ± 1.2 kJ mol^{-1}, and S = 240.6 ± 1.5 J K^{-1} mol^{-1}.[5] A simulation of the atomization reaction using the CCSD(T) method with the vTz-F12 and vQz-F12 basis sets led to $\Delta_f H_0^\circ$ = −193.2 ± 1.3 kJ mol^{-1} and $\Delta_f H^\circ_{298}$= −190.4 ± 1.3 kJ mol^{-1}.[1]

CHF_2 Derived from the kinetics and equilibria of the iodination reaction $CH_3F + I_2 \leftrightarrow CH_2FI + HI$.[11] A QCISD(T)/6-311+G(3df,2p) isodesmic study resulted in an enthalpy of –241.2 ± 4.1 kJ mol^{-1}.[16] A computational study with geometry optimization carried out at the CCSD(T) level of theory with the cc-pZQZ basis set, followed by an enthalpy calculation using the HEAT protocols, led to $\Delta_f H_0^\circ$ = −239.4 ± 2.6 kJ mol^{-1}, $\Delta_f H^\circ_{298}$= −243.0 ± 2.6 kJ mol^{-1}, and S = 255.8 ± 6.5 J K^{-1} mol^{-1}.[5] The enthalpy difference was used to calculate the 0 K value in the Table.

CH_2F_2 From review by Rodgers et al.[13] Pedley gives –452.3 ± 0.9 kJ mol^{-1}.[10] A computational study with geometry optimization carried out at the CCSD(T) level of theory with the cc-pZQZ basis set, followed by an enthalpy calculation using the HEAT protocols, led to $\Delta_f H_0^\circ$ = −442.6 ± 2.0 kJ mol^{-1}, $\Delta_f H^\circ_{298}$= −450.5 ± 2.0 kJ mol^{-1}, and S = 246.3 ± 1.5 J K^{-1} mol^{-1}.[5] The enthalpy difference was used to calculate the 0 K value in the Table.

CF_3 Enthalpy from a simultaneous solution of a thermochemical network for the CF_3X species, where X = nil, H, Cl, Br, I, CF_3, CN.[14] Entropy from recommendation of Gurvich et al.[6] A QCISD(T)/6-311+G(3df,2p) isodesmic study resulted in an enthalpy of –465.9 ± 4.1 kJ mol^{-1}.[16] A computational study with geometry optimization carried out at the CCSD(T) level of theory with the cc-pZQZ basis set, followed by an enthalpy calculation using the HEAT protocols, led

to $\Delta_f H_0^\circ$ = −464.8 ± 1.6 kJ mol^{-1}, $\Delta_f H_{298}^\circ$ = −467.6 ± 1.6 kJ mol^{-1}, and S = 264.1 ± 1.5 J K^{-1} mol^{-1}.[5] A simulation of the atomization reaction using the CCSD(T) method with the vTz-F12 and vQz-F12 basis sets led to $\Delta_f H_0^\circ$ = −468.4 ± 1.6 kJ mol^{-1} and $\Delta_f H_{298}^\circ$ = −469.3 ± 1.6 kJ mol^{-1}.[1]

CHF_3 Enthalpy from a simultaneous solution of a thermochemical network for the CF_3X species, where X = nil, H, Cl, Br, I, CF_3, CN.[14] Entropy from recommendation of Gurvich et al.[6] An enthalpy calculation from the atomization energy was obtained starting with a 'best estimated' structure from extensive calculations and analysis, followed by CCST with aug-cc-pVQZ and aug-cc-pV5Z basis sets, and CCSD(T) with aug-cc-pVTZ and aug-cc-pVQZ basis sets. Values of $\Delta_f H_0^\circ$ = –165.18 kcal mol^{-1} and $\Delta_f H_{298}^\circ$ = –166.86 kcal mol^{-1} were obtained.[2] A computational study with geometry optimization carried out at the CCSD(T) level of theory with the cc-pZQZ basis set, followed by an enthalpy calculation using the HEAT protocols, led to $\Delta_f H_0^\circ$ = −687.7 ± 2.0 kJ mol^{-1}, $\Delta_f H_{298}^\circ$ = −694.9 ± 2.0 kJ mol^{-1}, and S = 259.2 ± 1.5 J K^{-1} mol^{-1}.[5]

CF_4 CODATA Key Value.[4] The JANAF Tables give $\Delta_f H_0^\circ$ = –927.2 kJ mol^{-1}, $\Delta_f H_{298}^\circ$ = –933.2 kJ mol^{-1}, and S° = 261.419 J mol^{-1}.[3] A computational study with geometry optimization carried out at the CCSD(T) level of theory with the cc-pZQZ basis set, followed by an enthalpy calculation using the HEAT protocols, led to $\Delta_f H_0^\circ$ = −927.8 ± 2.0 kJ mol^{-1}, $\Delta_f H_{298}^\circ$ = −933.8 ± 2.0 kJ mol^{-1}, and S = 260.9 ± 1.5 J K^{-1} mol^{-1}.[5] A simulation of the atomization reaction using the CCSD(T) method with the vTz-F12 and vQz-F12 basis sets led to $\Delta_f H_0^\circ$ = −930.7 ± 2.0 kJ mol^{-1} and $\Delta_f H_{298}^\circ$ = −934.2 ± 2.0 kJ mol^{-1}.[1]

(1) Baranovskii, V. I.; Skorobogatov, G. A. Quantum-chemical simulation of the gas-phase molecular, thermodynamic, and kinetic parameters of CF, CF_2, and CF_3 radicals and CF_4, C_2F_2, C_2F_4, and C_2F_6 molecules. *Russ. J. Gen. Chem.* **2016**, *86*, 241-250, doi:10.1134/s1070363216020067.

(2) Breidung, J.; Cosleou, J.; Demaison, J.; Sarka, K.; Thiel, W. Ab initio anharmonic force field, molecular parameters, equilibrium structure and enthalpy of formation of fluoroform. *Mol. Phys.* **2004**, *102*, 1827-1841, doi:10.1080/00268970412331287089.

(3) Chase, M. W. NIST-JANAF thermochemical tables. *J. Phys. Chem. Ref. Data* **1998**, *Monograph 9*.

(4) Cox, J. D.; Wagman, D. D.; Medvedev, V. A. *CODATA Key Values for Thermodynamics*; Hemisphere Publishing Corp.: New York, 1989.

(5) Csontos, J.; Rolik, Z.; Das, S.; Kállay, M. High-accuracy thermochemistry of atmospherically important fluorinated and chlorinated methane derivatives. *J. Phys. Chem. A* **2010**, *114*, 13093-13103, doi:10.1021/jp105268m.

(6) Gurvich, L. V.; Veyts, I. V.; Alcock, C. B. *Thermodynamic Properties of Individual Substances,*, Fourth ed.; Hemisphere Publishing Corp.: New York, 1991; Vol. 2.

(7) Kormos, B. L.; Liebman, J. F.; Cramer, C. J. 298 K enthalpies of formation of monofluorinated alkanes: theoretical predictions for methyl, ethyl,isopropyl, and tert-butyl fluoride. *J. Phys. Org. Chem.* **2004**, *17*, 656-664, doi:10.1002/poc.801.

(8) Luo, Y. R.; Benson, S. W. Heats of formation of alkyl fluorides. *J. Phys. Chem. A* **1997**, *101*, 3042-3044, doi:10.1021/jp962641f.

(9) Matus, M. H.; Nguyen, M. T.; Dixon, D. A.; Christe, K. O. Thermochemical properties of CHFO and CF_2O. *J. Phys. Chem. A* **2008**, *112*, 4973-4981, doi:10.1021/jp800103y.

(10) Pedley, J. B. *Thermochemical Data and Structures of Organic Compounds*; Thermodynamics Data Center: College Station, TX, 1994.

(11) Pickard, J. M.; Rodgers, A. S. Kinetics of the gas-phase reaction $CH_3F + I_2 \leftrightarrows CH_2FI + HI$: The C-H bond dissociation energy in methyl and methylene fluorides. *Int. J. Chem. Kinet.* **1983**, *15*, 569-577, doi:10.1002/kin.550150607.

(12) Poutsma, J. C.; Paulino, J. A.; Squires, R. R. Absolute heats of formation of CHCl, CHF, and CClF. A gas-phase experimental and G2 theoretical study. *J. Phys. Chem. A* **1997**, *101*, 5327-5336, doi:10.1021/jp970778f.

(13) Rodgers, A. S.; Chao, J.; Wilhoit, R. C.; Zwolinski, B. J. Ideal gas thermodynamic properties of eight chloro- and fluoromethanes. *J. Phys. Chem. Ref. Data* **1974**, *3*, 117-140, doi:10.1063/1.3253135.
(14) Ruscic, B.; Michael, J. V.; Redfern, P. C.; Curtiss, L. A.; Raghavachri, K. Simultaneous adjustment of experimentally based enthalpies of formation of CF_3X, X = nil, H, Cl, Br, I, CF_3, CN, and a probe of G3 theory. *J. Phys. Chem. A* **1998**, *102*, 10889-10899, doi:10.1021/jp983237e.
(15) Schwartz, M.; Marshall, P. An ab initio investigation of halocarbenes. *J. Phys. Chem. A* **1999**, *103*, 7900-7906, doi:10.1021/jp9919213.
(16) Schwartz, M.; Peebles, L. R.; Berry, R. J.; Marshall, P. A computational study of chlorofluoro-methyl radicals *J. Chem. Phys.* **2003**, *118*, 557-564, doi:10.1063/1.1524157.

Note 24: *Compounds containing one C and one or more F and O*

Back to Table

CFH_2O and CFH_2OH

The enthalpies of formation are based on isodesmic reactions calculated at the MP2/6-31G(d,p) level of theory.[16]

FCO The enthalpy values are taken from a CCSDT(Q) calculation, with structure optimized using the cc-pVQZ basis set.[14] The previous $\Delta_f H_{298}^o = -174.1 \pm 2$ was from a CCSD(T) calculation with the aug-cc-pVnZ (n=D,T,Q,5) basis set extrapolated to the CBS limit.[13] The entropy value is from a MP2/aVTZ calculation.[13] The decomposition rate constant for FCO → F + CO,[9] combined with the rate constant $k = 2.4 \times 10^{-22}$ cm^6 s^{-1} [18] for the reverse reaction, results in an upper limit of $\Delta_f H_{298}^o < -153.1$ kJ mol^{-1}.[9] A. CCSD(T) calculation gives $\Delta_f H_{298}^o = -42.0 \pm 0.5$ kcal mol^{-1}.[4]

FCO_2, fluoroformyloxyl radical

Calculated at the CCSD(T) level of theory. CFO value from same work is –42.0 ± 0.5 kcal mol^{-1}, which differs from value in Table.[4]

CHFO The enthalpy values are taken from a CCSDT(Q) calculation, with structure optimized using the cc-pVQZ basis set.[14] The previous $\Delta_f H_{298}^o = -381.2 \pm 2$ was from a CCSD(T) calculation with the aug-cc-pVnZ (n = D,T,Q,5) basis set extrapolated to the CBS limit.[13] The entropy value is from a MP2/aVTZ calculation.[13] The earlier enthalpy value, –91.6 kcal mol^{-1}, was from an G2(MP2) calculation,[17] and the earlier entropy was from Gurvich et al.[8]

CF_2HFO and CF_2HOH

The enthalpies of formation are based on isodesmic reactions calculated at the MP2/6-31G(d,p) level of theory.[16]

CF_2O The enthalpy values are taken from a CCSDT(Q) calculation, with structure optimized using the cc-pVQZ basis set,[14] supported by several earlier computational studies discussed in that paper.[3,7,13] The previous $\Delta_f H_{298}^o = -623.8 \pm 5.9$ was a lower limit from a photoionization study.[1] Entropy from Gurvich et al.[8] Pedley review gives an enthalpy value of –639.8 ± 1.4 kJ mol^{-1}.[15] A CCSD(T) calculation with the aug-cc-pVnZ (n=D,T,Q,5) basis set extrapolated to the CBS limit gave $\Delta_f H_0^o = -143.9 \pm 0.5$ kcal mol^{-1}, $\Delta_f H_{298}^o = -144.7 \pm 0.5$ kcal mol^{-1}, and $S = 61.87$ cal $K^{-1}mol^{-1}$.[13]

CF_3O Re-analysis of data of Batt and Walsh, using new value for CF_2O.[1] The enthalpy of formation, $\Delta_f H_{298}^o = -154.5$ kcal mol^{-1} based on an isodesmic reaction calculated at the MP2/6-31G(d,p) level of theory.[16]

CF_2O_2 Determined on the basis of extensive ab initio calculations.[11] Isomeric forms F_2COO and FC(=O)OF are calculated to have enthalpies of –60 and –104 kcal $mole^{-1}$, respectively.

CF_3O_2 Two values for the C-O bond dissociation energy in CF_3O_2 are given in Lightfoot, et al., -144 ± 3.3 and –141 ± 10 kJ mol^{-1} at 0 K and adjusted to 298 K.[12] The value given is an average of the two resulting enthalpies.

CF_3OH Proton affinity obtained by using transitional energy threshold measurements on protonated trifluoromethanol. This was used in a thermochemical cycle to derive the enthalpy of formation.[6] Previous value was based on a photoionization study, where a lower limit of $\Delta_f H^{\circ}_{298} > -908.8 \pm 0.9$ kJ mol^{-1} was presented.[2] The enthalpy of formation, $\Delta_f H_{298}^{\circ} = -933.4$ kJ mol^{-1}, based on an isodesmic reaction calculated at the MP2/6-31G(d,p) level of theory.[16]

CF_3OF Based on photoionization of CF_3OF and an analysis of the CF_3^+ and CF_2O^+ fragments.[2] A G2 calculation led to an enthalpy of –774.5 kJ mol^{-1}.[5]

CH_2FOOH, CHF_2OOH, and CF_3OOH

Geometry optimization and frequency calculations were performed at the MP2/6-31G(d) and the B3LYP/6-311++G(d,p) levels of theory, with a single-point energy calculation at the CCSD(T)/6-311++G(d,p//B3LYP/6-311++G(d,p) level. The dissociation energy into HO_2 and the alkyl radical was then evaluated and used, after thermal correction, to calculate the enthalpy of formation at 298 K.[10] This was adjusted to the radical values from the present Table.

(1) Asher, R. L.; Appelman, E. H.; Ruscic, B. On the heat of formation of carbonyl fluoride, CF_2O. *J. Chem. Phys.* **1996**, *105*, 9781-9795, doi:10.1063/1.472848.

(2) Asher, R. L.; Appelman, E. H.; Tilson, J. L.; Litorja, M.; Berkowitz, J.; Ruscic, B. A photoionization study of trifluoromethanol, CF_3OH, trifluoromethyl hypofluorite, CF_3OF, and trifluoromethyl hypochlorite, CF_3OCl. *J. Chem. Phys.* **1997**, *106*, 9111-9121, doi:10.1063/1.474017.

(3) Bakowies, D. Ab initio thermochemistry with high-level isodesmic corrections: Validation of the ATOMIC protocol for a large set of compounds with first-row atoms (H, C, N, O, F). *J. Phys. Chem. A* **2009**, *113*, 11517-11534, doi:10.1021/jp9027782.

(4) Breidung, J.; Thiel, W. Thermochemistry of the fluoroformyloxyl radical: A computational study based on coupled cluster theory. *J. Phys. Chem. A* **2006**, *110*, 1575-1585, doi:10.1021/jp053883v.

(5) Brudnik, K.; Jodkowski, J. T.; Ratajczak, E. Kinetics of the formation reactions of trifluoromethanol and trifluoromethyl hypohalites in the gas phase. *J. Mol. Struct.* **2003**, *656*, 333-339, doi:10.1016/S0022-2860(03)00347-8.

(6) Chyall, L. J.; Squires, R. R. The proton affinity and absolute heat of formation of trifluoromethanol. *J. Phys. Chem.* **1996**, *100*, 16435-16440, doi:10.1021/jp961135n.

(7) Dixon, D. A.; Feller, D. Heats of formation of CF_2, FCO, and CF_2O. *J. Phys. Chem. A* **1998**, *102*, 8209-8216, doi:10.1021/jp982655g.

(8) Gurvich, L. V.; Veyts, I. V.; Alcock, C. B. *Thermodynamic Properties of Individual Substances,*, Fourth ed.; Hemisphere Publishing Corp.: New York, 1991; Vol. 2.

(9) Knyazev, V. D.; Bencsura, A.; Slagle, I. R. Unimolecular decomposition of the FCO radical. *J. Phys. Chem. A* **1997**, *101*, 849-852, doi:10.1021/jp9623296.

(10) Kosmas, A. M.; Mpellos, C.; Salta, Z.; Drougas, E. Structural and heat of formation studies of halogenated methyl hydro-peroxides. *Chem. Phys.* **2010**, *371*, 36-42, doi:10.1016/j.chemphys.2010.03.026.

(11) Kraka, E.; Konkoli, Z.; Cremer, D.; Fowler, J.; Schaefer, H. F. Difluorodioxirane: An unusual cyclic peroxide. *J. Am. Chem. Soc.* **1996**, *118*, 10595-10608, doi:10.1021/ja961983w.

(12) Lightfoot, P. D.; Cox, R. A.; Crowley, J. N.; Destriau, M.; Hayman, G. D.; Jenkin, M. E.; Moortgat, G. K.; Zabel, F. Organic peroxy radicals: Kinetics, spectroscopy and tropospheric chemistry. *Atmos. Environ.* **1992**, *26A*, 1805-1961, doi:10.1016/0960-1686(92)90423-I.

(13) Matus, M. H.; Nguyen, M. T.; Dixon, D. A.; Christe, K. O. Thermochemical properties of CHFO and CF_2O. *J. Phys. Chem. A* **2008**, *112*, 4973-4981, doi:10.1021/jp800103y.

(14) Nagy, B.; Csontos, J.; Kállay, M.; Tasi, G. High-accuracy theoretical study on the thermochemistry of several formaldehyde derivatives. *J. Phys. Chem. A* **2010**, *114*, 13213-13221, doi:10.1021/jp1085203.

(15) Pedley, J. B. *Thermochemical Data and Structures of Organic Compounds*; Thermodynamics Data Center: College Station, TX, 1994.

(16) Schneider, W. F.; Nance, B. I.; Wallington, T. J. Bond strengths in halogenated methanes: Evidence for negative hyperconjugation. *J. Am. Chem. Soc.* **1995**, *117*, 478-485, doi:10.1021/ja00106a055.

(17) Schneider, W. F.; Wallington, T. J. Thermochemistry of COF_2 and related compounds. *J. Phys. Chem.* **1994**, *98*, 7448-7451, doi:10.1021/j100082a009.
(18) Wallington, T. J.; Hurley, M. D.; Shi, J.; Maricq, M. M.; Shested, J.; Nielsen, O. J.; Ellermann, T. A kinetic study of the reaction of fluorine atoms with CH_3F, CH_3Cl, CH_3Br, CF_2H_2, CO, CF_3H, CF_3CHCl_2, CF_3CH_2F, CHF_2CHF_2, CF_2ClCH_3, CHF_2CH_3, and CF_3CF_2H at 295 ± 2 K. *Int. J. Chem. Kinet.* **1993**, *25*, 651-665, doi:10.1002/kin.550250806.

Note 25: *$CF_3O_2NO_2$ and CF_3CN*

Back to Table

$CF_3O_2NO_2$ The unimolecular decomposition rate constant, measured between 264 and 297 K, was combined with earlier measurements of the combination rate constants to obtain the equilibrium constant for the reaction.[2] Thermochemical values were derived from both second- and third-law evaluations.

CF_3CN Enthalpy from a simultaneous solution of a thermochemical network for the CF_3X species, where X = nil, H, Cl, Br, I, CF_3, CN.[3] Entropy from recommendation of Chen, et al.[1]

(1) Chen, S. S.; Rodgers, A. S.; Chao, J.; Wilhoit, R. C.; Zwolinski, B. J. Ideal gas thermodynamic properties of six fluoroethanes. *J. Phys. Chem. Ref. Data* **1975**, *4*, 441-456, doi:10.1063/1.555521.
(2) Mayer-Figge, A.; Zabel, F.; Becker, K. H. Thermal decomposition of $CF_3O_2NO_2$. *J. Phys. Chem.* **1996**, *100*, 6587-6593, doi:10.1021/jp953205g.
(3) Ruscic, B.; Michael, J. V.; Redfern, P. C.; Curtiss, L. A.; Raghavachri, K. Simultaneous adjustment of experimentally based enthalpies of formation of CF_3X, X = nil, H, Cl, Br, I, CF_3, CN, and a probe of G3 theory. *J. Phys. Chem. A* **1998**, *102*, 10889-10899, doi:10.1021/jp983237e.

Note 26: *Compounds containing two C and one or more F*

Back to Table

CH_2CHF Enthalpy from review of Pedley.[16]

CH_2CH_2F and CH_3CHF
Conformers and rotational barriers determined at the CCSD)T)/cc-pVTZ level of theory and the resulting equilibrium structure optimized at the CCSD(T)/cc-pVQZ level. The total electronic energy was calculated at the complete basis set limit (extrapolated from aug-cc-pVXZ (X = T, Q, 5)), corrected for correlation contributions, the core correlation, the zero-point energy, diagonal Born-Oppenheimer contributions, and the scalar relativistic effect.[8] The heat of formation was computed from the calculated enthalpies by using the elemental reaction approach, taking the gaseous atom as the standard state for carbon. For CH_2CH_2F, the value given is for the global minimum configuration. A local minimum with C_s symmetry is slightly higher in enthalpy, with $\Delta_f H_{298}^\circ$ = −58.7 ± 2.8 kJ mol^{-1}. Previous values of the enthalpy, $\Delta_f H_{298}^\circ(CH_2CH_2F)$ = −59.4 ± 8 kJ mol^{-1} and $\Delta_f H_{298}^\circ(CH_3CHF)$ = −70.3 ± 8 kJ mol^{-1}, were from photobromination studies.[14] The previous entropy value, $S(CH_2CH_2F)$ = 279.7 J K^{-1} mol^{-1} and $S(CH_3CHF)$ = 274.0 J K^{-1} mol^{-1}, were determined at the UHF/6-31G* level of theory.[3]

CH_3CH_2F Conformers and rotational barriers determined at the CCSD)T)/cc-pVTZ level of theory and the resulting equilibrium structure optimized at the CCSD(T)/cc-pVQZ level. The total electronic energy was calculated at the complete basis set limit (extrapolated from aug-cc-pVXZ (X = T, Q, 5)) energies, corrected for correlation contributions, the core correlation, the zero-point energy, diagonal Born-Oppenheimer contributions, and the scalar relativistic effect. The heat of formation was computed from the calculated enthalpies by using the elemental reaction approach, taking the gaseous atom as the standard state for carbon.[15] Previous value of $\Delta_f H_{298}^\circ$ = −278.2 ± 1.7 kJ mol^{-1} was based on enthalpies of reaction calculated at the MCG3//MCQCISD level of theory (up to 6-311++G(3d2f,2df,2p) basis set) for the homolytic fragmentation to the alkyl radical and fluoride atom, and for the atomization reaction and averaged. Enthalpy also

calculated for the heterolytic fragmentation into the alkyl cation and fluoride anion for support.[11] Previous entropy S^o = 265.1 J mol^{-1} from Gurvich et al. review.[9]

C_2F_2 Enthalpy values obtained from a computational study with CCSD(T)(FC) geometry optimization with the aug-cc-pVnZ(n = D, T, Q, 5-7) basis sets, checked by a CCSD(T)-F12 calculation followed by atomization energy calculation at the CCSD(T) level extrapolated to the complete basis set limit.[6] Note that these values are from a published correction: doi:10.1021/jp202158j. A simulation of the atomization reaction using the CCSD(T) method with the vTz-F12 basis set led to $\Delta_f H_0^o$ = 5.0 ± 2.0 kJ mol^{-1} and $\Delta_f H_{298}^o$= 9.0 ± 2.0 kJ mol^{-1}.[1]

CH_2CF_2 Enthalpy from review of Pedley.[16] A computational study with CCSD(T)(FC) geometry optimization with the aug-cc-pVnZ(n = D, T, Q, 5-7) basis sets, checked by a CCSD(T)-F12 calculation followed by atomization energy calculation at the CCSD(T) level extrapolated to the complete basis set limit, resulted in $\Delta_f H_0^o$ = −343.1 ± 2.5 kJ mol^{-1} and $\Delta_f H_{298}^o$= −350.2 ± 2.5 kJ mol^{-1}.[6] Note that these values are from a published correction: doi:10.1021/jp202158j.

***cis* and *trans* CHCHF**

Enthalpy values obtained from a computational study with CCSD(T)(FC) geometry optimization with the aug-cc-pVnZ(n = D, T, Q, 5-7) basis sets, checked by a CCSD(T)-F12 calculation followed by atomization energy calculation at the CCSD(T) level extrapolated to the complete basis set limit.[6] Note that these values are from a published correction: doi:10.1021/jp202158j.

CH_3CF_2 Conformers and rotational barriers determined at the CCSD)T)/cc-pVTZ level of theory and the resulting equilibrium structure optimized at the CCSD(T)/cc-pVQZ level. The total electronic energy was calculated at the complete basis set limit (extrapolated from aug-cc-pVXZ (X = T, Q, 5)), corrected for correlation contributions, the core correlation, the zero-point energy, diagonal Born-Oppenheimer contributions, and the scalar relativistic effect.[8] The heat of formation was computed from the calculated enthalpies by using the elemental reaction approach, taking the gaseous atom as the standard state for carbon.

CH_3CHF_2, 1,1-difluoroethane

Conformers and rotational barriers determined at the CCSD)T)/cc-pVTZ level of theory and the resulting equilibrium structure optimized at the CCSD(T)/cc-pVQZ level. The total electronic energy was calculated at the complete basis set limit (extrapolated from aug-cc-pVXZ (X = T, Q, 5)) energies, corrected for correlation contributions, the core correlation, the zero-point energy, diagonal Born-Oppenheimer contributions, and the scalar relativistic effect. The heat of formation was computed from the calculated enthalpies by using the elemental reaction approach, taking the gaseous atom as the standard state for carbon.[15] Previous value of $\Delta_f H_{298}^o$ = –497.0 ± 8.3 kJ mol^{-1} was from a review by Pedley.[16]

***anti-* and *gauche*-CH_2FCH_2F, 1,2-difluoroethanes**

The conformationally averaged values are $\Delta_f H_{298}^o$ = –446.9 ± 3.4 kJ mol^{-1} and S^o = 296.8 ± 2.8 J mol^{-1}. Conformers and rotational barriers determined at the CCSD)T)/cc-pVTZ level of theory and the resulting equilibrium structure optimized at the CCSD(T)/cc-pVQZ level. The total electronic energy was calculated at the complete basis set limit (extrapolated from aug-cc-pVXZ (X = T, Q, 5) energies, corrected for correlation contributions, the core correlation, the zero-point energy, diagonal Born-Oppenheimer contributions, and the scalar relativistic effect. The heat of formation was computed from the calculated enthalpies by using the elemental reaction approach, taking the gaseous atom as the standard state for carbon.[15] Previous enthalpy of $\Delta_f H_{298}^o$ = –232 ± 25 kJ mol^{-1} was based on an analysis of the thermal elimination of HF from CH_2FCH_2F, which led to a C-C bond dissociation energy of 88 ± 2 kcal mol^{-1}.[10]

CH_2FCHF Conformers and rotational barriers determined at the CCSD)T)/cc-pVTZ level of theory and the resulting equilibrium structure optimized at the CCSD(T)/cc-pVQZ level. The total electronic energy was calculated at the complete basis set limit (extrapolated from aug-cc-pVXZ (X = T, Q, 5)), corrected for correlation contributions, the core correlation, the zero-point energy, diagonal Born-Oppenheimer contributions, and the scalar relativistic effect.[8] The heat of formation was computed from the calculated enthalpies by using the elemental reaction

approach, taking the gaseous atom as the standard state for carbon. The enthalpy value given is for the global minimum synclinal configuration. A local minimum with antiperiplanar symmetry is slightly higher in enthalpy, with $\Delta_f H_{298}^o = -229.8 \pm 2.8$ kJ mol^{-1}. Previous thermodynamic properties, $\Delta_f H_{298}^o = -235.5$ kJ mol^{-1} and S = 293.3 J K^{-1} mol^{-1}, were determined at the UHF/6-31G* level, utilizing isodesmic/homodesmic reactions for enthalpy of formation.[5]

CHF_2CH_2 Conformers and rotational barriers determined at the CCSD)T)/cc-pVTZ level of theory and the resulting equilibrium structure optimized at the CCSD(T)/cc-pVQZ level. The total electronic energy was calculated at the complete basis set limit (extrapolated from aug-cc-pVXZ (X = T, Q, 5)), corrected for correlation contributions, the core correlation, the zero-point energy, diagonal Born-Oppenheimer contributions, and the scalar relativistic effect.[8] The heat of formation was computed from the calculated enthalpies by using the elemental reaction approach, taking the gaseous atom as the standard state for carbon. The value given is for the global minimum configuration. A local minimum, with C_s symmetry, is slightly higher with $\Delta_f H_{298}^o = -281.7 \pm 2.8$ kJ mol^{-1}. Previous thermodynamic properties, $\Delta_f H_{298}^o = -277$ kJ mol^{-1} and S = 297.8 J K^{-1} mol^{-1}, were determined at the UHF/6-31G* level, utilizing isodesmic/homodesmic reactions for enthalpy of formation.[3]

CH_3CF_2 The dissociation energy of CH_3CF_2-H of 99.5 ± 1 kcal mol^{-1} was derived from a study of the equilibrium $CH_3CF_2H + I_2 \leftrightarrow CH_3CF_2I + HI$.[17] Entropy calculated from molecular properties computed at the UHF/6-31* level of theory.[4]

CH_3CHF_2 Taken from a Thermodynamics Research Center review.[2]

***anti-* and *gauche*-CH_2FCHF_2, 1,1,2-trifluoroethanes**

The conformationally averaged values are, $\Delta_f H_{298}^o = -661 \pm 3.4$ kJ mol^{-1} and $S^o = 316.9 \pm 2.0$ J mol^{-1}. Conformers and rotational barriers determined at the CCSD)T)/cc-pVTZ level of theory and the resulting equilibrium structure optimized at the CCSD(T)/cc-pVQZ level. The total electronic energy was calculated at the complete basis set limit (extrapolated from aug-cc-pVXZ (X = T, Q, 5)) energies, corrected for correlation contributions, the core correlation, the zero-point energy, diagonal Born-Oppenheimer contributions, and the scalar relativistic effect. The heat of formation was computed from the calculated enthalpies by using the elemental reaction approach, taking the gaseous atom as the standard state for carbon.[15] Previous value of $\Delta_f H_{298}^o = -665 \pm 4$ kJ mol^{-1} was based on the heat of hydrogenation of CF_2CFCl.[12] Pedley gives an enthalpy value of –730.7 ± 20.8 kJ mol^{-1}.[16]

CH_2CF_3 Conformers and rotational barriers determined at the CCSD)T)/cc-pVTZ level of theory and the resulting equilibrium structure optimized at the CCSD(T)/cc-pVQZ level. The total electronic energy was calculated at the complete basis set limit (extrapolated from aug-cc-pVXZ (X = T, Q, 5)), corrected for correlation contributions, the core correlation, the zero-point energy, diagonal Born-Oppenheimer contributions, and the scalar relativistic effect.[8] The heat of formation was computed from the calculated enthalpies by using the elemental reaction approach, taking the gaseous atom as the standard state for carbon. The previous value, $\Delta_f H_{298}^o = -517.1 \pm 5$ kJ mol^{-1}, was calculated from the dissociation energy of CF_3CH_2-H, derived from a study of the equilibrium $CF_3CH_3 + I_2 \leftrightarrow CF_3CH_2I + HI$.[19] The previous entropy value, S^o = 306.8 J mol^{-1}, was calculated from molecular properties computed at the UHF/6-31* level of theory.[3]

CH_3CF_3, 1,1,1-trifluoroethane

Conformers and rotational barriers determined at the CCSD)T)/cc-pVTZ level of theory and the resulting equilibrium structure optimized at the CCSD(T)/cc-pVQZ level. The total electronic energy was calculated at the complete basis set limit (extrapolated from aug-cc-pVXZ (X = T, Q, 5)) energies, corrected for correlation contributions, the core correlation, the zero-point energy, diagonal Born-Oppenheimer contributions, and the scalar relativistic effect. The heat of formation was computed from the calculated enthalpies by using the elemental reaction approach, taking the gaseous atom as the standard state for carbon.[15] Previous values of $\Delta_f H_{298}^o = -445.6 \pm 1.7$ kJ mol^{-1} and S^o = 287.3 J mol^{-1} were from the Thermodynamics Research Center review.[2] Pedley review gives –744.6 ± 1.7 kJ mol^{-1}.[16]

CF_2CF_2 Enthalpy from review of Pedley.[16] A computational study with CCSD(T)(FC) geometry optimization with the aug-cc-pVnZ(n = D, T, Q, 5-7) basis sets, checked by a CCSD(T)-F12 calculation followed by an atomization energy calculation at the CCSD(T) level extrapolated to the complete basis set limit, resulted in $\Delta_f H_0^o = -669.4 \pm 3.3$ kJ mol^{-1} and $\Delta_f H_{298}^o = -672.8 \pm 3.3$ kJ mol^{-1}.[6] Note that these values are from a published correction: doi:10.1021/jp202158j. A simulation of the atomization reaction using the CCSD(T) method with the vTz-F12 basis set led to $\Delta_f H_0^o = -671.2 \pm 4.0$ kJ mol^{-1} and $\Delta_f H_{298}^o = -672.0 \pm 4.0$ kJ mol^{-1}.[1]

***anti-* and *gauche*-CHF_2CHF_2, 1,1,2,2-tetrafluoroethanes**

The conformationally averaged values are $\Delta_f H_{298}^o = -877.6 \pm 3.8$ kJ mol^{-1} and $S^o = 323.2 \pm 4.7$ J mol^{-1}. Conformers and rotational barriers determined at the CCSD)T)/cc-pVTZ level of theory and the resulting equilibrium structure optimized at the CCSD(T)/cc-pVQZ level. The total electronic energy was calculated at the complete basis set limit (extrapolated from aug-cc-pVXZ (X = T, Q, 5)) energies, corrected for correlation contributions, the core correlation, the zero-point energy, diagonal Born-Oppenheimer contributions, and the scalar relativistic effect. The heat of formation was computed from the calculated enthalpies by using the elemental reaction approach, taking the gaseous atom as the standard state for carbon.[15] Previous ,$\Delta_f H_{298}^o = -860 \pm 24$ kJ mol^{-1} calculated based on the C-C bond strength estimate of 91.4 ± 3.7 kcal mol^{-1}.[13] Previous $S^o = 320.3$ J mol^{-1} from Thermodynamics Research Center review.[7]

$CHFCF_3$ Conformers and rotational barriers determined at the CCSD)T)/cc-pVTZ level of theory and the resulting equilibrium structure optimized at the CCSD(T)/cc-pVQZ level. The total electronic energy was calculated at the complete basis set limit (extrapolated from aug-cc-pVXZ (X = T, Q, 5)), corrected for correlation contributions, the core correlation, the zero-point energy, diagonal Born-Oppenheimer contributions, and the scalar relativistic effect.[8] The heat of formation was computed from the calculated enthalpies by using the elemental reaction approach, taking the gaseous atom as the standard state for carbon. The previous value, $\Delta_f H_{298}^o = -690$ kJ mol^{-1}, was derived from isodesmic reactions and adjusted down by 2 kJ mol^{-1} to reflect the enthalpy value for CH_2FCF_3 in this Table.[5] The previous entropy, $S^o = 326.2$ J mol^{-1}, was calculated from molecular properties computed at the UHF/6-31* level of theory.

CH_2FCF_3, 1,1,1,2-tetrafluoroethane

Conformers and rotational barriers determined at the CCSD)T)/cc-pVTZ level of theory and the resulting equilibrium structure optimized at the CCSD(T)/cc-pVQZ level. The total electronic energy was calculated at the complete basis set limit (extrapolated from aug-cc-pVXZ (X = T, Q, 5)) energies, corrected for correlation contributions, the core correlation, the zero-point energy, diagonal Born-Oppenheimer contributions, and the scalar relativistic effect. The heat of formation was computed from the calculated enthalpies by using the elemental reaction approach, taking the gaseous atom as the standard state for carbon.[15] Previous values of $\Delta_f H_{298}^o = -896 \pm 8$ kJ mol^{-1} (estimated) and $S^o = 316.2$ J mol^{-1} were from the Thermodynamics Research Center review.[2]

CF_2CF_3 Conformers and rotational barriers determined at the CCSD)T)/cc-pVTZ level of theory and the resulting equilibrium structure optimized at the CCSD(T)/cc-pVQZ level. The total electronic energy was calculated at the complete basis set limit (extrapolated from aug-cc-pVXZ (X = T, Q, 5)), corrected for correlation contributions, the core correlation, the zero-point energy, diagonal Born-Oppenheimer contributions, and the scalar relativistic effect.[8] The heat of formation was computed from the calculated enthalpies by using the elemental reaction approach, taking the gaseous atom as the standard state for carbon. The previous value, $\Delta_f H_{298}^o = -891 \pm 5$ kJ mol^{-1}, was calculated from the dissociation energy of C_2F_5-I of 52.5 ± 1 kcal mol^{-1}, derived from a study of the reaction of pentafluoroethyl iodide with HI.[20]

CHF_2CF_3, pentafluoroethane

Conformers and rotational barriers determined at the CCSD)T)/cc-pVTZ level of theory and the resulting equilibrium structure optimized at the CCSD(T)/cc-pVQZ level. The total electronic energy was calculated at the complete basis set limit (extrapolated from aug-cc-pVXZ (X = T, Q, 5)) energies, corrected for correlation contributions, the core correlation, the zero-point energy, diagonal Born-Oppenheimer contributions, and the scalar relativistic effect. The heat of

formation was computed from the calculated enthalpies by using the elemental reaction approach, taking the gaseous atom as the standard state for carbon.[15] Previous values of $\Delta_f H_{298}^o$ = –1105 ± 5 kJ mol^{-1} and S^o = 333.7 J mol^{-1} were from the Thermodynamics Research Center review.[2] Pedley review gives an enthalpy value of –1100.4 ± 4.1 kJ mol^{-1}.[16]

C_2F_6, hexafluoroethane

Enthalpy from a simultaneous solution of a thermochemical network for the CF_3X species, where X = nil, H, Cl, Br, I, CF_3, CN.[18] Entropy from recommendation of Chen, et a.[2] A study in which conformers and rotational barriers determined at the CCSD)T)/cc-pVTZ level of theory and the resulting equilibrium structure optimized at the CCSD(T)/cc-pVQZ level. The total electronic energy was calculated at the complete basis set limit (extrapolated from aug-cc-pVXZ (X = T, Q, 5)) energies, corrected for correlation contributions, the core correlation, the zero-point energy, diagonal Born-Oppenheimer contributions, and the scalar relativistic effect led to $\Delta_f H_{298}^o$ = –1339.8 ± 3.2 kJ mol^{-1} and S^o = 331.0 ± 1.5 J mol^{-1}. The heat of formation was computed from the calculated enthalpies by using the elemental reaction approach, taking the gaseous atom as the standard state for carbon.[15]

(1) Baranovskii, V. I.; Skorobogatov, G. A. Quantum-chemical simulation of the gas-phase molecular, thermodynamic, and kinetic parameters of CF, CF_2, and CF_3 radicals and CF_4, C_2F_2, C_2F_4, and C_2F_6 molecules. *Russ. J. Gen. Chem.* **2016**, *86*, 241-250, doi:10.1134/s1070363216020067.

(2) Chen, S. S.; Rodgers, A. S.; Chao, J.; Wilhoit, R. C.; Zwolinski, B. J. Ideal gas thermodynamic properties of six fluoroethanes. *J. Phys. Chem. Ref. Data* **1975**, *4*, 441-456, doi:10.1063/1.555521.

(3) Chen, Y.; Rauk, A.; Tschuikow-Roux, E. Structures, barriers for internal rotation, vibrational frequencies, and thermodynamic functions of CH_2FCH_2, CHF_2CH_2, and CF_3CH_2 radicals: An *ab initio* study. *J. Chem. Phys.* **1990**, *93*, 6620-6629, doi:10.1063/1.458929.

(4) Chen, Y.; Rauk, A.; Tschuikow-Roux, E. Structures, barriers for rotation and inversion, vibrational frequencies, and thermodynamic functions of ethyl, α-fluoroethyl, and α-difluroroethyl radicals: An *ab initio* study. *J. Chem. Phys.* **1990**, *93*, 1187-1195, doi:10.1063/1.459182.

(5) Chen, Y.; Rauk, A.; Tschuikow-Roux, E. Structures, barriers for internal rotation, vibrational frequencies, and thermodynamic functions of CH_2FCHF, CHF_2CHF, and CF_3CHF radicals: An ab initio study. *J. Chem. Phys.* **1991**, *94*, 7299-7310, doi:10.1063/1.460214.

(6) Feller, D.; Peterson, K. A.; Dixon, D. A. Ab initio coupled cluster determination of the heats of formation of $C_2H_2F_2$, C_2F_2, and C_2F_4. *J. Phys. Chem. A* **2011**, *115*, 1440-1451, doi:10.1021/jp111644h; correction 10.1021/jp202158j.

(7) Frenkel, M.; Kabo, G. J.; Marsh, K. N.; Roganov, G. N.; Wilhoit, R. C. *Thermodynamics of Organic Compounds in the Gas State*; Thermodynamics Research Center: College Station, TX, 1994; Vol. I.

(8) Ganyecz, Á.; Kállay, M.; Csontos, J. Accurate theoretical thermochemistry for fluoroethyl radicals. *J. Phys. Chem. A* **2017**, *121*, 1153-1162, doi:10.1021/acs.jpca.6b12404.

(9) Gurvich, L. V.; Veyts, I. V.; Alcock, C. B. *Thermodynamic Properties of Individual Substances,*, Fourth ed.; Hemisphere Publishing Corp.: New York, 1991; Vol. 2.

(10) Kerr, J. A.; Timlin, D. M. A kinetic study of the thermal elimination of hydrogen fluoride from 1,2-dichloroethane. Determination of the bond dissociation energies *D*(CH_2F—CH_2F) and *D*(CH_2F—H). *Int. J. Chem. Kinet.* **1971**, *3*, 427-441, doi:10.1002/kin.550030505.

(11) Kormos, B. L.; Liebman, J. F.; Cramer, C. J. 298 K enthalpies of formation of monofluorinated alkanes: theoretical predictions for methyl, ethyl,isopropyl, and tert-butyl fluoride. *J. Phys. Org. Chem.* **2004**, *17*, 656-664, doi:10.1002/poc.801.

(12) Lacher, J. R.; Skinner, H. A. Bond energy additivity and bond interactions in fluoro-halogenated hydrocarbons. *J. Chem. Soc. A* **1968**, 1034-1038, doi:10.1039/J19680001034.

(13) Millward, G. E.; Hartig, R.; Tschuikow-Roux, E. Kinetics of the shock wave thermolysis of 1,1,2,2-tetrafluoroethane. *J. Phys. Chem.* **1971**, *75*, 3195-3201, doi:10.1021/j100690a001.

(14) Miyokawa, K.; Ozaki, S.; Yano, T. Kinetics of the photobromination of fluoroethane. Estimate of the C-H bond dissociation energies and the heats of formation of the CH_3CHF and CH_2CH_2F radicals. *Bull. Chem. Soc. Jpn.* **1996**, *69*, 869-873.

(15) Nagy, B.; Csontos, J.; Szakács, P.; Kállay, M. High-accuracy theoretical thermochemistry of fluoroethanes. *J. Phys. Chem. A* **2014**, *118*, 4824-4836, doi:10.1021/jp503492a.
(16) Pedley, J. B. *Thermochemical Data and Structures of Organic Compounds*; Thermodynamics Data Center: College Station, TX, 1994.
(17) Pickard, J. M.; Rodgers, A. S. The kinetics and thermochemistry of the reaction of 1,1-difluoroethane with iodine. The CF_2-H bond dissociation energy in 1,1-difluoroethane and the heat of formation of 1,1-difluoroethyl. *J. Am. Chem. Soc.* **1977**, *99*, 691-694, doi:10.1021/ja00445a005.
(18) Ruscic, B.; Michael, J. V.; Redfern, P. C.; Curtiss, L. A.; Raghavachri, K. Simultaneous adjustment of experimentally based enthalpies of formation of CF_3X, X = nil, H, Cl, Br, I, CF_3, CN, and a probe of G3 theory. *J. Phys. Chem. A* **1998**, *102*, 10889-10899, doi:10.1021/jp983237e.
(19) Wu, E. C.; Rodgers, A. S. Thermochemistry of gas-phase equilibrium $CF_3CH_3 + I_2 = CF_3CH_2I + HI$. The carbon-hydrogen bond dissociation energy in 1,1,1-trifluoroethane and the heat of formation of the 2,2,2-trifuloroethyl radical. *J. Phys. Chem.* **1974**, *78*, 2315-2317, doi:10.1021/j150671a002.
(20) Wu, E. C.; Rodgers, A. S. Kinetics of the gas phase reaction of pentafluoroethyl iodide with hydrogen iodide. Enthalpy of formation of the pentafluoroethyl radical and the pi bond dissociation energy in tetrafluoroethylene. *J. Am. Chem. Soc.* **1976**, *98*, 6112-6115, doi:10.1021/ja00436a007.

Note 27: *Compounds containing two C and one or more F and O*

Back to Table

CH_2FCH_2OH
The enthalpy of formation was calculated from a set of isodesmic and isogyric reactions at the CBS-QB3 level of theory and refers to the *gauche* configuration. Calculations with B3LYP/cc-pVTZ were in good agreement.[2]

CH_2FCOOH
The enthalpy of formation was calculated from a set of isodesmic and isogyric reactions at the CBS-QB3 level of theory. Calculations with B3LYP/cc-pVTZ were in good agreement.[2]

CF_3CO CBS-4 and G2(MP2,SVP) methods used to obtain thermodynamic properties. In addition, enthalpy was derived from isodesmic reaction calculations. Value listed is recommendation based on theoretical and experimental results. Entropy at the G2(MP2(full)//MP2(full)/6-31G(d) level treating internal rotations as harmonic oscillators.[8]

$CF_3C(O)H$ Thermodynamic properties calculated at the G2(MP2(full)//MP2(full)/6-31G(d) level of theory. Enthalpy from atomization energy and entropy calculated treating internal rotations as harmonic oscillators. Similar values obtained at the CBS-4//HF/3021G* level.[8]

$CH_3C(O)F$, acetyl fluoride
Enthalpy value from review of Pedley.[4]

$CF_3C(O)F$ Thermodynamic properties calculated for five isodesmic reactions at the MP2//6-31G(d) level of theory. In the same study, $\Delta H_f^\circ = -614 \pm 7$ kJ mol^{-1} for CF_2O and $\Delta H_f^\circ = -381 \pm 2$ kJ mol^{-1} for CHFO were calculated, both close to the recommended values.[7]

$CF_3C(O)OH$, trifluoroacetic acid
Enthalpy value from review of Pedley.[4]

CF_3OCO_2 An average of a result from an isodesmic reaction and an atomization energy, both calculated at the CBS-4 level of theory.[3]

CF_3OOCF_3
A thermal decomposition study from 575 to 900 K led to a BDE(O-O) of 47.5 ± 0.5 kcal

mol^{-1}.[5] An MP2//6-31G(d,p) calculation utilizing isodesmic and isogyric reactions resulted in –343 ± 3 kcal mol^{-1}.[6] A CBS-QB3 calculation led to a BDE(O-O) of 209.4 kJ mol^{-1}, and thus an enthalpy of –1479 kJ mol^{-1}.[1]

(1) Agapito, F.; Cabral, B. J. C.; Simoes, J. A. M. Oxygen-oxygen bond dissociation enthalpies of di-tert-butyl peroxide and di-trifluoromethyl peroxide. *J. Mol. Struct. - Theochem* **2005**, *729*, 223-227, doi:10.1016/j.theochem.2005.06.004.

(2) Bernardes, C. E. S.; Minas da Piedade, M. E.; Amaral, L. M. P. F.; Ferreira, A. I. M. C. L.; Ribeiro da Silva, M. A. V.; Diogo, H. P.; Costa Cabral, B. J. Energetics of C−F, C−Cl, C−Br, and C−I bonds in 2-haloethanols. Enthalpies of formation of XCH_2CH_2OH (X = F, Cl, Br, I) compounds and of the 2-hydroxyethyl radical. *J. Phys. Chem. A* **2007**, *111*, 1713-1720, doi:10.1021/jp0675678.

(3) Paci, M. A. B.; Argüello, G. A.; García, P.; Willner, H. Thermal decompositino of the perfluorinated peroxides $CF_3OC(O)OOC(O)F$ and $CF_3OC(O)OOCF_3$. *J. Phys. Chem. A* **2005**, *109*, 7481-7488, doi:10.1021/jp0528818.

(4) Pedley, J. B. *Thermochemical Data and Structures of Organic Compounds*; Thermodynamics Data Center: College Station, TX, 1994.

(5) Reints, W.; Pratt, D. A.; Korth, H. G.; Mulder, P. O-O bond dissociation enthalpy in di(trifluoromethyl) peroxide (CF_3OOCF_3) as determined by very low pressure pyrolysis. Density functional computations on O-O and O-H bonds in (fluorinated) derivatives. *J. Phys. Chem. A* **2000**, *104*, 10713-70720, doi:10.1021/jp994434w.

(6) Schneider, W. F.; Wallington, T. J. Thermochemistry of COF_2 and related compounds. *J. Phys. Chem.* **1994**, *98*, 7448-7451, doi:10.1021/j100082a009.

(7) Sudlow, K. P.; Woolf, A. A. Heats of formation of carbonyl, formyl and trifluoroacetyl fluorides. *J. Fluorine Chem.* **1999**, *96*, 141-145, doi:10.1016/S0022-1139(99)00067-6.

(8) Viskolcz, B.; Berces, T. Enthalpy of formation of selected carbonyl radicals from theory and comparison with experiment. *Phys. Chem. Chem. Phys.* **2000**, *2*, 5430-6436, doi:10.1039/b004548i.

Note 28: *Compounds containing more than two C and one or more F*

Back to Table

***iso*-C_3H_7F** Enthalpies of reaction calculated at the MCG3//MCQCISD level of theory (up to 6-311++G(3d2f,2df,2p) basis set) for the homolytic fragmentation to the alkyl radical and fluoride atom, and for the atomization reaction and averaged. Enthalpy also calculated for the heterolytic fragmentation into the alkyl cation and fluoride anion for support[2] $\Delta_f H^\circ_{298}$ = -318.8 ± 4.2 kJ mol^{-1} estimated by Luo and Benson.[3]

***tert*-C_4H_9F** Enthalpies of reaction calculated at the MCG3//MCQCISD level of theory (up to 6-311++G(3d2f,2df,2p) basis set) for the homolytic fragmentation to the alkyl radical and fluoride atom, and for the atomization reaction and averaged. Enthalpy also calculated for the heterolytic fragmentation into the alkyl cation and fluoride anion for support.[2] $\Delta_f H^\circ_{298}$ = -363.6 ± 4.2 kJ mol^{-1} estimated by Luo and Benson.[3]

$CF_3C(O)OCH_3$

The free energy of formation of methyl trifluoroacetate in solution was determined by measuring the equilibrium constant for the reaction of trifluoroacetic acid with methanol. The solubility was estimated from a linear free-energy relationship and the vapor pressure estimated from the boiling point, leading to a value of the free energy of formation in the gas phase. Combining this with the estimate of the standard entropy, also listed, leads to the cited value.[1] A density-functional calculation at the MPWB1K//6-31+G(d,p) level with two isodesmic reactions, led to to $\Delta_f H^\circ_{298} = -1020$ kJ mol^{-1}.[4]

(1) Guthrie, J. P. Thermodynamics of ester and orthoester formation from trifluoroacetic acid. *Can. J. Chem.* **1976**, *54*, 202-209, doi:10.1139/v76-032.

(2) Kormos, B. L.; Liebman, J. F.; Cramer, C. J. 298 K enthalpies of formation of monofluorinated alkanes: theoretical predictions for methyl, ethyl,isopropyl, and tert-butyl fluoride. *J. Phys. Org. Chem.* **2004**, *17*, 656-664, doi:10.1002/poc.801.

(3) Luo, Y. R.; Benson, S. W. Heats of formation of alkyl fluorides. *J. Phys. Chem. A* **1997**, *101*, 3042-3044, doi:10.1021/jp962641f.
(4) Mishra, B. K.; Chakrabartty, A. K.; Deka, R. C. Theoretical investigation of the gas-phase reactions of $CF_2ClC(O)OCH_3$ with the hydroxyl radical and the chlorine atom at 298 K. *J. Mol. Model* **2013**, *19*, 3263-3270, doi:10.1007/s00894-013-1865-1.

Note 29: *Inorganic compounds containing Cl*

Back to Table

Cl Enthalpy value is from the optimization of Ruscic et al.[20] Entropy is a CODATA Key Value[4] as was the previous enthalpy value of $\Delta_f H^\circ_{298} = 121.301 \pm 0.008$ kJ mol^{-1}.

Cl_2 CODATA Key Value[4]

HCl CODATA Key Value.[4] The active thermochemical tables optimization gives an enthalpy value of –92.1763 ± 0.0063 kJ mol^{-1}.[20] The most recent NIST-JANAF review gives and enthalpy of –92.31 ± 0.10 kJ mol^{-1} and an entropy of 186.901 ± 0.005 J K^{-1} mol^{-1}.[22]

ClO Both JANAF[3] and Gurvich et al.[9] use the dissociation energy from Coxan and Ramsay[5] of 265.380 ± 0.036 kJ mol^{-1}. The present recommendation is a recalculation using reference values from this Table. The entropy is a statistical mechanical calculation[1] using data from JANAF. The previous value of 101.63 ± 0.1 kJ mol^{-1} was from the JANAF recommendation.[3] A CCSD(T) calculation, extrapolated to the complete basis set limit, for the atomization energy leads to an enthalpy of formation of 24.8 kcal mol^{-1} at both 0 K and at 298 K.[16] Another CCSD(T) calculation of the dissociation energy, both directly and through a negative ion thermochemical cycle, led to enthalpy values of $\Delta_f H^\circ = 24.1 \pm 0.3$ and $\Delta_f H^\circ_{298}$ =24.1 ± 0.3 and 24.2 ± 0.3 kcal mol^{-1}.[18] Atomization energy was calculated using the Wn family of computational methods. A slight increase in the atomization energy was found going from W2.2 to W4.4. These results led to $\Delta_f H^\circ_{298} = 101.2 \pm 0.4$ kJ mol^{-1} and a 0 K value only 0.04 kJ mol^{-1} higher.[12]

ClOO Enthalpy and entropy values are from an analysis of equilibrium constant measurements (see Table 3-1, Note 11). More recent measurements over the temperature range 212–245 K[24] support these values. Previous enthalpy value of 98±4 kJ mol^{-1} and entropy value of 269.32±0.5 J K^{-1} mol^{-1} from JANAF. Enthalpy for the reaction HOOCl + FOO → HOOF + ClOO at the CCSD(T)/CBS(Q5) level of theory, adjusted for the Table value for FOO, leads to $\Delta_f H^\circ_{298}$ = 103.9 ± 6 kJ mol^{-1} and $\Delta_f H^\circ = 104.7 \pm 6$ kJ mol^{-1}.[8] Atomization energy was calculated using the Wn family of computational methods. Significant increases in the atomization energy were found going from W2.2 to W4.4. These results led to $\Delta_f H^\circ_{298} = 101.7 \pm 0.7$ kJ mol^{-1} and $\Delta_f H^\circ = 103.3 \pm 0.7$ kJ mol^{-1}.[12]

ClOOH Isodesmic reaction calculations done at MP2, CCSD, and CCSD(T) level with ANO basis sets to determine enthalpy of formation.[14]

OClO Near-threshold fragmentation studies led to a dissociation energy to O + ClO of 247.3±0.5 kJ mol^{-1}.[6] This leads to an enthalpy of formation at 0 K of 100.6 ± 0.6 kJ mol^{-1}. A computational study gives, at 0 K, 102.2 ± 6.5 kJ mol^{-1}.[13] Previous 298 K enthalpy of formation, 94.6 ± 1.2, derived from equilibrium constant for ClO + ClO ↔ Cl + OClO.[17] Entropy and enthalpy function are from JANAF.[3] A CCSD(T) calculation, extrapolated to the complete basis set limit, for the atomization energy leads to an enthalpy of formation of 24.5 kcal mol^{-1} at 0 K and 23.9 at 298 K.[16] An atomization energy calculated at the W4 level of theory led to $\Delta_f H^\circ_{298} = 99.0 \pm 0.7$ kJ mol^{-1} and $\Delta_f H_0^\circ = 101.5 \pm 0.7$ kJ mol^{-1}.[12]

ClO_3 A calculation of the isodesmic reaction ClO_3 + ClO → 2OClO at the W4.2 level of theory provided the selected enthalpy values.[12] The previous values, $\Delta_f H^\circ_{298} = 194 \pm 12$ kJ mol^{-1} and $\Delta_f H_0^\circ = 200 \pm 12$ kJ mol^{-1} were the JANAF recommendations, which were based on limited kinetic and theoretical studies.[3] A more recent density functional/G3 calculation led to a 298 K enthalpy of 43.1 kcal mol^{-1} (= 180.3 kJ mol^{-1}).[23]

ClClO A CCSD(T), extrapolated to the complete basis set limit, for the atomization energy leads to the recommended enthalpy of formation and a value of 32.2 kcal mol^{-1} at 0 K. For the ^{1}A' state. $\Delta_f H^\circ_{298}$ = 52.4 ± 1 kcal mol^{-1} for the ^{3}A" state.[16] The previous recommendation, 90 ± 30 kJ mol^{-1}, from the JANAF evaluation,[3] was based on an interpretation of the infrared spectrum and suggested that ClClO was less stable than ClOCl by ~9 kJ mol^{-1}. Several computational studies cited in the JANAF review indicated that the stability difference was considerably greater, typically about 60 kJ mol^{-1}. The present recommendation leads to a stability difference of 52 kJ mol^{-1}. Entropy and enthalpy difference calculated by a statistical mechanical calculation using vibrational frequencies from the WebBook and PM3 rotational moments.[1]

ClOCl Enthalpy value based on experimental reports on the equilibrium constant for the reaction $H_2O + Cl_2O \leftrightarrow 2HOCl$ and the recommended enthalpy of formation for HOCl.[10] Gurvich et al. recommended an enthalpy of formation at 298 K of 79±10 kJ mol^{-1}.[9] A CCSD(T) calculation, extrapolated to the complete basis set limit, for the atomization energy leads to an enthalpy of formation of 19.3 kcal mol^{-1} at 0 K and 18.9 at 298 K.[16]

ClOOCl Selected enthalpy value derived from a third-law calculation on the equilibrium constant for the dimerization reaction, ClO + ClO ↔ ClOOCl, presented in Table 3-1, note 20. Entropy value calculation is also discussed in Table 3-1. Previous Table value of $\Delta_f H^\circ_{298}$, 127.6±2.9 kJ mol^{-1}, was from the equilibrium constant of Nickolaisen, et al.[17] and the entropy was the JANAF recommendation.[3] A study of the fragmentation threshold of ClO^+ from the photoionization of ClOOCl yielded a 0 K enthalpy of 134.07 ± 2.8 kJ mol^{-1} and a 298 K value of 130.87 ± 2.8 kJ mol^{-1}.[19] A CCSD(T) calculation, extrapolated to the complete basis set limit, for the atomization energy leads to an enthalpy of formation of 32.9 kcal mol^{-1} at 0 K and 31.6 at 298 K.[16] A calculation using the isodesmic reactions $ClOOCl + H_2O \rightarrow H_2O_2 + Cl_2O$ and $ClOOCl + 2HOCl \rightarrow H_2O_2 + 2Cl_2O$ at the W4.2 level of theory leads to $\Delta_f H^\circ_{298}$ = 131.8 ± 1.3 kJ mol^{-1} and $\Delta_f H_0^\circ$ = 135.1 ± 1.3 kJ mol^{-1}.[12]

$ClClO_2$ Derived from a CCSD(T) calculation, extrapolated to the complete basis set limit, for the atomization energy.[16] See Table 3-1, note 21 for a more complete discussion. The previous value, 154.2 kJ mol^{-1} (36.9 kcal mol^{-1}), was calculated at Gaussian-2 level of theory.[15] Entropy from JANAF evaluation.[3] The same value resulted from a statistical mechanical calculation.

ClOClO Derived from a CCSD(T) calculation, extrapolated to the complete basis set limit, for the atomization energy[16] combined with G2 composite calculations.[26] See Table 3-1, note 20b for a more complete discussion. The previous value, 175.5 kJ mol^{-1} (41.9 kcal mol^{-1}), was calculated at Gaussian-2 level of theory[15] and the previous entropy (309±2 kJ mol^{-1}) was from the JANAF evaluation.[3]

Cl_2O_3 Selected enthalpy and entropy values derived from a third-law calculation on the equilibrium constant for the reaction, $ClO + OClO \leftrightarrow Cl_2O_3$, presented in Table 3-1, note 15. Previous values in Table, $\Delta_f H$ = 35.8 ± 1.5 kcal mol^{-1} and ΔS = 94 ± 5 cal K^{-1} mol^{-1}, were taken from a single study.[2] The most stable structure among the Cl_2O_3 isomers is calculated to be ClOCl(O)O.[27] A density functional/G3 calculation led to a 298 K enthalpy of 31.7 kcal mol^{-1}.[23]

HOCl Enthalpy value from an evaluation of the experimental data.[10] Entropy and the enthalpy difference from JANAF evaluation.[3] An enthalpy value of –18.1 ± 0.3 kcal mol^{-1} has been calculated by coupled-cluster theory with correlation consistent basis sets and corrections for core-valence, relativistic, and anharmonic effects.[7] A calculation of the isodesmic reaction HOF + OH → FO + H_2O at the W4.2 level of theory leads to $\Delta_f H^\circ_{298}$ = −76.1 ± 0.6 kJ mol^{-1} and $\Delta_f H_0^\circ$ = −73.4 ± 0.6 kJ mol^{-1}.[12] A re-evaluation of the spectroscopic results, along with a newer value for the OH enthalpy, has led to a recommended value of $\Delta_f H_0^\circ$ = −73.99 ± 0.12 kJ mol^{-1}.[11]

HOClO A calculation of the isodesmic reaction HOClO + ClO → HOCl + OClO at the W4lite level of theory provided the selected enthalpy values.[12]

$HOClO_2$ The total atomization energy was calculated at the W2.2 level of theory and then corrected to provide an estimated W4lite value, leading to the selected enthalpy values.[12]

$HOClO_3$ The total atomization energy was calculated at the W2.2 level of theory, leading to the selected enthalpy values.[12]

ClF Taken from review of Gurvich et al.[9] The JANAF Tables give $\Delta_f H_0^o = -50.2 \pm 0.4$ kJ mol^{-1}, $\Delta_f H_{298}^o = -50.3 \pm 0.4$ kJ mol^{-1}, and $S^o = 217.938$ J mol^{-1}.[3] A study in which the total atomization energy was calculated using a composite electronic structure approach based on CCSD(T) and extrapolated to the complete basis set limit with a two-point extrapolation scheme, Q5. Additional corrections included zero-point energy, core-valence effect, for scalar relativistic effects, and spin-orbit corrections, gave $\Delta_f H_{298}^o = -54.8$ kJ mol^{-1}.[25]

ClOF, ClO_2F

Enthalpy values derived from a weighted average of two isodesmic reactions and the atomization reaction, calculated at the CCSD(T) level of theory.[21] Previous values of $\Delta_f H_{298}^o = 24.3$ kJ mol^{-1} and $\Delta_f H_{298}^o = -34.3$kJ mol^{-1} were from the total atomization energy, which was calculated using a composite electronic structure approach based on CCSD(T) and extrapolated to the complete basis set limit with a two-point extrapolation scheme, Q5. Additional corrections included zero-point energy, core-valence effect, for scalar relativistic effects, and spin-orbit corrections.[25] Entropy values were from statistical mechanics calculations.[21] Thermodynamic parameters were also reported for $ClFO_3$, ClF_3O, ClF_2O_2, and ClF_5O.

(1) Barker, J. R.; Ortiz, N. F.; Preses, J. M.; Lohr, L. L.; Maranzana; Stimac, P. J.; Nguyen, L. T. MultiWell; 2009.1 ed.; University of Michigan: Ann Arbor, MI, 2009.

(2) Burkholder, J. B.; Mauldin, R. L.; Yokelson, R. J.; Solomon, S.; Ravishankara, A. R. Kinetic, thermodynamic, and spectroscopic study of Cl_2O_3. *J. Phys. Chem.* **1993**, *97*, 7597-7605, doi:10.1021/j100131a032.

(3) Chase, M. W. NIST-JANAF thermochemical tables. *J. Phys. Chem. Ref. Data* **1998**, *Monograph 9*.

(4) Cox, J. D.; Wagman, D. D.; Medvedev, V. A. *CODATA Key Values for Thermodynamics*; Hemisphere Publishing Corp.: New York, 1989.

(5) Coxon, J. A.; Ramsay, D. A. The $A^2\Pi_i$–$X^2\Pi_i$ band system of ClO: Reinvestigation of the absorption spectrum. *Can. J. Phys.* **1976**, *54*, 1034-1042, doi:10.1139/p76-122.

(6) Delmdahl, R. F.; Parker, D. H.; Eppink, A. T. J. B. Short wavelentgh photolysis of jet-cooled $OClO(^2A_2 v_1>20) \rightarrow ClO(X^2\Pi_\Omega,v,J) + O(^3P_J)$. *J. Chem. Phys.* **2001**, *114*, 8339-8346, doi:10.1063/1.1367393.

(7) Denis, P. A. Thermochemistry of the hypobromous and hypochlorous acids, HOBr and HOCl. *J. Phys. Chem. A* **2006**, *110*, 5887-5892, doi:10.1021/jp056950u.

(8) Grant, D. J.; Garner, E. B.; Matus, M. H.; Nguyen, M. T.; Peterson, K. A.; Francisco, J. S.; Dixon, D. A. Thermodynamic properties of the XO_2, X_2O, XYO, X_2O_2, and XYO_2 (X, Y = Cl, Br and I) isomers. *J. Phys. Chem. A* **2010**, *114*, 4254-4265, doi:10.1021/jp911320p.

(9) Gurvich, L. V.; Veyts, I. V.; Alcock, C. B. *Thermodynamic Properties of Individual Substances,*, Fourth ed.; Hemisphere Publishing Corp.: New York, 1991; Vol. 2.

(10) Hassanzadeh, P.; Irikura, K. K. Nearly ab initio thermochemistry: The use of reactions schemes. Application to IO and HOI. *J. Phys. Chem. A* **1997**, *101*, 1580-1587, doi:10.1021/jp963011g.

(11) Joens, J. A. The dissociation energy of $OH(X\ ^2P_{3/2})$ and the enthalpy of formation of $OH(X\ ^2\Pi_{3/2})$, ClOH, and BrOH from thermochemical cycles. *J. Phys. Chem. A* **2001**, *105*, 11041-11044, doi:10.1021/jp011833u.

(12) Karton, A.; Parthiban, S.; Martin, J. M. L. Post-CCSD(T) ab initio thermochemistry of halogen oxides and related hydrides XOX, XOOX, HOX, XO_n, and HXO_n (X = F, Cl), and evaluation of DFT methods for these systems. *J. Phys. Chem. A* **2009**, *113*, 4802-4816, doi:10.1021/jp8087435.

(13) Lee, S. Y. Computational study of enthalpies of formation of OXO (X = Cl, Br, and I) and their anions. *J. Phys. Chem. A* **2004**, *108*, 10754-10761, doi:10.1021/jp0467550.

(14) Lee, T. J.; Rendell, A. P. Ab initio characterization of ClOOH: Implications for atmospheric chemistry. *J. Phys. Chem.* **1993**, *97*, 6999-7002, doi:10.1021/j100129a014.

(15) Li, W. K.; Ng, C. Y. Gaussian-2 ab initio study of isomeric Cl_2O_2 and $Cl_2O_2^+$ and their dissociation reactions. *J. Phys. Chem. A* **1997**, *101*, 113-115, doi:10.1021/jp962253d.

(16) Matus, M. H.; Nguyen, M. T.; Dixon, D. A.; Peterson, K. A.; Francisco, J. S. $ClClO_2$ is the most stable isomer of Cl_2O_2. Accurate coupled cluster energetics and electronic spectra of Cl_2O_2 isomers. *J. Phys. Chem. A* **2008**, *112*, 9623-9627, doi:10.1021/jp806220r.
(17) Nickolaisen, S. L.; Friedl, R. R.; Sander, S. P. Kinetics and mechanism of the ClO + ClO reaction: Pressure and temperature dependences of the bimolecular and termolecular channels and thermal decomposition of chlorine peroxide, ClOOCl. *J. Phys. Chem.* **1994**, *98*, 155-169, doi:10.1021/j100052a027.
(18) Peterson, K. A.; Shepler, B. C.; Figgen, D.; Stoll, H. On the spectroscopic and thermochemical properties of ClO, BrO, IO, and their anions. *J. Phys. Chem. A* **2006**, *110*, 13877-13883, doi:10.1021/jp065887l.
(19) Plenge, J.; Kühl, S.; Vogel, B.; Müller, R.; Stroh, F.; von Hobe, M.; Flesch, R.; Rühl, E. Bond strength of chlorine peroxide. *J. Phys. Chem. A* **2005**, *109*, 6730-6734, doi:10.1021/jp044142h.
(20) Ruscic, B.; Pinzon, R. E.; Morton, M. L.; von Laszevski, G.; Bittner, S. J.; Nijsure, S. G.; Amin, K. A.; Minkoff, M.; Wagner, A. F. Introduction to active thermochemical tables: Several "key" enthalpies of formation revisited. *J. Phys. Chem. A* **2004**, *108*, 9979-9997, doi:10.1021/jp047912y.
(21) Sánchez, H. R.; Del Pla, J. Theoretical study of the thermochemistry of chlorine oxyfluorides. *Chem. Phys. Lett.* **2016**, *663*, 16-20, doi:10.1016/j.cplett.2016.09.045.
(22) Shenyavskaya, E. A.; Yungman, V. S. NIST-JANAF thermochemical tables. III. Diatomic hydrogen halide gases. *J. Phys. Chem. Ref. Data* **2004**, *33*, 923-957, doi:10.1063/1.1638781.
(23) Sicre, J. E.; Cobos, C. J. Thermochemistry of the higher chlorine oxides ClO_x (x = 3,4) and Cl_2O_x (x = 3 - 7). *J. Mol. Struct. (Theochem)* **2003**, *620*, 215-226, doi:10.1016/S0166-1280(02)00602-4.
(24) Suma, K.; Sumiyoshi, Y.; Endo, Y.; Enami, S.; Aloisio, S.; Hashimoto, S.; Kawasaki, M.; Nishida, S.; Matsumi, Y. Equilibrium constants of the reaction of Cl with O_2 in the formation of ClOO. *J. Phys. Chem. A* **2004**, *108*, 8096-8099, doi:10.1021/jp049124e.
(25) Thanthiriwatte, K. S.; Vasiliu, M.; Dixon, D. A.; Christe, K. O. Structural and energetic properties of closed shell XF_n (X = Cl, Br, and I; n = 1−7) and XO_nF_m (X = Cl, Br, and I; n = 1−3; m = 0−6) molecules and ions leading to stability predictions for yet unknown compounds. *Inorg. Chem.* **2012**, *51*, 10966-10982, doi:10.1021/ic301438b.
(26) Zhu, R. S.; Lin, M. C. *Ab initio* studies of ClO_x reactions. IV. Kinetics and mechanism for the self-reaction of ClO radicals. *J. Chem. Phys.* **2003**, *118*, 4094-4106, doi:10.1063/1.1540623.
(27) Zhu, R. S.; Lin, M. C. Ab initio studies of ClO_x reactions. VII. Isomers of Cl_2O_3 and their roles in the ClO + OClO reaction. *J. Chem. Phys.* **2003**, *118*, 8645-8655, doi:10.1063/1.1565315.

Note 30: *Inorganic compounds containing Cl, O, and N*

Back to Table

ClNO Taken from review of Gurvich et al.[4] The JANAF Tables give $\Delta_f H_0^\circ$ = 53.6 kJ mol^{-1}, $\Delta_f H_{298}^\circ$ = 51.7 kJ mol^{-1}[1], and S° = 261.680 J mol^{-1}.[2]

$ClNO_2$ The equilibrium geometry was calculated at the CCSD(T)/cc-pVQZ level of theory, while the energy was calculated by summing various contributions calculated at the CCSC(T) level with the use of various basis sets.[8] The previous value, $\Delta_f H_{298}^\circ$ = 52.7 ± 0.5 kJ mol^{-1}, was taken from review of Gurvich et al.[4] The JANAF Tables give $\Delta_f H_0^\circ$ = 17.5 kJ mol^{-1}, $\Delta_f H_{298}^\circ$ = 12.1 kJ mol^{-1}, and S° = 272.187 J mol^{-1}.[2]

***cis*-ClONO** The equilibrium geometry was calculated at the CCSD(T)/cc-pVQZ level of theory, while the energy was calculated by summing various contributions calculated at the CCSC(T) level with the use of various basis sets.[8] The previous value, $\Delta_f H_{298}^\circ$ = 64.6 kJ mol^{-1}, was predicted based on isodesmic reactions at the CCSD(T) level of theory.[5]

***trans*-ClONO**
The equilibrium geometry was calculated at the CCSD(T)/cc-pVQZ level of theory, while the energy was calculated by summing various contributions calculated at the CCSC(T) level with

the use of various basis sets.[8] The previous value, $\Delta_f H^\circ_{298}$ = 75.3 kJ mol^{-1}, was predicted based on isodesmic reactions at the CCSD(T) level of theory.[5]

***cis, perp*-ClO_2NO**

Enthalpy calculated at MP2 level of theory using basis sets ranging from 6-31G(d) to 6-311G(2df,2p).[7] A G3//B3LYP study gave enthalpies at 0 K and 298 K of 32.5 and 31.5 kcal mol^{-1}, respectively.[6]

***trans, perp*-ClO_2NO**

Enthalpy calculated at MP2 level of theory using basis sets ranging from 6-31G(d) to 6-311G(2df,2p).[7] A G3//B3LYP study gave enthalpies at 0 K and 298 K of 34.4 and 33.2 kcal mol^{-1}, respectively.[6]

$ClONO_2$ The equilibrium geometry was calculated at the CCSD(T)/cc-pVQZ level of theory, while the energy was calculated by summing various contributions calculated at the CCSC(T) level with the use of various basis sets.[8] The previous value, $\Delta_f H^\circ_{298}$ = 22.9 ± 2.0 kJ mol^{-1}, was derived from a study of the thermal dissociation of $ClONO_2$.[1] Enthalpy values obtained from the atomization energy obtained using the G3//B3LYP level of theory are $\Delta_r H_0^\circ$ = 7.0 kcal mol^{-1} and $\Delta_r H_{298}^\circ$ = 5.5 kcal mol^{-1}.[6]

***cis,perp*-ClOONO**

The equilibrium geometry was calculated at the CCSD(T)/cc-pVQZ level of theory, while the energy was calculated by summing various contributions calculated at the CCSC(T) level with the use of various basis sets.[8] The previous value, $\Delta_f H^\circ_{298}$ = 132 kJ mol^{-1}, was obtained from the atomization energy obtained using the G3//B3LYP level of theory.[6]

***trans, perp*-ClOONO**

The equilibrium geometry was calculated at the CCSD(T)/cc-pVQZ level of theory, while the energy was calculated by summing various contributions calculated at the CCSC(T) level with the use of various basis sets.[8] The previous value, $\Delta_f H^\circ_{298}$ = 132 kJ mol^{-1}, was obtained from the atomization energy obtained using the G3//B3LYP level of theory.[6]

***trans, perp*-OClONO**

Value obtained from the atomization energy obtained using the G3//B3LYP level of theory.[6]

O_2ClONO_2 Based on a study of the recombination of OClO and NO_3, leading to a bond strength of 18±3 kcal mol^{-1}.[3]

NH_2Cl, $NHCl_2$, NCl_3, chloramines

Geometries were optimized at the (AE)-CCSD(T)/AVQZ level of theory and zero-point energies computed at the B2PLYPD/AVQZ level. For the electronic energies, a calculational protocol termed TA14 was adapted from the W3, W4, and FPD protocols. Enthalpies of formation were determined from the total atomization energies.[9]

(1) Anderson, L. C.; Fahey, D. W. Studies with $ClONO_2$: Thermal dissociation rate and catalytic conversion to NO using an NO/O_3 chemiluminescence detector. *J. Phys. Chem.* **1990**, *94*, 644-652, doi:10.1021/j100365a027.

(2) Chase, M. W. NIST-JANAF thermochemical tables. *J. Phys. Chem. Ref. Data* **1998**, *Monograph 9*.

(3) Friedl, R. R.; Sander, S. P.; Yung, Y. L. Chloryl nitrate: A novel product of the OClO + NO_3 + M recombination. *J. Phys. Chem.* **1992**, *96*, 7490-7493, doi:10.1021/j100198a002.

(4) Gurvich, L. V.; Veyts, I. V.; Alcock, C. B. *Thermodynamic Properties of Individual Substances,*, Fourth ed.; Hemisphere Publishing Corp.: New York, 1991; Vol. 2.

(5) Lee, T. J. *Ab initio* characterization of $ClNO_2$, *cis*-ClONO, and *trans*-ClONO. *J. Phys. Chem.* **1994**, *98*, 111-115, doi:10.1021/j100052a019.

(6) Lesar, A.; Prebil, S.; Hodošček, M. Ab initio characterization of $ClNO_3$ isomers. *J. Phys. Chem. A* **2003**, *107*, 9168-9174, doi:10.1021/jp030192v.

(7) McGrath, M. P.; Rowland, F. S. Determination of the barriers to interneal rotatoin in ONOOX (X = H, Cl) and characterization of the minimum energy conformers. *J. Phys. Chem.* **1994**, *98*, 1061-1067, doi:10.1021/j100055a004.

(8) Szakács, P.; Csontos, J.; Das, S.; Kállay, M. High-accuracy theoretical thermochemistry of atmospherically important nitrogen oxide derivatives. *J. Phys. Chem. A* **2011**, *115*, 3144-3153, doi:10.1021/jp112116x.
(9) Trogolo, D.; Arey, J. S. Benchmark thermochemistry of chloramines, bromamines, and bromochloramines: halogen oxidants stabilized by electron correlation. *Phys. Chem. Chem. Phys.* **2015**, *17*, 3584-3598, doi:10.1039/c4cp03987d.

Note 31: *Compounds containing one C and one or more Cl and H* Back to Table

CCl Geometry optimization was carried out at the CCSD(T) level of theory with the cc-pZQZ basis set. Enthalpy was calculated using the HEAT protocols, which involves summing a number of individual CCSD(T) energies with the basis set limited HF energy, along with other contributions.[1]

CHCl Calculated for the X^1A' state. The triplet-singlet energy gap is estimated to be 2170±40 cm^{-1}. Enthalpy determined by calculating the enthalpy of the reaction $CH_2 + HCl \rightarrow HCCl + H_2$. Calculations involved the focal-point approach, based on methods up to CCSDTQ and basis sets ranging from aug-cc-pVDZ to aug-cc-pV6Z, extrapolated to the complete basis set limit.[12] Enthalpy obtained using the computed enthalpy of a reaction of the type: $CH_2(^1A_1) + CH_3X + CH_3Y \leftrightarrow CXY(^1A_1) + 2CH_4$ results in $\Delta_f H^\circ_{298}$ = 320 kJ mol^{-1} at the QCISD(T)/6-311+G(3df,2p)//QCISD/6-311G(d,p) level of theory. Calculations also done at the G2 level.[9] Previous recommendation was based on combining experimental chloride dissociation energies from the parent anion, prior experimental measurements, and G2 calculations.[7] Entropy values from Gurvich et al. review.[2] A computational study with geometry optimization carried out at the CCSD(T) level of theory with the cc-pZQZ basis set, followed by an enthalpy calculation using the HEAT protocols, led to $\Delta_f H_0^\circ$ = 320.1 ± 2.3 kJ mol^{-1}, $\Delta_f H^\circ_{298}$= 320.3 ± 2.3 kJ mol^{-1}, and S = 234.6 ± 1.5 J K^{-1} mol^{-1}.[1] The enthalpy difference was used to calculate the 0 K value in the Table.

CH_2Cl Measured rate constant for the reaction of the radical with HBr, combined with previous measurements on the reverse reaction, with thermodynamic values obtained through a second-law analysis.[11] A QCISD(T)/6-311+G(3df,2p) isodesmic study resulted in an enthalpy of 117.0 ± 4.1 kJ mol^{-1}.[10] A dissociative photoionization study of CH_2ClBr results in an enthalpy of 110.7 kJ mol^{-1}.[5] A computational study with geometry optimization carried out at the CCSD(T) level of theory with the cc-pZQZ basis set, followed by an enthalpy calculation using the HEAT protocols, led to $\Delta_f H_0^\circ$ = 119.4 ± 2.7 kJ mol^{-1}, $\Delta_f H^\circ_{298}$= 116.0 ± 2.7 kJ mol^{-1}, and S = 236.3 ± 1.5 J K^{-1} mol^{-1}.[1] The enthalpy difference was used to calculate the 0 K value in the Table.

CH_3Cl Enthalpy from Manion evaluation.[6] Entropy from Thermodynamics Research Center evaluation.[8] A computational study with geometry optimization carried out at the CCSD(T) level of theory with the cc-pZQZ basis set, followed by an enthalpy calculation using the HEAT protocols, led to $\Delta_f H_0^\circ$ = −74.3 ± 3.1 kJ mol^{-1}, $\Delta_f H^\circ_{298}$= −82.6 ± 3.1 kJ mol^{-1}, and S = 234.0 ± 1.5 J K^{-1} mol^{-1}.[1] The enthalpy difference was used to calculate the 0 K value in the Table.

CCl_2 Calculated for the X^1A' state. The triplet-singlet energy gap is estimated to be 7045 ± 60 cm^{-1}. Enthalpy determined by calculating the enthalpy of the reaction $CH_2 + 2HCl \rightarrow CCl_2 + 2H_2$. Calculations involved the focal-point approach, based on methods up to CCSDTQ and basis sets ranging from aug-cc-pVDZ to aug-cc-pV6Z, extrapolated to the complete basis set limit.[12] Enthalpy obtained using the computed enthalpy of a reaction of the type: $CH_2(^1A_1) + CH_3X + CH_3Y \rightarrow CXY(^1A_1) + 2CH_4$ results in $\Delta_f H^\circ_{298}$ = 230 kJ mol^{-1} at the QCISD(T)/6-311+G(3df,2p)//QCISD/6-311G(d,p) level of theory. Calculations also done at the G2 level.[9] Previous recommendation (55.0 ± 2.0 kcal mol^{-1}) based on combining experimental chloride dissociation energies from the parent anion, prior experimental measurements, and G2 calculations.[7] Entropy values from Gurvich et al. review.[2] A computational study with geometry optimization carried out at the CCSD(T) level of theory with the cc-pZQZ basis set, followed by an enthalpy calculation using the HEAT protocols, led to $\Delta_f H_0^\circ$ = 229.0 ± 1.9 kJ mol^{-1},

$\Delta_f H^\circ_{298}$= 230.1 ± 1.9 kJ mol^{-1}, and S = 264.5 ± 1.5 J K^{-1} mol^{-1}.[1] The enthalpy difference was used to calculate the 0 K value in the Table.

$CHCl_2$ Measured rate constant for the reaction of the radical with HBr, combined with previous measurements on the reverse reaction, with thermodynamic values obtained through a second-law analysis.[11] A QCISD(T)/6-311+G(3df,2p) isodesmic study resulted in an enthalpy of 91.1 ± 4.1 kJ mol^{-1}.[10] A computational study with geometry optimization carried out at the CCSD(T) level of theory with the cc-pZQZ basis set, followed by an enthalpy calculation using the HEAT protocols, led to $\Delta_f H_0^\circ$ = 91.2 ± 4.8 kJ mol^{-1}, $\Delta_f H^\circ_{298}$= 88.8 ± 5.8 kJ mol^{-1}, and S = 280.7 ± 6.5 J K^{-1} mol^{-1}.[1] The enthalpy difference was used to calculate the 0 K value in the Table.

CH_2Cl_2 Enthalpy from Manion evaluation.[6] Entropy from Thermodynamics Research Center evaluation.[8] A computational study with geometry optimization carried out at the CCSD(T) level of theory with the cc-pZQZ basis set, followed by an enthalpy calculation using the HEAT protocols, led to $\Delta_f H_0^\circ$ = −86.5 ± 4.2 kJ mol^{-1}, $\Delta_f H^\circ_{298}$= −93.7 ± 4.2 kJ mol^{-1}, and S = 269.7 ± 1.5 J K^{-1} mol^{-1}.[1] The enthalpy difference was used to calculate the 0 K value in the Table.

CCl_3 A third-law determination based on the reaction $CCl_3 + Br_2 \leftrightarrow CCl_3Br + Br$, re-evaluating the kinetics of the reverse reaction and using spectroscopic data to calculate the entropy.[4] A QCISD(T)/6-311+G(3df,2p) isodesmic study resulted in an enthalpy of 72.2 ± 4.1 kJ mol^{-1}.[10] A computational study with geometry optimization carried out at the CCSD(T) level of theory with the cc-pZQZ basis set, followed by an enthalpy calculation using the HEAT protocols, led to $\Delta_f H_0^\circ$ = 73.7 ± 4.9 kJ mol^{-1}, $\Delta_f H^\circ_{298}$= 73.1 ± 4.9 kJ mol^{-1}, and S = 301.3 ± 1.5 J K^{-1} mol^{-1}.[1] The enthalpy difference was used to calculate the 0 K value in the Table.

$CHCl_3$ Enthalpy from Manion evaluation.[6] Entropy from Thermodynamics Research Center evaluation.[8] A computational study with geometry optimization carried out at the CCSD(T) level of theory with the cc-pZQZ basis set, followed by an enthalpy calculation using the HEAT protocols, led to $\Delta_f H_0^\circ$ = 94.6±5.3 kJ mol^{-1}, $\Delta_f H^\circ_{298}$= −99.7 ± 5.3 kJ mol^{-1}, and S = 294.8 ± 1.5 J K^{-1} mol^{-1}.[1] The enthalpy difference was used to calculate the 0 K value in the Table.

CCl_4 Enthalpy from Manion evaluation.[6] Entropy from Thermodynamics Research Center evaluation.[8] A computational study with geometry optimization carried out at the CCSD(T) level of theory with the cc-pZQZ basis set, followed by an enthalpy calculation using the HEAT protocols, led to $\Delta_f H_0^\circ$ = −88.8 ± 6.4 kJ mol^{-1}, $\Delta_f H^\circ_{298}$= −91.0 ± 6.4 kJ mol^{-1}, and S = 308.6 ± 1.5 J K^{-1} mol^{-1}.[1] The enthalpy difference was used to calculate the 0 K value in the Table. Experimental data from threshold PEPICO studies of halogenated methanes were combined with *ab initio* calculations of isodesmic and exchange reactions into a thermochemical network, leading to $\Delta_f H_0^\circ$ = −94.0 ± 3.2 kJ mol^{-1}.[3]

(1) Csontos, J.; Rolik, Z.; Das, S.; Kállay, M. High-accuracy thermochemistry of atmospherically important fluorinated and chlorinated methane derivatives. *J. Phys. Chem. A* **2010**, *114*, 13093-13103, doi:10.1021/jp105268m.

(2) Gurvich, L. V.; Veyts, I. V.; Alcock, C. B. *Thermodynamic Properties of Individual Substances,*, Fourth ed.; Hemisphere Publishing Corp.: New York, 1991; Vol. 2.

(3) Harvey, J.; Tuckett, R. P.; Bodi, A. A halomethane thermochemical network from iPEPICO experiments and quantum chemical calculations. *J. Phys. Chem. A* **2012**, *116*, 9696-9705, doi:10.1021/jp307941k.

(4) Hudgens, J. W.; Johnson, R. D.; Timonen, R. S.; Seetula, J. A.; Gutman, D. Kinetics of the reactions of $CCl_3 + Br_2$ and thermochemistry of CCl_3 radical and cation. *J. Phys. Chem.* **1991**, *95*, 4400-4405, doi:10.1021/j100164a043.

(5) Li, J.; Yang, J.; Mo, Y. X.; Lau, K. C.; Qian, X. M.; Song, Y.; Liu, J. B.; Ng, C. Y. Combined vacuum ultraviolet laser and synchrotron pulsed field ionization study of CH_2BrCl. *J. Chem. Phys.* **2007**, *126*, 184304, doi:10.1063/1.2730829.

(6) Manion, J. A. Evaluated enthalpies of formation of the stable closed shell C1 and C2 chlorinated hydrocarbons. *J. Phys. Chem. Ref. Data* **2002**, *31*, 123-172, doi:10.1063/1.1420703.

(7) Poutsma, J. C.; Paulino, J. A.; Squires, R. R. Absolute heats of formation of CHCl, CHF, and CClF. A gas-phase experimental and G2 theoretical study. *J. Phys. Chem. A* **1997**, *101*, 5327-5336, doi:10.1021/jp970778f.
(8) Rodgers, A. S.; Chao, J.; Wilhoit, R. C.; Zwolinski, B. J. Ideal gas thermodynamic properties of eight chloro- and fluoromethanes. *J. Phys. Chem. Ref. Data* **1974**, *3*, 117-140, doi:10.1063/1.3253135.
(9) Schwartz, M.; Marshall, P. An ab initio investigation of halocarbenes. *J. Phys. Chem. A* **1999**, *103*, 7900-7906, doi:10.1021/jp9919213.
(10) Schwartz, M.; Peebles, L. R.; Berry, R. J.; Marshall, P. A computational study of chlorofluoro-methyl radicals *J. Chem. Phys.* **2003**, *118*, 557-564, doi:10.1063/1.1524157.
(11) Seetula, J. A. Kinetics and thermochemistry of the R + HBr ⇄ RH + Br (R = CH_2Cl, $CHCl_2$, CH_3CHCl or CH_3CCl_2) equilibrium. *J. Chem. Soc. Faraday Trans.* **1996**, *92*, 3069-3078, doi:10.1039/FT9969203069.
(12) Tarczay, G.; Miller, T. A.; Czakó, G.; Császár, A. G. Accurate ab initio determination of spectroscopic and thermochemical properties of mono- and dichlorocharbenes. *Phys. Chem. Chem. Phys.* **2005**, *7*, 2881-2893, doi:10.1039/b506790a.

Note 32: *Compounds containing one C and one or more Cl, H, and O* Back to Table

$CClH_2O$ and $CClH_2OH$

The enthalpies of formation based on isodesmic reactions calculated at the MP2/6-31G(d,p) level of theory.[11]

CClO Second- and third-law analyses of the equilibration kinetics for the reaction Cl + CO ↔ ClCO led to $\Delta_f H^\circ_{298}$ = -7.7 ± 0.6 kcal mol^{-1}, $\Delta_r H_0^\circ$ = -6.9 ± 0.7 kcal mol^{-1}, and $\Delta_r S^\circ_{298}$ = -23.8 ± 2.0 cal mol^{-1} K^{-1}.[9] See also Table 3-1, Note 12. (Previous enthalpy value had a sign error.) A shock-tube study of the thermal decomposition of $COCl_2$ led to a value of $\Delta_r H_0^\circ$ = -6.3 ± 1.0 kcal mol^{-1}.[7] Entropy value cited derived by using standard statistical mechanic methods.[9]

CHClO The enthalpy values are taken from a CCSDT(Q) calculation, with structure optimized using the cc-pVQZ basis set.[8] The previous $\Delta_f H_{298}^\circ$ = –164 ± 20 kJ mol^{-1} was estimated in the Gurvich et al. review.[3] Entropy was based on spectroscopic studies.[3]

CH_2OCl Molecular properties determined at the MP2/6-31G(p,d), B3LYP/6-31G(d,p), and MP2/6-31G(d) level with single-point energy calculations at B3LYP/6-311+G(3df,2p) levels. Enthalpy based on four isodesmic reactions calculated at the CBS-Q//MP2/6-31(G(d,p) level.[1]

CH_3OCl Molecular properties determined at the B3LYP/6-31G(d,p) level, with single-point calculations at this and the B3LYP/6-311+G(3df,2p), QCISD(T)/6-31G(d,p), and CBS-Q levels. Enthalpies determined using several working reactions.[4]

CH_2ClO_2 Based on a re-analysis of previous equilibrium data on R + O_2 ↔ RO_2 from the same laboratory.[5]

CH_2ClOOH

Molecular geometries determined at the B3LYP/6-31G(d,p) level of theory and electronic energies obtained through single-point calculations at the CBSQ level. Enthalpy of formation determined using five reaction schemes, three of which were isodesmic.[13] A study in which geometry optimization and frequency calculations were performed at the MP2/6-31G(d) and the B3LYP/6-311++G(d,p) levels of theory, with a single-point energy calculation at the CCSD(T)/6-311++G(d,p//B3LYP/6-311++G(d,p) level.[6] The dissociation energy into HO_2 and the alkyl radical was then evaluated and used, after thermal correction, to calculate $\Delta_f H^\circ_{298}$ = –174 kJ mol^{-1}, after adjustment to the values for CH_3 and HO_2 from the present Table.

CCl_2O Taken from "The Chemical Thermodynamics of Organic Compounds".[12] Pedley review gives an enthalpy value of –219.1±0.5 kJ mol^{-1}.[10]

CCl_2HO and CCl_2HOH

The enthalpies of formation are based on isodesmic reactions calculated at the MP2/6-31G(d,p) level of theory.[11]

$CHCl_2O_2$ Based on a re-analysis of previous equilibrium data on $R + O_2 \leftrightarrow RO_2$ from the same laboratory.[5]

CH_2ClOCl Molecular properties determined at the B3LYP/6-31G(d,p) level, with single-point calculations at this and the B3LYP/6-311+G(3df,2p), QCISD(T)/6-31G(d,p), and CBS-Q levels. Enthalpies determined using several working reactions.[4]

$CHCl_2OOH$

Molecular geometries determined at the B3LYP/6-31G(d,p) level of theory an d electronic energies obtained through single-point calculations at the CBSQ level. Enthalpy of formation determined using five reaction schemes, three of which were isodesmic.[13]

$CHCl_2OCl$

Molecular properties determined at the B3LYP/6-31G(d,p) level, with single-point calculations at this and the B3LYP/6-311+G(3df,2p), QCISD(T)/6-31G(d,p), and CBS-Q levels. Enthalpies determined using several working reactions.[4]

CCl_3O and CCl_3OH

Enthalpies of formation are based on isodesmic reactions calculated at the MP2/6-31G(d,p) level of theory.[11]

CCl_3O_2 Based on a re-analysis of previous equilibrium data on $R + O_2 \leftrightarrow RO_2$ from the same laboratory.[5]

CCl_3OOH Molecular geometries determined at the B3LYP/6-31G(d,p) level of theory an d electronic energies obtained through single-point calculations at the CBSQ level. Enthalpy of formation determined using five reaction schemes, three of which were isodesmic.[13]

CCl_3OCl Molecular properties determined at the B3LYP/6-31G(d,p) level, with single-point calculations at this and the B3LYP/6-311+G(3df,2p), QCISD(T)/6-31G(d,p), and CBS-Q levels. Enthalpies determined using several working reactions.[4] $\Delta_f H^\circ_{298}$ = -146.6 kJ mol^{-1} from a G2 calculation of the total energy of formation from the gas-phase elements.[2]

(1) Bozzelli, J. W.; Jung, D. Theoretical investigation on stability of the C•H_2OCl radical. *J. Phys. Chem. A* **2001**, *105*, 3941-3946, doi:10.1021/jp003401+.

(2) Brudnik, K.; Jodkowski, J. T.; Nowek, A.; Leszczynski, J. Kinetics of the formation reactions of trichloro- and tribromomethyl hypohalites and alcohols in the gas-phase: Theoretical study *Chem. Phys. Lett.* **2007**, *435*, 194-200, doi:10.1016/j.cplett.2006.12.079.

(3) Gurvich, L. V.; Veyts, I. V.; Alcock, C. B. *Thermodynamic Properties of Individual Substances,*, Fourth ed.; Hemisphere Publishing Corp.: New York, 1991; Vol. 2.

(4) Jung, D.; Chen, C. J.; Bozzelli, J. W. Structures, rotation barrier, and thermodynamic properties $\Delta H_f^\circ{}_{298}$, $S^\circ{}_{298}$, and C_p(T) of chloromethyl hypochlorites CH_3OCl, CH_2ClOCl, and CCl_3OCl. *J. Phys. Chem. A* **2000**, *104*, 9581-9590, doi:10.1021/jp001469j.

(5) Knyazev, V. D.; Slagle, I. R. Thermochemistry of the R-O_2 bond in alkyl and chloroalkyl peroxy radicals. *J. Phys. Chem. A* **1998**, *102*, 1770-1778, doi:10.1021/jp9726091.

(6) Kosmas, A. M.; Mpellos, C.; Salta, Z.; Drougas, E. Structural and heat of formation studies of halogenated methyl hydro-peroxides. *Chem. Phys.* **2010**, *371*, 36-42, doi:10.1016/j.chemphys.2010.03.026.

(7) Lim, K. P.; Michael, J. V. Thermal decomposition of $COCl_2$. *J. Phys. Chem.* **1994**, *98*, 211-215, doi:10.1021/j100052a035.

(8) Nagy, B.; Csontos, J.; Kállay, M.; Tasi, G. High-accuracy theoretical study on the thermochemistry of several formaldehyde derivatives. *J. Phys. Chem. A* **2010**, *114*, 13213-13221, doi:10.1021/jp1085203.

(9) Nicovich, J. M.; Kreutter, K. D.; Wine, P. H. Kinetics and thermochemistry of ClCO formation from the Cl + CO association reaction. *J. Chem. Phys.* **1990**, *92*, 3539-3544, doi:10.1063/1.457862.

(10) Pedley, J. B. *Thermochemical Data and Structures of Organic Compounds*; Thermodynamics Data Center: College Station, TX, 1994.

(11) Schneider, W. F.; Nance, B. I.; Wallington, T. J. Bond strengths in halogenated methanes: Evidence for negative hyperconjugation. *J. Am. Chem. Soc.* **1995**, *117*, 478-485, doi:10.1021/ja00106a055.
(12) Stull, D. R.; Westrum, E. F.; Sinke, G. C. *The Chemical Thermodynamics of Organic Compounds*; John Wiley & Sons: New York, 1969.
(13) Sun, H.; Chen, C. J.; Bozzelli, J. W. Structures, intramolecular rotation barriers, and thermodynamic properties (enthalpies, entropies, and heat capacites) of chlorinated methyl hydroperoxides (CH_2ClOOH, $CHCl_2OOH$, and CCl_3OOH). *J. Phys. Chem. A* **2000**, *104*, 8270-8282, doi:10.1021/jp0013917.

Note 33: *Compounds containing one C and one or more Cl and F* Back to Table

CHFCl Enthalpy derived from an analysis of thermochemical and kinetic data on the bromination of CH_2FCl.[12] A QCISD(T)/6-311+G(3df,2p) isodesmic study resulted in an enthalpy of -63.8 ± 4.1 kJ mol^{-1}.[11] A computational study with geometry optimization carried out at the CCSD(T) level of theory with the cc-pZQZ basis set, followed by an enthalpy calculation using the HEAT protocols, led to $\Delta_f H_0^o$ = −64.6 ± 3.7 kJ mol^{-1}, $\Delta_f H^o_{298}$= −67.8 ± 4.7 kJ mol^{-1}, and S = 273.5 ± 6.5 J K^{-1} mol^{-1} (used in the Table).[3] The enthalpy difference was used to calculate the 0 K value in the Table.

CH_2FCl Geometry optimization was carried out at the CCSD(T) level of theory with the cc-pZQZ basis set. Enthalpy was calculated using the HEAT protocols, which involves summing the CCSD(T) energy extrapolated to the complete basis set limit, along with several other contributions.[3] Previous enthalpy from Pedley review[7] and entropy from Thermodynamics Research Center review.[1]

CFCl Recommendation based on combining experimental chloride dissociation energies from the parent anion, prior experimental measurements, and G2 calculations.[8] Enthalpy obtained using the computed enthalpy of a reaction of the type: $CH_2(^1A_1) + CH_3X + CH_3Y \rightarrow CXY(^1A_1) + 2CH_4$ results in $\Delta_f H^o_{298}$ = 29.4 kJ mol^{-1} at the QCISD(T)/6-311+G(3df,2p)//QCISD/6-311G(d,p) level of theory. Calculations also done at the G2 level.[10] Entropy values from Gurvich et al. review.[4] A computational study with geometry optimization carried out at the CCSD(T) level of theory with the cc-pZQZ basis set, followed by an enthalpy calculation using the HEAT protocols, led to $\Delta_f H_0^o$ = 32.2 ± 2.3 kJ mol^{-1}, $\Delta_f H^o_{298}$= 32.0 ± 2.3 kJ mol^{-1}, and S = 258.9 ± 1.5 J K^{-1} mol^{-1}.[3] The enthalpy difference was used to calculate the 0 K value in the Table.

CF_2Cl Geometry optimization was carried out at the CCSD(T) level of theory with the cc-pZQZ basis set. Enthalpy was calculated using the HEAT protocols, which involves summing the CCSD(T) energy extrapolated to the complete basis set limit, along with several other contributions.[3] A photobromination study leads to D($CClF_2$-H) = 100.7 ± 2 kcal mol^{-1}.[6] A QCISD(T)/6-311+G(3df,2p) isodesmic study resulted in an enthalpy of –274.7 ± 4.1 kJ mol^{-1}.[11]

$CFCl_2$ Geometry optimization was carried out at the CCSD(T) level of theory with the cc-pZQZ basis set. Enthalpy was calculated using the HEAT protocols, which involves summing the CCSD(T) energy extrapolated to the complete basis set limit, along with several other contributions.[3] An enthalpy of –89.1±10 kJ mol^{-1} was derived from an analysis of thermochemical and kinetic data on the bromination of CH_2FCl.[12] A QCISD(T)/6-311+G(3df,2p) isodesmic study resulted in an enthalpy of –94.3 ± 4.1 kJ mol^{-1}.[11]

$CHFCl_2$ Geometry optimization was carried out at the CCSD(T) level of theory with the cc-pZQZ basis set. Enthalpy was calculated using the HEAT protocols, which involves summing the CCSD(T) energy extrapolated to the complete basis set limit, along with several other contributions.[3] Previous enthalpy value, from the Thermodynamics Research Center review,[1] was estimated.

CHF_2Cl Enthalpy from Pedley[7] review and entropy from Thermodynamics Research Center review.[1] A computational study with geometry optimization carried out at the CCSD(T) level of theory with the cc-pZQZ basis set, followed by an enthalpy calculation using the HEAT protocols, led to

$\Delta_f H_0^o$ = −475.7 ± 3.1 kJ mol^{-1}, $\Delta_f H_{298}^o$= −482.2 ± 3.1 kJ mol^{-1}, and S = 280.5 ± 1.5 J K^{-1} mol^{-1}.[3] The enthalpy difference was used to calculate the 0 K value in the Table.

$CFCl_3$ Enthalpy based on equilibrium measurements for the reaction $CClF_3 + 2CCl_4 \leftrightarrow 3CCl_3F$ leading to a heat of reaction of 10.59 kcal mol^{-1}, changed to reflect present enthalpy values.[2] Pedley review gives an enthalpy value of –268.3 ± 8.4 kJ mol^{-1}.[7] A computational study with geometry optimization carried out at the CCSD(T) level of theory with the cc-pZQZ basis set, followed by an enthalpy calculation using the HEAT protocols, led to $\Delta_f H_0^o$ = −286.0 ± 5.3 kJ mol^{-1}, $\Delta_f H_{298}^o$= −282.7 ± 5.3 kJ mol^{-1}, and S = 308.6 ± 1.5 J K^{-1} mol^{-1}.[3] The enthalpy difference was used to calculate the 0 K value in the Table. Experimental data from threshold PEPICO studies of halogenated methanes were combined with *ab initio* calculations of isodesmic and exchange reactions into a thermochemical network, leading to $\Delta_f H_0^o$ = −285.2 ± 3.2 kJ mol^{-1}.[5]

CF_2Cl_2 Enthalpy based on equilibrium measurements for the reaction $2CClF_3 + CCl_4 \leftrightarrow 3CCl_2F_2$ leading to a heat of reaction of 7.59 kcal mol^{-1}, changed to reflect present enthalpy values.[2] Pedley review gives an enthalpy value of –477.4 ± 7.2 kJ mol^{-1}.[7] A computational study with geometry optimization carried out at the CCSD(T) level of theory with the cc-pZQZ basis set, followed by an enthalpy calculation using the HEAT protocols, led to $\Delta_f H_0^o$ = −487.9 ± 4.2 kJ mol^{-1}, $\Delta_f H_{298}^o$= −492.1 ± 4.2 kJ mol^{-1}, and S = 300.2 ± 1.5 J K^{-1} mol^{-1}.[3] The enthalpy difference was used to calculate the 0 K value in the Table. Experimental data from threshold PEPICO studies of halogenated methanes were combined with *ab initio* calculations of isodesmic and exchange reactions into a thermochemical network, leading to $\Delta_f H_0^o$ = −487.8 ± 3.4 kJ mol^{-1}.[5]

CF_3Cl Enthalpy from a simultaneous solution of a thermochemical network for the CF_3X species, where X = nil, H, Cl, Br, I, CF_3, CN.[9] Entropy from recommendation of the Thermodynamics Research Center.[2] A computational study with geometry optimization carried out at the CCSD(T) level of theory with the cc-pZQZ basis set, followed by an enthalpy calculation using the HEAT protocols, led to $\Delta_f H_0^o$ = −703.4 ± 3.1 kJ mol^{-1}, $\Delta_f H_{298}^o$= −708.6 ± 3.1 kJ mol^{-1}, and S = 284.7 ± 1.5 J K^{-1} mol^{-1}.[3] The enthalpy difference was used to calculate the 0 K value in the Table. Experimental data from threshold PEPICO studies of halogenated methanes were combined with *ab initio* calculations of isodesmic and exchange reactions into a thermochemical network, leading to $\Delta_f H_0^o$ = −702.1 ± 3.5 kJ mol^{-1}.[5]

(1) Chen, S. S.; Rodgers, A. S.; Chao, J.; Wilhoit, R. C.; Zwolinski, B. J. Ideal gas thermodynamic properties of six fluoroethanes. *J. Phys. Chem. Ref. Data* **1975**, *4*, 441-456, doi:10.1063/1.555521.

(2) Chen, S. S.; Wilhoit, R. C.; Zwolinski, B. J. Ideal gas properties of six chlorofluoromethanes. *J. Phys. Chem. Ref. Data* **1976**, *5*, 571-580, doi:10.1063/1.555539.

(3) Csontos, J.; Rolik, Z.; Das, S.; Kállay, M. High-accuracy thermochemistry of atmospherically important fluorinated and chlorinated methane derivatives. *J. Phys. Chem. A* **2010**, *114*, 13093-13103, doi:10.1021/jp105268m.

(4) Gurvich, L. V.; Veyts, I. V.; Alcock, C. B. *Thermodynamic Properties of Individual Substances,*, Fourth ed.; Hemisphere Publishing Corp.: New York, 1991; Vol. 2.

(5) Harvey, J.; Tuckett, R. P.; Bodi, A. A halomethane thermochemical network from iPEPICO experiments and quantum chemical calculations. *J. Phys. Chem. A* **2012**, *116*, 9696-9705, doi:10.1021/jp307941k.

(6) Miyokawa, K.; Tschuikow-Roux, E. Reaction of atomic bromine with difluorochloromethane, The heat of formation of the $CClF_2$ radical and the $D^o(CClF_2\text{-H})$ bond dissociation energy. *J. Phys. Chem.* **1992**, *96*, 7328-7331, doi:10.1021/j100197a034.

(7) Pedley, J. B. *Thermochemical Data and Structures of Organic Compounds*; Thermodynamics Data Center: College Station, TX, 1994.

(8) Poutsma, J. C.; Paulino, J. A.; Squires, R. R. Absolute heats of formation of CHCl, CHF, and CClF. A gas-phase experimental and G2 theoretical study. *J. Phys. Chem. A* **1997**, *101*, 5327-5336, doi:10.1021/jp970778f.

(9) Ruscic, B.; Michael, J. V.; Redfern, P. C.; Curtiss, L. A.; Raghavachri, K. Simultaneous adjustment of experimentally based enthalpies of formation of CF_3X, X = nil, H, Cl, Br, I,

CF_3, CN, and a probe of G3 theory. *J. Phys. Chem. A* **1998**, *102*, 10889-10899, doi:10.1021/jp983237e.
(10) Schwartz, M.; Marshall, P. An ab initio investigation of halocarbenes. *J. Phys. Chem. A* **1999**, *103*, 7900-7906, doi:10.1021/jp9919213.
(11) Schwartz, M.; Peebles, L. R.; Berry, R. J.; Marshall, P. A computational study of chlorofluoro-methyl radicals *J. Chem. Phys.* **2003**, *118*, 557-564, doi:10.1063/1.1524157.
(12) Tschuikow-Roux, E.; Paddison, S. Bond dissociation energies and radical heats of formation in CH_3Cl, CH_2Cl_2, CH_3Br, CH_2Br_2, CH_2FCl, and $CHFCl_2$. *Int. J. Chem. Kinet.* **1987**, *19*, 15-24, doi:10.1002/kin.550190103.

Note 34: *Compounds containing one C and one or more Cl, F, and O* Back to Table

CFClO The enthalpy values are taken from a CCSDT(Q) calculation, with structure optimized using the cc-pVQZ basis set.[7] Previous enthalpy value of –429 ± 20 kJ mol^{-1} estimated in the Gurvich et al. review.[5] The recommended entropy is taken from the Gurvich et al. review.

CF_3OCl Based on photoionization study. Enthalpy presented as lower limit.[1] A G2 calculation led to an enthalpy of –768.3 kJ mol^{-1}.[4]

CCl_3OF Derived from a G2 calculation of the total energy of formation from the gas-phase elements.[3]

***cis*- and *trans*-FC(O)OCl**
Enthalpy computed at the G3//B3LYP/6-311++G(3df,3pd) level of theory with both atomization energies and isodesmic reactions.[2]

CHClFOOH and CCl_2FOOH
Geometry optimization and frequency calculations were performed at the MP2/6-31G(d) and the B3LYP/6-311++G(d,p) levels of theory, with a single-point energy calculation at the CCSD(T)/6-311++G(d,p//B3LYP/6-311++G(d,p) level. The dissociation energy into HO_2 and the alkyl radical was then evaluated and used, after thermal correction, to calculate the enthalpy of formation at 298 K.[6] This was adjusted to the radical values from the present Table.

(1) Asher, R. L.; Appelman, E. H.; Tilson, J. L.; Litorja, M.; Berkowitz, J.; Ruscic, B. A photoionization study of trifluoromethanol, CF_3OH, trifluoromethyl hypofluorite, CF_3OF, and trifluoromethyl hypochlorite, CF_3OCl. *J. Chem. Phys.* **1997**, *106*, 9111-9121, doi:10.1063/1.474017.
(2) Badenes, M. P.; Croce, A. E.; Cobos, C. J. Falloff curves for the recombination reaction Cl + FC(O)O + M → FC(O)OCl + M. *J. Phys. Chem. A* **2006**, *110*, 3186-3196, doi:10.1021/jp054591x.
(3) Brudnik, K.; Jodkowski, J. T.; Nowek, A.; Leszczynski, J. Kinetics of the formation reactions of trichloro- and tribromomethyl hypohalites and alcohols in the gas-phase: Theoretical study *Chem. Phys. Lett.* **2007**, *435*, 194-200, doi:10.1016/j.cplett.2006.12.079.
(4) Brudnik, K.; Jodkowski, J. T.; Ratajczak, E. Kinetics of the formation reactions of trifluoromethanol and trifluoromethyl hypohalites in the gas phase. *J. Mol. Struct.* **2003**, *656*, 333-339, doi:10.1016/S0022-2860(03)00347-8.
(5) Gurvich, L. V.; Veyts, I. V.; Alcock, C. B. *Thermodynamic Properties of Individual Substances,*, Fourth ed.; Hemisphere Publishing Corp.: New York, 1991; Vol. 2.
(6) Kosmas, A. M.; Mpellos, C.; Salta, Z.; Drougas, E. Structural and heat of formation studies of halogenated methyl hydro-peroxides. *Chem. Phys.* **2010**, *371*, 36-42, doi:10.1016/j.chemphys.2010.03.026.
(7) Nagy, B.; Csontos, J.; Kállay, M.; Tasi, G. High-accuracy theoretical study on the thermochemistry of several formaldehyde derivatives. *J. Phys. Chem. A* **2010**, *114*, 13213-13221, doi:10.1021/jp1085203.

Note 35: *Compounds containing two C and one or more Cl* Back to Table

C_2HCl Enthalpy from Manion evaluation based on calculations involving isodesmic reactions.[4]

C_2H_3Cl Enthalpy from Manion evaluation.[4] Pedley review gives an enthalpy value of 37.2 ± 1.2 kJ mol^{-1}.[7]

CH_2CH_2Cl Measured rate constant for the reaction of the radical with HBr, combined with previous measurements on the reverse reaction, with thermodynamic values obtained through a second-law analysis.[10]

CH_3CHCl Measured rate constant for the reaction of the radical with HBr, combined with previous measurements on the reverse reaction, with thermodynamic values obtained through a second-law analysis.[9]

CH_3CH_2Cl Enthalpy from Manion evaluation.[4] Entropy from a Thermodynamics Research Center evaluation.[1]

C_2Cl_2 Enthalpy from Manion evaluation based on calculations involving isodesmic reactions.[4]

CH_2CCl_2 Enthalpy from Manion evaluation.[4] Pedley review gives an enthalpy value of 2.8 ± 1.3 kJ mol^{-1}.[7]

***cis*-CHClCHCl**
Enthalpy from Manion evaluation.[4] Pedley review gives an enthalpy value of 4.6 ± 8.4 kJ mol^{-1}.[7]

***trans*-CHClCHCl**
Enthalpy from Manion evaluation.[4] Pedley review gives an enthalpy value of 5.0 ± 8.4 kJ mol^{-1}.[7]

CH_3CCl_2 Measured rate constant for the reaction of the radical with HBr, combined with previous measurements on the reverse reaction, with thermodynamic values obtained through a second-law analysis.[9]

CH_3CHCl_2 Enthalpy from Manion evaluation.[4] Entropy from a Thermodynamics Research Center evaluation.[1] Pedley review gives an enthalpy value of –127.7 ± 1.4 kJ mol^{-1}.[7]

$CHCl_2CH_2$ Measured rate constant for the reaction of the radical with HBr, combined with calculated (MP2(fc)/6-31G(d,p)) values for the reverse reaction, leading to thermodynamic values obtained through a second-law analysis.[11]

CH_2ClCH_2Cl
Enthalpy from Manion evaluation.[4] Pedley review gives an enthalpy value of −126.4 ± 2.3 kJ mol^{-1}.[7]

C_2HCl_3 Enthalpy from Manion evaluation.[4] Previous enthalpy from the heat of combustion of trichloroethene, $\Delta_f H^\circ_{298}$ = –19.1 ± 3.0 kJ mol^{-1}.[6] Entropy from review of Frenkel.[2] Pedley review gives an enthalpy value of −9.0 ± 8.8 kJ mol^{-1}.[7]

$CH_2ClCHCl_2$
Enthalpy from Manion evaluation.[4]

CH_2CCl_3 An analysis of the kinetic data from the bromine-catalyzed elimination of HCl from CH_3CCl_3 resulted in a C-H bond strength of 103.8 ± 2 kcal mol^{-1}.[8]

CH_3CCl_3 Enthalpy from Manion evaluation.[4] Entropy from a Thermodynamics Research Center evaluation.[1] Pedley review gives an enthalpy value of –144.4 ± 1.7 kJ mol^{-1}.[7]

C_2Cl_4 Enthalpy from Manion evaluation.[4] Pedley review gives an enthalpy value of -10.9 ± 8.3 kJ mol^{-1}.[7] Entropy from Gurvich et al.[3]

$CHCl_2CHCl_2$
Enthalpy from Manion evaluation.[4] Pedley review gives an enthalpy value of −149.3 ± 8.4 kJ mol^{-1}.[7]

CH_2ClCCl_3
Enthalpy from Manion evaluation.[4]

C_2Cl_5 Derived from both second- and third-law analyses of the equilibrium data for the reaction Cl + $C_2Cl_4 \leftrightarrow C_2Cl_5$, with the enthalpy adjusted for present reference values,[5] $\Delta_f H_0^\circ$ = 5.2 ± 1.5 kcal mol^{-1}.

C_2HCl_5 Enthalpy from Manion evaluation.[4] Pedley review gives an enthalpy value of −142.0 ± 9.0 kJ mol^{-1}.[7]

C_2Cl_6 Enthalpy from Manion evaluation.[4] Entropy from Gurvich et al.[3] Pedley review gives an enthalpy value of −143.6 ± 9.1 kJ mol^{-1}.[7]

(1) Chao, J.; Rodgers, A. S.; Wilhoit, R. C.; Zwolinski, B. J. Ideal gas thermodynamic properties of six chloroethanes. *J. Phys. Chem. Ref. Data* **1974**, *3*, 141-162, doi:10.1063/1.3253136.

(2) Frenkel, M.; Kabo, G. J.; Marsh, K. N.; Roganov, G. N.; Wilhoit, R. C. *Thermodynamics of Organic Compounds in the Gas State*; Thermodynamics Research Center: College Station, TX, 1994; Vol. I.

(3) Gurvich, L. V.; Veyts, I. V.; Alcock, C. B. *Thermodynamic Properties of Individual Substances,*, Fourth ed.; Hemisphere Publishing Corp.: New York, 1991; Vol. 2.

(4) Manion, J. A. Evaluated enthalpies of formation of the stable closed shell C1 and C2 chlorinated hydrocarbons. *J. Phys. Chem. Ref. Data* **2002**, *31*, 123-172, doi:10.1063/1.1420703.

(5) Nicovich, J. M.; Wang, L.; McKee, M. L.; Wine, P. H. Kinetics and thermochemistry of the $Cl(^2P_J) + C_2Cl_4$ association reaction. *J. Phys. Chem.* **1996**, *100*, 680-688, doi:10.1021/jp952396k.

(6) Papina, T. S.; Kolesov, V. P. Standard enthalpy of formation of trichloroethylene. *Russ. J. Phys. Chem.* **1985**, *59*, 1289-1292.

(7) Pedley, J. B. *Thermochemical Data and Structures of Organic Compounds*; Thermodynamics Data Center: College Station, TX, 1994.

(8) Rodgers, A. S.; Jerus, P. Kinetics of the bromine catalyzed elimination of HCl from 1,1,1-trichloroethane. *Int. J. Chem. Kinet.* **1988**, *20*, 565-575, doi:10.1002/kin.550200706.

(9) Seetula, J. A. Kinetics and thermochemistry of the R + HBr ⇄ RH + Br (R = CH_2Cl, $CHCl_2$, CH_3CHCl or CH_3CCl_2) equilibrium. *J. Chem. Soc. Faraday Trans.* **1996**, *92*, 3069-3078, doi:10.1039/FT9969203069.

(10) Seetula, J. A. Kinetics and thermochemistry of the R + HBr ⇄ RH + Br (R = C_2H_5 or β-C_2H_4Cl) equilibrium. *J. Chem. Soc. Faraday Trans.* **1998**, *94*, 891-898, doi:10.1039/A706440C.

(11) Seetula, J. A. *Ab initio* study of the transition states for determining the enthalpies of formation of alkyl and halogenated alkyl free radicals. *Phys. Chem. Chem. Phys.* **2000**, *2*, 3807-3812, doi:10.1039/b001350l.

Note 36: *Compounds containing two C and one or more F and Cl*

Back to Table

CH_3CHFCl
Review of the literature.[1]

CH_2CF_2Cl Derived from an exothermicity of 3.69 kcal mol^{-1} for the isodesmic reaction $CH_3CF_2Cl + CH_3CH_2 \rightarrow CH_2CF_2Cl + CH_3CH_3$, calculated at the HF/6-31G* level of theory.[3]

CH_3CF_2Cl Enthalpy from literature review.[1] Entropy calculated from experimental frequencies.[3] Enthalpy value calculated at the MP2/6-311G** level of theory is −128.41 kcal mol^{-1}.[2]

CH_3CFCl_2 Enthalpy calculated at the MP2/6-311G** level of theory.[2]

CF_2CFCl and CF_3CHFCl
Enthalpy values taken from review of Pedley.[4]

CF_3CH_2Cl, CF_3CHCl_2, and CF_3CCl_3
Enthalpy values calculated at the MP2/6-311G** level of theory.[2]

CF_2ClCF_2Cl, $CF_2ClCFCl_2$, and C_2F_5Cl
Enthalpy values taken from review of Pedley.[4]

(1) Kolesov, V. P.; Papina, T. S. Thermochemistry of haloethanes. *Russ. Chem. Rev.* **1983**, *52*, 425-439.

(2) Olleta, A. C.; Lane, S. I. Ab initio studies of the gas-phase thermodynamic properties and bond dissociation energies for haloethanes and halomethy radicals. *Phys. Chem. Chem. Phys.* **2001**, *3*, 811-818, doi:10.1039/b005375i.
(3) Paddison, S. J.; Chen, Y. H.; Tschuikow-Roux, E. An *ab initio* study of the structrures, barriers for internal rotation, vibrational frequencies, and thermodynamic functions of the hydrochlorofluorocarbon CH_3CF_2Cl and the corresponding radical CH_2CF_2Cl. *Can. J. Chem.* **1994**, *72*, 561-567, doi:10.1139/v94-079.
(4) Pedley, J. B. *Thermochemical Data and Structures of Organic Compounds*; Thermodynamics Data Center: College Station, TX, 1994.

Note 37: *Compounds containing two C and one or more Cl and O* Back to Table

$ClCH_2CH_2OH$

The enthalpy of formation of the liquid was determined by using rotating-bomb combustion calorimetry to be $\Delta_f H^\circ_{298}(l)$ =–315.5 ± 0.7 kJ mol^{-1}. The molar enthalpy of vaporization was then determined by use of Calvert-drop microcalorimetry as $\Delta_{vap}H^\circ_{298}$ = 48.32 ± 0.37 kJ mol^{-1}.[1]

CH_3CHClO_2

Based on a re-analysis of previous equilibrium data on R + O_2 ↔ RO_2 from the same laboratory.[4]

$CH_3C(O)Cl$, acetyl chloride

Enthalpy from review of Pedley.[6]

$CH_2ClC(O)OH$

Review of the literature.[2] Pedley review gives an enthalpy value of –435.2 ± 9.3 kJ mol^{-1}.[6]

$CH_2ClCOOH$

Geometries and frequencies calculated at the B3LYP/6-31G(d,p) level of theory. Enthalpy calculated from three isodesmic reactions at the CBSQ//B3LYP/6-31(Gd,p) level and corrected for mixing of rotational conformers.[7]

$CH_3CHClOOH$

Geometric parameters calculated at the RHF/6-31G* and MP2/6-31G* levels of theory, and the entropy obtained using the rigid-rotor/harmonic-oscillator approximation. Enthalpy calculated using the isodesmic reaction $CH_3OOH + C_2H_5Cl \leftrightarrow CH_3CHClOOH + CH_4$, adjusted with reference values from the present Table.[5]

CH_3CCl_2OOH

Geometric parameters calculated at the RHF/6-31G* and MP2/6-31G* levels of theory, and the entropy obtained using the rigid-rotor/harmonic-oscillator approximation. Enthalpy calculated using the isodesmic reaction $CH_3OOH + 1,1\text{-}C_2H_4Cl_2 \leftrightarrow CH_3CCl_2OOH + CH_4$, adjusted with reference values from the present Table.[5]

$CH_2ClC(O)OCl$, chloroacetyl chloride

Enthalpy value taken from review of Pedley.[6]

Cl(O)CC(O)Cl, ethanedioyl cichloride (oxalyl chloride)

Enthalpy value taken from review of Pedley.[6]

$CHCl_2C(O)Cl$, dichloroacetyl chloride

Enthalpy value taken from review of Pedley.[6]

CCl_3CH_2OOH

Geometries and frequencies calculated at the B3LYP/6-31G(d,p) level of theory. Enthalpy calculated from three isodesmic reactions at the CBSQ//B3LYP/6-31(Gd,p) level and corrected for mixing of rotational conformers.[7]

CCl_3CO Enthalpy is an average of values obtained at the CBS-4//HF/3-21G* and G2(MP2(full)//MP2(full)/6-31G(d) levels of theory, using both atomization energies and

formation from molecular species. Entropy at the G2(MP2(full)//MP2(full)/6-31G(d) level treating internal rotations as harmonic oscillators.[8]

$CCl_3C(O)H$

Thermodynamic properties calculated at the G2(MP2(full)//MP2(full)/6-31G(d) level of theory. Enthalpy from atomization energy and entropy calculated treating internal rotations as harmonic oscillators. Similar values obtained at the CBS-4//HF/3021G* level.[8]

$CCl_3C(O)Cl$, trichloroacetyl chloride

Enthalpy from review of Pedley.[6]

$CH_3CCl_2O_2$

Based on the equilibrium study using laser photolysis/PI mass spectrometry,[3] adjusted by using the enthalpy for CH_3CCl_2 cited in this Table.

$CHCl_2CH_2OOH$

Geometries and frequencies calculated at the B3LYP/6-31G(d,p) level of theory. Enthalpy calculated from three isodesmic reactions at the CBSQ//B3LYP/6-31(Gd,p) level and corrected for mixing of rotational conformers.[7]

(1) Bernardes, C. E. S.; Minas da Piedade, M. E.; Amaral, L. M. P. F.; Ferreira, A. I. M. C. L.; Ribeiro da Silva, M. A. V.; Diogo, H. P.; Costa Cabral, B. J. Energetics of C−F, C−Cl, C−Br, and C−I bonds in 2-haloethanols. Enthalpies of formation of XCH_2CH_2OH (X = F, Cl, Br, I) compounds and of the 2-hydroxyethyl radical. *J. Phys. Chem. A* **2007**, *111*, 1713-1720, doi:10.1021/jp0675678.

(2) Dorofeeva, O.; Novikov, V. P.; Neumann, D. B. NIST-JANAF thermochemical tables. 1. Ten organic molecules related to atmospheric chemistry. *J. Phys. Chem. Ref. Data* **2001**, *30*, 475-513, doi:10.1063/1.1364518.

(3) Knyazev, V. D.; Bencsura, A.; Slagle, I. R. Kinetics and thermochemistry of the reactions of CH_3CCl_2 and $(CH_3)_2CCl$ radicals with molecular oxygen. *J. Phys. Chem. A* **1998**, *102*, 1760-1769, doi:10.1021/jp9726089.

(4) Knyazev, V. D.; Slagle, I. R. Thermochemistry of the R-O_2 bond in alkyl and chloroalkyl peroxy radicals. *J. Phys. Chem. A* **1998**, *102*, 1770-1778, doi:10.1021/jp9726091.

(5) Lay, T. H.; Krasnoperov, L. N.; Venanzi, C. A.; Bozzelli, J. W.; Shokhirev, N. V. Ab initio study of α-chlorinated ethyl hydroperoxides CH_3CH_2OOH, CH_3ClOOH, and CH_3CCl_2OOH: Conformational analysis, internal rotation barriers, vibrational frequencies, and thermodynamic properties. *J. Phys. Chem.* **1996**, *100*, 8240-8249, doi:10.1021/jp952976h.

(6) Pedley, J. B. *Thermochemical Data and Structures of Organic Compounds*; Thermodynamics Data Center: College Station, TX, 1994.

(7) Sun, H.; Bozzelli, J. W. Structures, rotational barriers, and thermochemical properties of β-chlorinated ethyl hydroperoxides. *J. Phys. Chem. A* **2003**, *107*, 1018-1024, doi:10.1021/jp022298g.

(8) Viskolcz, B.; Berces, T. Enthalpy of formation of selected carbonyl radicals from theory and comparison with experiment. *Phys. Chem. Chem. Phys.* **2000**, *2*, 5430-6436, doi:10.1039/b004548i.

Note 38: *Compounds containing three C and, possibly, F, Cl, and O*

Back to Table

$CH_3CHClCH_3$

The measured onset energy for *i*-$C_3H_7^+$ from iPEPICO spectroscopy of *i*- C_3H_7Cl was used in conjunction with a new value of the ion enthalpy of formation to obtain the 0 K enthalpy of the chloride.[2]

$CF_2ClC(O)OCH_3$ and $CF_2ClC(O)OCH_3$

Geometry optimization carried out using the hybrid meta-density functional, MPWB1K with the 6-31+G(d,p) basis set. Energies refined using G2(MP2). Enthalpy of formation calculated by using two group-balanced isodesmic reactions.[1]

(1) Mishra, B. K.; Chakrabartty, A. K.; Deka, R. C. Theoretical investigation of the gas-phase reactions of $CF_2ClC(O)OCH_3$ with the hydroxyl radical and the chlorine atom at 298 K. *J. Mol. Model* **2013**, *19*, 3263-3270, doi:10.1007/s00894-013-1865-1.
(2) Stevens, W. R.; Bodi, A.; Baer, T. Dissociation dynamics of energy selected, propane, and *i*-$C_3H_7X^+$ ions by iPEPICO: Accurate heats of formation of *i*-$C_3H_7^+$, *i*-C_3H_7Cl, *i*-C_3H_7Br, and *i*-C_3H_7I. *J. Phys. Chem. A* **2010**, *114*, 11285-11291, doi:10.1021/jp104200h.

Note 39: *Inorganic compounds containing Br* Back to Table

Br CODATA Key Value.[2]

Br_2(g) CODATA Key Value.[2] A calculation of the atomization energy at the CCSD(T) level, extrapolated to the CBS limit, leads to $\Delta_f H^\circ_{298}$ = 33.1 ± 4 kJ mol^{-1} and $\Delta_f H^\circ$ = 47.7 ± 4 kJ mol^{-1}.[5]

HBr CODATA Key Value.[2] The most recent NIST-JANAF review gives and enthalpy of -36.29 ± 0.16 kJ mol^{-1} and an entropy of 198.699 ± 0.005 J K^{-1} mol^{-1}.[16]

BrO Enthalpy derived from a photodissociation dynamics study using velocity map ion imaging.[8] Previous enthalpy value of 30.2 ± 0.4 kcal mol^{-1} based on a Birge-Sponer extrapolation.[18] Entropy from the JANAF table for bromine oxides.[1] A CCSD(T) calculation of the dissociation energy, both directly and through a negative ion thermochemical cycle, led to enthalpy values of $\Delta_f H_0^\circ$ = 31.4 ± 0.4 and $\Delta_f H^\circ_{298}$ = 29.6 ± 0.4 kcal mol^{-1}.[15] A calculation of the atomization energy at the CCSD(T) level, extrapolated to the CBS limit, leads to $\Delta_f H^\circ_{298}$ = 128 ± 6 kJ mol^{-1} and $\Delta_f H_0^\circ$ = 136 ± 6 kJ mol^{-1}.[5]

OBrO Enthalpy based on the photoionization appearance energy of BrO^+ from OBrO, recalculated using the Table enthalpy for BrO.[9] A newer computational study gives an enthalpy at 0 K of 163.9 ± 7.1 kJ mol^{-1}.[10] Entropy taken from the JANAF table for bromine oxides.[1] A calculation of the atomization energy at the CCSD(T) level, extrapolated to the CBS limit, leads to $\Delta_f H^\circ_{298}$ = 169.9 ± 6 kJ mol^{-1} and $\Delta_f H^\circ_0$ = 179.5 ± 6 kJ mol^{-1}.[5]

BrOO Enthalpy for the reaction HOOBr + FOO → HOOF + BrOO at the CCSD(T)/CBS(Q5) level of theory, adjusted for the Table value for FOO, leads the cited enthalpy.[5] An estimate based on recombination rate constants for bromine atoms and subsequent calculations of interaction potentials, leads to a bond strength of about 1 kcal mol^{-1} and $\Delta_f H^\circ_{298}$ = 108 ± 40 kJ mol^{-1} and $\Delta_f H_0^\circ$ = 116 ± 10 kJ mol^{-1}.[1] These results have been supported by other computational studies.[14,17] CCSD(T)/AREP calculations predict, however, that BrOO lies below OBrO by about 5 kcal mol^{-1}, which appears to be inconsistent with these results.[14] Entropy value is taken from NIST-JANAF thermochemical tables for bromine oxides.[1]

BrO_3 Estimated values taken from the NIST-JANAF thermochemical tables for bromine oxides.[1]

BrOBr Enthalpy derived from a photoionization study. This value was accepted by the NIST-JANAF thermochemical tables for bromine oxides, which also discussed three related studies and recommended the entropy value.[1] A CCSD(T)/ANO4 result based on the isodesmic reaction 2HOBr → H_2O + Br_2O, adjusted for the present enthalpy values for the references, gives 26.9 ± 1.6 kcal mol^{-1}.[11] A calculation of the atomization energy at the CCSD(T) level, extrapolated to the CBS limit, leads to $\Delta_f H^\circ_{298}$ = 108.4 ± 6 kJ mol^{-1} and $\Delta_f H^\circ$ = 124.7 ± 6 kJ mol^{-1}.[5]

BrBrO The enthalpy is from a calculation of the atomization energy at the CCSD(T) level, extrapolated to the CBS limit. Listed value is for the ^{1}A' state. $\Delta_f H^\circ_{298}$ = 236.0 ± 6 kJ mol^{-1} for the ^{3}A" state and $\Delta_f H^\circ_{298}$ = 251.5 ± 6 kJ mol^{-1} for the ^{3}A' state.[5] Entropy from the NIST-JANAF thermochemical tables for bromine oxides, which estimated the enthalpy as 168 ± 20 kJ mol^{-1}.[1]

BrOOBr The enthalpy is from a calculation of the atomization energy at the CCSD(T) level, extrapolated to the CBS limit.[5] Calculated enthalpy for the reaction BrO + BrO → BrOOBr, ΔE = −16.93

kcal mol^{-1} by B3LYP/aug-cc-pVTZ method, leads to $\Delta_f H^{\circ}_{298}$ = 42.1 kcal mol^{-1}.[4] The dominant product observed in the matrix isolation/infrared spectroscopy study was BrOBrO.

BrOBrO The enthalpy is from a calculation of the atomization energy at the CCSD(T) level, extrapolated to the CBS limit.[5] Calculated enthalpy for the reaction BrO + BrO → BrOBrO, ΔE = −6.08 kcal mol^{-1} by B3LYP/aug-cc-pVTZ method, leads to $\Delta_f H^{\circ}_{298}$ = 52.9 kcal mol^{-1}.[4] The dominant product observed in the matrix isolation/infrared spectroscopy study was BrOBrO.

OBrBrO Calculated enthalpy for the reaction BrO + BrO → OBrBrO, ΔE = +13.44 kcal mol^{-1} by B3LYP/aug-cc-pVTZ method.[4] The dominant product observed in the matrix isolation/infrared spectroscopy study was BrOBrO.

$BrBrO_2$ The enthalpy is from a calculation of the atomization energy at the CCSD(T) level, extrapolated to the CBS limit.[5]

HOBr Enthalpy value from an evaluation of the experimental data.[6] An enthalpy value of –15.3±0.6 kcal mol^{-1} has been calculated by coupled-cluster theory with correlation consistent basis sets and corrections for core-valence, relativistic, and anharmonic effects.[3] Entropy value calculated from the experimental structure and vibrational frequencies.[13] A re-evaluation of the photoionization results, along with a newer value for the OH enthalpy, led to a value of $\Delta_f H_0^{\circ}$ = −47.7 ± 1.8 kJ mol^{-1}.[7]

BrOOH CCSD(T) calculation with spdfg one-particle basis set, using isodesmic reaction and present values of reference enthalpies.[12]

HOBrO and $HBrO_2$

Isomerization energy calculated at CCSD(T)/ANO4 level of theory, corrected for zero-point energy and to 298 K. BrOOH energy from present table.[12]

(1) Chase, M. W. NIST-JANAF thermochemical tables for the bromine oxides. *J. Phys. Chem. Ref. Data* **1996**, *25*, 1069-1111, doi:10.1063/1.555993.

(2) Cox, J. D.; Wagman, D. D.; Medvedev, V. A. *CODATA Key Values for Thermodynamics*; Hemisphere Publishing Corp.: New York, 1989.

(3) Denis, P. A. Thermochemistry of the hypobromous and hypochlorous acids, HOBr and HOCl. *J. Phys. Chem. A* **2006**, *110*, 5887-5892, doi:10.1021/jp056950u.

(4) Gálvez, O.; Zoermer, A.; Loewenschuss; Grothe, H. A combined matrix isolation and ab initio study of bromine oxides. *J. Phys. Chem. A* **2006**, *110*, 6472-6481, doi:10.1021/jp060586x.

(5) Grant, D. J.; Garner, E. B.; Matus, M. H.; Nguyen, M. T.; Peterson, K. A.; Francisco, J. S.; Dixon, D. A. Thermodynamic properties of the XO_2, X_2O, XYO, X_2O_2, and XYO_2 (X, Y = Cl, Br and I) isomers. *J. Phys. Chem. A* **2010**, *114*, 4254-4265, doi:10.1021/jp911320p.

(6) Hassanzadeh, P.; Irikura, K. K. Nearly ab initio thermochemistry: The use of reactions schemes. Application to IO and HOI. *J. Phys. Chem. A* **1997**, *101*, 1580-1587, doi:10.1021/jp963011g.

(7) Joens, J. A. The dissociation energy of OH(X $^2P_{3/2}$) and the enthalpy of formation of OH(X $^2\Pi_{3/2}$), ClOH, and BrOH from thermochemical cycles. *J. Phys. Chem. A* **2001**, *105*, 11041-11044, doi:10.1021/jp011833u.

(8) Kim, H.; Dooley, J. S.; Johnson, E. R.; North, S. W. Photodissociation of the BrO radical using velocity map ion imaging: Excited state dynamics and acurate D^0_0(BrO) evaluation. *J. Chem. Phys.* **2006**, *124*, 134304, doi:10.1063/1.2173265.

(9) Klemm, R. B.; Thorn, R. P.; Stief, L. J.; Buckley, T. J.; Johnson, R. D. Heat of formation of OBrO: Experimental photoionization study. *J. Phys. Chem. A* **2001**, *105*, 1638-1642, doi:10.1021/jp002397z.

(10) Lee, S. Y. Computational study of enthalpies of formation of OXO (X = Cl, Br, and I) and their anions. *J. Phys. Chem. A* **2004**, *108*, 10754-10761, doi:10.1021/jp0467550.

(11) Lee, T. J. Ab initio characterization of triatomic bromine molecules of potential interest in stratospheric chemistry. *J. Phys. Chem.* **1995**, *99*, 15074-15080, doi:10.1021/j100041a024.

(12) Lee, T. J. Ab initio characterization of $HBrO_2$ isomers: implications for stratospheric bromine chemistry. *Chem. Phys. Lett.* **1996**, *262*, 559-566, doi:10.1016/S0009-2614(96)01178-5.

(13) McGrath, M. P.; Rowland, F. S. Ideal gas thermodynamic properties of HOBr. *J. Phys. Chem.* **1994**, *98*, 4773-4775, doi:10.1021/j100069a001.
(14) Pacios, L. F.; Gómez, P. C. *Ab initio* study of bromine dioxides OBrO and BrOO. *J. Phys. Chem. A* **1997**, *101*, 1767-1773, doi:10.1021/jp963281z.
(15) Peterson, K. A.; Shepler, B. C.; Figgen, D.; Stoll, H. On the spectroscopic and thermochemical properties of ClO, BrO, IO, and their anions. *J. Phys. Chem. A* **2006**, *110*, 13877-13883, doi:10.1021/jp065887l.
(16) Shenyavskaya, E. A.; Yungman, V. S. NIST-JANAF thermochemical tables. III. Diatomic hydrogen halide gases. *J. Phys. Chem. Ref. Data* **2004**, *33*, 923-957, doi:10.1063/1.1638781.
(17) Suma, K.; Sumiyoshi, Y.; Endo, Y. Spectroscopic characterization of a molecule with a weak bond: The BrOO radical. *J. Chem. Phys.* **2005**, *123*, 024312, doi:10.1063/1.1953508.
(18) Wilmouth, D. M.; Hanisco, T. F.; Donahue, N. M.; Anderson, J. G. Fourier transform ultraviolet spectroscopy of the A $^2\Pi_{3/2} \leftarrow$ X $^2\Pi_{3/2}$ trasnsition of BrO. *J. Phys. Chem. A* **1999**, *103*, 8935-8945, doi:10.1021/jp991651o.

Note 40: *Inorganic compounds containing Br and F*

Back to Table

BrF Taken from a review of the literature.[1] A calculation of the total atomization energy using a composite electronic structure approach based on CCSD(T) and extrapolated to the complete basis set limit with a two-point extrapolation scheme, Q5 led to a value of $\Delta_f H^\circ_{298} = -58.9$ kJ mol^{-1}. Additional corrections included zero-point energy, core-valence effect, for scalar relativistic effects, and spin-orbit corrections.[2]

BrOF, BrO_2F
The total atomization energy was calculated using a composite electronic structure approach based on CCSD(T) and extrapolated to the complete basis set limit with a two-point extrapolation scheme, Q5. Additional corrections included zero-point energy, core-valence effect, for scalar relativistic effects, and spin-orbit corrections.[2]

(1) Gurvich, L. V.; Veyts, I. V.; Alcock, C. B. *Thermodynamic Properties of Individual Substances,*, Fourth ed.; Hemisphere Publishing Corp.: New York, 1991; Vol. 2.
(2) Thanthiriwatte, K. S.; Vasiliu, M.; Dixon, D. A.; Christe, K. O. Structural and energetic properties of closed shell XF_n (X = Cl, Br, and I; n = 1−7) and XO_nF_m (X = Cl, Br, and I; n = 1−3; m = 0−6) molecules and ions leading to stability predictions for yet unknown compounds. *Inorg. Chem.* **2012**, *51*, 10966-10982, doi:10.1021/ic301438b.

Note 41: *Inorganic compounds containing Br and Cl*

Back to Table

BrCl Review of the literature.[2] A calculation of the atomization energy at the CCSD(T) level, extrapolated to the CBS limit, leads to $\Delta_f H^\circ_{298} = 15.9 \pm 6$ kJ mol^{-1} and $\Delta_f H_0^\circ = 23.4 \pm 6$ kJ mol^{1}.[1]

ClOBr The enthalpy is from a calculation of the atomization energy at the CCSD(T) level, extrapolated to the CBS limit.[1] A CCSD(T)/ANO4 study, based on the isodesmic reaction HOBr + HOCl → H_2O +ClOBr, adjusted for the present enthalpy values for the references, led to $\Delta_f H^\circ_{298} = 98 \pm 7$ kJ mol^{-1}.[3]

ClBrO The enthalpy is from a calculation of the atomization energy at the CCSD(T) level, extrapolated to the CBS limit. $\Delta_f H^\circ_{298} = 145.2 \pm 6$ kJ mol^{-1} for the ^{3}A" state and $\Delta_f H^\circ_{298} = 252.7 \pm 6$ kJ mol^{-1} for the ^{3}A' state.[1]

BrClO The enthalpy is from a calculation of the atomization energy at the CCSD(T) level, extrapolated to the CBS limit. Listed enthalpy is for the ^{1}A' state. $\Delta_f H^\circ_{298} = 226.4 \pm 6$ kcal mol^{-1} for the ^{3}A' state.[1]

ClOOBr, BlOBrO, BrOClO, $ClBrO_2$, $BrClO_2$

The enthalpy values are from calculations of the atomization energy at the CCSD(T) level, extrapolated to the CBS limit.[1]

(1) Grant, D. J.; Garner, E. B.; Matus, M. H.; Nguyen, M. T.; Peterson, K. A.; Francisco, J. S.; Dixon, D. A. Thermodynamic properties of the XO_2, X_2O, XYO, X_2O_2, and XYO_2 (X, Y = Cl, Br and I) isomers. *J. Phys. Chem. A* **2010**, *114*, 4254-4265, doi:10.1021/jp911320p.

(2) Gurvich, L. V.; Veyts, I. V.; Alcock, C. B. *Thermodynamic Properties of Individual Substances,*, Fourth ed.; Hemisphere Publishing Corp.: New York, 1991; Vol. 2.

(3) Lee, T. J. Ab initio characterization of triatomic bromine molecules of potential interest in stratospheric chemistry. *J. Phys. Chem.* **1995**, *99*, 15074-15080, doi:10.1021/j100041a024.

Note 42: *Inorganic compounds containing Br, N, and O*

Back to Table

BrNO Taken from the NBS thermochemical tables.[6] A CCSD(T)/ANO4 result based on the homodesmic reaction $BrNO + H_2O \rightarrow HNO + HOBr$, adjusted for the present enthalpy values for the references, gives 22.7 ± 1.9 kcal mol^{-1}.[1]

***cis*-BrONO** Calculated using the isodesmic reaction H_2O + *cis*-BrONO → *cis*-HONO + HOBr at several levels of theory, leading to a reaction enthalpy of 7.6 kcal mol^{-1}.[2]

***trans*-BrONO**
Based on a calculated energy difference above $BrNO_3$ of 10.3 kcal mol^{-1} from calculations at several levels of theory.[2]

$BrNO_2$ Based on a calculated energy difference below *cis*-BrONO of 6.4 kcal mol^{-1} from calculations at several levels of theory.[2]

$BrONO_2$ The study of the thermal decomposition of $BrONO_2$ to BrO and NO_2 was used to obtain a reaction enthalpy of 28.2 ± 1.5 kcal mol^{-1} (118 ± 6.3 kJ mol^{-1}).[3] A computational study at the CCSD(T) level with a TZ2P basis set involving several isodesmic reactions[4] led to a value of $\Delta_f H^\circ_{298}$ = 42.3 kJ mol^{-1} whereas a CCSD(T)/cc-pV5Z calculation, extrapolated to the basis set limit, led to a BDE of 125.3 kJ mol^{-1}.[7]

$OBrONO_2$ and O_2BrONO_2
Enthalpy values from isodesmic reactions calculated at the CCSD(T) level of theory.[5]

(1) Lee, T. J. Ab initio characterization of triatomic bromine molecules of potential interest in stratospheric chemistry. *J. Phys. Chem.* **1995**, *99*, 15074-15080, doi:10.1021/j100041a024.

(2) Lee, T. J. Characterization of $BrNO_2$, *cis*-BrONO, and *trans*-BrONO. Implications for atmospheric chemistry. *J. Phys. Chem.* **1996**, *100*, 19847-19852, doi:10.1021/jp962605g.

(3) Orlando, J. J.; Tyndall, G. S. Rate coefficients for the thermal decomposition of $BrONO_2$ and the heat of formation of $BrONO_2$. *J. Phys. Chem.* **1996**, *100*, 19398-19405, doi:10.1021/jp9620274.

(4) Parthiban, S.; Lee, T. J. Ab initio investigation of the atmospheric molecule bromine nitrate: Equilibrium structure, vibrational spectrum, and heat of formation. *J. Chem. Phys.* **1998**, *109*, 525-530, doi:10.1063/1.476589.

(5) Parthiban, S.; Lee, T. J. Theoretical study of $XONO_2$ (X=Br, OBr, O_2Br): Implications for stratospheric bromine chemistry. *J. Chem. Phys.* **2000**, *113*, 145-152, doi:10.1063/1.481781.

(6) Wagman, D. D.; Evans, W. H.; Parker, V. B.; Schumm, R. H.; Halow, I.; Bailey, S. M.; Churney, K. L.; Nutall, R. L. The NBS tables of chemical thermodynamic properties. Selected values for inorganic and C_1 and C_2 organic substances in SI unites. *J. Phys. Chem. Ref. Data* **1982**, *11*, Suppl. No. 1, Erratum doi:10.1063/1.555845.

(7) Zou, P.; Derecskei-Kovacs, A.; North, S. W. Theoretical calculation of $ClONO_2$ and $BrONO_2$ bond dissociation energies. *J. Phys. Chem. A* **2003**, *107*, 888-896, doi:10.1021/jp021961y.

Note 43: *Bromoamines and Mixed Chlorobromoamines*

Back to Table

Geometries were optimized at the (AE)-CCSD(T)/AVQZ level of theory and zero-point energies computed at the B2PLYPD/AVTZ level. For the electronic energies, a calculational protocol termed TA14 was adapted from the W3, W4, and FPD protocols. Enthalpies of formation were determined from the total atomization energies.[1]

(1) Trogolo, D.; Arey, J. S. Benchmark thermochemistry of chloramines, bromamines, and bromochloramines: halogen oxidants stabilized by electron correlation. *Phys. Chem. Chem. Phys.* **2015**, *17*, 3584-3598, doi:10.1039/c4cp03987d.

Note 44: *Compounds containing one C and one or more Br* Back to Table

CBr Enthalpy from a CCSD(T) calculation extrapolated to the CBS limit.[2] A calculation at the W2DK level of theory gave an enthalpy of 118.51 kcal mol^{-1}.[7] Entropy obtained from the same study, using a DFT approach (B97-1/Aug-cc-pVTZ) for geometry optimization and frequency calculations.

CHBr Enthalpy from a CCSD(T) calculation extrapolated to the CBS limit.[2] A calculation at the DK-CCSD(T)/Aug-VTZ level, utilizing methyl bromide in an isodesmic reaction, resulted in an enthalpy value of 90.12 kcal mol^{-1}.[7] Entropy obtained from the same study, using a DFT approach (B97-1/Aug-cc-pVTZ) for geometry optimization and frequency calculations. Enthalpy obtained using the computed enthalpy of a reaction of the type: $CH_2(^1A_1) + CH_3X + CH_3Y \rightarrow CXY(^1A_1) + 2CH_4$ results in $\Delta_f H^\circ_{298}$ = 380 kJ mol^{-1} at the QCISD(T)/6-311+G(3df,2p)//QCISD/6-311G(d,p) level of theory. Calculations also done at the G2 level.[10]

CH_2Br Measured rate constant for the reaction of the radical with HBr, combined with previous measurements on the reverse reaction, with thermodynamic values obtained through a second-law analysis.[11] Recalculated from C-H bond strength of 427.2 kJ mol^{-1} and enthalpy for CH_3Br and H from this Table. Statistical thermodynamic methods also utilized. *Ab initio* calculations at the QCISD(T)/6-311+G(3df,2p) level of theory, utilizing an isodesmic reaction with methyl bromide, resulted in an enthalpy value of 166.6 ± 3 kJ mol^{-1}.[6]

CH_3Br Calculated from the dissociation of energy-selected CH_3Br^+ and its adiabatic ionization energy.[12] Enthalpy from Gurvich et al. review is –36.4 ± 0.5 kJ mol^{-1}.[3] Entropy taken from Ideal Gas Thermodynamic Properties, which gives an enthalpy of –37.7 ± 1.5 kJ mol^{-1}.[4] Pedley review gives an enthalpy of –35.4 ± 1.1 kJ mol^{-1}.[9]

CBr_2 Enthalpy from a CCSD(T) calculation extrapolated to the CBS limit.[2] Enthalpy obtained using the computed enthalpy of a reaction of the type: $CH_2(^1A_1) + CH_3X + CH_3Y \rightarrow CXY(^1A_1) + 2CH_4$ results in $\Delta_f H^\circ_{298}$ = 339 kJ mol^{-1} at the QCISD(T)/6-311+G(3df,2p)//QCISD/6-311G(d,p) level of theory. Calculations also done at the G2 level.[10] A calculation at the W2DK level of theory gave an enthalpy of 82.10 kcal mol^{-1}.[7] Entropy obtained from the same study, using a DFT approach (B97-1/Aug-cc-pVTZ) for geometry optimization and frequency calculations.

$CHBr_2$ Enthalpy derived from an analysis of thermochemical and kinetic data on the bromination of CH_2FCl.[13] *Ab initio* calculations at the QCISD(T)/6-311+G(3df,2p) level of theory, utilizing an isodesmic reaction with methyl bromide, resulted in an enthalpy value of 191.7±6 kJ mol^{-1}.[6] A calculation at the DK-CCSD(T)/Aug-VTZ level, again utilizing methyl bromide in an isodesmic reaction, resulted in an enthalpy value of 47.44 kcal mol^{-1}.[7] Entropy obtained from the same study, using a DFT approach (B97-1/Aug-cc-pVTZ) for geometry optimization and frequency calculations.

CH_2Br_2 Enthalpy taken from a dissociative photoionization study of a series of dihalomethanes, normalized using the experimental enthalpy of dichloromethane.[5] The reported value has been adjusted by +0.4 kJ mol^{-1} to agree with the present enthalpy for CH_2Cl_2. Previous value of –11.1 kJ mol^{-1} from Allen bond-energy scheme.[1] Ab initio calculations at the QCISD(T)/6-311+G(3df,2p) level of theory, utilizing an isodesmic reaction with methyl bromide, resulted in an enthalpy value of 4.3 ± 6 kJ mol^{-1}.[6] Entropy from evaluation of Gurvich et al.[3]

CBr_3 Enthalpy value from ab initio calculations at the QCISD(T)/6-311+G(3df,2p) level of theory, utilizing an isodesmic reaction with methyl bromide.[6] A calculation at the DK-CCSD(T)/Aug-VTZ level, again utilizing methyl bromide in an isodesmic reaction, resulted in an enthalpy value of 55.50 kcal mol^{-1}.[7] This same study, using a DFT approach for geometry optimization and frequency calculations, reported an entropy value of 80.60 cal K^{-1}. Gurvich et al. review has 235 ± 25 kJ mol^{-1}. Entropy from Gurvich et al.[3]

$CHBr_3$ Enthalpy of formation derived from the heat of combustion of the liquid of 545.1±3.3 kJ mol^{-1} measured by bomb calorimetry.[8] An enthalpy value of 51.6±9 kJ mol^{-1} was obtained from *ab initio* calculations at the QCISD(T)/6-311+G(3df,2p) level of theory, utilizing an isodesmic reaction with methyl bromide.[6] A calculation at the DK-CCSD(T)/Aug-VTZ level, again utilizing methyl bromide in an isodesmic reaction, resulted in an enthalpy value of 12.97 kcal mol^{-1}.[7] This same study, using a DFT approach for geometry optimization and frequency calculations, reported an entropy value of 78.93 cal K^{-1}. Previous value of 5.7 kcal mol^{-1} from Allen bond-energy scheme.[1] Entropy from evaluation of Gurvich et al.[3] Pedley gives enthalpy as 23.8 ± 4.5 kJ mol^{-1}.[9]

CBr_4 Enthalpy from rotation-bomb calorimetry.[1] *Ab initio* calculations at the QCISD(T)/6-311+G(3df,2p) level of theory, utilizing an isodesmic reaction with methyl bromide, resulted in an enthalpy value of 110.6 ± 12 kJ mol^{-1}.[6] A calculation at the DK-CCSD(T)/Aug-VTZ level, again utilizing methyl bromide in an isodesmic reaction, resulted in an enthalpy value of 28.49 kcal mol^{-1}.[7] This same study, using a DFT approach for geometry optimization and frequency calculations, reported an entropy value of 85.61 cal K^{-1}. Entropy from Gurvich et al.[3]

(1) Bickerton, J.; da Piedade, M. E. M.; Pilcher, G. Enthalpy of formation of tetrabromomethane by rotating-bomb calorimetry. *J. Chem. Thermo.* **1984**, *16*, 661-668, doi:10.1016/0021-9614(84)90046-6.

(2) Dixon, D. A.; de Jong, W. A.; Peterson, K. A.; Francisco, J. S. Heats of formation of CBr, CHBr, and CBr_2 from ab initio chemistry. *J. Phys. Chem. A* **2002**, *106*, 4724-4728, doi:10.1021/jp0147067.

(3) Gurvich, L. V.; Veyts, I. V.; Alcock, C. B. *Thermodynamic Properties of Individual Substances,*, Fourth ed.; Hemisphere Publishing Corp.: New York, 1991; Vol. 2.

(4) Kudchadker, S. A.; Kudchadker, A. P. Ideal gas thermodynamic properties of the eight bromo- and iodomethanes. *J. Phys. Chem. Ref. Data* **1975**, *4*, 457-470, doi:10.1063/1.555522.

(5) Lago, A. F.; Kercher, J. P.; Bödi, A.; Sztáray, B.; Miller, B.; Wurzelmann, D.; Baer, T. Dissociative photoionization and thermochemistry of dihalomethane compounds studied by threshold photoelectron photoion coincidence spectroscopy. *J. Phys. Chem. A* **2005**, *109*, 1802-1809, doi:10.1021/jp045337s.

(6) Marshall, P.; Srinivas, G. N.; Schwartz, M. A computational study of the thermochemistry of bromine- and iodine-containing methanes and methyl radicals. *J. Phys. Chem. A* **2005**, *109*, 6371-6379, doi:10.1021/jp0518052.

(7) Oren, M.; Iron, M. A.; Burcat, A.; Martin, J. M. L. Thermodynamic properties of C_1 and C_2 bromo compounds and radicals: A relativistic ab initio study. *J. Phys. Chem. A* **2004**, *108*, 7752-7761, doi:10.1021/jp0475786.

(8) Papina, T. S.; Kolesov, V. P.; Golovanova, Y. G. The standard enthalpy of formation of bromoform. *Russ. J. Phys. Chem.* **1982**, *56*, 1666-1668.

(9) Pedley, J. B. *Thermochemical Data and Structures of Organic Compounds*; Thermodynamics Data Center: College Station, TX, 1994.

(10) Schwartz, M.; Marshall, P. An ab initio investigation of halocarbenes. *J. Phys. Chem. A* **1999**, *103*, 7900-7906, doi:10.1021/jp9919213.

(11) Seetula, J. A. Kinetics of the R + HBr ⇄ RH + Br (R = CH_2Br, CHBrCl or CCl_3) equilibrium. Thermochemistry of the CH_2Br and CHBrCl radicals. *Phys. Chem. Chem. Phys.* **2003**, *5*, 849-855, doi:10.1039/b210787m.

(12) Song, Y.; Qian, X. M.; Lau, K. C.; Ng, C. Y.; Liu, J. B.; Chen, W. W. High-resolution energy-selected study of the reaction $CH_3H^+ \rightarrow CH_3^+ + X$: Accurate thermochemistry for the CH_3X/CH_3X^+ (X=Br, I) system. *J. Chem. Phys.* **2001**, *115*, 4095-4104, doi:10.1063/1.1391268.

(13) Tschuikow-Roux, E.; Paddison, S. Bond dissociation energies and radical heats of formation in CH_3Cl, CH_2Cl_2, CH_3Br, CH_2Br_2, CH_2FCl, and $CHFCl_2$. *Int. J. Chem. Kinet.* **1987**, *19*, 15-24, doi:10.1002/kin.550190103.

Note 45: *Compounds containing one C and one or more F and Br*

Back to Table

CFBr Enthalpy obtained using the computed enthalpy of a reaction of the type: $CH_2(^1A_1) + CH_2F_2 + 2CH_3Y \rightarrow CFY(^1A_1) + 3CH_4$ at the QCISD(T)/6-311+G(3df,2p)//QCISD/6-311G(d,p) level of theory. Calculations also done at the G2 level.[4]

CH_2FBr Taken from review of Kudchadker and Kudchadker. Enthalpy estimated.[1]

CHF_2Br Enthalpy from review of Pedley.[2] Entropy from review of Kudchadker and Kudchadker, who also estimate an enthalpy of –102.66 kcal mol^{-1}.[1]

CF_3Br Enthalpy from a simultaneous solution of a thermochemical network for the CF_3X species, where X = nil, H, Cl, Br, I, CF_3, CN.[3] Entropy from review of Kudchadker and Kudchadker.[1]

CF_2Br_2 Taken from review of Kudchadker and Kudchadker. All parameters estimated.[1]

$CFBr_3$ Taken from review of Kudchadker and Kudchadker. Enthalpy estimated.[1]

(1) Kudchadker, S. A.; Kudchadker, A. P. Ideal gas thermodynamic properties of $CH_{4-(a+b+c+d)}F_aCl_bBr_cI_d$ halomethanes. *J. Phys. Chem. Ref. Data* **1978**, *7*, 1285-1307, doi:10.1063/1.555585.
(2) Pedley, J. B. *Thermochemical Data and Structures of Organic Compounds*; Thermodynamics Data Center: College Station, TX, 1994.
(3) Ruscic, B.; Michael, J. V.; Redfern, P. C.; Curtiss, L. A.; Raghavachri, K. Simultaneous adjustment of experimentally based enthalpies of formation of CF_3X, X = nil, H, Cl, Br, I, CF_3, CN, and a probe of G3 theory. *J. Phys. Chem. A* **1998**, *102*, 10889-10899, doi:10.1021/jp983237e.
(4) Schwartz, M.; Marshall, P. An ab initio investigation of halocarbenes. *J. Phys. Chem. A* **1999**, *103*, 7900-7906, doi:10.1021/jp9919213.

Note 46: *Compounds containing one C and one or more Cl and Br*

Back to Table

CClBr Enthalpy obtained using the computed enthalpy of a reaction of the type: $CH_2(^1A_1) + CH_3X + CH_3Y \rightarrow CXY(^1A_1) + 2CH_4$ at the QCISD(T)/6-311+G(3df,2p)//QCISD/6-311G(d,p) level of theory. Calculations also done at the G2 level.[4]

CHClBr Measured rate constant for the reaction of the radical with HBr, combined with previous measurements on the reverse reaction, with thermodynamic values obtained through a second-law analysis.[6]

CH_2ClBr Enthalpy taken from a dissociative photoionization study of a series of dihalomethanes, normalized using the experimental enthalpy of dichloromethane.[2] The reported value has been adjusted by +0.4 kJ mol^{-1} to agree with the present enthalpy for CH_2Cl_2.

CCl_2Br Measured rate constant for the reaction of the radical with HBr, combined with calculated (MP2(fc)/6-31G(d,p)) values for the reverse reaction, leading to thermodynamic values obtained through a second-law analysis.[5]

$CHCl_2Br$ Taken from review of Kudchadker and Kudchadker. All parameters estimated.[1]

CCl_3Br Enthalpy from review of Pedley.[3] Entropy and enthalpy difference from review of Kudchadker and Kudchadker.[1]

CCl_2Br Measured rate constant for the reaction of the radical with HBr, combined with calculated (MP2(fc)/6-31G(d,p)) values for the reverse reaction, leading to thermodynamic values obtained through a second-law analysis.[5]

CCl_2Br_2 and $CClBr_3$

Taken from review of Kudchadker and Kudchadker. All parameters estimated.[1]

(1) Kudchadker, S. A.; Kudchadker, A. P. Ideal gas thermodynamic properties of $CH_{4-(a+b+c+d)}F_aCl_bBr_cI_d$ halomethanes. *J. Phys. Chem. Ref. Data* **1978**, *7*, 1285-1307, doi:10.1063/1.555585.

(2) Lago, A. F.; Kercher, J. P.; Bödi, A.; Sztáray, B.; Miller, B.; Wurzelmann, D.; Baer, T. Dissociative photoionization and thermochemistry of dihalomethane compounds studied by threshold photoelectron photoion coincidence spectroscopy. *J. Phys. Chem. A* **2005**, *109*, 1802-1809, doi:10.1021/jp045337s.

(3) Pedley, J. B. *Thermochemical Data and Structures of Organic Compounds*; Thermodynamics Data Center: College Station, TX, 1994.

(4) Schwartz, M.; Marshall, P. An ab initio investigation of halocarbenes. *J. Phys. Chem. A* **1999**, *103*, 7900-7906, doi:10.1021/jp9919213.

(5) Seetula, J. A. *Ab initio* study of the transition states for determining the enthalpies of formation of alkyl and halogenated alkyl free radicals. *Phys. Chem. Chem. Phys.* **2000**, *2*, 3807-3812, doi:10.1039/b001350l.

(6) Seetula, J. A. Kinetics of the R + HBr ⇄ RH + Br (R = CH_2Br, CHBrCl or CCl_3) equilibrium. Thermochemistry of the CH_2Br and CHBrCl radicals. *Phys. Chem. Chem. Phys.* **2003**, *5*, 849-855, doi:10.1039/b210787m.

Note 47: *Compounds containing one C and one or more Cl and Br*

Back to Table

CHFClBr Taken from review of Kudchadker and Kudchadker. Enthalpy estimated.[2]

CF_2ClBr Experimental data from threshold PEPICO studies of halogenated methanes were combined with *ab initio* calculations of isodesmic and exchange reactions into a thermochemical network.[1] Previous enthalpy value of $\Delta_f H^\circ_{298} = -589.5$ kJ mol^{-1}, and the entropy, were estimated.[2]

$CFCl_2Br$ Taken from review of Kudchadker and Kudchadker. All parameters estimated.[2]

$CFClBr_2$ Taken from review of Kudchadker and Kudchadker. All parameters estimated.[2]

(1) Harvey, J.; Tuckett, R. P.; Bodi, A. A halomethane thermochemical network from iPEPICO experiments and quantum chemical calculations. *J. Phys. Chem. A* **2012**, *116*, 9696-9705, doi:10.1021/jp307941k.

(2) Kudchadker, S. A.; Kudchadker, A. P. Ideal gas thermodynamic properties of $CH_{4-(a+b+c+d)}F_aCl_bBr_cI_d$ halomethanes. *J. Phys. Chem. Ref. Data* **1978**, *7*, 1285-1307, doi:10.1063/1.555585.

Note 48: *Compounds containing one C, one or more O, and Br*

Back to Table

CBr_2O, carbonyl bromide

Enthalpy from review of Pedley.[4]

CBr_3O Derived from a G2 calculation of the total energy of formation from the gas-phase elements.[1]

CBr_3OX (X=H,F,Cl,Br)

Derived from a G2 calculation of the total energy of formation from the gas-phase elements.[2]

CCl_3OBr Derived from a G2 calculation of the total energy of formation from the gas-phase elements.[2]

CH_2BrOOH, CHFBrOOH, CHClBeOOH

Geometry optimization and frequency calculations were performed at the MP2/6-31G(d) and the B3LYP/6-311++G(d,p) levels of theory, with a single-point energy calculation at the CCSD(T)/6-311++G(d,p//B3LYP/6-311++G(d,p) level. The dissociation energy into HO_2 and the alkyl radical was then evaluated and used, after thermal correction, to calculate the enthalpy of formation at 298 K.[3] This was adjusted to the radical values from the present Table.

(1) Brudnik, K.; Jodkowski, J. T.; Nowek, A.; Leszczynski, J. Kinetics of the formation reactions of trichloro- and tribromomethyl hypohalites and alcohols in the gas-phase: Theoretical study *Chem. Phys. Lett.* **2007**, *435*, 194-200, doi:10.1016/j.cplett.2006.12.079.
(2) Brudnik, K.; Jodkowski, J. T.; Ratajczak, E. Kinetics of the formation reactions of trifluoromethanol and trifluoromethyl hypohalites in the gas phase. *J. Mol. Struct.* **2003**, *656*, 333-339, doi:10.1016/S0022-2860(03)00347-8.
(3) Kosmas, A. M.; Mpellos, C.; Salta, Z.; Drougas, E. Structural and heat of formation studies of halogenated methyl hydro-peroxides. *Chem. Phys.* **2010**, *371*, 36-42, doi:10.1016/j.chemphys.2010.03.026.
(4) Pedley, J. B. *Thermochemical Data and Structures of Organic Compounds*; Thermodynamics Data Center: College Station, TX, 1994.

Note 49: *Compounds containing two C and Br*

Back to Table

C_2Br An *ab initio* calculation at the W2DK level of theory.[9] Entropy obtained from the same study, using a DFT approach (B97-1/Aug-cc-pVTZ) for geometry optimization and frequency calculations.

C_2HBr, bromoacetylene
Enthalpy from measurements of the photodissociation of bromoacetylene, leading to dissociation energy of 91.0±1.2 kcal mol^{-1}.[8] $\Delta_f H_0^o$ = 71.3 ± 1.5 kcal mol^{-1}. A calculation at the W2DK level of theory gave an enthalpy of 67.50 kcal mol^{-1}.[9] Entropy obtained from the same study, using a DFT approach (B97-1/Aug-cc-pVTZ) for geometry optimization and frequency calculations.

C_2CHBr Enthalpy from review of Pedley.[10] An enthalpy of 74.1 ± 3.1 kJ mol^{-1} has been derived from a dissociative photoionization study of $CH_2BrCHBr_2$ with a computed vinyl cation enthalpy.[5]

CH_2CH_2Br
An experimental study of the reaction $Br + C_2H_4 \leftrightarrow C_2H_4Br$ led to an enthalpy of reaction of 6.8 ± 1.6 kcal mol^{-1}.[1]

CH_3CHBr A photobromination study leads to $D(CH_3CHBr\text{-}H)$ = 97.2 ± 1 kcal mol^{-1}.[6]

CH_3CH_2Br
Enthalpy obtained from a TPEPICO determination of the onset energy of the ethyl cation from the photodissociation of ethyl bromide, taking $\Delta_f H_0^o(C_2H_5^+)$ = 915.5 ± 1.3 kJ mol^{-1}.[2] Previous enthalpy value, –61.5 ± 1.0 kJ mol^{-1}, was taken from review of the literature.[3] Entropy calculated by Kudchadker and Kudchadker.[4]

C_2Br_2 An *ab initio* calculation at the W2DK level of theory.[9] Entropy obtained from the same study, using a DFT approach (B97-1/Aug-cc-pVTZ) for geometry optimization and frequency calculations.

***trans*-CHBrCBr, *trans*-dibromovinyl radical**
A calculation at the DK-CCSD(T)/Aug-VTZ level, utilizing methyl bromide in an isodesmic reaction.[9] Entropy obtained from the same study, using a DFT approach (B97-1/Aug-cc-pVTZ) for geometry optimization and frequency calculations.

CH_3CBr_2 A photobromination study leads to $D(CClF_2\text{-}H)$ = 94.9 ± 1.2 kcal mol^{-1}.[7]

CH_3CBr_2H Taken from a review of the literature.[3]

$CHBrCBr_2$, tribromoethene
A calculation at the DK-CCSD(T)/Aug-VTZ level, utilizing methyl bromide in an isodesmic reaction.[9] Entropy obtained from the same study, using a DFT approach (B97-1/Aug-cc-pVTZ) for geometry optimization and frequency calculations.

CH_2BrCH_2Br
Enthalpy from review of Pedley.[10]

C_2Br_3 A calculation at the DK-CCSD(T)/Aug-VTZ level, utilizing methyl bromide in an isodesmic reaction.[9] Entropy obtained from the same study, using a DFT approach (B97-1/Aug-cc-pVTZ) for geometry optimization and frequency calculations.

$CH_2BrCHBr_2$
Enthalpy derived from a dissociative photoionization study of $CH_2BrCHBr_2$ and a computed vinyl cation enthalpy.[5]

CH_3CBr_3 Taken from a Thermodynamics Research Center review. Enthalpy estimated.[4]

C_2Br_4, $CHBr_2CBr_2$, CBr_3CHBr, C_2Br_5, C_2Br_6
A calculation at the DK-CCSD(T)/Aug-VTZ level, utilizing methyl bromide in an isodesmic reaction.[9] Entropy obtained from the same study, using a DFT approach (B97-1/Aug-cc-pVTZ) for geometry optimization and frequency calculations.

(1) Bedjanian, Y.; Poulet, G.; Le Bras, G. Low-pressure study of the reactions of Br atoms with alkenes. 2. Reactions with ethene and trans-2-butene. *J. Phys. Chem. A* **1999**, *103*, 4026-4033, doi:10.1021/jp9903007.
(2) Borkar, S.; Sztaray, B. Self-consistent heats of formation for the ethyl cation, ethyl bromide, and ethyl iodide from threshold photoelectron photoion coincidence spectroscopy. *J. Phys. Chem. A* **2010**, *114*, 6117-6123, doi:10.1021/jp102162f.
(3) Kolesov, V. P.; Papina, T. S. Thermochemistry of haloethanes. *Russ. Chem. Rev.* **1983**, *52*, 425-439.
(4) Kudchadker, S. A.; Kudchadker, A. P. Ideal gas thermodynamic properties of selected bromoethanes and iodoethane. *J. Phys. Chem. Ref. Data* **1979**, *8*, 519-526, doi:10.1063/1.555601.
(5) Lago, A. F.; Baer, T. A photoelectron photoion coincidence study of the vinyl bromide and tribromoethane ion dissociation dynamics: Heats of formation of $C_2H_3^+$, C_2H_3Br, $C_2H_3Br^+$, $C_2H_3Br_2^+$, and $C_2H_3Br_3$ *J. Phys. Chem. A* **2006**, *110*, 3036-3041, doi:10.1021/jp053943x.
(6) Miyokawa, K.; Tschuikow-Roux, E. Kinetics of α- and β- hydrogen abstraction from C_2H_5Cl by Br atoms. Estimate of C-H bond dissociation energies and heats of formation of CH_3CHCl and CH_2CH_2Cl radicals. *J. Phys. Chem.* **1990**, *94*, 715-717, doi:10.1021/j100365a037.
(7) Miyokawa, K.; Tschuikow-Roux, E. Kinetics of photobromination of dichloro- and dibromoethane. Estimate of the C-H bond dissociation energies and the heats of formation of the CH_3CCl_2 and CH_3CHBr_2 radicals. *Bull. Chem. Soc. Jpn.* **1999**, *72*, 1-5.
(8) Okabe, H. Photodissociation of acetylene and bromoacetylene in the vacuum ulraviolet: Production of electronically excited C_2H and C_2. *J. Chem. Phys.* **1975**, *62*, 2782-2787, doi:10.1063/1.430813.
(9) Oren, M.; Iron, M. A.; Burcat, A.; Martin, J. M. L. Thermodynamic properties of C_1 and C_2 bromo compounds and radicals: A relativistic ab initio study. *J. Phys. Chem. A* **2004**, *108*, 7752-7761, doi:10.1021/jp0475786.
(10) Pedley, J. B. *Thermochemical Data and Structures of Organic Compounds*; Thermodynamics Data Center: College Station, TX, 1994.

Note 50: *Compounds containing two C and Br and F and/or Cl*

Back to Table

All enthalpy values taken from the review of Pedley et al.[1]

(1) Pedley, J. B. *Thermochemical Data and Structures of Organic Compounds*; Thermodynamics Data Center: College Station, TX, 1994.

Note 51: *Compounds containing two C, O and Br*

Back to Table

$CH_3C(O)Br$, acetyl bromide
Enthalpy from review of Pedley.[3]

$CH_2BrCOOH$
Review of the literature by Dorofeeva et al.[2]

$BrCH_2CH_2OH$

The enthalpy of formation of the liquid was determined by using rotating-bomb combustion calorimetry to be $\Delta_f H^\circ_{298}(l)$ =–275.8 ± 0.6 kJ mol^{-1}. The molar enthalpy of vaporization was then determined by use of Calvert-drop microcalorimetry as $\Delta_{vap}H^\circ_{298}$ = 54.08 ± 0.40 kJ mol^{-1}.[1]

(1) Bernardes, C. E. S.; Minas da Piedade, M. E.; Amaral, L. M. P. F.; Ferreira, A. I. M. C. L.; Ribeiro da Silva, M. A. V.; Diogo, H. P.; Costa Cabral, B. J. Energetics of C−F, C−Cl, C−Br, and C−I bonds in 2-haloethanols. Enthalpies of formation of XCH_2CH_2OH (X = F, Cl, Br, I) compounds and of the 2-hydroxyethyl radical. *J. Phys. Chem. A* **2007**, *111*, 1713-1720, doi:10.1021/jp0675678.

(2) Dorofeeva, O.; Novikov, V. P.; Neumann, D. B. NIST-JANAF thermochemical tables. 1. Ten organic molecules related to atmospheric chemistry. *J. Phys. Chem. Ref. Data* **2001**, *30*, 475-513, doi:10.1063/1.1364518.

(3) Pedley, J. B. *Thermochemical Data and Structures of Organic Compounds*; Thermodynamics Data Center: College Station, TX, 1994.

Note 52: *Compounds containing three C and Br*

Back to Table

$CH_3CHBrCH_3$

The measured onset energy for *i*-$C_3H_7^+$ from iPEPICO spectroscopy of *i*- C_3H_7Br was used in conjunction with a new value of the ion enthalpy of formation to obtain the 0 K enthalpy of the bromide.[1]

(1) Stevens, W. R.; Bodi, A.; Baer, T. Dissociation dynamics of energy selected, propane, and *i*-$C_3H_7X^+$ ions by iPEPICO: Accurate heats of formation of *i*-$C_3H_7^+$, *i*-C_3H_7Cl, *i*-C_3H_7Br, and *i*-C_3H_7I. *J. Phys. Chem. A* **2010**, *114*, 11285-11291, doi:10.1021/jp104200h.

Note 53: *Compounds containing one I and 0 or 1 H*

Back to Table

I CODATA Key Values.[2] The JANAF values are $\Delta_f H^\circ_{298}$ = 106.76 kJ mol^{-1}, $\Delta_f H_0^\circ$ = 107.16 kJ mol^{-1}, and S = 180.786 J K^{-1} mol^{-1}.[1]

I_2 CODATA Key Values.[2] The JANAF values are $\Delta_f H^\circ_{298}$ = 62.42 kJ mol^{-1}, $\Delta_f H_0^\circ$ = 65.50 kJ mol^{-1}, and S = 260.685 J K^{-1} mol^{-1}.[1] A calculation of the atomization energy at the CCSD(T) level, extrapolated to the CBS limit, leads to $\Delta_f H^\circ_{298}$ = 61.9 ± 6 kJ mol^{-1} and $\Delta_f H_0^\circ$ = 65.3 ± 6 kJ mol^{-1}.[3]

HI Taken form a NIST-JANAF review.[4] CODATA Key Value enthalpy at 298 K is identical.[2]

(1) Chase, M. W. NIST-JANAF thermochemical tables. *J. Phys. Chem. Ref. Data* **1998**, *Monograph 9*.

(2) Cox, J. D.; Wagman, D. D.; Medvedev, V. A. *CODATA Key Values for Thermodynamics*; Hemisphere Publishing Corp.: New York, 1989.

(3) Grant, D. J.; Garner, E. B.; Matus, M. H.; Nguyen, M. T.; Peterson, K. A.; Francisco, J. S.; Dixon, D. A. Thermodynamic properties of the XO_2, X_2O, XYO, X_2O_2, and XYO_2 (X, Y = Cl, Br and I) isomers. *J. Phys. Chem. A* **2010**, *114*, 4254-4265, doi:10.1021/jp911320p.

(4) Shenyavskaya, E. A.; Yungman, V. S. NIST-JANAF thermochemical tables. III. Diatomic hydrogen halide gases. *J. Phys. Chem. Ref. Data* **2004**, *33*, 923-957, doi:10.1063/1.1638781.

Note 54: *Compounds containing I and O*

Back to Table

IO The photodissociation dynamics of expansion-cooled IO was investigated, using velocity map ion imaging. This led to D_0 = 54.9 (+0.2 -0.4) kcal mol^{-1} and to the recommended enthalpy values.[3] Previous recommendation of the enthalpy, $\Delta_f H_0^\circ$ = 127.2 ± 2.5 kJ mol^{-1}, $\Delta_f H^\circ_{298}$= 125.1 ± 2.5 kJ mol^{-1}, was from a CCSD(T) calculation of the dissociation energy, both directly

and through a negative ion thermochemical cycle.[10] The NIST-JANAF thermochemical tables for iodine oxides recommends $\Delta_f H^\circ_{298} = 126 \pm 18$ kJ mol^{-1} and $\Delta_f H^\circ_0 = 128 \pm 18$ kJ mol^{-1}, based on molecular beam studies.[2] The earlier spectroscopic studies are also discussed here. An equilibrium constant derived from the forward and reverse rate constants for IO + ClO ↔ I + OClO leads to an enthalpy at 298 K of about 28.6 kcal mol^{-1} (using reference values from this table) and 27.5 kcal mol^{-1} from the equilibrium Cl + IO ↔ I + ClO.[1] Enthalpy of reaction obtained using CCSD(T) calculations at B3LYP geometries, with corrections for spin-orbit coupling, for I + O → IO, using Table reference values, leads to $\Delta_f H^\circ_{298} = 117.3$ kJ mol^{-1}.[7] A calculation of the atomization energy at the CCSD(T) level, extrapolated to the CBS limit, leads to $\Delta_f H^\circ_{298} = 128.0 \pm 6$ kJ mol^{-1} and $\Delta_f H^\circ_0 = 130.1 \pm 6$ kJ mol^{-1}.[5] Entropy based on extensive calculations.[6]

OIO The enthalpy value was from a determination of the threshold for the appearance of IO upon pulsed photolysis of OIO, indicating a bond strength of D_0(O-IO) = 248.8 ± 1 kJ mol^{-1}.[4] The previous values of $\Delta_f H^\circ_{298} = 117.7 \pm 6$ kJ mol^{-1} and $\Delta_f H^\circ_0 = 123.4 \pm 6$ kJ mol^{-1} were from a calculation of the atomization energy at the CCSD(T) level, extrapolated to the CBS limit.[5] Molecular properties calculated at the MP2/6-31G(d) and MP2/6-311+G(3df) levels of theory provided the entropy and, with this information, an enthalpy of $\Delta_f H^\circ_{298} = 75$ kJ mol^{-1} was derived using approximate QCISD(T)/6-311+G93df) energies coupled with isodesmic reactions.[9] A more recent computational study gives an enthalpy at 0 K of 113.9 ± 10.3 kJ mol^{-1}.[8] Enthalpy of reaction obtained using CCSD(T) calculations at B3LYP geometries, with corrections for spin-orbit coupling, for 2IO → OIO + I leads to a 298 K enthalpy of 110.1 kJ mol^{-1}.[7]

IOO Enthalpy for the reaction HOOI + FOO → HOOF + IOO at the CCSD(T)/CBS(DTQ) level of theory, adjusted for the Table value for FOO, leads the cited enthalpy.[5] Entropy from molecular properties calculated at the MP2/6-31G(d) and MP2/6-311+G(3df) levels of theory and, with this information, an enthalpy of $\Delta_f H^\circ_{298} = 96$ kJ mol^{-1} was derived using approximate QCISD(T)/6-311+G93df) energies coupled with isodesmic reactions.[9]

IO_3 Enthalpy at 298 K of reaction obtained using CCSD(T) calculations at B3LYP geometries, with corrections for spin-orbit coupling, for OIO + IO_3 → I_2O_5.[7] Entropy and enthalpy difference from NIST-JANAF thermochemical tables for iodine oxides.[2] Previous enthalpy value of 242 kJ mol^{-1} was estimated.

IOI The enthalpy is from a calculation of the atomization energy at the CCSD(T) level, extrapolated to the CBS limit.[5] Entropy from molecular properties calculated at the MP2/6-31G(d) and MP2/6-311+G(3df) levels of theory and, with this information, an enthalpy of $\Delta_f H^\circ_{298} = 92.5 \pm 17$ kJ mol^{-1} was derived using approximate QCISD(T)/6-311+G93df) energies coupled with isodesmic reactions.[9]

IIO The enthalpy is from a calculation of the atomization energy at the CCSD(T) level, extrapolated to the CBS limit. Listed value is for the ^{1}A' state. $\Delta_f H^\circ_{298} = 234.3 \pm 6$ kJ mol^{-1} for the $^3A_2$ state.[5] Entropy from molecular properties calculated at the MP2/6-31G(d) and MP2/6-311+G(3df) levels of theory and, with this information, an enthalpy of $\Delta_f H^\circ_{298} = 134 \pm 17$ kJ mol^{-1} was derived using approximate QCISD(T)/6-311+G93df) energies coupled with isodesmic reactions.[9]

IOOI The enthalpy is from a calculation of the atomization energy at the CCSD(T) level, extrapolated to the CBS limit.[5] Entropy from molecular properties calculated at the MP2/6-31G(d) and MP2/6-311+G(3df) levels of theory and, with this information, an enthalpy of $\Delta_f H^\circ_{298} = 157$ kJ mol^{-1} was derived using approximate QCISD(T)/6-311+G93df) energies coupled with isodesmic reactions.[9] Enthalpy of reaction obtained using CCSD(T) calculations at B3LYP geometries, with corrections for spin-orbit coupling, for IO + IO → IOOI leads to a 298 K enthalpy of 179.9 kJ mol^{-1}.[7]

IIO_2 The enthalpy is from a calculation of the atomization energy at the CCSD(T) level, extrapolated to the CBS limit.[5] Entropy from molecular properties calculated at the MP2/6-31G(d) and

MP2/6-311+G(3df) levels of theory and, with this information, an enthalpy of $\Delta_f H^\circ_{298}$ = 103 kJ mol^{-1} was derived using approximate QCISD(T)/6-311+G93df) energies coupled with isodesmic reactions.[9] Enthalpy of reaction obtained using CCSD(T) calculations at B3LYP geometries, with corrections for spin-orbit coupling, for IO + IO → IIO_2, using Table reference values, leads to a 298 K enthalpy of 157.9 kJ mol^{-1}.[7]

IOIO The enthalpy is from a calculation of the atomization energy at the CCSD(T) level, extrapolated to the CBS limit.[5] Entropy from molecular properties calculated at the MP2/6-31G(d) and MP2/6-311+G(3df) levels of theory and, with this information, an enthalpy of $\Delta_f H^\circ_{298}$ = 124 kJ mol^{-1} was derived using approximate QCISD(T)/6-311+G93df) energies coupled with isodesmic reactions.[9] Enthalpy of reaction obtained using CCSD(T) calculations at B3LYP geometries, with corrections for spin-orbit coupling, for IO + IO → IOIO leads to a 298 K enthalpy of 141.3 kJ mol^{-1}.[7]

OIIO The enthalpy is from a calculation of the atomization energy at the CCSD(T) level, extrapolated to the CBS limit.[5] Molecular properties calculated at the MP2/6-31G(d) and MP2/6-311+G(3df) levels of theory. Enthalpy derived using approximate QCISD(T)/6-311+G93df) energies coupled with isodesmic reactions gives $\Delta_f H^\circ_{298}$ = 224 kJ mol^{-1}.[9]

I_2O_3 Enthalpy of reaction obtained using CCSD(T) calculations at B3LYP geometries, with corrections for spin-orbit coupling, for IO + OIO → I_2O_3.[7]

I_2O_4 Enthalpy of reaction obtained using CCSD(T) calculations at B3LYP geometries, with corrections for spin-orbit coupling, for 2OIO → I_2O.[7]

I_2O_5 Enthalpy of reaction obtained using CCSD(T) calculations at B3LYP geometries, with corrections for spin-orbit coupling, for I_2O_4 + O_3 → I_2O_5 + O.[7]

(1) Bedjanian, Y.; Le Bras, G.; Poulet, G. Kinetics and mechanism of the IO + ClO reaction. *J. Phys. Chem. A* **1997**, *101*, 4088-4096, doi:10.1021/jp963947p.

(2) Chase, M. W. NIST-JANAF thermochemical tables for the iodine oxides. *J. Phys. Chem. Ref. Data* **1996**, *25*, 1297-1340, doi:10.1063/1.555994.

(3) Dooley, K. S.; Geidosch, J. N.; North, S. W. Ion imaging study of IO radical photodissociation: Accurate bond dissociation energy determination. *Chem. Phys. Lett.* **2008**, *457*, 303-306, doi:10.1016/j.cplett.2008.04.009.

(4) Gómez Martín, J. C.; Plane, J. M. C. Determination of the O–IO bond dissociation energy by photofragment excitation spectroscopy. *Chem. Phys. Lett.* **2009**, *474*, 79-83, doi:10.1016/j.cplett.2009.04.052.

(5) Grant, D. J.; Garner, E. B.; Matus, M. H.; Nguyen, M. T.; Peterson, K. A.; Francisco, J. S.; Dixon, D. A. Thermodynamic properties of the XO_2, X_2O, XYO, X_2O_2, and XYO_2 (X, Y = Cl, Br and I) isomers. *J. Phys. Chem. A* **2010**, *114*, 4254-4265, doi:10.1021/jp911320p.

(6) Hassanzadeh, P.; Irikura, K. K. Nearly ab initio thermochemistry: The use of reactions schemes. Application to IO and HOI. *J. Phys. Chem. A* **1997**, *101*, 1580-1587, doi:10.1021/jp963011g.

(7) Kaltsoyannis , N.; Plane, J. M. C. Quantum chemical calculations on a selection of iodine-containing species (IO, OIO, INO_3, $(IO)_2$, I_2O_3, I_2O_4 and I_2O_5) of importance in the atmosphere. *Phys. Chem. Chem. Phys.* **2008**, *10*, 1723-1733, doi:10.1039/b715687c.

(8) Lee, S. Y. Computational study of enthalpies of formation of OXO (X = Cl, Br, and I) and their anions. *J. Phys. Chem. A* **2004**, *108*, 10754-10761, doi:10.1021/jp0467550.

(9) Misra, A.; Marshall, P. Computational investigation of iodine oxides. *J. Phys. Chem. A* **1998**, *102*, 9056-9060, doi:10.1021/jp982708u.

(10) Peterson, K. A.; Shepler, B. C.; Figgen, D.; Stoll, H. On the spectroscopic and thermochemical properties of ClO, BrO, IO, and their anions. *J. Phys. Chem. A* **2006**, *110*, 13877-13883, doi:10.1021/jp065887l.

Note 55: *Compounds containing I and O* Back to Table

HOI Reaction enthalpies for a set of isogyric reactions were calculated using CR-CCSD(T) with single and double excitation and with second-order spin-free Douglas-Kroll-Hess Hamiltonian applied to account for the scalar relativistic effects. The listed values are from a recalculation using the present Table values, which are particularly different for IO and OH. The authors report: $\Delta_f H^\circ_{298} = -69.0 \pm 3.7$ kJ mol^{-1}.[7] A computational study of the OH + $CH_2BrI \rightarrow$ HOI + CH_2Br reaction at the DK-CCSD(T)/ANO-RCC-L(1)//MP2/ccpVTZ level of theory led to $\Delta_f H^\circ_{298} = -62.9$ kJ mol^{-1}.[6] The previous values of $\Delta_f H^\circ_{298} = -69.6 \pm 5.4$ kJ mol^{-1} and $\Delta_f H_0^\circ = -64.9 \pm 5.4$ kJ mol^{-1} was based on the measured activation energy of the reaction OH + $CF_3I \rightarrow CF_3$ + HOI and G2(MP2) calculation indicating a negligible barrier for the reverse reaction.[2] Entropy based on extensive calculations.[3] Enthalpy values have also been calculated using the isogyric reaction HOOH + IO → HOO + HOI with density functional theory (GP96PW91 level), leading to –58.6 kJ mol^{-1} and –63.3 kJ mol^{-1} at 0 and 298 K, employing reference enthalpies from this Table.[1] A calculation involving a pair of isodesmic reactions at the CCSD(T) level of theory in conjunction with the aug-cc-pVTZ-PP and aug-cc-pVQZ-PP basis sets led to $\Delta_f H^\circ_{298} = -59.2 \pm 3.9$ kJ mol^{-1} and $\Delta_f H_0^\circ = -54.5 \pm 3.9$ kJ mol^{-1}.[5]

HIO Enthalpy difference calculated HOI → HIO with density functional theory (GP96PW91 level).[1]

HOIO Enthalpy differences were calculated for IO + OH → HIO_2, I + HO_2 → HIO_2, HIO_2 + HI → H_2O_2 + I_2 at the CCSD(T) level for B3LYP geometries.[4] Previous enthalpy value $\Delta_f H^\circ_{298} = -17.4$ kJ mol^{-1} calculated from the difference for HOOI → HOIO with density functional theory (GP96PW91 level), $\Delta_f H_0^\circ = -11.0$ kJ mol^{-1}.[1]

HOOI Enthalpy differences were calculated for IO + OH → HIO_2, I + HO_2 → HIO_2, HIO_2 + HI → H_2O2 + I_2 at the CCSD(T) level for B3LYP geometries.[4] Previous enthalpy value $\Delta_f H^\circ_{298} = 36.9$ kJ mol^{-1} calculated using the isogyric reaction HOOH + IO → HO + HOOI with density functional theory (GP96PW91 level), employing reference enthalpies from this Table.[1]

(1) Begović, N.; Marković, Z.; Anić, S.; Kolar-Anić, L. Computational investigation of HIO and HIO_2 isomers. *J. Phys. Chem. A* **2004**, *108*, 651-657, doi:10.1021/jp034492o.

(2) Berry, R. J.; Yuan, Y.; Misra, A.; Marshall, P. Experimental and computational investigations of the reaction of OH with CF_3I and the enthalpy of formation of HOI. *J. Phys. Chem. A* **1998**, *102*, 5182-5188, doi:10.1021/jp980645+.

(3) Hassanzadeh, P.; Irikura, K. K. Nearly ab initio thermochemistry: The use of reactions schemes. Application to IO and HOI. *J. Phys. Chem. A* **1997**, *101*, 1580-1587, doi:10.1021/jp963011g.

(4) Khanniche, S.; Louis, F.; Cantrel, L.; Černušák, I. Thermochemistry of HIO_2 species and reactivity of iodous acid with OH radical: A computational study. *Earth Space Chem.* **2017**, *1*, 39-49, doi:10.1021/acsearthspacechem.6b00010.

(5) Marshall, P. Computational studies of the thermochemistry of the atmospheric iodine reservoirs HOI and $IONO_2$. *Advances in Quantum Chemistry* **2008**, 159-175.

(6) Šulka, M.; Šulková, K.; Louis, F.; Neogrády, P.; Černušák, I. A theoretical study of the X-abstraction reactions (X = H, Br, or I) from CH_2IBr by OH radicals: Implications for atmospheric chemistry. *Z. Phys. Chem.* **2013**, *227*, 1337-1359, doi:10.1524/zpch.2013.0391.

(7) Šulková, J.; Federič, J.; Louis, F.; Cantrel, L.; Demovič, L.; Černušák, I. Thermochemistry of small iodine species. *Phys. Scr.* **2013**, *88*, 058304, doi:10.1088/0031-8949/88/05/058304.

Note 56: *Di-halo compounds containing I*

Back to Table

IF The total atomization energy was calculated using a composite electronic structure approach based on CCSD(T) and extrapolated to the complete basis set limit with a two-point extrapolation scheme, Q5. Additional corrections included zero-point energy, core-valence effect, for scalar relativistic effects, and spin-orbit corrections.[4]

ICl Taken from review of Gurvich et al.[3] The JANAF Tables give $\Delta_f H_0^\circ = 19.141 \pm 0.105$ kJ mol^{-1}, $\Delta_f H_{298}^\circ = 17.506 \pm 0.105$ kJ mol^{-1}, and $S^\circ = 247.567$ J mol^{-1}.[1] A calculation of the atomization

energy at the CCSD(T) level, extrapolated to the CBS limit, leads to $\Delta_f H^\circ_{298}$ = 18.8 ± 4 kJ mol^{-1} and $\Delta_f H_0^\circ$ = 20.5 ± 4 kJ mol^{-1}.[2]

IBr Taken from review of Gurvich et al.[3] The JANAF Tables give $\Delta_f H_0^\circ$ = 49.815 ± 0.08 kJ mol^{-1}, $\Delta_f H_{298}^\circ$ = 40.878 ± 0.08 kJ mol^{-1}, and S° = 258.95 J mol^{-1}.[1] A calculation of the atomization energy at the CCSD(T) level, extrapolated to the CBS limit, leads to $\Delta_f H^\circ_{298}$ = 41.4 ± 4 kJ mol^{-1} and $\Delta_f H_0^\circ$ = 50.2 ± 4 kJ mol^{-1}.[2]

(1) Chase, M. W. NIST-JANAF thermochemical tables. *J. Phys. Chem. Ref. Data* **1998**, *Monograph 9*.

(2) Grant, D. J.; Garner, E. B.; Matus, M. H.; Nguyen, M. T.; Peterson, K. A.; Francisco, J. S.; Dixon, D. A. Thermodynamic properties of the XO_2, X_2O, XYO, X_2O_2, and XYO_2 (X, Y = Cl, Br and I) isomers. *J. Phys. Chem. A* **2010**, *114*, 4254-4265, doi:10.1021/jp911320p.

(3) Gurvich, L. V.; Veyts, I. V.; Alcock, C. B. *Thermodynamic Properties of Individual Substances,*, Fourth ed.; Hemisphere Publishing Corp.: New York, 1991; Vol. 2.

(4) Thanthiriwatte, K. S.; Vasiliu, M.; Dixon, D. A.; Christe, K. O. Structural and energetic properties of closed shell XF_n (X = Cl, Br, and I; n = 1−7) and XO_nF_m (X = Cl, Br, and I; n = 1−3; m = 0−6) molecules and ions leading to stability predictions for yet unknown compounds. *Inorg. Chem.* **2012**, *51*, 10966-10982, doi:10.1021/ic301438b.

Note 57: *Compounds containing I, O, and F*

Back to Table

IOF, IO_2F The total atomization energy was calculated using a composite electronic structure approach based on CCSD(T) and extrapolated to the complete basis set limit with a two-point extrapolation scheme, Q5. Additional corrections included zero-point energy, core-valence effect, for scalar relativistic effects, and spin-orbit corrections.[1]

(1) Thanthiriwatte, K. S.; Vasiliu, M.; Dixon, D. A.; Christe, K. O. Structural and energetic properties of closed shell XF_n (X = Cl, Br, and I; n = 1−7) and XO_nF_m (X = Cl, Br, and I; n = 1−3; m = 0−6) molecules and ions leading to stability predictions for yet unknown compounds. *Inorg. Chem.* **2012**, *51*, 10966-10982, doi:10.1021/ic301438b.

Note 58: *Compounds containing I, O, and Cl*

Back to Table

ClOI The enthalpy is from a calculation of the atomization energy at the CCSD(T) level, extrapolated to the CBS limit.[1] Enthalpy derived using molecular properties calculated at the MP2/6-311+G(3df) level of theory, with Gaussian-2 energies coupled with isodesmic reactions, resulted in $\Delta_f H^\circ_{298}$ = 76.1 kJ mol^{-1}.[2]

ClIO The enthalpy is from a calculation of the atomization energy at the CCSD(T) level, extrapolated to the CBS limit. This value is for the ^{1}A' state. $\Delta_f H^\circ_{298}$ = 164.0 ± 6 kJ mol^{-1} for the ^{3}A" state.[1] Enthalpy derived using molecular properties calculated at the MP2/6-311+G(3df) level of theory, with Gaussian-2 energies coupled with isodesmic reactions, resulted in $\Delta_f H^\circ_{298}$ = 68.2 kJ mol^{-1}.[2]

ClClO The enthalpy is from a calculation of the atomization energy at the CCSD(T) level, extrapolated to the CBS limit.[1] Calculations using molecular properties at the MP2/6-311+G(3df) level of theory and Gaussian-2 energies, coupled with isodesmic reactions and reference enthalpies changed to correspond to values in this Table, resulted in $\Delta_f H^\circ_{298}$ = 166 kJ mol^{-1}.[2]

$ClIO_2$ The enthalpy is from a calculation of the atomization energy at the CCSD(T) level, extrapolated to the CBS limit.[1] Calculations using molecular properties at the MP2/6-311+G(3df) level of theory and Gaussian-2 energies, coupled with isodesmic reactions and reference enthalpies changed to correspond to values in this Table, resulted in $\Delta_f H^\circ_{298}$ = 10.9 kJ mol^{-1}.[2]

ClOIO The enthalpy is from a calculation of the atomization energy at the CCSD(T) level, extrapolated to the CBS limit.[1] Calculations using molecular properties at the MP2/6-311+G(3df) level of

theory and Gaussian-2 energies, coupled with isodesmic reactions and reference enthalpies changed to correspond to values in this Table, resulted in $\Delta_f H^\circ_{298}$ = 107 kJ mol^{-1}.[2]

ClOOI The enthalpy is from a calculation of the atomization energy at the CCSD(T) level, extrapolated to the CBS limit.[1] Calculations using molecular properties at the MP2/6-311+G(3df) level of theory and Gaussian-2 energies, coupled with isodesmic reactions and reference enthalpies changed to correspond to values in this Table, resulted in $\Delta_f H^\circ_{298}$ = 126 kJ mol^{-1}.[2]

IOClO The enthalpy is from a calculation of the atomization energy at the CCSD(T) level, extrapolated to the CBS limit.[1] Calculations using molecular properties at the MP2/6-311+G(3df) level of theory and Gaussian-2 energies, coupled with isodesmic reactions and reference enthalpies changed to correspond to values in this Table, resulted in $\Delta_f H^\circ_{298}$ = 154 kJ mol^{-1}.[2]

IClO_2 The enthalpy is from a calculation of the atomization energy at the CCSD(T) level, extrapolated to the CBS limit.[1] Calculations using molecular properties at the MP2/6-311+G(3df) level of theory and Gaussian-2 energies, coupled with isodesmic reactions and reference enthalpies changed to correspond to values in this Table, resulted in $\Delta_f H^\circ_{298}$ = 188 kJ mol^{-1}.[2]

(1) Grant, D. J.; Garner, E. B.; Matus, M. H.; Nguyen, M. T.; Peterson, K. A.; Francisco, J. S.; Dixon, D. A. Thermodynamic properties of the XO_2, X_2O, XYO, X_2O_2, and XYO_2 (X, Y = Cl, Br and I) isomers. *J. Phys. Chem. A* **2010**, *114*, 4254-4265, doi:10.1021/jp911320p.

(2) Misra, A.; Marshall, P. Computational studies of the isomers of ClIO and $ClIO_2$. *J. Chem. Soc. Faraday Trans.* **1997**, *93*, 3301-3304, doi:10.1039/a702360j.

Note 59: *Compounds containing I, O, and Br*

Back to Table

For all: The enthalpy values are from calculation of the atomization energies at the CCSD(T) level, extrapolated to the CBS limit.[1] For BrIO, the value is for the ^{1}A' state. $\Delta_f H^\circ_{298}$ = 190.0 ± 6 kJ mol^{-1} for the ^{3}A" state.

(1) Grant, D. J.; Garner, E. B.; Matus, M. H.; Nguyen, M. T.; Peterson, K. A.; Francisco, J. S.; Dixon, D. A. Thermodynamic properties of the XO_2, X_2O, XYO, X_2O_2, and XYO_2 (X, Y = Cl, Br and I) isomers. *J. Phys. Chem. A* **2010**, *114*, 4254-4265, doi:10.1021/jp911320p.

Note 60: *Compounds containing I, O, and N*

Back to Table

INO Thermodynamic parameters from a third-law analysis of the equilibrium reaction I + NO (+He) ↔ INO (+He).[4] Enthalpy of reaction obtained using CCSD(T) calculations at B3LYP geometries, with corrections for spin-orbit coupling, for I + NO → INO, using Table reference values, leads to a 298 K enthalpy of 134.2 kJ mol^{-1}.[1]

INO_2 Thermodynamic parameters from a third-law analysis of the equilibrium reaction I + NO_2 (+He) ↔ INO_2 (+He).[4]

IOONO Derived from CCSD(T) single-point calculations at B3LYP geometries for the interconversion of the two isomers.[3] The dissociation energy for IONO_2 was also calculated to be 131.4 kJ mol^{-1}, leading to an enthalpy at 298 K for that isomer of 24.8 kJ mol^{-1}, whereas a value of 37.5 kJ mol^{-1} has been selected for this Table.

IONO_2 The enthalpy values were derived from the average of the IO – NO_2 bond dissociation energies calculated by Kaltsoyannis and Plane[1] and by Marshall.[2] See Table 3-1, note 32 for more details. The selected entropy value is also discussed in that note.

(1) Kaltsoyannis , N.; Plane, J. M. C. Quantum chemical calculations on a selection of iodine-containing species (IO, OIO, INO_3, $(IO)_2$, I_2O_3, I_2O_4 and I_2O_5) of importance in the atmosphere. *Phys. Chem. Chem. Phys.* **2008**, *10*, 1723-1733, doi:10.1039/b715687c.

(2) Marshall, P. Computational studies of the thermochemistry of the atmospheric iodine reservoirs HOI and IONO_2. *Advances in Quantum Chemistry* **2008**, 159-175.

(3) Papayannakos, N.; Kosmas, A. M. The conformational potential energy surface of IOONO and the isomerization and decomposition processes. *Chem. Phys.* **2005**, *315*, 251-258, doi:10.1016/j.chemphys.2005.04.014.
(4) van den Bergh, H.; Troe, J. Kinetic and thermodynamic properties of INO and INO_2 intermediate complexes in iodine recombination. *J. Chem. Phys.* **1976**, *64*, 736-742, doi:10.1063/1.432220.

Note 61: *Compounds containing one C and I and H* Back to Table

CI Enthalpy computed from atomization energies at the CBS limit using valence correlated (R/U)CCSD(T) with au-cc-pVxZ (x=T,Q,5) basis sets, with relativistic and spin-orbit corrections. Geometries and vibrational frequencies obtained at the CCSD level with the cc-pVTZ basis set.[1]

CHI Enthalpy computed from atomization and dissociation energies at the CBS limit using valence correlated (R/U)CCSD(T) with aug-cc-pVxZ (x=T,Q,5) basis sets, with relativistic and spin-orbit corrections.[1] Geometries and vibrational frequencies obtained at the CCSD level with the cc-pVTZ basis set. Previous value of $\Delta_f H^\circ_{298}$ = 425 kJ mol^{-1} was obtained using the computed enthalpy of a reaction of the type: $CH_2(^1A_1)$ + CH_3X + CH_3Y = $CXY(^1A_1)$ + $2CH_4$ at the QCISD(T)/6-311+G(3df,2p)//QCISD/6-311G(d,p) level of theory. Calculations also done at the G2 level.[10]

CH_2I Enthalpy value from *ab initio* calculations at the QCISD(T)/6-311+G(3df,2p) level of theory, utilizing an isodesmic reaction with methyl bromide.[9] A computational study of the OH + CH_3I → H_2O + CH_2I reaction at the DK-CCSD(T)/ANO-RCC-L(1)//MP2/ccpVTZ level of theory led to $\Delta_f H^\circ_{298}$ = 215.9 kJ mol^{-1} and $\Delta_f H_0^\circ$ = 220.2 kJ mol^{-1}.[8] These values provided the enthalpy difference utilized. A subsequent study on the reaction OH + CH_2IBr → HOBr + CH_2I led to $\Delta_f H^\circ_{298}$ = 218.4 kJ mol^{-1} and $\Delta_f H_0^\circ$ = 223.3 kJ mol^{-1}.[14] Previous enthalpy value of 228.0±2.8 kJ mol^{-1} from *ab initio* calculations used to determine the entropies of the reactants and the transition state for Br + CH_3I → HBr + CH_2I. Arrhenius parameters were then calculated by transition state theory. The kinetics of the reverse reactions were measured in a flow system. The enthalpy value was obtained from a second-law analysis.[11]

CH_3I Enthalpy values from an imaging PEPICO study of the dissociative photoionization of methyl iodide, using both room temperature and supersonically cooled gas.[3] The previously recommended value, $\Delta_f H^\circ_{298}$= 13.22 ± 0.5 kJ mol^{-1}, was calculated from the dissociation of energy-selected CH_3I^+ and its adiabatic ionization energy.[12] Enthalpy from rotating combustion calorimetry is 14.4 ± 1.4 kJ mol^{-1}.[4] A review of the literature gave $\Delta_f H^\circ_{298}$= 13.8 ± 1.2 kJ mol^{-1} and the enthalpy difference; the entropy is from ideal gas thermodynamic properties.[5]

CI_2 Enthalpy computed from atomization and dissociation energies at the CBS limit using valence correlated (R/U)CCSD(T) with aug-cc-pVxZ (x=T,Q,5) basis sets, with relativistic and spin-orbit corrections.[1] Geometries and vibrational frequencies obtained at the CCSD level with the cc-pVTZ basis set. Previous value of $\Delta_f H^\circ_{298}$ = 450 kJ mol^{-1} was obtained using the computed enthalpy of a reaction of the type: $CH_2(^1A_1)$ + CH_3X + CH_3Y → $CXY(^1A_1)$ + $2CH_4$ at the QCISD(T)/6-311+G(3df,2p)//QCISD/6-311G(d,p) level of theory. Calculations also done at the G2 level.[10]

CHI_2 Enthalpy value from *ab initio* calculations at the QCISD(T)/6-311+G(3df,2p) level of theory, utilizing an isodesmic reaction with methyl bromide.[9] A computational study of the OH + CH_3I → HOI + CHI_2 reaction at the CCSD(T)/ANO-RCC-Large//MP2/ccpVTZ level of theory led to $\Delta_f H^\circ_{298}$ = 309.2 kJ mol^{-1} and $\Delta_f H_0^\circ$ = 298.9 kJ mol^{-1}.[13] These values provided the enthalpy difference utilized. A computational study of the OH + CH_2I_2 → H_2O + CHI_2 reaction at the DK-CCSD(T)/ANO-RCC-L(1)//MP2/ccpVTZ level of theory led to $\Delta_f H^\circ_{298}$ = 298.7 kJ mol^{-1} and $\Delta_f H_0^\circ$ = 303.5 kJ mol^{-1}.[8] Previous enthalpy value of 314.4 ± 3.3 kJ mol^{-1} from *ab initio* calculations used to determine the entropies of the reactants and the transition state for Br + CH_2I_2 → HBr + CHI_2. Arrhenius parameters were then calculated by transition state theory.

The kinetics of the reverse reactions were estimated. The enthalpy value was obtained from a second-law analysis.[11]

CH_2I_2 Enthalpy taken from a dissociative photoionization study of a series of dihalomethanes, normalized using the experimental enthalpy of dichloromethane.[7] The reported value has been adjusted by +0.4 kJ mol^{-1} to agree with the present enthalpy for CH_2Cl_2. Previous value of 119.5 ± 2.2 kJ mol^{-1} from rotating combustion calorimetry.[4] *Ab initio* calculations at the QCISD(T)/6-311+G(3df,2p) level of theory, utilizing an isodesmic reaction with methyl iodide, resulted in an enthalpy value of 108.1 ± 6 kJ mol^{-1}.[9] A review of the literature gave $\Delta_f H^\circ_{298}$= 117.6 ± 4.2 kJ mol^{-1} and the enthalpy difference; the entropy is from ideal gas thermodynamic properties.[6] In a more recent study, involving a TPEPICO determination of the heat of formation of 1,2-$C_2H_4I_2$, an analysis of the *ab initio* isodesmic reactions energies of four reactions led to a recommendation that the enthalpy values be reduced to $\Delta_f H_0^\circ$ = 123.1 ± 2.0 kJ mol^{-1} and $\Delta_f H^\circ_{298}$= 113.5 ± 2.0 kJ mol^{-1}.[2]

CHI_3 *Ab initio* calculations at the QCISD(T)/6-311+G(3df,2p) level of theory, utilizing an isodesmic reaction with methyl iodide.[9] Previous enthalpy value of 251.1 ± 1.4 kJ mol^{-1} from rotating combustion calorimetry.[4] A review of the literature gave $\Delta_f H^\circ_{298}$= 210.9 ± 4.2 kJ mol^{-1} and the enthalpy difference; the entropy is from ideal gas thermodynamic properties.[5]

CI_3 Enthalpy value from *ab initio* calculations at the QCISD(T)/6-311+G(3df,2p) level of theory, utilizing an isodesmic reaction with methyl bromide.[9] A computational study of the OH + CH_3I → H_2O + CI_3 reaction at the CCSD(T)/ANO-RCC-Large//MP2/ccpVTZ level of theory led to $\Delta_f H^\circ_{298}$ = 387.4 kJ mol^{-1} and $\Delta_f H_0^\circ$ = 384.4 kJ mol^{-1}.[13] These values provided the enthalpy difference utilized. Previous enthalpy value of 424.9 ± 2.8 kJ mol^{-1} from *ab initio* calculations used to determine the entropies of the reactants and the transition state for Br + CH_2I_2 → HBr + CHI_2. Arrhenius parameters were then calculated by transition state theory. The kinetics of the reverse reactions were estimated. The enthalpy value was obtained from a second-law analysis.[11] The uncertainty in the *ab initio* was suggested to be ±9 kJ mol^{-1}. We have expanded that considerably due to these obvious disagreements.

CI_4 *Ab initio* calculations at the QCISD(T)/6-311+G(3df,2p) level of theory, utilizing an isodesmic reaction with methyl iodide.[9] Previous enthalpy value of 474 ± 13 kJ mol^{-1} from rotating combustion calorimetry.[4] A review of the literature estimated $\Delta_f H^\circ_{298}$= 268 ± 4.2 kJ mol^{-1} and the enthalpy difference; the entropy is from ideal gas thermodynamic properties.[6] The uncertainty in the *ab initio* was suggested to be ±12 kJ mol^{-1}. We have expanded that considerably due to these obvious disagreements.

(1) Bacskay, G. B. Quantum chemical characterization of the X($^1A_1$), a($^3B_1$), A($^1B_1$) and B(2^1A_1) states of diiodomethylene and the enthalpies of formation of diiodomethylene, iodomethylene and iodomethylidyne. *Theor. Chem. Acc.* **2016**, 267-275, doi:10.1007/978-3-662-48148-6_24.

(2) Baer, T.; Walker, S. H.; Shuman, N. S.; Bodi, A. One- and two-dimensional translational energy distributions in the iodine-loss dissociation of 1,2-$C_2H_4I_2^+$ and 1,3-$C_3H_6I_2^+$: What does this mean? *J. Phys. Chem. A* **2012**, *116*, 2833-2844, doi:10.1021/jp2121643.

(3) Bodi, A.; Shuman, N. S.; Baer, T. On the ionization and dissociative photoionization of iodomethane: a definitive experimental enthalpy of formation of CH_3I. *Phys. Chem. Chem. Phys.* **2009**, *11*, 11013-11021, doi:10.1039/b915400k.

(4) Carson, A. S.; Laye, P. G.; Pendley, J. B.; Welsby, A. M. The enthalpies of formation of iodomethane, diiodomethane, triiodomethane, and tetraiodomethane by rotating combustion calorimetry. *J. Chem. Thermo.* **1993**, *25*, 261-269, doi:10.1006/jcht.1993.1025.

(5) Kudchadker, S. A.; Kudchadker, A. P. Ideal gas thermodynamic properties of the eight bromo- and iodomethanes. *J. Phys. Chem. Ref. Data* **1975**, *4*, 457-470, doi:10.1063/1.555522.

(6) Kudchadker, S. A.; Kudchadker, A. P. Erratum: Ideal gas thermodynamic properties of eight bromo- and iodomethanes. *J. Phys. Chem. Ref. Data* **1976**, *5*, 529-530, doi:10.1063/1.555537.

(7) Lago, A. F.; Kercher, J. P.; Bödi, A.; Sztáray, B.; Miller, B.; Wurzelmann, D.; Baer, T. Dissociative photoionization and thermochemistry of dihalomethane compounds studied by threshold photoelectron photoion coincidence spectroscopy. *J. Phys. Chem. A* **2005**, *109*, 1802-1809, doi:10.1021/jp045337s.

(8) Louis, F.; Černušák, I.; Canneaux, S.; Mečiarová, K. Atmospheric reactivity of CH_3I and CH_2I_2 with OH radicals: A comparative study of the H- versus I-abstraction. *Comp. Theor. Chem.* **2011**, *965*, 275-284, doi:10.1016/j.theochem.2010.09.022.
(9) Marshall, P.; Srinivas, G. N.; Schwartz, M. A computational study of the thermochemistry of bromine- and iodine-containing methanes and methyl radicals. *J. Phys. Chem. A* **2005**, *109*, 6371-6379, doi:10.1021/jp0518052.
(10) Schwartz, M.; Marshall, P. An ab initio investigation of halocarbenes. *J. Phys. Chem. A* **1999**, *103*, 7900-7906, doi:10.1021/jp9919213.
(11) Seetula, J. A. Kinetics of the R + HBr → RH + Br (R = CH_2I or CH_3) reaction. An ab initio study of the enthalpy of formation of the CH_2I, CHI_2 and CI_3 radicals. *Phys. Chem. Chem. Phys.* **2002**, *4*, 455-460, doi:10.1039/b107407p.
(12) Song, Y.; Qian, X. M.; Lau, K. C.; Ng, C. Y.; Liu, J. B.; Chen, W. W. High-resolution energy-selected study of the reaction $CH_3H^+ \rightarrow CH_3^+ + X$: Accurate thermochemistry for the CH_3X/CH_3X^+ (X=Br, I) system. *J. Chem. Phys.* **2001**, *115*, 4095-4104, doi:10.1063/1.1391268.
(13) Sudolská, M.; Louis, F.; Černušák, I. Reactivity of CHI_3 with OH radicals: X-abstraction reaction pathways (X = H, I), atmospheric chemistry, and nuclear safety. *J. Phys. Chem. A* **2014**, *118*, 9512-9520, doi:10.1021/jp5051832.
(14) Šulka, M.; Šulková, K.; Louis, F.; Neogrády, P.; Černušák, I. A theoretical study of the X-abstraction reactions (X = H, Br, or I) from CH_2IBr by OH radicals: Implications for atmospheric chemistry. *Z. Phys. Chem.* **2013**, *227*, 1337-1359, doi:10.1524/zpch.2013.0391.

Note 62: *Compounds containing one C and I, H and O*

Back to Table

CH_2IOOH, CHI_2OOH

Geometry optimization and frequency calculations were performed at the MP2/6-31G(d) and the B3LYP/6-311++G(d,p) levels of theory, with a single-point energy calculation at the CCSD(T)/6-311++G(d,p//B3LYP/6-311++G(d,p) level. The dissociation energy into HO_2 and the alkyl radical was then evaluated and used, after thermal correction, to calculate the enthalpy of formation at 298 K.[1] This was adjusted to the radical values from the present Table.

(1) Kosmas, A. M.; Mpellos, C.; Salta, Z.; Drougas, E. Structural and heat of formation studies of halogenated methyl hydro-peroxides. *Chem. Phys.* **2010**, *371*, 36-42, doi:10.1016/j.chemphys.2010.03.026.

Note 63: *Compounds containing one C, F, and I*

Back to Table

CFI Enthalpy values calculated from atomization energies by using the (R/U)CCSD(T) level of theory.[1] Basis sets from cc-pVTZ to aug-cc-pV5Z and cc-pwCVQZ were employed. Small-core relativistic pseudopotentials were used as needed. Geometric parameters and frequencies were computed using the CCSD method. A singlet-triplet spacing of 114.2 kJ mol^{-1} was also obtained. The previously listed enthalpy value of $\Delta_f H^{\circ}_{298}$= 154 kJ mol^{-1} was obtained using the computed enthalpy of a reaction of the type: $CH_2(^1A_1) + CH_2F_2 + 2CH_3Y \rightarrow CFY(^1A_1) + 3CH_4$ at the QCISD(T)/6-311+G(3df,2p)//QCISD/6-311G(d,p) level of theory, with calculations also done at the G2 level.[5]

CF_3I Enthalpy from a simultaneous solution of a thermochemical network for the CF_3X species, where X = nil, H, Cl, Br, I, CF_3, CN.[4] Entropy from recommendation of Gurvich et al.[2]

CF_2I_2 Taken from review of Kudchadker and Kudchadker. All parameters estimated.[3]

(1) Bacskay, G. B. Spectroscopy and heats of formation of CXI (X = Br, Cl, F) iodocarbenes: quantum chemical characterisation of the , and states. *Mol. Phys.* **2015**, *113*, 1608-1617, doi:10.1080/00268976.2014.1000991.
(2) Gurvich, L. V.; Veyts, I. V.; Alcock, C. B. *Thermodynamic Properties of Individual Substances,*, Fourth ed.; Hemisphere Publishing Corp.: New York, 1991; Vol. 2.

(3) Kudchadker, S. A.; Kudchadker, A. P. Ideal gas thermodynamic properties of $CH_{4-(a+b+c+d)}F_aCl_bBr_cI_d$ halomethanes. *J. Phys. Chem. Ref. Data* **1978**, *7*, 1285-1307, doi:10.1063/1.555585.
(4) Ruscic, B.; Michael, J. V.; Redfern, P. C.; Curtiss, L. A.; Raghavachri, K. Simultaneous adjustment of experimentally based enthalpies of formation of CF_3X, X = nil, H, Cl, Br, I, CF_3, CN, and a probe of G3 theory. *J. Phys. Chem. A* **1998**, *102*, 10889-10899, doi:10.1021/jp983237e.
(5) Schwartz, M.; Marshall, P. An ab initio investigation of halocarbenes. *J. Phys. Chem. A* **1999**, *103*, 7900-7906, doi:10.1021/jp9919213.

Note 64: *Compounds containing one C, Cl, and I*

Back to Table

CClI Enthalpy values calculated from atomization energies by using the (R/U)CCSD(T) level of theory.[1] Basis sets from cc-pVTZ to aug-cc-pV5Z and cc-pwCVQZ were employed. Small-core relativistic pseudopotentials were used as needed. Geometric parameters and frequencies were computed using the CCSD method. A singlet-triplet spacing of 60.2 kJ mol^{-1} was also obtained. The previously listed enthalpy value of $\Delta_f H^\circ_{298}$= 343 kJ mol^{-1} was obtained using the computed enthalpy of a reaction of the type: $CH_2(^1A_1) + CH_3X + CH_3Y \rightarrow CXY(^1A_1) + 2CH_4$ at the QCISD(T)/6-311+G(3df,2p)//QCISD/6-311G(d,p) level of theory. Calculations also done at the G2 level.[4]

CH_2CClI Enthalpy taken from a dissociative photoionization study of a series of dihalomethanes, normalized using the experimental enthalpy of dichloromethane.[3] The reported value has been adjusted by +0.4 kJ mol^{-1} to agree with the present enthalpy for CH_2Cl_2.

CCl_3I Taken from review of Kudchadker and Kudchadker. All parameters estimated.[2]

(1) Bacskay, G. B. Spectroscopy and heats of formation of CXI (X = Br, Cl, F) iodocarbenes: quantum chemical characterisation of the , and states. *Mol. Phys.* **2015**, *113*, 1608-1617, doi:10.1080/00268976.2014.1000991.
(2) Kudchadker, S. A.; Kudchadker, A. P. Ideal gas thermodynamic properties of $CH_{4-(a+b+c+d)}F_aCl_bBr_cI_d$ halomethanes. *J. Phys. Chem. Ref. Data* **1978**, *7*, 1285-1307, doi:10.1063/1.555585.
(3) Lago, A. F.; Kercher, J. P.; Bödi, A.; Sztáray, B.; Miller, B.; Wurzelmann, D.; Baer, T. Dissociative photoionization and thermochemistry of dihalomethane compounds studied by threshold photoelectron photoion coincidence spectroscopy. *J. Phys. Chem. A* **2005**, *109*, 1802-1809, doi:10.1021/jp045337s.
(4) Schwartz, M.; Marshall, P. An ab initio investigation of halocarbenes. *J. Phys. Chem. A* **1999**, *103*, 7900-7906, doi:10.1021/jp9919213.

Note 65: *Compounds containing one C, Br, and I*

Back to Table

CHBrI Enthalpy values from ab initio calculations at the QCISD(T)/6-311+G(3df,2p) level of theory, utilizing an isodesmic reaction with methyl bromide and methyl iodide.[3] Enthalpy value from ab initio calculations at the QCISD(T)/6-311+G(3df,2p) level of theory, utilizing an isodesmic reaction with methyl bromide.[3] A computational study of the OH + $CH_2BrI \rightarrow H_2O$ + CHBrI reaction at the DK-CCSD(T)/ANO-RCC-L(1)//MP2/ccpVTZ level of theory led to $\Delta_f H^\circ_{298}$ = 252.2 kJ mol^{-1} and $\Delta_f H_0^\circ$ = 262.5 kJ mol^{-1}.[5] These values provided the enthalpy difference utilized.

CH_2BrI Enthalpy taken from a dissociative photoionization study of a series of dihalomethanes, normalized using the experimental enthalpy of dichloromethane.[2] The reported value has been adjusted by +0.4 kJ mol^{-1} to agree with the present enthalpy for CH_2Cl_2. *Ab initio* calculations at the QCISD(T)/6-311+G(3df,2p) level of theory, utilizing an isodesmic reaction with methyl bromide and methyl iodide, resulted in an enthalpy value of 56.8 ± 6 kJ mol^{-1}.[3]

CBr_2I and $CHBr_2I$

Enthalpy value from *ab initio* calculations at the QCISD(T)/6-311+G(3df,2p) level of theory, utilizing an isodesmic reaction with methyl bromide and methyl iodide.[3]

CBrI Enthalpy values calculated from atomization energies by using the (R/U)CCSD(T) level of theory.[1] Basis sets from cc-pVTZ to aug-cc-pV5Z and cc-pwCVQZ were employed. Small-core relativistic pseudopotentials were used as needed. Geometric parameters and frequencies were computed using the CCSD method. A singlet-triplet spacing of 56.9 kJ mol^{-1} was also obtained. The previously listed enthalpy value of $\Delta_f H^\circ_{298}$= 395 kJ mol^{-1} was obtained using the computed enthalpy of a reaction of the type: $CH_2(^1A_1) + CH_3X + CH_3Y \rightarrow CXY(^1A_1) + 2CH_4$ at the QCISD(T)/6-311+G(3df,2p)//QCISD/6-311G(d,p) level of theory. Calculations also done at the G2 level.[4]

$CBrI_2$ and $CHBrI_2$
Enthalpy value from *ab initio* calculations at the QCISD(T)/6-311+G(3df,2p) level of theory, utilizing an isodesmic reaction with methyl bromide and methyl iodide.[3]

(1) Bacskay, G. B. Spectroscopy and heats of formation of CXI (X = Br, Cl, F) iodocarbenes: quantum chemical characterisation of the , and states. *Mol. Phys.* **2015**, *113*, 1608-1617, doi:10.1080/00268976.2014.1000991.
(2) Lago, A. F.; Kercher, J. P.; Bödi, A.; Sztáray, B.; Miller, B.; Wurzelmann, D.; Baer, T. Dissociative photoionization and thermochemistry of dihalomethane compounds studied by threshold photoelectron photoion coincidence spectroscopy. *J. Phys. Chem. A* **2005**, *109*, 1802-1809, doi:10.1021/jp045337s.
(3) Marshall, P.; Srinivas, G. N.; Schwartz, M. A computational study of the thermochemistry of bromine- and iodine-containing methanes and methyl radicals. *J. Phys. Chem. A* **2005**, *109*, 6371-6379, doi:10.1021/jp0518052.
(4) Schwartz, M.; Marshall, P. An ab initio investigation of halocarbenes. *J. Phys. Chem. A* **1999**, *103*, 7900-7906, doi:10.1021/jp9919213.
(5) Šulka, M.; Šulková, K.; Louis, F.; Neogrády, P.; Černušák, I. A theoretical study of the X-abstraction reactions (X = H, Br, or I) from CH_2IBr by OH radicals: Implications for atmospheric chemistry. *Z. Phys. Chem.* **2013**, *227*, 1337-1359, doi:10.1524/zpch.2013.0391.

Note 66: *Compounds containing two C and I*

Back to Table

***cis*- and *trans*-CHICHI**
Enthalpy values from review of Pedley.[5]

CH_3CH_2I Enthalpy obtained from a TPEPICO determination of the onset energy of the ethyl cation from the photodissociation of ethyl iodide, taking $\Delta_f H_0^\circ(C_2H_5^+)$ = 915.5 ± 1.3 kJ mol^{-1}.[2] Previous enthalpy value of –7.5 ± 0.9 kJ mol^{-1} from review of the literature.[3] Pedley gives –8.1 ± 2.2 kJ mol^{-1}.[5] Entropy calculated by Kudchadker and Kudchadker.[4]

CH_2ICH_2I Based on a TPEPICO study of the sequential photodissociation of $C_2H_4I_2^+$ coupled with theoretical calculations involving four isodesmic reactions.[1] Previous enthalpy value of 75 ± 4 kJ mol^{-1} from review of Pedley et al.[5]

(1) Baer, T.; Walker, S. H.; Shuman, N. S.; Bodi, A. One- and two-dimensional translational energy distributions in the iodine-loss dissociation of 1,2-$C_2H_4I_2^+$ and 1,3-$C_3H_6I_2^+$: What does this mean? *J. Phys. Chem. A* **2012**, *116*, 2833-2844, doi:10.1021/jp2121643.
(2) Borkar, S.; Sztaray, B. Self-consistent heats of formation for the ethyl cation, ethyl bromide, and ethyl iodide from threshold photoelectron photoion coincidence spectroscopy. *J. Phys. Chem. A* **2010**, *114*, 6117-6123, doi:10.1021/jp102162f.
(3) Kolesov, V. P.; Papina, T. S. Thermochemistry of haloethanes. *Russ. Chem. Rev.* **1983**, *52*, 425-439.
(4) Kudchadker, S. A.; Kudchadker, A. P. Ideal gas thermodynamic properties of selected bromoethanes and iodoethane. *J. Phys. Chem. Ref. Data* **1979**, *8*, 519-526, doi:10.1063/1.555601.

(5) Pedley, J. B. *Thermochemical Data and Structures of Organic Compounds*; Thermodynamics Data Center: College Station, TX, 1994.

Note 67: *Compounds containing two C, F and I*

Back to Table

CF_3CH_2I and CF_3CF_2I

Enthalpy values taken from review of Pedley.[1]

(1) Pedley, J. B. *Thermochemical Data and Structures of Organic Compounds*; Thermodynamics Data Center: College Station, TX, 1994.

Note 68: *Compounds containing two C, O and I*

Back to Table

$CH_3C(O)I$, acetyl iodide

Enthalpy value taken from review of Pedley.[2]

ICH_2CH_2OH

The enthalpy of formation of the liquid was determined by using rotating-bomb combustion calorimetry to be $\Delta_f H^\circ_{298}(l) = -207.3 \pm 0.7$ kJ mol^{-1}. The molar enthalpy of vaporization was then determined by use of Calvert-drop microcalorimetry to be $\Delta_{vap} H^\circ_{298} = 57.03 \pm 0.20$ kJ mol^{-1}.[1]

(1) Bernardes, C. E. S.; Minas da Piedade, M. E.; Amaral, L. M. P. F.; Ferreira, A. I. M. C. L.; Ribeiro da Silva, M. A. V.; Diogo, H. P.; Costa Cabral, B. J. Energetics of C−F, C−Cl, C−Br, and C−I bonds in 2-haloethanols. Enthalpies of formation of XCH_2CH_2OH (X = F, Cl, Br, I) compounds and of the 2-hydroxyethyl radical. *J. Phys. Chem. A* **2007**, *111*, 1713-1720, doi:10.1021/jp0675678.

(2) Pedley, J. B. *Thermochemical Data and Structures of Organic Compounds*; Thermodynamics Data Center: College Station, TX, 1994.

Note 69: *Compounds containing two C, N and I*

Back to Table

CH_2ICN From a PEPICO study of the neutral using the known enthalpy of CH_3CN.[1]

(1) Lafleur, R. D.; Szatary, B.; Baer, T. A photoelectron-photoion coincidence study of the ICH_2CN ion dissociation: Thermochemistry of CH_2CN, $^+CH_2CN$, and ICH_2CN. *J. Phys. Chem. A* **2000**, *104*, 1450-1455, doi:10.1021/jp993569z.

Note 70: *Compounds containing three C and I*

Back to Table

CH_3CHICH_3

The measured onset energy for *i*-$C_3H_7^+$ from iPEPICO spectroscopy of *i*- C_3H_7I was used in conjunction with a new value of the ion enthalpy of formation to obtain the 0 K enthalpy of the iodide.[1]

(1) Stevens, W. R.; Bodi, A.; Baer, T. Dissociation dynamics of energy selected, propane, and *i*-$C_3H_7X^+$ ions by iPEPICO: Accurate heats of formation of *i*-$C_3H_7^+$, *i*-C_3H_7Cl, *i*-C_3H_7Br, and *i*-C_3H_7I. *J. Phys. Chem. A* **2010**, *114*, 11285-11291, doi:10.1021/jp104200h.

Note 71: *Compounds containing S and H*

Back to Table

S CODATA Key Value.[2] The JANAF Tables give $\Delta_f H_0^\circ = 274.735$ kJ mol^{-1}, $\Delta_f H_{298}^\circ = 276.98$ kJ mol^{-1}, and $S^\circ = 167.828$ J mol^{-1}.[1]

S_2 CODATA Key Value.[2] The JANAF Tables give $\Delta_f H_0^\circ = 128.3$ kJ mol^{-1}, $\Delta_f H_{298}^\circ = 128.6$ kJ mol^{-1}, and $S^\circ = 228.165$ J mol^{-1}.[1]

HS Updated and corrected NIST-JANAF thermochemical tables.[7] Enthalpy calculated at the CCSD(T)/CBS level of theory is 34.4 kcal mol^{-1}.[9] Thermodynamic parameters calculated at the CCSDT(Q)/cc-pV(T+d)Z level of theory give $\Delta_f H_0^o$ = 142.6 kJ mol^{-1}, $\Delta_f H_{298}^o$ = 143.4 kJ mol^{-1}, and S^o = 195.4 J mol^{-1}.[8] A computational study of S-centered radicals, with geometry and conformational optimization at the M06-2X/6-31G(d) level of theory and energies determined using the G3(MP2)-RAD composite method, obtained $\Delta_f H_{298}^o$ = 140.89 kJ mol^{-1}, taking H_2S and H enthalpy values from the present Table.[3]

H_2S CODATA Key Value.[2] The JANAF Tables give $\Delta_f H_0^o$ = −17.58 kJ mol^{-1}, $\Delta_f H_{298}^o$ = −20.50 kJ mol^{-1}, and S^o = 205.757 J mol^{-1}.[1]

HSS A UCCSD(T)/cc-pV(n+d)Z(n=D,T,Q,5) calculation with correlation-consistent basis sets results in 3.63 ± 1.0 kcal mol^{-1}.[4] Atomization energy calculated by the CCSD(T) extrapolated to the CBS limit, with geometry optimized at the CCSD(T)/aV(n+d)Z (n = D,T,Q,5) level gives $\Delta_f H_{298}^o$ = 24.3 ± 1 kcal mol^{-1} and $\Delta_f H_0^o$ = −25.0 ± 1 kcal mol^{-1}.[6] A computational study of S-centered radicals, with geometry and conformational optimization at the M06-2X/6-31G(d) level of theory and energies determined using the G3(MP2)-RAD composite method, obtained $\Delta_f H_{298}^o$ = 106.3 kJ mol^{-1}, taking H_2S_2 and H enthalpy values from the present Table.[3]

HSSH Thermodynamics Center recommendation.[5] A UCCSD(T) calculation with correlation-consistent basis sets results in 3.63±1.0 kcal mol^{-1}.[4] The atomization energy calculated by the CCSD(T) extrapolated to the CBS limit, with geometry optimized at the CCSD(T)/aV(n+d)Z (n = D,T,Q,5) level, gives $\Delta_f H_{298}^o$ = 3.4 ± 1 kcal mol^{-1} and $\Delta_f H_0^o$ = 4.8 ± 1 kcal mol^{-1}.[6] Lowest energy configuration is the *syn* isomer. Values for the *trans* isomer are $\Delta_f H_{298}^o$ = 7.8 ± 1 kcal mol^{-1} and $\Delta_f H_0^o$ = 9.3 ± 1 kcal mol^{-1} and for the *cis* isomer $\Delta_f H_{298}^o$ = 10.0 ± 1 kcal mol^{-1} and $\Delta_f H_0^o$ = 11.5 ± 1 kcal mol^{-1}.

HSSS Atomization energy calculated by the CCSD(T) extrapolated to the CBS limit, with geometry optimized at the CCSD(T)/aV(n+d)Z (n = D,T,Q,5) level.[6] Lowest energy configuration is the *syn* isomer. Values for the *cis* isomer are $\Delta_f H_{298}^o$ = 27.0 ± 1 kcal mol^{-1} and $\Delta_f H_0^o$ = 28.1 ± 1 kcal mol^{-1} and for the *trans* isomer $\Delta_f H_{298}^o$ = 27.0 ± 1 kcal mol^{-1} and $\Delta_f H_0^o$ = 27.7 ± 1 kcal mol^{-1}.

HSSSH Atomization energy calculated by the CCSD(T) extrapolated to the CBS limit, with geometry optimized at the CCSD(T)/aV(T+d)Z level.[6] Lowest energy configuration is the *syn* isomer.

(1) Chase, M. W. NIST-JANAF thermochemical tables. *J. Phys. Chem. Ref. Data* **1998**, *Monograph 9*.

(2) Cox, J. D.; Wagman, D. D.; Medvedev, V. A. *CODATA Key Values for Thermodynamics*; Hemisphere Publishing Corp.: New York, 1989.

(3) Degirmenci, I.; Coote, M. L. Effect of substituents on the stability of sulfur-centered radicals. *J. Phys. Chem. A* **2016**, *120*, 7398-7403, doi:10.1021/acs.jpca.6b08223.

(4) Denis, P. A. Theoretical characterization of the thiosulfeno radical, HS_2 *Chem. Phys. Lett.* **2006**, *422*, 434-438, doi:10.1016/j.cplett.2006.02.107.

(5) Frenkel, M.; Kabo, G. J.; Marsh, K. N.; Roganov, G. N.; Wilhoit, R. C. *Thermodynamics of Organic Compounds in the Gas State*; Thermodynamics Research Center: College Station, TX, 1994; Vol. I.

(6) Grant, D. J.; Dixon, D. A.; Francisco, J. S.; Feller, D.; Peterson, K. A. Heats of formation of the $H_{1,2}O_mS_n$ (m,n = 0-3) molecules from electronic structure calculations. *J. Phys. Chem. A* **2009**, *113*, 11343-11353, doi:10.1021/jp905847e.

(7) Lodders, K. Revised and updated thermochemical properties of the gases mercapto (HS), disulfur monoxide (S_2O), thiazyl (NS), and thioxophosphino (PS). *J. Phys. Chem. Ref. Data* **2004**, *33*, 357-367, doi:10.1063/1.1611178.

(8) Nagy, B.; Szakács, P.; Csontos, J.; Rolik, Z.; Tasi, G.; Kallay, M. High-accuracy theoretical thermochemistry of atmospherically important sulfur-containing molecules. *J. Phys. Chem. A* **2011**, *115*, 7823-7833, doi:10.1021/jp203406d.

(9) Resende, S. M.; Ornellas, F. R. Thermochemistry of atmospheric sulfur compounds. *Chem. Phys. Lett.* **2003**, *367*, 489-494, doi:10.1016/S0009-2614(02)01738-4.

Note 72: *Compounds containing S and O* Back to Table

SO Enthalpy value based on the dissociation energy of SO.[4]

SOO Atomization energy calculated by the CCSD(T) extrapolated to the CBS limit, with geometry optimized at the CCSD(T)/aV(n+d)Z (n = D,T,Q,5) level, $\Delta_f H_0^o$ = 49.5 ± 1 kcal mol^{-1}.[3]

SO_2 CODATA Key Value.[2] The JANAF Tables give $\Delta_f H_0^o$ = –294.3 kJ mol^{-1}, $\Delta_f H_{298}^o$ = –296.8 kJ mol^{-1}, and S^o = 248.212 J mol^{-1}.[1]

SO_3 Taken from a review of the literature.[4] The JANAF Tables give $\Delta_f H_0^o$ = –390.0 kJ mol^{-1}, $\Delta_f H_{298}^o$ = –395.8 kJ mol^{-1}, and S^o = 256.769 J mol^{-1}.[1]

SSO Updated and corrected NIST-JANAF thermochemical tables.[5] Atomization energy calculated by the CCSD(T) extrapolated to the CBS limit, with geometry optimized at the CCSD(T)/aV(n+d)Z (n = D,T,Q,5) level gives $\Delta_f H_{298}^o$ = –13.1 ± 1 kcal mol^{-1} and $\Delta_f H_0^o$ = –13.1 ± 1 kcal mol^{-1}.[3]

SOS Atomization energy calculated by the CCSD(T) extrapolated to the CBS limit, with geometry optimized at the CCSD(T)/aV(n+d)Z (n = D,T,Q,5) level.[3]

(1) Chase, M. W. NIST-JANAF thermochemical tables. *J. Phys. Chem. Ref. Data* **1998**, *Monograph 9*.

(2) Cox, J. D.; Wagman, D. D.; Medvedev, V. A. *CODATA Key Values for Thermodynamics*; Hemisphere Publishing Corp.: New York, 1989.

(3) Grant, D. J.; Dixon, D. A.; Francisco, J. S.; Feller, D.; Peterson, K. A. Heats of formation of the $H_{1,2}O_mS_n$ (m,n = 0-3) molecules from electronic structure calculations. *J. Phys. Chem. A* **2009**, *113*, 11343-11353, doi:10.1021/jp905847e.

(4) Gurvich, L. V.; Veyts, I. V.; Alcock, C. B. *Thermodynamic Properties of Individual Substances,*, Fourth ed.; Hemisphere Publishing Corp.: New York, 1991; Vol. 2.

(5) Lodders, K. Revised and updated thermochemical properties of the gases mercapto (HS), disulfur monoxide (S_2O), thiazyl (NS), and thioxophosphino (PS). *J. Phys. Chem. Ref. Data* **2004**, *33*, 357-367, doi:10.1063/1.1611178.

Note 73: *Compounds containing S, H and O* Back to Table

HSO An enthalpy at 0 K determined to be –0.9 ± 0.7 kcal mol^{-1} (–3.8±2.9 kJ mol^{-1}) from crossed beam reactive scattering of O + H_2S.[2] This was the value recommended in the previous Table. In a more recent study, the authors suggested that the lower bound to the uncertainty could be as much as –3 kcal mol^{-1}, but confirmed the upper bound as 0.7 kcal mol^{-1}.[3] A number of computational studies have converged on the significantly lower value presently recommended, which is taken from a study where the atomization energy was calculated by CCSD(T) extrapolated to the CBS limit, with geometry optimized at the CCSD(T)/aV(n+d)Z (n = D,T,Q,5) level.[7] This value was chosen for consistency with the other HxOySz species from the same work included in the table. In a more recent study, at the CCSDT(Q)/cc-pV(T+d)Z level, led to a value of $\Delta_f H_{298}^o$ = –22.6 ± 2.3 kJ mol^{-1}, in close agreement, and to the entropy value cited.[8]

HOS Atomization energy calculated by the CCSD(T) extrapolated to the CBS limit, with geometry optimized at the CCSD(T)/aV(n+d)Z (n = D,T,Q,5) level.[7] In a more recent study, at the CCSDT(Q)/cc-pV(T+d)Z level, led to a value of $\Delta_f H_{298}^o$ = –5.3 ± 2.3 kJ mol^{-1}, in close agreement, and to the entropy value cited.[8]

HSO_2 Enthalpy obtained with DFT calculations on dissociation, atomization, and isodesmic reactions.[5] Value supported by a calculation of the H + SO_2 dissociation asymptote.[1] The latter study shows that HOSO is the more stable configuration, with HSO(O) as a local minimum.

HOSO Atomization energy calculated by the CCSD(T) extrapolated to the CBS limit, with geometry optimized at the CCSD(T)/aV(n+d)Z (n = D,T,Q,5) level.[7] Lowest energy configuration is the

cis isomer. Values for the *trans* isomer are $\Delta_f H^\circ_{298} = -56.2 \pm 1$ kcal mol^{-1} and $\Delta_f H^\circ_0 = -55.1 \pm 1$ kcal mol^{-1}. Another CCSD(T) calculation to the CBS limit, with additional corrections, including correlation through the CBSDT(Q) level, resulted in values for these isomers (identified as the *syn* and *anti* isomers) of $\Delta_f H^\circ_0 = -58.0$ kcal mol^{-1} and $\Delta_f H^\circ_0 = -55.7$ kcal mol^{-1}, respectively.[9]

HSOO Enthalpy for the reaction HOOSH + FOO → HOOF + HSOO at the CCSD(T)/CBS(Q,5) level of theory is 18.00 kcal mol^{-1}. Adjusted for the Table reference values, this gives the cited enthalpy of formation.[7] Lowest energy configuration is the *syn* isomer. Values for the *cis* isomer are $\Delta_f H^\circ_{298} = 29.9 \pm 1$ kcal mol^{-1} and $\Delta_f H^\circ_0 = 31.3 \pm 1$ kcal mol^{-1} and for the *trans* isomer $\Delta_f H^\circ_{298} = 29.8 \pm 1$ kcal mol^{-1} and $\Delta_f H^\circ_0 = 31.2 \pm 1$ kcal mol^{-1}.

HOSH Atomization energy calculated by the CCSD(T) extrapolated to the CBS limit, with geometry optimized at the CCSD(T)/aV(n+d)Z (n = D,T,Q,5) level. $\Delta_f H^\circ_0 = -26.5 \pm 1$ kcal mol^{-1}.[7] Lowest energy configuration is the *syn* isomer. Values for the *trans* isomer are $\Delta_f H^\circ_{298} = -24.3 \pm 1$ kcal mol^{-1} and $\Delta_f H^\circ_0 = -22.7 \pm 1$ kcal mol^{-1} and for the *cis* isomer $\Delta_f H^\circ_{298} = -22.6 \pm 1$ kcal mol^{-1} and $\Delta_f H^\circ_0 = -21.0 \pm 1$ kcal mol^{-1}.

HOOS Enthalpy for the reaction HOOSH + FOO → HOOF + HOOS at the CCSD(T)/CBS(Q,5) level of theory is 5.14 kcal mol^{-1}. Adjusted for the Table reference values, this gives the cited enthalpy of formation, $\Delta_f H^\circ_0 = 15.3 \pm 1.5$ kcal mol^{-1}.[7]

HOOSH Atomization energy calculated by the CCSD(T) extrapolated to the CBS limit, with geometry optimized at the CCSD(T)/aV(T+d)Z level.[7] Lowest energy configuration is the *syn* isomer.

HOSOH Atomization energy calculated by the CCSD(T) extrapolated to the CBS limit, with geometry optimized at the CCSD(T)/aV(T+d)Z level.[7] Lowest energy configuration is the *syn* isomer.

$HOSO_2$ Thermodynamic parameters calculated at the CCSDT(Q)/cc-pV(T+d)Z level of theory.[8] A third-law analysis of equilibrium data for the reaction OH + SO_2 ↔ $HOSO_2$ (extrapolated from data over the temperature range 523 to 603 K) led to $\Delta_f H_{298}^\circ = 373 \pm 6$ kJ mol^{-1}, in good agreement with the computed value.[4]

H_2SO_4 Taken from review of Dorofeeva et al.[6]

HOSS Atomization energy calculated by the CCSD(T) extrapolated to the CBS limit, with geometry optimized at the CCSD(T)/aV(T+d)Z level.[7] Lowest energy configuration is the *cis* isomer. Values for the *trans* isomer are $\Delta_f H^\circ_{298} = -13.6 \pm 1$ kcal mol^{-1} and $\Delta_f H_0^\circ = -12.7 \pm 1$ kcal mol^{-1}.

HSSO Atomization energy calculated by the CCSD(T) extrapolated to the CBS limit, with geometry optimized at the CCSD(T)/aV(T+d)Z level.[7] Lowest energy configuration is the *syn* isomer. Values for the *cis* isomer are $\Delta_f H^\circ_{298} = -9.1 \pm 1$ kcal mol^{-1} and $\Delta_f H_0^\circ = -7.8 \pm 1$ kcal mol^{-1} and for the *trans* isomer $\Delta_f H^\circ_{298} = -8.7 \pm 1$ kcal mol^{-1} and $\Delta_f H_0^\circ = -7.8 \pm 1$ kcal mol^{-1}.

HSOS Enthalpy for the reaction HSOSH + FOO → HOOF + HSOS at the CCSD(T)/CBS(Q,5) level of theory is 8.81 kcal mol^{-1}. Adjusted for the Table reference values, this gives the cited enthalpy of formation.[7] Lowest energy configuration is the *syn* isomer. Values for the *cis* isomer are $\Delta_f H^\circ_{298} = 27.5 \pm 1$ kcal mol^{-1} and $\Delta_f H_0^\circ = 28.9 \pm 1$ kcal mol^{-1} and for the *trans* isomer $\Delta_f H^\circ_{298} = 28.1 \pm 1$ kcal mol^{-1} and $\Delta_f H_0^\circ = 28.9 \pm 1$ kcal mol^{-1}.

HOSSH Atomization energy calculated by the CCSD(T) extrapolated to the CBS limit, with geometry optimized at the CCSD(T)/aV(T+d)Z level.[7] Lowest energy configuration is the *syn* isomer.

HSOSH Atomization energy calculated by the CCSD(T) extrapolated to the CBS limit, with geometry optimized at the CCSD(T)/aV(T+d)Z level.[7] Lowest energy configuration is the *syn* isomer.

(1) Ballester, M. Y.; Varandas, A. J. C. Double many-body expansion potential energy surface for ground state HSO_2. *Phys. Chem. Chem. Phys.* **2005**, *7*, 2305-2317, doi:10.1039/b500990a.

(2) Balucani, N.; Casavecchia, P.; Stranges, D.; Volpi, G. G. The enthalpy of formation of the HSO radical. *Chem. Phys. Lett.* **1993**, *211*, 469-472, doi:10.1016/0009-2614(93)87092-H.

(3) Balucani, N.; Stranges, D.; Casavecchia, P.; Volpi, G. G. Crossed beam studies of the reactions of atomic oxygen in the ground ^3P and first electronically excited ^1D states with hydrogen sulfide. *J. Chem. Phys.* **2004**, *120*, 9571-9582, doi:10.1063/1.1714809.
(4) Blitz, M. A.; Huges, K. J.; Pilling, M. J. Determination of the high-pressure limiting rate coefficient and the enthalpy of reaction for OH + SO_2. *J. Phys. Chem. A* **2003**, *107*, 1971-1978, doi:10.1021/jp026524y.
(5) Denis, P. A.; Ventura, O. N. Density functional investigation of atmospheric sulfur chemistry II. The heat of formation of the XSO_2 radicals X = H, CH_3. *Chem. Phys. Lett.* **2001**, *344*, 221-228, doi:10.1016/S0009-2614(01)00684-4.
(6) Dorofeeva, O.; Iorish, V. S.; Novikov, V. P.; Neumann, D. B. NIST-JANAF thermochemical tables. II. Three molecules related to atmospheric chemistry: HNO_3, H_2SO_4, and H_2O_2. *J. Phys. Chem. Ref. Data* **2003**, *32*, 879-901, doi:10.1063/1.1547435.
(7) Grant, D. J.; Dixon, D. A.; Francisco, J. S.; Feller, D.; Peterson, K. A. Heats of formation of the $H_{1,2}O_mS_n$ (m,n = 0-3) molecules from electronic structure calculations. *J. Phys. Chem. A* **2009**, *113*, 11343-11353, doi:10.1021/jp905847e.
(8) Nagy, B.; Szakács, P.; Csontos, J.; Rolik, Z.; Tasi, G.; Kallay, M. High-accuracy theoretical thermochemistry of atmospherically important sulfur-containing molecules. *J. Phys. Chem. A* **2011**, *115*, 7823-7833, doi:10.1021/jp203406d.
(9) Wheeler, S. E.; Schaefer, H. F. Thermochemistry of the HOSO radical, a key intermediate in fossil fuel combustion. *J. Phys. Chem. A* **2009**, *113*, 6779-6788, doi:10.1021/jp9029387.

Note 74: *Compounds containing S, H, N and O*

Back to Table

***trans*-HSNO**

Thermodynamic parameters calculated at the CCSDT(Q)/cc-pV(T+d)Z level of theory.[2] In an analysis of the fall-off curve for HS + NO → HSNO, a bond strength of 139 kJ mol^{-1} was required to match the experimental data, leading to $\Delta_f H^\circ_{298}$ = 95 kJ mol^{-1}.[1] The expected conformation was not indicated.

***cis*-HSNO** Thermodynamic parameters calculated at the CCSDT(Q)/cc-pV(T+d)Z level of theory.[2]

(1) Black, G.; Patrick, R.; Jusinski, L. E.; Slanger, T. G. Rate coefficients for the reaction HS + NO + M(M = He, Ar, and N_2) over the temperature range 250- 445 K. *J. Chem. Phys.* **1984**, *80*, 4065-4070, doi:10.1063/1.447287.
(2) Nagy, B.; Szakács, P.; Csontos, J.; Rolik, Z.; Tasi, G.; Kallay, M. High-accuracy theoretical thermochemistry of atmospherically important sulfur-containing molecules. *J. Phys. Chem. A* **2011**, *115*, 7823-7833, doi:10.1021/jp203406d.

Note 75: *Compounds containing halogens, S and O or H*

Back to Table

FSH Enthalpy from isodesmic reactions calculated at the MPW1K/6-311G(d,p) with single-point calculations at QCISD(T)/6-311G(3df,2dp).[2]

F_2SO, F_2SO_2, FClSO, $FClSO_2$

The enthalpies were determined from both atomization energies and through isodesmic reactions, after geometric properties were determined by using B3LYP, B1LYP, and mPW1PW91/6-311+G(3df) methods. The isodesmic results using G3, G3B3, CBS-Q, and CBS-QB3 were averaged to yield the recommended values.[1]

(1) Tucceri, M. E.; Badenes, M. P.; Cobos, C. J. Ab initio and density functional theory study of the enthalpies of formation of F_2SO_x and $FClSO_x$ (x=1, 2). *J. Fluorine Chem.* **2002**, *116*, 135-141, doi:10.1016/S0022-1139(02)00123-9.
(2) Wang, L.; Liu, J. Y.; Li, Z. S.; Sun, C. C. Dual-level direct dynamics study on the reactions of SH (SD) with F_2. *Int. J. Chem. Kinet.* **2005**, *37*, 710-716, doi:10.1002/kin.20124.

Note 76: *NS and PS*

Back to Table

NS Updated and corrected NIST-JANAF thermochemical tables.[1] $\Delta_f H_0^o$ = 277.3 ± 2 kJ mol^{-1} and $\Delta_f H_{298}^o$ = 278.0 ± 2 kJ mol^{-1} calculated from three working reactions at the CCSD(T) level of theory, extrapolated to CBS limit, with corrections for anharmonic ZPE, scalar and vector relativistic terms, and core-valence electron correlation.[2]

PS Updated and corrected NIST-JANAF thermochemical tables.[1]

(1) Lodders, K. Revised and updated thermochemical properties of the gases mercapto (HS), disulfur monoxide (S_2O), thiazyl (NS), and thioxophosphino (PS). *J. Phys. Chem. Ref. Data* **2004**, *33*, 357-367, doi:10.1063/1.1611178.

(2) Peebles, L. R.; Marshall, P. A coupled-cluster study of the enthalpy of formation of nitrogen sulfide, NS. *Chem. Phys. Lett.* **2002**, *366*, 520-524, doi:10.1016/S0009-2614(02)01619-6.

Note 77: *Compounds containing one C and S, H*

Back to Table

CS Taken from review of Gurvich et al.[6] The JANAF tables give $\Delta_f H_0^o$ = 277.1 kJ mol^{-1}, $\Delta_f H_{298}^o$ = 280.3 kJ mol^{-1}, and S^o = 210.554 J mol^{-1}.[2]

CS_2 Taken from review of Gurvich et al.[6] The JANAF tables give $\Delta_f H_0^o$ = 116.1 kJ mol^{-1}, $\Delta_f H_{298}^o$ = 116.9 kJ mol^{-1}, and S^o = 237.977 J mol^{-1}.[2]

HCS Enthalpy $\Delta_f H_0^o$ = 71.7 ± 2.0 kcal mol^{-1} obtained from a photoionization study of CH_2S and CHS, obtained by sequential abstraction from CH_3SH.[11] 298 K value from Berkowitz et al.[1]

CH_2S Enthalpy $\Delta_f H_0^o$ = 28.3 ± 2.0 kcal mol^{-1} obtained from a photoionization study of CH_2S and CHS, obtained by sequential abstraction from CH_3SH.[11] Integrated heat capacity from Berkowitz et al.[1]

CH_3S Second- and third-law analysis were utilized to obtain an enthalpy of reaction of –0.14±0.28 kcal mol^{-1} for the reaction Br + CH_3SH ↔ HBr + CH_3S.[8] Enthalpy calculated at the CCSD(T)/CBS level of theory is 29.7 kcal mol^{-1}.[10] DFT calculations support an enthalpy value of 29.78±0.44 kcal mol^{-1}.[4] A computational study of S-centered radicals, with geometry and conformational optimization at the M06-2X/6-31G(d) level of theory and energies determined using the G3(MP2)-RAD composite method, obtained $\Delta_f H_{298}^o$ = 120.6 kJ mol^{-1}, taking CH_3SH and H enthalpy values from the present Table.[3]

CH_2SH A photoionization study[11] leads to a recommended value for H-CH_2SH of 93.9 ± 2.0 kcal mol^{-1}.[1] The enthalpy is from this and the present values for H and CH_3SH. Enthalpy values calculated at the CCSDT(Q)/cc-pV(T+d)Z level of theory give $\Delta_f H_0^o$ = 142.6 kJ mol^{-1} and $\Delta_f H_{298}^o$ = 143.4 kJ mol^{-1}.[7] The entropy value is also from this reference.

CH_3SH Enthalpy from Pedley[9] entropy from Frenkel et al.[5] Enthalpy calculated at the CCSD(T)/CBS level of theory is –5.31 kcal mol^{-1}.[10]

(1) Berkowitz, J.; Ellison, G. B.; Gutman, D. Three methods to measure RH bond energies. *J. Phys. Chem.* **1994**, *98*, 2744-2765, doi:10.1021/j100062a009.

(2) Chase, M. W. NIST-JANAF thermochemical tables. *J. Phys. Chem. Ref. Data* **1998**, *Monograph 9*.

(3) Degirmenci, I.; Coote, M. L. Effect of substituents on the stability of sulfur-centered radicals. *J. Phys. Chem. A* **2016**, *120*, 7398-7403, doi:10.1021/acs.jpca.6b08223.

(4) Denis, P. A.; Ventura, O. N. Density functional investigation of atmospheric sulfur chemistry II. The heat of formation of the XSO_2 radicals X = H, CH_3. *Chem. Phys. Lett.* **2001**, *344*, 221-228, doi:10.1016/S0009-2614(01)00684-4.

(5) Frenkel, M.; Kabo, G. J.; Marsh, K. N.; Roganov, G. N.; Wilhoit, R. C. *Thermodynamics of Organic Compounds in the Gas State*; Thermodynamics Research Center: College Station, TX, 1994; Vol. I.

(6) Gurvich, L. V.; Veyts, I. V.; Alcock, C. B. *Thermodynamic Properties of Individual Substances,*, Fourth ed.; Hemisphere Publishing Corp.: New York, 1991; Vol. 2.

(7) Nagy, B.; Szakács, P.; Csontos, J.; Rolik, Z.; Tasi, G.; Kallay, M. High-accuracy theoretical thermochemistry of atmospherically important sulfur-containing molecules. *J. Phys. Chem. A* **2011**, *115*, 7823-7833, doi:10.1021/jp203406d.
(8) Nicovich, J. M.; Kreutter, K. D.; van Dijk, C. A.; Wine, P. H. Temperature dependent kinetics studies of the reactions $Br(^2P_{3/2}) + H_2S \leftrightarrow SH + HBr$ and $Br(^2P_{3/2}) + CH_3SH \leftrightarrow CH_3S + HBr$. Heats of formation of SH and CH_3S radicals. *J. Phys. Chem.* **1992**, *96*, 2518-2528, doi:10.1021/j100185a025.
(9) Pedley, J. B. *Thermochemical Data and Structures of Organic Compounds*; Thermodynamics Data Center: College Station, TX, 1994.
(10) Resende, S. M.; Ornellas, F. R. Thermochemistry of atmospheric sulfur compounds. *Chem. Phys. Lett.* **2003**, *367*, 489-494, doi:10.1016/S0009-2614(02)01738-4.
(11) Ruscic, B.; Berkowitz, J. Photoionization mass spectrometry of CH_2S and HCS. *J. Chem. Phys.* **1993**, *98*, 2568-2579, doi:10.1063/1.464139.

Note 78: *Compounds containing one C and S, H, O*

Back to Table

CS_2OH The temperature dependence of the equilibrium constant for the reaction $OH + CS_2 \leftrightarrow CS_2OH$ resulted in a heat of reaction of -10.9 ± 1.0 kcal mol^{-1} and an entropy change of -24.0 ± 4.4 cal K^{-1} mol^{-1}.[6]

CH_2SO Thermodynamic parameters calculated at the CCSDT(Q)/cc-pV(T+d)Z level of theory.[7] An enthalpy value of $\Delta_f H_{298}^o = -30$ kJ mol^{-1} was derived from CBS-QB3 calculations on 10 reactions (one isodesmic).[9]

$CH_2S(O)O$ Enthalpy derived from B3PW91 and OBS-QB3 calculations on 3 reactions (one isodesmic).[11]

CH_3SO Derived from an reaction enthalpy of -22.88 kcal mol^{-1} for the isodesmic reaction $CH_3S + SO_3 \rightarrow CH_3SO + SO_2$ calculated at the CCSD(T) level extrapolated to the CBS limit.[8]

$CH_3S(O)O$ Enthalpies of formation determined using five isodesmic reactions, with structures, vibrational frequencies, and rotational energies calculated at the B3LYP/6-311G(2p,d) level of theory, while the enthalpies were calculated at the CBS-QB3 level.[4] Heat of atomization, dissociation, and three isodesmic reactions calculated at the G2(MP2) level of theory gave $\Delta_f H^o_{298} = -211$ kJ mol^{-1}, used in the previous Table.[3] Enthalpy calculated at the CCSD(T)/CBS level of theory is -52.2 kcal mol^{-1}.[8] A DFT estimate gives -56.3 kcal mol^{-1}.[2]

CH_3OSO Heat of atomization, dissociation, and two isodesmic reactions calculated at the G2(MP2) level of theory to yield the enthalpy of formation.[3]

CH_3SOO The equilibrium constant for the reaction $CH_3S + O_2 \leftrightarrow CH_3SOO$ was measured between 216 to 258 K and resulted in a bond strength of 11.7 ± 0.9 kcal mol^{-1}.[10]

CH_3SO_3 Computations leading to the equilibrium constant for the reaction $CH_3 + SO_3 \rightarrow CH_3SO_3$ are discussed in Table 3.1 of Section 3 of this report. The selected enthalpy value was obtained from the calculated value of ΔrH0 = 78 kJ mol−1 obtained by Zhu, et al.12 by using the CBS-QB3 composite method. This group also obtained a value of ΔrH0 = 59.5 kJ mol−1 using CCST(T)/6-311++G(3df,2p). The entropy value is taken from Table 3 of Section X, as is the estimated uncertainty in the enthalpy value. Other theoretical calculations leading to the enthalpy of CH3SO3 are also discussed in that Table.

$CH_2S(O)OH$ and $CH_3S(O)OH$
Enthalpies of formation determined using five isodesmic reactions, with structures, vibrational frequencies, and rotational energies calculated at the B3LYP/6-311G(2p,d) level of theory, while the enthalpies were calculated at the CBS-QB3 level.[4]

OCS Taken from review of Gurvich et al.[5] The JANAF Tables give $\Delta_f H_0^o = -138.5$ kJ mol^{-1}, $\Delta_f H_{298}^o = -138.4$ kJ mol^{-1}, and $S^o = 231.581$ J mol^{-1}.[1]

SCSOH and S_2COH

Thermodynamic parameters calculated at the CCSDT(Q)/cc-pV(T+d)Z level of theory [7]

(1) Chase, M. W. NIST-JANAF thermochemical tables. *J. Phys. Chem. Ref. Data* **1998**, *Monograph 9*.

(2) Denis, P. A.; Ventura, O. N. Density functional investigation of atmospheric sulfur chemistry II. The heat of formation of the XSO_2 radicals X = H, CH_3. *Chem. Phys. Lett.* **2001**, *344*, 221-228, doi:10.1016/S0009-2614(01)00684-4.

(3) Frank, A. J.; Turecek, F. Methylsulfonyl and methoxysulfinyl radicals and cations in the gas phase. A variable-time and photoexcitation neutralization-reionization mass spectrometric and ab initio/RRKM study. *J. Phys. Chem. A* **1999**, *103*, 5348-5361, doi:10.1021/jp990946z.

(4) Gunturu, A.; Asatryan, R.; Bozzelli, J. W. Thermochemistry, bond energies and internal rotor barriers of methyl sulfinic acid, methyl sulfinic acid ester and their radicals. *J. Phys. Org. Chem.* **2011**, *24*, 366-377, doi:10.1002/poc.1766.

(5) Gurvich, L. V.; Veyts, I. V.; Alcock, C. B. *Thermodynamic Properties of Individual Substances,*, Fourth ed.; Hemisphere Publishing Corp.: New York, 1991; Vol. 2.

(6) Murrells, T. P.; Lovejoy, E. R.; Ravishankara, A. R. Oxidation of CS_2 by reaction with OH. 1. Equilibrium constant for the reaction OH + CS_2 ⇄ CS_2OH and the kinetics of the CS_2OH + O_2 reaction. *J. Phys. Chem.* **1990**, *94*, 2381-2386, doi:10.1021/j100369a036.

(7) Nagy, B.; Szakács, P.; Csontos, J.; Rolik, Z.; Tasi, G.; Kallay, M. High-accuracy theoretical thermochemistry of atmospherically important sulfur-containing molecules. *J. Phys. Chem. A* **2011**, *115*, 7823-7833, doi:10.1021/jp203406d.

(8) Resende, S. M.; Ornellas, F. R. Thermochemistry of atmospheric sulfur compounds. *Chem. Phys. Lett.* **2003**, *367*, 489-494, doi:10.1016/S0009-2614(02)01738-4.

(9) Ruttink, P. J. A.; Burgers, P. C.; Trikoupis, M. A.; Terlouw, J. K. The heat of formation of sulfine, CH_2=S=O, revisited: a CBS-QB3 study. *Chem. Phys. Lett.* **2001**, *342*, 447-451, doi:10.1016/S0009-2614(01)00610-8.

(10) Turnipseed, A. A.; Barone, S. B.; Ravishankara, A. R. Observation of CH_3S addition to O_2 in the gas phase. *J. Phys. Chem.* **1992**, *96*, 7502-7505, doi:10.1021/j100198a006.

(11) Ventura, O. N.; Kieninger, M.; Denis, P. A. Density functional computational thermochemistry: Determination of the enthalpy of formation of methanethial-S,S-dioxide (sulfene). *J. Phys. Chem. A* **2003**, *107*, 518-521, doi:10.1021/jp021661g.

(12) Zhu, B.; Zeng, X.; Beckers, H.; Francisco, J. S.; Willner, H. The methylsulfonyloxyl radical, CH_3SO_3. In *Angew. Chem. Int. Ed.*, 2015; Vol. 54; pp 11404-11408.

Note 79: *Compounds containing two C and S, H*

Back to Table

CH_3SCH_2 An analysis of the equilibrium constant for the reaction Br + CH_3SCH_3 ↔ HBr + CH_3SCH_2 resulted in a heat of reaction of 6.11 ± 1.37 kcal mol^{-1},[3] which was combined with present enthalpy values.

CH_3SCH_3 Enthalpy value from Pedley,[4] entropy value from Frenkel et al.[2]

CH_3SSCH_3 Enthalpy value from Pedley,[4] entropy value from Frenkel et al.[2]

C_2H_5S Enthalpy value determined from a computational study of S-centered radicals, with geometry and conformational optimization at the M06-2X/6-31G(d) level of theory and energies determined using the G3(MP2)-RAD composite method, taking C_2H_5SH and H enthalpy values from the present Table.[1]

C_2H_5SH Enthalpy value from Pedley.[4]

$HSCH_2CH_2SH$, 1,2-ethanedithiol
Enthalpy value from Pedley.[4]

(1) Degirmenci, I.; Coote, M. L. Effect of substituents on the stability of sulfur-centered radicals. *J. Phys. Chem. A* **2016**, *120*, 7398-7403, doi:10.1021/acs.jpca.6b08223.

(2) Frenkel, M.; Kabo, G. J.; Marsh, K. N.; Roganov, G. N.; Wilhoit, R. C. *Thermodynamics of Organic Compounds in the Gas State*; Thermodynamics Research Center: College Station, TX, 1994; Vol. I.
(3) Jefferson, A.; Nicovich, J. M.; Wine, P. H. Temperature-dependent kinetics studies of the reactions $Br(^2P_{3/2}) + CH_3SCH_3 \leftrightarrow CH_3SCH_2 + HBr$. Heat of formation of the CH_3SCH_2 radical. *J. Phys. Chem.* **1994**, *98*, 7128-7135, doi:10.1021/j100080a006.
(4) Pedley, J. B. *Thermochemical Data and Structures of Organic Compounds*; Thermodynamics Data Center: College Station, TX, 1994.

Note 80: *Compounds containing two C and S, H,O*

Back to Table

$CH_3S(O)CH_3$, dimethyl sulfoxide
Enthalpy value from Pedley.[2]

$CH_3S(O)OCH_3$
Enthalpies of formation determined using five isodesmic reactions, with structures, vibrational frequencies, and rotational energies calculated at the B3LYP/6-311G(2p,d) level of theory, while the enthalpies were calculated at the CBS-QB3 level.[1]

$CH_3C(O)SH$, ethanethioic acid
Enthalpy value from Pedley.[2]

(1) Gunturu, A.; Asatryan, R.; Bozzelli, J. W. Thermochemistry, bond energies and internal rotor barriers of methyl sulfinic acid, methyl sulfinic acid ester and their radicals. *J. Phys. Org. Chem.* **2011**, *24*, 366-377, doi:10.1002/poc.1766.
(2) Pedley, J. B. *Thermochemical Data and Structures of Organic Compounds*; Thermodynamics Data Center: College Station, TX, 1994.

Note 81: *Compounds containing Li*

Back to Table

Li CODATA Key Value.[2] The Lamoreaux and Hildenbrand review gives $\Delta_f H^\circ_{298}$ = 159.4±0.4 kJ mol^{-1} and S° = 138.69 J mol^{-1}.[4]

Li_2 Enthalpy and entropy values from the JANAF tables, adopting the $\Delta_f H^\circ_{298}$ value from the NBS table.[1] The Lamoreaux and Hildenbrand review gives $\Delta_f H^\circ_{298}$ = 214.9 ± 1.2 kJ mol^{-1} and S° = 96.89 J mol^{-1}.[4]

LiH Enthalpy and entropy values from the JANAF tables. A calculation of the atomization energy at the CCSD(T) level, extrapolated to the CBS limit, leads to $\Delta_f H^\circ_{298}$ = 138.9 ± 4 kJ mol^{-1} and $\Delta_f H_0^\circ$ = 139.3 ± 4 kJ mol^{-1}.[6]

LiF Enthalpy and entropy values from the JANAF tables.[1] A calculation of the atomization energy at the CCSD(T) level, extrapolated to the CBS limit, leads to $\Delta_f H^\circ_{298}$ = –340.6 ± 4 kJ mol^{-1} and $\Delta_f H_0^\circ$ = –340.6 ± 4 kJ mol^{-1}.[6]

LiCl Enthalpy and entropy values from the JANAF tables.[1] A calculation of the atomization energy at the CCSD(T) level, extrapolated to the CBS limit, leads to $\Delta_f H^\circ_{298}$ = –192.9 ± 4 kJ mol^{-1} and $\Delta_f H_0^\circ$ = –192.9 ± 1 kJ mol^{-1}.[6]

LiBr Enthalpy and entropy values from the JANAF tables.[1]

LiOH From an extensive evaluation from the Thermocenter of the RAS.[3] The JANAF Tables give $\Delta_f H_0^\circ$ = –234 ± 6 kJ mol^{-1}, $\Delta_f H_{298}^\circ$ = –234 ± 4 kJ mol^{-1}, and S° = 210.66 ± 2.1 J mol^{-1}.[1] A calculation of the atomization energy at the CCSD(T) level, extrapolated to the CBS limit, leads to $\Delta_f H^\circ_{298}$ = –239.7 ± 4 kJ mol^{-1} and $\Delta_f H_0^\circ$ = –237.7 ± 1 kJ mol^{-1}.[6]

LiO The enthalpy is from a calculation of the atomization energy at the CCSD(T) level, extrapolated to the CBS limit. Cited values are for the $^2\Pi$ state. Enthalpy at both 0 K and 298 K for the $^2\Sigma^+$ state is 89.5 ± 4 kJ mol^{-1}.[6] The JANAF values are $\Delta_f H^\circ_{298}$ = 84 ± 21 kJ mol^{-1} and $\Delta_f H_0^\circ$ = 84

± 21 kJ mol^{-1}, and the cited entropy.[1] The Pedley and Marshall review gives $\Delta_f H^{\circ}_{298}$ = 75 ± 8 kJ mol^{-1}.[5] The Lamoreaux and Hildenbrand review gives $\Delta_f H^{\circ}_{298}$ = 69.0 ± 4.2 kJ mol^{-1} and S° = 211.11 J mol^{-1}.[4]

LiO_2 and LiO_3
Atomization energy calculated by the CCSD(T) extrapolated to the CBS limit.[6]

Li_2O The enthalpy is from a calculation of the atomization energy at the CCSD(T) level, extrapolated to the CBS limit.[6] The JANAF values, calculated from the enthalpy of the crystal and the enthalpy of sublimation, are $\Delta_f H^{\circ}_{298}$ = −167 ± 10 kJ mol^{-1} and $\Delta_f H_0^{\circ}$ = −166 ± 10 kJ mol^{-1}, and the cited entropy.[1] The Lamoreaux and Hildenbrand review gives $\Delta_f H^{\circ}_{298}$ = −172.8 ± 3.7 kJ mol^{-1} and S° = 229.15 J mol^{-1}.[4]

Li_2SO_4 Enthalpy and entropy values from the JANAF tables.[1]

(1) Chase, M. W. NIST-JANAF thermochemical tables. *J. Phys. Chem. Ref. Data* **1998**, *Monograph 9*.
(2) Cox, J. D.; Wagman, D. D.; Medvedev, V. A. *CODATA Key Values for Thermodynamics*; Hemisphere Publishing Corp.: New York, 1989.
(3) Gurvich, L. V.; Bergman, G. A.; Borokhov, L. N.; Iorish, V. S.; Leonidov, V. Y.; Yungman, V. S. Thermodynamic properties of alkali metal hydroxides. Part 1. Lithium and sodium hydroxides. *J. Phys. Chem. Ref. Data* **1996**, *25*, 1211-1276, doi:10.1063/1.555982.
(4) Lamoreaux, R. H.; Hildenbrand, D. L. High temperature vaporization behavior of oxides. 1. Alkali metal binary oxides. *J. Phys. Chem. Ref. Data* **1984**, *13*, 151-173, doi:10.1063/1.555706.
(5) Pedley, J. B.; Marshall, E. M. Thermochemical data for gaseous monoxides. *J. Phys. Chem. Ref. Data* **1983**, *12*, 967-1032, doi:10.1063/1.555698.
(6) Vasiliu, M.; Li, S. G.; Peterson, K. A.; Feller, D.; Gole, J. L.; Dixon, D. A. Structures and heats of formation of simple alkali metal compounds: Hydrides, chlorides, fluorides, hydroxides and oxides for Li, Na and K. *J. Phys. Chem. A* **2010**, *114*, 4272-4281, doi:10.1021/jp911735c.

Note 82: *Compounds containing Na*

Back to Table

Na CODATA Key Value.[2] The Lamoreaux and Hildenbrand review gives $\Delta_f H^{\circ}_{298}$ = 107.1±0.4 kJ mol^{-1} and S° = 153.57 J mol^{-1}.[4]

Na_2 Enthalpy and entropy values from the JANAF tables.[1]

NaH Enthalpy and entropy values from the JANAF tables.[1]

NaF Enthalpy and entropy values from the JANAF tables.[1] A calculation of the atomization energy at the CCSD(T) level, extrapolated to the CBS limit, leads to $\Delta_f H^{\circ}_{298}$ = –291.6 ± 4 kJ mol^{-1} and $\Delta_f H_0^{\circ}$ = –290.0 ± 4 kJ mol^{-1}.[6]

NaCl Enthalpy and entropy values from the JANAF tables.[1] A calculation of the atomization energy at the CCSD(T) level, extrapolated to the CBS limit, leads to $\Delta_f H^{\circ}_{298}$ = –180.3 ± 4 kJ mol^{-1} and $\Delta_f H_0^{\circ}$ = –178.7 ± 4 kJ mol^{-1}.[6]

NaBr Enthalpy and entropy values from the JANAF tables.[1]

NaOH From an extensive evaluation from the Thermocenter of the RAS.[3] The JANAF Tables give $\Delta_f H^{\circ}_{298}$ = –198 ± 12 J mol^{-1} and $\Delta_f H_0^{\circ}$ = –194 ± 12 J mol^{-1}, and S° = 228.44 1 J mol^{-1}.[1] A calculation of the atomization energy at the CCSD(T) level, extrapolated to the CBS limit, leads to $\Delta_f H^{\circ}_{298}$ = –187.0 ± 4 kJ mol^{-1} and $\Delta_f H_0^{\circ}$ = –184.1 ± 4 kJ mol^{-1}.[6]

NaO The enthalpy is from a calculation of the atomization energy at the CCSD(T) level, extrapolated to the CBS limit.[6] Cited values are for the $^2\Pi$ state. For the $^2\Sigma^+$ state $\Delta_f H^{\circ}_{298}$ = 113.8 ± 4 kJ mol^{-1} and $\Delta_f H_0^{\circ}$ = 115.5 ± 4 kJ mol^{-1}. The JANAF values are $\Delta_f H^{\circ}_{298}$ = 84 ± 40 kJ mol^{-1} and $\Delta_f H_0^{\circ}$ = 85 ± 40 kJ mol^{-1}, and the cited entropy.[1] The Pedley and Marshall review gives $\Delta_f H^{\circ}_{298}$

= 100 ± 17 kJ mol^{-1}.[5] The Lamoreaux and Hildenbrand review gives $\Delta_f H^\circ_{298}$ = 104.6 ± 4.2 kJ mol^{-1} and S° = 228.48 J mol^{-1}.[4]

NaO_2 and NaO_3
Atomization energy calculated by the CCSD(T) extrapolated to the CBS limit.[6]

Na_2O Atomization energy calculated by the CCSD(T) extrapolated to the CBS limit.[6] The Lamoreaux and Hildenbrand review gives $\Delta_f H^\circ_{298}$ = −31.8 ± 3.7 kJ mol^{-1} and the cited entropy.[4]

Na_2SO_4 Enthalpy and entropy values from the JANAF tables.[1]

(1) Chase, M. W. NIST-JANAF thermochemical tables. *J. Phys. Chem. Ref. Data* **1998**, *Monograph 9*.
(2) Cox, J. D.; Wagman, D. D.; Medvedev, V. A. *CODATA Key Values for Thermodynamics*; Hemisphere Publishing Corp.: New York, 1989.
(3) Gurvich, L. V.; Bergman, G. A.; Borokhov, L. N.; Iorish, V. S.; Leonidov, V. Y.; Yungman, V. S. Thermodynamic properties of alkali metal hydroxides. Part 1. Lithium and sodium hydroxides. *J. Phys. Chem. Ref. Data* **1996**, *25*, 1211-1276, doi:10.1063/1.555982.
(4) Lamoreaux, R. H.; Hildenbrand, D. L. High temperature vaporization behavior of oxides. 1. Alkali metal binary oxides. *J. Phys. Chem. Ref. Data* **1984**, *13*, 151-173, doi:10.1063/1.555706.
(5) Pedley, J. B.; Marshall, E. M. Thermochemical data for gaseous monoxides. *J. Phys. Chem. Ref. Data* **1983**, *12*, 967-1032, doi:10.1063/1.555698.
(6) Vasiliu, M.; Li, S. G.; Peterson, K. A.; Feller, D.; Gole, J. L.; Dixon, D. A. Structures and heats of formation of simple alkali metal compounds: Hydrides, chlorides, fluorides, hydroxides and oxides for Li, Na and K. *J. Phys. Chem. A* **2010**, *114*, 4272-4281, doi:10.1021/jp911735c.

Note 83: *Compounds containing K*

Back to Table

K CODATA Key Value.[2] The Lamoreaux and Hildenbrand review gives $\Delta_f H^\circ_{298}$ = 89.2 ± 0.2 kJ mol^{-1} and the cited entropy.[4]

KH Enthalpy and entropy values from the JANAF tables.[1] A calculation of the atomization energy at the CCSD(T) level, extrapolated to the CBS limit, leads to $\Delta_f H^\circ_{298}$ = 132.2 ± 4 kJ mol^{-1} and $\Delta_f H_0^\circ$ = 134.7 ± 4 kJ mol^{-1}.[6]

KF Enthalpy and entropy values from the JANAF tables.[1] A calculation of the atomization energy at the CCSD(T) level, extrapolated to the CBS limit, leads to $\Delta_f H^\circ_{298}$ = –326.8 ± 4 kJ mol^{-1} and $\Delta_f H_0^\circ$ = –324.7 ± 4 kJ mol^{-1}.[6]

KCl Enthalpy and entropy values from the JANAF tables.[1] A calculation of the atomization energy at the CCSD(T) level, extrapolated to the CBS limit, leads to $\Delta_f H^\circ_{298}$ = –215.5 ± 4 kJ mol^{-1} and $\Delta_f H_0^\circ$ = –213.4 ± 4 kJ mol^{-1}.[6]

KBr Enthalpy and entropy values from the JANAF tables.[1]

KOH From an extensive evaluation from the Thermocenter of the RAS.[3] The JANAF Tables give $\Delta_f H^\circ_{298}$ = –233 ± 12 J mol^{-1} and $\Delta_f H_0^\circ$ = –228 ± 12 J mol^{-1}, and S° = 236.379 ± 1.31 J mol^{-1}.[1] A calculation of the atomization energy at the CCSD(T) level, extrapolated to the CBS limit, leads to $\Delta_f H^\circ_{298}$ = –221.8 ± 4 kJ mol^{-1} and $\Delta_f H_0^\circ$ = –218.0 ± 4 kJ mol^{-1}.[6]

KO The enthalpy is from a calculation of the atomization energy at the CCSD(T) level, extrapolated to the CBS limit.[6] Cited values are for the $^2\Pi$ state. For the $^2\Sigma^+$ state $\Delta_f H^\circ_{298}$ = 59.8 ± 4 kJ mol^{-1} and $\Delta_f H_0^\circ$ = 61.9 ± 4 kJ mol^{-1}. The JANAF values are $\Delta_f H^\circ_{298}$ = 71 ± 40 kJ mol^{-1} and $\Delta_f H_0^\circ$ = 73 ± 40 kJ mol^{-1}, and the cited entropy.[1] The Pedley and Marshall review gives $\Delta_f H^\circ_{298}$ = 61 ± 21 kJ mol^{-1}.[5] The Lamoreaux and Hildenbrand review gives $\Delta_f H^\circ_{298}$ = 59.9 ± 4.2 kJ mol^{-1} and S° = 237.88 J mol^{-1}.[4]

KO_2 and KO_3

Atomization energy calculated by the CCSD(T) extrapolated to the CBS limit.[6]

K_2O Atomization energy calculated by the CCSD(T) extrapolated to the CBS limit.[6] The Lamoreaux and Hildenbrand review gives $\Delta_f H^\circ_{298}$ = -58.61 ± 2.2 kJ mol^{-1} and the cited entropy.[4]

K_2SO_4 Enthalpy and entropy values from the JANAF tables.[1]

(1) Chase, M. W. NIST-JANAF thermochemical tables. *J. Phys. Chem. Ref. Data* **1998**, *Monograph 9*.

(2) Cox, J. D.; Wagman, D. D.; Medvedev, V. A. *CODATA Key Values for Thermodynamics*; Hemisphere Publishing Corp.: New York, 1989.

(3) Gurvich, L. V.; Bergman, G. A.; Borokhov, L. N.; Iorish, V. S.; Leonidov, V. Y.; Yungman, V. S. Thermodynamic properties of alkali metal hydroxides. Part II. Potassium, rubidium, and cesium hydroxides. *J. Phys. Chem. Ref. Data* **1997**, *26*, 1031-1110, doi:10.1063/1.555996.

(4) Lamoreaux, R. H.; Hildenbrand, D. L. High temperature vaporization behavior of oxides. 1. Alkali metal binary oxides. *J. Phys. Chem. Ref. Data* **1984**, *13*, 151-173, doi:10.1063/1.555706.

(5) Pedley, J. B.; Marshall, E. M. Thermochemical data for gaseous monoxides. *J. Phys. Chem. Ref. Data* **1983**, *12*, 967-1032, doi:10.1063/1.555698.

(6) Vasiliu, M.; Li, S. G.; Peterson, K. A.; Feller, D.; Gole, J. L.; Dixon, D. A. Structures and heats of formation of simple alkali metal compounds: Hydrides, chlorides, fluorides, hydroxides and oxides for Li, Na and K. *J. Phys. Chem. A* **2010**, *114*, 4272-4281, doi:10.1021/jp911735c.

Note 84: *Compounds containing Hg and H or O*

Back to Table

Hg^0 CODATA key values,[2] with the 0 K value calculated in JANAF.[1] The NBS Tables give $\Delta_f H^0$(298 K) = 61.32 kJ mol^{-1} and S^0 = 179.03 J mol^{-1} K^{-1}.[11] The review of Hepler and Olofsson accept the NBS value, but also discuss some more recent vapor pressure measurements.[6]

HgH Chosen values from the JANAF Table,[1] based on results reported by Herzberg.[7] Also selected by Hepler and Olofsson.[6] The NBS Tables give $\Delta_f H^0$(298 K) = 239.32 kJ mol^{-1} and S^0 = 219.49 J mol^{-1}K^{-1}.[11] A calculation using NESC/CCSD(T) in combination with triple-zeta basis sets, gave BDE = 38.5 kJ mol^{-1}, which leads to $\Delta_f H^0$(0 K) = 238.76 kJ mol^{-1}.[3]

HgH_2 The cited enthalpy values are an average of those calculated for the atomization energy and for the bond-dissociation reaction, $HgH_2 \rightarrow HgH + H$, both done at the NESC/B3LYP level of theory.[3]

HgO The selected enthalpy of formation is derived from computational determinations of the bond dissociation energy. Dissociation from both the $^1\Sigma^+$ (to Hg^1S and O^1D) and $^3\Pi$ (to Hg^1S and O^3P) states of HgO have been reported, with some disagreement about which is the ground state. From a relativistically-corrected MP4/CCSD(T) calculation, D_0 = 9.2 kJ mol^{-1} from a triplet ground state by Filatov and Cremer.[4] A subsequent study from the same group, adding the normalized elimination of the small component technique to improve the treatment of scalar relativistic effects, found the $^3\Pi$ state 5.4 kJ mol^{-1} lower than the $^1\Sigma^+$ state, and also calculated BDEs of 16.1 kJ mol^{-1} along the triplet surface and 202.9 kJ mol^{-1} along the singlet surface, both adjusted to 298 K.[3] At 0 K, the calculated triplet BDE was 14.6 kJ mol^{-1}. In contrast, a MRCI + Q/CBS level calculation by Peterson et al.[8] found a singlet ground state and computed a BDE of 203.3 kJ mol^{-1} at 0 K. This result is in agreement with earlier calculations from the same laboratory which resulted in a BDE to ground-state atoms of 17 and 19.1 kJ mol^{-1}.[9,10]

There has been an experimental determination of the dissociation energy of HgO by using high-temperature mass spectrometry.[5] In strong disagreement with the computational studies, a value of 222±33 kJ mol^{-1} was determined. Filatov and Cremer[4] have made a compelling case that the species detected in the mass spectrometer being a dimer, either or both HgO_2Hg and OHg_2O. There is clearly a great need for additional experimental work on HgO, but at this point, we accept the theoretical argument.

(1) Chase, M. W. NIST-JANAF thermochemical tables. *J. Phys. Chem. Ref. Data* **1998**, *Monograph 9*.
(2) Cox, J. D.; Wagman, D. D.; Medvedev, V. A. *CODATA Key Values for Thermodynamics*; Hemisphere Publishing Corp.: New York, 1989.
(3) Cremer, D.; Kraka, E.; Filatov, M. Bonding in mercury molecules described by the normalized elimination of the small component and coupled cluster theory. *ChemPhysChem* **2008**, *9*, 2510-2521, doi:10.1002/cphc.200800510.
(4) Filatov, M.; Cremer, D. Revision of the dissociation energies of mercury chalcogenides—unusual types of mercury bonding. *ChemPhysChem* **2004**, *5*, 1547-1557, doi:10.1002/cphc.200301207.
(5) Grade, M.; Hirschwald, W. Energetics and stabilities of the IIB/VIA-compounds at high-temperature equilibrium conditions. *Ber. Bunsen. Phys. Chem.* **1982**, *86*, 899-907, doi:10.1002/bbpc.19820861006.
(6) Hepler, L. G.; Olofsson, G. Mercury: Thermodynamic properties, chemical equilibria, and standard potentials *Chem. Rev.* **1975**, *75*, 585-602, doi:10.1021/cr60297a003.
(7) Herzberg, G. *Molecular Spectra and Molecular Structure. Vol.1: Spectra of Diatomic Molecules*; Van Nortrand Reinhold, 1950.
(8) Peterson, K. A.; Shepler, B. C.; Singleton, J. M. The group 12 metal chalcogenides: an accurate multireference configuration interaction and coupled cluster study. *Mol. Phys.* **2007**, *105*, 1139-1155, doi:10.1080/00268970701241664.
(9) Shepler, B. C.; Balabanov, N. B.; Peterson, K. A. Ab initio thermochemistry involving heavy atoms: An investigation of the reactions Hg + IX (X = I, Br, Cl, O). *J. Phys. Chem. A* **2005**, *109*, 10363-10372, doi:10.1021/jp0541617.
(10) Shepler, B. C.; Peterson, K. A. Mercury monoxide: A systematic investigation of its ground electronic state. *J. Phys. Chem. A* **2003**, *107*, 1783-1787, doi:10.1021/jp027512f.
(11) Wagman, D. D.; Evans, W. H.; Parker, V. B.; Schumm, R. H.; Halow, I.; Bailey, S. M.; Churney, K. L.; Nutall, R. L. The NBS tables of chemical thermodynamic properties. Selected values for inorganic and C_1 and C_2 organic substances in SI unites. *J. Phys. Chem. Ref. Data* **1982**, *11*, Suppl. No. 1, Erratum doi:10.1063/1.555845.

Note 85: *Mono- and Di-halides of Hg*

Back to Table

HgF, HgCl, HgBr, HgI, HgF_2, $HgCl_2$, $HgBr_2$, HgI_2

At this time, we accept the JANAF values.[3] More recent experimental and computational results scatter around these values, with no clear pattern. These are discussed below.

HgF The JANAF enthalpy value has a stated uncertainty of ±50 kJ mol^{-1}. We have reduced this to ±20 kJ mol^{-1} in light of the additional results discussed below. The JANAF enthalpy value leads to a BDE of 134 ± 20 kJ mol^{-1} at 0 K. A MP4/CCSD(T) calculation, including a normalized elimination of the small component (NESC) technique to improve the treatment of scalar relativistic effects, resulted in a BDE of 129 kJ mol^{-1},[4] while another CCSD(T) study led to values of 137 and 115 kJ mol^{-1} with the CRENBL and AVTZ-PP relativistic effective core potentials, respectively.[6]

HgCl The JANAF enthalpy value leads to a BDE of 102 ± 10 kJ mol^{-1} at 0 K. A reanalysis of the spectral data suggested a value of ~106 kJ mol^{-1}.[9] A more recent spectral study led to an upper limit on the BDE of 98 kJ mol^{-1},[8] although an analysis of these data by using empirical potential energy functions led to BDE = 107 kJ mol^{-1}.[2] Computational results tend to be lower: A CCSD(T)/CBS with relativistic pseudopotentials, corrected for spin-orbit coupling, gave a BDE of 96 kJ mol^{-1},[7] whereas a MP4/CCSD(T) calculation, including a normalized elimination of the small component (NESC) technique to improve the treatment of scalar relativistic effects, resulted in a BDE of 89.5 kJ mol^{-1}.[4] Another CCSD(T) study led to values of 94 and 78 kJ mol^{-1} with the CRENBL and AVTZ-PP relativistic effective core potentials, respectively.[6]

HgBr The JANAF enthalpy value has a stated uncertainty of ±38 kJ mol^{-1}. We have reduced this to ±10 kJ mol^{-1} in light of the additional results discussed below. The JANAF enthalpy value leads to a BDE of 67±10 kJ mol^{-1} at 0 K. A reanalysis of the spectral data suggested a value of ~72

kJ mol^{-1}.[9] A more recent spectral study led to a BDE of 66.1 kJ mol^{-1},[8] although an analysis of these data by using empirical potential energy functions led to BDE = 61.75 kJ mol^{-1}.[2] A CCSD(T)/CBS with relativistic pseudopotentials, corrected for spin-orbit coupling, gave a BDE of 68 kJ mol^{-1},[7] whereas a MP4/CCSD(T) calculation, including a normalized elimination of the small component (NESC) technique to improve the treatment of scalar relativistic effects, resulted in a BDE of 60 kJ mol^{-1}.[4] Another CCSD(T) study led to values of 21 and 59 kJ mol^{-1} with the CRENBL and AVTZ-PP relativistic effective core potentials, respectively.[6] A slightly different BDE of 66.3 kJ mol^{-1} was used in the analysis of the equilibrium constant data in Table 3-1, Note 33.

HgI The JANAF enthalpy value leads to a BDE of 32.9 ± 5 kJ mol^{-1} at 0 K. A reanalysis of the spectral data suggested a value of 37.3 kJ mol^{-1}.[9] A more recent spectral study led to a BDE of 33.5 kJ mol^{-1},[8] although an analysis of these data by using empirical potential energy functions led to BDE = 37.3 kJ mol^{-1}.[2] A CCSD(T)/CBS calculation with relativistic pseudopotentials, corrected for spin-orbit coupling,[7] gave a BDE of 36 kJ mol^{-1} whereas a MP4/CCSD(T) calculation, including the normalized elimination of the small component (NESC) technique to improve the treatment of scalar relativistic effects, resulted in a BDE of 46 kJ mol^{-1}.[4] Another CCSD(T) study led to values of 15 and 38.5 kJ mol^{-1} with the CRENBL and AVTZ-PP relativistic effective core potentials, respectively.[6]

HgF_2 In this case, the values listed in the JANAF Table are estimated. Enthalpy values have been calculated for the atomization energy and for the bond-dissociation reaction, $HgF_2 \rightarrow HgF + F$ at the NESC/B3LYP level of theory, leading to average values of $\Delta_fH^0(298\ K) = -288$ kJ mol^{-1} and $\Delta_fH^0(0\ K) = -296$ kJ mol^{-1}.[4] A CCSD(T) study led to $\Delta_fH^0(0\ K) = -302$ and -285 kJ mol^{-1} with the CRENBL and AVTZ-PP relativistic effective core potentials, respectively.[6]

$HgCl_2$ The values listed in the JANAF Table are based on a third-law analysis. A CCSD(T) calculation utilizing small-core relativistic effective core potentials for the reaction $Hg + Cl_2 \rightarrow HgCl_2$ led to $\Delta_fH^0(0\ K) = -139$ kJ mol^{-1}.[1] Another CCSD(T) study led to $\Delta_fH^0(0\ K) = -134$ and -122 kJ mol^{-1} with the CRENBL and AVTZ-PP relativistic effective core potentials, respectively.[6] A third CCSD(T) study, with the ECP60MDF relativistic core potential and B3LYP/aVTZ structures gave -135 kJ mol^{-1}.[5]

$HgBr_2$ The values listed in the JANAF Table are based on a third-law analysis. A CCSD(T) calculation utilizing small-core relativistic effective core potentials for the reaction $Hg + Br_2 \rightarrow HgBr_2$ led to $\Delta_fH^0(0\ K) = -67$ kJ mol^{-1}.[1] Another CCSD(T) study led to $\Delta_fH^0(0\ K) = -42$ and -34 kJ mol^{-1} with the CRENBL and AVTZ-PP relativistic effective core potentials, respectively.[6] A third CCSD(T) study, with the ECP60MDF relativistic core potential and B3LYP/aVTZ structures gave $\Delta_fH^0(0\ K) = -81$ kJ mol^{-1}.[5]

HgI_2 The values listed in the JANAF Table are based on a third-law analysis. A calculated enthalpy for the reaction $HgI_2 \rightarrow Hg + I_2$ at the CCSD(T)/CBS limit with corrections for core-valence correlation, spin-orbit coupling, Lamb shift, and scalar relativity leads to the value $\Delta_fH^0(0\ K) = -16$ kJ mol^{-1}.[7] Another CCSD(T) study led to $\Delta_fH^0(0\ K) = 9.6$ and 20 kJ mol^{-1} with the CRENBL and AVTZ-PP relativistic effective core potentials, respectively.[6]

(1) Balabanov, N. B.; Peterson, K. A. Mercury and reactive halogens: The thermochemistry of Hg + (Cl_2, Br_2, BrCl, ClO, and BrO). *J. Phys. Chem. A* **2003**, *107*, 7465-7470, doi:10.1021/jp035547p.

(2) Bhartiya, J. B.; Behere, S. H.; Rao, M. L. P. Dissociation energies of HgCl, HgBr and HgI from potential energy curves. *J. Quant. Spec. Radiat. Transf,* **1990**, *43*, 95-98, doi:10.1016/0022-4073(90)90070-M.

(3) Chase, M. W. NIST-JANAF thermochemical tables. *J. Phys. Chem. Ref. Data* **1998**, *Monograph 9*.

(4) Cremer, D.; Kraka, E.; Filatov, M. Bonding in mercury molecules described by the normalized elimination of the small component and coupled cluster theory. *ChemPhysChem* **2008**, *9*, 2510-2521, doi:10.1002/cphc.200800510.

(5) Dibble, T. S.; Zelie, M. J.; Mao, H. Thermodynamics of reactions of ClHg and BrHg radicals with atmospherically abundant free radicals. *Atmos. Chem. Phys.* **2012**, *12*, 10271-10279, doi:10.5194/acp-12-10271-2012.
(6) Kim, J.; Ihee, H.; Lee, Y. S. Spin-orbit density functional and *ab initio* study of HgX_n (X = F, Cl, Br, and I; *n* = 1, 2, and 4). *J. Chem. Phys.* **2010**, *133*, 144309, doi:10.1063/1.3497189.
(7) Shepler, B. C.; Balabanov, N. B.; Peterson, K. A. Ab initio thermochemistry involving heavy atoms: An investigation of the reactions Hg + IX (X = I, Br, Cl, O). *J. Phys. Chem. A* **2005**, *109*, 10363-10372, doi:10.1021/jp0541617.
(8) Tellinghuisen, J.; Tellinghuisen, P. C.; Davies, S. A.; Berwanger, P.; Viswanathan, K. S. B → X transitions in HgCI and HgI. *Appl. Phys. Lett.* **1982**, *41*, 789-791, doi:10.1063/1.93704.
(9) Wilcomb, B. E.; Bernstein, R. B. Dissociation energies of ground-state HgX molecules (X = I, Br, Cl) from analysis of vibrational level spacings. *J. Molec. Spectrosc.* **1976**, *62*, 442-448, doi:10.1016/0022-2852(76)90282-4.

Note 86: *Mixed di-halides of Hg*

Back to Table

ClHgBr, ClHgI, BrHgI

The mixed di-halides of mercury. 0 K enthalpy values from calculated reaction enthalpies at the CCSD(T)/CBS limit with corrections for core-valence correlation, spin-orbit coupling, Lamb shift, and scalar relativity.[1] The enthalpy value for HgI_2 in this study is about 6.5 kJ mol^{-1} lower than that selected above. Entropy values from NBS 270-4.[2]

(1) Shepler, B. C.; Balabanov, N. B.; Peterson, K. A. Ab initio thermochemistry involving heavy atoms: An investigation of the reactions Hg + IX (X = I, Br, Cl, O). *J. Phys. Chem. A* **2005**, *109*, 10363-10372, doi:10.1021/jp0541617.
(2) Wagman, D. D.; Evans, W. H.; Parker, V. B.; Halow, I.; Bailey, S. M.; Schumm, R. H. Selected Values of Chemical Thermodynamic Properties. Tables for Elements 35 through 53 in the Standard Order of Arrangement. *NBS Technical Note 270-4* **1969**.

Note 87: *Compounds containing Hg, a halogen, and O*

Back to Table

IHgO 0 K enthalpy value from calculated reaction enthalpies at the CCSD(T)/CBS limit with corrections for core-valence correlation, spin-orbit coupling, Lamb shift, and scalar relativity.[1]

(1) Shepler, B. C.; Balabanov, N. B.; Peterson, K. A. Ab initio thermochemistry involving heavy atoms: An investigation of the reactions Hg + IX (X = I, Br, Cl, O). *J. Phys. Chem. A* **2005**, *109*, 10363-10372, doi:10.1021/jp0541617.

Note 88: *Addition compounds formed in the reactions of HgCl and HgBr with free radicals*.

Back to Table

Bond energies obtained at the CCSD(T) level of theory with the ECP60MDF relativistic core potential and B3LYP/aVTZ structures. Results at the B3LP and CCSD levels also reported.[1] The same set of calculation led to $\Delta_f H^0(0\ K) = -135$ and -81 kJ mol^{-1} for $HgCl_2$ and $HgBr_2$, respectively.

(1) Dibble, T. S.; Zelie, M. J.; Mao, H. Thermodynamics of reactions of ClHg and BrHg radicals with atmospherically abundant free radicals. *Atmos. Chem. Phys.* **2012**, *12*, 10271-10279, doi:10.5194/acp-12-10271-2012.

Note 89: *Organo-mercury compounds*

Back to Table

$HgCH_3$ From a calculation carried out at the RCCSD(T)//QCISD/A level of theory.[1] The NBS Table recommends a value of 168 kJ mol^{-1}.[3]

$Hg(CH_3)_2$ Enthalpy of formation taken from a review of experimental studies.[2] The NBS Table recommends a value of 94.8 kJ mol^{-1}.[3] This was also the source of the entropy value.

$Hg(C_2H_5)_2$ Enthalpy of formation taken from a review of experimental studies.[2] The NBS Table recommends a value of 75.3 kJ mol^{-1}.[3]

(1) Lee, E. P. F.; Wright, T. G. Thermochemistry of $HgCH_3$ and $HgCH_3^+$ and the ionization energy of $HgCH_3$. *Chem. Phys. Lett.* **2003**, *376*, 418-423, doi:10.1016/S0009-2614(03)01022-4.

(2) Skinner, H. A. The strengths of metal-to-carbon bonds. *Adv. Organometallic Chem.* **1964**, *2*, 49-114.

(3) Wagman, D. D.; Evans, W. H.; Parker, V. B.; Halow, I.; Bailey, S. M.; Schumm, R. H. Selected Values of Chemical Thermodynamic Properties. Tables for Elements 35 through 53 in the Standard Order of Arrangement. *NBS Technical Note 270-4* **1969**.

Note 90: *Halo-organo-mercury compounds*

Back to Table

$ClHgCH_3$ Enthalpy of formation taken from a review of experimental studies.[1] The NBS Table recommends a value of −52.3 kJ mol^{-1}.[2]

$BrHgCH_3$ Enthalpy of formation taken from a review of experimental studies.[1] The NBS Table also recommends a value of −18.4 kJ mol^{-1}.[2]

$IHgCH_3$ Enthalpy of formation taken from a review of experimental studies.[1] The NBS Table recommends a value of 21.8 kJ mol^{-1}.[2]

$ClHgC_2H_5$ Enthalpy of formation taken from a review of experimental studies.[1] The NBS Table recommends a value of −62.8 kJ mol^{-1}.[2]

$BrHgC_2H_5$ Enthalpy of formation taken from a review of experimental studies.[1] The NBS Table recommends a value of −30.1 kJ mol^{-1}.[2]

$IHgC_2H_5$ Enthalpy of formation taken from a review of experimental studies.[1] The NBS Table recommends a value of 13.8 kJ mol^{-1}.[2]

(1) Skinner, H. A. The strengths of metal-to-carbon bonds. *Adv. Organometallic Chem.* **1964**, *2*, 49-114.

(2) Wagman, D. D.; Evans, W. H.; Parker, V. B.; Halow, I.; Bailey, S. M.; Schumm, R. H. Selected Values of Chemical Thermodynamic Properties. Tables for Elements 35 through 53 in the Standard Order of Arrangement. *NBS Technical Note 270-4* **1969**.

7.5 Bibliography – Thermodynamic Parameters

Abramowitz, S.; Chase, M. W. Thermodynamic properties of gas phase species of importance to ozone depletion. *Pure App. Chem.* **1991**, *63*, 1449-1454, doi:10.1351/pac199163101449.

Acree, W. E.; Pilcher, G.; da Silva, M. The dissociation enthalpies of terminal (N-O) bonds in organic compounds. *J. Phys. Chem. Ref. Data* **2005**, *34*, 553-572, doi:10.1063/1.1851531.

Agapito, F.; Cabral, B. J. C.; Simoes, J. A. M. Oxygen-oxygen bond dissociation enthalpies of di-tert-butyl peroxide and di-trifluoromethyl peroxide. *J. Mol. Struct. - Theochem* **2005**, *729*, 223-227, doi:10.1016/j.theochem.2005.06.004.

Alecu, I. M.; Marshall, P. Computational study of the thermochemistry of N_2O_5 and the kinetics of the reaction $N_2O_5 + H_2O \rightarrow 2\ HNO_3$. *J. Phys. Chem A* **2014**, *118*, 11405-11416, doi:10.1021/jp509301t.

Allodi, M. A.; Dunn, M. E.; Livada, J.; Kirschner, K. N.; Shields, G. C. Do hydroxyl radical-water clusters, $OH(H_2O)_n$, n = 1-5, exist in the atmosphere? *J. Phys. Chem. A* **2006**, *110*, 13283-13289, doi:10.1021/jp0644681.

An, X. W.; Mansson, M. Enthalpies of combustion and formation of acetonitrile. *J. Chem. Thermo.* **1983**, *15*, 287-293, doi:10.1016/0021-9614(83)90121-0.

Anderson, L. C.; Fahey, D. W. Studies with $ClONO_2$: Thermal dissociation rate and catalytic conversion to NO using an NO/O_3 chemiluminescence detector. *J. Phys. Chem.* **1990**, *94*, 644-652, doi:10.1021/j100365a027.

Anderson, W. R. Oscillator strengths of NH_2 and the heats of formation of NH and NH_2. *J. Phys. Chem.* **1989**, *93*, 530-536, doi:10.1021/j100339a009.

Anderson, W. R. Heats of formation of HNO and some related species. *Comb. Flame* **1999**, *117*, 394-403, doi:10.1016/S0010-2180(98)00077-7.

Anglada, J. M.; Hoffman, G. J.; Slipchenko, L. V.; Costa, M. M.; Ruiz-López, M. F.; Francisco, J. S. Atmospheric significance of water clusters and ozone−water complexes. *J. Phys. Chem. A* **2013**, *117*, 10381-10396, doi:10.1021/jp407282c.

Asatryan, R.; Bozzelli, J. W.; da Silva, G.; Swinnen, S.; Nguyen, M. T. Formation and decomposition of chemically activated and stabilized hydrazine. *J. Phys. Chem. A* **2010**, *114*, 6235-6249, doi:10.1021/jp101640p.

Asatryan, R.; Bozzelli, J. W.; Simmie, J. M. Thermochemistry for enthalpies and reaction paths of nitrous acid isomers. *Int. J. Chem. Kinet.* **2007**, *39*, 378-398, doi:10.1002/kin.20247.

Asatryan, R.; Bozzelli, J. W.; Simmie, J. M. Thermochemistry of methyl and ethyl nitro, RNO_2, and nitrite, RONO, organic compounds. *J. Phys. Chem. A* **2008**, *112*, 3172-3185, doi:10.1021/jp710960u.

Asatryan, R.; Silva, G. d.; Bozzelli, J. W. Quantum chemical study of the acrolein (CH_2CHCHO) + OH + O_2 reactions. *J. Phys. Chem. A* **2010**, *114*, 8302-8311, doi:10.1021/jp104828a.

Asher, R. L.; Appelman, E. H.; Ruscic, B. On the heat of formation of carbonyl fluoride, CF_2O. *J. Chem. Phys.* **1996**, *105*, 9781-9795, doi:10.1063/1.472848.

Asher, R. L.; Appelman, E. H.; Tilson, J. L.; Litorja, M.; Berkowitz, J.; Ruscic, B. A photoionization study of trifluoromethanol, CF_3OH, trifluoromethyl hypofluorite, CF_3OF, and trifluoromethyl hypochlorite, CF_3OCl. *J. Chem. Phys.* **1997**, *106*, 9111-9121, doi:10.1063/1.474017.

Atkinson, R.; Baulch, D. L.; Cox, R. A.; Hampson, R. F.; Kerr, J. A.; Rossi, M. J.; Troe, J. Evaluated kinetic, photochemical, and heterogeneous data for atmospheric chemistry: Supplement V, IUPAC subcommittee on gas kinetic data evaluation for atmospheric chemistry. *J. Phys. Chem. Ref. Data* **1997**, *26*, 521-1011, doi:10.1063/1.556011.

Bacskay, G. B. Spectroscopy and heats of formation of CXI (X = Br, Cl, F) iodocarbenes: quantum chemical characterisation of the , and states. *Mol. Phys.* **2015**, *113*, 1608-1617, doi:10.1080/00268976.2014.1000991.

Bacskay, G. B. Quantum chemical characterization of the $X(^1A_1)$, $a(^3B_1)$, $A(^1B_1)$ and $B(2^1A_1)$ states of diiodomethylene and the enthalpies of formation of diiodomethylene, iodomethylene and iodomethylidyne. *Theor. Chem. Acc.* **2016**, 267-275, doi:10.1007/978-3-662-48148-6_24.

Badenes, M. P.; Croce, A. E.; Cobos, C. J. Falloff curves for the recombination reaction Cl + FC(O)O + M → FC(O)OCl + M. *J. Phys. Chem. A* **2006**, *110*, 3186-3196, doi:10.1021/jp054591x.

Baer, T.; Walker, S. H.; Shuman, N. S.; Bodi, A. One- and two-dimensional translational energy distributions in the iodine-loss dissociation of $1,2\text{-}C_2H_4I_2^+$ and $1,3\text{-}C_3H_6I_2^+$: What does this mean? *J. Phys. Chem. A* **2012**, *116*, 2833-2844, doi:10.1021/jp2121643.

Bakowies, D. Ab initio thermochemistry with high-level isodesmic corrections: Validation of the ATOMIC protocol for a large set of compounds with first-row atoms (H, C, N, O, F). *J. Phys. Chem. A* **2009**, *113*, 11517-11534, doi:10.1021/jp9027782.

Balabanov, N. B.; Peterson, K. A. Mercury and reactive halogens: The thermochemistry of Hg + (Cl_2, Br_2, BrCl, ClO, and BrO). *J. Phys. Chem. A* **2003**, *107*, 7465-7470, doi:10.1021/jp035547p.

Ballester, M. Y.; Varandas, A. J. C. Double many-body expansion potential energy surface for ground state HSO_2. *Phys. Chem. Chem. Phys.* **2005**, *7*, 2305-2317, doi:10.1039/b500990a.

Balucani, N.; Casavecchia, P.; Stranges, D.; Volpi, G. G. The enthalpy of formation of the HSO radical. *Chem. Phys. Lett.* **1993**, *211*, 469-472, doi:10.1016/0009-2614(93)87092-H.

Balucani, N.; Stranges, D.; Casavecchia, P.; Volpi, G. G. Crossed beam studies of the reactions of atomic oxygen in the ground ^3P and first electronically excited ^1D states with hydrogen sulfide. *J. Chem. Phys.* **2004**, *120*, 9571-9582, doi:10.1063/1.1714809.

Baranovskii, V. I.; Skorobogatov, G. A. Quantum-chemical simulation of the gas-phase molecular, thermodynamic, and kinetic parameters of CF, CF_2, and CF_3 radicals and CF_4, C_2F_2, C_2F_4, and C_2F_6 molecules. *Russ. J. Gen. Chem.* **2016**, *86*, 241-250, doi:10.1134/s1070363216020067.

Barker, J. R.; Ortiz, N. F.; Preses, J. M.; Lohr, L. L.; Maranzana; Stimac, P. J.; Nguyen, L. T. MultiWell; 2009.1 ed.; University of Michigan: Ann Arbor, MI, 2009.

Becerra, R.; Carpenter, I. W.; Walsh, R. Time-resolved studies of the kinetics of the reactions of CHO with HI and HBr: Thermochemistry of the CHO radical and the H-C bond strengths in CH_2O and CHO. *J. Phys. Chem.* **1997**, *101*, 4185-4190, doi:10.1021/jp970443y.

Bedjanian, Y.; Le Bras, G.; Poulet, G. Kinetics and mechanism of the IO + ClO reaction. *J. Phys. Chem. A* **1997**, *101*, 4088-4096, doi:10.1021/jp963947p.

Bedjanian, Y.; Poulet, G.; Le Bras, G. Low-pressure study of the reactions of Br atoms with alkenes. 2. Reactions with ethene and trans-2-butene. *J. Phys. Chem. A* **1999**, *103*, 4026-4033, doi:10.1021/jp9903007.

Begović, N.; Marković, Z.; Anić, S.; Kolar-Anić, L. Computational investigation of HIO and HIO_2 isomers. *J. Phys. Chem. A* **2004**, *108*, 651-657, doi:10.1021/jp034492o.

Berkowitz, J.; Ellison, G. B.; Gutman, D. Three methods to measure RH bond energies. *J. Phys. Chem.* **1994**, *98*, 2744-2765, doi:10.1021/j100062a009.

Bernardes, C. E. S.; Minas da Piedade, M. E.; Amaral, L. M. P. F.; Ferreira, A. I. M. C. L.; Ribeiro da Silva, M. A. V.; Diogo, H. P.; Costa Cabral, B. J. Energetics of C−F, C−Cl, C−Br, and C−I bonds in 2-haloethanols. Enthalpies of formation of XCH_2CH_2OH (X = F, Cl, Br, I) compounds and of the 2-hydroxyethyl radical. *J. Phys. Chem. A* **2007**, *111*, 1713-1720, doi:10.1021/jp0675678.

Berry, R. J.; Yuan, Y.; Misra, A.; Marshall, P. Experimental and computational investigations of the reaction of OH with CF_3I and the enthalpy of formation of HOI. *J. Phys. Chem. A* **1998**, *102*, 5182-5188, doi:10.1021/jp980645+.

Bhartiya, J. B.; Behere, S. H.; Rao, M. L. P. Dissociation energies of HgCl, HgBr and HgI from potential energy curves. *J. Quant. Spec. Radiat. Transf.* **1990**, *43*, 95-98, doi:10.1016/0022-4073(90)90070-M.

Bickerton, J.; da Piedade, M. E. M.; Pilcher, G. Enthalpy of formation of tetrabromomethane by rotating-bomb calorimetry. *J. Chem. Thermo.* **1984**, *16*, 661-668, doi:10.1016/0021-9614(84)90046-6.

Black, G.; Patrick, R.; Jusinski, L. E.; Slanger, T. G. Rate coefficients for the reaction HS + NO + M(M = He, Ar, and N_2) over the temperature range 250- 445 K. *J. Chem. Phys.* **1984**, *80*, 4065-4070, doi:10.1063/1.447287.

Blitz, M. A.; Huges, K. J.; Pilling, M. J. Determination of the high-pressure limiting rate coefficient and the enthalpy of reaction for OH + SO_2. *J. Phys. Chem. A* **2003**, *107*, 1971-1978, doi:10.1021/jp026524y.

Bodi, A.; Hemberger, P.; Gerber, T. A robust link between the thermochemistry of urea and isocyanic acid by dissociative photoionization. *J. Chem. Thermo.* **2013**, *58*, 292-299, doi:10.1016/j.jct.2012.11.013.

Bodi, A.; Kercher, J. P.; Bond, C.; Meteesatien, P.; Sztaray, B.; Baer, T. Photoion photoelectron coincidence spectroscopy of primary amines RCH_2NH_2 (R=H, CH_3, C_2H_5, C_3H_7, *i*-C_3H_7): Alkylamine and alkyl radical heats of formation by isodesmic reaction networks *J. Phys. Chem. A* **2006**, *110*, 13425-13433, doi:10.1021/jp064739s.

Bodi, A.; Shuman, N. S.; Baer, T. On the ionization and dissociative photoionization of iodomethane: a definitive experimental enthalpy of formation of CH_3I. *Phys. Chem. Chem. Phys.* **2009**, *11*, 11013-11021, doi:10.1039/b915400k.

Borkar, S.; Sztaray, B. Self-consistent heats of formation for the ethyl cation, ethyl bromide, and ethyl iodide from threshold photoelectron photoion coincidence spectroscopy. *J. Phys. Chem. A* **2010**, *114*, 6117-6123, doi:10.1021/jp102162f.

Bouchoux, G.; Chamot-Rooke, J.; Leblanc, D.; Mourgues, P.; Sablier, M. Proton affinity and heat of formation of vinyloxy $[CH_2CHO]^{\cdot}$ and acetonyl $[CH_2COCH_3]^{\cdot}$ radicals. *ChemPhysChem* **2001**, *2*, 235-241, doi:10.1002/1439-7641(20010417)2:4<235::AID-CPHC235>3.0.CO;2-S.

Bozzelli, J. W.; Jung, D. Theoretical investigation on stability of the $C{\bullet}H_2OCl$ radical. *J. Phys. Chem. A* **2001**, *105*, 3941-3946, doi:10.1021/jp003401+.

Breidung, J.; Cosleou, J.; Demaison, J.; Sarka, K.; Thiel, W. Ab initio anharmonic force field, molecular parameters, equilibrium structure and enthalpy of formation of fluoroform. *Mol. Phys.* **2004**, *102*, 1827-1841, doi:10.1080/00268970412331287089.

Breidung, J.; Thiel, W. Thermochemistry of the fluoroformyloxyl radical: A computational study based on coupled cluster theory. *J. Phys. Chem. A* **2006**, *110*, 1575-1585, doi:10.1021/jp053883v.

Brudnik, K.; Jodkowski, J. T.; Nowek, A.; Leszczynski, J. Kinetics of the formation reactions of trichloro- and tribromomethyl hypohalites and alcohols in the gas-phase: Theoretical study *Chem. Phys. Lett.* **2007**, *435*, 194-200, doi:10.1016/j.cplett.2006.12.079.

Brudnik, K.; Jodkowski, J. T.; Ratajczak, E. Kinetics of the formation reactions of trifluoromethanol and trifluoromethyl hypohalites in the gas phase. *J. Mol. Struct.* **2003**, *656*, 333-339, doi:10.1016/S0022-2860(03)00347-8.

Buendía-Atencio, C.; Leyva, V.; González, L. Thermochemistry and UV spectroscopy of alkyl peroxynitrates. *J. Phys. Chem. A* **2010**, *114*, 9537-9544, doi:10.1021/jp103854y.

Burgess, D. R. An evaluation of gas phase enthalpies of formation for hydrogen-oxygen (H_xO_y) species. *J. Res. Natl. Inst. Sci. Technol.* **2016**, *121*, 108-138, doi:10.6028/jres.121.005.

Burke, S. M.; Simmie, J. M.; Curran, H. J. Critical evaluation of thermochemical properties of C1–C4 species: Updated group-contributions to estimate thermochemical properties. *J. Phys. Chem. Ref. Data* **2015**, *44*, 013101, doi:10.1063/1.4902535.

Burkholder, J. B.; Mauldin, R. L.; Yokelson, R. J.; Solomon, S.; Ravishankara, A. R. Kinetic, thermodynamic, and spectroscopic study of Cl_2O_3. *J. Phys. Chem.* **1993**, *97*, 7597-7605, doi:10.1021/j100131a032.

Cacace, F.; de Petris, G.; Pepi, F.; Troiani, A. Experimental detection of hydrogen trioxide. *Science* **1999**, *285*, 81-82, doi:10.1126/science.285.5424.81.

Carson, A. S.; Laye, P. G.; Pendley, J. B.; Welsby, A. M. The enthalpies of formation of iodomethane, diiodomethane, triiodomethane, and tetraiodomethane by rotating combustion calorimetry. *J. Chem. Thermo.* **1993**, *25*, 261-269, doi:10.1006/jcht.1993.1025.

Chao, J.; Hall, K. R.; Marsh, K. N.; Wilhoit, R. C. Thermodynamic properties of key organic oxygen compounds in the carbon range C1 to C4. Part 2. Ideal gas properties. *J. Phys. Chem. Ref. Data* **1986**, *15*, 1369-1436, doi:10.1063/1.555769.

Chao, J.; Rodgers, A. S.; Wilhoit, R. C.; Zwolinski, B. J. Ideal gas thermodynamic properties of six chloroethanes. *J. Phys. Chem. Ref. Data* **1974**, *3*, 141-162, doi:10.1063/1.3253136.

Chao, J.; Wilhoit, R. C.; Zwolinski, B. J. Ideal gas thermodynamic properties of ethane and propane. *J. Phys. Chem. Ref. Data* **1973**, *2*, 427-437, doi:10.1063/1.3253123.

Chao, J.; Zwolinski, B. J. Ideal gas thermodynamic properties of ethylene and propylene. *J. Phys. Chem. Ref. Data* **1975**, *4*, 251-261, doi:10.1063/1.555518.

Chao, J.; Zwolinski, B. J. Ideal gas thermodynamic properties of methanoic and ethanoic acids. *J. Phys. Chem. Ref. Data* **1978**, *7*, 363-377, doi:10.1063/1.555571.

Chase, M. W. NIST-JANAF thermochemical tables for the bromine oxides. *J. Phys. Chem. Ref. Data* **1996**, *25*, 1069-1111, doi:10.1063/1.555993.

Chase, M. W. NIST-JANAF thermochemical tables for the iodine oxides. *J. Phys. Chem. Ref. Data* **1996**, *25*, 1297-1340, doi:10.1063/1.555994.

Chase, M. W. NIST-JANAF thermochemical tables for the oxygen fluorides. *J. Phys. Chem. Ref. Data* **1996**, *25*, 551-603, doi:10.1063/1.555992.

Chase, M. W. NIST-JANAF thermochemical tables. *J. Phys. Chem. Ref. Data* **1998**, *Monograph 9*.

Chen, S. S.; Rodgers, A. S.; Chao, J.; Wilhoit, R. C.; Zwolinski, B. J. Ideal gas thermodynamic properties of six fluoroethanes. *J. Phys. Chem. Ref. Data* **1975**, *4*, 441-456, doi:10.1063/1.555521.

Chen, S. S.; Wilhoit, R. C.; Zwolinski, B. J. Ideal gas properties of six chlorofluoromethanes. *J. Phys. Chem. Ref. Data* **1976**, *5*, 571-580, doi:10.1063/1.555539.

Chen, Y.; Rauk, A.; Tschuikow-Roux, E. Structures, barriers for internal rotation, vibrational frequencies, and thermodynamic functions of CH_2FCH_2, CHF_2CH_2, and CF_3CH_2 radicals: An *ab initio* study. *J. Chem. Phys.* **1990**, *93*, 6620-6629, doi:10.1063/1.458929.

Chen, Y.; Rauk, A.; Tschuikow-Roux, E. Structures, barriers for rotation and inversion, vibrational frequencies, and thermodynamic functions of ethyl, α-fluoroethyl, and α-difluroroethyl radicals: An *ab initio* study. *J. Chem. Phys.* **1990**, *93*, 1187-1195, doi:10.1063/1.459182.

Chen, Y.; Rauk, A.; Tschuikow-Roux, E. Structures, barriers for internal rotation, vibrational frequencies, and thermodynamic functions of CH_2FCHF, CHF_2CHF, and CF_3CHF radicals: An ab initio study. *J. Chem. Phys.* **1991**, *94*, 7299-7310, doi:10.1063/1.460214.

Chyall, L. J.; Squires, R. R. The proton affinity and absolute heat of formation of trifluoromethanol. *J. Phys. Chem.* **1996**, *100*, 16435-16440, doi:10.1021/jp961135n.

Clifford, E. P.; Wenthold, P. G.; Gareyev, R.; Lineberger, W. C.; DePuy, C. H.; Bierbaum, V. M.; Ellison, G. B. Photoelectron spectroscopy, gas phase acidity, and thermochemistry of tert-butyl hydroperoxide: Mechanism for the rearrangement of peroxyl radicals. *J. Chem. Phys.* **1998**, *109*, 10293-10310, doi:10.1063/1.477725.

Cox, J. D.; Wagman, D. D.; Medvedev, V. A. *CODATA Key Values for Thermodynamics*; Hemisphere Publishing Corp.: New York, 1989.

Coxon, J. A.; Ramsay, D. A. The $A^2\Pi_i$–$X^2\Pi_i$ band system of ClO: Reinvestigation of the absorption spectrum. *Can. J. Phys.* **1976**, *54*, 1034-1042, doi:10.1139/p76-122.

Cremer, D.; Kraka, E.; Filatov, M. Bonding in mercury molecules described by the normalized elimination of the small component and coupled cluster theory. *ChemPhysChem* **2008**, *9*, 2510-2521, doi:10.1002/cphc.200800510.

Császár, A. G.; Furtenbacher, T. From a network of computed reaction enthalpies to atom-based thermochemistry (NEAT). *Chem. Eur. J.* **2010**, *16*, 4826-4835, doi:10.1002/chem.200903252.

Császár, A. G.; Szalay, P. G.; Leininger, M. L. The enthalpy of formation of $^2\Pi$ CH. *Mol. Phys.* **2002**, *100*, 3879-3883, doi:10.1080/0026897021000016684.

Csontos, J.; Rolik, Z.; Das, S.; Kállay, M. High-accuracy thermochemistry of atmospherically important fluorinated and chlorinated methane derivatives. *J. Phys. Chem. A* **2010**, *114*, 13093-13103, doi:10.1021/jp105268m.

Czakő, G.; Nagy, B.; Tasi, G.; Somogyi, A.; Šimunek, J.; Noga, J.; Braams, B. J.; Bowman, J. M.; Császár, A. Proton affinity and enthalpy of formation of formaldehyde. *Int. J. Quantum Chem.* **2009**, *109*, 2393-2409, doi:10.1002/qua.22009.

da Silva, G.; Bozzelli, J. W. Thermochemistry, bond energies, and internal rotor potentials of dimethyl tetraoxide. *J. Phys. Chem A* **2007**, *111*, 12026-12036, doi:10.1021/jp075144f.

da Silva, G.; Kim, C. H.; Bozzelli, J. W. Thermodynamic properties (enthalpy, bond energy, entropy, and heat capacity) and internal rotor potentials of vinyl alcohol, methyl vinyl ether, and their corresponding radicals. *J. Phys. Chem. A* **2006**, *110*, 7925-7934, doi:10.1021/jp0602878.

Davis, H. F.; Kim, B.; Johnston, H. S.; Lee, Y. T. Dissociation energy and photochemistry of NO_3. *J. Phys. Chem.* **1993**, *97*, 2172-2180, doi:10.1021/j100112a018.

Degirmenci, I.; Coote, M. L. Effect of substituents on the stability of sulfur-centered radicals. *J. Phys. Chem. A* **2016**, *120*, 7398-7403, doi:10.1021/acs.jpca.6b08223.

Delmdahl, R. F.; Parker, D. H.; Eppink, A. T. J. B. Short wavelentgh photolysis of jet-cooled $OClO(^2A_2\nu_1>20) \rightarrow ClO(X^2\Pi_\Omega,v,J) + O(^3P_J)$. *J. Chem. Phys.* **2001**, *114*, 8339-8346, doi:10.1063/1.1367393.

Denis, P. A. Theoretical characterization of the thiosulfeno radical, HS_2 *Chem. Phys. Lett.* **2006**, *422*, 434-438, doi:10.1016/j.cplett.2006.02.107.

Denis, P. A. Thermochemistry of the hypobromous and hypochlorous acids, HOBr and HOCl. *J. Phys. Chem. A* **2006**, *110*, 5887-5892, doi:10.1021/jp056950u.

Denis, P. A., and O. N. Ventura CCSDT study of the fluoroperoxyl radical, FOO. *Chem. Phys. Lett.* **2004**, *385*, 292-297, doi:10.1016/j.cplett.2003.12.081.

Denis, P. A.; Kieniger, M.; Ventura, O. N.; Cachau, R. E.; Diercksen, G. H. F. Complete basis set and density functional determination of the enthalpy of formation of the controversial HO_3 radical: a discrepancy between theory and experiment. *Chem. Phys. Lett.* **2002**, *365*, 440-449, doi:10.1016/S0009-2614(02)01432-X.

Denis, P. A.; Ornellas, F. R. Theoretical characterization of hydrogen polyoxides: HOOH, HOOOH, HOOOOH, and HOOO. *J. Phys. Chem. A* **2009**, *113*, 199-506, doi:10.1021/jp808795e.

Denis, P. A.; Ventura, O. N. Density functional investigation of atmospheric sulfur chemistry II. The heat of formation of the XSO_2 radicals X = H, CH_3. *Chem. Phys. Lett.* **2001**, *344*, 221-228, doi:10.1016/S0009-2614(01)00684-4.

Dibble, T. S.; Zelie, M. J.; Mao, H. Thermodynamics of reactions of ClHg and BrHg radicals with atmospherically abundant free radicals. *Atmos. Chem. Phys.* **2012**, *12*, 10271-10279, doi:10.5194/acp-12-10271-2012.
Diogo, H. P.; Minas de Piedada, M. E.; Simões, J. A. M.; Nagano, Y. Standard enthalpy of formation and enthalpy of vaporization of di-1,1-dimethylethyl peroxide: Re-evaluation of the standard enthalpy of formation of the di-1,1-dimethylethoxy radical *J. Chem. Thermo.* **1995**, *27*, 597-604, doi:10.1006/jcht.1995.0061.
Dixon, D. A.; de Jong, W. A.; Peterson, K. A.; Francisco, J. S. Heats of formation of CBr, CHBr, and CBr_2 from ab initio chemistry. *J. Phys. Chem. A* **2002**, *106*, 4724-4728, doi:10.1021/jp0147067.
Dixon, D. A.; de Jong, W. A.; Peterson, K. A.; McMahon, T. B. Methyl cation affinities of rare gases and nitrogen and the heat of formation of diazomethane. *J. Phys. Chem. A* **2005**, *109*, 4073-4080, doi:10.1021/jp044561e.
Dixon, D. A.; Feller, D. Heats of formation of CF_2, FCO, and CF_2O. *J. Phys. Chem. A* **1998**, *102*, 8209-8216, doi:10.1021/jp982655g.
Dixon, D. A.; Francisco, J. S.; Alexeev, Y. Thermochemical properties of H_xNO molecules and ions from ab initio electronic structure theory. *J. Phys. Chem. A* **2006**, *110*, 185-191, doi:10.1021/jp054642q.
Dóbé, S.; Bérces, T.; Turányi, T.; Márta, F.; Grussdorf, J.; Temps, F.; Wagner, H. G. Direct kinetic studies of the reactions Br + CH_3OH and CH_2OH + HBr: The heat of formation of CH_2OH. *J. Phys. Chem.* **1996**, *100*, 19864-19873, doi:10.1021/jp961398h.
Dooley, K. S.; Geidosch, J. N.; North, S. W. Ion imaging study of IO radical photodissociation: Accurate bond dissociation energy determination. *Chem. Phys. Lett.* **2008**, *457*, 303-306, doi:10.1016/j.cplett.2008.04.009.
Dorofeeva, O.; Iorish, V. S.; Novikov, V. P.; Neumann, D. B. NIST-JANAF thermochemical tables. II. Three molecules related to atmospheric chemistry: HNO_3, H_2SO_4, and H_2O_2. *J. Phys. Chem. Ref. Data* **2003**, *32*, 879-901, doi:10.1063/1.1547435.
Dorofeeva, O.; Novikov, V. P.; Neumann, D. B. NIST-JANAF thermochemical tables. 1. Ten organic molecules related to atmospheric chemistry. *J. Phys. Chem. Ref. Data* **2001**, *30*, 475-513, doi:10.1063/1.1364518.
Dorofeeva, O. V.; Osina, E. L. Performance of DFT, MP2, and composite ab initio methods for the prediction of enthalpies of formations of CHON compounds using isodesmic reactions. *Comput. Theor. Chem.* **2017**, *1106*, 28-35, doi:10.1016/j.comptc.2017.03.006.
Dorofeeva, O. V.; Suntsova, M. A. Enthalpies of formation of nitromethane and nitrobenzene: Theory *vs* experiment. *J. Chem. Thermo.* **2013**, *58*, 221-225, doi:10.1016/j.jct.2012.11.008.
Du, S.; Francisco, J. S.; Schenter, G. K.; Iordanov, T. D.; Garrett, B. C.; Dupris, M.; Li, J. The OH radical-H_2O molecular interaction potential. *J. Chem. Phys.* **2006**, *124*, 224318, doi:10.1063/1.2200701.
Duncan, T. V.; Miller, C. E. The HCO_2 potential energy surface: Stationary point energetics and the HOCO heat of formation. *J. Chem. Phys.* **2000**, *113*, 5138-5140, doi:10.1063/1.1312824.
El-Nahas, A. M.; Bozzelli, J. W.; Simmie, J. M.; Navarro, M. V.; Black, G.; Curran, H. J. Thermochemistry of acetonyl and related radicals. *J. Phys. Chem. A* **2006**, *110*, 13618-13623, doi:10.1021/jp065003y.
Ervin, K. M.; Gronert, S.; Barlow, E. E.; Gilles, M. K.; Harrison, A. G.; Bierbaum, V. M.; DePuy, C. H.; Lineberger, W. C.; Ellison, G. B. Bond strengths of ethylene and avetylene. *J. Am. Chem. Soc.* **1990**, *112*, 5750-5759, doi:10.1021/JA00171A013.
Espinosa-Garcia, J.; Dóbé, S. Theoretical enthalpies of formation for atmospheric hydroxycarbonyls. *J. Mol. Struct. - Theochem* **2005**, *713*, 119-125, doi:10.1016/j.theochem.2004.11.002.
Fabian, W. M. F.; Janoschek, R. Thermochemical properties of the hydroxy-formyl radical HO-CO, and the formyloxy radical, HC(O)O, and their role in the reaction OH + CO → H + CO_2. Computational G3MP2B3 and CCSD(T)-CBS studies. *J. Mol. Struct. - Theochem* **2005**, *713*, 227-234, doi:10.1016/j.theochem.2004.08.065.
Farkas, E.; Kovács, G.; Szilágyi, I.; Dóbé, S.; Bérces, T.; Márta, F. Rate constant for the reaction of $CH_3C(O)CH_2$ radical with HBr and its thermochemical implication. *Int. J. Chem. Kinet.* **2006**, *38*, 32-37, doi:10.1002/kin.20135.
Feller, D.; Dixon, D. A. Coupled cluster theory and multireference configuration interaction study of FO, F_2O, FO_2, and FOOF. *J. Phys. Chem. A* **2003**, *107*, 9641-9651, doi:10.1021/jp030267v.
Feller, D.; Dixon, D. A.; Francisco, J. S. Coupled cluster theory determination of the heats of formation of combustion-related compounds: CO, HCO, CO_2, HCO_2, HOCO, HC(O)OH, and HC(O)OOH. *J. Phys. Chem. A* **2003**, *107*, 1604-1617, doi:10.1021/jp030267v.
Feller, D.; Peterson, K. A.; Dixon, D. A. A survey of factors contributing to accurate theoretical predictions of atomization energies and molecular structures. *J. Chem. Phys.* **2008**, *129*, 204105, doi:10.1063/1.3008061.

Feller, D.; Peterson, K. A.; Dixon, D. A. Refined theoretical estimates of the atomization energies and molecular structures of selected small oxygen fluorides. *J. Phys. Chem. A* **2010**, *114*, 613-623, doi:10.1021/jp908128g.

Feller, D.; Peterson, K. A.; Dixon, D. A. Ab initio coupled cluster determination of the heats of formation of $C_2H_2F_2$, C_2F_2, and C_2F_4. *J. Phys. Chem. A* **2011**, *115*, 1440-1451, doi:10.1021/jp111644h; correction 10.1021/jp202158j.

Feller, D. F.; Bross, D.; Ruscic, B. Enthalpy of formation of N_2H_4 (hydrazine) revisited. *J. Phys. Chem. A* **2017**, doi:10.1021/acs.jpca.7b06017.

Filatov, M.; Cremer, D. Revision of the dissociation energies of mercury chalcogenides—unusual types of mercury bonding. *ChemPhysChem* **2004**, *5*, 1547-1557, doi:10.1002/cphc.200301207.

Frank, A. J.; Turecek, F. Methylsulfonyl and methoxysulfinyl radicals and cations in the gas phase. A variable-time and photoexcitation neutralization-reionization mass spectrometric and ab initio/RRKM study. *J. Phys. Chem. A* **1999**, *103*, 5348-5361, doi:10.1021/jp990946z.

Frenkel, M.; Kabo, G. J.; Marsh, K. N.; Roganov, G. N.; Wilhoit, R. C. *Thermodynamics of Organic Compounds in the Gas State*; Thermodynamics Research Center: College Station, TX, 1994; Vol. I.

Friedl, R. R.; Sander, S. P.; Yung, Y. L. Chloryl nitrate: A novel product of the OClO + NO_3 + M recombination. *J. Phys. Chem.* **1992**, *96*, 7490-7493, doi:10.1021/j100198a002.

Fulle, D.; Hamann, H. F.; Hippler, H.; Jänsch, C. P. The high pressure range of the addition of OH to C_2H_2 and C_2H_4. *Ber. Bunsenges. Phys. Chem.* **1997**, *101*, 1433-1442, doi:10.1002/bbpc.199700004.

Gálvez, O.; Gómez, P. C. An ab initio study on the structure and energetics of the ClO hydrates. *Chem. Phys. Lett.* **2007**, *448*, 16-23, doi:10.1016/j.cplett.2007.09.072.

Gálvez, O.; Zoermer, A.; Grothe, H. Theoretical study on the structure of the BrO hydrates. *J. Phys. Chem. A* **2006**, *110*, 8818-8825, doi:10.1021/jp062048q.

Gálvez, O.; Zoermer, A.; Loewenschuss; Grothe, H. A combined matrix isolation and ab initio study of bromine oxides. *J. Phys. Chem. A* **2006**, *110*, 6472-6481, doi:10.1021/jp060586x.

Ganyecz, Á.; Csontos, J.; Nagy, B.; Kállay, M. Theoretical and thermochemical network approaches to determine the heats of formation for HO_2 and its ionic counterparts. *J. Phys. Chem. A* **2015**, *119*, 1164-1176, doi:10.1021/jp5104643.

Ganyecz, Á.; Kállay, M.; Csontos, J. Accurate theoretical thermochemistry for fluoroethyl radicals. *J. Phys. Chem. A* **2017**, *121*, 1153-1162, doi:10.1021/acs.jpca.6b12404.

Gierczak, T.; Jimenez, E.; Riffault, V.; Burkholder, J. B.; Ravishankara, A. R. Thermal decomposition of HO_2NO_2 (peroxynitric acid, PNA): Rate coefficient and determination of the enthalpy of formation. *J. Phys. Chem. A* **2005**, *109*, 586-596, doi:10.1021/jp046632f.

Glarborg, P.; Miller, J. A.; Ruscic, B.; Klippenstein, S. J. Modeling nitrogen chemistry in combustion. *Progress in Energy and Combustion Science* **2018**, *67*, 31-68, doi:10.1016/j.pecs.2018.01.002.

Gómez Martín, J. C.; Plane, J. M. C. Determination of the O–IO bond dissociation energy by photofragment excitation spectroscopy. *Chem. Phys. Lett.* **2009**, *474*, 79-83, doi:10.1016/j.cplett.2009.04.052.

Grade, M.; Hirschwald, W. Energetics and stabilities of the IIB/VIA-compounds at high-temperature equilibrium conditions. *Ber. Bunsen. Phys. Chem.* **1982**, *86*, 899-907, doi:10.1002/bbpc.19820861006.

Grant, D. J.; Dixon, D. A.; Francisco, J. S.; Feller, D.; Peterson, K. A. Heats of formation of the $H_{1,2}O_mS_n$ (m,n = 0-3) molecules from electronic structure calculations. *J. Phys. Chem. A* **2009**, *113*, 11343-11353, doi:10.1021/jp905847e.

Grant, D. J.; Garner, E. B.; Matus, M. H.; Nguyen, M. T.; Peterson, K. A.; Francisco, J. S.; Dixon, D. A. Thermodynamic properties of the XO_2, X_2O, XYO, X_2O_2, and XYO_2 (X, Y = Cl, Br and I) isomers. *J. Phys. Chem. A* **2010**, *114*, 4254-4265, doi:10.1021/jp911320p.

Gunturu, A.; Asatryan, R.; Bozzelli, J. W. Thermochemistry, bond energies and internal rotor barriers of methyl sulfinic acid, methyl sulfinic acid ester and their radicals. *J. Phys. Org. Chem.* **2011**, *24*, 366-377, doi:10.1002/poc.1766.

Gurvich, L. V.; Bergman, G. A.; Borokhov, L. N.; Iorish, V. S.; Leonidov, V. Y.; Yungman, V. S. Thermodynamic properties of alkali metal hydroxides. Part 1. Lithium and sodium hydroxides. *J. Phys. Chem. Ref. Data* **1996**, *25*, 1211-1276, doi:10.1063/1.555982.

Gurvich, L. V.; Bergman, G. A.; Borokhov, L. N.; Iorish, V. S.; Leonidov, V. Y.; Yungman, V. S. Thermodynamic properties of alkali metal hydroxides. Part II. Potassium, rubidium, and cesium hydroxides. *J. Phys. Chem. Ref. Data* **1997**, *26*, 1031-1110, doi:10.1063/1.555996.

Gurvich, L. V.; Veyts, I. V.; Alcock, C. B. *Thermodynamic Properties of Individual Substances,*, Fourth ed.; Hemisphere Publishing Corp.: New York, 1991; Vol. 2.

Guthrie, J. P. Thermodynamics of ester and orthoester formation from trifluoroacetic acid. *Can. J. Chem.* **1976**, *54*, 202-209, doi:10.1139/v76-032.
Harvey, J.; Tuckett, R. P.; Bodi, A. A halomethane thermochemical network from iPEPICO experiments and quantum chemical calculations. *J. Phys. Chem. A* **2012**, *116*, 9696-9705, doi:10.1021/jp307941k.
Hassanzadeh, P.; Irikura, K. K. Nearly ab initio thermochemistry: The use of reactions schemes. Application to IO and HOI. *J. Phys. Chem. A* **1997**, *101*, 1580-1587, doi:10.1021/jp963011g.
Hassouna, M.; Delbos, E.; Devolder, P.; Viskolcz, B.; Fittschen, C. Rate and equilibrium constant of the reaction of 1-methylvinoxy radicals with O_2: $CH_3COCH_2 + O_2 \leftrightarrow CH_3COCH_2O_2$. *J. Phys. Chem. A* **2006**, *110*, 6667-6672, doi:10.1021/jp0558270.
Henry, D. J.; Parkinson, C. J.; Mayer, P. M.; Radom, L. Bond dissociation energies and radical stabilization energies associated with substituted methyl radicals. *J. Phys. Chem. A* **2001**, *105*, 6750-6756, doi:10.1021/jp010442c.
Hepler, L. G.; Olofsson, G. Mercury: Thermodynamic properties, chemical equilibria, and standard potentials *Chem. Rev.* **1975**, *75*, 585-602, doi:10.1021/cr60297a003.
Herzberg, G. *Molecular Spectra and Molecular Structure. Vol.1: Spectra of Diatomic Molecules*; Van Nortrand Reinhold, 1950.
Hildenbrand, D. L.; Lau, K. H.; Chandra, D. Revised thermochemistry of gaseous ammonium nitrate, NH_4NO_3(g). *J. Phys. Chem. A* **2010**, *114*, 11654-11655, doi:10.1021/jp105773q.
Hocking, W. H. The other rotamer of formic acid, *cis*-HCOOH. *Z. Naturforsch.* **1976**, *31a*, 1113-1121, doi:10.1515/zna-1976-0919.
Holmes, J. L.; Lossing, F. P.; Terlouw, J. K. Heats of formation and homolytic bond dissociation energies in the keto-enol tautomers C_2H_4O, C_3H_6O. *J. Am. Chem. Soc.* **1986**, *108*, 1086-1087, doi:10.1021/ja00265a042.
Hoy, E. P.; Schwerdtfeger, C. A.; Mazziotti, D. A. Relative energies and geometries of the *cis*- and *trans*-HO_3 radicals from the parametric 2-electron density matrix method. *J. Phys. Chem A* **2013**, *117*, 1817-1825, doi:10.1021/jp3105562.
Huang, M.-J.; Watts, J. D. Theoretical characterization of the F_2O_3 molecule by coupled-cluster methods. *J. Phys. Chem. A* **2010**, *114*, 10197-10201, doi:10.1021/jp101106n.
Huber, K. P.; Herzberg, G. *Constants of Diatomic Molecules*; National Institute of Standards and Technology, 1998.
Hudgens, J. W.; Johnson, R. D.; Timonen, R. S.; Seetula, J. A.; Gutman, D. Kinetics of the reactions of $CCl_3 + Br_2$ and thermochemistry of CCl_3 radical and cation. *J. Phys. Chem.* **1991**, *95*, 4400-4405, doi:10.1021/j100164a043.
Irikura, K. K. Thermochemistry of ammonium nitrate, NH_4NO_3, in the gas phase. *J. Phys. Chem. A* **2010**, *114*, 11651-11653, doi:10.1021/jp105770d.
Jacox, M. E. *Vibrational and Electronic Energy Levels of Polyatomic Transient Molecules*; National Institute of Standards and Technology, 1998.
Janoschek, R.; Rossi, M. J. Thermochemical properties of free radicals from G3MP2B3 calculations. *Int. J. Chem. Kinet.* **2002**, *34*, 550-560, doi:10.1002/kin.20035.
Janoschek, R.; Rossi, M. J. Thermochemical properties from G3MP2B3 calculations, set 2: Free radicals with special consideration of CH_2=CH-C$^{\bullet}$=CH_2, cyclo-$^{\bullet}C_5H_5$, $^{\bullet}CH_2OOH$, HO-$^{\bullet}$CO, and HC(O)O$^{\bullet}$. *Int. J. Chem. Kinet.* **2004**, *36*, 661-686, doi:10.1002/kin.20035.
Jefferson, A.; Nicovich, J. M.; Wine, P. H. Temperature-dependent kinetics studies of the reactions Br($^2P_{3/2}$) + $CH_3SCH_3 \leftrightarrow CH_3SCH_2$ + HBr. Heat of formation of the CH_3SCH_2 radical. *J. Phys. Chem.* **1994**, *98*, 7128-7135, doi:10.1021/j100080a006.
Joens, J. A. The dissociation energy of OH(X $^2P_{3/2}$) and the enthalpy of formation of OH(X $^2\Pi_{3/2}$), ClOH, and BrOH from thermochemical cycles. *J. Phys. Chem. A* **2001**, *105*, 11041-11044, doi:10.1021/jp011833u.
Johnson, R. D.; Hudgens, J. W. Structural and thermochemical properties of hydroxymethyl (CH_2OH) radicals and cations derived from observations of $B^2A'(3p) \leftarrow X^2A''$ electronic spectra and from ab initio calculations. *J. Phys. Chem.* **1996**, *100*, 19874-19890, doi:10.1021/jp961399+.
Jung, D.; Chen, C. J.; Bozzelli, J. W. Structures, rotation barrier, and thermodynamic properties $\Delta H_f^o{}_{298}$, $S^o{}_{298}$, and C_p(T) of chloromethyl hypochlorites CH_3OCl, CH_2ClOCl, and CCl_3OCl. *J. Phys. Chem. A* **2000**, *104*, 9581-9590, doi:10.1021/jp001469j.
Kaiser, E. W.; Wallington, T. J. Kinetics of the reactions of chlorine atoms with C_2H_4 (k_1) and C_2H_2 (k_2): A determination of $\Delta H_{f,298}°$ for C_2H_3. *J. Phys. Chem.* **1996**, *100*, 4111-4119, doi:10.1021/jp953178u.

Kaltsoyannis , N.; Plane, J. M. C. Quantum chemical calculations on a selection of iodine-containing species (IO, OIO, INO_3, $(IO)_2$, I_2O_3, I_2O_4 and I_2O_5) of importance in the atmosphere. *Phys. Chem. Chem. Phys.* **2008**, *10*, 1723-1733, doi:10.1039/b715687c.

Karton, A.; Parthiban, S.; Martin, J. M. L. Post-CCSD(T) ab initio thermochemistry of halogen oxides and related hydrides XOX, XOOX, HOX, XO_n, and HXO_n (X = F, Cl), and evaluation of DFT methods for these systems. *J. Phys. Chem. A* **2009**, *113*, 4802-4816, doi:10.1021/jp8087435.

Kerr, J. A.; Timlin, D. M. A kinetic study of the thermal elimination of hydrogen fluoride from 1,2-dichloroethane. Determination of the bond dissociation energies $D(CH_2F—CH_2F)$ and $D(CH_2F—H)$. *Int. J. Chem. Kinet.* **1971**, *3*, 427-441, doi:10.1002/kin.550030505.

Khanniche, S.; Louis, F.; Cantrel, L.; Černušák, I. Thermochemistry of HIO_2 species and reactivity of iodous acid with OH radical: A computational study. *Earth Space Chem.* **2017**, *1*, 39-49, doi:10.1021/acsearthspacechem.6b00010.

Kim, H.; Dooley, J. S.; Johnson, E. R.; North, S. W. Photodissociation of the BrO radical using velocity map ion imaging: Excited state dynamics and acurate D^0_0(BrO) evaluation. *J. Chem. Phys.* **2006**, *124*, 134304, doi:10.1063/1.2173265.

Kim, J.; Ihee, H.; Lee, Y. S. Spin-orbit density functional and *ab initio* study of HgX_n (X = F, Cl, Br, and I; *n* = 1, 2, and 4). *J. Chem. Phys.* **2010**, *133*, 144309, doi:10.1063/1.3497189.

King, K. D.; Golden, D. M.; Benson, S. W. Kinetics of the gas-phase thermal bromination of acetone. Heat of formation and stabilization energy of the acetonyl radical. *J. Am. Chem. Soc.* **1970**, *92*, 5541-5546, doi:10.1021/ja00722a001.

Kiselev, V. G.; Gritsan, N. P. Theoretical study of the nitroalkane thermolysis. 1. Computation of the formation enthalpy of the nitroalkanes, their isomers and radical products. *J. Phys. Chem. A* **2008**, *112*, 4458-4464, doi:10.1021/jp077391p.

Klemm, R. B.; Thorn, R. P.; Stief, L. J.; Buckley, T. J.; Johnson, R. D. Heat of formation of OBrO: Experimental photoionization study. *J. Phys. Chem. A* **2001**, *105*, 1638-1642, doi:10.1021/jp002397z.

Knyazev, V. D.; Bencsura, A.; Slagle, I. R. Unimolecular decomposition of the FCO radical. *J. Phys. Chem. A* **1997**, *101*, 849-852, doi:10.1021/jp9623296.

Knyazev, V. D.; Bencsura, A.; Slagle, I. R. Kinetics and thermochemistry of the reactions of CH_3CCl_2 and $(CH_3)_2CCl$ radicals with molecular oxygen. *J. Phys. Chem. A* **1998**, *102*, 1760-1769, doi:10.1021/jp9726089.

Knyazev, V. D.; Slagle, I. R. Thermochemistry of the R-O_2 bond in alkyl and chloroalkyl peroxy radicals. *J. Phys. Chem. A* **1998**, *102*, 1770-1778, doi:10.1021/jp9726091.

Kolesov, V. P.; Papina, T. S. Thermochemistry of haloethanes. *Russ. Chem. Rev.* **1983**, *52*, 425-439.

Kormos, B. L.; Liebman, J. F.; Cramer, C. J. 298 K enthalpies of formation of monofluorinated alkanes: theoretical predictions for methyl, ethyl,isopropyl, and tert-butyl fluoride. *J. Phys. Org. Chem.* **2004**, *17*, 656-664, doi:10.1002/poc.801.

Kosmas, A. M.; Mpellos, C.; Salta, Z.; Drougas, E. Structural and heat of formation studies of halogenated methyl hydro-peroxides. *Chem. Phys.* **2010**, *371*, 36-42, doi:10.1016/j.chemphys.2010.03.026.

Kraka, E.; Konkoli, Z.; Cremer, D.; Fowler, J.; Schaefer, H. F. Difluorodioxirane: An unusual cyclic peroxide. *J. Am. Chem. Soc.* **1996**, *118*, 10595-10608, doi:10.1021/ja961983w.

Kudchadker, S. A.; Kudchadker, A. P. Ideal gas thermodynamic properties of the eight bromo- and iodomethanes. *J. Phys. Chem. Ref. Data* **1975**, *4*, 457-470, doi:10.1063/1.555522.

Kudchadker, S. A.; Kudchadker, A. P. Erratum: Ideal gas thermodynamic properties of eight bromo- and iodomethanes. *J. Phys. Chem. Ref. Data* **1976**, *5*, 529-530, doi:10.1063/1.555537.

Kudchadker, S. A.; Kudchadker, A. P. Ideal gas thermodynamic properties of $CH_{4-(a+b+c+d)}F_a,Cl_b,Br_c,I_d$ halomethanes. *J. Phys. Chem. Ref. Data* **1978**, *7*, 1285-1307, doi:10.1063/1.555585.

Kudchadker, S. A.; Kudchadker, A. P. Ideal gas thermodynamic properties of selected bromoethanes and iodoethane. *J. Phys. Chem. Ref. Data* **1979**, *8*, 519-526, doi:10.1063/1.555601.

Lacher, J. R.; Skinner, H. A. Bond energy additivity and bond interactions in fluoro-halogenated hydrocarbons. *J. Chem. Soc. A* **1968**, 1034-1038, doi:10.1039/J19680001034.

Lafleur, R. D.; Szatary, B.; Baer, T. A photoelectron-photoion coincidence study of the ICH_2CN ion dissociation: Thermochemistry of CH_2CN, $^+CH_2CN$, and ICH_2CN. *J. Phys. Chem. A* **2000**, *104*, 1450-1455, doi:10.1021/jp993569z.

Lago, A. F.; Baer, T. A photoelectron photoion coincidence study of the vinyl bromide and tribromoethane ion dissociation dynamics: Heats of formation of $C_2H_3^+$, C_2H_3Br, $C_2H_3Br^+$, $C_2H_3Br_2^+$, and $C_2H_3Br_3$ *J. Phys. Chem. A* **2006**, *110*, 3036-3041, doi:10.1021/jp053943x.

Lago, A. F.; Kercher, J. P.; Bödi, A.; Sztáray, B.; Miller, B.; Wurzelmann, D.; Baer, T. Dissociative photoionization and thermochemistry of dihalomethane compounds studied by threshold photoelectron photoion coincidence spectroscopy. *J. Phys. Chem. A* **2005**, *109*, 1802-1809, doi:10.1021/jp045337s.

Lamoreaux, R. H.; Hildenbrand, D. L. High temperature vaporization behavior of oxides. 1. Alkali metal binary oxides. *J. Phys. Chem. Ref. Data* **1984**, *13*, 151-173, doi:10.1063/1.555706.

Lay, T. H.; Bozzelli, J. W. Enthalpies of formation and group additivity of alkyl peroxides and trioxides. *J. Phys. Chem. A* **1997**, *101*, 9505-9510, doi:10.1021/jp972103i.

Lay, T. H.; Krasnoperov, L. N.; Venanzi, C. A.; Bozzelli, J. W.; Shokhirev, N. V. Ab initio study of α-chlorinated ethyl hydroperoxides CH_3CH_2OOH, CH_3ClOOH, and CH_3CCl_2OOH: Conformational analysis, internal rotation barriers, vibrational frequencies, and thermodynamic properties. *J. Phys. Chem.* **1996**, *100*, 8240-8249, doi:10.1021/jp952976h.

Lee, E. P. F.; Wright, T. G. Thermochemistry of $HgCH_3$ and $HgCH_3^+$ and the ionization energy of $HgCH_3$. *Chem. Phys. Lett.* **2003**, *376*, 418-423, doi:10.1016/S0009-2614(03)01022-4.

Lee, S. Y. Computational study of enthalpies of formation of OXO (X = Cl, Br, and I) and their anions. *J. Phys. Chem. A* **2004**, *108*, 10754-10761, doi:10.1021/jp0467550.

Lee, T. J. *Ab initio* characterization of $ClNO_2$, *cis*-ClONO, and *trans*-ClONO. *J. Phys. Chem.* **1994**, *98*, 111-115, doi:10.1021/j100052a019.

Lee, T. J. Ab initio characterization of triatomic bromine molecules of potential interest in stratospheric chemistry. *J. Phys. Chem.* **1995**, *99*, 15074-15080, doi:10.1021/j100041a024.

Lee, T. J. Ab initio characterization of $HBrO_2$ isomers: implications for stratospheric bromine chemistry. *Chem. Phys. Lett.* **1996**, *262*, 559-566, doi:10.1016/S0009-2614(96)01178-5.

Lee, T. J. Characterization of $BrNO_2$, *cis*-BrONO, and *trans*-BrONO. Implications for atmospheric chemistry. *J. Phys. Chem.* **1996**, *100*, 19847-19852, doi:10.1021/jp962605g.

Lee, T. J.; Rendell, A. P. Ab initio characterization of ClOOH: Implications for atmospheric chemistry. *J. Phys. Chem.* **1993**, *97*, 6999-7002, doi:10.1021/j100129a014.

Leplat, N.; Federič, J.; Šulková, K.; Sudolská, M.; Louis, F.; Černušák, I.; Rossi, M. J. The Kinetics of the reaction $C_2H_5\bullet + HI \rightarrow C_2H_6 + I\bullet$ over an extended temperature range (213–623 K): Experiment and modeling. *Z. Phys. Chem.* **2015**, *229*, 1475, doi:10.1515/zpch-2015-0607.

Lesar, A.; Prebil, S.; Hodošček, M. Ab initio characterization of $ClNO_3$ isomers. *J. Phys. Chem. A* **2003**, *107*, 9168-9174, doi:10.1021/jp030192v.

Li, J.; Yang, J.; Mo, Y. X.; Lau, K. C.; Qian, X. M.; Song, Y.; Liu, J. B.; Ng, C. Y. Combined vacuum ultraviolet laser and synchrotron pulsed field ionization study of CH_2BrCl. *J. Chem. Phys.* **2007**, *126*, 184304, doi:10.1063/1.2730829.

Li, W. K.; Ng, C. Y. Gaussian-2 ab initio study of isomeric Cl_2O_2 and $Cl_2O_2^+$ and their dissociation reactions. *J. Phys. Chem. A* **1997**, *101*, 113-115, doi:10.1021/jp962253d.

Lightfoot, P. D.; Cox, R. A.; Crowley, J. N.; Destriau, M.; Hayman, G. D.; Jenkin, M. E.; Moortgat, G. K.; Zabel, F. Organic peroxy radicals: Kinetics, spectroscopy and tropospheric chemistry. *Atmos. Environ.* **1992**, *26A*, 1805-1961, doi:10.1016/0960-1686(92)90423-I.

Lim, K. P.; Michael, J. V. Thermal decomposition of $COCl_2$. *J. Phys. Chem.* **1994**, *98*, 211-215, doi:10.1021/j100052a035.

Litorja, M.; Ruscic, B. A photoionization study of the hydroperoxyl radical, HO_2, and hydrogen peroxide, H_2O_2. *J. Electron.Spec. Rel. Phenom.* **1998**, *97*, 131-146, doi:10.1016/S0368-2048(98)00264-3.

Lodders, K. Revised and updated thermochemical properties of the gases mercapto (HS), disulfur monoxide (S_2O), thiazyl (NS), and thioxophosphino (PS). *J. Phys. Chem. Ref. Data* **2004**, *33*, 357-367, doi:10.1063/1.1611178.

Louis, F.; Černušák, I.; Canneaux, S.; Mečiarová, K. Atmospheric reactivity of CH_3I and CH_2I_2 with OH radicals: A comparative study of the H- versus I-abstraction. *Comp. Theor. Chem.* **2011**, *965*, 275-284, doi:10.1016/j.theochem.2010.09.022.

Luo, Y. R.; Benson, S. W. Heats of formation of alkyl fluorides. *J. Phys. Chem. A* **1997**, *101*, 3042-3044, doi:10.1021/jp962641f.

Lyman, J. Thermodynamic properties of dioxygen difluoride (O_2F_2) and dioxygen fluoride (O_2F). *J. Phys. Chem. Ref. Data* **1989**, *18*, 799-807, doi:10.1063/1.555830.

Manion, J. A. Evaluated enthalpies of formation of the stable closed shell C1 and C2 chlorinated hydrocarbons. *J. Phys. Chem. Ref. Data* **2002**, *31*, 123-172, doi:10.1063/1.1420703.

Marshall, P. Computational studies of the thermochemistry of the atmospheric iodine reservoirs HOI and $IONO_2$. *Advances in Quantum Chemistry* **2008**, 159-175.

Marshall, P.; Srinivas, G. N.; Schwartz, M. A computational study of the thermochemistry of bromine- and iodine-containing methanes and methyl radicals. *J. Phys. Chem. A* **2005**, *109*, 6371-6379, doi:10.1021/jp0518052.

Martin, J. M. L.; François, J. P.; Gijbels, R. First principles computation of thermochemical properties beyond the harmonic approximation. II. Application to the amino radical NH_2. *J. Chem. Phys.* **1992**, *97*, 3530, doi:10.1063/1.462987.

Matus, M. H.; Arduengo, A. J.; Dixon, D. A. The heats of formation of diazene, hydrazine, $N_2H_3^+$, $N_2H_5^+$, N_2H, and N_2H_3 and the methyl derivatives CH_3NNH, CH_3NNCH_3, and $CH_3HNNHCH_3$. *J. Phys. Chem. A* **2006**, *110*, 10116-10121, doi:10.1021/jp064086f.

Matus, M. H.; Nguyen, M. T.; Dixon, D. A. Theoretical prediction of the heats of formation of C_2H_5O radicals derived from ethanol and of the kinetics of β-C-C scission in the ethoxy radical. *J. Phys. Chem. A* **2007**, *111*, 113-126, doi:10.1021/jp064086f.

Matus, M. H.; Nguyen, M. T.; Dixon, D. A.; Christe, K. O. Thermochemical properties of CHFO and CF_2O. *J. Phys. Chem. A* **2008**, *112*, 4973-4981, doi:10.1021/jp800103y.

Matus, M. H.; Nguyen, M. T.; Dixon, D. A.; Peterson, K. A.; Francisco, J. S. $ClClO_2$ is the most stable isomer of Cl_2O_2. Accurate coupled cluster energetics and electronic spectra of Cl_2O_2 isomers. *J. Phys. Chem. A* **2008**, *112*, 9623-9627, doi:10.1021/jp806220r.

Mayer-Figge, A.; Zabel, F.; Becker, K. H. Thermal decomposition of $CF_3O_2NO_2$. *J. Phys. Chem.* **1996**, *100*, 6587-6593, doi:10.1021/jp953205g.

McGrath, M. P.; Rowland, F. S. Determination of the barriers to interneal rotatoin in ONOOX (X = H, Cl) and characterization of the minimum energy conformers. *J. Phys. Chem.* **1994**, *98*, 1061-1067, doi:10.1021/j100055a004.

McGrath, M. P.; Rowland, F. S. Ideal gas thermodynamic properties of HOBr. *J. Phys. Chem.* **1994**, *98*, 4773-4775, doi:10.1021/j100069a001.

McMillen, D. F.; Golden, D. M. Hydrocarbon bond dissociation energies. *Ann. Rev. Phys. Chem.* **1982**, *33*, 493-532.

Miller, C. E.; Lynton, J. I.; Keevil, D. M.; Franscisco, J. S. Dissociation pathways of peroxyacetyl nitrate (PAN). *J. Phys. Chem. A* **1999**, *103*, 11451-11459, doi:10.1021/jp992667h.

Millward, G. E.; Hartig, R.; Tschuikow-Roux, E. Kinetics of the shock wave thermolysis of 1,1,2,2-tetrafluoroethane. *J. Phys. Chem.* **1971**, *75*, 3195-3201, doi:10.1021/j100690a001.

Mishra, B. K.; Chakrabartty, A. K.; Deka, R. C. Theoretical investigation of the gas-phase reactions of $CF_2ClC(O)OCH_3$ with the hydroxyl radical and the chlorine atom at 298 K. *J. Mol. Model* **2013**, *19*, 3263-3270, doi:10.1007/s00894-013-1865-1.

Misra, A.; Marshall, P. Computational studies of the isomers of ClIO and $ClIO_2$. *J. Chem. Soc. Faraday Trans.* **1997**, *93*, 3301-3304, doi:10.1039/a702360j.

Misra, A.; Marshall, P. Computational investigation of iodine oxides. *J. Phys. Chem. A* **1998**, *102*, 9056-9060, doi:10.1021/jp982708u.

Miyokawa, K.; Ozaki, S.; Yano, T. Kinetics of the photobromination of fluoroethane. Estimate of the C-H bond dissociation energies and the heats of formation of the CH_3CHF and CH_2CH_2F radicals. *Bull. Chem. Soc. Jpn.* **1996**, *69*, 869-873.

Miyokawa, K.; Tschuikow-Roux, E. Kinetics of α- and β- hydrogen abstraction from C_2H_5Cl by Br atoms. Estimate of C-H bond dissociation energies and heats of formation of CH_3CHCl and CH_2CH_2Cl radicals. *J. Phys. Chem.* **1990**, *94*, 715-717, doi:10.1021/j100365a037.

Miyokawa, K.; Tschuikow-Roux, E. Reaction of atomic bromine with difluorochloromethane, The heat of formation of the $CClF_2$ radical and the $D^o(CClF_2\text{-}H)$ bond dissociation energy. *J. Phys. Chem.* **1992**, *96*, 7328-7331, doi:10.1021/j100197a034.

Miyokawa, K.; Tschuikow-Roux, E. Kinetics of photobromination of dichloro- and dibromoethane. Estimate of the C-H bond dissociation energies and the heats of formation of the CH_3CCl_2 and CH_3CHBr_2 radicals. *Bull. Chem. Soc. Jpn.* **1999**, *72*, 1-5.

Moore, C. E. *Atomic Energy Levels*; NSRDS: Washington. DC, 1971; Vol. 1.

Murray, C.; Derro, E. L.; Sechler, T. D.; Lester, M. I. Stability of the hydrogen trioxide radical via infrared action spectroscopy. *J. Phys. Chem. A* **2007**, *111*, 4727-4730, doi:10.1021/jp071473w.

Murrells, T. P.; Lovejoy, E. R.; Ravishankara, A. R. Oxidation of CS_2 by reaction with OH. 1. Equilibrium constant for the reaction $OH + CS_2 \rightleftarrows CS_2OH$ and the kinetics of the $CS_2OH + O_2$ reaction. *J. Phys. Chem.* **1990**, *94*, 2381-2386, doi:10.1021/j100369a036.

Nagy, B.; Csontos, J.; Kállay, M.; Tasi, G. High-accuracy theoretical study on the thermochemistry of several formaldehyde derivatives. *J. Phys. Chem. A* **2010**, *114*, 13213-13221, doi:10.1021/jp1085203.

Nagy, B.; Csontos, J.; Szakács, P.; Kállay, M. High-accuracy theoretical thermochemistry of fluoroethanes. *J. Phys. Chem. A* **2014**, *118*, 4824-4836, doi:10.1021/jp503492a.
Nagy, B.; Szakács, P.; Csontos, J.; Rolik, Z.; Tasi, G.; Kallay, M. High-accuracy theoretical thermochemistry of atmospherically important sulfur-containing molecules. *J. Phys. Chem. A* **2011**, *115*, 7823-7833, doi:10.1021/jp203406d.
Nguyen, M. T.; Matus, M. H.; Lester, W. A., Jr.; Dixon, D. A. Heats of formation of triplet ethylene, ethylidene, and acetylene. *J. Phys. Chem. A* **2008**, *112*, 2082-2087, doi:10.1021/jp074769a.
Nguyen, M. T.; Nguyen, T. L.; Ngan, V. T.; Nguyen, H. M. T. Heats of formation of the Criegee formaldehyde oxide and dioxirane. *Chem. Phys. Lett.* **2007**, *448*, 183-188, doi:10.1016/j.cplett.2007.10.033.
Nguyen, T. L.; Baraban, J. H.; Ruscic, B.; Stanton, J. F. On the HCN – HNC energy difference. *J. Phys. Chem. A* **2015**, *119*, 10929-10934, doi:10.1021/acs.jpca.5b08406.
Nickolaisen, S. L.; Friedl, R. R.; Sander, S. P. Kinetics and mechanism of the ClO + ClO reaction: Pressure and temperature dependences of the bimolecular and termolecular channels and thermal decomposition of chlorine peroxide, ClOOCl. *J. Phys. Chem.* **1994**, *98*, 155-169, doi:10.1021/j100052a027.
Nicovich, J. M.; Kreutter, K. D.; van Dijk, C. A.; Wine, P. H. Temperature dependent kinetics studies of the reactions $Br(^2P_{3/2}) + H_2S \leftrightarrow SH + HBr$ and $Br(^2P_{3/2}) + CH_3SH \leftrightarrow CH_3S + HBr$. Heats of formation of SH and CH_3S radicals. *J. Phys. Chem.* **1992**, *96*, 2518-2528, doi:10.1021/j100185a025.
Nicovich, J. M.; Kreutter, K. D.; Wine, P. H. Kinetics and thermochemistry of ClCO formation from the Cl + CO association reaction. *J. Chem. Phys.* **1990**, *92*, 3539-3544, doi:10.1063/1.457862.
Nicovich, J. M.; Wang, L.; McKee, M. L.; Wine, P. H. Kinetics and thermochemistry of the $Cl(^2P_J) + C_2Cl_4$ association reaction. *J. Phys. Chem.* **1996**, *100*, 680-688, doi:10.1021/jp952396k.
Okabe, H. Photodissociation of HNCO in the vacuum ultraviolet; Production of NCO $A^2\Sigma$ and $NH(A^3\pi, \pi C^1)$. *J. Chem. Phys.* **1970**, *53*, 3507-3515, doi:10.1063/1.1674525.
Okabe, H. Photodissociation of acetylene and bromoacetylene in the vacuum ulraviolet: Production of electronically excited C_2H and C_2. *J. Chem. Phys.* **1975**, *62*, 2782-2787, doi:10.1063/1.430813.
Olleta, A. C.; Lane, S. I. Ab initio studies of the gas-phase thermodynamic properties and bond dissociation energies for haloethanes and halomethy radicals. *Phys. Chem. Chem. Phys.* **2001**, *3*, 811-818, doi:10.1039/b005375i.
Oren, M.; Iron, M. A.; Burcat, A.; Martin, J. M. L. Thermodynamic properties of C_1 and C_2 bromo compounds and radicals: A relativistic ab initio study. *J. Phys. Chem. A* **2004**, *108*, 7752-7761, doi:10.1021/jp0475786.
Orlando, J. J.; Tyndall, G. S. Rate coefficients for the thermal decomposition of $BrONO_2$ and the heat of formation of $BrONO_2$. *J. Phys. Chem.* **1996**, *100*, 19398-19405, doi:10.1021/jp9620274.
Paci, M. A. B.; Argüello, G. A.; García, P.; Willner, H. Thermal decompositino of the perfluorinated peroxides $CF_3OC(O)OOC(O)F$ and $CF_3OC(O)OOCF_3$. *J. Phys. Chem. A* **2005**, *109*, 7481-7488, doi:10.1021/jp0528818.
Pacios, L. F.; Gómez, P. C. *Ab initio* study of bromine dioxides OBrO and BrOO. *J. Phys. Chem. A* **1997**, *101*, 1767-1773, doi:10.1021/jp963281z.
Paddison, S. J.; Chen, Y. H.; Tschuikow-Roux, E. An *ab initio* study of the structrures, barriers for internal rotation, vibrational frequencies, and thermodynamic functions of the hydrochlorofluorocarbon CH_3CF_2Cl and the corresponding radical CH_2CF_2Cl. *Can. J. Chem.* **1994**, *72*, 561-567, doi:10.1139/v94-079.
Papayannakos, N.; Kosmas, A. M. The conformational potential energy surface of IOONO and the isomerization and decomposition processes. *Chem. Phys.* **2005**, *315*, 251-258, doi:10.1016/j.chemphys.2005.04.014.
Papina, T. S.; Kolesov, V. P. Standard enthalpy of formation of trichloroethylene. *Russ. J. Phys. Chem.* **1985**, *59*, 1289-1292.
Papina, T. S.; Kolesov, V. P.; Golovanova, Y. G. The standard enthalpy of formation of bromoform. *Russ. J. Phys. Chem.* **1982**, *56*, 1666-1668.
Parthiban, S.; Lee, T. J. Ab initio investigation of the atmospheric molecule bromine nitrate: Equilibrium structure, vibrational spectrum, and heat of formation. *J. Chem. Phys.* **1998**, *109*, 525-530, doi:10.1063/1.476589.
Parthiban, S.; Lee, T. J. Theoretical study of $XONO_2$ (X=Br, OBr, O_2Br): Implications for stratospheric bromine chemistry. *J. Chem. Phys.* **2000**, *113*, 145-152, doi:10.1063/1.481781.
Pedley, J. B. *Thermochemical Data and Structures of Organic Compounds*; Thermodynamics Data Center: College Station, TX, 1994.
Pedley, J. B.; Marshall, E. M. Thermochemical data for gaseous monoxides. *J. Phys. Chem. Ref. Data* **1983**, *12*, 967-1032, doi:10.1063/1.555698.

Peebles, L. R.; Marshall, P. A coupled-cluster study of the enthalpy of formation of nitrogen sulfide, NS. *Chem. Phys. Lett.* **2002**, *366*, 520-524, doi:10.1016/S0009-2614(02)01619-6.
Peterson, K. A.; Shepler, B. C.; Figgen, D.; Stoll, H. On the spectroscopic and thermochemical properties of ClO, BrO, IO, and their anions. *J. Phys. Chem. A* **2006**, *110*, 13877-13883, doi:10.1021/jp065887l.
Peterson, K. A.; Shepler, B. C.; Singleton, J. M. The group 12 metal chalcogenides: an accurate multireference configuration interaction and coupled cluster study. *Mol. Phys.* **2007**, *105*, 1139-1155, doi:10.1080/00268970701241664.
Pickard, J. M.; Rodgers, A. S. The kinetics and thermochemistry of the reaction of 1,1-difluoroethane with iodine. The CF_2-H bond dissociation energy in 1,1-difluoroethane and the heat of formation of 1,1-difluoroethyl. *J. Am. Chem. Soc.* **1977**, *99*, 691-694, doi:10.1021/ja00445a005.
Pickard, J. M.; Rodgers, A. S. Kinetics of the gas-phase reaction $CH_3F + I_2 \leftrightarrows CH_2FI + HI$: The C-H bond dissociation energy in methyl and methylene fluorides. *Int. J. Chem. Kinet.* **1983**, *15*, 569-577, doi:10.1002/kin.550150607.
Pittam, D. A.; Pilcher, G. Measurements of heats of combustion by flame calorimetry. Part 8. Methane, ethane, propane, n-butane and 2-methylpropane. *J. Chem. Soc. Faraday Trans. 1* **1972**, *68*, 2224-2229, doi:10.1039/F19726802224.
Plenge, J.; Kühl, S.; Vogel, B.; Müller, R.; Stroh, F.; von Hobe, M.; Flesch, R.; Rühl, E. Bond strength of chlorine peroxide. *J. Phys. Chem. A* **2005**, *109*, 6730-6734, doi:10.1021/jp044142h.
Poutsma, J. C.; Paulino, J. A.; Squires, R. R. Absolute heats of formation of CHCl, CHF, and CClF. A gas-phase experimental and G2 theoretical study. *J. Phys. Chem. A* **1997**, *101*, 5327-5336, doi:10.1021/jp970778f.
Ramachandran, R.; Vegesna, N. S.; Peterson, K. A. Effects of electron correlation and scalar relativistic corrections on the thermochemical and spectroscopic properties of HOF. *J. Phys. Chem. A* **2003**, *107*, 7938-7944, doi:10.1021/jp035266h.
Ramond, T. M.; Blanksby, S. J.; Kato, S.; Bierbaum, V. M.; Davico, G. E.; Schwartz, R. L.; Lineberger, W. C.; Ellison, G. B. Heat of formation of the hydroperoxyl radical HOO via negative ion studies. *J. Phys. Chem. A* **2002**, *106*, 9641-9647, doi:10.1021/jp014614h.
Regimbal, J. M.; Mozurkewich, M. Peroxynitric acid decay mechanisms and kinetics at low pH. *J. Phys. Chem. A* **1997**, *101*, 8822-8829, doi:10.1021/jp971908n.
Reints, W.; Pratt, D. A.; Korth, H. G.; Mulder, P. O-O bond dissociation enthalpy in di(trifluoromethyl) peroxide (CF_3OOCF_3) as determined by very low pressure pyrolysis. Density functional computations on O-O and O-H bonds in (fluorinated) derivatives. *J. Phys. Chem. A* **2000**, *104*, 10713-70720, doi:10.1021/jp994434w.
Resende, S. M.; Ornellas, F. R. Thermochemistry of atmospheric sulfur compounds. *Chem. Phys. Lett.* **2003**, *367*, 489-494, doi:10.1016/S0009-2614(02)01738-4.
Rissanen, M. P.; Amedro, D.; Eskola, A. J.; Kurten, T.; Timonen, R. S. Kinetic (T = 201−298 K) and equilibrium (T = 320−420 K) measurements of the $C_3H_5 + O_2 \leftrightarrows C_3H_5O_2$ reaction. *J. Phys. Chem. A* **2012**, *116*, 3969-3978, doi:10.1021/jp209977h.
Rodgers, A. S.; Chao, J.; Wilhoit, R. C.; Zwolinski, B. J. Ideal gas thermodynamic properties of eight chloro- and fluoromethanes. *J. Phys. Chem. Ref. Data* **1974**, *3*, 117-140, doi:10.1063/1.3253135.
Rodgers, A. S.; Jerus, P. Kinetics of the bromine catalyzed elimination of HCl from 1,1,1-trichloroethane. *Int. J. Chem. Kinet.* **1988**, *20*, 565-575, doi:10.1002/kin.550200706.
Rodriquez, C. F.; Williams, I. H. Ring strain energy and enthalpy of formation of oxiranone: an ab initio theoretical determination. *J. Chem. Soc.-Perkin Trans. 2* **1997**, 953-957, doi:10.1039/A606820K
Ruscic, B. Active thermochemical tables: Water and water dimer. *J. Phys. Chem. A* **2013**, *117*, 11940-11953, doi:10.1021/jp403197t.
Ruscic, B. Active thermochemical tables: Sequential bond dissociation enthalpies of methane, ethane, and methanol and the related thermochemistry. *J. Phys. Chem. A* **2015**, *119*, 7810-7837, doi:10.1021/acs.jpca.5b01346.
Ruscic, B.; Berkowitz, J. Photoionization mass spectrometry of CH_2S and HCS. *J. Chem. Phys.* **1993**, *98*, 2568-2579, doi:10.1063/1.464139.
Ruscic, B.; Boggs, J. E.; Burcat, A.; Csaszar, A. G.; Demaison, J.; Janoschek, R.; Martin, J. M. L.; Morton, M. L.; Rossi, M. J.; Stanton, J. F.; Szalay, P. G.; Westmoreland, P. R.; Zabel, F.; Berces, T. IUPAC critical evaluation of thermochemical properties of selected radicals. Part I. *J. Phys. Chem. Ref. Data* **2005**, *34*, 573-656, doi:10.1063/1.1724828.

Ruscic, B.; Feller, D.; Peterson, K. Active Thermochemical Tables: dissociation energies of several homonuclear first-row diatomics and related thermochemical values. *Theor. Chem. Acc.* **2014**, *133*, 1415, doi:10.1007/s00214-013-1415-z.

Ruscic, B.; Litorja, M. Photoionization of HOCO revisited: a new upper limit to the adiabatic ionization energy and lower limit to the enthalpy of formation. *Chem. Phys. Lett.* **2000**, *316*, 45-50, doi:10.1016/S0009-2614(99)01267-1.

Ruscic, B.; Litorja, M.; Asher, R. L. Ionization energy of methylene revisited: Improved values for the enthalpy of formation of CH_2 and the bond dissociation energy of CH_3 via simultaneous solution of the local thermochemical network. *J. Phys. Chem. A* **1999**, *103*, 8625-8633, doi:10.1021/jp992403v.

Ruscic, B.; Michael, J. V.; Redfern, P. C.; Curtiss, L. A.; Raghavachri, K. Simultaneous adjustment of experimentally based enthalpies of formation of CF_3X, X = nil, H, Cl, Br, I, CF_3, CN, and a probe of G3 theory. *J. Phys. Chem. A* **1998**, *102*, 10889-10899, doi:10.1021/jp983237e.

Ruscic, B.; Pinzon, R. E.; Morton, M. L.; Srinivasan, N. K.; Su, M.-C.; Sutherland, J. W.; Michael, J. V. Active thermochemical tables: Accurate enthalpy of formation of hydroperoxyl radical, HO_2. *J. Phys. Chem. A* **2006**, *110*, 6592–6601, doi:10.1021/jp056311j.

Ruscic, B.; Pinzon, R. E.; Morton, M. L.; von Laszevski, G.; Bittner, S. J.; Nijsure, S. G.; Amin, K. A.; Minkoff, M.; Wagner, A. F. Introduction to active thermochemical tables: Several "key" enthalpies of formation revisited. *J. Phys. Chem. A* **2004**, *108*, 9979-9997, doi:10.1021/jp047912y.

Ruttink, P. J. A.; Burgers, P. C.; Trikoupis, M. A.; Terlouw, J. K. The heat of formation of sulfine, CH_2=S=O, revisited: a CBS-QB3 study. *Chem. Phys. Lett.* **2001**, *342*, 447-451, doi:10.1016/S0009-2614(01)00610-8.

Sánchez, H. R.; Del Pla, J. Theoretical study of the thermochemistry of chlorine oxyfluorides. *Chem. Phys. Lett.* **2016**, *663*, 16-20, doi:10.1016/j.cplett.2016.09.045.

Saraf, S. R.; Rogers, W. J.; Mannan, M. S.; Hall, M. B.; Thomson, L. M. Theoretical thermochemistry: Ab initio heat of formation for hydroxylamine. *J. Phys. Chem. A* **2003**, *107*, 1077-1081, doi:10.1021/jp026027h.

Schneider, W. F.; Nance, B. I.; Wallington, T. J. Bond strengths in halogenated methanes: Evidence for negative hyperconjugation. *J. Am. Chem. Soc.* **1995**, *117*, 478-485, doi:10.1021/ja00106a055.

Schneider, W. F.; Wallington, T. J. Thermochemistry of COF_2 and related compounds. *J. Phys. Chem.* **1994**, *98*, 7448-7451, doi:10.1021/j100082a009.

Schwartz, M.; Marshall, P. An ab initio investigation of halocarbenes. *J. Phys. Chem. A* **1999**, *103*, 7900-7906, doi:10.1021/jp9919213.

Schwartz, M.; Peebles, L. R.; Berry, R. J.; Marshall, P. A computational study of chlorofluoro-methyl radicals *J. Chem. Phys.* **2003**, *118*, 557-564, doi:10.1063/1.1524157.

Sebbar, N.; Bozzelli, J. W.; Bockhorn, H. Thermochemical properties, rotation barriers, bond energies, and group additivity for vinyl, phenyl, ethynyl, and allyl peroxides *J. Phys. Chem. A* **2004**, *2004*, 8353-8366, doi:10.1021/jp031067m.

Sebbar, N.; Bozzelli, J. W.; Bockhorn, H. Enthalpy of formation and bond energies on unsaturated oxygenated hydrocarbons using G3MP2B3 calculation methods. *Int. J. Chem. Kinet.* **2005**, *37*, 633-648, doi:10.1002/kin.20086.

Seetula, J. A. Kinetics and thermochemistry of the R + HBr ⇄ RH + Br (R = CH_2Cl, $CHCl_2$, CH_3CHCl or CH_3CCl_2) equilibrium. *J. Chem. Soc. Faraday Trans.* **1996**, *92*, 3069-3078, doi:10.1039/FT9969203069.

Seetula, J. A. Kinetics and thermochemistry of the R + HBr ⇄ RH + Br (R = C_2H_5 or β-C_2H_4Cl) equilibrium. *J. Chem. Soc. Faraday Trans.* **1998**, *94*, 891-898, doi:10.1039/A706440C.

Seetula, J. A. Kinetics and thermochemistry of the C_3H_5 + HBr ⇌ C_3H_6 + Br equilibrium. *Phys. Chem. Chem. Phys.* **1999**, *1*, 4727-4731, doi:10.1039/A905347F.

Seetula, J. A. *Ab initio* study of the transition states for determining the enthalpies of formation of alkyl and halogenated alkyl free radicals. *Phys. Chem. Chem. Phys.* **2000**, *2*, 3807-3812, doi:10.1039/b001350l.

Seetula, J. A. Kinetics of the R + HBr → RH + Br (R = CH_2I or CH_3) reaction. An ab initio study of the enthalpy of formation of the CH_2I, CHI_2 and CI_3 radicals. *Phys. Chem. Chem. Phys.* **2002**, *4*, 455-460, doi:10.1039/b107407p.

Seetula, J. A. Kinetics of the R + HBr ⇄ RH + Br (R = CH_2Br, CHBrCl or CCl_3) equilibrium. Thermochemistry of the CH_2Br and CHBrCl radicals. *Phys. Chem. Chem. Phys.* **2003**, *5*, 849-855, doi:10.1039/b210787m.

Seetula, J. A.; Slagel, I. R. Kinetics and thermochemistry of the R + HBr ⇄ RH + Br (R = n-C_3H_7, isoC_3H_7, isoC_4H_9, sec-C_4H_9, or tert-C_4H_9) equilibrium. *J. Chem. Soc. Faraday Trans.* **1997**, *93*, 1709-1719, doi:10.1039/a608224f.

Shapley, W. A.; Bacskay, G. B. Ab initio quantum chemical studies of the formaldiminoxt (CH_2NO) radical: 1. Isomerization reactions. *J. Phys. Chem. A* **1999**, *103*, 4505-4513, doi:10.1021/jp984817e.
Shenyavskaya, E. A.; Yungman, V. S. NIST-JANAF thermochemical tables. III. Diatomic hydrogen halide gases. *J. Phys. Chem. Ref. Data* **2004**, *33*, 923-957, doi:10.1063/1.1638781.
Shepler, B. C.; Balabanov, N. B.; Peterson, K. A. Ab initio thermochemistry involving heavy atoms: An investigation of the reactions Hg + IX (X = I, Br, Cl, O). *J. Phys. Chem. A* **2005**, *109*, 10363-10372, doi:10.1021/jp0541617.
Shepler, B. C.; Peterson, K. A. Mercury monoxide: A systematic investigation of its ground electronic state. *J. Phys. Chem. A* **2003**, *107*, 1783-1787, doi:10.1021/jp027512f.
Shi, J. C.; Shang, Y. L.; Du, S. Y.; Luo, S. N. Hydrogen abstraction from CH_3NH_2, $(CH_3)_2NH$, and $(CH_3)_3N$ by HO_2 radicals: A theoretical study. *Chem. Phys. Lett.* **2018**, *691*, 307-313, doi:10.1016/j.cplett.2017.11.034.
Sicre, J. E.; Cobos, C. J. Thermochemistry of the higher chlorine oxides ClO_x (x = 3,4) and Cl_2O_x (x = 3 - 7). *J. Mol. Struct. (Theochem)* **2003**, *620*, 215-226, doi:10.1016/S0166-1280(02)00602-4.
Simmie, J. M. A database of formation enthalpies of nitrogen species by compound methods (CBS-QB3, CBS-APNO, G3, G4). *J. Phys. Chem. A* **2015**, *119*, 10511-10526, doi:10.1021/acs.jpca.5b06054.
Simmie, J. M.; Black, G.; Curran, H. J.; Hinde, J. P. Enthalpies of formation and bond dissociation energies of lower alkyl hydroperoxides and related hydroperoxy and alkoxy radicals. *J. Phys. Chem. A* **2008**, *112*, 5010-5016, doi:10.1021/jp711360z.
Simmie, J. M.; Metcalfe, W. K.; Curran, H. J. Ketene thermochemistry. *ChemPhysChem* **2005**, *9*, 700-702, doi:10.1002/cphc.200800003.
Skinner, H. A. The strengths of metal-to-carbon bonds. *Adv. Organometallic Chem.* **1964**, *2*, 49-114.
Skorobogatov, G. A.; Dymov, B. P.; Pogosyan, Y. I.; Khripun, V. K.; Tschuikow-Roux, E. Molecular, thermodynamic, and kinetic parameters of the free radical C_2H_5· in the gas phase. *Russ. J. General Chem.* **2003**, *73*, 75-84.
Soldi-Lose, H.; Schröder, D.; Schwarz, H. Gas-phase chemistry of alkylcarbonate anions and radicals. *Int. J. Mass Spec.* **2008**, *270*, 68-80, doi:10.1016/j.ijms.2007.12.007.
Song, Y.; Qian, X. M.; Lau, K. C.; Ng, C. Y.; Liu, J. B.; Chen, W. W. High-resolution energy-selected study of the reaction $CH_3H^+ \rightarrow CH_3^+ + X$: Accurate thermochemistry for the CH_3X/CH_3X^+ (X=Br, I) system. *J. Chem. Phys.* **2001**, *115*, 4095-4104, doi:10.1063/1.1391268.
Speranza, M. Structure, stability, and reactivity of cationic hydrogen trioxides and thermochemistry of their neutral analogs. A Fourier-transform ion cyclotron resonance study. *Inorg. Chem.* **1996**, *35*, 6140-6151, doi:10.1021/ic960549s.
Spiglanin, T. A.; Pery, R. A.; Chandler, D. W. Photodissociation studies of HNCO: Heat of formation and product branching ratios. *J. Phys. Chem.* **1986**, *90*, 6184-6189, doi:10.1021/j100281a025.
Stevens, W. R.; Bodi, A.; Baer, T. Dissociation dynamics of energy selected, propane, and *i*-$C_3H_7X^+$ ions by iPEPICO: Accurate heats of formation of *i*-$C_3H_7^+$, *i*-C_3H_7Cl, *i*-C_3H_7Br, and *i*-C_3H_7I. *J. Phys. Chem. A* **2010**, *114*, 11285-11291, doi:10.1021/jp104200h.
Stull, D. R.; Westrum, E. F.; Sinke, G. C. *The Chemical Thermodynamics of Organic Compounds*; John Wiley & Sons: New York, 1969.
Sudlow, K. P.; Woolf, A. A. Heats of formation of carbonyl, formyl and trifluoroacetyl fluorides. *J. Fluorine Chem.* **1999**, *96*, 141-145, doi:10.1016/S0022-1139(99)00067-6.
Sudolská, M.; Louis, F.; Černušák, I. Reactivity of CHI_3 with OH radicals: X-abstraction reaction pathways (X = H, I), atmospheric chemistry, and nuclear safety. *J. Phys. Chem. A* **2014**, *118*, 9512-9520, doi:10.1021/jp5051832.
Šulka, M.; Šulková, K.; Louis, F.; Neogrády, P.; Černušák, I. A theoretical study of the X-abstraction reactions (X = H, Br, or I) from CH_2IBr by OH radicals: Implications for atmospheric chemistry. *Z. Phys. Chem.* **2013**, *227*, 1337-1359, doi:10.1524/zpch.2013.0391.
Šulková, J.; Federič, J.; Louis, F.; Cantrel, L.; Demovič, L.; Černušák, I. Thermochemistry of small iodine species. *Phys. Scr.* **2013**, *88*, 058304, doi:10.1088/0031-8949/88/05/058304.
Suma, K.; Sumiyoshi, Y.; Endo, Y. Spectroscopic characterization of a molecule with a weak bond: The BrOO radical. *J. Chem. Phys.* **2005**, *123*, 024312, doi:10.1063/1.1953508.
Suma, K.; Sumiyoshi, Y.; Endo, Y.; Enami, S.; Aloisio, S.; Hashimoto, S.; Kawasaki, M.; Nishida, S.; Matsumi, Y. Equilibrium constants of the reaction of Cl with O_2 in the formation of ClOO. *J. Phys. Chem. A* **2004**, *108*, 8096-8099, doi:10.1021/jp049124e.
Sumathi, R.; Green, W. H. Oxygenate, oxyalkyl and alkoxcarbonyl thermochemistry and rates for hydrogen abstraction from oxygenates. *Phys. Chem. Chem. Phys.* **2003**, *5*, 3402-3417, doi:10.1039/b307050f.

Sun, H.; Bozzelli, J. W. Structures, rotational barriers, and thermochemical properties of β-chlorinated ethyl hydroperoxides. *J. Phys. Chem. A* **2003**, *107*, 1018-1024, doi:10.1021/jp022298g.
Sun, H.; Chen, C. J.; Bozzelli, J. W. Structures, intramolecular rotation barriers, and thermodynamic properties (enthalpies, entropies, and heat capacites) of chlorinated methyl hydroperoxides (CH_2ClOOH, $CHCl_2OOH$, and CCl_3OOH). *J. Phys. Chem. A* **2000**, *104*, 8270-8282, doi:10.1021/jp0013917.
Szakács, P.; Csontos, J.; Das, S.; Kállay, M. High-accuracy theoretical thermochemistry of atmospherically important nitrogen oxide derivatives. *J. Phys. Chem. A* **2011**, *115*, 3144-3153, doi:10.1021/jp112116x.
Szalay, P. G.; Tajti, A.; Stanton, J. F. Ab initio determination of the heat of formation of ketenyl (HCCO) and ethynyl (CCH) radicals. *Mol. Phys.* **2005**, *103*, 2159-2168, doi:10.1080/00268970500131124.
Tabor, D. P.; Harding, M. E.; Ichino, T.; Stanton, J. F. High-accuracy extrapolated ab initio thermochemistry of the vinyl, allyl, and vinoxy radicals. *J. Phys. Chem. A* **2012**, *116*, 7668-7676, doi:10.1021/jp302527n.
Talipov, M. R.; Timerghazin, Q. K.; Safiullin, R. L.; Khursan, S. L. No longer a complex, not yet a molecule: A challenging case of nitrosyl O-hydroxide, HOON. *J. Phys. Chem. A* **2013**, *117*, 679-685, doi:10.1021/jp3110858.
Tang, X.; Hou, Y.; Ng, C. Y.; Ruscic, B. Pulsed field-ionization photoelectron-photoion coincidence study of the process $N_2 + h\nu \rightarrow N^+ + B + e^-$: Bond dissociation energies of N_2 anad N_2^+. *J. Chem. Phys.* **2005**, *123*, 074330, doi:10.1063/1.1995699.
Tarczay, G.; Miller, T. A.; Czakó, G.; Császár, A. G. Accurate ab initio determination of spectroscopic and thermochemical properties of mono- and dichlorocharbenes. *Phys. Chem. Chem. Phys.* **2005**, *7*, 2881-2893, doi:10.1039/b506790a.
Tellinghuisen, J.; Tellinghuisen, P. C.; Davies, S. A.; Berwanger, P.; Viswanathan, K. S. B → X transitions in HgCI and HgI. *Appl. Phys. Lett.* **1982**, *41*, 789-791, doi:10.1063/1.93704.
Thanthiriwatte, K. S.; Vasiliu, M.; Dixon, D. A.; Christe, K. O. Structural and energetic properties of closed shell XF_n (X = Cl, Br, and I; n = 1−7) and XO_nF_m (X = Cl, Br, and I; n = 1−3; m = 0−6) molecules and ions leading to stability predictions for yet unknown compounds. *Inorg. Chem.* **2012**, *51*, 10966-10982, doi:10.1021/ic301438b.
Tian, Z.; Lis, L.; Kass, S. R. Carbon−hydrogen bond dissociation energies: The curious case of cyclopropene. *J. Org. Chem.* **2013**, *78*, 12650-12653, doi:10.1021/jo402263v.
Trogolo, D.; Arey, J. S. Benchmark thermochemistry of chloramines, bromamines, and bromochloramines: halogen oxidants stabilized by electron correlation. *Phys. Chem. Chem. Phys.* **2015**, *17*, 3584-3598, doi:10.1039/c4cp03987d.
Tsang, W. Heats of formation of organic free radicals by kinetic methods. In *Energetics of Free Radicals*; Simoes, J. A. M., Greenberg, A., Liebman, J. F., Eds.; Blackie Academic & Professional: London, 1996; pp 22-58.
Tschuikow-Roux, E.; Paddison, S. Bond dissociation energies and radical heats of formation in CH_3Cl, CH_2Cl_2, CH_3Br, CH_2Br_2, CH_2FCl, and $CHFCl_2$. *Int. J. Chem. Kinet.* **1987**, *19*, 15-24, doi:10.1002/kin.550190103.
Tucceri, M. E.; Badenes, M. P.; Cobos, C. J. Ab initio and density functional theory study of the enthalpies of formation of F_2SO_x and $FClSO_x$ (x=1, 2). *J. Fluorine Chem.* **2002**, *116*, 135-141, doi:10.1016/S0022-1139(02)00123-9.
Turnipseed, A. A.; Barone, S. B.; Ravishankara, A. R. Observation of CH_3S addition to O_2 in the gas phase. *J. Phys. Chem.* **1992**, *96*, 7502-7505, doi:10.1021/j100198a006.
van den Bergh, H.; Troe, J. Kinetic and thermodynamic properties of INO and INO_2 intermediate complexes in iodine recombination. *J. Chem. Phys.* **1976**, *64*, 736-742, doi:10.1063/1.432220.
Vasiliu, M.; Li, S. G.; Peterson, K. A.; Feller, D.; Gole, J. L.; Dixon, D. A. Structures and heats of formation of simple alkali metal compounds: Hydrides, chlorides, fluorides, hydroxides and oxides for Li, Na and K. *J. Phys. Chem. A* **2010**, *114*, 4272-4281, doi:10.1021/jp911735c.
Ventura, O. N.; Kieninger, M.; Denis, P. A. Density functional computational thermochemistry: Determination of the enthalpy of formation of methanethial-S,S-dioxide (sulfene). *J. Phys. Chem. A* **2003**, *107*, 518-521, doi:10.1021/jp021661g.
Verevkin, S. P.; Emel'yanenko, V. N.; Diky, V.; Muzny, C. D.; Chirico, R. D.; Frenkel, M. New group-contribution approach to thermochemical properties of organic compounds: Hydrocarbons and oxygen-containing compounds. *J. Phys. Chem. Ref. Data* **2013**, *42*, 033102, doi:10.1063/1.4815957.
Villano, S. M.; Eyet, N.; Wren, S. W.; Ellison, G. B.; Bierbaum, V. M.; Lineberger, W. C. Photoelectron spectroscopy and thermochemistry of the peroxyformate anion. *J. Phys. Chem. A* **2010**, *114*, 191-200, doi:10.1021/jp907569w.

Viskolcz, B.; Berces, T. Enthalpy of formation of selected carbonyl radicals from theory and comparison with experiment. *Phys. Chem. Chem. Phys.* **2000**, *2*, 5430-6436, doi:10.1039/b004548i.
Wagman, D. D.; Evans, W. H.; Parker, V. B.; Halow, I.; Bailey, S. M.; Schumm, R. H. Selected Values of Chemical Thermodynamic Properties. Tables for Elements 35 through 53 in the Standard Order of Arrangement. *NBS Technical Note 270-4* **1969**.
Wagman, D. D.; Evans, W. H.; Parker, V. B.; Schumm, R. H.; Halow, I.; Bailey, S. M.; Churney, K. L.; Nutall, R. L. The NBS tables of chemical thermodynamic properties. Selected values for inorganic and C_1 and C_2 organic substances in SI unites. *J. Phys. Chem. Ref. Data* **1982**, *11*, Suppl. No. 1, Erratum doi:10.1063/1.555845.
Walker, L. C. The enthalpy of reaction of sulfur and nitrogen trifluoride. *J. Phys. Chem.* **1967**, *71*, 361-363, doi:10.1021/j100861a023.
Wallington, T. J.; Hurley, M. D.; Shi, J.; Maricq, M. M.; Shested, J.; Nielsen, O. J.; Ellermann, T. A kinetic study of the reaction of fluorine atoms with CH_3F, CH_3Cl, CH_3Br, CF_2H_2, CO, CF_3H, CF_3CHCl_2, CF_3CH_2F, CHF_2CHF_2, CF_2ClCH_3, CHF_2CH_3, and CF_3CF_2H at 295 ± 2 K. *Int. J. Chem. Kinet.* **1993**, *25*, 651-665, doi:10.1002/kin.550250806.
Wang, L.; Liu, J. Y.; Li, Z. S.; Sun, C. C. Dual-level direct dynamics study on the reactions of SH (SD) with F_2. *Int. J. Chem. Kinet.* **2005**, *37*, 710-716, doi:10.1002/kin.20124.
Wayner, D. D. M.; Clark, K. B.; Rauk, A.; Yu, D.; Armstrong, D. A. C-H bond dissociation energies of alkyl amines: Radical structures and stabilization energies. *J. Am. Chem. Soc.* **1997**, *119*, 8925-8932, doi:10.1021/ja971365v.
Wenthold, P. G.; Squires, R. R. Gas-phase properties and reactivity of the acetate radical anion. Determination of the C-H bond strengths in acetic acid and acetate ion. *J. Am. Chem. Soc.* **1994**, *116*, 11890-11897, doi:10.1021/ja00105a032.
Wheeler, S. E.; Schaefer, H. F. Thermochemistry of the HOSO radical, a key intermediate in fossil fuel combustion. *J. Phys. Chem. A* **2009**, *113*, 6779-6788, doi:10.1021/jp9029387.
Wilcomb, B. E.; Bernstein, R. B. Dissociation energies of ground-state HgX molecules (X = I, Br, Cl) from analysis of vibrational level spacings. *J. Molec. Spectrosc.* **1976**, *62*, 442-448, doi: 10.1016/0022-2852(76)90282-4.
Wilmouth, D. M.; Hanisco, T. F.; Donahue, N. M.; Anderson, J. G. Fourier transform ultraviolet spectroscopy of the $A\ ^2\Pi_{3/2} \leftarrow X\ ^2\Pi_{3/2}$ trasnsition of BrO. *J. Phys. Chem. A* **1999**, *103*, 8935-8945, doi:10.1021/jp991651o.
Wu, E. C.; Rodgers, A. S. Thermochemistry of gas-phase equilibrium $CF_3CH_3 + I_2 = CF_3CH_2I + HI$. The carbon-hydrogen bond dissociation energy in 1,1,1-trifluoroethane and the heat of formation of the 2,2,2-trifuloroethyl radical. *J. Phys. Chem.* **1974**, *78*, 2315-2317, doi:10.1021/j150671a002.
Wu, E. C.; Rodgers, A. S. Kinetics of the gas phase reaction of pentafluoroethyl iodide with hydrogen iodide. Enthalpy of formation of the pentafluoroethyl radical and the pi bond dissociation energy in tetrafluoroethylene. *J. Am. Chem. Soc.* **1976**, *98*, 6112-6115, doi:10.1021/ja00436a007.
Yu, D.; Rauk, A.; Armstrong, D. A. Radicals and ions of formic and acetic acids: An ab initio study of the structures and gas and solution phase thermochemistry. *J. Chem. Soc. Perkin Trans 2* **1994**, 2207-2215, doi:10.1039/p29940002207.
Zhu, B.; Zeng, X.; Beckers, H.; Francisco, J. S.; Willner, H. The methylsulfonyloxyl radical, CH_3SO_3. In *Angew. Chem. Int. Ed.*, 2015; Vol. 54; pp 11404-11408.
Zhu, R. S.; Lin, M. C. *Ab initio* studies of ClO_x reactions. IV. Kinetics and mechanism for the self-reaction of ClO radicals. *J. Chem. Phys.* **2003**, *118*, 4094-4106, doi:10.1063/1.1540623.
Zhu, R. S.; Lin, M. C. Ab initio studies of ClO_x reactions. VII. Isomers of Cl_2O_3 and their roles in the ClO + OClO reaction. *J. Chem. Phys.* **2003**, *118*, 8645-8655, doi:10.1063/1.1565315.
Zou, P.; Derecskei-Kovacs, A.; North, S. W. Theoretical calculation of $ClONO_2$ and $BrONO_2$ bond dissociation energies. *J. Phys. Chem. A* **2003**, *107*, 888-896, doi:10.1021/jp021961y.